# *Syntheses of Peptides Related to the N-Terminal Structure of Corticotropin. I. Synthesis of Ser-Tyr-Ser-Met Sequence*

By Ken INOUYE and Hideo OTSUKA

(Received May 31, 1960)

The hypophyseal polypeptide hormones, the corticotropin and melanocyte-stimulating hormone (MSH), have a common amino acid sequence within their structures[1,2].

By Harris and Lerner[1,3] it has been shown that hog $\alpha$-MSH is an *N*-acetyltridecapeptide amide and its amino acid sequence, Ser-Tyr-Ser-Met-Glu-His-Phe-Arg-Try-Gly-Lys-Pro-Val, is identical with that occurring in the first tridecapeptide portion of corticotropin. This evidence affords a chemical basis for the intrinsic MSH activity[4,5] of corticotropin.

Considerably large fragments can be enzymatically or chemically removed from the carboxyl end of the molecule of corticotropin without loss of its biological activity[6]. While it has been reported that periodate oxidation of the *N*-terminal serine of corticotropin[7] or the cleavage of peptide bonds in the *N*-terminal Ser-Tyr-Ser segment of the molecule[6] results in complete depression of its ACTH activity, at the same time significant increase in the melanocyte expanding activity is observed[7].

The further detailed relationship between the two biological activities and the chemical structure must await the synthetic studies of active polypeptides.

Synthesis of *N*-terminal twenty sequence of corticotropin was done by Boissonnas et al. and the product exhibited a positive though limited ACTH activity[8]. Guttmann and Boissonnas[9] have recently synthesized the complete structure of $\alpha$-MSH and the synthetic hormone has been shown to possess the same properties as those of the natural hog $\alpha$-MSH. Hofmann et al. have reported that the blocked tridecapeptide amide, Cbz-Ser-Tyr-Ser-Met-Glu($NH_2$)-His-Phe-Arg-Try-Gly-($\varepsilon$-Tos)-Lys-Pro-Val-$NH_2$, has $0.8\times10^8$ MSH units per gram[10] and the replacement of the carbobenzoxy group with an acetyl group results in some twenty-five fold increase in its activity[11]. The substituted polypeptide sequence of $\beta$-MSH has also been synthesized by Schwyzer et al.[12]

Here we wish to write concerning a part of our studies of synthetic peptides corresponding to the amino acid sequence common to corticotropin and $\alpha$-MSH. The synthesis of Ser-Tyr-Ser-Met sequence will be described.

In the syntheses of serine-containing peptides we used *O*-benzylserine[13,14] as a starting material in place of serine to avoid unexpected side reactions which may be caused by the presence of the free hydroxyl group of the latter.

Carbobenzoxy-*O*-benzylseryltyrosine and -*O*-benzylserylmethionine methyl esters were obtained in good yields as compared with the corresponding serylpeptide derivatives[15,16], though as for the method of coupling, the anhydride procedure was different from the procedures used by the others.

The advantageous effect of *O*-benzylserine is much more remarkable in saponification of the peptide esters with alkali. It has been reported that the saponification of carbobenzoxyseryltyrosine methyl[16] or ethyl[15] ester gave only a 50 per cent yield of the desired product and the yield of carbobenzoxyserylmethionine was also significantly low (67%)[15]. However, we could derive carbobenzoxy-*O*-benzylseryltyrosine and -*O*-benzylserylmethionine and formyl-*O*-benzylserylmethionine in very high yields (near 90%) from the preceding methyl esters. The peptide bonds adjacent to the serine residues in corticotropin are sensitive to any alkali treatment[6] and Guttmann and

1) J. I. Harris and A. B. Lerner, *Nature*, **179**, 1346 (1957).
2) J. I. Harris, ibid., **184**, 167 (1959).
3) J. I. Harris, *Biochem. J.*, **71**, 451 (1959).
4) P. H. Bell, *J. Am. Chem. Soc.*, **76**, 5565 (1954); **78**, 5051 (1956).
5) H. B. F. Dixon, *Biochim. Biophys. Acta*, **19**, 392 (1956).
6) R. G. Shepherd, S. D. Willson, K. S. Howard, P. H. Bell, D. S. Davies, S. B. Davis, E. A. Eigner and N. E. Shakespeare, *J. Am. Chem. Soc.*, **78**, 5067 (1956).
7) H. B. F. Dixon, *Biochem. J.*, **62**, 25p (1956).
8) R. A. Boissonnas, St. Guttmann, J. -P. Waller and P. -A. Jaquenoud, *Experientia*, **12**, 446 (1956).
9) St. Guttmann and R. A. Boissonnas, *Helv. Chim. Acta*, **42**, 1257 (1959).
10) K. Hofmann, M. E. Woolner, H. Yajima, G. Spühler, T. A. Thompson and E. T. Schwartz, *J. Am. Chem. Soc.*, **80**, 6458 (1958).
11) K. Hofmann, H. Yajima and E. T. Schwartz, *Biochim. Biophys. Acta*, **36**, 252 (1959).
12) R. Schwyzer, H. Kappeler, B. Iselin, W. Rittel and H. Zuber, *Helv. Chim. Acta*, **42**, 1702 (1959).
13) K. Okawa and H. Tani, *J. Chem. Soc. Japan, Pure Chem. Sec.* (*Nippon Kagaku Zasshi*), **75**, 1199 (1954).
14) K. Okawa, This Bulletin, **29**, 486 (1956).
15) K. Hofmann, A. Jöhl, A. E. Furlenmeier and H. Kappeler, *J. Am. Chem. Soc.*, **79**, 1636 (1957).
16) St. Guttmann and R. A. Boissonnas, *Helv. Chim. Acta*, **41**, 1852 (1958).

Boissonnas[16] have, moreover, shown the fact that the saponification of serine peptide esters is accompanied by the cleavage of peptide bond at the carboxyl side of serine residue. However, we could not observe such a fact in regard to the *O*-benzylserine peptides.

On removal of carbobenzoxy and *O*-benzyl groups from carbobenzoxy-*O*-benzylserylmethionine methyl ester by hydrobromic acid/acetic acid or catalytic hydrogenation we failed to obtain the desired dipeptide ester, presumably because of the instability of the thioether bond. Sheehan and Yang[17] have shown that a formyl group, which is easily removed by mild acid solvolysis, can be used on peptide syntheses as an amino protecting function in conjugation with the carbodiimide procedure without racemization of the products. Following this procedure, formyl-*O*-benzylserine and methionine methyl ester were coupled with *N*, *N'*-dicyclohexylcarbodiimide (DCCI) to give formyl-*O*-benzylserylmethionine methyl ester which could be deformylated to *O*-benzylserylmethionine methyl ester without any difficulties.

Coupling of carbobenzoxy-*O*-benzylseryltyrosine with *O*-benzylserylmethionine methyl ester by DCCI yielded almost quantitatively the acyltetrapeptide ester, carbobenzoxy-*O*-benzylseryltyrosyl-*O*-benzylserylmethionine methyl ester in crystalline form.

## Experimental

All amino acids used are of L-configuration. The melting point was determined in a capillary tube in a sulfuric acid bath and not corrected.

**O-Benzylserine Methyl Ester Hydrochloride.**—To 20 ml. of anhydrous methanol previously cooled below −10°C, was added dropwise 1.33 ml. (0.0184 mol.) of thionylchloride and then 3 g. (0.0154 mol.) of *O*-benzylserine was introduced[13,14]. The mixture was stirred for 1.5 hr. at room temperature and then allowed to stand overnight. The resulting clear solution was evaporated under reduced pressure. The residue was crystallized from acetone-ether to give 3.44 g. (91%). Recrystallization from methanol-ether yielded needles, m. p. 141.5~142°C with decomposition.

Found: N, 5.86; Cl, 14.41. Calcd. for $C_{11}H_{16}O_3 \cdot NCl$: N, 5.69; Cl, 14.43%.

***N*-Formyl-*O*-benzylserine.**—This was prepared after the usual procedure for optically active formylamino acids of Sheehan and Yang[17]. 1.95 g. of *O*-benzylserine was formylated and the product was recrystallized from water to give 1.77 g., m. p. 137.5~138.5°C, $[\alpha]_D^{26} = +52.9 \pm 1°$ (*c* 2.613 in ethanol).

Found: C, 59.31; H, 6.03; N, 6.39. Calcd. for $C_{11}H_{13}O_4N$: C, 59.3; H, 5.88; N, 6.29%.

***N*-Carbobenzoxy-*O*-benzylseryltyrosine Methyl Ester.**—To a solution of 8.23 g. (0.025 mol.) of *N*-carbobenzoxy-*O*-benzylserine[18] (m. p. 100.5~101°C, $[\alpha]_D^{22} = +12.0 \pm 2°$ (*c* 2.448 in acetic acid)) in 75 ml. of tetrahydrofuran/dioxane (1 : 4) were added 6.56 ml. (0.0275 mol.) of tri-*n*-butylamine and 2.63 ml. (0.0275 mol.) of ethylchloroformate at −5°C. After 15 min. a solution of tyrosine methyl ester (prepared from 6.37 g. (0.0275 mol.) of the hydrochloride[19] and 4.23 ml. (0.030 mol.) of triethylamine) in 8 ml. water and 32 ml. dioxane was introduced. The reaction mixture was stirred at room temperature for 4 hr. and evaporated under reduced pressure. The residue dissolved in 150 ml. of ethyl acetate was successively washed with 1N hydrochloric acid, water, 5% sodium bicarbonate and water and dried over sodium sulfate. The solution was evaporated to a syrupy residue which was crystallized from methanol-ethyl acetate-petroleum ether, 12.3 g. (97.2%), m.p. 108~111.5°C. Recrystallization from ethyl acetate-petroleum ether yielded 10.2 g. (80.6%), m. p. 112~114.5°C, $[\alpha]_D^{19} = +14.6 \pm 2°$ (*c* 3.068 in 99% ethanol). (lit.[18] m. p. 111~112°C, $[\alpha]_D^{15} = +15.5°$ (*c* 2.84 in 99% ethanol).

Found: C, 66.32; H, 6.13; N, 5.41. Calcd. for $C_{28}H_{39}O_7N_2$: C, 66.3; H, 5.97; N, 5.53%.

***N*-Carbobenzoxy-*O*-benzylseryltyrosine.**—2.533 g. (0.005 mol.) of *N*-carbobenzoxy-*O*-benzylseryltyrosine methyl ester was saponified in 12.5 ml. of methanol with 5.0 ml. (0.01 mol.) of 2N Sodium hydroxide at room temperature for one hour, yielding 2.34 g. (95.0%). Recrystallization from ethyl acetate-petroleum ether gave 2.20 g. (89.5%), m. p. 158.5~159.5°C, $[\alpha]_D^{23} = +39.4 \pm 1°$ (*c* 2.086 in ethanol).

Found: C, 65.38; H, 5.88; N, 5.72. Calcd. for $C_{27}H_{28}O_7N_2$: C, 65.6; H, 5.74; N, 5.70%.

***N*-Carbobenzoxy-*O*-benzylserylmethionine Methyl Ester.**—4.12 g. (0.0125 mol.) of *N*-carbobenzoxy-*O*-benzylserine and methionine methyl ester (prepared from 2.80 g. (0.014 mol.) of the hydrochloride) were coupled in a tetrahydrofuran/dioxane solution almost exactly as in the case of *N*-carbobenzoxy-*O*-benzylseryltyrosine methyl ester. Yield 5.1 g. (86%), m. p. 69.0~70.5°C. Recrystallization for analysis from ethyl acetate-petroleum ether gave a sample with m. p. 69.5~71°C.

Found: C, 60.56; H, 6.48; N, 5.76. Calcd. for $C_{24}H_{30}O_6N_2S$: C, 60.8; H, 6.38; N, 5.91%.

***N*-Carbobenzoxy-*O*-benzylserylmethionine.**—3.56 g. (0.0075 mol.) of *N*-carbobenzoxy-*O*-benzylserylmethionine methyl ester was saponified in 18 ml. of methanol with 4.2 ml. of 2N sodium hydroxide at room temperature for 30 min. The product was recrystallized from ethyl acetate-ether to yield 3.17 g. (92%), m. p. 152~152.5°C.

Found: N, 5.95; S, 7.00. Calcd. for $C_{23}H_{28}O_6 \cdot N_2S$: N, 6.09; S, 6.97%.

***N*-Formyl-*O*-benzylserylmethionine Methyl Ester.**—To a suspension of 6.59 g. (0.033 mol.) of methionine methyl ester hydrochloride in 50 ml. of ether was added 20 ml. of ice-cold 50% potassium carbonate. The mixture was shaken at 0°C until the solid disappeared. The ether layer which separated was dried over sodium sulfate at 0°C and concentrated

17) J. C. Sheehan and D-D. H. Yang, *J. Am. Chem. Soc.*, **80**, 1154 (1958).

18) K. Okawa, This Bulletin, **29**, 488 (1956).

19) R. A. Boissonnas, St. Guttmann, P. -A. Jaquenoud and J. -P. Waller, *Helv. Chim. Acta*, **38**, 1491 (1955).

in vacuo to an oil. This oily residue was dissolved in 50 ml. of methylene chloride and the solution was mixed with a suspension of 6.69 g. (0.03 mol.) of *N*-formyl-*O*-benzylserine in 50 ml. of methylene chloride. To the resulting clear solution was added at 0°C 6.20 g. (0.03 mol.) of dicyclohexylcarbodiimide dissolved in 15 ml. of methylene chloride. The reaction mixture was stirred at room temperature for 5 hr. and then refrigerated. The separated dicyclohexylurea was collected by filtration, yielding 6.45 g. (95.8%). The filtrate was cooled in ice, washed with ice-cold 1 N hydrochloric acid, ice-water, 5% sodium bicarbonate and finally with water and dried over sodium sulfate. The concentration of the solution gave a syrupy residue which was crystallized from tetrahydrofuran-ether to yield colored needles, 7.55 g., m. p. 73~76°C. An additional 1.0 g. of crystal was obtained from the mother liquor. Total yield, 8.55 g. (77.4%). These crops, reddish orange in color, were combined and dissolved in ethyl acetate and chromatographed on 125 g. of aluminum oxide. Elution with the same solvent gave colorless fractions which were combined and concentrated in vacuo. Crystallization of the resulting syrup from ethyl acetate ether yielded colorless and odorless needles, 7.025 g. (63.5%), m. p. 78.5~79.5°C, $[\alpha]_D^{25} = -23.2 \pm 1°$ (*c* 2.08 in methanol).

Found: C, 55.84; H, 6.84; N, 7.42; S, 8.69. Calcd. for $C_{17}H_{24}O_5N_2S$: C, 55.5; H, 6.57; N, 7.61; S, 8.70%.

***N*-Formyl-*O*-benzylserylmethionine.** — 1.54 g. (0.0042 mol.) of *N*-formyl-*O*-benzylserylmethionine methyl ester was saponified in 11 ml. of dioxane with an equivalent amount of 1 N sodium hydroxide at room temperature for one hour. The resulting solution was diluted with ice-water to 30 ml. and neutralized with ice-cold 1 N hydrochloric acid to a separate crystalline precipitate, 1.30 g. (87.8%), m. p. 161~162°C. Recrystallization from ethanol-water gave 1.19 g. of needles, m. p. 163°C, $[\alpha]_D^{16} = -8.8 \pm 2°$ (*c* 2.095 in methanol).

Found: C, 54.49; H, 6.41; N, 7.96; S, 9.13. Calcd. for $C_{16}H_{22}O_5N_2S$: C, 54.20; H, 6.24; N, 7.88; S, 9.03%.

***O*-Benzylserylmethionine Methyl Ester.**—4.42 g. (0.012 mol.) of formyl-*O*-benzylserylmethionine methyl ester was dissolved in 40 ml. of *N*-methanolic hydrochloric acid and stored at room temperature overnight. After most of the methanol had been removed in vacuo the resulting colored syrup was dissolved in 40 ml. of water and washed several times with ethyl acetate. The colorless aqueous solution was concentrated in vacuo to a small volume and mixed with 15 ml. of 50% potassium carbonate and 40 ml. of ether at 0°C. The ether layer was separated and the alkaline phase was twice extracted with ether. The combined ether solution was dried over sodium sulfate at 0°C and concentrated to give a colorless and clear oil, 3.95 g. (97%). A sample was chromatographed on paper in the system of *n*-butanol-acetic acid-water (2 : 1 : 2) and only one spot positive to both ninhydrin and $PtI_6^{2-}$ reagent[20] was detected.

***N*-Carbobenzoxy-*O*-benzylseryltyrosyl-*O*-benzylserylmethionine Methyl Ester.**—4.925 g. (0.01 mol.) of *N*-carbobenzoxy-*O*-benzylseryltyrosine and 3.95 g. of *O*-benzylserylmethionine methyl ester were dissolved in 80 ml. of methylene chloride. To this birefringent solution was added 2.063 g. (0.01 mol.) of dicyclohexylcarbodiimide in 20 ml. of methylene chloride at 0°C and the reaction mixture was stirred at room temperature. The birefringence of flow almost completely disappeared in about 10 min. as the crystalline dicyclohexylurea separated. After the stirring had been continued for 3 hr. the mixture was stored at room temperature overnight to turn into a semi-solid state. It was returned to a solution by gentle warming at the boiling point and the insoluble urea was filtered off. The filtrate was concentrated to dryness in vacuo and the resulting solid was recrystallized from ethyl acetate-ether to yield 8.03 g. (98.7%), m. p. 163~167°C. Repeated recrystallization from methylene chloride-ether afforded 7.00 g. (86%), m. p. 166~169°C. A sample for analyses was further recrystallized from methanol to needles, m. p. 171~173°C, $[\alpha]_D^{20} = -12.9 \pm 0.1°$ (*c* 1.986 in methanol), $[\alpha]_D^{26} = -16.1 \pm 1°$ (*c* 2.008 in dimethylformamide).

Found: C, 63.54; H, 6.34; N, 6.95; S. 3.87. Calcd. for $C_{43}H_{50}O_{10}N_4S$: C, 63.5; H, 6.19; N, 6.88; S, 3.84%.

## Summary

1. Carbobenzoxy-*O*-benzylseryltyrosyl-*O*-benzylserylmethionine methyl ester, which has the *N*-terminal tetrapeptide sequence of corticotropin and $\alpha$-MSH, has been synthesized.

2. It has been shown that the *O*-benzylseryl peptide bond is very stable to an alkali treatment.

3. Syntheses of the relating serine peptide derivatives have been described.

The authors are indebted to Mr. Makoto Kanayama for valuable technical assistance.

*Division of Biochemistry*
*Research Laboratory of*
*Shionogi & Co., Ltd.*
*Imafuku, Amagasaki*

20) R. J. Block, E. L. Durrum and G. Zweig, "A Manual of Paper Chromatography and Paper Electrophoresis", Academic Press Inc., Publishers, New York (1955), p. 94.

# *Syntheses of Peptides Related to the N-Terminal Structure of Corticotropin. II. Synthesis of Gly-Lys-Pro-Val Sequence*

By Ken INOUYE and Hideo OTSUKA

(Received June 27, 1960)

The sequence, Gly-Lys-Pro-Val is found at positions 10 to 13 in corticotropin and α-MSH[1]. Boissonnas et al.[2,3] synthesized this sequence in the form of tritylglycyl-ε-carbobenzoxylysylprolylvaline methyl ester from the preceding intermediates, tritylglycyl-ε-carbobenzoxylysine (methyl ester) and (carbobenzoxy-)prolylvaline methyl ester, none of which have yet been obtained in any crystalline states.

In connection with our synthetic studies on the *N*-terminal structure of corticotropin we have now obtained this tetrapeptide sequence in another form, formylglycyl-ε-carbobenzoxylysylprolylvaline benzyl ester.

Formylglycine and ε-carbobenzoxylysine methyl ester were coupled in methylene chloride by the use of *N, N'*-dicyclohexylcarbodiimide to give formylglycyl-ε-carbobenzoxylysine methyl ester which was converted by saponification into formylglycyl-ε-carbobenzoxylysine. Both of these dipeptide derivatives were obtained in good yields and in crystalline states. When the coupling was done in dimethylformamide solution the yield of the desired product was less than 30 per cent and in addition a side product, formylglycyl-*N, N'*-dicyclohexylurea was isolated. The mixed acid anhydride procedure also notably lowered the yield and purity of the product.

Carbobenzoxypropoline was condensed with valine benzyl ester by the mixed anhydride method to carbobenzoxyprolylvaline benzyl ester which was easily crystallized. This was then decarbobenzoxylated with hydrogen bromide in glacial acetic acid and the resulting ester hydrobromide was treated with potassium carbonate to the free base.

Coupling of formylglycyl-ε-carbobenzoxylysine with prolylvaline benzyl ester by *N, N'*-dicyclohexylcarbodiimide yielded the tetrapeptide, formylglycyl-ε-carbobenzoxylysylprolylvaline benzyl ester as an amorphous solid. This product was negative to the ninhydrin test and after deformylation with *N*-methanolic hydrochloric acid gave only one spot on the paperchromatogram sprayed with ninhydrin. The complete acid hydrolysate was subjected to the quantitative amino acid analysis and was shown to be composed of glycine, lysine proline and valine in the molar ratio as expected.

## Experimental

All amino acids used are of L-configuration. The melting point was determined in a capillary tube in a sulfuric acid bath and not corrected.

**Formylglycine.**—This was prepared after the usual procedure for DL-formylamino acids of Sheehan and Yang[4]. 3.75 g. of glycine was formylated and the product was recrystallized from water to give 4.20 g. (81.6%), m. p. 149°C with decomposition.

Found: C, 35.12; H, 4.99; N, 13.35. Calcd. for $C_3H_5O_3N$: C, 35.0; H, 4.89; N, 13.6%.

**Formylglycyl-ε-carbobenzoxylysine Methyl Ester.**—To a suspension of 9.10 g. (0.0275 mol.) of ε-carbobenzoxylysine methyl ester hydrochloride[5] in ether was added 23 ml. of ice-cold 50% potassium carbonate. The mixture was shaken and the organic layer separated was dried over sodium sulfate at 0°C. After removal of the solvent in vacuo the oily residue was dissolved in 115 ml. of methylene chloride and 2.58 g. (0.025 mol.) of formylglycine was added. As soon as most of the formylglycine had dissolved, 5.16 g. (0.025 mol.) of *N, N'*-dicyclohexylcarbodiimide in 25 ml. of methylene chloride was quickly added. The mixture was stirred for five hours and allowed to stand overnight at room temperature and refrigerated. The separated dicyclohexylurea was collected by filtration, yielding 5.45 g. (97.2%). The filtrate was cooled at 0°C, washed successively with ice-cold 1 N hydrochloric acid, water, 5% sodium bicarbonate and water and dried over sodium sulfate. Evaporation of the solvent in vacuo gave a clear syrup which was crystallized from methylene chloride-ether. Yield 8.93 g. (94.3 %). This was recrystallized from ethyl acetate-ether to give 8.40 g. (88.7%), m. p. 76~78°C, $[\alpha]_D^{24} = -10.3 \pm 2°$ (*c* 2.901 in methanol).

Found: C, 57.02; H, 6.81; N, 10.89. Calcd. for $C_{18}H_{25}O_6N_3$: C, 57.1; H, 6.60; N, 11.0%.

When dimethylformamide was used as a solvent for this coupling reaction there was obtained, in

1) See the References of the preceding paper of this work. This Bulletin, **34**, 1 (1961).

2) R. A. Boissonnas, St. Guttmann, J. -P. Waller and P. -A. Jaquenoud, *Experientia*, **12**, 446 (1956).

3) R. A. Boissonnas, St. Guttmann, R. L. Huguenin, P. -A. Jaquenoud and Ed. Sandrin, *Helv. Chim. Acta*, **41**, 1867 (1958).

4) J. C. Sheehan and D-D. H. Yang, *J. Am. Chem. Soc.*, **80**, 1154 (1958).

5) M. Bergmann, L. Zervas and W. F. Ross, *J. Biol. Chem.*, **111**, 245 (1935).

addition to the desired peptide (in a 30% yield), a side product, formylglycyl-*N*,*N'*-dicyclohexylurea, m. p. 164.5~165.5°C.

Found: C, 62.46; H, 8.97; N, 13.69. Calcd. for $C_{16}H_{27}O_3N_3$: C, 62.2; H, 8.81; N, 13.6%.

**Formylglycyl-ε-carbobenzoxylysine.**—To a solution of 3.79 g. (0.01 mol.) of formylglycyl-ε-carbobenzoxylysine methyl ester in 27.5 ml. of dioxane was added 11 ml. of 1 N sodium hydroxide and the mixture was stirred at room temperature for one hour. After removal of a slight amount of insoluble precipitates the solution was diluted with water to about 80 ml., neutralized with 11 ml. of ice-cold 1 N hydrochloric acid and concentrated to about 25 ml. under reduced pressure. The concentrate was stored at 0°C overnight to complete the separation of crystals, 3.47 g. (95.1%). Recrystallization from water gave 3.28 g. (89.8%), m. p. 144~146°C, $[\alpha]_D^{24} = +13.1 \pm 0.2°$ (*c* 1.358 in methanol).

Found: C, 56.27; H, 6.33; N, 11.56. Calcd. for $C_{17}H_{23}O_6N_3$: C, 56.0; H, 6.35; N, 11.5%.

**Carbobenzoxyproline**[6]. — 4.6 g. (0.04 mol.) of proline was carbobenzoxylated with 8 g. of benzylchloroformate in 30 ml. of 2 N sodium hydroxide at 0°C. When the reaction was over the solution was washed with ether to remove an excess of benzylchloroformate and acidified. The product was taken up into ethyl acetate and the extract was shaken with 5% sodium bicarbonate. The aqueous solution was acidified and reextracted with ethyl acetate. The organic extract was dried over sodium sulfate and concentrated in vacuo to a syrup which was crystallized from carbon tetrachloride-petroleum ether (1 : 2) to give 9.47 g. (95.3%), m. p. 75~78°C. Recrystallization from the same solvent afforded 9.30 g., m. p. 76~78°C, $[\alpha]_D^{29} = -57.7 \pm 2°$ (*c* 0.975 in glacial acetic acid) (in lit.[6], m. p. 76~77°C, $[\alpha]_D^{20} = -61.7°$ (*c* 5.3 in glacial acetic acid).

Found: C, 62.98; H, 6.05; N, 5.89. Calcd. for $C_{13}H_{15}O_4N$: C, 62.75; H, 6.08; N, 5.63%.

**Valine Benzyl Ester Hydrochloride.**—A mixture of 4 g. of valine and 10 g. of *p*-toluenesulfonic acid monohydrate in 40 ml. of benzyl alcohol was stirred on an oil bath at 100°C (internal temperature). To this solution were added 40 ml. portions of carbon tetrachloride at one hour intervals and distilled out from a side-arm. After 8 hr. the remaining carbon tetrachloride was completely removed under reduced pressure and the crude ester *p*-toluenesulfonate was precipitated with the addition of ether, 10.0 g., m. p. 157~159°C. 10.0 g. of the crystal obtained above was suspended in 150 ml. of ether and mixed with 40 ml. of ice-cold 50% potassium carbonate. The insoluble precipitate was filtered off and the ether layer was dried over sodium sulfate at 0°C. Dry hydrogen chloride gas was bubbled into this ether solution to separate the desired ester hydrochloride, 6.3 g., m. p. 137~139.5°C. Recrystallization from chloroform-ether afforded 6.1 g., m. p. 139~141°C, $[\alpha]_D^{29} = -12.7 \pm 4°$ (*c* 0.495 in 0.1 N hydrochloric acid).

Found: N, 5.76; Cl, 14.50. Calcd. for $C_{12}H_{18}O_2NCl$: N, 5.75; Cl, 14.60%.

6) A. Berger, J. Kurtz and E. Katchalski, *J. Am. Chem. Soc.*, **76**, 5552 (1954).

**Carbobenzoxyprolylvaline Benzyl Ester.**—To a mixture of 2.49 g. (0.01 mol.) of carbobenzoxyproline and 2.39 ml. (0.01 mol.) of tri-*n*-butylamine in 10 ml. of tetrahydrofuran was added 0.96 ml. (0.01 mol.) of ethylchloroformate at −10°C. After 15 min. a solution of 2.44 g. (0.01 mol.) of valine benzyl ester hydrochloride and 2.39 ml. (0.01 mol.) of tri-*n*-butylamine in 10 ml. of tetrahydrofuran was introduced and the reaction mixture was then stirred at room temperature for 5 hr. and concentrated under reduced pressure. The syrupy residue was dissolved in 35 ml. of ethyl acetate, successively washed with 1 N hydrochloric acid, 15% sodium chloride, 5% sodium bicarbonate, and with 15% sodium chloride, and dried over sodium sulfate. The ethyl acetate solution was concentrated to about 10 ml. in vacuo and to this was added petroleum ether to separate an oily precipitate which was soon crystallized in needles, 4.0 g. (91.3%), m. p. 87~91°C. Recrystallization from the same solvent gave thin needles, m. p. 91~92°C, $[\alpha]_D^{29} = -78.6 \pm 1°$ (*c* 1.749 in methanol).

Found: C, 68.40; H, 6.96; N, 6.37. Calcd. for $C_{25}H_{30}O_5N_2$: C, 68.4; H, 6.90; N, 6.39%.

**Prolylvaline Benzyl Ester.**—2.63 g. (0.006 mol.) of carbobenzoxyprolylvaline benzyl ester was dissolved in 15 ml. of 21.2% (w/w) hydromromic acid/glacial acetic acid and the mixture was allowed to stand at room temperature for 50 min. at the end of which time about 80 ml. of anhydrous ether was added. The supernatant was decanted and an oily residue was dissolved in 10 ml. of water and washed twice with ether. A small aliquot of this aqueous solution was chromatographed on paper in the system of *n*-butanol-acetic acid-water (4 : 1 : 2) and there were detected two components which gave yellow spots with ninhydrin. The minor component with the lower $R_f$ value is possibly due to prolylvaline, and it may be found that the benzyl ester is cleaved to some extent under the conditions used, but no other side reactions take place.

The aqueous solution of the crude ester hydrobromide was then concentrated to a small volume in vacuo and shaken with 20 ml. of ether and 10 ml. of 50% potassium carbonate at −10°C. The aqueous phase was extracted with additional ether. The combined ether extract was dried over sodium sulfate at 0°C and evaporated in vacuo to an oil, 1.47 g. which was directly used for the following coupling reaction.

**Formylglycyl-ε-carbobenzoxylysylprolylvaline Benzyl Ester.**—The prolylvaline benzyl ester obtained above was dissolved in 30 ml. of methylene chloride and 1.28 g. (0.0035 mol.) of formylglycyl-ε-carbobenzoxylysine was adedd. The mixture was stirred at 0°C to give a homogeneous but somewhat cloudy solution in 15 min. To this solution was then added 0.723 g. (0.0035 mol.) of *N*,*N'*-dicyclohexylcarbodiimide and the reaction mixture was stirred at room temperature for five hours and allowed to stand overnight at 4°C. Separated dicyclohexylurea was removed by filtration, 0.739 g. (94.3%) and the filtrate was concentrated in vacuo. A syrupy residue was dissolved in ethyl acetate and washed with ice-cold 1 N hydrochloric acid, water, 5% sodium bicarbonate and finally with water and

dried over sodium sulfate. Concentration of the ethyl acetate solution in vacuo gave a foamy residue which was dried over phosphorus pentoxide at room temperature in high vacuum to afford 2.22 g. (97.5%) as colorless powder, $[\alpha]_D^{18} = -62.2 \pm 0.1°$ (*c* 2.505 in methanol).

Found: C, 62.13; H, 7.43; N, 10.54. Calcd. for $C_{34}H_{45}O_8N_5$: C, 62.7; H, 6.97; N, 10.7%.

This product gave a negative ninhydrin test and after treatment with 1N methanolic hydrochloric acid for 16 hr. only one spot[7] was visible on a paper-chromatogram which was developed in *n*-butanol-acetic acid-water (4 : 1 : 2) and sprayed with ninhydrin.

A sample of the tetrapeptide derivative was hydrolyzed with 6N hydrochloric acid at 100°C for 20 hr. and the hydrolysate was subjected to quantitative amino acid analysis by the method of Levy[8]. It was found that the product had a composition of Gly/Lys/Pro/Val in a molar ratio of 1.0/1.1/0.9/1.1.

7) The color of this spot changed with time from yellow to purple. Such a phenomenon has often been observed in glycylpeptides (K. Narita, *J. Chem. Soc. Japan, Pure Chem. Sec.* (*Nippon Kagaku Zasshi*), **75**, 487 (1954)).

## Summary

Formylglycyl-ε-carbobenzoxylysylprolylvaline benzyl ester, which has a sequence occurring in corticotropin and α-MSH, has been synthesized.

The authors are indebted to Mr. Makoto Kanayama for valuable technical assistance.

*Division of Biochemistry*
*Research Laboratory of*
*Shionogi & Co., Ltd.*
*Imafuku, Amagasaki*

8) A. L. Levy, *Nature*, **174**, 126 (1954).

# *Calculation on the Electronic States of the Acrolein Molecule by the Semi-Empirical Molecular Orbital Method*

By Kōzō Inuzuka

(Received May 31, 1960)

It is known that the semi-empirical molecular orbital method proposed by Pariser and Parr[1] gives good agreement with observation for the $\pi-\pi^*$ transitions of conjugated hydrocarbons and heteromolecules. Anno et al.[2-4] used the Pariser-Parr method to calculate the electronic state energies of some molecules containing C=O and N atoms, obtaining reasonably good agreement between calculated and observed values. Eastwood and Snow[5] have carried out a detailed vibrational analysis for the $n-\pi^*$ absorption spectrum of acrolein, while the experiment in vacuum ultraviolet region was done by Walsh[6]. In a previous paper[7] we were not certain whether or not the very weak band at 24647 $cm^{-1}$ in acrolein spectrum was due to a singlet-triplet transition. In order to get some information about the electronic state energies of the acrolein molecule, we calculated the electronic states of acrolein by the Pariser-Parr method which is expected also to yield successful results for the electronic state energies of some molecules exhibiting $n-\pi^*$ transitions.

## Calculation and Results

The calculation of the electronic state energies of acrolein was done with the semi-empirical method proposed by the previous authors[1-3]. The $\pi$-MO's take in this paper are

$$\phi_1=1/2(\chi_1^O+\chi_2^C+\chi_3^C+\chi_4^C)$$
$$\phi_2=1/2(\chi_1^O+\chi_2^C-\chi_3^C-\chi_4^C)$$
$$\phi_3=1/2(\chi_1^O-\chi_2^C-\chi_3^C+\chi_4^C)$$
$$\phi_4=1/2(\chi_1^O-\chi_2^C+\chi_3^C-\chi_4^C)$$

where $\chi_1^O$, $\chi_2^C$, $\chi_3^C$ and $\chi_4^C$ are $2p\pi$AO's of the oxygen and carbon atoms.

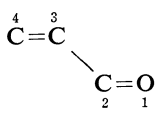
In addition to the above orbitals the acrolein molecule has a nonbonding orbital which can approximately be represented as follows:

$$\phi_n=\chi_n^O$$

$\chi_n^O$ being the $2p\pi$AO of the oxygen atom, the nodal plane of which is perpendicular to the

1) R. Pariser and R. G. Parr, *J. Chem. Phys.*, **21**, 466, 767 (1953).
2) T. Anno, I. Matubara and A. Sadō, This Bulletin, **30**, 168 (1957).
3) T. Anno, I. Matubara and A. Sadō, *J. Chem. Phys.*, **26**, 967 (1957).
4) T. Anno and A. Sadō, ibid., **26**, 1759 (1957).
5) E. Eastwood and C. P. Snow, *Proc. Roy. Soc.*, **149A**, 446 (1935).
6) A. D. Walsh, *Trans. Faraday Soc.*, **41**, 498 (1945).
7) K. Inuzuka, This Bulletin, **33**, 678 (1960).

molecular plane and contains the CO axis. The electron diffraction study of the acrolein molecule in the ground electronic state[8] shows that it is planar, having the following bond lengths and bond angles



$r_{12}=1.21\pm0.02$ Å
$r_{23}=1.46\pm0.03$ Å
$r_{34}=1.36\pm0.02$ Å
$\angle\gamma_{123}=\angle\gamma_{234}=120\pm3°$

Since the molecule belongs to the point group Cs, all the transition are symmetry-allowed. The energy integrals which appear in this calculation were evaluated according to the equation derived by Roothaan[9] and by Anno et al.[2] for the case of $r>2.80$ Å and of $r<2.80$ Å, respectively. We used Kon's formula[10] for the conculation of core integral $\beta_{CO}$ between carbon and oxygen atoms, and the Pariser-Parr formula for $\beta_{CC}$ between carbon and carbon atoms. For the evaluation of core integrals the Coulomb penetration integrals between next-neighboring neutral atoms were taken into consideration, and since we restricted the calculation of energy state up to 10 eV., singly and doubly excited electronic configurations[11] were taken in the calculation of energies for the excited electronic state. Since it is known that the calculation of energy state in $\pi-\pi^*$ transition usually results in a good agreement with the observed value without configuration interaction[12], we did not include the configuration interaction. On the other hand, as for $n-\pi^*$ transition the configuration interaction was taken into account but all the configurations more than 10 eV. higher than the ground configuration were neglected. Even for the configurations considered, we imposed the condition to reduce the order of the C. I. matrix: $(H_{ij}/H_{ii}-H_{jj})^2>1/10$, where $H_{ij}$ is the interaction matrix element between the configurations i and j. Neglected configurations within the 10 eV. energy range were taken into account by the second order perturbation theory. Calculated energy values are shown in Table I. From this result it is seen that in acrolein the $(n, \pi^*)$ triplet state is the lowest excited electronic state.

TABLE I. TRANSITION ENERGIES OF $n-\pi^*$ AND $\pi-\pi^*$ TRANSITIONS OF ACROLEIN MOLECULE

| Orbital jump | Electronic transition | Transition energy no C.I. eV. | Transition energy including C.I. eV. | Experimental eV. |
|---|---|---|---|---|
| $n-\pi_3$ | $^3A'\leftarrow{}^1A''$ | 5.55 | 2.85 | |
| $n-\pi_3$ | $^1A'\leftarrow{}^1A''$ | 5.98 | 3.85 | 3.71 |
| $n-\pi_4$ | $^3A'\leftarrow{}^1A''$ | 7.23 | 6.00 | |
| $n-\pi_4$ | $^1A'\leftarrow{}^1A''$ | 7.66 | 6.53 | |
| $\pi_2, n-\pi_3$, $\pi_3$ | $^3A'\leftarrow{}^1A''$ | 10.68 | 7.86 | |
| $\pi_2, n-\pi_3$, $\pi_3$ | $^1A'\leftarrow{}^1A''$ | 11.11 | 8.36 | |
| $\pi_2-\pi_3$ | $^3A'\leftarrow{}^1A'$ | 4.17 | | |
| $\pi_2-\pi_3$ | $^1A'\leftarrow{}^1A'$ | 6.08 | | 5.96 |
| $\pi_2-\pi_4$, $\pi_1-\pi_3$ | $^3A'\leftarrow{}^1A'$ | 5.85 | | |
| $\pi_2-\pi_4$, $\pi_2-\pi_3$ | $^1A'\leftarrow{}^1A'$ | 7.76 | | |
| $\pi_1-\pi_4$ | $^3A'\leftarrow{}^1A'$ | 7.53 | | |
| $\pi_1-\pi_4$ | $^1A'\leftarrow{}^1A'$ | 9.44 | | |

## Discussion

Acrolein in *n*-hexane solution has three absorption maxima in the 1800~4000 Å region, $\lambda$'s$_{max}$ 2078 Å (5.96 eV., $\log\varepsilon_{max}=3.89$), 3345 Å (3.71 eV., $\log\varepsilon_{max}=1.13$) and 4020 Å (3.08 eV., $\log\varepsilon_{max}=\bar{1}.13$). The last two absorption bands are assigned to the $n-\pi^*$ transition from the solvent effect. The first absorption band has the extinction coefficient of 7700, showing that this transition may be regarded as an allowed one. It is assigned to a $\pi-\pi^*$ transition from the red-shift in the solvent effect.

From these observations the absorption bands at 5.96 and 3.71 eV., may be assigned to the $^1A'\leftarrow{}^1A'$ and $^1A'\leftarrow{}^1A''$ transitions, respectively. In Table I they correspond to the calculated 6.07 eV. $(\pi, \pi^*)$ and 3.85 eV. $(n, \pi^*)$ transitions. The third absorption band may correspond to the lowest calculated singlet-triplet transition 2.85 eV. To account for this small discrepancy we tried to obtain the phosphorescence spectrum of acrolein in cyclohexane and ethyl alcohol solutions at liquid air temperature, but failed. The *n*-hexane solution of acrolein

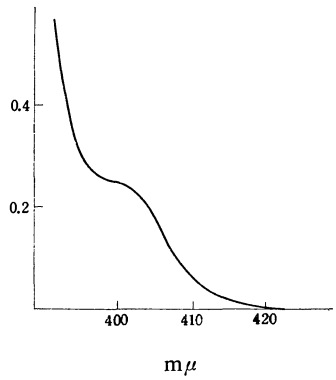



Fig. 1. Absorption band of acrolein in *n*-hexane solution (1.71 mol./l.) at 10°C.

8) H. Mackle and L. E. Sutton, *Trans. Faraday Soc.*, **47**, 691 (1951).
9) C. C. J. Roothaan, *J. Chem. Phys.*, **19**, 116 (1951).
10) H. Kon, This Bulletin, **28**, 275 (1955).
11) J. N. Murrell and K. L. McEwen, *J. Chem. Phys.*, **25**, 1143 (1956).
12) J. W. Sidman, ibid., **27**, 429 (1957).

has an absorption maximum at 4020 Å ($\varepsilon = 0.136, f = 1.16 \times 10^{-7}$) as shown in Fig. 1. These values of $\varepsilon$ and $f$ are somewhat greater than those usually given for a singlet-triplet absorption. According to Kasha[13] it may be expected to have increased intensity in ethyl iodide solution because of the spin-orbit coupling. However, we could not observe any increase of the absorption, due to the overlapping of an intense absorption of the iodine molecule which exists in the solution. On the other hand, this band in ethyl alcohol solution showed a remarkable decrease of intensity at dry ice temperature compared with that at 10°C. Hence, we assigned this 4000 Å band as a hot band. Fig. 2 shows the temperature dependence of this band in ethyl alcohol solution. This weak band lies at 1226 $cm^{-1}$ on the red side of the 0−0 band in vapor state.

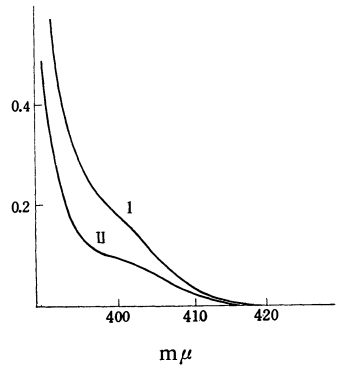



Fig. 2. The effect of temperature on the absorption band of acrolein in ethyl alcohol solution (0.956 mol./l.), curve I at 10°C, curve II at dry ice temperature.

The corresponding frequency could not be found in the infrared and Raman spectra[14], and we could not decide the vibrational mode of this band.

## Summary

It was found that the semi-empirical method proposed by Pariser and Parr can be applied to the $n-\pi^*$ transition as well as the $\pi-\pi^*$ transition in acrolein. In acrolein the $(n, \pi^*)$ triplet state is the lowest state. A weak band in the red side of the 0−0 band is a hot band and it is not the $n-\pi^*$ singlet-triplet transition band. The $n-\pi^*$ triplet band anticipated from calculation could not be found.

The author expresses his sincere thanks to Professor S. Imanishi and Dr. Y. Kanda for their kind encouragement throughout this work. He is also indebted to Dr. M. Ito and Mr. A. Sadō for their kind guidance, and also to Mr. R. Shimada for obtaining the phosphorescence spectrum of acrolein.

*Department of Chemistry*
*Faculty of Science*
*Kyushu University*
*Hakozaki, Fukuoka*

13) M. Kasha, *J. Chem. Phys.*, **20**, 71 (1952).

14) K. Inuzuka, This Bulletin, to be published.

# *Studies on D-Glucosamine Derivatives. VI. α-1-C-Phenyl-2-acetamido-2-deoxy-D-glucopyranoside and its Derivatives**

By Juji YOSHIMURA

(Received June 16, 1960)

The glucosylation of hydrocarbons with a carbohydrate moiety in which the pyranose ring is preserved has been accomplished by using glycosyl halides in two familiar organic reactions, i. g. the Friedel-Crafts and the Grignard reactions. Both approaches were originated by Hurd and Bonner[1] and extended by them[2]. Since then the glycosylation of organometallics has been applied to a variety of carbohydrates[3] and Grignard reagents[3-8] as well as

* Part V, This Bulletin, **33**, 1404 (1960).

1) C. D. Hurd and W. A. Bonner, *J. Am. Chem. Soc.*, **67**, 1664, 1972 (1945).

2) W. A. Bonner, Friedel-Crafts and Grignard Process, "Advances in Carbohydrate Chemistry" Vol., 6, Academic Press, Inc., New York (1951), p. 251.

3) C. D. Hurd and R. P. Holysz, *J. Am. Chem. Soc.*, **72**, 1732 (1950).

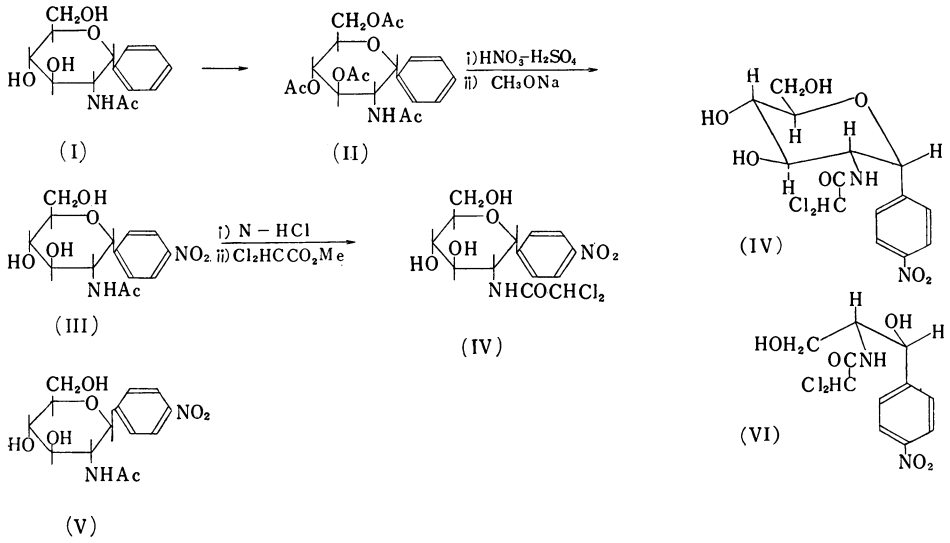
4) Yu. A. Zhdanov, L. I. Shcherbakova and T. N. Egorova, *Doklady Akad. Nauk S. S. S. R.*, **83**, 403 (1952).

5) Yu. A. Zhdanov and L. I. Shcherbakova, ibid., **90**, 185 (1953); *Chem. Abstr.*, **48**, 5114 (1954).

6) Yu. A. Zhdanov, L. I. Shcherbakova and R. V. Golovnya, *Doklady Akad. Nauk S. S. S. R.*, **107**, 259 (1956); *Chem. Abstr.*, **50**, 15476 (1956).

7) Yu. A. Zhdanov and G. F. Drofeenko, *Doklady Akad. Nauk S. S. S. R.*, **112**, 433 (1957).

8) R. Zelinski and R. E. Meyer, *J. Org. Chem.*, **23**, 810 (1958).




to organocadmium[9] and organoalkali[10] compounds. In earlier works of this series, the glycosylation of D-glucosamine was examined by the Friedel-Crafts[11] and Grignard reactions[12], and crystalline β-1-*C*-substituted-2-acetamido-2-deoxy-3, 4, 6-tri-*O*-acetyl-D-glucopyranosides (R; Me, Et, *n*-Pr, *n*-Bu, phenyl, benzyl) were obtained in the latter case. These crystalline substances were designated as β-anomers on the basis of their low rotations, and their pyranose ring systems were confirmed by periodate oxidation. The present investigation centers about the α-1-*C*-phenyl-2-acetamido-2-deoxy-3, 4, 6-tri-*O*-acetyl-D-glucopyranoside (II), produced as a by-product of the crystalline β-anomer when acetobromo-D-glucosamine hydrobromide reacts with phenylmagnesium bromide.

For the isolation of II from the crystallization mother liquors of the β-anomer, an attempt was first made to fractionate the sirupy materials obtained by concentration of the mother liquors using a magnesol-celite column. The existence of II was, however, scarcely deduced from the rotation of an effluent, though α- and β-pentaacetyl-D-glucosamine, and the β-anomer were separated in pure crystalline form. Secondly, the sirupy materials were de-*O*-acetylated by treatment with sodium in methanol and chromatographed on the same column. As is shown in Fig. 1, α-1-*C*-phenyl-2-acetamido-2-deoxy-D-glucopyranoside (I), m.p. 113~114°C, $[\alpha]_D^{24}$ 75.3°, was successfully isolated from the β-anomer and *N*-acetyl-D-glucosamine.

The proportions of the β-anomer to the α one, listed in Table II[13], are shown about ten to one in two cases. This is also ture for D-glucose derivatives[13].

On acetylation of I with acetic anhydride and pyridine, II was obtained as a thick sirup. Although all attempts to induce crystallization of this sirupy material failed, the values of elementary analysis were consistent with the theoretical values.

Nitration of II with a mixture of concentrated sulfuric and nitric acid affords again a sirupy material. However, the crystalline α-1-*C*-(*p*-nitrophenyl)-2-acetamido-2-deoxy-D-glucopyranoside (III) was obtained from it, by treating it with sodium methylate and afterwards by fractionation using a magnesol-celite column. The position of the nitro group of III was deduced from its ultraviolet absorption spectrum[14] as shown in Fig. 2.

For purposes of comparison with the compounds to be reported later, the β-anomer of III (V) was also prepared from β-1-*C*-(*p*-nitrophenyl)-2-acetamido-2-deoxy-3, 4, 6-tri-*O*-acetyl-D-glucopyranoside[14] by deacetylation.

Compound III was converted into sirupy *N*-dichloroacetyl derivative (IV) by treating with *N*-hydrochloric acid and methyl dichloroacetate in turn. The conformation at the position of *C*-1 and 2 of IV is very similar to that of chloramphenicol (VI), but IV showed no antibiotic activities.

Having several available anomeric glycosyl

9) C. D. Hurd and R. P. Holysz, *J. Am. Chem. Soc.*, **72**, 2005 (1950).
10) C. D. Hurd and R. P. Holysz, ibid., **72**, 1735 (1950).
11) J. Yoshimura, A. Kojima, S. Watanabe and T. Sato, *J. Chem. Soc. Japan, Pure Chem. Sec.* (*Nippon Kagaku Zasshi*), **80**, 1472 (1956).
12) J. Yoshimura, N. Muramatsu and T. Sato, ibid., **79**, 1503 (1958).
13) W. A. Bonner and J. M. Craig, *J. Am. Chem. Soc.*, **72**, 3480 (1950).
14) J. Yoshimura, T. Nakagawa and T. Sato, *J. Chem. Soc. Japan, Pure Chem. Sec.* (*Nippon Kagaku Zasshi*), **80**, 1475 (1959).

TABLE I. ISOROTATION RULE VALUES FOR ANOMERIC GLUCOSAMINE DERIVATIVES

| D-Glucosamine pyranoside-derivatives | | [M]D | T, °C | Approx. concn. g./100 ml. | Solvent | *A* | *B* |
|---|---|---|---|---|---|---|---|
| α-1-*C*-Phenyl-*N*-acetyl- | | 21180 | 24 | 0.65 | EtOH | 8790 | 12390 |
| β-1-*C*-Phenyl-*N*-acetyl- | | 3600 | 20 | 1.0 | EtOH | | |
| α-1-*C*-(*p*-Nitrophenyl)-*N*-acetyl- | | 31940 | 22 | 1.0 | MeOH | 19395 | 12545 |
| β-1-*C*-(*p*-Nitrophenyl)-*N*-acetyl- | | −6850 | 23 | 0.9 | MeOH | | |
| α-1-*C*-(*p*-Nitrophenyl)-*N*-dichloroacetyl- | | 23710 | 23 | 0.9 | MeOH | 13040 | 10670 |
| β-1-*C*-(*p*-Nitrophenyl)-*N*-dichloroacetyl- | | −2370 | 27 | 0.8 | EtOH | | |
| *N*-Acetyl-α- | b) | 18200 | 22 | 1.5 | $H_2O$ | 11475 | 6725 |
| *N*-Acetyl-β- | a) | −4750 | 22 | 0.054 | $H_2O$ | | |
| Methyl *N*-acetyl-α- | c) | 30800 | 25 | 1.0 | $H_2O$ | 20450 | 10350 |
| Methyl *N*-acetyl-β- | d) | −10100 | 22 | 2.0 | $H_2O$ | | |
| Phenyl *N*-acetyl-α- | e) | 63320 | 25 | 1.0 | $H_2O$ | 33160 | 30130 |
| Phenyl *N*-acetyl-β- | e) | −3060 | 25 | 1.3 | $H_2O$ | | |
| α-1-*C*-Phenyl-*N*, *O*-tetraacetyl- | | 27900 | 25 | 0.7 | $CHCl_3$ | 21650 | 6250 |
| β-1-*C*-Phenyl-*N*, *O*-tetraacetyl- | | −15400 | 20 | 1.2 | $CHCl_3$ | | |
| *N*, *O*-Pentaacetyl-α- | f) | 36400 | 20 | 5.0 | $CHCl_3$ | 17965 | 18435 |
| *N*, *O*-Pentaacetyl-β- | f) | 470 | 20 | 4.3 | $CHCl_3$ | | |
| Methyl *N*, *O*-tetraacetyl-α- | d) | 31790 | 22 | 2.0 | $CHCl_3$ | 19690 | 12100 |
| Methyl *N*, *O*-tetraacetyl-β- | g) | −7590 | 20 | 0.3 | EtOH | | |
| Phenyl *N*, *O*-tetraacetyl-α- | e) | 58330 | 25 | 2.0 | $CHCl_3$ | 33610 | 24720 |
| Phenyl *N*, *O*-tetraacetyl-β- | e) | −8890 | 25 | 2.0 | $CHCl_3$ | | |

a) R. Kuhn and F. Haber, *Ber.*, **86**, 722 (1953).
b) C. Niemann and J. T. Hays, *J. Am. Chem. Soc.*, **67**, 1302 (1945).
c) R. Kuhn, *Ber.*, **86**, 466 (1953).
d) A. Neuberger and R. P. Rivers, *J. Chem. Soc.*, **1939**, 122.
e) S. Roseman and A. Dorfman, *J. Biol. Chem.*, **191**, 609 (1951).
f) C. S. Hudson and J. K. Dale, *J. Am. Chem. Soc.*, **38**, 1431 (1916).
g) W. H. Myers and G. J. Robertson, ibid., **56**, 8 (1943).

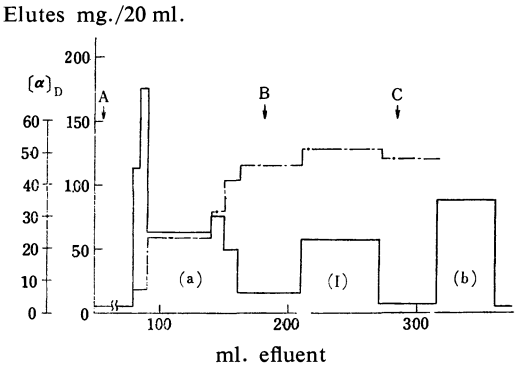



Fig. 1. Chromatographic separation of I on a magnesol-celite column.
A, B and C are a mixture of benzene and ethanol used for elution in which the ratios of benzene to ethanol are 10, 5 and 1, respectively.; ——- rotation of elutes, —— weight of elutes, (a) the β anomer of I, (b) *N*-acetyl-D-glucosamine.

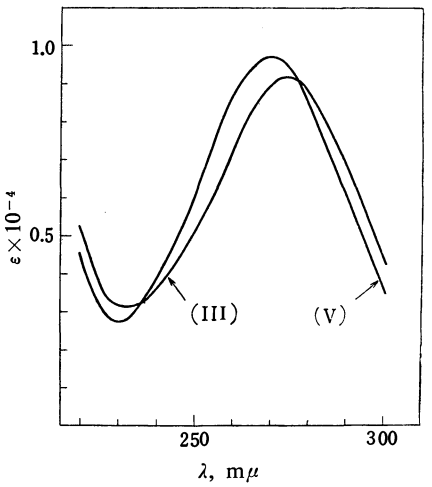



Fig. 2. Ultraviolet absorption spectra of III and V in methanol.

derivatives of D-glucosamine, it is interesting to apply Hudson's rules[15] of isorotation to them. The *A* values, referring to the molecular rotatory contribution of *C*-1 containing the phenyl group, and the *B* values, referring to the free or substituted remainder of the molecule, are presented in Table I.

For comparative purposes we have included in Table I, *B* values for other appropriately substituted anomeric D-glucosamine derivatives. Table I shows that the *A* and *B* values of glucosyl derivatives of D-glucosamine are very

15) C. D. Hudson, *J. Am. Chem. Soc.*, **31**, 66 (1909).

TABLE II. YIELDS AND RATIO OF PRODUCTS

| Starting material g. | | Crude yield g. (%) | Acetylderivative of the β-anomer, g. | Residual syrup, g. (β, α) | Ratio of β to α |
|---|---|---|---|---|---|
| Acetobromo-D-glucosamine | | 2.9 | | 0.5 | |
| hydrobromide | (5.0) | (64.0) | 2.1 | (0.2, 0.18) | 12.8 |
| 〃 | (45.0) | 24.1 | | 11.0 | |
| | | (59.3) | 12.6 | (3.69, 1.65) | 9.9 |
| α-Acetochloro-D-glucose[13] | | 19.5 | | 4.2 | |
| | (27.4) | (63.6) | 15.0 | (1.98, 1.58) | 10.7 |

similar to that of the corresponding glucosyl derivatives of D-glucose[13], and behave almost normally.

It is interesting to compare the values $A_{ph}$ and $A_{pho}$ for 1-*C*-phenyl derivatives and phenyl glycosides, substances differing only in the presence or absence of an oxygen atom at *C*-1.

The $A_{pho}$ value is seen to be higher than the $A_{ph}$ by a factor of about two to four.

Apparently, the conjugation with the aromatic nucleus of the unshared electrons on the glycosidic oxygen in the phenyl glycosides produces a considerably higher partial rotatory contribution of the *A*-portion of the molecule than is the case when the aromatic nucleus alone is present.

The substitution of the *p*-nitro group in the aromatic nucleus of 1-*C*-phenyl derivative, however, leads to an anomalously high *A* value which is analogous to that of phenyl glucosides[16].

## Experimental

**Reaction of Acetobromo-D-glucosamine Hydrobromide with Phenylmagnesium Bromide.** — The reaction was performed in the manner described previously[12], using a ninefold increase (45 g.) in the quantities of starting material. The crude product was isolated, after acetylation, as a thick brown sirup in about 60% yield. It was crystallized from a minimum of 2-propanol, yielding β-1-*C*-phenyl-2-acetamido-2-deoxy-3, 4, 6-tri-*O*-acetyl-D-glucopyranoside. The mother liqors were concentrated to dryness, leaving a sirup which contains the α-anomer.

In Table II are tabulated two results of such preparations.

**α-1-*C*-Phenyl-2-acetamido-2-deoxy-D-glucopyranoside (I).**—The entire residual sirup from the second run in Table II was deacetylated with sodium in methanol. Evaporation of methanol affords 7.2 g. of sirupy materials. A part of the sirup (2.5 g.) was dissolved in 10 ml. of benzene-ethanol (10 : 1 mixture) and insoluble *N*-acetyl-D-glucosamine (0.29 g.) was filtered off. The filtrate was chromatographed at room temperature on a column packed with 25 g. of magnesol-celite (5 : 1 mixture). The solvents used for elution were benzene and ethanol of successively increasing concentrations in benzene. The effluents were examined as to the weight of elutes and their rotation. As is shown in Fig. 1, 0.98 g. of the β-anomer, 0.51 g. of the α-anomer and 0.51 g. of crystalline *N*-acetyl-D-glucosamine were obtained. The α and β anomers were again chromatographed, and 0.395 g. and 0.88 g. of pure crystals were obtained respectively. The α-anomer had m. p. 113~114°C, $[\alpha]_D^{24}$ 75.3° (*c* 0.65, chloroform).

Found: C, 59.93; H, 7.02; N, 4.63. Calcd. for $C_{14}H_{19}O_5N$(281.3): C, 59.77; H, 6.81; N, 4.98%.

**α-1-*C*-Phenyl-2-acetamido-2-deoxy-3, 4, 6-tri-*O*-acetyl-D-glucopyranoside (II).**—Compound I (200 mg.) was acetylated with acetic anhydride (10 ml.) and pyridine (5 ml.) at 25°C for one day. Processing in the usual manner gave 290 mg. of a clear sirup. $[\alpha]_D^{25}$ 68.5° (*c* 0.69, ethanol).

Found: C, 58.36; H, 6.45; N, 3.34. Calcd. for $C_{20}H_{25}O_8N$(407.4): C, 58.69; H, 6.18; N, 3.44%.

**α-1-*C*-(*p*-Nitrophenyl)-2-acetamido-2-deoxy-D-glucopyranoside (III).**—A sirupy material of II (1.5 g.) was dissolved in a mixture of 7 ml. of concentrated sulfuric acid (sp. gr. 1.8) and 7 ml. of concentrated nitric acid (sp. gr. 1.38) on cooling with ice-salt bath. After 30 min. the reaction mixture was left to stand for 1 hr. at 0°C, and for 15 min. at room temperature. About 20 ml. of dry chloroform were added and the mixture was poured gradually into ice-water including an excess amount (about 20 g.) of sodium carbonate. The chloroform layer was separated from the water layer, and the latter was extracted with chloroform in the usual manner. Evaporation of the solvent afforded about 1.5 g. of a pale yellow sirup. A small grain of sodium was added to the solution of this sirup and 15 ml. of methanol, and was left to stand for 3 hr. at room temperature. The methanol solution was diluted with 10 ml. of water and treated with 15 ml. of cation-exchanger (IRA 120) and concentrated in vacuo to dryness. The residual sirup was chromatographed on 10 g. of magnesol-celite column (5 : 1 mixture) in a manner similar to that of I shown in Fig. 1. The fractions eluted with benzene-ethanol mixtures the ratios of which were five to one and two to one were crystallized. Yield 200 mg., m. p. 170~171°C, $[\alpha]_D^{22}$ 97.5° (*c* 1.0, methanol).

Found: C, 51.18; H, 5.23; N, 8.25. Calcd. for $C_{14}H_{18}O_7N_2$(326.3): C, 51.53; H, 5.56; N, 8.59%.

**α-1-*C*-(*p*-Nitrophenyl)-2-dichloroacetamido-2-deoxy-D-glucopyranoside (IV).**—A mixture of 1.3 g. of III, 10 ml. of 2 N hydrochloric acid and 10 ml. of

16) W. W. Pigman, *J. Research Natl. Bur. Standards*, 33, 129 (1944).

ethanol was refluxed 3 hr. on a steam bath. The reaction mixture was concentrated in vacuo, and the residual sirup (ca. 1 g.) was neutralized with about 0.072 g. of sodium in methanol. The solution was filtered and concentrated in vacuo, and the residual sirup was refluxed in 8 ml. of *n*-butanol and 3 ml. of methyl dichloroacetate for 5 hr. The precipitate (a small amount) was filtered off, and the filtrate was concentrated to a thick sirup. An attempt was made to fractionate this on a magnesol-celite column, but no crystalline material could be obtained. The main fraction was about 0.8 g., $[\alpha]_D^{23}$ 60.0° (*c* 0.9, methanol).

Found: C, 42.88; H, 4.25; N, 7.34; Cl, 17.32. Calcd. for $C_{14}H_{16}O_7N_2Cl_2$ (395.2): C, 42.52; H, 4.08; N, 7.09; Cl, 17.94%.

**β-1-*C*-(*p*-Nitrophenyl)-2-acetamido-2-deoxy-D-glucopyranoside (V).**—β-1-*C*-(*p*-Nitrophenyl)-2-acetamido-2-deoxy-3, 4, 6-tri-*O*-acetyl-D-glucopyranoside (0.5 g.) was deacetylated with sodium in methanol. Processing in the usual manner gave 0.3 g. of crystals. m. p. 269~271°C, $[\alpha]_D^{27}$ −21.0° (*c* 0.8, ethanol).

Found: C, 51.33; H, 5.47; N, 8.52. Calcd. for $C_{14}H_{18}O_7N_2$ (326.3): C, 51.53; H, 5.56; N, 8.59%.

**Summary**

The sirup obtained as a by-product with β-1-*C*-phenyl-2-acetamido-2-deoxy-3,4,6-tri-*O*-acetyl-D-glucopyranoside by the action of phenylmagnesium bromide on acetobromo-D-glucosamine hydrobromide has been deacetylated and chromatographed to yield the α-anomer. Several α-derivatives have been described, among which, α-1-*C*-(*p*-nitrophenyl)-2-dichloroacetamido-2-deoxy-D-glucopyranoside which is a chloramphenicol derivative showed no antibiotic activities. The application of Hudson's rules of isorotation to the anomeric compounds in this series is discussed.

The author would like to express his gratitude to Professor T. Sato for his encouragement in carrying out this study. He also thanks Mr. H. Ono for his help during the experiment.

*Laboratory of Organic Chemistry*
*Tokyo Institute of Technology*
*Meguro-ku, Tokyo*

# *Studies on Lactone Formation in Vapor Phase. I. Synthesis of γ-Butyrolactone*

By Shinzaburo OKA

(Received June 1, 1960)

Dehydrogenation of aliphatic glycols to the corresponding lactones with a copper catalyst was originated by Reppe[1,2] and later investigated by several investigators[3-5]. The reaction was generally carried out in the following two ways: (1) Heating glycol and a small amount of copper chromite under continuous stirring at 200~250°C until hydrogen evolution ceased, (2) passing glycol with hydrogen over reduced copper supported on silica gel or pumice at the same temperature.

In Germany, γ-butyrolactone had been manufactured from 1,4-butanediol by the second method, and Copenhaver[6] has described its outline in "Acetylene and Carbon Monoxide Chemistry". The yield of γ-butyrolactone (90%) was satisfactory but its space time yield was very small (about 0.015).

In order to find a more active catalyst for the vapor phase catalytic dehydrogenation of 1,4-butanediol to γ-butyrolactone, the activities of reduced copper supported on various carriers, the effects of the catalyst composition, and the reaction conditions have been examined.

## Experimental

**Catalyst.**—The catalyst consisting of 20% copper and 80% zinc oxide was prepared as follows.

An aqueous solution 300 ml. containing 51 g. of cupric nitrate trihydrate was slowly added to 300 ml. of water in which 109 g. of zinc carbonate was suspended with stirring. Stirring was continued until the deposition of basic copper carbonate on zinc carbonate with evolution of carbon dioxide had ceased. The material was then washed three times with one liter of water, filtered and dried at 70°C. The final decomposition to copper oxide was carried out in a porcelain dish with frequent stirring and cautious heating at 300°C until the color of the

1) W. Reppe et al., Ger. Pat., 699945 (1940); *Chem. Abstr.*, **35**, 6977 (1941).
2) W. Reppe et al., *Ann.*, **596**, 158 (1955).
3) L. P. Kyrides and F. B. Zienty, *J. Am. Chem. Soc.*, **68**, 1385 (1946).
4) R. I. Longley et al., ibid., **74**, 2012 (1952).
5) R. I. Longley et al., *Org. Synth.*, **35**, 87 (1955).
6) J. W. Copenhaver and M. H. Bigelow, "Acetylene and Carbon Monoxide Chemistry", Reinhold Publishing Corp. (1949), p. 152.

TABLE I. EFFECTS OF CARRIERS ON YIELD

| Carrier | B. D.* used | Product | T. H. F.** obtained | Yield of B. L.*** | | B. D. recovered | Conversion |
|---|---|---|---|---|---|---|---|
| | g. | g. | g. | g. | % | g. | % |
| AlO(OH) | 24.8 | 19.5 | 3.0 | 9.0 | 45 | 1.8 | 93 |
| $SiO_2$ | 23.0 | 20.0 | — | 15.4 | 77 | 2.2 | 91 |
| MgO | 20.0 | 19.0 | — | 15.5 | 92 | 2.3 | 89 |
| ZnO | 23.4 | 22.0 | — | 20.9 | 95 | 0.4 | 98 |

* 1,4-Butanediol, ** Tetrahydrofuran, *** $\gamma$-Butyrolactone.

catalyst turned from light blue into dark brown.

When magnesium oxide was used as carrier, the catalyst was prepared similarly. In the case of alumina, copper hydroxide and aluminum hydroxide were coprecipitated with ammonia from the solution of copper nitrate and aluminum nitrate. In the case of silica gel, the catalyst was prepared from copper nitrate and sodium silicate by the usual manner. These catalysts were put in tablets, 8 mm. in diameter and 2 mm. in thickness. About 70 ml. of the tablets was used in each experiment.

**Apparatus and Procedure.** — The apparatus used is shown in Fig. 1. The dehydrogenation tube

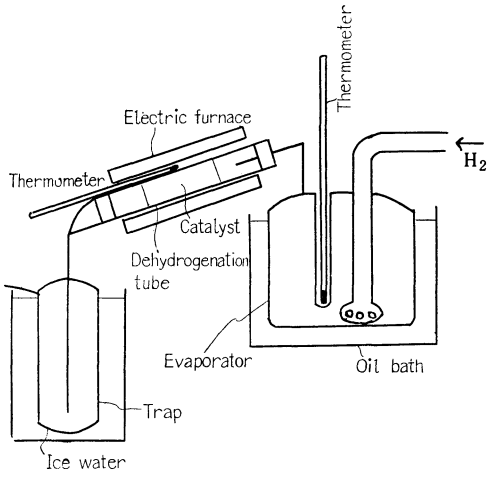



Fig. 1. Apparatus.

(60 cm.×15 mm.) was made from silica and heated in a furnace. Activation of the catalyst was carried out at 220°C in a stream of hydrogen until reduction was completed. The sample was passed in with a steady current of hydrogen. The evaporator containing 1,4-butanediol ($n_D^{25}$ 1.4452, $d_4^{25}$ 1.0130) was immersed in an oil bath and the feed speed of the sample was adjusted by regulating the temperature of the oil bath and rate of hydrogen. The evaporator was weighed before and after a run to determine the weight of material used. The reaction products were collected in a trap cooled by ice water, weighed and fractionated under a reduced pressure. $\gamma$-Butyrolactone (b. p. 98~100°C/25 mmHg) was easily fractionated from unreacted 1,4-butanediol (b. p. 142°C/25 mmHg). $\gamma$-Butyrolactone was a colorless liquid of $n_D^{25}$ 1.4350, $d_4^{25}$ 1.1264 and gave a hydrazide melting at 92°C.

Found : C, 40.92 ; H, 8.79. Calcd. for $C_4H_{10}O_2N_2$ : C, 40.66 ; H, 8.53%.

## Results and Discussion

Typical results for four carriers are tabulated in Table I.

The catalyst 70 ml. containing 20% copper was used. The reaction temperature was maintained at 230~240°C and the reaction time was one hour. The velocity of hydrogen passed with sample was 20 l. per hour. The yields of $\gamma$-butyrolactone were based upon the amount of butanediol consumed. With any carriers used, the conversion was very good. In the case of alumina, the yield was decreased owing to dehydration of butanediol to tetrahydrofuran. Magnesium oxide or zinc oxide was a superior carrier in respect to the yield

TABLE II. EFFECTS OF COPPER CONTENTS TO MAGNESIUM OXIDE

| Cu-cont. | B. D. used | Yield of B. L. | | B. D. recovered | Conversion |
|---|---|---|---|---|---|
| % | g. | g. | % | g. | % |
| 10 | 25.5 | 20.6 | 96 | 3.0 | 88 |
| 20 | 20.0 | 15.5 | 92 | 2.3 | 89 |
| 30 | 23.0 | 19.4 | 95 | 1.6 | 93 |
| 40 | 25.0 | 22.0 | 94 | 0.5 | 98 |

TABLE III. EFFECTS OF COPPER CONTENTS TO ZINC OXIDE

| Cu-cont. | B. D. used | Yield of B. L. | | B. D. recovered | Conversion |
|---|---|---|---|---|---|
| % | g. | g. | % | g. | % |
| 5 | 25.8 | 19.2 | 94 | 3.5 | 86 |
| 10 | 22.0 | 19.0 | 95 | 1.0 | 95 |
| 20 | 23.4 | 20.9 | 95 | 0.4 | 98 |
| 30 | 23.0 | 20.4 | 96 | 0.7 | 97 |
| 40 | 23.0 | 20.5 | 96 | 0.7 | 97 |

TABLE IV. EFFECTS OF THE REACTION TEMPERATURE

| Reaction temp. | B. D. used | Yield of B. L. | | B. D. recovered | Conversion |
|---|---|---|---|---|---|
| °C | g. | g. | % | g. | % |
| 210 | 23.7 | 17.0 | 97 | 5.3 | 78 |
| 220 | 23.8 | 18.7 | 98 | 3.8 | 84 |
| 240 | 23.0 | 18.8 | 96 | 2.5 | 89 |
| 260 | 24.8 | 20.5 | 95 | 2.1 | 92 |
| 280 | 26.5 | 21.3 | 90 | 1.8 | 93 |
| 300 | 26.5 | 21.3 | 87 | 1.0 | 96 |
| 330 | 27.2 | 20.8 | 83 | 0.8 | 97 |

TABLE V. EFFECTS OF HYDROGEN VELOCITY AND LIQUID SPACE VELOCITY OF BUTANEDIOL

| Velocity of $H_2$ l./hr. | S. V.* of $H_2$ | Reaction time min. | B. D. used g. | L. S. V.** of B. D. | Yield of B. L. g. | Yield of B. L. % | S. T. Y.** of B. L. | B. D. recovered g. | Conversion % |
|---|---|---|---|---|---|---|---|---|---|
| 10 | 145 | 70 | 25.2 | 0.34 | 21.2 | 92 | 0.26 | 1.0 | 96 |
| 20 | 290 | 60 | 24.0 | 0.34 | 19.4 | 95 | 0.28 | 2.5 | 90 |
| 30 | 435 | 60 | 23.5 | 0.34 | 18.2 | 93 | 0.26 | 3.0 | 87 |
| 20 | 290 | 120 | 26.0 | 0.19 | 21.0 | 92 | 0.15 | 2.0 | 92 |
| 20 | 290 | 40 | 26.0 | 0.57 | 18.5 | 96 | 0.40 | 5.8 | 78 |
| 10 | 145 | 120 | 23.7 | 0.17 | 19.0 | 87 | 0.14 | 0.8 | 97 |
| 30 | 435 | 40 | 27.3 | 0.58 | 19.0 | 93 | 0.41 | 6.0 | 77 |

* Space velocity, ** Liquid space velocity, *** Space time yield.

and undesirable side reaction. These catalysts were prepared by the new method described in the experimental part.

Effects of the catalyst composition, relative ratio of copper to magnesium oxide and to zinc oxide, are shown in Tables II and III, respectively. The reaction conditions were the same as those in Table I. The suitable contents of copper were about 10~20%. The higher contents of copper did not improve the yield and conversion. Effects of the reaction temperature in the case of 20% copper-zinc oxide is shown in Table IV. The reaction time and the hydrogen velocity were the same as those of the above experiments. The conversion increased with the elevation of the reaction temperature and $\gamma$-butyrolactone was obtained in a good yield at 210~260°C. At above 280°C the product decreased owing to undesirable decompositions.

Finally, in use of the same catalyst as the above, effects of space velocity of hydrogen and liquid space velocity of butanediol on yield, space time yield and conversion were examined at 230~240°C and the results were summarized in Table V.

The yield was hardly affected with varying velocity of hydrogen and butanediol, but the long contact with the catalyst lowered the yield to some extents. With increase of liquid space velocity from 0.17 to 0.58, the space time yield increased from 0.14 to 0.41, but the conversion decreased from 97% to 77%.

No final information was yet available as to the life of the catalyst, but its activity hardly decreased after several hours.

## Summary

Vapor phase catalytic dehydrogenation of 1, 4-butanediol to $\gamma$-butyrolactone with reduced copper supported on various carriers was studied. It was found that copper supported on zinc oxide or magnesium oxide was a superior catalyst. In the case of a catalyst consisting of 20% copper and 80% zinc oxide, the yield and space time yield of $\gamma$-butyrolactone were 95% and 0.28 at 230~240°C, respectively.

The author wishes to thank Professor S. Kunichika of Kyoto University, for valuable advices and criticism.

*Institute for Chemical Research*
*Kyoto University*
*Kosobe, Takatsuki*

# *Studies on Leucomycin. IV. Isolation of Mycaminose from the Acid Hydrolysate*

By Tetzuo WATANABE

(Received July 6, 1960)

Recent studies in this laboratory have demonstrated that the leucomycin complex produced by Streptomyces kitasatoensis Hata[1-3], can be resolved into six basic antibiotics by elution chromatography[4] or by counter current distribution[5]. The present paper will describe the presence of a mycaminose residue[6] as the basic moiety in each leucomycin component. Leucomycin A1 ($C_{46}H_{81}NO_{17}$, m. p. 135~138°C), the main component of this antibiotics complex, possessed a $pK_a'$ of 7.1 and did not reduce Fehling's solution. It gave no color with carbohydrate reagents such as anthrone under the usual conditions[7]. Upon hydrolysis with 2 N hydrochloric acid at 100C°, however, there was produced an appreciable amount of reducing sugars which became colored with sulfuric acid-anthrone reagent[8], together with some humic substances. By the elution chromatography of the hydrolysate from a column of Dowex-50 of H-phase with 2 N hydrochloric acid, the anthrone reaction-positive components were separated into three fractions, as shown in Fig. 1. The first fraction possessed no nitrogen, while the second fraction (IIa) contained a basic sugar, which was crystallized as a hydrochloride ($C_8H_{17}NO_4 \cdot HCl$, m. p., 114~116°C) from the alcoholic solution by the addition of ether.

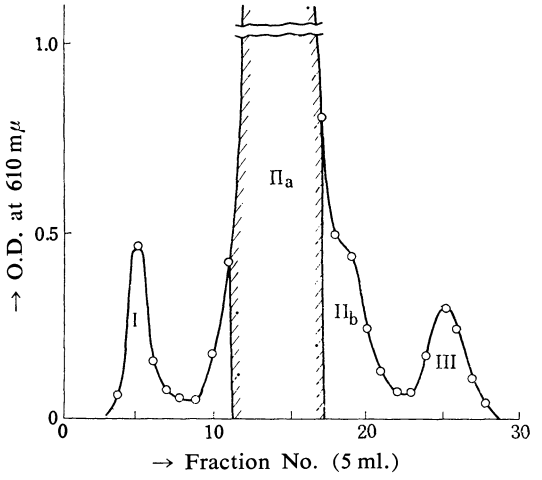



Fig. 1. Elution chromatogram of sugar components derived from leucomycin A1 with hydrochloric acid. The acid hydrolysate corresponding to 20 g. of leucomycin, was eluted from a column of Dowex-50 (H-phase) of 1×30 cm. with 2 N hydrochloric acid. The concentration of sugar was determined photocolorimetrically with sulfuric acid-anthrone reagent[8].

This basic sugar rapidly consumed one mole of slight alkaline iodine at room temperature, indicating that it was an aldose[9].

The aldose possessed one *C*-methyl group and showed a characteristic iodoform reaction, too. By the action of 3 N sodium hydroxide at 50°C, the basic group of this aldose was easily split as dimethylamine, which was identified as 2, 4-dinitro-*N*-dimethyl aniline after coupling with 1-fluoro-2, 4-dinitrobenzene[10]. These results seemed to indicate that the basic sugar isolated from leucomycin A1 was an aldomethylpentose having a dimethylamino group.

As shown in Fig. 2, the dimethylamino-aldomethylpentose consumed 4 mol. of periodate in aqueous solution at room temperature : one

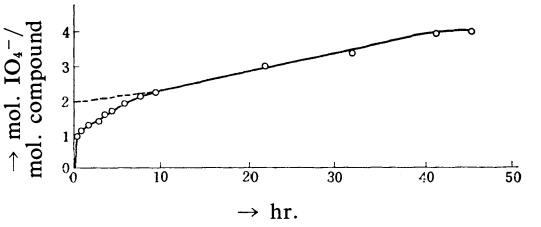
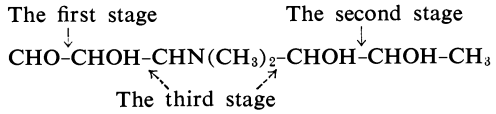



Fig. 2. Periodate consumption by the basic sugar isolated from leucomycin A1.

1) T. Hata et al., *J. Antibiotics Ser.*, A6, No. 2, 87 (1953).
2) T. Hata, F. Koga and H. Kanamori, ibid., A6, No. 3, 109 (1953).
3) J. Abe, Y. Suzuki, T. Watanabe and K. Satake, *J. Chem. Soc. Japan, Pure Chem. Sec.* (*Nippon Kagaku Zasshi*), 81, 969 (1960).
4) T. Watanabe, This Bulletin, 33, 1100 (1960).
5) T. Watana,de H. Nishida and K. Satake, ibid., 33, 1104 (1960).
6) F. A. Hochstein and P. P. Regar, *J. Am. Chem. Soc.*, 77, 3033 (1955).
7) Y. Sano, T. Hoshi and T. Hata, *J. Antibiotics, Ser.*, A7, No. 3, 88 (1954).
8) D. L. Morris., *Science*, 107, 254 (1948).
9) G. L. Miller and A. L. Burton, *Anal. Chem.*, 31, 1790 (1959).
10) F. Sanger, *Biochem. J.*, 39, 507 (1945).

mole very rapidly, one mole with moderate speed, and the additional two moles very slowly. During the initial stage of the oxidation, formic acid was produced at a rate approximating one mole per mole of periodate consumed: while the formation of acetaldehyde which was identified as the 2,4-dinitrophenylhydrazone and assayed photocolorimetrically with *p*-hydroxydiphenyl[11], was observed mainly during the second stage of oxidation. During the final stage of the oxidation, there was observed the formation of dimethylamine and an increase of the amount of formic acid with the increase of periodate consumption. No formation of formaldehyde was confirmed with the use of chromotropic acid[12]. These results suggested that the basic sugar possessed the following structure.




As already described in the present paper, the dimethyl amino group of this sugar was rather easily split as dimethylamine under the action of alkali. Fig. 3 illustrates the velocity of liberation. As a control, was used $C_7$-dimethylamino aldose, which had been derived from the original $C_8$-sugar with the action of one mole of periodate (presumably possessing methyltetrose structure[6,9]; see Fig. 2). A marked difference observed between the stabilities of both dimethylamino sugars in alkaline solution, seemed not to be inconsistent with the structure presumed above; thus the original $C_8$-sugar possessed the dimethylamino group at the $\beta$-position, while the oxidation product possessed it at the $\alpha$-position from the aldehyde group, respectively. As to the steric configuration of the 3,6-deoxy-3-dimethyl amino aldohexose isolated from leucomycin A1, the present author had no experimental data. The physical constants of this sugar, however, were very close to those reported on a 3,6-deoxy-3-dimethylaminoaldohexose, mycaminose which had been previously obtained from the acid hydrolysate of magnamycin and the infrared absorption spectra of both sugars were essentially the same, as shown in Fig. 4. These results indicated that mycaminose was a basic moiety of leucomycin A1.

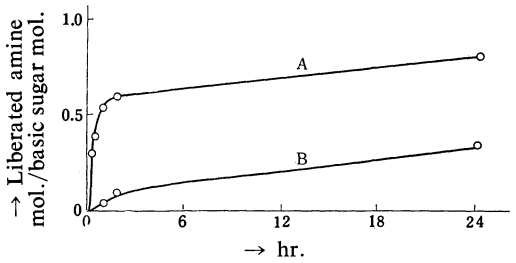



Fig. 3. Liberation of dimethylamine from dimethylamino sugar under the action of 3 N sodium hydroxide at 50°C.
A: CHO-CHOH-CHN$(CH_3)_2$-CHOH-CHOH-$CH_3$ from leucomycin A1.
B: CHO-CHN$(CH_3)_2$-CHOH-CHOH-$CH_3$ derived from A with the action of one mole of periodate.
The amount of dimethylamine was determined spectrophotometrically, after the coupling with 1-fluoro-2,4-dinitrobenzene.

It should be emphasized here that p$K_a'$ value of mycaminose (8.1) was somewhat higher than that of intact leucomycin A1 (7.1). Such a difference between their p$K_a'$ values may suggest that the hydroxyl group adjacent to the dimethylamino group of mycaminose residue in intact leucomycin A1, was blocked with other groups in the same way as magnamycin[13]. The p$K_a'$ of leucomycin, magnamycin, and their related compounds are listed in Table I.

Other components of leucomycin, A2 ($C_{65}H_{111}NO_{22}$, m. p., 142~144°C), B1 ($C_{35}H_{59}NO_{13}$,

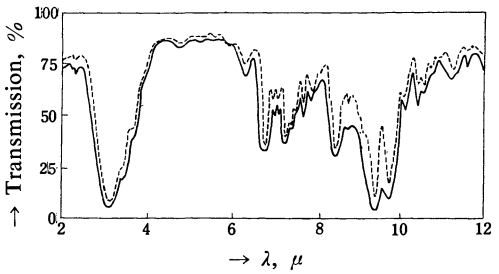



Fig. 4. Infrared absorption spectra of the basic sugars from leucomycin A1 and from magnamycin.

TABLE I. p$K_a'$ OF LEUCOMYCIN, MAGNAMYCIN AND THE RELATED COMPOUNDS

| | Leucomycin A1, A2 | Leucomycin B1, B2, B3, B4 | Magnamycin |
|---|---|---|---|
| Intact antibiotics | 7.1 | 6.6~6.8 | 7.0 |
| Basic sugar obtained with 6 N HCl hydrolysis | | 8.1 | 8.1 |
| A basic moiety obtained with methanolysis | 8.1* | 7.8* | 8.3 |

* T. Watanabe, unpublished.

11) B. A. Neidig and W. C. Hess, *Anal. Chem.*, **24**, 1627 (1952).
12) M. J. Boyd and M. A. Logan, *J. Biol. Chem.*, **146**, 279 (1942).
13) R. B. Woodward, *Angew. Chem.*, **68**, 13 (1956).

m. p., 214.5～216.5°C), B2 ($C_{38}H_{65}NO_{16}$, m. p., 214～216°C), B3 ($C_{34}H_{53}NO_{13}$, m. p., 216～217°C), B4 ($C_{38}H_{59}NO_{16}$, m. p., 221～223.8°C), also gave a basic sugar which was absorbed on a column of Dowex-50 of H-phase, on their acid hydrolysis. Although the isolation of the basic sugar in preparative scale was impossible, due to the limited amounts of these minor antibiotics, the paper chromatographic $R_f$ values was just the same as that of mycaminose and differed from that of desosamine which had been reported as another basic moiety of macrolides[14,15].

## Experimental

**Leucomycin.**—The leucomycin complex used in this experiment, was a commerical bulk, Lot No. 9LM-44, which was kindly offered from the Research Institute, Toyo Jozo Co. Ltd. Leucomycin components, A1, A2, B1, B2, B3 and B4, were isolated from the complex by the previous fractionation with benzene, followed by the further minute resolution with the use of counter current distribution technique, as already reported by the present author[5].

**Isolation of Basic Sugar from the Acid Hydrolysate of Leucomycin A1.**—Twenty grams of leucomycin A1 (m. p. 135～138°C, Found: C, 60.99; H, 8.72; N, 1.52. Calcd. for $C_{46}H_{81}NO_{17}$: C, 60.13; H, 8.75; N, 1.54%.) were disolved into 300 ml. of 2 N hydrochloric acid, and the solution was heated at 100°C for 3 hr. The dark brown solution so produced, after repeated washing with chloroform (five times, 30 ml. each) to remove humic substances, was concentrated to syrup under reduced pressure. The residue, dissolved in 10 ml. of water, was added to a column of Dowex-50 (H-phase, 150～200 mesh) of 1×30 cm. As soon as the applied sample solution had been allowed to flow into the column, elutions with 50 ml. of water, then with 2 N hydrochloric acid were initiated. Throughout these procedures, the rate of flow was maintained to be 10±2 ml. per hour. The concentration of sugar in the effluent, which had been collected in 5 ml. fractions by means of an automatic fraction collector, was determined spectrophotometrically with sulfuric acid-anthrone reagent, as follows. A half millilitre of the solution to be analyzed was mixed with 2 ml. of 2 per cent anthrone in concentrated sulfuric acid, and the mixture was heated for 15 min. in boiling water bath. The optical density of the resulting blue color was measured at 610 mμ.

The combined fractions, corresponding to the second main peak component (from No. 11 to No. 16; see Fig. 1), were concentrated to dryness under reduced pressure. The crystalline residues were dissolved into a minute amount of ethyl-alcohol and recrystallized out by the addition of ether. m. p. 114～116°C $[\alpha]_D^{25}$ +30° (*c* 1 in water 24 hr.) Yield 2.8 g.

Found: C, 42.18; H, 8.09; N, 5.94. Calcd. for $C_8H_{17}NO_4 \cdot HCl$: C, 42.19; H, 7.81; N, 5.59%.

**Periodate Oxidation of the Basic Sugar Isolated from Leucomycin A1.**—The oxidation was achieved in 0.1 per cent acetic acid at 25°C, with the uses of 3～7 mM of basic sugar hydrochloride and of 25～30 mM sodium metaperiodate, and an aliquot of the reaction mixture was pipetted out after a definite period, for the following analysis. The periodate consumption was determined, after the addition of potassium iodide by the titration with thiosulfate, and the amounts of acetaldehyde and of formaldehyde were determined spectrophotometrically with *p*-hydroxybiphenyl-[11] and chromotropic acid-[12] reagents, according to the method described in the cited reference, respectively. The amount of formic acid was assayed by the alkali-titration, on the oxidation mixture in aqueous solution instead of 0.1 per cent acetic acid solution. Acetaldehyde, formic acid, and dimethylamine produced by the periodate oxidation, were identified as the 2,4-dinitrophenylhydrazone (m. p. 160～161°C), *p*-bromophenacyl ester (m. p. 100～101°C) and dinitrophenyl derivative (m. p. 78°C), respectively.

**Alkali Degradation of the Basic Sugar from Leucomycin A1.**—Four hundred milligrams of the basic sugar hydrochloride was dissolved into 25 ml. of 3 N sodium hydroxide at 45°C. A 5 ml. portion of the solution, after a definite period, was immediately cooled and neutralized, and dinitrophenylated with 1-fluoro-2, 4-dinitrobenzene according to the method of Sanger[10].

The dinitrophenylation mixture, was directly added to a column of Amberlite IRC-50 of H-phase (100～150 mesh, 1×20 cm.)[16] and the column was washed with water. The unreacted reagent and 2,4-dinitrophenol, a main by-product, were removed in the filtrate and the washing. 2, 4-Dinitro-*N*-dimethylaniline derived from dimethylamine, was then eluted from the column with a mixture of acetone and water (1 ; 1 *V/V*) and the amount was determined by the spectrophotometry at 380 mμ. The absorption spectrum of the effluent was essentially the same as that of the authentic specimen in a wavelength range between 250 to 450 mμ.

As a control, a reaction mixture derived from the basic sugar with the equimolecular amount of sodium periodate (see Fig. 2) was used.

**Other Analysis of the Basic Sugar Isolated from Leucomycin.**—Aldose-reaction with alkaline iodine[9] 2-deoxyaldose reaction with perchloric acid-vanilline reagent[17], dinitrophenylation with 1-fluoro-2,4-dinitrobenzene for the detection of primary and secondary amino groups[10], were achieved under the conditions reported in the references cited, respectively.

Paper-chromatographic analysis was performed by the usual ascending method, with the uses of isopropanol-pyridine-acetic acid-water (8 : 8 : 1 : 4 *V/V*), *n*-butanol-pyridine-water (6 : 4 : 5 *V/V*) and collidine-pyridine-water (2 : 1 : 1 *V/V*) as the solvent

14) R. K. Clark, Jr., *Antibiotics and Chemotherapy*, 3, 663 (1953).
15) C. Djerassi and A. Bowers, *J. Am. Chem. Soc.*, 78, 1729 (1956).
16) T. Seki, *J. Chem. Soc. Japan, Pure Chem. Sec.* (*Nippon Kagaku Zasshi*), 75, 1297 (1954).
17) A. P. MacLennan, H. M. Randall and D. W. Smith, *Anal. Chem.*, 31, 2020 (1959).

systems. Ammonial silver nitrate was used for the detection of the spot, in both cases.

The author desires especially to thank Professor K. Satake for his constant support and encouragement throughout this work, and also gratitude to Mr. S. Kurioka and Mr. K. Fujii for their assistance.

*Research Institute*
*Toyo Jozo Co. Ltd.*
*Ohito, Tagata, Shizuoka*

# *Polyaddition Reaction of Diphenylsilane to Diallyl Carboxylate*

By Kuniharu KOJIMA

(Received June 21, 1960)

The monofunctional addition reaction of phenylsilane or methyl diethoxysilane to allyl acetate was first studied by Speier and coworkers[1,2], and 3-(phenylsilyl) propyl acetate and 3-(diethoxy methylsilyl)propyl acetate were prepared by this method under the influence of *tert*-butyl hydroperoxide. The addition reaction of trichlorosilane and methyl dichlorosilane to allyl acetate was also studied under the influence of platinum catalyst[3].

As an example of the bifunctional addition reaction, we have reported in the previous short communication, the polyaddition reaction of diphenylsilane to diallyl phthalate[4].

In the present work we have tried to extend the reaction in order to obtain larger molecules which might have more interesting properties. Some experiments using diallyl phthalate and diphenylsilane at various reaction conditions (reaction temperature, catalyst concentration and monomer concentration) are summarized in Tables II—VI.

The new method of polymer synthesis was further extented to the polyaddition reaction of diphenylsilane and the following diallyl carboxylate : diallyl oxalate, malonate, succinate, adipate, sebacate, phthalate, isophthalate and terephthalate.

## Experimental

**Materials.**—*Diphenylsilane.* — Diphenylsilane was prepared from diphenyldichlorosilane and lithium aluminum hydride by ordinary method[5]. Three hundred and four grams (1.2 mol.) of diphenyldichlorosilane was added to 25 g. (0.68 mol.) of lithium aluminum hydride in 300 ml. of anhydrous ether. The solution was refluxed for several hours and hydrolyzed with 260 ml. of dilute hydrochloric acid. The ethereal layer was distilled to give 215 g. of diphenylsilane b. p. 109°C/7 mmHg, $n_D^{20}$ 1.5799, $d_4^{20}$ 0.9970.

*Diallyl Phthalate.* — The commercial product was distilled under reduced pressure before use. The portion boiling at 155°C/6 mmHg, $n_D^{20}$ 1.5205, $d_4^{20}$ 1.1205, was used in the polyaddition reaction.

*Other Diallyl Carboxylates.* — Diallyl carboxylates were prepared by the method described previously[6]. Their physical properties were listed in Table I.

TABLE I. PHYSICAL PROPERTIES OF DIALLYL CARBOXYLATES

| Diallyl carboxylates | B. p. °C/mmHg | $n_D^{20}$ | $d_4^{20}$ |
|---|---|---|---|
| Oxalate | 104～106/15 | 1.4470 | 1.0890 |
| Malonate | 115/4 | 1.4480 | 1.0643 |
| Succinate | 112～113/8 | 1.4514 | 1.0559 |
| Adipate | 136～138/8 | 1.4539 | 1.0226 |
| Sebacate | 181～183/9 | 1.4564 | 0.9788 |
| Phthalate | 155/6 | 1.5205 | 1.1205 |
| Isophthalate | 163/8 | 1.5250 | 1.1213 |
| Terephthalate | 166～167/8 | — | — |

*Catalyst.* — Prepared by dissolving 0.518 g. of commercial $H_2PtCl_6 \cdot 6H_2O$ ($10^{-3}$ mol.) in 100 ml. *tert*-butyl alcohol.

**Polyaddition Reaction.**—To the equimolar mixture of diphenylsilane, and to diallyl carboxylate in a glass tube was added a constant amount of chloroplatinic acid solution. The tube was then sealed in a nitrogen atmosphere, and heated for several hours in a dry oven of constant temperature. The reaction product was dissolved in 100 ml. of acetone, and filtered. To the filtrate 30 ml. of water was added and reprecipitated. The precipitates were separated by decantation and dried in a vaccum desiccator at 50°C for 7 days until it reached constant weight.

**Determination of Molecular Weight.**—The molecular weight was calculated from the freezing point depression in benzene.

1) J. L. Speier et al., *J. Am. Chem. Soc.*, **78**, 2278 (1956).
2) J. L. Speier et al., ibid., **79**, 974 (1957).
3) L. G. Goodman et al., ibid., **79**, 3073 (1957).
4) K. Kojima., This Bulletin, **31**, 666 (1958).
5) R. A. Benkeser et al., *J. Am. Chem. Soc.*, **74**, 648 (1952).
6) K. Kojima et al., *Reports of the Research Institute of Dental Materials Japan*, **8**, 136 (1957).

**Determination of Inherent Viscosity.**—One fifth of a gram of solvent free polymer was dissolved in 50 ml. of benzene and the viscosity was determined by an Ostwald type viscosimeter at 25°C.

## Results and Discussion

The preliminary experiment for determing conditions which favor formation of polyaddition products were carried out using diphenylsilane and diallyl phthalate.

**Temperature Dependence.**—Polymerization of diphenylsilane with diallyl phthalate was carried out at various temperatures. The results are given in Tables II, III and IV.

The largest polymer was prepared at 120°C, 48 hr. and 0.1 ml. catalyst. The degree of polymerization increased as the conversion became higher. Higher reaction temperature also seemed to increase the degree of polymerization. It became clear that the addition

Table II. Polyaddition reaction of diphenylsilane with diallyl phthalate at 80°C

| Reaction time, hr. | Conversion % | Mot. wt. | $[\eta]$ |
|---|---|---|---|
| 3 | 3.5 | 421 | 0.5 |
| 6 | 5.1 | 482 | 0.5 |
| 12 | 9.8 | 718 | 0.6 |
| 24 | 17.9 | 789 | 0.6 |
| 48 | 24.8 | 877 | 0.6 |

Diphenylsilane 4.519 g., diallyl phthalate 6.041 g. and catalyst $5\times10^{-8}$ mol./ml. were used.

Table III. Polyaddition reaction of diphenylsilane with diallyl phthalate at 100°C

| Reaction time, hr. | Conversion % | Mol. wt. | $[\eta]$ |
|---|---|---|---|
| 3 | 5.2 | 498 | 0.5 |
| 6 | 9.7 | 663 | 0.6 |
| 12 | 18.8 | 880 | 0.6 |
| 24 | 31.9 | 1288 | 0.7 |
| 48 | 46.4 | 1394 | 0.7 |

Diphenylsilane 4.519 g., diallyl phthalate 6.041 g. and catalyst $5\times10^{-8}$ mol./ml. were used.

Table IV. Polyaddition reaction of diphenylsilane with diallyl phthalate at 120°C

| Reaction time, hr. | Conversion % | Mol. wt. | $[\eta]$ |
|---|---|---|---|
| 3 | 10.9 | 510 | 0.6 |
| 6 | 22.9 | 783 | 0.6 |
| 12 | 34.7 | 1079 | 0.6 |
| 24 | 55.9 | 1583 | 0.7 |
| 48 | 70.6 | 1688 | 0.7 |

Diphenylsilane 4.519 g., diallyl phthalate 6.041 g. and catalyst $5\times10^{-8}$ mol./ml. were used.

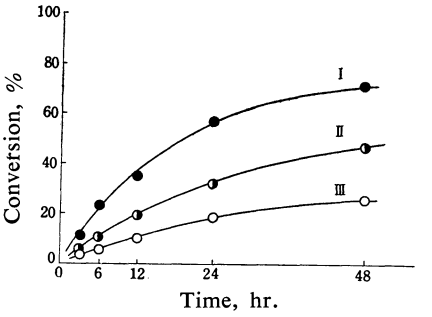



Fig. 1. Correlation of conversion percent with time.
I for reaction temperature 120°C (●), II for 100°C (◑), III for 80°C (○).

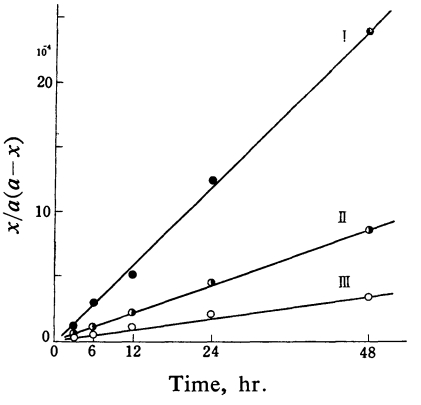



Fig. 2. Correlation of $x/a(a-x)$ with time.
I for reaction temperature 120°C (●), II for 100°C (◑), III for 80°C (○).

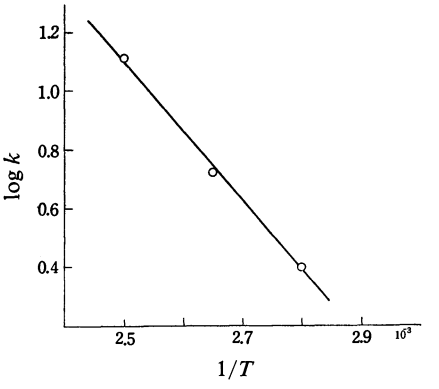



Fig. 3. Correlation of $\log k$ with $1/T$.

reaction was of second order at the initial stage (Figs. 1 and 2), and the $k$ values were $k_{80}=2.5$, $k_{100}=5.2$ and $k_{120}=13.2\times10^{-8}$ g./sec. mol. When the logarithm of the initial rates of polymerization was plotted against reciprocals of temperatures ($1/T$), a good straight line was obtained (Fig. 3). The over-all activation energy calculated from the slope in

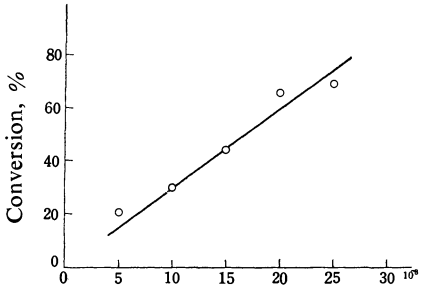
Fig. 3 was found to be 12 kcal./mol. for this reaction.

**Effect of the Catalyst Concentration.** — The data for the effect of the catalyst concentration is given in Table V, and the dependence of the initial rate of polymerization upon the concentration of catalyst are shown in Fig. 4.

TABLE V. EFFECTS OF CATALYST CONCENTRATION IN ADDITION REACTION OF DIPHENYLSILANE WITH DIALLYL PHTHALATE

| Catalyst conc. mol./ml. | Conversion % | Mol. wt. | $[\eta]$ |
|---|---|---|---|
| $5\times10^{-3}$ | 21.2 | 758 | 0.6 |
| 10 | 29.7 | 836 | 0.6 |
| 15 | 44.9 | 746 | 0.6 |
| 20 | 65.5 | 660 | 0.6 |
| 25 | 68.6 | 773 | 0.6 |

Diphenylsilane 4.519 g., diallyl phthalate 6.041 g. were used and were heated at 110°C., 6 hr.




Catalyst concentration, mol./ml.

Fig. 4. Effect of catalyst concentration.

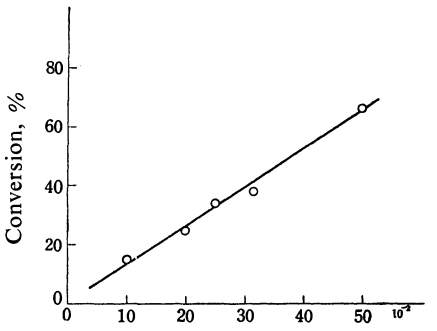
It is evident that the initial rate of polymerization is proportional to the concentration of chloroplatinic acid solution. The molecular weight of the polymer, however, is almost independent of the concentration of the catalyst.

**Effect of Initial Monomer Concentration.** — The relationship between initial rate of polymerization and the concentration of diphenylsilane-diallyl phthalate mixture in toluene

TABLE VI. EFFECTS OF INITIAL MONOMER CONCENTRATION IN ADDITION REACTION OF DIPHENYLSILANE WITH DIALLYL PHTHALATE

| Monomer conc. g./ml. | Conversion % | Mol. wt. | $[\eta]$ |
|---|---|---|---|
| $50\times10^{-2}$ | 66.3 | 870 | 0.6 |
| 33 | 36.7 | 627 | 0.6 |
| 25 | 33.5 | 597 | 0.5 |
| 20 | 24.6 | 545 | 0.5 |
| 10 | 15.5 | 463 | 0.5 |

Diphenylsilane 4.519 g., diallyl phthalate 6.041 g. and catalyst $20\times10^{-3}$ mol./ml. were used and were heated at 110°C, 24 hr.




Monomer concentration, g./ml.

Fig. 5. Effect of initial monomer concentration.

was studied at 110°C. The data for the rate of diminution of monomer concentration are given in Table VI and Fig. 5.

It is clear that the initial rate is proportional to the concentration of diphenylsilane—diallyl phthalate mixture.

The above result indicates that the over-all rate of polyaddition reaction, $k_p$ of diphenylsilane with diallyl phthalate is proportional to the initial monomer concentration (M) and to the catalyst concentration (C).

$$k_p \propto (M)(C)$$

The molecular weight of the polymer is proportional to the initial monomer concentration, but independent of the catalyst concentration.

**Polyaddition Reaction of Diphenylsilane to Diallyl Carboxylates.** — Similar experiments of diphenylsilane to diallyl oxalate, malonate, succinate, adipate, sebacate, phthalate, isophthalate, and terephthalate were carried out. The results obtained are shown in Table VII.

TABLE VII. ADDITION REACTION OF DIPHENYLSILANE WITH DIALLYL CARBOXYLATES

| Diallyl carboxylate | Conversion % | Mol. wt. | $[\eta]$ | Si Calc. % | Si Found % |
|---|---|---|---|---|---|
| Oxalate | 27.5 | 650 | 0.6 | 7.93 | 8.64 |
| Malonate | 59.5 | 990 | 0.6 | 7.62 | 7.36 |
| Succinate | 64.9 | 1080 | 0.6 | 7.34 | 7.38 |
| Adipate | 55.8 | 1120 | 0.6 | 6.84 | 7.58 |
| Sebacate | 76.3 | 1170 | 0.6 | 6.02 | 5.45 |
| Phthalate | 73.6 | 1860 | 0.7 | 6.52 | 6.24 |
| Isophthalate | 66.5 | — | — | 6.52 | 6.49 |
| Terephthalate | 53.0 | — | — | 6.52 | 6.35 |

Diallyl carboxylate 0.02 mol. and diphenylsilane 0.02 mol. were used and were heated at 110°C, 50 hr.

Addition products were viscous oily liquids, but the adducts of diphenylsilane to diallyl phthalate and isophthalate and terephthalate

were light yellow, glassy solid, and were useful as adhesives. Their softening temperatures were ca. 108°, 120°and >200°C.

## Summary

The polyaddition reaction of diphenylsilane to diallyl phthalate was studied. The reaction was found to be of the second order at the initial stage. The over-all rate is proportional to the initial monomer and catalyst concentration. The over-all activation energy calculated for this reaction was found to be 12 kcal./mol. at 80~120°C.

By a similar method following polyesters have been prepared from diphenylsilane and diallyl carboxylates: Polydiphenylsilylene 3, 3′-bis(trimethylene)oxalate, malonate, succinate, adipate, sebacate, phthalate, isophthalate and terephthalate. Their molecular weight and inherent viscosity were determined and properties have been described.

The author is much indebted to Professor Yoshio Iwakura for his many useful suggestions and to Mr. Niro Tarumi for his help in the experiments. Appreciation is also expressed to Shin-etu Chem. Co. for their kindness in supplying the diphenyldichlorosilane.

*Tokyo Medical and Dental University*
*Yushima, Bunkyo-ku Tokyo*

# *Absorption Spectra of Unstable Colored Intermediates from Picryl Chloride by the Action of Sodium Hydroxide*

By Takehiro ABE

(Received July 9, 1960)

In a previous paper[1], it was reported that on treatment of an aqueous solution of picryl chloride with a drop of aqueous solution of sodium hydroxide, a red solution was instantaneously formed and in a few minutes changed into a yellow solution which showed a spectrum closely resembling a spectrum of picric acid. At room temperature the red color faded away so fast that its spectrum could not be measured. It has, however, been found that the red solution containing a small quantity of ethanol is relatively stable. An attempt has, therefore, been made to measure the spectrum of the red solution prepared by adding a sodium hydroxide solution to an aqueous picryl chloride solution containing a small quantity of ethanol, together with spectra of colored solutions of picryl chloride in ethanol and in acetone in the presence of sodium hydroxide. These spectra have been compared to investigate a solvent effect on them.

## Experimental

Picryl chloride of Tokyo Kasei Co. guaranteed grade was recrystallized twice from methanol-water; m. p. 82.5°C (lit. 83°C). Commercial pure picric acid was recrystallized three times from water; m. p. 122.6°C (lit. 122.5°C). Commercial guaranteed ethanol and acetone were fractionally distilled after usual treatments. The spectra of the solutions were measured with a Hitachi EPU-2 spectrophotometer at room temperature. Path length of absorption celles was 1 cm.

## Results and Discussion

**Absorption Spectra of the Red-Colored Solution in Water Containing a Small Quantity of Ethanol.** — The orange aqueous solution of picryl chloride was made by pipetting 1 cc. of an aqueous sodium hydroxide solution and 5 cc. of ethanol into 1 cc. of a paleyellow ethanolic solution of picryl chloride and diluting the solution with water to 25 cc. The orange solution changed into a paleyellow solution by addition of a dilute aqueous solution of hydrochloric acid immediately after the preparation. When it was allowed to stand at room temperature, the orange solution changed gradually into a yellow solution. The spectra of the orange solution are shown in Fig. 1. Picryl chloride in water, in ethanol and in acetone dose not show an absorption maximum in a range of wavelengths from 300 mμ to 600 mμ[1]. The orange solution gives absorption bands at about 360, 416 and 490 mμ immediately after the preparation, but an only intense absorption band at about 397 mμ when the solution is allowed to stand at room temperature for more than six hours.

1) T. Abe, This Bulletin, 32, 339 (1959).

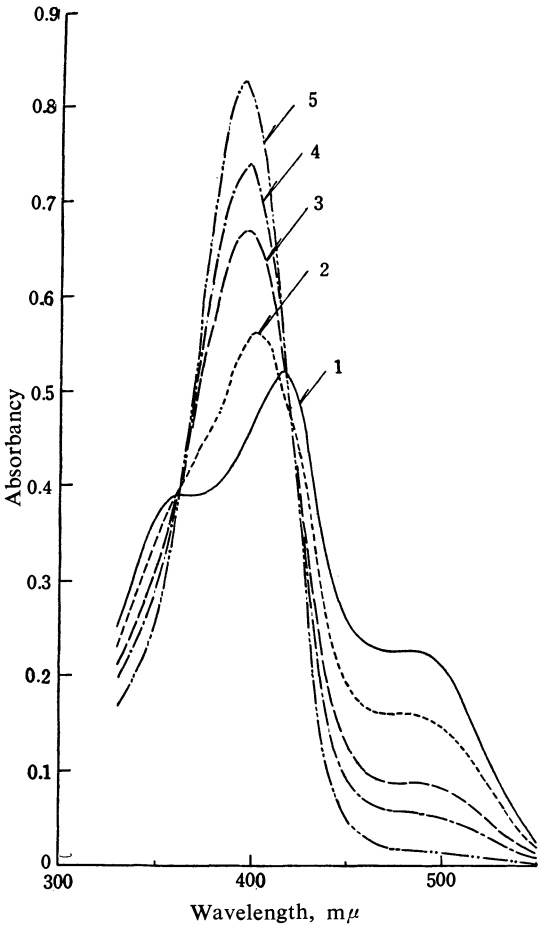



Fig. 1. Absorption spectra of picryl chloride ($3.15\times10^{-5}$ mol.) in water containing ethanol (24% by volume) in the presence of sodium hydroxide (0.377 N) at room temperature.
1 immediately after the preparation,
2 after 2.5 hr.,
3 after 6 hr.,
4 after 9 hr.,
5 after 20 hr.

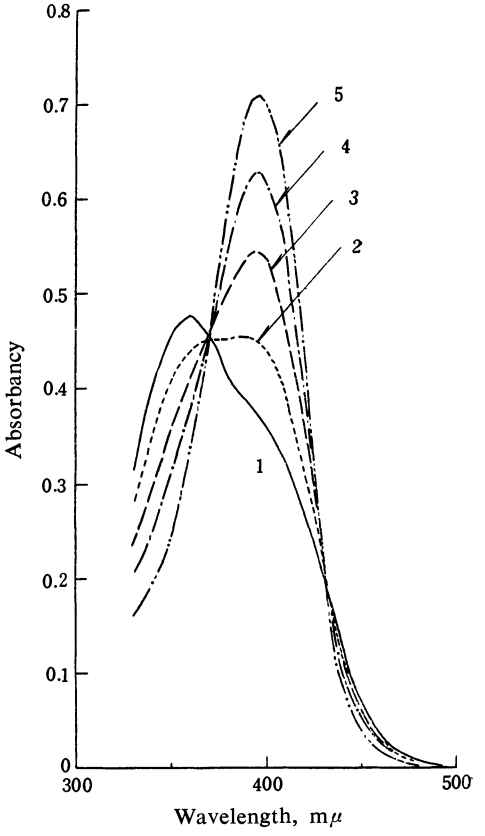



Fig. 2. Absorption spectra of picric acid ($3.12\times10^{-5}$ mol.) in water containing ethanol (24% by volume) in the presence of sodium hydroxide (0.377 N) at room temperature.
1 immediately after the preparation,
2 after 2 hr.,
3 after 5 hr.,
4 after 9 hr.,
5 after 20 hr.

Spectra of a solution of picric acid under the same condition in which the orange aqueous solution of picryl chloride was prepared, are indicated in Fig. 2. The solution of picric acid shows absorption bands at about 360 and 400 mμ, due to picrate anion, immediately after the preparation. However, when it is allowed to stand for many hours, the solution gives a 396 mμ band similar to the absorption curves 3-5 in Fig. 1. On addition of an aqueous hydrochloric acid solution, the 396 mμ band of the solution of picric acid disappears, as indicated in Fig. 3. Neither a spectrum of an aqueous picric acid solution ($3.12\times10^{-5}$ mol.) only in the presence of sodium hydroxide of 0.377 N nor a spectrum of an aqueous picric acid solution ($3.12\times10^{-5}$ mol.) containing only 24% ethanol by volume changed at all, although the solutions were allowed to stand at room temperature for more than ten hours. The intense 396 mμ bands in Fig. 2 closely resemble those of aqueous concentrated sodium hydroxide solutions of picric acid[2]. Both of the latter also disappeared when hydrochloric acid was added to the solutions. Accordingly, the 396 mμ bands in Fig. 2 may be due to a complex between picric acid and sodium hydroxide.

From the above results, the 397 mμ band of the solution in Fig. 1 can be considered to be due to picric acid produced from picryl chloride, in water containing both ethanol and sodium hydroxide. The 360 mμ band of the absorption curve 1 in Fig. 1 appears to be

2) T. Abe, *Nature*. **187**, 234 (1960).

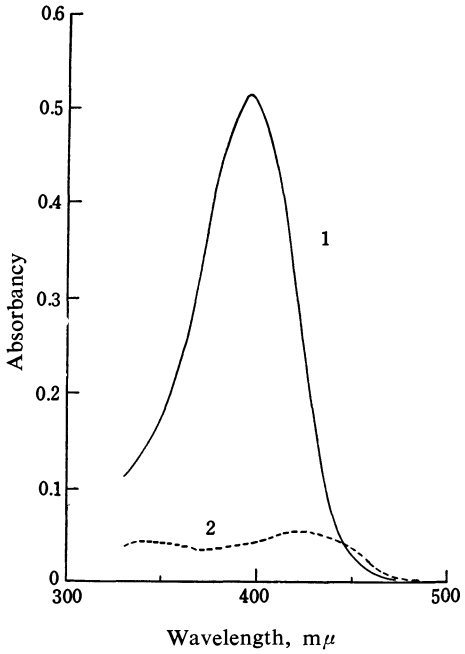
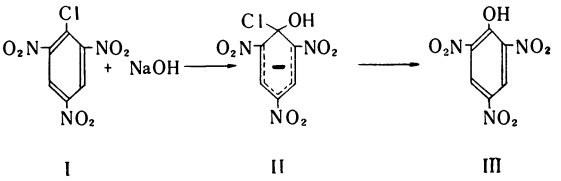



Fig. 3. Absorption spectra of solutions obtained by adding 2 cc. of water and 2 cc. of an aqueous hydrochloric acid solution (6.24 N), respectively, to 5 cc. of the solution of Fig. 2, stood for 25 hr.
1 water,
2 hydrochloric acid.

due to picric acid that changes later into the complex giving the 397 mμ band. Therefore, the 416 and 490 mμ bands of the curve 1 in Fig. 1 can be considered to be due to an labile intermediate that appears in the process of the substitution reaction of picryl chloride (I) to picric acid (III). This intermediate may be expected to be the same addition product II of Meisenheimer's type as presented for many colored products of polynitrobenzene derivatives with alkalies[1-15].




The absorption curve 1 at 416 and 490 mμ in Fig. 1 closely resembles those of red aqueous solutions of 1, 3, 5-trinitrobenzene, 2, 4, 6-trinitrotoluene and tetryl in the presence of sodium hydroxide[1,7]. The intense 416 mμ band lies at the wavelength close to that of

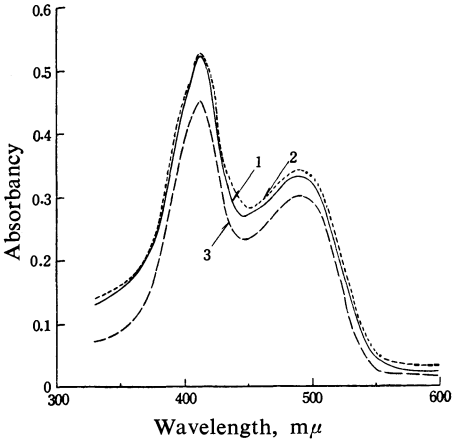



Fig. 4. Absorption spectra of picryl chloride ($1.77\times10^{-5}$ mol.) in ethanol (containing 4% water by volume) in the presence of sodium hydroxide ($4.16\times10^{-2}$ N) at room temperature.
1 immediately after the preparation,
2 after 2 hr.,
3 after 20 hr.

the maximum for an aqueous solution of a red complex obtained from an acetone solution of picryl chloride in the presence of ammonia water[6].

**Absorption Spectra of the Red-Colored Solution in Ethanol.**—The orange ethanolic solution of picryl chloride was made by pipetting 1 cc. of an aqueous sodium hydroxide solution into an ethanolic picryl chloride solution and diluting the solution to 25 cc. As indicated in Fig. 4, the orange ethanolic solution shows two absorption maxima at about 412 and 490 mμ close to those of the bands for the orange aqueous solution of picryl chloride. Yellow crystals began to precipitate from the orange ethanolic solution allowed to stand at room temperature for two hours. As shown in Fig. 4, the part of the solution gives the absorption maxima at the same wavelengths.

3) J. Meisenheimer, *Ann.*, **323**, 205, 214, 241 (1902).
4) R. Foster and D. LL. Hammick, *J. Chem. Soc.*, **1954**, 2153; R. Foster, *Nature*, **176**, 746 (1955); **183**, 1042 (1959).
5) J. B. Ainscough and E. F. Caldin, *J. Chem. Soc.*, **1956**, 2528.
6) T. Abe, This Bulletin, **32**, 997 (1959).
7) T. Abe, ibid., **33**, 41 (1960).
8) R. C. Farmer, *J. Chem. Soc.*, **1959**, 3425.
9) R. C. Farmer, ibid., **1959**, 3430, 3433.
10) M. Kimura, *J. Pharm. Soc. Japan* (*Yakugaku Zasshi*), **73**, 1219 (1953); M. Kimura and M. Thoma, ibid., **78**, 1401 (1958).
11) M. Kimura, *Pharm. Bull.* (*Japan*), **3**, 75 (1955).
12) M. Akatsuka, *J. Pharm. Soc. Japan* (*Yakugaku Zasshi*), **80**, 378, 384, 390 (1960).
13) S. Nagakura, S. Oosawa and H. Tsubomura, presented at the Symposium on Electronic States of Molecules, Kyoto, October, 1958.
14) S. Nagakura and S. Oosawa, presented at the 12th Annual Meeting of the Chemical Society of Japan, Kyoto, April, 1959.
15) S. Nagakura and S. Oosawa, presented at the 13th same Meeting, Tokyo, April, 1960.

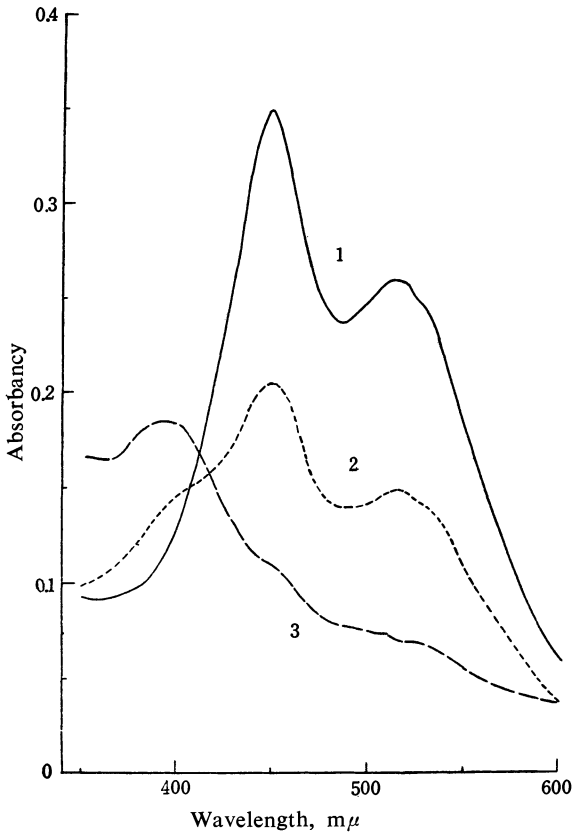



Fig. 5. Absorption spectra of picryl chloride ($1.73\times10^{-5}$ mol.) in acetone (containing 4% water by volume) in the presence of sodium hydroxide ($4.16\times10^{-2}$ N) at room temperature.
1 immediately after the preparation,
2 after 1 hr.,
3 after 3 hr.

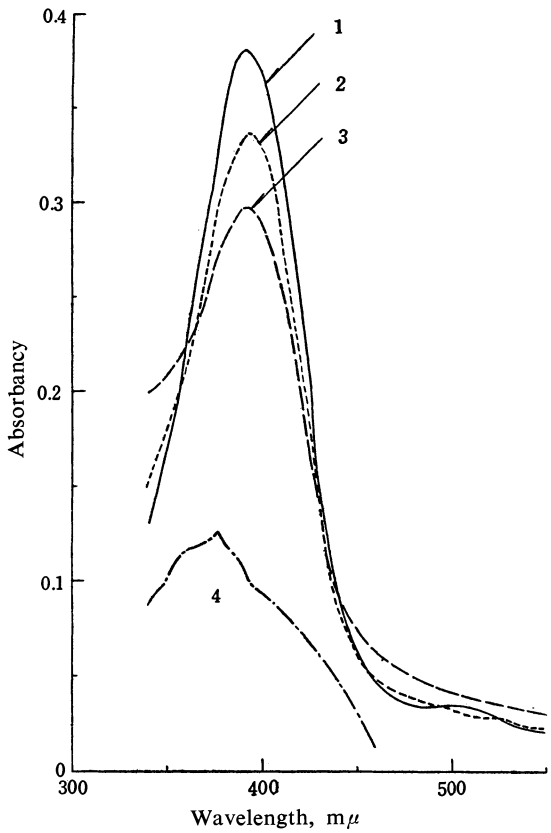



Fig. 6. Absorption spectra of picric acid ($1.81\times10^{-5}$ mol.) in acetone (containing 4% water by volume) in the presence of sodium hydroxide ($4.16\times10^{-2}$ N) at room temperature.
1 immediately after the preparation,
2 after 1 hr.,
3 after 3 hr.,
4 a solution of picric acid ($1.81\times10^{-5}$ mol.) in acetone.

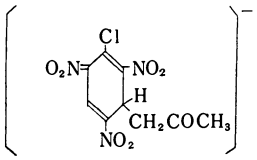
It was reported by Farmer[8] that on treatment of picryl chloride with methanolic potash, Meisenheimer's anion of [Picryl chloride·$OCH_3$]$^-$ was produced. It was reported by Nagakura and Oosawa[15] that when methoxide ion was added to a methanolic solution of chloro-dinitrobenzene, a red color appeared immediately and soon disappeared, and that chloro-dinitrobenzene was almost completely converted into dinitroanisole. The visible absorption curves in Fig. 4 would be due to Meisenheimer's product II. These absorption curves do not resemble that (showing an intense absorption band at about 425 mμ) of an ethanolic solution of the red complex obtained from the acetone solution of picryl chloride in the presence of ammonia water[6].

**Absorption Spectra of the Red-Colored Solution in Acetone.**—The reddishorange solution of picryl chloride in acetone was made by pipetting 1 cc. of an aqueous sodium hydroxide solution into an acetone solution of picryl chloride and diluting the solution to 25 cc. As indicated in Fig. 5, the reddishorange solution gives two absorption maximum bands at longer wavelengths of about 450 and 515 mμ, as compared with the orange aqueous solution in Fig. 1 and the orange ethanolic solution in Fig. 4. When allowed to stand, the reddishorange solution gradually changed into a decolorized solution giving a band at about 390 mμ. About three hours after the preparation the reddishorange solution became turbid. The spectra of the solution could not, therefore, be measured after that time.

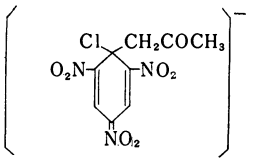
Spectra of a solution of picric acid under the same condition as when the reddishorange solution was prepared, are indicated in Fig. 6. The solution of picric acid showed an intence band at about 390 mμ immediately after the

preparation and also became turbid after about three hours. Absorbancy of the 390 mμ band decreases as the solution is allowed to stand.

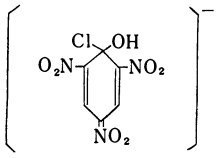
Kimura[11] reported that picryl chloride in a mixture of acetone and methanol (50% by volume) gave an intense 450 mμ band and weak 520~530 mμ ones, and stated that the following four products were responsible for the color, where the product IV was predominant.



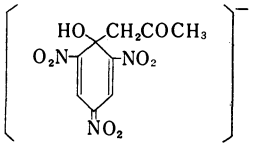
IV



V



VI



VII

The color reactions of trinitrobenzene derivatives with alkalies, however, occur instantaneously at room temperature even in the absence of acetone[1-9,13-15]. The absorption curve 1 in Fig. 5 closely resembles that of 1 in Fig. 1. In addition, the 360 mμ band of the absorption curve 3 in Fig. 5 seems to be due to picric acid produced in comparison with the absorption curves 1-3 in Fig. 6. Accordingly, the curve 1 in Fig. 5 would be due to the product II described above.

The curve (1) in Fig. 5 closely resembles that of a red solution prepared by adding a drop of aqueous sodium hydroxide solution to 1, 3, 5-trinitrobenzene in acetone[16].

## Summary

The red solution prepared by adding sodium hydroxide to an aqueous picryl chloride solution containing a small quantity of ethanol, was relatively stable even at room temperature. The red solution showing the two bands at about 416 and 490 mμ, changed into the yellow solution showing the band similar to that of picric acid under the same condition. Accordingly, the 416 and 490 mμ bands may be due to the intermediate of Meisenheimer's type in the process of the substitution reaction of picryl chloride to picric acid.

In the presence of sodium hydroxide, picryl chloride in ethanol as well as in acetone finally gave the absorption bands analogous to that of picric acid in water containing ethanol. The red solutions in ethanol and in acetone, therefore, would be due to the same intermediate.

The author is particularly indebted to Professor Yōkan Nomura for helpful discussions.

*Department of Chemistry*
*Defense Academy*
*Yokosuka*

16) T. Abe, This Bulletin, 32, 778 (1959).

# *Vinyl Polymerization XLVII*. Polymerization of Acenaphthylene with Ziegler-Type Catalysts*

By Minoru IMOTO and Isamu SOEMATSU

(Received July 22, 1960)

Recently it was patented by Baxter et al.[1] that indene and acenaphthylene were polymerized in the presence of catalysts containing a titanium, vanadium or molybdenum halide in conjunction with a lithium alkyl, lithium aluminum hydride or lithium aluminum tetraalkyl. Partially crystalline homopolymers as well as copolymers of these polymers with ethylene, propylene or 1-hexadecene were described in the patent examples.

Before the patent was published, a kinetic study on polymerization of acenaphthylene in the presence of catalyst of $Ti(OBu)_4$-$AlEt_3$ or $Ti(OBu)_4$-$LiAlH_4$ was undertaken by the present authors. In this paper, the results obtained are described. In literature, polymerization of vinyl monomer with $Ti(OBu)_4$-$AlEt_3$ is found[2]. However, the system of $Ti(OBu)_4$-$LiAlH_4$ was little investigated.

## Experimental

**Materials.**—Aluminum triethyl was obtained from Mitsui Petroleum Co. It was specified to contain 25.87% Al and 74.10% $C_2H_5$. The material was used without further purification. The lithium aluminum hydride was of commercial grade. *n*-Butyl titanate was prepared by the descriptions in literature[3]; b. p. 189~189.1°C (16 mmHg), Ti 13.82% (as $Ti(OC_4H_9)_4$, 14.07%). Acenaphthylene was obtained from acenaphthene by its dehyrogenation; m. p. 92~93°C, b. p., 106~107°C/3 mmHg. *n*-Heptane and toluene, pure grade, was purified as usual.

## Results

**Polymerization of Acenaphthylene with $AlEt_3$-$Ti(OC_4H_9)_4$.**—*Procedure.*—Freshly distilled *n*-heptane was added to a 200 ml. three-necked flask with a mercury seal stirrer, an inlet tube for nitrogen and monomer, and a thermometer. The system was flushed with dry nitrogen. A solution of $(BuO)_4Ti$ in heptane and then a solution of $AlEt_3$ in heptane were added under vigorous stirring. Color appeared immediately, varying from light red to deep green. No precipitate was formed. After 10 min. stirring, the monomer solution was introduced dropwise.

The polymerization system was poured into a large excess of methanol and the precipitate was repeatedly purified by reprecipitation from benzene solution with methanol. The polymer thus obtained contained no trace of ash.

*Effects of Al/Ti Molar Ratio on Conversion of Monomer and on* $[\eta]$ *of Polymer.*—Keeping

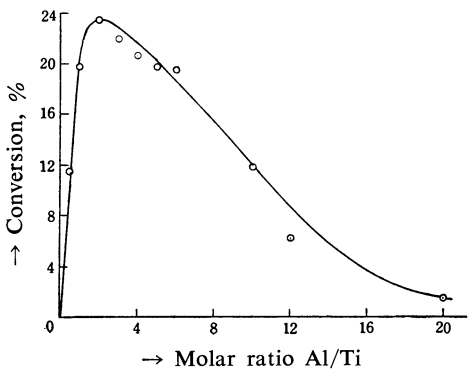



Fig. 1. Conversion of monomer vs. molar ratio of Al/Ti (at 80±0.5°C).

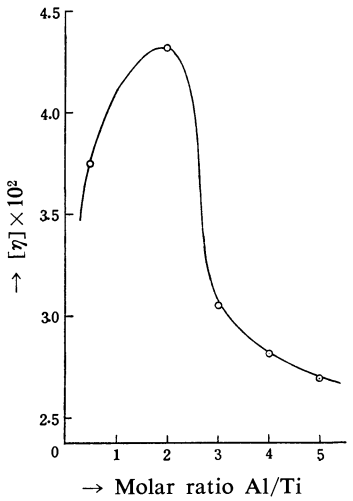



Fig. 2. $[\eta]^{30°}_{Benzene}$ of polyacenaphthylene vs. molar ratio of Al/Ti.

* XLVI of this series: M. Imoto and M. Matsuda, *High Polymer Chem.* (*Kobunshi Kagaku*), **17**, 472 (1960).

1) W. N. Baxter, I. M. Robinson and L. H. Rombach (to duPont) U. S. Pat., 2850488, Spt. 4, 1958.

2) N. G. Gaylord and H. F. Mark, "Linear and Stereoregular Addition Polymers", Interscience Pub., New York (1959), pp. 338, 362.

3) F. Bischoft and H. Adkins, *J. Am. Chem. Soc.*, **46**, 256 (1946).

the quantity of $AlEt_3$ constant at 0.376 g, the quantity of tetrabutyl titanate was varied. 5.00 g. of acenaphthylene was taken. The total volume was 100 ml.

Polymerization was carried out for 10 hr. The results obtained were illustrated in Figs. 1 and 2.

A maximum of conversion appeared at the molar ratio of Al/Ti of 2 : 1.

*Estimation of Activation Energy.* — The concentrations of aluminum triethyl and acenaphthylene were 0.376 g. and 5.00 g. in 100 ml. of the reacting solution. The molar ratio of Al/Ti was kept constant at 2 : 1. The conversions were shown in Fig. 3.

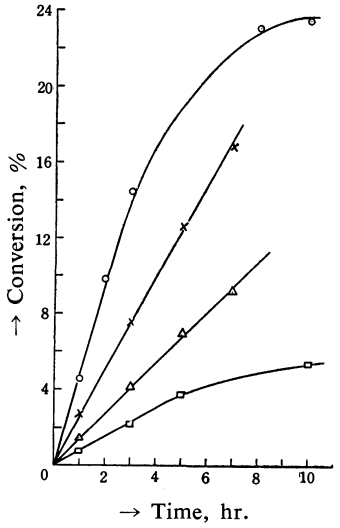



Fig. 3. Conversion of monomer vs. polymerization time.

From the slopes of the conversion curves, the initial rates of polymerisation were computed as Table I.

Table I. Rates of polymerization

| | $Rp$(mol./l. sec.) |
|---|---|
| 50±0.05°C | $0.723\times10^{-6}$ |
| 60 | 1.300 |
| 70 | 2.438 |
| 80 | 4.775 |

From Table I the activation energy for the polymerization of acenaphthylene with $AlEt_3$-$Ti(OC_4H_9)_4$ was computed as 14.3 kcal./mol. (c. f. Fig. 4).

Using collodion film, molecular weight of a polymer was measured by the method of osmotic pressure, as shown in Table II. Intrinsic viscosity was also measured in benzene ($c$=g./100 ml.).

Even if polyacenaphthylene had the small value of $[\eta]$, its molecular weight measured

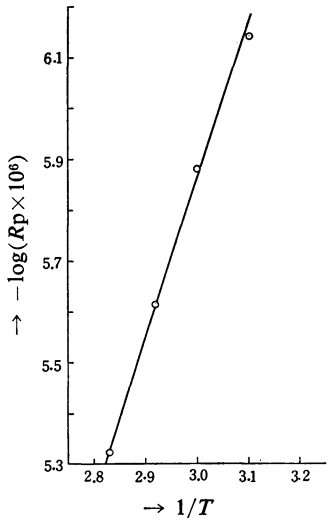



Fig. 4. Estimation of activation energy.

Table II.

| Polymer | Mol. wt. | $[\eta]^{30°}_{Benzene}$ | Literature |
|---|---|---|---|
| Al/Ti=3 : 1 80°C, 10 hr. | 108000 | 0.035 | This paper |
| $BF_3Et_2O$ (60°C) | 125000 | 0.040 | Imoto, Takemoto[4] |

by the method of osmotic pressure was very great. As Table II shows, this characteristic figure coincided with the result obtained in the previous paper[4].

**Polymerization of Acenaphthylene with $LiAlH_4$-$Ti(OC_4H_9)_4$.** — In a tube, 0.0671 g. of $LiAlH_4$, 1.00 g. of acenaphthylene and various quantities of $Ti(OC_4H_9)_4$ in 10 ml. of toluene were sealed. The tubes were heated at 100± 1°C for 2 hr. and then treated as described above. The results were illustrated in Fig. 5.

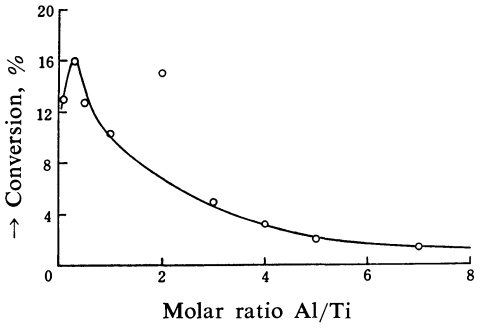



Fig. 5. Conversion of monomer vs. molar ratio of Al/Ti.

The initial rates of polymerization at several reaction temperatures were measured from the conversion curves, as shown in Fig. 6.

4) M. Imoto and K. Takemoto, *J. Polymer Sci.*, **15**, 271 (1955). (The value of $[\eta]$ was not described.)

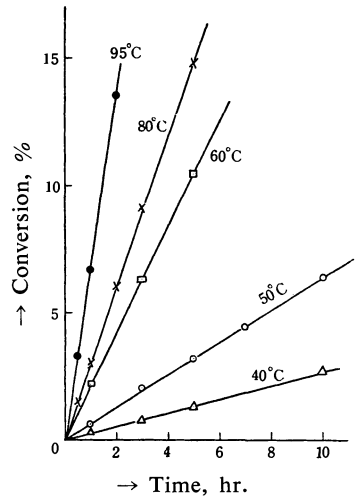



Fig. 6. Conversions of monomer at various temperatures vs. polymerization time.

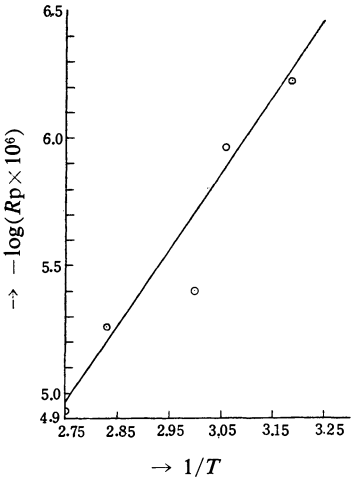



Fig. 7. Estimation of activation energy.

TABLE III. THE INITIAL RATES

| Temp. | $[Rp]_0$ |
|---|---|
| 40±0.05°C | $0.603\times10^{-6}$ mol./l. sec. |
| 50 | 1.15 |
| 60 | 3.99 |
| 80 | 5.55 |
| 95 | 12.2 |

These observations were made in the condition as follows: $LiAlH_4$ 0.25 g., acenaphthylene 1.00 g., toluene 10 ml. and the molar ratio of Al/Ti 2:1. The computed values of the initial rates are tabulated in Table III.

From the values of $[Rp]_0$ in Table III, the apparent activation energy was estimated at about 13 kcal./mol., as in Fig. 7.

After ten hours polymerization, five kinds of polymers were obtained. As to these polymers, the intrinsic viscosities were measured in benzene at 30±0.1°C and the apparent softening points were observed in sealed tubes. The results were shown in Table IV.

TABLE IV. $[\eta]$ AND SOFTENING POINTS

| Temp. | $[\eta]$ | Soften. pt. |
|---|---|---|
| 40°C | 0.0259 | 303°C |
| 50 | 0.0260 | 305 |
| 60 | 0.0268 | 302 |
| 80 | 0.0278 | 309 |
| 95 | 0.0406 | 305 |

**Polymerization of Styrene and Methyl Methacrylate with $LiAlH_4$-$Ti(OB_4H_9)_4$.**—The procedure for polymerization was the same as that described above. 0.0256 g. of $LiAlH_4$ and 0.5 mol. equivalents of $Ti(OB_4H_9)_4$, i.e., the Al/Ti molar ratio 2:1, were used as catalyst. The temperature was 80±1°C and the duration of reaction was 20 hr. The results obtained in toluene were shown in Table V.

TABLE V.

| | Methyl metacrylate g. | Styrene g. | Acenaphthylene, g. | Yield g. |
|---|---|---|---|---|
| Copolymerization | 1.980 | — | 1.000 | 1.1235 |
| | — | 2.040 | 1.000 | 0.1065 |
| Polymerization | 1.980 | — | — | 0.3360 |
| | — | 2.040 | — | 0.6980 |

## Summary

Polymerization of acenaphthylene was studied kinetically in heptane or toluene in the presence of titanium butanate-aluminum triethyl or titanium butanate-lithium aluminum hydride at 40~95°C. Activation energy was computed as 14.3 and about 13 kcal./mol.

Molecular weight of the polymer obtained was 125000, while $[\eta]^{30°}_{\text{Benzene}}$ was only 0.035 ($c$=g./100 ml.).

*Faculty of Engineering*
*Osaka City University*
*Minami-Ogi-machi*
*Kita-ku, Osaka*

# *Studies on the Mucilage of the Root of "Tororo-aoi" (Abelmoschus manihot, MEDIC). III. On the Mechanism of the Characteristic Colloidal Nature of the Mucilage*

By Saburo INOKAWA

(Received April 28, 1960)

In the previous paper[1] it has been shown that in the freshly purified mucilage there exists a network structure built by a very strong interaction between the mucin molecular chains, and that an irreversible marked loss of the interaction occurs by heat treatment although the change in average molecular weight measured by osmotic pressure is small[2]. The present investigation was undertaken in order to explain the mechanism of the network structure in the fresh mucilage and its breaking by heat treatment. Details are shown as follows.

## Experimental

**1) Material.**—Roots of "*Tororo-aoi*" were stored in 0.5% formalin.

**2) Crude Mucilage, Purified Mucin, and Purified Mucilage.**—These preparations were similar to those described in the previous paper[3].

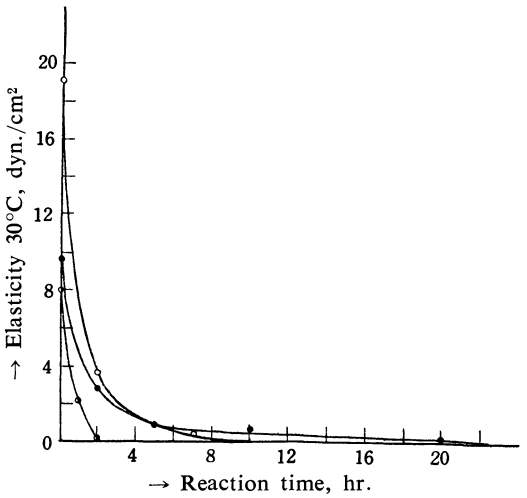



Fig. 1. Effect of addition of $H_2O_2$, $H_2SO_4$, or $H_2O_2$–$H_2SO_4$ on the elasticity of the purified mucilage.
Concentration of mucilage: 0.53%
○, $H_2O_2$ (0.12%)
●, $H_2SO_4$ (9.8%)
◑, $H_2O_2$–$H_2SO_4$ (0.06% : 9.8%)

**3) Elasticity and Intrinsic Viscosity.**—These determinations were the same as those described in the previous paper[3].

**4) Action of Hydrogen Peroxide on the Mucilage.**—The elasticity changes (at 15°C) in the purified mucilage in the presence of hydrogen peroxide, sulfuric acid, or the mixture of both, are shown in Fig. 1.

Acetone was added into the mucilage to precipitate the mucin, just when the elasticity could hardly be observed in the above experiments. The mucin thus obtained was washed with acetone, dried up in vacuo and redissolved in water. In the experiment using sulfuric acid, the redissolved mucilage was neutralized with a dilute sodium hydroxide solution. Table I gives the results of measurement of intrinsic viscosity of the redissolved mucilage.

TABLE I. INTRINSIC VISCOSITY OF THE PURIFIED MUCILAGE JUST WHEN THE ELASTICITY COULD HARDLY BE OBSERVED BY ADDITION OF HYDROGEN PEROXIDE, SULFURIC ACID, OR BOTH

| Treatment by | Intrinsic viscosity l./g. | | | | Mean value l./g. |
|---|---|---|---|---|---|
| $H_2O_2$ | 1.7 | 1.2 | 1.8 | 1.6 | 1.6 |
| $H_2SO_4$ | 0.47 | 0.55 | 0.58 | 0.50 | 0.53 |
| $H_2O_2$–$H_2SO_4$ | 1.8 | 1.7 | 1.4 | 1.7 | 1.7 |
| Heating at 80°C for 2 hr. | 1.5 | 1.6 | 1.4 | 1.4 | 1.5 |

The intrinsic viscosity of the mucilage treated with hydrogen peroxide or hydrogen peroxide-sulfuric acid is about the same as that of the heated mucilage. However, that of the mucilage treated with sulfuric acid is 0.52, and is considerably smaller than the above-mentioned values.

**5) Effect of Oxygen in the Air upon the Mucilage and the Mucin.**—a) The purified mucins, one in nitrogen atmosphere and the other in the air, were

TABLE II. EFFECT OF OXYGEN UPON THE INTRINSIC VISCOSITY LOSS OF THE PURIFIED MUCIN BY HEAT TREATMENT

| Heated in | Intrinsic viscosity, l./g. | |
|---|---|---|
| | Before heating | After heating at 80°C for 120 min. |
| $N_2$ atmosphere | 2.86 | 2.77 |
| Air | 2.86 | 1.83 |

1) S. Inokawa, This Bulletin, **33**, 1476 (1960).
2) S. Inokawa, R. Goto and I. Morimoto, *J. Chem. Soc. Japan, Pure Chem. Sec.* (*Nippon Kagagu Zasshi*), **81**, 783 (1960).
3) S. Inokawa, This Bulletin, **33**, 1472 (1960).

TABLE III. EFFECT OF OXYGEN UPON THE INTRINSIC VISCOSITY LOSS OF THE PURIFIED MUCILAGE BY HEAT TREATMENT

| Condition | Method | Intrinsic viscosity, l./g. | | |
|---|---|---|---|---|
| | | Before heating | After heating 80°C, 90 min. | After heating 80°C, 150 min. |
| Oxygen-free mucilage | High vacuum | 2.64 | 2.23 | 2.10 |
| | $N_2$-blowing | 2.55 | 2.20 | 2.08 |
| Air-containing mucilage | | 2.80 | 1.47 | 1.38 |

heated at 80°C for 120 min. by the high vacuum method described in the previous paper[4]. Both the heated mucins were dissolved in water and the viscosity was measured. As shown in Table II the intrinsic viscosity of the mucin heated in nitrogen atmosphere does not decrease practically. b) The purified oxygen-free mucilage prepared by the high vacuum method[4] was heated at 80°C and the intrinsic viscosity was measured. As shown in Table III the intrinsic viscosity loss of the purified oxygen-free mucilarge by heating is much smaller than that of the usual air-containing mucilage.

For the purpose of obtaining oxygen-free mucilage more simply, oxygen-free nitrogen[5] was blown for 10 hr. into the purified mucilage in the glass tube shown in Fig. 2, and then the glass tube was sealed off first at A and next at B. The viscosity loss of the obtained oxygen-free mucilage by heating was similar to that of oxygen-free mucilage prepared by the high vacuum method as shown in Table III. Then, the effect of oxygen upon the elasticity loss of the purified mucilage by heating was examined

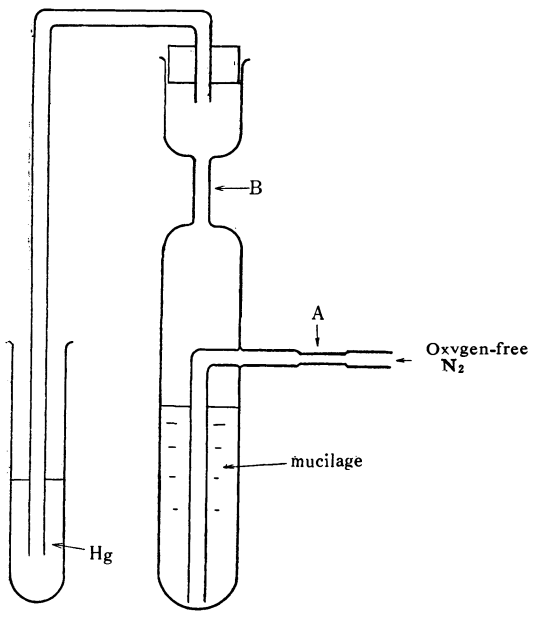



Fig. 2. Apparatus for the blowing method.

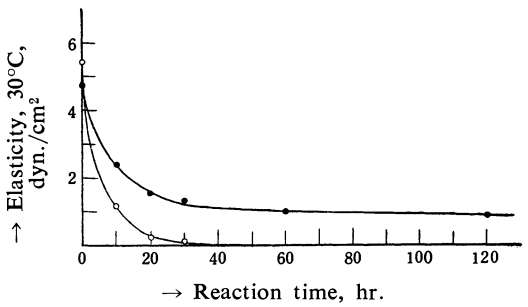



Fig. 3. Effect of oxygen on the elasticity fall of the purified mucilage by heating.
Concentration of mucilage: 0.31%.
○, air-containing mucilage
●, oxygen-free mucilage

by this nitrogen-blowing method. The elasticity loss of nitrogen-blowing mucilage by heating as shown in Fig. 3 is much smaller than that of the air-containing mucilage.

**6) Muddy Matter Produced by Heating.**—It has been reported[1], from the observation of sedimentation diagrams of the heated purified mucilage in an ultracentrifuge that there was something which sedimented rapidly in the initial few minutes. A precipitate[6] (ca. 1.1 wt. % of mucin), which was dispersed easily by irradiation of ultrasonic wave, was obtained from the purified mucilage heated at 95°C for 16 hr. The dispersed precipitate was mounted on a specimen holder for electron microscopy with a formvar supporting-film and dried.

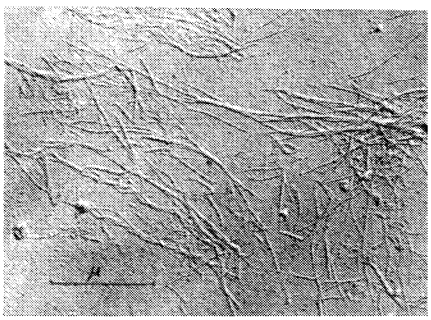


Fig. 4. Electron micrograph of the precipitate produced by heating the purified mucilage.
(dispersed by ultrasonic wave)
(Cr-shadowing)

4) S. Inokawa, R. Goto and E. Fujimoto, *J. Chem. Soc. Japan, Pure Chem. Sec. (Nippon Kagaku Zasshi)*, **81**, 678 (1960).

5) By blowing of carbon dioxide instead of nitrogen, similar results were obtained.

6) This precipitate did not show reactions of starch.

After chromium-shadowing the specimen was observed by an electron microscope of the type Akashi TRS-50 B, showing a fine fiber-like picture as shown in Fig. 4. The nitrogen content of the precipitate was 1.9%. After hydrolysis of the precipitate in 2 N hydrochloric acid at 100°C for 22 hr. in a sealed tube, the hydrolyzed solution was diluted with water, filtered, passed through a cation-exchange resin Amberlite IR-112, evaporated, and dried, in vacuo. From the residue only glucose was detected by paper chromatography using the solvent system: ethyl acetate: pyridine: water (12 : 5 : 4).

**7) Effect of Potassium Thiocyanate, Sodium Lauryl Sulfate, Guanidine Hydrochloride, and Dichloro acetic Acid on the Elasticity of the Purified Mucilage.**—Fig. 5 shows the elasticity curves plotted against concentrations of four sorts of reagents. It is observed that the elasticity is practically uninfluenced by the addition of these reagents[7].

**8) Periodate Oxidation of the Mucilage.**—The mucilage (0.448 g.) was dissolved in water (in 500 ml. bottle), and sodium periodate solution (0.2 M, 10 ml.) was added, followed by water to the requisite volume. Formic acid was yielded, and uptake of periodate of the solution followed. The results are tabulated in Table IV. It is clear that 1 M of formic acid was produced by consuming 2 M of periodate.

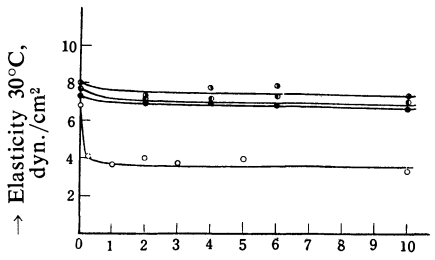



Fig. 5. Effect of addition of potassium thiocyanate sodium lauryl sulfate, guanidine hydrochloride, and dichloroacetic acid on the elasticity of the purified mucilage.
Concentration of mucilage: 0.36%.
●, potassium thiocyanate
◐, sodium lauryl sulfate
◑, guanidine hydrochloride
○, dichloroacetic acid

TABLE IV. PERIODATE OXIDATION OF THE MUCILAGE AT 15°C[8]

| Time, hr. | Formic acid produced mol./G mol.[9] | Consumed $IO_4^-$ mol./G mol. |
|---|---|---|
| 0 | 0 | 0 |
| 10 | 0.72 | 1.21 |
| 24 | 1.09 | 1.64 |
| 52 | 1.19 | 2.02 |
| 75 | 1.23 | 2.07 |
| 125 | 1.24 | 2.14 |

## Discussion

It is said that the mucin of "*Tororo-aoi*" is a polysaccharide consisting of rhamnose and galacturonic acid linked in straight chains[10] and the molecular weight is very high, that is, the value is 150000~200000[2]. The relative amounts of the components vary, depending on the source. However, it is shown from the results of periodate-oxidation (experiment 8) that the mucin molecule has branched chains. Thus, it seems to be plausible that the mucin molecule is a long chain polysaccharide with many short branched chains. Also, it has been shown that in the fresh purified mucilage there exists a network structure like a gel[1]. Considering that the elasticity is little changed by the electrolysis[3] or the addition of sodium chloride[3], the network structure may not be built by intermolecular ionic bonds of the mucin. Moreover, the elasticity is little influenced by the addition of potassium thiocyanate, sodium lauryl sulfate, guanidine hydrochloride, and dichloroacetic acid (experiment 7). Therefore the network structure may not be built by hydrogen bonds between mucin molecules. Also, the agitation of mucilage causes an irreversible diminution of the elasticity[3]. From the consideration of these experimental results, it seems to be most reasonable to suppose that the network structure is built by interlocking or entanglement of mucin molecules.

By heating, the elasticity of the purified mucilage diminishes and at the same time muddy matters consisting of fibrous glucosans and proteins were produced (experiment 6) but the molecular weight change is slight[2]. These experimental results mentioned above would lead to the conclusion that the mucin molecules are entangled between short branched chains of the mucin molecules, fibrous glucosans and proteins. On heating, the entanglement is broken by oxidation (experiment 5).

## Summary

1) The colloidal characteristics of the mucilage from "*Tororo-aoi*" such as the elasticity, spinnability, and so on are caused by the network built by interlocking between short branched chains of the mucin molecules, fibrous glucosans and proteins.

7) It seems to be reasonable that a little loss in elasticity by the addition of dichloroacetic acid was caused by a change of pH in the mucilage because the elasticity loss was identical with the case in which acetic acid or oxalic acid was added.

8) P. F. Fleury and J. Lange, *J. pharm. Chim.*, [8], **17**, 107, 196 (1933).

9) The value of G mol. was assumed to be 161, which is the mean value of molecular weight of rhamnose and galacturonic acid.

10) S. Machida and N. Uchino, *J. Chem. Soc. Japan, Pure Chem. Sec.* (*Nippon Kagaku Zasshi*), **74**, 183 (1953).

2) The remarkable change of the colloidal nature by heating is caused by breaking down the interlocking by oxidation.

Finally the writer wishes to express his hearty thanks to Professor R. Goto, Kyoto University, for his invaluable advice and encouragement throughout this work. He is also indebted to Professor E. Suito and Dr. K. Takiyama of Kyoto University for their help in the preparation of the electron micrographs, and further to Mr. A. Sera, Mr. A Takatsuki, Mr. I. Morimoto and Mr. E. Fujimoto for their kind co-operation in this research. It is a pleasure to thank Koshin Kogyo Co. for the generous supply of roots of "*Tororo-aoi*".

*Department of Chemistry*
*Faculty of Science*
*Kyoto University*
*Sakyo-ku, Kyoto*

# *Hydrogenation and Hydrogenolysis. V*[1]*. Rhodium-Platinum Oxide as a Catalyst for the Hydrogenation of Organic Compounds*[2]

By Shigeo NISHIMURA

(Received July 26, 1960)

In previous papers[1,2], it was reported that rhodium-platinum oxide, prepared by fusion of the mixture of rhodium chloride and chloroplatinic acid or ammonium chloroplatinate in a ratio of 3 : 1 by the weights of the metals with sodium nitrate exactly in the same way as in the preparation of Adams platinum oxide, can be reduced with hydrogen to the metal form under ordinary conditions and also that the resulting rhodium-platinum black is an excellent catalyst retaining the nature of pure rhodium catalysts and is substantially superior to Adams platinum oxide both in activity and in selectivity in the hydrogenation of various aromatic compounds. The present paper describes the use of the rhodium-platinum oxide as a catalyst and also the comparisons with platinum oxide and with palladous oxide in the hydrogenation of various organic compounds under ordinary conditions.

## Experimental

**Materials.** — The oxide catalysts were prepared according to the procedures described in the preceding paper[1]. Glacial acetic acid of Wakō Pure Chemical Industries G. R. grade was used without further purification. Commercial 95% ethanol was used after distillation. All the substrates were carefully purified before use by recrystallization or by distillation.

**Hydrogenation.**—Hydrogenation was carried out under atmospheric pressure and at room temperature (24~26°C). After the oxide was reduced to metal, the substance was added with a small amount of solvent, and the mixture was shaken with hydrogen at about 350~400 oscillations per minute.

## Results and Discussion

**Catalytic Reduction, where the C-O Linkage is Liable to Hydrogenolysis.** — As already reported in previous papers[1,2], the compounds, which have C-O linkages susceptible to hydrogenolysis, are less hydrogenolyzed and much more rapidly hydrogenated in acetic acid with rhodium-platinum oxide than with platinum oxide[3]. Further results are shown in Tables I and II, and also the hydrogenation of acetophenone in Table III and furfuryl alcohol in Table IV. If less hydrogenolysis is desired, it is preferable to use ethanol with a small amount of acetic acid as the solvent, as shown in the hydrogenation of benzyl methyl ether[4]. Benzyl acetate is almost completely hydrogenolyzed even under these conditions. The addition of a slight amount of hydrochloric acid increases the hydrogenolysis as shown in the hydrogenation of hydroquinone with platinum oxide[5].

Aliphatic and alicyclic ketones are also less hydrogenolyzed and much more rapidly hydrogenated with rhodium-platinum oxide than with platinum oxide in acetic acid (Table II).

1) Part IV of this series: S. Nishimura, T. Onoda and A. Nakamura, This Bulletin, 33, 1356 (1960).
2) Cf. Part III of this series: S. Nishimura, ibid., 33, 566 (1960).
3) Cf. H. A. Smith and R. G. Thompson, "Advances in Catalysis", Vol. 9, Academic Press Inc., New York (1957), p. 727.
4) Cf. S. Nishimura, This Bulletin, 32, 1155 (1959).
5) For the effect of the solvent on the hydrogenation and hydrogenolysis, see, for instance, Ref. 1.

TABLE I. CATALYTIC REDUCTION OF AROMATIC COMPOUNDS WHERE THE C-O LINKAGE IS LIABLE TO HYDROGENOLYSIS

| Compound, g. | Solvent, ml. | Catalyst, g. | Hydrogen uptake mol./mol. | Time for hydrogenation min. |
|---|---|---|---|---|
| Benzyl methyl ether, 0.611 | EtOH, 20 | Rh-Pt oxide, 0.10 | S.* | |
| 〃 | 〃 | Pt oxide, 0.20 | S.* | |
| 〃 | EtOH, 20+ AcOH, 0.02 | Rh-Pt oxide, 0.10 | 3.13 | 120 |
| 〃 | 〃 | Pt oxide, 0.20 | 3.13 | 240 |
| 〃 | AcOH, 20 | Rh-Pt oxide, 0.05 | 3.48 | 80 |
| 〃 | 〃 | Pt oxide, 0.05 | 3.89 | 130 |
| Benzyl alcohol, 0.541 | 〃 | Rh-Pt oxide, 0.05 | I.** | |
| 〃 | 〃 | Pt oxide, 0.05 | 3.95 | 120 |
| Benzyl acetate, 0.751 | 〃 | Rh-Pt oxide, 0.05 | 3.94 | 14 |
| 〃 | 〃 | Pt oxide, 0.05 | 3.99 | 60 |
| Hydroquinone, 1.101 | AcOH, 30 | Rh-Pt oxide, 0.05 | 3.25 | 40 |
| 〃 | 〃 | Pt oxide, 0.05 | 4.01 | 110 |
| 〃 | AcOH, 30+ 3 N HCl, 0.1 | 〃 | 4.59 | 120 |
| Methyl salicylate, 0.761 | AcOH, 20 | Rh-Pt oxide, 0.10 | 3.13 | 65 |
| 〃 | 〃 | Pt oxide, 0.10 | 3.26 | 200 |
| α-Naphthol, 0.721 | 〃 | Rh-Pt oxide, 0.10 | 5.17 | 270 |
| 〃 | 〃 | Pt oxide, 0.10 | 5.16 | 300 |
| β-Naphthol, 0.721 | 〃 | Rh-Pt oxide, 0.10 | 5.21 | 85 |
| 〃 | 〃 | Pt oxide, 0.10 | 5.37 | 275 |

* Slow reduction.

** Incomplete reduction because of the decreasing rate.

TABLE II. CATALYTIC REDUCTION OF ALIPHATIC AND ALICYCLIC KETONES

| Compound, g. | Solvent, ml. | Catalyst, g. | Hydrogen uptake mol./mol. | Time for hydrogenation min. |
|---|---|---|---|---|
| Diethyl ketone, 0.861 | AcOH, 20 | Rh-Pt oxide, 0.05 | 1.01 | 140 |
| 〃 | 〃 | Pt oxide, 〃 | 1.01 | 150 |
| Cyclohexanone, 0.981 | 〃 | Rh-Pt oxide, 〃 | 1.03 | 7 |
| 〃 | EtOH, 20 | Pt oxide, 〃 | 1.00 | 80 |
| 〃 | AcOH, 20 | 〃 〃 | 1.27 | 30 |
| 〃 | AcOH, 20+ 3 N HCl, 0.1 | 〃 〃 | 1.31 | 24 |
| Cyclopentanone, 0.841 | AcOH, 20 | Rh-Pt oxide, 〃 | 1.08 | 40 |
| 〃 | 〃 | Pt oxide, 〃 | 1.56 | 200 |
| Ethyl acetoacetate, 1.302 | 〃 | Rh-Pt oxide, 〃 | 1.11 | 15 |
| 〃 | 〃 | Pt oxide, 〃 | 1.56 | 300 |

In neutral ethanolic solution these ketones are hydrogenated quantitatively with platinum oxide to the corresponding alcohols with the absorption of just one mole of hydrogen, and the addition of hydrochloric acid increases hydrogenolysis, though only to a small extent, as shown in the hydrogenation of cyclohexanone. As is well known, palladous oxide is practically ineffective for the hydrogenation of these ketones. Details of the hydrogenation and hydrogenolysis of aliphatic and alicyclic ketones will be published later.

**Catalytic Reduction of Acetophenone (Table III).**—Acetophenone is reduced with rhodium-platinum oxide to cyclohexylmethylcarbinol quantitatively in ethanol and almost quantitatively in acetic acid. The hydrogenation is especially rapid in the latter solvent accompanied only by a slight hydrogenolysis (6%). With platinum oxide, in ethanol as the solvent, one mole of hydrogen is absorbed rather rapidly and further reduction occurs only very slowly, and in acetic acid as the solvent, as much as 84% is hydrogenolyzed to give ethylcyclohexane as indicated by the hydrogen uptake. Both platinum oxide and palladous oxide show the greatest activity for the reduction to ethylbenzene in the presence of acetic acid with

TABLE III. CATALYTIC REDUCTION OF ACETOPHENONE

| Acetophenone g. | Solvent, ml. | Catalyst, g. | Hydrogen uptake mol./mol. | Time for hydrogenation min. |
|---|---|---|---|---|
| 0.601 | EtOH, 20 | Rh-Pt oxide, 0.05 | 3.98 | 8/1 mol.<br>130/4 mol. |
| 〃 | 〃 | Pt oxide, 〃 | S. after 1 mol. | 25/1 mol. |
| 〃 | AcOH, 20 | Rh-Pt oxide, 〃 | 4.06 | 24 |
| 〃 | 〃 | Pt oxide, 〃 | 4.84 | 110 |
| 〃 | AcOH, 20+ 3 N HCl, 0.1 | Rh-Pt oxide, 〃 | S. | |
| 〃 | 〃 | Pt oxide, 〃 | 5.03 | 16/2 mol.<br>120/5 mol. |
| 1.201 | EtOH, 20 | Pd oxide, 〃 | 1.98 | 20/1 mol.<br>200/2 mol. |
| 〃 | AcOH, 20 | 〃 〃 | 1.98 | 15/1 mol.<br>60/2 mol. |
| 〃 | AcOH, 20+ 3 N HCl, 0.1 | 〃 〃 | 1.99 | 14/1 mol.<br>30/2 mol. |

Reduction on a preparative scale

| Acetophenone g. | Solvent ml. | Catalyst, g. | Reactivation with air | Hydrogen uptake mol./mol. | Time hr. | Time min. | Product |
|---|---|---|---|---|---|---|---|
| 12.01 | AcOH, 50 | Rh-Pt oxide, 0.2 | twice | 4.06 | 3 | 30 | Cyclohexyl-methylcarbinol, 80%. B.p. 91°C/ 22 mmHg; $n_D^{19}$ 1.4652 |

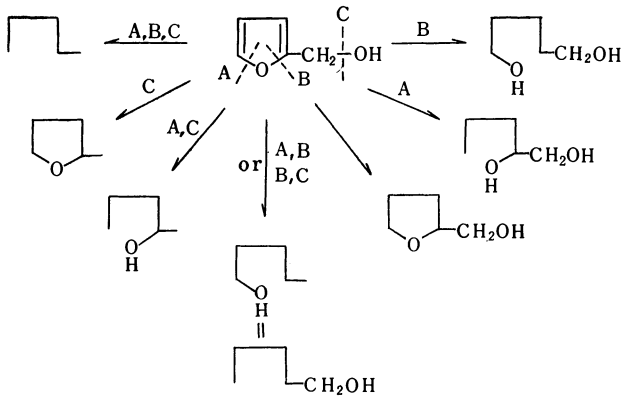



Fig. 1. Catalytic reduction of furfuryl alcohol.

added hydrochloric acid, while the reduction proceeds only very slowly with rhodium-platinum oxide in the same medium. As is well known, palladium is a catalyst preferred for the selective reduction of the side chain because of its low activity for the hydrogenation of the benzene nucleus. Like platinum and palladium catalysts, deactivated rhodium-platinum is also reactivated by shaking with air, and this process is very effective in the hydrogenation of a larger amount of a substrate.

**Catalytic Reduction of Furfuryl Alcohol (Table IV).**—The complete hydrogenation of furfuryl alcohol under mild conditions is generally expected to give the seven compounds as the result of various competitive reactions between the hydrogenation of the double bonds and the hydrogenolysis of the three C–O linkages indicated by A, B and C, as illustrated in Fig. 1. The kinds and amounts of the products largely depend on the nature of the catalyst and the solvent used. Both rhodium-platinum oxide and palladous oxide give tetrahydrofurfuryl alcohol quantitatively in acetic acid as well as in ethanol with the absorption of two moles of hydrogen. The reduction proceeds most rapidly with rhodium-platinum oxide in acetic acid. With platinum oxide the reduction could not be completed in ethanol because of the decreasing rate of the hydrogenation. But in acetic acid the reduction proceeds smoothly to completion

TABLE IV. CATALYTIC REDUCTION OF FURFURYL ALCOHOL

| Furfuryl alcohol g. | Solvent, ml. | Catalyst, g. | Hydrogen uptake mol./mol. | Time for hydrogenation min. |
|---|---|---|---|---|
| 0.981 | EtOH, 20 | Rh-Pt oxide, 0.05 | 1.96 | 42 |
| 〃 | 〃 | Pt oxide, 〃 | I. | |
| 〃 | 〃 | Pd oxide, 〃 | 1.95 | 105 |
| 〃 | AcCH, 20 | Rh-Pt oxide, 〃 | 1.97 | 28 |
| 〃 | 〃 | Pt oxide, 〃 | 2.86 | 115 |
| 〃 | 〃 | Pd oxide, 〃 | 1.96 | 45 |
| 〃 | EtOH, 20+ 3 N HCl, 0.1 | Pt oxide, 〃 | 3.11 | 120 |
| 〃 | AcOH, 20+ 3 N HCl, 0.1 | 〃 〃 | 3.38 | 85 |
| 〃 | 〃 | Pd oxide, 〃 | S. after 2.03 mol. | 35/2 mol. |

TABLE V. PRODUCTS OF CATALYTIC REDUCTION OF FURFURYL ALCOHOL WITH PLATINUM OXIDE IN ETHANOL (OR TETRAHYDROFURFURYL ALCOHOL) WITH HYDROCHLORIC ACID

| Product | Yield, % | B. p., °C | $n_D^{20}$ |
|---|---|---|---|
| Pentane* | 0.8 | 35 | |
| 2-Methyltetrahydrofuran* | 14.8 | 75～84 | 1.4031 |
| 2-Pentanol | 5.5 | 120～123 | 1.4047 |
| 1-Pentanol | 11.6 | 137～139 | 1.4096 |
| Tetrahydrofurfuryl alcohol | 20.6 | 173～177 | 1.4505 |
| 1,2-Pentanediol | 13.3 | 110～113/21 mmHg | 1.4402 |
| 1,5-Pentanediol | 3.3 | 138～142/21 mmHg | 1.4499 |

* These compounds were isolated with the use of tetrahydrofurfuryl alcohol as the solvent.

with an extensive hydrogenolysis as indicated by the absorption of 2.86 mol. of hydrogen[6]. On the other hand, in the presence of hydrochloric acid and ethanol (or tetrahydrofurfuryl alcohol), all the seven compounds were obtained with absorption of 3.11 mol. of hydrogen as shown in Table V[7]. The portion of hydrogenolysis increases further in the presence of acetic acid and hydrochloric acid. With palladous oxide, even in the presence of hydrochloric acid, no hydrogenolysis occurs before the saturation of the double bonds.

**Catalytic Reductions of Other Aromatic and Heterocyclic Compounds (Table VI).**—Rhodium-platinum oxide is as effective for the hydrogenation of pyridine and quinoline as for aromatic compounds, and substantially more active than platinum oxide also in these hydrogenations. The rhodium-platinum catalyst is also the most active of the three oxides in the hydrogenation of the double bond of the side chain as shown in the hydrogenation of ethyl cinnamate (Table VI) and cinnamyl alcohol (Ref. 1). Palladous oxide is more active in these hydrogenations than platinum oxide.

**Catalytic Reduction of Nitrobenzene (Table VII).**—Rhodium-platinum oxide is also the most active catalyst in the hydrogenation of nitrobenzene to aniline. Contrary to platinum oxide and palladous oxide, rhodium-platinum oxide is more active in acetic acid than in ethanol. The subsequent hydrogenation of the benzene nucleus proceeds rather slowly both with rhodium-platinum oxide and with platinum oxide in acetic acid. Palladous oxide is almost entirely ineffective for the hydrogenation.

The present results with those reported previously show that the rhodium-platinum (3 : 1) oxide is a substantially more active catalyst than platinum oxide and palladous oxide in the hydrogenation of various organic compounds under ordinary conditions[8], and especially effective where it is desired to avoid hydrogenolysis. Decrease of the platinum in the rhodium-platinum oxide depresses the hydrogenolysis further, but only to a small extent. On

6) H. A. Smith and J. F. Fuzek, *J. Am. Chem. Soc.*, **71**, 415 (1949), report that 1, 2-pentanediol was obtained almost quantitatively under similar conditions.

7) W. E. Kaufmann and R. Adams, *J. Am. Chem. Soc.*, **45**, 3029 (1923), reported that 1-pentanol, 1, 2- and 1, 5-pentanediols and tetrahydrofurfuryl alcohol were obtained with platinum oxide in the presence of ethanol and a small amount of ferrous chloride with the absorption of 2.5 mol. of hydrogen. Their results show that only the C-O linkages A and B were hydrogenolyzed under these conditions.

8) The metal content of rhodium-platinum (3 : 1) oxide is only 65% of its weight. The value is considerably smaller than those of platinum oxide (80%) and palladous oxide (87%). Therefore, the activity of the rhodium-platinum oxide is much greater when compared in a unit weight of the metal.

TABLE VI. CATALYTIC REDUCTIONS OF OTHER AROMATIC AND HETEROCYCLIC COMPOUNDS

| Compound, g. | Solvent, ml. | Catalyst, g. | Hydrogen uptake mol./mol. | Time for hydrogenation min. |
|---|---|---|---|---|
| Toluene, 0.921 | AcOH, 20 | Rh-Pt oxide, 0.05 | 3.02 | 28 |
| 〃 | 〃 | Pt oxide, 〃 | 3.01 | 110 |
| Biphenyl, 0.771 | 〃 | Rh-Pt oxide, 〃 | 5.99 | 180 |
| 〃 | 〃 | Pt oxide, 〃 | 6.01 | 440 |
| Ethyl cinnamate, 1.762 | 〃 | Rh-Pt oxide, 〃 | 4.06 | 6/1 mol.<br>65/4 mol. |
| 〃 | 〃 | Pt oxide, 〃 | 4.01 | 30/1 mol.<br>250/4 mol. |
| 〃 | 〃 | Pd oxide, 〃 | 1.02 | 10/1 mol. |
| Pyridine, 0.791 | 〃 | Rh-Pt oxide, 〃 | 3.01 | 28 |
| 〃 | 〃 | Pt oxide, 〃 | 3.01 | 170 |
| Quinoline, 0.646 | 〃 | Rh-Pt oxide, 〃 | 5.02 | 80 |
| 〃 | 〃 | Pt oxide, 〃 | 4.98 | 200 |

Reduction on a preparative scale

| Toluene g. | Solvent ml. | Catalyst, g. | Reactivation with air | Hydrogen uptake mol./mol. | Time hr. | Time min. | Product |
|---|---|---|---|---|---|---|---|
| 9.21 | AcOH, 50 | Rh-Pt oxide, 0.2 | once | 2.99 | 1 | 50 | Methylcyclohexane, 79%. B. p. 100～101°C |

TABLE VII. CATALYTIC REDUCTION OF NITROBENZENE

| Nitrobenzene g. | Solvent, ml. | Catalyst, g. | Hydrogen uptake mol./mol. | Time for hydrogenation min. |
|---|---|---|---|---|
| 1.231 | EtOH, 20 | Rh-Pt oxide, 0.05 | S. after 3 mol. | 10/3 mol. |
| 〃 | 〃 | Pt oxide, 〃 | 〃 | 14/3 mol. |
| 〃 | 〃 | Pd oxide, 〃 | 3.00 | 24 |
| 〃 | AcOH, 20 | Rh-Pt oxide, 〃 | 6.00 | 6/3 mol.<br>190/6 mol. |
| 〃 | 〃 | Pt oxide, 〃 | 5.97 | 20/3 mol.<br>230/6 mol. |
| 〃 | 〃 | Pd oxide, 〃 | 3.00 | 40 |

the other hand, the decrease of platinum causes the following disadvantages: (a) It takes a longer time for the reduction of the oxide to the metal. (b) The recovery of the catalyst becomes more difficult, because the residue insoluble in aqua regia increases with the decrease of the platinum[9]. For the reasons mentioned above, the present author chooses the proportion 3 : 1 of the two metals in the rhodium-platinum oxide as satisfactory for most hydrogenations and convenient for practical use. The fact that the rhodium-platinum oxide is not identical with a mere mixture of rhodium oxide and platinum oxide, the former being reduced with hydrogen much more rapidly and uniformly than the latter, was further confirmed by an X-ray diffraction of these oxides. The peak of rhodium oxide at $2\theta=28°$ (Cu-$K_\alpha$ radiation) disappers completely and most of other peaks of the oxide are greatly deformed in the pattern of rhodium-platinum (3 : 1) oxide, while the peak of rhodium oxide at 28° and the peak of platinum oxide at 33.3° are clearly detected in the pattern of a mechanical mixture of rhodium oxide and platinum oxide in a ratio of 3 : 1 by the weights of the metals.

The author wishes to express his hearty thanks to Professor Yoshiyuki Urushibara for his valuable suggestions and encouragement. The author is also indebted to Dr. Hiroshi Takahashi for the measurement of the X-ray diffraction and to the Ministry of Education for a Grant-in-Aid for Scientific Research.

9) This insoluble residue can be dissolved, e. g., by heating with hydrobromic acid and bromine at 100°C in a sealed tube ("Gmelins Handbuch der Anorganischen Chemie", Vol. 64, Verlag Chemie, G. m. b. H., Berlin (1938), p. 43.).

*Department of Chemistry*
*Faculty of Science*
*The University of Tokyo*
*Hongo, Tokyo*

# *Molecular Orbital Theory of Reactivity in Non-Alternant Hydrocarbons*

By Kenichi FUKUI, Teijiro YONEZAWA and Chikayoshi NAGATA

(Received July 11, 1960)

In the past decades there have been proposed not a few theoretical indexes for explaining chemical reactivity of a conjugated system. These are such as $\pi$-electron density[1], self-polarizability[2], free valence[3], localization energy[4], Dewar's approximate localization energy[5], frontier electron density[6], super-delocalizability[7], and so forth[8,9]. These quantities were derived from entirely different physical grounds. Nevertheless, predictions of the position of chemical attack by these quantities agreed well with known experimental results. This remarkable fact has attracted the attention of theoretical chemists, and several authors have attempted to interrelate these quantities[3,5,10-12]. The mathematical relations underlying these quantities in alternant hydrocarbons and hetero-alternant molecules have been clarified by the present authors[13] and Baba[14]. That is, as far as some conditions are satisfied, theoretical indexes in static, localization, and frontier electron methods were found to be entirely parallel. If this were so, good coincidence between the indexes and experiments does not always mean that each one of these indexes is the true reflection of the process of reaction. Rather, a possibility might exist that some of them are not qualified as the "good" index in the most general sense and the coincidence of such quantities with experimental facts may due mainly to the existing mathematical relations.

In this connection we should compare the theoretical prediction of an index with experimental data with regard to the compounds in which no such mathematical interrelation as found in alternant hydrocarbons exists. This will serve as testing the availability of theories and finding out the theory closest to the true mechanism of reaction. For this purpose the most suitable material may be non-alternant hydrocarbons in which less intimate relations than in alternant molecules are expected between these theoretical indexes.

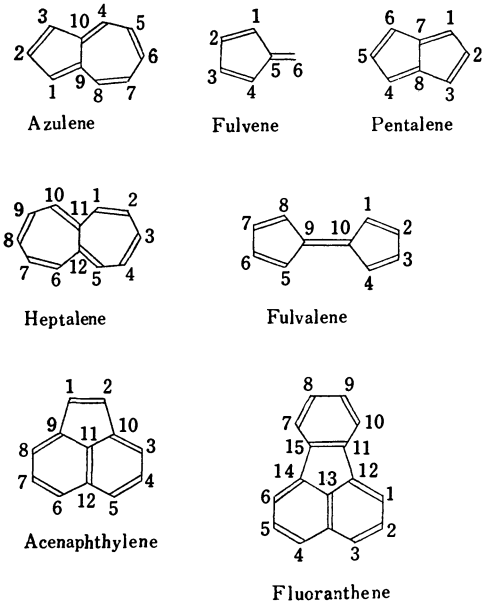



Fig. 1. Structure and numbering of non-alternant hydrocarbons.

In the present paper frontier electron density and superdelocalizability for several non-alternant hydrocarbons were calculated. The structure and numbering of these hydrocarbons are shown in Fig. 1. The calculated values of frontier electron density and superdelocalizability were compared with known experimental results, together with other theoretical indexes.

## Results and Discussion

Theoretical indexes of non-alternant hydrocarbons were compared with experiments for three cases of reactions, that is, for electrophilic, radical and nucleophilic reactions, respectively.

1) G. W. Wheland and L. Pauling, *J. Chem. Phys.*, **1**, 606 (1933), etc.
2) C. A. Coulson and H. C. Longuet-Higgins, *Proc. Roy. Soc.*, **A191**, 39 (1947); **A192**, 16 (1947).
3) F. H. Burkitt, C. A. Coulson and H. C. Longuet-Higgins, *Trans. Faraday Soc.*, **47**, 553 (1951).
4) G. W. Wheland, *J. Am. Chem. Soc.*, **64**, 900 (1940).
5) M. J. S. Dewar, ibid., **74**, 3341 (1952).
6) K. Fukui, T. Yonezawa and H. Shingu, *J. Chem. Phys.*, **20**, 722 (1952); K. Fukui, T. Yonezawa, C. Nagata and H. Shingu, ibid., **22**, 1433 (1954).
7) K. Fukui, T. Yonezawa and C. Nagata, ibid., **27**, 1247 (1957).
8) S. Nagakura and J. Tanaka, *J. Chem. Soc. Japan, Pure Chem. Sec. (Nippon Kagaku Zasshi)*, **75**, 993 (1954).
9) T. Nakajima, *J. Chem. Phys.*, **25**, 587 (1955).
10) H. H. Greenwood, *Trans. Faraday Soc.*, **48**, 585 (1952); *J. Chem. Phys.*, **20**, 1333 (1952).
11) B. Pullman, *Cahier d. phys.*, **48**, 42 (1954).
12) R. D. Brown, *Quart. Rev. Chem. Soc.*, **6**, No. 1, 63 (1952).
13) K. Fukui, T. Yonezawa and C. Nagata, *J. Chem. Phys.*, **26**, 831 (1957).
14) H. Baba, This Bulletin, **30**, 147, 154 (1957).

**Reaction with an Electrophilic Reagent.**—In Table I, the values of localization energy, frontier electron density and superdelocalizability for an electrophilic attack and the value of $\pi$-electron density were listed and compared with known experimental results. The values corresponding to the predicted position of attack are specified by italic letters. Experiments were once carried out for azulene, acenaphthylene and fluoranthene. As is seen in Table I, all indexes predict the same position as the most reactive for azulene and for acenaphthylene in accordance with experiments[15,16]. For fluoranthene, however, the situation is different. That is, the experiments showed that the bromination reaction occurred at two positions giving 3, 8-dibromo fluoranthene[17,18]. The prediction of frontier

TABLE I. LOCALIZATION ENERGY ($L_r^{(E)}$), FRONTIER ELECTRON DENSITY ($f_r^{(E)}$), AND SUPERDELOCALIZABILITY ($S_r^{(E)}$) FOR ELECTROPHILIC ATTACK AND $\pi$-ELECTRON DENSITY ($Q_r$) IN COMPARISON WITH EXPERIMENTS

| Compounds (Experimental position of attack) | Position | $f_r^{(E)}$ | $S_r^{(E)}$ | $L_r^{(E)}$ | $Q_r$ |
|---|---|---|---|---|---|
| Azulene | 1 | *0.590* | *1.760* | *1.352* | *1.173* |
| (1) | 2 | 0.000 | 1.017 | 1.728 | 1.047 |
| | 4 | 0.051 | 0.706 | 1.808 | 0.855 |
| | 5 | 0.225 | 1.035 | 1.659 | 0.986 |
| | 6 | 0.000 | 0.680 | 1.959 | 0.870 |
| | 9 | 0.134 | 0.951 | — | 1.027 |
| Fulvene | 1 | *0.724* | *1.850* | *2.002* | *1.092* |
| | 2 | 0.276 | 1.399 | 2.238 | 1.073 |
| | 5 | 0.000 | 0.894 | 2.994 | 1.047 |
| | 6 | 0.000 | 0.675 | 2.230 | 0.623 |
| Pentalene | 1 | 0.029 | 0.467 | 2.380 | 0.815 |
| | 2 | *0.526* | *1.365* | *2.027* | *1.173* |
| | 7 | 0.416 | 1.241 | — | 1.198 |
| Heptalene | 1 | *0.333* | *0.816*[a] | *1.660* | *1.125* |
| | 2 | 0.000 | 0.000 | 2.032 | 0.882 |
| | 3 | *0.333* | *0.816* | 1.715 | 1.119 |
| | 11 | 0.000 | 0.000 | — | 0.867 |
| Fulvalene | 1 | *0.361* | *1.351* | *1.987* | *1.097* |
| | 2 | 0.138 | 0.966 | 2.236 | 0.976 |
| | 9 | 0.000 | 0.569 | — | 0.853 |
| Acenaphthylene | 1 | *0.529* | *1.564* | *2.124* | *1.066* |
| (1) | 3 | 0.089 | 0.922 | 2.525 | 0.909 |
| | 4 | 0.005 | 1.026 | 2.513 | 1.008 |
| | 5 | 0.119 | 1.032 | 2.417 | 0.926 |
| | 10 | 0.069 | 1.041 | — | 1.044 |
| | 11 | 0.356 | 1.355 | — | 1.095 |
| | 12 | 0.021 | 0.819 | — | 0.998 |
| Fluoranthene | 1 | 0.083 | 0.779 | 1.77 | 0.947 |
| (3 and 8) | 2 | 0.057 | 0.820 | 1.82 | *1.005* |
| | 3 | *0.185* | *1.289* | *1.67* | 0.958 |
| | 7 | 0.150 | 1.078 | *1.71* | 0.997 |
| | 8 | *0.152* | *1.105* | 1.76 | *1.008* |

a) Calculated according to the formula of Eq. 27 of Ref. 7.

TABLE II. FRONTIER ELECTRON DENSITY ($f_r^{(R)}$), SUPERDELOCALIZABILITY ($S_r^{(R)}$) AND LOCALIZATION ENERGY ($L_r^{(R)}$) FOR RADICAL ATTACK AND FREE VALENCE IN COMPARISON WITH EXPERIMENTS

| Compounds (Experimental position of attack) | Position | $f_r^{(R)}$ | $S_r^{(R)}$ | Free valence | $L_r^{(R)}$ |
|---|---|---|---|---|---|
| Azulene | 1 | *0.299* | *1.186* | 0.480 | 1.721 |
| (1) | 2 | 0.100 | 0.962 | 0.420 | 1.728 |
| | 4 | 0.246 | 1.132 | *0.482* | *1.520* |
| | 5 | 0.123 | 0.986 | 0.429 | 1.655 |
| | 6 | 0.261 | 1.105 | 0.454 | 1.620 |
| | 9 | 0.161 | 0.901 | 0.149 | 2.710 |
| Fulvene | 1 | 0.485 | 1.378 | 0.505 | 2.002 |
| | 2 | 0.216 | 1.091 | 0.434 | 2.238 |
| | 5 | 0.036 | 0.746 | 0.075 | 2.994 |
| | 6 | *0.562* | *1.688* | *0.623* | *1.612* |
| Pentalene | 1 | *0.264* | *0.364*[a] | *0.558* | *1.959* |
| | 2 | 0.263 | 0.363 | 0.432 | 2.027 |
| | 7 | 0.208 | 0.322 | 0.153 | 2.828 |
| Heptalene | 1 | *0.183* | *0.303*[a] | *0.524* | *1.926* |
| | 2 | 0.166 | 0.288 | 0.441 | 2.032 |
| | 3 | 0.167 | 0.289 | 0.494 | 2.026 |
| | 11 | 0.137 | 0.262 | 0.158 | 2.817 |
| Fulvalene | 1 | *0.242* | *1.593*[b] | *0.510* | *1.676* |
| | 2 | 0.180 | 1.402 | 0.498 | 1.848 |
| | 9 | 0.156 | 1.823 | 0.243 | — |
| Acenaphthylene | 1 | *0.368* | *1.564* | 0.37 | *2.124* |
| (1 and 2) | 3 | 0.195 | 1.046 | 0.41 | 2.262 |
| | 4 | 0.017 | 0.873 | 0.38 | 2.513 |
| | 5 | 0.238 | 1.112 | *0.48* | 2.193 |
| | 10 | 0.088 | 0.853 | 0.02 | — |
| | 11 | 0.088 | 0.947 | 0.11 | — |
| | 12 | 0.011 | 0.717 | 0.14 | — |
| Fluoranthene | 1 | 0.124 | 0.904 | 0.454 | 1.61 |
| | 2 | 0.069 | 0.798 | 0.398 | 1.82 |
| | 3 | *0.284* | *1.139* | *0.470* | *1.54* |
| | 7 | 0.136 | 1.066 | 0.438 | 1.71 |
| | 8 | 0.086 | 0.929 | 0.409 | 1.76 |

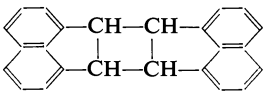
a) Calculated according to the modified formula of Eq. 27 of Ref. 7.
b) Calculated according to the formula of Eq. IV—4 of Ref. 7 (the constant term, $|\lambda_f|$ was omitted).

15) R. D. Brown, *J. Chem. Soc.*, **1959**, 2232.
16) A. G. Anderson, Jr., R. Scotoni, Jr., E. J. Cowles and C. G. Fritz, *J. Org. Chem.*, **22**, 1193 (1957); W. Treibs, *Angew. Chem.*, **67**, 70 (1955).
17) N. Campbell, W. W. Easton and J. Rayment, *Nature*, **165**, 76 (1950).
18) R. Tobler, T. Holbro, P. Sutter and W. Kern, *Helv. Chim. Acta*, **24**, 100 (1941).

electron theory agreed well with this fact because the values of frontier electron density and superdelocalizability at 3 and 8 positions are larger than the other positions. On the other hand, the total $\pi$-electron density method (the static method) predict 8 and 2 positions as the most susceptible to an electophilic attack, and localization method 3 and 7 positions. Other compounds such as fulvene, pentalene, heptalene and fulvalene have never been synthesized and accordingly no available experimental data have hitherto been obtained. The prediction of all indexes agreed entirely with each other in these compounds.

**Reaction for a Radical Reagent.**—In Table II, localization energy, frontier electron density and superdelocalizability for radical attack and the values of free valence were shown in comparison with known experimental data. For azulene the experiments showed that radical reagents attack position 1[19]. As is clearly seen in Table II, the values of frontier electron density and superdelocalizability explain the experimental fact well, whereas other indexes such as free valence and localization energy predict that position 4 will be the most reactive. Some doubts have been pointed out in connection with the reliability of the free valence as a chemical reactivity index[5,20]. Not a few cases appeared in which this index failed to explain the experiments; for example, in phenanthrene and 2-pentene[21]. On the other hand, localization energy has proved to be a good index in the case of alternant hydrocarbons. It may be of theoretical interest to observe in non-alternant hydrocarbons the inability of localization energy to explain the experimental results of, for example, the electrophilic reaction of fluoranthene and radical attack of azulene stated above.

Acenaphthylene has been found to make a colorless dimer, and it has been suggested that the mechanism of formation is not a simple "collisional" one, but depends on the existence of van der Waals complexes and Crawford and Coulson considered that the formation of these complexes is probably facilitated by the presence of a high free valence at the reacting carbon atoms. They calculated the free valence in this molecule and found that the values of 5, 6 positions are larger than that of 1, 2 positions[20]. On the other hand, experiments showed that the dimer has the following structure indicating that the 1, 2 positions have greater reactivity than 5, 6 positions[20,22].



Hence, the free valence, as is stated by Crawford and Coulson[20], is not a sufficient guide to reactivity. Frontier electron method and localization method both predict that the 1, 2 positions will be more reactive than 5, 6 positions. This result coincides with the experiment although there may remain some questions as to the applicability of the reactivity indexes to such a dimer-forming reaction.

TABLE III. FRONTIER ELECTRON DENSITY ($f_r^{(N)}$), SUPERDELOCALIZABILITY ($S_r^{(N)}$) AND LOCALIZATION ENERGY ($L_r^{(N)}$) FOR NUCLEOPHILIC ATTACK AND $\pi$-ELECTRON DENSITY ($Q_r$)

| Compounds | Position | $f_r^{(N)}$ | $S_r^{(N)}$ | $L_r^{(N)}$ | $Q_r$ |
|---|---|---|---|---|---|
| Azulene | 1 | 0.008 | 0.613 | 2.090 | 1.173 |
| | 2 | 0.199 | 0.907 | 1.728 | 1.047 |
| | 4 | 0.442 | *1.559* | *1.231* | *0.855* |
| | 5 | 0.021 | 0.937 | 1.655 | 0.986 |
| | 6 | *0.522* | 1.530 | 1.280 | 0.870 |
| | 9 | 0.169 | 0.851 | — | 1.027 |
| Fulvene | 1 | 0.246 | 0.906 | 2.002 | 1.092 |
| | 2 | 0.156 | 0.783 | 2.238 | 1.073 |
| | 5 | 0.073 | 0.597 | 2.994 | 1.047 |
| | 6 | *1.124* | *2.701* | *0.984* | *0.623* |
| Pentalene | 1 | *0.500* | *1.000*[a] | *1.531* | *0.815* |
| | 2 | 0.000 | 0.000 | 2.027 | 1.173 |
| | 7 | 0.000 | 0.000 | — | 1.198 |
| Heptalene | 1 | 0.032 | 0.529 | 2.193 | 1.125 |
| | 2 | *0.332* | *1.401* | *2.032* | *0.882* |
| | 3 | 0.000 | 0.401 | 2.357 | 1.119 |
| | 11 | 0.271 | 1.252 | — | 0.867 |
| Fulvalene | 1 | 0.123 | 1.835[b] | *1.365* | 1.097 |
| | 2 | *0.221* | *1.837* | 1.452 | *0.976* |
| | 9 | 0.312 | 1.797 | — | 0.853 |
| Acenaphthylene | 1 | 0.208 | 0.861 | 2.124 | 1.066 |
| | 3 | 0.301 | 1.170 | 1.999 | *0.909* |
| | 4 | 0.029 | 0.719 | 2.513 | 1.008 |
| | 5 | *0.356* | *1.191* | *1.969* | 0.926 |
| | 10 | 0.106 | 0.664 | — | 1.044 |
| | 11 | 0.000 | 0.539 | — | 1.095 |
| | 12 | 0.000 | 0.616 | — | 0.998 |
| Fluoranthene | 1 | 0.243 | 1.028 | 1.46 | *0.947* |
| | 2 | 0.045 | 0.776 | 1.82 | 1.005 |
| | 3 | *0.326* | *1.197* | *1.41* | 0.958 |
| | 7 | 0.031 | 1.054 | 1.71 | 0.997 |
| | 8 | 0.079 | 0.793 | 1.76 | 1.008 |

a) See the first footnote of Table I.
b) Calculated according to the formula of Eq. IV—2 of Ref. 7 (the constant term, $2\lambda_{m+1}$, was omitted).

19) K. Hafner, *Angew. Chem.*, **70**, 419 (1958); H. Arnold and K. Pahls, *Chem. Ber.*, **89**, 121 (1956).
20) V. A. Crawford and C. A. Coulson, *J. Chem. Soc.*, 1948. 1990.
21) S. Sato and R. J. Cvetanovic, *J. Am. Chem. Soc.*, **81**, 3223 (1959).
22) E. L. Bowen and L. D. F. Marsh, *J. Chem. Soc.*, 1947, 109.

For other compounds such as fulvene, pentalene, heptalene, fulvalene and fluoranthene there are no available data. The prediction of the most reactive position of these molecules by theoretical indexes agreed entirely with each other.

**Reaction for a Nucleophilic Reagent.**—Braun and Manz heated fluoranthene and CuCN for 6 hr. at 260°C and got 3-CN derivative[23]. The nature of this reaction has not been determined. The reaction may be nucleophilic or otherwise radical in nature. Provided that the reaction proceeds in radical mechanism the theories agree with the experiment because free valence, localization energy, frontier electron density and superdelocalizability all predict position 3 as the most reactive, as is seen in Table II. On the other hand if the reagent attacks the substrate molecule as a nucleophilic reagent, the $\pi$-electron density method fails to predict the correct position as is shown in Table III, whereas the localization and frontier electron methods both succeed also in this case.

For other molecules no experiment seems to have been carried out and all indexes predict the same position as the most reactive center except for acenaphthylene and fulvalene. Some experimental information may be looked for in relation to acenaphthylene; position 5 is predicted by the localization method and the frontier electron method, and position 3 by $\pi$-electron density method. In the case of fulvalene, disagreement of predictions by the localization method and the static method has been pointed out by Brown[12] in connection with the "chemical non-crossing rule"; that is, the former predict position 1, whereas the latter, position 2. The frontier electron density and the superdelocalizability predict position 2 as the most reactive center toward nucleophilic reagents in agreement with the static method.

As was stated above, the static method fails to explain the experimental results of fluoranthene with regard to the electrophilic attack and the radical reaction of azulene and acenaphthylene. The localization method also could not correctly predict the position of attack in the case of electrophilic reaction of fluoranthene and radical reaction of azulene. On the other hand, the predictions by the frontier electron method were entirely consistent with experiments for all molecules so far tested.

Since no ambiguous parameter has been used in the calculations stated above, such a comparison of availability of various theoretical indexes may be of significance in the sense that it may be able to afford us a clue to search for the "true" feature of substitution process in conjugated molecules.

*Department of Fuel Chemistry*
*Faculty of Engineering*
*Kyoto University*
*Sakyo-ku, Kyoto*

23) J. V. Braun and G. Manz, *Ann.*, **488**, 111 (1931).

# *The Formation and the Reactions of 3α-Chloro-5, 6β-epoxy-5β-cholestane**

By Michio SHIOTA, Taeko OGIHARA** and Yumi WATANABE***

(Received July 26, 1960)

The present paper describes a study on the configuration of the epoxide derived from 3α-chlorocholest-5-ene[1] by oxidation with monoperphthalic acid and also on the reaction of the epoxide with boron trifluoride-ether complex.

Oxidation of 3α-chlorocholest-5-ene with monoperphthalic acid gave an epoxide. The epoxide could not be reduced with lithium aluminum hydride in the usual way, but it was catalytically reduced with platinum oxide to afford, besides other products, 5β-cholestane (II) and 5β-cholestan-6β-ol (IIIa). The formation of the 5β-cholestane derivatives is of interest, and this reduction is analogous to the catalytic reduction of 5, 6β-epoxy-5β-cholestan-3α-ol[2]. The reductive cleavage of the

* Presented at the 11th Annual Meeting of the Chemical Society of Japan, Tokyo, April, 1958 and at the 13th Annual Meeting of the Chemical Society of Japan, Tokyo, April, 1960.

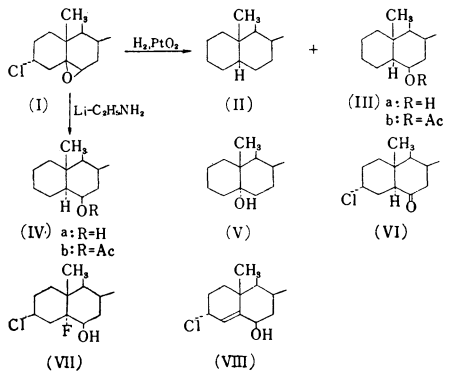
** Present address, The Textile Research Institute of the Japanese Government, Kanagawa-ku, Yokohama.

*** Present address, Tokyo Yushi Kogyo Co., Nagashima-chō, Edogawa-ku, Tokyo.

1) C. W. Shoppee and G. H. R. Summers, *J. Chem. Soc.*, **1952**, 1790.

2) Y. Urushibara and K. Mori, This Bulletin, **31**, 1068 (1958).

3α-chlorocholest-5-ene oxide with lithium-ethylamine[3] was also effected to give 5α-cholestan-6-β-ol (IVa) as the major product, along with an unsaturated material. In both of the above reductions, no 5α-cholestan-5-ol (V) was found in the products. On the basis of these observations, it was concluded that the epoxide is 3α-chloro-5,6β-epoxy-5β-cholestane




(I). An isomeric α-oxide was not obtained by the peracid oxidation of 3α-chlorocholest-5-ene.

The reaction of the epoxide with boron trifluoride-ether complex was investigated to complement the study by Henbest[4,5]. This lacks the reaction of a 3α-substituted 5,6β-epoxide with the reagent.

On treatment with boron trifluoride-ether complex, the epoxide was easily isomerized to 3α-chloro-5α-cholestan-6-one (VI) in a 35% yield. A "non-polar" oil[6] (13%) and an unsaturated substance (36%) were also produced. The yield of the 6-ketone was considerably lower than in the case of 3α-acetoxy-5,6α-epoxy-5α-cholestane[5]. It is probably because the resulting 6-ketone is a 5α-cholestane derivative (cis migration of $C_6$-hydrogen[4]) with 3α-chlorine and the 3-axial substituent decreases the yield of the 6-ketone. Since 5β-cholestane-3,6-dione was not transformed into 5α-cholestane-3,6-dione under the same condition, 3α-chloro-5α-cholestan-6-one was formed directly from 3α-chloro-5,6β-epoxy-5β-cholestane and, therefore, the above assignment of a β-configuration to the epoxide is further confirmed.

The formation of a diaxial fluorohydrin (5α-fluoro,6β-hydroxy) (VII) was probably discouraged because 1,3-diaxial interaction between 3α-chlorine and 5α-fluorine was involved.

3) A. S. Hallsworth, H. B. Henbest and T. I. Wrigley, *J. Chem. Soc.*, **1957**, 1969, 4604.
4) H. B. Henbest and T. I. Wrigley, ibid., **1957**, 4596.
5) H. B. Henbest and T. I. Wrigley, ibid., **1957**, 4765.
6) An oily substance which was not adsorbed on alumina.

## Experimental****

**3α-Chloro-5,6β-epoxy-5β-cholestane (I).**—A mixture of 200 mg. of 3α-chlorocholest-5-ene and 2 equivalents of monoperphthalic acid in 10 ml. of dry ether was allowed to stand at room temperature overnight. The solution was washed with 5% aqueous sodium hydroxide and then with water to neutral reaction. Removal of the solvent from the dried (sodium sulfate) solution afforded a colorless crystalline residue. Recrystallization from methanol gave 120 mg. of 3α-chloro-5,6β-epoxy-5β-cholestane in needles, m. p. 98~99°C. Filtration through alumina, followed by recrystallization from methanol, raised the m. p. to 101.5~103°C. $[\alpha]_D^{16}$ −7° (*c* 2.65, chloroform).

Found: C, 77.06; H, 10.92. Calcd. for $C_{27}H_{45}ClO$: C, 77.01; H, 10.77%.

**Reductive Cleavage of the Epoxide I.**—*Catalytic Reduction.*—A mixture of 150 mg. of I and 20 mg. of Adams platinum oxide in 10 ml. of acetic acid was agitated with hydrogen at room temperature. In 1.5 hr. the hydrogen uptake was complete (2 mol.). The catalyst was removed by filteration and the solvent was evaporated under reduced pressure. The colorless oily residue was acetylated in the usual way and the product was chromatographed on 4.5 g. of alumina. Fractions eluted with petroleum ether gave oily residues (108 mg. in total), some of which were crystallized from methanol to give 3 mg. of 5β-cholestane (II), m. p. 63~65°C (recrystallized from methanol) and 20 mg. of 5β-cholestan-6β-ol acetate[7] (IIIb), m. p. 108~108.5°C (recrystallized three times from methanol; the yield of the crude product was 46 mg.). These compounds were identified by the mixed melting point test with authentic samples. Further elution of the column with benzene-petroleum ether (1:9) afforded a small amount of a halogen-containing substance in needles, m. p. 117~124°C, which was not further investigated. The oily residues from other fractions failed to crystallize, and 5α-cholestan-5-ol was not isolated from them.

*Reduction with Lithium-Ethylamine.*—A solution of 150 mg. of I in 4.3 g. of ethylamine was treated with 100 mg. of lithium at room temperature. A deep blue color appeared after 20 min., and persisted during 40 min. The reaction product was isolated according to the procedure of Benkeser[8] to give 137 mg. of a pale yellow oily product, which gave a yellow color with tetranitromethane and showed a negative Beilstein test. The oil (81 mg.) was acetylated in the usual way and the resulting yellow oil (80.5 mg.) was treated with monoperphthalic acid, and the resulting epoxide was subjected to hydrolytic cleavage with phosphomolybdic acid[9]. An oily product (75.4 mg.), which did not give a yellow color with tetranitromethane, was chromatographed on 2.1 g. of alumina, and from the fractions

**** All melting points were not corrected.
7) D. N. Jones, J. R. Lewis, C. W. Shoppee and G. H. Summers, ibid., **1955**, 2876.
8) R. A. Benkeser, R. E. Robinson, D. M. Sauve and O. H. Thomas, *J. Am. Chem. Soc.*, **77**, 3230 (1955).
9) By this procedure, the unsaturated material was converted into a 1,2-*trans*-glycol (M. Sawai, presented at the 10th Annual Meeting of the Chemical Society of Japan, Tokyo, April, 1957).

eluted with petroleum ether, 43.9 mg. of an oily residue was obtained. This was crystallized from methanol to give 34 mg. of 5α-cholestan-6β-ol acetate[10] (IVb) in needles, m. p. and mixed m. p. 74~75°C. The amount of the unsaturated material in the above reduction products was estimated by catalytic reduction. From the amount of hydrogen uptake, it was inferred that the unsaturated material amounted to about 30% of the total.

*Attempted Reduction with Lithium Aluminum Hydride.* — I was treated with lithium aluminum hydride at the boiling point of ether in the usual way, but the reduction was not effected. An attempt to effect the reduction at the boiling point of benzene was also unsuccessful.

**Reaction of I with Boron Trifluoride-Ether Complex.** — Freshly distilled boron trifluoride-ether complex (4 drops) was added to a solution of 200 mg. of I in 20 ml. of dry benzene. After 4 min. at room temperature, the solution was treated with aqueous sodium bicarbonate, and washed with water. Removal of the solvent from the dried (sodium sulfate) solution afforded a semi-solid residue, which was crystallized from acetone to give 3α-chloro-5α-cholestan-6-one (VI), m. p. 178~180°C. Under the same condition, 5β-cholestane-3,6-dione was not converted into 5α-cholestane-3,6-dione.

The chromatography of the above semi-solid residue (200 mg.) afforded 26.9 mg. of a "non-polar" oil, 69 mg. of 3α-chlorocholestan-6-one, and 73.2 mg. of an oily material. The oily substance gave an intense yellow color with tetranitromethane and showed a positive Beilstein test and hydroxyl infrared absorption. Since it was readily acetylated in the usual way, and the 3α-chlorine in 3α-chlorocholest-5-ene and in 3α-chloro-5α-cholestan-6-one was not eliminated with boron trifluoride-ether complex to give unsaturated compounds, it is probable that the oily material consisted mainly of 3α-chlorocholest-4-en-6β-ol (VIII).

The authors express their thanks to Professor Y. Urushibara of the University of Tokyo for his valuable advice, and to Mrs. Y. Fujita for her assistance in the preliminary course of this study. The authors are also indebted to the Ministry of Education for the Grant in Aid for the Fundamental Scientific Research.

*Chemical Laboratory*
*Ochanomizu University*
*Bunkyo-ku, Tokyo*

10) C. W. Shoppee and G. H. R. Summers, *J. Chem. Soc.*, **1952**, 3361.

# *Studies on Pyridotropolones. VI*[1]. *Rearrangement Reactions of Brominated 8-Isopropyl-pyrido[3, 2-d]tropolones to 7-Isopropyl-6-quinolinols*

By Kameji YAMANE

(Received July 13, 1960)

Previously the author[2] reported that nitroso-, amino-, quinoxalo- and oxazolo-compounds were obtained from 2-methyl-8-isopropyl-pyrido[3, 2-*d*]tropolone. The present work was carried out for the purpose of elucidating the chemical reactivity of pyrido[3, 2-*d*]tropolone, and the rearrangement reactions of brominated 8-isopropyl-pyrido[3, 2-*d*]tropolones to 7-isopropyl-6-quinolinols were studied.

Bromination of 2-methyl-8-isopropyl-pyrido-[3, 2-*d*]tropolone (Ia) with 1 molar equivalent of NBS gave 5-bromo-compound IIa. IIa showed brownish yellow coloration in benzene layer with ferric chloride solution. Heating IIa in 2 N potassium hydroxide solution afforded pale yellow (nearly colorless) needles, m. p. 229.5~230°C (IIIa), 2-methyl-8-isopropyl-pyrido-[3, 2-*d*]-tropolone (Ia) and a red oily matter. IIIa gave no Beilstein test, whose analytical values agreed with formula $C_{13}H_{15}ON$. Its ultraviolet absorption spectrum (Fig. 1) closely resembled that of 6-quinolinol[3]. The infrared spectrum of IIIa exhibited several absorption bands (2980 $cm^{-1}$ for CH stretching vibrations, 1530, 1568, 1607 and 1630 $cm^{-1}$ for C=C and C=N streching vibrations, and 1245 $cm^{-1}$ for phenolic OH deformations). Furthermore, the compound IIIa readily underwent some typical electrophilic substitution reactions. Namely, IIIa was readily brominated in acetic acid solution to form a monobromo compound

1) This work was presented at the 13th Annual Meeting of the Chemical Society of Japan, Tokyo, April 1960.

2) K. Yamane, *J. Chem. Soc. Japan, Pure Chem. Sec.* (*Nippon Kagaku Zasshi*), **80**, 1175 (1959).

3) G. W. Ewing and E. A. Steck, *J. Am. Chem. Soc.*, **68**, 2181 (1946).

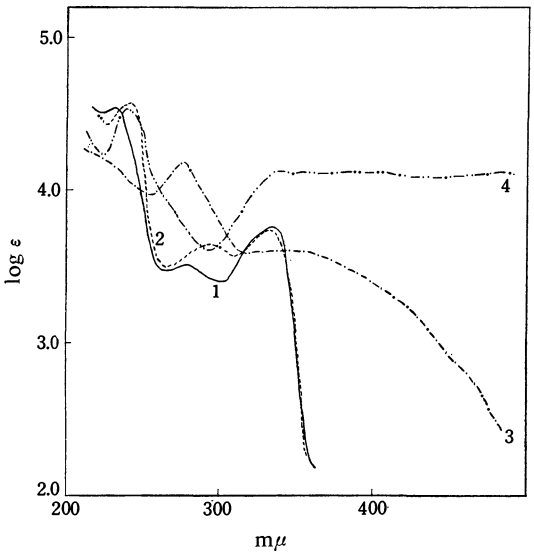



Fig. 1. Ultraviolet absorption spectra (in methanol).

1 : 2-Methyl-7-isopropyl-6-quinolinol (IIIa)
2 : 2-Methyl-5-bromo-7-isopropyl-6-quinolinol (IVa)
3 : 2-Methyl-5-nitroso-7-isopropyl-6-quinolinol (Va)
4 : 2-Methyl-5-(*p*-tolylazo)-7-isopropyl-6-quinolinol (VIa)

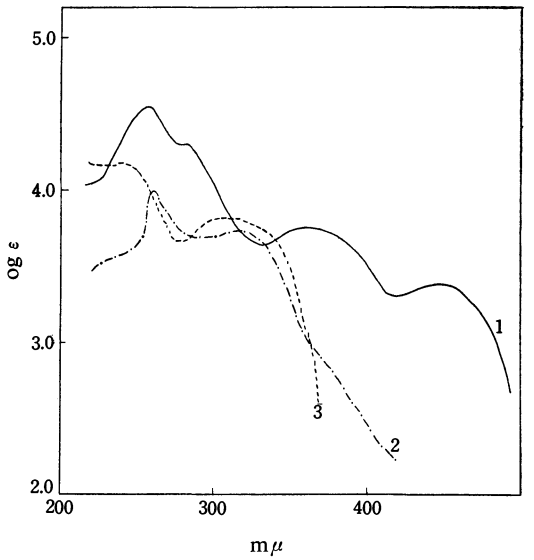



Fig. 2. Ultraviolet absorption spectra.

1 : 2-Methyl-5-bromo-8-isopropyl-pyrido-[3,2-*d*]tropolone (IIa) (in methanol)
2 : Dibromo-compound VIIa (in carbon tetrachloride)
3 : Dibromo-compound VIIa (in methanol)

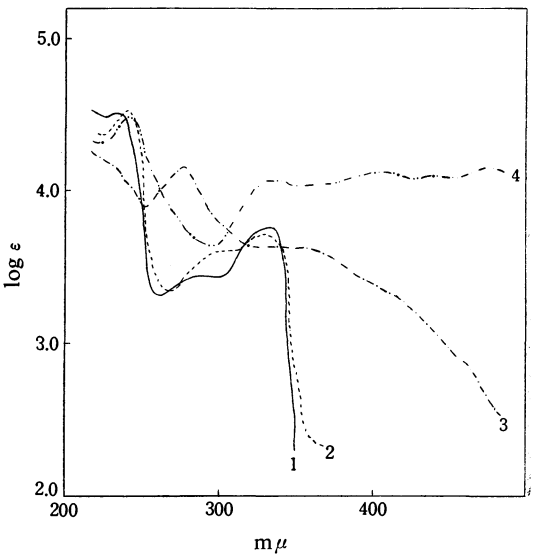



Fig. 3. Ultraviolet absorption spectra (in methanol).

1 : 7-Isopropyl-6-quinolinol (IIIb)
2 : 5-Bromo-7-isopropyl-6-quinolinol (IVb)
3 : 5-Nitroso-7-isopropyl-6-quinolinol (Vb)
4 : 5-(*p*-Tolylazo)-7-isopropyl-6-quinolinol (VIb)

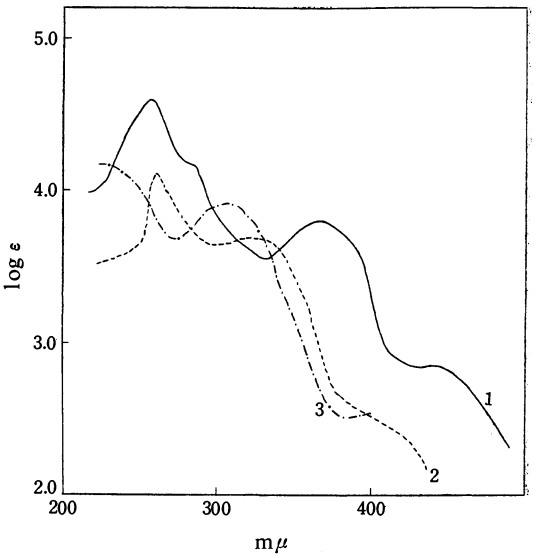
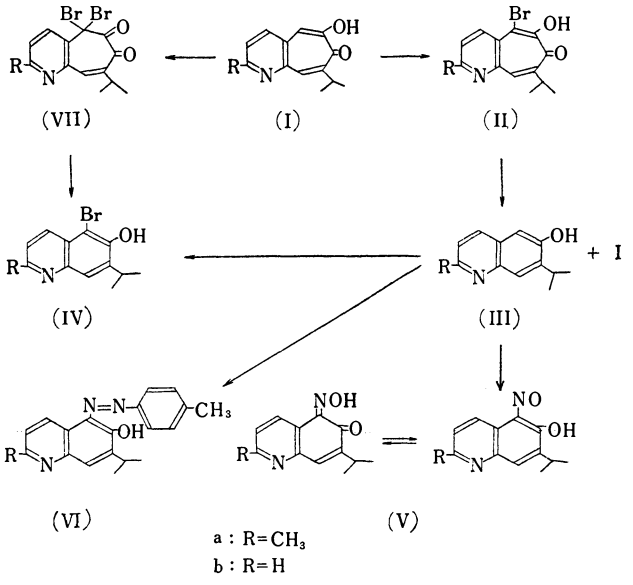



Fig. 4. Ultraviolet absorption spectra.

1 : 5-Bromo-7-isopropyl-pyrido[3,2-*d*]-tropolone (IIb) (in methanol)
2 : Dibromo-compound VIIb (in carbon tetrachloride).
3 : Dibromo-compound VIIb (in methanol)

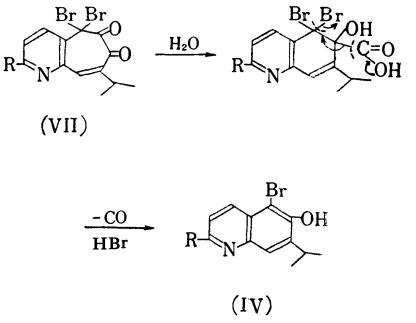
(IVa). Nitrosation of IIIa in acetic acid solution gave nitroso compound Va. The compound IIIa coupled with diazotized *p*-toluidine in alkaline solution to yield an azo compound VIa. From these facts shown above, IIIa was assumed to be 2-methyl-7-isopropyl-6-quinolinol.

Bromination of 2-methyl-8-isopropyl-pyrido-[3, 2-*d*] tropolone gave dibromo compound as yellow rhombic prisms, m. p. 129~130°C (VIIa). The analytical values of this compound agreed with formula $C_{14}H_{13}O_2NBr_2$, and its ultraviolet absorption spectrum (Fig. 2) differed from that of 2-methyl-5-bromo-8-isopropyl-pyrido [3, 2-*d*] tropolone (IIa). Moreover, the infrared spectrum of VIIa exhibited two bands at 1742 and 1684 $cm^{-1}$ due to the carbonyl group, and no bands in the hydroxyl region. The compound VIIa was unstable against water, acid, alkali and alcohols. In fact when heated with water, it dissolved gradually under foaming and gave 2-methyl-5-bromo-7-isopropyl-6-quinolinol (IVa) which was obtained by bromination of IIIa described above. Heating VIIa with 1 N hydrochloric acid also gave IVa in good yield. VIIa, however, gave 2-methyl-5-bromo-8-isopropyl-pyrido [3, 2-*d*] tropolone (IIa) when it was heated with 2 N potassium hydroxide solution. These facts indicated that the dibromo compound VIIa possessed the structure shown as *o*-diketone formula (VIIa).




8-Isopropyl-pyrido [3, 2-*d*] tropolone (Ib)[4] showed almost the similar reactions as in the case of Ia. Namely, Ib was readily brominated with NBS to form 5-bromo-compound (IIb) and dibromo compound (VIIb). Heating IIb in 2 N potassium hydroxide solution afforded 7-isopropyl-6-quinolinol (IIIb). IIIb afforded bromo compound (IVb), nitroso compound (Vb) and *p*-tolylazo-compound (VIb). Furthermore VIIb was rearranged to 5-bromo-7-isopropyl-6-quinolinol (IVb) when treated with water or 1 N hydrochloric acid, and or 2 N potassium hydroxide solution.

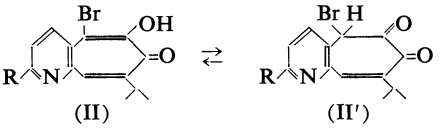
It is thought that the mechanism of this interesting rearrangement of VII to 5-bromo-7-isopropyl-6-quinolinols (IV) goes on first through benzilic acid rearrangement, followed by decarboxylation and dehydrobromination as follows:




In the case of the rearrangement reaction of 5-bromo-8-isopropyl-pyrido [3, 2-*d*] tropolones (II) to 7-isopropyl-6-quinolinols (III) with potassium hydroxide solution, it is thought

4) K. Yamane, *J. Chem. Soc. Japan, Pure Chem. Sec.* (*Nippon Kagaku Zasshi*), **81**, 509 (1960).

that II undergoes rearrangement in like manner as VII via its tautomeric structure II'.



(II) (II')

## Experimental

**2-Methyl-5-bromo-8-isopropyl-pyrido[3,2-*d*]tropolone (IIa).**—A mixture of 0.2 g. of 2-methyl-8-isopropyl-pyrido[3,2-*d*]-tropolone (Ia) and 0.18 g. of NBS in 4 cc. of carbon tetrachloride was refluxed for 2 hr. After cooling, succinimide and the solvent were removed and the residue was recrystallized from ethanol to give 0.25 g. of yellow needles, m. p. 145~145.5°C.

Found: C, 54.37; H, 4.65; N, 4.84. Calcd. for $C_{14}H_{14}O_2NBr$: C, 54.54; H, 4.58; N, 4.55%.

**5-Bromo-8-isopropyl-pyrido[3,2-*d*]tropolone (IIb).**—A mixture of 0.7 g. of 8-isopropyl-pyrido-[3,2-*d*]tropolone (Ib) and 0.64 g. of NBS in 40 cc. of carbon tetrachloride was refluxed for 2 hr. After cooling, succinimide and the solvent were removed and the residue was recrystallized from ethanol to give 0.72 g. of yellow needles, m. p. 155.5~156°C.

Found: C, 53.22; H, 4.02; N, 4.92. Calcd. for $C_{13}H_{12}O_2NBr$: C, 53.07; H, 4.11; N, 4.76%.

**2-Methyl-7-isopropyl-6-quinolinol (IIIa).—a)** A solution of 1 g. of IIa in 3 cc. of 2 N potassium hydroxide solution was heated for 2 hr. on a water bath. After cooling, 10 cc. of water was added and acidified with 1 N hydrochloric acid to deposite dark brown precipitates. The precipitates were collected and sublimated, yielding yellow sublimates, which were recrystallized from ethanol in pale yellow needles, m. p. 127~128°C, about 0.1 g. These did not depress by admixture with 2 methyl-8-isopropyl-pyrido[3,2-*d*]tropolone (Ia). The mother liquor of the dark brown precipitates was evaporated on a water bath to dryness and the residue was extracted with acetone. Acetone extracts were purified by passing through an alumina column to give about 30 mg. of crystals. Recrystallization from alcohol gave pale yellow (nearly colorless) needles, m. p. 229.5~230°C.

Found: C, 77.32; H, 7.19; N, 6.84. Calcd. for $C_{13}H_{15}ON$: C, 77.58; H, 7.51; N, 6.96%.

**b)** A solution of 0.4 g. of IIa in 3 cc. of 2 N potassium hydroxide solution was heated on a water bath for 2 hr. After cooling, the solution was slightly acidified with acetic acid to deposit brown precipitates (20 mg., m. p. 240°C). The filtrate of the precipitates was evaporated on a water bath to dryness and the residue was sublimated to give 130 mg. of pink prisms. Recrystallization from alcohol gave red needles, m. p. 228~229°C, undepressed by admixture with IIIa. Furthermore, the red needles were dissolved in acetone and purified by passing through an alumina column to give pale yellow (nearly colorless) needles, m. p. 229~230°C.

**7-Isopropyl-6-quinolinol (IIIb).**—A solution of 0.4 g. of IIb in 2.3 cc. of 2 N potassium hydroxide solution was heated on a water bath and acidified with 2 N hydrochloric acid to deposite pale brown precipitates. The precipitates were recrystallized from methanol to give yellow needles, m. p. 160~161°C, undepressed by admixture with Ib. Mother liquor of the pale brown precipitates was evaporated on a water bath to dryness and the residue was extracted with acetone. Acetone extracts were purified by passing through an alumina column to give colorless plates, m. p. 193°C. Yield 90 mg.

Found: C, 76.67; H, 6.85; N, 7.46. Calcd. for $C_{12}H_{13}ON$: C, 76.97; H, 7.00; N, 7.48%.

*Picrate*, yellow plates, m. p. 229~230°C (decomp.) from methanol.

Found: N, 13.43. Calcd. for $C_{18}H_{16}O_8N_4$: N, 13.46%.

**2-Methyl-5-bromo-7-isopropyl-6-quinolinol (IVa).**—To a solution of 0.13 g. of IIIa in 2 cc. of acetic acid, a solution of 0.1 g. of bromine in 0.5 cc. of the same solvent was added dropwise with stirring. When the addition had been nearly completed some yellow crystals were deposited. After removal of the crystals, water was added and neutralized with ammonia to give precipitates, which were recrystallized from dilute alcohol in pale yellow (nearly colorless) needles, m. p. 129~130°C.

Found: C, 55.84; H, 4.79; N, 4.92. Calcd. for $C_{13}H_{14}ONBr$: C, 55.72 H, 5.04; N, 5.00%.

**5-Bromo-7-isopropyl-6-quinolinol (IVb).**—To a solution of 20 mg. of IIIb in 0.5 cc. of acetic acid, 20 mg. of bromine dissolved in 0.5 cc. of the same solvent was added dropwise with stirring. After standing for 2 hr., water was added and neutralized with ammonia to give colorless precipitates, which were recrystallized from acetone in pale yellow needles, m. p. 128~129°C. Yield about 25 mg.

Found: C, 54.04; H, 4.26; N, 5.24. Calcd. for $C_{12}H_{12}ONBr$: C, 54.15; H, 4.55; N, 5.26%.

**2-Methyl-5-nitroso-7-isopropyl-6-quinolinol (Va).**—To a solution of 0.15 g. of IIIa in 1 cc. of acetic acid, a solution of 0.08 g. of sodium nitrite in a small amount of water was added dropwise. The yellow crystals that separated out were collected by filtration and washed with water. Yield 0.15 g. Recrystallization from methanol yielded yellow prisms, m. p. 181°C (decomp.).

Found: C, 67.76; H, 5.72; N, 11.59. Calcd. for $C_{13}H_{14}O_2N_2$: C, 67.81; H, 6.13; N, 12.17%.

**5-Nitroso-7-isopropyl-6-quinolinol (Vb).**—To a solution of 41 mg. of IIIb in 1 cc. of acetic acid, 23 mg. of sodium nitrite in a small amount of water was added dropwise. The yellow crystals that separated out were collected by filtration and washed with water. Recrystallization from methanol yielded bright yellow scales, m. p. 156°C (decomp.). Yield about 45 mg.

Found: C, 66.66; H, 5.76; N, 13.02. Calcd. for $C_{12}H_{12}O_2N_2$: C, 66.65; H, 5.59; N, 12.96%.

**2-Methyl-5-(*p*-tolylazo)-7-isopropyl-6-quinolinol (VIa).**—To a cold solution of 45 mg. of *p*-toluidine in 2 cc. of 3 N hydrochloric acid, a solution of 42 mg. of sodium nitrite in 0.5 cc. of water was dropped, and the resultant cold diazonium solution was added dropwise to the cold solution of 80 mg. of IIIa in 10 cc. of 2 N-potassium hydroxide solution. The red precipitates thereby formed were collected by filtration. These were recrystallized from methanol

in orange red needles, m. p. 109.5~110°C. Yield 90 mg.

Found: C, 75.46; H, 6.35; N, 13.57. Calcd. for $C_{20}H_{21}ON_3$: C, 75.21; H, 6.63; N, 13.16%.

**5-(*p*-Tolyl-azo)-7-isopropyl-6-quinolinol (VIb).**—A cold solution of diazonium salt prepared from 35 mg. of *p*-toluidine, 1 cc. of 3 N hydrochloric acid and 55 mg. of sodium nitrite was added dropwise to a solution of 60 mg. of IIIb in 2 cc. of 2 N sodium hydroxide solution. The reddish brown precipitates which formed were recrystallized from methanol in red needles, m. p. 122~123°C. Yield 50 mg.

Found: C, 74.62; H, 6.02; N, 13.92. Calcd. for $C_{19}H_{19}ON_3$: C, 74.73; H, 6.27; N, 13.76%.

**Bromination of 2-Methyl-8-isopropyl-pyrido[3, 2-*d*]tropolone (Ia) with 2 Molar Equivalents of NBS. (Dibromo-Compound VIIa).**—A mixture of 1.43 g. of Ia and 2.21 g. of NBS in 30 cc. of carbon tetrachloride was refluxed on a water bath for 2 hr. After cooling, succinimide and the solvent were removed, the residue was recrystallized from carbon tetrachloride to give 1.16 g. of yellow rhombic prisms, m. p. 129~130°C.

Found: C, 43.37; H, 3.56; N, 3.56. Calcd. for $C_{14}H_{13}O_2NBr_2$: C, 43.44; H, 3.39; N, 3.62%.

**Bromination of 8-Isopropyl-pyrido[3, 2-*d*]tropolone (Ib) with 2 Molar Equivalents of NBS. (Dibromo-Compound VIIb).**—A mixture of 1.72 g. of Ib and 2.85 g. of NBS in 100 cc. of carbon tetrachloride was refluxed on a water bath for 2 hr. After cooling, succinimide and the solvent were removed, and the residue was recrystallized from chloroform or carbon tetrachloride to give 2.21 g. of dibromo compound VIIb in yellow polyhedrones, m. p. 142~143°C.

Found: C, 42.09; H, 2.90; N, 3.69. Calcd. for $C_{13}H_{11}O_2NBr_2$: C, 41.85; H, 2.97; N, 3.76%.

**Rearrangement Reaction of Dibromo Compound VIIa to 2-Methyl-5-bromo-7-isopropyl-6-quinolinol (IVa).—a) By Water.**—When a mixture of 0.39 g. of dibromo compound VIIa and 3 cc. of water was heated on a water bath, VIIa slowly dissolved under foaming. The mixture was further heated for 2 hr. After removal of a small amount of brownish yellow resinous matter which appeared during the heating, the solution gradually deposited orange needles (hydrochloride of IVa) on standing. The needles were dissolved in 6 cc. of hot water and neutralized with 2 N potassium hydroxide solution to give precipitates, which were recrystallized from dilute alcohol in pale yellow (nearly colorless) needles, m. p. 129~130°C. Yield, 0.1 g. No depression in m. p. was observed on admixture of 2-methyl-5-bromo-7-isopropyl-6-quinolinol (IVa) which was obtained by bromination of IIIa described above.

**b) By 1 N Hydrochloric Acid.**—A mixture of 0.39 g. of VIIa and 3 cc. of 1 N hydrochloric acid solution was heated on a water bath for 30 min. On cooling, 0.31 g. of yellow crystals, m. p. 223~224°C (decomp.) were obtained. The crystals were dissolved in 5 cc. of hot water and neutralized with a 2 N potassium hydroxide solution to give colorless precipitates, which were recrystallized from dilute methanol in pale yellow (nearly colorless) needles, m. p. 129~130°C. Yield, 0.13 g. The needles were undepressed on admixture with IVa.

**Reaction of Dibromo Compound VIIa with 2 N Potassium Hydroxide Solution.**—When 0.16 g. of VIIa was mixed with 0.68 cc. of 2 N potassium hydroxide solution, an exothermic reaction began immediately to give a dark greenish yellow solution. After being heated for 20 min., the solution was slightly acidified with acetic acid to give yellow precipitates, which were recrystallized from alcohol in yellow prisms, m. p. 145~146°C, undepressed by admixture with 2-methyl-5-bromo-8-isopropyl-pyrido-[3,2-*d*]tropolone (IIa). Yield, about 0.04 g.

**Rearrangement Reaction of Dibromo Compound VIIb to 5-Bromo-7-isopropyl-6-quinolinol (IVb).—a) By Water.**—A mixture of 0.37 g. of VIIb and 1 cc. of water was heated on a water bath for 2 hr. After cooling, a small amount of water was added and neutralized with 2 N potassium hydroxide solution to deposit brown precipitates. Recrystallization from acetone yielded 0.17 g. of colorless needles, m. p. 128.5~129°C. No depression in m. p. was observed on admixture with the authentic sample of IVb which was obtained by bromination of IIIb described above.

**b) By 1 N Hydrochloric Acid.**—A mixture of 0.37 g. of VIIb and 3 cc. of 1 N hydrochloric acid solution was heated on a water bath for 1 hr. After cooling, the resultant red solution was neutralized with a 2N potassium hydroxide solution to give precipitates, which were recrystallized from acetone in colorless needles, m. p. 127~128°C. Yield 0.2 g. The needles also were undepressed on admixture with the authentic sample of IVb.

**c) By 1 N Potassium Hydroxide Solution.**—A mixture of 0.3 g. of VIIb and 3 cc. of 1 N potassium hydroxide solution was heated on a water bath for 10 min. After cooling, the mixture was neutralized with acetic acid to give brown precipitates, which were recrystallized from acetone in pale yellow needles, m. p. 129°C. The mother liquor was evaporated on a water bath to dryness and the residue was extracted repeatedly with acetone. The extracts were purified by passing through an alumina column. After removal of the solvent, the residue was crystallized from a dilute acetone to yield another crop of yellow needles, m. p. 129°C. Total yield 43 mg. These were found to be identical with IVb by mixed fusion.

The author takes this opportunity to express his sincere gratitude to Professor T. Nozoe (Tohoku University) and Professor A. Yokoo for their guidance and encouragement. Thanks are also due to Assistant Professor J. Iwasa for measurements of infrared spectra. The author is also grateful to Mrs. K. Kodaira, Mr. S. Azumi and Miss A. Iwanaga (Nozoe laboratory) for measurements of ultraviolet spectra and for carrying out micro analyses, and to Mr. Y. Shimoyama for his cooperation in these experiments.

*Chemical Institute*
*Faculty of Science*
*Okayama University*
*Tsushima, Okayama*

# *Partition Equilibria of 2-Methyl 5-Ethyl Pyridine in the Systems of Benzene-Water and Chloroform-Water*

By Tokio KATO and Yasugoro TSUNODA

(Received February 27, 1960)

It is well known that 2-methyl 5-ethyl pyridine (M. E. P.) is prepared through the condensation of paraldehyde with aqueous ammonia[1], where benzene and chloroform are used to extract M. E. P. from the reaction product[2,3].

This paper presents a brief discussion on the partition equilibria of M. E. P. in the above-mentioned systems.

## Experimental

A thermostat adjusted to ±0.1°C, and conical flasks of 300 cc. with tight stoppers were used. M. E. P. was prepared by catalytic condensation of paraldehyde with aqueous ammonia[1]. The crude M. E. P. was rectified for several times; b. p. 74°C/20 mmHg, $n_D^{20}$, 1.4966.

Benzene and chloroform were rectified, and their boiling points were 80~81°C and 61~62°C respectively. Several solutions, being varied in concentration of M. E. P. (less than 3.0 mol./l.) in benzene and chloroform (50 cc.) were prepared in the flasks. Distilled water (150 cc.) was added to each of them, and they were settled for a certain time after being subjected to vigorous shaking every 5~6 min.

Each group of five samples was brought side by side in the thermostat for 2 hr. at 10, 20, 30, 40 and 50°C, and used for analysis.

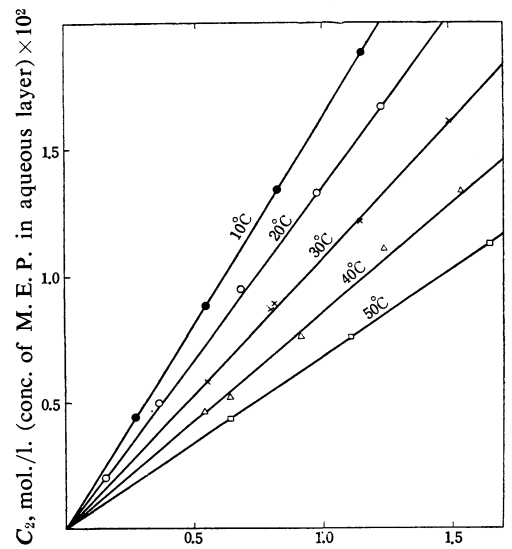
The concentration of M. E. P. was easily determined by titration with N/2 HCl, where methyl orange was used as an indicator.

Volumes of samples employed for analysis were 5 cc. for benzene and chloroform layer and 100 cc. for the aqueous layer, where the former was titrated in the mixed solvent (100 cc.) of isopropyl benzene and ethylene glycol.

## Results and Discussion

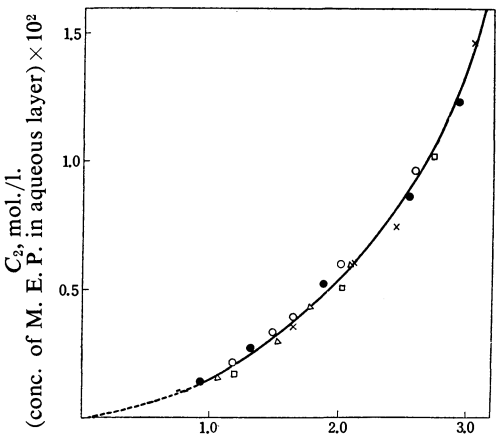
In Fig. 1 (2), $C_1$ and $C_2$ are the concentrations of M. E. P. in benzene (chloroform) and aqueous layers and both of them were calculated from volumes of consumed N/2 HCl (cc.), while titrating volumes were corrected by blank tests.

In the system of benzene-water, the constancy of $K(C_2/C_1)$ with the change of $C_1$ or $C_2$ at each temperature is confirmed, and the linear relation between $\log K$ and $1/T$ ($T$: absolute temperature, °K) shown in Fig. 3 suggests that it satisfies the following thermodynamic formula.




$C_1$, mol./l. (conc. of M. E. P. in benzene layer)

Fig. 1. Equilibrium concentrations of M. E. P. in benzene and water.




$C_1$, mol./l. (conc. of M. E. P. in chloroform layer)

Fig. 2. Equilibrium concentrations of M. E. P. in chloroform and water.

—●— 10°C —△— 40°C
—○— 20 〃 —□— 50 〃
—×— 30 〃

1) U. S. Pat., 2,615,022 (1952).
2) U. S. Pat., 2,703,804 (1955).
3) U. S. Pat., 2,769,007 (1956).

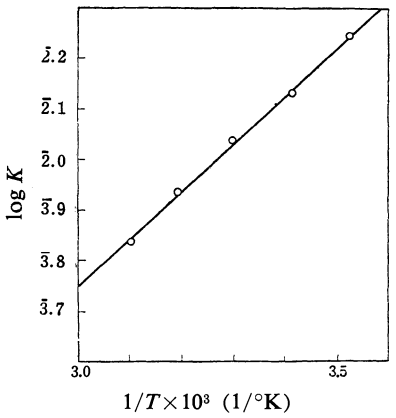



Fig. 3. Equilibrium constant $K$ (benzene-water).

$$\ln K_2/K_1 = -Q/R(1/T_1 - 1/T_2)$$

where $R$ is gas constant, and $Q$ the heat of transference of 1 mol. M. E. P. from benzene to water under equilibrium state.

Thus $Q$ was determined to be 4.3 kcal./mol. Therefore the equilibrium constant $K$ of M. E. P. between benzene and water satisfies the following formula

$$K = 7.7_6 \times 10^{-6}\, e^{2.19 \times 10^3/T}$$

In the system of chloroform-water, the parabolic relation between $C_1$ and $C_2$ was found (Fig. 2) and the constancy of $K$ ($\sqrt{C_2}/C_1$) at each temperature was confirmed, as shown in Fig. 4.

This means that the molecular weight of M. E. P. in chloroform is half of that in water

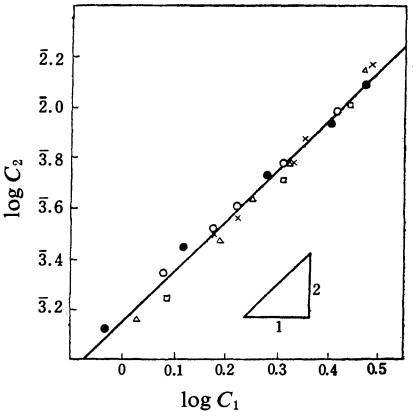



Fig. 4. Linear relation of $\sqrt{C_2}$ to $C_1$ (chloroform-water).

—●— 10°C —△— 40°C
—○— 20 〃 —□— 50 〃
—×— 30 〃

or benzene, so the molecules of M. E. P. in latter solvents seem to associate with each other. Furthermore, the values of $K$ in each temperature are uniformly equal to $3.7 \times 10^{-2}$, and their changes with temperatures (10～50°C) are negligibly small.

The authors are grateful to Dr. H. Sobue, Professor of the Tokyo University and Dr. A. Tomita, chief of the Laboratory Institute, for their valuable advice.

*Laboratory Institute of*
*Tokai Electrode Mfg. Co. Ltd.*
*Daigiri, Fujisawa*

# *On the Reaction of Aromatic Dinitriles and Formaldehyde*

By Toshihisa TACHIKAWA

(Received June 20, 1960)

The nitrile group is known to be hydrolysed to acid amide according to the following mechanism,

$$R\text{-}C{\equiv}N \xrightarrow{HCl} R\text{-}\underset{\displaystyle Cl}{\underset{|}{C}}{=}NH$$

$$R\text{-}\underset{\displaystyle Cl}{\underset{|}{C}}{=}NH \xrightarrow{H_2O} R\text{-}\underset{\displaystyle OH}{\underset{|}{C}}{=}NH + HCl$$

$$R\text{-}\underset{\displaystyle OH}{\underset{|}{C}}{=}NH \longrightarrow R\text{-}CONH_2$$

the reaction being caused by the polar structure of nitrile group. Therefore it is possible to synthesize the compounds having amide linkage by the reaction between nitrile compounds and the compounds which form carbonium cation readily. If the compounds having two nitrile radicals in a molecule are used as the starting material, it is possible to synthesize macromolecules having amide linkages.

Magat[1] and Ritter[2] have studied such

1) E. E. Magat, *J. Am. Chem. Soc.*, **73**, 1028, 1367 (1951).
2) J. J, Ritter, ibid., **70**, 4045 (1948).

reactions. Magat synthesized the polyamide known as 1, 6-nylon having the following structure by reacting adiponitrile and formaldehyde in concentrated sulfuric acid at normal temperature

$$n\,CN(CH_2)_4CN + n\,CH_2O \rightarrow CN\text{-}(CH_2)_4\text{-}\left[\text{-}CONHCH_2NHCO(CH_2)_4\cdot CONHCH_2NHCO(CH_2)_4\right]_n\text{-}CN$$

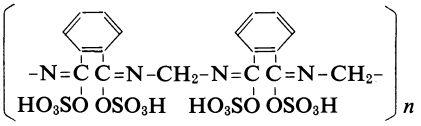
It is reported that this compound had the following properties: m. p. 225°C, mol. wt., 10,000~20,000 (by the osmotic pressure method) and the intrinsic viscosity $[\eta_{sp}/c] = 0.7 \sim 1.3$ (solvent: *m*-cresol). Magat also reported that this compound had good solvent resistance and fiber-forming ability. In his study on the dinitriles, aliphatic dinitriles have been used, but aromatic dinitriles have not been studied. However, it is probable that a new characteristic polyamide having a benzene nucleus and -CONH- linkage will be obtained by the reaction of the aromatic dinitrile and the formaldehyde.

In the present paper the reaction of aromatic dinitriles such as ortho-, iso-, tere-phthalonitrile and *p*-xylylene cyanide, with the formaldehyde has been investigated by means of Magat's method and as a result the author has been able to synthesize a new polyamide having benzene nucleus and -CONH- linkages.

The condensation polymers having -CONH- linkages in the molecule are obtained from all the above dinitriles except orthophthalonitrile. Condensation polymer from terephthalonitrile and formaldehyde has the largest intrinsic viscosity.

## Results and Discussion

In the reaction of aromatic dinitriles and formaldehyde in concentrated sulfuric acid, the effect of the substituted position of two nitrile groups is shown in Table I. In the case of orthophthalonitrile, it does not react with formaldehyde. This is believed to be due to the steric hindrance of the neighboring two nitrile groups in the intermediate polymer in the sulfuric acid.




In the case of terephthalonitrile on the other hand, it reacts easily with formaldehyde without the effect of steric hindrance and the product which has the highest condensation polymerization degree is formed. Further, *p*-xylylene cyanide with difficulty causes condensation polymerization reaction with formaldehyde. This is believed to be due to the high reactivity of the methylene hydrogen between the nitrile groups and the benzene nucleus of *p*-xylylene cyanide, which easily causes the side reaction with formaldehyde.

The infrared absorption spectra of the isophthalonitrile and the terephthalonitrile condensation polymer is shown in Fig. 1.

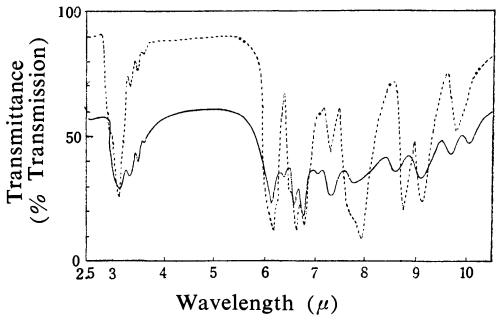



Fig. 1. Infrared spectra
—— Isophthalonitrile+$(HCHO)_n$ polymer
---- Terephthalonitrile+$(HCHO)_n$ polymer

As shown in Fig. 1, a C≡N stretching vibration at 4.5 $\mu$ disappears and an N-H stretching vibration at 3.05, 3.30, 3.45 $\mu$, an N-H deformation vibration at 6.6 $\mu$ and a C=O stretching vibration at 6.1 $\mu$ appears as in 6,6-nylon. Furthermore, a $-CH_2-$ deformation vibration at 6.75 $\mu$ is observed. So it is now clear that both of these polymers have -CONH $-CH_2-NHCO-$ linkages, as expected. The result of elementary analysis indicated that these polymers have the following structures;

Table I. Reaction conditions and results

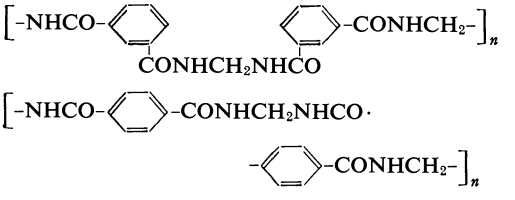
| Nitriles (g.) | HCHO (g.) | 95% $H_2SO_4$ (g.) | React. temp. (°C) | React. periods (hr.) | Product (g.) | $\eta_{sp}/c$ |
|---|---|---|---|---|---|---|
| Ortho- 11.30 | 2.75 | 90.70 | 20 | 3 | No product | — |
| Iso- 11.30 | 2.75 | 90.70 | 20 | 3 | Condensation polymer 15.0 | 0.258 |
| Tere- 11.30 | 2.75 | 90.70 | 20 | 3 | Condensation polymer 15.0 | 0.443 |
| *p*-Xylylene 4.70 | 1.00 | 30.00 | 20 | 3 | Condensation polymer 6.1 | — |

TABLE. II. SOLUBILITY

| Solvents | Isophthalonitrile polymer | | Terephthalonitrile polymer | | *p*-Xylylene cyanide polymer | |
|---|---|---|---|---|---|---|
| | Under room temp. | Under heating | Under room temp. | Under heating | Under room temp. | Under heating |
| 95% Sulfuric acid | Sol. | Sol. | Sol. | Sol. | Sol. | Sol. |
| 85% Phosphoric acid | Sol. | Sol. | Insol. | Insol. | Insol. | Insol. |
| 90% Formic acid | Insol. | Insol. | 〃 | 〃 | 〃 | 〃 |
| Acetic acid | 〃 | 〃 | 〃 | 〃 | 〃 | 〃 |
| Monochloroacetic acid | 〃 | 〃 | 〃 | 〃 | 〃 | 〃 |
| Methyl alcohol | 〃 | 〃 | 〃 | 〃 | 〃 | 〃 |
| Acetone | 〃 | 〃 | 〃 | 〃 | 〃 | 〃 |
| Ethyl ether | 〃 | 〃 | 〃 | 〃 | 〃 | 〃 |
| Chloroform | 〃 | 〃 | 〃 | 〃 | 〃 | 〃 |
| Chlorobenzene | 〃 | 〃 | 〃 | 〃 | 〃 | 〃 |
| Benzene | 〃 | 〃 | 〃 | 〃 | 〃 | 〃 |
| *n*-Hexane | 〃 | 〃 | 〃 | 〃 | 〃 | 〃 |
| Phenol | 〃 | Sol. | 〃 | 〃 | 〃 | 〃 |
| *m*-Cresol | 〃 | Sol. | 〃 | 〃 | 〃 | 〃 |
| Carbon disulfide | 〃 | Insol. | 〃 | 〃 | 〃 | 〃 |
| Dimethyl formamide | Sol. | Sol. | 〃 | 〃 | 〃 | 〃 |
| Dimethyl sulfoxide | Sol. | Sol. | 〃 | 〃 | 〃 | 〃 |
| Aniline | Insol. | Insol. | 〃 | 〃 | 〃 | 〃 |
| Pyridine | 〃 | 〃 | 〃 | 〃 | 〃 | 〃 |

TABLE III. EFFECT OF ADDITION CONDITION

| Addition condition | $\eta_{sp}/c$ |
|---|---|
| Adding terephthalonitrile into the sulfuric acid solution of formaldehyde. | 0.229 |
| Adding paraformaldehyde into the the sulfuric acid solution of terephthalonitrile. | 0.174 |
| Adding the mixture of terephthalonitrile and paraformaldehyde into the sulfuric acid. | 0.428 |




From these findings, it is understood that the aromatic dinitrile compounds are also capable of forming polyamide as in the case of aliphatic dinitrile compounds.

As benzene rings and -NHCO- linkages are arranged alternately in such polyamide, the crystallization will be accelerated by the intermolecular hydrogen bonds between -CONH- groups and the molecules will be oriented easily. The insolubility of these condensation polymers in almost all organic solvents as shown in Table II and the higher decomposition point above 300°C without melting or softening may be attributed to this crystalline structure.

In concentrated sulfuric acid, aromatic dinitrile is easily hydrolysed into acid amide and formaldehyde forms carbonium cation and becomes very reactive. Therefore, it is believed that the molar ratio between these two reagents

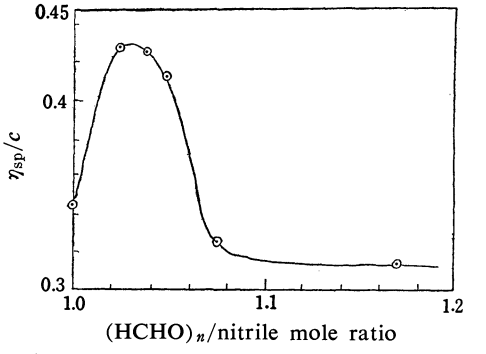
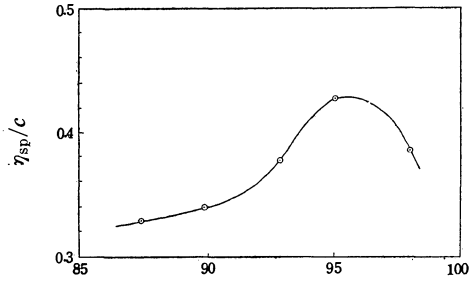



Fig. 2. Effect of the molar ratio of formaldehyde to terephthalonitrile.

greatly influences the condensation polymerization reaction in sulfuric acid. As shown in Fig. 2 and Table III, the product which has the highest condensation polymerization degree is obtained when the equimolecular mixture of terephthalonitrile and formaldehyde is added into sulfuric acid.

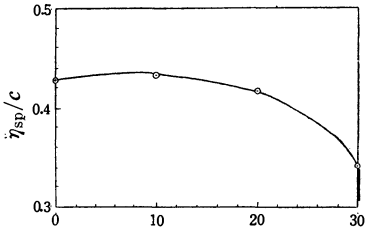
When terephthalonitrile is added into the sulfuric acid solution of formaldehyde and when the molar ratio of formaldehyde to terephthalonitrile is large, formaldehyde is always in excess to the dinitrile in the reaction

solution. In this condition the side reaction with activated formaldehyde becomes so predominant that the condensation polymerization reaction is impeded and consequently the intrinsic viscosity of the reaction product becomes low. Similarly when formaldehyde is added into the sulfuric acid solution of terephthalonitrile and the molar ratio is small, the intrinsic viscosity of the reaction product becomes low. It is considered that this fact is due to the hydrolysis of terephthalonitrile into terephthalamide. It is probably for the same reason that the condensation polymerization product of great intrinsic viscosity can not be obtained when the concentration of sulfuric acid is lower than 95% and the reaction temperature is higher, as shown in Figs. 3 and 4.



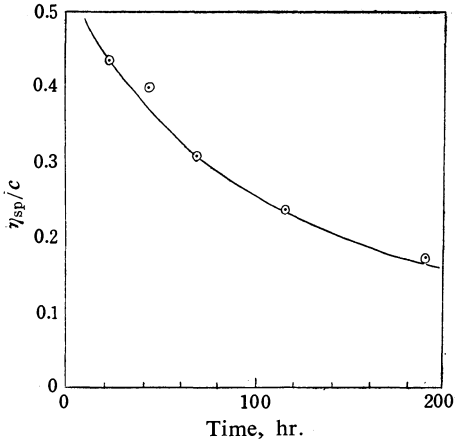

Concentration of sulfuric acid, %

Fig. 3. Effect of concentration of sulfuric acid.



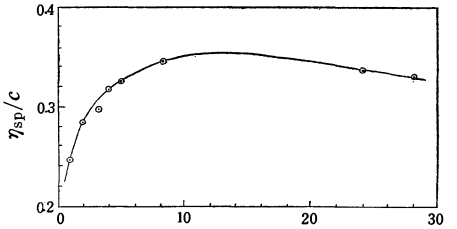

Reaction temperature, °C

Fig. 4. Effect of reaction temperature.




Time, hr.

Fig. 5. Degradation by sulfuric acid.




Time, hr.

Fig. 6. Effect of reaction time.

The condensation polymer from terephthalonitrile and formaldehyde rapidly degrades in the presence of sulfuric acid at room temperature as shown in Fig. 5. This behavior is somewhat unexpected since the condensation polymer itself is prepared in the concentrated sulfuric acid. Although the mechanism of degradation is not clear, -CONH- linkage may be hydrolysed by acid. As it is probable that the condensation polymerization reaction is accompanied by a simultaneous degradation reaction, the degree of condensation polymerization of the product becomes lower when the reaction time is longer, as shown in Fig. 6.

On the other hand no condensation polymer can be obtained by reacting terephthalamide with formaldehyde under the same reaction conditions as in the case of the terephthalonitrile. Thus it is clear that the mechanism of this reaction is not considered as the formation of acid amide by the hydrolysis of nitrile group in sulfuric acid followed by the methylol condensation as in urea resins, but is considered as follows.

$$CH_2O + H_2SO_4 \rightarrow CH_2OH^+ + HSO_4^-$$

$$CN\text{-}C_6H_4\text{-}CN + CH_2OH^+ + HSO_4^- \rightarrow CN\text{-}C_6H_4\text{-}C(OSO_3H)=N\cdot CH_2OH$$

(I)

$$I + H_2SO_4 \rightarrow CN\text{-}C_6H_4\text{-}C(OSO_3H)=N\cdot CH_2^+ + HSO_4^- + H_2O$$

(II)

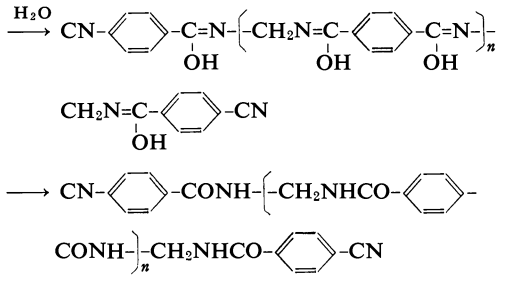
$$II + HSO_4^- + CN\text{-}C_6H_4\text{-}CN \rightarrow CN\text{-}C_6H_4\text{-}C(OSO_3H)=N\cdot CH_2\cdot N=C(OSO_3H)\text{-}C_6H_4\text{-}CN$$

$$\vdots$$

$$CN\text{-}C_6H_4\text{-}C(OSO_3H)=N\text{-}\left[\text{-}CH_2N=C(OSO_3H)\text{-}C_6H_4\text{-}C(OSO_3H)=N\text{-}\right]_n\text{-}CH_2N=C(OSO_3H)\text{-}C_6H_4\text{-}CN$$

TABLE IV. ELEMENTARY ANALYSIS

| Dinitrile | Found | | | Calcd. | | | |
|---|---|---|---|---|---|---|---|
| | C | H | N | C | H | N | |
| Isophthalonitrile | 58.6 | 4.7 | 15.5 | 61.4 | 4.6 | 15.9 | for $(C_9H_8N_2O_2)_n$ |
| Terephthalonitrile | 58.9 | 4.7 | 16.6 | 61.4 | 4.6 | 15.9 | for $(C_9H_8N_2O_2)_n$ |
| *p*-Xylylene cyanide | 62.3 | 6.0 | 13.0 | 64.7 | 5.9 | 13.7 | for $(C_{11}H_{12}N_2O_2)_n$ |



## Experimental

**Synthesis of Orthophthalonitrile.** — Phthalamide was prepared from phthalic anhydride and aqueous ammonia by the standard method, and then phthalamide (68 g.) was dehydrated to phthalonitrile with acetic anhydride (425 g.) in chlorobenzene (88 g.) by the known method[3]. Yield 26.5 g. (50% of theoretical yield). After recrystallizing from water, a colorless crystal was obtained, m. p. 141~142°C.

**Sntheysis of Isophthalonitrile.** — Isophthalyl chloride was prepared from isophthalic acid and thionyl chloride, and transformed to isophthalamide with aqueous ammonia. Isophthalamide (32.8 g.) and phosphorus pentachloride (41.6 g.) were mixed in chlorobenzene (200 g.) and the mixture was heated gradually. It was heated for an hour at 98°C. until a homogeneous solution was obtained. After pouring the solution into ice water, 20 g. of crude isophthalonitrile was obtained with 78% yield. The crude material was recrystallized from water. The pure material melted at 160.5°C.

**Synthesis of Terephthalonitrile.**—Terephthalyl chloride was prepared from terephthalic acid and phosphorus pentachloride and transformed to terephthalamide with aqueous ammonia and then terephthalamide was dehydrated to terephthalonitrile with phosphorus pentachloride in chlorobenzene, using the same methods as in the case of the isophthalonitrile. The crude terephthalonitrile was recrystallized from benzene to needle crystals, m. p. 221.5~222.0°C.

**Synthesis of *p*-Xylylene Cyanide.**—A solution of potassium cyanide (13 g.) in 25 g. of water was added dropwise into a solution of *p*-xylene bromide (13 g.) in 200 cc. of ethanol at 80°C and the mixture was heated under reflux for three hours. After the reaction was completed, ethanol was distilled off and the residue was poured into ice water and filtered. The precipitate was recrystallized from ethanol and hot water to get pure *p*-xylylene cyanide (4.7 g.), m. p. 96~97.5°C.

3) E. Koike; *J. Chem. Soc. Japan. Ind. Chem. Sec.* (*Kogyo Kagaku Zasshi*), **57**, 925 (1954).

**Condensation Polymerization of Aromatic Dinitriles and Formaldehyde.**—A mixture of paraformaldehyde and dinitriles was added in small portions with stirring at a constant temperature into sulfuric acid which was placed in a 100 cc. three-necked flask equipped with thermometer and stirrer. External cooling was necessary to maintain the constant temperature at 0°C because the reaction was exothermic. After the exothermic reaction was over, the mixture began to thicken gradually. The stirring was continued for two hours after the nitrile was added, to complete the reaction. The reaction product was poured into ice water with stirring to precipitate the condensation polymer. The precipitate was washed with water and the remaining acid was removed by washing with sodium bicarbonate solution (1%), then it was dried at 60°C until it was posssible to get constant weight under reduced pressure. The result of the elementary analysis is shown in Table IV.

**Infrared Absorption Spectrum.**—A specimen film of the condensation polymer of isophthalonitrile was prepared by evaporating the *m*-cresol solution of the polymer under reduced pressure. The specimen film of the condensation polymer of terephthalonitrile was prepared by squeezing the viscous reaction product between the two glass plates followed by washing the thin layer of polymer with water. The clear thin film thus obtained was dried under reduced pressure. The infrared absorption spectra were observed on these films using a Perkin-Elmer Model 21 spectrophotometer.

**Intrinsic Viscosity.**—Four hundred milligrams of the condensation polymer was added into 1000 cc. of 85% sulfuric acid and dissolved completely. This was left at 11~12°C for 24 hr. with shaking. The specific viscosity was measured on this solution by using Ostwald's viscosimeter at 30°C and the intrinsic viscosity was calculated.

**The Reaction of Terephthalamide and Formaldehyde.**—A mixture of terephthalamide (8.2 g.) and paraformaldehyde (1.5 g.) was added into concentrated sulfuric acid (98%, 75 g.) with stirring at 20°C. Although the stirring was continued for two hours after addition, the viscosity of the reaction mixture did not increase. When the reaction mixture was poured into the ice water, white precipitates (8.0 g.) were obtained.

Found: C, 58.41; H, 4.99; N, 17.10. Calcd. for $C_8H_8N_2O_2$: C, 58.53; H, 4.91; N, 17.07%

## Summary

1. Like aliphatic dinitriles, polyamide having benzene nucleus and -CONH- linkages was synthesized by condensation polymerization reaction of aromatic dinitriles and formaldehyde in concentrated sulfuric acid.

2. The condensation polymer obtained from terephthalonitrile had the greatest intrinsic viscosity among ortho-, iso-, tere-phthalonitrile and *p*-xylylene cyanide. A product of the highest condensation polymerization degree was obtained, by adding the 1.025 : 1 molar mixture of paraformaldehyde and terephthalonitrile in small portions into ten molar amounts of 95% sulfuric acid at 0°C and then stirring for ten hours at the same temperature.

3. These condensation polymers were insoluble in almost all organic solvents and had no melting and softening point. They decomposed above 300°C.

The author wishes to express his sincere thanks to Professor Ryozo Goto of Kyoto University for his kind advice, and also to Mr. Murataro Nakashima, President of Kunoshima Chemical Co., for his permission to publish this paper.

*Research Laboratory of Kunoshima Chemical Industry Co., Ltd.*
*En-ichi-cho, Mihara*

# *Ultraviolet Spectra of N-Heterocyclic Systems. I. The Anions of Uracils**

By Koji NAKANISHI, Noboru SUZUKI and Futaba YAMAZAKI

(Received July 26, 1960)

The keto-enol equilibria of uracil and its anions have been studied in order to clarify the nature of the tautomerism encountered in the complicated derivatives of a natural product[1,2]. Moreover, besides being of interest because of its relation to nucleic acids, uracil contains two potentially dissociable protons, and accordingly it was felt that this simple molecule might provide a convenient means for more complex systems. The keto-enol equilibria of various monohydroxy *N*-heterocyclic bases have already been studied extensively by means of infrared, ultraviolet, and Raman spectroscopy, and other methods[3]. The studies with dihydroxy compounds are much more limited, and although the phenomena have indeed been investigated with uracil, especially by Shugar and Fox[4], the tautomeric equilibrium constants $K_T$ were not taken into consideration.

Six tautomeric forms are conceivable for uracil. However, the following evidence shows that it exists predominantly in the diketo form I (Plate 1) in solution as well as in the solid state. The solid infrared spectrum of uracil (Table I) in the double bond stretching region is very similar to 1, 3-dimethyluracil (VIII) which has a fixed structure; 1-methyluracil (IV) and 3-methyluracil (VI), for which three tautomeric forms are possible, respectively, also show very similar absorptions. The dioxane solution spectra of uracil, 1-methyluracil, and 3-methyluracil are also quite similar to 1, 3-dimethyluracil. Hence, it is easily seen that all four compounds can be represented by the diketo forms both in dioxane and in the solid state. It is well-known that among the possible tautomers, the more polar forms are favored in the solid state and in solutions of high dielectric constants. The fact that the tautomers present in dioxane, a solvent of low dielectric constant (2.101 at 25°C)[5], and in the solid state, are the diketo forms (I, IV, VI) suggests that the same diketo forms are also predominant

TABLE I. INFRARED ABSORPTIONS (in $cm^{-1}$)

| | KBr | Dioxane |
|---|---|---|
| Uracil (I) | 1715, 1670 | 1720 sh, 1698 |
| 1-Methyluracil (IV) | 1695, 1675 | 1712 sh, 1694 |
| 3-Methyluracil (VI) | 1705, 1630 | 1726, 1670 |
| 1, 3-Dimethyluracil (VIII) | 1712, 1655 | 1713, 1673 |

* Paper read in part at the 13th Annual Meeting of the Chemical Society of Japan, Tokyo, April, 1960.

1) K. Nakanishi, M. Ohashi, S. Kumasaki and S. Yamamura, *J. Am. Chem. Soc.*, **81**, 6339 (1959).

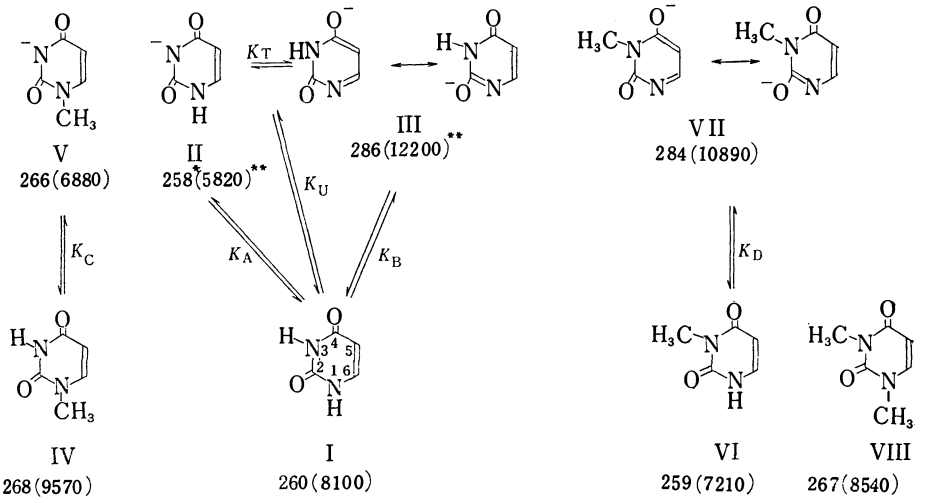
2) Results pertaining to the natural derivatives will be reported shortly.

3) Some recent papers on this subject: (a) H. Shindo, *Chem. and Pharm. Bull.*, **7**, 407 (1959); (b) K. Nakamoto and A. E. Martell, *J. Am. Chem. Soc.*, **81**, 5857 (1959); (c) A. Albert and E. Spinner, *J. Chem. Soc.*, **1960**, 1221.

4) D. Shugar and J. J. Fox, *Biochem. et Biophys. Acta*, **9**, 199 (1952); see also J. J. Fox and I. Wempen in "Advances in Carbohydrate Chemistry", Vol. 14, Academic Press, New York (1959), p. 283.

5) H. S. Harned and B. B. Owen, "Physical Chemistry of Electrolytic Solutions", Reinhold Publishing Co., New York (1958), p. 161.

Plate 1. Proton equilibria of uracils in water




Data for neutral molecules and anions are for pH 6.86 and 12.0, respectively.
Peak positions (m$\mu$) and intensities ($\varepsilon$) are given.
* Obtained after wing correction (Fig. 4).
** Calculated (see text).

TABLE II. ULTRAVIOLET SPECTRA OF URACILS (25°C)
Wavelengths given in m$\mu$; numbers in parentheses are $\varepsilon \times 10^{-3}$
$\Delta\lambda$ (in m$\mu$) = $\lambda$ (pH 12.0) − $\lambda$ (pH 6.86)

| | | Dioxane | pH 6.86 | pH 9.71 | pH 12.0 | $\Delta\lambda$ | p$K$ |
|---|---|---|---|---|---|---|---|
| 1. | Uracil | 257(8.35) | 260 (8.10) | 265(5.47) | 286 (6.01) | +26 | 9.51 (at 25°C) |
| 2. | Thymine[a] | | 265 (7.89) | | 291 (5.44) | +26 | 9.9 |
| 3. | 1-Methyluracil | 266(9.70) | 268 (9.57) | 267(7.64) | 266 (6.88) | − 2 | 9.77 (at 25°C) |
| 4. | Uridine[a] | | 262(10.1) | | 262 (8.5) | 0 | 9.25 |
| 5. | Uracil deoxyriboside[a] | | 262(10.2) | | 262 (7.63) | 0 | 9.3 |
| 6. | Thymidine[a] | | 267 (9.65) | | 267 (7.38) | 0 | 9.8 |
| 7. | 3-Methyluracil | 257(7.31) | 259 (7.21) | 255(5.74) | 284(10.89) | +25 | 10.00 (at 25°C) |
| 8. | 1,3-Dimethyl uracil | 265(8.71) | 267 (8.54) | | | | |

a) Data from D. Shugar and J. J. Fox, *Biochem. et Biophys. Acta*, **9**, 199 (1952).

in water, a solvent of higher dielectric constant[6]. This was supported by measuring the ultraviolet spectra in dioxane-water mixtures. Isosbestic points, suggestive of an equilibrium mixture, were absent, and in all cases the only trend observed was a slight red shift in going from 100 percent dioxane to water (pH 6.86, Table II, intermediate dioxane concentrations are omitted); it is well-known that in neutral uncharged molecules the $\pi-\pi^*$ bands are shifted towards the red as the dielectric constant of the solvent is increased.

The ultraviolet spectra are recorded in Figs. 1—3. In going from the neutral to the anionoid

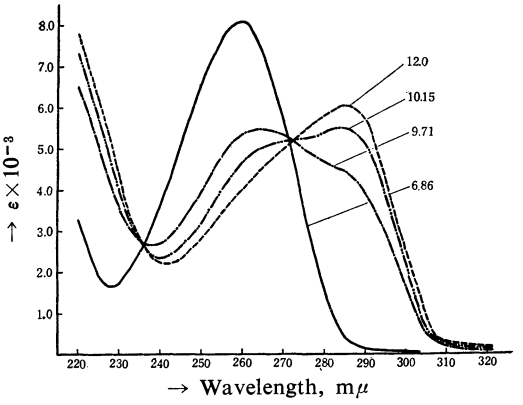



Fig. 1. Ultraviolet spectra of uracil at various pH (numbers beside curves).

6) Infrared measurements have shown that uridine and uridylic acid exist in the diketo form in $D_2O$: H. T. Miles, *Biochim. et Biophys. Acta*, **22**, 247 (1956).

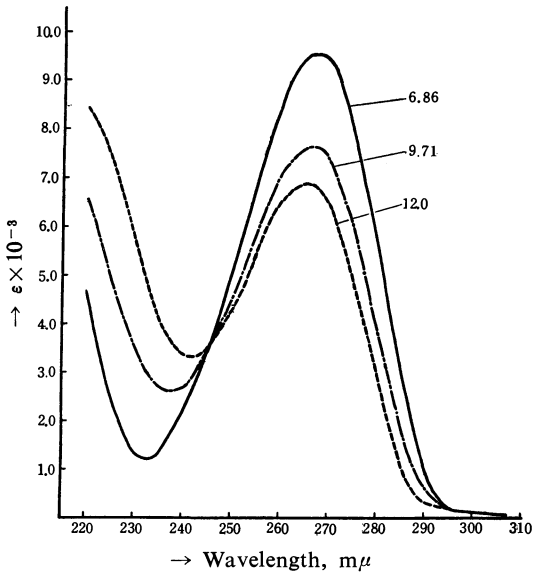



Fig. 2. Ultraviolet spectra of 1-methyluracil at various pH (numbers beside curves).

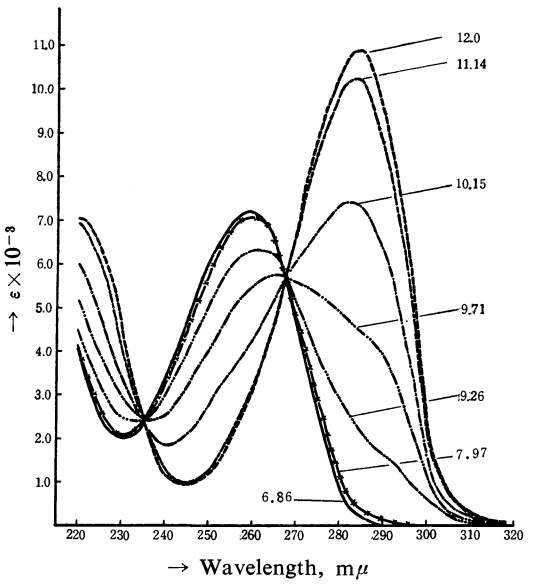
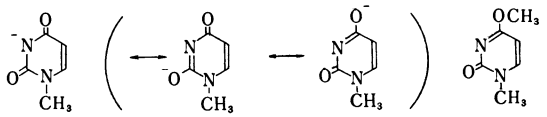



Fig. 3. Ultraviolet spectra of 3-methyluracil at various pH (numbers beside curves).

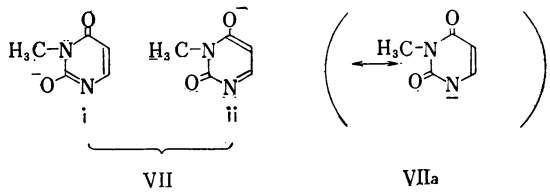
species in the case of 1-methyluracil, the peak intensity is lowered, but the wavelength is almost unaffected (Fig. 2 and Table II). This rules out the contribution of canonical structures such as Va or Vb; because of a more extended conjugated system, Va and Vb should show absorption at much longer wavelengths than the original species. For example, 1-methyl-4-methoxy-2-pyrimidone (IX) (cf., Experimental), which contains the O=C–N=C–$OCH_3$ system, already absorbs at 275 mμ, and accordingly Va and Vb containing the O=C–N=



V Va Vb IX

275 mμ
(ε 5,890)
at pH 6.86

C–$O^-$ system would be expected to show absorption at a still longer wavelength. Localization of the negative charge on the nitrogen atom has recently been suggested for the anion of 2-hydroxypyridine[8]. The cause for this localization is probably due to the fact that the intrinsic stability of the two carbonyl bonds outweigh the stabilization gained by an extended conjugation. Similar trends, i. e., lowering of peak intensity and constancy or slight blue shift of band position, are encountered upon anion formation in other 1-substituted uracils (Table II, nos. 4—6) and various uridine phosphates[9] such as uridine-5′-diphosphate (262 mμ, ε 10,000 vs. 261 mμ, 7,900), and uridine-5′-triphosphate (262 mμ, ε 10,000 vs. 261 mμ, 8,100). The anion of 3-methyluracil, on the other hand, shows a considerable red shift and increases in peak intensity. This behavior can be accounted for by canonical structures VII-i or VII-ii[10] but not by VIIa; in VII a conjugated system more extended than Va or Vb is present, and this probably compensates for the carbonyl bond energy.



i ii VII VIIa

The anion of uracil (Fig. 1) has its peak at 286 mμ (ε 6,010) with a broad hump around 260 mμ (ε ca. 4,000). The peak undoubtedly corresponds to the 284 mμ (ε 10,890) peak of VII; if wing correction (Fig. 4) is carried out by subtracting the curve of 3-methyluracil anion multiplied by 6,010/10,890, a peak is revealed at 258 mμ (ε 2,490). This peak is due to the anion II, the equivalent of V (266 mμ). Thus, the following empirical rule is apparent

7) H. McConnell, *J. Chem. Phys.*, **20**, 700 (1952).
8) E. Spinner, *J. Chem. Soc.*, **1960**, 1232.
9) R. M. C. Dawson, D. C. Elliott, W. H. Elliott and K. M. Jones, ed., "Data for Biochemical Research," Oxford Univ. Press, London (1959), p. 78.
10) At present, no conclusion can be drawn as regards the relative weights of contributions of structures VII-i and VII-ii.

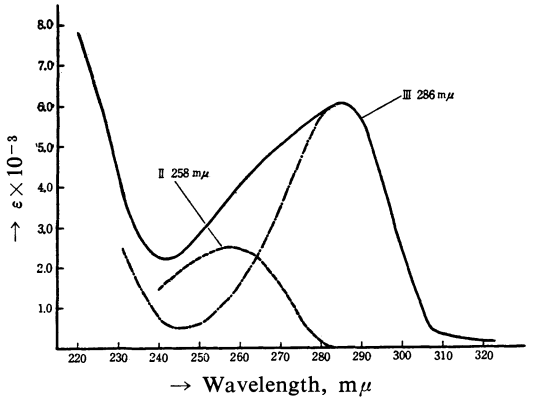



Fig. 4. Ultraviolet absorptions of uracil anions at pH 12.0.

in the ultraviolet spectra of uracils (Plate 1, see also Table II): (1) Alkylation at N-1 results in a red shift of ca. 8 mμ (I vs. IV, II vs. V). (2) Deprotonation at N-1 similarly results in a red shift of ca. 26 mμ (I vs. III, VI vs. VII). (3) Alkylation at N-3 results in a slight blue shift of 1~2 mμ (I vs. VI, III vs. VII). (4) Deprotonation at N-3 similarly results in a slight blue shift of ca. 2 mμ (IV vs. V, I vs. II). It is interesting to note that this simple calculation is also applicable to the disubstituted 1,3-dimethyluracil (VIII): calculated $\lambda_{max}$ 266~267 mμ; observed 267 mμ. The ultraviolet absorption curves of thymine

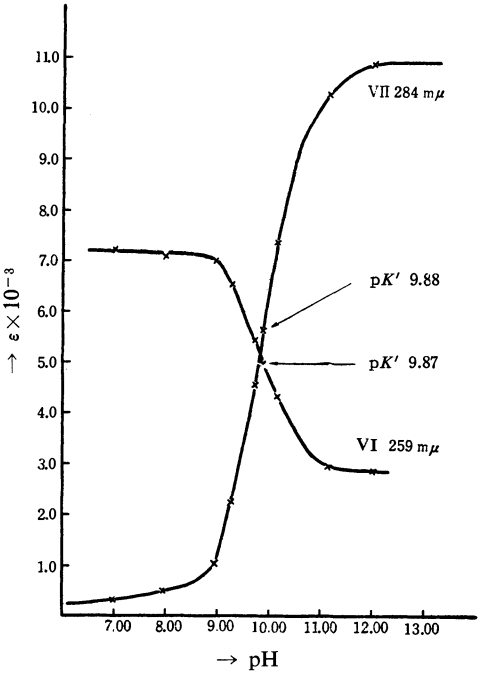



Fig. 5. 3-Methyluracil; variation of peak intensities with pH.

(5-methyluracil) and thymidine[4] show that this general trend is apparent in this series also.

The p$K$ of uracil (p$K_U$), 1-methyluracil (p$K_C$), and 3-methyluracil (p$K_D$) were obtained by spectroscopic measurement of the p$K'$ from the curves at pH 6.86, 9.71 and 12.0 (Figs. 1—3), and correction to thermodynamic p$K$ values (Table II). The p$K'$ values were also obtained by graphical plotting of extinction coefficients versus pH as shown in Fig. 5 for 3-methyluracil; the results are identical with the calculated values and, therefore, are omitted for other samples. The extinction coefficients for the anions II and III, which cannot be obtained experimentally, were calculated as follows:

$$\varepsilon_{III}/\varepsilon_I = \varepsilon_{VII}/\varepsilon_{VI}$$

hence, $\varepsilon_{III} = 8100 \times 10890/7210 = 12200$

and the percentage of III present in the uracil anion is

$$\text{III (percentage)} = 6010/12200 \times 100 = 49$$

Accordingly, the ratio of II to III, $K_T$, is 51/49=1.0.

Similarly,

$$\varepsilon_{II}/\varepsilon_I = \varepsilon_V/\varepsilon_{IV}$$

hence, $\varepsilon_{II} = 8100 \times 6880/9570 = 5820$

The percentage of II may be estimated from the intensity of the 258 mμ peak (Fig. 4):

$$\text{II (percentage)} = (2490/5820) \times 100 = 43$$

hence, $K_T = \text{II}/\text{III} = 43/57 = 0.8$

The agreement with the ratio 1.0 calculated from the 286 mμ peak is not quite satisfactory, but the 1.0 value is probably more correct because no wing correction is necessary.

If $K_A$ and $K_B$ are the individual dissociation constants leading from I to II and III, respectively (Plate 1), it can be readily shown[11] that

$$K_u = K_A + K_B \quad \text{and} \quad K_T = \text{II}/\text{III} = K_A/K_B$$

Substitution of $K_T = 1.0$ gives $pK_A = pK_B = 9.81$.

Occasionally[11,12], $K_T$ is calculated by assuming that $K_C$ or $K_D$ is approximately equal to $K_A$ or $K_B$, respectively, since substitution of a methyl group for a hydrogen atom would have a minor effect. However, the above results show that the approximation is not so satisfactory. Since the ultraviolet spectra of the other compounds listed in Table II and of the uridine phosphates[9] closely resemble those of the uracils treated in the present paper, the tautomeric behavior can be handled in an identical manner.

11) G. F. Tucker and J. L. Irvin, *J. Am. Chem. Soc.*, **73**, 1923 (1951).

12) E. J. Cohn and J. T. Edsall, "Proteins, Amino Acids and Peptides," Reinhold Publ. Corp., New York (1943), p. 96.

## Experimental

**Materials.**—1-Methyluracil[13] was prepared from uracil through 2,4-dichloropyrimidine, 2,4-dimethoxypyrimidine and 1-methyl-4-methoxy-2-pyrimidone (hydrolysis). The structure of the product as 1-methyluracil has been confirmed by Brown et al.[14].

3-Methyluracil[15] was prepared from ethyl ethoxy methylenemalonate[16] through 3-methyl-5-carbethoxyuracil and 3-methyl-5-carboxyuracil(decarboxylation). Product confirmed by Brown et al.[14]

1,3-Dimethyluracil[17] was prepared by methylation of uracil with dimethyl sulfate.

**Spectral Measurements.** — The infrared spectra were recorded with a Koken model 301 spectrophotometer. The ultraviolet spectra were recorded with a Hitachi model EP-1 spectrophotometer; a pair of 1 cm. quartz cells with stoppers was used and the cell temperature was maintained at 25±1°C. The error in absorbancy is ±0.002.

**Measurement of p*K*.**—All pH measurements were carried out at 25±1C° with a Horiba model P pH meter equipped with extension glass and calomel electrodes; the meter was calibrated with a standard Horiba buffer solution of pH 6.86 at 25°C($KH_2PO_4$+$Na_2HPO_4$). The following buffers were used for the pH indicated: pH 7.97, $KH_2PO_4$+$Na_2HPO_4$; pH 8.95, 9.26, 9.71 and 10.15, $Na_2CO_3$+$NaHCO_3$; pH 11.14 and 12.0 (uncorrected), $Na_2HPO_4$+NaOH. The ionic strength of the solutions was 0.1. The apparent p$K'$ was calculated from:

$$pK' = pH - \log (\varepsilon_{HX} - \varepsilon_{obs})/(\varepsilon_{obs} - \varepsilon_X)$$

where $\varepsilon_{HX}$ and $\varepsilon_X$ are the molecular extinction coefficients ($\varepsilon$) measured in pH 6.86 and pH 12.0 buffer solutions, respectively, and $\varepsilon_{obs}$ is the $\varepsilon$ measured in an intermediate pH solution where the pH was chosen so that the value of $(\varepsilon_{HX}-\varepsilon_{obs})/(\varepsilon_{obs}-\varepsilon_X)$ was near unity, i. e., pH 9.71. The wavelength chosen was 260 m$\mu$ and 285 m$\mu$ for uracil, 265 m$\mu$ for 1-methyluracil, and 259 m$\mu$ and 284 m$\mu$ for 3-methyluracil.

The p$K'$ was also obtained graphically as shown in Fig. 5. These apparent constants were corrected to the thermodynamic scale with the aid of the Debye-Hückel relationship,

$$pK = pK' + \log f_{HX} - \log f_X \quad (1)$$

$$\log f_X = -0.509(\sqrt{I}/1+\sqrt{I}) \text{ (at 25°C)}$$

where $f$ and $I$ represent the activity coefficient and the ionic strength. Since for neutral molecules $f_{HX}$ is approximately unity, the correction becomes

$$pK = pK' - \log f_X = pK' + 0.12$$

## Summary

In aqueous solutions uracil exists predominantly in the diketo form, whereas in alkaline solutions it exists as an approximately 1 : 1 mixture of two deprotonated forms. The two deprotonated anions show ultraviolet absorptions similar to the anions of 1-methyluracil and 3-methyluracil, and the main contributing canonical structures which give rise to the general absorption feature of the anions are discussed. The peak shifts accompanying N-alkylation or deprotonation may be summarized in a simple empirical rule. Individual ionization constants have also been estimated.

The results of uracil can be extended to thymine, uridine, thymidine, and their phosphates. The pesent method can probably be extended to other systems containing two dissociable protons.

The authors are indebted to Professor F. Egami, the University of Tokyo, for his initial suggestion of the problem and interests. Part of the expenses have been covered by the Grant in Aid for Fundamental Scientific Research, Ministry of Education.

*Department of Chemistry*
*Faculty of Science*
*Tokyo University of Education*
*Bunkyo-ku, Tokyo*

13) G. E. Hilbert and T. B. Johnson, *J. Am. Chem. Soc.*, 52, 2001 (1930).
14) D. J. Brown, E. Hoerger, and S. F. Mason, *J. Chem. Soc.*, 1955, 211.
15) C. E. Whitehead, *J. Am. Chem. Soc.*, 74, 4267 (1952).
16) "Organic Syntheses", Coll. Vol. 3, John Wiley and Sons, Inc., New York (1955), p. 395.
17) D. Davidson and O. Baudisch, *J. Am. Chem. Soc.*, 48, 2382 (1926).

# *Secondary Electron Emission from Copper-Beryllium (4%) Surface by Bombardment of Various Positive Ions*

By Toshio SUGIURA and Teruo HAYAKAWA

(Received July 4, 1960)

According to the development of the mass spectrometric investigations, the necessities for the measurements of the minute ion intensity are rapidly increasing. The secondary electron multiplier has now widely been used as an excellent ion detector for the measurements of ionization potentials and the microanalysis of many isotopes. Many reports on the secondary electron emission from the metal surfaces by the bombardment of high energy ions were already published. But unfortunately, some results of them disagree with each other[1,2], and these discrepancies might be caused by the different surface conditions of the ion targets for the secondary electron emission.

Recently, Hagstrum[3-6] has reported the many important results of the Auger ejection process of secondary electrons from the atomically clean surfaces of transition metals by the bombardment of the noble gas ions, and he suggested that the existence of the adsorbed layer causes the remarkable influence on the mechanism of the secondary electron ejection. But the target surfaces are not always atomically clean under the ordinary operating conditions, and the influence of the adsorbed layer seems considerably complicated since the semiconductor surfaces are usually used for obtaining the large electron yield.

The characteristics necessary for the secondary electron multiplier are the large electron yield per impinged ion or electron and the excellent stability for the electron yield under the usual operating conditions. The electron yield mainly depends upon the following factors:

(1) the mass, energy, electronic charge and configuration of the incident particle;

(2) the chemical and physical properties of the metal surface; and

(3) the angle with which the incident particle strikes the metal surface.

The present investigation was undertaken in order to find the optimum condition of the preparation of the sensitive and stable surface of the copper-beryllium target suitable for the secondary electron multiplier. This paper reports the main results of the following studies:

(1) the dependency of the electron yield of the non-activated and activated target surfaces upon the kinetic energy of various noble gas and hydrocarbon ions;

(2) the determination of the surface structures of the ion targets by means of electron diffraction analysis; and

(3) the influence of the temperature of treatment upon the electron yield and the stability of the target surfaces.

## Experimental

**Mass Analyser and Ion Targets.** — The present experiments were performed by a mass spectrometer self-constructed in our laboratory. This mass spectrometer is a single focusing 90° sector type and the radius of curvature of the ion path is 135 mm., and the ion source of the usual electron bombardment type was installed in this instrument. In the present experiments two kinds of simple detectors were used. The constructions of the target assembly of them are schematically shown in Figs. 1a and 1b.

In Fig. 1a, $T_1$ indicates the ion target, $C_1$ the collecting plate of secondary electrons, $S_1$ the enclosing cage of the detector, and $E_1$ the collector slit. The other detector shown in Fig. 1b was constructed in order to measure the electron yield of the copper-beryllium surface by the bombardment of secondary electrons. But in the present experiments this detector shown in Fig. 1b was also used for the measurements of the electron yield by the bombardment of various positive ions. In Fig. 1b, $T_2$ indicates the ion traget, D and $C_2$ the collecting plates of sencondary electrons, $S_2$ the enclosing cage of the detector, $E_2$ the collector slit.

The geometries of the ion tragets ($T_1$ and $T_2$) and the collecting plate of secondary electrons (D) are similar to those of the electron multiplier of the Nier type[7]. The width of the collector slit was fixed to 2 mm., while the width of the exit slit of

1) M. G. Inghram, "Mass Spectroscopy in Physical Research", NBS Circular No. 522, 257 (1953).
2) M. G. Inghram, "A Handbook on Mass Spectroscopy", National Academy Sciences (1954), p. 41.
3) H. D. Hagstrum, *Phys. Rev.* **89**, 244 (1953).
4) H. D. Hagstrum, ibid., **91**, 543 (1953).
5) H. D. Hagstrum, ibid., **96**, 325, 336 (1954).
6) H. D. Hagstrum, ibid.. **104**, 317, 672, 1516 (1956).
7) K. S. Quisenberry, T. T. Scolman and A. O. Nier, ibid., **102**, 1071 (1956), W. H. Johnson, Jr. and A. O. Nier, ibid., **105**, 1014 (1957).

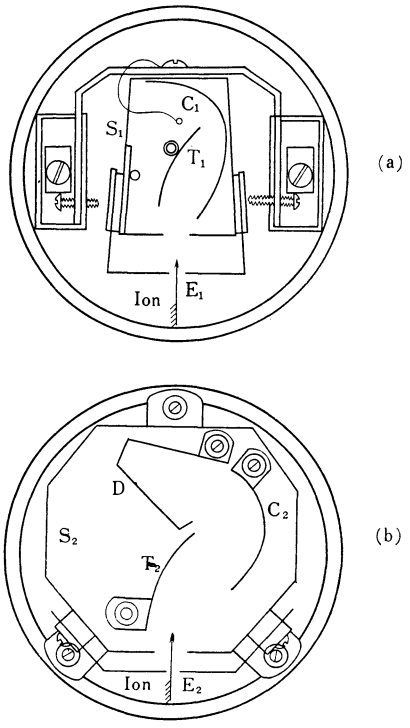



Fig. 1. Schematic diagrams of the ion collectors of the mass spectrometer. $T_1$(a) and $T_2$(b) are the ion targets, $C_1$ (a) and D(b) are the electron collectors, $C_2$(b) is Cu-Be dynode, $S_1$(a) and $S_2$(b) are the enclosing cages, and $E_1$(a) and $E_2$(b) are the collector slits.

the ion source is 0.2 mm. The ion targets were formed from the copper-beryllium plates* of 0.16 mm. in thickness, and the collecting plates of secondary electrons, the enclosing cages and the collector slits were all shaped from the molybdenum plates of 0.15 mm. in thickness.

For the measurements of the ion currents the collector slit ($E_1$ or $E_2$) and the ion target ($T_1$ or $T_2$) were kept to the earth potential and the electron suppressor voltage of $-20$ V. was supplied to all collecting plates ($C_1$ and $S_1$ in Fig. 1a; D, $C_2$ and $S_2$ in Fig. 1b). On the other hand, for the measurements of the secondary electron currents the collecting plates of secondary electrons were all kept to the earth potential and the potential of $-270$ V. was supplied to the ion target. It has been experimentally confirmed that these two types of detectors show the same value in the electron yield under the same experimental conditions.

A UX-54 tube was used as the primary tube of the d. c. amplifier, and the output currents were recorded by two galvanometers that have different sensitivities. The end vacuum under the ordinary experimental conditions was somewhat better than $1\times10^{-6}$ mm Hg.

**Treatment of Ion Targets.** — The non-activated targets were treated in the following manner. After being tempered, the alloy plates were mechanically polished with the fine emery papers of No. 0000 to 0005. After that the ion targets were formed and then electropolished in the polishing solution** for about one minute.

The treatment of activation of the ion targets was carried out in a quartz tube (25 mm. in outer diameter and 300 mm. in length) which was connected by the water-cooled taper joint to the vacuum system, the reservoir of purified oxygen and a McLeod gauge. The quartz tube was heated in an electric furnace and the temperature was measured by a copper-constantan thermocouple enclosed in this quartz tube. The electropolished targets were put into the quartz tube and evacuated to lower than $5\times10^{-6}$ mmHg at about 800°C for three hours. After the evacuation the temperature was lowered to each required temperature (i. e. 350, 420, or 480°C), and then the known quantity of oxygen was introduced into the quartz tube. The initial pressure of oxygen for each treatment was about $2\times10^{-2}$ mmHg, and the pressure decrease in each time was measured by a McLeod gauge.

The results are shown in Fig. 2. As seen in

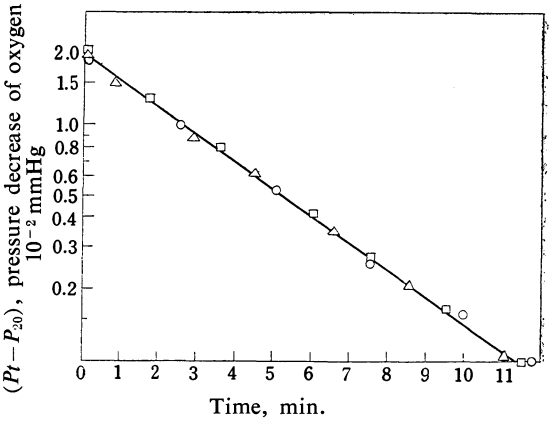



Fig. 2. Rate of the pressure decrease of the oxygen, by the treatment of the Cu-Be at the various temperatures: □; 350°C, △; 420°C and ○; 480°C.

Fig. 2, the present results indicate that the initial rate of the pressure decrease is independent of the temperature of treatment. After the treatment of 20 min. the quartz tube was evacuated and gradually cooled to the room temperature, and then the targets were taken out and mounted in the ion collector of the mass spectrometer.

**Determination of Surface Structure.** — The surface structure of the non-activated and activated ion targets was analysed by means of a commercial Hitachi E. D. C. type electron diffraction apparatus.

**Gaseous Materials.** — Oxygen was prepared by the thermal decomposition of potassium permanganate, and purified by passing through the trap

* The copper-beryllium plates of 0.16 mm. in thickness were prepared from a copper-beryllium(4%) alloy rod of the Beryllico Co., U. S. A.

** The electropolishing solution was prepared by mixing four volumes of phosphoric acid, four volumes of glycerin and three volumes of water.

cooled by liquid nitrogen. Spectroscopically pure argon and neon of the Teikoku Oxygen Co. were used without any further purification. The mass spectrometric analyses of these gaseous samples revealed that the total impurities were less than 0.005 per cent in volume. The research grade ethylene and ethane of the Philips Petroleum Co. were used in the present experiments, and the purity was also checked by means of the mass spectrometer.

## Results

**Surface Structure of Copper-Beryllium Targets.** — The surface structures of the copper-beryllium targets examined by the electron diffraction apparatus are summarized in Tables I and II. The main results of the analysed interplanar distances for the three kinds of ion targets — i. e. (a) tempered at about 800°C and mechanically polished, (b) tempered, mechanically polished, and then electropolished, and (c) tempered, mechanically polished, electropolished, and then bombarded by various positive ions for five hours — are listed in Table I together with that of Cu, $Cu_2O$ and CuO by X-ray diffraction analysis[8] for the sake of comparison. As seen in Table I, the oxide films of copper (mainly $Cu_2O$) are partially left on the mechanically polished surface (a). The electropolished surface (b) shows that the mechanically polished surface was re-oxidized by electropolishing, while the surface bombarded by various positive ions (c) indicates that the electropolished surface was partially reduced during the prolonged bombardments of various positive ions.

TABLE I. INTERPLANAR SPACINGS (Å) OF Cu-Be SURFACES MEASURED BY ELECTRON DIFFRACTION

(1) NOT TREATED SURFACES

(a) Mechanical polished surface, (b) electropolished surface, (c) after ion irradiation of the electropolished surface, and included the X-ray data of Cu, $Cu_2O$ and CuO.

| (a) | (b) | (c) | Cu | $Cu_2O$ | CuO |
|---|---|---|---|---|---|
| 2.998 | 2.501 | 2.992 | 2.08 | 3.00 | 2.51 |
| 2.443 | 2.166 | 2.623 | 1.81 | 2.45 | 2.21 |
| 2.207 | 1.758 | 2.395 | 1.277 | 2.12 | 1.70 |
| 2.010 | 1.522 | 2.180 | 1.228 | 1.51 | 1.57 |
| 1.816 | 1.273 | 1.766 | 1.089 | 1.283 | 1.50 |
| 1.540 | 1.131 | 1.649 | 1.043 | 1.065 | 1.408 |
| 1.356 | 0.956 | 1.577 | 0.905 | 0.971 | 1.370 |
| 1.235 | 0.874 | 1.176 | | 0.869 | 1.254 |
| 1.155 | | | | 0.819 | 1.159 |
| 1.070 | | | | | 1.086 |
| 1.030 | | | | | 1.007 |
| 0.864 | | | | | 0.855 |

8) K. Kubo, "The Method of Chemical Analysis by Meanes of X-ray Diffraction", Shukyosha Co., Tokyo (1947), pp. 118, 152, 156.

TABLE II. INTERPLANAR SPACINGS (Å) OF Cu-Be SURFACES MEASURED BY ELECTRON DIFFRACTION

(2) TREATED SURFACES BY OXYGEN

Included the X-ray data of BeO and CuO.

| Treated temperature | | | BeO | CuO |
|---|---|---|---|---|
| 480°C | 420°C | 350°C | | |
| 2.477 | 2.470 | 2.476 | 2.34 | 2.51 |
| 2.283 | 2.317 | 2.290 | 2.19 | 2.31 |
| 2.218 | 2.161 | 2.172 | 2.06 | 1.85 |
| 2.096 | 1.993 | 2.031 | 1.59 | 1.70 |
| 2.001 | 1.565 | 1.497 | 1.350 | 1.57 |
| 1.808 | 1.523 | 1.313 | 1.239 | 1.50 |
| 1.566 | 1.315 | 1.272 | 1.170 | 1.408 |
| 1.429 | 1.200 | 1.217 | 1.150 | 1.37 |
| 1.312 | 1.124 | 1.174 | 1.130 | 1.298 |
| 1.275 | 1.060 | 1.123 | 1.032 | 1.254 |
| 1.171 | 0.919 | 1.057 | 0.915 | 1.159 |
| 1.163 | 0.888 | 1.036 | 0.884 | 1.086 |
| 1.123 | 0.855 | 0.969 | 0·870 | 1.007 |
| 1.074 | 0.796 | 0.863 | 0.822 | 0.978 |
| 1.053 | 0.753 | 0.796 | 0.780 | 0.885 |
| 1.038 | | 0.741 | 0.758 | |
| 0.975 | | | | |
| 0.874 | | | | |
| 0.849 | | | | |
| 0.789 | | | | |
| 0.758 | | | | |

The interplanar distances analysed for the activated surfaces treated at various temperatures are summarized in Table II together with the X-ray diffraction data[8] of BeO and CuO. As seen in Table II, the difference in the surface structure between each temperature of the treatment is not clear, but the diffraction patterns peculiar to BeO are clearly observed for all specimens. This fact may be interpreted to mean that beryllium ions (or atoms) in the alloy rapidly migrate through the lattice and arrive at the surface at these temperatures of the treatment, and that since they easily react with oxygen and are fixed as beryllium oxide the concentration of this compound in the neighborhood of the alloy surface will be considerably increased by the treatments of activation.

**Dependency of Electron Yield upon Ion Kinetic Energy.**—In Figs. 3 and 4, the electron yield for the non-activated and activated (treated at 420°C) target surfaces is plotted as a function of the kinetic energy of singly- and doubly-charged argon ions and the five different ions from ethylene, respectively. The variation of the electron yield with the kinetic energy of the parent and fragment ions from ethane for the activated target surface treated at 420°C is shown in Fig. 5. Fig. 6. shows

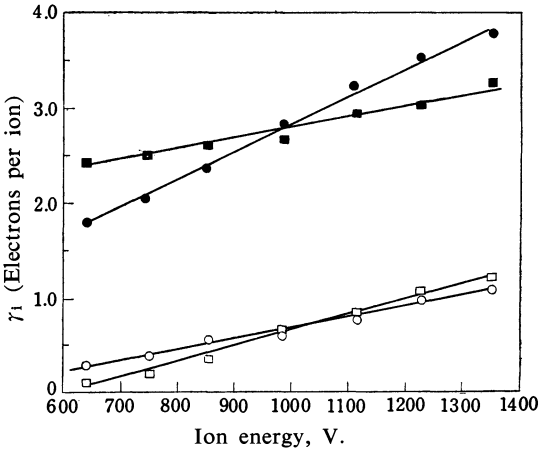



Fig. 3. Plot of experimental data giving electron yield $\gamma_i$, as a function of ion kinetic energy for $A^+$(● activated, and ○ non-activated) and $A^{2+}$(■ activated and □ non-activated) on 420°C activated and non-activated Cu-Be targets.

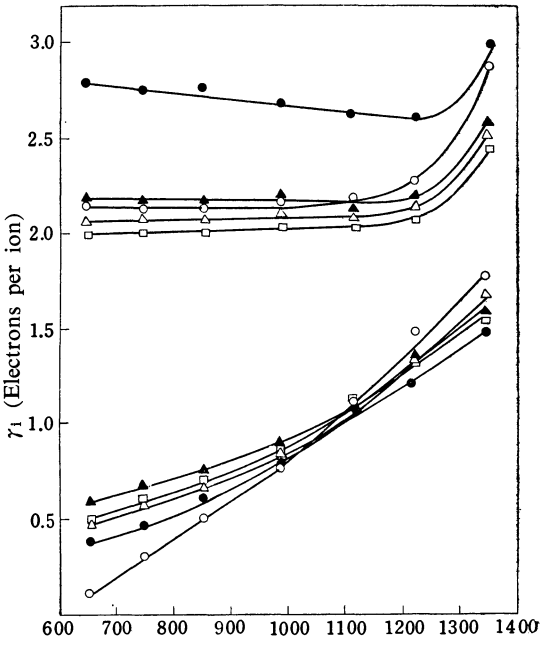



Fig. 4. Plot of experimental data giving electron yield $\gamma_i$, as a function of ion kinetic energy for parent and fragment ethylene ions; upper five curves are data on the 420°C activated Cu-Be target and lower are data on the non-activated Cu-Be target. ○; $C_2H_4^+$, △; $C_2H_3^+$, □; $C_2H_2^+$, ▲; $C_2H^+$, and ●; $C_2^+$.

the influence of the temperature of the treatment (480, 420 and 350°C) on the variation of the electron yield with the kinetic energy of singly- and doubly-charged neon ions.

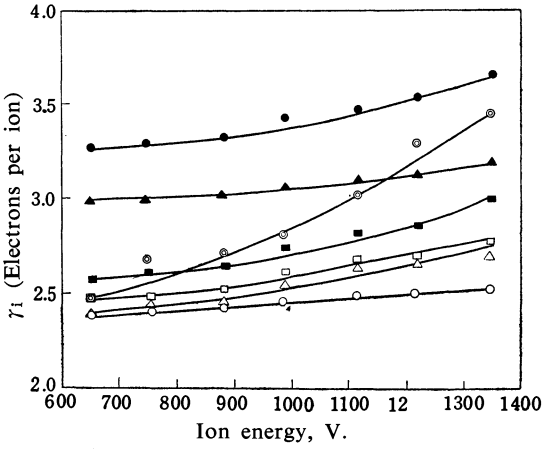



Fig. 5. Plot of experimental data giving electron yield $\gamma_i$, as a function of ion kinetic energy for parent and fragment ethane ions: ◎; $C_2H_6^+$, ■; $C_2H_5^+$, ○; $C_2H_4^+$, △; $C_2H_3^+$, □; $C_2H_2^+$, ▲; $C_2H^+$, and ●; $C_2^+$, on activated target treated at 420°C.

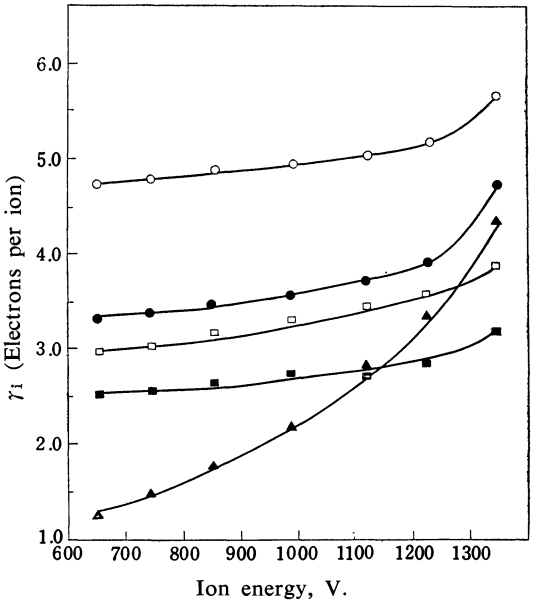



Fig. 6. Plot of experimental data giving electron yield $\gamma_i$, as a function of ion kinetic energy for singly- and doubly-neon ions on activated target treated at various temperatures.
○; $Ne^{2+}$, 420°C, ●; $Ne^+$, 420°C, □; $Ne^{2+}$, 350°C, ■; $Ne^+$, 350°C, ▲; $Ne^+$, 480°C.

**Stability of Electron Yield by Ion Impacts.** —Under the present experimental conditions, the electron yield for the non-activated surface gradually decreased and reached about 80 per cent of its initial value by the prolonged

TABLE III. THE SECONDARY ELECTRON YIELDS ($\gamma_i$) AND THE IONIZATION POTENTIALS (I. P.) AND THE APPEARANCE POTENTIALS (A. P.)

The values of $\gamma_i$ are shown for 980 volts ion energy and for the target surface activated at 420°C.

| Ion | Ethane | | | Ethylene | |
|---|---|---|---|---|---|
| | I. P.[9] eV. | $\gamma_i$ electrons/ion | A. P.[9] eV. | $\gamma_i$ electrons/ion | A. P.[9] eV. |
| $C_2H_6^+$ | 11.6 | 2.75 | 11.6 | — | — |
| $C_2H_5^+$ | 8.7 | 2.90 | 12.9 | — | — |
| $C_2H_4^+$ | 10.8 | 2.50 | 12.1 | 2.20 | 10.8 |
| $C_2H_3^+$ | 9.9 | 2.55 | 15.2 | 2.09 | 14.1 |
| $C_2H_2^+$ | 11.2 | 2.50 | 15.0 | 2.04 | 13.4 |
| $C_2H^+$ | 11.3 | 3.05 | 27.0 | 2.20 | 19.2 |
| $C_2^+$ | — | 3.05 | 31.5 | 2.70 | 26.4 |

bombardments of the various positive ions mentioned above for five hours. On the other hand, no measurable decrease in the electron yield for the activated target surface treated at 420°C was obtained within the limit of the experimental errors by the prolonged bombardments of various ions for ten hours.

## Discussion

As seen in Figs. 3 and 4, the electron yield of the activated surface treated at 420°C for the argon ions or the various ions of ethylene is considerably larger and more stable than that of the non-activated surface. Moreover, as seen in Figs. 3—6 (excepting the results obtained for the activated surface at 480°C in Fig. 6), the increment of the electron yield for each activated surface with the kinetic energy of various ions in the range 600 to 1000 V. is very small, while that for the non-activated surface in the same energy range is considerably large. The typical results shown in Fig. 6 indicate that the electron yield and the increment of it with the kinetic energy of ions are greatly influenced by the temperature of the treatment. It is worth while to notice that the electron yield curve of the singly-charged neon ions for the target surface activated at 480°C is markedly different from those activated at 350 and 420°C.

These characteristics in the electron yield of the activated target surfaces might be correlated with the structure and the concentration of beryllium oxide formed in the neighborhood of the target surface. But unfortunately, the present results of the electron diffraction analyses shown in Tables I and II can not elucidate the fine structures of the oxide layers, and the more detailed measurements of the surface structure are necessary in order to discuss the correlation mentioned above.

The detailed experiments and theoretical treatise on the mechanism of the electron ejection by the impacts of various noble gas ions from both atomically clean surfaces of molybdenum and tungsten and the surfaces of tungsten covered by various foreign gases have been reported by Hagstrum[5,6]. From his results it has been suggested that the probability of the electron ejection in a non-Auger process may begin at low ion energies when a monolayer is present on the target surface and that even for the atomically clean surface there is strong evidence of a non-Auger process setting in at energies above 400 eV. with the singly-charged helium ions.

The present results shown in Figs. 3—6 indicate that the electron yield for the activated surface of copper-beryllium by various noble gas and hydrocarbon ions is only slightly influenced by the kinetic energy of ions, while for the non-activated target surface there is a marked increase in the electron yield with the increase in the ion kinetic energy. But since we must recall that under the present experimental conditions the considerable part of the target surface might be covered by the residual gases, it seems unreasonable to simply correlate the mechanism of the electron ejection from the activated and non-activated surfaces to the Auger and a non-Auger processes, respectively.

Hagstrum[3] also reported that when the electron ejection from the target surface is mainly dominated by the Auger neutralization process the electron yield is proportional to the value of the ionization potential minus twice the work functions of the target surface. The present results of the electron yield for the target surface activated at 420°C and the literature values[9] of the ionization potentials are summarized in Table III. When we assume that the electron ejection from the activated target surface of copper-beryllium simply obeys the Auger neutralization process and that the work function was unchanged throughout the

9) G. C. Eltenton, *J. Chem. Phys.*, 15, 455 (1947).

measurements, it is reasonable to expect that the electron yield is proportional to the ionization potential. Table III indicates that the present results are somewhat complicated and do not simply satisfy the proportionality mentioned above.

Since the present experimental conditions are considerably complicated, it is necessary to continue more detailed experiments on the dependency of the electron yield upon the ion energy and energy distribution of secondary electrons both for the activated and non-activated target surfaces which are atomically clean and covered by foreign gases in order to discuss the mechanism of the electron ejection process.

## Summary

The secondary electron emission from the non-activated and activated surfaces of copper-beryllium (4%) by the impacts of various noble gas and hydrocarbon ions was studied together with the determination of the surface structure by the electron diffraction analysis. The main results obtained are as follows.

(1) The considerably thick layer of beryllium oxide is formed in the neighborhood of the target surface activated by oxygen at the temperature range of 350 to 480°C.

(2) The oxide films of copper are formed on the target surface by electropolishing, but these oxides easily undergo reduction by the prolonged ion bombardments.

(3) The optimum temperature of activation for the electron yield seems to be about 420°C, and the electron yield for the activated target surface treated at 350 or 420°C is only slightly dependent upon the ion kinetic energy.

(4) No measurable decrease in the electron yield for the activated surface treated at 420°C was obtained by the prolonged bombardments of various positive ions for ten hours, while the electron yield for the non-activated surface decrease about 20 per cent by the prolonged bombardments of ions for five hours.

(5) Under the present experimental conditions, the mechanism of the electron ejection process seems to be considerably complicated and it is difficult to deduce any definite conclusion for the electron ejection process.

The authors wish to express their sincere thanks to Professor N. Sasaki of Koyto University, Professor T. Chitani of Tokyo Metropolitan University, Professor O. Toyama of the University of Osaka Prefecture and Professor K. Ogata of Osaka University for their kind encouragement and discussions. The authors' thanks are also due to Mr. A. Iwata of the Central Research Laboratory of Hitachi Factory who kindly offered the copper-beryllium (4%) alloy and to Mr. M. Mera for his kind helpfulness in the course of the electron diffraction analysis.

The expense has been defrayed in part from a grant given by the Ministry of Education to which the authors thanks are due.

*Department of Chemistry*
*College of General Education*
*and*
*Department of Applied Chemistry*
*College of Engineering*
*University of Osaka Prefecture*
*Sakai, Osaka*

# *Inorganic Extraction Studies on the System between Bis(2-ethyl hexyl)-orthophosphoric Acid and Hydrochloric Acid. II*

By Kan KIMURA

(Received July 25, 1960)

In the previous paper[1], was reported the influence of acid concentration on the solvent extraction of about fifty elements in the system of 50 percent bis(2-ethyl hexyl) orthophosphoric acid (HDEHP)-aqueous hydrochloric acid. As is well known in solvent extraction studies[2], the distribution ratio, $K_d$, is much affected by the solvent concentration in a way similar to that by the acid concentration.

Accordingly, a study on the influence of solvent concentration in organic phase is very important for the purpose of determining the suitable concentration for a given separation procedure. Besides that, the relationship

1) K. Kimura, This Bulletin, 33, 1038 (1960).
2) G. H. Morrison and H. Freiser, "Solvent Extraction in Analytical Chemistry", John Wiley & Sons Inc., New York (1957), p. 52.

between $K_d$ values of a given ion and solvent concentrations gives some suggestions on the chemistry of the extraction.

Along this line, have been published many studies[3-5] on the chemical mechanisms of thenoyltrifluoroacetone extraction or the chemical composition of the thenoyltrifluoroacetates. Concerning HDEHP extraction, the solvent dependence of the distribution ratios was already studied for lanthanide elements[6-8], uranium[8-9], iron and a few other chemical elements[8]. However, no comprehensive study on the extraction from a given mineral acid solution has been reported. In the present paper, the influence of solvent concentration is presented, discussing the extraction carried out from hydrochloric acid solution of a given acidity containing each of about fifty elements.

## Experimental

**Sources of Materials.** — The bis(2-ethyl hexyl)-orthophosphoric acid received from Virginia Chemicals Co. was purified and checked on its purity as reported in the previous study[1]. The work reported here was carried out using HDEHP diluted with toluene of guaranteed reagent grade.

Radioisotopes used were the same as those which were reported previously[1] except for the following: The nuclides 19day $^{86}$Rb and 40day $^{103}$Ru were imported and used as received. The radioactive tracers of neodymium, samarium, europium, gadolinium, terbium, dysprosium, holmium, erbium, thulium and lutetium contributed for counting were mainly 11.3day $^{147}$Nd, 47 hr. $^{153}$Sm, 9.2hr. $^{152}$Eu, 18.0hr. $^{159}$Gd, 73day $^{160}$Tb, 2.32hr. $^{165}$Dy, 9.4day $^{169}$Er, 129day $^{170}$Tm and 6.8day $^{177}$Lu, respectively[10]. These were prepared by the neutron irradiation of highly-purified oxides in JRR-1. In the cases of gadolinium and erbium, the radioactivities caused by the radioactive daughters (6.75day $^{161}$Tb and 680day $^{171}$Tm) of simultaneously yielded short half-lived nuclides (3.73 min. $^{161}$Gd and 7.5hr. $^{171}$Er) were corrected from the total activities of gadolinium and erbium by the results of their decay measurements, respectively. The nuclide 27.4day $^{233}$Pa was obtained as a by-product of uranium-233 processings[11].

The radiochemical purity of these nuclides was checked by their half-lives, $\gamma$-ray spectra, and/or $\beta$-ray absorption curves with aluminum foils.

**Determination of Distribution Ratios.**—The distribution ratio, $K_d$, of a given nuclide was radiometrically determined. The details and some remarks of the method written about in the previous report[1] were also adopted in the present study. Most of the data in this experiment were obtained after shaking the two layers for three minutes.

Although the HDEHP concentration in the organic layer was varied usually in the range from 0.5 to 50 volume percent, it was extended to 0.01 volume percent in some cases. The extraction with barren toluene containing no HDEHP was also checked. On the other hand the acidity in the aqueous layer was kept constant in a series of extractions of a given element.

## Results and Discussion

The results are summarised in Fig. 1 as a series of graphs of $\log K_d$ vs. log (% HDEHP) where $K_d$ is the distribution ratio and % HDEHP the concentration of HDEHP in volume percentage.

As reported previously[1], $K_d$ values for each cation usually depend on inverse power of hydrogen ion concentration, and furthermore $K_d$ values for mono-, di-, tri-, and tetra-valent cation decrease with the following general sequence; $M^{4+} > M^{3+} > M^{2+} > M^{+}$. Meanwhile, $K_d$ values for the ion ready to form an anion are usually low. Therefore, it is desired that the acidity should be changed according to the valence of the ion concerned.

Although the acidity of aqueous phase was kept constant at 0.5 N for most of the elements, it was 0.05 N for the alkali and alkaline earth elements, 0.3 N for the rare earth elements, and 0.1 N or 2 N for some other elements. In some cases, the extractions of ion from the solutions of two different acidities were undertaken. The Arabic numeral in each graph shows the acidity taken.

Fig. 1 was compiled from some published and unpublished results. Data for lead and bismuth were taken from the observation of Ishimori[12]. Data for yttrium, promethium, thulium and americium were taken from the work of Peppard et al[6]. The $K_d$ values for selected lanthanide cation(III) in HDEHP-hydrochloric acid system are inverse third power dependent on the hydrogen ion concentration of the aqueous phase. Therefore, $K_d$ values for yttrium, promethium, thulium and americium were obtained correcting Peppard's value (at 0.552 M, 0.146 M, 0.552 M, and 0.275 M, respectively) for 0.3 N hydrochloric acid solution.

As is seen in Fig. 1, the $K_d$ values for each

3) R. E. Connick and W. H. McVey, *J. Am. Chem. Soc.*, **71**, 3128 (1949).
4) E. H. Hyffman and L. J. Beaufait, ibid., **71**, 3179 (1949).
5) J. C. Sullivan and J. C. Hindman, ibid., **76**, 5931 (1954).
6) D. F. Peppard, G. W. Mason, J. L. Maier and W. J. Driscoll, *J. Inorg. Nucl. Chem.*, **4**, 334 (1957).
7) D. F. Peppard, G. W. Mason, W. J. Driscoll and R. J. Sironen, ibid, **7**, 276 (1958).
8) C. A. Blake, Jr., C. F. Baes, Jr., K. B. Brown, C. F. Coleman and J. C. White, "Proceedings of the International Conference on the Peaceful Uses of Atomic Energy", Vol. 28, United Nations, Geneva (1958), p. 289.
9) C. F. Baes, Jr., R. A. Zingaro and C. F. Coleman, *J. Phys. Chem.* **62**, 129 (1958).
10) K. Kimura, "Hoshasen Data Book", Chijin Shokan, Tokyo (1958) p. 92.
11) T. Ishimori et al., unpublished.
12) T. Ishimori, unpublished.

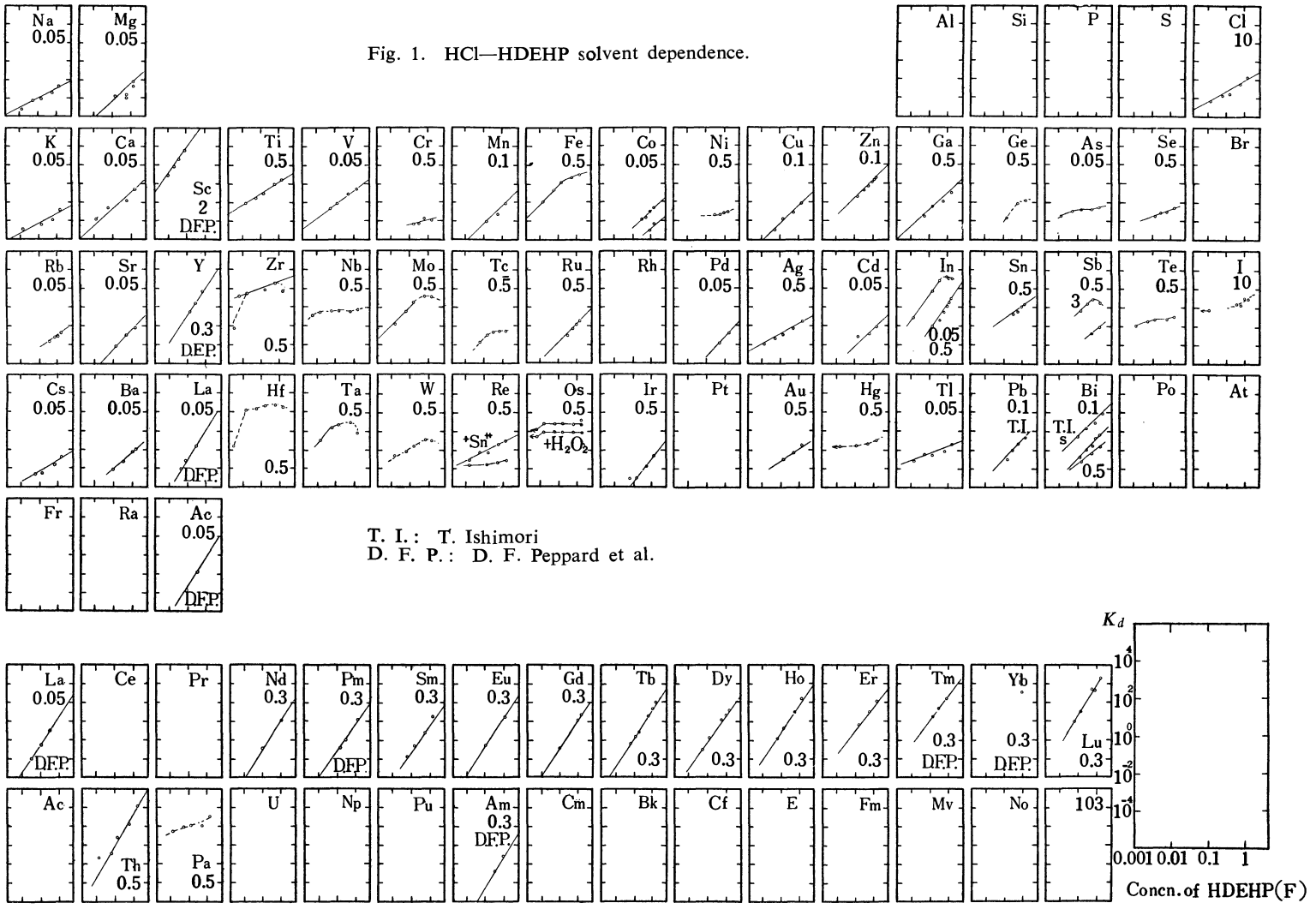



Fig. 1. HCl—HDEHP solvent dependence.

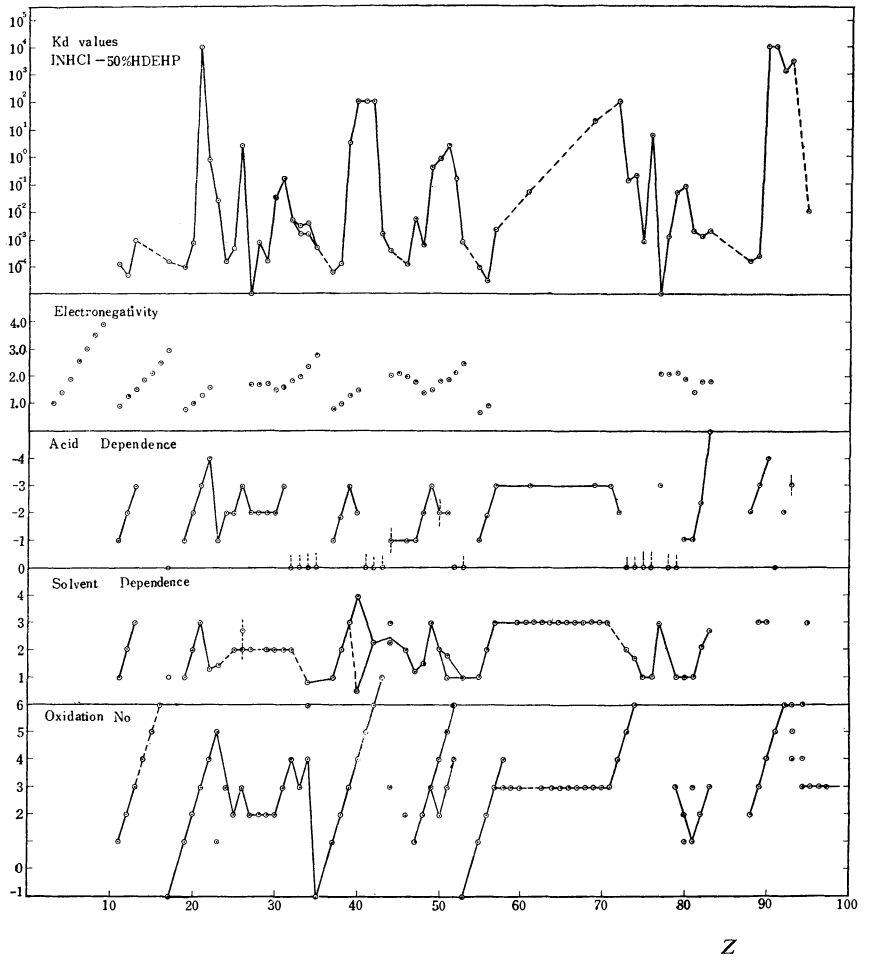



Fig. 2. $Z$ dependences.

of almost all the elements increase as the concentration of HDEHP in the toluene phase increases. A similar relationship is observed generally in many solvent extraction systems.

The $K_d$ values for alkali metals, alkaline earth metals and lanthanide elements show the first, second and third power dependence on the HDEHP concentration in the toluene phase, respectively. A similar relationship holds for some other elements: silver and thallium(I) indicate the first power solvent dependence, manganese, cobalt, copper, zinc and cadmium the second dependence, and indium indicates the third. The $K_d$ values for iron and gallium follow the second power solvent dependence and those for thorium the third dependence.

The $K_d$ values for zirconium remain nearly constant in almost the whole range of the solvent concentration. Although the strange behavior of zirconium is not clearly explained, it might be caused by both the hydrolysis of zirconium ion and its high $K_d$ values. Scadden and Ballou[13] reported that only zirconium and indium are completely extracted with 0.06 M dibutylphosphoric acid (HDBP) for 1 M nitric, hydrochloric, or perchloric acid; and Ishimori et al[14] reported that only zirconium is extracted with dilute tributyl phosphate (1%. toluene diluent) from 8 M hydrochloric acid solution of the fission products. Furthermore, White[15] reported that zirconium is completely extractable from 1 M hydrochloric acid solution with 0.1 M trioctylphosphine oxide and partially extractable with 0.1 M tris-2-ethylhexyl phosphine oxide. This high extractability of zirconium with many alkyl phosphorous reagents is noteworthy as compared with the very low solubility of zirconium phosphate in mineral acids. Hafnium, niobium and protactinium resemble zirconium in the solvent dependence of their $K_d$ values.

13) E. M. Scadden and N. E. Ballou, *Anal. Chem.*, **25**, 1602 (1953).
14) T. Ishimori K. Umezawa and K. Watanabe, *J. Atomic Energy Soc. Japan* **1**, 299 (1955).
15) J. C. White, USAEC TID-7555, 249 (1958).

The $K_d$ values for osmium are relatively high and kept nearly constant. Besides that, osmium can be extracted with pure toluene fairly well, giving the $K_d$ value of 1.31. This $K_d$ value is as low as about one tenth of the $K_d$ values for toluene containing HDEHP. The $K_d$ value is shown with open circles attached with arrow in Fig. 1. The addition of hydrogen peroxide to the tracer solution makes all the $K_d$ values for osmium low, keeping the shape of the curve unchanged. This would be explained as a partial reduction of the readily extractable species of osmium. Thus, the relatively high $K_d$ values for osmium might be explained assuming the extraction of a neutral molecule such as osmium tetroxide. Futhermore, the higher $K_d$ values with the HDEHP toluene solution might indicate that HDEHP promotes the extraction to some extent.

The $K_d$ value for mercury with pure toluene is also high. It appears as if the extraction of mercury is partially based on the extraction of a neutral molecule such as $HgCl_2$, which is slightly ionized in the low concentration region of chloride.

In the case of iodine, the $K_d$ values for the acid range up to 5 N were very low[15]. However, the slightly high $K_d$ value is obtained at 10 N. Similarly the $K_d$ value for pure toluene at 10 N hydrochloric acid remains high. It may be based on the oxidation of tracer quantity of iodide ion with the micro-amount of chlorine. Scadden and Ballou[13] reported that the neutral iodine molecule, $I_2$, showed a high extractability with dibutyl phosphate.

The different slopes of solvent dependence curve for bismuth are obtained varying the acid concentration of aqueous phase. Because it is known that bismuth forms a series of chloride complexes in hydrochloric acid solution[16], and that the ratios among these chloride complexes vary with the chloride concentration, it may be natural that the slope is changed according to the acid concentration.

On the other hand, the slopes of the $K_d$ curves for indium and rare earth elements are not dependent on the acid concentration. For instanse, the $K_d$ values for thulium follow the third power solvent dependence both at 0.552 M[6] and at 0.3 N hydrochloric acid. Concerning the $K_d$ values for indium, a similar relationship also holds at 0.5 N and 0.05 N hydrochloric acid. The $K_d$ values for cobalt are very low, but similar results are obtained at 0.5 N and 0.05 N, using a larger amount of radioactive cobalt-60.

The slopes of the solvent dependence and of the acid dependence and the oxidation number are plotted against the atomic number, $Z$, in Fig. 2. The graph of the "best values of electronegativity"[17] vs. $Z$ and that of the $K_d$ values between 50% HDEHP and 1 N hydrochloric acid vs. $Z$ are attached to Fig. 2. The values of electronegativity of cobalt, nickel, ruthenium, rhodium, palladium, iridium and platinum are taken from Haïsinsky's data[18].

As mentioned above, the solvent dependence is studied at one of the several definite acidities. Accordingly the data of the solvent dependence may not be suitable for detailed discussion, because the formation of chloro-complexes differs both with the acidity and with the element. However, the data may be applicable to general discussion. The vertical dotted lines indicate that the slope could not be clearly obtained. Almost all of the elements showed the slope defined as "the second type" in the previous paper indicate the slope of zero in the graph of the acid dependence vs. $Z$.

As is seen in Fig. 2, the slopes and the oxidation numbers vary regularly in Na-Mg-(Al), K-Ca-Sc, Rb-Sr-Y, and Cs-Ba-La, showing the increasing lines with increasing $Z$. Although the Fr-Ra-Ac-line is not studied, it may follow the similar relationship. Concerning the Ib-IIb-IIIb group of the periodic table, only the Ag-Cd-In line is satisfied with this increasing relation. On the other hand, the Cr-Zn line or La-Lu line is nearly horizontal. The curves indicate some complicated relationships for the ranges of the IVb-Vb-VIb group and of the platinum group in the periodic table.

Fig. 2 shows that the relation among the slopes of the dependences and the oxidation number is roughly divided into two types.

The first type is characteristic in the fact that the relation which the slope of the solvent dependence has equals that of the acid dependence and further that the oxidation number does so also. Scandium, yttrium, or lanthanum are satisfied with this relationship. This tendency is generally observed in the solvent extraction system where chelation plays an important role:

$$M^{m+}{}_{(aq.)} + mHR_{(org.)} \rightleftarrows MR_{m(org.)} + mH^{+}{}_{(aq.)} \quad (1)$$

In Eq. 1, the distributio ration of M is given:

$$K_d = K[HR]^{m}{}_{(org.)}[H^{+}]^{-m}{}_{(aq.)} \quad (2)$$

Baes and Peppard[6,7] assumed the following

16) L. S. Newman and D. N. Hume, *J. Am. Chem. Soc.*, 79, 4576 (1957).

17) H. O. Pritchard and H. A. Skinner, *Chem. Revs.* 55, 767 (1955).

18) M. Haïsinsky, *J. Phys.* 7, 7 (1946); *J. Chim. Phys.* 46, 298 (1949).

equilibrium for the reaction between uranium(VI) or lanthanide elements in perchloric acid solution and HDEHP, considering that the HDEHP molecule is essentially completely dimerized in the toluene phase:

$$M^{m+}_{(aq.)} + m(HDEHP)_{2\,(org.)} \rightleftarrows MH_m(DEHP)_{2m\,(org.)} + mH^+_{(aq.)} \quad (3)$$

where the $K_d$ value of M is given as:

$$K_d = K[(HDEHP)_{2\,(org.)}]^m [H]^{-m}_{(aq.)} \quad (4)$$

It is assumed that the alkali metal cation(I) and the alkaline earth metal cations(II) follow Eq. 3, showing the first and second power solvent dependence and the inverse first and second power acid dependence, respectively. Because manganese(II), cobalt(II), copper(II), zinc(II), silver(I), cadmium(II), indium(III) and thallium(I) also show the relationship of equal figures, it seems that they are also satisfied with Eq. 3.

$K_d$ values of iron(III) are approximately second-power dependent on the HDEHP concentration for 0.5~0.05% HDEHP in the organic phase and are inverse third-power dependent on the acid concentration in the aqueous phase. Thus, iron belongs to a modified first type. Blake et al.[8] postulate the following equilibrium for the partition of ferric iron:

$$Fe^{3+} + 2(HDEHP)_2 + HOH \rightleftarrows Fe(OH)H_2(DEHP)_4 + 3H^+ \quad (5)$$

Besides that, Peppard and Ferraro[19] mentioned that the solvent extraction of thorium is approximately third-power dependent on the HDEHP concentration and inverse forth-power dependent on the HDEHP concentration and inverse forth-power dependent on the acid concentration, and that these tentative dependencies are consistent with either or both of the following equilibria:

$$M^{4+}_{(aq.)} + 3H_2DEHP_{2\,(org.)} \rightleftarrows MDEHP_2(HDEHP_2)_{2\,(org.)} + 4H^+_{(aq.)} \quad (6)$$

and

$$M^{4+}_{(aq.)} + 3H_2DEHP_{2\,(org.)} + HOH \rightleftarrows M(OH)(HDEHP_2)_{3\,(org.)} + 4H^+_{(aq.)} \quad (7)$$

It seems that the solvent extraction of gallium also follows similar equilibria, showing the second-power solvent dependence and the inverse third-power acid dependence. A similar relationship also holds for the extraction of titanium.

On the other hand, the second type is characteristic both in the acid dependence with the slope of zero defined as "the second type"[1] and in the solvent dependence with the slope of one or more. These tendencies are commonly seen in the solvent extraction, in which the ion association plays an important role[20] such as TBP extraction of uranyl ion[21].

Chlorine, selenium, molybdenum, tungsten and gold, which form anions easily and have a relatively high value of electronegativity, are typical for the second type. Accordingly, it appears that the solvent extraction of these elements is based on partition as is found in the extraction with TBP. As for the electonegativity, it is noticed that the more extractable element generally has a value between 1.0 and 2.0.

Thanks are due to Dr. Tomitaro Ishimori for his guidance and suggestions, to Dr. Kenjiro Kimura and Dr. Toshio Nagai for their encouragement, and also to Mr. Ikuo Suzuki for his assistance.

*Japan Atomic Energy Research Institute*
*Tokai, Ibaraki-ken*

19) D. F. Peppard and J. R. Ferraro, *J. Inorg. Nucl. Chem.*, **10**, 275 (1959).

20) G. H. Morrison and H. Freiser, Ref. 2, p. 59.

21) K. Naito, This Bulletin, **33**, 363 (1960).

# *Studies on Antibiotics and Related Substances. XI. Methylated Amino-sugar Moieties from Methylated Kanamycin*[1]

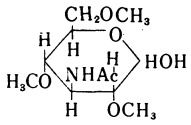
By Sumio UMEZAWA and Yukio ITŌ

(Received July 25, 1960)

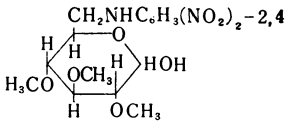
In a previous paper[2] we described the fact that 1,3-diamino-4,6-dihydroxy-5-methoxycyclohexane was isolated from the hydrolyzate of exhaustively methylated *N*-acetyl kanamycin. It was therefore concluded that both of the two aminohexose moieties in kanamycin are directly joined to deoxystreptamine through 4- and 6-hydroxyl groups by glucosidic linkages, the structure of kanamycin[3] being established. Subsequently, attempts have been made to isolate amino-sugar moieties from the same hydrolyzate. The present paper is concerned with the isolation of methylated derivatives of 3-amino-3-deoxy glucose and 6-amino-6-deoxyglucose.

Separation of 1,3-diamino-4,6-dihydroxy-5-methoxycyclohexane from acid-hydrolyzate was accomplished as described in a previous paper[2]. The residue from the mother liquor was chromatographed on a column of cellulose powder with butanol–ethanol–water (4 : 1 : 5). Repetition of the chromatography resulted in the isolation of 3-acetamido-3-deoxy-2,4,6-tri-*O*-methyl-D-glucose (I). The new derivative was converted into a methyl glucoside, which has been identified with the synthetic specimen prepared from D-glucose by the route of Peat and Wiggins[4].

On the other hand, an aqueous solution of



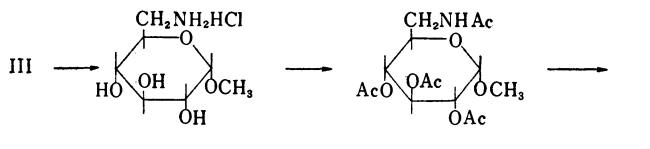
I



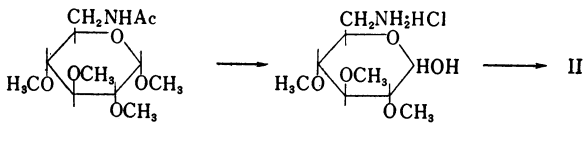
II

the above-mentioned residue from the mother liquor was passed through a column of Amberlite IRC-50 ($Na^+$ form) to remove *N*-acetylated amino-sugar moieties and developed with dilute hydrochloric acid. The combined residues from the early fractions were subjected to a cellulose powder chromatography to give fractions which showed a single ninhydrin-positive spot and positive Tollens and aniline phthalate reaction. The product was chromatographically identical with the synthetic specimen of 6-amino-6-deoxy-2,3,4-tri-*O*-methyl-D-glucose hydrochloride, the synthesis of which is mentioned below. The product could not be caused to crystallize. However, condensation with 2,4-dinitrofluorobenzene afforded yellow needles of 6-(2,4-dinitrophenylamino)-6-deoxy-2,3,4-tri-*O*-methyl-D-glucose (II).

The synthetic specimen of II has been prepared from 6-amino-6-deoxy-3,5-benzylidene-1,2-isopropylidene-D-glucose[5] (III) by the following scheme.



IV V



VI VII

1) Presented before the division of Organic Chemistry of the Annual Meeting of the Chemical Society of Japan at Kyoto, April, 1959 and at Tokyo, April, 1960.

2) S. Umezawa, Y. Ito and S. Fukatsu, This Bulletin, **32**, 81 (1959).

3) Ref. 2, p. 82.

4) S. Peat and L. F. Wiggins, *J. Chem. Soc.*, **1938**, 1810.

5) B. Helferich and R. Mittag, *Ber.*, **71**, 1588 (1938).

In the course of our synthesis of II, an alternative synthesis of methyl 6-amino-6-deoxy-α-D-glucoside hydrochloride (IV) was performed by Cramer et al.[6] The glucoside prepared by our method has been identified with a sample prepared by the alternative method by the mixed melting point method and infrared absorption spectra.

The mixed melting point determination of the natural and synthetic specimens of II was undepressed and the respective infrared spectra were completely superimposable.

## Experimental

**Isolation of 3-Acetamido-3-deoxy-2, 4, 6-tri-*O*-methyl-D-glucose (I).**—The exhaustively methylated tetra-*N*-acetyl-kanamycin was hydrolyzed with 6 N hydrochloric acid and 1, 3-diamino-4, 6-dihydroxy-5-methoxycyclohexane was separated from the hydrolyzate, details of which were described in a previous paper[1]. The mother liquor was evaporated to dryness. Paperchromatographic studies of the residue (brown syrup) showed ninhydrin-positive spots of $R_f$ 0.54 (violet) 0.41 (violet), 0.31 (orange) 0.23 (violet) and 0.08 (brown) using butanol-ethanol-water (4 : 1 : 5). The residue (9.67 g.) was dissolved in the above-mentioned solvent, chromatographed on a column (3×51 cm.) of cellulose powder and developed with the same solvent. One hundred and fourteen fractions were cut into 10 ml. each, evaporated to dryness, weighed and tested for $R_f$ values. The combined fractions of tube Nos. 27—37 (6.89 g., $R_f$ 0.48, 0.41, 0.36) were again chromatographed in the same manner and the combined fractions of tube Nos. 13-30 were evaporated to yield a crystalline residue (600 mg.). Recrystallization from absolute ethanol afforded needles of m. p. 229~230°C (decomp.), $[\alpha]_D^{15}$+107.1° (*c* 0.98, methanol).

Found: C, 49.89; H, 7.90; N, 5.49; $OCH_3$, 35.20; $COCH_3$, 14.70. Calcd. for $C_{11}H_{21}NO_6$: C, 50.18; H, 8.04; N, 5.32; $OCH_3$, 35.36; $COCH_3$, 16.35%.

The product feebly reduced Fehling's solution and showed a negative ninhydrin reaction. On hydrolysis by refluxing with 6 N hydrochloric acid for 2 hr., the product gave a hydrolyzate which showed a ninhydrin-positive spot of $R_f$ 0.29 (orange). These results indicated that the product was an *N*-acetylated derivative of methylated hexosamine. By refluxing in excess absolute methanol (40 ml.) in the presence of hydrogen chloride (2%), the product (350 mg.) afforded a methyl glucoside (120 mg.) of m. p. 156~157°C, $[\alpha]_D^{15}$+120.7° (*c* 0.41, chloroform), which had nearly the same m. p. with the methyl 3-acetamido-3-deoxy-2, 4, 6-tri-*O*-methyl-α-D-glucoside reported by Peat and Wiggings[4].

Found: C, 51.87; H, 8.10; N, 5.18; $OCH_3$, 44.00. Calcd. for $C_{12}H_{23}NO_6$: C, 51.97; H, 8.36; N, 5.05; $OCH_3$, 44.76%.

The synthetic specimen was therefore prepared from D-glucose by the route of the above authors. The mixed m. p. determination of the natural and synthetic specimen (m. p. 157~158.5°C) was undepressed and the respective infrared spectra were completely superimposable.

**Isolation of 6-Amino-6-deoxy-2, 3, 4-tri-*O*-methyl-D-glucose.**—The residue (4.89 g.) obtained by evaporation of the mother liquor from 1, 3-diamino-4, 6-dihydroxy-5-methoxycyclohexane was dissolved in water (20 ml.) and passed through a column of Amberlite IRC-50 ($Na^+$ form, 80 ml.) to remove *N*-acetylated amino-sugar moieties and developed with 0.5 N hydrochloric acid. Thirty-one fractions of eluate were cut into 20 ml. each, evaporated to dryness and tested for $R_f$ values. Fractions of tube Nos. 4-9 showed ninhydrin-positive spots of $R_f$ 0.44~0.46, 0.23~0.24*. The combined residues (4.54 g.) from the fractions were treated with absolute ethanol (30 ml.) to separate off the sodium chloride and the solution was evaporated to dryness to give a syrup (1.60 g.), which was treated with active charcoal in absolute ethanol (20 ml.). To the filtrate was added absolute ether (30 ml.) to precipitate sodium chloride and the filtrate was evaporated. A solution of the resulting syrup (1.39 g.) in methanol (2 ml.) was passed through a column (2×70 cm.) of cellulose powder and developed with *n*-butanol-acetic acid-water (10 : 2 : 5); fifty-seven fractions were cut into 5.0 ml. each. A residue (0.70 g.) obtained from tube Nos. 35-45 showed a single ninhydrin-positive spot of $R_f$ 0.33~0.38 and gave positive Tollens and aniline phthalate reactions. The combined residue (0.60 g.) obtained was mixed with cellulose powder (1.0 g.) in a small quantity of methanol, placed on a column (2×70 cm.) of cellulose powder, washed with *n*-butanol-ligroin-water (19 : 30 : 1) and developed with *n*-butanol-acetic acid-water (10 : 2 : 5); eighty-nine fractions were cut into 5.0 ml. each. Fractions of tube Nos. 43—55 showed a single ninhydrin-positive spot of $R_f$ 0.40 and were chromatographically identical with the synthetic specimen of 6-amino-6-deoxy-2, 3, 4-tri-*O*-methyl-D-glucose hydrochloride.

The combined residues (170 mg.) obtained from the above fractions were dissolved in an aqueous solution (3.0 ml.) of sodium bicarbonate (100 mg.) and to the solutions was added 2, 4-dinitrofluorobenzene (100 mg.) dissolved in absolute ethanol (2.0 ml.); the solution was stirred at room temperature for 1 hr. to give yellow needles. After standing overnight, the needles (180 mg.) were separated and treated with ether to remove a trace of any insoluble part. The ethereal solution was passed through a column of alumina** (10.0 g.) and eluted with ether-petroleum ether and ether in turn. Evaporation of the combined eluates gave a crystalline residue (92 mg.); recrystallization from absolte methanol afforded a pure sample (72 mg.) of 6-(2, 4-dinitrophenylamino)-6-deoxy-2, 3, 4-tri-*O*-methyl-D-glucose (II), m. p. 97~99°C sintered from 92°C), $\lambda_{max}^{EtOH}$ 261.5 (ε 3833), 348 mμ (ε 8293).

6) F. Cramer, H. Otterbach and H. Springmann, *Chem. Ber.*, **92**, 384 (1959).

* Unless otherweise indicated, the solvent system of *n*-butanol-acetic acid-water (10 : 2 : 5) and Toyo filter paper No. 51 were used.

** Aluminum Oxide, Merck.

Found: C, 46.31; H, 5.20. Calcd. for $C_{15}H_{21}N_3O_9$: C, 46.51; H, 5.46%.

**6-Amino-6-deoxy-D-glucose Hydrochloride (IV).**—6-Amino-6-deoxy-3,5-benzylidene-1,2-isopropylidene-D-glucose[5] (21.0 g.) was hydrolyzed by refluxing with 75% acetic acid (300 ml.) for 3 hr. and followed by treatment with active charcoal (1.0 g.). The filtrate was evaporated to dryness to give a residue (14.1 g.) which reduced Fehling's solution. To the residue (14.0 g.) which was dried over phosphorus pentoxide in a vacuum desiccator were added silver acetate (10.6 g.), acetic anhydride (11.5 g.) and methanol (141 ml.). The mixture was stirred at room temperature for 3 hr. and refluxed on a water bath for an additional 5 min. The reaction mixture was filtered and washed with hot water; the filtrate was acidified with concentrated hydrochloric acid to Thymol blue to precipitate silver salt. The filtrate was evaporated up to give a crude *N*-acetylated product***, which was dried over phosphorus pentoxide in a vacuum desiccator. The product as converted into a methyl glucoside by refluxing with 300 ml. of methanolic hydrochloride (2%) for 10 hr. The hydrolyzate was neutralized with basic lead carbonate (100 g.), filtered, and the filtrate was evaporated up in vacuo to give a dark syrup, which showed a positive ninhydrin reaction, indicating that de-*N*-acetylation occurred as well as the glucoside formation. The dark product was dissolved in methanol (26 ml.) and the solution was passed through a column of alumina (40 g.), washed with 1 N hydrochloric acid, and developed with methanol; early fractions (170 ml.) were combined and evaporated up to give a brown residue (7.88 g.), An aqueous solution (100 ml.) of the residue was passed through a column of Amberlite IRA-410 (base form, 100 ml.) and the early effluent (77 ml.) was treated with active charcoal (2 g.) and followed by evaporation to dryness to give crude methyl 6-amino-6-deoxy-D-glucoside (3.85 g., overall yield 23%). A solution of the crude product in absolute methanol was acidified with hydrogen chloride and evaporated to dryness. Recrystallization of the resulting solid from absolute methanol-ether afforded colorless crystals (1.5 g.) of methyl 6-amino-6-deoxy-α-D-glucoside hydrochloride, m. p. 200°C. (decomp.).

**Methyl 6-Acetamido-6-deoxy-2, 3, 4-tri-*O*-methyl-α-D-glucoside (VI).**—A mixture of methyl 6-amino-6-deoxy-α-D-glucoside hydrochloride (3.9 g.), acetic anhydride (15.5 g.) and pyridine (20.7 g.) was stirred at room temperature for 43 hr. The reaction mixture was added to ice water, stirred for 4.5 hr. and then extracted thrice with chloroform (100 ml.). The combined extracts were washed thrice with 35% potassium bisulfate (50 ml.) to remove the pyridine and further washed with a saturated solution (50 ml.) of sodium bicarbonate and water (90 ml.) in turn. The chloroform solution was dried with calcium chloride and evaporated to dryness. To a vigorously stirred solution of the acetylated product (5.90 g.) in methanol (6.0 ml.) was added a solution of dimethyl sulfate (60 ml.) in carbon tetrachloride (24 ml.) and water (4.0 ml.). During this and the subsequent addition of alkali, the temperature of the reaction was kept at about 40°C. A solution of sodium hydroxide (12.5 N, 60 ml.) was added dropwise over a 25 min. period. Again, dimethyl sulfate (20 ml.) was added and 12.5 N sodium hydroxide solution (80 ml.) was added gradually during one-hour period. The reaction mixture was kept at 75°C for 1 hr. and then heated on a boiling water bath for an additional 30 min. The temperature was lowered to about 40°C and the mixture was extracted with two 250-ml. portions of chloroform. After drying with calcium chloride, the combined extract was evaporated to give a crystalline solid (3.80 g. 96.3%). Recrystallization from ethyl acetate gave colorless needles of methyl 6-acetamido-6-deoxy-2,3,4-tri-*O*-methyl-α-D-glucoside, m. p. 121~121.5°C, $[\alpha]_D^{18}$ +250.8° (*c* 1.03, chloroform).

Found: C, 52.13; H, 8.06; N, 5.10; $OCH_3$, 44.36. Calcd. for $C_{12}H_{23}NO_6$: C, 51.97; H, 8.36; N, 5.05; $OCH_3$, 44.76%.

**6-Amino-6-deoxy-2, 3, 4-tri-*O*-methyl-D-glucose Hydrochloride (VII).**—A solution of VI (1.47 g.) in 3 N hydrochoric acid (30 ml.) was refluxed for 6 hr. and treated with active charcoal (100 mg.); the filtrate was evaporated in vacuo. The residue obtained was dissolved in water (30 ml.) and again the solution was evaporated in vacuo. The residue was dried over phosphorus pentoxide in a vacuum desiccator and crystallized from absolute ethanol-absolute ether; colorless needles (1.70 g., 99.6%). Recrystallization from the same solvent gave a pure sample of 6-amino-6-deoxy-2,3,4-tri-*O*-methyl-D-glucose hydrochloride, m. p. 179~180°C (decomp.), $[\alpha]_D^6$ +27.25° → +65.3° (*c* 1.32, water).

Found: C, 42.27; H, 7.56; N, 5.43; $OCH_3$, 36.37. Calcd. for $C_9H_{20}NO_5Cl$: C, 41.94; H, 7.82; N, 5.43; $OCH_3$, 36.13%.

**6-Deoxy-6-(2, 4-dinitrophenylamino)-2, 3, 4-tri-*O*-methyl-D-glucose.**—Condensation of VII with 2,4-dinitrofluorobenzene was accomplished in the same manner as described in the end of the second clause. The crude product (52%) was washed with ether and dissolved in absolute methanol to remove a trace of any insolube part. The residue from the methanol solution was recrystallized from a small quantity of absolute methanol to give an analytically pure sample of m. p. 97~99°C (sintered at about 90°C), $[\alpha]_D^{11}$ +37.7° (*c* 0.61, methanol); $\lambda_{max}^{EtOH}$ 261.5 (ε 3833), 348 mμ (ε 8393).

Found: C, 46.38; H, 5.24; N, 11.04. Calcd. for $C_{15}H_{21}N_3O_4$: C, 46.51; H, 5.46; N, 10.85%.

## Summary

1) 3-Acetamido-3-deoxy-2,4,6-tri-*O*-methyl-D-glucose (I) and *N*-(2,4-dinitrophenyl) derivative (II) of 6-amino-6-deoxy-2,3,4-tri-*O*-methyl-D-glucose have been isolated from the hydrolyzate of exhaustively methylated *N*-acetyl kanamycin.

2) II has been synthesized from 6-amino-6-deoxy-3,5-benzylidene-1,2-isopropylidene-D-glucose.

*** As direct formation of glucoside from free hexosamine seemed difficult, the glucoside formation was preceded by *N*-acetylation. See T. White, *J. Chem. Soc.*, **1940**, 428.

The authors are indebted to Mr. S. Fukatsu for technical assistance in some of the preparations here described and to Mr. S. Nakada for microanalyses.

*Department of Applied Chemistry*
*Engineering Faculty*
*Keio University*
*Koganei, Tokyo*

# *Spectrophotometric Determination of Beryllium, Copper and Iron with Sodium-2'', 6''-dichloro-4'-hydroxy-3, 3'-dimethylfuchsone-5, 5'-dicarboxylate*

By Yukiteru KATSUBE, Katsuya UESUGI and John H. YOE

(Received May 9, 1960)

Several organic compounds which have the hydroxydimethylfuchsone dicarboxylic acid structure have been used as the reagents for the determination of certain trace metals. Typical of these are eriochrome cyanine R for the colorimetric determination of aluminum[1] and beryllium[2], and chrome azurol S as an indicator for the complexometoric titration of aluminum, copper, iron and zirconium[3-5]. Sodium-2'', 6''-dichloro-4'-hydroxy-3, 3'-dimethylfuchsone-5, 5'-dicarboxylate (pontachrome azure blue B) has been examined spectrophotometrically for the determination of beryllium in an alkaline solution[2], but was not satisfactory because of the overlap of the absorption peak of the reagent with that of its beryllium complex. This paper reports an extensive study of the color reaction between the compound and metallic ions and procedures for its use as a reagent for the spectrophotometric determination of beryllium, copper and iron.

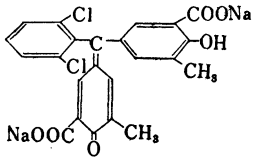



Fig. 1. Sodium-2'', 6''-dichloro-4'-hydroxy-3, 3'-dimethylfuchsone-5, 5'-dicarboxylate.

## Experimental

**Apparatus and Reagent.**—A Shimadzu spectrophotometer model QB-50, with 1.00 cm. glass cells and a Hitachi photoelectric photometer Type-FPW 4 with 1.00 cm. glass cells were used.

Amberlite IRA 410 (50 to 100 mesh) was used in a goose-neck type column (30 cm. in height and 10 mm. in inside diameter).

The reagent solution was prepared by dissolving 0.2 g. of sodium-2'', 6''-dichloro-4'-hydroxy-3, 3'-dimethylfuchsone-5, 5'-dicarboxylate in 100 ml. of 99% ethanol and filtering off the residue.

The standard solution containing 0.1 mg. of beryllium per milliliter was prepared by dissolving beryllium chloride (analytical grade) in distilled water. The standard copper solution containing 0.1 mg. of copper per milliliter was prepared by dissolving pure crystals of $CuSO_4 \cdot 5H_2O$ in distilled water. The standard iron(III) solution was prepared by dissolving crystals of pure $Fe_2(SO_4)_3(NH_4)_2SO_2 \cdot 24H_2O$ in dilute sulfuric acid to give a solution containing 0.1 mg. of iron per milliliter. Five grams of 8-hydroxyquinoline was dissolved in 12 ml. of 17 N acetic acid and diluted to 100 ml. with distilled water.

Concentrated ammonium hydroxide (130 ml.) was neutralized with 120 ml. of glacial acetic acid and diluted to 100 ml. with distilled water to give ammonium acetate solution.

**Determination of Beryllium.**—*Separation of Beryllium.*—Acidify slightly a solution, containing interfering ions such as $Al^{3+}$, $Co^{2+}$, $Cu^{2+}$, $Fe^{2+,3+}$ and $Ni^{2+}$, with dilute acetic acid, and warm it on a steam bath to 60~70°C. Add the oxine-acetic acid solution in 50% excess, and then add the ammonium acetate solution slowly, until precipitation is complete. Let stand for one hour with frequent stirring, filter off the precipitate and wash with dilute acetic acid. Determine the beryllium in the filtrate.

*Procedure of Determination.*—Transfer the solution (not more than 1.5 ml.) containing 2 to 20 p.p.m. of beryllium to a 25 ml. volumetric flask, add about 10 ml. of the acetate-acetic acid buffer solution (pH 5.8) and mix well. Then add 1 ml. of the 0.2% reagent solution, shake well, and make up to the

1) F. J. Welcher, "Organic Analytical Reagents", Vol. IV, D. Van Nostrand Co., Inc., New York (1949), p. 355.
2) S. Umemoto, This Bulletin, **29**, 845 (1956).
3) M. R. Lewis and P. P. Goland, *Cancer Research*, **13**, 130 (1953).
4) J. S. Fritz and C. L. Ford, *Anal. Chem.*, **25**, 1640 (1953).
5) M. Theis, *Z. anal. Chem.*, **144**, 275 (1955).
6) K. A. Kraus and G. E. Moore, *J. Am. Chem. Soc.*, **75**, 1460 (1953).

mark with the buffer solution. After 20 min., measure the absorbance at 570 mμ, using a reagent blank solution (or distilled water) as a reference.

**Determination of Copper and Iron(III).**—*Separation of Copper and Iron.*—Separate copper and iron(III) by the method of Kraus[6], using an anion exchange resin. (Copper and iron do not interfere with each other's determination if the solution is adjusted to pH 7.2 for copper and 3.5 for iron.)

*Procedure of Determination.*—Transfer 1.00 ml. of the neutralized sample solution containing 10 to 100 p.p.m. of copper (or iron) to a 25 ml. volumetric flask containing about 10 ml. of borax-succinic acid buffer solution (pH 7.2 for copper or 3.5 for iron). Then add 2 ml. of the reagent solution, mix thoroughly, and fill up to the mark with the buffer solution. After 20 min., measure the absorbance at 610 mμ, using a reagent blank solution (or distilled water) as a reference.

For all these measurements, a photoelectric photometer equipped with 570 and 610 mμ filters was used.

## Results and Discussion

**Color Reactions.**—Sodium-2'', 6''-dichloro-4'-hydroxy-3, 3'-dimethylfuchsone-5, 5'-dicarboxylate is a red-brown solid, soluble in water and ethanol. It was stable indefinitely in the solid state and for at least one month when dissolved in ethanol. The effect of pH on the reagent solution is shown in Fig. 2. Its color reaction was tested on a spot plate with 52 ions. Some metallic ions in an acid or a neutral medium reacted with it to give the colors shown in Table I. In an ammoniacal solution, only large amounts of calcium, magnesium and nickel ions gave blue solutions.

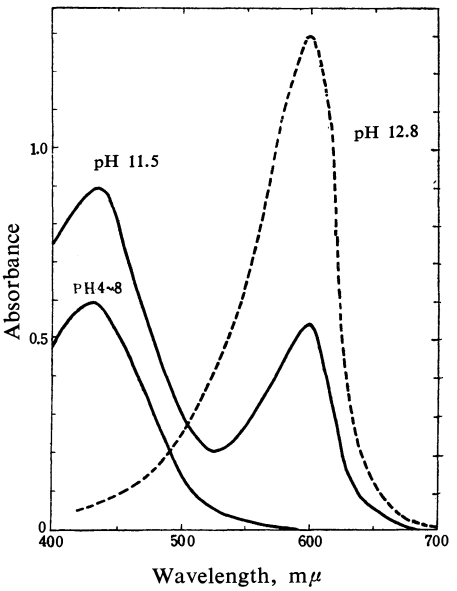



Fig. 2. Effect of pH on the reagent. Reagent: 40 ppm. pH was adjusted by HCl and NaOH solutions.

Seven of the colored complexes were examined spectrophotometrically. The results are summarized in Table II.

**Absorption Spectra.** — *Beryllium Complex.* — Absorption spectra of the reagent solution and

Table I. Color produced with ions in an acid or a neutral solution

| | | | | | | | | | | | | | | |
|---|---|---|---|---|---|---|---|---|---|---|---|---|---|---|
| $Li^+$ | *$Be^{2+}$* | | | | | | | | | | | | | |
| | $Mg^{2+}$ | | | | | | | | | | *$Al^{3+}$* | | | |
| $K^+$ | $Ca^{2+}$ | *$Sc^{3+}$* | $Ti^{4+}$ | $Cr^{3+}$ | $Mn^{2+}$ | **$Fe^{3+}$** | $Co^{2+}$ | $Ni^{2+}$ | **$Cu^{2+}$** | $Zn^{2+}$ | **$Ga^{3+}$** | | $As^{3+}$ | $SeO_3^{2-}$ | $Br^-$ |
| | | | | | | **$Fe^{2+}$** | | | | | | | | | |
| $Rb^+$ | $Sr^{2+}$ | **$Y^{3+}$** | $Zr^{4+}$ | | | $Ru^{3+}$ | $Rh^{3+}$ | $Pd^{3+}$ | $Ag^+$ | | $In^{3+}$ | $Sn^{2+,4+}$ | $Sb^{3+}$ | | |
| $Cs^+$ | $Ba^{2+}$ | | $Hf^{4+}$ | | | | $Ir^{4+}$ | | | $Hg^+$ | $Tl^{3+}$ | $Pb^{2+}$ | $Bi^{3+}$ | | |
| | | | | $UO_2^{2+}$ | | | | | | | | | | | |
| *$La^{3+}$ | $Ce^{3+}$ | **$Pr^{3+}$** | **$Nd^{3+}$** | | $Eu^{3+}$ | **$Gd^{3+}$** | | $Dy^{3+}$ | | $Er^{3+}$ | $Tm^{3+}$ | $Yb^{3+}$ | | | |
| | $Ce^{4+}$ | | | | | | | | | | | | | | |

Three ions shown in italic types give green solution.
Ten ions shown in gothic types give blue solution.

Table II. Optimum conditions for analytical use

| Ion | Optimum pH | Wavelength at max. absorbance | Buffer soln. | Ion p.p.m. per 0.1 abs. unit |
|---|---|---|---|---|
| $Fe^{3+}$ | 2.8~4.2 | 610 mμ | B. S.* | 0.22 |
| $Be^{2+}$ | 5.6~6.2 | 570 | A. A.** | 0.02 |
| $Al^{3+}$ | 5.6~6.2 | 600 | B. S. | 0.06 |
| $UO_2^{2+}$ | 5.2 | 610 | — | 1.04 |
| $Cu^{2+}$ | 6.8~7.8 | 610 | B. S. | 0.42 |
| $Ca^{2+}$ | 9.0 | 580 | $NH_4OH$-$NH_4Cl$ | 20.0 |
| $Mg^{2+}$ | 11.0 | 570 | $NH_4OH$-$NH_4Cl$ | 0.71 |

* Borax-succinic acid ** Acetate-acetic acid

of its beryllium complex solution are shown in Fig. 3. All solutions were adjusted to pH 5.8, using the acetate-acetic acid buffer solution. The beryllium complex had a maximum absorption at 570 mμ. However, the reagent appreciably absorbed light at 570 mμ when its concentration was more than 50 p.p.m.

*Copper and Iron(III) Complex.* — The copper complex in a solution of pH 7.2 had a maximum absorption at 610 mμ; the reagent did not appreciably absorb light at this wavelength when its concentration was less than 100 p.p.m. The iron(III) complex in a solution of pH 3.5 had also a maximum absorption at 610 mμ.

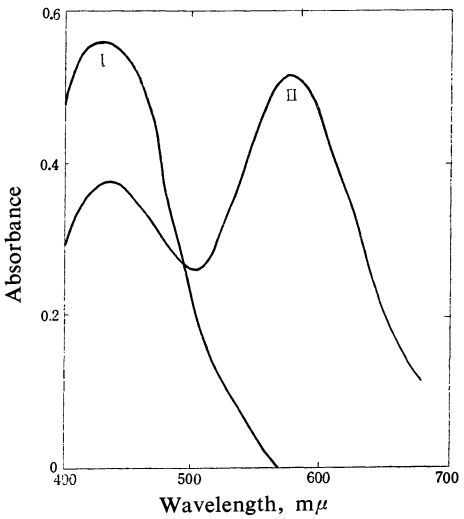



Fig. 3. Absorption spectra.
I: Reagent, 30 p.p.m.
II: Reagent (30 p.p.m.)+Be(0.1 p.p.m.)
pH: 5.8

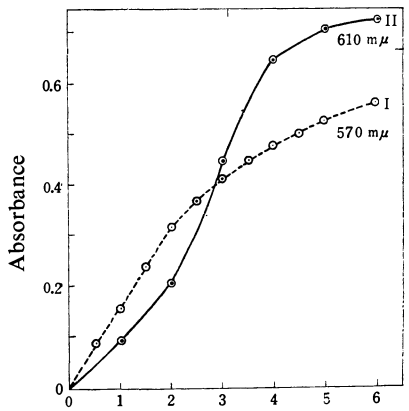



Fig. 4. Application of the mole ratio method.
I: Beryllium complex (pH 5.8)
II: Copper complex (pH 7.2)

**Mole Ratio Studies.**—*Beryllium Complex.*— Application of the mole ratio method[7] showed no sharp break or leveling-off to a constant absorbance for ratios up to as high as one mole of beryllium to six moles of reagent. The results are shown in Fig. 4.

Obviously the colored complex is appreciably dissociated and hence a large excess of the reagent is required to cause the reaction to proceed completion. By the application of the continuous variation method[8], the ratio of beryllium to the reagent was shown to be 1 to 2 (see Fig. 5).

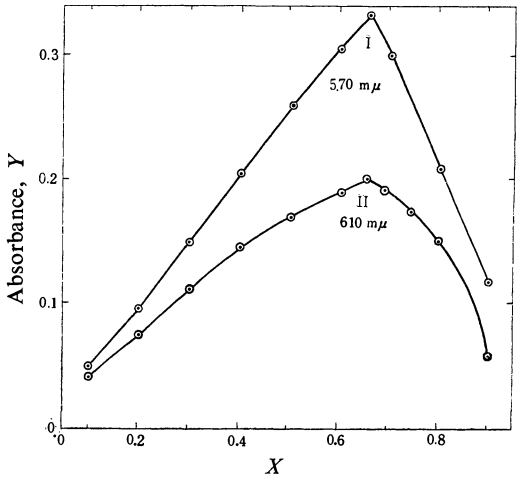



Fig. 5. Application of the method of continuous variation.
I: Be-complex (pH 5.8), II: Cu-complex (pH 7.2).

The best analytical results were obtained when the concentration of unreacted reagent was between 50 and 80 p.p.m.

*Copper and Iron(III) Complexes.*—Mole ratio studies for copper complex solution (pH 7.2) gave results similar to those for beryllium; the copper complex was appreciably dissociated and the ratio of copper to the reagent was 1 to 2 (see Figs. 4 and 5). The iron complex was also studied in a solution of pH 3.5. The ratio of iron to the reagent was 1 to 3.

**Effect of pH.** — Borax-succinic acid buffer and acetate-acetic acid buffer were satisfactory for the determination of beryllium, copper and iron. For an accurate measurement it was necessary to hold the pH fairly constant. The effect of pH on the color intensities of the metal complexes is shown in Fig. 6. The optimum pH range for the determination is listed in Table II.

**Effect of Temperature.**—There was no variation in the absorbance of the color systems

7) J. H. Yoe and A. I. Jones, *Ind. Eng. Chem., Anal. Ed.*, **16**, 111 (1944).

8) W. C. Vosburgh and G. R. Cooper, *J. Am. Chem. Soc.*, **63**, 437 (1941).

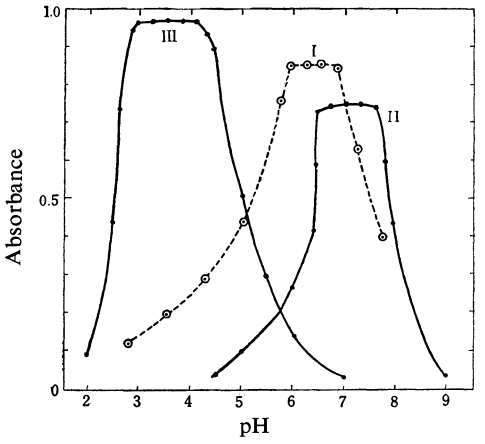



Fig. 6. Effect of pH.
I: $Be^{+2}$, 0.17 p.p.m., II: $Cu^{+2}$, 3.0 p.p.m., III: $Fe^{+3}$, 2.0 p.p.m.

over a temperature range of 15 to 30°C Hence, normal temperature changes in the laboratory introduce no error.

**Rate of Color Development.** — At room temperature the color intensities increased during the first 20 min. then remained constant for 40 to 50 min.

**Interfering Ions.**—Color reactions of 52 ions are listed in Table I. The limiting concentrations of seven ions in the determination of beryllium are given in Table III. The concentration of an ion that causes a diviation of 0.01 unit in the absorbance of a solution containing 0.1 p.p.m. of beryllium was taken to be the limiting concentration.

TABLE III. LIMITING CONCENTRATIONS OF INTERFERING IONS FOR DETERMINATION OF BERYLLIUM

| Ion | Added as | Limiting concentration p.p.m. |
|---|---|---|
| $Al^{+3}$ | $K_2SO_4Al_2(SO_4)_3$ | 0.09 |
| $Co^{+2}$ | $Co(NO_3)_2$ | 20.0 |
| $Cr^{+3}$ | $Cr_2(SO_4)_3$ | 3.0 |
| $Cu^{+2}$ | $CuSO_4$ | 0.22 |
| $Fe^{+3}$ | $K_2SO_4Fe_2(SO_4)_3$ | 0.27 |
| $Ni^{+2}$ | $Ni(NO_3)_2$ | 16.4 |
| $UO_2^{+2}$ | $UO_2(NO_3)_2$ | 1.9 |

Several methods were tried to eliminate the interfering ions for the determination of beryllium. The 8-hydroxyquinoline method[9] effected a good separation of beryllium. Interfering ions for the determination of copper and iron, such as $Al^{+3}$, $Be^{+2}$, $Co^{+2}$ and $Cr^{+3}$, were eliminated by the method of Kraus[6].

9) E. B. Sandell, "Colorimetric Determination of Traces of Metals", 3rd Ed., Interscience Publishers, Inc., New York (1959), p. 306.

**Beer's Law.**—As a large excess of the reagent required for the determination of beryllium, was copper and iron, the calibration curves of water blank did not pass through the origin because of the absorption of the reagent solution at 570 or 610 mμ. The use of these curves provided satisfactory results whenever the same concentration of the reagent was used for

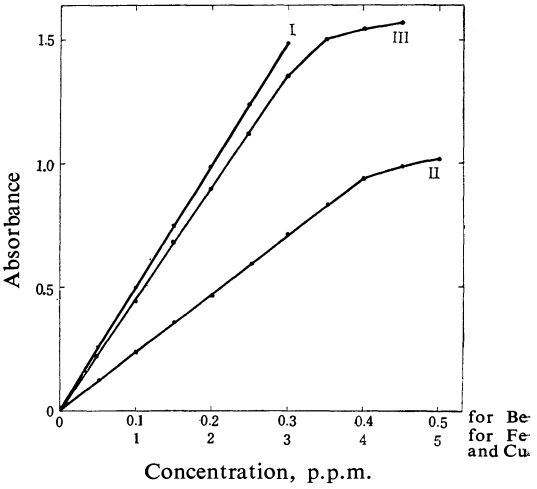



Fig. 7. Calibration curves for the determination.
I: $Be^{+2}$, pH 5.8, II: $Cu^{+2}$, pH 7.2, III: $Fe^{+3}$, pH 3.5, reference: reagent blank.

TABLE IV. DETERMINATION OF BERYLLIUM

| | Solution analized | | Found Be* p.p.m. | Error % |
|---|---|---|---|---|
| | Ion | Added p.p.m. | | |
| 1) | $Al^{+3}$ | 0.16 | | |
| | $Fe^{+2}$ | 0.16 | | |
| | $Co^{+2}$ | 0.16 | | |
| | $Ni^{+2}$ | 10.00 | | |
| | $Cu^{+2}$ | 20.00 | | |
| | $Zn^{+2}$ | 20.00 | | |
| | $Be^{+2}$ | 0.16 | 0.16 | 0.0 |
| 2) | $Al^{+3}$ | 8.00 | | |
| | $Fe^{+3}$ | 10.00 | | |
| | $Co^{+2}$ | 10.00 | | |
| | $Ni^{+2}$ | 20.00 | | |
| | $Cu^{+2}$ | 20.00 | | |
| | $Ti^{+4}$ | 20.00 | | |
| | $Be^{+2}$ | 0.16 | 0.15 | −6.3 |
| 3) | $Al^{+3}$ | 10.00 | | |
| | $Cr^{+3}$ | 10.00 | | |
| | $Cu^{+2}$ | 10.00 | | |
| | $Fe^{+3}$ | 20.00 | | |
| | $Ca^{+2}$ | 20.00 | | |
| | $Mg^{+2}$ | 20.00 | | |
| | $Ni^{+2}$ | 10.00 | | |
| | $Be^{+2}$ | 0.08 | 0.08 | 0.0 |

* These values are the averages of six repeated determinations.

standards and unknowns. However, color intensities measured with the reagent solution as a blank obeyed Beer's law better than those with a water blank; Beer's law was obeyed up to about 0.3 p.p.m. of beryllium, about 4.0 p.p.m. of copper and about 3.0 p.p.m. of iron (see Fig. 7). In addition, the absorbances were sufficiently reproducible to permit beryllium to be determined up to 0.4 p.p.m., but for the best precision the concentration range should be 0.05 to 0.3 p.p.m.

TABLE V. DETERMINATION OF COPPER AND IRON

| | Solution analyzed | | Found* | | Error |
|---|---|---|---|---|---|
| | Ion | Added p.p.m. | Cu p.p.m. | Fe | % |
| 1) | $Cu^{2+}$ | 2.00 | 2.01 | | +0.5 |
| | $Fe^{3+}$ | 2.00 | | 1.96 | −2.0 |
| 2) | $Al^{3+}$ | 20.00 | | | |
| | $Ca^{2+}$ | 20.00 | | | |
| | $Be^{2+}$ | 2.00 | | | |
| | $Cu^{2+}$ | 1.00 | 1.01 | | +1.0 |
| | $Fe^{3+}$ | 1.00 | | 0.97 | −3.0 |
| 3) | $Al^{3+}$ | 200.00 | | | |
| | $Ca^{2+}$ | 200.00 | | | |
| | $Mg^{2+}$ | 200.00 | | | |
| | $Cu^{2+}$ | 2.00 | 1.88 | | −6.0 |
| | $Fe^{3+}$ | 2.00 | | 1.86 | −7.0 |

* These values are the averages of three repeated determinations.

**Determination of Beryllium in Solutions Containing Various Ions.** — Beryllium has been determined in three solutions containing various amounts of certain foreign ions, after separation of the latter by oxine precipitation. The results are listed in Table IV.

**Determination of Copper and Iron in Solutions Containing Various Ions.**—Copper and iron(III) have been determined in three solutions, after separation of the foreign ions by the exchange resin. The results are given in Table V.

## Summary

Procedures have been developed for the spectrophotometric determination of trace amounts of beryllium, copper and iron(III) with sodium-2″, 6″-dichloro-4′-hydroxy-3, 3′-dimethylfuchsone-5,5′-dicarboxylate. Certain ions that interfere with the beryllium determination are removed by an oxine precipitation. Ions that interfere with the analysis of copper and iron(III) are removed with an anion exchange resin column.

Accuracy and precision are good. Beer's law is obeyed up to about 0.3 p.p.m. of beryllium, about 4 p.p.m. of copper and about 3 p.p.m. of iron.

*Himeji Technical College (Y. K. & K. U.)*
*Idei, Himeji*
*John Lee Pratt Trace Analytical Laboratory*
*University of Virginia*
*Charlottesville, Va., U. S. A. (J. H. Y.)*

# *Electronic Spectra of Substituted Aromatic Hydrocarbons. I. Phenol and Aniline*

BY Hiroaki BABA

(Received July 22, 1960)

Recent advances in both theoretical[1-4] and experimental[5,6] studies have made it possible to understand fully the origin of the electronic spectra of aromatic hydrocarbons. On the other hand, it appears that no satisfactory interpretations have been given to the spectra of substitution products of the aromatics other than benzene. The present series of papers are concerned with systematic analyses of the electronic spectra of substituted aromatic hydrocarbons, especially hydroxyl and amino derivatives.

As to the spectra of monosubstituted benzenes, a number of theoretical investigations have been carried out[7-13]. There remain, however, unsettled problems even concerning

1) J. R. Platt, *J. Chem. Phys.*, **17**, 484 (1949).
2) J. A. Pople, *Proc. Phys. Soc.*, **A68**, 81 (1955).
3) R. Pariser, *J. Chem. Phys.*, **24**, 250 (1956).
4) N. Mataga, K. Nishimoto and S. Mataga, This Bulletin, **32**, 395 (1959).
5) H. B. Klevens and J. R. Platt, *J. Chem. Phys.*, **17**, 470 (1949).
6) D. S. McClure, ibid., **22**, 1668 (1954); J. W. Sidman, ibid., **25**, 115 (1956).
7) A. L. Sklar, ibid., **7**, 984 (1939).
8) K. F. Herzfeld, *Chem. Revs.*, **41**, 233 (1947).
9) F. A. Matsen, *J. Am. Chem. Soc.*, **72**, 5243 (1950).
10) S. Nagakura and H. Baba, ibid., **74**, 5693 (1952).
11) L. Goodman and H. Shull, *J. Chem. Phys.*, **27**, 1388 (1957).
12) K. Nishimoto and R. Fujishiro, This Bulletin, **31**, 1036 (1958).
13) Y. I'Haya, *J. Am. Chem. Soc.*, **81**, 6120, 6127 (1959).

the qualitative assignment of the observed absorption bands. In this paper, a molecular orbital (MO) calculation has been made of the $\pi$-electronic spectra of phenol and aniline. Herein a semiempirical method of calculation is developed, which will be applied also to naphthalene derivatives in the next paper.

## Method of Calculation

The so-called simple LCAO MO theory originally proposed by Hückel is inadequate for dealing with molecules in their excited states. The more rigorous theoretical method, which is based on the correct many-electron Hamiltonian, has been developed to account for the electronic spectra of unsaturated compounds. Although the latter method has been simplified by Pariser and Parr[14] and Pople[2], it seems troublesome to apply it directly to such complex molecules as monosubstituted naphthalenes.

In this calculation an eclectic method is adopted; namely, the simplicity of the Hückel theory is retained, and at the same time it is somewhat modified by reference to the rigorous theoretical method so as to allow for electronic interaction. Thus, MO's are determined by the simple LCAO procedure; configurational wave functions are built up as antisymmetrized products of these MO's, configuration interaction being taken into account.

In the simple LCAO procedure, the energy of an MO is expressed in termes of the resonance integral $\beta[\equiv\beta_{CC}]$. In the present calculation, the evaluation of this integral is made, after the scheme of Goodman and Shull[11], in the following way.

According to the simple LCAO MO theory, the energy required for exciting an electron from an occupied MO $\phi_i$ to an unoccupied MO $\phi_k$ is given by

$$\Delta E=e_k-e_i=(m_k-m_i)\beta \qquad (1)$$

Here, $e_i$ and $e_k$ are the energies of the MO's $\phi_i$ and $\phi_k$, respectively; $e_i=\alpha+m_i\beta$ and $e_k=\alpha+m_k\beta$, where $\alpha[\equiv\alpha_C]$ is the Coulomb integral of a carbon atom.

In the rigorous theory, configurational wave functions are obtained as antisymmetrized products of molecular spin-orbitals. Such wave functions for the lowest energy configuration and for the singlet configuration resulting from the excitation $\phi_i\rightarrow\phi_k$ are denoted by $V_0$ and $V_{ik}$, respectively. The energies associated with these wave functions are

$$E(V_0)=\int V_0^*\mathbf{H}V_0\,d\nu, \quad \text{etc.}$$

where **H** is the complete many-electron Hamiltonian. Deriving an expression for the excitation energy $\Delta E=E(V_{ik})-E(V_0)$ by the self-consistent field method, Mulliken pointed out that the energy quantity which is acceptable as the energy of the excited MO $\phi_k$ is dependent not only upon the MO $\phi_k$, but also upon the MO $\phi_i$ from which the excitation occurs[15]. On the contrary, the orbital energy $e_k$ in Eq. 1 does not depend on $\phi_i$.

In view of this situation, let the resonance integral be regarded as a quantity depending upon both $i$ and $k$, and be designated as $\beta_{i\rightarrow k}$ instead of $\beta$. Then, the following relation may be assumed to hold[16]

$$(m_k-m_i)\beta_{i\rightarrow k}=E(V_{ik})-E(V_0) \qquad (2)$$

If the purely theoretical quantity, $E(V_{ik})-E(V_0)$, is replaced by an appropriate experimental one, $\beta_{i\rightarrow k}$ will immediately be determined, for the values of $m_i$ and $m_k$ can be obtained from the simple MO procedure.

In this study only the singlet transitions will be treated.

## Results of Calculation

**Molecular Orbitals.** — The MO's have been determined by the simple LCAO MO theory with neglect of overlap integrals.

In the parent hydrocarbon, benzene, the following four MO's are responsible for the lower electronic transitions:

$$\phi_2^0=(1/2)(\chi_2+{}_3\chi-\chi_5-\chi_6) \qquad (3a)$$

$$\phi_3^0=(1/\sqrt{12})(2\chi_1+\chi_2-\chi_3-2\chi_4-\chi_5+\chi_6) \qquad (3b)$$

$$\phi_4^0=(1/\sqrt{12})(2\chi_1-\chi_2-\chi_3+2\chi_4-\chi_5-\chi_6) \qquad (3c)$$

$$\phi_5^0=(1/2)(-\chi_2+\chi_3-\chi_5+\chi_6) \qquad (3d)$$

where $\chi_p$ is the $p$th carbon $2p\pi$ atomic orbital; the superscript zeros refer to the parent hydrocarbon; $\phi_2^0$, $\phi_3^0$ and $\phi_4^0$, $\phi_5^0$ are degenerate pairs of MO's, viz., $e_2^0=e_3^0=\alpha+\beta$, $e_4^0=e_5^0=\alpha-\beta$.

In the calculation of the MO's of a monosubstituted benzene, the Coulomb integral $\alpha_X$ of the substituent X is taken as

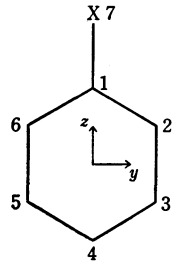



Fig. 1.

14) R. Pariser and R. G. Parr, *J. Chem. Phys.*, **21**, 466, 767 (1953).

15) R. S. Mulliken, *J. chim. phys.*, **46**, 497 (1949); R. G. Parr and R. S. Mulliken, *J. Chem. Phys.*, **18**, 1338 (1950).

16) A more detailed discussion on this point is given in H. Baba and S. Suzuki, ibid., **32**, 1706 (1960).

$$\alpha x = \alpha + \delta x \beta$$

The MO's and their energies are calculated for various values of the parameter $\delta x$. Let the MO of the monosubstituted benzene corresponding to $\phi_i^0$ of the parent hydrocarbon be designated as $\phi_i$, and suppose that the substituent X is attached to the carbon atom 1, as shown in Fig. 1. Then, the MO's $\phi_2$ and $\phi_5$ of symmetry type $a_2$ are identical with $\phi_0^2$ and $\phi_5^0$, respectively[17]; the MO's $\phi_3$ and $\phi_4$ are of symmetry type $b_1$. The variation of the MO energies with the magnitude of $\delta x$ was reported by Matsen[9].

**Configuration Energies.**—Owing to the high symmetry ($D_{6h}$) of benzene, $V_{24}^0$, $V_{35}^0$ and $V_{25}^0$, $V_{34}^0$ are degenerate pairs of configurations, and the interaction of the configurations of each pair is automatically introduced to give excited states, the characteristics of which are shown in Table I. Referring to this table, one obtains

TABLE I. EXCITED STATES OF BENZENE

| Symmetry $D_{6h}$ | Symmetry $C_{2v}$* | Wave function | Observed excitation energy**, eV. |
|---|---|---|---|
| $B_{2u}$ | $B_2^-$ | $\frac{1}{\sqrt{2}}(V_{24}^0 - V_{35}^0)$ | 4.88 |
| $B_{1u}$ | $A_1^+$ | $\frac{1}{\sqrt{2}}(V_{25}^0 + V_{34}^0)$ | 6.14 |
| $E_{1u}$ | $B_2^+$ | $\frac{1}{\sqrt{2}}(V_{24}^0 + V_{35}^0)$ | 6.74 |
| | $A_1^-$ | $\frac{1}{\sqrt{2}}(V_{25}^0 - V_{34}^0)$ | |

* In this column are given symmetry types for the subgroup $C_{2v}$ of $D_{6h}$. The plus or minus sign refers to the manner in which two configurations combine with each other.

** Taken from Ref. 18.

$$E(V_{24}^0) = E(V_{35}^0) = \frac{1}{2}\{W^0(B_{2u}) + W^0(E_{1u})\}$$
$$= E(V_0^0) + 5.81 \text{ eV}.$$
$$E(V_{25}^0) = E(V_{34}^0) = \frac{1}{2}\{W^0(B_{1u}) + W^0(E_{1u})\}$$
$$= E(V_0^0) + 6.44 \text{ eV}.$$

in which $W^0(B_{2u})$, for instance, represents the energy of the $B_{2u}$ state of the parent hydrocarbon, benzene. Since $m_2^0 = m_3^0 = 1$, $m_4^0 = m_5^0 = -1$, it follows from Eq. 2 that

$$\beta_{2\to4}^0 = \beta_{3\to5}^0 = -2.905 \text{ eV}. = \beta^0(B_2) \quad (4a)$$
$$\beta_{2\to5}^0 = \beta_{3\to4}^0 = -3.22 \text{ eV}. = \beta^0(A_1) \quad (4b)$$

In the monosubstituted benzene, the energies of the $B_2$ configurations, $V_{24}$ and $V_{35}$, are no longer equal to each other; the same is the case with the energies of the $A_1$ configurations, $V_{25}$ and $V_{34}$. In evaluating the energies of these configurations, the assumption is made that

$$\beta_{2\to4} = \beta_{3\to5} = \beta^0(B_2) \quad (5a)$$
$$\beta_{2\to5} = \beta_{3\to4} = \beta^0(A_1) \quad (5b)$$

Then the energies $E(V_{ik})$'s for the configurations $V_{ik}$'s are readily derived on the basis of Eq. 2, since $m_i$ and $m_k$ can be obtained from the simple MO calculation.

**Configuration Interaction.**—The matrix element of the total Hamiltonian **H** between $V_{ik}$ and $V_{jl}$ is, in general, given by

$$\{V_{ik} \mid V_{jl}\} = \int V_{ik}^* \mathbf{H} V_{jl}\, dv$$
$$= 2[ki \mid jl] - [kl \mid ji] \quad (i \neq j,\ k \neq l) \quad (6)$$

with

$$[ij \mid kl] = \int \phi_i^*(1)\phi_k^*(2)(e^2/r_{12})\phi_j(1)\phi_l(2)\,dv \quad (7)$$

The orthonormal MO's determined by the simple MO theory are used for the calculation of the above matrix element. On the assumption of zero differential overlap, the integral $[ij \mid kl]$ may be expressed in terms of integrals over atomic orbitals of the form

$$(pp \mid qq) = \int \chi_p^*(1)\chi_q^*(2)(e^2/r_{12})\chi_p(1)\chi_q(2)\,dv \quad (8)$$

The integrals of this type were evaluated by Pariser and Parr's method[14]. Necessary values of the valence-state ionization potentials and electron affinities for carbon, oxygen and nitrogen atoms were taken from the table of Pritchard and Skinner[19]. The values of the integrals $(11 \mid 11)_{CC}$ and $(11 \mid 22)_{CC}$ were slightly modified in the following manner.

To the approximation adopted in the present calculation, one obtains

$$\{V_{24}^0 \mid V_{35}^0\} = (1/12)\{(11 \mid 11)_{CC} + 3(11 \mid 22)_{CC} - (11 \mid 33)_{CC} - 3(11 \mid 44)_{CC}\}$$
$$= (1/2)\{W^0(E_{1u}) - W^0(B_{2u})\} \quad (9a)$$
$$\{V_{25}^0 \mid V_{34}^0\} = (1/12)\{(11 \mid 11)_{CC} - 9(11 \mid 22)_{CC} + 11(11 \mid 33)_{CC} - 3(11 \mid 44)_{CC}\}$$
$$= (1/2)\{W^0(B_{1u}) - W^0(E_{1u})\} \quad (9b)$$

17) Monosubstituted benzenes belong to symmetry group $C_{2v}$. The group-theoretical notation used in this paper is the same as that of G. Herzberg, "Infrared and Raman Spectra of Polyatomic Molecules", D. Van Nostrand Company, Inc., New York (1945), p. 106. The y and z axes are chosen as in Fig. 1 and the x axis is perpendicular to the molecular plane.

18) H. B. Klevens and J. R. Platt, "Technical Report, Laboratory of Molecular Structure and Spectra. Univ. of Chicago", Part One (1953-1954), p. 145.

19) H. O. Pritchard and H. A. Skinner, *Chem. Revs.*, 55, 745 (1955).

in which the superscript zeros refer, as before, to benzene. Pariser and Parr's method gives $(11 \mid 33)_{cc}=5.470$ eV. and $(11 \mid 44)_{cc}=4.894$ eV. Inserting these values into Eqs. 9a and 9b and using the experimental values, quoted in Table I, for $W^0(B_{2u})$, etc., one may determine those values of $(11 \mid 11)_{cc}$ and $(11 \mid 22)_{cc}$ which simultaneously satisfy Eqs. 9a and 9b. The result is

$$\left.\begin{aligned}(11 \mid 11)_{cc}&=11.212\text{ eV.}\quad(10.84\text{ eV.})\\(11 \mid 22)_{cc}&=\ 6.700\text{ eV.}\quad(7.392\text{ eV.})\end{aligned}\right\} \tag{10}$$

the values obtained by the method of Pariser and Parr being given in parentheses.

The matrix elements $\{V_{24} \mid V_{35}\}$ and $\{V_{25} \mid V_{34}\}$ for the monosubstituted benzene are calculated to be

$$\begin{aligned}&\{V_{24} \mid V_{35}\}\\&=(1/2)(-g_{22}+g_{33})\{(11 \mid 11)_{cc}-(11 \mid 33)_{cc}\}\\&+(3/2)(g_{32}-g_{23})\{(11 \mid 22)_{cc}-(11 \mid 44)_{cc}\}\end{aligned} \tag{11a}$$

$$\begin{aligned}&\{V_{25} \mid V_{34}\}\\&=(-g_{22}+g_{33})\{(1/2)(11 \mid 11)_{cc}-(11 \mid 22)_{cc}\\&+(3/2)(11 \mid 33)_{cc}-(11 \mid 44)_{cc}\}\\&+(1/2)(g_{32}-g_{23})\{(11 \mid 22)_{cc}-(11 \mid 44)_{cc}\}\\&-(g_{11}-g_{44})\{(11 \mid 22)_{cc}-(11 \mid 33)_{cc}\}\\&-g_{77}\{(22 \mid 77)_{cx}-(33 \mid 77)_{cx}\}\end{aligned} \tag{11b}$$

Here $g_{pq}=c_{3p}c_{4q}$, in which $c_{ip}$ is the coefficient of the atomic orbital $\chi_p$ in MO $\phi_i$. The matrix elements have been computed for various values of $\delta_X$, the results being shown in Fig. 2. Actually, the curve for $\{V_{25} \mid V_{34}\}$ was obtained by assuming X to be $NH_2$. It should be noted in this connection that, while $\{V_{24} \mid V_{35}\}$ does not contain any terms associated with the substituent X, $\{V_{25} \mid V_{34}\}$ does contain such terms (see Eq. 11b). Accordingly, a deviation from the above-mentioned curve may occur when X is taken to be OH instead of $NH_2$. An examination on this point, however, revealed that the deviation is so small as to be virtually negligible. Consequently the curve in question can be applied to the case of the hydroxyl substituent as well as to the amino substituent.

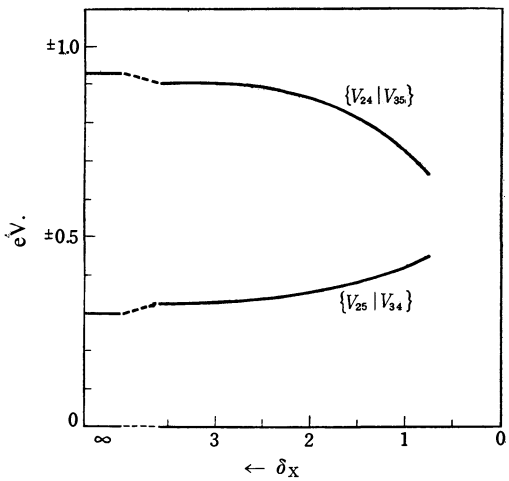



Fig. 2. Relation of the configuration interaction integrals to $\delta_X$. The plus and minus signs on the scale numbers of the ordinate correspond to $\{V_{24} \mid V_{35}\}$ and $\{V_{25} \mid V_{34}\}$, respectively.

**State Energies.**—The interaction between the two $B_2$ configurations, $V_{24}$ and $V_{35}$, gives two $B_2$ states, $B_2^+$ and $B_2^-$. Similarly $A_1^+$ and $A_1^-$ states arise from the interaction of $V_{25}$ and $V_{34}$. The dependencies of the energies of these states upon $\delta_X$ are shown in Fig. 3, together with the observed excitation energies[18,20] for phenol and aniline.

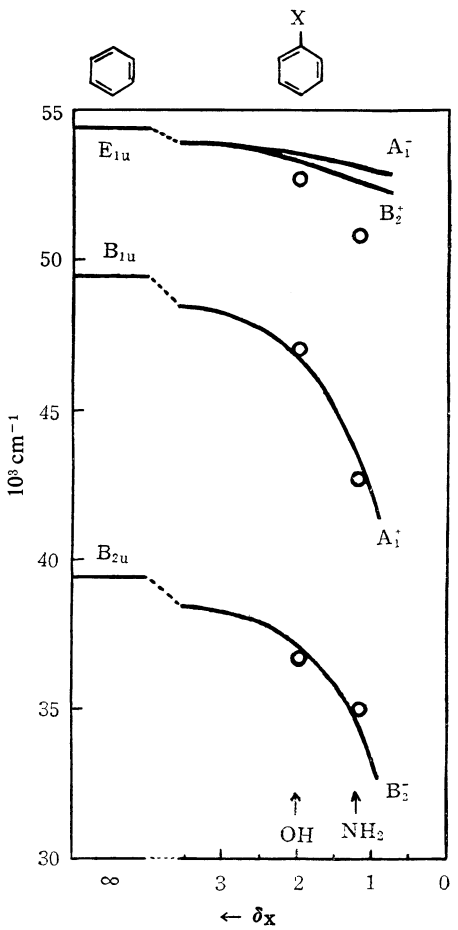



Fig. 3. Relation of the energies of the excited states to $\delta_X$. The observed energies are represented by circles.

20) American Petroleum Institute Research Project 44, Ultraviolet Spectral Data, Serial No. 171.

**Oscillator Strengths.**—The oscillator strengths, $f$, have been calculated by the use of the well-known relation[21]

$$f = 1.085 \times 10^{11} \nu \mathbf{Q}^2 \qquad (12)$$

where $\nu$ is wave number in $cm^{-1}$ and $\mathbf{Q}$ is transition moment in cm. The results are graphed in Fig. 4. The directions of the

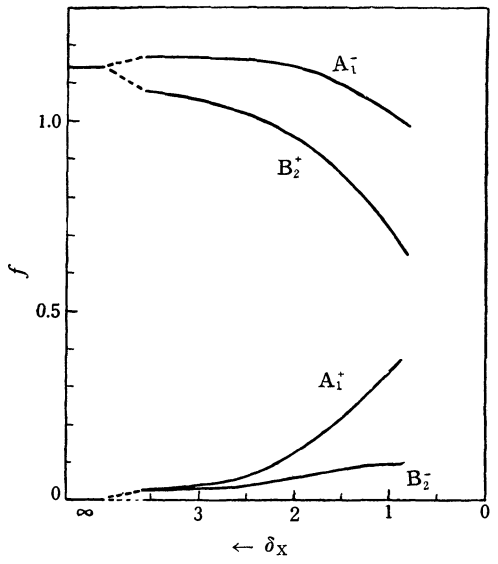



Fig. 4. Relation of $f$ values to $\delta_X$.

transition moments are known from the symmetry types of the excited states concerned. Thus the moments of the transitions to the $B_2^{\pm}$ states are perpendicular to the $C_1$-X axis, while those of the transitions to the $A_1^{\pm}$ states lie along the direction of the $C_1$-X axis.

**Changes of Electron Density Accompanying Electronic Transitions.**—The changes of the $\pi$-electron density at the substituent X, $\Delta q_X$, accompanying the electronic transitions have been calculated as functions of $\delta_X$. The results

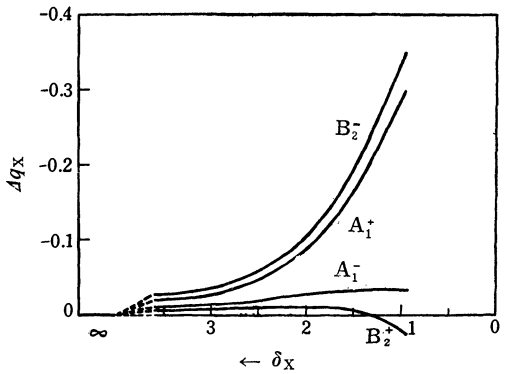



Fig. 5. Relation of $\Delta q_X$ values to $\delta_X$.

21) R. S. Mulliken and C. A. Rieke, *Repts. Progr. Phys.*, **8**, 231 (1941).

are shown in Fig. 5. The calculation of the electron density is based on the definition of Pariser[3].

**Summary of Calculation.**—In the preceding sections several theoretical quantities, e. g., configuration interaction integrals and energies of excited states, have been given as functions of the parameter $\delta_X$ to see the general trend of the substitution effects. However, in order to find the values of these quantities for a particular molecule, one must assign a suitable value to $\delta_X$. In this calculation the values of $\delta_X$ for phenol and aniline have been determined in such a way that the calculated excitation energies might be in best agreement with the observed. This led to the following parameter values (cf. Fig. 3):

$$\text{phenol}, \quad \delta_O = 2.0 \qquad (13a)$$

$$\text{aniline}, \quad \delta_N = 1.2 \qquad (13b)$$

Other theoretical quantities than the excitation energies are also derived by using these parameter values. The calculated results thus obtained for phenol and aniline are summarized in Tables II and III, together with available experimental data.

## Discussion

It is seen from Table III that the degrees of configuration mixing in the wave functions of the excited states are considerably changed upon substitution. As was pointed out by Goodman and Shull[11], this fact is of basic importance in discussing the effect of substitution on the excitation energies and intensities.

In making the assignment of the electronic transitions of the substituted benzenes, particularly of aniline, a problem is raised concerning the nature of the excited state for the transition corresponding to the $A_{1g} \rightarrow B_{1u}$ transition of benzene. Murrell[22] regarded the absorption band at 42700 $cm^{-1}$ in aniline as due to a transition to an electron transfer state characteristic of this molecule. According to the present calculation, the above band is attributed to the transition to the $A_1^+$ state of aniline which corresponds to the $B_{1u}$ state of benzene. As is seen from the data on $\Delta q_N$ of Table III, this transition is accompanied by an electron transfer, but its amount is much smaller than that in the electron transfer transition of Murrell. Moreover, there occurs an electron transfer also in the transition to the $B_2^-$ state, the amount of which is comparable to that in the case of the transition to the $A_1^+$ state. Inspection of the calculated values of $\Delta q_X$ will show that there is no substantial difference between the natures of

22) J. N. Murrell, *Proc. Phys. Soc.*, **A68**, 969 (1955).

TABLE II. ORBITAL ENERGIES AND ORBITALS FOR PHENOL AND ANILINE

| | $i$ | Orbital energy $(e_i-\alpha)/\beta$ | Orbital $\phi_i$ |
|---|---|---|---|
| Phenol | 3 | 0.755 | $0.477\chi_1+0.372(\chi_2+\chi_6)-0.197(\chi_3+\chi_5)-0.520\chi_4-0.384\chi_7$ |
| | 4 | −1.108 | $0.569\chi_1-0.224(\chi_2+\chi_6)-0.321(\chi_3+\chi_5)+0.580\chi_4-0.183\chi_7$ |
| Aniline | 3 | 0.575 | $0.356\chi_1+0.387(\chi_2+\chi_6)-0.133(\chi_3+\chi_5)-0.463\chi_4-0.569\chi_7$ |
| | 4 | −1.143 | $0.559\chi_1-0.200(\chi_2+\chi_6)-0.330(\chi_3+\chi_5)+0.577\chi_4-0.238\chi_7$ |

TABLE III. EXCITED STATES OF PHENOL AND ANILINE

| | Symmetry | Wave function | Excitation energy, $cm^{-1}$ | | $f$ | | $\Delta q_X$ |
|---|---|---|---|---|---|---|---|
| | | | calcd. | obs.* | calcd. | obs.** | calcd. |
| Phenol | $B_2^-$ | $0.495V_{24}-0.869V_{35}$ | 37200 | 36700 | 0.059(0.018) | 0.0213 | −0.103 |
| | $A_1^+$ | $0.487V_{25}+0.873V_{34}$ | 46800 | 47000 | 0.125(0.037) | 0.103 | −0.087 |
| | $B_2^+$ | $0.869V_{24}+0.495V_{35}$ | 53400 | 52700 | 0.956(0.29) | | −0.011 |
| | $A_1^-$ | $0.873V_{25}-0.487V_{34}$ | 53600 | | 1.142(0.34) | | −0.027 |
| Aniline | $B_2^-$ | $0.366V_{24}-0.931V_{35}$ | 34500 | 35000 | 0.091(0.027) | 0.026 | −0.273 |
| | $A_1^+$ | $0.356V_{25}+0.935V_{34}$ | 43400 | 42700 | 0.289(0.087) | 0.17 | −0.233 |
| | $B_2^+$ | $0.931V_{24}+0.366V_{35}$ | 52700 | 50800 | 0.773(0.23) | | +0.006 |
| | $A_1^-$ | $0.935V_{25}-0.356V_{34}$ | 53200 | | 1.051(0.32) | | −0.034 |

* Taken from Refs. 18 and 20.
** Values for phenol are obtained from the unpublished data of the present author, and those for aniline from the data of Ref. 20.

the 42700 $cm^{-1}$ band of aniline and of the 47000 $cm^{-1}$ band of phenol. Thus, as to the origin of the aniline band, the present interpretation is somewhat different from Murrell's. A further experimental examination is desirable for reaching a final conclusion.

In both phenol and aniline, the calculated energy levels of the $B_2^+$ and $A_1^-$ states are situated close to each other. This suggests that the 52700 $cm^{-1}$ band of phenol, or the 50800 $cm^{-1}$ band of aniline, consists of two absorptions corresponding to the excitations to the $B_2^+$ and $A_1^-$ states.

The calculated values of the oscillator strengths may account for the general feature of the effect of the substitution on the band intensities, but their absolute values are too high. A correction factor of 0.30 was introduced, which is the ratio of $f_{obs}$ to $f_{calcd}$ for the $A_{1g}\rightarrow E_{1u}$ transition in benzene; the corrected values are given in parentheses in Table III.

In making a comparison of the calculated and observed $f$ values, one should keep the following point in mind. Both the $A_{1g}\rightarrow B_{2u}(B_2^-)$ and $A_{1g}\rightarrow B_{1u}(A_1^+)$ transitions in benzene are theoretically forbidden, i.e., $f_{calcd}=0$; whereas $f_{obs}$ values for these transitions were found to be 0.0014 and 0.10, respectively[18]. This discrepancy was shown to be due to the distortion of the ring by unsymmetrical vibrations[23]. A part of the $f_{obs}$ values for the corresponding transitions of the substituted benzenes may come from such a ring distortion effect[24]. This is not taken into consideration in deriving the $f_{calcd}$ values. If allowance is made for the contribution from the ring distortion effect, the $f_{obs}$ values for phenol and aniline are known to be in fairly good agreement with the corrected values of $f_{calcd}$.

The calculation of $\Delta q_X$ provides useful information about the charge distributions in the excited states. It is seen in Table III that all the $\Delta q_X$ values are negative except for that associated with the $B_2^+$ state of aniline, and that the magnitudes of $\Delta q_X$ for the $B_2^-$ and $A_1^+$ states are noticeably greater than those for the $B_2^+$ and $A_1^-$ states. In the ground state of the substituted benzenes under consideration, the substituent has a formal positive charge on account of the migration of the non-bonding pair of electrons into the benzene ring[25]. It will be expected from the calculation that the transitions to the $B_2^-$ and $A_1^+$ states are accompanied by an appreciable increase of the said positive charge. This expectation is consistent with the observation that the absorption bands corresponding to the transitions to the $B_2^-$ and $A_1^+$ states are distinctly shifted to the longer wavelengths by the formation of a hydrogen bond between phenol or aniline and

23) A. L. Sklar, *J. Chem. Phys.*, **5**, 669 (1937); M. Goeppert-Mayer and A. L. Sklar, ibid., **6**, 645 (1938); H. Sponer, G. Nordheim, A. L. Sklar and E. Teller, ibid., **7**. 207 (1939).
24) A. L. Sklar, ibid., **10**, 135 (1942).
25) The charge distribution in the ground state of aniline will be shown in the next paper.

a proton-accepting substance, e. g., dioxane[26].

In consideration of the electronegativities of oxygen and nitrogen, the magnitudes of the Coulomb integral parameters $\delta_O$ and $\delta_N$, given in Eqs. 13a and 13b, appear to be reasonable. However in the present treatment no allowance has been made for the inductive effect of the substituent group on the ring carbon atoms, which is to be taken into account in a more precise calculation; further, the resonance integral $\beta_{CX}$ has been assumed to be equal to $\beta_{CC}$. Accordingly, the values of $\delta_O$ and $\delta_N$ should be regarded as effective ones. At any rate, in view of its practical nature, the present method of calculation is expected to be useful for dealing with the spectra of substitution products of complex organic compounds.

26) H. Baba and S. Suzuki, to be published in *J. Chem. Phys.*

**Summary**

The electronic spectra of monosubstituted benzenes are examined from the viewpoint of semi-empirical MO theory. To allow for electronic interaction, the simple LCAO method is refined in the light of purely theoretical procedure, configuration interaction being included. The refined method is particularly convenient for dealing with the spectra of substituted organic compounds.

The origins of the absorption bands for phenol and aniline are clarified on the basis of the calculated excitation energies, oscillator strengths and changes of charge distribution accompanying electronic transitions. The nature of the second excited state of aniline is discussed in detail, in connection with the problem of electron transfer.

*Research Institute of Applied Electricity*
*Hokkaido University, Sapporo*

# *Electronic Spectra of Substituted Aromatic Hydrocarbons. II. Naphthols and Naphthylamines**

By Hiroaki BABA and Satoshi SUZUKI

(Received July 22, 1960)

The effect of substitutions on the electronic spectrum of a conjugated molecule depends upon the positions at which the substituents are attached to the molecule. With naphthalene, there is a noticeable difference between the spectral changes caused by substitutions at $\alpha$- and $\beta$-positions. Several theoretical studies have been made to account for this interesting phenomenon[1]. The treatments, however, were limited to the framework of the LCAO molecular orbital (MO) theory in its simplest form, because substituted naphthalenes are complex molecules which have only low symmetry or none at all.

In the present study, the ultraviolet absorption spectra of naphthols and naphthylamines have been newly measured, and the effects of hydroxyl and amino substitutions upon the naphthalene spectrum have been examined on the basis of a calculation which was carried out according to the same method as that used in the preceding paper[2] (hereafter referred to as I).

## Experimental

**Materials.**—$\alpha$-Naphthol was recrystallized from ligroin, and $\beta$-naphthol from water and ligroin. Both were further purified by vacuum sublimation; m. p. 93.0~93.5°C and 119.0~119.5°C, respectively. $\alpha$-Naphthylamine and $\beta$-naphthylamine were repeatedly recrystallized from ligroin, and were sublimed in vacuo; m. p. 48.5~49.0°C and 110.0~110.5°C, respectively. Each of the four samples was subjected to vacuum sublimation whenever it was used for a measurement.

Isooctane (2,2,4-trimethylpentane; Enjay Co., Inc., U. S. A.) was carefully purified by distillation and by being passed through a chromatography tube filled with dried silica-gel powder. The isooctane thus purified is transparent down to 200 m$\mu$.

**Measurement of Spectra and Results.**—Ultraviolet absorption spectra were measured at controlled

* Read in part at the Symposium on Electronic States in Molecules, held by the Chem. Soc. Japan, Oct. 1958. (See Abstract of the Meeting, p. 73).

1) D. Peters, *J. Chem. Soc.*, 1957, 646, 1993, 4182; K. Nishimoto and R. Fujishiro, This Bulletin, 32, 445 (1959); R. Fujishiro and K. Nishimoto, Abstract of the Symposium on Electronic States in Molecules, held by the Chem. Soc. Japan, Sept. 1959, p. 14.

2) H. Baba, This Bulletin, 34, 76 (1961).

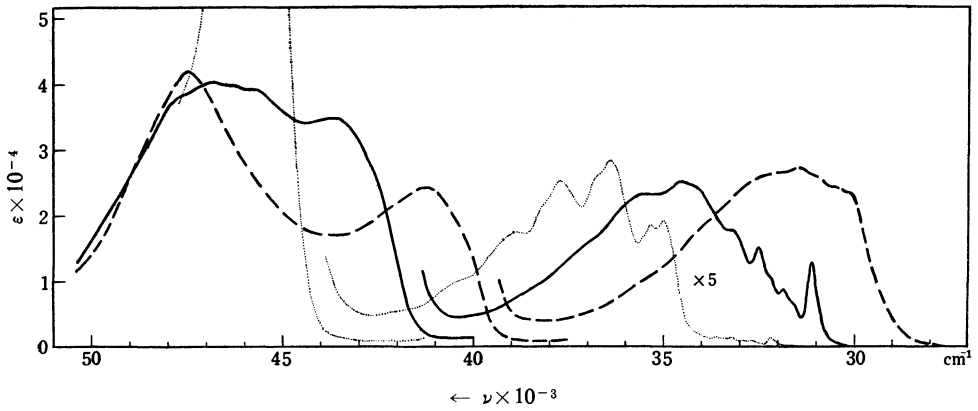



Fig. 1. Ultraviolet absorption spectra of α-naphthol (——), α-naphthylamine (----) and naphthalene (·····) in isooctane.

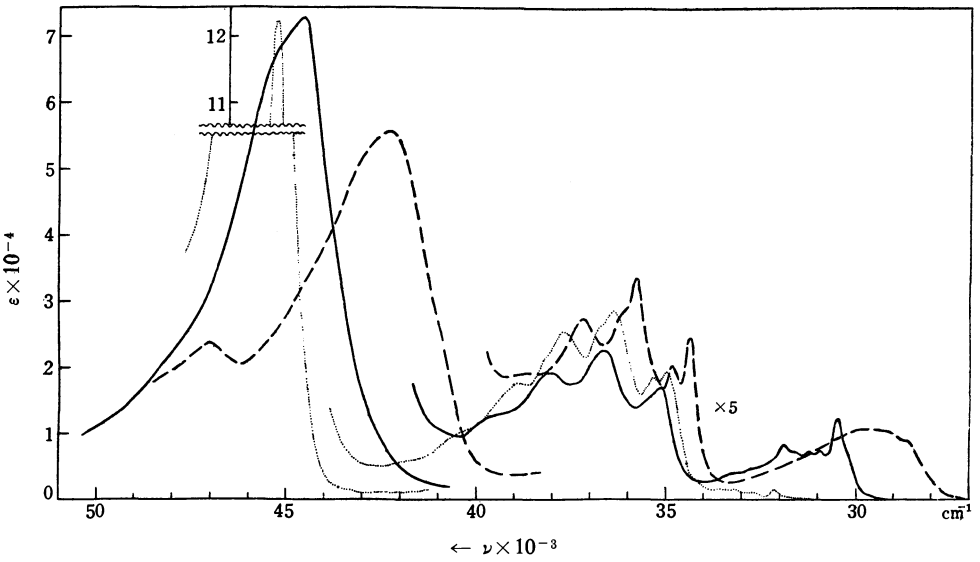



Fig. 2. Ultraviolet absorption spectra of β-naphthol (——), β-naphthylamine (----) and naphthalene (·····) in isooctane.

temperatures with a Hitachi quartz spectrophotometer of type EPU-2A. Attention was paid to the width of the slit so that the effective band width of the exit beam came to be sufficiently narrow as compared with the width of the absorption bands. Silica cells of 10 mm. and 2.5 mm. lengths were used, each of which was fitted with a ground-glass stopper. It was confirmed that Beer's law holds for all the substances in isooctane over the range of concentrations ($10^{-4}$~$10^{-5}$ mol./l.) used in the present measurement.

The absorption spectra of the α- and β-derivatives are shown, respectively, in Figs. 1 and 2. The spectra were observed at 20°C except for that of α-naphthylamine, which was obtained at 17.5°C. In the figures the spectrum of naphthalene[3] is also given for ready comparison.

3) American Petroleum Institute Research Project 44, Ultraviolet Spectral Data, Serial No. 640, 654.

## Calculation

Calculations have been made for α-, β-naphthols and α-, β-naphthylamines by following the same procedure as in I. Various theoretical quantities are at first presented as functions of the parameter $\delta_X$; and then the values of the quantities for naphthols and naphthylamines are derived by assuming $\delta_O$ and $\delta_N$ to

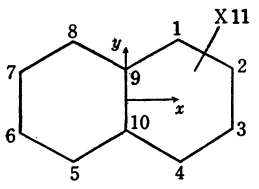



Fig. 3.

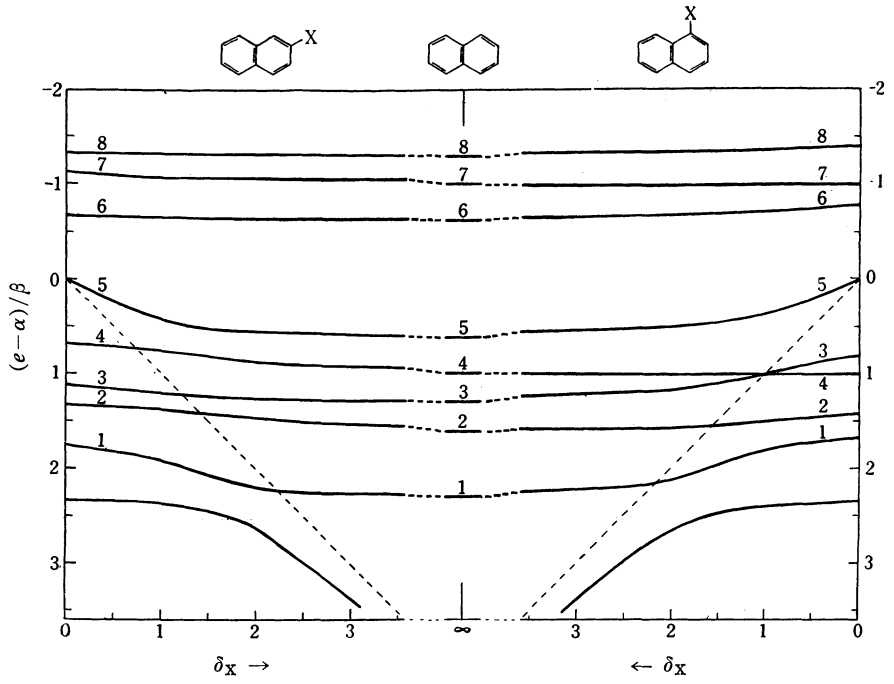



Fig. 4. Relation of MO energies to $\delta_X$.

be equal to the corresponding parameter values determined in I for phenol and aniline. The notation used in this paper is the same as in I.

**Molecular Orbitals.**—The MO's of the parent hydrocarbon, naphthalene, are designated as $\phi_1^0, \phi_2^0, \cdots\cdots$ in the sequence of ascending energy. Among these the following MO's are primarily associated with the lower electronic transitions[4].

$$\phi_4^0 = a(\chi_2+\chi_3+\chi_6+\chi_7) - a(\chi_9+\chi_{10}), \quad e_4^0 = \alpha+\beta \tag{1a}$$

$$\phi_5^0 = b(\chi_1-\chi_4+\chi_5-\chi_8) + c(\chi_2-\chi_3+\chi_6-\chi_7), \quad e_5^0 = \alpha+0.6180\beta \tag{1b}$$

$$\phi_6^0 = b(\chi_1+\chi_4-\chi_5-\chi_8) - c(\chi_2+\chi_3-\chi_6-\chi_7), \quad e_6^0 = \alpha-0.6180\beta \tag{1c}$$

$$\phi_7^0 = -a(\chi_2-\chi_3-\chi_6+\chi_7) + a(\chi_9-\chi_{10}), \quad e_7^0 = \alpha-\beta \tag{1d}$$

where $a=0.4082$, $b=0.4253$, $c=0.2629$; $\chi_p$ is the $p$th atomic orbital (see Fig. 3 for the numbering of the positions); the superscript zeros refer to the parent hydrocarbon.

The energies of the ground-state MO's and of the lower excited MO's for the monosubstituted naphthalenes are plotted against $\delta_X$ in Fig. 4.

**Configuration Interaction.**—With naphthalene, configurations $V_{46}^0$ and $V_{57}^0$ belong to $B_{3u}$, and $V_{47}^0$ and $V_{56}^0$ to $B_{2u}$ species of the symmetry group $D_{2h}$[5]. According to the simple LCAO treatment, the configuration $V_{46}^0$ and $V_{57}^0$ are degenerate, but $V_{47}^0$ and $V_{56}^0$ are not (cf. Eqs. 1a—1d). To a first approximation, interaction is included only between the degenerate configurations, $V_{46}^0$ and $V_{57}^0$[6]. The wave functions thus obtained for the lower excited states of naphthalene are shown in Table I. Using the observed excitation energies, given in Table I, one obtains

Table I. Excited states of naphthalene

| Symmetry | Wave function | Observed excitation energy* (eV.) |
|---|---|---|
| $B_{3u}^-$ | $\frac{1}{\sqrt{2}}(V_{46}^0 - V_{57}^0)$ | 3.99 |
| $B_{2u}$ | $V_{56}^0$ | 4.51 |
| $B_{3u}^+$ | $\frac{1}{\sqrt{2}}(V_{46}^0 + V_{57}^0)$ | 5.62 |

* Taken from Ref. 3.

$$E(V_{46}^0) = E(V_{57}^0) = \frac{1}{2}\{W^0(B_{3u}^-) + W^0(B_{3u}^+)\} = E(V_0^0) + 4.80 \text{ eV}.$$

$$E(V_{56}^0) = E(V_0^0) + 4.51 \text{ eV}.$$

4) R. Pariser, *J. Chem. Phys.*, **24**, 250 (1956).

5) The group-theoretical notation is the same as that used in G. Herzberg, "Infrared and Raman Spectra of Polyatomic Molecules," D. Van Nostrand Company, Inc., New York (1945), p. 108. The x and y axes are chosen as in Fig. 3 and the z axis is perpendicular to the molecular plane.

6) M. J. S. Dewar and H. C. Longuet-Higgins, *Proc. Phys. Soc.* (*London*), **A67**, 795 (1954).

Hence it follows from Eq. 2 of I

$$\beta^0_{4\to6}=\beta^0_{5\to7}=-2.97\text{ eV.}=\beta^0(B_{3u}) \quad (2a)$$

$$\beta^0_{5\to6}=-3.65\text{ eV.} \quad (2b)$$

With the naphthalene derivatives, even the energies of $V_{46}$ and $V_{57}$ are no longer equal. In this calculation, only the interaction is taken into account between those configurations of the derivatives which are degenerate in the parent hydrocarbon. Thus the interaction of $V_{46}$ and $V_{57}$ is included; on the other hand, $V_{56}$ is assumed to represent the wave function for an excited state without mixing with any other configurations. The energies of these configurations are obtained from Eq. 2 of I on the assumption that $\beta_{4\to6}=\beta_{5\to7}=\beta^0(B_{3u})$ and $\beta_{5\to6}=\beta^0_{5\to6}$.

The calculation of the matrix element $\{V_{46}\mid V_{57}\}$ is made in exactly the same way as in I. The integral values used in the present calculation are the same as those used in I. As a result, it follows that

naphthalene, $\{V^0_{46}\mid V^0_{57}\}=0.918$ eV.

$\alpha$-derivative, $\{V_{46}\mid V_{57}\}=0.866$ and 0.782 eV.

$\beta$-derivative, $\{V_{46}\mid V_{57}\}=0.824$ and 0.693 eV.

where the values for each derivative correspond, respectively, to the paramater values $\delta_X=2.0$ and 1.2.

**State Energies.**—The calculated energies of the excited states are shown in Fig. 5 as functions of $\delta_X$; the observed excitation energies of naphthalene, naphthols and naphthylamines are also indicated in the figure. In the parent hydrocarbon, naphthalene, the calculated and observed energies of the $B_{2u}$ state are, of course, in accord with each other. The energies of the $B^-_{3u}$ and $B^+_{3u}$ states are calculated, respectively, to be 3.89 and 5.72 eV., both being in good agreement with the observed excitation energies (see Table I). This may be regarded as a proof that the used integrals are of suitable values.

The monosubstituted naphthalenes have no symmetry, apart from their symmetry with respect to the molecular plane. However, the wave functions or energy levels of the derivatives may be denoted by the analogy of the notation for the corresponding quantities of the parent hydrocarbon. Thus, for example, the lowest excited state of the derivatives will be designated as $(B^-_{3u})$, where the symbol of the symmetry type for the parent hydrocarbon is inclosed in parentheses.

**Oscillator Strengths.** — Oscillator strengths, $f$, are calculated from Eq. 12 of I. Plots of $f_{calc}$ vs. $\delta x$ are given in Fig. 6. It may be noted that $f_{calc}$ values for the transitions to $B^-_{3u}$, $B_{2u}$ and $B^+_{3u}$ states in naphthalene are, respectively, 0, 0.52 and 2.14, corresponding $f_{obs}$ values being 0.002, 0.11 and 1.70[3,7].

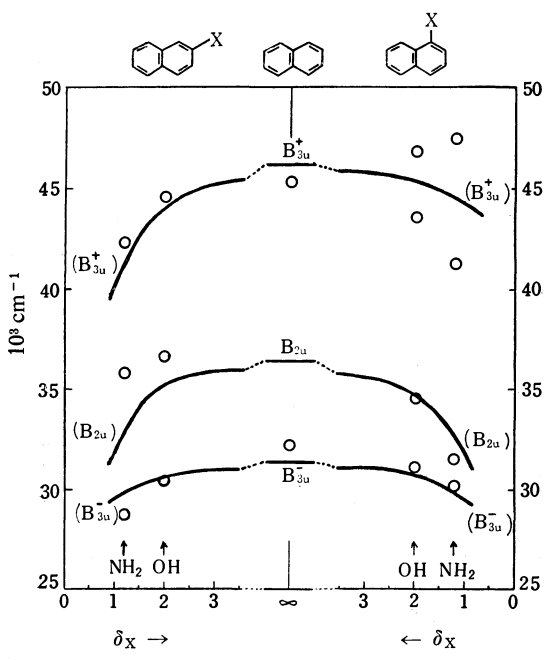



Fig. 5. Relation of the energies of the excited states to $\delta_X$. The observed energies are represented by circles.

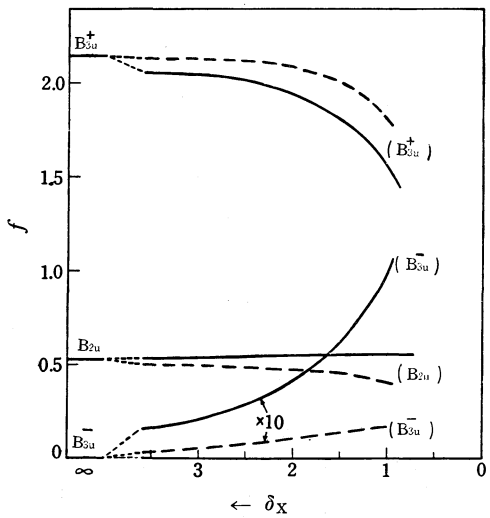



Fig. 6. Relation of $f$ values to $\delta_X$.
——, $\alpha$-derivative; ----, $\beta$-derivative.

**Summary of Calculation.**—As the most appropriate values for the Coulomb integral parameters of the oxygen and nitrogen atoms,

7) H. B. Klevens and J. R. Platt, *J. Chem. Phys.*, **17**, 470 (1949).

TABLE II. EXCITED STATES OF NAPHTHOLS AND NAPHTHYLAMINES

| | State | Wave function | Excitation energy ($cm^{-1}$) | | $f$ | | $\Delta q_X$ |
|---|---|---|---|---|---|---|---|
| | | | calc. | cbs. | calc. | obs.* | |
| | ($B_{3u}^-$) | $0.591V_{46}-0.807V_{57}$ | 30800 | 31100 | 0.042 | 0.016 | −0.038 |
| α-Naphthol | ($B_{2u}$) | $V_{56}$ | 34800 | 34570 | 0.55 | 0.102 | −0.049 |
| | ($B_{3u}^+$) | $0.807V_{46}+0.591V_{57}$ | 45400 | {43570<br>46820 | 1.94 | {0.328<br>0.892 | −0.010 |
| | ($B_{3u}^-$) | $0.766V_{46}-0.643V_{57}$ | 30600 | 30470 | 0.011 | 0.0211 | −0.056 |
| β-Naphthol | ($B_{2u}$) | $V_{56}$ | 35200 | 36600 | 0.48 | 0.0811 | −0.043 |
| | ($B_{3u}^+$) | $0.643V_{46}+0.766V_{57}$ | 44100 | 44580 | 2.08 | 1.06 | −0.049 |
| | ($B_{3u}^-$) | $0.502V_{46}-0.865V_{57}$ | 29900 | 30100 | 0.082 | 0.13 | −0.13 |
| α-Naphthyl-amine | ($B_{2u}$) | $V_{56}$ | 32700 | 31500 | 0.55 | | −0.14 |
| | ($B_{3u}^+$) | $0.865V_{46}+0.502V_{57}$ | 44500 | {41250<br>47440 | 1.68 | {0.34<br>0.82 | −0.011 |
| | ($B_{3u}^-$) | $0.778V_{46}-0.628V_{57}$ | 29900 | 28740 | 0.016 | 0.033 | −0.13 |
| β-Naphthyl-amine | ($B_{2u}$) | $V_{56}$ | 33000 | 35790 | 0.43 | 0.10 | −0.16 |
| | ($B_{3u}^+$) | $0.628V_{46}+0.778V_{57}$ | 41300 | 42340 | 1.91 | 0.86 | −0.14 |

* For the details of the determination of the observed $f$ values see Ref. 8.

$\delta_O=2.0$ and $\delta_N=1.2$ were obtained in I. Application of these values to the case of the naphthalene derivatives leads to the results summarized in Table II, where the changes of the $\pi$-electron density, $\Delta q_X$, accompanying the electronic transitions are also given. The observed excitation energies and oscillator strengths are cited in the table.

In connection with the $\Delta q_X$ values it is instructive to know the charge distribution in the ground state. Thus, from the ground-state MO's corresponding to $\delta_X=1.2$, quantities related to the charge distribution in the ground state were derived for naphthylamines. The results are collected in the molecular diagrams of Fig. 7, in which the analogous diagram for aniline is shown for the sake of comparison.

## Discussion

Inspection of Fig. 4 reveals several features of the MO's of the naphthalene derivatives. In the α-derivative, orbital energies $e_4$ and $e_7$ are completely identical with $e_4^0$ and $e_7^0$, respectively, regardless of the value of $\delta_X$; $e_3$ is raised with decreasing magnitude of $\delta_X$, and consequently the sequence of the heights of $e_3$ and $e_4$ is reversed at $\delta_X=1$; $e_5$ is most affected by the α-substitution. In the β-derivative $e_4$ is strongly influenced by the substitution, while $e_3$ remains almost unaltered. When $\delta x$ is large $e_5$ is little changed upon the β-substitution, but it is considerably affected by a substituent with a small magnitude of $\delta_X$, i.e., by a strongly conjugating substituent. The behaviors of the orbital energies in the α- and β-derivatives may, at least in part, be understood in terms of the coefficients of the atomic orbitals in the MO's of the parent hydrocarbon (cf. Eqs. 1a—1d).

Regarding the wave functions of the excited states, it is to be noted that the degrees of configuration mixing in the wave functions of the ($B_{3u}^{\pm}$) states are appreciably changed by the substitutions.

Before proceeding to a discussion of the excitation energies, mention should be made of the spectra shown in Fig. 1. In the spectrum of α-naphthol, several minor peaks are present on the lower frequency side of the 34570 $cm^{-1}$ band. In the light of the spectrum of naphthalene it is reasonable to regard these peaks as showing a fine structure of a definite electronic band which corresponds to the lowest frequency band of the parent hydrocarbon. No analogous band is found, at first sight, in the α-naphthylamine spectrum. However, the 31500 $cm^{-1}$ band of α-naphthylamine exhibits relatively high extinction at the shoulder of 30100 $cm^{-1}$, as compared with the corresponding bands of α-naphthol and naphthalene. In view of this fact, the present authors tentatively assumed that the band in question is hidden under the more intense band of 31500

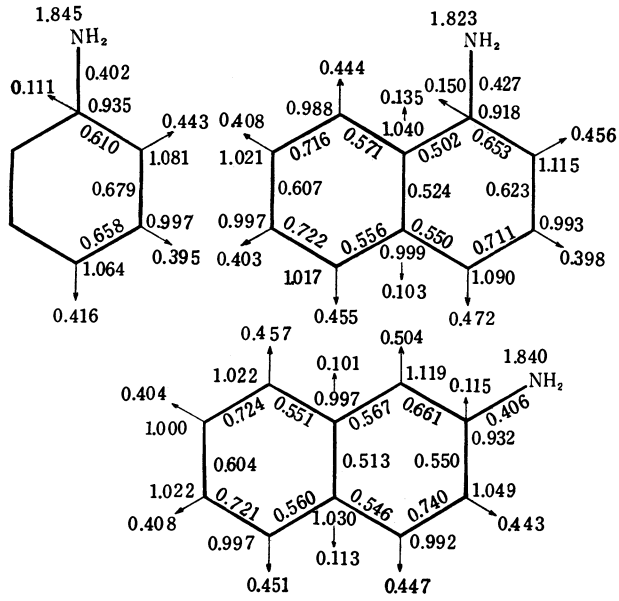



Fig. 7. Molecular diagrams for aniline, $\alpha$-naphthylamine and $\beta$-naphthylamine. The $\pi$-electron density, $\pi$-bond order and free valence are shown in the usual manner for each molecule.

$cm^{-1}$ in the neighborhood of the said shoulder.

$\alpha$-Naphthol has two absorption bands ($\nu_{max}$ =43570 and 46820 $cm^{-1}$) in the higher frequency region, which are not fully separated from each other. It has been observed that, when a hydrogen bond is formed between $\alpha$-naphthol and dioxane, these bands exhibit quite different behaviors: that is, the lower frequency band is displaced to the red and the other to the blue[8]. This observation conclusively indicates that the bands under consideration are due to two distinct electronic transitions.

The calculated excitation energies for the ($B_{3u}^-$) and ($B_{2u}$) states of the $\alpha$-derivatives are in good accord with the observed. A difficulty arises in the fact that two levels are observed near the calculated ($B_{3u}^+$) level of the $\alpha$-derivatives. A tentative explanation for this will be given below.

According to Pariser's calculation for naphthalene, there exists a $B_{1g}^+$ state slightly below the $B_{3u}^+$ state[4]. A plus state in general favors the transition from the ground state[4], but in the case of the $B_{1g}^+$ state the transition is forbidden, because $A_g \rightarrow B_{1g}$ is not allowed by the selection rule. To a first approximation, the $B_{1g}^+$ state is represented by $(1/\sqrt{2})(V_{36}^0 + V_{58}^0)$. As has already been shown, $\phi_3^0$ and $\phi_5^0$ are profoundly influenced by the $\alpha$-substitution, so that the $B_{1g}^+$ state will be subjected to a considerable distortion. It is therefore probable that the $B_{1g}^+$ state comes to be allowed in the $\alpha$-derivatives, and that a fairly strong interaction occurs between the ($B_{3u}^+$) and ($B_{1g}^+$) states to give two mixed states which can be assigned to the observed levels mentioned above. It seems reasonable to conclude that, of the two observed bands in question, the one of higher intensity, i.e., that of higher frequency, primarily corresponds to the ($B_{3u}^+$) state and the other to the ($B_{1g}^+$) state, for the transition to the $B_{3u}^+$ state is allowed even in the parent hydrocarbon.

Next, discussion will be turned to the excitation energies in the $\beta$-derivatives. There is a discrepancy between the calculated and observed energies of the ($B_{2u}$) state. It is generally accepted that the $p$ band of naphthalene, which arises from the $A_g \rightarrow B_{2u}$ transition, is makedly shifted to the red by $\alpha$-substitution, whereas it exhibits almost no shifts due to $\beta$-substitution[1]. The $B_{2u}$ state of naphthalene is approximately represented by $V_{56}^0$. Also, for the coefficients of the atomic orbitals in $\phi_5^0$ and $\phi_6^0$, the relation $b^2 \gg c^2$ is seen to hold. Accordingly, so far as the behaviors of the $p$ band are treated from the viewpoint of the perturbation theory, the calculation will lead to a result which is compatible with the observation. This is substantiated by the

8) H. Baba and S. Suzuki, to be published in *J. Chem. Phys.*

results of Peters' perturbation treatment[1]. However, quite a different situation may be produced for strongly conjugating substituents, to which the perturbation theory fails to apply. In fact, in cases $\delta_X < 2$ the orbital energy $e_5$ is noticeably raised even in the $\beta$-derivatives, and hence the calculated excitation energy for $\phi_5 \rightarrow \phi_6$ becomes considerably smaller than the observed. This discrepancy is the most serious is the most serious difficulty involved in the present calculation.

From the spectra of Figs. 1 and 2, the effect of substitutions on the band intensities may be summarized as follows: the intensity of the transitions to the ($B_{3u}^-$) state is greatly enhanced, while that of the transition to the ($B_{3u}^+$) state is lowered; the transition to the ($B_{2u}$) state is subject to only a slight change in its intensity. These remarks are applicable to each of the $\alpha$- and $\beta$-derivatives. It may be said that the $f_{calc}$ values account, at least qualitatively, for the observed intensity variations due to the substitutions.

One may predict from the calculation of $\Delta q_X$ that all transitions in both the $\alpha$- and $\beta$-derivatives are accompanied by an increase of the positive charge at the substituent, and that the increment of the charge is extremely small as regards the transition to the ($B_{3u}^+$) state of the $\alpha$-derivatives. This prediction has been verified in its essential points by experimental studies of the hydrogen bonding effect on the spectra of naphthols and naphthylamines[8].

By comparing the diagrams of Fig. 7, which are based on the molecular orbital method, with those obtained by the valence bond method[9,10], it is found that the two theoretical methods lead to essentially the same results in respect of both the charge distributions and the bond orders for aniline and the amines. It may be worthy of note that the $\pi$-electron densities at the nitrogen atoms are in the order

aniline> $\beta$-naphthylamine> $\alpha$-naphthylamine

The present calculation is based on the assumption of the transferability of the parameters $\delta_N$ and $\delta_O$ from the benzene derivatives to the naphthalene derivatives. This assumption is seen to be reasonable on the inspection of Table II and Fig. 5.

## Summary

The ultraviolet absorption spectra of $\alpha$-, $\beta$-naphthols and $\alpha$-, $\beta$-naphthylamines have been newly measured down to 200 m$\mu$. On the basis of a calculation which was carried out in the same manner as in the preceding paper, the effect of substitutions at $\alpha$- and $\beta$-positions upon the spectrum of napthalene has been explained and the assignment of the observed absorption bands has been made. It is suggested that, upon substitution at the $\alpha$-position, the $A_u \rightarrow B_{3u}^+$ band of naphthalene splits into two electronic bands because of the interaction of the $B_{3u}^+$ state with a $B_{1g}^+$ state. Molecular diagrams are given for naphthylamines and for aniline.

*Research Institute of Applied Electricity*
*Hokkaido University, Sapporo*

9) B. Pullman, *Bull. soc. chim. France*, **1948**, 533.
10) R. Daudel and M. Martin, ibid., **1949**, 83.

# *Thermal Decomposition of Potassium Chlorate*

By Shōtarō Tobisawa

(Received June 22, 1960)

The thermal decomposition of potassium chlorate has been investigated mostly by measuring the volume of oxygen gas evolved[1-4]. The present author has studied this reaction from the viewpoint of the loss in weight ($x$), due to oxygen gas released in the progress of the decomposition. The measurement of loss in weight was made at definite intervals of 45 sec. with a thermal balance of automatic recording type. Plots of $dx/dt$ against time ($t$) were obtained accurately.

## Experimental

Commercial guaranteed potassium chlorate was recrystallized four times from water. A single crystal and a polycrystal were selected from the recrystallized samples under a microscope. A powdered sample was obtained by carefully squeezing the recrystallized sample in an agate mortar with a pestle. The detail of the thermal balance was already described in a previous report[5]. This balance was modulated to be able to indicate distinct differences of 0.022 mg. on a recording chart.

## Results

When the temperature of the powdered sample was raised at constant rate, 250°C per hour, it decomposed at 500°C, evolving oxygen gas. Although the measurements were made for the powdered samples of different weights and also at different rates of heating, these samples decomposed at the same temperature of 500°C which was higher than the decomposition temperature obtained by Vitoria[6]. Since the melting point of potassium chlorate has been found to be 352[7] or 356°C[6], it is reasonable to consider that the thermal decomposition of potassium chlorate takes place in liquid state.

The kinetic measurements were made at several temperatures above 500°C. The reactant sample could reach these constant temperatures within five minutes. Fig. 1 shows the plots

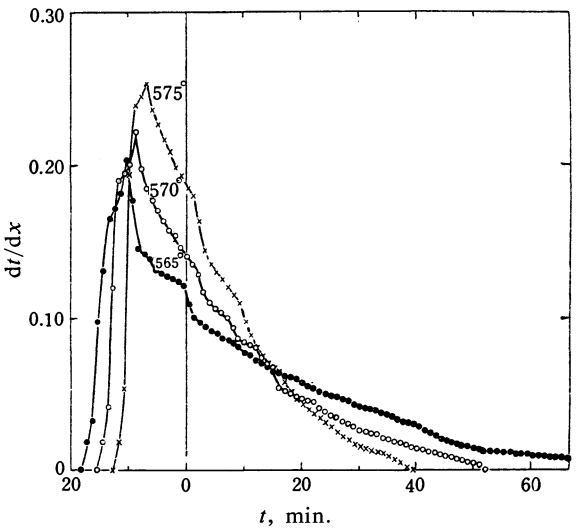



Fig. 1. Plots of $dx/dt$ against time for the powdered samples (12.0 mg. in weight).

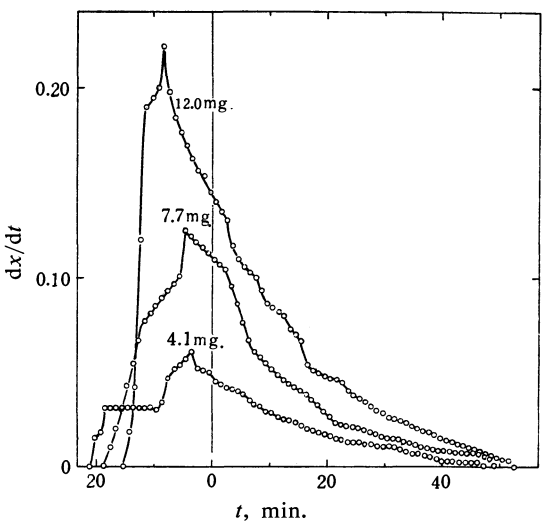



Fig. 2. Plots of $dx/dt$ against time for the powdered samples at 570°C.

of $dx/dt$ against $t$ for the powdered samples of 12.0 mg. at 565, 570 and 575°C, respectively. The time of zero in Fig. 1 was set at the point where half of the weight of the sample was decomposed. In the figure, the acceleratory period is extremly short in comparison with the decay period. From the curves of $dx/dt$

1) J. Scobai, *Z. physik. Chem.*, **44**, 319 (1903).
2) W. Farmer and J. B. Firth, *J. Chem. Soc.*, **125**, 82 (1924).
3) C. E. Otto and H. S. Fry, *J. Am. Chem. Soc.*, **46**, 272 (1924).
4) A. Glasner and L. Weidenfeld, ibid., **74**, 2464 (1952).
5) S. Tobisawa, This Bulletin, **32**, 1173 (1959).
6) A. P. Vitoria, *Anales soc. españ. fis. quim.*, **27**, 787 (1929); *Chem. Abstr.*, **24**, 773 (1930).
7) S. Tobisawa, to be published.

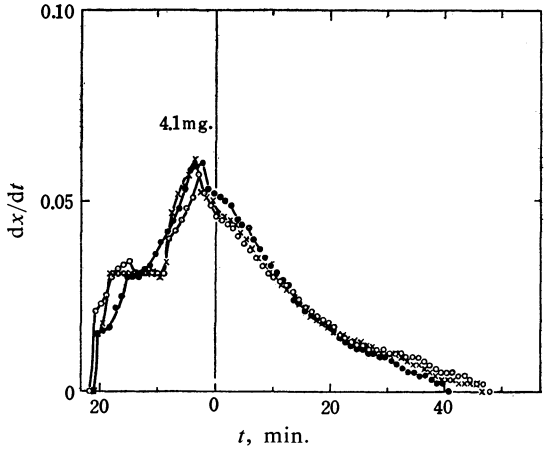



Fig. 3. Plots of $dx/dt$ against time at 570°C.
—○—: Single crystal,
—●—: Polycrystal,
—×—: Powdered sample.

against $t$ at the same temperature in Fig. 2, it is seen that, as the weight of the sample decreases, the acceleratory period becomes long and the shape of the curve of $dx/dt$ against $t$ in the acceleratory period becomes complicated. Fig. 3 shows the plots of $dx/dt$ against $t$ for the single crystal, the polycrystal and the powdered sample, all in the same weight of 4.1 mg. at the same temperature, 570°C. In the figure, the curves of $dx/dt$ against $t$ for the three samples show different shapes in the acceleratory period, while the curves in the decay period show analogous shapes. In each measurement, total losses in weight, due to the exhausted decomposition, agreed with the amount of oxygen calculated from the equation, $2KClO_3=2KCl+3O_2$, within the error of about one per cent.

## Discussion

As shown in Figs. 1, 2 and 3, each curve of $dx/dt$ against $t$ shows a complicated shape, and such complication tends to disappear as the decomposition progresses. It has been reported by Otto et al.[3] that the reaction, $2KClO_3 \rightarrow 2KCl+3O_2$, is a monomolecular reaction. Glasner et al.[4] have also stated that the decomposition at high temperature is of the first order. However, as is evident from Figs 1, 2 and 3, the thermal decomposition of potassium chlorate is so complicated that a rate-equation can not be determined.

In a microscopic study of the sample undergoing the thermal decomposition, zig-zag bubbles of oxygen gas were observed in the liquid. Moreover, by visual observation of a reaction vessel at the end of the experiment, specks which were considered to be owing to the splashing of the liquid, were recognized along the wall. The bubbling of gas causes the splashing of the liquid. On the liquid-phase decomposition of potassium perchlorate, Bircumshaw et al.[8] have stated that the composition of the liquid which consists of perchlorate, chlorate and chloride, will not be constant on account of the spreading of the liquid along the tube, owing to bubbling, and thus variations in the rate of evolution of gas may be expected, depending on how much splashing takes place. On the thermal decomposition of potassium chlorate, it has been known that the reaction system consists of chlorate, chlorite, perchlorate and chloride, and that the chlorate, the chlorite and the perchlorate convert into chloride with the evolution of oxygen gas[9]. The bubbling and splashing under such a complicated condition will take place very irregularly. The complication of the curves of $dx/dt$ against $t$ may, therefore, be associated with the irregularities of the bubbling and splashing. As the decomposition progresses, the bubbling and splashing will become difficult to take place on account of the accumulation of chloride in the liquid. Consequently, the complication of the curves of $dx/dt$ against $t$ may be expected to disappear.

## Summary

The curves of $dx/dt$ against $t$ were obtained with accuracy; in consequence, the complication of the curves appeared, and the complication may be associated with the irregularities of the bubbling and splashing.

The author is particularly indebted to Professor Y. Nomura for his suggestion and encouragement throughout this work. Thanks are also due to Mr. S. Shimoyama for his kind assistance.

*Department of Chemistry*
*Defense Academy*
*Yokosuka*

8) L. L. Bircumshaw and T. R. Phillips, *J. Chem. Soc.*, 1953, 703.
9) H. Osada, *J. Ind. Explosives Soc. Japan*, 15, 324 (1954).

# *Infrared Spectra of Troponoid Compounds. II. Absorption Band of O–H Stretching Vibration in Some Tropolones**

By Yusaku IKEGAMI

(Received February 10, 1960)

In the previous report[1], it was shown that the absorption bands assignable to O–H stretching vibration in tropolone (I) appear at around 3210 $cm^{-1}$ in solid and around 3140 $cm^{-1}$ in solution or gaseous state, indicating the characteristic properties in absorbing at a lower wave number in dilute solution or gaseous state than in solid. This fact has been explained[1-3] on the basis of the intermolecular or intramolecular hydrogen bonding in tropolone, but the nature of these bands was not studied in detail. In this paper, the examinations were made on O–H stretching absorption bands of tropolone, by using a calcium fluoride prism, to see how the absorption bands changed with different concentrations and states. The same examinations were also made on 4-isopropyltropolone (hinokitiol) (II) and 3-bromotropolone (III).

## Experimental

Infrared absorption spectra were measured with a Perkin-Elmer model 21 infrared spectrophotometer with a calcium fluoride prism. The solid spectra were obtained by potassium bromide disk or sandwich method, and a cell of 0.109, 0.508, 11.10 or 50.30 mm. thick with potassium chloride windows was used to obtain solution spectra.

## Results and Discussion

Fig. 1 shows the infrared spectra of tropolone in the region of 3600~2600 $cm^{-1}$, measured for solid, liquid and solution in carbon tetrachloride, and shows that there are more absorption bands in this region than had been expected. It also reveals the change in the spectrum accompanying variation of the concentration in solution and of the phase. The two bands in the ranges of 3051~3049 and 3020~3003 $cm^{-1}$ in these spectra correspond to the C–H stretching vibration in the seven-membered ring, which appear with comparative regularity in many of the troponoids[4]. Absorption bands other than these two must be those of O–H stretching vibration in respective states since corresponding bands do not appear in 2-deuteroxytropone[5] and metal tropolonate[4].

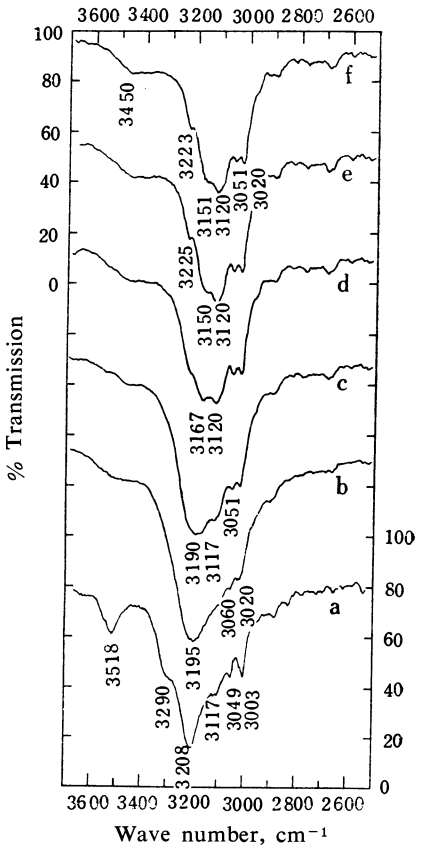



Fig. 1. Infrared spectra of tropolone in the states of solid, liquid and carbon tetrachloride solution (3600~2600 $cm^{-1}$ range): a; solid (crystalline film), b; liquid, c; ca. 1.5 mol./l. in $CCl_4$ (0.109 mm. thickness), d; 0.29 (0.508), e; 0.014 (11.10), f; 0.0029 (50.30).

From the spectra shown in Fig. 1, the following characteristics can be pointed out. a) When measured in the most dilute solution shown in Fig. 1 f, there is no sharp absorption

* A part of this work was presented at the 10th Annual Meeting of the Chemical Society of Japan, April 4, 1957.

1) Part I: S. Kinumaki, K. Aida and Y. Ikegami, *Sci. Repts. Research Inst. Tohoku Univ., Ser.* A, **8**, 263 (1956).

2) K. Kuratani, M. Tsuboi and T. Shimanouchi, This Bulletin, **25**, 250 (1952).

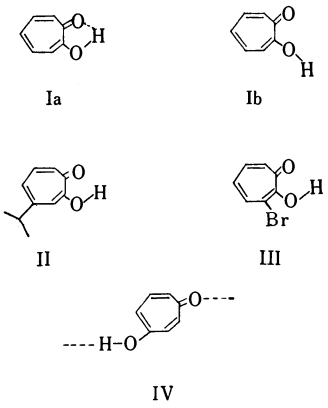
3) H. P. Koch, *J. Chem. Soc.*, **1951**, 512.

4) Y. Ikegami, unpublished data.

5) Y. Ikegami, This Bulletin, **34**, 94 (1961).

and there are bands at 3151 and 3223 $cm^{-1}$ besides the strongest one at 3120 $cm^{-1}$ and a broad band at 3500~3300 $cm^{-1}$. b) The O-H stretching absorption is dependent of the concentration in solution, although it had been reported that the spectrum is independent[2], and the bands at 3151 and 3223 $cm^{-1}$ increase their intensity gradually with increasing concentration, which finally merge into the comparatively broad absorption at 3195 $cm^{-1}$ in liquid. c) The spectrum in solid state exhibits shoulders at 3117 and 3290 $cm^{-1}$, besides the strongest band at 3208 $cm^{-1}$, and a distinct band at 3518 $cm^{-1}$. The spectrum obtained in gaseous state[1] is the same as that of Fig. 1 f.

Such characters of the O-H stretching absorption band in dilute solution are not essentially different from those of chelated hydroxyquinones[6] and enolized $\beta$-diketones[7] possessing a conjugated chelate system, and can be taken as the characteristics indicating tropolone structure. It is seen from Fig. 1 that the absorption bands shift to the higher wave number side as the concentration increases and as the compound transits liquid or solid. On the other hand, the absorption band at 1618 $cm^{-1}$ in solution appears at a wave number 5 $cm^{-1}$ higher than that in solid[1]. This is contrary to the direction of the shift of $\nu_{C=O}$ anticipated from that of $\nu_{O-H}$ in the hydrogen bonding of -O-H···O=C< type, and then the shift of O-H stretching absorption band can not be explained merely by the strength of hydrogen bonding in this type. Considering the fact that the direction of the shift of C=O stretching absorption band in tropolone according to changes in the states agrees with that in tropone[1], it is assumed that the cycloheptatrienone part in tropolones interacts in a manner similar to that in the case of tropone[8] and the intramolecular




hydrogen bonding is weakend by this interaction. Kuratani et al.[2] assumed a dimer form for tropolone in the solid state. However, a wave number 3208 $cm^{-1}$ in tropolone is approximately 700 $cm^{-1}$ higher than that in

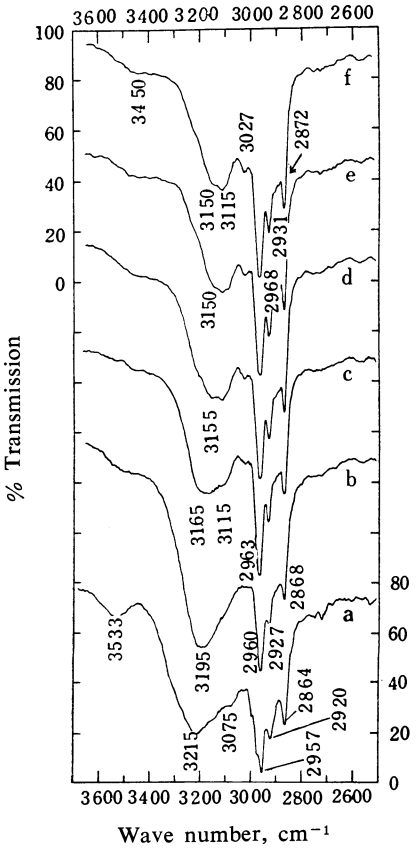



Fig. 2. Infrared spectra of 4-isopropyltropolone in the states of solid, liquid and carbon tetrachloride solution (3600~2600 $cm^{-1}$ range): a; solid (crystalline film), b; liquid, c; ca. 1.2 mol./l. in $CCl_4$ (0.109 mm. thickness), d; 0.29 (0.508), e; 0.014 (11.10), f; 0.0029 (50.30).

6) D. Hadzi and N. Sheppard, *Trans. Faraday Soc.*, **50**, 911 (1954).

7) S. Bratoz, D. Hadzi and G. Rossmy, ibid., **52**, 464 (1956).

8) Unpublished data. Infrared spectra of tropone in the region of 1700~1500 $cm^{-1}$ were measured in the states of vapor, liquid and solutions in various solvents. Two strong absorption bands in this region indicated the following wave-numbers, e. g.

| | | |
|---|---|---|
| vapor | 1651 $cm^{-1}$ | 1613 $cm^{-1}$ |
| in *n*-heptane | 1645 $cm^{-1}$ | 1602 $cm^{-1}$ |
| in acetonitril | 1634 $cm^{-1}$ | 1585 $cm^{-1}$ |
| in ethanol | 1633 $cm^{-1}$ | 1574 $cm^{-1}$ |
| pure liquid | 1634 $cm^{-1}$ | 1580 $cm^{-1}$. |

Also the shape of their bands in liquid tropone is similar to that in such a solvent as acetonitril, differing from it in the vapor state (cf. Ref. 1). From these facts, it is assumed that the tropone in liquid state associates by its polar character of B type as also shown in its large dipole moment (4.17D) (cf. Y. Kurita, S. Seto, T. Nozoe and M. Kubo, This Bulletin, **26**, 272 (1953)).



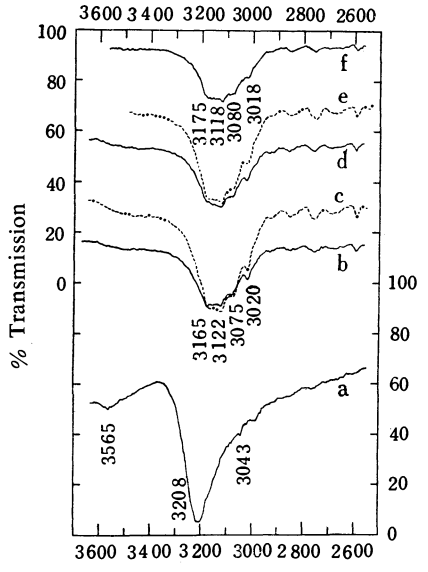



Fig. 3. Infrared spectra of 3-bromotropolone in the states of solid and carbon tetrachloride solution (3600~2600 $cm^{-1}$ range): a; solid (KBr disk), b; 0.1 mol./l. in $CCl_4$ (0.508 mm. thickness), c; 0.01 (11.10), d; 0.005 (11.10), e; 0.002 (50.30), f; 0.001 (50.30).

4-hydroxytropone[9,10] (IV) ($\nu_{O-H}$; 2920 (w.) and 2530 $cm^{-1}$ (v. s., broad)) and 3-hydroxytropone[11], which form a strong intermolecular hydrogen bond in solid and show the higher melting points and less volatilities than those of tropolone. Therefore, even though solid tropolone forms a dimer, it is not easy to explain why the hydrogen bonding in the dimer form is weaker than that in hydroxytropones. In addition, a distinct band at 3518 $cm^{-1}$ in Fig. 1a indicates the existence of unchelated O-H group as Ib type.

The absorption spectra of 4-isopropyltropolone (II) and 3-bromotropolone (III) are respectively indicated in Figs. 2 and 3. The spectra in Fig. 2 are essentially the same, with the exception of the bands due to isopropyl group, as the spectra in Fig. 1. 3-Bromotropolone is sparingly soluble in carbon tetrachloride. Its spectra in higher concentrations have not been measured, but the mode of change in the form of absorption can be learned similarly. It is therefore possible to discuss the absorption of these compounds in the same manner as in the case of tropolone.

The characters of O-H absorption bands above-mentioned will generally be observed in compounds possessing the skeletal structure of tropolone[12], but those forming a strong intermolecular hydrogen bonding such as 4- and 5-hydroxytropolones[13] and those showing extremely low intensity such as 3,7-dibromo- and 3,5,7-tribromo-tropolones[14] do not show the typical O-H absorption band of tropolones.

## Summary

Infrared spectra of tropolone, 4-isopropyltropolone and 3-bromotropolone in the solid, liquid and solution in carbon tetrachloride were measured with a calcium fluoride prism in the region of 3600~2600 $cm^{-1}$. The absorptions of O-H stretching vibration in these compounds in dilute solution are strongest at around 3120 $cm^{-1}$ with numerous branches, and these bands shift gradually to the higher wave number side with 100~88 $cm^{-1}$, as the concentration increases and the compound transits to the liquid or solid state. This character was explained by the assumption that the tropolone skeleton has a stable chelate system and that the intermolecular action increases with the increase of concentration. In the solid state, a distinct band corresponding to the O-H group of Ib type was also observed at around 3540 $cm^{-1}$.

The author deserves to express his deep gratitude to Professor Susumu Kinumaki and Assistant Professor Koyo Aida for their unfailing guidance during the course of this work, and to Professor Tetsuo Nozoe and members of his laboratory for the donation of valuable samples.

*The Chemical Research Institute of Non-Aqueous Solutions*
*Tohoku University*
*Katahira-cho, Sendai*

9) T. Nozoe, T. Mukai, Y. Ikegami and T. Toda, *Chem. & Ind.*, **1955**, 66; R. S. Coffey and A. W. Johnson, *J. Chem. Soc.*, **1958**, 1741.
10) Y. Ikegami, *J. Japan. Chem.* (*Kagaku-no-Ryoiki*), Extra No. 38, 46 (1959).
11) R. B. Johns, A. W. Johnson and M. Tisler, *J. Chem. Soc.*, **1954**, 4605.
12) Unpublished data. According to the results of spectral measurement made on about 40 kinds of tropolones, the O-H absorption bands appear in the region of 3260~3160 $cm^{-1}$ (s.) in the solid state, and in the region of 3225~3095 $cm^{-1}$ (m. or w.) in solution. Further, a very weak band generally appears in the region of 3640~3500 $cm^{-1}$ in the solid.
13) Y. Kitahara, *Sci. Repts. Tohoku Univ., Ser.* I, **39**, 258 (1956).
14) K. Ogura and Y. Ikegami, *Bull. Chem. Research Inst. Non-Aqueous Solutions, Tohoku Univ.*, **9**, 23 (1959); Ref. 10, p. 60.

# *Infrared Spectra of Troponoid Compounds. III. Tropolone and 2-Deuteroxytropone**

By Yusaku IKEGAMI

(Received February 10, 1960)

Absorption of O–H stretching vibration of tropolone (I) in solid, liquid and carbon tetrachloride solution was described in the preceding paper[1]. In the present paper the spectra of tropolone, chiefly in finger-print region, will be described. Infrared spectra of tropolone have been reported earlier by Koch[2], Kuratani[3], Kinumaki[4] and others, and its Raman spectrum by Imanishi and Ito[5], but only a few vibrations, such as those of C=O, C=C and C–H out-of-plane, have been assigned in the finger-print region. In order to clarify the absorption bands originating in C–O–H group in the spectrum of tropolone, an infrared spectrum of 2-deuteroxytropone (II) was measured and compared with that of I. On heating I with heavy water, a compound III, in which the deuterium atom had entered the seven-membered ring, was obtained and brief mention will be made of this compound. Further, some considerations were given to the spectrum of I in the finger-print region.

## Results and Discussion

**Comparison of the Infrared Spectra of 2-Deuteroxytropone and Tropolone.**—2-Deuteroxytropone (II) was obtained by recrystallization of tropolone (I) from heavy water. The infrared spectra of I and II in carbon tetrachloride and carbon disulfide solutions are shown in Fig. 1, a and b. The presence of an absorption due to hydroxyl compound can not be denied in the spectrum of Fig. 1b but most of it is in the spectrum of II.

In the spectral curve of Fig. 1b, the O–H stretching absorption around 3150 $cm^{-1}$ in 1a has shown drastic decrease of its intensity and a new absorption originating in the O–D bond has appeared at around 2400 $cm^{-1}$. This band has two peaks at 2400 and 2342 $cm^{-1}$ and the shape of this band is similar to that of tropolone in which the O–H stretching absorption is not sharp even in the state of dilute solution. The ratio of the wave numbers of $\nu_{O-H}$ and $\nu_{O-D}$ is indicated in Table I together with values obtained in 3-bromo- and 3-methyl-tropolones. These values are in good agreement with the values (1.33~1.34) obtained by Keussler et al.[6] on deuteration of phenols

TABLE I. $\nu_{O-H}/\nu_{O-D}$ VALUES FOR SOME TROPOLONES

| Compounds | | $\nu_{O-H}$ $cm^{-1}$ | $\nu_{O-D}$ $cm^{-1}$ | $\nu_{O-H}/\nu_{O-D}$ |
|---|---|---|---|---|
| Tropolne | solid | 3208 | 2385 | 1.345 |
| | in $CCl_4$ | 3167 | 2400 | 1.320 |
| | | 3120 | 2342 | 1.332 |
| 3-Bromotropolone | solid | 3208 | 2390 | 1.342 |
| 3-Methyltropolone | solid | 3202 | 2394 | 1.338 |

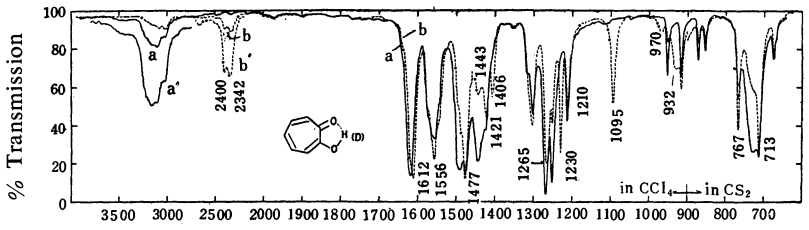



Fig. 1. Infrared spectra of tropolone (a: 3%, a': 10%) and 2-deuteroxytropone (b: 3%, b': 9%) in the solution of carbon tetrachloride (4000~900 $cm^{-1}$ range) and of carbon disulfide (900~650 $cm^{-1}$) (0.12 mm. thickness).

* A part of this work was presented at the 10th Annual Meeting of the Chemical Society of Japan, April 4, 1957.

1) Part II: Y. Ikegami, This Bulletin, **34**, 91 (1961).
2) H. P. Koch, *J. Chem. Soc.*, **1951**, 512.
3) K. Kuratani, M. Tsuboi and T. Shimanouchi, This Bulletin, **25**, 250 (1952).
4) Part I: S. Kinumaki, K. Aida and Y. Ikegami, *Sci. Repts. Research Inst. Tohoku Univ., Ser.* A, **8**, 263 (1956).
5) S. Imanishi and M. Ito, This Bulletin, **28**, 75 (1955); **29**, 632 (1956).
6) V. von Keussler und G. Rossmy, *Z. Elektrochem.*, **60**, 136 (1956).

possessing a conjugated chelate structure as tropolone.

In the region of 1700~650 $cm^{-1}$ : — In this region, the absorption band at 1618 $cm^{-1}$ in I shifts to the lower wave number side by 6 $cm^{-1}$ in II, and a certain amount of difference is observed between I and II below 1500 $cm^{-1}$. New bands have appeared at 1406, 1230, 1095, 970 and 932 $cm^{-1}$ in the spectrum of Fig. 1b. On the other hand, the absorption bands at 1490, 1444, 1251, 953 and 726 $cm^{-1}$ in I do not appear in II, and the intensity of the absorption at 1267 $cm^{-1}$ is weaker. These bands in Fig. 1a are considered to have some relation, either directly or comparatively closely, to the vibration of the C–O–H group.

Identification of absorption bands originating in the C–O–H group by conversion of hydroxyl to deuteroxyl compound has been reported already by Hadzi, Mecke and others in carboxylic acids[7], chelated hydroxyquinones[8], enolized β-diketones[9,10] and phenols[11]. These results point out that the distribution of absorption bands which shift by deuteration and their interpretation vary according to the shape of a molecule, even in the same C–O–H group. In the case of tropolone, a storng absorption band at 1490 $cm^{-1}$ disappeared and a new band appeared at 1095 $cm^{-1}$ (1086 $cm^{-1}$ in solid) by deuteration, and these wave numbers are close to those which were assigned to the O–H and O–D deformation vibrations in enolized β-diketones (around 1435 and 1090 $cm^{-1}$ respectively)[9]. Moreover, the other band which can be assigned to the O–D deformation vibration appeared at

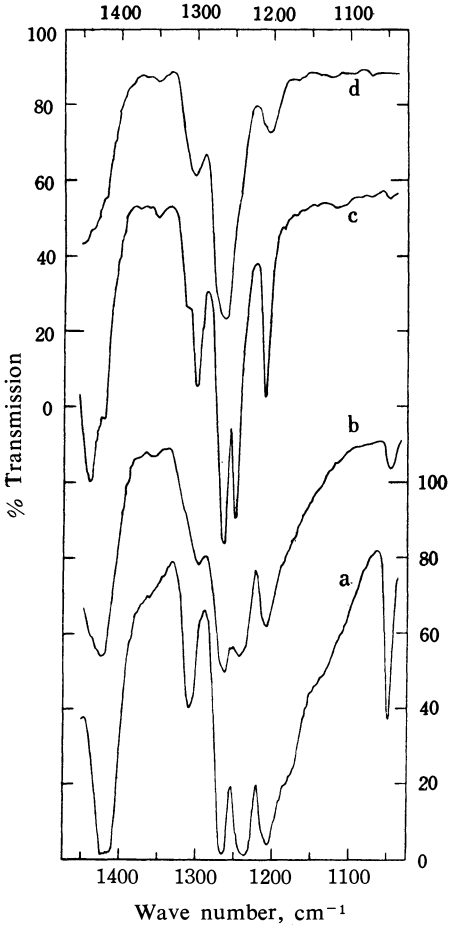



Fig. 2. Infrared spectra of tropolone in the states of solid (a), liquid (b), $CCl_4$ solution (c) and vapor (d) (1450~1050 $cm^{-1}$ range).

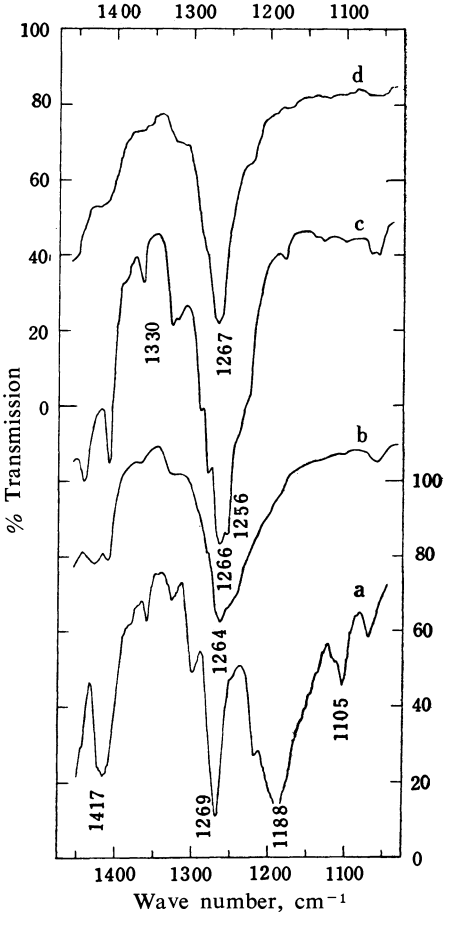
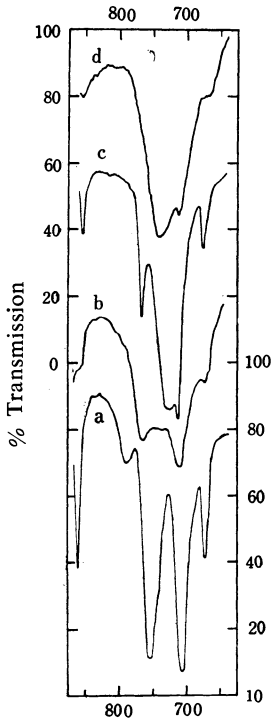



Fig. 3. Infrared spectra of 4-isopropyltropolone in the states of solid (a), liquid (b), $CCl_4$ solution (c) and vapor (d) (1450~1050 $cm^{-1}$ range).

7) D. Hadzi and N. Sheppard, *Proc. Roy. Soc.*, **216A**, 247 (1953).
8) Idem., *Trans. Faraday Soc.*, **50**, 911 (1954).
9) S. Bratoz, D. Hadzi and G. Rossmy, ibid., **52**, 464 (1956).
10) R. Mecke and E. Funck, *Z. Elektrochem.*, **60**, 1124 (1956).
11) R. Mecke and G. Rossmy, ibid., **59**, 866 (1955).

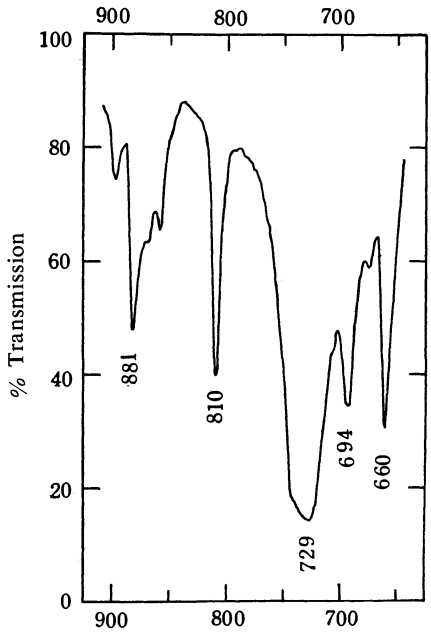
932 $cm^{-1}$ (896 $cm^{-1}$ in solid) by deuteration, while the band at 1267 $cm^{-1}$ weakened. These wave numbers are close to those of chelated hydroxyanthraquinones, in which two bands characteristic to the deuteroxyl group had been recognized at around 980 and 930 $cm^{-1}$ [8]. Anyway, these facts indicate that the bands at 1490 and 1267 $cm^{-1}$ in tropolone originate in the C–O–H group, although the definite assignments of these bands are indistinct.

It is clear that the bands at 1490 and 1267 $cm^{-1}$ in Fig. 1a are related to the vibration of the C–O–H group, not only because these bands shift by deuteration but because 2-halotropones, which have no C–O–H group, do not have strong absorptions this wavenumber region[12]. The fact that the absorption at around 1267 $cm^{-1}$ in tropolone has the character of O–H deformation is also understandable by comparing the spectra in solid, liquid, solution and gaseous states. The spectra in these states in the region of 1450～1050 $cm^{-1}$ are shown in Fig. 2, and the spectra of 4-isopropyltropolone, for the comparison with those, are also shown in Fig. 3. From the spectra in Fig. 3, it is clear that the broad absorption




Wave number, $cm^{-1}$

Fig. 4. Infrared spectra of tropolone in the states of solid (a), liquid (b), $CS_2$ solution (c), and vapor (d) (850～650 $cm^{-1}$ range).




Wave number, $cm^{-1}$

Fig. 5. Infrared spectrum of deuterated tropolone (III) in carbon disulfide (ca. 8%) (900～650 $cm^{-1}$ range).

at 1188 $cm^{-1}$ in solid has shifted to the higher wave number side, merging in the position at around 1265 $cm^{-1}$ in other states. In the same manner, the broad absorption in the region of 1208～1100 $cm^{-1}$ in solid tropolone (Fig. 2a) shifts to the higher wave number side in other states and is assumed to correspond to the strong absorption at 1265 $cm^{-1}$ in the gaseous. The direction of such a shift of absorptions according to changes in the state agrees with the direction of the shift of $\delta_{O-H}$ anticipated from that of $\nu_{O-H}$ as stated in the preceding report[1].

The absorption bands which shift by deuteration are recognized at 1444, 1251 and 953 $cm^{-1}$, but these bands have also disappeared in the compound III, as will be described below. In these bands, the absorption at 1251 $cm^{-1}$ is assumed to correspond to that at 1230 $cm^{-1}$ in Fig. 1b, from their similar shape.

In the region of 800～700 $cm^{-1}$, there are three strong absorption bands in the state of solution. Of these, the band at around 720 $cm^{-1}$ was assigned by Koch[2] and Kuratani et al.[3] to the out-of-plane vibration of hydrogen atoms in the seven-membered ring. On the other hand, Imanishi and Ito[5,13] assigned the Raman line at 743 $cm^{-1}$ to the breathing vibration of the seven-membered ring. Moreover, the following considerations are possible

12) Y. Ikegami, unpublished data.

13) S. Imanishi and M. Ito, *J. Chem. Phys.*, **24**, 1272 (1956).

from the spectra indicated in Fig. 1. The comparatively broad absorption at 726 $cm^{-1}$ in I is no longer visible in II and, therefore it can be assigned to the out-of-plane deformation vibration of C–O–H expected in this region. Analogous absorption bands have been recognized in carboxylic acids[7], chelated β-diketones[9] and hydroxyquinones[8]. This is also understandable since a broad absorption is seen in this region in tropolones in general but not in tropones[12]. The absorption at 767 $cm^{-1}$ can be assigned to the C–H out-of-plane deformation vibration as the majority of 1,2-disubstituted troponoids show strong absorption in this region[12] and because this absorption band has disappeared in deuterated tropolone (III), as shown in Fig. 5. Aside from such considerations in solution, the spectra in other states show a marked difference in shape, as shown in Fig. 4, and this fact indicates that such absorptions are easily affected by intermolecular action.

**On Deuterated Tropolone.** — Deuterated tropolone was obtained by heating a mixture of I and heavy water in a sealed tube at 150°C for a few hours. The compound III, obtained

Table II. Observed frequencies ($cm^{-1}$) of tropolone

| Infrared | | | | Raman[d] | |
|---|---|---|---|---|---|
| Solid[a] | Liquid[a] | Solution[b,a] | Vapor[c] | In benzene | |
| 3518 w | 3450 vw | 3450 vw | | | |
| | | | 3245 sh | | O–H stretch. |
| | | 3151 m | | | |
| 3208 s | 3195 s | | 3140 w | | |
| | | 3120 m | | | |
| 3049 vw | 3060 vw | 3051 sh | 3055 w | | C–H stretch. |
| 3003 vw | 3023 vw | 3020 sh | 3030 w | | |
| 1613 s | 1614 vs | 1618 vs | 1628 vs | 1610 (5) | C=O and C=C stretch. |
| 1548 vs | 1553 s | 1555 s | 1573 s | | |
| 1480 vs | | 1490 vs | 1490 vs | | C–O–H |
| | 1476 vs | | | | |
| 1469 sh | | 1476 vs | 1470 sh | | C–C stretch. |
| | | 1444 s | 1450 s | 1418 (5) | |
| 1425 vs | 1426 vs | | | | |
| | | 1425 sh | 1425 sh | | |
| 1363 vw | 1360 vw | 1355 vw | 1357 vw | | 2×675 |
| | | 1317 sh | | | |
| 1310 m | 1300 m | 1304 m | 1305 s | | |
| 1266 vs | 1264 vs | 1267 vs | 1265 vs | 1262 (4) | C–O–H or C–H in-plane deform. |
| 1238 vs | 1245 vs | 1251 vs | 1250 sh | | |
| 1208 vs | 1210 s | 1213 m | 1208 m | 1208 (2) | |
| 1049 m | 1048 w | 1048 vw | | | 357+679[d] |
| 1009 vw | 990 vw | 1000 vw | | | |
| 958 m | 956 m | 953 m | 940 m | 959 (1) | |
| 919 m | 920 m | 917 m | 908 m | | |
| 874 w | 871 m | 873 w | | | 2×436[d] |
| 860 m | 860 sh | 854 w | 860 w | | |
| 789 w | | | | | 357+436 |
| | 769 s | 767 m | | | |
| 754 s | | | 738 s | 743 (3) | CH out-of-plane deform. C–C stretch.[d] |
| | 740 s | 726 s | | | |
| 708 s | | | 710 m | | OH out-of-plane deform. |
| | 711 s | 713 s | | | |
| 672 m | 675 m | 675 w | 675 w | 679 (2) | C–C–C ring deform. |
| 531 vw | | | | | |
| 433[e] m | | | | 436 (1) | C–C–C ring deform. |
| | | | | 357 (2) | C–C–C ring deform. |

(vs: very strong, s: strong, m: medium, w: weak, vw: very weak, sh: shoulder)

a) The region of 3600~2600 $cm^{-1}$ was measured by using $CaF_2$ prism; see Ref. 1.

b) Fig. 1a. c) Ref. 4. d) Ref. 5.

e) The region of 650~400 $cm^{-1}$ was measured by using KBr prism only in solid (KBr disk).

by treating I twice with 99.78% heavy water for 5 hr., melted at 50°C, alone and in admixture with I. The ultraviolet spectrum of III is also very similar to that of I but their infrared spectra are very different. The absorption bands of III appeared at 3180, 1616, 1556, 1472, 1227 (in carbon tetrachloride) and 729 $cm^{-1}$ (in carbon disulfide), all corresponding to those in Fig. 1a with similar shape. The absorption of C–H stretching vibration in I has become indistinct and appears as a weak band of C–D stretching vibration at 2266 $cm^{-1}$ in III. Further, the strong absorptions at 1444, 1251 and 767 $cm^{-1}$ in I have all disappeared and appear at around 1370, 1084 and 810 $cm^{-1}$ in III (partly shown in Fig. 5), also indicating that these bands are closely related to the C–H bond in the seven-membered ring in I. However, there is not sufficient evidence to determine the position and number of deuteration.

**Considerations Regarding Vibrational Spectrum of Tropolone.**—The infrared absorption bands of tropolone, wave numbers of Raman lines reported by Imanishi[5], and their assignments are summarized in Table II. These assignments were chiefly based on the considerations of the foregoing deuteration and previously reported data[2-5]. Further, the weak absorptions at 1355 and 789 $cm^{-1}$ were assumed to correspond respectively to the overtone, $2\times675$ $cm^{-1}$, and combination tone, $357+436$ $cm^{-1}$. The spectrum of tropylium cation[14], which has the most fundamental form among tropoids, was compared with that of tropolone and bands corresponding well were recognized in the lower wave number region. The vibration due to the seven-membered ring in the cation should not differ greatly from that of tropolone. It is expected to indicate similar wave numbers. Therefore, the absorptions at 675 and 433 $cm^{-1}$ and Raman line at 357 $cm^{-1}$ can be assigned to the ring deformation vibration. The few medium intensity bands observed clearly in the region of 1300~1200 $cm^{-1}$, which are characteristics of tropoids, may be assigned to the C–H deformation vibration of the seven-membered ring.

## Experimental

**Materials.** — Recrystallization of tropolone (I), m. p. 50~51°C, was repeated several times from a mixed solvent of dioxane, dehydrated by metallic sodium, and 99.78% heavy water or from heavy water alone and 2-deuteroxytropone (II) was obtained as colorless needles, m. p. 51°C. Admixture of II and I showed no depression of the melting point. II easily reverted to I by the presence of a slight amount of moisture. Corresponding deuteroxyl compounds were also obtained by the same procedure from 3-bromotropolone, m. p. 108°C, and 3-methyltropolone, m. p. 50°C.

A mixture of 100 mg. of I and ca. 2 ml. of heavy water was heated in a sealed tube at 150°C for 5 hr. This procedure was repeated twice with fresh heavy water each time. The product purified by sublimation and recrystallization to colorless prisms (III), m. p. 50°C alone and in admixture with I.

U. V. $\lambda_{max}^{cyclohexane}$: 226, 239, 247 (sh.), 308 (sh.), 322, 355 and 374 m$\mu$[15].

**Infrared Absorption Spectra.**—All infrared spectra were measured by a Perkin-Elmer model 21 infrared spectrophotometer equipped with a sodium chloride prism. The solid spectra were obtained by the potassium bromide disk method and solution spectra in carbon tetrachloride, purified several times by dehydration with phosphorus pentoxide, or carbon disulfide.

## Summary

In order to find infrared absorption of tropolone, especially the absorption that can be assigned to the C–O–H group, the spectrum of 2-deuteroxytropone was measured and there were discussions chiefly on absorptions in the finger-print region. The absorption bands at around 3150, 1490, 1267 and 726 $cm^{-1}$ were assigned to the vibration of C–O–H group. In this connection, some mention was made on deuterated tropolone and considerations were made on the assignment of vibrational spectra of tropolone, as summarized in Table II.

The author expresses his deep gratitude to Professor Susumu Kinumaki and Assistant Professor Koyo Aida, both of this institute, for their valuable guidance throughout the course of this work.

*The Chemical Research Institute of Non-Aqueous Solutions*
*Tohoku University*
*Katahira-cho, Sendai*

14) K. Aida, *Sci. Repts. Research Inst. Tohoku Univ., Ser.* A, 8, 361 (1956); W. G. Fateley, B. Curnutte and E. R. Lippincott, *J. Chem. Phys.*, 26, 1471 (1957).

15) U. V. spectrum was measured by a Hitachi EPU-2A spectrophotometer.

# *The Dehydration Reactions by Means of Esters of Phosphoric Acid*

By Teruaki MUKAIYAMA and Tsujiaki HATA

(Received July 9, 1960)

Dehydration reactions of primary nitroparaffins and aldoximes by means of organic reagents, such as isocyanates, carbodiimides, ketene acetals and vinylogs, have been described in preceding papers[1-3]. In the present study, dehydration reactions using esters of phosphoric acid have been investigated in order to extend the scope of dehydrating reagents.

In general, the dehydrating reagents can be classified in three classes according to their abilities of dehydration: The first class involves well known strong dehydrating reagents, such as sulfuric acid and phosphorus pentoxide, which remove the hydrogen atom and the oxygen atom at the ratio of 2:1 irrespective of the structures of the compounds to be dehydrated. The second class involves very weak dehydrating reagents, such as calcium chloride and sodium sulfate, which can not remove a water molecule other than that included in the form of water, such as the water of crystallization or adhering water. The third class involves organic dehydrating reagents, such as carboxylic acid anhydrides, carboxylic acid chlorides, isocyanates, carbodiimides and vinylogs, which show that moderate dehydrating abilities and selective intramolecular or intermolecular dehydration of organic compounds are affected with these reagents.

These three classes of dehydrating reagents can be modified by strengthening or weakening their respective dehydrating abilities. For example, it is possible to weaken the strong dehydrating ability of sulfuric acid or phosphorus pentoxide till it is moderate. Recently, it was reported[4] that polyphosphoric acid which is considered to be a mixture of hydrates of phosphorus pentoxide is a very useful dehydrating reagent under moderate conditions.

Esters of phosphoric acid used as dehydrating reagents in the present study are prepared by the reaction of phosphorus pentoxide with alcohols instead of phosphoric acid in the preparation of polyphosphoric acid:

$$n\ P_2O_5 + m\ ROH \rightarrow P{-}R\ (n{-}m),$$

where P—R($n$—$m$) denotes an ester of phosphoric acid prepared by the reaction of $n$ mol. of phosphorus pentoxide with $m$ mol. of alcohol ROH. In general, the molar ratio of phosphorus pentoxide to monohydric alcohols is favorable when it is more than 1/3.

Esters of phosphoric acid are prepared very readily by adding alcohols to phosphorus pentoxide with vigorous agitation. In the preparation of these esters, it is desirable to make the reaction mixture as homogeneous as possible. For this purposes the addition of a pre-formed ester of phosphoric acid to phosphorus pentoxide in advance is favorable, just as shown in the preparation of polyphosphoric acid by the reaction of phosphorus pentoxide with phosphoric acid instead of water.

Monohydric alcohols, such as methyl, ethyl, *n*-propyl, isopropyl and *tert*-butyl alcohols, and also dihydric alcohol, and ethylene glycol, react with phosphorus pentoxide to give viscous esters of phosphoric acid, except in the case of *tert*-butyl alcohol. This does not form a homogeneous ester with phosphorus pentoxide, but the product separates into two layers, probably because of the branched structure of the alcohol. The esters of phosphoric acid thus formed, except that from *tert*-butyl alcohol, show nearly the same reactions. As an example of the dehydration reactions, the dehydrations using P—Et (2—5) prepared from 2 mol. of phosphorus pentoxide and 5 mol. of ethyl alcohol are described.

The reactions of benzaldoxime and heptanaldoxime with P—Et (2—5) give corresponding nitriles in quantitative yields without any accompanying side reactions:

$$RCH{=}NOH + P{-}Et\ (2{-}5) \rightarrow RC{\equiv}N$$

On the other hand, it was reported that the same dehydration reaction of an aldoxime could scarcely be observed with polyphosphoric acid and an acid amide formed by the Beckmann rearrangement of the aldoxime was mainly obtained because of the strong acid character of polyphosphoric acid. The yield of benzonitrile is maximum when benzaldoxime reacts with P—Et (2—5) for 15 min. and then it decreases with the time of heating as shown in Table I.

The dehydration of cyclohexanol to cyclohexene results by a simple treatment with

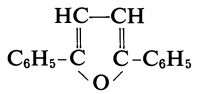
1) T. Mukaiyama and T. Hoshino, *J. Am. Chem. Soc.*, **82**, 5339 (1960).
2) T. Mukaiyama and T. Hata, This Bulletin, **33**, 1382 (1960).
3) T. Mukaiyama and T. Hata, ibid., **33**, 1712 (1960).
4) F. D. Popp and W. E. McEwen, *Chem. Revs.*, **58**, 321 (1958).

esters of phosphoric acid in a yield higher than when other dehydrating reagents, such as a catalytic amount of phosphoric acid, are used[5].

$$C_6H_{11}OH + P—Et\ (2—5) \rightarrow C_6H_{10}$$

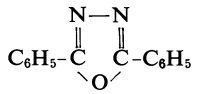
The reaction of dibenzoylethane with P—Et (3—4) gives 2, 5-diphenylfuran in a nearly quantitative yield:

$$C_6H_5COCH_2CH_2COC_6H_5 + P—Et\ (3—4) \rightarrow$$



Similarly, the reaction of dibenzoylhydrazine with P—Et (2—5) gives 2, 5-diphenyl-1, 3, 4-oxadiazole in a good yield:

$$C_6H_5CONHNHCOC_6H_5 + P—Et\ (2—5) \rightarrow$$



The results of the dehydrations of benzaldoxime and cyclohexanol with the other esters are listed in Tables I and II. It should be noted that the reactivities of the five esters are nearly the same irrespective of their nature, except the ester of *tert*-butyl alcohol. It is also noted that the yield increases as the molar ratio of phosphorus pentoxide to alcohols increases and the maximum yield is obtained when benzaldoxime reacts with P—Et (3—4). P—Et (3—4), being a highly viscous liquid, is made to react more smoothly with benzaldoxime in a separate layer of a benzene solution.

Moreover, the esters of phosphoric acid possess several obvious advantages over polyphosphoric acid: 1) Since esters of phosphoric acid are less acidic than polyphosphoric acid, side reactions other than dehydration do not take place as shown in the dehydration of benzaldoxime. 2) In contrast to polyphosphoric acid, esters of phosphoric acid are soluble in organic solvents, such as chloroform, and reactions of organic compounds are conducted in homogeneous systems. 3) By the change of the molar ratio of phosphorus pentoxide to alcohols, the dehydrating ability of the esters is properly controlled.

The dehydrations by means of esters of phosphoric acid are considered to proceed through the bond fission of the pyrophosphate linkage by an attack of compounds containing a hydroxyl group to form 2 mol. of phosphates, and it is established that tetraethyl pyrophosphate reacts with benzaldoxime to give benzonitrile in a 76% yield along with 2 mol. of diethyl phosphate (95% yield).

$$(EtO)_2POOPO(OEt)_2 + C_6H_5CH{=}NOH \rightarrow 2(EtO)_2POOH + C_6H_5C{\equiv}N$$

Dehydrations of aldoximes, cyclohexanol, dibenzoylethane and dibenzoylhydrazine are well conducted with esters of phosphoric acid and also mostly with polyphosphoric acid, but dehydration of an acid amide with these reagents does not succeed and, when benzamide reacts with P—Et (2—5), ethyl benzoate is obtained in an 18% yield instead of the dehydrated product, benzonitrile, probably because of a replacement reaction of the alkoxyl group of the esters with the amino group of the acid amide.

$$C_6H_5CONH_2 + P—Et\ (2—5) \rightarrow C_6H_5COOEt$$

Since esters of phosphoric acid contain alkoxyl groups and form a carboxylic ester by the reaction with an acid amide, polyphosphonic acid is prepared from phosphorus pentoxide and benzenephosphonic acid.

$$C_6H_5PO(OH)_2 + P_2O_5 \rightarrow \text{polyphosphonic acid}$$

When benzamide reacts with the polyphosphonic acid, the dehydrated product, benzonitrile, is obtained, as expected, in a 60% yield.

## Experimental

**Preparation of Esters of Phosphoric Acid [P—R(*n*—*m*)].**—To *n* mol. of phosphorus pentoxide was added *m* mol. of a monohydric alcohol or *m*/2 mol. of a dihydric alcohol dropwise with continuous stirring. When unchanged phosphorus pentoxide remained in a viscous ester, the whole was further heated on a boiling water bath until phosphorus pentoxide was completely dissolved. In general, the resulting esters, P—R (*n*—*m*), are viscous homogeneous liquids, but the ester from *tert*-butyl alcohol separated into two layers. P—Me (*n*—*m*)

TABLE I. THE REACTIONS OF α-BENZALDOXIME WITH VARIOUS ALKYL ESTERS OF PHOSPHORIC ACID, P—R (*n*—*m*), AT 100°C

| P—R (*n*—*m*) | Reaction time, min. | Benzonitrile, yield % |
|---|---|---|
| P—Et (2—5) | 5 | 60 |
| | 15 | 92 |
| | 60 | 70 |
| | 120 | 48 |
| P—Et (1—3) | 15 | 48 |
| P—Et (2—5) | 15 | 92 |
| P—Et (1—2) | 15 | 92 |
| P—Et (3—4) | 15 | 98 |
| P—Me (2—5) | 15 | 68 |
| P—*n*Pr (2—5) | 15 | 90 |
| P—iso Pr (2—5) | 15 | 92 |
| P—*t*Bu (2—5) | 15 | 53 |
| P—EG (3—4) | 15 | 87 |

5) L. F. Fieser, "Experiments in Organic Chemistry", D. C. Heath & Co., Boston (1955), p. 61.

and P—EG (*n*—*m*), prepared by the reactions of phosphorus pentoxide with methyl alcohol and ethylene glycol, respectively, were dark brown liquids, but they showed similar reactions to the other esters.

**Reactions of α-Benzaldoxime with Esters of Phosphoric Acid.**—A solution of α-benzaldoxime (5.0 g., 0.05 mol.) in 10 ml. dry benzene was added to 7.5 g. of P—Et (3—4) and the mixture was heated at 90°C with continuous stirring for 15 min. After removal of benzene, 4.2 g. (98% of the theoretical) of benzonitrile, b. p. 65~66°C (8 mmHg), was obtained. The results of the dehydration of α-benzaldoxime with P—R (*n*—*m*) are summarized in Table I.

**Reaction of Heptanaldoxime with P—Et (3—4).**—A solution of heptanaldoxime (2.6 g., 0.02 mol.) in 10 ml. dry benzene was added to 25 g. of P—Et (3—4). The mixture was heated on a boiling water bath for 30 min. with continuous stirring. After removal of benzene, 1.8 g. (80%) of heptanenitrile, b. p. 71~73°C (20 mmHg), was obtained.

**Reactions of Cyclohexanol with Esters of Phosphoric Acid.**—Cyclohexanol (6.0 g., 0.06 mol.) was added to 8.0 g. of P—Et (2—5) and the mixture was heated at 90°C with continuous stirring for 2 hr. 4.5 g., (92%) of cyclohexene, b. p. 47°C (200 mmHg), was obtained. The results of the dehydration of cyclohexanol with P—R (*n*—*m*) are summarized in Table II.

**Reaction of Dibenzoylethane with P—Et (3—4).**—Dibenzoylethane (1.0 g., 0.004 mol.) was added to P—Et (3—4) (5.0 g.) and the mixture was heated at 100°C with continuous stirring until the viscous mixture became brownish yellow in color. Then the mixture was poured into 150 ml. of ice water with vigorous stirring and the precipitate was collected by filtration. It was recrystallized from 95% ethanol and 0.86 g. (93%) of 2,5-diphenylfuran, m. p. 88~90°C, was obtained.

Table II. The reactions of cyclohexanol with various alkyl esters of phosphoric acid at 100°C

| P—R (*n*—*m*) | Reaction time, hr. | Cyclohexene, yield, % |
|---|---|---|
| P—Et (2—5) | 1.0 | 68 |
| | 1.5 | 92 |
| | 2.0 | 88 |
| | 3.0 | 93 |
| P—Me (2—5) | 2.0 | 88 |
| P—*n*Pr (2—5) | 2.0 | 99 |
| P—iso Pr (2—5) | 2.0 | 99 |
| P—*t*Bu (2—5) | 2.0 | 52 |

**Reaction of Dibenzoylhydrazine with P—Et (3—4).**—A solution of 1.0 g. (0.004 mol.) of dibenzoylhydrazine in 10 ml. dimethylformamide was added to 10 g. of P—Et (3—4). Then, the mixture was heated at 100°C for 2 hr. and poured into 200 ml. of ice water with vigorous stirring. The precipitate was collected by filtration and recrystallized from benzene to give 0.6 g. (65%) of 2,5-diphenyl-1,3,4-oxadiazole, m. p. 136°C.

**Reaction of α-Benzaldoxime with Tetraethyl Pyrophosphate.**—A mixture of tetraethyl pyrophosphate (2.9 g., 0.01 mol.) and α-benzaldoxime (1.21 g., 0.01 mol.) was heated at 95°C for 14 hr. and 0.78 g. (76%) of benzonitrile, b. p. 42~44°C (2 mmHg), and 2.92 g. (95%) of diethyl phosphate, b. p. 120~123°C (0.02 mmHg), were obtained.

**Reaction of Benzamide with Polyphosphonic Acid.**—To fused benzenephosphonic acid (2.0 g., 0.013 mol.) was added phosphorus pentoxide (3.0 g., 0.021 mol.) little by little with stirring during a period of 20 min. To the viscous polyphosphonic acid thus prepared was added benzamide (1.0 g., 0.008 mol.) with continuous stirring. After heating the mixture for 30 min. at 130°C, it was cooled at room temperature. Then it was dissolved in 20 ml. of water and extracted twice with 20 ml. of chloroform. The chloroform layers were combined and distilled under reduced pressure to give 0.5 g. (60%) of benzonitrile, b. p. 87~89°C (25 mmHg).

The authors wish to express their hearty thanks to Miss Hiroko Takahashi for her help throughout the course of this experiment. Thanks are also due to Mr. Asaji Kondo for the microanalyses.

*Tokyo Institute of Technology*
*Meguro-ku, Tokyo*

# *Oxidizing Action of Hydroperoxides. V. On the Oxidation of Ketones*

By Kazuhiro MARUYAMA

(Received June 14, 1960)

In the previous paper of this series[1], it has been reported that hydroperoxides have a strong oxidizing action cooperating with alkali hydroxides. For example, alkylbenzenes are oxidized to the corresponding alcohols, ketones and carboxylic acids. Further, alkyl aryl ketones are split very smoothly to benzoic acid derivatives and alcohols,—but diaryl ketones are not cleft by these oxidizing agents[2]. Furthermore, in order to obtain more extensive knowledge of the reaction, the same kinds of reactions were examined on some ketones; isopropyl phenyl ketone, cyclohexyl phenyl ketone *p*-chloroacetophenone, desoxybenzoin, phenyl *p*-chlorobenzyl ketone, benzoin, benzil, $\alpha$-tetralon, 3-pentanone, 3-heptanone and cyclohexanone were examined. All these reactions were performed in nonaqueous solvent and the examined ketones were also cleft smoothly with the one exception of cyclohexanone. An outstanding difference between this cleavage reaction mechanism and the Baeyer-Villiger mechanism is that any C–C linkage between carbonyl carbon and aromatic carbon in alkyl aryl ketones, is never attacked.

## Experimental

**Reagents.**—The reagents cited in Table I were synthesized by the Friedel-Crafts reaction.

Benzoin was prepared by condensation of benzaldehyde, m. p. 137°C; semicarbazone, m. p. 206°C. Benzil was prepared by nitric acid oxidation of benzoin, m. p. 95°C. $\alpha$-Tetralon was synthesized from tetralin after Thompson's method, checked by Shriner and Poland[3], b. p. 107°C/2 mmHg, $n_D^{15}$, 1.5640; semicarbazone, m. p. 217°C. 3-Pentanone and 3-heptanone, the commercially available guaranteed grade reagent was used without further purification. *tert*-Butylhydroperoxide was snythesized by the action of 30% hydrogen peroxide on *tert*-butanol according to Milas and Surgenor's method[4] and purified by fractional distillation under reduced pressure. B. p. 36°C/19 mmHg, $n_D^{27}$ : 1.3967. Cyclohexanone, the commercially available guaranteed grade reagent was treated with potassium permanganate and was purified by distillation. b. p. 157°C, Semicarbazone, m. p. 155°C.

**Reaction Procedure.**—The reaction apparatus and the treatments of reaction mixture are quite the same as that described in the previous paper[2]. With the exception of the case with benzil and $\alpha$-tetralon the experiment was conducted as following.

The weighed ketone was dissolved in purified monochlorobenzene (150 cc.). Carbonate free powdered potassium hydroxide was added to the mixture after the air in the reaction vessel was completely exchanged with dry pure nitrogen. As soon as the temperature of the reaction mixture reached 70°C, *tert*-butylhydroperoxide was added. The temperature raising of about 10°C was observed. After six hours, the reaction mixture was extracted with 100 g. of water three times. The water extract was acidified with 2 N-sulphric acid and the precipitated benzoic acid derivative was collected and weighed. The filtrate was neutralized with conc. ammonia

TABLE I

| Ketones | (B. p.) or [m. p.] °C | $n_D^{15}$ | Semicarbazones m. p., °C | Oxime m. p., °C | Synthesized from |
|---|---|---|---|---|---|
| Isopropyl phenyl | (95/10 mmHg) | 1.5196 | 181 | | benzene and isobutyl chloride |
| Cyclohexyl phenyl | [59~60] | | 175 | | benzene and cyclohexyl chloride |
| *p*-Chloroaceto-phenone | (99/7 mmHg) [19~20] | | 148 | | chlorobenzene and acetyl chloride |
| Desoxybenzoin | (177/12 mmHg) [60] | | 148 | | benzene and phenyl acetyl chloride |
| Phenyl *p*-chlorobenzyl | [138] | | | 95~96 | benzene and *p*-chlorophenylacetyl chloride |

1) K. Maruyama, R. Goto and H. Suzuki, *J. Chem. Soc. Japan, Pure Chem. Sec. (Nippon Kagaku Zasshi)*, **80**, 521 (1959).
2) This Bulletin, **33**, 1516 (1960).
3) Organic Syntheses, **20**, 94 (1940).
4) N. A. Milas and D. Sūrgenor, *J. Am. Chem. Soc.*, **68**, 205, 643 (1946).

TABLE II. OXIDATION OF KETONES WITH *tert*-BUTYLHYDROPEROXIDE
(Temp. 60°C, 6 hr.)

| Ketone | Hydroperoxide g. (mol.) | Ketone recovered | Reaction product |
|---|---|---|---|
| 1. Isopropyl phenyl ketone 10.0 g. | *tert*-Butylhydroperoxide 2.0 g. | 8.5 g. | Benzoic acid 1.05 g., isopropanol (*tert*-butanol, methanol) |
| 2. Cyclohexyl phenyl ketone 10.0 g. | *tert*-Butylhydroperoxide 2.0 g. | 9.0 g. | Benzoic acid 0.30 g., adipic acid, non-identified acid (*tert*-butanol, methanol) |
| 3. *p*-Chloroaceto-phenone 10.0 g. | *tert*-Butylhydroperoxide 2.0 g. | 7.0 g. | *p*-Chlorobenzoic acid 1.2 g. (*tert*-butanol, methanol) |
| 4. Desoxybenzoin 10.0 g. | *tert*-Butylhydroperoxide 2.0 g. | 8.3 g. | Benzoic acid 1.50 g. (*tert*-butanol, methanol) |
| 5. Phenyl *p*-chloro-benzyl ketone 10.0 g. | *tert*-Butylhydroperoxide 2.0 g. | 8.0 g. | Benzoic acid 0.30 g., *p*-chlorobenzoic acid 0.40 g. (*tert*-butanol, methanol) |
| 6. Benzoin* 10.0 g. | *tert*-Butylhydroperoxide 2.0 g. | 8.0 g. | Benzoic acid 1.9 g. (*tert*-butanol, methanol) |
| 7. Benzil** 10.0 g. | *tert*-Butylhydroperoxide 2.0 g. | 8.0 g. | Benzoic acid 1.8 g., benzilic acid (trace) (*tert*-butanol, methanol) |
| 8. $\alpha$-Tetralon*** 8.2 g. | *tert*-Butylhydroperoxide 2.0 g. | — | *O*-Carboxyhydrocinnamic acid 0.43 g., *O*-carboxycinnamic acid 0.07 g., phthalonic acid 0.01 g., resin. |
| 9. 3-Pentanone 8.6 g. (0.1 mol.) | *tert*-Butylhydroperoxide 5.4 g. (0.06 mol.) | — | Propionic acid (main), acetic acid } total acid 0.02 mol. |
| 10. 3-Heptanone 11.4 g. (0.1 mol.) | *tert*-Butylhydroperoxide 5.4 g. (0.06 mol.) | — | *n*-Valeric acid (main), propionic acid, *n*-butyric acid, acetic acid } total acid 0.016 mol. |
| 11. Cyclohexanone 9.8 g. (0.1 mol.) | *tert*-Butylhydroperoxide 5.4 g. (0.06 mol.) | almost completely recovered | No reaction (oxygen, *tert*-butanol, methanol) |

* In this case, the solution of benzoin suspended with potassium hydroxide was deeply colored violet before the addition of hydroperoxide. As the peroxide was dropped, however, the violet color disappeared.

** In this reaction, potassium hydroxide was added in the mixture of benzil and hydroperoxide in order to avoid the so-called "benzilic acid rearrangement." By this precaution, the rearrangement was in practice avoided.

*** In this case, benzene was used as a solvent and its solution of $\alpha$-tetralon and hydroperoxide were dropped to suspension of potassium hydroxide in benzene. However, a large quantity of resinous product was not avoided.

and was concentrated to 10 cc. and subjected to a paper chromatographic analysis.

The obtained experimental results are shown in Table II.

**Benzoic Acid.**—In the reaction 1, 2, 4, 5, 6 and 7 benzoic acid was obtained by the acidifying of the water extraction of the reaction mixture. The crude products were recrystallized from the water-alcohol mixture. The acid was identified by the mixed melting point method and paper chromatography.

**Isopropanol.** — In reaction 1, isopropanol was collected in a trap cooled by ice-salt mixture. This was identified as its phenylurethan derivative (from ligroin m. p. 88°C) and also verified by gas chromatography.

Found: C, 66.98; H, 7.22. Calcd. for $C_{10}H_{13}\cdot NO_2$: C, 67.02; H, 7.31%.

**Adipic Acid.**—In reaction 2, the acid was found in the solid acid of reaction products and in the concentrated part of the filtrate. Adipic acid was identified by paper chromatography ($R_f$ 0.22, solvent: 5% ammonia 1 vol.+isopropanol 4 vol., temp. 15~20°C). Another acid ($R_f$ 0.44) was found on the paper chromatogram accompanying benzoic acid and adipic acid. But, this acid could not be identified.

***p*-Chlorobenzoic Acid.**—In reaction 3, acid was obtained by the acidifying of the water extract of the reaction mixture, and was identified as *p*-chlorobenzoic acid by the mixed melting point method and paper chromatography (m. p. 243°C).

Found: C, 53.77; H, 3.11. Calcd. for $C_7H_5O_2Cl$: C, 53.69; H, 3.21%.

In reaction 5, *p*-chlorobenzoic acid was obtained by the acidifing of the water extract of the reaction mixture accompanying benzoic acid, and was easily separated from benzoic acid by crystallization from hot water. The obtained crude acid was recrystallized from the water-alcohol mixture, m. p. 242~243°C and was identified by the mixed melting point method and paper chromatography.

**Benzilic Acid.**—In reaction 7, a trace of benzilic acid was found in the acid products, and was detected paperchromatographically and identified by comparison with a known sample.

***o*-Carboxyhydrocinnamic Acid.** — In reaction 8, the acid was obtained as the main reaction product. The water extract of the reaction mixture was acidified and the obtained precipitation was recrystallized from hot water. *o*-Carboxyhydrocinnamic acid is slightly soluble in hot water and separated from insoluble acid. Repeated recrystallization resulted in the paperchromatographically pure product, and was identified by the mixed melting point method and paper chromatography ($R_f$ 0.21 solvent: 5% ammonia 1 vol. isopropanol 4 Vol., room temp.) m. p. 166~167°C.

Found: C, 62.14; H, 5.30. Calcd. for $C_{10}H_{10}O_4$: C, 61.85; H, 5.19%.

***o*-Carboxycinnamic Acid.** — In reaction 8, this acid was obtained as a product insoluble in hot water, but soluble in hot alcohol, m. p. 173~174°C and was identified by the mixed melting point method and paper chromatography.

**Phthalonic Acid.**—In reaction 8, phthalonic acid was obtained as the benzene soluble part of acid products, m. p. 150~151°C and was identified by the mixed melting point method and on a paper chromatogram by comparison with a known sample.

**Methanol and *tert*-Butanol.**—These products were collected in a trap cooled by ice-salt, and analyzed gaschromatographically. *tert*-Butanol was separated as its phenylurethan, m. p. 136°C.

Found: C, 68.86; H, 7.93. Calcd. for $C_{11}H_{15}\cdot NO_2$: C, 68.40; H, 7.80%.

***n*-Valeric Acid, *n*-Butyric Acid, Propionic Acid and Acetic Acid.**—These acids were detected by paper chromatography and their total acid contents were determined by titration.

## Discussion

It was discussed in the previous paper[1], almost all of the examined ketones, there being only one exception, are subjected to a cleavage reaction by *tert*-butylhydroperoxide. These reactions are summarized in the next equations.

i) Aromatic ketone

$$\mathrm{Ar\text{-}CO\text{-}R} \xrightarrow[\mathrm{KOH}]{t\text{-BuOOH}} \mathrm{ArCOOH + ROH} \qquad (1)$$

R=alkyl

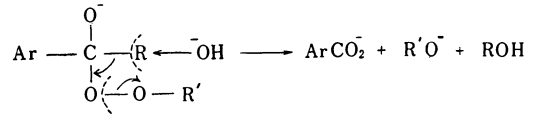
ii) Aromatic $\alpha,\beta$-diketone

$$\mathrm{ArCO\cdot COAr'} \xrightarrow[\mathrm{KOH}]{t\text{-BuOOH}} \mathrm{ArCOOH + Ar'COOH} \qquad (2)$$

iii) Aliphatic ketone

$$\mathrm{RCOR'} \rightarrow \begin{cases}\mathrm{RCOOH + R'OH}\\ \mathrm{R'COOH + ROH}\end{cases} \qquad (3)$$

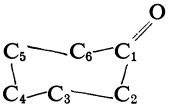
From results of Table II, it could be confirmed that in general, an alkyl aryl ketone can be cleft to benzoic acid derivative and alcohol by hydroperoxide cooperating with alkali hydroxide. The hydroperoxide was reduced to alcohol — e. g. *tert*-butylhydroperoxide → *tert*-butanol. Furthermore, aromatic $\alpha,\beta$-diketone was also cleft by the same oxidizing reagent to benzoic acid derivatives. It was a outstanding difference from the cleavage of aromatic ketones by peracids according to Baeyer-Villiger reaction that phenolic product was not found in the oxidation products. This difference, of course, is ascribed to the different reaction mechanism, for this kind of reactions are performed in alkaline medium. As it was briefly discussed in the previous paper, the reason of the absence of phenolic product may be due to a difficulty of formation of phenyl cation (or of $S_N2$-type reaction at nucleus carbon) at the moment of scission from the complex [I], which is consisted of ketone and hydroperoxide.



[I] (4)

The same kind of cleavage reaction occurred even in the aliphatic ketones, but in this case, the two linkages on both sides of carbonyl carbon have a chance of scission. The chance of scission, however is determined by the stability of the alkyl group as a cation*.

For cyclohexanone, which is only one exception to the cleavage reaction, it may be guessed that the complex can not be formed. This is because, in the alkaline medium the attack of the hydroperoxide anion to the positively polarized carbonyl carbon atom will be most easily performed on the opposite side of the negatively polarized oxygen atom and the steric hindrance which will be caused by the axial hydrogens on $C_2$, $C_6$, $C_3$ and $C_5$ and by the $C_3$, $C_4$ and $C_5$ carbon atom, against the attack of the hydroperoxide anion makes the formation of complex [I] impossible.



The author is indebted to Professor Ryozo Goto for discussion and encouragement throughout this investigation.

*Department of Chemistry*
*Faculty of Science*
*Kyoto University*
*Sakyo-ku, Kyoto*

* This was confirmed in the case of methyl ethyl ketone and of methyl isopropyl ketone in the homogeneous system (O. Soga, K. Maruyama and R. Goto, *J. Chem. Soc. Japan, Pure Chem. Sec.* (*Nippon Kagaku Zasshi*), **81**, 668 (1960).

# *Oxidizing Action of Hydroperoxides. VI. On the Oxidation of Ketones*

By Kazuhiro MARUYAMA

(Received June 20, 1960)

In the previous work[1], it was reported that hydroperoxides acted as a strong oxidizing agent in the presence of alkali hydroxide, and especially a vigorous reaction occurred with alkyl aryl ketone and resulted in a cleavage of C–C linkage between the carbonyl carbon and the alkyl carbon. The mechanism of this reaction must be different from the "Baeyer-Villiger" mechanism, because alkyl aryl ketone does not produce any phenolic products and diaryl ketone affords none of its reaction products.

From this point of view, the following three points were examined:

i) In the first place, it must be decided that the cleavage reaction of ketone with hydroperoxide can proceed by way of an intermediate complex, in which the hydroperoxide anion will be added to the carbonyl carbon atom of the ketone. And, if not, an active oxygen atom isolated from the hydroperoxide anion will be responsible for the cleavage reaction. In order to examine these points, a method of competitive reaction was employed; that is, with the selection of acetophenone-1-$^{14}$C (carbonyl $^{14}$C) as a standard ketone, the reactivity among methyl derivatives of acetophenone, substituted on the methyl group, was compared.

ii) The influence of *p*-substituent to acetophenone towards the reactivity was confirmed.

iii) The progression of cleavage reaction was traced for some ketones — acetophenone, ethyl phenyl ketone and isopropyl phenyl ketone.

## Experimental

**Reagent.** — Ketones used as reagents are all synthesized, as can be seen from the following tabulation.

Acetophenone-1-$^{14}$C was prepared from benzene and acetyl-1-$^{14}$C chloride. Acetyl-1-$^{14}$C chloride was synthesized from sodium acetate-1-$^{14}$C according to Anker's method.[2] The obtained acetophenone-1-$^{14}$C has b. p. 196~199°C (yield 75%). *tert*-Butyl-hydroperoxide was prepared from *tert*-butanol and

TABLE I

| Ketones | (B. p.), [m. p.] °C | Semicarbazone m. p. °C | Oxime m. p. °C | 2,4-Dinitrophenylhydrazone m. p. | Synthesized from |
|---|---|---|---|---|---|
| Ethyl phenyl | (105/20 mmHg), [21] | | | | benzene and propionyl chloride |
| *p*-Chlorobenzyl phenyl | [138] | | 95~96 | | benzene and *p*-chlorophenylacetyl chloride |
| Isopropyl phenyl | [59~60] | 175 | | | benzene and isobutyloyl chloride |
| *tert*-Butyl phenyl | (220~222) (104~106/17 mmHg) | | | 166~168 | isopropyl phenyl ketone and methyl iodide (Halle's method)* |
| *p*-Methylacetophenone | (222) | 205 | | | toluene and acetyl chloride |
| *p*-Methoxyacetophenone | (138/14 mmHg) [38~39] | 195 | | | anisole and acetyl chloride |
| *p*-Phenylacetophenone | [120~121] | | 184~185 | | biphenyl and acetyl chloride |
| *p*-Chloroacetophenone | (99/7 mmHg), [20] | 202~204 | | | chlorobenzene and acetyl chloride |
| *p*-Bromoacetophenone | (130~131/12 mmHg) (51] | | | | bromobenzene and acetyl chloride |

* M. A. Halle and E. Bauer, *Compt. rend.*, **148**, 72 (1909).

1) K. Maruyama, This Bulletin, 33, 1516 (1960).

2) H. S. Anker, *J. Biol. Chem.*, **176**, 1333 (1948).

30% hydrogen peroxide according to Milas's method[3], b. p. 36°C/19 mmHg, $n_D^{27}$ 1.3967.

**Reaction Procedure.** — *1) Competitive Reaction with Acetophenone-1-$^{14}$C.*—A three-necked 200cc. flask, equipped with a thermometer, a dropping funnel and a reflux condenser was placed in a thermostat, controlled to (70±1°C). A mixture of 0.01 mol. of acetophenone-1-$^{14}$C and 0.01 mol. of testing ketone, dissolved together in 50 g. of monochlorobenzene, was charged in the flask and the contents were agitated vigorously with a magnetic stirrer. When the temperature of the contents became constant, 0.062 mol. of finely powdered pure potassium hydroxide* was added and 0.06 mol. of *tert*-butylhydroperoxide, dissolved in 10 g. of monochlorobenzene, was dropped through a dropping funnel within three minutes. After one hour, the reaction was finished. The contents were cooled with ice, added with 50 cc. of ether and extracted with 20 cc. of water three times. The water extract was collected and acidified with 6N hydrochloric acid, and then precipitated benzoic acid was collected and purified. A hundred milligrams of the obtained benzoic acid was used for the counting** of the activity in each reaction.

*2) Comparison of Reactivity of p-Substituted Acetophenone.*—The same reaction apparatus as that described above was employed. A mixture of 0.02 mol. of ketone, 0.062 mol. of finely powdered pure potassium hydroxide dissolved in 50 g. of monochlorobenzene and a solution of 0.06 mol. of *tert*-butylhydroperoxide dissolved in 10 g. of monochlorobenzene was caused to react in the reaction vessel. After one hour, the reaction was ceased, the mixture was immediately cooled with ice, added with 50 cc. of ether, and extracted three times with 20 cc. of water each. The water extract was acidified with 14 cc. of 6N hydrochloric acid and extracted three times with 20 cc. of ether each. The ether extract was washed with 5 cc. of water three times, and then the ether extract was added with pure ethanol till the total volume became just 100 cc., and titrated with 0.054 N sodium hydroxide solution. Thus the obtained benzoic acid was determined.

*3) Measurement of Progression of Cleavage Reaction.*—In these reactions, 0.042 mol. of ketone, 0.056 mol. of *tert*-butylhydroperoxide and 0.056 mol. of finely powdered pure potassium hydroxide were used and reaction procedures were the same as in 2. The reaction mixture was not completely homogeneous, hence a pipetting-out method could not be used, and so the total reaction mixture was used for analysis after the definite time of reaction had elapsed. Therefore, to determine the cleavage velocity of a ketone, five reactions under the same conditions should be performed. In this method, the accuracy of the measurements was fairly good (see Fig. 2).

## Results and Discussion

**Competitive Reaction with Acetophenone-1-$^{14}$C.** —The results are given in Table II. A relative reactivity derived from counting the amount of the benzoic acid obtained in each reaction is cited in column 4.

TABLE II. COMPETITIVE REACTION WITH ACETOPHENONE-1-$^{14}$C

| | Ketone | Counting number*) (c. p. m.) | Reactivity |
|---|---|---|---|
| 1. | $C_6H_5\cdot C(=O)\cdot CH_3$ | 1000±19 | 1 |
| 2. | $C_6H_5\cdot C(=O)\cdot CH_2CH_3$ | 514±15 | 2.9 |
| 3. | $C_6H_5\cdot C(=O)\cdot CH_2C_6H_4Cl(p)$ | 860±19 | 1.3 |
| 4. | $C_6H_5\cdot C(=O)\cdot CH(CH_3)_2$ | 707±19 | 1.8 |
| 5. | $C_6H_5\cdot C(=O)\cdot CH(CH_2{-}CH_2{-}CH_2{-}CH_2)$ | 1706±27 | 0.2 |
| 6. | $C_6H_5\cdot C(=O)\cdot C(CH_3)_3$ | 1111±19 | 0.8 |

*) A hundred milligrams of the obtained benzoic acid was used for the counting of the activity in every reaction.

Conditions of reactions: Temp. 70°C, reaction time 1 hr.

{acetophenone-1-$^{14}$C 0.01 mol. + ketone 0.01 mol.; *tert*-butyl hydroperoxide 0.06 mol.; powdered potassium hydroxide 0.062 mol.} dissolved in 60 g. of monochlorobenzene.

3) N. A. Milas and D. Sūrgenor, *J. Am. Chem. Soc.*, **68**, 205, 643 (1946).

* After potassium hydroxide was added, the contents were slightly colored in brown, but soon decolorizeb when hydroperoxide was added.

** A G-M counter was applied.

TABLE III. COMPARISON OF REACTIVITY OF *p*-SUBSTITUTED ACETOPHENONE

| | Ketone | Substituent | Titration neeeded volume of 0.054 N-NaOH soln. ($V$) |
|---|---|---|---|
| 1. | $C_6H_5\cdot C(=O)\cdot CH_3$ | -H | 63.3 |
| 2. | $p$-$CH_3\cdot C_6H_4\cdot C(=O)\cdot CH_3$ | $-CH_3$ | 34.0 |
| 3. | $p$-$CH_3O\cdot C_6H_4\cdot C(=O)\cdot CH_3$ | $-OCH_3$ | 33.8 |
| 4. | $p$-$C_6H_5\cdot C_6H_4\cdot C(=O)\cdot CH_3$ | $-C_6H_5$ | 65.0 |
| 5. | $p$-$Cl\cdot C_6H_4\cdot C(=O)\cdot CH_3$ | -Cl | 170.5 |
| 6. | $p$-$Br\cdot C_6H_4\cdot C(=O)\cdot CH_3$ | -Br | 212.4 |

Conditions of reactions: Temp. 70°C, reaction time 1 hr.
{ketone 0.02 mol., *tert*-butylhydroperoxide 0.06 mol., powdered potassium hydroxide 0.062 mol.} dissolved in 60 g. of monochlorobenzene.

From the above results, it may be seen that the successive methyl substitution on the methyl group of acetophenone produces a ketone which has the maximum reactivity upon *tert*-butylhydroperoxide in the series of acetophenone derivatives; that is, the relative reactivities of acetophenone, ethyl phenyl ketone, isopropyl phenyl ketone and *tert*-butyl phenyl ketone were about 1 : 3 : 2 : 1. On the other hand, the reactivity of *p*-chlorobenzyl phenyl ketone is one third of that of ethyl phenyl ketone. The same result is also seen in the comparison between isopropyl phenyl ketone and cyclohexyl phenyl ketone. The latter is about one tenth of the former in its reactivity. Moreover, *tert*-butyl phenyl ketone is even more reactive upon *tert*-butylhydroperoxide than cyclohexyl phenyl ketone is.

These results obtained above would lead to the conclusion that the steric effect of the alkyl group and the effect of the stability of the alkyl group as its cation are conversely responsible for the reactivity of alkyl phenyl ketone, that is, the size of the alkyl group obviously increases in the following order, $CH_3 < CH_2CH_3 < CH(CH_3)_2 < C(CH_3)_3$ and so the more bulky the alkyl group is, the larger is the steric hindrance of alkyl groups against the attack of *tert*-butylhydroperoxide on the carbonyl group (F-strain). On the other hand, the stability of the alkyl group as a cation is in the following order $CH_3 < CH_2CH_3 < CH(CH_3)_2 < C(CH_3)_3$. If the alkyl group of an alkyl aryl ketone is cleft as a cation*, the same order of the relative reactivity may be expected. Then, based on these considerations, it seems reasonable to suppose that the appearance of maximum reactivity in ethyl phenyl ketone depends upon the overlap of the conversely acting two effects.

**Comparison of Reactivity of *p*-Substituted Acetophenones.**—Relative reactivities of *p*-substituted acetophenones are given in Table III and their relation to Hammett's $\sigma_p$ value is shown in Fig. 1. From the results obtained, it can be deduced that the more electron attractive the substituent of an acetophenone, the

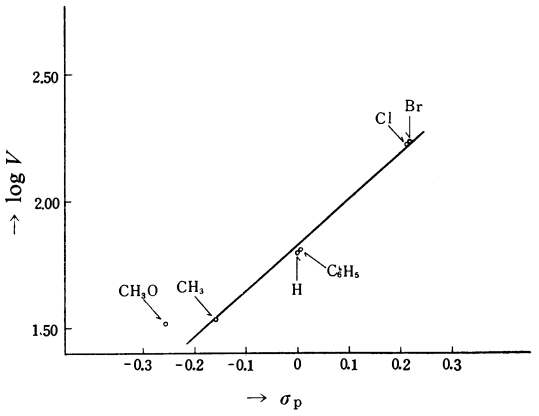



Fig. 1. The relation between $\sigma_p$ value and reactivity of *p*-substituted acetophenones.

* This is also supported from the following facts: i) alcohol derived from the alkyl group was confirmed as a reaction product and ii) diaryl ketones could not be cleft by these reagents.

more reactive is the acetophenone derivative. Furthermore, Hammett's plot of log $V$ to $\sigma_p$ gives straight line (see Fig. 1). It may be deduced that, in general, an electron attractive substituent on the phenyl group raises the reactivity of acetophenone derivatives for *tert*-butylhydroperoxide.

**Measurement of Progression of Cleavage.**—In order to study the progression of reaction and to elucidate its mechanism, the cleavage reaction of acetophenone, ethyl phenyl ketone and isopropyl phenyl ketone was examined. From the results obtained, the following may be written (see Fig. 2).

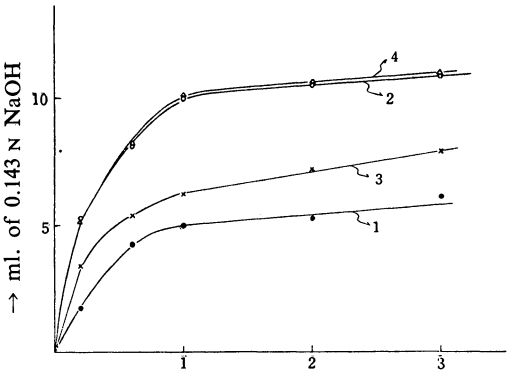



Fig. 2. Progression curve of reaction derived from titration curve of produced benzoic acid.

(1) $C_6H_5COCH_3$ 0.042 mol.
(2) $C_6H_5COC_2H_5$ 0.042 mol.
(3) $C_6H_5COCH\langle^{CH_3}_{CH_3}$ 0.042 mol.
(4) $\{^{C_6H_5COC_2H_5}_{As_2O_3}$ 0.042 mol. / 0.0005 mol.

Conditions of reactions: Temp. 70°C
{ketone 0.042 mol. / *tert*-butylhydroperoxide 0.056 mol. / powdered potassium hydroxide 0.056 mol.} dissolved in 60 g. of monochlorobenzene.

i) There is no induction period for any reaction.

ii) The addition of arsenious acid to the reaction mixture has no effect.

iii) The reproducibility of these reactions is fairly good.

From the above three points, it might be possible to obtain the conclusion that the cleavage of ketones with hydroperoxides in the presence of alkali hydroxide is not a chain reaction.

**Reaction Mechanism.**—On the examination of reaction mechanism, the followings should be born in mind:

i) Alkyl aryl ketone is cleft with hydroperoxide cooperating with alkali hydroxide and produces benzoic acid derivative and alcohol derived from the alkyl group of ketone.

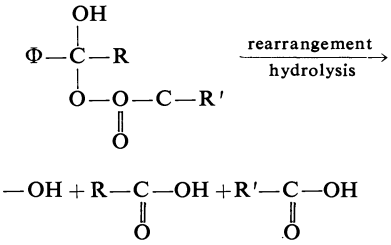
ii) Diaryl ketone (e. g. benzophenone, *p*-nitrobenzophenone and fluorenone) can not be cleft with this oxidizing reagent.

iii) In the series of methyl substituted derivatives of acetophenone having the substituent on the methyl group, a maximum reactivity is observed in ethyl phenyl ketone.

iv) In *p*-substituted derivatives of acetophenone, the more electron attractive the *p*-substituent is, the larger is the reactivity upon hydroperoxide.

v) These reactions have no induction period, and arsenious acid which is known as an inhibitor of the chain reaction has no effect.

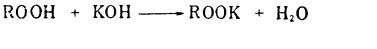
In view of i) — iii), this cleavage reaction of ketone should be different from the "Baeyer-Villiger" reaction, which is a cleavage reaction of ketone by peracid, for the cleavage of ketone according to "Baeyer-Villiger" mechanism is of a rearrangement of carbanion to oxygen cation.



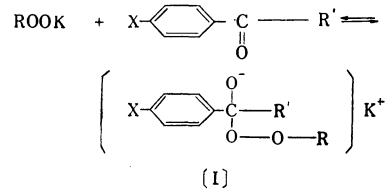

(1)

If this reaction, which is an oxidizing action of hydroperoxide cooperating with alkali hydroxide upon ketone, is supposed to follow the same mechanism as that of B. V., phenolic derivative and fatty acid must be produced, but, in fact, only benzoic acid derivative and fatty alcohol are obtained and so the C–C linkage between carbonyl carbon and phenyl carbon is not cleft. In order to explain these results conveniently, the following reaction mechanism seems very probable.

This mechanism implies that the hydroperoxide, first produces its potassium salt, and then this salt attacks carbonyl carbon and gives a complex (I), which is cleft by hydroxide anion to acid and alcohol. Reaction 3 should be a reversible reaction and the position of equilibrium would probably be settled under

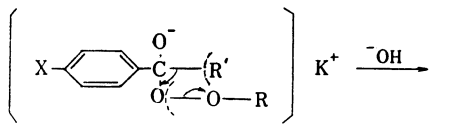


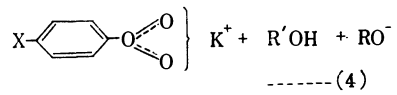

(2)



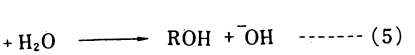

(3)

(I)



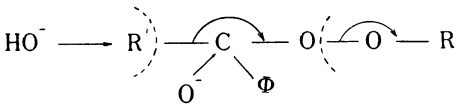


-------(4)



-------(5)

the influence of the size of alkyl group. F-Strain of alkyl group against the attack of hydroperoxide anion on the carbonyl carbon may act as a factor inhibiting the formation of complex [I]. On the other hand, the back-side attack of hydroxide anion on the alkyl group may play an important role* (Eq. 4) for the cleavage of complex I. The same equilibrium as in Eq. 3 may exist in the case of diaryl ketone, but the succeeding back-side attack of hydroxide anion would not act effectively, so that diaryl ketones could not be cleft. However, the cleavage reaction may be started by the scission of R'-cation from complex I, and a promoting action of $HO^-$ anion for this, too, may act and at the same time the scission of $RO^-$ anion may take place concertedly with the above process, that is:



As the result of this cleavage reaction, benzoic acid derivatives, R'OH and ROH are produced. According to this mechanism, it is quite possible that a maximum reactivity observed in ethyl phenyl ketone (discussion 3) is caused by a result of two counter-acting effects which are effects of R' cation and steric hindrance for the back-side attack of $HO^-$ anion. Moreover, the increase of of F-strain, caused by the increase in size of the alkyl group, for the formation of complex I (Eq. 3) may contribute to the decrease of reactivity. On the other hand, the promoting action of an electron attracting substituent on the phenyl group can be explained as follows; that is, the increase of stability of the *p*-substituted benzoate anion by an electron attracting substituent may cause an increase of driving force for the cleavage reaction of the complex [I].

Contrary to the above mechanism, i) the possibility of contribution of radicals for the cleavage reaction of the complex [I], ii) the possibility of contribution of enol-type of ketone this cleavage reaction, and iii) the possibility of contribution of atomic oxygen isolated completely from $ROO^-$ may be doubted. However, i) diaryl ketones can not be cleft and phenolic derivatives are not produced in any cleavage reaction, ii) *tert*-butyl phenyl ketone is cleft almost easily as acetophenone, and iii) when formaldehyde, acetaldehyde, propionaldehyde, acetone and methyl ethyl ketone are selected as carbonyl compounds, the decomposition velocity of hydroperoxide is strikingly different according to the structure of carbonyl compounds[5]. For example, *tert*-butylhydroperoxide did not decompose in the reaction with acetone (at 30°C), but the same hydroperoxide was decomposed in the reaction with methyl ethyl ketone under the same condition. If the isolated oxygen atom acts as an oxidizing agent, there must be no such phenomena.

The author is indebted to Professor Ryozo Goto for discussion and encouragement throughout this investigation.

*Department of Chemistry*
*Faculty of Science*
*Kyoto University*
*Sakyo-ku, Kyoto*

* In fact, it was confirmed that an increase of hydroxide anion, in homogeneous alkaline solution, accelerates the cleavage of the complex, which is inferred from the decomposition velocity of hydroperoxide, in the case of methyl ethyl ketone. The decomposition velocity of hydroperoxide was studied on the next two reaction mixtures;

A: methyl ethyl ketone 0.05 mol., *tert*-butylhydroperoxide 0.028 mol. and potassium hydroxide 0.03 mol. are all dissolved in 250 ml. of water.

B: methyl ethyl ketone 0.05 mol., *tert*-butylhydroperoxide 0.028 mol. and potassium hydroxide 0.06 mol. are all dissolved in 250 ml. of water.

The decomposition velocity of the hydroperoxide was in A: 0.30 mol./1 hr., in B: 0.40 mol./1 hr. at 35.0°C and in A: 0.49 mol./1 hr., in B: 0.60 mol./1 hr. at 40.2°C (unpublished work).

Cf. Maruyama, Goto and Kitamura, Oxidizing Action of Hydroperoxide III. under the contribution to *J. Chem. Soc. Japan, Pure Chem. Soc.* (*Nippon Kagaku Zasshi*).

5) O. Soga, K. Maruyama and R. Goto, *J. Chem. Soc. Japan, Pure Chem. Sec.* (*Nippon Kagaku Zasshi*), **81**, 668 (1960).

# *Rates of Solvolysis of Di-p-toluenesulfoxycyclohexanes*

By Nobuo MORI

(Received May 23, 1960)

In the previous paper[1] it was reported that *trans*-1,3-di-*p*-toluenesulfoxycyclohexane, in which one of two toluenesulfoxyl groups was axial and the other equatorial in stable form, was solvolyzed more rapidly than the cis form, in which two toluenesulfoxyl groups were equatorial in stable form, in agreement with the general rule as described below. However, it was unexpectedly observed that solvolysis of *trans*-4-hydroxy- or -acetoxy-cyclohexyl *p*-tosylate in which two substituents were equatorial proceeded at a rate twice as fast as that of the corresponding cis isomer in which one of two substituents was axial and the other equatorial[2]. In connection with the unexpected result mentioned above it was desirable to study further the configuration and the reactivity of the 4-substituted cyclohexyl *p*-tosylates.

In the present work, also in relation to the problem mentioned above, the solvolysis of 1,2- and 1,4-di-*p*-toluenesulfoxycyclohexanes (described as ditosylates in this paper) has been made.

## Experimental

**Samples.** — *cis*- and *trans*-Cyclohexane-1,2- and -1,4-diols used as starting materials were those which were previously prepared[2,3]. Each of them was treated in pyridine at 0 to 5°C with two equivalent quantities of *p*-toluenesulfonyl chloride according to the conventional method, and the resulting ditosylate was recrystallized from a mixture of benzene and ligroin. The ditosylates obtained in this way had respectively the following melting points.

| Position of tosyl groups | M. p. (reported m. p.), °C |
|---|---|
| *cis*-1,2 | 129～130 (128.5～129.5[4]) |
| *trans*-1,2 | 109～110 (109[4]) |
| *cis*-1,4 | 98～98.5 (98～99[5]) |
| *trans*-1,4 | 159 (159°[5]) |

**Procedure for Rate Measurements.**—Solvolysis rates were measured at 99.8°C in ethanol (98.5% by weight), in methanol (99.5% by weight) and in acetic acid containing a slight excess of acetic anhydride, by the usual ampoule technique[1,2]. Concentrations (all given at room temperature) of ditosylates were in the range from 0.005 to 0.01 mol./l., since they are less soluble in these solvents, especially in alcohol. Solvolysis of 1,4-ditosylates was performed in 0.01 mol./l. in acetic acid and also in 0.005 mol./l. in methanol since the solubility of the compounds in ethanol was very small, and that of 1,2-ditosylates was performed in ethanol. The reactions were followed by titrating at intervals for the sulfonic acid liberated or the alkali consumed during the solvolysis. Titrations in acetic acid were carried out with a 0.05 N solution of anhydrous sodium acetate or *p*-toluenesulfonic acid in acetic acid using bromophenol blue as indicator. In methanol and ethanol, a 0.05 N aqueous solution of sodium hydroxide or hydrogen chloride was used as a standard solution for titration with phenolphthalein as indicator. Rate constants were calculated from the formula:

$$k_1 = (1/t)\ln\{a/(a-x)\}$$

in which $a$ was the initial concentration of ditosylate and $x$ was the concentration of sulfonic acid liberated at time $t$.

## Results and Discussion

The solvolysis of the di-tosylates will proceed substantially in two steps as described below, and therefore a real solvolysis rate constant for each of them is not shown by the averaged value of the rate constants calculated from the formula. In fact, a calculated rate constant increased gradually during the alcoholysis and the acetolysis, and decreased gradually during the alcoholysis in the presence of a small amount of sodium alcoholate, in agreement with the behavior of 3-methylcyclohexyl *p*-tosylate and 1,3-di-*p*-toluenesulfoxycyclohexanes previously reported[1]. But, in all cases, since the differences between the rate constants and the averaged rate constant in the solvolysis were within 5%, the solvolysis could be approximately expressed as the first order reaction. Table I lists the data for a run with *cis*-1,4-ditosylate in acetic acid. It is seen that, though the first order rate constant increases gradually during the solvolysis, it is approximately constant.

The mean rate constants of the acetolysis of the 1,4-ditosylates were not substantially changed by the addition of a small quantity

1) N. Mori, *J. Chem. Soc. Japan, Pure Chem. Sec.* (*Nippon Kagaku Zasshi*), **80**, 1458 (1959).
2) N. Mori, This Bulletin, **33**, 1332 (1960).
3) N. Mori, ibid., **33**, 1144 (1960).
4) R. Criegee and H. Stanger, *Ber.*, **69**, 2753 (1936).
5) L. N. Owen and P. A. Robins, *J. Chem. Soc.*, **1949**, 320.

Table I. Acetolysis of *cis*-1,4-di-*p*-toluenesulfoxycyclohexane at 99.8°C

| Time, min. | Ditosylate, mol.×10² | $k_1\times10^2$/min. |
|---|---|---|
| 0.0 | 1.03 | |
| 40.0 | 0.92 | 0.269 |
| 100.0 | 0.786 | 0.267 |
| 160.0 | 0.666 | 0.269 |
| 280.0 | 0.448 | 0.294 |
| 400.0 | 0.304 | 0.303 |
| | | Mean 0.280 |

of anhydrous sodium acetate, and therefore the acetolysis is predominantly of the unimolecular type. On the other hand, since the mean rate constants of the alcoholysis were decreased by the addition of sodium alcoholate, and under this condition the rate constant decreased during the solvolysis as described above, a part of the alkaline alcoholysis consists of the bimolecular displacement and elimination reactions based on a back-side attack on carbon and hydrogen coincident with the departure of the toluenesulfoxyl group. The rate constants and the relative rates for the isomeric di-tosylates are summarized in Tables II and III.

Table II. Rate constants of solvolysis of di-*p*-toluenesulfoxycyclohexanes

| Position of tosyl groups | Tosylate, mol./l. | Solvent | Alkali, mol./l. | $k_1\times10^2$/min. |
|---|---|---|---|---|
| *cis*-1,4 | 0.005 | M | 0.020 a | 2.8 |
| 〃 | 0.005 | M | 0.013 a | 1.7 |
| 〃 | 0.005 | M | | 1.1 |
| 〃 | 0.010 | A | 0.023 b | 0.292 |
| 〃 | 0.010 | A | | 0.280 |
| *trans*-1,4 | 0.005 | M | 0.018 a | 1.7 |
| 〃 | 0.005 | M | 0.013 a | 1.5 |
| 〃 | 0.005 | M | | 1.2 |
| 〃 | 0.010 | A | 0.023 b | 0.603 |
| 〃 | 0.010 | A | | 0.614 |
| *cis*-1,2 | 0.005 | E | 0.015 c | 0.39 |
| *trans*-1,2 | 0.005 | E | 0.015 c | 0.069 |
| *cis*-1,3[1] | 0.010 | E | 0.025 c | 1.5 |
| 〃 | 0.010 | A | 0.026 b | 0.195 |
| *trans*-1,3[1] | 0.010 | E | 0.025 c | 3.5 |
| 〃 | 0.011 | A | 0.027 b | 0.209 |
| *trans*-4-acetoxy cyclohexyl tosylate[2] | 0.026 | A | | 1.61 |

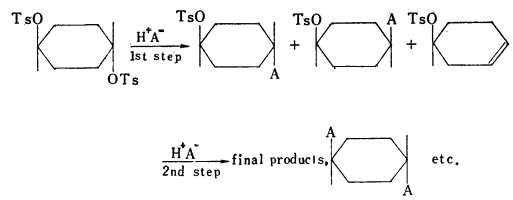
A, acetic acid; M, methanol; E, ethanol; a, sodium methoxide; b, sodium acetate; c, sodium ethoxide.

Table III. Relative rates of solvolysis of 1,4-di-*p*-Toluenesulfoxycyclohexanes

| | MeOH[a] | MeOH[b] | MeOH[c] | AcOH[d] | AcOH[c] |
|---|---|---|---|---|---|
| $k_{cis}$ | 10.0 | 6.0 | 4.0 | 1.04 | 1.0 |
| $k_{trans}$ | 2.8 | 2.4 | 2.0 | 0.98 | 1.0 |
| $k_{cis}/k_{trans}$ | 1.6 | 1.1 | 0.9 | 0.48 | 0.45 |

a, contained sodium methoxide in 0.02 mol./l.
b, contained sodium methoxide in 0.013 mol./l.
c, not contained alkali.
d, contained sodium acetate in 0.023 mol/l.

**Mechanism of Solvolysis.**—The solvolysis of the ditosylates proceeds substantially in two steps where in the first step three monotosylates are produced and in the second step they are converted into final products. For example, in the case of *trans*-1,4-ditosylate, the process is illustrated by the following formula:



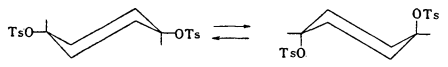

where $H^+A^-$ is the solvent and Ts is the tosyl group.

In the present work, it has been observed that a calculated rate constant increased gradually during the neutral alcoholysis and the acetolysis. The increase in the rate constants is probably due to the fact that the reaction rate in the second step is higher than that in the first step, as explained for the similar behavior of 1,3-di-*p*-toluenesulfoxycyclohexanes[1]. This suggestion is supported for example by the experimental facts that the acetolysis rate of *trans*-4-acetoxycyclohexyl *p*-tosylate is 1.7 times that of the *trans*-1,4-ditosylate and 3.4 times that of the *cis*-1,4-ditosylate, and that 2-acetoxycyclohexyl *p*-tosylates[6] and 2-hydroxycyclohexyl *p*-brosylates[3] are rapidly solvolyzed, but 1,2-ditosylates are not acetolyzed.

**Relative Rate $k_{cis}/k_{trans}$.**—The relation between conformation and reactivity in a rigid cyclohexane system is very important. An axial group is sterically more strained and therefore, in general, more ionizable or easier to depart than an equatorial group. In the labile cyclohexane system, the trans form of cyclohexyl *p*-tosylate with a group such as the acetoxyl group[6] at the $\beta$-position is solvolyzed more rapidly than the cis isomer, but *trans*-2-substituted cyclohexyl *p*-tosylates and *p*-brosylates with a group such as *p*-bromobenzenesulfoxyl[6], nitroxyl[7], and hydroxyl[3] group are solvolyzed at a slightly faster or slower rate than the corresponding cis forms. *trans*-3-Alkyl[8],

6) S. Winstein, E. Grunwald and L. L. Ingraham, *J. Am. Chem. Soc.*, **70**, 821 (1948).
7) S. J. Cristol and B. Franzus, ibid., **79**, 2488 (1957).
8) S. Winstein and H. J. Holmess, ibid., **77**, 5562 (1955).

hydroxy[1], acetoxy[1] or methoxycarbonyl[9] cyclohexyl *p*-tosylate is solvolyzed more rapidly than the corresponding cis from. Further, *cis*-4-alkylcyclohexyl *p*-tosylate is solvolyzed more rapidly than the trans form[8]. The *trans*-1, 4-ditosylate has the two possible chair conformations as follows:



trans (e, e) trans (a, a)

The trans (e, e) is more stable than the trans (a, a). On the other hand, the cis form has only one chair conformation as follows:



cis (e, a) cis (a, e)

where Ts is the toluenesulfonyl group.

Similarly, also in the case of the 1, 2-ditosylates, the cis form has two chair conformations and the trans form only one. From those facts it is expected that the solvolysis rates of the *cis*-1, 2- and 1, 4-ditosylates are higher than that of the corresponding trans forms.

In the present work, the 1, 2-ditosylates were not solvolyzed in acetic acid after being heated for 20 hr. at 100°C, as reported by Criegee[4]. They were, however, sowewhat ethanolyzed and especially solvolyzed more rapidly in the presence of sodium alcoholate and the relative rate $k_{cis}/k_{trans}$ was 5.6 (see Table II). Winstein[6] reported that the relative rate of acetolysis (75°C) of 1, 2-dibromobenzenesulfoxycyclohexanes was 1.1, although the rate constants of those brosylates were very low. Those facts are in agreement with the expectation described above.

In the solvolysis of the 1, 4-ditosylates, the trans form was solvolyzed in acetic acid unexpectedly at a rate 2.2 times faster than the cis form. Also, a similar result was obtained in the acetolysis of 1, 4-dibromobenezenesulfoxycyclohexanes[10] and the ratio of $k_{cis}$ to $k_{trans}$ was 0.78. Those facts are substantially similar to the results previously obtained in the solvolysis of 4-hydroxy- and 4-acetoxycyclohexyl tosylates[2], and are not explained by the rule as described above. Up to the present, the author can not give reasons for the fact that the trans form was acetolyzed more rapidly than the cis form. However, the methanolysis of the ditosylates, especially in the presence of alkali, proceeded more rapidly than their acetolysis and the cis form was methanolyzed more rapidly than the trans form. Thus, the ratio of $k_{cis}$ to $k_{trans}$ was 0.9 in methanol without alkali, 1.1 in methanol with NaOMe in 0.013 mol./l. and 1.6 in methanol with NaOMe in 0.02 mol./l.

**Solvent and Alkali Effects.**—In general, in unimolecular reaction solvation with solvent is very important, and the solvolysis rate in acetic acid is higher than that in ethanol. Further, such an enhancement in the rate in going from ethanol to acetic acid is nicely shown in the case of unsubstituted and substituted cyclohexyl tosylates. For example, the ratio of $k_{EtOH}$ to $k_{AcOH}$ for the cis form (with a-tosyl group) of 4-*tert*-butylcyclohexyl tosylate is 0.87 and that for the trans form (with e-tosyl group) 0.72[8]. On the other hand, primary alkyl tosylates, which are sensitive to a nucleophilic attack, are more reactive in ethanol than in acetic acid, such as those shown by the solvent-rate sequences[11] (EtOH : AcOH) for MeOTs, EtOTs and *iso*-BuOTs respectively to be 80 : 1, 39 : 1 and 6.2 : 1 at 75°C.

Furthermore, a carbon atom having an a-tosyl group is more easily attacked by a nucleophilic agent than that having an e-tosyl group, and the bimolecular reaction[12] of *cis*-*tert*-butylcyclohexyl tosylate with phenolate ion proceeds more rapidly than that of the trans form.

In the present work, however, the ditosylates were solvolyzed more rapidly in alcohol, especially in the presence of alkali, than in acetic acid and the solvolysis rate of the cis forms with the a-tosyl group was enhanced more than that of the trans forms without such a group, in going from acetic acid to alcohol containing alkali. Therefore, the alcoholysis and the alkaline alcoholysis of the di-tosylates probably involve bimolecular nucleophilic attack on carbon or hydrogen in the rate-determining step, similar to the primary alkyl tosylates, but in contrast to the general cyclohexyl tosylates.

## Summary

Rates of solvolysis of *cis*- and *trans*-1, 2- and -1, 4-di-*p*-toluenesulfoxycyclohexanes were measured at 99.8°C in methanol or in acetic acid. In all cases, the solvolysis was approximately of first order.

Mean rate constants of the solvolysis increased in going from acetic acid to alcohol, and were enhanced by the addition of a small

9) D. S. Noyce and H. J. Weingarten, ibid., **79**, 3103 (1957).

10) N. Mori, unpublished work. The $k_1$ of the cis form was 1.13 and that of the trans form 1.44 at 99.8°C.

11) S. Winstein and H. Marshall, *J. Am. Chem. Soc.*, **74**, 1120 (1952).

12) E. L. Eliel and R. S. Ro, ibid., **79**, 5995 (1958).

amount of alkali, in agreement with the behavior in solvolysis of primary alkyl tosylates.

The 1, 2-isomers were not solvolyzed in acetic acid in 20 hr., and in ethanol containing EtONa in 0.02 mol./l., the ratio of $k_{cis}$ to $k_{trans}$ was 5.6.

In the case of the 1, 4-isomers, the ratio was ca. 0.5 in acetic acid, 0.9 in methanol without alkali, 1.1 in methanol with MeONa in 0.013 mol./l. and 1.6 in methanol with MeONa in 0.02 mol./l.

The author wishes to express his hearty thanks to Professor Y. Tsuzuki for his advice.

*Tokyo College of Science*
*Kagurazaka, Shinjuku-ku*
*Tokyo*

# *Phase Relationship in System $3CaO \cdot P_2O_5$-MgO-$SiO_2$*

By Toshiyuki SATA

(Received July 6, 1960)

The author already presented in 1958 the result of a study on system $3CaO \cdot P_2O_5$–MgO·$SiO_2$–$SiO_2$ in this Bulletin[1]. This is a partial system at high silica portion in the three-component system $3CaO \cdot P_2O_5$–MgO–$SiO_2$. The present report concerns a basic portion in the system $3CaO \cdot P_2O_5$–MgO–$SiO_2$, and its phase relationships are important for the study of a composition of fused phosphate fertilizer[2] and a corrosion problem of magnesia-containing basic refractories against the molten fertilizer. This report consists of four parts; system $3CaO \cdot P_2O_5$–MgO, system $3CaO \cdot P_2O_5$–$2MgO \cdot SiO_2$, system $3CaO \cdot P_2O_5$–MgO–$2MgO \cdot SiO_2$, and the synthesis of these to system $3CaO \cdot P_2O_5$–MgO–$SiO_2$. Phase equilibria studies in these systems have never been published in any paper.

## Experimental

Tricalcium phosphate ($3CaO \cdot P_2O_5$), forsterite ($2MgO \cdot SiO_2$), and magnesia (MgO) were used as raw materials. The first was prepared by the reaction of calcium carbonate with phosphoric acid at 1350°C as mentioned in the previous paper[1]. The second was prepared by calcining the stoichiometric mixture of magnesia and silica constituents at 1300°C. The magnesia and silica fired from 1200 to 1300°C were used as raw materials respectively. After weighing, the batches were thoroughly mixed in an agate mortar with some methyl alcohol until they became dry. They were heated in a platinum crucible or in a platinum envelope above their melting points. Then they were rapidly cooled in air or water. For batches having the melting point above 1600°C, perfect glassification was impossible. These mixing, heating, and quenching processes were repeated once more.

The silicon carbide resister furnace with an inner diameter of 25 mm. was used for this study. The sample in a platinum envelope (8×8 mm.) was suspended by a platinum wire (0.5 mm. in diameter, 200 mm. in length) at the center of the furnace tube, and quenched together with the wire in water after holding for some minutes at constant temperature (±1°C). For measuring the temperature, two kinds of thermocouples (Pt-PtRh 10% and PtRh 5%-PtRh 20%) were used. These were calibrated with the melting point of silver, copper, diopside, and palladium.

The quenched samples were powdered and examined by a polarizing microscope and by an X-ray diffractometer. Pure silicon metal was used as a standard material in X-ray examination, its accuracy being ±0.003 Å

## Results and Discussion

**System $3CaO \cdot P_2O_5$–MgO.** — In the first place, specimens slowly cooled from 1650°C were examined in their microstructure. The specimen containing 3.20% of MgO consisted of a primary crystal part of $\beta$-tricalcium phosphate and an eutectic part which is a turbid phase containing periclase spots surrounded by tricalcium phosphate matrix. The specimen containing 5.28% of MgO revealed the eutectic structure only. The specimen containing 7.98% of MgO consisted of the eutectic part and large periclase grains. The softening temperatures of small cones of these three compositions were measured on platinum plates in the usual way. It was found that their temperatures decreased in order of contents of MgO ranging from 1620 to 1530°C.

1) T. Sata, This Bulletin, **31**, 408 (1958).
2) T. Sata and R. Kiyoura, *J. Chem. Soc. Japan, Ind. Chem. Sec.* (*Kogyo Kagaku Zasshi*), **62**, 63 (1959).

TABLE I. QUENCHING DATA IN THE SYSTEM $3CaO \cdot P_2O_5$–MgO

| No. | Composition | | | Holding | | Phases present |
|---|---|---|---|---|---|---|
| | $C_3P$ wt. % | MgO | MgO mol. % | temp. °C | time min. | |
| 193 | 99 | 1.0 | 7.2 | 1470 | 60 | $\beta$-$C_3P$, $\alpha$-$C_3P$ |
| 19 | 98.58 | 1.42 | 10.0 | 1450 | 60 | $\beta$-$C_3P$ |
| 20 | 96.8 | 3.2 | 20.0 | 1568 | 15 | $\beta$-$C_3P$, small $\alpha$-$C_3P$, periclase, glass |
| | | | | 1450 | 60 | $\beta$-$C_3P$, periclase |
| 21 | 94.7 | 5.3 | 30.0 | 1568 | 15 | $\beta$-$C_3P$, periclase |
| 22 | 92.1 | 7.9 | 40.0 | 1568 | 15 | $\beta$-$C_3P$, periclase |
| | | | | 1555 | 10 | 〃 |
| | | | | 1524 | 10 | 〃 |

The subsequent quenching runs, as listed in Table I, indicated that the specimen containing 3.20% of MgO, quenched from 1568°C, consisted of tricalcium phosphate ($\beta$ and small amount of $\alpha$), periclase, and glass. It is estimated from these results that this $3CaO \cdot P_2O_5$–MgO system is a binary one and its eutectic occurred at a composition of 4～7% of MgO and at a temperature near 1570±20°C, as shown in Fig. 1.

It is noted from Fig. 2, in which some X-ray diffraction lines of $\beta$-tricalcium phosphate quenched from 1450°C are plotted, that 15±3 mol. % of MgO is apparently dissolved into $\beta$-tricalcium phosphate as a solid solution. Another fact is that the transition temperature of $\beta$-$\alpha$ modification is considerably elevated nearly to 1550°C with increasing magnesia contents. These facts concerning tricalcium phosphate are difficult to discuss further without direct examination by a high-temperature X-ray technique. There is a new presentation of super $\alpha$-$3CaO \cdot P_2O_5$ phase by Nurse et al.[3]

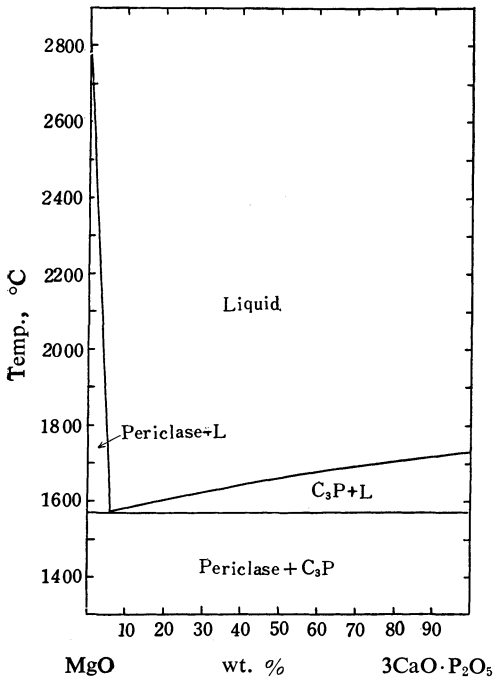



Fig. 1. The system $3CaO \cdot P_2O_5$–MgO.

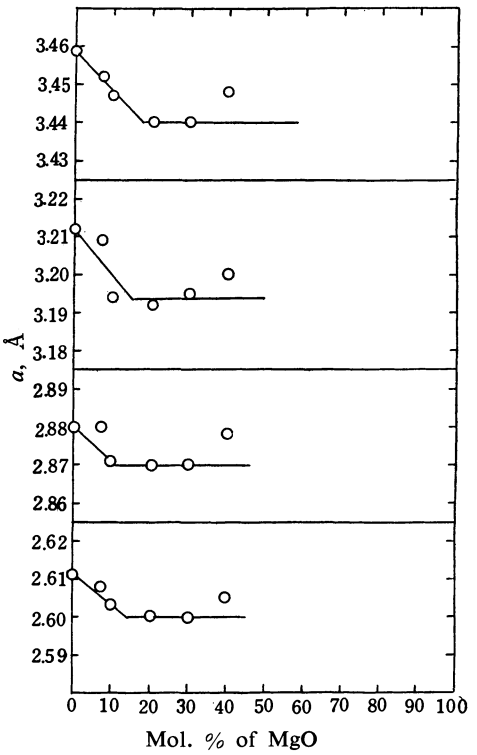



Fig. 2. The change in spacings of $\beta$-tricalcium phosphate at 1450°C in the system $3CaO \cdot P_2O_5$–MgO.

**System $3CaO \cdot P_2O_5$–$2MgO \cdot SiO_2$.** — Fasting and Haroldsen[4] have made X-ray tests of specimens in this system fired at 1000～1500°C, and Bobrownicki and Swiecki[5] have measured

3) R. W. Nurse, J. H. Welch and W. Gutt, *J. Chem. Soc.*, **1959**, 1077.
4) J. P. Fasting and H. Haroldsen, *Tid. Kjemi., Bergvesen Met.*, 3, 48 (1943); *Chem. Abstr.*, **39**, 13419 (1945).
5) W. Bobrownicki and Z. Swiecki, *Bull. Acad. Polon. Sci., Classe* III, 3, 232 (1955); *Chem. Abstr.*, **49**, 15419 (1955).

TABLE II. QUENCHING DATA IN THE SYSTEM $3CaO \cdot P_2O_5$-$2MgO \cdot SiO_2$

| No. | Composition | | Holding | | Phases present |
|---|---|---|---|---|---|
| | $C_3P$ wt. % | $M_2S$ | temp. °C | time min. | |
| 191 | 98 | 2 | 1342 | 60 | $\beta$-$C_3P$ only |
| 75 | 95 | 5 | 1370 | 60 | $\beta$-$C_3P$, gl. |
| | | | 1340 | 40 | $\beta$-$C_3P$ |
| | | | 1290 | 120 | $\beta$-$C_3P$ |
| | | | 1242 | 180 | $\beta$-$C_3P$, faint forst. |
| 192 | 93 | 7 | 1342 | 60 | $\beta$-$C_3P$ only |
| 71 | 90 | 10 | 1517 | 30 | $\alpha$-$C_3P$, $\beta$-$C_3P$, gl. |
| | | | 1467 | 60 | $\alpha$-$C_3P$, $\beta$-$C_3P$, gl. |
| | | | 1442 | 50 | $\beta$-$C_3P$, $\alpha$-$C_3P$, gl. |
| | | | 1392 | 60 | $\beta$-$C_3P$, gl. |
| | | | 1372 | 540 | $\beta$-$C_3P$, gl. |
| | | | 1340 | 40 | $\beta$-$C_3P$ |
| | | | 1312 | 40 | $\beta$-$C_3P$ |
| | | | 1290 | 40 | $\beta$-$C_3P$, forst. |
| 70 | 80 | 20 | 1545 | 20 | Ng., gl. |
| | | | 1442 | 20 | Ng., gl. |
| | | | 1392 | 60 | Ng., $\beta$-$C_3P$, gl. |
| | | | 1372 | 60 | $\beta$-$C_3P$, Ng., gl. |
| | | | 1357 | 40 | $\beta$-$C_3P$, gl. |
| | | | 1352 | 300 | $\beta$-$C_3P$, forst., small gl. |
| | | | 1342 | 60 | $\beta$-$C_3P$, forst. |
| 72 | 75 | 25 | 1575 | 15 | gl. |
| | | | 1566 | 15 | Ng., gl. |
| | | | 1515 | 15 | Ng., gl. |
| | | | 1374 | 40 | $\beta$-$C_3P$, Ng., gl. |
| | | | 1352 | 40 | $\beta$-$C_3P$, forst. |
| 73 | 72.5 | 27.5 | 1548 | 15 | Ng., gl. |
| | | | 1528 | 15 | Ng., gl. |
| | | | 1442 | 60 | Ng., gl. |
| | | | 1382 | 40 | $\beta$-$C_3P$, Ng., gl. |
| | | | 1372 | 40 | $\beta$-$C_3P$, Ng., forst., gl. |
| | | | 1365 | 50 | $\beta$-$C_3P$, forst., small gl. |
| | | | 1352 | 40 | $\beta$-$C_3P$, forst. |
| 66 | 70 | 30 | 1398 | 40 | gl. |
| | | | 1392 | 40 | $\beta$-$C_3P$, Ng., faint forst., gl. |
| | | | 1372 | 40 | $\beta$-$C_3P$, Ng., forst., gl. |
| | | | 1347 | 40 | $\beta$-$C_3P$, forst. |
| 74 | 67.5 | 32.5 | 1432 | 60 | gl. |
| | | | 1407 | 50 | $\beta$-$C_3P$, small forst., gl. |
| | | | 1374 | 40 | $\beta$-$C_3P$, forst. |
| 67 | 60 | 40 | 1465 | 40 | gl. |
| | | | 1458 | 20 | forst. gl. |
| | | | 1452 | 40 | Ng., forst., gl. |
| | | | 1400 | 60 | Ng., small forst. |
| | | | 1382 | 50 | Ng., forst. |
| | | | 1342 | 60 | $\beta$-$C_3P$, forst. |
| | | | 1300 | 60 | $\beta$-$C_3P$, forst. |
| 68 | 50 | 50 | 1537 | 20 | gl. |
| | | | 1522 | 20 | forst., gl. |
| | | | 1507 | 20 | forst., gl. |
| | | | 1442 | 60 | Ng., forst., gl. |
| 69 | 40 | 60 | 1442 | 60 | Ng., forst., gl. |

Abbreviations: $C_3P = 3CaO \cdot P_2O_5$, $M_2S = 2MgO \cdot SiO_2$, Ng. = nagelschmidtite forst. = forsterite, gl. = glass.

the softening points of this system. But the phase relationships of this system have not been presented.

Results of the quenching runs of this two-component system are summarized in Table II, from which a preliminary phase diagram of this system was obtained as shown in Fig. 3. Nagelschmidtite[6] (which was identified by a hexagonal X-ray pattern similar to that in $3CaO \cdot P_2O_5$–$2CaO \cdot SiO_2$ system) appeared over a wide range of this system above a temperature of 1350°C, and was crystallized primarily in the composition range of $3CaO \cdot P_2O_5$ side.

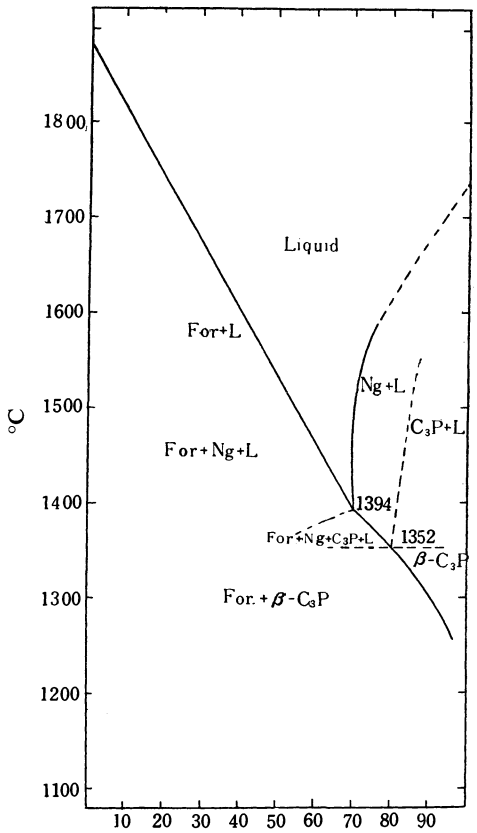



Fig. 3. The system $3CaO \cdot P_2O_5$–$2MgO \cdot SiO_2$.

The liquidus line falls very steeply to a temperature minimum at 1394°C and a composition of 70% $3CaO \cdot P_2O_5$ and 30% $2MgO \cdot SiO_2$. Below this temperature 1394°C, the secondary crystallization temperature of forsterite from nagelschmidtite and liquid decreases. Below 1352°C, nagelschmidtite and liquid disappeared, and forsterite and β-tricalcium phosphate phase only appeared. The meaning of this disappearance temperature 1352°C is not clear now. β-Tricalcium phosphate seems to contain magnesia component, judging from the fact that the crystallization temperature of forsterite from β-tricalcium phosphate phase descends with increasing contents of $3CaO \cdot P_2O_5$, and *d*-spacings of β-tricalcium phosphates in their X-ray patterns decrease till the content of 15 mol. % (7.4 weight %) of $2MgO \cdot SiO_2$ is attained, as shown in Fig. 4. Below about 1200°C, this two-component system is a binary one consisting of forsterite and β-tricalcium phosphate.

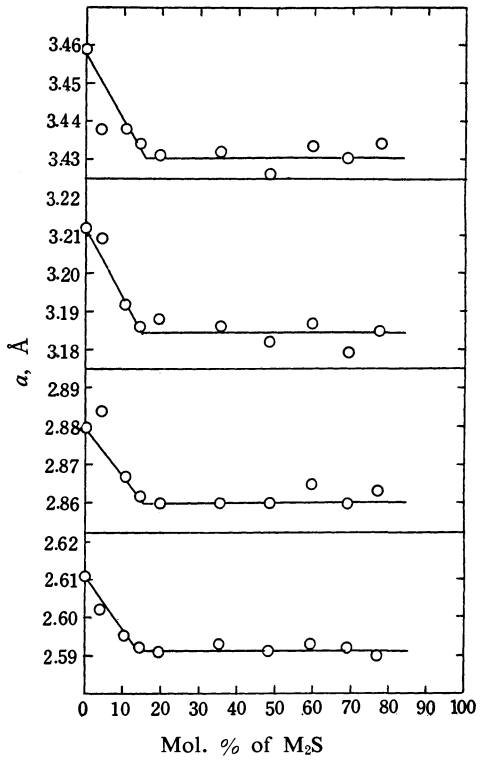



Fig. 4. The change in spacings of β-tricalcium phosphate in the system $3CaO \cdot P_2O_5$–$2MgO \cdot SiO_2$.

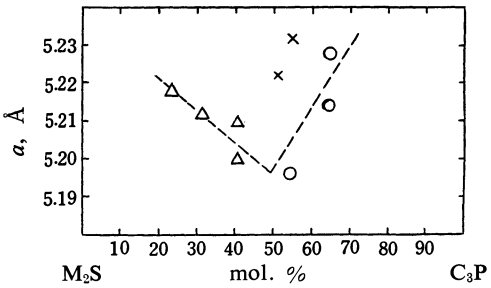



Fig. 5. The change in lattice constants of nagelschmidtite in the system $3CaO \cdot P_2O_5$–$2MgO \cdot SiO_2$ at 1370~1490°C.
○ Ng.+L, △ Ng.+forst.+L,
× Ng.+β-$C_3P$+L

6) G. Nagelschmidt, *J. Chem. Soc.*, 1937, 865.

When the lattice constants $a$ of hexagonal negelschmidtite are calculated from their (110) peak and plotted against molar compositions, a valley-type change are obtained, whose bottom may occur at the composition of temperature minimum of liquidus as shown in Fig. 5.

From the results mentioned above, this system was found to be complex, owing to the formation of nagelschmidtite above 1350°C, below which it is considered to be binary.

**System $3CaO \cdot P_2O_5$ – MgO – $2MgO \cdot SiO_2$.** — Although all of the specimens of this system slow-cooled to room temperature consisted of $\beta$-tricalcium phosphate, periclase, and forsterite, the primary crystal in the area of high content of $3CaO \cdot P_2O_5$ was nagelschmidtite, being the same as that mentioned in the system $3CaO \cdot P_2O_5$–$2MgO \cdot SiO_2$. But it was found by the preliminary quenching test that a ternary eutectic among their three components seems to be present. This paragraph described results of quenching experiments made to decide the position of a three-component eutectic.

The twelve compositions, which are expected to locate near the eutectic, were taken on the two tie lines connecting No. 24 ($60C_3P$–40M) with No. 72 ($75C_3P$–$25M_2S$) and No. 74 ($67.5C_3P$–$32.5M_2S$) along the $C_3P$–$M_2S$ join, as represented in Fig. 6. Results obtained are listed in Table III, from which a eutectic position was graphically decided to locate at the composition of 70% $3CaO \cdot P_2O_5$, 21% MgO and 9% $SiO_2$, and at 1362±5°C.

This eutectic temperature is close to the transition point between nagelschmidtite and $\beta$-tricalcium phosphate. It was, however, found that $\beta$-tricalcium phosphate was present at this eutectic temperature. The primary field of nagelschmidtite was approximately estimated as a dotted boundary from the previous results of the investigation in the systems $C_3P$–MS and $C_3P$–$M_2S$. The facts that a small amount of periclase was present even in the specimens quenched above liquidus temperatures of all compositions, and that nagelschmidtite was present even in the primary field of periclase or forsterite above eutectic

TABLE III. QUENCHING DATA IN THE SYSTEM $3CaO \cdot P_2O_5$–MgO–$2MgO \cdot SiO_2$

| No. | Composition wt. % | | $C_3P$ | M wt. % | S | Holding temp. °C | Holding time min. | Phases present (peri. = periclase) |
|---|---|---|---|---|---|---|---|---|
| | No. 74 | No. 24 | | | | | | |
| 78 | 95 | 5 | 67.1 | 19.7 | 13.2 | 1442 | 60 | gl. (faint peri.) |
| | | | | | | 1407 | 40 | small forst., peri., gl. |
| | | | | | | 1364 | 60 | $\beta$-$C_3P$, forst., peri. |
| 80 | 90 | 10 | 66.8 | 20.7 | 12.5 | 1442 | 60 | small peri., gl. |
| | | | | | | 1412 | 50 | small forst., gl. |
| | | | | | | 1392 | 50 | $\beta$-$C_3P$, forst., gl. |
| 81 | 85 | 15 | 66.4 | 21.8 | 11.8 | 1407 | 50 | small peri., gl. |
| | | | | | | 1382 | 50 | $\beta$-$C_3P$, small forst., gl. |
| 82 | 80 | 20 | 66.0 | 22.9 | 11.1 | 1422 | 40 | gl. |
| | | | | | | 1392 | 60 | peri., gl. |
| | | | | | | 1382 | 50 | $\beta$-$C_3P$, forst., gl. |
| 83 | 75 | 25 | 65.6 | 24.0 | 10.4 | 1390 | 50 | peri., gl. |
| | | | | | | 1382 | 50 | $\beta$-$C_3P$, forst., peri., gl. |
| 101 | 65 | 35 | 64.9 | 26.1 | 9.0 | 1382 | 40 | peri., gl. |
| | | | | | | 1372 | 40 | peri., $\beta$-$C_3P$, forst. |
| 102 | 55 | 45 | 64.2 | 28.2 | 7.6 | 1365 | 20 | peri., gl. |
| | | | | | | 1356 | 60 | peri., $\beta$-$C_3P$, forst. |
| 103 | 45 | 55 | 63.3 | 30.4 | 6.3 | 1375 | 40 | peri., gl. |
| | | | | | | 1356 | 40 | $\beta$-$C_3P$, forst., peri. |
| 104 | 35 | 65 | 62.6 | 32.5 | 4.9 | 1356 | 50 | $\beta$-$C_3P$, forst., peri. |
| | No. 72 | No. 24 | | | | | | |
| 151 | 90 | 10 | 73.5 | 16.9 | 9.6 | 1372 | 60 | peri., gl. |
| 152 | 80 | 20 | 72.0 | 19.5 | 8.5 | 1398 | 40 | Ng., peri., gl. |
| | | | | | | 1372 | 50 | Ng., peri., gl. |
| | | | | | | 1369 | 40 | $\beta$-$C_3P$, peri., forst., gl. |
| | | | | | | 1364 | 25 | no gl. |
| 153 | 70 | 30 | 70.5 | 22.0 | 7.5 | 1372 | 60 | peri., Ng., gl. |
| | | | | | | 1364 | 40 | peri., $\beta$-$C_3P$, forst., gl. |

temperature, were neglected in drawing this phase diagram at the step of this study, Detailed studies of the system containing nagelschmidtite will be made in future, because of the interesting scope of nagelschmidtite structure (super $\alpha$-tricalcium phosphate by Nurse or its solid solution containing MgO and $SiO_2$).

**System $3CaO \cdot P_2O_5$–MgO–$SiO_2$.** — The preliminary phase diagram, as shown in Fig. 6, was obtained from the results of previous paragraphs and the separate report of the system $3CaO \cdot P_2O_5$–$MgO \cdot SiO_2$–$SiO_2$[1]. The probable boundary curve between the phosphate and the forsterite fields in the $3CaO \cdot P_2O_5$–$2MgO \cdot SiO_2$–$MgO \cdot SiO_2$ triangle was drawn from the results without a cooling experiment.

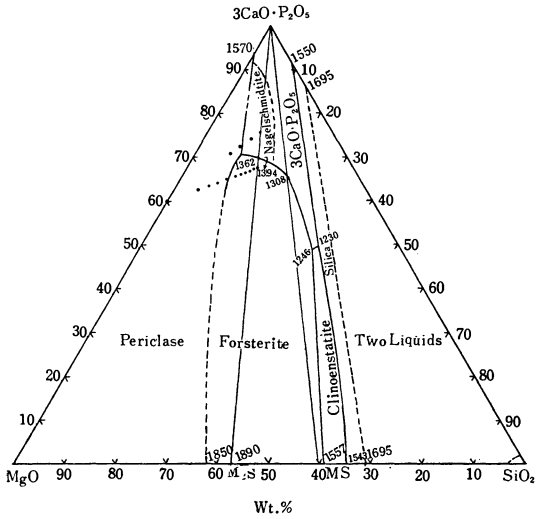



Fig. 6. The system $3CaO \cdot P_2O_5$–MgO–$SiO_2$.

## Summary

The phase relationship in the system $3CaO \cdot P_2O_5$–MgO–$SiO_2$ was investigated by a cooling experiment in the usual manner. The system $3CaO \cdot P_2O_5$–MgO, a side of this triangle, is a simple binary one, its eutectic being located at the composition of 4~7% by weight of magnesia and 1570±20°C. The system $3CaO \cdot P_2O_5$–$2MgO \cdot SiO_2$ is not binary over the temperature of about 1350°C, below which it is considered as binary. Above 1350°C, nagelschmidtite is formed over the whole composition range and crystallized primarily from liquid at a high $3CaO \cdot P_2O_5$ portion. The minimum liquidus temperature is 1394°C, which is located at the composition of 70% $C_3P$ and 30% $M_2S$. The system $3CaO \cdot P_2O_5$–MgO–$2MgO \cdot SiO_2$ was considered to be complex owing to the presence of nagelschmidtite, but the eutectic among their three components is located at the composition of 70% $3CaO \cdot P_2O_5$, 21% MgO, and 9% $SiO_2$, and 1362±5°C.

From the results described above and from those of the author's previous reports, the preliminary phase diagram of the system $3CaO \cdot P_2O_5$–MgO–$SiO_2$ was constructed. In this diagram the problem that nagelschmidtite is formed in the composition range which is rich in $3CaO \cdot P_2O_5$ was not mentioned in detail. In addition to this, it was found by X-ray examination that $\beta$-tricalcium phosphate may be apparently stabilized at a higher temperature than $\beta$-$\alpha$ transition point, and has the appearance of dissolving magnesia component.

The author acknowledges the constant help and encouragement given by Professor R. Kiyoura, Tokyo Institute of Technology. This work was conducted as a part of a program to investigate the corrosion problems of various refractory bricks in the manufacture of fused phosphate fertilizer.

*Research Laboratory of Engineering Materials*
*Tokyo Institute of Technology*
*Meguro-ku, Tokyo*

# *Interactions of Surface Active Agents with Congo Red*

By Makoto HAYASHI

(Received April 11, 1960)

Interactions between various surface active agents and many substances such as protein, dyes and polymers have been studied for contribution to the elucidation of fundamental properties of surface active agents to or extend their applications[1-4]. It has been reported that some dyes such as azo, thiazine or triphenylmethane dyes were changed in their spectra with the addition of various substances such as agar, chondroitin sulfate, nucleic acid or albumin[5-9]. The similar effects of surface active agents, though the greater part of these are ionic ones, on the spectral changes of some dyes have also been studied in recent years[10-15]. In the case of non-ionic detergents, a complex formation has been predicted between dyes and detergents[12,15], but details are not known.

In this paper, the metachromatic effects of a non-ionic surface active agent, Tween 80 and a cationic one, cetyl pyridinium chloride on the absorption spectrum of Congo Red solution are reported.

## Experimental

**Reagents.**—The Congo Red used in this experiment was purified by salting out with sodium acetate and recrystallizing several times from water. Tween 80 (Atlas Powder Co.) was dissolved in water to about 5%, ionic impurities were removed by means of ion-exchange resins (Amberlite IR-120, IRA-400), then evaporated and dried in vacuo at about 50°C. Other reagents were recrystallized from water before use.

**Absorption Spectra.**—The absorption spectra of the solutions were measured with a Beckman type spectrophotometer using a 1 cm. glass absorption cell.

**Procedures.**—The procedure used in the preparation of the dye solutions to be measured was as follows: 1 ml. of the Congo Red stock solution ($2.34\times10^{-3}$ mol./l.) was measured in a 100 ml. volumetric flask. Then 1 ml. of the concentrated buffer solution was pipetted in and an appropriate amount of 4.9% Tween 80 solution was added to the flask to obtain the desired pH and detergent concentrations. The entire contents of the flask were then diluted to 100 ml. and stirred sufficiently. It was left to stand for about 30 min. after the preparation in order to secure an equilibrium (it had been confirmed that 30 min. was sufficient for the equilibrium), then the spectrum was measured using an aliquot part of the solution. Another part of solution was used to determine the pH of the solution. In the experiments of cetyl pyridinium chloride, the sample solutions prepared were centrifuged and then the supernatant solutions were used to measure the spectra.

## Results

Fig. 1 represents the absorption spectra of Congo Red solution of $2.34\times10^{-5}$ mol./l. in the presence of various amounts of Tween 80 at the fixed pH of 3.4. The spectrum varies gradually with the addition of Tween 80 and the new absorption peak appears at about 510 m$\mu$. This peak increases in height with increasing concentration of Tween 80 and it becomes constant above the Tween 80 concentration of 0.309%. The isosbestic point is clearly observed among these spectra, which may suggest that there is a definite molecular constitution of the product. An isosbestic point of this kind was also observed in other reports[3,13,15] which studied the interaction between some dyes such as Methyl Orange, Benzopurpurine 4B and Erythrosine and non-ionic or cationic detergents.

Fig. 2 shows the results measured at pH 4.3. As a whole the spectra are similar to those in Fig. 1, but the spectral change occurs with the addition of a smaller amount of Tween 80 than in the case of that at pH 3.4. The wavelength of the absorption peak of the product is the same in both cases.

Fig. 3 shows the change of the absorbance at the absorption peak with the concentration

1) H. B. Bull, *J. Am. Chem. Soc.*, **67**, 10 (1945).
2) S. Mizushima and S. Akabori, "Chemistry of Proteins (Tampaku-shitsu Kagaku)", Vol. II, Kyoritsu Shuppan Co., Ltd, Tokyo (1954), p. 336.
3) C. F. Hiskey and T. A. Downey, *J. Phys. Chem.*, **58**, 835 (1954).
4) M. L. Corrin and W. D. Harkins, *J. Am. Chem. Soc.*, **69**, 679 (1947).
5) L. Michaelis and S. Granick, ibid., **67**, 1212 (1945).
6) A. Levine and M. Schubert, ibid., **74**, 91 (1952).
7) N. Weissman, W. H. Carnes, P. S. Rubin and J. Fisher, ibid., **74**, 1423 (1952).
8) I. M. Klotz, R. K. Burkhard and J. M. Urquhart, ibid., **74**, 202 (1952).
9) J. T. Martin and H. A. Standing, *J. Textile Inst.*, **40**, 671 (1949).
10) A. Levine and M. Schubert, *J. Am. Chem. Soc.*, **74**, 5702 (1952).
11) P. Mukerjee and K. J. Mysels, ibid., **77**, 2937 (1955).
12) T. Nakagawa, K. Tori and K. Kuriyama, *J. Chem. Soc. Japan, Pure Chem. Sec. (Nippon Kagaku Zasshi)*, **77**, 1563, 1684 (1956).
13) T. Kondo, ibid., **76**, 1374 (1955).
14) K. Meguro, ibid., **77**, 72 (1956).
15) J. T. Martin and H. A. Standing, *J. Textile Inst.*, **40**, 689 (1949).

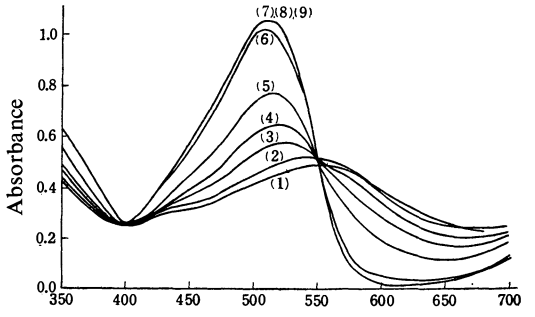



Fig. 1. Absorption spectra of Congo Red solutions containing various amounts of Tween 80 at fixed pH of 3.4; concentration of Congo Red, $2.34\times10^{-5}$ mol./l.; concentration of Tween 80 (%): (1), 0.00; (2), 0.00483; (3), 0.0193; (4), 0.0386; (5), 0.078; (6), 0.155; (7), 0.309; (8), 0.525; (9), 1.05.

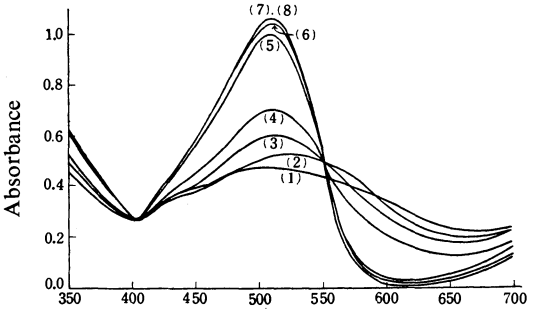



Fig. 2. Absorption spectra of Congo Red solutions containing various amouts of Tween 80 at pH 4.3; concentration of Congo Red, $2.34\times10^{-5}$ mol./l.; concentration of Tween 80 (%): (1), 0.00; (2), 0.005; (3), 0.02; (4), 0.04; (5), 0.08; (6), 0.15; (7), 0.29; (8), 0.58.

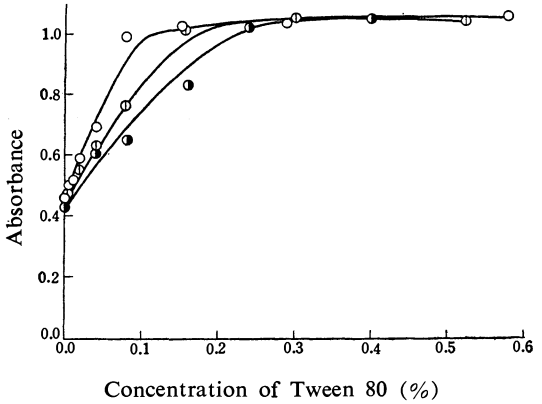



Fig. 3. The absorbances at 510 mμ of Congo Red solutions plotted against increasing concentrations of Tween 80 at three values of pH; ◑ pH 3.0; ◫ pH 3.4; ○ pH 4.3.

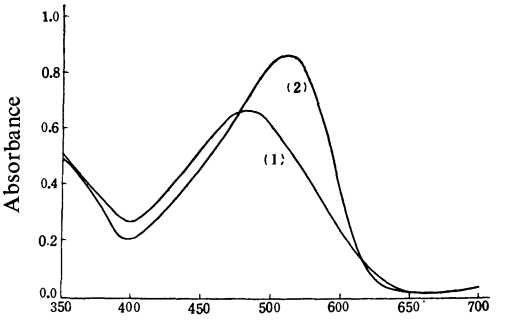



Fig. 4. Effect of the addition of Tween 80 on the absorption spectrum of Congo Red solution at pH 7.0; concentration of Congo Red, $1.87\times10^{-5}$ mol./l.; conccentration of Tween 80 (%): (1), 0.00; (2), 0.35.

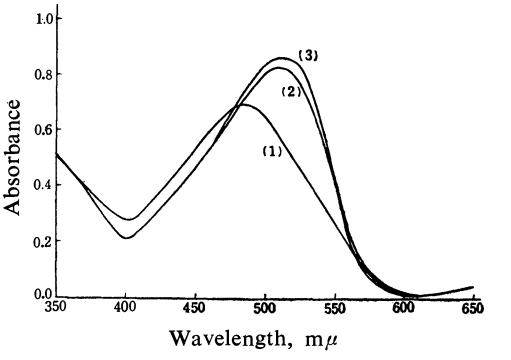



Fig. 5. Effect of the addition Tween 80 on the absorption spectrum of Congo Red solution at pH 9.2; concentration of Congo Red, $1.87\times10^{-5}$ mol./l.; concentration of Tween 80 (%): (1), 0.00; (2), 0.016; (3), 0.16.

of Tween 80 at three values of pH of the dye solution.

The identical effects of Tween 80 are also observed in either the neutral or basic medium, the results being shown in Figs. 4 and 5. In these cases the absorbance at 510 mμ became constant with the addition of a very small amount of the detergent and their spectral changes were not remarkable as compared with that in the acidic medium.

When cetyl pyridinium chloride (c. p. c.) is added to the Congo Red solution at pH 4.2, a spectral shift occurs and indicates the presence of an interaction product between c. p. c. and Congo Red, as shown in Fig. 6. In this case, Congo Red is dispersed by a small quantity of c. p. c., and has an absorption peak at about 660 mμ. When the concentration of the detergent increases, a new peak appears at 460 mμ which may be assigned to the interaction product between Congo Red and c. p. c. This peak increases in height with increasing

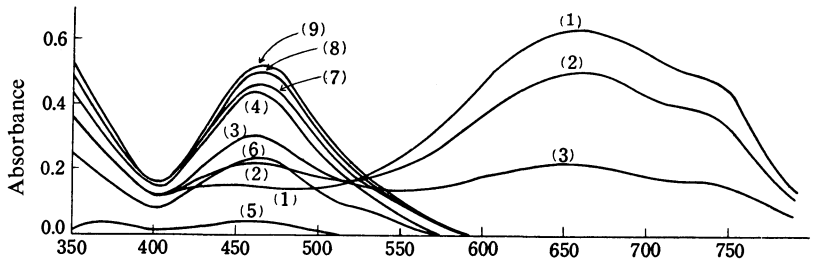



Fig. 6. Absorption spectra of Congo Red solutions containing various amounts of cetyl pyridinium chloride at fixed pH of 4.2; concentration of Congo Red, $2.17\times10^{-5}$ mol./l.; concentration of cetyl pyridinium chloride (mol./l.$\times10^{5}$): (1), 0.725; (2), 1.45; (3), 2.90; (4), 3.63; (5), 4.35; (6), 10.1; (7), 11.6; (8), 14.5; (9), 160.

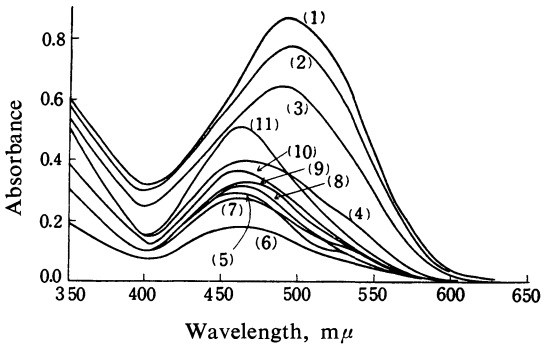



Fig. 7. Absorption spectra of Congo Red solutions containing various amounts of cetyl pyridinium chloride at fixed pH of 7.0; concentration of Congo Red, $2.17\times10^{-5}$ mol./l.; concentration of cetyl pyridinium chloride (mol./l.$\times10^{5}$): (1), 0.00; (2), 0.685; (3), 1.37; (4), 2.74; (5), 3.43; (6), 8.22; (7), 9.59; (8), 11.0; (9), 16.4; (10), 27.4; (11), 68.5.

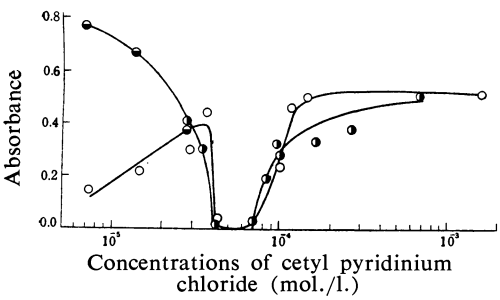



Fig. 8. The absorbances at 464 mμ and 490 mμ (pH 7.0) of Congo Red solutions (from which the precipitates are removed) plotted against the concentrations of cetyl pyridinium chloride at two values of pH: ○, 464 mμ, pH 4.2; ◑, 464 mμ, pH 7.0; ◒, 490 mμ, pH 7.0; concentration of Congo Red, $2.17\times10^{-5}$mol./l.

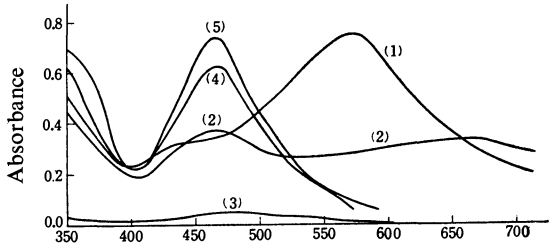



Fig. 9. Effect of the addition of cetyl pyridinium chloride at pH 3.8; concentration of Congo Red, $2.88\times10^{-5}$ mol./l.; concentration of cetyl pyridinium chloride (mol./l.$\times10^{5}$): (1), 0.00; (2), 1.5; (3), 4.5; (4), 30.0; (5), 300.

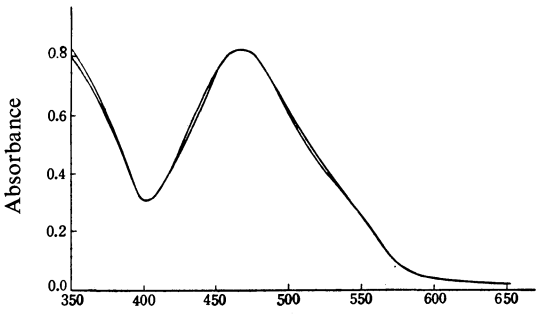



Fig. 10. Effect of the addition of cetyl pyridinium chloride at pH 1.45; concentration of Congo Red, $2.88\times10^{-5}$ mol./l; concentration of cetyl pyridinium chloride, 7.3 and $14.5\times10^{-5}$ mol./l.

concentration of c. p. c. The interaction products are precipitated in the presence of a certain amount of the detergent and then dispersed again with further increase of the concentration of c. p. c. The same effect of c. p. c. is observed in the neutral medium as shown in Fig. 7. In either case the interaction products are completely precipitated in the concentration range where the mole ratio of Congo Red to c. p. c. is about 1/2 and begins to be dispersed with further increase of c. p. c. concentration as shown in Fig. 8. Figs. 9 and 10 show that the same interaction product is also formed in the more acidic medium.

## Discussion

The absorption peak at 510 mμ, as seen from Figs. 1, 2, 4 and 5, is considered to indicate that Congo Red and Tween 80 make a definite molecular compound irrespective of the pH of the solution. The results of Fig. 3 show that the hydrogen ion in the medium plays an important role in the equilibrium of the interaction between Congo Red and Tween 80. Either the acid or the base form of Congo Red is similarly varied in its spectrum and well dispersed by the addition of a sufficient amount of Tween 80. However, the amount of detergent required to show just sufficient change increases with lowering the pH of the medium. Although in acidic Congo Red solutions containing insufficient Tween 80 (below 0.309% of Tween 80 concentration at pH 3.4), precipitates appear by aging (about 24 hr. after preparation), in the systems containing sufficient detergent, no precipitation occurs. This is probably due to a kind of solubilization, but the precise mechanism is not known at the present.

In view of these results, it may be considered as follows: in an acidic medium, an acid form of Congo Red is equilibrated to a base form as in the following formula,

$$R\begin{matrix}NH_2\\NH_2\end{matrix} + 2H^+ \rightleftharpoons R\begin{matrix}NH_3^+\\NH_3^+\end{matrix} \qquad (1)$$

It is possible to assume the following equilibrium process for the spectral change,

$$R\begin{matrix}NH_2\\NH_2\end{matrix} + 2\,\text{Tween 80} \rightleftharpoons R\begin{matrix}NH_2-\text{Tween 80}\\NH_2-\text{Tween 80}\end{matrix} \qquad (2)$$

In this expression $R\begin{matrix}NH_2\\NH_2\end{matrix}$, $R\begin{matrix}NH_3^+\\NH_3^+\end{matrix}$ and $R\begin{matrix}NH_2-\text{Tween 80}\\NH_2-\text{Tween 80}\end{matrix}$ represent the base form of Congo Red, the acid one and the interaction product respectively.

The effect of pH (Fig. 3) may be interpreted qualitatively by these assumptions as follows. When the pH of the medium is lowered, the concentration of the base form decreases according to the formulation 1, which results in an increase of the amount of Tween 80 required to give a definite absorbance. In either neutral or basic medium, the same processes are probably considered to occur from the results of Figs. 4 and 5. In these cases, however, the concentrations of the base form become so great that the process is mainly represented by the formulation 2 and the same effect is produced with a smaller amount of Tween 80 than that in the acidic medium.

Thus, the amino groups of Congo Red molecule are considered to be blocked with Tween 80 and the products are well dispersed, since the aggregation of Congo Red molecules is prevented by the attachement of Tween 80. It has been observed that the adsorption of Congo Red for filter paper or cotton (which is considered to have a negative surface), was reduced remarkably by the addition of Tween 80, which may also be interpreted by a similar process.

In the case of cetyl pyridinium chloride, the wavelength of the new peak is 460 mμ, the position of which is not affected by the medium pH as shown in Figs. 6 and 7.

When the concentration of the detergent is $4.2\times10^{-5}$ mol./l., at which the mole ratio of Congo Red to detergent is 1/2, the products are most hydrophobic and precipitated. They have a trend to be dispersed both sides of this ratio. In the lower concentrations of the detergent, in which the mole ratio is below about 1/1, neither precipitation nor metachromatic color is oberved. In the higher concentrations above the mole ratio of about 1/4, the products are well dispersed. The dispersion in the latter case is not considered to be due always to solubilization[11], since the system being dispersed with sufficient c. p. c. produces no precipitation even by means of dilution.

From these facts, it is considered that Congo Red is bound at the anionic loci, sulfonates, with c. p. c. by ionic force. It is probable that the products whose sulfonates are blocked become hydrophobic, but with further c. p. c. they will become hydrophilic again owing to the adsorption of the excess of c. p. c. with the hydrophilic groups towards water.

## Summary

The spectral changes of Congo Red solution with the addition of Tween 80 and cetyl pyridinium chloride were measured at various pH.

The wavelength of the absorption peak of

the interaction product between Congo Red and Tween 80 is 510 mμ in the acidic medium as well as those in the neutral and the basic ones, from which it is considered that they produce a molecular compound of a definite constitution irrespective of the medium pH. However, since the amount of Tween 80 required to show the same effect in spectra increases with lowering pH, it is considered that only a base form of Congo Red is probably active and binds with Tween 80 at the amino groups.

The solutions of Congo Red containing sufficient cetyl pyridinium chloride have an absorption peak at 460 mμ. The product is completely precipitated as the ratio of Congo Red to cetyl pyridinium chloride is 1/2 and dispersed in both sides of this ratio, which depends little on the medium pH. This is considered to show that cetyl pyridinium chloride binds with Congo Red at the sulfonate groups, the product becomes most hydrophobic as two sulfonates in a molecule are blocked and hydrophilic with an excess of the detergent.

In conclusion, the author wishes to express his sincere thanks to Professor R. Matsuura of Kyushu University for his kind guidance and encouragement during this experiment, and also to Dr. H. Kimizuka of Kyushu University for his supply of the cationic detergent and discussion concerning this work.

*Department of Pharmacology*
*Faculty of Medicine*
*Nagasaki University*
*Nagasaki*

# *Studies on the Chemical Forms of the Recoil Products in Some Neutron-Irradiated Phosphorus Compounds*

By Kenji YOSHIHARA and Tetsuyoshi YOKOSHIMA

(Received July 22, 1960)

The Szilard-Chalmers effect in the neutron-irradiated phosphorus compounds is rather complicated. This phenomenon was studied by several authors, but some important problems seem to be still left without any clear solution. In 1940, Libby[1] studied the Szilard-Chalmers effect in phosphate and phosphite, and found that phosphite is formed in neutron-irradiated phosphate. The retention of phosphate was about 50%. Thomas et al.[2] studied similar effects. In 1951, Fiskell[3] discovered some formation of hypophosphite in neutron-irradiated phosphate.

Fiskell et al.[4] continued further investigation on the Szilard-Chalmers effect of calcium phosphates, and found that pyro- and meta-phosphate are formed besides hypophosphate. Aten et al[5]. also investigated the formation of the polyatomic species in several neutron-irradiated phosphorus compounds, and demonstrated the presence of pyrophosphate in the recoil products. In the papers mentioned above the precipitation method was used for the analysis of the irradiated phosphorus compounds, and therefore exact determination of the complicated products was difficult.

Recently, the technique of paperelectrophoresis has been developed and has been applied successfully to the separation of many components in the complicated system. Sellers et al.[6] studied the chemical form of the recoil products in various phosphorus compounds by this method. Sato et al.[7] further investigated the question in the same way. These authors[6,7] reported that the principal component in each case was the parent species, and besides this principal component several components appeared in the chromatogram in small percentages. They argued that neutron-irradiation of various phosphates does not bring about extensive disruption of the P-O bonds or the P-O-P linkage.

Although paper electrophoresis is an excellent method for the separation and the determination of various phosphorus compounds, it

1) W. F. Libby, *J. Am. Chem. Soc.*, **62**, 1930 (1940).
2) W. D. E. Thomas and D. J. D. Nicholas, *Nature*, **163**, 719 (1949).
3) J. G. A. Fiskell, *Science*, **113**, 244 (1951).
4) J. G. A. Fiskell, W. A. Delong and W. F. Oliver, *Can. J. Chem.*, **30**, 9 (1952).
5) A. H. W. Aten, Jr., H. van der Straaten and P. C. Riesbos, *Science*, **115**, 267 (1952).
6) P. A. Sellers, T. R. Sato and H. H. Strain, *J. Inorg. Nucl. Chem.*, **5**, 31 (1957).
7) T. R. Sato, P. A. Sellers and H. H. Strain, ibid., **7**, 84 (1959).

should be limited to the analysis of the species which are stable to the electric current and to the heat liberated on the paper for several hours. Therefore we felt it would be necessary to compare the results with those by ordinary paper chromatography. We were particularly interested in the formation of polyatomic species which might be produced by the heat liberated in the neighborhood of the recoil atom. Sato et al.[7] detected a component presumably corresponding to pyrophosphate in neutron-irradiated phosphate, but they did not show the percentage of this component. Aten et al.[5] showed that an appreciable fraction of pyrophosphate is formed from phosphate. However, the formation of higher polyphosphates than pyrophosphate might occur, but this has not been shown so far. Thus we studied the chemical form of the recoil products in the neutron-irradiated phosphorus compounds by paper chromatography, and found several new facts.

## Experimental

**Target Materials.**—The target materials used in this work are as follows: $H_3PO_4$; $NaH_2PO_4$, $NaH_2PO_4 \cdot H_2O$, $NaH_2PO_4 \cdot 2H_2O$, $NH_4H_2PO_4$, $KH_2PO_4$, $Na_2HPO_4$, $Na_2HPO_4 \cdot 12H_2O$, $(NH_4)_2HPO_4$; $Na_3PO_4$, $Na_3PO_4 \cdot 12H_2O$, $Zn_3(PO_4)_2$; $Na_4P_2O_7$, $Na_4P_2O_7 \cdot 10H_2O$; $Na_2HPO_3 \cdot 5H_2O$.

These substances are guaranteed reagents of the Kanto Chemical Co. or of the Wako Pure Chemical Ind. Before the experiment the purity of each substance was tested by means of radioactivation analysis; the sample was dissolved in water (zinc phosphate was dissolved in dilute hydrochloric acid), and one drop of the solution was put on the filter paper for chromatography; this was developed with *n*-butanol which had been shaken with the same volume of 2 N nitric acid; the filter paper was dried and irradiated in a nuclear reactor; after appropriate cooling time, the radioautogram of the filter paper was prepared. Each test gave no impure component.

**Irradiation.**—Solid targets were irradiated in the Irradiation Hole No. 3, 12 or 15 in the nuclear reactor JRR-1 (homogeneous solution type). Hole No. 16 was used for short irradiation of solid targets. Liquid targets were irradiated in Hole No. 6. The standard thermal neutron flux in each hole is given as follows[8].

| | |
|---|---|
| No. 3. | $0.48 \times 10^{12}$ n/cm$^2$/sec. |
| 6. | 0.40 〃 |
| 12. | 0.38 〃 |
| 15. | 0.22 〃 |
| 16. | 0.51 〃 |

These values were given at the operation of 40 kW. per hour. In the whole period of this work the reactor was operated at 40 kW. per hour. It is desirable to irradiate the sample in the same position of the same hole, but this could not be realized for all cases. Presumably the variation of neutron flux in these experiments will not bring about any difference in the results. In Hole No. 16 (the nearest from the reactor core) the contribution of fast neutrons to the total radioactivation was tested by the cadmium foil absorption method. The result showed that about 5% of the radioactivity was produced by fast neutrons (residual 95% by slow and thermal neutrons). In the other holes contribution of neutrons to the total radioactivation will be smaller. Perhaps the contribution of fast neutrons will not greatly affect the results in all the experiments. Except in the case of short irradiation, the targets were usually irradiated for 5 hr. a day, and for successive three days a week. The irradiation temperature did not exceed about 50°C in any of the experiments.

**Analysis.**—*Paper chromatography.*—The irradiated target was dissolved in water, and one drop of the solution was put on the starting point of the filter paper, Tôyô No. 53 (2 cm × 40 cm). Other sorts of filter paper such as Tôyô No. 50, 51, 51A, 52 and 54 were tested, but No. 53 gave the best results. Several developing solvents were tested, and the best results were obtained by the use of *n*-butanol which had been shaken with the same volume of 2 N nitric acid. Development was made by the one-dimensional ascending method for about 15 hr., the travelling distance being 23~27 cm.

*Detection of Radioactive Zones.* — After development the filter paper was dried well and the radioautogram was taken on Fuji X-ray film. For the determination of the components on the chromatogram, the paper was cut in sections of 0.5 cm. width, and the radioactivity was measured by a proportional counter (Radiation Counter Laboratories, Inc.; an end-window type; flow gas, methane; counting efficiency about 30%,). When other radionuclides such as $^{24}$Na and $^{42}$K were produced, decay curves were investigated to distinguish them from $^{32}$P.

**Miscellaneous.**—Experiments on the time-dependency of $^{32}$P were carried out at room temperature (about 20°C) in air (under atmospheric pressure). Enrichment of $^{32}$P was roughly examined by the coloration test on the chromatogram obtained. A solution of ammonium molybdate was sprayed on the filter paper. In the cases of phosphate, pyrophosphate and higher polyphosphates a yellow color appeared, and in the cases of phosphite and hypophosphite a pale blue color appeared after the filter paper was heated. Thus amounts of the phosphorus compounds were roughly estimated.

## Result

There were small changes in $R_f$ values according to the experimental condition, but they did not exceed 0.02. In Fig. 1, chromatograms of several species are shown. The $R_f$ values of phosphate, phosphite* and pyrophosphate

8) K. Takahashi, M. Imai and Y. Kato, *JAERI-1004* (1958).

* The $R_f$ value of hypophosphite is nearly the same as that of phosphite and they could not be distinguished from each other. The sum of these fractions are shown in the tables.

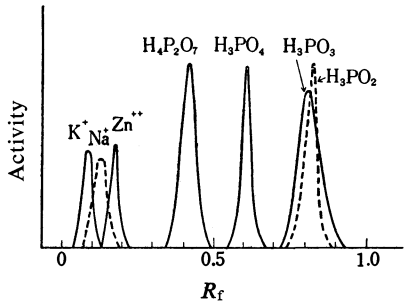



Fig. 1. $R_f$ values of some phosphorus compounds.

were referred to in each experiment. In some cases an unknown species was developed at an $R_f$ value of 0.95~1.0. This was usually observed as a very small spot. In almost all the experiments, spots appeared at the $R_f$ value of 0.05~0.4. Usually these were not clear but diffused and trailing. Sometimes two or three spots appeared in these parts. On the other hand, when a disodium hydrogen phosphate sample was heated and dehydrated into pyrophosphate and higher polyphosphate, this sample always showed the spots at the $R_f$ value of 0.05~0.4 besides a spot of pyrophosphate. Moreover, trimetaphosphate and hexametaphosphate were developed at the $R_f$ value of 0.05~0.1. Therefore the spots at the $R_f$ value of 0.05~0.4 were considered to be due to higher polyphosphates. In some experiments a spot appeared at the starting point of the chromatogram. This small fraction seems to be due to elementary phosphorus as was suggested by previous authors[6,7]. Oxidation of phosphorus might occur because the targets were irradiated in air. In the tables the sum of the percentages of the fractions is not always 100%, because the fractions of the tailing part of each spot, of the spot at the starting point, and of the spot at the $R_f$ value of 0.95~1.0 are omitted. Errors shown in the tables include not only counting errors but errors based on incomplete separation of the spots.

The enrichment of $^{32}P$ was examined by the coloration already mentioned. Except for the target compound the chemical species which appeared in the chromatogram were not detected by the test. Comparing it with the radioactivity data in the tables, this result shows that the chemical species other than the target compound are enriched by the Szilard-Chalmers effect.

The test for radioactive gases such as phosphine and diphosphine was omitted in this work. As shown in Sellers's work[6] these were present only in a very small percentage.

**Phosphoric Acid.** — Liquid phosphoric acid was irradiated in Hole No. 6 (neutron flux: $0.40\times10^{12}$n/cm$^2$/sec.) in JRR-1 for 5 hr. The results are shown in Table I. Small changes in the distribution are observed with the time elapsed. Most of $^{32}P$ atoms are present as phosphoric acid, and small portions are present as phosphorous and pyrophosphoric acids. Phosphorous acid and pyrophosphoric acid seem to change slowly into phosphoric acid. Besides these, higher polyphosphates fractions were detected.

**Potassium Dihydrogen Phosphate.**—The target was irradiated in Hole No. 15 (neutron flux: $0.22\times10^{12}$n/cm$^2$/sec.) in JRR-1 for 15 hr. The results are shown in Table II.

In this experiment higher polyphosphates

Table I. Szilard-Chalmers effect in phosphoric acid

| Chemical forms of $^{32}P$ | Time elapsed after irradiation (days) | | | |
|---|---|---|---|---|
| | 1 | 5 | 8 | 15 |
| | % | % | % | % |
| $H_3PO_4$ | 89.2±0.4 | 92.6±0.5 | 93.9±0.5 | 95.7±0.5 |
| $H_3PO_3$(+$H_3PO_2$) | 5.1±0.1 | 2.9±0.06 | 2.2±0.06 | 0.3±0.01 |
| $H_4P_2O_7$ | 2.5±0.07 | 1.4±0.04 | 1.2±0.04 | 1.0±0.04 |
| Higher polyphosporic acid | 2.0±0.09 | Trace | Trace | Trace |

Table II. Szilard-Chalmers effect in potassium dihydrogen phosphate

| Chemical forms of $^{32}P$ | | Time elapsed after irradiation (days) | | |
|---|---|---|---|---|
| | | 7 | 14 | 26 |
| | | % | % | % |
| Phosphate | | 43.5±0.4 | 43.7±0.4 | 45.4±0.5 |
| Phosphite (+hypophosphite) | | 13.9±0.3 | 13.2±0.3 | 13.1±0.3 |
| Pyrophosphate | | 11.8±2.0 | 14.7±2.6 | 15.2±2.6 |
| Higher polyphosphates | $R_f$ 0.09 | 19.6±3.3 | 9.6±1.6 | 21.5±3.7 |
| | Others | 9.9±3.2 | 14.9±4.8 | 4.5±1.5 |

TABLE III. SZILARD-CHALMERS EFFECT IN AMMONIUM DIHYDROGEN PHOSPHATE

| Chemical forms of $^{32}P$ | Time elapsed after irradiation (days) | | | |
|---|---|---|---|---|
| | Sample I | Sample II | | |
| | 0 | 5 | 7 | 17 |
| | % | % | % | % |
| Phosphate | 47.8±0.7 | 54.1±0.8 | 56.4±0.9 | 55.9±0.8 |
| Phosphite (+hypophosphite) | 13.1±0.6 | 7.1±0.3 | 6.2±0.3 | 6.5±0.3 |
| Pyrophosphate | 8.4±1.6 | 18.1±2.8 | 15.0±2.8 | 15.3±2.8 |
| Higher polyphosphates | 29.3±4.8 | $R_f$ 0.09: 12.7±2.8; Others: 7.0±3.6 | 8.7±1.9; 13.5±7.0 | 17.4±2.9 |

TABLE IV. SZILARD-CHALMERS EFFECT IN $NaH_2PO_4 \cdot 2H_2O$

| Chemical forms of $^{32}P$ | Time elapsed after irradiation (days) | | | |
|---|---|---|---|---|
| | 4 | 6 | 8 | 10 |
| | % | % | % | % |
| Phosphate | 78.2±0.6 | 83.5±0.7 | 83.0±0.7 | 77.8±0.6 |
| Phosphite (+hypophsphite) | 2.4±0.1 | — | — | — |
| Pyrophosphate | 16.8±2.0 | 9.9±1.2 | 9.9±1.2 | 11.7±1.4 |
| Higher polyphosphates | 2.4±0.2 | 6.5±0.7 | 6.9±0.7 | 10.4±1.0 |

TABLE V. SZILARD-CHALMERS EFFECT IN $NaH_2PO_4 \cdot H_2O$

| Chemical forms of $^{32}P$ | Time elapsed after irradiation (days) |
|---|---|
| | 4 |
| | % |
| Phosphate | 78.6±1.3 |
| Phosphite (+hypophosphite) | 4.7±0.2 |
| Pyrophosphate | 8.6±1.9 |
| Higher polyphosphates | 7.9±1.0 |

TABLE VI. SZILARD-CHALMERS EFFECT IN $NaH_2PO_4$

| Chemical forms of $^{32}P$ | Time elapsed after irradiation (days) | | | |
|---|---|---|---|---|
| | 1 | 7 | 8 | 10 |
| | % | % | % | % |
| Phosphate | 21.2±0.8 | 28.6±1.0 | 23.4±0.8 | 27.1±1.0 |
| Phosphite (+hypophosphite) | 17.3±0.3 | 14.9±0.2 | 18.8±0.3 | 15.7±0.3 |
| Pyrophosphate | 25.9±5.5 | 20.7±4.4 | 25.2±5.4 | 24.6±5.3 |
| Higher polyphosphates | $R_f$ 0.09: 19.1±3.2; Others: 15.8±8.2 | 35.9±0.6 | 32.4±0.5 | 31.7±5.5 |

TABLE VII. SZILARD-CHALMERS EFFECT IN $(NH_4)_2HPO_4$

| Chemical forms of $^{32}P$ | Time elapsed after irradiation (days) | | |
|---|---|---|---|
| | 5 | 7 | 17 |
| | % | % | % |
| Phosphate | 34.2±1.0 | 35.3±1.1 | 36.4±1.2 |
| Phosphite (+hypophosphite) | 22.6±0.3 | 25.1±0.4 | 23.8±0.4 |
| Pyrophosphate | 13.3±4.2 | 16.0±5.1 | 15.0±4.8 |
| Higher polyphosphates | 24.8±5.3 | 14.3±3.0 | 15.3±3.3 |

TABLE VIII. SZILARD-CHALMERS EFFECT IN $Na_2HPO_4 \cdot 12H_2O$

| Chemical forms of $^{32}P$ | Time elapsed after irradiation (days) | | |
|---|---|---|---|
| | 4 | 7 | 9 |
| | % | % | % |
| Phosphate | 70.3±1.2 | 77.8±1.3 | 84.3±1.4 |
| Phosphite (+hypophosphite) | — | — | — |
| Pyrophosphate | 28.1±0.7 | 22.2±0.6 | 15.6±0.4 |
| Higher polyphosphate | 1.5±0.2 | — | — |

TABLE IX. SZILARD-CHALMERS EFFECT IN $Na_2HPO_4$

| Chemical forms of $^{32}P$ | Time elapsed after irradiation (day) | | | | | | |
|---|---|---|---|---|---|---|---|
| | 1 | 2 | 3 | 7 | 8 | 9 | 10 |
| | % | % | % | % | % | % | % |
| Phosphate | 24.3±1.7 | 22.4±1.5 | 19.8±1.4 | 22.0±1.5 | 25.1±1.7 | 28.1±1.9 | 21.7±1.5 |
| Phosphite (+hypophosphite) | 20.2±0.4 | 20.7±0.4 | 24.3±0.5 | 21.7±0.4 | 21.3±0.4 | 21.2±0.4 | 23.7±0.5 |
| Pyrophosphate | 16.5±2.0 | 23.8±2.8 | 19.4±2.3 | 22.5±2.7 | 22.4±2.7 | 19.1±2.3 | 23.5±2.8 |
| Higher polyphosphates | 37.5±2.6 | 31.5±2.1 | 34.6±2.4 | 32.4±2.2 | 31.0±2.1 | 31.1±2.1 | 29.6±2.0 |

TABLE X. SZILARD-CHALMERS EFFECT IN $Na_3PO_4 \cdot 12H_2O$

| Chemical forms of $^{32}P$ | Time elapsed after irradiation (days) | | | | |
|---|---|---|---|---|---|
| | 1 | 2 | 5 | 8 | 12 |
| | % | % | % | % | % |
| Phosphate | 45.8±1.1 | 45.2±1.1 | 53.4±1.3 | 58.8±1.5 | 57.6±1.4 |
| Phosphite (+hypophosphite) | 47.3±1.2 | 44.6±1.1 | 37.2±0.9 | 30.9±0.8 | 32.2±0.8 |
| Pyrophosphate<br>Higher polyphosphates | 6.7±0.4 | 10.0±0.7 | 9.3±0.6 | 9.8±0.6 | 9.8±0.6 |

were not completely separated. Phosphate and phosphite fractions did not show remarkable change with standing time.

**Ammonium Dihydrogen Phosphate.** — Two samples were tested. Sample I was irradiated in Hole No. 16 (neutron flux: $0.51 \times 10^{12}$n/cm$^2$/sec.) for 1 hr. and Sample II was irradiated, in Hole No. 12 (neutron flux: $0.38 \times 10^{12}$n/cm$^2$/sec.) for 15 hr. The results are shown in Table III. The sum of the fractions of phosphate and phosphite in Table III is almost constant, 61~62%, and the sum of pyrophosphate and higher polyphosphates is 37~38% except for the result after 17 days for Sample II.

**Sodium Dihydrogen Phosphates.** — Hydrous and anhydrous salts were tested. The results were markedly different from each other.

i) *$NaH_2PO_4 \cdot 2H_2O$.*—The target was irradiated in the Hole No. 12 (neutron flux: 0.38 $10^{12}$n/cm$^2$/sec.) for 15 hr. The results are tabulated in Table IV. The data show some irregularities especially in the fractions of pyrophosphate and higher polyphosphates, but time dependency of the distribution seems to be small. The experiment was not done immediately after irradiation because of the formation of $^{24}Na$ (half-life: 15.0 hr.).

ii) *$NaH_2PO_4 \cdot H_2O$.*—The target was irradiated in Hole No. 15 (neutron flux: $0.22 \times 10^{12}$n/cm$^2$/sec.) for 15 hr. The result shown in Table V are similar to those for $NaH_2PO_4 \cdot 2H_2O$.

iii) *$NaH_2PO_4$.*—The anhydrous salt was irradiated in Hole No. 3 (neutron flux: $0.48 \times 10^{12}$ n/cm$^2$/sec.) for 5 hr. The results shown in Table VI are different from those for the hydrous salts. The difference is as follows. 1) The retention for the anhydrous salt is smaller than those for the hydrous salts. 2) The sum of the pyrophosphate and higher polyphosphate fractions for the anhydrous salt is larger than those for the hydrous salts. 3) The phosphite fraction for the anhydrous salt is larger than that for the hydrous salts.

**Diammonium Hydrogen Phosphate.**—The target was irradiated in Hole No. 12 (neutron flux: $0.38 \times 10^{12}$n/cm$^2$/sec.) for 15 hr. The results are shown in Table VII.

The sum does not attain to 100% because of the presence of tailing between the spots of pyro- and orthophosphate. The time dependency of distribution seems to be small. Three peaks appear in the fractions of polyphosphates.

**Disodium Hydrogen Phosphates.** — Both hydrous and anhydrous salts were tested.

i) *$Na_2HPO_4 \cdot 12H_2O$.*—The target was irradiated in Hole No. 3 (neutron flux: $0.48 \times 10^{12}$n/cm$^2$/sec.) for 5 hr. The results shown in Table VIII are different from the data for $Na_2HPO_4 \cdot 2H_2O$ and $Na_2HPO_4 \cdot 5H_2O$ in Aten's experiments[5]. Phosphite or hypophosphite can not be detected in Table VIII, while a large percentage of phosphite (or hypophosphite) appeared for $Na_2HPO_4 \cdot 2H_2O$ and $Na_2HPO_4 \cdot 5H_2O$ in Aten's work. In the table, the percentage of phosphate slowly increases with standing time while the percentage of pyrophosphate slowly decreases. Apparently, this is likely to be hydrolysis of pyrophosphate in to phosphate.

ii) *$Na_2HPO_4$.*—The target was irradiated in Hole No. 3 (neutron flux: $0.48 \times 10^{12}$n/cm$^2$/sec.) for 5 hr. The results are listed in Table IX. These are somewhat different from those in Aten's[5] and Sellers's work[6].

The distribution shows similar tendencies as those for $NaH_2PO_4$ (Table VI). These results are markedly different from those for the hydrous salt. 1) The retention for the anhydrous salt is smaller than that for the hydrous salt. 2) Fraction of pyrophosphate and higher polyphosphates in the anhydrous salt is larger than that in the hydrous salt. 3) An appreciable fraction of phosphite appears in the anhydrous salt, while it does not appear in the hydrous salts.

**Trisodium Phosphates.**—Both hydrous and anhydrous salts were tested.

i) *$Na_3PO_4 \cdot 12H_2O$.*—The target was irradiated in Hole No. 3 (neutron flux: $0.48 \times 10^{12}$n/cm$^2$/sec.) for 5 hr. The results are listed in Table X.

Fractions of phosphate and phosphite show remarkable changes with standing time. In Fig. 2, these changes are shown. Phosphite is slowly converted into phosphate.

ii) *$Na_3PO_4$.*—The target was irradiated in Hole No. 3 (neutron flux: $0.48 \times 10^{12}$n/cm$^2$/sec.) for 5 hr. The results are shown in Table XI.

Changes of fractions of phosphate and phosphate are shown in Fig. 3. The difference between the results of the hydrous and of the anhydrous salts is as follows. 1) Time dependency is remarkable in the hydrous salt, while it is scarcely ever observed in the anhydrous salt. 2) Retention in the hydrous salt is greater than that in the anhydrous salt. 3) Fractions of pyrophosphate and higher polyphosphates for the anhydrous salts are larger than that those in the hydrous salt.

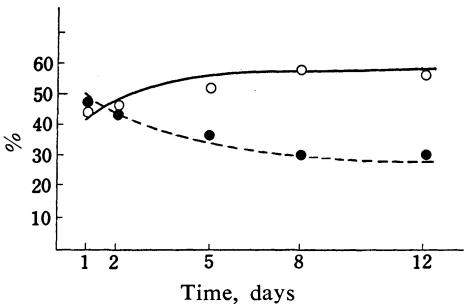



Fig. 2. Variation of percentages of $^{32}$P components in $Na_3PO_4 \cdot 12H_2O$. (The phosphate content in % is shown by the solid line and the phosphite (+hypophosphite) content in % is shown by the broken line).

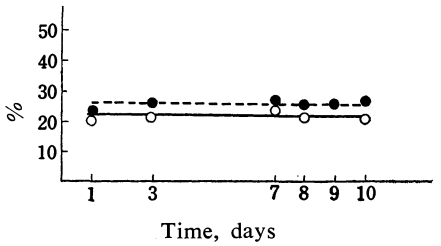



Fig. 3. Variation of percentages of $^{32}$P components in $Na_3PO_4$. (The phosphate content in % is shown by solid line and the phosphite (+hypophosphite) content in shown by the broken line).

**Zinc Phosphate.**—The target was irradiated in Hole No. 3 (neutron flux: $0.48 \times 10^{12}$n/cm$^2$/sec.) for 5 hr. The results are shown in Table XII. The results were similar to those for $Na_3PO_4$ (anhydrous).

**Sodium Phosphite** ($Na_2HPO_3 \cdot 5H_2O$). — The target was irradiated in Hole No. 3 (neutron flux: $0.48 \times 10^{12}$n/cm$^2$/sec.) for 5 hr. The results are tabulated in Table XIII.

TABLE XI. SZILARD-CHALMER EFFECT IN $Na_3PO_4$

| Chemical forms of $^{32}$P | Time elapsed after irradiation (days) | | | | | |
|---|---|---|---|---|---|---|
| | 1 | 3 | 7 | 8 | 9 | 10 |
| | % | % | % | % | % | % |
| Phosphate | 20.7±0.5 | 22.1±0.6 | 23.5±0.6 | 22.2±0.6 | 25.9±0.7 | 28.4±0.7 |
| Phosphite (+hypophosphite | 24.2±0.6 | 26.3±0.6 | 27.3±0.6 | 25.9±0.6 | 25.7±0.6 | 23.2±0.6 |
| Pyrophosphate | 18.3±5.0 | 47.0±1.0 | 48.2±1.0 | 16.8±4.8 | 18.2±5.0 | 19.4±5.2 |
| Higher polyphosphates | 35.1±7.7 | | | 32.2±7.0 | 28.8±6.3 | 28.4±6.2 |

TABLE XII. SZILARD-CHALMERS EFFECT IN $Zn_3(PO_4)_2$

| Chemical forms of $^{32}P$ | Time elapsed after irradiation (days) | |
|---|---|---|
| | 1 | 7 |
| | % | % |
| Phosphate | 29.6±1.1 | 34.5±1.3 |
| Phophate (hypophosphite) | 36.2±1.4 | 35.7±1.2 |
| Pyrophosphite | 9.3±0.9 | 28.8±0.6 |
| Higher polyphosphates | 24.8±2.0 | |

TABLE XIII. SZILARD-CHALMERS EFFECT IN $Na_2HPO_3 \cdot 5H_2O$

| Chemical forms of $^{32}P$ | Time elapsed after irradiation (days) | | | |
|---|---|---|---|---|
| | 2 | 5 | 12 | 15 |
| | % | % | % | % |
| Phosphate | 4.5±0.1 | 4.3±0.1 | 4.0±0.1 | 2.9±0.1 |
| Phosphite (+hypophosphite) | 77.2±8.3 | 76.0±8.2 | 77.9±8.4 | 82.0±8.9 |
| Pyrophosphate | 9.6±0.9 | 7.6±0.7 | 5.4±0.5 | 4.8±0.5 |
| Higher polyphosphates | 7.6±0.7 | 10.9±1.0 | 7.6±0.7 | 7.5±0.7 |

TABLE XIV. SZILARD-CHALMERS EFFECT IN $Na_4P_2O_7 \cdot 10H_2O$

| Chemical forms of $^{32}P$ | Time elapsed after irradiation (days) | | | | |
|---|---|---|---|---|---|
| | 2 | 5 | 12 | 15 | 22 |
| | % | % | % | % | % |
| Phosphate | 47.9±2.4 | 44.2±2.2 | 51.4±2.5 | 53.9±2.7 | 50.2±2.5 |
| Phosphite (+hypophosphite) | — | — | — | — | — |
| Pyrophosphate | 45.3±2.3 | 43.4±2.2 | 35.5±1.8 | 34.5±1.8 | 38.1±1.9 |
| Higher polyposphates | 7.1±0.5 | 12.1±0.9 | 12.8±0.9 | 11.0±0.8 | 11.6±0.8 |

TABLE XV. SZILARD-CHALMERS EFFECT IN $Na_4P_2O_7$

| Chemical forms of $^{32}P$ | Time elapsed after irradiation (days) |
|---|---|
| | 4 |
| | % |
| Phosphate | 9.4±1.6 |
| Phosphite (+hypophosphite) | 24.8±0.9 |
| Pyrophosphate | 36.2±4.2 |
| Higher polyphosphates | 26.5±2.3 |

Several components also appear in the chromatogram, but the major component is the parent substance. Pyrophosphate and higher polyphosphates are detected in appreciable quantities. Changes by standing time are not great.

**Sodium Pyrophosphates.**—Both hydrous and anhydrous salts were tested.

i) *$Na_4P_2O_7 \cdot 10H_2O$.*—The target was irradiated in Hole No. 3 (neutron flux: $0.48 \times 10^{12}$ n/cm$^2$/sec.) for 5 hr. The results are listed in Table XIV.

The distribution slightly changed by standing time.

ii) *$Na_4P_2O_7$.*—The anhydrous salt was irradiated in Hole No. 12 (neutron flux: $0.38 \times 10^{12}$ n/cm$^2$/sec.) for 15 hr. The result is shown in Table XV.

There are great differences between the results of the hydrous and of the anhydrous salt. 1) The phosphate fraction in the anhydrous salt is much smaller than that in the hydrous salt. 2) The phosphite fraction is not detected for the hydrous salt, while it is more than 20% for the anhydrous salt.

## Discussion

On the study on the Szilard-Chalmers effect, the exchange reaction between the separated atoms and parent substance is an important factor. If this exchange reaction occurred rapidly, we could not observe the Szilard-Chalmers effect. Several exchange reactions of phosphorus acids have been investigated so far. No isotopic exchange of phosphorus was

detected in the systems: $H_3PO_4+H_3PO_2$[9,10], $H_3PO_4+H_3PO_3$[10,11], $H_3PO_4+(HPO_3)_3$[12], $(NaPO_3)_3+(NaPO_3)_6$ and $(NaPO_3)_3$[13], $NaH_2PO_4+(NaPO_3)_6$[13]. Therefore, the effect of the exchange reaction between the parent substance and the daughter species can be ignored in the present paper. The phosphite fraction seems to become larger in the order of the targets of phosphoric acid, primary, secondary and tertiary phosphate. But this is not applicable to the hydrous salts.

Ammonium chromate[14] and iodate[15] show a much lower retention value in the Szilard-Chalmers effect than other alkali chromates and iodates do. Namely, the yield of the reduced form for the ammonium salts is much higher than that for other alkali salts. Therefore, Harbottle et al.[16] suggested that the ammonium ion may act as a reducing agent in the hot zone. However, in the present case the yield of the reduced forms for ammonium phosphates is not markedly higher than that for the corresponding alkali phosphates. Perhaps the ammonium ion does not act as a reducing agent to phosphate in the hot zone. This may be attributed to the difference in oxidation potential of phosphate and chromate or iodate to their reduced forms.

Remarkable differences are present between the Szilard-Chalmers effects of anhydrous and hydrous phosphates. Retention in the Szilard-Chalmers effect of the hydrous salt is generally greater than that of the anhydrous salt. In the cases of $NaH_2PO_4\cdot 2H_2O$, $NaH_2PO_4\cdot H_2O$ and $Na_2HPO_4\cdot 12H_2O$, the fraction of phosphite (or hypophosphite) is smaller than that in the anhydrous salts. Similar effects are observed in the cases of hydrous and anhydrous sodium pyrophosphates. The water molecule seems to act as an oxidizing agent for these salts. However, in the case of $Na_3PO_4\cdot 12H_2O$, the fraction of phosphite (+hypophosphite) is larger than that for the anhydrous salt. This seems to be inconsistent with the fact that the water molecule apparently acts as an oxidizing agent in the former cases, but the reason is not yet clear. Usually phosphite (or hypophosphite) changes slowly into phosphate by standing in the case of the hydrous salt, while it scarcely changes in the case of the anhydrous salt. This time dependency may be attributable to the formation of any oxidizing agent in the presence of the water molecule. Phosphite (or hypophoshite) may react slowly with this oxidizing agent and change into phosphate. Fractions of pyrophosphate and higher polyphosphates are smaller for the hydrous salt than those of the anhydrous salt. This fact may be interpreted by the dilution effect (or any other hindrance effect) of the water molecule on the condensation of phosphate in the solid state.

Formation of pyrophosphate and higher polyphosphates occurs in all phosphorus acids and their salts which have been tested. The presence of higher polyphosphates has not been pointed out clear by so far. The condensation reaction of phosphate to condensed polyphosphates usually occurs at a high temperature. For example, orthophosphoric acid is converted into pyrophosphoric acid by heating at 250°C. Therefore, the experiments may suggest that the high temperature reactions play important roles in the present cases. Really, at the event of the recoil a large amount of heat is liberated, and it is expected that the neighbor of the recoil atom is raised up to a high temperature[17]. According to the calculation based on the theory of Hatbottle et al.[17], the hot zone in an ionic crystal includes about 1000 atoms at 1000°K, and about 2000 atoms at 500°K, provided that the recoil energy is about 300 eV.

The spot at the $R_f$ value of 0.09 appears only in the primary phosphates. This is likely to correspond to polymetaphosphate. This may be produced by the following reaction:

$$nMH_2PO_4 \rightarrow (MPO_3)_n + nH_2O.$$

In the cases of the molecular and ionic crystals which are unstable to heat, the mechanism of the thermal reaction in the hot-zone is likely to be very important. This localized thermal reaction or high temperature reaction may be necessary to explain some complicated phenomena in the Szilard-Chalmers effect.

The authors wish to express their hearty thanks to Dr. Kenjiro Kimura, the Director of this Institute, for his encouragement.

*Radioisotope Production Laboratory*
*Japan Atomic Energy*
*Research Institute*
*Tokai, Ibaraki-ken*

9) C. Perrier and E. Segrè, *Ric. Sci.*, **9**, 1, 638 (1938).
10) V. D. Ionin, A. F. Lukovnikov, M. B. Neiman and A. N. Nesmeyanov, *Doklady Akad. Nauk. S. S. S. R.*, **67**, 463 (1949).
11) J. N. Wilson, *J. Am. Chem. Soc.*, **60**, 2697 (1938).
12) D. E. Hull, ibid., **63**, 1269 (1941).
13) R. C. Vogel and H. Podall, ibid., **72**, 1420 (1950).
14) G. Harbottle, *J. Chem. Phys.*, **22**, 1083 (1954).
15) R. E. Cleary, W. H. Hamill and R. R. Williams, *J. Am. Chem. Soc.*, **74**, 4675 (1952).
16) G. Harbottle and N. Sutin, "The Szilard-Chalmers Reaction in Solids" in "Advances in Inorganic Chemistry and Radiochemistry", Vol. I, (Editor, H. J. Emeléus and A. G. Sharpe), Academic Press, New York (1959), p. 267.
17) G. Harbottle and N. Sutin, *J. Phys. Chem.*, **62**, 1344 (1958).

# *Natural Furan Derivatives. V*[1]. *The Number of Double Bonds in Obacunone*

By Takashi TOKOROYAMA, Tadao KAMIKAWA and Takashi KUBOTA

(Received July 21, 1960)

Obacunone ($C_{26}H_{30}O_7$) is known as the bitter principle contained in the plants of the *Rutaceae* family, together with limonin[2] and nomilin[3]. It has been studied by many investigators[3-6] since the beginning of this century. Casimirolid, isolated from *Casimiroa edulis* Lave et Lex, was recently proved to be identical with obacunone[7-10].

Studies made to date have revealed the presence of one ketone group and two lactone groups, one being opened reversibly and the other being an $\alpha,\beta$-unsaturated lactone group which suffers irreversible fission. Of the remaining two oxygen atoms, one has been proved by Kubota and Tokoroyama[11] to be present in $\beta$-substituted furan ring and the other is considered to be present as an oxide bond from its inert nature.

Dean and Geissman[6] concluded from spectroscopic studies on obacunone and nomilin (acetoxydihydroobacunone with an acetoxyl group in the $\beta$-position of the unsaturated lactone group in obacunone)[3] and from the complicated behavior of these two compounds toward catalytic reduction* that obacunone had another double bond besides the three in the furan ring and the $\alpha,\beta$-unsaturated lactone group, and that it is a monocarbocyclic compound. The present paper presents evidences that obacunone possesses only three double bonds.

Obacunone (I) easily undergoes the addition of one mole of hydrogen chloride to form obacunone hydrochloride (II)[6]. Since this compound does not show the characteristics of an $\alpha,\beta$-unsaturated lactone and easily regenerates obacunone on being heated with pyridine, it is clear that the addition of hydrogen chloride has taken place at the double bond in the $\alpha,\beta$-unsaturated lactone group[6].

Ozonolysis of obacunone hydrochloride at room temperature affords an acid, $C_{23}H_{28}O_8\cdot HCl$, by losing three carbon atoms. The acid has been named etioobacunoic acid hydrochloride (III) which is characterized as its methyl ester (IV), $C_{24}H_{30}O_8\cdot HCl$. III and IV do not show infrared absorption characteristics of the furan ring at 3.18, 6.66 and 11.42 $\mu$[12]. Treatment of III with pyridine results in dehydrochlorination and a dilactone-carboxylic acid, etioobacunoic acid (V), $C_{23}H_{28}O_8$, is formed. Etioobacunoic acid shows the absorption of a double bond conjugated with a carboxyl group at 6.18 $\mu$ and an absorption maximum at 214.5 m$\mu$ ($\varepsilon$ 11,500) indicating that the $\alpha,\beta$-unsaturated lactone system has been regenrated as in the case of the conversion of obacunone hydrochloride to obacunone. It follows, therefore, that the change of obacunone to etioobacunoic acid may be indicated as follows:

$$(C_{22}H_{27}O_6)\text{-}\underset{\diagdown O \diagup}{\overset{\|}{\square}}\overset{\|}{\square} \rightarrow (C_{22}H_{27}O_6)\text{-}CO_2H$$

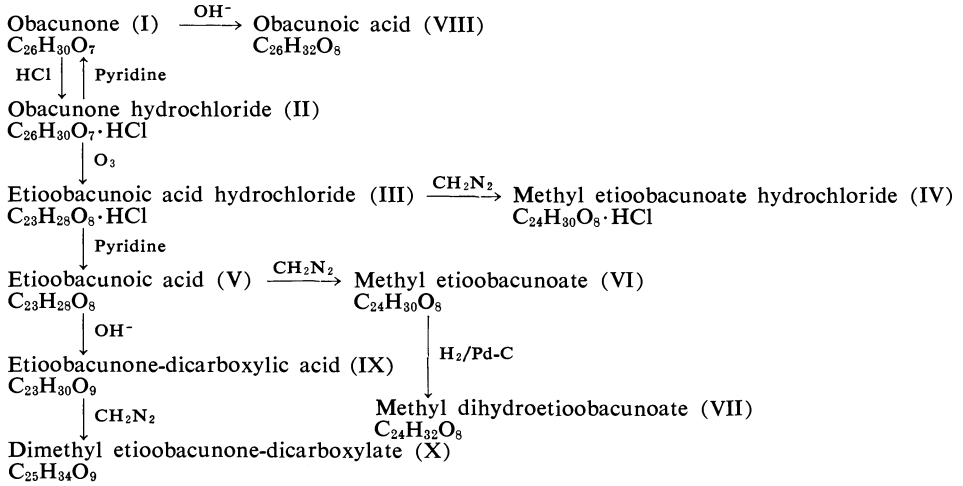
I V

Hydrolysis of obacunone results in the irreversible fission of the unsaturated lactone ring and an unsaturated hydroxy acid, obacunoic acid (VIII), is formed[5]. Mild hydrolysis of etioobacunoic acid (V) also gives an unsaturated hydroxy-dicarboxylic acid $C_{23}H_{30}O_9$, which has been named etioobacunone-dicarboxylic acid (IX) and shows absorptions at 2.96 (hydroxyl) and 6.18 $\mu$ (conjugated double bond). Careful methylation of IX with diazomethane affords a dimethyl ester (X) corresponding to methyl obacunoate[5].

Methyl etioobacunoate hydrochloride (IV) gives no coloration with tetranitromethane.

1) Part IV: T. Tokoroyama, *J. Chem. Soc. Japan, Pure Chem. Sec.* (*Nippon Kagaku Zasshi*), **79**, 319 (1958).
2) D. Arigoni et al., *Experientia*, **16**, 41 (1960).
3) O. H. Emerson, *J. Am. Chem. Soc.*, **70**, 545 (1948); **73**, 2621 (1951).
4) Y. Murayama and J. Takata, *J. Pharm. Soc. Japan* (*Yakugaku Zasshi*), **47**, 1037 (1928).
5) a) T. Kaku, C. Cho and T. Orita, ibid., **52**, 594 (1932). b) T. Kaku and P. Ri, ibid., **55**, 1153 (1935).
6) F. M. Dean and T. A. Geissman, *J. Org. Chem.*, **23**, 596 (1958).
7) F. B. Power and T. Callan, *J. Chem. Soc.*, **99**, 2004 (1911).
8) A. Aebi, *Helv. Chim. Acta*, **39**, 1495 (1956).
9) F. A. Kincl, J. Romo, G. Rosenkranz and F. Sondheimer, *J. Chem. Soc.*, **1956**, 4163.
10) F. Sondheimer et al., *J. Org. Chem.*, **23**, 762 (1958); **24**, 870 (1959).
11) T. Kubota and T. Tokoroyama, *Chem. & Ind.* **1957**, 1298. See also Ref. 1.

* Catalytic reduction of obacunone and its allied compounds will be reported in subsequent papers.
12) T. Kubota, *Tetrahedron*, **4**, 68 (1958); M. Yamaguchi, *Japan Analyst* (*Bunseki Kagaku*), **7**, 211 (1958).




Also its ultraviolet absorptions are weak in intensity, being end absorptions at 207 m$\mu$ ($\varepsilon$ 520) and at 210 m$\mu$ ($\varepsilon$ 400). If acid III should retain a double bond of poor reactivity with ozone and with tetranitromethane and thus a double bond of a tetrasubstituted ethylene, compound IV should show an absorption maximum of strong intensity of several thousands in $\varepsilon$ at around 205 m$\mu$[13]. Catalytic reduction of methyl etioobacunoate (VI) results in absorption of one mole of hydrogen to form methyl dihydroetioobacunoate (VII), which does not color with tetranitromethane and shows an end absorption of low intensity at 205 m$\mu$ ($\varepsilon$ 850). Consequently, it follows that IV and VII are completely saturated and therefore it is concluded that obacunone possesses three double bonds, two in the furan ring and one in the $\alpha,\beta$-unsaturated lactone group, and that it possesses a bicarbocyclic ring.

## Experimental

**Etioobacunoic Acid Hydrochloride (III).**— Obacunone hydrochloride (2.0 g.), which was prepared according to the method of Dean and Geissman[6], was dissolved in methylene chloride (50 ml.) and ozonized until the solution was saturated with ozone. The mixture was poured into water (50 ml.) and allowed to stand for several days with occasional swirling. The separated crystals were filtered and recrystallized from acetone-water as needles (1.1 g.), m. p. 238~240°C (decomp.). Infrared absorption (Nujol): 3.6~4.1 (carboxylic group), 5.74 (lactone goups), 5.96~6.00 $\mu$ (ketone and carboxylic groups).

Found: C, 58.61; H, 6.43. Calcd. for $C_{23}H_{29}O_8Cl$: C, 58.91; H, 6.23%.

**Methyl Etioobacunoate Hydrochloride (IV).**— A solution of etioobacunoic acid hydrochloride in acetone was methylated with an ether solution of diazomethane. Repeated recrystallization of the product from acetone-water gave needles, m. p. 202°C (decomp.). Infrared absorption (Nujol): 5.74 ~5.77 (lactone and ester groups), 5.83 $\mu$ (ketone group).

Found: C, 59.53; H, 6.61. Calcd. for $C_{24}H_{31}O_8Cl$: C, 59.68; H, 6.47%.

**Etioobacunoic Acid (V).** — Etioobacunoic acid hydrochlorid (150 mg.) was dissolved in pyridine (2 ml.) and the solution refluxed for 1 hr. After removal of the solvent under reduced pressure, the residue was dissolved in water and the solution was acidified with dilute sulfuric acid. Recrystallization of the resulting precipitates (132 mg.) from acetone-water gave needles, m. p. 236°C (decomp.). Infrared absorption (Nujol): 3.3~4.1 (carboxylic group), 5.74 (lactone groups), 6.00~6.05 (carboxylic group, ketone and $\alpha,\beta$-unsaturated lactone group), 6.18 $\mu$ (conjugated double bond).

Found: C, 63.76; H, 6.80. Calcd. for $C_{23}H_{28}O_8$: C, 63.88; H, 6.53%.

Neutralization equivalent: 423 (Calcd. value 432.5). Saponification equivalent: 150 (Calcd. value: 144.2).

**Methyl Etioobacunoate (VI).** — A solution of etioobacunoic acid in a mixture of acetone and methanol was methylated with an excess of diazomethane in ether. Recrystallization of the product from acetone-water gave needles, m. p. 275~277°C, in a practically quantitative yield. Infrared absorption (Nujol): 5.69 (lactone group), 5.75 (ester group), 5.89~5.92 $\mu$ (ketone and $\alpha,\beta$-unsaturated lactone groups).

Found: C, 64.52; H, 6.67. Calcd. for $C_{24}H_{30}O_8$: C, 64.56; H, 6.77%.

**Methyl Dihydroetioobacunoate (VII).** — Methyl etioobacunoate (500 mg.) dissolved in a mixture of ethyl acetate (25 ml.) and dioxane (10 ml.) was shaken with hydrogen at 31°C in the presence of 10% palladium-charcoal (100 mg.). Absorption of 1 mol. (31 ml.) of hydrogen was completeted in $4\frac{1}{8}$ hr. After filtration of the catalyst, the solvent was evaporated under reduced pressure. Recrystallization of the residue from acetone-water or from ethanol gave prisms, m. p. 236~237°C. Infrared

13) P. Blauden, H. B. Henbest and G. W. Wood, *J. Chem. Soc.*, **1952**, 2737.

absorption (Nujol): 5.72~5.88 $\mu$ (lactones, ester and ketone groups). Ultraviolet absorption: $\lambda_{205}^{EtOH}$, $\varepsilon$ 850; $\lambda_{210}^{EtOH}$, $\varepsilon$ 525.

Found: C, 63.81; H, 7.50. Calcd. for $C_{24}H_{32}O_8$: C, 64.27; H, 7.19%.

Saponification equivalent: 146 (Calcd. value: 149).

The dihydroester (VII) was also obtained by the hydrogenation of methyl etioobacunoate in the presence of palladium-alumina[14] in dioxane.

**Etioobacunone-Dicarboxylic Acid (IX).** — Etioobacunoic acid (2 g.) was dissolved in 1 N potassium hydroxide (20 ml.) and the solution heated below 80°C for 1 hr. After cooling the solution was acidified with 1 N hydrochloric acid (Congo Red). The separated crystals were collected and recrystallized twice from dilute methanol as needles (0.9 g.), m. p. 192~193°C (decomp.). Infrared absorption (Nujol): 2.97 (hydroxyl group), 3.07 (hydroxyl group), 5.74 (lactone group), 5.84 (ketone and carboxylic groups), 6.18 $\mu$ (conjugated double bonds). Ultraviolet absorption: $\lambda_{205}^{EtOH}$ $\varepsilon$ 5,500; $\lambda_{210}^{EtOH}$, $\varepsilon$ 5,500.

Found: C, 61.24; H, 6.89. Calcd. for $C_{23}H_{30}O_9$: C, 61.32; H, 6.71%.

**Dimethyl Etioobacunone-dicarboxylate (X).**—To a solution of etioobacunone-dicarboxylic acid (IX) in methanol was added an ethereal solution of diazomethane in an amount less than the theoretical. Immediately after the addition of diazomethane, the solvent evaporated under reduced pressure. The residue was dissolved in chloroform and the solution was shaken with aqueous bicarbonate to remove an acidic material. The chloroform layer was washed with water, dried and evaporated. Recrystallization of the residue from acetone-water, then from ethanol, gave needles, m. p. 177~178°C. Infrared absorption (Nujol): 2.81 (hydroxyl group), 5.73 (lactone and ester groups), 5.82 ($\alpha,\beta$-unsaturated ester group), 5.88 (ketone group), 6.15 $\mu$ (conjugated double bond).

Found: C, 62.61; H, 7.43. Calcd. for $C_{25}H_{34}O_9$: C, 62.75; H, 7.16%.

14) A. C. Johnston, *Chem. Abstr.*, **39**, 2001 (1945).

## Summary

Obacunone has only three double bonds in total, two in its furan ring and one in its $\alpha,\beta$-unsaturated lactone group and, therefore, it possesses a bicarbocyclic ring.

*Institute of Polytechnics*
*Osaka City University*
*Minamiogi-machi, Kita-ku, Osaka*

# *The Use of Radioactive Fission Product Rare Gases for the Study of the Change in Crystal Structure*

By Seishi YAJIMA, Sumio ICHIBA, Yuichiro KAMEMOTO and Koreyuki SHIBA

(Received July 14, 1960)

In our previous paper[1], the possible correlation between released fission rare gas which was captured in a sample of hematite by its recoil energy and the crystal structure change was reported, and the use of radioactive fission product rare gas for the emanation method in place of radon was proposed. In our present work, the experiment was carried out more extensively using the high temperature X-ray diffraction method to confirm the correlation. The usefullness of this emanation method using radioactive fission rare gas in place of radon for the studies in the field of physical chemistry is also discussed.

1) S. Yajima, S. Ichiba, Y. Kamemoto and K. Shiba, This Bulletin, 33, 426 (1960).
2) e. g., D. Strominger, J. M. Hollander and G. T. Seaborg, *Rev. Mod. Phys.*, 30, 585 (1958).

## Experimental

**Usable Nuclides in Fission Product Rare Gases for the Emanation Method.**—A major fraction of Uranium-235 thermal fission products consist of gaseous materials and the sum of independent and primary cumulative yields of all gaseous fission products, including iodine, bromine, xenon and krypton, amount to 52.3%. Of this value 55.3%, or a yield of 28.9%, is attributed to xenon and krypton.

Referring to a table of isotopes[2], krypton-85m, xenon-135 and xenon-133 have considerably long half-lives and large fission yields. To investigate the interference of the precursor and the radioactivity of the other nuclides, the changes of the radioactivity of the krypton-85m, xenon-135 and xenon-133 after two hours' irradiation with time are measured and these changes are plotted in Fig. 1. In these experiments, a closed polyethylene sheet containing 20 mg. of uranium dioxide was irradiated

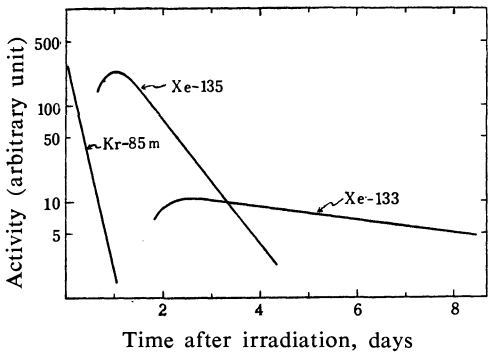



Fig. 1. Change of the radioactivities of the fission product krypton and xenon with time after two hour irradiation.

by thermal neutrons (flux,$\sim 5\times 10^{11}$ n/cm$^2$ sec.) for two hours. The sample is placed in a small flask after each cooling period and the sheet is broken, and the uranium dioxide is dissolved in concentrated nitric acid. Helium is made to flow through the flask, a trap is cooled by dry ice (for iodine) and a charcoal trap is cooled by liquid nitrogen (for xenon and krypton) during treatments and for ten minutes after the uranium has been dissolved. The radioactivities of the krypton and xenon trapped in charcol are measured by a multi-channel gamma ray spectrometer. Their gamma-ray spectra are shown in Fig. 2. The cooling periods to minimize the interference of precursor and radioactitvity of the other nuclides are found to be 1.5 and 4 days for xenon-135 and xenon-133, respectively. The use of one of these nuclides depends on the nature of the sample and the function of the measuring instrument, and the cooling period is therefore determined by the nuclide thus selected.

**Preparation of the Heating Curve and X-ray Diffraction Measurement.** — In the emanation method, the samples containing radioactive rare gases were heated at a constant rate and the radioactivity of the escaping rare gases was measured (heating curves), or the samples were heated at various temperatures and kept at these temperatures while the changes in escaped radioactivity with time were followed (isothermal curves). In the present

TABLE I. THE HEMATITE SAMPLES AND THEIR PREPARATION METHODS

| Sample No. | Chemical form | Preparation method |
|---|---|---|
| 1 | $\alpha$-$Fe_2O_3$ | Dehydration of $\alpha$-FeO·OH at 250°C |
| 2 | $\alpha$-$Fe_2O_3$ | Dehydration of $\alpha$-FeO·OH at 300°C |
| 3 | $\alpha$-$Fe_2O_3$ | Thermal decomposition of $FeSO_4\cdot 7H_2O$ at 780°C |
| 4 | $\gamma$-$Fe_2O_3$ | Oxidation of $Fe_3O_4$ at 250°C |
| 5 | $\gamma$-$Fe_2O_3$ | Pure $\gamma$-$Fe_2O_3$ |

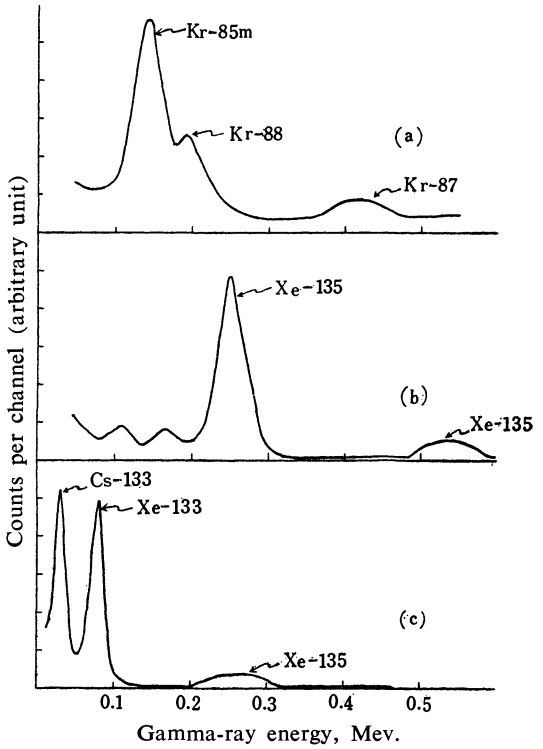



Fig. 2. Gamma-ray spectra of the fission product rare gases.
(a) 2 hr. irradiation and 8 hr. cooling.
(b) 2 hr. irradiation and 1.5 day colling.
(c) 2 hr. irradiation and 5 day cooling.

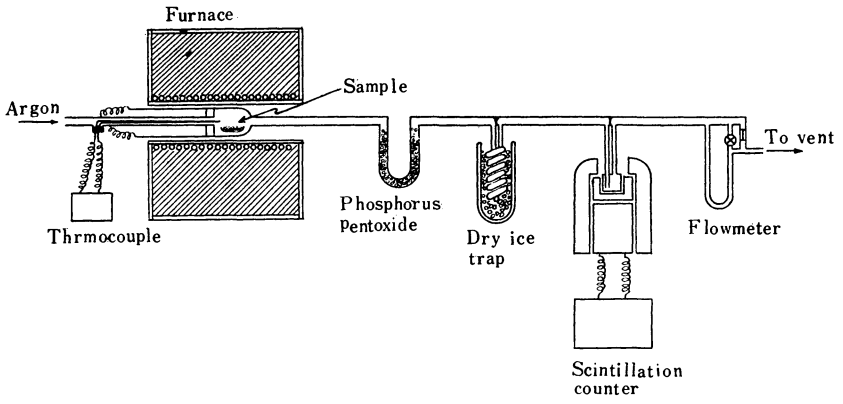



Fig. 3. Schematic diagram of the heating apparatus.

work, the crystal structure change of $\gamma$-hematite to $\alpha$-hematite is studied by the heating curve. An X-ray diffraction method is also employed to identify the crystal structures. The samples of hematites to be examined are shown in Table I.

Two hundred milligrams of thin film of formvar, in a small size, containing uranium dioxide of which the weight ratio to formvar is 1 : 5 was mixed with 500 mg. of hematite and irradiated by thermal neutron flux $\sim 5\times 10^{11}$ n/cm$^2$ sec. for 2 hr. in an experimental hole of JRR-1 reactor. Then the fission recoil energy enables the fission products to be caught by the surrounding solid powder through the film[4-6]. After 1.5 days' cooling ethyl alcohol was added to the sample and the solid powder retaining fission products was separated by a wire gauze and filter paper and was dried. The solid powder was placed in a quartz boat in a quartz tube which was connected to a phosphorus pentoxide drying tube, a dry ice trap for radioactive iodine, a counting cell inserted into an NaI scintillation crystal well of a $\gamma$-ray spectrometer and a flow rate meter, in the order mentioned. The schematic diagram of the apparatus is shown in Fig. 3. Solid powder was heated by a furnace at a rate 5°C/min. in a current of argon (100 ml. per min.). The radioactive xenon-135 escaping from hematite was carried by argon and the radioactivity was measured with the scintillation counter. Plots of the radioactivity of xenon-135 escaped from the sample versus temperature are shown in Fig. 4.

The correlations between the observed peaks in the heating curves and the crystal structure changes were studied by the high temperature X-ray diffraction method at temperatures below and over the temperatures where the peaks appear. $\gamma$-Hematite samples (Nos. 4 and 5) were investigated by the continuous recording method, by the use of the peaks (220) of $\gamma$-hematite and (104) of $\alpha$-hematite. The charts are shown in Figs. 5 and 6.

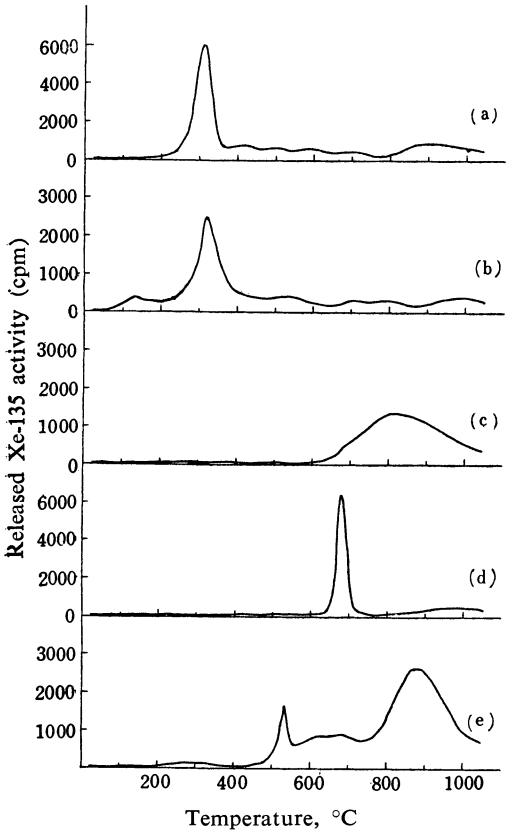



Fig. 4. Heating curves (5°C/min.) of hematite samples.
(a) No. 1 $\alpha$-hematite sample.
(b) No. 2 $\alpha$-hematite sample.
(c) No. 3 $\alpha$-hematite sample.
(d) No. 4 $\gamma$-hematite sample.
(e) No. 5 $\gamma$-hematite sample.

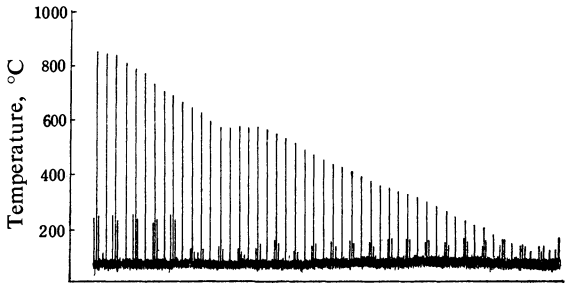



Fig. 5. Continuous recording chart of high temperature X-ray diffraction of No. 4 $\gamma$-hematite sample. Successive vertical lines indicate temperature.

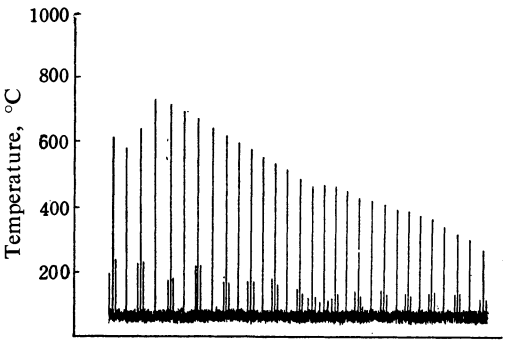



Fig. 6. Continuous recording chart of high temperature X-ray diffraction of No. 5 $\gamma$-hematite sample. Successive vertical lines indicate temperature.

## Results and Discussion

The peaks in the heating curves of Nos. 1 and 2 samples are considered to be related to the dehydration of FeO·OH, although the X-ray diffraction chart shows that the No. 2 sample is in $\alpha$-hematite form at room temperature. In the heating curve of No. 3 sample, no sharp peak is observed because no change

4) R. Wolfgang, *J. Inorg. Nucl. Chem.*, **2**, 180 (1956).
5) R. Henry and C. Herczeg, UNESCO/NS/RIC/14 (1957).
6) T. Nakai and S. Yajima, *J. Chem. Soc. Japan, Pure Chem. Sec. (Nippon Kagaku Zasshi)*, **79**, 1267 (1958).

in structure takes place. The slow ascendant of the curve probably shows that the xenon trapped in the dislocation of the crystal is released. The samples of Nos. 4 and 5 are identified to be $\gamma$-hematite at room temperature by the X-ray diffraction method but their heating curves of Fig. 4 are considerably different from each other. The charts of the continuous recording method of Figs. 5 and 6 show that peaks at 680°C and 530°C are the temperatures of the crystal structure change of $\gamma$-hematite of samples Nos. 4 and 5 to $\alpha$-hematite, respectively. The difference of their crystal structures might be investigated in detail by other methods, e. g., electron diffraction method.

The heating curves of the emanation method will suggest the temperature at which the crystal-structure change, dehydration and decomposition occur and also the detailed difference of the crystal structure for which the X-ray diffraction method does not give sufficient informaton. The heating curves may also suggest the possible existence of the dislocation of the crystal.

On the basis of the following reasons, the proposed method will promise a future development in various fields of the study.

1) This method will be applicable to many solids because the samples are prepared without chemical treatments.

(2) Different radioactive rare gases can be used at the same time. For example, prior to the reaction, if different nuclides of radioactive rare gas were retained in the reactants, the more detailed knowledge of the reaction between solids would be obtained.

3) When most of the rare gas is released at the first peak, it is possible to investigate the emanation at the higher temperature above the peak by means of the decay products of the precursor.

The radiation damage of the crystal will be negligible because the radioactivity of the fission rare gases is detected very sensitively and the sample does not require so much irradiation, as radiation damage occurs. The fission products captured in the solid will be also negligible as impurities.

The proposed method will be useful for the studies of crystal-structure change, reaction between solids and other problems of physical chemistry when the X-ray diffraction method and electron diffraction method are employed at the same time.

The authors wish to thank Professor S. Kachi of Kyoto Uuiversity for invaluable suggestions to this work and also for providing the hematite samples.

*Division of Chemistry*
*Japan Atomic Energy Research Institute*
*Tokai, Ibaraki-ken*

# SHORT COMMUNICATIONS

## *Rapid Separation of Nuclides in Fission Products and their Determinations by Focussing Chromatographic Method*

By Mutsuaki SHINAGAWA, Yoshiyuki KISO and Akira OYOSHI

(Received October 14, 1960)

Although many procedures such as ion exchange, extraction, paper chromatographic and precipitation methods etc. have been applied to the separation of nuclides in fission products, the present focussing chromatographic method has been proved to be more rapid and convenient for their determinations comparing with other methods mentioned above.

The apparatus and its manipulation were the same as in previous paper[1]. As the complexing agent of cathodic solution, 0.1 M citric, oxalic, malonic, malic, maleic, lactic, succinic and tartaric acid, 0.05 M sodium triphosphate, 0.01 M EDTA and NTA were used and hydrochloric acid was used as cathodic solution in the present experiment.

The separation of several kinds of nuclide in fission products (imported from U. S. A.) were possible in a few minutes by the adjustment of pH value between both solutions of hydrochloric acid and complexing agent under suitable conditions of initial dipped width of sample solution (1~3 cm.) and applied voltage (750~1000 V./20 cm. of strip length). The autoradiographic method was used to decide the position of separated lines. Identification of nuclides was carried out by measuring their half-lives and energies.

Autoradiogram exemplified in Fig. 1, shows the situation of separation obtained by hydrochloric acid-citric acid system. Fig. 2 shows the general view of the separated patterns obtained with several complexing agents.

Separated lines of $^{137}Cs$ and $^{95}Zr$ in fission products were formed with the complexing agent without mutual contaminations. Quantitative determinations of $^{137}Cs$ and $^{95}Zr$ proved

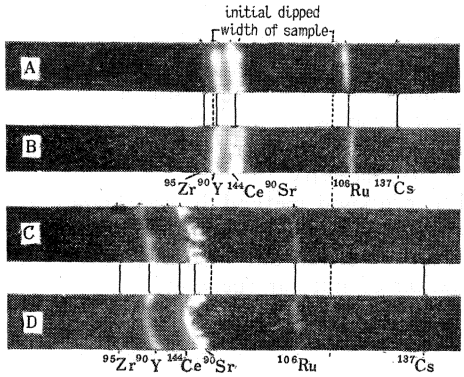



Fig. 1. Autoradiogram of separated lines of nuclides in fission product.
Complexing agent: 0.5 M citric acid (pH 4.5), hydrochloric acid: pH 1.5, initial dipped width of sample: 3 cm., sample volume: 0.05 ml. at A and B, 0.1 ml. at C and D, applied voltage: 1000 V./20 cm., duration time of applied voltage: 5 min. at A and B, 10 min. at C and D, autoradiographic exposure time: 2 hr., X-ray film: Fuji medical, 25 cm.×30 cm., paper strip: Toyo Roshi No. 50.

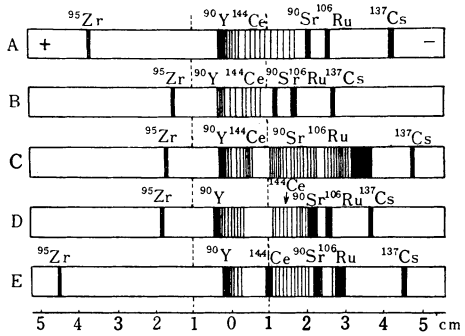



Fig. 2. General view of the separated pattern obtained with several complexing agents.
A: 0.1 M malonic acid, B: 0.1 M succinic acid, C: 0.1 M lactic acid, D: 0.1 M malic acid, E: 0.1 M maleic acid.
Anodic solution: 0.05 N hydrochloric acid and sodium chloride, cathodic solution: pH 7.0.
Applied voltage: 700 V./20 cm., duration time of applied voltage: 15 min., initial dipped width of sample: 2 cm., autoradiographic exposure time: 24 hr., paper strip: Toyo Roshi No. 50, X-ray film: Fuji medical, 25 cm.×30 cm.

1) *J. Chem. Soc. Japan, Pure Chem. Sec.* (*Nippon Kagaku Zasshi*), in press; (Presented at the 8th Annual Meeting of the Japan Society for Analytical Chemistry, Okayama, Oct., 1959).

to be effective by measuring $\gamma$-activity of their separated lines cut from the paper strip. The mean deviation rate of reproducibility of radioactivity obtained and recovery were found within $\pm 5\%$ and $95 \pm 5\%$ respectively, from the result of blank test using the standard sample solution prepared by mixing with known amounts of $^{95}Zr$ ($^{95}Nb$), $^{144}Ce$ ($^{144}Pr$), $^{90}Sr$ ($^{90}Y$) and $^{106}Ru$ ($^{106}Rh$). Even when the closeness or overlapping of separated lines of $^{90}Y$ and $^{144}Ce$, or $^{90}Sr$ and $^{106}Ru$, the determinations of $^{144}Ce$ and $^{106}Ru$ by $\gamma$ counting were feasible with an accuracy of the same order as $^{137}Cs$ and $^{95}Zr$, because $^{90}Y$ and $^{90}Sr$ have no $\gamma$-activity.

The proposed method is considered to be a new rapid and simple method for analysis of product; i.e. fall-out analysis, burn-up determination of nuclear fuels, etc.

*Department of Analytical Chemistry*
*Faculty of Science*
*Hiroshima University*
*Higashisendai-machi Hiroshima*

## *On the Constitution of Sulfo-Aluminous Clinker*

By Nobue FUKUDA

(Received October 26, 1960)

According to Lafuma[1], sulfo-aluminous clinker is produced by burning the mixture of gypsum, bauxite, and calcium carbonate, and is used as an expansive agent for the manufacture of expansive cement.

He succeeded in identifying the minerals, free anhydrous calcium sulfate, calcium aluminates particularly $5CaO \cdot 3Al_2O_3$, and $\gamma$ $2CaO \cdot SiO_2$ in the clinker, but he could not confirm the ternary compound, calcium-sulfo-aluminate.

In the course of previous studies[2] on the system $CaO$-$Al_2O_3$-$CaSO_4$, the author could conclusively establish the existence of a ternary compound of the composition $3CaO \cdot 3Al_2O_3 \cdot CaSO_4$ which gave the X-ray diffraction data as shown in Table I.

With the opinion that this ternary compound may be expected to exist in sulfo-aluminous clinker the author has carried out the following experiments.

1) Heating the mixture of bauxite, lime, and gypsum for 30 min. at 1350°C the clinker was prepared, which was similar in appearance as described by Lafuma.

2) A series of sulfo-aluminous clinkers with the mole ratios of $Al_2O_3/SO_3$, 8.2, 6.0, 3.5, 2.0 and 0.8, respectively, were prepared by heating the batches containing different amounts of gypsum under the same conditions as above.

The samples 1 and 2 were identified by the determination of their chemical composition, X-ray diffraction patterns (powder method), and quantitative X-ray analysis using standard substances.

The X-ray data and chemical composition of sample 1, and the chemical composition of sample 2 are given in Tables II, III and IV.

The results are summarized as follows:

a) The existence of $3CaO \cdot 3Al_2O_3 \cdot CaSO_4$ as the main constituent in sulfo-alminous clinker has definitely been established.

b) The amount of this ternary compound in clinkers estimated from the content of $Al_2O_3$ or $CaSO_4$ determined by the chemical

TABLE I. X-RAY DIFFRACTION DATA OF $3CaO \cdot 3Al_2O_3 \cdot CaSO_4$

| *d*, Å | 3.75 | 3.24 | 2.91 | 2.65 | 2.46 | 2.30 | 2.17 | 1.62 | 1.58 |
|---|---|---|---|---|---|---|---|---|---|
| Int. | 100 | 7 | 6 | 29 | 7 | 4 | 24 | 7 | 4 |

TABLE II. X-RAY DIFFRACTION DATA OF CLINKER

| *d*, Å | 3.75 | 3.49 | 3.25 | 2.91 | 2.85 | 2.79 | 2.71 | 2.65 | 2.46 | 2.34 | 2.17 | 1.63 |
|---|---|---|---|---|---|---|---|---|---|---|---|---|
| Int. | 100 | 59 | 10 | — | 12 | 20 | 4 | 30 | 11 | — | 37 | 13 |

TABLE III. CHEMICAL ANALYSIS OF CLINKER 1 (wt. %)

| | | | | | |
|---|---|---|---|---|---|
| $SiO_2$ | 7.08 | $TiO_2$ | 0.38 | CaO | 42.64 |
| $Al_2O_3$ | 21.82 | $Fe_2O_3$ | 5.38 | $SO_3$ | 22.26 |

Content of $3CaO \cdot 3Al_2O_3 \cdot CaSO_4$; Calcd. 43.50. By X-ray analysis. 39.20.

1) H. Lafuma, *Proc. of the 3rd. International Symposium on the Chemistry of Cement, London* (1952).

2) N. Fukuda, submitted to *J. Chem. Soc. Japan, Ind. Chem. Sec.*, (*Kogyo Kagaku Zasshi*).

TABLE IV. CHEMICAL ANALYSIS OF CLINKERS 2 (wt. %)

| | | | | | |
|---|---|---|---|---|---|
| $Al_2O_3$ | 35.30 | 34.27 | 30.84 | 28.41 | 21.80 |
| $SO_3$ | 3.36 | 4.52 | 7.02 | 10.98 | 21.12 |
| $Al_2O_3/SO_3$ mole ratio | 8.2 | 6.0 | 3.5 | 2.0 | 0.8 |
| $3CaO \cdot 3Al_2O_3\ CaSO_4$ | | | | | |
| Calcd. | 25.64 | 34.18 | 53.49 | 56.72 | 43.48 |
| By X-ray analysis. | 27.65 | 33.80 | 57.00 | 56.00 | 41.05 |

analysis is in fairly good agreement with the results of direct measurements by quantitative X-ray analysis. The author, furthermore, has found that the amount of this compound is in equivalent with $Al_2O_3$-content when $Al_2O_3/SO_3 < 3$, and with $CaSO_4$-content when $Al_2O_3/ > SO_3 > 3$.

c) As for the other constituents the existence of free anhydrous calcium sulfate was distinctly observed, while that of $\beta$ $2CaO \cdot SiO_2$ was not so clear.

*Cement Division*
*Tokuyama Soda Co., Ltd.*
*Oaza Tokuyama 8355, Tokuyama*

## *Einwirkung von Thionylchlorid auf Diaryläthinylcarbinolen*

Von Tsuneyuki NAGASE

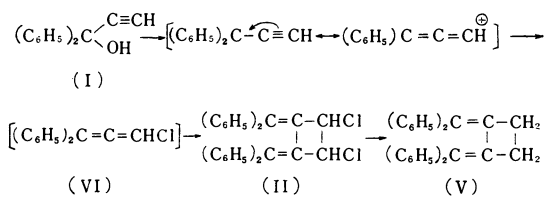
(Eingegangen am 22. Oktober, 1960)

Diphenyläthinylcarbinol (I) ergab bei der Einwirkung von Thionylchlorid in Äther-Pyridin-Lösung bei Zimmertemperatur ein gelbes nadelförmiges Produkt vom Schmp. 188 ~189°C (II) (UV. $\lambda_{Max}^{EtOH}$ m$\mu$ ($\varepsilon$) : 262(24,300), 372(18,100)) von der Zusammensetzung $C_{30}H_{22}\cdot Cl_2$ (Ber. C, 79.47; H, 4.89; Cl, 15.64; Mol. Gew., 453.4. Gef. C, 79.04; H, 4.92; Cl, 15.62%; Mol. Gew. (Rast), 435) mit der Ausbeute von ca. 40 proz. der Theorie. In seinem IR-Spektrum ist ein C–H Band von der Acetylenbindung bei 3300 $cm^{-1}$ verschwunden und bei 1950 $cm^{-1}$ ist nur eine schwache Bande bemerkbar, die scheinbar nicht der Allenbindung, sondern dem substituierten Benzolring zu zuschreiben ist. Seine 2 Chloratome sind durch die Acetoxylgruppe ersetzbar, wenn man II in Eisessig-Lösung mit wasserfreiem Kaliumacetat unter Rückfluss erhitzt. Das entstandene Diacetat (III) ($C_{34}H_{28}O_4$-Ber. C, 81.57; H, 5.64; Mol. Gew. 500. Gef. C, 80.95; H, 5.70%; Mol. Gew., 494. UV. $\lambda_{Max}^{EtOH}$ m$\mu$ ($\varepsilon$): 261(30,000), 363(20,000). IR. $\nu$ $cm^{-1}$ (in Nujol) : 1745 (Acetat)) bildet schwachgelbe Nadeln vom Schmp. 222°C und ergab beim Verseifen mit Salzsäure kein Produkt, das sich zu dem Brady'schen Reagens positiv verhält, sodaß die Enolacetat-Gruppe in ihm nicht vorhanden ist. Durch Ozon-Abbau von II konnte man ca. 1.6 Mol. Benzophenon erfassen und nebenbei eine chlorhaltige $\gamma$-Dicarbonsäure isolieren, die in das entsprechende Pyrrol übergeführt und durch die Ehrlich'sche Probe des letzteren bestätigt wurde. Diese Daten zeigen, daß II höchstwahrscheinlich einen Bisdiphenylmethylencyclobutan-Ring enthält.

II widersteht der Reduktion mit $LiAlH_4$, man konnte es jedoch durch katalytische Reduktion mit Pd-Kohle in methanolischer Kali-Lösung in das entsprechende entchlorierte Tetrahydroderivat (IV) als farblose Nadeln vom Schmp. 153~154°C ($C_{30}H_{28}$-Ber. C, 92.73; H, 7.27. Gef. C, 92.57; H, 7.23%) überführen. Andererseits ergab II beim Erhitzen mit frisch bereitetem Raney-Nickel W-7 in Tetrahydrofuran-Lösung das entsprechende entchlorierte Produkt (V) ($C_{30}H_{24}$-Ber. C, 93.70; H, 6.30. Gef. C, 93.31; H, 6.48) als schwachgelbe Nadeln vom Schmp. 180~181°C (UV. $\lambda_{Max}^{Dioxan}$ m$\mu$ ($\varepsilon$): 257(34,000), 352(28,000)), das mit der Beschreibung von 1,2-Bisdiphenylmethylencyclobutan[1] sehr ähnlich war. So wurde das letztere ausgehend von Adipinsäure über *trans*-Cyclobutandicarbonsäure[2] nach Alberman und Kipping[1] hergestellt und seine Identität mit V wurde durch eine Mischprobe sowie direkten Vergleich der IR-Spektren tatsächlich festgestellt. Die Konstitution von II ist dementsprechend 3,4-Dichlor-1,2-bisdiphenylmethylencyclobutan.

Die Entstehung von II aus I kann man nur in der Weise erklären, daß das zuerst durch eine anionotrope Umlagerung entstandene 1,1-Diphenyl-3-chlorallen (VI) dimerisiert hat. Zu bemerken ist dabei, daß in der Mutterlauge von II keine Allenverbindung IR-spektrographisch nachweisbar war.

1) K. B. Alberman und F. B. Kipping, *J. Chem. Soc.*, **1951**, 776.
2) E. R. Buchman, A. O. Reims, T. Skei und M. J. Schlatter, *J. Am. Chem. Soc.*, **64**, 2696 (1942).

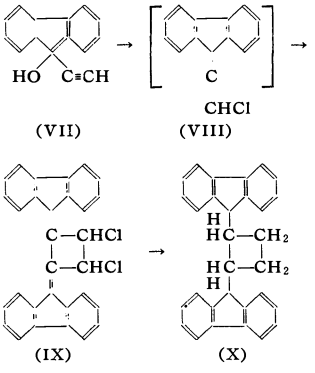


(I)



(VI) (II) (V)

Es ist daher merkwürdig, daß Hennion und seine Forschungsgruppe[3] bei analoger Reaktion von 9-Äthinyl-9-fluorenol (VII) mit Thionylchlorid 9-Chlorvinylidenfluoren (VIII) erhielten. So wurde VII aufs neue nach der Beschreibung von Hennion et al. in wasserfreier Äther-Lösung bei Gegenwart von wasserfreiem Pyridin mit Thionylchlorid behandelt und gelbe Nadeln vom Schmp. 223~224°C (u. Zers.) IX in einer Ausbeute von 71.5 proz. erhalten, die mit der literarischen Angabe[3] gut übereinstimmten. Dasselbe Produkt wurde auch durch Einwirkung von konz. Salzsäure auf VII in einer Ausbeute von 74 proz. erhalten. Die Zusammensetzung von IX stimmte jedoch nicht mit VIII ($C_{15}H_9Cl$) sondern mit $C_{30}H_{18}Cl_2$ (Ber. C, 80.18; H, 4.03; Cl, 15.78; Mol. Gew., 449.4. Gef. C, 79.92; H, 4.25; Cl, 15.78%; Mol. Gew. (Rast) 428) überein. Ferner im Gegensatz zur literarischen Angabe wurde im IR-Spektrum von IX keine scharfe Bande einer Allenbindung bei 1950 $cm^{-1}$ bemerkt, obwohl bei 2000~1650 $cm^{-1}$ Banden von einem substituierten Benzolring vorhanden waren. Außerdem ist das UV-Spektrum von IX (UV. $\lambda_{Max}^{CHCl_3}$ m$\mu$ ($\varepsilon$): 276(54,000), 375(30,000)) mit demjenigen von II sehr ähnlich und durch Ozon-Abbau von IX konnte man neben ca. 1.4 Mol. Fluorenon eine $\gamma$-Dicarbonsäure isolieren, wie bei dem Abbau von II. Diese Daten zeigen, daß IX kein 9-Chlorvinylidenfluoren sondern 3,4-Dichlor-1,2-bisfluorenylidencyclobutan ist, und daß die Reaktion von VII mit Thionylchlorid ganz analog wie beim I verläuft. Zur weiteren Bestätigung wurde IX mit Pd-Kohle katalytisch reduziert, wobei man kein 9-Äthylfluoren vom Schmp. 108°C, sondern ein halogenfreies Kristall vom Schmp. 167~168°C (X) ($C_{30}H_{24}$-Ber. C, 93.71; H, 6.29. Gef. C, 93.13; H, 6.06%.) unter 4 Mol. Wasserstoff-Aufnahme erhalten konnte.



(VII) (VIII)



(IX) (X)

Herrn Prof. Dr. E. Ochiai und Herrn Dr. T. Shimamoto für ihre freundliche Leitung dieser Arbeit und Herrn Dr. I. Iwai für den Literarischen Hinweis und die Diskussion danke ich verbindlichst.

*Synthetische Org. Chem. Laboratorium des Instituts für Physikalische und Chemische Forschungen Kamifujimaye, Komagome, Tokyo*

3) G. F. Hennion und B. R. Fleck, ebenda, **77**, 3253 (1955).
4) N. D. Zelinsky und M. W. Gawerdowskaja, *Ber.*, **61**, 1052 (1928).

# *Mechanism of the Recoil Phenomena in Hexamminecobalt(III) Chloride*

By Nagao IKEDA, Kenji YOSHIHARA and Shigeru YAMAGISHI

(Received August 18, 1960)

In the previous paper[1], we studied the heterogeneous extraction of recoil atoms in neutron-irradiated hexamminecobalt(III) nitrate target, and observed the anomalously high extraction yield with this compound. In the present paper, we studied the recoil effects in hexamminecobalt(III) chloride and found the following two interesting facts. 1) The recoil effects in hexamminecobalt(III) chloride involve more complicated processes than the simple replacement process. 2) A small percentage of the activity produced in the target is found in the form of chloropentamminecobalt(III) chloride as the result of recoil effect, and its radiochemical yield decreases on keeping it to stand even at room temperature; the rate determining step in this process is not diffusion, which has been usually considered to be responsible to the thermal annealing process of the recoil atom[2], but a chemical reaction.

Purified hexamminecobalt(III) chloride was subjected to neutron irradiation in the reactor, JRR-1 (neutron flux: $6\times10^{11}$ n/cm$^2$/sec.) for 10 min., and was dissolved in water in about

1) N. Ikeda, K. Yoshihara and N. Mishio, *Radioisotopes*, 8, 242 (1959).

2) G. Harbottle and N. Sutin, "The Szilard-Chalmers Reaction in Solids" in "Advances in Inorganic Chemistry and Radiochemistry" Edited by H. J. Emelius and A. G. Sharpe, Academic Press, New York (1959).

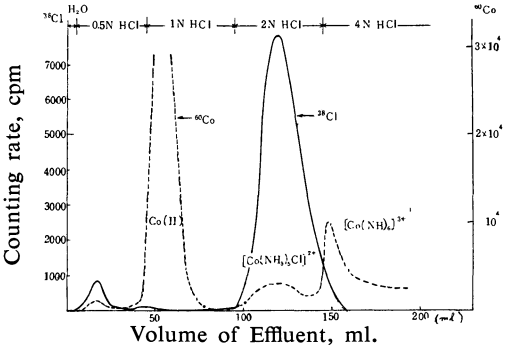



Fig. 1. Elution curve for recoil products in neutron-irradiated hexamminecobalt(III) chloride.

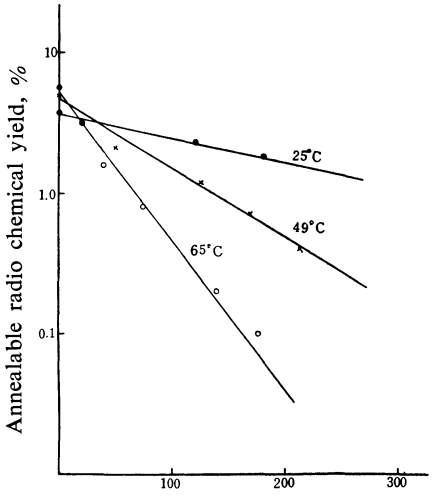



Fig. 2. Decrease of radiochemical yield of $[Co(NH_3)_5Cl^*]$ by standing irradiated hexamminecobalt(III) chloride at various temperatures.

30 min. after irradiation. The solution was passed through a cation-exchange resin column (Diaion SK #1, HR-form, 100~200 mesh, 1 cm. $\phi \times 4$ cm.). After being washed with a small quantity of water, the resin bed was eluted with hydrochloric acid of various concentrations. By the use of a pulse-height analyzoer, the $\gamma$-rays of $^{38}Cl$ and $^{60}Co$ in the eluted fractions were measured separately. The elution curve is shown in Fig. 1. The solid line shows the elution curve for $^{38}Cl$ activity and the dotted one shows that for $^{60}Co$ activity. The formation of $[Co(NH_3)_5Cl^*]^{2+}$ might be interpreted as simple replacement of $NH_3$ by $^{38}Cl$ recoil atom, but the formation of $[Co^*(NH_3)_5Cl]^{2+}$ can not be understood by this concept. Moreover, such a simple replacement can not explain the appearance of a peak at the earlier stage of the elution curve; a peak due to an unknown species containing both cobalt and chlorine atoms which might be a cobalt ammine complex, such as $[Co(NH_3)_4Cl_2]^+$.

The radiochemical yield of $[Co(NH_3)_5Cl^*]^{2+}$ was accurately measured after being separated from the luteo-salt. It was about 7% immediately after irradiation, but this value decreased on keeping the sample to stand in the solid state. At various temperatures, the relation between the standing time and the radiochemical yield of $[Co(NH_3)_5Cl^*]^{2+}$ was observed. The annealing curves for the earlier stage are shown in Fig. 2. The curves correspond to those of the first-order reaction. An apparent activation energy of 8.6 kcal. was obtained for this decreasing process of $[Co(NH_3)_5Cl^*] \cdot Cl_2$. Mori and Tsuchiya[3] studied the thermal decomposition of $[Co(NH_3)_6]Cl_3$ and reported the heat of formation $\Delta H = 9.6$ kcal./mol. and the activation energy $E_h = 18.0$ kcal./mol. for the reaction,

$$[Co(NH_3)_6]Cl_3 \rightleftarrows [Co(NH_3)_5Cl]Cl_2 + NH_3$$
(solid) (solid) (gas)

In the back-reaction, therefore, the activation energy $E_p = E_h - \Delta H = 8.4$ kcal./mol. is obtained. This value is very close to that obtained in this experiment. So that, one possible explanation of the annealing reaction observed by the present authors may be given by considering the back-reaction of the above-mentioned system provided that the quantity of ammonia is much larger compared with that of $[Co(NH_3)_5Cl]Cl_2$.

These results would lead us to the following model. In the neighborhood of the recoil atom, the chemical bonds of the molecules are broken and local fragmentation occurs. Unstable intermediate systems are formed. These are immediately rearranged into a group of several chemical species in the cooling step. However, some unbalances are still present in these systems, and slow changes occur by thermal annealing.

Details are to be reported in the full paper.

*Department of Chemistry*
*Faculty of Science*
*Tokyo University of Education*
*Bunkyo-ku, Tokyo*
*(N. I. & S. Y.)*

*Japan Atomic Energy Research Institute*
*Tokai, Ibaraki-ken (K. Y.)*

3) M. Mori and R. Tsuchiya, This Bulletin, **32**, 467 (1959).

# *Solvent Shift of Methyl Proton Nuclear Magnetic Resonance*

By Naoya NAKAGAWA and Shizuo FUJIWARA

(Received June 27, 1960)

The solvent effect of high resolution proton magnetic resonance has been investigated by many workers[1-3], recently. We also reported that the HCN, $-C\equiv CH$, and $-CH_3$ protons show quite large solvent shifts[4]. In this paper, we will show the results of the investigations for methyl protons in various compounds.

Chemical shifts of the NMR spectra of methyl protons in a number of organic compounds dissolved in solvents such as benzene, pyridine, dioxane, and carbon tetrachloride were measured by the internal reference method. Each sample consists of solute, solvent, and cyclohexane as the internal reference, with a molar ratio of 1 : 9 : 0.25, and is sealed in a glass tube of 3.5 mm. O. D. The apparatus of the NMR measurement is the one constructed by one of the authors (S. F.), and is operated at 27 Mc. The details of this set-up were reported elsewhere[5]. The chemical shifts of the methyl protons of the samples were measured on the recorded charts as the separations from cyclohexane by taking the separation between toluene $CH_3$ and cyclohexane as 0.75 p.p.m. This value of the reference was determined by the side-band technique[6].

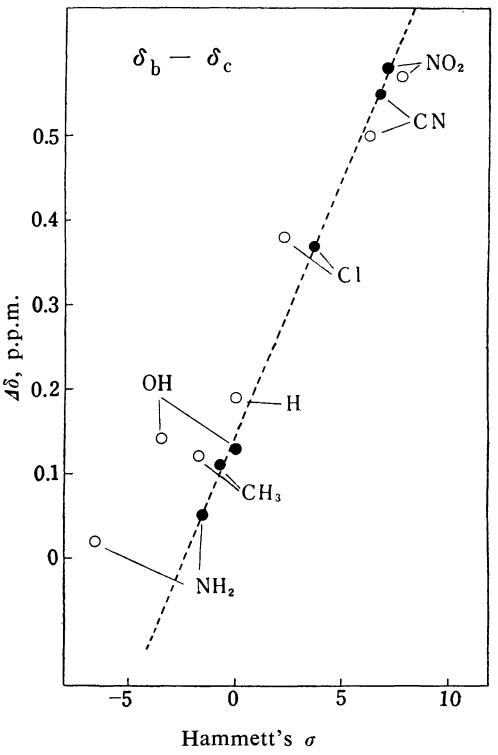



Fig. 1. Solvent shifts and Hammett's $\sigma$ of substituted toluenes.

● meta ○ para

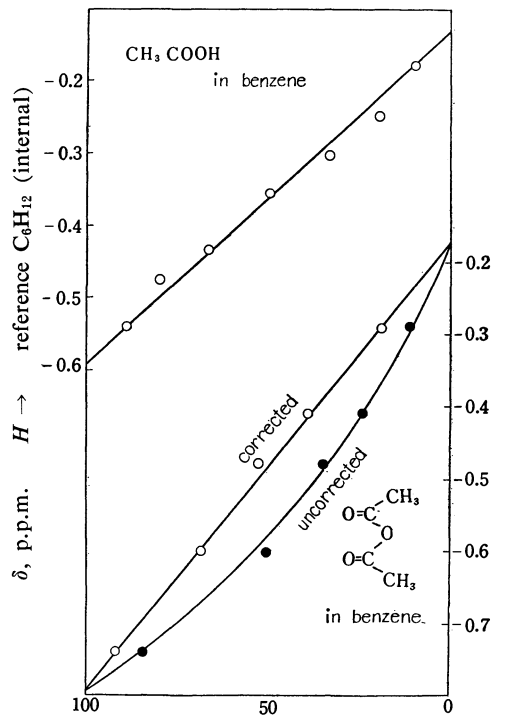



Fig. 2. Chemical shifts of $CH_3$ protons

1) As to the references of this effect before 1958, see, J. A. Pople, W. G. Schneider and H. J. Bernstein, "High-Resolution Nuclear Magnetic Resonance", McGraw-Hill, New York (1959), pp. 400—432.

2) E. B. Whipple, J. H. Goldstein, L. Mandell, G. S. Reddy and G. R. McClure, *J. Am. Chem. Soc.*, **81**, 1321 (1959).

3) R. E. Glick, D. F. Kates and S. J. Ehrenson, *J. Chem. Phys.*, **31**, 567 (1959).

4) N. Nakagawa and S. Fujiwara, to be published in *J. Org. Chem.*

5) S. Fujiwara and H. Shimizu, in press in *J. Chem. Phys.*

6) J. T. Arnold and M. G. Packard, *J. Chem. Phys.*, **19**, 1608 (1951).

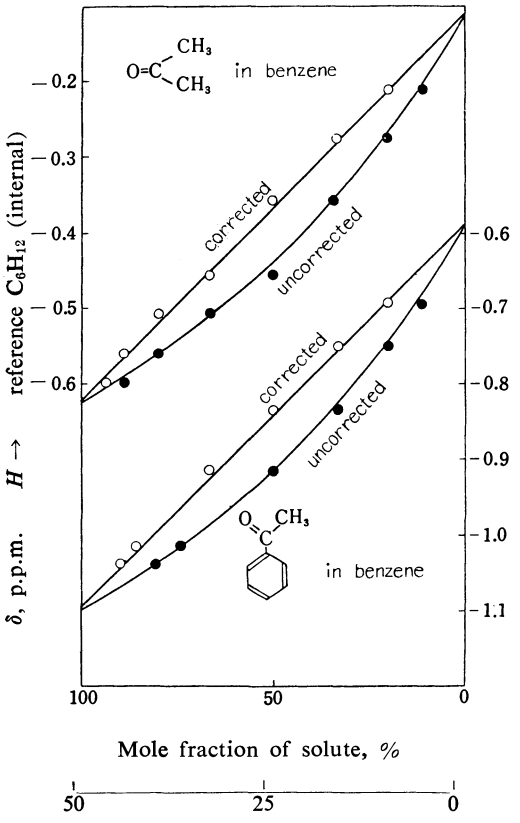



Fig. 3. Chemical shifts of $CH_3$ protons.

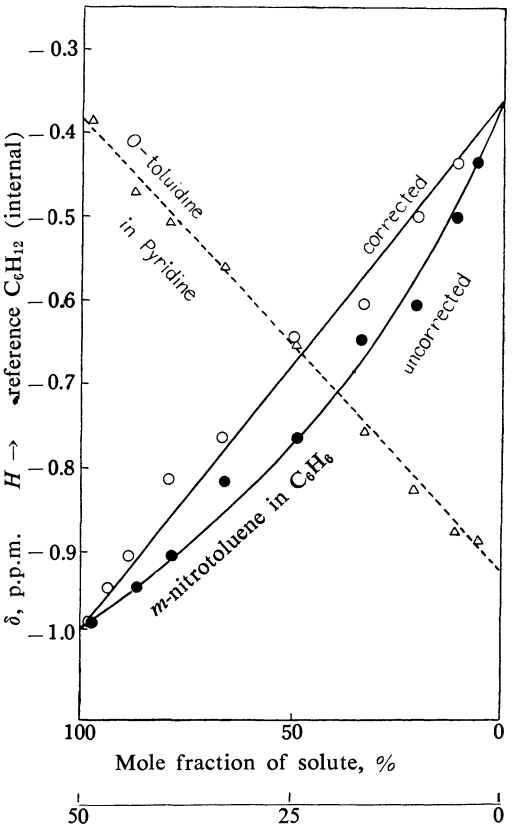



Fig. 4. Chemical shifts of $CH_3$ protons.

TABLE I. CHEMICAL SHIFTS OF METHYL PROTONS

Temperature: 11～12°C
Concentration: solute: solvent: cyclohexane=1 : 9 : 0.25 (mol.)
Unit of chemical shift: p.p.m. from cyclohexane

| Solute | Without solvent $-\delta_0$ | In $C_6H_6$ $-\delta_b$ | In $C_5H_5N$ $-\delta_p$ | In dioxane $-\delta_d$ | In $CCl_4$ $-\delta_c$ |
|---|---|---|---|---|---|
| Toluene | 0.75 | 0.71 | 0.81 | 0.89 | 0.90 |
| *p*-Nitrotoluene | — | 0.50 | 0.90 | 1.01 | 1.07 |
| *p*-Tolunitrile | 0.90 | 0.50 | 0.87 | 0.97 | 1.00 |
| p-Chlorotoluene | 0.65 | 0.50 | 0.75 | 0.85 | 0.88 |
| *p*-Xylene | 0.71 | 0.72 | 0.83 | 0.79 | 0.84 |
| *p*-Cresol* | 0.70 | 0.66 | 0.91 | 0.77 | 0.80 |
| *p*-Toluidine | — | 0.73 | 0.82 | 0.70 | 0.76 |
| *m*-Nitrotoluene* | 0.99 | 0.48 | 0.93 | 1.03 | 1.06 |
| *m*-Tolunitrile | 0.87 | 0.42 | 0.82 | 0.93 | 0.97 |
| *m*-Chlorotoluene | 0.64 | 0.48 | 0.77 | 0.85 | 0.84 |
| *m*-Xylene* | 0.71 | 0.75 | 0.86 | 0.83 | 0.86 |
| *m*-Cresol* | 0.66 | 0.67 | 0.89 | 0.83 | 0.80 |
| *m*-Toluidine | 0.66 | 0.72 | 0.83 | 0.75 | 0.76 |

TABLE I (Continued)

| | | | | | |
|---|---|---|---|---|---|
| *o*-Nitrotoluene | 1.09 | 0.80 | 1.14 | 1.18 | 1.16 |
| *o*-Tolunitrile | 0.99 | 0.73 | 1.02 | 1.12 | 1.11 |
| *o*-Chlorotoluene | 0.78 | 0.71 | 0.85 | 0.91 | 0.93 |
| *o*-Xylene | 0.61 | 0.61 | 0.74 | 0.77 | 0.81 |
| *o*-Cresol* | 0.76 | 0.69 | 1.11 | 0.74 | 0.77 |
| *o*-Toluidine | 0.37 | 0.39 | 0.88 | 0.61 | 0.58 |
| $\gamma$-Picoline | 0.75 | 0.41 | 0.79 | 0.87 | 0.93 |
| $\beta$-Picoline | 0.76 | 0.46 | 0.81 | 0.87 | 0.88 |
| $\alpha$-Picoline | 1.09 | 1.03 | 1.17 | 1.08 | 1.11 |
| Acetone | 0.65 | 0.24 | 0.66 | 0.62 | 0.67 |
| Acetophenone | 1.07 | 0.72 | 1.12 | 1.07 | 1.12 |
| Acetic acid | 0.60 | 0.17 | 0.80 | 0.52 | 0.62 |
| Acetic anhydride | 0.74 | 0.25 | 0.78 | 0.73 | 0.74 |
| Methyl iodide | 0.74 | 0.09 | — | 0.70 | 0.72 |
| Acetonitrile | 0.52 | −0.43 | 0.52 | 0.51 | 0.53 |
| Nitromethane | 2.87 | 1.75 | 3.00 | 2.88 | 2.88 |

* Measurements for the compounds with asterisks were made at 17°C.

TABLE II. "SOLVENT SHIFTS" $\Delta\delta$ OF METHYL PROTONS

Temperature: 11∼12°C
Concentration: solute: solvent: cyclohexane=1 : 9 : 0.25 (mol.)
Unit: p.p.m. ±0.03 p.p.m.

| Solute | $\Delta\delta\equiv\delta_b-\delta_p$ | $\delta_b-\delta_d$ | $\delta_b-\delta_c$ | $\delta_p-\delta_d$ | $\delta_p-\delta_c$ | $\delta_d-\delta_c$ |
|---|---|---|---|---|---|---|
| Toluene | 0.17 | 0.18 | 0.19 | 0.01 | 0.02 | 0.02 |
| *p*-Nitrotoluene | 0.40 | 0.51 | 0.57 | 0.11 | 0.17 | 0.06 |
| *p*-Tolunitrile | 0.37 | 0.47 | 0.50 | 0.10 | 0.13 | 0.03 |
| *p*-Chlorotoluene | 0.25 | 0.35 | 0.38 | 0.09 | 0.13 | 0.04 |
| *p*-Xylene | 0.11 | 0.07 | 0.12 | −0.04 | 0.01 | 0.05 |
| *p*-Cresol* | 0.25 | 0.11 | 0.14 | −0.14 | −0.11 | 0.03 |
| *p*-Toluidine | 0.08 | −0.03 | 0.02 | −0.11 | −0.06 | 0.05 |
| *m*-Nitrotoluene* | 0.45 | 0.55 | 0.58 | 0.09 | 0.13 | 0.03 |
| *m*-Tolunitrile | 0.40 | 0.51 | 0.55 | 0.11 | 0.15 | 0.04 |
| *m*-Chlorotoluene | 0.29 | 0.38 | 0.37 | 0.08 | 0.07 | −0.01 |
| *m*-Xylene* | 0.11 | 0.08 | 0.11 | −0.04 | 0.00 | 0.03 |
| *m*-Cresol* | 0.23 | 0.17 | 0.13 | −0.06 | −0.09 | −0.03 |
| *m*-Toluidine | 0.11 | 0.04 | 0.05 | −0.07 | −0.06 | 0.01 |
| *o*-Nitrotoluene | 0.33 | 0.37 | 0.35 | 0.04 | 0.02 | −0.02 |
| *o*-Tolunitrile | 0.30 | 0.40 | 0.39 | 0.10 | 0.09 | −0.01 |
| *o*-Chlorotoluene | 0.14 | 0.20 | 0.22 | 0.06 | 0.08 | 0.02 |
| *o*-Xylene | 0.13 | 0.16 | 0.19 | 0.03 | 0.07 | 0.03 |
| *o*-Cresol* | 0.42 | 0.05 | 0.07 | −0.37 | −0.35 | 0.02 |
| *o*-Toluidine | 0.49 | 0.22 | 0.20 | −0.27 | −0.30 | −0.03 |
| $\gamma$-Picoline | 0.38 | 0.46 | 0.52 | 0.08 | 0.14 | 0.06 |
| $\beta$-Picoline | 0.34 | 0.41 | 0.41 | 0.06 | 0.07 | 0.01 |
| $\alpha$-Picoline | 0.14 | 0.05 | 0.08 | −0.10 | −0.07 | 0.03 |
| Acetone | 0.42 | 0.38 | 0.43 | −0.04 | 0.01 | 0.05 |
| Acetophenone | 0.40 | 0.35 | 0.40 | −0.06 | 0.00 | 0.06 |
| Acetic acid | 0.64 | 0.35 | 0.45 | −0.29 | −0.19 | 0.10 |
| Acetic anhydride | 0.53 | 0.48 | 0.49 | −0.05 | −0.04 | 0.01 |
| Methyl iodide | — | 0.62 | 0.63 | — | — | 0.02 |
| Acetonitrile | 0.95 | 0.94 | 0.97 | −0.01 | 0.01 | 0.02 |
| Nitromethane | 1.26 | 1.13 | 1.13 | −0.13 | −0.13 | 0.02 |

* Values for the compounds with asterisks are for 17°C.

The results of measurements are summarized as shown in Table I. In meta- and para-substituted toluenes, the solvent shifts of the methyl protons, $\Delta\delta$, which are defined as the difference between the chemical shifts in any two solutions of different solvents, are linearly correlated with Hammett's sigma values as shown in Fig. 1. If we assume that the solvent shift of cyclohexane is constant, and if this is also the case with respect to the samples listed in the same column of Table II, the observed values of $\Delta\delta$ will mainly refer to the solvent shifts of the methyl protons.

In the results of Tables I and II, we notice that the magnitudes of the solvent shifts of the methyl protons are increased with the acidity of the methyl protons of the solute molecule. For example, the $\Delta\delta$ value of *p*-nitrotoluene for the benzene-$CCl_4$ system is 0.57 p.p.m. and that of *p*-toluidine is 0.02 p.p.m. This result coincides with the behavior of the solute parameter $x_1$ of the medium effect defined by Bothner-By[7].

According to the results of the measurements, we can conclude that the chemical shift of methyl proton in acetic acid is a linear function of the mole fraction solute (Fig. 2), as in the cases of nitromethane and of acetonitrile[5]. In acetic anhydride, or in acetone, the linear relation is not obtained with the simple mole fraction of the solute, but a fine linearity is obtained by taking the corrected mole fraction as abscissa, where one methyl group of the solute is taken into account as one solute molecule (cf. Figs. 2 and 3). In the cases of acetophenone and *m*-nitrotoluene, similar corrections are also necessary, and we have used the corrected mole fractions as shown in Figs. 3 and 4, where the number of the phenyl groups of the solute has been taken into account for the calculation as well as the solvent benzene.

In the case of *o*-toluidine, the chemical shifts of the methyl protons linearly depend on the simple mole fraction of the solvent (cf. Fig. 4) and, moreover, the magnitudes of the solvent shifts are anomalously large (cf. Table II). Similar results are observed with *o*-cresole.

The authors' thanks are due to Mr. Hiroshi Shimizu of the University of Tokyo and Professor Hajime Kashiwagi of Nagoya University for valuable discussions.

*University of Electro-communications*
*Chofu, Tokyo* (*N. N.*)

*Department of Chemistry*
*Faculty of Science*
*The University of Tokyo*
*Hongo, Tokyo* (*S. F.*)

7) A. A. Bothner-By: Private communication. The present authors are very grateful to Dr. Bothner-By for sending them the reprint.

# *Syntheses of Benzo[b]tropothiazine and its Derivatives*

By Tetsuo NOZOE, Toyonobu ASAO and Kazuko TAKAHASHI

(Received July 22, 1960)

The preparation of oxime and arylhydrazones of quinoxalotropone (I) by the condensation of 5-nitroso- or 5-arylazo-tropolones and *o*-phenylenediamine was reported earlier in this laboratory[1]. A parent compound II, named benzo[b]tropazine, was obtained also by condensation of 2-halo- or 2-methoxy-tropone, or 3-carboxy-tropolone and *o*-phenylenediamine[2]. In the present series of this work, several compounds having a new ring system IV containing sulfur and nitrogen atoms were synthesized and examinations were made on their properties.

A mixture of 2-halotropone (III) and *o*-aminothiophenol in methanol was allowed to stand at room temperature and red plates IV, m. p. 87°C, $C_{13}H_9NS$, were obtained. IV is stable to heating with alkali or hydrochloric acid, is easily soluble in various organic solvents and in dilute acid to form a deep red solution, and easily gives some molecular compounds such as picrate. The ultraviolet absorption spectrum of IV (Fig. 1) in hydrochloric acid solution shows a shift to a longer wavelength region compared with that in methanol.

Attempted catalytic hydrogenation of IV in

1) T. Nozoe, M. Sato and T. Matsuda, *Sci. Repts. Tohoku Univ., First Ser.*, **37**, 407 (1953); T. Nozoe, S. Ito, S. Suzuki and K. Hiraga, *Proc. Japan Acad.*, **32**, 344 (1956); S. Ito, *Sci. Repts. Tohoku Univ., First Ser.*, **42**, 236 (1958).

2) T. Nozoe, Y. Kitahara, K. Takase and M. Sasaki, *Proc. Japan Acad.*, **32**, 349 (1956).

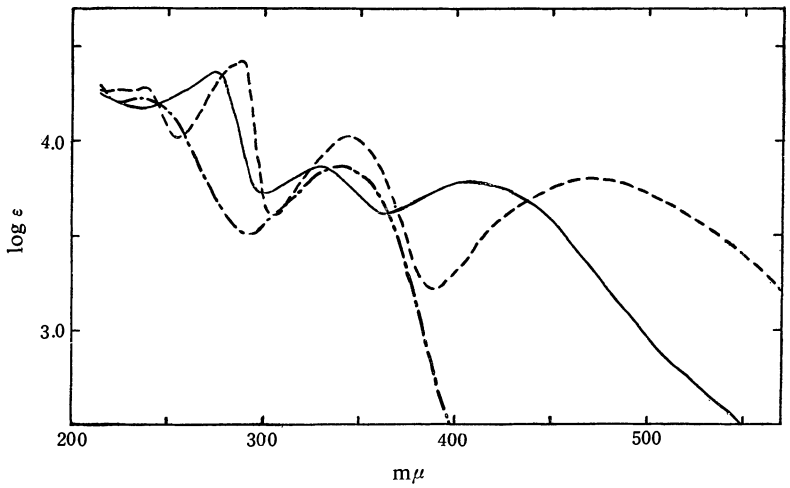
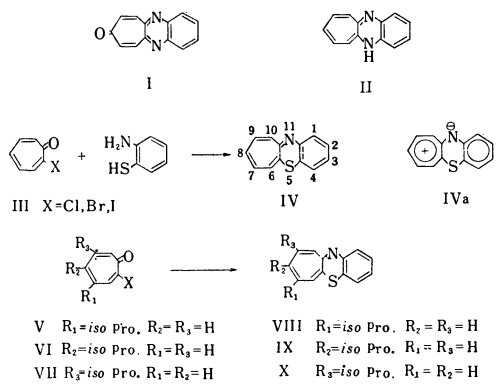



Fig. 1. Ultraviolet absorption spectra.
—·—· II (in methanol), —— IV (in methanol), ---- IV (in 0.1 N HCl).

the presence of palladium-carbon or Adams catalyst was unsuccessful with no hydrogen uptake and the complete recovery of the




original compound IV. The reaction of IV with methyl iodide did not give methiodide, but gave hydroiodide of IV. Hydrobromide of IV was also formed by treatment of IV with hydrobromic acid.

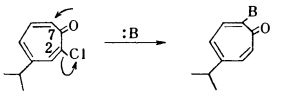
From these properties, the course of preparation, and the analytical values of IV and its several derivatives, the structure of IV could be proved to be cyclohepta[b]benzo-[e]-1,4-thiazine, for which the name of benzo[b]-tropothiazine is proposed.

It is interesting to compare compound IV with compound II. The latter compound II forms colorless prisms with poor solubility, and is unstable toward acids, reducible with palladium-carbon to 2,3-pentamethylene-quinoxaline. Also the ultraviolet spectrum of compound II is quite different from that of compound IV as shown in Fig. 1. These results would indicate that IV is stabilized by the resonance between IV and IVa.

Three kinds of isopropyl-2-halotropones (V, VI and VII)[3,4] were also reacted with *o*-aminothiophenol, easily affording 7-, 8- and 9-isopropylbenzo[b]tropothiazines (VIII, IX and X) as red oils. These isopropyl compounds have properties similar to those of the compound IV. In view of the fact that the abnormal nucleophilic substitution, which is frequently observed in troponoid chemistry*, does not occur in the reaction of 2-halotropone derivatives and methylmercaptane[5], it is considered that the same normal substitution occurs in the reaction of 2-halotropone derivatives and *o*-aminothiophenol; therefore it is assumed that the structure of VIII-X is correct.

2-Bromo-7-methoxytropone (XI)[6] gave a red oil XII, $C_{14}H_{11}ONS$, by the condensation with *o*-aminothiophenol. The compound XII, like IV, is soluble in dilute acid and gives molecular compounds such as picrate. Hydrolysis of XII with hydrochloric acid gave red needles XIII, m.p. 169°C, which were identical with a compound obtained by the reaction of 3-bromo-2-methoxytropone (XIV)[6]

3) S. Seto, *Sci. Repts. Tohoku Univ., First Ser.*, **37**, 286 (1953).
4) W. v. E. Docring and L. H. Knox, *J. Am. Chem. Soc.*, **75**, 297 (1953).
* It has been known that in the nucleophilic substitution reaction of 2-halotropones various reagents do not attack at the carbon-2 but at the carbon-7 in the majority of cases.




Cf. T. Nozoe, S. Seto and T. Sato, *Proc. Japan Acad.*, **30**, 473 (1954); T. Nozoe, "Non-Benzenoid Aromatic Compounds", Edited by D. Ginsburg, Interscience Publishers, Inc., New York (1959), p. 339.
5) K. Matsui, This Bulletin, **33**, 1448 (1960).
6) T. Nozoe, Y. Kitahara and S. Masamune, *Proc. Japan Acad.*, **27**, 649 (1951).

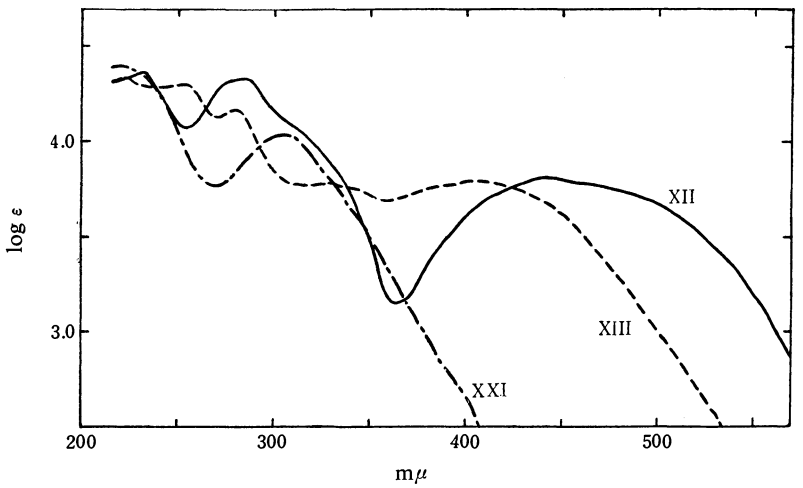
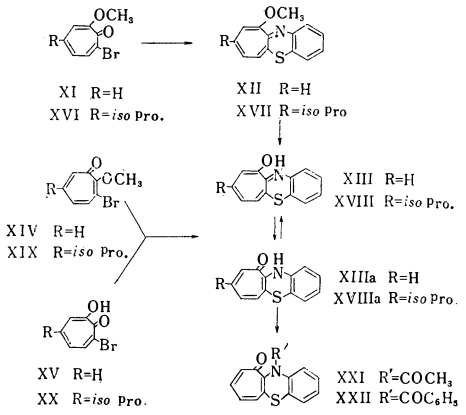



Fig. 2. Ultraviolet absorption spectra of XII, XIII and XXI in methanol.

and *o*-aminothiophenol. XIII was also obtained from 2-bromotropolone (XV) in good yield. From these results, it is assumed that the structure of XII is 10-methoxybenzo [b] tropothiazine and of XIII is 10-hydroxybenzo [b] - tropothiazine.

Attempted substitution of methoxyl in XII with amino or substituted amino group was not successful. The original compound XII was recovered unchanged.

2-Bromo-5-isopropyl-7-methoxytropone (XVI)[7] gave 7-isopropyl-10-methoxybenzo [b] tropothiazine (XVII) by the reaction with *o*-aminothiophenol. Hydrolysis of XVII with hydrochloric acid afforded 7-isopropyl-10-hydroxybenzo [b] - tropothiazine (XVIII). This was also obtained by the reaction of 3-bromo-6-isopropyl-2-methoxytropone (XIX)[7] or 7-bromohinokitiol (3-bromo-6-isopropyltropolone) (XX) with *o*-aminothiophenol. XIII and XVIII do not dissolve in dilute acids. XIII does not give molecular compounds such as picrate, but XVIII gives them.




It is considered that compounds XIII and XVIII could exist in two tautomeric forms respectively, i. e. 10-hydroxy derivatives of benzo [b] tropothiazine (XIII and XVIII) and benzothiazinotropone derivatives (XIIIa and XVIIIa). Information on this problem comes from the following data: 1) The ultraviolet spectrum of XII is similar to IV rather than to XIII as shown in Fig. 2. 2) The infrared spectrum of XIII shows $\nu_{NH}$ at 3218 $cm^{-1}$ and $\nu_{C=O}$ at 1607 $cm^{-1}$ (small peak). 3) XIII did not react with diazomethane, but gave yellow acetate XXI with acetic anhydride and orange benzoate XXII with benzoyl chloride in poor yield. The hydrolysis of these acyl derivatives converts them into XIII. $\nu_{C=O}$ at 1673 $cm^{-1}$ in infrared spectrum of XXI indicates that XXI is *N*-acetyl derivative. Remarkable shifts to a shorter wavelength region in the ultraviolet spectra of XXI and XXII (Fig. 2) seem to indicate that a conjugation of seven membered ring and benzene nucleus in XIII is broken by the introduction of the acyl group in the *N*-atom, as an additional reason for the decrease of the coplanarity of these nuclei is also considered.

From consideration of the above results, it seems reasonable to conclude that XIII would exist not as 10-hydroxybenzo [b] tropothiazine, but as its keto form, benzo-1, 4-thiazino [3,2-b] - tropone (XIIIa). XVIII would be named 8 - isopropylbenzo - 1, 4 - thiazino [3, 2-b] tropone (XVIIIa).

It is supposed that *N*-alkylation of the compound XII is possible as in the case of phenothiazine, but the attempted alkylations were not actually successful. Further experiments in this field will be reported in near future.

7) S. Seto, *Sci. Repts. Tohoku Univ., First Ser.*, 37, 298 (1953).

## Experimental**

**Benzo[b]tropothiazine (IV).** — A solution of 2 g. of 2-chlorotropone and 2 g. of *o*-aminothiophenol in 20 ml. of methanol was allowed to stand at room temperature for 3 hr. The solvent was distilled off and 100 ml. of water added to the residue, and the insoluble portion was filtered off. The filtrate was extracted with two 10 ml. portions of benzene. The mother liquor left after benzene extraction was adjusted to make it slightly alkaline with sodium carbonate solution, then was extracted with five 10 ml. portions of benzene. The latter benzene extract was dried over sodium sulfate and the benzene was distilled off, affording 2.4 g. of deep red crystals. Recrystallization of the crude crystals from petroleum (b. p. 60～70°C) gave 2.2 g. of IV as red plates, m. p. 86～87°C.

The reaction of 2-bromo- or 2-iodo-tropone with *o*-aminothiophenol gave the same compound IV.

Found: C, 74.05; H, 4.20; N, 6.61. Calcd. for $C_{13}H_9NS$: C, 73.92; H, 4.30; N, 6.63%.

$\lambda_{max}^{MeOH}$ mμ (log ε): 275 (4.37), 330 (3.86), 405 (3.79). $\lambda_{max}^{0.1N\ HCl}$ mμ (log ε): 224 (4.27), 238 (4.28), 289 (4.44), 343 (4.02), 470 (3.81).

*Picrate;* dark brown needles, m. p. 188～189°C (decomp.).

Found: C, 51.75; H, 3.16; N, 12.73. Calcd. for $C_{19}H_{12}O_7N_4S$: C, 51.82; H, 2.75; N.12.72%.

*Styphnate;* dark brown needles, m. p. 204～205°C (decomp.).

Found; C, 50.09; H, 2.75; N, 12.10. Calcd. for $C_{19}H_{12}O_8N_4S$: C, 50.00; H, 2.65; N, 12.10%.

*Hydriodide;* black violet needles, m. p. 194～195.5°C, 210～220°C (decomp.).

Found: C, 46.35; H, 3.42; N, 4.51. Calcd. for $C_{13}H_{10}NSI$: C, 46.00; H, 2.97; N, 4.13%.

*Hydrobromide*; black violet needles, m. p. 207°C (decomp.).

Found: C, 51.95; H, 3.37; N, 4.28. Calcd. for $C_{13}H_{10}NSBr$: C, 53.42; H, 3.45; N, 4.79%.

**7-Isopropylbenzo[b]tropothiazine (VIII).** — Reaction of 150 mg. of 2-chloro-4-isopropyltropone (V) with 100 mg. of *o*-aminothiophenol in methanol afforded 150 mg. of VIII as red oil.

*Picrate;* violet needles, m.p. 172～173°C(decomp.).

Found: C, 54.62; H, 3.68; N, 11.59. Calcd. for $C_{22}H_{18}O_7N_4S$: C, 54.77; H, 3.76; N, 11.62%.

*Styphnate;* dark violet needles, m.p. 169～170°C (decomp.).

Found: C, 53.15; H, 3.53; N, 11.22. Calcd. for $C_{22}H_{18}O_8N_4S$: C, 53.01; H, 3.63; N, 11.24%.

**8-Isopropylbenzo[b]tropothiazine (IX).** — IX as red oil was obtained from 2-halo-5-isopropyltropone (VI) and *o*-aminothiophenol.

*Picrate;* violet needles, m. p. 176～177°C.

Found: C, 54.74; H, 3.79; N, 11.52%.

*Styphnate;* violet needles, m.p. 176.5～177.5°C.

Found: C, 52.74; H, 3.42; N, 11.23%.

**9-Isopropylbenzo[b]tropothiazine (X).** — X as red oil was obtained from 2-halo-6-isopropyltropone (VII) and *o*-aminothiophenol.

*Picrate;* violet plates, m. p. 198～199°C (decomp.).

Found: C, 54.39; H, 3.27; N, 11.64%.

*Styphnate;* violet prisms, m. p. 191～192°C (decomp.).

Found: C, 53.19; H, 3.77; N, 10.97%.

**10-Methoxybenzo[b]tropothiazine (XII).** — A solution of 215 mg. of 2-bromo-7-methoxytropone (XI) and 130 mg. of *o*-aminothiophenol in 3 ml. of methanol was warmed for twenty minutes. After allowing it to stand at room temperature for 10 min., the solvent was distilled off, and 20 ml. of water was added and extracted with two 5 ml. portions of benzene. The water layer left after the benzene extraction was adjusted to slightly alkaline with sodium carbonate and was extracted with benzene. The latter benzene extract was dried over sodium sulfate and the solvent was removed, affording 150 mg. of XII as red oil, and was purified by chromatogram, using an alumina.

$\lambda_{max}^{MeOH}$ mμ (log ε): 222 (4.33), 253 (4.28), 280 (4.15), 328 (3.78), 408～410 (3.78).

*Picrate;* dark brown needles, m. p. 184～185°C.

Found: C, 51.01; H, 2.83; N, 11.76. Calcd. for $C_{21}H_{14}O_8N_4S$: C, 51.07; H, 3.00; N, 11.91%.

*Styphnate;* dark brown needles, m. p. 173～174°C.

Found: C, 49.55; H, 2.78; N, 11.25. Calcd. for $C_{21}H_{14}O_9N_4S$: C, 49.39; H, 2.90; N, 11.52%.

**Benzo-1,4-thiazino[3,2-b]tropone (XIII).** — a) A solution of 3 g. of 3-bromotropolone (XV) and 2 g. of *o*-aminothiophenol in 20 ml. of methanol was refluxed for 2 hr. The red needles which separated out by cooling thoroughly were collected by filtration and recrystallization from ethanol or acetic acid, giving 2.6 g. of XIII as red needles, m. p. 168～169°C.

Found: C, 68.84; H, 3.76; N, 6.11. Calcd. for $C_{13}H_9ONS$: C, 68.72; H, 3.99; N, 6.17%.

$\lambda_{max}^{MeOH}$ mμ (log ε): 233 (4.36), 285 (4.33), 440 (3.82). $\lambda_{max}^{0.1N\ HCl}$ mμ (log ε): 230 (4.37), 285 (4.35), 450 (3.81).

b) After allowing a solution of 215 mg. of 3-bromo-2-methoxytropone (XIV) and 130 mg. of *o*-aminothiophenol in 2 ml. of a methanol to stand under cooling, 220 mg. of XIII was obtained.

c) A solution of 50 mg. of XII in 3 ml. of 2 N hydrochloric acid was refluxed for 5 hr., and the crystals which separated out were recrystallized from ethanol, affording 30 mg. of XIII.

**10-Methoxy-8-isopropylbenzo[b]tropothiazine (XVII).** — A solution of 520 mg. of 2-methoxy-4-isopropyl-7-bromotropone (XVI) and 250 mg. of *o*-aminothiophenol in 2 ml. of methanol was refluxed for thirty minutes. The solvent was distilled off and 7 ml. of water was added to the residue and the solution was extracted with benzene. The mother liquor left after the benzene extraction was adjusted to slightly alkaline with sodium carbonate and was extracted with benzene. The latter benzene extract was dried and the removal of the solvent left 270 mg. of red oil. The oil was crystallized with methanol and the recrystallization from methanol gave XVII as orange prisms, m. p. 123～124°C.

---

** All the melting points were uncorrected. The microanalyses were carried out by Mr. S. Azumi and Miss A. Iwanaga, and I. R. spectra were measured with Perkin-Elmer Model 112 by the member of Professor Kinumaki's laboratory, Research Institute, Chemistry of Non-Aqueous Solution, Tohoku Univ., to whom the authors' sincere acknowledgements are hereby extended.

Found: C, 71.70; H, 5.84; N, 4.93, Caled. for $C_{17}H_{17}ONS$: C, 72.06; H, 6.05; N, 4.94%.

$\lambda_{max}^{MeOH}$ mμ (log ε): 225 (4.41), 255 (4.24 sh), 280 (4.14 sh), 333 (3.74), 408~410 (3.78).

*Picrate;* brown needles, m.p. 160~161°C.

Found: C, 53.99; H, 3.93; N, 10.85. Calcd. for $C_{23}H_{20}O_8N_4S$: C, 53.91; H, 3.93; N, 10.93%.

*Styphnate;* brown needles, m. p. 145~146°C.

Found: C, 52.74; H, 3.75; N, 10.60. Calcd. for $C_{23}H_{20}O_9N_4S$: C, 52.25; H, 3.81; N, 10.61%.

**8-Isopropylbenzo-1, 4-thiazino[3, 2-b] tropone (XVIII).** — a) A solution of 500 mg. of 7-bromohinokitiol (3-bromo-6-isopropyltropolone) (XX) and 250 mg. of *o*-aminothiophenol in 3 ml. of methanol was refluxed for an hour, the solvent was distilled off and 20 ml. of water was added to the residue, and then extracted six times with 3 ml. each of benzene. The benzene solution was dried over sodium sulfate, passed through an alumina column, and 440 mg. of oily substance was obtained after removal of the solvent from the effluent. The oil crystallized with cyclohexane and the recrystallization from cyclohexane afforded XVIII as red needles, m. p. 94~95°C.

Found: C, 71.01; H, 5.50; N, 5.27. Calcd. for $C_{16}H_{15}ONS$: C, 71.36; H, 5.61; N, 5.20%.

$\lambda_{max}^{MeOH}$ mμ (log ε): 237 (4.31), 277 (4.23), 430 (3.65).

*Picrate;* brownish violet plates, m.p. 141~142°C.

Found: C, 53.70; H, 3.98; N, 11.19. Calcd. for $C_{22}H_{18}O_8N_4S$: C, 53.01; H, 3.64; N, 11.24%.

*Styphnate;* brownish violet plates, m. p. 170~171°C.

Found: C, 51.47; H, 3.47; N, 10.39. Calcd. for $C_{22}H_{18}O_9N_4S$: C, 51.36; H, 3.53; N, 10.89%.

b) A solution of 260 mg. of 2-methoxy-3-bromo-6-isopropyltropone (XIX) and 130 mg. of *o*-aminothiophenol in 3 ml. of methanol was allowed to stand for an hour. 300 mg. of red crystals was obtained after treatment using the same method as (a). These crystals showed no depression of melting point on admixture with a specimen obtained in (a).

c) After refluxing a solution of 50 mg. of XVII in 3 ml. of 2 N hydrochloric acid for 5 hr., the solution was extracted with benzene and the benzene extract was passed through an alumina column, affording 30 mg. of red needles, m. p. 92~93°C. The crystals showed no depression of melting point on admixture with XVIII.

**Acetate (XXI) of XIII.** — One hundred mg. of XIII were dissolved in 0.5 ml. of acetic anhydride, to which one drop of concentrated sulfuric acid was added, and then the mixture was allowed to stand at room temperature. After removing the acetic anhydride, the residue was dissolved in benzene and the benzene solution was passed through an alumina layer. The first elution gave unreacted XIII, but the second effluent afforded yellow prisms. Recrystallization of the latter crystals from methanol gave XXI as yellow prisms, m.p. 169.5~170.5°C.

Found: C, 66.62; H, 3.71; N, 5.36. Calcd. for $C_{15}H_{11}O_2NS$: C, 66.91; H, 4.12; N, 5.20%.

$\lambda_{max}^{MeOH}$ mμ (log ε): 220 (4.39), 303 (4.04).

**Benzoate (XXII) of XIII.** — To a solution of 100 mg. of XIII in 1 ml. of pyridine, 0.2 ml. of benzoylchloride was added and heated for 20 min. The crystals separated out by adding water were dissolved into benzene and the insoluble portion was recrystallized from methanol, affording XXII as orange prisms, m. p. 193~194°C.

Found: C, 72.39; H, 3.71; N, 4.38. Calcd. for $C_{20}H_{13}O_2NS$: C, 72.50; H, 3.96; N, 4.23%.

$\lambda_{max}^{MeOH}$ mμ (log ε): 220 (4.49), 308 (4.01).

The authors wish to take this opportunity to express their gratitude for the donation of the Grant in Aid for Scientific Research from the Ministry of Education and for financial assistance from the Sankyô Co., Ltd.

*Department of Chemistry*
*Faculty of Science*
*Tohoku University*
*Katahira-cho, Sendai*

# *On Pyrazino[d, d']ditropone and its Derivatives*

By Toyonobu Asao

(Received July 22, 1960)

It is already known that 2, 5-diaminotroponimine reacts with formic acid and nitrous acid forming 1, 3-diazaazulene or 1,2,3-triazaazulene derivatives respectively[1,2].

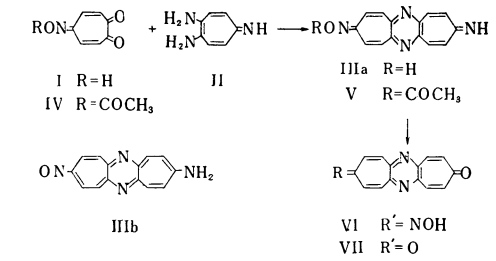
If one considers the facile condensation of 5-nitrosotropolone with 1, 2-diamine to form a troponeoxime with the heterocyclic system[3-6], it is expected that the formation of a new 7-6-7 hetrocyclic system in which N-atoms are located in a six-membered ring by application of 2, 5-diaminotroponimine, will make a tautomer of 4,5-diaminotroponimine.

An account of the attempt to synthesize such a 7-6-7 membered ring system is reported herein.

Heating of 5-nitrosotropolone (I)[7] in methanol afforded brown crystals, m. p. over 300°C, $C_{14}H_{11}ON_4Cl$, very easily with dihydrochloride of 2, 5-diaminotroponimine (II)[1]. Neutralization of the aqueous solution of these crystals with sodium hydrogencarbonate gave brown powder III, m. p. over 300°C, $C_{14}H_{10}ON_4$, indicating the former crystals to be monohydrochloride of III. III is insoluble in various organic solvents and recrystallized with difficulty. Ultraviolet spectra of III in acidic and alkaline media show a little shift to longer wavelength region compared with that in methanol.

The structural confirmation of III came from alkaline permanganate oxidation, in which pyrazine tetracarboxylic acid dihydrate, m. p. 205°C[8], was obtained. Its tetramethyl ester obtained by the reaction with diazomethane showed no depression of melting point on admixture with authentic tetramethyl pyrazinetetracarboxylate, m. p. 182°C, obtained by methylation of pyrazinetetracarboxylic acid, the latter being synthesized by oxidation of quinoxalotroponeoxime[3]. Therefore, together with its analytical value and the following reactions, it is clear that III is pyrazino [d, d'] - ditroponemonoiminemonooxime.

Attempted acetylation of III with acetic anhydride led to the formation of a black substance. However, acetate V was obtained by the reaction of acetate IV[3] of 5-nitrosotropolone with II.



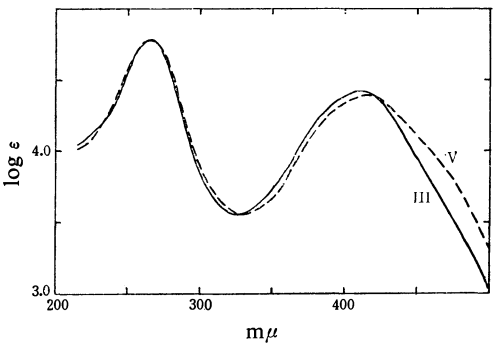




Fig. 1. Ultraviolet absorption spectra of III and V in methanol.

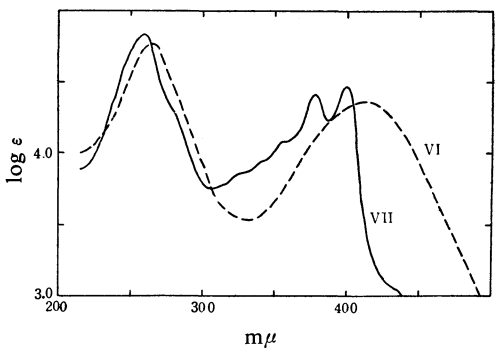



Fig. 2. Ultraviolet absorption spectra of VI and VII in methanol.

1) T. Nozoe, M. Sato, S. Ito, K. Matsui and T. Matsuda, *Proc. Japan Acad.*, **29**, 565 (1953).
2) T. Nozoe, S. Ito and K. Matsui, ibid., **30**, 313 (1954).
3) T. Nozoe, M. Sato and T. Matsuda, *Sci. Repts. Tohoku Univ., First Ser.*, **37**, 407 (1953).
4) T. Nozoe, S. Ito, S. Suzuki and K. Hiraga, *Proc. Japan Acad.*, **32**, 344 (1956).
5) S. Ito, *Sci. Repts. Tohoku Univ., First Ser.*, **42**, 236 (1958).
6) S. Ito, ibid., **43**, 247 (1959).
7) T. Nozoe, S. Seto, H. Takeda and T. Sato, ibid., **35**, 274 (1952).
8) F. D. Chattaway and W. G. Humphrey, *J. Chem. Soc.*, **1929**, 645.

From the similarity of the ultraviolet spectra of III and V shown in Fig. 1, compound III is assumed to have the structure IIIa rather than its tautomeric form IIIb.

Although III and V are easily soluble in aqueous alkali, acidification of these solutions with acetic acid afforded not the original substance but the same needles VI, m. p. 266°C, $C_{14}H_9O_2N_3$, from both III and V. The infrared spectrum of VI shows peaks at 3250 (O-H), at 1627 (C=O) and at 1585 $cm^{-1}$ (C=C). VI gives carbonyl derivatives such as oxime and 2, 4-dinitrophenylhydrazone. These results indicate VI to be pyrazino[d, d'] ditroponemonoxime, which is produced by hydrolysis of the acetyl group and or imino group in V or III.

The reaction of benzoate[3] of 5-nitrosotropolone and II afforded dark brown crystals. Although these crystals were unstable for further purification, VI was obtained by treatment of these crystals with alkaline.

Heating of III or VI in formic acid in the presence of copper carbonate[5,9] gave pyrazino-[d, d'] ditropone (VII), peaks of infrared spectrum at 1635 (C=O) and at 1598 $cm^{-1}$ (C=C), in poor yield. The ultraviolet spectrum of VII (Fig. 2) exhibits the characteristic fine structure compared with III and VI. This kind of fine structure has been observed in the case of quinoxalotropone or pyrazinotropone[5,6]. While being stable to acid, VII is unstable to alkali and gradually turns to brown in alkaline solution.

## Experimental*

**Pyrazino[d, d']ditroponemonoiminemonoxime (III.)**—A solution of 900 mg. of I and 1.1 g. of dihydrochloride of II dissolved in 40 ml. of methanol was refluxed for twenty minutes and brownish orange crystals separated out. After cooling, 1.3 g. of the crystals, m. p. over 300°C, were obtained by filtration. These crystals are positive to the halogen test and are insoluble in various organic solvents. Recrystallization of the crystals was carried out from a large amount of dilute hydrochloric acid.

Found: C, 58.55; H, 3.66; N, 18.93. Calcd. for $C_{14}H_{10}ON_4 \cdot HCl$: C, 58.64; H, 3.88; N, 19.54%.

Neutralization of these crystals dissolved in a large amount of water with aqueous sodium hydrogencarbonate gave brown powder III, m. p. over 300°C. Attempted recrystallization of III from various solvents was in vain.

Found: C, 66.98; H, 4.10; N, 22.10. Calcd. for $C_{14}H_{10}ON_4$: C, 67.19; H, 4.03; N, 22.39%.

*Picrate;* red needles, m. p. over 300°C, turn to black from about 225°C.

Found: C, 50.21; H, 3.00; N, 20.50. Calcd. for $C_{20}H_{13}O_8N_7$: C, 50.11; H, 2.73; N, 20.45%.

**Oxidation of III.**—To a solution of 500 mg. of III and 400 mg. of potassium hydroxide dissolved in 40 ml. of water, a solution of 5g. of potassium permanganate dissolved in 250 ml. of water was added at 80°C in a period of 6 hr. The excess of potassium permanganate was killed by a few drops of methanol and the resulting manganese dioxide was filtered. Manganese dioxide was washed with hot water thoroughly, and the combined solution of filtrate and washing was concentrated to about 15 ml., and was acidified with dilute hydrochloric acid affording colorless crystals, 230 mg. Recrystallization of the crystals from hydrochloric acid gave pyrazinetetracarboxylic acid as colorless plates, m. p. 205°C (decomp.).

Found: C, 32.72; H, 2.43; N, 9.81. Calcd. for $C_8H_4O_8N_2 \cdot 2H_2O$: C, 32.89; H, 2.76; N, 9.59%.

By the methylation reaction of 10 mg. of pyrazinetetracarboxylic acid with diazomethane, colorless needles, m. p. 181~182°C (from methanol-benzene) were obtained. This ester showed no depression of melting point on admixture with tetramethyl pyrazinetetracarboxylate obtained by another route.

Found: C, 46.32; H, 3.84; N, 8.92. Calcd. for $C_{12}H_{12}O_8N_2$: C, 46.16; H, 3.87; N, 8.97%.

**Acetate V.**—A solution of 200 mg. of acetate IV of 5-nitrosotropolone and 200mg. of dihydrochloride of II dissolved in 5 ml. of methanol was refluxed for 10 min., affording 300 mg. of red needles, which turn to black from around 250°C.

Found: C, 58.27; H, 3.77; N, 17.81. Calcd. for $C_{16}H_{12}O_2N_4 \cdot HCl$: C, 58.44; H, 3.98; N, 17.04%.

Neutralization of aqueous solution of the above crystals gave acetate V of III as brown powder, m. p. over 300°C.

Found: C, 65.60; H, 3.99; N, 19.07. Calcd. for $C_{16}H_{12}O_2N_4$: C, 65.75; H, 4.14; N, 19.17%.

**Pyrazino[d, d']ditroponemonoxime (VI).**—A solution of 100 mg. of hydrochloride of III dissolved in 1.5 ml. of 3 N sodium hydroxide solution was heated gently for 3 min. Ammonia gas evolved during this time. After allowing the solution to stand for 30 min. at room temperature, it was acidified with a few drops of acetic acid. Orange crystals, 70 mg., precipitated out were recrystallized from pyridine yielding, orange needles, m. p. 266°C (carbonize).

Found: C, 66.95; H, 3.77; N, 17.16. Calcd. for $C_{14}H_9O_2N_3$: C, 66.92; H, 3.61; N, 16.73%.

*Oxime;* red fine crystals (from pyridine), m. p. over 300°C.

Found: C, 63.79; H, 3.84; N, 20.62. Calcd. for $C_{14}H_{10}O_2N_4$: C, 63.15; H, 3.79; N, 21.04%.

*2, 4-Dinitrophenylhydrazone;* violet crystals, carbonize at about 265°C.

Found: C, 55.31; H, 3.24; N, 22.88. Calcd. for $C_{20}H_{13}O_5N_7$: C, 55.68; H, 3.04; N, 22.77%.

**Pyrazino[d, d']ditropone (VII).**—a) A mixture of 150 mg. of hydrochloride of III and 150 mg. of copper carbonate in 4.5 ml. of 80% formic acid was

9) R. Robinson, *Nature*, 173, 541 (1954).

* All the melting points were uncorrected. The microanalyses were carried out by Messrs. S. Oyama, S. Azumi and Miss A. Iwanaga, and I. R. spectra were measured with Perkin-Elmer Model 112 by a member of Professor Kinumaki's laboratory, Research Institute, Chemistry of Non-Aqueous Solution, Tohoku Univ., to whom the author's sincere acknowledgements are hereby extended.

heated at 80°C for 70 hr. The resulting brown precipitates were filtered affording 30 mg. of VI. By neutralization of the filtrate, 20 mg. of precipitates were obtained. Recrystallization from pyridine gave VII as gold-colored needles, m. p. 244~245°C (decomp.).

Found: C, 71.14; H, 3.43; N, 12.38. Calcd. for $C_{14}H_8O_2N_2$: C, 71.18; H, 3.41; N, 11.86%.

b) Three hundred milligrams of VI were heated at 75°C for 120 hr. with 300 mg. of copper carbonate and 10 ml. of 80% formic acid. After cooling, 150 mg. of undissolved VI was obtained. Neutralization of the filtrate with sodium hydrogencarbonate afforded 70 mg. of solid. Recrystallization from pyridine gave gold-colored needles VII, m. p. 244~245°C (decomp.).

The author takes this opportunity to express his sincere gratitude to Professor Tetsuo Nozoe for his kind guidance throughout these experiments, as well as to Assistant Professor Toshio Mukai and Dr. Sho Ito for their kind advice and suggestions.

*Department of Chemistry*
*Faculty of Science*
*Tohoku University*
*Katahiracho, Sendai*

# *The Mechanical Behavior of Swollen Polystyrene, Poly-p-chlorostyrene and their Copolymers in Benzene. II. Stress Relaxation under Constant Strain*

By Kazuyoshi OGINO

(Received May 2, 1960)

In the previous paper[1], the stress relaxation of swollen polymethylacrylate gels in several organic solvents was studied, and it was shown that the smaller the volume fraction of polymer is, the greater degree of relaxation, and the higher temperature dependency of stress relaxation are observed.

In this paper, the stress relaxation of gel swollen in benzene is studied as a function of intermolecular force which is controlled by changing the content of substituted chlorine atoms in the chain molecules[2].

When a viscoelastic body is strained quickly to a definite extent and kept at this state, the relaxation of stress is observed.

Tobolsky et al. have shown[3] that the relaxation curves at different temperatures can be superposed upon each other when plotted as the reduced stress, $g$, against the logarithmic time, and that a change in temperature corresponds to a shift of the curve along the logarithmic time scale. (In the present experiment, the stress is arbitrarily reduced to 20°C, and is denoted by $g_{20}$.)

The existence of this superposition principle of relaxation curves at different temperatures indicates that the relaxation curves for the same polymer at different temperatures are identical if plotted as the reduced stress vs. the logarithm of $(Kt)$ where $K$ is a function of temperature. Or we can express the reduced stress $g_{20}$, for example, as a function of $Kt$[3]; i. e.,

$$g_{20} \equiv g_{20}(Kt)$$

It is found that the temperature dependence on $K$ may be expressed by Arrhenius's equation[3]

$$K = A \exp.\ (-H/RT)$$

The apparent activation energy $H$ can therefore be calculated by plotting the logarithm of the time factor $K$ against the reciprocal of absolute temperature.

## Experimental

**Samples.**—About 4 cc. of styrene (for sample A), *p*-chlorostyrene (for sample D) or their mixtures (for samples B and C) which contains one drop (about 2 mg.) of divinylbenzene and about 10 mg. of benzoyl peroxide was polymerized thermally in bulk in a sealed glass tube. They were swollen in

TABLE I. VOLUMES OF STYRENE AND *p*-CHLOROSTYRENE MONOMER TAKEN INTO POLYMERIZATION

| Sample | *p*-Chlorostyrene, cc. | Styrene, cc. |
|---|---|---|
| A | 0 | 4 |
| B | 1.6 | 2.4 |
| C | 2.4 | 1.6 |
| D | 4 | 0 |

1) K. Ogino, This Bulletin, **31**, 580 (1958).
2) K. Ogino, ibid., **32**, 553 (1959).
3) A. V. Tobolsky et al., *J. Polymer Sci.*, **3**, 669 (1948).

benzene to the equilibrium state. Benzene was purified by shaking several times with concentrated sulfuric acid, and with distilled water, and was then dried over calcium chloride and redistilled.

Volumes of *p*-chlorostyrene and styrene monomer before polymerization are shown in Table I.

**Apparatus.** — The apparatus used to observe the change of stress with time is the same as was described in the previous paper[1], and is shown in Fig. 1; a definite strain (11.2%) is given to the specimen (A) and the stress, measured by the vertical component of the chain length, is recorded on a rotating drum. The chain corresponding to and following the decaying stress at each time is controlled by a balancing motor (E) which is connected to a relay (F) through an amplifier circuit (G).

## Results and Discussion

The experimental curves of the reduced stress against logarithmic time for each polymer are shown in Figs. 2, 3, 4 and 5.

The apparent activation energy for the relaxation obtained by plotting the logarithm of the time factor $K$ against the reciprocal temperature is also shown in each figure.

If these curves at different temperatures are superposed with each other by suitable translations along the logarithmic time axis, the master curves shown in Fig. 6 are obtained.

Four parameters in the mechanical model[1]

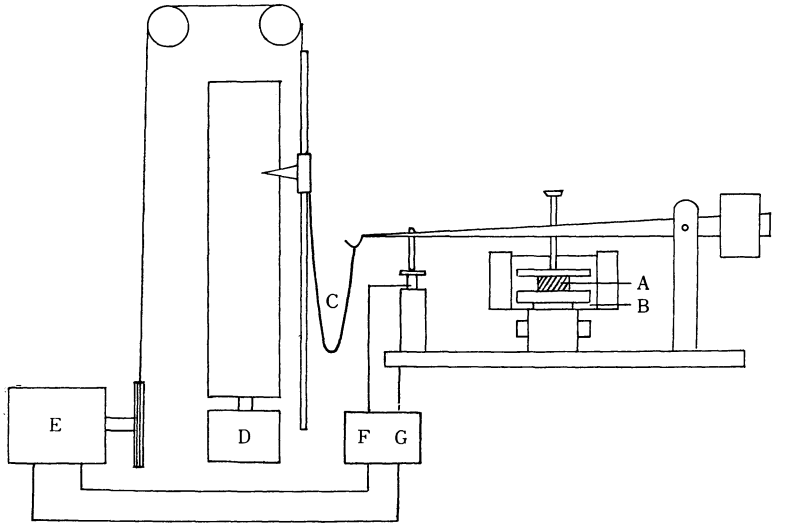



Fig. 1. Chainomatic balance.

(A): Specimen (B): Solvent (C): Chain (D): Rotating drum
(E): Balancing motor (F): Relay (G): Amplifier circuit

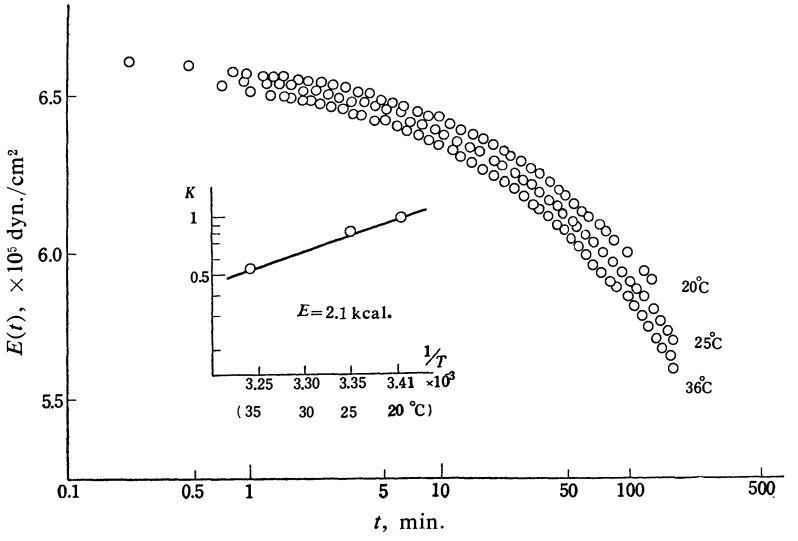



Fig. 2. Stress relaxation curves for sample A, $E$=2.1 kcal.

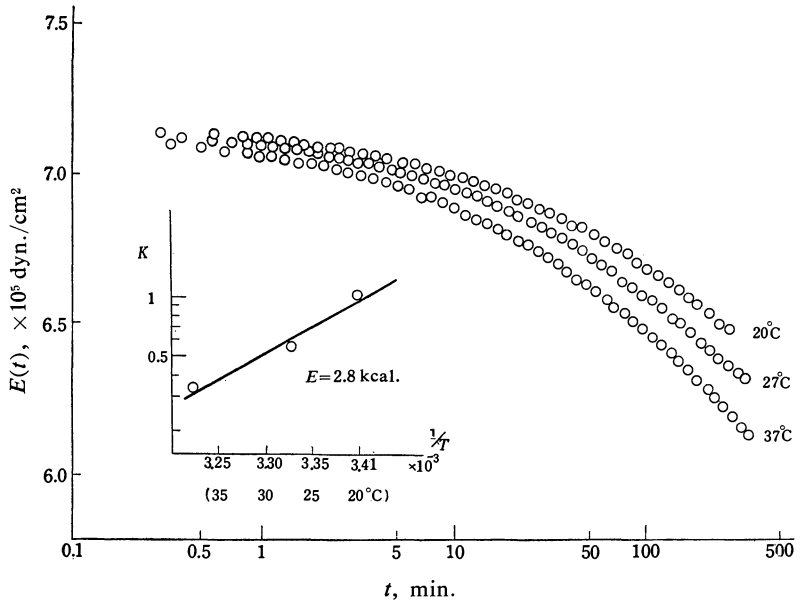



Fig. 3. Stress relaxation curves for sample B, $E$=2.8 kcal.

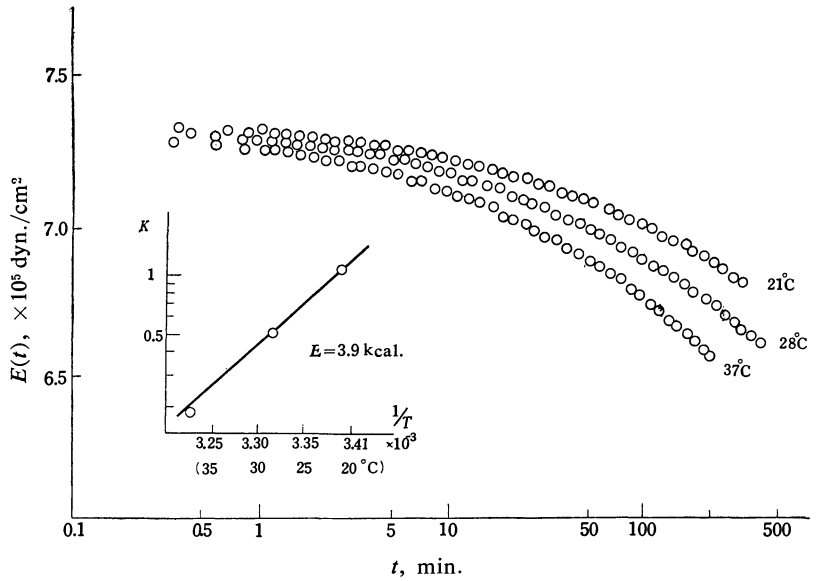



Fig. 4. Stress relaxation curves for sample C, $E$=3.9 kcal.

to express the curves of Fig. 6 are listed in Table II.

As these gels are cross-linked chemically by divinylbenzene, we can expect that the stress relaxation in the present case arises mainly from the breakage or slippage of some weak bonds such as entanglements or other secondary bonds present between junction points.

The value of $G_1$, in Table II, increases with the increase of chlorine content. Considering that these gels have nearly equal values of $v_r$, volume fraction of polymer at swelling equilibrium[4], the fact that the initial Young's modulus $G_1$ increases with the increase of chlorine content leads to the assumption that the stronger interaction force between chain molecules appears by the presence of chlorine atoms.

As each parameter in the four-element model for the chlorine rich gel, especially $\eta_2$ or $\eta_3$, is large, we can assume that the contribution of chlorine atoms to the relaxation or viscous

4) K. Ogino, This Bulletin, 31, 577 (1958).

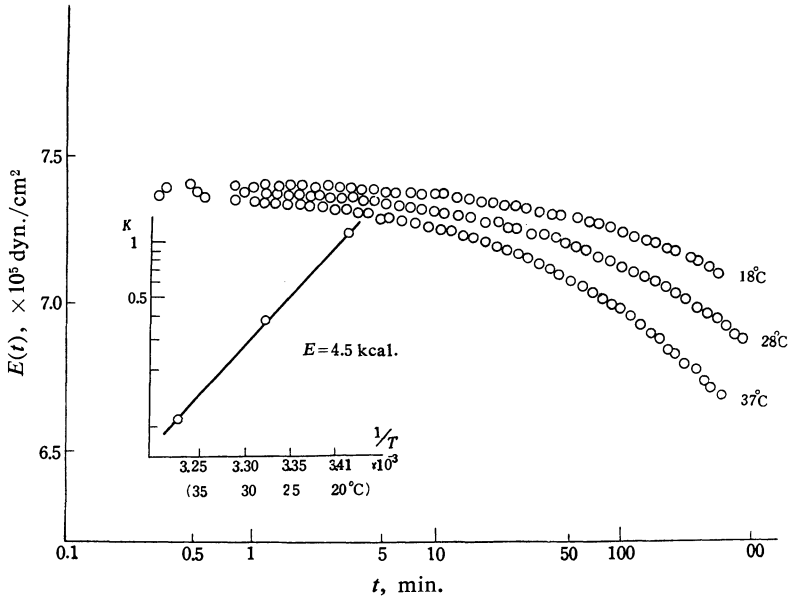
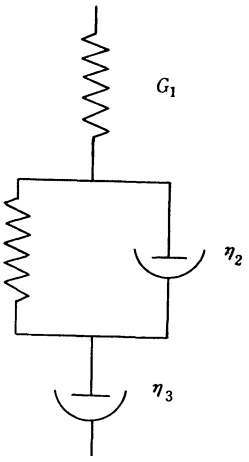



Fig. 5. Stress relaxation curves for sample D, $E$=4.5 kcal.

TABLE II. PARAMETER VALUES IN FOUR-ELEMENT MODEL

| Sample | $v_r$ | $G_1$ dyn./cm² | $G_2$ dyn./cm² | $\eta_2$ (poise) | $\eta_3$ (poise) | $\eta_3/G_1$, sec. | $\eta_2/G_2$, sec. |
|---|---|---|---|---|---|---|---|
| A | 4.3 | $5.90\times10^6$ | $2.54\times10^8$ | $3.90\times10^8$ | $8.55\times10^{11}$ | $1.45\times10^5$ | 1.5 |
| B | 4.1 | $6.35\times10^6$ | $7.50\times10^7$ | $4.70\times10^8$ | $3.75\times10^{12}$ | $5.95\times10^5$ | 6.7 |
| C | 4.0 | $6.54\times10^6$ | $1.23\times10^8$ | $2.39\times10^9$ | $3.35\times10^{12}$ | $5.12\times10^5$ | 19.4 |
| D | 4.4 | $6.63\times10^6$ | $3.00\times10^8$ | $2.95\times10^9$ | $3.99\times10^{12}$ | $6.03\times10^5$ | 10 |



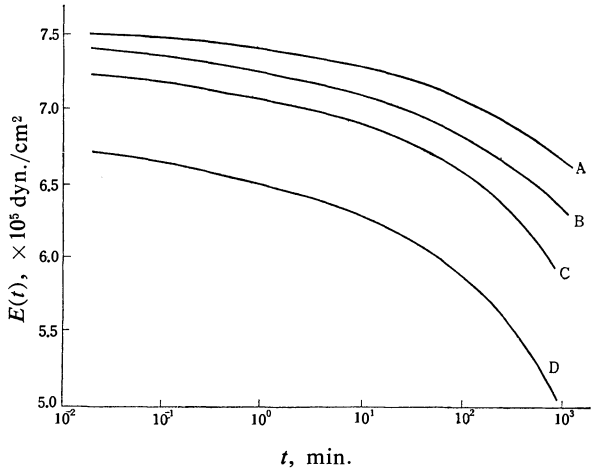




Fig. 6. Relaxation master curves.

property is, primarily, a decisive factor.

When we express these mechanical properties by this four-element model, the value of the retardation time $\eta_2/G_2$ can be expected to have a comparable value to the observation time scale, and values of these parameters in Table II can be considered to be reasonable from this point.

Hatfield and Rathmann assumed[5] that for swollen gels viscous flow or molecular slippage is brought about by chemical rupture of primary bonds. For the fact that $\eta_2/G_2$ in Table II has the order of about 10° sec., the author assumed that the retardation time of this order

5) M. R. Hatfield and G. B. Bathmann, *J. Appl. Phys.*, 25, 1082 (1951).

may correspond to the slippage of some secondary bonds in polymeric substances.

The values of $\eta_3$ in the four-element model for the other polymeric substances are much smaller than that of this gel (about $10^7$ poises is expected in the usual case). This parameter may be considered to correspond to a process of a longer retardation time. It will be possible to consider that for swollen gels most of the secondary bonds are set free by solvation, and that the number of bonds which are to slip off or to be liberated per unit time under constant strain are much fewer than those in the dry and undiluted states. The apparent rate of flow will therefore be smaller, and the viscosity will then be much greater ($10^{12}$ poises).

The apparent activation energy for relaxation process is also great when the chlorine content increases. The great activation energy means great temperature dependence. As the contribution of energy term to the elasticity or the value of $\mu$, polymer-solvent interaction parameter[4], increases with the increase of chlorine content[2], we can presume that the cause of the great temperature dependence may be the fact that the breaking of some secondary bonds are favored because the solvent-polymer contacts increase, or that these bonds come to be slipped off more easily as temperature rises. In the case of polystyrene gel, on the other hand, there may be no residual secondary bonds to be released by temperature rise.

These facts can be interpreted by considering the appearance of the interaction force by the introduction of chlorine atoms, as was mentioned here and in the previous paper[2].

In this discussion, the author considered that the nature of the solvent itself has no influence upon the relaxation phenomena of swollen gels, as it may not be affected by the different content of chlorine atoms in the swollen gels.

Acknowledgement is made to Professor H. Akamatu and Assistant Professor T. Nakagawa for their support and advice in this experiment.

*Department of Chemistry*
*Faculty of Science*
*The University of Tokyo*
*Hongo, Tokyo*

# *The Chemical Reaction in Silent Electric Discharge. I*

By Kihei MORINAGA and Momotaro SUZUKI

(Received June 16, 1960)

In a series of reports[1-3], it was proposed that in regard to the chemical processes in silent electric discharge, more significance should be put on the high frequency pulse current which accompanies the discharge, rather than on the basic current, usually 50 c/s, which sustains the whole discharge process.

In the present work some electrical, as well as geometrical conditions contributing significantly to the ozone formation process, were studied in more detail. This seems to have been helpful in realizing the actual feature of the reaction.

## Experimental

The discharge tube used was of the Siemens type with two concentric glass cylinders which served as dielectric electrodes. The whole length and diameter of the discharge tube was 35 cm. and 4 cm. respectively. The outer surface of the outer cylinder was patched with tin foil and the inner tube was filled with brine. The area covered by the foil patches varied from 50 to 200 $cm^2$ for the purpose of having the desired electrode area. To change the gap distance, several ozonizers of the same type with different gap distance of 1~3 mm. were used. The electrical system was a usual circuit. The current of 50 c/s city source was sent through a voltage regulator to a leakage transformer where the voltage was stepped up to the required value. The discharge current was side circuited by a cathode ray oscillograph (Toshiba ST-1651) for the observation of basic 50 c/s, as well as the high frequency pulse current.

The whole system of the circuit is shown diagrammatically in Fig. 1. A series of shots of each oscillogram were taken using the single sweep system. The time constant of the oscillogram circuit was $5.4\times10^{-6}$ sec.

1) M. Suzuki, *Proc. Japan Acad.*, **26**, 21 (1950).
2) M. Suzuki and Y. Naito, ibid., **28**, 429 (1951).
3) M. Suzuki, S. Okazaki and T. Yamamoto, *J. Am. Chem. Soc., Adv. Chem. Ser.*, **No. 26**, 331 (1957).

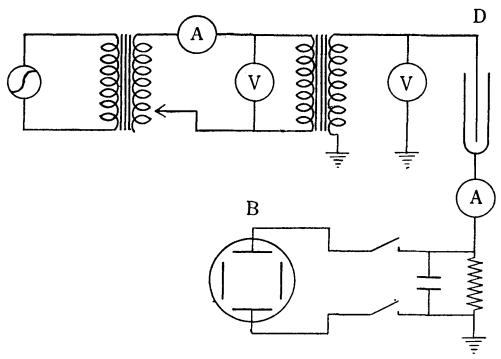



Fig. 1. The circuit system.
D, ozonizer; B, oscillograph

The sum of the height of each pulse current which appears as hairs on the base current diagram in an oscillogram, is due to the total electricity carried through the electric discharge during a cycle of base current which is simply noted here as pulse current[2]. The value of the sum in every run is an arithmetic mean of several successive shots of the oscillogram.

To obtain the yield of ozone in each run the leading glass tube distance from the discharge tube to the ozone absorption bulb was shortened as much as possible. The gas mixture submitted to the discharge was led through the neutral potassium iodide solution in the absorption bulb which was later analyzed by the usual known process. The oxygen, which served as a reactant, was taken from a cylinder and used after drying with calcium chloride.

## Results

Variation in ozone concentration in the oxygen gas after leaving the discharge vessel with apparent residence time $\tau$, is shown in Fig. 2. The ozone concentration increases at first linearly as the time of residence increases, until finally it reaches a saturation value. At a saturation state the rates of the ozone formation and of the ozone destruction by any of the chemical entities existing there have equal values. This leads to the stationary ozone concentration in the exit gas.

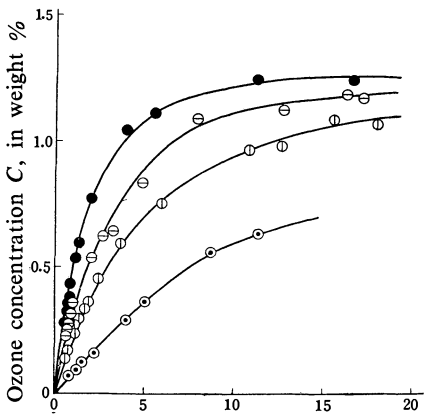



Fig. 2. The relation between the ozone concentration $C$ and the residence time $\tau$. Gap distance 2 mm. electrode area 100 cm².
● Pulse current 184~199 μamp.
⊖ 148~155 μamp.
⊕ 87~92 μamp.
⊙ 28~30 μamp.

The rate value of ozone formation $Y$ (mg./sec.) at $\tau=0$ where presumably hardly any destruction reaction takes place is referred to further in the results. This consideration will simplify the discussion to some extent, because the reaction, in that case, will be restricted simply to the formation of ozone.

The numerical value of the pulse current is obtainable from the comparison of the sum of length of a certain pulse current with an adequate standard current. In Fig. 3, the value of $Y$ (mg./sec. at $\tau=0$) is plotted against the pulse current in $\mu$amp. which was obtained through the above procedure. These curves manifest themselves again as a group of straight lines of which the inclination depends solely upon the physical conditions under which the experiments were carried out.

The dependence of ozone yield per unit pulse current $Y_I$ (mg./sec. $\mu$amp.) on $A/d$, where $A$ (cm²) is the area of the electrode,

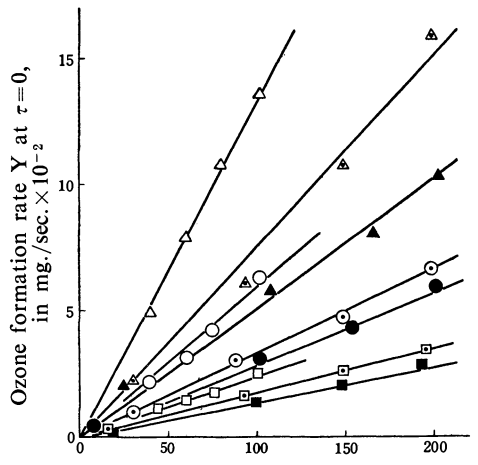



Fig. 3. The relation between the rate of ozone formation at $\tau=0$ in the various shape of ozonizers and the pulse current.
△ Area 200 cm². Gap 1 mm.
○ Area 100 cm². Gap 1 mm.
□ Area 50 cm². Gap 1 mm.
◬ Area 200 cm². Gap 2 mm.
⊙ Area 100 cm². Gap 2 mm.
⊡ Area 50 cm². Gap 2 mm.
▲ Area 200 cm². Gap 3 mm.
● Area 100 cm². Gap 3 mm.
■ Area 50 cm². Gap 3 mm.

and $d$ (mm.) is the gap distance between electrodes, is shown in Fig. 4. $Y_I$ values increase linearly with $A/d$, no matter how the individual value of $A$ or $d$ varies respectively, nor does it depend upon the total value of the current through the discharge vessel. The inclination of the straight lines has the value of $7.0\times10^{-7}$ (mg./sec. $\mu$amp. cm.).

In Figs. 5, 6 and 7, ozone concentration (weight %) at steady state was plotted against pulse current. It will be seen from the figures that the ozone concentration is the highest at a certain optimum value of electrode area, and above or under this value the ozone concentration becomes lower.

## Discussion

The behavior of the diagram which manifests itself in Fig. 4 seems to require some explanation from the chemical as well as the electrical viewpoint.

To begin with, under the experimental conditions during which the measurements were made, Paschen's law is applicable with virtual validity[4]. Then, as the pressure throughout the measurements is atmospheric and therefore constant, the sparking potential $E_s$, which initiates each individual small discharge at certain points on the electrode surface, depends solely on the gap distance $d$[2]. Further, $E_s$ should increase proportionally with $d$ within our experimental conditions[2].

With increasing $E_s$, the leaving of electrons from the electrode surface will be more difficult where on the oscillogram the hairs will shift to the upper part of the basic wave form and its placement will be more dense. Keeping ones sight on a certain definite number of electrons from the electrode, and taking into consideration the fact that the spots are distributed fairly uniformly and that the number of electrons issuing from each spot are virtually equal[2], the number of spots from which the individual small discharge starts will accordingly be less and the decrease of the number of spots in a unit area shows that the spots are located more sporadically. Or in our experimental conditions the greater the gap distance is, the greater the sparking potential, the less the number of spots in a unit area where the individual small discharge starts and finally the more the number of electrons which leave each spot, so long as one definite number of electrons which come into reactions are dealt with.

Now electrons leaving the electrode will collide with surrounding chemical molecules initiating some chemical change which leads to a chemical reaction.

Collisions which would cause some chemical reaction would seem to prevail as long the electrons travel along the spark gap distance. But actually the electrons, just after leaving the electrode, only then have sufficient energy to provoke a chemical effect such as dissociation. With the first collision, electron energy is virtually lost. Normally, the electron would regain energy in the electrical field; but, because of the very short mean free path, which is in the order of $10^{-6}$ cm. at atmospheric pressure[5], the electrons can not acquire sufficient energy to be able to react further chemically. Thus, further collisions between electron and molecule will hardly contribute to the initiation of the ozone formation. Accordingly, after the first collision, the distance traveled by the electron through gap distance may be disregarded in this discussion.

As far the change of Townsend's first coefficient $\alpha$ in relation to the gap distance; $\alpha/P$ is known to be the function of $X/P$ where $X$ is field strength. In this experiment the pressure is constant, $\alpha$ therefore, depends solely on $X$. As $X=E_s/d$ and $E_s$ increases proportionally with $d$, the $X$ value is independent of $d$. Thus the behavior of $\alpha$ along with change of $d$ can likely be neglected in this present case.

In Fig. 4 $Y_I$ is shown to be proportional to the electrode area $A$ and inversely proportional to the gap distance $d$. The increase of $A$, keeping the total electron number constant, leads to the increase of the total spot number in a whole discharge tube, because the increase

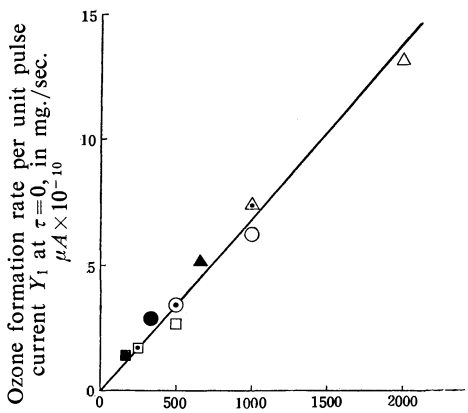



Fig. 4. The rate $Y_I$ of ozone formation per unit pulse current at various value of $A/d$.

4) K. S. Fitzsimons, *Phys. Rev.*, **58**, 197 (1940); W. R. Haseltine, ibid., **72**, 423 (1947).

5) R. H. Healey and J. W. Reed, "The Behaviour of Slow Electrons", Amalgamated Wireless Press, Sydney (1941).

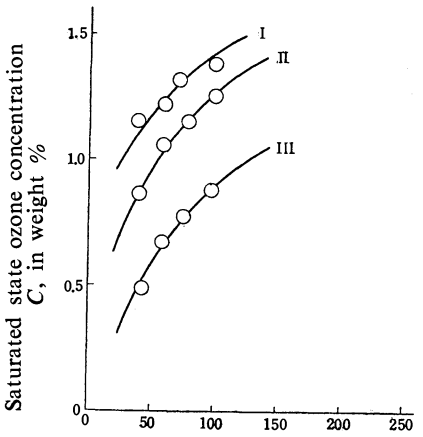



Fig. 5. Saturation ozone concentration against pulse current (Gap distance 1 mm.).
I Electrode area $A=100\,cm^2$; II $A=200\,cm^2$; III $A=50\,cm^2$

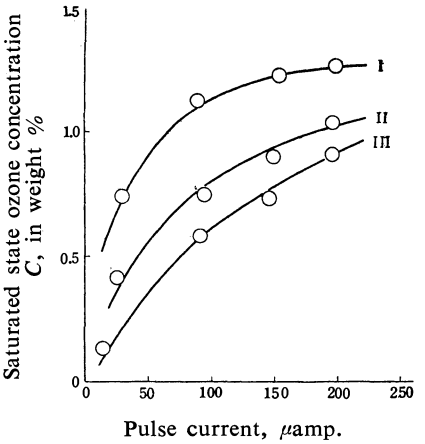



Fig. 6. Saturation ozone concentration against pulse current (Gap distance 2 mm.).
I Electrode area $A=100\,cm^2$; II $A=200\,cm^2$; III $A=50\,cm^2$

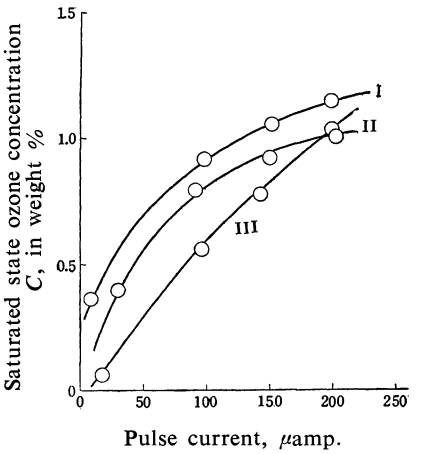



Fig. 7. Saturation ozone concentration against pulse current (Gap distance 3 mm.).
I Electrode area $A=100\,cm^2$; II $A=200\,cm^2$; III $A=50\,cm^2$

of the discharge area implies that the spots come to be distributed more sporadically and more chances are offered for the generation of more new spots. This corresponds to the effect of decreasing gap distance as just stated above. It might be conceivable if $Y_1$ be inversely proportional to $d$; then it should be proportional to $A$.

A tentative explanation of this phenomena is proposed as follows: In the experiment the average value of the pulse current is about 100 μamp., and the number of hairs on the half wave of 50 c/s base current from city source, in an oscillogram, is virtually 30~50. The number of spots involved in a hair, i. e. in one shot of pulse current, is about $10\sim10^{2}$ [2], thus the number of electrons ejected from a spot has the order of $10^{10}$. On the other hand, the area of each spot is $10^{-2}\sim10^{-4}\,cm^2$ [2], and the number of molecules just in front of this area is about $10^{10}$ or a little less, which means that the above number of gas molecules has almost the same number or a little fewer than those of ejected electrons from a spot.

Now the velocity of electrons, just after they leave the electrode, is estimated at $10^{8}\sim10^{9}$ cm./sec.[6] which features, because of the virtually instantaneous time of travel up to the first collision, that the electron beam from each spot might seem to suffer hardly any appreciable conical diversion and hit the molecule target covering almost the same dimension as the spot area.

In this pattern of collision, the more sporadically the spots are located, the more packed is the ejected stream electrons, which lead to the increase of the ineffective collision. The rate of the ineffectiveness will essentially be regarded to be linear to the rate of congestion of the electron stream. Thus the effective collision number for a definite number of electrons of $Y_1$ is proportional to the number of spots, or in other words, to the electrode area and the reciprocal of the gap distance.

The postulate appears qualitatively to make sense, but from the quantitative point of view further and more detailed investigation may be required.

6) N. E. Bradbury and R. A. Nielson, *Phys. Rev.*, **49**, 338 (1936); **51**, 69 (1937).

**Summary**

1. The ozone yield $Y$ from oxygen gas in the silent electric discharge in a Siemens ozonizer is proportional to the pulse current which was measured from an oscillogram where $Y$ is referred to $\tau=0$ value. The proportionality is valid independent of the gap distance $d$ between electrodes and the effective area $A$ of electrodes.

2. The above ozone yield $Y_1$ which is referred to $\tau=0$ and further to unit pulse current is proportional to $A/d$.

3. The reason of the above relationship is briefly discussed.

*Department of Chemistry*
*Defense Academy*
*Yokosuka*

# *Dehydrogenation of Secondary Alcohols with Reduced Copper. III*[1]. *Catalytic Dehydrogenation of Isopropyl Alcohol (Part 1)**

By Kazuaki KAWAMOTO**

(Received July 16, 1960)

Although there are a large number of patents and are latively small number of reports concerning the vapor phase dehydrogenation of isopropyl alcohol to acetone, the majority deal with the use of copper in some form as the catalysts. Sabatier[2] found that reduced copper heated at 200~300°C is a suitable catalyst for the dehydrogenation of alcohols to aldehydes or ketones with no side reaction, and he showed that isopropyl alcohol, in the presence of reduced copper, is dehydrogenated to acetone slowly at 150°C, and rapidly and smoothly in the whole range of temperatures between 250°C and 430°C without the formation of a large amount of propylene. This method was improved by Bouveault[3], Armstrong[4] and Palmer[5]. A remarkable addition to the knowledge of the contact action of reduced copper was made by Komatsu[6], who found that reduced copper has the property of promoting not only the dehydrogenation but also dehydration of alcohols and that isopropyl alcohol is transformed into acetone and propylene by exposure to high temperature (300°C). Platonow et al.[7] found that in the presence of copper dehydrogenation of isopropyl alcohol at 300°C furnishes 53.2% of the theoretical yield of acetone. Moreover, Katsuno[8] reported the synthesis of acetone from isopropyl alcohol, using copper-active-carbon or copper-kieselguhr as a catalyst. Dunbar and Arnold[9] also used a copper-chromium-oxide catalyst with considerable success in the dehydrogenation of isopropyl alcohol.

The reduced copper is little used at present for the industrial synthesis of ketones from alcohols. However, copper is considered as the most important component in the majority of widely used mixed catalysts. Therefore, the behavior of the reduced copper catalyst will be of special interest for the interpretation of the mechanism of catalysis with mixed copper catalysts.

Earlier, Frolich et al.[10] found that the copper catalyst prepared by precipitation with sodium hydroxide is more active in the decomposition of methanol than that precipitated with ammonia, and Fischer and Meyer[11] studied the influence of the precipitants on the

1) Previous paper, *J. Chem. Soc. Japan, Pure Chem. Sec.* (*Nippon Kagaku Zasshi*), **80**, 681 (1959).

* The major part of this research was presented at the 11th Annual Meeting of the Chemical Society of Japan, Tokyo, April 3, 1958.

** Present address, Institute of Commodities, Faculty of Economics, Kagawa University, Takamatsu Kagawa-ken.

2) P. Sabatier and J. B. Senderens, *Compt. rend.*, **136**, 738, 921, 983 (1903); P. Sabatier and J. B. Senderens, *Bull. soc. chim. France*, (3) **33**, 263 (1905); P. Sabatier, "Die Katalyse in der Organischen Chemie", Akademische Verlagsgesellschaft m. b. H., Leipzig (1927).

3) L. Bouveault, *Bull. soc. chim. France*, (4) **3**, 119 (1908).

4) E. F. Armstrong and T. P. Hilditch, *Proc. Roy. Soc.*, **A97**, 259 (1920).

5) W. G. Palmer, *Proc. Roy. Soc.*, **A98**, 13 (1920); W. G. Palmer, ibid., **A99**, 412 (1921); W. G. Palmer, ibid., **A101**, 175 (1922); W. G. Palmer and F. H. Constable, ibid., **A106**, 250 (1924).

6) S. Komatsu, *Mem. Coll. Sci. Kyoto Imp. Univ.*, **A7**, 85 (1924).

7) M. S. Platonow, S. B. Anissimow and W. M. Krascheninnikowa, *Ber.*, **69**, 1050 (1936).

8) M. Katsuno, *J. Soc. Chem. Ind. Japan*, (*Kogyo Kagaku Zasshi*), **45**, 1026 (1942); M. Katsuno, ibid., **46**, 109 (1943).

9) R. E. Dunbar and M. R. Arnold, *J. Org. Chem.*, **10**, 501 (1945).

10) P. K. Frolich, M. R. Fenske, L. R. Perry and N. L. Hurd, *J. Am. Chem. Soc.*, **51**, 187 (1929).

11) F. Fischer and K. Meyer, *Brennstoff Chem.*, **12**, 225 (1931).

nickel-thoria-kieselguhr catalyst, which is used as a catalyst for the Fischer-Tropsch synthesis. For this catalyst potassium carbonate was the best precipitant and the preparation using sodium hydroxide or potassium hydroxide was virtually inactive. Further, Niwa and Yamaguchi[12] reported that the activity of the copper catalyst prepared with sodium hydroxide is greater than that treated with ammonium carbonate.

As no comparative study of the action of reduced copper catalysts prepared with a number of precipitants upon secondary alcohols has been reported, the present work has been undertaken to discover how the reaction temperature and the precipitant influence the activity and the behavior of the catalysts, and furthermore to find the most suitable condition and the most suitable catalyst for the preparation of acetone from isopropyl alcohol. Experiments were carried out at several temperatures between 185°C and 325°C, and five different precipitants, i. e. sodium hydroxide, potassium hydroxide, potassium carbonate, sodium bicarbonate and potassium bicarbonate, were used.

## Experimental

**Purification of Isopropyl Alcohol and Acetone.**—The isopropyl alcohol used in this research was purified, after being dried with anhydrous potassium carbonate, by fractionation through a Widmer column: b. p. 82~82.5°C, $n_D^{25}$ 1.3753, $d_4^{25}$ 0.7811. Acetone was also purified in an analogous manner: b. p. 56.2~56.3°C, $n_D^{25}$ 1.3564, $d_4^{25}$ 0.7844.

**Preparation of Catalysts.**—Komatsu and Kurata[13] previously found that the reduced copper catalysts derived from copper sulfate and copper nitrate act to promote both dehydrogenation and dehydration of *l*-menthol. The degree of dehydration, however, was smaller with the catalyst prepared from copper nitrate than with that from copper sulfate under the same conditions. Consequently, the present author used copper nitrate as the starting material to prepare the dehydrogenation catalyst. Copper nitrate was prepared from electrolytic copper and nitric acid, and was purified by recrystallization. The catalysts are classified into Cu I, II, III, IV and V, as shown in Table I. These catalysts were prepared similarly except for the species and amount of the precipitant. For example, Cu I was prepared as follows: A solution of 30 g. of cupric nitrate hexahydrate in 900 ml. of distilled water was kept at 90°C. A sodium hydroxide solution, prepared from 300 ml. of distilled water and 15 g. of sodium hydroxide, was brought to the same temperature and added rapidly to the stirred copper nitrate solution. After the mixture was stirred at this temperature for 30 min., the precipitate was washed by decantation with a copious amount of warm water (at 70°C), collected on a glass filter, dried in an electric oven at 105°C for 10 hr., powdered in an agate mortar and finally stored in a stoppered bottle. It has been reported[14] that the occluded or absorbed impurities (mainly anions) in the preparation of reduced copper influence the activity. Accordingly, to minimize the inclusion of such impurities dilute solutions were used for precipitation and the resulting precipitates were then washed well with distilled water by decantation. The chemicals used were of the purest reagent grade and all vessels were washed with nitric acid and rinsed with distilled water.

TABLE I. PREPARATION OF CATALYSTS

| Catalyst | Precipitant | Amount of precipitant g. | Distilled water ml. | Color of catalyst |
|---|---|---|---|---|
| Cu I | NaOH | 15 | 300 | black |
| Cu II | KOH | 24 | 500 | black |
| Cu III | $K_2CO_3$ | 25 | 500 | dark brown |
| Cu IV | $NaHCO_3$ | 30 | 300 | yellowish green |
| Cu V | $KHCO_3$ | 40 | 400 | yellowish green |

**Apparatus.**—The apparatus, illustrated diagrammatically in Fig. 1, is designed to measure the ratio of dehydrogenation and dehydration by the catalysts. Hydrogen coming from the reservoir (A) was passed through a tube (C) containing heated copper gauze to remove the oxygen present in the hydrogen by converting it into water, and then through a bottle (D) containing a 30% sodium hydroxide solution

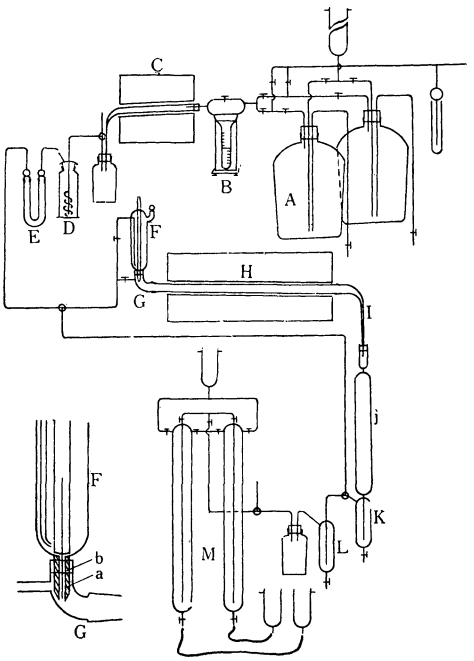



Fig. 1. Apparatus.

12) M. Niwa and M. Yamaguchi, *J. Chem. Soc. Japan, Pure Chem. Sec.* (*Nippon Kagaku Zasshi*), **73**, 159, 162 (1952).
13) S. Komatsu and M. Kurata, *Mem. Coll. Sci. Kyoto Imp. Univ.*, **A8**, 147 (1925).
14) H. Hasegawa, *J. Chem. Soc. Japan, Ind. Chem. Sec.* (*Kogyo Kagaku Zasshi*), **58**, 334 (1955).

and a solid sodium hydroxide tube (E). The hydrogen flow was measured by passing it through a calibrated flowmeter (B). The reaction tube (H) was a hard glass tube of 1 m. length and 18 mm. inside diameter, and was set in a combustion furnace and in this tube 10 g. of the catalyst to be used was spread in a length of approximately 70 cm. This tube was inclined at an angle of about 5° to insure proper drainage of the liquid product and the temperature was measured by a thermometer at a position of 30 cm. from the exit end of the catalyst bed. A rate of flow of the sample can be kept approximately constant by varying the extent of the insertion of the tungsten wire (a) into the capillary (b) (Fig. 1), and connecting the funnel (F) with a receiver (K) to keep the pressure equal. The sample is vaporized through a vaporizer (G) before reaching the catalyst. This vaporizer was made of a hard glass tube filled with glass wool and heated to a desired temperature by a heater. The reaction tube was connected with a condenser (J) by means of an adapter (I). The liquid product condensed was collected in a receiver (K) and uncondensed vapor was absorbed in water in a bottle (L). Noncondensable gas was collected in a gas-holder (M).

**Procedure.**—The catalyst was placed in the reaction tube and the apparatus was tested for gas-tightness. After the tube was filled with hydrogen, the furnace was heated to the reduction temperature, and was kept at this temperature for the period of reduction. Care was taken during the reduction to avoid the overheating of the catalyst as the reaction is exothermic, and the reduction temperature was always below 185°C. The standard flow rate of hydrogen (measured at room temperature) was 750~900 ml. per hour. The reduction was continued until the color of the catalyst changed from black or yellowish green to reddish purple and then the hydrogen supply was stopped and the resulting catalyst was heated to the operating temperature. Experiments were performed at 185, 250, 305 and 325°C under the ordinary pressure, and in the case of the copper catalyst precipitated with sodium hydroxide, further experiments were carried out at 220°C and 280°C, and during the run which lasted for several hours, the temperature was maintained within about ±5°C of the desired temperature. A definite weight of the alcohol or acetone was supplied from the dropping funnel (F) at the predetermined rate. The vapor coming out from the reaction tube was condensed by passing through a condenser cooled with ice water and the escaped gas from the condenser was passed into ice-cooled distilled water (50 ml.) to catch condensable products completely. The noncondensable gas which came out of the receiver (L) was collected in a gas-holder and its volume was measured from time to time. At the end of the run, the weight of liquid products collected in the receiver, that absorbed by water in the bottle, and the volume of noncondensable gas in the gas-holder were measured. The condensed product and the water solution in the bottle were combined. If an oily product

TABLE II. INFLUENCE OF PRECIPITANTS AND TEMPERATURES ON DEHYDROGENATION OF ISOPROPYL ALCOHOL

| Exp. no. | Precipitant | Temp. °C | Isopropyl alcohol g. | Velocity g./hr. | Acetone g. | Oily product g. | Gas collected l. | Percentage of conversion* % |
|---|---|---|---|---|---|---|---|---|
| 1 | NaOH | 185 | 39.69 | 10.82 | 21.78 | 0 | 8.57 | 57.9 |
| 2 | KOH | 185 | 38.81 | 12.25 | 19.71 | 0 | 7.95 | 54.9 |
| 3 | $K_2CO_3$ | 185 | 39.04 | 11.71 | 18.39 | 0 | 7.38 | 50.7 |
| 4 | $NaHCO_3$ | 185 | 38.83 | 11.95 | 19.95 | 0 | 8.06 | 55.7 |
| 5 | $KHCO_3$ | 185 | 39.02 | 12.01 | 20.55 | 0 | 8.26 | 56.7 |
| 6 | NaOH | 220 | 39.49 | 10.53 | 20.06 | 9.26 | 9.64 | 65.5 |
| 7 | NaOH | 250 | 39.59 | 10.55 | 18.60 | 11.53 | 9.07 | 61.4 |
| 8 | KOH | 250 | 38.66 | 12.21 | 19.69 | 9.97 | 9.91 | 68.7 |
| 9 | $K_2CO_3$ | 250 | 39.24 | 12.07 | 24.46 | 5.25 | 10.87 | 74.3 |
| 10 | $NaHCO_3$ | 250 | 38.87 | 11.66 | 30.92 | 0 | 12.35 | 85.2 |
| 11 | $KHCO_3$ | 250 | 38.78 | 11.08 | 30.96 | 0 | 12.36 | 85.5 |
| 12 | NaOH | 280 | 39.63 | 10.56 | 26.98 | 4.24 | 11.39 | 77.0 |
| 13 | NaOH | 305 | 39.18 | 11.47 | 33.55 | 0 | 13.63 | 93.3 |
| 14 | KOH | 305 | 38.86 | 11.96 | 33.51 | 0 | 13.63 | 94.1 |
| 15 | $K_2CO_3$ | 305 | 39.36 | 11.52 | 34.33 | 0 | 13.51 | 92.0 |
| 16 | $NaHCO_3$ | 305 | 38.93 | 12.29 | 34.77 | 0 | 13.75 | 94.7 |
| 17 | $KHCO_3$ | 305 | 38.82 | 11.65 | 35.11 | 0 | 13.89 | 95.9 |
| 18 | NaOH | 325 | 38.96 | 11.40 | 34.41 | 0 | 13.91 | 95.7 |
| 19 | KOH | 325 | 38.87 | 11.96 | 34.43 | 0 | 14.03 | 96.7 |
| 20 | $K_2CO_3$ | 325 | 39.32 | 11.80 | 35.15 | 0 | 13.87 | 94.6 |
| 21 | $NaHCO_3$ | 325 | 38.91 | 11.12 | 35.44 | 0 | 14.01 | 96.6 |
| 22 | $KHCO_3$ | 325 | 38.91 | 11.39 | 35.62 | 0 | 14.07 | 97.0 |

* Calculated from the volume of the gaseous product collected in each experiment on the assumption that original isopropyl alcohol is transformed completely into gases such as hydrogen or propylene.

was formed, this was separated from the water layer and washed with a known volume (20 ml.) of distilled water. If the oily product was not formed, the aqueous solution was analyzed by the method described below.

**Analysis of the Products.**—The aqueous solution was recognized to consist of acetone and unchanged isopropyl alcohol by the preparation of the 2,4-dinitrophenylhydrazone and the phenylurethan, respectively, and the content of the acetone was determined by the hydroxylamine method[15]. The reliability of this analytical method was checked by titrating a known sample of acetone and the result was found to be correct within experimental errors. The oily product, which was obtained in some of the experiments, was dried with anhydrous sodium sulfate and then fractionally distilled through a Widmer column. Isobutyl methyl ketone was present in a fraction that showed the properties: b. p. 110~125°C, $n_D^{25}$ 1.3963, $d_4^{25}$ 0.7908, and a semicarbazone, m. p. 133~133.5°C and a 2,4-dinitrophenylhydrazone, m. p. 93.5~94°C were obtained and showed no depression of the melting points when mixed with the known derivatives of isobutyl methyl ketone. Diisobutyl ketone was found mainly in a fraction as follows: b. p. 160~170°C, $n_D^{25}$ 1.4115, $d_4^{25}$ 0.8012, and it was identified on the basis of the preparation of the 2,4-dinitrophenylhydrazone, m. p. 92~92.5°C and the semicarbazone, m. p. 122~122.5°C which were shown to be the corresponding derivatives of diisobutyl ketone by the mixed melting point determination. The formation of unsaturated and hydroxy ketones such as mesityl oxide, phorone and diacetone alcohol, was not detected in the oily product.

## Results and Discussion

The influence of the precipitants and reaction temperatures on the activity and the selectivity of the copper catalysts is summarized in Table II. Experiments were controlled so as to regulate the reducing condition of the precipitate* with hydrogen as far as possible and further to maintain the constancy of the velocity of the isopropyl alcohol passing over the catalyst. To find the difference in the reaction products on varying the reaction temperature and the optimum temperature for dehydrogenation, the catalytic reaction was performed at 185, 250, 305 and 325°C. Since isopropyl alcohol was not changed in the absence of the catalysts over the range (185~325°C) of temperatures, the changes shown in Table II do not involve the simple pyrolysis of isopropyl alcohol. The yield of acetone shown in Table II does not necessarily represent the maximum yield but is an average of three or four experiments under the constant operating condition. However the fluctuation in the yields of acetone and of the oily product obtained by the repeated experiments was less than 1 per cent, and thus within the limit of experimental error in the determination of acetone.

**Influence of the Reaction Temperatures on the Dehydrogenating Activity of Reduced Copper.**—The dehydrogenating activity of the various copper catalysts depends upon the temperature at which the reaction is carried out. Using a copper catalyst, the equilibrium constant for the reaction of isopropyl alcohol to form acetone and hydrogen has been measured[16]. Though the results obtained by various workers show little agreement, it is accepted that the equilibrium transfers to the direction of dehydrogenation at the reaction temperature above 220°C. Consequently, at low temperatures the copper catalyst has a poor activity for dehydrogenation. In the present research all catalysts act to promote dehydrogenation of isopropyl alcohol at high temperatures, and at the highest reaction temperature (325°C) the dehydrogenation of isopropyl alcohol to acetone is the highest.

**Influence of the Precipitants on the Dehydrogenating Activity of Reduced Copper.**—As shown in Table II, the dehydrogenating activity of the copper catalysts varies considerably with the sort of precipitants, and the catalyst prepared by the treatment with potassium bicarbonate showed the largest activity. On the contrary, the catalyst prepared with sodium hydroxide showed the smallest activity. The dehydrogenating activity of the copper catalysts prepared with various precipitants is in the following order: $KHCO_3 > NaHCO_3 > K_2CO_3 > KOH > NaOH$.

The author presumed that the catalysts prepared with alkali bicarbonates possess a capillary or a porous structure on account of the evolution of carbon dioxide at precipitation or the hydrogen treatment, and this is one of the reasons for the large dehydrogenating activity of the catalysts.

**The Relation between the Amount of Gas Evolved and that of Acetone Produced.**—When the oily product was not formed, the difference between the theoretical yield of acetone and the percentage of conversion was a few per cent. Therefore, the dehydration of isopropyl alcohol to propylene seems to occur little at temperatures below 325°C. Accordingly, the dehydration is not an important factor from the viewpoint of dehydrogenation. When the

15) M. Katsuno, *J. Soc. Chem. Ind. Japan*, (*Kogyo Kagaku Zasshi*), **46**, 112 (1943).

* Copper compound prepared from copper nitrate by "precipitant".

16) G. S. Parks and H. M. Huffman, "Free Energies of Some Organic Compounds", Reinhold Pub. Corp., New York (1932), p. 22; H. J. Kolb and R. L. Burwell, Jr., *J. Am. Chem. Soc.*, **67**, 1084 (1945); A. H. Cubberley and M. B. Mueller, ibid., **68**, 1149 (1946).

oily product was not formed, a proportional relation was found between the amount of the gas evolved and that of acetone produced, namely the greater the amount of the evolved gas, the greater the amount of acetone. This is reasonably accounted for by considering that both the gas and acetone result from the dehydrogenation of isopropyl alcohol. Also the amount of the gas collected increased proportionally with the temperature rise.

**The Relation between the Amount of Gas Evolved and the Reaction Time.**—A test was made by the following method to see whether the catalytic activity is kept constant during the whole reaction time or not. The amount of gas evolved (Table II) was measured at intervals of 15~20 min. and the volumes of the evolved gas reduced to the normal state were plotted against the reaction time in Fig. 2. Since the evolution of the gas is constant during the reaction time as seen in Fig. 2, it is concluded that the sustained activity of the catalyst holds over the period of the operation. Thus the constancy of the activity of the catalyst can be detected by inspecting the amount of the gas evolved.

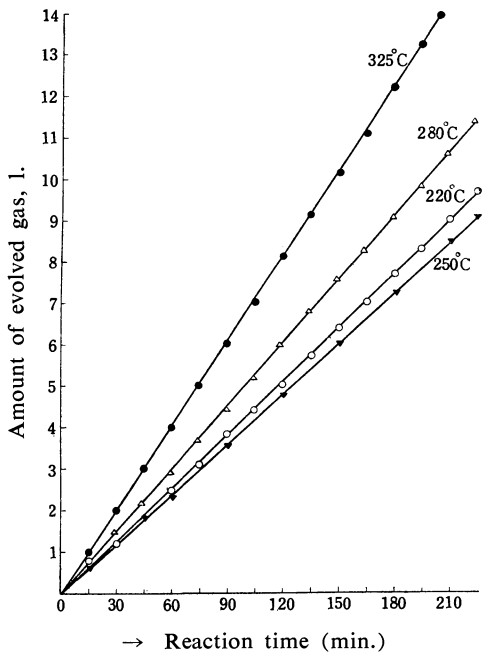
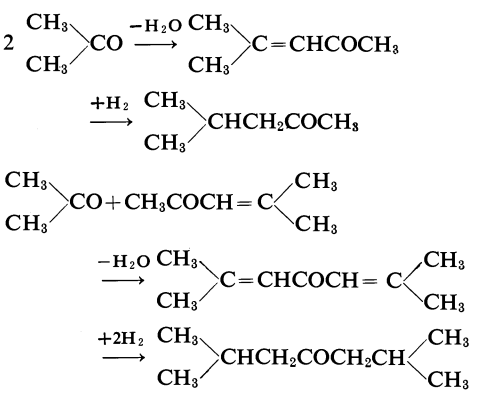



Fig. 2. The amount of evolved gas as a function of the reaction time for various temperatures (precipitant: NaOH)

**Two Types of Reduced Copper Catalysts.**—It was found that there are two distinct types of reduced copper catalysts. One of them catalyzes the decomposition of isopropyl alcohol to acetone and hydrogen; that is, promotes dehydrogenation. Cu IV and Cu V belong to this type. The other type catalyzes the conversion of isopropyl alcohol into isobutyl methyl ketone and diisobutyl ketone together with acetone and hydrogen, that is, promotes both dehydrogenation and condensation. Cu I, Cu II and Cu III belong to this type. Further, there is a distinct difference in color before reduction between these two types of catalysts. As shown in Table I, the precipitates prepared with sodium hydroxide, potassium hydroxide, and potassium carbonate are black or dark brown in color. On the contrary, those prepared with potassium bicarbonate and sodium bicarbonate have a yellowish green color. Cu I and Cu II were nearly equal in the activity for the production of both the oily product and acetone, and Cu III has a relatively poor activity for the formation of the oily product. Also Cu IV and Cu V were entirely inactive to the production of the oily product. There is thus a marked difference of activity between the copper catalysts prepared with alkali hydroxides and those prepared with alkali bicarbonates with respect to the relative amount of acetone formed. Cu I and Cu II are especially convenient for preparing isobutyl methyl ketone and diisobutyl ketone. The new synthetic process of these ketones, which consists in passing isopropyl alcohol over Cu I or Cu II under the atmospheric pressure at 220~250°C, is now proposed as one which has not yet been observed with a copper catalyst alone.

**Mechanism of the Condensation Reaction.**—Lassieur[17] found that a mixture of acetone and hydrogen, when it is passed over reduced nickel at 200~300°C, yields mesityl oxide, isobutyl methyl ketone, phorone and diisobutyl ketone. Concerning the mechanism of this reaction he showed that acetone undergoes condensation to give mesityl oxide and phorone, and these unsaturated ketones are then reduced by hydrogen.



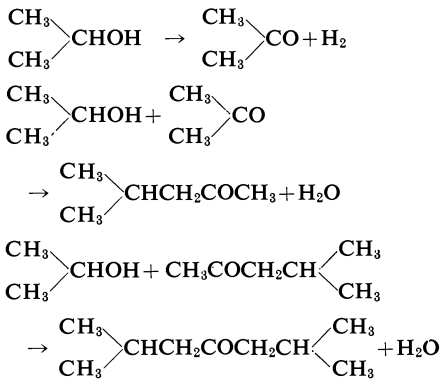

17) M. A. Lassieur, *Compt. rend.*, **156**, 795 (1913).

On the other hand, Ipatieff and Haensel[18] found that in the presence of a copper-alumina or a copper-zinc-oxide-alumina catalyst, a mixture of isopropyl alcohol and acetone is converted into isobutyl methyl ketone and diisobutyl ketone, and that in the absence of isopropyl alcohol, acetone reacts to give only small amounts of mesityl oxide and phorone, and they reported that isobutyl methyl ketone is obtained by a regular ketonic condensation of acetone to diacetone alcohol and then a hydrogen disproportionation between isopropyl alcohol and diacetone alcohol.

$$2\ CH_3COCH_3 \rightleftarrows (CH_3)_2COHCH_2COCH_3$$

$$(CH_3)_2COHCH_2COCH_3+CH_3CHOHCH_3 \rightarrow (CH_3)_2CHCH_2COCH_3+CH_3COCH_3+H_2O$$

In the present research, isobutyl methyl ketone and diisobutyl ketone were obtained from isopropyl alcohol with the copper catalyst prepared with sodium hydroxide or potassium hydroxide, but the formation of mesityl oxide, diacetone alcohol and phorone was not observed. Further, it was confirmed that, when the catalytic reaction is carried out with acetone alone under a condition similar to that in the experiment with isopropyl alcohol, acetone is not changed. It is generally recognized that hydrogen atoms of a methyl group adjacent to a carbonyl group are reactive. From these considerations, the formation of the reaction products obtained by the present author can be illustrated by the following schemes:



Further, the following results have been obtained by the present author: (1) Alicyclic alcohols (cyclohexanol and *l*-menthol) do not undergo alcohol-ketone condensation under a condition similar to that employed for isopropyl alcohol[1], consequently giving no higher ketones. (2) When *sec*-butyl alcohol is passed over reduced copper, 5-methyl-3-heptanone together with ethyl methyl ketone is formed.* From these results it seems that the condensation reaction takes place when three hydrogen atoms are attached to the alpha carbon atom of a carbonyl group, but is not favored when only two hydrogen atoms are attached. The alcohols which on dehydrogenation can yield ketones containing a methyl group adjacent to the carbonyl group can condense with the ketones produced.

Up to the present, isobutyl methyl ketone has been prepared by the following method: Acetone is first condensed in the presence of bases to give diacetone alcohol, and this diacetone alcohol is dehydrated by heating with an acid such as sulfuric acid to give mesityl oxide, and then the mesityl oxide thus formed is hydrogenated in the presence of a copper catalyst to give isobutyl methyl ketone. It is of interest that isobutyl methyl ketone can be prepared in one step by passing isopropyl alcohol over reduced copper as described above.

## Summary

In order to determine whether the dehydrogenating activity of reduced copper is affected by the species of precipitants in the preparation, the dehydrogenation of isopropyl alcohol to acetone was studied by using five different precipitants, i. e. sodium hydroxide, potassium hydroxide, potassium carbonate, sodium bicarbonate and potassium bicarbonate. The dehydrogenation was the highest with no side reaction at 305~325°C, especially when potassium bicarbonate was used as precipitant.

When the copper catalysts, prepared with sodium hydroxide, potassium hydroxide and potassium carbonate, were used, condensation together with dehydrogenation occurred. The formation of higher ketones is explained by the assumption of intermolecular dehydration between acetone and original isopropyl alcohol.

The author wishes to express his hearty thanks to Professor T. Matsuura for his kind guidance and valuable suggestions throughout this work.

*Department of Chemistry*
*Faculty of Science*
*Hiroshima University*
*Hiroshima*

18) V. N. Ipatieff and V. Haensel, *J. Org. Chem.*, 7, 189 (1942).

* Presented at the 13th Annual Meeting of the Chemical Society of Japan, April, 1960.

# *Studies on Tritium Labeled Compounds. II.*[1] *Preparation of Tritium Labeled Stearic Acid*

By Yoshishige SATO, Teruhiko MESHI and Tadao TAKAHASHI

(Received May 19, 1960)

In an attempt to prepare $^3$H-labeled stearic acid as a biochemical tracer, we have carried out three different methods; chemical method, electric discharge method and recoil tritium labeling method. Wolfgang, Pratt and Rowland[2] investigated the labeling of organic compounds by a electric discharge in tritium in 0.05 mmHg region on the assumption that accelerated tritium ions will be active transients required for labeling. Dorfman and Wilzbach[3] have recently conducted investigations on the labeling method by means of electric discharge in a 10 mmHg region. We have also studied the labeling method by electric discharge in tritium-hydrogen in 100 mmHg region[1].

Wolfgang and Rowland[4] have developed a $^3$H-labeling method of organic compounds. According to their reports, the compound to be labeled is mixed with lithium salt and the mixture is irradiated by slow neutrons in a reactor. A considerable fraction of the energetic tritium produced in the $^6Li(n, \alpha)T$ reaction will replace bound hydrogen in the molecules of stopping medium to form a radioactive form of the original hydrogenous molecule.

We have made investigations on the recoil tritium labeling method using a mixture of stearic acid and lithium carbonate in a reactor of the Japan Atomic Research Laboratory (JRR-1).

## Experimental and Results

**Chemical Method.**—*Reduction of Ethyl Linoleate*[5]. —154 mg. of ethyl linoleate, 5 mg. of platinum oxide catalyst and 2 ml. of ethyl acetate are mixed together in a reaction vessel connected with a vacuum apparatus. Then in the apparatus, H$^3$-labeled ethyl stearate was prepared by catalytic hydrogenation of ethyl linoleate with $^3$H-H gas liberated by electrolysis of $^3$HHO. After about 20 min., 23 ml. (theoretical: 22.4 ml.) of $^3$H-H was absorbed and the uptake of $^3$H-H has ceased. The catalyst was removed by filtration and after the solvent was evaporated, $^3$H-labeled ethyl stearate was hydrolyzed by heating under reflux for three hours with potassium hydroxide-methanol solution. The solution was acidified with 10 N-hydrochloric acid, cooled and filtered. Then, deposited $^3$H-stearic acid was extracted with ether. The yield of $^3$H-stearic acid was 90% on the basis of ethyl linoleate, with a specific activity of 0.9 $\mu$c/mg.

*Exchange Method in the Presence of Catalyst.* — In an attempt to prepare $^3$H-stearic acid, exchange method for deuterium labeling of fatty acid developed by Heyninger, Rittenberg and Schoenheimer[6] was employed. In a glass tube, 20 mg. of $PtO_2$ suspended in 1 ml. of ethyl alcohol was reduced in a hydrogen stream. After alcohol was distilled, 200 mg. of stearic acid, 5 mg. of potassium hydroxide and 0.4 ml. of $^3$HHO (50 mc./ml.) were added. The mixture was frozen, the tube was sealed and then heated at 135°C for a week. After the period of reaction, the tube was opened and connected with a vacuum apparatus, and the liquid was distilled in vacuo. The dried residue was dissolved in potassium hydroxide-ethyl alcohol solution and filtered, and the filtrate was acidified with hydrochloric acid. The deposited $^3$H-stearic acid was recrystallized from ether. The yield of $^3$H-stearic acid was 90% on the basis of stearic acid, with a specific activity of 6.2 $\mu$c/mg.

**Electric Discharge Method.** — Discharge was carried out in a sample cell of approximately 20 ml., with tungsten electrodes (15 mm. apart). A sample to be labeled was placed on the bottom of the glass cell. Discharge was normally run from 20 sec. to 180 sec. in $^3$H-H mixture gas under a constant pressure of 100 mm Hg. The following is the procedure: A quantity of approximately 20 mg. was placed on the bottom of a glass cell and the cell was degassed. After the degassing was completed, $^3$H-H gas liberated by electrolysis of tritiated water (30 mc./ml.) was introduced into the cell and the discharge was made to run. In running of the discharge, the electrodes were over-heated. The electrodes were cooled by stopping the discharge. The cell was again degassed and air was introduced into the cell.

The stearic acid was then assayed for tritium in a gas-flow counter. The following table summarize the results.

Table I shows activity levels obtained for stearic acid subjected to the discharge technique. The

1) Y. Sato, T. Meshi, T. Takahashi and N. Sugimoto, *Japanese J. Pharm. and Chem.* (*Yakugaku Kenkyu*), **32**, (5) 317 (1960).
2) R. Wolfgang, T. Pratt and F. S. Rowland, *J. Am. Chem. Soc.*, **78**, 5132 (1956).
3) L. M. Dorfman and K. E. Wilzbach, *J. Phys. Chem.*, **63**, 799 (1959).
4) F. S. Rowland, C. N. Turton and R. Wolfgang, *J. Am. Chem. Soc.*, **78**, 2354 (1956).
5) R. F. Glascock and L. R. Reinius, *Biochem. J.*, **62**, 529 (1956).
6) W. E. Van Heyningen, D. Rittenberg and R. Schoenheimer, *J. Biol. Chem.*, **125**, 495 (1938).

Chart I

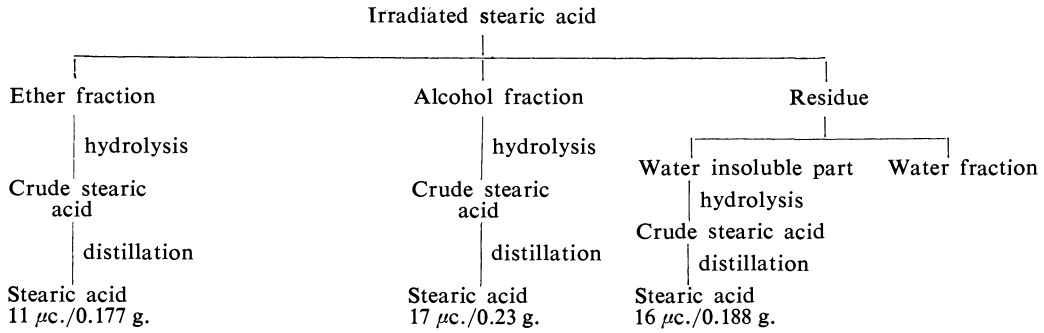



TABLE I. LABELING BY ELECTRIC DISCHARGE IN $^3$H-H GAS

| $^3$H-H Pressure, mm Hg | Discharge Time, sec. | Activity, μc./g. |
|---|---|---|
| 100 | 20 | 1.9 |
| 100 | 40 | 5.7 |
| 100 | 60 | 8.6 |
| 100 | 120 | 23.6 |
| 100 | 180 | 91.6 |

tritium content of the product increases approximately with the discharge time.

**Recoil Tritium Labeling Method.** — A mixture of 2 g. stearic acid and 1 g. lithium carbonate was irradiated with thermal neutrons for 17 hr. at a flux $2.5\times10^{11}$ n/cm$^2$ sec. The irradiated product was first extracted with anhydrous ether, and then with anhydrous ethyl alcohol. Infrared spectra of the ether fraction, alcohol fraction and the residue are shown in Fig. 1. It was recognized, that ester of fatty acid was produced by irradiation. Hydrolysis of each fraction was carried out by alcoholic potassium hydroxide. The hydrolyzed compounds were identified as stearic acid by infrared spectra, and they all distilled in vacuo (10 mm Hg) at 206~208°C.

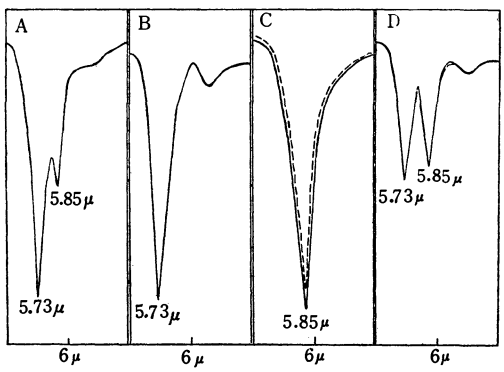



Fig. 1. Infrared absorption spectra of recoil tritiated stearic acid.
A: Residue, B: Alcohol fraction, C: —— Authentic stearic acid, ---- Hydrolyzed specimens of A, B and D, D: Ether fraction.

The stearic acid was assayed for tritium by means of a gas-flow counter. Chart I represents the experimental treatments described above.

The total yield of radio active stearic acid was about 0.6 g. (about 30%). Activity ($A$) of recoil tritium atoms produced by irradiation was calculated on the basis of the following equation.

$$A=\sigma Nf(1-e^{-0.693/t})$$

$\sigma$: Cross section 945 barn, $N$: Number of Li atom, $f$: Neutron flux, $T$: Half-life, $t$: Irradiation time.

When a mixture of stearic acid and lithium carbonate was irradiated by a $2.5\times10^{11}$ neutron flux, value of $A$ was 832 μc. The tritium content of the obtained stearic acid was therefore about 5% of the theoretical value.

**Radioactivity Measurement of Tritium Labeled Stearic Acid.** — Tritium activity was counted according to the Jackson and Lampe's method.[7] A windowless gas flow counter was used for radioassay of $^3$H-stearic acid. The self-absorption characteristics of tritium labeled stearic acid samples are given in Fig. 2.

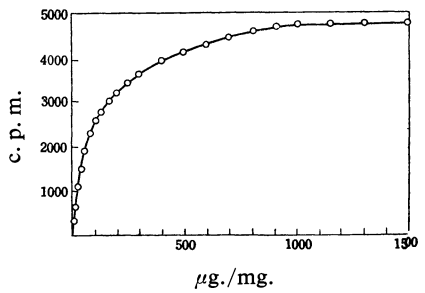



Fig. 2. Self-absorption curve of $^3$H-stearic acid.

These curves indicate that self-absorption is negligible up to sample weights of about 20 μg. per sq. cm.

7) F. L. Jackson and H. W. Lampe, *Anal. Chem.*, **28**, 1735 (1956).

## Discussion

By using tritium gas with higher specific activity than in above chemical process, it is easy to get a much higher specific activity. A higher specific activity can also be obtained using the discharge method when the discharge time is made prolonged and the tritium gas is of a higher specific activity. Tritium labeling in a reactor, on the other hand, is less usable, since this method gives rise to high destruction and lower specific activity. From the infrared absorption spectra of each fraction of irradiated products, it was recognized that the irradiated products contain fatty acid ester, because a 5.73 $\mu$ band of these products was identical with the carboxyl band of ethyl stearate.

## Summary

Chemical reduction method, exchange method, electric discharge method and recoil tritium labeling method were applied for preparing tritium labeled stearic acid. As the result of the recoil tritium labeling, the irradiated stearic acid was found to contain high destruction products which are mainly composed of esters of fatty acid.

*Osaka Research Laboratory*
*Tanabe Seiyaku Co., Ltd.*
*Kashima-cho, Higashiyodogawa-ku*
*Osaka*

# *Studies on Tritium Labeled Compounds. IV*. Preparation of Tritium Labeled Alanine by Means of Electric Discharge*

By Yoshishige SATO and Tadao TAKAHASHI

(Received July 4, 1960)

On the assumption that accelerated-tritium ions are the active transients required for labeling, Wolfgang, Pratt and Rowland[1] studied methods for preparing tritium labeled organic compounds using the electric discharge method. On the other hand, Dorfman and Wilzbach[2] investigated the labeling method under electric discharge in a 10 mmHg pressure region and reported that the labeling would be expected to occur as a result of the primary process of ionization, excitation and dissociation of tritium molecules in the gas phase. We recently reported[3] that the labeling would be produced in the same mechanism as that reported by Dorfman and Wilzbach. In this work, we carried out tritium labeling under electric discharge by employing $\alpha$-hydroximinopropionic acid as the sample and obtained DL-alanine of a high specific activity.

## Experimental and Results

About 50 mg. of $\alpha$-hydroximinopropionic acid was placed in the bottom of a glass cell which has two electrodes of tungsten as shown in Fig. 1. The cell was attached to a vacuum line and degassed. $^3$H-H gas, which was liberated by electrolysis of tritiated water (130 mc./ml.), was introduced into the cell and electric discharge (8000 V.) was struck at 40 mmHg for 10 min.

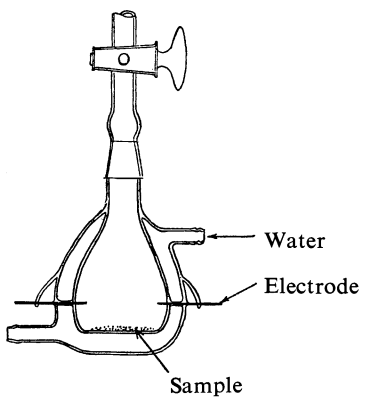



Fig. 1. Discharge cell.

During the discharge, the electrodes were overheated. In order to avoid over-heating, the electrodes were cooled by passing of cold water around the outside of the cell and by stopping further discharge. After the discharge the cell was degassed and air was introduced into the cell. As it was presumed that tritium labeled alanine was produced by this method, the discharged sample was extracted with ether. Almost all $\alpha$-hydroximinopropionic

* Part III; Y. Sato, T. Meshi and T. Takahashi, This Bulletin, 33, 1146 (1960).

1) R. Wolfgang, T. Pratt and F. S. Rowland, *J. Am. Chem. Soc.*, 78, 5132 (1956).

2) L. M. Dorfman and K. E. Wilzbach, *J. Phys. Chem.*, 63, 799 (1959).

acid being soluble in ether, was removed from the discharged sample by filtration. The amount of residue was about 5 mg. and was assayed for tritium in a gas flow counter. Its specific activity was 0.66 $\mu$c./mg.; on the other hand, the specific activity of ether soluble part was 0.71 $\mu$c./mg.

Paper chromatography of the residue, using *n*-butanol-acetic acid-water (4 : 1 : 1) as developing solvent, was performed. Owing to the low energy of the $\beta$-rays from tritium, the radioactivity from tritium could not be measured directly on the paper chromatogram. The paper was cut into pieces, and the active products were extracted with water. Water was evaporated in stainless steel dishes, and the activity of the extracted products was measured in a gas flow counter. Fig. 2 shows the results of the paper chromatogram and the radioactivity. As a comparison, parallel runs were made with ordinary DL-alanine and $\alpha$-hydroximinopropionic acid.

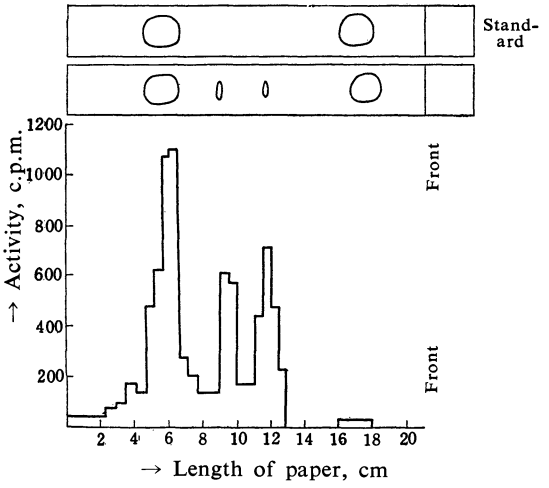



Fig. 2. Paper chromatography and the radioactivity of ether insoluble part. For comparison spots obtained with pure DL-alanine and $\alpha$-Hydroximinopropionic acid are shown.

Four hundred $\mu$g. of ether insoluble part of sample was employed as a sample of paper chromatography. DL-Alanine, the unidentified product A and B and, $\alpha$-hydroximinopropionic acid were obtained in the amounts and with activity values as shown in Table I.

TABLE I. SPECIFIC ACTIVITY OF THE PRODUCTS SEPARATED BY PAPER CHROMATOGRAPHY

| Compound | Activity c. p. m. | Amount $\mu$g. | Sp. act. $\mu$c./mg. | $R_f$ |
|---|---|---|---|---|
| DL-Alanine | 15600 | 20* | 4.4 | 0.28 |
| Unidentified product A | 4600 | 2* | 12.9 | 0.36 |
| B | 6450 | 2* | 17.2 | 0.45 |
| $\alpha$-Hydroximinopropionic acid | 100 | 350** | 0.0016 | 0.80 |

* Determination by spraying with ninhydrin.
** Determination by spraying with Bromophenyl Blue.

## Discussion

In the previous reports[3], it was reported that specific activity of tritium labeled DL-alanine obtained by means of electric discharge was only about 0.02 $\mu$c./mg. when DL-alanine was used as the sample. However, in this paper, tritium labeled DL-alanine with specific activity of 4.4 $\mu$c./mg. was obtained by using $\alpha$-hydroximinopropionic acid as the sample. A higher specific activity can be expected by using carrier free tritium gas.

## Summary

To obtain tritium labeled alanine of a high specific activity by means of electric discharge, $\alpha$-hydroximinopropionic acid was employed in place of alanine. After electric discharge, tritium labeled $\alpha$-hydroximinopropionic acid was removed by ether extraction and the residue was chromatographed. Tritium labeled alanine was obtained with a specific activity of 4.4 $\mu$c./mg. which was two hundred times as great as that obtained by the use of alanine.

*Osaka Research Laboratory*
*Tanabe Seiyaku Co., Ltd.*
*Kashimacho, Higashiyodogawa-ku*
*Osaka*

3) Y. Sato, T. Meshi. T. Takahashi and N. Sugimoto, *Tanabe Seiyaku Kenkyû Nempô*, 5, (1) 57 (1960).

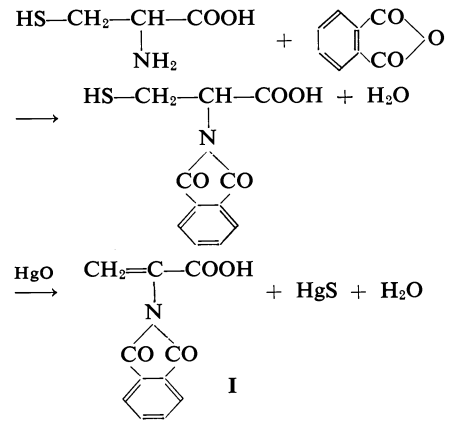
# *Studies on Dehydroalanine Derivatives. IV. Synthesis of N-Phthaloyl-Dehydroalanine by Thermal Decomposition of Cysteine and Serine in the Presence of Phthalic Anhydride*

By Shumpei SAKAKIBARA

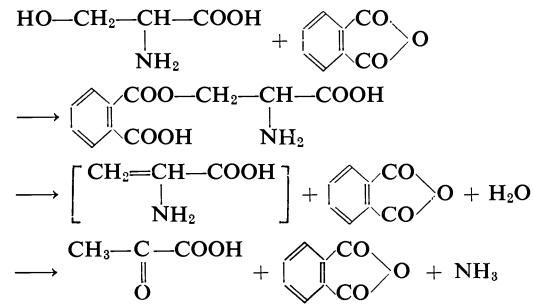
(Received July 13, 1960)

Bergmann et al.[1] reported, that in alkaline solution, serine- or cysteine- diketopiperazine (or peptide) was converted to dehydroalanine-diketopiperazine (or peptide). Weygand and Rinno[2] pointed out that *N*-trifluoroacetyl-serine was converted into *N*-trifluoroacetyl dehydroalanine, when it was distilled under high vacuum. In the present investigation, the thermal decomposition of cysteine and of serine in the presence of phthalic anhydride were studied.

Usually $\alpha$-amino acids are easily *N*-phthaloylated when heated with phthalic anhydride at 180°C for about half an hour[3]. However, cystine has not yet been tested owing to its poor solubility and reactivity. On the contrary, cysteine and serine were both very unstable to heat, and their *N*-phthaloyl derivatives have not been separated from the respective reaction mixtures after the thermal treatment. When a mixture of cysteine and phthalic anhydride was heated at or above 150°C, formation of hydrogen sulfide was detected by its characteristic odor and by using the lead acetate paper test. The thermal decomposition of cysteine at about 180°C was, however, not so great that its complete decomposition might not be expected within a short time. It was found experimentally that an equimolar amount of yellow mercuric oxide greatly accelerated the desulfhydration reaction and the reagent was rapidly converted into mercuric sulfide at 180°C. After purification of the reaction mixture, *N*-phthaloyl dehydroalanine (I) was obtained as colorless prisms (m. p. 171°C). Use of more than twice the molar equivalent of phthalic anhydride resulted in a better yield, because during the reaction, water is formed and the excess phthalic anhydride may compensate for the partial rehydrolysis of the newly-formed phthaloylimino groups.




When a mixture of serine and phthalic anhydride was heated at 180°C, vigorous evolution of water was observed, and the mixture changed to a dark brown syrup within a short time. At the same time, the formation of pyruvic acid was detected by its order. The purification of the reaction product was very difficult and the yield of substance I was poor. Perhaps part of the serine might have been converted into its *O*-phthalic acid monoester, which was then decomposed to pyruvic acid and ammonia at high temperature before the *N*-phthaloylation reaction occurred. Therefore it was necessary to establish conditions




in which the *N*-phthaloylation of serine was complete before such a dehydration reaction could occur. Sheehan et al. have shown[4] that usual amino acids could be *N*-phthaloylated in

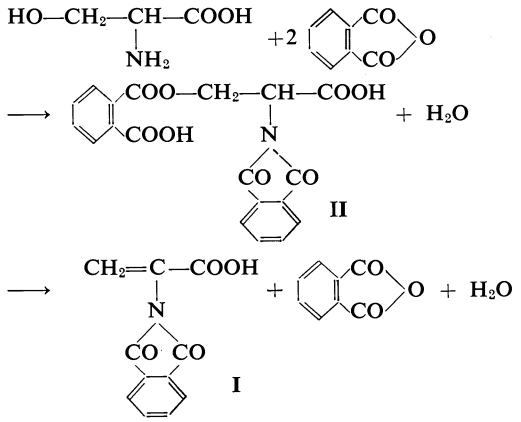
1) M. Bergmann and A. Miekeley, *Ann.*, **458**, 40 (1927); B. H. Nicolet, *J. Am. Chem. Soc.*, **53**, 3066 (1931); B. H. Nicolet, *J. Biol. Chem.*, **140**, 685 (1941).

2) F. Weygand and H. Rinno, *Chem. Ber.*, **92**, 517 (1959).

3) J. H. Billman and W. F. Harting, *J. Am. Chem. Soc.*, **70**, 1473 (1948).

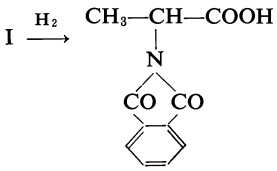
4) J. C. Sheehan, M. Goodman and G. P. Hess, ibid., **78**, 1367 (1956).

a gentle reaction in boiling dioxane. However, they did not mention such a reaction for serine. When serine and an equimolar amount of phthalic anhydride were boiled in dioxane for about five hours, a part of the serine remained in suspension, but twice the molar amount of phthalic anhydride readily solubilized the remaining serine in dioxane. Perhaps *O*, *N*-diphthaloylated serine (II) is formed under these conditions.

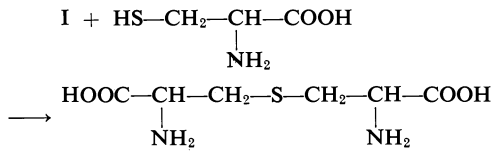


After the solvent had been distilled off, the residual syrup was heated gently in an oil bath at 200°C for about one hour under reduced pressure, and as in the case of cysteine, *N*-phthaloyl dehydroalanine (I) was obtained from the reaction mixture. The melting points of substance I from cysteine and serine were the same (m. p. 171°C), and no depression of the melting point was observed, when equal amounts of product I from cysteine and from serine were mixed. However, the yield of substance I from serine was inferior to that from cysteine. When substance I was recrystallized from dimethylformamide, crystals were obtained which melted at 84~88°C and contained one mole of dimethylformamide as crystallization solvent. Since the dimethylformamide complex was readily crystallizable, this procedure was suitable for purification of the product.

Hydrogenation of substance I gave rise to *N*-phthaloyl-DL-alanine, and lanthionine could also be formed from substance I by an addition reaction with L-cysteine under the conditions described by Schöberl[5].

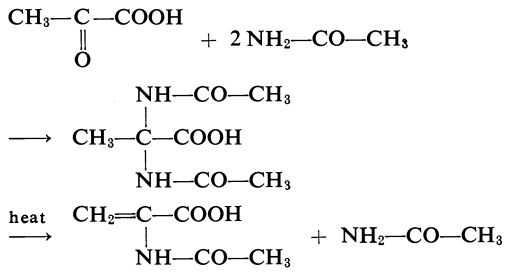


5) A. Schöberl, *Chem Ber.*, **80**, 379 (1947).



The properties of substance I all supported structure I.

Bergmann[6] first prepared *N*-acetyl dehydroalanine from pyruvic acid and acetamide as follows:



Many investigators utilized this procedure for preparing other *N*-acyl-dehydroalanine derivatives[7]. However, an attempt in the present work to prepare substance I by this procedure failed, because of the poor reactivity of phthalimide with pyruvic acid.

Substance I can polymerize to a vinylidene-type poly-$\alpha$-phthalimino acrylic acid, which may be converted into poly-$\alpha$-amino acrylic acid by hydrazinolysis.

## Experimental

***N*-Phthaloyl Dehydroalanine (I) from Cysteine.** —A mixture of freshly prepared cysteine (12 g.) and phthalic anhydride (37 g.) was placed in a round bottomed flask (300 ml.) fitted with a distillation adaptor. The flask was heated in an oil bath at 180°C (for about 20 min.) until a clear syrup was obtained, and then the water formed was distilled off under vacuum, using a water pump for about 10 min. more. An intimate mixture of yellow mercuric oxide (20 g.) and phthalic anhydride (22 g.) was added to the reaction mixture in one portion and then the flask was kept under vacuum for about 10~15 min. at 180~190°C. After being cooled to 50~60°C, the reaction mixture was extracted with hot ethyl acetate (300 ml.). The black precipitate was centrifuged off, and extracted three times with 40 ml. each of ethyl acetate. The combined extracts were concentrated to dryness under reduced pressure. The excess phthalic anhydride was separated by sublimation at 140°C in vacuo. The residue was dissolved in ethyl acetate (about 50 ml.) and the resinous products were precipitated by adding ether (about 150~200 ml.). The precipitates were centrifuged off and the supernatant was concentrated to dryness. The

6) M. Bergmann and K. Grafe, *Z. Phys. Chem.*, **187**, 187 (1930).

7) Cf. S. Sakakibara, This Bulletin, **32**, 13 (1959).

residue was recrystallized from toluene (about 30 ml.) to yield light-brown prisms (15 g.), which melt at 150~165°C. The small amount of phthalic anhydride remaining was sublimed out at 140°C in vacuo, and the remaining crystals were recrystallized from ethyl acetate after treatment with a small amount of active charcoal. The yield of slightly colored prisms with a melting point of 164~167°C was 60% (13.2 g.).

For final purification, the product was recrystallized from dimethyl formamide. The dimethyl formamide-complex (plates) formed melted at 84~88°C.

Found: C, 58.70; H, 4.98; N, 9.11. Calcd. for $C_{11}H_7O_4N \cdot C_3H_7ON$: C, 58.00; H, 4.84; N, 9.65%.

The complex was dried at 120°C in vacuo for about 3 hr. and recrystallized from ethyl acetate to yield colorless prisms with m. p. 169~171°C. The over-all yield was about 50~55%.

Found: C, 60.80; H, 3.17; N, 6.37. Calcd. for $C_{11}H_7O_4N$: C, 60.82; H, 3.24; N, 6.46%.

**I from Serine.**—A mixture of DL-serine (10.5 g.) and phthalic anhydride (37 g.) in dioxane (100 ml.) was refluxed until a clear solution was obtained (for about 5 hr.). The solution was concentrated to dryness in a flask, as shown in Fig. 1, under

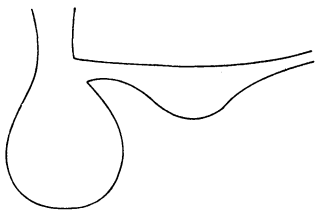


Fig. 1.

reduced pressure, and the residue was heated to 190~200°C under reduced pressure for about 20 min., during which time about 22 g. of phthalic anhydride distilled over. The residue was dissolved in ethyl acetate (50 ml.) and resinous products were precipitated by adding ether (150~200 ml.). The precipitates were centrifuged off, and the supernatant was concentrated to dryness. The residue was heated at 190~200°C for about 20 min. in vacuo and then the same procedures for separating the resinous products formed were repeated. The residue obtained was recrystallized from toluene (30 ml.) to yield light-brown prisms (9 g.) which melted at 150~160°C. The crystals were recrystallized from butanol-toluene (1 : 1) and then from dimethylformamide. The dimethylformamide complex (8.5 g., m. p. 82~88°C) was dried at 120°C in vacuo for about 3 hr. and recrystallized from ethyl acetate to yield colorless prisms (5 g.) with m. p. 169~171°C. The yield was 23%. The product was identified exactly with that obtained from cysteine by the mixed melting point test.

***N*-Phthaloyl DL-Alanine (II).**—A solution of I (1 g.) in ethanol (30 ml.) was hydrogenated in the presence of silk-palladium catalyst[8] (150 mg.) in an autoclave. The initial hydrogen pressure was 60 atm. The mixture was heated at 40°C for about 3 hr. and then at 70°C for additional 3 hr. After the reaction, the mixture was cooled to room temperature, and the catalyst was filtered off. The filtrate concentrated to dryness under reduced pressure. The residue was recrystallized from water-ethanol, and prisms with m. p. 159~161°C (650 mg.) and with m. p. 157~160°C (280 mg.) were obtained; the total yield was 93%. No depression of the melting point was observed, when the substance with m. p. 159~161°C was mixed with an authentic sample with m. p. 161~161.5°C. The infrared absorption spectrum of the product was also exactly the same as that of an authentic sample.

**Lanthionine (III).**—Substance I (3.3 g.) and L-cysteine hydrochloride (1.6 g.) were dissolved in aqueous N sodium hydroxide (24 ml.), and the solution was heated at 50°C for 1 hr. and then at 80°C for 2 hr. in an atmosphere of hydrogen. Concentrated hydrochloric acid (30 ml.) was added to the reaction mixture and the solution was boiled for about 6 hr. After colling to room temperature, the phthalic acid formed was filtered off, and the filtrate was concentrated to dryness under reduced pressure. The residue was dissolved in water, and recrystallized by neutralizing the solution with aqueous ammonia. After being kept overnight in a refrigerator, the crystals were filtered off and recrystallized from 6 N hydrochloric acid and aqueous ammonia as described above. The crystals formed were filtered off, washed with water, and alcohol, and dried; wt. 1.8 g., the yield was 86% (calcd. from cysteine).

Found: C, 34.18; H, 6.02; N, 13.44; S, 15.39. Calcd. for $C_6H_{12}O_4N_2S$: C, 34.61; H, 5.81; N, 13.45; S, 15.40%.

## Summary

*N*-Phthaloyl dehydroalanine (I) was synthesized by heating cysteine or serine in the presence of phthalic anhydride. Yellow mercuric oxide greatly accelerated the desulfhydration reaction. The yield of I from serine was inferior to that from cysteine. *N*-Phthaloyl-DL-alanine and lanthionine were derived from I.

The author wishes to express his thanks to Professor Shiro Akabori and Professor Shunsuke Murahashi for their valuable advice and encouragement.

*Institute for Protein Research*
*Osaka University*
*Kita-ku, Osaka*

8) Y. Izumi, This Bulletin, 32, 932 (1959).

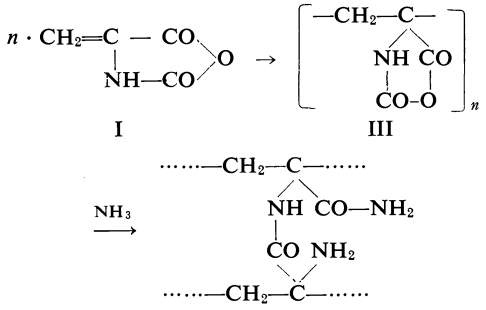
# *Studies on Dehydroalanine Derivatives. V. Radical Polymerization of N-Carboxy-dehydroalanine Anhydride and of N-Phthaloyl-dehydroalanine. Synthesis of a New Amphoteric Polymer*

By Shumpei SAKAKIBARA

(Received July 13, 1960)

Dehydroalanine derivatives such as *N*-carboxy-dehydroalanine anhydride (I)[1] and *N*-phthaloyl-dehydroalanine (II)[2] are considered as vinylidene derivatives. In the present communication, radical homo-polymerization and co-polymerization of compounds I and II are described.

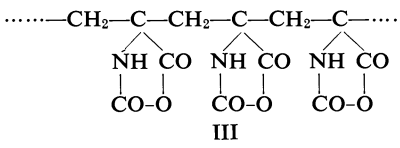
As reported previously[3], compound I is readily polymerized to poly-dehydroalanine in pyridine at 100°C with the evolution of carbon dioxide. The polymer obtained is dark brown because of the presence of conjugated double bonds. On the other hand, it was found in this study, that, when this same compound I was heated at 50°C in a dry inert solvent such as ethyl acetate or acetone in the presence of a radical initiator, the solution changed to an opaque jelly within 2 hr. Since, no evolution of carbon dioxide was observed during the polymerization reaction, it was considered that active *N*-carboxy anhydride groups were still present in the polymer obtained. This suggestion was supported by the fact that, when the polymer obtained was dissolved in aqueous ammonia, the solution rapidly turned into a clear gel. Perhaps intermolecular cross-linkages are formed in the solution due to a secondary polymerization reaction of the remaining *N*-carboxy anhydride groups.



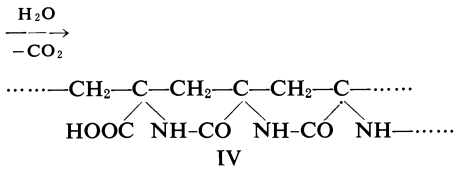
I III



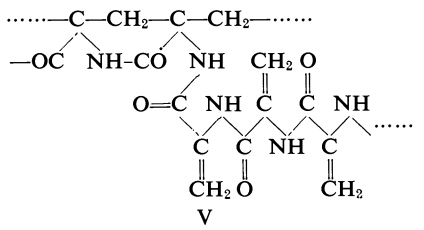
However, separation of analytically pure poly-*N*-carboxy-$\alpha$-amino acrylic acid anhydride (III) from the reaction mixture was unsuccessful because of the partial hydrolysis and secondary polymerization of the *N*-carboxy anhydride groups during the course of the purification of this compound. Actually, due to air humidity or impurities in the solvents used, analytical data of the polymers obtained from different experiments were between the theoretical values for formula III and those for the completely decarboxylated formula IV. Moreover, it was found that the nitrogen content of the compound gradually increased during storage over phosphorous pentoxide in a desiccator at room temperature. Since the *N*-carboxy anhydride groups should be in juxtaposition in polymer III, they may readily polymerize forming the poly-lactam IV.



III



IV



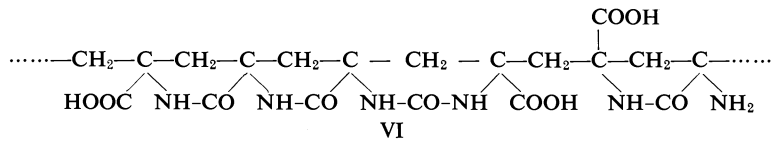
V

Structure V could scarcely be considered because polymerization of *N*-carboxy-dehydroalanine anhydride I to poly-dehydroalanine is very slow as described previously[3]. This is also supported by the color; that is, the polymer obtained was white, not dark brown like poly-dehydroalanine.

Polymer III was soluble in aqueous alkaline solution accompanied with decarboxylation reaction, but not in inert solvents. When the polymer was hydrolyzed with aqueous N potassium hydroxide at 100°C, the greater part of the hydrolyzed polymer was precipitated on acidification of the medium. As shown from

1) S. Sakakibara, This Bulletin, **32**, 13 (1959).
2) S. Sakakibara, ibid., **34**, 171 (1961).
3) S. Sakakibara, ibid., **32**, 814 (1959).

the pH-titration curve of the hydrolyzed polymer (Fig. 1), there were few amino groups and these were far exceeded by the number of carboxyl groups. Perhaps this is due to ureide formation as well as lactam formation, as described below (formula VI).



VI

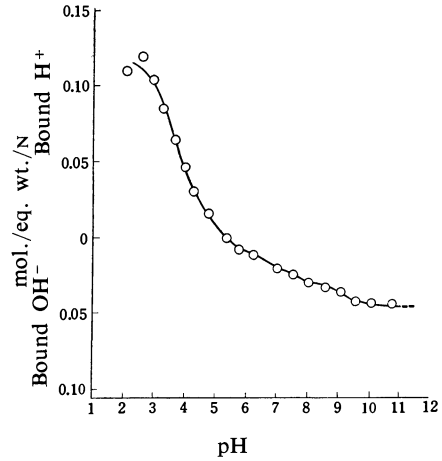
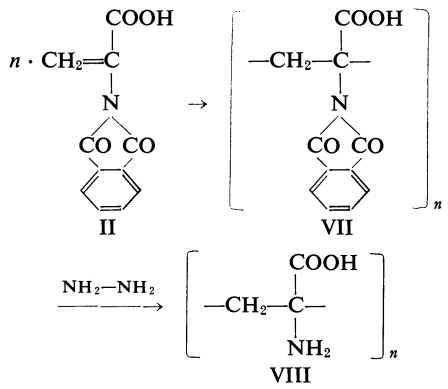



Fig. 1. pH-Titration curve of compound VI.

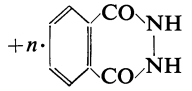
Frank[4] and Smets et al.[5] indicated that the equilibrium between a five-membered cyclic lactam and its open amino acid, in a polymer chain, tends to the former. Such a ureide-ring may be more stable against hydrolysis than a lactam.

Radical polymerizability of $\alpha$-phthalimido acrylic acid (II) was rather weak. When the monomer was heated in methanol at 60°C for about 200 hr. in the presence of azobisisobutylonitrile, a polymer(VII) was separated as a methanol-insoluble oil. The polymer was finally obtained as white powder, and it was soluble in dimethylformamide, and in hot acetic acid.



II VII VIII

4) H. P. Frank, *J. Polymer Sci.*, **12**, 570 (1954).



After hydrazinolysis, poly-$\alpha$-amino acrylic acid (VIII) was obtained in poor yield. To molecular weight of the starting polymer may not have been very high. The poly-$\alpha$-amino acrylic acid obtained was soluble in water. However, elementary analysis and pH-titration (Fig. 2) indicated that the content of ionizable groups was lower, than the calculated values, for the same reason as explained above.

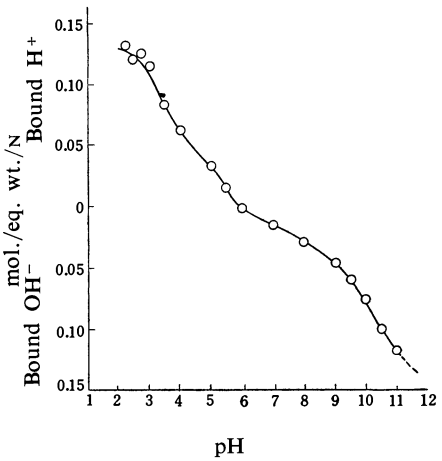
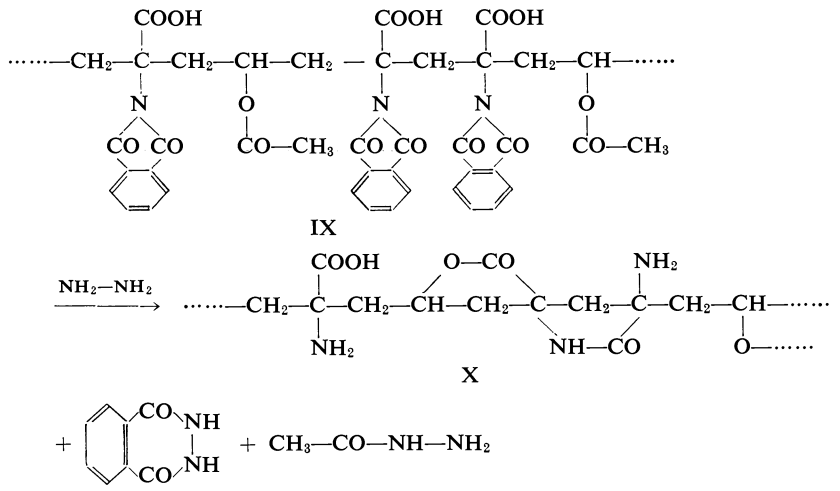



Fig. 2. pH-Titration curve of compound VIII.

Copolymerization of monomer II with vinyl acetate (V. Ac.) in methanol gave a gelatinous precipitate (IX-a). From the mother liquor, a second fraction (IX-b) was precipitated on addition of ether. Elementary analysis indicated that polymer IX-a was about 8 : 5-co-polymer (II : V. Ac.) and polymer IX-b was about 1 : 5-co-polymer (II : V. Ac.). The former was only soluble in dimethyl formamide, but the latter was soluble in pyridine, glacial acetic acid, dimethyl formamide, *m*-cresol, chloroform, hot ethanol, a mixture of methanol and acetone, and of ethyl acetate and acetone. Polymer IX-b was sparingly soluble in methanol, ethyl acetate and acetone, and insoluble in

5) M. Vrancken and G. Smets, ibid., **14**, 521 (1954); A. Conix, N. V. Mortsel and G. Smets, ibid., **15**, 221 (1955).

benzene, toluene and water. After hydrazinolysis of these copolymers, water soluble polyampholytes (X) were obtained. The pH-titration curves of these copolymers (Figs. 3 and 4) were of a typical polyampholyte-type, the structure of which was assumed to be as follows:



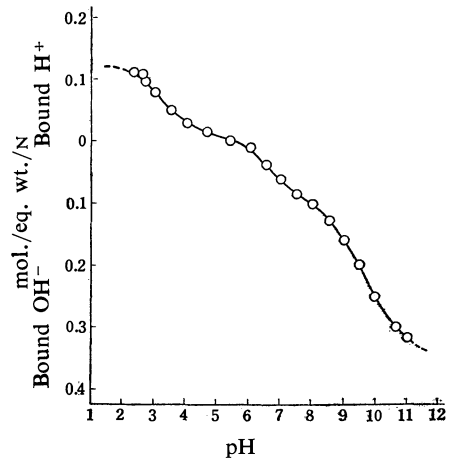




Fig. 3. pH-Titration curve of compound X-a.

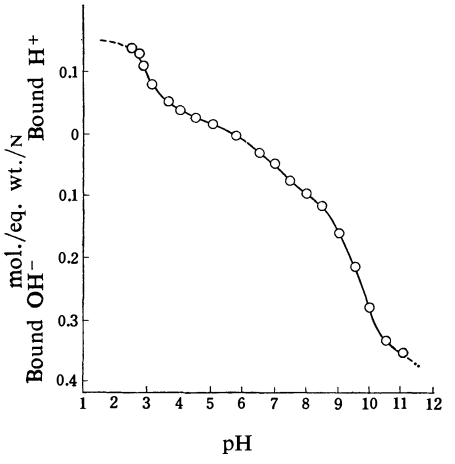



Fig. 4. pH-Titration curve of compound X-b.

If the sequence of co-monomer-segments was at random, five-membered lactam formation, as in poly-$\alpha$-amino acrylic acid, should not occur. As shown in Figs. 3 and 4 however, the number of ionizable groups was about 30% of the theoretical value. The values increased inversely with the number of amino acid segments. In this cases, the number of amino groups was greater than that of carboxyl groups. Perhaps, amino acid segments may have been localized in the molecule. Moreover, partial intramolecular lactone formation may have occurred.

If copolymerization of small amounts of compounds I or II with vinyl monomers such as acrylonitrile were possible, these would improve the affinity for dyeing of the parent polymers. Moreover, these would be useful as key-substances for preparing graft-copolymer of vinyl- and amino acid-polymers.

## Experimental*1

**Polymerization of I to III.**—A solution of I (2 g.) and azobisisobutylonitrile (0.1 g.) in purified ethyl acetate (20 ml.) was heated at 50°C in a sealed tube for about 4 hr. The opaque jelly formed, was crushed up finely and became powdery on addition of dry ether. The powder formed III was collected centrifugally, washed with ether and dried over phosphorus pentoxide in a desiccator; colored gradually above 180°C, sintered at about 250°C, yield 40% (0.8 g.).

Found*2: C, 44.5; H, 4.9; N, 15.8. Found*3:

*1 All melting points were determined by using capillary tubes in a Kanechlole-bath, maximum temperature of which was 300°C.

*2 Analyzed immediately after preparation.

*3 Analyzed after storing the same sample for 10 days in a desiccator over phosphorus pentoxide.

C, 46.9; H, 5.07; N, 16.9. Found*4 : C, 46.5; H, 4.1; N, 16.5. Calcd. for $C_4H_3O_3N$ (III): C, 42.5; H, 2.6; N, 12.4%. Calcd. for $C_3H_3ON$ (IV): C, 52.2; H, 4.35; N, 20.3%.

**Formation of VI from III.**—The polymer obtained above (0.5 g.) was dissolved in aqueous N potassium hydroxide (20 ml.) and the solution was heated in a sealed tube at 105°C for about 20 hr. The hydrolyzate was dialyzed against distilled water for 2 days and then lyophilized. White spongy material (0.4 g.) was obtained, which was soluble in water at above pH 6. For analysis, this materials was dissolved in distilled water, and reprecipitated by adding hydrochloric acid. The precipitates formed were washed with water, ethanol and, ether and dried; colored gradually above 250°C without melting.

Found: C, 49.1; H, 5.1; N, 17.3. Calcd. for $C_3H_3ON$-0.1·$CO_2$-0.2·$H_2O$ (VI): C, 48.5; H, 4.4; N, 18.2%; equiv. wt./N=77.0.

**Polymerization of II to VII.**—A solution of II (4 g.) and azobisisobutylonitrile (0.6 g.) in methanol (10 ml.) was heated in a sealed tube at 60°C for about 200 hr. The polymer formed (VII) precipitated on addition of ether and washed with methanol and ether, and dried; sintered at 250°C and melted at 270°C, yield 55% (2.2 g.).

Found: C, 60.3; H, 4.2; N, 6.8. Calcd. for $C_{11}H_7O_4N$ (VII): C, 60.8; H, 3.2; N, 6.4%.

**Hydrazinolysis of VII.**—The polymer VII (1.5 g.) was dissolved in hydrazine hydrate (15 ml.) and the solution was boiled for about 3 hr. The hydrazinolyzate was concentrated to drynes and the residue was redissolved in aqueous 0.1 N potassium hydroxide (5 ml.) and the phtaloyl hydrazide formed, precipitated on addition of enough acetic acid to reduce the pH to 5. The white precipitate formed was centrifuged off, and washed with water; 1.0 g. of phthaloyl hydrazide was recovered. The supernatant was concentrated to 5 ml. and poured into ethanol (about 100 ml.) to precipitate polymer VIII, which was centrifuged off, washed with ethanol, and dried in vacuo at room temperature; slightly brown powder (80 mg.) which colored gradually above 250°C.

Found: C, 43.9; H, 4.5; N, 17.5. Calcd. for $C_3H_3ON$-0.7·$H_2O$: C, 44.1; H, 5.4; N, 17.2%; equiv. wt./N=81.6.

**Copolymerization of II with Vinyl Acetate.**—A mixture of II (5 g.), vinyl acetate (20 g.) and azobisisobutylonitrile (0.5 g.) in methanol (20 ml.) was heated in a sealed tube at 60°C for about 100 hr. The gelatinous precipitates formed were centrifuged off, washed with methanol, and powdered from dimethyl formamide and ether (IX-a); m. p. 220~230°C, wt. 4.0 g.

Found: C, 56.9; H, 5.2; N, 5.0. Calcd. for $C_{11}H_7O_4N$-0.625·$C_4H_6O_2$-$H_2O$ (IX-a): C, 56.1; H, 4.5; N, 4.9%; eq. wt./N=289.

From the methanolic mother liquor, polymer IX-b was precipitated by addition of ether. It was centrifuged off, washed with ether and dried; sintered at 160~170°C and melted at 200°C, wt. 4.6 g.

Found: C, 56.6; H, 6.3; N, 2.2. Calcd. for $C_{11}H_7O_4N$-4.8·$C_4H_6O_2$-0.67·$H_2O$ (IX-b): C, 56.5; H, 5.8; N, 2.2%; equiv.wt./N=642.

**Hydrazinolysis of IX-a and IX-b.**—The polymer IX-a (3 g.) was dissolved in hydrazine hydrate (50 ml.) and the solution was boiled for about 3 hr. The hydrazinolyzate was concentrated to dryness, and the residue was redissolved in aqueous N potassium hydroxide (5 ml.) and the phthaloyl hydrazide formed precipitated on additon of acetic acid. The white precipitates were centrifuged off, and washed with water; about 1.6 g. of phthaloyl hydrazide was recovered. The supernatant and the washings were combined and after adding a few drops of N potassium hydroxide, the solution was dialyzed against distilled water for about 2 days. The dialyzed solution was lyophilized to yield a spongy material X-a; colored gradually above 250°C, wt. 0. 5 g.

Found: C, 48.5; H, 7.6; N, 13.5. Calcd. for $C_3H_3ON$-0.625·$C_2H_4O$-0.5·$H_2O$: C, 48.5; H, 6.2; N, 13.3%; equiv.wt./N=105.5.

The polymer IX-b (4 g.) was similarly treated with hydrazine hydrate (50 ml.) as described above, and material X-b) (1.1 g.) was obtained as a white spongy material; m. p. 200~210°C.

Found: C, 51.2; H, 8.1; N, 6.0. Calcd. for $C_3H_3ON$-3.5·$C_2H_4O$-0.67·$H_2O$ (X-b): C, 51.1; H, 7.8; N, 6.0%; equiv.wt./N=235.

**pH-Titrations.**—Each polyampholyte (VI, VIII, X-a or X-b) was weighed (50~150 mg.) and dissolved in 0.1 N potassium chloride (20.00 ml.) containing 0.30 ml. of 1.00 N potassium hydroxide. The solution was titrated with 1.00 N hydrochloric acid using an Agla micrometer-syringe under stirring in an atmosphere of nitrogen. Determination of pH-values was carried out by using a Beckman, GS pH-meter. The curves shown in Figs. 1, 2, 3 and 4 were obtained by Parke and Davis's method[6].

## Summary

Homopolymers of *N*-carboxy-dehydroalanine anhydride (I) and of *N*-phthaloyl-dehydroalanine (II), and copolymers of II with vinyl acetate were synthesized. Hydrolysis or hydrazinolysis was carried out to obtain polymers containing $\alpha$-amino acid structures. Actual structures of these polymers were discussed.

The author wishes to express his thanks to Professor Shiro Akabori and Professor Shunsuke Murahashi for their valuable advice and encouragement.

*Institute for Protein Research*
*Osaka University*
*Kita-ku, Osaka*

*4 Another example of analysis.

6) T. V. Parke and W. W. Davis, *Anal. Chem.*, **26**, 642 (1954).

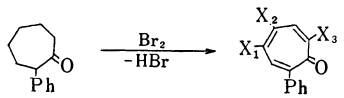
# *The Acid Product Obtained in the Synthesis of 2-Phenyltropone Derivatives from 2-Phenylsuberone*[1]

By Tadashi MUROI*

(Received February 20, 1960)

Previously Nozoe, Kitahara and others[2] reported that in the direct bromination-dehydrobromonation of suberone, a considerable amount of an acid product was sometimes obtained besides the 2,4,7-tribromotropone, and thereafter confirmed the structure of this acid product to be 2,4,7-tribromo-5-hydroxytropone[3].

The present author also reported[4] previously that by the application of 4~5 molar equivalents of bromine on 2-phenylsuberone (I), 4-bromo-and 4,7-dibromo-2-phenyltropone (II and III) were obtained in a good yield and that these products were occasionally accompanied by a considerable amount of an acid substance (A), assumed to be a mixture of bromo-derivatives of 4-hydroxy-2-phenyltropone (IV). This paper describes the details of A and the four methyl ethers derived from A.



(I) (II): $X_1$=Br, $X_2$=$X_3$=H
(III): $X_1$=$X_3$=Br, $X_2$=H
(IV): $X_1$=OH, $X_2$=$X_3$=H

Scheme I

The yield of A was found to increase remarkably, when somewhat impure I, or a solvent containing a trace of water was used, i.e. when fairly prolonged heating had to be applied in order to complete the reaction. Compound A separated as yellow needles or pale yellow scales of decomp. point ca. 200°C, and was sparingly soluble in chloroform, alcohol and acetic acid, and insoluble in benzene, ether and water. It gave no coloration with ferric chloride characteristic of tropolone or enol. It gave, however, a sparingly soluble yellow sodium salt when treated with sodium hydroxide or sodium carbonate solution. When treated with diazomethane, A afforded four kinds of methyl ethers; pale yellow needles (V), m.p. 173~174°C, yellow needles (VI), m.p. 131~132°C, yellow prisms (VII), m.p. 74~75°C, and pale yellow plates (VIII), m.p. 112~113°C. Their formation ratio was not constant but, in general, V and VI were always obtained in a better yield than VII or VIII and some times the yield of VII and VIII was so small that they can not be isolated.

Both V and VII had the molecular formula of $C_{14}H_{11}O_2Br$ and were obtained chiefly from the sparingly soluble portion of A in alcohol. On the other hand VI and VIII analyzed for $C_{14}H_{10}O_2Br_2$ and were obtained from the comparatively soluble portion of A.

Previously, Kitahara and others reported[5] that 2,4,7-tribromo-5-hydroxytropone (IXa) gave two kinds of methyl ethers and predicted from this fact that IXa existed as an equilibrium mixture of IXa and its tautomeric isomer, i.e. 2,4,6-tribromo-5-hydroxytropone (IXb).



(IXa) (IXb)

Scheme II

Acid hydrolysis of V gave yellow needles (X), $C_{13}H_9O_2Br$ m.p. ca. 210°C (decomp.), treatment of which with diazomethane afforded V and VII, with the former predominating. This fact indicates that X exists in a tautomeric mixture (Xa and Xb) and that V and VII are the respective methyl ethers of Xa and Xb.

When refluxed with sodium methoxide in absolute methanol, VII underwent aromatization, and the successive hydrolysis of its product yield pale yellow crystals (XI), m.p. 98~103°C. When treated with concentrated sulfuric acid, XI was converted to give yellow scales (XII), m.p. 93~94°C, which was proved to be 3-methoxyfluorenone[6] by mixed fusion with the authentic sample. It is, therefore, clear

* Present address, Hitachi Research Laboratory of Hitachi Ltd., Sukegawa-machi, Hitachi.

1) Presented at the 11th Annual Meeting of the Chemical Society of Japan, Tokyo, April, 3, 1958.

2) T. Nozoe, Y. Kitahara, T. Ando, S. Masamune and H. Abe, *Sci. Repts. Tohoku Univ., Ser.* I, **36**, 166 (1952).

3) T. Nozoe, Y. Kitahara and H. Abe, *Proc. Japan Acad.*, **29**, 347 (1953).

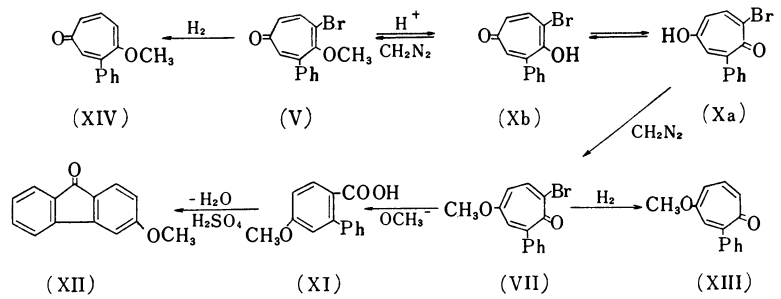
4) T. Muroi, This Bulletin, **33**, 1166 (1960).

5) Y. Kitahara, J. Shin and T. Toda, Presented at the Local Meeting of Tohoku District of the Chemical Society of Japan, Yamagata, Oct. 6, 1955.

6) F. Ullmann and H. Bleier, *Ber.*, **35**, 4272 (1902).

that XI is 4-methoxy-2-phenyl-benzoic acid and VII is 7-bromo-4-methoxy-2-phenyltropone, and X is a tautomeric mixture of 7-bromo-4-hydroxy-2-phenyltropone (Xa) and 5-bromo-4-hydroxy-3-phenyltropone (Xb).

Catalytic debromination of VII and V in the presence of palladium-carbon gave 4-methoxy-2-phenyltropone (XIII), m. p. 93~94°C, and 4-methoxy-3-phenyltropone (XIV), m. p. 75~76°C, respectively.



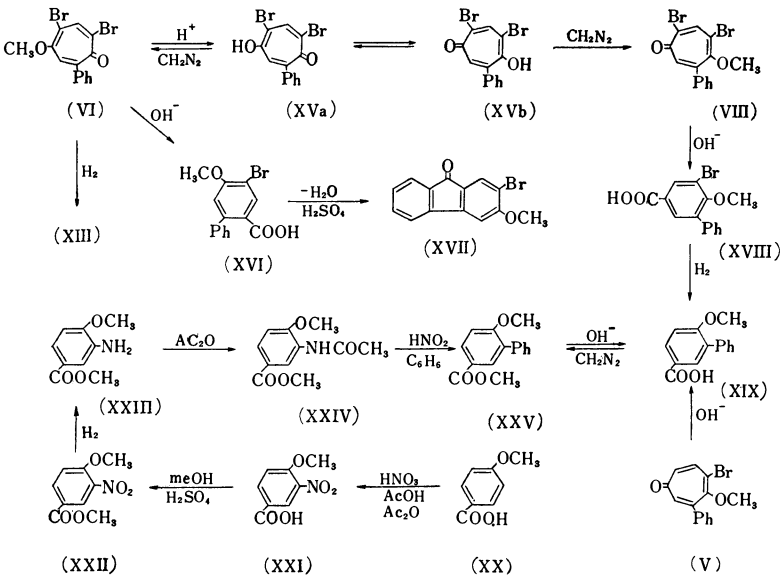
Scheme III

Acid hydrolysis of VI afforded pale yellow needles (XV), $C_{13}H_8O_2Br_2$ m. p. ca. 200°C (decomp.) which when treated with diazomethane, gave a mixture of VIII and VI. Catalytic debromination of VI gave XIII in a good yield. These facts indicate that XV also exists in a equilibrium mixture of two tautomeric forms (XVa and XVb) as in the case of IX and X, and moreover, that VI and VIII are respective methyl ethers of XVa and XVb.

When heated with alkali in alcohol, VI easily underwent aromatization to give colorless needles (XVI) m. p. 168~169°C, accompanied by a small amount of XV. When treated with concentrated sulfuric acid, XVI afforded yellow scales (XVII) m. p. 235~237°C, which was assumed to be monobromo-derivatives of XII. It follows therefore that one of the bromine atoms of VI occupies its C-7 position.

It was also found that VIII underwent aromatization very easily with alkali to give colorless needles (XVIII), m. p. 187~188°C, in a good yield. Catalytic debromination of XVIII gave colorless needles (XIX), m. p. 208~210°C. The structure of XIX is proved to be 4-methoxy-3-phenylbenzoic acid by the synthetic method shown in scheme IV.

These facts indicate, that VI and VIII are 5, 7-dibromo-4-methoxy-2-phenyltropone and 5, 7-dibromo-4-methoxy-3-phenyltropone, respectively, and XV is 5, 7-dibromo-4-hydroxy-2-phenyltropone as shown in the Scheme IV.



Scheme IV

From the fact mentioned above, the acid substance(A) is clarified to be a mixture of 7-bromo- and 5,7-dibromo-4-hydroxy-2-phenyltropone (Xa and XVa) and their respective tautomeric isomers. As the reaction of bromine on I is fairly complicated as reported previously[4], the mechanism of the formation of A can not be discussed at this stage. It is, however, assumed that A is derived through II or III by their hydroxylation or successive bromination during the reaction.

When treated with alkali, V was easily converted to give XIX in a good yield with the elimination of bromine at the C-5 position. Similar reaction was reported previously[7] by the present author, and this reaction is considered to be very interesting from the viewpoint that, in the rearrangement reaction of troponoid compound, the elimination of the substituents other than in C-2 (i. e. C-7) position has not been observed so far[8].

The synthesis and some reactions of IV and its bromoderivatives will be reported in the next paper.

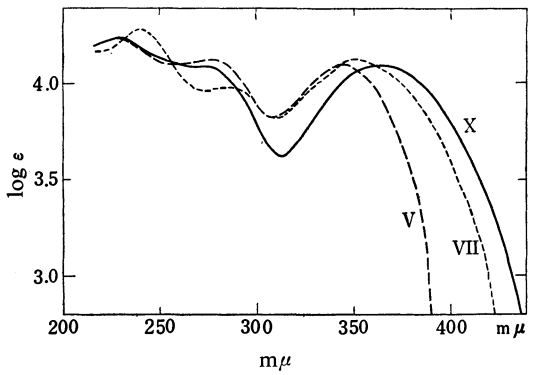



Fig. 1. Ultraviolet absorption spectra of V, VII and X in methanol.

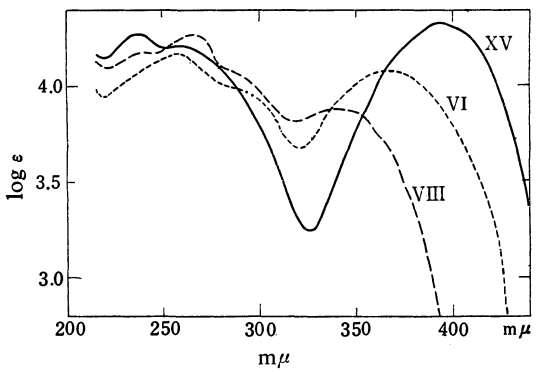



Fig. 2. Ultraviolet spectra of VI, VIII and XV in methanol.

7) T. Muroi, *J. Chem. Soc. Japan, Pure Chem. Sec.* (*Nippon Kagaku Zasshi*), **80**, 303 (1959).

## Experimentals[9]

**Formation of Acid Substance (A) from 2-Phenylsuberone(I).**—i) To a mixture of 4.7 g. of I, (b. p. 110~111°C/0.3~0.4 mmHg, $n_D^{25}$: 1.5390) 7.5 cc. of acetic acid and 1 cc. of water, a solution of 20 g. of bromine dissolved in 3.5 cc. of acetic acid was added dropwise over a period of 2 hr. at 50~80°C. The whole was heated on a water bath for about 3 hr. until there were no liberations of hydrogen bromide, cooled, and diluted with about 200 cc. of methanol, and yellow crystals (a) thereby separated were collected by filtration. Yield, ca. 4.3 g., m. p. 110~130°C. Crystalline residue, obtained after the evaporation of the solvent under reduced pressure, was digested with water and chloroform to give 0.25 g. of yellow crystals (b), m. p. 200°C (decomp.). The chloroform solution was shaken with 10% sodium carbonate solution and the aqueous layer was acidified with hydrochloric acid to give pale yellow crystals (c), m. p. 195°C (decomp.). Yield, 0.25 g.

The crystals (a) were digested with benzene and the insoluble portion (d), m. p. 195°C (decomp.) was collected by filtration. Yield, 0.85 g. The crystals (b), (c), and (d) were combined and dissolved in sodium carbonate solution. After treated with active carbon, the solution was acidified again and an acid product (A) was obtained as pale yellow crystals, m. p. 195~200°C (decomp.). Yield, 1.3 g.

The benzene soluble parts of (a) gave 2.8 g. of III. Similarly, chromatographic separation of the chloroform solution (aforementioned)[4] through a silica-gel column gave small amounts of III, II and 7-bromo-2-phenyltropone.

ii) To a solution of 4.7 g. of impure I (b. p. 140~149°C/2~3 mmHg, $n_D^{20}$: 1.5339) dissolved in 7.5 cc. of acetic acid, a solution of 16 g. of bromine in 3 cc. of acetic acid was added dropwise at 50~80°C. The whole was heated on a water bath for about 20 hr. till the liberation of hydrogen bromide was ceased. The solvent was evaporated under reduced pressure and the residue was washed with chloroform and water by which 1.8 g. of yellow crystals (a), m. p. 150~180°C (decomp.) were obtained. After the treatment of the chloroform solution with 10% sodium carbonate solution as in the above case, 0.2 g. of pale yellow crystals (b), m. p. ca. 175°C (decomp.) were obtained. The combined crystals (a) and (b) were repeatedly recrystallized from ethanol. Yellow needles ($A_1$) m. p. 207~210°C (decomp.) and pale yellow scales ($A_2$) m. p. 195~198°C (decomp.) were obtained from the sparingly soluble portion and comparatively easily soluble portion in alcohol, respectively.

Further recrystallization did not give pure substances and the analytical values of $A_1$ and $A_2$ were as below:

8) a) S. Seto, *Sci. Repts. Tohoku Univ., Ser.* I., **37**, 377 (1953). b) Y. Kitahara, ibid., **38**, 280 (1954). b) T. Mukai, ibid., **39**, 250 (1956). d) P. L. Pauson, *Chem. Revs*, **55**, 9 (1955).

9) Melting points are uncorrected. The micro analyses and the measurement of U. V. spectra were carried out by Mrs. K. Kodaira of Tohoku University, to whom deep gratitude is hereby expressed.

$A_1$: Found: C, 51.08; H, 2.88. Calcd. for $C_{13}H_9O_2Br$: C, 56.35; H, 3.27%.

$A_2$: Found: C, 44.11; H, 2.33. Calcd. for $C_{13}H_8O_2Br_2$: C, 45.15; H, 2.33%.

The neutral portion, when treated as in i), gave a small amount of the bromo derivatives of 2-phenyltropone whose structures were confirmed by mixed fusion with their authentic samples, respectively.

**Methylation of A.**—i) To a suspension of 1.15 g. of A, m. p. 185~190°C (decomp.) in 10 cc. of ether, ethereal diazomethane was added and the whole was kept standing overnight in a refrigerator. The crystals, m. p. 110~115°C, thereby separated, were collected by filtration and recrystallized from benzene or methanol to give 0.5 g. of VI as yellow needles m. p. 131~132°C.

Found: C, 46.00; H, 2.84. Calcd. for $C_{14}H_{10}O_2Br_2$: C, 45.44; H, 2.74%.

The filtrate was evaporated and the residue, dissolved in a mixture of benzene and petroleum ether, was chromatographed through a silica-gel column. This was eluted successively with benzene-petroleum ether mixture, benzene, and chloroform to give 0.15 g. of VI and 0.05 g. of V.

ii) A mixture of 0.7 g. of $A_1$ and 5 cc. of ether was treated with diazomethane as in i). The raw crystals thereby obtained were recrystallized from benzene or methanol to give 0.2 g. of V, as pale yellow needles, m. p. 173~174°C.

Found: C, 58.53; H, 4.14. Calcd. for $C_{14}H_{11}O_2Br$: C, 58.09; H, 3.81%.

The mother liquor, chromatographed as above, gave 0.1 g. of VI, 0.05 g. of V and a trace of VII as in their respective raw crystals.

iii) A mixture of 0.7 g. of $A_2$ and 5 cc. of ether was treated with diazomethane as above, and 0.3 g. of VI was separated. The chromathographic separation of the mother liquor through a silica-gel column gave 0.03 g. of VII, 0.05. of VI and 0.03 g. of V.

**Acid Hydrolysis of 5-Bromo-4-methoxy-3-phenyltropone (V).**—To a solution of 0.2 g. of V dissolved in 0.6 cc. of concentrated sulfuric acid, 6 cc. of water was added and the mixture was refluxed for 2 hr. After cooling, additional 10 cc. of water was added and the yellow crystals that separated were collected by filtration and washed with hot benzene. Yield 0.23 g. Recrystallization from ethanol gave X as yellow needles, m. p. 210~212°C (decomp.).

Found: C, 56.30; H, 3.40. Calcd. for $C_{13}H_9O_2Br$: C, 56.35; H, 3.27%.

From benzene solution 0.05 g. of V was recovered.

**Acid Hydrolysis of 5, 7-Dibromo-4-methoxy-2-phenyltropone (VI).**—A mixture of 0.37 g. of VI, 2 cc. of concentrated sulfuric acid and 4 cc. of water was refluxed for 30 min. After cooling the whole, the separated crystals were collected by filtration and washed with benzene. Yield 0.32 g. Recrystallization from ethanol gave XV as yellow scales, m. p. 195~198°C. (decomp.).

Found: C, 45.63; H, 2.46. Calcd. for $C_{13}H_8O_2Br_2$: C, 45.15; H, 2.33%.

**Methylation of 7-Bromo-4-hydroxy-2-phenyltropone (X).** — Treatment of X (0.3 g.) with diazomethane in ether followed by the removal of the solvent gave crystalline residue. Recrystallization from benzene gave 0.16 g. of raw crystals of V, m. p. 160~165°C. The mother liquor, after the removal of the solvent, was dissolved in a mixture of benzene and petroleum ether and chromatographed through a silica-gel column. About 0.07 g. of yellow crystals of VII, m. p. 62~65°C and a small amount of V were obtained. Recrystallization of VII from cyclohexane or dilute methanol gave yellow needles, m. p. 73~74°C.

VII: Found: C, 58.09; H, 3.60. Calcd. for $C_{14}H_{11}O_2Br$: C, 58.09; H, 3.81%.

**Methylation of 5,7-Dibromo-4-hydroxy-2-phenyltropone (XV).**—In the usual manner, 0.3 g. of XV was treated with diazomethane in ether. The crystals that separated were recrystallized from benzene or methanol to give 0.18 g. of VI as yellow needles, m. p. 129~130°C and 0.02 g. of VIII as pale yellow plates, m. p. 112~113°C.

VIII: Found: C, 45.51; H, 2.68. Calcd. for $C_{14}H_{10}O_2Br_2$: C, 45.44; H, 2.72%.

Chromatographic separation of the mother liquor through a silica-gel column gave additional 0.03 g. of VIII and a trace of VI.

**Reaction of 7-Bromo-4-methoxy-2-phenyltropone (VII) and Sodium Methoxide.**—To a solution of 0.04 g. of metallic sodium in 4 cc. of absolute methanol, 0.2 g. of VII was added and the solution was refluxed over a period of 20 hr. on an oil bath. After removal of the solvent, 5 cc. of water was added, and the solution was refluxed for an additional period of 3 hr. The solution was shaken with chloroform to remove the neutral portions and the water layer was acidified with dilute sulfuric acid. The acidic product that separated was extracted with chloroform. After removal of the solvent, the crystalline residue was recrystallized from cyclohexane to give 0.03 g. of XI as yellow crystals, m. p. 95~100°C. This was dissolved in 0.5 cc. of concentrated sulfuric acid and heated on a water bath for several min. After cooling, the solution was diluted with water and extracted with benzene. The benzene extract, after being washed with dilute sodium hydroxide solution, was evaporated and the residue was recrystallized from cyclohexane to give yellow needles, m. p. 95~97°C. This was proved to be identical by mixed fusion with the authentic sample of 3-methoxyfluorenone (XI).

**Reaction of 5, 7-Dibromo-4-methoxy-2-phenyltropone (VI) and Alkali.**—A mixture of 0.12 g. of VI, 3 cc. of ethanol and 1 cc. of 2 N sodium hydroxide was refluxed for 30 min. After removal of ethanol, the residue was acidified and extracted with benzene. Benzene extract gave 0.06 g. of pale yellow crystals which were digested, with a small amount of yellowish brown crystals, m. p. 185~193°C (decomp.). This was proved to be XV from its analytical value.

Found: C, 43.88; H, 2.20. Calcd. for $C_{13}H_8O_2Br_2$; C, 45.15; H, 2.33%.

The benzene solution was passed through a short silica-gel column to give 0.03 g. of raw crystals of m. p. 140~155°C. Recrystallization from dilute methanol gave XVI as colorless needles, m. p. 168~169°C.

Found: C, 54.51; H, 3.46. Calcd. for $C_{14}H_{11}O_3Br$: C, 54.75; H, 3.61%.

When XVI was heated with concentrated sulfuric

acid on a water bath for several minutes and then diluted with water, there were obtained yellow crystals of m. p. 235~237°C.

Found: C, 57.52; H, 3.04. Calcd. for $C_{14}H_9O_2Br$; C, 58.16; H, 3.14%.

**Reaction of 5, 7-Dibromo-4-methoxy-3-phenyltropone (VIII) and Alkali.**—A mixture of 0.06 g. of VIII, 3 cc. of methanol and 10 cc. of 2 N sodium hydroxide was refluxed on a water bath for 30 min. After treated as in the case of VII, 0.05 g. of raw crystals of m. p. 175~180°C were obtained. Recrystallization from methanol gave XVIII as colorless needles of m. p. 187~188°C.

Found: C, 55.28; H, 3.60. Calcd. for $C_{14}H_{11}O_3Br$: C, 54.75; H, 3.61%.

Debromination of 0.03 g. of XVIII dissolved in 3 cc. of methanol, in the presence of palladium carbon catalyst and sodium acetate, gave 0.02 g. of colorless crystals m. p. 190~200°C. This was recrystallized from methanol to give colorless needles of m. p. 210~211°C, which was proved to be identical with the authentic sample of XIX obtained from V.

**Reaction of 5-Bromo-4-methoxy-3-phenyltropone (V) and Alkali.**—A mixture of 0.14 g. of V, 2.5 cc. of ethanol and 0.8 cc. of 2 N sodium hydroxide was refluxed for 30 min. After treated as in the above cases, 0.12 g. of pale yellow acidic crystals were obtained. This was digested with hot benzene to give a minute amount of yellow crystals of m. p. 205~208°C (decomp.). Which was proved to be identical with X from its analytical value and ultraviolet spectrum.

Found: C, 56.28; H, 3.34. Calcd. for $C_{13}H_9O_2Br$: C, 56.35; 3.27%.

From the benzene solution, colorless needles of m. p. 207~209°C were obtained. This was proved to be identical with the sample of XIX obtained from 4-methoxybenzoic acid (XX).

Found: C, 73.97; H, 5.04. Calcd. for $C_{14}H_{12}O_3$: C, 73.67; H, 5.30%.

**Reduction of 7-Bromo-4-methoxy-2-phenyltropone (VII).**—Catalytic reduction of 0.11 g. of VII dissolved in 3 cc. of ethanol, in the presence of 0.02 g. of sodium acetate and 0.02 g. of palladium carbon, resulted in absorption of hydrogen at room temperature. After removal of the catalyst by filtration, the filtrate was diluted with water and extracted with benzene. This extract, evaporated under reduced pressure, gave crystalline residue which was recrystallized from cyclohexane to give XIII as pale yellow needles m. p. 91~92°C.

Found: C, 79.63; H, 5.80. Calcd. for $C_{14}H_{12}O_2$: C, 79.22; H, 5.70%.

**Reduction of 5, 7-Dibromo-4-methoxy-2-phenyltropone (VI).**—Catalytic reduction of 0.1 g. of VI, as in the case of VII, gave 0.02 g. of XIII.

**Reduction of 5-Bromo-4-methoxy-3-phenyltropone (V).**—Catalytic reduction of 0.1 g. of V dissolved in 40 cc. of ethanol, in the presence of 0.1 g. of palladium carbon and 0.1 g. of sodium acetate, resulted in absorption of hydrogen at room temperature. After removal of the catalyst and the solvent, the residue was diluted with water and extracted with benzene. This solution, passed through a silica-gel column, gave raw crystals of m. p. 70~74°C. Recrystallization from cyclohexane gave XIV, as pale yellow prisms, m. p. 75~76°C.

Found: C, 78.31; H, 5.81. Calcd. for $C_{14}H_{12}O_2$: C, 79.22; H, 5.70%.

**Synthesis of 4-Methoxy-3-phenylbenzoic Acid (XIX).**—4-Methoxy-3-nitrobenzoic acid (XXI)[10], m. p. 191~192°C, was obtained by the nitration of 4-methoxybenzoic acid (XX) in a mixture of acetic acid and acetic anhydride with concentrated nitric acid.

The methylation of XXI with methanol and concentrated sulfuric acid gave methyl-4-methoxy-3-nitrobenzoate (XXII)[11] m. p. 110~111°C in a good yield. Catalytic reduction of XXII in ethyl acetate in the presence of Raney nickel catalyst (W-5), gave methyl-3-amino-4-methoxy benzoate (XXIII)[12], m. p. 83~85°C.

A solution of 0.7 g. of acetic anhydride and 3 cc. of acetic acid was heated for 30 min. To the cold reaction mixture, nitrous fume generated by the action of concentrated nitric acid to solid sodium nitrate, was passed in for a period of 1 hr. at about 5°C. When diluted with water, the reaction mixture separated a yellow oily product, which was extracted with benzene. After washed with water and dried over anhydrous sodium sulfate, the benzene solution was poured on a mixture of 0.7 g. of anhydrous sodium carbonate and 0.7 g. of anhydrous sodium sulfate. The whole was stirred for a period of 5 hr. and then kept to stand for 2 days. After removal of solid materials, the filtrate was evaporated to give 0.6 g. of an oily product. This was distilled under reduced pressure and about 0.2 g. of yellow crystalline oil was obtained. Recrystallization from ether and methanol gave methyl 4-methoxy-3-phenylbenzoate (XXV) as colorless prisms, m. p. 88~89°C. Hydrolysis of XXV gave XIX as colorless needles of m. p. 115~117°C which was proved to be identical by mixed fusion with the sample obtained from V or VII. Methylation of 0.04 g. of XIX with diazomethane gave about 0.03 g. of XXV.

The author takes this opportunity to express his sincere gratitude to Professor Tetsuo Nozoe of Tohoku University for his guidance and encouragement throughout the course of this work, to Professor Shuichi Seto, Professor Yoshio Kitahara of Tohoku University and to Assistant Professor Katsuo Kikuchi of Yamagata University for their very helpful and kind discussions.

*Department of Chemistry*
*Faculty of Liberal Arts and Science*
*Yamagata University*
*Koshirakawa-machi, Yamagata*

10) *Beilsteins Handbuch. Org. Chem.*, **10**, 181.
11) ibid., **10**, 182.
12) ibid., **14**, 594.

# *A Study on Anion Exchange aud Amine Extraction of Rare Earth Elements in Nitric Acid*

By Fujio ICHIKAWA

(Received April 28, 1960)

The use of amine extraction for uranium, thorium and many other elements has recently been developed by a number of investigators[1-7]. It is reported that the mechanism of amine extraction is similar to that of anion exchange and the former is called commercially liquid anion exchanger. The author previously reported[8] the amine extraction and anion exchange of uranium, protactinium and thorium in nitric, hydrochloric and sulfuric acid. Peppard, Mckay and their coworkers[9-12] reported on the extraction of rare earth nitrates with tri-*n*-butyl phosphate.

In the present paper, the distribution coefficients of rare earth elements between anion exchange resin and nitric acid are compared with those between amine and nitric acid. Based on the resuls from these distribution studies, the mechanism of amine extraction is discussed.

## Experimental

**Materials.**—Dowex 1, X8 (100~200 mesh), converted into nitrate form by nitric acid, is used as an anion exchange resin. Primene JM-T, Amberlite LA-2 and tri-*n*-octyl amine are respectively used as primary, secondary and tertiary amine. Amines are diluted with kerosene, and octyl alcohol is added to this solution to avoid the third phase formation, making phase separation clear. These amine solutions are converted into the nitrate form with 8 N nitric acid, as shown in the following equation.

$$RR'NH + HNO_3 \rightleftarrows RR'NH_2NO_3$$

Promethium-147 is used as a tracer of Pm. Other radioactive tracers of rare earth elements are prepared by neutron irradiation of rare earth oxides in J. R. R.-1 Reactor or by separation from isotopes of alkaline earth elements which are in a state of equilibrium with their daughter nuclides. The irradiated oxides are dissolved in 8 N nitric acid. The $\gamma$-ray spectrograms of these samples are obtained with a single channel pulse height analyzer and the radioactivities of these samples are measured by $\gamma$-ray or $\beta$-ray counting.

Table I shows the radioisotopes used in this experiment and the method for radioactivity measurement.

TABLE I. RADIOISOTOPES OF RARE EARTH ELEMENTS

| Nuclide | Preparation | Counting method |
|---|---|---|
| $^{140}$La | Imported $^{140}$Ba→$^{140}$La, coprecipitation with $Fe(OH)_3$, extraction of Fe by Amberlite LA-1 from 6 N HCl | $\gamma$ |
| $^{141}$Ce | $(n, \gamma)$ | $\gamma$ |
| $^{142}$Pr | $(n, \gamma)$ | $\beta$ |
| $^{147}$Nd | $(n, \gamma)$ | $\gamma$ at 0.092 MeV. of $^{147}$Nd |
| $^{147}$Pm | imported | $\beta$ |
| $^{152}$Eu+$^{154}$Eu | $(n, \gamma)$ | $\gamma$ |
| $^{159}$Gd | $(n, \gamma)$ | $\gamma$ at 0.364 MeV. of $^{159}$Gd |
| $^{160}$Tb | $(n, \gamma)$ | $\gamma$ |
| $^{165}$Dy | $(n, \gamma)$ | $\gamma$ |
| $^{166}$Ho | $(n, \gamma)$ | $\gamma$ |
| $^{170}$Tm | $(n, \gamma)$ | $\gamma$ |
| $^{175}$Yb | $(n, \gamma)$ | $\gamma$ at 0.396 MeV. of $^{175}$Yb |
| $^{176m}$Lu+$^{177}$Lu | $(n, \gamma)$ | $\gamma$ |

Sm and Er are omitted from this experiment because their $\gamma$-ray spectra resemble those of the daughters'.

**Procedure.**—The distribution coefficients in both anion exchange and amine extraction are measured by the batch method. Half a gram of dried resin is immersed in 5 ml. of nitric acid solution of rare earth elements and then shaken for 20 hr. at a constant temperature so that a state of equilibrium is attained. Then the sample is filtered and the activity of 1 ml. of the filtrate is compared with that of a reference solution.

In the case of the amine extraction, 2 ml. of 30% kerosene solution of amine is shaken for 1 min. with 2 ml. of nitric acid solution of rare earth element. Then resulting solution is then centrifuged and two phases are separated. The activity of both organic and aqueous solutions are measured. The distribution coefficient is calculated from the data which are obtained in these experiments.

1) D. J. Crouse et al., ORNL-2099 (1956).
2) J. C. Sheppard, HW-51958 (1957).
3) C. F. Coleman et al., A/Conf. 15/p/510 (1958).
4) K. B. Brown et al., ORNL-2269 (1957).
5) A. Preuss and J. Saunders, RMO-2533 (1955).
6) A. S. Wilson, A/Conf. 15/p/544 (1958).
7) D. J. Crouse and J. O. Denis, ORNL-1859 (1955).
8) F. Ichikawa and S. Uruno, This Bulletin, 33, 569 (1960).
9) D. P. Peppard et al., *J. Phys. Chem.*, 57, 294 (1953).
10) D. F. Peppard et al., *J. Am. Chem. Soc.*, 75, 6063 (1953).
11) H. A. C. Mckay et al., *J. Inorg. Nucl. Chem.*, 4, 304 (1957).
12) H. A. C. Mckay et al., idid., 9, 279 (1959).

## Results

Distribution coefficients ($K_d$) of lanthanum, promethium and holmium are measured for the nitric acid solution of various concentrations.

Results are shown in Figs. 1—4. In the concentration range from 1 to 8 N nitric acid, the $K_d$ value of anion exchange increases slowly and then decreases in acidities over 8 N. The distribution coefficients in primary amine extraction increases with the increase in the concentration of nitric acid. As is shown in Fig. 1, the maximum value of $K_d$ decreases with increasing atomic number. In order to confirm this trend, values of $K_d$ for rare earth elements in 8 N nitric acid is determined at 20°C. Fig. 5 shows the result of this experiment. For rare earth elements from lanthanum to gadolinium the $K_d$ value decreases with increasing atomic number. The difference in the $K_d$ value for rare earth elements of higher atomic number is very small and the relation between the $K_d$ value and the atomic number is complicated.

In the case of amine extraction, the $K_d$ values for rare earth elements are very small. Results are shown in Figs. 6—8. $K_d$ decreases slowly from lanthanum to dysprosium in

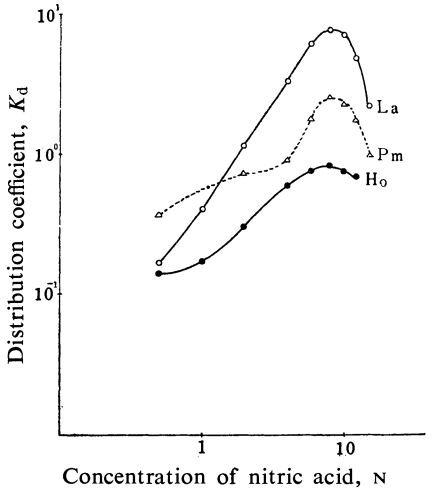



Fig. 1. Distribution coefficients of La, Pm and Ho between Dowex 1 and nitric acid.

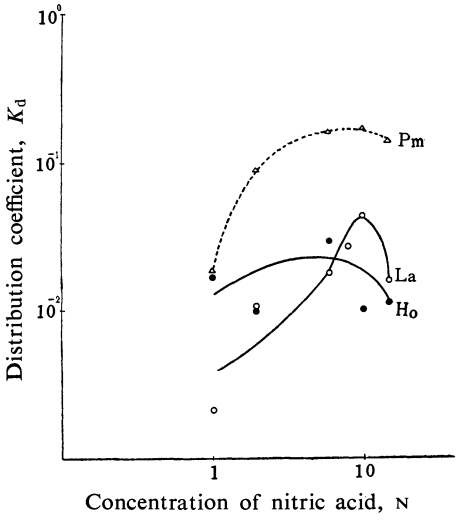



Fig. 3. Distribution coefficients of La, Pm and Ho between 30% Amberlite LA-2 and nitric acid.

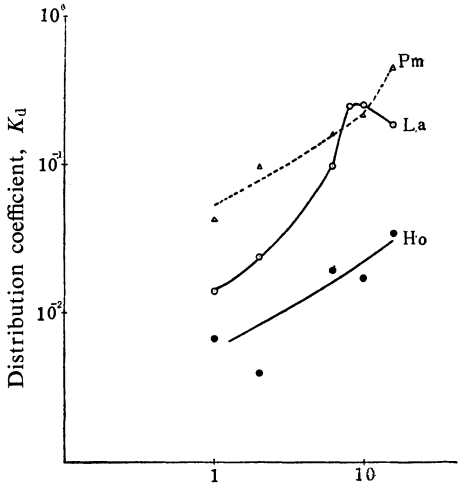



Fig. 2. Distribution coefficients of La, Pm and Ho between 30% Primene JM-T and nitric acid.

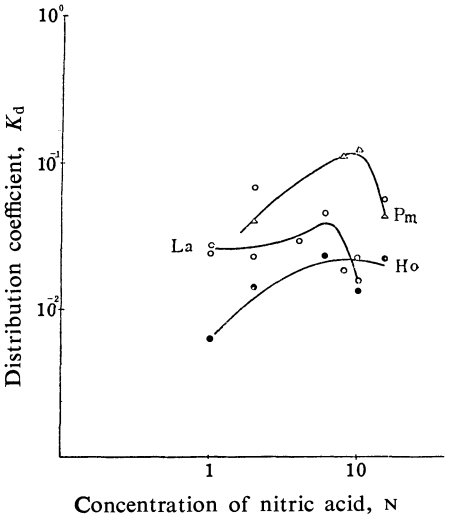



Fig. 4. Distribution coefficients of La, Pm and Ho between 30% tri-*n*-octyl amine and nitric acid.

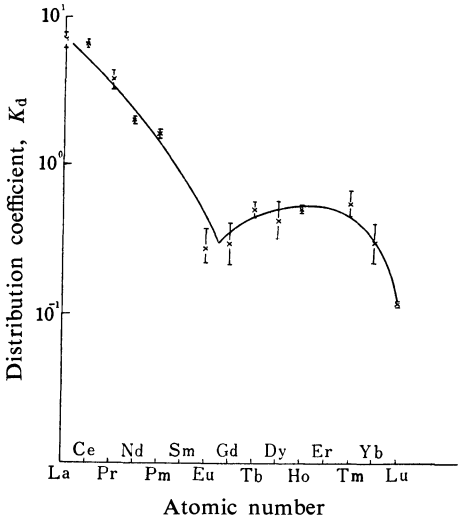



Fig. 5. Distribution coefficients of rare earth elements between Dowex 1 and 8 N nitric acid.

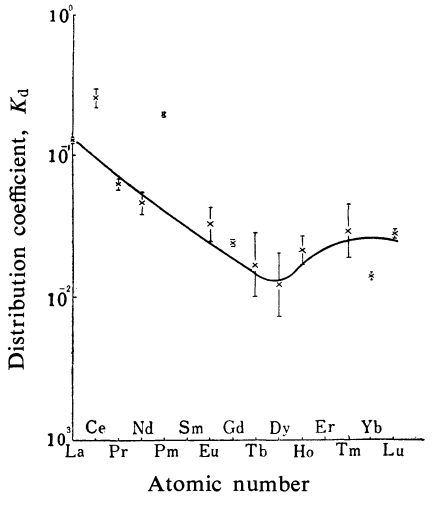



Fig. 6. Distribution coefficients of rare earth elements between 30% Primene JM-T and 8 N nitric acid.

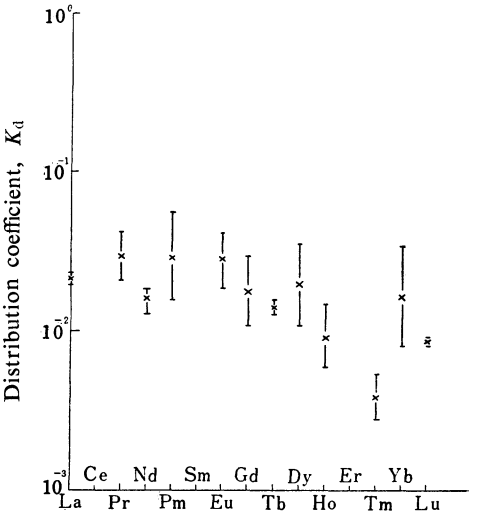



Fig. 7. Distribution coefficients of rare earth elements between 30% Amberlite LA-2 and 8 N nitric acid.

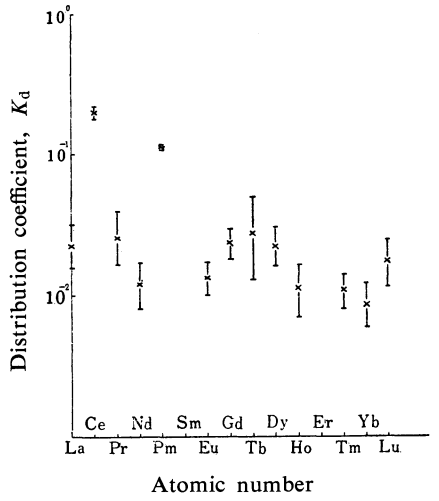



Fig. 8. Distribution coefficients of rare earth elements between 30% tri-*n*-octyl amine and 8 N nitric acid.

primary amine extraction. From holmium to lutetium, the difference in $K_d$ value is very small. This is a tendency similar to that observed in anion exchange. As to the secondary amine extraction, a small decrease in $K_d$ is found. But no significant variation in $K_d$ is observed in tertiary amine extraction.

To compare these results, the extraction of rare earth elements by 100% TBP from 8 N nitric acid solution is studied. Fig. 9 shows the result. $K_d$ value increases with increasing atomic number and this result is very different from those in anion exchange or amine extraction.

## Discussion

Peppard and his coworkers[9,10] found the tendency of the increase in the extractability of rare earth nitrates by TBP with increasing atomic number. Mckay and his coworkers[11,12] reported that this trend is not always found in the subgroup from Gd to Lu. In the present experiment, the extractability of rare earth elements by 100% TBP from 8 N nitric acid solution also increased with increasing atomic number and some difference is found between lower and higher subgroups.

On the contrary, anion exchange study shows

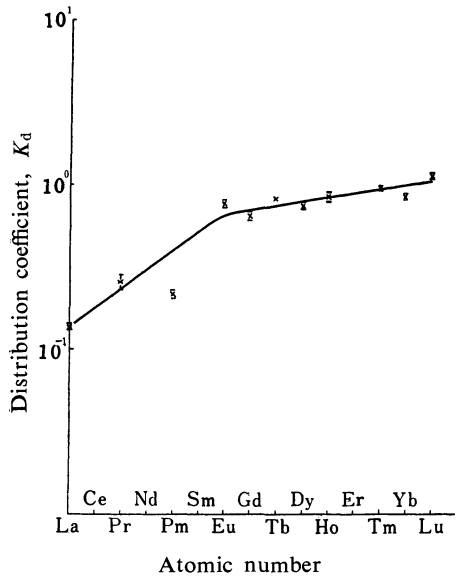



Fig. 9. Distribution coefficients of rare earth elements between 100% TBP and 8 N nitric acid.

decreasing of $K_d$ value with increasing atomic number for rare earth elements of lower subgroup.

The different behavior of these two subgroups is probably due to the ionic radius, electronic structure and other characters. The reverse trend observed in TBP extraction and anion exchange might be due to the different probability of neutral complex formation and anionic complex formation in each circumstance.

From these points of view, the amine extraction behavior of these elements is very interesting. As is shown in Figs. 6—8, the difference in $K_d$ value between rare earth elements of lower and higher atomic number is greater in the case of primary amine extraction than in secondary amine extraction. But, in both cases, decrease in $K_d$ value with increasing atomic number is observed. It is suggested from these facts that the mechanism of amine extraction of rare earth elements resembles more the mechanism of anion exchange than TBP extraction does.

## Summary

The amine extraction of rare earth elements in nitric acid is compared with anion exchange and TBP extraction with respect to the increase or decrease in $K_d$ value with increasing atomic number of rare earth elements.

Concerning the relationship between distribution coefficient and atomic number of rare earth element, a similar trend is observed in anion exchange and amine extraction. The distribution coefficient decreases with increase in the atomic number. In TBP extraction, however, the corresponding value increases with increasing atomic number. It seems that the mechanism of amine extraction for rare earth element is similar to that of anion exchange.

The author expresses his gratitude to Dr. T. Nakai for his encouragement in this work. He also wishes to thank Miss. S. Uruno for assistance with experimental work.

*Japan Atomic Energy Research Institute*
*Tokai, Ibaraki-ken*

# *Vinyl Polymerization. XLVIII.* Polymerization of Methylstyrenes and the Effect of Dimethylaniline on their Polymerization*

By Minoru IMOTO, Kiichi TAKEMOTO and Yuichi IIKUBO

(Received July 22, 1960)

Previously we have carried out polymerization of styrene and *p*-methylstyrene initiated by the azobisisobutyronitrile (ABIN)-dimethylaniline (DMA) system. Consequently a peculiar effect was observed in the polymerization of *p*-methylstyrene[1]. In this paper, the polymerization of *p*-methylstyrene with the ABIN-DMA system was studied repeatedly, and some different conclusions were obtained. The value of $k_1$ in this system was also measured by the ferric chloride method of Bamford et al.[2]

* XLVII of this series: M. Imoto and I. Soematsu, in contribution.

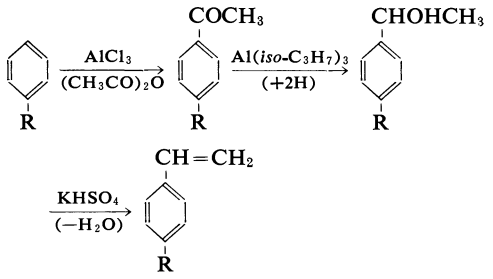
1) M. Imoto and K. Takemoto, *J. Polymer Sci.*, **19**, 205 (1956).

2) J. C. Bamford, A. D. Jenkins and R. Johnston, *Proc. Roy. Soc.*, **A241**, 364 (1957).

As the polymerization of other monomethyl- and dimethylstyrenes has been little investigated, it was interesting to carry out the polymerization of these monomers. The polymerization with ABIN was studied in benzene, and rates of polymerization and intrinsic viscosities were determined.

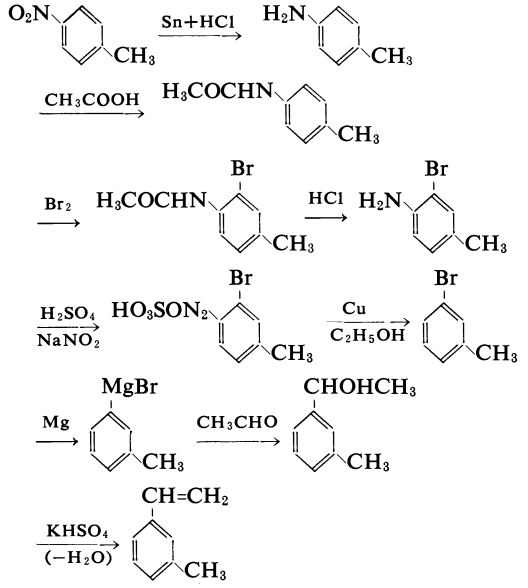
## Experimental

**Syntheses of Monomers.**—*Syntheses of p-Alkylstyrenes.*—*p*-Methyl-, *p*-ethyl- and *p-tert*-butylstyrene were synthesized from corresponding alkylbenzenes, according to the following sequence of reactions[3]:




(R : $CH_3$, $C_2H_5$, *tert*-$C_4H_9$)

*Synthesis of m-Methylstyrene.*—*m*-Methylstyrene was synthesized from *p*-nitrotoluene as follows[4]:




*Syntheses of Dimethylstyrenes.*—2,4-Dimethyl-, 2,5-dimethyl- and 3,4-dimethylstyrene were synthesized from corresponding xylenes in a manner similar to that used in the case of *p*-alkylstyrenes[5].

The Meerwein-Ponndorf reduction of the substituted acetophenones was found to be unsuccessful in the case of 3,4-dimethyl derivative. By the direct hydrogenation in autoclave, using copper-chromium oxide or Raney nickel as catalyst, 3,4-dimethylphenylcarbinol was obtained with yield of 90%.

*Purification of Monomers.*—All monomers were purified by distillation in vacuo under flushing of nitrogen after drying over calcium chloride. Before use, they were distilled again through a 40 cm. Stedman column. Reflux ratios were 10 : 1∼6 : 1. Physical constants of the monomers were shown in Table I. Infrared spectroscopic analyses were also made for all the monomers to ascertain their structures.

Styrene was purified by distillation in the same manner as the substituted styrenes (b. p. 145°C/760 mmHg).

**Purification of Reagents.**—2,2'-Azobisisobutyronitrile (ABIN) was purified by recrystallization from methanol and dried in vacuo (m. p. 103°C). Dimethylaniline (DMA) was distilled in a nitrogen atmosphere and stored. Before use, it was again distilled under reduced pressure through a Vigreux column (b. p. 68°C/10 mmHg). Benzene was distilled, after thiophene was removed, dried over calcium chloride and again distilled over metallic sodium (b. p. 80°C). Ferric chloride ($FeCl_3 \cdot 6H_2O$), commercial pure grade, was used after crushing. Benzoquinone was synthesized from hydroquinone by oxidation with sodium dichromate and purified by sublimation under reduced pressure twice before use (m. p. 113∼114°C). Nitrogen was purified by washing through alkaline pyrogallol solution and concentrated sulfuric acid and by passing over reduced copper at 550°C.

**Procedures.**—*Measurement of Rate of Polymerization.*—In order to determine the initial rate of polymerization, the dilatometric and usual sealed tube methods were adopted. In some experiments, the dilatometer reported earlier[6] was used. In another case, a dilatometer in a different form was used, the total capacity being about 4.5∼5.5 ml. and the diameter of the capillary tube about 0.3∼0.5 mm.

Polymerization was carried out as described in the previous paper. The polymerization temperature was regulated within ±0.02°C in the case of dilatometry, and ±0.05°C in the case of the sealed tube method.

*Measurement of Intrinsic Viscosity.*—Intrinsic viscosities [$\eta$] of polymers were measured in benzene solution at 30±0.1°C, using Ostwald's viscometer. Assuming that the following equation given by Tobolsky et al.[7] for polystyrene can also be available for substituted polystyrenes, the number-average polymerization degree $\bar{P}_n$ of all polymers was computed.

$$\bar{P}_n = 1770[\eta]^{1.40}$$

*Measurement of Rate of Decomposition of ABIN.*—The rate of decomposition of ABIN was measured, with the volume of nitrogen evolved[8].

3) C. G. Overberger, C. Frazier, J. Mandelman and H. G. Smith, *J. Am. Chem. Soc.*, **75**, 3326 (1951).
4) C. S. Marvel, C. G. Overberger, R. E. Allen and J. H. Saunders, ibid., **68**, 736 (1946).
5) C. S. Marvel, J. H. Saunders and C. G. Overberger, ibid., **68**, 1085 (1946).
6) M. Imoto and K. Takemoto, *J. Polymer Sci.*, **18**, 377 (1955).
7) D. H. Johnson and A. V. Tobolsky, *J. Am. Chem. Soc.*, **74**, 938 (1952).
8) M. Imoto, T. Otsu, T. Ota, H. Takatsugi and M. Matsuda, *J. Polymer Sci.*, **22**, 137 (1956).

TABLE I. PHYSICAL PROPERTIES OF SUBSTITUTED STYRENES

| Styrene | B. p., °C (mmHg) | S. g. | Refractive index |
|---|---|---|---|
| *p*-Methylstyrene | 58 ( 7) | $d_4^{25}=0.890$ | $n^{25}=1.5393$ |
| *p*-Ethylstyrene | 68 (10) | $d_4^{20}=0.9070$ | $n^{25}=1.5349$ |
| *p-tert*-Butylstyrene | 90~92 (10) | $d_4^{23}=0.8739$ | $n^{20}=1.5212$ |
| *m*-Methylstyrene | 90~91 (30) | $d_{25}^{25}=0.9032$ | $n^{24.5}=1.5392$ |
| 2,4-Dimethylstyrene | 90 (25) | $d_{25}^{25}=0.9048$ | $n^{20.5}=1.5425$ |
| 2,5-Dimethylstyrene | 81~83 (23) | $d_{25}^{25}=0.9050$ | $n^{20}=1.5389$ |
| 3,4-Dimethylstyrene | 86~88 (20) | $d_{25}^{25}=0.9200$ | $n^{20}=1.5420$ |

TABLE II. RATES OF POLYMERIZATION AND DEGREES OF POLYMERIZATION FOR SUBSTITUTED STYRENES

| Monomer | Rate of polymerization: Sealed tube method, 50°C (mol./l. sec.) | Rate of polymerization: Dilatometry, 70°C (mol./l. sec.) | Degree of polymerization $\bar{P}_n$ |
|---|---|---|---|
| Styrene | $11.13\times10^{-6}$ | $5.10\times10^{-6}$ | 700 |
| *p*-Methylstyrene | 14.30 | 5.32 | 190 |
| *p*-Ethylstyrene | — | 2.13 | — |
| *p-tert*-Butylstyrene | — | 1.73 | — |
| *m*-Methylstyrene | 4.20 | — | 280 |
| 2,4-Dimethylstyrene | 6.52 | — | 150 |
| 2,5-Dimethylstyrene | 6.86 | — | 300 |
| 3,4-Dimethylstyrene | 10.96 | — | 490 |

* Monomer concentration=3.43 mol./l., ABIN concentration=$1.097\times10^{-2}$ mol./l.
** Monomer concentration=0.455 mol./l., ABIN concentration=$2.50\times10^{-3}$ mol./l.

## Results

**Polymerization of Substituted Styrenes.**—*Polymerization of p-Alkyl- and Dimethylstyrenes.*— Polymerizations of styrene, *p*-methyl-, *p*-ethyl- and *p-tert*-butylstyrene were carried out dilatometrically in benzene at 70°C. The linear time-conversion relationship was obtained for all runs. Polymerization of *m*-methyl-, 2,4-dimethyl-, 2,5-dimethyl and 3,4-dimethylstyrene were also carried out in benzene at 50°C by the sealed tube method. Time-conversion curves were shown in Fig. 1 (including the curves of styrene and *p*-methylstyrene), where the concentrations of monomer and initiator were kept constant at 3.43, and $1.097\times10^{-2}$ mol./l., respectively. The linear time-conversion curves were also obtained. The rate for *p*-methylstyrene was greater than that for styrene. The rates for other monomers were smaller than that for styrene.

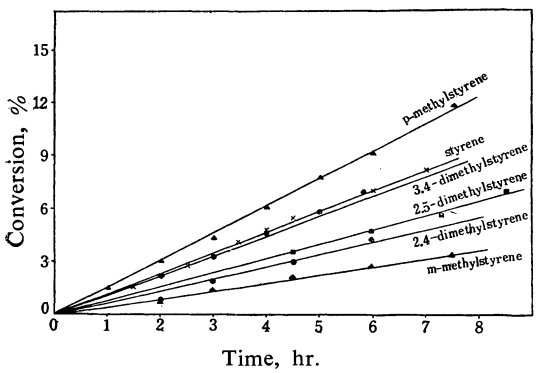


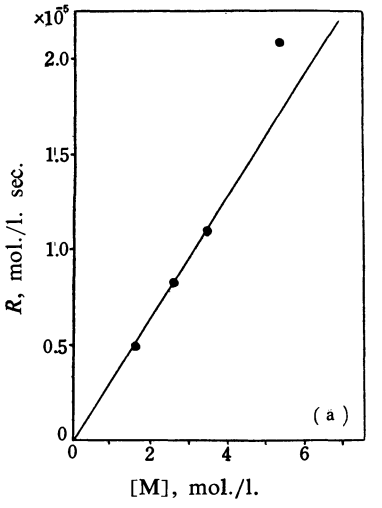

Fig. 1. Time-conversion curves for polymerization of substituted styrenes initiated by ABIN (sealed tube, in benzene, 50°C).
[M]=3.43 mol./l.
[ABIN]=$1,097\times10^{-2}$ mol./l.
50°C, in benzene

The values of the rate of polymerization obtained were tabulated in Table II. The table includes also the values of degree of polymerization. The polymers used for the determination of $[\eta]$ were obtained by 4.5 hr. polymerization.

Comparing the values of $\bar{P}_n$ and *Rp* of *p*-methylstyrene with these of styrene, it was assumed that *p*-methylstyrene easily underwent chain transfer reaction. This was because in spite of the larger value of *Rp*, the degree of polymerisation was smaller. In order to study the effect of solvents on reaction, polymerization of *p*-methylstyrene was carried out in acetone or dimethylformamide (DMF) in the same manner as in benzene. As shown in Table III, the rates of polymerization in acetone were nearly the same as that in benzene. But the value obtained in DMF was relatively low. Separation of the polymer from benzene or DMF solution was easy, because the polymer separated granulously when the reaction mixture was poured into an excess of methanol.

TABLE III. OVERALL RATES OF POLYMERIZATION OF *p*-METHYLSTYRENE IN SOME SOLVENTS (DILATOMETRY, 60°C)

| Exp. run | Solvent | Rate of polymerization mol./l. sec. |
|---|---|---|
| 1 | Dimethylformamide | $2.13\times10^{-5}$ |
| 2 | 〃 | 2.08 |
| 3 | Benzene | 2.47 |
| 4 | 〃 | 2.46 |
| 5 | 〃 | 2.56 |
| 6 | Acetone | 2.46 |
| 7 | 〃 | 2.47 |



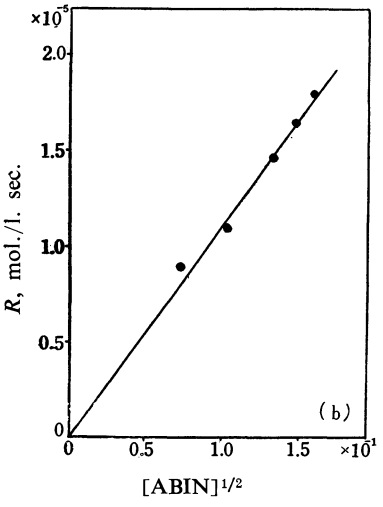




Fig. 2. Polymerization of 3,4-dimethylstyrene initiated by ABIN (sealed tube, in benzene, 50°C).
(a) Relationship of the initial rate of polymerization with the monomer concentration. ([ABIN] = $1.098\times10^{-2}$ mol./l.)
(b) Relationship of the initial rate of polymerization with the initiator concentration. ([M] = 3.49 mol./l.)

However, when acetone was used, a turbid emulsion was obtained and the separation by filtration was much more difficult.

**Rate Equation of Polymerization for Substituted Styrene.**—From the results of 3,4-dimethylstyrene as shown in Fig. 2, the following equation was derived. This was identical with that for styrene.

$$R_0 = k\,[\mathrm{M}]\,[\mathrm{ABIN}]^{1/2}$$

**Determination of Rate Constants for Initiation.**—The rate constants of initiation of the polymerization of styrene and *p*-methylstyrene were determined, according to the $FeCl_3$-method by Bamford et al.[2], using the following equation.

$$\tau = \frac{[FeCl_3\cdot 6H_2O]}{2f\cdot k_d\,[\mathrm{ABIN}]} = \frac{[FeCl_3\cdot 6H_2O]}{2k_i\,[\mathrm{ABIN}]}$$

where $\tau$ is the induction period (in minutes), $f$ the initiator efficiency, and $k_d$ and $k_i$ the rate constants for decomposition of initiator and for initiation, respectively. The measurement of the value of $\tau$ for *p*-methylstyrene was carried out in DMF at 60°C.

In Fig. 3, examples of the time-conversion curve were illustrated. In Fig. 4, the relationship between the induction period and the amount of ferric chloride was shown. In Fig. 5, the relationship between the concentration of ABIN and the reciprocal of induction period was shown. The rate constants of initiation

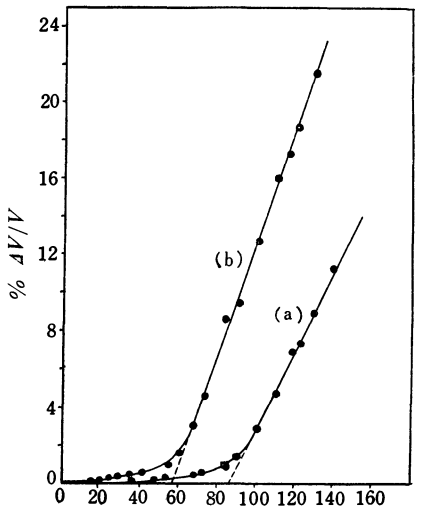



Fig. 3. Time-conversion curve for polymerization of *p*-methylstyrene initiated by ABIN in the presence of ferric chloride (in DMF, 60°C).
[M] = 2.17 mol./l.
[$FeCl_3\cdot 6H_2O$] = $4.46\times10^{-3}$ mol./l.
(a) [ABIN] = $6.12\times10^{-2}$ mol./l.
(b) [ABIN] = $1.00\times10^{-1}$ mol./l.

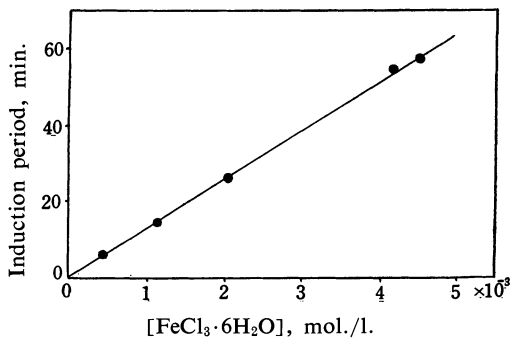



Fig. 4. Relationship between the induction period and the amount of ferric chloride in the polymerization of *p*-methylstyrene (in DMF, 60°C). [M]=2.17 mol./l., [ABIN]=$1.00\times10^{-1}$ mol./l.

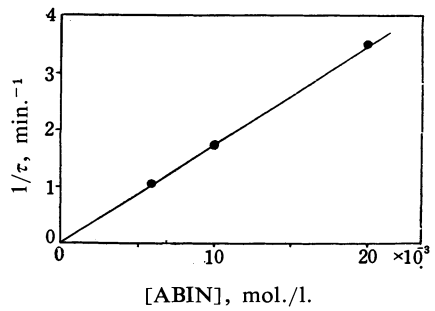



Fig. 5. Relationship between the induction period and the amount of ABIN in the polymerization of *p*-methylstyrene (in DMF, 60°C). [M]=2.17 mol./l., [$FeCl_3\cdot6H_2O$]=$4.46\times10^{-3}$ mol./l.

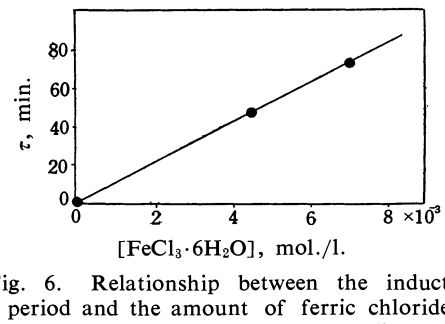



Fig. 6. Relationship between the induction period and the amount of ferric chloride in the polymerization of styrene (in DMF, 60°C). [M]=2.04 mol./l., [ABIN]=$1.00\times10^{-1}$ mol./l.

for the polymerization of *p*-methylstyrene were estimated as follows:

$$k_1=0.67\times10^{-5}\ (\mathrm{sec}^{-1})$$

Similar determination was also made for styrene in DMF at 60°C, and the result obtained was shown in Fig. 6. The value of $k_1$ was as follows:

$$k_1=0.76\times10^{-5}\ (\mathrm{sec}^{-1})$$

This value was in good agreement with the value, $k_1=0.70\times10^{-5}$ ($\mathrm{sec}^{-1}$), obtained by Bamford et al. From the agreement of our value with that by Bamford et al., the value of $k_1$ for *p*-methylstyrene seemed to be reasonable.

As for $k_1$, the value for *p*-methylstyrene was found to be rather smaller than that for styrene. As shown in the former section of this paper, however, the overall rate of the polymerization of *p*-methylstyrene was greater than that of styrene. These results imply that in the sase of *p*-methylstyrene the rate constant for the propagation would be greater than that for styrene, or, that the rate constant of the termination $k_t$ would be smaller. Further work will be done to clarify this point.

**Polymerization of Substituted Styrene in the Presence of Dimethylaniline.—Polymerization of Styrene and *p*-Methylstyrene.**—*a) Polymerization with $Bz_2O_2$-DMA.*—Polymerization of *p*-methylstyrene was carried out dilatometrically at 70°C, using a system of benzoyl peroxide ($Bz_2O_2$)-dimethylaniline (DMA) as initiator. Time-conversion curves were shown in Fig. 7, where the concentrations of monomer and $Bz_2O_2$ were kept constant at 0.455 and $2.50\times10^{-3}$ mol./l., respectively, and the concentration of DMA was varied from 0 to 0.02 mol./l. Fig. 8 shows the results obtained, where the concentration of monomer and DMA were kept constant at 0.455 and $2.50\times10^{-3}$ mol./l., respectively, and the concentration of $Bz_2O_2$ was varied from 0 to 0.085 mol./l. The initial rates of polymerization were determined by the extrapolation method previously reported[5].

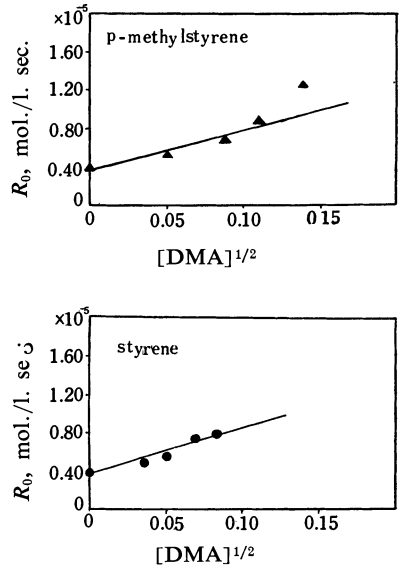



Fig. 7. Polymerization of styrene and *p*-methylstyrene initiated by $Bz_2O_2$ at 70°C (dilatometry).

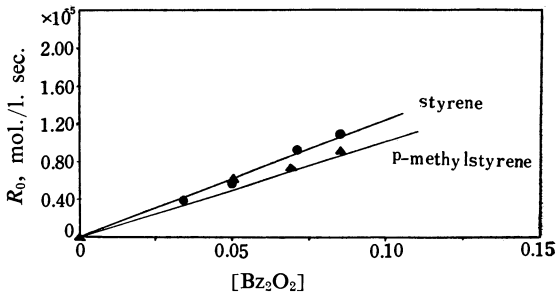



Fig. 8. Polymerization of styrene and *p*-methylstyrene initiated by $Bz_2O_2$ at 70°C (dilatometry).

The polymerization of styrene was carried out in parallel.

It was found that in the polymerization of *p*-methylstyrene, the initial rate of polymerization was also regarded as of 1/2-order with the concentrations of $Bz_2O_2$ and DMA, respectively.

$$R_0 = k'[Bz_2O_2]^{1/2}[DMA]^{1/2}$$

This agrees well with the results reported for the polymerization of several vinyl monomers[9].

*b) Polymerization with ABIN-DMA.*—Polymerizations of styrene and *p*-methylstyrene were carried out dilatometrically at 70°C by the ABIN-DMA system. Keeping the concentrations of monomer and ABIN constant at 0.455 and $2.50\times10^{-3}$ mol./l., respectively, and varying the concentration of DMA from 0 to $2.5\times10^{-2}$ mol./l., the initial rates of polymerization were measured.

Previously, two of the present authors, M. Imoto and K. Takemoto, published a paper on the polymerization of *p*-methylstyrene by ABIN-DMA[1]. There an apparent conclusion was obtained that the initial rate of polymerization increased with the addition of a small

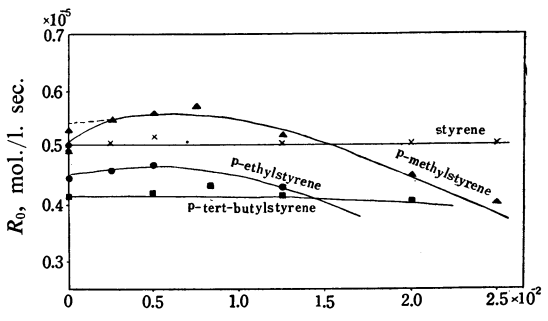



Fig. 9. Polymerization of styrene and *p*-alkylstyrenes initiated by ABIN in the presence of DMF at 70°C.
[M] = 0.455 mol./l.
[ABIN] = $2.50\times10^{-3}$ mol./l.

9) M. Imoto, T. Otsu and T. Ota, *Makromol. Chem.*, **16**, 10 (1955).

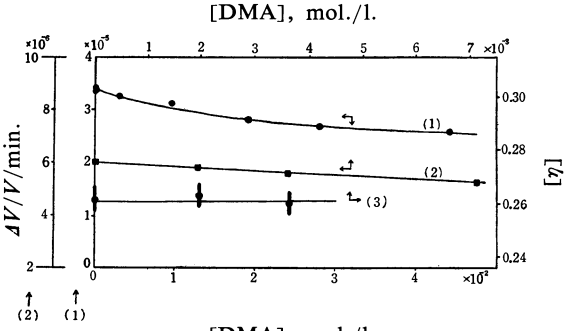



Fig. 10. Relationship of overall rate and intrinsic viscosity with the amount of DMA in the polymerization of *p*-methylstyrene initiated by ABIN at 60°C (in benzene). [M] = 2.17 mol./l., [ABIN], (1) $1.00\times10^{-1}$ mol./l., (2), (3) $2.68\times10^{-3}$ mol./l.

quantity of DMA and then decreased with the increasing quantity of DMA, after passing a maximum value (Fig. 9). It had been assumed that this phenomenon was due to the acceleration of the hyperconjugation effect of the *p*-alkyl group by DMA. For four years the study to ascertain this phenomenon was carried out repeatedly. In many cases, it was observed that no such accelerating effect by DMA existed as shown in Fig. 10.

Granting the dotted line in Fig. 9 to be correct, the former observations coincided with the results obtained in this paper. (As stated above, the rate of polymerization of *p*-methylstyrene was surely greater than that of styrene.) It was now concluded that an accelerating effect by hyperconjugation might be denied, and that the initial rates of polymerization seemed to decrease with DMA as seen from Figs. 9 and 10.

**Polymerization of Dimethylstyrenes and *m*-Methylstyrene.**—We have carried out further

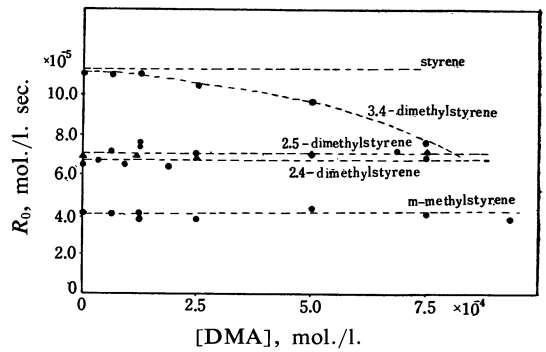



Fig. 11. Polymerization of *m*-methylstyrene and dimethylstyrenes initiated by ABIN in the presence of DMA at 50°C.
[M] = 3.43 mol./l.
[ABIN] = $1.097\times10^{-2}$ mol./l.

experiments on the polymerization of dimethylstyrenes in order to examine the effect of DMA on the polymerization initiated by ABIN.

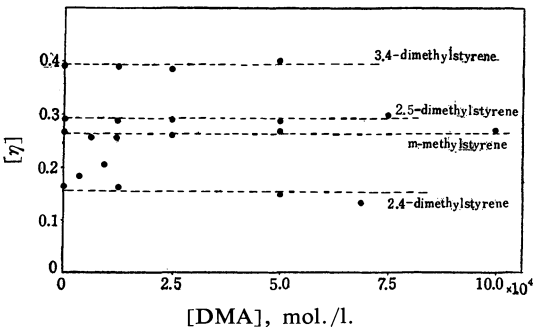
Polymerization was carried out by the sealed tube method at 50°C. The concentrations of the monomer and ABIN were kept constant at 3.43 and $1.097\times10^{-2}$ mol./l. respectively, while the concentration of DMA was varied from 0 to $1.0\times10^{-3}$ mol./l. As shown in Fig. 11, in the case of *m*-methylstyrene no effect of DMA on the initial rate was observed as in the case of styrene, while in the case of 2, 4- and 3, 4-dimethylstyrene a slight decrease with DMA was observed.

**Measurement of Intrinsic Viscosity.**—Intrinsic viscosities of the polymers obtained were measured in benzene at 30°C. Figs. 10 and 12 gave the plots of the intrinsic viscosities to the amounts of DMA added in the polymerization. From the results, it was concluded that no effect of DMA on the intrinsic viscosity was present.

**Rate of Decomposition of ABIN in the Presence of DMA and Monomer.**—The rate of decomposition of ABIN was measured at 50°C in benzene in the presence of monomer and DMA, using the apparatus described in the experimental part. The concentration of ABIN was kept constant at $9.84\times10^{-2}$ mol./l.

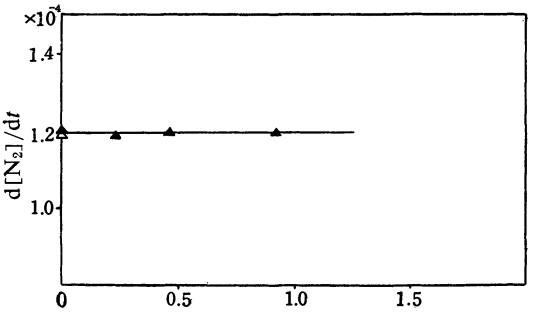
It was established that the rate of decomposition of ABIN was independent of the concentrations of styrene and DMA as shown in Fig. 13.

**Relationship between DMA and Induction Period.**—(*a*) *In DMF, with Ferric Chloride.*—We have already shown that an induction period was observed in the polymerization of styrene or *p*-methylstyrene in the presence of ferric chloride. We have studied further the effect of DMA on the induction period for the polymerization of *p*-methylstyrene initiated by ABIN in DMF, where the concentrations of ABIN and ferric chloride were kept constant at $1.00\times10^{-1}$ and $3.5\times10^{-3}$ mol./l. respectively, and the concentration of DMA was varied from 0 to 2.4 mol./l. As can be seen from Fig. 14 and Table IV, it was found that no effect of DMA on the induction period was observed.




[DMA], mol./l.

Fig. 12. Intrinsic viscosity for the substituted styrene polymers (30°C, in benzene).



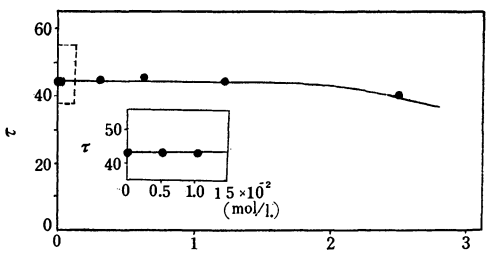

[DMA], mol./l.

Fig. 13. Decomposition rate of ABIN in the presence of monomer and DMA at 50°C (in benzene).
[M]=0.253 mol./l.
[ABIN]=$9.84\times10^{-2}$ mol./l.
△ In the absence of monomer
▲ In the presence of monomer

TABLE IV. RELATIONSHIP BETWEEN INDUCTION PERIOD AND THE AMOUNT OF DMA AT 60°C (IN DMF)

[ABIN]=$1.00\times10^{-1}$ mol./l., [M]=2.17 mol./l., [$FeCl_3\cdot6H_2O$]=$3.5\times10^{-3}$ mol./l.

| Amount of DMA mol./l. | Induction period min. |
|---|---|
| $5\times10^{-3}$ | 43.0 |
| $1\times10^{-2}$ | 43.0 |
| $3\times10^{-1}$ | 44.0 |
| $6\times10^{-1}$ | 44.5 |
| 1.2 | 43.5 |
| 2.4 | 39.0 |
| 0 | 43.0 |




[DMA], mol./l.

Fig. 14. Relationship between induction period and the amount of DMA in the polymerization of *p*-methylstyrene at 60°C (in DMF). [M]=2.17 mol./l., [ABIN]=$1.00\times10^{-1}$ mol./l., [$FeCl_3\cdot6H_2O$]=$3.5\times10^{-3}$ mol./l.

(*b*) *In Benzene, with p-Benzoquinone.*—It could not be completely denied, that DMF reacted with a free radical. Therefore, it was

considered that DMF was not the most suitable solvent. Thus, in the following runs, benzene was chosen as solvent. However, ferric chloride did not dissolve in benzene. We have studied finally the polymerization of *p*-methylstyrene in the presence of *p*-benzoquinone and DMA in benzene and studied the effect of DMA on the induction period, on the rate of polymerization after induction period and on the intrinsic viscosity of polymers. As can be seen from Fig. 15 and Table V, the induction period was decreased with the amount of DMA, which was somewhat different from the result obtained when the ferric chloride-DMA system was used. The rate of polymerization after the induction period had a tendency to increase,

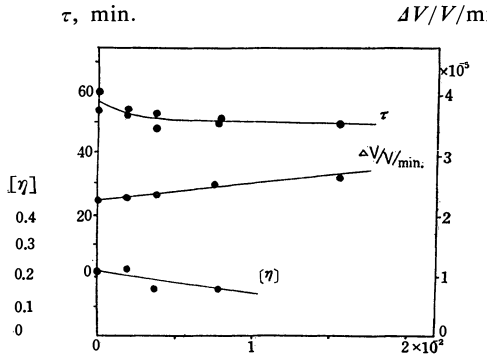



Fig. 15. Relationship of the amount of DMA with induction period, with over-all rate after induction period, and with intrinsic viscosity in the polymerization of *p*-methylstyrene at 60°C (in benzene). [M]=2.17 mol./l., [ABIN]=$7.05\times10^{-2}$mol./l., [*p*-Benzoquinone] =$1.06\times10^{-3}$ mol./l.

TABLE V. INDUCTION PERIOD, AND OVER-ALL POLYMERIZATION RATE AFTER INDUCTION PERIOD IN THE POLYMERIZATION OF *p*-METHYLSTYRENE IN THE PRESENCE OF DMA AT 60°C (IN BENZENE)

| DMA mol./l. | Induction period min. | Volume conversion $\Delta V/V$/min. | Rate$\times10^5$ mol./l./sec. |
|---|---|---|---|
| 0 | 56.0 | — | — |
| $2\times10^{-3}$ | 54.0 | — | — |
| $4\times10^{-3}$ | 49.0 | — | — |
| $8\times10^{-3}$ | 52.0 | — | — |
| 0 | 60.5 | 2.24 | 1.69 |
| $1.8\times10^{-3}$ | 53.5 | 2.27 | 1.71 |
| $3.8\times10^{-3}$ | 54.0 | 2.27 | 1.71 |
| $7.8\times10^{-3}$ | 51.5 | 2.43 | 1.82 |
| $15.6\times10^{-3}$ | 49.5 | 2.60 | 1.95 |

while the intrinsic viscosities decreased with DMA.

Determination of the individual rate constants in the polymerization of *p*-methylstyrene is in progress using the sector method. The results will be reported in near future.

## Summary

1. Solution polymerizations of styrene, *p*-methyl-, *p*-ethyl-, *p*-*tert*-butyl-, *m*-methyl-, 2,4-dimethyl-, 2,5-dimethyl- and 3,4-dimethylstyrene were carried out at 50 and 70°C by ABIN in benzene, and the rates of polymerization and $[\eta]$'s of the polymers were determined. For 3,4-dimethylstyrene, the same equation as for styrene was obtained:

$$R_0=k[\mathrm{M}][\mathrm{ABIN}]^{1/2}$$

2. Rate constants of initiation of the polymerizations of styrene and *p*-methylstyrene were determined, according to the $FeCl_3$-method as follows:

$$k_i=0.67\times10^{-5}\ (\mathrm{sec}^{-1})$$

(for *p*-methylstyrene)

$$k_i=0.76\times10^{-5}\ (\mathrm{sec}^{-1})$$ (for styrene)

3. Polymerizations of styrene and *p*-methylstyrene were carried out at 70°C by the $Bz_2O_2$-DMA system, and the same equation as styrene was derived for *p*-methylstyrene as follows:

$$R_0=k'[Bz_2O_2]^{1/2}[\mathrm{DMA}]^{1/2}$$

4. Polymerizations of styrene, *p*-methyl-, and dimethylstyrenes were carried out at 50 and 70°C by ABIN-DMA system, and the results for the rate of polymerization and the value of $[\eta]$ were discussed. A correction was made for the results previously obtained.

5. The effect of DMA on the induction period for the polymerization of *p*-methylstyrene was studied at 60°C. In the case of polymerization with $FeCl_3$ in DMF, no effect of DMA on the induction period was observed, while in the case of that with *p*-benzoquinone in benzene, the induction period was decreased with the amount of DMA.

*Faculty of Engineering*
*Osaka City University*
*Kita-ku, Osaka*
(*M. I. & K. T.*)

*Onoda Cement Co. Ltd.*
*Onoda Factory*
*Onoda-shi, Yamaguchi-ken*
(*Y. I.*)

# *Visco-elastic Behaviors of Aluminum Soap-Hydrocarbon Systems. I. Aluminum Stearate in Nujol*

By Sukekuni SHIBA

(Received August 6, 1960)

Aluminum soaps dispersed in hydrocarbon oils exhibit many interesting flow properties. Gelling characteristics of aluminum soaps and flow properties of aluminum soap-hydrocarbon systems have been studied by many authors[1-3].

Flow properties have been studied usually for viscous or plastic properties under static conditions. The conception of "elastic fluid" for these systems was adopted first by Goldberg and Sandvik[4], who studied visco-elastic properties (dynamic viscosity and shear modulus) of aluminum soaps gelled in varsol, and found breakdown under steady shear at audio frequency. Garner, Nissan and Wood[5], studying elasto-viscous properties of aluminum stearate in petrol, found the correlation of free energy with the mechanical shearing of the system. Weber and Bauer[6], studying flow properties of aluminum dilaurate-toluene gels, found from the initial elastic axial extension in a capillary that pronounced elastic properties appear abruptly in the gels as the concentration of soap increases, and a concentration of 1% by weight of aluminum dilaurate in toluene is reached.

In the preceding paper[7], flow properties of aluminum soaps in nujol and time effects of flow under shear were studied in static conditions. In the present paper, dynamic visco-elastic behaviors of aluminum stearate dispersed in nujol were studied in a region of low frequency, rangining from $10^0$ to $10^{-3}$ cycles/sec. to examine the correlation of the rheological properties and dispersed states of the soaps.

## Experimental

**Materials.** — Aluminum stearate was prepared from purified stearic acid by a metathetic process as described in the previous paper[7]. Stearic acid, found: m. p., 69.5°C; neutralization equivalent, 281.9. Analysis of the soap showed that the ratio of moles of acid per mole of aluminum was 1.72. Nujol, which was a paraffin-rich saturated hydrocarbon, was used as a vehicle. Physical constants were: $d_4^{25}=0.8429$; $\eta_{25}=0.217$ poise; $n_D^{20}=1.4672$. The purity of the materials was checked by infrared absorption measurements.

**Apparatus.** — A top-drive concentric cylinder rheometer, essentially the same as the apparatus designed by Nakagawa[8], was used. The outer cylinder was fixed in a thermostat; the inner cylinder was suspended coaxially on a torsion wire. The specimen was placed in the annular space between the two cylinders, and a sinusoidal torsional oscillation was applied at the top of the torsion wire. The oscillation of the inner cylinder was detected by a small mirror attached to the inner cylinder, and the oscillation was combined rectangularly with the driving oscillation optically. The resulting Lissajous' figure, which indicates the phase angle and amplitude ratio of the oscillations, was recorded on an oscillographic paper and analysed for visco-elasticity by an approximate method neglecting the inertia of the specimen. Details of the apparatus and analysis were reported elsewhere[9].

**Procedure.**—Aluminum stearate was added to the weighed portions of nujol and the mixture was heated at 110~120°C with stirring for 15 min. The resulting isotropic solution was cooled and kept in a desiccator over phosphorus pentoxide. The specimen thus prepared was aged more than 24 hr. at room temperature. Measurements were carried out under the following conditions:

Temperature; 15~100°C.
Period of oscillation; 2~1,000 sec.
Maximum shear strain; 0.01~0.3.
Soap concentration; up to 1 wt. %.

Experiments were performed avoiding effects of humidity as far as possible.

## Results and Discussion

The systems both in gel and sol states behave always as visco-elastic bodies. A relatively dilute system (sol) shows linear visco-elastic behaviors, whereas a more concentrated system (gel) shows non-linear behaviors as seen in the case of static measurements[7]. In this experiment, the systems were treated as linear visco-elastic bodies, because the shear strain was

1) V. R. Gray and A. E. Alexander, *J. Phys. & Colloid Chem.*, **53**, 9 (1949).
2) H. Sheffer, *Can. J. Research*, **B-26**, 481 (1948).
3) E. K. Rideal et al., *Proc. Roy. Soc.*, **A200**, 135 (1950).
4) H. Goldberg and O. Sandvik, *Anal. Chem.*, **19**, 123 (1947).
5) F. H. Garner, A. H. Nissan and G. F. Wood, *Phil. Trans. Roy. Soc.*, **A243**, 37 (1950).
6) N. Weber and W. H. Bauer, *J. Phys. Chem.*, **60**, 270 (1956).
7) S. Shiba, This Bulletin, **33**, 1563 (1960).
8) T. Nakagawa and M. Senō, This Bulletin, **29**, 471 (1956).
9) S. Shiba, *Railway Technical Research Report*, **No. 112** (Feb. 1960).

small and approximation by linear behaviors was possible.

**Aging.**—It is necessary to examine the effect of aging in order to get reproducible results. Changes in dynamic viscosity $\eta$ and shear modulus $G$ with time are shown in Fig. 1.

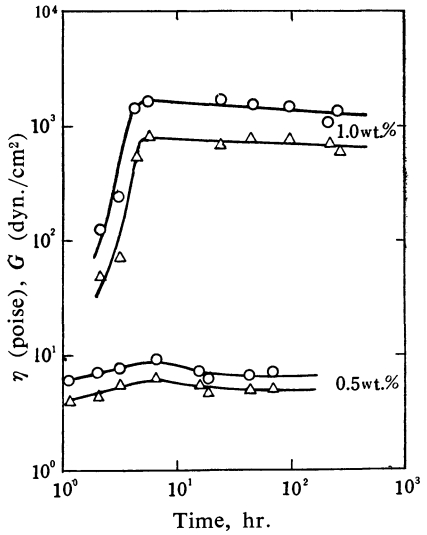



Fig. 1. Change in dynamic viscosity (○) and modulus (△) with time.
25°C, period $T=12$ sec.

Rapid increase in dynamic properties was found in the first stage of aging, then the properties approach constant values after they reach maximum values 4~6 hr. after preparation of the specimen. This result supports the results obtained by viscosity and flow birefringence measurements for benzene and nujol solutions of aluminum soaps[7,10]. However, the change in the properties of a gel was extraordinarily great compared with other cases. This fact indicates that the properties of the system which has not been disturbed by shear were measured in this experiment; whereas in the former reports, a state in which the weak structures formed by aging in the system had been broken, was measured.

**Amplitude Dependence.**—Effects of amplitude of oscillation which are a measure of non-linear behavior, were examined changing the amplitude of the oscillation given at the top of the torsion wire. Results are shown in Fig. 2, where $\gamma_{max}$ is the maximum shear strain at the wall of the internal cylinder expressed as follows;

$$\gamma_{max}=\left[\frac{2Ar_e^2r_i^2}{(r_e^2-r_i^2)r^2}\right]_{r=r_i}=\frac{2Ar_e^2}{r_e^2-r_i^2} \qquad (1)$$

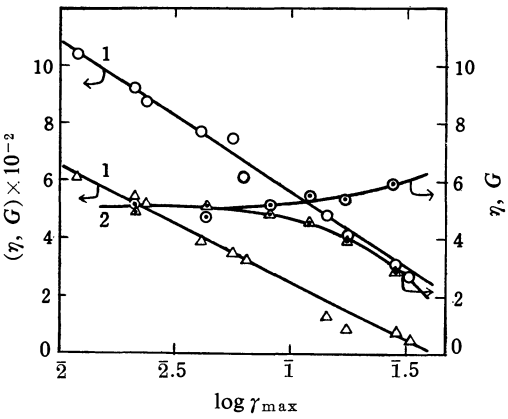



Fig. 2. Amplitude dependence of dynamic viscosity (○) and shear modulus (△), 25°C, period $T=12$ sec, 1. 1.0 wt. %, 2. 0.5 wt. %.

$A$ is the amplitude of the oscillation of the internal cylinder; $r_i$ and $r_e$ are the radii of internal and external cylinders, respectively. The 1 wt. % gel shows marked amplitude dependence; for the 0.5 wt. % sol dependence is found for large values of $\gamma$, but is negligible for usual measurements carried out in the region of $\gamma$ up to 0.1.

As was found from static measurements of viscosity[7], the aluminum soap-hydrocarbon gels undergo shear breakdown. Accordingly, amplitude dependence may be ascribed not only to the non-linearity but also to the shear breakdown of the rheological structures. In the first stage of flow, it requires a certain amount of work to begin deformation against the network structures in the gel, and this work results in the amplitude effect in this experiment. It is not clear, however, whether the effect is due completely to shear strain or to the rate of shear; because the maximum rate of shear changes proportionally to shear strain when other conditions are equal.

Because of this dependence, a series of experiments should be carried out under constant shear strain and shear rate, but the apparatus is not suitable for this purpose. The amplitude was kept as small and constant as possible to avoid these effects.

**Frequency Dependence.**—Frequency dependence of the dynamic rheological properties of the system was examined under various conditions. Fig. 3 shows the shear modulus, dynamic loss, and relaxation spectra of a gel containing 1 wt. % of soap in nujol. The spectra were obtained from shear modulus ($E'$) and dynamic loss ($E''$) by the approximation method[11],

10) J. W. McBain and E. B. Working, *J. Phys. & Colloid Chem.*, **51**, 974 (1947).

11) F. Schwarzl, "Proceedings of the Second International Congress on Rheology" (Edited by V. G. W. Harrison), Butterworths Sci. Pub., London (1954), p. 197.

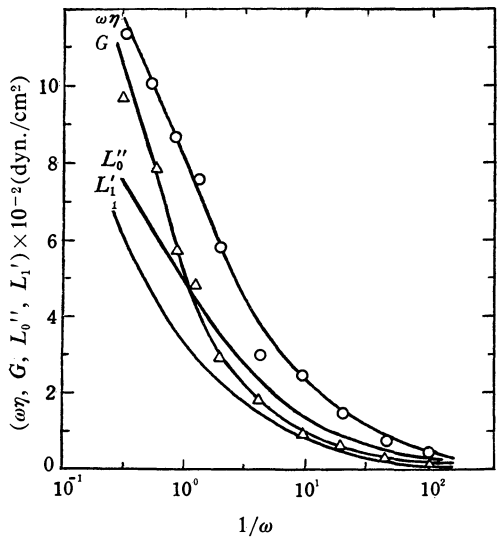



Fig. 3. Frequency dispersion of visco-elasticity and relaxation spectra, 25°C, 1.0 wt%.

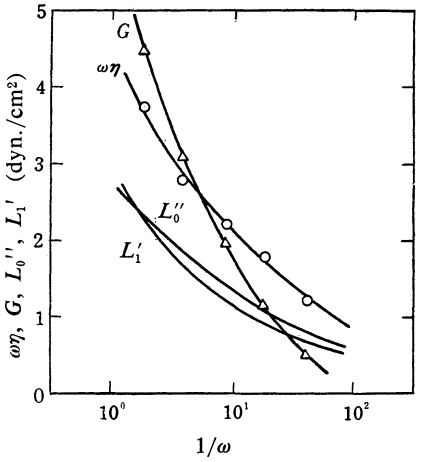



Fig. 4. Frequeny dispersion of visco-elasticity and relaxation spectra, 25°C, 0.5 wt. %.

$$L(t) \simeq L_1'(t) = [\mathrm{d}E'(\omega)/\mathrm{d}\log\omega]_{\omega=1/t} \quad (2)$$

$$L(t) \simeq L_0''(t) = (2/\pi)\,[E''(\omega)]_{\omega=1/t} \quad (3)$$

In these formulae $L$ without index is the exact spectrum, whereas $L$ with index indicates an approximation to the spectrum. The system shows typical visco-elastic properties. Curves of visco-elasticity show marked dispersion; the dynamic shear modulus and dynamic loss increase conspicuously with the increase of frequency. Relaxation spectra obtained from the two approximation methods show similar results. The spectra show a wedge type similar to the spectra found for polyisobutylene. This indicates that the gel resembles the polymer solution or gels in dynamic properties, accordingly the dispersed state of the soap crystallites as well. Fig. 4 shows the dispersion of a sol containing 0.5 wt. % of soap in nujol; similar results are observed in this case, although the visco-elasticity is far smaller than in the case of gel.

Frequency dependence at various temperatures is shown in Figs. 5 and 6. At each temperature, similar dispersion is found. It is possible to express these data by a single curve by the method of reduced variables[12]. The reduced curves for the dynamic shear modulus and dynamic loss are shown in Fig. 7. Good coincidence was found except for the data obtained at 80°C. The results suggest the

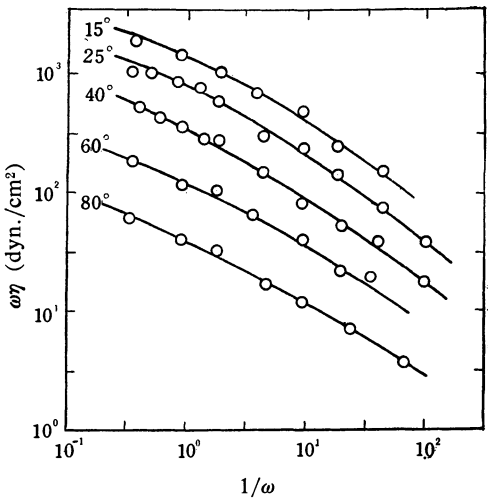



Fig. 5. Frequency dispersion of dynamic loss at various temperatures, aluminum stearate 1 wt. %.

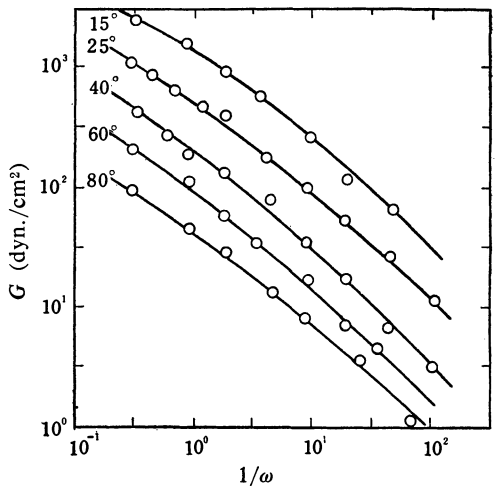



Fig. 6. Frequency dispersion of shear modulus at various temperatures, aluminum stearate 1 wt. %.

12) J. D. Ferry et al., *Ind. Eng. Chem.*, **44**, 703 (1952).

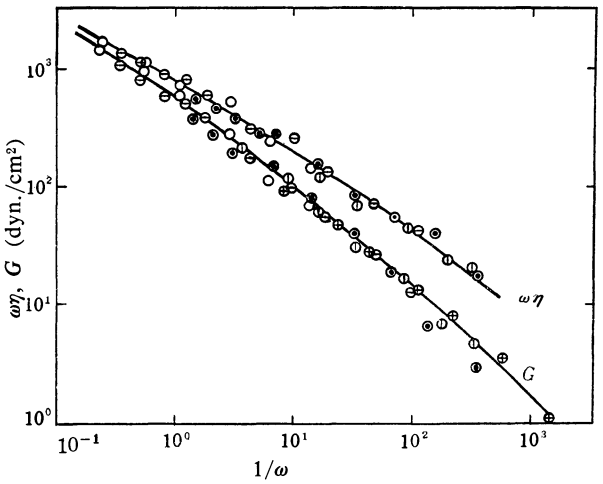



Fig. 7. Reduced curves.
○ 15°C ⊖ 25°C ⊙ 40°C ⏀ 60°C ⊕ 80°C

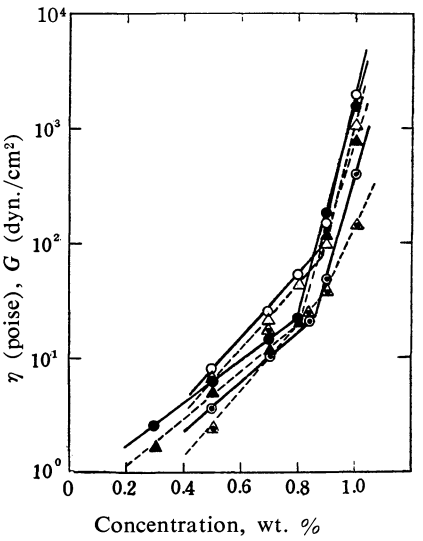



Fig. 8. Change in dynamic viscosity (—○—) and shear modulus (--△--) with concentration, period $T=12$ sec.
○ 15°C ● 25°C ⊙ 40°C

TABLE I. SHIFT FACTORS FOR ALUMINUM STEARATE-NUJOL GEL (1 wt. %)

| Temperature (°C) | $\log a_T$ |
|---|---|
| 15 | 0.52 |
| 25 | 0 |
| 40 | −0.53 |
| 60 | −0.97 |
| 80 | −1.38 |

absence of serious changes in rheological structures up to 60°C, that is, the system is thermo-rheologically simple in that temperature region. The shift factors for this transformation to 25°C are summarized in Table I. Change in the reducing factor with temperature is somewhat small compared with the data of usual polymers.

**Concentration Dependence.**—Change in shear modulus and dynamic viscosity with concentration at various temperatures is shown in Fig. 8. Modulus and viscosity show similar curves which are composed of two straight lines, and have a break point near concentration 1 wt. %. Above this point, modulus and viscosity increase abruptly. This point corresponds to the appearance of soft gel, therefore it is considered as the critical concentration for gel formation. Change in temperature has a minor effect both on the type of the curve and on the critical concentration. The critical concentrations of gel formation obtained from the curves at 15, 25 and 40°C are 0.86, 0.82, and 0.86 wt. % respectively. The curves were obtained from a single period of oscillation; however, these types of curves and critical concentrations are expected under various conditions, because the frequency dependence of the systems is similar,

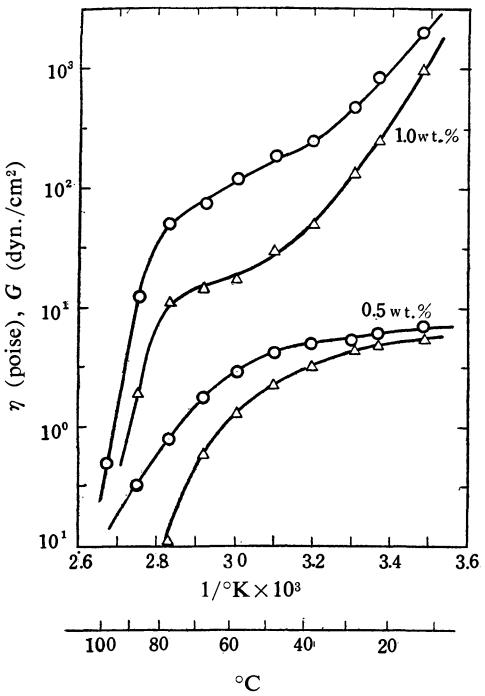



Fig. 9. Temperature dependence of dynamic viscosity (○) and shear modulus (△), period $T=12$ sec.

as shown in Figs. 5 and 6.

Below the critical concentration, the viscosity and elasticity change exponentially with concentration; this region corresponds to the sol in which the soap crystallites are dispersed with secondary interactions. Above the critical

concentration, an extraordinarily sudden increase in visco-elasticity occurs due to the strong network structures in the system, which is stable under a very low rate of shear. This was not observed in a static viscosity measurement carried out under a high rate of shear, owing to the degradation of the structure under shear.

**Effect of Temperature.** — Changes in visco-elasticity with temperature are shown in Fig. 9. Viscosity change of the vehicle is expressed approximately by the Andrade formula ; whereas the system shows complex thermal behaviors. The curves have deflection points near 80°C, which show some phase change in the structure of the systems, the transition from dispersion to isotropic solution. Below this transition temperature, the 1 wt. % gel shows greater temperature effect than the vehicle due to the effect of temperature on the strength of network structures; that is, the gel structures change continuously with temperature. On the other hand, a 0.5 wt. % sol undergoes less temperature effect than the vehicle, which shows that the rheological structures remain unchanged by temperature.

**Summary**

Dynamic visco-elastic behaviors of the aluminum stearate nujol system were studied, using a concentric cylinder type forced oscillation rheometer. The system behaves always as a typical visco-elastic body in a wide range of concentrations and temperatures, and manifests conspicuous amplitude and frequency dependence, which indicates non-linear visco-elastic properties. Wedge type relaxation spectra of the system were obtained, and it was found that the system is thermo-rheologically simple in a confined region of temperatures. The time effect of the specimen and temperature dependence of dynamic properties were examined, and the rheological structures in the system under various conditions were discussed.

The author wishes to express his thanks to Professor H. Akamatu and Dr. T. Nakagawa, both of the University of Tokyo, for their kind advice and encouragement throughout this investigation.

*Railway Technical Research Institute*
*Kunitachi, Tokyo*

# *Visco-elastic Behaviors of Aluminum Soap-Hydrocarbon Systems. II. Aluminum Soaps in Nujol*

By Sukekuni SHIBA

(Received August 6, 1960)

In the previous paper[1], dynamic behaviors of the aluminum stearate-nujol system were studied, and typical visco-elastic properties of the system were found. In this paper, visco-elastic behaviors of aluminum soaps from various fatty acids and aluminum stearates of different compositions dispersed in nujol were studied.

## Experimental

**Materials.**—Aluminum soaps from various parent fatty acids were prepared from purified fatty acids. The purity of the fatty acids and method of preparation were described in the previous paper[2]. Results of aluminum analysis of the soaps are shown in Table I. Aluminum stearates of different compositions were prepared, varying the amount of excess of sodium hydroxide during the precipitation

1) S. Shiba, This Bulletin, **34**, 194 (1961).
2) S. Shiba, ibid., **33**, 1563 (1960).

TABLE I. COMPOSITIONS OF ALUMINUM SOAPS

| Soap | No. of C atoms in acid | Al wt. % (analysed) | Mol. acid per mol. Al |
|---|---|---|---|
| Palmitate | 16 | 5.80 | 1.62 |
| Myristate | 14 | 5.96 | 1.77 |
| Laurate | 12 | 6.38 | 1.87 |
| Caprate | 10 | 7.36 | 1.87 |
| Caprylate | 8 | 9.17 | 1.72 |

TABLE II. COMPOSITIONS OF ALUMINUM STEARATES

| Excess NaOH % | Al wt. % (analysed) | Mol. acid per mol. Al |
|---|---|---|
| 10 | 4.09 | 2.18 |
| 18 | 4.40 | 2.01 |
| 25 | 4.68 | 1.89 |
| 35 | 5.04 | 1.72 |
| 50 | 5.46 | 1.56 |
| 75 | 5.96 | 1.41 |

of the soaps. Compositions of the aluminum stearates are summarized in Table II.

The vehicle was the same nujol as in the previous work. Infrared absorption measurements showed no free fatty acid for the soaps from various fatty acids, whereas the spectra of aluminum stearates containing more than 2 acid molecules per aluminum showed the presence of free fatty acids.

**Apparatus and Procedure.** — Forced oscillation rheometer and the experimental procedure are the same as in the previous work[1].

## Results and Discussion

Various aluminum soaps dispersed in nujol show thickening properties to some extent, and the system becomes an elastic gel at a high concentration or a viscous sol at lower concentrations. Gelling characteristics of the soaps were examined for varying fatty acids and soap compositions.

**Frequency Dependence.** — The frequency dependency of aluminum palmitate, caprate and caprylate in nujol is shown in Fig. 1. A gel

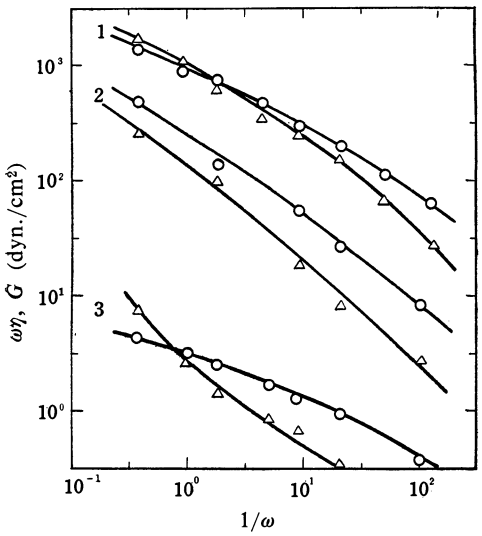



Fig. 1. Frequency dependence of dynamic loss (○) and shear modulus (△), aluminum soaps in nujol at 25°C.
1. Palmitate 1 wt. % 2. Caprate 2 wt. %
3. Caprylate 3 wt. %

containing 1 wt. % of palmitate shows frequency dispersion similar to stearate which indicates wedge type relaxation spectrum. A gel of aluminum caprate (2 wt. %) shows a dispersion which resembles that of palmitate as shown in Fig. 1, despite the higher concentration of the soap. Aluminum myristate and laurate show behaviors similar to palmitate; caprylate scarcely shows the elastic properties. That is to say, the visco-elastic properties of the systems decrease suddenly when the length of the fatty acid molecule decreases below ten carbon atoms.

**Concentration Dependence.** — The concentration dependences of visco-elastic properties for the systems are shown in Figs. 2 and 3.

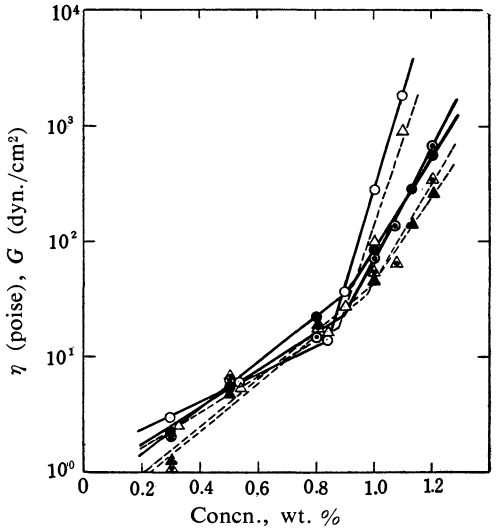



Fig. 2. Concentration dependence of dynamic viscosity (—○—) and shear modulus (--△--), 25°C period $T=12$ sec.
○ Palmitate ● Myristate ⊙ Laurate

Palmitate, myristate and laurate show curves similar to stearate, and each curve consists of two straight lines in the concentration range above and below the break point. The break points correspond to the critical concentrations necessary to form gels, and the two straight lines represent the concentration dependence of visco-elasticity of gels and sols respectively. These curves are expressed by empirical formulae;

$$\log \eta_s = a_s + b_s c, \qquad \log \eta_g = a_g + b_g c \tag{1}$$

$$\log G_s = a_s' + b_s' c, \qquad \log G_g = a_g' + b_g' c \tag{2}$$

where $\eta$ and $G$ are dynamic viscosity (poise) and shear modulus (dyn./cm²), the subscripts s and g mean that the values are referred to the sol and gel states. Changes in critical concentration and constant $b_g$ with soaps are summarized in Table III. The two values represent the gelling capacity of the soaps and the concentration dependence of the rheological properties of the resulting gel. The fatty acid of shorter hydrocarbon chain length gives an indistinct and higher critical concentration and a lower value of $b_g$. When the mole concentrations of the systems are considered, the difference will be larger. This tendency indicates the superiority of soaps from higher fatty acids as thickener. The results for laurate support those of Weber and Bauer[3], who found the appearance of pronounced elastic properties

TABLE III. CRITICAL CONCENTRATION AND CONSTANT $b_g$

| Soap | Crit. conc. wt. % | $b_g$ 1/wt. % |
|---|---|---|
| Stearate* | 0.81 | 10.2 |
| Palmitate | 0.85 | 8.3 |
| Myristate | 0.92 | 4.1 |
| Laurate | 0.91 | 4.9 |
| Caprate | 2.0 | 1.4 |
| Caprylate | — | — |

* Obtained from Ref. 1.

in the gels as the concentration of soap increased over 1 wt. %.

Caprate and caprylate show a somewhat different type of concentration dependence, as shown in Fig. 3. Caprate has a critical concentration near 2 wt. % and visco-elasticity

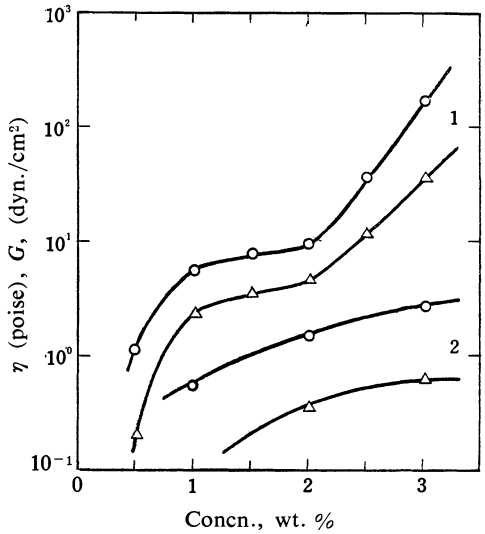



Fig. 3. Concentration dependence of dynamic viscosity (○) and shear modulus (△), 25°C period $T=12$ sec.

1. Caprate 2. Caprylate

decreases rapidly at a concentration below 1 wt. %. Caprylate shows neither conspicuous thickening effect nor gelling property. Thus, the aluminum soaps from fatty acid lower than capric acid, show remarkably different rheological behaviors.

A mixture of the stearate and palmitate shows intermediate concentration dependence of both soaps.

The experiments were carried out under definite conditions, however results similar to the case of stearate[1] are expected under various conditions, due to their relatively similar dependence on frequency and temperature.

3) N. Weber and W. H. Bauer, *J. Phys. Chem.*, **60**, 270 (1956).

**Temperature Dependence.**—Changes in visco-elastic properties of aluminum soap-nujol systems with temperature are shown in Fig. 4. The soaps examined do not show linear relation as described by the Andrade formula. In this temperature region, distinct transition was not

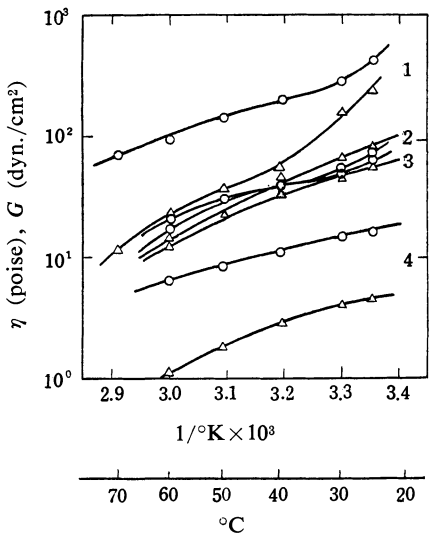



Fig. 4. Temperature dependence of dynamic viscosity (○) and shear modulus (△), aluminum soaps in nujol 1 wt. %, $T=12$ sec.

1. Palmitate 2. Myristate 3. Laurate 4. Caprate

observed; however, the transition from dispersion to solution found for stearate may exist in these cases. The curves show a convex type against temperature. This suggests that gradual transition or structural change occurs over a wide range of temperatures resulting in decrease in rheological properties. Therefore, the apparent activation energies of flow calculated from gradients of the curves are somewhat larger than that of the vehicle, nujol.

**Effect of Soap Composition.** — Aluminum stearate of different compositions that is, the soaps in which a different number of acids combined with the aluminum atom, in nujol were examined. Comparison of the results for 1 wt. % soaps in nujol is made in Fig. 5. An extraordinary difference was found; however, when the conspicuous concentration dependence of the systems as shown in Fig. 2 is considered, it is clear that the results expressed by single point observations on visco-elasticity do not reveal the full aspects of the properties of the soaps. The critical concentration was observed by a simple method: soap solutions of various concentrations were cooled in test tubes and kept still overnight; when the specimen did not flow in a minute after the

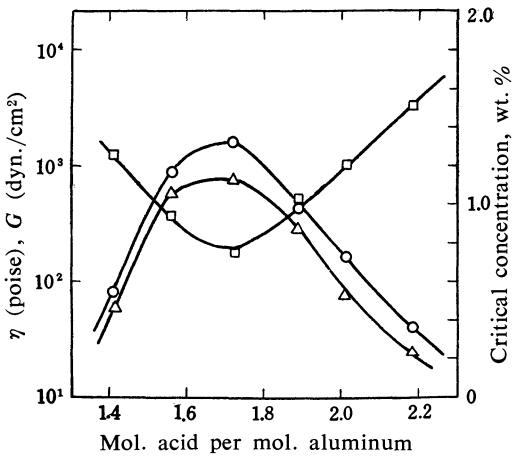



Fig. 5. Visco-elastic properties and critical concentrations of aluminum stearates in nujol at 25°C.

○ $\eta$, △ $G$ for 1 wt. % soaps in nujol, $T$=12 sec., □ critical concentration.

tube was laid down, the specimen was judged to be a gel. The results are also shown in Fig. 5, which shows the maximum effects as thickener near 1.7 mol. acid per aluminum.

**Rheological Structures in the Systems.**—Visco-elastic behaviors of the systems show evidence of strong rheological structures in the systems. The system is essentially a colloidal dispersion of elongated aluminum soap crystallites in hydrocarbon media as ascertained by electron microscope observation[4]. The system containing soaps in more than the critical concentration exhibits typical visco-elastic properties of gels indicating the network structures of soap crystallites by secondary interactions. At lower concentrations the network is incomplete, resulting in a sol with fluidity. At elevated temperatures, e. g. above 80°C, the soaps disperse homogeneously to a transparent solution. Transition from dispersion to solution is expected from conspicuous change in rheological properties.

Static flow properties of the system under constant shear were discussed elsewhere[2]. Network structures suffer a breakdown by shear and result in relatively high fluidity in that case. In this experiment, extraordinarily high values of visco-elasticity were obtained, since the specimen was treated so as not to be affected by shear. The effects of weak secondary interactions which undergo breakdown are recognized as the difference between the two results.

4) D. Evans and J. B. Matthews, *J. Colloid Sci.*, 9, 60 (1954).

## Summary

Dynamic visco-elastic behaviors of aluminum soaps from various fatty acids and aluminum stearates of different compositions in nujol were studied, using a forced oscillation rheometer. The systems behave always as typical visco-elastic bodies in a wide range of concentrations and temperatures. Aluminum palmitate, myristate, and laurate show properties similar to stearate, whereas caprate and caprylate show less effects on rheological properties. Optimum composition of aluminum stearate as thickener was obtained. Rheological structures in the systems were discussed and comparison of the results by static and dynamic measurements was made.

The author wishes to express his thanks to Professor H. Akamatu and Dr. T. Nakagawa, both of the University of Tokyo, for their kind advice and encouragement throughout this investigation.

*Railway Technical Research Institute*
*Kunitachi, Tokyo*

# *Infrared Studies of the Librations of Water Molecules in the Solid Matrices at 20°K*

By Tatsuo MIYAZAWA

(Received July 28, 1960)

The matrix isolation technique has been applied for the infrared absorption studies in the rocksalt or potassium bromide regions[1-4], however, not in the cesium iodide region so far. In the cesium iodide region (400~190 $cm^{-1}$) librational frequencies of small molecules in the crystalline state as well as internal rotation frequencies and bending frequencies are observed. These intramolecular vibrations are coupled with rotational motions in the vapor phase and quite complicated vibration-rotation bands are observed. In the solid matrices at sufficiently low temperatures, however, translational diffusion as well as rotational diffusion of trapped molecules are generally hindered, and the overall rotational motions are reduced to librational motions. No rotation envelope is apparent, and complicating effects frequently arising from rotational motions in the vapor phase are absent.

In carrying out matrix isolation experiments it is necessary to purify the matrix material carefully since the molar ratio (M/R) of the matrix (M) and the reactive species (R) may be as high as 1000 or more. It is not possible to remove the trace of water in nitrogen gas by simply passing the gas through a liquid nitrogen bath. It was necessary first to measure the spectra of water in the nitrogen matrix at various M/R ratios. Spectroscopic studies of water itself are also interesting in relation with hydrogen bonds and with the effects of matrix solids on the low frequency vibrations.

## Experimental Results

For spectroscopic measurements in the region 400~190 $cm^{-1}$ a Perkin Elmer Model 12C spectrometer was used with the cesium iodide optics[5]. The experimental technique of the matrix isolation method has been described[1]. The infrared spectra of water in the solid nitrogen matrix at 20°K were measured for the molar ratios ($N_2/H_2O$) of 1000, 200, 80 and 40. In each case 55 micromoles of water was dispersed in the matrix over an area of about 2 $cm^2$. The nitrogen gas used in the measurement was purified by being passed over copper at 600°C and then through a liquid nitrogen bath. The observed spectra are shown in Fig. 1. It may be seen that the intensity of the

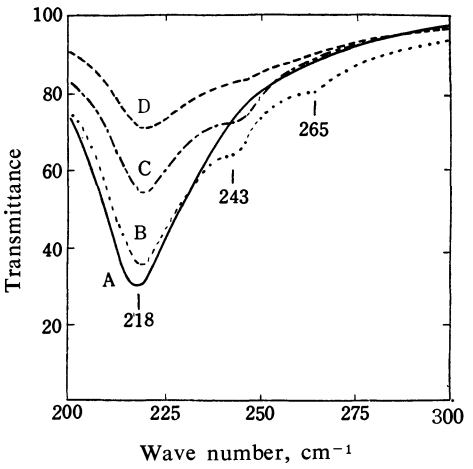



Fig. 1. Infrared spectra of water in the solid nitrogen matrix at 20°K. A: M/R =1000, B: M/R=200, C: M/R=80, D: M/R=40.

band at 218 $cm^{-1}$ increases as M/R is increased from 40 to 1000. The intensity of the band at 243 $cm^{-1}$ increases as M/R is increased from 40 to 80, reaches its maximum for M/R of 80~200 and then decreases as M/R is increased to 1000. The band at 265 $cm^{-1}$ appears to exhibit its intensity maximum for M/R of 200.

In order to measure the effect of isotopic substitution on the water bands, 55 micromoles of heavy water was also suspended in the solid nitrogen matrix for M/R of 200; however, in this case no bands were observed in the region above 190 $cm^{-1}$.

The infrared spectrum of water (55 micromoles, M/R of 200) was also measured in the solid argon matrix at 20°K. Argon gas was

1) E. Whittle, D. A. Dows and G. C. Pimentel, *J. Chem. Phys.*, **22**, 1943 (1954); E. D. Becker and G. C. Pimentel, ibid., **25**, 224 (1956).
2) M. Van Thiel, E. D. Becker and G. C. Pimentel, ibid., **27**, 486 (1957).
3) E. Catalano and D. E. Miligan, ibid., **30**, 45 (1959).
4) M. Van Thiel, E. D. Becker and G. C. Pimentel, ibid., **27**, 95 (1957); G. C. Prinental, *Spectrochim. Acta*, **12**, 94 (1958); T. Miyazawa and K. S. Pitzer, *J. Chem. Phys.*, **30**, 1076 (1959).
5) T. Miyazawa, ibid., **29**, 421 (1958). The measurements were made at the University of California.

purified by being passed over copper heated to 600°C and then through a dry ice-acetone bath. In this case no bands were observed in the region 400~190 $cm^{-1}$, in contrast with the case of the nitrogen matrix.

## Discussion

Infrared spectra of water in the solid nitrogen matrix have been measured in the region 3500~3000 $cm^{-1}$ by Van Thiel, Becker and Pimentel[2]. Eleven peaks have been observed at various M/R ratios, and the bands at 3725 $cm^{-1}$ and 3627 $cm^{-1}$ have been assigned to the monomeric species, and the other bands have been assigned to the dimeric, trimeric, and polymeric species.

**Assignment of Low Frequencies.** — In the present study in the cesium iodide region three bands were observed at 218, 243 and 265 $cm^{-1}$. The intensity of the band at 218 $cm^{-1}$ is plotted against M/R in Fig. 2, along with the corresponding curve for the 3725 $cm^{-1}$ band. It

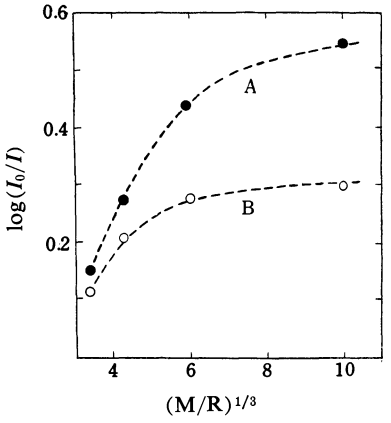



Fig. 2. Peak intensities vs. $(M/R)^{1/3}$.
A: 218 $cm^{-1}$, B: 3725 $cm^{-}$.

may be seen that the intensity of the 218 $cm^{-1}$ band changes in iust the same manner as the intensity of the 3725 $cm^{-1}$ band of the monomeric species. The 218 $cm^{-1}$ band is therefore assigned to the monomeric species. The 243 $cm^{-1}$ band is observed as a shoulder of the 218 $cm^{-1}$ band and its intensity change with M/R appears to correspond most closely with the 3691 $cm^{-1}$ band of the dimeric species[2].

**218 $cm^{-1}$ Band of Monomer.**—All the intramolecular vibrations of the monomeric species have already been observed[2] at 3725, 3627 and 1600 $cm^{-1}$. The 218 $cm^{-1}$ band is, therefore, undoubtedly due to translational or rotational modes in the solid matrix. The translational and rotational motions are restricted in the matrix and become vibrational motions giving rise to vibrational infrared bands.

**Lattice Vibrations of Ice.** — Prior to more detailed discussions of the matrix spectra the infrared bands of crystalline ice due to these translational or rotational vibrations will be briefly reviewed. The infrared bands due to the translational lattice vibrations of water and heavy water (at −190°C) have been observed at 229 and 222 $cm^{-1}$ respectively[6]. The observed frequency ratio ($\nu_{H_2O}/\nu_{D_2O}$) of 1.03 agrees with the theoretical ratio of $1.05=(M_{D_2O}/M_{H_2O})^{1/2}$ for the translational mode. On the other hand the rotational lattice vibrations (librations) of water and heavy water (at −170°C) have been observed at 850 and 630 $cm^{-1}$ respectively[7] and in this case the frequency ratio of 1.35 is much greater than the ratio of 1.03 for the translational mode.

**Three Librations in the Nitrogen Matrix.**— The 218 $cm^{-1}$ band in question disappears on deuteration and the corresponding band of heavy water has not been observed in the region above 190 $cm^{-1}$. The isotopic frequency ratio for this mode is definitely greater than the ratio of 1.05 expected for the translational mode. The 218 $cm^{-1}$ band may thus be assigned to a librational mode of the monomeric species in the nitrogen matrix.

So far we have not specified the types of librations in the matrix. For the monomeric species of water there are three types as shown in Fig. 3; one around the twofold axis (the B axis), one around the axis perpendicular to

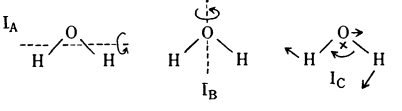



Fig. 3. Librational modes of monomer.

the molecular plane (the C axis), and the last one around the axis of the least moment of inertia (the A axis). The first one will not be infrared active since the B axis is parallel to the dipole moment of the molecule. The other two involve rotations of the molecular dipole moment and will give rise to strong infrared bands.

**Intensity of Libration Bands.**—The infrared intensities of these libration bands may be estimated assuming that the molecules carry out librations about the axes passing through the center of the mass. The moments of inertia about the three axes are

$$I_A = 2m_H r^2 (m_O/M_{H_2O}) \cos^2 \alpha$$

$$I_B = 2m_H r^2 \sin^2 \alpha$$

6) R. Zimmermann and G. C. Pimentel, unpublished.
7) K. B. Harvey and P. A. Giguère, *Can. J. Chem.*, **34**, 798 (1956); N. Ockman, *Advances in Physics*, **7**, 199 (1958); D. F. Hornig, H. F. White and F. P. Reding, *Spectrochim. Acta*, **12**, 338 (1958).

and $I_C = I_A + I_B$

where $m_H$ and $m_O$ are the masses of the hydrogen and oxygen atoms, respectively, $r$ the bond length and $2\alpha$ the interbond angle. Now if the monomeric species is randomly oriented in the matrix the infrared intensities, $D_A$ and $D_C$, of the A and C librations are expressed analogous to the vapor intensities, and

$$D_i \propto |\partial\mu/\partial Q_i|^2 = |\partial\mu/\partial\theta_i|^2 \cdot |\partial\theta_i/\partial Q_i|^2 = \mu^2/I_i$$

where $\mu$ is the dipole moment, $Q_i$ the $i$th normal coordinate, $\theta_i$ the angle of rotation around the $i$th axis, and $I_i$ the corresponding moment of inertia. The intensity ratio of the A and C bands is calculated to be $D_A/D_C = 2.7$ for the $H_2O$ molecule with the bond angle of 105°. The 218 $cm^{-1}$ band of the monomeric species is considered to be primarily due to the A librational mode.

**Librational Frequencies.** — The three librational frequencies may be estimated assuming that the potential energy arises from Cartesian displacements of the hydrogen atoms in the matrix. The potential energy possibly arising from Cartesian displacements of the oxygen atom was not considered in the present treatment. The Cartesian displacements of the hydrogen atoms, $\xi_A$, $\xi_B$ and $\xi_C$, due to the rotations around the three axes are

$$\xi_A = \theta_A (m_O/M_{H_2O}) r \cos\alpha$$

$$\xi_B = \theta_B r \sin\alpha$$

and

$$\xi_C = \theta_C r [\sin^2\alpha + (m_O/M_{H_2O})^2 \cos^2\alpha]^{1/2}$$

Taking into account the potential energies for the two hydrogen atoms, the librational frequencies, $\nu_A$, $\nu_B$ and $\nu_C$, are found to be

$$(2\pi\nu_A)^2 = (K/m_H)(m_O/M_{H_2O})$$

$$(2\pi\nu_B)^2 = (K/m_H)$$

and

$$(2\pi\nu_C)^2 = (K/m_H)\{\tan^2\alpha + (m_O/M_{H_2O})^2\}/\{\tan^2\alpha + (m_O/M_{H_2O})\}$$

whre $K$ is the potential constant. The value of $K$ is calculated to be 0.032 millidyne/A from the $\nu_A$ frequency (218 $cm^{-1}$) of water, and other librational frequencies were calculated to be $\nu_B = 231$ and $\nu_C = 226$ $cm^{-1}$ for $H_2O$ and $\nu_A' = 146$, $\nu_B' = 164$ and $\nu_C' = 157$ $cm^{-1}$ for $D_2O$.

The $\nu_C$ frequency of 226 $cm^{-1}$ is slightly higher than the observed $\nu_A$ frequency of 218 $cm^{-1}$ and the intensity of the $\nu_C$ band is considered to be weaker than the intensity of the $\nu_A$ band as mentioned before. In fact the 218 $cm^{-1}$ band has an ill-defined shoulder on the high frequency side around 230 $cm^{-1}$, in agreement with the result of the present treatment*. The librational frequencies calculated for $D_2O$ are much lower than 190 $cm^{-1}$, again in agreement with the result of the present measurement on $D_2O$.

**243 $cm^{-1}$ Band of the Ring Dimer.** — The structure of the dimeric species of water in the solid nitrogen matrix has been found to be a ring dimer by Van Thiel et al.[2] The ring dimer has a center of symmetry and there will be three infrared active low frequency vibrations as shown in Fig. 4. The $b_u$ vibration

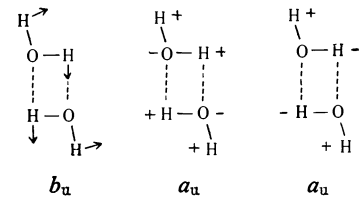



Fig. 4. Infrared active low frequency modes.

involves the stretching of the O···H hydrogen bonds and its frequency will be appreciably higher than the two $a_u$ frequencies involving only the bending of the hydrogen bonds. The observed frequency of 243 $cm^{-1}$ is slightly higher than the monomeric frequency and this is most probably due to either one of the two $a_u$ modes of the ring dimer.

**Libration in the Argon Matrix.** — The librational frequencies of water in the argon matrix have not been observed in the region above 190 $cm^{-1}$. It has been found that the nitrogen and argon matrices have different effects on the monomeric bands of water. Catalano and Milligan have observed seven sharp peaks (1654~1554 $cm^{-1}$) due to the bending vibration in the argon matrix but only one peak at 1600 $cm^{-1}$ in the nitrogen matrix[3]. The observed fine structure in the argon matrix has been ascribed to overall rotations of the monomeric species in the argon matrix**. The rotations may not be unrestricted of course; however, they should be much less restricted in the argon matrix than in the nitrogen matrix. The present observation in the cesium iodide region is in accord with the conclusion drawn by Catalano and Milligan[2].

The author wishes to thank Professor K. S. Pitzer and Professor G. C. Pimentel of the University of California for their interest and

* In crystalline ice the $\nu_A$ and $\nu_C$ librations give rise to a band at 850 $cm^{-1}$ (at −170°C). The two librations, however, have not been resolved from each other[7].

** It is interesting to note that $NH_2$ radical has been found to carry out almost free rotation in the argon matrix[8].

8) G. W. Robinson and M. McCarty, Jr., *J. Chem. Phys.* **30**, 999 (1959).

encouragement. The present work was partly supported by the American Petroleum Institute Research Project 50.

*Institute for Protein Research*
*Osaka University*
*Kita-ku, Osaka*

# *Studies on Dehydroalanine Derivatives. III. Formation of Amino Acids from Poly-dehydroalanine*

By Shumpei SAKAKIBARA

(Received July 13, 1960)

In the previous papers of this series[1,2], the synthesis of *N*-carboxy-dehydroalanine anhydride and of poly-dehydroalanine was described. However, the synthesis of analytically pure poly-dehydroalanine was unsuccessful, and it was found that the polymer contained only about 10% dehydroalanyl residues in the molecule[2]. This suggested that the dehydroalanyl groups in the polypeptide chain are very reactive. The present investigation is on the reactivity of dehydroalanyl residues in polypeptide chains. Poly-dehydroalanine was used as test material, and the reagents used for the reaction were potassium carbonate, potassium cyanide, benzyl mercaptane and acetonitrile. The amino acids derived from the poly-dehydroalanine were examined after hydrolysis of the reaction products.

## Experimental

**Meterial.**—Poly-dehydroalanine was prepared from *N*-carboxy-dehydroalanine anhydride[1]. It was polymerized in pyridine as described in the previous paper[2]. The freshly prepared polymer was used in these experiments.

**Reaction Conditions and Detection of Amino Acids Formed.**—The reaction mixtures shown in Table I were hydrolyzed for about 15 hr. at 105°C after addition of concentrated hydrochloric acid (an equal volume to that of the reaction mixture), and then concentrated to dryness. These concentrates were analyzed by Dowex 50 column chromatography using the conditions of Moore and Stein[3] (Fig. 1) and/or by two dimensional paper chromatrgraphy after dinitrophenylation under the improved conditions of Levy[4] (Fig. 2). Amino acids formed were analyzed quantitatively by Levy's method (Table II). The spot corresponding to DNP-aspartic or glutamic acid in Fig. 2 was rechromatographed on paper by descending method using 2.5 M phosphate buffer as solvent, as shown Fig. 4. Since the spot corresponding to DNP-aspartic acid from reaction mixture 3 contained a little DNP-glutamic acid, these two compounds were separated on a buffered celite column using 0.2 M phosphate-citric acid as buffer and chloroform-ether (90 : 10) as developer[5] (Fig. 3). Then, the bands corresponding to DNP-aspartic acid (A) and DNP-glutamic acid (B) were reconfirmed and repurified by paper

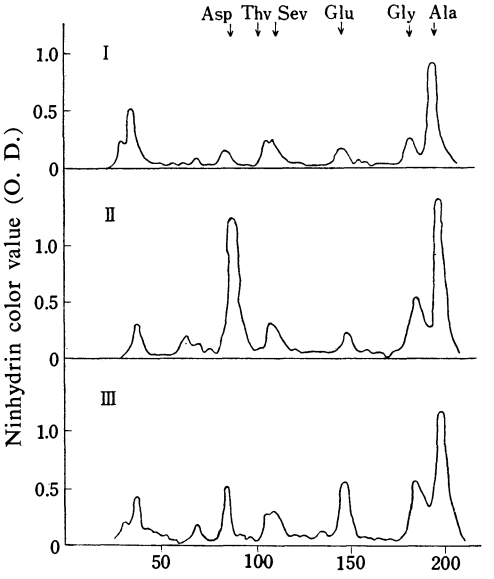



Fig. 1. Chromatographic analysis of ninhydrin-positive materials in the HCl-hydrolyzates (per 10 mg. of poly-dehydroalanine): I. Reaction mixture 1; II. Reaction mixture 3; III. Reaction mixture 5 (cf. Table I). Column: Dowex 50-X8, 100×0.9 cm.
Arrows indicate the position of the peaks of standard amino acids.

1) S. Sakakibara, This Bulletin, **32**, 13 (1959).
2) S. Sakakibara, ibid., **33**, 814 (1960).
3) S. Moore and W. H. Stein, *J. Biol. Chem.*, **192**, 663 (1951).
4) A. L. Levy, *Nature*, **174**, 126 (1954); G. Koch and W. Weidel, *Z. physiol. Chem.*, **303**, 213 (1956).
5) A. Courts, *Biochem. J.*, **58**, 70 (1954).

TABLE I. REACTIONS OF POLY-DEHYDROALANINE WITH VARIOUS REAGENTS

| Reaction No. | Poly-dehydroalanine* apparent wt. (calcd. wt.) mg. | Reagent g. | Water ml. | Reaction conditions |
|---|---|---|---|---|
| 1 | 5 ( 4.10) | $K_2CO_3$ 0.04 | 2 | A** |
| 2 | 10 ( 8.20) | $K_2CO_3$ 0.08 | 4 | B† |
| 3 | 65 (53.4) | KCN 0.4 | 20 | A** |
| 4 | 15 (12.3) | $K_2CO_3$ 0.12<br>Benzyl mercaptane 0.1 | 6 | C†† |
| 5 | 10 ( 8.20) | $K_2CO_3$ 0.08<br>$CH_3CN$ 1 | 4 | B† |

* Soluble poly-dehydroalanine contained 17.9% of volatile components. Since completely dry polymer was partially insoluble[2], the actual weight was calculated from the apparent weight.
** Kept at room temp. for about 15 hr. and then heated at 80°C for 1 hr. in a sealed tube.
† Irradiated with an UV-lamp (Mazda 15 W sterilizing lamp at the irradiation distance of 10 cm.) for 24 hr. at room temp. in a petridish (dia. 5 cm.) covered with cellophane (0.05 mm. thick).
†† Shaken at room temp. for about 15 hr. in a sealed tube.

TABLE II. QUANTITATIVE ESTIMATION OF DNP-AMINO ACIDS ANALYZED BY LEVY'S CHROMATOGRAPHICAL METHOD (FIG. 2) : $\mu$M/10 mg. OF DRIED POLY-DEHYDROALANINE

| Spot No. in Fig. 2 | | 1 | 2 | 3 | 4 | 5 | 6 | 7 | 8 | 9 | 10 | 11 | | 12 | 13 |
|---|---|---|---|---|---|---|---|---|---|---|---|---|---|---|---|
| Corresponding amino acid | | | Ala | Gly | Thr | Ser | | | | | | Asp | Glu | | *S*-Bz-CyS* |
| No. of reaction mixt.** | 1 | 2.24 | 1.81 | 0.18 | 0.05 | 0.13 | 0.05 | 0.07 | 0.10 | 0.07 | 0.14 | 0.29 | 0.42 | 0.25 | — |
| | 2 | 2.78 | 1.74 | 0.78 | 0.18 | 0.20 | 0.06 | 0.06 | 0.23 | 0.09 | 0.17 | 0.50 | 0.90 | 0.19 | — |
| | 3 | 0.88 | 2.15 | 0.24 | 0.03 | 0.11 | — | 0.03 | 0.17 | 0.07 | 0.16 | 2.11 | 0.44 | 0.27 | — |
| | 4 | 1.01 | 1.27 | 0.19 | 0.05 | 0.25 | — | 0.12 | 0.16 | 0.12 | 0.13 | 0.14 | 0.19 | 0.09 | 0.96 |
| | 5 | 2.47 | 1.89 | 1.93 | 0.15 | 0.29 | 0.06 | 0.04 | 0.23 | 0.16 | 0.13 | 0.74 | 1.09 | 0.27 | — |

* Bz=Benzyl
** Confer Table I

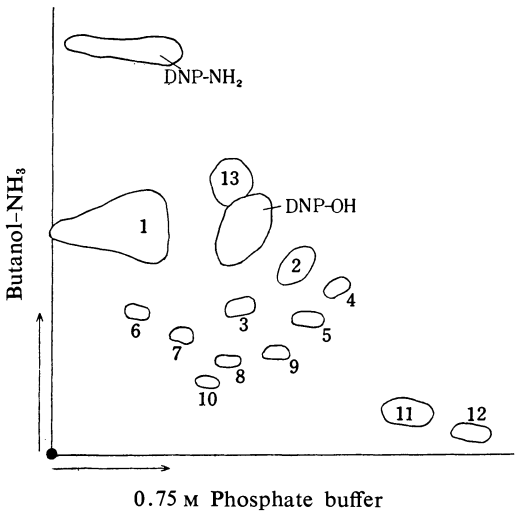



Fig. 2. Standard map of two-dimensional paper chromatogram of DNP-amino acids derived from every reaction mixture.
Details are listed on Table II.

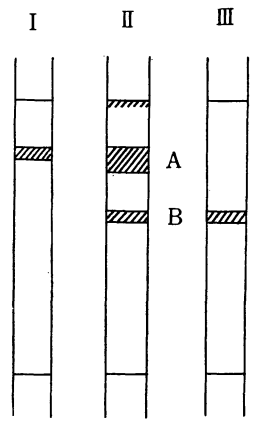



Fig. 3. Chromatographic separation of spot 11 in Fig. 2, reaction mixture 3; I. Standard DNP-aspartic acid; II. Spot 11 in Fig. 2, reaction mixture 3; III. Standard DNP-glutamic acid.
Column: Buffered celite; pH 4.2, 0.2 M phosphate-citric acid buffer.
Solvent: Chloroform-ether (90 : 10).

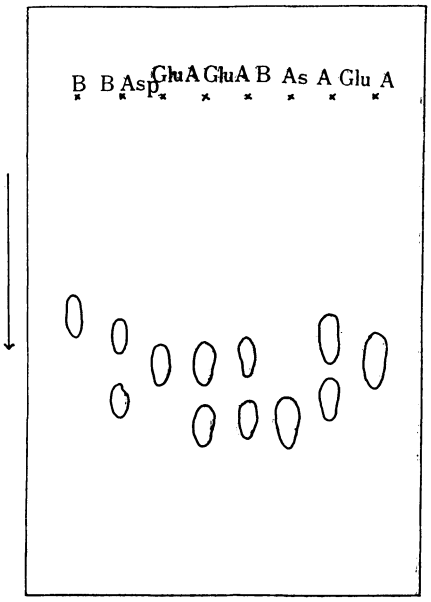



Fig. 4. Paper chromatogram for identification of bands A and B in Fig. 3 with authentic samples.
Solvent: 2.5 M phosphate buffer.
Descending method.

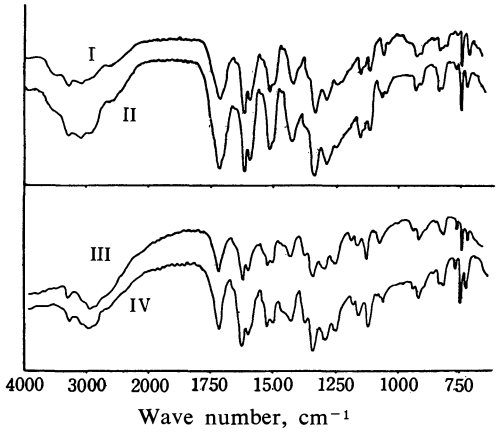



Fig. 5. Infrared absorption spectra of DNP-aspartic acid and DNP-alanine; I. Standard DNP-DL-aspartic acid; II. DNP-aspartic acid derived from the reaction mixture 3; III. Standard DNP-DL-alanine; IV. DNP-alanine derived from the reaction mixture 3.
Recorded on a Shimadzu IR spectrophotometer.
Liquid layer on KRS-5 plate.

chromatography (Fig. 4). The resulting DNP-aspartic acid was reconfirmed by comparison of its infrared absorption spectrum with that of an authentic sample (Fig. 5, I and II). The DNP-alanine formed in reaction mixture 3 was, like DNP-aspartic acid, identified by its infrared absorption spectrum (Fig. 5, III and IV).

In reaction mixture 4, *S*-benzyl cysteine was qualitatively detected by one-dimensional paper

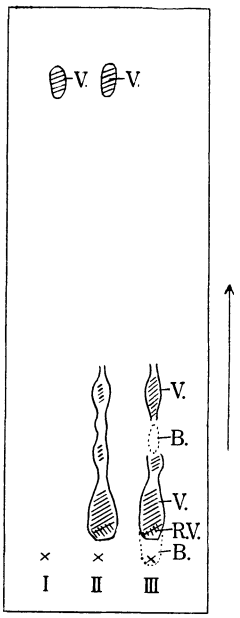
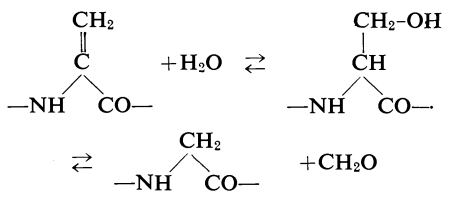



Fig. 6. One dimensional paper chromatogram of reaction mixtures 1 and 4. Identification of *S*-benzyl-cysteine formed in reaction mixture 4. I. Standard *S*-benzyl-cysteine; II. Reaction mixture 4; III. Reaction mixture 1.
V.···violet B.···brown R. V.···reddish violet

chromatography (butanol : acetic acid : water, 4:1:1) (Fig. 6).

## Results and Discussion

Before hydrolysis, reaction mixtures 1 and 3 were clear light-brown solutions, 2 and 5 were clear light-yellow solutions, and 4 was a stable white emulsion. The hydrochloric acid hydrolyzates of these reaction mixtures contained small amounts of huminic material as mentioned in the previous paper[2]. As can be seen in the chromatograms of each reaction mixture (Figs. 1 and 2), several unknown bands and spots were observed besides bands and spots corresponding to natural-type amino acids such as alanine, glycine, serine, threonine, glutamic acid and aspartic acid. Formation of glycine and serine in each case could be explained by the following scheme.

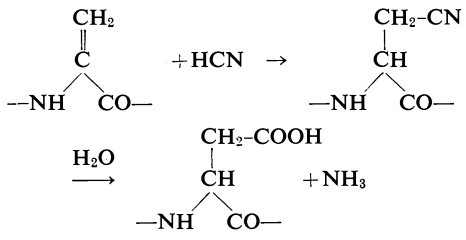



However, formation of amino acids such as alanine, glutamic acid, aspartic acid and threonine could not be explained. Perhaps, compounds such as carbon dioxide, formaldehyde,

ammonia and hydrochloric acid may react in various complex ways with the dehydroalanyl groups. It was very interesting to find spot 1 in the chromatogram shown in Fig. 2. This might correspond to di- or poly-DNP-derivative of some amino acid. Since the structure has not yet been confirmed, some kinds of basic amino acids or polyamino polycarboxylic acids may be derived from dehydroalanine.

Ultraviolet-radiation of dehydroalanyl groups resulted in the liberation of greater amounts of glycine.

As shown in Figs. 1, 2, 3, 4 and 5, and in Table II, formation of considerable amounts of aspartic acid in reaction mixture 3 was definitely confirmed, and this was explained by the following reactions:



In reaction mixture 5, the liberation of greater amounts of glycine, aspartic acid and glutamic acid was observed. However, the reason of their formation is as yet unknown.

*S*-Benzyl cysteine was clearly detected in reaction mixture 4 (Figs. 2 and 6). It was expected that cystine would have been found in some reaction mixtures containing sodium sulfide and thiosulfate, but this could not be confirmed. Similary, attempts to detect formation of tryptophane and tyrosine residues in the polymer using indol and phenol reagents, were unsuccessful because of the difficulty of detecting small amounts of these amino acids. Nevertheless, it was interesting that many kinds of amino acids were liberated from polydehydroalanine.

A few years ago, Akabori[6,7] proposed a hypothesis on the mechanism of formation of primordial protein. He suggested that initially polyglycine was formed by the polymerization of amino-acetonitrile[8] on the surface of clay. Then, many kinds of side chains were introduced into polyglycine through the reactions of this material with simple substances such as aldehydes or olefines. Subsequently, he confirmed experimentally the formation of serine, threonine[9] and leucine[7] from polyglycine, dispersed on kaolinite, on treatment with formaldehyde, acetoaldehyde and butene-2, respectively. If it is assumed that dehydroalanyl residues are formed from polyglycine during the dehydration reaction with formaldehyde, the formation of residues such as aspartic acid, glutamic acid, alanine and threonine, from polyglycine would be rationally explained. This suggestion is supported by the fact, as shown in the following communication, that *N*-phthaloyl-dehydroalanine can be derived from serine and phthalic anhydride. Furthermore, if experimental confirmation is possible, the formation of amino acids such as cystine, tryptophane and tyrosine could also be explained in a similar way.

## Summary

Reaction of poly-dehydroalanine with various reagents such as potassium carbonate, potassium cyanide, benzyl mercaptane and acetonitrile were studied. In every reaction mixture, alanine, glycine, serine, threonine, glutamic acid, aspartic acid and several unknown amino acids were detected. Ultraviolet-radiation resulted in the liberation of greater amounts of glycine. It was observed that considerable amounts of aspartic acid, *S*-benzyl-cysteine and glutamic acid were formed in reaction mixtures of potassium cyanide, benzyl mercaptane and acetonitrile, respectively.

The author wishes to express his thanks to Professor Shiro Akabori and Professor Shunsuke Murahashi for their valuable advice and encouragement.

*Institute for Protein Research*
*Osaka University*
*Kita-ku, Osaka*

6) S. Akabori, *Science* (*Kagaku*), **25**, 54 (1955).
7) S. Akabori, Proc. International Symposium on "The Origin of Life on the Earth", Pergamon Press, London (1959), p. 189.
8) H. Hanafusa and S. Akabori, This Bulletin, **32**, 626 (1959).
9) S. Akabori, K. Okawa and M. Sato, ibid., **29**, 608 (1956).

# *The Beckmann Rearrangement of the Geometrical Isomers of Cyclohexyl Phenyl Ketoxime in Liquid Sulfur Dioxide*[1]

Ritsuro TADA, Yoichi MASUBUCHI and Niichiro TOKURA

(Received May 21, 1960)

In the previous report[1] of this series some effects of reagents on the products of the Beckmann rearrangement have been reported. It is currently accepted[2] that the Beckmann rearrangement is accompanied by exclusive trans migration. However, Some anomalies on the migratory aptitude in this rearrangement have been observed. Recently, Brown, van Gulic and Schmid[3] have reported that when pivalophenoxime was subjected to the Beckmann rearrangement with hydrochloric acid in acetic acid, similar products were obtained either from the *syn*-oxime or from the *anti*-isomer. This phenomena could be accounted for by a preliminary isomerization of the oximes before the rearrangement. On the other hand, Yukawa, Hanabusa and Kin[4] have examined the Beckmann rearrangement of cyclohexyl phenyl ketoximes and found that the migratory aptitude varied according to the reagents applied.

In addition, in the light of the publications hitherto reported[5-7], the geometrical structures of the cyclohexyl phenyl ketoximes are still ambiguous. Contradictory geometrical structures have been assigned to the oximes by Meyer and Scharvin[5,6] and also by Meisenheimer and Theilacher[7]. Moreover, since its first synthesis in 1897 by Meyer and Scharvin[5], the establishment of the geometrical structures mainly depended upon the analysis of the migrated products of the Beckmann rearrangement and the above-mentioned random migratory aptitude was ignored.

It is the purpose of the present writers to carry out the rearrangement in liquid sulfur dioxide of this compound to obtain further information on the geometrical structures of this ketoxime and the migration tendency in the Beckmann rearrangement by subjecting it to a more moderate condition. The isomeric cyclohexyl phenyl ketoximes were prepared and separated by the well-known precedure[5], to give the $\alpha$-oxime, m. p. 156~157°C., and $\beta$-oxime, m. p. 113~114°C, respectively after repeated fractional precipitations from acetic acid solution by the addition of water.

The authentic specimens of the acid amides,

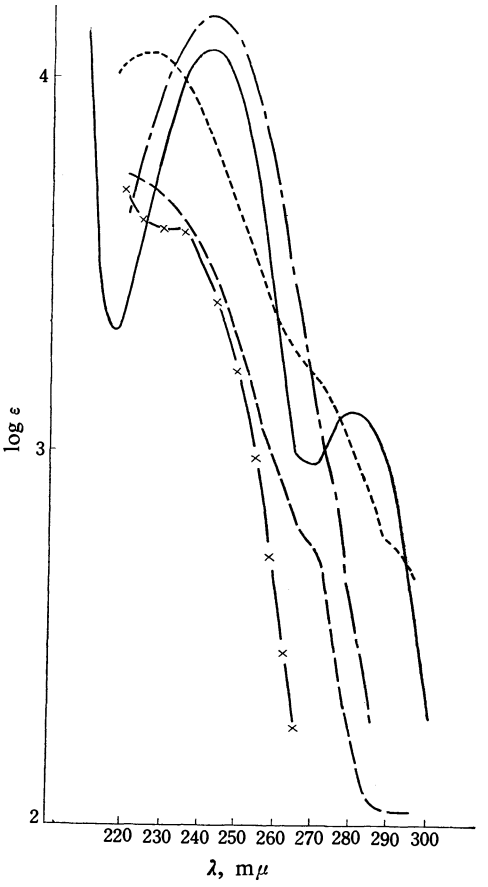



Fig. 1. Ultraviolet absorption spectra of cyclohexyl phenyl ketoximes and the derived acid amides.

---- $\alpha$-Cyclohexyl phenyl ketoxime (I)
-×- $\beta$-Cyclohexyl phenyl ketoxime (II)
------ *N*-Cyclohexyl benzamide (III)
—·— Cyclohexanecarboxyanilide (IV)
—— Cyclohexyl phenyl ketone (V)

1) Part VI; On the Beckmann rearrangement in liquid sulfur dioxide. Previous papers on this series: IV. R. Tada, H. Sakuraba and N. Tokura, This Bulletin, **31**, 1003 (1958). V. N. Tokura, R. Tada and H. Suzuki, ibid., **32**, 654 (1959).
2) B. Jones, *Chem. Revs.*, **23**, 335 (1944).
3) R. F. Brown, M. M. van Gulic and G. H. Schmid, *J. Am. Chem. Soc.*, **77**, 1094 (1955).
4) Y. Yukawa, "Jikken Kagaku Koza", Vol. 18, Maruzen Co. Ltd., Tokyo, (1957), p. 426.
5) V. Meyer and W. Scharvin, *Ber.*, **30**, 1942 (1897).
6) W. Scharvin, ibid., **30**, 2862 (1897).
7) J. Meisenheimer and W. Theilacher, "Stereochemie", edited by Freudenberg Leibzig (1933), p. 2103.

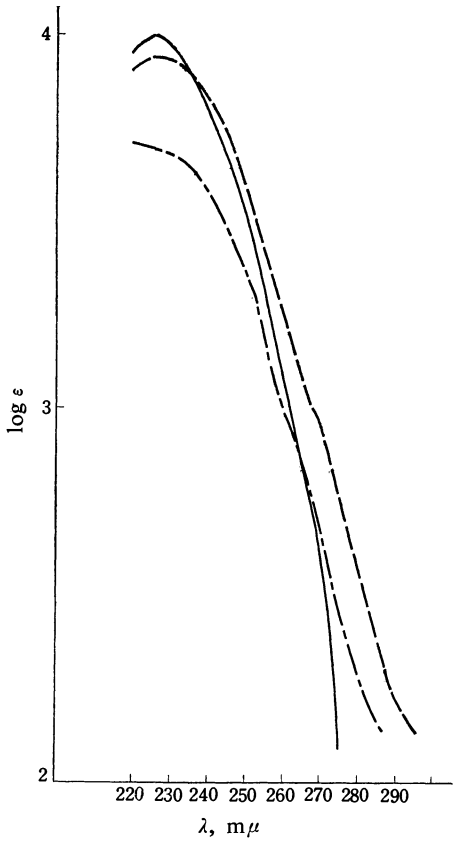



Fig. 2. Ultraviolet spectra of the reaction products from α-oxime I in liquid $SO_2$ at −70°C.
—— $SOCl_2$
—·— $SOCl_2$ in ether
---- Bromine

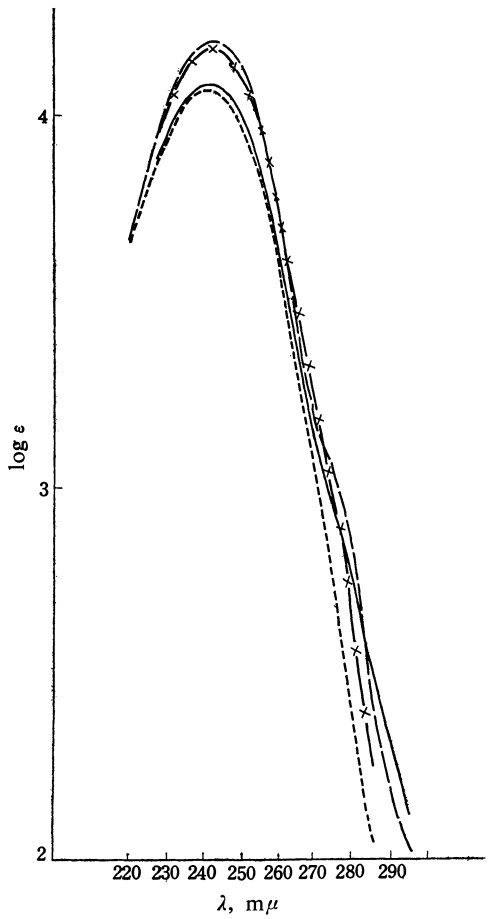



Fig. 3. Ultraviolet spectra of the reaction products from β-oxime II in liquid $SO_2$ at −70°C.
—— $SOCl_2$ in ether -×- $SOCl_2$
—— Bromine ------ $C_6H_5SO_2Cl$

which should be expected to produce by the Beckmann rearrangement from the ketoximes, *N*-cyclohexyl benzamide (III), m. p. 148~149°C (reportedly[8] 146°C) and cyclohexanecarboxyanilide (IV), m. p. 146.5~147°C (reportedly 139°C)[9] respectively, were also prepared for identification of the reaction product and the ultraviolet spectra of the respective amides were compared. Although the melting point of the two compounds were close to each other, the mixed melting point of the two authentic acid amides, III and IV, was depressed to 112 ~116°C.

A preliminary test was performed to confirm the stability of the oximes in liquid sulfur dioxide. In the range of this experimental condition the α-oxime was sufficiently stable whereas the β-oxime isomerized to the α-oxime gradually in liquid sulfur dioxide. Accordingly, special attention was paid to carry out the Beckmann rearrangement of the β-oxime.

Table I. Rearrangement of cyclohexyl phenyl ketoximes in liquid sulfur dioxide

| Reagent | −70±0.2°C, 1 hr. | |
|---|---|---|
| | Product | Rearrangement |
| α-Oxime I | | |
| $SOCl_2$ | III | trans |
| $C_6H_5SO_2Cl$ | I | No |
| Bromine | III | trans |
| HCl | I | No |
| HBr | I | No |
| $SOCl_2$ in ether | I | No |
| β-Oxime II | | |
| $SOCl_2$ | IV | trans |
| $C_6H_5SO_2Cl$ | IV | trans |
| Bromine | IV | trans |
| HCl | I+V | No, deoximation |
| HBr | I+V | No, deoximation |
| $SOCl_2$ in ether | IV | trans |

8) W. Markownikoff, *J. Chem. Soc.*, **87**, 92 (1892).
9) J. S. Lumsden, *Ann.*, **302**, 27 (1905).

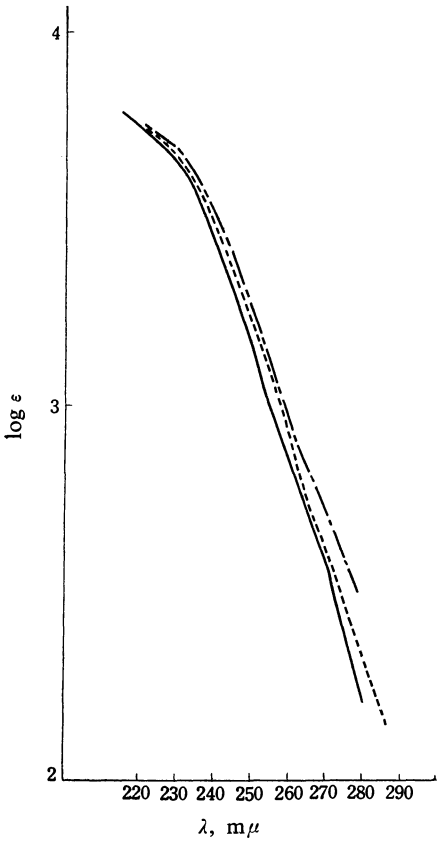



Fig. 4. Ultraviolet spectra of the reaction products from α-oxime I by hydrogen halides in liquid $SO_2$ at −70°C.
---- HCl —— HBr
—— α-Oxime (I)

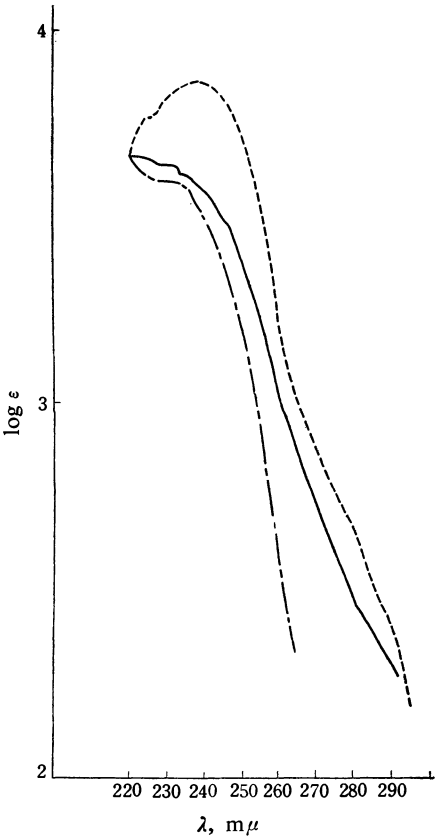


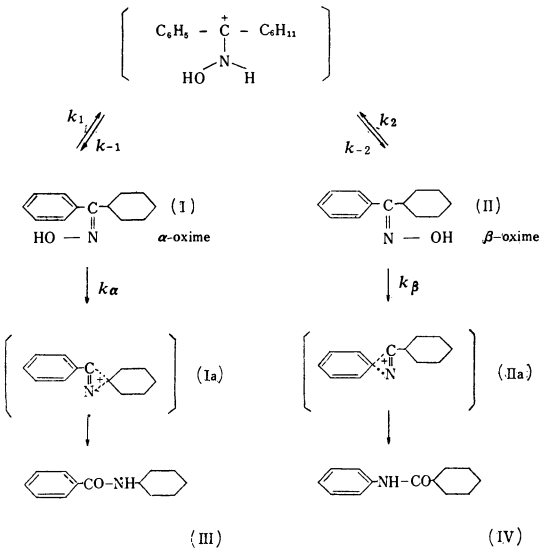

Fig. 5. Ultraviolet spectra of the reaction products from β-oxime II in liquid $SO_2$ at −70°C.
---- HCl —— HBr
—— β-oxime (II)

The Beckmann rearrangement were carried out in liquid sulfur dioxide at −70°C to avoid any undesirable side reaction. The reagents adopted for the rearrangement were thionyl chloride, benzenesulfonyl chloride, bromine and hydrogen halides. The result of the rearrangement is listed in Table I.

When the Beckmann rearrangement was carried out with thionyl chloride at −70°C in liquid sulfur dioxide, neither the α-oxime nor the β-oxime showed the random migratory aptitude, affording only *N*-cyclohexyl benzamide(III) from α-oxime I, and cyclohexanecarboxyanilide (IV) from β-oxime II, respectively. The mixed melting point and the superimposability of the ultraviolet spectra with those of the authentic specimen have proved that the rearrangement was progressing only in one direction, producing a single acid amide of the two.

The similar results were also obtained by other reagents, by which the different migratory aptitudes were not displayed in the rearrangements.

Chart 1.



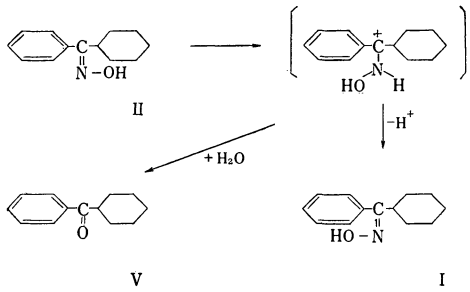

Thus, among a variety of reagents examined, within the range of these experimental conditions, thionyl chloride and bromine were only effective for the rearrangement of the α-oxime,

from which both reagents yielded the compound III exclusively as the result of trans migration.

As for the less stable β-oxime, the rearrangements were effected by thionyl chloride, benzenesulfonyl chloride and bromine to yield the amide IV exclusively, again the trans migration being predominant.

Hydrogen chloride and hydrogen bromide were both ineffective for the rearrangement, recovering the original α-oxime when it was started from the α-oxime or yielding a mixture of cyclohexyl phenyl ketoxime (V) and the α-oxime isomerized when the β-oxime was reacted. It is not surprising that the β-oxime unreacted was transformed to the more stable α-oxime (Chart 1, $k_2 > k_{-2}$ and $k_{-1} > k_1$) and the ketone V was recovered as the result of deoximation in liquid sulfur dioxide (Chart 2).

Chart 2.

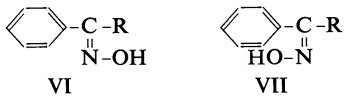



The ultraviolet spectra of the respective specimens and the crude products were recorded in methanol solutions and are seen in Fig. 1—5.

The products were obtained in the pure state or in a comparatively pure state. Sometimes the melting points of the crude products (after being washed with water and dried in vacuo) were in a range such as 135~142°C, but the ultraviolet spectra showed no contamination of another amide and were almost superimposable to the authentic acid amide. It is worthy to note that the formation of the ketone V and the possible contamination of the ketone in small quantity would make the quantitative analysis of the β-oxime impossible by ultraviolet spectrometry, because the ultraviolet spectrum of the ketone V was closely resembling that of the β-oxime. (Fig. 1)

It is a plausible conclusion that the more stable α-oxime I is in the *syn*-phenyl structure VII and the less stable β-oxime II is in the *anti*-phenyl structure VI.

When R (alkyl) is methyl[10], the structure of the oxime is principally of the *anti*-phenyl oxime VI,




because the Beckmann rearrangement affords mainly acetanilide, the phenyl groups migrating. Thus the *anti*-phenyl structure VI of the oxime is favored. As the bulkiness of the alkyl group increases, the presence of the *syn*-phenyl structure becomes more favorable[11].

When R is cyclohexyl, the *anti*-structure VII will be predominant because the steric interference between the hydroxyl group and the puckered cyclohexane ring will be more serious than that between the hydroxyl group and the planer phenyl group. Thus, the α-oxime, structure I, viz. *syn*-phenyl VII, is the more stable form, from which the Beckmann rearrangement should give III by the trans migration.

The rearrangement reaction in liquid sulfur dioxide was so rapid that the isomerization of one isomer to the other or the equilibration between the two oximes could not be competitive against the Beckmann rearrangement reaction, ($k_\alpha \gg k_1$, $k_\beta \gg k_2$, Chart 1). Even the labile β-oxime afforded only the trans migrated product IV on the Beckmann rearrangement. On this occasion the elucidation of Brown et al.[3] may again be recalled to account for the discrepancy of our result.

The complication of the result may be increased if the isomerization and the deoximation of the oxime were accompanied competitively with the rearrangement.

Another point of interest is that when the Beckmann rearrangement was carried out at −70°C in ether as the solvent in place of sulfur dioxide with thionyl chloride as the reagent, α-oxime could not be rearranged, whereas β-oxime rearranged to the acid amide IV smoothly with trans migration. The difference of the reactivity in these solvents and oximes may perhaps depend on the different solvations of the two solvents on oximes and the difference of the reactivity of the two oximes.

That the β-oxime II is more reactive than the α-oxime I is satisfactorily explicable by the facility of producing the intermediate azirinum cation[12] (IIa) by phenyl group participation, and the release of the steric hindrance by rearranging.

In conclusion, the assignment of Meisenheimer and Theilacher[7] has been verified for

10) D. E. Pearson and F. Ball, *J. Org. Chem.*, **14**, 118 (1949).

11) Y. Yukawa, Y. Tsuno and A. Tsukamoto, Abstracts of the 7th Annual Meeting of Chem. Soc. of Japan., April, 1954.

12) R. Huisgen, J. Witte and I. Ugi, *Chem. Ber.*, **90**, 1844, 1850 (1957).

the geometrical structure of cyclohexyl phenyl ketoximes, the $\alpha$-oxime being of the *syn*-phenyl and the $\beta$ being of the *anti*-structure.

## Experimental

**Material.**—The purification and the manipulation of the liquid sulfur dioxide has already been published elsewhere. Thionyl chloride and benzenesulfonyl chloride were used after one distillation respectively[1]. Bromine was washed with concentrated sulfuric acid and distilled.

**Preparation and Separation of Cyclohexyl Phenyl Ketoxime (I) and (II).**—Essentially the method of Meyerand Scharvin[5] was used and modified slightly. A Grignard reagent from cyclohexyl bromide was reacted with benzaldehyde to obtain the corresponding carbinol, b. p. 130~135°C (5 mmHg), 26%, which was spontaneously oxidized in the air to cyclohexyl phenyl ketone (V), fine crystals, m. p. 57~58°C. The oxidation of the ketone resulted in a mixture of the geometrical isomers in good yield. The oximes were dissolved in acetic acid and fractionally precipitated by adding water gradually to obtain first the $\beta$-oxime, fine crystals, m. p. 113~114°C (II), then the $\alpha$-isomer, fine needles, m. p. 156~157°C (I), respectively. For compound I. Found: N, 6.64. Calcd. for $C_{13}H_{17}ON$: N, 6.89%. For compound II. Found: N, 6.80. Calcd. for $C_{13}H_{17}ON$: N, 6.89%.

***N*-Cyclohexyl Benzamide(III).**—This material was prepared by the known method[8], from cyclohexyl amine and benzoyl chloride in a yield of 82.3%, fine needles, m. p. 148~149°C (methanol). Found: N, 6.51. Calcd. for $C_{13}H_{17}ON$: N, 6.89%.

**Cyclohexanecarboxyanilide (IV).**—Aniline and cyclohexanecarboxylic acid was refluxed for several hours and the resulting mass was twice recrystallized from ethanol[9], long pillars, m. p. 146.5~147°C. Found: N, 6.60. Calcd, for $C_{13}H_{17}ON$: N, 6.89%.

**Mixed Melting Point of III and IV.**—Though the melting points of the two acid amides III and IV, were very close to each other, the mixed melting point of the two materials, III and IV, was depressed to 112~126°C.

**Isomerization of $\alpha$- or $\beta$-Oxime, I or II in Liquid Sulfur Dioxide.**—$\alpha$-Oxime I, (1.0 g.) was dissolved in 300 ml. of liquid sulfur dioxide at $-70 \pm 0.2$°C and allowed to stand for 24 hr. No change of melting point of I, 156~157°C, was seen after the recovery of the material (0.89 g.), which showed no depression of mixed melting point with an authentic specimen. On the contrary, the same treatment on the $\beta$-oxime II was carried out at $-70$°C for 24 hr. and $\alpha$-oxime was obtained as the result of isomerization which was identified by the mixed melting point measurement with the authentic $\alpha$-oxime.

**The Beckmann Rearrangement.**—To a solution of 0.5g. (0.0025 mol.) of the $\alpha$-oxime in 100 ml. of liquid sulfur dioxide, a reagent (0.0025 mol.), e. g. 0.3 g. of thionyl chloride in a small ampoule was added and the vessel was cooled to a definite temperature in a constant temperature bath. After the mixture reacted to the temperature ($-70 \pm 0.2$°C) the vessel was vigorously shaken in order to break the ampoule in the mixture. The mixture was allowed to stand at this temperature for one hour. Then the mixture was filtered and the filtrate was poured into ice-water. The precipitate afforded was collected, washed with water and dried in vacuo. The product was examined as to its melting point and the mixed melting point with the authentic acid amide, and ultraviolet spectrum of the product was compared in methanolic solution.

As the $\beta$-oxime was so unstable in liquid sulfur dioxide that the oxime in a glass ampoule was placed in a mixture of a reagent and sulfur dioxide. The rearrangement by hydrogen chloride or hydrogen bromide was carried out by passing the dry hydrogen halide gas into the reaction mixture at $-70$°C, followed by the crushing of the ampoule of the oxime.

**Ultraviolet Spectra Measurement.**—A Hitachi EPU-2A type spectrophotometer was used. All the measurements were carried out in methanolic solution.

**Results of the Rearrangements.**—*$\alpha$-Oxime by Thionyl Chloride.*—The melting point of the product (0.42 g.) was 142~145°C, the mixed melting point with III being 144~147°C, whereas with IV, the melting point depressed to 112~116°C. The ultraviolet spectrum was superimposable with that of III. (Fig. 2)

*$\beta$-Oxime by Thionyl Chloride.*—The melting point of the product (0.43 g) was 145~146°C. No melting point depression with IV, whereas with III it was depressed. The ultraviolet spectrum was superimposable on that of IV. (Fig. 3)

*$\alpha$-Oxime by Benzenesulfonyl Chloride.*—The product was recovered $\alpha$-oxime (0.46 g), melting point and mixed melting point being 155~157°C.

*$\beta$-Oxime by Benzenesulfonyl Chloride.*—The reaction gave a product (0.44 g.) of meltng point 135~142°C. The mixed melting point with IV was 136~145°C. The ultraviolet spectrum was superimposable on that of IV. (Fig. 3) The wide range of the melting point will mean that the reaction was not complete in one hour.

*$\alpha$-Oxime by Bromine.*—The result in this case was somewhat complicated, as the Beckmann rearrangement of a phenyl ketoxime by bromine was often accompanied by a bromination of the benzene nucleus[13]. The ultraviolet spectrum of the crude product was close to that of III, (Fig. 2), however, the melting point of the product (0.43 g.) was 112~120°C. A fractional crystallization from alcohol yielded two crystals, one melting at 116~120°C and containing bromine (by the Beilstein test), but was a very small quantity for its further identification. The other was the acid amide III, m. p. 145~146°C (0.30 g.) and mixed melting point with III was 146~147°C.

*$\beta$-Oxime by Bromine.*—From the crude product (0.46 g.), the fractional precipitation (from acetic acid solution by adding water), yielded crystals of m. p. 131~139°C, which was negative for the Beilstein test but was not pure enough. However, the ultraviolet spectrum of this material was resembling well that of IV, (Fig. 3).

*$\alpha$-Oxime by Hydrogen Chloride.*—$\alpha$-Oxime (0.47

13) N. Tokura, R. Asami and R. Tada, *J. Am. Chem. Soc.*, **79**, 3135 (1957).

g.), melting point and mixed m. p. 154~157°C was recovered. (Fig. 4)

*β-Oxime by Hydrogen Chloride.*—The ultraviolet spectrum of the product was reproduced in Fig. 5. Two kinds of crystals were separated by fractional precipitation as above mentioned. One, melting point and mixed m. p. 55.56°C (0.40 g.) was the ketone V, 2,4-dinitrophenyl hyrazone, m. p. 198~199.5°C, Found: N, 15.68. Calcd. for $C_{10}H_{20}O_4N_4$: N, 15.21%. The other, (0.12 g.), melting point and mixed m. p. 156~158°C was the α-oxime[1] isomerized from the β-oxime II.

*α-Oxime by Hydrogen Bromide.*—α-Oxime (0.48 g.), melting point and mixed m. p., 155~157°C was recovered.

*β-Oxime by Hydrogen Bromide.*—The ketone V, (0.15 g.), meltng point and mixed m. p. 53~55°C, and the α-oxime (0.23 g.), melting point and mixed m. p. 156~158°C, were separated and identified respectively, as above.

*α-Oxime by Thionyl Chloride in Ether at −70°C.*—The α-oxime (0.33g.) was recovered, melting point and mixed m. p. 155~157°C, (ultraviolet spectrum, Fig. 2).

*β-Oxime by Thionyl Chloride in Ether at −70°C.*—The product (0.43 g.), melting point and mixed m. p. 142~143.5°C was proved to be the IV. The ultraviolet spectrum was superimposable. (Fig. 3)

## Summary

The Beckmann rearrangement of the isomeric cylcohexyl phenyl ketoximes was carried out in liquid sulfur dioxide at low temperature (−70°C) with thionyl chloride, benzenesulfonyl chloride, bromine and hydrogen halides. In liquid sulfur dioxide, the β-oxime was unstable and isomerized slowly to the α-oxime with no reagent. The α-oxime yielded *N*-cyclohexyl benzamide and the β-oxime yielded cyclohexanecarboxyanilide, respectively, by the Beckmann rearrangement in liquid sulfur dioxide. The geometrical structure of the isomers and isomerization between them were discussed. As for the β-oxime, the rate of the rearrangement by far surpassed the rate of the isomerization. The principle of the trans migration in the Beckmann rearrangement has been confirmed within the range of this experiment. The deoximation of the oxime to the parent ketone, cyclohexyl phenyl ketone was observed in the reaction of β-oxime with hydrogen chloride and bromide.

We are indebted to the Befu Chemical Industries Ltd., for the donation of liquid sulfur dioxide. The present authors are also grateful to Professor Y. Yukawa of Osaka University for his courtesy in carrying out this project.

*Chemical Research Institute of Non-Aqueous Solutions*
*Tohoku University, Sendai*

# *On the Reactivity of Various Silicate Minerals toward Acids*

By Hanzo MASE

(Received May 31, 1960)

As for the relative difficulty of dissolution of oxyacids and their salts toward water, a few qualitative rules have been proposed on the standpoint of ionic potential[1]. However, it is not too much to say that no comprehensive treatises on the reactivity of various silicate minerals toward ordinary acids (except hydrofluoric acid) have been reported, although the studies on the individual one have been undertaken by many investigators[2].

Previously, the author pointed out the requirements for the frothing reaction of silicate minerals toward water and concentrated sulfuric acid. Those requirements were summarized as follows: 1) the silicates belonging to either the neso- or the phyllo-silicates are generally reactive; 2) in the phyllosilicates, most of those of the 1 : 1 type (e. g., serpentine) are as a rule reactive, but those of the 2 : 1 type are not at all or only slightly reactive; and 3) the more electropositive the metallic components are, the more reactive the silicates become. But the electropositivity of metals was not discussed in detail.

1) G. H. Cartledge, *J. Am. Chem. Soc.*, **50**, 2855 (1928); V. M. Goldschmidt, *J. Chem. Soc.*, **1937**, 655; F. E. Wickman, *Arkiv. Kemi, Min. Geol.*, **19B**, No. 2 (1944); R. Tsuchida, *Chemistry (Kagaku)*, **6**, 6 (1951); **7**, 88 (1952).

2) W. Eitel, "The Physical Chemistry of the Silicates", The University of Chicago Press, Chicago, Illinois (1954), p. 965; S. Nagai and Y. Arai, *Gypsum and Lime (Sekko to Sekai)*, **34**, 7 (1958); J. Ando, *J. Chem. Soc. Japan, Ind. Chem. Sec. (Kogyo Kagaku Zasshi)*, **63**, 83 (1960).

In this paper, the author attempted to make this problem clear by using various terms concerning the combining forces between the cations and the silicate ions, and also to explain it energetically from the bonding energies of silicate minerals.

## Results from the Electropositivity of the Constituent Metals

It is well known in the field of crystal chemistry that the bonding force between various cations and silicate ions is related to the polarizing power of the cations or their tendencies to form covalent bonds with oxygen atoms. One may say that a cation with strong polarizing power or a pronounced tendency to make covalent bonds loosens bonds within a silicate ion, thus causing a splitting up of it into free acids. On the contrary, cations with small polarizing power allow strong bonds to form within the silicate ion and do therefore make stable silicate.

This polarizing power of cations is qualitatively or approximately measured with their ionic potentials (e. g., cation charge/cation radius), the ratio of cation charge to the square of cation radius (Goldschmidt's polarizing power), or the field strength around the cations[3], etc. (hereafter referred to as $\phi$, $\phi'$ or F. S., respectively.)

Therefore, the author tried to calculate and to view the above mentioned values of various cations contained in silicate minerals. The results were listed in the following table[4].

| | |
|---|---|
| $\phi$; more than 4 | Ti, Be, Al, Cr, V(III), Zr, Fe(III), Mn(III). |
| 3~4 | Th, Sc. |
| 2~3 | Y, Mg, Ni, Ce, La, Fe(II), Zn, Mn(II). |
| less than 2 | Cu, Ca, Sr, Pb, Ba, Li, Na, K. |
| $\phi'$; more than 6 | Be, Ti, Al, Cr, V(III), Fe(III), Mn(III). |
| 4~6 | Zr, Sc. |
| 2~4 | Th, Mg, Ni, Y, Fe(II), Zn, Mn(II), Ce, La. |
| less than 2 | Cu, Ca, Li, Sr, Pb, Na, Ba, K. |
| F. S.; more than 0.7 | Ti, Th, Al, Cr, Zr, V(III), Fe(III), Be, Mn(III). |
| 0.5~0.7 | Sc, Y. |
| 0.4~0.5 | Ce, La, Mg, Ni, Fe(II), Zn, Mn(II). |
| less than 0.4 | Cu, Ca, Sr, Pb, Ba, Li, Na, K. |

As shown in this table, the polarizing power of the following cations seems to be extremely great, and further the electropositivity of them to be small: e. g., Ti, Be, Al, Cr, V(III), Fe(III), Mn(III), Zr, etc. Thus the existence of these metals may contribute to the decrease of reactivity of silicate minerals. This conclusion is in agreement with the experimental results that kaolinite is not completely decomposed, although serpentine is easily attacked by acids.

As is generally known, all the silicate minerals were now divided into five classes structurally; namely, neso-, soro-, ino-, phyllo-, and tecto-silicate. According to this classification, it was at first in Tables I—V[5] examined whether or not the singularity of the above eight metal ions is applicable to those silicates. In Tables I—V the results of reactions toward acids are made an entry. Most of them are cited from the data of Lange's Handbook[6], Dana's Textbook of Mineralogy[7], and Mellor's Treatise[8]. The parenthesized passage is refered to the author's prediction.

**Nesosilicate Minerals.**—The nesosilicates are termed the silicates having the structures with separated tetrahedra $(SiO_4)^{4-}$ groups, and involve the following minerals listed in Table I.

Generally speaking, the results in Table I seem to indicate that the majority of nesosilicate minerals are able to react with acids, and to be decomposed with the formation of gelatinous silica, except the garnet group and a few particular complex silicate minerals. Also it is confirmed that one of the above eight metallic elements is inevitably contained in these insoluble nesosilicate minerals.

For example, phenacite ($Be_2SiO_4$) is not attacked by acids. This fact is probably due to the existence of Be atoms, which have very large $\phi$, $\phi'$ and F. S. For the same reason, the garnet group minerals, euclase, topaz, zunyite, andalusite, sillimanite, mullite, kyanite, sapphirine, etc. may be not decomposed by acids. Moreover titanosilicate minerals containing Ti atoms are inactive toward acids. Although

3) A. Dietzel, *Naturwiss.*, **29**, 537 (1941); *Electrochem.*, **48**, 9 (1942).

4) The values of the ionic radii of various cations were quoted from C. W. Stillwell's "Crystal Chemistry", McGraw-Hill Book Co., Inc., New York (1938).

5) The classification, species and structural formula of silicate minerals are based upon Sudo's system (which is primarily cited from Berman's and Swartz's systems and is revised and enlarged with the latest data.) and Strunz's Tables (H. Strunz, "Mineralogische Tabellen" (1958)).

H. Berman, *Am. Mineralogist*, **22**, 342 (1937); O. K. Swartz, ibid., **22**, 1073, 1161 (1937); T. Sudo, "Mineral Chemistry (Kobutsu Kagaku) (II)", Kyoritsu Shuppan Co., Ltd. (1959), p. 259.

6) Lange's Handbook of Chemistry (1949).

7) Dana's Textbook of Mineralogy (1959).

8) W. Mellor, "A Comprehensive Treatise on Inorganic and Theoretical Chemistry", Vol. VI (1925).

TABLE I. REACTIVITY OF NESOSILICATE MINERALS TOWARD ACIDS

| Minerals | Chemical formula | Reactivity toward acids | Bonding energy (kcal.) |
|---|---|---|---|
| Olivine series (Ca, Mn, Mg, Fe, Pb) (Mg, Fe, Mn, Zn) $SiO_4$ | | | |
| Forsterite | $Mg_2SiO_4$ | Gel. a. | 29796 |
| Olivine | $(Mg, Fe)_2SiO_4$ | Gel. a. | (29904)*1) |
| Hortonolite | $(Mg, Fe, Mn)_2SiO_4$ | Gel. a. | |
| Fayalite | $Fe_2SiO_4$ | Gel. a. | (29880) |
| Knebelite | $(Fe, Mn)_2SiO_4$ | Gel. a. | |
| Tephroite | $(Mn, Zn, Mg)_2SiO_4$ | Gel. a. | |
| Roepperite | $(Fe, Mn, Zn)_2SiO_4$ | Gel. HCl | |
| Glaucochroite | $CaMnSiO_4$ | Gel. HCl | |
| Monticellite | $CaMgSiO_4$ | Gel. HCl | (29358) |
| Larsenite | $PbZnSiO_4$ | Sol. $HNO_3$ | |
| Calcium Larsenite | $(Pb, Ca)ZnSiO_4$ | Sol. $HNO_3$ | |
| Larnite | $Ca_2SiO_4$ | Sol. HCl | (28920) |
| Merwinite | $Ca_3Mg(SiO_4)_2$ | Sol. HCl | (29139) |
| Phenacite group $X_2SiO_4$ | | | |
| Phenacite | $Be_2SiO_4$ | Insol. | |
| Willemite | $Zn_2SiO_4$ | Gel. a. | |
| Troostite | $(Zn, Mn)_2SiO_4$ | Gel. a. | |
| Trimerite | $CaMn_2(BeSiO_4)_3$ | Sol. HCl | |
| Humite group $nMg_2SiO_4 \cdot Mg(OH, F)_2$ | | | |
| Norbergite | $Mg_2SiO_4 \cdot Mg(OH, F)_2$ | Gel. a. | (27632)*2) |
| Chondrodite | 2 〃 · 〃 | Gel. a. | (28498)*2) |
| Humite | 3 〃 · 〃 | Gel. a. | (28869)*2) |
| Clinohumite | 4 〃 · 〃 | Gel. a. | (29075)*2) |
| Hodgkinsonite group $X_{2r+1}(SiO_4)_r(OH, F)_2$ | | | |
| Hodgkinsonite | $(Zn_2Mn)(SiO_4)(OH)_2$ | Sol. a. | |
| Alleghanyite | $Mn_5(SiO_4)_2(OH, F)_2$ | Sol. a. | |
| Leucophoenicite | $Mn_7(SiO_4)_3(OH)_2$ | Sol. a. | |
| Garnet group $X_3Y_2(ZO_4)_3$ X=Mg, Fe, Mn, Ca<br>Y=Al, Fe(III), Cr, Ti, Mn<br>Z=Si, Ti | | | |
| (1) Almandite series $(Mg, Fe, Mn)_3Al_2(SiO_4)_3$ | | | |
| Pyrope | $Mg_3Al_2(SiO_4)_3$ | Insol. | (31836) |
| Almandite | $Fe_3Al_2(SiO_4)_3$ | Insol. | 31878 |
| Spessartite | $Mn_3Al_2(SiO_4)_3$ | Insol. | |
| (2) Andradite series | | | |
| Grossularite | $Ca_3Al_2(SiO_4)_3$ | Insol. | (31398) |
| Andradite | $Ca_3Fe_2(SiO_4)_3$ | Insol. | |
| Uvarovite | $Ca_3Cr_2(SiO_4)_3$ | Insol. | |
| Titanium Garnet | $Ca_3(Al, Fe(III), Fe(II), Ti)_2[(Si, Ti)O_4]_3$ | Insol. | |
| Zircon group $XSiO_4$ | | | |
| Zircon | $ZrSiO_4$ | Mostly insol. | |
| Thorite | $ThSiO_4$ | Gel. a. | |
| Wöhlerite group $W_3X(ZO_4)_2(F, OH)$ | | | |
| Rosenbuschite | $(Na, Ca)_3(Fe, Ti, Zr)(SiO_4)_2F$ | Sol. HCl | |
| Wöhlerite | $(Ca, Na)_3(Zr, Ta)(SiO_4)_2F$ | Sol. HCl | |
| Hiortdahlite | $(Ca, Na)_3(Fe, Mn, Zr, Ti)(SiO_4)_2(F, OH)$ | (Sol. HCl) | |
| Guarinite | $(Ca, Na)_3(Fe, Mn, Zr, Ta)(SiO_4)_2(O, F, OH)$ | Gel. HCl | |
| Johnstrupite | $(Ca, Na, Ce)_3(Al, Mg, Ti, Ce)(SiO_4)_2(F, OH)$ | Sol. HCl | (29850)*3) |
| Rinkite | $(Ca, Na)_6(Ce, Zr, Ti)_7(SiO_4)_{10}F_7$ | Decomp. $H_2SO_4$ | |
| Rinkolite | $(Ca, Na)_6(Ce, Ti)_3(SiO_4)_4(F, OH)_4$ | (Decomp. a.) | |
| Mosandrite | $(Ca, Na)_{12}Ce_3(Zr, Ti, Mg)_4(SiO_4)_{10}F_5$ | Sol. HCl | |
| Låvenite | $(Ca, Na)(Zr, Ta, Fe, Ti, Mn)(SiO_4)F$ | Sl. sol. HCl | |
| Britholite | $Ca_3Ce_4[(Si, P)O_4]_4(OH, F)_3$ | (Decomp. a.) | |
| Hellandite | $Ca_3(Y, Er)_4(Al, Fe(III), Mn(III))_5(SiO_4)_6(OH)_9$ | Sol. HCl | |

TABLE I. (Continued)

| Minerals | Chemical formula | Reactivity toward acids | Bonding energy (kcal.) |
|---|---|---|---|
| Lessingite | $Ca_2(Ce, La, Na)_3(SiO_4)_3(OH, F)$ | (Decomp. a.) | |
| Beckelite | | Sol. a. | |
| Datolite group | | | |
| Datolite | $Ca_2B_2(SiO_4)_2(OH)_2$ | Gel. HCl | |
| Euclase | $Al(BeOH)SiO_4$ | Insol. | |
| Homilite | $Ca_2Fe(II)Be_2(SiO_4)_2O$ | Gel. HCl | |
| Gadolinite | $Y_2Fe(II)Be_2(SiO_4)_2O_2$ | Gel. a. | |
| Misc. | | | |
| Topaz | $Al_2SiO_4(F, OH)_2$ | Sl. decomp. $H_2SO_4$ | 31712 |
| Ilvaite | $Ca(Fe, Mn)_2Fe(III)(SiO_4)_2(OH)$ | Gel. a. | |
| Afwillite | $Ca_3(SiO_3OH)_2\cdot 2H_2O$ | (Decomp. a.) | |
| $\alpha$-Eucryptite | $\alpha$-$LiAl(SiO_4)$ | Gel. HCl | |
| Eulytite | $Bi_4(SiO_4)_3$ | Gel. HCl | |
| Zunyite | $Al_{12}(Si_2O_7)_2(SiO_4)(AlO_4)(OH, F)_{18}Cl$ | Insol. | |
| Quasi-silicates | | | |
| Aluminum silicates | | | |
| Andalusite | $Al_2SiO_5$ | Insol. | |
| Sillimanite | $Al_2SiO_5$ | Insol. | 31957 |
| Mullite | $(Al_2O)_6(SiO_4)_6(Al_2O_7)$ | Insol. | |
| Kyanite | $Al_2SiO_5$ | Insol. | |
| Staurolite | $Fe(II)Al_4Si_2O_{10}(OH)_2$ | Sl. decomp. $H_2SO_4$ | 31828 |
| Kentrolite group | | | |
| Kentrolite | $Pb_3Mn(III)_4Si_3O_{15}$ | Sol. a. | |
| Melanotekite | $Pb_3Fe(III)_4Si_3O_{15}$ | Decomp. $HNO_3$ | |
| Titanosilicates | | | |
| Titanite | $CaTiSiO_5$ | Sol. $H_2SO_4$ | (32942) |
| Lorenzenite | $Na_2(Zr, Ti)_2Si_2O_9$ | Insol. HCl | |
| Ramsayite | $Na_2Ti_2Si_2O_9$ | (Insol.) | (33845) |
| Lamprophyllite | $Na_3Sr_2Ti_3(SiO_4)_4(O, OH, F)_2$ | (Insol.) | |
| Fersmanite | $Ca_4Na_4Ti_4Si_3O_{18}F_2$ (?) | (Insol.) | |
| (App.) | | | |
| Dumortierite | $(Al, Fe)_7BSi_3O_{18}$ | Insol. HF | |
| Serendibite | $(Ca, Mg)_5Al_5BSi_3O_{20}$ | (Insol.) | |
| Sapphirine | $Mg_2Al_4SiO_{10}$ | Insol. | (31283) |
| Ardennite | $Mn_5Al_5(V, As)O_4Si_5O_{20}(OH)_2\cdot 2H_2O$ | (Insol.) | |
| Kornerupine | $(Mg, Fe, Al)_4(Al, B)_6Si_4O_{16}(O, OH)_{5\sim 6}$ | (Insol.) | |
| Cappelenite | $(Ba, Ca, Ce, Na)_3(Y, Ce, La)_6B_6Si_3O_{27}$ | Sol. HCl | |
| Melancocerite | $Ca_{16}Na_4(Y, La)_3(Zr, Ce)_6B_3Si_{12}O_{57}F_{12}$ | Decomp. HCl | |
| Uranosilicates | | | |
| Uranophane | $Ca(H_3O)_2(UO_2)(SiO_4)_2\cdot 3H_2O$ | Gel. HCl | |
| Sklodowskite | $MgU_2O_2(OH)_2(SiO_4)_2\cdot 4H_2O$ | Gel. HCl | |
| Kasolite | $PbUO_2SiO_4\cdot H_2O$ | Gel. a. | |
| Soddyite | $(UO_2)_2SiO_4\cdot 2H_2O$ (?) | Gel. HCl | |

(Abbreviations used in Tables I—V.)

a.: acids; abbr.: abbreviation; app.: appendix; conc.: concentrated; decomp.: decomposed (by); gel.: gelatinize; insol.: insoluble (in, or, in acids); misc.: miscellanea; sl.: slightly; sol: soluble (in); undecomp.: undecomposed (by).

(The minerals cited in the appendixes in these tables are unassigned up to the present.)

*1) This value was calculated regarding the compositional formula of olivine as $9Mg_2SiO_4\cdot Fe_2SiO_4$.

*2) These values were calculated regarding $nMg_2SiO_4\cdot Mg(OH, F)_2$ as $nMg_2SiO_4\cdot Mg(OH)_2$.

*3) This value was calculated regarding the chemical formula of johnstrupite as ideally $Ca_3Al(SiO_4)_2(OH)$.

Table II. Reactivity of sorosilicate minerals toward acids

| Minerals | Chemical formula | Reactivity toward acids | Bonding energy (kcal.) |
|---|---|---|---|
| Benitoite | $BaTi(Si_3O_9)$ | Sol. HF | |
| Rhodonite series | | | |
| Rhodonite | $(Mn, Ca)_5Si_5O_{15}$ | Sl. sol. HCl | |
| Pyroxmangite | $(Mn, Ca)_7Si_7O_{21}$ | Insol. a. | |
| Wollastonite group | | | |
| Wollastonite | $Ca_3Si_3O_9$ | Decomp. HCl | |
| Bustamite | $(Ca, Mn)_3Si_3O_9$ | (Decomp. HCl) | |
| Pectolite | $Ca_2NaH(SiO_3)_3$ | Gel. HCl | |
| Alamosite | $PbSiO_3$ | (Gel. $HNO_3$) | |
| Catapleiite series | | | |
| Catapleiite | $Na_2Zr(Si_3O_9)\cdot H_2O$ | Sol. HCl | |
| Eudialyte | $(Na, Ca, Fe)_6ZrSi_6O_{18}(OH, Cl)$ | Gel. HCl | |
| Steenstrupine | $(Ca, Na)_4Mn(Ce, La, Al, Fe(III))_6(Si, Ti)_9O_{27}(OH)_7\cdot 3H_2O$ (?) | Decomp. a. | |
| Tourmaline series | $WX_3Y_6(Z_3O_9)_3(O, OH, F)_4$ | | |
| Dravite | $NaMg_3B_3Al_3(Al_3Si_6O_{27})(OH)_4$ | Undecomp. a. | |
| Uvite | $CaMg_3B_3Al_3(Al_3Si_6O_{27})(O, OH)_4$ | Undecomp. a. | |
| Indigolite | $Na(Al, Fe(II), Li, Mg)_3B_3Al_3(Al_3Si_6O_{27})(O, OH, F)_4$ | Undecomp. a. | |
| Tourmaline | $(Na, Ca)(Mg, Fe(II), Fe(III))_3B_3Al_3(Al_3Si_6O_{27})(O, OH)_4$ | Undecomp. a. | |
| Schorl | $NaFe_3B_3Al_3(Al_3Si_6O_{27})(OH)_4$ | Undecomp. a. | |
| Misc. | | | |
| Dioptase | $Cu_6(Si_6O_{18})\cdot 6H_2O$ | Gel. HCl | |
| Axinite | $(Fe, Mn)Ca_2Al_2(BO_3)(Si_4O_{12})(OH)$ | Undecomp. a. | |
| Beryl | $Al_2Be_3Si_6O_{18}$ | Insol. | |
| Osumilite | $(K, Na, Ca)(Mg, Fe(II))_2(Al, Fe(III), Fe(II))_3(Si, Al)_{12}O_{30}\cdot H_2O$ | (Sl. decomp. a.) | |
| Indialite | $(Mg, Fe)_2Al_3(Si_5, Al)O_{18}$ | (Sl. decomp.) | (31920)*1) |
| Cordierlite | $(Mg, Fe)_2Al_3(Si_5, Al)O_{18}$ | Sl. decomp. a. | (31920)*1) |
| Thalenite group | | | |
| Thalenite | $Y_2Si_2O_7$ | (Insol. a.) | |
| Thortveiteit | $(Sc, Y)_2Si_2O_7$ | Insol. HCl | |
| Cerite | $(Ce, Y, Pr, Nd)_2Si_2O_7\cdot H_2O$ | Gel. HCl | |
| Rowlandite | $(Y, Ce, La)_4Fe(II)(Si_2O_7)_2F_2$ | Gel. HCl | |
| Melilite series | | | |
| Åkermanite | $Ca_2MgSi_2O_7$ | Gel. HCl | 30391 |
| Gehlenite | $Ca_2Al(AlSiO_7)$ | Gel. HCl | 26890 |
| Melilite | $(Ca, Na)_2(Al, Mg)(Si, Al)_2O_7$ | Gel. HCl | |
| Hardystonite | $Ca_2ZnSi_2O_7$ | Gel. HCl | |
| Leucophanite | $(Ca, Na, H)_2BeSi_2O_6(OH, F)$ (?) | Sol. HF | |
| Meliphanite | $(Ca, Na)_2(Be, Al)Si_2O_6F$ | (Insol.) | |
| Barysilite group | | | |
| Barysilite | $Pb_3Si_2O_7$ | Gel. $HNO_3$ | |
| Ganomalite | $Pb_6Ca_4(Si_2O_7)_3(OH)_2$ | Gel. $HNO_3$ | (27383)*2) |
| Nasonite | $Pb_6Ca_4(Si_2O_7)_3Cl_2$ | Gel. $HNO_3$ | |
| Hemimorphite group | | | |
| Hemimorphite | $Zn_4(OH)_2Si_2O_7\cdot H_2O$ | Gel. a. | |
| Clinohedrite | $Ca_2Zn_2Si_2O_7(OH)_2\cdot H_2O$ | Gel. HCl | |
| Bertrandite | $Be_4Si_2O_7(OH)_2$ | Insol. a. | |
| Cuspidine | $Ca_4Si_2O_7(F, OH)_2$ | (Gel. HCl, $HNO_3$) | (28427)*3) |
| Molybdophyllite | $Pb_2Mg_2Si_2O_7(OH)_2$ | (Gel. $HNO_3$) | |
| Murmanite | $NaTiSiO_4(OH)$ (?) | (Insol. a.) | (32,164) (?) |
| (App.) | | | |
| Barylite | $BaBe_2Si_2O_7$ | Insol. | |
| Lawsonite | $CaAl_2Si_2O_7(OH)_2\cdot H_2O$ | Insol. | (31,030) |
| Danburite | $CaB_2Si_2O_8$ | Sl. decomp. HCl | |

TABLE II. (Continued)

| Minerals | Chemical formula | Reactivity toward acids | Bonding energy (kcal.) |
|---|---|---|---|
| Astrophyllite | $(K_2, Na_2, Ca)(Fe, Mn)_4(Ti, Zr)Si_4O_{14}(OH)_2$ | Decomp. HCl | |
| Aenigmanite | $(Na, Ca, K)_4(Fe(II), Mn, Fe(III), Ti, Al)_{13}(Si_2O_7)_6$ (?) | Sl. sol. a. | |
| Vesuvianite | $Ca_{10}Al_4(SiO_4)_5(Si_2O_7)_2 \cdot 2(Mg, Fe)(OH)_2$ | Sl. decomp. HCl | |
| Epidote group | $W_2Y_3(ZO_4)(OH)(Z_2O_7)O$ | | |
| Zoisite | $Ca_2Al_3(SiO_4)(Si_2O_7)O(OH)$ | Insol.*4) | |
| Epidote series | | | |
| Clinozoisite | $Ca_2Al_3(SiO_4)(Si_2O_7)O(OH)$ | Insol. | |
| Epidote | $Ca_2(Al, Fe)_3(SiO_4)(Si_2O_7)O(OH)$ | Sl. decomp. HCl | |
| Piedmontite | $Ca_2(Al, Fe, Mn)_3(SiO_4)(Si_2O_7)O(OH)$ | (Sl. decomp. a.) | |
| Allanite series | | | |
| Allanite | $(Ca, Ce, La, Na)_2(Al, Fe, Mn, Be, Mg)_3(SiO_4)(Si_2O_7)O(OH)$ | Gel. HCl | |
| Nagatelite | $(Ca, Ce)_2(Al, Fe(III), Fe(II))_3[(P, Si)O_4][(P, Si)_2O_7]O(OH)$ | Sol. HCl, $HNO_3$ | |
| Pumpellyite | $Ca_4(Mg, Fe, Mn)(Al, Fe, Ti)_5Si_6O_{23}(OH)_3 \cdot 2H_2O$ | (Sol. HCl ) | |

*1) These values were calculated regarding $(Mg, Fe)_2Al_3(Si_5, Al)O_{18}$ as $Mg_2Al_3(Si_5, Al)O_{18}$.
*2) This value was calculated regarding the chemical formula of ganomalite as $Ca_{10}(Si_2O_7)_3(OH)_2$.
*3) This value was calculated regarding $\cdots\cdots(F, OH)_2$ as $\cdots\cdots(OH)_2$.
*4) The fine powder of zoisite is completely decomposed by boiling hydrochloric acid.

TABLE III. REACTIVITY OF INOSILICATE MINERALS TOWARD ACIDS

| Minerals | Chemical formula | Reactivity toward acids | Bonding energy (kcal.) |
|---|---|---|---|
| Pyroxene group $W(X, Y)(Z_2O_6)$ | W=Ca, Na, K, Mg, Mn. X, Y=Mg, Fe(II), Al, Ti, Li, Mn, Fe(III), Cr, Ni. Z=Si, Al. | | |
| (1) Enstatite series $WXZ_2O_6$ | | | |
| Enstatite | $Mg_2Si_2O_6$ | Insol. HCl | 32344 |
| Hyperthene | $(Mg, Fe)_2Si_2O_6$ | Insol. a. | |
| (2) Pigeonite series | | | |
| Clinoenstatite | $Mg_2Si_2O_6$ | Insol. a. | |
| Pigeonite | $(Ca, Mg)(Mg, Fe)Si_2O_6$ | (Insol. a.) | |
| (3) Diopside series $W(X, Y)Z_2O_6$ | | | |
| Diopside | $CaMgSi_2O_6$ | Insol. a. | 32052 |
| Hedenbergite | $CaFeSi_2O_6$ | Insol. HCl | (32080) |
| Augite | $(Ca, Mg)(Mg, Fe, Al)(Al, Si)_2O_6$ | Insol. a. | 30728 |
| Schefferite | $Ca(Mg, Fe, Mn)Si_2O_6$ | (Insol. a.) | |
| Jeffersonite | $Ca(Mg, Mn, Zn)Si_2O_6$ | (Insol. a.) | |
| (4) Acmite-Jadeite series $WYZ_2O_6$ | | | |
| Acmite | $NaFe(III)Si_2O_6$ | Very sl. sol. a. | |
| Jadeite | $NaAlSi_2O_6$ | Insol. a. | (33848) |
| Aegirite | $(Ca, Na)(Mg, Fe(III), Al)Si_2O_6$ | Insol. a. | |
| Spodumene | $LiAlSi_2O_6$ | Insol. a. | |
| (App.) | | | |
| Margarosanite | $(Pb, Ca, Mn)SiO_3$ | Gel. $HNO_3$ | |
| Babingtonite | $Ca_2Fe(II)Fe(III)Si_5O_{14}(OH)$ | Gel. HCl | |
| Taramellite | $BaFeSi_2O_6(OH)$ | Insol. a. | |
| Hyalotekite | $(Pb, Ca, Ba)_4BSi_6O_{17}(F, OH)$ | Insol. a. | |
| Neptunite | $Na_2FeTiSi_4O_{12}$ | Insol. HF | (33938) |

TABLE III. (Continued)

| Minerals | Chemical formula | Reactivity toward acids | Bonding energy (kcal.) |
|---|---|---|---|
| Calcium metasilicates | | | |
| Inesite | $Ca_2Mn_7H_2Si_{10}O_{30}\cdot 5H_2O$ | (Sol. HCl) | |
| Hillebrandite | $Ca_2SiO_4\cdot H_2O$ | Sol. HCl | (28027)*1) |
| Riversideite | $Ca_5H_2Si_6O_{18}\cdot 2H_2O$ | Sol. HCl | (31285) |
| Copper metasilicates | | | |
| Chrysocolla | $CuSiO_3\cdot nH_2O$ | Decomp. a. | |
| Shattuckite | $8CuSiO_3\cdot 4H_2O$ | (Decomp. a.) | |
| Plancheite | $14CuSiO_3\cdot 4H_2O$ | (Decomp. a.) | |
| The others | | | |
| Carpholite | $MnAl_2Si_2O_6(OH)_4$ | Insol. HCl | |
| Stokesite | $CaSnSi_3O_9\cdot 2H_2O$ | Insol. a. | |
| Searlesite | $NaBSi_2O_6\cdot H_2O$ | Decomp. HCl | |
| Bavenite | $Ca_4AlBe_3HSi_9O_{27}\cdot H_2O$ | (Sl. sol. a.) | |
| Cainosite | $Ca_2(Ce, Y)_2Si_4O_{12}CO_3\cdot 1\sim 2H_2O$ | Sol. HCl | |
| Epididymite | $NaBeSi_3O_7(OH)$ | Very sl. sol. a. | |
| Elpidite | $Na_2(Zr, Ti)Si_6O_{15}\cdot 3H_2O$ | (Sl. sol. a.) | |
| Leucosphenite | $Ba(Na, Ca)_4Ti_3BSi_8O_{27}$ | Decomp. HF | |
| Ussingite | $Na_2Al(Si_3O_8)(OH)$ | Gel. HCl | |
| Amphybole group $(W, X, Y)_{7\sim 8}(Z_4O_{11})_2(O, OH, F)_2$ | | | |
| (1) Anthophyllite series | | | |
| Anthophyllite | $(Mg, Fe)_7Si_8O_{22}(OH)_2$ | Insol. | |
| Gedrite | $(Mg, Fe, Al)_7(Al, Si)_8O_{22}(OH)_2$ | (Insol.) | |
| (2) Cummingtonite series $X_7(Z_4O_{11})_2(OH)_2$ | | | |
| Cummingtonite | $(Mg, Fe)_7Si_8O_{22}(OH)_2$ | (Insol.) | |
| Grunerite | $(Mg, Fe, Mn)_7Si_8O_{22}(OH)_2$ | Insol. a. | |
| Kupfferite | $Mg_7Si_8O_{22}(OH)_2$ | (Insol.) | (32430) |
| (3) Tremolite series | | | |
| Tremolite | $Ca_2Mg_5Si_8O_{22}(OH)_2$ | Insol. | 32284 |
| Actinolite | $Ca_2(Mg, Fe)_5Si_8O_{22}(OH)_2$ | Insol. | |
| (4) Hornblende series $W_6(X, Y)_{10}(Z_4O_{11})_4(O, OH, F)_4$ | | | |
| Edenite | $Ca_4Na_2Mg_{10}Al_2Si_{14}O_{44}(OH, F)_4$ | (Insol.) | (31272)*2) |
| Pargasite | $Ca_4Na_2Mg_9Al_4Si_{13}O_{44}(OH, F)_4$ | (Insol.) | (31088)*3) |
| Hastingsite | $Ca_4Na_2Mg_8Al_6Si_{12}O_{44}(OH, F)_4$ | (Insol.) | (30904)*3) |
| Hornblende | $Ca_4Na_2(Mg, Fe(II))_8(Al, Fe(III), Ti)_6Si_{12}O_{44}(OH, O)_4$ | Insol. a. | |
| Kaersutite | $Ca_4Na(Mg, Fe(II))_7(Al, Fe(III))_6Ti_2Si_{12}O_{46}(OH)_2$ | (Insol.) | |
| Arfvedosonite | $Na_6Mg_8Al_2Si_{16}O_{44}(OH, F)_4$ | Insol. a. | (32538)*2) |
| 〃 | $Ca_2Na_4Fe(II)_7(Al, Fe(III))_6Si_{13}O_{44}(OH)_4$ | Insol. a. | |
| Holmquistite | $CaNaLi_2Mg_6Al_5Si_{15}O_{44}(OH)_2$ | (Insol. a.) | |
| Glaucophane | $Na_4Mg_6Al_4Si_{16}O_{44}(OH, F)_4$ | Insol. a. | (33182)*2) |
| Riebeckite | $Na_6Fe(II)_6Fe(III)_4Si_{16}O_{46}(OH)_2$ | Insol. a. | |
| Narsarsukite | $Na_2(Ti, Fe(III))Si_4(O, OH, F)_{11}$ | Insol. a. | |
| Chrysotile | $(Mg, Fe)_6Si_4O_{11}(OH)_6\cdot H_2O$ | Decomp. $H_2SO_4$ | (29468)*3) |
| (App.) | | | |
| Sepiolite | $Mg_8H_2(Si_4O_{11})_3\cdot 3H_2O$ | Decomp. HCl | (32627) |
| Attapulgite | $Mg_5Si_8O_{20}(OH)_2\cdot 8H_2O$ | (Decomp. a.) | (31076) |

*1) This value was calculated regarding the chemical formula of hillebrandite as $Ca_2SiO_3(OH)_2$.
*2) These values were calculated regarding ……$(OH, F, or, OH, O)_4$ as …… $(OH)_4$.
*3) This value was calculated regarding $(Mg, Fe)_6$…… as $Mg_6$…….

TABLE IV. REACTIVITY OF PHYLLOSILICATE MINERALS TOWARD ACIDS

| Minerals | Chemical formula | Reactivity toward acids | Bonding energy (kcal.) |
|---|---|---|---|
| | Phyllosilicates of aluminum. $Y_pSi_4O_{10}(OH)_{3p-4}\cdot sH_2O$ Y=Al, Fe(III), rarely Cr; $p=2\sim3$; $s=0\sim4$. | | |
| 2 : 1 Type | | | |
| Pyrophyllite | $Al_2Si_4O_{10}(OH)_2$ | Sl. decomp. HCl | 32558 |
| 1 : 1 Type kaolin minerals | $Al_4Si_4O_{10}(OH)_8$ | | |
| Kaolinite | $Al_4Si_4O_{10}(OH)_8$ | Sl. decomp. HCl | |
| Dickite | 〃 | (Sl. decomp. HCl) | 32165 |
| Nacrite | 〃 | (Sl. decomp. HCl) | |
| | Phyllosilicates of iron, magnesium, calcium and manganese. | | |
| 2 : 1 Type | | | |
| Talc | $Mg_3Si_4O_{10}(OH)_2$ | Undecomp. a. | (32516) |
| Minnesotaite | $(Fe(II), Mg)_{5.5}$ $(Si, Al, Fe(III))_8O_{18.5}(OH)_{5.5}$ | (Undecomp. a.) | |
| Chlorite graup (abbr.) | | | |
| Clinochlore | (abbr.) | Decomp. $H_2SO_4$ | |
| Penninite | (abbr.) | Decomp. $H_2SO_4$ | |
| Prochlorite | (abbr.) | Decomp. hot $H_2SO_4$ | |
| Montmorillonite group | | | |
| Montmorillonite | (E. C.)*1)$_{0.67}(Al_{3.33}Mg_{0.67})Si_8O_{20}(OH)_4$ | Decomp. boiling a. | |
| Beidellite | (E. C.)*1)$_{0.67}Al_4(Si_{7.33}Al_{0.67})O_{20}(OH)_4$ | (Decomp. boiling a.) | |
| Nontronite | (E. C.)*1)$_{0.67}Fe_4(Si_{7.33}Al_{0.67})O_{20}(OH)_4$ | Gel. HCl | |
| Saponite | (E. C.)*1)$_{0.67}Mg_6(Si_{7.33}Al_{0.67})O_{20}(OH)_4$ | Decomp. $H_2SO_4$ | |
| Iron-saponite | (E. C.)*1)$_{0.67}(Mg, Fe)_6(Si_{7.33}Al_{0.67})O_{20}(OH)_4$ | (Decomp. a.) | |
| Sauconite | (E. C.)*1)$_{0.67}(Mg, Fe, Zn)_6(Si_{7.33}Al_{0.67})O_{20}(OH)_4$ | (Decomp. a.) | |
| Vermiculite group | | | |
| Vermiculite | $(Mg, Fe)_{2\sim3}(Si, Al, Fe(II))_4O_{10}(OH)_2\cdot4H_2O$ | (Decomp. a.) | |
| Brittle mica group | | | |
| Chalcodite | $(Mg, Fe)_{13}Al_4Si_{18}O_{50}(OH)_{10}\cdot10H_2O$ | (Decomp. a.) | |
| Epichlorite | $(Mg, Fe)_{10}Al_6Si_{18}O_{40}(OH)_{10}\cdot8H_2O$ | (Decomp. a.) | |
| Stilpnomelane | $(K, Na, Ca)_{0\sim1}(Fe(II), Mg, Al, Fe(III))_{7\sim8}Si_8O_{22\sim24}(OH)_{2\sim4}\cdot H_2O$ | (Decomp. a.) | |
| Margarite | $CaAl_2(Al_2Si_2)O_{10}(OH)_2$ | Sl. decomp. HCl | (30914) |
| Prehnite | $Ca_2Al_2Si_3O_{10}(OH)_2$ | Sl. decomp. HCl | (31496) |
| Chloritoid | $(Fe, Mg)_2Al_4Si_2O_{10}(OH)_4$ | Decomp. $H_2SO_4$ | (29976)*2) |
| Clintonite | $X_4Z_4O_{10}(OH)_2$ X=Mg : Ca : Al=3 : 2 : 1, Al : Si=2 : 1. | Decomp. hot & conc. a. | |
| Xanthophyllite | $(Mg, Ca, Al)_4(Si, Al)_4O_{10}(OH)_2$ | (Decomp. a.) | |
| Mica group | | | |
| (1) Muscovite series | | | |
| Muscovite | $KAl_2(AlSi_3)O_{10}(OH, F)_2$ | Insol. | 32494 |
| Phengite | $K_4Mg_2Al_8Si_{14}O_{40}(OH)_8$ | Insol. | (32858) |
| Alurgite | $K_4Mg_3Al_7Si_{14}O_{39}(OH)_9$ | (Insol.) | |
| Paragonite | $Na_4Al_{12}Si_{12}O_{40}(OH)_8$ | Insol. HCl | (32540) |
| Roscoelite | $K_4V_8Al_4Si_{12}O_{40}(OH)_8$ | Sl. decomp. $H_2SO_4$ | |
| (2) Biotite series | | | |
| Biotite | $K_4(Mg, Fe)_{12}Al_4Si_{12}O_{40}(OH)_8$ | Decomp. $H_2SO_4$ | 30475 |
| Phlogopite | $K_4Mg_{12}Al_4Si_{12}O_{40}(OH)_8$ | Decomp. $H_2SO_4$ | (30454) |
| Cryophyllite | $K_4Mg_{10}Al_8Si_{10}O_{40}(OH)_8$ | (Decomp. $H_2SO_4$) | (30090) |
| (3) Lepidolite series | | | |
| Lepidolite | $K_4Mg_4Li_4Al_8Si_{12}O_{40}(OH)_4F_4$ | Very sl. sol. HCl | |
| 〃 | $K_4Li_6Al_8Si_{14}O_{42}(OH)_4F_2$ | ( 〃 ) | |
| 〃 | $K_4Li_6Al_7Si_{14}O_{39}(OH)_2F_7$ | ( 〃 ) | |
| Zinnwaldite | $K_4Fe(II)_4Li_4Al_8Si_{12}O_{40}(OH)_4F_4$ | Sl. sol. HCl | |
| Polylithionite | $K_4Li_8Al_4Si_{16}O_{40}F_8$ | (Sl. sol. HCl) | |

Table IV. (Continued)

| Minerals | Chemical formula | Reactivity toward acids | Bonding energy (kcal.) |
|---|---|---|---|
| (Misc.) | | | |
| Glauconite | $K_{2\sim3}(Mg, Fe, Ca)_{1\sim3}(Fe(III), Al)_{3\sim6}(Si_{13\sim14}Al_{2\sim3})O_{38\sim40}(OH)_{6\sim10}$ | Decomp. HCl | |
| (App.) | | | |
| Pholiodolite | $KMg_6AlSi_7O_{20}(OH)_4\cdot3H_2O$ | (Decomp. HCl) | (30733) |
| Cookeite | $(Li, Al)_4(Si, Al)_4O_{10}(OH)_4\cdot2H_2O$ | Decomp. $H_2SO_4$ | |
| Bityite | $CaLiAl_3BeSi_2O_{10}(OH)_2$ | (Insol.) | |
| Ganophyllite | $NaMn_6Al_2(Si_4O_{10})_2(OH)_{11}$ (?) | (Decomp. a.) | |
| 1 : 1 Type | | | |
| Antigorite | $Mg_6Si_4O_{10}(OH)_8$ | Decomp. $H_2SO_4$ | (29445) |
| Greenalite | $(Fe(II), Mg)_9Fe(III)_2Si_8O_{22}(OH)_{12}\cdot2H_2O$ | (Decomp. $H_2SO_4$) | |
| Neponite | $(Mg, Ni)_6Si_4O_{10}(OH)_8$ | (Decomp. $H_2SO_4$) | |
| Connarite | $(Ni, Mg)_8(Si_4O_{10})_3(OH)_4\cdot6H_2O$ | (Decomp. $H_2SO_4$) | |
| Amesite | $(Mg, Al, Fe(II))_3(Si, Al)_2O_5(OH)_4$ | (Decomp. $H_2SO_4$) | |
| Cronstedite | $(Mg, Ca, Fe(II), Fe(III), Al)_{3\sim4}(Si, Al)_2O_5(OH)_4$ | (Decomp. $H_2SO_4$) | |
| Chamosite | $(Al, Fe(II), Fe(III), Mg, Ti)_3(Si, Al)_2O_5(OH)_4$ | (Decomp. $H_2SO_4$) | |
| (App.) | | | |
| Zeophyllite | $Ca_8Si_6O_{15}(OH, F)_{10}$ | (Decomp. HCl, $HNO_3$) | (29376)*3) |
| Friedelite | $Mn_8Si_6O_{15}(OH, Cl)_{10}$ | Gel. HCl | |
| Pyrosmalite | $(Mn, Fe)_8Si_6O_{15}(OH, Cl)_{10}$ | Gel. HCl | |
| Schallerite | $Mn_8(Si, Al)_6O_{15}(OH, Cl)_{10}$ | (Gel. HCl) | |
| Ferroschallerite | $(Fe, Mn)_8(Si, Al)_6O_{15}(OH, Cl)_{10}$ | (Gel. HCl) | |
| Centrallasite | $Ca_4Si_6O_{15}(OH)_2\cdot5H_2O$ | Decomp. HCl | (30844) |
| Truscottite | $(Ca, Mg)_4Si_6O_{15}(OH)_2\cdot5H_2O$ | (Decomp. HCl) | |
| Gyrolite | $Ca_4Si_6O_{15}(OH)_2\cdot3H_2O$ (?) | (Decomp. HCl, $HNO_3$) | (31457) (?) |
| Bementite | $Mn_5Si_4O_{10}(OH)_6$ | Gel. hot HCl | |
| Errite | $Mn_4Si_4O_{10}(OH)_4\cdot3H_2O$ | (Gel. a.) | |
| Apophyllite | $KCa_4(Si_4O_{10})_2F\cdot8H_2O$ | Decomp. a. | |
| Okenite | $Ca_2(Si_4O_{10})\cdot4H_2O$ | Gel. HCl | (31354) |
| | Anhydrous phyllosilicates containing no aluminum. | | |
| Gillespite | $BaFeSi_4O_{10}$ | (Decomp. HCl, $HNO_3$) | |
| Sanbornite | $Ba_2Si_4O_{10}$ | (Decomp. HCl, $HNO_3$) | |

*1) E. C.=Exchangeable cations (Na, K, Ca, etc.)
*2) This value was calculated regarding the chemical formula of chloritoid as $Fe_2Al_4Si_2O_{10}(OH)_4$.
*3) This value was calculated regarding $\cdots\cdots(OH, F)_{10}$ as $\cdots\cdots(OH)_{10}$.

Table V. Reactivity of tectosilicate minerals toward acids

| Minerals | Chemical formula | Reactivity toward acids | Bonding energy (kcal.) |
|---|---|---|---|
| | W=Ca, Na, K; Li, Cs(rare); Mn, Fe, Zn(very rare)<br>Z=Si, Al; Be(rare); N=S, Cl, $CO_3$, $SO_4$, $H_2O$ | | |
| Silica group | | | |
| Quartz | $SiO_2$ | Insol. | 37320 |
| Petalite group | | | |
| Petalite | $(Li, Na)AlSi_4O_{10}$ | Insol. | |
| Milarite | $KCa_2AlBe_2Si_{12}O_{30}\cdot\frac{1}{2}H_2O$ | Insol. | |
| Leifite | $Na_4Al_2Si_9O_{22}F_2$ | (Insol.) | |
| Feldspar group $WZ_4O_8$, W=Na, Ca, K, Ba; Z=Si, Al; Si : Al=3 : 1$\sim$1 | | | |
| (1) Monoclinic system | | | |
| Orthoclase | $KAlSi_3O_8$ | Insol. | 34266 |
| Soda orthoclase | $(K, Na)AlSi_3O_8$ | Insol. | |
| Hyalophane | $(K, Na, Ba)Al(Al, Si)Si_2O_8$ | Insol. | |
| Celsian | $BaAl_2Si_2O_8$ | Sol. HCl | |

TABLE V. (Continued)

| Minerals | Chemical formula | Reactivity toward acids | Bonding energy (kcal.) |
|---|---|---|---|
| (2) Triclinic system | | | |
| (a) Microcline series :— | | | |
| Microcline | $KAlSi_3O_8$ | Insol. | (34521) |
| Soda microcline | $(K, Na)AlSi_3O_8$ | (Insol.) | |
| Anorthoclase | $(Na, K)AlSi_3O_8$ | Insol. | |
| (b) Plagioclase series :— | | | |
| Albite | $NaAlSi_3O_8$ | Insol. | 34335 |
| Anorthite | $CaAl_2Si_2O_8$ | Decomp. HCl | 31935 |
| Leucite | $KAlSi_2O_6$ | Decomp. HCl | (33248) |
| Nepheline group $WZ_2O_4$ | | | |
| Nepheline | $KNa_3(AlSiO_4)_4$ | Gel. a. | (31465) |
| Kaliophyllite | $KAlSiO_4$ | Gel. a. | (31212) |
| $\beta$-Eucryptite | $\beta$-$LiAlSiO_4$ | Gel. HCl | |
| Cancrinite group | | | |
| Cancrinite | $(Na, K)_6Ca_2(SO_4)_2(AlSiO_4)_6$ | Sol. HCl | |
| Davyne | $(Na_2, Ca)_4(CO_3)(H_2O)_{0\sim3}(AlSiO_4)_6$ | Gel. HCl | |
| Sodalite group | | | |
| Sodalite | $Na_8Al_6Si_6O_{24}Cl_2$ | Sol. HCl | |
| Noselite | $Na_6(AlSiO_4)_6\cdot Na_2SO_4$ | Gel. HCl | |
| Hauyne | $(Na, Ca)_{8\sim4}(SO_4)_{2\sim1}(AlSiO_4)_6$ | Sol. HCl | |
| Helvite | $Mn_8S_2(BeSiO_4)_6$ | Sol. HCl | |
| Danalite | $Fe_8S_2(BeSiO_4)_6$ | Gel. HCl | |
| Scapolite series $W_4Z_{12}O_{24}N$ | | | |
| Marialite | $(Na, Ca)_4Al_3(Al, Si)_3Si_6O_{24}(Cl, CO_3, SO_4)$ | Sl. decomp. HCl | |
| Meionite | $(Ca, Na)_4Al_3(Al, Si)_3Si_6O_{24}(Cl, CO_3, SO_4)$ | Decomp. HCl | |
| Zeolite group | | | |
| Mordenite | $(Ca, K_2, Na_2)Al_2Si_{10}O_{24}\cdot 7H_2O$ | Decomp. a. | (32590) |
| Heulandite group | | | |
| Clinoptilolite | $Ca_2Na_3Al_7Si_{33}O_{80}\cdot 23H_2O$ (?) | Decomp. a. | (32974) (?) |
| Heulandite | $CaAl_2Si_7O_{18}\cdot 6H_2O$ | Decomp. a. | (32375) |
| Epistilbite | $CaAl_2Si_6O_{16}\cdot 5H_2O$ | Decomp. HCl | (32268) |
| Brewsterite | $(Sr, Ba, Ca)Al_2Si_6O_{16}\cdot 5H_2O$ | Decomp. HCl | |
| Desmine group | | | |
| Desmine | $CaAl_2Si_7O_{18}\cdot 7H_2O$ | Decomp. HCl | (32069) |
| Harmotome | $BaAl_2Si_6O_{16}\cdot 6H_2O$ | Decomp. HCl | |
| Phillipsite | $KCaAl_3Si_5O_{16}\cdot 6H_2O$ | Gel. HCl | (30815) |
| Gismondite | $CaAl_2Si_2O_8\cdot 4H_2O$ | Gel. HCl | (29530) |
| Erionite | $(K_2, Na_2, Ca)Al_2Si_6O_{16}\cdot 6H_2O$ (?) | Sol. HCl | |
| Chabazite group | | | |
| Chabazite | $(Ca, Na_2)Al_2Si_4O_{12}\cdot 6H_2O$ | Decomp. HCl | |
| Gmelinite | $(Na_2, Ca)Al_2Si_4O_{12}\cdot 6H_2O$ | Decomp. HCl | |
| Levynite | $CaAl_2Si_4O_{12}\cdot 6H_2O$ | Gel. a. | (30727) |
| Thomsonite group | | | |
| Thomsonite | $NaCa_2[Al_4(Al, Si)_2Si_4]O_{20}\cdot 5H_2O$ | Gel. HCl | |
| Gonnardite | $(Ca, Na)_3(Al, Si)_{10}O_{20}\cdot 6H_2O$ | (Gel. HCl) | |
| Ashcroffine | $KNa(Ca, Mg, Mn)Al_4Si_5O_{18}\cdot 8H_2O$ | (Gel. HCl) | |
| Natrolite group | | | |
| Natrolite | $Na_2Al_2Si_3O_{10}\cdot 2H_2O$ | Gel. a. | (31240) |
| Mesolite | $Na_2Ca_2Al_6Si_9O_{30}\cdot 8H_2O$ | Gel. a. | (31143) |
| Scolesite | $CaAl_2Si_3O_{10}\cdot 3H_2O$ | Gel. a. | (31098) |
| Edingtonite | $BaAl_2Si_3O_{10}\cdot 3H_2O$ | Gel. a. | |
| Unassigned | | | |
| Yugawaralite | $Ca_4Al_7Si_{20}O_{54}\cdot 14H_2O$ | (Gel. a.) | (32657) |
| Analcite | $NaAlSi_2O_6\cdot H_2O$ | Gel. HCl | (32109) |
| Faujasite | $CaNa_2Al_4Si_8O_{24}\cdot 16H_2O$ | Decomp. HCl | (30009) |
| Laumonite | $CaAl_2Si_4O_{12}\cdot 4H_2O$ | Gel. HCl | (31478) |
| Ferrierite | $(Na, K)_2MgAl_3Si_{15}O_{36}(OH)\cdot 9H_2O$ | (Gel. HCl) | |
| Questionable | | | |
| Didymolite | $(Ca, Mg, Fe)Al_2Si_3O_{10}$ | Insol. a. | |
| D'Achiardite | $(K, Na)CaH_3Al_2Si_9O_{24}\cdot 6H_2O$ | Decomp. HCl | |

trimerite contains Be, it is dissolved by hydrochloric acid. This fact may be due to the presence of a considerable amount of electropositive Mn(II) and Ca.

Generally, it may safely be assumed that 1) of the above-mentioned requirements and the singularity of the above eight metallic elements hold in the case of nesosilicates.

Furthermore, it is noteworthy that the nesosilicate minerals containing Ca, Sr, Ba and Pb react with difficulty with sulfuric acid, because sulfates of these metals are hardly soluble. Of these metals, lead chloride is soluble with difficulty in water, and so the silicate minerals containing Pb do not react easily with hydrochloric acid at ordinary temperatures.

**Sorosilicate Minerals.**—The results for the solosilicate minerals are listed in Table II. The above inductive rules appear also to be applicable in this case as well as in the case of the nesosilicate minerals. For example, osumilite, indialite, cordierite, the tourmaline and the epidote series minerals may be scarcely attacked by acids, because of the presence of great amounts of Al, and Fe(III); and then for the same reason, schorl probably appears to be undecomposed by acids. In the thalenite group minerals, the fact that thortveiteit is insoluble in acids, in spite of the reactivity of cerite toward acids, is presumably due to the existence of scandium atoms having comparatively large values of $\phi$, $\phi'$ or F. S. Similarly, the fact that bertrandite only in the hemimorphite group is undecomposed by acids appears to be due to the presence of Be. Beryl containing Al and Be is insoluble as shown from the above results. In addition, in the melilite series, leucophanite and meliphanite are slightly decomposed by hydrochloric acid (and perhaps nitric acid) owing to the existence of Be.

From this standpoint, it appears to be deducted that thalenite and rowlandite are probably attacked by acids. Moreover, it is noteworthy that dioptase ($Cu_6Si_6O_{18}\cdot 6H_2O$) having the structure identical with that of beryl[9] is easily decomposed by acids, because $Cu^{2+}$ has remarkably smaller $\phi$, $\phi'$ or F. S. than those of $Be^{2+}$. But the unreactivity of the rhodonite series[10] seems to be impossible to explain from this viewpoint, and appears to indicate the necessity of consideration for their structures, but now no satisfactory explanation has been offered as to this fact.

**Inosilicate Minerals.**—As is generally known, the inosilicate minerals are structurally classified in the pyroxene and the amphybole group. The former consists in structure with infinite single chain $(SiO_5)_\infty^{2-}$ of $(SiO_4)^{4-}$ tetrahedra with common corners, and the latter is characterized by the double chains of the type $(Si_4O_{11})_\infty^{6-}$.

The results are listed in Table III.

From Table III, it would be presumably derived that these inosilicate minerals could not for the most part be decomposed by acids. Taken in connection with their structures, this fact would seem to prove that these silicates are probably constructed by the compact arrangements of metallic ions and $(SiO_3)_\infty^{2-}$ or $(Si_4O_{11})_\infty^{-6}$ ions; in other words, their metal ions are compactly surrounded with the above-cited giant ions. Relating to this structure, it is noteworthy that the inosilicates containing alkali metals, e. g., the acmite-jadeite series and hornblende series, are not decomposed by acids. Therefore, it seems that the structural factor adds a striking effect to the reactivity toward acids in these cases. But the chemical composition of these silicates also has a comparative effect on their reactivity. For example, the inertness of the above-mentioned acmite-jadeite series and epididymite are probably in part due to the existence of Be and Al; and from the same viewpoint, it is presumably best to deduct the inertness of carpholite and bavenite. Furthermore, the fact that sepiolite and attapulgite are easily decomposed by acids would probably be due to the existence of large voids such as caves passing through between chains of $(Si_4O_{11})_\infty^{6-}$ ions[11].

**Phyllosilicate Minerals.** — As stated above, it is confirmed from the Table IV that all the 1 : 1 type phyllosilicate minerals are easily decomposed by acids, except the aluminum ones (e. g., the kaolin minerals) as was expected. On the contrary, in the 2 : 1 type phyllosilicate minerals, the magnesium type (talc) also is unattacked by acids, as well as the aluminum type (pyrophyllite). This seems to be mainly due to its 2 : 1 type structure; namely, all the magnesium ions in talc are compactly sandwiched with the two infinite layerous ions $(Si_2O_5)_\infty^{2-}$. Furthermore, the inertness of the muscovite and lepidolite series appears to be in part due to the above-cited structure and in part to the existence of aluminum. The biotite series contain no aluminum for positive ions, and then these would perhaps be attacked by acids.

**Tectosilicate Minerals.** — Table V seems to indicate that the reactivity of tectosilicate minerals toward acids are scarcely connected

9) N. V. Belov, *Compt. Rend. Acad. Sci. Russ.* **37**, 139 (1942).

10) E. H. Kraus, W. F. Hunt and L. S. Ramsdell, "Mineralogy, An Introduction to the Study of Minerals and Crystals", 3rd. Ed., McGraw-Hill Book Co., Inc., New York and London (1936), p. 368.

11) W. T. Grandquist and R. C. Amero, *J. Am. Chem. Soc.*, **70**, 3265 (1948).

with their chemical compositions. For example, the fact that orthoclase, microclire, and albite are insoluble to acids, and leucite and nepheline are decomposed by acids, cannot be explained from their chemical compositions. Therefore, in this case, it is suggested that their structures have an important effect on their reactivity.

As for their structures, the position and state of metallic ions in their crystal lattices would seem to carry on connection with their reactivity.

### Results from the Bonding Energies

It appears that the bonding energies of the silicate minerals are closely related to their reactivity. Especially the bonding energies of the tectosilicate minerals would seem to be important. As for this problem, Keller[12] made a computation by adding the energies of the bonds between their constituent cations and oxygen, starting with the elements in the gaseous state, on the basis of the data from Huggins and Sun[13].

The author computed the bonding energies of the various silicate minerals by adding the bonding energies of their constituent elements, utilizing data compiled by Huggins and Sun[13], and Keller[12]. Of the valuse in Tables I—V, those in parentheses are computed by the author, and the rest are reprinted from Keller's paper.

It is reasonable to assume that there are some deep relationships between the reactivity and the bonding energies of silicate minerals. Judging from the comparison of these two properties in Tables I—V, the following results were obtained. Generally speaking, the neso-, soro-, ino-, and phyllo-silicate minerals of which bonding energies are less than about 30500 kcal. and the tectosilicate minerals of which these energies are less than about 33500 kcal. seem to be decomposed by acids. The fact that the tectosilicate minerals alone are in particular different from others appears presumably to be relative to the singularity of themselves; namely, this seems to depend primarily upon their ultimately polymerized structures—the three-dimentional frameworks —constructed by complete sharing of all oxygens in all the tetrahedra contained in their structures.

12) W. D. Keller, *Am. Mineralogist*, **39**, 783 (1954).
13) M. L. Huggins and K-H. Sun, *J. Phys. Chem.*, **50**, 319 (1946).

### Summary

In this paper, the author proposed a classified table of metals contained in silicate minerals, and the qualitative and conventional rules in which it appeared possible to predict the reactivity of all the known silicate minerals toward ordinary mineral acids. In the classification and rules, ionic potential, Goldschmidt's polarizing power, and field strength of the metals in the silicate minerals play important roles.

The rules are summarized as follows: 1) the silicate minerals—especially, the neso- and soro-silicate ones composed of the comparative simple ionic crystal lattices—containing the less electropositive metals (e. g., Ti, Be, Al, Cr, V(III), Fe(III), Mn(III), Zr, etc.) are generally unattacked by acids; 2) in the ino-, phyllo-, and tecto-silicate minerals, which contain various polymerized and giant silicate ions, their structures exert a favorable influence upon their reactivity toward acids. Thus, in these minerals, it is necessary for us to take their structural effects into consideration, besides the above rule 1); and 3) the bonding energies of silicate minerals are closely related to their reactivity. In general, the neso-, soro-, ino-, and phyllo-silicate minerals of which bonding energies are less than about 30500 kcal. and the tectosilicate ones of which the energies are less than about 33500 kcal. seem to be decomposed by acids.

*Department of Applied Chemistry*
*Faculty of Industry*
*Iwate University*
*Ueda, Morioka*

# *Studies on Mass Spectra and Appearance Potentials of Acetic Acid and Deuteroacetic Acid $CD_3COOH$*

By Kozo HIROTA, Kazuo NAGOSHI* and Motoyoshi HATADA

(Received June 8, 1960)

Recently the data of mass spectra have often been utilized in the discussion of radiation-induced reactions of organic compounds[1]. On such an occasion it is indispensable to determine the chemical species corresponding to each peak in the spectra by some methods, e. g. by comparing the spectra of the compounds marked by isotopes. For the same purpose, ionization potentials of these compounds are required, if possible. Although the data of this kind have been accumulated to some extent, those of the appearance potentials which are necessary to produce fragment ions do not exist so much yet in spite of their increasing importance. Such being the situation, as a part of our research on radiation chemistry of oxygen-containing compounds, mass spectra of acetic acid and deuteroacetic acid $CD_3COOH$ were measured at several accelerating voltages and temperatures of the ion source on one hand, and also the appearance potentials of parent ions and main fragment ions of these acids on the other hand.

## Experimental

**Materials.**— The purest commercial acetic acid was used without any treatment. Deuteroacetic-$d_3$ acid was synthetized as follows; carbon suboxide $C_3O_2$ obtained by dehydrating commercial malonic acid with phosphorus pentoxide was reacted with deuterium oxide. The deuteromalonic acid thus produced was decomposed thermally into deutero-acetic-$d_3$ acid-d $CD_3COOD$. The deuterium atom of the carboxylic group of this acid was replaced by protium atom, bubbling gaseous hydrogen chloride through the acid. The result of mass spectrometric analysis of the acid thus obtained showed that the amount of $CD_3COOH$ in the deuterated acid was 95.6 atomic per cent, while $CD_2HCOOH$ was the major parts of the impurities, $CH_3COOH$ being negligibly small.

**Apparatus.** — The specifications of the mass spectrometer (Hitachi type RMU-5) are as follows: 90° focusing type, the temperature of the ion source is variable from 120 to 240°C, and electron accelerating voltage is also variable between 0 and 200 V. The standard conditions for gas analysis were as follows: electron accelerating voltage, 82 eV.: ion accelerating voltage, 1500 V., total emission current, 130 $\mu$A ; target current, 35 $\mu$A ; standard temperature of the ion source, 130°C.

## Results

**Mass Spectra.**—Mass spectra of both acids are shown in Table I, where each peak height is per cent of total ion yield. From the table, the peak heights of the ions produced from $CH_3COOH$ are in the order: $m/e=43>45>15>60>29$. The result is concordant with that of some other research[2], but not with that of Kambara[3] who found the ion of $m/e=28$ to be the most abundant followed by the ions of $m/e=43>45>15>14>12$ (cf. Table II). The discrepancy between the two data is too great to be explained by the discrimination peculiar to the respective apparatus. However, larger values of the peaks of $m/e=28$, 14 and 12 of Kambara may be explained by the contamination of carbon monoxide and nitrogen, and this explanation is supported by the fact that the peak at $m/e=28$ in the mass spectrum of

TABLE I. MASS SPECTRA OF $CH_3COOH$ AND $CD_3COOH$

| *m/e* | $CH_3COOH$ % | $CD_3COOH$ % | *m/e* | $CH_3COOH$ % | $CD_3COOH$ % |
|---|---|---|---|---|---|
| 1 | 0.9 | 0.6 | 30 | 0.3 | 1.9 |
| 2 | 0.03 | 0.6 | 31 | 2.0 | 0.1 |
| 3 | — | 0.03 | 32 | 0 | 0.1 |
| 4 | — | 0.03 | 33 | 0 | 0.6 |
| 12 | 0.7 | 0.5 | 40 | 0.4 | 0.2 |
| 13 | 1.8 | 0.1 | 41 | 1.3 | 0.1 |
| 14 | 4.0 | 1.5 | 42 | 4.5 | 0.8 |
| 15 | 11.0 | 0.6 | 43 | 26.5 | 0.7 |
| 16 | 1.7 | 3.6 | 44 | 1.0 | 3.3 |
| 17 | 1.4 | 2.7 | 45 | 21.2 | 19.9 |
| 18 | 2.6 | 13.8 | 46 | 0.9 | 28.4 |
| 19 | — | 1.4 | 47 | 0 | 0.3 |
| 24 | 0.2 | 0.1 | 60 | 9.4 | 0.3 |
| 25 | 0.4 | 0 | 61 | — | 0 |
| 26 | 0.4 | 0.4 | 62 | — | 0.7 |
| 27 | 0.1 | 0.1 | 63 | — | 13.0 |
| 28 | 1.6 | 1.9 | 64 | — | 0.3 |
| 29 | 4.7 | 1.0 | | | |

* Research fellow dispatched from Kurashiki Rayon Co. (1958~1959).

1) For instance, see, J. G. Burr, *J. Phys. Chem.*, **61**, 1483 (1957).

2) Catalog of Mass Spectral Data of the American Petroleum Institute, Project, 44, Spectrum Serial No. 640.

3) T. Kambara, *J. Phys. Soc., Japan*, **5**, 84 (1950).

TABLE II. MASS SPECTRA OF $CH_3COOH$ IN THE LITERATURE

| $m/e$ | Ions | Relative peak height* | | |
|---|---|---|---|---|
| | | Kambara[3] | API Table No. 640 | The present research |
| 12 | $C^+$ | 34 | | 4 |
| 13 | $CH^+$ | 16 | | 7 |
| 14 | $CH_2^+$ | 43 | | 15 |
| 15 | $CH_3^+$ | 64 | | 42 |
| 25 | $C_2H^+$ | 4 | | 2 |
| 26 | $C_2H_2^+$ | 5 | 1.3 | 2 |
| 27 | $C_2H_3^+$ | 5 | 0.40 | 0 |
| 28 | $C_2H_4^+$, $CO^+$ | 130 | 5.6 | 6 |
| 29 | $CHO^+$ | 33 | 15.6 | 18 |
| 30 | $CH_2O^+$ | 1 | 0.7 | 1 |
| 31 | $CH_3O^+$ | 8.5 | 4.5 | 8 |
| 32 | — | — | 0.1 | 0 |
| 41 | $C_2HO^+$ | 19 | 4.5 | 5 |
| 42 | $C_2H_2O^+$ | 28 | 14.5 | 17 |
| 43 | $C_2H_3O^+$ | 100 | 100 | 100 |
| 44 | $C_2H_4O^+$, $CO_2^+$ | 12 | 4.9 | 4 |
| 45 | $CHO_2^+$ | 81 | 93.6 | 80 |
| 46 | $CH_2O_2^+$ | — | 1.2 | 3 |
| 55 | | — | 0.08 | — |
| 56 | | — | 0.13 | — |
| 57 | | — | 0.06 | — |
| 60 | $C_2H_4O_2^+$ | 29 | 57.7 | 36 |

* The peak height of $m/e=43$ is normalized to 100.

$CD_3COOH$ obtained under the same experimental condition is also small. Moreover, the heights of the main peaks of both spectra of $CH_3COOH$ and $CD_3COOH$ can be explained without contradiction, i. e., the peaks at $m/e=43$, 15 and 60 in $CH_3COOH$, corresponding to $CH_3CO^+$, $CH_3^+$ and $CH_3COOH^+$, shift to those at $m/e=46$, 18 and 63 in $CD_3COOH$, corresponding to $CD_3CO^+$, $CD^+$ and $CD_3COOH^+$, while the peak of $COOH^+$ ($m/e=45$) occupies the second height in both spectra. Therefore it may be concluded that our spectra are free from the peaks due to some impurities or thermally decomposed products.

In Fig. 1, the effect of temperature on the mass spectrum of acetic acid is shown over a temperature range 130~230°C, taking the temperature of the ion source as abscissa and the percentage of the peak height as ordinate. It is found that the observed effect is not so large, as to be explained by such a mechanism as that the fragment ions are produced monomolecularly from the parent ions with some activation energies for bond breaking processes. However, considering that the gaseous acetic acid molecules may not be in thermal equilibrium completely with the wall of the ion

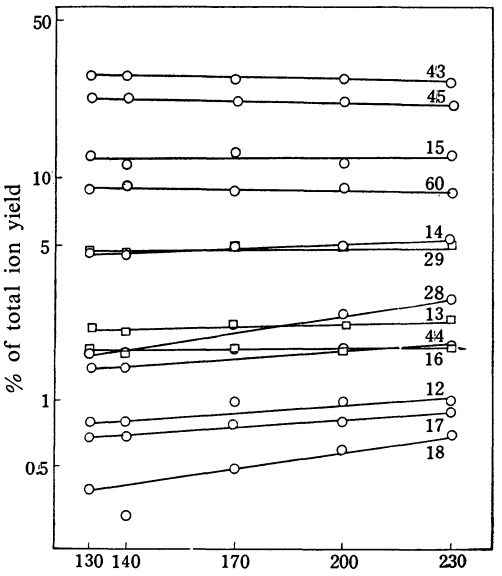



Fig. 1. The effect of ion source temperature on the mass spectrum of acetic acid.

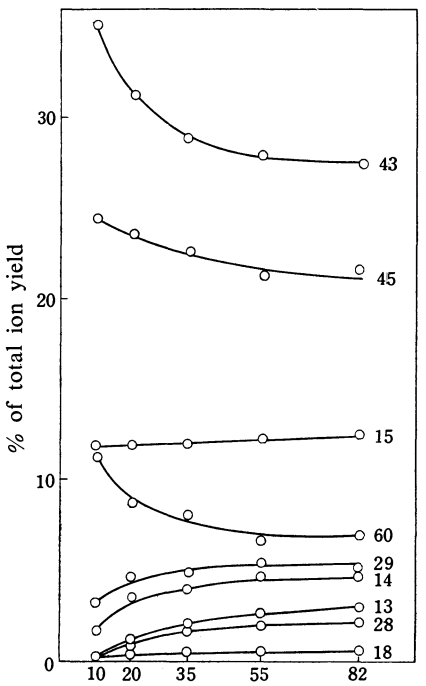



Fig. 2. The effect of electron accelerating voltage on the mass spectrum of acetic acid.

source this result may not be curious. But from this figure, it might be said that the temperature effect has the following tendencies: ions $m/e=15$, 43 and 45 are practically independent on temperature, while others

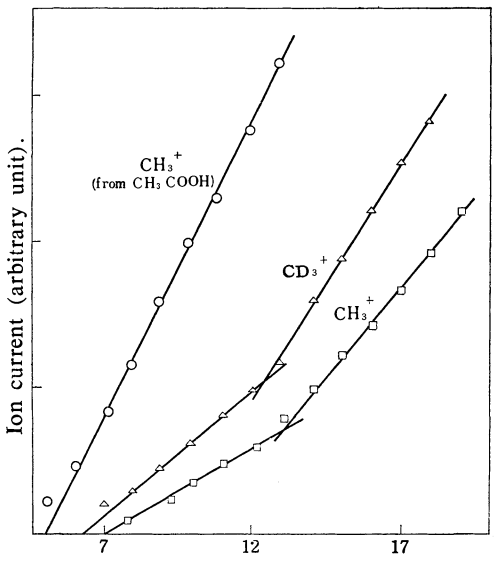



Fig. 3. Ionization efficiency curves of $CH_3^+$, $CD_3^+$ and $COOH^+$ ions.

increase, especially those of $CO_2^+$ ($m/e=44$), $CO^+$ ($m/e=28$) and $H_2O^+$ ($m/e=18$), $HO^+$ ($m/e=17$) and $C^+$ ($m/e=12$), which are the parent and fragment ions from molecules probably produced by the thermal decomposition of acetic acid.

The effect of electron accelerating voltage on the spectrum of acetic acid is shown in Fig. 2, where the voltage is varied from 9 to 82 V., and the sum of each peak height is normalized to 100 at each voltage. It is evident that the main peaks can be classified into three groups, i. e., the first group, $CH_3^+$ ion is practically constant, the second group, $CH_3COOH^+$ ($m/e=60$), $CH_3CO^+$ ($m/e=43$) and $COOH^+$ ($m/e=45$) ions, decreases and the residual third group, $COH^+$ ($m/e=29$) and $CH_2^+$ ($m/e=14$) increases with the increasing electron accelerating voltage. These tendencies may be reasonable if it is assumed, as is done by King and Long[4] on the mass-spectra of formic esters, that most of the ions which belong to the first and the third groups are produced from the ions of the second group. Detailed mechanism of production of $CH_3^+$ will be discussed again.

**Appearance Potential.**—As described above, the ions, $CH_3^+$, $CH_3CO^+$, $COOH^+$ and $CH_3COOH^+$ can be regarded as the main peaks in the spectrum of $CH_3COOH$, because the total contribution of the other ions to the spectrum is below 30%. The appearance potential of the above four ions were measured by the following procedure. The ionization efficiency curve for the ion under investigation was determined up to about 10 V. above the expected value of appearance potential and then the accurate one was determined by extrapolating the linear portion of the curve to the voltage axis. Thus, the obtained value of the ionization potential was calibrated by use of Moore's photo-ionization datum of argon ion, i. e., 15.76 V.[5]

In Fig. 3, the measurements on $CH_3^+$, $CD_3^+$ and $COOH^+$ are plotted against apparent voltage of electron acceleration. The results of these and other ions are summarized in Table III.

TABLE III. APPEARANCE POTENTIALS IN VOLT

| Ions | $CH_3COOH$ | $CD_3COOH$ |
|---|---|---|
| $CH_3COOH^+$ or $CD_3COOH^+$ | $10.7_2$ | $10.7_1$ |
| $CH_3CO^+$ or $CD_3CO^+$ | $12.6_8$ | $12.9_7$ |
| $COOH^+$ | $14.1_5$ | $14.0_8$ |
| $CH_3^+$ or $CD_3^+$ | $16.0_8$ | $15.5_6$ |
| Break point of $CH_3^+$ or $CD_3^+$ curve | 22.3 | 21.5 |

**General discussion.**—In order to confirm the reliability of our data, the appearance potential of the parent ion $CH_3COOH^+$ ($10.7_2$ V.) was compared with those in the literatures. Among the latter values, our appearance potential coincides fairly well with those obtained by the critical slope method of Honig ($10.70^6$ and $10.6_7$[7] V.), but is higher than the value $10.3_3\pm$ 0.03 V. obtained by the method of photo-ionization[8]. Such a situation may be plausible considering the generally accepted fact that the former method as well as our linear extrapolation method gave higher values than the latter.

Thus it has been found that the degree of accuracy of our measurement is sufficient for discussing the appearance potentials of other fragment ions and of other ions produced from $CD_3COOH$. The first point to be discussed will be the fact that the appearance potentials of the parent ions of both acids are $10.7_2$ and $10.7_1$ V.; i. e., they coincide with each other within the experimental errors, while those of the corresponding fragment ions differ definitely from each other.

Secondly, it may be noteworthy that the appearance potential of $CD_3CO^+$ ion is higher by 0.3 V. than that of $CH_3CO^+$ ion. On the other hand, the appearance potentials of $COOH^+$ (from deuterated acid) and $CD_3^+$ ions are lower than those of $COOH^+$ and $CH_3^+$ ions by 0.1 and 0.5 V., respectively. According

4) A. King and F. Long, *J. Chem. Phys.*, **29**, 374 (1958).

5) D. P. Stevenson, *Trans. Faraday Soc.*, **49**, 867 (1953).

6) J. D. Morrison and A. J. C. Nicholson, *J. Chem. Phys.*, **20**, 1021 (1952).

7) I. Omura, K. Higasi and H. Baba, This Bulletin, **29**, 504 (1956).

8) K. Watanabe, *J. Chem. Phys.*, **26**, 542 (1957).

to the results hitherto published, it seems to be a rule that the ionization potential of a molecule increases by deuteration; e. g. 13.04 V. for $CH_4^+$ against 13.21 V. for $CD_4^+$ [9]. Our data, therefore, seem to be an exceptional case. At present, such an anomaly can not be explained easily. The next point to be mentioned may be the breaks of the curves observed in cases of $CH_3^+$ and $CD_3^+$ ions. The breaks occur at about 6 V. higher than the corresponding appearance potentials in both cases.

The occurrence of these breaks might be explained by assuming that above this break point the simultaneous fragmentation process (1b) of the parent ion at two bonds occurs in addition to the single fragmentation process (1a) to form $CH_3^+$ ion:

$$CH_3COOH \rightarrow CH_3^+ + COOH \quad (1a)$$
$$\searrow CH_3^+ + CO_2 + H \quad (1b)$$

However, according to the theoretical result[10] which has been derived by the quasi-equilibrium theory, most of the $CH_3^+$ ions must be produced secondarily, i. e., by the decomposition of highly excited $CH_3CO^+$ ion. This explanation may not be extraordinary, because a similar shape of ionization efficiency curve of $CH_3NO_2$, in which a sharp break point occured about 4.3 V. above the first appearance potential of $NO_2^+$, was explained reasonably by the existence of a bent excited state of $NO_2^+$ [11]. Therefore, the mechanism of producing the $CH_3^+$ ions whose appearance potentials are different is not such as that described by Scheme 1, but both ions are produced by Scheme 2,

$$CH_3COOH \rightarrow CH_3CO^+ + OH$$
$$\rightarrow CH_3^+ + CO + OH \quad (2)$$

The states of the $CH_3^+$ produced below and above the break point in the curve are therefore different.

9) R. E. Honig, ibid., **16**, 105 (1948).
10) Cf. K. Fueki and K. Hirota, *J. Chem. Soc. Japan, Pure Chem. Sec.* (*Nippon Kagaku Zasshi*), **81**, 356 (1960).
11) J. Collin, *J. Chem. Phys.*, **30**, 1621 (1959).

**Summary**

In order to obtain information on the decomposition process of acetic acid in radiation chemistry, not only mass spectra of both acetic acid and deuteroacetic acid but also appearance potentials of parent and main fragment ions of both acids have been measured.

By studying the effects of ion source temperature and of electron accelerating voltage on the spectra, and by comparing the mass spectra of both acids, it has been possible to identify the chemical species produced by electron impact without ambiguity and also to estimate the process of their production to some extent.

It has been found that, although the appearance potentials of the parent ion of both acids coincide fairly well, those of $CH_3^+$ and $COOH^+$ from $CH_3COOH$ are higher than those of corresponding ions from deuterated acid. The breaks of ionization-efficiency curves have been observed in $CH_3^+$ and $CD_3^+$ ions at about 6 volts higher than the appearance potentials suggesting a possibility of the presence of an excited state of the product ions.

The authors express their sincere thanks to Dr. I. Kanomata of Tokyo Metropolitan University and also to Dr. K. Fueki of Osaka University for their discussions.

*Osaka Laboratory*
*Japanese Association for Radiation Research on Polymers*
*508, Mii, Neyagawa, Osaka*
*(K. H., K. N. & M. H.)*

*Faculty of Science*
*Osaka University*
*Nakanoshima, Osaka*
*(K. H.)*

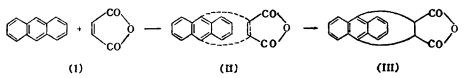
# *Theoretical Reactivity Index of Addition in the "Frontier Electron Theory"*

By Kenichi FUKUI, Chikayoshi NAGATA, Teijiro YONEZAWA and Keiji MOROKUMA

(Received August 8, 1960)

It is well known that many polycondensed aromatic hydrocarbons undergo addition such as that of the Diels-Alder type and oxidation with osmium tetroxide: the former is the addition of e. g. quinone or maleic anhydride to the reactive para position and the latter is the addition to the reactive ortho bond.

It is suggested that the frontier electron density and superdelocalizability which have been proved to be good indexes of substitution reaction in conjugated compounds[1-3] will also be applicable to interpreting the reactivity in simultaneous addition reactions stated above, because the substitution and addition seem to be not so greatly different in nature from each other, at least until the activated complex is formed. In substitution reaction, the hydrogen atom of the attacking position and the reagent was considered to form a pseudoatom and the hyperconjugation energy due to the charge transfer between the pseudoatom and the orbital at the attacking position was assumed to make the reaction easy[4]. The situation in the addition reaction can be considered to resemble the substitution reaction in the sense that the delocalization energy due to the charge transfer in the transition state play a dominant role in decreasing the activation energy of the reaction. The circumstances will be clearly seen in the following example: the addition of maleic anhydride to the para position of polycondensed aromatic hydrocarbon, e. g. anthracene is deemed to proceed by a one-step process as follows:



(I) (II) (III)

The charge transfer between the maleic anhydride and the substrate molecule through the orbitals at the ethylenic bond of the former and the para position of the latter will occur in the transition state (II), and the delocalization energy due to the charge transfer is naturally considered a measure of easiness of addition reaction because the activation energy is decreased according as the increase of delocalization energy. In this connection, the frontier electron density and the superdelocalizability which could be derived from the delocalization energy are expected to be a good measure of the addition reaction.

In the present paper, the theoretical index for addition reaction in the frontier electron theory is derived and the index is compared with the rate of reactions hitherto carried out.

## Theoretical Treatment

The secular equation of the $\pi$ part of the transition complex which includes the orbitals of reagent and substrate $\pi$ electron system is written as

$$D(\varepsilon) = \begin{vmatrix} \alpha_h-\varepsilon & 0 & 0 & \gamma & 0 & 0 & \cdots & 0 \\ 0 & \alpha_h-\varepsilon & \gamma & 0 & 0 & 0 & \cdots & 0 \\ 0 & \gamma & a_{11}-\varepsilon & a_{12} & a_{13} & a_{14} & \cdots & a_{1n} \\ \gamma & 0 & a_{21} & a_{22}-\varepsilon & a_{23} & a_{24} & \cdots & a_{2n} \\ 0 & 0 & a_{31} & a_{32} & a_{33}-\varepsilon & a_{34} & \cdots & a_{3n} \\ \cdots & \cdots & \cdots & \cdots & \cdots & \cdots & \cdots & \cdots \\ \cdots & \cdots & \cdots & \cdots & \cdots & \cdots & \cdots & \cdots \\ 0 & 0 & a_{n1} & a_{n2} & \cdots & \cdots & \cdots & a_{nn}-\varepsilon \end{vmatrix}$$

$$= (\alpha_h-\varepsilon)^2\Delta(\varepsilon) - \gamma^2[(\alpha_h-\varepsilon)\{\Delta_{rr}(\varepsilon) + \Delta_{ss}(\varepsilon)\}] + \gamma^4\Delta_{rrss}(\varepsilon) = 0 \qquad (1)$$

where

$$\Delta(\varepsilon) = \begin{vmatrix} a_{11}-\varepsilon & a_{12} & a_{13} & \cdots & a_{1n} \\ a_{21} & a_{22}-\varepsilon & a_{23} & \cdots & a_{2n} \\ a_{31} & a_{32} & a_{33}-\varepsilon & \cdots & a_{3n} \\ \cdots & \cdots & \cdots & \cdots & \cdots \\ \cdots & \cdots & \cdots & \cdots & \cdots \\ a_{n1} & a_{n2} & \cdots & \cdots & a_{nn}-\varepsilon \end{vmatrix}$$

is the secular determinant for the substrate $\pi$-electron system and $\Delta_{rr}(\varepsilon)$ and $\Delta_{ss}(\varepsilon)$ are the minors of $\Delta(\varepsilon)$ corresponding to the *rr*- and *ss*-elements, and $a_{ii}$ and $a_{ij}(i \neq j)$ are the

1) K. Fukui, T. Yonezawa and H. Shingu, *J. Chem. Phys.*, **20**, 722 (1952).
2) K. Fukui, T. Yonezawa, C. Nagata and H. Shingu, ibid., **22**, 1433 (1954).
3) K. Fukui, T. Yonezawa and C. Nagata, ibid., **27**, 1247 (1957).
4) K. Fukui, T. Yonezawa and C. Nagata, This Bulletin, **27**, 423 (1954).

Coulomb and the resonance integrals, respectively. For simplicity, the values of these integrals are assumed to be the same as those in an isolated molecule. $\alpha_h$ and $\gamma$ are the Coulomb integral of the reagent*, and the resonance integral between the reagent and the $r$th and the $s$th atom of the substrate molecule at which the reaction takes place, respectively.

When the conjugation between the substrate molecule and reagent is small, i. e., in the case of $0<\gamma\leqq 1$, the perturbed orbital energy of the complex are given by the following formula

$$\varepsilon_j' = \varepsilon_j + \delta\varepsilon_j\gamma^2 + 0(\gamma^4) + \cdots\cdots \quad (2a)$$

$$\alpha_h' = \alpha_h + \delta_h\gamma^2 + 0(\gamma^4) + \cdots\cdots \quad (2b)$$

The values of $\delta\varepsilon_j$ and $\delta\alpha_h$ are easily obtained by the perturbation treatment as

$$\delta\varepsilon_j = \frac{\Delta_{rr}(\varepsilon_j)+\Delta_{ss}(\varepsilon_j)}{(\alpha_h-\varepsilon_j)\Delta'(\varepsilon_j)}\gamma^2 + \cdots\cdots \quad (3)$$

$$\delta\alpha_h = -\frac{\{\Delta_{rr}(\alpha_h)+\Delta_{ss}(\alpha_h)\}}{2\Delta(\alpha_h)} \pm \frac{\sqrt{\{\Delta_{rr}(\alpha_h)-\Delta_{ss}(\alpha_h)\}^2+4\{\Delta_{rs}(\alpha_h)\}^2}}{2\Delta(\alpha_h)} \quad (4)$$

$\varepsilon_j'$ and $\alpha_h'$ are the roots of $D(\varepsilon)=0$ and they correspond to the energy of the molecular orbital of the unperturbed system $\Delta(\varepsilon)$ and the orbitals of the reagent, respectively. We assumed that $\Delta(\varepsilon)=0$ has no multiple roots here, but in the case in which $\Delta(\varepsilon)=0$ has double roots, the final result is not altered.

The delocalization energy $\mathcal{K}_{r+s}$ is derived by treatment analogous to the case of substitution reaction[3]. It is given according as the type of reaction as follows:

for electrophilic reaction,

$$\mathcal{K}_{r+s} \cong 2\sum_{j=1}^{m}\frac{\Delta_{rr}(\varepsilon_j)+\Delta_{ss}(\varepsilon_j)}{(\alpha_h-\varepsilon_j)\Delta'(\varepsilon_j)}\gamma^2 = 2\sum_{j=1}^{m}\frac{(C_r^j)^2+(C_s^j)^2}{\varepsilon_j-\alpha_h}\gamma^2 \quad (5)$$

for radical reaction**,

$$\mathcal{K}_{r+s} \cong \left[-\sum_{j=1}^{m}\frac{\Delta_{rr}(\varepsilon_j)+\Delta_{ss}(\varepsilon_j)}{(\varepsilon_j-\alpha_h)\Delta'(\varepsilon_j)} - \sum_{j=m+1}^{n}\frac{\Delta_{rr}(\varepsilon_j)+\Delta_{ss}(\varepsilon_j)}{(\alpha_h-\varepsilon_j)\Delta'(\varepsilon_j)}\right]\gamma^2$$

$$= \left[\sum_{j=1}^{m}\frac{(C_r^j)^2+(C_s^j)^2}{\varepsilon_j-\alpha_h} + \sum_{j=m+1}^{n}\frac{(C_r^j)^2+(C_s^j)^2}{-(\varepsilon_j-\alpha_h)}\right]\gamma^2 \quad (6)$$

for nucleophilic reaction,

$$\mathcal{K}_{r+s} \cong -2\sum_{j=m+1}^{n}\frac{\Delta_{rr}(\varepsilon_j)+\Delta_{ss}(\varepsilon_j)}{(\alpha_h-\varepsilon_j)\Delta'(\varepsilon_j)}\gamma^2 = 2\sum_{j=m+1}^{n}\frac{(C_r^j)^2+(C_s^j)^2}{-(\varepsilon_j-\alpha_h)}\gamma^2 \quad (7)$$

where $C_r^j$ is the coefficient of the $r$th atomic orbital of $j$th molecular orbital of non-perturbed substrate molecule and the relation $-\Delta_{rr}(\varepsilon_j)/\Delta'(\varepsilon_j)=(C_r^j)^2$ was used in deriving the last terms of the right hand side of the above equations.

When the value of $\alpha_h$ is equal to $\alpha$, the Coulomb integral of carbon atom in benzene, the coefficients of $\gamma^2$ in Eqs. 5, 6 and 7 are nothing but $(S_r+S_s)$ for electrophilic, radical and nucleophilic reactions, respectively. Therefore, the theoretical index for addition reaction at two positions $r$ and $s$ is the sum of the superdelocalizability at $r$ and $s$ positions. It is clearly seen in the expression in Eqs. 5, 6 and 7 that the contribution of the frontier orbital is the greatest, hence as in the case of the treatment of substitution reaction[3], the one term approximation taking into consideration the frontier orbital alone, will be allowed.

It is noted that the present treatment gives the same result regardless whether one considers the reaction as a simultaneous or two-step one. This indescernability is also seen in other treatments such as static and localization methods. Therefore, it is impossible to decide whether the reaction is one-step or not by comparing the theories and experimental results.

The theoretical index derived above is qualified as a good index for predicting the reactivity in simultaneous addition reaction as a result of comparison with the experiment. For instance, the data of the attacking positions in the Diels-Alder reaction are in agreement without an exception with the predicted most reactive position in a molecule (Table I). The relative rate of these compounds in the Diels-Alder reaction has not been measured in one

* In this treatment, the attacking reagent was assumed to be composed of two non-conjugating components. In other words, the reaction was considered to occur with two reagents. The one reagent attacks the $r$ position and the other the $s$ position simultaneously or stepwise. In the case of the addition of maleic anhydride to poly-condensed aromatic hydrocarbons, the reagent as well as the substrate is a conjugated system, and the whole $\pi$ electron system of maleic anhydride should be taken into consideration. In this case, however, the reaction was considered as an addition of two reagents to the substrate separately.

** For a radical reaction twice the second term (the energetically lower term) of Eq. 4 are omitted in deriving Eq. 6. It is because one may conclude that the term has no connection with the simultaneous addition reaction. That is to say, from the configuration interaction's point of view, it originates in the interaction between the initial configuration (initial state of reaction) and the configuration corresponding to one-electron transfer from a component of the reagent to another component. Not involving the charge transfer between the reagent and the substrate molecule but between the two components of reagents, this interaction seems to have no connection with the reaction.

TABLE I. SUM OF THE SUPERDELOCALIZABILITY AT PARA CARBON ATOMS IN SOME AROMATIC HYDROCARBONS ($S_r+S_s$) IN COMPARISON WITH EXPERIMENTS

| Compound | Para position | $S_r+S_s$ | Experiment; position of attack |
|---|---|---|---|
| Hexacene | 6,15 | 4.011 | 6,15[a] |
| | 5,16 | 3.459 | |
| | 1,4 | 2.355 | |
| Pentacene | 6,13 | 3.589 | 6,13[a] |
| | 5,14 | 3.269 | |
| | 1,4 | 2.308 | |
| Naphthacene | 5,12 | 3.010 | 5,12[a] |
| | 1,4 | 2.243 | |
| Anthracene | 9,10 | 2.627 | 9,10[b] |
| | 1,4 | 2.147 | |
| 1,2-Benzanthracene | 9,10 | 2.437 | 9,10[a,c] |
| | 5,8 | 2.098 | |
| | 1',4' | 1.915 | |
| 1,2,3,4-Dibenz-anthracene | 9,10 | 2.303 | 9,10[a,d,h] |
| | 5,8 | 2.056 | |
| | 1',4' | 1.853 | |
| 1,2,5,6-Dibenz-anthracene | 9,10 | 2.292 | 9,10[e] |
| | 1',4' | 1.919 | |
| Naphthalene | 1,4 | 1.989 | No addition[f] |
| Phenanthrene | 1,4 | 1.918 | No addition[g] |
| Chrysene | 1,12 | 1.907 | No addition[g] |
| Benzene | | 1.667 | No addition[f] |

a) E. Clar, *Ber.*, **64**, 2194 (1931); **65**, 503 (1932); **72**, 1817 (1939).
b) O. Diels, K. Alder and S. Beckmann, *Ann.*, **486**, 1191 (1931).
c) E. Clar, *Ber.*, **65**, 519 (1932).
d) E. Clar and L. Lombardi, *Ber.*, **65**, 1411 (1932).
e) J. W. Cook, *J. Chem. Soc.*, **1931**, 3273.
f) E. Clar, "Aromatische Kohlenwasserstoffe" p. 12 (1941).
g) R. N. Jones, C. J. Gogek and R. W. Sharpe, *Can. J. Res.*, **B26**, 719 (1948).
h) E. J. Moriconi, W. F. O'Conner and F. T. Wallenberger, *J. Am. Chem. Soc.*, **81**, 646 (1959).

TABLE II. SUM OF THE SUPERDELOCALIZABILITY AT TWO ADJACENT CARBON ATOMS IN SOME AROMATIC HYDROCARBONS ($S_r+S_s$) IN COMPARISON WITH EXPERIMENTS

| Compound | Bond ($r-s$) | $S_r+S_s$ | Experiment; position of attack |
|---|---|---|---|
| 1,2-Benzanthracene | 3,4 | 2.079 | 3,4[a] |
| | 5,6 | 1.963 | |
| | 7,8 | 1.953 | |
| | 3',4' | 1.849 | |
| | 1',2' | 1.832 | |
| | 6,7 | 1.818 | |
| | 2',3' | 1.766 | |
| 1,2,5,6-Dibenz-anthracene | 3,4 | 2.062 | 3,4[a,e] |
| | 3',4' | 1.848 | |
| | 1',2' | 1.842 | |
| | 2',3' | 1.771 | |
| Pyrene | 1,2 | 2.052 | 1.2[b] |
| | 3,4 | 1.944 | |
| Chrysene | 1,2 | 1.997 | 1.2[b] |
| | 3,4 | 1.857 | |
| | 5,6 | 1.852 | |
| | 4,5 | 1.762 | |
| Phenanthrene | 9,10 | 1.995 | 9,10[a,b,d] |
| | 1,2 | 1.837 | |
| | 3,4 | 1.832 | |
| Anthracene | 1,2 | 1.995 | 1,2,3,4[a,c] |
| | 2,3 | 1.843 | |
| Naphthalene | 1,2 | 1.867 | 1,2[c] |
| | 2,3 | 1.746 | |
| Benzene | | 1.667 | No addition[c] |

a) G. M. Badger, *J. Chem. Soc.*, **1949**, 456; Ref. 5.
b) J. W. Cook and R. Schoental, ibid., **1948**, 170.
c) J. W. Cook and R. Schoental, *Nature*, **161**, 237 (1948).
d) N. L. Drake and T. R. Sweeney, *J. Org. Chem.*, **11**, 67 (1946).
e) E. J. Moriconi, W. F. O'Conner, W. J. Schmitt, G. W. Cogswell and B. P. Fürer, *J. Am. Chem. Soc.*, **82**, 3441 (1960).

and the same condition. However, considering the experimental data which have been so far reported (cf. references in Table I), one can conclude that the following order of reactivity might exist : hexacene> pentacene> naphthacene >anthracene> 1, 2-benzanthracene> 1, 2, 5, 6-dibenzanthracene> naphthalene, phenanthrene, benzene. This is in excellent accord with the order of magnitude of $S_r+S_s$ of these compounds.

As is seen in Table II, the experimental position of attack of osmium tetroxide to the double bond of some polycondensed aromatic hydrocarbons agree very well with the prediction by the theory. The reactive rate of reaction of these compounds is not determined completely ; however, the experiment by Badger and Reed showed that 1, 2-benzanthracene reacts with osmium tetroxide faster than phenanthrene does[5]. This fact is explained well by our calculated result.

*Faculty of Engineering*
*Kyoto University*
*Sakyoku, Kyoto*

5) G. M. Badger and R. I. Reed, *Nature*, **161**, 238 (1948).

# *Diamagnetic Behavior of Some Aliphatic Molecules in Crystals*

By A. MOOKHERJI, S. N. MOOKHERJI and D. NEOGY

(Received May 18, 1960)

According to Pauling[1] the normal susceptibility in the plane of the aromatic molecules is due to the bound electrons, contributing to the susceptibility equally in all directions, and the electrons which are free to precess only in the plane of the molecule in orbits, provided by the entire molecular ring system, contribute only to the susceptibility along the normal to the molecular plane. When such anisotropic molecules are regularly arranged in crystals, the crystal as a whole will exhibit magnetic anisotropy. Hence anisotropy of the diamagnetic crystals is obviously due to the anisotropy of its constituent molecules.

Krishnan and Banerji[2] and Banerji[3] showed that, if the molecular anisotropy is known, it is possible to obtain much useful information regarding the orientation of the molecules in crystals relative to one another.

In a recent paper (Mookherji et al.)[4] studying the susceptibilities of a few dibasic aliphatic acids and their salts observed that,

a) Unlike the normal aliphatics the maximum diamagnetic susceptibility for the these salts lies normal to the plane of the carboxylic groups.

b) This extra diamagnetism could be attributed to resonance which exists in these molecules.

From X-ray studies and chemical considerations one may be led to think that the carboxylic groups in mono- and dibasic aliphatic acids and their salts can be represented by two or more structures and hence in these molecules resonance will exist. It would be therefore interesting to study the diamagnetic anisotropy of the crystals of the above mentioned acids and their salts and to find whether a similar diamagnetic behaviour like succinic and tartaric acids and their salts could be observed.

## Experimental

Crystals were grown out of aqueous solution at room temperature by slow evaporation. The chemicals used were Merk's extra pure reagent quality prewar variety.

The magnetic anisotropy and the orientation of the crystals in magnetic field were carried out by the well known method of Krishnan and Banerji[2]. The absolute susceptibility in any convenient direction was measured by a modified quartz balance (Bose)[5]. The magnetic field used for the purpose had a constant gradient over a considerable volume by using pole pieces as devised by Dutta Roy[6]. The standard crystal for calibration of this balance was a well developed crystal of naphthalene for which mass susceptibility is accurately known (Banerji)[7].

## Results

The results of measurements are collected in Tables I and II, and are expressed in the usual units i. e. c. g. s. E. M. units. $\chi_3$ is the gram molecular susceptibility along b-crystallographic axis of a monoclinic crystal; the algebraically greater of the two values in the symmetry plane (010) is denoted by $\chi_1$ and the smaller by $\chi_2$; $\phi$ is the angle that $\chi_1$-direction makes with c-crystallographic axis taken positive from c-axis towards a-axis through obtuse $\beta$.

In orthorhombic crystals, the gram molecular susceptibilities along the crystallographic axes a, b and c are represented by $\chi_a$, $\chi_b$ and $\chi_c$, respectively.

## Discussion

**Magnetic Analysis of Molecular Orientation in Crystals.**—We proceed now to discuss the magnetic anisotropy in the light of the orientation of the molecules in the unit cell of the crystal. The crystals are discussed individually.

*Oxalic Acid Dihydrate.* — Complete X-ray studies by Robertson and Woodword[8] revealed that the crystal is monoclinic in the space group $C_{2h}^5$ with two molecules in the unit cell. The molecules are centro symmetric, approximately plane, and are magnetically nearly uniaxial.

Let us represent the axes of symmetry of the two molecules by $Z_1$ and $Z_2$ and the principal susceptibilities of the molecule by $K_\perp$ and $K_\parallel$ in the plane of the molecule and normal to it respectively.

1) L. Pauling, *J. Chem. Phys.*, **4**, 673 (1936).
2) K. Krishnan and S. Banerji, *Philos. Trans.*, **A 234**, 265 (1935); *Z. Kristallogr*, **A 99**, 499 (1938).
3) S. Banerji, *Z. Kristallogr.*, **A 100**, 316 (1938).
4) A. Mookherji, R. Mittal and D. Neogy, *Bull. Nat. Inst. Sci. India*, No. 14 (1959).
5) A. Bose, *Ind. Jour. Phys.*, **21**, 275 (1947).
6) S. Datta Roy, idid., **29**, 429 (1955).
7) S. Banerji, *Report Symposium. Ind. Association for the cultivation of Science*, 19 (1957).
8) J. M. Robertson and J. Woodward, *J. Chem. Soc.*, **1936**, 1817.

TABLE I. MAGNETIC ANISOTROPY AT 30°C

| Sl. No. | Name and structural formula of the crystal | Crystallographic data | Mode of suspension | Orientation in the field | $\Delta\chi\times10^6$ | Magnetic anisotropy |
|---|---|---|---|---|---|---|
| 1 | 2 | 3 | 4 | 5 | 6 | 7 |
| 1. | Oxalic acid dihydrate | Monoclinic | "b" axis vertical | $\theta=15.2°$ | 2.1 | $\chi_1-\chi_2=2.10$ |
| | | $C_{2h}^5$ | "a" axis vertical | "b" axis normal to the field | 8.39 | $\chi_1-\chi_3=8.53$ |
| | COOH<br>\|<br>COOH $+2H_2O$ | $a=6.12$<br>$b=3.6$<br>$c=12.0$<br>$\beta=106°\ 12'$<br>$z=2$ | 001 Plane horizontal | "b" axis normal to the field | 6.56 | $\theta_{cal}=14.7°$<br>$\theta_{obs}=15.2°$ |
| 2. | Ammonium oxalate monohydrate | Orthorhombic | "c" axis vertical | "a" axis along the field | 1.108 | $\chi_a-\chi_b=1.108$ |
| | | $P_{2_12_12}$ | "a" axis vertical | "c" axis normal to the field | 13.17 | $\chi_b-\chi_c=13.17$ |
| | $COONH_4$<br>\|<br>$COONH_4$ $+H_2O$ | $a=8.04$<br>$b=10.27$<br>$c=3.82$<br>$z=2$ | "b" axis vertical | "a" axis along the field | 14.16 | Cal. $\Delta\chi=0.99$ |
| 3. | Potassium oxalate monohydrate | Monoclinic | "b" axis vertical | $\theta=61.0°$ | 1.6 | $\chi_1-\chi_2=1.6$ |
| | | $C_{2/c}$ | "b" & "c" axes horizontal | "b" axis normal to the field | 8.8 | $\chi_1-\chi_3=10.0$ |
| | COOK<br>\|<br>COOK $+H_2O$ | $a=9.32$<br>$b=6.17$<br>$c=10.65$<br>$\beta=110°\ 58'$<br>$z=4$ | "a" axis vertical | "b" axis normal to the field | 9.5 | $\theta_{cal}=59.5°$<br>$\theta_{obs}=61.0°$ |
| 4. | Ammonium bi-oxalate monohydrate | Orthorhombic | "b" axis vertical | "b" axis along the field | 9.09 | $\chi_c-\chi_a=9.09$ |
| | | $a:b:c=$<br>0.4524:1:0.5593 | "c" axis vertical | "b" axis along the field | 10.78 | $\chi_b-\chi_a=10.78$ |
| | $COONH_4$<br>\|<br>COOH $+H_2O$ | | "a" axis vertical | "b" axis along the field | 2.06 | Cal. $\Delta\chi=1.70$ |
| 5. | Potassium bi-oxalate monohydrate | Monoclinic | "b" axis vertical | $\varphi=4.0$ | 9.00 | $\chi_1-\chi_2=9.00$ |
| | | $P_{2_1/c}$ | "c" axis vertical | "b" axis along the field | 10.2 | $\chi_3-\chi_2=10.3$ |
| | COOK<br>\|<br>COOH $+H_2O$ | $a=4.32$<br>$b=12.88$<br>$c=10.32$<br>$\beta=133°\ 29'$<br>$z=4$ | "b" & "c" axes horizontal | "b" axis along the field | 1.4 | $\phi_{cal}=3.9$<br>$\phi_{obs}=4.0$ |
| 6. | Calcium formate | Orthorhombic<br>$P_{Cab}$ | "b" axis vertical | "c" axis along the field | 1.722 | $\chi_c-\chi_a=1.722$ |
| | H—COO<br>H—COO Ca | $Z=8$<br>$a=10.16$ | "c" axis vertical | "a" axis normal to the field | 1.287 | $\chi_b-\chi_a=1.287$ |
| | | $b=13.38$<br>$c=6.27$ | "a" axis vertical | "b" axis normal to the field | 0.3118 | Cal. $\Delta\chi=0.435$ |
| 7. | Barium formate | Orthorhombic | "c" axis vertical | "a" axis along the field | 0.621 | $\chi_a-\chi_b=0.621$ |
| | | $a:b:c=$<br>0.765:1:0.8638 | "b" axis vertical | "b" axis normal to the field | 1.729 | $\chi_c-\chi_b=1.729$ |
| | H—COO<br>H—COO Ba | | "b" axis vertical | "c" axis along the field | 0.9279 | Cal. $\Delta\chi=1.108$ |
| 8. | Barium acetate trihydrate | Monoclinic | "b" axis vertical | $\theta=33.5°$ | 1.18 | $\chi_1=\chi_2=1.18$ |
| | | $a:b:c=$<br>2.1362:1:1.222 | "a" axis vertical | "b" axis along the field | 0.776 | $\chi_1-\chi_3=0.458$ |
| | $CH_3$—COO<br>$CH_3$—COO Ba<br>$+3H_2O$ | $\beta=113°\ 27'$ | 001 Plane horizontal | "b" axis along the field | 1.27 | $\phi_{cal}=33.5°$ |

TABLE II. ABSOLUTE SUSCEPTIBILITIES

| Sl. No. | Name of the crystal | Temp. °C | Direction along which suscept. was measured | Volume suscept. | Corresponding $\chi_M$ | Principal gram molecular suscept. | Mean suscept. $\bar{\chi}_m$ | Pascal's value $\bar{\chi}_m$ |
|---|---|---|---|---|---|---|---|---|
| 1 | 2 | 3 | 4 | 5 | 6 | 7 | 8 | 9 |
| 1. | Oxalic acid dihydrate, Monoclinic | 33.00 | Along "b" axis | −0.4214 | −53.1 | $\chi_1=-53.1$<br>$\chi_2=-55.2$<br>$\chi_3=-61.63$ | −56.64 | −60.42 |
| 2. | Ammonium oxalate monohydrate, orthorhombic | 33.00 | Along "b" axis | −0.4257 | −60.4 | $\chi_a=-60.4$<br>$\chi_b=-61.51$<br>$\chi_c=-74.68$ | −65.33 | −68.20 |
| 3. | Potassium oxalate monohydrate, monoclinic | 33.00 | Along "b" axis | −0.3740 | −68.82 | $\chi_1=-68.82$<br>$\chi_2=-70.42$<br>$\chi_3=-78.82$ | −72.68 | −67.20 |
| 4. | Ammonium bi-oxalate monohydrate, orthorhombic | 33.00 | Along "b" axis | −0.3417 | −42.72 | $\chi_a=-42.72$<br>$\chi_b=-31.94$<br>$\chi_c=-33.63$ | −36.09 | −56.83 |
| 5. | Potassium bi-oxalate monohydrate, monoclinic | 33.00 | Along "b" axis | −0.2954 | −43.13 | $\chi_1=-43.13$<br>$\chi_2=-52.13$<br>$\chi_3=-41.93$ | −45.73 | −57.33 |
| 6. | Calcium formate orthorhombic | 33.00 | Along "b" axis | −0.2650 | −34.46 | $\chi_c=-34.46$<br>$\chi_a=-36.182$<br>$\chi_b=-34.895$ | −35.179 | −44.70 |
| 7. | Barium formate orthorhombic | 33.00 | Along "b" axis | −0.2892 | −65.77 | $\chi_c=-65.77$<br>$\chi_b=-67.50$<br>$\chi_a=-66.88$ | −66.71 | −65.40 |
| 8. | Barium acetate trihydrate, monoclinic | 33.00 | Along "b" axis | −0.3772 | −116.7 | $\chi_1=-116.7$<br>$\chi_2=-117.88$<br>$\chi_3=-116.242$ | −116.94 | −128.00 |

Then $\chi_1$ will lie in the direction, normal to the plane containing $Z_1$ and $Z_2$ axes and $\chi_2$ will be the internal bisector of the angle $2\Psi$ between $Z_1$ and $Z_2$ and hence,

$$\left.\begin{aligned}\chi_1&=K_\perp\\ \chi_2&=K_\parallel\cos^2\Psi+K_\perp\sin^2\Psi\\ \chi_3&=K_\parallel\sin^2\Psi+K_\perp\cos^2\Psi\end{aligned}\right\} \quad (1)$$

and $$\bar{\chi}=(\chi_1+\chi_2+\chi_3)/3=\frac{K_\parallel+2K_\perp}{3}$$

substituting the values of $(\chi_1-\chi_2)$ and $(\chi_1-\chi_3)$ in Eq. 1 we have $(K_\perp-K_\parallel)=10.7\times10^{-6}$ and $\Psi=63.5°$, which agrees well with X-ray findings, i. e. 61.9°.

*Ammonium Oxalate Monohydrate.*—Fine structure studies by X-ray methods (Hendricks, and Hendricks and Jefferson[9,10]) reveal that there are two molecules in the unit cell in space group $P_{2_12_12}$ and that the two parts of the COOH group are in planes making an angle of 20° whereas in oxalic acid both parts are in the same plane. The planes containing the oxygens of the oxalate groups are almost parallel to (001) plane. Following Mookherji[11] we can attribute the abnormal diamagnetism to oxygen atoms of the oxalate groups. Hence according to X-ray findings (001) plane should approximately be a plane of magnetic symmetry, whereas normal to this plane we should expect algebraically maximum susceptibility. From Table I we find that in the (001) plane $\Delta\chi=\chi_a-\chi_b=1.1\times10^{-6}$, whereas it is $14.2\times10^{-6}$ in the plane normal to it.

We may therefore conclude that for oxalate molecules, which are in strained condition because of its two parts being in two different planes $\Delta K=K_\perp-K_\parallel=14.0\times10^{-6}$, more by 4 units for the oxalate groups, where both the parts are in the same plane.

*Ammonium Bi-oxalate.*—From Table I it is seen that the two susceptibilities in the (001) plane are nearly equal and numerically less than the third susceptibility by about 10 units, which is almost equal to the value of the oxalate group in oxalic acid dihydrate. Thus we conclude that in this crystal all the oxalate groups are oriented parallel with (001) plane. At present no X-ray data are available to verify the above conclusions.

*Potassium Oxalate Monohydrate.*—Hendricks[9] by X-ray methods found that the crystal is

9) S. B. Hendricks, *Z. Kristallogr.*, **91**, 48 (1935).
10) S. B. Hendricks and M. E. Jefferson, *J. Chem. Phys.*, **4**, 102 (1936).
11) A. Mookherji, *Acta Cryst.*, **10**, 25 (1957).

monoclinic in the space group of $C_{2/c}$ with four molecules in the unit cell; they form a set of two pairs with the two molecular planes in each pair being parallel. If the slight tilt between the two pairs is neglected then the molecules may be taken oriented parallel to the plane (010).

Evidently, $K_{\parallel}=\chi_3$, $K_{\perp}\approx\chi_2\approx\chi_1$

Hence, $1/2[(\chi_1-\chi_3)+(\chi_2-\chi_3)]=K_{\perp}-K_{\parallel}$

Thus it is observed that $(K_{\perp}-K_{\parallel})$ for oxalate group in the crystal is 9.2 as against 10.7 for that in the oxalic acid. This is evidently due to the neglect of the tilt. On calculating the tilt comes out as 15.0° with the (010) plane.

*Potassium Bi-oxalate.* — According to Hendricks[9], the crystal has four molecules in the unit cell and the molecular planes are oriented parallel to (100) plane. Hence $K_{\perp}-K_{\parallel}=10.0\times10^{-6}$, which is almost the same as found with other oxalate groups.

*Calcium Formate.*—It crystallises in the orthorhombic system in the space group $P_{Cab}$ with eight molecules in the unit cell (Nitta and Osaki[12]). If $n$, $m$ and $l$ are the direction cosines of the normal to the formate group, following Banerji[3] we have,

$$l^2-m^2=\frac{\chi_b-\chi_a}{K_{\perp}-K_{\parallel}},\qquad l^2-n^2=\frac{\chi_c-\chi_a}{K_{\perp}-K_{\parallel}}$$

and $l^2+m^2+n^2=1$

In order to calculate $m$, $l$ and $n$ one must know $(K_{\perp}-K_{\parallel})=\Delta K$ for COOH group. This may be estimated as follows:

According to Pauling and Sherman[13] resonance energy in monobasic acids is 1.20 electron volts. Now according to Pauling[14], if one attributes to $\Delta K$ this resonance energy then,

$$\Delta K=\frac{E\times M}{3.22\times\rho}=8.36\times10^{-6}$$

where $E$ is kinetic energy, $M$ the molecular weight and $\rho$ the density. On substituting this value and $(\chi_b-\chi_a)$ and $(\chi_c-\chi_a)$ from Table I we find that the formate groups are inclined at 48.1, 56.0 and 59.8° to a, b and c crystallographic axes respectively.

*Barium Formate.*—The crystal is orthorhombic. The orientation of the formate group is calculated following the same method as in the case of calcium formate, which show that the normal to the formate group is inclined at 54.0° to a-axis 35.8° to b-axis and 38.8° to c-axis.

12) I. Nitta and K. Osaki, *X-Rays*, 5, 37 (1948).
13) L. Pauling and J. Sherman, *J. Chem. Phys.*, 1, 679 (1933).
14) L. Pauling, *Phys. Rev.*, 34, 954 (1929).

**Diamagnetic Anisotropy and Resonance Energy.**—According to Pauling, mono- and dicarboxylic acids and their salts exhibit resonance with two contributing forms and the actual resonance structure is a resonance hybrid intermediate between the contributing forms. Taking into account the empirical values of the polar effect and the dissociation constants of fatty acids Pauling calculated the resonance energy in carboxylic groups. One direct consequence of such resonance is the abnormal diamagnetism normal to the plane of the groups. Therefore it would be very interesting to correlate the measured abnormal diamagnetism with the resonance energy as obtained empirically. As already stated the kinetic energy $E$ of the resonating electron is related to $\Delta K$ by expression

$$E=3.22\times\frac{\Delta K\times\rho}{M}$$

Using the above relation we have calculated the resonance energy for formates, oxalates, succinates and tartrates using $\Delta K$-values which are given in Table III. We have also taken

TABLE III

| Substances | $\Delta K\times10^6$ | Extra resonance energy calculated By Pauling | Extra resonance energy calculated From magnetic values |
|---|---|---|---|
| | Aromatics | | |
| Diphenyl | 118.6 | 86.88 | 84.65 |
| Naphthalene | 114.0 | 74.66 | 82.62 |
| Anthracene | 182.6 | 104.70 | 100.30 |
| Stilbene | 141.6 | 94.26 | 101.00 |
| | Aliphatics | | |
| Succinic acid | 10.7 | 54.86 | 52.00 |
| Tartaric acid | 9.6 | 54.86 | 52.00 |
| Oxalic acid | 10.7 | 54.86 | 53.31 |

some of the $\Delta K$-values for some typical aromatics as determined by Krishnan and Banerji[2] and calculated resonance energy. The agreement between the observed and calculated values is very encouraging.

**Influence of Resonance Energy on Diamagnetism.**—Adopting the conventional structural formulae for oxalates, formates and acetates, we have calculated mean gram molecular susceptibilities $\bar{\chi}_m$ for them on the basis of Pascal's additive law which are given in Table II. On comparing with our measured values of $\bar{\chi}_m$ a lowering is observed. This lowering is well understood if we recall that the resonance occuring in these groups impart on them some amount of double bond character (unsaturated) which lowers $\bar{\chi}_m$. A similar comparison of $\bar{\chi}_m$ deduced on the basis of Pascal's law and those measured by Krishnan and Banerji[2] for a number of aromatic substances

points to the same findings. Matsunaga[15] found with azobenzene the same value as Banerji[3] which is lower than Pascal's value Thus one can safely conclude that resonance lowers diamagnetic values.

The above point of view is further strengthened by our findings that for molten oxalic acid dihydrate $\bar{\chi}_m$ is $-60.89\times10^{-6}$ (100°C) while that for the powder state is $-56.4\times10^{-6}$ (30°C). In molten state the crystal lattice completely breaks down so that the double bond character almost vanishes and hence there is an increment of $\bar{\chi}_m$ approaching Pascal's value.

## Summary

The principal magnetic susceptibilities of single crystals of some aliphatic mono- and di-basic acids and their salts have been measured and the results have been correlated with the fine structure studies of the crystals by X-ray methods. It is observed that the anisotropy per -COOH group is 5 units, which increases by nearly 2 units if two parts of $\begin{matrix}\text{COOH}\\|\\\text{COOH}\end{matrix}$ groups are not in the same plane.

The observed extra diamagnetism normal to the plane of the carboxylic groups, if attributed to resonance, the calculated energy compares very favourably with that deduced by Pauling from a consideration of the heat of formation of molecules and the lowering of the susceptibility from Pascal's value is then well understood.

We take this opportunity to thank the Ministry of Education, Govt. of India for the individual (A. M.) research grants and to U. P. S. R. G. C. for the award of scholarship to one of us (D. N.).

*Physics Labratries*
*Agra College*
*Agra, India*

15) Y. Matsunaga, This Bulletin, **29**, 308 (1956).

# *The Surface Tension and the Critical Micelle Concentration in Aqueous Solution of β-D-Alkyl Glucosides and their Mixtures*

By Kozo SHINODA, Tokio YAMAGUCHI and Ryohei HORI

(Received August 11, 1960)

There have not been many research works on the pure non-ionic agents[1-3]. Future progress in this field should be assured by the study of pure non-ionic agents. Some colloid chemical properties of a series of pure octyl polyol ethers in aqueous solution have been studied to determine the effect of differences in the hydrophilic group[3]. In the present paper, we have measured the surface tension vs. concentration of octyl, decyl and dodecyl glucosides in order to know the effect of paraffin chain length on the physico-chemical properties of alkyl glucosides. The CMC was determined from the inflexion of the surface tension vs. concentration curve. The surface tension of mixtures of alkyl glucosides solutions and the effect of added salts on the surface tension of octyl glucoside were also measured.

## Experimental

The procedures and purifications of alkyl glucosides were similar[4] as in the case of octyl glucoside[3]. The melting points and specific rotations of β-D-octyl, decyl and dodecyl glucosides were m. p. 63.8~65°C, $[\alpha]_D^{20} = -33.8°$ ($H_2O$); m. p. 135°C, $[\alpha]_D^{25} = -27.8°$ ($H_2O$); m. p. 143.5°C, $[\alpha]_D^{25} = -24.7°$ ($H_2O$), respectively.

The materials were further purified by foam fractionation. The concentration of the solution foam fractionated was chosen slightly below the CMC, because the foam stability and the efficiency of the elimination of highly surface active impurities were optimum in this concentration[5]. Surface

1) C. R. Bury and J. Browning, *Trans. Faraday Soc.*, **49**, 209 (1953).
2) T. Nakagawa et al., *J. Chem. Soc. Japan, Pure Chem. Soc.* (*Nippon Kagaku Zasshi*), **77**, 1563 (1956); **79**, 345, 348 (1958).
3) K. Shinoda, T. Yamanaka and K. Kinoshita, *J. Phys. Chem.*, **63**, 648 (1959).
4) R. Hori, Ph. D. Dissertation, Kyoto University (1959) (in Japanese).
5) K. Shinoda and K. Mashio, *J. Phys. Chem.*, **64**, 54 (1960).

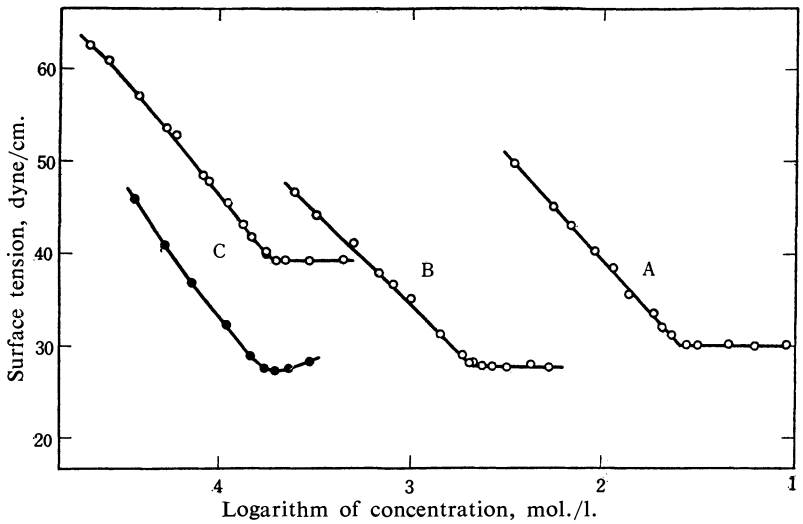



Fig. 1. The surface tension vs. log. concentration curves of β-D-alkyl glucosides at 25°C: A, octyl glucoside; B, decyl glucoside; C, dodecyl glucoside; ●, before foam fractionation.

tension was measured by the drop weight method, with a tip 0.576 cm. in diameter in an air thermostat at 25±0.2°C. The correction of Harkins et al.[6] was applied. There was appreciable change, 2~4 dyne cm. of surface tension, with time durations of 4~20 min. and 10~60 min. for decyl and dodecyl glucosides, respectively.

## Results

The surface tension vs. concentration relations are shown in Fig. 1 and summarized in Tables I, II and III. There was great change in surface tension between foam fractionated unfractionated solution of dodecyl glucoside. However, there was no appreciable change in solutions of octyl and decyl glucosides.

TABLE I. THE SURFACE TENSION IN AQUEOUS SOLUTION OF β-D-OCTYL GLUCOSIDE AT 25°C

| Concentration, mol./l. ×10² | Time per drop in min. | Number of measurements | Surface tension dyne/cm. | Mean variation dyne/cm. |
|---|---|---|---|---|
| 0.343 | 20 | 4 | 49.8 | 0.2 |
| 0.549 | 15 | 4 | 45.0 | 0.6 |
| 0.686 | 10 | 4 | 43.1 | 0.35 |
| 0.915 | 10 | 4 | 40.3 | 0.4 |
| 1.14 | 10 | 4 | 38.4 | 0.2 |
| 1.37 | 10 | 4 | 35.6 | 0.3 |
| 1.83 | 5 | 8 | 33.6 | 0.9 |
| 2.05 | 5 | 4 | 32.1 | 0.05 |
| 2.29 | 5 | 2 | 31.2 | 0.05 |
| 2.75 | 5 | 4 | 30.2 | 0.3 |
| 3.07 | 5 | 3 | 30.3 | 0.2 |
| 4.61 | 5 | 4 | 30.4 | 0.1 |
| 6.15 | 5 | 3 | 29.9 | 0.6 |
| 9.23 | 5 | 2 | 30.1 | 0.0 |

TABLE II. THE SURFACE TENSION IN AQUEOUS SOLUTION OF β-D-DECYL GLUCOSIDE AT 25°C

| Concentration, mol./l. ×10³ | Time per drop in min. | Number of measurements | Surface tension dyne/cm. | Mean variation dyne/cm. |
|---|---|---|---|---|
| 0.255 | 20 | 2 | 46.7 | 0.1 |
| 0.325 | 15 | 3 | 44.2 | 0.1 |
| 0.513 | 15 | 4 | 41.2 | 0.3 |
| 0.683 | 10 | 4 | 37.8 | 0.1 |
| 0.816 | 10 | 2 | 36.7 | 0.0 |
| 1.025 | 10 | 4 | 35.0 | 0.3 |
| 1.46 | 10 | 2 | 31.2 | 0.2 |
| 1.91 | 5 | 3 | 29.0 | 0.0 |
| 2.06 | 5 | 3 | 28.1 | 0.1 |
| 2.14 | 5 | 2 | 28.3 | 0.0 |
| 2.41 | 5 | 4 | 27.8 | 0.1 |
| 2.67 | 5 | 2 | 27.7 | 0.1 |
| 3.22 | 5 | 3 | 27.7 | 0.1 |
| 4.28 | 5 | 3 | 28.0 | 0.3 |
| 5.35 | 5 | 4 | 27.7 | 0.5 |

The inflexion in the surface tension vs. logarithm of concentration curve was distinct and there was no minimum in foam fractionated solution. The surface tension of mixtures of alkyl glucosides has been measured. The results are summarized in Fig. 2. The surface tension vs. concentration curve showed the minimum in the mixture of octyl-decyl glucosides. The effect of added sodium chloride, calcium chloride and sodium sulfate on the surface tensions of aqueous solution of octyl glucoside has also been measured. The results are shown in Fig. 3.

6) W. D. Harkins and F. E. Brown, *J. Am. Chem. Soc.*, **41**, 519 (1919).

Table III. The surface tension in aqueous solution of β-D-dodecyl glucoside at 25°C

| Concentration, mol./l. ×10⁴ | Time per drop in min. | Number of measurements | Surface tension dyne/cm. | Mean variation dyne/cm. |
|---|---|---|---|---|
| 0.213 | 60 | 3 | 62.5 | 0.1 |
| 0.270 | 60 | 3 | 60.8 | 0.3 |
| 0.385 | 60 | 3 | 57.0 | 1.0 |
| 0.540 | 50 | 3 | 53.6 | 1.1 |
| 0.609 | 40 | 3 | 52.8 | 0.1 |
| 0.835 | 30 | 3 | 48.5 | 0.1 |
| 0.900 | 20 | 3 | 47.9 | 0.2 |
| 1.13 | 20 | 4 | 45.4 | 0.4 |
| 1.35 | 15 | 4 | 43.1 | 0.3 |
| 1.51 | 15 | 4 | 41.8 | 0.4 |
| 1.81 | 10 | 4 | 40.2 | 0.2 |
| 1.82 | 10 | 4 | 39.8 | 0.9 |
| 2.00 | 10 | 4 | 39.3 | 0.25 |
| 2.26 | 10 | 4 | 39.3 | 0.1 |
| 3.01 | 10 | 4 | 39.4 | 0.15 |
| 3.77 | 10 | 4 | 39.4 | 0.4 |

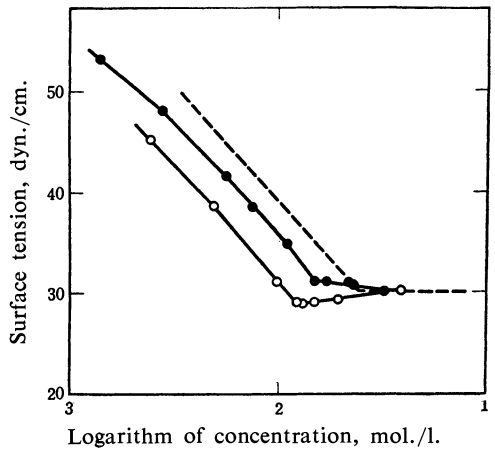



Fig. 2. The surface tension vs. log. concentration of mixtures of alkyl glucosides at 25°C: ○, decyl and octyl glucosides in mole ratio of 0.089 to 0.911; ●, dodecyl and octyl glucosides in mole ratio of 0.0084 to 0.9916; dotted curve shows pure octyl glucoside.

## Discussion

The CMC was obtained from the inflexions in the curves. As the surface tension remains constant, the activity of solute is constant over the flat portion of the surface tension vs. concentration curve. Because, in Gibbs adsorption isotherm,

$$\left(-\frac{\partial\gamma}{\partial \ln c_2}\right)_T\left(\frac{\partial \ln c_2}{\partial \ln a_2}\right)_T = -RT\Gamma_2 \qquad (1)$$

if $(\partial\gamma/\partial \ln c_2)_T=0$ and $\Gamma_2>0$, then $(\partial \ln a_2/\partial \ln c_2)_T=0$ and therefore $a_2$=const. with concentration.

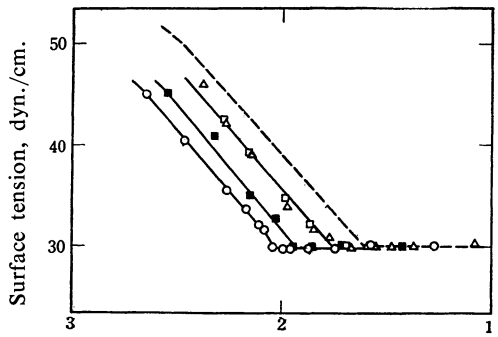



Fig. 3. The effect of added salts on the surface tension of β-D-octyl glucoside at 25°C: △, 0.93 N $CaCl_2$; □, 0.47 N NaCl; ■, 0.93 N NaCl; ○, 0.93 N $Na_2SO_4$.

The fact that the activity vs. concentration remains constant suggests that something similar to a phase separation is occurring in the solution. Namely, the micelle formation begins above the concentration of inflexion and the concentration of single species stays constant.

Table IV gives the CMC, surface excess and residual area per molecule calculated from the data in Tables I, II and III under the assumption that $(\partial \ln a_2/\partial \ln c_2)_T=1$ below the concentration of inflexion point.

Table IV. The CMC, surface excess and residual area of β-D-alkyl glucosides at 25°C

| Substance | CMC mol./l. | Surface excess $10^{-10}$ mol./cm² | Residual area Å² |
|---|---|---|---|
| Octyl glucoside | 0.025 | 3.9 | 42 |
| Decyl glucoside | 0.0022 | 3.5 | 47 |
| Dodecyl glucoside | 0.00019 | 4.6 | 36 |

The CMC of ionic agents was given as a function of hydrocarbon chain length and the concentration of gegenions[7-10],

$$\log \mathrm{CMC} = -\frac{m\omega}{kT} + K_6 \ln C_i + \text{const.} \qquad (2)$$

where $\omega$ is the cohesive energy change per methylene group passing from the bulk of the solution to the micelle, $m$ the number of carbon atoms in hydrocarbon chain, $K_6$ the experimental constant, $C_i$ the concentration of uni-valent gegenions.

As there is no electrical work accompanying

7) A. B. D. Cassie and R. C. Palmer, *Trans. Faraday Soc.*, 37, 156 (1941).
8) H. Lange, *Kolloid-Z.*, 117, 48 (1950).
9) M. E. Hobbs, *J. Phys. & Colloid Chem.*, 55, 675 (1951).
10) K. Shinoda, This Bulletin, 26, 101 (1953).

the formation of micelles of non-ionic agents, the electrical term in Eq. 2 disappears. The change in CMC as a function of the paraffin chain length may be expressed as,

$$\log \mathrm{CMC} = -\frac{m\omega}{kT} + \text{const.} \quad (3)$$

Actually the CMC of octyl, decyl and dodecyl glucosides decreased to 1/3.4 per one additional methylene group. This relation is similar to that of ionic agents under the condition of a definite concentration of gegenions[11] as will be expected from Eq. 2. In a case where no salt is added, the decrease in CMC of ionic agent is much smaller. Lange has found similar results for octyl, decyl and dodecyl polyoxyethylene ether[12].

The CMC's of mixtures of ionic agents have been studied and interpreted rather well[13,14]. As there is no electrical energy involved in micellization of non-ionic agent, the theoretical treatment is far simpler and the CMC is given as a function of the mole composition of the mixture.

$$\sum \mathrm{CMC}_{mi} \cdot x_i = \mathrm{CMC}_{\mathrm{mix}} \quad (4)$$

$$\sum \mathrm{CMC}_{mi} \frac{x_i' \exp(m_i\omega/kT)}{\sum x_i' \exp(m_i\omega/kT)} = \mathrm{CMC}_{\mathrm{mix}} \quad (5)$$

Where $x_i$ is the mole fraction of the $i$th component in the micelle and $x_i'$ the mole fraction of the $i$th component in the bulk of the solution. The comparison between the calculated and observed CMC values is shown in Table V.

Table V

| Substance | Mole fraction of the latter compound | CMC mol./l. | Calcd. CMC mol./l. |
|---|---|---|---|
| Octyl/Decyl glucoside | 0.089 | 0.0125 | 0.013 |
| Octyl/Dodecyl glucoside | 0.0084 | 0.015 | 0.012 |

It seems very interesting to us that the surface tension vs. concentration curve showed the minimum in the mixture of decyl and octyl glucoside, but the mixture of dodecyl octyl glucoside did not show the recognizable minimum as shown in Fig. 2. The existence of the minimum in the former and non-existence in the latter can be explained as being based on the change in composition at the surface. In the mixture of decyl and octyl glucosides, the more surface-active molecule, decyl glucoside, has lower suface tension over the flat portion, as shown in Fig. 1. The mole fraction of decyl glucoside is relatively large at the surface at the minimum, i. e., at the beginning of micelle formation, whereas the fraction of decyl glucoside decreases above the CMC, due to the increase of the micellar species, and the surface tension approaches that of pure octyl glucoside solution. This discussion may hold for the mixture of homologous compounds of non-ionic agents.

The addition of salts to solutions of non-ionic agents has a relatively small effect compared with ionic agents. Moreover, the slope of surface tension vs. logarithm of concentration curve does not change appreciably in contrast with ionic agents[15]. The effect is not electrical and probably rather indirect. Sodium chloride showed a greater effect than calcium chloride depressing the cloud point[16] and increasing relative viscosity and turbidity[17] of non-ionic agents. The same trend was observed in depressing the CMC. Sodium sulfate of the same concentration shows an even greater effect than sodium chloride. The CMC obtained from the inflexions of surface tension vs. concentration curves are summarized in Table VI.

Table VI. The effect of added salts on the CMC determined by surface tension measurements at 25°C

| Substance | Medium | CMC mol./l. |
|---|---|---|
| Octyl glucoside | $H_2O$ | 0.025 |
| 〃 | 0.93 N $CaCl_2$ | 0.017 |
| 〃 | 0.47 N NaCl | 0.017 |
| 〃 | 0.93 N NaCl | 0.012 |
| 〃 | 0.93 N $Na_2SO_4$ | 0.009 |

The salts of the same ionic strengths do not exhibit the same effect. The volume of salts added, including hydration water, may change the effective concentration of agents and the change in solvent property may decrease the hydration and the CMC decreases.

## Summary

The surface tension in aqueous solutions of β-D-alkyl glucoside and their mixtures at 25°C has been measured. The CMC was determined from the inflexions of the curves; octyl glucoside, 0.025 mol./l., decyl glucoside 0.0022 mol./l., dodecyl glucoside, 0.00019 mol./l. The effect of hydrocarbon chain length was explained theoretically. The CMC of mixtures has been also explained by the extension of the theory of ionic agents. The effect of added sodium chloride, calcium chloride and sodium sulfate

11) K. Shinoda, *J. Phys. Chem.*, **59**, 432 (1955).
12) H. Lange, *Kolloid-Z.*, **163**, 9 (1959).
13) H. Lange, ibid., **131**, 96 (1953).
14) K. Shinoda, *J. Phys. Chem.*, **58**, 1136 (1954).
15) H. Lange, *Kolloid-Z.*, **153**, 155 (1957).
16) W. N. Macley, *J. Colloid Sci.*, **11**, 272 (1956).
17) T. M. Doscher, G. E. Myers and D. C. Atkins, Jr., ibid., **6**, 223 (1951).

on the surface tension in aqueous solution of octyl glucoside has been measured. The effect of added salts on the CMC was determined from the inflexions of the surface tension vs. logarithm of concentration curves.

We wish to thank Mr. K. Ito for some of the measurements and the Ministry of Education for their support.

*Department of Chemistry*
*Faculty of Engineering*
*Yokohama National University*
*Minami-ku Yokohama*
*(K. S. & Y. T.)*

*Department of Pharmacy*
*Kyoto University*
*Sakyo-ku, Kyoto*
*(H. R.)*

# *Some Copper Complexes of Diazoaminobenzene Derivatives and their Properties**

By Hiraku YAMADA, Hiroshi OHTA, Masaru YAMAGUCHI and Tokuichi TSUMAKI

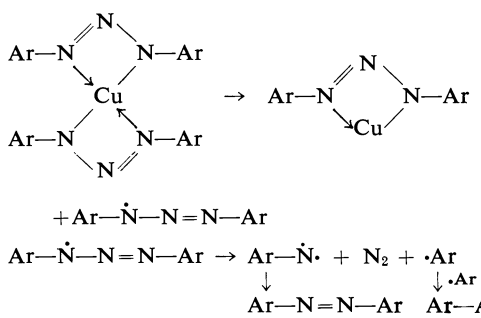
(Received August 13, 1960)

It is well known that the copper(I) complexes of diazoaminobenzene and its derivatives are, in some organic solvents, more stable than the copper(II) complexes. Dwyer et al.[1-6] found that in solution the copper(II) complex of diazoaminobenzene decomposed rapidly into the copper(I) complex by auto-reduction, splitting off the organic fragments. But they did not investigate these fragment. In the present paper are described the synthesis of the copper(II) complexes of diazoaminobenzene derivatives and the isolation and identification of their thermal decomposition products.

As the starting materials for the synthesis of the copper(II) complexes, we chose 4, 4'-dichloro-, 4, 4'-dimethoxy-, 4-chloro-, 4-methoxy- and 4-ethoxydiazoaminobenzenes. The synthesis of their copper(II) complexes was fairly difficult owing to their extreme instability in solution. The synthesis was, therefore, carried out successfully at low temperature, and, in some cases, at temperature as low as possible by cooling with an ethanol-dry ice bath. The complexes were obtained as dark green crystals or powder. In the dry state they are stable, but in solution they become much less stable; and, when heated, they decompose very rapidly into black brown solutions containing tarry substances.

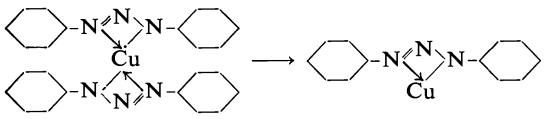
From the tarry substances we could obtain by chromatography on alumina, the copper(I) complexes as yellow to orange-red crystals. From the solution after the separation of the copper(I) complexes a considerable amount of azobenzene derivatives was obtained.

In order to obtain some knowledge concerning the decompositon mechanism, we furthermore investigated the thermal decomposition products of bis(diazoaminobenzene)copper(II) [or bis(1, 3-diphenyltriazenato)copper(II)] and estimated quantitatively nitrogen gas evolved by the thermal decomposition of the copper(II) complexes of diazoaminobenzene derivatives. From bis(diazoaminobenzene)copper(II), only biphenyl, not azobenzene, was obtained. Further it was ascertained that one molecule of nitrogen was evolved per molecule of each of the complexes during the decomposition. It is, therefore, considered most probable that the decomposition of the copper(II) complexes proceeds in the manner shown below.



* "Co-ordinate Valency Rings" XXIX. XXVIII of this series: Y. Kihara, H. Ohta and T. Tsumaki, *Mem. Faculty Sci., Kyushu Univ., Ser. C, Chem.*, **3**, 137 (1960).

1) F. P. Dwyer, *J. Soc. Chem. Ind.*, **58**, 110 (1939); *Chem. Abstr.*, 33. 5818 (1939).
2) F. P. Dwyer, *Australian Chem. Inst. J. and Proc.*, **6**, 348 (1939); *Chem. Abstr.*, **34**, 733 (1940).
3) F. P. Dwyer, ibid., **6**, 362 (1939); *Chem. Abstr.*, **34**, 734 (1940).
4) F. P. Dwyer, *J. Am. Chem. Soc.*, **63**, 79 (1941).
5) F. P. Dwyer et al., ibid., **63**, 81 (1941).
6) F. P. Dwyer et al., *Chemistry and Industry*, **1940**, 136; *Chem. Abstr.*, **34**, 3245 (1940).



## Experimental

The following diazoaminobenzene derivatives were synthesized:

4,4'-dichlorodiazoaminobenzene[7],
4,4'-dimethoxydiazoaminobenzene[8],
4,4'-diethoxydiazoaminobenzene[9],
4-chlorodiazoaminobenzene[10],
4-methoxydiazoaminobenzene[11],
and 4-ethoxydiazoaminobenzene[12]

**The Synthesis of the Copper(II) Complexes of Diazoaminobenzene Derivatives.**—*General Remarks*: Since the copper(II) complexes of diazoaminobenzene and its derivatives are very unstable in solution, the synthesis must always be carried out below 0°C.

**Bis(4, 4'-dichlorodiazoaminobenzene)copper(II).**—To a solution of 5 g. of 4,4'-dichlorodiazoaminobenzene in 50 cc. of ethanol is added a solution of 1.8 g. of copper acetate in 100 cc. of the same solvent. The solvent is removed in vacuo, till the precipitate deposits. The precipitate is filtered off and washed with water and then with ethanol. The precipitate is then dissolved in cold acetone and concentrated under reduced pressure at room temperature, when dark green crystals separate out. Dark green plates, which decompose violently at 114°C. Soluble in acetone, ethanol, benzene and chloroform.

Found: C, 48.02; H, 3.02; N, 18.18; Cu, 11.43. Calcd. for $C_{24}H_{16}N_6Cl_4Cu$: C, 48.54; H, 2.72; N, 14.15; Cu, 10.70%.

**Bis(4, 4' - dimethoxydiazoaminobenzene)copper(II).**—To a solution of 5.2 g. of 4,4'-dimethoxydiazoaminobenzene in 100 cc. of ether is added a solution of 1.8 g. of copper acetate in 200 cc. of ethanol, and the mixture is cooled in an ethanol-dry ice bath and stirred well. The color of the solution becomes green. After standing for an hour, the solvent is removed under reduced pressure at room temperature. The precipitate produced is filtered and washed successively with water, ethanol, acetone and ether, and dried. Dark green micro-crystals, which decompose at 200~204°C. Soluble in acetone, ethanol, benzene and chloroform. In solution it is extremely unstable.

Found: C, 58.45; H, 5.08; N, 14.47; Cu, 11.08. Calcd. for $C_{28}H_{28}N_6O_4Cu$: C, 58.37; H, 4.90; N, 14.59; Cu, 11.03%.

**Bis(4, 4'-diethoxydiazoaminobenzene)copper(II).**—To a solution of 5.7 g. of 4,4'-diethoxydiazoaminobenzene in 200 cc. of acetone is added a solution of 1.8 g. of copper acetate in 100 cc. of ethanol, and the mixture is maintained between −10~−20°C for an hour, and after that concentrated under reduced pressure. The precipitate is filtered and washed successively with water, acetone and ether, and dried. Dark green plates, which decompose at 150°C. Soluble in ether, acetone and ethanol.

Found: C, 60.28; H, 6.05; N, 13.20; Cu, 9.92. Calcd. for $C_{32}H_{36}N_6O_4Cu$: C, 60.79; H, 5.74; N, 13.29; Cu, 10.05%.

**Bis(4-chlorodiazoaminobenzene)copper(II).**—To a solution of 4.5 g. of 4-chlorodiazoaminobenzene in 100 cc. of ethanol is added a solution of 1.8 g. of copper acetate in 100 cc. of ethanol, and the mixture is maintained between −10~−20°C for an hour, and then concentrated under reduced pressure at room temperature. The precipitate is filtered, washed successively with water, ethanol, and ether, and dried. Dark green powder, which decomposes at 85~87°C. Soluble in acetone, ethanol and benzene.

Found: C, 57.07; H, 3.84; N, 15.97; Cu, 12.05. Calcd. for $C_{24}H_{18}N_6Cl_2Cu$: C, 54.92; H, 3.46; N, 16.01; Cu, 12.10%.

**Thermal Decomposition of the Copper(II) Complexes of Diazoaminobenzene Derivatives in Solution.**—One per cent solution of each of the copper(II) complexes in acetone, benzene or ether is refluxed on a water-bath. In 15~30 min. the color of the solution changes from green to black-brown, and a tarry precipitate is produced. After 1~3 hr. the decomposition is complete. The tarry precipitate is filtered off from the solution, dissolved in benzene-chloroform-petroleum ether mixture and chromatographed on alumina, when the copper(I) complexes were obtained. The effluent was combined with the filtrate from the tarry precipitate and the combined solution was used for the later operations.

The following copper(I) complexes were obtained.

**4, 4' - Dichlorodiazoaminobenzenecopper(I).**—Yellow needles, which decompose at 242°C explosively. Readily soluble in benzene and chloroform, soluble with difficulty in ether and acetone.

Found: C, 43,47; H, 2.46; N, 12.20; Cu, 19.34. Calcd. for $C_{12}H_8N_3Cl_2Cu$: C, 43.85; H, 2.45; N, 12.78; Cu, 19.33%.

**4, 4' - Dimethoxydiazoaminobenzenecopper(I).**—Orange-red needles, which decompose at 228°C, giving tarry substance. Readily soluble in benzene and chloroform, soluble with difficulty in ether and acetone.

Found: C, 52.95; H, 4.56; N, 13.88; Cu, 19.78. Calcd. for $C_{14}H_{14}N_3O_2Cu$: C, 52.58; H, 4.41; N, 13.14; Cu, 19.87%.

**4, 4'-Diethoxydiazoaminobenzenecopper(I).**—Orange-colored needles, which decompose at 240°C, giving tar. Readily soluble in benzene and ethanol, soluble with difficulty in ether and acetone.

Found: C, 55.59; H, 5.55; N, 12.01; Cu, 18.12. Calcd. for $C_{16}H_{18}N_3O_2Cu$: C, 55.24; H, 5.22; N, 12.08; Cu, 18.26%.

The above-mentioned combined solution was extracted with 1 N hydrochloric acid after the addition of 3~4 times its volume of ether. From this acid extract no identifiable substance was obtained. The remaining ether solution was chromatographed on alumina, using petroleum ether, petroleum benzine and acetone as eluents, when

7) R. Meldola et al., *J. Chem. Soc.*, **53**, 670 (1888).
8) M. Busch and E. Bergmann, *Chem. Zentr.*, **1905 I**, 1102.
9) R. Henriques, *Ber.*, **25**, 3064 (1892).
10) A. Hantzsch et al., ibid., **30**, 1413 (1897).
11) D. Vorländer, ibid., **62**, 2830 (1929).
12) D. Vorländer, ibid., **62**, 2825 (1929).

five fractions were obtained. From the first fraction the following azobenzene derivatives were obtained, and identified by the measurement of the mixed melting point with the authentic samples: 4,4'-dichloroazobenzene, 4,4'-dimethoxyazobenzene, and 4,4'-diethoxyazobenzene. From the fractions following we could not obtain any identifiable substances. We could, further, obtain biphenyl from the decomposition products of bis(diazoaminobenzene)copper(II) in benzene, but in this case we could not notice azobenzene.

**Determination of Nitrogen Gas Evolved during the Decomposition of the Copper(II) Complexes in Solution.**—The solution of 20~25 mg. of the complex in 10 cc. of benzene was heated in an airtight vessel in a stream of carbon dioxide. After removal of benzene vapour through the efficient trap cooled by dry ice, the nitrogen gas evolved was collected on an azotometer. The results are shown below:

| Copper(II) complexes (one mole) | Nitrogen gas evolved (mole) |
|---|---|
| Bis(4, 4'-dichlorodiazoaminobenzene)copper(II) | 0.754 |
| Bis(4, 4'-dimethoxydiazoaminobenzene)copper(II) | 0.952 |
| Bis(4, 4'-diethoxydiazoaminobenzene)copper(II) | 0.836 |
| Bis(4-chlorodiazoaminobenzene)-copper(II) | 0.748 |

The authors wish to express their gratitude to Mr. Michio Shido, Miss Sachiko Indo and Miss Takeko Tahara for the microanalyses.

*Department of Chemistry*
*Faculty of Science*
*Kyushu University*
*Hakozaki, Fukuoka*

# *Studies on Heavy-Nitrogen Labeled Compounds. III.*[1] *Preparation of $^{15}N$-Labeled α-Hydroximinopropionic Acid*

By Yoshishige SATO, Teruhiko MESHI and Norio SUGIMOTO

(Received July 16, 1960)

There are a number of methods of preparing $^{15}N$-labeled compounds by using $(^{15}NH_4)_2SO_4$ as a starting substance but there are not many methods which resort to $K^{15}NO_3$. However, the use of $K^{15}NO_3$ as a starting substance will be required, when reactions including diazotization are performed. In 1950, Clusius et al.[2] succeeded in preparing $Na^{15}NO_2$ by the reaction of aqueous solution of sodium hydroxide with a mixture of oxygen and nitric oxide obtained by decomposition of $K^{15}NO_3$. Using $Na^{15}NO_2$ obtained, they prepared potassium azide-$^{15}N$[3], phenyl hydrazine $^{15}N$[2] and diphenyl hydrazine-$^{15}N$[4]. Bothner-By and Friedman[5], in 1951, synthesized 3, 5-dinitrobenzoylazide-3-$^{15}N$ according to the same method as described above.

In this paper synthesis of α-hydroximinopropionic acid-$^{15}N$ was performed by using $K^{15}NO_3$ as a starting substance. For preliminary experiment, $K^{14}NO_3$, $K^{14}NO_2$ and $^{14}NH_2OH \cdot HCl$ were employed for preparing $K^{14}NO_2$, $^{14}NH_2OH \cdot (1/2)H_2SO_4$ and $CH_3C(^{14}NOH)COOH$, respectively. Then, using $K^{15}NO_3$, $CH_3C(^{15}NOH) \cdot COOH$ was prepared without separating the intermediate products: $K^{15}NO_2$ and $^{15}NH_2OH \cdot (1/2)H_2SO_4$.

## Experimental and Results

**Preliminary Experimental by Use of $^{14}N$-Compound.** — *Preparation of $K^{14}NO_2$ from $K^{14}NO_3$.* — In order to reduce $KNO_3$ to $KNO_2$, lead, copper, sodium bisulfite, sodium formate and zinc were used and potassium hydroxide was sometimes employed as an accelerating agent for the reduction in a fused state. The amount of potassium nitrite was measured by the titration with N/10-$KMnO_4$ solution. The data are shown in Table I.

When a mixture of potassium hydroxide with copper, sodium formate or zinc is employed as a reducing agent, a high yield can be obtained as seen from this table.

On the other hand, in the case of the reduction of the aqueous solution, it was found that potassium nitrite was obtained with a greater yield than in the case of the fusion method. The procedure is as follows. Ten milliliter of aqueous solution containing 4 g. of potassium nitrate was

1) Part II; Y. Sato, T. Meshi, T. Takahashi, I. Chibata, M. Kisumi and Y. Ashikaga, *Radiation and Isotops*, 3, 31 (1960).

2) K. Clusius and M. Hoch, *Helv. Chim. Acta.*, 33, 2122 (1950).

3) K. Clusius and H. Hurzeler, ibid., 36, 1326 (1953).

4) K. Clusius and M. Vecchi, ibid., 36, 933 (1953).

5) A. A. Bothner-By and L. Friedman, *J. Am. Chem. Soc.*, 73, 5391 (1951).

TABLE I. YIELD OF $KNO_2$, THE REDUCING AGENTS AND THE REDUCTION TIME

| Reducing agents | Yield of $KNO_2$ % | Amounts of reduction agents for 2 g. of $KNO_3$ g. | Fusion time, hr. |
|---|---|---|---|
| Pb | 64* | 2.4 | 2 [6] |
| Pb | 80.2* | 2 | [5] |
| Pb | 65~70* | 4 | [7] |
| Pb | 91~93* | 2.4 | [8] |
| Pb | 62 | 6 | 0.5 |
| Pb+KOH | 50 | Pb 4, KOH 1.2 | 2 |
| $NaHSO_3$ | 59 | 2 | |
| HCOONa +KOH | 80 | HCOONa 1.4, KOH 1 | 0.5 |
| Cu | 82 | 1.37 | 1 |
| Cu+KOH | 83 | Cu 1.37, KOH 1.2 | 1 |
| Zn+KOH | 79 | Zn 1.3, KOH 1.2 | 1 |

* From literature.

mixed with 30 ml. of 30% aqueous ammonia solution and the mixture was kept below 10°C. Then, 2.6 g. of zinc dust was added in small portions to the mixture. The zinc-oxide was filtered off and the filtrate was concentrated to 3 ml. under vacuo. The yield of potassium nitrite was found to be 85%, when measured by titration with potassium permanganate solution.

**Synthesis of Hydroxylamine Hydrochloride.** — Using potassium nitrite as a starting substance, hydroxylamine hydrochloride was synthesized according to the method of organic syntheses[9]. The aqueous solution of potassium carbonate saturated with sulfur dioxide gas was added to the aqueous solution containing 1.7 g. of potassium nitrite in a vessel, the temperature of which was kept at 0°C. The mixed solution was kept at pH 3 with 7% aqueous solution of sulfurous acid. Two milliliter of acetone was added to it. The acetoxime was hydrolized with concentrated hydrochloride. The yield of hydroxylamine hydrochloride was about 70%.

**Synthesis of α-Hydroximinopropionic Acid.**—In 4 ml. of aqueous solution containing 0.9 g. of pyruvic acid, 0.732 g. of hydroxylamine hydrochloride was added and allowed to stand for one hour. Hydrochloric acid was neutralized by addition of 0.7 g. potassium carbonate powder. After the aqueous solution was neutralized, the solution was concentrated to dryness in vacuo. The solid residue was extracted with 100 ml. of ether, and α-hydroximinopropionic acid was obtained by removing ether. The yield is 85% on the basis of hydroxylamine hydrochloride and about 50% on the basis of potassium nitrate.

**Synthesis of α-Hydroximinopropionic Acid-$^{15}$N.** —α-Hydroximinopropionic acid-$^{15}$N was synthesized by the method described above. The procedure is as follows. Two and a half grams of $K^{15}NO_3$ ($^{15}$N atom % : 88%) was dissolved in an aqueous ammonia solution and kept below 10°C. Zinc powder (1.6 g.) was added for the reduction of $K^{15}NO_3$ to $K^{15}NO_2$. After the deposited zinc oxide was removed by filtration, the solution was concentrated to 10 ml., kept at 0°C and made pH 3 with 7% sulfurous acid. Further 0.4 ml. of concentrated sulfuric acid was added to the solution in order to hydrolize the reaction product and refluxed for five hours. Into the hydrolized solution, 50% aqueous solution containing 1.5 g. pyruvic acid was added and allowed to stand for one hour. Using the powder of potassium carbonate, the liberated sulfuric acid was neutralized and its solution was concentrated to dryness in vacuo. The residue was extracted with 100 ml. of ether. Water in the extracted ether solution was removed by anhydrous sodium sulfate and ether was removed in vacuo to give α-hydroximinopropionic acid-$^{15}$N. The yield is 1.55 g. and 61.5% on the basis of $K^{15}NO_3$.

## Summary

By use of $K^{15}NO_3$ as a starting material, α-hydroximinopropionic acid-$^{15}$N was synthesized in accordance with the following reactions:

$$K^{15}NO_3 \rightarrow K^{15}NO_2 \rightarrow {}^{15}NH_2OH \rightarrow CH_3C(={}^{15}NOH)COOH$$

The above reactions were carried out without separating any intermediate products. The yield of α-hydroximinopropionic acid-$^{15}$N was about 61% on the basis of $K^{15}NO_3$.

*Osaka Research Laboratory*
*Tanabe Seiyaku Co., Ltd.*
*Kashimacho, Higashiyodogawa-ku*
*Osaka*

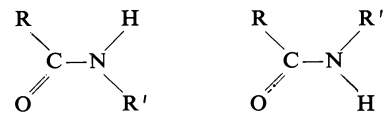
6) W. R. Vaughan, D. I. McCane and G. B. Sloan, ibid., **73**, 2298 (1951).
7) S. Feldhaus, *Ann.*, **126**, 71 (1863).
8) V. I. Maimind, B. V. Tokarev, E. Gomes, R. G. Vdovina, K. M. Ermolaev and M. M. Shemyakin, *J. Gen. Chem.* (*U. S. S. R.*), **26**, 2187 (1956).
9) Organic Syntheses, **3**, 61 (1923); W. L. Semon, *J. Am. Chem. Soc.*, **45**, 188 (1923).

# *The Resonance Effect of Amide Group on the Polymerizability of Lactam Derivatives. I. The Infrared Spectrum of N-Methyl Lactams**

By Naoya OGATA

(Received July 7, 1960)

The amide linkage of chain amide molecule tends to take a planar structure owing to the resonance in the molecule[1]. The two configurations of cis and trans forms shown below are possible:



trans form cis form

It it known that the trans form of an amide group is more stable than the cis form and monosubstituted acid amide RCONHR′ takes the trans[1,2] form, while lactams of less than 9 membered rings take the cis form owing to the steric hindrance[3].

It has been reported on the polymerizability of ε-caprolactam that the configuration of the amide group relates to its reactivity[4] and *N*-alkyl-substituted derivatives of the cis amide such as *N*-methyl-ε-caprolactam are too stable to polymerize[5].

The great stability of *N*-alkyl-substituted lactams can not be explained from the difference in the ring strain or in the thermodynamical character[6] caused by the intramolecular rotational isomerism, but it is supposed to be due to the increase of resonance in the amide group[7]. Therefore, the infrared spectra of several chain and cyclic amide compounds have been measured with special interest in the range of 1600~1800 $cm^{-1}$, and the effect of the resonance on the characteristic band of the amide group has been investigated.

## Experimental

The infrared spectra of several amide compounds were measured with a Hitachi model EPI-2 spectrophotometer in the range of 2~15 $\mu$, with a rock salt prism. The cell thickness was 0.01 mm.

The infrared spectra of chloroform solution of *N*-alkyl-substituted chain or cyclic amides were measured in the range of 5.5~6.5 $\mu$ at various concentrations and temperatures. The cell thickness was selected suitably so that the transmittance at the absorption maximum is within the range of 20 ~80%. Although it is desirable to use a nonpolar solvent such as carbon tetrachloride, *N*-methyl lactams do not dissolve in carbon tetrachloride.

## Results

The infrared spectra of several amide compounds are shown in Figs. 1—5. The frequencies of the carbonyl absorption (amide I band) of these compounds are shown in Table I, in which values in parentheses mean the frequencies of shoulders in the amide I band. The absorptions of the chloroform solution of *N*-methyl lactams are shown in Fig. 6. *N, N*-Disubstituted chain amide shows a sharp absorption at 1626 $cm^{-1}$ (Fig. 7), while the amide I band of *N*-methyl lactams splits into

Table I. The frequencies of the carbonyl absorption

| Kind of amide | Frequency, $cm^{-1}$ | State |
|---|---|---|
| *N*-Hexylacetamide | 1653 | Liquid |
| *N, N*-Dibutylacetamide | 1650 | 〃 |
| ε-Caprolactam | 1645 | KBr disk |
| *N*-Methyl-ε-caprolactam | (1739), 1634 | Liquid |
| α-Piperidone | 1664 | 〃 |
| *N*-Methyl-α-piperidone | (1739), 1672, 1631 | 〃 |
| α-Pyrrolidone | 1680 | 〃 |
| *N*-Methyl-α-pyrrolidone | 1681, (1629) | 〃 |

Table II. The molar extinction coefficient of *N*-methyl-ε-caprolactam in chloroform solution

| Concn. mol./l. | 1733 $cm^{-1}$ | | | 1634 $cm^{-1}$ | | |
|---|---|---|---|---|---|---|
| | 20°C | 40°C | 60°C | 20°C | 40°C | 60°C |
| 0.02 | 26.8 | 26.8 | 28.8 | 554 | 506 | 483 |
| 0.05 | 24.4 | 25.9 | 27.4 | 484 | 406 | 379 |
| 0.1 | — | 29.7 | — | 545 | 552 | 484 |
| 0.2 | — | 31.2 | 29.2 | 467 | 520 | 456 |
| 0.3 | — | 21.6 | 27.5 | — | — | — |
| 0.5 | — | 21.0 | 26.3 | — | — | — |
| 1.0 | — | 26.0 | 24.4 | — | — | — |
| Mean | 25.6 | 26.0 | 27.3 | 512 | 496 | 451 |

* Presented at the 13th Annual Meeting of the Chemical Society of Japan, Tokyo, April, 1960.

1) M. Tsuboi, This Bulletin, **22**, 215 (1949).
2) S. Mizushima et al., *J. Am. Chem. Soc.*, **72**, 3490 (1950).
3) R. Huisgen and H. Walz, *Chem. Ber.*, **89**, 2616 (1956).
4) N. Ogata, *Makromol. Chem.*, **30**, 212 (1959).
5) J. Procházka, *Chem. Listy*, **37**, 158 (1943).
6) H. Yumoto, *J. Chem. Phys.*, **29**, 1234 (1958).
7) N. Ogata, This Bulletin, **32**, 813 (1959).

TABLE III. THE MOLAR EXTINCTION COEFFICIENT OF *N*-METHYL-α-PIPERIDONE IN CHLOROFORM SOLUTION

| Concn. mol./l. | 1736 cm$^{-1}$ | | | 1669 cm$^{-1}$ | | | 1631 cm$^{-1}$ | | |
|---|---|---|---|---|---|---|---|---|---|
| | 20°C | 40°C | 60°C | 20°C | 40°C | 60°C | 20°C | 40°C | 60°C |
| 0.02 | 22.8 | — | — | 167 | — | 150 | 83 | 87 | 118 |
| 0.05 | 25.5 | 30.2 | — | 182 | 145 | 150 | 93 | 100 | 142 |
| 0.1 | 23.3 | 27.9 | 18.5 | 182 | 139 | 113 | 88 | 130 | 163 |
| 0.2 | 24.9 | 28.6 | 19.5 | 176 | 186 | — | 103 | 119 | — |
| 0.3 | — | — | 19.2 | 166 | 174 | 112 | 99 | 114 | 150 |
| 0.5 | — | — | 18.7 | 167 | 164 | — | 99 | 101 | — |
| 1.0 | — | — | 18.0 | 168 | 149 | — | 109 | 88 | — |
| Mean | 24.1 | 28.9 | 18.8 | 173 | 159 | 131 | 96 | 106 | 143 |

TABLE IV. THE MOLAR EXTINCTION COEFFICIENT OF *N*-METHYL-α-PYRROLIDONE IN CHLOROFORM SOLUTION

| Concn. mol./l. | 1675 cm$^{-1}$ | | | 1630 cm$^{-1}$ | | |
|---|---|---|---|---|---|---|
| | 20°C | 40°C | 60°C | 20°C | 40°C | 60°C |
| 0.01 | — | — | 538 | — | — | — |
| 0.02 | 583 | 562 | 538 | — | — | — |
| 0.05 | 464 | 438 | — | 42.1 | 37.0 | 35.8 |
| 0.1 | 634 | 636 | 473 | 45.5 | 41.3 | 36.4 |
| 0.2 | 512 | 644 | 425 | 46.2 | 40.6 | 36.0 |
| 0.3 | — | 582 | 441 | — | — | — |
| 0.5 | — | 497 | 426 | — | — | — |
| 1.0 | — | — | — | — | — | — |
| Mean | 548 | 560 | 474 | 44.6 | 39.6 | 36.1 |

TABLE V. THE MOLAR EXTINCTION COEFFICIENT OF CHAIN AMIDE IN CHLOROFORM SOLUTION

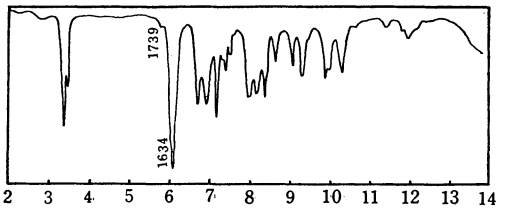
| Concn. mol./l. | *N*-Hexylacetamide 1653 cm$^{-1}$ | | *N*,*N*-Dibutylacetamide 1626 cm$^{-1}$ | | |
|---|---|---|---|---|---|
| | 20°C | 40°C | 20°C | 40°C | 60°C |
| 0.1 | 478 | 462 | 568 | 642 | 557 |
| 0.2 | 442 | 433 | 528 | 582 | — |
| 0.3 | 443 | 397 | 512 | 563 | — |
| 0.5 | 350 | — | 453 | — | — |
| 1.0 | — | — | 413 | — | — |
| Mean | 428 | 431 | 515 | 596 | 557 |

TABLE VI. THE FREQUENCIES OF THE AMIDE I BAND OF *N*-METHYL LACTAM

| Lactam | Ring member | I-a | I-b | I-c |
|---|---|---|---|---|
| *N*-Methyl-α-pyrrolidone | 5 | — | 1675* | 1630 |
| *N*-Methyl-α-piperidone | 6 | 1736 | 1669* | 1631 |
| *N*-Methyl-ε-caprolactam | 7 | 1733 | — | 1634* |

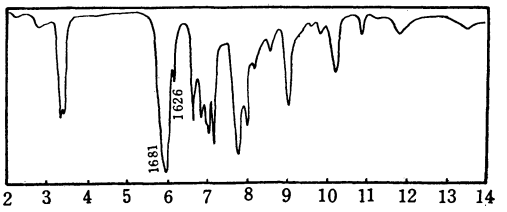
* Maximum absorption

two or three absorptions. The molar extinction coefficients at the absorption maximum of the amide I band for these *N*-methyl lactams are almost constant regardless of concentrations, but change with temperature, as shown in Tables II—V.



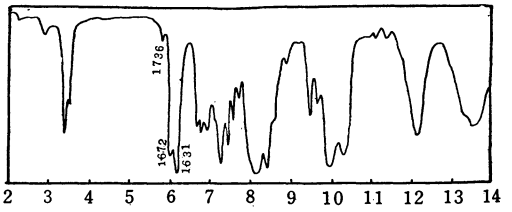

Wavelength, μ

Fig. 1. The infrared spectrum of *N*-methyl-ε-caprolactam (Liquid).



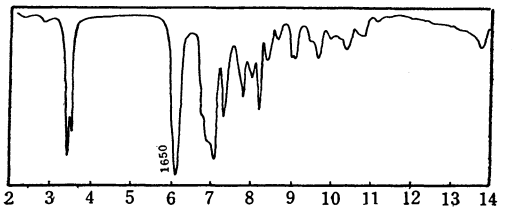

Wavelength, μ

Fig. 2. The infrared spectrum of *N*-methyl-α-pyrrolidone (Liquid).




Wavelength, μ

Fig. 3. The Infrared spectrum of *N*-methyl-α-piperidone (Liquid).




Wavelength, μ

Fig. 4. The infrared spectrum of *N*, *N*-dibutyl-acetamide (Liquid).

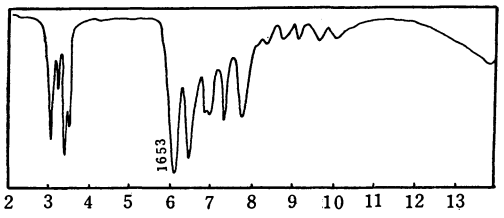
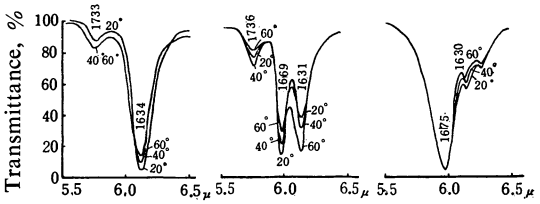



Fig. 5. The infrared spectrum of *N*-hexylacetamide (Liquid).




*N*-Methyl-ε-caprolactam *N*-Methyl-α-piperidone *N*-Methyl-α-pyrrolidone

Fig. 6. The carbonyl absorption of *N*-methyl lactams in chloroform solution at the concentration of 0.1 mol./l.

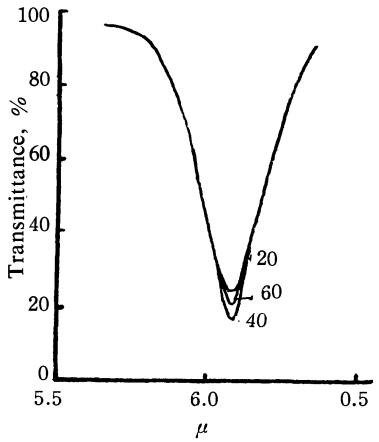



Fig. 7. The carbonyl absorption of *N*, *N*-dibutylacetamide in chloroform solution at the concentration of 0.1 mol./l.

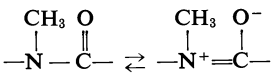
TABLE VII. THE INTEGRATED ABSORPTION INTENSITY OF THE AMIDE I BAND (5.5~6.5 μ) OF *N*-METHYL LACTAM

| Lactam | Temp. °C | Intensity, $mol^{-1}\,l.\,cm^{-2}$ |
|---|---|---|
| *N*-Methyl-α-pyrrolidone | 20 | $2.5\times10^4$ |
| | 40 | 2.5 〃 |
| | 60 | 2.0 〃 |
| *N*-Methyl-α-piperidone | 20 | $1.8\times10^4$ |
| | 40 | 1.7 〃 |
| | 60 | 1.8 〃 |
| ε-Caprolactam | 20 | $2.5\times10^4$ |
| | 40 | 2.5 〃 |
| | 60 | 2.4 〃 |

## Discussion

*N*-Methyl-ε-caprolactam is too stable to polymerize at a temperature over 200°C and *N*-methyl-ε-aminocaproic acid transforms easily into *N*-methyl-ε-caprolactam by heating[8].

The rate of hydrolysis[7] of *N*-methyl-ε-caprolactam into *N*-methyl-ε-aminocaproic acid is much slower than that of ε-caprolactam. Since the cyclic structure of *N*-methyl-ε-caprolactam is the same as that of ε-caprolactam, it is supposed that this stability of *N*-methyl-ε-caprolactam is not due to the change in the ring strain, but to the increase of the resonance in the amide group as shown below by the −I effect of the methyl group:




All *N*-monosubstituted acid amides show a strong absorption band usually near 1640 $cm^{-1}$ in the solid state[8,9]. The lower frequencies of the carbonyl absorption of these amides are considered to be due to the resonance with the ionic form. The shifts of the carbonyl absorption towards lower frequencies by the *N*-alkyl substitution, therefore, seem to suggest the increase of the resonance in the amide group.

As stated before, the infrared spectra of *N*-methyl lactams with less than 7 membered rings exhibit a doublet or triplet in the region of the amide I band, and this is not caused by the interaction among molecules or by the solvent effect, since the molar extinction coefficients of these amide I bands in the chloroform solution are hardly influenced by the change of the amide compounds. The changes with temperature of the molar extinction coefficients of these absorption peaks are different from each other, as can be seen from Fig. 6. The elucidation of the cause of this interesting fact requires further investigation. The frequency of the maximum intensity among these doublets or triplets shifts towards lower frequencies with the enlargement of the ring. These bands are now named amide I-a, I-b and I-c in the order of the increasing frequency, respectively. These are shown in Table VI.

The integrated intensity of these split amide I bands was measured as follows: a point by point measurement of $\log(I_0/I)$ was made at intervals of 0.02 μ in the range of 5.5~6.5 μ and these data were plotted against the wavelength and the area under the curve was

8) H. Yumoto, K. Ida and N. Ogata, ibid., 31, 249 (1958).
9) H. K. Hall, Jr. and R. Zbinden, *J. Am. Chem. Soc.*, 80, 6428 (1958).

graphically determined. The true integrated absorption intensities were obtained by the method proposed by Ramsey[10]. The integrated absorption of the amide I band is almost unaltered with the ring size, as shown in Table VII. Therefore, these split absorptions are estimated to be due to the amide group.

## Summary

The infrared spectra of several *N*-methyl lactams and acid amides have been measured in chloroform solution in order to investigate the correlation between the polymerizability of lactams and the frequencies of the carbonyl absorption of the amide group. The observed frequency lowering of the amide I band by *N*-methyl substitution can be related to the increasing contribution of the ionic structure to the resonance in the amide group, and to the low polymerizability. The infrared spectra of *N*-methyl lactams exhibit doublets or triplets in the carbonyl stretching region.

The author wishes to express his sincere gratitude to Dr. H. Kobayashi and Dr. H. Yumoto for their instruction in these studies and for their permission to publish the results. Thanks are also due to Mr. M. Nakata who collaborated with him in experiments.

*Research Department*
*Toyo Rayon Co., Ltd.*
*Minato-ku, Nagoya*

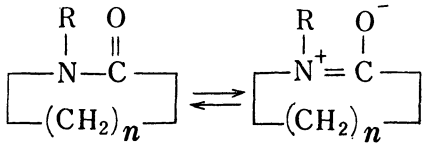
10) D. A. Ramsey, ibid., **74**, 72 (1952).

# *The Resonance Effect of Amide Group on the Polymerizability of Lactam Derivatives. II*. The Basicity of Amide Group of Lactams***

By Naoya OGATA

(Received July 23, 1960)

Th polymerizability of lactams becomes very small by *N*-alkyl substitution[1,2]. *N*-Methyl-ε-caprolactam, for instance, is too stable to polymerize at a temperature above 200°C and *N*-methyl-ε-aminocaproic acid converts easily into *N*-methyl-ε-caprolactam by heating. The increase in the stability of the ring structure by the *N*-alkyl substitution of lactams is explained[3] from the increase of resonance in the amide group as shown below:



If the resonance effect of the amide group increases by *N*-alkyl substitution, it is expected that the basicity of the amide group will decrease. In this connection, an addition reaction of hydrogen chloride with several cyclic or chain amides has been investigated by the measurement of the infrared spectrum.

## Experimental

**Measurement ot the Infrared Spectrum of Addition Products of Hydrogen Chloride and Amide Compounds.**—A chloroform solution of hydrogen chloride of 0.15 mol./l. was prepared by introducing dry hydrogen chloride gas into chloroform. This hydrogen chloride solution was diluted with chloroform to the concentrations of 0.08, 0.04, 0.02 and 0.01 mol./l. and 3.5 cc. of each of the solutions was mixed with 3.5 cc of a chloroform solution of several amide compounds of 0.04 mol./l.

The infrared spectra of the mixtures and the amide solutions were measured by a Hitachi model EPI-2 spectrophotometer with a rock salts prism, using hydrogen chloride-chloroform solution or pure chloroform as reference, respectively.

**Determination of Equilibrium Constant of the Addition Reaction between the Amide Group and Hydrogen Chloride.**—The equilibrium constants of the addition reaction between the amide group and hydrogen chloride were determined for several cyclic or chain amides by the intensity measurement of the carbonyl absorption in the infrared spectra.

The calibration curves for several amide compounds in chloroform were determined by measuring absorbances of the amide I band at 20°C which are shown in Figs. 1 and 2. The calibration curves at

* I, This Bulletin, **34**, 245 (1961).

** Presented at the 13th Annual Meeting of the Chemical Society of Japan, Tokyo, April, 1960.

1) J. Procházka, *Chem. Listy*, **37**, 202 (1943), *Chem. Abstr.*, **40**, 2113 (1946).

2) H. Yumoto, K. Ida and N. Ogata, This Bulletin, **31**, 249 (1948).

3) N. Ogata, ibid., **32**, 813 (1959).

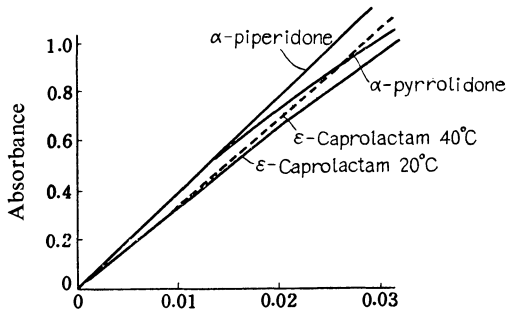



Fig. 1. The calibration curves for several lactams in chloroform solutions.

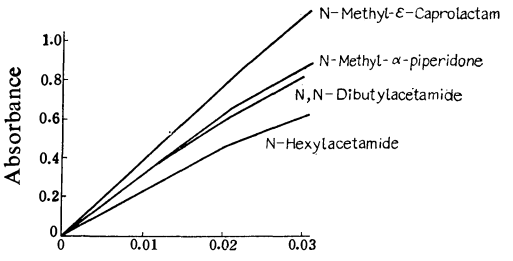



Fig. 2. The calibration curves for several amides in chloroform solutions.

40 and 55°C were almost the same as those at 20°C.

The concentrations of amide [-NHCO-] in chloroform solutions in the presence of hydrogen chloride were determined by these calibration curves. As hydrogen chloride has a tendency to be volatilized with rise of temperature, infrared spectra were measured for the narrow range of 1400~1800 $cm^{-1}$ to avoid the change of concentration. The concentration of hydrogen chloride in chloroform was determined by titrating with N/100 sodium hydroxide.

The equilibrium constant $K$ of the addition reaction between the amide group and hydrogen chloride can be calculated as follows:

$$[\text{-NH}_2^+\text{CO-}] = [\text{-NHCO-}]_0 - [\text{-NHCO-}]_{HCl}$$

$$[H^+] = [HCl] - [\text{-N}^+\text{H}_2\text{CO-}]$$

$[\text{-NHCO-}]_0$: Initial concentration of amide

$[\text{-NHCO-}]_{HCl}$: Concentration of amide in the presence of HCl

$$K = \frac{[\text{-N}^+\text{H}_2\text{CO-}]}{[\text{-NHCO-}][H^+]}$$

## Results

Figs. 3—9 show the spectra, where a solid line represents the spectrum of the chloroform solution of the amide compound in the presence of hydrogen chloride and a dotted line the spectrum of the amide compound only.

In the presence of equal moles of hydrogen chloride and amide, the N—H absorption of cyclic or chain amides in the 3400~3500 $cm^{-1}$ region is replaced by a broad absorption in the 2000~2400 $cm^{-1}$ region and the intensity of the C=O absorption near 1650 $cm^{-1}$ becomes weaker, accompanied by the appearance of a weak absorption in the 1750~1800 $cm^{-1}$ region as shown in Table I.

The whole infrared spectrum of secondary or tertiary chain amide is not much altered in the presence of hydrogen chloride, while that of cyclic amide is altered considerably, accompanying a new absorption in the 1560~1640 $cm^{-1}$ region.

The broad absorption in the 2000~2400 $cm^{-1}$ region which appears in the chloroform solution of the amides in the presence of hydrogen chloride is supposed to be due to the $\rangle N^+H_2$ stretching motion.

The values of $K$ at various concentrations of hydrogen chloride at 20, 40 and 55°C are shown in Table II. Table III shows the mean values of $K$ for several amide compounds. The value of $K$ decreases with the rise of temperature. $K$ for chain amides is considerably smaller than that for cyclic amides. The values of $K$ for cyclic amides increase with the enlargement of the lactam ring and those for tertiary amides are smaller than those for the corresponding secondary amides, especially for lactams.

From the slope of the linear relationship between the logarithm of $K$ and reciprocals of absolute temperatures as shown in Fig. 10, heats of the addition reaction of the amide with hydrogen chloride are obtained. These are shown in Table IV. The heats of the addition reaction for cyclic amides become lower

Table I. The carbonyl absorption of several amides in the presence of HCl

| Kind of lactam | Ring member | The C=O absorption band, $cm^{-1}$ | | | | |
|---|---|---|---|---|---|---|
| | | Lactam alone | In the presence of HCl | | | |
| α-Pyrrolidone | 5 | 1689 | 1800 | 1689* | 1639 | |
| α-Piperidone | 6 | 1658 | 1800 | 1658* | 1577 | 1565 |
| ε-Caprolactam | 7 | 1658 | 1800 | 1659* | 1575 | |

* Maximum absorption

TABLE II. THE VALUES OF $K$

| Sample | Temp. °C | Concn. of HCl mol./l. | Absorbance of C=O | Concn. of [-NHCO-] mol./l. | Concn. of [$H^+$] mol./l. | Concn. of [-$N^+H_2CO$-] mol./l. | $K$ |
|---|---|---|---|---|---|---|---|
| $\alpha$-Pyrrolidone | 20 | 0.0030 | 0.654 | 0.0174 | 0.0009 | 0.0021 | 134 |
| | | 0.0058 | 0.586 | 0.0157 | 0.0020 | 0.0038 | 121 |
| | | 0.0112 | 0.456 | 0.0117 | 0.0034 | 0.0078 | 196 |
| | | 0.0224 | 0.275 | 0.0069 | 0.0098 | 0.0126 | 186 |
| | 40 | 0.0030 | 0.552 | 0.0148 | 0.0018 | 0.0012 | 45 |
| | | 0.0058 | 0.514 | 0.0135 | 0.0033 | 0.0025 | 56 |
| | | 0.0114 | 0.421 | 0.0108 | 0.0062 | 0.0052 | 78 |
| | | 0.0220 | 0.283 | 0.0072 | 0.0132 | 0.0088 | 93 |
| $\alpha$-Piperidone | 20 | 0.0048 | 0.686 | 0.0175 | 0.0013 | 0.0035 | 154 |
| | | 0.0094 | 0.564 | 0.0143 | 0.0027 | 0.0067 | 174 |
| | 40 | 0.0054 | 0.632 | 0.0161 | 0.0025 | 0.0029 | 72 |
| | | 0.0084 | 0.548 | 0.0140 | 0.0041 | 0.0043 | 75 |
| | | 0.0106 | 0.495 | 0.0125 | 0.0041 | 0.0065 | 51 |
| | | 0.0168 | 0.376 | 0.0095 | 0.0080 | 0.0088 | 116 |
| | | 0.0330 | 0.266 | 0.0068 | 0.0215 | 0.0115 | 79 |
| $\varepsilon$-Caprolactam | 20 | 0.0098 | 0.721 | 0.0218 | 0.0016 | 0.0082 | 235 |
| | | 0.0132 | 0.697 | 0.0212 | 0.0035 | 0.0097 | 131 |
| | | 0.0264 | 0.419 | 0.0118 | 0.0073 | 0.0191 | 222 |
| | | 0.0375 | 0.353 | 0.0098 | 0.0173 | 0.0202 | 119 |
| | 40 | 0.0054 | 0.580 | 0.0173 | 0.0024 | 0.0030 | 72 |
| | | 0.0104 | 0.485 | 0.0140 | 0.0041 | 0.0063 | 110 |
| | | 0.0204 | 0.291 | 0.0080 | 0.0081 | 0.0123 | 190 |
| | 55 | 0.0040 | 0.586 | 0.0175 | 0.0017 | 0.0023 | 77 |
| | | 0.0076 | 0.529 | 0.0155 | 0.0033 | 0.0043 | 84 |
| | | 0.0280 | 0.269 | 0.0073 | 0.0155 | 0.0125 | 111 |
| *N*-Methyl-$\alpha$-piperidone | 20 | 0.0022 | 0.737 | 0.0192 | 0.0014 | 0.0008 | 30 |
| | | 0.0046 | 0.695 | 0.0182 | 0.0028 | 0.0018 | 35 |
| | | 0.0092 | 0.604 | 0.0158 | 0.0050 | 0.0042 | 53 |
| | | 0.0190 | 0.433 | 0.0112 | 0.0102 | 0.0088 | 77 |
| | 40 | 0.0036 | 0.609 | 0.0160 | 0.0023 | 0.0013 | 35 |
| | | 0.0071 | 0.577 | 0.0150 | 0.0048 | 0.0023 | 32 |
| | | 0.0144 | 0.479 | 0.0125 | 0.0096 | 0.0048 | 40 |
| | | 0.0286 | 0.355 | 0.0092 | 0.0205 | 0.0081 | 43 |
| *N*-Methyl-$\varepsilon$-caprolactam | 20 | 0.0060 | 0.616 | 0.0195 | 0.0043 | 0.0017 | 20 |
| | | 0.0124 | 0.530 | 0.0165 | 0.0077 | 0.0047 | 37 |
| | | 0.0246 | 0.395 | 0.0122 | 0.0156 | 0.0090 | 47 |
| | 40 | 0.0037 | 0.593 | 0.0188 | 0.0030 | 0.0007 | 12 |
| | | 0.0074 | 0.559 | 0.0175 | 0.0054 | 0.0020 | 21 |
| | | 0.0146 | 0.486 | 0.0151 | 0.0102 | 0.0044 | 29 |
| | | 0.0288 | 0.393 | 0.0141 | 0.0234 | 0.0054 | 16 |
| | 55 | 0.0060 | 0.569 | 0.0178 | 0.0050 | 0.0010 | 11 |
| | | 0.0114 | 0.548 | 0.0172 | 0.0098 | 0.0016 | 10 |
| | | 0.0200 | 0.492 | 0.0153 | 0.0165 | 0.0035 | 14 |
| | | 0.0374 | 0.423 | 0.0131 | 0.0317 | 0.0057 | 14 |
| *N*,*N*-Dibutyl-acetamide | 20 | 0.0028 | 0.627 | 0.0213 | 0.0016 | 0.0012 | 35 |
| | | 0.0054 | 0.602 | 0.0203 | 0.0032 | 0.0022 | 34 |
| | | 0.0106 | 0.548 | 0.0182 | 0.0063 | 0.0043 | 38 |
| | | 0.0222 | 0.467 | 0.0150 | 0.0147 | 0.0075 | 34 |
| | 40 | 0.0042 | 0.570 | 0.0190 | 0.0032 | 0.0010 | 17 |
| | | 0.0076 | 0.539 | 0.0178 | 0.0054 | 0.0022 | 23 |
| | | 0.0148 | 0.482 | 0.0155 | 0.0103 | 0.0045 | 28 |
| | | 0.0288 | 0.420 | 0.0135 | 0.0223 | 0.0065 | 22 |
| *N*-Hexyl-acetamide | 20 | 0.0034 | 0.422 | 0.0183 | 0.0017 | 0.0017 | 55 |
| | | 0.0067 | 0.382 | 0.0166 | 0.0033 | 0.0034 | 62 |
| | | 0.0130 | 0.329 | 0.0142 | 0.0072 | 0.0058 | 57 |
| | 40 | 0.0044 | 0.413 | 0.0180 | 0.0024 | 0.0020 | 46 |
| | | 0.0078 | 0.381 | 0.0165 | 0.0043 | 0.0035 | 49 |
| | | 0.0154 | 0.329 | 0.0143 | 0.0097 | 0.0057 | 41 |

TABLE III. THE EQUILIBRIUM CONSTANT OF THE ADDITION REACTION OF SEVERAL AMIDES AND HCl

| Sample | Configuration of amide | K | | |
|---|---|---|---|---|
| | | 20°C | 40°C | 60°C |
| α-Pyrrolidone | 5 membered cyclic cis amide | 159 | 68 | — |
| α-Piperidone | 6 membered cyclic cis amide | 164 | 79 | — |
| ε-Caprolactam | 7 membered cyclic cis amide | 177 | 124 | 91 |
| *N*-Methyl-α-piperidone | 6 membered cyclic tertiary amide | 49 | 38 | — |
| *N*-Methyl-ε-caprolactam | 7 membered cyclic tertiary amide | 35 | 20 | 12 |
| *N*, *N*-Dibutylacetamide | tertiary chain amide | 35 | 22 | — |
| *N*-Hexylacetamide | secondary trans amide | 58 | 48 | — |

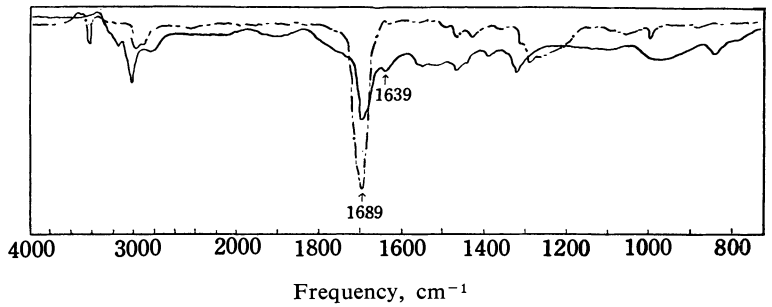



Fig. 3. The infrared spectrum of α-pyrrolidone in the presence of HCl (Chloroform solution).

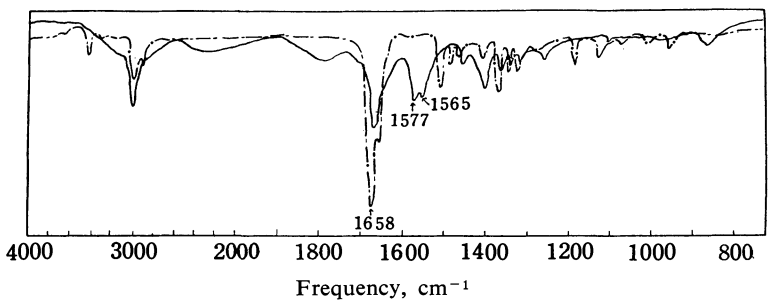



Fig. 4. The infrared spectrum of α-piperidone in the presence of HCl (Chloroform solution).

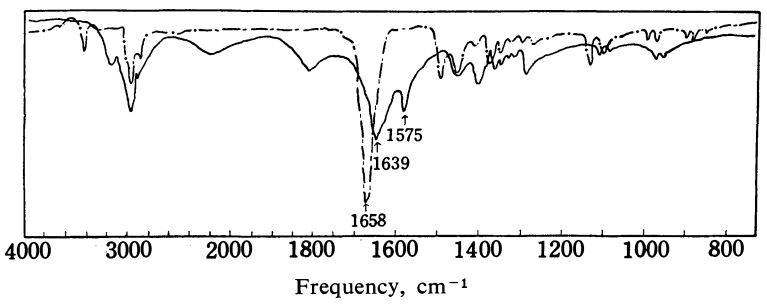



Fig. 5. The infrared spectrum of ε-caprolactam in the presence of HCl (Chloroform solution).

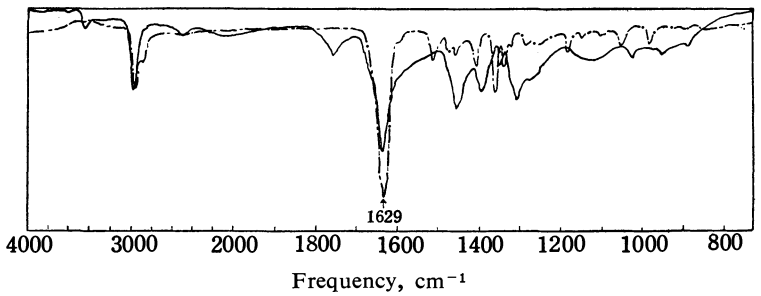



Fig. 6. The infrared spectrum of *N*-methyl-α-piperidone in the presence of HCl (Chloroform solution).

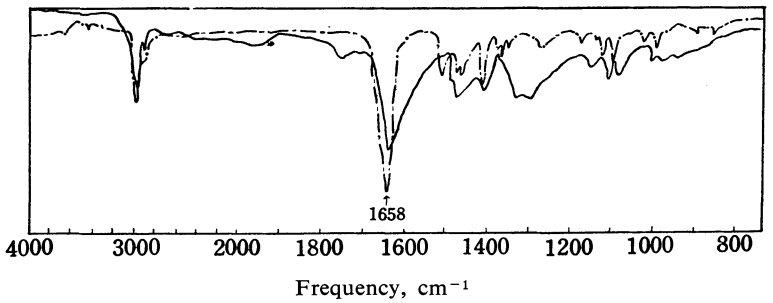



Fig. 7. The infrared spectrum of *N*-methyl-ε-caprolactam in the presence of HCl (Chloroform solution).

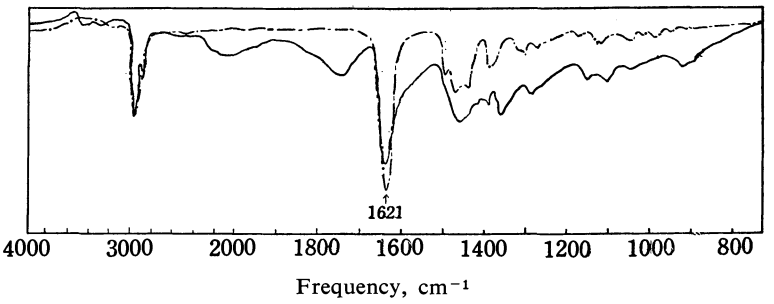



Fig. 8. The infrared spectrum of *N*, *N*-dibutylacetamide (Chloroform solution).

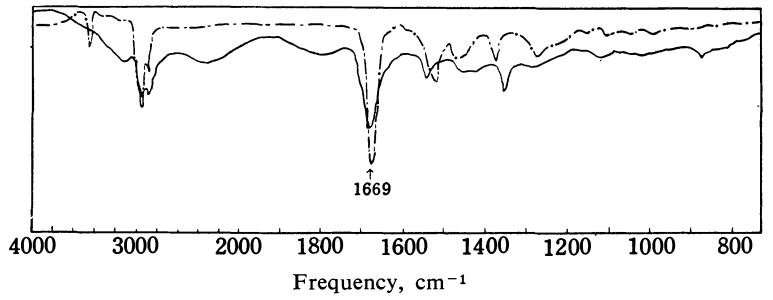



Fig. 9. The infrared spectrum of *N*-hexylacetamide in the presence of HCl (Chloroform solution).

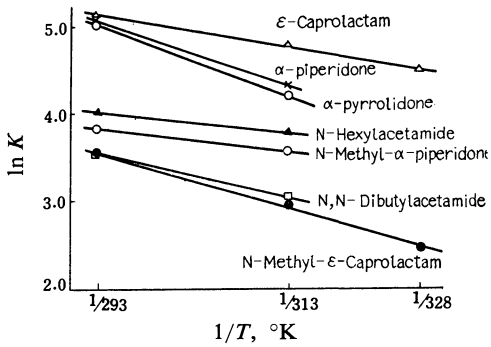



Fig. 10. The relationship between ln $K$ and $1/T$.

TABLE IV. THE HEAT OF ADDITION REACTION OF SEVERAL AMIDES AND HCl

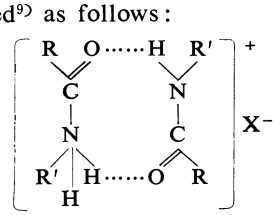
| Sample | $-\Delta H$, kcal./mol. |
|---|---|
| α-Pyrrolidone | 7.6 |
| α-Piperidone | 6.6 |
| ε-Caprolactam | 3.2 |
| *N*-Methyl-α-piperidone | 2.3 |
| *N*-Methyl-ε-caprolactam | 5.1 |
| *N*,*N*-Dibutylacetamide | 4.1 |
| *N*-Hexylacetamide | 2.2 |

with the enlargement of the ring and those for chain amides are generally lower than those for cyclic amides.

## Discussion

The configuration of the amide group takes a planar structure owing to the resonance and two configurations of trans and cis forms are possible. It is known[4-7] that chain amides take the trans form, while cyclic amides of less than 9 membered rings take the cis form.

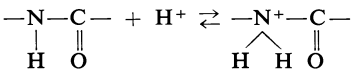
Although the basicity of the nitrogen atom of the amide becomes very weak by the +E effect of the carbonyl group, the amide group acts as a base, adding a proton[8]. It has been reported[9] that chain amide reacts with hydrogen chloride forming an addition product with 1/2 or 1 mol. of hydrogen chloride to 1 mol. of amide. The structure of the 1/2 mol. salt is proposed[9] as follows:




The intensity of the absorption which appears in lactams near 1800 $cm^{-1}$ in the presence of hydrogen chloride becomes stronger with the enlargement of the lactam ring. This absorption shifts towards 1759 $cm^{-1}$ in the case of *N*-methyl lactams or tertiary amide.

It has been presumed[10] that the higher frequencies of the carbonyl absorption of acid halide, which appears near 1800 $cm^{-1}$, is due to the strong +I effect of the halogen atom. Therefore, it is expected that the absorption near 1800 $cm^{-1}$ in the amide-hydrogen chloride addition product may be the free carbonyl absorption which shifts towards higher frequencies by the increase in the electron affinity of the nitrogen atom of the amide.

It is supposed that a proton adds to the nitrogen atom of the amide group as shown in the following equation, since the N—H absorption disappears and new absorption due to the $\rangle N^+H_2$ and the free C=O stretching motion (near 1800 $cm^{-1}$) appear in the infrared spectrum of the amide hydrogen chloride addition product.




Primary and secondary amides show a strong absorption in the 1600~1500 $cm^{-1}$ region, which is absent from those of cyclic lactams, and this band is refered to generally as the amide II band. The origin of the amid II band is generally supposed to be due to a mixed vibration which can be described as an out-of-phase combination of OCN and NH vibrations. The frequency of the amide II band of secondary amide shifts from 1530 $cm^{-1}$ to 1550 $cm^{-1}$ in the presence of hydrogen chloride, as shown in Fig. 9. This is explained from the increase in the ionic character of the N—H linkage by the addition of a proton.

The addition products of lactams and hydrogen chloride show a sharp absorption in the region of 1570~1640 $cm^{-1}$. This absorption does not appear in *N*-methyl lactams or tertiary chain amides in the presence of hydrogen chloride. It is supposed that this band may be assigned to the N—H deformation vibration. The assignment of this band to the C—N stretching motion is not accepted, since no absorption in the 1570~1640 $cm^{-1}$ region appears in tertiary cyclic or chain amides in the presence of hydrogen chloride.

4) M. Tsuboi, ibid., **22**, 215 (1949).
5) R. Huisgen and H. Walz, *Chem. Ber.*, **89**, 2616 (1956).
6) H. K. Hall, Jr., *J. Am. Chem. Soc.*, **80**, 6404 (1958).
7) N. Ogata, *Makromol. Chem.*, **30**, 212 (1959).
8) M. J. S. Dewar, "The Electronic Theory of Organic Chemistry", Oxford University Press, London (1949), p. 96.
9) E. H. White, *J. Am. Chem. Soc.*, **77**, 6215 (1955).
10) L. J. Bellamy, "The Infrared Spectra of Complex Molecules", John Wiley & Sons, Inc., New York (1958), p. 125.

The equilibrium constants $K$ of the addition reaction of hydrogen chloride and cyclic amide (cis form) are considerably greater than those of chain amide (trans amide). It is supposed that the basicity of the nitrogen atom of the cis amide may increase owing to the decrease of resonance in the amide group. The addition of hydrogen chloride to cyclic amide becomes easier with the enlargement of the ring, as shown by the greater value of $K$ and the lower heat of addition reaction.

The values of $K$ for $N$-methyl lactams are considerably smaller than those for the corresponding lactams and they are almost the same as those for tertiary chain amide. The heat of the addition reaction of hydrogen chloride with amide becomes higher with the $N$-methyl substitution of an amide hydrogen in lactams. This is expected to be due to the fact that the amide group is stabilized by hyperconjugation of methyl group as well as the increase in resonance by the $-I$ effect of methyl group. It is presumed that the small polymerizability of $N$-methyl-substituted lactams is due to the increase of resonance in the amide group.

## Summary

The addition reaction of hydrogen chloride with several cyclic or chain amides has been investigated by the infrared absorption measurement in order to study the correlation between the polymerizability of lactams and the resonance in the amide group. The equilibrium constant $K$ for the addition reaction with cyclic amide (cis form) is 150~180 and it becomes greater with enlargement of the ring size, while $K$ for $N$-methyl lactams is about 30~40. The $K$ value for secondary chain amide (trans form) is 60. The heat of the addition reaction of hydrogen chloride with lactams becomes lower with the enlargement of the lactam ring and also with the $N$-methyl substitution of the amide hydrogen.

The stronger basicity of the cis amide compared with the trans amide may be due to the decrease of resonance in the amide group, and the stabilization of the lactam ring by the $N$-methyl substituion may be ascribed to the increase in resonance by hyperconjugation of the methyl group.

The author wishes to express his sincere gratitude to Dr. H. Kobayashi and Dr. H. Yumoto who instructed him through these studies and permitted him to publish the results. Thanks are also due to Mr. M. Nakata for his collaboration in experiments.

*Research Department*
*Toyo Rayon Co. Ltd.*
*Minato-ku, Nagoya*

# *Studies on the Thiocarbamoylthiocarbonates. I. Synthesis of Aryl Thiocarbamoyldithiocarbonates*

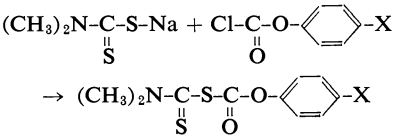
By Aritsune KAJI

(Received July 26, 1960)

*O*-Alkyl *S*-(*N*, *N*-disubstituted-thiocarbamoyl)-thiocarbonates were studied by Cambron[1] and Lo[2]. Lo reported that these alkyl esters, except isopropyl ester, were unstable and decomposed even at room temperature. No report on the aryl esters of this thiocarbonic acid has been given. The present author succeeded in the synthesis of these aryl esters.

## Results and Discussion

Aryl chloroformates reacted with sodium dimethyldithiocarbamate in acetone, giving *O*-aryl *S*-(*N*, *N*-dimethylthiocarbamoyl) thiocarbonates as shown in Table I.



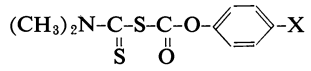
(X: -H, $-CH_3$, -Cl) (1)

But these esters were unstable and decomposed even at room temperature within a few weeks.

Aryl chlorothionoformates reacted with sodium or ammonium dialkyldithiocarbamates, giving various *O*-aryl *S*-(*N*, *N*-dialkylthiocarbamoyl) dithiocarbonates in good yields as

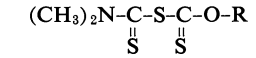
1) A. Cambron, *Can. J. Res.*, **2**, 341 (1930).
2) C. Lo and W. E. Craig, Japanese Pat. 253207 (1958).

TABLE I. *O*-ARYL *S*-(*N*,*N*-DIMETHYLTHIOCARBAMOYL) THIOCARBONATES



| X | M. p., °C | Yield, % | Formula | Anal. C% Found (Calcd.) | Anal. H% Found (Calcd.) |
|---|---|---|---|---|---|
| -H | 97.5~ 98.5 | 51.5 | $C_{10}H_{11}NO_2S_2$ | 49.79 (50.43) | 4.56 (4.32) |
| 4-$CH_3$ | 105.5~106.5 | 50.5 | $C_{11}H_{13}NO_2S_2$ | 51.76 (51.65) | 5.10 (4.99) |
| 3-Cl | 122 ~123 | 24 | $C_{10}H_{10}ClNO_2S_2$ | 43.56 (44.09) | 3.29 (3.80) |

TABLE II. *O*-ARYL *S*-(*N*,*N*-DIMETHYLTHIOCARBAMOYL) DITHIOCARBONATES



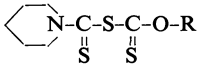
| R | Appearance | M. p., °C | Yield, % | Formula | Anal. C % Found (Calcd.) | Anal. H % Found (Calcd.) |
|---|---|---|---|---|---|---|
| Phenyl | Yellow pillars | 68 ~ 69 | 86 | $C_{10}H_{11}NOS_3$ | 46.30 (46.69) | 3.95 (4.28) |
| 2-Tolyl | Yellow prisms | 74 ~ 75 | 90 | $C_{11}H_{13}NOS_3$ | 48.20 (48.70) | 5.13 (4.80) |
| 4-Tolyl | Yellow needles | 88 ~ 89 | 78 | $C_{11}H_{13}NOS_3$ | 48.97 (48.70) | 4.71 (4.80) |
| 4-Methoxyphenyl | Yellow needles | 87.5~ 88.5 | 80 | $C_{11}H_{13}NO_2S_3$ | 46.03 (45.99) | 4.42 (4.53) |
| 4-Chlorophenyl | Yellow prisms | 104 ~105 | 80 | $C_{10}H_{10}ClNOS_3$ | 41.40 (41.17) | 3.56 (3.43) |
| 2,4-Dichlorophenyl | Yellow needles | 138 ~139 | 78 | $C_{10}H_9Cl_2NOS_3$ | 36.95 (36.80) | 2.54 (2.76) |
| 2,4,5-Trichlorophenyl | Yellow prisms | 113.5~114.5 | 75 | $C_{10}H_8Cl_3NOS_3$ | 33.34 (33.29) | 1.84 (2.22) |
| 4-Bromophenyl | Yellow needles | 110 ~111 | 74 | $C_{10}H_{10}BrNOS_3$ | 35.95 (35.71) | 2.60 (2.98) |
| 2,4,6-Tribromophenyl | Yellow needles | 118 (decomp.) | 69 | $C_{10}H_8Br_3NOS_3$ | 24.50 (24.30) | 1.49 (1.69) |
| 4-Chloro-2-tolyl | Yellow prisms | 113 ~113.5 | 56 | $C_{11}H_{12}ClNOS_3$ | 43.22 (43.20) | 3.73 (3.93) |
| 2-Chloro-4-tolyl | Yellow prisms | 131.5~132.5 | 52 | $C_{11}H_{12}ClNOS_3$ | 43.50 (43.20) | 3.63 (3.93) |
| 2,6-Dichloro-4-tolyl | Yellow prisms | 133 ~134 | 60 | $C_{11}H_{11}Cl_2NOS_3$ | 39.05 (38.82) | 3.47 (3.24) |
| 4,6-Dichloro-2-tolyl | Yellow needles | 115 ~116.5 | 56 | $C_{11}H_{11}Cl_2NOS_3$ | 39.30 (38.82) | 3.41 (3.24) |
| 3,5-Dimethyl-4-chlorophenyl | Yellow prisms | 113 ~114.5 | 85 | $C_{12}H_{14}ClNOS_3$ | 44.74 (45.07) | 4.25 (4.38) |
| 2-Phenyl-4-chlorophenyl | Yellow prisms | 107 ~108 | 61 | $C_{16}H_{14}ClNOS_3$ | 52.55 (52.24) | 3.68 (3.81) |
| 2-Biphenylyl | Yellow needles | 135 ~136 | 84 | $C_{16}H_{15}NOS_3$ | 57.83 (57.66) | 4.62 (4.50) |
| 4-Acetylphenyl | Yellow needles | 117.5~118 | 78 | $C_{12}H_{13}NO_2S_3$ | 48.50 (48.16) | 4.10 (4.35) |
| 2-Methoxycarbonyl-phenyl | Yellow prisms | 102.5~103.5 | 60 | $C_{12}H_{13}NO_3S_3$ | 45.80 (45.71) | 4.10 (4.13) |
| 4-Nitrophenyl | Yellow prisms | 114 ~115 | 90 | $C_{10}H_{10}N_2O_3S_3$ | 40.05 (39.75) | 3.52 (3.31) |
| 1-Chloro-2-naphthyl | Yellow prisms | 126.5~127 | 91 | $C_{14}H_{12}ClNOS_3$ | 49.20 (49.20) | 3.60 (3.51) |
| 1-Bromo-2-naphthyl | Yellow prisms | 141 ~142 | 76 | $C_{14}H_{12}BrNOS_3$ | 43.55 (43.52) | 2.92 (3.11) |

TABLE III. *O*-ARYL *S*-(*N*,*N*-DIETHYLTHIOCARBAMOYL) DITHIOCARBONATES

$(C_2H_5)_2N-\overset{\overset{S}{\|}}{C}-S-\overset{\overset{S}{\|}}{C}-O-R$

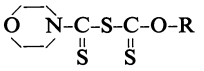
| R | Appearance | M. p., °C | Yield, % | Formula | Anal. C % Found (Calcd.) | Anal. H % Found (Calcd.) |
|---|---|---|---|---|---|---|
| 2-Biphenylyl | Yellow plates | 76 ~ 77 | 72 | $C_{18}H_{19}NOS_3$ | 60.30 (59.83) | 5.34 (5.26) |
| 2-Chloro-4-tolyl | Yellow needles | 93 ~ 94 | 81 | $C_{13}H_{16}ClNOS_3$ | 47.15 (46.78) | 5.15 (4.80) |
| 2,6-Dichloro-4-tolyl | Yellow needles | 91.5~ 93 | 70 | $C_{13}H_{15}Cl_2NOS_3$ | 42.85 (42.39) | 3.92 (4.08) |
| 3,5-Dimethyl-4-chlorophenyl | Yellow needles | 92 ~ 93 | 69 | $C_{14}H_{18}ClNOS_3$ | 48.45 (48.35) | 4.57 (5.18) |
| 2,4,6-Tribromophenyl | Yellow needles | 114 (decomp.) | 69 | $C_{12}H_{12}Br_3NOS_3$ | 27.40 (27.59) | 2.82 (2.30) |
| 2-Nitro-4-tolyl | Yellow scales | 104.5~105.5 | 84 | $C_{13}H_{16}N_2O_3S_3$ | 46.17 (45.35) | 4.75 (4.65) |
| 2-Naphthyl | Yellow prisms | 62 ~ 63 | 64.5 | $C_{16}H_{17}NOS_3$ | 57.08 (57.31) | 5.25 (5.07) |
| 1-Chloro-2-naphthyl | Yellow prisms | 143 ~144 | 60 | $C_{16}H_{16}ClNOS_3$ | 52.50 (51.96) | 4.40 (4.33) |
| 3-Chloro-2-naphthyl | Yellow needles | 107.5~108.5 | 72 | $C_{16}H_{16}ClNOS_3$ | 51.80 (51.96) | 4.57 (4.33) |
| 1-Bromo-2-naphthyl | Yellow prisms | 142 ~144 | 73 | $C_{16}H_{16}BrNOS_3$ | 46.10 (46.38) | 3.67 (3.86) |

TABLE IV. *O*-ARYL *S*-(PIPERIDINOTHIOCARBONYL) DITHIOCARBONATES



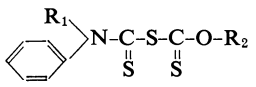
| R | Appearance | M. p., °C | Yield, % | Formula | Anal. C % Fonnd (Calcd.) | Anal. H % Found (Calcd.) |
|---|---|---|---|---|---|---|
| Phenyl | Yellow needles | 95~ 96 | 61 | $C_{13}H_{15}NOS_3$ | 52.70 (52.53) | 4.84 (5.05) |
| 4-Tolyl | Yellow needles | 102~103 | 74 | $C_{14}H_{17}NOS_3$ | 53.90 (54.02) | 5.15 (5.47) |
| 2-Naphthyl | Yellow needles | 127~128 | 71 | $C_{17}H_{17}NOS_3$ | 59.10 (58.79) | 4.85 (4.90) |
| 1-Chloro-2-naphthyl | Yellow needles | 131~132 | 76 | $C_{17}H_{16}ClNOS_3$ | 53.42 (53.47) | 4.25 (4.19) |

TABLE V. *O*-ARYL *S*-(MORPHOLINOTHIOCARBONYL) DITHIOCARBONATES



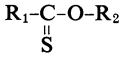
| R | Appearance | M. p., °C | Yield, % | Formula | Anal. C % Found (Calcd.) | Anal. H % Found (Calcd.) |
|---|---|---|---|---|---|---|
| 4-Tolyl | Yellow needles | 136 ~137 | 51.5 | $C_{13}H_{15}NO_2S_3$ | 50.20 (49.84) | 4.75 (4.79) |
| 4-Chlorophenyl | Yellow needles | 134 ~135 | 53.5 | $C_{12}H_{12}ClNO_2S_3$ | 43.55 (43.18) | 3.69 (3.60) |
| 2-Biphenylyl | Yellow needles | 130.5~131 | 53 | $C_{18}H_{17}NO_2S_3$ | 57.35 (57.60) | 4.15 (4.53) |
| 2-Methoxycarbonyl-phenyl | Yellow prisms | 115 ~116 | 72 | $C_{14}H_{15}NO_4S_3$ | 47.73 (47.06) | 3.75 (4.20) |
| 1-Chloro-2-naphthyl | Yellow needles | 149 ~150 | 73 | $C_{16}H_{14}ClNO_2S_3$ | 50.31 (50.07) | 3.78 (3.65) |

TABLE VI. *O*-ARYL *S*-(ARYLTHIOCARBAMOYL) DITHIOCARBONATES



| $R_1$ | $R_2$ | Appearance | M. p., °C | Yield, % | Formula | Anal. C % Found (Calcd.) | Anal. H % Found (Calcd.) |
|---|---|---|---|---|---|---|---|
| Methyl | 4-Toyl | Yellow prisms | 98~ 99 | 72 | $C_{16}H_{15}NOS_3$ | 57.95 (57.66) | 4.11 (4.50) |
| Methyl | 4-Chloro-phenyl | Yellow prisms | 133~134 | 85 | $C_{15}H_{12}ClNOS_3$ | 51.20 (50.92) | 3.72 (3.39) |
| Phenyl | 4-Tolyl | Orange needles | 110~111 | 73 | $C_{21}H_{17}NOS_3$ | 63.90 (63.80) | 4.51 (4.30) |
| Phenyl | 4-Chloro-phenyl | Orange prisms | 118~119 | 60 | $C_{20}H_{14}NOS_3$ | 58.00 (57.76) | 3.36 (3.37) |

TABLE VII. *O*-ARYL *N*, *N*-DISUBSTITUTED-THIONOCARBAMATES



| $R_1$ | $R_2$ | Appearance | M. p., °C | Yield, % | Formula | Anal. C, % Found (Calcd.) | Anal. H, % Found (Calcd.) |
|---|---|---|---|---|---|---|---|
| Dimethyl-amino | 4-Tolyl | Colorless pillar | 95 ~ 96 | 62 | $C_{10}H_{13}NOS$ | 61.80 (61.53) | 6.59 (6.67) |
| Dimethyl-amino | 4-Chlorophenyl | Colorless needles | 58 ~ 59 | 64 | $C_9H_{10}ClNOS$ | 50.45 (50.12) | 4.31 (4.64) |
| Dimethyl-amino | 2,4,5-Trichloro-phenyl | Colorless prisms | 136 ~137 | 72.5 | $C_9H_8Cl_3NOS$ | 38.38 (37.96) | 2.37 (2.81) |
| Dimethyl-amino | 4-Acetylphenyl | Slight amber needles | 102.5~103.5 | 61.5 | $C_{11}H_{13}NO_2S$ | 59.26 (59.19) | 5.83 (5.83) |
| Morpholino | 1-Chloro-2-naphthyl | Colorless plates | 138 ~139 | 81 | $C_{15}H_{14}ClNO_2S$ | 58.80 (58.54) | 4.23 (4.55) |
| *N*-Methyl-anilino | 4-Chloro-phenyl | Colorless needles | 104 ~105.5 | 78 | $C_{14}H_{12}ClNOS$ | 60.05 (60.54) | 4.19 (4.32) |

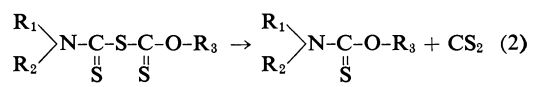
shown in Tables II—V. *O*-Aryl *S*-(*N*-alkyl-*N*-arylthiocarbamoyl) dithiocarbonates and *O*-aryl *S*-(*N*, *N*-diarylthiocarbamoyl) dithiocarbonates were also given by the similar reaction and listed in Table VI. In these reactions, water, methanol, ethanol, acetone and benzene can be used as the reaction medium. These aryl esters of *S*-(*N*, *N*-disubstituted-thiocarbamoyl)-dithiocarbonic acid, isolated as yellow or orange crystals when recrystallized from acetone-ethanol, were stable at room temperature.

*O*-Aryl *S*-(*N*-monosubstituted-thiocarbamoyl)-dithiocarbonates could not be isolated by the reaction between aryl chlorothionoformates and sodium *N*-monoalkyl- or *N*-monoaryl-dithiocarbamates, because of their decomposition during the reaction period.

It was concluded that both of the two hydrogen atoms connected with the nitrogen atom of the thiocarbamoyl group must be substituted to stabilize these dithiocarbonates.

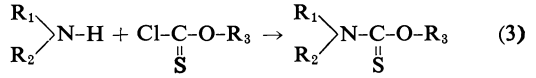
The substituents of the aryl group, as shown in Tables II—VI, did not have such strong effects on the stability of the esters which were kept at a lower temperature than their respective melting points.

Aryl esters of *S*-(*N*, *N*-disubstituted-thiocarbamoyl) dithiocarbonic acid decomposed when heated at the melting points for a long period, giving carbon disulfide and *O*-aryl *N*, *N*-disubstituted thionocarbamate as shown in Table VII.



(2)

These thionocarbamates showed no depression of the melting point on the admixture with *O*-aryl *N*, *N*-disubstituted-thionocarbamates prepared from *N*, *N*-disubstituted-amines and aryl chlorothionoformates.



(3)

## Experimental

**Starting Materials.**—Sodium or ammonium salts of *N*,*N*-disubstituted-dithiocarbamic acid were synthesized by the known methods[3]. Aryl esters of chlorothionoformic acid were prepared as follows: To a solution of 1 mol. of thiophosgen and 1 mol. of phenol in chloroform was added gradually 1 mol. of sodium hydroxide (5% aqueous solution) under vigorous agitation. The temperature was kept at 5~10°C during the reaction period of 30 min. The chloroform layer was washed with water and dried over calcium chloride. The removal of chloroform gave esters which could be used in the following reaction without further purification.

***O*-(3,5-Dimethyl-4-chlorophenyl) *S*-(*N*,*N*-dimethylthiocarbamoyl)dithiocarbonate.**—To a solution of 14.3 g. (0.1 mol.) of sodium dimethyldithiocarbamate in 100 cc. of water was added gradually 23.5 g. (0.1 mol.) of 3,5-dimethyl-4-chlorophenyl chlorothionoformate keeping the temperature at 10~15°C during the reaction period of 2 hr. By the filtration of the reaction mixture, 27.2 g. (yield, 85%) of yellow crystals with m. p. 112~114°C were obtained. Recrystallization from acetone-ethanol gave yellow prisms with m. p. 113~114.5°C.

3) Houben-Weyl, "Methoden der organischen Chemie", 9, Georg Thieme Verlag, Stuttgart (1955), p. 826.

***O*-(4-Chlorophenyl) *S*-(*N*-methyl-*N*-phenylthiocarbamoyl)dithiocarbonate.**—To a solution of 20 g. (0.1 mol.) of ammonium *N*-methyl-*N*-phenyldithiocarbamate in 200 cc. of acetone was added gradually 21 g. (0.1 mol.) of 4-chlorophenyl chlorothionoformate keeping the temperature at 5~10°C during the reaction period of 1 hr. The reaction mixture, poured into 500 cc. of cold water, gave 31 g. (yield, 85%) of yellow precipitates with m. p. 132~134°C. Recrystallization of the preceipitates from acetone-ethanol gave yellow prisms with m. p. 133~134°C.

The other esters shown in Tables II—VI were synthesized in the similar way.

**4-Tolyl *N*,*N*-dimethylthionocarbamate.**—In an oil bath, 0.45 g. of *O*-(4-tolyl) *S*-(*N*,*N*-dimethylthiocarbamoyl)dithiocarbonate was kept at 160°C for 1 hr. After the subsidence of evolution of carbon disulfide, the reaction mixture was cooled to room temperature. Twice repeated recrystallization of the reaction mixture from 0.5 cc. of ethanol, gave 0.2 g. (yield, 62%) of 4-tolyl *N*,*N*-dimethylthionocarbamate with m. p. 95~96°C.

The author wishes to express his sincere thanks to Professor Dr. Ryozo Goto, Kyoto University, for his guidance and encouragement throughout this work.

*Takaoka Factory, Nippon Soda Co., Ltd.*
*Mukaino-honmachi, Takaoka, Toyama-ken*

# *Spectrophotometric Determination of Submicrogram Quantities of Orthophosphate in Natural Waters*

By Ken SUGAWARA and Satoru KANAMORI

(Received August 13, 1960)

In advanced researches of natural waters, need is felt for a method of determining phosphate more sensitive than the current Dénigè's colorimetric method[1] especially when the quantity of the sample is limited. Such a need is partly filled with the radioactivation method[2,3]. However, a nuclear reactor is not easily accessible. Furthermore, irradiation and cooling are time-consuming. This situation initiated the present work.

It is true that there have been made various trials to increase the sensitivity of the determination of phosphate by the use of solvent extraction of phosphomolybdate[4-7] where the yellow complex is extracted with an organic solvent to be directly or after reduction to molybdenum blue subjected to spectrophotometry. These methods, however, are not sufficiently sensitive to determine submicrogram quantities of the compound. The authors' idea was to step up this increased sensitivity. Thus the phosphomolybdate which was once extracted in an *n*-butanol-chloroform mixture is decomposed into the components. Then, the

1) G. Dénigè, *Compt. rend.*, **171**, 802 (1920).
2) L. M. Foster and D. C. Gaitanis, *Anal. Chem.*, **27**, 1342 (1955).
3) J. A. James and D. H. Richards, *Nature*, **176**, 1062 (1955); **177**, 1230 (1956).
4) T. Kiba and M. Ura, *J. Chem. Soc. Japan, Pure Chem. Sec.* (*Nippon Kagaku Zasshi*), **76**, 520 (1955).
5) Coe Wadeline with M. G. Mellon, *Anal. Chem.*, **25**, 1668 (1953).
6) C. M. Proctor and D. W. Hood, *J. Marine Res.*, **13**, 122 (1954).
7) C. H. Lueck and D. F. Boltz, *Anal. Chem.*, **28**, 1168 (1956).

liberated molybdenum is separated to be spectrophotometrically determined as thiocyanate complex whereby 0.02~1.00 μg. of phosphorus as phosphate in a water sample less than 250 ml. can be determined with an accuracy of an error less than 5%.

## Experimental

**Apparatus.**—Absorbance was measured with a Beckman spectrophotometer model DU by using 10 mm. cells of Pyrex glass.

**Reagents.**—Hydrochloric acid, concentrated.

*n*-Butanol and chloroform, distilled.

*n*-Butanol-chloroform mixture: *n*-Butanol and chloroform are mixed in the proportion of 3 : 7 by volume.

Ammonium molybdate solution, 10%.

Washing solution. Thirty mlliliter of *n*-butanol is dissolved in 500 ml. of 0.5 N nitric acid.

Sodium hydroxide solution, 1N.

Ferrous ammonium sulfate solution: In 100 ml. of 0.2 N sulfuric acid 1 g. of the hexahydrate is dissolved.

Potassium thiocyanate solution, 10%.

Stannous chloride solution: In 100 ml. of 1 N hydrochloric acid 10 g. of the dihydrate is dissolved.

Phosphate standard solution: The stock solution which contains 1 mg. of phosphorus as phosphate per ml. is prepared by dissolving 0.439 g. of dihydrogen potassium phosphate in distilled water and making it up to 100 ml. The addition of a few drops of chloroform keeps the solution from mold growth. The working standard solutions are prepared by properly diluting the stock solution.

**Procedure.** — A sample is properly diluted or evaporated so that 250 ml. contains 0.02~1.0 μg. of phosphorus. After having been filtered, if necessary, this 250 ml. is placed in a 500 ml. separatory funnel. Then, 10 ml. of hydrochloric acid, 15 ml. of *n*-butanol and 10 ml. of the *n*-butanol-chloroform mixture are added. The funnel is shaken for 1 min. to saturate the aqueous phase with the mixed solvent. When two layers clearly separate, the organic layer is drawn out to be replaced by a new addition of 5 ml. of the ammonium molybdate solution and 5 ml. of the mixed solvent. Two minutes shaking follows whereby the phosphomolybdate is formed and extracted into the solvent. The extract is transferred into a 100 ml. funnel. The extraction is repeated by using another 5 ml. of the mixed solvent. The two extracts are combined and shaken for 1 min. with 50 ml. of the washing solution, whereby the uncombined molybdate is completely washed out. The remaining organic layer which contains exclusively phosphomolybdate is transferred into a 50 ml. separatory funnel. After the addition of 10 ml. of 1 N sodium hydroxide solution and 5 ml. of distilled water, the funnel is shaken for 1 min. to strip the phosphomolybdate completely from the oily phase by the aqueous alkali solution. After 15 min. standstill during which the decomposition of the phosphomolybdate into molybdate and phosphate is complete, the organic layer is drawn off. With swirling, 3 ml. of concentrated hydrochloric acid, 1 ml. of ferrous ammonium sulfate solution, 3 ml. of thiocyanate solution and 3 ml. of stannous chloride solution are added successively. An amber color develops immediately. This is extracted with two small portions of the mixed solvent and made up to 5 ml. To the joint extract a few small crystals of stannous chloride are recommended to be added to protect the ferrous iron from oxidation. Otherwise ferric thiocyanate is formed to cause a high blank value because of its red coloration. The quantity of phosphate is determined from the absorbance reading at 475 mμ in reference to the standard curve. The curve has previously been constructed by following the same procedure with the standard solutions at different dilutions.

## Discussion

**Extraction of Phosphomolybdate.** — The extraction must proceed on a condition where following two requirements are satisfied: 1) The extraction must be complete. 2) The possible contaminations of arseno-, germano- and silicomolybdate must be avoided. To this

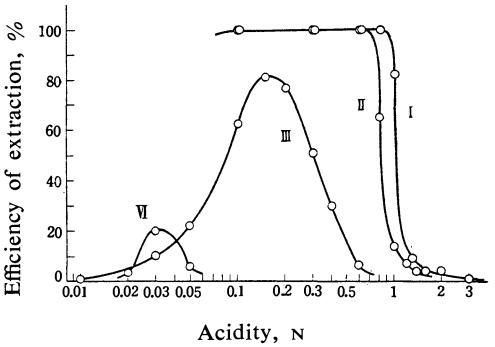



Fig. 1. Effect of the acidity on the extraction of heteromolybdates with *n*-butanol.
I Phosphomolybdate
II Arsenomolybdate
III Germanomolybdate
IV Silicomolybdate

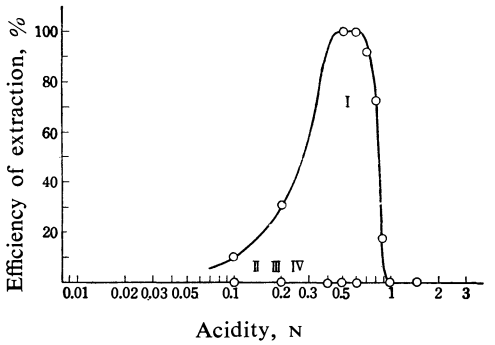



Fig. 2. Effect of the acidity on the extraction of heteromolybdates with the *n*-butanol-chloroform mixture.
I Phosphomolybdate
II Arsenomolybdate
III Germanomolybdate
IV Silicomolybdate

aim an appropriate solvent and the range of acidity where the solvent is most efficiently active were sought. Two sets of 50 ml. of arsenate, germanate and silicate solutions, each containing 10 $\mu$g. of one of the three elements, As, Ge and Si, were prepared and adjusted to various acidities with hydrochloric acid. Then, after the addition of 1 ml. of 10% ammonium molybdate solution, one of the sets was extracted with *n*-butanol, while another set with the *n*-butanol-chloroform mixture. The extracts were processed with 1.0% stannous chloride solution (1 N in hydrochloric acid) to reduce and strip the extracted heteropolyacids which were subjected to spectrophotometry to determine the efficiency of these extractions. As is seen from Figs. 1 and 2, the results point to the fact that the extraction is practically complete in a wider range of acidity from 0.1 to 0.8 N with *n*-butanol as compared with the range from 0.5 to 0.6 N with the mixed solvent. However, in these ranges, separation of phosphate from arsenate, germanate and silicate is not complete with *n*-butanol, while it is nearly complete with the mixed solvent. Thus the *n*-butanol-chloroform mixture is only acceptable as a solvent.

**Standard Curve***.—Standard curves for three different methods are compared in Fig. 3, where the high sensitivity of the authors' method is quite evident.

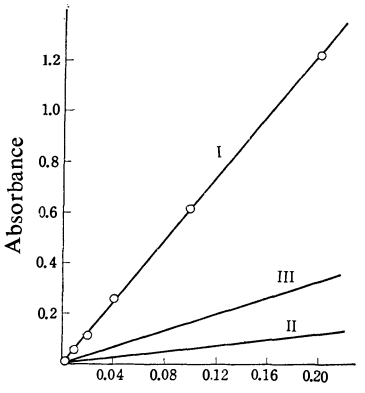



Fig. 3. Standard curves.

I The present method
II Molybdenum blue method (940 m$\mu$)
III Simple phosphomolybdate extraction method (245 m$\mu$)

**Washing of the Extract.**—This treatment is indispensable for removing the contamination of unbound moybdate which otherwise gives a higher apparent value at the final spectrophotometry. To check this point, samples containing 0.50 $\mu$g. of phosphorus and samples with

TABLE I. EFFECT OF THE WASHING ON THE BLANK VALUE AND RECOVERY OF PHOSPHORUS

| Times of washing | Blank value absorbance | Recovery of 0.50 $\mu$g. of phosphorus $\mu$g. |
|---|---|---|
| 1 | 0.005 | 0.49 |
| 1 | 0.001 | 0.51 |
| 2 | 0.000 | 0.50 |
| 2 | 0.001 | 0.50 |
| 3 | 0.000 | 0.50 |

TABLE II. THE INTERFERENCE OF VARIOUES IONS

| Ion | Added as | Quantity mg.-element | $PO_4^{3-}$ added $\mu$g.-P | $PO_4^{3-}$ recovered $\mu$g.-P |
|---|---|---|---|---|
| $AsO_4^{3-}$ | $As_2O_5$ in NaOH | 0.1 | 0.50 | 0.52 |
| $GeO_3^{2-}$ | $GeO_2$ in NaOH | 0.1 | 0.50 | 0.49 |
| $SiO_3^{2-}$ | $SiO_2$ in $Na_2CO_3$ | 5 | 0.50 | 0.50 |
| $Na^+$ | NaCl | 800 | 0.50 | 0.52 |
| $K^+$ | KCl | 500 | 0.50 | 0.50 |
| $Mg^{2+}$ | $MgSO_4$ | 400 | 0.50 | 0.50 |
| $Ca^{2+}$ | $Ca(NO_3)_2$ | 150 | 0.50 | 0.52 |
| $Fe^{3+}$ | $FeCl_3$ | 50 | 0.50 | 0.52 |
| $Al^{3+}$ | $Al_2(SO_4)_3$ | 25 | 0.50 | 0.51 |
| $Mn^{2+}$ | $MnSO_4$ | 10 | 0.50 | 0.50 |
| $Cl^-$ | NaCl | 1200 | 0.50 | 0.52 |
| $SO_4^{2-}$ | $MgSO_4$ | 500 | 0.50 | 0.50 |
| $NO_3^-$ | $Ca(NO_3)_2$ | 100 | 0.50 | 0.52 |
| $Cu^{2+}$ | $CuSO_4$ | 1 | 0.50 | 0.49 |
| $Ag^{+}$* | $AgNO_3$ | 1 | 0.50 | 0.48 |
| $Ba^{2+}$ | $BaCl_2$ | 1 | 0.50 | 0.50 |
| $Zn^{2+}$ | $ZnCl_2$ | 1 | 0.50 | 0.50 |
| $Cd^{2+}$ | $CdSO_4$ | 1 | 0.50 | 0.52 |
| $Hg^{2+}$ | $HgCl_2$ | 1 | 0.50 | 0.51 |
| $TiO^{2+}$ | $TiO_2$ in $H_2SO_4$ | 1 | 0.50 | 0.24 |
| | | 0.1 | 0.50 | 0.47 |
| | | 0.01 | 0.50 | 0.50 |
| $ZrO^{2+}$ | $ZrO(NO_3)_2$ | 1 | 0.50 | 0.52 |
| $Th^{4+}$ | $Th(NO_3)_4$ | 1 | 0.50 | 0.49 |
| $Pb^{2+}$ | $Pb(NO_3)_2$ | 1 | 0.50 | 0.50 |
| $VO_2^+$ | $NH_4VO_3$ | 1 | 0.50 | 0.20 |
| | | 0.1 | 0.50 | 0.49 |
| $SbO^+$ | $K(SbO)C_4H_4O_6$ | 1 | 0.50 | 0.49 |
| $BiO^+$ | Nitrate | 1 | 0.50 | 0.49 |
| $CrO_4^{2-}$ | $K_2CrO_4$ | 1 | 0.50 | 0.50 |
| $WO_4^{2-}$ | $Na_2WO_4$ | 1 | 0.50 | 0.37 |
| | | 0.1 | 0.50 | 0.50 |
| $UO_2^{2+}$ | $UO_2(CH_3CO_2)_2$ | 1 | 0.50 | 0.50 |
| $SeO_3^{2-}$ | $Na_2SeO_3$ | 1 | 0.50 | 0.52 |
| $Co^{2+}$ | $CoSO_4$ | 1 | 0.50 | 0.50 |
| $Ni^{2+}$ | $NiSO_4$ | 1 | 0.50 | 0.51 |

* Sulfuric acid was used in place of hydrochloric acid for the extraction of phosphomolybdate.

* The molar extinction coefficient of molybdenum thiocyanate under the present experimental condition was determined as $1.55\times10^4$ l. per mol. cm. and the corresponding value of phosphate $1.85\times10^5$ l. per mol. cm. Thus, the atom ratio of phosphorus to molybdenum is calculated to be 1/12 within an experimental error.

no phosphorus were processed according to the procedure in which they were subjected to one to three washings. The results listed in Table I show that the blank value is already nearly zero after one washing. This points to the fact that one washing is sufficient to completely remove free molybdate from the extract. On the other hand, the phosphate value remains constant even after three washings. This shows that there is no risk for the extracted phosphomolybdate to escape through the washing.

**Interference.** — The interference of various ions with the present determination of phosphate was examined with the results listed in Table II.

A) An error of 5% is found only with a concentration of 100 $\mu$g. As/50 ml. for arsenate, with 100 $\mu$g. Ge/50 ml. for germanate, and with 5 mg. Si/50 ml. for silicate. B) $Na^+$, $K^+$, $Mg^{2+}$, $Ca^{2+}$, $Cl^-$, $SO_4^{2-}$ and $NO_3^-$ cause no interference up to a considerable concentration. C) Tungstate and vanadate may be partly extracted in the mixed solvent to cause a considerable interference. However, the concentration of these elements in usual natural waters is too small to consider their interference. The same thing can be said in the case of titanium. In conclusion, the present method of phosphate determination can be safely applied to usual waters with no special consideration of the interference which might be caused by co-existing elements. Examples of the application of the method to several natural waters are listed in Table III.

TABLE III. APPLICATION OF THE METHOD TO NATURAL WATERS

| Description | Sample taken ml. | *P* added $\mu$g. | *P* recovered $\mu$g. |
|---|---|---|---|
| Ground water from a well on the campus of Nagoya University | 5.0 | | 0.28 |
| | 5.0 | 0.10 | 0.39 |
| Rain (March 20, 1956; Nagoya) | 200 | | 0.77 |
| | 200 | 0.05 | 0.83 |
| Snow (Feb. 3, 1956; Nagoya) | 100 | | 0.48 |
| | 100 | 0.10 | 0.58 |

*Chemical Institute, Faculty of Science*
*Nagoya University, Chikusa-ku*
*Nagoya*

# *Reduction of Organic Compounds with Urushibara Catalysts under High Pressure. VII*[1]*. Feature of Various Urushibara Catalysts as Revealed in the Reduction of Benzophenone*

By Shinichi TAIRA

(Received August 22, 1960)

In the previous paper[2] of this series, catalytic reductions of ketones under high pressure with Urushibara nickel B were reported. In the present paper, reduction of benzophenone with various Urushibara catalysts under various conditions was investigated.

The preparation of the Urushibara nickel catalyst has been successively modified, and some varieties of this catalyst were reported. Each of these Urushibara nickel catalysts is prepared by digesting precipitated nickel with alkali or acid. In the original preparation[3], nickel was precipitated from nickel chloride solution with zinc dust, and digested with caustic alkali to obtain U-Ni-B. The alternative catalyst U-Ni-A[4] was prepared by digesting the precipitated nickel with acetic acid or propionic acid instead of caustic alkali. The third catalyst U-Ni-BA[1,5] was developed by modifying the preparation of U-Ni-B, using aluminum grains instead of zinc dust for precipitating nickel metal from nickel chloride solution. Each of these Urushibara nickels has been found to have a comparable activity with the Raney nickel for the hydrogenation of various organic compounds.

Now it is expected that metallic cobalt and metallic copper prepared by the same procedure as to obtain the Urushibara nickel may have

1) Part VI. I. Motoyama, This Bulletin, **33**, 232 (1960).
2) K. Hata, S. Taira and T. Higase, *J. Chem. Soc. Japan, Pure Chem. Sec.* (*Nippon Kagaku Zasshi*), **78**, 186 (1957).
3) Y. Urushibara and S. Nishimura, This Bulletin, **27**, 480 (1954).
4) Y. Urushibara, S. Nishimura and H. Uehara, ibid., **28**, 446 (1955).
5) K. Hata, S. Taira and I. Motoyama, ibid., **31**, 776 (1958).

catalytic activities for hydrogenation. Actually it was already reported[6] that Urushibara cobalt B had a property similar to Raney cobalt and was recognized to be useful for the hydrogenation of nitriles. A similar copper catalyst was also reported[7] to be prepared from copper sulfate solution and zinc dust.

In case of catalytic reduction under high pressure, the reaction velocity may be influenced by various factors, namely, the nature of the groups to be reduced, the purity of substance, the activity and quantity of catalyst, the kind of solvent, the concentration and pH value of solution, the pressure of hydrogen, the temperature of reduction, the efficiency of agitation, etc. The temperature at which the absorption of hydrogen gas begins, or the time or the quantity of catalyst required for the completion of reduction, may be regarded as a measure to determine the activity of the catalyst.

In the present experiments, reduction of benzophenone is selected as an example for determining the activities of Urushibara catalysts prepared by various methods. The time required for reducing the ketone to benzhydrol was compared with each other under a similar condition.

## Experimental

**Apparatus.** — Reductions were carried out in a Sakashita SE-20, electro-magnetically stirring type autoclave having a capacity of 200 ml.

**Materials.** — Benzophenone was prepared from benzoyl chloride and benzene by the Friedel-Crafts reaction[8]. The raw product was submitted to vacuum distillation and then recrystallized twice from ethanol, b. p. 140~141°C/5 mmHg, m. p. 48°C.

**General Procedure for Reduction.**—The catalyst containing 1 g. of nickel, cobalt, or copper was carefully transferred with ethanol into the autoclave. Then air in the autoclave was replaced by hydrogen gas. Most operations were carried out under the following conditions: (1) benzophenone; 12.74 g. (0.07 mol.) (2) ethanol(99%); 110 ml. (3) pH; 9~11 (When Urushibara catalysts A and CA were used, 0.5 ml. of 10% sodium hydroxide solution was added.) (4) agitation; 40~50 strokes per minute (5) temperature; Since a remarkable reduction of carbonyl compounds was found to begin at about 60°C as was reported in the previous paper[2], agitation was started when the temperature in the autoclave was reached at 60°C, and it was kept between 58° and 70°C. (6) Pressures were observed at intervals of five minutes.

After the reduction was finished and the autoclave got cold, hydrogen gas was discharged and the contents were taken out with ethanol. The catalyst was filtered off and washed with ethanol. The major part of the combined solvent was distilled off and the hot residue was poured into 300 ml. of hot water with stirring. The crude benzhydrol was filtered off and dried. It was recrystallized from ligroin into colorless silky needles, m. p. 68~69°C. Yield, 90~95% of the theoretical. It did not depress the m. p. with an authentic sample.

**Preparation of Catalysts.**—The Urushibara nickel B[3], the Urushibara nickel A[4] and the Urushibara nickel BA[1,5] were prepared by the methods described in the references cited. Some new types of Urushibara catalysts were prepared as follows. The procedures described below are the methods for the preparation of the catalysts, each containing 1 g. of catalyst metal.

*(a) Urushibara Nickel B (U-Ni-B) Prepared from Nickel Acetate.*—On a boiling water bath 4.24 g. of nickel acetate ($Ni(CH_3CO_2)_2 \cdot 4H_2O$) is dissolved in 20 ml. of water. This hot solution is added at once with stirring by hand onto a hot mixture of zinc dust (10 g.) and water (10 ml.) placed in a 500 ml. beaker warmed on a boiling water bath. As a vigorous reaction takes place and the reaction mixture swells up, good agitation is required to prevent the contents running over. When the reaction subsides, 200 g. of 10% sodium hydroxide solution is cautiously added with stirring onto the reaction product (precipitated nickel). The temperature of the mixture is kept at about 50~55°C for fifteen minutes with occasional stirring. When solid matter settles down, the upper liquor is decanted. The solid is washed with two 100 ml. portions of hot water, and then with two 50 ml. portions of ethanol. In this way 8.5~10.5 g. of bulky catalyst, containing nickel (about 1 g.), zinc, zinc oxide and a very small amount of alkali, is obtained.

*(b) Urushibara Cobalt B (U-Co-B).* — To a hot mixture (90~100°C) of zinc dust (10 g.) and water (4 ml.) placed in a 100 ml. flask is added at once 10 ml. of hot aqueous solution (90~100°C) containing 4.04 g. of cobalt chloride ($CoCl_2 \cdot 6H_2O$) with vigorous stirring on a boiling water bath. The reaction product (precipitated cobalt) is transferred into a 300 ml. beaker and washed with 200 ml. of hot water. After 160 g. of 10% sodium hydroxide solution is added, the mixture is warmed at about 50~55°C on a water bath for fifteen minutes with occasional stirring. Then the upper liquor is decanted, and the residual solid is washed with two 100 ml. portions of hot water and then with two 50 ml. portions of ethanol. About 6.5~7 g. of catalyst, containing cobalt (about 1 g.), zinc, zinc oxide and a trace of alkali, is obtained.

*(c) Urushibara Nickel CB (U-Ni-CB).*—Ten milliliter of aqueous solution containing 4.04 g. of nickel chloride ($NiCl_2 \cdot 6H_2O$) is added to a mixture of zinc dust (10 g.) and water (4 ml.) placed in a 100 ml. flask. This mixture is stirred at room temperature or under cooling with water or ice until the green color of nickel ion disappears. This process requires about three to four hours. As the major part of the ion exchange reaction proceeds during the initial period, the reaction mixture may be left standing until the green color has disappeared

6) S. Saito, *J. Pharm. Soc. Japan* (*Yakugaku Zasshi*), **76**, 351 (1956).
7) Y. Urushibara, Japanese Pat., 203309.
8) Gattermann-Wieland, "Die Praxis des organischen Chemikers", Walter de Gruyter & Co., Berlin (1940), p. 340.

after stirring for an hour. When the preparation of a large quantity of precipitated nickel is required, the reaction mixture must be cooled with ice to remove the generated heat of the reaction. The slushy precipitated nickel is transferred into a 300 ml. beaker and washed with 200 ml. of cold water. After 160 g. of cold 10% sodium hydroxide solution is added, the mixture is stirred for an hour under cooling with water or ice if necessary. When the major part of solid settles down, the upper liquor is cautiously decanted, and the solid is washed with two 100 ml. portions of cold water and then with two 50 ml. portions of ethanol. About 8~11 g. of bulky catalyst, containing nickel (about 1 g.), zinc, zinc oxide and a very small quantity of alkali, is obtained.

*(d) Urushibara Cobalt CB (U-Co-CB).* — This catalyst is prepared from cobalt chloride by the same procedure as is described above.

*(e) Urushibara Nickel A (U-Ni-A) Prepared from Nickel Acetate.*—Precipitated nickel was prepared by the same procedure as is described in (a). Instead of caustic alkali, 160 ml. of 13% acetic acid is added with stirring onto the precipitated nickel. The mixture is stirred occasionally until the generation of hydrogen gas ceases and a solid comes up to the surface of the solution which is of green color. The solid is collected on a glass filter and washed with 200 ml. of hot water and then with 100 ml. of ethanol. About 0.7 g. of catalyst, containing nickel, small quantities of zinc and zinc oxide, is obtained.

*(f) Urushibara Cobalt A (U-Co-A).* — The precipitated cobalt prepared by the same way as is described in (b) is treated with 160 ml. of 13% acetic acid. The mixture is stirred for about five minutes until the generation of hydrogen gas ceases and a solid comes up to the surface of the solution which is rose-colored. This coloration is necessary to obtain an active catalyst. The solid is collected on a glass filter and washed with 200 ml. of hot water and then with 100 ml. of ethanol. About 1~1.2 g. of catalyst, containing cobalt (about 0.8 g.), small quantities of zinc and zinc oxide, is obtained.

*(g) Urushibara Copper (U-Cu).*—To a hot mixture (90~100°C) of zinc dust (10 g.) and water (5 ml.) placed in a 200 ml. flask is added at once 10 ml. of hot aqueous solution (90~100°C) containing 2.69 g. of cupric chloride ($CuCl_2 \cdot 2H_2O$) with vigorous stirring. The reaction ends at once. The upper liquor is decanted and the solid (precipitated copper) is transferred into a 300 ml. beaker and washed with 200 ml. of hot water. After the precipitated copper is treated with 160 ml. of 13% acetic acid at 70~75°C on a water bath for about thirty minutes, the upper liquor is decanted. The solid is washed with two 100 ml. portions of hot water and then with two 50 ml. portions of ethanol. About 2~2.5 g. of black catalyst, containing copper (about 1 g.) and zinc, is obtained.

*(h) Urushibara Nickel CA (U-Ni-CA).*—The precipitated nickel prepared by the same way as is described in (c) is transferred into a 500 ml. beaker and is carefully treated with 200 ml. of 10% acetic acid under cooling with water. After about five minutes the generation of hydrogen gas subsides and a solid comes up to the surface of the solution, which carries more deep green color than in case of Urushibara nickel A. The solid is collected on a glass filter and washed with 200 ml. of cold water and then with 100 ml. of ethanol. About 0.6~0.8 g. of fine catalyst, containing nickel (0.4~0.5 g.), small quantities of zinc and zinc oxide, is obtained.

*(i) Urushibara Cobalt CA (U-Co-CA).*—This catalyst is prepared from cobalt chloride by the same way as is described above, the volume of 10% acetic acid being modified to 150 ml. for the treatment of the precipitated cobalt.

*(j) Urushibara Copper C (U-Cu-C).*—During ten minutes 30 ml. of cold aqueous solution containing 2.69 g. of cupric chloride is added dropwise to a vigorously stirred mixture of zinc dust (10 g.) and water (10 ml.) placed in a 100 ml. flask under cooling with ice. The precipitated copper is transferred into a 300 ml. beaker and washed with 200 ml. of cold water. After the precipitated copper is treated with 160 ml. of 13% acetic acid for two hours at room temperature, the upper liquor is decanted and the residual solid is washed with two 100 ml. portions of cold water and then with two 50 ml. portions of ethanol. About 3~4 g. of black catalyst, containing copper (about 1 g.) and zinc, is obtained. Urushibara copper catalyst carries a black color before use, and it is changed in red-brown after use for reduction.

In cases of the preparations of the Urushibara catalysts B, the Urushibara copper and the Urushibara copper C, every washing is removed by decantation. In all procedures, distilled water is used for washing, and the solid must be protected from the contact with air as far as possible after the treatment of the precipitated metals with acid or alkali.

## Results and Discussion

The results obtained from the reduction of benzophenone which was purified by a single vacuum distillation are summarized in Tables I and II. A series of experiments shown in Table I were carried out to examine the effect of initial pressure, and to find the difference due to the kind of nickel salt or amount of zinc dust used for preparing the catalyst. The activities of U-Ni-B and U-Co-B were also compared. As seen from Table I, the velocity of reduction was affected only slightly, if any, by the initial pressure within 30~134 kg./cm$^2$. Therefore the effect of the initial pressure was ignored in the following operations. The use of potassium hydroxide solution for digesting the precipitated nickel in place of sodium hydroxide solution gave the similar result (Exp. No. 14). The U-Ni-B contains a large quantities of zinc and zinc oxide aside from nickel metal. To diminish these ingredients the precipitated nickel was prepared with less amount of zinc dust and was treated with much quantities of alkaline solution (Exp. No. 15). As the catalyst thus obtained was less active and the velocity of reduction was depressed in the course of the

TABLE I. REDUCTION OF BENZOPHENONE* WITH U-Ni-B OR U-Co-B

| Exp. No. | Catalyst[a] | pH | Total weight of catalyst g.[b] | Initial press. kg./cm² | Initial temp., °C | React. temp. °C | Time min. |
|---|---|---|---|---|---|---|---|
| 11 | U-Ni-B | 10.2 | | 40 | 20 | 58~65 | 95 |
| 12 | U-Ni-B | 11.1 | | 134 | 22 | 58~67 | 95 |
| 13 | U-Ni-B | 8.9 | 6.7 | 30 | 29 | 58~67 | 95 |
| 14 | U-Ni-B[c] | 8.3 | | 50 | 26 | 58~64 | 100 |
| 15 | U-Ni-B[d] | 11 | | 50 | 17 | 59~76 | 165 |
| 16 | U-Ni-B[e] | 10.8 | 9.5 | 45.5 | 20 | 58~66 | 55 |
| 17 | U-Ni-B[e] | 11.3 | | 35 | 23 | 58~64 | 55 |
| 18 | U-Ni-B[e,f] | 10.6 | 9 | 65 | 25 | 58~66 | 65 |
| 19 | U-Co-B | 10.1 | | 55 | 26 | 58~68 | 95 |

* Benzophenone, purified by a single vacuum distillation, was used.
a) Each catalyst was prepared so as to contain 1 g. of nickel or cobalt.
b) The figures were obtained by weighing the dried catalysts after use for reduction.
c) The precipitated nickel was treated with 200 g. of 14% potassium hydroxide solution.
d) The precipitated nickel, obtained from nickel chloride solution with 5 g. of zinc dust, was treated with two 150 g. portions of 10% sodium hydroxide solution.
e) The precipitated nickel was prepared from nickel acetate. The other was prepared from nickel chloride.
f) The precipitated nickel was treated with 150 g. of 20% sodium hydroxide solution.

reaction, higher temperature was required to complete the reaction. This may be partly due to the big size of the particles of nickel metal and partly to the contact with an alkali for a long time. Moreover, it must be considered that the zinc and zinc oxide contaminated in the U-Ni-B may act as carrier[9]. For the reduction of benzophenone, purified by a single vacuum distillation, the U-Ni-B prepared from nickel acetate was more effective than the catalyst obtained from nickel chloride (Exp. Nos. 16, 17, 18), but this was not always true, when more carefully purified benzophenone was used. The U-Ni-B prepared from nickel acetate weighs in dry state about 8.5~10.5 g. (for 1 g. of nickel), and is about three times as bulky as the catalyst obtained from nickel chloride. Therefore, it must contain more zinc oxide (cf. micro-photograph, Fig. 1 (d)), which may act as a sort of an effective carrier in the reduction of a less purified substance.

It was already reported[10], that the catalytic reduction of a carbonyl group with Raney nickel was accelerated by a trace of alkali. For the Urushibara nickel catalyst, the effect of an alkali was quantitatively investigated in the reduction of cyclohexanone under ordinary pressure[11]. The results of the reduction of benzophenone in neutral solution with the Urushibara catalyst A and the well washed Urushibara catalyst B are shown in Table II. From these results, it is obvious that the catalytic reduction of a carbonyl group with these catalyst is desirable to operate above pH 8 (S. Nishimura reported that the excess of alkali retarded the reaction[11]).

The results tabulated in Tables III, IV, V and VI were obtained by the use of more carefully purified benzophenone, which was recrystallized twice from ethanol after vacuum distillation. The effect of purification was remarkable when the U-Ni-B was used. The U-Ni-BA was reported to be specially useful in the hydrogenation of aromatic nucleus[1,5], but it was found to be not so particularly effective for the reduction of a carbonyl group (Table III, Exp. Nos. 37, 38). It was revealed by micro-photographs that the size of the particles of the U-Ni-BA catalyst is greater than that of the other Urushibara catalysts* as shown in Fig. 1. Also the X-ray diffraction of the U-Ni-BA gives a different pattern from that of the U-Ni-A. The U-Co-BA was proved to be less active for the reduction of benzophenone, and it required higher temperature and longer time to finish the reduction than the other Urushibara catalysts (Exp. No. 39). As was already described, the U-Ni-A in neutral solution was not suitable for the reduction of a carbonyl group. But an addition of a small amount of alkali promoted remarkably the reduction and such a nickel catalyst gave better results than those obtained with the U-Ni-B (Exp. Nos. 310—313). The reason may be partly supposed to be due to the dispersability of the catalyst.

9) Y. Urushibara, S. Yamaguchi and M. Kobayashi, This Bulletin, **29**, 816 (1956).
10) M. Delépine and A. Horeau, *Bull. soc. chim. France*, [5] **4**, 31 (1937).
11) S. Nishimura, *J. Chem. Soc. Japan, Pure Chem. Sec.* (*Nippon Kagaku Zasshi*), **79**, 56 (1958).
* The size of the particles of Urushibara copper catalyst is as large as that of the U-Ni-BA.

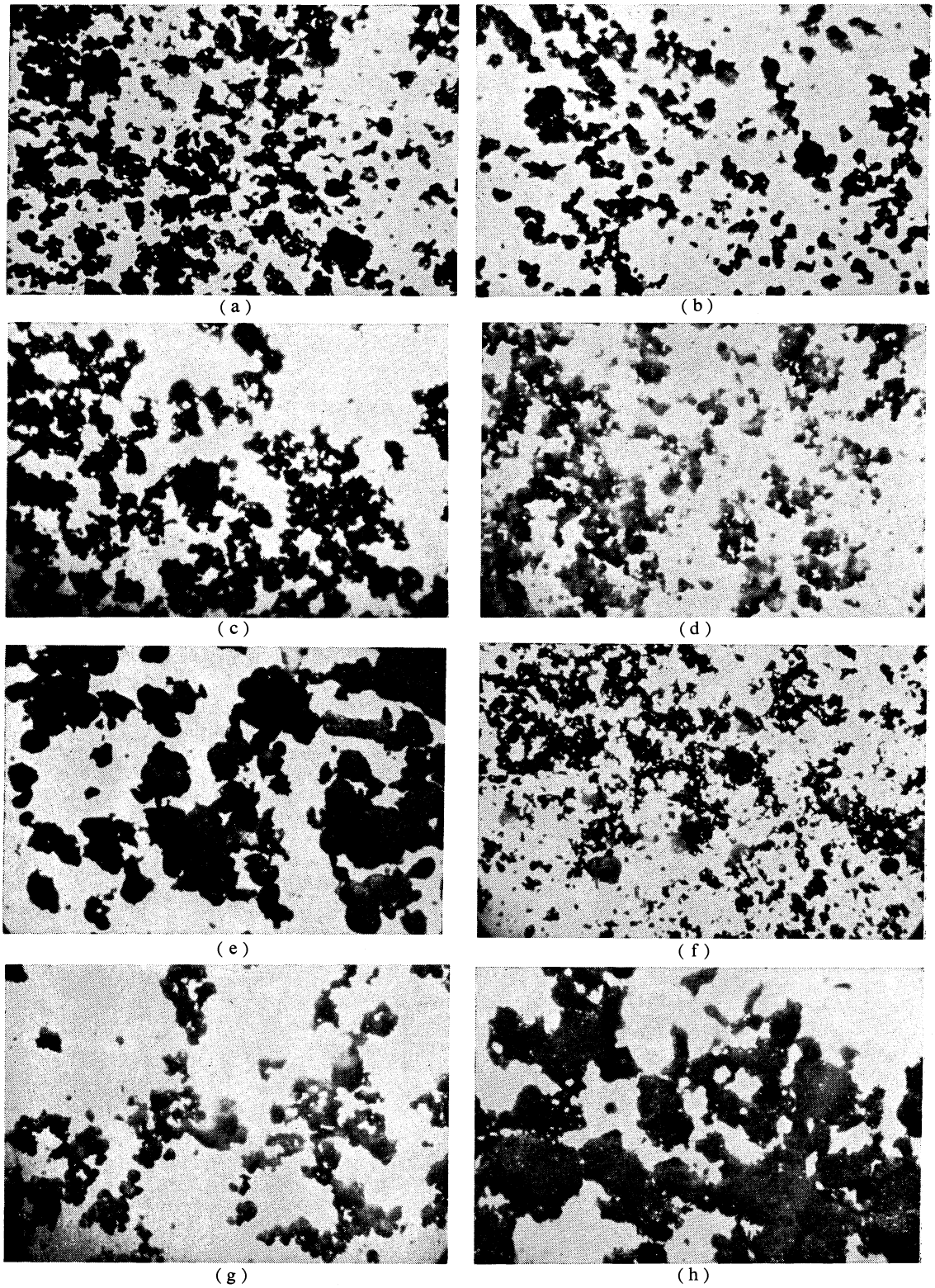



Fig. 1. Micro-photographs of Urushibara catalysts (×150).
(a) U-Ni-A (b) U-Ni-B (c) U-Ni-A (The precipitated nickel was prepared from nickel acetate.) (d) U-Ni-B (The precipitated nickel was prepared from nickel acetate.) (e) U-Ni-BA (f) U-Co-A (g) U-Co-B (h) U-Cu.

TABLE II. REDUCTION IN NEUTRAL SOLUTION

| Exp. No. | Catalyst[a] | pH | Total weight of catalyst g.[b] | Initial press. kg./cm² | Initial temp., °C | React. temp. °C | Time min. |
|---|---|---|---|---|---|---|---|
| 21 | U-Ni-B[c,d] | 7.5 | | 45 | 20 | 58～ 66 | 250 |
| 22 | U-Co-B[d] | 7.7 | 6.6 | 55 | 22 | 58～ 66 | 165 |
| 23 | U-Ni-A | 7 | | 55 | 22 | 58～ 64 | 155 |
| 24 | U-Ni-A[c] | 6.8 | 0.7 | 45 | 18 | 62～102 | 205 |
| 25 | U-Co-A | 6.7 | | 50 | 20 | 62～ 76 | 180 |

Benzophenone, purified by a single vacuum distillation, was used.

a) Each catalyst was prepared so as to contain 1 g. of nickel or cobalt.
b) The figures were obtained by weighing the dried catalysts after use for reduction.
c) The precipitated nickel was prepared from nickel acetate instead of nickel chloride.
d) The catalysts were thoroughly washed with water to remove a trace of alkali.

TABLE III. REDUCTION OF CAREFULLY PURIFIED BENZOPHENONE*

| Exp. No. | Catalyst[a] | pH | Total weight of catalyst g.[b] | Initial press. kg./cm² | Initial temp., °C | React. temp. °C | Time min. |
|---|---|---|---|---|---|---|---|
| 31 | U-Ni-B | 9.7 | 6.5 | 30 | 24 | 58～68 | 75 |
| 32 | U-Ni-B | 9.3 | 6.8 | 49.5 | 22 | 63～67 | 25 |
| 33 | U-Ni-B | 9.4 | 6.6 | 52.5 | 28 | 61～66 | 35 |
| 34 | U-Ni-B[c] | 11.1 | 11.2 | 50 | 16 | 63～66 | 30 |
| 35 | U-Co-B | 10.4 | 7 | 50 | 15 | 60～69 | 70 |
| 36 | U-Co-B | 9 | 6.2 | 56 | 24 | 61～65 | 65 |
| 37 | U-Ni-BA | 10.5 | 1.4 | 50 | 15 | 60～64 | 45 |
| 38 | U-Ni-BA | 10.6 | 1.8 | 45 | 14 | 62～66 | 35 |
| 39 | U-Co-BA | 10.2 | 0.8 | 45 | 16 | 72～84 | 115 |
| 310 | U-Ni-A | 10.5[d] | 1.1[e] | 52 | 25 | 60～63 | 10 |
| 311 | U-Ni-A | 10.3[d] | 1.4[e] | 46 | 26 | 59～62 | 8 |
| 312 | U-Ni-A | 10.1[d] | 1.4[e] | 48.5 | 20 | 59～63 | 6 |
| 313 | U-Ni-A | 10[d] | 1.3[e] | 46 | 29 | 60～62 | 12 |
| 314 | U-Ni-A[c] | 10.4[d] | 0.7 | 45 | 24 | 59～66 | 60 |
| 315 | U-Co-A | 10.1[d] | 1[e] | 45 | 22 | 61～66 | 45 |
| 316 | U-Co-A | 10.4[d] | 1.2[e] | 49.5 | 25 | 59～65 | 50 |

* Benzophenone, purified by a single vacuum distillation and then recrystallized twice from ethanol, was used.

a) Each catalyst was prepared so as to contain 1 g. of nickel or cobalt.
b) The figures were obtained by weighing the dried catalysts after use for reduction.
c) The precipitated nickel was prepared from nickel acetate. The other was prepared from nickel chloride.
d) 0.5 ml. of 10% sodium hydroxide solution was added.
e) The quantities of nickel or cobalt were about 0.75～0.85 g.

TABLE IV. REDUCTION WITH THE U-Ni-A OF LOW ACTIVITY

| Exp. No. | Weight of cat., g.[a] | pH[b] | Weight of sample, g. | Volume of ethanol ml. | Initial press. kg./cm² | Initial temp. °C | React. temp. °C | Time min. |
|---|---|---|---|---|---|---|---|---|
| 41 | 1 | 10.7 | 12.74 | 110 | 45 | 16 | 60～ 66 | 30 |
| 42 | 2 | 10 | 12.74 | 110 | 40 | 22 | 62～ 66 | 10 |
| 43 | 1 | 10.1 | 12.74 | 55 | 32 | 20 | 60～ 68 | 10 |
| 44 | 1 | 10.2 | 25.48 | 110 | 60 | 14 | 61～ 66 | 20 |
| 45 | 1 | 10.2 | 12.74 | 110 | 50 | 20 | 97～100[c] | 7 |
| 46 | 1 | 10.5 | 12.74 | 55 | 45 | 18 | 98～108[c] | 4 |

Benzophenone, purified by a single vacuum distillation and then recrystallized twice from ethanol, was used.

a) The figures are weight of nickel metal to be included in catalysts.
b) 0.5 ml. of 10% sodium hydroxide solution was added.
c) The time for heating the autoclave before starting agitation was equal to those of the other experiments.

TABLE V. REDUCTION WITH URUSHIBARA CATALYSTS C

| Exp. No. | Catalyst[a] | pH | Total weight of catalyst g.[b] | Initial press. kg./cm² | Initial temp., °C | React. temp. °C | Time min. |
|---|---|---|---|---|---|---|---|
| 51 | U-Ni-CB[c] | | 5.7 | 34.5 | 16 | 62~65 | 35 |
| 52 | U-Ni-CB[c] | 10.2 | 11.5 | 56 | 22 | 60~62 | 20 |
| 53 | U-Ni-CB[d] | 10.7 | 8.8 | 60 | 25 | 60~66 | 15 |
| 54 | U-Ni-CB[d] | 10 | 9.6 | 50 | 22 | 68~70 | 10 |
| 55 | U-Ni-CA[c] | 10.1[e] | 0.55 | 40 | 14 | 66~70 | 15 |
| 56 | U-Ni-CA[c] | 10.5[e] | 0.55 | 42 | 13 | 62~66 | 10 |
| 57 | U-Ni-CA[c] | 10.3[e] | 0.7 | 50 | 17 | 63~65 | 20 |
| 58 | U-Ni-CA[c] | 10[e] | 0.7 | 50 | 20 | 60~63 | 15 |
| 59 | U-Ni-CA[c] | 10[e] | | 60 | 26 | 61~65 | 10 |
| 510 | U-Ni-CA[d] | 10.2[e] | 0.6 | 52.5 | 20 | 62~64 | 10 |
| 511 | U-Ni-CA[d] | 9.8[e] | 0.5 | 42.5 | 24 | 58~60 | 30 |
| 512 | U-Ni-CA[d] | 10[e] | | 55 | 24 | 62~66 | 15 |
| 513 | U-Co-CB[c] | 10.5 | 8.5 | 60 | 20 | 60~62 | 35 |
| 514 | U-Co-CB[c] | 10.5 | 7.8 | 40 | 23 | 59~60 | 35 |
| 515 | U-Co-CB[d] | 10.6 | 3.4[f] | 60 | 20 | 62~66 | 35 |
| 516 | U-Co-CB[d] | 10.2 | 3.2[f] | 52 | 28 | 60~66 | 35 |
| 517 | U-Co-CA[c] | 10.7[e] | 1.1 | 55 | 22 | 60~64 | 30 |
| 518 | U-Co-CA[d] | 10.6[e] | 1.4 | 55.5 | 23 | 60~62 | 60[g] |
| 519 | U-Co-CA[c] | 10.4[e] | 1.4 | 37 | 22 | 59~62 | 80[g] |

Benzophenone, purified by a single vacuum distillation and then recrystallized twice from ethanol, was used.

a) Each catalyst was prepared so as to contain 1 g. of nickel or cobalt.
b) The figures were obtained by weighing the dried catalysts after use for reduction.
c) The precipitated metal was prepared at room temperature.
d) The precipitated metal was prepared under cooling with ice.
e) 0.5 ml. of 10% sodium hydroxide solution was added.
f) The precipitated cobalt was digested for 1.5 hr. under cooling with ice.
g) The major part of the catalyst proved to be deposited on the flange of copper packing after the reduction was finished. The reason was not clear, but the magnetic nature of this catalyst might be different from the other catalysts.

TABLE VI. REDUCTION WITH URUSHIBARA COPPER CATALYST

| Exp. No. | Catalyst[a] | pH[b] | Total weight of catalyst g.[c] | Initial press. kg./cm² | Initial temp., °C | React. temp. °C | Time min. |
|---|---|---|---|---|---|---|---|
| 61 | U-Cu | 10 | 2.2 | 40 | 16 | 100~118 | 40 |
| 62 | U-Cu | 9.5 | 2.4 | 53 | 24 | 110~120 | 65 |
| 63 | U-Cu-C | 10.3 | 4.2 | 50 | 28 | 110 | 10 |
| 64 | U-Cu-C | | 2.8 | 52.5 | 22 | 120~121 | 15 |

Benzophenone, purified by a single vacuum distillation and then recrystallized twice from ethanol, was used.

As a solvent 55 ml. of ethanol was used.

a) Each catalyst was prepared so as to contain 1 g. of copper.
b) 0.5 ml. of 10% sodium hydroxide solution was added.
c) The figures were obtained by weighing the dried catalyst after use for reduction.

As the apparent bulk of the U-Ni-A is much smaller than that of the U-Ni-B, the fine particles of the former may be easily dispersed into a solution by the up and down agitation employed in these experiments. However, the U-Ni-A prepared from nickel acetate was less active than the U-Ni-B prepared from the same salt (Exp. No. 314), and the reason is obscure. In alkaline solution the U-Co-A also gave better results than those obtained with the U-Co-B (Exp. Nos. 315, 316).

Reaction temperature, concentration of solution and quantity of catalyst are naturally expected to exert some influences on the rate of reduction. As a catalyst with high activity is not suitable for the purpose of this series of experiments, the U-Ni-A, which was specially prepared to have a lower activity, was used.

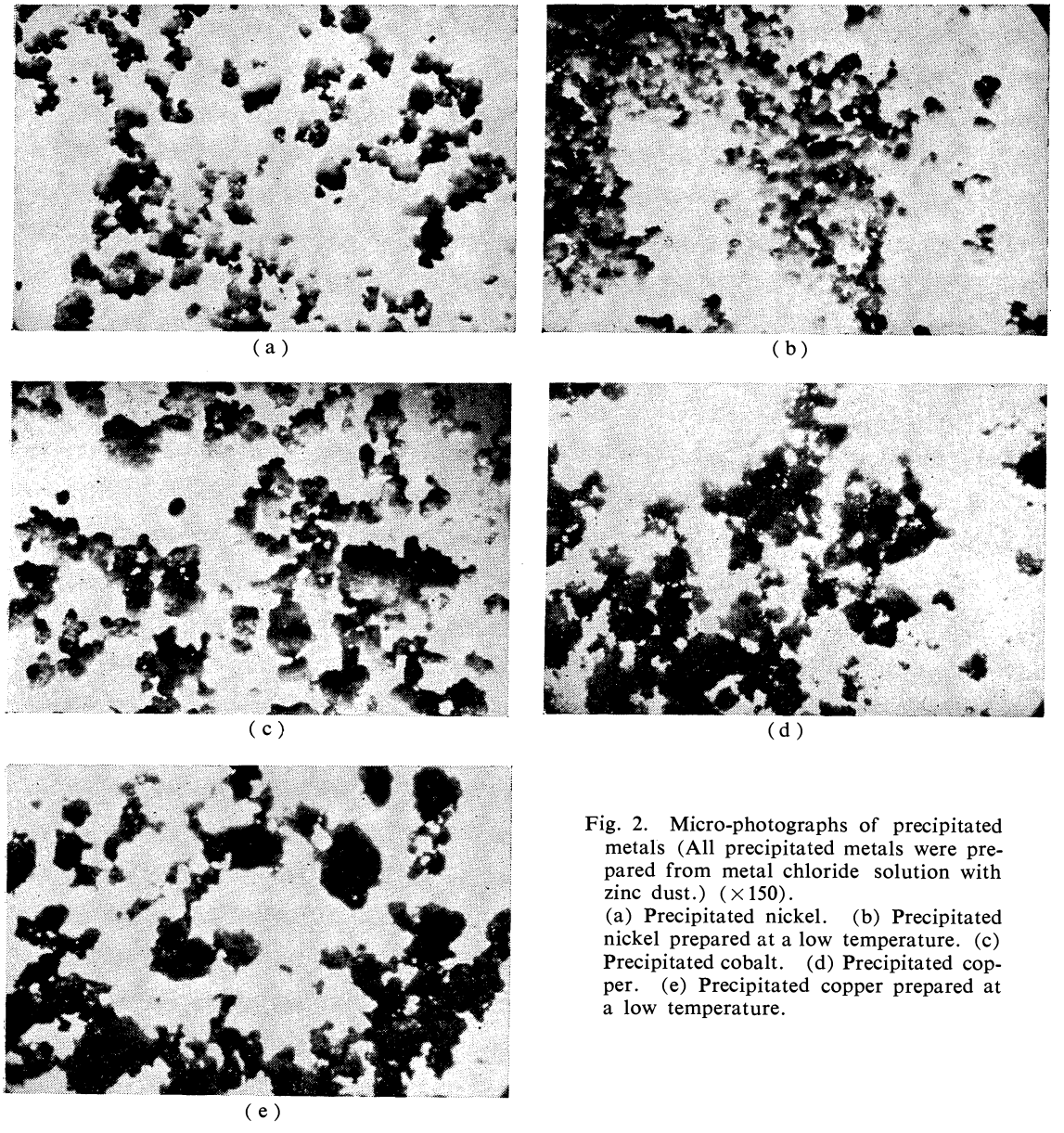



Fig. 2. Micro-photographs of precipitated metals (All precipitated metals were prepared from metal chloride solution with zinc dust.) (×150).
(a) Precipitated nickel. (b) Precipitated nickel prepared at a low temperature. (c) Precipitated cobalt. (d) Precipitated copper. (e) Precipitated copper prepared at a low temperature.

The results are listed in Table IV. To obtain a highly active U-Ni-A, the treatment of the precipitated nickel with diluted acetic acid should be continued until the solution acquires the green color of nickel ion. The U-Ni-A, used for these experiments, was prepared by interrupting the digestion before the solution was colored. The activity of this catalyst was considerably lower than that of the ordinary U-Ni-A. As shown in Table IV, the increment of either the concentration of solution or the amount of catalyst exerts a similar favorable effect on the reduction of benzophenone.

The first step of the preparation of Urushibara catalyst is to obtain precipitated metal by an ion exchange reaction. The so-called precipitated metal may consist of particles of metallic zinc covered with proper metal to be used as a catalyst, admixed with a quantity of zinc dust and zinc compounds. It can be said that the former is a true precipitated metal. Supposing that the size of the particles of a catalyst are decided mainly by those of the precipitated metal, it is necessary to prepare the fine particles of the precipitated metal for making the particles of catalyst to be fine. When a definite weight of zinc dust is used for preparing a definite weight of catalyst, the size of the particles of the precipitated metal may be decided by the size of the particles of

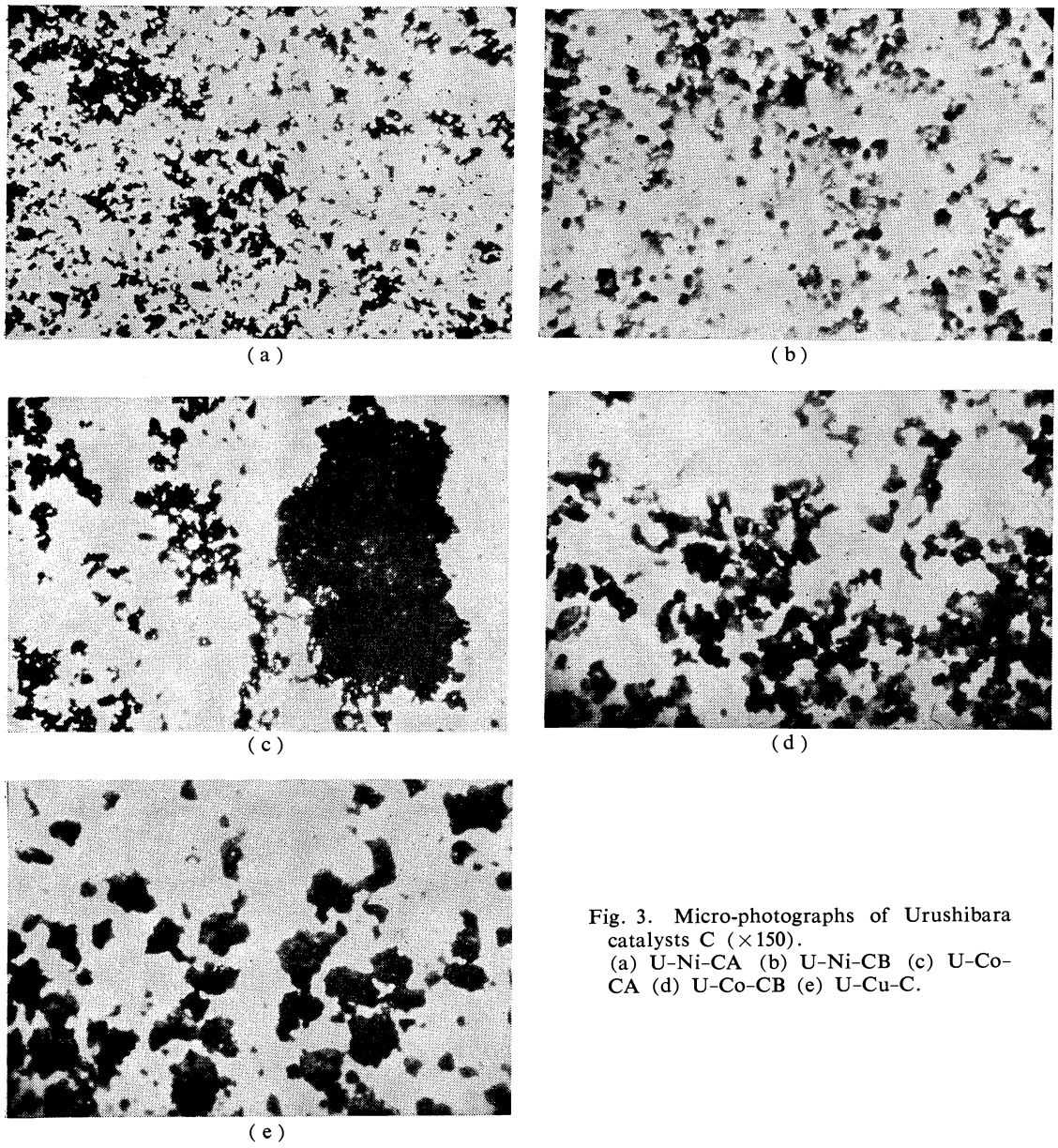


Fig. 3. Micro-photographs of Urushibara catalysts C (×150).
(a) U-Ni-CA (b) U-Ni-CB (c) U-Co-CA (d) U-Co-CB (e) U-Cu-C.

zinc dust and the rate of the ion exchange reaction. The rate of the ion exchange reaction may be affected by several factors, such as the difference of the standard electrode potential between zinc and the metal used to form a catalyst, the fineness of zinc dust, the concentration of the solution of metal chloride, the temperature and the efficiency of agitation when the precipitated metal is prepared. Of the above-mentioned factors, the size of the particles of zinc dust is difficult to change, so far as a commercially available product is used. The difference of the standard electrode potential is almost constant, and the improvement of the efficiency of agitation is limited to some extent. If the concentration of the solution of metal chloride is definite, only the temperature at which the ion exchange reaction is carried out can be freely varied. At a low temperature the ion exchange reaction occurs very slowly, and the influence of the efficiency of agitation can be minimized. Consequently, the metal may uniformly separate out on the surface of the particles of zinc dust and then fine particles of catalyst may be obtained (cf. micro-photographs, shown in Fig. 2).

Urushibara catalysts, thus prepared at a low temperature as described in the experimental part, are temporarily named Urushibara catalysts C and the abbreviations, such as U-Ni-CB,

U-Ni-CA, etc., are used. The results obtained with these catalysts are shown in Table V.

With the U-Ni-CB, better results were obtained than with the U-Ni-B. The dried U-Ni-CB is somewhat heavier in weight and more bulky than the U-Ni-B. The appearance of the U-Ni-CB resembles that of the U-Ni-B prepared from nickel acetate. A microphotograph (Fig. 3) shows that the size of the particles of this catalyst are somewhat smaller than that of the U-Ni-B, and that much zinc oxide remains undissolved. The U-Ni-CA was also proved to be effective, but somewhat longer time was necessary with this catalyst to finish the reduction than with the U-Ni-A. It is partly explained by the fact that the weight of the U-Ni-CA is about a half of that of the U-Ni-A. In the same manner, the U-Co-CB and the U-Co-CA were found to be superior to the corresponding ordinary cobalt catalyst.

To obtain a highly active Urushibara catalyst it has been claimed that the ion exchange reaction to obtain the precipitated metal should be carried out in a short time at a high temperature. Nevertheless, it was proved as mentioned above that the precipitated metal prepared in a long time at a low temperature gives an excellent catalyst. The X-ray diffraction of the U-Ni-CA gives a somewhat different pattern from that of the U-Ni-A, and it will be reported in another paper.

In Table VI the results obtained with copper catalyst are shown. As the precipitated copper does not react with 10% sodium hydroxide solution, only acid is a suitable reagent for treating the precipitated copper. The copper catalyst being considered not so active as a nickel catalyst for catalytic reduction, the condition of reduction was decided in consideration of the results obtained in Table IV. The results shown in Table VI are similar to those obtained with Raney copper[12]. Again, the U-Cu-C gave better results than those obtained with the ordinary U-Cu.

## Summary

High pressure reduction of benzophenone was examined with various Urushibara catalysts under various conditions. The purity of benzophenone, the concentration and pH of a solution, reaction temperature and quantity of the catalyst exerted considerable effects on the rate of reduction. Effective Urushibara catalysts were prepared from the precipitated metals which were obtained from the metal chlorides and zinc dust at a low temperature.

The author wishes to express his gratitude to Professor K. Hata for his helpful suggestions and encouragement throughout this work.

*Department of Chemistry*
*Faculty of Science*
*Tokyo Metropolitan University*
*Setagaya, Tokyo*

12) L. Faucounau, *Bull. soc. chim. France*, [5] 4, 58 (1937).

# *Formation of Cyclohexano[c]1, 2, 5-oxadiazole from 1, 2-Cyclohexanedione Dioxime. An Attempted Beckmann Rearrangement with Thionyl Chloride in Liquid Sulfur Dioxide*[1,2]

By Niichiro TOKURA, Ritsuro TADA and Kunio YOKOYAMA

(Received July 20, 1960)

It has already been shown by the present authors[2,3] and also by other writers[4] that the direction of the migratory aptitude in the Beckmann rearrangement was often changed by the circumstances, by the reagents or for other reasons. A transannular rearrangement was observed when 1, 6-cyclodecanedione dioxime was subjected to the rearrangement with thionyl chloride in place of sulfur trioxide in liquid sulfur dioxide[3].

1) The Beckmann rearrangement in liquid sulfur dioxide. Part VII.

2) Part VI; R. Tada, Y. Masubuchi and N. Tokura, This Bulletin, in press.

3) N. Tokura, R. Tada and K. Suzuki, ibid., 32, 654 (1959).

4) Y. Yukawa, "Jikken Kagaku Koza", Vol. 18, Maruzen, Tokyo (1958), p. 426; A. D. McLaren and R. E. Schat, *J. Org. Chem.*, 14, 254 (1959) : R. F. Brown, N. M. van Gulick and G. H. Schmid, *J. Am. Chem. Soc.*, 77, 1094 (1955) ; R. Huisgen, J. Witte and I. Ugi, *Ber.*, 90, 1844 (1957).

Tada, Masubuchi and Tokura[2] carried out the Beckmann rearrangement of the geometrical isomers of cyclohexyl phenyl ketoximes in liquid sulfur dioxide without any appreciable difference of the migratory aptitude by a variety of reagents at −70°C.

The Beckmann rearrangements of 1,2-diketone dioximes have scarcely been reported at all, but those of 1,2-diketone monoximes have been examined extensively to yield nitriles and carboxylic acid as the result of cleavage[5,6] of the dione monoximes. A number of trials of the Beckmann rearrangement on benzil dioximes have been reported since the turn of the last century[7-9] but the result were subjects of controversy[10] and the presence of geometrical isomers in the dioxime led the direction of the rearrangement to various products, for example, 3,5-diphenyl-1,2,4-oxadiazole, oxanilide and so on, among which the derivation of the 1,2,4-oxadiazole was ascribed to the Beckmann rearrangement of one of the two oximino groups, followed by dehydration. The reagents used were phosphorus pentachloride, phosphorus pentoxide, phosphoryl chloride and sulfuric acid. Of the three isomers, only the $\gamma$-isomer was reported to yield oxanilide, a product of the double Beckmann rearrangement, whereas the $\alpha$- and $\beta$-isomers gave the diphenyl-1,2,4-oxadiazole. Recently, Conley and Mikulski[6] have obtained the same oxadiazole with polyphosphoric acid as the reagent.

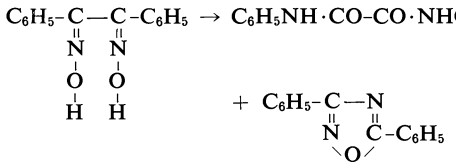


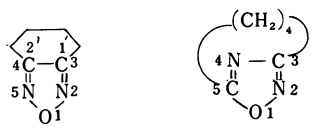
Chart 1.

The present paper describes the experiments which have been undertaken to throw light upon the nature and the migratory tendency of 1,2-cyclohexanedione dioxime in sulfur dioxide. The preparation of the 1,2-cyclohexane dioxime has been reported in a number of papers, of which the method of Belcher, Hoyle and West[11] has been adopted. This method, consisting in the oximation of 2-bromocyclohexanone (Ia), is essentially similar to that of Tokura and Oda[12] which was published earlier in 1943 and uses 2-chlorocyclohexane (Ib) as the starting material. The former method is however more convenient for laboratory work. To our regret, however, neither method was satisfactory enough to be a standard method of preparation owing to the formation of many resinous matters and unavoidable fluctuation in the yields.

1,2-Cyclohexanedione dioxime (II) was obtained in yields of 10~34% as crystals of m.p. 185~186°C (literature[11], 186~187°C), from which it was impossible further to separate the possible isomers by repeated crystallization or by repeated precipitation. Since the various reagents examined on this material have given no symptom of the geometrical isomers which will be reported in the following paper, the problem of the possible isomers was shelved in this project.

In this light of such a consideration, it is interesting to examine the direction of the Beckmann rearrangement, but contrary to expectation, the rearrangement was not caused by thionyl chloride in liquid sulfur dioxide. When thionyl chloride was used as the reagent, a low melting material III, m.p. 26°C, was obtained in a yield of 70% by ether extraction of the residue obtained on evaporation of sulfur dioxide from the reaction mixture. Although the elementary analysis was consistent with the anhydride of the dioxime II, there still remained another possibility of the presence of isomeric matters such as those produced by single and/or double rearrangement followed by dehydration. As cited above, benzil dioxime gave in such a case 3,4-diphenyl-1,2,4-oxadiazole and oxanilide, products of single and double rearrangement, respectively.

If the anhydride was formed by a simple dehydration without rearrangement, the structure must be a 1,2,5-oxadiazole derivative A, and not a 1,2,4-oxadiazole derivative B.



(A) (B)

The I.R. spectrum of III showed the characteristic absorption of a 1,2,5-oxadiazole (furazan)[13] at 1630 and 1588 $cm^{-1}$. This substance was very stable and resisted hydrolysis on refluxing with concentrated hydrochloric acid for 5 hr., with aqueous 25% caustic soda for 6.5 hr., with aqueous 40% sulfuric acid for 7 hr. and

5) D. Murakami and N. Tokura, This Bulletin, 31, 1044 (1958).
6) K. J. Conley and F. A. Mikulski, *J. Org. Chem.*, 24, 97 (1959).
7) K. Awers and V. Meyer, *Ber.*, 21, 810 (1888).
8) E. Beckmann and A. Koster, *Ann.*, 274, 18 (1893).
9) A. Günther, *Ber.*, 21, 517 (1888); *Ann.*, 257, 46 (1889).
10) J. Meisenheimer and W. Lamparter, *Ber.*, 57, 276 (1924).
11) R. Belcher, W. Hoyle and T. S. West, *J. Chem. Soc.*, 1958, 2743.
12) N. Tokura and R. Oda, *Sci. Papers Inst. Phys. Chem. Research (Tokyo)*, 22, 8501 (1943).
13) R. J. Gaughran et al., *J. Am. Chem. Soc.*, 76, 2233 (1954).

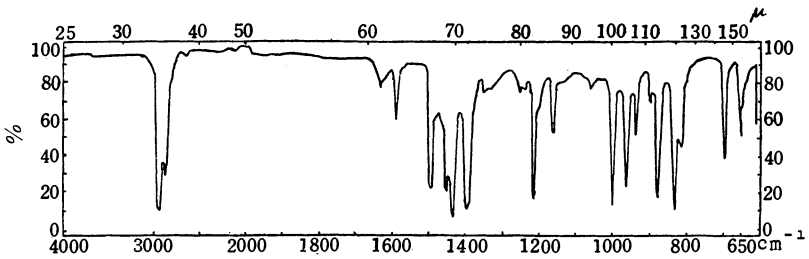



Fig. 1. I. R. spectrum of III.

heating with concentrated sulfuric acid for 5 hr. on a steam bath. Oxidation with chromic anhydride in acetic acid or with ozone in 50% acetic acid and reduction with tin and hydrochloric acid were all ended in the recovery of the starting compound. The compound underwent an oxidation only with potassium permanganate in dilute sulfuric acid to yield a dicarboxylic acid, $C_6H_6O_5N_2$, m. p. 147~148°C (decomp.), which showed no coloration with a nickel salt and is assigned to the structure of IVa. Another possible structure IVb is ruled out because the cleavage of this sort may be more difficult than the cleavage to afford IVa.

The exhaustive oxidation of the compound with the same oxidant gave a dicarboxylc acid, m. p. 178°C (decomp.), 1, 2, 5-oxadiazole-3, 4-dicarboxylic acid (V), (literature[14], m. p. 178°C), the structure being proved as V by elementary analysis and mixed melting point.

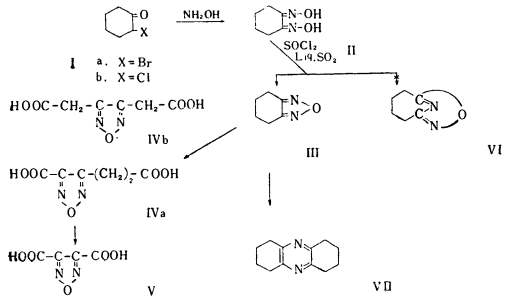



Chart 2.

Another evidence of structure III as the anhydride of the unrearranged dioxime was attained by reduction with sodium in ethanol. The use of lithium aluminum hydride was avoided because of the possible rearrangement[15] by this reagent. The reduction of III gave a basic compound, the analysis and the melting point corresponding to octahydrophenazine, $C_{12}H_{16}N_2$ (VII), m.p. 108~109°C, which was prepared by Wallach[17a], by Baumgarten and Bower[17b] and by Smith[16]. Wallach[17a] prepared the compound VII from II by reduction with zinc and alkali and a structure of decahydrophenazine was assigned, but recently[17b] it was found to be octahydrophenazine.

It was reported as early as in 1886 that 3, 4-diphenyl-1, 2, 5-oxadiazole[18] was synthesized from benzil dioxime by the reaction with potassium ferricyanide. The present authors have deviced a method of synthesis of compound III in a low yield by refluxing II in aqueous 10% sodium hydroxide. The coincidence of the melting point and the mixed melting point, and the I. R. spectra of the two materials confirmed the structure III unequivocally.

Thionyl chloride is one of the most powerful reagents to effect the Beckmann rearrangement. The failure of the rearrangement of II with thionyl chloride in liquid sulfur dioxide in contrast to benzil dioxime suggests some meaning. Benzil dioxime has presumably a coplanar structure favorable for a Beckmann rearrangement at least in one moiety of the molecule, whereas cyclohexanedione dioxime will prefer dehydration rather than a Beckmann rearrangement since it is sterically more restricted than benzil dioxime to build an intermediate azilinium cation[19] (aza-cyclopropenyl cation). In addition, the formation of the intermediate cation of benzil dioxime may be facilitated by the presence of phenyl ring participation in the rearrangement.

Gillis[20] recently reported that a cyclic sulfite derived from tetramethylene glycol and thionyl chloride gave tetrahydrofuran without stopping at the stage of a cyclic sulfone via the Bissinger rearrangement[21]. The formation of the anhydride III may likely proceed through cyclic sulfite IIa and sulfone IIIb (Chart 3).

14) L. Wolff, *Ber.*, **28**, 69 (1895): A. Quilico and M. Freri, *Gaz. chim. Ital.* **76**, 3 (1946), *Chem. Abstr.*, **41**, 382*d* (1947).
15) A. T. Blomquist, B. F. Hallam and A. D. Josey, *J. Am. Chem. Soc.*, **81**, 678 (1959).
16) P. A. S. Smith, ibid., **70**, 323 (1948).
17) a. A. Wallach, *Ann.*, **437**, 177 (1924); b. H. E. Baumgarten and F. A. Bower, *J. Am. Chem. Soc.*, **76**, 4561 (1954).
18) R. Koreff, *Ber.*, **19**, 176 (1886).
19) R. Huisgen, J. Witte and I. Ugi, *Ber.*, **90**, 1844 (1957).
20) R. G. Gillis, *J. Org. Chem.*, **25**, 651 (1960).
21) W. E. Bissinger, F. E. King and C. W. Hamilton, *J. Am. Chem. Soc.*, **70**, 3940 (1948).

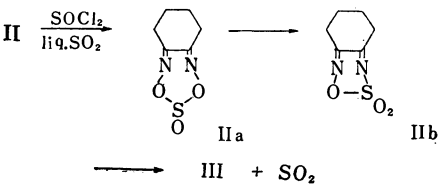



Chart 3.

A variety of products have also been obtained as the results of the attempted Beckmann rearrangement with some other reagents. The results will be reported elsewhere in near future.

## Experimental

**Material.**—Commercial sulfur dioxide was dried with concentrated sulfuric acid and distilled. A commercial thionyl chloride was redistilled.

**Apparatus and General Procedure.** — The procedure and manipulation for the Beckmann rearrangement were essentially the same as described earlier[1,2].

**1,2-Cyclohexanedione Dioxime (II).** — To a refluxed mixture of hydroxylamine hydrochloride (227 g.), sodium acetate (45 g.), methanol (400 ml.) and water (460 ml.) was added 128 g. of 2-bromocyclohexanone (Ia) gradually. After the mixture was refluxed for 45 min., it was condensed and diluted with water. The crystals were recrystallized from water, m. p. 186~187°C. Yield, 31 g. (34%).

Found: N, 19.66. Calcd. for $C_6H_{10}O_2N_2$: N, 19.71%.

**Reaction of II will Thionyl Chloride in Liquid Sulfur Dioxide.** — A mixture of the dioxime II (7.1 g.), thionyl chloride (13.0 g.) and 150 ml. of liquid sulfur dioxide was allowed to stand for an hour at room temperature. The solution was then poured into ice water, sulfur dioxide was evaporated and the residue was extracted with ether. The ether solution was washed with water, dried and condensed to give 5 g. (70%) of colorless crystals III, m. p. 26°C (recrystallized from ethanol), b. p. 99~101.5°C (13 mmHg). The substance was later identified as cyclohexano[c]1,2,5-oxadiazole.

Found: C, 58.19; H, 6.16; N, 22.10. Calcd. for $C_6H_8ON_2$: C, 58.05; H, 6.50; N, 22.57%. Mol. wt. Found: 139.5 (benzene). Calcd.: 124.

I. R. $\nu_{max}^{liq}$ 1588(m) (C=N-), and 2960(s), 2880(s) ($CH_2$=), $cm^{-1}$, U. V. $\lambda_{max}^{MeOH}$ 220 m$\mu$ ($\log \varepsilon = 3.56$). No significant amount of any other material was found in the residual solution after the ether extraction.

**Synthesis of III with Alkali.**—With 20 ml. of 10% aqueous sodium hydroxide, 3 g. of II was refluxed for 1.5 hr. The reaction mixture was extracted with ether. After the distillation of the ether, a small quantity of crystals was obtained as the residue. This was recrystallized from ethanol, m. p. 25.5~26.0°C, b. p. 180~196°C (18 mmHg), 0.3 g. (10%). This material showed no depression of melting point when mixed with III from II and thionyl chloride and gave an I. R. spectrum completely identical with that given by the specimen obtained from II and thionyl chloride.

**Oxidation of III with Potassium Permanganate.** —To 10 ml. of 10% aqueous solution of sulfuric acid was added 1.5 g. of III and the mixture was stirred and heated on a water bath. About 2.0 g. of potassium permanganate was added to the mixture bit by bit till the permanent red color remained. The precipitate of manganese dioxide was dissolved by introducing sulfur dioxide gas, and the mixture was extracted with ether, and the extract was condensed to give 1.3 g. (86.7%) of colorless fine crystals IVa, m. p. 147~148°C (decomp.) (from acetone-ligroin), IVa was soluble in hot water, alkali, alcohol and acetone, but insoluble in benzene.

Structure of 4-ethyl-1,2,5-oxadiazole-3,2'-dicarboxylic acid (IVa) was assigned.

Found: C, 38.08; H, 3.62; N, 14.78. Calcd. for $C_6H_6O_5N_2$: C, 38.72; H, 3.25; N, 15.02%. Acid value, Found: 628. Calcd. for 2-COOH: 617.0. I. R. $\nu_{max}^{KBr}$ 3400~3540 (-OH) and 1695 (>CO) $cm^{-1}$. White precipitates with $Ag^+$ and $Ba^{2+}$ ions. No red coloration with $Ni^{2+}$.

**Exhaustive Oxidation of IVa.** — A mixture of 0.5 g. of IVa, 1.0 g. of potassium permanganate and 10 ml. of 10% sulfuric acid was stirred and warmed for two days on a water bath. The precipitate of manganese dioxide was dissolved by passing sulfur dioxide gas. Extraction of the mixture with ether followed by condensing the ether solution yielded 0.1 g. of fine crystals V, m. p. 178°C (decomp.). (repeated recrystallization from alcohol.)

Found: N, 17.78. Calcd. for $C_4H_2O_5N_2$: N, 17.72%.

V was mixed with an authentic specimen of 1,2,5-oxadiazole-3,4-dicarboxylic acid prepared by the method of Wallach[17a] to show no melting point depression.

**Reduction of III with Sodium and Ethanol.**— To a solution of 2.0 g. of III in 100 ml. of ethanol was added 5 g. of metallic sodium with stirring. The mixture was further refluxed for 1.5 hr. and then a half of the ethanol was evaporated. The residual mixture was acidified with concentrated hydrochloric acid and was extracted with ether. Evaporation of the ether extract gave 0.4 g. of a product which was identified as the starting material III. The residual solution was again made alkaline with soda ash and the mixture was again extracted with ether. Evaporation of the ether extract gave colorless needles VII contaminated with a brown resinous matter. The needles sublimed at 60~80°C (15 mmHg). The needles were repeatedly recrystallized from ethanol to m. p. 108~109°C. Picrate, yellow needles, m. p. 155°C (decomp.).

Base: Found: C, 75.89; H, 8.10; N, 14.46. Calcd. for $C_{12}H_{16}N_2$: C, 76.55; H, 8.57; N, 14.88%. Picrate: Found: N, 16.83. Calcd. for $C_{18}H_{19}N_5O_7$: N, 16.78%.

The material VII was proved to be octahydrophenazine by admixing with an authentic sample prepared by reduction of II by the method of Wallach. No depression of the melting point[17a] was observed.

**Summary**

An attempted Beckmann rearrangement of 1, 2-cyclohexanedione dioxime with thionyl chloride in liquid sulfur dioxide resulted in the formation of cyclohexano [*c*] 1, 2, 5-oxadiazole in 70% yield. The structure of the oxadiazole was established by oxidation, reduction, and synthesis. The reason why the condensation was predominant over the rearrangement was discussed in comparison with the case of benzil dioxime.

The authors are indebted to the Befu Chemical Industries Co., for the donation of liquid sulfur dioxide.

*Research Institute of*
*Non-Aqueous Solutions*
*Tohoku University*
*Sendai*

# *A Synthesis of an Octahydrophenanthrene Derivative*[1]

By Takeshi MATSUMOTO and Akira SUZUKI

(Received August 22, 1960)

In the previous paper[2] synthesis of 2-methoxy-5-hydroxy-1-naphthylacetic acid and unsuccessful attempts to prepare therefrom 1, 2, 3, 4-tetrahydro-2-oxo-5-methoxy-1-naphthyl acetate (IIIb) were described. This paper reports a successful synthesis of the acetate IIIb from 5-methoxy-2-tetralone (I) and of a hydrophenanthrene derivative IX, a promising intermediate in the synthesis of certain diterpenoid skeletons, from IIIb.

The monoalkylation of $\beta$-tetralones had been in general difficult to achieve by direct alkylation since they tend to undergo partial or exclusive dialkylation[3]. However, the difficulty was recently overcome by the ingeneous procedure of Stork[4], which is concerned with alkylation of enamine derivatives of ketones with alkyl halides. In this study, the Stork method was adopted. The reaction of 5-methoxy-2-tetralone with pyrrolidine in boiling benzene afforded a previously undescribed enamine II, m. p. 78.5~79.5°C, in almost quantitative yield. II was then alkylated in benzene with ethyl bromoacetate and the intermediary ammonium salt was hydrolysed with water. Ethyl 1, 2, 3, 4-tetrahydro-2-oxo-5-methoxy-1-naphthyl acetate (IIIb), thus obtained in 74% yield, is a viscous liquid, boiling at 150~151°C (0.05 mmHg). Piperidine enamine of the methoxytetralone, on being treated in the same way, afforded a poor yield of IIIb. Hydrolysis of the ester IIIb with aqueous sodium hydroxide gave the acid IIIa, m. p. 172~173°C.

In hope of preparing a tricyclic $\alpha\beta$-unsaturated ketone V, the authors next examined the reaction of IIIb with 1-(*N*, *N*-diethylamino)-butan-3-one methiodide in benzene in the presence of potassium ethoxide. After chromatography on acid alumina, there could be isolated from the reaction mixture a compound $C_{19}H_{24}O_5$, m. p. 134~135°C, as the main product. The infrared spectrum (Fig. 1; nujol mull) of this compound exhibited absorption bands at 3400 (broad; OH), 1700 (six-membered ring ketone) 1735 and 1175 $cm^{-1}$ (ester). The authors supposed at this stage that they had ketol IV in hand. In several instances, the Robinson annelation reaction has been shown[5] to lead to intermediary ketol of type IV, which affords $\alpha\beta$-unsaturated ketone of type V by a $\beta$-elimination process. On treatment with isopropenyl acetate in the presence of *p*-toluenesulfonic acid, the ketol IV afforded an acetate

1) Approaches to the Synthesis of Diterpenoid Alkaloid Models, Part III. A portion of Ph. D. Dissertation (Hokkaido University) of Akira Suzuki. Read in part before the 12th Annual Meeting of the Chemical Society of Japan, Kyoto, April, 1959 and outlined in part in the preliminary communication; T. Matsumoto and A. Suzuki, This Bulletin, 33, 862 (1960).

2) T. Matsumoto and A. Suzuki, ibid., 32, 1283 (1959).

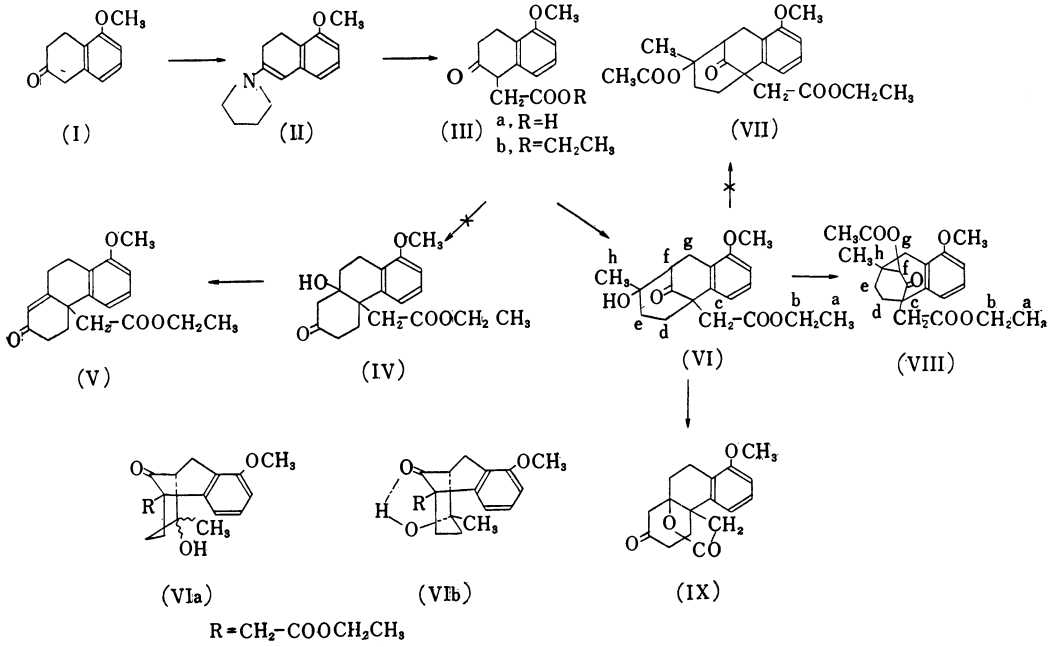
3) J. W. Cornforth, R. H. Cornforth and R. Robinson, *J. Chem. Soc.*, **1942**, 689; C. A. Grob and W. Jundt, *Helv. Chim. Acta*, **31**, 1691 (1948); J. W. Cornforth and R. Robinson, *J. Chem. Soc.*, **1946**, 676; J. D. Chanely, *J. Am. Chem. Soc.*, **70**, 244 (1948); M. D. Soffer, R. A. Stewart, J. C. Cavagnol, H. E. Gellerson and E. A. Bowler, ibid., **72**, 3704 (1950); G. Stork, ibid., **73**, 4748 (1951).

4) G. Stork, R. Terrell and J. Szmuszkovicz, ibid., **76**, 2024 (1954); E. D. Bergmann and R. Ikan, ibid., **78**, 1482 (1956); S. Hunig, E. Benzing and E. Lucke, *Ber.*, **90**, 2833 (1957).

5) C. Mannich, W. Koch and F. Borkowsky, ibid., **70**, 355 (1937); P. Wieland, H. Neberwasser, G. Anner and K. Misscher, *Helv. Chim. Acta*, **36**, 1231 (1953); C. Georgian, *Chem. & Ind.*, **1954**, 930; J. Colonge, J. Dreux and J. P. Kehlstadt, *Bull. soc. chim. France*, **1954**, 1404; G. Stork, ibid., **1955**, 256; F. J. McQuillin, *J. Chem. Soc.*, **1955**, 528; R. Howe and F. J. McQuillin, ibid., **1955**, 2423; W. S. Johnson, J. Ackerman. J. F. Eastham and H. A. Dewalt, Jr., *J. Am. Chem. Soc.*, **78**, 6302 (1956).

having a m. p. 97.5~98.5°C. Contrary to expectation, attempted pyrolytic elimination of acetic acid from the acetate to the $\alpha\beta$-unsaturated ketone did not occur, even though the reaction temperature was raised to 300°C.

Eventually, through the aid of N. M. R. spectroscopy, the ketol was shown to be actually a bridged ring compound VI. The N. M. R.



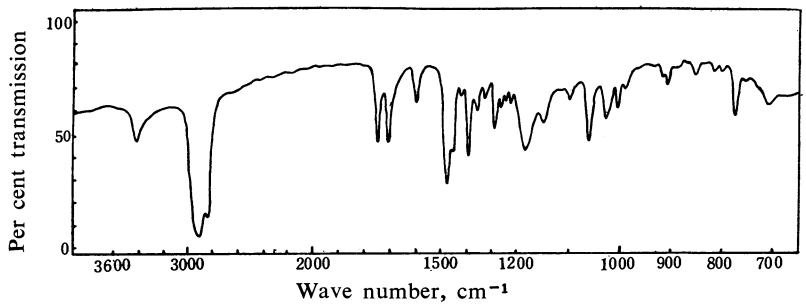




Fig. 1. Infrared spectrum of VI.

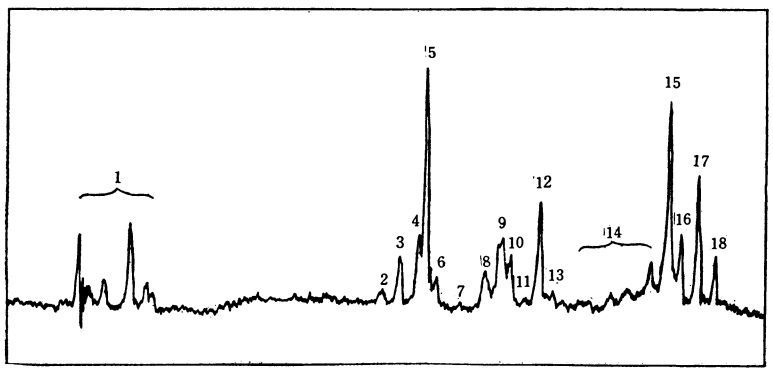



Fig. 2. N. M. R. spectrum of VI in $CDCl_3$

TABLE I. ASSIGNMENTS OF THE N. M. R. SPECTRUM OF VI

| Peak number in Fig. 2 | Chemical shift c. p. s. (stand. benzene) | Proton type | Number of protons | |
|---|---|---|---|---|
| | | | Calcd. for VI | Obs. from peak area |
| 1 | −21 | Aromatic H | 3 | 3.0 |
| 2, 3, 4, 6 | 100 | b-H | 2 | 2.5 |
| 5 | 105 | O-$CH_3$ | 3 | 2.9 |
| 8, 9, 10 | 136 | f, g-H and OH | 4 | 3.5 |
| 12 | 151 | c-H | 2 | 1.7 |
| 15 | 203 | h-H | 3 | 3.4 |
| 16, 17, 18 | 215 | a-H | 3 | 3.0 |
| 14 and others | | d, e-H | | |

spectrum[6] of the ketol (Fig. 2) showed one sharp maximum at a high applied magnetic field, characteristic of proton resonance for the $-\overset{|}{\underset{|}{C}}-CH_3$ group (203 c. p. s.; standard, benzene). This observation is clearly incompatible with structure IV, and the spectrum is completely accounted for in terms of structure VI (see Table I). A formula such as VIII and Xa would also explain the resonance line at 203 c. p. s., but would not give any explanation for the other lines. The formation of a bridged ketol system similar to VI through the Robinson annelation-reaction was first disclosed only quite recently by Johnson and his coworkers[7].

In order to elucidate the conformation the authors further examined the O-H stretching absorption band of the ketol in the 3300 $cm^{-1}$ region. The spectrum was measured in 0.0046 M[8] tetrachloroethylene solution[9] and as indicated in Fig. 3, was found to exhibit two bands at 3430 and 3590 $cm^{-1}$. The latter band corresponds to the vibration of aliphatic free OH group[10] while the former band may be attributed to OH group bonded to the carbonyl oxygen atom[11]. In structure VIa, in which the cyclohexanone ring takes a boat form, the hydroxyl group, be it either axial or equatorial, is unable to form an intramolecular hydrogen bond[12].

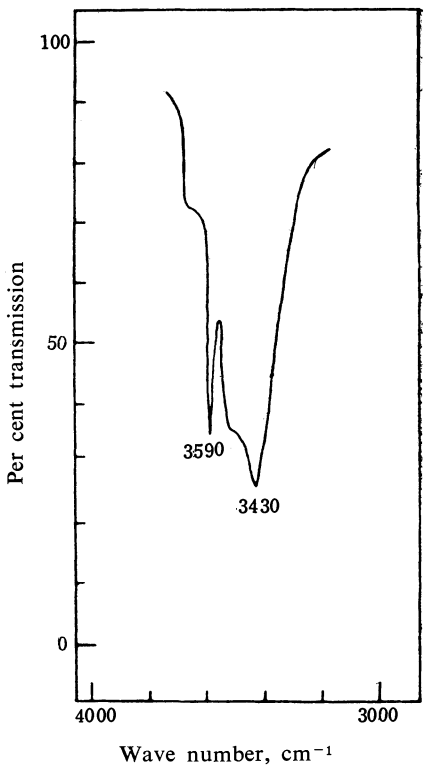



Fig. 3. ν O-H absorption of VI in tetrachloroethylene (0.0046 M).

The conformation VIb with chair cyclohexanone ring and axial OH group is the only one in which the formation of an intramolecular hydrogen bond is possible.

6) The N. M. R. spectra were taken on a Varian 40 MC instrument at the University of Illinois through the courtesy of Drs. Ben Shoulder and Masaji Ohno, to both of whom the authors are pleased to express their sincere thanks.

7) W. S. Johnson, J. J. Korst, R. A. Clement and J. Dutta, *J. Am. Chem. Soc.*, **82**, 614 (1960).

8) At this dilution the association of the solute molecule is neglegible. N. D. Coggeshall, *J. Chem. Phys.*, **18**, 978 (1958); F. A. Smith and E. C. Creitz, *J. Research Natl. Bur. Standards*, **46**, 145 (1951).

9) The infrared spectrum was taken with a Hilger H 800 infrared spectrophotometer with calcium fluoride optics. The authors wish to express their gratitude to Assistant Professor Sanjuro Matsushita and Miss Hisako Nakato of the Physical Chemistry Laboratory for the infrared spectral measurement. For the absence of interaction between hydroxyl group of solute and π-electrons of tetrachloroethylene, see L. L. Ingraham, J. Corse, G. F. Bailey and F. Stitt, *J. Am. Chem. Soc.*, **74**, 2297 (1952).

10) L. J. Bellamy, "The Infrared Spectra of Complex Molecules", Methuen and Co., Ltd., London (1958), p. 96.

11) In general, an intramolecularly bonded OH group exhibits a sharp band. The rather broad absorption band at 3430 $cm^{-1}$ might be caused by the overlapping of the absorption due to intramolecular hydrogen bond between the OH group and the ethoxy carbonyl oxygen atom (see formula VIb) and or by the rotatory isomerism of the hydroxyl group. For the latter effect, see R. Piccolini and S. Winstein, *Tetrahedron Letters*, No. 13, 4 (1959); M. Kahn, N. Lüttke and R. Mecke, *Z. anal. Chem.*, **170**, 106 (1959).

12) For example, L. Hunter, W. Klyne's "Progress in Stereochemistry", Vol. 1, Butterworths Scientific Publications, London (1954), p. 223.

TABLE II. ASSIGNMENTS OF THE N. M. R. OF VIII

| Peak number in Fig. 5 | Chemical shift c. p. s. (stand. benzene) | Proton type | Number of protons | |
|---|---|---|---|---|
| | | | Calcd. for VIII | Obs. from peak area |
| 1 | −22 | Aromatic H | 3 | 3.0 |
| 2, 3, 4, 6 | 100 | b-H | 2 | 2.2 |
| 5 | 104 | O-$CH_3$ | 3 | 2.9 |
| 8 | 129 | g-H | 2 | 1.8 |
| 9 | 138 | c-H | 2 | 1.7 |
| 11 | 178 | $COCH_3$ | 3 | 3.8* |
| 13 | 190 | h-H | 3 | 3.1 |
| 15, 16, 17 | 212 | a-H | 3 | 3.0 |
| 10, 12, 14 and others | | d and e-H | | |

* Absorption due to d and e-H may be overlapped.

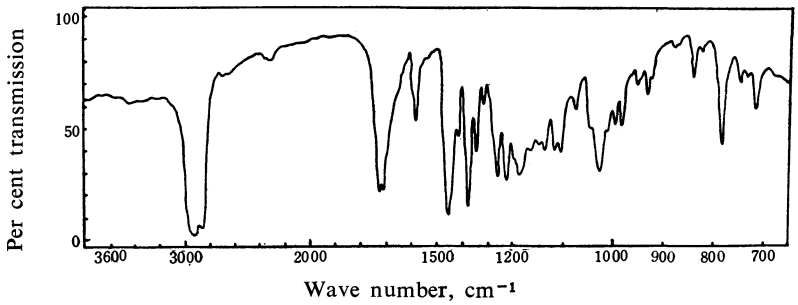



Fig. 4. Infrared spectrum of VIII.

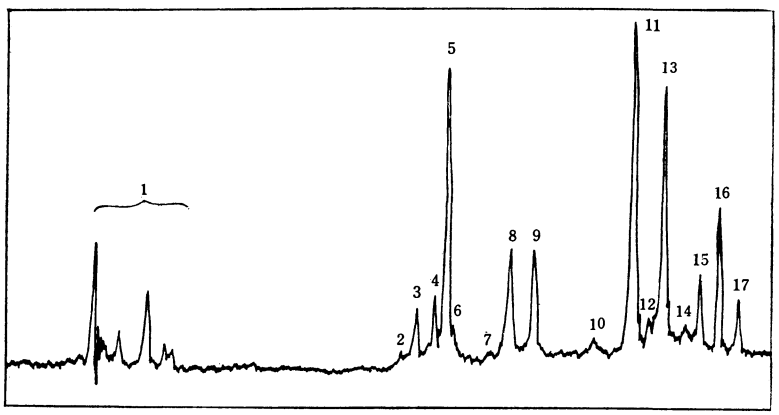



Fig. 5. N. M. R. spectrum of VIII in $CDCl_3$.

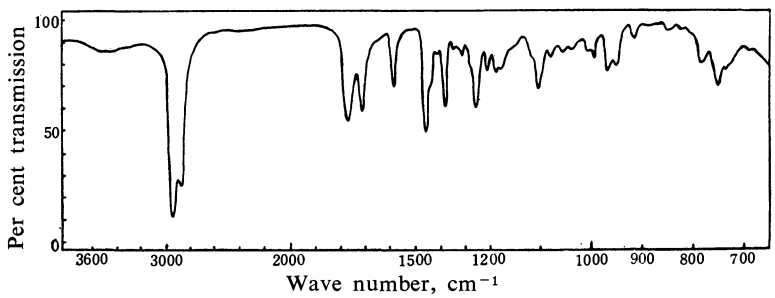
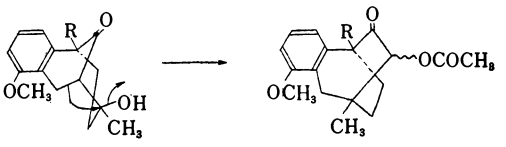



Fig. 6. Infrared spectrum of IX.

Next, examination was made of the structure of the acetylation product with m. p. 98.5°C (vide supra). The infrared spectrum (Fig. 4) of the acetate showed complete absence of hydroxyl function and presence of the following groups: saturated ester (1730 and 1175 $cm^{-1}$), acetate (1730 and 1230 $cm^{-1}$) and six-membered cyclic ketone (1715 $cm^{-1}$). Therefore a structural formula VII may be considered for this compound. Invalidity of this structure was however concluded from the N. M. R. spectrum, which is depicted in Fig. 5. The paramagnetic shift of the peak due to presence of $CH_3-\overset{|}{C}-$ protons to 190 c. p. s., disappearance of the peak at 151 c. p s. due to $-\overset{|}{C}-CH_2-CO_2$ protons and appearance of a new peak at 138 c. p. s. suggest a fundamental change in the framework of VI. The acetate may then be expressed by VIII, since an attack of proton upon the hydroxyl function of compound VIc would result in the formation of structure VIIIa through the well known 1, 2-shift as follows:




(VIc) (VIIIa)

R=$CH_2-COOCH_2CH_3$

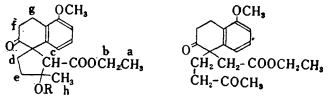
This structure is consistent with the N. M. R. spectrum; the interpretation of the spectrum in terms of formula VIII is summarized in Table II. The structure also explains the stability of the acetate to pyrolitic treatment, since in formula VIII elimination of an element of acetic acid would be impossible. Further, convincing evidences in favor of the formula VIII were provided by positive reactions with triphenyltetrazolium chloride and with the Tollens' reagent. On the basis of these findings the structure of the acetate may be concluded to be VIII[13].

Contrary to the case of acid treatment described above, treatment of VI with dilute aqueous alkali or with sodium ethoxide in ethanol, followed by acidification gave rize to a product $C_{17}H_{18}O_4$, to which a hydrophenanthrene structure IX was assigned on the basis of infrared (Fig. 6) and N. M. R. spectra. Although the product was amorphous and could not be crystallized by chromatography or by any other means, it was regarded homogeneous enough on the basis of the behavior in chromatography and of infrared spectrum. The infrared absorption spectrum showed complete absence of the hydroxyl group and presence of six-membered cyclic ketone (1720 $cm^{-1}$) and $\gamma$-lactone (1770 $cm^{-1}$). The formation of $\gamma$-lactone is impossible from the above mentioned skeletons VI and VIII and is possible only from the structure containing the hydrophenanthrene skeleton IX. The correctness of structure IX is further substantiated by the elemental analysis and by the N. M. R. spectrum. In the spectrum[14], the sharp maximum at high magnetic field characteristic for $-\overset{|}{C}-CH_3$ protons could not be recognized. This type of conversion from skeletons VI to IX by alkaline reagent has been recently described by Johnson and coworkers[7]. The authors were thus able to obtain an intermediate IX which seems to be promising for the synthesis of a certain diterpenoid skeleton.

## Experimental[15]

**Preparation of Pyrrolidine Enamine (II).** — A solution of 4.3 g. (0.0244 mol.) of 5-methoxy-2-tetralone, which was prepared from 2,5-dimethoxynaphthalene by the procedure of Cornforth and Robinson[16], and 3.5 g. (0.0488 mol.) of freshly distilled pyrrolidine in 40 ml. of dry benzene was refluxed on a water bath while water, distilled off as an azeotropic mixture with benzene, was separated with a Dean-Stark type apparatus[17]. The condensation reaction was completed after 3 hr. After removal of the solvent and excess pyrrolidine, the residue afforded a distillation under reduced pressure

13) In the preliminary report[1] a formula Xb was suggested as the structure of the acetate. The formation of the spirocyclic compound was explained through a reverse aldol condensation and a subsequent aldol condensation of an intermediary diketone XI. Peaks at 129 and 138 c. p. s. were interpreted to be attributable to f and g protons, although in general these four protons constitute an ABCD system and a rather simple absorption pattern as in Fig. 5 is not to be expected except in special cases.




(X) (XI)

a. R=H
b. R=COCH3

14) The spectrum was taken on a Varian 40 MC instrument at Tohoku University. The authors are very grateful to Professor Genjiro Hazato and his coworkers for the measurement.

15) All melting and boiling points are uncorrected. Unless otherwise specified, infrared spectra were taken in nujol mull on a Koken model DS-301 infrared spectrophotometer with sodium chloride optics. Ultraviolet spectra were measured in 95% ethanol or methanol solutions by means of a Beckmann model DK-2 spectrophotometer. The authors are indebted to Miss Noriko Fujino for microanalysis.

16) J. W. Cornforth and R. Robinson, *J. Chem. Soc.*, **1949**, 1861.

17) E. W. Dean and D. D. Stark, *Ind. Eng. Chem.*, **12**, 486 (1920); S. Natelson and S. Gottfried, *Org. Syntheses*, **23**, 37 (1943).

5.35 g. (95.5%) of a product, boiling at 159~160°C (0.09 mmHg). The enamine derivative II was a pale yellow viscous liquid, which crystallized on being allowed to stand. Recrystallization from petroleum ether yielded colorless prisms, m. p. 78.5~79.5°C.

$\nu_{max}^{nujol}$ [18] 1610, 1590 and 1565 $cm^{-1}$.

$\lambda_{max}^{MeOH}$ [18] 243 ($\varepsilon$ 13800) and 315 m$\mu$ ($\varepsilon$ 19300).

Found: C, 78.48; H, 8.21. Calcd. for $C_{15}H_{19}ON$: C, 78.56; H, 8.35%.

Piperidine enamine of 5-methoxy-2-tetralone was obtained under the same condition. The condensation of 5 g. (0.0284 mol.) of the tetralone with 5 g. (0.0588 mol.) of the amine in 30 ml. of dry benzene was complete in 3 hr.; yield 4.6 g. (67%), b. p. 135~140°C (0.001 mmHg).

Found: C, 79.16; H, 8.54. Calcd. for $C_{16}H_{21}ON$: C, 78.97; H, 8.70%.

**Ethyl 1,2,3,4-Tetrahydro-2-oxo-5-methoxy-1-naphthyl Acetate (IIIb).**—At room temperature and during 45 min., 3.9 g. of ethyl bromoacetate in 5 ml. of benzene was added to a solution of 5.3 g. of 3,4-dihydro-2-(*N*-pyrrolidyl)-5-methoxy naphthalene (II) in 10 ml. of benzene. After refluxing for 3 hr. on a water bath (ca. 70°C), the solution was cooled to room temperature and 20 ml. of water was added. The whole was vigorously stirred for one hour at room temperature and the organic layer was separated; the water layer was extracted twice with benzene. The combined organic layer was washed with water, dried over anhydrous sodium sulfate and distilled under reduced pressure; b. p. 150~151°C (0.05 mmHg.), colorless viscous liquid, yield 4.5 g. (74%).

$\nu_{max}^{film}$ 1725 (ketonic carbonyl) and 1735 $cm^{-1}$ (ester carbonyl).

Found: C, 68.36; H, 6.59. Calcd. for $C_{15}H_{18}O_4$: C, 68.68; H, 6.92%.

The keto ester IIIb was also prepared from the piperidine enamine derivative by the same procedure. The yield, however, was lower than the above case; there was obtained 2 g. (41%) of IIIb from 4.5 g. of the piperidine enamine and 3.1 g. of ethyl bromoacetate.

**Hydrolysis of the Ethyl Ester IIIb.**—A mixture of 300 mg. of IIIb, 3 ml. of 60% sodium hydroxide and 3 ml. of ethanol was heated on a water bath for one hour. The solution was then diluted with 5 ml. of water, acidified with 6 N hydrochloric acid and extracted with ethyl acetate three times. The combined extracts were washed with water and dried over anhydrous sodium sulfate. Removal of the solvent in vacuo left an oily pale brown residue, from which on trituration with ether, a crystalline material was obtained. For analysis the product was recrystallized from benzene to afford colorless prisms, m. p. 172~173°C.

$\nu_{max}^{nujol}$ 1695 (carboxylic carbonyl) and 1710 $cm^{-1}$ (ketonic carbonyl).

$\lambda_{max}^{MeOH}$ 271 ($\varepsilon$ 2200) and 278 m$\mu$ ($\varepsilon$ 2220).

Found: C, 66.77; H, 6.00. Calcd. for $C_{13}H_{14}O_4$: C, 66.65; H, 6.02%.

18) For the characteristic frequencies of enamine, see G. Opitz, H. Hellmann and H. W. Schubert, *Ann.*, 623, 112 (1959).

**Condensation of IIIb with 1-(*N*, *N*-Diethylamino)-butan-3-one Methiodide.** — Diethylaminobutanone (4.2 g.), prepared according to the Wilds and Shunk method[19] was swirled gently in a 200 ml. flask and cooled with ice during the addition of methyl iodide (4.2 g) in portions for 15 min. The swirling was regulated, so as to obtain crystalline methiodide as an even coating on the walls of the flask. When no more liquid remained, the flask was kept in ice for one hour. A solution of the keto ester IIIb (7 g.) in dry thiophen-free benzene (40 ml.) was added, air was expelled from the flask by dry nitrogen, and a solution of potassium (1.7 g.) in absolute ethanol (25 ml.) was added with ice cooling during 5 min. Swirling was continued until the methiodide had all dissolved (about one hour) and was replaced by a precipitate of potassium iodide. After it had been kept in ice for another hour, the mixture was heated gently for 30 min. An excess of 3 N sulfuric acid was then added and the nitrogen gas was stopped. After addition of enough water (60 ml.) to dissolve the potassium sulfate the benzene layer was separated and the aqueous layer extracted three times with ether. The united extracts were washed with water, cleared with a little sodium sulfate, and concentrated in vacuo to leave 3.5 g. of an oil which was chromatographed through a column of acid-washed alumina[20] (50 g.) packed and washed with benzene. The portions eluted with benzene-chloroform (volume ratio 1 : 1, 450 ml.) and with chloroform only (400 ml.) were viscous oils and gave no crystalline products. The fraction obtained by elution to a total of 450 ml. of ethanol, contained 1.8 g. (20.3%) of a solid, m. p. 124~130°C; recrystallization from ligroin yielded a pure sample of the bridged ring ketol VI as colorless prisms, m. p. 134~135°C.

$\lambda_{max}^{MeOH}$ 271 ($\varepsilon$ 1410) and 278 m$\mu$ ($\varepsilon$ 1310).

Found: C, 68.44; H, 7.10. Calcd. for $C_{19}H_{24}O_5$: C, 68.65; H, 7.28%.

The 2,4-dinitrophenylhydrazone of VI was crystallized from ethanol as orange needles and had m. p. 260°C (decomp.).

Found: C, 58.61; H, 5.43. Calcd. for $C_{25}H_{28}O_8N_4$: C, 58.58; H, 5.51%.

**Acetylation of the Ketol VI.**—A mixture of 300 mg. of VI, 6 mg. of *p*-toluenesulfonic acid and 3 ml. of isopropenyl acetate (Eastman) was heated on a water bath for 4 hr. After the acid was neutralized with a few drops of pyridine, the solution was concentrated in vacuo to leave a pale yellow brown oil, which on trituration with petroleum benzine completely crystallized; yield 300 mg. (89%), m. p. 77~85°C. Upon recrystallization from petroleum benzine, it formed colorless plates, m. p. 97.5~98.5°C.

Found: C, 67.10; H, 6.94. Calcd. for $C_{21}H_{26}O_6$: C, 67.36; H, 7.00%.

**Alkali Treatment of the Ketol VI.**—A mixture consisting of 300 mg. of VI, 35 mg. of sodium and 5 ml. of ethanol was refluxed on a water bath for 4 hr. and was then acidified with glacial acetic acid. After removal of most of the ethanol, the residue

19) A. L. Wilds and C. H. Shunk, *J. Am. Chem. Soc.*, 65, 471 (1943).

20) E. Lederer and M. Lederer. "Chromatography", Elsevier Publishing Company, Amsterdam (1954), p. 22.

was diluted with water and extracted with chloroform three times. The united extracts were washed with an aqueous solution saturated with sodium chloride, dried over anhydrous sodium sulfate and then concentrated in vacuo. There remained a pale brown oil which was chromatographed on acid-washed alumina[20] (ca. 30 g.) packed and washed with benzene. One hundred and six fractions were collected as in the following table.

| Fraction No. | Eluant | Residue |
|---|---|---|
| 1— 15 | Benzene-chloroform (1 : 1); 150 ml. | Colorless oil 24 mg. |
| 16— 36 | The same; 200ml. | Nil. |
| 37— 46 | Benzene-chloroform (1 : 2); 100 ml. | Colorless oil 8 mg. |
| 47— 51 | Benzene-chloroform (1 : 2); 100 ml. | Nil. |
| 52— 61 | Benzene-chloroform (1 : 3); 100 ml. | Colorless oil 10 mg. |
| 62— 71 | The same; 100ml. | Pale orange oil 7 mg. |
| 72— 91 | Chloroform, 200 ml. | Nil. |
| 92— 96 | Chloroform-ethanol (1 : 1); 50 ml. | Colorless oil 8 mg. |
| 97—101 | The same; 50 ml. | Colorless oil 120 mg. |
| 102—106 | The same; 50 ml. | Colorless oil 10 mg. |

Treatment of the fractions numbered 97 through 101 with ether-petroleum ether yielded an amorphous product which could not be turned into a crystalline substance by any means. The substance was however submitted to elemental, infrared and N. M. R. analysis.

Found: C, 70.64; H, 6.45. Calcd. for $C_{17}H_{18}O_4$: C, 71.31; H, 6.34%.

Infrared absorption spectrum is reproduced in Fig. 6.

## Summary

Ethyl 1, 2, 3, 4-tetrahydro-2-oxo-5-methoxy-1-naphthyl acetate (IIIb) has been synthesized. Condensation of IIIb with 1-diethylaminobutan-3-one methiodide afforded an anomalous product VI. Treatment of VI with isopropenyl acetate in the presence of *p*-toluenesulfonic acid gave rise to an acetate VIII, while on treatment with alkali and then with acid, a hydrophenanthrene lactone IX was obtained.

*Department of Chemistry*
*Faculty of Science*
*Hokkaido University*
*Sapporo*

# *Über die Kupfer-salze der ω-Aminosäure I. Zur Kenntnis des Kupfer-Glycins*

Von Ken-ichi TOMITA

(Eingegangen am 23. Juli, 1960)

Für die Kristallanalyse der Kupfer-Komplexe von ω-Aminosäuren haben wir den Kupfer-Glycin-Komplex als erste Stufe der Versuchsmaterialien ausgewählt und einige physikalisch-chemischen Versuche mit diesem Material unternommen, weil das Glycin einerseits die einfachste ω-Aminosäure und andererseits die einfachste α-Aminosäure ist.

Wenn das Cu-Ion mit verschiedenen ω-Aminosäuren einen Komplex bildet, ist es strukturchemisch sehr interessant zu sehen welche Rolle das Cu-Ion bei dieser Komplexbildung spielt und welche räumliche Konfiguration die um Cu-Ion koordinierte Gruppe hat. Überdies ist es weit bekannt, daß Kupfersalze der ω-Aminosäuren so häufig Kristallwasser enthält (z. B., daß Kupfer-salze von β-Alanin, Isoserin und γ-Aminobuttersäure jeder für sich sechs, drei und zwei Kristallwassermoleküle haben). Deshalb ist es von Bedeutung für Chemiker zu wissen wie das Kristallwassermolekül auf den Prozess der Kristallbildung und der geometrischen Anordnung der um das Cu-Ion koordinierten Atome wirkt.

Bei der Kristallstrukturbestimmung der ω-Aminosäuren selbst ist es uns auch sehr wichtig festzustellen, ob die "Schwer-atom" Methode in der röntgenographischen Kristallanalyse auch für die Kupfer-salze der ω-Aminosäuren gültig ist.

Neben dieser strukturchemischen Wichtigkeit gibt es auch noch andere biochemischen Gründe, warum wir die Kupfer-salze der ω-Aminosäuren als Versuchsmaterie gewählt haben: die verschiedenen ω-Aminosäuren wurden neuerdings in der Natur entdeckt und ihre physiologisch-chemischen Bedeutungen werden

mit grossem Interesse verfolgt. Ausserdem ist die Funktion der Cu-Ionen in den Tierkörpern sehr wichtig. Einige Beispiele dafür seien hier aufgeführt.

1) In dem Blut der Mollusken und Arthropoden findet sich Hämocyanin, welches aus einem Cu-Ion und dem Porphyrin bestehendes Farbstoffprotein ist.
2) Ferner gibt es unter den Metallproteiden einige Oxydationsenzyme mit einem Cu-Ion, z. B., Tyrosinase, Polyphenoloxydase und Ascorbinsäure-oxydase[1].
3) Wie aus der Bakteriologie bekannt, fördert das Cu-Ion die bakteriziden Wirkungen des N-haltigen Heilmittels, Isonicotinsäure-hydrazid (INH) gegen den Tuberkelbazillus[2].

### Darstellung des Kupfer-Glycins

Wenn man, wie bei der gewöhnlichen Darstellung[3] der Kupfersalze, eine wässerige Lösung von Glycin mit überschüssigem, gereinigtem Kupferhydroxyd im Wasserbad etwa 1 Stunde erhitzt und filtriert, so bekommt man eine tiefblaue Lösung. Um verschiedene Kristallisationen aus dieser Lösung zu erhalten, werden Ammonium-hydroxyd, Kohlensäure oder Methanol addiert; beim nachherigen Einengen des tiefblauen Filtrates scheidet sich daraus der Kupfer-Komplex entweder als tiefblauer, aus langer Nadel bestehender Kristall (Kristall I) oder als hellblauer pulveriger Kristall (Kristall II) ab.

a) Kristall I; tiefblaue, lange Nadel, die sich bei 213°C (unkorr.) zu verkohlen beginnt und sich bei 228°C unter Gasentwicklung zersetzt. Dieser Komplex enthält 1 Molekül Kristallwasser, das bei etwa 120°C nach 32 stündigem Erhitzen entweicht. Die Analyse gibt das folgende Resultat.
Gef. Cu, 28.12; C, 20.01; H, 4.39; N, 12.19; $H_2O$, 7.78. Ber. für $Cu(C_2H_4NO_2)_2+H_2O$(Mol. Gew. 229.54): Cu, 27.68; C, 20.91; H, 4.39; N, 12.19; $H_2O$, 7.84%.

b) Kristall II; hellblauer, pulveriger Kristall, der sich bei 222~225°C unter Gasentwicklung zersetzt. Aus den folgenden Analysendaten geht hervor, dass dieser Komplex 2 Moleküle Kristallwasser enthält, das nach 12 stündigem Erhitzen bei etwa 120°C grösstenteils entweicht. Gef. Cu, 27.67; C, 18.22; H, 4.36; N, 11.81; $H_2O$, 13.99. Ber. für $Cu(C_2H_4NO_2)_2+2H_2O$ (Mol. Gew. 247.54): Cu, 25.66; C, 19.39; H, 4.84; N, 11.31; $H_2O$, 14.54%.

Aus obiger Mikroanalyse bestätigt man dass das Kupfer-Glycin zwei Hydrate, nämlich Mono- und Di-hydrat, hat.

### Differential-thermoanalyse des Kupfer-Glycins

Um die Kristallwassermenge von Kristall I und II auf andere Weise zu bestimmen, wurde die Entwässerungswärme beobachtet, die in einem gewissen Verhältnis zur Kristallwassermenge steht.

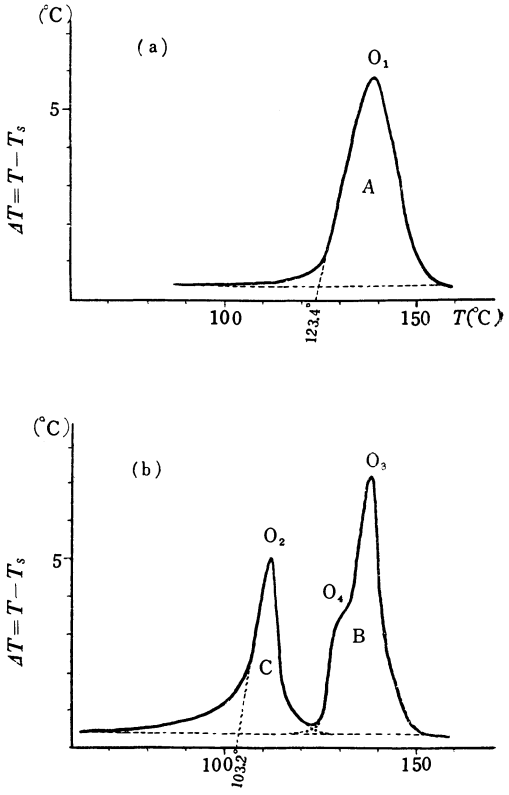



Abb. 1. Differential-thermoanalyse (DTA)-Kurven.
(a) Kupfer-Glycin-Monohydrat (Kristall I)
(b) Kupfer-Glycin-Dihydrat (Kristall II)
$T$: Temperatur von Normalsubstanz ($Al_2O_3$)
$T_s$: Temperatur von Versuchssubstanz.

Das Entweichen des Kristallwassers lässt sich leicht mit Hilfe der Differential-thermoanalyse (DTA) nachweisen und das Resultat wird in Abb. 1 gezeigt. Dabei gebrauchten wir $Al_2O_3$ als Normalsubstanz[4]. Bei dynamischem Erhitzen (z. B., 7.5°C/Min.) setzt die Reaktion für Kristall I bei $T=100$°C ein, durchläuft ein Maximum ($O_1$ in Abb. 1(a)) bei etwa $T=138$°C und klingt dann ab. Dieser endotherme Effekt wird durch die Entwässerung des 1 Molekülkristallwassers verursacht, welche durch die Messung der Verlustmenge von Kristallwasser nach der endothermen Reaktion bestätigt wird (Ber. 7.8%, Gef. 8.2%). Für Kristall II werden drei endotherme Reaktionen beobachtet, wie in Abb. 1(b) gezeigt, indem das erste Maximum

1) B. J. Ralph, *Rev. Pure and Appl. Chem.*, **4**, 85 (1954).
2) E. Sorkin, W. Roth und H. Erlenmeyer, *Helv. Chim. Acta*, **35**, 1736 (1952); J. Cymerman-Craig, G. N. Vaughan und D. Willis, *Nature*, **177**, 480 (1956).
3) E. Abderhalden und E. Schnitzler, *Z. physik. Chem.*, **163**, 96 (1927).
4) Über den automatischen Messungsapparat der Differential-thermoanalyse hat Herr H. Suga von unserem Institut eine baldige Veröffentlichung vorgesehen.

$O_2$ (Temperaturbereich von 80°C bis 120°C) durch die Bildung von Monohydrat (Verlustmenge: Ber. 6.5%, Gef. 7.8%) und das zweite Maximum $O_3$ durch das Entweichen von übrigem 1 Molekül-kristallwasser (Verlustmenge: Ber. 7.8%, Gef. 7.8%) verursacht wird.

Das Verhältnis der Entwässerungswärmemenge zwischen Kristall I und II wird wie dasselbe der Fläche zwischen Null-linie und DTA-Kurve beurteilt: d. h., das Verhältnis der Flächen zwischen A und B (Abb. 1(a) und 1(b)) ist ungefähr 1 : 1, dagegen ist das der Fläche zwischen A und C (Abb. 1(a) und 1(b)) ungefähr 1 : 0.58.

Daraus läßt sich ersehen, daß das erste Kristallwassermolekül von Kristall II leichter entwässert wird als das zweite Kristallwassermolekül von Kristall II. Die zwei Kristallwassermoleküle des Kupfer-Glycin-Dihydrates (Kristall II) unterscheiden sich voneinander durch ihre Verbindungsweise.

Es unterliegt also keinem Zweifel, daß es in Kupfer-Glycin-Komplexen zwei Hydrate gibt, nämlich Mono- und Di-hydrat.

Wie in Abb. 1 ersichtlich ist, ist die Entwässerungstemperatur für Kristall I (Maximum $O_1$) 123.4°C, und für Maximum $O_2$ des Kristall II 103.2°C. Für Maximum $O_3$ des Kristall II

TABELLE I. BEUGUNGSWINKEL UND NETZEBENENABSTÄNDE

| Kristall I vor Entwässerung | | Kristall I und II nach Entwässerung | | Kristall II vor Entwässerung | |
|---|---|---|---|---|---|
| $2\theta$ | $d$, Å | $2\theta$ | $d$, Å | $2\theta$ | $d$, Å |
| 10°30′ | 8,42 | 10°15′ | 8,62 | 12°00′ | 7,37 |
| 13 10 | 6,72 | 13 30 | 6,65 | 18 00 | 4,92 |
| 15 30 | 5,71 | 20 10 | 4,40 | 18 25 | 4,82 |
| 16 25 | 5,39 | 20 25 | 4,35 | 19 20 | 4,59 |
| 17 40 | 5,02 | 22 30 | 3,95 | 21 35 | 4,11 |
| 18 20 | 4,84 | 25 50 | 3,44 | 22 35 | 3,93 |
| 19 00 | 4,67 | 26 30 | 3,36 | 23 00 | 3,86 |
| 20 10 | 4,40 | 27 10 | 3,28 | 24 50 | 3,58 |
| 21 10 | 4,20 | 28 25 | 3,14 | 26 05 | 3,41 |
| 23 10 | 3,84 | 30 45 | 2,90 | 29 45 | 3,00 |
| 23 45 | 3,74 | 31 15 | 2,86 | 30 35 | 2,92 |
| 24 40 | 3,61 | 32 20 | 2,77 | 31 10 | 2,87 |
| 25 35 | 3,48 | 33 30 | 2,67 | 34 30 | 2,60 |
| 28 05 | 3,18 | 33 50 | 2,65 | 35 30 | 2,53 |
| 29 10 | 3,06 | 34 50 | 2,57 | 37 25 | 2,40 |
| 31 00 | 2,88 | 35 40 | 2,52 | 39 10 | 2,30 |
| 31 35 | 2,83 | 36 15 | 2,48 | 40 15 | 2,24 |
| 33 10 | 2,70 | 37 00 | 2,43 | 41 10 | 2,19 |
| 33 50 | 2,65 | 38 20 | 2,35 | 41 25 | 2,18 |
| 35 45 | 2,51 | 40 00 | 2,25 | 41 55 | 2,15 |
| 36 20 | 2,47 | 40 15 | 2,24 | 42 20 | 2,13 |
| 37 40 | 2,39 | 40 45 | 2,21 | 43 50 | 2,06 |
| 38 05 | 2,36 | 41 15 | 2,19 | 44 30 | 2,03 |
| 39 00 | 2,31 | 42 20 | 2,13 | 45 55 | 1,97 |
| 39 55 | 2,26 | 42 55 | 2,11 | 47 00 | 1,93 |
| 40 45 | 2,21 | 44 05 | 2,05 | 48 45 | 1,87 |
| 42 55 | 2,11 | 45 00 | 2,01 | 49 15 | 1,85 |
| 43 30 | 2,08 | 46 35 | 1,95 | 50 30 | 1,81 |
| 44 00 | 2,06 | 48 45 | 1,87 | 51 35 | 1,77 |
| 44 40 | 2,03 | 50 10 | 1,82 | 52 40 | 1,74 |
| 45 30 | 1,99 | 51 55 | 1,76 | 53 35 | 1,71 |
| 46 30 | 1,95 | 52 55 | 1,73 | 56 50 | 1,62 |
| 47 20 | 1,92 | 53 30 | 1,71 | 57 25 | 1,60 |
| 47 40 | 1,91 | 54 20 | 1,69 | | |
| 48 40 | 1,87 | 55 55 | 1,64 | | |
| 49 20 | 1,85 | | | | |
| 51 00 | 1,79 | | | | |
| 52 55 | 1,73 | | | | |
| 53 30 | 1,71 | | | | |

können wir aber die genaue Entwässerungstemperatur nicht festlegen, weil es noch ein anderes flaches Maximum $O_4$ zwischen 125°C und 130°C gibt, das vielleicht irgendeine Umwandlung im Kristall anzeigt.

### Röntgenographische Untersuchungen des Kupfer-Glycins nach Debye-Scherrer'scher Pulver-Methode

Von den röntgenographischen Untersuchungen der Kristalle I und II, und ihrer kristallwasserfreien Materie mußten wir uns auf die Debye-Scherrer'sche Pulver-Methode beschränken, weil es sehr schwierig war, einen Einkristall von Kristall II mit geeigneter Grösse zu bekommen. Bei dieser Untersuchung wurde die gewöhnliche zylindrische Kamera (Kameraradius: 50.6 mm) angewandt. Die Versuchsmaterien (Kristalle I und II) wurden

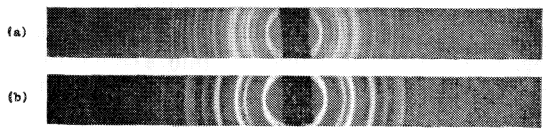



Abb. 2.
(a) Kupfer-Glycin-Monohydrat
(b) Kupfer-Glycin-Dihydrat

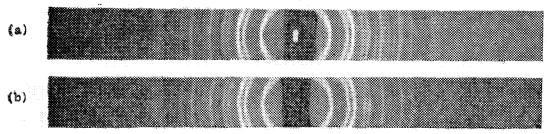



Abb. 3.
(a) Nach Entwässerung des Kristallwassers von Kupfer-Glycin-Monohydrat
(b) Nach Entwässerung des Kristallwassers von Kupfer-Glycin-Dihydrat

in die Glaskapillaren gepackt und nach Debye-Scherrer'scher Methode aufgenommen (Abb. 2). Nach etwa halb-stündigem Erhitzen bei 150°C im Vakuum wurden die Substanzen in diesen Kapillaren entwässert, sofort eingeschlossen und wieder photographiert. Abb. 3 zeigt die Debye-Scherrer'schen Aufnahmen nach Entzug des Kristallwassers.

Bei der Anwendung Norelco Diffraktometers (North American Philips Gesellschaft) wurden auch die Pulver-Diagramme von Kristallen I und II vor und nach Entwässerung erhalten und davon wurden die Beugungswinkel ($2\theta$) und die Netzebenenabstände ($d$) jeder Reflexion festgesetzt (Tabelle I).

Aus den obigen experimentalen Ergebnissen können die folgenden Schlussfolgerungen gezogen werden.

1) Die Kristallstrukturen der Kristalle I und II unterscheiden sich voneinander.
2) Bei der Entweichung des Kristallwassers zeigen die Debye-Scherrer'sche Aufnahmen von Kristallen I und II eine vollkommene Übereinstimmung, d. h., Kristalle I und II haben nach Entzug des Kristallwassers die gleiche Kristallstruktur.
3) Bei der Benutzung von Tabelle I und Hull-Davey-Harrington'schen Kurven[5] wurde vorausgesehen, daß Kristall I vor Entwässerung zu dem rhombischen System gehört, während Kristall II vor Entwässerung und Kristalle I und II nach Entzug des Kristallwassers nicht zu den vier Systemen (isometrischen, tetragonalen, hexagonalen, und rhombischen Systemen) gehören.

### Infrarotspektroskopische Untersuchungen des Kupfer-Glycins

Die Spektren wurden mittels eines Hilger H-800 Doppelstrahlspektrophotometers mit Kochsalz-optik bei Zimmertemperatur (23°C) untersucht. Die in Nujol (Messungsbereich von 650 $cm^{-1}$ bis 2000 $cm^{-1}$) oder Daifloil (Messungsbereich von 1500 $cm^{-1}$ bis 4500 $cm^{-1}$) suspendierten Substanzen von Kristallen I und II wurden benutzt (Abb. 4). Die Wellenzahlen jeder spektralen Lage von Kristallen I und II sind in der ersten und dritten Reihe von Tabelle II wiedergegeben.

Von S. Mizushima et al.[6] wurden infrarotspektroskopische Untersuchungen des Kupfer-

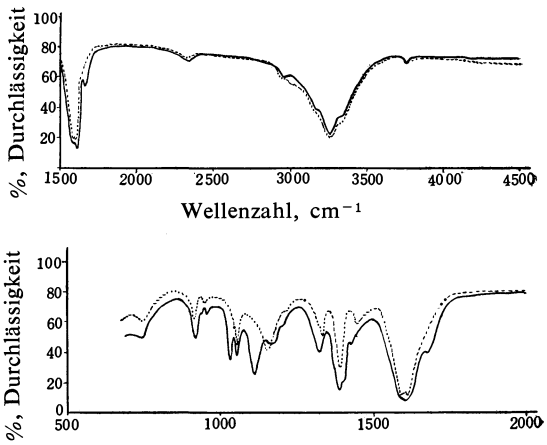



Abb 4. Infrarotabsorptionsspektren des Kupfer-Glycins.
—— : Kupfer-Glycin-Monohydrat (Kristall I).
------ : Kupfer-Glycin-Dihydrat (Kristall II).

5) J. C. Bell und A. E. Austin, „Battelle Indexing Charts for Diffraction Patterns of Tetragonal, Hexagonal and Orthorhombic Crystals", Battelle Memorial Institute, Columbus 1, Ohio, U. S. A.
6) D. N. Sen, S. Mizushima, C. Curran und J. V. Quagliano, *J. Am. Chem. Soc.*, 77, 211 (1955).

TABELLE II.

| Kupfer-Glycin-Monohydrat (Kristall I) Wellenzahl $cm^{-1}$ | Zuordnung nach K. Nakamura | Kupfer-Glycin-Dihydrat (Kristall II) Wellenzahl $cm^{-1}$ |
|---|---|---|
| 745 | COO-Scherenschwingung. | 745 |
| 924 | *sym.* C-N-Valenzschwingung+ | 917 |
| 935 | $CH_2$-Schaukelschwingung. | — |
| 959 | | 948 |
| 1036 | *antisym.* C-N-Valenzschwingung+ | — |
| 1057 | $NH_2$-Torsionsschwingung. | 1059 |
| 1118 | $NH_2$-Nickschwingung | — |
| — | | 1152 |
| 1167 | | — |
| 1179 | $CH_2$-Torsionsschwingung. | — |
| 1194 | | 1201 |
| 1323 | $CH_2$-Nickschwingung. | 1319 |
| — | | 1333 |
| 1391 | *sym.* COO-Valenzschwingung. | 1391 |
| 1403 | | — |
| 1424 | $CH_2$-Scherenschwingung. | 1435 |
| 1580 | | — |
| 1592 | *antisym.* COO-Valenzschwingung+ | 1590 |
| 1605 | $NH_2$-Scherenschwingung. | 1610 |
| 1672 | Scherenschwingung von Kristallwasser. | — |
| 2325 | | 2325 |
| 2935 | | 2935 |
| — | | 2980 |
| 3165 | | 3165 |
| 3254 | | 3254 |
| 3320 | | 3300 |
| 3754 | | 3754 |

Glycin-Monohydrates und Nickel-Glycin-Dihydrates durchgeführt. Ihre Messergebnisse über das Kupfer-Glycin-Monohydrat stimmen mit unserem Ergebnis des Kristall I überein.

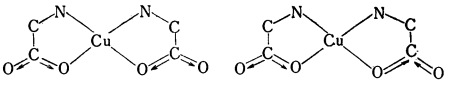
K. Nakamura[7] hat neulich die Isotopenverschiebungen der Infrarotspektren des Kupfer-Glycin-Monohydrates beim Substituieren des Wasserstoffs von Kristallwassermolekül und den $CH_2$- und $NH_2$-Gruppen des Glycinmoleküls durch das Deuterium untersucht und er hat die genauen Zuordnungen über jede Spektren ausgeführt, die in der zweiten Reihe von Tabelle II gezeigt werden.

Die Infrarotabsorptionsspektren von Kristall II sind etwas anders als Kristall I (vgl. Abb. 4 und Tabelle II).

Die infrarotspektroskopischen Unterschiede von Kristallen I und II beruhen, im allgemeinen gesagt, auf den Unterschieden der beiden Kristallsysteme, der Symmetrieeigenschaften von beiden Molekülen, der Zahlen des Kristallwassermoleküls, usw.

Ausgegangen nur von dem Unterschied der geometrischen Konfiguration von Molekül, d. h., cis und trans Konfiguration[8], muß sich deutlich dieser Unterschied in dem Band von symmetrischer COO-Valenzschwingung (Bereich : 1300 $\sim$1420 $cm^{-1}$) und in den Bändern von $NH_2$-Schaukelschwingung und COO-Deformationsschwingung (Bereich : 400$\sim$700 $cm^{-1}$, und diese Bänder können mit KBr-optik beobachtet werden) zeigen.

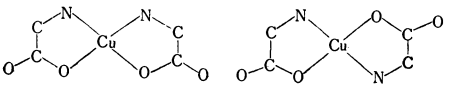
Bei der Benutzung unserer Messergebnisse über das Spektrum der symmetrischen COO-Valenzschwingung können wir den Unterschied der geometrischen Konfiguration von Kristallen I und II betrachten. Wenn das Kupfer-Glycin-Molekül eine cis oder trans Konfiguration hat, so gibt es folgende vier symmetrische COO-Valenzschwingungen :



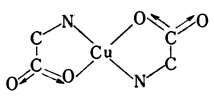
(I) (II)

7) K. Nakamura, *J. Chem. Soc. Japan, Pure Chem. Sec.* (*Nippon Kagaku Zasshi*), (in der Presse).

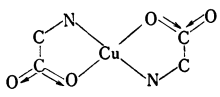
8) In diesem Fall bedeuten die cis und trans Konfigurationen den folgenden geometrischen Anordnungsunterschied der um zentrales Cu-Atom eben koordinierten N und O von zwei Glycin-Molekülen;



(cis) (trans)



(III)



(IV)

Während dabei (I), (II) und (IV) alle ultrarot-aktiv sind, ist aber (III) ultrarot-inaktiv. Es zeigt, dass der Kristall mit cis Konfiguration zwei symmetrische COO-Valenzschwingungen hat, während der Kristall mit trans Konfiguration nur einen Band hat.

Benutzt man diese Annahme auf Kristall I und II, so zeigt Kristall I zwei Spektren von symmetrischer COO-Valenzschwingung bei 1391 $cm^{-1}$ und 1403 $cm^{-1}$, während bei Kristall II nur ein Spektrum bei 1391 $cm^{-1}$ beobachtet wird. Demnach vermuten wir, dass Kristall I eine cis Konfiguration und Kristall II eine trans Konfiguration hat.

Rosenberg[9] hat schon beobachtet, dass der Unterschied zwischen cis und trans Konfiguration von Metall-Komplexen der verschiedenen Aminosäuren in den Infrarotabsorptionsspektren bei der Temperatur von flüssiger Luft (−170°C) in den Gebieten von 3$\mu$ und 6$\mu$ ($NH_2$-Valenzschwingungsband und antisymmetrischer COO-Valenzschwingungsband) erscheint. Aus unseren Messergebnissen konnten wir aber den Unterschied zwischen cis und trans Konfiguration in dieser Gebieten nicht feststellen, weil unsere Beobachtung nur bei Zimmertemperatur durchgeführt wurde und der gebrauchte Apparat kein genügendes Auflösungsvermögen hat, um die Differenz der Zahl der Spektren und die Verschiebung der Wellenzahl von cis und trans Konfigurationen in diesen breiten Bändern zu bestimmen.

## Schluss

Aus der obigen physikalisch-chemischen Untersuchung können wir die folgenden Schlüsse ziehen:

1) Bei Zimmertemperatur hat das Kupfer-Glycin zwei Hydrate, nämlich Mono- und Di-hydrat. Von diesen beiden ist das Kupfer-Glycin-Dihydrat (Kristall II), worüber bis heute keine Mitteilung erschien, ein neu gefundenes Hydrat.
2) Mit Hilfe der Differential-thermoanalyse findet sich, dass das Kupfer-Glycin-Monohydrat (Kristall I) eine endothermische Reaktion wegen der Entwässerung eines Kristallwassermoleküls zeigt, während die endothermischen Reaktionen des Kupfer-Glycin-Dihydrates (Kristalls II) drei Maxima haben, zwei davon durch die Entwässerungen von zwei Kristallwassermolekülen entstehen, und ein übriges Maximum vielleicht wegen irgendeiner Umwandlung im Kristall vorkommt. Die Entwässerungstemperaturen sind 123.4°C für Kristall I und 103.2°C für erstes Maximum von Kristall II, aber wir können die genauen Entwässerungstemperaturen für die zweite und dritte Maxima von Kristall II wegen der Überlappung der zwei Maxima nicht feststellen. Aus Kristall II wird das erste Kristallwassermolekül leichter entwässert als das zweite Kristallwassermolekül.
3) Das Kristallsystem des Kupfer-Glycin-Monohydrates (Kristalls I) gehört vor Entwässerung zu dem rhombischen System, das Kristallsystem des Kupfer-Glycin-Dihydrates (Kristalls II) ist aber vor Entzug des Kristallwassers noch nicht feststellbar. Nach Entwässerung haben diese beiden Kristalle die gleiche Kristallstruktur miteinander.
4) Von der infrarotspektroskopischen Untersuchung können wir vermuten, dass das Kupfer-Glycin-Monohydrat (Kristall I) eine cis Konfiguration hat, und das Kupfer-Glycin-Dihydrat (Kristall II) eine trans Konfiguration hat.
5) Aus der Tatsache des gleichzeitigen Entstehens zwei verschiedener Kristalle (Kristalle I und II) aus wässeriger Lösung wird vorausgesehen, dass die Differenz der freien Energie beider Hydrate also sehr klein ist und in wässeriger Lösung die zweierlei Komplexmoleküle (mit cis Konfiguration einerseits, und mit trans Konfiguration andererseits) vermutlich existieren.

Es scheint uns, dass die Strukturbestimmung dieser zwei Hydrate nicht nur zur Erweiterung der Kenntnis des geometrischen Verbindungszustandes des Glycin-Moleküls im Kristall, sondern auch zur Kenntnis der Wirkungsarten des Kristallwassermoleküls sehr wünschenswert ist.

Herrn Professor Dr. I. Nitta danke ich herzlichst für mannigfache Anregungen und seine Unterstützung bei der Durchführung dieser Arbeit, insbesondere für seine freundlichen Diskussionen. Mein Dank gilt auch Dr. Y. Sasada für seine hilfreichen Ratschläge bei der Durchführung dieser Arbeit. Zu danken habe ich ferner Dr. H. Suga für seine freundliche Mitwirkung bei Benutzung des Messungsapparates der Differential-thermoanalyse und den Herren T. Shiba, T. Inui und

9) A. Rosenberg, *Acta Chem. Scand.*, **10**, 840 (1956).

M. Okumiya und Fräulein K. Koike für ihre Messungen von Mikroanalyse und Infrarotspektren.

*Chemisches Institut*
*Naturwissenschaftliche Fakultät*
*Universität Osaka*
*Kita-ku, Osaka*

# *Über die Kupfer-salze der ω-Aminosäure. II. Über die Kristallstruktur des Kupfer-Glycin-Monohydrates*

Von Ken-ichi TOMITA und Isamu NITTA

(Eingegangen am 23 Juli, 1960)

Wie schon in Teil I gesagt[1], hat das Kupfer-Glycin zwei Hydrate, Mono- und Di-hydrat, die sich durch die Kristallstruktur unterscheiden. Während diese beiden Kristallstrukturen durch die röntgenographischen Untersuchungen bestimmt werden können, wurde zunächst das Kupfer-Glycin-Monohydrat (Kristall I in Teil I) als Strukturbestimmungsmaterie genommen, weil ein reiner Einkristall von Kupfer-Glycin-Dihydrat (Kristall II in Teil I) schwer zu bekommen war.

Vor kurzem erschien eine Mitteilung von Stosick[2,3], dass sowohl Nickel-Glycin-Dihydrat als auch Kupfer-*dl*-α-Aminobuttersäure eine plane trans Konfiguration haben. Schon vorher haben wir durch unsere infrarotspektroskopischen Untersuchungen[1] vermutet, daß das Kupfer-Glycin-Monohydrat eine plane cis Kofiguration und das Kupfer-Glycin-Dihydrat eine plane trans Konfiguration hat.

Im Anschluss daran haben wir die Kristallanalyse von Kupfer-Glycin-Monohydrat mit der röntgenographischen Methode unternommen, das Verhalten des Kristallfeldes um das zentrale Metallatom zu untersuchen, deren Ergebnisse im folgenden mitgeteilt werden.

## Experimentelles

Bei der gewöhnlichen Darstellungsmethode, wie schon in Teil I gesagt[1], konnte man der Kristall von Kupfer-Glycin-Monohydrat erhalten; die Grösse der angewandten Kristallnadeln bei der röntgenographischen Untersuchung ist ungefähr 0.2 mm × 0.2 mm × 0.6 mm. Mittelst der Oszillationsmethode, wobei die mit dünner Ni-Folie filtrierte Cu$K_\alpha$-Strahlung ($\lambda_{CuK\alpha}=1.542$ Å) gebraucht wurde, konnten die Gitterkonstanten dieses Kristalls wie folgt ausgemessen werden.

$$a=10.78\pm0.01\text{ Å}$$

$$b=5.208\pm0.004\text{ Å}$$

$$c=13.47\pm0.02\text{ Å}$$

Dabei wurden die genauen Werte der Gitterkonstanten nach der folgenden Methode bestimmt.

Bei der Benutzung des Norelco-Diffraktometers (von North American Philips Gesellschaft geliefert) haben wir zuerst die Beugungswinkel $2\theta_0$ von acht Reflexionen des pulverigen Silikon-Kristalls (normale Materie) beobachtet. Von dem Diagram des Winkels $2\theta_0$ versus $\Delta(2\theta)=2\theta_s-2\theta_0$, wobei Winkel $\theta_s$ den normalen Wert der Reflexion des Silikons (nach der Tabelle von Norelco-Gebrauchsanleitung) zeigt, wurde der Nullpunkt-fehler des Norelco-Diffraktometers mit der Methode der kleinsten Quadrate korrigiert. Zunächst wurden die Bragg-Winkel von acht Reflexionen des Kupfer-Glycin-Monohydrates beobachtet, die in dem Gebiet $10°<2\theta_0<20°$ erschienen, und nach der Berichtigung des Nullpunkt-fehlers, wie oben gesagt, wurden die genauen Werte der Gitterkonstanten mit der Methode der kleinsten Quadrate festgestellt.

Die Dichte dieses Kristalls beträgt nach einer Messung mittels der Schwebemethode (Äthylen-Dibromid/Benzol-Gemisch) bei 15°C 1.998 g/cc. Aus diesem Wert kann man annehmen, daß vier Moleküle von der Formel $Cu(C_2H_4NO_2)_2+H_2O$ in jedem Zellinhalt vorhanden sind (Die röntgenographishe Dichte dieses Kristalls beträgt 2.016 g/cc).

Die Auswertung der Weissenberg- und Sauter-Aufnahmen ergab folgende Auslöschungsgesetze:

($hkl$) in allen Ordnungen vorhanden,
($h00$), ($0k0$) und ($00l$) jeder für sich nur mit $h=2n$, $k=2n$ und $l=2n$ vorhanden.

Diese Auslöschungen kommen nur in der Raumgruppe $D_2^1$-$P2_12_12_1$ vor.

Mittels Äquator-Weissenberg-Aufnahmen um [010], [100] und Schwenkaufnahme um [001] mit Cu$K_\alpha$-Strahlung (Ni-Folie) werden die Intensitäten nach der „multiple-film method" aus vier Filmen im Vergleich zu einer Intensitätsskala geschätzt, und das Verhältnis der relativen Intensitäten von stärkster Reflexion zu schwächster Reflexion war ungefähr 3000 : 1 für ($h0l$) Zone, 1800 : 1 für ($0kl$) Zone, und 120 : 1 für ($hk0$) Zone. Unberücksichtigt

1) K. Tomita, Diese Zeitschrift, **34**, 280 (1961).
2) A. J. Stosick, *J. Am. Chem. Soc.*, **67**, 365 (1945).
3) A. J. Stosick, ebenda **67**, 362 (1945).

der Absorption und Extinktion wurden die Lorentz-Polarizationsfaktoren und die $(\sin\theta/\lambda)$-Werte für die einzelnen Reflexe mit der gewöhnlichen Weise ermittelt. Die totalen Zahlen der unabhängigen Äquator-Reflexionen, die in der Ausbreitungskugel enthalten sind, sind 190 für [010]-Projektion, 92 für [100]-Projektion und 74 für [001]-Projektion, während die beobachteten Zahlen jeder für sich 170, 75 und 26 sind.

## Strukturbestimmung

Es wurde eine Pattersonprojektion nach [010] gerechnet, die in Abb. 1 wiedergegeben ist. Eine „zugespitzte" („sharpened")[4] Synthese unter Verwendung „unitärer" Atomformamplituden wurde ausgeführt. Berücksichtigt man

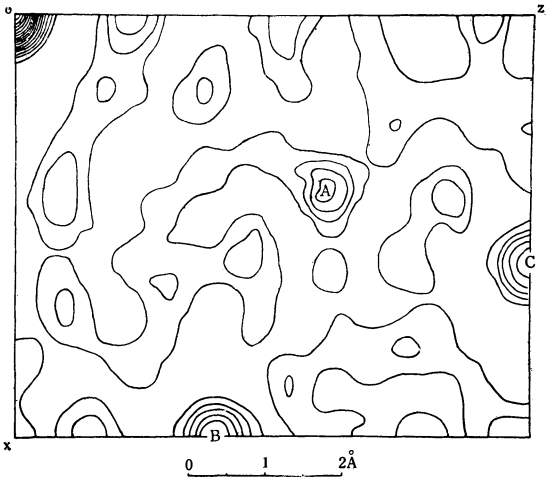



Abb. 1. „Zugespitzte" Pattersonprojektion nach [010].

die Raumgruppe und die Zahl der Formeleinheiten in der Elementarzelle von diesem Kristall, können alle Metallatome (Cu-Atome) eine allgemeine Lage in der Elementarzelle einnehmen. Aus den Maxima A, B und C in der Pattersonprojektion nach [010] kann aber der $x$- und $z$-Parameter des Kupferatoms leicht gefunden werden.

Raumgruppe $D_2^4$-$P2_12_12_1$ hat kein symmetrisches Zentrum im Kristall. Wird für jede Projektion dabei der Anfangspunkt auf der $2_1$-Achse aufgewährt, so steht dieser Anfangspunkt auf symmetrischem Zentrum in Projektion. Dann wurde eine vorläufige Fouriersynthese mit 87 $(h0l)$-Reflexen gerechnet (Abb. 2), und die Vorzeichen jedes Reflexes wurden von der mit Parameterswert des Cu-Atoms gerechneten Strukturfaktoren geführt. (Von den gebrauchten 87 Reflexen veränderten im

4) H. Lipson und W. Cochran, „The Determination of Crystal Structures", G. Bell & Sons, London (1953), S. 170.

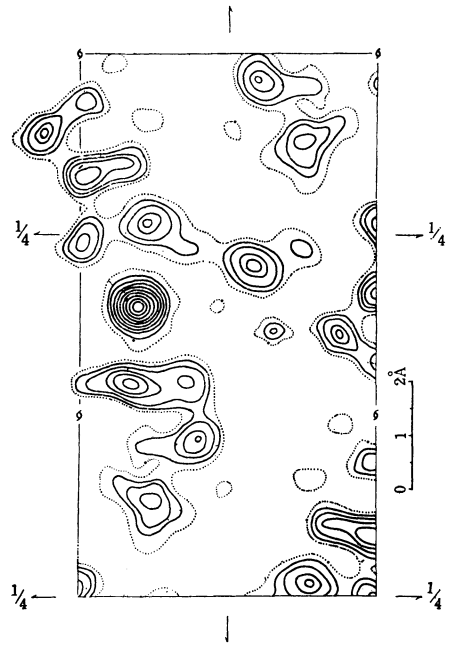



Abb. 2. Erste Fourierprojektion nach [010]. Es wurde die für die Kupferlagen berechneten Vorzeichen eingesetzt (Methode des schweren Atoms).

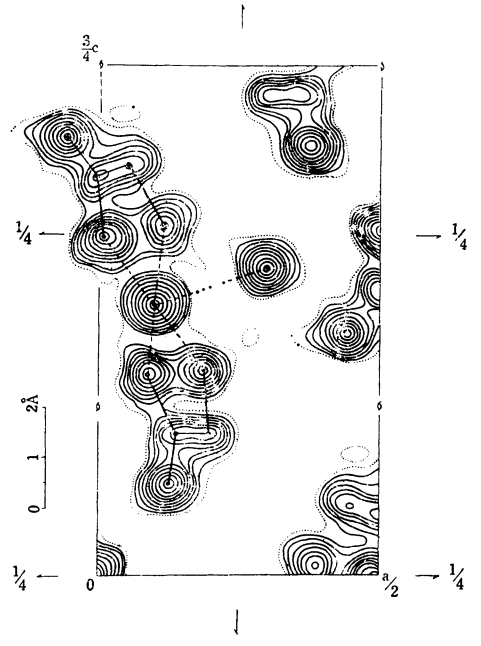



Abb. 3. Elektronendichteprojektion nach [010]. Das punktierte Niveau der Kurven geht durch $2\,e/Å^2$ und die Kurven gleicher Elektronendichte liegen um $1\,e/Å^2$ auseinander, ausgenommen in den Kupfermaxima, wo die Äquidistanz $5\,e/Å^2$ beträgt.

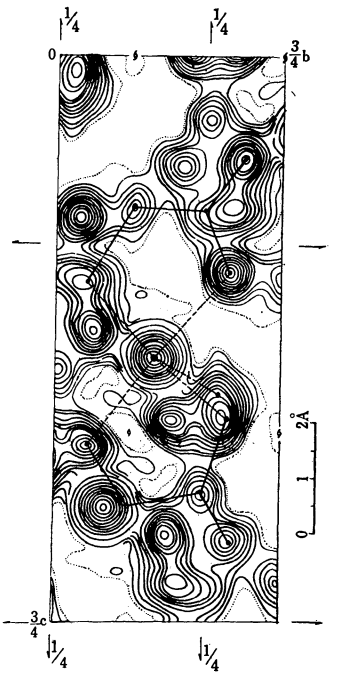


Abb. 4. Elektronendichteprojektion nach [100]. Das punktierte niedrigste Niveau der Kurven liegt bei $3\,e/Å^2$ und die Kurven gleicher Elektronendichte sind in Abständen von $1\,e/Å^2$ gezeichnet, von den Cu-Maxima abgesehen, wo diese Äquidistanz fünfmal grösser ist.

Vergleich zu den endgültigen $F_c$-Werten nur 7 Reflexe die Vorzeichen.)

Zur Berechnung der Strukturamplituden wurde die Atomstreukurve für Cu nach Berghuis et al.[5] gebraucht, die mit der genauen Berechnungsmethode gefunden wurde und im Vergleich zu den Werten von „Internationalen Tabellen„[6] bei weitem die besseren Werte zeigt. Für C, N und O benutzen wir die Atomstreukurven nach McWeeny[7].

Der $y$-Parameterswert des Kupferatoms kann auch mit der Pattersonsynthese nach [100] in gleicher Weise wie mit derselben nach [010] leicht gefunden werden. Die Parameterswerte von anderen leichten Atomen wurden schrittweise mit Fouriersynthese und sukzessiver Näherung („trial-and-error" method) gefunden und verfeinert, wie in Tabelle I gezeigt. Der Abbruchsfehler von Parameterswerten wurde im Vergleich von $F_0$- und $F_c$-Synthesen nach [010] und [100] korrigiert; dabei sind die Zahl und Vorzeichen der Reflexe von $F_0$- und $F_c$-Synthesen selbstverständlich gleich, und die Lagen der Maxima (Atome) von $F_0$- und $F_c$-Synthesen wurden nach Booth-Methode[8] gerechnet. Die letzten absoluten Fourierprojektionen nach [010] und [100] zeigen sich in Abb. 3 und 4, während die letzte absolute Fourierprojektion nach [001] nicht gezeigt wurde. Die isotropischen $B$-Werte nach [010], [100] und [001] betragen jeder für sich 3.0, 2.8 und 2.5. Werden die nicht beobachteten Reflexe berücksichtigt, so beträgt der Zuverlässigkeitsfaktor ($R=\Sigma||F_0|-|F_c||/\Sigma|F_0|$) 0.16 für [010]-Projektion und 0.17 für [100]-Projektion. Für [001]-Projektion wurde $R=0.17$ gerechnet; dabei wurden die aus dem Projektionen nach [010] und [100] gefundenen Parameterswerte und die beobachtbaren Reflexe benutzt. Die mit diesen endgültigen Parameterswerten (Tabelle I) berechneten $F_c$ und die beobachteten $F_0$ sind graphisch in Abb.

TABELLE I. PARAMETER

| Atomart | $x/a$ | $y/b$ | $z/c$ |
|---|---|---|---|
| Cu | 0.102 | 0.339 | 0.400 |
| $N^I$ | 0.185 | 0.110 | 0.302 |
| $N^{II}$ | 0.129 | 0.113 | 0.516 |
| $O_1^I$ | 0.083 | 0.572 | 0.290 |
| $O_2^I$ | 0.119 | 0.620 | 0.131 |
| $O_1^{II}$ | 0.016 | 0.572 | 0.490 |
| $O_2^{II}$ | −0.064 | 0.582 | 0.648 |
| $O_3$ | 0.292 | 0.538 | 0.450 |
| $C_1^I$ | 0.191 | 0.252 | 0.210 |
| $C_2^I$ | 0.126 | 0.494 | 0.211 |
| $C_1^{II}$ | 0.058 | 0.233 | 0.598 |
| $C_2^{II}$ | 0.004 | 0.487 | 0.578 |

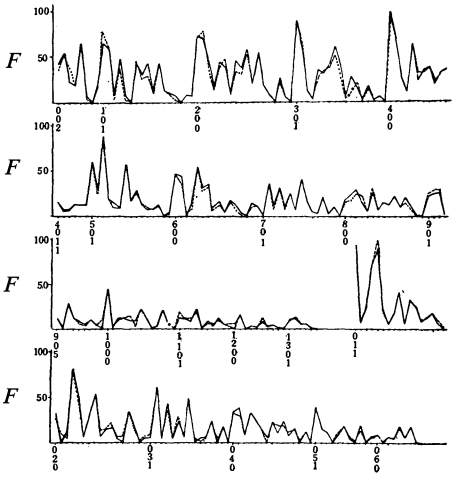


Abb. 5. Vergleich der beobachteten und berechneten $F$-Werte.
(——: $F_0$, ----: $F_c$)

5) J. Berghuis, I. M. Haanappel, M. Potters, B. O. Loopstra, C. H. MacGillavry und A. L. Veenendaal, *Acta Cryst.*, **8**, 478 (1955).

6) „Internationale Tabellen zur Bestimmung von Kristallstrukturen", Bornträger, Berlin (1935).

7) R. McWeeny, *Acta Cryst.*, **4**, 513 (1951).

8) A. D. Booth, "Fourier Technique in X-ray Organic Structure Analysis", Cambridge at the University Press (1948), S. 62.

5 zusammengestellt, wobei sich die $F_c$ auf vier Formeleinheiten in der Elementarzelle beziehen.

Zur Bestätigung der gefundenen Parameter wurde für jedes Atom und jede Bindungslänge noch mittlere Fehler nach Cruickshank[9] wie folgt gerechnet:

$\sigma(x) \fallingdotseq 0.005$ Å, $\sigma(y) \fallingdotseq 0.006$ Å,
$\sigma(z) \fallingdotseq 0.006$ Å für Cu,

$\sigma(x) \fallingdotseq 0.030$ Å, $\sigma(y) \fallingdotseq 0.025$ Å,
$\sigma(z) \fallingdotseq 0.030$ Å für N,

$\sigma(x) \fallingdotseq 0.025$ Å, $\sigma(y) \fallingdotseq 0.027$ Å,
$\sigma(z) \fallingdotseq 0.029$ Å für O,

$\sigma(x) \fallingdotseq 0.034$ Å, $\sigma(y) \fallingdotseq 0.043$ Å,
$\sigma(z) \fallingdotseq 0.043$ Å für C,

für Bindungslänge;

$\sigma(r) \fallingdotseq 0.03$ Å für Cu—N,
$\sigma(r) \fallingdotseq 0.03$ Å für Cu—O,
$\sigma(r) \fallingdotseq 0.06$ Å für N—C,
$\sigma(r) \fallingdotseq 0.06$ Å für C—C,
$\sigma(r) \fallingdotseq 0.05$ Å für C—O,
$\sigma(r) \fallingdotseq 0.04$ Å für O—O,
$\sigma(r) \fallingdotseq 0.04$ Å für N—O.

## Beschreibung der Struktur und Diskussion

Die Projektionen der Atomschwerpunkte nach [010] und [001] sind jeder für sich in Abb. 6 und 7 wiedergegeben. Die interatomaren Abstände und Bindungswinkel werden auch in Abb. 6 und 7 gezeigt.

Wie schon in Abb. 6 und 7 deutlich gezeigt, haben die um das zentrale Metallatom (Cu-Atom) koordinierten vier Atome der zwei Glycin-Molekülen (d. h., $O_1^I$, $O_1^{II}$, $N^I$ und $N^{II}$) in Beziehung auf dem zentralen Metallatom eine plane cis Konfiguration; das Kupfer-Glycin-Monohydrat hat eine andere Kristallstruktur als wie in Nickel-Glycin-Dihydrat, das eine plane trans Konfiguration hat.

Um das zentrale Metallatom wurde ein entstellter Oktaeder mit sechs Atomen, d. h., $O_1^I$, $O_1^{II}$, $N^I$, $N^{II}$, $O_3$ (ein Sauerstoffatom von Kristallwassermolekül) und $O_2^I$ (ein Sauerstoffatom der COO-Gruppe von einem anderen Salz, welches mit $2_1$-Achse zu dem zentralen Metallatom koordiniert wird) gebildet. In diesem entstellten Oktaeder gibt es eine intramolekulare Wasserstoffbindung zwischen $N^{II}$ und $O_3$ und damit wird $O_3$ Atom nach einem Glycin-Molekül (II) mehr oder weniger gezogen.

Von den infrarotspektroskopischen Untersuchungen haben schon Mizushima et al.[10] folgendes geschlossen: das Kupfer-Glycin-Monohydrat (Kristall I) hat wie Nickel-Glycin-Dihydrat eine plane trans Konfiguration, die mit *sp* Hybridisation geradlinig gebildet ist, und die Bindung zwischen COO-Gruppe von zwei Glycin-Molekülen und ein zentrales Metallatom (Cu-Atom) ist wesentlich eine Ionenbindung. Das Resultat unserer röntgenographischen Kristallanalyse stimmt aber nicht gänzlich mit ihrer Schlussfolgerung überein: das Kupfer-Glycin-Monohydrat hat eine um das zentrale Metallatom gebundene plane cis Konfiguration und deshalb können wir die Bindung zwischen der COO-Gruppe und dem zentralen Metallatom mit sp Hybridisation nicht anerkennen. Es scheint uns, dass diese, um das zentrale Metallatom gebildeten Bindungen auf $dsp^2$ oder $d^2sp^3$ Hybridisation beruhen, so daß ein planes Quadrat mit $O_1^I$, $O_1^{II}$, $N^I$ und $N^{II}$ gebildet wird.

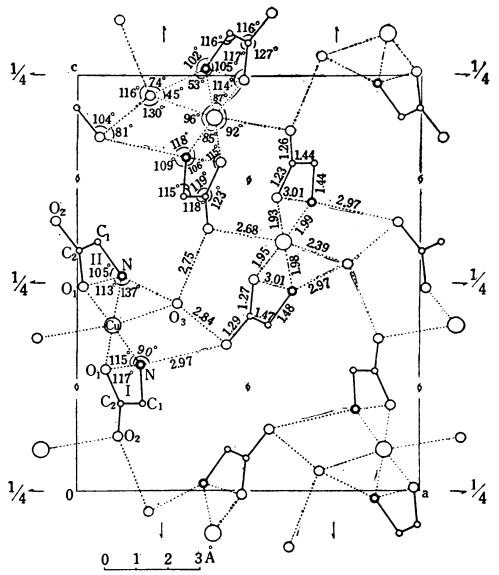



Abb. 6. Schematische Projektion der Atomschwerpunkte nach [010].

Die interatomaren Abstände von Cu—$O_3$ und Cu—$O_2^I$ weichen miteinander über die Grenze von mittlerem Fehler ab: dieser Unterschied wird vielleicht auf den folgenden Ursachen basieren, nämlich auf den Unterschied der molekularen Anordnungsweisen, der Ioneneigenschaften und der Zahlen der Wasserstoffbindung von $O_3$ und $O_2^I$, die jedes Sauerstoffatom ($O_3$ und $O_2^I$) bilden kann.

Wenn die Bildung von Cu—$O_1^I$ (oder Cu—$O_1^{II}$) wesentlich den Ionencharakter hat, soll sich diese Bindungslänge zwischen Cu und $O_1^I$ (oder $O_1^{II}$) im Vergleich zu der Kovalenzbindungslänge ziemlich verändern. Bis heute ist

9) D. W. J. Cruickshank, *Acta Cryst.*, **2**, 65 (1949).

10) D. N. Sen, S. Mizushima, C. Curran und J. V. Quagliano, *J. Am. Chem. Soc.*, **77**, 211 (1955).

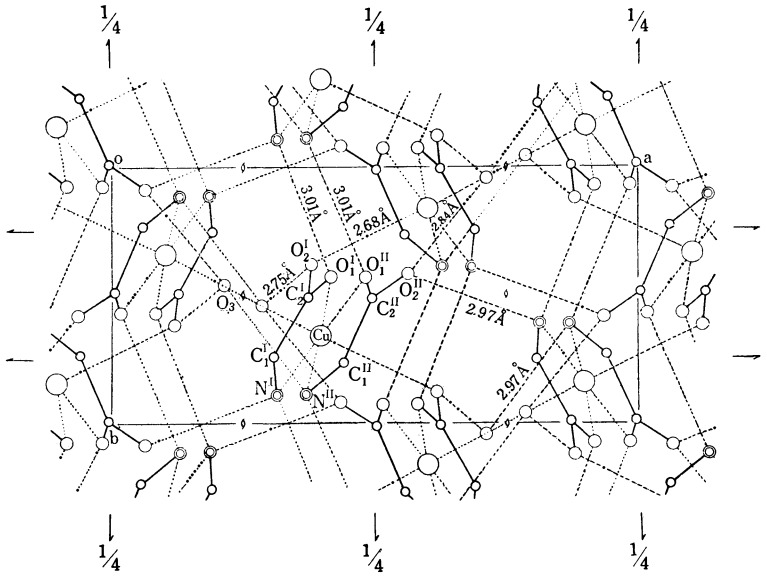



Abb. 7. Schematische Projektion der Atomschwerpunkte nach [001].

das genaue Resultat über den Ionenradius von $Cu^{2+}$-Ion noch nicht veröffentlicht geworden[11], und es ist undenkbar, dass das $Cu^{2+}$-Ion die vollkommende Kugel-Konfiguration hat, wenn sich das $Cu^{2+}$-Ion mit anderen Atomen im Kristall verbindet. Damit ist es unmöglich, den Unterschied zwischen Ionen- und Kovalenzradius über die Bindung von $Cu—O_1^I$ (oder $Cu—O_1^{II}$) zu vergleichen und die Menge des Ionencharakters von $Cu—O_1^I$ (oder $Cu—O_1^{II}$) Bindung zu bestimmen.

Werden auch die Verbindungsweise berücksichtigt, müssen sich die interatomaren Abstände von $Cu—O_1^I$ (oder $Cu—O_1^{II}$) und $Cu—N^I$ (oder $Cu—N^{II}$) sichtbar voneinander verändern, weil das Cu-Atom einerseits mit Stickstoffatom eine Kovalenzbindung oder Koordinationsbindung bildet und andererseits mit Sauerstoffatom von COO-Gruppe zum Teil eine Ionenbindung und zum Teil eine Kovalenzbindung bildet. Wir konnten aber den Unterschied von diesen beiden Bindungslängen nicht erklären, weil der Unterschied von beiden beobachteten Abständen weniger als die Grenze von einem mittlerem Fehler war.

Wie in Abb. 6 und 7 gezeigt, formiert der zentrale Cu-Atom mit $O_2^I$ von einem anderem Molekül die $Cu—O_2^I$-Bindung und das Molekül von Kupfer-Glycin-Monohydrat bildet mit der $2_1$-Operation die unendliche spiralförmige Konfiguration nach der *c*-Achse, wobei zwei N—H···O Wasserstoffbindungen ($N^I—H\cdots O_1^I$ und $N^{II}—H\cdots O_1^{II}$) die Bindungskraft nach der *c*-Richtung verstärken. Die intermolekularen Bindungskräfte nach *a*- und *b*-Richtungen werden mit verschiedenen Wasserstoffbindungen (N—H···O und O—H···O) zusammengesetzt.

Während dem, das Kupfer-Glycin-Monohydrat eine plane cis Konfiguration hat, was von uns festgestellt worden ist, können wir aber noch nicht bestätigen, welche Kristallstruktur das Kupfer-Glycin-Dihydrat hat. Obgleich wir den Schluss gezogen haben, daß das Kupfer-Glycin-Dihydrat (Kristall II von Teil I) der Analogie der Kristallstruktur des Nickel-Glycin-Dihydrates nach und aus dem Resultat der infrarotspektroskopischen Untersuchung von Teil I eine plane trans Konfiguration mit zwei N und zwei O von Glycin-Molekülen hat, kann man aber nicht bestimmen, ob die zwei Kristallwassermoleküle einander mit gleicher Bindungsweise zu dem zentralen Metallatom koordinieren oder nicht. Wie aus DTA-Kurve von Teil I festgestellt, entwässert sich ein Kristallwassermolekül (Maximum $O_2$ in Abb. 1 von Teil I) leichter als ein anderes Kristallwassermolekül (Maximum $O_3$ in Abb. 1 von Teil I), so daß die Bindungsweise von beiden Kristallwassermolekülen nicht gleich ist: d. h., in dem Fall des Kupfer-Glycin-Dihydrates (Kristall II von Teil I) ist es also undenkbar, daß die zwei Kristallwassermoleküle mit der gleichen Bindungsweise koordiniert sind. Aus den Tatsachen, daß die Entwässerungswärme von Maximum $O_1$ (von Kupfer-Glycin-Monohydrat) in DTA-Kurve mit derselben von

11) V. M. Goldschmidt, *Nature*, **157**, 192 (1949).

Maximum $O_3$ (von Kupfer-Glycin-Dihydrat) ungefähr gleich ist und die beiden Entwässerungstemperaturen voneinander ähnlich sind, kann man vermuten, daß das eine Kristallwassermolekül des Kupfer-Glycin-Dihydrates in seiner Bindungsweise dem Kristallwassermolekül des Kupfer-Glycin-Monohydrates ähnlich ist und das ein übriges Kristallwassermolekül des Kupfer-Glycin-Dihydrates mit einer anderen schwächeren Bindungskraft gebunden ist.

In Teil I haben wir schon bestimmt, daß das Kupfer-Glycin-Monohydrat (Kristall I von Teil I) und das Kupfer-Glycin-Dihydrat (Kristall II von Teil I) nach Entweichung des Kristallwassers eine vollkommen gleiche Kristallstruktur zeigt. Die Kristallstrukturen dieses Anhydrates und des Dihydrates sind noch nicht festgestellt. Berücksichtigt man aber das Resultat der DTA-Kurve von Teil I, so kann man vermuten, daß nach Entwässerung von erstem Wassermolekül der Kristall II eine Umwandlung von planer trans Konfiguration nach planer cis Konfiguration beginnt und nach dem Durchgang von Maximum $O_4$ in DTA-Kurve eine plane cis Konfiguration hat, so daß die Kristalle I und II bei dem Zustand von Anhydrat eine gleiche Kristallstruktur haben.

Herrn Professor Dr. T. Watanabe danken wir herzlichst für mannigfache Anregungen bei der Durchführung dieser Arbeit. Sei auch dabei Herrn Dr. Y. Sasada für seinen hilfreichen Rat gedankt.

*Chemisches Institut*
*Naturwissenchaftlche Fakultät*
*Universität Osaka*
*Kita-ku, Osaka*

# SHORT COMMUNICATIONS

## *Electron Spin Resonance and Electronic Absorption Spectra of the Radical Anions of Pyridine and Acridine*

By Keiji KUWATA, Teiichiro OGAWA and Kozo HIROTA

(Received December 20, 1960)

Recently a number of radical anions of aromatic hydrocarbons have been studied[1-3] extensively and their electronic structures have been elucidated to some extent. As for anions of conjugated heterocyclic compounds, however, the phenazine anion was the only one studied hitherto[4]. It seems to be interesting, therefore, to study the electronic structures of anions of heterocyclic compounds, giving special attention to hyperfine interaction between unpaired electron spins and nuclear moments of heteroatoms, and to compare the results with those of aromatic hydrocarbons. In the present communication a study on the anions of pyridine and acridine is reported briefly. The method of preparation of the anions was the same as reported in the previous paper[3]; that

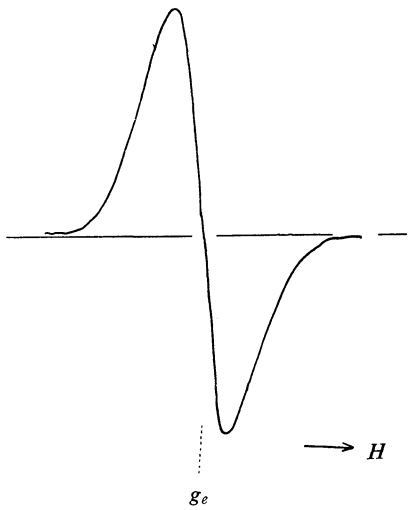



Fig. 1. ESR spectrum of the THF solution of the adduct of pyridine with sodium ($H_{msl}$= 10 gauss).

1) D. E. Paul, D. Lipkin and S. I. Weissman *J. Am. Chem. Soc.*, **78**, 116 (1956); T. R. Tuttle, Jr. and S. I. Weissman, ibid., **80**, 5342 (1958).
2) G. J. Hoijtinks and W. P. Wiyland, *Molecular Physics*, **1**, 231 (1958).
3) K. Morigaki, K. Kuwata and K. Hirota, This Bulletin, **33**, 952, 958 (1960); K. Kuwata, K. Morigaki and K. Hirota, ibid., **32**, 895 (1959).
4) Y. Fellion and J. Uebersfeld, *J. Arch. Sci.*, Geneve, **10**, 95 (1957); cf. D. J. E. Ingram, "Free Radicals as Studied by Electron Spin Resonance", Butterworths Scientific Publication, London (1955), p. 167.

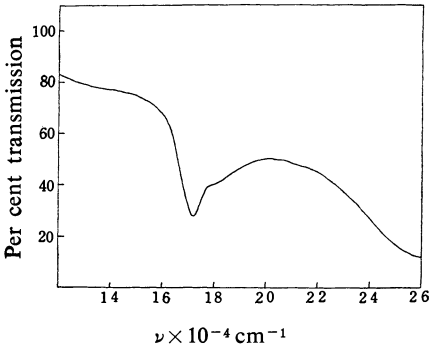



Fig. 2. Absorption spectrum for the THF solution of the adduct of pyridine with sodium.

is to say, all the procedures were carried out in an extremely evacuated system.

On heating pyridine with metallic sodium in tetrahydrofuran solution, a brownish yellow solution was obtained after evolution of a definite amount of gas[5]. This solution exhibited an ESR spectrum of a broad singlet as shown in Fig. 1. On continuing the procedure a red solution was obtained. Its absorption spectrum in the visible region is shown in Fig. 2, and the ESR spectrum obtained in this reaction stage was the same as that obtained in the early stage.

In the case of acridine a red solution of diamagnetic adduct was formed at the early stage of the reaction with sodium. The color of the solution changed to blue on heating it with sodium, and the ESR spectrum of a broad singlet was observed, the *g*-facter and the line width ($H_{msl}$) of which were 2.003 and 13 gauss, respectively.

In the previous investigation on the reaction of pyridine with alkali metals[6], formation of "sodium bipyridyl" was proposed on the basis of the results of chemical analysis of its decomposition product. However, according to our experiment described above, it is highly probable that radical anions of pyridine and also of acridine were formed.

Further studies will be published elsewhere.

The authors wish to express their sincere thanks to Professor M. Nakagawa of Osaka University for his helpful discussions.

*Department of Chemistry*
*Faculty of Science*
*Osaka University*
*Kita-ku, Osaka*

5) In the case of dimethoxyethane solution, a main part of the gas evolved was methane which may be formed from decomposition of the solvent.

6) B. Emmert, *Ber.*, **50**, 31 (1917).

## *Selectivity in Radiation-Induced Crosslinking and Scission of Polyvinyl Alcohol (PVA)*

By Yutaka HIRANO and Ayao AMEMIYA

(Received December 17, 1960)

The chemical structure of radiation-induced crosslinking of PVA irradiated in aqueous solution was supposed to be of 1, 2-glycol type and/or $\alpha$-oxy ketone type[1].

We studied the mechanism of scission and/or crosslinking of irradiated PVA. The samples were either dry or swollen with water, when irradiated.

We found a certain selectivity in scission and crosslinking in PVA. The samples were exposed to radiation from a cobalt-60 gamma source in air or in vacuo up to $10^8$ rad. at several temperatures and intensities.

We observed the influence of oxidation by periodic acid ($HIO_4$) upon the limiting viscosity number of irradiated PVA and, in particular, its variation with radiation dose.

In our experiments, the limiting viscosity number of PVA decreased with the increase in radiation dose. As shown in Fig. 1, there is a difference in the results between dry samples and swollen ones.

It should be noted that the limiting viscosity number after oxidation of dry samples is quite independent of radiation dose and agrees with the value of the sample, oxidized but not irradiated. But swollen samples show a different behavior of the limiting viscosity number after oxidation which definitely increases with radiation dose.

These results are inconsistent with the assumption of random scission and crosslinking, on which current theories[2,3] are based.

We are forced to conclude as follows: Only special types of bonds such as of 1, 2-glycol type which exists initially in usual samples[4], can be fractured selectively in either dry or swollen samples. Also, bonds formed by crosslinking in dry samples are definitely of the special types that are susceptible to oxidation by periodic acid. But in swollen samples we have at least two kinds of bonds formed by crosslinking, one susceptible and one not susceptible to oxidation.

---

1) M. Matsumoto and A. Danno, *Large Radiation Source in Industry*, Vol. 1, p. 331. Conference Proceedings, Warsaw, September 1959.
2) O. Saito, *J. Phys. Soc. Japan*, **13**, 198, 1451, 1465 (1958).
3) A. Charlesby, *Proc. Roy. Soc.*, **A222**, 542 (1954), **A224**, 120 (1954).
4) P. J. Flory and F. S. Leutner, *J. Polymer Sci.*, **3**, 880 (1948).

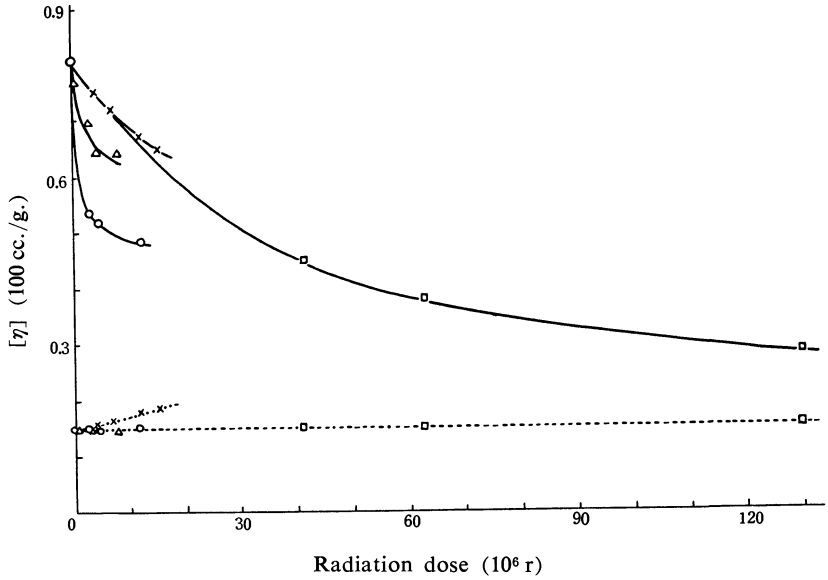



Fig. 1. The changes in the limiting viscosity number of irradiated PVA before and after oxidation by $HIO_4$ plotted against radiation dose: Full lines show the results before oxidation and dotted lines after oxidation by $HIO_4$.

△ Dry powder, irradiated in air at 95°C and $1\times10^5$ r/hr. and aged for 9 months.
○ Dry powder, irradiated in air at room temperature and $3\times10^4$ r/hr. and aged for 1.9 years.
□ Dry powder, irradiated in vacuo at room temperature and $2.9\times10^4$ r./hr. and aged for 1.1 years.
× Monofilament containing 6.7% water by weight, irradiated in air at room temperature and $4\times10^4$ r/hr.

Detailed results will be presented in a forthcoming paper.

*Department of Applied Physics*
*Faculty of Engineering*
*the University of Tokyo*
*Hongo, Tokyo*

## *A Method for Estimation of the Hydration Numbers of Ions in Ion Exchange Resins*

By Hitoshi Ohtaki, Kôzô Gonda and Hidetake Kakihana

(Received December 16, 1960)

A method for estimation of the hydration numbers of ions in ion exchange resins is proposed on the basis of the measurement of the amount of the solvent adsorbed isopiestically on the resin. The sulfonated cation exchange resins, Dowex 50-X4 (4% DVB resin), Diaion SK (8% DVB), Dowex 50-X16 (16% DVB) and Diaion SK-X24 (24% DVB) of sodium form, were used in mesh sizes of 50 to 200. They were dried at 50°C in vacuo. The resins were placed in the small dishes of stainless steel and were contacted with the solvent vapor under the pressure of about 3 mmHg. Ethanol-water and dioxane-water mixtures were used as the solvent systems. The concentrations of the organic solvents were in the range of 0 to 99.6% (v/v). The equilibrium of each isopiestic experiment had been attained in three days in a thermostat at 25 $\pm$0.5°C.

The total amount of solvents adsorbed on the resin was determined gravimetrically. The solvent composition on the resin was determined by the following ways: in the ethanol-water system the solvents adsorbed on the resin were eluted with water and the amount of ethanol in the eluate was measured colorimetrically[1]. In the dioxane-water system, the solvents on the resin were distilled completely

1) B. Lange, "Kolorimetrische Analyse", Verlag Chemie, Weinheim (1956), p. 334.

and the refractive index of the distilled solution was measured.

The distribution coefficient of the solvents, $K_o^w$, is defined as

$$K_o^w = \frac{\bar{m}_w \cdot m_o}{\bar{m}_o \cdot m_w} \quad (1)$$

where $\bar{m}$ and $m$ denote the concentrations of the solvents in the resin and the solution phases, respectively, and subscripts w and o represent water and the organic solvent.

The distribution of the solvents between the resin and the solution phases is thermodynamically given as follows*:

$$\ln \frac{\bar{a}_w \cdot a_o}{\bar{a}_o \cdot a_w} = \frac{\pi}{RT}(\bar{v}_o - \bar{v}_w) \quad (2)$$

where $\bar{a}$ and $a$ denote the activities of the solvents in the resin and the solution phases, respectively, and $\bar{v}$ is the partial molal volume of the solvent in the resin phase. $\pi$ is the swelling pressure of the resin.

It may be considered that the solvent adsorbed on the resin is devided to two different parts: the one I is the solvents solvating to the functional groups (sulfonic acid groups) and their counter ions (sodium ions), another II is the solvents condensed on the exchange sites which become solvophilic by the solvation of the exchange groups. The fact that the resin particles without functional groups do not adsorb the solvent shows that the solvent is not adsorbed on the resin skeleton. We assume that only water molecules can solvate to the ions even in the considerably high concentration of the organic solvent in the solution phase (probably up to about 80%).

From these considerations Eq. 1 may be rewritten as follows:

$$K_o^w = \frac{(\bar{m}_{w_I} + \bar{m}_{w_{II}})}{\bar{m}_{o_{II}}} \cdot \frac{m_o}{m_w} \quad (3)$$

where subscripts I and II denote part I and part II described above.

Being different from the case in which the resin is derectly dipped in the solvents, it is observed that the resin scarcely swells in the equilibrium with the solvent vapor. From this observation, we assume that $\pi$ in Eq. 2 is very small, or

$$\frac{\pi}{RT}(\bar{v}_o - \bar{v}_w) \simeq 0 \quad (4)$$

As the water molecules solvated to the functional groups are fixed and hardly move, the fugacities of the solvents in the resin phase which is equilibrated with the vapor phase may be proportional to the molar fractions of the solvents in part II. It is assumed that the activities of the solvents in the solution phase are proportional to their molar fractions, the following equation is derived from Eqs. 2 and 4:

$$\ln \frac{\bar{a}_{w_{I,II}} \cdot a_o}{\bar{a}_{o_{II}} \cdot a_w} \simeq \ln \frac{\bar{N}_{w_{II}} \cdot N_o}{\bar{N}_{o_{II}} \cdot N_w} = \ln \frac{\bar{m}_{w_{II}} \cdot m_o}{\bar{m}_{o_{II}} \cdot m_w} \simeq 0 \quad (5)$$

where $\bar{N}$ and $N$ denote the molar fractions of the solvents in the resin and the solution phases, respectively, and hence

$$\frac{\bar{m}_{w_{II}}}{\bar{m}_{o_{II}}} \simeq \frac{m_w}{m_o} \quad (6)$$

Applying Eqs. 3 and 6, the hydration number per one functional group and its counter ion (sodium ion), $\bar{H}$, is calculated readily by the following equation:

$$\bar{H} = \frac{(1-m_o)\bar{W}_o}{1000\, E M_w m_o}(K_o^w - 1) \quad (7)$$

where $\bar{W}_o$ is the weight of the organic solvent adsorbed on the resin (gram), $E$ denotes the exchange capacity (meq.) of the resin used, $M_w$ is the molecular weight of water and $m_o$ represents the concentration of the organic solvent given in the scale of weight percentage.

In Fig. 1 the hydration numbers are plotted against the concentrations of ethanol for the variously cross-linked resins. The similar results can be obtained in the dioxane-water system.

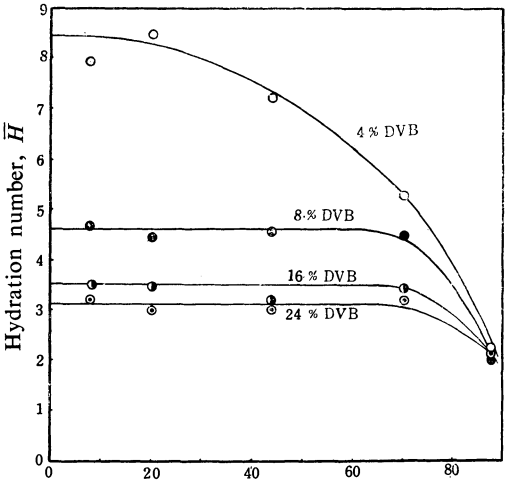



Fig. 1. Hydration number per one functional group and its counter ion (sodium ion) of the cross-linked sulfonic acid resins in the various concentrations of ethanol.

* Cf. H. Kakihana, H. Ohtaki and T. Nomura, *Bull. Tokyo Inst. Tech., Series-B*, No. 1, 1 (1960); H. Kakihana, T. Nomura and H. Ohtaki, ibid., No. 1, 14 (1960).

The numbers extrapolated to zero concentration of the organic solvents may correspond to the hydration numbers of the ions on the ion exchange resins equilibrated with the saturated water vapor. The values of the numbers are listed in Table I. The agreement of the results obtained in the cases of ethanol-water and dioxane-water systems is satisfactory.

TABLE I. HYDRATION NUMBERS, $\bar{H}$, EXTRAPOLATED TO ZERO CONCENTRATION OF THE ORGANIC SOLVENTS

| Resins | Ethanol-water | Dioxane-water | Mean |
|---|---|---|---|
| 4% DVB resin | 8.3 | 8.4 | 8.4 |
| 8% DVB resin | 4.6 | 4.5 | 4.6 |
| 16% DVB resin | 3.5 | 3.7 | 3.6 |
| 24% DVB resin | 3.1 | 3.0 | 3.1 |

*Tokyo Institute of Technology*
*Meguro-ku, Tokyo*

## *The Crystal Structure of* $[Cr(NH_3)_6]\,[CuCl_5]$*

By Masayasu MORI, Yoshihiko SAITO** and Tokunosuké WATANABE

(Received December 9, 1960)

Unstable halogen complexes of heavy metals sometimes exist in more than two forms having considerably different chemical constitutions and structures. Thus bromothallates(III) are found with compositions, $KTlBr_4 \cdot 2H_2O$, $Rb \cdot TlBr_4 \cdot H_2O$ and $CsTlBr_4$. These complexes have the octahedral, pyramidal and square configurations[1]. The interatomic distances Tl-Br in these complexes are considerably different from that found in a more stable complex, $[Co(NH_3)_6]\,[TlBr_6]$[2].

Such variety in ionic species is also found in the case of chlorocuprates, but the information seems much less satisfactory. A pentachlorocuprate(II) of hexamminechromium(III), $[Cr(NH_3)_6]\,[CuCl_5]$ has recently been prepared[3]. It occurred to the present authors that the crystal analysis of this compound would give a useful guide to the structural chemistry of chlorocuprates(II).

Weissenberg photographs for the equatorial, the first and fourth layer lines, and oscillation photographs were prepared using Cu$K\alpha$ ($\lambda$= 1.5418 Å) radiation. From these data, it was concluded that the crystals belong to the cubic system, and the systematic reflections were characteristic only for $O_h^8$-Fd3c. The exact reflection angles of several ($hk0$) reflections for Cu$K\alpha_1$ radiation ($\lambda$=1.5405 Å) were determined by means of a GM counter X-ray defractometer which was calibrated with a standard microcrystalline plate of metallic silicon ($a$=5.4301 Å). From these values the unit cube edge was determined to be $a$=22.265 ±0.01 Å. There are 32 formula units in each unit cell, the calculated density being 1.901 g. $cm^{-3}$, in good agreement with the observed value, 1.892 g. $cm^{-3}$. The relative intensities of reflections were visually estimated with a calibrated standard, and the Lorentz and polarization corrections were made using Cochran's chart[4].

There are 32 Cu, 32 Cr, 160 Cl and 192 N atoms in the unit cell. The observed intensities were best accounted for when these atoms are placed in the following equivalent positions:

32 Cu: (b) 1/4, 1/4, 1/4, etc.,
32 Cr: (c) 0, 0, 0, etc.,
64 Cl: (e) $u$, $u$, $u$, ($u$=0.190), etc.,
96 Cl: (g) 1/4, $v$, $-v$, ($v$=0.075), etc.,
192 N: (h) $x$, $y$, $z$, ($x$=0.070, $y$=0.050, $z$=−0.030), etc.

The parameters were obtained by the trial and error method, by comparing the calculated and observed structure factors, $F_c$ and $F_o$ at the each stage. At the final stage, corrections were made for extinction and the anomalous dispersion of copper and chromium atoms. The atomic coordinates given above, combined with the overall temperature factor, $B$=2.5, gave for the equatorial ($hk0$) Weissenberg data a reliability factor, $R$=0.136. The intensities of the unobserved reflections were taken equal to zero in this comparison. For 333 ($hkl$) reflections up to $l$=8 the $R$ value was 0.190 (in this case the unobserved reflections were excluded).

According to the above atomic coordinates, the crystal is composed of octahedral complex ion, $[Cr(NH_3)_6]^{3+}$ and trigonal bipyramidal complex ion, $[CuCl_5]^{3-}$ arranged the sodium chloride type. Because of the symmetry requirement, however, the unit cube edges are twice as much of a simple sodium chloride

* Presented at the Symposium on Coordination Chemistry, Sendai, September 1960.

** Present Address: Institute for Solid State Physics, the University of Tokyo, Shinryudo-cho, Azabu, Minato-ku, Tokyo.

1) T. Watanabe, Y. Saito, R. Shiono and M. Atoji, *Structure Repts.* 11, 393 (1947—8).
2) T. Watanabe, M. Atoji and C. Okazaki, *Acta Cryst*, 3, 405 (1950).
3) M. Mori, This Bulletin, 33, 985 (1960).
4) J. Cochran, *J. Sci. Instr.*, 25, 253 (1948).

arrangement. The threefold axis of the $[CuCl_5]^{3-}$ ion lies on the body diagonal of the cube cell, in accordance with the point symmetry of the Cu position, $D_3$–32. This structure of the $[CuCl_5]^{3-}$ ion is quite a new one, most chlorocomplexes of copper(II) being distorted octahedra. The only exception is the structure of $[CuCl_4]^{2-}$ ion in $Cs_2CuCl_4$ or its bromine analogue, in which case $[CuCl_4]^{2-}$ ion can be taken to be a flattened tetrahedron or a twisted square[5,6].

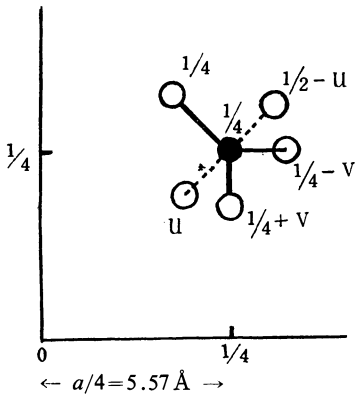



Fig. 1. The structure of $[CuCl_5]^{3-}$ with Cu at 1/4, 1/4, 1/4 (the figure refers to the $z$ coordinate).

The important characteristic of the trigonal bipyramidal structure of $[CuCl_5]^{3-}$ found in the present research is that the distance between the copper atom and the two chlorine atoms on the threefold axis (2.32 Å) is of the same order of magnitude as the distance between the copper atom and the three chlorine atoms at the corner of the triangle (2.35 Å) (Fig. 1). This is in a clear contrast to much greater distances (2.8~3.0 Å) between copper and chlorine atoms on the fourfold or nearly four fold axis found in many distorted octahedral chlorocomplexes.

The authors wish to express their sincere thanks to Dr. Yozo Chatani of Osaka University for the cooperation in preparing Weissenberg photographs.

*Institute of Polytechnics*
*Osaka City University*
*Kita-ku, Osaka*
*(M. M.)*

*Faculty of Science, Osaka University*
*Kita-ku, Osaka*
*(T. W.)*

5) L. Helmholz and R. F. Kruh, *J. Am. Chem. Soc.*, **74**, 1176 (1952).
6) B. Morosin and E. C. Lingafelter, *Acta Cryst.*, **13**, 80 (1960).

# *Über die Kupfersalze der ω-Amino-säuren. III. Über die Kristallstruktur von Kupfersalz des β-Alanins*

Von Ken-ichi TOMITA

(Eingegangen am 23. Juli, 1960)

In Teil II[1] wurde die Kristallstruktur des Kupferglycinmonohydrates dargestellt. Als zweite Stufe der Versuchsmaterialien haben wir dasKupfersalz des β-Alanins gewählt und die Kristallstruktur dieses Materials mit Hilfe der röntgenographischen Methode untersucht. Nach der Feststellung dieser Kristallstruktur können wichtige Erkenntnisse, nicht nur über den Koordinationszustand des Cu Atomes, sondern auch über die molekulare Konfiguration des β-Alanins selbst[2], abgeleitet werden.

Wir würden uns auf die Kristallanalyse des Kupfersalzes des Isoserins, das ein Derivat von β-Alanin ist, weiter einlassen, aber diese Kristallstruktur ist so kompliziert, daß wir diese Analyse unterbrechen mussten. Trotzdem fügen wir am Ende dieser Abhandlung die kristallographischen Daten bei, weil diese Substanz sehr wichtig ist.

## Experiment und Resultat

**Darstellungsweise.**—Das gereinigte, überschüssige Kupferhydroxyd wurde mit einer wässerigen Lösung von β-Alanin im Wasserbad etwa 2 Stunden erhitzt und filtriert. Beim nachherigem Einengen des tiefblauen Filtrates scheidet sich das Kupfersalz von β-Alanin als ein papierstreifenförmiger tiefblauer Kristall ab.

Wenn dieser Einkristall in der Atomsphäre liegen gelassen wird, verändert sich die Oberflächenfarbe zu hellblau. Dieses Ausbleichen beweist teilweise Entwässerung des Kristalles.

Die Mikroanalyse gibt folgende Resultate:

$Cu(C_3H_6NO_2)_2+6H_2O$ (Mol. Gew. 347.81)

Ber.: C, 20.72; H, 6.96; N, 8.06; $H_2O$, 31.08; Cu, 18.28. Gef.: C, 21.31; H, 7.02; N, 8.06; $H_2O$, 31.77; Cu, 18.12%.

Mit Hilfe der Schwebemethode (Benzoläthylendibromid Gemisch) ergibt sich ein spezifisches Gewicht von 1.50.

**Gitterkonstante.**—Mittels Rotation- und Weissenberg-Aufnahmen um [100] und [010] mit Cu$K\alpha$-Strahlung wurde die Intensität jeder Reflexion nach der sogenannten "multiple film method" aus vier Filmen im Vergleich zu einer gewöhnlichen Intensitätsskala bestimmt; die Schnittflächeneinheit des gebrauchten Einkristalls ist ungefähr $0.1\times0.2$ mm bei $(0kl)$-Reflexionen und ungefähr $0.8\times1.2$ mm bei $(h0l)$-Reflexionen. Das Verhältnis der relativen Intensitäten von stärkster zu schwächster Reflexion war ungefähr 1500 : 1 für $(0kl)$-Reflexion und 700 : 1 für $(h0l)$-Reflexion.

Wir nahmen keine Notiz von der Absorption, aber auf die Kompensation des primären Extinktioneffekts wurde der genaue $g$-Wert angewandt ($g=6.76\times10^{-4}$), der aus der Formel

$$I_r=I_o/(1-gI_o)$$

gerechnet wurde, wobei $I_o$ die beobachtete Intensität und $I_r$ die reale Intensität zeigt.

Die gesamten unabhängigen Zahlen der Äquator-Reflexionen, welche in der Ausbreitungskugel enthalten sind, sind 182 für [100]-Projektion und 133 für [010]-Projektion, während die beobachteten Zahlen 132 bzw. 125. Für die Bestimmung der Raumgruppe wurden die Auslöschungsgesetze für $(0kl)$, $(1kl)$ und $(h0l)$-Reflexionen benützt.

Die gefundenen Gitterkonstanten sind wie folgt:

$a=5.46$ Å, $b=7.71$ Å, $c=18.11$ Å,
$\beta=92°$ (Monoklinisches System).
Die Zahl der Moleküle pro Elementarzelle; $z=2$.
Raumgruppe: $C_{2h}^5-P2_1/c$.

## Strukturbestimmung und Betrachtung

Die Raumgruppe $C_{2h}^5-P2_1/c$ hat ein symmetrisches Zentrum auf dem Anfangspunkt; wenn das Molekül die allgemeine Lage einnimmt, ist die Zahl der Moleküle in der Elementarzelle vier. Beim Kupfersalz des β-Alanins, beträgt jedoch diese Zahl nur zwei; hierzu muss das Cu-Atom die spezielle Lage in der Elementarzelle, d. h., den Anfangspunkt, einnehmen, und die um das Cu-Atom koordinierten zwei Moleküle des β-Alanins haben daher selbstverständlich eine trans Konfiguration. Unmittelbar darnach wurde eine vorläufige Fouriersynthese um [100] und [010]-Projektionen kalkuliert, wobei die Vorzeichen jeder Reflexion nur mit den Parametern des Cu-Atoms berechneten Strukturfaktoren durchgeführt wurden. Aus den vielen Maxima, die sich in Fourier-projektionen um [100] und [010] zeigen, wurden einige, die gleiche $z$-Parameterwerte haben, gewählt und in Hinsicht auf den Valenzwinkel und die interatomaren Abstände wurden einige weitere schnittweise

1) K. Tomita und I. Nitta, diese Zeitschrift, **34**, 286 (1961).

2) Die Strukturanalyse von β-Alanin wurde schon ungefähr 1948 von Herrn Dr. M. Katayama durchgeführt, aber bis heute ist dieses Resultat noch nicht veröffentlicht worden.

TABELLE I.

| Atomart | $x/a$ | $y/b$ | $z/c$ |
|---|---|---|---|
| Cu | 0.000 | 0.000 | 0.000 |
| $C_1^I$ | −0.185 | −0.025 | 0.158 |
| $C_2^I$ | 0.065 | −0.118 | 0.185 |
| $C_3^I$ | 0.187 | −0.228 | 0.130 |
| $O_1^I$ | −0.205 | 0.005 | 0.095 |
| $O_2^I$ | −0.325 | 0.005 | 0.206 |
| $O_3^I$ | 0.187 | 0.280 | 0.040 |
| $O_4^I$ | 0.450 | 0.322 | 0.172 |
| $O_5^I$ | −0.258 | 0.445 | 0.060 |
| $N^I$ | 0.278 | −0.135 | 0.058 |

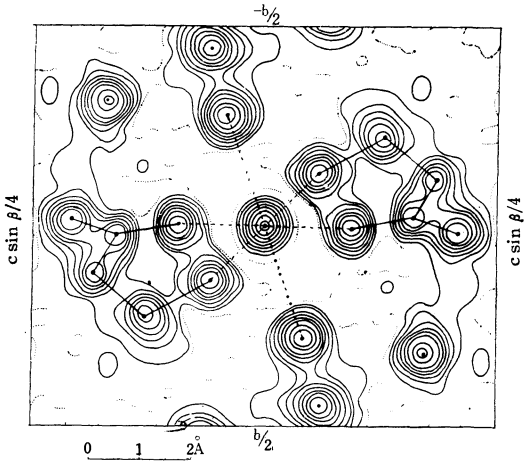



Abb. 1. Elektronendichteprojektion nach [100].
Das puntkierte Niveau der Kurven geht durch $1e/Å^2$ und die Kurve gleicher Elektronendichte liegen um $1e/Å^2$ auseinander, ausser im Kupfermaximum, wo die Äquidistanz $5e/Å^2$ beträgt.

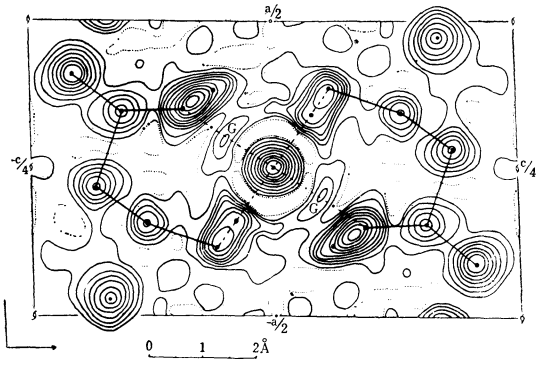



Abb. 2. Elektronendichteprojektion nach [010].
Das punktierte niedrigste Niveau der Kurven liegt bei $2e/Å^2$ und die Kurven gleicher Elektronendichte liegen um $1e/Å^2$ auseinander, ausser im Kupfermaximum, wo die Äquidistanz $5e/Å^2$ beträgt.

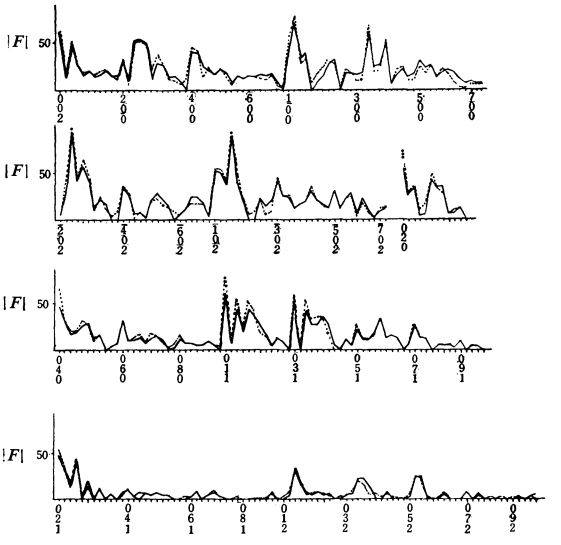



Abb. 3. Graphisches Vergleich der beobachteten und berechneten F-Werte.
(——: $|F_o|$, ------: $|F_c|$)

Fouriersynthesen unternommen. Zur Berechnung der Strukturamplituden wurde die Atomstreukurve für Cu nach Berghuis et al.[3] und für C, N und O nach McWeeny[4] angewandt. In Tabelle I sind die gefundenen Parameterwerte jedes Atoms zusammengestellt. Die letzte Elektronendichteprojektion nach [100] wird in Abb. 1, und nach [010] in Abb. 2 gezeigt, die ein weiteres Maximum G um das zentrale Cu-Atom vorweist; es scheint, daß dieses letztere Maximum von Abbruchs- oder Absorptionseffekt abhängt. In Abb. 3 sind die graphischen Vergleiche der beobachteten und berechneten F-Werte zusammengestellt. Die gefundenen isotropischen Temperaturfaktoren nach [100] und [010] betragen je 3.9 und 2.4, und für die [100]-Projektion wurde ein Zuverlässigkeitsindex $R$ von 0.19 berechnet und für die [010]-Projektion von 0.22, wobei die Kalkulation über alle Reflexionen in der Ausbreitungskugel durchgeführt wurde.

Aus der schematischen Projektion der Atomschwerpunkte (Abb. 4) kann man auch die interatomaren Abstände und Bindungswinkel ersehen. Wie Abb. 4 deutlich zeigt, haben die um das zentrale Cu-Atom koordinierten vier Atome der zwei β-Alanin Moleküle (d. h., $O_1^I$, $O_1^{II}$, $N^I$ und $N^{II}$) in Beziehung zu dem zentralen Metallatom eine plane trans Konfiguration; um das zentrale Metallatom wurde ein ungefähr planes gleichseitiges Viereck mit $O_1^I$, $O_1^{II}$, $N^I$ und $N^{II}$ gebildet und zwei Sauerstoffatome des Kristallwassermoleküls (d. h., $O_3^I$ und

3) J. Berghuis, IJ. M. Haanappel, M. Potters, B. O. Loopstra, C. H. MacGillavry und A. L. Veenendaal, *Acta Cryst.*, **8**, 478 (1955).
4) R. McWeeny, ibid., **4**, 513 (1951).

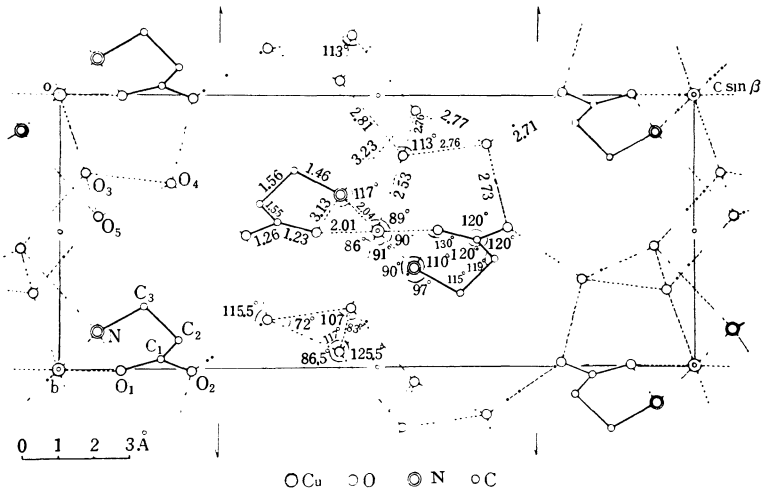



Abb. 4. Schematische Projektion der Atomschwerpunkte nach [100].

Tabelle 2a.

| Verbindung | Cu—O | Cu—N | Cu—O ($H_2O$) |
|---|---|---|---|
| Cu-Ameisensäure Tetrahydrat[5] | 2.00Å, 2.01 | — | 2.36Å |
| Cu-Prolin Dihydrat[6] | 2.03 | 1.99 | 2.52 |
| Cu-Glycin Monohydrat[1] | 1.93, 1.95 | 1.98, 1.99 | 2.39 |
| Cu-β-Alanin Hexahydrat | 2.01 | 2.04 | 2.53 |

Tabelle 2b.

| Verbindung | O—H···O | Typus |
|---|---|---|
| Cu-Ameisensäure Tetrahydrat[5] | 2.82Å | Wasser-Carboxyl |
| | 2.74, 2.78 | Wasser-Wasser |
| Cu-Prolin Dihydrat[6] | 2.94, 3.00 | Wasser-Carboxyl |
| Ni-Glycin Dihydrat[7] | 2.72, 2.72 | Wasser-Carboxyl |
| Cu-Glycin Monohydrat[1] | 2.75, 2.84 | Wasser-Carboxyl |
| Cu-β-Alanin Hexahydrat | 2.71, 2.73 | Wasser-Carboxyl |
| | 2.76, 2.76<br>2.77, 2.81 | Wasser-Wasser |

Tabelle 2c.

| Verbindung | N—H···O | Typus |
|---|---|---|
| Glycin[8] | 2.77, 2.85, 2.95, 3.07 | Amino-Carboxyl |
| *dl*-Alanin[9] | 2.80, 2.84, 2.88 | Amino-Carboxyl |
| Cu-Prolin Dihydrat[6] | 2.86 | Imino-Carboxyl |
| Ni-Glycin Dihydrat[7] | 2.96, 3.13 | Amino-Carboxyl |
| Cu-Glycin Monohydrat[1] | 2.97, 3.01 | Amino-Carboxyl |
| | 2.97 | Amino-Wasser |
| Cu-β-Alanin Hexahydrat | 3.13 | Amino-Carboxyl |
| | 3.23 | Amino-Wasser |

5) R. Kiriyama, H. Ibamoto und K. Matso, ibid., 7, 482 (1954).

$O_3^{II}$) nehmen zur gleichen Zeit die auf- und abgehenden Spitzen eines Oktaeders ein, das um das Cu-Atom gebildet wurde. Mit den übrigen vier Kristallwassermolekülen wurden die verschiedene Bindungen zwischen jedem Komplexmolekül in Form von Wasserstoffbrücken, d. h., N—H···O oder O—H···O, gebracht.

Es ist auch sehr interessant, die molekulare Struktur von β-Alanin selbst zu erkennen; Die $NH_2$- und COO-Gruppen des β-Alanin Moleküls haben eine sogenannte gauche Konfiguration in Beziehung zu der αC—βC Bindung. (Der Winkel zwischen der durch $C_1^I$, $C_2^I$ und $C_3^I$ und der durch $C_2^I$, $C_3^I$ und $N^I$ gebildeten Ebene ergab ungefähr 70°.) Bis heute wurde das Resultat über die Struktur des β-Alanins noch nicht veröffentlicht[2], aber wenn das Molekül des β-Alanins im Fall von Komplexbildung die gleiche molekulare Form als im freien Zustand beibehält, kann man daraus schliessen, dass es eine gauche Konfiguration hat.

Zum Schluss wird der Vergleich zwischen den verschiedenen interatomaren Abständen im Kupfersalz des β-Alanins mit denjenigen in anderen begleitenden Substanzen dargestellt (Tabelle 2a, 2b und 2c). Beim Kupfersalz der ω-Aminosäuren ist der Cu—O Abstand etwas kürzer als der Cu—N Abstand, während der Cu—O Abstand bei dem Kupfersalze des Prolins im Gegenteil etwas länger als der Cu—N Abstand ist. Wie in Tabelle 2b und 2c deutlich gezeigt wird, sind die O—H···O Abstände zwischen Wassermolekül und Car-

6) A. M. Mathieson und H. K. Welsh, ibid., 5, 599 (1952).
7) A. J. Stosick, *J. Am. Chem. Soc.*, 67, 365 (1945).
8) R. E. Marsh, *Acta Cryst.*, 11, 654 (1958).
9) J. Donohue, *J. Am. Chem. Soc.*, 72, 949 (1950).

boxylgruppe bei dem Kupfersalz des β-Alanins etwas kürzer als bei dem Kupfersalz des Glycins, aber die ersteren N—H···O Abstände sind etwas länger als die letzteren. Damit kann man vermuten, dass bei Kristallbildung des Kupfersalzes des Glycins die O—H···O und N—H···O Waserstoffbindungen zugleich die grössere Rolle spielen, während bei Kristallbildung von Kupfersalz des β-Alanins grösstenteils nur bei der O—H···O Wasserstoffbindung durchgeführt wird.

### Kristallographische Daten von Kupferisoserintrihydrat

$CuC_3H_5NO_3+3H_2O$ (Mol. Gew. 220.67)

Ber.: C, 16.33; H, 5.02; N, 6.35; $H_2O$, 24.48; Cu, 28.81. Gef.: C, 16.11; H, 4.92; N, 6.49; $H_2O$, 21.91; Cu, 28.50%.

Gitterkonstanten:

$a=7.06$ Å, $b=22.47$ Å, $c=15.77$ Å, $\beta=109°43'$.

Gefundene Dichte:

1.88 g/cc (Schwebemethode).

Die Zahl der Moleküle pro Elementarzelle:

$z=12$.

Raumgruppe: $C_{2h}^5-P2_1/c$ (Monoklinisch).

Bei dieser Raumgruppe ist die Zahl der Moleküle in jeder Elementarzelle vier, wenn das Molekül die allgemeine Lage einnimmt.

Demnach sind in diesem Kristall drei kristallographisch verschiedenartige Moleküle, jeder für sich vier, vorhanden.

Meinem verehrten Lehrer, Herrn Professor Dr. I. Nitta, danke ich herzlich für wertvolle Anregungen und für seine stete Unterstützung bei der Durchführung dieser Arbeit. Dabei sei auch Herrn Dr. Y. Sasada für seine hilfreichen Ratschläge gedankt.

*Chemisches Institut*
*Naturwissenschaftliche Fakultät*
*Universität Osaka*
*Nakanoshima Osaka*

# *Quinones. I. The Syntheses of Acetyl-p-benzoquinone Derivatives and 2-Acetylnaphthoquinone*

By Eturo KUROSAWA

(Received August 8, 1960)

Acetyl-*p*-benzoquinone derivatives are expected to show interesting chemical and biological properties, owing to the presence of an acetyl carbonyl group conjugated to quinone double bond. However, only acetyl-*p*-benzoquinone has been reported in the literature[1].

An attempt was made as described below to synthesize several acetyl-*p*-benzoquinone derivatives, e. g., 2-methyl-5-acetyl-*p*-benzoquinone (acetyltoluquinone), 2, 3-dimethyl-5-acetyl-*p*-benzoquinone (acetyl-*o*-xyloquinone) and 2-acetyl-1, 4-naphthoquinone by the oxidation of corresponding acetylhydroquinone derivatives with silver oxide.

Acetylhydroquinone has been synthesized by several methods: viz., i) by the action of zinc chloride on hydroquinone in glacial acetic acid[2], ii) by the Fries migration of hydroquinone diacetate[3], and iii) by the action of acetyl chloride on hydroquinone dimethyl ether in the presence of aluminum chloride followed by demethylation[1]. But because of the complicated procedures or low yield, these methods did not give good results.

It has been found that these acetylhydroquinone derivatives are obtained in good yield as a result of the action of boron trifluoride on hydroquinone derivatives in glacial acetic acid[4]. Acetylation was carried out by the saturation of boron trifluoride to the suspension of hydroquinone derivatives in excess glacial acetic acid. 2-Acetylhydroquinone (III, $R=R'=H$) was obtained directly by this method from hydroquinone (I, $R=R'=H$) in an almost quantitative yield. But in the cases of 2-methyl- and 2, 3-dimethylhydroquinone and naphthohydroquinone, there were obtained mono- or diacetates of corresponding acetyl derivatives. For example, acetylation of 2-

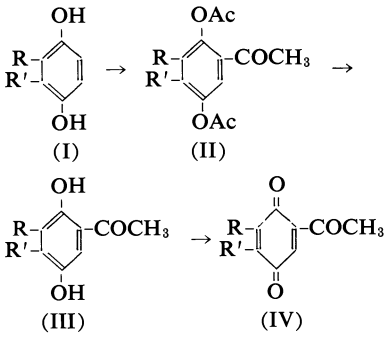
1) T. Irie and E. Kurosawa, presented at the 7th Annual Meeting of the Chemical Society of Japan, Tokyo, April, 1954; M. C. Kloetzel, R. P. Dayton and B. Y. Abadir, *J. Org. Chem.*, **20**, 38 (1955); N. N. Vorozhtsov and V. P. Makaev, *D. I. Statei obschei Khim. Akad. Nauk, U. S. S. R.*, **1**, 553 (1953).

2) M. Nencki and W. Schmidt, *J. Prakt. Chem.*, **23**, 546 (1881).

3) "Organic. Syntheses," Vol. 28, New York (1948), p. 42; R. D. Desai and C. K. Mavani, *Proc. Indian Acad. Sci.*, **29A**, 267 (1949); P. S. Rao and K. L. Gakhar, ibid., **30A**, 327 (1949).

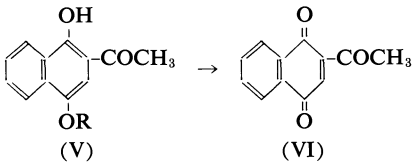
4) E. Kurosawa, *J. Chem. Soc. Japan, Pure Chem. Sec.* (*Nippon Kagaku Zasshi*), **78**, 312 (1957).

methylhydroquinone (I, R=H, R'=$CH_3$) afforded pale yellow crystals, then after several recrystallizations from dilute ethanol, colorless crystals were obtained. This material melted at 112°C and exhibited no coloration with ferric chloride in ethanol.



(I) (II) (III) (IV)

After saponification of this diacetate (II, R=H, R'=$CH_3$) with aqueous sodium hydroxide containing a small amount of sodium hydrosulfite, 2-methyl-5-acetylhydroquinone (III, R=H, R'=$CH_3$) was obtained; it melted at 145°C. Similarly, there was obtained 2, 3-dimethyl-5-acetylhydroquinone diacetate (II, R=R'=$CH_3$), m. p. 98°C, which was hydrolyzed to corresponding hydroquinone (III, R=R'=$CH_3$), m. p. 151°C. In the case of acetylation of naphthohydroquinone, 2-acetyl-4-acetoxynaphthol (V, R=$COCH_3$), m. p. 101°C, was obtained and it was hydrolyzed to 2-acetylnaphthohydroquinone (V, R=H).



(V) (VI)

2-Methyl-5-acetylhydroquinone was oxidized quantitatively to 2-methyl-5-acetyl-*p*-benzoquinone (IV, R=H, R'=$CH_3$) by being shaken with silver oxide and anhydrous potassium carbonate in dry benzene. When 2, 3-dimethyl-5-acetylhydroquinone was oxidized under the same conditions, an oily product was obtained. It gave the stimulative odor characteristic to quinone derivative and it was easily reduced to 2, 3-dimethyl-5-acetylhydroquinone by shaking its chloroform solution with aqueous sodium hydrosulfite. In infrared spectrum, this compound showed the band attributed to quinone carbonyl at 1640 $cm^{-1}$ as shown in Fig. 1, but no band in the region of about 3300 $cm^{-1}$. Similarly, 2-acetylnaphthohydroquinone was oxidized to 2-acetyl-1, 4-naphthoquinone (VI), m. p. 83~84°C, in good yield.

2-Acetyl-*p*-benzoquinone and 2-methyl-5-acetyl-*p*-benzoquinone have the bands attributed to quinone carbonyl at 1645 $cm^{-1}$ and 1635 $cm^{-1}$

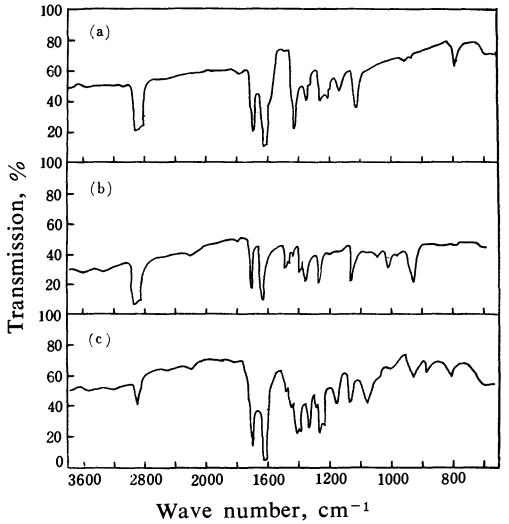



Fig. 1. IR spectra.
(a) Acetylbenzoquinone (Nujol)
(b) Acetyltoluquinone (Nujol)
(c) Acetyl-*o*-xyloquinone (direct)

in infrared spectrum as shown in Fig. 1. Likewise, 2, 3-dimethyl-5-acetyl-*p*-benzoquinone and 2-acetyl-1, 4-naphthoquinone have the bands attributed to quinone carbonyl at 1640 $cm^{-1}$ and 1662 $cm^{-1}$, respectively. In general, it has been reported[5], that *p*-benzoquinone has the band attributed to quinone carbonyl at 1663 $cm^{-1}$; when the substituent is a negative group as chlorine or bromine, the quinone carbonyl band shifts to a higher frequency, and when the substituent is positive, the band shifts to a lower frequency. The position of the absorption maximum can be qualitatively interpreted by the sum of I-effect and M-effect. Contrary to expectation that acetyl-*p*-benzoquinone derivatives would show the band attributed to quinone carbonyl at a higher frequency than that of *p*-benzoquinone, due to the influence of the acetyl carbonyl group, these compounds show the bands at a considerable lower frequency as shown in Fig. 1.

These results indicate the existence of a large M-effect in the molecules of acetyl-*p*-benzoquinone derivatives. For the confirmation of this fact, the author attempted to find the relationship between the frequency of quinone carbonyl in infrared spectrum and the other properties of quinone derivatives. L. J. Bellamy[6] reported the existence of a straight lineal relationship between the sum of electronegativity of substituents of ethylene derivatives and frequency of $CH_2$-deformation ($\delta CH_2$), and between the molecular refractions of

5) P. Yates, M. I. Ardao and L. F. Fieser, *J. Am. Chm. Soc.*, 78, 650 (1956).
6) L. J. Bellamy, *J. Chem. Soc.*, 1955, 4221.

functional derivatives and frequencies of the carbonyl band of carboxylic acids. The author gave attention to the oxidation-reduction potential of quinone derivatives which is one of the important properties of these compounds. It has been suggested that certain quinones, e. g., ubiquinone, play a part in the oxidation-reduction process of living matter[7] and the feature of the reactions is interpreted with the oxidation-reduction potential[8].

The oxidation-reduction potentials and the frequencies of quinone carbonyl bands of some benzoquinone derivatives are listed in Table I. When the oxidation-reduction potentials are plotted against the frequency of quinone carbonyl bands, the resulting curve is a nearly straight line as shown in Fig. 2.

This result indicates that the hypsochromic shift of the quinone carbonyl band resultant from the effect of the substituent linearly depends on the elevation of oxidation-reduction potential of the quinones.

TABLE I. CARBONYL FREQUENCIES AND OXIDATION-REDUCTION POTENTIALS OF BENZOQUINONE DERIVATIVES

| Benzoquinone | Frequency cm$^{-1}$[a] | | Potential V.[b] |
|---|---|---|---|
| | in $CS_2$ | Nujol | |
| Chlorobenzoquinone | 1678 | | 0.736[c] |
| Benzoquinone | 1668 | 1663 | 0.711 |
| Toluquinone | 1663 | 1663 | 0.656 |
| *o*-Xyloquinone | 1660 | 1660 | 0.588 |
| *p*-Xyloquinone | 1660 | 1668 | 0.597 |
| *m*-Xyloquinone | 1657 | 1653 | 0.592 |
| Thymoquinone | 1660 | | 0.589[c] |
| Pseudocumoquinone | 1657* | 1650 | 0.536 |
| Duroquinone | 1642 | 1639 | 0.471 |
| Ubiquinone[d] | 1653 | | 0.542 |

a) P. Yates, M. I. Ardao and L. F. Fieser, *J. Am. Chem. Soc.*, **78**, 650 (1956).
b) See Ref. 8.
c) Conant and Fieser, *J. Am. Chem. Soc.*, **45**, 2194 (1923).
d) J. F. Pennock, R. Ruegg, U. Schwieter and O. Wiss, *Helv. Chim. Acta*, **41**, 3243 (1958).
* Inflection.

TABLE II. CARBONYL FREQUENCIES AND OXIDATION-REDUCTION POTENTIALS OF ACETYL-*p*-BENZOQUINONE DERIVATIVES

| Benzoquinone | Frequency, cm$^{-1}$ | | Potential V. |
|---|---|---|---|
| | in $CS_2$ | Nujol | |
| Acetylbenzoquinone | 1668 | 1645 | 0.564 |
| Acetyltoluquinone | 1662 | 1645 | 0.539 |
| Acetyl-*o*-xyloquinone | 1654 | 1640 | 0.504 |

TABLE III. CARBONYL FREQUENCIES AND OXIDATION-REDUCTION POTENTIALS OF 1,4-NAPHTHOQUINONE DERIVATIVES

| Substituent | Frequency, cm$^{-1}$ in $CCl_4$ | Potential V.[a] |
|---|---|---|
| 2-Chloro- | 1684 | 0.510 |
| 2-Bromo- | 1686 | 0.509 |
| 2,3-Dichloro- | 1687 | 0.498 |
| None | 1675 | 0.483 |
| 2-Methyl- | 1670 | 0.422 |
| 2,3-Dimethyl- | 1660 | 0.340 |
| 2,6-Dimethyl- | 1668 | 0.405 |
| 2,7-Dimethyl- | 1673 | 0.407 |
| 2-Methoxy- | 1660 | 0.369 |

a) W. Mansfield Clark, "Oxidation-Reduction Potentials of Organic Systems", The Williams & Wilkins Company, Baltimore (1960), p. 376.

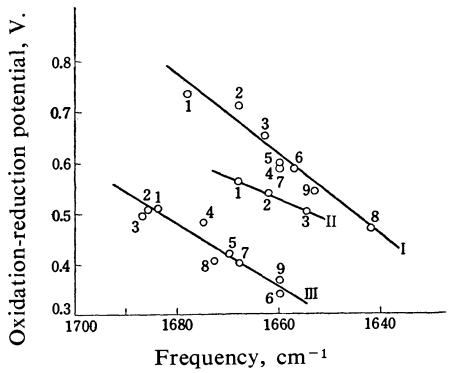



Fig. 2. Carbonyl frequency vs. oxidation-reduction potential.
I: Benzoquinone derivatives (in $CS_2$)
1. Chlorobenzoquinone
2. Benzoquinone
3. Toluquinone
4. *o*-Xyloquinone
5. *p*-Xyloquinone
6. *m*-Xyloquinone
7. Thymoquinone
8. Duroquinone
9. Ubiquinone
II: Acetylbenzoquinone derivatives (in $CS_2$)
1. Acetylbenzoquinone
2. Acetyltoluquinone
3. Acetyl-*o*-xyloquinone
III: Naphthoquinone derivatives (in $CCl_4$)
1. 2-Chloronaphthoquinone
2. 2-Bromonaphthoquinone
3. 2,3-Dichloronaphthoquinone
4. Naphthoquinone
5. 2-Methylnaphthoquinone
6. 2,3-Dimethylnaphthoquinone
7. 2,6-Dimethylnaphthoquinone
8. 2,7-Dimethylnaphthoquinone
9. 2-Methoxynaphthoquinone

7) R. H. Thomson, "Naturally Occurring Quinones". Butterworths Scientific Publications, London (1957), p. 1; W. Mansfield Clark, "Oxidation-Reduction Potentials of Organic Systems", The Williams and Wilkins Company. Baltimore (1960).
8) Fausto Ramirez, et al., *J. Am. Chem. Soc.* **81**, 4338 (1959).

The author determined the oxidation-reduction potentials of acetylbenzoquinone derivatives by the polarographic method. The buffer solution used was that of Smith et al.[9] The results, given in Table II and Fig. 2, show that these acetyl benzoquinone derivatives have relatively low potentials, but the quinone carbonyl frequencies are slightly higher than the other benzoquinone derivatives as compared with the potentials.

In general, the effect of substituents upon the oxidation-reduction potential has not been interpreted sufficiently, but in this case, the following explanation is possible. When the substituent of benzoquinone derivative gives a fairly large inductive effect in comparison with the M-effect against quinone carbonyl, a straight linear relationship between quinone-carbonyl frequency in the infrared spectrum and oxidation-reduction potential exists as shown in Fig. 2.

In the case of naphthoquinone and anthraquinone, however, relatively high frequencies of quinone carbonyl-bands against the oxidation-reduction potentials were observed as shown in Table III and Fig. 2. This fact is interpreted as due to the influence of the M-effect of an aromatic ring against quinone carbonyl.

Similarly, it is possible that in the cases of acetylbenzoquinone derivatives, deviation from the above linear relationship, as shown in Fig. 2, may be interpreted as due to the fairly large M-effect of the acetyl group against quinone carbonyl in comparison with the inductive effect.

From these results, it is expected that the interesting properties may be gained about acetylquinone derivatives by reason of the low oxidation-reduction potential and the lack of substituent in $\beta$-position toward quinone carbonyl and acetyl carbonyl.

Further investigation concerning the effect of the substituent upon the oxidation-reduction potential and the reactivity of acetylbenzoquinone derivatives is in progress.

## Experimental

**2-Methyl-5-acetylhydroquinone.** — Methylhydroquinone (5 g.) was suspended in glacial acetic acid (30 cc.) and warmed on a water bath. Boron trifluoride was passed into the mixture. The suspension slowly dissolved and a red color appeared. The saturation of boron trifluoride afforded a clear red solution which was heated for further 5 hr. on a water bath. The reaction mixture was then poured into ice water. The crystals thus separated (crude product) were collected by filtration and dried. After repeated recrystallizations from dilute ethanol, colorless needles were obtained, m. p. 112°C. (Found: C, 62.35; H, 5.78%). This material was found to be identical with 2-methyl-5-acetylhydroquinone diacetate[10] by use of the mixed melting point method.

The above crude product was treated with 2 N sodium hydroxide containing a small amount of sodium hydrosulfite for half an hour and then the alkaline solution was neutralized with 2 N hydrochloric acid. The crystals thus obtained were filtered and recrystallized from dilute ethanol. 2-Methyl-5-acetylhydroquinone was obtained as yellow needles, m. p. 145°C. (Found: C, 65.10; H, 6.17%).

**2-Methyl-5-acetylbenzoquinone.** — 2-Methyl-5-acetylhydroquinone (5 g.), anhydrous potassium carbonate (5 g.) and freshly prepared silver oxide (15 g.) were shaken in dry benzene (50 cc.) for 5 min. at 40°C. The reaction mixture was filtered and the solids were shaken with fresh benzene. On evaporation of the combined solution under reduced pressure, orange yellow crystals were obtained. After sublimation in vacuo or recrystallization from carbon disulfide, this substance melted at 79.5°C, yield 94%.

Found: C, 65.90; H, 4.95. Calcd. for $C_9H_8O_3$: C, 65.85; H, 4.88%.

**2, 3-Dimethyl-5-acetylhydroquinone.** — *o*-Xylohydroquinone (5 g.) was suspended in glacial acetic acid (30 cc.) and warmed on a water bath. Boron trifluoride was passed into the mixture. The suspension slowly dissolved and a yellow color appeared. After saturation of boron trifluoride, the reaction mixture was heated for further 5 hr. on a water bath. After the solution was poured into ice water, the resulting crystals (crude product) were collected and dried. After repeated recrystallizations from dilute ethanol, colorless needles were obtained, m. p. 97~98°C. This material exhibited no coloration with ferric chloride in ethanol and gave positive result to the iodoform test; by the mixed melting point method, it was found to be identical with 2,3-dimethyl-5-acetylhydroquinone diacetate (see below).

The above crude product was treated with 2 N alcoholic sodium hydroxide for 5 min. and then the alkaline solution was neutralized with 2 N hydrochloric acid. The crystals thus obtained were recrystallized from dilute ethanol. Yellow needles were obtained, m. p 151°C, yield 5.9 g. (91%).

Found: C, 66.83; H, 6.92. Calcd. for $C_{10}H_{12}O_3$: C, 66.67; H, 6.67%.

This material exhibited green coloration with ferric chloride in ethanol and a positive result to the iodoform test.

**Acetylation of 2,3-Dimethyl-5-acetylhydroquinone.** —2,3-Dimethyl-5-acetylhydroquinone (0.5 g.) was refluxed for 2 hr. in acetic anhydride (2 cc.). The solvent was removed under reduced pressure and the residue was sublimated in vacuo. Diacetate m. p. 97~98°C, was obtained as colorless needles.

Found: C, 63.64; H, 5.94. Calcd. for $C_{14}H_{16}O_5$: C, 63.64; H, 6.06%.

9) L. I. Smith, I. M. Kolthoff, S. Wawzonek and P. M. Ruoff, *J. Am. Chem. Soc.*, **63**, 1018 (1941).

10) R. D. Desai and C. K. Mavani, *Proc. Indian Acad. Sci.*, **29A**, 269 (1949).

**2,4-Dinitrophenylhydrazone of 2,3-Dimethyl-5-acetylhydroquinone.** — 2, 3-Dimethyl-5-acetylhydroquinone and 2,4-dinitrophenylhydrazine reacted in ethanol in the presence of a few drops of concentrated sulfuric acid. Crystals deposited were collected and recrystallized from butanol. Orange red needles were obtained, m. p. 271°C.

Found : C, 53.26 ; H, 4.55. Calcd. for $C_{16}H_{16}O_6N_4$ : C, 53.33 ; H, 4.45%.

**2,3 - Dimethyl - 5 - acetylbenzoquinone.** — 2,3 - Dimethyl-5-acetylhydroquinone (5 g.), anhydrous potassium carbonate (5 g.) and freshly prepared silver oxide (15 g.) were shaken in dry benzene (50 cc.) for 5 min. at 35°C. The reaction mixture was filtered and the solid was shaken with fresh benzene. On evaporation of combined solution under reduced pressure, 2,3-dimethyl-5-acetylbenzoquinone was obtained in yellow brown oily state, yield 92%.

Found : C, 67.52 ; H, 5.68. Calcd. for $C_{10}H_{10}O_3$ : C, 67.41 ; H, 5.62%.

**2 - Acetylnaphthohydroquinone.** — Naphthohydroquinone (5 g.) was suspended in glacial acetic acid (30 cc.) and under water cooling, boron trifluoride was passed into the suspension. Under heat evolution, hydroquinone dissolved slowly and a clear red-brown solution was obtained. After saturation with boron trifluoride the reaction mixture was immediately poured into ice water. The orange red product (crude product) was filtered ; after repeated recrystallizations from dilute ethanol, it melted at 101°C.

Found : C, 68.96 ; H, 5.00. Calcd. for $C_{14}H_{12}O_4$ : C, 68.85 ; H, 4.93%.

In the infrared spectrum, this material has the bands attributed to OH at 3300 $cm^{-1}$ (broad), acetate carbonyl at 1750 $cm^{-1}$ and carbonyl (bonded) at 1630 $cm^{-1}$. It exhibited greenish blue coloration with ferric chloride in ethanol solution and a positive result to the iodoform test.

The above crude product was dissolved in 2 N aqueous sodium hydroxide containing a small amount of sodium hydrosulfite. After 20 min., the insoluble materials were filtered off, the solution was neutralized with 2 N hydrochloric acid and the resulting crystals collected by filtration. After repeated recrystallizations from dilute ethanol, yellow crystals were obtained, m.p. 206～208°C, yield 3.5 g. (56%).

Found : C, 70.92 ; H, 4.96. Calcd. for $C_{12}H_{10}O_3$ : C, 71.29 ; H, 4.96%.

This material exhibited yellow brown coloration with ferric chloride in an ethanol solution and a positive result to the iodoform test. In the infrared spectrum, it has the bands attributed to OH at about 3300 $cm^{-1}$ (bonded) and acetyl carbonyl at 1618 $cm^{-1}$ (bonded.).

**2-Acetylnaphthoquinone**[11]. — 2-Acetylnaphthohydroquinone (1 g.), anhydrous potassium carbonate (1 g.) and freshly prepared silver oxide (3 g.) were shaken in dry benzene at 40°C for 15 min. The reaction mixture was filtered and the solvent was removed under reduced pressure. The residue was recrystallized from light petroleum ; golden yellow needles were obtained, m. p. 83～84°C, yield 0.84 g. (85%). (Found : C, 71.85 ; H, 3.87%).

**Determinations of Oxidation-Reduction Potential by Polargroaphic Method.** — Oxidation-reduction potential measurement was carried out by preparing 0.001 M solution of quinone derivatives in a buffer solution containing 0.1 N sodium acetate and 0.1 N acetic acid in 50% ethanol at pH 5.4. In order to find the standard normal hydrogen electrode the potentials were calculated for pH of zero, using 0.246 V. as the standard potential of the saturated calomel electrode.

The author wishes to thank Professor Tosi Irie of Hokkaido University for his kind guidance throughout this work.

*Department of Chemistry*
*Faculty of Science*
*Hokkaido University, Sapporo*

11) P. Friedländer, *Ber.*, **28**, 1950 (1895).

# *Interaction Polarization of the Hydrogen Bonded Complexes. II*

By Ko KIMURA and Ryoichi FUJISHIRO

(Recieved August 22, 1960)

An increase of the molecular polarization due to hydrogen bonding reported by Sutton et al.[1], by Tsubomura[2] and also by the present authors[3] is one of variations of dielectric properties arising from the molecular interaction. Many obstacles are present in the precise determination of the molecular polarizations for the hydrogen bonded complexes from the measurements of dielectric constants, specific volumes and refractive indexes of ternary solutions (proton donors, proton acceptors and inert solvents). The most important point is

1) J. R. Hulett, J. A. Pegg and L. E. Sutton, *J. Chem. Soc.*, **1955**, 3901.
2) H. Tsubomura, This Bulletin, **31**, 435 (1958).
3) K. Kimura and R. Fujishiro, ibid., **32**, 433 (1959).

whether or not Debye's equation holds even approximately in ternary solutions, because the measurements are carried out in such solutions that the interaction between proton donors and proton acceptors can take place. This problem will be discussd elsewhere. In so far as polarization values for the complexes are calculated by the use of Debye's equation, we must devise a way to make the difference as small as possible between the dielectric constant of a pure solvent and that of a ternary solution containing large quantities of a proton acceptor. Otherwise the polarization values obtained from observed dielectric constants and specific volumes are not reliable because of the solvent effect. In order to make the dielectric constants of ternary solutions with high concentrations of proton acceptors as low as possible, it is necessary to use nonpolar proton acceptors such as *p*-dioxane and bipyridyl. For example, it follows that when we want to investigate the polarization value of the phenol + pyridine complex, examination of the phenol + bipyridyl complex instead of the phenol + pyridine complex itself is more reasonable from consideration of the solvent effect.

In the previous paper, the dielectric measurements were carried out for some of the OH···O hydrogen bonded systems by using benzene as an inert solvent, and the analysis was performed based on a model with the covalent character of the hydrogen bonds[4]. This report describes first the results of dielectric measurements for the OH···N hydrogen bonded systems such as benzyl alcohol + bipyridyl, benzyl alcohol + triethylamine, phenol + bipyridyl and phenol + triethylamine by exactly the same procedure as in the previous report, and secondly the correlation between the dielectric data and the infrared spectra.

## Experimental

Materials used in this work were purified by the method described in Weissberger's text-book[5]. Benzene was used as a solvent throughout this work. It was frozen three times after being shaken with concentrated sulfuric acid and with dilute sodium hydroxide, dried over phosphorous pentoxide, and then fractionally distilled through a "Heli-Pack" column. Benzyl alcohol was purified by shaking with aqueous potassium hydroxide solution and extracting with ether, which had been freed from peroxides. The extract was treated with saturated sodium hydrogen sulfite solution and dried over potassium carbonate. After the removal of ether, benzyl alcohol was dried over lime and distilled under reduced pressure. $\alpha,\alpha'$-Bipyridyl (the special grade made by Wako Pure Chemicals Co., Ltd.) was dried in a desiccator and used without further purification. Its melting point was 70. 5°C. The measurements of dielectric constants $\varepsilon$, refractive indexes $n$ and specific volumes $v$ were carried out at 25°C with the apparatus already reported[3].

## Results

The results of the measurements of $\varepsilon$, $n^2$ and $v$ for the four ternary systems i. e., benzyl alcohol + $\alpha,\alpha'$-bipyridyl + benzene, benzyl

Table I. Polarization data and formation constants of the hydrogen bonded complexes

| | | | |
|---|---|---|---|
| Benzyl alcohol+$\alpha,\alpha'$-Bipyridyl | | Benzyl alcohol | |
| (The weight per cent of $\alpha,\alpha'$-bipyridyl is 4.011.) | | | |
| $\varepsilon=2.2988+3.36\,w$ | | | |
| $n^2=2.2555+0.07\,w$ | | | |
| $v=1.13442-0.163\,w$ | | | |
| $P'$ | 98.7 cc. | | |
| $K$ | 5.5 l./mol. | | |
| $P_1$ | 102.6 cc. | $P$ | 93.8 cc. |
| $R_D$ | 32.4 cc. | $R_D$ | 32.5 cc. |
| $\mu_1$ | 1.85 D | $\mu$ | 1.73 D |
| Benzyl alcohol+Triethylamine | | | |
| (The weight per cent of triethylamine is 9.300, | | or 29.95.) | |
| $\varepsilon=2.3025+5.70\,w$ | | $\varepsilon=2.3512+6.18\,w$ | |
| $n^2=2.2104+0.156\,w$ | | $n^2=2.1411+0.240\,w$ | |
| $v=1.16696-0.282\,w$ | | $v=1.21583-0.347\,w$ | |
| $P'$ | 145.6 cc. | $P'$ | 157.9 cc. |
| $K$ | 2.9 l./mol. | $K$ | 2.9 l./mol. |
| $P_1$ | 168.2 cc. | $P_1$ | 167.0 cc. |
| $R_D$ | 30.8 cc. | $R_D$ | 31.4 cc. |
| $\mu_1$ | 2.57 D | $\mu_1$ | 2.57 D |
| Phenol+$\alpha,\alpha'$-Bipyridyl | | Phenol | |
| (The weight per cent of $\alpha,\alpha'$-bipyridyl is 2.527.) | | | |
| $\varepsilon=2.2900+4.80\,w$ | | | |
| $n^2=2.2512+0.168\,w$ | | | |
| $v=1.13811-0.259\,w$ | | | |
| $P_1$ | 108.7 cc. | | |
| $K$ | 55 l./mol. | | |
| $P_1$ | 111.7 cc. | $P$ | 84.6 cc. |
| $R_D$ | 27.2 cc. | $R_D$ | 27.6 cc. |
| $\mu_1$ | 2.03 D | $\mu$ | 1.67 D |
| Phenol+Triethylamine | | | |
| (The weight per cent of triethylamine is 28.35.) | | | |
| $\varepsilon=2.3430+10.54\,w$ | | | |
| $n^2=2.1459+0.380\,w$ | | | |
| $v=1.21204-0.424\,w$ | | | |
| $P'$ | 214.2 cc. | | |
| $K$ | 83.8 l./mol. | | |
| $P_1$ | 214.8 cc. | | |
| $R_D$ | 28.0 cc. | | |
| $\mu_1$ | 3.02 D | | |

4) C. A. Coulson and U. Danielsson, *Arkiv Fysik*, **8**, 239, 245 (1954); H. Tsubomura, This Bulletin, **27**, 445 (1954).
5) A. Weissberger et al., "Organic Solvents", Interscience Publishers, New York (1955).

TABLE II

| | $\Delta\mu_T$ | $\Delta\mu_D$ | [III] | $\Delta\nu$ | |
|---|---|---|---|---|---|
| Benzyl alcohol+bipyridyl | 0.19D | 0.19D | 1.6% | 240 $cm^{-1}$ | a) |
| Benzyl alcohol+triethylamine | 1.17 | 1.17 | 10 | 400 | b) |
| Phenol+bipyridyl | 0.48 | 0.39 | 3.4 | 480 | c) |
| Phenol+triethylamine | 1.54 (1.00)* | 1.45 | 13 | 600 | d) |
| Benzyl alcohol+dioxane | 0.10 | 0.10 | 0.7 | 110 | e) |
| Phenol+dioxane | 0.29 | 0.21 | 1.5 | 250 | f) |

* This value reported by Sutton et al.[1] was calculated by the use of the formula $P=\sum f_i p_i$.

a) Measurements for the ethanol+pyridine system were carried out by the present authors with a Perkin-Elmer model 21 spectrophotometer.

b) C. H. Huggins and G. C. Pimental, *J. Phys. Chem.*, **60**, 1615 (1956).

c) N. Fuson, P. Pineau and M-L. Josien, *J. Chem. Phys.*, **55**, 454 (1958).

d) Measurements were carried out by the present authors with a Perkin-Elmer model 21 spectrophotometer.

e) N. D. Coggeshall and E. L. Saier, *J. Am. Chem. Soc.*, **73**, 5414 (1951).

f) H. Tsubomura, *J. Chem. Phys.*, **24**, 927 (1956).

alcohol + triethylamine + benzene, phenol + $\alpha,\alpha'$-bipyridyl + benzene and phenol + triethylamine + benzene, are expressed in Table I by formulae relating $\varepsilon$, $n^2$ and $v$ to $w$, respectively, where $w$ represents the weight fraction of the proton donors. The calculation of the molecular polarizations from these experimental data was performed according to the method described in the previous paper[3]. Polarization values $P'$ thus obtained are also shown in Table I, together with those for the corresponding binary systems already reported i. e., benzyl alcohol + benzene and phenol + benzene. $P'$ will contain the polarization for the free proton donor as well as that for the complex. If the fraction of the proton donor existing in the form of the complex in the limit $w\to 0$ is estimated by the use of the formation constant $K$ of the complex, the true polarization value $P_1$ for the complex is determined by both the polarization value $P$ for the free proton donor and $P'$. The formation constants of the complexes tabulated in Table I are either taken from literatures or measured by the present authors. As $K$ for the benzyl alcohol + $\alpha,\alpha'$-bipyridyl complex is expected to be of the same order as that for the ethanol + pyridine complex, we measured the ultraviolet spectra[6] of the latter system by using *n*-heptane as a solvent, and determined $K$ from the variation of the intensity of the $n\to\pi$ electronic transition of pyridine[7] due to the addition of ethanol. $K$ for the benzyl alcohol + triethylamine complex is reported to be about 2.9 l./mol.[8] by the measurement of infrared absorptions. When the content of triethylamine is 9.30 or 29.95 weight per cent, $P_1$ is calculated to be 168.2 cc. or 167.0 cc. The difference 1.2 cc. between these two values is attributable to the solvent effect. On the other hand, one can deduce both $K$ and $P_1$ from $P$'s in two concentrations of triethylamine. The calculated values of $K$ and $P_1$ are 3.2 l./mol. and 166.2 cc., respectively. This result indicates the fact that the reliable association constant can be obtained in the case of the complexes of the small $K$ and large $\Delta P=P_1-P$. As $K$ for the phenol + $\alpha,\alpha'$-bipyridyl complex, we used the formation constant for the phenol + pyridine[9] determined by the measurement of infrared absorptions. The value of $K$ for the phenol + triethylamine complex is reported to be about 83.8 l./mol.[10] by the measurement of ultraviolet absorptions.

If we assume that the distortion polarization does not vary with complex formation and is equal to the molecular refraction $R_D$ at the sodium D line, then we can calculate the permanent dipole moment $\mu_1$ for the proton donor forming the complex. This assumption is not always reasonable, because it is conceivable to ascribe $\Delta P$ to an increase of the atomic polarization. However, we shall carry out tentatively the analysis of experimental data under the assumption that $\Delta P$ arises from the intermolecular charge transfer. The vector subtraction of the dipole moment $\mu$ of the free proton donor from $\mu_1$ gives the increment of the dipole moment due to complex formation. The results of the vector calculations are summarized in Table II.

6) Ultraviolet absorption spectra were measured with a Beckman model DU spectrophotometer.

7) G. J. Brealey and M. Kasha, *J. Am. Chem. Soc.*, **77**, 4462 (1955).

8) G. M. Barrow and E. A. Yerger, ibid., **76**, 5247 (1954).

9) N. Fuson, P. Pineau and M-L. Josien, *J. chim. phys.*, **55**, 454 (1958).

10) S. Nagakura and M. Gouterman, *J. Chem. Phys.*, **26**, 881 (1957).

## Discussion

It is generally believed that the hydrogen bond is not only of the electrostatic, but also of the covalent character. If the hydrogen bond is somewhat of the covalent character, structure III among the following three

(I) $O \cdots H \cdots Y$

(II) $O^- \quad H^+ \cdots Y$

(III) $O^- \cdots H - Y^+$

will play a relatively important role. Then the observed increment of the dipole moment $\vec{\Delta\mu}_T = \vec{\mu}_1 - \vec{\mu}$ is considered to be due to the contribution of structure III in the case of benzyl alcohol + triethylamine, whereas in the phenol + triethylamine system, polarization of $\pi$-electrons of phenol will, to a certain extent, arise owing to the lone pair field of triethylamine. This induced moment will be of the magnitude of 0.16 D, as estimated from the detailed description for the phenol + dioxane system. In systems such as phenol + triethylamine, therefore, the vector subtraction of 0.16 D from $\Delta\mu_T$ gives the average increment of the dipole moment due to the contribution of the structure III. Furthermore, in the case of phenol + bipyridyl, it must be considered that polarization of $\pi$-electrons will be induced in pyridine owing to the proton field of phenol. This calculation is very difficult, and we could not estimate this value. The increase of the dipole moment $\Delta\mu_D$ arising from delocalization in this system, therefore, may be smaller than the tabulated $\Delta\mu_D$ which gives the upper limit.

If we estimate the O···Y distance from the shift of the wave number of the OH stretching vibration[11], the electric moment for structure III is evaluated. Moreover, when we suppose that the ratio of the weight of structure I to that of structure II is the same as in a free state, then we can estimate the contribution of structure III from the increment of the dipole moment. The results thus obtained are shown for all systems in Table II. The large contribution of structure III means the weakening of the OH bond, which is reflected on the decrease of the force constant of the OH bond, and hence leads to a decrease in the wave number of the OH stretching vibration. The wave number shift $\Delta\nu$ of the OH stretching vibration has often been correlated with the strengths of the hydrogen bonds. Therefore, we may expect the correlation of $\Delta\nu$ with the weight of structure III. The observed $\Delta\nu$'s for the OH stretching vibration are given in the last column in Table II. The weight of structure III is plotted against $\Delta\nu$ in Fig 1. The four complexes lie on a straight line except benzyl alcohol + triethylamine and phenol + triethylamine, but the latter two complexes show extraordinarily great values for the weight of structure III in spite of the small $\Delta\nu$. If the spectroscopic results are correct, it seems that there are some questions about the above-mentioned treatment of the dielectric data. This is because it is natural to expect that the weight of structure III varies continuously with $\Delta\nu$. However, it has already been found by Barrow[12] that when pyridine and triethylamine are used as proton acceptors, the latter shows a character considerably different from that of the former. He distinguished acetic acid + pyridine from acetic acid + triethylamine, and called the former and the latter the hydrogen bonded complex and the hydrogen bonded ion pair, respectively. If we accept the idea suggested by Barrow, the hydrogen bonded complex belongs to a different category from the hydrogen bonded ion pair, that is to say, there is a distinct boundary between the former and the latter. The dielectric data suggest this idea, but it seems difficult to understand even qualitatively that benzyl alcohol + triethylamine is of the ion pair character without showing an intermediate character. This point will be discussed elsewhere in near future.

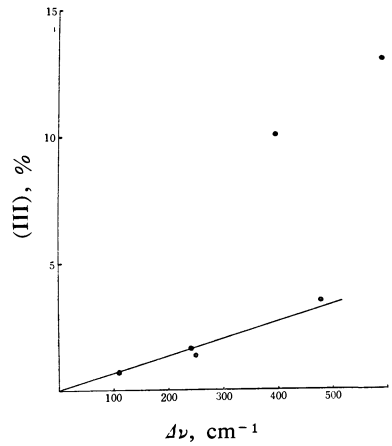



Fig. 1. The correlation of the weight of the structure III with $\Delta\nu$.

## Summary

The dielectric measurements were carried out for benzyl alcohol + $\alpha$, $\alpha'$-bipyridyl, benzyl alcohol + triethylamine, phenol + $\alpha$, $\alpha'$-bipyridyl and phenol + triethylamine by using

11) K. Nakamoto, M. Margoshes and R. E. Rundle, *J. Am. Chem. Soc.*, 77, 6480 (1955).

12) G. M. Barrow, ibid., 78, 5802 (1956).

benzene as a solvent, and the polarization value for each system was calculated. The additional moments due to complex formation were evaluated, as in the previous paper, from both the polarization data and the spectroscopically determined formation constants. Then the weight of structure III was estimated and correlated with the wave number shift $\Delta\nu$ of the OH stretching vibration.

The authors wish to express their thanks to Dr. M. Momotani and Mr. M. Shiro of the Momotani Juntenkan Co., Ltd. for their kind permission to use an infrared spectrometer. The expense of this work has been partly defrayed by a grant from the Ministry of Education.

*Department of Chemistry*
*Faculty of Science*
*Osaka City University*
*Kita-Ku, Osaka*

# *Studies on Antibiotics and Related Substances. XII. Syntheses of 10-Oxo-11-dodecenoic Acid and 11-Oxo-12-tridecenoic Acid, Antitumor Substances*[1]

By Mitsuhiro KINOSHITA and Sumio UMEZAWA

(Received August 18, 1960)

A recent publication[2] from this laboratory described the syntheses and antitumor activities of some methylene derivatives of ketocarboxylic acids, among which the calcium salt of 4-keto-5-hexene-1-carboxylic acid was found to have low toxicity as well as strong activity. The present paper is concerned with an extension of this work and presents the syntheses and antitumor activities of two higher members of even- and odd-numbered carbon acids of the above mentioned series. The syntheses have been worked out as shown in the accompanying chart.

$HO_2C(CH_2)_3CO_2C_2H_5$ → $Br(CH_2)_8CO_2C_2H_5$
I II

→ $CH_3CO\cdot CH(CO_2C_2H_5)\cdot(CH_2)_3CO_2C_2H_5$ → IVa
III

$CH_3CO(CH_2)_nCO_2H$
IVa, IVb

→ $HCl\cdot(CH_3)_2N(CH_2)_2CO(CH_2)_nCO_2H$
Va, Vb

→ $HCl\cdot(CH_3)_2N(CH_2)_2CO(CH_2)_nCO_2CH_3$
VIa, VIb

→ $I(CH_3)_3N(CH_2)_2CO(CH_2)_nCO_2CH_3$
VIIa, VIIb

→ $CH_2=CHCO(CH_2)_nCO_2CH_3$
VIIIa, VIIIb

→ $CH_2=CHCO(CH_2)_nCO_2H$
IXa, IXb

IVa, Va, VIa, VIIa, VIIIa, IXa: $n=9$;
IVb, Vb, VIb, VIIb, VIIIb, IXb: $n=8$

**11-Oxo-12-tridecenoic Acid (IXa).**—Ethyl 9-bromononanoate (II) was prepared from ethyl hydrogen sebacate by the method[3] used for methyl 5-bromovalerate. The bromoester was converted into 13-(dimethylamino)-11-oxotridecanoic acid hydrochloride (Va) by the sequence of acetoacetic ester condensation, decarboxylation and the Mannich reaction. The methyl ester VIa of the Mannich base hydrochloride was converted into its free base and then to the methiodide VIIa. Thermal degradation of the methiodide afforded the desired methylene derivative VIIIa in a yield of 75.5%. Hydrolysis of the ester VIIIa with hydrochloric acid in acetone afforded 11-oxo-12-tridecenoic acid IXa.

The ultraviolet absorptions of VIIIa and IXa in methanol solution showed peaks at 210, 317~318 and 210, 317 mμ, respectively, suggesting the presence of α, β-unsaturated ketone group (Fig. 1), The infrared absorption characteristics of VIIIa and IXa were just as expected,

1) Presented at the 13th Annual Meeting of the Chemical Society of Japan, Tokyo, April 1960.
2) M. Kinoshita and S. Umezawa, This Bulletin, 33, 1075 (1960).
3) C. F. H. Allen and C. W. Wilson, "Organic Syntheses," Coll. Vol. 3 (1955), p. 579.

showing the presence of double bond, conjugated carbonyl and carboxyl groups (Fig. 2 and Fig. 3).

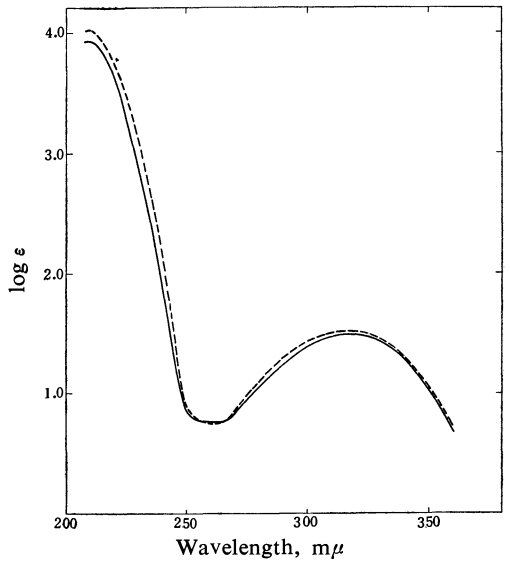



Fig. 1. Ultraviolet absorption spectra of methyl 11-oxo-12-tridecenoate (VIIIa) (----) and 11-oxo-12-tridecenoic acid (IXa) (——) in methanol.

Ozonolysis of the unsaturated keto-acid IXa gave formaldehyde, indicating the presence of a terminal methylene group.

As described above, 11-oxo-12-tridecenoic acid was obtained when the hydrolysis of methyl 11-oxo-12-tridecenoate (VIIIa) with hydrogen chloride in acetone was followed by adjustment of pH to feebly alkaline with a saturated solution of sodium bicarbonate and by removal of acetone at 60~65°C. However, it has been found that 13-chloro-11-oxotridecanoic acid was obtained by a similar procedure except that acetone was removed under cooling at about 5°C. On being treated with an aqueous acetone solution of sodium bicarbonate at 60~65°C, the saturated chloro derivative afforded IXa.

**10-Oxo-11-dodecenoic Acid (IXb).** — 12-(Dimethylamino)-10-oxododecanoic acid hydrochloride(Vb) was prepared from 10-oxo-undecanoic acid which had been described by J. Cason[4]. An analogous sequence of reactions as described above in the synthesis of IXa has been applied to yield the title compound.

Both 11-oxo-12-tridecenoic acid and 10-oxo-11-dodecenoic acid have been found to possess antitumor and antifungal activities. These compounds showed rather higher toxicity in

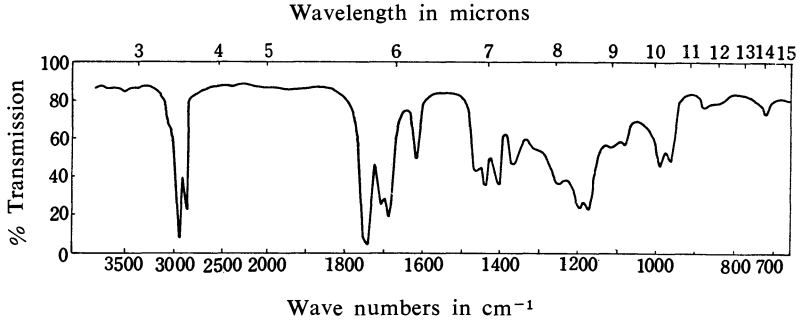



Fig. 2. Infrared absorption spectrum of methyl 11-oxo-12-tridecenoate (VIIIa) (liquid).

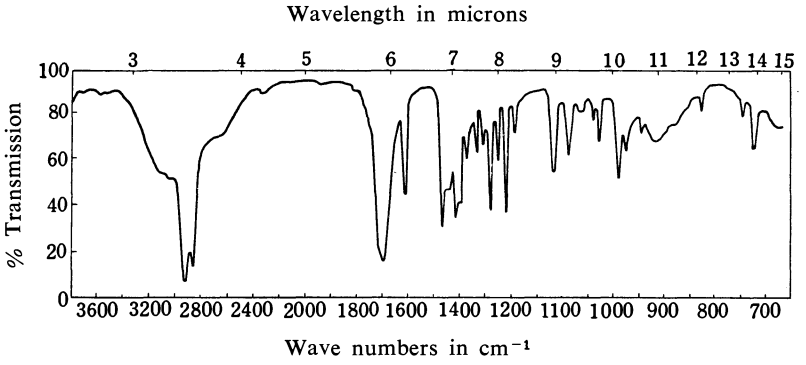



Fig. 3. Infrared absorption spectrum of 11-oxo-12-tridecenoic acid (IXa) (Nujol).

4) J. Cason, *J. Am. Chem. Soc.*, 68, 2078 (1946).

comparison with 4-keto-5-hexene-1-carboxylic acid, which was previously reported[2].

## Experimental

**Ethyl 9-Bromononanoate (II).**—This preparation was carried out according to the method used for methyl 5-bromovalerate[3]. Ethyl hydrogen sebacate (139 g.) was dissolved in a solution of potassium hydroxide (40 g.) in water (1.8 l.). A solution of silver nitrate (103 g.) in water (1.2 l.) was added under stirring. The precipitate of ethyl silver sebacate was collected, washed with methanol (400 ml.) and dried in a vacuum desiccator overnight. The silver salt was finely powdered, sieved through a 60-mesh screen and again dried in vacuo at 100°C over phosphorus pentoxide for 15 hr.; yield 183 g. (90%). To a stirred suspension of the dried salt in dry carbon tetrachloride (238 ml.) was added dry bromine (27.2 ml.) over a 45-min. period, and then the mixture was refluxed for 1 hr. on a water bath. The resulting mixture was filtered to remove silver bromide, which was washed with warm carbon tetrachloride (68 ml.). The filtrate was washed with 10% sodium carbonate and dried over sodium sulfate. The filtration followed by the removal of the solvent afforded a crude product of the title compound boiling at 148.5~151.8°C (9.8 mmHg), yield 80.1 g. (50% based upon ethyl hydrogen sebacate). Redistillation of the product gave an analytical sample, b. p. 147.5~148.5°C (8.9 mmHg), $n_D^{20}$ 1.4622.

Found: C, 50.02; H, 8.14; Br, 30.35. Calcd. for $C_{11}H_{21}O_2Br$: C, 49.81; 7.94; Br, 30.19%.

**Ethyl 10-Oxoundecane-1, 9-dicarboxylate (III).**—A solution of sodioacetoacetic ester was prepared from sodium (7.75 g.), absolute ethanol (135 ml.) and ethyl acetoacetate (43.9 g.). Ethyl 9-bromononanoate (II) was added at 40~45°C under stirring in a 45 min. period and then the mixture was refluxed on a water bath for 2 hr. After filtration of sodium bromide, the filtrate was concentrated under reduced pressure. Distillation of the residue gave ethyl 10-oxoundecane-1,9-dicarboxylate, b. p. 173~191°C (5 mmHg), yield 62.3 g. (58.8%). Redistillation gave an analytical sample; b. p. 188.5~191.4°C (1.8 mmHg), $n_D^{20}$ 1.4051.

Found: C, 64.80; H, 9.68. Calcd. for $C_{17}H_{30}O_5$: C, 64.94; H, 9.62%.

**11-Oxododecanoic Acid (IVa).**—A mixture of ethyl 10-oxoundecane-1,9-dicarboxylate (14.6 g.), 35% hydrochloric acid (26.3 ml.) and glacial acetic acid (50 ml.) was refluxed in an oil bath (125~130°C) for 1.5 hr. After cooling, the mixture was extracted with five 40 ml. portions of ether. The extract was evaporated to yield a crude solid of the title compound. Recrystallization from petroleum benzine (45~80°C) gave 82.5 g. (82.5%) of crystals. Repeated recrystallization from the same solvent gave an analytical sample, m. p. 62.8~63.7°C[5].

Found: C, 67.36; H, 10.08. Calcd. for $C_{12}H_{22}O_3$: C, 67.25; H, 10.35%.

5) J. Cason et al. recently reported m. p. 61~61.5°C of this compound which was prepared by an alternative method; see J. Cason and D. J. McLeod, *J. Org. Chem.*, 23, 1499 (1958).

**13-(Dimethylamino)-11-oxotridecanoic Acid Hydrochloride (Va).**—A mixture of 10-oxododecanoic acid (IV) (5.0 g.) and dimethylamine hydrochloride (1.9 g.) was heated at 110~115°C. To a resulting melt was added paraformaldehyde (0.7 g.) and the mixture was stirred at 105°C for 45 min. Evaporation under reduced pressure to remove moisture gave a solid, which was recrystallized from absolute ethanol to afford fine needles of 13-(dimethylamino)-11-oxotridecanoic acid hydrochloride, m. p. 145.0~146.5°C, yield 2.15 g. (31.2%). Repeated recrystallization from the same solvent gave an analytical sample, m. p. 145.5~146.5°C.

Found: C, 58.72; H, 9.70; N, 4.59. Calcd. for $C_{15}H_{30}O_3NCl$: C, 58.54; H, 9.83; N, 4.56%.

**Methyl 13-(Dimethylamino)-11-oxotridecanoate Hydrochloride (VIa).**—A mixture of 13-(dimethylamino)-11-oxotridecanoic acid hydrochloride (Va) (3.85 g.) in absolute methanol (40 ml.) was saturated with dry hydrogen chloride and allowed to stand overnight. Removal of the solvent under reduced pressure afforded the title compound as colorless fine needles, yield 3.85 g. (96.3%). An analytical pure sample was obtained by recrystallization from absolute methanol-ether followed by fractional sublimation under reduced pressure; m. p. 105~107°C.

Found: C, 59.44; H, 9.55; N, 4.28. Calcd. for $C_{16}H_{32}O_3NCl$: C, 59.67; H, 9.95; N, 4.38%.

**Methyl 13-(Dimethylamino)-11-oxotridecanoate Methiodide (VIIa).**—The crude methyl 13-(dimethylamino)-11-oxotridecanoate hydrochloride (2.55 g.) was triturated with water (3 ml.) and 50% aqueous potassium carbonate solution (5.5 ml.). The separated oil was extracted with eight 10 ml. portions of ether. After the extract was dried with fused potassium acetate, the ether was removed by distillation to give the crude crystalline solid of methyl 13-(dimethylamino)-11-oxo-tridecanoate melting at 22.0~23.0°C. Yield, 2.04 g. (90.4%). The product (2.0 g.) was dissolved in a mixture of absolute benzene (8.5 ml.) and absolute acetone (4.3 ml.) and to the solution was added methyl iodide (9.64 ml.) rapidly. The reaction was exothermic and immediately afforded a crystalline methiodide VIIa, which was washed with benzene-acetone (2:1); m. p. 142.5~144.8°C, yield, 3.05 g. (89.8%).

Found: C, 47.99; H, 7.59 N, 3.34. Calcd. for $C_{17}H_{34}O_3NI$: C, 47.79; H, 7.96; N, 3.28%.

**Methyl 11-Oxo-12-tridecenoate (VIIIa).**—A sample of the above methiodide VIIa (3.0 g.) was placed in a small distillation flask and heated at 164°C in an oil bath under highly reduced pressure (0.005 mmHg). The colorless crystals of methyl 11-oxo-12-tridecenoate were obtained in a receiver cooled in a dry ice-methanol bath; 1.27 g. (75.7%). Microdistillation gave an analytical sample; b. p. 85~90°C (bath temperature) (0.002 mmHg), m. p. 7.5~8.5°C.

Found: C, 69.88; H, 10.14. Calcd. for $C_{14}H_{24}O_3$: C, 69.96; H, 10.07%.

Maxima in the ultraviolet absorption spectrum were observed in methanol at 210 and 317~318 mμ with ε 10,360 and 32.8, respectively. The infrared absorption spectrum with liquid film showed maxima at 1747 (ester C=O), 1692 (conjugated C=O) and 1618 $cm^{-1}$ (C=C).

**11-Oxo-12-tridecenoic Acid (IXa).** — A solution of methyl-11-oxo-12-tridecenoate (VIIIa) (1.100 g.) in acetone (30 ml.) and 35% hydrochloric acid (5 ml.) was kept at 20°C for 20 hr. The solution was cooled in an ice bath and adjusted to pH 8.2~8.4 with a saturated solution of sodium bicarbonate (35 ml.) and with solid sodium bicarbonate (9 g.). After removal of acetone by distillation at 60~65°C, the solution was shaken with two 10 ml. portions of ether to remove any unreacted ester. The water-layer was adjusted to pH 1.8~2.0 with 3 N hydrochloric acid and extracted with five 10 ml. portions of ethyl acetate. After the extract was dried over sodium sulfate, the ethyl acetate was distilled off under reduced pressure to yield a crude product of 11-oxo-12-tridecenoic acid (IXa), which was crystallized from petroleum benzine (b. p. 45~80°C); yield 588 mg. (57.3%), m. p. 57.5~61.0°C. An analytical sample was prepared by fractional vacuum sublimation, m. p. 61.0~62.0°C. The substance gave a negative iodoform reaction. Maxima in the ultraviolet absorption spectrum were observed at 210 and 317 mμ with ε 8575 and 30.5 in methanol, respectively. The infrared absorption spectrum in Nujol showed maxima at 1700 (C=O) and 1616 $cm^{-1}$ (C=C).

Found: C, 68.58; H, 9.97. Calcd. for $C_{13}H_{22}O_3$: C, 68.99; H, 9.80%.

**Ozonolysis of IXa.**—A solution of IXa (100 mg.) in ethyl acetate (5 ml.) was treated with an approximately 2% (by weight) ozone-oxygen mixture at 0°C at a rate of 500 ml./min. for 2 hr. The resulting solution was mixed with water (5 ml.) and zinc dust (150 mg.) and the mixture was refluxed for 30 min. The reaction mixture was filtered while hot into a solution of methone (150 mg.) in ethanol (5 ml.). Dilution with 10 ml. of water afforded the needles of formaldehyde methone, m. p. 187~189°C; yield 22 mg. (17.1%). Admixing with an authentic specimen of formaldehyde methone showed no change of melting point.

**13-Chloro-11-oxotridecanoic Acid.**—A solution of methyl 11-oxotridecenoate (VIIIa) (1.0 g.) in acetone (30 ml.) and 35% hydrochloric acid (5 ml.) was kept at 20°C for 20 hr. The solution was cooled in an ice-bath and adjusted to pH 8.2~8.4 with a saturated solution of sodium bicarbonate (35 ml.) and with solid sodium bicarbonate (9 g.). After removal of acetone under reduced pressure at 5°C, the resulting solution was shaken with two 10 ml. portions of ether to remove any unchanged ester. The water layer was adjusted to pH 1.8~2.0 with 3 N hydrochloric acid and extracted with five 10 ml. portions of ethyl acetate. After the extract was dried over sodium sulfate, the solvent was distilled off in vacuo. The residue was crystallized from petroleum benzine (b. p. 45~80°C) to afford colorless fine plates of 13-chloro-11-oxotridecanoic acid; yield 639 mg. (58.4%), m. p. 58.5~61.0°C. They were recrystallized twice from petroleum benzine, m. p. 61.0~61.8°C. The substance gave a positive Beilstein's test. Admixing with a sample of IXa showed depression of melting point (m. p. 53.0~59.5°C). Only one maximum in the ultraviolet absorption spectrum was observed in methanol at 280 mμ (ε 47.0), which indicated a normal carbonyl group. The infrared absorption spectrum in Nujol showed a normal carbonyl band at 1710 $cm^{-1}$.

Found: C, 59.18; H, 9.01; Cl, 13.56. Calcd. for $C_{13}H_{23}O_3Cl$: C, 59.36; H, 8.74; Cl, 13.50%.

To a solution of the above product (850 mg.) in water (60 ml.) and acetone (60 ml.) was added an excess amount of sodium bicarbonate. Acetone was removed by distillation at 60~65°C. The residue was processed by the same procedure as that used for the preparation of IXa to afford 655 mg. (89.7%) of IXa, m. p. 57.5~60.7°C. Admixing with a sample of IXa showed no change of melting point.

**12-(Dimethylamino)-10-oxododecanoic Acid Hydrochloride (Vb).**—A mixture of 10-oxoundecanoic acid[4] (IVb) (9.60 g.) and dimethylamine hydrochloride (3.93 g.) was heated at 110°C. To the resulting melt was added paraformaldehyde (1.44 g.) and the mixture was stirred at 105°C for 45 min. Evaporation under reduced pressure to remove moisture gave a solid which was crystallized from absolute ethanol (24 ml.) and absolute acetone (24 ml.) to afford the crystals of 12-(dimethylamino)-10-oxododecanoic acid hydrochloride; yield 3.55 g. (25.2%), m. p. 138~139.5°C. From the mother liquor 0.3 g. of the additional crop was obtained, m. p. 137~139°C. The total yield was 27.3%. An analytical sample was obtained by repeated recrystallization from ethanol, m. p. 138.5~139.5°C.

Found: C, 57.17; H, 9.63; N, 4.85. Calcd. for $C_{14}H_{28}O_3NCl$: C, 57.23; H, 9.60; N, 4.77%.

**Methyl 12-(Dimethylamino)-10-oxododecanoate Methiodide (VIIb).** — A mixture of 12-(dimethylamino)-10-oxododecanoic acid hydrochloride (Vb) (4.5 g.) and absolute methanol (46 ml.) was saturated with dry hydrogen chloride and allowed to stand overnight. The solvent was removed by distillation under reduced pressure to afforded a crude product of methyl 12-(dimethylamino)-10-oxododecanoate hydrochloride, which was triturated with water (5.7 ml.) and 50% aqueous potassium carbonate solution (10.4 ml.). The separated oil was extracted with eight 18 ml. portions of ether. After the extract was dried over fused potassium acetate, the ether was removed by distillation to give colorless prisms of methyl 12-(dimethylamino)-10-oxododecanoate (VIb) melting at 34.0~35.5°C; yield 1.7 g. (40.5%). The crude free ester (1.7 g.) was dissolved in a mixture of absolute benzene (7.5 ml.) and absolute acetone (4.8 ml.) and to the solution was added methyl iodide (8.5 g.). The reaction was exothermic and immediately afforded a crystalline methiodide (VIIb), which was washed with benzene-acetone (2:1); m. p. 173°C (decomp., sintered at 141~142°C); yield 2.2 g. (34.7% based upon Vb).

Found: C, 45.97; H, 7.78; N, 3.80. Calcd. for $C_{16}H_{32}O_3NI$: C, 46.49; H, 7.80; N, 3.39%.

**Methyl 10-Oxo-11-dodecanoate (VIIIb).** — A sample of methiodide VIIb (2.20 g.) was placed in a small distillation flask and heated at 164°C in an oil bath under highly reduced pressure (0.005 mmHg). Colorless crystals of methyl 10-oxo-11-dodecenoate (VIIIb) were obtained in a receiver cooled in a dry ice-methanol bath; yield 1.02 g. (84.5%). Microdistillation gave an analytical sample, b. p. 95°C (bath temperature) (0.005 mmHg),

m. p. 12.2~13.2°C. Maxima in the ultraviolet absorption spectrum were observed in methanol at 209 and 317 mμ, with ε 9730 and 39.2, respectively. The infrared absorption spectrum in liquid film showed maxima at 1747 (ester C=O), 1692 (conjugated C=O), 1620 $cm^{-1}$ (C=C).

Found: C, 69.26; H, 9.65. Calcd. for $C_{13}H_{22}O_3$: C, 68.99; H, 9.80%.

**10-Oxo-11-dodecenoic Acid (IXb).**—A solution of methyl 10-oxo-11-dodecenoate (VIIIb) (1.112 g.) in acetone (36 ml.) and 35% hydrochloric acid (6 ml.) was kept at 21°C for 21 hr. The solution was cooled in an ice-bath and adjusted to pH 8.2~8.4 with a saturated solution of sodium bicarbonate (42 ml.) and with solid sodium bicarbonate (9 g.). After removal of acetone by distillation at 65°C the solution was shaken with two 10 ml. portions of ether to remove any unchanged ester. The water-layer was adjusted to pH 1.8~2.0 with 3 N hydrochloric acid and extracted with five 10 ml. portions of ethyl acetate. After the extract was dried over sodium sulfate, ethyl acetate was distilled off under reduced pressure to yield a crude product of 10-oxo-11-dodecenoic acid (IXb) (850 mg.) melting at 47~53.5°C, which was recrystallized from petroleum benzine (b. p. 45~80°C); yield 548 mg. (51%), m. p. 56.0~56.8°C. It gave a negative iodoform reaction. Maxima in the ultraviolet absorption spectrum were observed in methanol at 209~210 and 321 mμ with ε 8660 and 27.9, respectively. The infrared absorption spectrum in Nujol showed maxima at 1702 (C=O) and 1615 $cm^{-1}$ (C=C).

Found: C, 67.76; H, 9.36. Calcd. for $C_{12}H_{20}O_3$: C, 67.89; H, 9.50%.

**Bioassays.**—It is interesting to find that both 11-oxo-12-tridecenoic acid (IXa) and 10-oxo-11-dodecenoic acid (IXb) possess antitumor and antifungal activities. The minimum necessary concentrations of both IXa and IXb for the anti-HeLa cell effect were 125 mcg./ml. Against cells of Ehrlich cartinoma, IXa and IXb had potencies of 1.3 and 1.4 units/mg. (in terms of sarkomycin potency) by cylinder plate method, respectively. The daily intraperitoneal injection of 125 mcg. of IXa and IXb inhibited the ascites increase and prolonged the survival period of mice bearing ascities type of Ehrlich cartinoma by intraperitoneal route. Intravenous acute toxicity tests of IX and IXb in mice indicated the same $LD_{50}$ dose of 670 mcg./mouse.

Both IXa and IXb completely inhibited the growth of *Trichophyton mentagrophytes* and *Penicillium chrysogenum* in a concentration of 7.8 mg./ml., but had comparatively weak activities against other fungi and bacteria tested.

## Summary

1) 11-Oxo-12-tridecenoic acid (IXa) has been prepared from ethyl 9-bromononanoate (II) via 11-oxododecanoic acid (IVa) and the corresponding Mannich base Va.

2) 10-Oxo-11-dodecenoic acid (IXb) has been prepared from 10-oxoundecanoic acid (IVb) via the corresponding Mannich base Vb.

3) It has been found that IXa and IXb possess antitumor and antifugal activities.

The authors are indebted to Dr. H. Umezawa, National Institute of Health, Tokyo, for antitumor assays. Analyses of compounds were performed by Mr. S. Nakada of this laboratory. This work has been supported in part by the Cancer Research Grant of the Ministry of Education and by a grant from the Research Society of Microbiological Chemistry, to which the authors' thanks are due.

*Department of Applied Chemistry*
*Faculty of Engineering*
*Keio University*
*Koganei-shi, Tokyo*

# *On Oxazolo[5 : 4-b]tropones*[1]

By Tetsuo Nozoe, Kozo Doi* and Kazuo Kitahara**

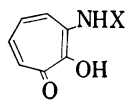
(Received August 29, 1960)

In the course of trying to prepare a pyridotropolone from 3-aminotropolone (I), it has been found that the condensation product of the aminotropolone and ethyl ethoxymethylenemalonate is not the anticipated vinylaminotropolone(II) but the dihydro-oxazolotropone (III), and that the latter III results in fission to form the oxazolotropone (IV) and ethyl malonate on pyrolysis[2]. An analogous observation has also been found in the

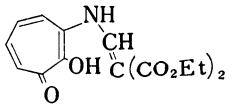
* Present address: The Chemical Research Institute of Non-Aqueous Solution, Tohoku University, Sendai.
** Present address, The Research Laboratory, Tokyo Tanabe Pharmaceutical Co., Tokyo.

1) This work in part was presented at the Tohoku Local Meeting of the Chemical Society of Japan, June, 1956.
2) T. Nozoe, K. Doi and K. Kitahara, This Bulletin, to be published.

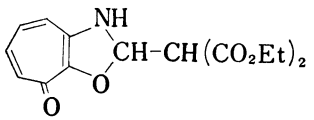
condensation product of *o*-aminophenol and ethoxymethylenemalonate[3]. The structure of the oxazolotropone (IV) was elucidated, at that time, from the similarity of its ultraviolet absorption to that of 2-methyloxazolo[5 : 4-b]-tropone (V) which had been obtained from the reaction of the aminotropolone and acetic anhydride[4].



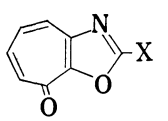
I : X=H
VI : X=CHO



II



III

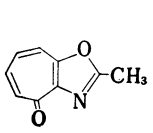


IV : X=H
V : X=$CH_3$

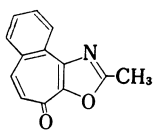
In this communication the present authors will deal with some reactions of the oxazolotropone (IV) and its derivatives, and with the condensation products of the aminotropolone and benzaldehydes in relation to the subject.

Oxazolo[5:4-b]tropone (IV) was also prepared readily by application of methods analogous to those used for the preparations of benzoxazole from *o*-aminophenol to the aminotropolone. Thus, IV was obtained easily on heating the aminotropolone and formamide[5] and on heating 3-formylaminotropolone (VI) in a sealed tube[6].

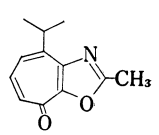
There have been known to date besides IV, the following oxazolotropones: 2-methyloxazolo-[5 : 4-b]tropone[4] (V) and its bromo derivatives, 2-methyloxazolo[4 : 5-b]tropone[7] (VII), and 2-methyloxazolo[5 : 4-b]benzo[d]tropone[8] (VIII). Recently preparations of 2-methyloxazolo[5 : 4-b]tropones from several diaminotropolones and acetic anhydride have been reported[9].



VII



VIII



IX

3) T. Nozoe and K. Doi, ibid., to be published.
4) Y. Kitahara, *Science Repts. Tohoku Univ., Ser. I*, **40**, 83 (1956).
5) S. Niementowski, *Ber.*, **30**, 3064 (1897).
6) A. Ladenburg, ibid., **10**, 1124 (1877).
7) A. W. Johnson and M. Tisler, *J. Chem. Soc.*, 1955, 1841.
8) C. A. Nicholls and D. S. Tarbell, *J. Am. Chem. Soc.*, **74**, 4935 (1951).
9) T. Nozoe, Y. Kitahara, K. Doi and M. Takahashi, *Bull. Chem. Research Inst. Non-Aqueous Solns.*, Tohoku Univ., **9**, 7 (1959).

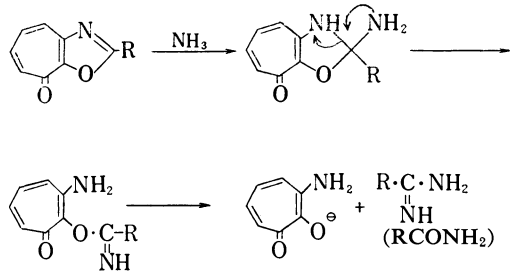
Nicholls and Tarbell[8] assigned the absorption maxima at 1617 and 1567 $cm^{-1}$ in the infrared spectrum of VIII to the tropone carbonyl and the conjugated C=N stretching vibration, respectively. The oxazolotropone (IV) has maxima at 1635 and 1588 $cm^{-1}$, and has a further sharp maximum at 3120 $cm^{-1}$, which is probably considered to originate in the CH vibration of the oxazole ring of IV, because a corresponding absorption is absent in the 2-methyloxazolotropones (V, VII and VIII); benzoxazole has also a maximum at 3125 $cm^{-1}$, whereas 2-methylbenzoxazole lacks this absorption[10].

It had been reported that 3-amino-4-isopropyltropolone affords a monoacetate of m. p. 70.5~73°C on being heated with acetic anhydride[11]. This monoacetate, however, was found to be an oxazolotropone (IX) because of the close resemblance of its ultraviolet absorption to that[2] of IV.

Oxazolotropone (IV), similarly to benzoxazole, was readily hydrolyzed by dilute acid or alkali to form 3-aminotropolone (I). In either case, the formylaminotropolone (V) was not isolated as the intermediate of the reaction.

It has been known that tropolone methyl ethers react with liquid ammonia to give 2-aminotropones. Oxazolotropone (IV) is also regarded as a methyl ether analogue of tropolone and an examination, therefore, was directed to find a possibility of formation of 1, 3-diazaazulene derivative from IV.

When oxazolotropone (IV) was allowed to stand in liquid ammonia overnight, there was obtained the aminotropolone (I) as an ammonolysis product. The 2-methyloxazolotropone (V) resulted in formation of I and additional acetamide on being treated in the same way as the above. The reaction mechanism is probably interpreted as follows:



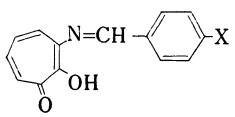
The proposed machanism seems to be endorsed by the following facts: a) While tropolone acetate was ammonolyzed under the same

10) H. M. Randall, R. G. Fowler, N. Fuson and J. R. Dangl, "Infrared Determination of Organic Molecules", Van Nostrand, New York (1949), p. 214.
11) T. Nozoe, Y. Kitahare, E. Kunioka and K. Doi, *Proc. Japan Acad.*, **26**, 38 (1950).

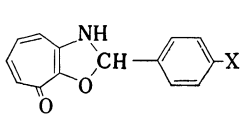
condition to give tropolone and acetamide, 3-acetylaminotropolone was recovered unreacted. b) While the dibenzoyl compound of the aminotropolone was also ammonolyzed readily to give the *N*-benzoylaminotropolone and benzamide under the same condition, the former was recovered likewise in an unreacted state. These facts suggest that the formation of *O*-acylated compound as an intermediate occurs in the respective reaction of the oxazolotropone and liquid ammonia. The cleavage of this kind of oxazole ring recalls the reaction of imino ethers and ammonia resulting in the formation of the corresponding alcohol and amidine[12].

In the subsequent papers[2,3], the authors are to discuss a ring-chain tautomerism between aromatic vinylamines possessing a hydroxyl group in the ortho position and oxazoline derivatives. According to Sachs and Brunetti[13], the reaction product of *o*-aminophenol and 2,4-dinitrobenzaldehyde exists in the form of 2-(2,4-dinitrophenyl)benzoxazoline in place of the expected 2,4-dinitrobenzylidene-*o*-aminophenol. It seems to be very interesting to find whether such a fact would also be applicable to the condensation products of the aminotropolone (I) and benzaldehydes.

Unlike 5-aminotropolone[14], 3-aminotropolone (I) did not give any reaction product when heated with benzaldehyde. Even on being heated with more reactive *p*-nitrobenzaldehyde at 150°C for one hour, a condensation product was not obtained. This difficulty, however, was overcome easily by the use of caustic alkali in the reaction. When an equimolar mixture of the aminotropolone, respective benzaldehyde and sodium hydroxide was heated in methanol, the azomethine derivative (X, XI and XII) could be readily prepared. These products showed red coloration with ferric chloride test and hydrolyzed readily to form the aminotropolone (I) with water or aqueous alcohol. These facts mean that they do not exist in the form of their ring-tautomers of XIII. The same reaction of the aminotropolone and *p*-nitrobenzaldehyde afforded 2-(*p*-nitrophenyl)oxazolotropone (XIV), the structure of which was assumed from the fact that it agreed with a reaction product of the aminotropolone and *p*-nitrobenzoyl chloride.

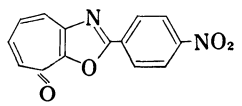



X: X=H
XI: X=Cl
XII: X=$OCH_3$




XIII

12) J. Houben et al., *J. prakt. Chem.*, **105**, 12 (1922).




XIV

While the reaction of the aminotropolone and benzoyl chloride in pyridine produced a mixture of the dibenzoylated and *N*-benzoylated compounds, the reaction of the aminotropolone and *p*-nitrobenzoyl chloride under the same condition resulted in the formation of the oxazolotropone (XIV), which showed no coloration with ferric chloride. An oxazole ring formation in the reaction with benzaldehydes or benzoyl chlorides seems to be more rapid in the case of the aminotropolone (I) than in the case of *o*-aminophenol[15].

## Experimental

The ultraviolet absorptions were measured in methanol solution with a Beckman model DU spectrophotometer. The infrared absorption was measured on potassium bromide disk with a Perkin-Elmer model 21 infrared spectrometer, using a rock salt prism.

**Oxazolo[5:4-b]tropone (IV).** — a) 3-Aminotropolone (I, 0.28 g.) and formamide (1 ml.) was heated under reflux at 220°C. Benzene (2 ml.) was added to the reaction mixture at room temperature and the residual solid was collected. It gave IV (0.1 g.), m. p. and mixed m. p.[2] 150~151°C, after sublimation in vacuo following recrystallization from benzene. b) A mixture of the aminotropolone (I, 1.4 g.) and 80% formic acid (30 ml.) was heated under reflux for 3 hr. The evaporated residue of the solvent was crystallized from ethanol to give 3-formylaminotropolone (VI, 1.2 g.) as yellow prisms, m. p. 167~168°C (reported[4] m. p. 168~169°C). When VI (0.3 g.) in a sealed tube was heated on an oil bath of 250°C for 30 min., the oxazolotropone (IV, 0.1 g.) was obtained.

**Hydrolysis of the Oxazolotropone (IV).** — A mixture of IV (30 mg.) and 3 N hydrochloric acid (1 ml.) or 2 N sodium hydroxide (1 ml.) was heated at 50°C for 30 min. Neutralization of the reaction mixture gave 3-aminotropolone (I), m. p. and mixed[4] m. p. 97~98°C.

**2-Methyl-4-isopropyloxazolo[5:4-b]tropone (IX).** —A mixture of 3-amino-4-isopropyltropolone[11] (30 mg.) and acetic anhydride (1 ml.) was heated under reflux for one hour. The evaporated residue of the solvent, after sublimation in vacuo following crystallization from petroleum ether (b. p. 40~60°C), gave the oxazolotropone (IX) as colorless prisms, undepressed on admixture with an authentic sample which had been reported[11] to be a monoacetate of the aminotropolone.

Found: C, 69.82; H, 6.21; N, 7.35. Calcd. for $C_{11}H_{11}O_2N$: C, 69.82; H, 5.86; N, 7.40%. $\lambda_{max}^{MeOH}$ m$\mu$ (log $\varepsilon$): 245 (4.51), 320 (3.91)

13) F. Sachs and W. Brunetti, *Ber.*, **40**, 3230 (1907).
14) T. Nozoe, S. Seto et al., *Proc. Japan Acad.*, **27**, 426 (1951).
15) R. D. Desai, *J. Chem. Soc.*, **1934**, 1186.

**Ammonolysis of the Oxazolotropone (IV).**—A solution of IV (0.7 g.) in liquid ammonia (50 ml.) was allowed to stand in a pressure bottle for 24 hr. at room temperature. Ammonia was allowed to evaporate, the residue was washed out with methanol (50 ml.), and the evaporated residue of the solvent was crystallized from benzene to give the aminotropolone (I, 0.53 g.).

**Ammonolysis of the 2-Methyloxazolotropone (V).**—A solution of V (0.5 g.) in liquid ammonia (50 ml.) was allowed to stand for 3 days at room temperature. The residual solid of evaporation of ammonia, afer recrystallization from dilute methanol, afforded the aminotropolone (I, 0.3 g.). The evaporated residue of the mother-liquor, after chromatographic purification (alumina—benzene) following crystallization from petroleum ether (b. p. 40~60°C), gave acetamide (50 mg.) of m. p. 80~81°C.

**Ammonolysis of Tropolone Acetate.**—A solution of tropolone acetate (0.4 g.), which prepared according to Doering's description[16], in liquid ammonia (40 ml.) was allowed to stand overnight at room temperature. The evaporated residue of ammonia was dissolved in water, the residual solution was acidified with dilute hydrochloric acid, and extracted with chloroform (20 ml.). The extract, after re-extraction with dilute alkali followed by evaporation in vacuo, gave acetamide (50 mg.). The alkaline extract, after acidification with dilute hydrochloric acid, and after being extracted with chloroform and subsequent evaporation of the solvent, gave tropolone (0.27 g.). The result similar to the above has been recently reported by Sato[17]. An experiment on ammonolysis of 3-acetylaminotropolone under the same condition ended in the recovery of unreacted material.

**Condensation of 3-Aminotropolone (I) and Benzaldehydes.**—To a solution of I (0.28 g.), respective benzaldehyde (0.02 mol.) and methanol (5 ml.), was added a solution of sodium hydroxide (80 mg.) in water (0.5 ml.), and the mixture was heated under reflux for 30 min. Then the reaction mixture was diluted with water (10 ml.), neutralized with acetic acid, and extracted with chloroform (30 ml.). The evaporated residue of the solvent was crystallized from a suitable solvent to give :

*3-Benzylideneaminotropolone (X):* yellow leaflets (chloroform), m. p. 142~143°C,

Found : N, 6.19. Calcd. for $C_{14}H_{11}O_2N$ : N, 6.22%.

*3-p-Chlorobenzylideneaminotropolone (XI):* yellow prisms (chloroform), m. p. 124~125°C,

Found : N, 5.68. Calcd. for $C_{14}H_{10}O_2NCl$ : N, 5.40%.

*3-Anisylideneaminotropolone (XII):* yellow prisms (benzene), m. p. 110~111°C.

Found : N, 5.34. Calcd. for $C_{15}H_{13}O_3N$ : N, 5.49%.

All of the three reaction products showed red coloration with alcoholic ferric chloride and hydrolyzed easily to form the aminotropolone (I) on being shaken with water or aqueous alcohol.

**2-*p*-Nitrophenyloxazolo[5 : 4-b]tropone (XIV).**—a) A solution of sodium hydroxide (0.1 g.) in water (0.5 ml.) was added to a solution of the aminotropolone (I, 0.35 g.), *p*-nitrobenzaldehyde (0.4 g.) and methanol (5 ml.), and heated under reflux for 30 min. The reaction mixture, treated as above, afforded the oxazolotropone (XIV, 0.2 g.) as yellow needles, m. p. 251~252°C. It did not show any coloration with ferric chloride.

Found : C, 62.69 ; H, 3.01 ; N, 10.45. Calcd. for $C_{14}H_8O_4N_2$ : C, 62.69 ; H, 3.12 ; N, 10.51%. $\lambda_{max}^{MeOH}$ mμ (log ε): 265 (4.44), 374 (4.06).

b) A mixture of the aminotropolone (0.14 g.), *p*-nitrobenzoyl chloride (0.19 g.), and pyridine (4 ml.) was stirred for one hour at room temperature. It was then diluted with water (10 ml.) and the residual solid was collected. Recrystallization of it from nitrobenzene gave the above XIV, m. p. and mixed m. p. 251~252°C.

**Benzoylation of 3-Aminotropolone (I).**—A solution of I (0.14 g.), benzoyl chloride (0.14 g.) and pyridine (2 ml.) was stirred for 20 min. at room temperature, then diluted with water (10 ml.), and the residual solid (0.19 g.) of m. p. 150~152°C, was collected. Its fractional recrystallization from a mixture of benzene and methanol afforded 3-benzoylaminotropolone benzoate from the less soluble portion, and 3-benzoylaminotropolone from the more soluble portion,

*3-Benzoylaminotropolone Benzoate :* pale yellow leaflets, m. p. 174°C, which showed no coloration with ferric chloride.

Found : C, 73.29 ; H, 4.40 ; N, 4.07. Calcd. for $C_{21}H_{15}O_4N$ : C, 73.29 ; H, 4.38 ; N, 4.06%.

*3-Benzoylaminotropolone :* pale yellow needles, m.p. 146°C, which showed red coloration with ferric chloride.

Found : C, 69.62 ; H, 4.72 ; N, 6.00. Calcd. for $C_{14}H_{11}O_3N$ : C, 69.70 ; H, 4.59 ; N, 5.80%.

When a mixture of the dibenzoylated compound (0.5 g.) and liquid ammonia (60 ml.) was allowed to stand for 7 days at room temperature, 3-benzoylaminotropolone and benzamide were obtained by treatment similar to the above description.

The authors express their gratitude to Messrs. K. Kato, S. Ohyama, A. Iwanaga and S. Azumi for microanalyses, and to Mr. Y. Ikegami for the infrared spectral measurement.

*Department of Chemistry*
*Faculty of Science*
*Tohoku University*
*Katahira-cho, Sendai*

16) W. von E. Doering and L. H. Knox, *J. Am. Chem. Soc.*, **73**, 828 (1951).
17) T. Sato, *J. Chem. Soc. Japan, Pure Chem. Sec.* (*Nippon Kagaku Zasshi*), **80**, 1058 (1959).

# *Colloid Chemical Studies on Starching Materials. III. Dynamic Viscosity and Dynamic Rigidity of Starch Solutions*

By Masayuki NAKAGAKI* and Kazuko MURAGISHI

(Received August 18, 1960)

In recent years, anomalous flow properties of colloidal systems have been investigated extensively in the field of rheology, in which the flow property is explained by a combination of rigidities and viscosities. Examples of the combination frequently used are so called Maxwell's model and Voigt's model. Even for fluid, it is required to presuppose some rigidity element to explain its flow property on the basis of these models. The existence of a kind of rigidity may be understood by considering the fact that the so-called structural viscosity of a solution can be explained by assuming a kind of yield value, as shown in a previous paper of this series on dilute solutions of polyvinyl alcohol[1].

In the present paper, starch solutions, also known to show structural viscosity, are examined by a rheometer to obtain the frequency dependencies of dynamic rigidity and dynamic viscosity, and an attempt is made to explain these by Maxwell's and Rouse's model.

## Experimental

**Rheometer.**—A top-drive coaxial rheometer was used. Details of the rheometer were described by Nakagawa and Seno[2]. The sample to be studied was put in the gap between the coaxial internal and external cylinders. The radius of the internal cylinder $r_1$ was 2.00 cm. and that of the external cylinder $r_2$ was 2.50 cm. The depth $l$ of the immersion of the internal cylinder was 15.0 cm., which was equal to the height of the cylinder. The moment of inertia $I$ of the internal cylinder was 3005 g. cm$^2$. The internal cylinder was hung by a quenched steel wire whose diameter was 1.0 mm., and whose length was 92.5 cm. The torsional constant of the wire determined from the period of the free torsional oscillation, $k$, was $0.90\times10^5$ dyne cm.

At the top of the wire, a sinusoidal torsional oscillation was applied and the oscillation of the internal cylinder was recorded on a photographic paper as a Lissajous' figure obtained by combining perpendicularly the oscillation of the internal cylinder and the oscillation at the top of the wire. The Lissajous' figure thus obtained was an ellipse.

The dynamic viscosity $\eta$ and the dynamic rigidity $G$ are calculated by the equations:

$$\left.\begin{aligned}\eta&=\frac{R}{4\pi l}\left(\frac{1}{r_1^2}-\frac{1}{r_2^2}\right)=47.8\times10^{-5}\times R(\text{poises})\\ G&=\frac{K}{4\pi l}\left(\frac{1}{r_1^2}-\frac{1}{r_2^2}\right)=47.8\times10^{-5}\times K(\text{dyne/cm}^2)\end{aligned}\right\}\quad(1)$$

where $R$ and $K$ are the quantities to be determined experimentally by using the equations:

$$\left.\begin{aligned}R&=k\sin\phi/\omega p\\ K&=k(\cos\phi/p-1)+I\omega^2\end{aligned}\right\}\quad(2)$$

Here, the lag angle $\phi$ and the amplitude ratio $p$ are to be obtained by the analysis of the photographic picture, and $\omega$ is the angular frequency. The latter is defined by

$$\omega=2\pi/T_f\quad(3)$$

where $T_f$ is the period of oscillation. All experiments were made in a thermostat at 30°C.

**A Check of the Rheometer by Using Distilled Water.**—Distilled water is an example of so-called Newtonian liquid, for which $G=0$ and $K=0$. All the Lissajous' figures obtained for distilled water by the present rheometer were linear, which give $\sin\phi=0$ and $R=0$. This means that the viscosity of distilled water was too small to be detected by this apparatus, that is $\eta\fallingdotseq0$. Since $\sin\phi=0$ and $\cos\phi=1$ for distilled water, Eq. 2 can be simplified to

$$1/p=1-(I/k)\omega^2\quad(4)$$

Therefore the relation between $1/p$ and $\omega^2$ should be expressed by a straight line which intersects with the ordinate at $1/p=1$ and has an inclination of $-0.0333$ according to the values of $I$ and $k$ given above. In Fig. 1, the experimental values are shown by open circles, while the theoretical relation give by Eq. 4 is shown by a straight line. The agreement is fairly good. Apparent values of the rigidity $G$ of distilled water calculated from the experimental values of $p$ will give the experimental error. The error in the worst case was about 18 dyne/cm$^2$ (for $\omega=11.5$).

**Materials and Preparation of Pastes.** — The materials used were potato starch, sweet potato starch, and rice starch of pharmaceutical grade. The starch, dried in a desiccator and weighed accurately, was put in a flask, water was added, and it was heated at 90°C for 30 min. stirring with a glass rod inserted through a hole in a rubber stopper fitted loosely to the flask. For the heating, the temperature of a water bath was raised gradually from room temperature to boiling, and kept boiling

* Present address: Faculty of Pharmacy, Koyto University, Sakyo-ku, Kyoto.

1) M. Nakagaki and A. Shimazaki, This Bulletin, **29**, 60 (1956).

2) T. Nakagawa and M. Seno, ibid., **29**, 471 (1956).

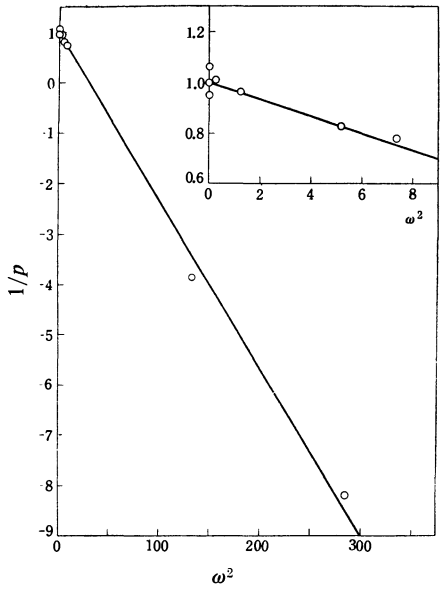



Fig. 1. Distilled water.

for 30 min. The temperature in the flask was 90°C when the bath water was boiling. Then, the flask was placed in cold water for cooling. The paste was used for the measurement immediately after it was cooled, and the measurement was finished in the same day.

## Results and Discussion

The values of the dynamic viscosity $\eta$ and the dynamic rigidity $G$ thus obtained are shown in the following figures. Fig. 2 is for 3% potato starch paste, Fig. 3 is for 5% potato starch paste, Fig. 4 is for 5% sweet potato

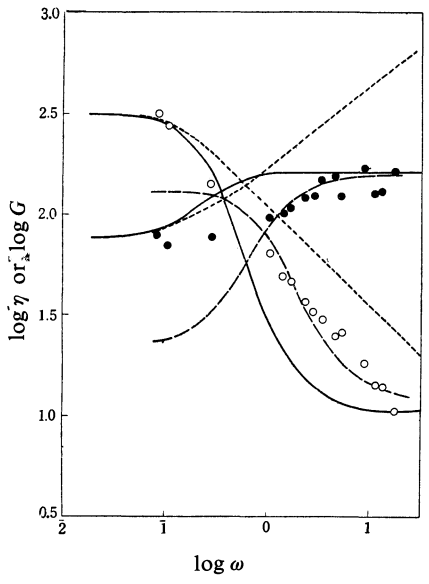



Fig. 2. $\eta(\bigcirc)$ and $G(\bullet)$ of 3% potato starch paste.

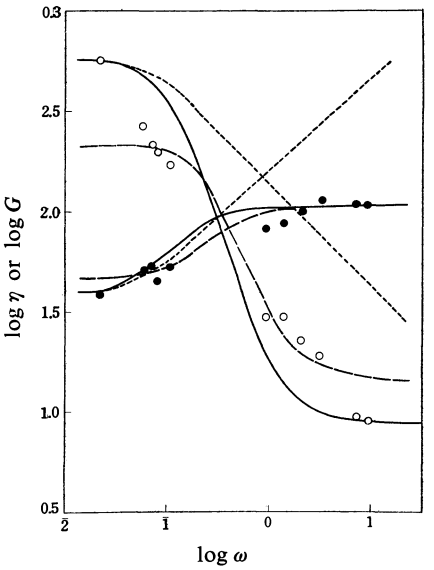



Fig. 3. $\eta(\bigcirc)$ and $G(\bullet)$ of 5% potato starch paste.

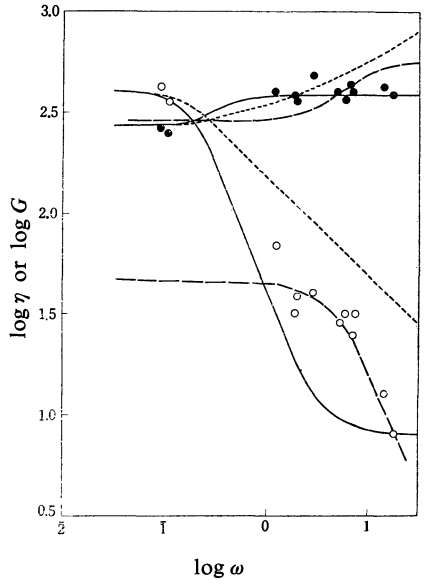



Fig. 4. $\eta(\bigcirc)$ and $G(\bullet)$ of 5% sweet potato starch paste.

starch paste, and Fig. 5 is for 5% rice starch paste. In these figures, the abscissa is $\log\omega$, while the ordinate is $\log\eta$ for open circles and is $\log G$ for closed circles.

For all these pastes, the dynamic viscosity decreased and the dynamic rigidity increased with the increase of the frequency. This is, as is well known, the usual viscoelastic behavior. To describe the viscoelastic behavior, Maxwell's four element model is often used. By this model the frequency dependence of

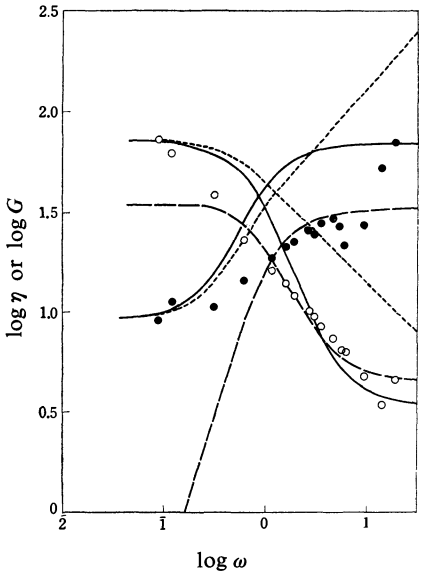



Fig. 5. $\eta$(○) and $G$(●) of 5% rice starch paste.

the dynamic viscosity and the dynamic rigidity are expressed by the equations,

$$\eta=\eta_2/(1+\tau_2^2\omega^2)+\eta_3 \quad (5)$$

$$G=G_1+G_2\tau_2^2\omega^2/(1+\tau_2^2\omega^2) \quad (6)$$

where, $\eta_2$, $\eta_3$, $G_1$ and $G_2$ are constants, and $\tau_2$ is also a constant called relaxation time, and is given by the relation,

$$\tau_2=\eta_2/G_2 \quad (7)$$

An attempt was made to see how well these equations can explain the experimental results.

In order to find out the values of the parameters, $G_1$, $G_2$, $\eta_2$, $\eta_3$ and $\tau_2$, attaching importance equally to both $\eta$ and $G$, the following procedure was at first used. By using Eqs. 5, 6 and 7,

$$\left.\begin{aligned}\eta&=B-\tau_2 G\\ B&=\eta_3+\eta_2+\tau_2 G_1\end{aligned}\right\} \quad (8)$$

can be derived. Therefore, if one plots experimental values of $\eta$ and $G$ of the same $\omega$ value on the ordinate and the abscissa, respectively, one should obtain a linear relationship and one can determine the value of $B$ and $\tau_2$. Then, by plotting experimentally obtained $\eta$ and $(B-\tau_2 G)$ on the ordinate (these quantities are not necessarily equal with each other because of experimental errors and any deviation from Maxwell's model), and $1/(1+\tau_2^2\omega^2)$ on the abscissa, one should again obtain another linear relationship which gives the value of $\eta_2$ and $\eta_3$. The parameter $G_1$ is obtained from these values on the basis of the second equation of Eq. 8. Thus, one should be able to determine the values of all the parameters, $\eta_2$, $\eta_3$, $G_1$, $G_2$, and $\tau_2$. However, the experimental data seemed not to agree with Maxwell's model in the present case, because two expected linear relationships were not exactly satisfied. By trying, however, to draw straight lines to satisfy the experimental plots as far as possible, the values of the parameters were determined, as shown in lines called I in Table I. Calculated values of $\log\eta$ and $\log G$ by using these values are shown in Figs. 2—5 with broken curves. It is seen that these curves partially satisfy the experimental plots but not in the whole range of the frequency.

The second method to determine the parameter values of Maxwell's four element model was used as follows, according to the experience that most curves in the previous case were already almost horizontal in the larger and smaller range of $\log\omega$. Eqs. 5 and 6 show that

$$\left.\begin{aligned}&\eta(\tau_2\omega\ll 1)=\eta_2+\eta_3\\ &\eta(\tau_2\omega\gg 1)=\eta_3\\ &G(\tau_2\omega\ll 1)=G_1\\ &G(\tau_2\omega\gg 1)=G_1+G_2\end{aligned}\right\} \quad (9)$$

On the basis of these equations, it was assumed that the experimental values of $\eta$ and $G$ for the smallest $\omega$ are $(\eta_2+\eta_3)$ and $G_1$, respectively, and those for the largest $\omega$ are $\eta_3$ and $(G_1+G_2)$. The values of the parameters thus obtained

Table I. Parameters in Maxwell's four element model
(in c. g. s. units)

| Starch | Concentration | No. | $G_1$ | $G_2$ | $\eta_2$ | $\eta_3$ | $\tau_2$ |
|---|---|---|---|---|---|---|---|
| Potato | 3% | I | 22.5 | 129 | 120 | 13.0 | 0.933 |
| | | II | 78.5 | 83.1 | 303 | 10.6 | 3.65 |
| Potato | 5% | I | 45.3 | 60.0 | 200 | 15.0 | 3.33 |
| | | II | 38.8 | 66.2 | 550 | 8.82 | 7.55 |
| Sweet potato | 5% | I | 290 | 287 | 43.2 | 3.17 | 0.150 |
| | | II | 268 | 120 | 411 | 8.01 | 3.43 |
| Rice | 5% | I | 0.32 | 32.6 | 30.5 | 4.60 | 0.937 |
| | | II | 9.21 | 59.6 | 67.6 | 3.41 | 1.13 |

are cited in line II of Table I. By using these values, solid curves in Figs. 2—5 were obtained. Comparing these curves with experimental plots, it is seen that $\log\eta$ decreases with the increase of $\log\omega$ more slowly in experimental plots than in Maxwell's model, and that $\log G$ increases at greater values of $\log\omega$ in experimental plots than in Maxwell's model. Moreover, it is by no means guaranteed experimentally that $\log\eta$ and $\log G$ curves are almost horizontal in the larger and smaller ranges of $\log\omega$.

Considering that these two attempts were not successful, it may be concluded that the viscoelastic behavior of starch paste can not be explained by Maxwell's four element model. Then, Rouse's model was examined. Rouse[3] studied the viscoelastic properties of high polymer solution and obtained theoretical equations. Neglecting the viscosity of solvent, $\eta_s$, because it is far smaller than the viscosity of paste, the equations are:

$$\left.\begin{aligned}\eta&=\eta_0 f_1(\tau\omega)\\ f_1&=(6/\pi^2)\sum_{p=1}^{N}[p^2/(p^4+\tau^2\omega^2)]\end{aligned}\right\}\quad(10)$$

and

$$\left.\begin{aligned}G&=(6/\pi^2)(\eta_0/\tau)f_2(\tau\omega)\\ f_2&=\sum_{p=1}^{N}[\tau^2\omega^2/(p^4+\tau^2\omega^2)]\end{aligned}\right\}\quad(11)$$

The values of $f_1$ and $f_2$ are given in Rouse's paper. These equations are essentially a modification of Maxwell's theory. On comparing these equations with experimental data, it turned out to be necessary to introduce a constant $G_0$ into Eq. 11 to give

$$G=G_0+(6/\pi^2)(\eta_0/\tau)f_2(\tau\omega)\quad(12)$$

Referring the results of the second method of Maxwell's four element model (the line II in Table I), the value of $\eta_0$ should be equal to $(\eta_2+\eta_3)$ and $G_0$ to $G_1$ in order to satisfy the experimental values for small $\omega$ values. If it is further assumed that the value of $\tau$ is equal to $\tau_2$ of the second method, the dotted curves in Figs. 2—5 are obtained. Values of both $\log\eta$ and $\log G$ thus calculated from Eqs. 10 and 12, respectively, are in all cases greater than experimental values. If the value of $\tau$ is to be changed to improve the agreement between the calculated values and the experimental values, the value of $\tau$ should be larger for $\log\eta$ (to shift the theoretical curves toward the left), and smaller for $\log G$ (to shift the curves to the right). Therefore, Rouse's equation can not explain both $\log\eta$ and $\log G$ simultaneously by using a common set of $\eta_0$, $G_0$, and $\tau$. The other feature of Rouse's curves to be mentioned here is that $\log\eta$ decreases with the increase of $\log\omega$ too slowly and $\log G$ increases too rapidly, if they are compared with the experimental data. This difficulty will be removed if one assumes that there are large aggregates of polymer molecules with large values of $\eta_0$ and $G_0$ in a paste under small frequency and that the aggregates change to smaller ones of smaller $\eta_0$ and $G_0$ with the increase of the frequency. Such an assumption of the structural change of paste with the frequency will be discussed in detail in a following paper of this series.

Comparing the values of parameters in the line II of Table I, it is seen that the rigidity of sweet potato starch paste is much greater than potato starch paste, and both the rigidity and viscosity of rice starch paste are smaller than those of potato and sweet potato starch pastes. These are comparisons for pastes prepared by heating at 90°C for 30 min. The viscoelastic properties of starch paste would change by changing the method of preparation, so that the above stated results do not exclude an expectation that rice starch paste would have larger $\eta$ and $G$ values than potato starch paste if the pastes are cooked at a higher temperature for a longer time.

The authors wish to thank Dr. Tsurutaro Nakagawa for his kind advice concerning the construction of the rheometer. The authors also thank Dainihon Ink Manufacturing Co. for supporting this project.

## Summary

The frequency dependences of dynamic viscosity and dynamic rigidity of (3 and) 5% starch pastes were measured by using a top-drive coaxial rheometer for potato starch, sweet potato starch and rice starch at 30°C. The results were compared with Maxwell's four element model and Rouse's model. Neither fit the experimental results. A structural change of the paste depending on the frequency was suggested.

*Faculty of the Science of Living*
*Osaka City University*
*Nishi-ku, Osaka*

3) P. E. Rouse, *J. Chem. Phys.*, **21**, 1272 (1953).

# *Dielectric Investigation on Coals. V. Microwave Dielectric Constant*

By Kazuo CHITOKU and Keniti HIGASI

(Received August 25, 1960)

Dielectric methods have been applied to the study of coals during these several years[1-4]. In the laboratory of the present writers[1,2] measurements were made directly on polished coal plates as well as on mixtures of coal powder and paraffin-wax, and a frequency range from 300 c./sec. to 50 Mc./sec. was employed. In contrast to the work by Groenewege et al.[3,4], special attention was paid to the frequency dependence of dielectric constants and losses of coals. In the present paper new and more complete information will be given which was obtained by use of a wider frequency range including a microwave measurement at 4.28 cm. wavelength. Representative coals were kindly selected and provided for this measurement by Dr. H. Honda, Resources Research Institute of Japan.

### Experimental Apparatus and Method

The dielectric measurement at the microwave frequency of 7000 Mc./sec. was made by use of the transmission method developed by von Hippel and others[5,6]. The block diagram of the apparatus is shown in Fig. 1.

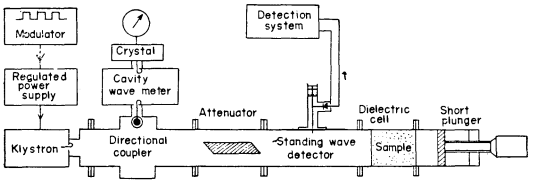



Fig. 1. Block diagram of the apparatus for measuring dielectric constant and loss at 7000 Mc./sec.

The complex dielectric constant $\varepsilon^* = \varepsilon' - j\varepsilon''$ is given by

$$\varepsilon' - j\varepsilon'' = \frac{(1/\lambda_c)^2 - (\gamma_2 d/2\pi d)^2}{(1/\lambda_c)^2 + (1/\lambda_g)^2} \qquad (1)$$

where $\lambda_c$ and $\lambda_g$ are the cut-off wavelength and the wavelength in the air-filled guide, respectively. $\gamma_2$ is the complex propagation factor of the coal sample and $d$ is the thickness of the sample. For determining $\gamma_2 d$ of the sample, the standing wave ratio $E_{min.}/E_{max.}$ and the distance from the sample

TABLE I. MICROWAVE DIELECTRIC CONSTANT OF COAL MIXTURE ESTIMATED BY THE METHOD OF DAKIN AND WORKS[7]

| No. | Specimen | Thickness cm. | Dielectric constant (Short) | (Open) | (Values taken) |
|---|---|---|---|---|---|
| 1 | Taihei | 0.41 | 2.845 | 2.840 | |
| | | 1.40 | 2.87 | 2.85 | 2.86 |
| 2 | Tempoku | 0.40 | 3.15 | 2.85 | |
| | | 1.40 | 2.946 | 2.84 | 2.89 |
| 3 | Nakago-kaso | 0.415 | 2.757 | 2.85 | |
| | | 1.415 | 2.908 | 2.802 | 2.86 |
| 4 | Nakago | 0.410 | 2.837 | 2.789 | |
| | | 0.310 | 2.884 | 2.854 | 2.81 |
| 5 | Kasima | 0.415 | 2.620 | 2.688 | |
| | | 0.910 | 2.726 | 2.692 | |
| | | 1.305 | 2.692 | 2.653 | 2.67 |
| 6 | Pocahontas | 0.40 | 2.926 | 2.720 | |
| | (USA) | 1.40 | 2.887 | 2.683 | 2.79 |
| 7 | Hutago | 0.40 | 2.908 | 2.695 | |
| | | 1.40 | 2.690 | 2.670 | 2.68 |
| 8 | Yubari | 0.40 | 2.923 | 2.700 | |
| | | 0.82 | 2.763 | 2.622 | |
| | | 1.40 | 2.680 | 2.365 | 2.69 |
| 9 | Hasima | 0.405 | 2.802 | 2.660 | |
| | | 0.305 | 2.940 | 2.722 | 2.73 |
| 10 | Kamati | 0.92 | 2.800 | 2.765 | |
| | | 1.40 | 2.812 | 2.765 | 2.79 |
| 11 | Yatake | 0.40 | 2.930 | 2.700 | |
| | | 1.40 | 2.796 | 2.738 | 2.77 |
| 12 | Onuki | 0.405 | 2.910 | 2.735 | |
| | | 1.310 | 2.854 | 2.730 | 2.79 |
| | Paraffin | 0.415 | 2.230 | 2.285 | |
| | | 0.320 | 2.302 | 2.248 | 2.26 |

1) a) I. Miyasita, R. Miura and K. Higasi, This Bulletin, **28**, 148 (1955); b) I. Miyasita and K. Higasi, ibid., **30**, 513 (1957); c) K. Higasi, I. Miyasita and Y. Ozawa, ibid., **30**, 546 (1957), d) I. Miyasita, K. Higasi and M. Kugo, ibid., **30**, 550 (1957); e) K. Higasi, Y. Higasi and I. Miyasita, ibid., **30**, 556 (1957); f) K. Higasi, *Kagaku*, **27**, 148 (1957); g. K. Higasi and Y. Higasi, ibid., **27**, 630 (1957).

2) a) I. Miyasita, *Bull. Res. Inst. Appl. Elec. Hokkaido Univ., (Oyodenki Kenkyujo Iho)*, **5**, 123 (1953); b) I. Miyasita, ibid., **6**, 117 (1954); c) I. Miyasita, ibid., **7**, 17 (1955); d) I. Miyasita, ibid., **9**, 122 (1957).

3) M. P. Groenewege, J. Schuyer and D. W. van Krevelen, *Fuel*, **34**, 339 (1955).

4) D. W. van Krevelen and J. Schuyer, "Coal Science", Elsevier Publ. Co., Amsterdam (1957).

5) S. Roberts and A. R. von Hippel, *J. Appl. Phys.*, **17**, 610 (1946).

6) A. R. von Hippel, "Dielectrics and Waves", John Wiley and Sons, New York, N. Y., (1954); A. R. von Hippel, "Dielectric Materials and Applications", John Wiley and Sons, New York, N. Y., (1954).

7) T. W. Dakin and C. N. Works, *J. Appl. Phys.*, **18**, 789 (1947).

TABLE II. CHEMICAL ANALYSIS OF COAL

| No. | Specimen | Moisture | Ash | Dry-ash-free basis | | | | |
|---|---|---|---|---|---|---|---|---|
| | | | | C% | H | O | N | S |
| 1 | Taihei | 12.86 | 5.84 | 65.10 | 4.93 | 28.43 | 0.93 | 0.62 |
| 2 | Tempoku | 12.80 | 1.52 | 70.37 | 4.74 | 23.79 | 1.10 | 0 |
| 3 | Nakago-kaso | 11.19 | 4.75 | 70.92 | 4.65 | 23.59 | 0.73 | 0.11 |
| 4 | Nakago | 13.32 | 3.96 | 74.33 | 5.26 | 19.29 | 0.95 | 0.17 |
| 5 | Kasima | 4.11 | 5.02 | 77.94 | 6.07 | 12.62 | 0.65 | 2.72 |
| 6 | Pocahontas (USA) | 2.09 | 2.59 | 82.79 | 6.02 | 8.86 | 2.01 | 0.32 |
| 7 | Hutago | 1.54 | 2.31 | 83.16 | 6.31 | 8.81 | 1.56 | 0.16 |
| 8 | Yubari | 1.13 | 2.67 | 84.85 | 6.16 | 7.20 | 1.78 | 0.01 |
| 9 | Hasima | 1.24 | 2.09 | 86.59 | 5.56 | 6.48 | 1.22 | 0.15 |
| 10 | Kamati | 1.05 | 2.47 | 89.47 | 4.61 | 3.43 | 1.84 | 0.65 |
| 11 | Yatake | 1.11 | 2.74 | 89.55 | 4.86 | 3.07 | 1.88 | 0.64 |
| 12 | Onuki | 1.68 | 1.80 | 91.16 | 3.97 | 2.56 | 1.78 | 0.53 |

boundary to the position $E_{min.}$ were measured[6]. The ambiguity in finding $\gamma_2 d$ can be avoided by carrying out both open and short circuit measurements by the standard method. Further, as the samples treated here had low dielectric losses the simplification due to Dakin and Works[7] could be introduced into the calculation. Values of $\varepsilon'$ obtained independently in this manner by open and short circuit methods were compared with each other (see Table I). A weighted mean value is taken for each sample.

The sample material which was made of coal powder and paraffin-wax was prepared in the form having the exact dimension required by the size of the wave guide, the possible error being $\pm 0.05$ mm. (see Fig. 1).

The measurement at the frequency range between 1~20 kc./sec. was made by a low frequency bridge (Yokogawa BV-z-103) (see Ref. 2 for further information.). For the frequency range between 1~50 Mc./sec. a Q-meter (Yokogawa CA-102) was used. In order to compare the values of dielectric constants obtained by three different apparatuses, the absolute determination of dielectric constants becomes necessary. For this purpose, standard reference materials of dielectric constants provided by the Government Electrotechnical Laboratory, Tokyo, were measured with the apparatuses described above and compared with the results on coals. The maximum error in the dielectric constant is believed to be 5% and reliability in values of dielectric losses are somewhat lower but the latter are not so important in the interpretation as dielectric constants. All the measurements were carried out at room temperature.

### Experimental Materials

All the coal specimens examined in these experiments were kindly provided by Dr. H. Honda, Resources Research Institute, Japan. The chemical analyses of the samples are given in Table II. The paramagnetic susceptibility has been examined by the present writers for the following specimens[8]: No. 4, 0.40; No. 8, 0.28; No. 11, 1.23; No. 12, 3.90 $10^{-8}$ c. g. s. electromagnetic units per gram.

On account of its exceptionally high dielectric constant, water is the greatest cause of error in the dielectric measurement. Great care was taken to eliminate any traces of moisture contained in the samples. The coal samples were reduced into powder form below 200 mesh and strongly dried by heating at 105°C and reduced pressure of $10^{-2}$ mmHg for 30 hr.

About 26 g. of dried powder of coal thus obtained was mixed with 20 g. of melted paraffin-wax, cooled in a mold and cut carefully into a shape suitable for the measurement. The volume percent of coal in the mixture was estimated for each sample by measuring the densities of coal and paraffin-wax. The properties of solid paraffin-wax used are: density 0.914/24°C, m. p. 58.5~60°C, dielectric constant 2.29/1 Mc., 2.26/7000 Mc. and $\tan\delta$ 0.000/1 kc.~7000 Mc.

### Results

Dielectric constants $\varepsilon'$ and $\tan\delta$ obtained for the coal mixture are recorded in Table III.

In order to determine the value of the dielectric constant of a coal from that of a mixture, Böttcher's equation[1,9,10] was employed, in which $\varepsilon'$, $\varepsilon_1'$ and $\varepsilon_2'$ are the dielectric constant

$$\frac{\varepsilon'-\varepsilon_1'}{3\varepsilon'} = v_2 \frac{\varepsilon_2'-\varepsilon_1'}{\varepsilon_2'+2\varepsilon'} \qquad (2)$$

of the mixture, the paraffin-wax and coal particles, respectively and $v_2$ is the volume fraction of the coal particle in the mixture. The value $\varepsilon_2'$ for each specimen of coal thus obtained is shown in parentheses below that for the mixture.

8) H. Honda, K. Chitoku, Y. Yokozawa and K. Higasi, This Bulletin, 31, 891 (1958).

9) C. J. F. Böttcher, *Rec. trav. chim.*, **64**, 47 (1945); C. J. F. Böttcher, "The Theory of Electric Polarisation", Elsevier, Amsterdam (1952), p. 417.

10) Y. Zyomoto, *J. Fuel Soc. Japan*, (*NenryoKyokaishi*), **37**, 248 (1958).

TABLE III. DIELECTRIC CONSTANTS ($\varepsilon'$) AND LOSS TANGENT (UNIT : $10^{-4}$) OF COAL MIXTURES MEASURED AT FREQUENCIES 1 kc./sec.~7000 Mc./sec. AND DIELECTRIC CONSTANTS OF COALS ESTIMATED ($\varepsilon_2'$)

| No. (Specimen) | Vol. % of coal | | 1 kc. | 3 kc. | 10 kc. | 20 kc. | 1 Mc. | 3 Mc. | 50 Mc. | 7000 Mc. |
|---|---|---|---|---|---|---|---|---|---|---|
| 1 | 40.1 | $\varepsilon'$ | 3.17 | 3.17 | 3.19 | 3.19 | 3.06 | 3.03 | 3.01 | 2.86 |
| | | $\varepsilon_2'$ | (4.75) | (4.75) | (4.82) | (4.82) | (4.51) | (4.44) | (4.38) | (3.95) |
| | | $\tan\vartheta$ | 238 | 169 | 113 | 83 | 92 | 101 | 108 | 142 |
| 2 | 49.0 | $\varepsilon'$ | 3.26 | 3.21 | 3.21 | 3.21 | 3.19 | 3.18 | 3.14 | 2.89 |
| | | $\varepsilon_2'$ | (4.45) | (4.32) | (4.32) | (4.32) | (4.35) | (4.34) | (4.24) | (3.66) |
| | | $\tan\vartheta$ | 91 | 67 | 58 | 72 | 72 | 84 | 127 | 158 |
| 3 | 46.0 | $\varepsilon'$ | 3.21 | 3.23 | 3.22 | 3.22 | 3.12 | 3.10 | 3.08 | 2.86 |
| | | $\varepsilon_2'$ | (4.48) | (4.53) | (4.51) | (4.51) | (4.33) | (4.29) | (4.24) | (3.69) |
| | | $\tan\vartheta$ | 64 | 72 | 61 | 49 | 68 | 76 | 95 | 134 |
| 4 | 48.0 | $\varepsilon'$ | 3.09 | 3.10 | 3.09 | 3.05 | 3.10 | 3.09 | 3.08 | 2.81 |
| | | $\varepsilon_2'$ | (4.07) | (4.09) | (4.07) | (3.97) | (4.17) | (4.16) | (4.14) | (3.50) |
| | | $\tan\vartheta$ | 83 | 64 | 50 | 61 | 52 | 53 | 67 | 99 |
| 5 | 47.4 | $\varepsilon'$ | 2.89 | 2.89 | 2.89 | 2.89 | 2.78 | 2.78 | 2.77 | 2.67 |
| | | $\varepsilon_2'$ | (3.59) | (3.59) | (3.59) | (3.59) | (3.40) | (3.42) | (3.39) | (3.18) |
| | | $\tan\vartheta$ | 32 | 58 | 55 | 40 | 39 | 37 | 50 | 92 |
| 6 | 48.4 | $\varepsilon'$ | 2.87 | 2.87 | 2.81 | 2.81 | 2.81 | 2.81 | 2.79 | 2.79 |
| | | $\varepsilon_2'$ | (3.52) | (3.52) | (3.38) | (3.38) | (3.45) | (3.46) | (3.41) | (3.44) |
| | | $\tan\vartheta$ | 229 | 143 | 138 | 97 | 44 | 41 | 48 | 70 |
| 7 | 50.4 | $\varepsilon'$ | 2.85 | 2.79 | 2.79 | 2.79 | 2.79 | 2.79 | 2.78 | 2.68 |
| | | $\varepsilon_2'$ | (3.42) | (3.29) | (3.29) | (3.29) | (3.35) | (3.36) | (3.34) | (3.14) |
| | | $\tan\vartheta$ | 106 | 65 | 43 | 47 | 22 | 25 | 31 | 59 |
| 8 | 49.6 | $\varepsilon'$ | 2.77 | 2.77 | 2.77 | 2.77 | 2.76 | 2.76 | 2.76 | 2.69 |
| | | $\varepsilon_2'$ | (3.26) | (3.26) | (3.26) | (3.26) | (3.30) | (3.31) | (3.31) | (3.18) |
| | | $\tan\vartheta$ | 68 | 10 | 26 | 22 | 17 | 19 | 16 | 51 |
| 9 | 49.5 | $\varepsilon'$ | 2.84 | 2.84 | 2.84 | 2.84 | 2.77 | 2.77 | 2.77 | 2.73 |
| | | $\varepsilon_2'$ | (3.42) | (3.42) | (3.42) | (3.42) | (3.32) | (3.34) | (3.34) | (3.27) |
| | | $\tan\vartheta$ | 66 | 75 | 81 | 65 | 25 | 21 | 33 | 75 |
| 10 | 47.2 | $\varepsilon'$ | 2.83 | 3.87 | 2.89 | 2.89 | 2.81 | 2.81 | 2.80 | 2.79 |
| | | $\varepsilon_2'$ | (3.45) | (3.55) | (3.60) | (3.60) | (3.48) | (3.49) | (3.47) | (3.47) |
| | | $\tan\vartheta$ | 67 | 120 | 46 | 23 | 19 | 21 | 21 | 25 |
| 11 | 45.9 | $\varepsilon'$ | 2.85 | 2.86 | 2.86 | 2.86 | 2.84 | 2.83 | 2.82 | 2.77 |
| | | $\varepsilon_2'$ | (3.54) | (3.57) | (3.57) | (3.57) | (3.59) | (3.58) | (3.56) | (3.46) |
| | | $\tan\vartheta$ | 152 | 68 | 72 | 48 | 21 | 18 | 13 | 26 |
| 12 | 40.0 | $\varepsilon'$ | 3.19 | 3.05 | 3.05 | 3.05 | 2.89 | 2.89 | 2.87 | 2.79 |
| | | $\varepsilon_2'$ | (4.83) | (4.37) | (4.37) | (4.37) | (3.98) | (4.00) | (3.94) | (3.73) |
| | | $\tan\vartheta$ | 886 | 563 | 311 | 192 | 60 | 37 | 21 | 40 |
| Paraffin[a] | | $\varepsilon_1$ | 2.34 | 2.34 | 2.34 | 2.34 | 2.29 | 2.28 | 2.28 | 2.26 |

a) Values of $\varepsilon_1$ used in calculating $\varepsilon_2$ by Eq. 2.

**Dielectric Constant and Oxygen Content.**— Dielectric constants obtained at 1 kc./sec. and 7000 Mc./sec. are plotted against oxygen content (Fig. 2). Intermediate frequency dielectric constants lie between the two curves.

Dielectric constants decrease sharply at first but increase regularly with increase in oxygen content after reaching a minimum at about 8%. From functional group analysis of coal it has been found that the amounts of hydroxyl groups, carboxyl groups, carbonyl groups and methoxyl groups increase with oxygen content[11]. Among them, the hydroxyl group is regarded as the most important*. From the infrared analysis, the absorption band at 3.0 $\mu$ is ascribed to the existence of associated OH and NH bonds[12]. One might infer from these

11) M. Ihnatowicz, *Prace Glownego Inst. Gornictwa* (Katowice) *Komun.*, 125 (1952); L. Blom, L. Edelhausen and D. W. van Krevelen, *Fuel*, **36**, 135 (1957) cited by Ref. 3, p. 217.

* According to private communication from Dr. H. Honda, functional analysis gives the following data. No. 2, Tempoku. O, 23.79%; $O_{OH}$; 10.3%; $O_{COOH}$, 0.4%. No. 6, Pocahontas: O, 8.86%; $O_{OH}$, 2.4%; $O_{COOH}$, 0.5%. No. 8, Yubari: O, 7.20%; $O_{OH}$, 0%; $O_{COOH}$, 0.9%. No. 10, Kamati: O, 3.43%; $O_{OH}$, 0%; $O_{COOH}$, 0%.

12) C. G. Cannon and G. B. B. Sutherland, *Trans. Faraday Soc.*, **41**, 279 (1945) and others, see Ref. 3, p. 185.

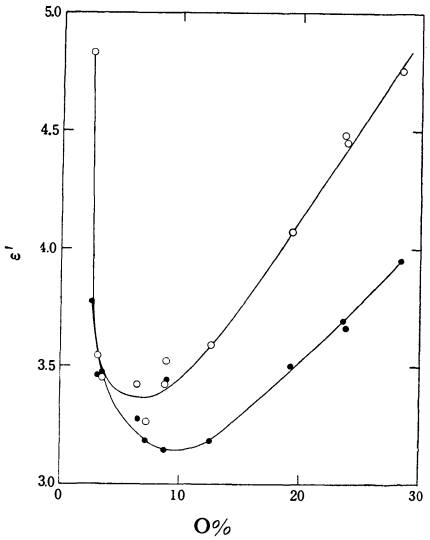



Fig. 2. Dielectric constants of coals ($\varepsilon_2'$) at frequencies 1 kc./sec. and 7000 Mc./sec. and oxygen content (dry-ash-free basis).
—○— 1 kc. —●— 7000 Mc.

pieces of evidence that polar groups which are closely associated with the oxygen content are mainly responsible for the dielectric constant of coal containing more than 10% oxygen. This seems parallelled by the fact that dielectric constants of polymers increase with the amount of polar groups contained in them[13,14]. Indeed, coals generally speaking are a sort of high-polymers having some polar groups.

**Dielectric Constant and Carbon Content.** — Dielectric constants obtained at three frequencies, 1 kc./sec., 1 Mc./sec. and 7000 Mc./sec. are plotted against carbon content (Fig. 3). For the sake of comparison, optical dielectric constants as defined by the refractive index $n$ and the absorption index $k$ for visible light of the wavelength 5460 Å.

$$\varepsilon_\infty = n^2(1-k^2) \qquad (3)$$

are plotted as dotted lines in the same graph. The optical measurement is due to Huntjens and van Krevelen[15]. There are available other optical measurements[16], but they are not recorded here in order to prevent the figure from becoming overcrowded with points.

From a glance at Fig. 3, it will be seen that in the region C 85~89% all the dielectric constants, at audio, radio and microwave frequencies converge so that they become almost identical to each other. The plotted curve for

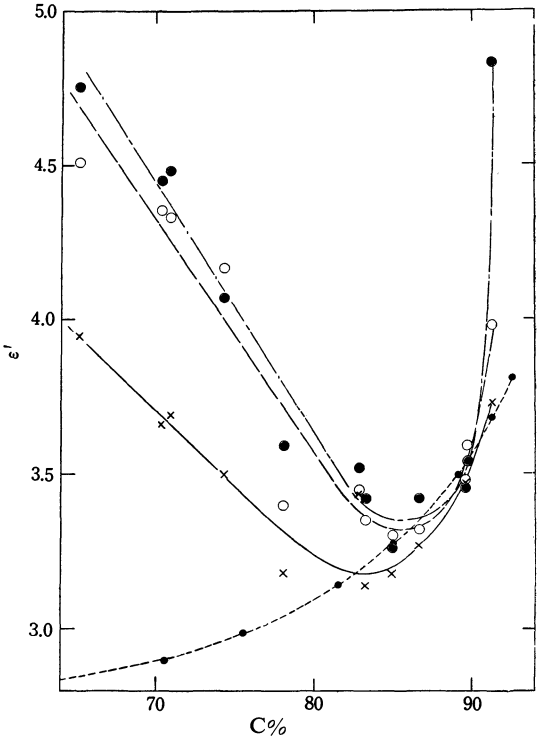



Fig. 3. Dielectric constants of coals ($\varepsilon_2'$) at various frequencies and carbon contents of coals.
—⊙— 1 kc.
—○— 1 Mc.
—×— 7000 Mc.
—●— van Krevelen $n^2(1-k^2)$

optical dielectric constants lies between these three curves. This is probably anomalous, but it must be remembered that optical dielectric constants were obtained for coals of different origins**. It may be reasonable to assume that microwave values in this region are almost identical with the optical dielectric constant.

With the decrease in carbon content (less than 80%) the difference between the optical and the microwave dielectric constants becomes significant. It was unexpected that there should be such a large difference between these values in this region. If this difference is due to the rotation of polar groups, these groups must have a small size[14]. One might infer from this that the perticular polar groups responsible for this phenomenon are hydroxyl groups situated at the periphery of the aromatic system, because the internal rotation of non-associated OH groups around the C-O axis will be least sterically hindered.

Fischer found that diphenyl ether has an anomalously small relaxation time[17]. Recently

13) R. M. Fuoss, *J. Am. Chem. Soc.*, **63**, 369 (1941).
14) C. P. Smyth, "Dielectric Behavior and Structure", McGraw-Hill Book Co., Inc., New York, N. Y., 1955.
15) F. J. Huntjens and D. W. van Krevelen, *Fuel*, **33**, 88 (1954).
16) D. G. Murchison, *Brennstoff Chem.*, **39**, 47 (1958); S. R. Broadbent and A. J. Shaw, *Fuel*, **34**, 385 (1955).

** In fact, Broadbent and Shaw[16] gave smaller optical dielectric constants than van Krevelen.
17) E. Fischer, *Z. Elektrochem.*, **53**, 16 (1949).

an explanation has been given for this observation as arising from the internal rotation of the two benzene rings around C-O axes[18]. Coal is sometimes considered as built up of aromatic ring complexes linked through oxygen or non-aromatic bridges containing oxygen atoms[19]. Possibly these units might provide certain contributions to the microwave dielectric constant, if a particular type of internal rotation is to occur. But roughly speaking the hydroxyl group will be mainly responsible for this effect.

It would be a matter of speculation to estimate dipole moments for coals. However, if coal may be regarded as a supercooled liquid[3], the Onsager equation for liquids may be used for this purpose[1e,f]. Further, on account of the low dielectric constant, the Debye equation will give practically the same moment values the Onsager equation[13]. It can be shown that the dipole moment $\mu$ for the unit having the molecular volume $M/d$ is

$$\mu = A\left[(\varepsilon_2' - \varepsilon_\infty)\frac{M}{d}\right]^{1/2} \qquad (4)$$

where $A$ for Debye equation is

$$A^2 = \frac{27kT}{4\pi N(\varepsilon_2'+2)(\varepsilon_\infty+2)}, \qquad (5)$$

in which $k$ is Boltzman constant, $N$ is Avogadro constant and $T$ is the absolute temperature. Further, at room temperature, $T=298°C$

$$A^2 = \frac{0.147\times10^{-36}}{(\varepsilon_2'+2)(\varepsilon_\infty+2)} \qquad \text{Debye}$$

In similar way it can be shown that

$$A^2 = \frac{0.147\times10^{-36}(2\varepsilon_2'+\varepsilon_\infty)}{3\varepsilon_1'(\varepsilon_\infty+2)^2} \qquad \text{Onsager}$$

There exist no reliable data for the molecular weight of coal. According to van Krevelen and Schuyer[3] the average molecular weight is in the vicinity of 2500. We shall assume an arbitrary molecular volume $M/d=2000$ for the purposes of the present calculation. For coal with a density of 1.3, this assumption gives a molecular weight of 2600.

Regarding the static dielectric constant $\varepsilon_2'$ in Eq. 1 we shall use values obtained at frequency of 1 kc. Optical dielectric constants $\varepsilon_\infty$ are calculated by Eq. 3 using van Krevelen's data, which are supposed to be somewhat higher than those of the coals considered here; the estimated dipole moment is consequently slightly smaller than the actual moment. Further, the $A$ value for the Debye equation will be used in the calculation of the moment. The result is shown in Table IV.

TABLE IV. DIPOLE MOMENTS OF COALS ($\mu$) FOR THE MOLECULAR VOLUME ($M/d=2000$)

| No. | Specimen | C% | $\varepsilon_2'$/1 kc. | $\varepsilon_\infty$ | $\mu$, D |
|---|---|---|---|---|---|
| 1 | Taihei | 65.10 | 4.75 | 2.85 | 4.1 |
| 2 | Tempoku | 70.37 | 4.45 | 2.90 | 3.8 |
| 3 | Nakago-kaso | 70.92 | 4.48 | 2.91 | 3.8 |
| 4 | Nakago | 74.33 | 4.07 | 2.96 | 3.3 |
| 5 | Kasima | 77.94 | 3.59 | 3.05 | 2.4 |
| 6 | Pocahontas (USA) | 82.79 | 3.52 | 3.20 | 1.8 |
| 7 | Hutago | 83.16 | 3.42 | 3.21 | 1.5 |
| 8 | Yubari | 84.85 | 3.26 | 3.28 | 0 |
| 9 | Hasima | 86.59 | 3.42 | 3.36 | ~0 |
| 10 | Kamati | 89.47 | 3.45 | 3.53 | 0 |
| 11 | Yatake | 89.55 | 3.54 | 3.54 | 0 |
| 12 | Onuki | 91.16 | 4.83 | 3.68 | — |

As an example we shall consider a dipole moment 3.8 D obtained for specimen No. 2 Tempoku brown coal. If this magnitude of moment arises only from OH groups which have complete freedom of rotation around C-O axis, the number of OH groups in a volume 2000 cc. will be estimated by

$$\mu^2_{obs} = n\cdot\mu^2_{OH} \qquad (6)$$

where $\mu_{obs}$ and $\mu_{OH}$ are moments observed and that of the OH group respectively. Putting $\mu_{obs}=3.8$ D and $\mu_{OH}=1.56$ D[20] we obtain $n=5.9$; there are about 6 OH groups capable of rotation.

On the other hand, functional analysis reveals that this particular coal specimen has a hydroxyl (phenolic) percentage of 10.3%. In molecular volume $M/d=2000$ ($d=1.41$), this gives 291 g. oxygen, that is 18 OH groups. Therefore, one may conclude that about one-third of the total OH groups can rotate freely. The hydroxyl percentage chemically determined does not represented the amount of OH group actually existing in coal. There is no strong reason for supposing that a certain fraction of OH groups has complete freedom of rotation while another fraction has not and that other polar groups can not make a contribution to dielectric constant. In fact, the estimation of the dipole moment described above and its related discussion has only qualitative significance.

## Summary

1. Using the transmission method, resonance method and bridge method, dielectric constants

18) K. Higasi and C. P. Smyth, to be published in *J. Am. Chem. Soc.*

19) S. G. Ward, *J. Inst. Fuel*, 21, 80 (1947); cited in Ref. 3, p. 207.

20) Y. Kurita and M. Kubo, This Bulletin, 27, 364 (1954). This is not the moment of OH group moment itself but the component of the phenolic OH moment perpendicular to the C-O axis.

and losses are measured on paraffin-wax mixtures of twelve specimens of coal ranging from C 65 to 92%.

2. Dielectric constants of coals are estimated for these coals by means of Böttcher's equation.

3. The relation between dielectric constant and oxygen content is discussed and it is shown that polar groups contribute to dielectric constant.

4. From the comparison with optical dielectric constant, the motion of dipoles in coals in the electric field can be discussed. Rough estimates of dipole moments are also given.

The present writers wish to thank Dr. H. Honda for his cooperation in this work and also Dr. H. Baba for his assistance in performing the calculation of microwave dielectric constants.

*Research Institute of Applied Electricity*
*Hokkaido University, Sapporo*

# *Polarographic Behavior of Vanadium and Iron in Thiocyanate*

By G. S. DESHMUKH and J. P. SRIVASTAVA

(Received June 13, 1960)

Thiocyanate has been used extensively as a complexing agent for a number of cations. Meite's[1] observation that iron (III) is reduced in a medium composed of 0.7 M KCNS, 0.02 M sulfuric acid and 0.004% gelatin with a half-wave potential >0.0 volt is contradicted by the data of the "Polarographic spectra"[2] giving $E_{1/2}$ vs. S. C. E. as −0.2 volt. The condition for the latter observation has not been defined.

Direct estimation of $VO^{2+}$ based on the catalytic action of the ion on potassium chlorate and potassium iodide reaction has been developed recently by Shiokawa[3]. Polarographic characteristics of vanadyl ion showed that it is reducible or oxidizable depending on the nature of the complex formed with the supporting electrolyte[4]. Syrokomskiĭ and Nazareva[5] devised a new type of coulometer to effect anodic oxidation of $VO^{2+}$ to $VO^{3+}$ which is titrable with Mohr's salt solution.

Preliminary investigations showed that thiocyanate in presence of mineral acids is capable of reducing vanadium(V) to lower valency states. Vanadium(V) and thiocyanate solution when mixed together developed the green coloration characteristics of trivalent vanadium ion, which on raising the acidity of the solution turned blue. The intermediate green state was initially mistaken to be vanadium green, corresponding to molybdenum blue, and was found to be very stable even on prolonged exposure to air. Spectrophotometric studies revealed that it is only the mixture of vanadium(V) and vanadium(IV). This conclusion was further confirmed when the green solution was shaken with isobutyl alcohol. The solution separated into two layers; the yellow aqueous layer and blue tetravalent vanadium in the organic layer.

The present communication reports in detail a study of polarographic behavior of vanadium (IV) thus obtained and iron(III) in potassium thiocyanate. Appropriate conditions for the simultaneous determination of the two elements in presence of each other have also been described.

## Experimental

Leeds and Northrup Electrochemograph Type E was used for recording the polarograms in conjunction with an external saturated calomel reference electrode connected through an agar-potassium chloride bridge to the electrolysis cell. The temperature was maintained throughout at 25±0.1°C. A Beckman zeromatic pH meter was used for measuring the pH of the solutions. The dropping mercury electrode had $m^{2/3}t^{1/6}$ value of 2.414 $mg^{2/3}/sec^{1/2}$ with open circuit.

Vanadyl sulfate solution was prepared by dissolving the reagent grade vanadium pentoxide in dilute sulfuric acid and reducing it by sulfur dioxide. Excess of sulfur dioxide was boiled off and the solution standardized against potassium permanganate. Iron solution was obtained by dissolving a weighed quantity of "A. R. ferric ammonium sulfate" in distilled water. This was

1) L. Meites, "Polarographic Technique", Interscience Publishers, New York, N. Y. (1955), p. 269.
2) L. Meites, loc. cit Front and back lining papers.
3) T. Shiokawa, *J. Chem. Soc. Japan, Pure Chem. Sec. (Nippon Kagaku Zasshi)*, **70**, 418 (1950).
4) I. M. Kolthoff and J. J. Lingane, "Polarography", Vol. II, Interscience Publishers, New York, N. Y. (1952), p. 449.
5) V. S. Syrokomskii and T. I. Nazareva, *Zhur. Anal. Khim.*, **6**, 15 (1951).

also standardized against potassium permanganate. All other chemicals used were of reagent grade.

## Results and Discussion

**Characteristics of Polarographic Waves.**—A number of vanadium(IV) and iron(III) polarograms were recorded at different pH values. It was observed that vanadium(IV) gets reduced at and below pH≈3. The two reduction stages of vanadium(IV) are well developed when the pH of the solution was below 2.0 but above 1.5. Further increase in acidity shifted the half-wave potentials of the first wave towards positive potentials. The wave was completely obliterated below a pH of 0.5. In less acidic solutions (between pH 2.0~3.5), the first wave was drawn out and ill defined. Iron polarograms also were well defined below pH 3.0 but the $E_{1/2}$ ($E_{1/2}=-0.17$ volt vs. S. C. E. in 1.0 M potassium thiocyanate containing 0.005% gelatin at pH 1) was not much affected by the pH of the solution (cf. Table I).

Thiocyanate concentration had considerable effect on the half-wave potential of vanadium. While the first wave was shifted towards negative potentials with increasing thiocyanate concentration, the $E_{1/2}$ of the second wave moved to more positive potentials. The polarograms of iron were also shifted towards negative potentials by the increased concentrations of the supporting electrolyte. The shift in both the cases i. e., the first wave of vanadium and the polarograms of iron, towards negative potentials with the increasing thiocyanate concentrations may possibly be attributed to the superimposition of the anodic wave of thiocyanate. During the course of experiments it was further observed that the half-wave potential of the iron wave was dependent not only on the thiocyanate concentrations but also on the iron and thiocyanate ratio. Conjugating it with the previous observation that the $E_{1/2}$ of iron polarograms remain unaffected by the pH of the solution, it may

TABLE I. EFFECT OF pH ON VANADIUM AND IRON POLAROGRAMS

| Solution No. | pH of solun. | $E_{1/2}$ of vanadium polarograms, volt vs. S. C. E. | | $E_{1/2}$ of iron polarograms, volt vs. S. C. E. |
|---|---|---|---|---|
| | | 1st wave | 2nd wave | |
| 1 | 0.5 | −0.20 | −0.57 | −0.20 |
| 2 | 0.8 | −0.21 | −0.57 | −0.18 |
| 3 | 1.1 | −0.23 | −0.56 | −0.18 |
| 4 | 1.3 | −0.25 | −0.56 | −0.18 |
| 5 | 1.5 | −0.27 | −0.57 | −0.18 |
| 6 | 1.8 | −0.30 | −0.57 | −0.17 |
| 7 | 2.0 | −0.32 | −0.57 | |
| 8 | 2.5 | Not defined | −0.57 | |
| 9 | 3.0 | Not reducible | −0.57 | −0.17 |
| 10 | 3.6 | Not reducible | | |

TABLE II. EFFECT OF SUPPORTING ELECTROLYTE'S CONCENTRATION ON VANADIUM AND IRON POLAROGRAMS

| Solution No. | Thiocyanate concentration M | $E_{1/2}$ of vanadium polarograms, volt vs. S. C. E. | | $E_{1/2}$ of iron polarograms, volt vs. S. C. E. |
|---|---|---|---|---|
| | | 1st wave | 2nd wave | |
| 1 | 5.0 | −0.30 | −0.49 | −0.31 |
| 2 | 3.75 | −0.28 | −0.51 | −0.29 |
| 3 | 2.50 | −0.24 | −0.53 | −0.26 |
| 4 | 1.25 | −0.25 | −0.56 | −0.20 |
| 5 | 1.00 | −0.25 | −0.56 | −0.17 |
| 6 | 0.50 | — | −0.57 | −0.15 |
| 7 | 0.25 | Washed off | −0.58 | −0.15 |

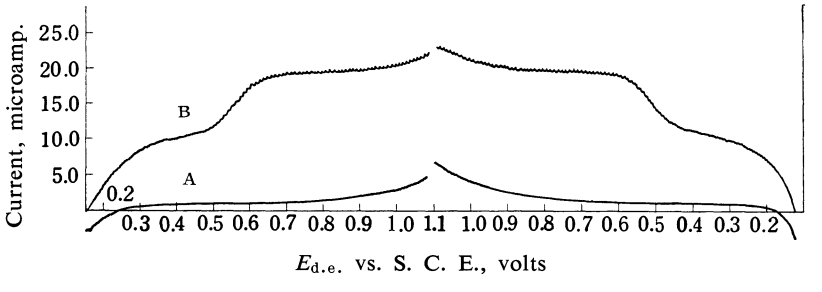



Fig. 1. Direct and reverse vanadium (2.19 mM) polarograms

Temperature 25±0.1°C
Drop time 3.33 sec.
Gelatin concn. 0.005%
Recorder damping 2.0
Recorder range 50 μA
pH of solution 1.6

| Waves | Zero line | $E_{1/2}$ of 1st wave | $E_{1/2}$ of 2nd wave |
|---|---|---|---|
| A | 0.0 | Blank | — |
| B | 2.5 | −0.21 | −0.537 |

be concluded that over the pH range studied a series of iron thiocyanate complexes are formed depending on the iron : thiocyanate ratio. Shifting of the second wave of vanadium towards more positive potentials with increasing thiocyanate concentrations suggest that the V(II)-NCS complex apparently has a lower dissociation constant than the V(III)-NCS complex (cf. Table II).

A study of the typical polarogram and its log plot shows that the vanadium waves are reversible (Fig. 1). The polarogram was obtained with a mixture of 2.19 mM vanadyl sulfate and 1.0 M potassium thiocyanate and 0.005% gelatin as maximum suppressor. In agreement with the general equation

$$E_{d.e.} = E_{1/2} - \frac{0.059}{n} \log \frac{i}{i_d - i}$$

the plot of $E_{d.e.}$ vs. $\log \frac{i}{i_d - i}$ is a straight line. The slope of 0.07 volt for the second wave suggests one electron transfer in reduction. As both the waves of vanadium have the same height, it was concluded that vanadium gets reduced first to vanadium(III) and finally to vanadium(II).

Iron polarograms exhibit only one reduction stage, and thus suggest the possibility of only one electron change. $E_{1/2}$ for iron reduction could not be assigned due to its dependence both on iron as well as on thiocyanate concentration but under the most restricted conditions of 2.00 mM iron and 1.0 M thiocyanate with 0.005% gelatin as maximum suppressor the $E_{1/2}$ observed was $-0.17$ volt vs. S. C. E.

The average $E_{1/2}$ for 2.19 mM vanadyl sulfate in 1.0 M potassium thiocyanate and 0.005% gelatin as maximum suppressor at pH 1.5 was found to be $-0.21$ volt, and to be $-0.54$ volt for the first and second wave respectively.

Under the conditions defined, a series of vanadium(IV) polarograms were run to plot the calibration curve. All the wave heights for the first wave were read from the plots at $-0.45$ volt and the corresponding values for the residual current were deducted to obtain the $i_d$ for vanadium(IV) alone. The wave heights for the second stage reduction were calculated by extrapolating the plateau of the two waves.

The values of $I$ obtained for different concentrations (cf. Table III) show that the reduction for both the waves are diffusion controlled. A linear concentration-current relationship is also followed by iron polarograms. The wave heights for iron polarograms were obtained by taking the difference of the actual and residual wave height at the same potential i. e., at $-0.45$ volt.

Table III. Diffusion current constant for vanadium polarograms

| Solution No. | Concentration of vanadium mM | $I(I=i_d/cm^{2/3}\ t^{1/6})$ of vanadium waves | |
|---|---|---|---|
| | | 1st wave | 2nd wave |
| 1 | 0.438 | 1.43 | 1.65 |
| 2 | 0.876 | 1.42 | 1.65 |
| 3 | 1.09 | 1.42 | 1.65 |
| 4 | 1.31 | 1.42 | 1.65 |
| 5 | 1.75 | 1.42 | 1.66 |
| 6 | 2.19 | 1.42 | 1.65 |
| 7 | 2.62 | 1.42 | 1.65 |
| 8 | 3.5 | 1.42 | 1.66 |
| 9 | 3.94 | 1.42 | 1.65 |
| 10 | 4.38 | 1.42 | 1.65 |

The effect of different cations on vanadium polarograms was also studied. Cobalt and manganese do not interfere with the polarogram. Nickel and chromium(III) develop their own waves at more negative potentials but the diffusion current plateau for vanadium is not appreciably distorted. The presence of molybdenum(VI) and tungsten(VI) is detrimental as these ions deteriorate the vanadium waves, thus making the measurement of diffusion current practically impossible. Cupric ion has a typical effect of shifting the vanadium waves to more negative potentials. This results in the formation of only one wave which is probably the resultant of the waves comprising the wave heights due to $Cu^{2+}$ and both the vanadium waves. The presence of nitrates, chlorides, bisulfates and ammonium ions has no effect on vanadium polarograms. None of these above mentioned ions except molybdenum and tungsten affect the iron polarograms. Molybdenum and tungsten completely distort the wave.

**Recommended Procedure of Analysis.**—The appropriate amount of unknown solution to give a final vanadium concentration above 0.4 mM and iron concentration above 0.5 mM is mixed with potassium thiocyanate. The overall potassium thiocyanate concentration is maintained at 1.0 M. The acidity of the solution is adjusted to pH 1.5 with hydrochloric acid and the mixture allowed to stand for 15 min. During this period vanadium(V) gets reduced to vanadium(IV). The appearance of violet color (being a mixture of blue due to vanadium(IV) and blood-red due to iron(III) thiocyanate) indicates the completion of the reduction. This solution when polarographed exhibits a two-step reduction, the first being the composite wave due to the reductions of iron(III) to iron(II) and vanadium(IV) to vanadium(III), and the second one being due to the degradation of vanadium(III) to vanadium(II). In order to derive the vanadium

content of the solution, the wave height of the second stage reduction is measured by extrapolating the plateaus and reading it from the calibration curve.

On subtracting the height of the first wave of vanadium as read from the calibration curve for the corresponding value of vanadium obtained previously, from that of the composite wave (the polarogram of the mixed iron and vanadium solution), the contribution due to iron alone is calculated. In the procedure adopted, wave heights of iron and vanadium polarograms are appreciable, only if the concentrations of corresponding elements are above the prescribed limit, i. e., 0.5 mM and 0.4 mM respectively.

TABLE IV. SIMULTANEOUS DETERMINATION OF IRON AND VANADIUM

| Solution No. | Vanadium added mM | Vanadium recovered, mM | Iron added, mM | Iron recovered mM |
|---|---|---|---|---|
| 1 | 0.438 | 0.438 | 0.4 | 0.42 |
| 2 | 0.87 | 0.87 | 0.8 | 0.81 |
| 3 | 1.31 | 1.33 | 1.2 | 1.21 |
| 4 | 1.75 | 1.79 | 1.6 | 1.62 |
| 5 | 2.19 | 2.21 | 2.0 | 2.0 |
| 6 | 2.62 | 2.66 | 2.4 | 2.4 |
| 7 | 3.16 | 3.16 | 2.8 | 2.82 |
| 8 | 3.50 | 3.50 | 3.2 | 3.18 |
| 9 | 3.94 | 4.10 | 3.6 | 3.6 |
| 10 | 4.38 | 4.42 | 4.01 | 4.01 |

Values obtained by the above procedure are reported in Table IV. It may be seen that the results are within the limits of experimental error. The method provides a convenient procedure for the simultaneous determination of iron and vanadium contents and may suitably be adopted to the analysis of vanadium steels provided copper(II), molybdenum(VI), and tangsten(VI) are sequestered.

The authors wish to express their sincere thanks to Professor S. S. Joshi for his advice and to Dr. G. B. Singh, Head of the Chemistry Department, for facilities during the course of this study. The financial aid by the Government of India to one of us (J. P. S.) is also gratefully acknowledged.

*Chemical Laboratories*
*Banaras Hindu University*
*Varanasi-5*

# *The Thermal Decomposition of Dimethyl Ether in the Presence of Hydrogen Sulfide*

By Naomi IMAI and Osamu TOYAMA

(Received August 23, 1960)

The catalytic action of hydrogen sulfide on the thermal[1] as well as photochemical[2] chain decomposition of acetaldehyde has been studied in this laboratory, and its catalytic effect has been attributed to the reactions between methyl radicals and hydrogen sulfide molecules and between hydrosulfide radicals and acetaldehyde molecules, both taking place faster than the reaction between methyl radicals and acetaldehyde molecules. Methanethiol was also found to have an analogous catalytic action on the thermal decomposition of acetaldehyde[3].

Dimethyl ether has been known to decompose thermally by a chain mechanism involving methyl radicals[4-6] and its decomposition may therefore be expected to be catalyzed by hydrogen sulfide like that of acetaldehyde. In the present work the kinetics of the thermal decomposition of dimethyl ether in the presence of hydrogen sulfide has been studied in the temperature range 360 to 440°C and compared with the results obtained in the absence of hydrogen sulfide.

## Experimental

*Materials.* — Dimethyl ether was prepared by dehydration of methyl alcohol by concentrated sulfuric acid at 80°C, decarbonated and dried by potassium hydroxide and calcium chloride, and purified by bulb-to-bulb distillation. Hydrogen sulfide was

1) N. Imai and O. Toyama, unpuhlished work.
2) N. Imai and O. Toyama, This Bulletin, 33, 1120 (1960).
3) N. Imai and O. Toyama, ibid., 33, 1408 (1960).
4) F. O. Rice and K. F. Herzfeld, *J. Am. Chem. Soc.*, 56, 284 (1934).
5) S. W. Benson, *J. Chem. Phys.*, 25, 27 (1956).
6) S. W. Benson and P. V. S. Jain, ibid., 31, 1008 (1959).

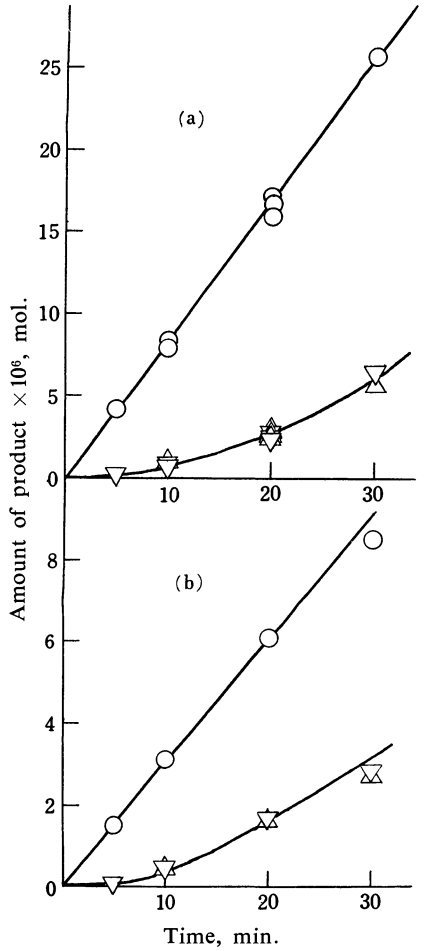



Fig. 1. Dependence of amount of product on reaction time. ○, $CH_4$; ▽, CO; △, $H_2$. (a) $[CH_3OCH_3]=2.13\times10^{-6}$ mol. $cc^{-1}$, $[H_2S]=0$, 440°C; (b) $[CH_3OCH_3]=2.32\times10^{-6}$, $[H_2S]=1.64\times10^{-6}$ mol. $cc^{-1}$, 380°C.

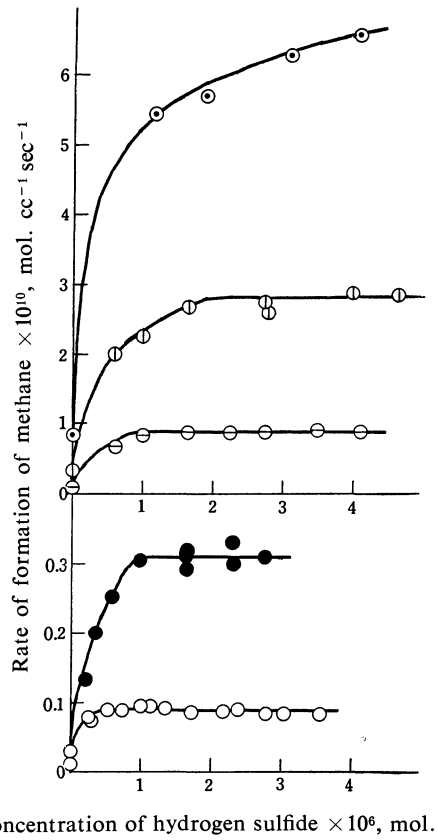



Fig. 3. Dependence of the rate of decomposition in the presence of hydrogen sulfide on its concentration. ○, $[CH_3O\cdot CH_3]=2.39\times10^{-6}$ mol. $cc^{-1}$, 360°C; ●, $[CH_3OCH_3]=2.32\times10^{-6}$ mol. $cc^{-1}$, 380°C; ⊖, $[CH_3OCH_3]=2.25\times10^{-6}$ mol. $cc^{-1}$, 400°C; ①, $[CH_3OCH_3]=2.19\times10^{-6}$ mol. $cc^{-1}$, 420°C; ⊙, $[CH_3OCH_3]=2.13\times10^{-6}$ mol. $cc^{-1}$, 440°C.

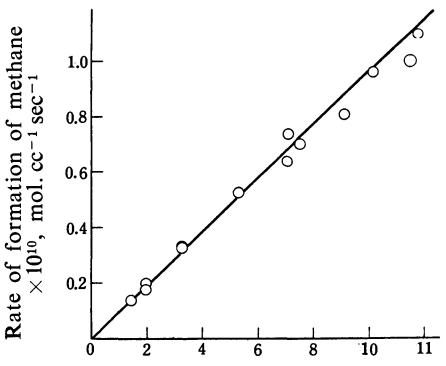



Fig. 2. Dependence of the rate of decomposition of the ether alone on its concentration at 420°C.

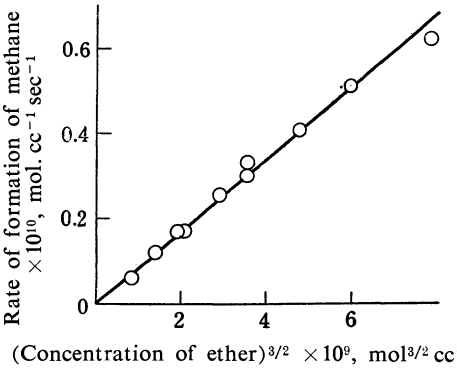



Fig. 4. Dependence of the rate of the decomposition of ether on its concentration in the presence of $2.32\times10^{-6}$ mol. $cc^{-1}$ of hydrogen sulfide at 380°C.

TABLE I. PYROLYSIS OF DIMETHYL ETHER IN THE ABSENCE AND PRESENCE OF HYDROGEN SULFIDE

| Temp. °C | Initial concentration $\times 10^6$ mol./cc. | | Reaction time min. | Amount of product $\times 10^6$ mol. | | |
|---|---|---|---|---|---|---|
| | $CH_3OCH_3$ | $H_2S$ | | $CH_4$ | CO | $H_2$ |
| 360 | 2.39 | 0 | 100 | 0.79 | 0.082 | — |
| | | 0 | 100 | 0.81 | 0.073 | — |
| | | 0.263 | 30 | 2.32 | 0.187 | — |
| | | 0.287 | 30 | 2.17 | 0.17 | — |
| | | 0.527 | 30 | 2.64 | 0.23 | — |
| | | 0.742 | 30 | 2.60 | 0.31 | — |
| | | 1.00 | 30 | 2.78 | 0.38 | — |
| | | 1.13 | 30 | 2.80 | 0.40 | — |
| | | 1.36 | 30 | 2.96 | 0.48 | — |
| | | 1.72 | 40 | 3.35 | 0.65 | — |
| | | 2.18 | 30 | 2.55 | 0.46 | — |
| | | 2.39 | 40 | 3.51 | 0.74 | — |
| | | 2.78 | 40 | 3.28 | 0.72 | — |
| | | 3.04 | 30 | 2.46 | 0.43 | — |
| | | 3.57 | 30 | 2.43 | 0.44 | — |
| 380 | 2.32 | 0 | 50 | 1.51 | 0.067 | — |
| | | 0 | 100 | 2.86 | 0.186 | — |
| | | 0 | 100 | 2.92 | 0.21 | — |
| | | 0.204 | 20 | 2.6 | 0.38 | — |
| | | 0.344 | 20 | 3.9 | 0.40 | — |
| | | 0.580 | 20 | 4.9 | 0.66 | — |
| | | 0.975 | 5 | 1.49 | 0.099 | — |
| | | 1.64 | 5 | 1.51 | 0.11 | — |
| | | 1.64 | 10 | 3.1 | 0.49 | 0.46 |
| | | 1.64 | 20 | 6.1 | 1.72 | 1.62 |
| | | 1.64 | 30 | 8.5 | 2.83 | 2.7 |
| | | 2.32 | 10 | 3.25 | 0.50 | — |
| | | 2.32 | 20 | 5.88 | 1.62 | 1.3 |
| | | 2.76 | 10 | 3.00 | 0.54 | — |
| | 0.91 | 2.32 | 20 | 1.21 | 0.237 | — |
| | 1.25 | | 20 | 2.32 | 0.676 | — |
| | 1.53 | | 20 | 3.28 | 0.76 | 0.6 |
| | 1.63 | | 20 | 3.33 | 0.78 | — |
| | 2.03 | | 20 | 4.94 | 1.06 | 0.9 |
| | 2.32 | | 10 | 3.25 | 0.50 | — |
| | 2.32 | | 20 | 5.88 | 1.60 | 1.3 |
| | 2.83 | | 20 | 8.00 | 1.90 | 1.7 |
| | 3.27 | | 20 | 10.0 | 2.46 | 1.7 |
| | 3.94 | | 10 | 6.13 | 0.97 | — |
| 400 | 2.25 | 0 | 50 | 4.61 | 0.34 | — |
| | | 0 | 100 | 8.86 | 1.03 | 1.1 |
| | | 0.61 | 12 | 7.9 | 1.06 | 1.2 |
| | | 1.00 | 10 | 8.1 | 1.35 | 1.4 |
| | | 1.65 | 10 | 8.3 | 1.64 | 1.5 |
| | | 2.25 | 20 | 16.9 | 5.68 | 5.4 |
| | | 2.75 | 10 | 8.6 | 1.72 | 1.5 |
| | | 3.49 | 10 | 8.8 | 2.08 | 2.1 |
| | | 4.12 | 10 | 8.6 | 2.09 | 1.9 |

TABLE I (Continued)

| | | | | | | |
|---|---|---|---|---|---|---|
| 420 | 1.27 | 0 | 30 | 4.00 | 0.376 | — |
| | 1.55 | 0 | 30 | 5.13 | 0.48 | 0.5 |
| | 1.56 | 0 | 30 | 5.79 | 0.68 | 0.5 |
| | 2.19 | 0 | 20 | 6.36 | 0.504 | 0.5 |
| | 2.19 | 0 | 40 | 12.8 | 1.72 | 1.5 |
| | 3.02 | 0 | 30 | 15.3 | 1.86 | 2.1 |
| | 3.67 | 0 | 30 | 18.6 | 2.31 | 1.6 |
| | 3.69 | 0 | 30 | 21.5 | 3.0 | 3.0 |
| | 3.83 | 0 | 30 | 20.4 | 2.14 | 2.6 |
| | 4.35 | 0 | 30 | 26.5 | 3.49 | 3.2 |
| | 4.68 | 0 | 20 | 18.8 | 5.02 | 2.2 |
| | 5.05 | 0 | 20 | 20.0 | 2.30 | 2.2 |
| | 5.16 | 0 | 20 | 21.4 | 2.24 | 1.7 |
| | 2.19 | 0.59 | 5 | 9.72 | 1.64 | 1.8 |
| | | 1.00 | 5 | 11.0 | 2.02 | 2.0 |
| | | 1.65 | 5 | 13.0 | 3.0 | 2.8 |
| | | 2.73 | 5 | 13.4 | 3.16 | 3.2 |
| | | 2.78 | 5 | 12.6 | 3.02 | 2.9 |
| | | 3.99 | 5 | 14.0 | 3.9 | 3.5 |
| | | 4.64 | 5 | 13.9 | 3.68 | 3.8 |
| 440 | 2.13 | 0 | 5 | 4.10 | 0.28 | — |
| | | 0 | 10 | 7.9 | 0.70 | 1.0 |
| | | 0 | 10 | 8.3 | 0.91 | — |
| | | 0 | 20 | 15.9 | 2.42 | 2.4 |
| | | 0 | 20 | 16.7 | 2.74 | 2.8 |
| | | 0 | 20 | 17.1 | 2.5 | 2.5 |
| | | 0 | 30 | 25.6 | 6.5 | 5.6 |
| | | 1.15 | 2 | 10.6 | 1.69 | 1.1 |
| | | 1.88 | 2 | 11.1 | 2.19 | 2.3 |
| | | 3.08 | 2 | 12.3 | 2.34 | 2.5 |
| | | 4.08 | 2 | 12.8 | 2.69 | 2.9 |

prepared by dropping water on aluminum sulfide in an evacuated vessel, dried by passing through a trap at −78°C and purified by bulb-to-bulb distillation. The cupric oxide used in analysis was a commercial sample.

*Apparatus.* — The apparatus used in the present work is similar to that described previously[8]. The reaction vessel is a glass cylinder of about 162 cc. capacity.

*Procedure.*—Required quantities of dimethyl ether and hydrogen sulfide were mixed and left at room temperature for about 30 min. before pyrolysis, and then introduced into the reaction vessel which had already been kept at the experimental temperature. After an appropriate time of reaction, usually corresponding to less than five per cent decomposition, the reaction mixture was expanded into an analytical system. Methane and carbon monoxide in products were analyzed quantitatively in the same way as described previously[7]. Hydrogen was oxidized by cupric oxide at 260°C to water vapor and the amount of the latter was determined from its pressure by an oil manometer. As it was found that the adsorption of the water on the glass wall led to incorrect estimates of hydrogen, calibration was made with known amounts of hydrogen. The amounts of hydrogen thus corrected seem to be still not very accurate. When the amount of hydrogen formed by the decomposition was very small, it was not determined.

## Results and Discussion

In Table I are listed the amounts of methane, carbon monoxide and hydrogen formed by the decomposition of dimethyl ether both in the absence and in the presence of hydrogen sulfide at various conditions. It has been well known that dimethyl ether decomposes thermally according to the following stoichiometric equations[6,8,9].

$$CH_3OCH_3 \rightarrow CH_4 + CH_2O$$

$$CH_2O \rightarrow CO + H_2$$

It is shown in Table I that, even in the presence of hydrogen sulfide, the amount of

7) N. Imai and O. Toyama, This Bulletin, 33, 652 (1960).

8) P. J. Askey and C. N. Hinshelwood, *Proc. Roy. Soc.*, A115, 251 (1927).

9) E. Leifer and H. C. Urey, *J. Am. Chem. Soc.*, 64, 994 (1942).

carbon monoxide formed is always equal to that of hydrogen within the experimental error and is always less than 30% of that of methane. Fig. 1 shows plots of the amounts of methane, carbon monoxide and hydrogen against the time obtained from series of runs (a) in the absence and (b) in the presence of hydrogen sulfide under otherwise constant conditions. It is seen in the figure that the rate of formation of methane remains constant for 30 min. during which 7.4 (a) and 2.3 (b) % of the ether have decomposed, while those of carbon monoxide and hydrogen increase with time. These observations indicate that carbon monoxide and hydrogen are produced by the decomposition of formaldehyde as represented by the above equation in the presence of hydrogen sulfide as well as in its absence.

It is generally agreed that the main feature of the thermal decomposition of dimethyl ether can be explained by the following chain mechanism[4].

$$CH_3OCH_3 \rightarrow CH_3 + OCH_3 \quad (1)$$

$$OCH_3 + CH_3OCH_3 \rightarrow CH_3OH + CH_3OCH_2 \quad (2)$$

$$CH_3 + CH_3OCH_3 \rightarrow CH_4 + CH_3OCH_2 \quad (3)$$

$$CH_3OCH_2 \rightarrow CH_2O + CH_3 \quad (4)$$

$$CH_3 + CH_3 \rightarrow C_2H_6 \quad (5)$$

The steady state equations derived from this scheme yield the rate equation

$$-d[CH_3OCH_3]/dt = R_{CH_4} = k_1^{1/2}k_3k_5^{-1/2}[CH_3OCH_3]^{3/2} \quad (I)$$

in general agreement with experimental results obtained by various workers[6,8,9]. Also in this work, the rate of decomposition of the ether alone was found to be proportional to the 3/2 power of the concentration of dimethyl ether at 420°C as seen in Fig. 2. From the slope of the straight line in the figure, the value of $k_1^{1/2}k_3k_5^{-1/2}$ was obtained. At other temperatures, values of $k_1^{1/2}k_3k_5^{-1/2}$ were calculated from the concentration of ether and the rate of formation of methane, making use of Eq. I. They are listed in Table II.

TABLE II. VALUES OF $k_1^{1/2}k_3k_5^{-1/2}$ AND $k_1^{1/2}k_7k_8^{-1/2}$

| Temp. °C | $k_1^{1/2}k_3k_5^{-1/2}\times10^3$ ($mol^{1/2}\,cc^{1/2}\,sec^{-1/2}$) | $k_1^{1/2}k_7k_8^{-1/2}\times10^2$ ($mol^{1/2}\,cc^{1/2}\,sec^{-1/2}$) |
|---|---|---|
| 360 | 0.223 | 0.240 |
| 380 | 0.855 | 0.847 0.864[a] |
| 400 | 2.73 | 2.60 |
| 420 | 9.68 | 8.75 |
| 440 | 28.8 | |

a) Obtained from a series of runs with varied ether concentrations and a constant hydrogen sulfide concentration (Fig. 4).

Now in the presence of a sufficient amount of hydrogen sulfide, the reactions of methyl and methoxyl radicals with hydrogen sulfide may be so much faster than those with dimethyl ether, that the latter reactions may be neglected compared to the former. Hence reaction 2 may be replaced by reaction 2′ and reaction 3 by reactions 6 and 7.

$$OCH_3 + H_2S \rightarrow CH_3OH + HS \quad (2')$$

$$CH_3 + H_2S \rightarrow CH_4 + HS \quad (6)$$

$$HS + CH_3OCH_3 \rightarrow H_2S + CH_3OCH_2 \quad (7)$$

If, in addition, the concentration of hydrosulfide radicals is much higher than that of methyl radicals, the chain will terminate by reaction 8, reaction 5 being negligible compared to reaction 8.

$$HS + HS \rightarrow \text{products} \quad (8)$$

The above chain mechanism consisting of reactions 1, 2′, 6, 7, 4 and 8 leads to the following rate equation.

$$-d[CH_3OCH_3]/dt = R_{CH_4} = k_1^{1/2}k_7k_8^{-1/2}[CH_3OCH_3]^{3/2} \quad (II)$$

If the chain is sufficiently long, it is readily shown that in the steady state

$$k_6[CH_3][H_2S] = k_7[HS][CH_3OCH_3]$$

or

$$[HS]/[CH_3] = (k_6/k_7)([H_2S]/[CH_3OCH_3]) \quad (III)$$

Therefore, when the quantity in the right-hand side of Eq. III is very large, the rate of decomposition will be represented by Eq. II.

Fig. 3 shows the dependence of the rate of formation of methane on the concentration of hydrogen sulfide at varied temperatures. The rate increases with the increase in the concentration of hydrogen sulfide, until it attains a constant value. Fig. 4 shows that the rate of formation of methane in the presence of $2.32\times10^{-6}$ mol. $cc^{-1}$ of hydrogen sulfide at 380°C is proportional to the 3/2 power of the concentration of the ether. Both Figs. 3 and 4 thus indicate that Eq. II holds when the ratio $[H_2S]/[CH_3OCH_3]$ is large. Values of $k_1^{1/2}k_7k_8^{-1/2}$ determined from the constant values of the rate in Fig. 3 and from the slope of the straight line in Fig. 4 are listed in Table II together with those of $k_1^{1/2}k_3k_5^{-1/2}$. The fairly good agreement of the two values of $k_1^{1/2}k_7k_8^{-1/2}$ at 380°C obtained by different methods shows again the validity of Eq. II.

The values given in Table II lead to the following Arrhenius expressions:

$$k_1^{1/2}k_3k_5^{-1/2} = 10^{15.16\pm0.13} \times \exp\{-(54{,}500\pm400)/RT\} \quad mol^{-1/2}\,cc^{1/2}\,sec^{-1/2}$$

$$k_1^{1/2}k_7k_8^{-1/2}=10^{15.26\pm0.24}\times\exp\{-(51{,}800\pm700)/\boldsymbol{RT}\}\ \mathrm{mol}^{-1/2}\,\mathrm{cc}^{1/2}\,\mathrm{sec}^{-1/2}$$

The expression for $k_1^{1/2}k_3k_5^{-1/2}$ shows a good agreement with that of $10^{15.11}\exp(-55{,}600/\boldsymbol{RT})$ $\mathrm{mol}^{-1/2}\,\mathrm{cc}^{1/2}\,\mathrm{sec}^{-1/2}$ obtained by Benson and Jain[6] who studied the thermal decomposition of dimethyl ether in the temperature range from 490 to 550°C.

The expression of $k_1^{1/2}k_3k_5^{-1/2}$ divided by that of $k_1^{1/2}k_7k_8^{-1/2}$ yields

$$(k_3/k_7)(k_8/k_5)^{1/2}=0.8\exp(-2{,}700/\boldsymbol{RT})$$

Assuming $k_8/k_5$ to be unity, $k_3/k_7=0.8\exp(-2{,}700/\boldsymbol{RT})$ and hence $E_7=E_3-2.7$ kcal./mol., $E$'s denoting activation energies. The result seems reasonable since hydrosulfide radicals have been shown to be more reactive towards organic molecules than methyl radicals. Reported values of $E_3$ are 8.4[10], 9.5[11] and 10.0[12] kcal./mol. and that of $A_3$ is of the order of $10^{11}\,\mathrm{mol}^{-1}\,\mathrm{cc.\,sec}^{-1}$. If we accept the intermediate value of 9.5 kcal./mol. for $E_3$, it follows that

$$k_7=10^{11}\exp(-6{,}800/\boldsymbol{RT})\ \ \mathrm{mol}^{-1}\,\mathrm{cc.\,sec}^{-1}$$

The present authors found previously that $k_6=10^{11}\exp(-2{,}600/\boldsymbol{RT})$[7]. The combination of these yields

$$k_6/k_7=\exp(4{,}200/\boldsymbol{RT})$$

It follows therefore that $k_6/k_7$ is much greater than unity at experimental temperatures although it decreases with the rise of temperature. This accounts for the fact that Eq. II holds even when the ratio $[H_2S]/[CH_3OCH_3]$ in Eq. III is not very large and that, the higher the temperature, the greater is the ratio $[H_2S]/[CH_3OCH_3]$ where Eq. II begins to be applicable, as seen in Fig. 3.

Benson and Jain have argued that the activation energy of the initial step, $E_1$, of 92 kcal./mol., obtained from their value of $E_{overall}=(1/2)E_1+E_3-(1/2)E_5=55.6$ kcal./mol. combined with $E_3=9.5$ kcal./mol., is too large compared with $E_1=81$ kcal./mol. obtained by Rice and Johnston[13], who decomposed dimethyl ether in the temperature range from 1010 to 1150°K and determined $E_1$ by an antimony mirror removal method. In order to explain this discrepancy, they suggest that the chain terminates not only by reaction 5 but also by reactions 9 and 10

$$CH_3+CH_2OCH_3\rightarrow C_2H_5OCH_3 \qquad (9)$$

$$2CH_2OCH_3\rightarrow (CH_3OCH_2)_2 \qquad (10)$$

and that reaction 4 is not unimolecular but bimolecular

$$CH_2OCH_3+\mathbf{M}\rightarrow CH_2O+CH_3+\mathbf{M} \qquad (4')$$

The rate of decomposition is then expressed as

$$-\mathrm{d}[CH_3OCH_3]/\mathrm{d}t=\frac{k_1^{1/2}k_3k_5^{-1/2}}{1+(k_{10}/k_5)^{1/2}(k_3/k_{4'})}[CH_3OCH_3]^{3/2}$$

Since $E_{10}=E_5=0$, $E_3=9.5$ and $E_4=19$ kcal./mol.[12], the denominator of the overall rate constant decreases with temperature. This situation, they believe, explains the overall activation energy greater than $(1/2)E_1+E_3-(1/2)E_5$.

However, if $E_1=81$ kcal./mol. and consequently $(1/2)E_1+E_3-(1/2)E_5=50$ kcal./mol. as they assume, $E_3-E_7=-1.8$ kcal./mol., i. e., $E_3<E_7$ and the catalysis such as shown by Eq. II cannot be expected to take place[14]. The interpretation given by Benson and Jain must therefore be regarded as incompatible with the results obtained in the present work. On the other hand, the agreement between the two overall $A$ factors in the absence and presence of hydrogen sulfide seems to support the idea that $k_{overall}=k_1^{1/2}k_3k_5^{-1/2}$, since it is probable that $A_3=A_7$ and $A_5=A_8$. The discrepancy between the overall activation energy in the pyrolysis of the ether alone and those of elementary reactions may therefore be attributed to the error in the estimation of $E_1$. Baughan et al.[15] estimated $E_1$ as 87 kcal./mol.

As seen in Table I, the time required to produce a definite amount of methane in the absence of hydrogen sulfide is about ten times as great as that in its presence, but the ratio of the amount of carbon monoxide to that of methane, compared with the same amount of the latter, is far less sensitive to the presence of hydrogen sulfide. This indicates that the decomposition of formaldehyde is also catalyzed by hydrogen sulfide. Kodama, Takezaki and Fujie[16] suggested that in the pyrolysis of dimethyl ether, formaldehyde decomposes by the following chain processes:

$$CH_3+CH_2O\rightarrow CH_4+CHO$$

$$CHO\rightarrow CO+H$$

$$H+CH_3OCH_3\rightarrow H_2+CH_3OCH_2$$

$$CH_3OCH_2\rightarrow CH_2O+CH_3$$

10) M. K. Phibbs and B. B. Darwent, *Can. J. Research*, **B28**, 395 (1950).
11) A. F. Trotman-Dickenson and E. W. R. Steacie, *J. Chem. Phys.*, **19**, 329 (1951).
12) R. A. Marcus, B. B. Darwent and E. W. R. Steacie, ibid., **16**, 983 (1948), recalculated in Ref. 11.
13) F. O. Rice and W. R. Johnston, *J. Am. Chem. Soc.*, **56**, 214 (1934).
14) Whether reaction 4 may be unimolecular or bimolecular, Eq. II holds when reactions 5, 9 and 10 are neglected compared with reaction 8.
15) E. C. Baughan, M. G. Evans and M. Polanyi, *Trans. Faraday Soc.*, **37**, 377 (1941).
16) S. Kodama, Y. Takezaki and R. Fujie, *J. Chem. Soc. Japan, Pure Chem. Sec.* (*Nippon Kagaku Zasshi*), **72**, 892 (1951).

In the presence of hydrogen sulfide, this scheme may be modified as follows:

$$HS+CH_2O \rightarrow H_2S+CHO$$
$$CHO \rightarrow CO+H$$
$$H+H_2S \rightarrow H_2+HS$$

## Summary

Dimethyl ether has been decomposed thermally in the presence and absence of hydrogen sulfide over the temperature range 360~440°C. The rate of decomposition is enhanced by the presence of hydrogen sulfide, but the rate law is unchanged, i. e., the rate is proportional to the 3/2 power of the ether concentration, irrespective of the presence of hydrogen sulfide.

The catalytic action of hydrogen sulfide is satisfactorily explained by the steps, $CH_3+H_2S \rightarrow CH_4+HS$ (6), $HS+CH_3OCH_3 \rightarrow H_2S+CH_3OCH_2$ (7) and $CH_3OCH_2 \rightarrow CH_2O+CH_3$ (4). Overall rate constants in the absence and presence of hydrogen sulfide are represented by $10^{15.16}\exp(-54{,}500/\boldsymbol{RT})$ and $10^{15.26}\exp(-51{,}800/\boldsymbol{RT})$ mol.$^{-1/2}$ cc$^{1/2}$ sec$^{-1/2}$ respectively. The combination of these gives $k_3/k_7=0.8\exp(-2{,}700/\boldsymbol{RT})$, where $k_3$ refers to the reaction $CH_3+CH_3OCH_3 \rightarrow CH_4+CH_3OCH_2$ (3). If, therefore, the activation energy of reaction 3 is 9.5 kcal./mol. as reported by Trotman-Dickenson and Steacie, that for reaction 7 is 6.8 kcal./mol. The results obtained indicate that the decomposition of the formaldehyde formed intremediately is also catalyzed by hydrogen sulfide.

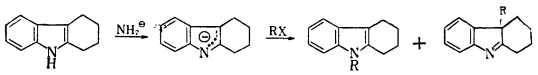
*Department of Applied Chemistry*
*College of Engineering*
*University of Osaka Prefecture*
*Sakai, Osaka*

# *Alkylation of Sodio-2, 3-dimethylindole and Sodio-tetrahydrocarbazole in Non-polar Solvent*

By Masao NAKAZAKI

(Received September 26, 1960)

In the previous paper[1], the formation of 11-alkyltetrahydrocarbazolenines (IV) and 9-alkyltetrahydrocarbazoles (III) by the alkylation of tetrahydrocarbazole (I) with sodium amide and alkyl halides in liquid ammonia was reported.

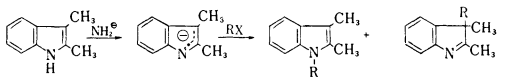


I II III IV

III a $R=CH_2C_6H_5$ IV a $R=CH_2C_6H_5$
b $R=CH_2-CH=CH_2$ b $R=CH_2-CH=CH_2$
c $R=CH_3$ c $R=CH_3$

The ratio of the yield of 11-alkyltetrahydrocarbazolenines (IV) to 9-alkyltetrahydrocarbazoles (III) was found to be affected by the halides employed: benzyl chloride gave the highest ratio and was followed by ally bromide, isopropyl iodide and methyl iodide.

The same sort of "ambident" alkylation[2,3] to give 1-alkyl-2, 3-dimethylindoles (VII) and 3-alkyl-2,3-dimethylindolenines (VIII) was observed in the alkylation of 2, 3-dimethylindole(V) in liquid ammonia with sodium amide and alkyl halides, and the ratio of *C*-alkyl/*N*-alkyl products were also found to depend on the nature of alkyl halides in the same sequence as that demonstrated in the alkylation of tetrahydrocarbazole. On the other hand, the alkylation of sodio-indole (IX) in non-polar solvent (benzene or without solvent) was studied by Funakubo[4], who reported the preparation of

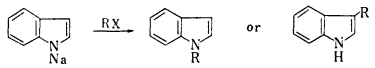


V VI VII VIII

VII a $R=CH_3$ VII a $R=CH_2C_6H_5$
b $R=CH_2-CH=CH_2$
c $R=CH_3$

1) M. Nakazaki and S. Isoe, *J. Chem. Soc. Japan, Pure Chem. Sec.* (*Nippon Kagaku Zasshi*), **76**, 1159 (1955).
2) M. Nakazaki, This Bulletin, **32**, 838 (1959).
3) The Grignard complex of I and V give 11-alkyltetrahydrocarbazolenines(IV) and 3-alkyl-2,3-dimethylindolenines (VIII) respectively, and there can be found no formation of *N*-substituted derivatives. T. Hoshino, *Ann.*, **500**, 35 (1932); B. Witkop, *J. Am. Chem. Soc.*, **72**, 614 (1950); Ref. 1.
4) E. Funakubo, *J. Chem. Soc. Japan, Pure Chem. Sec.* (*Nippon Kagaku Zasshi*), **48**, 652 (1927). Cf. R. Weisberger, *Ber.*, **42**, 3520 (1910).

*N*-alkyl indoles (X) (methyl, ethyl, *n*-propyl, isopropyl, allyl, *n*-butyl, isobutyl and isoamyl) by this method.



IX X XI

a $R=CH_2-CH=CH_2$
b $R=CH_2C_6H_5$
c $R=C(C_6H_5)_3$
d $R=CH_2COOC_2H_5$

But on our repetition of his experiment[1], his *N*-allylindole picrate (m. p. 169~170°C) turned out to be the picrate of recovered indole, and from the mother liquor was isolated another picrate (m. p. 105~106°C) which was established to be identical with the picrate of 3-allylindole (XIa)[5] prepared by the Grignard synthesis.

Kubota also found another example of β-alkylation of sodio-indole in non-polar solvent when he obtained 3-benzyl(XIb)[6], 3-triphenylmethyl-indole (XIc)[7] and ethyl β-indoleacetate (XId)[8] by heating a suspension of sodio-indole in dry benzene with benzyl chloride, triphenylmethyl chloride and ethyl chloroacetate respectively.

Unfortunately these authors did not dare to examine their alkylation method for 2, 3-disubstituted indoles, and this contribution is concerned with the alkylation of sodio-2, 3-disubstituted indoles in non-polar solvent as a natural extension of our alkylation studies in liquid ammonia.

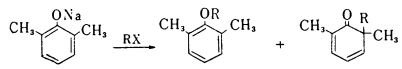
Tetrahydrocarbazole (I) and 2, 3-dimethylindole (V) were chosen as representatives of 2, 3-disubstituted indoles, because various 11-alkyltetrahydrocarbazlenines (IV), 3-alkyl-2, 3-dimethylindolenines (VIII) and *N*-alkyl derivatives III and VII have been prepared by our hands[1,2] and their structures were firmly established.

The general procedure carried out in our alkylation study was as follows: to a suspension of sodium amide in liquid ammonia (prepared in situ), a solution of indole derivatives (I or V) in toluene was added and the liquid ammonia was evaporated at room temperature. After residual ammonia was expelled by heating the solution up to the boiling point of toluene, a solution of halide in toluene was added under refluxing with stirring. The separation of indolenine derivatives and *N*-alkyl derivatives was worked out by the conventional method as in the case of alkylation in liquid ammonia.

The same directing effect of the alkylation reagents was confirmed in this alkylation in non-polar solvent; i. d. with benzyl chloride and allyl bromide, sodio-tetrahydrocarbazole afforded 11-alkyltetrahydrocarbazolenines (IV) predominantly, whereas with methyl iodide, *N*-methyl derivative was the sole product isolated; 2, 3-dimethyl-indole gave only indolenine derivatives VIII with benzyl chloride and allyl bromide, but with methyl iodide, *N*-methyl derivative VIIa accompanied with a small amount of indolenine derivative VIIIc.

It is noteworthy to compare these results with the directing effects of alkylation reagents in the alkylation of sodium salt of 2, 6-disubstituted phenols (XII) in non-polar solvent, which was studied strenuously by Curtin and his collaborators[9] recently.

To explain their observation that benzyl chloride and ally bromide give predominantly the *C*-alkyl derivative(6-alkyl-2, 6-dimethyl-2, 4-cyclohexadienone) XIII, whereas methyl iodide gives XIV with a trace of XIII, various factors which seem to control the direction of alkylation were considered, however, no decisive conclusion seems have to have been reached. We have proposed a reasonable mechanism to explain the marked directing effect of benzyl



XII XIV XIII

and ally halides in the alkylation of tetrahydrocarbazole in liquid ammonia, but this can not be advanced to rationalize the ambident alkylations in non-polar solvent without further experimental supports.

Studies of alkylation of 2, 6-dimethylphenol in liquid ammonia are now in progress in our laboratory, and should be the subject of a subsequent communication.

## Experimental

**Alkylation of Tetrahydrocarbazole (I).**—*1) With Benzylchloride.*—A mixture of 5 g. of tetrahydrocarbazole and 100 cc. of toluene was added to a suspension of sodium amide in lipuid ammonia

5) Authentic *N*-allylindole (b. p. 114~116°C/6 mmHg., picrate: m. p. 79~79.5°C) was prepared by the alkylation of indole in liquid ammonia with sodium amide and allyl bromide. Ref. 1.

6) T. Kubota, *J. Chem. Soc. Japan, Pure Chem. Sec.* (*Nippon Kagaku Zasshi*), **59**, 407 (1938).

7) T. Kubota and I. Mita, ibid., **59**, 409 (1936). This 3-triphenylmethyl-indole was found to be identical with the compound which had been prepared by E. Funakubo and T. Hirotani (*Ber.*, **69**, 2123 (1936)) by the reaction of the Grignard complex of indole with triphenylmethyl chloride and had been assigned the structure of *N*-triphenylmethyl derivative by them.

8) T. Kubota, Japan Pat., 166925 (1934).

9) D. Y. Curtin et al., *J. Am. Chem. Soc.*, **79**, 3156 (1957); **80**, 1391, 4339, 6016 (1958); *J. Org. Chem.*, **23**, 9 (1958).

prepared from 0.5 g. of sodium and 200 cc. of liquid ammonia. The liquid ammonia was evaporated at room temperature and the resulting suspension of sodio-tetrahydrocarbazole in toluene was refluxed in order to expel the last trace of ammonia. A solution of 4 g. of benzyl chloride in 20 cc. of toluene was added dropwise. After the solution was stirred and refluxed for 1.5 hr., the toluene was distilled with steam, and the residue was extracted with ether. The ether solution was washed with 2 N hydrochloric acid to separate the basic and neutral fractions.

*N-Benzyltetrahydrocarbazole (IIIa)*: — The ethereal extract was washed with water twice and dried over anhydrous sodium sulfate. Removal of the solvent gave a semisolid which was washed with petroleum ether-ether to give 0.5 g. of recovered tetrahydrocarbazole. The washing was concentrated to afford a pale yellow oil, which was distilled in vacuo, 0.4 g. b. p. 170~180°C/2 mmHg (literature[1]: b. p. 195°C/2 mmHg). The picrate was recrystallized from ethanol to give red needles which melted at 110~111°C, alone and admixed with an authentic sample of *N*-benzyltetrahydrocarbazole (m. p. 110~111°C).

Found: N, 11.49. Calcd. for $C_{19}H_9N \cdot C_6H_3O_7N_3$: N, 11.42%.

*11-Benzyltetrahydrocarbazolenine (IVa)*:—After the acidic solution was washed with ether, 4 N sodium hydroxide solution was added to precipitate the basic material which was extracted with ether.

The extract was washed with water and dried over anhydrous sodium sulfate. The solvent was removed to give a semisolid which was filtered free from viscous mother liquor. The crystals were recrystallized from ethanol-water to afford prisms melting at 84~85°C, which was found identical with 11-benzyltetrahydrocarbazolenine by the mixed melting point determination with an authentic specimen (literature: m. p. 85~86°C[1]). The picrate was recrystallized from ethanol to give yellow prisms, m. p. 176~177.5°C (literature: 176~177°C[1]). The mixed melting point with an authentic specimen was 176~177.5°C.

Found: N, 11.53. Calcd. for $C_{19}H_{19}N \cdot C_6H_3O_7N_3$: N, 11.42%.

*2) With Allyl Bromide.* — To a suspension of sodio-tetrahydrocarbazole in toluene prepared from 200 cc. of liquid ammonia, 0.7 g. of sodium, 5 mg. of ferric nitrate, 5 g. tetrahydrocarbazole (I) and 100 cc. of toluene, as described previously, a solution of 4 g. of ally bromide in 20 cc. of toluene was added dropwise with stirring and refluxing in a period of 2 hr. After the reaction mixture was refluxed for an additional 5 hr., the solvent was removed by steam distillation and the residue was extracted with ether. The neutral and basic fractions were separated as described above.

*N-Allyltetrahydrocarbazole(IIIb)*:—From the neutral fraction, 0.5 g. of tetrahydrocarbazole was recovered (m. p. 110~116°C). The residue was distilled in vacuo to afford a viscous pale yellow liquid, b. p. 125~128°C/2 mmHg (literature[1]: b. p. 157°C/3 mmHg). The picrate was recrystallized to give red needles melting at 76~77°C, which were found to be identical with the picrate of *N*-allyltetrahydrocarbazole by the mixed melting point determination with an authentic sample, m. p. 76~77°C[1].

Found: N, 13.05. Calcd. for $C_{15}H_{17}N \cdot C_6H_3O_7N_3$: N, 12.73%.

*11-Allyltetrahydrocarbazolenine (IVb)*: — The basic fraction gave 2.0 g. of crystals which were recrystallized from petroleum ether to afford 11-allyltetrahydrocarbazolenine, m. p. 54~56°C, identified by the mixed melting point determination with an authentic sample (literature[1]: m. p. 57~58°C). The picrate was recrystallized from ethanol to give yellow prisms, m. p. 139~142°C, the identity of which with the picrate of 11-allytetrahydrocarbazolenine was established by the mixed melting point determination with an authentic sample (literature[1]: m. p. 142~143°C).

Found: N, 12.94. Calcd. for $C_{15}H_{17}N \cdot C_6H_3O_7N_3$: N, 12.72%.

*3) With Methyl Iodide.* — The alkylation with methyl iodide was carried out following the general procedure described above. A solution of 8 g. of methyl iodide in 40 cc. of toluene was added dropwise during 6 hr. in a suspension of sodio-tetrahydrocarbazole (0.02 mol.) on toluene prepared from 200 cc. of liquid ammonia, 0.7 g. of sodium, 3.4 g. of sodium and 80 cc. of toluene. After the usual work up, the basic and neutral fractions were separated.

*N-Methyltetrahydrocarbazole (IIIc)*: — The vacuum distillation of the neutral fraction gave 1.4 g. of viscous pale yellow oil, b. p. 124~126°C/2 mmHg. The picrate was recrystallized from ethanol to give brown-red needles melting at 109~112°C. The mixed melting point with an authentic specimen[1] (m. p. 113~114°C) was 109~112°C.

Found: N, 13.79. Calcd. for $C_{13}H_{15}N \cdot C_6H_3O_7N_3$: N, 13.52%.

*The Basic Fraction*: — Removal of the ether afforded an amber yellow solid which was sparingly soluble in dilute sodium hydroxide, dilute hydrochloric acid, ethanol and ether respectively add could not be converted into crystalline picrate. This substance was not studied further.

**Alkylation of 2, 3-Dimethylindole (V).**—*1) With Benzylchloride*:—A solution of 5 g. of 2,3-dimethylindole (V) in 100 cc. of toluene was added dropwise into a suspension of sodium amide in liquid ammonia prepared from 200 cc. of liquid ammonia, 1 g. of sodium and 5 mg. of ferric nitrate. The liquid ammonia was evaporated and the remaining mixture was refluxed with stirring. To the reaction mixture, a solution of 5.3 g. of benzyl chloride in 20 cc. of toluene was added and refluxing with stirring was continued for 8 hr. After the reaction mixture was worked up as described in the alkylation of tetrahydrocarbazole, the basic and the neutral fractions were separated.

*2, 3-Dimethyl-3-benzylindolenine (VIIIa)*:—Removal of the solvent afforded 4.6 g. of a solid, which was recrystallized from petroleum ether to give crystals melting at 48~49°C, alone and admixed with an authentic specimen (m. p. 48~49°C[10]).

The picrate was recrystallized from ethanol to give

10) M. Nakazaki, S. Isoe and K. Tanno, *J. Chem. Soc. Japan, Pure Chem. Sec.* (*Nippon Kagaku Zasshi*), **76**, 1262 (1955).

yellow prisms, m. p. 137~139°C, the mixed melting point of which with an authentic sample[10] was found 137~140°C.

Found: N, 12.20. Calcd. for $C_{17}H_{17}N \cdot C_6H_3O_7N_3$: N, 12.06%.

*The Neutral Fraction:* — A small amount of 2,3-dimethylindole was recovered, but the search for *N*-benzyl derivative was fruitless.

*2) With Allyl Bromide.*—Using 5 g. of allyl bromide, the alkylation was carried out exactly as the procedure described above.

*2,3-Dimethyl-3-allylindolenine (VIIIb):* — The crude basic fraction (1 g.) was distilled in vacuo to give a yellow liquid, b. p. 125~128°C/12 mmHg. The picrate was recrystallized from ethanol to afford yellow needles m. p. 158~160°C, the mixed melting point with an authentic sample[2] (m. p. 156~157°C) showed 159~160°C.

Found: N, 13.65. Calcd. for $C_{13}H_{15}N \cdot C_6H_3O_7N_3$: N, 13.52%.

*Neutral Fraction:* — The crude neutral fraction (2 g.) was distilled in vacuo to give two fractions: 1. 1.4 g. b. p. 100~125°C/2 mmHg. which was proved as 2,3-dimethylindole recovered, 2. 0.5 g. b. p. 125~130°C/2 mmHg which did not give crystalline picrate and was not studied further.

*3) With Methyl Iodide.* — The alkylation was carried out using 12 g. of methyl iodide, and the basic and neutral fractions were separated as described above.

*2,3,3-Trimethylindolenine (VIIIc):*—The crude basic fraction (1.1 g.) was distilled in vacuo to give 0.4 g. of VIIIc, b. p. 80°C/1 mmHg, the characteristic odor of which resembles that of jasmin. The picrate was recrystallized from ethanol to afford yellow needles melting at 158°C, which was found identical with the picrate of 2,3,3-trimethylindolenine (literature[2]: m. p. 158°C) by the mixed melting point determination.

Found: N, 14.54. Calcd. for $C_{11}H_{13}N \cdot C_6H_3O_7N_3$: 14.43%.

*1,2,3-Trimethylindole (VIIa):* — From the neutral fraction, a small amount of 2,3-dimethylindole was recovered by recrystallization from petroleum ether. The mother liquor, after removal of the solvent, was distilled in vacuo to give 1.1 g. of yellow liquid, b. p. 90~93°C/2 mmHg (literature[2]: b. p. 117~120°C/6 mmHg). The picrate was recrystallized from ethanol to afford brownish-black needles, m. p. 145~147°C which was not depressed on admixing with an authentic specimen[2] of the picrate of 1,2,3-trimethylindole (m. p. 148~149°C).

Found: N, 14.70. Calcd. for $C_{11}H_{13}N \cdot C_6H_3O_7N_3$: N, 14.43%.

The author is very grateful to Mr. Sachio Itaba for his technical assistance.

*Institute of Polytechnics*
*Osaka City University*
*Kita-ku, Osaka*

# *Microwave Spectrum and Molecular Structure of Monochloroacetonitrile, $CH_2ClCN$*

By Kaname WADA, Yoshikazu KIKUCHI, Chi MATSUMURA, Eizi HIROTA and Yonezo MORINO

(Received September 5, 1960)

Since the structure of the monochloroacetonitrile molecule $CH_2ClCN$ is similar to that of propargyl chloride $CH_2ClC{\equiv}CH$, it is of some interest to compare the structure of the two molecules with each other in detail. In particular, the C—Cl bond length is important in the respect because it will give some information concerning the electronic structure of the molecule. The quadrupole coupling constant of chlorine nucleus is also important for discussing the nature of the C—Cl bond.

When the present investigation was coming nearly to the end, a paper was published by Graybeal on the structure of the $CH_2ClCN$ molecule by the microwave absorption spectrum[1]. But his result seems to involve a number of unreliable data and moreover only two isotopic species, $CH_2{}^{35}ClCN$ and $CH_2{}^{37}ClCN$, were used in his study. The molecular structure and the molecular constants obtained in the present paper would be more reliable than those by Graybeal.

## Experimental

The rotational spectra of monochloroacetonitrile, $CH_2{}^{35}ClCN$, $CH_2{}^{37}ClCN$, $CD_2{}^{35}ClCN$, and $CD_2{}^{37}ClCN$, were observed at room temperature by using the recording microwave spectrometer with a 100 Kc. Stark modulation described in the previous paper[2]. The microwave was supplied by klystrons,

1) J. D. Graybeal, *J. Chem. Phys.*, **32**, 1258 (1960).
2) E. Hirota and Y. Morino, This Bulletin, to be published.

TABLE I. OBSERVED AND CALCULATED CENTER FREQUENCIES

| | $CH_2{}^{35}ClCN$ | | $CH_2{}^{37}ClCN$ | | $CD_2{}^{35}ClCN$ | | $CD_2{}^{37}ClCN$ | |
|---|---|---|---|---|---|---|---|---|
| | obs. | calcd. | obs. | calcd. | obs. | calcd. | obs. | calcd. |
| a-Type | | | | | | | | |
| $2_{1,2}\rightarrow 3_{1,3}$ | 17545 | 17544.20 | | | 17190.80 | 17190.34 | 16832.86 | 16833.12 |
| $3_{0,3}\rightarrow 4_{0,4}$ | 23966.23 | 23968.50 | | | | | | |
| $3_{1,3}\rightarrow 4_{1,4}$ | 23385.72 | 23388.83 | | | 22914.78 | 22914.49 | | |
| $4_{1,4}\rightarrow 5_{1,5}$ | 29227.24 | 29230.41 | 28611.54 | 28612.16 | 28633.16 | 28633.68 | 28038.14 | 28039.38 |
| $5_{1,5}\rightarrow 6_{1,6}$ | 35065.78 | 35068.33 | 34324.38 | 34326.95 | 34346.03 | 34346.84 | 33636.16 | 33634.53 |
| b-Type | | | | | | | | |
| $1_{0,1}\rightarrow 1_{1,0}$ | 22422.50 | 22422.48 | 22332.96 | 22332.97 | | | | |
| $3_{0,3}\rightarrow 3_{1,2}$ | 23192.78 | 23191.36 | 23074.41 | 23074.49 | 17585.67 | 17584.56 | | |
| $4_{0,4}\rightarrow 4_{1,3}$ | 23821.51 | 23820.40 | | | 18304.48 | 18304.23 | 18187.47 | 18185.99 |
| $5_{0,5}\rightarrow 5_{1,4}$ | 24625 | 24623.42 | | | 19234.33 | 19232.49 | | |
| $6_{0,6}\rightarrow 6_{1,5}$ | 25614.88 | 25612.08 | 25409 | 25405.55 | 20389.63 | 20387.74 | 20192.84 | 20191.62 |
| $7_{0,7}\rightarrow 7_{1,6}$ | 26801 | 26799.24 | 26549 | 26547.20 | 21791.27 | 21790.80 | 21541.20 | 21540.40 |
| $8_{0,8}\rightarrow 8_{1,7}$ | 28201 | 28199.58 | 27894 | 27892.79 | 23465.04 | 23463.98 | 23148.64 | 23147.47 |
| $9_{0,9}\rightarrow 9_{1,8}$ | 29831 | 29828.87 | 29458 | 29457.20 | 25429.58 | 25429.40 | 25034.94 | 25033.99 |
| $10_{0,10}\rightarrow 10_{1,9}$ | 31706 | 31703.42 | 31253 | 31255.89 | 27708.01 | 27706.52 | 27222.44 | 27219.00 |
| $11_{0,11}\rightarrow 11_{1,10}$ | 33842 | 33839.15 | 33303 | 33304.09 | 30318.90 | 30308.94 | | |
| $12_{0,12}\rightarrow 12_{1,11}$ | | | | | 33273.50 | 33239.82 | 32562.24 | 32531.71 |
| $13_{0,13}\rightarrow 13_{1,12}$ | | | | | | | 35734.94 | 35655.44 |
| $0_{0,0}\rightarrow 1_{1,1}$ | 28120.10 | 28120.11 | 27912.08 | 27912.07 | | | | |
| $1_{0,1}\rightarrow 2_{1,2}$ | 33818.58 | 33817.76 | 33492.20 | 33491.20 | | | | |
| $4_{0,4}\rightarrow 4_{1,3}$ | 23821.51 | 23820.40 | | | | | | |
| $5_{1,5}\rightarrow 6_{0,6}$ | 15794.49 | 15800.49 | 15038.47 | 15042.88 | | | | |
| $6_{1,6}\rightarrow 7_{0,7}$ | 22551.95 | 22559.80 | | | | | | |
| $11_{2,10}\rightarrow 12_{1,11}$ | 16468.89 | 16502.57 | 14790.03 | 14823.01 | | | | |

TABLE II. ROTATIONAL CONSTANTS AND ASYMMETRY PARAMETERS

| | $CH_2{}^{35}ClCN$ | $CH_2{}^{37}ClCN$ | $CD_2{}^{35}ClCN$ | $CD_2{}^{37}ClCN$ |
|---|---|---|---|---|
| $A$ | 25271.30 Mc./sec. | 25122.52 Mc./sec. | 19494.88 Mc./sec. | 19377.44 Mc./sec. |
| $B$ | 3151.01 | 3081.13 | 3119.94 | 3051.63 |
| $C$ | 2848.80 | 2789.56 | 2780.81 | 2724.15 |
| $b_P$ | $-6.78471\times10^{-3}$ | $-6.57069\times10^{-3}$ | $-1.02490\times10^{-2}$ | $-9.92993\times10^{-3}$ |

Varian X-12 and X-13, and the frequency was multiplied by a silicon crystal. The frequency range covered was 15000 Mc./sec. to 35000 Mc./sec.

The deuterated samples were prepared as follows: a mixture of the normal monochloroacetonitrile, heavy water and a trace of anhydrous sodium carbonate was kept on a hot water bath for a day and then distilled out. The infrared absorption spectrum showed neither the C-H stretching nor the $CH_2$ deformation bands.

## Results

Monochloroacetonitrile is a nearly prolate symmetric top molecule and both a- and b-type transitions were observed. The transitions of the b-type Q-branch, $J_{0,J}\rightarrow J_{1,J-1}$, were most easily identified because of their characteristic hyperfine patterns due to the quadrupole moment of the chlorine nucleus ($I=3/2$) and confirmed by plotting the values of $A-(B+C)/2$ and $b_P=(C-B)/(2A-B-C)$. For $CH_2ClCN$ a-type, and b-type R-branch transitions and for $CD_2ClCN$ a-type R-branch transitions were also measured. The observed center frequencies are given in Table I.

The rotational constants of $CH_2ClCN$ were determined by using the transitions, $0_{0,0}\rightarrow 1_{1,1}$, $1_{0,1}\rightarrow 1_{1,0}$, and $3_{0,3}\rightarrow 3_{1,2}$. Unfortunately none of these transitions were measured for $CD_2ClCN$ and the rotational constants were determined by using relatively low-$J$ transitions. The values are listed in Table II. The center frequencies calculated by using these constants are compared with the observed ones in Table I. (a rigid rotor calculation).

For $CH_2{}^{35}ClCN$ rough estimation of centrifugal effect is made (Table III) by assuming the expression for a symmetric top molecule, $-D_JJ^2(J+1)^2-D_{JK}J(J+1)K_{-1}{}^2-D_KK_{-1}{}^4$. The transitions used for determining the centrifugal constants are $4_{0,4}\rightarrow 4_{1,3}$, $5_{1,5}\rightarrow 6_{1,6}$, $5_{1,5}\rightarrow 6_{0,6}$, $6_{1,6}\rightarrow 7_{0,7}$, and $11_{2,10}\rightarrow 12_{1,11}$. The center frequencies calculated with the centrifugal distortion correction are compared with the observed

TABLE III. EFFECT OF THE CENTRIFUGAL DISTORTION FOR $CH_2{}^{35}ClCN$

($D_J=0.004399$ Mc./sec., $D_{JK}=-0.02340$ Mc./sec., $D_K=0.3398$ Mc./sec.)

| | $\nu_{rigid}$ | $D_{corr.}$ | $\nu_{corr.}$ | $\nu_{obs.}$ |
|---|---|---|---|---|
| $2_{1,2}\rightarrow 3_{1,3}$ | 17544.20 | −0.33 | 17543.87 | 17545 |
| $3_{0,3}\rightarrow 4_{0,4}$ | 23968.50 | −1.13 | 23967.37 | 23966.23 |
| $3_{1,3}\rightarrow 4_{1,4}$ | 23388.83 | −0.94 | 23387.89 | 23385.72 |
| $4_{1,4}\rightarrow 5_{1,5}$ | 29230.41 | −1.97 | 29228.44 | 29227.24 |
| $5_{1,5}\rightarrow 6_{1,6}$ | 35068.33 | −3.52 | 35064.81 | 35065.78 |
| $1_{0,1}\rightarrow 1_{1,0}$ | 22422.48 | −0.29 | 22422.19 | 22422.50 |
| $3_{0,3}\rightarrow 3_{1,2}$ | 23191.36 | −0.06 | 23191.30 | 23192.78 |
| $4_{0,4}\rightarrow 4_{1,3}$ | 23820.40 | 0.13 | 23820.53 | 23821.51 |
| $5_{0,5}\rightarrow 5_{1,4}$ | 24623.42 | 0.36 | 24623.78 | 24625 |
| $6_{0,6}\rightarrow 6_{1,5}$ | 25612.08 | 0.64 | 25612.72 | 25614.88 |
| $7_{0,7}\rightarrow 7_{1,6}$ | 26799.24 | 0.97 | 26800.21 | 26801 |
| $8_{0,8}\rightarrow 8_{1,7}$ | 28199.58 | 1.35 | 28200.93 | 28201 |
| $9_{0,9}\rightarrow 9_{1,8}$ | 29828.87 | 1.77 | 29830.64 | 29831 |
| $10_{0,10}\rightarrow 10_{1,9}$ | 31703.42 | 2.23 | 31705.65 | 31706 |
| $11_{0,11}\rightarrow 11_{1,10}$ | 33839.15 | 2.75 | 33841.90 | 33842 |
| $0_{0,0}\rightarrow 1_{1,1}$ | 28120.11 | −0.31 | 28119.80 | 28120.10 |
| $1_{0,1}\rightarrow 2_{1,2}$ | 33817.76 | −0.34 | 33817.42 | 33818.58 |
| $4_{0,4}\rightarrow 4_{1,3}$ | 23820.40 | 0.12 | 23820.52 | 23821.51 |
| $5_{1,5}\rightarrow 6_{0,6}$ | 15800.49 | −4.16 | 15796.33 | 15794.49 |
| $6_{1,6}\rightarrow 7_{0,7}$ | 22559.80 | −6.63 | 22553.17 | 22551.95 |
| $11_{2,11}\rightarrow 12_{1,11}$ | 16502.57 | −34.01 | 16468.56 | 16468.89 |

TABLE IV. MOLECULAR CONSTANTS OF MONOCHLOROACETONITRILE

(Graybeal's values are also given for comparison.)

Present

Calculated

C—Cl 1.7815 Å, C—H 1.0881 Å, H···H 1.7812 Å, ∠CCCl 111°29′, ∠CCH 107°27′, $\Delta=0.2194$ amu Å$^2$, $\chi_{aa}=-32.8$ Mc./sec., $\chi_{bb}=-7.2$ Mc./sec.

Assumed

C—C 1.458 Å, C—N 1.158 Å, ∠CCN 180°,

Graybeal

Calculated

C—Cl 1.767 Å, C—C 1.472 Å, H···H 1.728 Å, ∠CCCl 111°24′, $\chi_{aa}=-30.45$ Mc./sec., $\chi_{bb}=-7.73$ Mc./sec.,

Assumed

C—H 1.070 Å, C—N 1.158 Å, ∠CCN 180°, ∠CCH 109°30′.

ones in Table III. It is seen that the discrepancy found in the rigid rotor calculation is largely reduced, even for high-$J$ transitions.

Since only two hydrogen atoms are located above and below the symmetry plane, the distance between them $r$ is given by[2]

$$r=[(I_a+I_b-I_c+\Delta)/m]^{1/2}$$

where $\Delta$ is a quantity similar to the inertia defect and $m$ is the mass of hydrogen or deuterium atom. The values of $\Delta$ and $r$ (Table IV) were determined by means of the method of least-squares using the four equations given by the four isotopic species.

The number of the rotational constants obtained is twelve. Four of them are used in obtaining the hydrogen to hydrogen distance, hence there remain eight constants for determining the other structural parameters, $d_{C-C}$, $d_{C-Cl}$, $d_{C-H}$, $d_{C\equiv N}$, ∠CCCl, ∠CCH, and ∠CCN. Since isotopes of carbon and nitrogen atoms were not available, none of these parameters could be determined. The C-C bond length adjacent to the triple bond is usually about 1.458 Å, and the C≡N bond length in cyano group is reported for a number of molecules to be 1.158 Å[3]. The assumption of the linear structure for the C—C≡N group may not influence the other structural parameters. Thus the following values were assumed: $d_{C-C}=1.458$ Å,

3) C. C. Costain and B. P. Stoicheff, *J. Chem. Phys.*, **30**, 777 (1959).

TABLE V. COMPARISON OF THE CENTER FREQUENCIES ($CH_2{}^{35}ClCN$) GIVEN BY GRAYBEAL AND BY THE PRESENT AUTHORS

| | obs. | | calcd. | |
|---|---|---|---|---|
| | Graybeal | Present | Graybeal* | Present** |
| a-Type | | | | |
| $2_{1,2}\rightarrow 3_{1,3}$ | 17550 | 17545 | 17549.40 | 17550.06 |
| $3_{0,3}\rightarrow 4_{0,4}$ | 23974 | 23966.23 | 23975.39 | 23975.42 |
| $3_{2,2}\rightarrow 4_{2,3}$ | 24002 | | 24003.65 | 24003.66 |
| $3_{3,1}\rightarrow 4_{3,2}$ | 24011 | | 24012.09 | 24012.11 |
| $3_{3,0}\rightarrow 4_{3,1}$ | 24011 | | 24012.21 | 24012.23 |
| $3_{2,1}\rightarrow 4_{2,2}$ | 24036 | | 24034.28 | 24034.28 |
| b-Type | | | | |
| $5_{1,5}\rightarrow 6_{0,6}$ | 15794.54 | 15794.49 | 15794.54 | 15795.07 |
| $10_{1,10}\rightarrow 9_{2,7}$ | 16347.33 | | 16347.34 | 16337.31 |
| $11_{2,10}\rightarrow 12_{1,11}$ | 16469.00 | 16468.89 | 16469.00 | 16467.53 |
| $6_{1,6}\rightarrow 7_{0,7}$ | 22554.00 | 22551.95 | 22553.57 | 22555.14 |
| $4_{0,4}\rightarrow 4_{1,3}$ | 23829.80 | 23821.51 | 23830.09 | 23830.39 |

* Values cited from Graybeal's paper. No corrections for centrifugal effects.

** Values calculated by using the rotational constants given by Graybeal. No corrections for centrifugal effects.

$d_{C\equiv N}=1.158$ Å, and $\angle CCN=180°$. The remaining five parameters were determined by the method of least-squares using the values of $A$ and $B$, as shown in Table IV.

Nuclear quadrupole coupling constant is calculated for $CH_2{}^{35}ClCN$ from the transitions $1_{0,1}\rightarrow 1_{1,0}$, $3_{0,3}\rightarrow 3_{1,2}$, and $6_{0,6}\rightarrow 6_{1,5}$, and given in Table IV. If the electronic charge distribution about the C—Cl bond is assumed to be cylindrical, the quadrupole coupling constant along the C—Cl bond axis is $-80$ Mc./sec. The value is consistent with that observed in the solid state, 76.25 Mc./sec.[4] The hyperfine structures due to the nitrogen nucleus were not resolved.

## Discussion

A quite normal value 1.7815 Å is obtained for the C—Cl bond length, which is very close to the value obtained for propargyl chloride, 1.780 Å[2], hence it is sure that neither a double bond structure nor an ionic structure contributes so much to the electronic configuration in the ground state of this molecule.

The center frequencies measured by Graybeal[1] are shown in Table V. Some of them are confirmed by the present investigation within the experimental error, but others show a definite discrepancy. Graybeal calculated the center frequencies by using the rotational constants given in Table VI. However, some of them are also in error by as much as 10 Mc./sec. It is found that the $\delta$ expansion formula he used[5] is insufficient for calculating the energy of the rotational states with $J$ as high as ten. As a result his values of $A$ are larger than the present ones by about 13 Mc./sec. (Table VI). On the other hand the constants of the present paper reproduce the

TABLE VI. COMPARISON OF THE ROTATIONAL CONSTANTS (IN Mc./sec) OBTAINED BY GRAYBEAL AND BY THE PRESENT AUTHORS

| | $CH_2{}^{35}ClCN$ | | $CH_2{}^{37}ClCN$ | |
|---|---|---|---|---|
| | Graybeal | Present | Graybeal | Present |
| $A$ | 25284.77 | 25271.30 | 25135.17 | 25122.52 |
| $B$ | 3151.61 | 3151.01 | 3081.77 | 3081.13 |
| $C$ | 2849.90 | 2848.80 | 2790.84 | 2789.56 |

frequencies of low-$J$ transitions in good agreement with the observed ones. If the centrifugal distortion is taken into account, the rotational constants given in the present paper would account even for high-$J$ transitions (Table III).

Graybeal reported the C—Cl bond length to be 1.767 Å and the C—C bond length to be 1.472 Å (Table IV). If isotopic species of carbon or nitrogen atoms were not available as in his study, it would be difficult to determine these two parameters separately. The correction due to the inertia defect has not been taken in the H···H distance obtained by Graybeal, thus the structure of the $CH_2$ group reported by him is not reliable.

The value of the quadrupole coupling constant of chlorine nucleus is observed to be $-80$ Mc./sec., which is slightly higher than that of propargyl chloride ($-75.8$ Mc./sec.)[2]

4) J. D. Graybeal and C. D. Cornwell, *J. Phys. Chem.*, 62, 483 (1958).

5) Graybeal used likely the expansion formula given by King, Hainer and Cross [*J. Chem. Phys.*, 11, 27 (1943)].

or of ethyl chloride (−70.07 Mc./sec.)[6]. This fact may be accounted for by the presence of the electronegative cyano group, since this reduces the ionic structure of the C—Cl bond. The present value of the quadrupole coupling constant of chlorine nucleus would be more reasonable than Graybeal's value −76.36 Mc./sec., since the (absolute) value obtained in the vapor phase is usually larger than that in the solid phase by several megacycles and the coupling constant of monochloroacetonitrile is 76.25 Mc./sec. in the solid state.

6) R. S. Wagner and B. P. Dailey, ibid., **26**, 1588 (1957).

The authors wish to express their sincere thanks to Dr. Makoto Shima, Institute for Physical and Chemical Research, for supplying them with heavy water. The expenses for this research were defrayed from the Scientific Research Encouragement Grant of the Ministry of Education to which the authors' thanks are also due.

*Department of Chemistry*
*Faculty of Science*
*The University of Tokyo*
*Hongo, Tokyo*

# *Microwave Spectrum of Propargyl Halides. I. Molecular Structure, Dipole Moment, and Quadrupole Coupling Constant of Propargyl Chloride*

By Eizi HIROTA and Yonezo MORINO

(Received September 5, 1960)

The C—Cl bond length in propargyl chloride $CH_2ClC \equiv CH$ was found by Pauling, Gordy and Saylor[1] to be $1.82 \pm 0.02$ Å. It is remarkably longer than C—Cl lengths observed in a number of other aliphatic chlorides. However, the value obtained in the previous paper[2], 1.7802 Å, was close to the usual C—Cl bond length.

The present paper will include the observation and the analysis of rotational spectra of two other isotopic species, $CH_2{}^{35}ClC{\equiv}CD$ and $CH_2{}^{37}ClC \equiv CD$, and will give a molecular structure more reliable than the previous one.

## Experimental

The spectrometer used was similar to that reported by Shimoda, Nishikawa and Itoh[3]. A 100 Kc. sine wave modulation was used. The microwave was generated by klystrons, 2K26, 2K25, 8V77, X-12, and X-13, and the frequency was multiplied by a silicon crystal. The frequency range covered was from 7000 Mc./sec. to 36000 Mc./sec. An X-band absorption cell of 3 m. in length was employed, and the Stark electrode was supported by Teflon tape grooved at its center. The spacing between the electrode and the cell was not measured, but the calibration was made by observing the Stark effect of the $J=1 \rightarrow 2$ lines of carbonyl sulfide $^{16}O^{12}C^{32}S$ at 24325.94 Mc./sec.[4]. The vacuum system was designed in such a way that the sample flew continuously through the cell, its pressure being estimated by a Pyrani gauge. The cell was cooled with dry ice when necessary. The frequency of microwave was measured by the technique developed by Shimoda[5]. The out-put power of microwave was detected by another silicon crystal and fed into a narrow band amplifier tuned with 100 Kc./sec. and then detected by a phase-sensitive detector. The signal was amplified by a low-frequency amplifier and observed on a cathode ray oscilloscope or on a recorder. The ultimate sensitivity was about $5 \times 10^{-9}$ cm$^{-1}$ when the recorder was used[6].

Propargyl chloride was synthesized by Dr. T. Shimozawa by the chlorination of propargyl alcohol[7]. The deuterated species $CH_2ClC{\equiv}CD$ was obtained by mixing normal propargyl chloride with heavy water which was made slightly alkaline by adding a small quantity of anhydrous sodium carbonate.

## Results

**Rotational Spectra and Rotational Constants.** —Propargyl chloride is a nearly prolate symmetric top, and the a- and b- axes are in the

1) L. Pauling, W. Gordy and J. H. Saylor, *J. Am. Chem. Soc.*, **64**, 1753 (1942).
2) E. Hirota, T. Oka and Y. Morino, *J. Chem. Phys.*, **29**, 444 (1958).
3) K. Shimoda, T. Nishikawa and T. Itoh, *J. Phys. Soc. Japan*, **9**, 974 (1954).
4) S. A. Marshall and I. Weber, *Phys. Rev.*, **105**, 1502 (1957).
5) K. Shimoda, *J. Phys. Soc. Japan*, **9**, 378 (1954).
6) C. Matsumura, E. Hirota and Y. Morino, This Bulletin, to be published.
7) T. Chiba, T. Shimozawa, I. Miyagawa and Y. Morino, This Bulletin, **30**, 223 (1957).

TABLE I. OBSERVED AND CALCULATED FREQUENCIES OF THE SPECTRA IN THE GROUND VIBRATIONAL STATE (Mc./sec.)*

| | $CH_2{}^{35}ClC{\equiv}CH$ | | $CH_2{}^{37}ClC{\equiv}CH$ | | $CH_2{}^{35}ClC{\equiv}CD$ | | $CH_2{}^{37}ClC{\equiv}CD$ | |
|---|---|---|---|---|---|---|---|---|
| | Obs. | Calcd. | Obs. | Calcd. | Obs. | Calcd. | Obs. | Calcd. |
| a-Type | | | | | | | | |
| $2_{0,2}\rightarrow 3_{0,3}$ | 17559.47 | 17559.49 | 17194.93 | 17195.16 | 16494.03 | 16494.16 | 16153.62 | 16153.69 |
| $2_{1,2}\rightarrow 3_{1,3}$ | 17117.51 | 17117.56 | 16769.44 | 16767.89 | 16085.85 | 16085.84 | 15758.59 | 15758.66 |
| $2_{1,1}\rightarrow 3_{1,2}$ | 18023.22 | 18023.67 | 17643.00 | 17644.90 | 16919.85 | 16922.17 | 16567.43 | 16567.27 |
| $3_{0,3}\rightarrow 4_{0,4}$ | 23397.48 | 23397.50 | | | | | 21526.20 | 21525.66 |
| $3_{1,3}\rightarrow 4_{1,4}$ | 22819.59 | 22819.50 | | | 21444.19 | 21444.31 | 21008.84 | 21008.26 |
| $3_{1,2}\rightarrow 4_{1,3}$ | 24028.26 | 24027.56 | 23520.91 | 23520.66 | | | | |
| $3_{2,2}\rightarrow 4_{2,3}$ | 23429.$2_0$ | 23428.80 | | | | | | |
| $3_{2,1}\rightarrow 4_{2,2}$ | 23460.52 | 23460.76 | | | | | | |
| $4_{0,4}\rightarrow 5_{0,5}$ | 29222.29 | 29222.55 | 28617.83 | 28618.03 | 27452.20 | 27452.01 | 26887.05 | 26886.87 |
| $4_{1,4}\rightarrow 5_{1,5}$ | 28518.24 | 28518.16 | 27936.00 | 27936.02 | 26800.23 | 26779.84 | 26255.39 | 26255.11 |
| $4_{2,3}\rightarrow 5_{2,4}$ | 29281.78 | 29281.64 | 28672.8 | 28673.52 | 27504.77 | 27504.40 | 26936.60 | 26936.20 |
| $4_{2,2}\rightarrow 5_{2,3}$ | 29345.$7_0$ | 29345.55 | | | 27560.52 | 27560.76 | 26988.42 | 26989.13 |
| $4_{3,1}\rightarrow 5_{3,2}$, $4_{3,2}\rightarrow 5_{3,3}$ | 29302.15 | 29302.58 | 28694.4 | 28693.31 | 27523.16 | 27523.20 | 26953.83 | 26954.03 |
| $4_{1,3}\rightarrow 5_{1,4}$ | | | 29394.00 | 29394.71 | 28193.52 | 28193.40 | | |
| b-Type | | | | | | | | |
| $2_{0,2}\rightarrow 2_{1,1}$ | | | | | 21067.5 | 21067.11 | | |
| $3_{0,3}\rightarrow 3_{1,2}$ | | | | | 21495.43 | 21495.16 | 21364.7 | 21365.02 |
| $4_{0,4}\rightarrow 4_{1,3}$ | 22921.58 | 22921.47 | | | | | | |
| $5_{0,5}\rightarrow 5_{1,4}$ | 23727.87 | 23726.87 | | | 22816.32 | 22817.10 | | |
| $6_{0,6}\rightarrow 6_{1,5}$ | 24719.31 | 24719.17 | 24508.91 | 24508.92 | 23728.20 | 23729.56 | 23520.15 | 23521.57 |
| $7_{0,7}\rightarrow 7_{1,6}$ | 25911.16 | 25911.93 | 25656.94 | 25657.54 | 24822.98 | 24825.12 | 24575.30 | 24577.65 |
| $8_{0,8}\rightarrow 8_{1,7}$ | 27319.22 | 27320.31 | 27011.07 | 27012.77 | 26114.84 | 26117.23 | 25819.24 | 25822.33 |
| $9_{0,9}\rightarrow 9_{1,8}$ | 28958.40 | 28960.73 | 28587.43 | 28590.16 | 27615.44 | 27620.62 | 27263.97 | 27269.54 |
| $0_{0,0}\rightarrow 1_{1,1}$ | 27077.01 | 27077.01 | 26868.46 | 26868.46 | 26008.25 | 26008.25 | 25797.49 | 25797.49 |
| $7_{1,7}\rightarrow 8_{0,8}$ | 29132.01 | 29130.87 | | | | | | |
| $11_{2,10}\rightarrow 12_{1,11}$ | 17442.95 | 17435.36 | | | | | | |
| $12_{2,11}\rightarrow 13_{1,12}$ | 25079.7 | 25072.4 | | | | | | |

* The centrifugal distortion is assumed to be $-D_{JK}J(J+1)K^2{}_1-D_JJ^2(J+1)^2$, with $D_{JK}=-0.057$ Mc./sec. and $D_J=0.0021$ Mc./sec.

TABLE II. ROTATIONAL CONSTANTS AND PRINCIPAL MOMENT OF INERTIA IN THE GROUND VIBRATIONAL STATE*

| | $CH_2{}^{35}ClC{\equiv}CH$ | (Calcd.)** | $CH_2{}^{37}ClC{\equiv}CH$ | (Calcd.)** | $CH_2{}^{35}ClC{\equiv}CD$ | (Calcd.)** | $CH_2{}^{37}ClC{\equiv}CD$ | (Calcd.)** |
|---|---|---|---|---|---|---|---|---|
| $A$ | 24299.28 | (24300.75) | 24146.48 | (24144.91) | 23396.70 | (23396.74) | 23238.18 | (23236.39) |
| $B$ | 3079.77 | (3080.72) | 3013.80 | (3014.82) | 2890.33 | (2890.24) | 2828.85 | (2828.84) |
| $C$ | 2777.73 | (2778.31) | 2721.98 | (2722.64) | 2611.55 | (2611.56) | 2559.31 | (2550.40) |
| $b_P$ | $-7.06709\times10^{-3}$ | | $-6.85720\times10^{-3}$ | | $-6.75178\times10^{-3}$ | | $-6.56026\times10^{-3}$ | |
| $I_a$ | 20.80436 | | 20.93601 | | 21.60694 | | 21.75433 | |
| $I_b$ | 164.146 | | 167.739 | | 174.904 | | 178.705 | |
| $I_c$ | 181.994 | | 185.722 | | 193.575 | | 197.526 | |

* Rotational constants are given in Mc./sec. and principal moments of inertia in amu Å$^2$. Conversion factor 505531 Mc./sec. amu Å$^2$ is used.

** Values are calculated by using the set of structure parameters (I) given in Table V.

symmetry plane. Thus the dipole moment has components along the a- and b-axes, and transitions of both a- and b-types are observed. The observed spectra are listed in Table I, where center frequencies are given. The assignment is made mainly by the b-type Q-branch series, $J_{0,J}\rightarrow J_{1,J-1}$. The quadrupole hyperfine structure due to chlorine atom is of some use to check the assignment.

The b-type Q-branch series mentioned above give the rotational constants $[A-(B+C)/2]$ and the asymmetry parameters $b_P$, whereas the constants $B+C$ and $B-C$ are obtained by measuring the a-type R-branch lines. The

$0_{0,0}\rightarrow 1_{1,1}$ lines are important since their frequencies are equal to $A+C$. The rotational constants and the asymmetry parameters are given in Table II, where the moments of inertia are calculated by using the conversion factor 505531 Mc./sec. amu Å$^2$. The frequencies calculated by using these rotational constants are compared with the observed ones in Table I.

In the course of searching, the spectra of two excited vibrational states were found. By comparing their intensities with those of the ground state, one is assigned to the CCCl bending mode and the other to one of the C—C≡C bending modes. The center frequencies and the rotational constants derived from them are listed in Table III.

Table III. Observed and calculated frequencies of the spectra and rotational constants in the excited vibrational states ($CH_2{}^{35}ClC{\equiv}CH$) (Mc./sec.)

| | State I ($\delta$CCCl) | | State II ($\delta$CC≡C) | |
|---|---|---|---|---|
| | Obs. | Calcd. | Obs. | Calcd. |
| $2_{0,2}\rightarrow 3_{0,3}$ | 17597.0 | 17592.7 | 17545.4 | 17545.4 |
| $0_{0,0}\rightarrow 1_{1,1}$ | 27230.76 | 27230.8 | | |
| $6_{0,6}\rightarrow 6_{1,5}$ | 24926.32 | 24926.7 | | |
| $7_{0,7}\rightarrow 7_{1,6}$ | 26141.31 | 26142.4 | | |
| $8_{0,8}\rightarrow 8_{1,7}$ | 27576.77 | 27578.2 | 27184.66 | 27185.2 |
| $9_{0,9}\rightarrow 9_{1,8}$ | | | 28809.18 | 28810.5 |
| $A(\alpha_i)$ | 24450.2 | (−150.9) | 24214.6 | (84.7) |
| $B(\beta_i)$ | 3088.1 | (−8.3) | 3076.09 | (3.68) |
| $C(\gamma_i)$ | 2780.6 | (−2.9) | 3776.60 | (1.13) |
| $b_P$ | $-7.14570\times10^{-3}$ | | $-7.03413\times10^{-3}$ | |

**Structure Analysis.** — The structure of propargyl chloride is specified by eight parameters: C—Cl, C—C, C≡C, methylenic C—H, and acetylenic C—H bond lengths, and CCCl, HCH and CCH bond angles, the C—C≡C—H group being assumed to be linear. The distance between two hydrogen atoms in methylene group is directly given by the quantity $[(I_a+I_b-I_c)/m_H]^{1/2}$. The four kinds of isotopic species give fairly close values for the distance, as shown in Table IV. However, as Laurie pointed out[8], the inertia defect $\Delta$ makes this distance short and the angle HCH apparently small. Since the data on the isotopic molecules for which deuterium is substituted in the methylene group were not available, it was difficult to see how much the inertia defect was. If the value is assumed to be 0.2194 amu Å as found for chloroacetonitrile[9], the distance H···H becomes 1.7715 Å. In the following the molecular structure is calculated by assuming $\Delta$ equal to zero or 0.2194 amu Å$^2$.

8) V. W. Laurie, *J. Chem. Phys.*, **28**, 704 (1958).
9) K. Wada, Y. Kikuchi, C. Matsumura, E. Hirota, and Y. Morino, This Bulletin, **34**, 337 (1961).

Table IV. The hydrogen to hydrogen distance in methylene group

| | $I_a+I_b+I_c$ (amu Å$^2$) | H···H (Å) |
|---|---|---|
| $CH_2{}^{35}ClC{\equiv}CH$ | 2.956 | $1.712_3$ |
| $CH_2{}^{37}ClC{\equiv}CH$ | 2.953 | $1.711_4$ |
| $CH_2{}^{35}ClC{\equiv}CD$ | 2.936 | $1.706_5$ |
| $CH_2{}^{37}ClC{\equiv}CD$ | 2.933 | $1.705_6$ |

The inertia defect arises from the zero-point vibration, and it is accepted from the case of water molecule[10] that the contribution of low-frequency vibrations to inertia defect is larger than those of high-frequency ones. The CCCl and C—C≡C bending modes are mentioned as the low-frequency vibrations in propargyl chloride, and the rotational constants are obtained in the excited states of these two vibrations as stated above. It is interesting to see how much the inertia defect and the distance H···H are changed if the rotational constants are corrected for these two vibrations. The corrected rotational constants, $A'$, $B'$, and $C'$, are given by

$$A' = A_0 + (1/2)(\alpha_1+\alpha_2)$$
$$B' = B_0 + (1/2)(\beta_1+\beta_2)$$
and $$C' = C_0 + (1/2)(\gamma_1+\gamma_2)$$

where $\alpha_1$, $\beta_1$, $\gamma_1$ and $\alpha_2$, $\beta_2$, $\gamma_2$ denote the changes of rotational constants due to the two vibrations. Their observed values are 24266.2 Mc./sec., 3077.5 Mc./sec. and 2776.8 Mc./sec., respectively. The H···H distance, 1.738 Å, calculated by using $A'$, $B'$ and $C'$ is in fact fairly larger than that obtained by $A_0$, $B_0$ and $C_0$, 1.709 Å, but still smaller than 1.772 Å which was obtained by assuming $\Delta=0.2194$ amu Å$^2$.

The parameters other than the H···H distance, seven in number, are to be determined by the remaining eight constants. Not all parameters can be determined by the present data, hence several assumptions are necessary. It is recognized that the C≡C bond length is relatively constant, irrespective of the attached groups. The value 1.207 Å is assumed for this length[11,12]. The acetylenic C—H bond length makes a small contribution to the rotational constants, hence the value 1.06 Å is assumed for this distance without strong influence upon other parameters to be obtained[12]. The lengths, C—H and C—D, are assumed to be the same. The groups C—C≡C and C—C≡N are usually considered linear, though the detailed investigations gave slightly bent structures[13]. Here the

10) B. T. Darling and D. M. Dennison, *Phys. Rev.*, **57**, 128 (1940). See also Ref. 8.
11) G. Herzberg and B. P. Stoicheff, *Nature*, **175**, 79 (1955).
12) C. C. Costain and B. P. Stoicheff, *J. Chem. Phys.*, **30**, 777 (1959).
13) C. C. Costain and J. R. Morton, ibid., **31**, 389 (1959); E. Hirota and Y. Morino, This Bulletin, **33**, 158, 705 (1960).

linear structure is also assumed. Two additional assumptions are the methylenic C—H bond length equal to 1.09 Å and the CCH bond angle equal to 111°30′. These two parameters, especially the latter, affect considerably the rotational constant $A$, in spite of the light weight of a hydrogen atom. Hence some precaution must be taken for selecting the assumed values for these parameters.

First, the inertia defect is set equal to zero. The methylenic C—H bond length and the CCH bond angle are assumed to be 1.09 Å and 111°30′, respectively. The eight rotational constants, $A$ and $C$ for each isotopic molecule, are used to determine the C—Cl and the C—C bond lengths, and the CCCl bond angle. They are found to be 1.7800 Å, 1.4582 Å, and 112°9′, respectively (Table V). If the bond lengths C—Cl and C—C become longer, both $A$ and $C$ decrease, on the other hand the $A$ increases and the $C$ decreases with the increase of the

TABLE V. STRUCTURE PARAMETERS UNDER VARIOUS ASSUMPTIONS

| Set | Assumption | | Result | | |
|---|---|---|---|---|---|
| | $\Delta$ amuÅ$^2$ | ∠CCH | C—Cl Å | C—C Å | ∠CCCl |
| I | 0 | 111°30′ | 1.7800 | 1.4582 | 112° 9′ |
| $II_a$ | 0.2194 | 107°30′ | 1.7728 | 1.4766 | 111°43′ |
| $II_b$ | 0.2194 | 109°30′ | 1.7768 | 1.4724 | 111°45′ |
| $II_c$ | 0.2194 | 111°30′ | 1.7808 | 1.4690 | 111°44′ |

Other assumptions
C≡C 1.207Å
C—H (methylenic) 1.09Å
C—H=C—D (acetylenic) 1.06Å
C—C≡C—H(D) linear

CCCl angle. Thus the determination of the CCCl angle is definite, but it is somewhat difficult to determine two bond lengths separately. Still it is feasible to obtain fairly good results for the two bond lengths. The fitting of the calculated constants with the observed is carried out by the least-squares method, the mean deviation is 0.00051 Å for the C—Cl bond length, 0.00062 Å for the C—C bond length, and 0.54′ for the CCCl bond angle. If the assumed value for the C≡C length, 1.207 Å, is in error by 0.01 Å, the C—Cl is changed by 0.001 Å, the C—C by 0.007 Å, and the CCCl by 2.5′.

Thus far, the analysis gives reasonable results. However, the inertia defect is by no means equal to zero, and its effect is obvious if the HCH angle is calculated to be 103°14′ by using the observed H···H distance 1.709 Å and the assumed C—H (methylenic) distance 1.09 Å.

In the second place, the inertia defect is assumed to be 0.2194 amu Å$^2$. This value is borrowed from the result for the chloroacetonitrile molecule. An analysis by the least-squares method is carried out by using three values for the CCH angle, 107°30′, 109°30′ and 111°30′. The methylenic C—H length is fixed to 1.09 Å. As stated above, the HCH angle becomes 108°42′, a quite reasonable value. The results obtained for the C—Cl and the C—C lengths, and the CCCl angle are listed in Table V. The CCCl bond angle is relatively independent of the values assumed for the CCH angle; however, the two bond lengths are varied by 0.008 Å. It is difficult to say which case is the most reasonable, but the length of the C—C bond adjacent to the triple bond is reported about 1.460 Å in a number of related molecules[11,12]. In this respect the case 111°30′ for the CCH angle is the most favorable, where the C—C length is 1.4690 Å. It is yet by no means clear whether or not the assumed value for the inertia defect is reasonable. It is felt that the inertia defect slightly less than 0.2194 amu Å$^2$ is more reasonable, since the C—C bond length then becomes somewhat shorter than 1.4690 Å. The parameter values, which are considered the most reasonable at present, are given in the last column of Table VI, where errors are attached by taking into account the zero-point vibration, inadequacy of the assumed parameters, and so on.

TABLE VI. MOLECULAR STRUCTURE

| | |
|---|---|
| C—Cl | 1.780±0.003Å |
| C—C | 1.465±0.007Å |
| CCCl | 111°50′±20′ |
| HCH | 108°42′±1° |
| CCH | 111°30′±1°30′ |

Assumptions
C≡C 1.207Å
C—H (methylenic) 1.09Å
C—H(D) (acetylenic) 1.06Å
C—C≡C—H(D) linear

**Quadrupole Coupling Constant of Chlorine Atom.** — The chlorine nuclear quadrupole coupling constant is determined by measuring the hyperfine structure of eight rotational transitions of the most abundant species $CH_2{}^{35}ClC{\equiv}CH$. By the lack of accidental degeneracy in rotational energy only the two components of the coupling constant, $\chi_{aa}$ and $\chi_{bb}$, are obtained. The least-squares method gives $\chi_{aa}=-30.4$ Mc./sec. and $\chi_{bb}=-7.5$ Mc./sec. The hyperfine structures calculated by using these values are compared with the observed ones in Table VII.

A similar analysis is carried out on the hyperfine structures of eight transitions of $CH_2{}^{35}ClC{\equiv}CD$, but it is found that the values −28.2 Mc./sec. and −9.7 Mc./sec., which are

TABLE VII. HYPERFINE STRUCTURES OF THE CHLORINE NUCLEAR QUADRUPOLE COUPLING CONSTANT (Mc./sec.)

| Transition | $F'' \rightarrow F'$ | $CH_2{}^{35}ClC{\equiv}CH$ | | | $CH_2{}^{35}ClC{\equiv}CD$ | | |
|---|---|---|---|---|---|---|---|
| | | Obs. | Calcd.* | Calcd.−Obs. | Obs. | Calcd.** | Calcd.−Obs. |
| $2_{12}\rightarrow 3_{13}$ | 7/2 9/2 | +1.08 | +1.09 | +0.01 | +1.08 | +1.05 | −0.03 |
| | 5/2 7/2 | −0.88 | −0.83 | +0.05 | −0.57 | −0.74 | −0.17 |
| | 3/2 5/2 | −2.34 | −2.28 | +0.06 | −2.56 | −2.25 | +0.31 |
| | 1/2 3/2 | −0.28 | −0.36 | −0.08 | | | |
| $3_{21}\rightarrow 4_{22}$ | 9/2 11/2 | +0.97 | +1.05 | +0.08 | | | |
| | 7/2 9/2 | −1.82 | −1.85 | −0.03 | | | |
| | 5/2 7/2 | −0.74 | −0.81 | −0.07 | | | |
| | 3/2 5/2 | +2.08 | +2.09 | +0.01 | | | |
| $3_{13}\rightarrow 4_{14}$ | 9/2 11/2 | | | | +0.80 | +0.98 | +0.18 |
| | 7/2 9/2 | | | | −0.07 | −0.13 | −0.06 |
| | 5/2 7/2 | | | | −1.00 | −1.17 | −0.17 |
| $3_{03}\rightarrow 3_{12}$ | 7/2 7/2 | | | | +5.63 | +5.26 | −0.34 |
| | 5/2 5/2 | | | | +1.58 | +1.58 | 0.00 |
| | 9/2 9/2 | | | | −2.92 | −2.63 | +0.29 |
| | 3/2 3/2 | | | | −6.52 | −6.31 | +0.21 |
| $4_{04}\rightarrow 4_{13}$ | 9/2 9/2 | +4.51 | +4.52 | +0.01 | | | |
| | 7/2 7/2 | +1.95 | +2.03 | +0.08 | | | |
| | 11/2 11/2 | −2.40 | −2.59 | −0.19 | | | |
| | 5/2 5/2 | −5.16 | −5.08 | +0.08 | | | |
| $5_{05}\rightarrow 5_{14}$ | 11/2 11/2 | +4.07 | +4.23 | +0.16 | +4.29 | +4.37 | +0.08 |
| | 9/2 9/2 | +2.38 | +2.29 | −0.09 | +2.15 | +2.37 | +0.22 |
| | 13/2 13/2 | −2.69 | −2.65 | +0.04 | −2.55 | −2.73 | −0.18 |
| | 7/2 7/2 | −4.45 | −4.59 | −0.14 | −4.61 | −4.73 | −0.12 |
| $6_{06}\rightarrow 6_{15}$ | 13/2 13/2 | +4.21 | +4.10 | −0.11 | +4.24 | +4.25 | +0.01 |
| | 11/2 11/2 | +2.65 | +2.49 | −0.16 | +2.67 | +2.57 | −0.10 |
| | 15/2 15/2 | −2.94 | −2.74 | +0.20 | −2.92 | −2.83 | +0.09 |
| | 9/2 9/2 | −4.45 | −4.35 | +0.10 | −4.51 | −4.50 | +0.01 |
| $7_{07}\rightarrow 7_{16}$ | 15/2 15/2 | +4.02 | +4.06 | +0.04 | +4.10 | +4.21 | +0.11 |
| | 13/2 13/2 | +2.67 | +2.66 | −0.01 | +2.67 | +2.75 | +0.08 |
| | 17/2 17/2 | −2.84 | −2.84 | 0.00 | −2.86 | −2.95 | −0.09 |
| | 11/2 11/2 | −4.25 | −4.25 | 0.00 | −4.30 | −4.40 | −0.10 |
| $8_{08}\rightarrow 8_{17}$ | 17/2 17/2 | +4.10 | +4.08 | −0.02 | +4.30 | +4.23 | −0.07 |
| | 15/2 15/2 | +2.85 | +2.82 | −0.03 | +2.98 | +2.92 | −0.06 |
| | 19/2 19/2 | −3.02 | −2.97 | +0.05 | −3.09 | −3.08 | +0.01 |
| | 13/2 13/2 | −4.24 | −4.23 | +0.01 | −4.51 | −4.38 | +0.12 |
| $9_{09}\rightarrow 9_{18}$ | 19/2 19/2 | +4.06 | +4.14 | +0.08 | +4.30 | +4.29 | −0.01 |
| | 17/2 17/2 | +2.98 | +2.98 | 0.00 | +3.13 | +3.09 | −0.04 |
| | 21/2 21/2 | −3.06 | −3.11 | −0.05 | −3.22 | −3.22 | 0.00 |
| | 15/2 15/2 | −4.21 | −4.26 | −0.05 | −4.46 | −4.42 | +0.04 |

* $\chi_{aa}=-30.4$ Mc./sec. and $\chi_{bb}=-7.5$ Mc./sec. are used.
** $\chi_{aa}=-28.2$ Mc./sec. and $\chi_{bb}=-9.7$ Mc./sec. are used.

calculated from coupling constants of $CH_2{\cdot}{}^{35}ClC{\equiv}CH$ by transforming the principal axes, explain the hyperfine structures sufficiently well.

If the values of $\chi_{aa}$ and $\chi_{bb}$ were accurate, the rotation of the principal axes due to the deuterium substitution might give the asymmetry parameter, but the present data do not warrant such a procedure. On the other hand, the second-order effect observed for the bromine nuclear quadrupole hyperfine structure of rotational spectra of propargyl bromide $CH_2BrC{\equiv}CH$ indicated that the asymmetry parameter was small[14]. The values of $\chi_{aa}$ and $\chi_{bb}$ obtained above give $\chi_{bond}=-75.8$ Mc./sec., under the assumption of the cylindrical symmetry of charge distribution about the C—Cl bond. The result is consistent with the value in the solid state, 71.6246 Mc./sec.[15]

**Dipole Moment.** — The dipole moment has two components; one along the a-axis and the other along the b-axis. The Stark effect of the $0_{0,0}\rightarrow 1_{1,1}$ transition of $CH_2{}^{35}ClC{\equiv}CH$ is measured to obtain the two components of the

14) Y. Kikuchi, E. Hirota and Y. Morino, *J. Chem. Phys.*, **31**, 1139 (1959); This Bulletin, **34**, 348 (1961).

15) T. Shimozawa, T. Chiba, I. Miyagawa and Y. Morino, ibid., to be published.

dipole moment. The presence of the chlorine nuclear quadrupole moment makes the Stark effect complicated, but it is possible to analyze the Stark effect of the $0_{0,0}\rightarrow 1_{1,1}$ transition, since the $J$ number associated is small[16].

The quadrupole energy of the state $1_{1,1}$ is small, hence the weak, the intermediate, and the strong field cases are successively met with the increase of the Stark electric field. The quadrupole energy is zero for the state $0_{0,0}$.

The calculation of the Stark effect and the quadrupole effect is carried out by taking the wave function, $|IJ\tau M_J M_I>$, as the basis. The matrix elements of the Hamiltonian for the Stark effect $H_E$ are diagonal in $M_J$ and $M_I$, but they connect different rotational states. The state $0_{0,0}$ couples with states $1_{0,1}$ and $1_{1,1}$, and the state $1_{1,1}$ with states $1_{1,0}$, $2_{1,2}$, $0_{0,0}$, $2_{2,0}$ and $2_{0,2}$ by the Hamiltonian $H_E$. The differences in rotational energies are greater than the Stark or quadrupole energies, so that the second-order perturbation is sufficient to calculate the Stark effect[17]. Thus, it is reduced to the form;

$$\sum_{J'\tau'} \frac{|(IJ\tau M_J M_I|H_E|IJ'\tau' M_J M_I)|^2}{E_{J\tau}-E_{J'\tau'}} = (\alpha+\beta M_J^2)\varepsilon^2$$

where $\varepsilon$ is the Stark field strength, and $\alpha$ and $\beta$ are constants depending upon the rotational constants, the rotational quantum numbers, and the dipole moment.

The Hamiltonian for the quadrupole energy, $H_Q$, has matrix elements, diagonal as well as nondiagonal with respect to $M_J$ and $M_I$. Matrix elements between different rotational states are ignored, since the first-order perturbation is sufficient enough to treat the quadrupole energy. The matrix elements appropriate at present are as follows:

$$\begin{aligned}
&(IJ\tau M_J M_I|H_Q|IJ\tau M_J' M_I')\\
&=P[3M_I^2-I(I+1)]\,[3M_J^2-J(J+1)]\\
&\qquad (M_J'=M_J,\ M_I'=M_I)\\
&=P[3/2+3M_I M_J+3(M_I\mp 1)(M_J\pm 1)]\\
&\quad\times\{[I(I+1)-M_I(M_I\mp 1)]\\
&\quad\times[J(J+1)-M_J(M_J\pm 1)]\}^{1/2}\\
&\qquad (M_J'=M_J\pm 1,\ M_I'=M_I\mp 1)\\
&=P(3/2)\{[J(J+1)-M_J(M_J\pm 1)]\\
&\quad\times[J(J+1)-(M_J\pm 1)(M_J\pm 2)]\\
&\quad\times[I(I+1)-M_I(M_I\mp 1)]\\
&\quad\times[I(I+1)-(M_I\mp 1)(M_I\mp 2]\}^{1/2}\\
&\qquad (M_J'=M_J\pm 2,\ M_I' M_I\mp 2)
\end{aligned}$$

where $P$ is given by

$$\begin{aligned}
P=\{&\chi_{aa}[J(J+1)+E(\kappa)-(\kappa+1)(\partial E(\kappa)/\partial\kappa)]\\
&+2\chi_{bb}(\partial E(\kappa)/\partial\kappa)\\
&+\chi_{cc}[J(J+1)-E(\kappa)\\
&+(\kappa-1)(\partial E(\kappa)/\partial\kappa)]\}/\\
&[4J(J+1)(2J-1)(2J+3)I(2I-1)]
\end{aligned}$$

which is reduced for the state $1_{1,1}$ to

$$P(1_{1,1})=-(1/60)\chi_{bb}$$

Secular determinant for the state $1_{1,1}$ factors into three groups, corresponding to $M_F=M_J+M_I=5/2$, $3/2$ and $1/2$, respectively. Secular determinants are all doubly degenerate. The case $M_F=5/2$ is the simplest, since the wave function belonging to $M_F=5/2$ is $|M_J, M_I>=|1, 3/2>$ or $|-1, -3/2>$. The secular equation is

$$3P+(\alpha+\beta)\varepsilon^2-W=0$$

The two pairs of wave functions, $[|\pm 1, \pm 1/2>, |0, \pm 3/2>]$, belong to $M_F=3/2$ and give rise to a two-dimensional secular equation:

$$\begin{vmatrix} -3P+(\alpha+\beta)\varepsilon^2-W & 3\sqrt{6}\,P \\ 3\sqrt{6}\,P & -6P+\alpha\varepsilon^2-W \end{vmatrix}=0$$

The wave functions corresponding to $M_F=1/2$ are $|\pm 1, \mp 1/2>$, $|0, \pm 1/2>$ and $|\mp 1, \pm 3/2>$, and the secular equation is

$$\begin{vmatrix} 3P+(\alpha+\beta)\varepsilon^2-W & -3\sqrt{6}\,P & 6\sqrt{3}\,P \\ -3\sqrt{6}\,P & 6P+\alpha\varepsilon^2-W & 0 \\ 6\sqrt{3}\,P & 0 & -3P+(\alpha+\beta)\varepsilon^2-W \end{vmatrix}=0$$

If the field strength $\varepsilon$ is equal to zero, the secular equations give the following energy states:

| | | |
|---|---|---|
| $W_1=3P$ | $F=5/2$, | $M_F=5/2$ |
| $W_{21}=3P$ | $5/2$, | $3/2$ |
| $W_{22}=-12P$ | $3/2$, | $3/2$ |
| $W_{31}=3P$ | $5/2$, | $1/2$ |
| $W_{32}=-12P$ | $3/2$, | $1/2$ |
| $W_{33}=15P$ | $1/2$, | $1/2$ |

Here the representation $|IFM_I M_F>$ rather than $|IJM_I M_J>$ is good. There are only two states $|F, M_F>=|3/2, 1/2>$ and $|3/2, 3/2>$ possible in the rotational state $0_{0,0}$. Since the selection rule is $\Delta M_F=0$, transition to the state $W_1$ is forbidden and two pair states $W_{21}$ and $W_{31}$, and $W_{22}$ and $W_{32}$ are degenerate, there are three hyperfine lines. If the Stark field increases so that the Stark energies $\alpha\varepsilon^2$ or $\beta\varepsilon^2$ are larger than $P$, the strong field case is apropppriate. The secular determinantes described above give the following states:

16) F. Coester, *Phys. Rev.*, **77**, 454 (1950).
17) S. Golden and E. B. Wilson, Jr., *J. Chem. Phys.*, **16**, 669 (1948).

$$W_1=(\alpha+\beta)\varepsilon^2+3P \quad M_J=1, \quad M_I=3/2$$
$$W_{21}=(\alpha+\beta)\varepsilon^2-3P \quad 1, \quad 1/2$$
$$W_{22}=\alpha\varepsilon^2-6P \quad 0, \quad 3/2$$
$$W_{31}=(\alpha+\beta)\varepsilon^2+3P \quad 1, \quad 3/2$$
$$W_{32}=\alpha\varepsilon^2+6P \quad 0, \quad 1/2$$
$$W_{33}=(\alpha+\beta)\varepsilon^2-3P \quad 1, \quad 1/2$$

This case can be expressed by the representation $|IJM_IM_J>$. The rotational state $0_{0,0}$ involves two states $|M_J, M_I>=|0, 1/2>$ and $|0, 3/2>$. Two transitions to the states $W_{22}(M_J=0, M_I=3/2)$ and $W_{32}(M_J=0, M_I=1/2)$ are allowed by the selection rules, $\Delta M_J=0$ and $\Delta M_I=0$.

The solutions for the intermediate case are obtained by solving the secular determinants given above. Eigenfunctions are obtained to calculate the transition probabilities. The change of the hyperfine patterns with the electric field, the frequencies and the intensities, is given in Fig. 1.

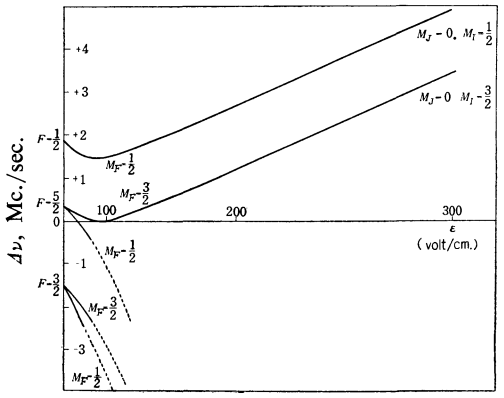



Fig. 1. Stark effect of the $0_{0,0}\rightarrow 1_{1,1}$ transition ($CH_2{}^{35}ClC\equiv CH$).

It is interesting to note that the transition to the state $W_{21}$ in case $\varepsilon=0$ shifts first to lower frequency with increasing electric field, stops at some field strength $\varepsilon_0$, and then moves to a higher frequency. The observed intensity reduces to zero at $\varepsilon_0$, because the Stark modulation is used for the measurement. This is also the case for the transition to the state $W_{33}$ at $\varepsilon=0$. The case $M_F=3/2$ is considered. The solutions are obtained by solving the secular equation, that is

$$W^{\pm}=-(1/2)\,[9P-(2\alpha+\beta)\varepsilon^2] \pm[(1/4)\,(3P+\beta\varepsilon^2)^2+54P^2]^{1/2}$$

The line mentioned above corresponds to the transition to the state $W^+$ and its frequency is given by

$$\nu=(W^++\alpha_0\varepsilon^2)/h$$

where $-\alpha_0\varepsilon^2$ is the Stark effect of the state $0_{0,0}$. Then the electric field $\varepsilon_0$, at which the Stark effect of the line changes its sign from minus to plus, is given by

$$\varepsilon_0{}^2=(P/\beta)\{-3-[216(2\alpha_0+2\alpha+\beta)^2/[\beta^2-(2\alpha_0+2\alpha+\beta)^2]\,]^{1/2}\}$$

The constants, $\alpha_0$, $\alpha$ and $\beta$, are functions of two components of dipole moments, $\mu_a$ and $\mu_b$. The Stark effect of the strong field case gives $\alpha_0+\alpha+\beta$ and $\varepsilon_0$ thus obtained provides another information on $\alpha_0$, $\alpha$ and $\beta$.

The two components thus found are $\mu_a=0.98_5$ D and $\mu_b=1.36_0$ D, and the total moment $\mu_t=1.68$ D. There are four choices for the direction of the dipole moment, but it seems most plausible that the negative direction of the dipole moment lies between the C—Cl and the C—C≡C—H bonds, at an angle of 16±7° from the former. The total dipole moment 1.68 D is compared favorably with the value obtained by the dielectric constant measurement, 1.65 D[7].

## Discussion

Pauling, Gordy and Saylor[1] explained the long C—Cl bond length by assuming a resonance structure $Cl-CH_2=C=C^+-H$, but the present result clearly shows that it is unnecessary to consider such a resonance structure. The C—Cl bond was found to be a normal value of 1.780 Å. In addition to this, the resonance structure given above predicts a small quadrupole coupling constant and a large dipole moment. These are not found in the present data either. Laurie and Lide observed the C—Cl bond length in 1-chloro-2-butyne to be

Table VIII. Comparison of molecular structures

| | Propargyl chloride $CH_2ClC\equiv CH$ | Methyl chloride $CH_3Cl$ | Ethyl chloride $CH_3CH_2Cl$ |
|---|---|---|---|
| C—Cl (Å) | 1.780[a] | 1.781[b] | 1.7785[e] |
| C—C (Å) | 1.465[a] | — | 1.5495[e] |
| $\chi_{bond}$ ($Cl^{35}$) (Mc./sec.) | −75.8[a] | −74.740[c] | −70.07[e] |
| $\mu$ (D) | 1.68[a] | 1.869[d] | 2.05[f] |

a) The present paper.
b) S. L. Miller, L. C. Aamodt, G. Dousmanis, C. H. Townes and J. Kraitchman, *J. Chem. Phys.*, **20**, 1112 (1952).
c) S. Geschwind, R. Gunther-Mohr and C. H. Townes, *Phys. Rev.*, **81**, 288 (1951).
d) R. G. Shulman, C. H. Townes and B. P. Dailey, ibid., **78**, 145 (1950).
e) R. S. Wagner and B. P. Dailey, *J. Chem. Phys.*, **26**, 1588 (1957).
f) C. P. Smyth, "Dielectric Behavior and Structure" McGraw-Hill Book Co., New York, N. Y. (1955), p. 269.

$1.79_8$ Å[18]. The data were, however, not sufficiently accurate and in addition the presence of internal rotation complicated the problem.

It is of some help to compare the constants of the propargyl chloride molecules with those of some other molecules. Table VIII shows such a comparison, where methyl and ethyl chlorides are taken as reference substances.

The authors are greatly indebted to Professor K. Shimoda, Mr. H. Hirakawa, and their coworkers at the Department of Physics for their advice in constructing the apparatus. They should like to thank Mr. T. Oka who collaborated with them in the early stage of this investigation. They wish also to express their sincere thanks to Dr. M. Shima, Institute for Physical and Chemical Research, for supplying them with heavy water. The expenses for this research were defrayed from the Scientific Research Encouragement Grant of the Ministry of Education to which the authors' thanks are also due.

*Department of Chemistry*
*Faculty of Science*
*The University of Tokyo*
*Hongo, Tokyo*

18) V. W. Laurie and D. R. Lide, Jr., ibid., 31, 939 (1959).

# *Microwave Spectrum of Propargyl Halides. II. Molecular Structure and Second-Order Quadrupole Effect of Propargyl Bromide*

By Yoshikazu KIKUCHI, Eiji HIROTA and Yonezo MORINO

(Received September 5, 1960)

In the previous papes[1] the C—Cl distance in propargyl chloride was reported to be close to the usual C–Cl bond length, 1.780±0.002 Å. The determination of the C—Br length in propargyl bromide is also of interest to obtain an additional assurance to the conclusion obtained in the previous paper.

An anomaly due to accidental degeneracy in rotational energy has been observed in bromine nuclear quadrupole hyperfine structure of some b-type Q-branch transitions[2]. The deviation from the first-order theory amounted to several megacycles. An analysis using the second-order perturbation has enabled us to know the direction of the principal axes and principal values of the quadrupole coupling constant of the bromine atom. It was found that the direction of the largest principal value of the coupling constants coincided with that of the C—Br bond and the asymmetry parameter was very small*.

1) E. Hirota and Y. Morino, This Bulletin, 34, 341 (1961).
2) Preliminary account is given in the paper, Y. Kikuchi, E. Hirota and Y. Morino, *J. Chem. Phys.*, 31, 1139 (1959).
* Recently the microwave spectrum of ethyl iodide was measured by Kasuya and Oka[3]. They found a hyperfine structure of the iodine atom deviating from the first-order theory.
3) T. Kasuya and T. Oka, *J. Phys. Soc., Japan*, 15, 296 (1960).

## Experimental

The spectra of propargyl bromide, $CH_2{}^{79}BrC{\equiv}CH$, $CH_2{}^{81}BrC{\equiv}CH$, $CH_2{}^{79}BrC{\equiv}CD$ and $CH_2{}^{81}BrC{\equiv}CD$, were observed by a Stark modulation spectrometer described in the previous paper. The two isotopic species of bromine have almost equal natural abundance, hence no special preparation was necessary. The deuterated samples were obtained by the method used for the preparation of deuterated propargyl chloride.

## Results

**Rotational Spectra and Rotational Constants.** —Propargyl bromide is also a nearly prolate symmetric top, similar to the chloride. The symmetry plane includes a- and b-axes, hence a- as well as b-type transitions are expected to be observed.

Table I gives the observed center frequencies. Preliminary assignment is based on frequencies expected for the assumed structure and hyperfine patterns. Transitions of a-type R-branch, $J_{1,J} \rightarrow J+1_{1,J+1}$, split into four lines and are easily identified by their characteristic hyperfine structures. The assignment of b-type Q-branch transitions is confirmed by plotting the asymmetry parameter $b_P$ versus the quantity $A-(B+C)/2$.

The rotational constants and the asymmetry

Table I. Observed and calculated center frequencies (Mc./sec.)

| Transition | $CH_2{}^{79}BrC{\equiv}CH$ | | $CH_2{}^{81}BrC{\equiv}CH$ | | $CH_2{}^{79}BrC{\equiv}CD$ | | $CH_2{}^{81}BrC{\equiv}CD$ | |
|---|---|---|---|---|---|---|---|---|
| | Obs. | Calcd. | Obs. | Calcd. | Obs. | Calcd. | Obs. | Calcd. |
| a-Type | | | | | | | | |
| $6_{0,6}\rightarrow 7_{0,7}$ | 29035.53 | 29035.59 | 28843.44 | 28843.46 | 27359.91 | 27359.92 | 27178.13 | 27178.01 |
| $6_{1,6}\rightarrow 7_{1,7}$ | 28460.66 | 28460.76 | 28275.01 | 28274.95 | 26820.29 | 26820.65 | 26644.31 | 26644.52 |
| $6_{1,5}\rightarrow 7_{1,6}$ | 29721.56 | 29721.58 | 29520.15 | 29520.46 | | 28001.53 | 27811.32 | 27811.37 |
| $6_{2,5}\rightarrow 7_{2,6}$ | 29099.90 | 29099.97 | 28906.35 | 28906.25 | 27419.44 | 27419.53 | 27235.99 | 27236.07 |
| $6_{2,4}\rightarrow 7_{2,5}$ | 29171.76 | 29171.81 | 28976.40 | 28976.40 | 27485.36 | 27485.50 | 27301.11 | 27300.52 |
| $5_{0,5}\rightarrow 6_{0,6}$ | 24903.78 | 24904.57 | 24739.83 | 24739.50 | | 23466.94 | | 23310.34 |
| $5_{1,5}\rightarrow 6_{1,6}$ | 24399.30 | 24399.29 | 24240.00 | 24239.93 | 22993.25 | 22993.14 | 22841.84 | 22841.79 |
| $5_{1,4}\rightarrow 6_{1,5}$ | 25479.55 | 25480.30 | 25308.40 | 25307.79 | | 24005.60 | | 23842.20 |
| $4_{1,4}\rightarrow 5_{1,5}$ | 20335.98 | 20335.82 | 20203.04 | 20202.97 | 19163.99 | 19163.81 | | 19037.41 |
| $3_{1,3}\rightarrow 4_{1,4}$ | 16270.72 | 16270.71 | 16164.26 | 16164.38 | 15332.75 | 15332.94 | 15231.60 | 15231.63 |
| b-Type | | | | | | | | |
| $13_{0,13}\rightarrow 13_{1,12}$ | 28406.9 | 28414.0 | 28270.2 | 28275.0 | 26945.4 | 26945.9 | 26815.7 | 26816.0 |
| $12_{0,12}\rightarrow 12_{1,11}$ | 26906.93 | 26911.78 | 26791.33 | 26794.45 | 25545.00 | 25545.56 | 25435.05 | 25435.40 |
| $11_{0,11}\rightarrow 11_{1,10}$ | 25563.6 | 25566.2 | 25466.9 | 25468.0 | 24290.1 | 24290.0 | 24197.6 | 24197.4 |
| $10_{0,10}\rightarrow 10_{1,9}$ | 24367.0 | 24368.6 | 24286.7 | 24287.3 | 23171.6 | 23171.9 | 23095.0 | 23094.6 |
| $9_{0,9}\rightarrow 9_{1,8}$ | 23309.9 | 23310.7 | 23243.9 | 23243.9 | 22184.3 | 22183.7 | 22120.1 | 22119.7 |
| $8_{0,8}\rightarrow 8_{1,7}$ | 22384.6 | 22384.2 | 22330.7 | 22330.0 | 21318.0 | 21317.9 | 21265.6 | 21265.4 |
| $7_{0,7}\rightarrow 7_{1,6}$ | 21578.3 | 21581.5 | 21538.3 | 21538.0 | | | | |
| $6_{0,6}\rightarrow 6_{1,5}$ | 20896.0 | 20895.5 | 20861.7 | 20861.0 | | | | |
| $5_{0,5}\rightarrow 5_{1,4}$ | 20319.5 | 20319.8 | 20292.9 | 20292.7 | | | | |
| $9_{1,9}\rightarrow 10_{0,10}$ | 26159.13 | 26164.36 | 25854.17 | 25860.54 | | | | |

Table II. Rotational constants, asymmetry parameters, and centrifugal distortion constants

| | | $CH_2{}^{79}BrC{\equiv}CH$ | $CH_2{}^{81}BrC{\equiv}CH$ | $CH_2{}^{79}BrC{\equiv}CD$ | $CH_2{}^{81}BrC{\equiv}CD$ |
|---|---|---|---|---|---|
| $A$ | obs. | 21010.0±3 Mc./sec. | 20986.5±3 Mc./sec. | 20045.8±3 Mc./sec. | 20021.0±3 Mc./sec. |
| | calcd. | 21012.0 | 20987.9 | 20047.3 | 20022 |
| $B$ | obs. | 2169.31±0.2 | 2154.37±0.2 | 2043.49±0.2 | 2029.28±0.2 |
| | calcd. | 2169.41 | 2154.51 | 2043.06 | 2028.96 |
| $C$ | obs. | 1989.09±0.2 | 1976.34±0.2 | 1874.70±0.2 | 1862.50±0.2 |
| | calcd. | 1989.19 | 1976.44 | 1874.36 | 1862.27 |
| | $b_P$ | $-4.7600\times10^{-3}$ | $-4.7045\times10^{-3}$ | $-4.6662\times10^{-3}$ | $-4.6136\times10^{-3}$ |
| | $D_J$ | 0.001 Mc./sec. | 0.001 Mc./sec. | 0.001 Mc./sec. | ~0 Mc./sec. |
| | $D_{JK}$ | −0.0455 | −0.0432 | −0.0505 | −0.0460 |

Table III. The hydrogen to hydrogen distance in methylene group (Å)

| | $CH_2{}^{79}BrC{\equiv}CH$ | $CH_2{}^{81}BrC{\equiv}CH$ | $CH_2{}^{79}BrC{\equiv}CD$ | $CH_2{}^{81}BrC{\equiv}CD$ |
|---|---|---|---|---|
| $r$(H···H) | 1.7098 | 1.7108 | 1.7092 | 1.7084 |

parameters are given in Table II, and the frequencies calculated by using these constants are compared with the observed ones in Table I. A rough correction is made for the centrifugal distortion by assuming the expression $-D_J J^2(J+1)^2 - D_{JK} J(J+1) K_{-1}^2$. The observed values of $D_J$ and $D_{JK}$ are given in Table II.

**Structure Analysis.**—The number of structural parameters is the same as that of the chloride. Again the H···H distance in methylene group is given by

$$r(\mathrm{H\cdots H}) = [(I_a + I_b - I_c)/m_{\mathrm{H}}]^{1/2} \qquad (1)$$

The values for the four isotopic species given in Table III are close to each other, their average being 1.7096 Å. The eight constants are left to calculate other structural parameters. Since the mass ratio of two bromine isotopes $^{79}Br$ and $^{81}Br$ is almost equal to unity and the bromine atom is located so close to the a-axis, the data are not sufficient to calculate seven parameters. The following values are assumed: methylene C—H is equal to 1.090 Å, ∠CCH to 111°30′, C≡C to 1.207 Å, and acetylene C—H to 1.060 Å. The acetylene C—H and C—D bond lengths are assumed to be equal. The linearity of the group C—C≡C—H is again assumed. By means of the method of least-squares the

bond lengths C—Br and C—C and the bond angle CCBr are found to be 1.9415 Å, 1.4549 Å, and 111°59′, respectively.

Thus far, the effect of inertia defect is ignored, but, as mentioned in the previous paper, the results given above for the three parameters do not change appreciably even by taking account of the inertia defect. In addition, since the weight of a bromine atom is more than twice as great as that of a chlorine atom, errors in the parameters C—Br and ∠CCBr may be small. The results are given in Table IV.

TABLE IV. MOLECULAR STRUCTURE

| | | | |
|---|---|---|---|
| C—Br | 1.9415 Å | H···H* | 1.7096 Å |
| C—C | 1.4549 Å | ∠CCBr | 111°59′ |

Assumed values

C—H (methylene) 1.090 Å

C—H, C—D (acethylene) 1.060 Å

| | | | |
|---|---|---|---|
| C≡C | 1.207 Å | ∠CCH | 111°30′ |

* Correction for the inertia defect is not made.

**Second-Order Quadrupole Effect.** — Theory[4] indicates that the quadrupole energy is expressed as follows, averaging over rotational states of an asymmetric molecule

$$E_Q=(IJ\tau F|H_Q|IJ\tau F)+\sum_{J'\tau'}\frac{|(IJ\tau F|H_Q|IJ'\tau'F)|^2}{E_{J\tau}-E_{J'\tau'}} \quad (2)$$

Usually the difference in rotational energies $E_{J\tau}-E_{J'\tau'}$, is much larger than the quadrupole energy hence the second terms may be omitted. For a nearly prolate symmetric top the first-order energy

$$(IJ\tau F|H_Q|IJ\tau F)=\frac{1}{J(J+1)}\{\chi_{aa}[3K_{-1}^2-J(J+1)-3\sum_n(n-1)C_nb_P^n-\sum_n nC_nb_P^{n-1}]-2\chi_{bb}\sum_n nC_nb_P^{n-1}\}\cdot\boldsymbol{f}(IJF) \quad (3)$$

is a good approximation for the quadrupole energy, where $\chi_{ff}=eQ\partial^2V/\partial f^2$, $f=a$, $b$ and $c$ are molecule-fixed axes chosen as the principal axes of inertia, and $\boldsymbol{f}(IJF)$ is Casimir's function. However, if rotational energies $E_{J\tau}$ and $E_{J'\tau'}$ are almost degenerate, the second-order terms can not be ignored. The matrix elements have been derived by Bragg[5]:

$$(IJ\tau F|H_Q|IJ+A\tau'F)=\boldsymbol{g}_\alpha(IJF)(J\tau M_J=J|\chi_{ZZ}|J+A\tau'M_J=J) \quad (4)$$

where $\chi_{ZZ}=eQ\partial^2V/\partial Z^2$ ($Z$ is a space-fixed axis), $\alpha=0$, $\pm1$, $\pm2$, and

$$\boldsymbol{g}_0=[3C(C+1)-4I(I+1)J(J+1)]\div[8I(2I-1)J(2J-1)] \quad (5a)$$

$$\boldsymbol{g}_1=[F(F+1)-I(I+1)-J(J+2)]\times[(I+J+F+2)(I-J+F)\times(J-I+F+1)(J+I-F+1)]^{1/2}\div\{8I(2I-1)J[(2J+1)]^{1/2}\} \quad (5b)$$

$$\boldsymbol{g}_2=[(I+J+F+2)(I+J+F+3)(I-J+F-1)\times(I-J+F)(J-I+F+1)(J-I+F+2)\times(I+J-F+1)(I+J-F+2)]^{1/2}\div\{16I(2I-1)[(2J+1)(J+1)]^{1/2}\} \quad (5c)$$

where $C=F(F+1)-I(I+1)-J(J+1)$. The $(J|J-1)$ and $(J|J-2)$ elements may be determined from equations given above by the Hermitian property of $H_Q$. The tensor component $\chi_{ZZ}$ is expressed in terms of direction cosines $\Phi_{Zf}$ and $\chi_{aa}$, etc., the components of $eQq$ tensor referred to the principal axes a, b and c. The result is

$$\chi_{ZZ}=(\Phi_{Za}^2-\Phi_{Zc}^2)\chi_{aa}+(\Phi_{Zb}^2-\Phi_{Zc}^2)\chi_{bb}+2\Phi_{Za}\Phi_{Zb}\chi_{ab}+2\Phi_{Zb}\Phi_{Zc}\chi_{bc}+2\Phi_{Zc}\Phi_{Za}\chi_{ca} \quad (6)$$

The asymmetric top wave functions as well as direction cosines belong to the representation of the four group[6]. Thus the matrix element of $\chi_{ZZ}$ is zero unless the direct product of the representation of the two rotational states is equal to that of $\Phi_{Zf}$ $\Phi_{Zf'}$. Table V gives the symmetry of the direction cosines and the wave functions.

The rotational wave function for a slightly asymmetric top molecule is approximately given by

$$\Psi_K^{(1)}=S_K+\alpha S_{K-2}+\beta S_{K+2} \quad (7)$$

where $S_K$ is Wang's symmetric top wave function, and the coefficients $\alpha$ and $\beta$ are given by Lide[7]. For propargyl bromide the wave function of this type is sufficient to calculate the second-order quadrupole energy, since the asymmetry parameter of the molecule is small.

Transitions of b-type Q-branches are observed to split into four lines by the quadrupole effect of bromine nucleus. For transitions of high $J$ the first-order theory predicts that the splitting $\nu_4-\nu_3$ is equal to $\nu_2-\nu_1$, but the deviation was observed, in particular, for the transition $12_{0,12}\rightarrow12_{1,11}$ (Table VI).

In applying the second-order theory described above the energies of the states which couple with the states $12_{0,12}$ and $12_{1,11}$ are first calculated. The result is shown in Tables VII

4) See, for example, M. W. P. Strandberg, "Microwave Spectroscopy", Methuen & Co., Ltd., London (1954), Chapter IV.

5) J. K. Bragg, *Phys. Rev.*, **74**, 533 (1948). See also G. Racah, ibid., **62**, 438 (1942).

6) G. W. King, R. M. Hainer and P. C. Cross, *J. Chem. Phys.*, **11**, 27 (1943).

7) D. R. Lide, Jr., ibid., **20**, 1761 (1952).

TABLE V. SYMMETRY OF DIRECTION COSINES AND WAVE FUNCTIONS

| Direction cosine | $K_{-1}$ | $K_1$ | | E | $C_2^a$ | $C_2^b$ | $C_2^c$ |
|---|---|---|---|---|---|---|---|
| $\Phi_{Za}^2$, $\Phi_{Zb}^2$, $\Phi_{Zc}^2$ | e | e | A | 1 | 1 | 1 | 1 |
| $\Phi_{Zc}\Phi_{Zb}$, $\Phi_{Za}$ | e | o | $B_a$ | 1 | 1 | −1 | −1 |
| $\Phi_{Zc}\Phi_{Za}$, $\Phi_{Zb}$ | o | o | $B_b$ | 1 | −1 | 1 | −1 |
| $\Phi_{Za}\Phi_{Zb}$, $\Phi_{Zc}$ | o | e | $B_c$ | 1 | −1 | −1 | 1 |

TABLE VI. LINE SEPARATIONS OF HYPERFINE STRUCTURES OF b-TYPE Q-BRANCH LINES

| Transition | $CH_2{}^{79}BrC{\equiv}CH$ | | | $CH_2{}^{81}BrC{\equiv}CH$ | | | $CH_2{}^{79}BrC{\equiv}CD$ | | | $CH_2{}^{81}BrC{\equiv}CD$ | | |
|---|---|---|---|---|---|---|---|---|---|---|---|---|
| | $\nu_2-\nu_1$ | $\nu_3-\nu_2$ | $\nu_4-\nu_3$ | $\nu_2-\nu_1$ | $\nu_3-\nu_2$ | $\nu_4-\nu_3$ | $\nu_2-\nu_1$ | $\nu_3-\nu_2$ | $\nu_4-\nu_3$ | $\nu_2-\nu_1$ | $\nu_3-\nu_2$ | $\nu_4-\nu_3$ |
| $13_{0,13}\rightarrow13_{1,12}$ | 4.14 | 41.43 | 6.99 | 3.30 | 35.04 | 5.40 | 3.71 | 43.70 | 7.69 | 3.04 | 36.60 | 6.09 |
| $12_{0,12}\rightarrow12_{1,11}$ | 10.47 | 40.59 | ~0 | 6.81 | 33.48 | 1.71 | 8.55 | 42.58 | 2.42 | 6.25 | 35.15 | 2.80 |
| $11_{0,11}\rightarrow11_{1,10}$ | 6.51 | 38.97 | 4.98 | 5.52 | 32.37 | 4.29 | 6.87 | 40.80 | 5.21 | 5.59 | 33.88 | 4.50 |
| $10_{0,10}\rightarrow10_{1,9}$ | 6.51 | 37.95 | 5.58 | 5.52 | 31.23 | 4.86 | 7.06 | 39.36 | 6.54 | 5.76 | 33.34 | 4.82 |
| $9_{0,9}\rightarrow9_{1,8}$ | 7.32 | 36.36 | 6.51 | 5.76 | 30.39 | 5.37 | 7.74 | 38.38 | 6.86 | 6.21 | 31.42 | 5.84 |
| $8_{0,8}\rightarrow8_{1,7}$ | 7.65 | 35.28 | 7.29 | 6.72 | 29.49 | 6.24 | 8.29 | 36.83 | 8.09 | 6.94 | 31.03 | 6.49 |
| $7_{0,7}\rightarrow7_{1,6}$ | 4.89 | 40.74 | 2.37 | 4.35 | 34.74 | 2.10 | | | | | | |
| $6_{0,6}\rightarrow6_{1,5}$ | 9.99 | 34.05 | 8.49 | 8.46 | 28.26 | 7.65 | | | | | | |
| $5_{0,5}\rightarrow5_{1,4}$ | 16.08 | | | 13.9 | 28.0 | | | | | | | |

TABLE VII. STATES COUPLING WITH $12_{0,12}$ AND THEIR ENERGY DIFFERENCES IN Mc./sec.

| State | $E(12_{0,12})-E(J'\tau')$ | | | |
|---|---|---|---|---|
| | $CH_2{}^{79}BrC{\equiv}CH$ | $CH_2{}^{81}BrC{\equiv}CH$ | $CH_2{}^{79}BrC{\equiv}CD$ | $CH_2{}^{81}BrC{\equiv}CD$ |
| $10_{0,10}$ | 95006.7 | 94384.4 | 89533.3 | 88939.3 |
| $10_{2,8}$ | 18110.3 | 17554.3 | 16109.0 | 15586.0 |
| $11_{2,10}$ | −26955.9 | −27223.1 | −26370.1 | −26616.9 |
| $12_{2,10}$ | −78067.2 | −77973.8 | −74500.4 | −74405.1 |
| $13_{2,12}$ | −130783.8 | −130361.7 | −124203.3 | −123792.9 |
| $14_{0,14}$ | −111267.7 | −110542.5 | −104862.6 | −104170.4 |
| $14_{2,12}$ | −191185.0 | −190324.8 | −181064.9 | −180239.9 |
| $10_{1,10}$ | 80545.6 | 79884.1 | 75641.6 | 75014.2 |
| $11_{1,10}$ | 23982.4 | 23756.1 | 22405.3 | 22188.0 |
| $12_{1,12}$ | −12875.3 | −12928.3 | −12397.7 | 12444.1 |
| $13_{1,12}$ | −82010.7 | −81522.4 | −77457.7 | −76994.7 |
| $14_{1,14}$ | −122480.5 | −121820.7 | −115690.4 | −115056.0 |

TABLE VIII. STATES COUPLING WITH $12_{1,11}$ AND THEIR ENERGY DIFFERENCES IN Mc./sec.

| State | $E(12_{1,11})-E(J'\tau')$ | | | |
|---|---|---|---|---|
| | $CH_2{}^{79}BrC{\equiv}CH$ | $CH_2{}^{81}BrC{\equiv}CH$ | $CH_2{}^{79}BrC{\equiv}CD$ | $CH_2{}^{81}BrC{\equiv}CD$ |
| $10_{1,9}$ | 97547.1 | 96888.9 | 91904.6 | 91277.9 |
| $10_{3,7}$ | −49195.1 | −49830.0 | −48378.4 | −48962.1 |
| $11_{1,11}$ | 62763.7 | 62276.3 | 59067.8 | 58608.9 |
| $11_{3,9}$ | −94962.1 | −95291.8 | −91501.1 | −91794.0 |
| $12_{3,9}$ | −144934.8 | −144930.2 | −138584.9 | −138559.3 |
| $13_{3,13}$ | −38752.5 | −38579.1 | −36601.2 | −36429.1 |
| $13_{1,11}$ | −199018.7 | −198653.7 | −189544.5 | −189175.5 |
| $14_{1,13}$ | −114429.1 | −113658.5 | −107812.3 | −107078.5 |
| $14_{3,11}$ | −257371.4 | −256614.8 | −244522.1 | −243780.1 |
| $10_{2,9}$ | 45646.4 | 44958.5 | 42227.2 | 41581.5 |
| $11_{0,11}$ | 76446.2 | 76005.1 | 72226.3 | 71807.5 |
| $11_{2,9}$ | −962.0 | −1324.9 | −1668.2 | −2005.4 |
| $12_{2,11}$ | −49895.0 | −49948.2 | −47797.5 | −47838.1 |
| $13_{0,13}$ | −26703.6 | −26470.8 | −24983.3 | −24758.8 |
| $13_{2,11}$ | −105599.8 | −105254.7 | −100246.0 | −99909.3 |
| $14_{2,13}$ | −162004.1 | −161313.4 | −153434.4 | −152765.8 |

TABKE IX. HYPERFINE STRUCTURES OF a-TYPE R-BRANCH LINES (Mc./sec.)

| $J''\tau''\rightarrow J'\tau'$ | $F''\rightarrow F'$ | $CH_2{}^{79}BrC\equiv CH$ | | $CH_2{}^{81}BrC\equiv CH$ | | $CH_2{}^{79}BrC\equiv CD$ | | $CH_2{}^{81}BrC\equiv CD$ | |
|---|---|---|---|---|---|---|---|---|---|
| | | Calcd. | Obs. | Calcd. | Obs. | Calcd. | Obs. | Calcd. | Obs. |
| $6_{1,6}-7_{1,7}$ | 15/2−17/2 | −1.99 | −2.00 | −1.63 | −1.52 | −0.91 | −1.76 | −1.63 | −1.59 |
| | 13/2−15/2 | −0.29 | −0.26 | −0.24 | −0.22 | −0.30 | −0.19 | −0.26 | −0.16 |
| | 9/2−11/2 | +1.26 | +1.11 | +1.03 | +0.90 | +1.23 | +1.10 | +1.05 | +0.98 |
| | 11/2−13/2 | +2.95 | +3.04 | +2.42 | +2.31 | +2.84 | +2.70 | +2.43 | +2.30 |
| $5_{1,5}-6_{1,6}$ | 13/2−15/2 | −2.65 | −2.59 | −2.17 | −2.17 | −2.54 | −2.54 | −2.17 | −2.10 |
| | 11/2−13/2 | −0.15 | −0.19 | −0.12 | −0.10 | −0.16 | −0.08 | −0.15 | −0.12 |
| | 7/2− 9/2 | +1.65 | +1.62 | +1.36 | +1.30 | +1.62 | +1.55 | +1.39 | +1.34 |
| | 9/2−11/2 | +4.15 | +4.12 | +3.40 | +3.43 | +4.00 | +3.97 | +3.41 | +3.37 |
| $4_{1,4}-5_{1,5}$ | 11/2−13/2 | −3.76 | −3.76 | −3.08 | −3.08 | −3.61 | −3.64 | −3.08 | |
| | 9/2−11/2 | +0.40 | +0.31 | +0.32 | +0.31 | +0.34 | +0.11 | +0.28 | |
| | 5/2− 7/2 | +2.13 | +2.32 | +1.75 | +1.80 | +2.11 | +2.01 | +1.81 | |
| | 7/2− 9/2 | +6.28 | +6.11 | +5.15 | +5.14 | +6.05 | +6.41 | +5.17 | |
| $3_{1,3}-4_{1,4}$ | 9/2−11/2 | −5.80 | −5.72 | −4.76 | −4.90 | −5.57 | −5.55 | −4.75 | −4.76 |
| | 7/2− 9/2 | +2.25 | +2.26 | +1.84 | +1.87 | +2.09 | +2.23 | +1.76 | +1.90 |
| | 3/2− 5/2 | +2.38 | | +1.95 | | +2.41 | | +2.08 | |
| | 5/2− 7/2 | +10.43 | +10.37 | +8.55 | +8.84 | +10.06 | +10.18 | +8.59 | +8.60 |

TABLE X. HYPERFINE STRUCTURES OF $12_{0,12}\rightarrow 12_{1,11}$ TRANSITION (Mc./sec.)

| $J''\rightarrow J'$ | $F''\rightarrow F'$ | $CH_2{}^{79}BrC\equiv CH$ | | $CH_2{}^{81}BrC\equiv CH$ | | $CH_2{}^{79}BrC\equiv CD$ | | $CH_2{}^{81}BrC\equiv CD$ | |
|---|---|---|---|---|---|---|---|---|---|
| | | Calcd. | Obs. | Calcd. | Obs. | Calcd. | Obs. | Calcd· | Obs. |
| $12_{0,12}-12_{1,11}$ | 27/2−27/2 | −30.54 | −30.71 | −23.50 | −23.53 | −29.92 | −29.85 | −23.71 | −23.80 |
| | 25/2−25/2 | −20.43 | −20.24 | −16.67 | −16.72 | −21.39 | −21.30 | −17.43 | −17.55 |
| | 29/2−29/2 | +20.39 | +20.35 | +16.71 | +16.76 | +21.36 | +21.28 | +17.47 | +17.60 |
| | 23/2−23/2 | +20.34 | +20.35 | +18.43 | +18.47 | +23.77 | +23.70 | +20.30 | +20.40 |

TABLE XI. QUADRUPOLE COUPLING CONSTANTS OF THE BROMINE ATOM

| | $CH_2{}^{79}BrC\equiv CH$ | $CH_2{}^{81}BrC\equiv CH$ | $CH_2{}^{79}BrC\equiv CD$ | $CH_2{}^{81}BrC\equiv CD$ |
|---|---|---|---|---|
| $\chi_{aa}$ | 316 Mc./sec. | 259 Mc./sec. | 300 Mc./sec. | 255 Mc./sec. |
| $\chi_{bb}$ | −16 | −13 | −8 | −5 |
| $\chi_{cc}$ | 403 | 336 | 415 | 342 |
| $\chi_{xx}$ | −286 | −238 | −295 | −241 |
| $\chi_{yy}$ | −301 | −246 | −292 | −250 |
| $\chi_{zz}$ | 587 | 484 | 587 | 491 |
| $\theta$ | 33°48′ | 33°59′ | 34°49′ | 34°36′ |
| $\theta'$ | 34° 2′ | 33°58′ | 35° 7′ | 35° 3′ |
| $\eta$ | 0.03 | 0.02 | −0.01 | 0.02 |

TABLE XII. COMPARISON OF THE MOLECULAR CONSTANTS

| Compound | $r$(C—Br) | $eQ_q$ | |
|---|---|---|---|
| | | $^{79}Br$ | $^{81}Br$ |
| Propargyl bromide | 1.9415 Å | 587 Mc./sec. | 484 Mc./sec. |
| Methyl bromide | 1.939 Å* | 577.3** | 482.4** |
| Ethyl bromide | 1.9400 Å*** | 416.5*** | 349.1*** |

* J. W. Simmons and W. E. Anderson, *Phys. Rev.*, **80**, 338 (1950).
** A. H. Sharbaugh and J. Mattern, ibid., **75**, 1102 (1949).
*** R. S. Wagner, B. P. Dailey and N. Solimene, *J. Chem. Phys.*, **26**, 1593 (1957).

and VIII where the states are chosen by symmetry consideration.

It is to be noted that the state $11_{2,9}$ is nearly degenerate with the state $12_{1,11}$, while the energies of other states differ by more than 10000 Mc./sec. from that of the state $12_{0,12}$ or $12_{1,11}$. Since the symmetry of the state $11_{2,9}$ is $B_a$ and that of the state $12_{1,11}$ $B_b$ while that of $\Phi_{Za}\Phi_{Zb}$ is $B_c$ as is given in Table V, the state $11_{2,9}$ couples with the state $12_{1,11}$ by the quadrupole Hamiltonian of the form $\Phi_{Za}\Phi_{Zb}\chi_{ab}$. This coupling is dominant in the second-order terms, thus the second-order energy is nearly proportional to $\chi_{ab}{}^2$. The other terms $\chi_{bc}$ and

$\chi_{ca}$ are equal to zero by the symmetry of the molecule.

The line separations given in Table VI, $\nu_2-\nu_1$ and $\nu_4-\nu_3$, are expressed as

$$\nu_2-\nu_1=K\chi_{aa}+L\chi_{bb}+M\chi_{ab}^2 + (\text{small terms involving } \chi_{aa}^2,\ \chi_{bb}^2 \text{ and } \chi_{aa}\chi_{bb}) \quad (8a)$$

$$\nu_4-\nu_3=K\chi_{aa}+L\chi_{bb}+N\chi_{ab}^2 + (\text{small terms involving } \chi_{aa}^2,\ \chi_{bb}^2 \text{ and } \chi_{aa}\chi_{bb}) \quad (8b)$$

where $K$, $L$, $M$ and $N$ are constants. In these expressions the first two terms are the first-order energies and the others are the second-order energies. It is to be noted that the first two terms are the same for both equations. In employing Eq. 7 the second-order terms of $\delta$ in the coefficients, $\alpha$ and $\beta$, are neglected. After appropriate correction is made for the last term, $\chi_{ab}$ is obtained by subtracting Eq. 8b from Eq. 8a. By substituting the value of $\chi_{ab}$ into Eq. 8a or 8b, a linear equation of $\chi_{aa}$ and $\chi_{bb}$ is obtained. Another linear relation is given by well-resolved a-type R-branch transitions (Table IX), for which the second-order effect seems to be small. From these relations $\chi_{aa}$ and $\chi_{bb}$ are calculated. The results are compared with the observed ones in Tables IX and XI.

By use of $\chi_{aa}$, $\chi_{bb}$ and $\chi_{ab}$ the principal values of the $\chi$-tensor and the directions of the principal axes (x, y and z) are determined without any assumptions. The $\theta$ designates the angle between the a- and z-axes and the $\theta'$ that between the direction of the C—Br bond and the a-axis. The two angles are found to agree within experimental errors. The asymmetry parameter $\eta$, which is given by $(\chi_{xx}-\chi_{yy})/\chi_{zz}$, is close to zero for the four isotopic species, where the x-axis is taken in the (ab) plane. The average value of $\eta$ is $+0.015\pm0.013$.

## Discussion

The C—Br bond length obtained, 1.9415 $\pm$0.005 Å, is close to the values usually observed in saturated hydrocarbon bromides. Table XII shows comparison of this value with those of methyl and ethyl bromides. It is to be noted that the values for the C—Br length in those three compounds are of the same order of magnitude within experimental errors.

The z-direction of the quadrupole coupling constant coincides with the direction of the C—Br bond within errors involved in the present experiment. It is a good confirmation of the current assumption usually made. The value of $\chi_{zz}$ is compared with those of methyl and ethyl bromides in Table XII. The three values of the coupling constant are also close to each other.

The authors wish to express their sincere thanks to Dr. Makoto Shima, Institute for Physical and Chemical Research, for supplying them with heavy water. The expenses for this research were defrayed from the Scientific Research Encouragement Grant of the Ministry of Education to which the authors' thanks are also due.

*Department of Chemistry*
*Faculty of Science*
*The University of Tokyo*
*Hongo, Tokyo*

# *Nuclear Magnetic Resonance Study of Hydrogen Bond in Salicylaldehyde*

By Ichiro YAMAGUCHI

(Received August 7, 1960)

It is well accepted that a strong intramolecular hydrogen bond is formed between the hydroxyl and aldehyde groups in a salicylaldehyde molecule. This evidence was obtained by various molecular spectroscopic methods[1] and dipole moment measurements,[2] and some characteristic structures for this hydrogen-bonded system were suggested on the basis of these measurements. Nuclear magnetic resonance (NMR) measurement is expected to give further informations concerning the

1) a) M. Tsuboi, This Bulletin, **25**, 60 (1952); b) H. Yamada, ibid., **32**, 1051 (1959); c) A. E. Martin, *Nature*, **166**, 474 (1950); d) P. D. Simova and B. Skorchev, *Izvest. Bulgar. Akad. Nauk., Otdel. Fiz.-Mat. i Tekh. Nauki Ser. Fiz.*, **4**, 47 (1954).

2) a) H. Lumbroso and P. Rumpf, *Bull. soc. chim. France*, **1950**, 371; b) R. Mecke and A. Reuter, *Z. Naturforsch.*, **4a**, 368 (1949).

hydrogen bond in this molecule.

Compounds with intramolecular hydrogen bond so far well investigated by the NMR method are *o*-chlorophenol[3,4], *o*-bromophenol[5], and *o*-cresol[3,5]. The resonance field for the OH proton in these compounds was comparatively dependent on concentration in various solutions. This suggests that the intermolecular hydrogen bond in these compounds is easily disrupted by dilution of solutions. On the other hand, the intramolecular hydrogen bond in compounds such as *o*-nitrophenol or salicylaldehyde is so strong that it would scarcely form a intermolecular hydrogen bond. It is expected therefore that the OH lines of NMR for these compounds would not show remarkable concentration dependence[6].

In the present experiment, the measurement of the OH resonance shift in NMR spectrum of salicylaldehyde was carried out in solutions of several solvents with various concentrations. In addition to this, the concentration dependence of the resonance spectrum of the ring protons was also investigated.

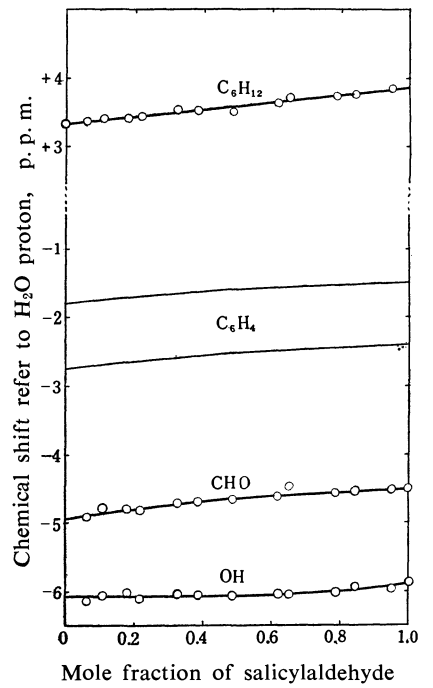
## Experimental

NMR measurements were made at 20°C with a Varian NMR spectrometer operating at 56.4 Mc./sec. Salicylaldehyde was a guaranteed grade reagent and used without further purification. Solvents chosen in this experiment were cyclohexane and carbon tetrachloride (inert solvents), and chloroform, methanol, benzene, acetone, ether and pyridine (proton donors and acceptors). These solvents were purified for eliminating extra lines in their NMR spectra.

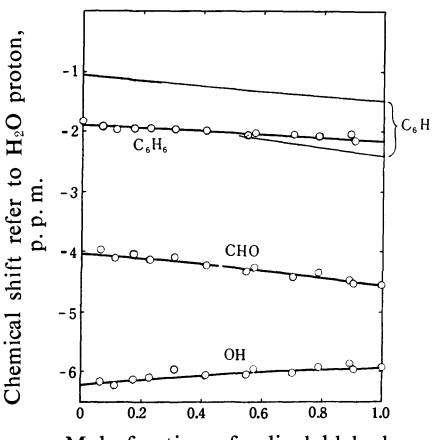
The sweep rate was calibrated by taking the value of the chemical shift between the methyl group proton and the benzene ring proton in toluene as 4.90 p. p. m.[7] The value of chemical shift of each line was obtained referring to an external reference of water in a capillary, and the correction for bluk diamagnetic susceptibility was made. Solutions of twelve stages of concentrations between 0.05 and 0.95 mole fractions were prepared for each solvent.

## Results and Discussion

Fig. 1a shows the concentration dependence of the chemical shifts for protons of salicylaldehyde in cyclohexane solution. The lowest curve was assigned to the OH proton by reasoning which will be described later. The next lowest is for the CHO proton. The resonance lines for the ring protons are very complex as shown later. However the corresponding magnetic fields are expressed by two lines for simplicity in the figure, showing decrease with decreasing concentration. The displacement of the lines to a higher field at higher concentration is caused by the interaction among benzene molecules. The decrease of the resonance field for the OH group on dilution seems to correspond to a charge migration from the proton to the ring. Most of the chemical




(a)




(b)

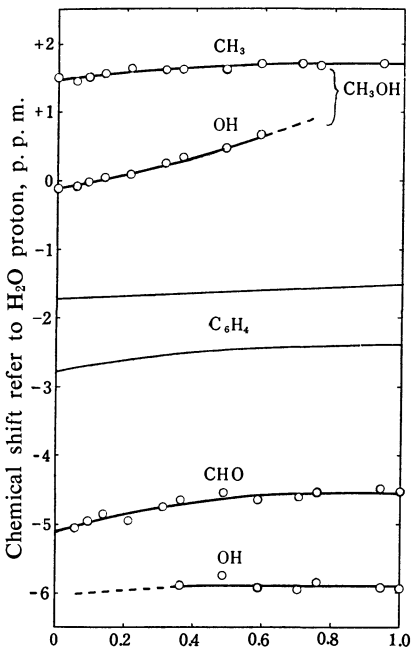
3) C. M. Huggins, G. C. Pimentel and J. N. Shoolery, *J. Phys. Chem.*, **60**, 1311•(1956).

4) I. Gränacher, *Helv. Phys. Acta*, **31**, 734 (1958); M. Martin and F. Hérail, *Compt. rend.*, **248**, 1994 (1954).

5) R. L. Batdorf, Ph. D. thesis, Univ. of Minnesota, 1955.

6) Puranik and Ramavataram observed the slight shift in the C=O vibrational frequency for salicylaldehyde in the presence of proton donor or acceptor group. This shift was attributed to the minute weakening of the intramolecular hydrogen bond. P. G. Puranik, *J. Chem. Phys.*, **23**, 761 (1955); K. Ramavataram, *Proc. Indian Acad. Sci.*, **45A**, 47 (1957).

7) N. F. Chamberlain, *Anal. Chem.*, **31**, 56 (1959).




(c)

Fig. 1. Chemical shift diagrams of salicylaldehyde in several solutions;
(a) cyclohexane solution, (b) benzene solution, and (c) methanol solution.

shift diagrams observed for the other solutions have much the same feature as that for cyclohexane solution except for benzene and pyridine solutions.

Fig. 1b. shows the proton resonance in benzene solution. The field for the CHO group increases with decreasing concentration in contrast to the other observed solutions. This may be due to a hydrogen bond formation between the acidic proton in the CHO group and the $\pi$ electron system of a solvent benzene molecule; the proton is located in a region where the effect of the benzene ring is diamagnetic as in the case of chloroform in benzene solution[8].

Fig. 1c. shows the chemical shift diagram for methanol solution. The OH proton resonance line of alcohol disappears in the concentrated region. The some is true for the OH proton of salicylaldehyde but in the dilute region. This implies the exchange of protons between OH group of alcohol and that of phenol. The broadening of these two lines over all the concentration range may also be an additional evidence for this exchange process. From the separation of the above two lines for both groups, the upper limit for the exchange rate was estimated as about 330 c. p. s. It is therefore probable that even a proton contributing to a strong intramolecular hydrogen bond formation is also able to exchange.

Fig. 2 shows the concentration dependence of the chemical shift of proton resonance lines for the OH group in various solutions. Batdorf[5] measured the chemical shift of the OH proton in various phenol derivatives in saturated solutions of acetone. He showed that among the OH lines for various phenol derivatives the OH line for salicylic acid derivatives appeared at the lowest field region (around $-6$ p. p. m. referring to water proton). The OH proton lines for the other phenol derivatives appeared at considerably higher fields than that for salicylaldehyde. In general, the OH line for phenol derivatives forming merely intermolecular hydrogen bond appears in the range of about $-2$ to $-4$ p. p. m. from the water proton line. Comparing these values with those for salicylic acid derivatives with intramolecular hydrogen bond, it may be said that the strength of the intramolecular hydrogen bond in salicylic acid derivatives is ranked to be considerably high.

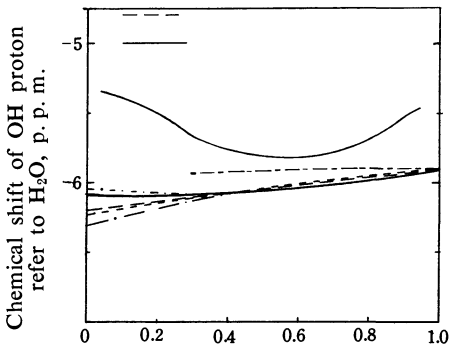



Fig. 2. OH proton resonance shift in salicylaldehyde of various solutions.
Solvent
——— Cyclohexane
—·—· Carbon tetrachloride
-·-·-· Chloroform
— — — Methanol
- - - - Benzene
—— —— Acetone
——— Pyridine

For various solutions observed, the concentration dependence of the OH lines are almost the same except pyridine solution which will be discussed later. This fact is somewhat surprising because it may suggest that the nature of the OH proton in salicylaldehyde is scarcely affected at all by the solvents with high hydrogen bond forming ability. The above fact also suggests that the intramolecular hydrogen

8) L. W. Reeves and W. G. Schneider, *Can. J. Chem.*, 35, 251 (1957).

bond in salicylaldehyde is considerably strong and does not allow a hydrogen bond to form with the other molecular species.

The resonance field of the OH proton is observed to decrease slightly as the concentration of the solution decreases. In general dilution of a phenol with some moderate solvent, intermolecularly hydrogen-bonded polymerized molecules dissociate to dimer molecules showing a decrease of the OH proton resonance field. However dissociation of dimerized ones to monomers shows an increase of the field. Thus, for intermolecularly hydrogen-bonded compounds the variation of the OH proton resonance field generally has a minimum, where the most effectively and strongly hydrogen-bonded species is seemed to form. In contrast to phenol, the field for the OH proton line of salicylaldehyde decreases monotonously with dilution of solution showing no increase even on extreme dilution. This suggests that the bonding becomes stronger as the concentration decreases and the hydrogen bond remains even in the solution of extremely low concentration. Therefore, for salicylaldehyde, the free single molecule with the intramolecular hydrogen bond is considered to be the most effectively hydrogen-bonded species. This result also suggests that in concentrated solutions there exist dimerized or polymerized molecules[9] which dissociate to monomer molecules on dilution. The broadening of the OH lines observed in concentrated range in almost all the solutions may be attributed to a rather slow exchange process of OH protons among several kinds of polymerized species.

An exceptional behavior of OH line was observed for pyridine solution. The curve in Fig. 2 shows apparently anomalous behavior. First, the resonance occurs at higher field than that for the other solutions. This may be ascribed to some change in its electronic configuration caused by interaction with a pyridine molecule. Secondly, the magnetic field decreases with decreasing concentration in concentrated range. This may arise from the same dissociation process as that the other solutions show and simultaneously from the formation of strong hydrogen bond between salicylaldehyde and pyridine. Thus the minimum resonance field appears at the equimolecular composition of the solution. The third is the increase of the curve in dilute range. This may be attributed to the formation of multiply hydrogen-bonded species with pyridine. This experimental result may suggest that the hydrogen bond between salicylaldehyde and pyridine is stronger than the intramolecular hydrogen bond in salicylaldehyde.

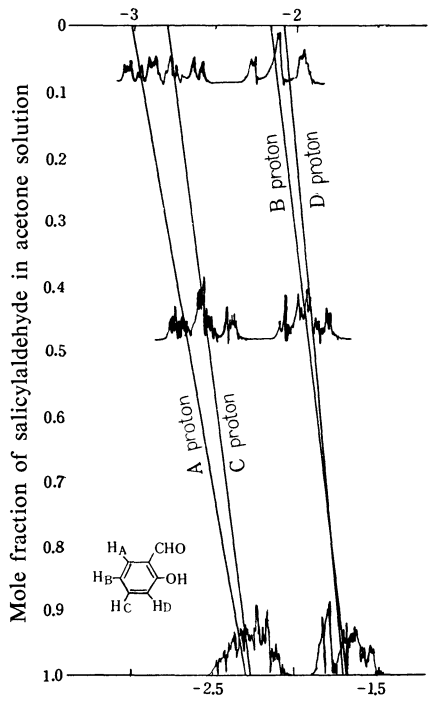



Fig. 3. Concentration dependent behavior of ring proton resonance lines of salicylaldehyde in acetone solution.

A remarkable solvent effect was also observed in the resonance spectra of ring protons, especially in the systems with proton donor or acceptor solvents. Although the spectrum of the ring protons could not be exactly analyzed, it was possible to assign the spectral lines to each proton by tracing the change in the spectral figure of the system on dilution. Fig. 3. shows an example of this solvent effect on the ring protons in acetone solution.

The whole spectrum of the ring protons displaces to lower field on dilution. This displacement is considered to arise from change in the interaction among benzene rings as mentioned previously. In a series of the spectra of solutions with different concentrations, the lines due to A proton (ortho to CHO group) and D proton (ortho to OH group) exhibit opposed dilution displacement to each other. The A proton lines displace to lower field while those of D to higher field on dilution relative to the displacement of the whole ring proton spectrum. Various effects may be attributed to these shift changes of dilution[10]. However, the essential feature to cause the

9) Simova and Skorchev also suggested the existence of dimerized molecules. See Ref. 1d.

10) A. D. Buckingham, T. Schaefer and W. G. Schneider, *J. Chem. Phys.*, 32, 1227 (1960).

spectral change, especially that for A and D protons, would probably be a charge migration in the molecule affected by the change in the hydrogen bonding situation of this molecule.

**Summary**

The concentration dependent behavior of the proton resonance spectra of salicylaldehyde in several solution systems were measured. The behavior of the OH resonance line for the solution systems showed the evidence of the existence of considerably strong intramolecular hydrogen bond in the molecule. The behavior of the ring proton spectrum on dilution suggested the occurrence of the charge migration in the ring affected by the change in the hydrogen bonding situation.

The author wishes to express his sincere thanks to Professor S. Fujiwara and Dr. A. Danno for their kind encouragement and suggestions on this work and also to Dr. H. Shimizu, N. Nakagawa and N. Hayakawa for their valuable discussions.

*Radiation Application Division*
*Japan Atomic Energy Research Institute*
*Tokai Ibaraki-ken*

# *Non-benzenoid Aromatic Heterocycles. IV* [1]. An Attempted Synthesis of Indolo[3, 2-b]indole: A Hetero-pentalene*

By Hiroshi KATO and Masaki OHTA

(Received September 19, 1960)

Since the proposal of pentalene (I) by Robinson[2] as a possible aromatic substance, it has been the subject of many studies. Although dibenzopentalene and a few other condensed pentalene derivatives have recently been synthesized (showing non-aromatic polyene properties), the synthesis of pentalene or even benzopentalene is still awaited, and the results of theoretical treatments on the stability of these compounds by several groups of workers are not in accordance[3].

It has been found that substitution of –C=C– groups in a conjugated compound by hetero-atoms results in a system which shows properties of the original compound to a certain extent. These facts led the authors to attempt a synthesis of indolo[3, 2-b]indole (II) as a model of diazadibenzopentalene in order to add some experimental data concerning the stability of the proposed pentalene ring system[4]. As possible routes to indolo[3, 2-b]indole, intramolecular dehydration of 2-(*o*-aminophenyl)-indolone (III) or dehydrogenation of *N*, *N'*-dihydroindolo[3, 2-b]indole (dindole) (IV) may be considered. These two compounds, III and IV, have been prepared[5] by reduction of *o*, *o'*-dinitrobenzil by Raney nickel or by zinc and hydrochloric acid, respectively.

An attempted intramolecular condensation of 2-(*o*-aminophenyl)indolone has been briefly reported by Ruggli et al.[5], but as nothing has been described about the condensation reagent, the present authors tried to dehydrate it using a variety of condensation catalysts, none of which gave an identifiable product.

Next, the dehydrogenation of dindole was tried. When dindole was refluxed with chloranil in *n*-butanol, an intense violet coloration took place, but the color faded away gradually and tetrachlorohydroquinone was isolated from the reaction mixture. Neither, in this case, was the expected indolo[3, 2-b]indole, obtained, and an amorphous polymeric product was obtained. The elemental composition of this substance is not very far from $C_{14}H_{10}ON_2$. Attempts to isolate this colored substance were not successful, but the absorption curve of this substance in the visible region is quite similar to 2-(*o*-aminophenyl)indolone and the $R_f$ value of this compound is the same as 2-(*o*-aminophenyl)-indolone. From these facts and the supplemental data described in the experimental

* Presented at the meeting of the Chemical Society of Japan, Tokyo, October, 1959.

1) Part III, H. Kato, T. Ogawa and M. Ohta, This Bulletin, 33, 1468 (1960).

2) J. W. Armit and R. Robinson, *J. Chem. Soc.*, **1922**, 827.

3) Cf. for example, W. Baker and J. F. W. McOmie, "Non-benzenoid Aromatic Compounds" in "Progress in Organic Chemistry", Vol. 3, Butterworths Scientific Publications, London (1955), p. 44.

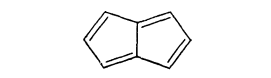
4) During the course of this investigation, a series of condensed azapentalenes have been prepared by Treibs. W. Treibs, *Naturwissenschaften*, **46**, 170 (1959).

5) P. Ruggli et al., *Helv. Chim. Acta*, **18**, 845 (1935).

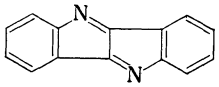
part, it may be concluded that the colored compound is 2-(*o*-aminophenyl)indolone.

These experimental data, although negative, indicate that at least some interaction exists between the two compounds (IV and chloranil) and dehydrogenation has occurred in dindole. On the basis of these data, it seemed reasonable to assume that dehydrogenation of dindole gave indolo[3, 2-b]indole as an intermediate product, but this compound is so unstable that it took up traces of water present in butanol and gave 2-(*o*-aminophenyl)indolone. When rigidly dehydrated *n*-butanol was used as solvent, the beginning of coloration required a longer period and on addition of a small amount of water, the coloration took place at once. This fact also lends some support to the above described assumption.

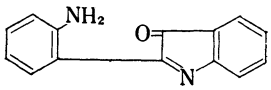
During the course of this investigation, the authors have known that Treibs[6] also attempted dehydrogenation of dindole using many catalysts, but indolo[3, 2-b]indole was not prepared.



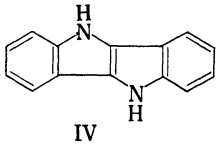
I



II



III



IV

## Experimental

**Attempted Cyclodehydration of 2-(*o*-Aminophenyl) indolone.**—2-(*o*-Aminophenyl)indolone[5] was treated with the following reagents under warming or at room temperature: polyphosphoric acid, concentrated sulfuric acid, acetic acid, triethylamine, and piperazine. Polyphosphoric acid and sulfuric acid gave a yellow amorphous substance, accompanied by the starting material. Acetic acid yielded a yellow polymeric substance, and in the case of triethylamine the starting material was recovered unchanged.

6) W. Treibs, private communication.

**Reaction of Dindole with Chloranil.**—a) A butanolic solution (30 ml.) of dindole[5] (0.5 g.) and chloranil (0.6 g.) was gently refluxed for four hours. At first a deep violet coloration took place, but it faded away gradually, and after four hours the solution became pale brown. The solvent was removed under reduced pressure and the residue was washed with ether and purified by chromatography (alumina-benzene). The yellow powder from the eluate was repeatedly recrystallized first from benzene-benzine and then from benzene giving yellow amorphous powder. It does not show a distinct melting point (about 300°C).

Found: C, 74.02; H, 4.40. Calcd. for $C_{14}H_{10}ON_2$: C, 75.65; H, 4.54%.

The ether washings in the above experiment were extracted with 10% aqueous sodium hydroxide and the aqueous layer was acidified which hydrochloric acid. The white crystals (0.47 g.) which separated out were recrystallized from acetic acid giving white needles, m. p. 234°C (in a sealed tube), undepressed on admixture with tetrachlorohydroquinone.

b) When chloranil or dindole alone was refluxed in *n*-butanol, no coloration took place, and chloranil gave no tetrachlorohydroquinone.

c) Dindole and chloranil was heated cautiously until the coloration took place, and the colored solution in situ was used for spectroscopic measurement. ($\lambda_{max}$ 550 m$\mu$; with a small shoulder at about 490 m$\mu$; intensity unspecified). The shape of the curve in the visible region is the same with 2-(*o*-aminophenyl)indolone. Attempts to isolate this colored substance (by chromatography) were unsuccessful. The colored substance and 2-(*o*-aminophenyl)indolone gave the same spot in paper chromatography ($R_f$=0.95, solvent: butanol-pyridine-water, 4 : 1 : 2). This colored substance seemed a little more unstable than 2-(*o*-aminophenyl)indolone, but when 2-(*o*-aminophenyl)indolone was heated with chloranil in *n*-butanol, it decomposed rapidly to give a yellow solution.

d) When rigidly dehydrated *n*-butanol (freshly twice distilled) was used as solvent, the beginning of coloration was delayed and the intensity of the color was feeble and on addition of a small amount of water, the color was intensified immediately.

The authors are indebted to Mr. Asaji Kondo for microanalyses.

*Laboratory of Organic Chemistry*
*Tokyo Institute of Technology*
*Meguro-ku, Tokyo*

# *Normal Coordinate Treatment and Assignment of Infrared Absorption Bands of Polyvinyl Chloride*

By Takehiko SHIMANOUCHI and Mitsuo TASUMI

(Received September 16, 1960)

In the analysis of infrared absorption spectra it is often of considerable importance to calculate the frequencies of the normal vibrations.

Recent developments in high-speed computers have made it possible to calculate the normal vibrations of complex molecules. We have calculated the frequencies of the polyvinyl chloride molecule using the force constants transferred from simple molecules. These results suggest a modification of the assignment proposed in former studies[1,2] and will be reported in the present paper.

## Method of Calculation and Results

The normal coordinate treatment was carried out on assuming that the polyvinyl chloride molecule is syndyotactic and takes the extended zigzag form with the repeating unit made up of two monomer units. The unit cell for this structure is shown in Fig. 1. This model belongs to a group isomorphous with to the point group $C_{2v}$[1], and in Table I symmetry species, selection rules, and dichroic properties are given.

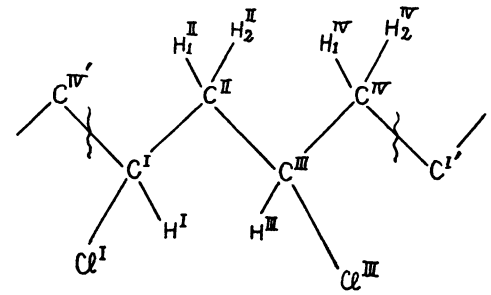


Fig. 1. Unit cell for syndyotactic structure of polyvinyl chloride.

TABLE I. SYMMETRY SPECIES, SELECTION RULES, AND DICHROISM FOR SYNDYOTACTIC POLYVINYL CHLORIDE*

| $C_{2v}$ | $E$ | $C_2$ | $\sigma_v$ | $\sigma_g$ | Number of frequencies | IR (Dichroism) | R |
|---|---|---|---|---|---|---|---|
| $A_1$ | 1 | 1 | 1 | 1 | 9 | $\sigma$ | active |
| $A_2$ | 1 | 1 | −1 | −1 | 7 | inactive | active |
| $B_1$ | 1 | −1 | 1 | −1 | 9 | $\sigma$ | active |
| $B_2$ | 1 | −1 | −1 | 1 | 7 | $\pi$ | active |

* As to the notation, see Ref. 1.

TABLE II. INTERNAL COORDINATES

| Bond lengths; | | Bond angles; | | | |
|---|---|---|---|---|---|
| $R^{I}$ | $C^{I}$–$C^{II}$ | $\theta^{I}$ | $C^{IV\prime}$–$C^{I}$–$C^{II}$ | $\varphi_1^{II}$ | $C^{I}$–$C^{II}$–$H_1^{II}$ |
| $R^{II}$ | $C^{II}$–$C^{III}$ | $\theta^{II}$ | $C^{I}$–$C^{II}$–$C^{III}$ | $\varphi_2^{II}$ | $C^{I}$–$C^{II}$–$H_2^{II}$ |
| $R^{III}$ | $C^{III}$–$C^{IV}$ | $\theta^{III}$ | $C^{II}$–$C^{III}$–$C^{IV}$ | $\varphi_3^{II}$ | $C^{III}$–$C^{II}$–$H_1^{II}$ |
| $R^{IV}$ | $C^{IV}$–$C^{I\prime}$ | $\theta^{IV}$ | $C^{III}$–$C^{IV}$–$C^{I\prime}$ | $\varphi_4^{II}$ | $C^{III}$–$C^{II}$–$H_2^{II}$ |
| $r_1^{I}$ | $C^{I}$–$Cl^{I}$ | $\theta^{I}$ | $Cl^{I}$–$C^{I}$–$H^{I}$ | $\varphi_1^{III}$ | $C^{II}$–$C^{III}$–$H^{III}$ |
| $r_2^{I}$ | $C^{I}$–$H^{I}$ | $\theta^{II}$ | $H_1^{II}$–$C^{II}$–$H_2^{II}$ | $\varphi_2^{III}$ | $C^{II}$–$C^{III}$–$Cl^{III}$ |
| $r_1^{II}$ | $C^{II}$–$H_1^{II}$ | $\theta^{III}$ | $H^{III}$–$C^{III}$–$Cl^{III}$ | $\varphi_3^{III}$ | $C^{IV}$–$C^{III}$–$H^{III}$ |
| $r_2^{II}$ | $C^{II}$–$H_2^{II}$ | $\theta^{IV}$ | $H_1^{IV}$–$C^{IV}$–$H_2^{IV}$ | $\varphi_4^{III}$ | $C^{IV}$–$C^{III}$–$Cl^{III}$ |
| $r_1^{III}$ | $C^{III}$–$H^{III}$ | $\varphi_1^{I}$ | $C^{IV\prime}$–$C^{I}$–$Cl^{I}$ | $\varphi_1^{IV}$ | $C^{III}$–$C^{IV}$–$H_1^{IV}$ |
| $r_2^{III}$ | $C^{III}$–$Cl^{III}$ | $\varphi_2^{I}$ | $C^{IV\prime}$–$C^{I}$–$H^{I}$ | $\varphi_2^{IV}$ | $C^{III}$–$C^{IV}$–$H_2^{IV}$ |
| $r_1^{IV}$ | $C^{IV}$–$H_1^{IV}$ | $\varphi_3^{I}$ | $C^{II}$–$C^{I}$–$Cl^{I}$ | $\varphi_3^{IV}$ | $C^{I\prime}$–$C^{IV}$–$H_1^{IV}$ |
| $r_2^{IV}$ | $C^{IV}$–$H_2^{IV}$ | $\varphi_4^{I}$ | $C^{II}$–$C^{I}$–$H^{I}$ | $\varphi_4^{IV}$ | $C^{I\prime}$–$C^{IV}$–$H_2^{IV}$ |

1) S. Krimm and C. Y. Liang, *J. Polymer Sci.*, **22**, 95 (1956).

2) S. Narita, S. Ichinohe and S. Enomoto, ibid., **37**, 273, 281 (1959).

TABLE III. INTERNAL SYMMETRY COORDINATES

$A_1$

$$S_1 = \frac{1}{2}(\Delta R^{I} + \Delta R^{II} + \Delta R^{III} + \Delta R^{IV})$$

$$S_2 = \frac{1}{2}(\Delta r_1^{II} + \Delta r_2^{II} + \Delta r_1^{IV} + \Delta r_2^{IV})$$

$$S_3 = \frac{1}{\sqrt{2}}(\Delta r_2^{I} + \Delta r_1^{III})$$

$$S_4 = \frac{1}{\sqrt{2}}(\Delta r_1^{I} + \Delta r_2^{III})$$

$$S_5 = \frac{1}{\sqrt{2}}(\Delta \Theta^{I} + \Delta \Theta^{III})$$

$$S_6 = \frac{1}{\sqrt{2}}(\Delta \Theta^{II} + \Delta \Theta^{IV})$$

$$S_7 = \frac{1}{\sqrt{2}}(\Delta \theta^{I} + \Delta \theta^{III})$$

$$S_8 = \frac{1}{\sqrt{2}}(\Delta \theta^{II} + \Delta \theta^{IV})$$

$$S_9 = \frac{1}{\sqrt{8}}(\Delta \varphi_1^{II} + \Delta \varphi_2^{II} + \Delta \varphi_3^{II} + \Delta \varphi_4^{II} + \Delta \varphi_1^{IV} + \Delta \varphi_2^{IV} + \Delta \varphi_3^{IV} + \Delta \varphi_4^{IV})$$

$$S_{10} = \frac{1}{\sqrt{8}}(\Delta \varphi_1^{II} - \Delta \varphi_2^{II} - \Delta \varphi_3^{II} + \Delta \varphi_4^{II} - \Delta \varphi_1^{IV} + \Delta \varphi_2^{IV} + \Delta \varphi_3^{IV} - \Delta \varphi_4^{IV})$$

$$S_{11} = \frac{1}{2}(\Delta \varphi_2^{I} + \Delta \varphi_4^{I} + \Delta \varphi_1^{III} + \Delta \varphi_3^{III})$$

$$S_{12} = \frac{1}{2}(\Delta \varphi_1^{I} + \Delta \varphi_3^{I} + \Delta \varphi_2^{III} + \Delta \varphi_4^{III})$$

Four redundancies are included among these coordinates.

$A_2$

$$S_1 = \frac{1}{2}(\Delta R^{I} + \Delta R^{II} - \Delta R^{III} - \Delta R^{IV})$$

$$S_2 = \frac{1}{2}(\Delta r_1^{II} + \Delta r_2^{II} - \Delta r_1^{IV} - \Delta r_2^{IV})$$

$$S_3 = \frac{1}{\sqrt{2}}(\Delta \Theta^{II} - \Delta \Theta^{IV})$$

$$S_4 = \frac{1}{\sqrt{2}}(\Delta \theta^{II} - \Delta \theta^{IV})$$

$$S_5 = \frac{1}{\sqrt{8}}(\Delta \varphi_1^{II} + \Delta \varphi_2^{II} + \Delta \varphi_3^{II} + \Delta \varphi_4^{II} - \Delta \varphi_1^{IV} - \Delta \varphi_2^{IV} - \Delta \varphi_3^{IV} - \Delta \varphi_4^{IV})$$

$$S_6 = \frac{1}{\sqrt{8}}(\Delta \varphi_1^{II} - \Delta \varphi_2^{II} - \Delta \varphi_3^{II} + \Delta \varphi_4^{II} + \Delta \varphi_1^{IV} - \Delta \varphi_2^{IV} - \Delta \varphi_3^{IV} + \Delta \varphi_4^{IV})$$

$$S_7 = \frac{1}{2}(\Delta \varphi_2^{I} - \Delta \varphi_4^{I} - \Delta \varphi_1^{III} + \Delta \varphi_3^{III})$$

$$S_8 = \frac{1}{2}(\Delta \varphi_1^{I} - \Delta \varphi_3^{I} - \Delta \varphi_2^{III} + \Delta \varphi_4^{III})$$

One redundancy is included.

$B_1$

$$S_1 = \frac{1}{2}(\Delta R^{I} - \Delta R^{II} - \Delta R^{III} + \Delta R^{IV})$$

$$S_2 = \frac{1}{2}(\Delta r_1^{II} - \Delta r_2^{II} + \Delta r_1^{IV} - \Delta r_2^{IV})$$

$$S_3 = \frac{1}{\sqrt{2}}(\Delta r_2^{I} - \Delta r_1^{III})$$

$$S_4 = \frac{1}{\sqrt{2}}(\Delta r_1^{I} - \Delta r_2^{III})$$

$$S_5 = \frac{1}{\sqrt{2}}(\Delta \Theta^{I} - \Delta \Theta^{III})$$

$$S_6 = \frac{1}{\sqrt{2}}(\Delta \theta^{I} - \Delta \theta^{III})$$

$$S_7 = \frac{1}{\sqrt{8}}(\Delta \varphi_1^{II} + \Delta \varphi_2^{II} - \Delta \varphi_3^{II} - \Delta \varphi_4^{II} - \Delta \varphi_1^{IV} - \Delta \varphi_2^{IV} + \Delta \varphi_3^{IV} + \Delta \varphi_4^{IV})$$

$$S_8 = \frac{1}{\sqrt{8}}(\Delta \varphi_1^{II} - \Delta \varphi_2^{II} + \Delta \varphi_3^{II} - \Delta \varphi_4^{II} + \Delta \varphi_1^{IV} - \Delta \varphi_2^{IV} + \Delta \varphi_3^{IV} - \Delta \varphi_4^{IV})$$

$$S_9 = \frac{1}{2}(\Delta \varphi_2^{I} + \Delta \varphi_4^{I} - \Delta \varphi_1^{III} - \Delta \varphi_3^{III})$$

$$S_{10} = \frac{1}{2}(\Delta \varphi_1^{I} + \Delta \varphi_3^{I} - \Delta \varphi_2^{III} - \Delta \varphi_4^{III})$$

One redundancy is incuded.

$B_2$

$$S_1 = \frac{1}{2}(\Delta R^{I} - \Delta R^{II} + \Delta R^{III} - \Delta R^{IV})$$

$$S_2 = \frac{1}{2}(\Delta r_1^{II} - \Delta r_2^{II} - \Delta r_1^{IV} + \Delta r_2^{IV})$$

$$S_3 = \frac{1}{\sqrt{8}}(\Delta \varphi_1^{II} + \Delta \varphi_2^{II} - \Delta \varphi_3^{II} - \Delta \varphi_4^{II} + \Delta \varphi_1^{IV} + \Delta \varphi_2^{IV} - \Delta \varphi_3^{IV} - \Delta \varphi_4^{IV})$$

$$S_4 = \frac{1}{\sqrt{8}}(\Delta \varphi_1^{II} - \Delta \varphi_2^{II} + \Delta \varphi_3^{II} - \Delta \varphi_4^{II} - \Delta \varphi_1^{IV} + \Delta \varphi_2^{IV} - \Delta \varphi_3^{IV} + \Delta \varphi_4^{IV})$$

$$S_5 = \frac{1}{2}(\Delta \varphi_2^{I} - \Delta \varphi_4^{I} + \Delta \varphi_1^{III} - \Delta \varphi_3^{III})$$

$$S_6 = \frac{1}{2}(\Delta \varphi_1^{I} - \Delta \varphi_3^{I} + \Delta \varphi_2^{III} - \Delta \varphi_4^{III})$$

As only the vibrations in which corresponding atoms in all the unit cells move in phase are optically active for such high polymers, the calculation was done for these modes of vibration according to the method applied to polyethylene[3]. The internal coordinates and the internal symmetry coordinates used are given in Tables II and III. For the internal coordinates only the bond lengths and angles are taken and the angles of internal rotation about the C-C bond are excluded. Therefore, in this calculation the torsional vibrations of the zigzag chain are not considered, but this has comparatively little effect on the other calculated frequencies.

The potential field used is the Urey-Bradley type[4].

$$2V = K(\text{C-C})\sum_{R}(\Delta R)^2 + K(\text{C-H})_{\text{CHH}}\sum_{ra}(\Delta r_a)^2 + K(\text{C-H})_{\text{CHCl}}\sum_{rb}(\Delta r_b)^2$$

3) T. Shimanouchi and S. Mizushima, *J. Chem. Phys.*, **17**, 1102 (1949).

4) T. Shimanouchi, ibid., **17**, 245, 734, 848 (1949).

$$+K(\text{C-Cl})\sum_{r_c}(\Delta r_c)^2$$
$$+H(\text{C-C-C})\times(1.54)^2\sum_{\Theta}(\Delta\Theta)^2$$
$$+H(\text{H-C-H})\times(1.09)^2\sum_{\theta_a}(\Delta\theta_a)^2$$
$$+H(\text{H-C-Cl})\times(1.09)\times(1.77)\sum_{\theta_b}(\Delta\theta_b)^2$$
$$+H(\text{H-C-C})_{\text{CHH}}\times(1.09)\times(1.54)\sum_{\varphi_a}(\Delta\varphi_a)^2$$
$$+H(\text{H-C-C})_{\text{CHCl}}\times(1.09)\times(1.54)\sum_{\varphi_b}(\Delta\varphi_b)^2$$
$$+H(\text{Cl-C-C})\times(1.77)\times(1.54)\sum_{\varphi_c}(\Delta\varphi_c)^2$$
$$+F(\text{C}\cdots\text{C})\sum_{Q}(\Delta Q)^2+F(\text{H}\cdots\text{H})\sum_{q_a}(\Delta q_a)^2$$
$$+F(\text{H}\cdots\text{Cl})\sum_{q_b}(\Delta q_b)^2$$
$$+F(\text{H}\cdots\text{C})_{\text{CHH}}\sum_{q_c}(\Delta q_c)^2$$
$$+F(\text{H}\cdots\text{C})_{\text{CHCl}}\sum_{q_d}(\Delta q_d)^2$$
$$+F(\text{Cl}\cdots\text{C})\sum_{q_e}(\Delta q_e)^2+\text{linear terms}$$

where $R$, $r_a$, $r_b$, $r_c$, $\Theta$, $\theta_a$, $\theta_b$, $\varphi_a$, $\varphi_b$, $\varphi_c$, $Q$, $q_a\cdots q_e$ represent the following bond lengths, bond angles, and interatomic distances indicated in parentheses.

$R(R^{\text{I}}, R^{\text{II}}, R^{\text{III}}, R^{\text{IV}})$
$r_a(r_1^{\text{II}}, r_2^{\text{II}}, r_1^{\text{IV}}, r_2^{\text{IV}})$
$r_b(r_2^{\text{I}}, r_1^{\text{III}})$
$r_c(r_1^{\text{I}}, r_2^{\text{III}})$
$\Theta(\Theta^{\text{I}}, \Theta^{\text{II}}, \Theta^{\text{III}}, \Theta^{\text{IV}})$
$\theta_a(\theta^{\text{II}}, \theta^{\text{IV}})$
$\theta_b(\theta^{\text{I}}, \theta^{\text{III}})$
$\varphi_a(\varphi_1^{\text{II}}, \varphi_2^{\text{II}}, \varphi_3^{\text{II}}, \varphi_4^{\text{II}}, \varphi_1^{\text{IV}}, \varphi_2^{\text{IV}}, \varphi_3^{\text{IV}}, \varphi_4^{\text{IV}})$
$\varphi_b(\varphi_2^{\text{I}}, \varphi_4^{\text{I}}, \varphi_1^{\text{III}}, \varphi_3^{\text{III}})$
$\varphi_c(\varphi_1^{\text{I}}, \varphi_3^{\text{I}}, \varphi_2^{\text{III}}, \varphi_4^{\text{III}})$
$Q(\text{C}^{\text{IV}'}\cdots\text{C}^{\text{II}}, \text{C}^{\text{I}}\cdots\text{C}^{\text{III}}, \text{C}^{\text{II}}\cdots\text{C}^{\text{IV}}, \text{C}^{\text{III}}\cdots\text{C}^{\text{I}'})$
$q_a(\text{H}_1^{\text{II}}\cdots\text{H}_2^{\text{II}}, \text{H}_1^{\text{IV}}\cdots\text{H}_2^{\text{IV}})$
$q_b(\text{H}^{\text{I}}\cdots\text{Cl}^{\text{I}}, \text{H}^{\text{III}}\cdots\text{Cl}^{\text{III}})$
$q_c(\text{C}^{\text{I}}\cdots\text{H}_1^{\text{II}}, \text{C}^{\text{I}}\cdots\text{H}_2^{\text{II}}, \text{C}^{\text{III}}\cdots\text{H}_1^{\text{II}}, \text{C}^{\text{III}}\cdots\text{H}_2^{\text{II}}, \text{C}^{\text{III}}\cdots\text{H}_1^{\text{IV}}, \text{C}^{\text{III}}\cdots\text{H}_2^{\text{IV}}, \text{C}^{\text{I}'}\cdots\text{H}_1^{\text{IV}}, \text{C}^{\text{I}'}\cdots\text{H}_2^{\text{IV}})$
$q_d(\text{C}^{\text{IV}'}\cdots\text{H}^{\text{I}}, \text{C}^{\text{II}}\cdots\text{H}^{\text{I}}, \text{C}^{\text{II}}\cdots\text{H}^{\text{III}}, \text{C}^{\text{IV}}\cdots\text{H}^{\text{III}})$
$q_e(\text{C}^{\text{IV}'}\cdots\text{Cl}^{\text{I}}, \text{C}^{\text{II}}\cdots\text{Cl}^{\text{I}}, \text{C}^{\text{II}}\cdots\text{Cl}^{\text{III}}, \text{C}^{\text{IV}}\cdots\text{Cl}^{\text{III}})$

For the first calculation we used the force constants transferred from polyethylene[3], 1,2-dichloroethane[5], and 1,1,2,2-tetrachloroethane[6]. These force constants are indicated as Set 1 in Table IV. The molecular constants assumed are also given in Table IV. From these values the characteristic values, L-matrix, potential energy distribution, and Jacobian $\partial(\nu_1\cdots\nu_k)/\partial(K_1\cdots K_n)$ were calculated with the use of the PC-1 computer built in the Department of Physics, The University of Tokyo. In the next calculation, taking into account the results of the first calculation and the observed values, we introduced the new force constants, Sets 2 and 3 given in Table IV, and repeated the calculation in the same way. In the case of Set 2 the force constants are adjusted so that the calculated frequencies show the best agreement with the observed values of polyvinyl chloride. Set 3 was obtained by modifying the former sets in such a way as to make the calculated frequencies correspond reasonably to the observations for deuterated polyvinyl chloride also.

The calculated frequencies are compared with the observed in Tables V and VI, in which the assignments of bands based on the calculated potential energy distribution are also given.

TABLE IV. FORCE CONSTANTS (in millidyn./Å)[a] AND INTRAMOLECULAR TENSION ($\kappa$) (in millidyn. Å)

| | | Set 1 | Set 2 | Set 3 |
|---|---|---|---|---|
| 1 | $K$(C-C) | 2.8[b] | 3.10 | 3.00 |
| 2 | $K$(C-H)$_{\text{CHH}}$ | 4.2[b] | 4.15 | 4.15 |
| 3 | $K$(C-H)$_{\text{CHCl}}$ | 3.90[d] | 4.10 | 4.10 |
| 4 | $K$(C-Cl) | 1.81[c] | 1.65 | 1.70 |
| 5 | $\kappa$(-CHH-) | 0.2[b] | 0.21 | 0.20 |
| 6 | $\kappa$(-CHCl-) | 0.10[c] | 0.10 | 0.10 |
| 7 | $H$(C-C-C) | 0.2[b] | 0.20 | 0.20 |
| 8 | $H$(H-C-H) | 0.4[b] | 0.36 | 0.38 |
| 9 | $H$(H-C-C)$_{\text{CHH}}$ | 0.15[b] | 0.09 | 0.12 |
| 10 | $H$(H-C-Cl) | 0.05[c] | 0.06 | 0.06 |
| 11 | $H$(H-C-C)$_{\text{CHCl}}$ | 0.15[c] | 0.15 | 0.15 |
| 12 | $H$(Cl-C-C) | 0.10[c] | 0.10 | 0.10 |
| 13 | $F$(C···C) | 0.3[b] | 0.50 | 0.45 |
| 14 | $F$(H···H) | 0.1[b] | 0.06 | 0.08 |
| 15 | $F$(H···C)$_{\text{CHH}}$ | 0.4[b] | 0.43 | 0.41 |
| 16 | $F$(H···Cl) | 0.80[c] | 0.80 | 0.80 |
| 17 | $F$(H···C)$_{\text{CHCl}}$ | 0.40[c] | 0.45 | 0.45 |
| 18 | $F$(Cl···C) | 0.60[c] | 0.50 | 0.55 |

Molecular constants
$r$(C-C)=1.54 Å, $r$(C-H)=1.09 Å, $r$(C-Cl)=1.77 Å,
All the bond angles=109°28′

a $F'$ is assumed to be $-0.1F$.
b Transferred from polyethylene[3].
c Transferred from 1,2-dichloroethane[5].
d Transferred from 1,1,2,2-tetrachloroethane[6].

## Discussion

**Polyvinyl Chloride (PVC).** — Of the three infrared active species, $A_1$, $B_1$ and $B_2$, only $B_2$

5) S. Mizushima, I. Nakagawa, I. Ichishima and T. Miyazawa, ibid., 22, 1614 (1954).
6) K. Naito, I. Nakagawa, K. Kuratani, I. Ichishima and S. Mizushima, ibid., 23, 1907 (1955).

TABLE V. CALCULATED AND OBSERVED FREQUENCIES OF POLYVINYL CHLORIDE (in $cm^{-1}$) and assignments

| Calcd. 1[a] | Calcd. 2[b] | Calcd. 3[c] | Obs.[d] | | Assignment |
|---|---|---|---|---|---|
| 2891<br>2880 | 2969<br>2969 | 2969}<br>2968} | 2967 | w $\sigma$ | CH str. ($B_1$), ($A_1$) |
| 2921<br>2919 | 2911<br>2910 | 2905}<br>2905} | 2920 | m $\sigma$ | $CH_2$ antisym. str. ($B_1$), ($B_2$) |
| 2905 | 2871 | 2873 | 2849 | w $\sigma$ | $CH_2$ sym. str. ($A_1$) |
| | | | 2820 | vvw $\sigma$ | |
| 1501 | 1425 | 1459 | 1427 | s $\sigma$ | $CH_2$ bend. ($A_1$) |
| 1392 | 1340 | 1360 | 1381 | vw $\pi$ | $CH_2$ wag. ($B_2$) |
| 1397 | 1343 | 1367 | 1352 | vw $\sigma$ | $CH_2$ wag. ($B_1$) |
| 1225 | 1246 | 1245 | 1330 | m $\sigma$ | CH bend. ($A_1$) |
| 1227 | 1245 | 1244 | 1250 | s $\sigma$ | CH bend. ($B_1$) |
| | | | 1243 | vvw $\sigma$ | |
| 1190 | 1210 | 1208 | 1228 | w $\pi$ | CH bend. ($B_2$) |
| | | | 1197 | w $\pi$ | |
| 1030 | 1063 | 1054 | 1125 | vw $\pi$ | CC str. ($B_2$) |
| 1076<br>1028 | 1103<br>1089 | 1100}<br>1071} | 1096 | m $\sigma$ | CC str. ($A_1$), ($B_1$) |
| 1016 | 976 | 993 | 963 | m $\sigma$ | $CH_2$ rock. ($B_1$) |
| 1026 | 930 | 977 | 926 | vw $\sigma$ | $CH_2$ twist. ($A_1$) |
| 874 | 832 | 849 | 833 | w $\pi$ | $CH_2$ rock. ($B_2$) |
| | | | 693 | m $\sigma$ | |
| 663 | 639 | 651 | 635 | s $\sigma$ | CCl str. ($A_1$) |
| | | | 615 | s $\sigma$ | |
| 639 | 624 | 633 | 603 | w $\sigma$* | CCl str. ($B_1$) |
| | | | 487 | vw | |
| 444 | 458 | 452 | 430 | w | CCC def. ($B_1$) |
| 343 | 328 | 338 | 363 | w | CCl bend. ($A_1$) |
| 313<br>290 | 294<br>283 | 303}<br>290} | 315 | vw | {CCl bend. ($B_2$)<br>{CCl bend. ($B_1$) |
| | | | 182<br>160 | w}<br>w} | torion ($A_1$, $B_2$) |
| | | | 102 | vw | |

a Calculated from the force constants, Set 1.
b Calculated from the force constants, Set 2.
c Calculated from the force constants, Set 3.
d See Refs. 1, 2, 7—11.
* As to the dichroism of the 603 $cm^{-1}$ band we shall report later.

should have parallel dichroism when the molecular chains are oriented along the stretching direction. As shown in Table V the observed parallel bands correspond reasonably to the calculated $B_2$ frequencies. The perpendicular bands, also, show good correspondence with the calculated $A_1$ and $B_1$ frequencies. The main points of the present assignment are summarized as follows:

1) Both of the two CH stretching frequencies which belong to the $A_1$ and $B_1$ species are assigned to the band at 2967 $cm^{-1}$. The former assignment[1] of the CH stretching mode ($A_1$) to the 2820 $cm^{-1}$ band is improper because of the weak interaction between the two CH bonds. This is also the case for 1, 1, 2, 2-tetrachloroethane, in which the two CH bonds are situated nearer than in polyvinyl chloride. The CH stretching frequency of this compound appears only at 2990 $cm^{-1}$ in infrared spectra and at 2989 $cm^{-1}$ in Raman spectra[6].

2) Krimm and Liang[1] assigned the $A_1$ and $B_1$ CH bending modes to the bands at 1330 $cm^{-1}$ and 1250 $cm^{-1}$, respectively, However, because of the weak interaction between the two CH bonds such great splitting can not be expected. This expectation is confirmed clearly by our calculation. The calculated Jacobian shows that both of these frequencies depend similarly on the force constants $H$(H-C-Cl), $H(\text{H-C-C})_{\text{CHCl}}$, $F(\text{H}\cdots\text{Cl})$, $F(\text{H}\cdots\text{C})_{\text{CHCl}}$, and $\kappa_{\text{CHCl}}$, and it is impossible to separate them. The corresponding frequencies are found in 1, 1, 2, 2-tetrachloroethane at 1304 $cm^{-1}$ ($A_u$)

TABLE VI. CALCULATED AND OBSERVED FREQUENCIES OF DEUTERATED POLYVINYL CHLORIDE (in $cm^{-1}$) AND ASSIGNMENTS

| Calcd. 1[a] | Calcd. 3[b] | Obs.[c] | Assignment |
|---|---|---|---|
| 2120<br>2111 | 2177<br>2169 | 2228 m $\sigma$ | CD str. ($A_1$, $B_1$) |
| 2164<br>2163 | 2151<br>2152 | 2159 vw $\sigma$ | $CD_2$ antisym. str. ($B_1$, $B_2$) |
| 2095 | 2090 | 2122 vw $\sigma$ | $CD_2$ sym. str. ($A_1$) |
| 1218 | 1225 | 1273 w $\sigma$ | CC str.+$CD_2$ bend. ($A_1$) |
| 1254 | 1261 | 1251 m $\pi$ | CC str.+$CD_2$ wag. ($B_2$) |
| 1170 | 1189 | 1112 s $\sigma$ | CC str.+$CD_2$ wag. ($B_1$) |
| | | 1091 sh ? | |
| 1024 | 1028 | 1041 sh $\sigma$ | CD bend.+CC str. ($B_1$) |
| 998 | 986 | 1017 vs $\sigma$ | $CD_2$ bend.+CD bend. ($A_1$) |
| | | 958 sh $\sigma$ | |
| 938 | 930 | 937 s $\pi$ ? | $CD_2$ wag.+CD bend. ($B_2$) |
| 909 | 905 | 904 sh $\pi$ ? | $CD_2$ rock.+$CD_2$ wag. ($B_1$) |
| 844 | 858 | 886 vw ? | CD bend.+$CD_2$ bend. ($A_1$) |
| | | 836 w $\pi$ ? | |
| 806 | 807 | 806 w $\pi$ | CD bend.+$CD_2$ wag.+$CD_2$ rock. ($B_2$) |
| 820<br>805 | 822<br>771 | 787 s $\sigma$ | CD bend.+$CD_2$ rock.+CCl str. ($B_1$)<br>$CD_2$ twist.+CCl str. ($A_1$) |
| 685 | 672 | 680 vw $\pi$ | $CD_2$ rock. ($B_2$) |
| | | 628 m $\sigma$ | |
| 591 | 574 | 594 m $\sigma$ | CCl str.+$CD_2$ twist. ($A_1$) |
| | | 573 w $\sigma$ | |
| 586 | 575 | 568 m $\sigma$ | CCl str.+$CD_2$ rock. ($B_1$) |
| 374 | 391 | | CCC def. ($B_1$) |
| 330 | 322 | | CCl bend. ($A_1$) |
| 279 | 272 | | CCl bend. ($B_2$) |
| 260 | 260 | | CCl bend. ($B_1$) |

a Calculated from the force constants, Set 1.
b Calculated from the force constants, Set 3.
c See Ref. 2.

and 1308 $cm^{-1}$ ($B_g$) for the trans from, and at 1280 $cm^{-1}$ (A) and 1243 $cm^{-1}$ (B) for the gauche form. Even in the gauche form the splitting does not exceed 40 $cm^{-1}$. So, at first it seemed reasonable to assign the 1250 $cm^{-1}$ band to both $A_1$ and $B_1$ CH bending modes and the 1330 $cm^{-1}$ band to the $CH_2$ wagging mode ($B_1$). On the other hand the change of the dichroism observed for PVC films of varying degrees of stretching (which will be reported later) shows that the 1330 and 1250 $cm^{-1}$ bands should belong to $A_1$ and $B_1$ species, respectively. This fact can be understood if we assume that strong coupling takes place between one of the CH bending modes and the $CH_2$ wagging or twisting mode, and the large splitting of frequencies occurs, though it is inconsistent with the results of our calculation. This deviation may be due to the incompleteness of the force constants given in Table IV. Ambiguity is still remaining as to this point; our final assignments are shown in Table V.

3) The bands at 1228, 963 and 833 $cm^{-1}$ are assigned to CH bending ($B_2$), $CH_2$ rocking ($B_1$), and $CH_2$ rocking ($B_2$) frequencies, respectively, according to the results of the calculation. The 1228 $cm^{-1}$ band was assigned by Krimm et al.[7] to the overtone of the 615 $cm^{-1}$ band. However, this band remains definitely in the spectrum of the highly syndyotactic polymer for which the 615 $cm^{-1}$ band is observed as a shoulder of the 603 $cm^{-1}$ band. Kawasaki et al.[8] suggested that the very weak band found at 1243 $cm^{-1}$ may be assignable to the overtone of the 615 $cm^{-1}$ band.

4) The bands at 2820, 1197, 693 and 615 $cm^{-1}$ are not assigned. The 693 $cm^{-1}$ band is associated with the atactic structure and the 615 $cm^{-1}$ band with the syndyotactic structure, which is not in the ordered configuration,

7) S. Krimm, A. R. Berens, V. L. Folt and J. J. Shipman, *Chem. & Ind.*, **1958**, 1512.
8) A. Kawasaki et al., *Abstr. of Symposium on the Infrared and Raman Spectroscopy (Tokyo)*, p. 41 (1959).

because they can not be observed for the sample prepared by radiation-induced polymerization of a urea-vinyl chloride complex[7,9-11]. The band at 1197 $cm^{-1}$ seems to behave analogously, but in a less distinct manner.

5) The band at 926 $cm^{-1}$ is only tentatively assigned to the $CH_2$ twisting frequency. It is known that for some vibrational modes, such as $CH_3$ rocking vibrations in ethane and $CH_2$ twisting vibrations in 1,2-dichloroethane, the calculated frequencies deviate considerably from the observed[4,12-14]. Therefore, it may be undesirable to assign the 926 $cm^{-1}$ band to the $CH_2$ twisting mode simply because it corresponds to the calculated value of 977 $cm^{-1}$. More detailed investigation of the intramolecular potential field seems to be necessary to settle this problem.

**Deuterated Polyvinyl Chloride.**—1) The infrared spectrum of deuterated PVC was reported by Enomoto et al.[2] Compared with the spectrum of normal PVC, it is quite complicated and hard to analyze, as many bands are found in the 800 $cm^{-1}$ to 1300 $cm^{-1}$ region. From the results of the present calculation and the observed dichroism tentative assignments are proposed for the main bands. The calculated potential energy distribution and L-matrix indicate that a strong coupling of two or more modes occurs for most bands of deuterated PVC. For example, for the calculated 858 $cm^{-1}$ ($A_1$) vibration, in-phase coupling of the $CD_2$ and CD bending modes occurs while in the case of the calculated 986 $cm^{-1}$ ($A_1$) vibration, out-of-phase coupling occurs. This is shown in Fig. 2. The in-phase mode is expected to be weak in intensity, and it probably corresponds to the very weak band at 886 $cm^{-1}$. The intensity of the out-of-phase mode is strong and it undoubtedly corresponds to the very strong band at 1017 $cm^{-1}$. A similar situation is found for the calculated 807 $cm^{-1}$ ($B_2$) and 930 $cm^{-1}$ ($B_2$) vibrations (see Fig. 3). The 930 $cm^{-1}$ mode is expected to be strong and corresponds to the strong parallel band at 937 $cm^{-1}$, and the 807 $cm^{-1}$ mode is weak and corresponds to the weak band at 806 $cm^{-1}$.

2) The bands at 594 $cm^{-1}$ and 568 $cm^{-1}$ are assigned to the CCl stretching frequencies ($A_1$ and $B_1$). These bands correspond to those at

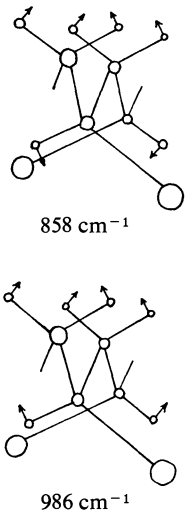
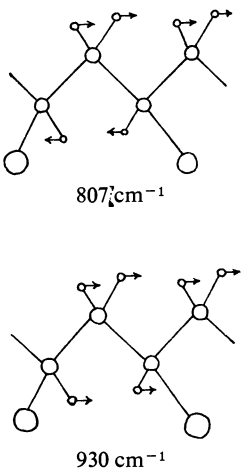



Fig. 2. Vibrational modes of 858 $cm^{-1}$ and 986 $cm^{-1}$.




Eig. 3. Vibrational modes of 807 $cm^{-1}$ and 930 $cm^{-1}$.

635 $cm^{-1}$ and 603 $cm^{-1}$, respectively, of normal PVC. Asahina and Enomoto[15] showed that the 628 $cm^{-1}$ band disappears in the sample obtained by irradiation-induced polymerization of a urea-vinyl chloride-$d_3$ complex. Therefore, this band is the contribution of the atactic structure and corresponds to the 690 $cm^{-1}$ band of normal PVC. The deuterated PVC prepared by Enomoto et al. was kindly made available to us. We measured the spectrum of this sample using a grating spectrometer (Perkin-Elmer Model 112G) and found a new band at about 573 $cm^{-1}$, which probably corresponds to the 615 $cm^{-1}$ band of normal PVC. All four bands of deuterated PVC are perpendicular.

As stated above the observed infrared absorption bands, including their dichroism, can

9) T. Shimanouchi, S. Tsuchiya and S. Mizushima, *J. Chem. Phys.*, **30** 1365 (1959).
10) T. Shimanouchi, S. Tsuchiya and S. Mizushima, *The High Polymer* (*Kobunshi*), **8**, 202 (1959).
11) S. Krimm, A. R. Berens, V. L. Folt, and J. J. Shipman, *Chem. & Ind.*, **1959**, 433.
12) I. Nakagawa and S. Mizushima, *J. Chem. Phys.*, **21**, 2195 (1953).
13) I. Nakagawa, *J. Chem. Soc. Japan, Pure Chem. Sec.* (*Nippon Kagaku Zasshi*), **74**, 848 (1953).
14) I. Nakagawa, ibid., **77**, 1030 (1956).
15) M. Asahina and S. Enomoto, ibid., **81**, 1374 (1960).

be satisfactorily accounted for on the basis of the calculation of normal vibrations. This gives a further confirmation of the syndyotactic configuration for the crystalline part of polyvinyl chloride. The remaining important problem is to study the potential field more thoroughly, and for this purpose the comparative investigation of other polymers and related compounds will be indispensable.

We wish to thank Professor H. Takahashi for making available the PC-1 computer. Thanks are also due to Dr. K. Nambu and Mr. S. Enomoto, who kindly gave us various samples of polyvinyl chloride.

*Department of Chemistry*
*Faculty of Science*
*The University of Tokyo*
*Hongo, Tokyo*

# *Molecular Structure of Epibromohydrin and Glycidol by Electron Diffraction*

By Masato IGARASHI

(Received September 26, 1960)

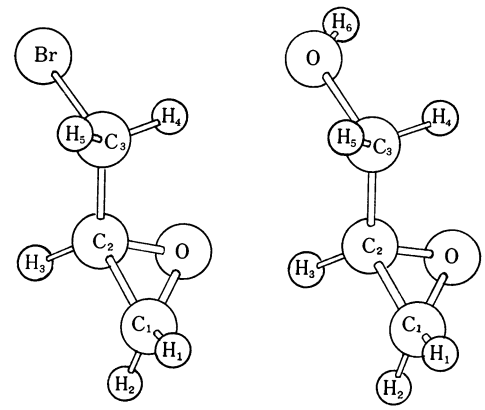
The molecular structure of ethylene oxide[1], propylene oxide and epichlorohydrin[2] has been studied previously by the electron diffraction method. As for the size of the CCO ring, the electron diffraction results have agreed almost perfectly with that of microwave spectrum study of ethylene oxide[3]. The C–C distance was 1.46±0.03 Å and the C–O distance were about 1.44 Å, whereas the values by microwave spectroscopy were 1.472 Å and 1.436 Å, respectively.

In propylene oxide and epichlorohydrin, the C–C (methyl) distance was about 1.52 Å and the angle between C–C (methyl) and CCO ring plane was about 58°. The chlorine atom in epichlorohydrin was the farthest apart from the CCO ring.

In the present paper the structures of epibromohydrin and glycidol are reported especially in regard to the configuration of the bromine atom and of the oxygen atom of alcohol in each molecule.

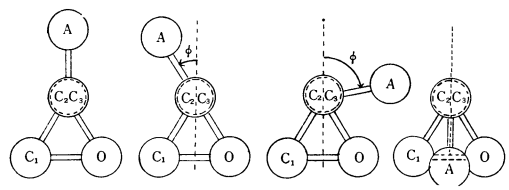
## Experimental

Epibromohydrin was prepared according to the procedure described in "Organic synthesis"[4]. The boiling point was 61°C at 50 mmHg. Glycidol was prepared from glycerol monochlorohydrin by the procedure of Nef[5]. The boiling point was 52°C at 10 mmHg. The apparatus of electron diffraction and the procedures of experiment were the same as those of the previous reports[1,2]. Visual intensity curves are shown in Figs. 3 and 5.




Epibromohydrin Glycidol

Fig. 1. Perspective pictures of epibromohydrin and glycidol.




$\phi=0$ $\phi=33°$ $\phi=-80°$ $\phi=180°$

Fig. 2. Various configurations of epibromohydrin and glycidol showing internal rotations, which were projected along $C_2$–$C_3$ axis (cf. Fig. 1). A stands for bromine or oxygen atom. Hydrogen atoms are omitted for convenience.

## Analysis

Radial distribution and theoretical intensity curves were calculated using the same formulas

1) M. Igarashi, This Bulletin, **26**, 330 (1953).
2) M. Igarashi, ibid., **28**, 58 (1955).
3) G. L. Cunningham, A. W. Boyd, R. J. Myer, W. D. Gwinn and W. I. Le Van, *J. Chem. Phys.*, **19**, 676 (1951).
4) Organic Synthesis, **14**, 42; **16**, 31.
5) J. U. Nef, *Ann.*, **335**, 231 (1904).

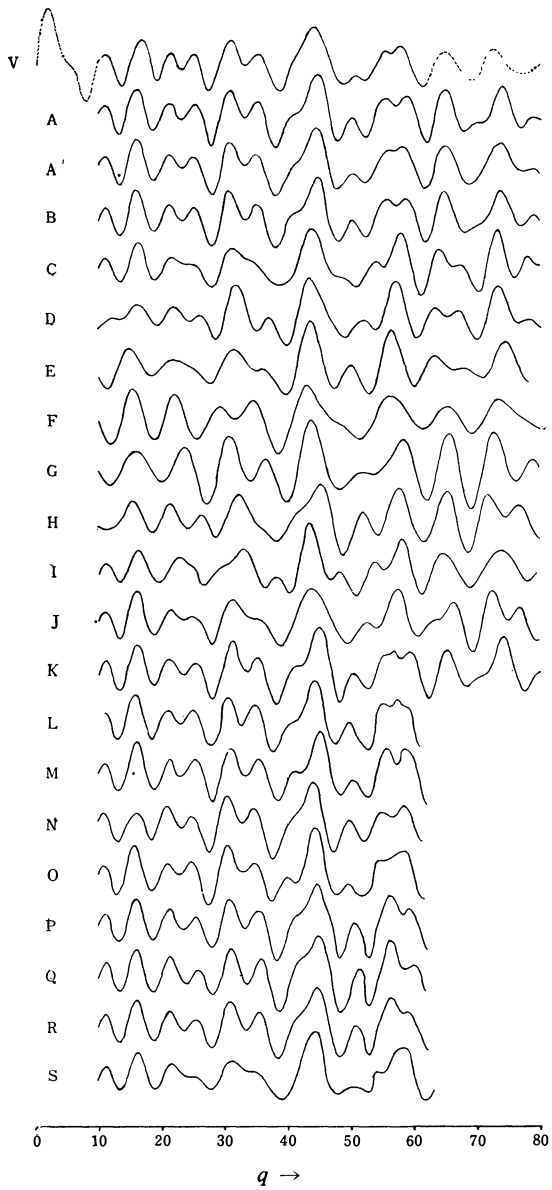



Fig. 3. Visual intensity curve (V) and theoretical intensity curves for the models from A to S (Table I) of epibromohydrin. Curve A' is drawn using thermal factor $b_{ij}=-0.0002$ instead of zero in curve A for the atomic pairs $C_1\cdots Br$ and $O\cdots Br$.

as before[2]. Making reference to the previous reports[1-3], some parameters of the molecular models for the theoretical intensity curves were assumed as follows: the CCO ring size and C-H distances adjacent, attached to the ring, are equal to those of ethylene oxide, the other C-H distances 1.09 Å, the angles $C_2C_3Br$ and $C_2C_3O$ are both 109.5°, and the angle between $C_1C_2$ and $C_3C_2H_3$ plane is 21° (Fig. 1). Other parameters such as $C_2$-$C_3$ distance and its inclination from the ring plane, $C_3$-Br and $C_3$-O distances, and the angles of internal rotation (Fig. 2) were examined.

**Epibromohydrin.**—The visual intensity curve in the region of $q=60\sim80$ was uncertain, therefore in the correlation method the maxima and minima in the region of $q=10\sim60$ were compared with the theoretical intensity curves, and radical distribution curves were calculated, using several different intensity values in the former region. On account of the damping factor $\exp(-aq^2)$ the positions of the peaks in radial distribution curves were not so much affected by the intensity in such a region. The radial distribution curve is nearly consistent with models A and K (Table I).

Molecular models for the theoretical intensity curves were constructed in the following ranges: $C_2$-$C_3$: 1.50~1.58 Å, $C_3$-Br: 1.88~1.96 Å, angle between $C_2$-$C_3$ and CCO ring: 45~70°, rotational angle $\phi$ around $C_2$-$C_3$ axis: 0~360° (Table I).

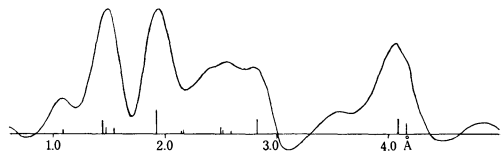



Fig. 4. Radial distribution curve of epibromohydrin. Vertical lines show the interatomic distances of model A.

The theoretical intensity curves of the models in which the rotational angles drawn in Fig. 2 are smaller than ±15° have features which resemble the observed. But as those having the other rotational angles are very far from the observed, these models can be rejected. $C_2$-$C_3$ and $C_3$-Br bond distances and the inclination of $C_2$-$C_3$ were examined mainly by the $q_{calcd}/q_{obs}$ values (Table I).

The results are as follows: $C_2$-$C_3=1.53\pm0.03$ Å, $C_3$-$Br=1.91\pm0.02$ Å, angle between $C_2$-$C_3$ and CCO ring is 58±8°, rotational angle $\phi$ is 0±15°, i. e. the bromine atom is almost trans against the midpoint of $C_1$-O.

**Glycidol.** — Theoretical intensity curves of the models in which the rotational angles are about 0° and 80° have features which resemble the observed, although the maximum of the model of 80° at about $q=33$ is not predominant compared with that of 0° (Fig. 5). The models of the other $\phi$ values such as G, H, L and M may be excluded because the apperances of the intensity curves at about $q=30$ and 50 are very different in comparison with the observed.

The radial distribution curve $RD_1$ calculated using the visual intensity curve which is shown by the solid line in Fig. 5 and spliced by the

TABLE I. MODELS FOR EPIBROMOHYDRIN AND $q_{calcd}/q_{obs}$ VALUES

| Model | $C_2$–$C_3$ Å | $C_3$–Br Å | Inclination of $C_2$–$C_3$ | Rotational angle, $\phi$ | Mean value of $q_{calcd}/q_{obs}$ | Average deviation |
|---|---|---|---|---|---|---|
| A | 1.54 | 1.92 | 58° | 0° | 0.993 | 0.015 |
| B | 1.54 | 1.92 | 58° | 15° | 0.996 | 0.017 |
| C | 1.54 | 1·92 | 58° | 33° | — | — |
| D | 1.54 | 1.92 | 58° | 90° | — | — |
| E | 1.54 | 1.92 | 58° | 147° | — | — |
| F | 1.54 | 1.92 | 58° | 180° | — | — |
| G | 1.54 | 1.92 | 58° | −147° | — | — |
| H | 1.54 | 1.92 | 58° | −90° | — | — |
| I | 1.54 | 1.92 | 58° | −33° | — | — |
| J | 1.54 | 1.92 | 58° | −15° | 0.998 | 0.015 |
| K | 1.50 | 1.92 | 58° | 0° | 1.003 | 0.015 |
| L | 1.58 | 1.92 | 58° | 0° | 0.991 | 0.015 |
| M | 1.54 | 1.88 | 58° | 0° | 1.005 | 0.019 |
| N | 1.54 | 1.96 | 58° | 0° | 0.986 | 0.015 |
| O | 1.54 | 1.92 | 45° | 0° | 0.987 | 0.015 |
| P | 1.54 | 1.92 | 65° | 0° | 0.998 | 0.019 |
| Q | 1.54 | 1.92 | 70° | 0° | 1.011 | 0.016 |
| R | 1.54 | 1.92 | 65° | 15° | — | — |
| S | 1.54 | 1.92 | 65° | 33° | — | — |

TABLE II. MODELS FOR GLYCIDOL AND $q_{calcd}/q_{obs}$ VALUES

| Model | $C_2$–$C_3$ Å | $C_3$–O Å | Inclination of $C_2$–$C_3$ | Rotational angle, $\phi$ | Mean value of $q_{calcd}/q_{obs}$ | Average deviation |
|---|---|---|---|---|---|---|
| A | 1.54 | 1.43 | 58° | 0° | 0.998 | 0.016 |
| B | 1.50 | 1.40 | 58° | 0° | 1.005 | 0.020 |
| C | 1.54 | 1.46 | 58° | 0° | 0.992 | 0.022 |
| D | 1.58 | 1.43 | 58° | 0° | — | — |
| E | 1.50 | 1.43 | 58° | 0° | 1.005 | 0.013 |
| F | 1.50 | 1.43 | 58° | −15° | 1.006 | 0.008 |
| G | 1.50 | 1.43 | 58° | −33° | — | — |
| H | 1.50 | 1.43 | 58° | −60° | — | — |
| I | 1.50 | 1.43 | 58° | −75° | — | — |
| J | 1.50 | 1.43 | 58° | −80° | 1.003 | 0.008 |
| K | 1.50 | 1.43 | 58° | −90° | 1.010 | 0.005 |
| L | 1.50 | 1.43 | 58° | −120° | — | — |
| M | 1.50 | 1.43 | 58° | 180° | — | — |
| N | 1.50 | 1.43 | 58° | 33° | 1.007 | 0.011 |
| O | 1.54 | 1.43 | 58° | −85° | 0.998 | 0.007 |
| P | 1.50 | 1.40 | 58° | −85° | 1.010 | 0.008 |
| Q | 1.54 | 1.46 | 58° | −85° | 0.995 | 0.008 |
| R | 1.50 | 1.43 | 50° | 0° | — | — |
| S | 1.50 | 1.43 | 50° | 85° | — | — |
| T | 1.50 | 1.43 | 65° | 0° | — | — |
| U | 1.50 | 1.43 | 65° | 85° | — | — |

theoretical intensity of model E at small $q$ values has a slight peak at about 3.0 Å, which might be regarded as a ghost and a somewhat larger peak at about 3.6 Å, which should correspond to the configuration $\phi=0°$.

But another radial distribution curve $RD_2$ calculated using the dashed intensity curve in the region of about $q=35$ instead of solid intensity curve and the theoretical intensity curve of model J at small $q$ values in Fig. 5, shows a more predominant peak at about 3.0 Å which corresponds to the existence of the configuration of about $\phi=80°$ (Fig. 6).

Whether the configuration of the oxygen atom of alcohol is at about $\phi=0°$, or about $\phi=80°$, or at the both positions, could not be determined by the present visual method.

The parameters other than the internal rotation were examined in the following ranges: $C_2$–$C_3$: 1.50∼1.58 Å, $C_3$–O: 1.40∼1.46 Å, angle

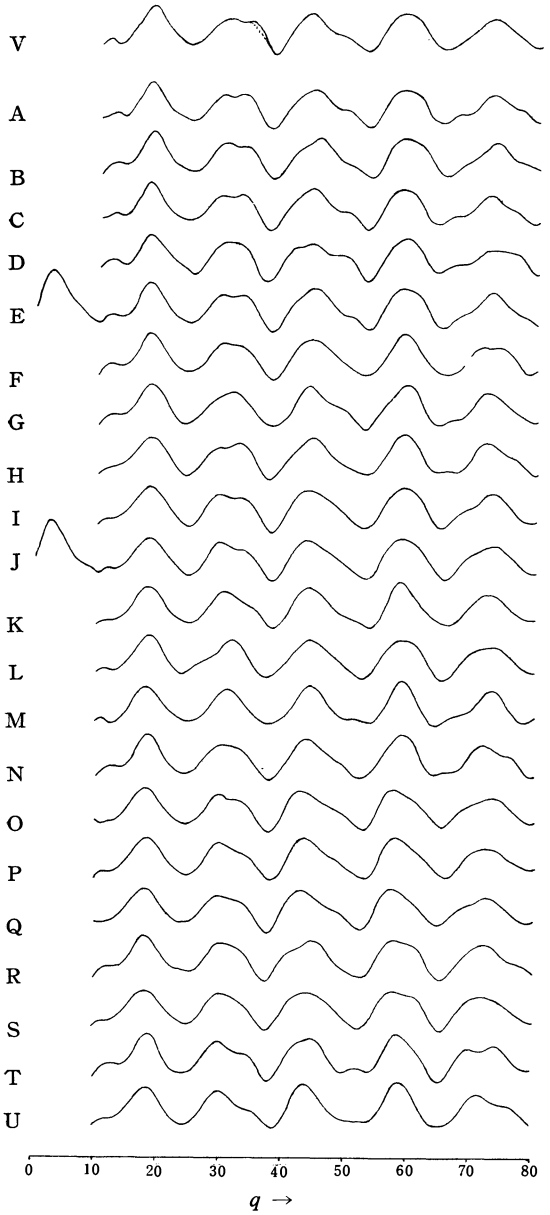



Fig. 5. Visual intensity curve (V) and theoretical intensity curves for the models from A to U (Table II) of glycidol.

between $C_2$–$C_3$ and CCO ring: 50~65° (Table II).

As the features of the theoretical intensity curves of the models in which $C_2$–$C_3$ inclinations against CCO ring plane are 50° and 65° are considerably different from the visual, both models can be excluded as inadequate. $C_2$–$C_3$ and $C_3$–O bond distances were examined mainly by the $q_{calcd}/q_{obs}$ values (Table II). The results are as follows: $C_2$–$C_3$ = 1.53±0.03 Å, $C_3$–O = 1.43±0.03 Å, angle between $C_2$–$C_3$ and CCO ring is 58±5°.

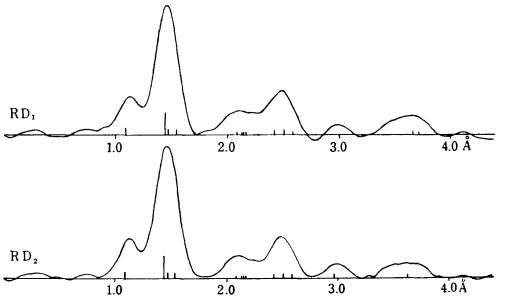



Fig. 6. Radial distribution curves of glycidol. Vertical lines show the interatomic distance of models A ($RD_1$) and O ($RD_2$).

## Discussion

As mentioned in the previous report[2] about epichlorohydrin and the present report about epibromohydrin, chlorine and bromine atoms in these compounds are almost at the trans position against the midpoint of $C_1$–O, i. e. these atoms are fathest apart from the CCO ring.

Therefore it can be thought that there is a strong steric repulsion between chlorine atom or bromine atom and ethylene oxide ring.

If the same steric repulsion is present between oxygen atom of alcohol and ethylene oxide ring and moreover no intramolecular hydrogen bond between two oxygen atoms, the oxygen atom of alcohol will be at trans too. Contrarily, if there is a stronger intramolecular hydrogen bond than the steric repulsion, the oxygen atom of alcohol will be nearer to the oxygen atom in the ring than the trans position and $\phi$ will be equal to about 80°.

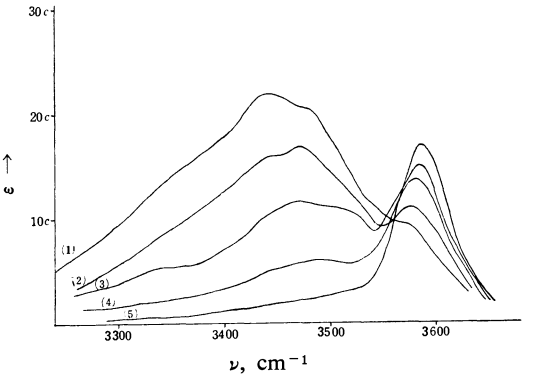



Fig. 7. Infrared absorption spectra of glycidol in carbon tetrachloride solutions. $\varepsilon$ is molecular extinction coefficient, $c$ is the concentration of satulated solution at room temperature and $\nu$ is wave number. Curves from (1) to (5) are absorption spectra of solutions of the following concentratrations; (1): $c$, (2): $1/2\,c$, (3): $1/5\,c$, (4): $1/18\,c$, (5): $1/54\,c$.

Unfortunately as the theoretical intensity curves of both the models rather resemble each other in the features which are characteristic of internal rotations, the above two cases could not be determined unambiguously.

However infrared absorption spectrums of glycidol in dilute carbon tetrachloride solutions using lithium fluoride prism did not show a deviation of O-H stretching vibration by which the intramolecular hydrogen bond can be recognized (Fig. 7). It may be supposed that in the vapor state at room temperature there exists no intramolecular hydrogen bond either, so the oxygen atom of alcohol will be almost at trans against the midpoint of $C_1$-O.

The author wishes to express his sincere gratitude to Professor A. Kotera for his guidance throughout this research and to Dr. K. Nukada and Miss. U. Maeda, Government Chemical Industrial Research Institute of Tokyo, for the infrared investigation of glycidol solution. He is also indebted to Mr. T. Wada for his help during the experiment.

*Department of Chemistry*
*Faculty of Science*
*Tokyo University of Education*
*Koishikawa, Tokyo*

# *An Electron Diffraction Investigation of the Molecular Structure of Ethylenimine*

By Masato IGARASHI

(Received September 26, 1960)

In the three membered ring compounds such as cyclopropane, ethylene oxide, ethylene sulfide and ethylenimine, the isoelectronic groups $H_2C<$, $O<$, $S<$ and $HN<$ bear a resemblance to each other, so that the structural features for these molecules are identical except for these groups.

Since two sp hybrid atomic orbitals may not be at an angle less than 90° to each other, the bonding orbitals which constitute rings CCC, CCO, CCS and CCN can not point directly at each other, but they are bent, forming the "banana bond"[1].

Electron diffraction and microwave spectrum investigations have reported the molecular structures of these ring compounds in which the nuclear distances of C–C were in most cases shorter than the normal C–C single bond distance, 1.54 Å.

By the electron diffraction method, the C–C distances were 1.53±0.03 Å[2], 1.54 Å[3] and 1.515 ±0.02 Å[4] in cyclopropane, and 1.46±0.03 Å[5] in ethylene oxide. Further, by the microwave spectroscopy the C–C distance was 1.472 Å[6] in ethylene oxide, 1.492 Å[6] in ethylene sulfide and 1.480 Å[7] in ethylenimine respectively. The HCH angles have been found to be about 116°[4] and 117°[6,7], which are larger than the tetrahedral angle, 109.5°.

In this report the results of the electron diffraction study of ethylenimine by the sector-microphotometer method are described and compared with those of the microwave spectrum study[7] (Table I).

TABLE I. MOLECULAR STRUCTURE OF ETHYLENIMINE BY MICROWAVE SPECTROSCOPY[7]

| | | |
|---|---|---|
| C–C | 1.480 Å | $\angle C_2NH$ 112° |
| C–N | 1.488 Å | $\angle CCH_2$ 159°25′ |
| C–H | 1.083 Å | $\angle HCH$ 116°41′ |
| H–H | 1.000 Å (assumed) | |

## Experimental

Ethylenimine was kindly furnished by Professor Y. Iwakura, Tokyo Institute of Technology; its boiling point was 55°C.

The electron diffraction instrument in the Department of Chemistry, Faculty of Science, the University of Tokyo[8] was used for the diffraction experiment. It incorporates with $r^2$-sector which

1) C. A. Coulson and W. E. Moffit, *Phil. Mag.*, **40**, 1 (1949).
2) L. Pauling and L. O. Brockway, *J. Am. Chem. Soc.*, **59**, 1223 (1937).
3) O. Bastiansen and O. Hassel, *Tids. Kjemi Bergvesen Met.*, **6**, 71 (1946).
4) H, Pfeiffer, Ph. D. thesis, California Institute of Technology, 1948.
5) M. Igarashi, This Bulletin, **26**, 330 (1953).
6) G. L. Cunningahm, A. W. Boyd, R. J. Mayer, W. D. Gwinn and W. I. LeVan, *J. Chem. Phys.*, **19**, 679 (1951).
7) T. E. Turner, V. C. Fiora, W. M. Kendrick and B. L. Hicks, ibid., **21**, 564 (1953); T. E. Turner, V. C. Fiora and W. M. Kendrick, ibid., **23**, 1966 (1955).
8) K. Kuchitsu, This Bulletin, **30**, 391 (1956).

is rotated rapidly during exposure. Diffraction photographs were obtained on Fuji Process Hard plates. During the diffraction experiment the liquid sample reservoir has been cooled by a freezing mixture of ice and sodium chloride to reduce the amount of the sample vapor. The camera length was 11.82 cm. and the wave length of electron was 0.0578 Å, which was determined by measuring the transmission patterns of a gold foil.

Two pairs of photographs of the exposures of 25 and 50 sec., and of 30 and 60 sec. were used for intensity measurement. The optical densities of these plates were measured by the microphotometer. The photographic plates were rotated rapidly around the center of the diffraction pattern while being scanned by the microphotometer.

## Analysis

Optical densities of each pair of the diffraction photographs were converted to relative intensity by Karle's procedure[9]. A smooth background line was drawn through the intensity curve multiplied by $q$ and molecular intensity curve $M(q)$ was obtained by the following formula

$$M(q)=(I_T-I_B)/I_B, \qquad (1)$$

where $I_T$ is the total intensity and $I_B$ is the background intensity.

**Radial Distribution Curve.** — The radial distribution carve was calculated from the molecular intensity curve $M(q)$ according to the following equation:

$$f(r)=\sum_{q=1}^{90} qM(q)\exp(-aq^2)\sin(\pi qr/10) \qquad (2)$$

where the value of $a$ is chosen as 0.000284 to make the integrand of Eq. 2 converge rapidly and $q=(40/\lambda)\sin(\theta/2)$, where $\theta$ is the angle of scattering and $\lambda$ is the wavelength of the electron beam. The intensity curve from $q=0$ to $q=18$ was spliced by the theoretical intensity curve calculated for an assumed model.

A few steps of successive approximation were made to get a reasonable background line which would satisfy Karle's criterion of non-negativeness in the radial distribution curve as closely as possible. The final molecular intensity curve is shown in Fig. 1 and the radial distribution curve in Fig. 2.

The radial distribution curve consists of three peaks at about 1.09 Å, 1.49 Å and 2.19 Å. The first peak is due to bonded C-H and N-H distances, the second to bonded C-C and C-N distances and the third to non-bonded N···cH, C···cH and C···nH distances. It is difficult to separate the first and the second peaks into two components and the third into three components respectively, because these component peaks overlap each other heavily. The first peak can be resolved into its components by three distinct sets of parameters (Fig. 3 and Table II). Sets A and C are the extreme cases for the differences between C-H and N-H

9) J. Karle and I. L. Karle, *J. Chem. Phys.*, **18**, 957, 963 (1950).

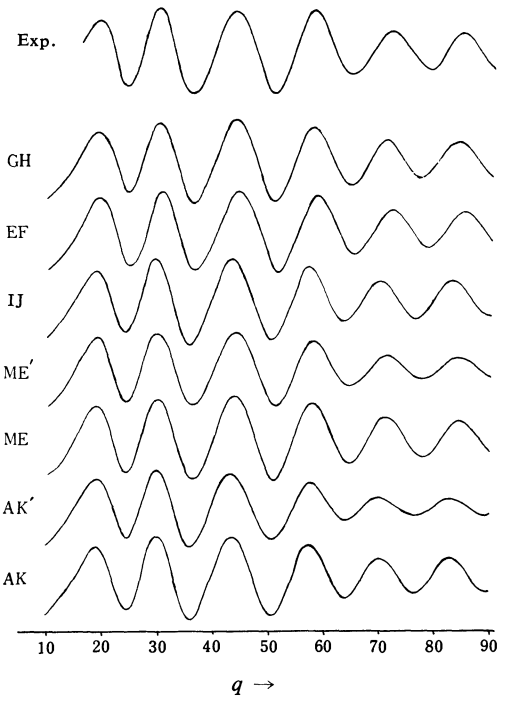



Fig. 1. Experimental and theoretical intensity curves.

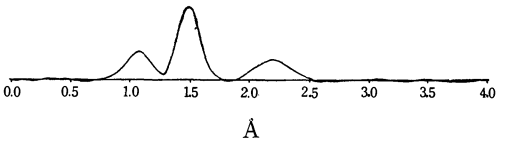



Fig. 2. The radial distribution curve.

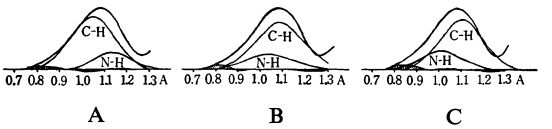



Fig. 3. Analysis of the first peak of the radial distribution curve.

TABLE II. ANALYSIS OF THE FIRST PEAK OF RADIAL DISTRIBUTION CURVE

| Set | Atomic pair | Equilibrium distance, Å | Mean amplitude, Å |
|---|---|---|---|
| A | C-H | 1.05 | 0.065 |
| | N-H | 1.14 | 0.03 |
| B | C-H | 1.09 | 0.075 |
| | N-H | 1.04 | 0.07 |
| C | C-H | 1.11 | 0.06 |
| | N-H | 1.01 | 0.04 |

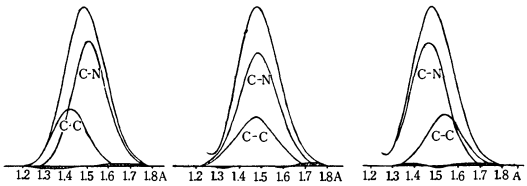



Fig. 4. Analysis of the second peak of the radial distribution curve.

TABLE III. ANALYSIS OF THE SECOND PEAK OF RADIAL DISTRIBUTION CURVE

| Set | Atomic pair | Equilibrium distance, Å | Mean amplitude, Å |
|---|---|---|---|
| D | C-N | 1.51 | 0.02 |
| | C-C | 1.42 | 0.02 |
| E | C-N | 1.49 | 0.05 |
| | C-C | 1.48 | 0.05 |
| F | C-N | 1.47 | 0.03 |
| | C-C | 1.54 | 0·03 |

equilibrium distances. So the reasonable ranges of equilibrium distances are C-H=1.05～1.11 Å and N-H=1.01～1.14 Å.

The second peak can also be resolved into two component peaks by three distinct sets of parameters (Fig. 4 and Table III).

Sets D and F are the extreme cases for the differences between C-N and C-C equilibrium distances. There is an intimate relation between the difference of atomic distances and their mean amplitudes, that is when the difference becomes larger, the assumed mean amplitudes must be smaller in order to explain the peak of radial distribution curve well. This relation shall be discussed once more later at the correlation method. Here the reasonable equilibrium distances are thought to be C-N=1.47～1.51 Å and C-C=1.42～1.54 Å.

The third peak is the lowest among the three and consists of three component peaks of non-bonded C···cH, N···cH and C···NH. Therefore there may be many reasonable sets of resolution into its components. Some probable examples are listed in Fig. 5 and Table IV. In set G the atomic distances are equivalent to $\angle CCH_2=160°$, $\angle HCH=117°$ and $\angle C_2NH=122°$, assuming C-C=1.48 Å, C-N=1.49 Å, C-H=1.08 Å and N-H=1.04 Å. In set H they are equivalent to $\angle CCH_2=130°$, $\angle HCH=117°$ and $\angle C_2NH=126°$ and in set I to $\angle CCH_2=170°$,




Fig. 5. Analysis of the third peak of the radial distribution curve.

TABLE IV. ANALYSIS OF THE THIRD PEAK OF RADIAL DISTRIBUTION CURVE

| Set | Atomic pair | Equilibrium distance, Å | Mean amplitude, Å |
|---|---|---|---|
| G | C···cH | 2.22 | 0.12 |
| | C···NH | 2.16 | 0.12 |
| | N···cH | 2.17 | 0.12 |
| H | C···cH | 2.11 | 0.11 |
| | C···NH | 2.21 | 0.11 |
| | N···cH | 2.25 | 0.11 |
| I | C···cH | 2.24 | 0.11 |
| | C···NH | 2.20 | 0.11 |
| | N···cH | 2.16 | 0.11 |

$\angle HCH=117°$ and $\angle C_2NH=125°$. Other sets of resolution show different atomic distances, so different bond angles. But by several attempts of resolution, the values $\angle HCH\approx117°$ and $\angle C_2NH=120\sim130°$ seem to be probable. When N···cH distances become longer, C···cH distances become shorter and vice versa, assuming the bonded distances are constant, and at that time a reasonable resolution of the peak is obtained, so $\angle CCH_2$ can not be determined more accurately than the range 130～170°.

**Correlation Method.**—The theoretical intensity curves were calculated using the following equation:

$$qM(q)=\sum_{i,j}Z_iZ_j/r_{ij}\exp(-b_{ij}q^2)\sin(\pi qr_{ij}/10) \qquad (3)$$

where $r_{ij}$ is the equilibrium distance between atoms $i$ and $j$ and $Z_i$ is the atomic number of atom $i$, apart from the value 1.25 for the hydrogen atom. The constant $b_{ij}$ is equal to $(\langle\Delta r_{ij}^2\rangle/2)(\pi/10)^2$, where $\langle\Delta r_{ij}^2\rangle$ is the mean square amplitude of the atomic pair $i$ and $j$.

Making reference to the results of radial distribution curve, various molecular models were selected for the theoretical intensity curves. At first in order to determine the acceptable C-C and C-N nuclear distances, theoretical intensity curves were drawn for the models in which both distances were varied in and out of the range found by the analysis of the second peak of radial distribution curve, assuming C-H=1.08 Å, N-H=1.04 Å, $\angle CCH_2=160°$ and $\angle C_2NH=120°$. In Table V the constants of the models which were examined and mean values and average deviations of $q_{calcd}/q_{obs}$ were listed. In Fig. 1 some of the intensity curves were drawn. The features of the theoretical intensity curves of these models resembled each other, so the $q_{calcd}/q_{obs}$ ratios were used to select reasonable models.

If the mean amplitudes of both C-C and C-N are assumed to be 0.05 Å, which is nearly equal to those of the normal single bonds in most cases, the most reasonable model is such

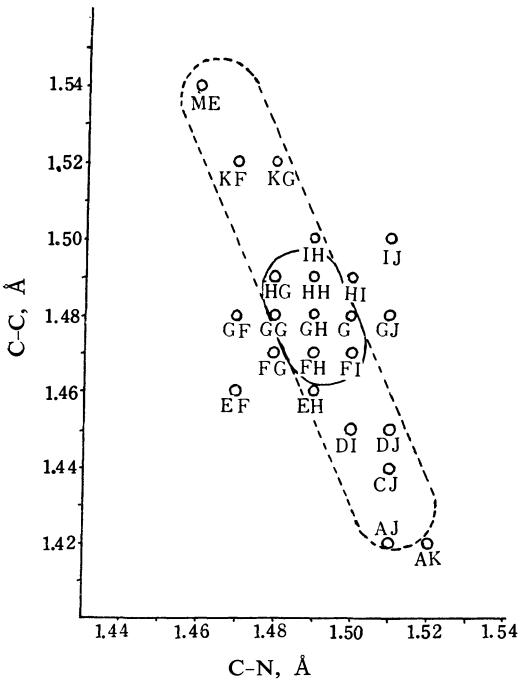



Fig. 6. The parameter chart. The area surrounded by a solid line is an acceptable region when the mean amplitudes are assumed to be 0.05Å, and the area surrounded by a broken line includes an acceptable region when the smaller mean amplitudes than 0.05Å are assumed.

that the C-C equilibrium distance is 1.48 Å and the C-N equilibrium distances are 1.49 Å. When C-N distances become longer than 1.49 Å, the acceptable model is such that the C-C distance becomes shorter than 1.48 Å and at that time the mean amplitudes of the atomic pairs should be smaller than 0.05 Å. If we fix the mean amplitudes as 0.05 Å, then in the case when the difference between C-N and C-C distances becomes larger, the amplitudes of the theoretical intensity curve become smaller at large $q$ values compared to the experimental intensity curve, as the curve ME′ and AK′ in Fig. 1. So there is an intimate relation between the difference of the two distances and their mean amplitudes. From Fig. 6 and Table V reasonable C-C and C-N distances and acceptable regions of uncertainty are concluded as follows;

$$\text{C-C} = (1.48 \pm 2d) \pm 0.02 \text{ Å}$$

$$\text{C-N} = (1.49 \mp d) \pm 0.01 \text{ Å}$$

The parameter $d$ is dependent upon the assumed mean amplitudes, M. A., of the atomic pairs. There is the following rough relation between them;

$$d = 0.05 - \text{M.A.}$$

TABLE V. LIST OF MEAN VALUES OF $q_{calcd}/q_{obs}$ AND THEIR AVERAGE DEVIATIONS WHEN C-C AND C-N DISTANCES WERE VARIED, ASSUMING THE OTHER PARAMETERS TO BE CONSTANT

| Model | C-C Å | C-N Å | Mean amplitude | Mean value of $q_{calcd}/q_{obs}$ | Average deviation of $q_{calcd}/q_{obs}$ |
|---|---|---|---|---|---|
| GH | 1.48 | 1.49 | 0.05 | 1.000 | 0.004 |
| GG | 1.48 | 1.48 | 0.05 | 1.004 | 0.006 |
| GI | 1.48 | 1.50 | 0.05 | 0.995 | 0.005 |
| GF | 1.48 | 1.47 | 0.05 | 1.008 | 0.004 |
| GJ | 1.48 | 1.51 | 0.05 | 0.990 | 0.006 |
| FH | 1.47 | 1.49 | 0.05 | 1.001 | 0.006 |
| HH | 1.49 | 1.49 | 0.05 | 0.997 | 0.007 |
| EH | 1.46 | 1.49 | 0.05 | 1.003 | 0.006 |
| IH | 1.50 | 1.49 | 0.05 | 0.993 | 0.006 |
| FG | 1.47 | 1.48 | 0.05 | 1.006 | 0.005 |
| FI | 1.47 | 1.50 | 0.05 | 0.997 | 0.006 |
| HG | 1.49 | 1.48 | 0.05 | 1.001 | 0.006 |
| HI | 1.49 | 1.50 | 0.05 | 0.993 | 0.007 |
| EF | 1.46 | 1.47 | 0.05 | 1.013 | 0.005 |
| IF | 1.50 | 1.47 | 0.05 | 1.004 | 0.005 |
| IJ | 1.50 | 1.51 | 0.05 | 0.986 | 0.006 |
| EJ | 1.46 | 1.51 | 0.04 | 0.994 | 0.007 |
| DI | 1.45 | 1.50 | 0.04 | 0.999 | 0.007 |
| KF | 1.52 | 1.47 | 0.04 | 1.001 | 0.004 |
| KG | 1.52 | 1.48 | 0.04 | 0.996 | 0.007 |
| DJ | 1.45 | 1.51 | 0.03 | 0.996 | 0.008 |
| CJ | 1.44 | 1.51 | 0.03 | 0.996 | 0.006 |
| KE | 1.52 | 1.46 | 0.03 | 1.006 | 0.004 |
| ME | 1.54 | 1.46 | 0.03 | 1.003 | 0.004 |
| ME′ | 1.54 | 1.46 | 0.05 | 1.003 | 0.004 |
| AJ | 1.42 | 1.51 | 0.02 | 0.998 | 0.008 |
| AK | 1.42 | 1.52 | 0.02 | 0.993 | 0.007 |
| AK′ | 1.42 | 1.52 | 0.05 | 0.993 | 0.009 |

Next C-H and N-H bond distances were investigated. There are similar relations among C-H and N-H bond distances and their mean amplitudes as in the case of C-C and C-N distances. But as the contributions of the former ones to the intensity curves are smaller than those of the latter ones, the above relation is somewhat obscure. The mean values of $q_{calcd}/q_{obs}$ and their average deviations for the models in which C-H and N-H distances have been varied, are represented in Table VI. Reasonable ranges of C-H and N-H distances are 1.05～1.11 Å and 1.00～1.11 Å, respectively.

Finally the angles HCH, $CCH_2$ and $C_2NH$ were investigated. When ∠HCH is varied from 109.5° to 130°, the $q_{calcd}/q_{obs}$ values change but slightly (Table VII). The model of 117° seems to be the best, but the above range of angles will be within the experimental error. When the angles $CCH_2$ increase, C···cH distances increase and N···cH distances decrease, consequently the $q_{calcd}/q_{obs}$ values remain

Table VI. List of mean values of $q_{calcd}/q_{obs}$ and their average deviations when C-H and N-H distances were varied, assuming the other parameters to be equal to model GH

| Model | C-H Å | C-N Å | Mean amplitude | Mean value of $q_{calcd}/q_{obs}$ | Average deviation of $q_{calcd}/q_{obs}$ |
|---|---|---|---|---|---|
| MO | 1.08 | 1.00 | 0.075 | 1.000 | 0.004 |
| GH | 1.08 | 1.04 | 0.075 | 1.000 | 0.004 |
| MN | 1.08 | 1.12 | 0.075 | 0.998 | 0.004 |
| LP | 1.05 | 1.04 | 0.075 | 1.000 | 0.005 |
| LN | 1.05 | 1.12 | 0.06 | 0.999 | 0.006 |
| NP | 1.12 | 1.04 | 0.06 | 0.997 | 0.004 |
| ON | 1.12 | 1.00 | 0.06 | 0.998 | 0.006 |

Table VII. List of mean values of $q_{calcd}/q_{obs}$ and their average deviations when the angles HCH were varied, assuming the other parameters to be equal to model GH

| Model | ∠HCH | Mean value of $q_{calcd}/q_{obs}$ | Average deviation of $q_{calcd}/q_{obs}$ |
|---|---|---|---|
| Q | 109.5° | 0.999 | 0.005 |
| GH | 117° | 1.000 | 0.004 |
| R | 130° | 1.000 | 0.006 |

Table VIII. List of mean values of $q_{calcd}/q_{obs}$ and their average deviations when the angles $CCH_2$ were varied, assuming the other parameters to be equal to model GH

| Model | $\angle CCH_2$ | Mean value of $q_{calcd}/q_{obs}$ | Average deviation of $q_{calcd}/q_{obs}$ |
|---|---|---|---|
| S | 130° | 0.999 | 0.005 |
| T | 140° | 0.999 | 0.005 |
| U | 150° | 0.999 | 0.005 |
| GH | 160° | 1.000 | 0.004 |
| V | 170° | 1.000 | 0.005 |

Table IX. List of mean values of $q_{calcd}/q_{obs}$ and their average deviations when the angle $C_2NH$ was varied, assuming the other parameters to be equal to model GH

| Model | $\angle C_2NH$ | Mean value of $q_{calcd}/q_{obs}$ | Average deviation of $q_{calcd}/q_{obs}$ |
|---|---|---|---|
| W | 90° | 0.999 | 0.006 |
| GH | 120° | 1.000 | 0.004 |
| Y | 180° | 0.998 | 0.005 |

almost unchanged (Table VIII). So the angles $CCH_2$ may be determined only in the range 130~170°, as having been mentioned in the radial distribution analysis. As the contribution of C···NH atomic pairs to the total molecular intensity curve is the smallest except that of H···H atomic pairs which is negligibly small in this case, and their distances are comparable to those of C···CH and N···CH, the angle $C_2NH$ can not be determined unambiguously. But from the $q_{calcd}/q_{obs}$ values (Table IX), the reasonable value seems to be about 120°.

## Summary and Discussion

By the radial distribution and correlation methods, the molecular structure of ethylenimine was obtained as follows;

$$C\text{-}C = (1.48 \pm 2d) \pm 0.02\ \text{Å}$$

$$C\text{-}N = (1.49 \mp d) \pm 0.01\ \text{Å}$$

where

$$d = 0.05 - \text{M.A.}$$

$$C\text{-}H = 1.08 \pm 0.03\ \text{Å},\quad N\text{-}H = 1.05 \pm 0.07\ \text{Å}$$

The angles $CCH_2$ could not be determined accurately. They seem to be in the range 130~170°. The angles HCH and $C_2NH$ also could not be determined unambiguously, but $\angle HCH \approx 117°$ and $\angle C_2NH \approx 120°$ seem to be probable.

The above values of C-C and C-N nuclear distances are consistent with the values obtained by microwave spectroscopy (Table I). They are especially consistent when their mean amplitudes are assumed to be 0.05 Å.

As for the N-H bond distance and the angle $C_2NH$, the present values coincide with those of microwave spectroscopy within the extents of uncertainty, but the most probable values of the former are somewhat larger than the latter.

The C-C distance 1.48 Å is considerably shorter than the single bond distance 1.54 Å of normal chain compounds as the other three-membered ring compounds.

The author wishes to express his gratitude to Professor A. Kotera for his guidance and encouragement throughout the course of this research, to Professor Y. Morino, the University of Tokyo for the use of the diffraction apparatus, to Dr. K. Kuchitsu and Dr. E. Hirota, the University of Tokyo for their kind aid during the experiment and calculation by the Punched Card Machine, and to Dr. S. Shibata and Dr. H. Morimoto, Nagoya University, for the microphotometer tracing.

*Department of Chemistry*
*Faculty of Science*
*Tokyo University of Education*
*Koishikawa, Tokyo*

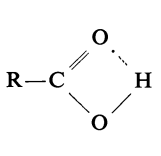
# *Intramolecular Hydrogen Bonding in α-Keto and α-Alkoxycarboxylic Acids. III*. Comparison of the Spectra in the Carbonyl Region with Those in the O–H Stretching Region*

By Michinori Ōki and Minoru Hirota

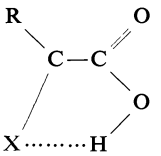
(Received July 13, 1960)

It was previously reported[1] that the O–H stretching absorption of carboxylic acids with a proton accepting group at α-position, such as monoesters of oxalic acid, α-ketocarboxylic acid, α-alkoxycarboxylic acid and α-aryloxycarboxylic acid, had two maxima. The maximum at the higher frequency has been assigned to the free O–H stretching mode and the other at the lower frequency to the O–H of the hydrogen bonded form.

Since it is a well known fact that the C=O stretching absorption ($\nu_{C=O}$) shifts to the lower frequency on hydrogen bonding formation, the frequency shift of $\nu_{C=O}$ to the lower side is also expected in a carboxylic acid which forms hydrogen bonding. Alternately, a trans carboxyl group should show $\nu_{C=O}$ at the higher frequency, because the carbonyl group becomes free on hydrogen bonding formation between the carboxylic hydroxyl group and the hydrogen accepting group at α-position. In this respect, the authors measured $\nu_{C=O}$ together with the O–H stretching absorption ($\nu_{O-H}$) and compared the spectra, thus establishing the assignment of the $\nu_{O-H}$ and $\nu_{C=O}$.



cis structure (I)



trans structure (II)

## Experimental

**Measurement and Calculation.** — All spectral measurements were carried out with a Perkin Elmer 112G grating infrared spectrophotometer as a carbon tetrachloride solution. The absorption curves were regared as an overlap of the bands with Lorentzian type envelopes and separated graphically. The half-width ($\Delta\nu^{a}_{1/2}$) and extinction coefficients at the absorption maxima ($\varepsilon_{max}$) are obtained by the above calculation and the apparent integrated intensities are obtained. The concentration of the solution is about 0.002 mol./l. for the measurements in the $\nu_{O-H}$ region and 0.0005 mol./l. for the $\nu_{C=O}$ region. The measurements are carried out through the ranges of 3580~3350 $cm^{-1}$ for the $\nu_{O-H}$ region and 1830~1690 $cm^{-1}$ for the $\nu_{C=O}$ region.

**Materials.**—The compounds used for the measurement are known unless otherwise described and their physical constants were checked prior to the measurements.

*β-Phenoxypropionic Acid.* — A solution of 250 g. (1.6 mol.) of β-phenoxyethyl chloride and 120 g. (1.85 mol.) of potassium cyanide in 600 ml. of ethanol was refluxed for four hours with stirring and the insoluble material was removed by filtration after cooling. The solvent was evaporated and the residue hydrolyzed by refluxing with 1000 ml. of 20% aqueous sodium hydroxide. The acidification followed by recrystallization from aqueous ethanol gave colorless leaves, m. p. 97°C, in 55% overall yield.

Found: C, 65.21; H, 6.30. Calcd. for $C_9H_{10}O_3$: C, 65.05; H, 6.07%.

*γ-Phenoxybutyric Acid.* — To a sodium ethoxide solution prepared from 38.5 g. (1.67 mol.) of sodium and 700 ml. of ethanol, was added 520 g. (3.3 mol.) of diethyl malonate followed by 260 g. (1.67 mol.) of β-phenoxyethyl chloride and the reaction mixture was refluxed for six hours. The solvent was evaporated and the residue poured into water. The organic material was taken up in ether, dried over anhydrous sodium sulfate and then fractionated. A fraction boiling at 195~200°C/16 mmHg was collected, being crude diethyl α-(2-phenoxyethyl)-malonate (360 g.), which was refluxed with 1100 ml. of 60% acetic acid containing 85 g. of sulfuric acid. The product was treated according to the literature[2]. The acid was obtained as colorless needles, m. p. 64°C in 65% overall yield.

Found: C, 66.48; H, 6.75. Calcd. for $C_{10}H_{12}O_3$: 66.65; H, 6.71%.

## Results and Discussion

**Comparison in the Homologous Series.**—The $\nu_{O-H}$ and the $\nu_{C=O}$ absorption spectra of some compounds are shown in Figs. 1 to 4 and the data obtained by assuming that the band envelopes are expressed by the Lorentz function are given in Table I.

Among the homologs of phenoxyacetic acid, the only compound which shows two $\nu_{O-H}$ maxima is phenoxyacetic acid. The band at

* Part II: This Bulletin, 33, 119 (1960).

1) M. Ōki and M. Hirota, *J. Chem. Soc. Japan, Pure Chem. Sec.* (*Nippon Kagaku Zasshi*), **81**, 855 (1960).

2) E. B. Vliet, C. S. Marvel and C. M. Husen, "Organic Syntheses" Col. Vol. 2, John Wiley & Sons, New York (1943), p. 416.

TABLE I. THE $\nu_{O-H}$ AND THE $\nu_{C=O}$ ABSORPTION SPECTRA OF VARIOUS CARBOXYLIC ACIDS WITH HYDROGEN-ACCEPTING GROUPS

| Compound | $\nu_{O-H}$, $cm^{-1}$ | | $\nu_{C=O}$, $cm^{-1}$ | | |
|---|---|---|---|---|---|
| Phenoxyacetic acid | 3526.9 | 3487.5 | 1790.6 | 1762.9 | 1737.4 |
| β-Phenoxypropionic acid | 3531.7 | — | — | 1760.8 | 1719.0 |
| γ-Phenoxybutyric acid | 3534.2 | — | — | 1760.0 | 1715.8 |
| Methoxyacetic acid | 3526.7 | 3450.8 | 1791.3 | 1761.3 | 1730.9 |
| Isopropyloxyacetic acid | 3533.6 | 3437.4 | 1787.6 | 1760.8 | 1731.7 |
| *tert*-Butoxyacetic acid | 3528.0 | 3424.2 | 1788.5 | 1759.3 | 1733.3 |
| α-Phenoxypropionic acid | 3526.3 | 3475.1 | 1785.7 | 1758.7 | 1731.4 |
| α-Phenoxyisobutyric acid | 3526.3 | 3431.6 | 1786.1 | 1754.4 | 1716.4 |
| Pyruvic acid | — | 3430.7 | 1788.5 | — | 1725 |

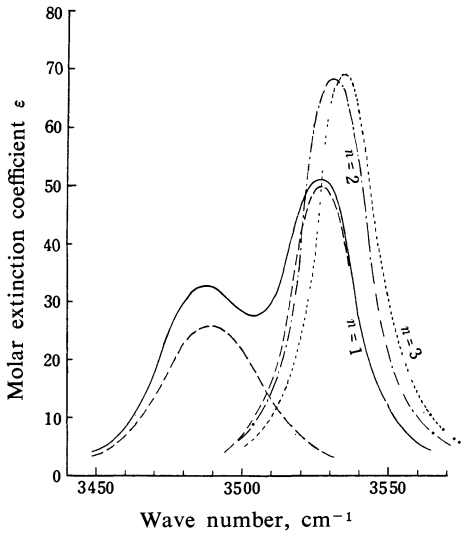



Fig. 1. The $\nu_{O-H}$ bands of $C_6H_5O\cdot(CH_2)_nCO_2H$
$n=1$ —— $n=2$ —·— $n=3$ ·····
The curve of phenoxyacetic acid is separated into the two symmetrical absorptions. (— — —)

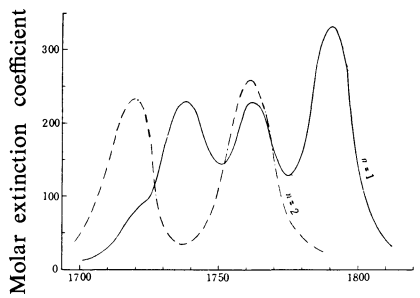



Fig. 2. The $\nu_{C=O}$ absorptions of $C_6H_5O(CH_2)_n\cdot CO_2H$. $n=1$ —— $n=2$ —·—

higher frequency has been assigned to the $\nu_{O-H}$ of the monomeric acid, whereas the band at lower frequency has been assigned to the monomeric acid with an intramolecular hydrogen bonding. The higher homologs exhibit one band at ca. 3530 $cm^{-1}$ which can doubtless be assigned to the usual $\nu_{O-H}$ mode of monomeric acid. The results are indicative of the absence of hydrogen bonding between the carboxylic hydroxyl group and the oxygen atom of the phenoxyl group in β-phenoxypropionic and γ-phenoxybutyric acids.

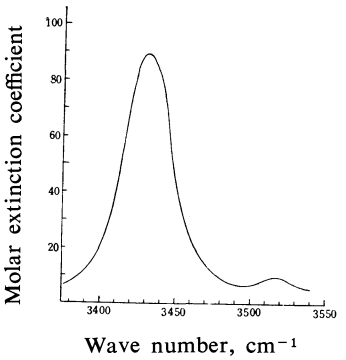



Fig. 3. The $\nu_{O-H}$ absorption of pyruvic acid.

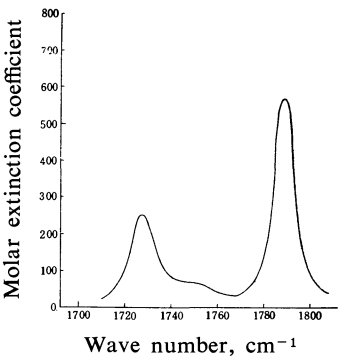



Fig. 4. The $\nu_{C=O}$ absorption of pyruvic acid.

In the carbonyl region, phenoxyacetic acid shows three maxima and a shoulder at ca. 1715 $cm^{-1}$, while β-phenoxypropionic and γ-phenoxybutyric acids exhibit only two bands. Acetic acid and benzoic acid also possess similar absorptions with the latter two compounds. Comparison of these data together with the study of the change in concentration as described later indicates that the band at about 1760 $cm^{-1}$ is arising from the cis structure of

TABLE II. COMPARISON OF THE SPECTRA OF CARBOXYLIC ACIDS CARRYING $\alpha$-HYDROGEN ACCEPTING GROUPS WITH THOSE OF THEIR ESTERS

| Compound | R | $\nu_{C=O}$, $cm^{-1}$ | | | | |
|---|---|---|---|---|---|---|
| $CH_3COCOOR$ | H | 1788.5 | | — | | 1725 |
| | Ethyl | | | | | 1733.0 |
| $C_6H_5OCH_2COOR$ | H | 1790.6 | | 1762.9 | | 1737.4 |
| | Ethyl | | | 1766.8 | | 1739.4 |
| $\begin{matrix}COOR\\ \vert\\ COOCH_3\end{matrix}$ | H | 1808.2 | 1788.9 | 1758.3 | | 1739.9 |
| | Methyl | | 1780.2 | | 1752.3 | |
| $C_6H_5COOR$ | H | — | | 1744 | | 1700 |
| | Ethyl | | | | | 1722.6 |
| $CH_3COOR$ | H | — | | 1769.3 | | 1714.8 |
| | Ethyl | | | 1754 | | |

a monomeric carboxylic acid illustrated by I, whereas the band at 1790 $cm^{-1}$ must correspond to the trans structure.

The difference ($\Delta\nu_{max}$) of the wave number between the band maxima corresponding to the cis and the trans structures is about 30 $cm^{-1}$ and may be explained in the following way. That is, the peak for the cis isomer shifts to the lower frequency because of the formation of the hydrogen bonding between the carboxylic hydroxyl and carbonyl groups, a non-planar[3] four-membered ring being formed. Although this may be taken as a peculiar phenomenon, a support is found in the accumulated data in this laboratory[4]. None of the phenylacetic, diphenylacetic and triphenylacetic acids show intramolecular interaction between the hydroxyl group and $\pi$-electrons, the existence of which is naturally expected from the analogy of *N*-methylphenylacetamide[5]. The absence of the interaction must be interpreted by considering that there is a favorable structure over the intramolecular O-H$\cdots\pi$ interaction, the energy of which is estimated as about 1 kcal./mol. The stabilization may be afforded by the presence of O-H$\cdots$O=C hydrogen bonding in the cis structure of the carboxylic acid.

The homologs of methoxyacetic acid which carries methyl groups show some variation in the $\nu_{C=O}$ absorptions according to the degree of substitution. Although the authors cannot comment precisely on the cause of the variation at the present time, it is probable that the electronic effect of the introduced methyl groups is playing an important role.

Pyruvic acid possesses two peaks at 1788.5 $cm^{-1}$ and 1725 $cm^{-1}$ and a shoulder at 1735 $cm^{-1}$ but the band at 1760 $cm^{-1}$ which is common for the other acids failed to appear. This is reasonable, since the band at 1760 $cm^{-1}$ corresponds to the cis species, the absorption of which in the $\nu_{O-H}$ region is negligibly small. The band at the highest frequency is assigned to the free carbonyl group of the carboxyl group which is due to the hydrogen bonding formation between the carboxylic hydroxyl and the $\alpha$-carbonyl groups. The origin of the two bands at the lower frequencies is determined through the study of concentration effects on the intensities. The band at 1735 $cm^{-1}$ is assigned to the dimeric carboxyl group and the other at 1725 $cm^{-1}$ to the $\alpha$-carbonyl group.

It is well known that the $\alpha$-ketocarboxylic acid has the monomer $\nu_{C=O}$ absorption at abnormally high frequency. The phenomenon has been attributed to the inductive and the field effects of the $\alpha$-keto group. However, it is now evident that pyruvic acid exclusively exists as the trans monomer with the free carbonyl group of the carboxyl group which causes the absorption at the high frequency.

**Comparison of the Spectra of the Acids with those of the Esters.**—In Table II are listed the $\nu_{C=O}$ spectra of esters together with the corresponding acids. Since the esterification cancels all posibilities of hydrogen bonding, esters of the carboxylic acids which carry the hydrogen accepting group at $\alpha$-position are expected to be normal when compared with the ordinary esters and this is proved to be the case. None of the esters show $\nu_{C=O}$ band as high as 1790 $cm^{-1}$.

Ethyl pyruvate shows one somewhat unsymmetrical $\nu_{C=O}$ band at 1733 $cm^{-1}$, which is believed to be an overlap of the ester and ketone bands. The band intensity is nearly twice that of the normal esters. Ethyl phenoxyacetate possesses two absorptions in the carbonyl region, the intensities being nearly equal. This phenomenon may be attributed to the

3) C. P. Smyth, "Dielectric Behavior and Structure", McGraw-Hill Book Co., Inc., New York (1955), p. 306,
4) H. Iwamura, unpublished work.
5) I. Suzuki, M. Tsuboi and T. Shimanouchi, *Spectrochim. Acta*, **16**, 467 (1960).

TABLE III. THE EFFECT OF THE CONCENTRATION ON THE INTENSITIES OF THE ABSORPTION BANDS OF PHENOXYACETIC ACID

| Concentration mol./l. | Intensity of the absorption band | | | |
|---|---|---|---|---|
| | $\nu_{C=O}$ of the trans structure of the monomer ($\varepsilon_t$) at 1790.6 $cm^{-1}$ | $\nu_{C=O}$ of the cis structure of the monomer ($\varepsilon_t$) at 1762.9 $cm^{-1}$ | $\nu_{C=O}$ of the dimer at 1737.4 $cm^{-1}$ | $\varepsilon_t/\varepsilon_c$ |
| 0.00092 | 204 | 153 | 281 | 1.33 |
| 0.00046 | 248 | 185 | 252 | 1.34 |
| 0.00023 | 300 | 226 | 221 | 1.33 |
| 0.000058 | 390 | 278 | 185 | 1.40 |

existence of the rotational isomers or to some other cause. The decisive comment cannot be made at the present stage.

**The Effects of Concentration on the $\nu_{C=O}$ Bands of Phenoxyacetic Acid.**—As was already pointed out, phenoxyacetic acid possesses three $\nu_{C=O}$ bands, the intensities of which are measured at various concentrations in carbon tetrachloride. The results are shown in Table III.

It is recognized that the intensities of the bands at 1762.9 $cm^{-1}$ and 1790.6 $cm^{-1}$ increase with the decreasing concentration, while the band at 1737 $cm^{-1}$ decreases on lowering the concentration. These behaviors indicate that two bands at the higher frequencies must be attributed to the monomeric forms of the carboxylic acid and the other at 1737 $cm^{-1}$ to the dimeric form. It is also found that the ratio of the intensities of the bands at 1762.9 $cm^{-1}$ and 1790.6 $cm^{-1}$ is almost constant at the various concentrations. This fact suggests that the equilibrium between the cis and the trans forms is not influenced by the concentration.

TABLE IV. ASSIGNMENT OF THE $\nu_{O-H}$ AND THE $\nu_{C=O}$ BANDS OF A CARBOXYLIC ACID WITH AN α-HYDROGEN-ACCEPTING GROUP

| Structure | Monomer | | Dimer $cm^{-1}$ |
|---|---|---|---|
| | Cis structure $cm^{-1}$ | Trans structure $cm^{-1}$ | |
| $\nu_{O-H}$ | 3550～3500 | 3490～3390 | 3300～2500 |
| $\nu_{C=O}$ | ca. 1760 | ca. 1790 | 1730～1710 |

**Assignment of the Band.** — From the above discussion, it is apparent that the bands can be assigned as shown in Table IV.

## Summary

The $\nu_{C=O}$ and the $\nu_{O-H}$ absorption of carboxylic acids were measured and the following conclusion was obtained; 1) The carboxylic acids carrying a proton-accepting group at α-position give three absorption bands at ca. 1790 $cm^{-1}$, ca. 1760 $cm^{-1}$ and 1740～1710 $cm^{-1}$, which can be assigned to the trans form of the monomeric acid, the cis form of the monomeric acid and the dimer, respectively. 2) The $\Delta\nu_{max}$ between the cis and the trans forms can be explained from an intramolecular hydrogen bonding between carboxylic hydroxyl and carbonyl groups.

The authors wish to express their hearty thanks to Professor Y. Urushibara for his encouragement and advice throughout this work. The authors are also indebted to Mr. H. Iwamura and Mr. K. Mutai for their technical assistance.

*Department of Chemistry*
*Faculty of Science*
*The University of Tokyo*
*Hongo, Tokyo*

# *Intramolecular Hydrogen Bonding in α-Keto and α-Alkoxycarboxylic Acids. IV*[1]. *Electronic Effect in Aryloxyacetic Acids*

By Michinori Ōki and Minoru Hirota

(Received July 26, 1960)

The authors measured[1,2] the O-H stretching ($\nu_{O-H}$) and the C=O stretching ($\nu_{C=O}$) bands of various carboxylic acids and concluded that there is a hydrogen bonding in the acids carrying a hydrogen-accepting group at α-position. The hydrogen bonding is doubtlessly formed between the carboxylic hydroxyl group and the hydrogen-accepting group. Phenoxyacetic acid satisfies the above conditions and is found to exist as "free" and "bonded"[3] species, from the data obtained in O-H stretching and carbonyl regions.

The strength of the hydrogen-accepting power of the oxygen atom in the phenoxyl group may be assumed to be proportional to the electron density on the oxygen atom. Since it is known that Hammett's σ constants and the $pK_a$ values of phenols are in linear relation, it can be seen that the σ constant[4] is a measure of the electron density of the oxygen atom in the aryloxy group. Thus the electron-repelling group will enrich the electron-density on the oxygen atom to be favorable as a hydrogen acceptor and the contrary situation is expected for the electron-attracting group.

The present paper deals with the effect of the substituent in the phenyl group on the $\nu_{O-H}$ and the $\nu_{C=O}$ absorptions, thus giving another verification for the existence of a hydrogen bonding between the carboxylic hydroxyl group and the hydrogen-accepting group at α-position.

## Experimental

**Preparation of the Materials.** — Aryloxyacetic acids[5] were prepared in the following way. Equivalent amounts of sodium aryloxide and sodium chloroacetate in water were heated on a water bath for one to two hours. The reaction mixture was acidified and extracted with ether. The ethereal extract was shaken with aqueous sodium bicarbonate and the aqueous layer was acidified. The aryloxyacetic acid was recrystallized from benzene. Those which are not listed in Table I are known compounds and their physical constants agreed with the literature.

Table I. Aryloxyacetic acid ($RC_6H_4OCH_2COOH$)

| R | M. p. °C | Analyses C, % Found | C, % Calcd. | H, % Found | H, % Calcd. |
|---|---|---|---|---|---|
| *m*-$NO_2$ | 151 | 48.80 | 48.74 | 7.19 | 7.11 |
| *p*-Cl* | 158.5 | 51.62 | 51.47 | 3.96 | 3.75 |
| *m*-$CH_3O$ | 119 | 59.35 | 59.33 | 5.41 | 5.33 |
| *p*-$CH_3O$ | 112 | 59.48 | 59.33 | 5.60 | 5.33 |

* Since the melting point (152°C) reported in the literature disagreed with that measured in this work, the purity was checked by elemental analysis.

**Measurement and Calculation.**—The measurement of the spectra were carried out with a Perkin Elmer 112G grating spectrophotometer. The materials were dissolved in carbon tetrachloride to make up concentration of ca. 0.002 mol./l. for the $\nu_{O-H}$ and ca. 0.0005 mol./l. for the $\nu_{C=O}$ measurements[6]. The spectral slit width was 1.0 $cm^{-1}$ for the $\nu_{O-H}$ region and 0.6 $cm^{-1}$ for the $\nu_{C=O}$ region. The absorption curves were assumed to be an overlap of the bands which obey the Lorentz function and the half band-widths ($\Delta\nu^a_{1/2}$) and the extinction coefficients ($\varepsilon^a_{max}$) at the maxima were obtained by Ramsay's first method[7]. That is, the approximate absorption maxima, $\Delta\nu^a_{1/2}$'s and $\varepsilon^a_{max}$ were obtained by dividing the curves graphically and the characteristic numericals were corrected by the trial and error method.

## Results and Discussion

Locations of the absorption maxima and the integrated intensities of the bands of aryloxyacetic acids are summarized in Table II.

1) Part III: M. Ōki and M. Hirota, This Bulletin, **34**, 374 (1961).

2) M. Ōki and M. Hirota, *J. Chem. Soc. Japan, Pure Chem. Sec.* (*Nippon Kagaku Zasshi*), **81**, 855 (1960).

3) Although C. P. Smyth ("Dielectric Behavior and Structure", McGrawHill Book Co, Inc., New York (1955), p. 307) used the name cis and trans for the carboxyl group which has hydrogen atom between the two oxygen atoms and the other of which hydrogen atom is located outside the two oxygen atoms, respectively, "free" and "bonded" are used in this paper because of the nature of situation. However, as pointed out previously (Ref. 1), existence of a hydrogen bonding has been deduced in the cis form. Thus quotation marks are used to distinguish between the situation in this work and purely free form.

4) H. H. Jaffé, *Chem. Revs.*, **53**, 191 (1953).

5) A. Michael, *J. Am. Chem. Soc.*, **9**, 180 (1887).

6) *p*-Nitrophenoxyacetic, *m*-nitrophenoxyacetic and *h*-benzyloxyphenoxyacetic acids were exceptions, of which poor solubility in carbon tetrachloride did not allow to measure at this level of concentration. The measurements of the nitro compounds were run with the saturated solutions.

7) D. A. Ramsay, *J. Am. Chem. Soc.*, **74**, 72 (1952).

TABLE II. THE $\nu_{O-H}$ ABSORPTIONS OF SUBSTITUTED PHENOXYACETIC ACIDS

| Substituent | $\sigma$ | $\nu_f$, $cm^{-1}$ | $A_f$** | $\nu_b$, $cm^{-1}$ | $A_b$** | $\Delta\nu_{max}$ | $A_b/A_f$ | $\log(10 \cdot A_b/A_f)$ | Concentration $10^{-3}$ mol./l. |
|---|---|---|---|---|---|---|---|---|---|
| *p*-$NO_2$ | 0.778 | 3521.8 | — | not found | — | — | — | — | —* |
| *m*-$NO_2$ | 0.710 | 3522.3 | — | 3493.8 | — | 28.5 | 0.10 | 0.00 | —* |
| *m*-Br | 0.391 | 3522.5 | 7.59 | 3484.7 | 1.48 | 37.8 | 0.180 | 0.255 | 1.30 |
| *p*-Br | 0.232 | 3525.1 | 7.64 | 3494.0 | 2.95 | 31.1 | 0.386 | 0.587 | 0.828 |
| *p*-Cl | 0.227 | 3524.3 | 9.77 | 3492.8 | 2.58 | 31.5 | 0.264 | 0.422 | 1.09 |
| *m*-$CH_3O$ | 0.115 | 3525.7 | 6.15 | 3484.0 | 2.60 | 41.7 | 0.426 | 0.629 | 1.71 |
| H | 0 | 3526.9 | 5.57 | 3487.5 | 2.69 | 39.4 | 0.484 | 0.685 | 1.18 |
| *m*-$CH_3$ | −0.069 | 3527.5 | 4.49 | 3486.7 | 3.15 | 40.8 | 0.698 | 0.844 | 1.47 |
| *p*-$CH_3$ | −0.170 | 3528.8 | 4.99 | 3484.5 | 3.48 | 44.3 | 0.699 | 0.845 | 1.60 |
| *p*-$CH_3O$ | −0.268 | 3527.7 | 4.72 | 3481.3 | 4.19 | 46.4 | 0.886 | 0.947 | 1.61 |
| *p*-$C_6H_5CH_2O$ | −0.41 | 3527.6 | — | 3482.4 | — | 45.2 | 0.993 | 0.997 | —* |

* Saturated solution.

** The integrated intensity can be calculated by the equation $A = 2.30 \times \frac{\pi}{2} \frac{1}{Cl} \log_{10}(T_0/T)_{max} \times \Delta\nu^a{}_{1/2}$, because the correction factors[7] are almost unity under the conditions for the measurement.

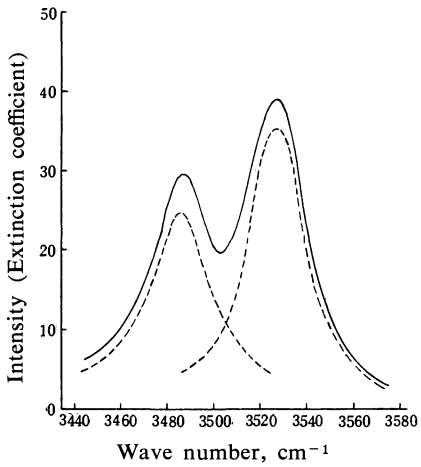



Fig. 1. The $\nu_{OH}$ absorption of *m*-methylphenoxyacetic acid.

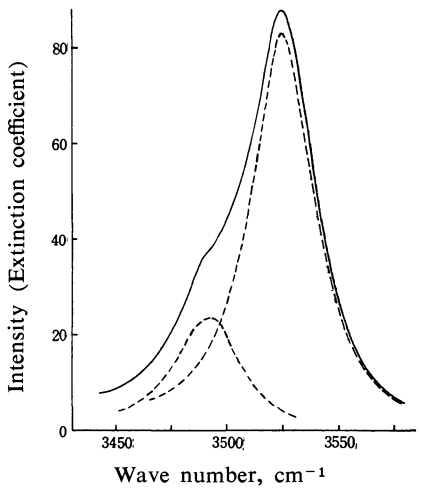
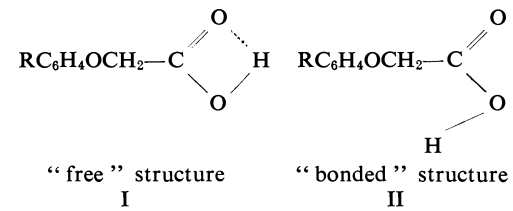



Fig. 2. The $\nu_{OH}$ absorption of *p*-chlorophenoxyacetic acid.

The aryloxyacetic acid with a substituent whose $\sigma$ value is smaller than 0.115 (for meta-methoxyl) shows two apparent maxima, as exemplified by *m*-methylphenoxyacetic acid in Fig. 1. The separation of the two absorption maxima is fairly large. According to the previous paper, the band at ca. 3525 $cm^{-1}$ is assigned to the cis structure (I) and the other at ca. 3490 $cm^{-1}$ to the trans (II). Therefore, it can be said that the electron-repelling groups enhance the contribution of the trans, "bonded" form. If it can be assumed that the larger $\Delta\nu_{max}$ represents the more stabilization, then it is also clear that the aryloxyacetic acids carrying the electron-repelling group forms the more stable hydrogen bonding.




"free" structure I "bonded" structure II

As to the substitution of the electron-attracting group, the aryloxyacetic acids do not show two maxima. *p*-Chlorophenoxyacetic and *p*-bromophenoxyacetic acids possess absorption bands with a peak and a shoulder as shown in Fig. 2, *p*-chlorophenoxyacetic acid being taken as a representative. *m*-Nitrophenoxyacetic acid shows a somewhat unsymmetrical absorption, while *p*-nitrophenoxyacetic acid a nearly symmetrical band. The error caused by the poor solubility of *p*-nitrophenoxyacetic acid prevents the division of the band into two.

The bands at higher and at lower wave numbers are undoubtedly assigned to the "free" and to the "bonded" OH's, respectively, as

reported in the previous paper. Then it is evident that the electron repelling groups favor the "bonded" form and the electron-attracting groups the "free" form.

Since an equilibrium between the "free" and the "bonded" forms is considered to be operative, an equilibrium constant $K_h$ may be expressed by Eq. 1.

$$K_h = \frac{[\text{bonded}]}{[\text{free}]} \qquad (1)$$

On the other hand, the concentrations of each of the species are proportional to the intensities of the respective $\nu_{O-H}$, as far as Beer's law is applicable. Therefore, Eq. 1 may be transformed to

$$K_h = a\frac{A_b}{A_f} \qquad (2)$$

where $A_b$ and $A_f$ are the integrated intensities due to the "bonded" and the "free" molecules, respectively, and $a$ is a constant pertaining to the magnifying power of the absorption intensity per molecule, when hydrogen bonding is formed. The value "$a$" is assumed to be equal for the series of compound.

Hammett's $\sigma$ value is defined as

$$\sigma \equiv \log (K/K_0) \qquad (3)$$

where $K_0$ and $K$ are dissociation constants of benzoic acid and the substituted benzoic acid, respectively. Thus a linear relation is expected between $\sigma$ value and $\log (A_b/A_f)$ from Eqs. 2 and 3, because $\sigma$ value is also a measure of the basicity of the oxygen atom in the aryloxyl group. The $\log (A_b/A_f)$ versus $\sigma$ diagram is shown in Fig. 3 and the relation is linear as expected.

The frequency shift ($\Delta\nu_{max}$) from the "free" molecule to the "bonded" is also plotted against the $\sigma$ value. The result (Fig. 4) may be considered as linear relation. The larger the the $A_b/A_f$ value, the more is the $\Delta\nu_{max}$. Since it is accepted that the energy of a hydrogen

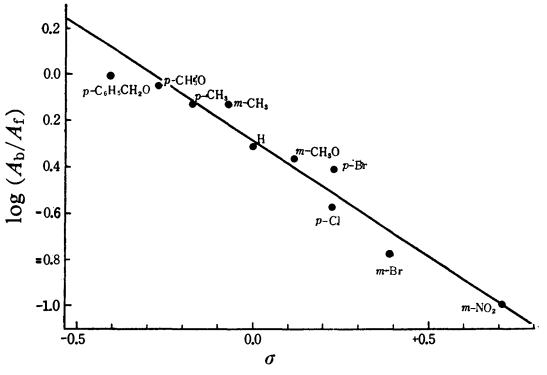



Fig. 3. The relation between the intensity ratio $A_b/A_f$ and the Hammett's substituent constant.

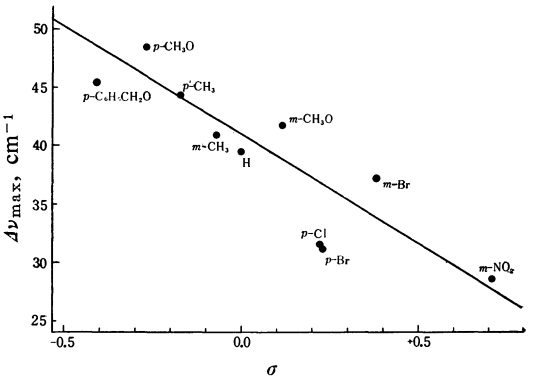



Fig. 4. The relation between the $\Delta\nu_{max}$ and the Hammett's substituent constant.

bonding is proportional to the shift of the the wave number as a rough approximation, this $\Delta\nu_{max} - \sigma$ relation seems to be reasonable.

The measurement was extended to the carbonyl region and the band at 1790 $cm^{-1}$ which is assigned[1] to the "bonded" form and the band at 1790 $cm^{-1}$ which is assigned[1] to the "bonded" form and the other at 1760 $cm^{-1}$ due to the "free" form are also found in every case.

Although these bands are nearly symmetrical, the dimer band at ca. 1730 $cm^{-1}$ always overlaps with these, making it hard to obtain the integrated intensities. $\varepsilon_b/\varepsilon_f$ is obtained in this regard, where $\varepsilon_b$ and $\varepsilon_f$ are the extinction coefficients of the "bonded" and the "free" molecules at the corresponding peaks. The results are summarized together with other data in Table III. The result indicates that, when the $\sigma$ value is large with a plus sign, $\varepsilon_b/\varepsilon_f$ is small and agrees with the tendency obtained in the $\nu_{O-H}$ measurement.

TABLE III. THE $\nu_{C=O}$ ABSORPTION OF ARYLOXYACETIC ACIDS

| Substituent | $\nu_{C=O}$ of the "free" structure | $\nu_{C=O}$ of the "bonded" structure | $\varepsilon_b/\varepsilon_f$ |
|---|---|---|---|
| *m*-$NO_2$ | 1768.9 | 1788.9 | 1.20 |
| *m*-Br | 1764.2 | 1789.8 | 1.19 |
| *p*-Cl | 1763.6 | 1790.2 | 1.27 |
| H | 1762.9 | 1790.6 | 1.37 |
| *p*-$CH_3$ | 1763.0 | 1791.0 | 1.55 |
| *p*-$CH_3O$ | 1760.5 | 1790.4 | 1.63 |

The $\nu_{O-H}$ band of the dimeric carboxylic acid is known to be a very broad band and is often masked by the $\nu_{C-H}$ band. However, the $\nu_{C=O}$ band of the dimetric acid is easily observable and it is known in this measurement that the contribution of the dimer is fairly large even in a dilute solution. From this result, the direct comparison of the absolute

intensities of the bands corresponding to the "free" and the "bonded" forms becomes less significant. Thus, the ratio $A_b/A_f$ or $\varepsilon_b/\varepsilon_f$ is exclusively used for the present discussion. The concentrations of the solutions are also included in Table III, because the contribution of the dimers may insert influence upon other data. The detailed discussion on the effect of concentration will be reported elsewhere in connection with the dissociation constant of the dimer.

## Summary

The electronic effect on the hydrogen bonding formation in aryloxyacetic acid was examined. It is found that the electron-repelling groups enhance the band at the lower frequency in O-H stretching region and the band at ca. 1790 $cm^{-1}$. The result is completely agreeable with the expectation that the electron density on the oxygen atom in the aryloxyl group controls the hydrogen bonding formation.

The authors are grateful to Professor Y. Urushibara for his encouragement throughout this work.

*Department of Chemistry*
*Faculty of Science*
*The University of Tokyo*
*Hongo, Tokyo*

# *Stereoregular Polymers. VII.*[1] *Infrared Spectra of Isotactic Polystyrene, Isotactic Poly-α, β, β-trideuterostyrene and Isotactic Poly-p-deuterostyrene*[*1]

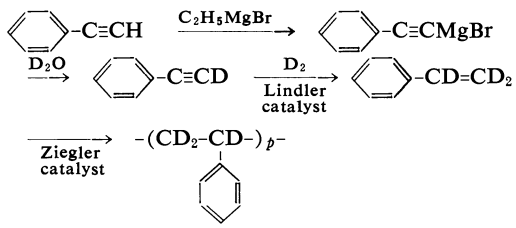
By Hiroyuki TADOKORO, Yoshiyuki NISHIYAMA,[*2] Shun'ichi NOZAKURA and Shunsuke MURAHASHI

(Received September 12, 1960)

Isotactic polystyrene is a very interesting polymer from the point of view of fine structure and fine texture. Its crystallinity can be varied over wide range, from amorphous to highly crystalline state by heat-treatments, and also a highly oriented sample can be made by hot stretching. We are now studying this substance by use of the X-ray, infrared and density measurements. In this paper we wish to present a report on the results obtained from the changes of infrared spectra with crystallization and the infrared dichroism of isotactic polystyrene (IPS), isotactic poly-α, β, β-trideuterostyrene (IPTDS), $-(-CD_2-\underset{\displaystyle C_6H_5}{\underset{|}{CD}}-)_p-$ and isotactic poly-*p*-deuterostyrene (IPPDS), $-(CH_2-\underset{\displaystyle D}{\underset{|}{CH}}-)_p-$.

Natta[2] measured the infrared spectra of IPS both at solid and molten states. He showed that the spectrum of IPS at the molten state is similar to that of atactic polystyrene (APS), but did not discuss it further in detail. Liang and Krimm[3] reported the detailed analysis of the infrared spectrum of polystyrene. Their analysis was, however, based only on the commercial ASP, and they have not yet examined the dicroism and the deuteration of this polymer. Deuteropolystyrenes (probably atactic) were prepared by Beachell and Nemphos[4], but the infrared spectra of their products seem not to be published yet.

**Samples.** — The samples used in this work are IPS, IPTDS and IPPDS polymerized with Ziegler catalyst. The deuterated polymers were prepared according to the following schemes:




1) Part I of this series, S. Murahashi, S. Nozakura, M. Sumi and K. Hatada, This Bulletin, **32**, 1094 (1959).

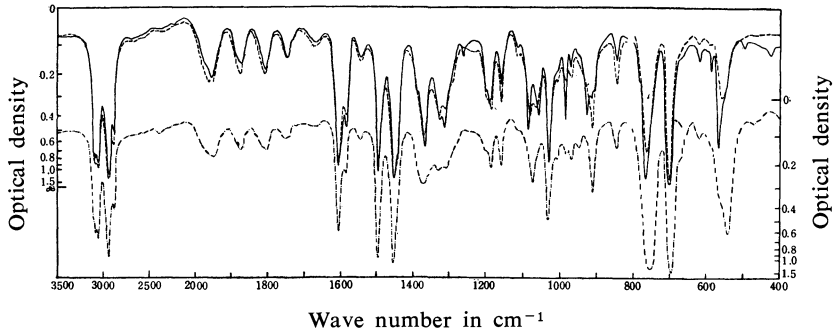
*1 Presented at the Annual Meeting of the Society of High Polymer Science in Tokyo, June, 1958, and at the Symposium on High Polymers in Osaka, October, 1958.

*2 Present Address: Tôhô Rayon Co., Ltd., Research Institute, Tokushima.

2) G. Natta, *Makromol. Chem.*, **16**, 213 (1955).

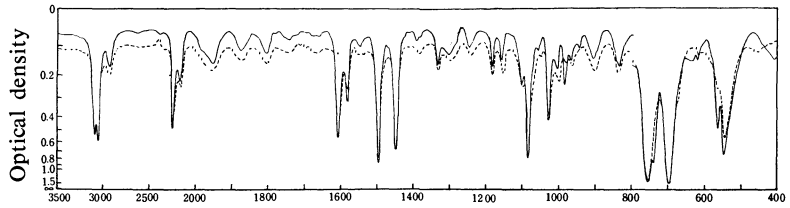
3) C. Y. Liang and S. Krimm, *J. Polymer Sci.*, **27**, 241 (1958).

4) H. C. Beachell and S. P. Nemphos, ibid., **25**, 173 (1957).



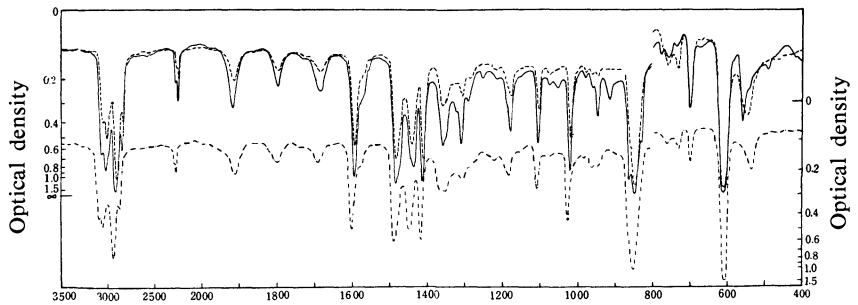

Wave number in $cm^{-1}$

Fig. 1a. Infrared spectra of isotactic polystyrene (—— sample subjected to heat-treatment; - - - - quenched sample) and atactic polystyrene (-·-·-).



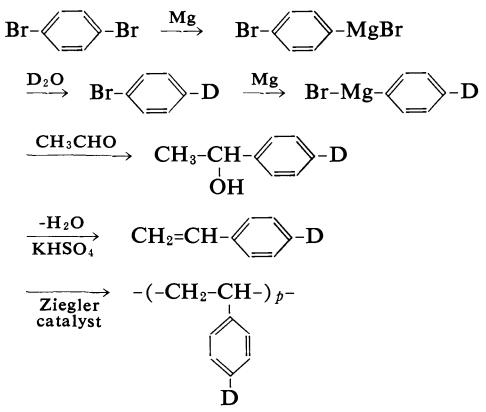

Wave number in $cm^{-1}$

Fig. 1b. Infrared spectra of isotactic poly-$\alpha$, $\beta$, $\beta$-trideuterostyrene (—— sample subjected to heat-treatment; - - - - quenched sample).




Wave number in $cm^{-1}$

Fig. 1c. Infrared spectra of isotactic poly-*p*-deuterostyrene (—— sample subjected to heat-treatment; - - - - quenched sample) and atactic poly-*p*-deuterostyrene (-·-·-).




The films for the infrared measurements were cast on a metal plate*3 from toluene solution, and were subjected to one of the following treatments: 1) quenching, 2) heat-treatment after quenching, and 3) elongation and subsequent heat-treatment. The quenched sample was prepared by heating in Wood's alloy at about 240°C*4 for 15~30 sec., and subsequent quenching in cold water. The oriented sample was prepared by stretching very slowly in boiling water, until it could be stretched no more (about 5 times of the original length). Heat-treatment was taken in Wood's alloy at about 180°C for 30 min. The crystallization and the

*3 A glass plate and the surface of water were also used for casting the film.

*4 The melting point of IPS is reported to be 230°C[2].

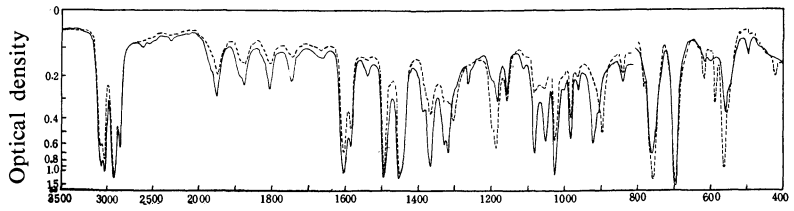



Fig. 2a. Infrared dichroism of isotactic polystyrene: —— electric vector perpendicular to elongation, - - - - electric vector parallel to elongation.

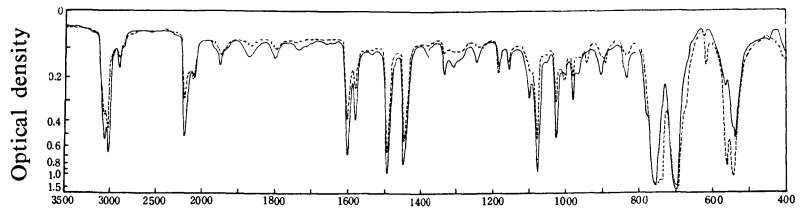



Fig. 2b. Infrared dichroism of isotactic poly-$\alpha$, $\beta$, $\beta$-trideuterostyrene: —— electric vector perpendicular to elongation, - - - - electric vector parallel to elongation.

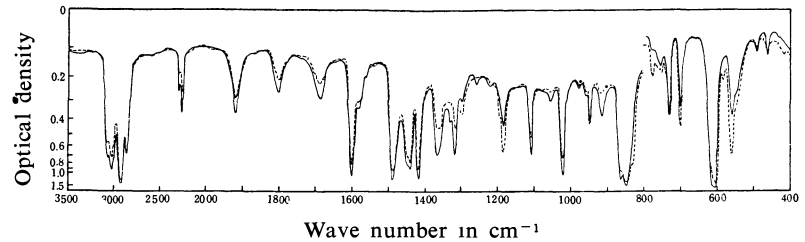



Fig. 2c. Infrared dichroism of isotactic poly-*p*-deuterostyrene: —— electric vector perpendicular to elongation, - - - - electric vector parallel to elongation.

orientation of the samples were confirmed by the X-ray photographs.

Infrared spectra were measured by using a Hitachi Model EPI-2 recording infrared spectrophotometer with sodium chloride and potassium bromide prisms and silver chloride polarizers.

## Results and Discussion

**Features of the Spectra.** — Fig. 1 shows the spectra of IPS (a), IPTDS (b) and IPPDS (c), together with those of atactic samples (lower curve in Figs. 1a and 1c) for reference. In the figures the solid lines are for the samples subjected to heat-treatment and broken lines for the quenched samples. In Fig. 2, polarized infrared spectra of the oriented samples of IPS (a), IPTDS (b) and IPPDS (c) were shown. The solid lines represent transmission with the electric vector perpendicular to the stretching direction, and the broken lines that with the electric vector parallel to the stretching direction. In Figs. 1 and 2, the films used for the absorption measurements with sodium chloride prism are not all the same as those for the measurements with potassium bromide prism. The spectral data and the tentative assignments were also shown in Tables I—III.

As shown in Fig. 1, the spectra exhibit considerable changes with crystallization. The bands at 1364, 1314, 1297 and 1185 $cm^{-1}$ in the spectrum of IPS are very sensitive to crystallization, and have strong dichroic nature. These four bands appear in weak intensity even in the spectrum of quenched samples of IPS, while do not appear in the spectrum of APS. On the other hand, the spectra of IPTDS do not show any bands at these four positions. The band at 1070 $cm^{-1}$ of APS which splits slightly into two bands in the spectrum of the quenched IPS, undergoes large splitting with increase in intensity and sharpness in the spectrum of the crystallized IPS. The resulting two bands are at 1080 and 1048 $cm^{-1}$, showing strong perpendicular dichroism. The spectrum of the quenched IPS is similar

TABLE Ia. SPECTRAL DATA AND TENTATIVE ASSIGNMENT OF IPS (CRYSTALLIZED)

| Frequency in $cm^{-1}$ | Intensity[a] | Dichroism | Tentative assignment[b] |
|---|---|---|---|
| 3103 | w | ⊥ | |
| 3082 | m | ⊥ | |
| 3060 | s | ⊥ | $\nu(CH)_{ph}$ |
| 3026 | s | ⊥ | |
| 3002 | w | ⊥ | |
| 2924 | vs | ⊥ | $\nu_a(CH_2)$ |
| 2849 | m | | $\nu_s(CH_2)$ |
| 1946 | w | ⊥ | |
| 1872 | w | ⊥ | |
| 1801 | w | ⊥ | combination of $\gamma(CH)_{ph}$ |
| 1748 | w | ⊥ | |
| 1675 | w | ⊥ | |
| 1602 | s | ⊥ | $\nu(CC)_{ph}$, k ($A_1$) |
| 1583 | m | ⊥ | $\nu(CC)_{ph}$, l ($B_1$) |
| 1542 | w | | |
| 1493 | s | ⊥ | $\nu(CC)_{ph}$, m ($A_1$) |
| 1452 | vs | ⊥ | $\nu(CC)_{ph}$, n ($B_1$) |
| 1444 | sh | | $\delta(CH_2)$ |
| 1387 | sh | ⊥ | |
| 1364 | s | ⊥ | associated with helical configuration |
| 1324 | m | ⊥ | |
| 1314 | m | ⊥ | associated with helical configuration |
| 1297 | m | ∥ | associated with helical configuration |
| 1260 | w | | |
| 1197 | sh | | |
| 1185 | m | ∥ | associated with helical configuration |
| 1181 | w | ∥ | $\beta(CH)_{ph}$, a ($A_1$) |
| 1154 | w | ∥ | $\beta(CH)_{ph}$, c ($B_1$) |
| 1111 | w | ⊥ | |
| 1080 | m | ⊥ | $\beta(CH)_{ph}$, d ($B_1$) |
| 1048 | m | ⊥ | |
| 1028 | s | ⊥ | $\beta(CH)_{ph}$, b ($A_1$) |
| 1004 | vw | ∥ | |
| 985 | m | ⊥ | $\gamma(CH)_{ph}$, j ($B_2$) |
| 965 | w | | $\gamma(CH)_{ph}$, h ($A_2$) |
| 920 | m | ⊥ | |
| 906 | w | | $\gamma(CH)_{ph}$, i ($B_2$) |
| 898 | m | ∥ | |
| 842 | w | | $\gamma(CH)_{ph}$, g ($A_2$) |
| 775 | sh | ∥ | |
| 755 | vs | ∥ | $\gamma(CH_{ph})$, f ($B_2$) |
| 697 | vs | | |
| 620 | w | ∥ | |
| 586 | m | ∥ | |
| 566 | s | ∥ | |
| 550 | sh | | |
| 499 | w | ⊥ | |
| 429 | w | ∥ | |

a) vs : very strong, s : strong, m : medium, w :weak, vw : very weak.

b) Whiffen's notations for the vibrational modes of the monosubstituted benzenes were used in this table.
$\nu(CH)_{ph}$ : phenyl CH stretching, $\nu(CC)_{ph}$ : phenyl CC stretching, $\beta(CH)_{ph}$ : phenyl CH in-plane deformation, $\gamma(CH)_{ph}$ : phenyl CH out-of-plane deformation, $\nu_a(CH_2)$: $CH_2$ asymmetric stretching, $\nu_s(CH_2)$ : $CH_2$ symmetric stretching, $\delta(CH_2)$ : $CH_2$ bending.

Table Ib. Spectral changes of polystyrene with crystallization

| APS | Quenched IPS | Crystallized IPS | Changes with crystallization |
|---|---|---|---|
| 1583 (m) | 1583 (m) | 1583 (m) | increase intensity |
| — | — | 1444 (sh) | appear |
| — | — | 1387 (sh) | 〃 |
| 1370 (m) | 1367 (s) | 1365 (s) | |
| 1328 (m) | 1324 (m) | 1324 (m) | |
| 1306 (m) | 1312 (m) | 1314 (m) | increase intensity |
| — | 1297 (vw) | 1297 (m) | |
| — | — | 1260 (w) | appear |
| — | — | 1185 (m) | |
| 1070 (m) | 1075 (m)<br>1056 (m) | 1080 (m)<br>1048 (m) | |
| — | — | 985 (s) | |
| 980 (w) | 980 (w) | — | |
| 943 (w) | — | — | (APS only) |
| 906 (m) | 906 (m) | 920 (m)<br>906 (m)<br>898 (m) | |
| — | — | 775 (sh) | appear |
| 755 (vs) | 755 (s) | 755 (vs) | increase intensity |
| 620 (w) | 620 (w) | 620 (w) | 〃 |
| — | 590 (w) | 586 (m) | 〃 |
| 557 (sh)<br>542 (s) | 557 (m) | 566 (s)<br>550 (sh) | |
| — | — | 499 (w) | appear |
| — | — | 429 (w) | 〃 |

Table II. Spectral data of IPTDS

| Frequency in $cm^{-1}$ a) | Intensity | Dichroism | Changes with crystallzation |
|---|---|---|---|
| 3102 | w | ⊥ | |
| 3083 | m | ⊥ | |
| 3058 | s | ⊥ | |
| 3021 | s | ⊥ | |
| 2997 | w | ⊥ | |
| 2910 | w | ⊥ | |
| 2195 | s | ⊥ | |
| 2095 | m | (∥) | |
| 1950 | w | ⊥ | |
| 1875 | w | ⊥ | |
| 1805 | w | ⊥ | |
| 1602 | s | ⊥ | |
| 1581 | m | ⊥ | increase intensity |
| 1537 | vw | ⊥ | |
| 1493 | s | ⊥ | |
| 1447 | s | ⊥ | |
| 1385 | w | ⊥ | increase intensity |
| 1328 | w | ⊥ | |
| 1303 | w | ⊥ | |
| 1292 | vw(broad) | | |
| 1240 | w | ⊥ | |
| 1179 | w | ∥ | |
| 1154 | w | ⊥ | |
| 1100 | m | ⊥ | increase intensity |
| 1077 | s | ⊥ | |
| 1052 | vw | ⊥ | increase intensity |
| 1025 | m | ⊥ | |
| 1006 | w | ∥ | increase intensity |
| 1000 | vw | ⊥ | |

TABLE II (Continued)

| | | | |
|---|---|---|---|
| 980 | m | ⊥ | increase intensity |
| 965 | w | ⊥ | |
| 940 | w | ∥ | appear |
| 903 | w | ⊥ | 898 $cm^{-1}$ (quenched IPTDS) |
| 891 | w | ∥ | |
| 840 | w | ⊥ | |
| 834 | w | ⊥ | |
| 774 | sh | ⊥ | appear |
| 754 | vs | ∥ | |
| 740 | s | ∥ | appear |
| 697 | vs | ⊥ | |
| 620 | w | ∥ | |
| 562 | m | ∥ | increase intensity |
| 548 | s | ∥ | 545 $cm^{-1}$ (quenched IPTDS) |

a) Data on the crystallized IPTDS.

TABLE III. SPECTRAL DATA OF IPPDS

| Frequency in $cm^{-1}$ a) | Intensity a) | Dichroism | Changes with crystallization |
|---|---|---|---|
| 3071 | s | ⊥ | |
| 3024 | s | ⊥ | |
| 2997 | sh | ⊥ | |
| 2925 | vs | ⊥ | |
| 2850 | s | | |
| 2290 | w | ⊥ | |
| 2264 | m | ⊥ | |
| 1920 | m | ⊥ | |
| 1803 | w | ⊥ | |
| 1689 | w | ⊥ | |
| 1600 | s | ⊥ | |
| 1578 | sh | ⊥ | |
| 1487 | s | ⊥ | |
| 1441 | s | ⊥ | 1446 $cm^{-1}$ (quenched IPPDS) |
| 1417 | s | ⊥ | |
| 1363 | m | ⊥ | increase intensity |
| 1355 | sh | | |
| 1325 | vw | ⊥ | increase intensity |
| 1314 | m | ⊥ | 〃 |
| 1297 | w | ∥ | 〃 |
| 1265 | w | ⊥ | appear |
| 1220 | w | ⊥ | |
| 1183 | m | ∥ | increase intensity |
| 1107 | m | ⊥ | |
| 1077 | | | (toluene ?) |
| 1055 | w | ⊥ | appear |
| 1021 | s | ⊥ | |
| 980 | w | | |
| 960 | w | | |
| 948 | m | ∥ | increase intensity |
| 915 | w | ⊥ | appear |
| 862 | m | ⊥ | increase intensity |
| 846 | vs | ⊥ | |
| 830 | sh | ∥ | appear |
| 776 | w | ⊥ | |
| 730 | | | (toluene ?) |
| 699 | m | ∥ | |
| 609 | vs | ⊥ | 605 $cm^{-1}$ (quenched IPPDS) |
| 560 | m | ∥ | 545 $cm^{-1}$ (quenched IPPDS and APPDS) |
| 493 | vw | ⊥ | |

a) Data on the crystallized IPPDS.

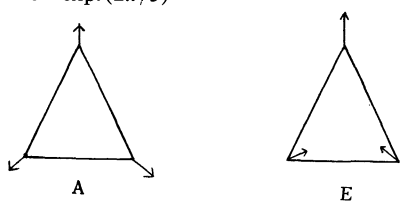
on the whole to that of APS, but is different on the points that 1) the 1070 $cm^{-1}$ band splits in the quenched IPS and 2) the 542 $cm^{-1}$ band in APS shifts to 557 $cm^{-1}$ in the quenched IPS. These cases may be considered to be the examples that the infrared spectrum indicates the existence of localized regularity in some narrow region, which can be hardly observed from the X-ray photographs. The band at 985 $cm^{-1}$ shows marked change of intensity with heat-treatment.*5 It is an interesting fact that a band which shows behavior similar to this band in the spectrum of IPS (crystallization-sensitive and perpendicular natures) appears also at the same wave number (980 $cm^{-1}$) in the case of IPTDS. This fact suggests that these bands appear from the similar origins and it would be considered that the bands can be used for the determination of the degree of crystallinity. In the spectra of IPPDS (Figs. 1c and 2c), the band at 948 $cm^{-1}$ is also very sensitive to crystallization, but has parallel dichroism, differing from the 985 $cm^{-1}$ band of IPS. The band which appears at about 906 $cm^{-1}$ in the spectrum of APS as well as the quenched IPS splits with crystallization into two bands, i. e. the perpendicular band at 920 $cm^{-1}$ and the parallel one at 898 $cm^{-1}$ (Fig. 2a). The intensity of the 755 $cm^{-1}$ band increases remarkably with crystallization.

**Treatment with Factor Group.** — The crystal structure of IPS analyzed by Natta et al.[5] and Bunn et al.[6] belongs to trigonal symmetry class. The molecular chain in the crystalline state has a structure of three-fold screw axis. An infinitely extended molecule of three-fold screw symmetry may be represented by a one-dimensional space group. When the interchain interaction is negligible, it is adequate to consider its factor group $C(2\pi/3)$ shown in Table IV[7]. The symmetry operation, $C^1$, bringing any structural unit into coincidence with an adjacent unit, consists of a rotation of $2\pi/3$ about the screw axis followed by a translation of 1/3 of the identity period of 6.65 Å along the axis. In the case of this group $C(2\pi/3)$, there appear the species A and E. In species A whole structural units vibrate in the same phase, and the direction of the transition moment is parallel with the screw axis. In species E, the phase of the vibration of a structural unit is different from that of the adjacent structural unit by $2\pi/3$, and consequently the direction of the transition moment is perpendicular to the screw axis. In the cases in which the interaction among the structural units is so strong that the frequencies of the A and the E modes clearly split, these bands should show strong dichroism. On the contrary, in the cases in which the interaction among the structural units is not so strong, and the frequencies of the A and the E modes are nearly equal, both bands, i. e. the parallel band of the species A and the perpendicular band of the species E, superpose in the same location of the spectrum. In this case the dichroism of the more intense component will appear. Which dichroism appears may be decided by the angle between the direction of the transition moment in each structural unit and the screw axis. It should be mentioned here that the vibrational modes, in which the interaction between the neighboring helical molecules is strong, can not be interpreted by the aforementioned method of factor group for a single molecular chain.

Table IV. Symmetry species, irreducible representations, number of normal modes, and selection rules for isotactic polystyrene under the group $C(2\pi/3)$

| | E | $C^1$ | $C^2$ | Null | vib. | $n$ | I. R. | Raman |
|---|---|---|---|---|---|---|---|---|
| A | 1 | 1 | 1 | $T_\parallel$ | R | 46 | active ($\parallel$) | active |
| E | 1 | $\varepsilon$ | $\varepsilon^2$ | $T_\perp$ | | 47 | active ($\perp$) | active |
| | 1 | $\varepsilon^{-1}$ | $\varepsilon^{-2}$ | $T_\perp$ | | 47 | | |

$\varepsilon = \exp i(2\pi/3)$




**Methylene Group Vibrations.**—The $CH_2$ antisymmetric stretching band at 2924 $cm^{-1}$ shows a distinguished perpendicular nature, which is explainable by the fact that the direction of the transition moment of this vibrational mode of each structural unit is nearly perpendicular to the screw axis. On the other hand, the $CH_2$ symmetric stretching band at 2849 $cm^{-1}$ shows only very weak dichroism. The direction of the transition moment of this vibrational mode is on the bisector of the angle H-C-H of the methylene group. The angle between this direction and the screw axis is considered to be about 58° from the angle 116° of the C-C-C of the main chain of this polymer estimated by Natta et al.[8]

*5 In the spectra of APS and quenched IPS, a weak band is observed at 980 $cm^{-1}$.

5) G. Natta and P. Corradini, *Makromol. Chem.*, **16**, 77 (1955).

6) C. W. Bunn and E. R. Howells, *J. Polymer Sci.*, **18**, 307 (1955).

7) A detailed description on the factor group analysis of a helical molecule will be found in C. Y. Liang and S. Krimm, *J. Chem. Phys.*, **25**, 563 (1956).

8) G. Natta and P. Corradini, *J. Polymer Sci.*, **20**, 251 (1956).

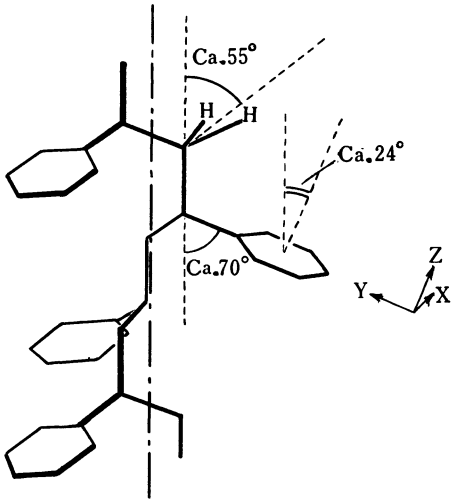



Fig. 3. The molecular structure of isotactic polystyrene in the crystalline state.

(Fig. 3). For perfect uniaxial orientation, the dichroic ratio, $R$, defined as the ratio of the optical densities with electric vector respectively parallel and perpendicular to the orientation direction, is given by $R=2\cot^2\varphi$, where $\varphi$ is the angle between the transition moment and the orientation direction. If $\varphi=54°44'$, $R=1$, i. e., the band exhibits no dichroism. The critical angle for $R=1$ is considered to increase only a small amount, when the orientation deviates from the perfect one. For instance, if the transition moments are uniformly distributed in a 20° angular range, the critical angle is 54°54'.[9] Thus the absence of the dichroic nature of the $CH_2$ symmetric stretching band could be explained, since the aforementioned angle 58° is near this critical angle. These dichroic natures of $CH_2$ stretching bands are hence considered to be characteristic of the helical structure (alternate sequence of trans and gauche conformations) of isotactic polystyrene. The same feature was found in the case of $CD_2$ stretching bands of IPTDS (2195 and 2095 $cm^{-1}$).

In the region of 1400~1100 $cm^{-1}$ the spectra of IPS and IPPDS change remarkably by heat-treatment (crystallization) and show distinguished dichroism as shown in Figs. 1 and 2. On the other hand, the absorption bands of IPTDS in this region which have comparatively weak dichroism, are not affected appreciably by heat-treatment, and are considerably different from those of IPS and IPPDS. The four bands (1364, 1314, 1297 and 1185 $cm^{-1}$), appearing in weak intensity in the spectra of quenched IPS and IPPDS, increase their intensity with crystallization, while they do not appear in the spectra of APS and APPDS (atactic poly-*p*-deuterostyrene). As these bands are absent in the spectra of IPTDS, these bands are considered to be not directly associated with the vibrations of the phenyl group, but mainly with that of the main chain. These four bands are also supposed to be closely associated with the helical structure of the IPS molecule in crystalline region, the detailed discussions of which we will report in the subsequent paper. On this problem we have briefly reported already.[10]

**Phenyl Group In-plane Vibrations.**—Now we wish to discuss the vibrational modes associated with the benzene ring. By calculating from the X-ray data of Natta et al.[5], it is estimated that the $y$ and the $z$ axes of the benzene ring shown in the figure in Table V are at an angle of about 70° and about 24° to the screw axis, respectively, and the $x$ axis at an angle of about 14° from the plane normal to the screw axis as shown in Fig. 3.

The vibrations of monosubstituted benzene which has point symmetry of $C_{2v}$ are useful for a step to the assignments of the bands due to phenyl group of polystyrene as studied by Liang et al.[3] in the case of APS previously. On the spectra and the vibrations of monosubstituted benzenes, a number of works have been done by many workers.[11-17] In Table V, we reproduce the symmetry species, the total number of normal vibrations associated with each species, $n$, and the infrared and the Raman activity to be expected, from the paper by Liang and Krimm[3]. As shown in this table, the transition moment for $A_1$ species is in the $y$ direction, that for $B_1$ in the $x$ direction and that for $B_2$ in the $z$ direction, which is the out-of-plane vibration. We may presume the dichroism of the bands, placing these phenyl groups on the three-fold screw axis. In the cases of $A_1$ and $B_1$ species (of $C_{2v}$), the component E (of $C(2\pi/3)$) must be more intense than the component A and so the dichroism should be perpendicular. On the contrary in the case of species $B_2$, the component A must be more intense and thus the parallel nature should appear.

The fact that the bands mainly due to the

9) C. Y. Liang and S. Krimm, *J. Chem. Phys.*, **27**, 1437 (1957).

10) H. Tadokoro, S. Nozakura, T. Kitazawa, Y. Yasuhara and S. Murahashi, This Bulletin, **32**, 313 (1959).

11) C. R. Bailey et al., *J. Chem. Soc.*, **1946**, 299.

12) E. K. Plyler, *Discussions Faraday Soc.*, No. **9**, 100 (1950).

13) D. H. Whiffen, *J. Chem. Soc.*, **1956**, 1350.

14) R. R. Randle and D. H. Whiffen, "Molecular Spectroscopy", Institute of Petroleum, London (1955), p. 111.

15) Y. Kakiuchi, *J. Chem. Soc. Japan, Pure Chem. Sec.* (*Nippon Kagaku Zasshi*), **77**, 1591 (1956).

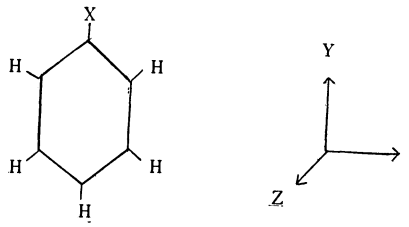
16) Y. Kakiuchi, ibid., **77**, 1839 (1956).

17) D. H. Whiffen, *Spectrochim. Acta*, **7**, 253 (1955).

TABLE V. SYMMETRY SPECIES AND NUMBER OF NORMAL MODES FOR MONOSUBSTITUTED BENZENE[3]

| $C_{2v}$ | E | $C_2(y)$ | $\sigma(xy)$ | $\sigma(yz)$ | Null vib. | $n$ | IR | R |
|---|---|---|---|---|---|---|---|---|
| $A_1$ | 1 | 1 | 1 | 1 | $T_y$ | 12 | a | a |
| $A_2$ | 1 | 1 | −1 | −1 | $R_y$ | 4 | f | a |
| $B_1$ | 1 | −1 | 1 | −1 | $T_x$, $R_z$ | 12 | a | a |
| $B_2$ | 1 | −1 | −1 | 1 | $T_z$, $R_x$ | 8 | a | a |

f=forbidden a=active




z-Axis is normal to the plane of the benzene ring.

CH stretching modes of phenyl group at about 3000 $cm^{-1}$ show perpendicular dichroism, is in good agreement with the presumption described above, because these bands should belong to $A_1$ or $B_1$ symmetry species.

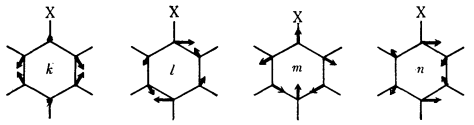
The bands at 1946, 1872, 1801, 1748 and 1675 $cm^{-1}$ (IPS and IPTDS) all show perpendicular dichroism. The similar bands in the spectra of monosubstituted benzenes have been assigned to the binary combinations of the CH out-of-plane deformation vibrations of phenyl group as shown in Table VI by Whiffen[17] and Kakiuchi[16] independently. Liang and Krimm[3] have assigned these bands in the case of polystyrene as shown in the same table. The assignments of these bands to symmetry species $A_1$ or $B_1$ by all these authors are in accord with the perpendicular dichroism of the bands. But the assignments of the component fundamental frequencies 906 and 755 $cm^{-1}$ by Liang and Krimm[3] are different from those by Whiffen[17] and Kakiuchi[16]. On this problem more detailed discussion will appear later.

TABLE VI. ASSIGNMENTS OF THE MAIN COMBINATION BANDS IN 2000~1700 $cm^{-1}$ REGION BY LIANG ET AL., WHIFFEN AND KAKIUCHI

| Wave number $cm^{-1}$ | Assignments | |
|---|---|---|
| | Liang and Krimm[3] | Whiffen[17] and Kakiuchi[16] |
| 1946 | $\nu_{17A}(A_2)+\nu_5(B_2)$, $B_1$ | $j(B_2)+h(A_2)$, $B_1$ |
| 1872 | $\nu_{17B}(B_2)+\nu_5(B_2)$, $A_1$ | $i(B_2)+h(A_2)$, $B_1$ |
| 1801 | $\nu_{10A}(A_2)+\nu_{17A}(A_2)$, $A_1$ | $g(A_2)+h(A_2)$, $A_1$ |
| 1748 | $\nu_{10A}(A_2)+\nu_{17B}(B_2)$, $B_1$ | $i(B_2)+g(A_2)$, $B_1$ |

Notations of the vibrations in this table are those of Liang et al. and of Whiffen, respectively.

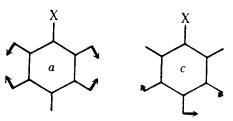
The four bands at 1602, 1583, 1493 and 1452 $cm^{-1}$ (IPS and IPTDS) show perpendicular dichroism, and are not affected appreciably by deuteration. These facts are consistent with the assignments to the in-plane C–C stretching vibrations of phenyl group by Whiffen et al.[13,14] as follows*6.




| | ($A_1$) | ($B_1$) | ($A_1$) | ($B_1$) |
|---|---|---|---|---|
| IPS | 1602 | 1583 | 1493 | 1452 $cm^{-1}$ |

Liang et al.[3] also have assigned these four bands to the C–C stretching model, except the assignments of 1602 and 1583 $cm^{-1}$ bands (to the l and k modes, respectively).

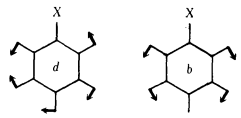
In the region of 1400~1100 $cm^{-1}$ the hydrogen deformation vibrations ($CH_2$ wagging and twisting, and CH wagging) of the main chain may couple to some extent with the in-plane vibrations of the benzene ring, showing the complex nature of the spectrum in the case of non-deuterated sample. In the spectrum of IPTDS the bands due to the vibrations of the deuterium of the main chain would shift to lower frequency region, and thus the aforementioned coupling may be removed. Accordingly the bands in this region may be considered to be mainly due to the vibrational modes of the benzene ring in the case of IPTDS. Thus the 1179 and 1154 $cm^{-1}$ bands of IPTDS may be assigned to the a and c modes of monosubstituted benzene according to the Whiffen's notation.[9] It is difficult to settle the assignments of the 1328 and 1240 $cm^{-1}$ bands from the present data.




| | ($A_1$) | ($B_1$) |
|---|---|---|
| IPS | 1185 | 1158 $cm^{-1}$ |
| IPTDS | 1179 | 1154 |

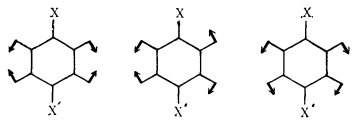
The 1070 $cm^{-1}$ band (APS) may be assigned to the d($\nu_{18B}$)($B_1$) mode. The splitting of this band in the case of IPS may be explained by the intramolecular interaction. The 1028 $cm^{-1}$ band may be assigned to the b ($\nu_{18A}$)($A_1$) mode, as Whiffen and Liang et al. assigned.

*6 In this paper the notation of the vibrational modes of the monosubstituted benzene by Whiffen (shown with h, j.···) will be mainly used for convenience, but those by Liang and Krimm ($\nu_{10A}$, $\nu_{17A}$,···) will also be added if necessary.



| | ($B_1$) | ($A_1$) |
|---|---|---|
| IPS | 1080, 1048 | 1028 $cm^{-1}$ |
| APS | 1070 | 1028 |

The 1183, 1107 and 1021 $cm^{-1}$ bands of IPPDS are considered to be the following CH in-plane modes, as Whiffen[14] and Ingold[11] assigned in the cases of *p*-substituted benzenes.



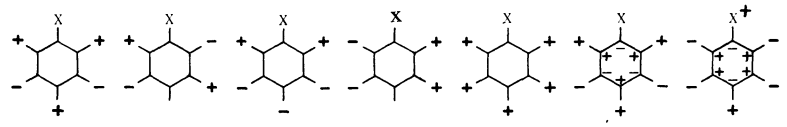
| | ($A_1$) | ($B_1$) | ($A_1$) |
|---|---|---|---|
| IPPDS | 1183 | 1107 | 1021 $cm^{-1}$ |
| PPMS | 1184 | 1110 | 1017 |

Here we have shown the data of poly-*p*-methylstyrene (PPMS) from our paper[10] for reference. The vibrational modes of the 1185 and 1028 $cm^{-1}$ band of IPS are the same with those of the 1183 and 1021 $cm^{-1}$ bands of IPPDS (and of the 1184 and 1017 $cm^{-1}$ band of PPMS) respectively. In the cases of these two vibrational modes the hydrogen atom of the *p*-position does not move significantly. Thus, the experimental fact that the substitution of the *p*-hydrogen atom with deuterium or methyl group does not affect these two bands appreciably may be reasonably explained. The 1106 $cm^{-1}$ band of IPPDS and the 1110 $cm^{-1}$ of PPMS are supposed to be characteristic of the *p*-substituted benzenes. It is natural that the bands which correspond to the c and d modes of IPS do not appear in the spectra of IPPDS and PPMS, since these modes contain the displacement of *p*-hydrogen atom.

**Phenyl Group Out-of-plane Vibrations.** — As mentioned in the previous section, the assignments of the two bands at 906 and 755 $cm^{-1}$ by Liang et al. are different from other authors (Whiffen[13] and Kakiuchi[16]), although the assignments of the other three bands (985, 965 and 842 $cm^{-1}$) in this region by all these authors are the same. They assigned these bands as shown in Table VII. The crystallization-sensitive 985 $cm^{-1}$ band may be assigned to the j mode by considering the position. The 906 $cm^{-1}$ band which splits into two bands of different polarizations with crystallization is assigned to the $\nu_{17B}$ vibration by Liang et al., while the band at 908±10 $cm^{-1}$ of monosubstituted benzenes was assigned to the i mode by Whiffen. Kakiuchi has calculated the frequency of this i mode to be 897 $cm^{-1}$ assuming the mass of the substituent atom to be infinite, and has made the similar assignment as Whiffen's. On the other hand, Liang and Krimm have assigned the 755 $cm^{-1}$ band to this i mode. The 755 $cm^{-1}$ band (the 751±15 $cm^{-1}$ band of monosubstituted benzene) was assigned to the f mode known as the "umbrella" vibrational mode by Whiffen. Kakiuchi has calculated the frequency of this mode to be 716 $cm^{-1}$, and has made similar assignment. To this f vibrational mode, Liang and Krimm have assigned the band at 700 $cm^{-1}$. Although it is difficult to decide which

TABLE VII. CH OUT-OF-PLANE VIBRATIONS OF IPS

| IPS | | | Monosubstituted benzene | | | |
|---|---|---|---|---|---|---|
| Frequency in $cm^{-1}$ | Intensity | Dichroism | Average frequency and intensity (Whiffen) | Vibrational mode (sym. species) (Whiffen) | Calculated frequency (Kakiuchi) | Polystyrene (Liang et al.) |
| 985 | m | ⊥ | 982±6 vw | j($B_2$) | 1004 | $\nu_5$=j |
| 965 | w | ⊥ | 962±6 w | h($A_2$) | 984 | $\nu_{17A}$=h |
| 906 { 920 | m | ⊥ | 908±10 mw | i($B_2$) | 897 | $\nu_{17B}$[a] |
| 906 { 898 | m | ∥ | | | | |
| 842 | w | ⊥ | 837±10 w | g($A_2$) | 837 | $\nu_{10A}$=g |
| 760 | vs | ∥ | 751±15 vvs | f($B_2$) | 716 | $\nu_{10B}$=i |
| 700 | vs | — | 697±11 vs | v($B_2$) | — | $\nu_{11}$=f |

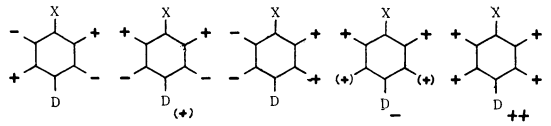


j h i g f v $\nu_{17B}$

a) No vibrational mode which corresponds to the $\nu_{17B}$ of Liang and Krimm's notation is in Whiffen's assignment.

TABLE VIII. CH OUT-OF-PLANE VIBRATIONS OF IPPDS

| IPPDS | | | *p*-Deuterotoluene (Kakiuchi[18]) | | |
|---|---|---|---|---|---|
| | | | Frequency in $cm^{-1}$ | | Vibrational mode |
| Frequency in $cm^{-1}$ | Intensity | Dichroism | Calculated | Assigned | |
| 960 | w | — | 984 | 951 | e |
| 948 | m | ∥ | 963 | 944 | c |
| 846 | vs | ⊥ | 837 | 840 | d |
| | | | 835 | 838 | b |
| 609 | vs | ⊥ | 630 | 607 | a |



e c d b a

assignment we should accept for polystyrene, it seems to be more favorable to apply Kakiuchi's assignment for this case, because of the agreement of the calculated value with the observed. Here we should mention the unexplainable dichroism of the 985 and 906 $cm^{-1}$ bands, which are expected to have parallel dichroism because of their symmetry species $B_2$. These complexities of the bands sensitive to crystallization, would have occurred from the interaction between the molecules in the crystalline lattice and could not be explained by the treatment on a single helical chain, which is a first approximation for the interpretation of the spectra of crystalline polystyrene.

The assignment of the CH out-of-plane vibrations of IPPDS can be made as shown in Table VIII on the basis of the work on *p*-deuterotoluene by Kakiuchi. Although the vibrational mode assigned to the 948 $cm^{-1}$ band of IPPDS is similar to that of the 983 $cm^{-1}$ band of IPS, the dichroisms of these two bands are different from each other, as described in the previous section. This difference may be explained by the change of the nature of the interaction between the molecular chains in the crystalline lattice owing to the deuteration of the *p*-position.

For detailed interpretation of the spectrum and the elucidation of the nature of intermolecular interaction in crystalline region, further accumulation of the experimental data is going on.

The authors express their sincere thanks to Professor T. Shimanouchi and Dr. M. Tsuboi of the University of Tokyo for helpful discussions and the measurements of parts of spectra by use of the Perkin-Elmer 112G spectrophotometer.

*Department of Polymer Science*
*Faculty of Science*
*Osaka University*
*Nakanoshima, Osaka*

18) Private communication.

# *An X-ray Study on the Phase Transition of Aniline Hydrobromide, $C_6H_5NH_3Br$*

By Inao TAGUCHI*

(Received August 1, 1960)

Crystal structures of amine halides can be divided into two groups. To the first group belong methylammonium chloride[1] and *n*-propylammonium halides[2], in which the nitrogen atoms are surrounded by four halogen atoms. To the second group belong adenine hydrochloride[3], hexamethylenediamine dihalides[4], aniline hydrochloride[5] and cyclohexamine hydrochloride[6], in which the nitrogen atoms are surrounded by three halogen atoms. It is interesting to note that those crystals belonging to the first group always exhibit a phase transition at low temperature, whereas no report has ever been made of any phase transition in crystals belonging to the second group.

A preliminary report on the crystal structure of aniline hydrobromide, $C_6H_5NH_3Br$, has been published[7], in which it was shown that the nitrogen atom in this crystal is surrounded by four bromine atoms. During the course of refinement, it was found that the crystal exhibits a peculiar type of phase transition in the neighbourhood of room temperature. Detailed structure analyses of the crystal below and above the transition temperature will soon be reported[8]. In the present paper, an account of an X-ray study on the phase transition of aniline hydrobromide will be given.

**Outline of the Phase Transition.** — Large crystals of aniline hydrobromide in the form described by Groth[9] are easily obtained by evaporation from methanol, ethanol or acetic acid solutions. Preliminary X-ray examinations showed that most of these crystals contained stacking disorder as revealed by diffuse scattering. Crystals free from stacking disorder were found to be obtainable by slow evaporation from methanol solutions. The crystals obtained are long along the [010] axis, and the planes (001) and (100) are predominant. A sharp cleavage is found parallel with (001).

Using these 'single crystals', a series of oscillation and Weissenberg photographs were prepared, using Cu $K$ radiations, about the three principal axes. It was found that not all but many reflections are split into two closely separated spots, appearing more or less blurred. If we ignore these splittings, all the reflections could be indexed based on an orthorhombic unit cell, in accord with the axial ratios given by Groth. It is suggested that these crystals are not really single crystals, but that they consist of repeated twins or polysynthetic twins[10], such as are found in orthorhombic pyroxene[11]. All the reflections appearing on oscillation photographs are split into two along the same $\zeta$-lines, except those of ($hk0$) and ($00l$). These can be interpreted, if we assume that the twin components or domains are oriented to two different directions, and that each domain is in fact monoclinic with an axial angle $\beta$ slightly deviated from 90°, and that all the domains have their $b$- and $c$-axes in common directions. All the reflections appearing on oscillation and Weissenberg photographs were satisfactorily indexed without any ambiguity by two axial systems, as schematically shown in Fig. 1.

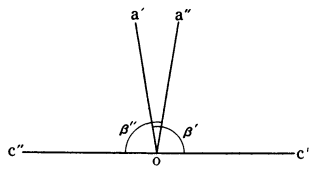



Fig. 1. Schematic representation of the orientations of the principal axes of the two components of the domains.

It was noticed that Weissenberg photographs prepared at different seasons of the year, using one and the same crystal, showed differences in detail. We were led to an assumption that these differences might be caused by a slight

* Deceased, May, 26 1959.

1) E. W. Hughes and W. N. Lipscomb, *J. Am. Chem. Soc.*, **63**, 1737 (1946).
2) M. V. King and W. N. Lipscomb, *Acta Cryst.*, **3**, 222, 227 (1950).
3) W. Cochran, ibid., **4**, 81 (1951).
4) W. P. Binne and J. M. Robertson, ibid., **2**, 180, 116 (1949).
5) C. J. Brown, ibid., **2**, 228 (1949).
6) A. Shimada, Y. Okaya and I. Nitta, ibid., **8**, 819 (1955).
7) I. Nitta, T. Watanabé and I. Taguchi, *X-rays*, **5**, 31 (1948).
8) I. Nitta, T. Watanabé and I. Taguchi, to be published in this Bulletin.
9) P. Groth, "Chemische Krystallographie" **IV**, (1917) p. 170.
10) I. Ito, "X-ray Studies on Polymorphism", (1950) p. 122.
11) T. Ito, *Z. Krist.*, **90**, 151 (1935).

variation of temperature. A series of Weissenberg photographs were taken at various temperatures, using a carefully designed temperature control camera[12], and confirmed the fact that they are really sensitive to temperature in the neighborhood of room temperature. Split reflections observed at 18°C became degenerated into a single one at 25°C, and blurred reflections at 18°C became more or less distinct. These changes were more marked at 50°C. From these observations, it was concluded that the crystal would undergo a phase transition in this temperature range, the splitting and blurring of reflections being associated with the formation of domains. The crystal does not shutter on passing the transition range.

**Variation of the Axial Angle $\beta$ with Temperature.** — From the preliminary experiments stated in the preceding paragraphs, it became clear that the splitting distances of reflections depend upon temperature, implying that the axial angle $\beta$ varies gradually with temperature. The variation of the axial angle $\beta$ with temperature was determined from the splitting distances of the reflection (002), which is the largest and most intense. The results are shown in Fig. 2. It was also found that the

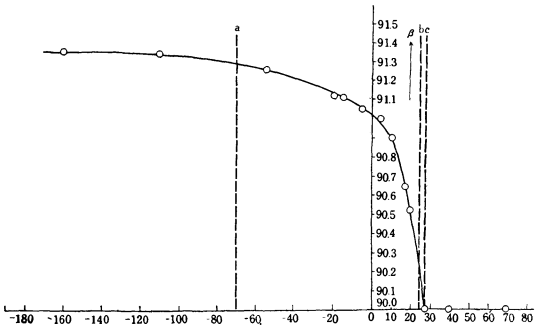



Fig. 2. Variation of the axial angle $\beta$ with temperature.

relative intensities of reflections vary with temperature, parallel with the variation of $\beta$ with temperature. The intensity variation ceases practically outside the range from +30°C to −70°C. The axial angle $\beta$ also remains unchanged outside this region. There was found to be no other phase transition down to −160°C as far as X-ray methods were employed.

The temperature variations of the axial angle $\beta$, of the relative intensities and of the fine structure of reflections were found to be reversible. Photographs taken after cooling or heating are practically the same as those taken before heat treatment.

12) I. Taguchi, *Annual Report Inst. Fiber Research, Osaka Univ.*, **8**, 45 (1954).

Now, in order to investigate the variation of the axial angle $\beta$ with temperature more precisely and to determine the transition temperature of the high temperature side, experiments at smaller temperature intervals were carried out at temperatures, ranging from 15°C to 30°C. Measurements for cooling were made after keeping the temperature of the crystal at 30°C for twenty hours. The results are shown in Fig. 3, where crosses and small circles are the values obtained for heating and cooling respectively. From all the observations and results obtained therefrom the following conclusions are made. (1) The transition temperature range is as wide as 100°C, i. e., from 27.5°C to ca. −70°C. (2) The phase change is perfectly reversible within the experimental error. (3) The phase transition is of a higher order. It was suggested that the specific heat curve would show the $\lambda$ type anomaly. The temperature range between −40°C and 24.5°C, as is shown by dotted lines a and b, might correspond to the ascending part of the specific heat curve, and the range between 24.5°C and 27.5°C as is shown by curves b and c might correspond to the declining part of the same curve. This view was recently verified by a calorimetric measurement[13].

**The Unit Cell Dimensions and Space Groups of the High and Low Temperature Modifications.** —Above 27.5°C, the crystal is orthorhombic, and below this temperature it is monoclinic. The unit cell dimensions and space groups of the two modifications, determined at 70°C and at −110°C, respectively, are given in Table I. There are four formula units in each unit cell.

Table I. The unit cell dimensions and space groups of the high and low temperature modifications

| | 70°C | −110°C |
|---|---|---|
| $a$ | 16.77±0.06 Å | 16.725±0.06 Å |
| $b$ | 6.05±0.03 | 5.95 ±0.03 |
| $c$ | 6.86±0.03 | 6.81 ±0.03 |
| $\beta$ | 90° | 91°22′ |
| Space group | $D_{2h}^{10}$-Pnaa | $C_{2h}^{5}$-$P2_1/a$ |

**Nature of the Domain Structure.**—It was found that the axis [010] and the plane (001) are in common with the two modifications and remain unaltered on passing the transition temperature. These features are illustrated schematically in Fig. 4. Since there are no appreciable changes in the axial parameters, the change of the axes can be taken as a kind of shear, which can be expressed by $\Delta\beta$ as is shown in Fig. 4.

13) H. Suga, This Bulletin, **34**, 426 (1961).

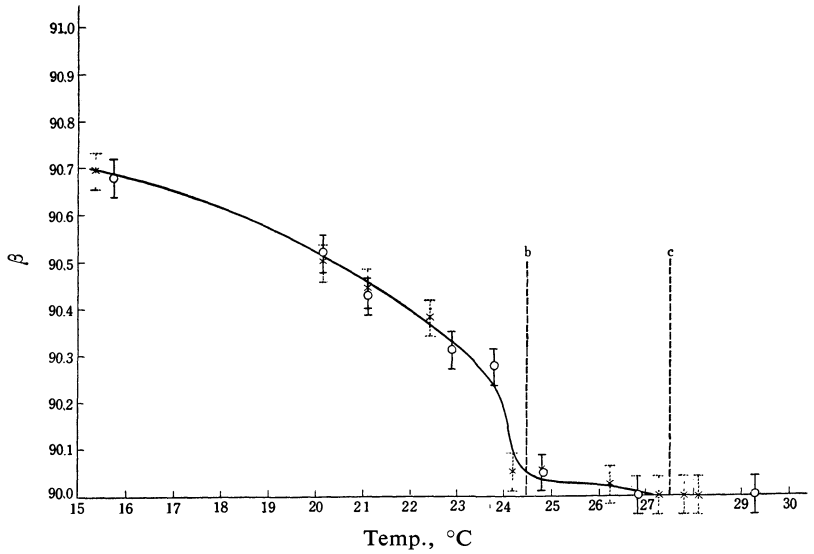



Fig. 3. Details of the variation of the axial angle $\beta$ with temperature.
○ : heating × : cooling

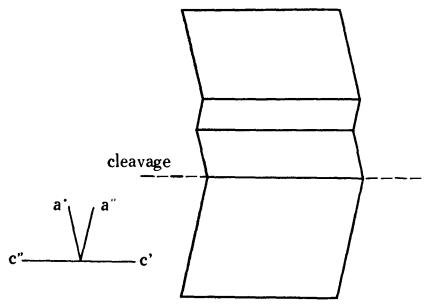



Fig. 4. Cleavage planes and the domain structure.

Below the transition temperature, the crystal is built up by domains which are oriented to the two directions, as shown in Fig. 4. These domains can be seen under a polarized microscope in certain specimens[14].

It was found that the ratios of the intensities within a pair of split reflections vary from specimen to specimen. For numerous specimens these ratios are found to be nearly at unity, as the formation of the two orientations of the domains is expected to occur with equal probability, though we have once found a specimen which is made of nearly a single domain.

Quite independent of these intensity ratios, or the abundance of the two orientations of the domains, each of a pair of split reflections shows a similar fine structure. There were found no complementary features in intensity in these split reflections, suggesting that these domains are interpenetrated.

On passing the transition temperature, no line broadening was ever found. This is in contrast to the observations reported for cobalt oxide[15], CoO, or potassium dihydrogen phosphate[16], $KH_2PO_4$. Thus the lower limit of the size of domains is of the order of $10^{-6}$ cm. No diffuse scattering associated with the splitted reflections was found, hence the domains are distributed in such a way that they are incoherent to X-ray. In this connection, it must be mentioned that in the cases of ferroelectric crystals there has never been reported any polysynthetic twinning associated with the domain formation.

As stated earlier, the (001) plane gives a perfect cleavage. The (100) plane also gives a cleavage at low temperature. It was observed that this latter cleavage becomes poorer as temperature increases, and finally vanishes at 30°C. This cleavage plane is the twinning plane between the two adjacent domains, as shown in Fig. 4. The vanishing of cleavage can be taken as a measure of the coalescence of the domain structure.

**The Mechanism of the Phase Transition.**—It will be interesting to discuss the structural change taking place during the transformation from symmetry considerations. There are four formula units in the unit cell, both of the high and low temperature modifications. The space group, $D_{2h}^{10}$-Pnaa, to which the high temperature modification belongs, requires that the anilinium ion, or more precisely the axis of anilinium ion passing through $N\text{-}C_1\cdots\cdots C_4$ atoms, should lie on a digonal axis. This

14) T. Iwai, to be published.

15) S. Greenwald, *Acta Cryst.*, 6, 396 (1953).
16) A. R. Ubbelohde and I. Woodward, *Proc. Roy. Soc.*, A188, 358 (1947).

implies that the three hydrogen atoms bound to the nitrogen atom are arranged in a statistical way so that the anilinium ion assumes a digonal symmetry in a statistical sense. In the low temperature modification, the anilinium ion is no more restricted by the digonal symmetry by virtue of the low symmetry of the crystal, $C_{2h}^5$-$P2_1/a$. Above the transition temperature, the $-NH_3^+$ group assumes two (or a multiple of two) equally stable orientations with respect to the C-N bond, or it may be flipping among different orientations. When the crystal is cooled down and passes the transition temperature, all the atoms move onto new equilibrium positions and the flipping ceases. These will be the most essential features of this phase transition.

The author would like to express his sincere thanks to Professors I. Nitta and T. Watanabé for their continued interest, and to Dr. Suga for valuable discussions.

*Department of Chemistry*
*Faculty of Science*
*Osaka University*
*Nakanoshima, Osaka*

# *The Effect of Alcohols on the Solubilization of Oleic Acid in the Aqueous Solution of Sodium Dodecyl Sulfate*

By Ryohei MATUURA, Kazuo FURUDATE, Hidetoshi TSUTSUMI and Seido MIIDA

(Received July 14, 1960)

It may well be established that the solubilizing power of the detergent towards hydrocarbons, such as *n*-heptane[1] and benzene[2], increases by adding alcohols in the detergent solution, the more markedly the longer the hydrocarbon chains of the added alcohols are. The solubilization of polar materials in the presence of alcohols in the detergent solution, however, has not been known well. Kolthoff and Graydon[3] studied the effect of *n*-amyl alcohol and *n*-octyl alcohol on the solubilization of some dyes in the potassium soap solutions and found no such regular and simple relations as for nonpolar substances. Some other studies also reported the complicated nature of the solubilization of polar materials in the presence of additives[4]. In order to make the situation clearer we have investigated the effect of various alcohols on the solubilization of oleic acid in the aqueous solution of sodium dodecyl sulfate.

## Experimental

**Materials.**—Sodium dodecyl sulfate (SDS) used was synthesized from fractionally distilled *n*-dodecyl alcohol and purified by repeated ether extraction. Its purity was confirmed by elementary analysis and surface tension measurements. The alcohols used were purified by distillation and their boiling points were as follows: *n*-butyl alcohol (117°C), *n*-hexyl alcohol (157°C), *n*-amyl alcohol (137.5~138.5°C), *iso*-amyl alcohol (132°C), *n*-octyl alcohol (194°C), *n*-dodecyl alcohol (127°C/7 mmHg) and *n*-hexadecyl alcohol (190°C/15 mmHg). Oleic acid was obtained by distillation at 211°C/6 mmHg.

**Method.** — The solubilization end point was measured by the turbidity method using a Shimadzu AKA photoelectric nephelometer. The experiment was performed at a constant temperature of 25.0°C.

## Results

In Fig. 1 the amount of oleic acid solubilized in the aqueous solution of SDS is plotted against the concentration of the latter. An almost linear relationship has been obtained. When an alcohol is added to the detergent solution beforehand, the solubilization of oleic acid decreases as shown in Figs. 2, 3 and 4 for the case of *n*-butyl, *n*-hexyl and *n*-hexadecyl alcohol, respectively. In Fig. 5 the amount of oleic acid solubilized is plotted against the amount of alcohols added to the detergent solution of 0.05 mol./l. It is seen that the solubilization of oleic acid decreases monotonously as the amount of alcohols added increases and this effect of decreasing the solubilization of oleic acid increases as the chain length of the alcohol increases.

1) H. B. Klevens, *J. Am. Chem. Soc.*, **72**, 3780 (1950).
2) K. Shinoda and H. Akamatsu, This Bulletin, **31**, 497 (1958).
3) I. M. Kolthoff and W. F. Graydon, *J. Phys. Chem.*, **55**, 699 (1951).
4) M. E. L. McBain and E. Hutchinson, "Solubilization", Academic Press Inc., New York (1955), p. 85.

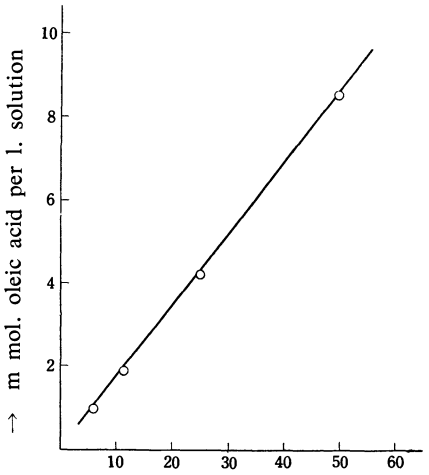



Fig. 1. The relation between the solubilized amount of oleic acid and the concentration of SDS.

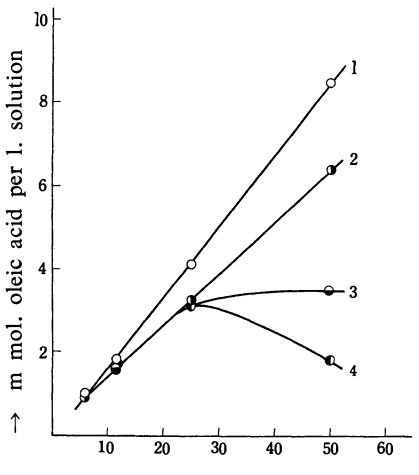



Fig. 2. The relation between the solubilized amount of oleic acid and the concentration of SDS containing *n*-butyl alcohol. Mol. SDS: mol. alcohol is 1, 1 : 0; 2, 1 : 1; 3, 1 : 2; 4, 1 : 3.

## Discussion

It may be a general agreement that alcohols added can cause a decrease in cmc of the detergent solution and an increase in micelle volume by penetration into the micelle surface. In the case of SDS solutions, Hutchinson et al.[5] measured the cmc in the presence of *n*-hexyl, *n*-heptyl and *n*-octyl alcohols and found that the cmc decreases as the amount of alcohols added increases. When hydrocarbon is solubilized in the detergent solution in the presence of alcohols, therefore, it is evident that its solubilization increases as the amount of alcohols added increases, since hydrocarbon is considered to dissolve in the micelle interior which has been made larger by the presence of alcohols. A typical example of the solubilization of hydrocarbon in the detergent solution in the presence of alcohols may be given by the result obtained by Klevens[1], which is reproduced in Fig. 6. This shows

5) E. Hutchinson, A. Inaba and L. G. Bailey, *Z. phys. Chem., N. F.*, 5, 344 (1955).

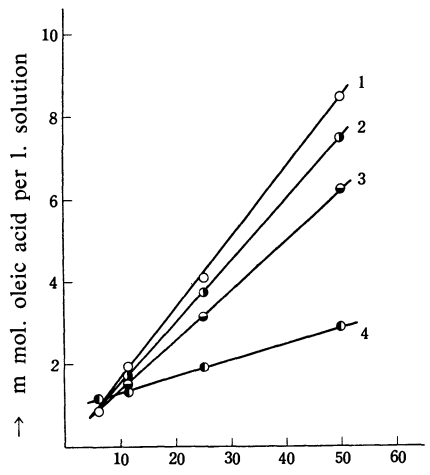



Fig. 3. The relation between the solubilized amount of oleic acid and the concentration of SDS containing *n*-hexyl alcohol. Mol. SDS: mol. alcohol is 1, 1 : 0; 2, 1 : 0.2; 3, 1 : 0.4; 4, 1 : 0.8.

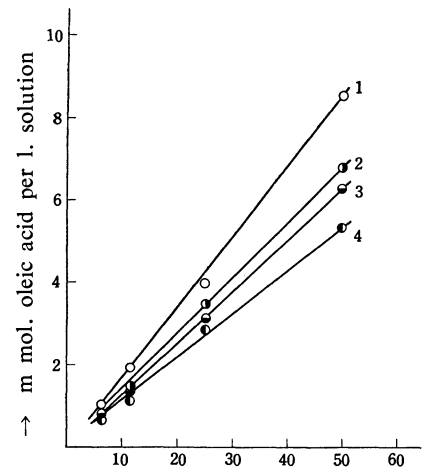



Fig. 4. The relation between the solubilized amount of oleic acid and the concentration of SDS containing *n*-hexadecyl alcohol. Mol. SDS: mol. alcohol is 1, 1 : 0; 2, 1 : 0.0081; 3, 1 : 0.0168; 4, 1 : 0.0276.

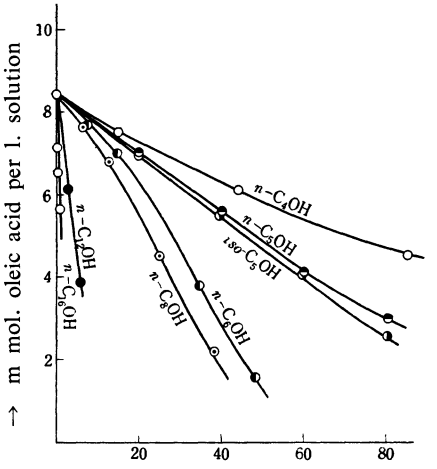



Fig. 5. The Effect of alcohols on the solubilization of oleic acid in 0.05 M SDS solution.

the effect of alcohols on the solubilization of *n*-heptane in the aqueous solution of potassium tetradecanoate. It is clearly seen that the solubilized amount of *n*-heptane increases as the amount of added alcohols increases, and that the effect of alcohols to increase the solubilization of the hydrocarbon increases with the chain length of the alcohols. The result shown in Fig. 6 is quite contrary to the result obtained in the present experiment which is shown in Fig. 5. The solubilized amount of oleic acid decreases as the amount of alcohols added increases, the more markedly the longer the hydrocarbon chain of the alcohols is. It will be reasonable to ascribe this difference to the fact that hydrocarbon dissolves in the micelle interior, while polar materials, such as oleic acid in the present experiment, dissolve in the palisade layer of the micelle. Since alcohols also dissolve in the palisade layer, oleic acid will be hindered from dissolving in the same place by already existing alcohol molecules, the result being that the solubilization of oleic acid decreases as the amount of alcohols increases in the detergent solution, as shown in Fig. 5.

In connection with the above explanation it may be interesting to note the effect of electrolytes on the solubilization of nonpolar and polar materials in the detergent solution. Klevens[6] studied the solubilization of *n*-heptane and *n*-octyl alcohol in the aqueous solution of potassium myristate in the presence of potassium chloride, potassium sulfate and potassium ferrocyanate. He found that the solubility of *n*-octyl alcohol decreases, while that of *n*-heptane increases, with the increasing electrolyte concentration in the detergent solution. Klevens explained this difference as follows. The increased aggregation of the micelles in the presence of electrolytes results in an increase in micelle interior volume which is available to a nonpolar solute, butre sults in a decrease in the micellar area which is available for penetration by a polar solute. Richards and McBain[7] also report that the presence of sodium chloride and potassium chloride decreases the solubilizing power of cetyl pyridinium chloride towards polar materials such as *n*-octyl alcohol and benzaldehyde, but increases that towards nonpolar materials such as benzene and *n*-octane. These results

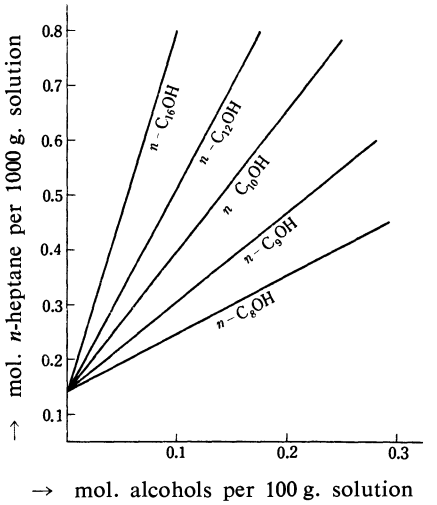



Fig. 6. The Effect of alcohols on the solubilization of *n*-heptane in 0.35 M K tetradecanoate solution (reproduced from Kleven's paper[1]).

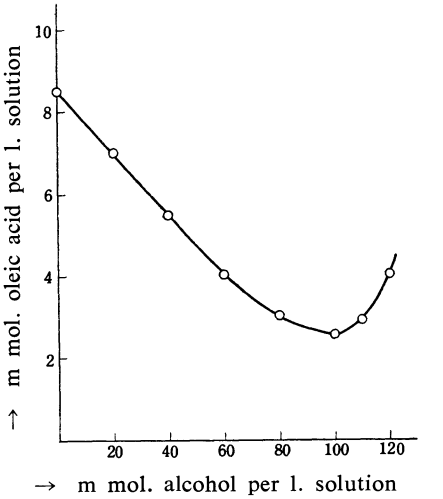



Fig. 7. The Effect of *n*-amyl alcohol on the solubilization of oleic acid in 0.05 M SDS solution.

6) H. B. Klevens, *J. Am. Chem. Soc.*, **72**, 3780 (1950).
7) R. H. Richards and J. W. McBain, ibid., **70**, 1338 (1948).

conform in their behaviors to the result obtained in the present experiment, the same explanation being applied, although the additives are electrolytes in the former and alcohols in the latter experiments.

It is to be noted that the concentration of alcohols in the detergent solution shown in Fig. 5 is not so great as that in Fig. 6. We found that, in the case of *n*-butyl and *n*-amyl alcohol, when the amount of alcohols in the detergent solution becomes greater than that shown in Fig. 5 the solubilization of oleic acid turns out to increase with the concentration of the alcohols in the detergent solution. The case of *n*-amyl alcohol is shown in Fig. 7. Since these alcohols are fairly soluble in water, the solvent property of water will alter as the amount of the alcohol in it becomes greater, the result being that the solubility of oleic acid in the solvent liquid will become appreciable. Also it may be probable that the micelle-forming property of the detergent is lessened by the presence of water soluble alcohols in fairly large concentrations, the result being that the solubilization of oleic acid in the detergent micelle will decrease. These two factors counteract each other in the determination of solubility of oleic acid in the detergent plus alcohol solutions. We see in Fig. 2 that the solubilization of oleic acid decreases when the concentration of the detergent containing *n*-butyl alcohol (mole ratio 1 : 3) exceeds a certain value. This may be attributed to the predomination of the factor of lessening the solubilization in the detergent micelle. On the contrary the result obtained in Fig. 7 may be attributed to the predomination of the factor of increasing the solubility of oleic acid in the water-alcohol mixture.

## Summary

The solubilization of oleic acid in the aqueous solution of sodium dodecyl sulfate was studied in the presence of various kinds of alcohols in various concentrations. When the concentration of alcohols in the detergent solution is not so great, the solubility of oleic acid decreases as the amount of alcohols increases. This is explained by the solution of oleic acid and alcohols in the same place in the micelle, i. e., in the palisade layer. When the water soluble alcohols are used the solubilization of oleic acid turns out to increase at a certain concentration of the alcohols in the detergent solution. This is explained by the solution of oleic acid in the solvent liquid as well as in the detergent micelles.

*Department of Chemistry*
*Faculty of Science*
*Kyushu University*
*Fukuoka*

# *Synthesis and Physical Properties of Normal Higher Primary Alcohols. III. Synthesis of Normal Higher Primary Alcohols of Even Carbon Numbers from Dodecanol to Hexatriacontanol*

By Akira WATANABE*

(Received July 23, 1960)

In the previous investigation of this series[1,2] the author confined his attention to the synthesis of normal higher alcohols of odd carbon numbers. In view of the interesting results on the physical properties, especially the transition phenomena of these alcohols in the solid state, it was felt desirable to extend the study to alcohols of even carbon numbers, and thirteen members with even carbon atoms ranging from $C_{12}$ to $C_{36}$ were synthesized and their transition points were observed.

The alcohols were all prepared by the lithium aluminum hydride reduction of the corresponding fatty acids or their ethyl esters, of which acids from $C_{12}$ to $C_{22}$ were obtained by careful purification of commercial specimens.

Tetracosanoic acid ($C_{23}H_{47}CO_2H$) was synthesized from docosyl bromide ($C_{22}H_{45}Br$) by the modified malonic ester synthesis[3]. The method employed for the synthesis of the fatty

* Some parts of this work were performed at the Department of Chemistry, Faculty of Science, Kyoto University, Sakyo-ku, Kyoto.

1) A. Watanabe, This Bulletin, **32**, 1295 (1959).
2) A. Watanabe, ibid., **33**, 531 (1960).
3) W. Bleyberg et al., *Ber.*, **64**, 2506 (1931).

acids with more than 24 carbon atoms is Bowman's synthesis:

$$C_2H_5O_2C(CH_2)_nBr \xrightarrow{\text{Ethyl malonate}}$$
(I)

$$C_2H_5O_2C(CH_2)_nCH(CO_2C_2H_5)_2 \xrightarrow{\text{Benzyl alcohol}}$$
(II)

$$C_6H_5CH_2O_2C(CH_2)_nCH(CO_2CH_2C_6H_5)_2 \xrightarrow{RCOCl}$$
(III)

$$C_6H_5CH_2O_2C(CH_2)_nC(CO_2CH_2C_6H_5)_2COR \xrightarrow{H_2(Pd)}$$
(IV)

$$HO_2C(CH_2)_nC(CO_2H)_2COR \xrightarrow{\text{Decarboxylation}}$$
(V)

$$RCO(CH_2)_{n+1}CO_2H \xrightarrow[\text{reduction}]{\text{Huang-Minlon}}$$
(VI)

$$R(CH_2)_{n+2}CO_2H \xrightarrow[LiAlH_4]{\text{Esterification}} R(CH_2)_{n+3}OH$$
(VII) (VIII)

Although this method was extensively applied in the preparation of odd members[1,2], the yields of the ketonic acids were low and fluctuated (maximum 37%) compared with those obtained by Bowman (70%). Nunn[4] and Hougen[5] reported similar low yields, and ascribed them to the ketonic hydrolysis of the ketoesters, although their studies appeared not to be extensive. Since it was felt necessary to increase the yield and convenience in order to develop the present study, several improvements in the synthetic technique were made and the results are reported in this paper.

It was found that partial hydrolysis of triester II occurred in spite of precautions during the reaction of alcoholysis as evidenced by the isolation of the carboxylic acid from the reaction mixture in an amount of 30% to the starting triester and by the recovery of a nearly corresponding amount of benzyl alcohol. It seemed quite probable that the presence of this acid and the alcohol was detrimental to the subsequent malonic ester condensation. The procedures were then improved as follows, giving the desired product with a fairly good and consistent yield.

After the alcoholysis the acid was removed with a sodium carbonate solution and benzyl alcohol was distilled off under reduced pressure. Tribenzyl ester III, freed from the acid and benzyl alcohol and obtained as an oil, was condensed with an acid chloride by means of sodium ethoxide to give compound IV. Hydrogenolysis of compound IV and subsequent decarboxylation yielded ketonic acid VI in a yield of 65% based on the acid chloride. Details of the procedures are given in the Experimental Part.

In order to avoid the hydrolysis of triester II, the use of sulfuric acid, hydrogen chloride, and zinc chloride as the catalysts for the alcoholysis were attempted with no success. Metallic sodium, instead of sodium ethoxide, was used in the malonic ester condensation without success, probably because the hydrogen from the reaction of sodium with the malonic ester cleaved the benzyl groups.

Another factor which affects the yield is the instability of compound IV as shown by the fact that this compound was decomposed even at room temperature by the hydrochloric acid liberated from the unchanged acid chloride on washing the reaction mixture with water. At temperature low enough to be harmless to the compound it was quite difficult to decompose the acid chloride with water when the carbon chain of the acid was long. Therefore, it is advisable to use slightly less than one equivalent of the acid chloride to obtain a good yield.

It has been known that Bowman's synthesis suffers from the catalyst poisoning which can not be avoided on account of the difficulty in purification of compound IV, and it was experienced in the previous study[2] that a long period was required for complete hydrogenolysis when the intermediate acid chloride could not be purified by distillation. However, in the present experiments, it was found advantageous to purify compound IV with activated aluminum oxide, permitting the complete hydrogenolysis with great saving in time and catalysts and with no lowering of the yield of ketonic acid V.

The ketonic acids thus obtained were all converted into the corresponding fatty acids by Huang-Minlon reduction[6] and the desired alcohols were obtained easily by the lithium aluminum hydride reduction of the fatty acids or their ethyl esters. The alcohols were purified with great care to obtain the final products with sharp melting points and excellent analytical values. For hexacosanol $C_{26}H_{53}OH$ and higher alcohols high vacuum ($2\times10^{-3}$ mmHg) distillation as well as recrystallization was employed.

An alternative chain-lengthening process for the synthesis of octacosanol $C_{28}H_{57}OH$ is Cason's method[7], which consists in the condensation of a dialkyl cadmium with a halfester-acid chloride. The accompanying flow chart indicates the reaction:

4) J. R. Nunn, *J. Chem. Soc.*, **1951**, 1742.
5) F. W. Hougen et al., ibid., **1953**, 98.
6) Huang-Minlon, *J. Am. Chem. Soc.*, **66**, 839 (1944).
7) J. Cason, ibid., **68**, 2078 (1946).

TABLE I

| Alcohol | Formula | Calcd. C | Calcd. H | Found C | Found H | M. p., °C | F. p., °C | T. p., °C |
|---|---|---|---|---|---|---|---|---|
| Dodecyl | $C_{12}H_{26}O$ | 77.35 | 14.07 | 77.46 | 14.00 | 22.5(24.0[a]) | 22.3 | |
| Tetradecyl | $C_{14}H_{30}O$ | 78.43 | 14.11 | 78.36 | 13.90 | 39.0(37.7[b]) | 37.5 | 33.5 |
| Hexadecyl | $C_{16}H_{34}O$ | 79.26 | 14.14 | 79.02 | 14.22 | 48.5(49.0[c]) | 48.0 | 42.5 |
| Octadecyl | $C_{18}H_{38}O$ | 79.92 | 14.16 | 80.11 | 14.25 | 58.5(58.5[d]) | 58.0 | 50.0 |
| Eicosyl | $C_{20}H_{42}O$ | 80.46 | 14.18 | 80.41 | 14.02 | 65.3(66.5[e]) | 64.2 | 55.5 |
| Docosyl | $C_{22}H_{46}O$ | 80.90 | 14.20 | 80.86 | 14.07 | 70.4(70.8[e]) | 69.3 | 61.0 |
| Tetracosyl | $C_{24}H_{50}O$ | 81.28 | 14.21 | 81.43 | 14.29 | 76.0(75.3[e]) | 75.7 | 68.0 |
| Hexacosyl | $C_{26}H_{54}O$ | 81.60 | 14.22 | 81.70 | 14.48 | 78.8(79.2[e]) | 78.2 | 73.0 |
| Octacosyl | $C_{28}H_{58}O$ | 81.87 | 14.23 | 81.75 | 14.10 | 82.5(82.6[e]) | 82.0 | |
| Triacontyl | $C_{30}H_{62}O$ | 82.11 | 14.24 | 82.22 | 14.19 | 86.3(86.5[e]) | 85.5 | |
| Dotriacontyl | $C_{32}H_{66}O$ | 82.32 | 14.25 | 82.40 | 14.21 | 88.2(89.2[e]) | 87.0 | |
| Tetratriacontyl | $C_{34}H_{70}O$ | 82.51 | 14.26 | 82.35 | 14.20 | 91.0(91.7[e]) | 89.5 | |
| Hexatriacontyl | $C_{36}H_{74}O$ | 82.68 | 14.26 | 82.40 | 14.22 | 91.6(92.6[e]) | 89.5 | |

Melting points are uncorrected.

When a sample was cooled below its freezing point from the melt, a transition appeared with the change of the transparent waxy material into the opaque crystalline state. Transition points of the alcohols higher than hexacosanol could not be observed.

a) F. Krafft, *Ber.*, **16**, 1718 (1883).
b) W. E. Garner et al., *J. Chem. Soc.*, **1927**, 1357.
c) F. Krafft, *Ber.*, **16**, 1721 (1883).
d) P. A. Levene et al., *J. Biol. Chem.*, **59**, 914 (1924).
e) F. Francis et al., *Proc. Roy. Soc.*, A **158**, 691 (1937).

TABLE II

| Ethyl alkane-tricarboxylates | Acid chlorides (Cno.) | Ketonic acid (Cno.) | M. p., °C | Fatty acid | M. p., °C |
|---|---|---|---|---|---|
| *n*-Undecane | Myristoyl ($C_{14}$) | $CH_3(CH_2)_{12}CO(CH_2)_{11}CO_2H(C_{26})$ | 95.5 | Hexacosanoic | 86.5(87.7)* |
| 〃 | Palmitoyl ($C_{16}$) | $CH_3(CH_2)_{14}CO(CH_2)_{11}CO_2H(C_{28})$ | 99.5 | Octacosanoic | 90.2(90.9) |
| 〃 | Stearoyl ($C_{18}$) | $CH_3(CH_2)_{16}CO(CH_2)_{11}CO_2H(C_{30})$ | 102.6 | Triacontanoic | 93.0(93.6) |
| *n*-Octane | Tricosanoyl ($C_{23}$) | $CH_3(CH_2)_{21}CO(CH_2)_8CO_2H(C_{32})$ | 105.5 | Dotriacontanoic | 96.0(96.2) |
| *n*-Undecane | Docosanoyl ($C_{22}$) | $CH_3(CH_2)_{20}CO(CH_2)_{11}CO_2H(C_{34})$ | 107.5 | Tetratriacontanoic | 97.8(98.2) |
| 〃 | Tetracosanoyl ($C_{24}$) | $CH_3(CH_2)_{22}CO(CH_2)_{11}CO_2H(C_{36})$ | 110.0 | Hexatriacontanoic | 98.5(99.9) |

* F. Francis et al., *Proc. Roy. Soc.*, A **158**, 691 (1937).

$$C_{18}H_{37}OH \xrightarrow{HBr} C_{18}H_{37}Br \rightarrow C_{18}H_{37}MgBr \xrightarrow{CdCl_2} (C_{18}H_{37})_2Cd \xrightarrow{ClOC(CH_2)_8CO_2C_2H_5}$$

$$C_{18}H_{37}CO(CH_2)_8CO_2C_2H_5 \xrightarrow[\text{reduction}]{\text{Huang-Minlon}}$$

$$C_{27}H_{55}CO_2H \xrightarrow[LiAlH_4]{\text{Ethyl ester}} C_{28}H_{57}OH$$

The alcohol obtained by this method was shown to be identical with that obtained by Bowman's method by the mixed melting point and the X-ray data[8].

Melting points, transition points and analytical data of the alcohols synthesized here are given in Table I. The transition points of the alcohols with more than 22 carbon atoms have been unknown. All the alcohols described in this paper and two previous papers, namely odd and even members from $C_{11}$ to $C_{37}$, are being studied for their physical properties and part of the results has been published from the Department of Physics of Kyoto University[9-11]. Thermal data will be reported in this Bulletin in near future.

## Experimental

Since the reactions used for the synthesis of the lower members are well known, descriptions of the experiments are omitted. Bowman's[4] method was applied with some improvements for the synthesis of the alcohols with more than 24 carbon atoms. As the conditions except those for isolation of the products, were essentially the same throughout the series, the synthesis of octacosanol is described as an illustration. Combinations of the starting materials and the intermediates are listed in Table II.

*Ethyl n-Undecane-1, 1, 11-tricarboxylate.* — It was

8) A. Watanabe, unpublished.

9) K. Tanaka, T. Seto and T. Hayashida, *Bull. Inst. Chem. Res. Kyoto Univ.*, **35**, 123 (1957).
10) K. Tanaka, T. Seto, A. Watanabe and T. Hayashida, ibid., **37**, 281 (1959).
11) K. Asai, *J. Phys. Soc. Japan*, **14**, 1084 (1959).

prepared by condensation of ethyl bromoundecanoate with ethyl malonate as already described[2].

B. p. 187°C/1 mmHg, $n_D^{28}$ 1.4435.

*Benzyl n-Undecane-1, 1, 11-tricarboxylate*.—In a 200 ml. three-necked flask, equipped with a mechanical stirrer, a dropping funnel and a reflux condenser fitted with a calcium chloride tube, were placed 0.65 g. of sodium sand (finely powdered in toluene) and 50 ml. of thiophene-free dry benzene. To the mixture was added from the dropping funnel 10 g. of ethyl *n*-undecane-1, 1, 11-tricarboxylate. The mixture was allowed to stand at room temperature for about 6 hr. with stirring and then moderately heated to the complete disappearance of the sodium. After 8.7 g. of freshly distilled benzyl alcohol was added, the condenser was replaced by a Fenske column and the mixture was heated to distill off ethanol as the benzene ethanol azeotrope. During the distillation reflux-ratio was controlled from 6 : 1 to 20 : 1 (2~3 drops per minute). When no more ethanol distilled over, the boiling point reaching 79°C and the absence of the ethanol in the final portion of the distillate being confirmed by the index of refraction, the mixture was cooled and acidified with dilute sulfuric acid. The benzene layer was separated, washed with water, with sodium carbonate solution, again with water to neutral reaction, and dried over sodium sulfate.

After evaporating the benzene, the residue was heated to 120°C in an oil bath under reduced pressure (3 mmHg), the flask being immersed into the bath as deeply as possible to remove the benzyl alcohol completely. Recovered benzyl alcohol weighed 2.5 g. The Tribenzyl ester III remained in the flask as an oil which weighed 11 g. On acidification of the above alkali washing with sulfuric acid, an oily substance separated out which gradually crystallized on standing several days. Recrystallization from ethyl acetate-petroleum ether gave the product in white crystals, m. p. 89°C. It was found not to depress the melting point when mixed with the acid obtained by hydrolysis of the triester.

*13-Keto-octacosanoic Acid* $C_{15}H_{31}CO(CH_2)_{11}CO_2H$.—In a 200 ml. three-necked flask, 0.41 g. of freshly cut sodium was placed. Absolute ethanol (5 ml.) was added to give a clear solution. All excess of the ethanol was distilled off until a crust of sodium ethoxide was formed on the surface of the residue. Then 15 ml. of dry thiophene-free benzene was added from the dropping funnel. To this suspension a solution of 11 g. of the tribenzyl ester in 10 ml. of benzene was added and the mixture was allowed to stand at room temperature with occasional shaking, while the solid gradually went into solution. The benzene was removed under reduced pressure at room temperature, leaving a brown syrup in the flask. Two portions of 10 ml. of fresh benzene were added and removed under reduced pressure to remove the last traces of ethanol. Thus the sodium salt of the tribenzyl ester was obtained as a brown viscous material, to which 30 ml. of fresh benzene was added, giving a colored solution. Then the flask was equipped with a stirrer and a reflux condenser fitted with a calcium chloride tube. A solution of 5.2 g. of palmitoyl chloride (prepared from pure acid and thionyl chloride, b. p. 148°C/1.5 mmHg) in 10 ml. of benzene was added from the dropping funnel with stirring and the mixture was refluxed for 30 min. with continued stirring.

After the reaction mixture attained room temperature the flask was immersed in an ice bath. Ice-cooled water containing 1 g. of sulfuric acid was added gradually with vigorous stirring, the temperature of the mixture being maintained at 3 to 5°C. The contents of the flask were then transfered to a separating funnel. The layers were separated with the aid of a small amount of ethanol and the benzene layer was washed with water to neutral reaction with occasional cooling to prevent the temperature from rising above 5°C. After the solution was dried over sodium sulfate the benzene was removed under reduced pressure at about 30°C of bath temperature. The condensation product remained as an oil (15 g.). A solution of 5 g. of the above product in a mixture of 15 ml. of ethyl acetate and 15 ml. of absolute ethanol was shaken with Pd-C (0.2 g.) and Pd-$SrCO_3$ (0.2 g.) in a hydrogen atmosphere at room temperature. Catalyst poisoning was so often encountered that it was necessary to add fresh catalysts frequently until a nearly theoretical amount of hydrogen was absorbed. The total amount of the catalyst used was 2.7 g. The time required for the complete hydrogenolysis was about 4 hr. The solution freed from the catalyst was refluxed for 30 min. to decarboxylate the product. Upon cooling the solution to room temperature white crystals appeared. These were collected and washed with ethyl acetate. The ketonic acid obtained showed the melting point of 91 to 94°C. Yield was 1.5 g. The filtrate and washing were combined and concentrated to a syrup. To this was added 10 ml. of acetic acid containing 1 ml. of sulfuric acid and the mixture was refluxed for 40 min. The solid residue obtained on removing acetic acid was taken up in benzene and the solution was washed and dried over sodium sulfate. Concentration and subsequent cooling of the benzene solution gave white crystals which melted at 93 to 97°C and weighed 0.6 g. The substance was combined with the acid obtained from the ethyl acetate solution and the combined crystals were recrystallized twice from benzene. The pure ketonic acid showed the melting point of 99.5°C. The yield was 1.8 g. or 65% based on palmitoyl chloride.

Found : C, 76.60 ; H, 12.45. Calcd. for $C_{28}H_{54}O_3$: C, 76.65 ; H, 12.41%.

Palmitic acid (0.15 g.) was recovered from the filtrate of the ketonic acid.

*Purification of the Condensation Product (IV)*.—The product (5 g.) was dissolved in 20 ml. of pure benzene (dried over sodium wire) and the solution was shaken with active alumina for a short period. The alumina was filtered off and the filtrate was evaporated under reduced pressure at about 30°C of bath temperature to give a colorless liquid. This was hydrogenated in the same manner as described above. Absorption of the first 280 ml. of hydrogen proceeded rapidly (30 min.) with 0.4 g. of the catalyst. The second 140 ml. was absorbed in about 1 hr. with the addition of 0.3 g. of the catalyst. The product was treated in the same way as the

above. The yield of the pure ketonic acid was 1.8 g. (65%).

*Octacosanol* $C_{28}H_{57}OH$. — Octacosanoic acid ($C_{27}H_{55}CO_2H$) was obtained from 3 g. of the ketonic acid by the Huang-Minlon reduction[6] in a yield of 77% (2.2 g.). Details were given in the previous paper[2] for the reaction of other higher alcohols. The melting point was 90.2°C (recrystallized from toluene).

Found: C, 79.10; H, 13.34. Calcd for $C_{28}H_{56}O_2$: C, 79.18; H, 13.29%.

The acid was converted into its ethyl ester by a usual method. The lithium aluminum hydride reduction[2] of 2 g. of the pure ester (recrystallized from benzene, m. p. 64°C) afforded 1.4 g. of the desired alcohol after recrystallization from benzene. The melting point was 82.5°C. Further purification of the alcohol was tried by high vacuum distillation ($2\times10^{-3}$ mmHg) followed by recrystallizations. Although the melting point and analytical data were not changed, the physical data[8] indicated that these procedures seemed to be necessary to obtain a pure sample.

The author expresses his sincere thanks to Professor Ryozo Goto, Kyoto University, for his kind guidance throughout this study. Thanks are also due to Mr. T. Araki and Mr. H. Horino for their assistance in some of the experiments. The cost of this work was partly defrayed from a grant (Shigenkagaku Kenkyuhi) from the Ministry of Education.

*Department of Applied Chemistry*
*Himeji Technical College*
*Idei, Himeji*

# *Distribution of Neptunium between Di-(2-ethyl hexyl)-phosphoric Acid and Mineral Acids*

By Eiko NAKAMURA

(Received June 28, 1960)

Solvent extraction studies on neptunium have been carried out using tri-*n*-butyl phosphate[1-4], tertiary amines[5], thenoyl tri-fluoro acetone[6], diethyl ether[7] or methyl isobutyl ketone[7], as an extractant.

However, the extraction behavior of neptunium using di-(2-ethyl hexyl)-phosphoric acid, HDEHP, has not been reported. The experimental results in the works referred to above have usually been complicated unless careful precautions were taken, because the neptunium tracer solution often contains neptunium in two or three oxidation states. Giving special attention to the oxidation states of neptunium, the extraction behavior of quadri-, quinqui- and sexi-valent neptunium in the system of diluted HDEHP vs. hydrochloric or perchloric acid was studied in this work.

Di-(2-ethyl hexyl)-phosphoric acid has been proved to be useful as a solvent extracting agent for uranium(VI) and other metals. Some works about this extracting agent have been published by a number of investigators[8-10]. Recently a comprehensive study on the extraction of metal ions from hydrochloric acid solution has been reported by Kimura[11]. According to these previous works, it seems that HDEHP behaves as a cation extracting reagent in the low acidity region. In other words, HDEHP-metal ion complex is formed with the inorganic cation in the aqueous phase, and extracted into the organic phase which is composed of the organic diluent and HDEHP. The neptunium(IV), (V) and (VI) cations also seemed to be extracted as the HDEHP-neptunium(IV), (V) or (VI) cation complex.

## Experimental

**Reagents.**—The HDEHP received from Virginia Chemicals, Co. Ltd. was purified by the method of Peppard et al.[12] It was diluted with toluene, C. P.

1) T. Ishimori and E. Nakamura, This Bulletin, **32**, 713 (1959).
2) H. A. C. McKay, J. S. Nairn and M. B. Waldron, *Second United Nations International Conference on the Peaceful Uses of Atomic Energy*, p/304 (1958).
3) J. S. Nairn, D. A. Collins, H. A. C. McKay and A. G. Maddock, ibid, p/1458 (1958).
4) W. H. Lewis, ibid, p/537 (1958).
5) J. C. Sheppard, HW-51958 (1957).
6) L. B. Magnusson, J. C. Hindman and T. J. LaChapell, ANL-4066 (1947).
7) J. Kooi, *First United Nations International Conference on the Peaceful Uses of Atomic Energy*, Vol. VII, p/929, United Nations Publication, New York (1956).
8) C. F. Baes, Jr., R. A. Zingaro and C. C. Coleman, *J. Phys. Chem.*, **62**, 129 (1958).
9) D. F. Peppard, G. W. Mason. W. J. Driscoll and R. J. Sironen, *J. Inorg. & Nucl. Chem.*, **7**, 276 (1958).
10) D. F. Peppard and J. R. Ferraro, ibid., **10**, 275 (1959).
11) K. Kimura, This Bulletin, **33**, 1038 (1960).
12) D. F. Peppard, G. W. Mason, J. L. Maier and W J. Driscoll, *J. Inor. & Nucl. Chem.*, **4**, 334 (1957).

grade, in this work. Hydrochloric and perchloric acids, analytical grade, were used as received.

Carrier-free 2.3d-neptunium-239, 27.5d-protactinium-233 and 24.1d-thorium-234 were prepared as described in the previous paper[1,13]. The activities of these nuclides were measured by a gamma-scintillation counter. Zirconium-niobium-95 imported from the Oak Ridge National Laboratory, Tenn. USA, was used as received and measured the hard beta-rays of zirconium-95 cutting off the soft beta-rays of niobium-95.

The radiochemical purity of the tracers was checked by gamma-spectrometry, beta-ray absorption and decay.

According to the method written in the previous work[1], the quadri-, quinqui- and sexi-valent neptunium tracers were prepared. In the case of quadrivalent neptunium, hydrochloric acid was used as the aqueous medium, because neptunium(IV) is unstable in a perchloric medium[1].

**Distribution Measurement.**—All experiments were carried out with radioactive tracers. The distribution ratio, $K_d$, of a given nuclide was determined in the usual way[1,11]. The scrubbing techniques were used in every case in order to obtain the $K_d$ values exactly. In all cases both acid and solvent dependence of the $K_d$ values were determined.

## Results and Discussion

**Distribution of Sexivalent Neptunium in the System of HDEHP vs. Perchloric Acid.**—The distribution ratios of sexivalent neptunium were determined in the system of about 0.6% (v/v) HDEHP-toluene vs. perchloric acid varying the acidity from 0.1 to 0.5 N. Experimental results are shown in Fig. 1 where the curve for uranium(VI), taken from the work of Baes et al.[8], is also given for comparison. Baes et al. determined the distribution ratio of uranium in the system of 0.1 M (3.33% v/v) HDEHP-hexane vs. perchloric acid changing the acidity from 0.01 to 2.0 N.

From these results it is found that both sexivalent neptunium and uranium are extracted very well with HDEHP from perchloric acid solution. As Fig. 1 shows, both lines for neptunium and uranium have the slope of −2, suggesting a close similarity between uranium (VI) and neptunium(VI) ions.

The solvent dependence of $K_d$ values for sexivalent neptunium was determined at 0.52 N perchloric acid concentration using toluene as the diluent. Experimental results for neptunium(VI) are shown in Fig. 2 together with the solvent dependence curve for uranium at 1 N perchloric acid, which is quoted from the work of Baes et al.[8] The distribution ratios of neptunium(VI) and uranium(VI) show the second power dependence on the HDEHP concentration, again suggesting the similarity

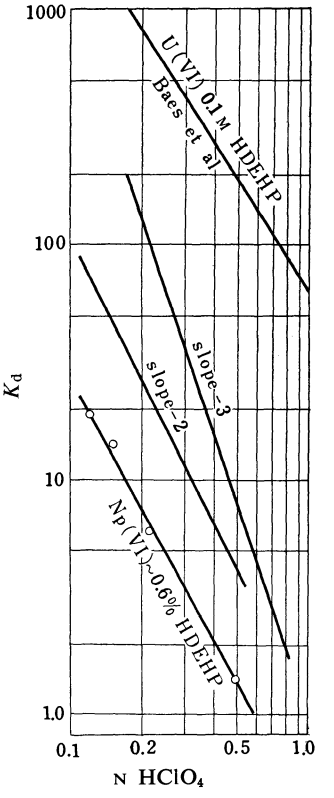



Fig. 1. The acid dependence of $K_d$ values for neptunium(VI) and uranium(VI).

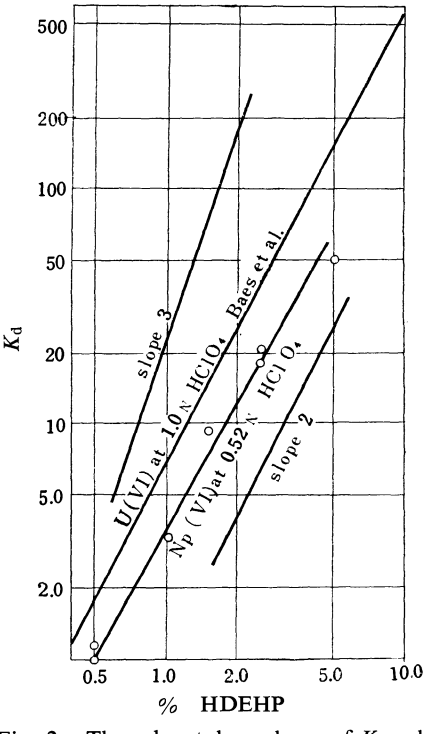



Fig. 2. The solvent dependence of $K_d$ values for neptunium(VI) and uranium(VI).

13) T. Ishimori, K. Watanabe and E. Nakamura, This Bulletin, 33, 636 (1960).

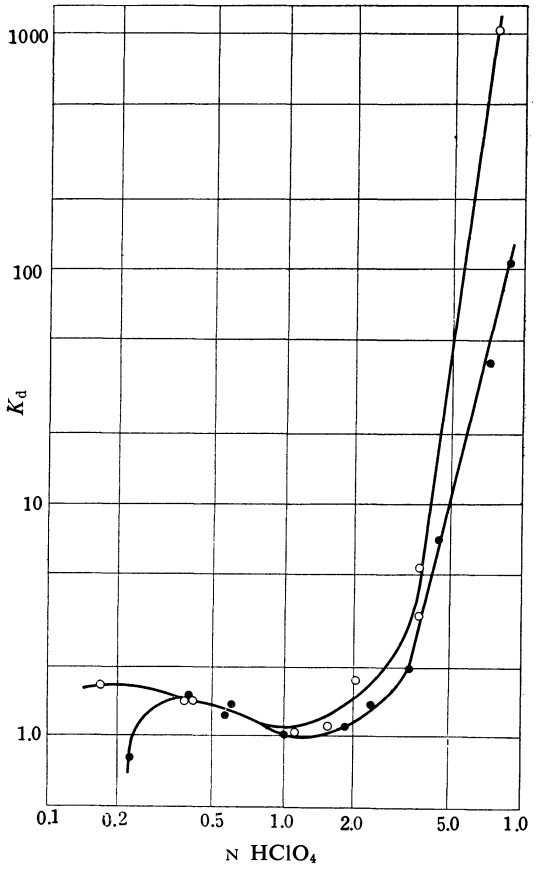



Fig. 3. The variation of the $K_d$ values for sexivalent neptunium[5] and uranium[14] in the system of 100% TBP vs. perchloric acid.
—○— U(VI) by Naitō —●— Np(VI)

between the chemistry of sexivalent neptunium and uranium in an acid solution.

The similarity between sexivalent neptunium and uranium is also found in other systems:

The acid dependence curves for neptunium-(VI)[1] and uranium(VI) in the system of 100% TBP vs. perchloric acid are given in Fig. 3 which shows that the behavior of sexivalent neptunium resembles that of uranium quite well, where the uranium curve is taken from the work of Naito[14]. Besides that found in the perchloric acid system similar behavior is also found in the nitric acid system. The acid dependence curve for neptunium(VI) also resembles that for uranium(VI)[1,2] in 100% TBP* vs. nitric acid system or in the trioctylamine vs. nitric acid system[5]. Thus it is likely that sexivalent ions of neptunium and uranium show almost the same behavior in the distribution experiments discussed above. In

* Tri-*n*-butyl phosphate.
14) K. Naito, This Bulletin, 33, 363 (1960).

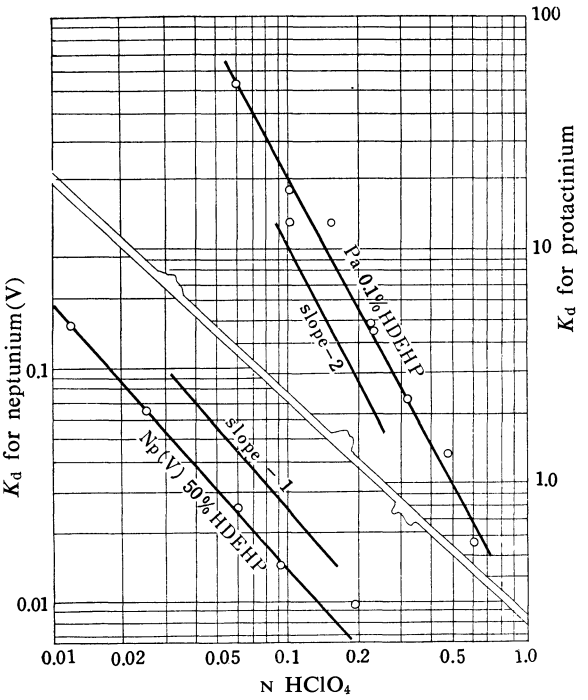



Fig. 4. The acid dependence of $K_d$ values for neptunium(V) and protactinium.

other words, the extraction mechanism of neptunium(VI) seems to be analogous to that of uranium(VI).

According to Baes et al.[8], who discussed the composition of uranium-HDEHP complex based on the acid and the solvent dependence of the $K_d$ values for uranium in the system of HDEHP vs. perchloric acid, the uranium-HDEHP complex is $UO_2A_4H_2$, where HA represents HDEHP molecule. As mentioned above, both acid and solvent dependence of $K_d$ values for neptunium-(VI) in the HDEHP vs. perchloric acid system coincide with those of uranium(VI), so that it is presumed that the neptunium(VI) ion is extracted forming the neptunium(VI)-HDEHP complex, $NpO_2A_4H_2$.

**Distribution of Quinquivalent Neptunium in the System of HDEHP vs. Perchloric Acid.**— The distribution ratios of quinquivalent neptunium were determined in the system of 50% HDEHP-toluene vs. perchloric acid varying the acidity from 0.01 to 0.2 N. The results obtained are given in Fig. 4, where the $K_d$ values for protactinium are also shown. The $K_d$ values for protactinium were so high that the relationship between the acidity and the $K_d$ values for protactinium could not be found clearly using 50% HDEHP with which the extraction of neptunium(V) was studied. Therefore, 0.1% HDEHP-toluene was chosen as the extractant in the determination of the $K_d$ values for

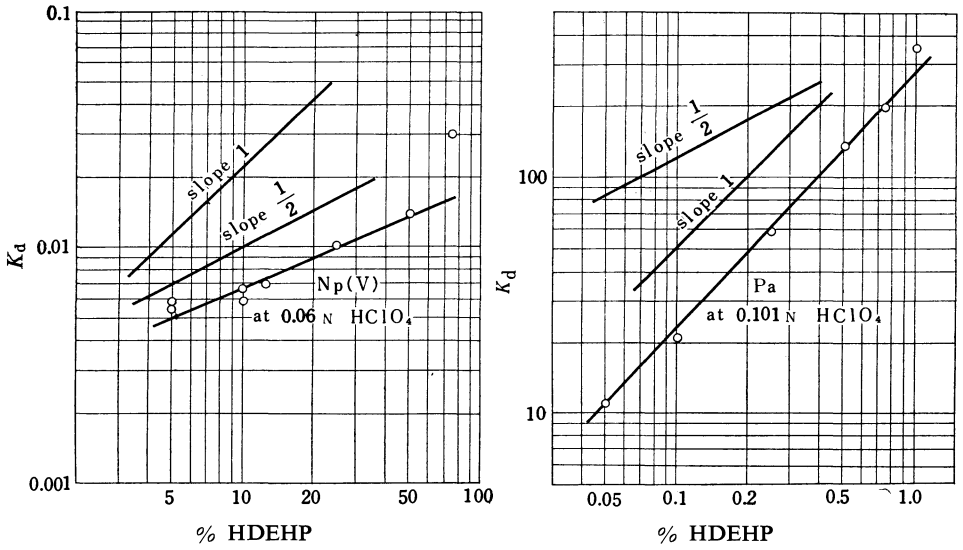



Fig. 5. The solvent dependence of $K_d$ values for neptunium(V) and protactinium.

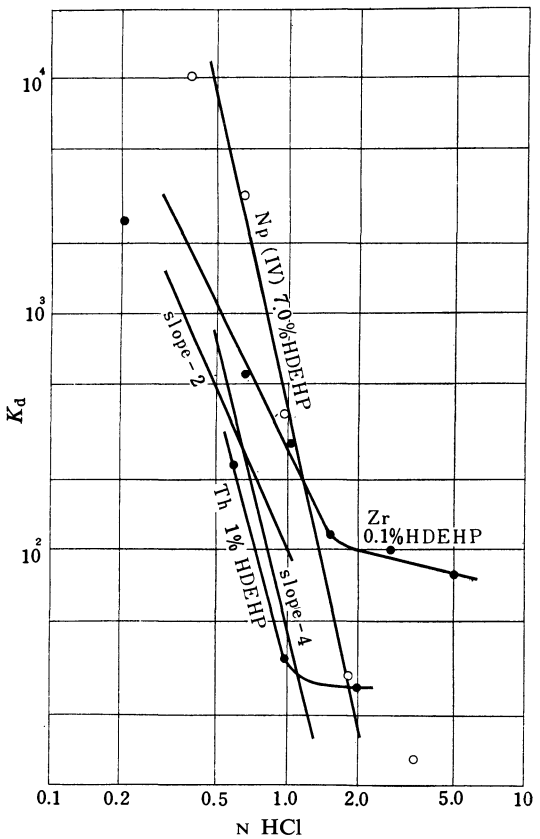



Fig. 6. The acid dependence of $K_d$ values for neptunium(IV), thorium and zirconium.

protactinium varying the acidity of perchloric acid from 0.05 to 1.0 N. As Fig. 4 shows, the slope of the line for neptunium(V) is −1, whereas that for protactinium is −2. Thus it is likely that the neptunium(V) ion behaves differently from the protactinium ion in a dilute perchloric acid medium.

The variation of the $K_d$ values of neptunium-(V) and protactinium with the concentration of HDEHP in the organic phase, keeping the concentration of perchloric acid in the aqueous phase constant, is shown in Fig. 5. As Fig. 5 shows, the line for neptunium(V) has the slope of 1/2, whereas that for protactinium has the slope of 1. Assuming that the solvent dependence of $K_d$ values for protactinium is kept at the first power up to 50% HDEHP at 0.1 N perchloric acid solution, it is calculated that the $K_d$ value for protactinium is about $10^4$, 500 times that of the $K_d$ value shown in Fig. 4. On the other hand, in the 0.1 N perchloric acid-50% HDEHP system quinquivalent neptunium shows the $K_d$ value of about $10^{-2}$ (Fig. 4). The difference of the $K_d$ values between neptunium(V) and protactinium, $10^4$ and $10^{-2}$, shows that quinquivalent neptunium is less extractable than protactinium with the organic extractant from the aqueous phase. Similar relationships are seen in other cases like the system of 100% TBP vs. some mineral acids[1].

As mentioned above, the both acid and solvent dependence of $K_d$ values for neptunium-(V) show different values from those of protactinium. These facts suggest the difference between the chemistry of quinquivalent neptunium and protactinium.

**Distribution of Quadrivalent Neptunium in the System of HDEHP vs. Hydrochloric Acid.** —The distribution ratio of quadrivalent neptunium was determined in the system of 7.0%

HDEHP vs. hydrochloric acid varying the acidity from 0.5 to 3.0 N. The results are shown in Fig. 6, where the $K_d$ values for thorium and zirconium are also given. The behavior of thorium was studied in the acidity range from 0.6 to 2.0 N using 1% HDEHP-toluene solution. Although zirconium is not a member of the actinide elements, the behavior of zirconium was studied as a quadrivalent species in the system of 0.1% HDEHP vs. hydrochloric acid varying the acidity from 0.2 to 4.0 N, where the $K_d$ values for zirconium are so high that HDEHP-toluene solution had to be diluted to 0.1%.

From these results, it is found that thorium and zirconium are more extractable than quadrivalent neptunium. As is shown in Fig. 6, the lines for neptunium(IV) and thorium both have the slope of −4. The behavior of thorium had been studied by Peppard and Ferraro who had also found negative fourth power dependence of the $K_d$ values on the acidity of hydrochloric acid[10]. On the other hand, zirconium shows a negative second power dependence on the acidity. The difference between the neptunium(IV) and zirconium ion seems to be greater than that between the neptunium(IV) and thorium ion.

The $K_d$ values for quadrivalent neptunium in the system of 0.5 N hydrochloric acid vs. HDEHP-toluene are studied, the HDEHP concentration being varied. In Fig. 7, the neptunium(IV) curve is compared with those for thorium and zirconium. The behavior of thorium is taken from the work of Ishimori[15] in the system of 0.5 N perchloric acid vs. HDEHP-toluene. Peppard and Ferraro had also given a third power dependence of the $K_d$ values for thorium on the hydrochloric or perchloric acid concentration. On the other hand, the results for zirconium obtained presently fall on a line of slope 2 in Fig. 7. Thus it is shown again that the quadrivalent neptunium ion behaves in a manner more nearly similar to thorium ion than to zirconium ion in the hydrochloric acid solution.

It is likely that the HDEHP extraction mechanism of neptunium(IV) from hydrochloric acid is similar to that of thorium ion, because both acid and solvent dependence of $K_d$ values for neptunium(IV) coincide with those of thorium. That is to say, neptunium-(IV)-HDEHP complex is supposed to have an

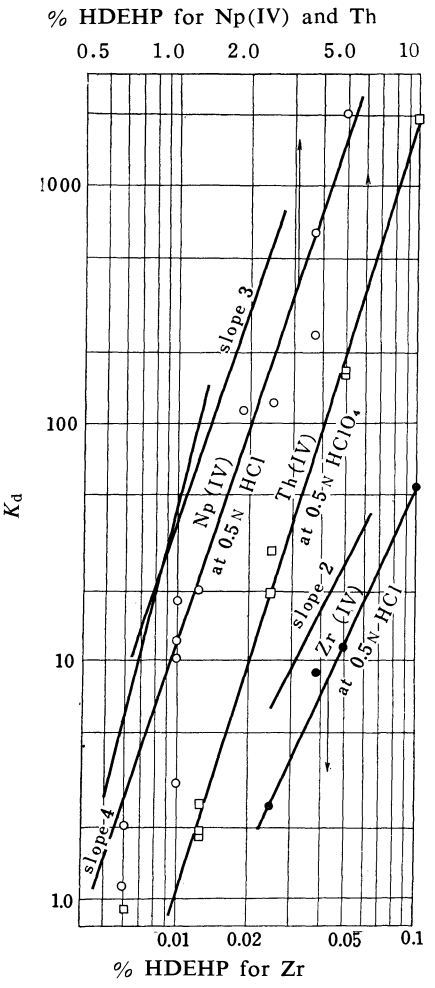



Fig. 7. The solvent dependence of $K_d$ values for neptunium(IV), thorium and zirconium.

iso-morphous structure with that of thorium-(IV)-HDEHP complex. As the formula for the thorium complex, Peppard and Ferraro gave $ThA_2(HA_2)_2$ which was proposed from the results of the infrared spectra and the elementary analysis, where HA denotes the HDEHP molecule. Therefore it might be reasonable to give $NpA_2(HA_2)_2$ for the neptunium(IV)-HDEHP complex.

The author wishes to thank Dr. Tomitaro Ishimori for criticism and suggestions which made a major contribution to this work.

*Chemistry Division, Tokai Laboratory*
*Japan Atomic Energy*
*Research Institute*
*Tokai, Ibaraki-Ken*

15) Unpublished work performed during the writer's stay in the Argonne National Laboratory, Lemont, Illinois, USA.

# *The Competitive Reduction of Nitrobenzene and para-Substituted Nitrobenzenes with Nickel Catalysts*

By Akira SUGIMORI*

(Received July 26, 1960)

Several approaches to the elucidation of the mechanism of catalytic reduction may be possible. The present paper describes the competitive reduction of nitrobenzene and substituted nitrobenzenes with nickel catalysts. In all the cases examined, the nitro compounds with an electron attracting group in para position were reduced preferentially to those with an electron repelling group in the same position.

## Experimental

**Materials.** — Nitro compounds were purified by recrystallization or redistillation. The melting points and boiling points are listed in Table I.

TABLE I

| Compound | M. p. | B. p. |
|---|---|---|
| Nitrobenzene | | 95.5～97°C/ 17～18 mmHg |
| *p*-Nitrophenol | 113°C | |
| *p*-Nitroanisole | 52 ～ 53°C | |
| *p*-Nitroaniline | 145.5～146.5°C | |
| Ethyl *p*-nitrobenzoate | 55 ～ 56°C | |
| *p*-Nitrobenzaldehyde | 105 ～105.5°C | |

**Preparation of Catalysts.** — a) Raney nickel catalyst. The method of Adkins and Billica[1] was modified in order to obtain stable catalytic activity. One gram of nickel-aluminum alloy (Ni 40%) was treated with 7 ml. cf. 20% aqueous sodium hydroxide at 50°C for 50 min. Then the catalyst was washed ten times by decantation with 20 ml. of cold water. The pH of the last washing wad 8.5～9.0. The catalyst was then washed twice with 20 ml. of 95% ethanol.

b) Urushibara nickel A (U-Ni-A) was prepared according to Urushibara, Nishimura and Uehara[2].

**Catalytic Reduction.**—A suspension of the Raney nickel (0.4 g.) from 1 g. of the alloy in 30 ml. of 95% ethanol was shaken with hydrogen under ordinary pressure in a shaking type catalytic reduction apparatus until the catalyst absorbed no more hydrogen. Then 5 mM of a nitro compounds in 30 ml. of ethanol was added to the catalyst suspension, hydrogen was charged, and the reaction was started by shaking the reaction vessel. The temperature was maintained at 25°C, and the rate of hydrogen absorption was measured. In the reduction with U-Ni-A catalyst, 1.67 mM of a nitro compound, 1.0 g. of the catalyst and 20 ml. of 95% ethanol were used.

**Competitive Reduction.**—An equimolar mixture of two nitro compounds (each 5 mM) was reduced under the condition described above until 8～13 mM of hydrogen was absorbed, whereas complete reduction to amines requires 30 mM of hydrogen. The catalyst was removed by filtration and was washed several times with ether. The products in the filtrate and washings were analysed. In the reduction with U-Ni-A, 6.67 mM each of two nitro compounds, 1.0 g. of the catalyst and 80 ml. of 95% ethanol were used.

**Analysis of Products.**—*Competitive Reduction of Nitrobenzene and p-Nitrophenol.* — Amines were removed from the ethereal solution of the products by shaking with dilute hydrochloric acid. Then the ethereal solution was extracted with dilute aqueous sodium hydroxide, the alkaline solution was acidified with hydrochloric acid and extracted with ether, and *p*-nitrophenol, m. p. 113°C, was obtained after removal of ether from the extract. The quantity of unchanged nitrobenzene was estimated from the volume of absorbed hydrogen in the catalytic reduction of the ethereal mother liquor of the alkaline extraction.

*Competitive Reduction of Nitrobenzene and p-Nitroaniline.* — *p*-Nitroaniline, *p*-phenylenediamine and aniline were separated from unchanged nitrobenzene by extracting ten times the ethereal solution of the reaction products with hydrochloric acid. Then the ethereal solution containing the unchanged nitrobenzene was evaporated in vacuum and the residue was catalytically reduced in alcoholic solution. The quantity of absorbed hydrogen was the same as that of unchanged nitrobenzene. The acidic extract was basified with aqueous sodium hydroxide and shaken with ether. The residue from the ethereal extract was catalytically reduced in alcoholic solution to know the quantity of unchanged *p*-nitroaniline.

*Competitive Reduction of Ethyl p-Nitrobenzoate and Nitrobenzene.*—After the solvent was distilled off from the reaction products, the residue was dissolved in a mixture of 30 ml. of dioxan and 40 ml. of concentrated hydrochloric acid. The solution was heated under reflux for 5 hr. The solution was made alkaline with aqueous sodium carbonate. Then nitrobenzene was steam-distilled, and the distillate was extracted with ether. After removal of ether from the extract, the residue was dissolved in alcohol and catalytically reduced to estimate the

* Present address: Division of Radiation Applications, Japan Atomic Energy Research Institute, Tokai, Ibaraki-Ken, Japan.

1) H. Adkins and H. R. Billica, "Organic Syntheses" Vol., 29, John Wiley & Sons, Inc., New York (1949), p. 24.

2) Y. Urushibara, S. Nishimura and H. Uehara. This Bulletin, **28**, 446 (1955).

quantity of nitrobenzene. The quantity of reduced ethyl *p*-nitrobenzoate was estimated by weighing *p, p'*-diethoxycarbonylazoxy-benzene which precipitated on exposure of the reaction mixture to air.

*Competitive Reduction of p-Nitrobenzaldehyde and Nitrobenzene.*—The unchanged nitrobenzene and *p*-nitrobenzaldehyde were steam-distilled from the mixture produced, and the nitro compounds were extracted from the distillate with ether. The ethereal solution was divided into two portions of known volume. The total molar quantity of the nitro compounds was calculated from the quantity of absorbed hydrogen in catalytic reduction of one portion. An acidic solution of 2,4-dinitrophenylhydrazine was added to another portion. The quantity of *p*-nitrobenzaldehyde in the unchanged nitro compounds was obtained from that of the 2,4-dinitrophenylhydrazone. The quantity of nitrobenzene was given by the difference of the quantities of the total nitro compounds and *p*-nitrobenzaldehyde.

*Competitive Reduction of Ethyl p-Nitrobenzoate and p-Nitroanisole.*—The solution resulting from the competitive reduction was left under exposure to air for two days, and ethyl *p*-hydroxylaminobenzoate was changed to the corresponding azoxy compound[3]. After the precipitated *p, p'*-diethoxycarbonylazoxybenzene was collected by filtration, the solution was analysed chromatographically, and *p*-nitroanisole was obtained in white crystals. The quantity of *p, p'*-diethoxycarbonylaxoxybenzene gave the quantity of reduced ethyl *p*-nitrobenzoate, and the unchanged *p*-nitroanisole was directly weighed.

## Results and Discussion

**Separate Reduction Rates of Nitro Compounds.** — The hydrogenation curves of several nitro compounds were given in the preceding paper[3]. The increasing rates towards the end of the hydrogenation of nitrobenzene and of ethyl *p*-nitrobenzoate with Raney nickel catalyst are due to stepwise hydrogenation. Namely, the nitro compounds are reduced first to the hydroxylamines with $2H_2$, and then the hydroxylamines to amines with $H_2$, the latter process being faster than the former. In the hydrogenation of *p*-nitrobenzaldehyde and of ethyl *p*-nitrobenzoate with U-Ni-A the hydrogenation rates go down, making a break after 2 mol. of hydrogen has been consumed. This is also due to stepwise hydrogenation and here hydroxylamines are reduced more slowly than the parent compounds.

**Competitive Reduction.** — In the competitive catalytic reduction, a more reactive substance is not necessarily reduced in a greater quantity than a less reactive competitor. For example, in separate reduction nitrobenzene is reduced three times as quickly as ethyl *p*-nitrobenzoate with Raney nickel. But, when a mixture of nitrobenzene and ethyl *p*-nitrobenzoate was catalytically reduced, more ethyl *p*-nitrobenzoate was reduced than nitrobenzene. While nitrobenzene and *p*-nitrophenol are almost equally reactive in separate reduction with U-Ni-A catalyst, nitrobenzene was reduced exclusively at first in the competition with *p*-nitrophenol.

These phenomena can be explained by the difference in the affinities of substrates to nickel catalysts. In the above example, ethyl *p*-nitrobenzoate must be adsorbed, and thus reduced, preferentially to nitrobenzene. The same interpretation applies to the competitive reduction of nitrobenzene and *p*-nitrophenol with U-Ni-A catalyst.

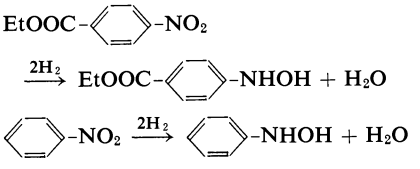
In order to find out the sequence, if any exists, in the strengths of affinities of nitrobenzene and substituted nitrobenzenes, the following considerations will be made:

To make the matter simple, any difference in the adsorption areas of the molecules of a pair of nitro compounds is neglected until later discussion.

If it is assumed that there was no selectivity in the adsorption of the nitro compounds, each component being adsorbed with equal ease, the rates of separate hydrogenation of the two compounds will give the quantities of both compounds to be reduced in a partial hydrogenation of their mixture, and comparison of the false values calculated in this way with observed ones will give a suggestion regarding the different affinities of the two nitro compounds to the nickel catalyst.

One or two examples will be illustrated below:

A mixture of 5 mM each of ethyl *p*-nitrobenzoate and nitrobenzene was hydrogenated with Raney nickel until 251 ml. of hydrogen was absorbed, and 2.60 mM of the former was reduced and 3.15 mM of the latter remained unchanged. Both ethyl *p*-nitrobenzoate and nitrobenzene are hydrogenated stepwise and, therefore, the competing reactions are:



As the initial rates of separate hydrogenation of ethyl *p*-nitrobenzoate and nitrobenzene are 73 ml./5 min. and 216 ml./5 min., respectively, the quantity of hydrogen to be consumed for the hydrogenation of ethyl *p*-nitrobenzoate would be from the above assumption:

$$H_1 = \frac{73}{73+216} \times 251 = 63 \text{ ml.}$$

that for nitrobenzene:

$$H_2 = \frac{216}{73+216} \times 251 = 188 \text{ ml.}$$

3) A. Sugimori, submitted to this Bulletin.

The quantities of the nitro compounds to be hydrogenated would respectively be:

$$R_1=\frac{63}{2\times22.4}=1.41 \text{ mM}$$

$$R_2=\frac{188}{2\times22.4}=4.19 \text{ mM}$$

Accordingly, the quantities of the nitro compounds left unchanged would be:

$$L_1=5.00-1.41=3.59 \text{ mM}$$

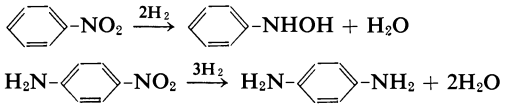
$$L_2=5.00-4.19=0.81 \text{ mM}$$

The calculated values are compared with the observed values in Table II, which is interpreted as showing that ethyl *p*-nitrobenzoate has a stronger affinity with the nickel catalyst than nitrobenzene has.

TABLE II

| Compound | | Calcd. mM | Obs. mM |
|---|---|---|---|
| Ethyl *p*-nitrobenzoate | reduced | 1.41 | 2.60 |
| | unchanged | 3.59 | — |
| Nitrobenzene | reduced | 4.19 | — |
| | unchanged | 0.81 | 3.15 |

The competitive hydrogenation of nitrobenzene and *p*-nitroaniline with Raney nickel catalyst is more complicated, because the former gives phenylhydroxylamine while the latter is reduced to *p*-phenylenediamine:



The separate hydrogenation rates of nitrobenzene and *p*-nitroaniline are 216 ml./5 min. and 134 ml./5 min., respectively. The hydrogenation of a mixture of 5 mM each of nitrobenzene and *p*-nitroaniline was stopped when 291 ml. of hydrogen was absorbed, and 4.10 mM of *p*-nitroaniline remained unchanged. From the above assumption, the quantities of hydrogen to be consumed by nitrobenzene and *p*-nitroaniline would respectively be:

$$H_1=\frac{216}{216+134}\times291=180 \text{ ml.}$$

$$H_2=\frac{134}{216+134}\times291=111 \text{ ml.}$$

The quantity of nitrobenzene to be hydrogenated to phenylhydroxylamine with 180 ml. of hydrogen is:

$$R_1=\frac{180}{2\times22.4}=4.24 \text{ mM}$$

and the quantity of *p*-nitroaniline to be hydrogenated to *p*-phenylenediamine with 111 ml. of hydrogen is:

$$R_2=\frac{111}{3\times22.4}=1.65 \text{ mM}$$

Table III gives the comparison, which shows that nitrobenzene has a stronger affinity to the nickel catalyst than *p*-nitroaniline.

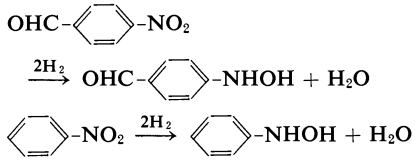
TABLE III

| Compound | | Calcd. mM | Obs. mM |
|---|---|---|---|
| Nitrobenzene | reduced | 4.24 | |
| | unchanged | 0.76 | |
| *p*-Nitroaniline | reduced | 1.65 | |
| | unchanged | 3.35 | 4.10 |

Similar treatments of the other competitions are shown in Table IV.

TABLE IV

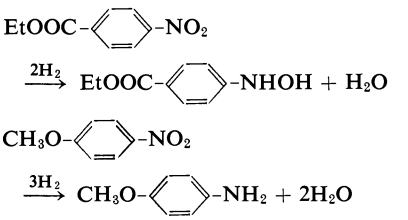
i) Nitrobenzene and *p*-nitrobenzaldehyde with Raney nickel.



| Compound | | Calcd. mM | Obs. mM |
|---|---|---|---|
| *p*-Nitrobenzaldehyde | reduced | 1.18 | |
| | unchanged | 3.82 | 0.52 |
| Nitrobenzene | reduced | 4.78 | |
| | unchanged | 0.22 | 3.10 |

Affinity to the catalyst: *p*-Nitrobenzaldehyde >Nitrobenzene

ii) Ethyl *p*-nitrobenzoate and *p*-nitroanisole with Raney nickel.



| Compound | | Calcd. mM | Obs. mM |
|---|---|---|---|
| Ethyl *p*-nitrobenzoate | reduced | 1.83 | 3.15 |
| | unchanged | 3.17 | |
| *p*-Nitroanisole | reduced | 2.54 | |
| | unchanged | 2.46 | 2.85 |

Affinity to the catalyst: Ethyl *p*-nitrobenzoate >*p*-Nitroanisole

Separate and competitive hydrogenation of the nitro compounds were also studied with U-Ni-A catalyst. Results are shown in Table V.

TABLE V

(A) Initial hydrogenation rates of separate hydrogenations.

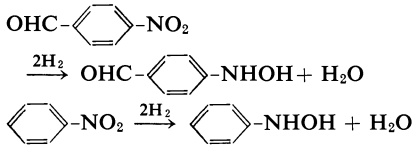
| | |
|---|---|
| Nitro compound | 1.67 mM |
| U-Ni-A | 1.0 g. |

| Compound | Rate of hydrogen absorption |
|---|---|
| Nitrobenzene | 126 ml./5 min. |
| *p*-Nitrobenzaldehyde | 126 ml./2.5 min. |
| Ethyl *p*-nitrobenzoate | 141 ml./5 min. |
| *p*-Nitrophenol | 138 ml./5 min. |
| *p*-Nitroaniline | 68 ml./5 min. |

(B) Competitive reduction

| | |
|---|---|
| Nitro compounds | 6.67 mM each |
| U-Ni-A | 1.0 g. |

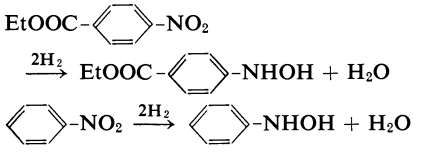
i) *p*-Nitrobenzaldehyde and nitrobenzene.



| Compound | | Calcd. mM | Obs. mM |
|---|---|---|---|
| *p*-Nitrobenzaldehyde | reduced | 4.74 | |
| | unchanged | 1.93 | |
| Nitrobenzene | reduced | 2.37 | |
| | unchanged | 4.30 | 5.60 |

Affinity to the catalyst: *p*-Nitrobenzaldehyde >Nitrobenzene

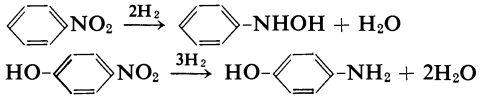
ii) Nitrobenzene and ethyl *p*-nitrobenzoate.



| Compound | | Calcd. mM | Obs. mM |
|---|---|---|---|
| Ethyl *p*-nitrobenzoate | reduced | 3.82 | |
| | unchanged | 2.85 | |
| Nitrobenzene | reduced | 3.37 | |
| | unchanged | 3.30 | 5.13 |

Affinity to the catalyst: Ethyl *p*-nitrobenzoate >Nitrobenzene

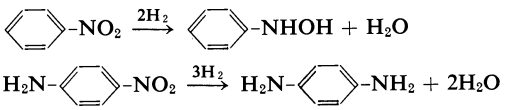
iii) Nitrobenzene and *p*-Nitrophenol



| Compound | | Calcd. mM | Obs. mM |
|---|---|---|---|
| Nitrobenzene | reduced | 4.80 | |
| | unchanged | 1.87 | 0.34 |
| *p*-Nitrophenol | reduced | 3.47 | |
| | unchanged | 3.20 | 5.10 |

Affinity to the catalyst: Nitrobenzene >*p*-Nitrophenol

iv) Nitrobenzene and *p*-nitroaniline.



| Compound | | Calcd. mM | Obs. mM |
|---|---|---|---|
| Nitrobenzene | reduced | 5.47 | |
| | unchanged | 1.20 | 0.47 |
| *p*-Nitroaniline | reduced | 1.92 | |
| | unchanged | 4.70 | 6.10 |

Affiinity to the catalyst: Nitrobenzene >*p*-Nitroaniline

To examine further the selectivity in adsorption, the initial rates of hydrogenation of mixtures were measured and compared with the initial rates of separate reduction in Table VI.

TABLE VI

| Compound | Initial rate of separate reduction (ml. of $H_2$/5 min.) | Initial rate of the reduction of mixture (ml. of $H_2$/5 min.) |
|---|---|---|
| Nitrobenzene | 216 | 54 |
| Ethyl *p*-nitrobenzoate | 73 | |
| Nitrobenzene | 216 | 63 |
| *p*-Nitrobenzaldehyde | 52 | |
| Nitrobenzene | 216 | 208 |
| *p*-Nitroaniline | 134 | |

Table VI shows that the reduction rate of a mixture is almost the same as that of the component which is considered to have a stronger affinity to the catalyst. These data also indicate that the difference in affinities of the two components of each combination is great enough to cause completely selective adsorption.

The comparisons of the affinities of the nitro compounds to the nickel catalysts are summarized in Table VII.

TABLE VII

| Raney nickel | U-Ni-A |
|---|---|
| Ethyl *p*-nitrobenzoate >Nitrobenzene | Ethyl *p*-nitrobenzoate >Nitrobenzene |
| *p*-Nitrobenzaldehyde >Nitrobenzene | *p*-Nitrobenzaldehyde >Nitrobenzene |
| Nitrobenzene >*p*-Nitroaniline | Nitrobenzene >*p*-Nitrophenol |
| Ethyl *p*-Nitrobenzoate >*p*-Nitroanisole | Nitrobenzene >*p*-Nitroaniline |

In all the systems studied, an aromatic nitro compound with an electron attracting group in para position has a stronger affinity to the nickel catalysts than the compound with an electron repelling group in the same position.

Other factors that might have effects on the affinities of nitro compounds to the nickel catalysts must also be examined.

*Cross Section in Adsorption.*—The cross section in adsorption has been neglected in the above discussion but it might affect the apparent affinity of the nitro compound to the nickel catalysts. The molecule with a larger cross section in adsorption may be adsorbed in a smaller number than the molecule with a smaller cross section. Therefore, the same observed rate of separate hydrogenation with U-Ni-A catalyst may suggest that the hydrogenation of one molecule of *p*-nitrophenol is more rapid than that of nitrobenzene. Thus, if there were no selectivity in adsorption, *p*-nitrophenol might be reduced to a greater extent than nitrobenzene in the competitive reduction, but this was not true, and so the selectivity in adsorption rather than the molecular cross section governs the results.

Carbonyl group in ethyl *p*-nitrobenzoate and *p*-nitrobenzaldehyde can attack the active centers of the nickel catalysts, and the strong affinity of *p*-nitrobenzaldehyde and ethyl *p*-nitrobenzoate to the catalyst might be attributed to the adsorption of the carbonyl group. But this is denied, because the partial reduction of *p*-nitrobenzaldehyde gave *p*-hydroxylaminobenzaldehyde, and nitro group is preferentially adsorbed to carbonyl group by the catalysts.

The author wishes to express his hearty thanks to Professor Y. Urushibara for his kind guidance and encouragement throughout this work. He is also very grateful to Dr. M. Kobayashi and Dr. S. Nishimura for their helpful discussion.

*Department of Chemistry*
*Faculty of Science*
*The University of Tokyo*
*Hongo, Tokyo*

# *Studies on Extraction of Polonium(IV) by Hexone from Acid Solution*

By Niro MATSUURA, Akira OUCHI* and Masuo KOJIMA**

(Received June 10, 1960)

Solution chemistry of polonium(IV) with a weighable quantity of polonium was developed by Bagnall et al.[1] for several years past. However, one of the present authors found that polonium(VI), having a higher oxidation potential with regard to polonium(IV), was not stable, owing to its own $\alpha$ radiation[2]. Accordingly, it is necessary to employ a minute quantity of this element (which does not cause any radiolysis) in order to distinguish the results from self radiolysis. The extraction study of polonium(IV) was undertaken, therefore, with quantities of less than one microcurie of polonium per millilitre. In the course of the present studies on polonium extraction with hexone (methyl isobutyl ketone,) some peculiarities in the extraction characteristics were observed in a certain range of acidity, suggesting that there will be one or more unestablished complex species of polonium other than $PoX_6^{2-}$[3,4]. These phenomena appeared to be closely related with the history of employed polonium sources as well as with the acid nature of the aqueous phase from which polonium was extracted[3,5-7]. In order to find out new species of polonium(IV) responsible for this peculiarity in aqueous medium, the experiments were carried out under well defined conditions concerning the history of polonium source and the acidity of the extraction system.

## Experimental

**1) Materials.**—Polonium received from Amersham, England, dated June 1959, was in the form of nitrate in 1 N nitric acid. It was used after purification in our laboratory as described below:

A portion of polonium solution was converted into 0.3 N hydrochloric acid solution from which

* A. Ouchi (formerly A. Iguchi).

** Present address: Government Chemical Industrial Research Institute of Tokyo, Yoyogi P. O., Tokyo.

1) K. W. Bagnall, "Chemistry of the Rare Radioelements", Butterworths Scientific Publications, London, (1957), pp. 3—94.

2) N. Matsuura and M. Haissinsky, *J. chim. phys.*, **55**, 475 (1958).

3) M. Guillot, ibid., **28**, 107 (1931).

4) K. W. Bagnall, R. W. M. D'Eye and J. H. Freeman, *J. Chem. Soc.*, **1955**, 3959.

5) G. Hevesy, *Phys. Z.*, **14**, 49, 1202 (1913).

6) K. W. Bagnall and D. S. Robertson, *J. Chem. Soc.*, **1957**, 509.

7) T. Ishimori, This Bulletin, **27**, 520 (1954).

polonium was deposited on a silver foil by electrochemical displacement. The deposited polonium was redissolved in 1 N nitric acid together with metallic silver and was freed from silver by precipitating silver as chloride. The supernatant liquid thus obtained was evaporated to dryness, while the residue was extracted with hot dilute hydrochloric acid. After this purification procedure was repeated several times, the extracted polonium solution was stored in 6 N hydrochloric acid. The resulting solution was the usual starting source of our experiments, though other solutions of different kinds of acid and acidities were sometimes used as well.

**2) Activity Measurement.**—Twenty microlitres of the solution, containing polonium, was pipetted by a glass micro-syringe furnished with a micrometer. In order to obtain the homogeneity of the samples for the $\alpha$ counting of polonium, two different methods were applied, one by evaporating the pipetted sample directly on a glass plate and the other depositing the polonium on a silver foil by the electrochemical displacement. The simple evaporation method was not suitable for obtaining consistent $\alpha$ activity of polonium, especially when some non-volatile material was present. In the electrochemical method it was desirable to make preliminary extraction with hexone from acid solution in the presence of an excess amount of potassium iodide. By this method all polonium activities could be transferred to an organic phase as hexa-iodo polonium complex, $PoI_6^{2-}$. The hexone solution thus obtained was placed on a silver foil, while polonium was deposited electrochemically for activity measurement. The discharge rate of electroscope, 5.575 div./min. was standardized against the counting rate of $4\pi$ flow counter for the same sample under the same condition of measurement. This yielded 977 counts/min. against 5.575 div./min., i. e., 1 div./min. corresponds to $4.7\times10^{-3}$ microcurie of $^{210}Po$.

**3) Partition of Polonium between Two Liquid Phases.** — For determining the distribution of polonium between hexone and aqueous acid solution the sample solution was shaken at room temperature in a stoppered glass test tube with the same volume of solvent, preliminarily saturated with the acid of the same concentration. The correction of volume change after extraction was needed when the extraction was made from concentrated acid solution. Although in our measurements only several ten micro microlitres of the sample was taken, the errors fell within the limit of 10%. The equilibrium of partition was established in less than 5 min. at the temperature of $20\pm5$°C.

**4) Aging of Polonium Solution.**—About 80 microlitres of the stock solution which contained a known amount of polonium was taken in 4 ml. of hydrochloric, sulfuric or nitric acid. Just after mixing a portion of polonium was extracted with hexone from the mixture. This provided the data at time 0. The rest of the polonium solution was boiled in a glass flask with reflux condenser for several hours on a steam bath, before it was cooled to room temperature. This aged solution was used as a sample for extraction of polonium.

## Results and Discussion

**1) Adsorption of Polonium on Glass Wall.**—Polonium is generally adsorbed strongly on a number of substances. For example, the adsorption on ion-exchange resins, either cationic or anionic, is so strong that polonium is hardly eluted even by an eluant of high ionic concentration. In this respect, ion-exchange technique did not give any reliable data for studying the complex chemistry of polonium. It seemed to us that the partition method was rather preferable. In the extraction method, however, the adsorption on a glass wall caused another difficulty in the accurate determination of polonium activity. In order to obtain a correct partition coefficient, it is necessary to know the loss of polonium by adsorption from the extraction system. In Fig. 1 the actual adsorption loss was shown in

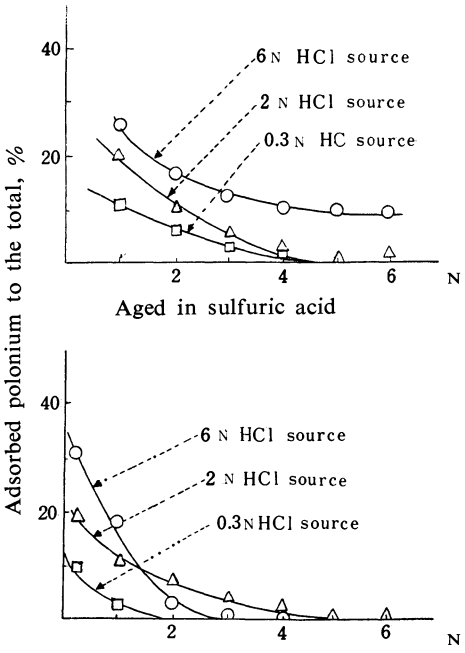



Fig. 1. Adsorption of polonium(IV) on the wall of 1 ml. glass stoppered vessel for hexone extraction.

(Po lost/Total Po used) $\times$ 100% as the function of acidity of the medium from which polonium was extracted. In the hydrochloric acid vs. hexone system the adsorption on a glass wall was very small, if the acid was stronger than 2 N. On the other hand in sulfuric acid-hexone system several hundredths of polonium was left on the surface of the glass wall regardless of the acidity so far as we examined it. Therefore, the adsorption loss cannot be neglected for the correct extraction data.

**2) Aging Effect on Nitric Acid.**—The amount of polonium extracted from nitric acid solution was nearly constant, 80% being found in the organic phase. This constant value of extraction coefficient can be obtained if the polonium source stored in 6 N nitric acid is employed for extraction after immediate dilution to a given concentration of the acid. Much lower extraction coefficients were observed, on the other hand, if polonium in 0.4 N nitric acid was extracted. In Fig, 2, the extraction

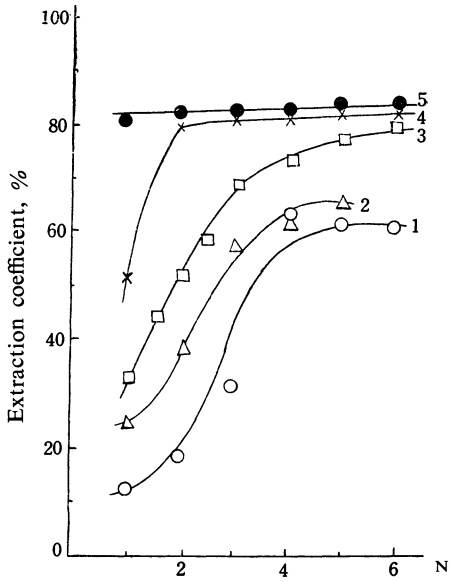



Fig. 2. Aging effect on polonium(IV) extraction with hexone from nitric acid medium for the source stored in 0.4 N (1~4) and in 6 N (5).
-○- 1. Extraction immediately after dilution.
-△- 2. Extraction after 1 hr.'s heating.
-□- 3. Extraction after 2 hr.'s heating.
-×- 4. Extraction after 12 hr.'s heating.
-●- 5. Extraction without aging.

coefficient curve 1 for polonium source in 0.4 N nitric acid fell with decreasing acidity. The aging before extraction by heating under reflux for 1, 2 and 12 hr. at 80°C increased the extraction coefficients up to 80% as shown in corresponding curves 2, 3 and 4 in Fig. 2. This fact suggests that polonium(IV) nitrate complex $Po(NO_3)_6^{2-}$ or $Po(NO_3)_5^-$ [8,9], which is stable in 6 N nitric acid, can be readily extracted by hexone, whereas the hydrolysed complex produced in weak nitric acid below

8) J. Danon and A. A. L. Zamith, *J. Phys. Chem.*, **61**, 431 (1957).
9) K. W. Bagnall, D. S. Robertson and M. A. A. Stewart. *J. Chem. Soc.*, **1958**, 3633.

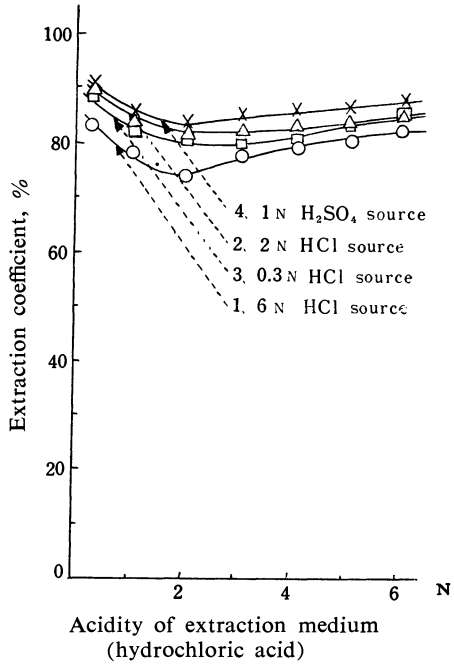



Fig. 3A. Aging effect on extraction coefficients. (Immediately after dilution.) 1. 6 N HCl source 2. 2 N HCl source 3. 0.3 N HCl source 4. 1 N $H_2SO_4$ source

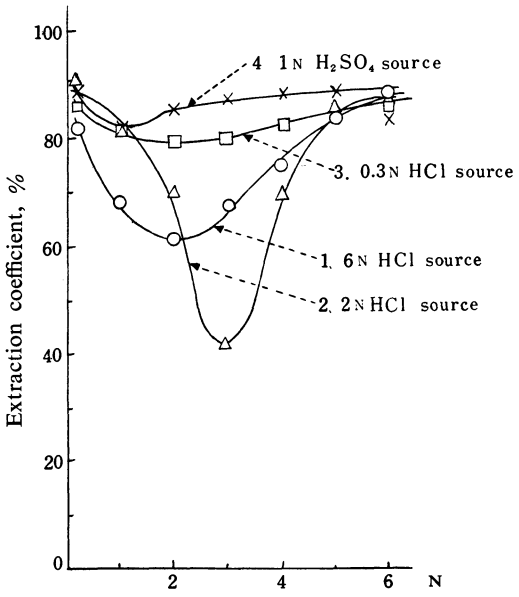



Fig. 3B. Aging effect on extraction coefficients. (Aged for 6 hr. at boiling point.)
1. 6 N HCl source 2. 2 N HCl source 3. 0.3 N HCl source 4. 1 N $H_2SO_4$ source

1 N is hardly extracted at all. The form of the latter hydrolysed ionic species cannot be detected in our experiments, though some authors suggest that the ionic formula is $PoO^{2+}$ or $Po(OH)_2$ $(NO_3)_4^{2-}$ [7].

**3) Aging Effect in Hydrochloric Acid.**— Aging effect on the extraction characteristics of polonium was also observed in hydrochloric acid as well as in nitric acid. The results were represented in Fig. 3 for the several different polonium sources aged and stored in 0.3, 2 or 6 N hydrochloric acid. In this case polonium was extracted from hydrochloric acid of 0.3~6 N for the samples aged 6 hr. under reflux (A) and non-aged (B). The minimum extraction coefficient was observed at about 2 N hydrochloric acid. This minimum appeared only in the extraction from hydrochloric acid medium. Hence, it was assumed that in hydrochloric acid there would be two different ionic species of polonium complex easily soluble in hexone. A well-established form of polonium(IV) complex in hydrochloric acid is $PoCl_6^{2-}$ which is believed to be formed easily in hydrochloric acid of higher than 6 N and stable even in more dilute acid after it was formed[10,11]. But by aging in more dilute acid solution for prolonged time, the solubility of polonium in hexone decreased as it formed some kinds of hydrolytic products which were hardly soluble in hexone.

**4) Ionic Species of Hydrolytic Product.**— It is very interesting to estimate the ratio of insoluble species to soluble species from the data of Fig. 3B. This ratio depends not only on the acidity of the extraction system but also on the history of the polonium source. Then, for example, the curve 2 in Fig. 3B, having a sharp minimum at nearly 2 N, can be analysed into two separated curves, as shown in Fig. 4 with dotted lines. These separated curves indicate two different hexone soluble complex species contributed to the extraction at the same time, though in different ways, in the acidity region, one in the range over 3 N and the other in the acidities less than 2 N. The dependence of each curve on the acidity of the extraction system can be shown in Fig. 5 by the logarithmic plots of Polonium soluble/Polonium insoluble or $E'/(1+E')$ as a function of acidity in linear scale. Here, $E'$ denotes the extraction coefficient for separated species. These plots have linear character with the tangential increment 4. Applying mass action law to this system for the hydrolytic reaction given by (1), an equilibrium relation (2) is obtained between two polonium species, soluble and insoluble, which shows dependence on the fourth power of acidity.

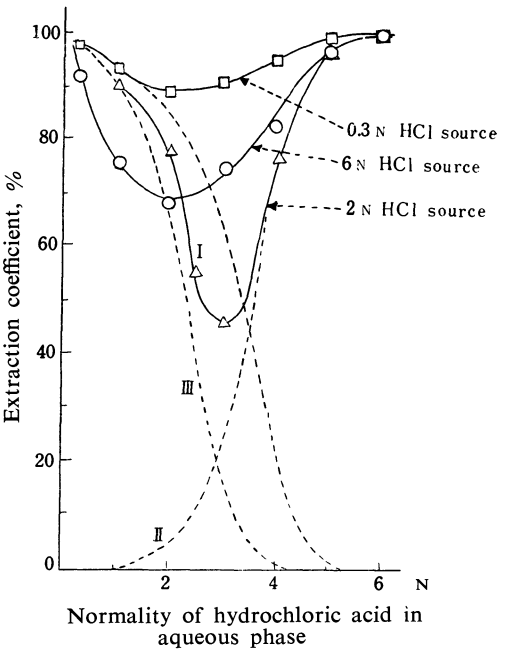



Fig. 4. Analysis of the extraction coefficient curve.

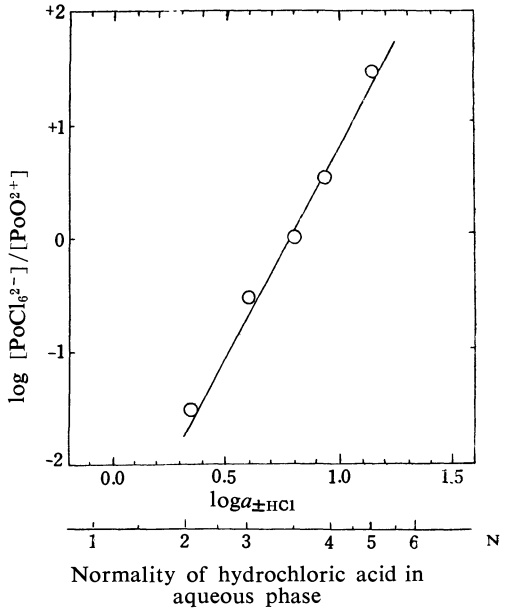



Fig. 5. Logarithmic plots of curve II in Fig. 4.

$$PoCl_6^{2-} + 2H_2O = Po(OH)_2Cl_4^{2-} + 2H^+ + 2Cl^- \quad (1)$$

$$\frac{PoCl_6^{2-}\ \text{soluble in hexone}}{Po(OH)_2Cl_4^{2-}\ \text{insoluble}} = K\cdot[H^+]^2\cdot[Cl^-]^2$$

10) D. J. Hunt, *Amer. Rep.*, MLM, 979 (1954).
11) K. W. Bagnall and J. H. Freeman, *J. Chem. Soc.*, 1956, 2770.

$$\text{or} \quad \frac{\text{Po(IV) soluble}}{\text{Po(IV) insoluble}} = \frac{E'}{1-E'} = K \cdot a^2_{\pm HCl}$$

Where, $a_{\pm HCl}$ is the mean activity of hydrochloric acid. It seemed from the above consideration that the species of $Po(OH)_2Cl_4^{2-}$ or $PoO^{2+}(H_2O+4Cl^-)$ is responsible for the appearance of minimum extraction from hydrochloric acid medium at the concentration about 2 N.

However, the idea is not entirely excluded that polonium nitrate complex formed in the purification process is partly extracted even from hydrochloric acid. Accordingly, it is possible to assume that the minimum value of extraction appears in the acidity most favorable to hydrolytic reaction succeeded by the following schema:

$$Po(NO_3)_6^{2-} + 2H_2O = PoO^{2+} + 2H^+ + 6NO_3^- + H_2O$$

$$\frac{PoO^{2+} + 2H^+ + 6Cl^- + H_2O = PoCl_6^{2-} + 2H_2O}{Po(NO_3)_6^{2-} + 6Cl^- = PoCl_6^{2-} + 6NO_3^-}$$

Here, unconverted nitrate complex contributes to the extraction in the concentration range of hydrochloric acid lower than 2 N. In this hypothesis, an assumption of an uncertain soluble complex of polonium is not necessary.

However, there is no reason to believe that the nitrate complex is more stable than chloro-complex nor that the conversion of nitrate complex into chloro-complex is incomplete.

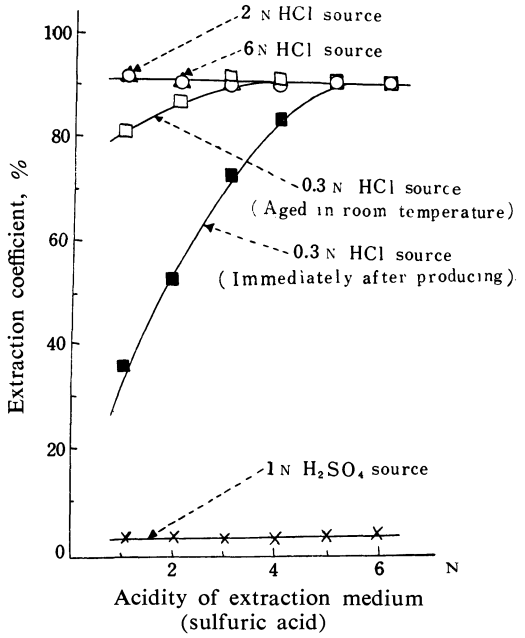



Fig. 6A. Aging effect on extraction coefficient. (Immediately after dilution.)

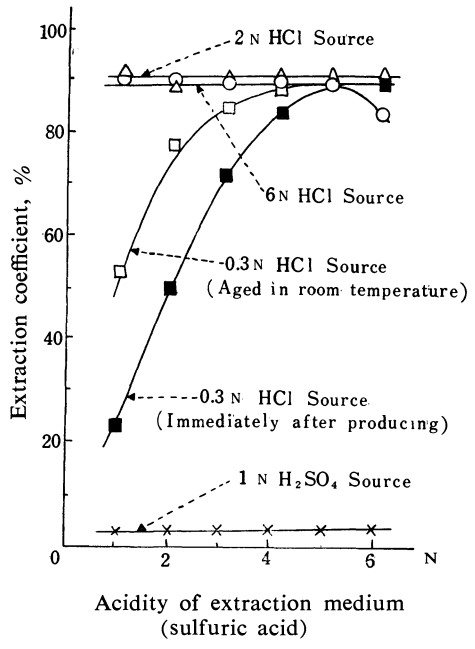



Fig. 6B. Aging effect on extraction coefficient. (Aged for 6 hr. at boiling point.)

**5) Aging Effect on the Extraction from Sulfuric Acid Medium.**—Partition equilibrium of polonium(IV) between hexone and aqueous solution of sulfuric acid was also studied with the different sources of polonium, stored in 6, 2 and 0.3 N hydrochloric acid and 1 N sulfuric acid, respectively. The results were shown in Fig. 6. Among them only the polonium source prepared and stored in sulfuric acid

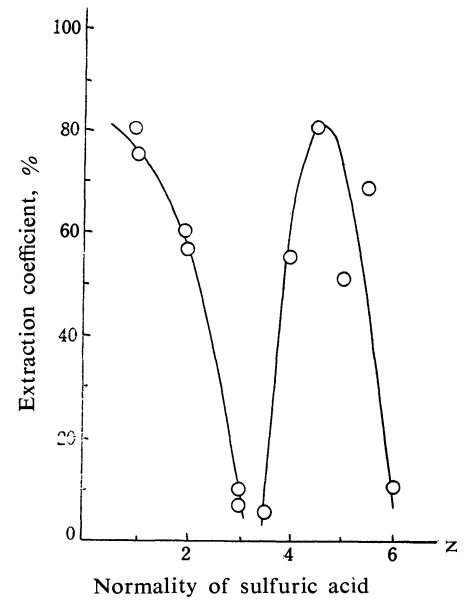



Fig. 7. Extraction of polonium(IV) in sulfuric acid.

gives extraction coefficient nearly nul in the entire range of acidity examined. This indicates that a trace quantity of chloride, if present in sulfuric acid, causes a remarkable increase of extraction yield and that the yield attains the maximum value corresponding to that of hexachloro-polonium(IV) complex, $PoCl_6^{2-}$. It can be said that one of the complex species, $PoCl_6^{2-}$ is readily formed in the presence of a minimum quantity of chloride in sulfuric acid. In our latest publication on polonium the extraction of polonium(IV) from sulfuric acid medium passed through maximum and minimum phases as shown in Fig. 7. This was observed by using the polonium source of 6 N hydrochloric acid after diluting 100 times with sulfuric acid before extraction. In this case the aging was made at 80°C for one hour by heating on a steam bath. A minimum value of extraction that appeared in the proximity of 2 N sulfuric acid is consistent with the results obtained for the extraction from hydrochloric acid by using an aged polonium source as already mentioned in 3). From this consideration the present authors prefer the ionic form $PoO^{2+}$ as the stable species of polonium(IV) in sulfuric acid to that of $PoO_3^{2-}$ which is regarded as stable in less acidic solution according to the analogy of $Te(IV)O_3^{2-}$.

## Summary

The ionic state of polonium(IV) in hydrochloric and sulfuric acid solution was studied by the solvent extraction with hexone (methyl isobutyl ketone).

1) The polonium solution stored in 0.4 N nitric acid is strongly hydrolysed by aging. The low extraction coefficient caused by hydrolysis became higher by heating the polonium solution in stronger nitric acid. On the other hand, the polonium stored in 6 N nitric acid can be extracted with constant extraction coefficient, about 80%, through the entire acidity range from 1 to 6 N., if the extraction was carried out without any aging.

2) The aging effect of polonium(IV) in hydrochloric acid is rather complicated. A minimum extraction appeared in the acidity range near 2 N hydrochloric acid. By applying mass action law the probable form of polonium(IV) in that range was $Po(OH)_2Cl_4^{2-}$ or $PoO^{2+}$, assuming that $PoCl_6^{2-}$ was the stable form of polonium(IV) in 6 N hydrochloric acid which is readily soluble in hexone.

3) Almost no polonium(IV) was extracted by hexone from sulfuric acid solution. Here, the polonium(IV) in sulfuric acid exists probably as $PoO^{2+}$ rather than as $PoO_3^{2-}$.

The authors wish to express their thanks to Professor T. Shirai and to their colleagues in the laboratory for their helpful discussions. A part of the expenses of these studies was defrayed by a grant from the Ministry of Education.

*College of General Education*
*The University of Tokyo*
*Meguro-ku, Tokyo*

# *On the Differences in Monolayer Properties of Poly-γ-benzyl-L-glutamate and Poly-β-benzyl-L-aspartate*

By Shoichi IKEDA and Toshizo ISEMURA

(Received July 28, 1960)

Recently great progress has been made in the studies on synthetic polypeptides, especially concerninig their solutions. Among them, the solutions of poly-γ-benzyl-L-glutamate in various solvents have been investigated extensively and it is found that this polymer has a right-handed α-helical configuration in some solvents[1]. More recently it has been reported, however, that poly-β-benzyl-L-aspartate, the side chain of which has a length by one methylene group less than that of poly-γ-benzyl-L-glutamate, is quite different from poly-γ-benzyl-L-glutamate in its behavior and that the α-helix of the former polymer may be left-handed rather than right-handed[2].

1) P. Doty, J. H. Bradbury and A. M. Holtzer, *J. Am. Chem. Soc.*, **78**, 947 (1956); J. T. Yang and P. Doty, ibid., **79**, 761 (1957); E. R. Blout, P. Doty and J. T. Yang, ibid., **79**, 749 (1957).

2) E. R. Blout and R. H. Karlson, ibid., **80**, 1259, 6701 (1958); E. M. Bradbury, L. Brown, A. R. Downie, A. Elliott, W. E. Hanby and T. R. R. McDonald, *Nature*, **183**, 1736 (1959); R. H. Karlson, K. S. Norland, G. D. Fasman and E. R. Blout, *J. Am. Chem. Soc.*, **82**, 2268 (1960).

According to the surface chemical studies, synthetic polypeptides with non-polar or unionized side chains are known to give monolayers of condensed type on aqueous surfaces, the surface viscosity of which is manifest at a very low surface pressure region, but only those which contain prolyl residues in some high amounts give monolayers of expanded type, the surface viscosity of which is manifest first at a very high surface pressure region[3,4]. In general, therefore, the monolayers of ordinary unionized polypeptides are of condensed type and exhibit high surface viscosities, and the only difference among those which are composed of different amino acid residues are reflected explicitly in the behavior of the surface potential, according to the difference in polarities or electric moments of their side chains. Considering the striking difference in properties of poly-γ-benzyl-L-glutamate and poly-β-benzyl-L-aspartate in crystals or in solutions, as cited above, however, it is expected that the two polymers behave in a different way in their spread monolayers, since the difference of the two polymers in solutions and in crystals will be based on the different kinds of interactions of side chain with main chain or with other side chains and such an effect of side chain of polymers will be most distinctly revealed in monolayer states.

We have thus studied the monolayers of poly-γ-benzyl-L-glutamate (PBLG) and poly-β-benzyl-L-aspartate (PBLA) by the measurements of surface pressure, potential and viscosity. We will report any marked differences in their behavior and propose possible chain configurations of these polymers in monolayers and then discuss the differences on the basis of these configurations. Further we have examined the monolayer of a copolymer of γ-benzyl-L-glutamate and β-benzyl-L-aspartate, copoly-1: 1-(γ-benzyl-L-glutamate, β-benzyl-L-aspartate) (CP(BLG, BLA)), and the equimolar mixture of PBLG and PBLA.

## Experimental

PBLG (Code No. J11A) and PBLA (J826) were prepared by polymerizing *N*-carboxy-anhydrides of the corresponding L-amino acids in dioxane with triethylamine and CP(BLG, BLA) (A227B) by copolymerizing the equimolar mixture of *N*-carboxy-anhydrides of these amino acids in (1 : 1 v/v) chloroform-dioxane with triethylamine. Their intrinsic viscosities in dichloroacetic acid solution at 25°C were 0.13, 0.11 and 0.34, respectively. Their solutions in (1 : 4 v/v) dichloroacetic acid-benzene were spread on aqueous surfaces. The equimolar mixed monolayer of PBLG and PBLA was spread from their mixed solution in the same solvent.

The surface pressure was measured by a surface balance of the hanging plate type, the surface potential by a vibrating electrode and the surface viscosity by a rotatory oscillating disk[3,4]. The temperature was regulated by heating the inside of the shielding box with a voltage controlled lamp, if necessary.

## Results

The surface pressure, $\Pi$, surface potential, $\Delta V$, and surface viscosity, $\eta$, of PBLG, PBLA and CP(BLG, BLA) are plotted against the area, expressed in the unit of Å$^2$ per (average)

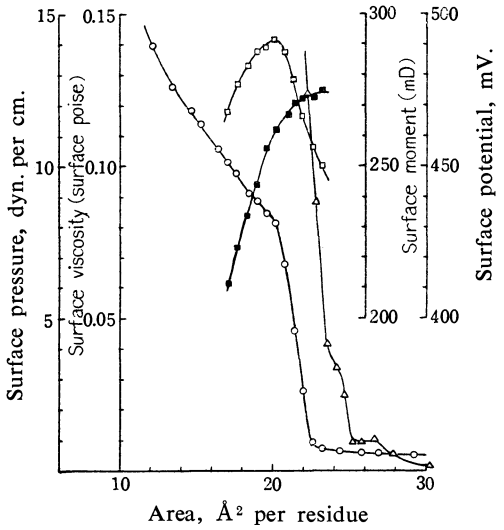



Fig. 1. Monolayer of PBLG at 9.0°C. ○, surface pressure; □, surface potential; ■, surface moment; △, surface viscosity.

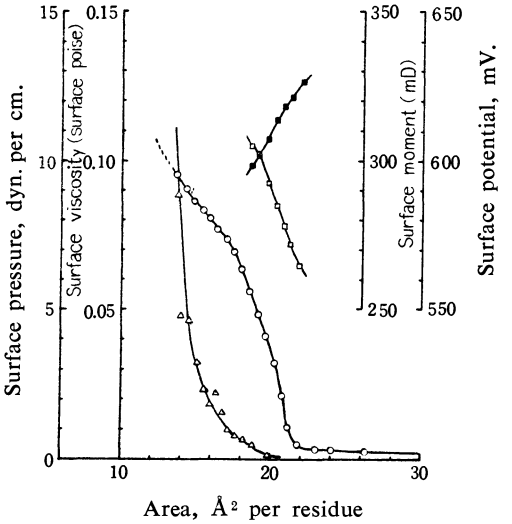



Fig. 2. Monolayer of PBLA at 10.8°C. ○, surface pressure; □, surface potential; ■, surface moment; △, surface viscosity.

3) T. Isemura and S. Ikeda, This Bulletin, 32, 178 (1959).
4) S. Ikeda and T. Isemura, ibid., 32, 659 (1959).

TABLE I. MONOLAYER CHARACTERISTICS OF POLYPEPTIDES

| | $A_{\Pi\to 0}$, Å$^2$ | $A_{\Delta V}$, Å$^2$ | $\mu_{21\text{Å}^2}$, mD | $A_{\eta=0.10}$, Å$^2$ |
|---|---|---|---|---|
| PBLG | 22.8 | 23.2 | 270 | 22.7 ( 9.0°C) |
| PBLA | 21.5 | 22.0 | 322 | 13.5 (10.8°C) |
| CP(BLG, BLA) | 23.0 | 22.6 | 305 | 23.4 (12.3°C) |
| 1 : 1 PBLG+PBLA | 22.4 | 22.5 | 240 | 13.4 (19.3°C) |

TABLE II. SURFACE COMPRESSIBILITIES

| | $\delta_1$, cm./dyn. | $\delta_2$, cm./dyn. | $\delta_3$, cm./dyn. |
|---|---|---|---|
| PBLG | 0.0126 (22.8~20.3Å$^2$) | 0.0855 (20.3~ca. 11.4Å$^2$) | — |
| PBLA | 0.0222 (21.5~20.3Å$^2$) | 0.0329 (20.3~ca. 17Å$^2$) | 0.129 (ca. 17~14.0Å$^2$) |
| CP(BLG, BLA) | 0.0195 (23.0~18.3Å$^2$) | 1.21 (18.3~ca. 12Å$^2$) | — |
| 1 : 1 PBLG+PBLA | 0.0191 (22.4~19.5Å$^2$) | 0.114 (19.5~ca. 14Å$^2$) | — |

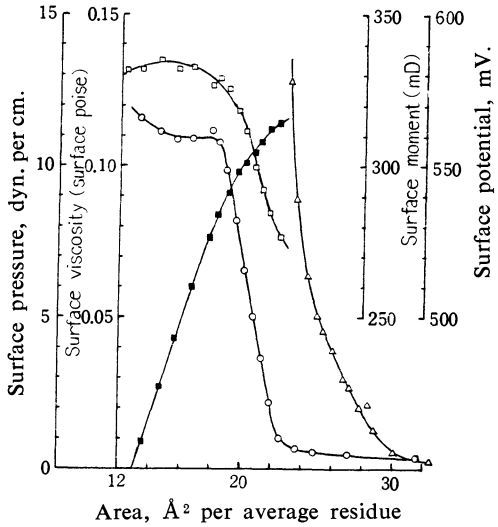



Fig. 3. Monolayer of CP(BLG, BLA) at 12.3°C. ○, surface pressure; □, surface potential; ■, surface moment; △, surface viscosity.

amino acid residue, as shown in Figs. 1, 2 and 3. All the monolayers are of condensed type. The surface potential was not definite but fluctuated from time to time at the region of large areas. However, reproducible values were observed as the surface pressure began to rise. Values of the area, $A_{\Pi\to 0}$, at which the surface pressure steeply increases on compression, and of the area, $A_{\Delta V}$, at which the surface potential becomes reproducible on compression, are tabulated in Table I. The surface pressure and potential were scarcely at all influenced by temperature. The $A_{\Pi\to 0}$ is nearly equal to $A_{\Delta V}$ for each polymer and they will represent the actual area occupied by an (average) amino acid residue.

The values of surface compressibility calculated by

$$\delta = -\frac{1}{A}\frac{\partial A}{\partial \Pi}$$

are given in Table II, which shows clearly the difference in surface pressure-area curves of the three polymers. In the region of low surface pressure the surface compressibility is in the order: PBLA> CP(BLG, BLA) >PBLG. The surface pressure-area curve of CP(BLG, BLA) is characterized by the region of very high surface compressibility such as that observed for poly-$\gamma$-benzyl-DL-glutamate[5].

The surface moments per amino acid residue calculated by the Helmholtz equation

$$\mu = \frac{A\cdot\Delta V}{4\pi}$$

are plotted against the area, as is also shown in Figs. 1, 2 and 3, and the values at 21 Å$^2$ are also listed in Table I. It is noticed that the surface moment of PBLA is about 50 mD higher than that of PBLG and CP(BLG, BLA) has an intermediate value of these two.

Although some differences are observed in surface pressure and potential between PBLG and PBLA, as described above, they are most distinctly reflected in surface viscosity behavior. The surface viscosity of PBLG is very high at very low surface pressure region, but that of PBLA is manifest first at high surface pressure region; the surface viscosity of the former is much lower than that of the latter. It is remarkable that, in spite of the condensed nature of monolayer reflected in surface pressure, PBLA has a very low surface viscosity. A monolayer of polymer with such composite properties, i. e., a monolayer of condensed type with a low surface viscosity, has never been reported. The surface viscosity-area curve of CP(BLG, BLA) is similar to that of PBLG rather than being an intermediate between PBLG and PBLA.

The surface viscosities of PBLG and PBLA were markedly influenced by temperature and they were higher as the temperature was high.

5) T. Isemura and K. Hamaguchi, ibid., 27, 125 (1954).

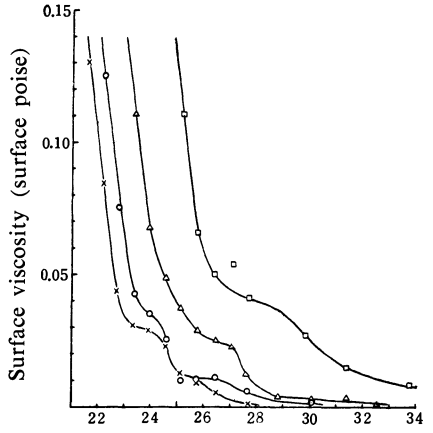



Fig. 4. Variation of surface viscosity of PBLG with temperature. □, 24.0°C; △, 16.2°C; ○, 9.0°C; ×, 5.6°C.

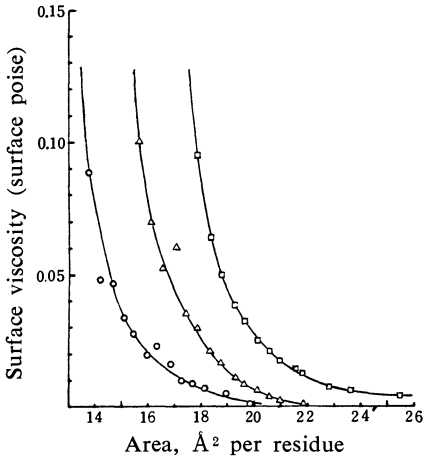



Fig. 5. Variation of surface viscosity of PBLA with temperature. □, 24.5°C; △, 17.9°C; ○, 10.8°C.

The variations of surface viscosity with temperature are shown in Figs. 4 and 5. Contrary to the common nature of the expanded monolayer[4], PBLA has a positive temperature coefficient of surface viscosity rather than a negative one.

Values of the area, $A_{\eta=0.10}$, at which the surface viscosity reaches 0.10 surface poise, are also given in Table I.

## Discussion

**Chain Configurations of PBLG and PBLA in Monolayer.**—The values of the limiting area, $A_{\Pi\to 0}$, derived from the surface pressure-area curves imply that these three polymers assume a configuration such as the β-form in monolayers. Although the limiting area, 22 Å², of these polymers is somewhat larger than that of some other polypeptides such as poly-DL-alanine, 15 Å² [3,6], this suggests that the area occupied by a residue is not defined by the main chain only but by the large side chain for these polymers. As the polymers are composed of L-amino acid residues exclusively, the side chains are oriented up and down alternatively when spread on an aqueous surface, assuming a β-configuration[6,7] but the hydrophilic or hydrophobic nature and the orientation of side chain should be different from that of non-polar polypeptides owing to the presence of two oxygen atoms.

Since the three polymers have polar groups on a side chain as well as on the main chain and then the side chain has both hydrophilic and hydrophobic nature, the side chain can change its orientation with greater ease sometimes rising into the air, sometimes lying on the surface and sometimes submerging into the water. The fluctuation of surface potential at large areas might be ascribed to such a thermal motion of the side chain. On high compression, however, the orientation of the side chain is forced to be fixed into a definite position, as given below. Thus the area, $A_{\Delta V}$, at which the surface potential gives a definite value, is nearly equal to the limiting area, $A_{\Pi\to 0}$.

As shown in Table I, the surface moments of these three polymers are much higher than those of polypeptides with non-polar side chains such as poly-DL-alanine, 160 mD[3]. This can be attributed to the contributions of the polar groups on side chain, i. e., the electric moments of the carbonyl group and the $H_2C$–O bond, to the surface moment besides that of the main chain. If the carbonyl group on the side chain is directed towards the aqueous surface with an angle $90° - \theta$, then the 'surface moment' of the side chain of PBLG and PBLA is given by

$$\text{(A)} \qquad \mu_{C=O}\cos\theta - \mu_{C-O}\cos(\theta + 30°)$$

if all the bonds on the side chain are assumed to be in trans form, or by

$$\text{(B)} \qquad \mu_{C=O}\cos\theta + \mu_{C-O}\cos(\theta + 30°)$$

if the O–C$\lesssim$O bond alone takes cis form. About half of the side chains are submerged into the aqueous subphase and surrounded by water molecules; this does not contribute to the surface moment[8]. Thus the total surface moment observed experimentally consists of

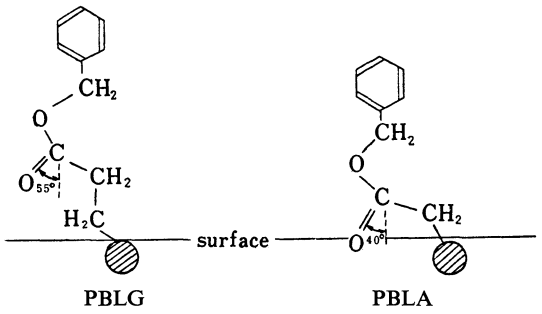
6) C. W. N. Cumper and A. E. Alexander, *Trans. Faraday Soc.*, **46**, 235 (1950).
7) J. T. Davies, *Biochim. Biophys. Acta*, **11**, 165 (1953).
8) J. T. Davies, *Trans. Faraday Soc.*, **49**, 949 (1953).

TABLE III. CALCULATED VALUES OF SURFACE MOMENTS

$\mu = 160\,\text{mD} + 1/2\,\mu(\text{side chain})$

| $\theta$ (°) | | 0 | 30 | 35 | 40 | 45 | 50 | 55 | 60 | 90 |
|---|---|---|---|---|---|---|---|---|---|---|
| $\mu$(mD) | (A) | 242 | 274 | 272 | 269 | 266 | 261 | 252 | 250 | 203 |
| | (B) | 439 | 359 | 344 | 327 | 309 | 291 | 271 | 250 | 117 |

the contributions of the main chain, 160 mD[3], and of half the 'surface moment' of the side chain. If it is assumed that $\mu_{C=O} = 360$ mD and $\mu_{C-O} = 170$ mD[9], the total surface moment can be calculated for various values of $\theta$ in either case, (A) or (B). The results are given in Table III. Comparing these calculated values with the observed values in Table I, it is found that the side chain of PBLA has a configuration with $\theta = 40°$ in which all the bonds are trans except that the O–C(=O) bond is cis. On the other hand, the configuration of the side chain of PBLG has two possible configurations from the data on surface moment alone, but it is confined to the one with all the bonds being trans other than the O–C(=O) bond and with $\theta = 55°$, if the limiting area derived from the surface pressure is taken into account. The configurations deduced thus are illustrated as follows:




It can be seen that the orientations of side chains of PBLG and PBLA are quite different from each other, although the difference in their structure is only by one methylene group in side chain length. In other words, the carbonyl group on the side chain of PBLG seems to play the role of a hydrophobic part and does not serve for the hydrophility of the side chain very well, but that of PBLA is submerged into the aqueous subphase and is indistinguishable from the carbonyl group on the main chain, thus greatly increasing the hydrophilic nature of the side chain.

The value of surface moment of CP(BLG, BLA) intermediate between PBLG and PBLA supports the configuration similar to the $\beta$-form for these three polymers in monolayer and the value, 305 mD, slightly higher than the mean value, 296 mD, suggests that the side chains of $\gamma$-benzyl-L-glutamate residue are influenced by $\beta$-benzyl-L-aspartate residue in this copolymer.

The observed value of surface moment of $\gamma$-benzyl-L-glutamate residue in PBLG, $\mu_{21A^2} = 270$ mD, may be compared with that of $\gamma$-methyl-L-glutamate residue in copoly-1 : 1-($\gamma$-methyl-L-glutamate, DL-phenylalanine). The latter copolymer has a surface moment per amino acid residue, $\mu_{19A^2} = 197$ mD[8]. Since the surface moment of poly-DL-phenylalanine is 110 mD[7], the contribution of $\gamma$-methyl-L-glutamate residue to the surface moment of the copolymer should be 284 mD, which is in accord with the surface moment of $\gamma$-benzyl-L-glutamate residue in PBLG.

**Relation of Surface Viscosity with Surface Pressure.**—As was noted before, whereas PBLG gives a high surface viscosity at areas larger than the area at which the surface pressure begins to rise steeply or the limiting area, i. e., at a very low surface pressure region, PBLA shows a high surface viscosity only at areas far smaller than the limiting area, i. e., at a high surface pressure region. In other words, the surface viscosity is much higher for PBLG than for PBLA. The behavior as was observed for PBLG has the general characteristics of monolayers of condensed type. However, that for PBLA has not been noticed for monolayers of any polymers so far examined, but only for monolayers of long chain fatty acids[10] and their mixtures with each other or with long chain alcohols[11]. This striking difference between PBLG and PBLA may be interpreted on the basis of the configurations of side chains presented above.

The monolayer of PBLG would correspond to the glassy state polymers in three dimensional state in which the interaction between segments are very strong, and consequently the monolayer is condensed and the surface viscosity is very high[4]. In this case the interaction between segments would mainly be the hydrogen bonding between peptide bonds in the main chain. The monolayer of PBLA would also correspond to the glassy state. In the case of PBLA, however, the carbonyl group on the side chain is submerged into water like

9) A. E. Alexander and J. H. Schulman, *Proc. Roy. Soc.*, A161, 115 (1937).

10) G. E. Boyd and W. D. Harkins, *J. Am. Chem. Soc.*, 61, 1188 (1939).

11) G. E. Boyd and F. Vaslow, *J. Colloid Sci.*, 13, 275 (1958).

the one on the main chain, as referred to before, and, therefore, the interactions between segments are not necessary ascribed to the hydrogen bonding between peptide bonds but also possibly to the hydrogen bonding of the carbonyl group on the side chain with the imino group on the main chain. The monolayer configuration of PBLA would be less stable than that of other polypeptides and a part of the molecular chain can easily be submerged into the aqueous subphase under compression or under shear flow. Further, the hydrophilic nature of the side chain is greatly enhanced owing to the carbonyl group in contact with water and would be responsible for reducing the resistance against compression or shear. Thus the high surface compressibility and the low surface viscosity of PBLA will be exhibited after the surface pressure begins to rise or the monolayer is compressed to the limiting area.

The specific nature of the side chain of PBLA seems to be related to its reactivity when it is reduced to remove the benzyl group on the side chain. By this treatment, PBLA does not produce poly-α-L-aspartic acid but gives poly-anhydro-L-aspartic acid[12], while PBLG gives poly-α-L-glutamic acid. This also suggests that the carbonyl group on the side chain is scarcely distinguishable from that on the main chain.

The variations of surface viscosity with temperature for PBLG and PBLA are given in Figs. 4 and 5. If the logarithms of surface viscosity of PBLA at different temperatures are plotted against surface pressure, a part of each curve gives a straight line expressed by

$$\log \eta = \log \eta_0 + c\Pi$$

as shown in Fig. 6. The same type of equation has been found for some other monolayers[4,10,11,13]. The constants of this equation for PBLA are tabulated in Table IV. No further implication of these constants is clear.

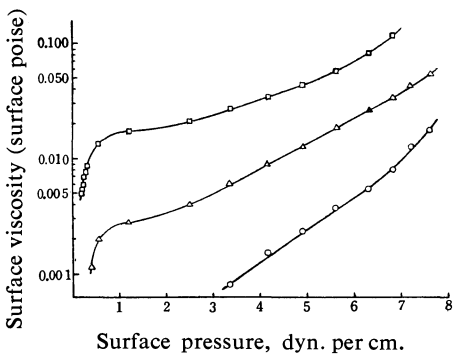



Fig. 6. The log η-Π plots for PBLA at different temperatures. □, 24.5°C; △, 17.9°C; ○, 10.8°C.

TABLE IV. CONSTANTS OF THE log η-Π RELATION FOR PBLA

| Temperature, °C | log $\eta_0$ | $c$ | Π, dyn./cm. |
|---|---|---|---|
| 24.5 | −1.99 | 0.124 | 2.0∼5.0 |
| 17.9 | −2.92 | 0.207 | 2.2∼6.5 |
| 10.8 | −3.77 | 0.249 | 2.2∼7.0 |

**The Equimolar Mixed Monolayes of PBLG and PBLA.** — The monolayer characteristics of the equimolar mixture of PBLG and PBLA are shown in Fig. 7. The limiting areas

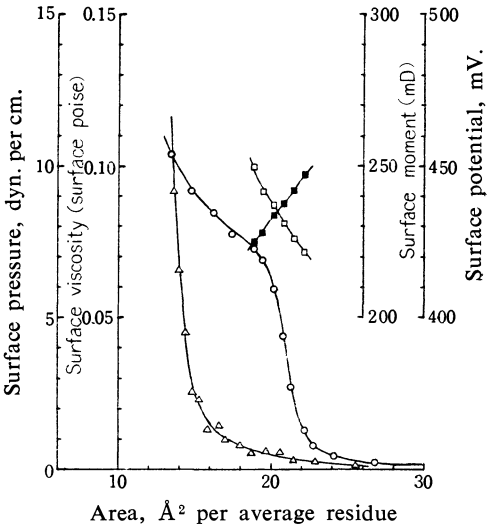



Fig. 7. Equimolar mixed monolayer of PBLG and PBLA at 19.3°C. ○, surface pressure; □, surface potential; ■, surface moment; △, surface viscosity.

derived from the surface pressure and from the surface potential are equal to each other and are about 22 Å², and the surface compressibility at the region of rise of surface pressure is intermediate between those for PBLG and PBLA and almost equal to that of CP(BLG, BLA). However, the surface moment and viscosity are much lower than those of CP(BLG, BLA). These characteristics are also given in Tables I and II. The reason for the low surface moment and the low surface viscosity of the mixed monolayer is not clear, since the dipole-dipole interaction would not be strong enough to influence monolayer properties very appreciably[14].

12) J. Noguchi, T. Saito and M. Asai, *J. Chem. Soc. Japan, Pure Chem. Sec.* (*Nippon Kagaku Zasshi*), **81**, 620 (1960).

13) T. Isemura and K. Fukuzuka, *Mem. Inst. Sci. Ind. Res., Osaka Univ.*, **13**, 137 (1956).

14) J. Marsden and J. H. Schulman, *Trans. Faraday Soc.*, **34**, 748 (1938); W. D. Harkins and R. T. Florence, *J. Chem. Phys.*, **6**, 847 (1938).

**Summary**

In view of the marked differences of PBLG and PBLA in crystals and in solutions, we have investigated their differences in monolayer states and further examined the monolayers of CP(BLG, BLA) and of the equimolar mixture of PBLG and PBLA.

All these polymers were found to be of condensed type and their limiting areas to be about 22 Å$^2$. The surface compressibility at the region of rise of surface pressure was in the order: PBLA>CP(BLG, BLA)>PBLG. The surface moments of all these polymers were considerably higher than those of non-polar polypeptides. The surface moment of PBLA was 50 mD higher than that of PBLG, and that of CP(BLG, BLA) gave a value intermediate between them. PBLG and CP(BLG, BLA) exhibited high surface viscosities at a very low surface pressure region, but, in spite of the condensed nature of the monolayer, PBLA showed appreciable surface viscosity first at a high surface pressure region. The surface viscosities of PBLG and PBLA were higher at higher temperatures.

From the data on surface pressure and surface moment, all these polymers were considered to have a configuration similar to the $\beta$-form in the spread state and possible configurations of side chains of PBLG and PBLA were deduced. It was found that the carbonyl group on the side chain of PBLG is far from the aqueous surface but that of PBLA is in contact with the surface and scarcely distinguishable from the carbonyl group on the main chain. Accordingly, PBLG can take a stable configuration like the $\beta$-form in monolayer, but the correspounding configuration of PBLA will be less stable owing to possible hydrogen bonding of the carbonyl group on the side chain with the imino group on the main chain and the resulting enhanced hydrophility of the side chain. This might be ascribed to the differences in surface compressibility and surface viscosity of PBLG and PBLA.

The surface pressure behavior of the mixed monolayer of PBLG and PBLA was such as was expected, but its behavior in surface potential and viscosity was very anomalous.

We wish to acknowledge to Professor J. Noguchi of Kanazawa University our indebtedness for his kind guidance in preparing the polypeptides.

*Faculty of Science (S. I. & T. I.) and*
*Institute for Protein Research (T. I.)*
*Osaka University*
*Osaka*

# *Monolayer Studies on Polyanhydro-L-glutamic and Polyanhydro-L-aspartic Acids*

By Shoichi IKEDA and Toshizo ISEMURA

(Received August 15, 1960)

When poly-$\gamma$-benzyl-L-glutamate is reduced to remove the benzyl group in an anhydrous state, poly-$\alpha$-L-glutamic acid is obtained[1]. However, even if poly-$\beta$-benzyl-L-aspartate is treated in the same way, no poly-$\alpha$-L-aspartic acid but only polyanhydro-L-aspartic acid can be obtained[2]. Berger et al.[3] has reported that poly-$\alpha$-L-aspartic acid is prepared by this method, but Noguchi et al.[2] has suggested that the polymer obtained by Berger et al. would be a copolymer of L-aspartic acid with its andydride. Furthermore, Asai et al.[4] has shown that polyanhydro-L-glutamic acid can be produced by dehydrating poly-$\alpha$-L-glutamic acid with acetic anhydride. Polyanhydro-L-glutamic acid may be identified with either poly-L-glutarimide (I) or poly-L-pyrrolidone-2-carboxylic acid (II), and polyanhydro-L-aspartic acid with either poly-L-succinimide (III) or poly-L-propiolactam-2-carboxylic acid (IV). Noguchi et al.[2,4] has demonstrated from the

1) W. E. Hanby, S. G. Waley and J. Watson, *J. Chem. Soc.*, **1950**, 3239; E. R. Blout and M. Idelson, *J. Am. Chem. Soc.*, **78**, 497 (1956); M. Idelson and E. R. Blout, ibid., **80**, 4631 (1958).

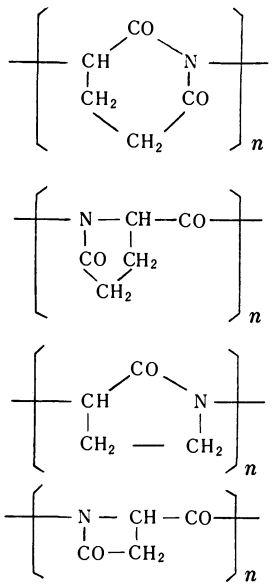
2) J. Noguchi, T. Saito and M. Asai, *J. Chem. Soc. Japan, Pure Chem. Sec.* (*Nippon Kagaku Zasshi*), **81**, 622 (1960).

3) M. Frankel and A. Berger, *J. Org. Chem.*, **16**, 1513 (1951); A. Berger and E. Katchalski, *J. Am. Chem. Soc.*, **73**, 4084 (1951).

4) M. Asai, K. Imai and J. Noguchi, *J. Chem. Soc. Japan, Pure Chem. Sec.* (*Nippon Kagaku Zasshi*), **81**, 624 (1960).

syntheses of appropriate polymers and the comparison of their infrared spectra that polyanhydro-L-glutamic acid is poly-L-glutarimide itself and polyanhydro-L-aspartic acid is poly-L-succinimide.

We have examined the monolayers of polyanhydro-L-glutamic acid, poly-DL-pyrrolidone-2-carboxylic acid, polyanhydro-L-aspartic acid and poly-L-succinimide at air-water interfaces and attempted to obtain further information concerning the structure of the polyanhydro acids. Some of these polymers are interesting in themselves for monolayer studies, since they are composed of chains of rings directly connected with each other and expected to have highly rigid structures.



## Experimental

Polyanhydro-L-glutamic acid and poly-DL-pyrrolidone-2-carboxylic acid were prepared by Professor Noguchi and his collaborators[4]. Polyanhyro-L-aspartic acid was prepared by reducing poly-$\beta$-benzyl-L-aspartate[5] in glacial acetic acid with anhydrous hydrobromic acid. Poly-L-succinimide was also prepared by Professor Noguchi et al.[2]

Surface pressure, potential and viscosity were measured by the methods as described previously[5]. Surface moment was calculated by the usual Helmholtz equation. Area was expressed in the unit of $Å^2$ per residue, a residue being assumed to consist of an anhydro acid residue plus a water molecule. The spreading solvent was a mixture of dichloroacetic acid-benzene (1 : 1 v/v) throughout the present investigation.

## Results and Discussion

**Polyanhydro-L-glutamic Acid.**—Two kinds of polymers, i. e., poly-L-glutarimide and poly-L-pyrrolidone-2-carboxylic acid, are possibly assumed as polyanhydro-L-glutamic acid. The former has a structure composed of rings exclusively, each connected directly by a C–N linkage, and is expected to be rigidly folded. The latter has a structure similar to poly-L-proline but is different from poly-L-proline by the presence of a carbonyl group in the pyrrolidone ring and expected to be highly hydrophilic. Poly-DL-pyrrolidone-2-carboxylic acid did not spread on distilled water but gave stable films on aqueous salt solutions, as illustrated in Fig. 1. The films of poly-DL-

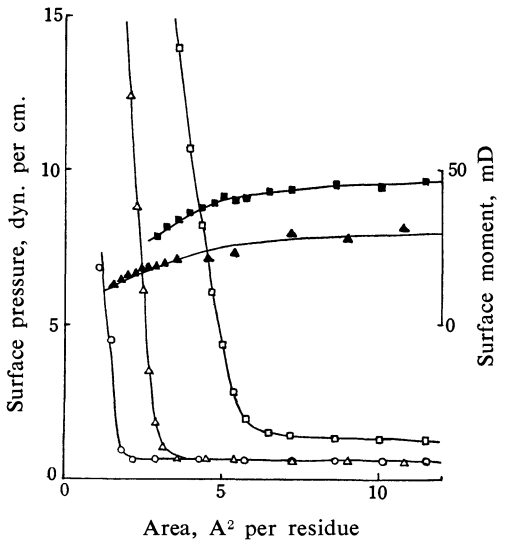



Fig. 1. Plots of surface pressure and surface moment of poly-DL-pyrrolidone-2-carboxylic acid against area (10°C). Aqueous subphases: potassium chloride solutions; ○, 0.01 M; △, ▲, 0.1 M; □, ■, 1 M.

pyrrolidone-2-carboxylic acid are of condensed type, in contrast to the expanded nature of poly-L-proline film. The reason why the film is condensed is not clear, since an expanded nature of polypeptide monolayer is ascribed to the structure devoid of hydrogen bonding[6] and polypyrrolidone carboxylic acid can include no hydrogen bond as polyproline.

On the other hand, polyanhydro-L-glutamic acid gave a stable monolayer of condensed type on distilled water, as shown in Fig. 2. This already indicates that polyanhydro-L-glutamic acid is not identical with poly-L-pyrrolidone-2-carboxylic acid but is poly-L-glutarimide itself. The limiting areas from surface pressure and surface viscosity were equally 13 $Å^2$, which was smaller than those assigned to a

5) S. Ikeda and T. Isemura, This Bulletin, 34, 416 (1961).
6) T. Isemura and S. Ikeda, ibid., 32, 178 (1959).

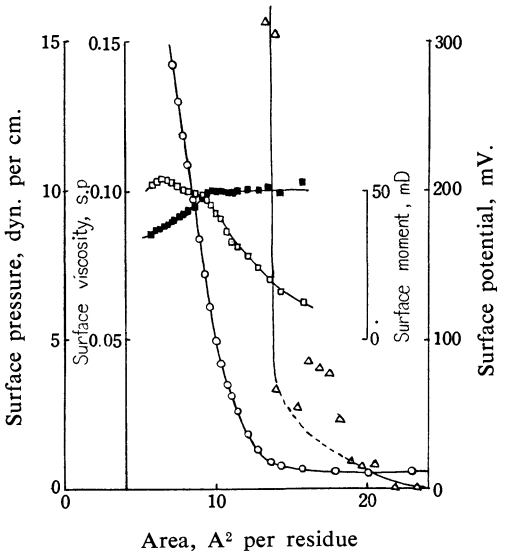



Fig. 2. Monolayer of polyanhydro-L-glutamic acid on distilled water (10°C).
○, surface pressure; □, surface potential; ■, surface moment; △, surface viscosity.

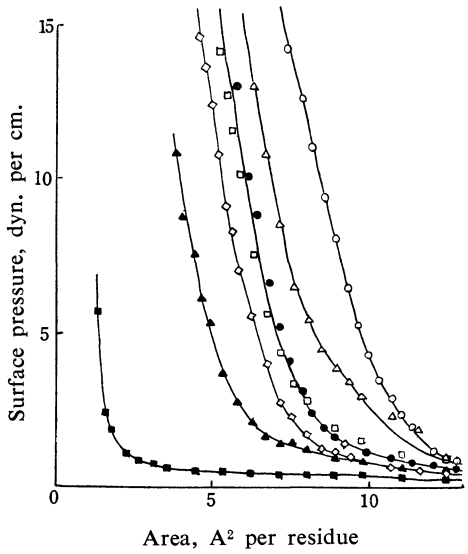



Fig. 3 Variation of surface pressure-area curves of polyanhydro-L-glutamic acid with alkalinity of aqueous subphase (10°C).
○, $H_2O$; △, 0.01 M, □, 0.1 M; ◇, 0.2 M $K_2CO_3$; ●, 0.01 M; ▲, 0.02 M; ■, 0.05 M KOH.

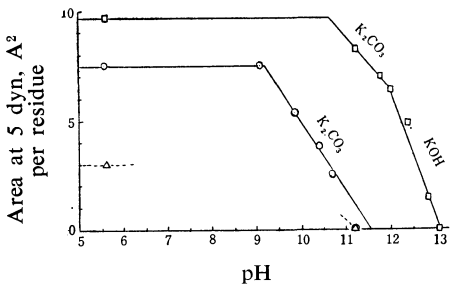



Fig. 4. Plots of area at 5 dyn. per cm. against pH.
□, polyanhydro-L-glutamic acid; ○, poly-L-succinimide; △, polyanhydro-L-aspartic acid.

β-configuration[6,7]. The surface potential was also low and the surface moment was about 50 mD. The low values of limiting area and surface moment also suggest that polyanhydro-L-glutamic acid might be poly-L-glutarimide, which can not be spread on aqueous surface as a monomolecular layer but has a folded configuration in film, as expected from its structure consideration.

The condensed nature of the monolayer of poly-L-glutarimide may be attributed to the rigid structure of this polymer, i. e., to its low configurational entropy. On the contrary, poly-L-proline has a relatively loose configuration in film, since its film is of an expanded type. Thus the pyrrolidine rings would not influence the flexibility of polymer chain in film very profoundly.

As referred to later, the monolayer of polyanhydro-L-glutamic acid behaves very similarly to that of poly-L-succinimide; this also supports the identity of polyanhydro-L-glutamic acid with poly-L-glutarimide. All these are consistent with the results of Asai et al.[4] and Bruckner et al.[8]

Since the ring of poly-L-glutarimide can be cleaved by dilute alkali[8,9], we have examined the monolayers of polyanhydro-L-glutamic acid on alkaline solutions of different pH's. The results on surface pressure-area relations are shown in Fig. 3 and the areas at 5 dyn. per cm. are plotted against the pH in Fig. 4. It can be seen that the film occupies smaller area as the rise of pH at the region of pH higher than 10.5 and no film can be formed at pH 13. This indicates that poly-L-glutamic acid produced by the cleavage of ring of polyanhydro-L-glutamic acid does not cause any expansion of film. When polyanhydro-L-glutamic acid was spread from its alkaline solution, no film was obtained on distilled water and even on 0.01 N hydrochloric acid or on potassium chloride solution. This suggests that the poly-L-glutamic acid thus formed should be composed of both α- and γ-linkages of peptide bonds, because poly-α-L-glutamic acid

7) C. W. N. Cumper and A. E. Alexander, *Trans. Faraday Soc.*, **46**, 235 (1950).
8) V. Bruckner, J. Kovács and K. Medzihradszky, *Naturwiss.*, **42**, 96 (1955).
9) V. Bruckner, M. Szekerke and J. Kovács, ibid., **42**, 179 (1955).

can make films on the acid side[10], but poly-γ-L-glutamic acid forms no film on aqueous subphases of various compositions[11]. Although the cupric salt of the poly-L-glutamic acid is insoluble[8], the poly-L-glutamic acid spread from an alkaline solution gave no film on cupric sulfate solution.

**Polyanhydro-L-aspartic Acid.**—We will proceed to examine the relation of polyanhydro-L-aspartic acid with poly-L-succinimide. The behavior of the monolayer of poly-L-succinimide on distilled water is shown in Fig. 5. The

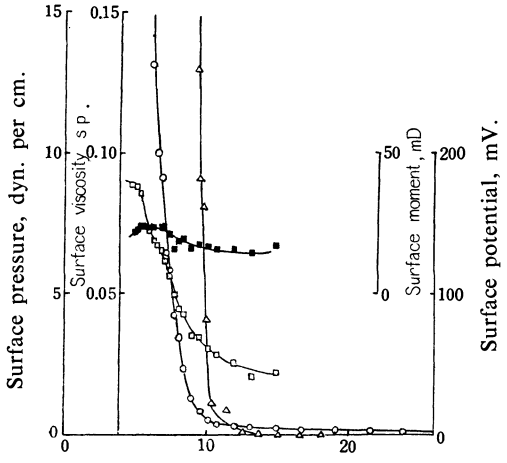



Fig. 5. Monolayer of poly-L-succinimide on distilled water (17°C).
○, surface pressure; □, surface potential; ■, surface moment; △, surface viscosity.

monolayer was of a condensed type and the limiting area determined from both surface pressure and viscosity was about 11 Å², and the surface potential was low and the surface moment was 20 to 25 mD. These low values may be attributed to the rigidly folded configuration of this polymer, which is maintained even in the spread state. Since poly-L-succinimide can be converted into poly-L-aspartic acid by dilute alkaline solutions[12-14], as poly-L-glutarimide to poly-L-glutamic acid[8,9], we have examined the monolayer properties on alkaline solutions of different pH's. The results are shown in Figs. 6 and 4. The cleavage of ring occurred at less alkaline pH for poly-L-succinimide than for poly-L-glutarimide; the

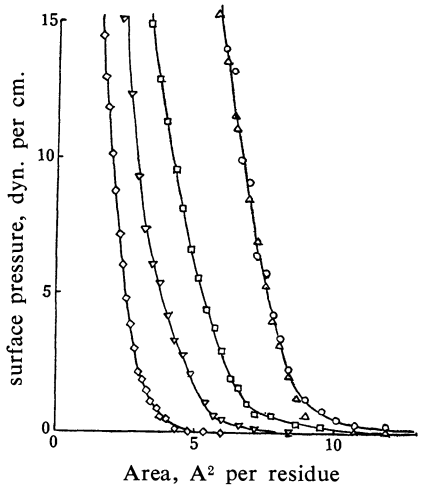



Fig. 6. Variation of surface pressure-area curves of poly-L-succinimide with alkalinity of aqueous subphase (17°C).
○, $H_2O$; △, 0.0002 M; □, 0.001 M; ▽, 0.003 M; ◇, 0.005 $K_2CO_3$.

film spreads less completely as the rise of pH at the region of pH higher than 9.0 and no film can be formed at pH 11. By the same procedures as for poly-L-glutarimide, it was found that the poly-L-aspartic acid thus formed might include both α- and β-linkages. This is in accord with the result of Kovács et al.[14]

Polyanhydro-L-aspartic acid gave a stable monolayer on distilled water, as shown in Fig. 7. The spreading of this polymer was far less than that of poly-L-succinimide, and it could not be increased by the addition of salt into the aqueous subphase. Except for the

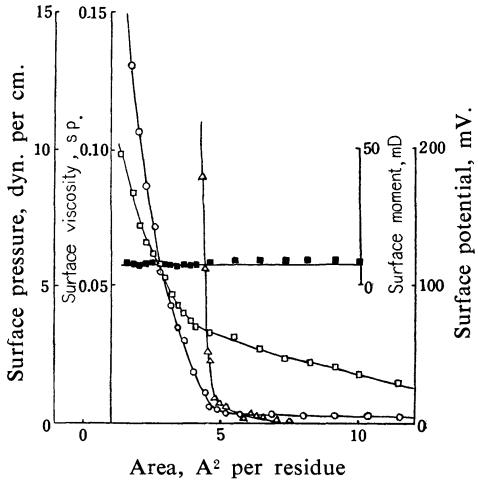



Fig. 7. Monolayer of polyanhydro-L-aspartic acid on distilled water (12°C). ○, surface pressure; □, surface potential; ■, surface moment; △, surface viscosity.

10) T. Isemura and K. Hamaguchi, This Bulletin, **27**, 339 (1954).
11) T. Yamashita, personal communication.
12) J. Kovács, J. Könyves and J. Császár, *Naturwiss.*, **41**, 575 (1954).
13) A. Vegotsky, K. Harada and S. W. Fox, *J. Am. Chem. Soc.*, **80**, 3361 (1958).
14) J. Kovács, I. Könyves and A. Pustzai, *Experientia*, **9**, 459 (1953); J. Kovács and I. Könyves, *Naturwiss.*, **41**, 333 (1954).

poorer spreading, however, polyanhydro-L-aspartic acid behaved very similarly to poly-L-succinimide in the monolayer state; e. g., no film was formed on an alkaline solution of pH 11, as shown in Fig. 4. Noguchi et al.[2] has confirmed that polyanhydro-L-aspartic acid is just poly-L-succinimide itself but never poly-L-propiolactam-2-carboxylic acid. Further they have referred to the Berger's polyaspartic acid[3] and concluded that it might be a copolymer of L-succinimide and L-aspartic acid. Our polyanhydro-L-aspartic acid might also be the same kind of copolymer since it occupies smaller area than poly-L-succinimide.

## Summary

To examine the structures of polyanhydro-L-glutamic acid and polyanhydro-L-aspartic acid, we have studied their monolayer properties and compared them with those of poly-DL-pyrrolidone-2-carboxylic acid and poly-L-succinimide. It was found that polyanhydro-L-glutamic acid is not identical with polypyrrolidone carboxylic acid but with poly-L-glutarimide, which has a rigidly folded configuration even in monolayer. This conclusion is in agreement with the results obtained by other methods. It was shown, however, that polyanhydro-L-aspartic acid can not be identified with poly-L-succinimide but it might be a copolymer of L-succinimide and L-aspartic acid.

We are grateful to Professor J. Noguchi of Kanazawa University for the gift of the polymers as well as for his guidance in preparing polyanhydro-L-aspartic acid.

*Faculty of Science and*
*Institute for Protein Research*
*Osaka University*
*Kita-ku, Osaka*

# *On the Orientational Order-Disorder Transition in Crystalline Aniline Hydrobromide*

By Hiroshi SUGA*

(Received August 1, 1960)

In the course of X-ray structural analyses[1] of aniline hydrobromide, Taguchi[2] has recently observed a phase transition from the orthorhombic to the monoclinic system, which occurs on cooling at about 27°C. He also found that the monoclinic angle $\beta$, between the a and c axes, is not constant below the critical temperature but varies continuously over a wide range of temperature as the temperature is lowered. The detailed analyses of crystal structures above and below the transition temperature range were carried out by the same author. He found further anomalous spectra in oscillation and Weissenberg photographs below the critical temperature associated with the appearance of a hybrid structure. The detailed knowledge concerning the crystal structures above and below the transition temperature range, the unusual variation of the monoclinic angle, and the appearance of a hybrid structure stimulated us to study the thermal properties of this compound to look into the mechanism of this peculiar phase transition.

## Experimental

**Material.** — Aniline (extra pure grade manufactured by Wakō Chem. Ind., Ltd.) was added to an excess of an aqueous solution of hydrobromic acid (1st grade, the same company). The precipitated salt was washed with cold distilled water and then recrystallized from warm ethanol. The crude product thus obtained was slightly colored and found to have some lattice imperfection as revealed by X-ray photographs[1]. In order to purify the product further, it was finally subjected to fractional sublimation under high vacuum ($10^{-5}$ mmHg). The final product obtained by this procedure is colorless powder. Single crystals were also obtained by sublimation. They are transparent and colorless

* Present address: Department of Physics, Osaka University, Osaka.

1) I. Nitta, T. Watanabé and I. Taguchi, *X-rays*, 5, 31 (1948); to be published in this Bulletin.

2) I. Taguchi, This Bulletin 34, 392 ((1961).

and are found to be free from lattice imperfection; m. p. 283°C.

**Apparatus and Procedure.**—For the preliminary study to ascertain the occurrence of the phase transition, a differential thermal analysis was carried out in the temperature range from −150 to +300°C. The apparatus was the same in its main feature as the one used hitherto in this laboratory[3] except for attachment of an automatic recording of the temperature difference between the sample and the reference substance (in this case, KCl). The detailed description of the recorder was recently given[4]. To determine the accurate transition temperature and to study the thermal behavior more in detail, measurements of heat capacity were also carried out in the temperature range from −80 to +60°C by the use of the conduction calorimeter[5]. For the heat capacity measurements 4.4 g. of the material was used, the heating rate being 0.25~0.30°C/min. over the full temperature range. Further, the relative thermal expansion below and above the transition temperature as well as the hysteresis phenomenon associated with the phase transition were studied by employing a simple double-walled glass-made dilatometer filled with mercury as the confining liquid. About 29 g. of the material was used, and the heating and cooling rates were about 0.2°C/min.

## Results

One of the typical curves of the differential thermal analysis is reproduced in Fig. 1. From this curve it was found that there is a comparatively broad thermal anomaly over the temperature range from −50 to +25°C, with sufficient reproducibility in the repeated measurements and also there is no detectable hysteresis either in the heating or in the cooling direction. The data of heat capacity

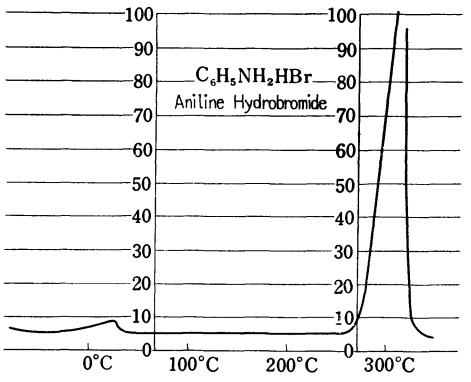



Fig. 1. Automatic recording curve of the differential thermal analysis for aniline hydrobromide.

TABLE I. HEAT CAPACITY DATA OF ANILINE HYDROBROMIDE

| $t$°C | $C_p$(cal./mol. deg.) | $t$°C | $C_p$(cal./mol. deg.) |
|---|---|---|---|
| −73.93 | 28.62 | 2.63 | 40.64 |
| −71.27 | 28.84 | 5.27 | 41.10 |
| −68.08 | 29.24 | 7.88 | 41.80 |
| −66.78 | 29.51 | 10.46 | 42.52 |
| −63.28 | 29.93 | 13.01 | 43.16 |
| −58.60 | 30.31 | 15.57 | 43.98 |
| −53.91 | 30.98 | 18.10 | 44.69 |
| −50.90 | 31.42 | 20.62 | 45.72 |
| −47.83 | 31.81 | 23.18 | 42.60 |
| −44.85 | 32.04 | 24.43 | 38.54 |
| −41.85 | 32.41 | 25.60 | 38.13 |
| −38.92 | 32.91 | 28.22 | 38.13 |
| −36.01 | 33.34 | 31.98 | 38.26 |
| −33.10 | 33.92 | 34.43 | 38.39 |
| −30.23 | 34.39 | 38.12 | 38.60 |
| −27.35 | 35.00 | 41.80 | 39.18 |
| −24.58 | 35.56 | 44.21 | 39.31 |
| −18.98 | 36.62 | 47.80 | 39.74 |
| −16.21 | 36.99 | 50.22 | 40.22 |
| −13.43 | 37.34 | 52.63 | 40.29 |
| −10.73 | 38.11 | 55.03 | 40.64 |
| − 8.04 | 38.54 | 61.00 | 41.63 |
| − 5.35 | 39.11 | 64.53 | 42.00 |
| − 2.67 | 39.71 | 66.88 | 41.81 |

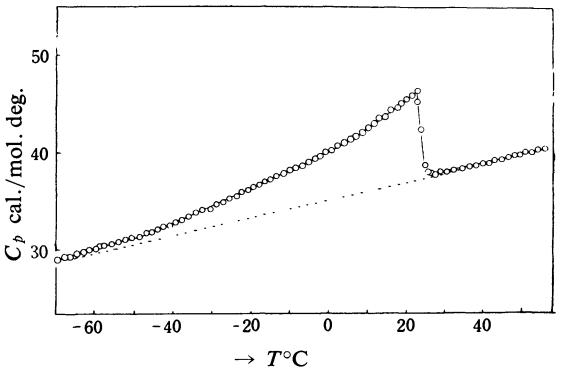



Fig. 2. Heat capacity versus temperature curve of aniline hydrobromide.

in this temperature range are given in Table I and they are plotted in Fig. 2. As this figure shows, the excess heat capacity starts to rise gradually at about −70°C, reaches a maximum value at 22°C (critical temperature), and then drops down abruptly by as much as 9 cal./mol. deg. The general trend of the heat capacity versus temperature curve reminds us of the similarity to that of the order-disorder phase transition of binary alloy systems[6]. Table II gives enthalpy and entropy of the

3) H. Chihara and S. Seki, ibid. **26**, 88 (1953); I. Nitta, S. Seki and H. Chihara, *J. Chem. Soc. Japan, Pure Chem. Sec.* (*Nippon Kagaku Zasshi*), **70**, 387 (1949).
4) H. Suga, H. Chihara and S. Seki, ibid., **82**, 24 (1961).
5) I. Nitta, S. Seki and M. Momotani, *Proc. Japan Acad.*, **26-9**, 25 (1950); S. Seki, M. Momotani, K. Nakatsu and T. Ōshima, This Bulletin, **28**, 411 (1955).
6) H. Moser, *Physik. Z.*, **37**, 737 (1936); F. W. Jones and C. Sykes, *Proc. Roy. Soc.*, **A167**, 440 (1937).

TABLE II. HEAT AND ENTROPY OF TRANSITION AND DIFFERENCE OF HEAT CAPACITIES AT $T_c$

| | |
|---|---|
| $\Delta H$ (transition) | $297 \pm 10$ cal./mol. |
| $\Delta S$ (transition) | $1.10 \pm 0.05$ e. u. |
| $\Delta C_p$ (at $T_c$) | $\sim 9$ cal./mol. deg. |

transition and the difference of heat capacities at the critical temperature. To evaluate the enthalpy of transition, the excess heat capacities over the dotted line given in the figure are integrated graphically. Here the dotted line is drawn as the normal contribution of the lattice vibration to the heat capacity. By dividing the abnormal part into many sections of temperature intervals, the entropy of transition was evaluated by summing up the quotients obtained by dividing each area of these sections with the corresponding mean absolute temperature. The entropy of transition thus obtained, 1.10 e. u. is comparable in magnitude with those of $NH_4Cl$ and $ND_4Cl$[7] at their lambda point, 1.30~1.40 e. u. As is evident from Fig. 2, the heat capacity curve is of typical lambda type and there is no indication of the latent heat at the critical temperature, showing that this transition is of higher order nature.

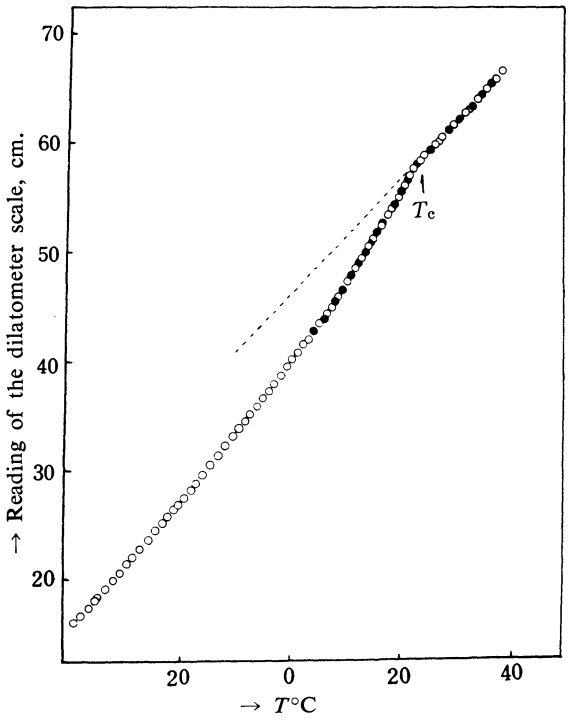



Fig 3. Volume versus temperature curve of aniline hydrobromide.

○ heating direction ● cooling direction

7) C. C. Stephenson, R. W. Blue and J. W. Stout, *J. Chem. Phys.*, **20**, 1046 (1952).

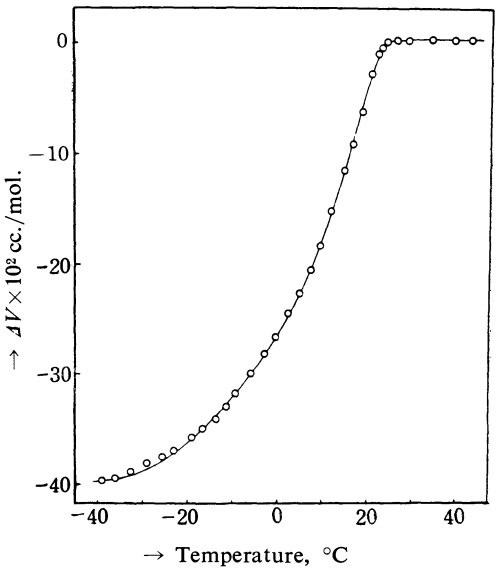



Fig. 3a. Anomalous thermal contraction of aniline hydrobromide.

Dilatometric studies revealed also the existence of abnormal expansion over the same transition range, as shown in Fig. 3. In this figure one can see that all the observed points in the heating and cooling directions can be represented by one and the same curve, showing again no hysteresis phenomenon. The dotted line in this figure means the thermal contraction extrapolated from the curve above the critical temperature by the use of the method of least squares. Fig. 3a gives the excess contraction $\Delta V$ below the dotted line and Fig. 4 the "abnormal" expansion coefficient calculated by $(1/V_0)\mathrm{d}(\Delta V)/\mathrm{d}T$, where $V_0$ is the molar volume of the crystal at the critical temperature. Although the expansion coefficient changes discontinuously at the critical point, the volume itself changes continuously over the whole range of measurements. These facts

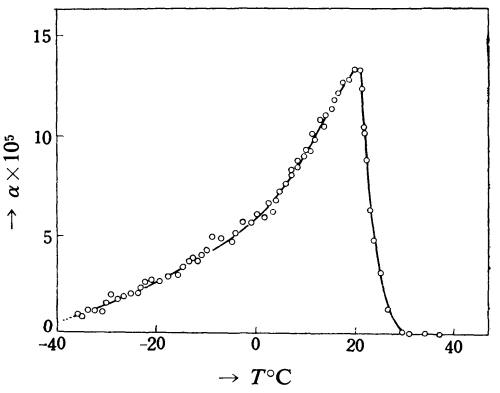



Fig. 4. Abnormal expansion coefficient of aniline hydrobromide.

also reasonably support the proposition that the transition is of higher order nature. The fact of non-existence of hysteresis phenomenon in the higher order phase transition was interpreted by Staveley et al.[8] from the point of view of lattice strain energy accompanying the phase transition.

## Discussion

Prior to the discussion of the plausible mechanism of this phase transition, it is necessary to give a brief account of the crystal structure[1,2] above and below the critical temperature. The high temperature phase belongs to the orthorhombic system ($D_{2h}^{10}-Pnaa$). In this structure, it is required from the crystal symmetry that both the principal axis of anilinium ion ($N-C_1\cdots C_4$ axis) and the $Br^-$ ion are found to lie on two different two-fold symmetry axes along the a axis. Although the positions of hydrogen atoms attached to the nitrogen atom are not yet determined, $-NH_3^+$ ionic group is surrounded by four $Br^-$ ions, of which two are slightly more distant than the other two. On cooling the crystal through the critical temperature, it is transformed into the monoclinic system ($C_{2h}^5-P2_1/a$); the monoclinic angle deviates gradually from 90° and reaches 91°22′ asymptotically in a manner shown in Fig. 8, where the unit of the ordinate is twice the quantity $\Delta\beta(=\beta-90°)$, for convenience. In the structure of the low temperature modification, the requirement of two-fold symmetry imposed to the C-N axis is lost. In this phase, in response to the variation of $\beta$, the positions of $Br^-$ ions and $-NH_3^+$ ionic groups are displaced with respect to each other, with the following sequence that the interionic distances between $Br^-$ ions and an $-NH_3^+$ ionic group become different from each other, and also that the pseudo electric dipole moments due to the displacements of the two kinds of ions in the neighboring ionic array along the a axis may be found to be antiparallel with each other in a similar manner as in the anti-ferroelectric crystal which was proposed originally by Kittel[9].

Considering the crystal structures as well as the thermal behaviors above and below the critical temperature described above it is suggested that a mechanism of orientational order-disorder of the $-NH_3^+$ group as an interpretation of this phase transition be given, based on the reason given below. In the first place, it will be natural to assume the pyramidal configuration ($C_{3v}$) of the $-NH_3^+$ ionic group. In the high temperature phase, since the C-N axis should lie on the two-fold symmetry axis, the potential energy of $-NH_3^+$ group associated with the rotational motion of this group will also have the same two-fold axial symmetry around this axis. Therefore, one has to consider necessarily some statistical randomness for the azimuthal orientation of $-NH_3^+$ group with respect to the C-N bond so far as one puts an $-NH_3^+$ group having three-fold symmetry on the axis of two-fold symmetry. On the other hand, in the low temperature phase such a requirement of two-fold symmetry is lost owing to the different crystal symmetry. Taking into account the possible formation of the N-H···Br weak hydrogen bond, possible orientations of the $-NH_3^+$ group with respect to the hydrogen atoms may be expected to be such as are represented in Fig. 5.

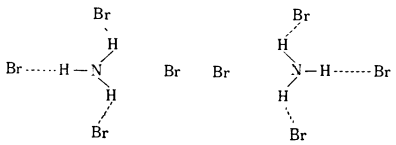



Fig. 5. Possible orientations of $-NH_3^+$ group (a- and b-types).

It is obvious from the symmetry consideration that these a- and b-type orientations are equally probable in the orthorhombic phase, whereas in the monoclinic phase one of these two types would be stabilized. We shall call this the a-type for convenience. Then, the requirement of two-fold axial symmetry in the high temperature phase will be satisfied if we distribute the $-NH_3^+$ groups between these two equilibrium orientations (a- and b-types), statistically in space and time. Thus, we may call tentatively this transition the "orientational order-disorder" type in the sense that an equal number of the a- and b-type orientations of $-NH_3^+$ groups can exist above the critical temperature whereas the number of the a-type orientation is predominant below the critical temperature. A simplified hindering potential energy curve for such a rotational motion of the $-NH_3^+$ group in the lattice may be represented schematically as in Fig. 6. This potential energy curve has 60° periodicity in the high temperature phase, while that corresponding to the low temperature phase will have 120° periodicity. As is shown in the figure, the degree of increase or decrease in depth of potential minima is assumed to be a linear function of $\Delta\beta$. Since the extent of displacement of the atomic position is assumed to be proportional to the variation of macroscopic quantity $\beta$ in a first approximation, some of the physical properties of the present crystal

8) D. G. Thomas and L. A. K. Staveley, *J. Chem. Soc.*, 1951, 2572.
9) C. Kittel, *Phys. Rev.*, **82**, 729 (1951).

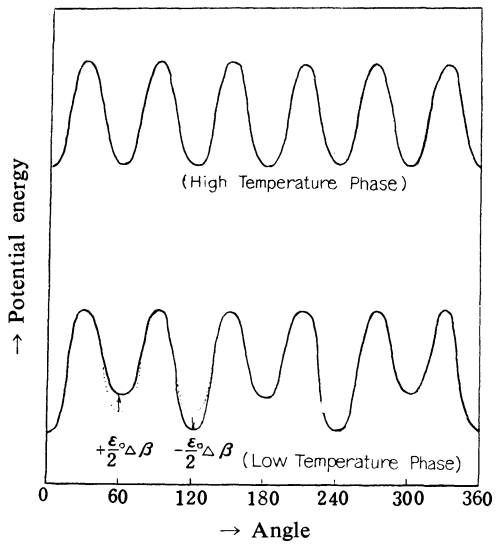



Fig. 6. Schematic representation of hindering potential for the rotational motion of $-NH_3^+$ group.

associated with the variation of $\beta$ may be considered to change proportionally with the variation of $\beta$. As a matter of fact, Horie et al.[10] have recently given an example of the temperature dependence of the angle between optic elasticity axes, $\gamma$, in adjacent domains in the hybrid structure of aniline hydrobromide in the vicinity of the critical temperature (Fig. 7); one can see here a fairly linear relationship between the temperature variation of $\Delta\beta$ and $\gamma$.

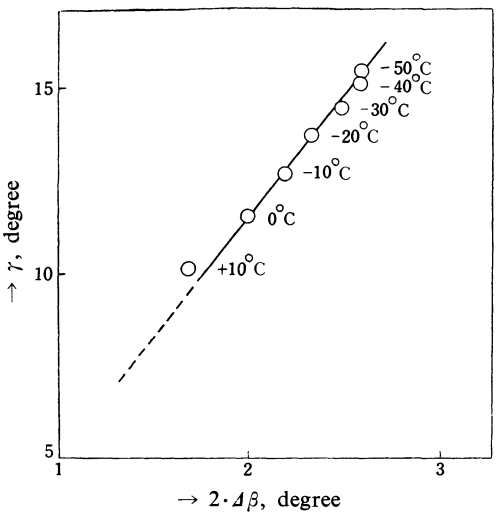



Fig. 7. Linear relationship between the temperature variation of $\Delta\beta$ and of the angle $\gamma$ between the two optic elasticity axes in adjacent domains (after Horie et al.[10]).

10) T. Horie. T. Iwai and I. Taguchi, Annual Meeting of Phys. Soc. Japan, 1956,: To be published in near future. The author would like to express his appreciation for their permission to refer to their result before its publication.

Now, let us calculate the temperature dependence of $\Delta\beta$ on the basis of the proposed model in order to compare the result with the experimental value reported by the X-ray method[2]. We define the degree of order $s$ as follows; let it be assumed that in a state specified by a set of values $(T, s)$, $N(1+s)/2$ $-NH_3^+$ groups in the a-type orientation and $N(1-s)/2$ in the b-type are distributed over the whole $N$ lattice points. The order parameter $s$ thus defined has the same character as the one proposed for the theory of order-disorder phase transition of binary alloy[11]. That is, when $s=1$ all the $-NH_3^+$ groups are in the a-type orientation; this corresponds to the state of perfect order. When $s=0$ there are as many a-type groups as b-type groups; the state of complete disorder. It is somewhat difficult to calculate the hindering potential energy for rotational motion of the $-NH_3^+$ group in the crystalline field owing to an ambiguity in the estimation of effective charge distribution of the $-NH_3^+$ group, the unknown N-H distance and also the complexity of the crystal structure, so that we shall confine our calculation at the present stage only to the differences in the energy and entropy between the two phases. The notation $\Delta$ used in the following calculation stands for the excess of any thermodynamic quantities of the ordered state over that of the completely disordered state extrapolated above the transition point. The difference in the internal energy $\Delta U$ will consist of two parts in its origins; one is the contribution from the variation of the arrangements of ions and ionic groups and the other is that from the change of orientations of $-NH_3^+$ ionic groups when the ordered state changes to the disordered state. The first part of energy difference, $\Delta U_1$, may be expressed formally by a power series in $\Delta\beta$ of which all the odd terms are omitted by the requirement that $\Delta U$ should be an even function of $\Delta\beta$, because the gradual change of either direction from the orthorhombic to the monoclinic crystal system should produce the same energy change. For example, the electro-static part of $\Delta U_1$, which is the mutual interaction energy between the pseudo electric dipole moments produced by the displacements of ions and ionic groups, is expressed by

$$-1/2\sum_{i>j}\frac{\mu_i\mu_j}{r^3_{ij}}\{3\cos(\theta_i+\theta_j)+\cos(\theta_i-\theta_j)\}$$

11) W. L. Bragg and E. L. Williams, *Proc. Roy. Soc.*, A145, 699 (1934); A151, 540 (1935); F. C. Nix and W. Shockley, *Rev. Mod. Phys.*, 10, 1 (1938).

where $\mu_i$, $\mu_j$, $\theta_i$, $\theta_j$ and $r_{ij}$ have the usual meanings. Since $\mu_i$ and $\mu_j$ may be reasonably considered to be proportional to $\Delta\beta$, the term may be rewritten by $J(\Delta\beta)^2$, where $J$ is a constant. If the higher terms in $\Delta\beta$ can be neglected, then $\Delta U_1=A(\Delta\beta)^2$, where $A$ is another constant. The second part of energy difference $\Delta U_2$, which is due to the change of potential energy at an $-NH_3^+$ group caused by the variation of the degree of order $s$, may be expressed by $\frac{1+s}{2}N\left(-\frac{\varepsilon_0}{2}\Delta\beta\right)+\frac{1-s}{2}N\left(\frac{\varepsilon_0}{2}\Delta\beta\right)$ In this case it has been assumed that the change in the depth of potential minima is proportional to the change in $\Delta\beta$ with a constant of proportionality $\varepsilon_0/2$ (see Fig. 6). Thus,

$$\Delta U=\Delta U_1+\Delta U_2=A(\Delta\beta)^2-sE\Delta\beta/2 \qquad (1)$$

where $E=N\varepsilon_0$.

On the other hand, the entropy difference $\Delta S$ is given approximately by the possible number of $N(1+s)/2$ a-type and $N(1-s)/2$ b-type arrangements of $-NH_3^+$ groups over the $N$ whole lattice points.

$$\Delta S=\boldsymbol{k}\ln\frac{N!}{\left(\frac{1+s}{2}N\right)!\left(\frac{1-s}{2}N\right)!}-\boldsymbol{R}\ln 2$$

$$=-\boldsymbol{R}\left\{\frac{1+s}{2}\ln\frac{1+s}{2}+\frac{1-s}{2}\ln\frac{1-s}{2}+\ln 2\right\} \qquad (2)$$

Here, the additional term $\boldsymbol{R}\ln 2$ appears since the completely disordered state was taken as the reference. Accordingly, the difference of Helmholtz free energy $\Delta F$ between the two phases is given by

$$\Delta F=\Delta U-T\Delta S=A(\Delta\beta)^2-sE\Delta\beta/2+\boldsymbol{RT}\left\{\frac{1+s}{2}\ln\frac{1+s}{2}+\frac{1-s}{2}\ln\frac{1-s}{2}+\ln 2\right\} \qquad (3)$$

By the equilibrium conditions, we can obtain the following set of equations. From $\partial(\Delta F)/\partial(\Delta\beta)=0$ (since there is no external shear stress), it follows

$$\Delta\beta=Es/(4A) \qquad (4)$$

$$\Delta U=-E^2s^2/(16A) \qquad (4')$$

Eq. 4′ shows that the present treatment corresponds formally to the Bragg-Williams approximation. From $\partial(\Delta F)/\partial s=0$, we have

$$s=\tanh E^2s/(8\boldsymbol{R}AT) \qquad (5)$$

$$T_c=E^2/(8\boldsymbol{R}A) \qquad (6)$$

where $T_c$ is the critical temperature, above which $s$ becomes zero. Inserting the value of $s$ derived from 5 into 2, we get a calculated total entropy change 0.83 e. u. ($-70\sim+35$°C) in comparison with the observed value 1.10 e. u. In this case, the additional entropy increment due to the increase of the available volume of ion, which may be reasonably given by $\boldsymbol{R}\ln(V+\Delta V)/V$, is quite negligible in magnitude, less than 0.01 e. u., in the same temperature interval. Combination of Eqs. 5 and 6 with Eq. 4 gives the temperature dependence of $\Delta\beta$ including the numerical factor $E/(4A)$, which can be determined, for example, by fitting the calculated value with the observed value of $\Delta\beta$ at a single temperature, say $-40$°C. The temperature dependence of $\Delta\beta$ obtained in this way is given by the dotted line in Fig. 8. Although qualitative agreement is obtained, the details are

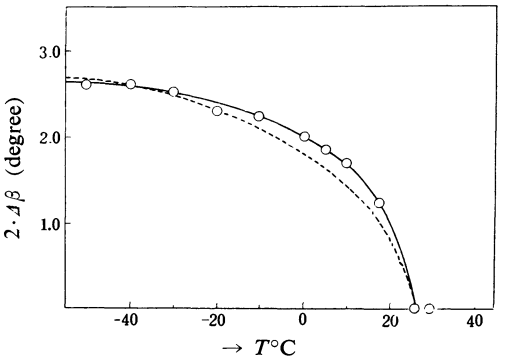



Fig. 8. Comparison of observed temperature variation of $\Delta\beta$ with the theoretical one.
○ Observed by Taguchi[2]
---- Theoretical curve ignoring volume effect.
—— Theoretical curve including volume effect.

not fully explained especially in the following points; one is that the degree of covergence of this curve to the critical point is not so steep as that of the experimental curve, and another point is that the calculated $\Delta\beta$ should increase to 1.37 times as large a value as that at $-40$°C if the curve is extrapolated to 0°K, while the corresponding value obtained by experiment[2] is only 1.12.

As already mentioned, an anomalous thermal expansion in the vicinity of the critical point appears (see Fig. 3). According to the results by Eisenschitz[12], Sato[13] and Nagamiya[14], the temperature dependence of the order parameter is appreciably affected by taking into account the anomalous thermal expansion accompanied

12) R. Eisenschitz, *Proc. Roy. Soc.*, **A168**, 546 (1938).
13) Y. Sato, *J. Phys. Soc. Japan*, **2-1**, 17 (1947).
14) T. Nagamiya, "Kotai-ron (Solid State Physics)", 1, Kyōritsu, Tokyo (1951), p. 20.

with the order-disorder phase transition in the case of binary alloy systems. We have then attempted to examine the effect of volume change in the present case as the next stage of refinement. After Sato's treatment, we can get the following expression for the abnormal expansion coefficient

$$\Delta\alpha=\alpha(s)-\alpha(0)=\kappa_0 \mathrm{d}s^2/\mathrm{d}T\cdot E_0 \mathrm{d}(E/E_0)/\mathrm{d}V$$
$$=\kappa_0 \boldsymbol{R}T_c/2\cdot \mathrm{d}s^2/\mathrm{d}T\cdot \mathrm{d}(E/E_0)/\mathrm{d}V \qquad (7)$$

Here, $\kappa_0$ is isothermal compressibility of the disordered phase; $V$ the molar volume; $E$ and $E_0$ the ordering energy at $T$°K and 0°K, respectively. Then, the abnormal expansion over $V^\circ$, the molar volume at 0°K, is given by

$$v=\int_0^T V^0\Delta\alpha \mathrm{d}T=\int_1^s V^0 C\mathrm{d}s^2=-CV^0(1-s^2) \qquad (8)$$

where the following abbreviations were used

$$\mathrm{d}(E/E_0)/\mathrm{d}V=B, \qquad \boldsymbol{R}T_c=C$$

By using the observed $v_{max}$ value 0.41 cc./mol. and $V_0=110$ cc.*, $C$ becomes $-3.76\times10^{-3}$.

Based on these expressions the following thermodynamic functions are derived as functions of $s$, $v$ and $T$.

$$U(s,\ v,\ T)=E_0-Es^2=E_0\{1-(1+Bv)s^2\} \qquad (9)$$

$$G(s,\ v,\ T)=E_0\{1-(1+Bv)s^2\}$$
$$+\boldsymbol{R}T/2\{(1+s)\ \ln\ (1+s)+(1-s)\ \ln\ (1-s)$$
$$-2\ \ln\ 2\} \qquad (10)$$

Here, $G$ is the Gibbs free energy**. From $\partial G/\partial s=0$ and $\partial^2 G/\partial s^2=0$, we have

$$s=\tanh 2E_0 s\{(1+Bv)+BCV_0 s^2\}/\boldsymbol{R}T \qquad (11)$$

$$\boldsymbol{R}T_c/E_0=2(1+Bv_{max}) \qquad (12)$$

The differentiation of $U(s,\ v,\ T)$ with $T$ gives an expression for excess heat capacity over that arising from lattice vibration. The maximum value is obtained from the limitation of $s\to0$.

$$C_{max}=\lim_{s\to0}(\partial U/\partial s)/(\partial T/\partial s)$$
$$=3\boldsymbol{R}/2\{1-(6BCV_0)/(1+Bv_{max})\}^{-1} \qquad (13)$$

On the assumption that the $C_{max}$ value thus defined is identical with the experimentally observed $\Delta C_p$, the following set of values can be obtained: $B=-2.44\times10^{-1}$ cc$^{-1}$, $\kappa_0=1.25\times10^{-6}$ atm$^{-1}$. By using these numerical values and the observed volume change, the refined $\Delta\beta-T$ curve is calculated and drawn by the full line in Fig. 8, where a fairly satisfactory agreement between this curve and the observed points is seen. It is to be noted that the calculated total entropy change 1.06 e. u. (from $-70$ to $+35$°C) is in good agreement with the observed one 1.10 e. u., if the same numerical values for parameters are used. The value of $\kappa_0$ obtained above seems to be somewhat smaller for this kind of crystal including organic complex ion, since the compressibility is in the range of $(2\sim7)\times10^{-6}$ atm$^{-1}$ for usual ionic crystals. Although the model proposed here is merely a possible one, it may be said that rather satisfactory results were obtained.

A preliminary study of proton magnetic resonance absorption of the powdered specimen of this crystal was recently made by Yamagata* over the temperature range between $-190$ and $+40$°C and there was no detectable change in the line width at the critical point. The observed second moment 8.35 Gauss$^2$ almost coincides with 7.82 Gauss$^2$ of the calculated value obtained by assuming the isolated $-NH_3^+$ group (the value 1.032 Å for N-H distance and tetrahedral angle were assumed) with rotational flipping motion about the C-N axis. The situations are very similar in the cases of ammonium halides[15].

## Summary

Measurements of the heat capacity ($-80\sim+60$°C) and the thermal expansion ($-40\sim+60$°C) of aniline hydrobromide were carried out covering the transition temperature which has been observed recently by X-ray methods. The observed heat capacity versus temperature curve was of the $\lambda$-shape, similar to that of the order-disorder phase transition of binary alloy systems. The following results were obtained; $T_c$ (the temperature corresponding to the heat capacity peak) 22°C, $\Delta H$ (heat of transition, $-70\sim+35$°C) $297\pm10$ cal./mol., $\Delta S$ (entropy of transition, the same temperature interval) $1.10\pm0.05$ e. u., $\Delta C_p$ (drop of heat capacity at $T_c$) $\sim9$ cal./mol. deg. Also the anomalous behavior of thermal expansion was observed in the vicinity of the critical temperature. These observations showed that the transition was of higher order nature.

Based on the lits of knowledge of the crystal structures above and below the critical temperature, the author has discussed the main feature of the phase transition from the sandpoint of the orientational order-disorder of the $-NH_3^+$ ionic group and obtained fairly satisfactory results.

* This value was taken from $d_{25}=1.58$, by the picnometric measurement of Taguchi et al.[1]

** The $G$ function expressed here does not correspond exactly to the Gibbs free energy, since the $PV$ term was neglected.

* Private communication.

15) H. S. Gutowsky, G. E. Pake and R. Bersohn, *J. Chem. Phys.*, **22**, 643 (1954); R. Bersohn and H. S. Gutowsky, ibid., **22**, 651 (1954).

The author wishes to express his sincere thanks to Professor I. Nitta, Professor T. Watanabe and Dr. I. Taguchi for their valuable advice and continued interest in the present study, to Professor T. Nagamiya for his valuable suggestion, and to Professor S. Seki for his kind guidance and illuminating discussion. He is also grateful to Dr. H. Chihara for his kind support, and to Mr. K. Nakatsuka for his technical assistance.

*Department of Chemistry*
*Faculty of Science*
*Osaka University*
*Nakanoshima, Osaka*

# *Optical Properties of Colored Colloidal Systems. II. Apparent Refractive Index and Extinction Coefficient of the System of Small Spherical Particles*

By Masayuki NAKAGAKI* and Tomiko FUJII

(Received September 26, 1960)

In the preceding paper of this series[1], the extinction of light by the system of colored small spheres were theoretically calculated. As a result, it was concluded that the scattering of light by colored spheres is affected by the absorption of light, the latter being expressed by the imaginary part of the refractive index of the dispersed phase. In the present paper, the calculation will be extended to the apparent refractive index of the system. The result thus obtained will be applied to the system of infinitesimally small particles, and will be used to discuss the optical properties of a dyestuff solution as an example.

## Theoretical Calculations

**Principle of the Calculation.** — The relation between the refractive index of a colloidal system or a solution, $\mu_{12}$, and the refractive indices and compositions of the components is usually given by the following equation called a mixture rule,

$$\mu_{12}=\mu_1\varphi_1+\mu_2\varphi_2 \tag{1}$$

where $\mu_1$ and $\mu_2$ are the refractive indices of the solvent and dispersed phases, respectively, and $\varphi_1$ and $\varphi_2$ are the volume fractions of the respective phases. If the concentration of the dispersed phase, $c$, is given in mol./l. unit, Eq. 1 may be rewritten as,

$$\mu_{12}=\mu_1+(M/1000\rho_2)(\mu_2-\mu_1)c \tag{2}$$

where $M$ is the molecular weight of the material of the dispersed phase and $\rho_2$ is the specific gravity of the same phase. The linear relationship between $\mu_{12}$ and $c$ as predicted by Eq. 2 has been verified experimentally by many investigators, but the value of $\mu_2$ is not equal[2] to the refractive index in bulk of the dispersed phase, $\mu_2$ (bulk). Therefore the value of $\mu_2$ obtained experimentally on the basis of Eq. 2 is an apparent refractive index of the dispersed phase. If the apparent relative refractive index $m'$ defined by

$$m'=\mu_2/\mu_1 \tag{3}$$

is used, the inclination of the straight line to give the variation of $\mu_{12}$ with the concentration $c$ is expressed as

$$\partial\mu_{12}/\partial c=(M\mu_1/1000\rho_2)(m'-1) \tag{4}$$

This equation is to be used to determine the value of $m'$ experimentally.

On the other hand, $(m'-1)$ is given theoretically by the equation[2],

$$m'-1=(3/2)\mathrm{R}[j_\perp(180)]/\alpha^3 \tag{5}$$

where $\alpha$ is a parameter defined by

$$\alpha=2\pi a/\lambda \tag{6}$$

Here, $a$ is the radius of the sphere and $\lambda$ is the wave length of light in the medium. The sign R in Eq. 5 means the real part of a complex function $j_\perp(180)$, the latter being

$$j_\perp(180)=\frac{m^2-1}{m^2+2}\alpha^3+\left(\frac{m^2-1}{m^2+2}\right)^2\times\frac{(m^4+27m^2+38)}{15(2m^2+3)}\alpha^5-i\frac{2}{3}\left(\frac{m^2-1}{m^2+2}\right)^2\alpha^6 \tag{7}$$

* Present address: Faculty of Pharmacy, Kyoto University, Sakyo-ku, Kyoto.

1) M. Nakagaki, This Bulletin, 31, 980 (1958).

2) M. Nakagaki and W. Heller, *J. Appl. Phys.*, 27, 975 (1956).

as already given in the previous paper[1], where $m$ is a complex quantity in the case of colored particles:

$$m=\mu_2^*(\text{bulk})/\mu_1=m_0-ik_0 \tag{8}$$

where $\mu^*$ means the complex refractive index.

**Apparent Refractive Index as a Function of Particle Size.**—If $k_0 \ll m_0$, the theoretical equation may be expanded in a power series,

$$m'-1=M_1-M_2k_0+M_3k_0^2+\cdots\cdots \tag{9}$$

where

$$\left.\begin{aligned} M_1&=(3/2)(X_1+Y_1\alpha^2)\\ M_2&=(3/2)Z_2\alpha^3\\ M_3&=(3/2)(X_3-Y_3\alpha^2)\end{aligned}\right\} \tag{10}$$

Here,

$$\left.\begin{aligned} X_1&=\frac{m_0^2-1}{m_0^2+2}\\ Y_1&=\frac{1}{15}\left(\frac{m_0^2-1}{m_0^2+2}\right)^2\frac{(m_0^4+27m_0^2+38)}{(2m_0^2+3)}\\ Z_2&=8m_0\frac{m_0^2-1}{(m_0^2+2)^3}\\ X_3&=\frac{3(3m_0^2-2)}{(m_0^2+2)^3}\\ Y_3&=\frac{\left\{\begin{array}{l}4m_0^{18}+66m_0^{16}-1104m_0^{14}-5033m_0^{12}\\ +12966m_0^{10}+105525m_0^8+218152m_0^6\\ +182376m_0^4+37824m_0^2-16176\end{array}\right\}}{15(m_0^2+2)^6(2m_0^2+3)^3}\end{aligned}\right\} \tag{11}$$

The results of the numerical computation are shown in Fig. 1. Crosses in the figure are the values for colorless particles calculated on the basis of the Mie theory without any approximation[2]. The agreements between these Mie values and the values obtained from Eqs. 9, 10 and 11 and shown with open circles for colorless particles are very good, although a small discrepancy can be seen in the case where both $\alpha$ and $m_0$ are large ($\alpha=0.8$, $m_0=1.3$). When $k_0$(which shows the absorption of light) is small, the apparent relative refractive index $m'$ increases with $\alpha$ (or particle size), but when $k_0$ is large, the value of $m'$ decreases (after passing a flat maximum when $m_0$ is large) with the increase of $\alpha$.

**Optical Properties of Infinitesimally Small Particles.**—The equation used in the preceding paper as well as in the preceding paragraphs of this paper are for small values of $k_0$. In the present paragraph, equations for infinitesimally small particles ($\alpha \to 0$) are examined without any restriction on $k_0$. The equations are

$$m'-1=\frac{3}{2}-\frac{9}{2}\times\frac{(m_0^2+2-k_0^2)}{(m_0^2+k_0^2+2)^2-8k_0^2} \tag{12}$$

and

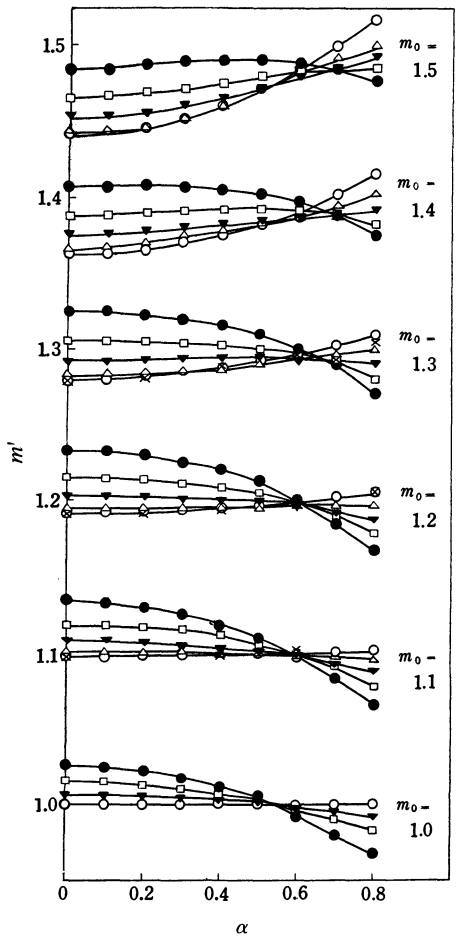



Fig. 1. $m'-\alpha$ relation for $k_0=0$ (○); 0.1 (△); 0.2 (▼); 0.3 (□); 0.4 (●). Mie's values are shown with (×).

$$\left.\begin{aligned} x&\equiv(\lambda\rho_2/3\pi)\varepsilon=\frac{12m_0k_0}{(m_0^2+k_0^2+2)^2-8k_0^2}\\ x(\text{bulk})&=(4/3)k_0\end{aligned}\right\} \tag{13}$$

where $x$ is a quantity proportional to the extinction coefficient $\varepsilon$ as already introduced in the preceding paper[1].

The numerical values of $m'$ as a function of $k_0$ were calculated for various values of $m_0$ from 0.88 to 1.24 with the interval of 0.02. A part of the results is shown in Fig. 2. Although the apparent relative refractive index $m'$ and the relative refractive index in bulk $m_0$ are parallel when $k_0$ is small, the sequence is inverted when $k_0$ is larger than about 1.4. The smaller $m'$ the larger is the $m_0$. Moreover, the value of $m'$ approaches 2.5 when $k_0$ becomes infinitely large. These results shown in Fig. 2 have not been expected by any previous investigator.

The numerical values of $x$ as a function of

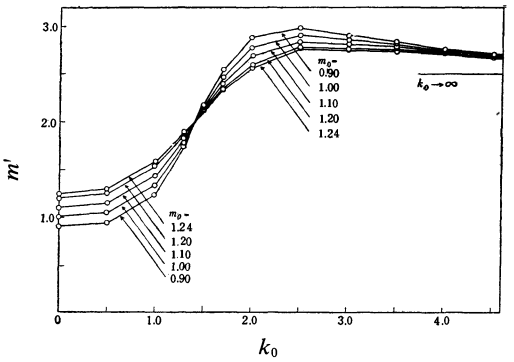



Fig. 2. $m'-k_0$ relation calculated theoretically.

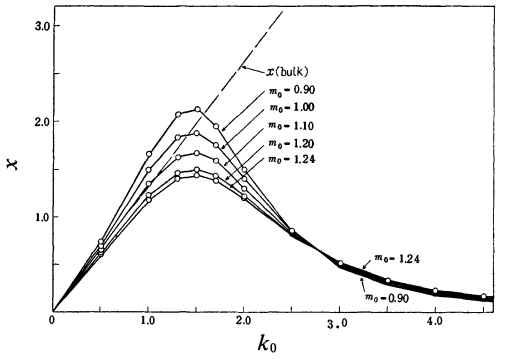



Fig. 3. $x-k_0$ relation calculated theoretically.

$k_0$ were calculated for various values of $m_0$ from 0.88 to 1.24 with the interval of 0.02. A part of the results is shown in Fig. 3. The curves have the maximum at the $k_0$ value of about 1.5. The apparent extinction coefficient or $x$ decreases for the larger value of $k_0$ and approaches zero when $k_0$ becomes infinitely large.

These results, too, have not been expected by any previous investigator[3].

## An Example for the Treatment of Experimental Data

**Materials.**—It is generally believed that acid dyes dissolve in water monomolecularly, showing a small tendency to form micelles in contradistinction to direct cotton dyes which form micelles when the temperature is not high. Therefore, an acid dye solution is used as a model of the system of colored infinitesimally small particles.

The acid dye used in this experiment was Acid Orange R (C. I. 15575, Acid Orange 8) purified by the sodium acetate-alcohol method. The purity determined by titanium trichloride titration was 96.32%.

3) In Figs. 2 and 3, theoretically calculated points were connected with straight lines for the convenience of the drawings. The actual theoretical curves should, of course, be curved smoothly.

**Determination of Refractive Index.**—The difference of the refractive index between the solution and the solvent was measured by using a differential refractometer of modified Brice type as shown in Fig. 4. Light from a

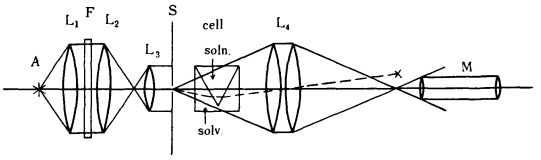



Fig. 4. Schematic diagram of differential refractometer of modified Brice type.

tungsten lamp A was collimated with lenses $L_1$ and $L_2$ ($f_1=6$ cm., $f_2=6$ cm.), filtered with a gelatine filter F, made parallel with a lens $L_3$ ($f_3=3$ cm.) and projected to a slit S. The image of the slit focused by a lens $L_4$ ($f_4=15$ cm. lens for a slide projector was used) was observed with a microscope M of the magnification of 40 times ($4\times10$). The location of the image of the slit was shifted when a solution was put in the prism cell containing solvent outside the prism in the cell. The shift of the image of the slit was measured by a micrometer in the eyepiece of the microscope M. The reading $\theta$ is proportional to the difference of the refractive index,

$$\mu_{12}-\mu_1=K\theta \qquad (14)$$

The proportionality constant $K$ was determined to be $K=4.15\times10^{-5}$ by using potassium chloride solution as a standard, the refractive index of the latter being cited in the literature[4]. The value of $\mu_1$ is also given in the literature[5].

In order to convert the experimental values of $(\partial\mu_{12}/\partial c)$ to $m'$ according to Eq. 4, the value of the density of dye, $\rho_2$, should be known. The density was assumed to be 1.5 by Robinson[6] and to be 1.0 by Atherton et al.[7] Since the accurate value of the density for the dispersed state can not be known, calculations were made here for both these density values. The results are shown in Fig. 6 with broken lines. A typical anomalous dispersion was observed as already reported for some other dye solutions[7]. In Fig. 6 and also Fig. 7, $\lambda_0$ is wavelength in vacuum.

**Determination of Extinction Coefficient.**—The extinction coefficient was determined by Shimazu spectrophotometer QR-50. The results were recalculated to $x$ by Eq. 13 for $\rho_2=1.0$ and $\rho_2=1.5$. The results are shown in Fig. 7 with broken lines.

4) "International Critical Tables", VII, 13, 75 (1930).
5) "International Critical Tables", VII, 13 (1930).
6) C. Robinson, *Trans. Faraday Soc.*, **31**, 245 (1935).
7) E. Atherton and E. Cowill, *J. Soc. Dyers Colorists*, **70**, 116 (1954).

**Calculation of $m_0$ and $k_0$.** — The quantities obtainable by experiments are $m'$ and $x$, but the fundamental quantities of theoretical interest are $m_0$ and $k_0$. To determine $m_0$ and $k_0$ from $m'$ and $x$, a graphical method is shown in Fig. 5. The $m'-x$ relation calculated theoretically for systematically varied values of parameters $m_0$ and $k_0$ make a network. A pair of experimental values of $m'$ and $x$ give one plot on this chart. Then, the values of $m_0$ and $k_0$ corresponding to this plot can be read off by interpolation. The values of $m_0$ thus obtained are shown in Fig. 6 with solid lines, and the values of $x$(bulk) calculated by Eq. 13 from the values of $k_0$ thus obtained are shown in Fig. 7 with solid lines.

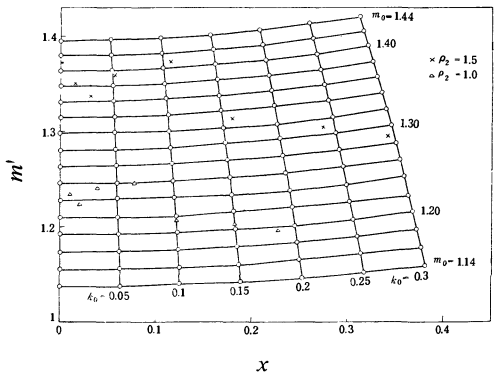



Fig. 5. $m'-x$ relation. Network shown with (○) is theoretical. Experimental data for $\rho_2=1.0$ (△) and for $\rho_2=1.5$ (×) are also ploted.

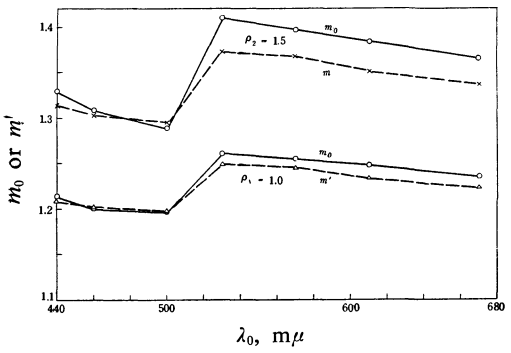



Fig. 6. Dependencies of $m_0$ and $m'$ on $\lambda_0$.

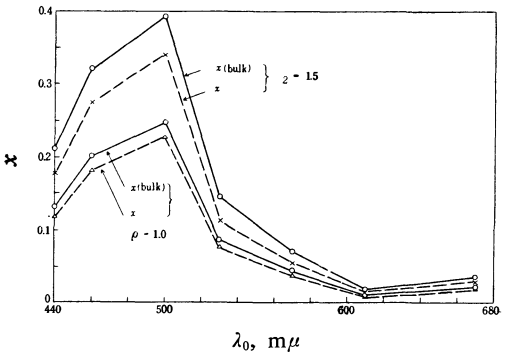



Fig. 7. Dependencies of $x$(bulk) and $x$ on $\lambda_0$.

The discrepancies between solid curves and broken curves in Fig. 6 and Fig. 7 show the error committed if one assume that the experimental $m'$ and $x$ values are equal to $m_0$ and $x$(bulk)—the latter is equal to $(4/3)k_0$—of the dispersed phase in bulk. The errors in this sense are given in Table I for the present solutions. The table shows that the error in $m'$ is less than 2.6% at the greatest, but the error in $x$ reaches as far as 21% at the greatest.

TABLE I. ERRORS COMMITTED BY IGNORING THE PRESENT THEORY

| $\lambda_0$ | $\rho_2=1.5$ | | $\rho_2=1.0$ | |
|---|---|---|---|---|
| | $\Delta m$ | $\Delta x$ | $\Delta m$ | $\Delta x$ |
| mμ | % | % | % | % |
| 440 | −1.27 | −15.7 | −0.43 | − 9.6 |
| 460 | −0.37 | −14.4 | −0.24 | − 9.0 |
| 500 | 0.55 | −13.1 | 0.08 | − 8.0 |
| 530 | −2.56 | −20.6 | −0.96 | −11.5 |
| 570 | −2.51 | −19.6 | −1.10 | −10.4 |
| 610 | −2.41 | −19.5 | −1.05 | − 8.1 |
| 670 | −2.10 | −17.7 | −0.91 | − 8.7 |

## Summary

The theoretical values of apparent relative refractive index $m'$ of colored particles was calculated as a function of particle size for various values of $m_0$ and $k_0$.

The theoretical values of $m'$ as well as $x$ were calculated for infinitesimally small particles. It was shown that $m'$ increases and, after passing a maximum point, approaches a limiting value of 2.5 with the increase of $k_0$, and that $x$ approaches zero, after passing a maximum, with the increase of $k_0$.

The values of $m'$ and $x$ of Acid Orange R solutions were measured by a modified Brice type differential refractometer and by a spectrophotometer. A method to convert $m'$ and $x$ values into $m_0$ and $k_0$ values was illustrated. The errors committed by assuming experimental $m'$ and $x$ values as $m_0$ and $(4/3)k_0$ values of bulk phase are estimated for the dye solution. The error of $x$ reached 21%, while the error of $m'$ was not larger than 2.6%.

*Faculty of the Science of Living*
*Osaka City University*
*Nishi-ku, Osaka*

# *A Diffusion Mechanism for Liesegang Rings*. I. Spacing Law*

By Prem Behari MATHUR**

(Received August 18, 1960)

Jablczynski's equation for spacings between Liesegang rings

$$x_n = ak^n \tag{1}$$

where $x_n$ is the distance of $n$th ring from the diffusion level, and $a$ and $k$ are constants, may be written as

$$\frac{x_{n-1}}{x_n} = \frac{1}{R} \tag{2}$$

or $$1-\frac{x_{n-1}}{x_n} = \left(1-\frac{1}{R}\right)$$

or $$(x_n - x_{n-1}) = kx_n \tag{3}$$

From statistical consideration, Eq. 3 is more sensitive form of Jablczynski's relation 1. According to the Eq. 3 the plot of $(x_n - x_{n-1})$ against $x_n$ should be straight line curves passing through the origin. In practice the curves are not found to pass through the origin when the distances of the rings are measured from diffusion level for which Eq. 1 stands. The author has advanced a theory and deduced from Fick's diffusion law a few general expressions for the Liesegang phenomenon. The theory reflects light on the mechanism of ring formation, fine structure, influence of various environmental conditions, etc.

Fick's diffusion equation

$$\frac{\partial c}{\partial t} = D\frac{\partial^2 c}{\partial x^2} \tag{4}$$

may have a solution

$$c = a\,e^{-\alpha x}\cos(\omega t + \beta x + y) \tag{5}$$

given by Riemann[2] for similar type of differential equations. Such a solution would be possible under conditions analogous to those operating in the propagation of sound in air, discharge of a current through a condenser and a resistance, where the motion of the matter is met by an opposing force.

In the phenomenon of Liesegang rings the two electrolytes meet and get precipitated and thus forms a new phase at the boundary of the diffusing salt and the medium. By virtue of the electrical forces at its surface and the fine nature of the particles distributed there, the boundary phase or say 'membrane' will have the tendency in certain cases to oppose the diffusion of salt and so to develop a situation where diffusion may be governed by Eq. 6.

The concentration distribution at a particular instant $t_i$ may be given by

$$c = a\,e^{-\alpha x}\cos(\beta x + \phi) \tag{6}$$

where $\phi$ is another constant equal to $(\omega t_i + y)$.

During the process of Liesegang ring formation of say silver chromate rings, the diffusion wave front of silver ions moves forward and gives rings one after another. The latter changes in concentration at the preceeding levels when one of the precipitating ions is completely removed cannot influence a ring position. By determining the values of arbitrary constants $a$ and $\phi$ in Eq. 6 from the known boundary conditions of reacting ions the equations for their concentration distribution can be obtained.

For silver ions, when $x=0$, $C \rightarrow$ maximum. In Eq. 6 $C$ will be maximum, when $\cos(\beta x+\phi)$ is unity or $(\beta x+\phi)=0$. Since $x=0$, $\phi$ must be zero to satisfy the above condition. Hence

$$c = a\,e^{-\alpha x}\cos(\beta x) \tag{7}$$

Now, the limiting maximum value of $C$ at $x=0$ is the same as the initial bulk concentration $C_0$ of silver ions; substituting this value into above equation we have $a=C_0$. Eq. 7 reduces to

$$c = C_0\,e^{-\alpha x}\cos(\beta x) \tag{8}$$

Relation 8 geometrically represents a simple harmonic curve whose amplitude $C_0\,e^{-\alpha x}$ diminishes exponentially to zero with increasing distance. As the chromate ions diffuse in the upward direction their distribution may be represented by the equation

$$C' = C_1\,e^{\alpha' x}\sin(\beta' x) + C_2\,e^{\alpha' x}\cos(\beta' x) \tag{9}$$

where damping coefficient $\alpha'$ has a positive sign. The constants $C_1$ and $C_2$ in the above equation can be determined from boundary conditions of chromate ions.

In a thin region of the precipitate the concentration of chromate ions may be taken to be equal to zero because the traces of ions

* This work is the part of author's Ph.D thesis submitted to the University of Allahabad (1956).

** Present address: Senior Scientific Officer, Central Electrochemical Research Institute, Karaikudi-3, India.

1) K. Jablczynski, *Bull. soc. chim., France* (4), 33, 1592 (1923).

2) Riemann, "Particlle Differentialgleichungen", Edit Hattendorff (1938), p. 110.; P. B. Mathur, *Bull. Acad. Polona. Sci.*, 8, 8, 429 (1960).

left there after precipitation get absorbed by the precipitates rendering practically a complete disappearance of the ions. Hence at $x=0$, $C'=0$. Substituting this condition into Eq. 9, we have $C_2=0$, so we have,

$$C'=C_1 e^{\alpha' x} \sin(\beta' x) \quad (10)$$

Let us suppose, when $x=x_0$, $C' \rightarrow$ maximum. So, in Eq. 10, $C'$ is maximum when $\sin(\beta' x_0)$ is unity or $\beta' x_0=\pi/2$ or $x_0=\pi/2\,\beta'$ and so

$$C'=C_1 e^{(\alpha'\pi/2\beta')}$$

Now the limiting maximum value of $C'$ at a distance of $x_0$ is the same as the initial bulk concentration $C_0'$ of chromate ions. Substituting this value into the above equation we have

$$C_1=C_0' e^{-(\alpha'\pi/2\beta')}$$

Eq. 10 thus reduces to the form,

$$C'=(C_0' e^{-(\alpha'\pi/2\beta')}) e^{\alpha' x} \sin(\beta' x) \quad (11)$$

Eq. 11 represents the distribution of chromate ions where $x$ is measured from zero concentration level.

Let us now suppose that $(n-1)$ rings have already formed and $n$th ring is in the process of formation. So the concentration of chromate ions at $(n-1)$th level has fallen to zero. Let $C_n$ and $C_n'$ be the concentrations of silver and chromate ions respectively at $n$th rings, and $x_n$ and $x_{n-1}$, the distances of $n$th and $(n-1)$th levels respectively from the initial diffusion level. The reference line for chromate ions corresponding to the $n$th ring is $(n-1)$th ring level, while for silver ions it is the initial diffusion level. In order that the two equations could be combined, the line of reference for the two ions must be the same. Substituting $x=(x_n-x_{n-1})$ into Eq. 11 for chromate ions and $x=x_n$ in Eq. 8 for silver ions and corresponding concentrations in the two equations, we get the following equations for silver and chromate ions respectively,

$$C_n=C_0 e^{-\alpha x_n} \cos(\beta x_n) \quad (12)$$

$$C_n'=C_0' e^{-(\alpha'\pi/2\beta')} e^{\alpha'(x_n-x_{n-1})} \times \sin[\beta'(x_n-x_{n-1})] \quad (13)$$

The distribution of the concentration product of silver and chromate ions can be obtained by combining Eqs. 12 and 13

$$C_nC_n'=C_0C_0' e^{-(\alpha'\pi/2\beta')} e^{-\alpha x_n} e^{\alpha'(x_n-x_{n-1})} \times \sin[\beta'(x_n-x_{n-1})]\cos(\beta x_n) \quad (14)$$

The above equation represents the curve shown in Fig. 1. The periodic terms cos. and sin. alternate between the limits $\pm 1$, and the concentration curve shows two types of periodicities one by broad wave PQRS and the other by narrow waves. By putting $\cos(\beta x_n)=1$, we get the curve PQRS which is the locus

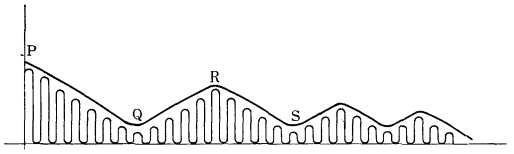


Fig. 1

of the points of maxima of narrow curves, and by putting $\sin(\beta'(x_n-x_{n-1}))=1$, the remaining equation represents only the finer structures of a half wave PQ.

The condition for the precipitation at the place is that the ionic product should exceed or be equal to the solubility product of the sparingly soluble salt at the level

$$C_nC_n' \geq S$$

In critical case $C_nC_n'=S$; so substituting the condition into Eq. 14, we have

$$S=[C_0C_0' e^{-(\alpha'\pi/2\beta')} e^{-\alpha x_n} e^{\alpha'(x_n-x_{n-1})} \times \sin[\beta'(x_n-x_{n-1})]\cos(\beta x_n) \quad (15)$$

The above equation represents the phenomenon of Liesegang Rings in general form. The graphical representation of the equation is made in Fig. 2. The dotted liness in Fig.

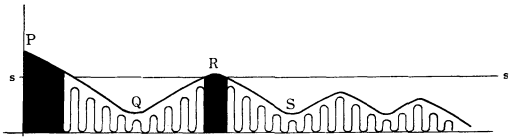


Fig. 2

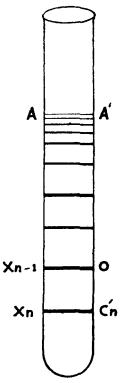


Fig. 3

2 indicates the solubility product of sparingly soluble salt. The spaces where the ionic product curve falls below SS' level indicates void regions while those places where the curve crosses the line SS' indicates the precipitate regions. Void spaces and precipitate regions have been represented in the figure by clear and dark areas respectively. The broader band structure of Liesegang systems will be given by

$$S=[C_0C_0'\,e^{-(\alpha'\pi/2\beta')}\,e^{-\alpha x_n}\,e^{\alpha'(x_n-x_{n-1})}]\times\sin\{\beta'(x_n-x_{n-1})\} \quad (16)$$

In case where the modulus of decay $\alpha$ and frequency factor $\beta'$ of the wave profile of chromate ions are sufficiently small, Eq. 16 can be simplified further by putting $e^{\alpha'(x_n-x_{n-1})}$ =unity, and

$$\sin[\beta'(x_n-x_{n-1})]=\beta'(x_n-x_{n-1})$$

So, we get

$$S=(C_0C_0'\,e^{-(\alpha'\pi/2\beta')})e^{-\alpha x_n}\,\beta'(x_n-x_{n-1}) \quad (17)$$

or $$(x_n-x_{n-1})=\left(\frac{S\,e^{(\alpha'\pi/2\beta')}}{C_0C_0'}\right)e^{\alpha x_n} \quad (18)$$

or $$(x_n-x_{n-1})=\left[P\left(\frac{S}{C_0C_0'}\right)\right]e^{\alpha x_n} \quad (19)$$

$P$ is a constant.

Since $\beta'=2\pi/\lambda'$, $\lambda'$ being the wave length of chromate ions wave, Eq. 18 can be written as

$$(x_n-x_{n-1})=\left(\frac{S\lambda'\,e^{\alpha'\lambda'/4}}{2\pi C_0C_0'}\right)e^{\alpha x_n} \quad (20)$$

or $$(x_n-x_{n-1})=\psi\,e^{\alpha x_n} \quad (21)$$

Taking the logarithm, we have

$$\log(x_n-x_{n-1})=A+\alpha x_n \quad (22)$$

where $A$ is another constant.

It may be noted here that the nature of Eq. 22 is not affected by changing the line of reference in the measurement of the rings. If $d$ is the distance of $n'$ order ring from a new reference level, then

$$x_n=(x_{n'}-d)$$

or $$\log(x_{n'}-x_{n'-1})=A+\alpha(x_n-d)$$

or $$\log(x_{n'}-x_{n'-1})=A'+\alpha' x_{n'} \quad (23)$$

Two Eqs. 22 and 23 differ only in constants.

In a Liesegang ring system $\alpha x_n$ may be considered as a small quantity for first few rings and so $e^{\alpha x_n}$ can be expanded and higher terms may be neglected. Eq. 21 thus reduces to

$$(x_{n'}-x_{n'-1})=\beta'+\alpha' x_{n'} \quad (24)$$

Eq. 24 differs from Eq. 3 in the constant $\beta$. The derivations here thus lead to an equation which is a corrected form of Jablczynski's empirical relation 1 or 3 which has already been studied by several workers. It may be noted that even Eq. 24 is a special case of more general expressions (15, 19, 20 and 23) for the phenomenon of Liesegang rings.

## Discussion

Eq. 15 has graphically been represented in Fig. 1. The figure predicts the presence of fine structure between precipitate bands. Such structures have already been reported by Riegel and Reinhands[4], Hedges[5] and Friend[6] for the silver chromate system in gelatin gel. The author also made studies on the growth of rings. Liesegang rings of silver chromate were obtained by diffusing 2.5, 5, 7.5 and 10% silver nitrate solutions through test tubes containing 2, 4, 6 and 8% gelatin gels impregnated with 0.01 M chromate. The temperature was maintained befow 16°CF during the experiment. Distinct fringes of bright yellow color closely packed rings were seen when gelatin was dilute. The rings obtained were watched continuously for 12 hr. and it was found that even precipitate rings developed not as one single ring but as an aggregate of two or more closely packed fine rings which grew thicker and thicker with time and finally small gaps in between them gradually disappeared and thick layers of precipitates were formed. The observation proves the validity of Eqs. 14 and 15. For close study of the phenomenon, it is always useful to carry out experiments at low temperature and with low concentrations of gel.

Eq. 19 indicates that the rings would get more and more packed as the initial concentrations of ions increase and solubility product decreases. The effect of solubility on silver chromate rings has been studied by Varma and Ghosh[7] and influence of ionic concentration by several other workers[8]. Their results are in conformity with the conclusions drawn above.

The theory indicates that the nature of diffusion is mainly responsible for rhythmic phenomenon; a proper type of membrane[9] however becomes a necessary condition for the occurance of the process. Several factors such as colloidal formation super-saturation, etc., may help or hinder the formation of a proper type of membrane, but they themselves cannot be considered as the cause for Liesegang rings. The phenomenon may occur even in the absence of any of these conditions.

The experimental support of various expressions obtained above for Liesegang rings justifies the use of Raimann solution for Fick's diffusion equation. The theory thus indirectly throws light on the mechanism of diffusion.

In subsequent communications other aspects

3) R. Matalon and A. Packter, *J. Colloid Sci.*, **10**, 1, 46 (1955).
4) E. R. Riegel and M. C. Reinhard, *J. Phys. Chem.*, **31**, 713 (1927).
5) E. S. Hedges and R. V. Henley, *J. Chem. Soc.*, **1928**, 2715.
6) J. A. N. Friend, ibid., **121**, 472 (1922).
7) K. K. Varma and S. Ghosh, *Kolloid-Z.*, **133**, 1, 32 (1953).
8) R. Metalon and A. Packter, *Loc. Cit.* A. Packter, *Kolloid-Z.*, **142**, 109 (1955).
9) P. B. Mathur, *J. Sci. Ind. Research, (India)*, **14B**, 12, 668 (1955).

of Liesegang ring phenomenon will be treated quantitatively.

The author takes this opportunity to thank Professor S. Ghosh for discussions and for his interest and encouragement during the course of this research work and also to the Scientific Research Committee uttar Pradesh Government for granting a research scholarship during the period of the work.

*Department of Chemistry*
*Allahabad University*
*Allahabad India*

# *Structural Analysis of Liesegang Ring Systems**

By Prem Behari MATHUR**

(Received May 17, 1960)

Since the discovery of the phenomenon of Liesegang ring several types of ring systems have been produced which on the structural basis may be broadly classified into the following categories:

a) Direct and revert systems
b) Macro and micro ring systems
c) Void spaced and continuous banded systems.

In the present paper these classifications have been analyzed in the light of the quantitative theory advanced by the author[1] in an earlier communication to this journal for the phenomenon of Liesegang rings.

## Direct and Revert Systems

In the previous communication, the author obtained the following equations for Liesegang ring phenomenon,

$$(x_n - x_{n-1}) = a\left(\frac{S}{C_0 C'_0}\right)e^{\alpha x_n} \qquad (1)$$

or

$$(x_n - x_{n-1}) = K \qquad (2)$$

where $x_n$ and $x_{n-1}$ represent the distances of $n$th and $(n-1)$th rings respectively from the initial level of diffusion, $S$ the solubility product, $C_0$ and $C_0'$ the initial concentrations of the two ions and $a$, $\alpha$ and $K$ the characteristic constants.

It can be seen that the two different types of ring systems are possible as $\alpha$ in Eq. 1 is negative or positive. When $\alpha$ is positive the distances between the successive rings $(x_n - x_{n-1})$ would increase with the increase of $x_n$ as is commonly observed for this phenomenon. When $\alpha$ is negative the rings separation would decrease in the direction of diffusion of flocculating solution. Thus two different types of ring systems, which may be called a "Direct" and Revert" systems respectively could be produced.

Mathur and Ghosh[2] noted that if a diffusing electrolyte renders high peptizing influence or dissolves out the precipitate formed as a result of the interaction of the two ions, the decrease in the concentration of the peptizing ion along the diffusion path would lead to the "Revert" system of rings. The authors have noted that the ferricyanides of copper, iron, nickel and silver are peptized by the excess of the same metal ions, and this effect is more marked in the case of copper, iron, nickel and uranium ferricyanides and at the same time the revert systems have also been observed to be more prominent in these precipitate systems. Pactor[3] obtained a revert type of rings system by diffusing a solution of ammonia through a silver chromate solution peptized by acitic acid in gelatin gel. Hook[4] has obtained revert type of Liesegang ring systems of zinc, nickel, cobalt, ferrocyanides, nickel, zinc and iron cyanides, barium and mercury vandates and cerrous oxalate in gelatin medium and of chromium hydroxide and uranyl carbonate in agar-agar gel.

Periodic precipitations of "Direct" nature are of common occurrence. Silver chromate system in gelatin gel is a well known example of this type of banded structure.

* This work is the part of the Ph. D. Thesis submitted by the author to the University of Allahabad in September, 1956.

** Present Address: Senior Scientific Officer, Central Electrochemical Research Institute, Karaikudi-3, S. India.

1) P. B. Mathur, This Bulletin, **34**, 437 (1961); Ph. D. Thesis, Allahabad University, p. 25—51, (1956); *J. Colloid Sci.*, June (1960).

2) P. B. Mathur and S. Ghosh, *Kolloid-Z*, **159**, 2, 143 (1958).

3) A. Packter, *Nature*, **175**, 556 (1955).

4) A. van Hook, *J. Phys. Chem.*, **41**, 593 (1937).

### Macro and Micro Ring Systems

Gel or other peptizing agents influence the precipitation of an sparingly soluble salt by keeping the coarser matter in colloidal state. The nature of the distributed matter in a system of periodic precipitation under the influence of environmental conditions can be ascertain from Fig. 1 which is a graphical representation of the ionic product relation obtained in the previous communication[5].

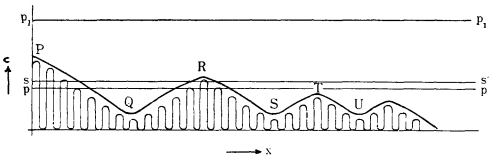



Fig. 1

$$C_nC_n' = [C_0C_0'e^{-(\alpha'\pi/2\beta')}]\, e^{\alpha'(x_n-x_{n-1})} \times \sin\{\beta'(x_n-x_{n-1})\} \times \cos(\beta' x_n)e^{-\alpha x_n} \quad (3)$$

or

$$C_nC_n' = a\, e^{[\alpha'(x_n-x_{n-1})]}e^{-(\alpha x_n)} \times \sin[\beta'(x_n-x_{n-1})]\cos(\beta x_n) \quad (4)$$

where $C_nC'_n$ is the ionic product and $\alpha$, $\alpha'$, $\beta'\beta$ and $a$ are characteristic constants. In Fig. 1, SS′ represents the solubility product level and PP′ the peptizing level. The insoluble substance formed by interaction of diffusing ions would exist in precipitate or in peptized form according as PP′ is very close to or high above the SS′ level.

When the peptizing level PP′ is little above SS′ and cuts the ionic product curve at several places, the sparingly soluble matter will precipitate out in the regions where the ionic product curve rises above PP′. Thus, at P, R, T regions the precipitate bands would appear. At intermediate spaces Q, S, U etc., where the ionic curve falls below PP′ the residual matter will exist in colloidal state. The distribution of this colloidal matter along the diffusion column would also be of periodic nature following the curve 1. Thus, translucent micro-sealed ring systems of tracer colloidal material would be produced in between the precipitate bands. Such a type of structure has been observed by several workers notedly Hedges and Henley[6], Dounin and Shamyakin[7] and Mathur and Ghosh with silver chromate in gelatin medium.

5) P. B. Mathur, *Loc. cit.*
6) E. S. Hedges and R. V. Henley, *J. Chem. Soc.*, **1928**, 2715.
7) M. S. Dounin and F. M. Shemyakin, *Kolloid-Z*, **48**, 167 (1928).

The possibility of another type of such fine system is also apparent from Eq. 4. If in Eq. 4 the damping coefficients $\alpha$ and $\alpha'$ are almost negligible the factor

$$\exp[\alpha'(x_n-x_{n-1})-\alpha x_n]$$

tends to unity and Eq. 4 reduces to the form

$$C_nC_n' = a\sin[\beta'(x_n-x_{n-1})]\cos(\beta x_n)$$

which is an equation of the Simple Harmonic Curve (Fig. 2). In such systems whatsoever be the position of PP′ closely packed fine rings without any large size void spaces in between them, would be discerned. The fine ring systems will be of precipitated material when PP′ would cut the ionic produt curve, and of colloidal matter when PP′ would be situated above it. Mathur and Ghosh have been able to obtain the micro-sized Liesegang ring systems of cobalt and silver ferricyanide under suitable experimental conditions.

### Void Spaced and Continuous Banded Systems

Let us now consider the case where damping factor $\exp(\alpha x_n)$, in Eq. 4 is large enough and at the same time the peptizing influence of the medium or of the ions present therein is moderately high on the insoluble substances. Such a system will graphically be represented by the curve P, Q, R, S and $P_1P_1'$ shown in Fig. 1. If, due to high peptizibility of the

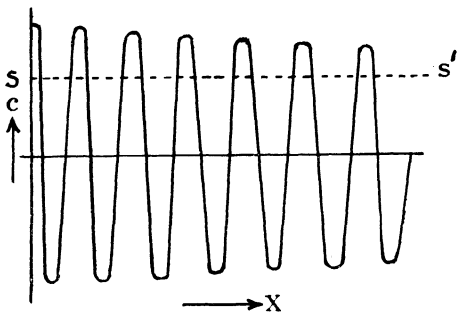



Fig. 2

insoluble salt the position of PP′ is just above the ionic product curve or if PP′ cuts the curve at some of its maxima points, the insoluble substance will exist both in colloidal as well as in precipitate form showing a continuous deposition of matter throughout the diffusion column. Due to the fact that the concentrations of ions in the regions of maxima and minima points very markedly, the colloidal particles in the neighbourhood of maxima points P, R, T will be much coarser due to the high concentration of the peptizing matter in this region in comparison to that in the minima regions. Such a system will therefore form bands of different size particles within a

continuous deposition, which will appear as alternate bands of different colors.

In cases where peptizing level is very high so much so that high concentration of a stable colloid may be produced, a very fine ring structure of colloidal matter, may appear but if it is too packed it may be left undetected.

Dhar and Chatterji[8] obtained a continuous banded system for mercuric iodide in agar gel, where a thick red color precipitate bands are followed by yellow ones and vice versa. Hatschek[9] noted a similar structure for cadmium sulphide in gelatin gel; Rastogi and Chatterji[10] reported for certain insoluble rare earth salts; Mathur and Ghosh for silver ferrocyanide and uranium ferricyanide.

Void spaced systems have already been discussed in the earlier communication. From Fig. 1, it can be seen that when peptizing level PP′ is close to the ionic product curve P, Q, R, S, the precipitate regions will be followed by void spaces and not by thick colloid bands, and so a void spaced ring system will be obtained.

It may, therefore, be concluded that the factors which control the Shape of Liesegang ring systems in gel media are (a) the damping coefficients $\alpha$ and $\alpha'$ of Eq. 3, and (b) the peptizability of the precipitate in particular environment, or say, the stability of the colloid formed under the conditions of the system. However, it may clearly be understood that colloidal formation like other factors simply influence the shape of rings in gel media, but it itself is not the cause of rhythemic phenomenon. The nature of diffusion is mainly responsible for the phenomenon, as explained in the earlier communication.

My thanks are due to Professor S. Ghosh, Head of the Department of Chemistry, Allahabad University for his keen interest in the work and valuable suggestions and also to the Scientific Research Committee of Uttar Pradesh for granting a research scholarship during the period of the work.

*Department of Chemistry*
*Allahabad University*
*Allahabad India*

8) N. R. Dhar and A. C. Chatterji, *J. Phys. Chem.*, **28**, 41 (1924); *Kolloid-Z.*, **37**, 2 (1925).
9) E. Hatschek, *Kolloid-Z*, **37**, 297 (1925).
10) M. C. Rastogi and A. C. Chatterji, *J. Indian Chem. Soc.*, **28**, 283 (1951).

# "Frontier Electron Density" in Saturated Hydrocarbons

By Kenichi FUKUI, Hiroshi KATO and Teijiro YONEZAWA

(Received August 8, 1960)

Several simple quantum-mechanical methods have been proposed to discuss the physical properties of aliphatic compounds[1-3], but they were not always successful in interpreting quantum-chemically the chemical reactivity of these compounds.

In our previous papers treating aliphatic compounds, we calculated the ionization potential, the bond energy[4] and the reactivity in nucleophilic substitution[5] by using Yoshizumi's C-C skeleton method[6].

In the present paper, we have investigated the chemical reactivity of several aliphatic hydrocarbons in a metathetical reaction by using the simple LCAO MO method including all of the atomic orbitals which participate in forming C-C and C-H $\sigma$ bonds in these compounds. The molecular orbital of aliphatic hydrocarbons, $\phi_j$, may be represented by a linear combination of 1s orbitals of hydrogen atoms, $\phi_{Hl}$, and $sp^3$ orbitals of carbon atoms, $\phi_{Cr}$.

$$\phi_j=\sum_r C_{rj}\phi_{Cr}+\sum_l C_{lj}\phi_{Hl}$$

where $C_{rj}$, $C_{lj}$ are the coefficients of the $r$th $sp^3$ orbital of carbon atom and the $l$th 1s orbital of hydrogen atom in the $j$th molecular orbital, respectively.

The resonance integrals between neighboring atomic orbitals are assumed

$$\int \phi_{C,n} H \phi_{H,n+1} d\tau = b\beta$$

1) R. D. Brown, *J. Chem. Soc.*, **1953**, 2615.
2) M. J. S. Dewar and R. Pettit, ibid., **1954**, 1625.
3) J. Lennard-Jones and G. G. Hall, *Disc. Faraday Soc.*, **53**, 127 (1957).
4) K. Fukui, H. Kato and T. Yonezawa, This Bulletin, **33**, 1197 (1960).
5) K. Fukui, H. Kato and T. Yonezawa, ibid., **33**, 1202 (1960).
6) H. Yoshizumi, *Trans. Faraday Soc.*, **53**, 125 (1957).

the $sp^3$ orbital of carbon and the 1s orbital of hydrogen in a C–H $\sigma$ bond:

$$\int \phi_{C,r} H \phi_{C,r+1} d\tau = \beta$$

between two $sp^3$ orbitals of two adjacent carbon atoms each:

$$\int \phi_{C,r} H \phi_{C,r+1} d\tau = m\beta$$

between two $sp^3$ orbitals belonging to one and the same carbon atom:

The Coulomb integrals are taken as

$$\int \phi_{Hl} H \phi_{Hl} d\tau = \alpha + a\beta$$

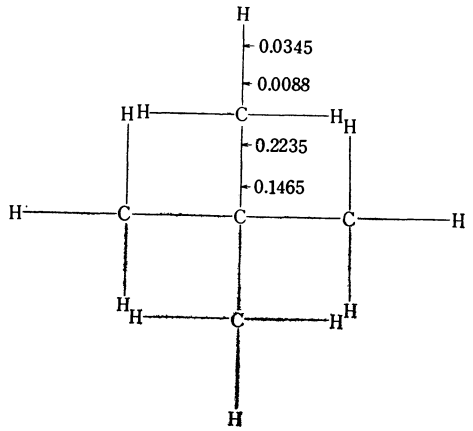
$$\int \phi_{C,r} H \phi_{C,r} d\tau = \alpha$$

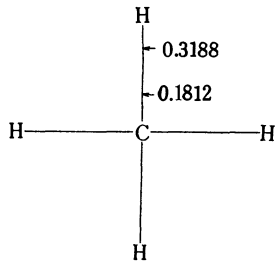
All overlap integrals are neglected.

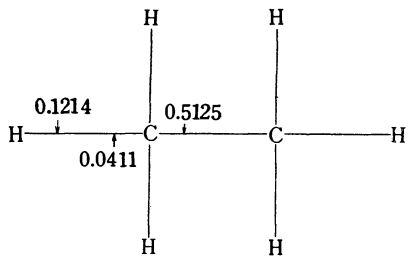
The values of $m$ is taken as 0.34 determined by Yoshizumi, $a$ is put equal to $-0.2$ referring the value of C–H bond moment ($C^{-\delta}$–$H^{+\delta}$, 0.4 D),* and $b$ is put 1.1 which is the ratio of the overlap integral $S_{C-H}$ to $S_{C-C}$[7].

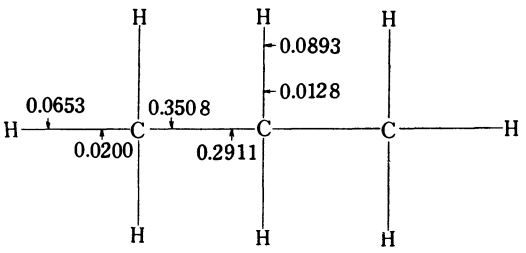
The calculated values of ionization potential and heat of formation of several compounds are listed in Table I, where the values of $\alpha$ and $\beta$ are taken as $-5.05$ eV. and $-8.8$ eV., tentatively.

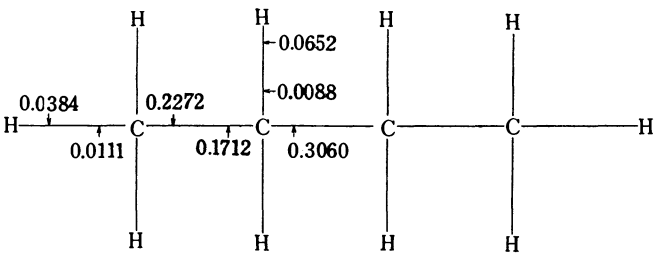
Since a good agreement between the calculated and experimental values is observed in this table, the numerical estimation of these parameters is considered to be reasonable.




7) R. S. Mulliken, C. A. Rieke, D. Orloff and H. Orloff, *J. Chem. Phys.*, 17, 1248 (1949).

* The value of $a$ varies according as the hydrogen atom is primary, secondary or tertiary. In the present treatment $a$ is taken as the same for simplicity's sake. Future improvement is expected with regard to this point.

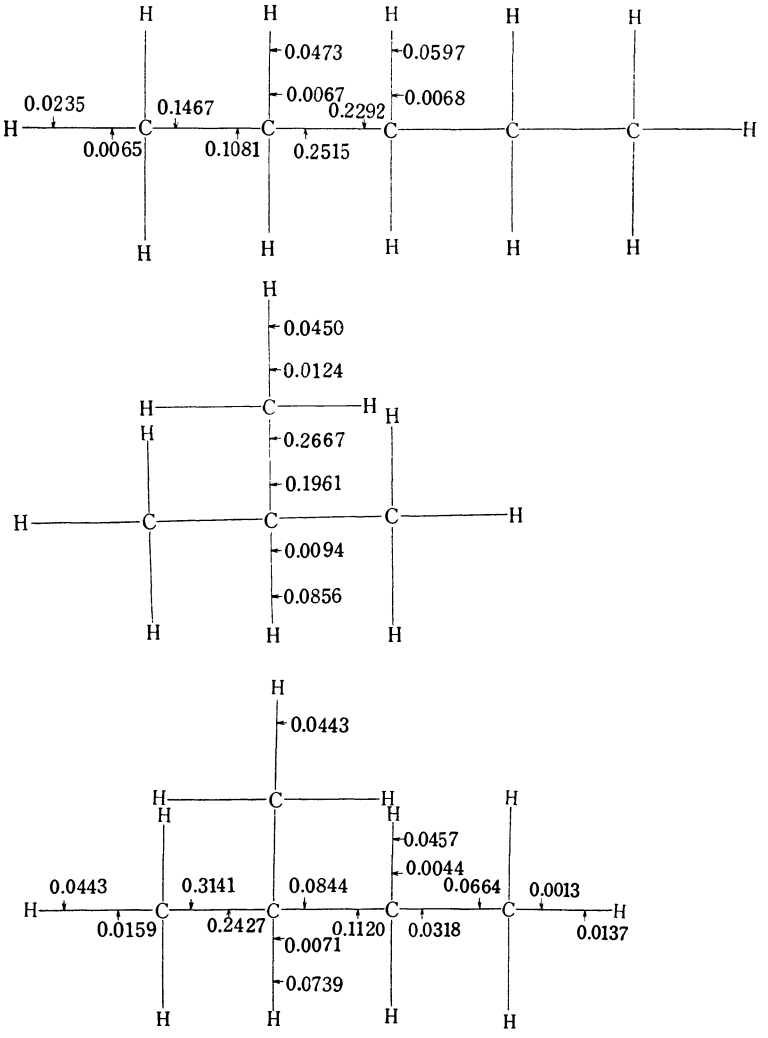



Fig. 1. The values of $f^{(R)}$ in several saturated hydrocarbons.

TABLE Ia. IONIZATION POTENTIAL

| | Calcd. I. P. | | Obs. I. P.[a] |
|---|---|---|---|
| | $\lambda_{ho}$ | $\varepsilon_{ho}$ eV. | eV. |
| $CH_4$ (1st) | 0.8322 | 12.37 | 13.16 |
| $CH_4$ (2nd) | 1.6546 | 19.61 | 19.80 |
| $C_2H_6$ | 0.7254 | 11.43 | 11.76 |
| $C_3H_8$ | 0.7009 | 11.22 | 11.21 |
| $C_4H_{10}$ | 0.6871 | 11.10 | 10.80 |

where $\lambda_{ho}$ is the coefficient $\varepsilon_{ho}=\alpha+\lambda_{ho}\beta$, $\varepsilon_{ho}$ is the highest occupied orbital energy.

The metathetical reaction of paraffins is expressed by the equation

$$R\text{-}H+\cdot X \rightarrow R\cdot + H\text{-}X$$

where R is an alkyl group and $\cdot X$ is an attacking radical.

We previously proposed the frontier electron

TABLE Ib. TOTAL ENERGY AND HEAT OF FORMATION

| | Calcd. | Obs. heat of formation[b] kcal./mol. | Difference: Calcd. $-\beta$ | Difference: Obs. kcal. |
|---|---|---|---|---|
| $CH_4$ | $8\alpha+8.329\beta$ | −17.9 | | |
| | | | 6.334 | −2.3 |
| $C_2H_6$ | $14\alpha+14.663\beta$ | −20.2 | | |
| | | | 6.337 | −4.6 |
| $C_3H_8$ | $20\alpha+21.000\beta$ | −24.8 | | |
| | | | 6.368 | −5.4 |
| $C_4H_{10}$ | $26\alpha+27.368\beta$ | −30.2 | | |

a) R. E. Hornig, *J. Chem. Phys.*, **16**, 105 (1948).
b) F. D. Rossini, K. S. Pitzer et al., "Selected Values of Physical and Thermodynamic Properties of Hydrocarbons and Related Compounds", Carnegie Press (1953).

density[8], $f^{(R)}$, as an excellent reactivity index for a radical reaction of conjugated systems. Now we can show that $f^{(R)}$ is found to be also available as the reactivity index of saturated compounds.* The calculated values of $f^{(R)}$ in several compounds are listed in Fig. 1. It is observed that the values of $f^{(R)}$ on hydrogen atoms in these compounds is parallel with the experimental results. That is to say, the activity of hydrogen-extraction in saturated hydrocarbons increases in the order *prim.* H $<$*sec.* H $<$*tert.* H[9].

Thus, the frontier electron density has been found to relate with the experimental chemical reactivity of aliphatic saturated molecules.

An application of this fact to explaining the reaction mechanism of oxidation or pyrolysis in aliphatic hydrocarbons seems to be possible.

*Faculty of Engineering*
*Kyoto University*
*Sakyo-ku, Kyoto*

8) K. Fukui, T. Yonezawa, C. Nagata and H. Shingu, ibid., **22**, 1432 (1954).

* According to the electronegativity of the attacking radical, $f^{(E)}$ or $f^{(N)}$ (frontier electron densities for electrophilic or nucleophilic attack) may be used in lieu of $f^{(R)}$. In the present case we are imagining e. g.·$CH_3$ for the attacking radical, whose energy level seems to lie between the highest occupied and the lowest vacant orbitals of R-H.

9) A. F. Trotman-Dickenson, *Quart. Revs.*, **7**, 198 (1953).

# *Studies on the Catalytic Double Wave of Cystine by Oscillographic Polarography*

By Mutsuaki SHINAGAWA, Hideo IMAI and Hiroyuki NEZU

(Received July 16, 1960)

Brdicka[1] has reported that in a conventional polarography cystine and cysteine develop a pronounced single catalytic wave in an ammonia buffer containing divalent cobalt. In the previous paper[2] it was reported that this catalytic wave gives a rounded maximum of good reproducibility by the addition of gelatin and that the maximum wave is split off into two waves by the addition of methyl cellulose (cf. Fig. 1). The form of these double waves resembles that of the catalytic double wave of protein, and the evolution of hydrogen as the electrolytic reductant is facilitated by the catalytic action of the cobalt(II)-cysteine complex* adsorbed on the surface of the dropping mercury electrode (DME). Accordingly, one can expect to clarify the nature of the protein wave from the analogy to the cystine wave.

The present experiment was carried out as a tentative model of the protein wave, and a possible mechanism of the cystine wave is proposed from the consideration of the adsorption equilibria among three surface active substances, i. e., the cobalt(II)-cysteine complex anion, methyl cellulose and gelatin.

1) R. Brdicka, *Collection Czechoslov. Chem. Communs.*, **4**, 148 (1933).

2) M. Shinagawa and H. Nezu, This Bulletin, **33**, 272 (1960).

* This catalytic wave occurs at a more negative potential than the potential of the reduction of cystine to cysteine, and therefore, must be caused by the reduced form, cystein.

## Experimental

A Sevcik type oscillographic polarograph[3] constructed in our laboratory[4] was used. Effects of the mercury head and the frequency of the applied triangular sweep on the oscillographic current voltage pattern were observed. The mercury head was changed from 25 to 65 cm., when the life-time of the DME changed from 5.4. to 2.0 sec. under the applied span voltage from $-0.28$ to $-2.16$ V. vs. S. C. E. (20 cycles/sec.). The rate of the mercury flow was 0.755 mg./sec. at the mercury head of 25 cm. The frequency applied was 20~60 cycles/sec., when the rate of potential change was 75~225 V./sec.

All the reagents were of analytical grade. The test solutions used are tabulated as follows:

| Test solution No. | Constituent |
|---|---|
| 0 | 0.1 F $NH_3$-$NH_4Cl$ buffer |
| 1 | $1\times10^{-3}$ F $CoCl_2$+$2\times10^{-5}$ F cystine in solution 0 |
| 2 | 0.02% methyl cellulose in solution 1 |
| 3 | 0.01% gelatin in solution 1 |
| 4 | 0.02% methyl cellulose+0.01% gelatin in solution 1 |
| 5 | 0.005~0.08% methyl cellulose in solution 0 |

3) A. Sevcik, *Collection. Czechoslov. Chem. Communs.*, **13**, 349 (1948).

4) M. Shinagawa, H. Imai and S. Chaki, *J. Electrochem. Soc. Japan*, **23**, 132 (1955); H. Imai, This Bulletin, **29**, 276 (1956).

An H-cell with low impedance was used, and the dissolved oxygen in the test solution was not removed. The temperature was 29±0.5°C.

## Results and Discussion

Under the experimental conditions described in the preceding section, the cobalt(II)-ammine complex behaves irreversibly at the DME, and the charging current, which flows when the adsorption or desorption of surface active substances occurs, becomes markedly great. The effect of the mercury head on the peak current gives information concerning the difference between the electrolytic current and the charging current and also concerning the irreversibility of an electrode process. One can obtain similar information from the effect of the sweep frequency on the peak current and the peak potential**.

**The Oscillographic Current-Voltage Pattern.** — The oscillographic current-voltage pattern of solutions 1, 2, 3 and 4 are illustrated in Figs. 2-A, B, C and D, respectively. In Fig. 2-A, two reduction steps represented by $i_p1$ and $i_p2$ are noticeable***. $i_p1$, the peak potential of which is −1.27 V. vs. S. C. E., corresponds to the reduction of the cobalt(II)-ammine complex ion. The peak height of $i_p1$ is decreased and rounded off by the addition of methyl cellulose and gelatin as is illustrated in Figs. 2-B, C and D, simultaneously the peak potential being shifted toward more negative potentials ($E_p$=−1.27, −1.31 and −1.36 V. vs. S. C. E. in solutions 2, 3 and 4, respectively.).

The second step ($E_p$=ca. −1.7 V. vs. S. C. E.)

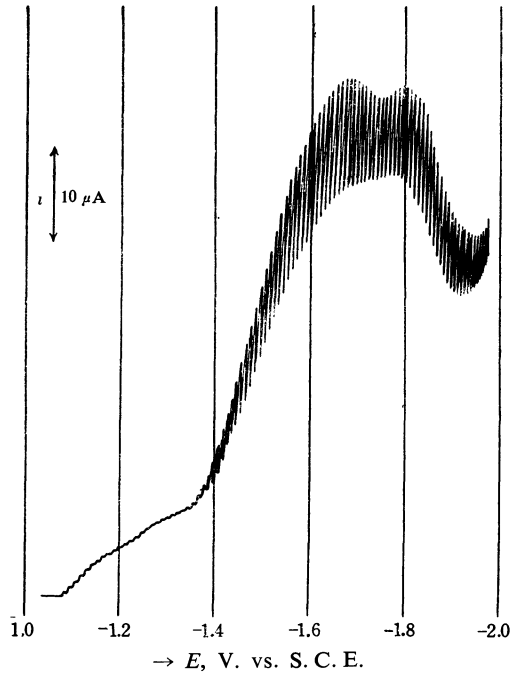



Fig. 1. The catalytic double wave of cystine by a conventional polarograph. Solution: $1\times10^{-3}$ F $CoCl_2$, $2\times10^{-5}$ F cystine, 0.002% methyl cellulose in 0.1 F $NH_3$-$NH_4Cl$ buffer. $m$=2.46 mg./sec., $t$=3.5 sec.

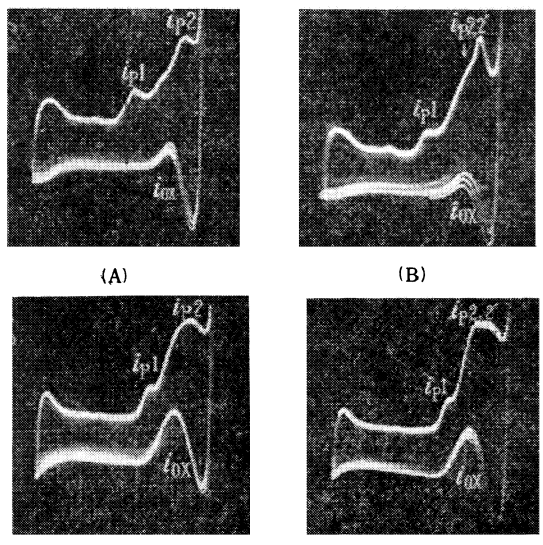



Fig. 2. The oscillographic current-voltage pattern of $1\times10^{-3}$ F $CoCl_2$ and $2\times10^{-5}$ F cystine in 0.1 F ammonia buffer (A). (B): +0.02% methyl cellulose, (C): +0.01% gelatine, (D): +0.02% methyl cellulose and 0.01% gelatin, Sweep frequency=20 cycles/sec., v=75 V./sec., $h$=25 cm., $t$=4.9 sec.

** These points of view are summarized in detail as follows in order to help the subsequent considerations.

(1) The peak of the oscillographic pattern is rounded off and the peak potential ($E_p$) is shifted toward more negative potentials in the cathodic branch as the electrode process becomes irreversible[5].

(2) No reoxidation peak can be observed in the anodic branch unless the DME forms the amalgam with the reductant.

(3) The maximal peak current (i. e. the peak current just before the electrode mercury droplet falls) of a reversible electrode process ($i_{p,r}$) is independent of the mercury head, while that of an irreversible one ($i_{p,ir}$) varies with the mercury head[6].

(4) $i_{p,r}$ is proportional to the square root of the rate of the potential change (v)[6], while $i_{p,ir}$ deviates from this proportionality[7].

(5) The maximal charging current is independent of the mercury head, and it is linearly proportional to v.

(6) The peak potential of the charging current, which flows at the adsorption or the desorption potential of surface active substances, will be shifted by the change in the concentration of the adsorbed substance.

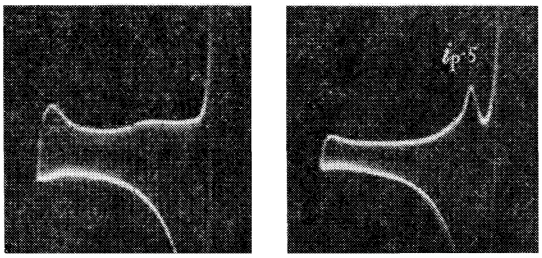
5) P. Delahay, *J. Am. Chem. Soc.*, **75**, 1190 (1953); H. Matsuda and Y. Ayabe, *Z. Elektrochem.*, **59**, 494 (1955).

6) P. Delahay, *J. Phys. Colloid Chem.*, **54**, 630 (1950); H. Imai, *J. Electrochem. Soc. Japan*, **23**, 530 (1955).

7) P. Delahay and G. Perkins, *J. Phys. Colloid Chem.*, **55**, 586, 1146 (1951).

*** $i_p2$ is accompanied by a barely perceptible peak at −1.5 V. vs. S. C. E. This peak corresponds to an irregular wave observed at the same potential by a conventional polarograph. The nature of this wave is unknown at this stage.

represented by $i_p2$ in Fig. 2 is the catalytic current. This catalytic current is accompanied by a sharp peak at $-1.72$ V. vs. S. C. E. in the presence of methyl cellulose. Since a similar sharp peak is developed at $-1.7$ V. vs. S. C. E. by the desorption of methyl cellulose in solution 5 (cf. Fig. 3), the above-mentioned sharp




(A) (B)

Fig. 3. The oscillographic current-voltage pattern of 0.1 F ammonia buffer (A) and 0.06% methyl cellulose in 0.1 F ammonia buffer (B). Sweep frequency=20 cycles/sec., v=75V./sec., $h$=45 cm., $t=2.4_5$ sec.

peak of solution 2 can be assigned to the charging current change caused by the desorption of methyl cellulose. By the addition of gelatin, the catalytic current is rounded off ($E_p=1.72$ V. vs. S. C. E.) as is illustrated in Fig. 2-C, and this wave is split off into two waves by the addition of methyl cellulose (Fig. 2-D), the potential of the first and the second peak being $-1.62$ and $-1.73$ V. vs. S. C. E., respectively. Undoubtedly, these double peaks are different in nature from the catalytic double waves developed by a conventional polarograph (Fig. 1), because the charging current becomes predominant in an oscillographic method. It may safely be assumed, however, from the coincidence of the peak potential of $i_p2'$ with the desorption potential of methyl cellulose that the desorption of methyl cellulose is closely connected with the occurrence of $i_p2'$ and presumably with that of the second maximum wave in the conventional polarography.

In the anodic branch, the current change represented by $i_{ox}$ is noteworthy. The pattern of $i_{ox}$ is pronounced by the addition of gelatin, and in this case it can be seen from Figs. 2-C and 2-D that this current is obviously cathodic (the reduction current). A cathodic current of a similar character has been observed in the solution containing indium(III) and chloride[8], corresponding to the well-known minimum wave in the conventional polarography. It is supposed that this minimum wave is caused by the electrostatic repulsion of $InCl_6^{3-}$ from the negatively charged electrode. By analogy, it can be assumed that the cobalt(II)-cysteine complex anion behaves likewise. When the electrode potential is shifted toward less negative values in the anodic branch after the repulsion of the complex anion in the cathodic branch, the complex anion will be readsorbed on the electrode surface and contributes to the catalytic reduction of the hydrogen ion. Thus, the mechanism of $i_{ox}$ leads to the idea of the repulsion of the cobalt(II)-cysteine complex anion at the potential more negative than $-1.63$ V. vs. S. C. E.

**The Variation of the Peak Current with the Mercury Head.**—The peak current is plotted against the mercury head in Fig. 4, where the

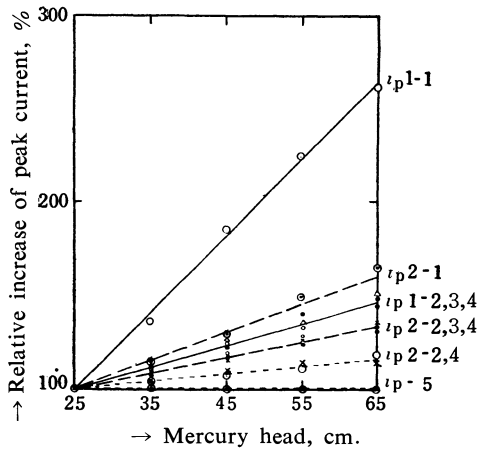



Fig. 4. The relative variation of the peak current with the mercury head. The symbols of the peak current are given in Fig. 2, and the second figure of the symbol represents the solution number given in the section of the experimental. Sweep frequency=20 cycles/sec., v=75 V./sec.

peak current is represented by the same symbols as those used in Fig. 2, and the second figure in the symbols represents the solution number given in the section of Experimental. In Fig. 4 three groups are classified according to their inclination. The first group involves $i_p1$-1 and $i_p2$-1 which have the steepest inclination among $i_p1$'s and $i_p2$'s, respectively. When the recovery of the diffusion layer in each cycle of the voltage sweep imperfect owing to the imcomplete reoxidation of the reductant (Note that $i_p1$ and $i_p2$ give no reoxidation peak in Fig. 2.), the repetition of the reduction process during the life-time of the DME results in the depletion of the oxidant at the vicinity of the electrode surface except for the supply due to the duffusion from the bulk of solution. Under

8) M. Shinagawa, H. Imai and H. Sunahara, *J. Chem. Soc. Japan, Pure Chem. Sec. (Nippon Kagaku Zasshi)*, **77**, 1482 (1956).

this condition, the thickness of the diffusion layer will be markedly decreased by the rapid rate of the DME growth. Moreover, the fresh surface of the DME is increased by the rapid rate of the DME growth. Since the rate of the DME growth increases as the mercury head is increased, it is easy to see why these currents increase as the mercury head is increased.

The second groups involves $i_p1$-2, 3, 4 and $i_p2$-2, 3, 4, which show a moderate change with the mercury head. In this group, the effect of the drop growth seems to be retarded by the presence of the surface active substances.

The third group involves $i_p$-5. This desorption peak current of methyl cellulose is practically independent of the mercury head.

The peak heights of $i_p2'$-2 and $i_p2'$-4 were measured from the height of the charging current without paying any attention to the superposition of the preceding peak current, $i_p2$, which is markedly affected by the mercury head. Keeping this fact in mind, one can assign the slight inclination of $i_p2'$ to the superposition of the intrinsic current of $i_p2'$ on the decreasing current of $i_p2$. Accordingly, it is assumed that $i_p2'$ is practically independent of the mercury head and will be tacitly controlled by the desorption of methyl cellulose. This assumption is best realized from Fig. 5 which illustrates the relative change of $i_p2$-4 and $i_p2'$-4 with the mercury head.

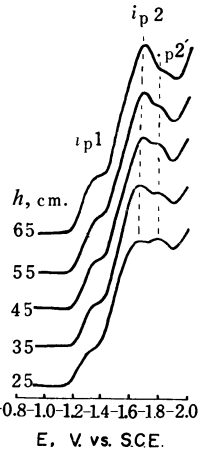



Fig. 5. The variation of the oscillographic current-voltage pattern of $1\times10^{-3}$ F $CoCl_2$ and $1\times10^{-5}$ F cystine in 0.1 F ammonia buffer containing 0.02% methyl cellulose and 0.01% gelatin with the mercury head ($h$, cm.). Sweep frequency=20 cycles/sec., v=75 V./sec.

**The Effect of the Sweep Frequency.** — The effect of the sweep frequency on the cathodic peak current is illustrated in Fig. 6. Any peak, except for the desorption peak of methyl cellulose, becomes more rounded and the peak

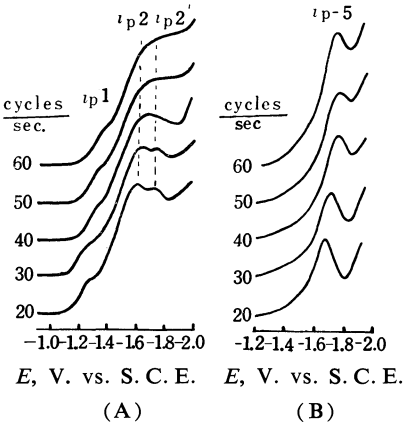



Fig. 6. The variation of the oscillographic current-voltage pattern of $1\times10^{-3}$ F $CoCl_2$ and $1\times10^{-5}$ F cystine in 0.1 F ammonia buffer containing 0.02% methyl cellulose and 0.01% gelatin (A) and the desorption charging current of 0.06% methyl cellulose (B) with the sweep frequency. $h$=45 cm.

potentional is shifted toward more negative potentials as the sweep frequency is increased. This result indicates that all of these electrode processes are irreversible. It must be pointed out here that the electrode process of $i_p2'$-4 is irreversible in nature, though it relates to the desorption of methyl cellulose as is described in the preceding section.

## Conclusion

By a conventional polarograph, cystine develops the pronounced double maximum in an ammonia buffer containing divalent cobalt, gelatin and methyl cellulose. This double wave is of interest because of the resemblance to the protein wave in the wave form and in the catalytic behavior. In the following description, it is explained why the cystine wave is developed in the form of the double maximum.

In this experiment, it was confirmed that cobalt(II)-cysteine complex, which acts as a catalyser for the depolarization of the hydrogen

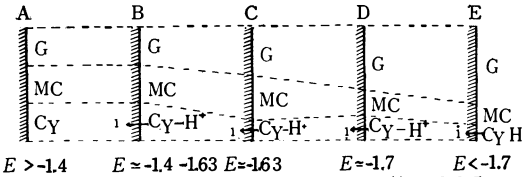



Fig. 7. The schematic representation of the adsorbed quantities of gelatin (G), methyl cellulose (MC) and the cobalt(II)-cysteine complex (Cy) on the unit surface area of the DME at each electrode potential. In this figure, i←Cy-H$^+$ means that Cy behaves as a catalysis of the hyrogen ion depolarization.

ion, desorbs from the electrode surface at about −1.63 V. vs. S. C. E. When the electrode potential becomes more negative than −1.7 V. vs. S. C. E., methyl cellulose also desorbs from the electrode surface. Accordingly, the quantity of the surface active substances adsorbed on the unit surface area of the DME at each electrode potential can be schematically expressed as is illustrated in Fig. 7.

In Fig. 7, G, MC and Cy represent the adsorbed quantity of gelatin, methyl cellulose and cobalt(II)-cysteine complex anion, respectively, on the unit surface area of the DME. The quantity of G, MC and Cy depends on each adsorbed concentration, which is in equilibrium with each concentration of the bluk of the solution and on the mutual equilibria among G, MC and Cy on the electrode surface. When the electrode potential is less negative than −1.6 V. vs. S. C. E., all of the surface active substances are adsorbed on the electrode surface as is illustrated in Fig. 7-A. As the electrode potential becomes more negative than −1.5 V. vs. S. C. E., the catalytic current gradually increases (Fig. 7-B). The cobalt(II)-cysteine complex anion, however, begins to desorb at −1.63 V. vs. S. C. E. and results in the decrease of the catalytic current (Fig. 7-C). Thus, the first maximum wave will be developed by the conventional polarograph. It is noteworthy, here, that the quantity of G and MC will be increased, corresponding to the desorption of Cy-complex. This is because the surface area to be occupied by G and MC will increase when Cy-complex desorbs.

At the potential of −1.7 V. vs. S. C. E. methyl cellulose begins to desorb from the electrode surface (Fig. 7-D). In this case, the quantity of G and Cy-complex will be increased, though the increase of Cy-complex is limited in the potential region where the desorption of methyl cellulose appreciably proceeds. Accordingly, the catalytic current will temporarily increase near the potential of −1.7 V. vs. S. C. E. (Fig. 7-E). Thus, the second maximum wave will be developed.

In the above-mentioned conclusion, the present authors proposed a possible mechanism of the cystine double wave from the consideration of the adsorption equilibria among gelatin, methyl cellulose and cobalt(II)-cystein complex anion. The criticism of this idea and its application to the protein wave is left for future.

Part of the expenses has been covered by the Grant in Aid for Fundamental Scientific Research, Ministry of Education.

*Laboratory of Analytical Chemistry*
*Faculty of Science and Minami College*
*Hiroshima University*
*Higashisendamachi, Hiroshima*

# SHORT COMMUNICATIONS

## *Radiolysis of Crystalline Oxalato Complexes*

By Akira SUGIMORI and Gen-ichi TSUCHIHASHI

(Received December 2, 1960)

The effects of metal ions on the radiolysis of organic compounds have mainly been studied in aqueous solutions[1]. The present authors previously studied the radiation chemistry of aqueous metal salicylate complexes, and found that chelated $Fe^{3+}$ and $Cu^{2+}$ effectively increase the decarboxylation of salicylic acid[2]. The study on the radiolysis of crystalline metal complexes was also considered to be very helpful for the elucidation of the mechanism of the reaction affected by metal ions. In this paper, the radiolysis of various crystalline metal oxalato complexes is repoted.

Oxalic acid ($H_2C_2O_4 \cdot 2H_2O$), anhydrous oxalic acid ($H_2C_2O_4$), ferrous oxalate ($Fe(C_2O_4) \cdot 2H_2O$), sodium oxalate ($Na_2C_2O_4$), potassium trisoxalatoaluminate ($K_3Al(C_2O_4)_3 \cdot 3H_2O$), potassium trisoxalatochromate ($K_3Cr(C_2O_4)_3 \cdot 3H_2O$), potassium trisoxalatocobaltate ($K_3Co \cdot (C_2O_4)_3 \cdot 3H_2O$) and potassium trisoxalatoferrate ($K_3Fe(C_2O_4)_3 \cdot 3H_2O$) were irradiated with Co-60 gamma rays at room temperature, mainly

1) J. H. Baxendale and D. Smithies, *J. Chem. Phys.*, **23**, 604 (1955); *J. Chem. Soc.*, **1959**, 779.

2) A. Sugimori and G. Tsuchihashi, This Bulletin, **33**, 713 (1960).

TABLE I. THE ANALYSIS OF THE GASEOUS PRODUCTS

| Compound | Dose rate r./hr. | Dose, r. | $G$(gas) | $CO/CO_2$ |
|---|---|---|---|---|
| $H_2C_2O_4 \cdot 2H_2O$ | $4.4\times10^5$ | $1.45\times10^8$ | 1.1 | 0.0 |
| $Na_2C_2O_4$ | $4.4\times10^5$ | $1.45\times10^8$ | 0.03 | 0.1 |
| $K_3Al(C_2O_4)_3 \cdot 3H_2O$ | $4.4\times10^5$ | $1.31\times10^8$ | 2.0 | 0.1 |
| $K_3Cr(C_2O_4)_3 \cdot 3H_2O$ | $4.4\times10^5$ | $1.45\times10^8$ | 1.5 | 0.6 |
| $K_3Fe(C_2O_4)_3 \cdot 3H_2O$ | $4.4\times10^5$ | $1.45\times10^8$ | 7.5 | 0.0 |
| $K_3Co(C_2O_4)_3 \cdot 3H_2O$ | $4.4\times10^5$ | $1.45\times10^8$ | 9.8 | 0.0 |

TABLE II. THE DECOMPOSITION OF THE COMPLEXES

| Compound | Condition | Dose rate r./hr. | Dose, r. | $G$(-complex) |
|---|---|---|---|---|
| $K_3Cr(C_2O_4)_3 \cdot 3H_2O$ | vacuum | $4.4\times10^5$ | $1.45\times10^8$ | 0.7 |
| | air | $4.6\times10^5$ | $1.46\times10^8$ | 0.7 |
| $K_3Co(C_2O_4)_3 \cdot 3H_2O$ | vacuum | $4.4\times10^5$ | $1.31\times10^8$ | 8.9 |
| | air | $4.6\times10^8$ | $1.46\times10^8$ | 9.1 |

TABLE III. THE DECOMPOSITION OF $C_2O_4^{2-}$

| Compound | Condition | Dose rate r./hr. | Dose, r. | $G(-C_2O_4^{2-})$ |
|---|---|---|---|---|
| $H_2C_2O_4 \cdot 2H_2O$ | vacuum | $4.6\times10^5$ | $1.46\times10^8$ | 2.3 |
| | air | $2.6\times10^5$ | $5.15\times10^7$ | 5.1 |
| $H_2C_2O_4$ | vacuum | $4.6\times10^5$ | $1.46\times10^8$ | 3.6 |
| | air | $4.6\times10^5$ | $1.46\times10^8$ | 4.3 |
| $Na_2C_2O_4$ | vacuum | $4.6\times10^5$ | $1.46\times10^8$ | $<0.03$ |
| | air | $2.6\times10^5$ | $5.15\times10^7$ | $<0.3$ |
| $K_3Al(C_2O_4)_3 \cdot 3H_2O$ | vacuum | $4.4\times10^5$ | $1.31\times10^8$ | 4.6 |
| | air | $4.4\times10^5$ | $1.46\times10^8$ | 5.5 |
| $Fe(C_2O_4) \cdot 2H_2O$ | vacuum | $1.6\times10^5$ | $1.46\times10^8$ | 0.1 |

at a does rate of $4.4\times10^5$ r./hr. and at a total dose of $1.5\times10^8$ r. both in the presence and in the absence of air.

After the quantity of evolved gas was measured, the gas was analyzed mass-spectrometrically. The quantity of decomposed complex was measured by visible light absorption spectrometry of aqueous solutions of irradiated complexes. The quantity of decomposed oxalate was measured by titrating the solutions of irradiated samples with acid permanganate solution. $G$(gas) (the number of the molecules of evolved gas), the ratio of CO to $CO_2$ in the evovled gas, $G$(−complex) (the number of the decomposed molecules of the complex) and $G$ ($-C_2O_4^{2-}$) are shown in Tables I, II and III. From the experimental results, the followings are concluded.

(1) Oxalate ions such as in sodium oxalate and ferrous oxalate are very stable to gamma ray irradiation, compared with those in metal oxalato complexes. The fairly large reactivity of oxalic acid and potassium trisoxalatoaluminate toward gamma irradiation might be attributed to the covalent character of oxalate-M (M=metal ion or hydrogen) bond. Oxalate ions with larger covalent character decompose more easily by gamma irradiation.

(2) The much larger $G$ values of $Fe^{3+}$ and $Co^{3+}$ complex than those of $Al^{3+}$ complex can not be explained only by the covalent character of oxalato-metal bond. They seem to be related with the reduction of metal ions. On gamma irradiation of $Fe^{3+}$ and $Co^{3+}$ complex, the reduction of the metal ions also occurs, and ferrous and cobaltous oxalate precipitates when the irradiated complexes are dissolved in water. Therefore, the electron transfer from oxalate to metal ions might increase the radiation-induced decomposition of oxalate.

(3) Chromium is stable in the state $Cr^{3+}$ and Cr(VI) whereas very unstable in the state $Cr^{2+}$; therefore on gamma irradiation of $K_3Cr(C_2O_4)_3 \cdot 3H_2O$ the electron transfer from oxalato to metal ion might be difficult and this might cause the lower $G$ values of $Cr^{3+}$ complex than those of $Fe^{3+}$ and $Co^{3+}$ complex. But on the reaction of $Cr^{3+}$ complex, the oxidation of $Cr^{3+}$ to Cr(VI) might occur, and a fairly large amount of CO is formed in place of $CO_2$ which is the main product in the gamma irradiation of oxalic acid and the oxalate complexes other than those with $Cr^{3+}$.

Details of this study will be published later.

*Radiation Applications Division*
*Japan Atomic Energy Research Institute*
*Tokai, Ibaraki-ken*

## *Steric Effects of ortho-Groups on Hydrogen Bond Formation in Phenol Derivatives as Studied by Nuclear Magnetic Resonance*

By Ichiro YAMAGUCHI

(Received December 20, 1960)

In the previous report[1], the author pointed out that the chemical shift of the OH proton depends greatly on the relative position of the methyl groups to the OH group in dimethyl phenol isomers, and this was attributed to the steric effects of the methyl group on the formation of intermolecular hydrogen bond. The present report shows a dependence of the OH proton chemical shift on the size of the ortho-group.

The compounds investigated are 2, 6-dichlorophenol, 2, 6-dimethyl phenol and 2, 6-di-*t*-butyl-*p*-cresol. The chemical shifts of the OH proton in various solutions were determined by the side band technique refering to water as an external standard. The correction for the bulk diamagnetic susceptibility was not applicable except to the values extrapolated to infinite dilution because reliable data of the susceptibility for these compounds were not available.

In Figs. 1a and 1b, the OH resonance shifts (in p.p.m.) are plotted against the concentration of the solutions (in mole fraction). The curves for various solutions are comparatively separated in a wide range of the magnetic field from one another for 2, 6-dichlorophenol and 2, 6-dimethyl phenol, but not for 2, 6-di-*t*-butyl-*p*-cresol. This suggests that the size of the ortho-group would be a factor which affects the ability of the formation of an intermolecular hydrogen bond of a phenol. This effect was qualitatively pointed out by Batdorf with his NMR measurements[2].

As a measure of the extent of the ability of the hydrogen bond formation, the difference between the chemical shift at infinite dilution (extrapolated and then corrected for bulk diamagnetic susceptibility of the solvents) for carbon tetrachloride solution and that for acetone solution is taken. In Fig. 2, the values of the difference, $\Delta$, are plotted against the size of the ortho-groups, for instance the Van der Waals radii. The data for phenol[2,3] are also plotted.

In Fig. 2, the followings are observed: First, the $\Delta$ value is larger as the radius is smaller. Secondly, the $\Delta$ value for 2, 6-dichlorophenol is found above the line connecting the points for phenol and dimethyl phenol. This discrepancy may be due to weak intramolecular hydrogen bond between OH and Cl groups. Linear extrapolation of the

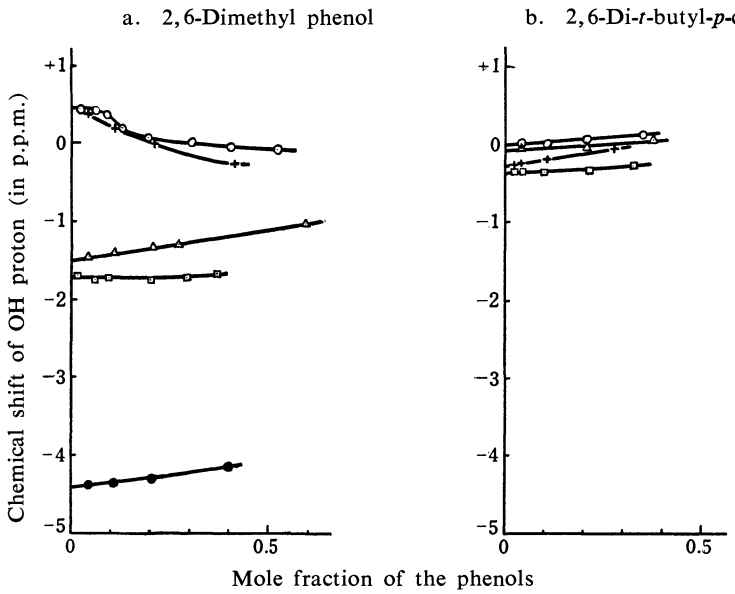



Fig. 1. OH proton resonance shift refer to $H_2O$ proton (susceptibility correction is not applied.).
Solvent: -○- $CCl_4$ -+- $CHCl_3$ -△- Ether -□- Acetone -●- Pyridine

1) I. Yamaguchi, This Bulletin, **34**, 353 (1961).
2) R. L. Batdorf, Ph. D. thesis, Univ. of Minnesota, 1955.
3) C. M. Huggins, G. C. Pimentel and J. N. Shoolery, *J. Phys. Chem.*, **60**, 1311 (1956).

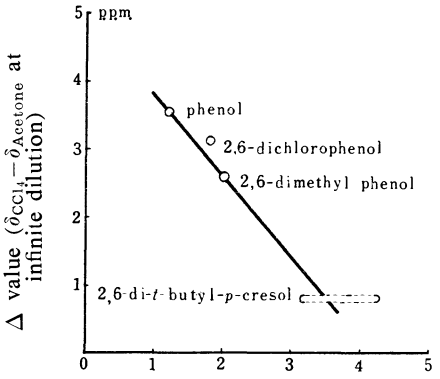



Fig. 2. Dependence of the ability of hydrogen bond formation of phenols on the size of ortho-group.

line connecting two points for 2, 6-di-alkyl phenols (alkyl=H and $CH_3$) to the $\Delta$ value of 0.8 gives a value approximately 3.5 Å as the Van der Waals radius corresponding to the size of the *t*-butyl group. This value seems to be reasonable for this group. Therefore it may be concluded that the ability of the formation of an intermolecular hydrogen bond in phenol derivatives is a linear function of the size of the ortho-group.

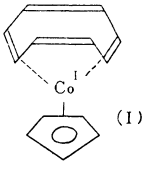
*Radiation Applications Division*
*Japan Atomic Energy Research Institute*
*Tokai, Ibaraki-ken*

## *New Stable Olefin Complexes of Cobalt(I)*

By Akira NAKAMURA and Nobue HAGIHARA

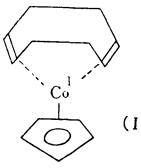
(Received December 8, 1960)

In a previous communication the authors described the synthesis of cyclopentadienyl cobalt cyclooctatetraene (I)[1]. In that report the authors reported that I took up 2 mol. of hydrogen on catalytic hydrogenation to give orange crystals (II), m. p. 102°C. The authors supposed this compound II to be cyclopentadienyl cobalt 1, 5-cyclooctadiene considering from the proposed structure of I (cf. Fig. 1). In order to determine the correct structure of II, an attempt was made to obtain the same compound from 1, 5-cyclooctadiene. Thus 1, 5-cyclooctadiene was refluxed with cyclopentadienyl cobalt dicarbonyl in xylene under nitrogen for 15 hr. After removal of the unreacted starting materials, orange crystals were obtained by sublimation at 80°C under reduced pressure in 30% yield. These crystals were recrystallized from petroleum ether, m. p. 102.5°C. Found: C, 67.05; H, 6.76. Calcd. for $C_{13}H_{17}Co$: C, 67.24; H, 7.38%. The infrared spectrum of this compound was identical with that of II and showed the presence of $\pi$-cyclopentadienyl group. No absorption was observed at usual C=C stretching region. These facts indicate the structure of II to be $(C_8H_{12})Co(C_5H_5)$ which is shown in Fig. 2.




(I)

Fig. 1




(II)

Fig. 2

1, 3, 5-Cyclooctatriene yielded brown crystals (III), m. p. 90°C, by the similar reaction with cyclopentadienyl cobalt dicarbonyl. The infrared spectrum of III showed C=C stretching absorption at 1625 cm.$^{-1}$ III also gave II on catalytic hydrogenation.

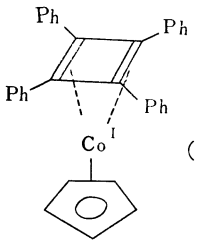
II was stable in air, soluble in organic solvents and readily decomposed by bromine or by iodine in carbon tetrachloride. It also reacted with carbon monoxide (50 atm.) to give cyclopentadienyl cobalt dicarbonyl. The ultraviolet spectrum of II showed maximum at 361 m$\mu$(log $\varepsilon$: 2.87, in alcohol) and had shoulders at 235, 267 and 420 m$\mu$, as well as increasing absorption in the shorter wavelengths. I and II reacted with diphenyl acethylene in refluxing xylene to give yellowish brown crystals (IV), m. p. 256°C, in 40 and 47% yield respectively. These crystals were purified by recrystallization from benzene or by chromatography on alumina. Found: C, 81.82; H, 5.2. Calcd. for $C_{33}H_{25}Co$: C, 82.48; H, 5.24%. The analysis conformed to the composition, $(C_5H_5C{\equiv}CC_6H_5)_2Co(C_5H_5)$. IV was soluble in organic solvents and was quite stable in air. IV was thermally stable up to ca. 360°C under nitrogen and surprisingly oxidation resistant as a univalent cobalt compound. For example the solution of IV in benzene was oxidized neither by air on heating nor by iodine on warming. The ultraviolet spectrum of IV showed maxima at 241, 257 and 278 m$\mu$ (log $\varepsilon$: 4.51, 4.50, 4.46, in alcohol) and had shoulders at 287, 295 and 400 m$\mu$.

The infrared spectrum of IV showed the

1) A. Nakamura and N. Hagihara, This Bulletin, 33, 425 (1960).

presence of $\pi$-cyclopentadienyl group and mono-substituted phenyl group.

IV was reduced by sodium in liquid ammonia to give 1, 2, 3, 4-tetraphenylbutane, m. p. 181°C. IV did not react with concentrated hydrochloric acid, alcoholic potassium hydroxide and lithium aluminum hydride. It was attacked neither by carbon monoxide (100 atm.) at 290°C, by triphenyl phosphine at 150°C nor by acetylene dicarboxylic acid ester at 200°C. This remarkable stability of the compound IV together with its chemical and spectroscopic properties seems to indicate its structure involving a cyclobutadiene ring as shown in Fig. 3. Alternative structures such as those involving Co–C sigma bonds or involving tetraphenylbutadiene are less probable.




(IV)

Fig. 3

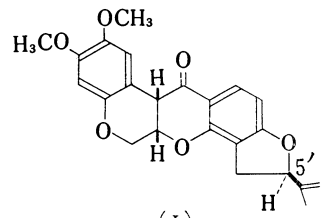
*The Institute of Scientific and Industrial Research*
*Osaka Unversity*
*Sakai-shi, Osaka*

## *The Absolute Configuration of Rotenone*

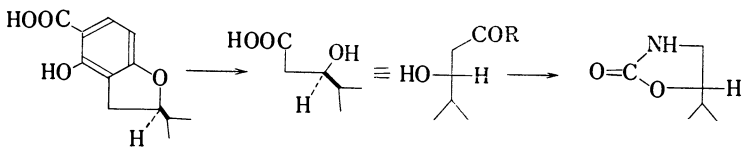
By Masao NAKAZAKI and HISAO ARAKAWA

(Received December 22, 1960)

A recent short communication by Büchi et al.[1] on the absolute configuration of rotenone (I) prompts us to report our current work in this field. They submitted (−)dihydrotubaic acid (II) to exhaustive ozonolysis and obtained (+)3-hydroxy-4-methylpentanoic acid. In order to secure enough starting material, they synthesized (±)3-hydroxy-4-methylpentanoic acid and resolved it through the quinine salt to obtain the (−)acid (enantiomer of III, or IVa in Fischer projection), which they converted, via three steps into (−)2-methylpenta-3-ol with a known absolute configuration[2]. They thus established the (R) configuration[3] at position 5′ of rotenone. We also exhaustively ozonolysed (−)dihydrotubaic acid[4], m. p. 166°C, $[\alpha]_D^{25}$ −103.7° (methanol), then oxidized it with peracetic acid following our previous method[5]. The resulting hydroxy acid III was treated with diazomethane to afford the methyl ester IVb, b. p. 77∼86°C/18 mmHg $[\alpha]_D^{20}$ +19° (ethanol), which was converted into (−)3-hydroxy-4-methylpentanohydrazide IVc,



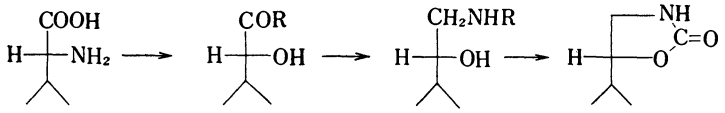
(I)



(II) (III) (IV) (V)

(a) R=OH
(b) R=$OCH_3$
(c) R=$NHNH_2$

1) G. Büchi, J. S. Kaltenbronn, L. Crombie, P. L. Godin and D. A. Whiting, *Proc. Chem. Soc.*, **1960**, 274.
2) See the footnote 4 and 5 of Büchi and Crombie's paper 1).
3) R. S. Cahn, C. K. Ingold and V. Prelog, *Experientia*, **12**, 18 (1956).
4) S. Takei and M. Koide, *Ber.*, **62**, 3030 (1929).
5) H. Arakawa and M. Nakazaki, *Ann.*, **636**, 111 (1960).



(VI) (VII) (VIII) (IX)

(VII): (a) R=OH, (b) R=$OCH_3$, (c) R=$NH_2$

(VIII): (a) R=H, (b) R=$COOC_2H_5$

m. p. 152~153°C, $[\alpha]_D^{19}$+43° (ethanol) with hydrazine. To relate this hydrazide IVc with D-valine, IVc was treated with nitrous acid[6] to afford (−)5-isopropyloxazolidone (V), m. p. 113~114°C, $[\alpha]_D^{18}$−44.5° (ethanol). Found: C, 55.93; H, 8.55; N, 10.98. Calcd. for $C_6H_{11}O_2N$: C, 55.79; H, 8.58; N, 10.84%.

Racemic hydrazide IVc, m. p. 149~150°C, was prepared from ethyl 3-hydroxy-4-methylpentanoate which was prepared by the reduction of ethyl 3-oxo-4-methylpentanoate with sodium borohydride. Reaction with nitrous acid converted the racemic hydrazide IVc into the oxazolidone V, m. p. 87~88°C, the I. R. spectrum of which was found sound superimposable on that of the (−)oxazolidone V from rotenone.

(−)Methyl 2-hydroxy-3-methylbutanoate[7], b. p. 62~63°/15 mmHg, $[\alpha]_D^{17}$−1.4° (etahnol) prepared from D-valine[8], $[\alpha]_D^{16}$−27.6° (6 N hydrochloric acid), was treated with liquid ammonia to give the amide VIIc, m. p. 99~100°C, $[\alpha]_D^{15}$+65.1° (methanol) (racemic compound, m. p. 104~105°C), which in turn was reduced with lithium aluminumhydride to the aminoalcohol VIIIa.

Reaction of sodium methoxide with the ethyl carbamate drivative VIIIb, which was obtained from the aminoalcohol VIIIa by the action of ethyl chlorocarbonate in pyridine, gave (+)5-isopropyloxazolidone (IX), m. p. 113~114°C, $[\alpha]_D^{14}$+44.2° (ethanol). Found: C, 56.18; H, 8.68; N, 11.13%.

(−)5-Isopropyloxazolidone (V) derived from rotenone and (+)5-isopropyloxazolidone (IX) prepared from D-valine exhibited I. R. spectra which could be superimposed in every detail.

In order to make sure that they are enantiomorphic, an equal amount of (+) and (−) oxazolidone were mixed and recrystallized to give the racemic 5-isopropyloxazolidone which melted at 87~88°C, alone and admixed with the synthetic racemic oxazolidone from the racemic hydrazide.

Thus we could confirm Büchi and Crombie's result that rotenone has the (R) configuration at position 5'.

*Department of Chemistry*
*Institute of Polytechnics*
*Osaka City University*
*Kita-ku, Osaka*

6) Cf. C. Schöpf, G. Dummer and W. Wüst, ibid., **626**, 134 (1959); C. Schöpf and W. Wüst, ibid., **626**, 150 (1959).

7) E. Fischer and H. Scheibler, *Ber.*, **41**, 2891 (1908); P. D. Bartlett, M. Kuna and P. A. Leven, *J. Biol. Chem.*, **118**, 303 (1937); W. Klyne, "Progress in Stereochemistry", Vol. I, Butterworth, London (1950), p. 195.

8) We are indebted to Dr. Setsuji Sakurai, Ajinomoto Co., for his generous gift of D-valine.

# *On Some Dark-colored Chlorocuprates(I, II) and Related Compounds. II. Magnetic Susceptibility and Color at Liquid Helium Temperatures*

By Masayasu MORI

(Received December 19, 1960)

A series of dark-colored chloroplumbates(II, IV) and chlorocuprates(I, II) of hexammine-chromium(III) and hexamminecobalt(III) were reported in previous papers[1]. In the present paper a study on the magnetic susceptibility and the color of some of these compounds at liquid helium temperatures will be reported.

The samples studied in this research were "mixed valence compounds", $[Co(NH_3)_6]\cdot[PbCl_6]$ (I), $[Co(NH_3)_6][CuCl_5]_x[CuCl_4]_{1-x}$ ($x\sim0.75$) (II) and a single valence compound, $[Co(NH_3)_6][CuCl_5]$ (III). Measurements of magnetic susceptibility were carried out by the a. c. method[2] using a Hartshorn bridge in the temperature range, 1.3~4.2°K. The frequency used was 90 cycles/sec. The reciprocal values of the molar susceptibility ($\chi_M$) of II and III obtained in this way are plotted against absolute temperature $T$ in Fig. 1.

It is seen that the susceptibility obeys the Curie-Weiss law, $\chi_M=C/(T-\Theta)$, down to the temperature of about 2°K. The Weiss constant, ca. −2.3°K, for both II and III as seen from

1) M. Mori, This Bulletin, 24, 285 (1951); 33, 985 (1960).
2) C. J. Gorter, "Paramagnetic Relaxation", Elsevier, Amsterdam (1947).

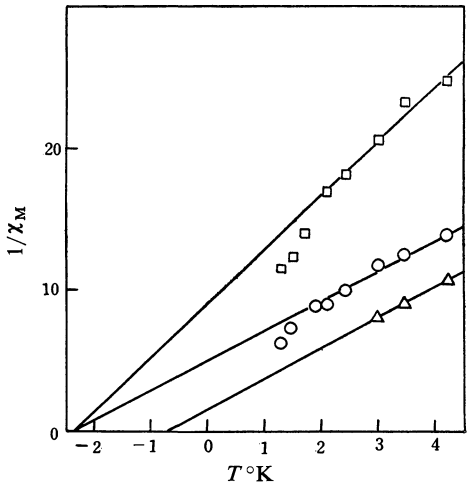



Fig. 1. Plots of $1/\chi_M$ vs. $T$°K.
—△— $CuSO_4 \cdot 5H_2O$
—○— $[Co(NH_3)_6][CuCl_5]_x[CuCl_4]_{1-x}$
—□— $[Co(NH_3)_6][CuCl_5]$

Fig. 1 is considerably different from that of $CuSO_4 \cdot 5H_2O$ (ca. −0.7°K). The magnetic moments per each bivalent copper atom calculated from the slopes are 1.57 B. M. for II and 1.47 B. M. for III*. These values are also abnormal as compared with the value of $CuSO_4 \cdot 5H_2O$, 1.92 B. M. These anomalies seem to be due to the trigonal-bipyramidal structure[3] of chlorocuprate ion, $[CuCl_5]^{3-}$, and not to the $Cu^{I}$–$Cu^{II}$ interaction, since II and III exhibit similar magnetic behaviors.

No marked change of color was observed when II (brownish black) and III (yellowish orange) were dipped in liquid helium except that the color of III appeared a little lighter. On the other hand the color of I (brownish black) changed into brown in liquid air and brick red in liquid helium. The cause and reason of such different behaviors of chloroplumbate(II, IV) and chlorocuprate(I, II) are not yet clear.

The author is very grateful to Professor Taiichiro Haseda of Tohoku University for his kind guidance and valuable suggestions in the magnetic measurement. The experiment has never been possible without the offer of the laboratory facilities for liquid helium experiments at the Research Institute for Iron, Steel and Other Metals in the Tohoku University.

*Institute of Polytechnics*
*Osaka City University*
*Kita-ku, Osaka*

* In the calculation of this value the ratio of $Cu^{II}$ content to the total copper was assumed to be $x = 0.75$.

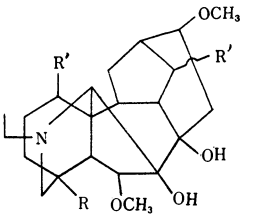
3) M. Mori, Y. Saito and T. Watanabe, This Bulletin, to be published.

# *The Nuclear Magnetic Resonance Spectra of Some Aconite Bases: Lucaconine and Lucidusculine*

By Akira SUZUKI, Takashi AMIYA and Takeshi MATSUMOTO

(Received December 26, 1960)

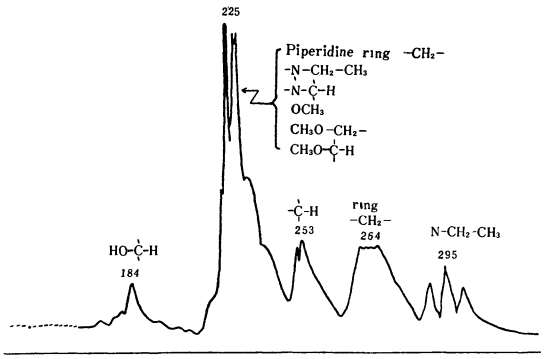
An alkaloid lucaconine has beeen isolated from *Aconitum luciduscul*um, Nakai[1]. Recently, the alkaloid was identified[2] as delcosine[3] obtained from *Delphinium conolida* L. Based on several reactions of delcosine, Marion and others[4] assumed that the alkaloid possesses the same carbon-nitrogen framework and oxygen pattern as lycoctonine II[5] and suggested a tentative structure I. However, there has been no direct evidence for this substance bearing the $CH_2OCH_3$ group for R.




I R=$CH_2OCH_3$, R'=OH
II R=$CH_2OH$, R'=$OCH_3$

In *Aconitum* and *Delphinium* alkaloids, R is generally the methyl, hydroxymethyl or methoxymethyl group[6]. However, the possibility of the presence of the hydroxymethyl group in lucaconine can be excluded, since corresponding aldehydic or acidic products have not been obtained by the oxidation conditions which are expected to lead to these products[1,4,7]. The observation of NMR spectrum of lucaconine has been made to determine whether R is methyl or methoxymethyl. The NMR spectrum at 40 Mc. of lucaconine in pyridine solution is shown in Fig. 1. In this figure, although the other *Aconitum* alkaloids in which R is methyl have a strong singlet absorption characteristic of

1) H. Suginome, S. Kakimoto, J. Sonoda and S. Noguchi, *Proc. Japan Acad.*, **22**, 122 (1946); H. Suginome and S. Furusawa, This Bulletin, **32**, 352 (1959); S. Furusawa, ibid., **32**, 399 (1959); T. Amiya and T. Shima, ibid., **31**, 1083 (1958).
2) T. Amiya and T. Shima, in preparation.
3) L. N. Markwood, *J. Am. Pharm. Assoc.*, **13**, 696 (1924).
4) R. Anet, D. W. Clayton and L. Marion, *Can. J. Chem.*, **35**, 397 (1957); R. Anet and L. Marion, ibid., **36**, 766 (1958); V. Skaric and L. Marion, *J. Am. Chem. Soc.*, **80**, 4434 (1958).
5) M. Przybylska and L. Marion, *Can. J. Chem.*, **34**, 185 (1956).
6) O. E. Edwards, L. Marion and K. H. Palmer, *Can. J. Chem.*, **36**, 1097 (1958); K. Wiesner, D. L. Simmons and L. R. Fowler, *Tetrahedron Letters*, **No. 18**, 1 (1959).
7) E. Ochiai, T. Okamoto and M. Kaneko, *Chem. Pharm. Bull.*, **6**, 730 (1958).

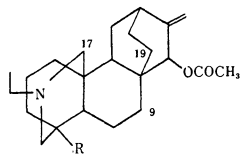



| | | | | | | |
|---|---|---|---|---|---|---|
| Relative area | Found | 1.6 | 19 | 4.8 | 7.6 | 3 |
| | (Calcd. on formula I) | (2) | (18) | (4) | (8) | (3) |

Fig. 1. The proton spectrum of lucaconine (taken on Varian 40 Mc. instrument).

$-\overset{|}{\underset{|}{C}}-CH_3$ group at about 318 c. p. s. from the signal of $\alpha$-proton of pyridine[8], such absorption can not be recognized for lucaconine. Accordingly, R is concluded to be $CH_2OCH_3$ in lucaconine. The anticipated singlet peak due to the methylene group of $-\overset{|}{\underset{|}{C}}-CH_2-OCH_3$ is, however, obscure[9] in Fig. 1, probably because of the overlapping with strong peaks of methoxyl groups, and of possible broadening due to the unequivalence of two methylene protons caused by the neighbouring asymmetric carbon atom[10]. A tentative interpretation based on the suggested structure I is also given in Fig. 1[11].

We next examined NMR spectrum of an aconite base lucidusculine[12]. Recently, one of us (T. A.) proposed formula III for the partial structure of lucidusculine on the basis of some chemical transformations[13].




III R=$CH_2OH$, one secondary OH group on the ring. Possible linkage between $C_{17}$-$C_{19}$ or $C_{17}$-$C_9$.

IV R=$CH_3$, two secondary OH groups on the ring. Possible linkage between $C_{17}$-$C_{19}$ or $C_{17}$-$C_9$.

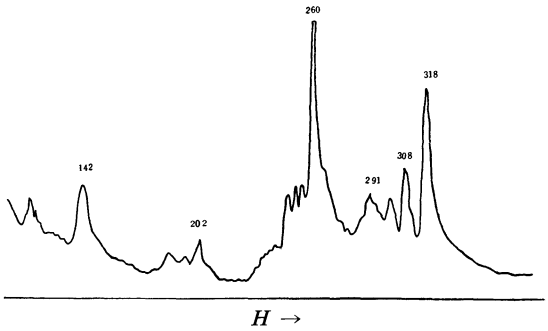



Fig. 2. The proton spectrum of lucidusculine.

The NMR trace at 40 Mc. of lucidusculine in pyridine is shown in Fig. 2. Clearly, the singlet band at 318 c. p. s. is to be ascribed to the methyl group on a quaternary carbon atom. This observation forces one to the conclusion that in lucidusculine R is actually the methyl group. The two hydroxyl groups in lucidusculine may both be secondary, since they are easily acetylated[12]. From above described results, a modified formula IV is now suggested as the partial structure of lucidusculine.

The authors express thier sincere thanks to Professor Genjiro Hazato and Dr. Kensuke Takahashi of Tohoku University for the measurement of NMR spectra. They are also grateful to Professor Harusada Suginome for his encouragement in this work.

*Department of Chemistry*
*Faculty of Science*
*Hokkaido University*
*Sapporo*

8) A. Suzuki, T. Amiya, K. Takahashi and T. Matsumoto, unpublished work.

9) In the NMR spectrum of lycoctonine[8], the absorption due to methylene group of $-\overset{|}{\underset{|}{C}}-CH_2OH$ is also obscure.

10) L. M. Jackman, "Applications of Nuclear Magnetic Resonance Spectroscopy in Organic Chemistry", Pergamon Press, London (1959), p. 102.

11) The signal of the methine proton of methoxycyclohexanes (H-C-$OCH_3$) has been shown to appear at a position very close to the methoxyl group. R. U. Lemieux, R. K. Kullning, H. J. Bernstein and W. G. Schneider, *J. Am. Chem. Soc.*, **80**, 6098 (1958).

12) R. Majima and S. Morio, *Ber.*, **65**, 599 (1932); H. Suginome, S. Kakimoto and J. Sonoda, *J. Fac. Sci. Hokkaido Univ.*, Ser. III, Chem., **4**, 25 (1950); H. Suginome and S. Kakimoto, This Bulletin, **32**, 352 (1959): T. Amiya, ibid., **32**, 1133 (1959).

13) T. Amiya, This Bulletin, **33**, 1175 (1960).

## *The Interaction of a Surfactant with a Monolayer Studied by Radiotracer Method*

By Ryosuke SHIMOZAWA and Ryohei MATUURA

(Received February 6, 1961)

The adsorption of sodium alkyl sulfates at the solution-air interface was studied by radiotracer method and the result was already reported[1-3]. In this case if an insoluble monolayer is present on the surface of the solution, the surface count of the radioactive detergent may be different from that of the free surface, and it is expected that we may be able to know the interaction of the detergent with the monolayer substance from this difference in the surface count. We measured the interaction of sodium dodecyl sulfate (SDS) with the monolayer of octadecyl amine, octadecyl alcohol and nylon 6 spread on the surface of the solution by tracing sulfate sulfur tagged with $^{35}S$. The apparatus was almost the same as that used for measuring the adsorption of the detergent at the free surface[1]. The radioactivity of the surface of the SDS solution in the lucite tray was measured first. Then the monolayer was spread on this solution and the surface area was kept constant with the surface pressure of about 10 dyn./cm. The radioactivity of the surface in this state was measured with the same geometry as above. The spreading solvents used were a mixture of one volume ethanol and two volume benzene for octadecyl amine and octadecyl alcohol and a mixture of one volume phenol and three volume benzene for nylon 6. The result is shown in Fig. 1, in which the abscissa represents the time after spreading the monolayer on the surface and the ordinate is the surface count.

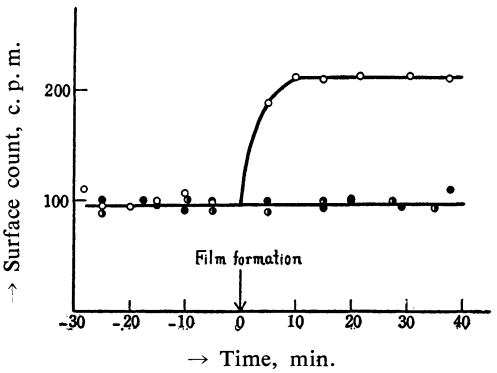



Fig. 1. Change in surface counting rate before and after film formation. Substrate is $8\times10^{-5}$ mol./l. SDS solution.
○ Octadecyl amine-SDS series
◑ Octadecyl alcohol-SDS series
● Nylon 6-SDS series

From this figure it is evident that in the presence of octadecyl amine monolayer the surface count increases to more than twice the value of the free surface, while in the case of octadecyl alcohol and nylon 6 no change is observed after spreading the monolayer of these substances. These results may show that the monolayer of octadecyl amine interacts with the molecule of SDS in the substrate solution remarkably but that of octadecyl alcohol and nylon 6 affects no such interaction as the amine monolayer. Goddard and Schulman[4] measured the surface pressure of an eicosyl amine monolayer at constant area on the surface of water and found that a remarkable increase in pressure took place by injecting sodium hexadecyl sulfate (SHS) into the substrate solution beneath the monolayer. They explained the result in terms of penetration of SHS into the monolayer and formation of a 1 to 1 stoichiometric complex. The present experiment confirms directly the strong interaction of the long chain amine monolayer with sodium alkyl sulfate in the solution. However, we found that the surface pressure of the monolayer of octadecyl alcohol and nylon 6 increases appreciably by the presence of SDS in the solution just as is the case with the amine monolayer, but the surface count with the monolayer of the former substances does not differ from the value without the monolayer contrary to the case of the latter substance, as shown in Fig. 1. These results suggest that the mechanism of the interaction of the long chain amine monolayer with SDS is different from that of the monolayer of long chain alcohol or nylon 6 with it. The quantitative treatment of the data and the detailed discussion will be reported in future.

*Department of Chemistry*
*Faculty of Science*
*Kyushu University*
*Hakozaki, Fukuoka*

1) R. Matuura, H. Kimizuka, S. Miyamoto and R. Shimozawa, This Bulletin, 31, 532 (1958).
2) R. Matuura, H. Kimizuka, S. Miyamoto, R. Shimozawa and K. Yatsunami, ibid., 32, 404 (1959).
3) R. Matuura, H. Kimizuka and K. Yatsunami, ibid., 32, 646 (1959).
4) E. D. Goddard and J. H. Schulman, *J. Colloid Sci.*, 8, 309 (1953).

## *Electron Spin Resonance Study on Photolysis of Acetone and Benzophenone*

By Keiji KUWATA and Kōzō HIROTA

(Received December 24, 1960)

Recently several trapped radicals formed in photolysis have been identified with organic compounds of low molecular weight by the ESR method[1]. By the use of a X-band spectrometer of high sensitivity it became possible to study the radical intermediates formed in photolysis of some ketones. Preliminary investigation on acetone and benzophenone will be reported here.

According to the kinetic studies on the photolysis of gaseous acetone, formation of several types of free radicals was proposed[2]:

$$CH_3COCH_3 + h\nu \rightarrow \dot{C}H_3CO + \dot{C}H_3$$

$$(\dot{C}H_3CO \rightarrow \dot{C}H_3 + CO)$$

$$\dot{C}H_3 + CH_3COCH_3 \rightarrow CH_4 + \dot{C}H_2COCH_3$$

$$\dot{C}H_2COCH_3 \rightarrow \dot{C}H_3 + CH_2CO$$

$$\dot{C}H_3 + \dot{C}H_2COCH_3 \rightarrow CH_3COCH_2CH_3$$

In the liquid phase photolysis of the both ketones, formation of the active intermediates was proposed[5], but their natures were not well known. Observation of ESR for these free radical intermediates will give a confirmative evidence for such mechanisms.

The spectrometer used was a type of high frequency field modulation, being similar to that of Fujimoto and Ingram, but the frequency of the field modulation was 455 kilocycles/sec. Design of a low temperature resonant cavity is shown in Fig. 1.

After an irradiation of ultraviolet light for several hours, any signal could not be observed in pure acetone, while a broad singlet was observed in pure benzophenone and in 0.1~1% solutions of the both ketones. However, the intensity of the signal decreased rapidly in the case of acetone, a half life being 50 min. at about 77°K. The characteristics of the signals observed are shown in Table I.

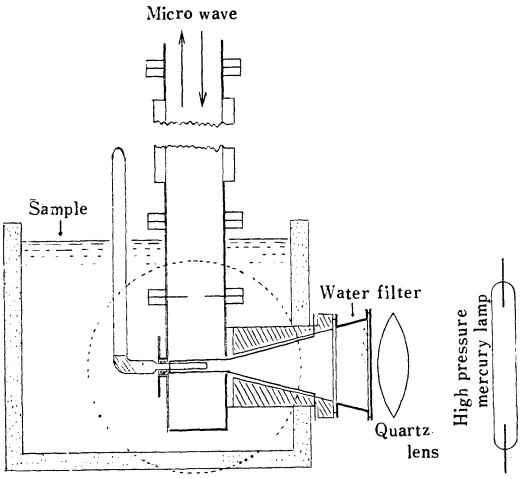



Fig. 1

TABLE I. ESR OF TRAPPED RADICALS AT ABOUT 77°K

| | Line width ($H_{msl}$) | Line shape | $g$-Factor |
|---|---|---|---|
| Acetone in ethanol and EPA (Ether, iso-Pentane and Alcohol) | 30 gauss | (gaussian) | 2.003 |
| Benzophenone | 23 gauss | 〃 | 2.003 |
| Benzophenone in ethanol and EPA | 24 gauss | 〃 | 2.003 |

An unstable free radical in the solution of acetone would be the methyl radical, but confirmative evidence for this assignment was not yet given since no hyperfine structure was observed. In the case of benzophenone a hyperfine structure neither of a quartet for the phenyl radical nor of a quartet with the small separations for the benzoyl radical was observed. The result indicates that two types of free radicals were present together or broadning of the line width occurred by some reasons, so that the hyperfine structure was smeared out. Detailed research will be published elsewhere.

The authors wish to express their thanks to Dr. M. Fujimoto and also to Dr. K. Morigaki of Osaka University for their suggestions on design of the low temperature cavity.

*Department of Chemistry*
*Faculty of Science*
*Osaka University*
*Nakanoshima, Osaka*

1) Cf. A. M. Bass and H. P. Broida, "Formation and Trapping of Free Radicals", Academic Press, New York (1960), p. 239.
2) Cf. J. A. Leermakers, *J. Am. Chem. Soc.*, **16**, 1899 (1934).
3) H. H. Glazebrock and T. G. Pearson, *J. Chem. Soc.*, **1937**, 557.
4) S. W. Benson and G. S. Fordes, *J. Am. Chem. Soc.*, **65**, 1399 (1943).
5) E. J. Bowen and E. de la Prandiere, *J. Chem. Soc.*, **1934**, 1503.

## *Reaction of Tetraphenyl Titanate with Amines*

By Takeshi Yoshino, Ichiro Kijima and Miyoko Ochi

(Received on December 26, 1960)

In the previous paper, the reaction of tetraphenyl titanate with ammonia, phenols, acetophenone and esters have been reported[1]. In the course of the synthetical studies on the organo titanium compounds, it has been found that the addition compounds of tetraphenyl titanate were more stable than that of tetraalkyl titanates. In the present communication, the reaction of tetraphenyl titanate (TPhT) with aliphatic or aromatic amines are described.

When TPhT was made to react with aliphatic amines (*n*-butylamine, tri-ethylamine, tri-*n*-butylamine) in toluene solution, addition compounds of TPhT could not be isolated. However, when aromatic amines (aniline, $\alpha$-naphthylamine, pyridine) were used, they gave addition compounds with TPhT (molar ratio of 1 : 1). When the addition compound of TPhT with phenol I reacted with aromatic amines, the addition compound I was converted into the addition compounds of the corresponding amines used. They also were converted into the addition compound of TPhT with ammonia. The reaction of TPhT with hexamethylenediamine gave yellow crystals, which were considered as the addition compound of TPhT with hexamethylenediamine (molar ratio of 2 : 1).

### Experimental

**1) Addition Compounds of TPhT with Aromatic Amines.** — Into a solution of TPhT (8.0 g.) in toluene (50 ml.), freshly distilled aniline (2.1 g.) was added and refluxed for 15 min. After the reaction mixture was allowed to stand at room temperature, the crystals separated out were collected by filtration and dried under reduced pressure, 8.0 g. of yellowish orange crystals were obtained. They were recrystallized from toluene. M. p. 181~183°C. (Found: Ti, 9.64; N, 2.80. Calcd. for $C_{30}H_{27}O_4NTi$: Ti, 9.33; N, 2.73%). In a similar way the following addition compounds were obtained: $Ti(OC_6H_5)\cdot C_{10}H_7NH_2$, orange crystals, m. p. 168~169°C. (Found: Ti, 8.49; N, 2.60. Calcd. for $C_{34}H_{29}O_4NTi$: Ti, 8.50; N, 2.49%); $Ti(OC_6H_5)_4\cdot C_5H_5N$, reddish orange crystals, m. p. 191~192°C. (Found: Ti, 9.53; N, 2.83. Calcd. for $C_{29}H_{25}O_4NTi$: Ti, 9.59; N, 2.80%).

When aliphatic amines (*n*-butylamine, tri-ethylamine, tri-*n*-butylamine) were used, addition compound of TPhT could not be isolated.

**2) Reaction of the Addition Compound $Ti(OC_6H_5)_4\cdot C_6H_5OH$ (I) and Aromatic Amines.**— To a solution of the addition compound I (4.0 g.), in toluene (15 ml.), aniline (2.0 g.) was added and the solution was refluxed for 15 min. After allowed to stand at room temperature, it deposited yellowish orange crystals. They were purified as described under (1), m. p. 183°C. (Found: Ti, 9.08; N, 2.86. Calcd. for $C_{30}H_{27}O_4NTi$; Ti, 9.33; N. 2.73%). $Ti(OC_6H_5)_4\cdot C_6H_5OH+C_6H_5NH_2 \rightarrow Ti(OC_6H_5)_4\cdot C_6H_5NH_2+C_6H_5OH$. In a similar way, by the use of $\alpha$-naphthylamine or pyridine, the addition compound I was converted into the corresponding addition compounds of TPhT with the above amines respectively: $Ti(OC_6H_5)_4\cdot C_{10}H_7NH_2$, m. p. 167~168°C. (Found: Ti, 8.91; N, 2.63, Calcd. for $C_{34}H_{29}O_4NTi$: Ti, 8.50; N, 2.49%); $Ti(OC_6H_5)_4\cdot C_5H_5N$, m. p. 191~192°C. (Found: Ti, 9.67; N, 2.88. Calcd. for $C_{29}H_{25}O_4NTi$: Ti, 9.59; N, 2.80%).

**3) Reaction of the Addition Compound $Ti(OC_6H_5)_4\cdot C_6H_5NH_2$ (II) and Ammonia.** — When excess of dry ammonia gas was passed at room temperature to a solution of the addition compound II (2.5 g.), in toluene (10 ml.), the addition compound II was converted into the addition compound of TPhT with ammonia III, (molar ratio of 1 : 1). M. p. 201~202°C. (Found: Ti, 10.89; N, 3.17. Calcd. for $C_{24}H_{23}O_4NTi$: Ti, 10.95; N. 3.20%).

$$Ti(OC_6H_5)_4\cdot C_6H_5NH_2+NH_3 \rightarrow Ti(OC_6H_5)_4\cdot NH_3+C_6H_5NH_2$$

In a similar way, the addition compounds $Ti(OC_6H_5)_4\cdot C_{10}H_7NH_2$ and $Ti(OC_6H_5)_4\cdot C_5H_5N$ were converted into III.

**4) Reaction of TPhT with Hexamethylenediamine.**—Into a solution of TPhT (8.7 g.) in toluene (60ml.), hexamethylenediamine (0.6 g.) was added and refluxed for 30 min. After the reaction mixture was allowed to stand at room temperature, the crystals were collected by filtration, washed with toluene and dried under reduced pressure, 4.7 g. of powdery yellow crystals were obtained. M. p. 237~239°C. The analytical data showed this compound to be an addition compound of TPhT with hexamethylenediamine (molar ratio of 2 : 1), (Found: Ti, 10.13; N, 3.45. Calcd. for $C_{54}H_{56}O_8N_2Ti_2$: Ti, 10.01; N, 2.92%).

*Department of Applied Chemistry*
*Tokyo College of Science*
*Shinjuku-ku, Tokyo*

1) T. Yoshino et al., *J. Chem. Soc. Japan, Ind. Chem. Sec.* (*Kogyo Kagaku Zasshi*), **63**, 1758 (1960).

# *On the Oxidation of β-Aminopropionitrile. II*

By Toshihisa TACHIKAWA

(Received June 16, 1960)

In the previous paper of this series[1], it was reported that β-aminopropionitrile became viscous and yielded a resinous material, when it had been stored in the air for a prolonged period. This resinous material was also obtained by bubbling air through β-aminopropionitrile and the following structure has been proposed for the oxidation product:

$$\begin{matrix}\bar{O}\text{-}\overset{+}{N}\text{-}CH_2CH_2CONHCH_2CH_2CONH_2 \\ \quad\| \\ \quad N\text{-}CH_2CH_2CONHCH_2CH_2CONH_2\end{matrix}$$

During the course of oxidation experiments, the evolution of a small amount of hydrogen peroxide was noticed. This phenomenon suggests that the oxidation reaction may be accelerated in the presence of hydrogen peroxide. The present work has been carried out to clarify the effect of hydrogen peroxide in the oxidation processes.

The effect of hydrogen peroxide on the oxidation of β-aminopropionitrile was investigated by means of ultraviolet absorption spectrum. As is shown in Fig. 1, the oxidation product similar to that in the air was obtained in the presence of 1 mol. of hydrogen peroxide per mole of β-aminopropionitrile. This result agrees quite well with that obtained from the infrared absorption measurement. Further-

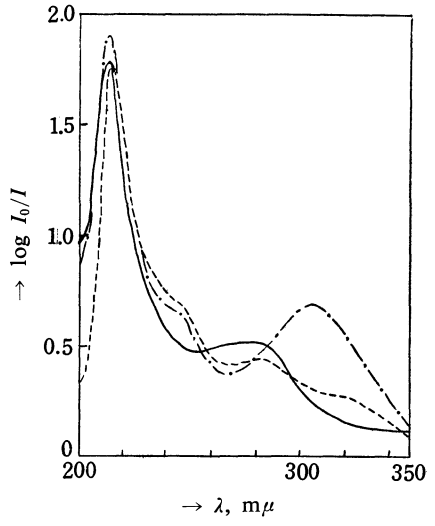



Fig. 1. Effect of mole ratios ($H_2O_2$/β-aminopropionitrile).

- · - Mole ratio 0.5
---- 〃 0.83
—— 〃 1.0

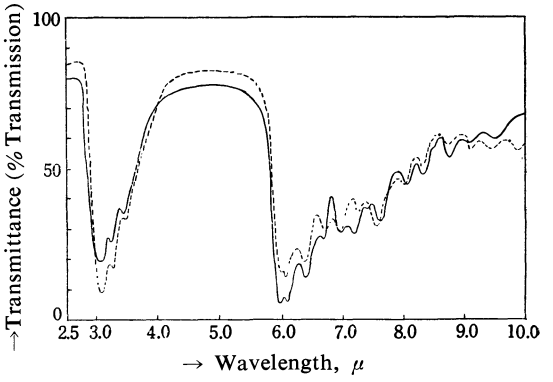



Fig. 2. Infrared absorption spectrum.

---- Air oxidation
—— $H_2O_2$ oxidation

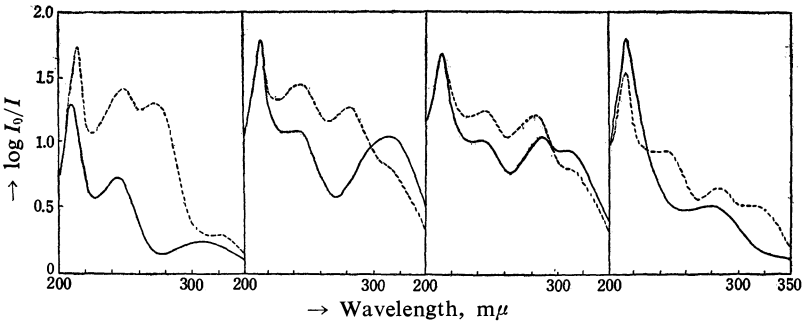
more, the evidence that the oxidation product by hydrogen peroxide is the same as that in the air was also confirmed by the rapid evolution of gaseous nitrogen when this product was decomposed with sulfuric acid and by the formation of β-alanine when this product was reduced with tin and concentrated hydrochloric acid. It is understood from Table I, that 1 mol. of ammonia was evolved from 2 mol. of β-aminopropionitrile in the course of this oxidation reaction by hydrogen peroxide as was observed in the oxidation by air. Therefore, there results strongly suggest that the oxidation of β-aminopropionitrile by hydrogen peroxide proceeds through the same mechanism as that by air. At the mole ratio of 0.50 (hrdrogen peroxide/β-aminopropionitrile), a characteristic ultraviolet absorption spectrum was obtained, which may correspond to some intermediates of this oxidation reaction. Thus, ultraviolet absorption spectra were measured at different mole ratios.

It is understood from Fig. 3 that the spectra taken immediately after sampling show the presence of absorptions at 212～215, 240～242 and 307～310 mμ regardless of their mole ratios. However, on standing for 48 hr., absorptions at 212～215, 240～242 and 307～310 mμ were obtained only at mole ratios smaller than 0.7

1) T. Tachikawa, This Bulletin, 33, 1181 (1960).

TABLE I. $NH_3$ GENERATED

| Nitrile g. used | 25% $H_2O_2$ g. used | $\frac{H_2O_2}{\text{Nitril}}$ mole ratio | $NH_3$ generated g. | $\frac{\text{moles of } NH_3}{\text{moles of nitrile}}$ |
|---|---|---|---|---|
| 1.0 | 1.6 | 0.83 | 0.130 | 0.535 |
| 1.0 | 1.6 | 0.83 | 0.125 | 0.514 |
| 10.0 | 19.4 | 1.00 | 1.399 | 0.566 |




Mole ratio 0.1 Mole ratio 0.3 Mole ratio 0.7 Mole ratio 1.0

Fig. 3. Ultraviolet spectra of the reaction intermediates.
---- Immediately after sampling —— After 48 hr.

(hydrogen peroxide/β-aminopropionitrile), and at mole ratios greater than 0.7 an absorption at 280 mμ appears as an absorption at 307~310 mμ decreases.

Since several reaction intermediates were probably contained in a sample when measurements were performed right after sampling, it was not possible to postulate a reasonable reaction process and products. However it was inferred from the spectral measurements of samples which were allowed to stand for more than 48 hr. after sampling that the second reaction took place in the presence of 0.7 mol. of hydrogen peroxide against one mole of β-aminopropionitrile.

The mechanism proposed for the oxidation of β-aminopropionitrile is as follows:

1) In the first step of the oxidation reaction, β-aminopropionitrile is presumably transformed into β-hydroxylaminopropionitrile. This reaction process agrees with the known fact that an amino group is oxidized by hydrogen peroxide to yield a hydroxylamine group[2,3]. β-Hydroxylaminopropionitrile which was synthesized from hydroxylamine and acrylonitrile, was very unstable and transformed into a viscous substance in air. An infrared absorption spectrum of this viscous material showed six bands at 3.1, 3.35, 3.45, 6.05, 6.45, 6.75 μ, as shown in Fig. 4. This spectrum was similar to that of the oxidation product by air or hydrogen peroxide.

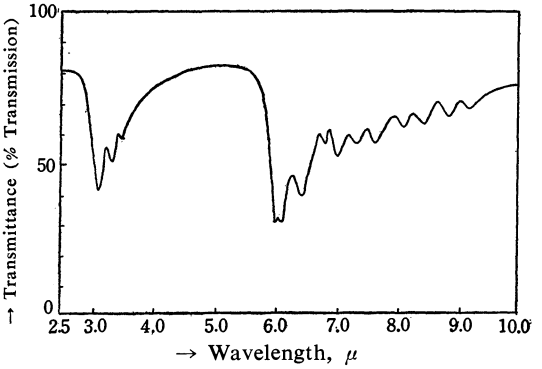



Fig. 4. Infrared absorption spectrum of the oxidation product of β-hydroxylaminopropionitrile.

2) At the next stage, β-hydroxylaminopropionitrile (or β-aminopropionitrile itself) may be hydrolyzed to yield β-hydroxylaminopropioamide (or β-aminopropioamide). This postulate is considered to be reasonable because a nitrile radical undergoes hydrolysis to produce an acid amide group in the presence of hydrogen peroxide as a catalyst[4].

3) An acid amide group thus formed reacts with a hydroxylamino group as the third step of the reaction. This reaction is well known as the reaction for the qualitative test of an acid amide group.

4) It is known that a hydroxylamino compound is a strong reducing agent and is oxidized

2) L. Mamlock and R. Wolffenstein, *Ber.*, 33, 159 (1900).
3) R. A. Henry and W. M. Dehn, *J. Am. Chem. Soc.*, 72, 2780 (1950).
4) S. Soloway and A. Lipschiz, *Anal. Chem.*, 24, 898 (1952).

to a nitroso compound. Therefore, a hydroxamic acid produced in the reaction process shown by Eq. 1 may be reduced to -CONH- group.

$$R\text{-}CONH_2 + R'\text{-}NHOH \rightarrow R\text{-}\underset{\underset{O}{\|}}{C}\text{-}\underset{\underset{OH}{|}}{N}\text{-}R' + NH_3 \quad (1)$$

$$R\text{-}\underset{\underset{O}{\|}}{C}\text{-}\underset{\underset{OH}{|}}{N}\text{-}R' + R'\text{-}NHOH \rightarrow R\text{-}\underset{\underset{O}{\|}}{C}\text{-}NH\text{-}R' + R'\text{-}NO + H_2O \quad (2)$$

5) The final product of this oxidation reaction is considered to be an azoxy compound. This final reaction process may be considered reasonable accordance to the work by Bamberger[5], who reported, that the formation of azoxy compound from a hydroxylamino compound has taken place with the evolution of hydrogen peroxide, assuming a nitroso compound as an intermediate.

The oxidation process mentioned above is formulated as follows:

$$CNCH_2CH_2NH_2 + 1/2\ O_2(H_2O_2) \rightarrow CNCH_2CH_2NHOH + (H_2O) \quad (3)$$

$$CNCH_2CH_2NHOH + H_2O \rightarrow NH_2COCH_2CH_2NHOH \quad (4)$$

$$3NH_2COCH_2CH_2NHOH \rightarrow \underset{(I)}{NH_2COCH_2CH_2NHCOCH_2CH_2NHOH} + NH_2COCH_2CH_2NO + NH_3 + H_2O \quad (5)$$

$$(I) + 1/2\ O_2(H_2O_2) \rightarrow \underset{(II)}{NH_2COCH_2CH_2NHCOCH_2CH_2NO} + H_2O(2H_2O) \quad (6)$$

$$(I) + (II) + 1/2\ O_2(H_2O_2) \rightarrow \overset{-}{O}\text{-}\overset{+}{N}CH_2CH_2CONHCH_2CH_2CONH_2 \quad \underset{\|}{N}CH_2CH_2CONHCH_2CH_2CONH_2 + H_2O_2(H_2O + H_2O_2) \quad (7)$$

The secondary reaction process observed at higher mole ratios of hydrogen peroxide may be shown by Eq. 5 which corresponds to the reduction reaction by a hydroxylamino radical.

## Experimental

**Oxidation Reaction of β-Aminopropionitrile with Hydrogen Peroxide.**—To β-aminopropionitrile (15 g.) which was placed in a 100 cc. three-necked flask equipped with a thermometer, a dropping funnel and a capillary, 25% hydrogen peroxide (29.3 g.) was added dropwise at below 5°C and at reduced pressure to removed ammonia gas as soon as it was reduced during the course of the reaction. The reaction was exothermic and ammonia gas was evolved violently as hydrogen peroxide was added to the reaction mixture. The reaction mixture become viscous as the reaction proceeded. After the addition of hydrogen peroxide was completed, the temperature of the reaction mixture was brought up to 90°C to remove water and β-aminopropionitrile unreacted. The yellow, amorphous, and hydroscopic solid (17 g.) was obtained from the residue, which decomposed at 120°C.

Found: C, 43.53; H, 6.25; N, 24.62. Calcd. for $C_{12}H_{22}N_6O_5$: C, 43.63; H, 6.71; N, 24.22%.

By means of the same method in the previous paper[1], nitrogen gas (6.77 ml.) was evolved from this sample (0.1014 g.) by the decomposition with sulfuric acid and β-alanine (9.1 g.) was obtained from this sample (20 g.) by the reduction with tin (19.1 g.) and 35% hydrochloric acid (75 g.).

Found: C, 40.62; H, 7.65; N, 15.77. Calcd. for $C_3H_7NO_2$: C, 40.44; H, 7.92; N, 15.72%.

**Ultraviolet Absorption Spectrum.**—The Shimazu spectrophotometer model QR 51 equipped with a cell of 1 cm. path length was used throughout this work. Ultraviolet spectral measurements of the reaction intermediates were performed as follows: The 50% aqueous solution of β-aminopropionitrile (10 g.) through which nitrogen gas was bubbled was kept at below 5°C with stirring. After a known amount of hydrogen peroxide was added, nitrogen gas was introduced further into the reaction mixture and the ammonia gas which evolved was removed. Then, 0.01~0.03 cc. of the reaction mixture was pipetted out and measured spectroscopically after dilution to 50 cc. with water. Samples which were allowed to stand for over 48 hr. were also measured, at which time the reaction stopped completely.

**Infrared Absorption Spectrum.** — A sample for the spectral measurement was prepared in the following procedure: A sample was dissolved in methanol to obtain 3% solution. Then, a piece of thin film was prepared on a cell by evaporating methanol from the solution. The infrared spectrum was obtained with a Perkin-Elmer spectrophotometer model 21 equipped with a sodium chloride prism.

**Synthesis of β-Hydroxylaminopropionitrile.** — Acrylonitrile (80 g.) is added slowly while cooling to about 10°C into freshly prepared solution of hydroxylamine (33 g.) in methyl alcohol. After being allowed to stand for two hours at room temperature the methanol and unchanged acrylonitrile are distilled off. The residue consists of a practically quantitative yield of β-hydroxylamino-propionitrile. It is a thick liquid which decomposes when distilled even under a pressure of a few millimeters of mercury. It is extremely sensitive to oxidation; it becomes viscous in the air. The colorless amorphous and hygroscopic solid was obtained by treating this viscous material with anhydrous acetone. An infrrared absorption spectrum was recorded with a Perkin Elmer spectrophotometer model 21 on the sample film which was prepared by evaporating 2~3 drops of 3% methanolic solution on the sodium chloride window.

The author wishes to express his sincere thanks to Professor Ryozo Goto of Kyoto University for his kind advice, and also to

5) E. Bamberger, *Ber.*, 33, 113 (1900).

Mr. Murataro Nakashima, President of Kunoshima, Chemical Co., for his permission to publish this paper.

*Research Laboratory of Kunoshima Chemical Industry Co., Ltd.*
*En-ichi-cho, Mihara*

# *On the Oxidation of β-Aminopropionitrile. III*

By Toshihisa TACHIKAWA

(Received June 16, 1960)

In the previous papers of this series[1,2], the structure of a resinous oxidation product of β-aminopropionitrile was proposed. β-Aminopropionitrile was oxidized using either air or hydrogen peroxide as an oxidizing agent. In the previous paper[2], it was proposed that in the first step of this oxidation process β-aminopropionitrile was oxidized into β-hydroxylaminopropionitrile which was hydrolyzed to produce an acid amide compound and in the second step, these intermediates reacted to form a compound with azoxy group and -CONH- linkage.

In the present investigation, five different derivatives of β-aminopropionitrile were prepared and the effect of the substituents in the oxidation reaction was studied in addition to the identification of oxidation products of these derivatives and to the investigation of reaction mechanisms. These five derivatives of β-aminopropionitrile are as follows:

α-Methyl-β-aminopropionitrile (I)
β-Methyl-β-aminopropionitrile (II)
β-Ethylaminopropionitrile (III)
β-Dimethylaminopropionitrile (IV)
β-Methyl-α-aminopropionitrile (V)

These derivatives did not undergo any change either on standing in the open air or by bubbling air through the materials. On the other hand, these materials were oxidized with hydrogen peroxide and the results are summarized in Table I. Hygroscopic materials were obtained as oxidation products of compounds I and II. These products are quite similar to the oxidation product of β-aminopropionitrile in their hygroscopic properties. The oxidation products of I and II have their softening points at 110°C. Their infrared absorption spectra are shown in Figs. 1 and 2.

As observed in the oxidation product of β-aminopropionitrile, an absorption band at

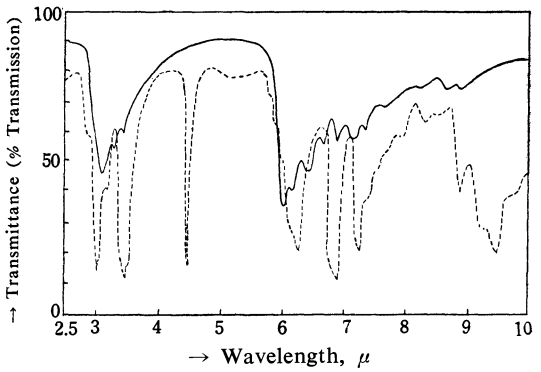



Fig. 1. Infrared absorption spectrum.
---- α-Methyl-β-aminopropionitrile
—— Oxidation product

TABLE I. PRODUCTS BY $H_2O_2$ OXIDATION

| Amino-nitrile | Yield % | Property of the product | Analysis Found C | H | N | Calcd. C | H | N | |
|---|---|---|---|---|---|---|---|---|---|
| I | 45.2 | Yellow hygroscopic solid | 49.9 | 7.9 | 21.2 | 49.7 | 7.7 | 21.8 | for $C_{16}H_{30}N_6O_5$ |
| II | 47.8 | Yellow hygroscopic solid | 49.2 | 7.8 | 21.0 | 49.7 | 7.7 | 21.8 | for $C_{16}H_{30}N_6O_5$ |
| III | No change | — | | | | | | | |
| IV | 46.2 | Needle crystal m. p. above 250°C | 44.9 | 9.5 | 21.0 | 45.4 | 9.2 | 21.2 | for $C_5H_{12}N_2O_2$ |
| V | No change | — | | | | | | | |

1) T. Tachikawa, This Bulletin, 33, 1181 (1960).
2) T. Tachikawa, ibid., 34, 461 (1961).

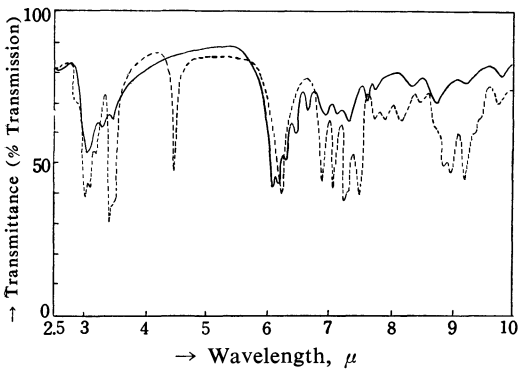
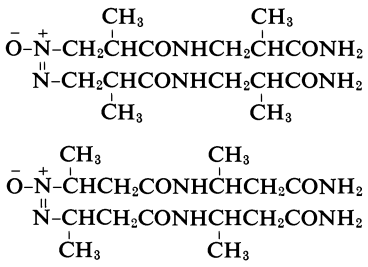



Fig. 2. Infrared absorption spectrum.
---- β-Methyl-β-aminopropionitrile
—— Oxidation product

4.5 μ due to C≡N stretching vibration disappeared and absorption bands at 3.1, 3.3, 3.4 and 6.5 μ which were caused by -CONH- vibrations and at 6.70 μ by the stretching vibration of an azoxy group appeared.

Accordingly, it seems reasonable to propose the following structures for their oxidation products:

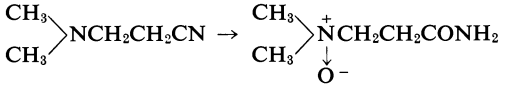




The oxidation reaction of β-aminopropionitrile, proceeded at below 5°C to yield a viscous substance. On the contrary, it was necessary to raise the reaction temperature up to 20°C in the oxidation of compounds I and II. This means presumably that one methyl substituent introduced in β-aminopropionitrile interferes with the oxidation of an amino group.

A tertiary amino compound IV did not yield resinous material, but a crystalline substance in oxidation reaction. Recrystallization of this product from butanol gave a compound with melting point above 250°C and the composition, $C_5H_{12}N_2O_2$, which was obtained from its elemental analysis. The infrared absorption spectrum of this compound does not possess an absorption band at 4.5 μ due to C≡N stretching vibration, while the absorption bands, which correspond to C=O stretching vibration and $NH_2$ bending vibrations, appeared at 6.0 and 6.15 μ, respectively, as shown in Fig. 3. This result thus indicates the complete hydrolysis of the nitrile to the corresponding acid amide compound.

The strong absorption bands at 7.8 and 10.45 μ present a strong support to the presence of a *N*-oxide group in the molecule. These absorption bands were observed also by Parker[3] and Koelsch[4] to be caused by *N*-oxide vibrations. *N*, *N*-dimethyl-β-alanine was obtained by treating this compound with sodium hydrosulfite and hydrochloric acid. Thus, it is understood from these studies that the compound IV was transformed into β-dimethylaminopropioamide *N*-oxide as shown by the following equation:



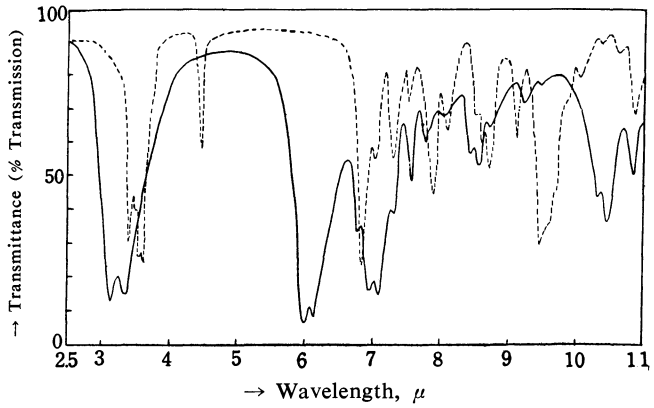



Fig. 3. Infrared absorption spectrum.
---- β-Dimethylaminopropionitrile
—— β-Dimethylaminopropionitrile *N*-oxide

3) E. D. Parker and A. Furst, *J. Org. Chem.*, **23**, 201 (1958).

4) C. F. Koelsch and W. H. Gumprecht, *J. Org. Chem.*, **23**, 1603 (1958).

From this fact it is clear that amino groups of these β-aminopropionitrile derivatives are not oxidized to aldehydes or ketones but to hydroxylamino groups.

β-Dimethylaminopropioamide *N*-oxide is comparatively unstable in the air and undergoes a gradual transformation into a reddish substance when it is stored in the air for a prolonged period. As Rogers[5] reported previously, phthalates of the *N*-oxides of β-dimethylaminopropionic esters or nitrile were prepared by the reaction of β-dimethylaminopropionic esters or nitrile with monoperphthalic acids. However, nothing has been reported about the synthesis of an *N*-oxide compound itself. It is very interesting to know that a new *N*-oxide was prepared in the present investigation. This *N*-oxide was prepared by hydrogen peroxide oxidation of the compound IV, a nitrile group which underwent hydrolysis simultaneously to yield an acid amide group. Since the compound V did not yield a resinous substance by the oxidation with hydrogen peroxide, it seems that β-aminonitrile compounds are oxidized with hydrogen peroxide by the mechanism as described in the previous paper[1], but α-aminonitrile compounds are not oxidized by the same mechanism.

## Experimental

**Preparation of α-Methyl-β-aminopropionitrile[6].**—Thirty-three grams of methacrylonitrile and 110 g. of 28% aqueous ammonia were placed in a Carius-type tube heated for 8 hr. at 70~75°C. Then, unreacted methacrylonitriles which lay above an aqueous phase were separated. α-Methyl-β-aminopropionitrile, $n_D^{20.2}$ 1.4340, $d_4^{20.2}$ 0.9180, b. p. 76.5~77.5°C/16.8 mmHg, was obtained from the aqueous phase; yield, 17.5 g.

Found: N, 33.63. Calcd. for $C_4H_8N_2$: N, 33.83%.

**Preparation of β-Methyl-β-Aminopropionitrile[7].**—A Carius-type tube containing 41 g. of allyl cyanide and 200 g. of 28% aqueous ammonia was heated for one hour at 70°C. The reaction mixture became homogeneous after this treatment and then distilled in vacuo to give the product, β-methyl-β-aminopropionitrile; yield, 34.5 g., b. p. 84.7~85.0°C/23 mmHg.

**Preparation of β-Dimethylaminopropionitrile[8].**—This was prepared from 60 g. of 50% aqueous dimethylamine and 35 g. of acrylonitrile. Yield, 33.1 g., b. p. 83~85°C/37 mmHg.

**Preparation of β-Ethylaminopropionitrile[8].**—This was prepared from 70% aqueous ethylamine and 45.0 g. of acrylonitrile. Yield, 13.0 g., b. p. 78~80°C/16 mmHg.

**Preparation of α-Methyl-α-aminopropionitrile.**—To a mixture containing 110 g. of acetonecyanhydrine and 400 ml. of methanol, ammonia gas was introduced at 15°C with stirring until the solution was saturated with ammonia. After being allowed to stand for 2 days in an ice bath, the reaction mixture was distilled in vacuo to yield α-methyl-α-aminopropionitrile; 35 g., b. p. 48.7~50.2°C/12 mmHg.

**Oxidation Reaction with Hydrogen Peroxide.**—Twenty-five per cent hydrogen peroxide was added dropwise to aminonitrile placed in a 100 ml. flask equipped with a thermometer, a dropping funnel and a capillary, keeping the reaction temperature below 5°C. This reaction proceeded under reduced pressure to remove ammonia gas. After the addition of hydrogen peroxide was completed, the reaction temperature was raised gradually up to 50°C, and the ammonia and water were removed. Unreacted aminonitrile was also displaced from the reaction mixture by treating it with anhydrous acetone. When β-dimethylaminopropionitrile was employed as an aminonitrile compound and treated as described above at 50°C, a crystalline product was obtained. Recrystallization of this product from butanol gave glittering needle-like crystals.

**Reduction and Hydrolysis of the β-Dimethylaminopropioamide *N*-Oxide.**—β-Dimethylaminopropioamide *N*-oxide (13.2 g.) in 50 cc. methanol was boiled with 30% hydrochloric acid (20 g.) for an hour. After cooling and basification with aqueous sodium hydroxide, the reacted solution was stirred with sodium hydrosulfite (25 g.) for 2 hr. at room temperature. The reacted solution was acidified with hydrochloric acid and evaporated at reduced pressure. The residue was extracted with cold ethanol. Evaporation of the ethanol left a crystalline residue which was recrystallized from ethanol and formed leaflets (8.6 g.) m. p. 186.5~188°C[9]. The melting point was not depressed by admixture with *N*, *N*-dimethyl-β-alanine hydrochloride.

**Infrared Absorption Spectrum.**—A sample of the oxidation products of the compounds I and II were dissolved in methanol to obtain 3% solution. Then, a piece of thin film was prepared on a cell by evaporating methanol from the solution. The potassium bromide disk method was employed to prepare a sample of the oxidation product of IV.

The Perkin-Elmer model 21 spectrophotometer was used to obtain spectral data.

The author wishes to express his sincere thanks to Professor Ryozo Goto of Kyoto University for his kind advice, and also to Mr. Murataro Nakashima, President of Kunoshima Chemical Co., for his permission to publish this paper.

*Research Laboratory of Kunoshima Chemical Industry Co., Ltd.*
*En-ichi-cho, Mihara*

5) M. A. T. Rogers, *J. Chem. Soc.*, **1955**, 769.
6) J. B. Dickey, U. S. Pat. 2659739 (1953); *Chem. Abstr.*, **48**, 3036 (1954).
7) B. Bruyland, *Bull. soc. chim. Belg.*, **32**, 257.
8) F. C. Whitmore and H. S. Mosher, *J. Am. Chem. Soc.*, **66**, 725 (1944).
9) T. L. Gresham et al., ibid., **73**, 3168 (1951).

# *Effect of Solvent on Carbonyl Stretching Frequency of Ketones*

By Kōzō Inuzuka, Mitsuo Ito and Sunao Imanishi

(Received July 29, 1960)

It is well known that ketones and aldehydes show characteristic infrared absorption bands assignable to the C=O stretching vibration of molecule. In our previous works[1,2] we studied the solvent effect on $n-\pi^*$ absorption bands of some ketones on the basis of a theoretical equation proposed by McRae[3]. In these studies we found a certain relationship between the solvent-induced shift of the ultraviolet $n-\pi^*$ absorption frequencies and that of infrared C=O frequency. It is found in the present work that the same McRae's equation can also be applied to the interpretation of the solvent shift of the C=O stretching frequency for both nonpolar and polar solvents. The intensity of the C=O stretching vibration is influenced by the polarity of the solvent. The magnitude of the bond moment derivative measuring the infrared absorption intensity increases for polar solvents, especially for solvents which tend to form hydrogen bonds with the solute molecules. However, this intensification for the C=O bands is not so large as for the OH bands. In this paper we intend to estimate the bond moment derivative for the C=O bond and its increase on hydrogen bonding.

## Experimental

Infrared absorption measurements of ketones were made with a Hitachi E. P. I double beam spectrophotometer with an sodium chloride prism, using 0.1 mm. cell. Solvent effects were observed for acetone, mesityl oxide, acetophenone and benzophenone. The solvents used were *n*-hexane, ethyl ether, carbon tetrachloride, benzene, dioxane, acetonitrile, chloroform, *iso*-butyl alcohol and ethyl alcohol. They were purified by the methods recommend by Weissberger and Proskauer[4]. Special care was taken to remove contaminating water in the solvents. Acetone was purified by the above method. Highest quality commercial mesityl oxide and acetophenone were further purified by repeated distillations. Benzophenone was recrystallized several times from ethanol.

## Results and Discussion

The positions of the carbonyl bands of four ketones in the different solvents are given in Table I. The refractive index and dielectric constant of the solvents are given in Table II. It is seen that the carbonyl frequency in a given solvent decreases in the order of acetone, mesityl oxide, acetophenone and benzophenone. This is just the order of increase of the amount of conjugation in the respective molecules. The observed parallelism between the carbonyl frequency and the extent of conjugation may be interpreted as a result of the lowering of the double bond character of the carbonyl bond with increasing conjugation. Kirkwood and Magat[5] related the frequency shift in the infrared absorption of a solution to the dielectric constant $D$ of the solvent by a formula

Table I. Frequencies ($cm^{-1}$) of C=O vibration bands of ketones in various solvents

| Solvent | Acetone | Mesityl oxide | Aceto-phenone | Benzo-phenone |
|---|---|---|---|---|
| *n*-Hexane | 1727 | 1702 | 1701 | 1673 |
| Ethyl ether | 1725 | 1699 | 1697.5 | 1671 |
| Carbon tetrachloride | 1723 | 1697.5 | 1695 | 1669 |
| Benzene | 1721.5 | 1695 | 1693 | 1667 |
| Dioxane | 1720 | 1694 | 1693 | 1667 |
| Acetonitrile | 1718 | 1692.5 | 1691 | 1664 |
| Chloroform | 1715.5 | 1690 | 1687 | 1662 |
| *iso*-Butyl alcohol | 1714.5 | 1687 | 1684 | 1658 |
| Ethyl alcohol | 1713.5 | 1686 | 1683 | 1657 |

Table II. Refractive index and dielectric constant of the solvents

| Solvent | $n_D$ | $D$ |
|---|---|---|
| *n*-Hexane | 1.375 | 1.89 |
| Carbon tetrachloride | 1.460 | 2.238 |
| Dioxane | 1.422 | 2.209 |
| Benzene | 1.501 | 2.284 |
| Ethyl ether | 1.356 | 4.335 |
| Acetonitrile | 1.344 | 37.5 |
| Chloroform | 1.449 | 4.806 |
| *iso*-Butyl alcohol | 1.398 | 17.7 |
| Ethyl alcohol | 1.361 | 24.3 |

1) M. Ito, K. Inuzuka and S. Imanishi, *J. Am. Chem. Soc.*, **82**, 1317 (1960).
2) M. Ito, K. Inuzuka and S. Imanishi, *J. Chem. Phys.*, **31**, 1694 (1959).
3) E. G. McRae, *J. Phys. Chem.*, **61**, 562 (1957).
4) A. Weissberger and E. S. Proskauer, "Organic Solvents", Interscience Publishers, Inc., New York, N. Y. (1955).
5) W. West and R. T. Edwards, *J. Chem. Phys.*, **5**, 14 (1937); E. Bauer and M. Magat, *J. Physique Radium*, **9**, 319 (1938).

$$\Delta\nu/\nu = C(D-1)/(2D+1)$$

where $\nu$ is the frequency of an absorption band, and $C$ is a constant. This equation has been checked experimentally for a number of substances, and it generally holds only for nonpolar solvents. The linear relation is shown in Fig. 1, in which the shift of the carbonyl stretching frequency of the ketones investigated is plotted against the value $(D-1)/(2D+1)$ of nonpolar solvents. However, such a linearity is no longer seen for polar solvents. In the case of non-hydrogen bonding polar solvents, the dipole moment effect of the

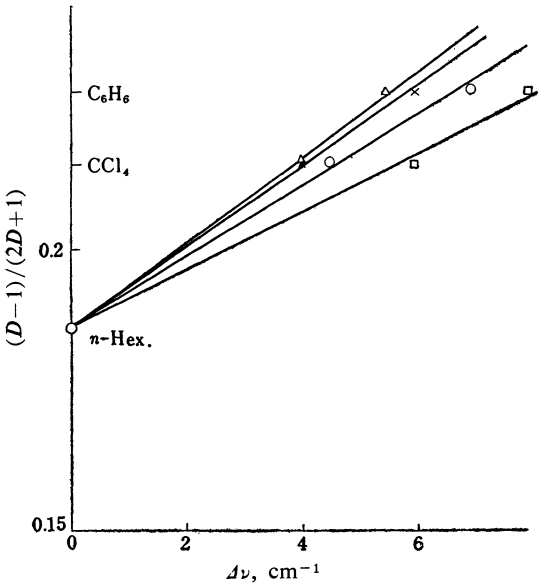


Fig. 1

solvent must be taken into consideration. In our previous paper[1] on the solvent effect on the $n-\pi^*$ absorption of ketones, observed shifts were well explained by McRae's equation as mentioned above. In the same paper it was found that the solvent induced shift of the infrared carbonyl frequency relates linearly in turn with that of the ultraviolet $n-\pi^*$ absorption frequency of the same ketone. It is then expected that the solvent effect on the carbonyl frequency itself may also be explained by the same McRae's equation. With polar solvents for which $D$ is no longer equal to $n^2$, the above equation tells us that if $n$ of all the solvents used are nearly equal, the solvent induced frequency shift must be proportional to $(D-1)/(D+2)$. We took mixtures of ethyl ether and acetonitrile in various ratios as the solvents satisfying the above condition. While the $n$ values of ethyl ether and acetonitrile are nearly the same, their $D$ values are quite different from each other. The $\Delta\nu$ vs. $(D-1)/(D+2)$ relations are shown in Figs. 2—5 for the ketones investigated, in which the approximate linearity is clearly seen for each substance.

From the above results it may be understood that the following McRae's equation holds well for both the cases of polar and nonpolar solvents.

$$\Delta\nu = A(n^2-1)/(2n^2+1) + B\{(D-1)/(D+2) - (n^2-1)/(n^2+2)\}$$

in which $A$ and $B$ are constants characteristic of the solute molecule. For nonpolar solvents $D$ is nearly equal to $n^2$, thus the second term

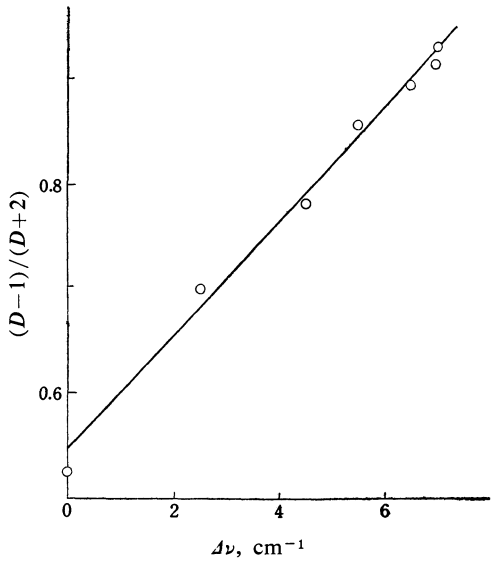


Fig. 2

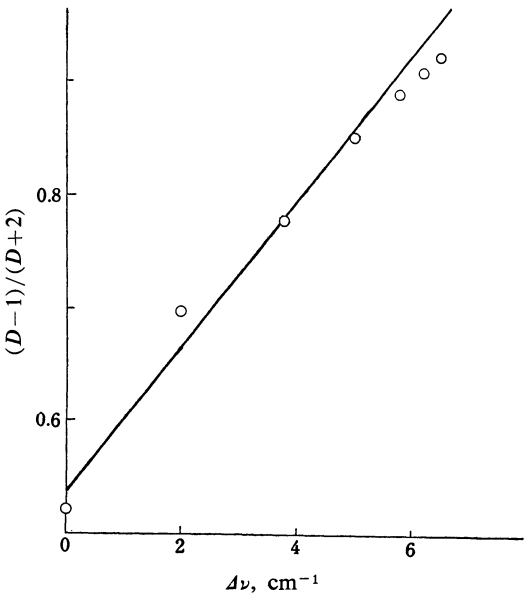


Fig. 3

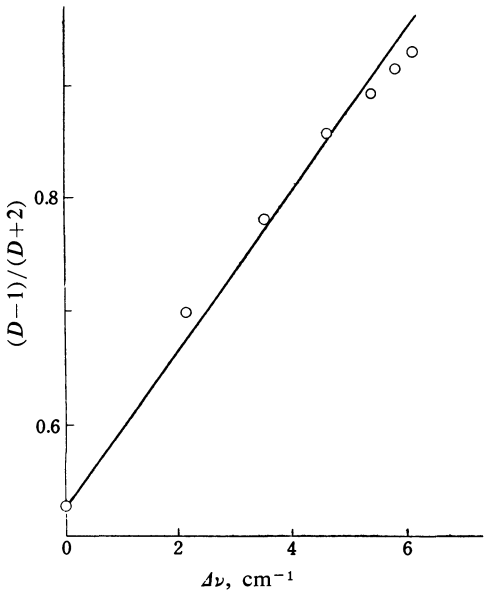



Fig. 4

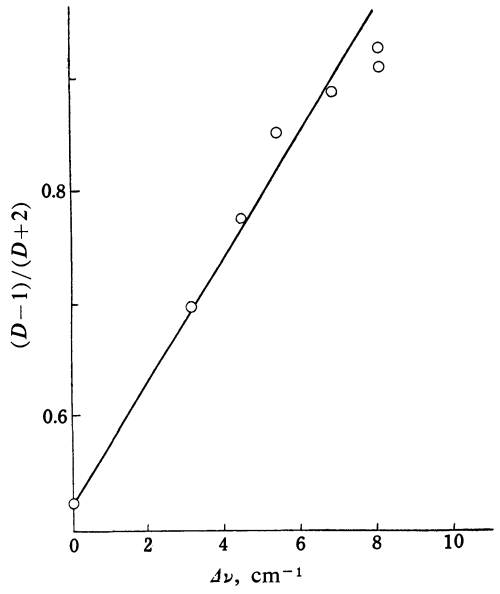



Fig. 5

vanishes. Substituting $n^2$ with $D$ in the first term we obtain an equation identical with the one derived by Kirkwood and Magat. Fig. 6 shows a comparison between the observed shifts for benzophenone and those calculated from the McRae's equation, putting 65 and 9 $cm^{-1}$ for $A$ and $B$, respectively. It is seen that the points for most solvents, except those having possibilities for forming hydrogen bonds with the solute molecule, drop near to the theoretical line. For hydrogen bonding systems large deviations occur, which may be interpreted as due to the hydrogen bonding, as this effect

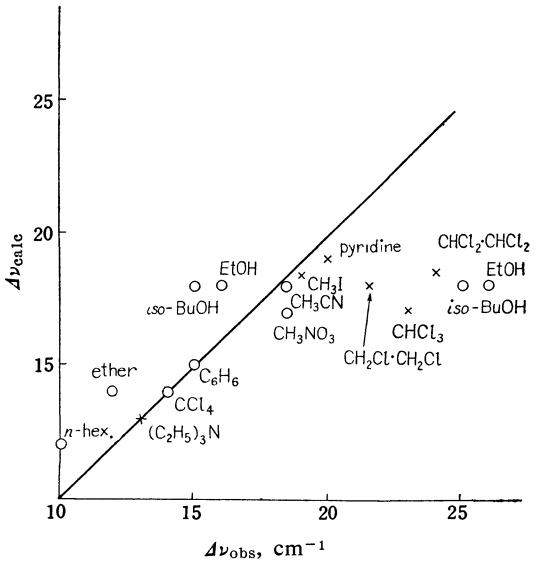



Fig. 6

is not taken care of at all by the McRae's equation. The carbonyl frequency suffers larger shifts in hydrogen bonding than in nonhydrogen bonding solvents, but this shift is much smaller than that of the hydroxyl frequency due to the same cause. In the benzophenone and ethyl alcohol system the hydroxyl frequency of the alcohol diminishes by about 150 $cm^{-1}$, while the decrease of the carbonyl frequency of benzophenone is only about 15 $cm^{-1}$. Recently Bellamy et al.[6,7] studied the solvent effect on C=O and OH bands of several molecules in various mixed solvents, suggesting that the local association effect is the dominant factor in producing the frequency shift, and that the electrostatic properties of the medium as a whole does not play an important role. If the solvent effect is principally due to the local association, two different bands will be expected for a system in which two kinds of solvents are present. Fig. 7 shows the change of the C=O frequency of mesityl oxide on changing the mixing volume ratio of ethyl ether and acetonitrile in the solvent. The band maximum changes in succession with the mixing ratio suggesting that the shift depends on the dielectric constant of the medium. The same situation obtains for acetophenone, acetone and benzophenone. These observations favor the view emphasizing the importance of dielectric constant in the solvent effect. However, the possibility of local association may not be excluded, as our experiment is not accurate enough for it.

6) L. J. Bellamy and H. E. Hallam, *Trans. Faraday Soc.*, 55, 220 (1959).
7) L. J. Bellamy and R. L. Williams, ibid., 55, 14 (1959).

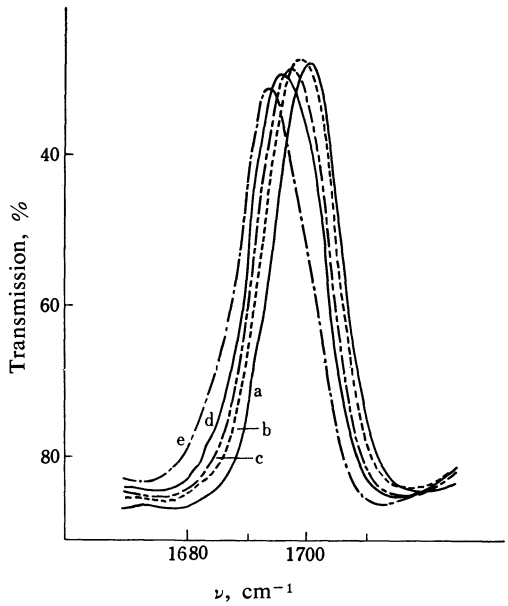



Fig. 7

On the other hand, for simplification we assumed that the C=O stretching vibration in these ketones is localized at this group and almost independent of the rest of the molecule. Therefore the normal coordinate $Q$ contains only the pure carbonyl stretching vibration.

Then

$$d\mu/dr=(1/m_c+1/m_o)^{-1/2}d\mu/dQ$$

where $\mu$ is the dipole moment, $Q$ the normal coordinate, $m_c$ and $m_o$ the masses of the carbon and oxygen atoms and $r$ the distance between the C and O atoms.

From the observed intensities $A$ in l. mol$^{-1}$ cm$^{-2}$ the change in the dipole moment with respect to the normal coordinate $Q$ is given by

$$d\mu/dQ=\pm(3c^2\times1000\,A/N\pi)^{1/2}$$

where $c$ is the light velocity and $N$ is the Avogadro number. Table III summarizes the values of $d\mu/dr$ calculated as above. They fall in the range between 4 and 6 D/Å, and show that the bond moment derivative increases with the increasing polarity of the solvent as well as with the increasing amount of conjugation, with the exception of mesityl oxide. However, the difference of the bond moment derivative for the bond of ketones in nonpolar and polar solvents is only about 1 D/Å, much smaller than the corresponding change of the OH bond moment derivatives of alcohols.

Table III. Bond moment ($\times10^{-10}$ e.s.u./cm.) derivatives of ketones in various solvents

| Solvent | Acetone | Mesityl oxide | Aceto-phenone | Benzo-phenone |
|---|---|---|---|---|
| *n*-Hexane | 4.54 | 4.10 | 4.80 | 5.36 |
| Ethyl ether | 4.67 | 4.13 | 5.09 | 5.45 |
| Dioxane | 4.67 | 4.41 | 5.28 | 5.58 |
| Benzene | 4.70 | 4.41 | 5.29 | 5.45 |
| Carbon tetrachloride | 4.87 | 4.50 | 5.45 | 5.32 |
| Acetonitrile | 4.87 | 4.28 | 5.64 | 5.60 |
| *iso*-Butyl alcohol | 5.07 | 4.41 | 6.72 | 5.56 |
| Ethyl alcohol | 5.11 | 4.41 | 5.81 | 5.60 |
| Chloroform | 5.28 | 4.54 | 5.81 | 5.81 |

**Theoretical Calculation of $d\mu/dr$ for Ketones.**—According to Coulson the value of $d\mu/dr$ can be evaluated from the bond polarizability defined on the simple MO theory for a $\pi$ electron system. We have assumed that there is no appreciable change in the $\sigma$ electron cloud during the C=O stretching vibration. Treating the acetone molecule as diatomic $d\mu/dr$ is expressed by

$$d\mu/dr=d(qer)/dr=r_0e(dq/dr)_o+q_oe$$

where $e$ is the electronic charge, $q$ the formal charge density on the oxygen atom, $r_o$ the equilibrium distance of the C=O bond and $q_o$ the formal charge density for $r=r_o$. As $q$ is a function of the exchange integral for the carbonyl bond

$$dq/dr=dq/d\beta\cdot d\beta/dr=\pi_{o,co}d\beta/dr$$

where $\beta$ is the exchange integral between the oxygen and carbon atoms, and $\pi_{o,co}$ the atom-bond polarizability defined by Coulson et al.[8], which is calculable from the coefficients in the molecular orbital function. If we use the relation $\beta_{co}=k/r^6$ as given by Kon[9] we obtain

$$d\mu/dr=r_0e\pi_{o,co}(-6\,\beta_{co}/r_0)+q_oe$$

for which $\pi_{o,co}$ and $q_o$ have been calculated by the simple MO treatment for the C=O group*. If we take $r_0=1.23$ Å we obtain

$$d\mu/dr=8.4\text{ D/Å}$$

Instead, if the SCF molecular orbital calculated by Nagakura[10] is employed,

$$d\mu/dr=8.3\text{ D/Å}$$

is obtained. These calculated values are different from the observed 5 D/Å but the discrepancy is due to the rough approximation. As mentioned previously $d\mu/dr$ tends to be increased with the increase of the polarity of the solvent, the value of $d\mu/dr$ for solvents forming hydrogen

8) C. A. Coulson and H. C. Longuet-Higgins, *Proc. Roy. Soc.*, **A191**, 39 (1947).
9) H. Kon, This Bulletin, **28**, 275 (1955).
* Using the values of Coulomb integrals of carbon and oxygen atoms $\alpha_c=\alpha+0.2\beta$ and $\alpha_o=\alpha+2\beta$, respectively, and the carbonyl exchange integral $\beta_{co}=1.4\beta$[11], 3.1D is obtained as the value of the dipole moment of acetone, in agreement with the experimental 2.7D.
10) S. Nagakura, ibid., **25**, 164 (1952).
11) L. E. Orgel, T. L. Cottrell, W. Dick and L. E. Sutton, *Trans. Faraday Soc.*, **47**, 113 (1951).

bonds with the ketone molecule increases by about 1 D/Å compared with the case of non-polar solvents.

Now, we may assume for a hydrogen bonding system the following two resonance forms

$$O\text{-}H\cdots O{=}C \qquad \Phi_n \qquad I$$

$$O^-\text{-}H\text{-}O^+{=}C \qquad \Phi_p \qquad II$$

and represent the ground state wave function of the hydrogenbonded complex by

$$\Phi = \Phi_n + c_p\Phi_p$$

where $c_p$ measures the extent of the charge-transferred form II to the system. During the C=O vibration $c_p$ changes continuously. If the dipole of $\Phi_p$ is represented by $\mu_p$, the dipole moment $\mu_T$ contributed by II is given by

$$\mu_T = \mu_p \cdot c_p^2$$

yielding

$$d\mu_T/dr_{co} = d(\mu_p c_p^2)/dr_{co}$$
$$= \mu_p dc_p^2/dr_{co} + c_p^2 d\mu_p/dr_{co}$$

For simplicity of calculation, we assume that firstly a C atom is fixed in a C=O vibration of acetone molecule $(CH_3)_2{=}C{=}O$ because of the great mass ratio of a $(CH_3)_2{=}C$ group to an O atom, and secondly a hydrogen bond OH···O=C is linear.

Since $dr_{co} = -dr_{o\cdots o}$ in the present approximation,

$$d\mu_T/dr_{co} = -\mu_p dc_p^2/dr_{o\cdots o} - c_p^2 d\mu_p/dr_{o\cdots o}$$

Substituting $r_{OH}=1$ Å, $r_{o\cdots o}=3$ Å, and the estimated $c_p$ value[12] into the above equation, we obtain

$$d\mu_T/dr_{co} = 1.2 \text{ D/Å}$$

Thus the increase of intensity due to hydrogen bonding is 1.2 D/Å, in good agreement with the observed 1 D/Å.

## Summary

The C=O stretching frequencies in acetone, mesityl oxide, acetophenone and benzophenone were measured in various solvents and the frequency shifts induced by solvents were interpreted by McRae's theoretical equation. Results show that the observed shifts can be explained in terms of the coöperating interactions between solute and solvent molecules.

Next, the intensity of the C=O group vibration bands of these ketones was observed and compared with bond moment derivatives calculated by diatomic molecular appoximation. Small changes of about 1 D/Å were observed for polar and nonpolar solvents. The increase of the bond moment derivative value in a hydrogen bonding system was attributed to the charge transfer force.

*Department of Chemistry*
*Faculty of Science*
*Kyushu University*
*Hakozaki, Fukuoka*

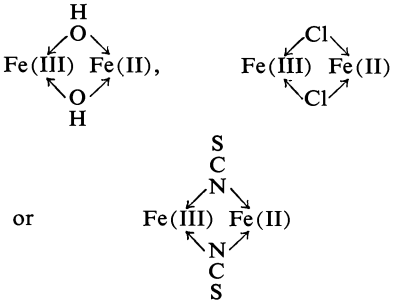
12) C. A. Coulson and U. Danielsson, *Arkiv Fysik*, **8**, 245 (1954).

# *Magnetic and Spectrophotometric Studies on the Decoloration of Thiocyanatoiron(III) Complexes in Solutions. II. Effect of Acids*

By Chie MIYAKE*

(Received February 11, 1960)

In order to account for magnetic observations on the reaction between iron(III) and thiocyanate ions, the present writer has proposed the formations of three kinds of dimers in solutions and discussed their roles in reactions. The results have been reported in the previous paper[1].




* Present address: Nuclear Engineering Department, Faculty of Engineering, Osaka University, Miyakojima-ku, Osaka.

1) C. Miyake, This Bulletin, **33**, 867 (1960).

There seems to be much remaining to be investigated. One of the problems to be clarified first is which dimer of the three is the most abundant and stable one in the solution. In this paper are reported the experimental data which are conceivably useful for considering the above-mentioned problems.

## Experimental

**Materials.** — The iron(III) solution and potassium thiocyanate solution were prepared by the same method as that previously described. Acetic acid was purified by distillation until it became negative for the test of the iron ion. Sulfuric acid of analytical grade was used without further purification. It was confirmed that the test of the iron ion was negative. The sample solution was prepared by adding appropriate amounts of sulfuric acid (or acetic acid) and potassium thiocyanate to the iron stock solution. Before each measurement, the solution was diluted to the desired concentration.

**Measurements.** — The methods of measurements are the same as those described in the previous paper.

## Experimental Results

**Magnetic Data.** — Fig. 1 shows that the magnetic moment of iron in solutions of various acids with the same normality decreases with time. Fig. 2 shows that the magnetic moment of iron in sulfuric acid of various normalities decreases with time.

**Spectrophotometric Data.** — The spectral curves of thiocyanatoiron(III) complexes in solutions of sulfuric acid or acetic acid are shown in Fig. 3. The absorption maxima at about 460 mμ are due to thiocyanatoiron(III) complexes in the solutions. Other maxima at about 300 mμ seem to be due to sulfatoiron(III) and acetatoiron(III) complexes. The curves of thiocyanatoiron(III) complexes in sulfuric acid of various normalities are shown in

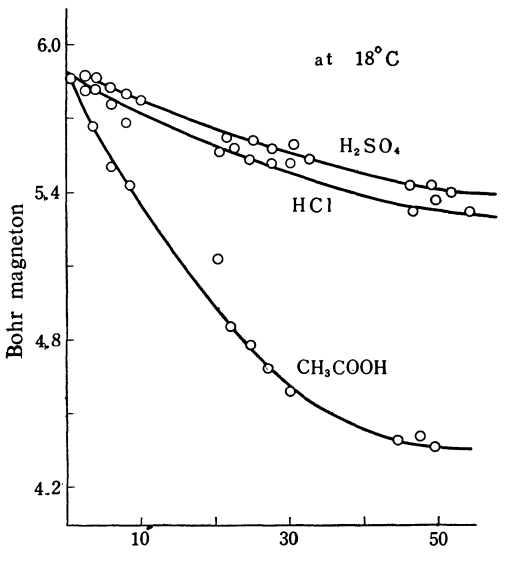



Fig. 1. Dependency of decrease in magnetic moment of iron upon kind of acid. (0.005 M iron(III), 0.5 M thiocyanate ion, 0.12 N-each acid solutions).

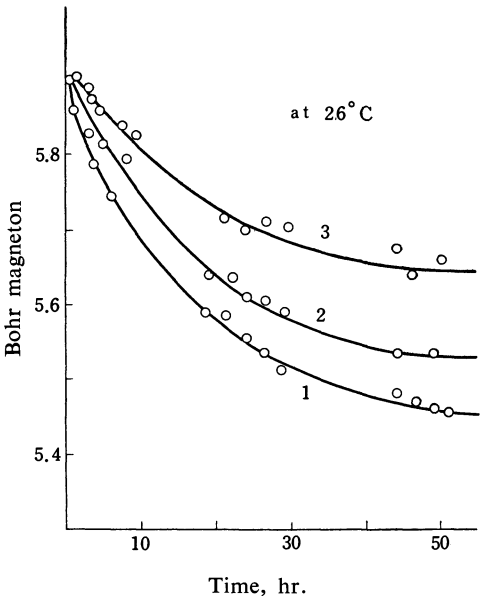



Fig. 2. Dependency of decrease in magnetic moment of iron upon concentration of sulfuric acid (0.005 M iron(III), 0.05 M thiocyanate ion solutions).
1 : 0.012 N $H_2SO_4$, 2 : 0.12 N $H_2SO_4$, 3 : 1.2 N $H_2SO_4$.

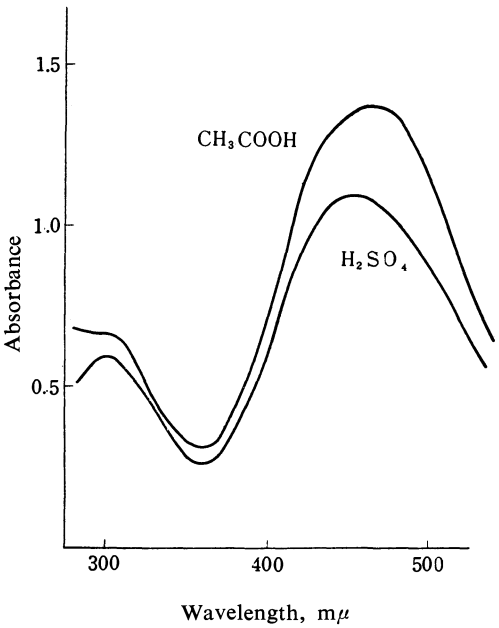



Fig. 3. Absorption spectra of thiocyanato iron(III) complexes in sulfuric or acetic acid solutions.

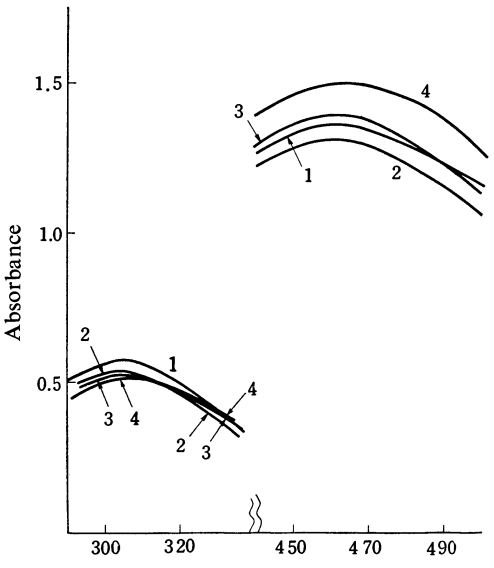



Fig. 4. Absorption spectra of thiocyanatoiron(III) complexes in solutions with varying concentration of sulfuric acid (0.005 M iron(III), 0.05 M thiocyanate ion solutions).
1: 3.6N, 2: 1.2 N, 3: 0.6 N, 4: 0.12 N.

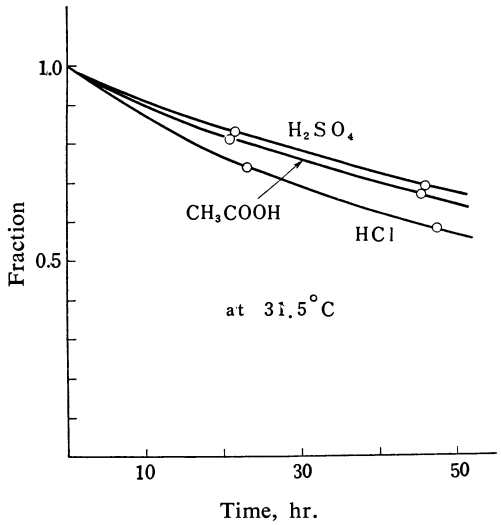



Fig. 5. Dependency of decrease in absorbance at about 470 mμ upon kind of acid (0.005 M iron(III), 0.5 M thiocyanate iron, 1.2 N each acid solutions).

Fig. 4. Fig. 5 shows the time dependency of absorbance values at the peak wavelength, about 460 mμ of the complexes in various acid solutions having the same normality. Fig. 6 represents the time dependency of absorbance values at the peak wavelength, about 460 mμ of the complexes whose time dependency of magnetic moment values is already shown in Fig. 2. The relations between

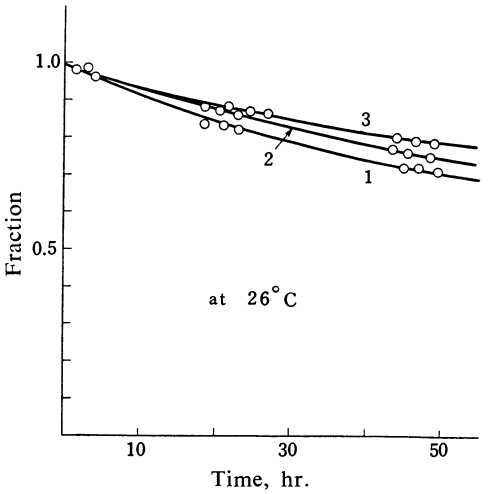



Fig. 6. Decrease of absorbance at about 460 mμ of thiocyanatoiron(III) complexes in solutions.
1: corresponds to 1 in Fig. 2.
2: 〃 2 〃
3: 〃 3 〃

the concentration of the hydrogen or thiocyanate ion and the above-mentioned absorbances at about 460 mμ and 320 mμ are tabulated in Table I, which can afford some knowledge about the effects of hydrochloric and sulfuric acids upon the nature of decoloration and of the formation of the dimer.

## Discussion

The magnetic moment of thiocyanatoiron(III) complexes in sulfuric acid and acetic acid solutions, when measured within fifteen minutes after the preparation, was found to be 5.91 and 5.88 Bohr magnetons, respectively. The values are characteristic of the outer orbital type of binding of the iron(III) complexes as in the case of the complexes in hydrochloric acid. As is seen in Fig. 3, no noticeable difference from the absorption for the complexes in hydrochloric acid solutions can be seen with respect to the absorption at about 460 mμ. As shown in Figs. 1 and 5, the decrease of the magnetic moment with time, which suggests the formation of complexes having the inner orbital type of binding, is also remarkable in both the solutions. However, the decrease is rather conspicuous in the acetic acid solution. This seems to be due to the unknown magnetic interaction between iron ions and acetate ions. Werbel et al.[2] pointed out that this kind of interaction makes the magnetic moment of the solution smaller while other authors proposed the formation of trimers. Some interpretation

2) B. Werbel, V. Debeler and W. C. Vosborgh, *J. Am. Chem. Soc.*, 65, 2329 (1943).

TABLE I. EFFECTS OF CONCENTRATIONS OF BOTH HYDROGEN IONS AND THIOCYANATE IONS TO ABSORBANCES AT ABOUT 470 mμ AND 320 mμ

| | Increase of $[NCS^-]$ | Increase of $[H^+]$ |
|---|---|---|
| | Absorbance at about 470 mμ | |
| Wavelength of max. absorbance | Bathochromic | Constant* |
| Absorbance | Increase | Decrease* |
| Rate of decrease in absorbance | Increase | Decrease |
| | Absorbance at about 320 mμ | |
| Wavelength of max. absorbance | Bathochromic* | Bathochromic |
| Absorbance | Decrease* | Increase |
| Rate of decrease in absorbance | Constant* | Decrease |

* The absence of any noticeable effect.

for the time dependency of the magnetic moment of the acetic acid solution should be postponed to the future when sufficient data are available.

In the present paper the discussion will be conducted with the data of sulfuric and hydrochloric acid solutions. The most important fact is to determine which dimer of the three is most likely existing and prevailing during the course of reaction. According to the present author's results shown in Figs. 2 and 5 or those also given in Table I, the increase in the acidity of the solution suppresses the progress of reactions which conceivably brings about the decrease of the magnetic moment. If it is assumed that the second type of dimers containing chloride or sulfate ions may exist, the formation of dimers should increase with the increasing concentrations of acids, resulting in a great decrease of the magnetic moment. This expected relation can not be supported by the afore-mentioned experimental results. Consequently the existence of the second type of dimers is thought to be very unlikely.

A question is raised whether the dimer with hydroxo bridges or that with thiocyanate bridges is more stable. The latter dimer may tentatively be considered to be stable in the solution in which the magnetic moment decreases with the increasing concentrations of thiocyanate ions (as shown in Fig. 2 in the previous paper). However, it should be noticed that the degree of decrease of the magnetic moment can increase even at a constant concentration of the thiocyanate ion, if the acidity of the solution decreases. Therefore, it will be safely concluded that the existence of dimers through hydroxo bridges is more likely than their existence through thiocyanate bridges.

## Summary

Magnetic and spectrophotometric measurements have been carried out for the purpose of determining which of the proposed three types of dimers is most probable. The results obtained show that the second one with chloride ion bridges can safely be neglected. The existence of the first type with hydroxo bridges can be considered to be plausible.

The author wishes to express her sincere thanks to Professor H. Takaki for his interest and encouragement throughout this experiment. Her acknowledgment is also due to Dr. Y. Yamamoto for his helpful discussion and advice given in this experiment.

*Department of Chemistry*
*Faculty of Science*
*Kyoto University*
*Sakyo-ku, Kyoto*

# *Magnetic and Spectrophotometric Studies on the Decoloration of Thiocyanatoiron(III) Complexes in Solutions. III. Structure of Thiocyanatoiron(III) Complex in Organic Solvents*

By Chie MIYAKE*

(Received July 11, 1960)

The present writer has reported the nature of the reaction between iron(III) ion and thiocyanate ions in aqueous solution in detail[1,2]. The experimental data obtained so far are rather consistently explained when we consider hypothetically the formation of a dimer containing iron(II) and iron(III) coupled by hydroxo bridges during the course of chemical reaction. However, there still remains a question whether the magnetic time change we observed is attributable to the above-mentioned dimer, or to the higher complexes, such as $Fe(NCS)_2^+$, $Fe(NCS)_3$, $Fe(NCS)_4^-$,..., which are formed by the prolonged replacement of the coordinated $H_2O$, $Cl^-$ ion etc. of the preexisting complexes with thiocyanate ions whose binding is of the so-called inner orbital type. In order to elucidate this, it is necessary at least to extract a definite species of complex having a known chemical formula by using an organic solvent and then to measure its magnetic property, because in the aqueous solution there are so many species of complexes, as shown in the previous paper[1], that it is difficult to consider which species is responsible for the measured magnetism and absorption. This paper deals with the results of measurements and the inferred structure of thiocyanatoiron(III) complex extracted by organic solvent.

## Experimental

**Materials.** — Ferric perchlorate was prepared by dissolving an appropriate amount of electrolytic iron in perchloric acid (about 4 N), oxidizing with hydrogen peroxide (30%), and evaporating the solution until crystals appeared. After perchloric acid was added to dissolve the deposit, the solution was evaporated again. The procedure was repeated until the solution gave a negative test for chloride and iron(II) ions. Violet crystals separated on cooling were filtered off with a sintered glass filter and recrystallized twice from distilled water. The stock solution of iron was prepared by dissolving the crystal of ferric perchlorate in water to the concentration of 1000 p. p. m.

The peroxides were removed from ether by shaking with a solution of ferrous sulfate acidified with sulfuric acid, until the organic phase no longer gave the test for peroxides and then the ether was purified by distillation.

Ethyl acetate used was of analytical grade.

Extraction of thiocyanatoiron(III) complex was carried out by adding the proper amount of potassium thiocyanate and shaking the iron solution with a given volume of organic solvent. After standing the whole solutions for fifteen minutes, the organic phase was separated from the aqueous solution.

**Measurements.**—Magnetic and spectrophotometric measurements were made as described previously[1].

## Results and Discussion

The magnetic moment for total iron in the ether solution of thiocyanatoiron(III) complex was found to be 6.0 Bohr magnetons. This value indicates that thiocyanatoiron(III) complex in the organic phase possesses a magnetic moment corresponding to five unpaired electrons, showing the outer orbital type of binding. Fig. 1 shows the spectral

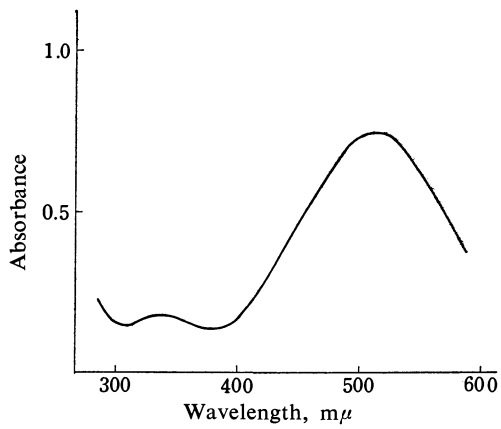



Fig. 1. Absorption spectrum of thiocyanatoiron(III) complex in ethyl acetate.

curve of the complex in organic solvents, such as ether or ethyl acetate. The absorption maximum found at 511 mμ is slightly longer in wavelength as compared to the already reported value of the complexes having one or two thiocyanate ions in term.

* Present address: Nuclear Engineering Department, Faculty of Engineering, Osaka University, Miyakojima-ku, Osaka.

1) C. Miyake, This Bulletin, 33, 867 (1960).
2) C. Miyake, ibid., 34, 471 (1961).

As to the constitution of extracted thiocyanatoiron(III) complex, no definite conclusion can be drawn as yet relating to the ratio of thiocyanate ions to iron in the complex. Babko[3] has reported the existence of $HFe(NCS)_4$ in an ether phase analogously to $HFeCl_4$ [4]. Other authors have postulated a complex having the chemical formula of $Fe(NCS)_3$ [5-8]. In our attempt to determine the ratio by gravimetric analysis of iron and sulfur as ferric oxide and barium sulfate, respectively, the values obtained are ranged over 3 to 4, the mean value being 3.6. On the other hand, repeated attempts were made to prepare crystalline thiocyanatoiron(III) complex by the evaporation of organic solutions. In no case was a pure product obtained, as the product always contained an insoluble residue whose magnetic moment was slightly smaller than that expected for a complex having five unpaired electrons. These problems are going to be studied in our laboratory and will be reported in the future. But, at least it is clearly concluded that what was extracted by the organic solvent was a higher complex possessing three or four thiocyanate ions in it. The fact that the absorption maximum in the ether phase shifts to longer region than that in the aqueous solution, that is, about 470 m$\mu$ to 511 m$\mu$, supports the existence of the higher complex in the organic phase, when we take into account the bathochromic effect due to the increase of thiocyanate ions in the complexes.

Thus, the remarkable time change of the magnetic moment of thiocyanatoiron(III) complexes which we confronted in the aqueous solution and reported previously can be attributed to the dimer possessing hydroxo bridges and the inner orbital type of binding with the smaller magnetic moment.

3) A. K. Babko, *Chem. Abstr.*, **51**, 4121 *b* (1957).
4) R. J. Myers, D. E. Metzler and E. H. Swift, *J. Am. Chem. Soc.*, **72**, 3767 (1950).
5) J. Y. McDonald, K. M. Mitchell and A. T. S. Mitchell, *J. Chem. Soc.*, **1951**, 1574.
6) K. M. Mitchell and J. Y. McDonald, ibid., **1951**, 1310.
7) L. Melnik, H. Fraser and H. F. Beeghly, *Anal. Chem.*, **25**, 867 (1953).
8) A. Okáč and M. Hniličková, *Collection Czechoslov. Chem. Communs.*, **25**, 68 (1960).

**Summary**

Thiocyanatoiron(III) complex was extracted by organic solvents. The magnetic moment of the complex was found to be 6.0 Bohr magnetons which is characteristic of the iron(III) complexes possessing the outer orbital type of binding. The absorption spectrum in the visible region of the complex shows the maximum of absorbance at 511 m$\mu$.

The writer's hearty thanks are due first to Professor H. Takaki for his supervision and guidance throughout this work. She would like to express her thanks to Dr. N. Kawai for his advice and help in constructing the magnetometer. The author desires to extend her sincere thanks to Dr. Y. Yamamoto whose discussion and encouragement given throughout the experiments were so fruitful. She also thanks Mrs. F. Morii and Mr. M. Mekata who kindly helped with the measurements.

*Department of Chemistry*
*Faculty of Science*
*Kyoto University*
*Sakyo-ku, Koyto*

# *The Effects of Various Spinning Processes on the Fine Structure of Viscose Rayon Staples (Distribution of Chain Length of Oxidizing-hydrolyzed Residue)*

By Taketoshi KŌSHIRO and Toshikazu FUJIMURA

(Received September 29, 1959)

The object of this paper is to study the effects of various spinning processes on the fine structure of viscose rayon staples.

In the preceding paper[1], it was suggested that the distribution of crystalline size could be shown by the chain-length distribution of oxidizing-hydrolyzed residue. Determination of the average crystalline size expressed by the average degree of polymerization of acid hydrolyzed residue has been reported by many

* This paper was partially presented at the 23rd Viscose Symposium, Takatsuki, September, 1958.

1) T. Kōshiro, K. Yagami, E. Shiratsuchi and T. Fujimura, This Bulletin, 31, 606 (1958).

authors[2]. These methods, however, except for electron-microscopy[3], give little information on the distribution of crystalline size.

The oxidizing-hydrolysis conditions employed in the preceding report were so mild that it took a long time to obtain the crystalline portion of cellulose fibers. Therefore, the modification of the oxidizing-hydrolysis conditions was studied at first and revised. Various types of rayon staples (spun in concentrated sulfuric acid, dilute sulfuric acid, high zinc per cent Müller's bath etc.) were then compared by the improved method.

Carboxyl groups of oxdizing-hydrolyzed residue were determined to clarify the cause of abnormally low iodine sorption.

The relation between the distribution of crystalline size and the lateral-order distribution by Yurugi-Maeda's method was discussed.

## Experimental

**Oxidizing-hydrolysis.**—The samples were refluxed at 100±1°C in the mixture of 4 N sulfuric acid and 0.3 N potassium dichromate for 30 min. After the predetermined time, the residues were filtered off with a glass-filter and washed with hot water and methanol, and then dried in vacuo at 60°C for five hours and their yields were determined.

**Chain-length Distribution.**—The oxidizing-hydrolyzed residue was nitrated and fractionated as in the preceding report[1].

**Carboxyl Group.** — The carboxyl content was determined by titration with EDTA[4].

## Results

**Oxidizing-hydrolysis.**—Since the logarithm of the yield of residues decreases inverse-proportionally to the reaction time, as shown in Fig. 1, crystallinity $C$ is obtained by the extraporation of this time curve to zero. The crystallinity and the characteristics of crystalline portions of various rayons are given in Table I, where $R_5$ is the yield of residue after 5 hr.-hydrolysis, $\bar{P}$ is the average size of crystalline portion expressed by degree of polymerization, $U$ is the uniformity of the degree of polymerization, $P_m$ is the mode of D. P. distribution, which corresponds to the peak in the crystalline size distribution curve. The samples, which were spun in Müller's bath or in its modifications (B, Z and C) have lower crystallinity.

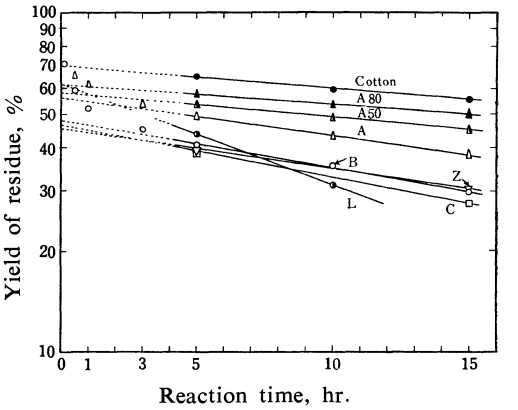



Fig. 1. Oxidizing-hydrolysis behavior of various types of rayons and cotton.

| Mark | Type of rayon |
|---|---|
| B | Ordinary rayon, spun in Müller's bath. |
| C | Commercial tire cord, |
| Z | High tenacity rayon, spun in high zinc per cent Müller's bath. |
| L | Toramomen type, spun in dilute sulfuric acid. |
| A | Lilienfeldt type, spun in concentrated sulfuric acid. |
| A50 A, A80 | treated with aqueous alkali solution, 50 and 80 g./l. of NaOH, respectively. |

TABLE I. CRYSTALLINITY AND THE CHARACTERISTICS IN CRYSTALLINE PORTIONS OF VARIOUS TYPES OF RAYON

| Mark of fiber | $R_5$ % | $C_0$ % | $\bar{P}$ | $U$ | $P_m$ |
|---|---|---|---|---|---|
| B | 41.1 | 49 | 14.1 | 0.31 | 10~13 |
| C | 39.5 | 47 | 7.4 | 0.09 | 6~7.5 |
| Z | 39.5 | 46 | 8.3 | 0.25 | 8 |
| L | 43.9 | 62 | 11.0 | 0.11 | 9 |
| A | 49.6 | 56 | 17.5 | 0.27 | 11~15 |
| A50 | 53.6 | 58 | 19.1 | 0.16 | 15 (32) |
| A80 | 56.8 | 62 | 28.2 | 0.66 | 10~20(41) |

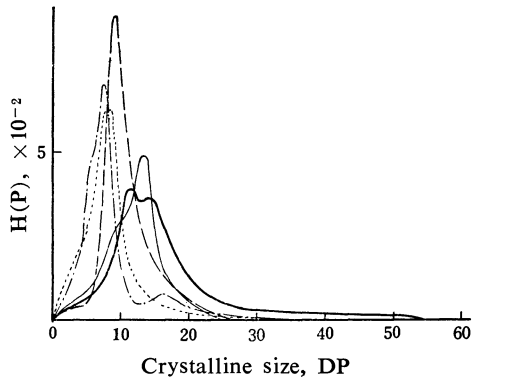



Fig. 2. Crystalline size distribution of various types of rayons.

—— B, ---- Z, —·— C, ——— L, ▬ A

2) See e. g., R. F. Nickerson, *Ind. Eng. Chem.*, **33**, 1022 (1941): **34**, 85, 1480 (1942); T. Yurugi, *Bull. Textile Research Inst. Japan*, No. 19 (1951); F. F. Morehead, *Textile Research J.*, **20**, 549 (1950); A. Sharples, *Trans. Faraday Soc.*, **53**, 1003 (1957); **54**, 113 (1958).

3) B. G. Rånby and E. A. Immergut, *Ind. Eng. Chem.*, **48**, 1183 (1956).

4) K. Ueno and Y. Yamaguchi, *J. Japan. Chem.* (*Kagaku-no-Ryoiki*), **6**, 38 (1952).

**Distribution of Crystalline Size.**—As shown in Fig. 2, the distribution curves have only one peak. From Fig. 3, some correlations between the average size of crystallites and the peak $P_m$ may generally be observed. It is noteworthy that by alkali treatment, $P_m$ of Lilienfeldt-type rayon shifts to a higher D. P. showing two peaks in its distribution chart and the longer one with almost twice the length of the shorter one (Fig. 4).

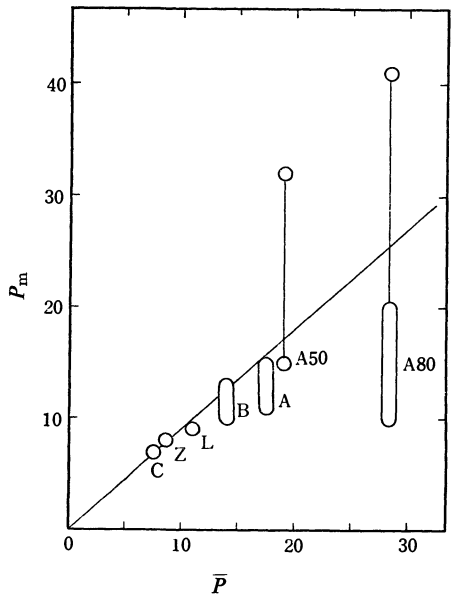



Fig. 3. Correlation between average crystalline size $\bar{P}$ and the crystalline size with maximum frequency in distribution ($P_m$).

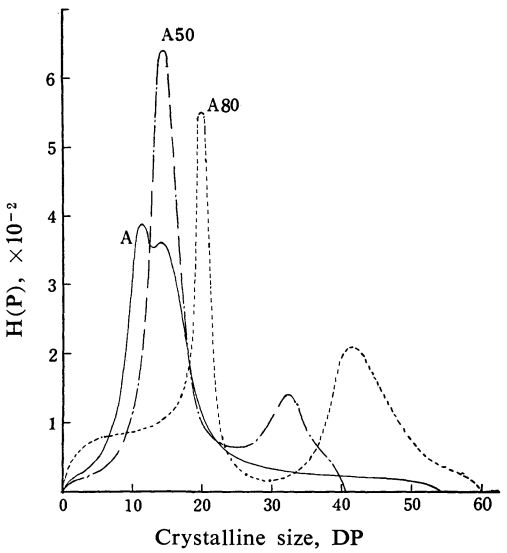



Fig. 4. Change of crystalline size distribution of Lilienfeldt-type rayon (sample A) by alkali treatment.

**Effect of Alkali Treatment.**—Lilienfeldt-type rayon and Müller's bath-type rayon which have clearly different fine structures, were immersed in alkaline solutions of various concentrations and then oxidizing-hydrolyzed. The results given in Fig. 5-a show that the apparent crystallinity that is, the yield of crystalline residue calculated on the basis of sample weight after alkali treatment increases in both Lilienfeldt and ordinary rayon after alkali treatment, and

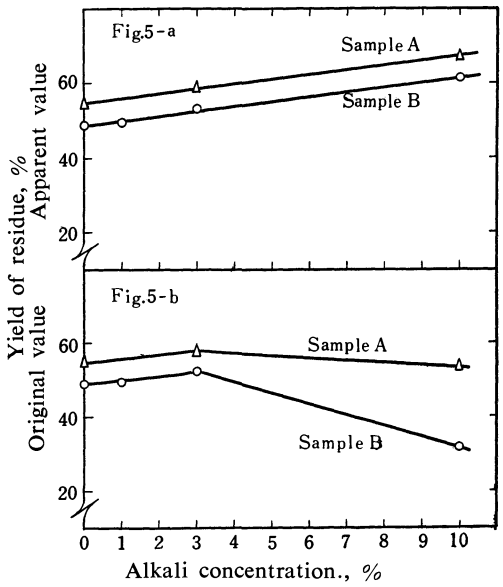



Fig. 5. Effect of alkali treatment on the yield of residue, calculated on the basis of sample weight after alkali treatment (Fig. 5-a) and untreated sample weight (Fig. 5-b).

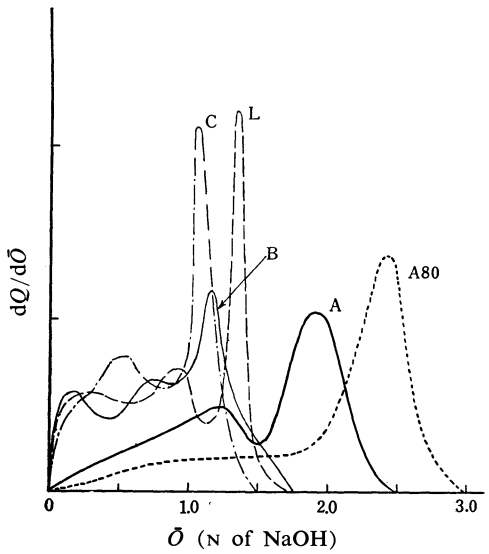



Fig. 6. Lateral-order distribution of various types of rayons by Yurugi-Maeda's method.

the tendency for recrystallization appears to be entirely the same. However, a different tendency is observed between Lilienfeldt and ordinary rayon when calculated on the basis of untreated sample weight. (Fig. 5-b)

**Relation between Crystalline Size Distribution and Lateral Order Distribution by Yurugi-Maeda**[5].—The lateral order distributions given in Fig. 6 are compared with the crystalline size distributions shown in Fig. 4. It is found that the modes of lateral order distribution, $O_m$, increase with $P_m$ or $\bar{P}$ (Fig. 7). The higher $P_m$ might correspond to the higher $O_m$.

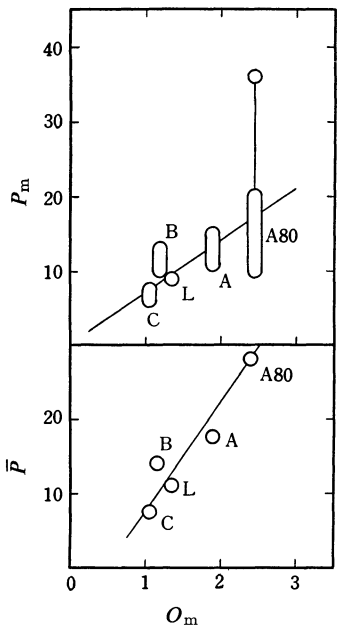



Fig. 7. The relationship between lateral-order distribution and crystalline size distribution characteristics.

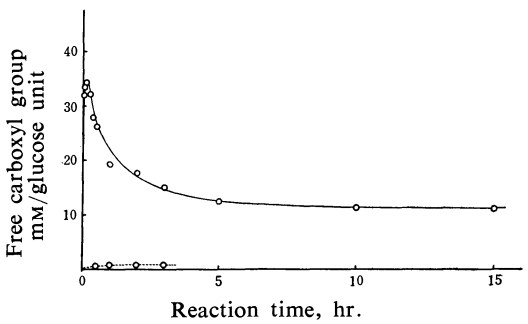



Fig. 8. Rise and fall of amount of carboxyl group during oxidizing-hydrolysis.

—— Oxidizing-hydrolysis
--- Ordinary hydrolysis with 4 N $H_2SO_4$ alone.

5) H. Maeda, *J. Soc. Textile Cellulose Ind., Japan (Sen-i Gakkai-shi)*, **12**, 6 (1956), etc.

**Carboxyl Group of Oxidizing-Hydrolyzed Residue.**—As shown in Fig. 8, the carboxyl group in oxidizing-hydrolyzed residue of Müller's bath-type rayon increased rapidly to a maximum value in the initial five minutes and decreased gradually to a levelling-off value after 5~8 hr.

## Discussion

The chief reason why the crystalline size in our experiment was smaller than the measured values by small angle X-ray scattering, electron microscope or viscosity of cuprammonium solution of the hydrolysis residue, may be due to the fact that the Staudinger's $K_m$ constant used for calculation was not appropriate, but it is justifiable for the purpose of comparing sizes. According to this experiment, not only the mean size of crystallites but also their distribution is indicated with rayons produced by different methods—particularly, spun in various kind of spinning baths. High tenacity rayon of high percentage zinc bath is generally composed of uniform and small crystallites but the size of crystallites of the Lilienfeldt-type rayon is large and also the distribution is not perfectly uniform indicating two distribution peaks, large and small. It is well known that when viscose rayon is treated with aqueous alkali solution of appropriate concentration, generally, the orientation of crystallites is disturbed, the strength is reduced and the elongation is improved, and it has also been confirmed by electron microscopy, X-ray and acid hydrolysis that the mean length of crystallites increases[6].

However, when seen from the viewpoint of distribution of length of crystallites, the entire distribution tends to increase in length of crystallites when Lilienfeldt-type rayon is treated with alkali and also, other peaks in the vicinity of about twice the peak of short particles become higher. This probably indicates the possibility that within the crystalline region of Lilienfeldt-type rayon, there is originally a defective part in short crystals which swells and relaxes by alkali treatment, next it deswells and recrystallizes during drying and fuses into one crystal. Of course, this manner of assumption is ideological and it is natural to assume that the distribution of crystallite length is not necessarily the fusion of two crystallites which recrystallize but growth occurs at the terminating part of the crystallites.

6) See e. g., P. H. Hermans and A. Weidinger, *Nature*, **165**, 238 (1950); *J. Polymer Sci.*, **6**, 533 (1951); K. Katō and K. Yamada, *High Polymer Chemistry (Kōbunshi Kagaku)*, **16**, 627 (1959); *Textile Research J.*, **29**, 368 (1959).

**Crystalline Size Distribution and Lateral Order Distribution.** — There are many low lateral order parts in fibers with many small crystallites and many high lateral order parts in fibers with large crystallites. Also, as the mode of lateral order distribution of Lilienfeldt-type rayon will shift to the high order side when its crystalline size moves to the larger side by alkali treatment, it can be assumed that lateral order distribution is affected by distribution of length of crystallites, in addition to hydrogen bond density. The small difference between both distributions may be due to the difference in the degree of depolymerization.

**Accessibility of Oxidizing-hydrolysis Residue.** —In view of the fact that, at first, carboxyl group increases rapidly and then reduces to its levelling-off value, it seemed reasonable to assume that, at first, the amorphous part is rapidly oxidized, then the oxidized amorphous part is removed by hydrolysis and finally a part of the carboxyl radicals remain on the surface of the crystallites. Therefore, it is possible that the iodine absorption accessibility of the residue is much lower than that for the residue of ordinary hydrolyzed residue due to the repulsion of iodine anion by carboxyl radicals.

**Summary**

The fractionation of oxidizing-hydrolyzed residue was applied to study the fine structure of various types of rayons.

It was assured that tirecord, high-tenacity rayon spun in high zinc percent Müller's bath, Toramomen and ordinary rayon have one sharp peak in each crystalline size distribution curve and smaller crystallites than Lilienfeldt-type rayon which shows two peaks in the crystalline size distribution curve.

The alkali-treatment of Lilienfeldt-type rayon increases not only its crystallinity but also the crystalline size, probably owing to the fusion of two adjacent crystallities.

There can be a correlation between the crystalline size distribution by oxidizing-hydrolysis and the lateral-order distribution; namely, the higher lateral-order portion may consist of the longer crystallite.

The carboxyl group in the oxidizing-hydrolyzed residue increases rapidly in the initial stage of hydrolysis and then decreases to an equilibrium value. The apparently lower accessibility by iodine sorption may be due to the negative carboxyl group remaining.

*Yatsushiro Laboratory*
*Kokoku Rayon and Pulp Co., Ltd.*
*Yatsushiro-shi, Kumamoto-ken*

# *On the Studies of the Friedel-Crafts Acylation. II. The Relative Reactivity for Some Acyl Halides*

By Yoshiaki YAMASE

(Received August 29, 1960)

In Part I[1] the relative reactivities for benzoyl halides, phenylacetyl halides, and mesitoyl halides were measured by Calloway's method and Olivier's method; it was confirmed that the order of reactivity observed is not always in agreement with the order for acetyl halides obtained by Calloway,

$$CH_3COF < CH_3COCl < CH_3COBr < CH_3COI$$

In the present study the relative reactivities for acetyl halides, propionyl halides, isobutyryl halides, cyclohexanecarbonyl halides, and trimethylacetyl halides in the Friedel-Crafts acylation were measured by Calloway's method, and the effect of structure on the order of reactivity for acyl halides was examined. From the observation, it was found that on replacement of the methyl group in acetyl halides with a group with great steric requirement, the order of reactivity for acyl halides varies and does not agree with the order for acetyl halides, but when the methyl group is replaced with a group with a greater steric requirement, the order of reactivity for acyl halides again agrees with the order for acetyl halides.

On the other hand, it was observed that the order of reactivity for acyl halides remains the same in acylation of various aromatic compounds, even when a sterically hindered

1) Y. Yamase and R. Goto, *J. Chem. Soc. Japan, Pure Chem. Sec.* (*Nippon Kagaku Zasshi*), **81**, 1906 (1960).

or activated aromatic position is to be substituted, and is influenced by the structure of acyl halides.

## Experimental

**Methods.** — In measuring the relative reactivity for acyl halides by Calloway's method, the apparatus was the same as that used in Part I, and also in the same manner as that mentioned in Part I the measurement of the temperature was carried out at which the velocity of reaction for various acyl halides becomes sufficient to cause visible bubbles to be evolved. The temperature at which the first visible evolution of hydrogen halide occurred was taken as the temperature at which the measurable reaction began, and it was designated as the temperature of incipient reaction. The inverse order of this temperature, therefore, was regarded as the order of reactivity for the acyl halides.

**Materials.** — The acyl halides used in the acylation were acetyl halides(I), propionyl halides(II), isobutyryl halides (III) cyclohexanecarbonyl halides (IV), and trimethylacetyl halides (V). The fluorides of I, II, and IV were prepared by the reaction between the acyl chlorides and antimony trifluoride, and those of III and V by the interaction between the corresponding carboxylic acids and benzoyl fluoride. The chlorides of II, III, and V were prepared by the interaction between the corresponding carboxylic acids and benzoyl chloride, and that of IV by the interaction between the corresponding carboxylic acid and thionyl chloride. The bromides of I, III, and IV were prepared by the interaction between the corresponding carboxylic acids and phosphorous tribromide, and that of V by the interaction between the corresponding carboxylic acid and benzoyl bromide. The iodides of I, II, III and IV were prepared by the interchange of halogens between the acyl chlorides and hydrogen iodide. The physical constants of these compounds are summarized in Table I.

Table I. Boiling points acyl halides

| | Acyl halides | | |
|---|---|---|---|
| X | $CH_3COX$ | $CH_3CH_2COX$ | $(CH_3)_2CHCOX$ |
| F | 22°C | 42.5~43.5°C | 55~56°C |
| | (20~23°C) | (44°C) | (—) |
| Cl | 50~51°C | 77~78°C | 90°C |
| | (50.9°C) | (80°C) | (92°C) |
| Br | 75~76°C | 98~100°C | 114~115°C |
| | (76.7°C) | (96~98°C) | (116~118°C) |
| I | 104~105°C | 32~34°C/ 16 mmHg | 43~44°C/ 21 mmHg |
| | (108°C) | (127~128°C) | (—) |

| | Acyl halides | |
|---|---|---|
| X | $C_6H_{11}COX$ | $(CH_3)_3CCOX$ |
| F | 146~148°C | 67.5~68°C |
| | (—) | (—) |
| Cl | 180~182°C | 102~104°C |
| | (184°C) | (104°C) |
| Br | 197~198°C | 124~126°C |
| | (—) | (—) |
| I | 103~105°C/11 mmHg | — |
| | (—) | (—) |

The values in parentheses are those reported in the literature.

## Results and Discussion

The orders of reactivity of various acyl halides obtained by Calloway's method are described below.

**Reactivity of Acetyl Halides.** — *Acylation of Benzene.* — A mixture of aluminum chloride (0.1 mol.), benzene (0.3 mol.), and carbon disulfide (95 ml.) was cooled to about −60°C. To the solution was added the acetyl halide (0.1 mol.) in carbon disulfide (5 ml.). After addition, the mixture was warmed slowly and the temperature of incipient reaction was measured. Results are shown in Table II.

*Acylation of Mesitylene.*—A mixture of aluminum chloride (0.01 mol.), mesitylene (0.01 mol.), and carbon disulfide (150 ml.) was cooled to about −60°C. To the solution was added the acetyl halide (0.01 mol.) in carbon disulfide (10 ml.). After addition, the mixture was warmed slowly and the temperature of incipient reaction was measured. Results are shown in Table II.

*Acylation of Anisole.*—A mixture of aluminum chloride (0.01 mol.), anisole (0.01 mol.), and carbon disulfide (150 ml.) was cooled to about −60°C. To the solution was added the acetyl halide (0.01 mol.) in carbon disulfide (10 ml.). After addition, the mixture was warmed slowly and the temperature of incipient reaction was measured. Results are shown in Table II.

From these results, the order of reactivity of the acetyl halides is independent of the nature of aromatic compounds to be acylated and increases in the following order,

$$CH_3COF < CH_3COCl < CH_3COBr < CH_3COI.$$

This order is consistent with that of acetyl halides observed by Calloway[2].

**Reactivity of Propionyl Halide.** — A mixture of aluminum chloride (0.1 mol.), benzene (13.4 g.), and carbon disulfide (100 ml.) was cooled to about −60°C. To the solution was added the propionyl halide (0.1 mol.) in benzene (10 g.). After addition, the mixture was warmed slowly and the temperature of incipient reaction was measured. The reaction mixture was warmed to 30°C over a period of 5 min. from the initiation of hydrogen halide evolution and was maintained at 30°C for 55 min. The yields of ketone from various propionyl halides were obtained by the ordinary method. Results are shown in Table III.

2) N. O. Calloway, *J. Am. Chem. Soc.*, **59**, 1474 (1937).

TABLE II. REACTIVITY OF ACETYL HALIDES

| | Acetyl halides | | | |
|---|---|---|---|---|
| The temp. of incipient reaction | $CH_3COF$ | $CH_3COCl$ | $CH_3COBr$ | $CH_3COI$ |
| In acylation of benzene, °C | 13 | 6 | 0 | −5 |
| In acylation of mesitylen, °C | 15 | 0 | −5 | —* |
| In acylation of anisole, °C | 5; 3 | −10; −8 | −14; −14 | —* |

* The temperature of incipient reaction for acetyl iodide could not be measured, as only a very small amount of it was used in the acylation and also it was readily hydrolyzed.

TABLE III. REACTIVITY OF PROPIONYL HALIDES

| | Propionyl halides | | | |
|---|---|---|---|---|
| | $CH_3CH_2COF$ | $CH_3CH_2COCl$ | $CH_3CH_2COBr$ | $CH_3CH_2COI$ |
| The temp. of incipient reaction, °C | 5 | −1 | −5 | −2 |
| The max. reaction temp. reached, °C | 30 | 30 | 30 | 30 |
| Reaction time, hr. | 1 | 1 | 1 | 1 |
| Ketone isolated, g. | 8.0 | 11.0 | 12.0 | 2.5 |
| Yields of ketone, % | 59.7 | 82.2 | 89.6 | 18.7 |

TABLE IV. REACTIVITY OF ISOBUTYRYL HALIDES

| | Isobutyryl halides | | | |
|---|---|---|---|---|
| | $(CH_3)_2CHCOF$ | $(CH_3)_2CHCOCl$ | $(CH_3)_2CHCOBr$ | $(CH_3)_2CHCOI$ |
| The temp. of incipient reaction, °C | 12 | 5 | 6 | 20 |
| The max. reaction temp. reached, °C | 30 | 30 | 30 | 30 |
| Reaction time, hr. | 1 | 1 | 1 | 1 |
| Ketone isolated, g. | 5.9 | 11.2 | 11.0 | 1.0 |
| Yields of ketone, % | 39.8 | 75.7 | 74.3 | 6.8 |

TABLE V. REACTIVITY OF CYCLOHEXANECARBONYL HALIDES

| | Cyclohexanecarbonyl halides | | | |
|---|---|---|---|---|
| | $C_6H_{11}COF$ | $C_6H_{11}COCl$ | $C_6H_{11}COBr$ | $C_6H_{11}COI$ |
| The temp. of incipient reaction, °C | 12 | 0 | 2 | 22 |
| The max. reaction temp. reached, °C | 30 | 30 | 30 | 30 |
| Reaction time, hr. | 1 | 1 | 1 | 1 |
| Ketone isolated, g. | 4.4 | 10.5 | 10.0 | 1.0 |
| Yields of ketone, % | 23.4 | 55.9 | 53.2 | 5.3 |

From these results, the order of reactivity of the propionyl halides is given as follows,

$$CH_3CH_2COF < CH_3CH_2COCl < CH_3CH_2COBr > CH_3CH_2COI$$

The yields of ketone were in good agreement with the reactivity observed.

**Reactivity of Isobutyryl Halides.**—A mixture of aluminum chloride (0.1 mol.), benzene (18.4 g.), and carbon disulfide (100 ml.) was cooled to about −60°C. To the solution was added the isobutyryl halide (0.1 mol.) in benzene (5 g.). After addition, the mixture was warmed slowly and the temperature of incipient reaction was measured. The yield of ketone was obtained in the usual manner. Results are shown in Table IV.

From these results, the order of reactivity of the isobutyryl halides is as follows,

$$(CH_3)_2CHCOF < (CH_3)_2CHCOCl \fallingdotseq (CH_3)_2CHCOBr > (CH_3)_2CHCOI$$

The yields of ketone were in good agreement with the reactivity observed.

**Reactivity of Cyclohexanecarbonyl Halides.**—A mixture of aluminum chloride (0.1 mol.), benzene (15.4 g.), and carbon disulfide (100 ml.) was cooled to about −60°C. To the solution was added the cyclohexanecarbonyl halide (0.1 mol.) in benzene (8 g.). After addition, the mixture was warmed slowly and the temperature of incipient reaction was measured. The yield of ketone was obtained by the same method. Results are shown in Table V.

From these results, the order of reactivity of the cyclohexanecarbonyl halides is given

Table VI. Reactivity of trimethylacetyl halides

| | Trimethylacetyl halides | | |
|---|---|---|---|
| | $(CH_3)_3CCOF$ | $(CH_3)_3CCOCl$ | $(CH_3)_3CCOBr$ |
| The temp. of incipient reaction, °C | −10 | −19 | −30 |

Table VII. Reactivity of benzoyl halides

| | Benzoyl halides | | | |
|---|---|---|---|---|
| The temp. of incipient reaction, | $C_6H_5COF$ | $C_6H_5COCl$ | $C_6H_5COBr$ | $C_6H_5COI$ |
| In acylation of mesitylene, °C | 15 | 0 | 0 | 10 |
| In acylation of anisole, °C | 13 ; 15 | 3 ; 4 | 4 ; 4 | 12 ; 12 |

Table VIII. Reactivity of acyl halides

| Acyl halides | Compounds to be acylated | Solvents | The orders of reactivity for acyl halides |
|---|---|---|---|
| $CH_3COX$ | Benzene | $CS_3$ | F<Cl<Br<I |
| 〃 | Mesitylene | 〃 | 〃 |
| 〃 | Anisole | 〃 | 〃 |
| $CH_3CH_2COX$ | Benzene | 〃 | F<Cl<Br>I |
| $C_6H_5CH_2COX$ | 〃 | 〃 | 〃 |
| 〃 | 〃 | $C_6H_5NO_2$ | F<Cl>Br>I |
| $(CH_3)_2CHCOX$ | 〃 | $CS_2$ | F<Cl=Br>I |
| $C_6H_{11}COX$ | 〃 | 〃 | 〃 |
| $C_6H_5COX$ | 〃 | 〃 | 〃 |
| 〃 | Mesitylene | 〃 | 〃 |
| 〃 | Anisole | 〃 | 〃 |
| $2,4,6\text{-}(CH_3)_3C_6H_2COX$ | 〃 | 〃 | F<Cl<Br<I |
| 〃 | 〃 | $C_6H_5NO_2$ | 〃 |
| $(CH_3)_3CCOX$ | 〃 | $CS_2$ | 〃 |

as follows,

$$C_6H_{11}COF < C_6H_{11}COCl \fallingdotseq C_6H_{11}COBr > C_6H_{11}COI$$

The yields of ketone were in good agreement with the reactivity observed.

**Reactivity of Trimethylacetyl Halides.** — A mixture of alminum chloride (0.005 mol.), anisole (0.005 mol.), and carbon disulfide (140 ml.) was cooled to about −60°C. To the solution was added the trimethylacetyl halide (0.005 mol.) in carbon disulfide (10 ml.). After addition, the mixture was warmed slowly and the temperature of incipient reaction was measured. Results are shown in Table VI.

From these results, the order of reactivity of the trimethylacetyacetyl halides is given as follows,

$$(CH_3)_3CCOF < (CH_3)_3CCOCl < (CH_3)_3CCOBr (< (CH_3)_3CCOI)$$

**Reactivity of benzoyl halides.** — *Acylation of Mesitylene.* — A mixture of aluminum chloride (0.01 mol.) and carbon disulfide (90 ml.) was cooled to about −60°C. To the solution were added the benzoyl halide (0.01 mol.) and mesitylene (0.01 mol.) in carbon disulfide (10 ml.). After addition, the mixture was warmed slowly and the temperature of incipient reaction was measured. Results are shown in Table VII.

*Acylation of Anisole.*—A mixture of aluminum chloride (0.01 mol.), anisole (0.01 mol.), and carbon disulfide (100 ml.) was cooled to about −60°C. To the solution was added the benzoyl halide (0.01 mol.) in carbon disulfide (10 ml.). After addition, the mixture was warmed slowly and the temperature of incipient reaction was measured. Results are shown in Table VII.

From these results, it is seen that the order of reactivity for the benzoyl halides is independent of the nature of aromatic compounds to be acylated and is given as follows,

$$C_6H_5COF < C_6H_5COCl \fallingdotseq C_6H_5COBr > C_6H_5COI$$

These orders of reactivity for the acyl halides obtained in the present study and in Part I are summarized in Table VIII.

To summarize, it was observed that when R group in acyl halides RCOX is replaced successively with $CH_3$- group, $CH_3CH_2$- and $C_6H_5CH_2$- groups, and $(CH_3)_2CH$-, $C_6H_{11}$-, and $C_6H_5$- groups, the orders of reactivity vary as follows as a result of the steric hindrance of R group, RCOF < RCOCl < RCOBr < RCOI ($R=CH_3$-), RCOF < RCOCl < RCOBr > RCOI

($R=CH_3CH_2-$ and $C_6H_5CH_2-$), and RCOF $>$ RCOCl $\fallingdotseq$ RCOBr $>$ RCOI ($R=(CH_3)_2CH-$, $C_6H_{11}-$, and $C_6H_5-$) respectively. In the acylation by mesitoyl halides and trimethylacetyl halides, the orders of reactivity were observed as follows, RCOF $<$RCOCl $<$RCOBr $<$RCOI, in spite of the large steric hindrance of $(CH_3)_3C_6H_2-$ and $(CH_3)_3C-$ groups.

On the other hand, it was observed that in acylation of benzene, anisole, and mesitylene the orders of reactivity for benzoyl halides and acetyl halides do not change, and are given as follows, $C_6H_5COF < C_6H_5COCl \fallingdotseq C_6H_5COBr > C_6H_5COI$ and $CH_3COF < CH_3COCl < CH_3CBr < CH_3COI$ respectively.

Thus it may be suggested that the order of reactivity of acyl halides does not change even when a sterically hindered or activated aromatic position is to be substituted; that is, the order of reactivity depends only on the structure of acyl halides.

The author wishes to thank Professor Ryozo Goto, Kyoto University, for his helpful discussions and criticisms.

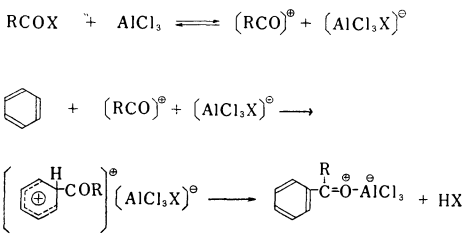
*Chemistry Institute*
*Faculty of Science*
*Kyoto University*
*Sakyo-ku, Kyoto*

# *On the Studies of the Friedel-Crafts Acylation. III. The Reaction Mechanism*

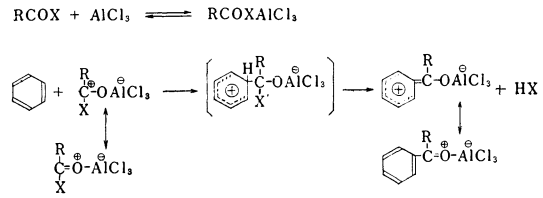
By Yoshiaki YAMASE

(Received September 12, 1960)

The two types of mechanism, ionic and substitution mechanisms, are generally accepted at the present time for the Friedel-Crafts acylation. The concept of an ionic mechanism[1-3] is that the attacking agent is an acylium ion produced by ionization of an acyl halide under the catalytic influence of aluminum chloride. The concept of a substitution



mechanism[4-8] is that the attacking agent is an addition complex produced by the interaction of an acyl halide and aluminum chloride.



Since some evidence exists for both ionic and substitution mechanisms, they may not be dismissed.

Recently, a duality of mechanism for the Friedel-Crafts acylation, the concept of which is that the acylation by acyl halides under the influence of aluminum chloride takes place by both ionic and substitution mechanisms, seems to offer an attractive hypothesis[9-12], and it appears likely that the acylation by acyl halides under the influence of aluminum chloride takes place by one of two mechanisms, depending on the reactivity of aromatic substances and acyl halides; that is, the normal Friedel-Crafts acylation may proceed mainly by the substitution mechanism, but when a sterically hindered acyl halide is used, or when a sterically hindered aromatic position is to

1) F. Fairbrother, *J. Chem. Soc.*, **1937**, 503.
2) G. Baddeley et al., ibid., **1954**, 418.
3) F. Fairbrother, *Trans. Faraday Soc.*, **37**, 763 (1941).
4) R. Pajean, *Bull. soc. chim. France* [5] **13**, 544 (1946).
5) J. C. Butler et al., *J. Am. Chem. Soc.*, **76**, 1906 (1954).
6) H. Burton et al., *J. Chem. Soc.*, **1950**, 2034.
7) P. H. Groggins, "Unit Processes in Organic Synthesis" McGraw-Hill, New York (1952), p. 866.
8) H. C. Brown et al., *J. Am. Chem. Soc.*, **76**, 605 (1954).
* The above formulas were quoted from P. H. Gore, *Chem. Revs.*, **54**, 232 (1955).
9) H. Burton et al., *Chemistry & Industry*, **1954**, 90.
10) J. M. Tedder, ibid., **1954**, 630.
11) P. H. Gore, ibid., **1954**, 1385.
12) P. H. Gore, *Chem. Revs.*, **54**, 229 (1955).

be substituted, the ionic mechanism becomes important.

The order of reactivity for acetyl halides in the Friedel-Crafts acylation has been found by Calloway to be $CH_3COF < CH_3COCl < CH_3COBr < CH_3COI$, and it has been inferred from this evidence that the order of reactivity for acyl halides is the same as that for acetyl halides[13,14].

Now, if the Friedel-Crafts acylation proceeds by the ionic mechanism, the reactivity for acyl halides depends on the equilibrium concentration of the acylium ion produced by ionization of acyl halides in the presence of aluminum chloride,

$$RCOX + AlCl_3 \rightleftarrows [RCO]^+ + [AlCl_3X]^-$$

and the concentration of the acylium ion depends on the lability of the carbon-halogen bond in acyl halides. Therefore, the order of reactivity of acyl halides should be

$$RCOF < RCOCl < RCOBr < RCOI$$

On the other hand, if the Friedel-Crafts acylation proceeds by the substitution mechanism, the reactivity for acyl halides should be identical with the reactivity for the addition complexes produced from acyl halides and aluminum chloride, because the attacking agent in this case is the addition complex. Then, the reactivity for acyl halides must be influenced not only by the lability of the carbon-halogen bond, but also by the steric effect of the halogen atom which reduces the reactivity of acyl halides as follows,

$$RCOF > RCOCl > RCOBr > RCOI$$

Therefore, it is possible that the order of reactivity for acyl halides does not always agree with the order of reactivity for acetyl halides.

Taking the above facts into consideration, the determinations of reactivities for some acyl halides in the presence of aluminum chloride in the Friedel-Crafts acylation have been carried out in Parts I[15] and II[16], and it has been observed that the order of reactivity for acyl halides may be influenced by the structure of acyl halides.

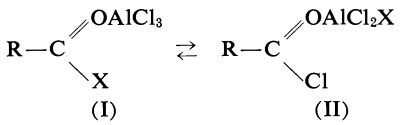
On the replacement of the methyl group in acetyl halides with a group with great steric requirement, the order of reactivity for acyl halides does not consist with the order for acetyl halides. But, when the methyl group is replaced with a group with greater steric requirement, the order of reactivity for acyl halides becomes consistent with the order for acetyl halides.

These phenomena can be explained reasonably on the basis of the concept that the normal Friedel-Crafts acylation proceeds mainly by the substitution mechanism, but when a sterically hindered acyl halide is used, the acylation proceeds by the ionic mechanism.

## Discussion

The halogen exchange reactions have been observed between acetyl chloride and aluminum chloride in which some of the chlorine atoms are radioactive isotopes[1], and also between 2, 4, 6-tribromobenzoyl chloride, or 2, 4, 6-trimethylbenzoyl chloride and aluminum bromide[2].

If the acylation proceeds by the substitution mechanism, it is conceivable that the attacking agents are the complexes I and II, and in the complete halogen exchange the ratio of the concentration of the complexes I and II will be 1/3.




On the assumption that there is scarcely any difference between the catalytic ability of $AlCl_3$ and $AlCl_2X$, it may be considered that of the two different kinds of complexes produced by the interaction between aluminum chloride and various acyl halides, the complexes II, $RCOClAlCl_2X$, have similar reactivities regardless of the nature of X (F, Cl, Br and I).

From this assumption, the difference of reactivities of acyl halides is nothing but that of reactivities of the complex, I, $RCOXAlCl_3$, and the order of reactivity of acyl halides can be explained by considering the difference of reactivity of the complex I.

The reactivity of the complex I is influenced by the lability of the carbon-halogen bond and the steric hindrance of the halogen atom; the effect of the carbon-halogen bond energy on the reactivity for the complex I increases in the following order, $F < Cl < Br < I$, and the steric hindrance of the halogen atom may reduce the reactivity of the complex I as follows, $F > Cl > Br > I$.

In the substitution mechanism, the order of reactivity of acyl halides is influenced by both the lability of the carbon-halogen bond and the steric hindrance of the halogen atom simultaneously and does not always agree with the order of acetyl halides.

On the other hand, in the ionic mechanism the reactivity of acyl halides depends on the equilibrium concentration of the acylium ion

13) N. O. Calloway, *J. Am. Chem. Soc.*, **59**, 1474 (1937).
14) N. O. V. Sonntag, *Chem. Revs.*, **52**, 345 (1953).
15) Y. Yamase, R. Goto, *J. Chem. Soc. Japan, Pure Chem. Sec.* (*Nippon Kagaku Zasshi*), **81**, 1906 (1960).
16) Y. Yamase, This Bulletin, **34**, 480 (1961).

TABLE I. REACTIVITY OF ACYL HALIDES

| Acyl halides | Compound to be acylated | Solvent | The order of reactivity of acyl halides |
|---|---|---|---|
| $CH_3COX$ | Benzene | $CS_2$ | F<Cl<Br<I |
| 〃 | Mesitylene | 〃 | 〃 |
| 〃 | Anisole | 〃 | 〃 |
| $CH_3CH_2COX$ | Benzene | 〃 | F<Cl<Br>I |
| $C_6H_5CH_2COX$ | 〃 | 〃 | 〃 |
| 〃 | 〃 | $C_6H_5NO_2$ | F<Cl>Br>I |
| $(CH_3)_2CHCOX$ | 〃 | $CS_2$ | F<Cl=Br>I |
| $C_6H_{11}COX$ | 〃 | 〃 | 〃 |
| $C_6H_5COX$ | 〃 | 〃 | 〃 |
| 〃 | Mesitylene | 〃 | 〃 |
| 〃 | Anisole | 〃 | 〃 |
| 2,4,6-$(CH_3)_3C_6H_2COX$ | 〃 | 〃 | F<Cl<Br<I |
| 〃 | 〃 | $C_6H_5NO_2$ | 〃 |
| $(CH_3)_3CCOX$ | 〃 | $CS_2$ | 〃 |

which, in turn, depends on the lability of the carbon-halogen bond in acyl halides. Then, the order of reactivity of acyl halides is influenced by the magnitude of the carbon-halogen bond energy and increases as follows

$$F < Cl < Br < I$$

Upon these considerations, the experimental data of reactivities for some acyl halides summarized in Table I can be reasonably explained.

**Acylation of Benzene in Carbon Disulfide or Benzene.**—In acylation of benzene in a nonpolar solvent, carbon disulfide or benzene, the order of reactivity of acetyl halides was RCOF < RCOCl <RCOBr<RCOI; for propionyl and phenylacetyl halides it was RCOF<RCOCl < RCOBr>RCOI, and for isobutyryl, cyclohexanecarbonyl, and benzoyl halides it was RCOF< RCOCl≒RCOBr>RCOI.

These results may be explained reasonably by the substitution mechanism. It has generally been considered that in the substitution mechanism the addition complex $RCOXAlCl_3$ attacks the aromatic substance by the displacement reaction of $S_N2$ type. Then, it must be considered how much effect the lability of the carbon-halogen bond and the steric hindrance of the $OAlCl_3$, R, and X groups have on the reactivity of the complex. The $OAlCl_3$ group in the addition complex may be considerably bulky and be common to various addition complexes.

In acylation by acetyl halides the reactivity of the addition complex is influenced by the lability of the carbon-halogen bond alone, since the steric hindrance of the methyl group is small. Therefore, the order of reactivity for acetyl halides is F<Cl <Br<I.

In acylation by propionyl and phenylacetyl halides, the steric hindrances of ethyl and phenylmethyl groups become great, and the reactivities of the addition complexes are influenced not only by the lability of the carbon-halogen bond but also by the steric hindrance of the halogen atom caused by the sterically hindered R groups. Consequently, the orders of reactivities of these acyl halides become F<Cl<Br>I.

In acylation by isobutyryl, cyclohexanecarbonyl, and benzoyl halides, the steric hindrances of isopropyl, cyclohexyl, and phenyl groups become considerably great, and the orders of reactivities of these addition complexes are influenced not only by the lability of the carbon-halogen bond but also by the steric hindrance of the halogen atom caused by the sterically hindered R groups. Accordingly, the orders of reactivities for these acyl halides become F<Cl≒Br>I.

**Acylation of Anisole by Mesitoyl Halides and Trimethylacetyl Halides.**—In acylation of anisole by mesitoyl[2] and trimethylacetyl halides[17], the reaction has been believed to occur by the ionic mechanism. As reported in the previous reports, in spite of the large steric hindrance of mesityl and *tert*-butyl groups, the orders of reactivities for these acyl halides were as follows, RCOF <RCOCl<RCOBr<RCOI.

These results are explained reasonably by the ionic mechanism; as a result of the great steric hindrance of acyl halides, the addition complex is not formed and the halide is completely ionized, giving the acylium ion. The acylium ion attacks anisole as an acylating agent, and the order of reactivities for these acyl halides agrees with the order of the lability of the carbon-halogen bond, F <Cl < Br <I.

**Acylation of Benzene by Phenylacetyl Halides and Anisole by Mesitoyl Halides.**—In acylation of benzene by phenylacetyl halides the reaction is believed to proceed by the substitution

17) E. Rothstein et al., *J. Chem. Soc.*, **1949**, 1950.

mechanism, and the order of reactivity of phenylacetyl halides was RCOF< RCOCl< RCOBr>RCOI in a non-polar solvent (carbon disulfide) and RCOF <RCOCl> RCOBr> RCOI in a polar solvent (nitrobenzene).

When the polar solvent, nitrobenzene, is used in place of the non-polar solvent, carbon disulfide, aluminum chloride is solvated with nitrobenzene and it forms bulkier addition complexes with acyl halides. Then, the influence of the steric hindrance of the halogen atom on the reactivity of phenylacetyl halides becomes greater, and consequently the above orders are observed.

On the other hand, in acylation of anisole by mesitoyl halides the reaction is believed to proceed by the ionic mechanism. The order of the lability of the carbon-halogen bond would always be the same regardless of the nature of the solvent and, in fact, the order of reactivity of mesitoyl halides was RCOF<RCOCl< RCOBr<RCOI.

**Acylation of Benzene, Mesitylene, and Anisole by Acetyl Halides and Benzoyl Halides.**—In acylation of benzene, mesitylene, and anisole by acetyl and benzoyl halides, the orders of reactivities of these acyl halides were $CH_3COF < CH_3COCl < CH_3COBr < CH_3COI$, and $C_6H_5COF < C_6H_5COCl \fallingdotseq C_6H_5COBr > C_6H_5COI$, respectively.

These results show that the orders of reactivities of these acyl halides are not influenced even when a sterically hindered or activated aromatic position is to be substituted and these acylations proceed by the same substitution mechanism.

From the above results, it may be considered that the normal Friedel-Crafts acylation by acyl halides proceeds mainly by the substitution mechanism. However, when sterically hindered acyl halides are used, the ionic mechanism becomes important as the formation of the addition complexes becomes difficult; that is, the mechanism of the Friedel-Crafts acylation by acyl halides is influenced by the structure of acyl halides, and not by the nature of the aromatic substances to be acylated.

The author wishes to express his sincere appreciation to Professor Ryozo Goto, Kyoto University, for his helpful discussions and criticisms.

*Chemistry Institute*
*Faculty of Science*
*Kyoto University*
*Sakyo-ku, Kyoto*

# *Iodine-Catalyzed Thermal cis-trans Isomerization of Stilbene*

By Shigeru YAMASHITA

(Received August 16, 1960)

It is well known[1-3] that iodine is an efficient catalyst in the cis-trans isomerization of ethylenic compounds. However, there few studies have been undertaken in the case of stilbene. The present work has been carried out to compare these results with the results of iodine-catalyzed photochemical isomerization[4] of stilbene which is under investigation. For this purpose, just as in photochemical work, *n*-hexane has been used for the solvent and the kinetics of isomerization have been studied in as low a temperature range as possible. From the results obtained the mechanism of isomerization is discussed.

## Experimental

**Materials.**—*cis- and trans-Stilbene and n-Hexane.*—The purification of these compounds has already been described in a previous paper[5].

*Iodine.*—A commercially available reagent was used after several repetitions of sublimation.

**Apparatus and Procedure.**—To exclude the photochemical contribution, the reaction vessel, made of a brown stoppered glass tube 8 cm. long and 1 cm. in diameter, was shielded from any light source[6]. The extent of isomerization in each run, confined to a low conversion, was determined by a spectrophotometric analysis of the reaction mixture after the iodine was removed by a copper coil as described by Dickinson et al.[7] The dependence of rate on

1) G. M. Wyman, *Chem. Revs.*, **55**, 625 (1955).
2) B. Tamamushi, This Bulletin, **19**, 147 (1944).
3) R. E. Wood and R. G. Dickinson, *J. Am. Chem. Soc.*, **61**, 3259 (1939).
4) To be published shortly.
5) S. Yamashita, This Bulletin, **32**, 1212 (1959).
6) A photographic paper which had been left in the reaction vessel for two hours was not blackened on developing.
7) R. G. Dickinson, R. F. Wallis and R. E. Wood, *J. Am. Chem. Soc.*, **71**, 1238 (1949).

TABLE I. RATE MEASUREMENTS AT 68.8, 65.0 AND 62.0°C WITH VARIED CONCENTRATIONS

| Reaction temperature °C | Initial concentration $\times 10^4$ mol./l. Iodine | *cis*-Stilbene | Reaction time hr. | Reaction rate $\times 10^4$ mol./l. hr. |
|---|---|---|---|---|
| 68.8 | 10.0 | 10.0 | 2.0 | 0.19 |
| 68.8 | 10.0 | 5.0 | 2.0 | 0.09 |
| 68.8 | 10.0 | 12.5 | 2.0 | 0.24 |
| 68.8 | 15.0 | 10.0 | 2.0 | 0.23 |
| 68.8 | 5.0 | 10.0 | 2.0 | 0.15 |
| 65.0 | 10.0 | 10.0 | 2.0 | 0.11 |
| 65.0 | 10.0 | 5.0 | 2.0 | 0.05 |
| 65.0 | 10.0 | 12.5 | 2.0 | 0.15 |
| 65.0 | 15.0 | 10.0 | 2.0 | 0.14 |
| 62.0 | 10.0 | 10.0 | 2.0 | 0.09 |
| 62.0 | 10.0 | 12.5 | 2.0 | 0.11 |
| 62.0 | 15.0 | 10.0 | 2.0 | 0.10 |

the concentrations of stilbene and iodine was obtained from the initial rates thus determined for solutions of varied compositions. In some preliminary experiments it was confirmed that in the absence of iodine no conversion to *trans*-stilbene takes place in this temperature range.

## Results and Discussion

The experimental results obtained in the present work are summarized in Table I. Figs. 1 and 2 show the dependence of the rate of isomerization on concentrations of *cis*-stilbene and of iodine, respectively.

These results conform to the rate expression

$$-\mathrm{d}(C)/\mathrm{d}t = k(C)(I_2)^{1/2}$$

where $(C)$ and $(I_2)$ are the concentrations of *cis*-stilbene and iodine, respectively. The Arrhenius plot of rate constant $k$ is shown in Fig. 3, from which the following expression is obtained:

$$k = 9.53 \times 10^{11} \times \exp(-25\ \mathrm{kcal.\ mol^{-1}}/\boldsymbol{RT})$$

$$(\mathrm{l^{1/2}/mol^{1/2}\ sec.})$$

A probable mechanism that explains the above rate equation is analogous to the one that Dickinson and his coworker proposed for the iodine-catalyzed thermal isomerization of cinnamic acid[8]:

$$\mathrm{I_2} \rightleftarrows 2\mathrm{I} \qquad (1)$$

$$\mathrm{C} + \mathrm{I} \rightarrow \mathrm{CI} \qquad (2)$$

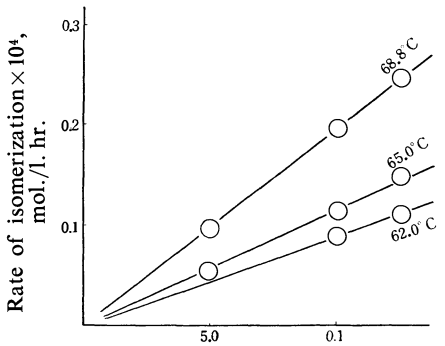



Fig. 1. Dependence of the reaction rate on the concentration of *cis*-stilbene.

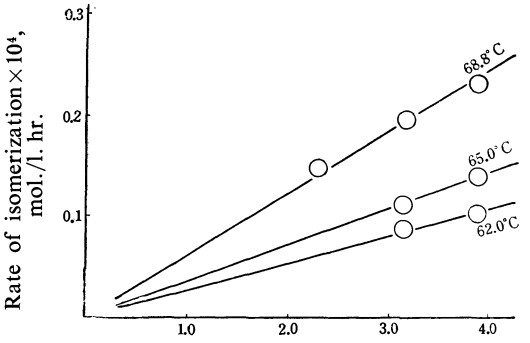



Fig. 2. Dependence of the reaction rate on the concentration of iodine.

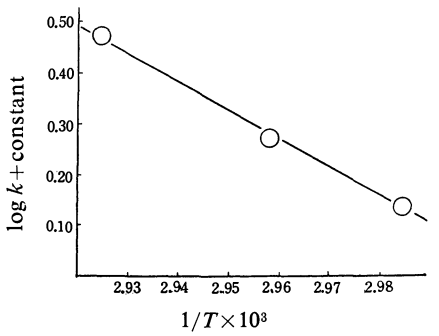



Fig. 3. Temperature dependence of the rate constant.

8) R. G. Dickinson and H. Lotzker, ibid., 59, 472 (1937).

$$CI \rightarrow C + I \quad (3)$$

$$CI \rightarrow TI \quad (4)$$

$$TI \rightarrow T + I \quad (5)$$

Here C and T represent the *cis*- and *trans*-stilbene, respectively. Assuming that reaction (1) is always in equilibrium and that the concentrations of the intermediate complexes CI and TI are sufficiently small in the stationary state, the sequence of reactions (1)—(5) lead to the following rate expression which is in good agreement with the experimental one:

$$-d(C)/dt = K^{1/2}k_2k_4/(k_3+k_4)\cdot(C)(I_2)^{1/2} \quad (6)$$

where $K$ represents the equilibrium constant of reaction (1) and also the $k_1-k_4$ rate constants for respective process (1)—(4). When combined with the dissociation energy of iodine molecules 36 kcal./mol., the overall activation energy of 25 kcal./mol. found above means that the term $k_2k_4/(k_3+k_4)$ in equation (6) has a temperature dependence corresponding to an activation energy of 7 kcal./mol. Accordingly, if $k_3$ is much greater than $k_4$, the activation energy of the step(4) may be represented as follows;

$$E_4 = 7 + Q_{CI} \text{ (kcal./mol.)}$$

where $Q_{CI}$ is the heat of formation of CI.

The present work offers no direct evidence for the intermediate complex CI. However, the formation of such a transient complex has recently been demostrated by a flash technique[9]: by flashing a solution of iodine in benzene, the formation and subsequent decay of a transient complex probably of the composition $C_6H_6\cdot I$ was observed spectroscopically[10].

It has been suggested by a number of workers[11-14] that the cis-trans isomerization catalyzed by paramagnetic molecules and atoms takes place through a triplet state of the substrate. It is therefore not unlikely that a triplet state of stilbene is involved in reaction (4), though the kinetic results obtained in the present work offer no information in favor of such an interpretation.

## Summary

The iodine-catalyzed thermal cis → trans conversion of stilbene has been studied kinetically in *n*-hexane in temperature range 62.0~68.8°C. The reaction rate obtained spectrophotometrically has been found to be proportional to the concentration of *cis*-stilbene and to the square root of iodine concentration. The overall activation energy has been found to be 25 kcal./mol. The results have been interpreted in terms of the thermal dissociation of iodine molecules followed by the formation of a transient complex between *cis*-stilbene and atomic iodine.

The author is particularly indebted to Professor O. Toyama of the College of Engineering and to Dr. T. Hayakawa for their discussions and encouragement during this investigation. The author wishes to thank Mr. H. Matsuda for his assistance.

*Department of Chemistry*
*College of General Education*
*The University of Osaka Prefecture*
*Mozu-Umemachi, Sakai, Osaka*

9) S. J. Rand and R. L. Strong, ibid., **82**, 5 (1960).

10) The present author has studied the formation of 1:1 molecular complexes between iodine and *cis*- and *trans*-stilbene in *n*-hexane and carbon tetrachloride in the temperature range 10~30°C[5]. It may be of interest to investigate whether such a molecular complex participates in the isomerization. Unfortunately, the present study can not give any clue to this problem. In the temperature range in which the isomerization has been studied, the molecular complex $CI_2$ has such a low concentration that its contribution, if any, can not be detected.

11) R. A. Harman and H. Eyring, *J. Chem. Phys.*, **10**, 557 (1942).

12) H. McConnell, ibid., **20**, 1043 (1952).

13) C. Schulte-Frohlinde, *Ann.*, **615**, 131 (1958).

14) J. P. Simons, *Quart. Rev.*, **13**, 3 (1959).

# *Photochemical cis-trans Isomerizatin of Stilbene*

By Shigeru YAMASHITA

(Received August 16, 1960)

The photoisomerization of stilbene has been studied by Lewis and his coworkers[1] using the 254 mμ line of mercury and isooctane as the solvent. In the present investigation which was carried out with *n*-hexane solution, in connection with the study of the iodine-catalyzed photoisomerization of stilbene[2], mercury lines of longer wavelengths i. e., 313 and 334 mμ were employed.

Reaction rates and quantum yields were measured for both cis→trans and trans→cis conversions. Combining the results obtained with other information on stilbene such as fluorescence and phosphorescence, a plausible mechanism for the isomerization is presented.

## Experimental

**Materials.**—*cis-Stilbene.*—The method of preparation described in Ref. 3 was followed. The purified stilbene (b. p. 114~119°C/3.5~4.0 mmHg) was stored in the dark under reduced pressure. The absorption curve obtained with an *n*-hexane solution is given in Fig. 1 which is in good agreement with previous ones obtained with similar solvents[4,5].

*trans-Stilbene.*—The commercial reagent (m. p. 119~120°C) was used without further purification. The absorption curve given in Fig. 1 is again in good agreement with those previously reported[4,5].

*n-Hexane.*—The commercial reagent of chemically pure grade was treated with fuming sulfuric acid, concentrated sulfuric acid, and an aqueous solution of potassium permanganate, successively. After drying over anhydrous calcium chloride, the product was fractionally distilled.

**Apparatus and Procedure.**—For the light source, Mazda SHL-100 type mercury lamp was used. Through collimating quartz lens and appropriate combination of filters, a parallel light beam of a desired wavelength was projected upon the quartz reaction cell of 4-cm. diameter and 2-cm. thickness, immersed in a thermostat, which had a window for irradiation. The light intensity of the mercury lamp was kept constant within 1% by using a voltage stabilizing power supply. Care was taken to exclude scattering light, for it was found to give rise to a considerable error. For experiments with varied light intensities a required mesh of blackened copper gauze previously calibrated for its transmittance was used.

For the cis→trans conversion, Mazda UV-D2 filter combined with a potassium chromate aqueous solution (concentration, 0.2 g./l.; depth, 1.0 cm.) was used, which allowed the light in the range of wavelength 300~350 mμ to be transmitted. Principal lines of mercury which lie in this range and are expected to be effective in the isomerization are 313 and 334 mμ. For the conversion in the reverse direction, a combination of Mazda UV-D2 filter with a copper nitrate aqueous solution (concentration, 83.5 g./l.; depth, 1.0 cm.) served to allow the light in the wavelength range 310~400 mμ to be transmitted*. However, in view of the absorption curve of *trans*-stilbene given in Fig. 1, the mercury lines lying in this range and expected to be effective in the isomerization are again 313 and 334 mμ.

In every run freshly distilled *n*-hexane was used as a solvent, although the effect of the dissolved air in the reaction solution seemed to be practically negligible. Stirring of the reaction mixture in a reaction cell was not devised, because stirring or

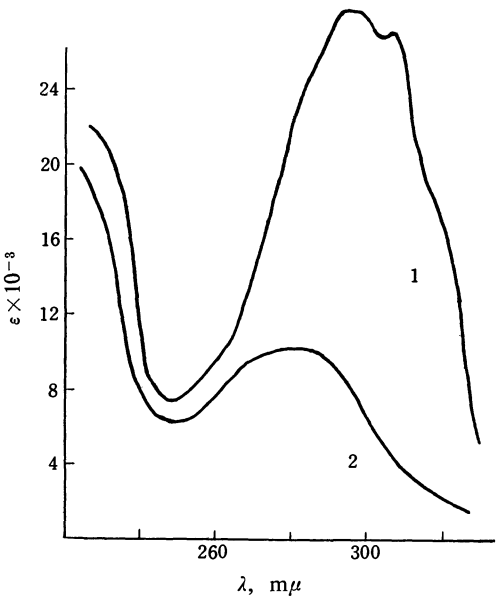



Fig. 1 Molar extinction coefficient for *trans*-stilbene (curve 1) and for *cis*-stilbene (curve 2).

1) G. N. Lewis, T. T. Magel and Lipkin, *J. Am. Chem. Soc.*, **62**, 2973 (1940).
2) To be published shortly.
3) R. E. Buckles and N. G. Wheeler, "Organic Syntheses", Vol. 33, John Wiley & Sons, New York, N. Y. (1953), p. 88.
4) R. N. Beale and E. M. F. Roe, *J. Chem. Soc.*, **1955**, 2755.
5) M. Orchin et al., *J. Chem. Educ.*, **34**, 496 (1957).

* This combination of filters was used to enable the results obtained to be compared with those in the presence of iodine which are to be reported in a later paper.

vibrating of the reaction mixture was found to have no influence on the reaction rate.

Throughout the series of experiments the rate of isomerization was measured only in the initial stage of reaction so that the reverse reaction may be neglected. The change in concentrations of *cis*- and *trans*-stilbene due to the isomerization was determined by Hitachi a EPB-U types pectrophotometer.

The absorbance of the solution was very small in the present work, the concentration of stilbene being of the order of $10^{-5}\sim10^{-4}$ mol./l. Hence the rate of light absorption $I_a$ is given by

$$I_a = I_0(1-\exp(-\alpha cd)) \simeq I_0\alpha cd$$

where $I_0$, $\alpha$, $c$ and $d$ represent incident light quanta per unit time, molar absorption coefficient, concentration of the solute and cell thickness, respectively. $I_0$ was determined actinometrically, using potassium ferrioxalate solution[6]. From such actinometric results and from transmittancy of the reaction mixtures, quantum yields for isomerization were determined.

## Results and Discussion

Fig. 2 shows the dependence of the rates of cis→trans and trans→cis isomerization on light intensity. Fig. 3 shows the dependence of the rates on the concentrations of the two isomers of stilbene. Dependence of the rate on temperature was investigated between 10 and 30°C with the result that the isomerization in both directions was practically independent of temperature. On the other hand, there exists an appreciable difference between the quantum yields in the two directions: $\phi_{cis\rightarrow trans}$ and $\phi_{trans\rightarrow cis}$ were found to be 0.04 and 0.27 when solutions of $4\times10^{-5}$ M *cis*-stilbene and $2.5\times10^{-5}$ M *trans*-stilbene absorbed the light of $2.3\times10^{-8}$ and $0.90\times10^{-8}$ einstein/min. at 25°C, respectively.

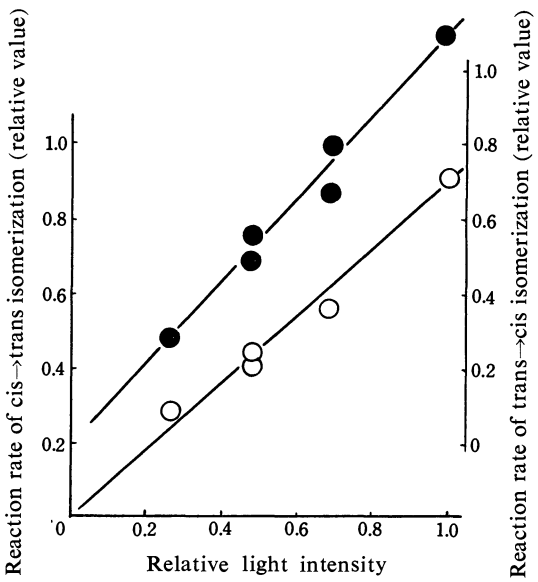



Fig. 2 Dependence of the rate of cis→trans (-○-) and trans→cis (-●-) isomerization on light intensity at 25°C.

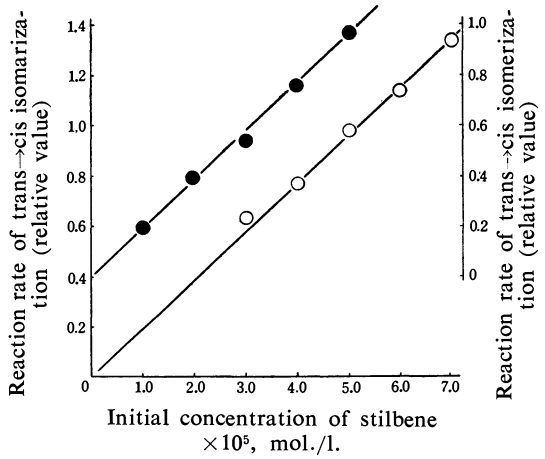



Fig. 3 Dependence of the initial rate of cis→trans (-○-) and trans→cis (-●-) isomerization on the initial concentrations of the two isomers of stilbene at 25°C.

Lewis and his coworkers have studied the reaction in isooctane solution under the irradiation with 254 mμ and obtained the quantum yield of 0.32 for the cis→trans and 0.35 for the trans→cis conversion[1]. Comparing these values with those obtained in the present work, values of $\phi_{trans\rightarrow cis}$ are in fairly good agreement, while the value of $\phi_{cis\rightarrow trans}$ is much smaller than that obtained by Lewis and his coworkers. They observed a yellow product accumulating under a prolonged irradiation of *cis*-stilbene with 254 mμ. In the present work with *cis*-stilbene, although the conversion was followed only in the initial stage, the concentration sum of *trans*-stilbene produced and *cis*-stilbene remaining was found to be constant within the experimental error of ±1% and equal to the initial concentration of *cis*-stilbene. Hence there was no need to take any side reaction into account. Presumably, these differences between the results of Lewis and his coworkers and of the present investigation are ascribed to the difference in wavelength of the light used.

As seen in Fig. 1, the absorption curve of *trans*-stilbene in solution shows a vibrational fine structure while that of *cis*-stilbene has no significant structure even at −90°C[1]. Hence, as is pointed out by Lewis and his coworkers, the excited state of *cis*-stilbene probably has a very short life.

It is known that *trans*-stilbene in solution

6) C. A. Parker, *Proc. Roy. Soc.*, **A220**, 104 (1955); C. G. Hatchard and C. A. Parker, ibid., **A235**, 518 (1956).

shows fluorescence under irradiation, but *cis*-stilbene does not. Lewis and his coworkers[1] have shown that the fluorescence obtained by a continued irradiation of *cis*-stilbene is explained by the existence of *trans*-stilbene produced by photoisomerization. Contrary to fluorescence, *cis*-stilbene shows phosphorescence while it is absent in the case of *trans*-stilbene[7,8]. Considering from the results observed in stilbene and its derivatives, the phosphorescent metastable state seems to be a triplet[9,10]. It was shown by Mulliken[11] that the potential energy curve for the lowest triplet state of ethylene has a minimum when the molecule takes a 90° twisted structure about the C=C double bond while for the singlet ground state the potential curve has a maximum at this configuration. In the case of molecules having conjugated double bonds such as stilbene and azobenzene, the situation is somewhat different. The triplet state now shows a rather flat potential energy curve which has a slight hump for the 90° twisted structure[12].

On the basis of quantum yields and absorption and fluorescence characteristics of *cis*- and *trans*-stilbene, Lewis and his coworkers presented a mechanism for the isomerization, according to which the electronic energy of excited molecules of either *cis*- or *trans*-stilbene is converted into rotational and vibrational energies in the ground state; one can discriminate neither cis- nor trans-form in this state. The normal cis- or trans-form, however, is produced as the excess energy is dissipated.

Results obtained in the present work are not necessarily incompatible with Lewis's mechanism. However, in view of the appreciable difference between the quantum yields in opposite directions and of the phosphorescence characteristics which are not taken into account in Lewis's mechanism, the following one seems to be more probable for the present case.

In Fig. 4 transitions d and h represent the light absorption and fluorescence of *trans*-stilbene respectively. Transition a represents the light absorption of *cis*-stilbene, and f an internal conversion to the ground state of *cis*-stilbene since no fluorescence is observed with *cis*-stilbene as described above. Similar radiationless transition may also be involved in h. The phosphorescent state M is produced by an internal conversion b. In solution, transitions

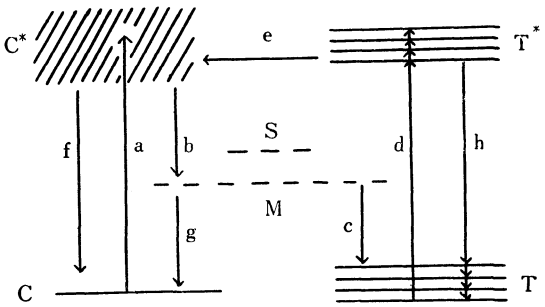



Fig. 4 Energetic schema for the photoisomerization of stilbene. C and T, the ground state of *cis*- and *trans*-stilbene respectively; C* and T*, the excited state of *cis*- and *trans*-stilbene respectively; M, the metastable state; S, the potential barrier separating *cis*- and *trans*-stilbene in the singlet ground state. The height of S relative to C is about 40 kcal./mol. so that S situates probably higher than M[12].

to the ground states, g and c, may also be principally internal conversions. The potential barrier separating the cis- and trans-forms of ethylenic compounds is generally considered to be much lower in the excited state than in the ground state[13]. On irradiating *trans*-stilbene, therefore, isomerization to cis-form may proceed via def or debg. In the case of *cis*-stilbene, the excited state is very short-lived and will be deactivated instantly through process b or f; hence the isomerization of *cis*- to *trans*-stilbene probably proceeds via abc.

The mechanism here presented appears to be consistent with the experimental findings that the rate of isomerization in both directions is proportional to the concentration of stilbene and to the light intensity and shows negligible dependence on temperature. Moreover, provided that the internal conversion f has a sufficiently large probability, the scheme given above may explain the greater value of $\phi_{\text{trans}\rightarrow\text{cis}}$ than $\phi_{\text{cis}\rightarrow\text{trans}}$, and also it may not be incompatible with the fact that phosphorescence has not been observed for *trans*-stilbene.

## Summary

The photochemical isomerization of *cis* as well as *trans*-stilbene in *n*-hexane was studied kinetically in the temperature range 10~30°C using the mercury lines of 313 and 334 mμ. Quantum yields were found to be 0.04 for the cis→trans, and 0.27 for the trans→cis conversion. Conversion rates for both directions obtained spectrophotometrically were found to be of the first order with respect to the substrate concentration, proportional to the light intensity, and nearly independent of temperature.

7) G. N. Lewis and M. Kasha, *J. Am. Chem. Soc.*, **66**, 2100 (1944).
8) B. Rosenberg, *J. Chem. Phys.*, **31**, 238 (1959).
9) G. N. Lewis, M. Kasha and M. Calvin, ibid., **17**, 804 (1949).
10) C. Reid, *Quart. Revs.*, **12**, 205 (1958).
11) R. S. Mulliken and C. C. Roothan, *Chem. Revs.*, **41**, 219 (1947).
12) P. P. Birnbaum and D. W, G. Style, *Trans. Faraday Soc.*, **50**, 1192 (1954).
13) R. S. Mulliken, *Phys. Rev.*, **41**, 751 (1932).

Moreover, in view of the differences in quantum yields and in optical properties of *cis*- and *trans*-stilbene, it seems probable that the reaction paths for the conversions in the two opposite directions are different from each other.

The author wishes to express his sincere thanks to Professor O. Toyama of the College of Engineering and to Dr. T. Hayakawa for their discussions and encouragement throughout this work.

*Department of Chemistry*
*College of General Education*
*University of Osaka Prefecture*
*Mozu-Umemachi, Sakai, Osaka*

# *The Behavior of Fission Products Captured in Graphite Powder by Nuclear Recoil. III. Diffusion of Iodine-133 and Tellurium-132 in Graphite at High Temperatures*

By Seishi YAJIMA, Sumio ICHIBA, Yuichiro KAMEMOTO and Koreyuki SHIBA

(Received September 3, 1960)

One of the distinctive features of a semi-homogeneous reactor is its use of a fuel element of the mixture of graphite and uranium dioxide. It was stated in the previous paper[1] that most of the fission products were captured in graphite by recoil energy. The diffusion of fission products captured in graphite at high temperatures is an important subject from the standpoint mentioned below. The release of fission products from a fuel element causes contamination of the coolant and its facilities. On the other hand, it is desirable from the viewpoint of neutron economy to remove fission products to some extent.

But the high velocity of diffusion results in the release of the fission products emitting delayed neutrons that are important in reactor control.

This paper describes the diffusion of iodine and tellurium, following the description of the diffusion of xenon in the previous paper[1].

In operating a reactor, the behavior of iodine-135, precursor of xenon-135, must be taken into consideration as well as that of xenon-135, which has an abnormally large neutron absorption cross-section. Because of the short half-life of iodine-135, iodine-133 was used as a tracer in this experiment. On the diffusion of tellurium which shows a chemical behavior similar to iodine, tellurium-132 was used as a tracer.

## Experimental

**Preparation of Samples.**—A mixture of 1 g. of graphite powder and 50 mg. of uranium dioxide was irradiated with thermal neutrons (thermal neutron flux, about $5\times10^{11}$ neutron/cm$^2$/sec.) for 2 hr. in an experimental hole of a JRR-1 reactor. After irradiation the mixture was treated with hot 4 N nitric acid solution to dissolve the uranium dioxide and neptunium-239 produced. The graphite was washed with distilled water and dried at 100°C. It was already reported that the fission products captured in graphite were not leached out by being treated with 4 N nitric acid solution in a short period of time[2]. In order to allow short-lived

TABLE I. PARTICLE SIZES OF GRAPHITE SAMPLES AND THE ANALYTICAL DATA OF IMPURITIES

| | Sample | | |
|---|---|---|---|
| | AG (Artificial graphite) | NG-1 (Natural graphite-1) | NG-2 (Natural graphite-2) |
| Paticle size | | | |
| $\mu$ | 30 | 1 | 50 |
| Impurity | | | |
| Ash (total) | 0.07% | 0.3% | 0.8% |
| $SiO_2$ | 250 p.p.m. | 220 p.p.m. | 3700 p.p.m. |
| $Al_2O_3$ | 210 | 60 | 3500 |
| $Fe_2O_3$ | 130 | 24 | 300 |
| MgO | 15 | 24 | 100 |
| CaO | 70 | 36 | 300 |
| $V_2O_5$ | — | 0.12 | 0.5 |
| MnO | — | — | — |
| $Na_2O$ | 20 | 12 | 25 |
| $K_2O$ | 15 | 12 | 20 |
| NiO | — | 0.06 | — |
| $ThO_2$ | — | 2.4 | — |
| CuO | — | — | — |
| $B_2O_3$ | 0.1 | 0.02 | 0.5 |

1) T. Nakai, S. Yajima, K. Shiba, J. Osugi and D. Shinoda, This Bulletin, 33, 497 (1960).

2) T. Nakai, S. Yajima, K. Shiba, J. Osugi and D. Shinoda, ibid., 33, 494 (1960).

fission iodine nuclides to decay, the irradiated graphite samples were cooled for about forty hours before use. The particle sizes of graphite samples used in this experiment and analytical data on impurities are given in Table I.

**Flow System.**—*Diffusion of Iodine-133.*—A flow system is illustrated in Fig. 1. The furnace consisted of a heater of silicon carbide. The temperature of the furnace was measured with a platinum-platinum rhodium thermocouple with a

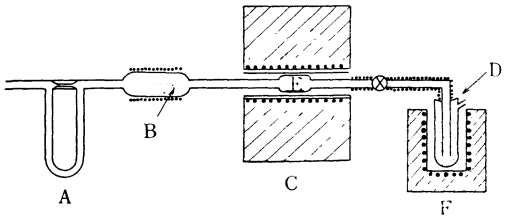



Fig. 1 Flow system.
A, Flow meter
B, Sponge titanium
C, Furnace
D, Copper trap
E, Diffusion cell
F, Heater

regulator control. The whole assembly was made of silica. The sponge titanium heated at 800°C served to remove a trace amount of oxygen in helium to avoid oxidation of the graphite surface. The silica tube from the diffusion cell to a copper trap was heated at over 300°C with a nichrome winding to prevent fission iodine from deposition on the wall of the tube. A copper trap was heated at 430°C in a furnace, because it was experimentally confirmed that fission iodine was completely captured in a copper net at 400 to 450°C.

The graphite powder mentioned above was placed in the diffusion cell. Helium gas was introduced into it. After confirming the fact that gas took the place of air, the diffusion cell with the graphite powder was slid into the preheated furnace, when the temperature was kept constant at 400, 800 and 1200°C (or 1100°C). Helium gas swept over the sample at a constant flow rate (100 ml./min.) and carried the volatile fission products diffusing out of graphite. The iodine-133 used as a measure of diffusion was separated from the fission products and was captured in a copper trap together with other fission iodine nuclides. The trap was exchanged for a new one at appropriate intervals.

*Diffusion of Tellurium-132.*—The apparatus was almost similar to that for diffusion of iodine-133. A copper trap was used to capture tellurium-132. It was found in advance that fission tellurium was completely captured in copper at 700 to 720°C. Therefore, the copper trap was heated at 710°C.

The silica tube from the diffusion cell to a trap was heated at about 700°C with a nichrome winding to avoid the deposition of fission tellurium on the wall of the tube.

**Determination of Iodine-133 and Tellurium-132 Activities.**—Activities of iodine-133 and tellurium-132 were measured with a RCL 256 channel gamma-ray

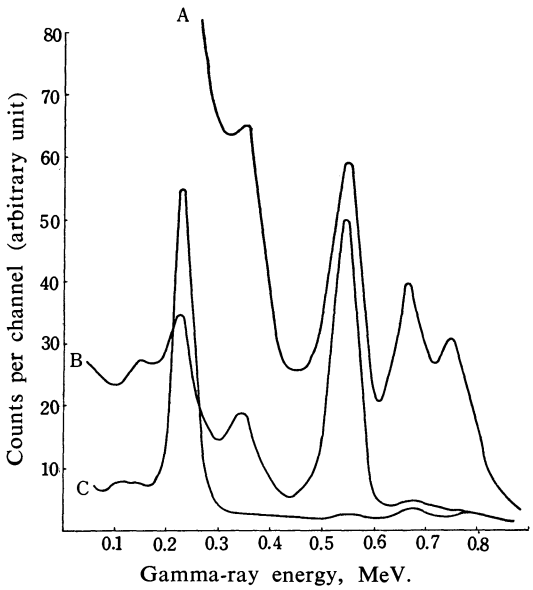



Fig. 2. Gamma-ray spectra of (A) fission products in graphite sample and (B) iodine-133 and (C) tellurium-132 in copper trap.

spectrometer with a well type sodium iodide scintillator (2 inch diameter×1.75). The gamma-ray spectra of the fission products in the graphite sample, iodine-133 and tellurium-132 in a copper trap, all cooled for forty hours after irradiation, are illustrated in Fig. 2. Iodine-132, the daughter of tellurium-132, exists in a trap in the state of transient equilibrium. Because the height of a photoelectric peak is proportional to the activity of the iodine-133 released and thus to the amount of iodine-133, the percentage of iodine released was calculated by comparing the height of the gamma-ray spectrum of the graphite sample, which was not heat-treated, with that of a trap. It was impossible to measure directly the activity of tellurium-132 in the graphite sample. Therefore, radiochemically pure tellurium was separated from the sample by the following radiochemical procedure. After burning the sample the residue was dissolved in nitric acid. The tellurium released from the sample on burning was caught in nitric acid solution and the resulting solution was combined with the solution with the residue. A tellurium carrier was then added to the solution, reduced with sulfur dioxide and precipitated as a metal. Then the activity of the tellurium metal was measured. The percentage of tellurium released was calculated as described in the case of iodine.

## Results and Discussion

Isothermal curves of the diffusion of iodine-133 and tellurium-132 in four kinds of graphite are illustrated in Figs. 3—10. These figures show that with these nuclides the respective curve apparently consists of a rapid diffusion lasting for about 30 min. and a slow diffusion

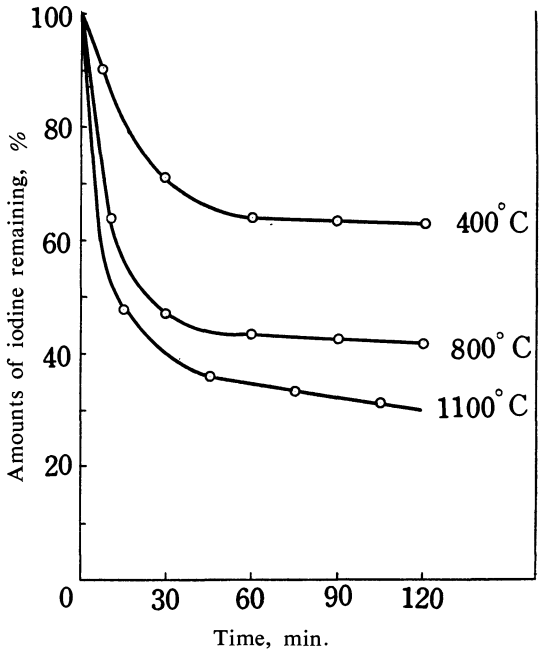



Fig. 3 Isothermal curves of diffusion of iodine-133 in natural graphite-1.

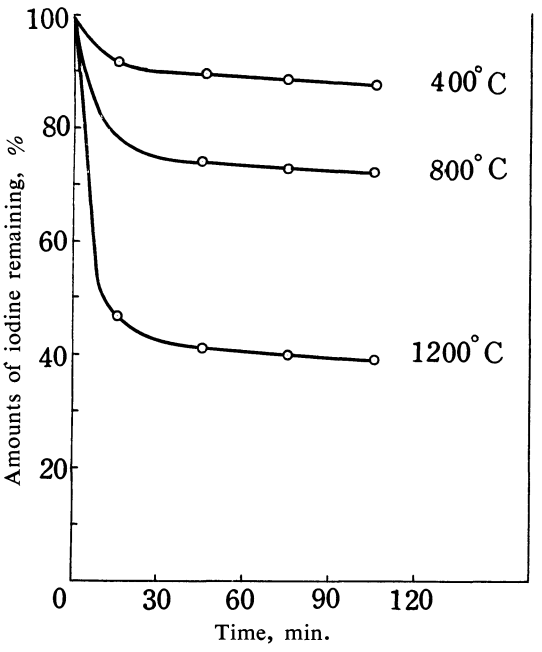



Fig. 4 Isothermal curves of diffusion of iodine-133 in natural graphite-2.

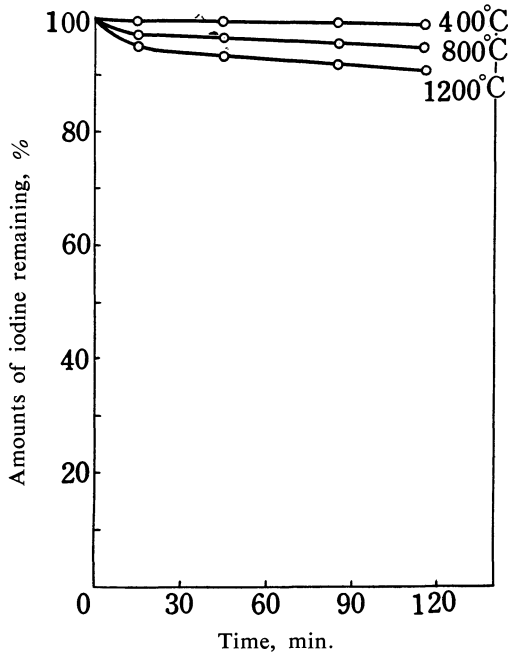



Fig. 5 Isothermal curves of diffusion of iodine-133 in artificial graphite.

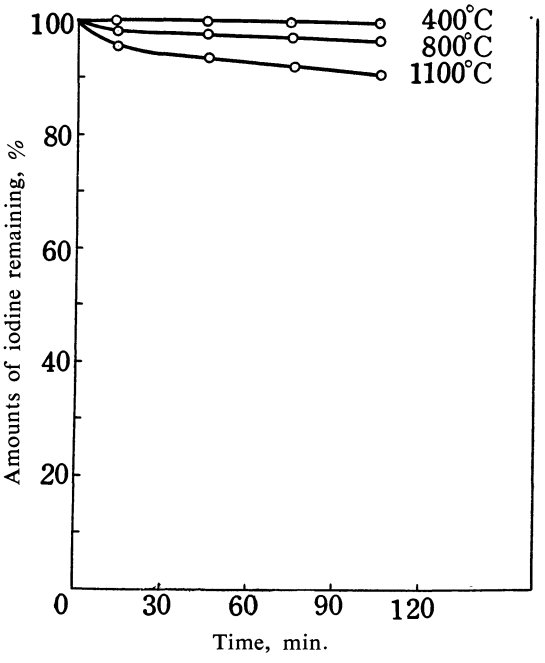



Fig. 6 Isothermal curves of diffusion of iodine-133 in amorphous carbon.

following it. This tendency is the same as that observed in the diffusion of xenon-135, where the activation energy of interlaminar diffusion of xenon-135 in graphite was calculated from a slow diffusion[1].

It has, however, been expected that there are several activation energies in diffusion in graphite. In fact, it is difficult to interpret the diffusion in graphite only from the interlaminar activation energy. A study is being continued on this subject with the use of a new method, and interesting information has

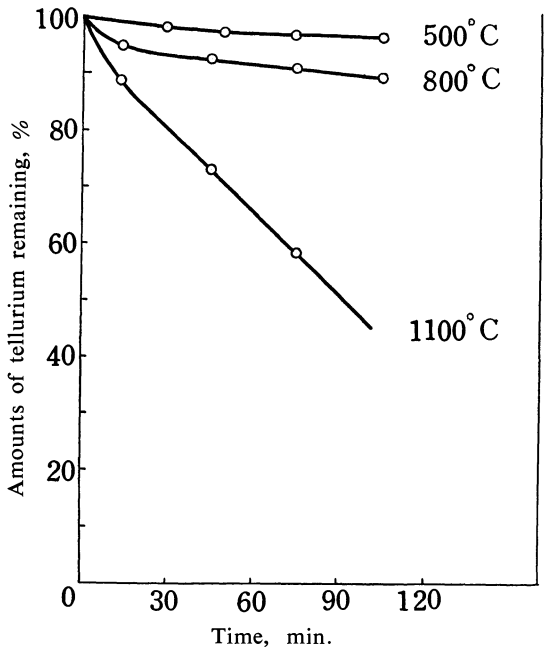



Fig. 7 Isothermal curves of diffusion of tellurium-132 in natural graphite-1.

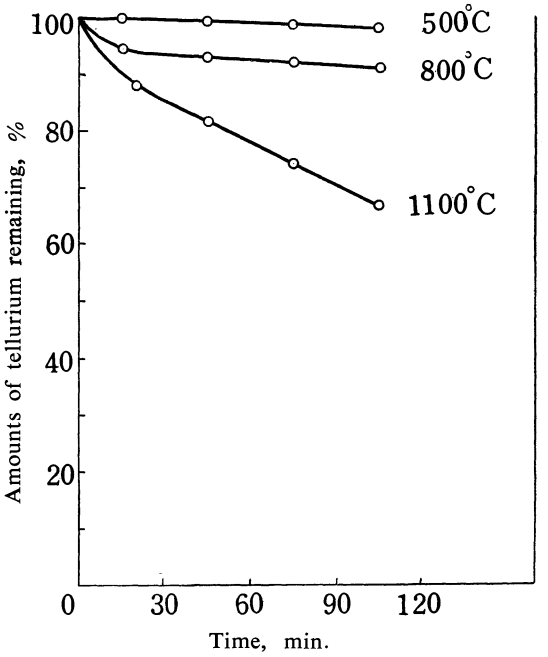



Fig. 8 Isothermal curves of diffusion of tellurium-132 in natural graphite-2.

been obtained. Details of the study will be reported later[3].

The rates of diffusion of iodine-133 and tellurium-132 in natural graphite are greater

3) S. Yajima, S. Ichiba, Y. Kamemoto and K. Shiba, This Bulletin, in press.

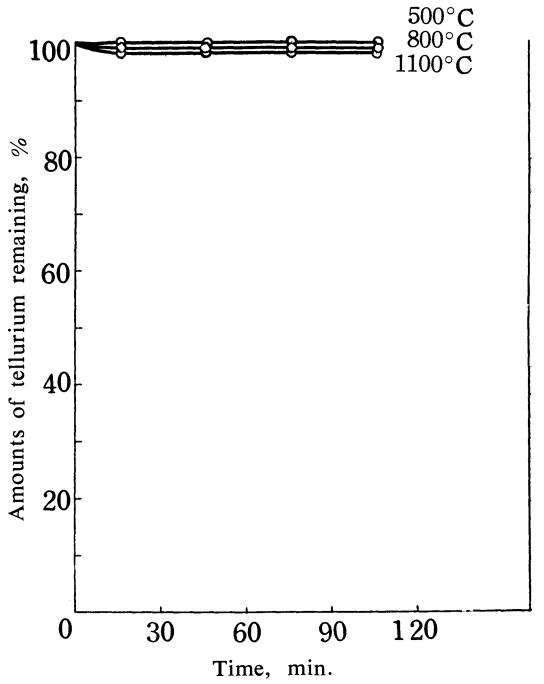



Fig. 9 Isothermal curves of diffusion of tellurium-132 in artificial graphite.

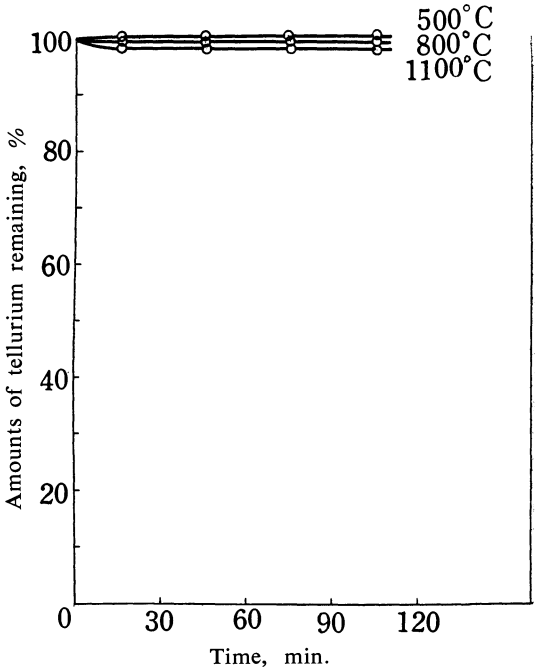



Fig. 10 Isothermal curves of diffusion of tellurium-132 in amorphous carbon.

than those in artificial graphite. This result is similar to the diffusion of xenon-135 in graphite observed in the previous work[1]. According to the X-ray diffraction and electron diffraction studies, natural graphite has a large

mosaic structure and artificial graphite has a small one. From this observation, it will be concluded that natural graphite has a lower density of dislocation than artificial graphite and that the trapping centers which are distributed along the dislocation line are less in natural graphite than in artificial graphite. Consequently, it is expected that the rates of the diffusion of iodine-133 and tellurium-132 in natural graphite, which has only a few trapping centers, are greater than in artificial graphite which has many trapping centers.

*Division of Chemistry*
*Japan Atomic Energy Research Institute*
*Tokai, Ibaraki-ken*

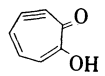
# *Preparation of 4-Aminotropolones by Amination of 3-Iodotropolones with Alkali Amides in Liquid Ammonia**

By Kozo Doi

(Received September 2, 1960)

Elimination-addition mechanisms involving intermediates of benzyne or dehydrobenzene ($C_6H_4$) type have been established in the rearrangement reactions occurring in the amination of non-activated aryl halides[1], high-temperature alkaline hydrolysis of aryl halides[2], and the coupling of aryl halides and phenyllithium[3]. Further, such mechanism has been extended to the rearrangement reaction in the amination of 3-bromopyridine[4] and the coupling of 1-chlorocyclohexene and phenyllithium[5].

The possibility of the extension of the elimination-addition mechanism involving dehydrotropolone (I), an intermediate corresponding to benzyne, in the field of tropolones has been suggested in the formation of 4-hydroxytropolone[6,7] (VII) and 4-hydroxy-6-isopropyltropolone[8] (XVII) on respective high-temperature alkaline hydrolysis of 3-bromotropolone (II) and 3-bromo-6-isopropyltropolone (V), and the formation of 4-cyanotropolone[6,9] (VIII) on high-temperature treatment of 3-bromotropolone (II) with potassium cyanide. Johnson and his co-workers[10] stated, with no experimental evidence, that dehydrotropolone (I) would be liable to form more easily than benzyne because of a decrease of the steric strain.




I

For the purpose of synthesizing 4-aminotropolones, examinations were made on the amination of 3-iodotropolones with alkali amides in liquid ammonia, the results of which will be described below in this paper.

Reaction of 3-iodotropolone (III) with three moles of potassium amide in liquid ammonia resulted in 4-aminotropolone (IX) in low yield. In order to confirm its structure, the same aminotropolone was synthesized through the Curtius reaction from 4-carboxytropolone (X), the structure of which had been established. The tropolone X was converted to 4-ethoxycarbonyltropolone (XI) in a good yield on being heated with ethanolic hydrogen chloride. The melting point (91°C) and the ultraviolet spectrum of XI were in agreement with those of the authentic sample[11] which had been obtained from the ring-enlargement of veratrole with ethyl diazoacetate. When treated with hydrazine hydrate under the ordinary condition, XI yielded the hydrazide XII which was converted with nitrous acid to the corresponding azide less soluble in water. Hydrolysis of the azide in an acidic medium afforded 4-aminotropolone (IX) in a poor yield.

* This work was presented in part at the 12th Annual Meeting of the Chemical Society of Japan, Kyoto, April, 1959.

1) J. D. Roberts, H. E. Simmons, L. A. Carlsmith and C. W. Vaughan, *J. Am. Chem. Soc.*, **75**, 3290 (1953); ibid., **78**, 601 (1956).

2) A. T. Bottini and J. D. Roberts, ibid., **79**, 1458 (1957).

3) G. Wittig and L. Pohmer, *Angew. Chem.*, **67**, 348 (1955).

4) R. Levine and W. W. Leake, *Science*, **121**, 780 (1955).

5) F. Scardiglia and J. D. Roberts, *Tetrahedron*, **1**, 343 (1957).

6) T. Nozoe and Y. Kitahara, *Proc. Japan Acad.*, **30**, 204 (1954).

7) Y. Kitahara, *Science Repts. Tohoku Univ., Ser. I*, **39**, 258 (1956).

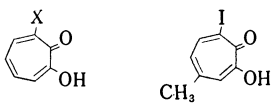
8) T. Toda, private communication.

9) Y. Kitahara, *Science Repts. Tohoku Univ., Ser. I*, **40**, 74 (1956).

10) R. B. Johns, A. W. Johnson and M. Tisler, *J. Chem. Soc.*, **1954**, 4605.

11) J. R. Bartels-Keith, A. W. Johnson and W. I. Taylor, ibid., **1951**, 2352.

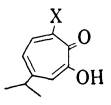
Amination of 3-iodo-6-methyltropolone[12] (IV) and 3-iodo-6-isopropyltropolone (VI) with potassium amide under the same condition as that described above resulted in the formation



II : X=Br
III : X=I



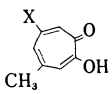
IV



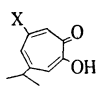
V : X=Br
VI : X=I



VII : X=OH
VIII : X=CN
IX : X=$NH_2$
X : X=COOH
XI : X=COOEt
XII : X=$CONHNH_2$



XIII : X=$NH_2$
XIV : X=COOH
XV : X=COOEt
XVI : X=$CONHNH_2$



XVII : X=OH
XVIII : X=$NH_2$

of 4-amino-6-methyltropolone (XIII) and 4-amino-6-isopropyltropolone (XVIII), respectively. The structure of the former XIII was confirmed by the synthesis of XIII from 4-carboxy-6-methyltropolone[13] (XIV) according to an authentic method[14]. The structure of XVIII was deduced from the close resemblance of its ultraviolet absorption to those of IX and XIII.

It has been known to date that the halogen atom in 3-halotoropolone is reactive and undergoes various anionoid substitutions such as the following: nitrile formation with cuprous cyanide[6], methoxylation with sodium methoxide[6], phenoxylation with sodium phenoxide[6], arylsulfonamidation with potassium arylsulfonamide[6], hydroxylation with concentrated caustic alkali[7], with aqueous sodium naphthalene-$\beta$-sulfonate[15] and with hydrochloric acid[10], and alkylation with some active methylene compounds[16]. In this reaction with potassium amide in liquid ammonia, however, the normal substitution products, 3-aminotropolones, were not isolated. This means probably that the elimination of iodide ion precedes the substitution in this reaction and the subsequent addition results in formation of 4-aminotropolones. The use of sodium amide instead of potassium amide and the use of 3-bromotropolones in place of the iodo compounds caused a marked decrease in the yield of the aminotropolones. Secondary and tertiary amines are expected to be produced as by-products[17], but no such products were separated in pure states.

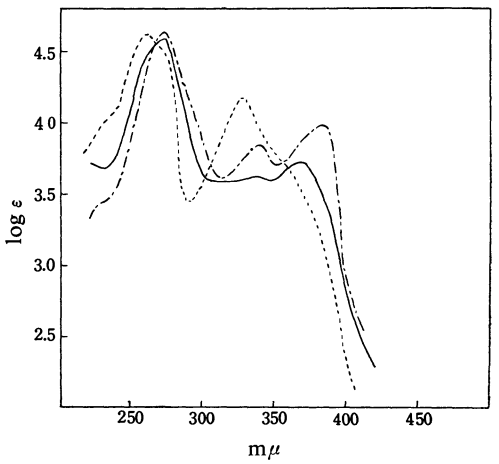



Fig. 1. The ultraviolet absorption spectra of 4-aminotropolone (IX) ; curve ——, in methanol, curve ----, in 0.1 N HCl, curve —·—·, in 0.1 N NaOH.

Fig. 1 indicates the ultraviolet absorption spectra of 4-aminotropolone (IX). In acid solution, the band near 350 m$\mu$ in the neutral solution shows a blue shift to give a tropone-type spectrum, whereas in alkaline solution it shows a red shift to give a tropolone-type spectrum. The ultraviolet spectra of the other two aminotropolones (XIII and XVIII) are also essentially similar to those of IX. These facts suggest that the aminotropolones possess an amphoteric character.

In Table I are listed some principal absorption bands in the infrared spectra of the aminotropolones.

Table I. Main absorptions of 4-aminotropolones in the infrared spectra ($cm^{-1}$)

| | $\nu_{NH_2}$ | | $\nu_{OH}$ | I | II | $\delta_{C-N}$ |
|---|---|---|---|---|---|---|
| IX | 3410 | 3325 | 3185 | 1640 | 1596 | 1335 |
| XIII | 3400 | 3340 | 3190 | 1648 | 1592 | 1325 |
| XVIII | 3400 | 3330 | 3195 | 1640 | 1588 | 1338 |

According to the result of Kinumaki, Ikegami and Aida[18], the carbonyl frequencies, measured in the solid state, of aminotropolones (3- and

12) T. Nozoe, K. Doi, K. Kitahara and K. Omura, This Bulletin, to be published.
13) W. D. Crow and R. D. Haworth, *J. Chem. Soc.*, **1951**, 1325.
14) W. D. Crow, R. D. Haworth and P. R. Jefferies ibid., **1952**, 3705.
15) T. Nozoe, K. Doi and T. Hashimoto, This Bulletin, **33**, 1071 (1960).
16) K. Takase, to be published.
17) J. F. Bunnett and T. K. Brotherton, *J. Org. Chem.*, **23**, 904 (1958).
18) S. Kinumaki, Y. Ikegami and K. Aida, *Bull. Chem. Research Inst. Tohoku Univ.*, **6**, 49 (1956).

5-aminotropolones, and 3, 5- and 3, 7-diaminotropolones) appear in the region of 1660～1609 $cm^{-1}$, whereas 4-aminotropolones have two bands (I and II bands in Table I) in the same region, and the II band of these two is stronger in its intensity and, therefore, it may be taken as the band due to the carbonyl stretching vibration in the respective aminotropolones. This assumption appears to be reasonably supported from the following observation on the relationship between frequencies of the II band and substituent constants.

It has been elucidated by many investigators[19] that the carbonyl frequencies of acetophenones, benzophenones, benzaldehydes and benzoic acids, and the substituent constants are in good linear relationship. It has also been found[20] in the tropolone field that Hammett's rule is satisfied between the dissociation constants and the substituent constants in a way similar to the case of benzene derivatives. It follows, naturally, that there would also be the same relationship between carbonyl frequencies of 4- and 5-substituted tropolones and substituent constants.

In Table II are shown the values of carbonyl frequency of several of the 4- and 5-substituted tropolones and substituent constants, $\sigma$, concerned.

Table II. Relationship between carbonyl frequencies and substituent constants in several substituted tropolones

| Substituent | 4-$NH_2$ | 4-Me | 4-iso-$C_3H_7$ | H |
|---|---|---|---|---|
| $\nu_{C=O}$*, $cm^{-1}$ | 1056 | 1610[21] | 1605[22] | 1613[23] |
| $\sigma$*[2] | −0.161 | −0.069 | −0.120*[3] | 0.000 |

| Substituent | 4-Cl | 4-Br | 4-$COCH_3$ | 5-Me |
|---|---|---|---|---|
| $\nu_{C=O}$, $cm^{-1}$ | 1615[24] | 1613[24] | 1620[24] | 1603[21] |
| $\sigma$ | 0.373 | 0.391 | 0.306 | −0.17 |

* All were measured in solid state.

*[2] L. P. Hammett, "Physical Organic Chemistry", McGraw-Hill Book Co., New York, N. Y. (1940).

*[3] $\sigma_m$ for *tert*-$C_4H_9$ was used.

Graphically, a fairly good linear relationship is observed between $\nu$ and $\sigma$. Therefore, the II band in Table I is considered to correspond to the carbonyl stretching frequencies of the 4-aminotropolones. The use of the values measured in solution makes it probable to expect the existence of a better linear relationship between them.

## Experimental

The ultraviolet absorptions were determined with a Beckman model DU spectrophotometer. The infrared spectra were measured on potassium bromide disks with a Perkin-Elmer model 21 infrared spectrometer, using a rock salt prism.

*Amination of 3-Iodotropolones with Potassium Amide.*

**4-Aminotropolone (IX).**—To a solution of liquid ammonia (100 ml.) and potassium amide obtained from potassium (2.6 g.), 3-iodotropolone[25] (III, 5.5 g.) was added during about 10 min., and the reaction mixture was allowed to reflux at the boiling point of ammonia. For the reaction was used a 300 ml. three-necked, round-bottomed flask equipped with a dry ice reflux condenser, an efficient mechanical stirrer and an Erlenmeyer flask fitted to one of the tubulatures of the reaction vessel by a section of rubber tubing for adding the iodotropolone. After 2 hr., ammonium chloride (2.4 g.) was added to the mixture and the ammonia was allowed to evaporate. The residual solid was dissolved in water (200 ml.), acidified to Congo red with concentrated hydrochloric acid, and extracted with chloroform (300 ml.). The extract was shaken with three 50 ml. portions of 6 N hydrochloric acid. This acid solution was combined with the foregoing aqueous solution, neutralized with sodium carbonate, and extracted continuously with ether for 5 hr. The ether extract, after evaporation of the solvent, sublimation in vacuo, and subsequent crystallization from methanol, yielded 4-aminotropolone (IX, 0.7 g.) as colorless needles, m. p. 187～188°C.

Found: C, 61.25; H, 5.08; N, 10.19. Calcd. for $C_7H_7O_2N$: C, 61.31; H, 5.15; N, 10.21%.

$\lambda_{max}$ m$\mu$ (log $\varepsilon$): 274 (4.60), 338 (3.62), 367 (3.72), in methanol; 260 (4.61), 328 (4.16) in 0.1 N HCl; 273 (4.64), 338 (3.86), 385 (4.00) in 0.1 N NaOH.

*Picrate:* A mixture of the aminotropolone (IX, 35 mg.), picric acid (120 mg.), and methanol (5 ml.) was heated under reflux for 5 min., cooled, and the residual precipitate was collected. Yellow prisms, m. p. 202～203°C.

Found: N, 15.08. Calcd. for $C_7H_7O_2N \cdot C_6H_3O_7N_3$: N, 15.06%.

**4-Amino-6-methyltropolone (XIII).**—To a stirred mixture of liquid ammonia (300 ml.) and potassium amide prepared from potassium (4.7 g.) was added 3-iodo-6-methyltropolone[12] (IV, 10 g.) at −50°C for 5 min. and the reaction mixture was allowed to reflux for 2 hr. When the following procedure was carried out essentially as described in the preceding experiment, the aminotropolone (XIII, 1.7 g.) was obtained as colorless needles (from methanol) of m. p. 199～200°C (reported[13] m. p. 199～200°C).

Found: C, 63.59; H, 5.85; N, 8.85. Calcd. for $C_8H_9O_2N$: C, 63.56; H, 6.00; N, 9.27%.

$\lambda_{max}$ m$\mu$ (log $\varepsilon$): 274 (4.64), 340 (3.67), 360 (3.68) in methanol; 260 (4.54), 328 (4.06) in 0.1 N HCl; 273 (4.62), 340 (3.84), 380 (3.95) in 0.1 N NaOH.

19) N. Fuson et al., *J. Am. Chem. Soc.*, **76**, 2526 (1954); R. N. Johns et al., *Can. J. Chem.*, **35**, 504 (1957); H. W. Thompson et al., *Spectrochim. Acta*, **9**, 208 (1957); M. St. Flett, *Trans. Faraday Soc.*, **44**, 767 (1948).

20) N. Yui, *Science Repts. Tohoku Univ., Ser. I*, **40**, 114 (1956).

21) T. Nozoe, T. Mukai et al., ibid., **35**, 242 (1951).

22) K. Kuratani et al., This Bulletin, **25**, 250 (1952).

23) S. Kinumaki, K. Aida and Y. Ikegami, *Science Repts. Research Inst. Tohoku Univ.*, **A8**, 263 (1956).

24) K. Doi, This Bulletin, to be published.

25) Y. Kitahara and T. Arai, *Proc. Japan Acad.*, **27**, 423 (1951).

*Picrate:* Yellow needles (from methanol), m. p. 178~180°C.

Found: N, 14.64. Calcd. for $C_8H_9O_2N \cdot C_6H_3O_7N_3$: N, 14.94%.

**4-Amino-6-isopropyltropolone (XVIII).** — To a stirred mixture of liquid ammonia (400 ml.) and potassium amide obtained from potassium (8 g.) was added 3-iodo-6-isopropyltropolone[26] (VI, 19 g.) during 10 min. When the procedure which followed was carried out as the above, the aminotropolone (XVIII, 3.7 g.) was isolated from benzene as colorless needles of m. p. 145~146°C.

Found: C, 67.32; H, 7.18; N, 8.00. Calcd. for $C_{10}H_{13}O_2N$: C, 67.02; H, 7.31; N, 7.82%.

$\lambda_{max}$ mμ (log ε): 275 (4.63), 340 (3.68), 360 (3.66) in methanol; 263 (4.55), 328 (4.08) in 0.1 N HCl; 273 (4.74), 338 (3.96), 385 (4.10) in 0.1 N NaOH.

*Picrate:* Yellow needles (from benzene-methanol), m. p. 96~97°C.

Found: N, 13.49. Calcd. for $C_{10}H_{13}O_2N \cdot C_6H_3O_7N_3$: N, 13.72%.

*Preparation by the Curtius Reaction.*

**4-Aminotropolone (IX).** — After dry hydrogen chloride was saturated in a mixture of 4-carboxytropolone (X, 1.1 g.) and ethanol (20 ml.), the mixture was heated under reflux for one hour. The solution was evaporated to dryness under reduced pressure, the residue was sublimed in vacuo, and the sublimate was recrystallized from cyclohexane to give 4-ethoxycarbonyltropolone (XI, 0.95 g.) as yellow needles, m. p. 91°C (reported[11] m. p. 90~91°C).

Found: C, 61.74; H, 5.23. Calcd. for $C_{10}H_{10}O_4$: C, 61.85; H, 5.19%.

$\lambda_{max}^{MeOH}$ mμ (log ε): 250 (4.43), 313 (3.69), 325 (3.73), 375 (3.72), 388 (3.68).

A solution of XI (1.5 g.), 80% hydrazine hydrate (1 ml.) and ethanol (10 ml.) was heated under reflux for 3 hr.; the solution was concentrated to a small volume under reduced pressure, and the residue so obtained was recrystallized from ethanol to form tropolone-4-carbohydrazide (XII, 0.7 g.) as yellow needles, m. p. 258°C (decomp.).

Found: N, 15.63. Calcd. for $C_8H_8O_3N_2$: N, 15.55%.

$\lambda_{max}^{MeOH}$ mμ (log ε): 230 (4.16), 245 (4.18), 297 (4.41), 386 (4.29), 440 (4.01).

To a cold stirred solution of XII (0.54 g.), concentrated hydrochloric acid (1 ml.) and water (3 ml), was added dropwise a solution of sodium nitrite (0.21 g.) in water (1 ml.), and the deposited colorless azide was collected. The crude azide was then added to a solution of acetic acid (5 ml.), concentrated hydrochloric acid (1 ml.) and water (0.5 ml.), and the mixture was heated under reflux for 2 hr. This was evaporated under reduced pressure to a small volume, diluted with water (40 ml.), neutralized with sodium carbonate, and extracted with ether continuously for 5 hr. The ether extract, after evaporation of the solvent and crystallization from methanol, afforded the aminotropolone (IX, 0.25 g.), m. p. and mixed m. p. 187~188°C.

**4-Amino-6-tropolone (XIII).**—A cold mixture of 4-carboxy-6-methyltropolone (XIV, 1.8 g.) and ethanol (10 ml.), was saturated with dry hydrogen chloride, and the mixture was heated under reflux for 2 hr. By the procedure as described in the preceding experiment 4-ethoxycarbonyl-6-methyltropolone (XV, 1.92 g.) was obtained as pale yellow needles (from cyclohexane), m. p. 103~104°C.

Found: C, 63.62; H, 5.63. Calcd. for $C_{11}H_{12}O_4$: C, 63.45; H, 5.81%.

$\lambda_{max}^{MeOH}$ mμ (log ε): 251 (4.46), 312 (3.66), 330 (3.72), 378 (3.72), 388 (3.72).

A mixture of XV (0.21 g.) and 80% hydrazine hydrate (0.19 g.) was heated on a boiling water bath for 20 min., acidified with dilute acetic acid, and an insoluble solid was collected. Recrystallization of it from ethanol gave 6-methyltropolone-4-carbohydrazide (XVI, 0.13 g.) as yellow leaflets, m. p. 177~178°C (decomp.) (reported[13] m. p. 171~172°C (decomp.)).

Found: N, 14.76. Calcd. for $C_9H_{10}O_3N_2$: N, 14.43%.

$\lambda_{max}^{MeOH}$ mμ (log ε): 247 (4.19), 300 (4.43), 389 (4.28), 444 (3.99).

XVI was derived, by the reported experimental procedures[13], to the aminotropolone (XIII), m. p. and mixed m. p. 199~200°C.

The author wishes to express his gratitude to Professor Y. Kitahara for his helpful guidance throughout the course of this work, to Professor T. Nozoe for his unfailing encouragement, and to Professors S. Seto and Y. Matsuki for providing experimental facilities. The author gratefully ackonwledges his debt to Mr. S. Ohyama and Miss Y. Endo for microanalyses and to Mr. Y. Ikegami for infrared spectral measurements.

*The Chemical Research Institute of Non-Aqueous Solutions*
*Tohoku University*
*Katahira-cho, Sendai*

26) T. Nozoe et al., *Science Repts. Tohoku Univ., Ser. I*, 36, 299 (1952).

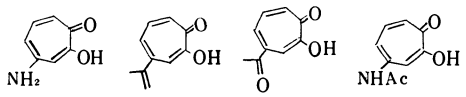
# *The Schmidt Reaction in Some Tropolone Derivatives**

By Kozo Doi

(Received September 9, 1960)

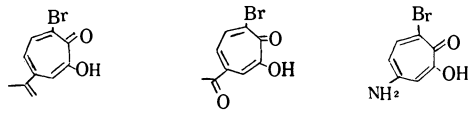
In the preceding paper[1] the author has described the syntheses of 4-aminotropolone (I) and its alkyl derivatives by the extended application of the elimination-addition mechanism involving a benzyne-type intermediate[2] to the tropolone field. As the general method for synthesizing 4-aminotropolones, however, this synthetic method, included amination of 3-iodotropolones with potassium amide in liquid ammonia, appeared to be still unsatisfactory in respect to the yield. Therefore attempts were made for the synthesis of 4-aminotropolones by application of the Schmidt reaction[3] to 4-isopropenyltropolone (β-dolabrin)[4] (II), 4-acetyltropolone[4] (III), and their derivatives.

Addition of both a solution of hydrazoic acid in chloroform and of sodium azide to a cold stirred solution of 4-acetyltropolone (III) in concentrated sulfuric acid resulted in instantaneous reaction to give 4-aminotropolone sulfate, having a composition of $C_7H_7O_2N \cdot 1/2\ H_2SO_4 \cdot H_2O$, instead of the anticipated acetylaminotropolone (IV). The desired aminotropolone (I) was readily obtained when this product was treated with sodium hydrogen carbonate. The use of excess hydrazoic acid in this reaction did not afford the tetrazole derivative, observed in the reactions with acetone and benzophenone[5]. The fact that 4-acetylaminotropolone (IV), which will be described in the subsequent paper[6], readily forms 4-aminotropolone sulfate on treatment with concentrated sulfuric acid makes it certain that IV arises as an intermediate in the reaction with III.



I II III IV

It was reported that bromination of the isopropenyltropolone (II) with *N*-bromosuccinimide yielded 3-bromo-6-isopropenyltropolone[7,8] (V) and its oxidation with hydrogen peroxide in formic acid, followed by that with sodium periodate, afforded 6-acetyl-3-bromotropolone[7] (VI). Application of sodium azide to a concentrated sulfuric acid solution of VI produced the corresponding aminotropolone (VII), in which case the sulfate of VII was not obtained owing to the decreased basicity by the introduction of the bromine atom in the molecule.



V VI VII

Fig. 1 indicates the ultraviolet absorption of VII, which possesses a maximum at a longer wavelength region than in the case of I[1].

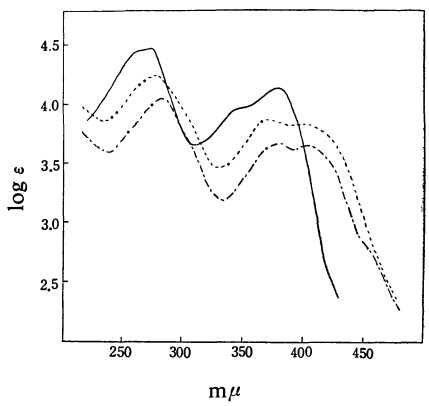



Fig. 1. Ultraviolet absorption spectra.

—— 6-Amino-3-bromotropolone (VII)
---- 4-Amino-5-nitrotropolone (X, log ε +0.2)
—·— 6-Amino-3-bromo-5-nitrotropolone (XI, log ε +0.4)

In order to obtain further derivatives of the aminotropolone, nitrations with fuming nitric acid were carried out on the acetyltropolones (III and VI). Thus, 4-acetyl-5-nitrotropolone

* This work was presented in part at the 12th Annual Meeting of the Chemical Society of Japan Kyoto, April, 1959.

1) K. Doi, This Bulletin, **34**, 497 (1961).

2) J. D. Roberts, H. E. Simmons, L. A. Carlsmith and C. W. Vaughan, *J. Am. Chem. Soc.*, **75**, 3290 (1953); J. D. Roberts, D. A. Semenow, H. E. Simmons and L. A. Carlsmith, ibid., **78**, 601 (1956).

3) A review of the Schmidt reaction is given by H. Wolff, in "Organic Reactions", edited by R. Adams, Vol. III, p. 307, John Wiley and Sons, New York, N. Y. (1946).

4) T. Nozoe, K. Takase and M. Ogata, *Chem. & Ind.*, 1957, 1070.

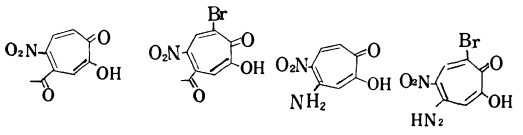
5) K. F. Schmidt, *Ber.*, **57**, 704 (1924).

6) K. Doi, This Bulletin, to be published.

7) Y. Kitahara and M. Funamizu, unpublished work.

8) K. Takase, T. Kusunose and T. Meguro, Abstracts of the 12th Annual Meeting of the Chemical Society of Japan, p. 232 (1959).

(VIII) and 6-acetyl-3-bromo-5-nitrotropolone (IX) were obtained from the respective compound. The positions of the nitro group in VIII and IX are supported from the similarity of their ultraviolet absorption spectra (Fig. 2) to that of 5-nitrotropolone[9]. It has been found that the presence of an alkyl group (especially isopropyl) in the 4-position of a tropolone effects preferential orientation of the nitro group towards the 3- or 7-position instead of the 5-position[10]. In spite of such a fact, nitration of III and VI, possessing a meta-directing acetyl group, has caused substitution of the nitro group into the adjacent position of the acetyl group. This means probably that the acetyl group is not in full conjugation with the tropolone ring. This conclusion is also supported reasonably from the fact that the absorption maximum at 437 mμ (log ε 4.42) in the longest wavelength of the ultraviolet spectrum of VIII is approximately the same value as that of 5-nitrotropolone, 435 mμ (log ε 4.41).



VIII IX X XI

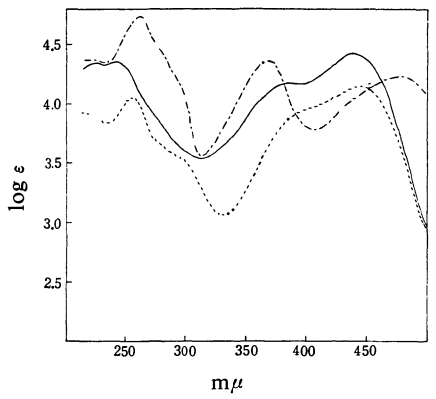
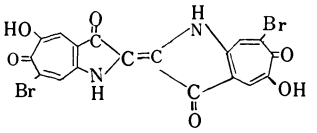



Fig. 2. Ultraviolet absorption spectra.

—— 4-Acetyl-5-nitrotropolone (VIII)
---- 6-Acetyl-3-bromo-5-nitrotropolone (IX, log ε +0.3)
—·— Indigo-type tropolone (XII)

When treated with sodium azide in a concentrated sulfuric acid solution, the above nitroacetyltropolones (VIII and IX) also yielded 4-amino-5-nitrotropolone (X) and 6-amino-3-bromo-5-nitrotropolone (XI), respectively. Their ultraviolet absorptions, indicated in Fig. 1, show that an introduction of a bromine atom in the 3-position of I, VII and IX causes a red shift of the longest wavelength maximum by 13, 8 and 7 mμ respectively, the fact of which is in approximate agreement with the observation of Tsuboi[11].

Catalytic hydrogenation of the bromo-acetyltropolone (IX) over palladized charcoal was found to give instead of the expected debromination product (VIII) an orange red product, which had its ultraviolet maximum in a longer wavelength region than that of the starting compound (cf. Fig. 2). The infrared absorption of this reaction product shows peaks at 3350 ($\nu_{NH}$) and 1648 $cm^{-1}$ ($\nu_{C=O}$). It follows, therefore, that this hydrogenation product of IX is probably an indigo-type tropolone (XII),



XII

the conclusion of which appears to be supported by the fact that 5,5′-dibromoindigo[12] has infrared peaks at 3300 ($\nu_{NH}$) and 1634 ($\nu_{C=O}$) $cm^{-1}$.

It was found that the Schmidt reaction was applicable satisfactorily to also 4-formyltropolone (XIII). Thus on being treated with an excess of sodium azide in concentrated sulfuric acid, XIII afforded the aminotropolone (I) and also 4-cyanotropolone (XIV). It has been well known in the reaction with benzaldehyde that the relative yields of the reaction products, benzonitrile and formanilide, vary



XIII XIV

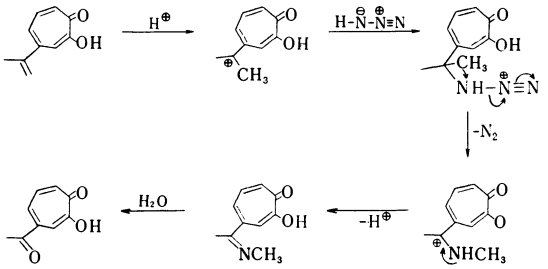
according to the amount of sulfuric acid used[3], but in the reaction with XIII further detailed examinations could not be made owing to difficulty in preparing the starting material.

Some kinds of unsaturated compounds have been reported to react with hydrazoic acid[3]. For instance, amylene forms a Schiff base in high yield, while cyclopentene and camphene undergo ring-enlargement. McEven and Mehta[13] investigated in detail an application of the Schmidt reaction to 1,1-diphenylethylene and its derivatives. The author's attention

9) T. Nozoe, Y. Kitahara, K. Doi and T. Arai, *Bull. Chem. Research Inst. Non-Aqueous Solns. Tohoku Univ.*, **7**, 13 (1957).
10) T. Nozoe, Y. Kitahara, E. Kunioka and K. Doi, *Proc. Japan Acad.*, **26**, 38 (1950).
11) M. Tsuboi, This Bulletin, **25**, 369 (1952).
12) J. Weinstein and G. M. Wymann, *J. Am. Chem. Soc.*, **78**, 2387 (1956).
13) W. E. McEven and N. B. Mehta, ibid., **74**, 526 (1952).

was directed to examine this reaction in 4-isopropenyltropolones (II and V), since there is no example of application of the Schmidt reaction to asymmetrically 1, 1-disubstituted ethylenes.

On being treated with one equivalent of hydrazoic acid in concentrated sulfuric acid solution, II afforded the acetyltropolone (III) in a fairly good yield, whereas on being treated with an excess of the reagent II yielded the aminotropolone (I). A similar phenomenon was recognized also in the reaction with the bromo derivative V. A Schiff base XV, as shown in the following mechanism, is expected to form as an intermediate in these reactions, but has not been isolated, since it is probably too hydrolyzable to be isolated under the reaction conditions.



XV

It has been elucidated from the above description that the Schmidt reaction can be satisfactorily applied to the acetyl, isopropyl, and formyl derivatives of tropolone. On the other hand, it has been found that not only 4-carboxytropolone but also 3- and 5-carboxytropolones are entirely inert to the same reaction, and that neither use of trifluoroacetic acid[14] instead of sulfuric acid nor the application of the method for preparing amines by the action of hydroxylamine sulfate with carboxylic acids[15] produce aminotropolones from the carboxytropolones.

## Experimental

The ultraviolet absorption spectra were measured in methanol solution with a Beckman model DU quartz spectrophotometer, and the infrared absorption spectrum was determined on potassium bromide disk with a Perkin-Elmer model 21 infrared spectrometer, using rock salt prism.

**Reaction of 4-Acetyltropolone (III).**—To a stirred solution of III (16.4 g.) and concentrated sulfuric acid (50 ml.), was added a solution of chloroform (200 ml.) and hydrazoic acid, prepared from sodium azide (13 g.), during 1 hr. at room temperature. After 1 hr's stirring, the acid layer was diluted with ice water (200 ml.) and the colorless solid thereby separated was crystallized from methanol to give 4-aminotropolone sulfate as colorless needles, m. p. 146~147°C (decomp.).

Found: C, 41.16; H, 4.89; N, 6.83; water of crystallization, 8.64. Calcd. for $(C_7H_7O_2N)_2 \cdot H_2SO_4 \cdot 2H_2O$: C, 41.17; H, 4.94; N, 6.86; water of crystallization, 8.82%.

The sulfate was digested with saturated sodium carbonate solution to an alkaline point, acidified with acetic acid, and the deposited solid was crystallized from methanol to afford 4-aminotropolone (I, 11.8 g.), m. p. 187~188°C, undepressed on admixture with an authentic specimen[1].

**Reaction of 6-Acetyl-3-bromotropolone (VI).**—To a stirred mixture of VI[7] (0.24 g.), concentrated sulfuric acid (1 ml.) and chloroform (6 ml.), was added sodium azide (0.2 g.) for 5 min. at room temperature. After 1 hr., the acid layer was diluted with water (5 ml.), the precipitated solid was collected, and crystallized from methanol to form 6-amino-3-bromotropolone (VII) as pale yellow needles, m. p. 214~215°C.

Found: N, 6.19. Calcd. for $C_7H_6O_2NBr$: N, 6.48%. $\lambda_{max}^{MeOH}$ m$\mu$ (log $\varepsilon$): 273 (4.48), 380 (4.14).

**4-Acetyl-5-nitrotropolone (VIII).** — To a stirred mixture of III (1.64 g.) and acetic acid (2 ml.), was added dropwise a solution of fuming nitric acid ($d$=1.8, 0.7 g.) and acetic acid (2 ml.) at room temperature, and resulting deep red solution was diluted with water (25 ml.). The precipitated solid was collected and recrystallized from a mixture of acetic acid and methanol to yield 4-acetyl-5-nitrotropolone (VIII, 0.14 g.) as yellow prisms, m. p. 213°C (decomp.).

Found: C, 51.68; H, 3.37; N, 6.70. Calcd. for $C_9H_7O_5N$: C, 51.92; H, 3.27; N, 6.68%. $\lambda_{max}^{MeOH}$ m$\mu$ (log $\varepsilon$): 225 (4.33), 245 (4.34), 385 (4.17), 437 (4.42).

**Reaction of 4-Acetyl-5-nitrotropolone (VIII).**—Sodium azide (0.1 g.) was added at room temperature to a stirred mixture of VIII (0.1 g.), concentrated sulfuric acid (0.5 ml.) and chloroform (3 ml.). The initial red color of the acid layer changed gradually to yellow with progress of the reaction. The acid layer, after dilution with water (5 ml.), filtration of the resulting solid and subsequent crystallization from acetic acid, gave 4-amino-5-nitrotropolone (X, 0.07 g.) as yellow needles, which turned black at around 270°C and did not melt up to 300°C.

Found: C, 46.24; H, 3.38; N, 15.36. Calcd. for $C_7H_6O_4N_2$: C, 46.16; H, 3.32; N, 15.38%. $\lambda_{max}^{MeOH}$ m$\mu$ (log $\varepsilon$): 275 (4.45), 370 (4.09), 397 (4.04).

**6-Acetyl-3-bromo-5-nitrotropolone (IX).** — Nitration of VI (2.2 g.), which was carried out essentially as described in the case of III, resulted in formation of IX (1.0 g.) as yellow needles from acetic acid, m. p. 164~165°C.

Found: C, 37.85; H, 2.07; N, 4.92. Calcd. for $C_9H_6O_5NBr$: C, 37.67; H, 2.10; N, 4.92%. $\lambda_{max}^{MeOH}$ m$\mu$ (log $\varepsilon$): 255 (4.35), 445 (4.46).

**Reaction of 6-Acetyl-3-bromo-5-nitrotropolone (IX).**—To a stirred mixture of IX (0.15 g.), concentrated sulfuric acid (1 ml.) and chloroform (4

14) K. G. Rutherford and M. S. Newman, ibid., 79, 213 (1957).
15) H. R. Snyder, C. T. Elston and D. B. Kellom, ibid., 75, 2014 (1953).

ml.) was added sodium azide (0.1 g.). The followed procedure was carried out as described in the preceding Schmidt reaction, and then 6-amino-3-bromo-5-nitrotropolone (XI) was obtained as yellow prisms (from dimethylformamide), having m. p. 250°C (decomp.).

Found: N, 10.57. Calcd. for $C_7H_5O_4N_2Br$: N, 10.73%. $\lambda_{max}^{MeOH}$ mμ (log ε): 284 (4.46), 380 (4.08), 404 (4.06).

**Hydrogenation of IX.**—A mixture of IX (0.29 g.), sodium acetate trihydrate (0.14 g.), 5% palladium-on-charcoal (0.04 g.), and methanol (15 ml.) was shaken in hydrogen atmosphere until 30 ml. of hydrogen was absorbed at room temperature. The catalyst was removed by filtration, the solvent was evaporated from the filtrate, and the residue, after washing with dilute hydrochloric acid, was recrystallized from methanol to afford an indigo-type tropolone (XII) as orange red needles, m. p. 209°C (decomp.).

Found: C, 42.37; H, 1.41; N, 5.48. Calcd. for $C_{18}H_8O_6N_2Br_2$: C, 42.54; H, 1.59; N, 5.51%. $\lambda_{max}^{MeOH}$ mμ (log ε): 260 (4.72), 370 (4.36), 480 (4.23).

**Reaction of 4-Formyltropolone (XIII).**—To a stirred mixture of XIII[16] (0.15 g.), concentrated sulfuric acid (0.5 ml.) and chloroform (5 ml.) was added sodium azide (0.08 g.) at room temperature. After 2 hr's stirring, the acid layer was diluted with water (3 ml.), neutralized to pH 7 with sodium carbonate, and the resulting solid was collected. Fractional recrystallization of the solid from methanol afforded 4-cyanotropolone (XIV, 0.03 g.), m. p. and mixed[17] m. p. 194~195°C, from the less soluble portion, and 4-aminotropolone (I, 0.08 g.), m. p. and mixed[1] m. p. 187~188°C, from the more soluble portion.

**Reaction of 4-Isopropenyltropolone (II).**—Sodium azide (0.97 g.) was added to a stirred mixture of II[4] (1.62 g.), concentrated sulfuric acid (5 ml.) and chloroform (5 ml.) at room temperature, and then the mixture was stirred at 40~50°C for 3 hr. The acid layer was diluted with water (20 ml.) and the resulting acetyltropolone (III, 1.0 g.), m. p. 129°C, undepressed on admixture with an authentic specimen[4], was collected. The use of excess of sodium azide gave 4-aminotropolone (I) in this reaction.

**Reaction of 3-Bromo-6-isopropenyltropolone (V).**—The Schmidt reaction with V[7,8] (0.24 g.) was carried out essentially as described in the preceding experiment. As the reaction product 3-bromo-6-acetyltropolone (VI, 0.13 g.), m. p. and mixed[7] m. p. 132~133°C, was obtained. The use of excess of sodium azide in this reaction yielded 6-amino-3-bromotropolone (VII), similarly in the case of II.

The author wishes to express his sincere gratitude to Professor Y. Kitahara for his unfailing guidance throughout the course of this work, to Dr. K. Takase for helpful advice, and to Mr. M. Funamizu for experimental assistance. Grateful acknowledgements are also made to Mr. S. Ohyama and Miss Y. Endo for microanalyses, and to the Ogawa Perfumery Company for the supply of the source of β-dolabrin.

*The Chemical Research Institute of Non-Aqueous Solutions*
*Tohoku University*
*Katahira-cho, Sendai*

16) R. D. Haworth and J. D. Hobson, *J. Chem. Soc.*, **1951**, 561.
17) K. Doi, This Bulletin, to be published.

# *Partial Debromination of Polybromotropolones with Cuprous Cyanide and Some Reactions of 4-Bromotropolone*

By Kozo Doi

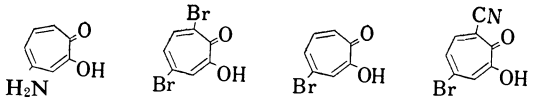
(Received September 30, 1960)

In the previous papers the author reported that amination of 3-iodotropolones with potassium amide in liquid ammonia, whose process is an example of extensive application of the elimination-addition mechanism[1] involving benzyne-type intermediate to the tropolone field, resulted in the formation of 4-aminotropolone (I) and its derivatives[2]. Further, he reported that an application of the Schmidt reaction to the acetyl, formyl, and isopropenyl derivatives of tropolone resulted also in the formation of the aminotropolones in satisfactory yields[3].

The present study was undertaken in order to derive 3, 6-dibromotropolone (II), which is obtainable comparatively[4], to 4-bromotropolone

1) J. D. Roberts, H. E. Simmons, L. A. Carlsmith and C. W. Vaughan, *J. Am. Chem. Soc.*, **75**, 3290 (1953); **78**, 601 (1956).
2) K. Doi, This Bulletin, **34**, 488 (1961).
3) K. Doi, ibid., **34**, 501 (1961).
4) T. Nozoe, Y. Kitahara et al., *Science Repts. Tohoku Univ. Ser. I*, **36**, 166 (1952); S. Iseda, This Bulletin, **28**, 617 (1955); T. Nozoe, K. Doi and S. Endo, ibid., **33**, 1285 (1960).

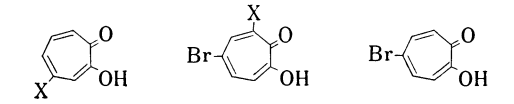
(III) and to convert it to the aminotropolone (I) by a suitable method.



I II III IV

It has been found that treatment of alkali salt of 3-bromotropolones with cuprous cyanide in pyridine produces 3-cyanotropolone[5,6] in general. The author's attention, therefore, was directed towards obtaining 6-bromo-3-cyanotropolone (IV), which is expected to be derived to 4-bromotropolone (III) on its hydrolysis and subsequent decarboxylation, by application of this synthetic process to 3, 6-dibromotropolone (II).

It was found in practice, however, that, when the copper salt, in place of alkali salt, of the dibromotropolone (II) was heated with cuprous cyanide in pyridine, the anticipated 6-bromo-3-cyanotropolone (IV) did not form but 4-bromotropolone (III) and 4-cyanotropolone (V) resulted in formation as the reaction products. The structure of III was proved by the mixed melting point determination and comparison of the ultraviolet spectrum with that of an



V : X=CN VI : X=Br VII
XIV : X=NHSO$_2$Ts VIII : X=CN



IX : X=Br XI : X=Br
X : X=CN XII : X=NHSO$_2$Ts
XIII : X=NH$_2$

authentic specimen[7]. The direct formation of the cyanotropolone (V) from the dibromotropolone (II) in the above reaction is probably due to a secondary reaction of the bromotropolone (III) with cuprous cyanide, since the reaction of III and cuprous cyanide in the same condition was proved to give the cyanotropolone (V) really.

With the reaction of 3, 5-dibromotropolone (VI) in the same condition, both a partially debrominated product, 5-bromotropolone (VII), and a substitution product, 5-bromo-3-cyanotropolone (VIII), were obtained as the reaction products. The structure of the latter (VIII) is proved from the formation of VII on hydrolyzing it with sulfuric acid followed by decarboxylation and from the resemblance of its ultraviolet spectrum (Fig. 1) to that of 3-cyanotropolone[6].

A similar result was also recognized in the reaction of 3, 5, 7-tribromotropolone (IX). Thus the reaction products were a partially debrominated product, 3, 5-dibromotropolone (VI), and a substitution product, 5-bromo-3, 7-dicyanotropolone (X), which derived to 5-bromotropolone (VII) on hydrolysis with sulfuric acid followed by decarboxylation.

The ultraviolet absorption spectra of the above two cyanotropolones are shown in Fig. 1.

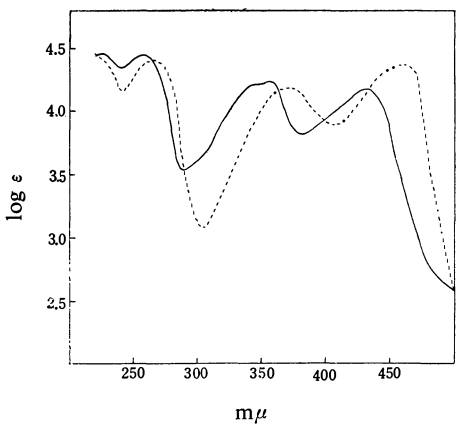



Fig. 1. The ultraviolet absorption spectra.
(——) : 5-Bromo-3-cyanotropolone (VIII)
(------) : 5-Bromo-3,7-dicyanotropolone(X)

It has now been clarified, as shown in the above description, that the reaction of copper salt of some polybromotropolones with cuprous cyanide in pyridine results in the formation of a partially debrominated product in general. On the other hand, it is noteworthy that such a fact has not been observed in the case of the reaction with alkali salt, not copper, of bromotropolones. For instance, the alkali salt of 3-bromotropolone (XI) was reported to give only a corresponding nitrile in a fairly good yield in a reaction with cuprous cyanide in pyridine[5,6]. However, it has now been ascertained that the copper salt of the bromotropolone (XI) gives not only a substitution product, 3-cyanotropolone, but also a debrominated product, tropolone itself, although in an extremely poor yield, in the reaction with cuprous cyanide.

There have already been reported a few

5) a) B. J. Abadir, J. W. Cook, J. D. Loudon and D. K. V. Steel, *J. Chem. Soc.*, **1952**, 2350. b) T. Nozoe, Y. Kitahara and S. Masamune, *Proc. Japan Acad.*, **29**, 17 (1953). c) T. Nozoe and Y. Kitahara, ibid., **30**, 204 (1954).

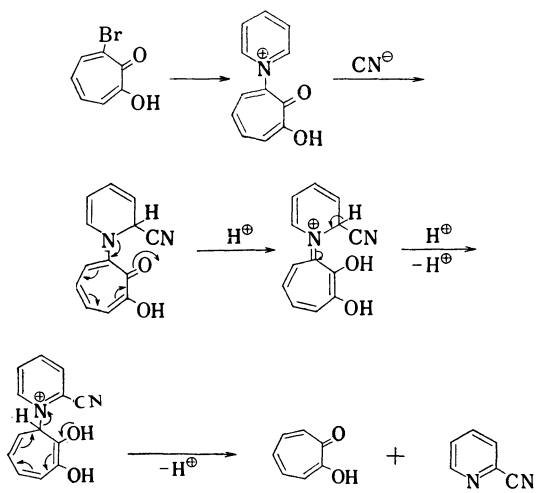
6) Y. Kitahara, *Science Repts. Tohoku Univ. Ser. I*, **40**, 74 (1956).

7) T. Sato, *J. Chem. Soc. Japan, Pure Chem. Sec.* (*Nippon Kagaku Zasshi*), **80**, 1171 (1959).

examples of obtaining a dehalogenated product in place of a corresponding nitrile in a reaction of halogenated compound and cuprous salt-pyridine complex. Edwards and Stewart[8] found that the treatment of 5-bromoacenaphthene, α-bromonaphthalene, bromobenzene or chlorobenzene with cuprous acetate in pyridine led not to the objective acetoxyl compound but to the corresponding dehalogenated product, all in yields of about 60 per cent of the theory. In the same reaction, Campbell, McKail and Muir[9] used cuprous cyanide instead of cuprous acetate and obtained a similar result, attributing this mechanism to nitrile formation, hydrolysis, and subsequent decarboxylation to a dehalogenated product.

However, the application of such a mechanism to the case of the debromination of polybromotropolones previously described seems not to be reasonable from the following points of view: (1) dehydrated pyridine was used in this series of experiments, whereas in the reported conditions[8] pyridine containing a small amount of water was used; (2) only a bromine atom, which is activated by the adjacent carbonyl group, in the 3 (or 7)-position is removed, whereas bromine in the 5-position is not; (3) 3-cyanotropolone was inert at least to cuprous cyanide in pyridine under the condition employed; (4) copper salt of bromotropolones is very soluble in pyridine, while alkali salt is scarcely soluble.

The author supposes that the debromination of bromotropolones can probably be explained by a mechanism similar to the formation of benzaldehyde by hydrolytic decomposition of Reisert compounds[10], although this is not founded on any concrete basis.




It was reported that the reaction of copper salt of 3-bromotropolone (XI) and its derivatives with potassium salt of arylsulfonamide in pyridine produced 3-arylsulfonylaminotropolones (XII), which hydrolyzed to 3-aminotropolones (XIII)[5c,11]. Application of this process to 4-bromotropolone (III) for the purpose of preparing 4-aminotropolone (I), however, resulted in no formation of any reaction product.

On the other hand, the bromine atom of III was replaced by the amino group to form the aminotropolone (I), though in a poor yield, on being treated with concentrated ammonia in the presence of cupric sulfate, the process of which had been used to prepare an aminophenol from a bromophenol[12]. The amino compound I gave easily, under a condition of the Schotten-Baumann method, 4-*p*-toluenesulfonylaminotropolone (XIV), which returned back to I on action of concentrated sulfuric acid, likewise in the case of the 3-analogue.

An attempt to synthesize 4,4′-bitropolonyl by treatment of copper salt of 4-bromotropolone (III) with copper powder in pyridine did not succeed unfortunately, whereas in the same condition 3,3′-bitropolonyls have been synthesized satisfactorily from 3-iodotropolones[13].

That the bromine atom of 4-bromotropolone (III) was replaced by the amino or cyano group to form a corresponding substituted product is clarified from the above description, but its reactivity against anionoid reagents seems to be smaller than that of isomeric 3-bromotropolone (XI). This is probably due to the fact that the mesomeric effect of the bromine of 4-bromotropolone (III) predominates its inductive effect to result in the decrease of activation of the bromine, whereas the inductive effect of the bromine of 3-bromotropolone (XI) becomes stronger through a hydrogen bond with the hydroxyl group of the molecule and in consequence the electron density at the 3- (or 7-)position is much decreased to result in promotion of anionoid substitutions.

Some electrophilic substitutions were also attempted on the bromotropolone (III). Nitration of III afforded in a poor yield 6-bromo-3-nitrotropolone (XV), whose structure was proved by its derivation to 3,6-dibromotropolone (II) on treatment with hydrobromic

8) W. G. H. Edwards and R. G. Stewart, *Chem. & Ind.*, **1952**, 472.

9) N. Campbell, J. E. McKail and J. Muir, ibid., **1952**, 739.

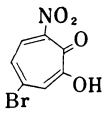
10) W. E. McEven and R. N. Hazlett, *J. Am. Chem. Soc.*, **71**, 1949 (1949).

11) Y. Kitahara, *Science Repts. Tohoku Univ. Ser. I*, **40**, 83 (1956); T. Nozoe, Y. Kitahara and K. Doi, ibid., **40**, 121 (1957).

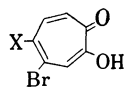
12) H. E. Podall and W. E. Foster, *J. Org. Chem.*, **23**, 280 (1958).

13) T. Nozoe, K. Doi and K. Kitahara, *Proc. Japan Acad.*, **32**, 480 (1956).

acid in acetic acid[14], and by the resemblance of its ultraviolet absorption (Fig. 2) to that of 3-nitrotropolone[14].



XV



XVI: X=-N=N-Ph
XVII: X=$NH_2$

Similarly to many tropolones, III underwent azo-coupling to give 4-bromo-5-phenylazotropolone (XVI), which was hydrogenolyzed to 5-aminotropolone via 5-amino-4-bromotropolone (XVII). The ultraviolet absorptions of XVI and XVII resemble closely those of the respective debrominated compound (Fig. 2).

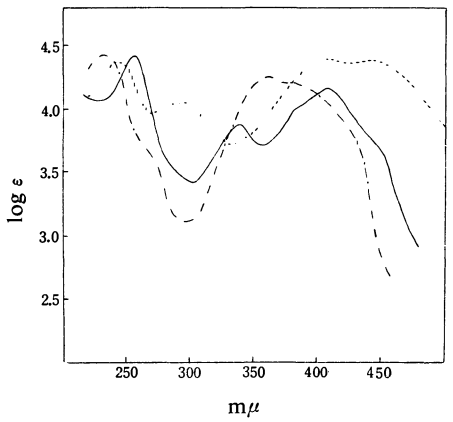



Fig. 2. The ultraviolet absorption spectra.
(——) : 6-Bromo-3-nitrotropolone (XV)
(----) : 4-Bromo-5-phenylazotropolone (XVI)
(—·—) : 5-Amino-4-bromotropolone (XVII)

## Experimental

All of the ultraviolet absorption spectra were measured in methanol solution with a Beckman model DU quartz spectrophotometer.

**Reactions of Bromotropolones with Cuprous Cyanide.**—*Reaction of 3, 6-Dibromotropolone (II).*—A mixture of the copper salt (7g.) of II, cuprous cyanide (2.2g.) and pyridine (26 ml.), distilled over solid potassium hydroxide, was heated under reflux for 2 hr., acidified to Congo red with dilute hydrochloric acid; then chloroform (100 ml.) was added to this mixture. After hydrogen sulfide was introduced into it, copper sulfide was removed by filtration and the chloroform layer was evaporated in vacuo to dryness. The residual solid, after sublimation in vacuo and subsequent recrystallization, yielded 4-bromotropolone (III, 1.2 g), from the soluble part in cyclohexane, as pale yellow needles, m. p. 86~87°C, undepressed on admixture with an authentic specimen which was kindly supplied by Dr. Teruko Sato[7]. The less soluble part in cyclohexane was recrystallized from ethanol to give 4-cyanotropolone (V, 0.17 g.) as yellow needles, m. p. and mixed m. p.[6] 194~195°C.

*Reaction of 3, 5-Dibromotropolone (VI).*—A mixture of the copper salt (1.5 g.) of VI[4], cuprous cyanide (0.47 g.) and pyridine (10 ml.) was heated under reflux for 2 hr. The following procedure was essentially as described in the previous experiment and the evaporated solid of the chloroform extract was recrystallized from ethanol to separate into more soluble 5-bromotropolone (VII, 0.2 g.), undepressed on admixture with an authentic sample[14], and less soluble 5-bromo-3-cyanotropolone (VIII, 0.05 g.) as yellow prisms, m. p. 168~170°C.

Found: N, 5.82. Calcd. for $C_8H_4O_2NBr$: N, 6.19%. $\lambda_{max}$ mμ (log ε): 225 (4.45), 257 (4.45), 355 (4.25), 435 (4.18).

A mixture of VIII (40 mg.) and 75% sulfuric acid (0.2 ml.) was heated on an oil bath at 150°C for 30 min., diluted with water (1 ml.), and the residual crystals were collected by filtration. This product, which corresponds to 5-bromo-3-carboxytropolone melted at 166~170°C, 25 mg., without any further purification, was heated at reflux for 30 min. in pyridine (0.5 ml.), acidified to Congo red with dilute hydrochloric acid, and the residual solid was crystallized from cyclohexane to afford 5-bromotropolone (VII, 5 mg.), m. p. and mixed m. p.[14] 189~190°C.

*Reaction of 3, 5, 7-Tribromotropolone (IX).*—A mixture of the copper salt (3.5 g.) of IX, cuprous cyanide (0.9 g.) and pyridine (5 ml.) was heated at reflux for 2 hr. The chloroform extract obtained by the usual procedure was evaporated in vacuo and the residue was recrystallized fractionally from ethanol. The more soluble portion yielded 3, 5-dibromotropolone (VI, 0.12 g.) as pale yellow needles, m. p. and mixed m. p. 154~155°C. The less soluble portion afforded 5-bromo-3, 7-dicyanotropolone (X, 60 mg.) as yellow needles, m. p. 231~232°C.

Found: N, 11.07. Calcd. for $C_9H_3O_2N_2Br$: N, 11.15%. $\lambda_{max}$ mμ (log ε): 265 (4.41), 370 (4.19), 460 (4.39).

A mixture of X (50 mg.) and 75% sulfuric acid (0.5 ml.) was heated at 150°C for 1 hr., acidified with dilute mineral acid, and the residual solid, which corresponded to 5-bromo-3, 7-dicarboxytropolone, m. p. 233~235°C (decomp.), 40 mg., without any further purification, was heated in pyridine (1 ml.), giving 5-bromotropolone (VII, 5 mg.), undepressed on admixture with an authentic specimen.

*Reaction of 3-Bromotropolone (XI).*—A mixture of the copper salt (11.6 g.) of XI, cuprous cyanide (6.5 g.) and pyridine (50 ml.) was heated under reflux for 3 hr., acidified to Congo red with dilute hydrochloric acid, and the solid deposited was collected by filtration. Hydrogen sulfide was bubbled through the suspension of this solid in chloroform (200 ml.), copper sulfide was removed by filtration, the chloroform solution was evaporated in vacuo to dryness, and the residue, after washing with cyclohexane, was crystallized from methanol

14) T. Nozoe, Y. Kitahara, K. Doi and T. Arai, *Bull. Chem. Research Inst. Non-Aqueous Solns. Tohoku Univ.*, 7, 13 (1957).

to give 3-cyanotropolone (5.4 g.) as yellow needles, m. p. and mixed m. p.[5] 174~174.5°C. From the part soluble in cyclohexane, tropolone (0.1 g.) was obtained, after evaporation of the extract and sublimation in vacuo followed by crystallization from petroleum ether.

**Reaction of 4-Bromotropolone (III).**—*4-Cyanotropolone (V).*—A mixture of the copper salt (0.47 g.) of III, cuprous cyanide (0.21 g.) and pyridine (3 ml.) was heated under reflux for 2 hr. and the following procedure was carried out essentially as described in the preceding experiments. The chloroform extract was evaporated in vacuo and the residue therefrom was recrystallized from methanol to afford 4-cyanotropolone (V, 0.05 g), undepressed on admixture with an authentic specimen. From the mother-liquor of recrystallization unreacted bromotropolone (III, 0.07 g.) was recovered.

*4-Aminotropolone (I).*—A mixture of III (0.4 g.), cupric sulfate pentahydrate (10 mg.) and concentrated ammonia (4 ml.) was heated at 130~140°C for 1 hr. in an autoclave. The reaction mixture was diluted with water (10 ml.), acidified with mineral acid to pH 6, and then extracted continuously with ether. The ether extract, after evaporation of the solvent, yielded 4-aminotropolone (I, 0.12 g.) as colorless needles, m. p. 187~189°C, undepressed on admixture with an authentic specimen[2].

*4-p-Toluenesulfonylaminotropolone (XIV).*—To a stirred solution of the aminotropolone (I, 70 mg.), pyridine (1 ml.) and water (2 ml.) was added *p*-toluenesulfonyl chloride (100 mg.), and then the reaction mixture was stirred for 1 hr. This was neutralized with dilute hydrochloric acid, the deposited solid was collected and recrystallized from a mixed solvent of methanol and acetic acid to yield XIV (80 mg.) as pale yellow prism, m. p. 195~196°C.

Found: C, 57.27; H. 4.63; N, 4.97. Calcd. for $C_{14}H_{13}O_4NS$: C, 57.73; H, 4.50; N, 4.82%.

A mixture of XIV (60 mg.) and concentrated sulfuric acid (0.2 ml.) was heated at 50°C for 30 min., diluted with water (1 ml.), and neutralized with sodium carbonate, by which 4-aminotropolone (I), m. p. and mixed m. p. 187~188°C, was deposited.

*6-Bromo-3-nitrotropolone (XV).*—A solution of nitric acid (0.3 g., $d=1.42$) and acetic acid (1 ml.) was added dropwise at room temperature to a stirred solution of III (0.79 g.) and acetic acid (4 ml.). The resulting solution was then diluted with water (10 ml.) and extracted with ether (20 ml.×2). The extract, after evaporation of the solvent, sublimation in vacuo followed by recrystallization from ethanol, gave XV as yellow prisms, m. p. 159~160°C, in 13% yield.

Found: N, 6.09. Calcd. for $C_7H_4O_4NBr$: N, 5.69%. $\lambda_{max}$ mμ (log ε): 256 (4.42), 338 (3.88), 407 (4.16).

A solution of XV (50 mg.), concentrated hydrobromic acid (1 ml.) and acetic acid (1 ml.) was heated in a sealed tube at 120°C for 1 hr., the resulting solution was evaporated to dryness, and the residue, after sublimation in vacuo followed by recrystallization from ethanol, afforded 3, 6-dibromotropolone (II, 10 mg.), m. p. and mixed m. p.[4] 120~121°C.

*4-Bromo-5-phenylazotropolone (XVI).*—To a stirred solution of the bromotropolone (III, 0.2 g.) and pyridine (1.5 ml.) was added dropwise when cold a solution of benzenediazonium chloride obtained from aniline (95 mg.). The reaction mixture was acidified to Congo red with dilute hydrochloric acid and the precipitated solid was recrystallized from ethyl acetate to yield XVI (0.3 g.) as red needles, m. p. 194~195°C.

Found: N, 9.64. Calcd. for $C_{13}H_9O_2N_2Br$: N, 9.18%. $\lambda_{max}$ mμ (log ε): 245 (4.37), 295 (4.40), 410 (4.38), 444 (4.37).

*5-Amino-4-bromotropolone (XVII).*—A solution of XVI (0.9 g.), 5% palladium-on-carbon (0.5 g.) and ethanol (100 ml.) was shaken in hydrogen atmosphere until the uptake of hydrogen had reached one mole equivalent. The reaction mixture, from which the catalyst was removed, was evaporated in vacuo and the residue was crystallized from benzene to give XVII (0.12 g.) as yellow needles, m. p. 116~117°C.

Found: N, 6.39. Calcd. for $C_7H_6O_2NBr$: N, 6.48%. $\lambda_{max}$ mμ (log ε): 235 (4.42), 360 (4.25).

When a mixture of XVII (100 mg.), 5% palladium-on-carbon (100 mg.), and sodium acetate trihydrate (70 mg.), and methanol (15 ml.) was shaken in hydrogen atmosphere until no further hydrogen was absorbed, 5-aminotropolone, undepressed on admixture with an authentic specimen[15], was obtained from the reaction mixture.

The author expresses his sincere gratitude to Professor Y. Kitahara for his unfailing guidance throughout the course of this work, to Mr. S. Endo and Mr. T. Terasawa for their helpful assistance with experiments, and to Messrs. K. Kato, S. Ohyama, A. Iwanaga and S. Azumi for microanalyses.

*The Chemical Research Institute of Non-Aqueous Solutions*
*Tohoku University*
*Katahira-cho, Sendai*

15) T. Nozoe, S. Seto, S. Ebine and S. Ito, *J. Am. Chem. Soc.*, 73, 1895 (1951).

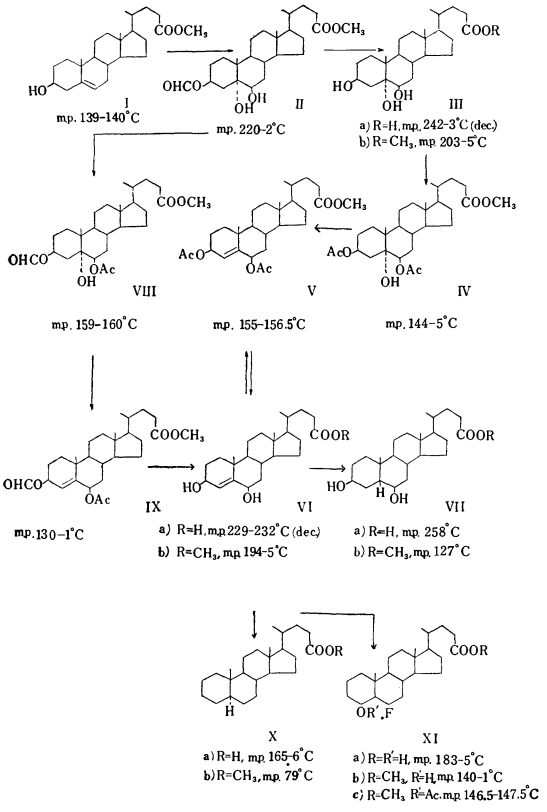
# *Bile Acids and Steroids. XX*[1]*. Studies on the Hog Bile Acids (Part 4)*[2]*. Synthesis of 3β, 6β-Dihydroxy-5β-cholanoic Acid and 3β, 6α-Dihydroxy-5α-cholanoic Acid*

By Jun'ichi KAWANAMI

(Received September 30, 1960)

**3β, 6β-Dihydroxy-5β-cholanoic Acid.** — Although 3β, 6β-dihydroxy-5β-cholanoic acid has been synthesized earlier[3-5], the methods then used were unprofitable for the preparation because the yield was low and the treatment difficult. The most convenient method for this purpose was as follows (chart 1). The starting

Chart I




material, methyl 3β-hydroxy-$\Delta^5$-cholenoate (I) was prepared from methyl α-hyodeoxycholate in high yield according to Bharucha's method[6]. A trans-hydroxylation of the double bond was done according to the method that was performed in the cholesterol series by Fieser[7] and the trans triol III (acid, m. p. 242~243°C with decomp.; methyl ester, m. p. 203~205°C) was obtained in a comparatively good yield. As seen in Table I, it is clear that the configuration of the hydroxyl group at position 6 in the triol III thus obtained belongs to the β-series by comparison with the molecular rotations[8] of the analogous derivatives in the cholesterol series. By acetylation with acetic anhydride, the triol IIIb afforded a diacetate IV with m. p. 144~145°C which was followed by dehydration according to the Darzens' method[9] to afford an unsaturated derivative V with m. p. 155~156.5°C in a quantitative yield. The unsaturated diacetate V was saponified with alkali to yield an unsaturated diol VIa, m. p. 229~232°C (decomp.), in high yield. This acid VIa was esterified with an ethereal diazomethane to furnish its methyl ester VIb, m. p. 194~195°C, in 89% yield, which was sparingly soluble in ether. This methyl ester VIb was also obtained from the monoformate IX by the following route: When the 6-acetate VIII, m. p. 159~160°C, obtained from the monoformate II was dehydrated according to Darzens' method[9] as in the previous case, it afforded an unsaturated derivative IX, m.p. 130~131°C, which was saponified to give the identical diol VI with that obtained from the diacetate V. Since all of the unsaturated derivatives, V, VI and IX described above were positive to the Rosenheim test[10], it shows that these compounds have acetyl, formyl or hydroxyl group at the allyl position[11]. The ultraviolet ($\lambda_{max}$ 205.5 mμ) and the infrared absorption spectrum ($\nu_{max}$ 1658 $cm^{-1}$) show the presence of a double bond at position 4-5. The unsaturated diol VIb obtained on the above

1) Part XIX: K. Takeda, H. Ōsaka and A. Horiki, *J. Pharm. Soc. Japan* (*Yakugaku Zasshi*), in press.
2) Part 3 of this series: K. Takeda, T. Kubota and J. Kawanami, *J. Biochem.* (*Japan*), **44**, 51 (1957).
3) M. Tsukamoto, ibid., **32**, 451 (1940).
4) M. Tsukamoto, ibid., **32**, 467 (1940).
5) J. S. Moffatt, *J. Chem. Soc.*, **1947**, 812.
6) K. R. Bharucha, G. C. Buckley, C. K. Cross, L. J. Rubin and P. Ziegler, *Can. J. Chem.*, **34**, 982 (1956).
7) L. F. Fieser and S. Rajagopalan, *J. Am. Chem. Soc.*, **71**, 3938 (1949).
8) L. F. Fieser and M. Fieser, "Steroids", Reinhold Publish. Co., New York (1959), p. 204.
9) G. Darzens, *Compt. rend.*, **152**, 1601 (1911).
10) O. Rosenheim, *Biochem. J.*, **23**, 47 (1929).
11) R. Schoenheim and E. A. Evans, Jr., *J. Biol. Chem.* **114**, 567 (1936).

TABLE I. MOLECULAR ROTATIONS OF 6-EPIMERS

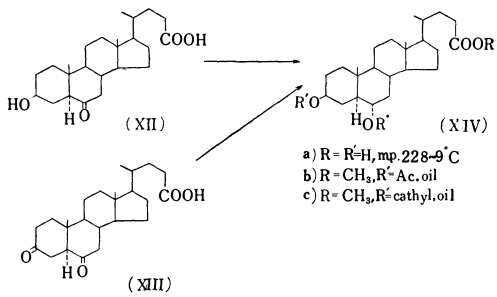
| Substituent | Skeletal | 6β | 6α* | $\Delta^{\alpha-\beta}$ |
|---|---|---|---|---|
| 3β,6-Diol | 5α-Cholestane | + 53 | +154 | +101 |
| | 5α-Cholanoic acid | 0 (Py.) | +135 | +135 |
| 3β,5α,6-Triol | Cholestane | + 4 (Di.) | + 88 (Di.) | + 84 |
| | Cholanoic acid | − 41 (Py.) | + 94 (Py.) | +135 |
| | Methyl cholanoate | − 34 (Py.) | +346 (Me.) | +370 |
| 3β,5α,6-Triol 3,6-diacetate | Cholestane | −232 | + 28 | +260 |
| | Methyl cholanoate | −243 | + 41 (Di.) | +283 |
| $\Delta^4$-3β,6-Diol | Cholestane | − 53 | +117 | +170 |
| | Cholanoic acid | 0 (Py.) | +109 (Py.) | +109 |
| $\Delta^4$-3β,6-Diacetate | Cholestane | − 58 | + 89 | +147 |
| | Methyl cholanoate | − 78 | + 78 | +156 |

* Molecular rotations of the 6α-derivatives, in bile acid are unpublished data by the author. Unless otherwise noted, the solvent is chloroform. Di., Py. and Me. are dioxane, pyridine and methanol, respectively.

saponification was again acetylated back to the parent unsaturated diacetate V. Hence, it was defined that allyl rearrangement or epimerization did not take place in the course of the saponification. In absolute ethanol the unsaturated diol VIb was hydrogenated with the Adams' catalyst to absorb hydrogen very rapidly (1 hr.) in comparison with the case in cholestene diol (28 hr.)[12] yielding the anticipated methyl 3β,6β-dihydroxy-5β-cholanoate VIIb, m. p. 127°C, in a quantitative yield. This compound shows the absence of the double bond in both the ultraviolet and the infrared absorption spectrum and it was also negative to the Rosenheim test. The methyl ester VIIb was saponified with methanolic potassium hydroxide to give 3β,6β-dihydroxy-5β-cholanoic acid VIIa, m. p. 258°C, in 87% yield. While catalytic hydrogenation was carried out in 95% ethanol solution, there occurred simultaneous hydrogenolysis as in the case of the diacetate[13] and the following reduction products were separated after acetylation: 45.5% of methyl 5α-cholanoate, Xb m. p. 79°C, 27% of methyl acetoxy cholenoate, XIc m. p. 146.5~147.5°C and an oil which was saponified to afford 5% of 3β,6β-dihydroxy-5β-cholanoic acid, VIIa m. p. 255°C. In the above methyl acetoxycholenoate XIc, the positions of both the hydroxyl group and the double bond could not be determined on account of the scarcity of the substance.

**3β, 6α-Dihydroxy-5α-cholanoate.** — Reduction of the steroid six-membered ketone by metal and alcohol generally produces almost exclusively equatorial alcohols. Then the reduction of 3β-hydroxy-6-oxo-5α-cholanoic acid (XII) with sodium and *n*-butanol was carried out and it

Chart 2




gave an acid with m. p. 228~229°C. This reduction product afforded a diacetate XIVb and a dicathylate XIVc by treatment in the usual method[14]. Since the attempted partial saponification of the diacetate XIVb was unsuccessful, it was assumed that the newly formed hydroxyl group is equatorial. Also, as seen in Table I, comparison of molecular rotations shows that this product belongs to the 6α-series. With the above observation, it could be deduced that this reduction product is 3β, 6α-dihydroxy-5α-cholanoic acid. The identical compound was also obtained from 3,6-dioxo-5α-cholanoic acid (XIII) by the same reduction.

## Experimental[15]

**3β, 6β-Dihydroxy-5β-cholanoic Acid.**—*Methyl 3β, 5α, 6β-trihydroxy-cholanoate 3-Formate (II).* — This preparation corresponded to the treatment on the

12) V. Prelog and E. Tagmann, *Helv. Chim. Acta*, **27**, 1880 (1944).

13) O. Mancera, G. Rosenkranz and C. Djerassi, *J. Org. Chem.*, **16**, 192 (1951); S. Nishimura and K. Mori, This Bulletin, **32**, 103 (1959).

14) L. F. Fieser et al., *J. Am. Chem. Soc.*, **74**, 3309 (1952).

15) All melting points are uncorrected. Infrared spectra were recorded in Nujol mulls with a Koken DS 301 double beam infrared spectrophotometer, unless otherwise noted, and the ultraviolet spectra were taken in 95% ethanol solution using a Hitachi EPS 2 spectrophotometer. Optical rotations were determined in a 1-dm. tube for chloroform solutions, unless otherwise specified. The alumina used for chromatography in this experiment was Merck's reagent grade standardized according to Brockmann and the chromatography was usually performed according to the method described by T. Reichstein. (T. Reichstein and W. Schopee, *Discussions Faraday Soc.*, No. 7, (1949)) The extracts were dried over anhydrous sodium sulfate before evaporation unless stated otherwise.

study of cholesterol series[7]. Methyl 3β-hydroxy-$\Delta^5$-cholenoate (I), m. p. 139~140°C, (5.871 g.) (prepared from methyl α-hyodeoxycholate ditosylate according to Bharucha's method[6]) was added to 88% of formic acid (59 ml.) and warmed for 5 min. on a boiling water bath, and so the crystals precipitated were dissolved to separate as oil. To this reaction mixture cooled to room temperature, 30% of aqueous hydrogen peroxide (6 ml.) was added. The white deposit initially precipitated was dissolved by occasionally shaking for 30 min. After standing overnight at room temperature, the reaction mixture was diluted with water to separate an oily precipitate. The extract with ether-chloroform mixture (4 : 1) was washed successively with water, dilute hydrochloric acid and again water. The extract was evaporated to afford an oily product (9.448 g.). Trituration of the oily residue with methanol (45 ml.) coupled with 5% methanolic hydrochloric acid (5 ml.) caused the crystallization of II as cubes. After standing overnight at room temperature, the crystals obtained were collected and washed thoroughly with methanol to give methyl 3β,5α,6β-trihydroxycholanoate 3-formate (II), 1.657 g. (24.4%), cubes, m. p. 220~222°C. The melting point was not elevated by further recrystallization from methanol. $[\alpha]_D^{19}=-17.7\pm2°$ (*c* 0.962). infrared spectrum: $\nu_{max}$ 3939, 3454 (OH); 1722, 1710 (C=O); 1183, 1169 $cm^{-1}$ (C-O).

Found: C, 69.43; H, 9.46. Calcd. for $C_{26}H_{42}O_6$: C, 69.30; H, 9.40%.

*Methyl 3β,5α,6β-Trihydroxycholanoate (IIIb).*—i) From the above filtrate—The filtrate was concentrated under diminished pressure to cause the crystallization. After cooling well the crystals were collected and washed with cold methanol to give crystals with m. p. 193~202°C (1.947 g.: 30.5%) as a first crop and those with m. p. 168~172°C as a second crop (1.086 g.: 17%) were obtained on concentration of the mother liquor. These are combined and recrystallized from methanol to methyl 3β,5α,6β-trihydroxycholanoate (IIIb), cubes, m. p. 203~205°C. $[\alpha]_D^{20}=-7.6\pm2°$ (*c*=0.996, pyridine). Infrared spectrum: $\nu_{max}$ 3568, 3488 (OH); 1740 (C=O); 1173 $cm^{-1}$ (C-O).

Found: C, 70.95; H, 9.86. Calcd. for $C_{25}H_{42}O_5$: C, 71.05; H, 10.02%.

ii) From the formate II — The formate II (591 mg.) was dissolved in methanol (3 ml.) coupled with ten drops of 10% methanolic hydrochloric acid and allowed to stand overnight at room temperature (22~25°C). After removal of the solvent under reduced pressure, the crystals obtained were collected and washed with methanol to afford methyl 3β,5α,6β-trihydroxycholanoate (IIIb), 497 mg. (90%), m. p. 202~205°C. The sample showed no depression on admixture with the triol (IIIb) obtained above and the infrared spectrum of the sample was also identical with that of IIIb.

*3β,5α,6β-Trihydroxycholanoic Acid (IIIa).*—After a solution of the formate II (591 mg.) in 0.5 N methanolic potassium hydroxide (25 ml.) was allowed to stand overnight at room temperature, the solvent was removed under reduced pressure, water was added and it was acidified with dilute hydrochloric acid under cooling. After being kept for 1 hr. at room temperature, the precipitate was collected by filtration, washed thoroughly with water and dried in vacuo overnight at 100°C. The crude acid obtained in 96% yield (167 mg.) was recrystallized from acetone-methanol to yield 3β,5α,6β-trihydroxycholanoic acid (IIIa), 64 mg., m. p. 242~243°C (decomp.). $[\alpha]_D^{21}=-10.3\pm2°$ (*c* 0.987, pyridine). Infrared spectrum: $\nu_{max}$ 3575, 3433, about 3000 (OH); 1710, 1692, 1674 $cm^{-1}$ (C=O).

Found: C, 70.67; H, 9.89. Calcd. for $C_{24}H_{40}O_5$: C, 70.55; H, 9.87%.

*Methyl 3β,5α,6β-Trihydroxycholanoate 3,6-Diacetate (IV).*—In warming with acetic anhydride (4 ml.) on a boiling water bath for 30 min., the triol methyl ester III (415 mg.) was dissolved. After further warming for 2 hr., the mixture was cooled, water was added carefully and it was occasionally shaken to crystallize it. After being kept for 30 min. at room temperature, the precipitate was collected and washed successively with water and methanol to furnish 3,6-diacetate, 491 mg. (99%), m. p. 142~143°C. This was further recrystallized from methanol to methyl 3β,5α,6β-trihydroxycholanoate 3,6-diacetate (IV), 296 mg. (59.5%), long prisms, m. p. 144~145°C. $[\alpha]_D^{24}=-48.1\pm2°$ (*c* 0.998). Infrared spectrum: $\nu_{max}$ 3540 (OH); 1741, 1724, 1710 (C=O); 1270, 1250, 1164, 1030 $cm^{-1}$ (C-O).

Found: C, 68.76; H, 9.11. Calcd. for $C_{29}H_{46}O_7$: C, 68.74; H, 9.15%.

*Methyl 3β,6β-Diacetoxy-$\Delta^4$-cholenoate (V).*—To a solution of the diacetate IV (1.215 g.) in pyridine (7 ml.), thionyl chloride (0.28 ml.) was added dropwise under cooling and shaking to give needles immediately. After shaking for ten min. at 0°C, the mixture was carefully diluted with 100 ml. of water and allowed to stand for 1 hr. at room temperature. The crystals thus obtained were collected and washed thoroughly with water and a little methanol to afford methyl 3β,6β-diacetoxy-$\Delta^4$-cholenoate (V), 1.112 g. (95%), prismatic needles, m. p. 155~156.5°C. The Rosenheim test gave blue coloration. $[\alpha]_D^{18}=-16.3\pm2°$ (*c* 1.011). Infrared spectrum: $\nu_{max}$ 1738, 1726, (C=O); 1658 (C=C); 1242, 1200, 1164, 1034, 1023 $cm^{-1}$ (C-O).

Found: C, 71.55; H, 9.08. Calcd. for $C_{29}H_{44}O_6$: C, 71.28; H, 9.08%.

*3β,6β-Dihydroxy-$\Delta^4$-cholenoic Acid (VIa).*—A solution of the above ester V (3.365 g.) in 0.5 N methanolic potassium hydroxide (670 ml.) was heated under reflux for 5 hr. on a boiling water bath. After removal of the solvent under reduced pressure, the residue was diluted with water and acidified with dilute hydrochloric acid under cooling. After standing, the precipitate was collected by filtration, washed well with water and dried in vacuo overnight at 100°C to furnish a crude acid (2.662 g.: 99%). For analysis, 59 mg. of the crude acid was recrystallized from methanol to 3β,6β-dihydroxyl-$\Delta^4$-cholenoic acid (VIa), 32 mg., scales, m. p. 229~232°C (decomp.). The Rosenheim test gave violet-blue coloration. $[\alpha]_D^{19}=0\pm2°$ (*c* 0.913, pyridine). I. R. spectrum: $\nu_{max}$ 3436 (broad), 3256, about 3000 (OH); 1706 (C=O); 1658 $cm^{-1}$ (C=C).

Found: C, 73.61; H, 9.36. Calcd. for $C_{24}H_{38}O_4$: C, 73.80; H, 9.81%.

*3β,6β-Dihydroxy-Δ⁴-cholenoic Acid (VIa) from Methyl 3β-Formoxy-6β-acetoxy-Δ⁴-cholenoate (IX).*—Methyl 3β-formoxy-6β-acetoxy-Δ⁴-cholenoate (289 mg.) which will be described in the next section, was saponified under reflux with 0.5 N methanolic potassium hydroxide (75 ml.) for 2 hr. Isolation in the usual way gave a crude acid (187 mg.) in 79% yield. The product was recrystallized from chloroform-methanol to 3β,6β-dihydroxy-Δ⁴-cholenoic acid (VIa), 153 mg., cubes, m. p. 228~230°C (decomp.). The resenheim test gave violet-blue coloration. Its infrared spectrum was satisfactorily identical with that of the acid from diacetate V.

Found: C, 74.03; H, 9.77. Calcd. for $C_{24}H_{38}O_4$: C, 73.80; H, 9.81%.

*Methyl 3β,6β-Dihydroxy-Δ⁴-cholenoate (VIb).*—Being esterified with ethereal diazomethane the above crude acid (2.603 g.) was violently bubbled to react and afforded a precipitate. After collecting and washing with ether, the precipitate was recrystallized from acetone to methyl 3β,6β-dihydroxy-Δ⁴-cholenoate (VIb), 2.477 g. (89%), cubes, m. p. 194~195°C. The Rosenheim test gave blue coloration and the Liebermann test violet to blue and to green. $[\alpha]_D^{22}=+22\pm2°$ (*c* 0.948). Ultraviolet spectrum: $\lambda_{max}$ 205.5 mμ (ε=5800). Infrared spectrum: $\nu_{max}$ 3292 (OH); 3029 (shoulder) (C=C); 1742 (C=O); 1659 $cm^{-1}$ (C=C).

Found: C, 74.22; H, 9.95. Calcd. for $C_{25}H_{40}O_4$: C, 74.21; H, 9.97%.

*Methyl 3β,6β-Diacetoxy-Δ⁴-cholenoate (V) from the above Ester (VIb).*—The above ester VIb (85 mg.) was warmed with pyridine (1 ml.) and acetic anhydride (1 ml.) for 2 hr. on a boiling water bath. After cooling, water was carefully addded to the mixture to furnish needles which after filtering and washing, were recrystallized from methanol to methyl 3β,6β-diacetoxy-Δ⁴-cholenoate (V), 65 mg. (82.6%), fine needles, m. p. 154~155°C. The compound was identified by a mixed melting point and the infrared spectrum with the specimen described above.

*Methyl 3β-Formoxy-5α,6β-dihydroxycholanoate 6-Acetate (VIII).*—On warming with acetic anhydride (6 ml.) on a boiling water bath for 2 hr., the 3-formyl derivative II (580 mg.) described above had dissolved completely. After warming for a further 2 hr., the mixture was cooled and water was added carefully to give crystals which after filtering and washing with water and a little methanol, were recrystallized from methanol to methyl 3β-formoxy-5α,6β-dihydroxycholanoate 6-acetate (VIII), 500 mg. (80%), fine needles, m. p. 159~160°C. $[\alpha]_D^{18}=-46\pm2°$ (*c* 1.006). Infrared spectrum: $\nu_{max}$ 3495 (OH); 1733, 1721, 1711 (C=O); 1282, 1185, 1040 $cm^{-1}$ (C-O).

Found: C, 68.09; H, 9.01. Calcd. for $C_{28}H_{44}O_7$: C, 68.26; H, 9.00%.

*Methyl 3β-Formoxy-6β-acetoxy-Δ⁴-cholenoate (IX).*—To a solution of the above 5α-hydroxy derivative VIII (431 mg.) in pyridine (2 ml.), thionyl chloride (0.1 ml.) was added dropwise under cooling and shaking to give needles immediately. After shaking for ten min. at 0°C, 50 ml. of water was added carefully to the mixture and it allowed to stand for 1 hr. at room temperature. The crystals obtained after filtering and washing thoroughly with water and a little methanol, were further recrystallized from methanol to methyl 3β-formoxy-6β-acetoxy-Δ⁴-cholenoate (IX), 334 mg. (80.7%), needles, m. p. 130~131°C, sinter at 123~124°C. $[\alpha]_D^{18}=-5\pm2°$ (*c* 0.911). Infrared spectrum: $\nu_{max}$ 1738, 1725 (C=O); 1659 (C=C); 1248, 1183, 1161, 1038 $cm^{-1}$ (C-O).

Found: C, 70.98; H, 8.96. Calcd. for $C_{28}H_{42}O_6$; C, 70.85; H, 8.92%.

*Methyl 3β,6β-Dihydroxy-5β-cholanoate (VIIb).*—A suspension of Adams catalyst (73 mg.) in absolute ethanol (20 ml.) was prereduced with hydrogen at 20°C to absorb 18 ml. of hydrogen for 20 min. To the above mixture, the methyl 3β,6β-dyhydroxy-Δ⁴-cholenoate (VIb) (1.134 g.) which was dissolved in absolute ethanol (150 ml.) by warming and successively being cooled to room temperature, was added and shaken under hydrogen for 1 hr. to uptake 63.5 ml. of hydrogen. (calcd. for 1 mol. equiv. 67.5 ml. at 20°C). The filtrate from platinum moll was evaporated under reduced pressure to give a sirup which was recrystallized from methanol to methyl 3β,6β-dihydroxy-5β-cholanoate (VIIb), 1.096 g. (96.3%), needles, m. p. 127°C, softening at 78~80°C. The Rosenheim test was negative and the Liebermann test gave cherry-red to bordeaux coloration. $[\alpha]_D^{21}=+17\pm2°$ (*c* 1.062). No appreciable absorption in the ultraviolet spectrum. Infrared spectrum: $\nu_{max}$ 3602, 3377 (OH); 1740 (C=O); 1174, 1023 $cm^{-1}$ (C-O).

Found: C, 73.89; H, 10.41. Calcd. for $C_{25}H_{42}O_4$: C, 73.85; H, 10.41%.

*3β,6β-Dihydroxy-5β-cholanoic Acid (VIIa).*—After a solution of the saturated ester VIIb (150 mg.) in 0.2 N methanolic potassium hydroxide (15 ml.) was heated under reflux for 2 hr., the mixture was evaporated, diluted with water and acidified with dilute hydrochloric acid to Congo red to give a crude acid. The precipitate after filtering and washing thoroughly with water, was recrystallized from a large volume of acetone to 3β,6β-dihydroxy-5β-cholanoic acid (VIIa), 126 mg. (87%), scales, m. p. 258°C. The Liebermann test gave pink coloration. $[\alpha]_D^{20}=+21\pm2°$ (*c* 1.004, methanol). Infrared spectrum: $\nu_{max}$ 3497, about 3000 (OH); 1710 $cm^{-1}$ (C=C).

Found: C, 73.53; H, 10.33. Calcd. for $C_{24}H_{40}O_4$: C, 73.43; H, 10.27%.

*On the Hydrogenation of Methyl 3β,6β-Dihydroxy-Δ⁴-cholenoate (VIb) in 95% of Ethanol.*—A suspension of methyl 3β,6β-dihydroxy-Δ⁴-cholenoate (VIb) (460 mg.) in 95% of ethanol (40 ml.) was dissolved by warming and successively cooled to room temperature and then shaken with prereduced Adams catalyst (35 mg.) under hydrogen atmosphere for 24 hr. at 26°C to absorb 30.9 ml. of hydrogen (calcd. for 1 mol. equiv., 28 ml.). The filtrate from the catalyst was evaporated under diminished pressure to give a residue which was recrystallized from methanol to methyl 5α-cholanoate (Xb), 130 mg. scales, m. p. 78~79°C. The filtrate from the above crystals was evaporated to dryness to afford an oil (326 mg.) which was acetylated with pyridine (3 ml.) and acetic anhydride (3 ml.) by being kept overnight at room temperature. Working up in the usual way gave an oil (341 mg.) which was followed by chromatography on alumina. The petroleum ether eluate gave methyl 5α-cholanoate, 63 mg., scales,

m. p. 78~79°C. The fractions eluted with petroleum ether and petroleum ether-benzene (9 : 1 and 8 : 2) gave fine needles from methanol, 129 mg. (27%), m. p. 146.5~147.5°C. The last fractions eluted with petroleum ether-benzene (1 : 1), benzene and benzene-chloroform (9 : 1) gave an oil (39 mg.).

*Methyl 5α-Cholanoate (Xb).*—Methyl 5α-cholanoate was both scales (130 mg.) obtained by the recrystallization from methanol and scales (63 mg.) from the first elution on the chromatography described above. The total yield was 45.4%. The Liebermann test was negative. A mixed melting point with methyl 5β-cholanoate showed definite depression, melting at 60~61°C. The infrared spectrum of this compound was different from that of the normal series. $[\alpha]_D^{18}=+21\pm2°$ (*c* 1.018). Infrared spectrum: $\nu_{max}$ 1736 (C=O); 1197, 1167 $cm^{-1}$ (C-O).

Found: C, 80.31; H, 11.32. Calcd. for $C_{25}H_{42}O_2$: C, 80.15; H, 11.30%.

*5α-Cholanoic Acid (Xa).*—After a solution of the above ester Xb (103 mg.) in 0.5 N methanolic potassium hydroxide (2 ml.) was heated under reflux for 2 hr., the mixture was diluted with water, acidified with dilute hydrochloric acid and extracted with ether. The ethereal layer was washed with water and evaporated to give crystals which were recrystallized from methanol to 5α-cholanoic acid, 82 mg. (83%), scales, m. p. 165~166°C. $[\alpha]_D^{23}=+21\pm2°$ (*c* 1.013). Infrared spectrum: $\nu_{max}$ about 3000 (broad) (OH); 1710 $cm^{-1}$ (C=O).

Found: C, 80.03; H, 11.27. Calcd. for $C_{24}H_{40}O_2$: C, 79.94; H, 11.18%.

*The Second Elution on the Chromatography.*—This compound was assumed to be methyl ?-acetoxy-$\Delta^?$-cholenoate from both the elementary analysis and the infrared spectrum. The Liebermann test gave from red to violet and to brown coloration successively. $[\alpha]_D^{22}=+14\pm2°$ (*c* 1.009). Infrared spectrum: $\nu_{max}$ 1738 (C=O); 1694 (C=C); 1254, 1167, 1036 $cm^{-1}$ (C-O).

Found: C, 75.50; H, 10.19. Calcd. for $C_{27}H_{42}O_4$: C, 75.31; H, 9.83%.

*Acid from the above Ester XIa.*—After a solution of the above ester acetate XIc (51 mg.) in 0.2 N methanolic potassium hydroxide was heated under reflux for 2 hr., the mixture was cooled, diluted with water and acidified with dilute hydrochloric acid to afford a precipitate which was collected, washed will with water and dried in vacuo at 100°C to yield a crude acid. The crude acid was recrystallized from methanol to furnish the pure acid, 33 mg. (74.5%), fine needles, m. p. 183~185°C. The Liebermann test gave from red to bordeaux coloration. Infrared spectrum: $\nu_{max}$ 3397, about 3000 (broad) (OH); 1693 $cm^{-1}$ (C=O).

Found: C, 73.50; H, 10.52. Calcd. for $C_{24}H_{38}O_3\cdot CH_3OH$: C, 73.85; H, 10.41%.

*Ester from the above Acid XIb.* — Being esterified with ethereal diazomethane in the usual manner, the above acid (21 mg.) gave fine needles from methanol, 7 mg., m. p. 140~141°C. The Rosenheim test was negative. No appreciable absorption in the ultraviolet spectrum. Infrared spectrum: $\nu_{max}$ 3541 (OH); 3013 (shoulder) (C=C); 1712 (C=O); 1619 $cm^{-1}$ (C=C).

*3β,6β-Dihydroxy-5β-cholanoic Acid (VIIa) from the Third Elution on the Chromatography.*—Since attempts to crystallize the oil failed, the oil (39 mg.) wasaaponified with 0.2 N methanolic potassium hydroxide in the usual way to give 3β,6β-dihydroxy-5β-cholanoic acid (VIIa), 23 mg. (5%), scales, (from acetone-methanol), m. p. 250~255°C. This compound was identified by a mixed melting point and the infrared spectrum with 3β,6β-dihydroxy-5β-cholanoic acid described above. I. R. spectrum: $\nu_{max}$ 3480, about 3000 (broad) (OH); 1710 $cm^{-1}$ (C=O).

Found: C, 73.53; H, 10.25. Calcd. for $C_{24}H_{40}O_4$: C, 73.43; H, 10.27%.

**3β, 6α-Dihydroxy-5α-cholanoic Acid.** — *Reduction of 3β-Hydroxy-6-oxo-5α-cholanoic Acid.*—To a boiling solution of 3β-hydroxy-6-oxo-5α-cholanoic acid (397 mg.) in absolute *n*-buthanol (8 ml.), sodium (0.8 g.) was added dropwise. After completion of addition, the mixture was further heated for 3 hr. After the addition of water, removal of the solvent and cooling, the alkaline solution was acidified with dilute hydrochloric acid to yield a crude acid (268 mg.) which was recrystallized from ethyl acetate to crystals with m. p. 228~229°C. $[\alpha]_D^{29}=+35\pm2°$ (*c* 1.104, methanol).

Found: C, 73.03; H, 10.26. Calcd. for $C_{24}H_{30}O_4$: C, 73.43; H, 10.27%.

Its dicathylate—After esterification with ethereal diazomethane, the cathylation acording to Fieser's method[14] gave dicathylate XIV as an oil which would not crystallize. No hydroxyl band in the infrared spectrum. Its diacetate XIVb—After esterification with etheral diazomethane and acetylation with acetic anhydride and pyridine overnight at room temperature, the acid gave a diacetate XIVb as an oil which would not crystallize. Infrared spectrum shows no hydroxyl band. This diacetate was saponified with methanolic potassium carbonate overnight at room temperature to afford 3β, 6α-dihydroxy-5α-cholanoic acid with m. p. 228~229°C.

Reduction of 3,6-dioxo-5α-cholanoic acid with sodium and absolute *n*-buthanol as in the previous case gave identical acid in the mixed melting point and the infrared spectrum.

Found: C, 73.50; H, 10.29%.

## Summary

(1) 3β, 6β-Dihydroxy-5β-cholanoic acid was synthesized from methyl 3β-hydroxy-$\Delta^5$-cholenoate in high yield.

(2) 3β, 6α-Dihydroxy-5α-cholanoic acid was also synthesized from 3β-hydroxy-6-oxo-5α-cholanoic acid or 3, 6-dioxo-5α-cholanoic acid.

The author is particularly indebted to Dr. K. Takeda, Director of this Laboratory, for his discussions and encouragement during this work. Thanks are also due to Mr. M. Takasuka for infrared spectral measurements, to Messrs T. Ieki, K. Miyahara, K. Daikatsu, T. Takaoka and Miss U. Kasugai for elementary analyses and to Mr. T. Iwata for measurements of optical rotation.

*Research Laboratory*
*Shionogi & Co., Ltd.*
*Imafuku, Amagasaki, Hyogo-ken*

# *Oxidation of l-Dihydrocarveol and its Acetate with Selenium Dioxide*

By Yoshitsugu SAKUDA

(Received Sepetmber 14, 1960)

It was previously reported that in the oxidation of β-terpineol[1] and its acetate[2] with selenium dioxide at room temperature (about 30°C), the use of *tert*-butyl alcoholic solution of the oxidant as an oxidizing agent appeared to be favorable both as to yield and as to quality of product. In this paper *l*-dihydrocarveol and its acetate were taken up as the sample and oxidized with selenium dioxide in a manner similar to that in the case of β-terpineol. A solution of selenium dioxide dissolved in *tert*-butyl alcohol by heating to 70~75°C under stirring was used as an oxidizing agent. The conditions and the results in oxidations are shown in Table I.

In the case of *l*-dihydrocarveol, the active methyl group of $C_9$ position outside the ring was oxidized mainly. The reaction products, in Exp. 1, consisted of 8(9)-*p*-menthen-2, 10-diol (I), 8(9)-*p*-menthen-2-ol-10-al (II) and a small amount of dihydrocarvone (III) which was produced by the oxidation of the secondary alcohol group of the sample. In Exp. 2, I and II were obtained.

In the case of *l*-dihydrocarvyl acetate. the active methylidyne group of $C_4$ position in the ring was oxidized mainly, and the conjugated diene compound was obtained as the result of dehydration of the tertiary alcohol formed[3]. As the reaction products, in Exp. 3, *trans*-8(9)-*p*-menthen-2, 4-diol (IV) monoacetate and a small amount of II-acetate were obtained. In addition to these compounds, 3, 8(9)-*p*-menthadien-2-ol (V) was identified in the saponified reaction mixture. In Exp. 4, the reaction mixture was saponified, and IV and V were identified. Excepting III these four products are new compounds. In each oxidation the total yield of crude materials was about 6~9% to the sample used, and unchanged samples was recovered in amounts ranging from 60 to 70%.

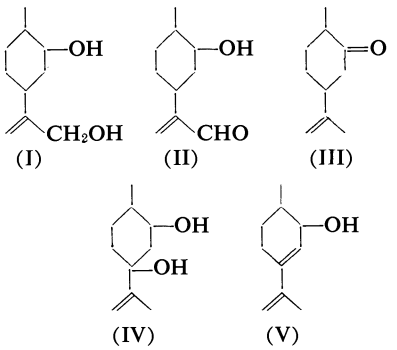



Fig. 1

Each reaction product was identified by the following procedures.

**(8)9-*p*-Menthen-2, 10-diol.**—In Exp. 1 and 2, crystals melting at 66°C were obtained. It was previously observed that the infrared spectrum of (8)9-*p*-menthen-1, 10-diol showed, in addition to the band due to a bonded hydroxyl group at 3275 $cm^{-1}$, characteristic bands due to the endmethylene group[1]. That is to say, the band based on the -C=C- stretching vibrations was at 1650 $cm^{-1}$, normal region, but the band

TABLE I. CONDITIONS AND RESULTS IN OXIDATION OF DIHYDROCARVEOL AND ITS ACETATE

| Exp. | Sample g. | $CH_3COOH$ g. | $(CH_3CO)_2O$ g. | $SeO_2$ g. | *t*-BuOH g. | Benzene g. | Temp.* °C | Time hr. | Reacton product** | Yield*** % |
|---|---|---|---|---|---|---|---|---|---|---|
| 1 | 26 | 50 | 50 | 9.3 | 77 | 70 | R.T.<br>45 | 15 | I II III | 8 |
| 2 | 31 | 50 | / | 12.0 | 90 | 90 | 40~43<br>R.T. | 4<br>20 | I II | 9 |
| | Acetate | | | | | | | | | |
| 3 | 39 | 50 | 50 | 12.0 | 90 | 90 | 45~47<br>R.T. | 4<br>20 | II IV V | 6 |
| | 〃 | | | | | | | | | |
| 4 | 66 | / | / | 18.5 | 148 | / | 48~50 | 8 | IV V | 8 |

* R.T.: Room temperature
** I—V are shown in Fig. 1.
*** Yields represent wt% to sample used.

1) Y. Sakuda, *J. Chem. Soc. Japan, Pure Chem. Sec.* (*Nippon Kagaku Zasshi*), **82**, 117 (1961).
2) Y. Sakuda, ibid., **81**, 1891 (1960).
3) A. Guillemonat, *Ann. chim.*, **11**, 143 (1939).

based on the =C-H bending vibrations shifted slightly to higher frequency than in 1,4-diol, and was at 900 $cm^{-1}$. The infrared spectrum of the crystals melting at 66°C (Fig. 2) has similar bands at 900, 1646 and 3280 $cm^{-1}$. Moreover, in the oxidation of $\beta$-terpineol with selenium dioxide, the methyl group of $C_9$ position was oxidized mainly, but in the case of its acetate, the methylidyne group of $C_4$ position was oxidized[1]. In the oxidation of dihydrocarveol and its acetate, the same phenomenon is observed. By analogy with these facts, it is assumed that the crystal melting at 66°C is 8(9)-*p*-menthen-2, 10-diol.

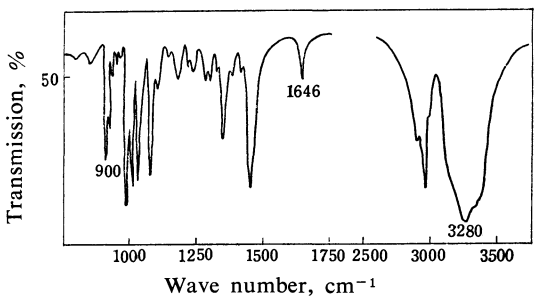



Fig. 2 Infrared spectrum of 8(9)-*p*-Menthen-2,10-diol (KBr).

**8(9)-*p*-Menthen-2-ol-10-al.**—In Exps. 1 and 2, in addition to I, the carbonyl compound was obtained as the main product. The infrared spectrum of the carbonyl compound (Fig. 3) shows the bands at 900, 1621 and 3092 $cm^{-1}$ attributable to the conjugated endmethylene group[4], at 1689 $cm^{-1}$ to the unsaturated carbonyl group, and at 3405 $cm^{-1}$ to the hydroxyl group. The ultraviolet spectra of derivatives of the carbonyl compound, semicarbazone gives $\lambda_{max}^{alc}$ 262 m$\mu$ and 2,4-dinitrophenylhydrazone gives $\lambda_{max}^{alc}$ 372 m$\mu$ which are identical with the absorption maxima of those of 8(9)-*p*-menthen-1-ol-10-al[1]. The carbonyl compound is easily oxidized with silver oxide to give the corresponding carboxylic acid. From these facts it seems that the carbonyl compound is 8(9)-*p*-menthen-2-ol-10-al.

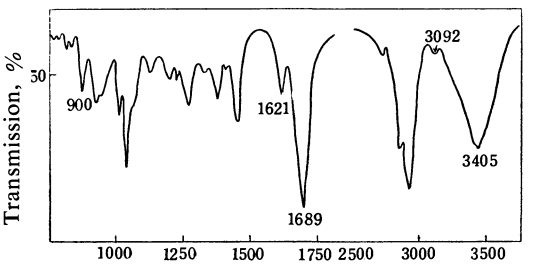



Fig. 3 Infrared spectrum of 8(9)-*p*-menthen-2-ol-9-al (liquid film).

***trans*-8(9)-*p*-Menthen-2, 4-diol.** — In the oxidation of *l*-dihydrocarvyl acetate, Exps. 3 and 4, the crystal melting at 128°C was obtained.

Naves[5] and Simonsen[6] deduced that dihydrocarveol had each equatorial group of methyl at $C_1$, hydroxyl at $C_2$ and isopropenyl at $C_4$ in chair conformations, based on the known fact[7] that on hydrogenation the alcohol gave carvomenthol. If the conformation of dihydrocarveol is maintained during the oxidation procedure, it is expected that 2,4-diol formed from dihydrocarveol is a *trans*-compound with one equatorial hydroxyl group at $C_2$ and one axial hydroxyl group at $C_4$. The conformational assignment of 2,4-diol may be supported by the infrared spectrum. Pickering and Price[8] empirically assumed that in *cis*-4-*tert*-butylcyclohexanol having a pure axial C-OH, a strong absorption band based on the C-OH stretching vibrations was at 955 $cm^{-1}$; and in *trans*-4-*tert*-butylcyclohexanol having a pure equatorial C-OH, at 1062 $cm^{-1}$. Choe and Tsutsumi[9] assumed that in *cis*-1,2-cyclohexanediol having one axial and one equatorial hydroxyl group, absorption bands based on the axial and equatorial C-OH stretching vibrations were at 950 and 1075 $cm^{-1}$ respectively. The infrared spectrum of the crystals melting at 128°C (Fig. 4) shows, in addition to the usual bands due to the endmethylene group at 895 and 1645 $cm^{-1}$, two bands characteristic of the hydroxyl groups. One, at 930 $cm^{-1}$, is attributed to the axial C-OH stretch, although it shifts slightly to lower frequency; and the other, at 1077 $cm^{-1}$, is attributed to the equatorial C-OH stretch. From these facts, the crystals melting at 128°C seem to be *trans*-8(9)-*p*-menthen-2, 4-diol.

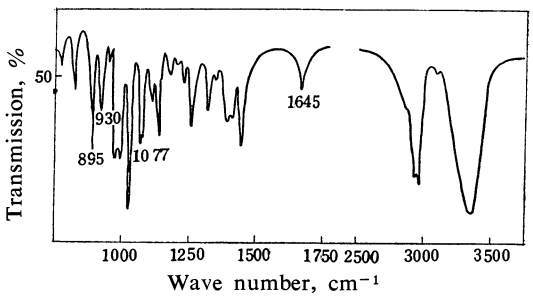



Fig. 4 Infrared spectrum of 8(9)-*p*-menthene-2,4-diol (KBr).

4) E. R. Blout et al., *J. Am. Chem. Soc.*, **70**, 194 (1948).
5) Y. R. Naves, *Bull. soc. chim. France*, **1956**, 1020.
6) J. Simonsen, "The Terpenes", University Press, Cambridge, Vol. III, (1952), p. 520.
7) R. G. Johnston and J. Read, *J. Chem. Soc.*, **1934**, 233.
8) R. A. Pickering and C. C. Price, *J. Am. Chem. Soc.*, **80**, 4931 (1958).
9) S. Choe and S. Tsutsumi, *J. Chem. Soc. Japan, Pure Chem. Sec.*, (*Nippon Kagaku Zasshi*), **81**, 785 (1960).

**3, 8(9)-*p*-Menthadien-2-ol.**—In Exps. 3 and 4, the ultraviolet spectrum of each reaction mixture gives $\lambda_{max}^{alc}$ 233 m$\mu$ which is identical with the absorption maximum of 3, 8(9)-*p*-menthadien-1-ol[1]. The reaction mixture showing $\lambda_{max}^{alc}$ 233 m$\mu$ reacts easily with maleic anhydride and the adduct is obtained.

## Experimental

**Materials and Reaction Procedure.**—*l-Dihydrocarveol.*—*l*-Carvone was synthesized from *d*-limonene via limonene nitrosochloride and carvoxime[10]. *l*-Dihydrocarveol, the sample, was prepared by a reduction of carvone thus obtained with sodium and alcohol. The process is schematically shown in Fig. 5.

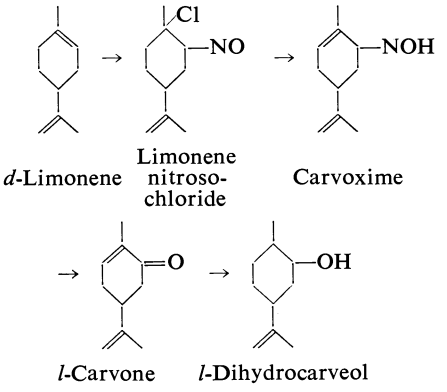



Fig. 5

The overall yield of *l*-dihydrocarveol is about 20% of the limonene used. As the crude *l*-dihydrocarveol thus obtained contained a small amount of non-reduced *l*-carvone, it was purified as follows. Crude *l*-dihydrocarveol was esterified with benzoyl chloride in a pyridine solution and the ester produced was steam-distilled. The remaining part of steam-distillation was saponified by 10% alcoholic sodium hydroxide solution. The saponification product was fractionated under reduced pressure. Rectified *l*-dihydrocarveol showed the following properties; b.p.$_6$ 95~97°C, $n_D^{25}$ 1.4783, $d_4^{25}$ 0.9296, $[\alpha]_D$ −33.2; 3,5-dinitrobenzoate m.p. 122°C, $[\alpha]_D$ −55.0 (in chloroform).

*l-Dihydrocarvyl acetate.* — *l*-Dihydrocarvyl acetate was prepared by refluxing *l*-dihydrocarveol with acetic anhydride and anhydrous sodium acetate, and rectifying the product. The sample thus obtained showed the following properties; b.p.$_5$ 95~97°C, $n_D^{25}$ 1.4611, $d_4^{25}$ 0.9490, $[\alpha]_D$ −67.1, E. V. 286.5 (Calcd. for $C_{10}H_{17}OOCCH_3$: 285.9).

*Oxidizing Agent.* — Pulverized selenium dioxide was dissolved in *tert*-butyl alcohol by heating to 70~75°C under continuous stirring for two hours in a current of carbon dioxide. In exception of Exp. 4, the *tert*-butyl alcoholic solution of selenium dioxide was employed by diluting with benzene and drying with anhydrous sodium sulfate.

10) E. E. Royals and S. E. Horne, *J. Am. Chem. Soc.*, **73**, 5856 (1951). C. Bordenca et al., *Ind. Eng. Chem.*, **43**, 1196 (1951).

*Reaction Procedure.* — Under each condition as shown in Table I the solution of the oxidizing agent was added to the sample solution in one lot, and stirred from time to time. When the reaction was over, in Exp. 1, the reaction mixture was heated to 45°C and the solvent was removed in vacuo, and the remaining product was fractionated under reduced pressure. In Exps. 2—4, each reaction mixture was diluted with water and extracted twice with ether. The combined ether solution was treated with aqueous alkali and with water successively and dried. After removal of the solvent, the remaining product was fractionated under reduced pressure. The fractions thus obtained were treated by chromatography, and each reaction product was identified as follows.

**Identification of the Reaction Products.** — *Dihydrocarvone.* — The result of distillation of the reaction product obtained in Exp. 1 is shown in Table II.

TABLE II

| Fraction | b. p., °C /3 mmHg | Yield, g. | $n_D^{25}$ | $d_4^{25}$ |
|---|---|---|---|---|
| 1 | 73~ 78 | 2.0 | 1.4775 | 0.9293 |
| 2 | 78~ 80 | 8.0 | 1.4780 | 0.9285 |
| 3 | 80~ 83 | 3.0 | 1.4792 | 0.9314 |
| 4 | 83~ 85 | 1.7 | 1.4816 | 0.9381 |
| 5 | 85~106 | 1.5 | 1.4852 | 0.9500 |
| 6 | 106~119 | 2.6 | 1.4985 | 1.0367 |

Fraction 1 was chromatographed over 55 g. of silica gel. The column was eluted with petroleum ether-ethyl acetate (volume ratio 7 : 3). The initial elute gave 0.5 g. ($n_D^{25}$ 1.4780, $d_4^{25}$ 0.9274) of a faintly yellow oil possessing a carvone-like odor. The oil gave a semicarbazone, m.p. 188~189°C, $[\alpha]_D$ −14.6 (in chloroform).

Found: N, 20.25. Calcd. for $C_{11}H_{19}ON_3$: N, 20.27%. The ultraviolet spectrum of the semicarbazone gave $\lambda_{max}^{alc}$ 228 m$\mu$ (log $\varepsilon$ 4.14) which corresponded to the absorption maximum of that of the simple carbonyl compounds.

*8(9)-p-Menthen-2-ol-10-al.* — Fractions 5 and 6 of Table II were combined and chromatographed in the same way as in the case of fraction 1. A viscid yellow oil was obtained, which amounted to about 35% of these combined two fractions. The infrared spectrum of the oil (Fig. 3) showed the bands due to the conjugated carbonyl, endmethylene and hydroxyl groups.

Derivatives: Semicarbazone, m.p. 201~202°C; U. V. $\lambda_{max}^{alc}$ 262 m$\mu$, log $\varepsilon$ 4.27.

Found: N, 18.49. Calcd. for $C_{11}H_{19}O_2N_3$: N, 18.65%. 2,4-dinitrophenylhydrazone, m. p. 188°C; U. V. $\lambda_{max}^{alc}$ 372 m$\mu$, log $\varepsilon$ 4.49.

Found: C, 54.87; H, 5.95; N, 16.00. Calcd. for $C_{16}H_{20}O_5N_4$: C, 55.16; H, 5.79; N, 16.08%.

*Oxidation with Silver Oxide.* — A solution of the carbonyl compound 0.13 g. ($0.8\times10^{-3}$ mol.) in 1 cc. alcohol was added dropwise under rapid stirring to a mixture of sodium hydroxide 0.5 g., water 5 cc. and silver oxide ($0.6\times10^{-3}$ mol. equiv.) which was newly prepared from silver nitrate 0.43 g. and sodium hydroxide 0.12 g. The combined mixture

was stirred at room temperature for 30 min. The reaction mixture was acidified with dilute hydrochloric acid and extracted repeatedly with ether. The combined extract was washed with water and dried. After removal of the solvent, it was distilled under reduced pressure, and 0.05 g. of a very viscid acidic material was obtained. The infrared spectrum thereof showed the bands due to the endmethylene group at 1621 $cm^{-1}$ and that of the carboxylic acid group at 1690 $cm^{-1}$. From this oil *p*-bromophenacyl ester was prepared as white needles of m. p. 99~100°C.

*8(9)-p-Menthen-2, 10-diol.*—In the chromatography above described, the crystal was eluted after 8(9)-*p*-menthen*l*-2-ol-10-al as the final eluate. Recrystallization of the crystals from a mixed solvent of ethyl acetate and petroleum ether gave long white needles of m. p. 66°C.

Found: C, 67.22; H, 10.81. Calcd. for $C_{10}H_{18}O_2 \cdot 1/2H_2O$: C, 67.01; H, 10.68%.

Identification of the crystals has been described.

In Exp. 2, the reaction product was fractionated under reduced pressure, and was separated into four fractions. The fourth fraction, b. p.$_2$ 110~125°C, $n_D^{25}$ 1.4990, $d_4^{25}$ 1.0261, yield 6.2 g., was chromatographed in the same way as in the case of Exp. 1. 8(9)-*p*-Menthen-2-ol-10-al and 8(9)-*p*-menthen-2,10-diol were yielded in about 50 and 5% of this fraction respectively.

TABLE III

| Fraction | b.p.°C/2 mmHg | Yield g. | $n_D^{25}$ | $d_4^{25}$ | E.V.* |
|---|---|---|---|---|---|
| 1 | 90~ 94 | 1.6 | 1.4640 | 0.9522 | |
| 2 | 94~ 95 | 19.8 | 1.4625 | 0.9490 | |
| 3 | 95~ 98 | 6.0 | 1.4630 | 0.9533 | 282.2 |
| 4 | 98~130 | 8.3 | 1.4704 | 1.0260 | 270.4 |

* E. V. calcd. for $C_{10}H_{16}(OH)OOCCH_3$: 265.0.

*3,8(9)-p-Menthadien-2-ol.*—The results of distillation of the oxidation product of *l*-dihydrocarvyl acetate, in Exp. 3, is shown in Table III.

Fraction 4 was chromatographed over 350 g. of silica gel, and the column was eluted with petroleum ether-ethyl acetate (8 : 2), and the elutes were separated into five fractions. Saponification of the initial elute gave 1.2 g. of the oil. The ultraviolet spectrum of the oil gave $\lambda_{max}^{alc}$ 233 mμ which corresponded to the absorption maximum of 3,8(9)-*p*-menthadien[11]. The infrared spectrum of the oil showed the bands due to the endmethylene group at 887, 1643 and 3078 $cm^{-1}$, and that of the conjugated double bond[12] at 1609 and 1643 $cm^{-1}$, and that of the hydroxyl group at 3354 $cm^{-1}$. A solution consisting of 1.0 g. of the oil, 0.3 g. of maleic anhydride, a very small amount of hydroquinone and 3.0 g. of ether was refluxed for two hours. The ether solution was washed with water to remove the excess of maleic anhydride and was steam-distilled. The remaining part of the steam-distillation was recrystallized from 50% aqueous methyl alcohol. A colorless needle adduct, m. p. 190~191°C, was obtained.

Found: C, 67.41; H, 7.30. Calcd. for $C_{14}H_{18}O_4$: C, 67.18; H, 7.24%.

In Exp. 4, the ultraviolet spectrum of the reaction product showed $\lambda_{max}^{alc}$ 233 mμ. The reaction product was fractionated under reduced pressure, and the distillate was saponified. The oil thus obtained was treated with maleic anhydride in the same way as that described above, and the adduct of m. p. 191°C was obtained.

*8(9)-p-Menthen-2-ol-10-al Acetate.* — In chromatography of fraction 4 in Table III, a small amount of the carbonyl compound was obtained as the second eluate, and it gave 2,4-dinitrophenylhydrazone as yellow needles of m. p. 183°C.

Found: N, 14.08. Calcd. for $C_{18}H_{22}O_6N_4$: N, 14.35%.

The ultraviolet spectrum of 2,4-dinitrophenylhydrazone gave $\lambda_{max}^{alc}$ 372 mμ, log ε 4.43, which was identical with the absorption maximum of that of 8(9)-*p*-menthen-2-ol-10-al. From this fact, it is assumed that the carbonyl compound is 8(9)-*p*-menthen-2-ol-10-al acetate.

*trans-8(9)-p-Menthen-2, 4-diol Monoacetate.* — In the chromatography above described, the crystalline mass was obtained as the final eluate. Recrystallization of the mass from a mixed solvent of petroleum ether and ethyl acetate gave white crystals of m. p. 78°C. The infrared spectrum thereof showed the bands due to the acetate group at 1268 and 1705 $cm^{-1}$, and that of the hydroxyl group at 3478 $cm^{-1}$. Saponification of the crystals gave *trans*-8(9)-*p*-menthen-2,4-diol mentioned next.

Found: C, 68.15; H, 9.75. Calcd. for $C_{12}H_{20}O_3$: C, 67.89; H, 9.49%.

*trans-8(9)-p-Menthen-2,4-diol.* — In the fractional distillation of the oxidation product obtained in Exp. 4, a very viscid residue having the following constants was obtained; b. p.$_7$ above 147°C, yield 8.5 g., $n_D^{25}$ 1.4885, $d_4^{25}$ 1.0593, E. V. 262.4 (Calcd. for $C_{10}H_{16}(OH)OOCCH_3$: 265.0). Saponification of the residue by 10% alcoholic sodium hydroxide solution gave 4.7 g. of the resinous mass. The mass was eluted through a column packed with silica gel using petroleum ether-ethyl acetate (55 : 45) as a moving phase. Recrystallizaton of the crystals thus obtained from ethyl acetate gave long white needles of m. p. 128°C. Identification of the crystals has been described.

Found: C, 70.36; H, 10.80. Calcd. for $C_{10}H_{18}O_2$: C, 70.58; H, 10.58%.

## Summary

*l*-Dihydrocarveol and its acetate were oxidized with a solution of selenium dioxide dissolved in *tert*-butyl alcohol, in the range of 15~50°C. In the case of *l*-dihydrocarveol, the active methyl group of $C_9$ position outside the ring was oxidized mainly. As the reaction products, dihydrocarvone, 8(9)-*p*-menthene-2,10-diol and 8(9)-*p*-menthen-2-ol-10-al were obtained. In the case of *l*-dihydrocarvyl

11) H. Pines and H. E. Eching, *J. Am. Chem. Soc.*, **77**, 6314 (1955).

12) J. L. H. Allan et al., *J. Chem. Soc.*, **1955**, 1874.

acetate, the active methylidyne group of $C_4$ position in the ring was oxidized mainly. *trans*-(8)9-*p*-Menthen-2,4-diol and its monoacetate, 8(9)-*p*-menthen-2-ol-10-al acetate and 3,8(9)-*p*-menthadien-2-ol were identified. Excepting dihydrocarvone, these products are new compounds.

The author wishes to express his deep gratitude to Professor Tamon Matsuura of Hiroshima University for his kind and constant guidance throughout this study and to Dr. T. Suga for the measurement of infrared spectra.

*Kochi Women's University*
*Kochi*

# *Polarographic Investigations of Vitamin C. III. Reduction Waves of the Condensation Products of Dehydro-L-ascorbic Acid and its Related Compounds with o-Phenylenediamine. Application to the Simultaneous Determination of L-Ascorbic Acid, Dehydro-L-ascorbic Acid and their Related Compounds**

BY Tamotsu WASA, Masanosuke TAKAGI and Sôzaburo ONO

(Received September 19, 1960)

It has been previously reported[1-3] that the reduction waves of dehydro-L-ascorbic acid (DAA), dehydroreductic acid(DRA), mesoxalaldehyde(MOA) and alloxan are all typically kinetic in nature and the limiting currents are very small, compared with their expected diffusion currents. These reduction waves are therefore not suited for the analytical purpose.

In order to obtain the diffusion currents corresponding to the above named substances, the experiments have been carried out under conditions where the substances may form condensation products with *o*-phenylenediamine (OPD). The diffusion controlled reduction waves have been obtained, which are characteristic of each substance.

In the present paper, the authors describe the polarographic behavior of these condensation products and some considerations are made on their molecular structures. Further, as an application of these reduction waves, a method of the simultaneous determination of L-ascorbic acid(AA), DAA and their related compounds is presented.

## Experimental

**Materials.**—AA, reductic acid (RA), triose-reductone (TR) and alloxan were the same specimens as those used for the previous works[1-3]. For the preparation of aqueous solutions of DAA, DRA and MOA, 1 ml. of $10^{-2}$ M aqueous solution of each of the above endiols, that is, AA, RA and TR, was taken in a 10 ml. volumetric flask and 1 ml. of $2\times10^{-2}$ M aqueous solution of silver nitrate was added. After the oxidation of the endiol with silver nitrate had been completed, the volumetric flask was filled up to 10 ml. with appropriate buffer solution (pH below 4) and the precipitate of silver was filtered off and the filtrate was used as $10^{-3}$ M aqueous solution of the oxidized form, that is DAA, DRA and MOA, respectively. The solution was used as a stock solution for the experiments with more dilute concentrations of the oxidized form. For the stock solutions containing both the endiol and its oxidized form, the above endiols were treated with an equimolar amount of silver nitrate, consequently the filtrates of the resulting mixtures were expected to contain both the endiol and its oxidized form in equal amouts. To check the concentrations of the endiol and its oxidized form in the above prepared solution, polarograms were sometimes taken with the standard solution containing only the endiol of known concentration, and by comparing both the limiting current obtained with the standard solution and that obtained with the above stock solution, corrections were made, when necessary.

For DAA, the preparation according to Pecherer[4] was also used, but it was only for the qualitative purpose because of its less degree of purity, compared with the above preparation.

2,3-Diketogulonic acid (DGA) was prepared as barium salt according to Penney and Zilva[5].

* This paper is the thesis submitted by Tamotsu Wasa for the Degree of Master the University of Osaka Prefecture.

1) S. Ono, M. Takagi and T. Wasa, *J. Am. Chem. Soc.*, 75, 4369 (1953).

2) S. Ono, M. Takagi and T. Wasa, This Bulletin, 31, 356 (1958).

3) S. Ono, M. Takagi and T. Wasa, ibid., 31, 364 (1958).

4) B. Pecherer, *J. Am. Chem. Soc.*, 73, 3827 (1951).

5) J. R. Penney and S. S. Zilva, *Biochem. J.*, 39, 1 (1945).

Dialuric acid was prepared according to Tipson[6] by reducing alloxan with hydrogen sulfide.

Stock solutions of alloxan, dialuric acid and DGA were prepared by dissolving the specimens directly into buffer solutions.

OPD was a commercial product of analytical grade and was checked to give no reduction waves under the present experimental conditions, unless the oxidized form of the endiols existed.

**Buffer solutions.**—Walpole's buffer for pH 0.5 to 5.0, McIlvain's buffer for pH 2.2 to 8.0 and the mixtures of disodium hydrogen phosphate with sodium hydroxide for pH above 8, were used, investigating the effect of pH and, at the same time, checking the effect of the components of the buffer solutions.

**Apparatus and Procedure.**—The polarograph used was the same one as that used for the previous works[1-3]. The characteristics of the capillaries used were, a) $m=2.652$ mg./sec., $t=3.09$ sec., b) $m=1.987$ mg./sec., $t=2.85$ sec. at open circuit, at 25°C, when the height of the mercury reservoir was 60 cm.

For the temperature control by using a thermostat, an electrolytic cell with potassium nitrate saturated agar bridge, was used. The accuracy of the temperature control was ±0.05°C. As the reference electrode, a normal calomel electrode was used. The cell resistance was less than 500 ohm.

The experimental procedure is as follows: a given volume (usually 5 to 8 ml.) of the sample solution diluted with a given volume of a buffer solution is taken in an electrolytic cell and the cell is kept in the thermostat of a given temperature for about 20 min., while the dissolving oxygen in the solution is removed by bubbling nitrogen gas. After the removal of dissolving oxygen, a given volume of OPD solution of known concentration, which had been separately freed from oxygen, is taken and added into the electrolytic cell. The cell is then kept in the thermostat for a given time, during which the bubbling of nitrogen gas is still continued, and after the given period, polarograms are taken.

## Results

**Reduction Waves of the Condensation Products of DAA with OPD.**—*Effect of the Concentration of OPD.*—As the first attempt to see the polarographic behavior of the condensation products of DAA with OPD, the concentration of DAA was kept constant (approximately $1\times10^{-3}$ M) and the concentration of OPD was changed in the acetate buffer solution of pH 3.6. Polarograms were taken at about one hour after the addition of OPD into the electrolytic solution. For this experiment, no thermostat was used and the room temperature was about 20°C. The polarograms are shown in Fig. 1, from which it can be seen that polarograms of the condensation products of DAA with OPD show three different reduction waves and the ratio of the limiting currents of the three is changed, depending on the concentration of OPD. The limiting currents of the three waves have also been observed to change with time. The half-wave potentials of the three waves at pH 3.60 are −0.26, −0.44 and −0.67 V. (vs. N.C.E.), respectively. Fig. 2 shows the relationships

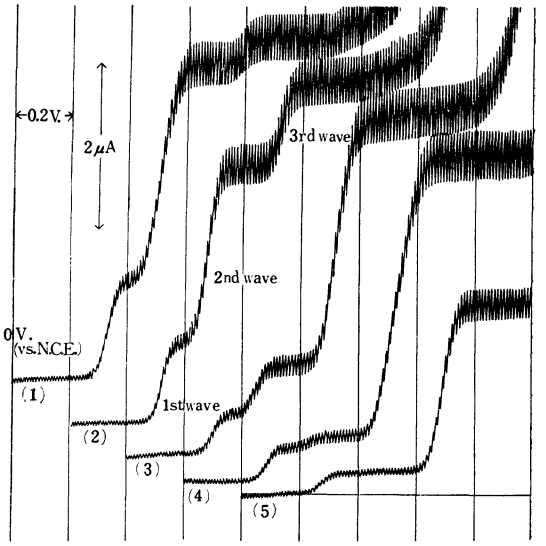



Fig. 1. Polarograms of the condensation products of DAA with OPD. Concn. of DAA: $1\times10^{-3}$ M. Concn. of OPD: (1) $2\times10^{-2}$ M, (2) $1\times10^{-2}$ M, (3) $2\times10^{-3}$ M, (4) $1\times10^{-3}$ M, (5) $5\times10^{-4}$ M. Capillary (b). pH 3.6, temp. 20°C.
Polarograms were taken at one hour after the addition of OPD.

between the limiting currents, the concentration of OPD and the time elapsed after the addition of OPD. As seen from Fig. 2, when the concentration of OPD is equal to or less than that of DAA, the third wave prevails and the ratio of the three waves remains almost unchanged with time even after 24 hr., while with increasing concentration of OPD, the growing velocities of the first and the second wave increase at the expense of the third wave. The total height of the three waves has been observed to increase for the first one hour and remain almost constant for a further 24 hr.

*Effect of pH.*—Fig. 3 shows the limiting currents of the three waves at one hour after the addition of OPD at 25°C, when the concentrations of DAA and OPD were kept constant and only the pH of the electrolytic solution was changed. Under the present experimental conditions, the limiting current of the third wave reached its maximum value in pH between 3 and 4, and decreased with further increasing pH. The first wave was observed in all the pH range studied and increased

6) R. S. Tipson, "Organic Syntheses", Coll. Vol. 33, J. Wiley & Sons, New York (1953), p. 3.

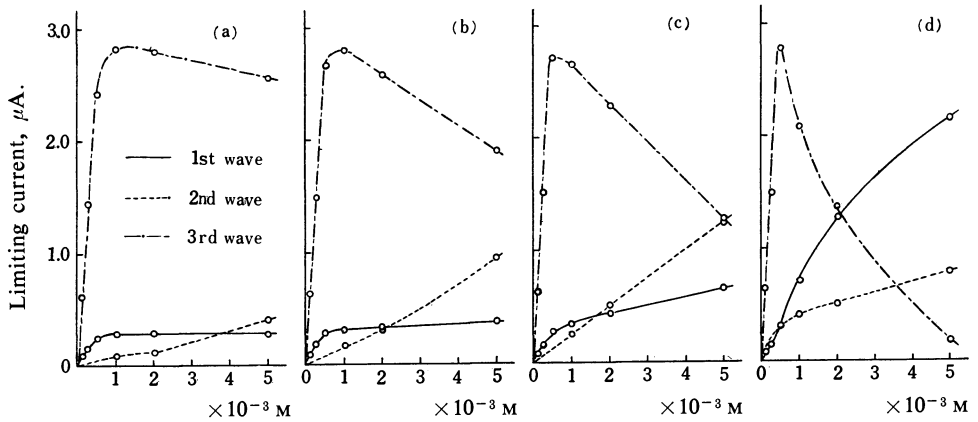



Fig. 2. Effects of the concentration of OPD and the condensation time on the reduction waves of the condensation products of DAA with OPD.
Concn. of DAA: $5\times10^{-4}$ M in acetate buffer of pH 3.59, temp. 25°C, capillary (a).
Polarograms were taken a) at one hour after the addition of OPD, b) 3 hr., c) 6 hr., and d) 25 hr., respectively.

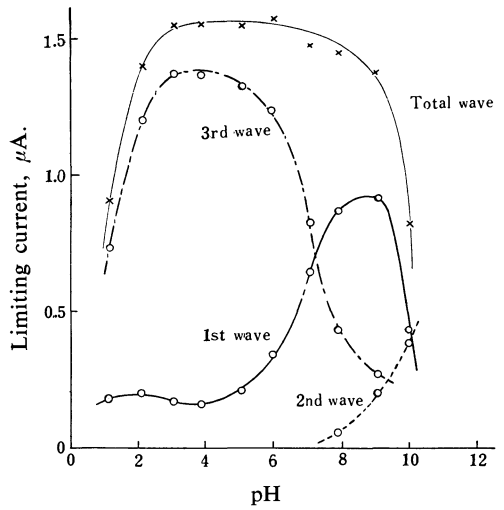



Fig. 3. Effects of pH on the reduction waves of the condensation products of DAA with OPD.
Concn. of DAA: $2.5\times10^{-4}$ M, concn. of OPD: $1\times10^{-3}$ M, temp. 25°C. Polarograms were taken at one hour after the addition of OPD. Capillary (a).

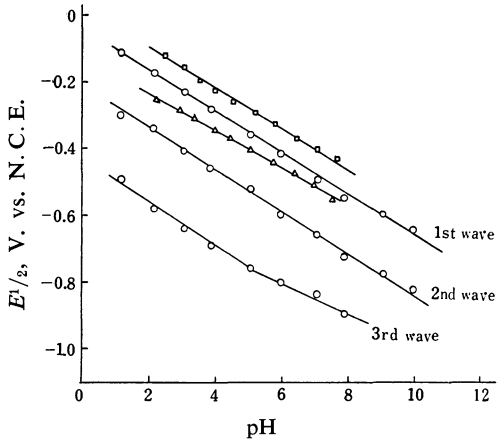



Fig. 4. pH-Dependence of the half-wave potentials of the condensation products of DAA, DRA and alloxan with OPD.
Temp. 25°C.
□ DRA △ alloxan ○ DAA

rapidly in pH above 4, showing its maximum value in pH near 9. The second wave was hardly observed in pH below 7, but increased rapidly in pH above 7.

The fact that the total height of the three waves was decreased with decreasing pH in acid range, may be related with the rates of the condensation reactions, while another decrease in alkaline range may be due to the instability of DAA.

The changes of the half-wave potentials of the three waves with changing pH are presented in Fig. 4, in which the half-wave potentials of the condensation products of DRA and alloxan with OPD are also shown. From Fig. 4, it can be seen that the first wave for DAA shows half-wave potentials close to those of DRA and alloxan, while the other two waves for DAA show considerably more negative half-wave potentials in all the pH range studied.

*Effect of Temperature.*—When the concentration of DAA was kept constant and the temperature was raised, the time required for the condensation was observed to be shortened depending on the concentration of OPD. Fig. 5 shows the relationships between the ratio of each of the three waves to the total, the concentration of OPD and the experimental

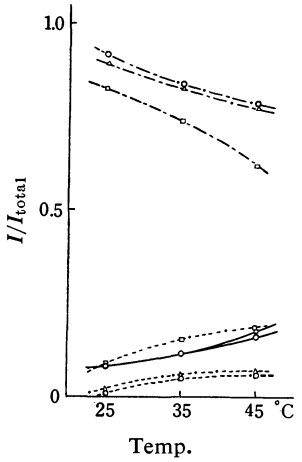



Fig. 5. Effects of temperature on the reduction waves of the condensation products of DAA with OPD.
Concn. of DAA: $2\times10^{-4}$ M, pH 3.09.
Capillary (b).
Concn. of OPD: ○ $4\times10^{-4}$ M, △ $1\times10^{-3}$ M, □ $4\times10^{-3}$ M.
Each wave height is expressed as its ratio to the total wave.
—— 1st wave ---- 2nd wave
-·-· 3rd wave

temperature at one hour after the addition of OPD.

*Effect of the Presence of AA.* — It has been found that in pH between 3 and 4, the oxidation wave of AA is observed independently of the reduction waves of the condensation products of DAA with OPD in one polarogram, if OPD freed from oxygen is added into the electrolytic solution containing both AA and DAA, which has been freed from oxygen, as seen in Fig. 6. However here it should be noticed that, though AA has been known to be stable against the oxidation with atmospheric oxygen in such pH as that used for the present case, a considerable increase of the limiting current for DAA was observed at the expense of that for AA, unless the removal of oxygen from the electrolytic solution had been completed before the addition of OPD solution, which had been also separately freed from oxygen.

**Reduction Waves of the Condensation Products of DRA and Alloxan with OPD.**—A simple and well defined reduction wave was obtained, when DRA or alloxan was treated with OPD in acid buffer solutions in the same way as in the case of DAA, as seen in Fig. 7. The half-wave potentials of the reduction waves for alloxan and DRA at pH 3.60 are −0.32 and −0.19 V. (vs. N. C. E), respectively.

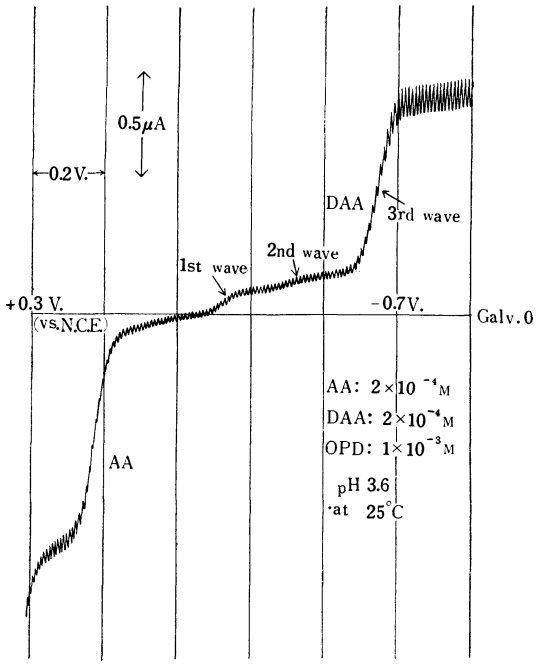



Fig. 6. A polarogram taken with an electrolytic solution containing both AA and DAA in equal amounts in the presence of excess OPD. The polarogram was taken at one hour after the addition of OPD. Capillary (b).

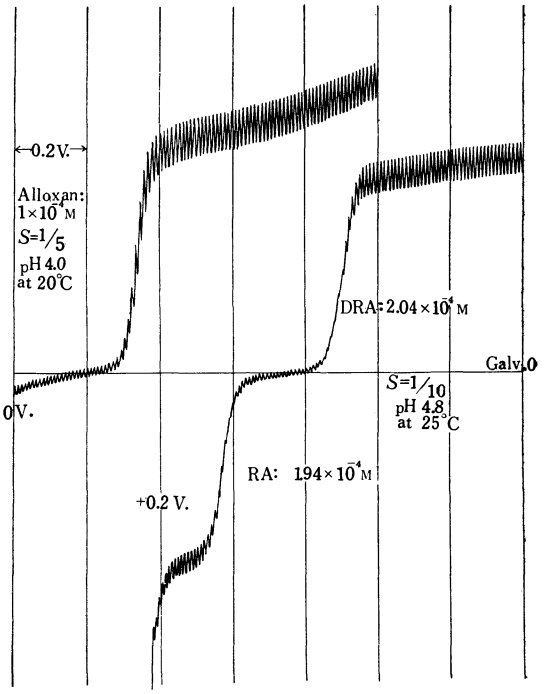



Fig. 7. A polarogram of the condensation product of alloxan with OPD and that of the condensation product of DRA with OPD, with the anodic wave of RA. Capillary (b).

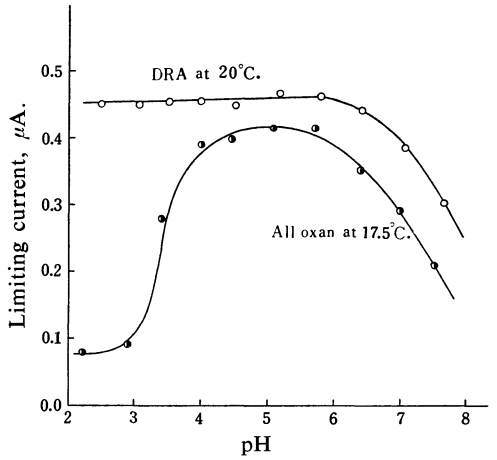



Fig. 8. Effect of pH on the reduction wave of the condensation product of alloxan with OPD and that of DRA with OPD. Concn. of alloxan and DRA: $1\times10^{-4}$ M. Concn. of OPD: $1\times10^{-3}$ M, capillary (b). The polarograms were taken at one hour after the addition of OPD.

Fig. 8 shows the relationship between the limiting current and pH, when the concentrations of DRA, alloxan and OPD were kept constant and polarograms were taken at one hour after the addition of OPD at 20°C. The limiting current of the condensation product of alloxan with OPD shows its maximum value in pH between 4 and 6 under the present experimental conditions. In pH above 6 the splitting of the reduction wave into two waves was observed. The limiting current of the condensation product of DRA with OPD reached its maximum value very rapidly in pH below 6, and in pH above 6 the rate of the condensation reaction was observed to decrease with increasing pH, but no splitting of the wave was seen as in the case of alloxan.

The pH-dependence of the half-wave potentials of the above two waves for alloxan and DRA is as already presented in Fig. 4.

When the electrolytic solution contained both DRA and its reduced form RA, polarograms of both the anodic wave of RA and the cathodic wave of the condensation product of DRA with OPD were obtained in one polarogram as in the case of DAA, if the removal of oxygen from the solution was complete. On the contrary, when OPD was added into the electrolytic solution containing the reduced form of alloxan, i. e., dialuric acid, the oxidation of dialuric acid was observed to be greatly accelerated and no stable polarograms of its anodic wave were obtained even with a careful removal of atmospheric oxygen.

**Reduction Waves of the Condensation Products of MOA with OPD.** — The condensation

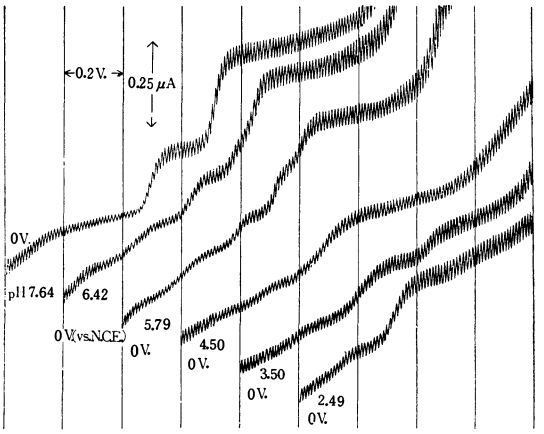



Fig. 9. Polarograms of the condensation products of MOA with OPD.
Concn. of MOA: $1\times10^{-4}$ M. Concn. of OPD: $1\times10^{-3}$ M, temp. 25°C, capillary (b). Polarograms were taken at one hour after the addition of OPD.

products of MOA with OPD showed no well defined waves in acid pH and with increasing pH two reduction waves were observed to be more distinct, as seen in Fig. 9. The reduction waves in acid pH were somewhat complicated and the limiting current was considerably small, compared with the above three cases. No further experiments have been made with MOA.

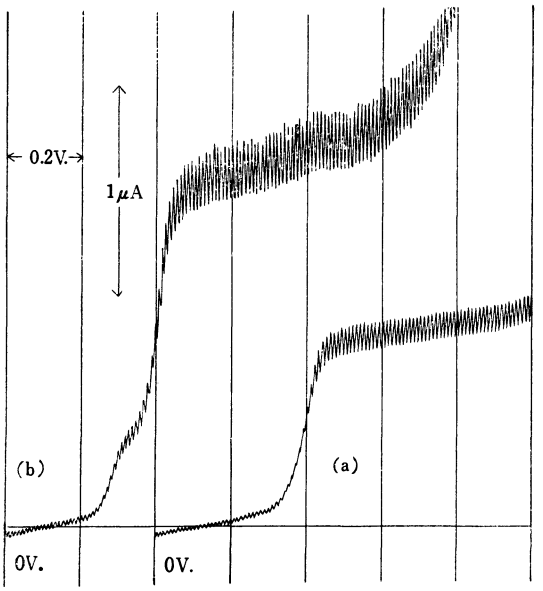



Fig. 10. Polarograms of the condensation products of DGA with OPD. Concn. of DGA: $4\times10^{-4}$ M. Concn. of OPD: $1\times10^{-3}$ M. Capillary: $m=1.261$ mg./sec., $t=2.84$ sec. Polarograms were taken at 128 min. at 25°C (a) and at 6 days at about 15°C (b), after the addition of OPD. pH 3.44.

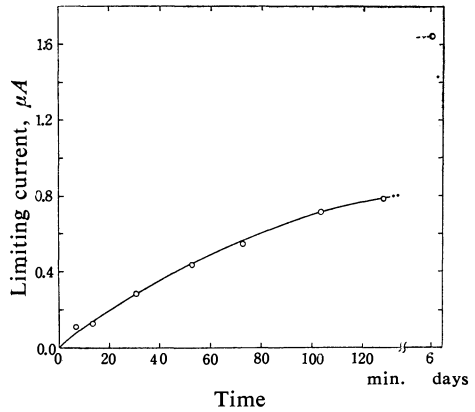
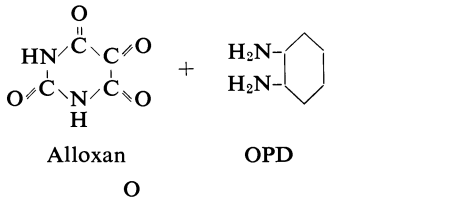



Fig. 11. Change of the limiting current of the reduction wave of the condensation product of DGA with OPD. The experimental conditions are the same as for Fig. 10. The limiting current after 6 days is that for the total wave in Fig. 10 (b).

**Reduction Waves of the Condensation Products of DGA with OPD.** — When OPD was added into the electrolytic solution containing DGA, a well defined reduction wave ($E_{1/2}=-0.40$ V. vs. N. C. E. at pH 3.44) was observed as seen in Fig. 10. However, the time required for the condensation was much longer than those required for the cases of DAA, DRA and alloxan, as seen in Fig. 11. After the same electrolytic solution was left for several days at room temperature, a more positive reduction wave was observed ($E_{1/2}=-0.27$ V. vs. N. C. E. at pH 3.44).

## Discussion

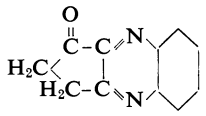
According to Kühling[7] and Archibald[8], the most probable condensation product of alloxan with OPD in acid pH may be considered to be alloxazine and the reaction may be written as



Alloxan + OPD → Alloxazine (I) + $2H_2O$ (1)

On the other hand, alloxazine has been polarographically studied by Koide[9] and the half-wave potential obtained is practically identical with that of the present case.

Analogously to the case of alloxan, the condensation product of DRA with OPD may be assumed to be



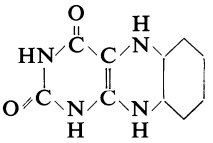
(II)

Since the limiting current of each of the above condensation products is observed to be almost equal to the anodic limiting current of the corresponding reduced form, i. e., RA or dialuric acid, of the same concentration, a two-electron transfer has been supposed to exist for the electrode reaction, referring to the two-electron transfer for the electrode oxidation of RA, dialuric acid and many other endiols[10]. The slight difference between the cathodic and the corresponding anodic limiting current can be well understood as due to their diffusion coefficients.

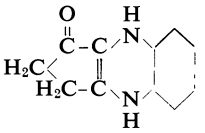
The mechanisms of the electrode reactions of the two substances may possibly be assumed to be expressed as follows.

(I) + $2H^+$ + 2e → (III) (2)

(II) + $2H^+$ + 2e → (IV) (3)



(III)

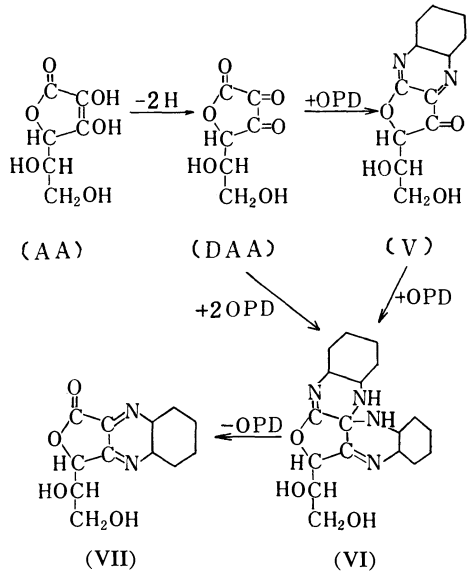


(IV)

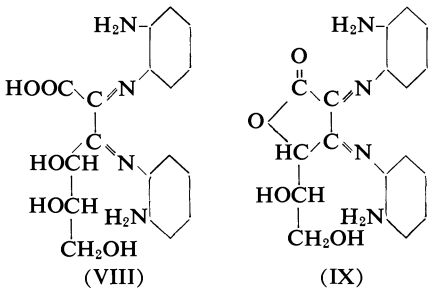
In contrast with DRA and alloxan, at least three different types of the condensation products for DAA should be considered, which would correspond to the three waves obtained (see Fig. 1).

Erlbach and Ohle[11] studied the condensation products of iso-DAA and DAA with OPD. Hasselquist[12] investigated the condensation products of OPD, aniline, etc., especially in respect to the characteristics of the lactone ring of the products. Ogawa[13] also studied this kind of condensation of DAA with OPD for the purpose of the determination of total vitamin C, in which he measured the fluorescence of one of the condensation products of DAA with OPD, referring to those of iso-DAA studied by Erlbach and Ohle[11].

7) O. Kühling, *Ber.*, **24**, 2364 (1891).
8) R. M. Archibald, *J. Biol. Chem.*, **158**, 347 (1945).
9) S. Koide, a private communication to the authors.
10) R. Brdicka and P. Zuman, *Collection Czechoslov Chem. Communs., Suppl.*, **15**, 766 (1950).
11) H. Erlbach and H. Ohle, *Ber.*, **67**, 555 (1934).
12) H. Hasselquist. *Arkiv Kemi*, **4**, 369 (1952).
13) S. Ogawa, *J. Pharm. Soc. Japan* (*Yakugaku Zasshi*), **73**, 54, 59, 94, 309, 316, 324 (1953).




The mechanism of the condensation reactions in the present experiments may be profitably considered with the reaction diagram which was given by Ogawa for DAA and is analogous to the one originally presented for the condensation of iso-DAA with OPD by Erlbach and Ohle. According to Erlbach and Ohle, and also Ogawa, OPD reacts stoichiometrically with DAA to transform to V, when the concentration of OPD is equal to or less than that of DAA, and V corresponds to the product whose fluorescence was utilized by Ogawa for the determination of total vitamin C. From the polarograms in Fig. 1, it would be reasonable to say that the product corresponding to the third wave may be identical with the one described as V, since the third wave is much larger than the other two waves and considerably stable for a relatively long period, under conditions similar to those described for V by the above authors. Further the above authors' diagram shows that when the concentration of OPD is sufficiently greater than that of DAA, VI and VII are produced and their final equilibrium ratio is about 1/3. Since our polarographic results showed that when an excess of OPD to DAA was used, the first and the second wave increased with time at the expense of the third wave and the final ratio of the second wave to the first was found to be about 1/3, the first and the second wave may be considered to correspond to the reductions of the products described as VII and VI, respectively, if a two-electron transfer is assumed for both the first and the second wave. However, according to Hasselquist[12], when freshly prepared DAA was treated with excess OPD, VIII was produced instead of IX. This he could obtain by treating VIII with various solvents.




He also observed the separation of one mole of OPD from VIII or IX in about 1 N hydrochloric acid solution.

As the reduction wave first obtained with DGA in our experiments seemed to be identical with the second wave for DAA (see Fig. 10), the possibility that VI in the above diagram can be replaced with VIII, may be considered. Further, the appearance of a more-positive reduction wave in the case of DGA after a long period, may suggest the conversion from VIII to VII, though the results are not sufficient for full discussion.

On the other hand, there still remain some difficulties, in interpreting the difference between the half-wave potentials of the three waves for DAA: V and VII would be expected to be reduced at very near potentials to each other. It seems therefore necessary to study further on the configuration of the product corresponding to the third wave. The reduction wave due to the condensation product of an oxidation product of AA (probably DGA) with ammonia studied by Zuman[14] seems also to be interesting in comparison with the present case.

However, as the present results are insufficient for a complete revision of the diagram, for the time being, only the importance of the third wave for DAA will be emphasized; the wave is characteristic of DAA and the separation of the half-wave potential from those of the condensation products of other related compounds is considerably large in the wide pH range.

Though the electrode reaction corresponding to each wave can not be discussed in detail, a two-electron transfer for each wave is readily understood by comparing the limiting currents with the anodic limiting current of AA of the same concentration, as for the cases of alloxan and DRA.

As for the condensation products of MOA with OPD, though several types of the reaction may be supposed, discussions are not made on this problem, since the polarograms of the products themselves were not well defined and moreover the limiting currents in acid pH

14) P. Zuman, *Collection Czechoslov Chem. Communs., Suppl.*, 15, 839 (1950).

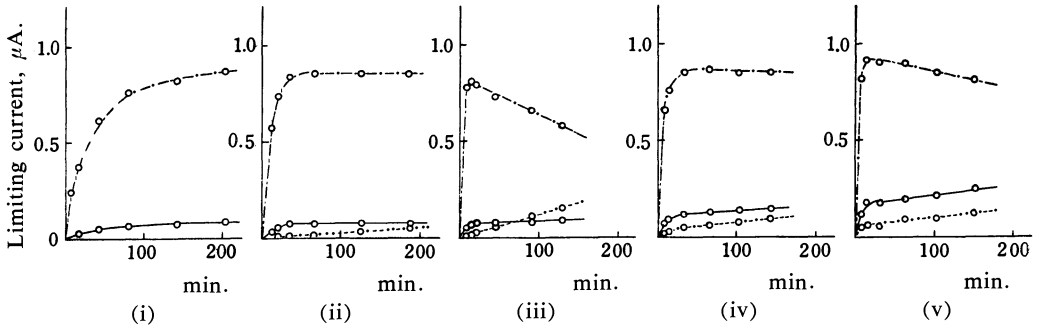
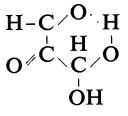



Fig. 12. Time-dependences of the limiting currents of the condensation products of DAA with OPD. Concn. of DAA: $2\times10^{-4}$ M. Concn. of OPD: i) $4\times10^{-4}$ M; ii), iv), v) $1\times10^{-3}$ M; iii) $4\times10^{-3}$ M. Temp: i), ii), iii) 25°C; iv) 35°C; v) 45°C. pH 3.6. Capillary (b).
—— 1st wave ---- 2nd wave ---- 3rd wave

range were considerably smaller than those of other related substances. These facts may be qualitatively interpreted partly by the hydration of carbonyl group and partly by the hydrogen bonding in hydrated MOA, one of whose possible structures may be X.



(X)

**Application to the Simultaneous Determination of AA, DAA and their Related Compounds.** —As described above, the reduction waves of the condensation products of the oxidized forms of the endiols with OPD are readily obtained, and especially the third wave for the condensation product of DAA with OPD is so characteristic of DAA, that an application of these polarographic phenomena to the simultaneous determination of AA, DAA and their related compounds has been attempted.

In order to establish the most practical conditions for the determination of DAA by utilizing the third wave, the following additional experiments have been carried out. Since the third wave has been found to be comparatively stable in acid pH range (pH 3~5), when the concentration of OPD is low (see Fig. 2), the change of the limiting currents of the condensation products of DAA with OPD has been investigated for the first one hour after the addition of OPD, by changing the concentration of OPD in a limited low concentration range and the temperature for the condensation also in a practical range. The data are presented in Fig. 12. From such experiments as the above, for the concentration of OPD, the temperature and time for the condensation, $1\sim2\times10^{-3}$ M, 25°C and 50~60 min., respectively, may be recommended. The linearity of the limiting current of the third wave with the concentration of DAA has also been tested, as shown in Fig. 13, for which the stock solution containing both AA and DAA in equal amounts, was used, consequently

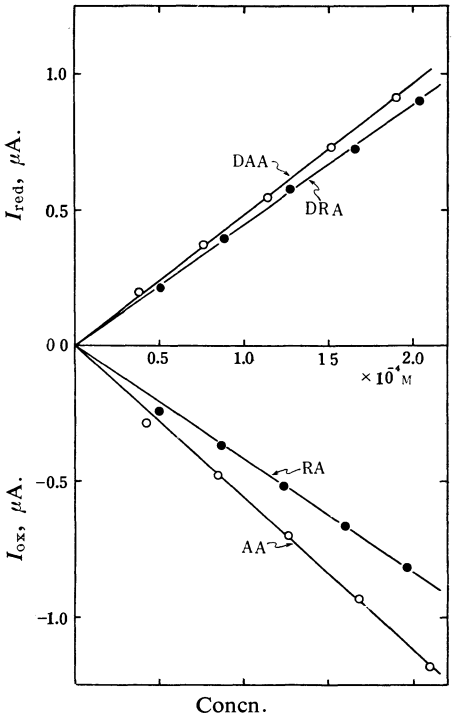



Fig. 13. Linear relationships between the limiting currents and the concentrations for AA and DAA or for RA and DRA, when the electrolytic solutions contain AA and DAA, or RA and DRA. Concn. of OPD: $2\times10^{-3}$ M. Temp. 25°C, pH: 3.6 for AA and DAA, 4.8 for RA and DRA. Capillary: (a) for AA and DAA, (b) for RA and DRA. Polarograms were taken at one hour after the addition of OPD for AA and DAA. $I_{red}$: the cathodic limiting current, $I_{ox}$: the anodic limiting current.

the linearity of the limiting current of the oxidation wave with the concentration of AA could be seen simultaneously, without any interference with that of the third wave for DAA, under the present experimental conditions.

For RA and DRA, experiments similar to those for AA and DAA have been carried out. The linearity of the limiting currents with the concentration of RA and DRA, respectively, is presented in Fig. 13. In this case, the time required for the condensation was not considered strictly, since the growth of the reduction wave of the condensation product of DRA with OPD has been observed to be much faster than that of the third wave for DAA, and moreover the limiting current has been seen to be quite stable for a long period.

For dialuric acid and alloxan, a linearity of the limiting current with the concentration for alloxan similar to those for DAA or DRA, was obtained, when the electrolytic solutions contained no dialuric acid (Fig. 14). However, as already stated, dialuric acid is very readily oxidized to alloxan, when OPD is added into the electrolytic solution even under conditions where the atmospheric oxygen is excluded from the solution as carefully as possible. Consequently the oxidation wave of dialuric acid could not be obtained with the reduction wave of the condensation product of alloxan with the OPD in one polarogram.

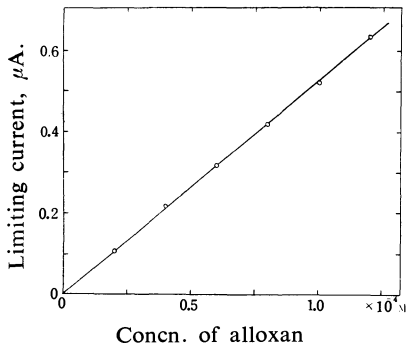



Fig. 14. Linear relationship between the limiting current of the condensation product of alloxan with OPD and the concentration of alloxan. Concn. of OPD: $2\times10^{-3}$ M, temp. 20°C, pH 4.0. Capillary (a). Polarograms were taken at one hour after the addition of OPD.

**Simultaneous Determination of AA and DAA in Natural Products.** —For the determination of AA and DAA in natural products by using the present polarographic method, the following procedure has been used; 10 g. of the sample and about 1 g. of quartz sand are taken in a mortar and 40 ml. of 2% metaphosphoric acid aqueous solution is added into it. The mixture is crushed and ground, and then filtered or centrifuged. The filtrate or the supernatant is expected to be an extract, in which AA and DAA in the starting material are diluted five times. Now, in a run, 2 ml. of the extract is taken in an electrolytic cell and 7 ml. of McIlvain's buffer of pH 4.7 is added. The electrolytic cell is immersed in a thermostat of 25°C and the oxygen dissolving in the electrolytic solution is chased out by bubbling nitrogen gas for 20 min. One milliliter of $2\times10^{-2}$ M OPD aqueous solution which has been separately freed from oxygen by bubbling nitrogen gas is added, and the electrolytic cell is kept in the thermostat for a further 50 min. during which time the bubbling of nitrogen gas is still continued. After that, a polarogram is taken in the usual way (A). In another run, 2 ml. of the extract is taken in an electrolytic cell and 6.4 McIlvain's buffer pH 4.7 and 0.6 ml. of the standard solution containing both AA and DAA of $1\times10^{-3}$ M, are added. After that, the common procedure with that of the former run is carried out and a polarogram is taken (B). Comparing the polarograms (A) and (B), AA and DAA can be calculated with the anodic and the cathodic limiting currents, respectively. When *A* and *B* represent the values of the limiting currents of the polarograms (A) and (B) respectively, the contents

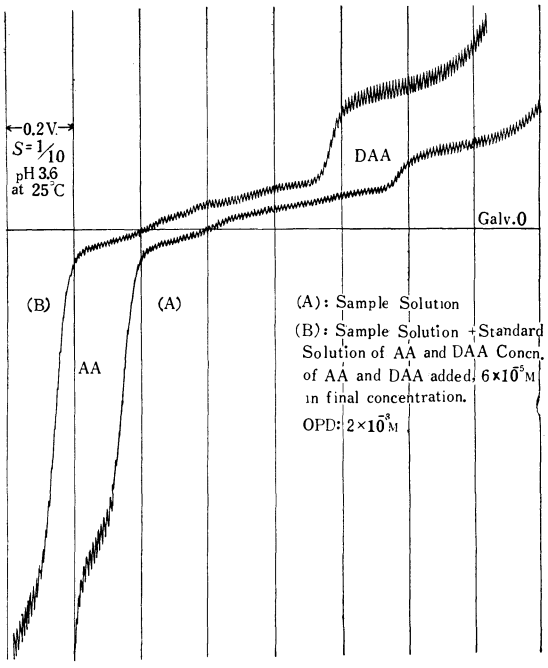



Fig. 15. Polarograms for the simultaneous determination of AA and DAA in radish leaves by means of polarographic OPD method.

$C$ of AA and DAA in the natural material may be calculated as follows.

$$C_{AA}=A_{ox}/(B_{ox}-A_{ox})\times 1.056\times 25 \text{ (mg. \%)}$$

and

$$C_{DAA}=A_{red}/(B_{red}-A_{red})\times 1.044\times 25 \text{ (mg. \%)}$$

where suffix ox and red represent the anodic and the cathodic limiting currents, respectively. In Fig. 15, an example of the polarograms obtained with radish leaves is presented. Some of the analytical results obtained by using the present method are listed in Table I, together with those obtained by the 2,4-dinitrophenylhydrazine method[15-18]. The results by both methods are in good agreement with each other.

TABLE I. AA AND DAA IN NATURAL PRODUCTS DFTERMINED BY MEANS OF POLAROGRAPHIC OPD METHOD

| Sample | AA mg. % | DAA mg. % | Note |
|---|---|---|---|
| Radish leaves | 102.8 | 20.6 | |
| | 106.5 | 17.3 | DNP method* |
| Spinach | 58.6 | 5.5 | |
| | 57.8 | 9.8 | DNP method* |
| Mizuna | 68.9 | 8.3 | |
| Mandarin orange | 28.1 | 5.1 | |

* Determined by 2,4-dinitrophenylhydrazine method.

In the above described OPD method, although the addition of the standard solution into the sample solution was utilized, the calibration curve may also be used, with which the procedure may be more simplified, when a number of samples are treated.

**Determination of AA in the Presence of One of the Other Endiols.** — When two or more endiols are in a sample solution, their oxidation waves are not suited for the analytical purpose, since their half-wave potentials are usually very close to each other[10]. In such cases, the present OPD method may be recommended, especially for the determination of AA coexisting with other endiols. As a demonstration of this method, the following procedure has been employed by the present authors; a given volume of the sample solution (usually 1 ml.) is taken in a 10 ml. volumetric flask and an excess of silver nitrate aqueous solution is added. After the oxidation of the endiols has been completed, the excess of silver ions is precipitated by adding a sodium chloride solution. Then 1 ml. of $1\times10^{-2}$ M OPD solution is added and the volumetric flask is filled up to 10 ml. with an appropriate buffer solution. The mixture is filtered and the filtrate is taken in an electrolytic cell. The cell is kept at 25°C for 50 min., during which oxygen is chased out by bubbling nitrogen gas, and after that polarograms are taken in the usual way. Examples of the polarograms taken with the solutions containing DAA and one of the oxidized forms of different endiols are presented in Fig. 16. As seen from the Fig. 16, the simultaneous determination of AA and DRA is possible. The figure may also indicate that AA can be determined even in the presence of triose-reductone, though the method itself is not suitable for the determination of the latter substance.

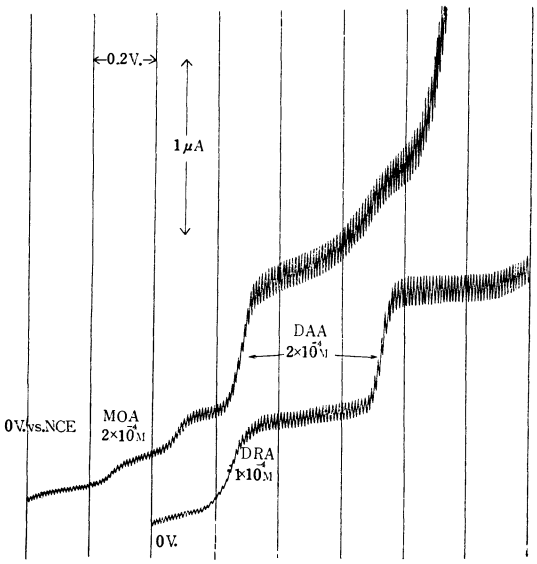



Fig. 16. Polarograms taken with the electrolytic solutions containing DAA and MOA (a) or DAA and DRA (b). Concn. of OPD: $1\times10^{-3}$ M, pH 4.2. Capillary: $m=1.261$ mg./sec. $t=2.84$ sec, temp. 25°C.

**Comparison with Other Determination Methods.** —In the determination of vitamin C by using either one of the previously reported methods i. e. 2, 6-dichlorophenolindophenol method[19], usual polarographic method[20], colorimetric method[15-18], etc., either AA or DAA can be directly determined. Therefore, in order to determine both AA and DAA, either one of the two forms should be converted into the other in a preliminary treatment. Further, when other endiols exist in the same sample

15) J. H. Roe and C. A. Kuether, *J. Biol. Chem.*, **147**, 399 (1943).
16) J. H. Roe and M. J. Oesterling, ibid., **152**, 511 (1944).
17) J. H. Roe, M. B. Mills, M. J. Oesterling and C. M. Damron, ibid., **174**, 201 (1948).
18) J. Teruuchi, *Kitasato Arch. Experimental Med.*, **23**, 37 (1950).
19) J. Tillmans: *Z. Unters. Lebensm.*, **60**, 34 (1930); **63**, 1, 21, 241, 267, 276 (1932); See also H. v. Euler and H. Hasselquist, "Die Reduktone", Stuttgart, Enke (1950).
20) See, for example, M. Brezina and P. Zuman, "Die Polarographie in der Medizin, Biochemie und Pharmazie", Akademische Verlagsgesellschaft, Leipzig (1956), p. 370.

solution, the contents of AA and DAA are in most cases overestimated, since endiols have closely resembling chemical properties; all of the endiols reduce 2, 6-dichlorophenolindophenol and the half-wave petentials of the oxidation waves of the endiols are very close to each other. Also the colorization of the oxidized forms of the endiols with 2, 4-dinitrophenylhydrazine resembles one another.

In recent years, Ogawa[13] reported his fluorometric determination method of vitamin C, in which he measured the fluorescence of the condensation product of DAA with OPD described as V. However, as reported in his paper, the presence of TR causes the overestimation of vitamin C. Moreover, in order to obtain a satisfying reproducibility of the results, stricter experimental conditions seem to be required[21] than those recommended by Ogawa.

In our polarographic OPD method, firstly, for the simultaneous determination of AA and DAA, no need for the conversion of one of the two forms into the other may be emphasized. Secondly, when two or more endiols are in the same sample solution, there is still a possibility of determining these endiols separately as described above. Of course, the method may not be applicable to all of the endiols, but it is interesting that the third wave for DAA is considerably more negative than the reduction waves corresponding to the oxidized forms of the endiols tested, and even MOA (or TR) and DGA may not seriously interfere with the determination of AA and DAA.

## Summary

The polarographic behavior of dehydro-L-ascorbic acid (DAA), dehydroreductic acid (DRA), alloxan, mesoxalaldehyde (MOA) and 2, 3-diketogulonic acid (DGA) in acid buffer solutions containing *o*-phenylenediamine (OPD), has been investigated.

DAA shows three diffusion controlled reduction waves, whose half-wave potentials ($E_{1/2}$) at pH 3.60 are $-0.26$, $-0.44$ and $-0.67$ V. (vs. N. C. E.), respectively. The limiting currents of the three waves depend on the time after the addition of OPD into the electrolytic solution, the concentration of OPD. pH and the temperature. When the electrolytic solution contains both AA and DAA, the oxidation wave of L-ascorbic acid (AA) can be obtained independently of the three waves for DAA in one polarogram.

DGA shows two reduction waves whose $E_{1/2}$ at pH 3.44 are $-0.27$ and $-0.40$ V., respectively. The $E_{1/2}$ of the first wave is very close to that of the first wave for DAA and the second wave seems to be identical with the second wave for DAA, but the velocities of the condensation reactions of DGA with OPD are much slower than those of DAA with OPD.

Alloxan and DRA show single well defined reduction waves, whose $E_{1/2}$ at pH 3.60 are $-0.32$ and $-0.19$ V., respectively. The oxidation wave of reductic acid (RA) can be obtained with the reduction wave for DRA in one polarogram, while the oxidation wave of dialuric acid decreases very fast when alloxan and OPD are added into the electrolytic solution even after the careful removal of the atmospheric oxygen.

MOA shows a somewhat complicated behavior. In acid pH, the waves are not well defined and are considerably smaller than those of the above substances of the same concentration.

Discussions are made on the structures of the condensation products corresponding to their reduction waves.

Since the linear relationship between the limiting current and the concentration has been obtained, for DAA (the 3rd wave), DRA and alloxan, these polarographic phenomena have been applied to the simultaneous determination of AA and DAA, and to that of RA and DRA and further to that of AA and RA. The method is also applicable to the determination of alloxan, but not to those of MOA (or TR) and DGA, none of which, however, seriously interfere with the determination of DAA (or AA) by means of this polarographic OPD method.

*Laboratory of Biophysical Chemistry*
*College of Agriculture*
*University of Osaka Prefecture*
*Sakai, Osaka*

21) M. Taki, a private communication to the authors.

# *Simultaneous Polarographic Determination of a System of o-Nitroanisole, o-Chloronitrobenzene and o-Nitrophenol*

By Kenichi HONDA and Shin-ichi KIKUCHI

(Received September 27, 1960)

*o*-Nitroanisole is industrially synthesized as a dyestuff intermediate by the reaction of *o*-chloronitrobenzene, sodium hydroxide and methanol. In this process, *o*-nitrophenol is often formed as a by-product. The final solution thus contains *o*-nitroanisole, unreacted *o*-chloronitrobenzene and *o*-nitrophenol as a by-product. From the industrial point of view, it is desired to determine these three compounds in the final solution with the greatest possible simplicity and rapidity. The present study deals with the polarographic method applied to the above determination.

In general, the aromatic nitro compounds are easily reduced at a dropping mercury electrode and numerous investigations upon each of these compounds have already been reported. *o*-Nitroanisole in 10% ethanol-buffer or 30% methanol-buffer solutions of various pH values[1,2], *o*-chloronitrobenzene in 50% ethanol-buffer or 30% methanol-buffer solutions[3,2] and *o*-nitrophenol in ethanol-buffer[4,5] or tetraethylammonium bromide solution[6] have been studied polarographically. It is accordingly known that they can be determined independently, but in the case they are mixed, the condition becomes quite different. As was expected, the half-wave potentials of such compounds are so close that their waves often overlap each other and it seems difficult to get their well-defined waves with good separation. The chief efforts of the present study were exerted to find out the optimum condition of the supporting electrolytes under which the waves of three compounds might be obtained with satisfactory separation.

From this point of view, the effects of pH and various kinds of electrolytes, such as the components of buffer solutions, the effect of mixing of organic solvents such as methanol, ethanol and acetone were thoroughly investigated. The optimum condition is obtained with sodium hydroxide-methanol solution in which the wave of *o*-nitrophenol is so well separated from those of the others that it can easily be determined. The separation of the waves of *o*-nitroanisole and *o*-chloronitrobenzene in this solution is not, however, satisfactory, though better than in other solutions. To improve the wave form, the compensation of residual current was then tried and it was found that by passing the compensating current very excessively, the separation of two reduction waves became distinct.

## Expriemental

Three nitro compounds were obtained from Toa Gosei Company and were further purified. *o*-Nitroanisole the purity of which was more than 99% was redistilled under reduced pressure. *o*-Chloronitrobenzene and *o*-nitrophenol were recrystallized from methanol of which m. p.'s were 33.0 and 45.7°C respectively. 0.01M ethanol, methanol and acetone solutions of each compound were prepared as master solutions. Sørensen's borate-citrate and phosphate buffer solutions of various pH values ranging from 1.17 to 12.16 and other indifferent electrolyte solutions, were also prepared from reagents of analytical grade. The sample solution to be electrolyzed was prepared by mixing the master solution and the indifferent salt solution in an appropriate ratio. Inactive gelatin was added till it was 0.01% of the solution. To remove oxygen, nitrogen was passed through the solution.

The electrolysis was carried out in a liquid paraffin bath which was regulated at 25°C. Both the photographic methods using a Yanagimoto's polarograph apparatus and the pen-writing method using a direct-current amplifier which had been conceived in this laboratory[7] were used. The compensating method of residual current was also applied in further studies by using the circuit proposed by Ishibashi, Shinagawa and Sasabe[8].

## Results

As the results of the preliminary experiments treating the solutions of three components in

1) J. E. Page, J. W. Smith and J. G. Waller, *J. Phys. & Colloid. Chem.*, **53**, 545 (1949).
2) H. Iida and K. Kayahara, *J. Chem. Soc. Japan, Ind. Chem. Sec.* (*Kogyo Kagaku Zasshi*), **60**, 289 (1957).
3) S. F. Dennis, A. S. Powell and M. J. Astle, *J. Am. Chem. Soc.*, **71**, 1484 (1949).
4) J. Pearson, *Trans. Faraday Soc.*, **44**, 692 (1948).
5) M. J. Astle and W. V. McConnell, *J. Am. Chem. Soc.*, **65**, 35 (1943).
6) E. Gergely and T. Iredale, *J. Chem. Soc.*, **1953**, 3226.
7) S. Kikuchi, Y. Sakaguchi and K. Honda, This Bulletin, **25**, 98 (1952).
8) M. Ishibashi, M. Shinagawa and T. Sasabe, *J. Chem. Soc. Japan, Pure Chem. Sec.* (*Nippon Kagaku Zasshi*), **64**, 1441 (1943).

an arbitrary ratio, it was confirmed that the reduction waves appear in the order of *o*-chloronitrobenzene, *o*-nitroanisole and *o*-nitrophenol and the latter can easily be measured because its wave is distinctly separated from those of the two others in most of the tested solutions (Fig. 1). But the reductions of *o*-

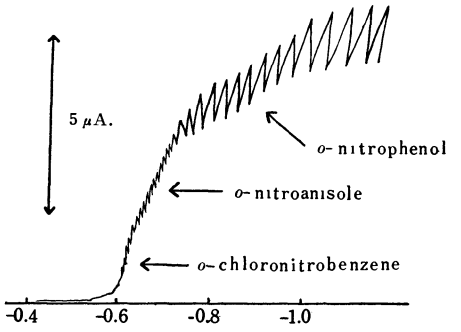



Fig. 1. Polarogram of *o*-nitroanisole ($5\times10^{-4}$M/l.), *o*-chloronitrobenzene ($5\times10^{-4}$M/l.) and *o*-nitrophenol ($2\times10^{-4}$M/l.) in 1 N NaOH-methanol (4 : 1).

chloronitrobenzene and *o*-nitroanisole take place at such close potentials that their waves appear to coincide considerably. Hence it seems difficult to determine them directly on a polarogram. The problem is, therefore, reduced to the polarographic determination of the system of *o*-nitroanisole and *o*-chloronitrobenzene.

**The System of *o*-Nitroanisole and *o*-Chloronitrobenzene.** — Müller[9] described that when two components in a solution the waves of which are assumed to be reversible, are both measurable, their half-wave potentials must differ at least by $(RT/nE)$ ln 1000. In general it would be unwise to presume the separation of waves from the reported values of half-wave potentials of the components to be reduced. It seems desirable to examine the above system under every possible condition.

Here the system of two compounds in mole ratio of 1 : 1 in various electrolyte solutions was investigated to observe the feature of overlapping of waves. In the solutions of various pH values ranging from 1 to 12, containing methanol, ethanol or acetone 2～50%, their reduction waves overlap completely and there is no possibility of determining them directly. In the case of strong basic solutions, the overlapped wave shows a slight tendency to split into two parts, which indicates the possibility of simultaneous determination. Further investigation was then carried out, varying the alkaline concentration and the ratio of organic solvent. The results are summarized in Table I.

TABLE I. SEPARATION OF REDUCTION WAVES OF *o*-NITROANISOLE AND *o*-CHLORONITROBENZENE IN VARIOUS ELECTROLYTE SOLUTIONS

| Concentration of NaOH | Solvent | | Separation of waves |
|---|---|---|---|
| N | | % | |
| 0.1 | Methanol | 10 | ** |
| 1 | Acetone | 2 | * |
| | 〃 | 10 | ** |
| | 〃 | 20 | * |
| | Methanol | 40～50 | ** |
| | 〃 | 10～30 | *** |
| | 〃 | 2～ 5 | * |
| 2 | Acetone | 20 | No separation |
| | Methanol | 50 | ** |
| | 〃 | 20～30 | *** |
| | 〃 | 5～10 | ** |
| 3 | Methanol | 50 | ** |
| | 〃 | 5～30 | *** |
| 4 | Methanol | 50 | * |
| | 〃 | 20～30 | ** |
| | 〃 | 10 | * |
| 5 | Methanol | 30 | * |
| 10 | Methanol | 20～50 | * |

*** ; favorable
** ; fairly good
* ; not good

By examining the results in Table I and considering the practical condition, a solution of four parts of 1 N sodium hxdroxide and one part of methanol was selected as the most suitable solution. In Fig. 2, curve (a) shows an overlapped wave and curve (b) the separated wave.

**Use of the Compensating Method of Residual Current.**—As mentioned above, it is possible to determine *o*-nitroanisole and *o*-chloronitrobenzene in the solution hitherto described when their molar concentrations are equal or nearly equal. But with the increase of differences of their concentrations, the separation of waves becomes again unsatisfactory and it cannot be expected to obtain accurate results. To resolve this difficulty, the compensating method of residual current was tested and it was found that the current compensation gave rise to an apparent separation of waves. For the present purpose, the compensating current must be applied so excessively that the zero-current inclines downwards with the potential increase, resulting in an abnormal form of polarogram. The shape of the polarogram is shown in Fig. 2, curve (c).

By the application of this method, the difference of concentrations of both compounds may

9) O. H. Müller, "The Polarographic Method of Analysis", Chemical Education Co., Easton, Pa. (1950), p. 156.

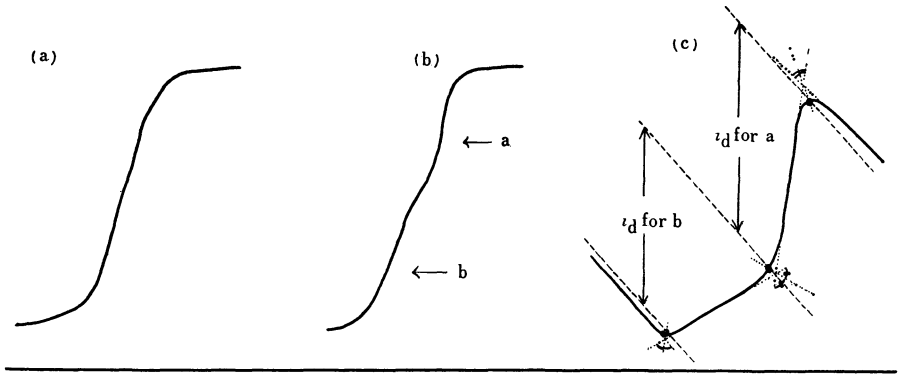



Fig. 2. Wave forms of *o*-nitroanisole (a) and *o*-chloronitrobenzene (b):
(a) in neutral media, (b) in alkaline media,
(c) in alkaline media, compensating current is passed excessively.

be extended over a considerable range. The separation of the waves is noticeable even when their concentration ratio is 10:1 and vice versa. A calibration curve must be made for each compensating condition, because the wave-height of this abnormal polarogram measured by an appropriate drawing method usually presents a little lower value than that of a normal polarogram. The relation between the concentrations of *o*-nitroanisole and *o*-chloronitrobenzene in 1 N sodium hydroxide-methanol (volume ratio 4:1) and their wave-heights are shown in Tables II and Fig. 3.

Table II. Concentrations and wave-heights ($i_d$) for the 1 N sodium pydroxide methanol (4:1) solutions of *o*-nitroanisole and for that of *o*-chloronitrobenzene

| Concentration $C$ | *o*-Nitroanisole | | *o*-Chloronitrobenzene | |
|---|---|---|---|---|
| M/l. | $i_d$ μA. | $i_d/Cm^{2/3}t^{1/6}$ | $i_d$ μA. | $i_d/Cm^{2/3}t^{1/6}$ |
| $10\times10^{-4}$ | $6.1_3$ | 5.92 | $5.7_3$ | 5.53 |
| $8\times10^{-4}$ | $4.7_8$ | 5.77 | $4.9_1$ | 5.93 |
| $6\times10^{-4}$ | $3.7_3$ | 5.99 | $3.5_8$ | 5.77 |
| $4\times10^{-4}$ | $2.5_3$ | 6.10 | $2.2_0$ | 5.32 |
| $2\times10^{-4}$ | $1.1_3$ | 5.45 | $1.1_8$ | 5.69 |

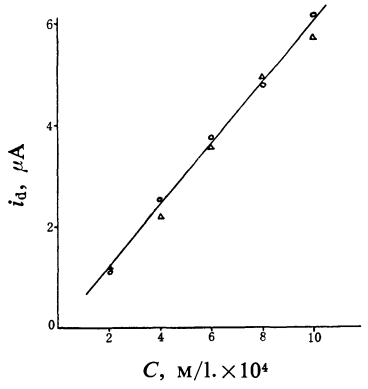



Fig. 3. Relation between wave-heights and concentrations.
○ *o*-Nitroanisole
△ *o*-Chloronitrobenzene

**System of Three Components.**—As described before, *o*-nitrophenol can be determined directly on the ordinary polarogram. The relation between concentrations and wave-heights is shown in Table III and Fig. 4. Once *o*-nitrophenol is determined by the usual polarography, the electrolysis is repeated, using the compensating current. On this second polarogram *o*-nitroanisole and *o*-chloronitrobenzene are

Table III. Concentrations and wave-heights ($i_d$) for the 1N sodium hydroxide methanol (4:1) solutions of *o*-nitrophenol

| Concentration, $C$ M/l. | $i_d$ μA. | $i_d/Cm^{2/3}t^{1/6}$ |
|---|---|---|
| $10\times10^{-4}$ | $8.1_4$ | 7.76 |
| $5\times10^{-4}$ | $4.1_8$ | 7.84 |
| $2\times10^{-4}$ | $1.8_4$ | 8.88 |
| $5\times10^{-5}$ | $0.4_9$ | 9.45 |

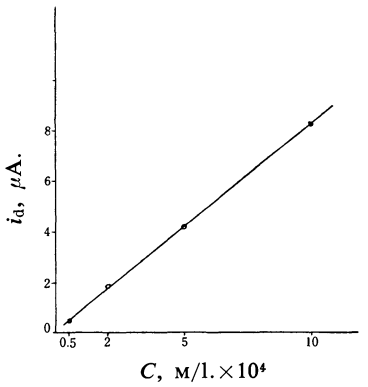



Fig. 4. Relation between wave-heights and concentrations of *o*-nitrophenol.

TABLE IV. SIMULTANEOUS DETERMINATION OF *o*-NITROANISOLE (a), *o*-CHLORONITROBENZENE (b) AND *o*-NITROPHENOL (c)

(1) Concentration of a is varied, while those of b and c remain constant.

| Concentration, calculated M/l. | Wave-height μA. | Concentration, found M/l. | Difference % |
|---|---|---|---|
| a $8\times10^{-4}$ | 4.7 | $7.9\times10^{-4}$ | − 1.5 |
| b $1\times10^{-3}$ | 4.8 | $8.4\times10^{-4}$ | −16 |
| c $2\times10^{-4}$ | 1.8 | $2.0\times10^{-4}$ | − 2 |
| a $6\times10^{-4}$ | 3.3 | $5.3\times10^{-4}$ | −11 |
| b $1\times10^{-3}$ | 4.9 | $8.6\times10^{-4}$ | −14 |
| c $2\times10^{-4}$ | 1.9 | $2.1\times10^{-4}$ | + 3 |
| a $4\times10^{-4}$ | 2.7 | $4.2\times10^{-4}$ | + 6 |
| b $1\times10^{-3}$ | 4.9 | $8.6\times10^{-4}$ | −14 |
| c $2\times10^{-4}$ | 1.7 | $1.8\times10^{-4}$ | − 9 |
| a $2\times10^{-4}$, b $1\times10^{-3}$ | Measurement is not possible | | |
| c $2\times10^{-4}$ | 1.7 | $1.8\times10^{-4}$ | − 9 |

(2) Concentration of b is varied, while those of a and c remain constant.

| | | | |
|---|---|---|---|
| a $1\times10^{-3}$ | 6.1 | $9.9\times10^{-4}$ | − 1 |
| b $8\times10^{-4}$ | 3.7 | $6.3\times10^{-4}$ | −22 |
| c $2\times10^{-4}$ | 1.9 | $2.1\times10^{-4}$ | + 4 |
| a $1\times10^{-3}$ | 6.4 | $1.1\times10^{-3}$ | + 8 |
| b $5\times10^{-4}$ | 2.5 | $4.2\times10^{-4}$ | −16 |
| c $2\times10^{-4}$ | 1.8 | $2.0\times10^{-4}$ | − 2 |
| a $1\times10^{-3}$ | 5.6 | $9.2\times10^{-4}$ | − 8 |
| b $3\times10^{-4}$ | 1.5 | $2.7\times10^{-4}$ | − 9 |
| c $2\times10^{-4}$ | 1.9 | $2.0_6\times10^{-4}$ | + 3 |
| a $1\times10^{-3}$ | 5.8 | $9.4\times10^{-4}$ | − 6 |
| b $2\times10^{-4}$ | 0.9 | $1.5\times10^{-4}$ | −24 |
| c $2\times10^{-4}$ | 1.7 | $1.8\times10^{-4}$ | −11 |

(3) Concentration of c is varied, while those of a and b remain constant.

| | | | |
|---|---|---|---|
| a $5\times10^{-4}$ | 2.6 | $4.2\times10^{-4}$ | −16 |
| b $5\times10^{-4}$ | 2.7 | $4.2\times10^{-4}$ | −16 |
| c $1\times10^{-3}$ | 8.6 | $1.0_5\times10^{-3}$ | + 5 |
| a $5\times10^{-4}$ | 2.6 | $4.1\times10^{-4}$ | −17 |
| b $5\times10^{-4}$ | 2.3 | $3.9\times10^{-4}$ | −23 |
| c $5\times10^{-4}$ | 4.0 | $4.8\times10^{-4}$ | − 4 |
| a $5\times10^{-4}$ | 2.7 | $4.3\times10^{-4}$ | −15 |
| b $5\times10^{-4}$ | 2.3 | $3.8\times10^{-4}$ | −24 |
| c $2\times10^{-4}$ | 1.7 | $1.8\times10^{-4}$ | −10 |
| a $5\times10^{-4}$ | 2.8 | $4.5\times10^{-4}$ | −11 |
| b $5\times10^{-4}$ | 2.4 | $4.1\times10^{-4}$ | −18 |
| c $5\times10^{-5}$ | $0.4_4$ | $4.5\times10^{-5}$ | −10 |

determined by reference to the data of Table II. Experiments are carried out, varying the concentration of one of three components, while those of two others remain constant. The results, summarized in Table IV, are, therefore, classified in three groups according to the compound of which the concentration is varied.

## Summary

1) The solution of *o*-nitroanisole, *o*-chloronitrobenzene and *o*-nitrophenol is investigated polarographically with the intention of their simultaneous determination.

2) The most suitable supporting electrolyte solution for the above object is the mixture of 4 parts of 1 N sodium hydroxide and 1 part of methanol.

3) Although this solution is not buffered, the variation of concentration of one component does not exert appreciable influence upon the wave-heights and the relative positions of the waves of other two components.

4) *o*-Nitrophenol can be determined directly from the ordinary polarogram. The accuracy of determination is under ±10%.

5) The residual current compensation gives aid to the determination of *o*-nitroanisole and *o*-chloronitrobenzene. By passing the compensating current very excessively, their reduction waves become better defined. The accuracy of determination is +8～−17% for *o*-nitroanisole and −24～−9% for *o*-chloronitrobenzene.

6) The half-wave potentials of three compounds, $5\times10^{-4}$ M/l. in 1 N sodium hydroxide-methanol (4 : 1) solution are as follows;

| | $E_{1/2}$(vs. S.C.E.) V. | Difference V. |
|---|---|---|
| *o*-Chloronitrobenzene | −0.645 | 0.114 |
| *o*-Nitroanisole | −0.759 | 0.179 |
| *o*-Nitrophenol | −0.938 | |

These values would give some indications for the estimation of the separation of waves.

The authors wish to express grateful thanks to Mr. H. Hara for his technical assistance in the present study.

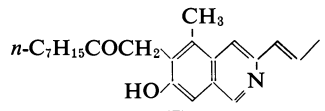
*Institute of Industrial Science*
*The University of Tokyo*
*Chiba*

# *Ultraviolet Spectra of N-Heterocyclic Systems. II*. The Spectra of 5~8-Hydroxyisoquinolines and Related Compounds*

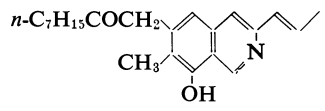
By Koji NAKANISHI, Mamoru OHASHI, Shoichiro KUMASAKI and Hisashi KOIKE

(Received October 6, 1960)

The mold pigment, monascorubrin, when treated with ammonia gives monascamine, which in turn, when reacted with, zinc affords monascaminone, a key degradation product for structural studies[1,2]. Preliminary spectroscopic measurements showed it to be an isoquinoline derivative hydroxylated at the 5-, 6-, 7- or 8-position. The four hydroxyisoquinolines have accordingly been synthesized and the ultraviolet spectra of the free hydroxy compounds, the methoxylated compounds, and the methiodides have been measured in neutral, acid, and basic methanol solutions; these curves have been compared with the curves of the corresponding derivatives prepared from the natural monascaminone in order to determine, if possible, which of the two alternative structures I, II is more appropriate[3].



(I)



(II)

The spectra of hydroxyisoquinolines, hydroxyquinolines, and their derivatives have been compared under a variety of conditions in the present paper so that there may be deduced general qualitative characteristics useful in structural studies. The azanaphthalenes with the hydroxyl group either at the $\alpha$- or $\gamma$-position with respect to the ring nitrogen atom exist predominantly in the amide form in solvents of low dielectric constant[4-7], a behavior which is similar to the well known 2-hydroxy- and 4-hydroxypyridines[8-10]. These hydroxyazanaphthalenes have been omitted from the present paper; only those in which the hydroxy group is not placed $\alpha$ or $\gamma$ to the ring nitrogen atom will be considered.

The spectra of the compounds measured are shown in Table I and Figs. 1—9; the peaks reported previously by Mason for 8-hydroxyisoquinoline[7] do not seem to be correct. The measurements were undertaken under limiting conditions, i. e., conditions in which the presence of a tautomeric mixture or an equilibrium between species with different net charge need not be taken into consideration. For example, in methanol, unlike in water of the isoelectric pH value, the parent compounds exist solely as one species and not as a tautomeric mixture. On the other hand, the methiodide of 7-hydroxyisoquinoline in methanol shows a complex absorption of seven peaks, which was shown to be due to the presence of a mixture

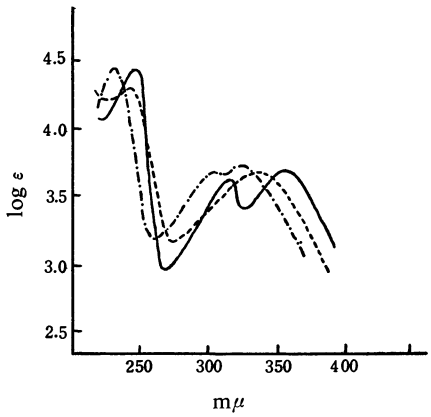



Fig. 1. Ultraviolet spectra of 5-hydroxyisoquinoline.
———: in 0.1 N HCl-MeOH
·—·—·: in MeOH
------: in 0.1 N NaOH-MeOH

* Presented in part at the 1st IUPAC Symposium on Natural Products, Australia, August, 1960.

Part I, K.Nakanishi, N. Suzuki and F. Yamazaki, This Bulletin, **34**, 53 (1961).

1) M. Ohashi, S. Kumasaki, S. Yamamura, K. Nakanishi and H. Koike, *J. Am. Chem. Soc.*, **81**, 6339 (1959).

2) B. C. Fielding, F. J. Haws, J. S. E. Holker, A. D. G. Powell, A. Robertson, D. N. Stanway and W. B. Whalley, *Tetrahedron Letters*. No. 5, 24 (1960).

3) To be published soon. NMR spectroscopy could not clearly differentiate between the two alternative structures: M. Ohashi, A. Terahara and K. Nakanishi, This Bulletin, **33**, 1311 (1960).

4) G. W. Ewing and E. A. Steck, *J. Am. Chem. Soc.*, **68**, 2181 (1946).

5) G. F. Tucker and J. L. Irvin, ibid., **73**, 1923 (1951).

6) A. Albert and J. N. Phillips, *J. Chem. Soc.*, **1956**, 1294.

7) S. Mason, ibid., **1957**, 5010.

8) A. Albert, *Chem. Soc. Spec. Publ.*, No. 3, 124 (1955).

9) A. Albert and E. Spinner, *J. Chem. Soc.*, **1960**, 1221.

10) E. Spinner, ibid., **1960**, 1226, 1232.

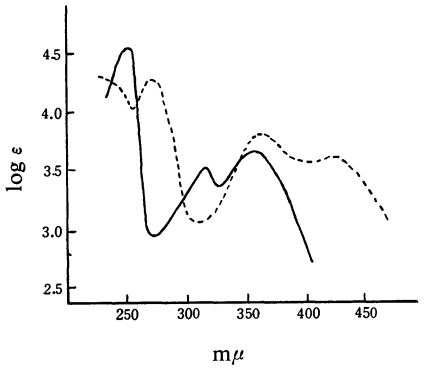



Fig. 2. Ultraviolet spectra of 5-hydroxy-isoquinoline methiodide.
———: in 0.1 N HCl-MeOH
------: in 0.1 N NaOH-MeOH

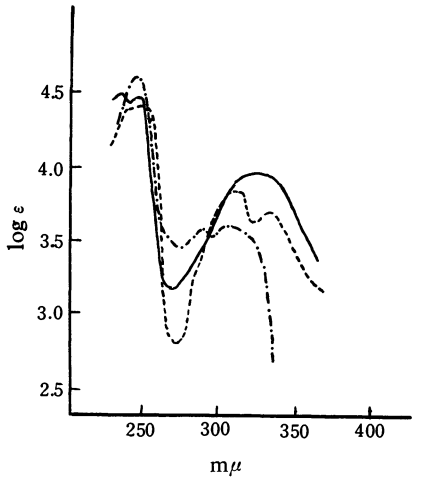



Fig. 3. Ultraviolet spectra of 6-hydroxy-isoquinoline.
———: in 0.1 N HCl-MeOH
·—·—: in MeOH
------: in 0.1 N NaOH-MeOH

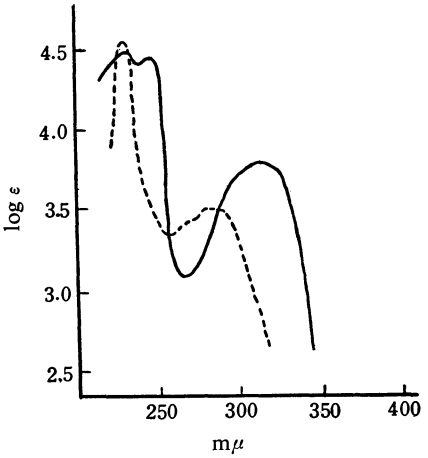



Fig. 4. Ultraviolet spectra of 6-methoxy-isoquinoline.
———: in 0.1 N HCl-MeOH
------: in 0.1 N NaOH-MeOH

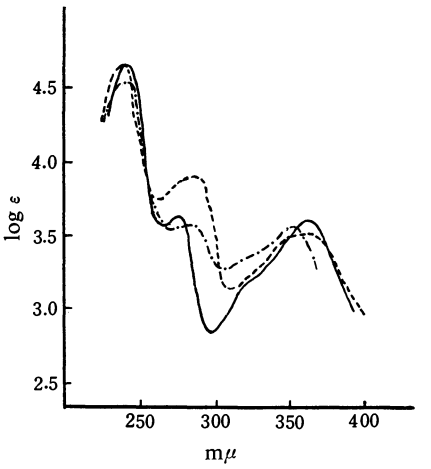



Fig. 5. Ultraviolet spectra of 7-hydroxy-isoquinoline.
———: in 0.1 N HCl-MeOH
·—·—: in MeOH
------: in 0.1 N NaOH-MeOH

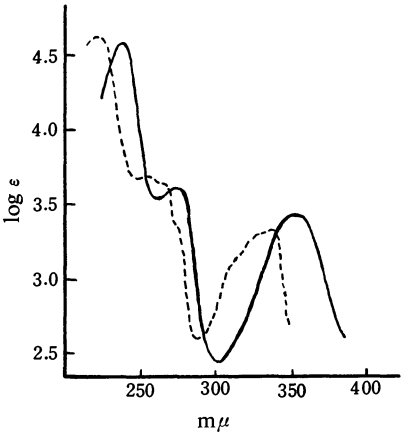



Fig. 6. Ultraviolet spectra of 7-methoxy-isoquinoline.
———: in 0.1 N HCl-MeOH
------: in 0.1 N NaOH-MeOH

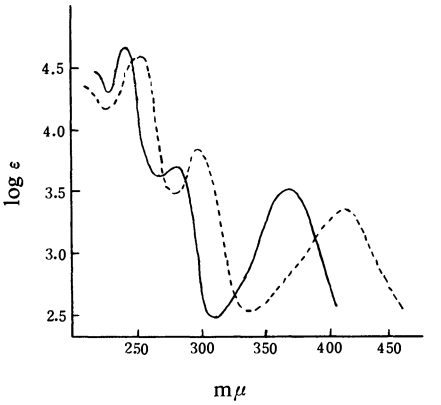



Fig. 7. Ultraviolet spectra of 7-hydroxy-isoquinoline methiodide.
———: in 0.1 N HCl-MeOH
------: in 0.1 N NaOH-MeOH

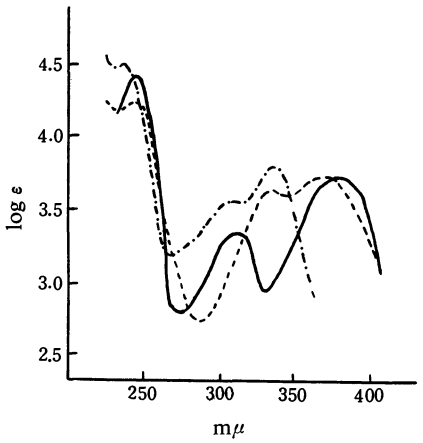



Fig. 8. Ultraviolet spectra of 8-hydroxyisoquinoline.
———: in 0.1 N HCl-MeOH
•—•—: in MeOH
------: in 0.1 N NaOH-MeOH

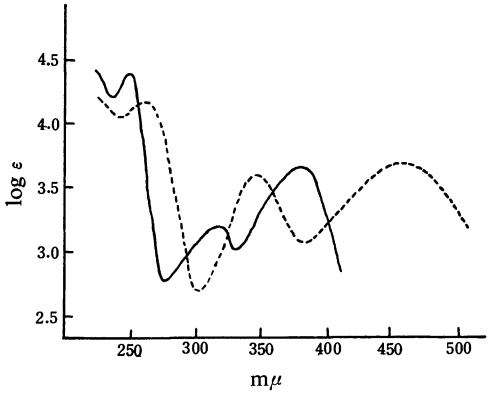



Fig. 9. Ultraviolet spectra of 8-hydroxyisoquinoline methiodide.
———: in 0.1 N HCl-MeOH
------: in 0.1 N NaOH-MeOH

of neutral (zero net charge, No. 17) and cationic (No. 16) species. Thus in comparing spectra of compounds capable of existing as mixtures, the conditions should be chosen so that complicating factors are not called into play. The spectra of other hydroxyazanaphthalenes[4,7] are also considered in the following discussion, but those of 6-hydroxyisoquinoline and derivatives (Nos. 6—10) seem to constitute a special type and will be mentioned later. Figs. 1—9 and the data published so far show that, excepting the 6-hydroxyisoquinoline derivatives (Figs. 3 and 4), all curves are roughly made up from three major absorptions; the peaks of monoazanaphthalenes are known to

Table I. Spectra of 5~8-hydroxyisoquinolines and derivatives

| No. | Comp. | Solv. | $\lambda_{max}$ | log ε | Fig. | Ionic species | Type |
|---|---|---|---|---|---|---|---|
| 1 | 5-OH | N | 234/303 328 | 4.45/3.65 3.70 | 1 | a | $\pi_3/\pi_2$ $\pi_1$ |
| 2 | 〃 | A | 251/318 367 | 4.47/3.63 3.70 | 1 | b | 〃 |
| 3 | 〃 | B | 248/340 | 4.28/3.81 | 1 | c | 〃 |
| 4 | 5-OH, $CH_3I$ | A | 255/322 368 | 4.51/3.46 3.66 | 2 | f | 〃 |
| 5 | 〃 | B | 245(sh) 274/362 430 | 4.22 4.26/3.87 3.52 | 2 | g | 〃 |
| 6 | 6-OH | N | 229/266+286+300 | 4.65/3.62+3.65+3.63 | 3 | a | $\pi_3$ $\pi_2/\pi_1$ |
| 7 | 〃 | A | 228+247/321 | 4.55+4.51/3.84 | 3 | b | 〃 |
| 8 | 〃 | B | 241+253/276(sh) 308 332 | 4.46+4.40/3.20 3.87 3.65 | 3 | c | 〃 |
| 9 | 6-$OCH_3$ | A | 230+247/311 | 4.49+4.45/3.76 | 4 | d | $\pi_3$ $\pi_2/\pi_1$ |
| 10 | 〃 | B | 231/266+280+290 | 4.65/3.40+3.49+3.50 | 4 | e | $\pi_3/\pi_2$ $\pi_1$ |
| 11 | 7-OH | N | 224 260+268+273/301(sh) 333 | 4.55 3.59+3.59+3.42/ 3.31 3.58 | 5 | a | $\pi_3$ $\pi_2/\pi_1$ |
| 12 | 〃 | A | 241 278/318(sh) 362 | 4.64 3.65/3.16 3.63 | 5 | b | 〃 |
| 13 | 〃 | B | 238 282+289/360 | 4.64 3.85+3.88/3.51 | 5 | c | 〃 |
| 14 | 7-$OCH_3$ | A | 241 268+275/354 | 4.58 3.58+3.61/3.46 | 6 | d | 〃 |
| 15 | 〃 | B | 233 255+263/326+337 | 4.67 3.69+3.66/3.32+3.33 | 6 | e | 〃 |
| 16 | 7-OH, $CH_3I$ | A | 217 243 280/367 | 4.48 4.71 3.72/3.54 | 7 | f | 〃 |
| 17 | 〃 | B | 217 265 308/424 | 4.39 4.64 3.86/3.38 | 7 | g | 〃 |
| 18 | 8-OH | N | 233/304+334 | 4.47/3.57+3.79 | 8 | a | $\pi_3/\pi_2$ $\pi_1$ |
| 19 | 〃 | A | 245/310 378 | 4.47/3.39 3.72 | 8 | b | 〃 |
| 20 | 〃 | B | 247/328 370 | 4.28/3.66 3.78 | 8 | c | 〃 |
| 21 | 8-OH, $CH_3I$ | A | 217 250/315 378 | 4.48 4.31/3.22 3.68 | 9 | f | 〃 |
| 22 | 〃 | B | 263/347 460 | 4.21/3.59 3.69 | 9 | g | 〃 |

N; MeOH, A; 0.1 N HCl-MeOH, B; 0.1 N NaOH-MeOH
/; location of the lowest trough,
+; multiplets, sh: shoulder

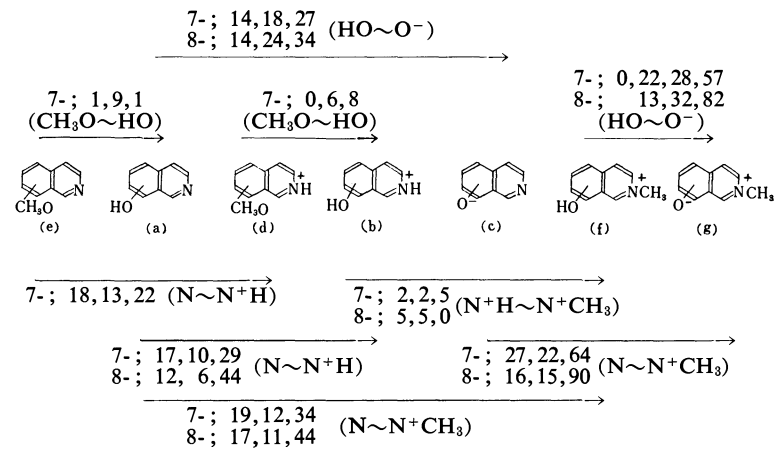



Plate 1. $\Delta\lambda_{max}$ between the ionic species of 7- and 8-hydroxyisoquinolines in methanol. (Figures denote $\Delta\lambda_{max}$ of $\pi_3$ $\pi_2$ and $\pi_1$ bands; for multiplets. the middle peak or the mean wavelength is taken.)

be $\pi\rightarrow\pi^*$ bands[11], and they will hereafter be abbreviated as $\pi_1$, $\pi_2$ and $\pi_3$-bands (in order of decreasing wavelengths).

The shifts of the bands accompanying change in media and derivatives parallel those observed for 3-hydroxypyridine[7,12-14], and the main species as shown in Plate 1 account consistently for these shifts. The species (a—g) are arranged in the order of increasing wavelengths of the peaks (from left to right).

The following common trends are apparent: (a) ionization of the phenolic group causes a red shift, a vs. c, f vs. g, (b) methylation of the phenolic group causes a slight blue shift, a vs. e, b vs. d; (c) *N*-protonation causes a red shift, e vs. d, a vs. b, (d) the change $N\rightarrow N^+CH_3$ causes a red shift larger than that due to *N*-protonation, c vs. g, a vs. f, compare also b vs. f, (e) in general, the shift for the $\pi_1$-band ($\Delta\pi_1$) is the largest, and $\Delta\pi_2 > \Delta\pi_3$ for ionization of the phenolic group, while $\Delta\pi_3 > \Delta\pi_2$ for changes involving *N*-protonation or *N*-quaternarization, (f) published data show that this general tendency is also observable in other hydroxyquinolines and hydroxyisoquinolines[4,7]. In addition to this generalization the compounds fall broadly into the $\alpha$-naphthol or the $\beta$-naphthol' type as already noted by Ewing and Steck[4], which can be further refined into the form as summarized in Table II. This general classification may be observed in all of the simple hydroxylated monoazanaphthalenes (excepting 6-hydroxyisoquinoline). Full data for the methoxy and *N*-methyl compounds are missing but since the general aspects of the curves are not greatly altered by the changes of $OH\sim OCH_3$ and $N^+H\sim N^+CH_3$, excepting roughly parallel shifts of the entire curve, it can be presumed that the same relation holds for these derivatives also. Indeed, this is seen in the limited examples shown in Figs. 5, 6 and 7. The most apparent distinction between the $\alpha$- and $\beta$-naphthol series is that in the former the lowest trough in the curve is located between the $\pi_3$ and $\pi_2$ bands, whereas in the latter, with the exception of the cation of the isoquinolines, the trough lies between the $\pi_2$ and $\pi_1$ bands. The exceptional behavior of the $\beta$-naphthol type quinoline cations is

TABLE II. CLASSIFICATION OF THE ULTRAVIOLET SPECTRA OF HYDROXYQUINOLINES AND HYDROXYISOQUINOLINES IN METHANOL

**$\alpha$-Naphthol type**

5- and 8-Hydroxy-Q, 5- and 8-hydroxy-isoQ

| | | |
|---|---|---|
| Neutral (a, e) | ; | $\pi_3/\pi_2+\pi_1$ |
| Cation (b, d, f) Q | ; | $\pi_3/\pi_2$(doublet) $\pi_1$ |
| iso Q | ; | $\pi_3/\pi_2$ $\pi_1$ |
| Anion (c) | | $\pi_3/\pi_2+\pi_1$ |

**$\beta$-Naphthol type**

3-, 6- and 7-Hydroxy-Q[4], 7-hydroxy-isoQ (6-hydroxy-isoQ)

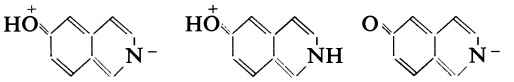
| | | |
|---|---|---|
| Neutral (a, e) | ; | $\pi_3\pi_2$(multiplet)/$\pi_1$ |
| Cation (b, d, f) Q | ; | $\pi_3/\pi_2$ $\pi_1$ |
| iso Q | ; | $\pi_3$ $\pi_2/\pi_1$ |
| Anion (c) | ; | $\pi_3$ $\pi_2/\pi_1$ |

Q; Quinoline
/; Location of lowest trough
+; Poorly resolved or coalesced bands
( ); Alphabets in parentheses denote species shown in Plate 1.

11) S. F. Mason, *Chem. Soc. Spec. Publ.*, **No. 3**, 139 (1955).
12) D. E. Metzler and E. E. Snell, *J. Am. Chem. Soc.*, **77**, 2431 (1955).
13) K. Nakamoto and A. E. Martell, ibid., **81**, 5857 (1959).
14) S. F. Mason, *J. Chem. Soc.*, **1959**, 1253.

caused by the fact that upon *N*-protonation the shift of the $\pi_2$-band is much larger (35～50 m$\mu$) than those of the $\pi_1$- or $\pi_3$-bands (0～20 m$\mu$) (see Figs. 9—11 in Ref. 4).

The spectra of 6-hydroxyisoquinolines (Nos. 6—10, Figs. 3 and 4) do not fall into the general differentiation described in Table II, although the shifts accompanying changes in the species fall in line with the sequence shown in Plate 1. This could possibly be due to the fact that the nitrogen and oxygen functions are located in positions favorable for the contribution of "para-para-quinonoid" canonical structures[7] such as:




Neutral Cation Anion

However, it can be stated that these canonical structures do not make a major contribution since if this were the case, they would rather behave like pyridones or quinolones (e. g., 4-hydroxyquinoline[5]) which do not fall into the pattern outlined in Plate 1. It is interesting to note, that whereas the $K_t$ constant ($K_t$= [N-H form]/[O-H form]) of other hydroxyazanaphthalenes in aqueous solutions buffered to the isoelectric pH are much less than the unity, those of 6-hydroxyisoquinoline and 4-hydroxyisoquinoline are exceptionally high (1.92 and 3.76, respectively)[7]. In view of the high value of 3.76 for 4-hydroxyisoquinoline, the spectra of this compound might also fail to agree with the generalizations of Table II. The theoretical implications of these trends are still not clear, but it is hoped that the empirical generalizations shown in Plate 1 and Table II will be of assistance in structural studies of natural products.

## Experimental

**Materials.**—The hydroxyisoquinolines and their methyl ethers were prepared according to following literatures:

5-Hydroxyisoquinoline; R. A. Robinson, *J. Am. Chem. Soc.* **69**, 1942 (1947):
6-Hydroxyisoquinoline and 6-methoxyisoquinoline; idem., ibid., **69**, 1936, 1944 (1947):
7-Hydroxyisoquinoline and 7-methoxyisoquinoline; R. D. Woodward and W. E. Doering, ibid., **67**, 868 (1945):
8-Hydroxyisoquinoline; R. A. Robinson, ibid., **69**, 1944 (1947).

The methiodides were prepared by treating a solution of 100 mg. of the hydroxyisoquinoline in 10 ml. of 1 : 1 acetone-benzene with 3 ml. of methyl iodide, refluxing for 1 hr., collecting the precipitate after cooling, and recrystallizing from ethanol. The 5-, 7-, and 8-hydroxyisoquinoline methiodides melted at 235～237°C, 218～220°C and 217～219°C, respectively.

**Measurement of Spectra.**—The absorption spectra were measured with a Beckman DK-2 and a Hitachi Model EP-2 spectrophotometer in the solvents listed in Table I.

## Summary

The spectra of monohydroxymonoazanaphthalenes in which the hydroxyl group is neither $\alpha$ nor $\gamma$ to the ring nitrogen atom have been compared under various conditions. Shifts of peaks accompanying changes in the species involved have been generalized and a distinction between the spectra of the $\alpha$- and $\beta$-naphthol type hydroxyazanaphthalenes has been made.

*Department of Chemistry*
*Faculty of Science*
*Tokyo University of Education*
*Bunkyo-ku, Tokyo*
*(K. N. & M. O.)*

*Chemical Institute*
*Nagoya University*
*Chikusa, Nagoya*
*(S. K.*)*

*Pharmacy Department*
*Nagoya City University*
*Mizuho, Nagoya*
*(H. K.)*

* Present address: Research Laboratory, Daikyo Oil Co., 1 Daikyo-cho, Yokkaichi, Mie.

# *Dehydration of Bile Acid and their Derivatives. VIII. Synthesis of 3α-Hydroxy-Δ$^{8(14)}$-cholenic and 3α-Hydroxy-Δ$^{14}$-cholenic Acids. A Note on "β"-Cholenic Acid*

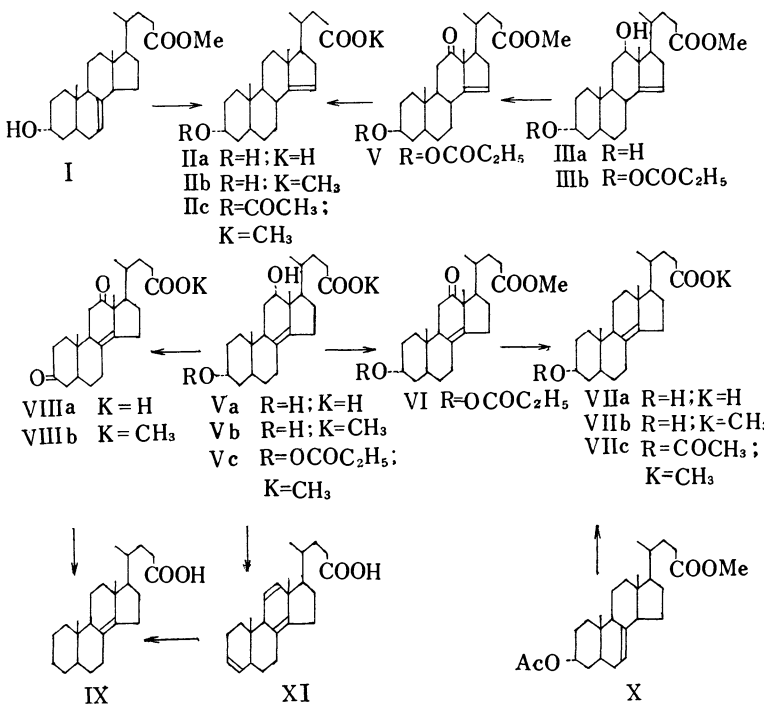
By Fujinori NAKADA, Ryuzaburo OSAWA and Kazumi YAMASAKI

(Received October 12, 1960)

In the preceding[1] paper it has been reported that methyl 3α-hydroxy-Δ$^{7}$-cholenate (I) in chloroform was isomerized into 3α-hydroxy-Δ$^{14}$-cholenate (IIb) by means of hydrochloric acid gas. It is here shown that this new hydroxycholenic acid can also be prepared by another route: methyl dihydroxycholenate (IIIa) of Bödecker[2], 3-hydroxy group of which was selectively protected by its conversion into an ethoxycarbonyloxy grouping IIIb, was oxidized and the resulting 12-keto compound IV was then subjected to the Huang-Minlon reduction. The physical properties of the product obtained as well as of its derivatives were in fairly good agreement with those of the hydroxycholenic acid prepared by the isomerization[1].

Apocholic acid[2], 3α, 12α-dihydroxy-Δ$^{8(14)}$-cholenic acid (Va), 12-hydroxy group of which was eliminated by a procedure similar to that mentioned above, was found to be converted into another 3α-hydroxycholenic acid (VIIa) of melting point 167~168°C, $\alpha_D^{15} = +41 \pm 2°$ (chf.). It is reasonably assumed that during the Huang-Minlon reduction cource of methyl 3α-ethoxycarbonyloxy-12-keto-Δ$^{8(14)}$-cholenate(VI), one of the intermediary products of this route, no shift of its double bond did happen to occur, since the same reduction procedure of methyl 3, 12-diketocholenate (VIIIb) derived from apocholic acid (Va) gave "β"-cholenic acid (IX) without shift of its double bond (see below).

This assumption was further confirmed by the fact that the extinction quotient in the ultraviolet region of the above-mentioned hydroxycholenic acid was high enough ($\varepsilon_{max}^{EtOH} =$




1) R. Osawa and K. Yamasaki, This, Bulletin, 32, 1302 (1959).

2) Fr. Bödecker, *Ber.*, 53, 1852 (1920).

TABLE I. $\Delta^{8(14)}$-CHOLENIC ACID

| Designated as | M. p., °C | $[\alpha]_D$ | Preparative method | Starting material | Ref. |
|---|---|---|---|---|---|
| Apocholanic acid | 144.5～145.5 | +37.0° (chf.) | $CrO_3$-oxidation +Clemmensen reduction | Apocholic acid | 6 |
| β-Cholenic acid | 142～143 | +38.0°(chf.)* | Pyrolysis+Hydrogenation | Apocholic acid | 7 |
| β-Cholenic acid | 141～142 | +40.7°(alc.) | Pyrolysis+Hydrogenation | Apochenodeoxy-cholic acid | 5 |
| β-Cholenic acid | 145～146 | +37.0°(chf.) | Hydrogenation | α-Cholatrienic acid (II) | 9 |
| $\Delta^{8(14)}$-Cholenic acid | 140～141 | +38.8±5° (chf.) | $CrO_3$-oxydation+Huang-Minlon reduction | Apocholic acid | |

* H. Wieland and E. Dane, *Z. physiol. Chem.*, **210**, 268 (1932).

5550) to indicate that its double bond was tetra-substituted[3], (Bladon et al.) like its mother substance, apocholic acid.

According to Reichstein et al.[4] 3α,12α-dihydroxy-$\Delta^7$-cholenic acid is easily isomerized into apocholic acid by treating it with platinum and hydrogen gas. It was found, however, that isomerization of methyl 3α-acetoxy-$\Delta^7$-cholenate (X) by the same treatment was unexpectedly slow in rate, and that even with a 30 hrs' shaking with the catalyst in hydrogen-atmosphere not more than 40% of the starting material was isomerized into 3α-hydroxy-$\Delta^{8(14)}$-cholenate (VIIc).

"α-Apochenodeoxycholic acid[5]" had been obtained by hydrolysis of a crystalline taurine-conjugated acid (m. p. 210°C) which separated from the chicken bile treated with a higher concentrated hydrochloric acid (about 18%). Notwithstanding some discrepancies in physical property, this acid must be identical with the above-mentioned hydroxycholenic acid (VIIa) derived from apocholic acid, because the former was reported[5] to give just the same cholenic acid, "β"-cholenic acid (IX) as apocholic acid gave[6,7].

"β"-Cholenic acid had been first derived from apocholic acid, two hydroxyl groups of which were eliminated either by the usual chromium trioxide-oxidation VIIIa followed by the Clemmensen reduction[6] or by pyrolytic dehydration XI followed by catalytic hydrogenation[6,7]. As shown in Table I, apocholic acid (Va) afforded the same cholenic acid, "β"-cholenic acid, by the methods involving even such drastic procedure as pyrolysis or heating in concentrated hydrochloric acid.

While Borsche et al.[6] had failed to obtain any of the diketo derivatives of apocholic acid in a crystalline state, the chromium trioxide-sulfuric acid oxidation of its methyl ester gave a crystalline diketo ester VIIIb which was converted into "β"-cholenic acid (IX) by the Huang-Minlon reduction.

## Experimental

**$\Delta^{8(14)}$-Cholenic Acid from Apocholic Acid.**—*Methyl Apocholate (Vb).*—Apocholic acid (m. p. 171～173°C) was methylated with diazomethane as usual and recrystallized from methanol, m. p. 88～90°C.

*Methyl 3,12-Diketo-$\Delta^{8(14)}$-cholenate (VIIIb).*—Methyl apocholate (1 g.) in acetone was oxidized with the $CrO_3$-$H_2SO_4$ mixture (Bladon et al.[8]). The reaction product was extracted with ether, the extract was washed successively with dilute sodium carbonate solution and water, and dried over magnesium sulfate. To the concentrated ether extract was added a small volume of petroleum ether, and the deposited crystals were collected and washed with small portions of a petroleum ether-ether mixture (1 : 1). The crystals melted at 114～115°C. From the filtrate a second crop of m. p. 113～115°C was obtained. The total yield was 0.61 g. After recrystallization from methanol, the product melted at 119～120°C.

Found: C, 74.17; H, 9.19. Calcd. for $C_{25}H_{36}O_4$ (400.563): C, 74.96; H, 9.05%.

*$\Delta^{8(14)}$-CholenicAcid (IX).*—Methyl 3,12-diketo-$\Delta^{8(14)}$-cholenate (0.21 g.) (VIIIb) in 2.0 ml. of triethylene glycol was reduced together with 1 ml. of hydrazine and 0.8 g. of potassium hydroxide according to the Huang-Minlon method. The product melted at 140～141°C after recrystallization from acetone or acetic acid; $\alpha_D^{24}=+38.8\pm5°$ (chf.); $\varepsilon_{max}^{EtOH}=6170$.

Found: C, 79.68; H, 10.49. Calcd. for $C_{24}H_{38}O_2$ (358.568): C, 80.39; H, 10.68%.

**Preparation of 3α-Hydroxy-$\Delta^{8(14)}$-cholenic Acid.**—*Methyl 3α-Ethoxycarbonyloxy-12α-hydroxy-$\Delta^{8(14)}$-cholenate (Vc).*—Methyl apocholate (5 g.) (Vb) was dissolved in 25 ml. of dioxane and 4 ml. of pyridine, and then 5 ml. of ethyl chlorocarbonate was added with cooling. The reaction mixture was allowed to stand at room temperature for 30 min. and then diluted with water; 2 ml. of concentrated hydrochloric acid was added and heated on a water bath for 30 min. The product was extracted with ether and the ether extract was washed with water, dried over sodium sulfate and then evaporated in vacuo.

3) P. Bladon, H. B. Henbest, and G. W. Wood, *J. Soc., Chem.*, **1952**, 2737.
4) E. Berner, A. Lardon and T. Reichstein, *Helv. Chim. Acta*, **30**, 1542 (1947).
5) K. Takahashi, *Z. physiol. Chem.*, **255**, 277 (1938).
6) W. Borsche and A. R. Todd, ibid., **197**, 173 (1931).
7) H. Wieland and V. Deulofeu, ibid., **198**, 127 (1931).
8) P. Bladon, J. M. Favian, H. B. Henbest, H. P. Koch and G. W. Wood, *J. Chem. Soc.*, **1951**, 2402.
9) T. Shimizu, T. Oda and H. Makino, *Z. physiol. Chem.*, **213**, 136 (1932).

Yield, 5.5 g. The product was subjected to the following procedure without crystallization.

*Methyl 3α-Ethoxycarbonyloxy-12-keto-$\Delta^{8(14)}$-cholenate (VI).*—The above-mentioned ester (5.5 g.) was dissolved in 550 ml. of acetone and the $CrO_3$-$H_2SO_4$ mixture of Bladon et al.[8] was added carefully in 3 min. at 30~35°C, and the excess of chromic acid was reduced with methanol. The mixture was diluted with water and a crystalline matter deposited. After several recrystallizations from methanol a pure substance melting at 116~117°C was obtained. Yield, 2 g.

Found: C, 70.67; H, 9.09. Calcd. for $C_{28}H_{42}O_6$ (474.644): C, 70.85; H, 8.91%.

*Methyl 3α-Acetoxy-$\Delta^{8(14)}$-cholenate (VIIc).*—Methyl 3α-ethoxycarbonyloxy-12-keto-$\Delta^{8(14)}$-cholenate (1.2 g.) (VI) was subjected to the Huang-Minlon reduction (triethylene glycol, 12 ml.; potassium hydroxide, 1.2 g.; and 80% hydrazine hydrate, 1.2 ml.). The reaction mixture was acidified with dilute hydrochloric acid and a crystalline precipitate was collected. Yield, about 1 g. The product was converted into methyl ester (amorphous) with an ethereal solution of diazomethane, and the ester in 10 ml. of acetic anhydride was heated for 1 hr. on a water bath. After several recrystallizations from methanol, colorless crystals of m. p. 81~82°C were obtained. Yield, 0.5 g. $\alpha_D^{27}=+56\pm2°$ (chf.); $\varepsilon_{max}^{EtOH}=5410$ ($\lambda_{max}=215$ mμ).

Found: C, 75.09; H, 9.77. Calcd. for $C_{27}H_{42}O_4$ (430.633): C, 75.30; H, 9.83%.

*3α-Hydroxy-$\Delta^{8(14)}$-cholenic Acid (VIIa).*—The acetyl methyl ester mentioned above was dissolved in 2% alcoholic solution of potassium hydroxide and let stand at room temperature for 24 hr. The free acid so obtained was recrystallized from methanol. Colorless plates of m. p. 167~168°C; $\alpha_D^{15}=+41\pm2°$ (chf.); $\varepsilon_{max}^{EtOH}=5550$ ($\lambda_{max}=214$ mμ).

Found: C, 77.01; H, 10.24. Calcd. for $C_{24}H_{38}O_3$ (374.568): C, 76.95; H, 10.22%.

*Taurine-conjugation of 3α-Hydroxy-$\Delta^{8(14)}$-cholenic Acid.*—The above-mentioned acid (100.25 mg.) was treated with a mixture of tri-*n*-butylamine (0.06 ml.) in 0.5 ml. of dioxane and ethyl chlorocarbonate (0.024 ml.). The mixture was allowed to stand at room temperature for 15 min., and cooled down to 10°C; a solution of taurine (33.6 mg.) in 0.25 ml. of 1 N sodium hydroxide was added and left for 1 hr. One milliliter of water was added and then the solvent was removed by reduced pressure. The residue was dissolved in water and acidified with dilute hydrochloric acid. Crystalline substance so obtained was collected and recrystallized from dilute alcohol. M. p. 207°C. Yield, 30 mg.

Found: N, 2.87. Calcd. for $C_{26}H_{43}O_5NS$ (481.701): N, 2.90%.

"Tauroapochenodeoxycholic acid" of Takahashi[5] was reported to melt at 210°C.

**Isomerization of Methyl 3α-Acetoxy-$\Delta^{7}$-cholenate into its $\Delta^{8(14)}$-Isomer.**—*Methyl 3α-Acetoxy-$\Delta^{8(14)}$-cholenate (VIIc).*—Methyl 3α-acetoxy-$\Delta^{7}$-cholenate (m. p. 123~124°C) (300 mg.) (X) in 10 ml. of glacial acetic acid was shaken with platinum dioxide (300 mg.) for 30 hr. in hydrogen atmosphere. The catalyst was filtered off. The filtrate was diluted with water and crystals separated.

The first crop (230 mg.) melted at 90~95°C and repeated recrystallization gave 80 mg. of the pure starting material (m. p. 123~124°C).

From the combined filtrate fractions of recrystallization a crude crystalline matter (m. p. of 90~100°C) weighing 120 mg. was obtained, and a carefull repetition of recrystallization afforded silky crystals of m. p. 84~85°C, $\alpha_D^{23}=+61\pm2°$ (chf.). They showed no melting point depression on admixture with methyl 3α-acetoxy-$\Delta^{8(14)}$-cholenate mentioned above.

Found: C, 75.19; H, 9.69. Calcd. for $C_{27}H_{42}O_4$ (430.633): C, 75.30; H, 9.83%.

*3α-Hydroxy-$\Delta^{8(14)}$-cholenic Acid (VIIa).*—The above-mentioned ester (220 mg.) was dissolved in 10 ml. of methanol with 3 ml. of 10% solution of potassium hydroxide, and refluxed on a water bath for 30 min. After cooled, the product was deposited with dilute hydrochloric acid and collected. Yield, 130 mg. The free acid was recrystallized from methanol and melted at 168~169°C, exactly like the acid prepared from apocholic acid. $\alpha_D^{25}=+33\pm5°$ (di.).

**Preparation of 3α-Hydroxy-$\Delta^{14}$-cholenic Acid.**—*Methyl 3α,12α-Dihydroxy-$\Delta^{14}$-cholenate (IIIa).*—3α,12α-Dihydroxy-$\Delta^{14}$-cholenic acid (700 mg.) was methylated with ethereal solution of diazomethane as usual. Colorless prisms of m. p. 91~92°C. Yield, 500 mg.

*Methyl 3α-Ethoxycarbonyloxy-12α-hydroxy-$\Delta^{14}$-cholenate (IIIb).*—Methyl 3α,12α-dihydroxy-$\Delta^{14}$-cholenate was dissolved in 0.8 ml. of pyridine, 1.0 ml. of ethyl chlorocarbonate was added with cooling in ice-water, and allowed to stand at room temperature for 2 hr. On addition of water, the reaction mixture was extracted with ether, and the extract was washed with water, dried over sodium sulfate and then evaporated to dryness. Crystallization from methanol gave 400 mg. of a pure ethoxycarbonyloxy compound (m. p. 150°C).

Found: C, 70.49; H, 9.34. Calcd. for $C_{28}H_{44}O_6$ (476.66): C, 70.55; H, 9.30%.

It must be pointed out here that under the same condition as methyl apocholate was treated (see above), the conversion of the isomer IIIa into the ethoxycarbonyloxy compound did not occur, almost all the starting material being recovered unchanged. It seemed to be harmful to add dioxane to the reaction mixture.

*Methyl 3α-Ethoxycarbonyloxy-12-keto-$\Delta^{14}$-cholenate (IV).*—Methyl 3α-ethoxycarbonyloxy-12α-hydroxy-$\Delta^{14}$-cholenate (350 mg.) (IIIb) in 50 ml. of acetone was oxidized exactly as the corresponding ester of apocholic acid was done. The oxidation product was recrystallized from methanol. M. p. 144~145°C; yield, 300 mg.

Found: C, 70.95; H, 8.91. Calcd. for $C_{28}H_{42}O_6$ (474.644): C, 70.85; H, 8.91%.

*3α-Hydroxy-$\Delta^{14}$-cholenic Acid (IIa).*—The above-mentioned ketocholenate (250 mg.) was reduced according to the Huang-Minlon method and the crude product was purified as acetyl methyl ester (see below), and hydrolyzed in 2% of alcoholic potassium hydroxide. The free acid was recrystallized from acetone-water. M. p. 171~172°C. $\alpha_D^{14}=+65\pm2°$ (chf.); $\varepsilon_{max}^{EtOH}=2270$ ($\lambda_{max}=210$ mμ).

Found: C, 76.39; H, 10.17. Calcd. for $C_{24}H_{38}O_4$ (374.568): C, 76.96; H, 10.22%.

The physical constants of the corresponding product isomerized from methyl 3$\alpha$-hydroxy-$\Delta^7$-cholenate (Osawa et al.[1]) are as follows: m. p. 161°C, $\alpha_D^{24}=+62.8°$ (chf.).

*Methyl 3α-Hydroxy-$\Delta^{14}$-cholenate (IIb).* — 3$\alpha$-Hydroxycholenic acid above mentioned (20 mg.) was methylated with diazomethane as usual. The ester was recrystallized from methanol and melted at 141~142°C, undepressed on admixture with the sample obtained by Osawa et al.[1]

Found: C, 76.86; H, 10.28. Calcd. for $C_{25}H_{40}O_3$ (388.595): C, 77.27; H, 10.37%.

*Methyl 3α-Acetoxy-$\Delta^{14}$-cholenate (IIc).*—Methyl 3$\alpha$-hydroxy-$\Delta^{14}$-cholenate (200 mg.) was acetylated with a mixture of acetic anhydride (3 ml.) and pyridine (0.2 ml.) as usual.

Recrystallizations from methanol gave a pure sample melting at 106~107°C, $\alpha_D^{14}=+87\pm2°$ (chf.). $\varepsilon_{max}^{EtOH}=2230$ ($\lambda_{max}=209$ m$\mu$).

Found: C, 75.45; H, 9.90. Calcd. for $C_{27}H_{42}O_4$ (430.633): C, 75.30; H, 9.83%.

The physical properties of the product are in fairly good agreement with those of the sample obtained by Osawa et al.[1] (M. p. 110°C; $\alpha_D^{20}=+86.7°$ (chf.)).

Of the experiments mentioned above, the conversion of methyl 3, 12-diketo-$\Delta^{8(14)}$-cholenate as well as the isomerization of methyl 3$\alpha$-acetoxy-$\Delta^7$-cholenate were carried out by one of us (K. Y.) in Fieser's Laboratory during his stay at the Harvard University, U. S. A.

Deep gratitude is due to the memberes of the Microbiological Research Institute, the University of Tokyo, by whom elementary analysis of most of the samples was carried out.

*Department of Biochemistry*
*Tottori University*
*School of Medicine*
*Yonago (F. N. & K. Y.)*

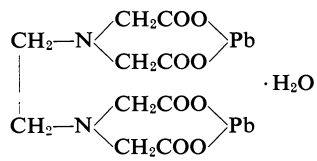
*Laboratory of the Nippon*
*Eiyō Kagaku Co.*
*Katsushika-ku, Tokyo (R. O.)*

# *The Composition and the Solubility Product Constant of Lead(II) Ethylenediaminetetraacetatoplumbate(II)*

By Nobuyuki TANAKA, Minoru KAMADA and Gen SATÔ

(Received October 13, 1960)

Although most metal-ethylenediaminetetraacetate (EDTA) complexes are very soluble in water, a few metal-EDTA complexes which are insoluble or slightly soluble have been reported[1-4]. Schwarzenbach[1] obtained two kinds of slightly soluble compounds when he oxidized cobalt(II)-EDTA complexes with lead dioxide. He concluded from the results of chemical analysis that those compounds had compositions represented by $Pb[CoY]_2 \cdot 7H_2O$ and $Co[CoY]_2 \cdot 10H_2O$. Schmid and Reilley[2] reported that when a mercury electrode was immersed in solutions containing mercury(II)-EDTA complexes, slightly water-soluble materials, such as Hg[HgY] and $Hg_2[HgY]$, were deposited on its surface. Moreover, there have been two reports concerning slightly soluble compounds which are composed of lead(II) and EDTA. One was given by Tanaka, Kato and Tamamushi[3], who suggested, from their preliminary study of the solubility product constant, that the compound was represented as lead(II) ethylenediaminetetraacetatoplumbate(II). The other report was made by Brintzinger, Thiele and Müller[4], who assumed their slightly soluble lead(II)-EDTA compound to be of the formula,



Because of the discrepancy between these two reports, the present authors are concerned in this communication with the reinvestigation on the composition and the solubility product constant of the slightly soluble white crystals which precipitate from the solution containing lead(II) and EDTA.

1) G. Schwarzenbach, *Helv. Chim. Acta*, **32**, 839 (1949).
2) R. W. Schmid and C. N. Reilley, *J. Am. Chem. Soc.*, **78**, 5513 (1956).
3) N. Tanaka, K. Kato and R. Tamamushi, This Bulletin, **31**, 283 (1958).
4) H. Brintzinger, H. Thiele and U. Müller, *Z. anorg. allgem. Chem.*, **251**, 285 (1943).

## Experimental

**Reagents.**—A stock solution of lead(II) nitrate was prepared by dissolving an appropriate amount of lead(II) nitrate of guaranteed reagent grade in distilled water and standardized with the authentic EDTA solution by amperometric titration, using a dropping mercury electrode as an indicator electrode[5]. The EDTA solution was prepared from disodium ethylenediaminetetraacetate (DOTITE 2NA) and standardized amperometrically[5] against the standard copper(II) nitrate solution. A solution of lead(II)-EDTA complex was obtained by mixing lead(II) nitrate and an equivalent EDTA solution. The pH of the solution was adjusted to be 4.8 by addition of sodium carbonate solution. Acetic acid-sodium acetate buffers were prepared with acetic acid and sodium carbonate of guaranteed reagent grade. All the other chemicals used were of guaranteed reagent grade.

The slightly soluble crystals of lead(II) ethylenediaminetetraacetatoplumbate(II) were obtained by following procedure. The lead(II) solution and the lead(II)-EDTA solution were mixed in acetate buffers (0.05 M acetate) of appropriate pH and ionic strength 0.2, when white crystalline compounds appeared in the solution. The solution with the crystals was shaken on the shaker in a thermostat of a given temperature. After being shaken for a week, the crystals were filtered with the aid of suction, and then washed several times with cold water. The crystals were kept in a desiccator at room temperature (15°C).

**Apparatus.**—A manual apparatus similar to that of Kolthoff and Lingane[6] was used for the precise measurement of current-voltage curves. A dropping mercury electrode used as an indicator electrode had an $m$ value of 2.57 mg./sec. and a drop time $\tau$ of 3.52 sec., being measured in a de-aerated acetate buffer solution of pH 4.7 containing 0.1 M potassium nitrate, 0.1 M sodium acetate and 0.01% gelatin at 25°C with open circuit. A saturated calomel electrode (SCE) was used as a reference electrode, which was connected to the electrolytic solution through a Hume and Harris' type salt bridge[7]. The pH of the solution was measured with a Hitachi Model EHP-1 pH meter with glass electrode within the accuracy of 0.02 pH unit.

**Determination of the Concentrations of $Pb^{2+}$ and $PbY^{2-}$ Ions in the Solution.**—Since preliminary experiments showed that when the crystals were dissolved in water all the lead(II) existed partly as $Pb^{2+}$ ions and partly as $PbY^{2-}$ ions, the method for determining these two species in the solution was examined and established.

The current-voltage curves of the mixture of $Pb^{2+}$ and $PbY^{2-}$ ions were obtained in the acetate buffers of pH 4.8 and of ionic strength 0.2 containing acetate ions of 0.05 M to 0.10 M and 0.01% gelatin. In this supporting electrolyte, $PbY^{2-}$ ions do not dissociate appreciably and therefore the diffusion current measured at −0.60 volt vs. SCE must correspond only to the concentration of Pb(II) ions which are not complexed with EDTA. On the other hand, $PbY^{2-}$ ions are thought to dissociate completely in 1 M nitric acid solution. After measuring the current-voltage curves of the mixture of $Pb^{2+}$ and $PbY^{2-}$ ions in 50 ml. solution of the above-mentioned supporting electrolyte of pH 4.8, 5 ml. of 11 M nitric acid was added to the solution drop by drop and the current-voltage curves were measured again. The diffusion current at −0.60 volt vs. SCE corresponds to the concentration of the total concentration of lead(II). The concentration of the $PbY^{2-}$ ions present in the original solution can be obtained from the difference of these two measurements.

A linear relation was obtained between the concentration of $Pb^{2+}$ ions and the diffusion current in the supporting electrolyte of pH 4.8 in the absence

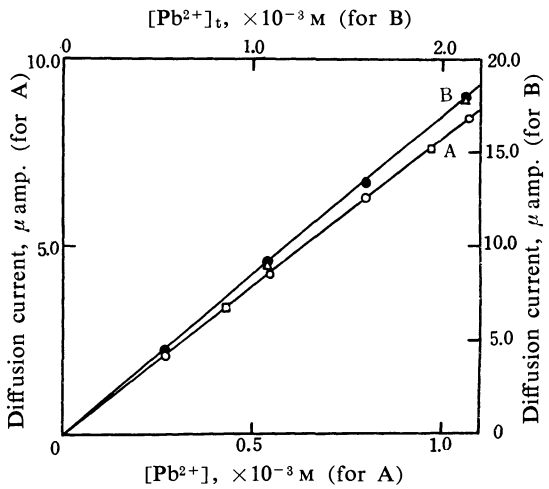



Fig. 1. Relation between the diffusion currents and the concentration of lead(II) ions at 25°C and ionic strength 0.2 before (A) and after (B) the addition of nitric acid: (A) In acetate buffer of pH 4.85 containing 0.08 M acetate without (○) and with $1.177\times10^{-3}$ M $PbY^{2-}$ (□); (B) In 1 M nitric acid containing 0.16 M acetic acid without (●) and with $0.970\times10^{-3}$ M EDTA (△).

Table I. Polarographic determinations of $[Pb^{2+}]$ and $[PbY^{2-}]$

| Species | Concentration added $\times10^3$ mol./l. | Concentration found $\times10^3$ mol./l. | Error % |
|---|---|---|---|
| $[Pb^{2+}]$ | 0.801 | 0.795 | −0.7 |
| $[PbY^{2-}]$ | 0.810 | 0.814* | +0.5 |
| $[Pb^{2+}]_t$ | 1.611* | 1.609 | −0.1 |
| $[Pb^{2+}]$ | 0.494 | 0.495 | +0.2 |
| $[PbY^{2-}]$ | 0.499 | 0.499* | 0.0 |
| $[Pb^{2+}]_t$ | 0.993* | 0.994 | +0.1 |

* Values calculated with the equation, $[Pb^{2+}]_t=[Pb^{2+}]+[PbY^{2-}]$.

5) N. Tanaka, M. Kodama, M. Sasaki and M. Sugino, *Japan Analyst (Bunseki Kagaku)*, **6**, 86 (1957).
6) I. M. Kolthoff and J. J. Lingane, "Polarography," Vol. I, Interscience Publishers, New York (1952), p. 297.
7) D. N. Hume and W. E. Harris, *Ind. Eng. Chem., Anal. Ed.*, **15**, 465 (1943).

and the presence of $PbY^{2-}$ ions. This is indicated in Fig. 1. In Fig. 1 is also shown a linear relation between the lead concentration and the diffusion current which was obtained in 1 M nitric acid solution containing 0.16 M acetic acid in the absence and the presence of EDTA. These relations clearly indicate that the procedure can be used for the determination of the concentrations of $Pb^{2+}$ and $PbY^{2-}$ ions present in the solution. Two of the examples in which $[Pb^{2+}]$ and $[Pb^{2+}]_t$ were determined in the acetate buffers and in the 1 M nitric acid solution respectively are given in Table I with the $[PbY^{2-}]$ calculated from the $[Pb^{2+}]_t$ and $[Pb^{2+}]$.

## Results

**Composition of the Compounds.**—The slightly soluble white crystals which were prepared in the solution of pH 4.50 were dissolved in the above-mentioned acetate buffers of pH 4.8 and the concentrations of $Pb^{2+}$ and $PbY^{2-}$ ions present in the solution were determined by the polarographic method. From the results shown in Table II, the molar ratio

Table II. The molar ratio of $PbY^{2-}$ to $Pb^{2+}$ in the crytals*

| | $[Pb^{2+}]\times10^3$ mol./l. | $[PbY^{2-}]\times10^3$ mol./l. | $[PbY^{2-}]/[Pb^{2+}]$ |
|---|---|---|---|
| A | 0.922 | 0.931 | 1.01 |
| | 0.891 | 0.893 | 1.00 |
| | 0.502 | 0.509 | 1.01 |
| B | 0.786 | 0.793 | 1.01 |
| | 0.304 | 0.306 | 1.01 |

* The crystals were prepared at 25°C in the solutions of ionic strength 0.2 and pH 4.50 (A) and pH 3.53 (B) containing 0.05 M acetate ions.

of $Pb^{2+}$ to $PbY^{2-}$ ions in the solution was determined as one to one. This suggested that the crystals might contain $Pb^{2+}$ and $PbY^{2-}$ ions at the ratio of one to one. The same molar ratio of $Pb^{2+}$ to $PbY^{2-}$ ions was obtained with the crystals prepared at pH 3.53. This excluded any possibility of the existence of such related species as $Pb[PbHY]_2$

The crystals dried at 15°C lost 3.22% of the water when being kept at 160°C in the air oven. Since the theoretical value of water content for monohydrate of lead(II) ethylenediaminetetraacetatoplumbate(II) is 2.56%, the crystals were considered to be of the monohydrate. The discrepancy between the theoretical and the experimental values may be attributed to the small amount of hygroscopic water contained in the crystals.

**Solubility Product Constant of Pb[PbY].**—In aqueous solution, the lead(II) ethylenediaminetetraacetatoplumbate(II), Pb[PbY], is in equilibrium according to the equation,

$$Pb[PbY] \rightleftarrows Pb^{2+} + PbY^{2-} \quad (1)$$

As Pb[PbY] is slightly soluble in water, its solubility product constant ($K_{sp}$) is represented as,

$$K_{sp} = [Pb^{2+}][PbY^{2-}] \quad (2)$$

In the acetate buffers of pH 4.6 containing acetate ions of 0.02 M to 0.08 M the concentrations of $Pb^{2+}$ and $PbY^{2-}$ ions which are determined polarographically are apparent concentrations[8], $[Pb^{2+}]_{app}$ and $[PbY^{2-}]_{app}$, respectively which are represented by the equations,

$$[Pb^{2+}]_{app} = [Pb^{2+}] + [PbOAc^+] + [Pb(OAc)_2] \quad (3)$$

$$[PbY^{2-}]_{app} = [PbY^{2-}] + [PbHY^-] \quad (4)$$

Consequently, the solubility product constant calculated with these concentrations is considered to be the apparent constant, $K_{sp,app}$, which is given by the equation,

$$K_{sp,app} = [Pb^{2+}]_{app}[PbY^{2-}]_{app} \quad (5)$$

Using the overall formation constants of acetatolead(II) complexes $K_{Pb(OAc)_n}$ and the equilibrium constant, $K^H_{PbHY}$, Eqs. 3 and 4 are rewritten as

$$[Pb^{2+}]_{app} = [Pb^{2+}]\{1 + \sum_{n=1}^{2} K_{Pb(OAc)_n}[OAc^-]^n\} \quad (6)$$

$$[PbY^{2-}]_{app} = [PbY^{2-}]\{1 + K^H_{PbHY}[H^+]\} \quad (7)$$

where

$$K_{Pb(OAc)_n} = \frac{[Pb(OAc)_n^{(2-n)+}]}{[Pb^{2+}][OAc^-]^n} \quad (8)$$

$$K^H_{PbHY} = \frac{[PbHY^-]}{[PbY^{2-}][H^+]} \quad (9)$$

With Eqs. 2, 6 and 7, the apparent solubility product constant $K_{sp,app}$ given by Eq. 5 is expressed as

$$K_{sp,app} = K_{sp}\{1 + \sum_{n=1}^{2} K_{Pb(OAc)_n}[OAc^-]^n\} \times \{1 + K^H_{PbHY}[H^+]\} \quad (10)$$

The apparent solubility product constants were obtained at pH 4.6 and ionic strength 0.2 but at various acetate concentrations. The relation between the $K_{sp,app}$ and the acetate concentration is shown in Fig. 2. The solubility product constant ($K_{sp}$) at ionic strength 0.2 was calculated with Eq. 10 from the apparent solubility product constants observed at various acetate concentrations. The results obtained at 25°C are exemplified in Table III. A satisfactory agreement in the $K_{sp}$'s obtained at various acetate concentrations clearly indicates

8) N. Tanaka and K. Kato, This Bulletin, 33, 417 (1960).

TABLE III. $K_{sp,app}$ AND $K_{sp}$ ($\mu=0.2$) OBTAINED AT VARIOUS ACETATE CONCENTRATIONS AT 25°C

| $[OAc^-]$ mol./l. | $[Pb^{2+}]_{app}\times10^3$ mol./l. | $[PbY^{2-}]_{app}\times10^3$ mol./l. | $K_{sp,app}\times10^5$ $(mol./l.)^2$ | $\alpha$* | $K_{sp}\times10^6$ $(mol./l)^2$ |
|---|---|---|---|---|---|
| 0.0621 | 6.07 | 7.69 | 4.67 | 10.54 | 4.37 |
| 0.0564 | 5.74 | 7.20 | 4.13 | 9.56 | 4.27 |
| 0.0452 | 4.08 | 8.42 | 3.44 | 7.66 | 4.43 |
| 0.0443 | 5.04 | 6.68 | 3.37 | 7.51 | 4.43 |
| 0.0434 | 6.64 | 4.73 | 3.14 | 7.34 | 4.23 |
| 0.0248 | 4.04 | 4.84 | 1.96 | 4.45 | 4.34 |

* $\alpha=1+\sum_{n=1}^{2}K_{Pb(OAc)_n}[OAc^-]^n$

TABLE IV. $K_{sp,app}$ AND $K_{sp}$ ($\mu=0.2$) OBTAINED AT DIFFERENT pH's*

| pH | $\frac{K_{sp,app}}{1+\sum_{n=1}^{2}K_{Pb(OAc)_n}[OAc^-]^n}$ $(mol./l.)^2$ | $1+K^{H}_{PbHY}[H^+]$ | $K_{sp}$ $(mol./l.)^2$ |
|---|---|---|---|
| 3.50 | $4.15\times10^{-6}$ | 1.16 | $3.58\times10^{-6}$ |
| 4.67 | $3.63\times10^{-6}$ | 1.01 | $3.59\times10^{-6}$ |

* The measurements were made at 15°C in the solution containing 0.035 M acetate ions.

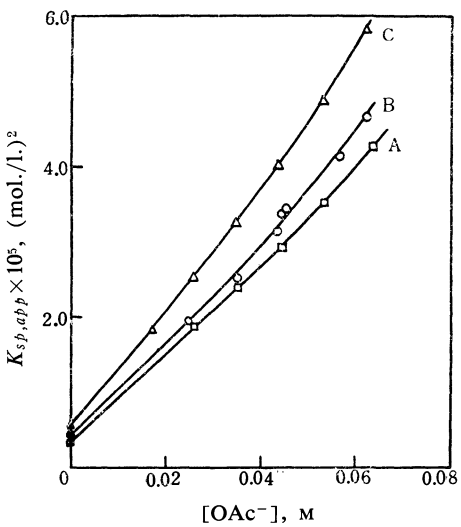



Fig. 2. Relation between the apparent solubility product constant $K_{sp,app}$ and the concentration of acetate ions, determined at pH approximately 4.6, ionic strength 0.2 and at (A) 15°, (B) 25° and (C) 35°C. ■, ● and ▲ indicate the values of $K_{sp}$ calculated with Eq. 10.

the validity of Eq. 10 as well as of the treatment presented in this paper. The validily is further confirmed by the fact that the solubility product constant which was calculated from the $K_{sp,app}$ obtained at pH 3.5 is in satisfactory agreement with the $K_{sp}$ obtained at pH 4.6. One of the examples is shown in Table IV. The formation constants, $K_{PbOAc}$ and $K_{Pb(OAc)_2}$, used in these calculations were those reported by Tanaka and Kato[8]. For the equilibrium constant, $K^{H}_{PbHY}$, the value given by Schwarzenbach, Gut and Anderegg[9] was used after correction for ionic strength[3]. The activity coefficient of hydrogen ion was estimated to be 0.80 at ionic strength 0.2.

In Table V are given the solubility product constants of lead(II) ethylenediaminetetraacetatoplumbate(II) at 15, 25 and 35°C.

TABLE V. THE SOLUBILITY PRODUCT CONSTANT AT IONIC STRENGTH 0.2

| Temp., °C | $K_{sp}$, $(mol./l.)^2$ |
|---|---|
| 15 | $3.54\times10^{-6}$ |
| 25 | $4.34\times10^{-6}$ |
| 35 | $5.72\times10^{-6}$ |

## Discussion

The slightly soluble crystals which contain lead(II) and EDTA at molar ratio of two to one were prepared by Brintzinger, Thiele and Müller[4] by adding an excessive amount of lead(II) nitrate to the EDTA solution. They reported that when the crystals were dissolved in water, the solution reacted with hydrogen sulfide, sulfuric acid, potassium dichromate and potassium iodide in the same fashion as the solution containing only hydrated lead(II) ions did. From this observation, they concluded that all lead(II) present in the solution had characteristics of hydrated lead(II) ions, but not those of lead(II)-EDTA complexes.

9) G. Schwarzenbach, R. Gut and G. Anderegg, *Helv. Chim. Acta*, 37, 937 (1954).

However, if a suitable condition is chosen[10], $PbY^{2-}$ ions give precipitates by the reaction with hydrogen sulfide, although they give no precipitate generally by that reaction. Furthermore, lead sulfate can be formed when $PbY^{2-}$ ions react with sulfuric acid, because $PbY^{2-}$ ions dissociate to a considerable extent in a strong acid solution[11]. Therefore, the formation of the precipitate is no longer a guarantee that lead(II) ions exist in the form of hydrated lead(II) ions.

Some qualitative observations were made also in the present study. When a sufficient amount of potassium dichromate solution was added to the solution which was obtained by dissolving the crystals prepared at pH 4.50, yellow precipitates were observed. After the precipitates were filtered off, sulfuric acid was added to the filtrate when white precipitates appeared in the solution. The yellow precipitates were lead chromate that was formed from the hydrated lead(II) ions present in the solution. The white precipitates, on the other hand, were identified to be lead sulfate which was formed with the lead(II) ions resulting from the dissociation of $PbY^{2-}$ ions in the solution. It should be noted here that lead chromate did not precipitate when potassium dichromate was added to the solution which contained only $PbY^{2-}$ ions. These observations and considerations contradict the conclusion given by Brintzinger et al., but support the interpretation that the solution of the crystals in question contains both $Pb^{2+}$ and $PbY^{2-}$ ions. Consequently, it may be reasonable to conclude that the crystals in question also contain both $Pb^{2+}$ and $PbY^{2-}$ ions. The solubility product constants obtained and the analysis of the composition support the idea that the crystals are lead(II) ethylenediaminetetraacetatoplumbate(II) monohydrate.

10) R. Pribil, *Collection Czechoslov. Chem. Communs.*, **16**, 86 (1951).
11) C. N. Reilley and R. W. Schmid, *Anal. Chem.*, **30**, 947 (1958).

## Summary

The slightly soluble white crystals which form when lead(II) nitrate is added to the lead(II) ethylenediaminetetraacetate complexes in acetate buffer solution have been investigated. From the chemical analysis, it was found that the crystals have the composition of lead(II) ethylenediaminetetraacetatoplumbate(II) monohydrate. The solubility product constant,

$$K_{sp} = [Pb^{2+}][PbY^{2-}]$$

where $Y^{4-}$ means an ethylenediaminetetraacetate anion was determined at ionic strength 0.2 as $3.54\times10^{-6}$(mol./l.)$^2$ at 15°C, $4.34\times10^{-6}$ (mol./l.)$^2$ at 25°C and $5.72\times10^{-6}$ (mol./l.)$^2$ at 35°C.

The authors are grateful to the Ministry of Education for the financial support grated for this research.

*Department of Chemistry*
*Faculty of Science*
*Tohoku University*
*Katahira-cho, Sendai*

# *Infrared Spectra of Acyclic Imides. I. Two Modifications of Diacetamide in the Crystalline State*

By Toyozo UNO and Katsunosuke MACHIDA

(Received October 13, 1960)

There have been two reports concerning the vibrational spectra of diacetamide. Kohlrausch et al.[1] have reported the Raman bands in the liquid state. Orr et al.[2] have measured the infrared spectrum as a solution in chloroform. However, the vibrational frequencies below 1600 $cm^{-1}$ have not yet been assigned. Regarding the infrared spectra for the crystalline state, no literature has been available.

The purpose of this series is to determine and assign the characteristic bands of acyclic imides (R-CONHCO-R′) and to inquire into the relation between the structures and the characteristic bands of the -CONHCO- group. Since diacetamide is the first member of homologs which have the structure R-CONHCO-R′ (R, R′=alkyl), we have taken up the infrared spectra of this compound. In the course of

1) K. W. F. Kohlrausch, A. Pongratz and R. Seka, *Ber.*, **66**, 1 (1933).
2) S. F. D. Orr, P. Sims and D. Manson, *J. Chem. Soc.*, **1956**, 1338.

the measurements in the crystalline state, we have found that there are at least two modifications depending on the recrystallizing solvents. The infrared spectra of these two forms are markedly different from each other in the region 3600 to 400 $cm^{-1}$ for each of the undeuterated and the *N*-deuterated species. A discussion will be made for the origin of the difference between the infrared spectra of these two forms of diacetamide.

## Results and Discussion

**Dimorphism of Diacetamide.** — Crystals of diacetamide recrystallized from ethanol, ether, chloroform and carbon tetrachloride show an identical infrared spectrum with that of crystals from molten liquid. The recrystallization from water, however, gives another crystal form which shows a markedly different infrared spectrum from that of the former. Hereafter, the former and the latter will be called the form A and the form B respectively. The form B seems to be a metastable form, since a slow change to the form A often takes place when it is allowed to stand over several days at room temperature. Although the factors which affect this change are still uncertain, we have found that crystals obtained by the freeze-drying method from an aqueous solution always show the identical infrared spectrum with that of the form A. Owing to this fact, diacetamide-*d* in both the form A and the

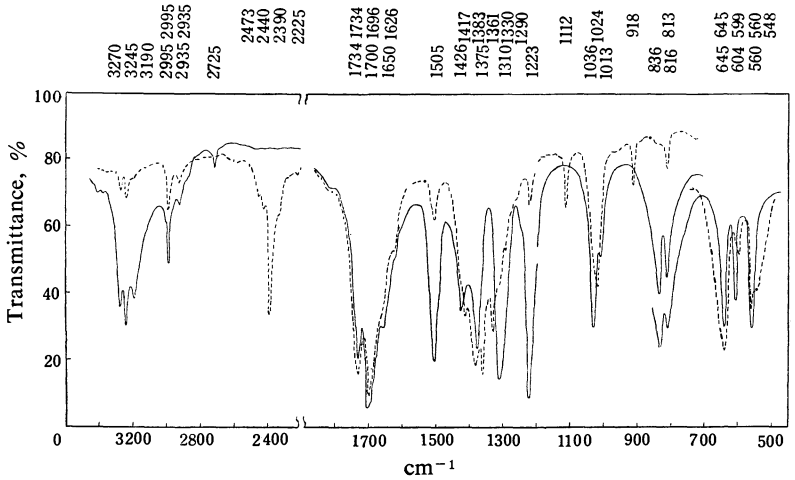



Fig. 1. Infrared spectra of diacetamide (solid line) and diacetamide-*d* (broken line) in the form A*.

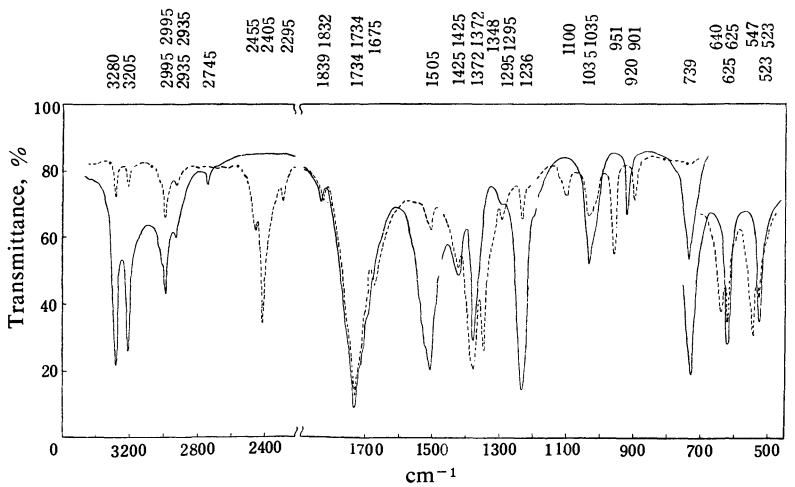



Fig. 2. Infrared spectra of diacetamide (solid line) and diacetamide-*d* (broken line) in the form B*.

* (3600~2300 $cm^{-1}$ and 1480~1200 $cm^{-1}$): hexachlorobutadiene pastes.
(1900~1480 $cm^{-1}$ and 1200~400 $cm^{-1}$): Nujol pastes.

form B has been obtained by the usual exchange reaction with deuterium oxide.

As shown in Figs. 1 and 2, many differences are observed between the infrared spectra of the form A and the form B. In the region 3300 to 3150 $cm^{-1}$, two sharp strong bands are observed for the undeuterated species in the form B while there is a medium triplet for that in the form A. As for the C=O stretching bands, the intensity of the band near 1734 $cm^{-1}$ increases while the band near 1700 $cm^{-1}$ almost disappears on going from the form A to the form B. Furthermore, there is no correspondence of absorption bands between these two forms below 1000 $cm^{-1}$. However, several correspondences of absorption bands are also observed between these two forms. Both the form A and the form B of the undeuterated species show a strong band near 1500 $cm^{-1}$ which disappears on deuteration. A band near 1035 $cm^{-1}$ is observed for each of these two forms of the undeuterated and the *N*-deuterated species.

To interpret these observations, the structural or the rotational isomerism must be considered since the difference only in crystal lattice can hardly give rise to such a remarkable spectral difference as is seen between the form A and the form B of diacetamide. Isoimide (R-C(=NH)-O-CO-R′), a structural isomer of imide (R-CO-NH-CO-R′), has been proposed to correspond to an unstable isomer (m.p. 68~69°C) of *N*-butyrylbenzamide (m.p. 104°C) and a slow change of this unstable form to the stable one has been reported[3]. Another author[4] has regarded it as an intermediate in the pyrolytic formation of acyclic imides from primary amides.

As for the unstable form of diacetamide (the form B), the C=O stretching frequency (1734 $cm^{-1}$) is as high as those of fatty acid esters. The strong band at 1236 $cm^{-1}$ seems to correspond to the C-O-C antisymmetric stretching band of acetic acid esters. These features favor the isoimide structure which contains the group $-O-CO-CH_3$ for the form B. However, the disappearance of the band at 1236 $cm^{-1}$ on deuteration cannot be explained by the assignment of this band to the C-O-C antisymmetric stretching vibration of the isoimide structure, because *N*-deuterated isoimide has also the group $-O-CO-CH_3$ and must show a similar strong band in this region. On the other hand, if the imide structure is assumed, the above fact can be reasonably explained in analogy with the case of the amide III band of monosubstituted amides since a considerable coupling between the C-N stretching modes and the N-H deformation mode is expected for the imide structure.

On the other hand, the imide structure of diacetamide in the form A has been proved by the X-ray diffraction study[5], which has revealed that every two molecules of diacetamide form a ring dimer by means of a pair of the hydrogen-oxygen hydrogen bond. The oxygen atom not involved in the hydrogen bond is in the trans position with respect to the hydrogen atom as shown in Fig. 3. Thus, the

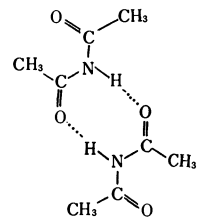


Fig. 3. Dimeric structure of diacetamide in the form A.

isoimide structure has been ruled out from both of these two forms. These facts suggest that the difference in the infrared spectra between the form A and the form B of diacetamide is due to the rotational isomerism among imide structures.

**Internal Rotation in the Imide Structure.**—It has been well established that there are marked differences in the characteristic bands between the trans and the cis configurations for monosubstituted amides[6,7]. In the case of imides, the presence of two (O=C)-N links differentiates three configurations shown in Fig. 4 among the planar structure of the -CONHCO- group. However, possibility for several non-planar structures must not be neglected in this case since the C-N bond order of the (O=C)-N

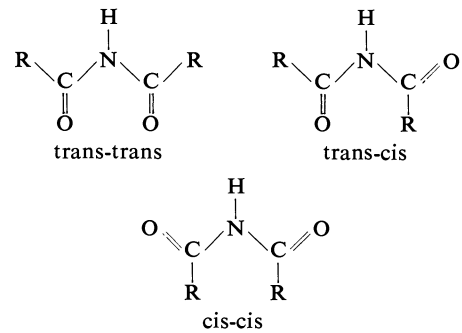



Fig. 4. Planar configurations of imide structure.

3) P. Dunn, E. A. Parkes and J. B. Polya, *Rec. trav. chim.*, **71**, 680 (1952).
4) D. Davidson and M. Karten, *J. Am. Chem. Soc.*, **78**, 1066 (1956).
5) T. Watanabé and K. Osaki, unpublished.
6) T. Miyazawa, T. Shimanouchi and S. Mizushima, *J. Chem. Phys.*, **24**, 408 (1956).
7) T. Miyazawa, *J. Mol. Spectroscopy*, **4**, 155 (1960).

link may be less for imides than for amides. Since there is the close similarity between the amide and the imide structure, it is reasonably expected that the infrared spectra of those isomers whose differences are in the configuration of the -CONHCO- group may be presumably different from one another. Consequently, if acyclic imides take the configuration other than the cis-cis one which can be regarded approximately as the configuration of five- or six-membered cyclic imides, the infrared spectra of the former will be markedly different from those of the latter. Comparison of the infrared spectrum of succinimide[8,9] with those of the form A and the form B of diacetamide suggests that this is the case.

Monosubstituted amides with the trans -CONH- group show the amide II band in the region 1600 to 1450 $cm^{-1}$ while those with the cis -CONH- group does not. This simple but well-known rule seems to be applicable to the -CONHCO- group in somewhat modified form. For instance, succinimide[8,9] and glutarimide[10], which are in the cis-cis configuration, exhibit no strong band in the region 1600 to 1450 $cm^{-1}$ while the form A of diacetamide, which is in the trans-cis configuration, show a strong band which disappears on deuteration near 1500 $cm^{-1}$. Thus, it is seen that a distinguished band analogous to the amide II band of monosubstituted amides arises from the -CONHCO- group provided that the trans -CONH- group is contained in it. The form B of diacetamide also shows the band in question near 1500 $cm^{-1}$ while that of diacetamide-*d* does not. Consequently, it seems quite probable that the trans -CONH- group is contained in the -CONHCO- group of diacetamide not only in the form A but also in the form B. The spectral difference between these two forms may be due to the difference in the configuration of the remaining C=O bond with respect to the N-H bond in the -CONHCO- group.

**The Bands in the Potassium Bromide Region.** —Another information concerned with the symmetry of a molecule can be obtained from the behavior of the absorption bands on deuteration in the potassium bromide region. From the analogy to monosubstituted amides, the band at 739 $cm^{-1}$ observed for the form B is assigned to the N-H deformation mode perpendicular to the plane of the C-N-C link. This band shifts to 547 $cm^{-1}$ on deuteration. The corresponding N-H deformation vibration in the form A is reasonably assigned to the broad doublet (836 and 816 $cm^{-1}$) which disappears on deuteration. The splitting of this band may result from Fermi resonance with an overtone or a combination tone of some lower fundamentals. For the *N*-deuterated species, the alternative N-D deformation band appears at 645 $cm^{-1}$, where the band splitting is not observed. Since these N-H (or N-D) deformation frequencies are within the region where the usual C=O deformation frequencies occur, the more or less coupling of the N-H or the N-D deformation mode in question with appropriate C=O deformation modes can be expected as long as the condition of the same symmetry is satisfied. However, if the molecule has a plane of symmetry or a two-fold axis along the N-H or the N-D bond, at least two C=O deformation modes are free from the possibility of such a coupling with the N-H or the N-D deformation mode. Thus, the number of the C=O deformation bands which undergo no frequency shift on deuteration may be used to estimate the symmetry of the molecule. The bands between 700 and 450 $cm^{-1}$ observed for the undeuterated species should be attributed to the C=O deformation modes. Regarding the form A, three bands are observed at 645, 604 and 560 $cm^{-1}$ for the undeuterated species. The change of these bands on deuteration is such that the band at 645 $cm^{-1}$ is overlapped by the N-D deformation band without any apparent frequency shift, the band at 604 $cm^{-1}$ shifts to 599 $cm^{-1}$ and a shoulder not well resolved from the band at 560 $cm^{-1}$ appears near 548 $cm^{-1}$. This fact may be taken as indicating that the band at 560 $cm^{-1}$ observed for the undeuterated species is the overlap of two bands, one of which arises from a vibrational mode belonging to the same symmetry species as the N-H deformation mode and the other does not. Thus, except for the band at 645 $cm^{-1}$ whose frequency shift on deuteration is uncertain owing to the overlap of the broad N-D deformation band, there is at least one band undergoing no frequency shift on deuteration. Therefore, a molecular structure with no symmetry is improbable for the form A. In fact, as an approximation, the planar structure (the presence of a plane of symmetry) has been shown by the X-ray diffraction study[5].

On the other hand, two bands are observed at 625 and 523 $cm^{-1}$ for the undeuterated species of the form B, both of which undergo no frequency shift on deuteration. The *N*-deuterated species shows, besides these bands, a broad band near 640 $cm^{-1}$. Namely, the high-frequency shift of one component of the overlapped band at 625 $cm^{-1}$ for the undeuteuterated species takes place on deuteration. Thus, there are two bands which do not shift

8) J. Chouteau, *Bull. soc. chim. France*, (5) **20**, 1149 (1953).
9) A. W. Baker, *J. Phys. Chem.*, **61**, 453 (1957).
10) R. L. Frank and J. B. McPherson, Jr., *J. Am. Chem. Soc.*, **71**, 1389 (1949).

TABLE I. DEFORMATION FREQUENCIES IN THE KBr REGION OF THE FORM A AND THE FORM B OF DIACETAMIDE

| Crystal form | Absorption frequencies (in $cm^{-1}$) Undeuterated species | *N*-deuterated species | Assignments | Symmetry species |
|---|---|---|---|---|
| A | 836, 816 m** | | N-H out-of-plane | A'' |
| | | 645 m | N-D out-of-plane | A'' |
| | 645 m | (645)* | C=O in-plane | A' |
| | 560 m | 560 m | | |
| | 604 w | 599 w | C=O out-of-plane | A'' |
| | (560) | 548 w, sh. | | |
| B | 739 m | | N-H out-of-plane | $B_2$ |
| | | 547 m | N-D out-of-plane | $B_2$ |
| | 625 m | 625 m | C=O in-plane | $A_1$ or $B_1$ |
| | 523 m | 523 m | | |
| | (625) | | C=O out-of-plane | $B_2$ |
| | | 640 w, sh. | | |

* Parentheses indicate the overlapping frequencies.
** m : medium, w : weak, sh. : shoulder

on deuteration and a plane of symmetry or a two-fold axis is necessarily required for this form. As suggested in the previous section, if the configuration of a C=O bond with respect to the N-H bond is not far from the trans one, the other C=O bond must also take the trans configuration with respect to the same N-H bond. Any other configuration with a trans -CONH- group has no symmetry except for the trans-cis one which has already been given to the form A. The fact that only one band shifts on deuteration is consistent with the trans-trans planar structure which has the symmetry $C_{2v}$, where only one C=O deformation mode belongs to the same symmetry species ($B_2$) as the N-H out-of-plane deformation mode.

These considerations made it possible to assign all the bands observed in the potassium bromide region to appropriate C=O and N-H (or N-D) deformation modes for both the form A and the form B of diacetamide and diacetamide-*d*. These results were summarized in Table I. Thus, it seems reasonable at least qualitatively that the configurations of the -CONHCO- group in the form A and the form B are not far from the trans-cis and the trans-trans ones respectively. This conclusion may be confirmed by the application of the product rule for the isotopic molecules.

**The Product Rule.**—The product rule for the out-of-plane vibrations for each of the trans-cis and the trans-trans planar structure is represented by the equations

$$\frac{\Pi\nu(A'')}{\Pi\nu'(A'')}=\left(\frac{m_D M I_x I_z}{m_H M' I'_x I'_z}\right)^{1/2} \quad (1)$$

and

$$\frac{\Pi\nu(B_2)}{\Pi\nu'(B_2)}=\left(\frac{m_D M I_x}{m_H M' I'_x}\right)^{1/2} \quad (2)$$

respectively[11], where the primes indicate the *N*-deuterated species, $\nu$'s are the observed frequencies, the multiple products are taken over those belonging to the symmetry species indicated in the parentheses, $m_H$ and $m_D$ are the masses of hydrogen and deuterium atoms respectively, $M$ is the total mass of the molecule, $I_x$ and $I_z$ are the moments of inertia with respect to the principal axes in the molecular plane. As for the trans-trans planar structure, Eq. 2 shows that the principal moment of inertia with respect to the two-fold axis ($I_z$) is not related to the $B_2$ species. In calculation of the moments of inertia, the bond lengths were assumed to be the same as those used in the normal vibration calculation of *N*-methylacetamide[12], and all the bond angles were assumed to be 120°. The observed and the theoretical values are shown in Table II, where the out-of-plane frequencies other than those shown in Table I were assumed to be unchanged on deuteration. As the N-H out-of-plane deformation frequency of the form A, the mean value (826 $cm^{-1}$) of the listed frequencies was used. As seen from Table II, the agreement between the observed and the theoretical values is rather reasonable, since the uncertainly in frequencies due to the broadening and the

11) E. B. Wilson, Jr., J. C. Decius and P. C. Cross, "Molecular Vibrations", McGraw-Hill, New York (1955), p. 183.
12) T. Miyazawa, T. Shimanouchi and S. Mizushima, *J. Chem. Phys.*, **29**, 612 (1958).

Table II. Product rule for the out-of-plane frequencies of diacetamide

| Crystal form | Configuration of the -CONHCO- group | Symmetry species | Product rule ratio ( undeuterated species theoretical / *N*-deuterated species observed ) |
|---|---|---|---|
| A | trans-cis | A'' | 1.38 / 1.34 |
| B | trans-trans | $B_2$ | 1.38 / 1.32 |

overlapping of bands may result in deviations up to 4%. These results give supports to the assignments of the bands in the potassium bromide region as well as the planar structures of the form A and the form B of diacetamide in the crystalline state. On the basis of these structures, the bands in the sodium chloride region will be discussed in successive papers.

## Experimental

**Materials.** — Diacetamide was prepared by the acetylation of acetamide with acetic anhydride in the presence of ammonium chloride[13], distilled in vacuo and recrystallized twice from ether. Then each of two crystal forms was obtained as follows. The form A was crystallized from ether. M.p. 81°C. (Found: C, 47.43; H, 7.217; N, 13.56. Calcd. for $C_4H_7NO_2$: C, 47.52; H, 6.98; N, 13.86%). Recrystallization from water, at 30~35°C under the reduced pressure (5~10 mmHg) produces the form B. M.p. 81°C. (Found: C, 47.43; H, 7.08; N, 13.86%). The form B was identified before and after the elementary analyses by the infrared spectra.

Diacetamide-*d* was prepared by the exchange reaction with deuterium oxide. The form A was obtained when deuterium oxide was removed by the freeze-drying method with the mixture of acetone and dry ice at 1~2 mmHg. The form B was obtained when deuterium oxide was removed under the same conditions as those applied to obtain the form B of the undeuterated species.

**Measurements.** — The Koken DS-301 infrared spectrophotometer was used with sodium chloride (3600 to 600 $cm^{-1}$) or potassium bromide (900 to 400 $cm^{-1}$) prisms. Ammonia and polystyrene were used for the frequency calibration. The errors were within 5 $cm^{-1}$ in 3600~2000 $cm^{-1}$, 2 $cm^{-1}$ in 2000~1200 $cm^{-1}$ and 1 $cm^{-1}$ in 1200~400 $cm^{-1}$. The measurements of infrared spectra were carried out for hexachlorobutadiene (3600 to 1200 $cm^{-1}$) or Nujol (2300 to 400 $cm^{-1}$) pastes. A current of dry nitrogen gas was introduced into the spectrophotometer in order to exclude the effect of $CO_2$ absorption from the bands in the region 2400 to 2300 $cm^{-1}$ for the *N*-deuterated species.

13) D. Davidson and M. Karten, *J. Am. Chem. Soc.*, **78**, 1068 (1956).

## Summary

Two crystal forms have been found for diacetamide (the form A and the form B). Infrared spectra of these two forms of diacetamide and diacetamide-*d* have been measured in the region 3600 to 400 $cm^{-1}$ and many differences of absorption bands have been observed. It has been shown that these differences of absorption bands can be explained to result from rotational isomerism. The trans-trans planar structure of the -CONHCO- group has been proposed to correspond approximately to the molecular structure of the unstable form (the form B) of diacetamide. The frequency shifts of absorption bands on deuteration in the potassium bromide region has been discussed to give support to this interpretation. An assignment has been given to each absorption band in the potassium bromide region for the form A and the form B of diacetamide and diacetamide-*d*.

The authors express their thanks to Dr. T. Miyazawa and Dr. K. Nakamura for their kind advice throughout this work. Thanks are also due to Miss I. Uchida for technical assistance and to Dr. K. Hozumi and his associates for elementary analyses.

*Faculty of Pharmacy*
*Kyoto University*
*Sakyo-ku, Kyoto*

# *Infrared Spectra of Acyclic Imides. II. The Characteristic Absorption Bands of Saturated Acyclic Imides in the Crystalline State*

By Toyozo UNO and Katsunosuke MACHIDA

(Received October 13, 1960)

The infrared spectra of four saturated aliphatic acyclic imides and their *N*-deuterated compounds in the crystalline state have been measured and compared with those of diacetamide and diacetamide-*d* reported previously[1]. The crystals of these higher homologs show the same characteristic absorption bands as those of the form B of diacetamide. This suggests that in the crystalline state, these higher homologs take a configuration similar to that in the form B of diacetamide. Vibrational assignments have been given to the characteristic bands in the sodium chloride region in analogy with the case of monosubstituted amides[2,3]. The influence of an adjacent carbonyl group on the characteristic frequencies of the -CONH- group has been discussed. The present result gives support to the trans-trans planar structure for the crystals of these higher homologs as well as for the form B of diacetamide.

## Results and Discussion

The infrared spectra of these acyclic imides and their absorption frequencies are shown in Fig. 1 [4] and Table I[4]. As seen from Fig. 1, the infrared spectra of the crystals of those

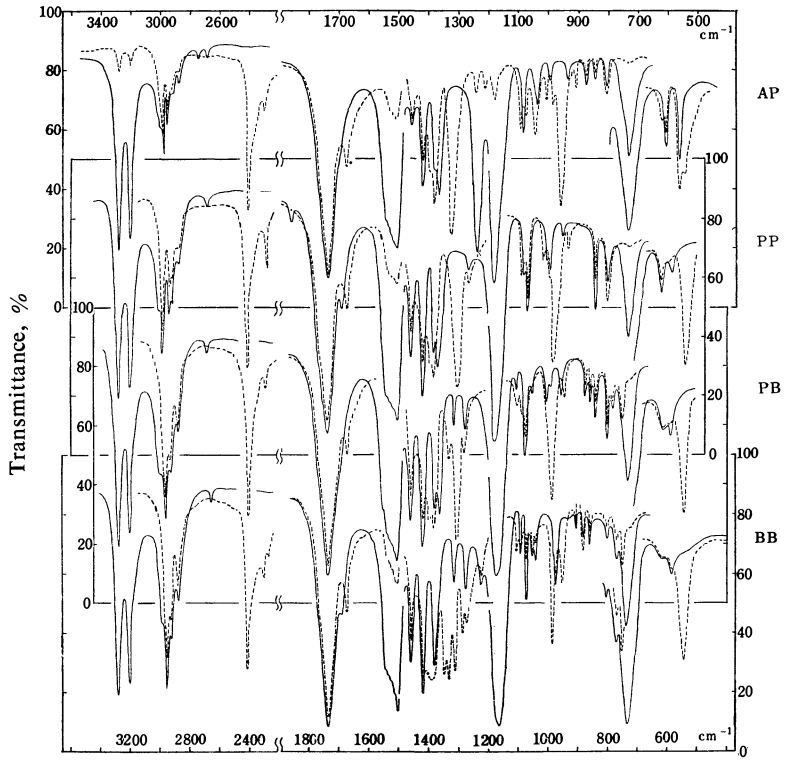



Fig. 1. Infrared spectra of higher homologs of diacetamide in the crystalline state.
Solid line: the undeuterated species, broken line: the *N*-deuterated species.
(3600~2300 $cm^{-1}$ and 1480~1200 $cm^{-1}$) hexachlorobutadiene pastes
(1900~1480 $cm^{-1}$ and 1200~400 $cm^{-1}$) Nujol pastes.

1) T. Uno and K. Machida, This Bulletin, **34**, 545 (1961).
2) T. Miyazawa, T. Shimanouchi and S. Mizushima, *J. Chem. Phys.*, **24**, 408 (1956); ibid., **29**, 611 (1958).
3) T. Miyazawa, *J. Chem. Soc. Japan, Pure Chem. Sec.*, (*Nippon Kagaku Zasshi*), **77**, 171, 321, 526, 619 (1956).
4) Abbreviations used in Fig. 1 and Tables I—IV are: AA: diacetamide, AP: *N*-acetylpropionamide, PP: dipropionamide, PB: *N*-propionyl-*n*-butyramide, BB: di-*n*-butyramide.

TABLE I. INFRARED ABSORPTION FREQUENCIES OF ACYCLIC IMIDES (in $cm^{-1}$)

| Undeuterated species | | | | *N*-Deuterated species | | | |
|---|---|---|---|---|---|---|---|
| AP | PP | PB | BB | AP | PP | PB | BB |
| 3280 vs | 3280 vs | 3280 vs | 3280 vs | 2978 m | 2992 s | 2960 s | 2958 s |
| 3205 vs | 3200 vs | 3205 vs | 3200 vs | 2960 w | 2948 w | 2939 m, sh. | 2935 m, sh. |
| 3000 w, sh. | 3005 w, sh. | 3000 w, sh. | 2995 w, sh. | 2920 w, sh. | | | |
| 2978 m | 2992 s | 2960 s | 2958 s | 2875 w | 2875 w, sh. | 2875 w | 2875 w |
| 2960 w | 2948 m | 2939 m | 2935 w, sh. | 2410 s | 2416 s | 2415 s | 2410 s |
| 2920 w, sh. | 2923 w | | | 2300 w | 2283 m | 2290 w | 2300 w |
| 2875 w | 2875 w | 2875 w | 2875 w | | | | 2283 w |
| 2750 w | | | | 1734 vs | 1736 vs | 1737 vs | 1733 vs |
| 2690 w | 2693 w | 2695 w | 2678 w | 1674 w | 1673 w | 1674 w | 1673 w |
| | 1860 w | | | 1458 w | 1459 m | 1460 m | 1460 m |
| 1734 vs | 1736 vs | 1737 vs | 1733 vs | 1419 m | 1420 m | 1423 m | 1415 s |
| | 1690 w | | 1695 w, sh. | 1405 m, sh. | 1395 m, sh. | 1404 m, sh. | |
| 1504 vs, br. | 1504 vs, br. | 1507 vs, br. | 1503 vs, br. | 1381 s | 1380 s | 1380 s | 1385 s, br. |
| 1458 w | 1459 m | 1460 m | 1460 m | | | | 1348 m |
| 1419 m | 1420 s | 1423 s | 1415 s | 1329 s | | 1334 w | 1332 m |
| 1380 m, sh. | 1384 m | 1380 m | 1378 m | | 1304 s | 1307 s | 1314 m |
| 1370 s | 1367 s | 1367 s | | | | 1284 w | 1285 w |
| | | 1311 w | 1306 w | | | | 1275 w |
| | | 1275 w | 1272 w | 1212 w | 1263 w | | 1230 w |
| 1240 vs, br. | 1263 w | | 1230 w | | | 1105 w | 1112 w |
| 1180 vs, br. | 1180 vs, br. | 1180 vs, br. | 1167 vs, br. | 1090 m | 1088 w | | 1098 w |
| | 1080 w, sh. | 1105 w | 1098 m | 1073 w | 1075 m | 1075 m | 1076 w |
| 1081 m | 1075 m | 1075 m | 1076 m | 1048 m | | | 1055 w |
| | | 1050 w | 1055 w | 1008 w | 1016 w | | 1044 w |
| 1035 w | 1009 w | 1007 w | 1044 w | 988 w | 994 w, sh. | | |
| 994 w | 994 w | 994 w, sh. | | 969 m | 986 m | 987 m | 985 m |
| | 955 w | 964 w | 971 m | | 934 w | 945 w | 954 w |
| 938 w | | | 903 w | 914 w | | | 903 w |
| 879 w | | 879 w | 880 w | 879 w | | 879 w | 880 w |
| | | 861 w | 862 w | | | 861 w | 862 w |
| 845 w | 843 m | 842 w | | 845 w | 843 w | 842 w | |
| 808 w | 806 w | 807 m | 802 w | 808 w | 806 m | 807 w | 802 w |
| | | 787 w | 770 w, sh. | | | 787 w | 770 w |
| 734 m, br. | 732 m, br. | 733 m, br. | 733 m, br. | | | 752 w | 750 w |
| 609 w | 614 w, br. | 616 w | 620 w, sh. | 620 w | | | |
| 559 m | 590 w | 590 w, br. | 589 w, br. | 609 w | 612 w, br. | 610 w, br. | 620 w, sh. |
| | | | | 559 m | 590 w, sh. | 586 w, sh. | 580 w, sh. |
| | | | | 541 m, sh. | 540 m | 542 m | 542 m |

vs : very strong, s : strong, m : medium, w : weak, sh. : shoulder, br. : broad

higher homologs of diacetamide measured in the present study are quite similar to that of the form B of diacetamide, so that these crystals will also be called form B hereafter. Since both acyclic imides R-CONHCO-R′ and monosubstituted amides R-CONH-R′ contain the -CONH- group, their infrared spectra are expected to be closely related with each other. In fact, these acyclic imides and *N*-deuterated acyclic imides exhibit a number of absorption bands whose frequencies and intensities correspond to those of the characteristic bands of monosubstituted amides and their *N*-deuterated compounds[2,3]. Thus, it appears that similar vibrational modes are responsible for the corresponding absorption bands of acyclic imides and monosubstituted amides. The characteristic frequencies and their vibrational assignments of these imides are shown in Table II[4] along with those of *N*-methylacetamide[2] for comparison. Detailed discussion for each characteristic frequency is as follows.

**Imide I (Carbonyl Stretching) Band.**—All the undeuterated and *N*-deuterated species of these acyclic imides show a strong band clearly due to the C=O stretching vibration near 1735 $cm^{-1}$.

TABLE II. THE CHARACTERISTIC FREQUENCIES OF ACYCLIC IMIDES (in $cm^{-1}$)

Undeuterated species

| | AA | AP | PP | PB | BB | MA* |
|---|---|---|---|---|---|---|
| Imide I | | | | | | |
| (sym.) | 1734 | 1734 | 1736 | 1737 | 1733 | 1653 |
| (antisym.) | — | — | 1690 | — | 1695 | |
| Imide II | 1505 | 1504 | 1504 | 1507 | 1503 | 1567 |
| C-N-C sym. stretch. | 1295 | — | 1263 | — | 1230 | — |
| Imide III | 1236 | 1240 | | | | 1299 |
| | | 1180 | 1180 | 1180 | 1167 | |
| Imide V | 739 | 734 | 732 | 733 | 733 | 725 |
| Imide IV | 625 | 609 | | | | |
| | 523 | 559 | 614 | 616 | 620 | 627 |
| | | | 590 | 590 | 589 | |
| Imide VI | (625)** | (609) | | | | 600 |

*N*-Deuterated species

| | AA | AP | PP | PB | BB | MA |
|---|---|---|---|---|---|---|
| Imide I | | | | | | |
| (sym.) | 1734 | 1734 | 1736 | 1737 | 1733 | 1642 |
| (antisym.) | 1675 | 1674 | 1673 | 1674 | 1673 | |
| Imide II′ | 1348 | | | | 1348 | |
| | | 1329 | | 1334 | 1332 | 1475 |
| | | | 1304 | 1307 | 1314 | |
| C-N-C sym. stretch. | 1295 | — | 1263 | — | 1230 | — |
| Imide III′ | 951 | 969 | 986 | 987 | 985 | 960 |
| Imide V′ | 547 | 541 | 540 | 542 | 542 | 510 |
| Imide IV | 625 | 609 | ? | ? | ? | 627 |
| | 523 | 559 | | | | |
| Imide VI′ | 640 | 620 | ? | ? | ? | (627) |

* The corresponding amide characteristic frequencies of *N*-methylacetamide (liquid)[2].

** Parentheses indicate the overlapping frequencies.

TABLE III. THE C-H DEFORMATION FREQUENCIES OF ACYCLIC IMIDES (in $cm^{-1}$)

| | AA | AP | PP | PB | BB |
|---|---|---|---|---|---|
| $CH_3(\alpha)$* asym. | 1425 | 1419 | | | |
| $CH_3(\alpha)$ sym. | 1372 | 1380 | | | |
| $CH_2(\alpha)$ bend. | | (1419)** | 1420 | 1423 | 1415 |
| $CH_2(\beta)$ bend. | | | | 1460 | 1460 |
| $CH_3(\beta)$ or $(\gamma)$ asym. | | 1458 | 1459 | (1460) | (1460) |
| $CH_3(\beta)$ or $(\gamma)$ sym. | | (1380) | 1384 | 1380 | 1378 |

* $\alpha$, $\beta$ and $\gamma$ indicate the position of the methyl or the methylene group with respect to the carbonyl group.

** Parentheses indicate the overlapping frequencies.

Such high C=O frequencies have been reported[5-8] for a number of imides and explained as resulting from the appreciable double bond character of the imide C=O bond. To distinguish the C=O stretching bands of imides from the amide I band whose lower frequencies indicate the decreased double bond character of the amide C=O bond, we may call the former the imide I bands. In contrast with amides, imides may show two bands in the 6$\mu$ region as many other dicarbonyl compounds do. In fact, the duplication of the C=O stretching band of several diacyl derivatives of aromatic amines have been reported and attributed to a vibrational coupling between two C=O stretching modes[6]. In general, an acyclic imide can exhibit the symmetric and the antisymmetric imide I band if the molecule

5) B. Witkop and J. B. Patrick, *J. Am. Chem. Soc.*, **74**, 3861 (1952).
6) R. A. Abramovitch, *J. Chem. Soc.*, **1957**, 1413.
7) J. F. Grove, P. W. Jeffs and D. W. Rustidge, ibid., **1956**, 1956.
8) S. F. D. Orr, P. Sims and D. Manson, ibid., **1956**, 1338.

has a symmetry operation permuting those two C=O bonds. Furthermore, if the transition moment of the stretching vibration of each C=O bond is nearly parallel to the bond itself, the intensity ratio of the antisymmetric imide I band to the symmetric one will increase with the angle between those two equivalent C=O bonds. In the present study, besides the above mentioned strong band near 1735 $cm^{-1}$, the undeuterated species of some imides show a weak band near 1700 $cm^{-1}$, which disappears on deuteration. On the other hand, a weak band near 1675 $cm^{-1}$ is observed for all the *N*-deuterated acyclic imides in form B regardless of the presence of the band near 1700 $cm^{-1}$ for the corresponding undeuterated species. Weak as it is, the band near 1675 $cm^{-1}$ must be a fundamental one because it is unlikely to expect a constant overtone or combination frequency in this region throughout all the *N*-deuterated species of these acyclic imides. Thus, a similar fundamental frequency for the undeuterated species can be expected and it is quite probable that the band near 1700 $cm^{-1}$ actually exists for all the undeuterated species of these acyclic imides although in some cases this band is covered with the shoulder of the strong band near 1735 $cm^{-1}$. These considerations lead to a reasonable assignment of the above bands to the symmetric and the antisymmetric C=O stretching vibration on the basis of the trans-trans planar structure proposed for the form B in the preceding paper[1]. Thus, the antisymmetric imide I band (near 1700 $cm^{-1}$) is expected to be weak, just as is observed, since in this configuration two C=O bonds are nearly parallel to each other. The low-frequency shift of this weak band on deuteration may be due to some contribution of the N-H deformation mode, whereas the strong symmetric imide I band (near 1735 $cm^{-1}$) does not shift on deuteration because there is no coupling between the C=O symmetric stretching and the N-H in-plane deformation mode. As will be discussed later, the antisymmetric imide I band near 1700 $cm^{-1}$ is considered to combine with the band near 1500 $cm^{-1}$ and to give rise to a combination band near 3200 $cm^{-1}$.

**Imide II and II′ Bands.**—Detailed discussions have been given to the band near 1500 $cm^{-1}$ observed for the form A and the form B of diacetamide[1]. All higher homologs of diacetamide in the present study show a similar band near 1505 $cm^{-1}$ which disappears on deuteration. On the basis of the trans-trans planar structure, this band is assigned to the vibration in which the coupling between the C-N-C antisymmetric stretching and the N-H in-plane deformation mode is considerable, and will be called the imide II band hereafter. As seen from the frequency difference between the imide I and the amide I bands, the double bond character of the C=O bond is greater for acyclic imides than for monosubstituted amides. Consequently, the C-N bond order of acyclic imides should be less than that of monosubstituted amides, and it is quite reasonable that the imide II frequency of acyclic imides in the trans-trans configuration is lower than the amide II frequency of monosubstituted amides in the trans configuration, since the C-N stretching force constant is one of the important factors which determine the imide II and the amide II frequency. Further studies such as normal vibration calculations are necessary for a more detailed elucidation of the nature of the imide II band since the structural differences between the –CONH– and the –CONHCO– group must be taken into account.

As is the case of the C=O stretching vibrations, the trans-trans configuration of the –CONHCO– group must exhibit the C-N-C symmetric stretching vibration as well as the antisymmetric one. Since there is no possibility of remarkable vibrational coupling, which would give rise to the high imide II frequency for the antisymmetric vibration, the C-N-C symmetric stretching frequency is expected to be considerably lower than the imide II frequency. In fact, diacetamide, dipropionamide and di-*n*-butyramide show a weak band due probably to the C-N-C symmetric stretching mode at 1295, 1263 and 1230 $cm^{-1}$ respectively. These bands do not shift on deuteration. Since the angle between two C-N bonds in the imide group is nearly 120°, the vibrational transition moment of the C-N-C symmetric stretching mode is expected to be so small as to result in these weak bands.

The form B of diacetamide-*d* shows a band at 1348 $cm^{-1}$, which clearly corresponds to the amide II′ band of *N*-deuterated monosubstituted amides. This band, which may be called the imide II′ band, is assigned to the C-N-C antisymmetric stretching mode. It is obvious that the difference in the C-N bond order between imides and amides contributes to the frequency difference between the imide II′ and the amide II′ bands. As for the *N*-deuterated species of the higher homologs of diacetamide, the imide II′ band appears in the region 1350 to 1300 $cm^{-1}$, taking somewhat complicated features. In this case, there are several vibrational modes belonging to $B_2$ species in this region and they may contribute to the imide II′ band in various ways. This effect results in the splitting of the imide II′ band in the case of di-*n*-butyramide-*d*. The antisymmetric $CH_2$ wagging modes may be examples of such participating vibrational modes.

**Imide III and III′ Bands.** — As previously reported[1], the form B of diacetamide shows a strong band at 1236 $cm^{-1}$. *N*-Acetylpropionamide also shows an analogous band at 1240 $cm^{-1}$ together with another strong band at 1180 $cm^{-1}$. The other three higher homologs containing no acetyl group show only one strong band near 1180 $cm^{-1}$. All these bands disappear on deuteration and an alternative medium band appears in the region 990 to 950 $cm^{-1}$ for each of these *N*-deuterated acyclic imides. In analogy with the case of monosubstituted amides, these bands of the undeuterated species of acyclic imides in the region 1250 to 1150 $cm^{-1}$ may be assigned to the vibration to which both the C-N-C antisymmetric stretching and the N-H in-plane deformation mode mainly contribute and the medium band of the *N*-deuterated species in the region 990 to 950 $cm^{-1}$ to the vibration to which the N-D in-plane deformation mode mainly contributes. Thus, these bands are considered to be characteristic of the -CONHCO- or the -CONDCO- group. Hereafter, the former and the latter bands will be called the imide III and the imide III′ bands of acyclic imides respectively. To explain the appearance of two strong imide III bands for *N*-acetylpropionamide, somewhat different fashions of vibrational coupling between the N-H in-plane deformation and the C-N streching vibrations must be considered. Because the C-N bond order of acyclic imides is less than that of monosubstituted amides, the imide III frequencies are lower than the amide III frequencies. On the other hand, it is noticed that there is no appreciable difference between the imide III′ and the amide III′ frequencies. Since there are many factors affecting such deformation frequencies, estimation of the difference in the deformation force constant of the angle C-N-H between monosubstituted amides and acyclic imides is not so simple as that in the stretching force constants. These problems will be discussed later with the aid of the normal vibration calculation for diacetamide.

**Imide V and V′ Bands.**—There is a medium band near 735 $cm^{-1}$ for the undeuterated species while there is a somewhat weaker band near 540 $cm^{-1}$ for the *N*-deuterated species of each higher homolog of diacetamide in the present study. The presence of these bands clearly indicates that the crystal form of higher homologs corresponds rather to the form B than to the form A of diacetamide. These two bands correspond to the amide V and the amide V′ band of monosubstituted amides and their *N*-deuterated compounds respectively. The N-H or the N-D out-of-plane deformation mode is considered to contribute mainly to these bands. Hereafter, the band of the undeuterated species near 735 $cm^{-1}$ and the band of the *N*-deuterated species near 540 $cm^{-1}$ will be called the imide V and the imide V′ band, respectively, of acyclic imides. A discussion concerning these bands has already been made in the preceding paper on diacetamide[1]. There are few differences between the imide V and the the amide V frequency and between the imide V′ and the amide V′ frequency. Namely, together with the case of the imide III′ and the amide III′ frequencies, it can be said that no appreciable frequency difference is observed between the bands of trans monosubstituted amides and those of trans-trans acyclic imides as far as nearly pure N-H deformation modes are concerned.

**Imide IV, VI and VI′ Bands.**—The other bands in the potassium bromide region observed for diacetamide and diacetamide-*d* were assigned before[1]. The correspondence between these bands and the amide IV, VI and VI′ bands of monosubstituted amides is obvious. In analogy with the case of monosubstituted amides, the C=O in-plane and the C=O out-of-plane deformation bands of the undeuterated species will be called the imide IV and the imide VI bands respectively, and the C=O out-of-plane deformation bands of the *N*-deuterated species will be called the imide VI′ bands. The imide IV bands which do not shift on deuteration are observed at 609 and 559 $cm^{-1}$ for *N*-acetylpropionamide and the weak imide VI′ band appears at 620 $cm^{-1}$ for *N*-acetylpropionamide-*d*. For the other three acyclic imides containing no acetyl group, two weak bands are observed near 610 and 590 $cm^{-1}$ for the undeuterated species. They are probably due to some C=O deformation modes. However, because of ambiguous spectral change on deuteration in this region, the assignment of these bands is still uncertain.

**N-H and N-D Stretching Bands.**—Two strong bands near 3280 and 3200 $cm^{-1}$ are observed for the undeuterated species of these acyclic imides in the form B. These bands are related to the N-H stretching vibration, and their frequencies clearly show the presence of hydrogen bonds. Their distinguished sharpness, however, together with the high C=O stretching frequencies previously mentioned, suggests that the nature of hydrogen bonds involved in the form B is markedly different from those known for monosubstituted amides and related compounds. As for the N-D stretching vibration, except for the band near 2410 $cm^{-1}$, *N*-deuterated acycilc imides in the form B show no strong band in the region 2500 to 2300 $cm^{-1}$. Thus, it is seen that the remarkable band splitting observed for the undeuterated species vanishes

TABLE IV. ANALYTICAL DATA AND MELTING POINTS OF ACYCLIC IMIDES

| | Calcd., % | | | Found., % | | | M. p., °C | |
|---|---|---|---|---|---|---|---|---|
| | C | H | N | C | H | N | Exp. | Lit. |
| AP | 52.16 | 7.88 | 12.17 | 52.31 | 7.86 | 12.08 | 86 | 86[11] |
| PP | 55.79 | 8.58 | 10.85 | 56.03 | 8.70 | 10.61 | 154 | 154[12] |
| PB | 58.72 | 9.15 | 9.28 | 58.47 | 8.95 | 9.90 | 116 | 109[13] |
| BB | 61.12 | 9.62 | 8.91 | 60.82 | 9.67 | 9.17 | 115 | 111[9] |

on deuteration. This situation will be discussed in the next paper, where the dichroic properties of those two bands of the undeuterated species will also be treated.

**C-H Deformation Bands.**—Two or three bands are observed for each of the undeuterated species of these acyclic imides in the region 1460 to 1370 $cm^{-1}$. These bands are assigned to the $CH_3$ or the $CH_2$ deformation modes in analogy with the case of other compounds containing acyl groups. The results are summarized in Table III[4], where it is noticed that acyclic imides which contain the ethyl or the *n*-propyl group, show a sharp and strong band due to the bending vibrations of the $\alpha$-methylene group near 1420 $cm^{-1}$. For the molecules containing the structure $-C-CH_2-CONHCO-CH_2-C-$, this band is the strongest among the C-H deformation bands in this region. Changes in features and intensities of these C-H deformation bands also take place on deuteration. In general, the intensity of the band near 1420 $cm^{-1}$ decreases while that of the band near 1380 $cm^{-1}$ increases. This fact shows that, in connection with the complicated features of the imide II′ bands of these higher homologs, certain C-H deformation vibrations may be involved in the couplings which give rise to the imide characteristic bands in this region.

## Conclusion

On the basis of the trans-trans planar structure of the -CONHCO- group, almost all the assignments as well as the interpretation of the frequencies and the intensities have been given to the characteristic bands of those saturated acyclic imides in the form B. These results give support to the internal rotation mechanism for the dimorphism of diacetamide by confirming the configuration of the -CONHCO- group in the form B. There are few deviations in the imide I, II, V and V′ frequencies of these acyclic imides while the difference in the alkyl residues affects the imide II′, III and III′ frequencies as well as their band features. Further evidences of the trans-trans planar structure for form B will be given in the next paper which deals with the infrared dichroism of some acyclic imides.

## Experimental

The four acyclic imides in the present paper were prepared by the acylation of primary amides with the mixture of acid chlorides and acid anhydrides according to Polya's method[9]. In the preparation of asymmetric acyclic imides, the smaller acyl groups were chosen to be in primary amides. These acyclic imides were recrystallized two or three times from petroleum ether[10]. Table IV[4] shows the analytical data for these preparations and their melting points together with those in the literatures. The *N*-deuterated species of these acyclic imides were prepared by the exchange reaction with deuterium oxide[10]. These preparations were subjected to measurements with the same instrument and technique as those described in the preceding paper[1].

The authors express their thanks to Dr. T. Miyazawa and Dr. K. Nakamura for their kind advice. Thanks are also due to Mr. H. Goto for technical assistance and to Dr. K. Hozumi and his associates for elementary analyses.

*Faculty of Pharmacy*
*Kyoto University*
*Sakyo-ku, Kyoto*

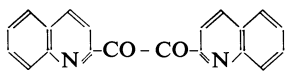
9) P. Dunn, E. A. Parkes and J. B. Polya, *Rec. trav. chim.*, **71**. 676 (1952).
10) Crystals from water show the identical infrared spectra with those of crystals from petroleum ether.
11) Q. E. Thompson, *J. Am. Chem. Soc.*, **73**, 5844 (1951).
12) D. Davidson and M. Karten, ibid., **78**, 1066 (1956).
13) M. Tarbouriech, *Compt. rend.*, **137**, 326 (1903).

# *Reactions of Quinaldil and its Related Compounds with Alkali. I. Quinaldil and Phenyl-2-quinolyl Diketone*

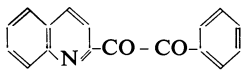
By Daihei ODA

(Received October 11, 1960)

Previous investigations[1,2] have shown that under the action of aqueous alkali, the pyridil containing 2- or 4-pyridyl group was subjected to the fission of the C-C bond of dicarbonyl and simultaneously the decomposition of these groups, accompanied with the evolution of ammonia. In the present paper, the reaction of quinaldil (I) or phenyl-2-quinolyl diketone (II) with alkali was investigated, and compared with that of pyridil.



I

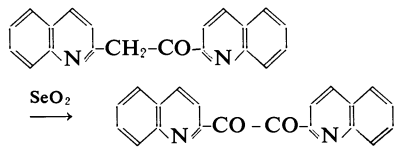


II

Hammick and Brown[3] have reported that I reacts with aqueous alkali to yield 60% of quinaldic acid. From this fact and some other properties of I, i. e., its high melting point, its low solubility and its lack of properties associated with the carbonyl group, these investigators have proposed a meso-ionic structure named "Quinocoll" for I, instead of the usual benzil structure and suggested that the structure I-a, similar to that of a quinol ion, should readily undergo autoxidation to yield a quinone, which is the cation of an acylquinolinium hydroxide and hence would be expected to hydrolyse readily to quinaldic acid:

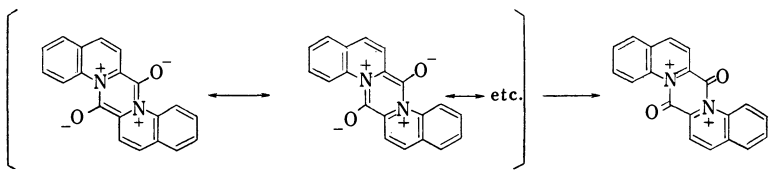
Buehler and Harris[4], however, have obtained different results that I forms various carbonyl derivatives, and its infrared absorption spectrum has the characteristic CO band, and so they doubted the validity of the structure I-a, but did not refer to the reaction with alkali.

Now, in order to confirm the structure of I, it was independently prepared from desoxyquinaldoin as follows:

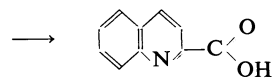


and compared with Hammick's "Quinocoll" and usual "Quinaldil". Then, all these products were proved to be identical with each other in melting point, mixed melting point and infrared absorption spectrum respectively. This means the validity of benzil structure of I and thus Hammick's explanation about the reaction of I with alkali seems to be inadequate. II was also prepared from phenacyl quinaldine by the same way as above.

These diketones were reacted with alkali under several conditions shown in Tables I and II. In these reactions, the evolution of ammonia observed in pyridil did not occur at all. I was certainly found to afford quinaldic acid as Hammick had reported, while in II benzoic acid was alternatively obtained in about 90% yield. These results seem to be quite



I-a (meso-ionic structure)



1) D. Oda, *J. Chem. Soc. Japan, Pure Chem. Sec.* (*Nippon Kagaku Zasshi*), **82**, 478 (1961).
2) D. Oda, ibid., **82**, 480 (1961).
3) D. Ll. Hammick and B. R. Brown, *J. Chem. Soc.*, **1950**, 628.
4) C. A. Buehler and J. O. Harris, *J. Am. Chem. Soc.*, **72**, 5015 (1950).

TABLE I. REACTION OF QUINALDIL (I) WITH ALKALI

| Sample Quinaldil g. | Conditions Temp. °C | Time hr. | Atmosphere | Products Quinaldic acid, g. | III g. | Hydroquinaldoin, g. |
|---|---|---|---|---|---|---|
| 3.1 | 20 | 2 | $N_2$ | 1.3 | 1.1 | 0.18 |
| 3.1 | 50 | 1 | $N_2$ | 1.3 | 1.3 | 0.20 |
| 3.1 | 80 | 1 | — | 1.5 | 1.1 | 0.20 |

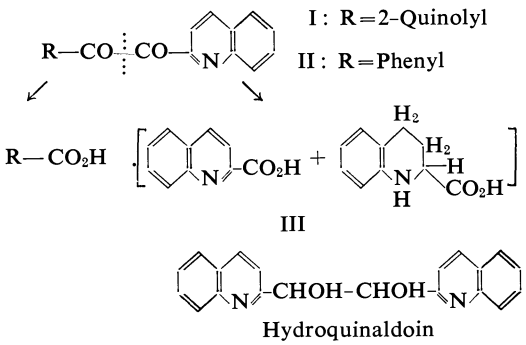
TABLE II. REACTION OF PHENYL-2-QUINOLYL DIKETONE (II) WITH ALKALI

| Sample Diketone g. | Conditions Temp. °C | Time hr. | Atmosphere | Products Benzoic acid, g. | III g. | Hydroquinaldoin, g. |
|---|---|---|---|---|---|---|
| 3.2 | 20 | 5 | $N_2$ | 1.2 | 1.1 | 0.05 |
| 3.2 | 50 | 2 | $N_2$ | 1.3 | 1.4 | 0.08 |
| 3.2 | 50 | 2 | — | 1.3 | 1.3 | 0.07 |
| 3.2 | 80 | 1 | — | 1.3 | 1.1 | 0.05 |

parallel to the facts that picolic acid was obtained from 2,2'-pyridil and that benzoic acid was obtained from phenyl-2-pyridyl diketone, each as main product. So these carboxylic acids should be derived from the half parts of the diketones respectively, and also indicated not to be yielded through oxydative cleavage of these diketones as Hammick described, because in either nitrogen atmosphere or not, the results obtained were shown to be scarcely affected.

In addition to these carboxylic acids, a red-orange compound III and small amount of hydroquinaldoin were obtained from I or II equally. III is an acidic compound, soluble in both acid and alkali and easily reduces Tollens' reagent at room temperature. Its melting point was not clear, i. e. 130~135°C, even after repeated crystallizations from benzene or water. A mixture of III and quinaldic acid melted at 120~150°C, so it might be suggested that III consists of quinaldic acid and other compounds; the latter may be of reducing property with color. On the other hand, the elementary analysis and molecular weight determination revealed that the formula of III closely resembled to $C_{10}H_9O_2N$, for example that of dihydroquinaldic acid, though III was much more stable than other dihydro compounds. Direct benzoylation or acetylation of III yielded only dark red resinous paste, from which not any compound could be isolated. However, preliminary esterification of III and then benzoylation of the resulting viscous oil yield methyl 1-benzoyl-1,2,3,4-tetrahydroquinaldate and methyl quinaldate, so it was suggested that III contained 1,2,3,4-tetrahydroquinaldic acid (IV) and quinaldic acid. In fact, it was found that when the aqueous solutions of equi-molecular amounts of IV and quinaldic acid were mixed, a red color immediately appeared and a red-orange compound was precipitated. It was identical with III, in melting point and other properties. These results indicate that III consists of IV and quinaldic acid; III might be an addition compound of these components.* Hammick and Brown have experimented in a small scale (0.5 g. of I was treated) and isolated quinaldic acid as hydrochloride, which must also contain that of the component of III; for, according to their analytical procedure, only quinaldic acid hydrochloride was precipitated and IV remained in the acid solution.

Then, the reactions of these diketones are summarized as follows:




It seems probable that these results were brought about not through benzilic acid rearrangement, but through the fission of C-C bond of dicarbonyl, analogously in pyridil. The formation of hydroquinaldoin in both cases is very interesting in connection with this suggestion. The mechanism of these reaction will be discussed later.

## Experimental

**Quinaldil (I) from Desoxyquinaldoin.**—Desoxyquinaldoin was prepared, according to the method

* *N*-Phenyl glycine, the structure of which is analogous to IV, was also found to give a yellow compound on mixing with quinaldic acid.

of Weiss and Hauser[5], by the condensation of quinaldine and ethyl quinaldate with potassium amide in liquid ammonia. Recrystallization from dioxane gave yellow crystals, m.p. 218.5~220°C, yield 31.5% (lit.[4] 221°C).

Three grams of desoxyquinaldoin was dissolved in 50 cc. of hot dioxane and oxidized with 1.4 g. of selenium oxide under reflux and stirring for 4 hr. The liquid was filtered hot from precipitated selenium, and the latter washed with hot dioxane. After removal of the solvent from the combined filtrate in vacuo, ca. 20 cc. of saturated sodium bicarbonate solution was added to the resulting viscous oil. Acid contaminates were dissolved foaming and insoluble oil was solidified. The dark brown solid was collected, washed with water and recrystallized from pyridine to yield 2.2 g. (71%) of yellow-brown crystals, m.p. 265~272°C. Successive crystallizations from dioxane gave pale yellow needles, m.p. 271~272°C.

Found: C, 76.87; H, 3.92; N, 8.86. Calcd. for $C_{20}H_2O_2N_2$: C, 76.92; H, 3.84; N, 8.97%.

The product showed no melting point depression when mixed with that obtained by the decarboxylation of picolic acid in quinoline-2-aldehyde (Hammick's method) or by the oxidation of quinaldoin (Buehler's and usual method). The identity of these products was further confirmed by the comparison of their infrared absorption spectra which could be overlapped in every detail.

**Phenyl-2-quinolyl Diketone (II).**—Similarly as in the case of I, 19.1 g. of phenacylquinaldine prepared by the method of Weiss and Hauser[5] was oxidized with selenium oxide. After removal of the solvent and treatment of the residue with sodium bicarbonate solution, extraction of the resulting dark brown solid with hot ligroin yielded 9.9 g. (49%) of yellow crystals. Recrystallization from ligroin gave pale yellow crystals, m.p. 109~110°C.

Found: C, 77.84; H, 4.25; N, 5.35. Calcd. for $C_{17}H_{11}O_2N$: C, 78.14; H, 4.24; N, 5.36%.

**Reaction of Quinaldil (I) with Alkali.**—A typical procedure is as follows: to a suspension of 3.1 g. of I in 10 cc. of ethanol, a 30% aqueous solution of 3.1 g. of potassium hydroxide was added. The mixture was heated at 50°C under nitrogen atmosphere. The initially appearing red-brown color was gradually turned to light orange, while I disappeared and new precipitates began to deposit. After the reaction was continued for 2 hr., the precipitates were filtered, washed with water and dried, amounting 0.2 g. Recrystallization from pyridine gave colorless crystals, m.p. 215~217°C (decomp.). The melting point showed no depression when mixed with an authentic sample of hydroquinaldoin[4].

Found: C, 75.47; H, 5.03; N, 8.89. Calcd. for $C_{20}H_{16}O_2N_2$: C, 75.93; H, 5.10; N, 8.86%.

The filtrated was extracte with ether or chloroform. Evaporation of the solvent from the extract yielded but a little amount of residue, from which not any compound could be isolated. Acidification of the mother liquor to pH 3 with concentrated hydrochloric acid gave precipitates, which were washed with water, and dried, m.p. 110~114°C. The precipitates were boiled with ether and the solution was filtered while hot. Cooling the filtrate yielded 0.2 g. of pale orange crystals, m.p. 130~150°C. Recrystallization from benzene gave colorless crystals, m.p. 154~155°C, which were proved identical with quinaldic acid. The orange substance (1.3 g.) insoluble in ether was recrystallized from benzene and water to give beautiful red-orange crystals III, which melted at 130~135°C. Repeated crystallization could not improve the melting point. A mixture of this compound and quinaldic acid melted at 120~150°C. Analytical results were shown below together with reference data:

| | C, % | H, % | N, % | Mol. wt. |
|---|---|---|---|---|
| Found: | 68.69 | 5.12 | 7.81 | 180.2 (Rast) |
| | 68.68 | 5.24 | 7.88 | 182.6 (titration) |
| Calcd. for | | | | |
| $C_{10}H_7O_2N$: (quinaldic acid) | 69.36 | 4.07 | 8.09 | 173.17 |
| $C_{10}H_9O_2N$: | 68.56 | 5.17 | 7.99 | 175.19 |

To the weak acid filtrate from these compounds a saturated aqueous solution of cupper sulfate was added. Green-blue cupper salt was precipitated, washed with water and treated with hydrogen sulfide. The filtrated from the precipitated cupper sulfide was evaporated to dryness in vacuo to give a pale orange residue (1.2 g.), which melted at 120~150°C and consisted mostly of quinaldic acid.

**Reaction of Phenyl-2-quinolyl Diketone (II) with Alkali.**—The procedure is substantially the same as used with I: in the reaction mixture there was also an insoluble substance, which melted at 215~217°C and was found identical with hydroquinaldoin by the mixed melting point determination.

Found: N, 8.92. Calcd. for $C_{20}H_{16}O_2N_2$: N, 8.86%.

The precipitates obtained by acidification (pH 3) of the filtrate were boiled with petroleum ether and the solution was filtered while hot. Cooling the filtrate gave colorless crystals, m.p. 120~121°C, which were proved to be identical with benzoic acid. The insoluble fraction in petroleum ether was recrystallized from water to give red-orange crystals, which melted at 130~135°C and were found identical with III obtained in the case of I. From the weak acid filtrate, a small amount of quinaldic acid was detected via the cupper salt.

**Formation of Methyl 1-Benzoyl-1, 2, 3, 4-tetrahydroquinaldate and Methyl Quinaldate from (III).**—A solution of 1.5 g. of III in 20 cc. of absolute methanol was saturated with dry hydrogen chloride. After standing at room temperature for 24 hr. the mixture was concentrated in vacuo and the residue was poured into about 10 cc. of ice water. The solution was made alkaline with sodium bicarbonate, the separating oil was taken up in ether and dried over anhydrous sodium sulfate. The ether was distilled off and 1.1 g. of viscous brown oil was obtained which did not solidify even after standing in the refrigerator for 2 days. The oil was dissolved in 10 cc. of pyridine, then 1 g. of freshly distilled benzoyl chloride was added and the mixture allowed to stand at room temperature for 4 days under

5) M. J. Weiss and C. R. Hauser, *J. Am. Chem. Soc.*, 71, 2023 (1949).

seal. After removal of the solvent in vacuo, the residue was poured into excess of sodium bicarbonate solution and the mixture was extracted with ether, washed with dilute hydrochloric acid, and sodium bicarbonate solution, and dried over anhydrous sodium sulfate. On evaporation of ether, there remained 0.4 g. of semi-solid substance. The product was boiled with petroleum ether and the solution filtered while hot. Cooling the filtrate gave colorless crystals which melted at 78~80°C. Recrystallization from petroleum ether improved the melting point to 81~82°C, which showed no depression, when mixed with an authentic sample of methyl quinaldate.

Found: N, 7.59. Calcd. for $C_{11}H_9O_2N$: N, 7.49%.

The semi-solid insoluble in petroleum ether was pressed on a clay plate and recrystallized from a ligroin-benzene mixture (1 : 1) to give long crystals, which melted at 109.5~110.5°C when alone and admixed with an authentic sample of methyl 1-benzoyl-1, 2, 3, 4-tetrahydroquinaldate[6].

Found: C, 73.00; H, 5.63; N, 4.74. Calc. for $C_{18}H_{17}O_3N$: C, 73.54; H, 5.80; N, 4.75%.

**Formation of III from Quinaldic Acid and 1, 2, 3, 4-Tetrahydroquinaldic Acid.**—A solution of 2.1 g. (0.01 mol.) of pure 1, 2, 3, 4-tetrahydroquinaldic acid hyrochloride[6] in 10 cc. of water was brought to pH 3 with sodium bicarbonate, and 1.7 g. (0.01 mol.) of quinaldic acid was dissolved in 10 cc. of hot water. When both solutions were combined, red color immediately appeared, and then a red-orange compound was precipitated, washed with a little water and dried, m. p. 125~133°C. Recrystallization from water gave beautiful red-orange crystals, m. p. 130~135°C. The melting point showed no change when admixed with the reaction product of the diketone with alkali.

## Summary

In the reaction of quinaldil or phenyl-2-quinolyl diketone with alkali, the fission of C-C bond of dicarbonyl occurred and from the half part of diketone common to each, a red-orange compound and a small amount of hydroquinaldoin were obtained and the other half gave the corresponding acid. The colored compound was found to be consisting of quinaldic acid and 1, 2, 3, 4-tetrahydroquinaldic acid. These results refuse to accept Hammick's explanation about the reaction of quinaldil with alkali, in which there is a mistake fundamentally.

The author wishes to express his sincere thanks to Professor Ryozo Goto, Kyoto University, and Professor Kotaro Shimo, Defense Academy, for their valuable advice and encouragement.

*Department of Chemistry*
*Defense Academy*
*Yokosuka*

9) H. Wieland, et al., *Ber.*, **61**, 2371 (1928).

# *Infrared Spectra of Some Deuterated Crystalline Polystyrenes. II. Isotactic Poly-$\beta d_1$-, Poly-$\alpha, \beta d_2$- and Poly-$\beta, \beta d_2$-styrene*

By Masamichi KOBAYASHI

(Received October 18, 1960)

In the previous paper[1] were made the assignments of some absorption bands which have been regarded as characteristic of the helical conformation of the isotactic polystyrene (IPS) molecule, and it was concluded that the 1364 $cm^{-1}$ band ($\sigma$) was assumed to be due mainly to the CH deformation, the 1297 $cm^{-1}$ band ($\pi$) to the $CH_2$ wagging, the 1195 $cm^{-1}$ band ($\pi$) to the CH wagging, and 1185 $cm^{-1}$ band ($\pi$) to the stretching of the carbon skeletal chain. But some other bands which are also characteristic of the isotactic polymer remained as unassigned (E. X. the bands at near 1070 $cm^{-1}$ and 900 $cm^{-1}$).

In order to gain more information for the assignments of the bands, in this paper some deuterated derivatives of IPS were synthesized, in which some of the hydrogen atoms attached to the skeletal chain were substituted with deuterium, such as poly-$\beta d_1$-styrene ($I\beta d_1$), poly-$\alpha, \beta d_2$-styrene ($I\alpha, \beta d_2$) and poly-$\beta, \beta d_2$-styrene ($I\beta, \beta d_2$), and their infrared spectra were investigated.

The characteristic bands showed considerable changes depending on the site and the number of the deuterium atoms in the molecule. On the basis of the results, the discussions were made on the assignments of these bands. But, for some of them, the dependences on deuteration were too complicated to assign them to

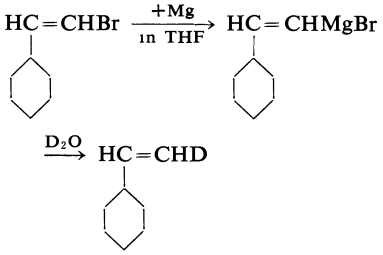
1) M. Kobayashi, This Bulletin, 33, 1416 (1960).

the simple vibrational modes of the molecucle.

The molecule of I$\beta d_1$ or I$\alpha, \beta d_2$ contains two assymmetric carbon atoms in one repeating unit, and the stereoregular polymer of this type has been termed recently "diisotactic polymer" by Natta[2]. Since the monomers used in this research were mixtures of the two geometrical isomers, although detailed discussions on the structure of the polymers of the new type could not be made, a few spectroscopic evidences were gained reflecting the differences in structure between so called threo and erythro diisotactic structures.

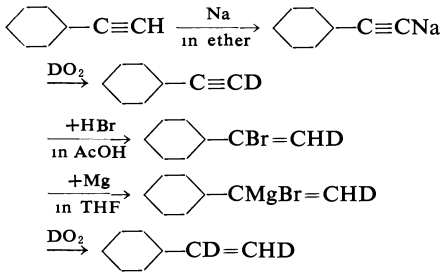
## Experimental

**Preparations of the Monomers.** — $\beta d_1$-Styrene was synthesized by hydrolysis with deuterium oxide of the Grignard-reagent of $\beta$-bromostyrene;



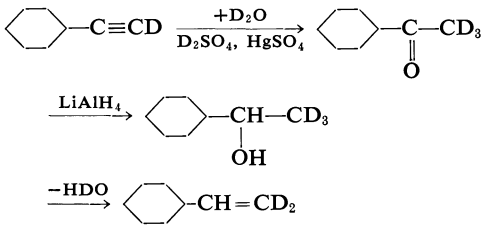

For this deuterated monomer, two geometrical isomers, cis and trans, are considered. Although it has been known that *trans*-$\beta$-bromostyrene can be prepared from cinnamic acid dibromide by Nef's method[3], according to which our sample was synthesized, the product usually contains a considerable amount of the cis-isomer. Moreover, it has still been uncertain whether the deuterium atom is substituted at the same position as the bromine by the reactions described above. Therefore, our deuterated monomer may be a mixture of cis- and trans-isomers. The NMR spectroscopic data of the sample showed that the latter was the predominant component (see Fig. 1).

$\alpha, \beta d_2$-Styrene was prepared by the following scheme;




Since the hydrogen atom is assumed to be added to cis and trans position with the same probability in the addition reaction of hydrogen bromide to the deuterated phenylacetylene, the product may be a 1 : 1 mixture of two geometrical isomers. This was confirmed by the NMR measurement as shown in Fig. 1.

$\beta, \beta d_2$-Styrene was prepared as following;



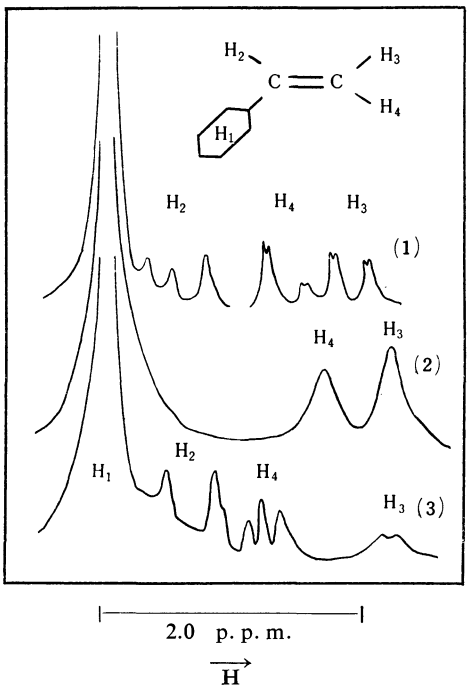




Fig. 1. Proton magnetic resonance spectra of styrene and its deuterated derivatives.
(1) Styrene (2) $\alpha, \beta d_2$-Styrene
(3) $\beta d_1$-Styrene

**Polymerization.** — The monomers were polymerized with Ziegler type catalyst and the samples of the crystalline polymers for infrared measurements were prepared according to the same method as that described in the previous paper.

**Infrared Spectra Measurements.** — The infrared spectra of each sample was measured using a Hilger H800 infrared spectrometer and the polarized spectra were measured with a selenium polarizer.

## Experimental Results

The polarized spectra in the regions of 3500~1600 $cm^{-1}$ and 1600~650 $cm^{-1}$ of the oriented samples are shown in Fig. 2 and Figs. 3a—3c respectively.

Depending on the site and the number of the deuterium atoms substituted in the polymer molecule, some remarkable differences in

2) G. Natta, *Makromol. Chem.*, 35, 94 (1960).
3) J. V. Nef, *Ann.*, 308, 267 (1899).

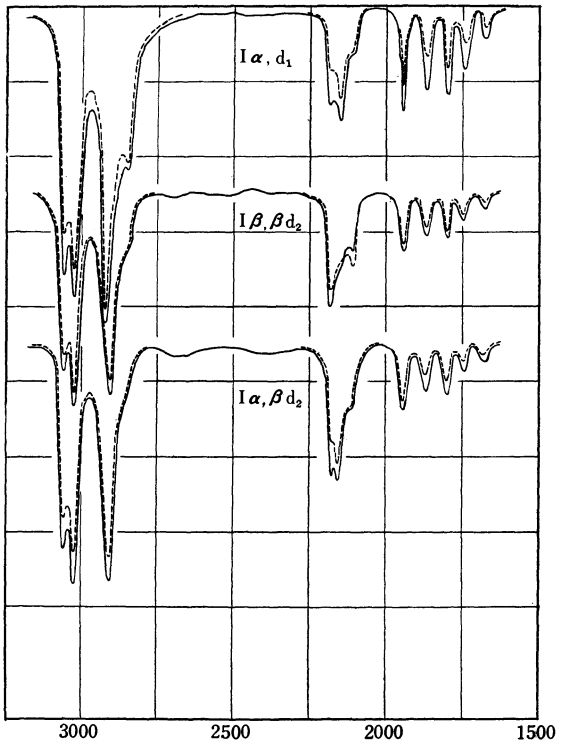



Fig. 2. Infrared dichroisms of the deuterated derivatives of isotactic polystyrene.
—— Electric vector perpendicular to elongation
---- Electric vector parallel to elongation

spectrum among the samples were observed, mainly in the regions of 2500~2000 $cm^{-1}$ (associated with the stretching vibrations of the CD and the $CD_2$ groups), 1450~1180 $cm^{-1}$ (the deformational vibrations of the CH and the $CH_2$ groups), 1100~1040 $cm^{-1}$ and 920~890 $cm^{-1}$. In Table I the main bands of the samples in these regions are compared with each other. The data of IPS and I$\alpha d_1$ are cited for comparison.

## Discussion

**The Bands due to the Stretchings of the CD and the $CD_2$ Groups.** — The CD (and $CD_2$) stretching bands appear in the region of 2200~2100 $cm^{-1}$. The well-known three-fold helical structure of the molecule of IPS is reflected by the polarization properties of the bands; (1) all bands due to the CD stretching show a remarkable $\sigma$ nature, and (2) 2186 $cm^{-1}$ band (corresponding to the $CD_2$ assymmetric stretching) and the 2106 $cm^{-1}$ band (the $CD_2$ symmetric stretching) of I$\beta$, $\beta d_2$ show $\sigma$ and $\pi$ nature respectively.

The frequency of the CD stretching depends on the position of the deuterium in the molecule. While the band of I$\alpha d_1$ appears at 2134 $cm^{-1}$, two $\sigma$ bands appear at 2183 and 2150 $cm^{-1}$ in I$\beta d_1$.

As described in the introduction, two kinds of isotactic structure can be considered for the molecule of I$\beta d_1$. On the basis of the results of the factor group analysis for the three-fold helical polymer, although two bands due to the CD stretching are expected to be observed in I$\beta d_1$, they should be of opposite dichroism. Therefore, the two $\sigma$ bands of our sample may predict the presence of the two stereo-isomers in the sample. These bands differ in intensity with each other (the 2150 $cm^{-1}$ band

TABLE I. ABSORPTION BANDS CHARACTERISTIC OF THE HELICAL CONFORMATION OF ISOTACTIC POLYSTYRENE

| IPS | | | Iα$d_1$ | | | Iβ$d_1$ | | | Iβ, β$d_2$ | | | Iα, β$d_2$ | | | Assignment |
|---|---|---|---|---|---|---|---|---|---|---|---|---|---|---|---|
| Freq. $cm^{-1}$ | | RI | Freq. $cm^{-1}$ | | RI | Freq. $cm^{-1}$ | | RI | Freq. $cm^{-1}$ | | RI | Freq. $cm^{-1}$ | | RI | |
| | | | | | | 2183 | $\sigma$ | m | 2186 | $\sigma$ | ms | 2187 | $\sigma$ | ms | $\nu$ (CD) or $\nu$ ($CD_2$) |
| | | | | | | 2150 | $\sigma$ | m | 2150 | $\sigma$ | msh | 2155 | $\sigma$ | ms | |
| | | | 2134 | $\sigma$ | m | 2102 | — | wsh | 2106 | $\pi$ | m | 2102 | — | m | |
| 1444 | — | ssh | 1440 | — | ssh | | | | | | | | | | $\delta$ ($CH_2$) A+E |
| 1364 | $\sigma$ | ms | | | | 1363 | $\sigma$ | ms | 1356 | $\sigma$ | mw | | | | $\delta$ (CH) (mainly) |
| | | | 1334 | $\sigma$ | ms | | | | | | | 1332 | $\sigma$ | ms | |
| 1314 | $\sigma$ | m | 1311 | $\sigma$ | m | 1311 | $\sigma$ | m | 1301 | $\sigma$ | m | 1311 | $\sigma$ | m | $\delta$ (CH) |
| 1297 | $\pi$ | mw | 1295 | $\pi$ | mw | (1297) | $\sigma$ | wsh | (1297) | $\sigma$ | wsh | (1295) | $\sigma$ | mw | w ($CH_2$) A |
| 1195 | $\pi$ | mw | | | | 1195 | $\pi$ | mw | 1195 | $\pi$ | vw | | | | w (CH) A |
| 1185 | $\pi$ | mw | 1183 | $\pi$ | mw | 1185 | $\pi$ | mw | 1181 | $\pi$ | mw | 1180 | $\pi$ | mw | $\nu$ (CC) A |
| 1180 | $\pi$ | mw | | | | | | | | | | | | | |
| 1080 | $\sigma$ | m | 1084 | $\sigma$ | m | 1084 | $\sigma$ | ms | 1080 | $\sigma$ | s | 1080 | $\sigma$ | s | skeletal mode + in-plane deformation |
| | | | 1072 | $\sigma$ | m | 1071 | $\sigma$ | msh | | | | 1070 | $\sigma$ | msh | |
| 1048 | $\sigma$ | m | | | | | | | | | | | | | |
| 920 | $\sigma$ | m | 910 | — | m | 912 | $\sigma$ | m | 908 | $\sigma$ | m | 908 | $\sigma$ | m | i-mode + r($CH_2$) |
| 906 | — | m | | | | | | | | | | | | | |
| 898 | $\pi$ | w | 891 | $\pi$ | mw | 903 | $\pi$ | m | 905 | $\pi$ | m | 905 | $\pi$ | m | |

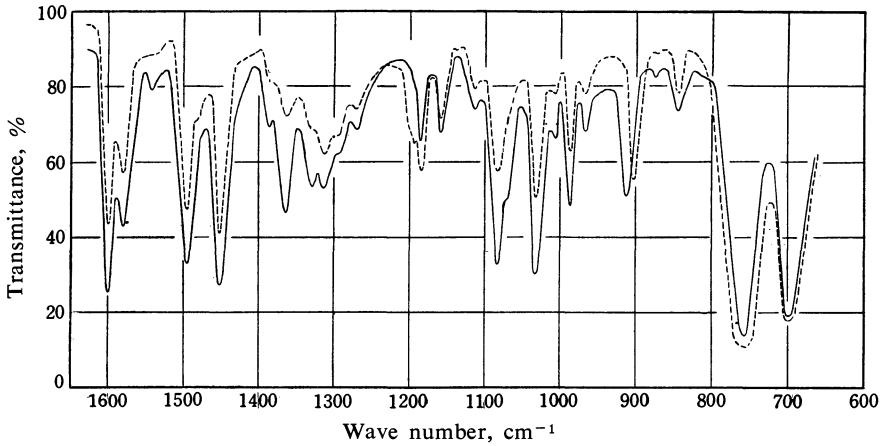



Fig. 3a. Infrared dichroisms of I$\beta d_1$.

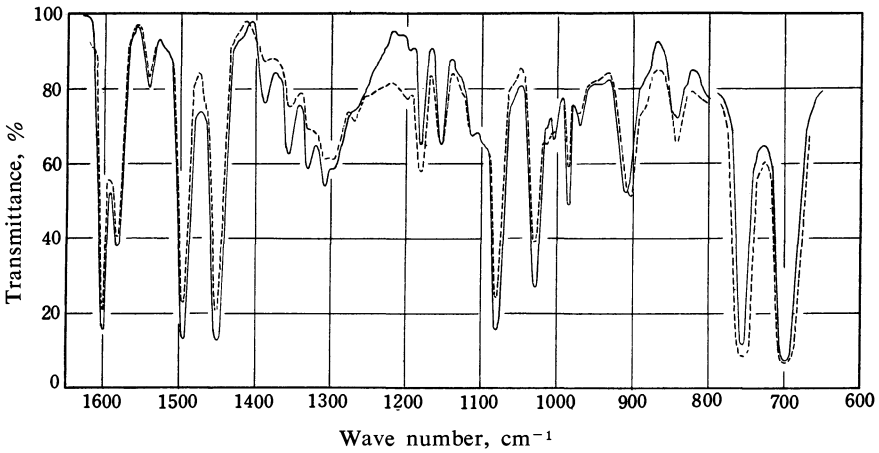



Fig. 3b. Infrared dichroisms of I$\beta, \beta, d_2$.

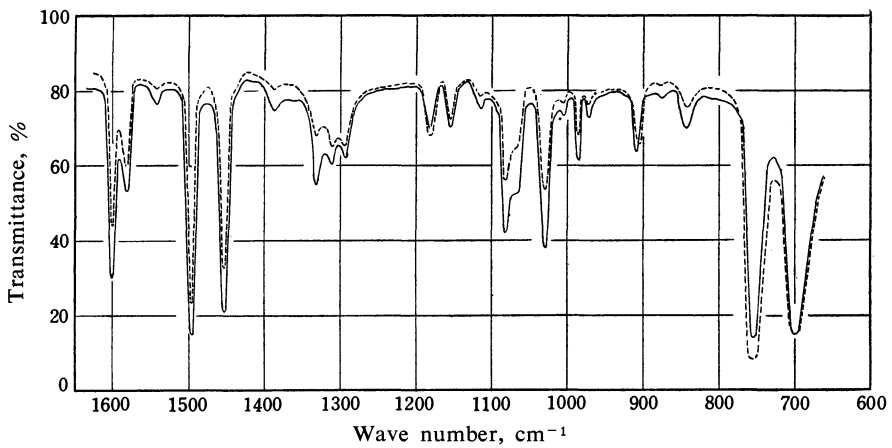



Fig. 3c. Infrared dichroisms of I$\alpha, \beta d_2$.

—— Electric vector perpendicular to elongation
---- Electric vector parallel to elongation

is greater than the 2183 $cm^{-1}$ band) and this fact is assumed to result from the composition of the geometrical isomers of the monomer used.

The same discussions should be undertaken about I$\alpha$, $\beta d_2$, nevertheless, in this case, we could not make a simple assignment because of the complexity resulting from an interaction between the neighboring CD groups.

**The Bands in the Region of 1450~1180cm$^{-1}$.**—The spectra of the region are very important since the absorption bands characteristic of the isotactic polymers appear mainly in this region. The strong shoulder at 1440 $cm^{-1}$ appearing in IPS and I$\alpha d_1$ is not observed in the other deuterated samples. This fact supports the conclusion assigning the band to the $CH_2$ bending. The 1364 $cm^{-1}$ $\sigma$ band of IPS is affected by deuteration; it appears at slightly lower frequency (1363 $cm^{-1}$) in I$\beta d_1$, appears at 1356 $cm^{-1}$ and decreases its intensity in I$\beta$, $\beta d_2$, appears at 1334 $cm^{-1}$ in I$\alpha d_1$, and at 1332 $cm^{-1}$ in I$\alpha$, $\beta d_2$.

Although the greater effect of the substitution of $\alpha$-hydrogen on the frequency may suggest a validity of assigning the band of IPS mainly to the CH deformation, the changes in frequency and intensity on $\beta$-deuteration show that this band should be assigned to a more complicated vibrational mode.

Admitting a few differences in frequency, the 1314 $cm^{-1}$ $\sigma$ band of IPS observed in each of the deuterated derivatives; 1311 $cm^{-1}$ in I$\alpha d_1$, I$\beta d_1$ and I$\alpha$, $\beta d_2$, and 1301 $cm^{-1}$ in I$\beta$, $\beta d_2$. Since the corresponding band does not appear in poly-$\alpha$, $\beta$, $\beta d_3$-styrene (I$\alpha$, $\beta$, $\beta d_3$)[4], this band may be assumed to be associated with a deformational mode of the CH group of the skeletal chain.

From the fact that the 1297 $cm^{-1}$ band of IPS was not observed in the deuterated derivatives except I$\alpha d_1$ (the $\sigma$ bands appearing at the same frequency in $\beta$-deuterated derivatives should be distinguished from it because of the discrepancy of polarization property), this may be assigned to the $CH_2$ wagging.

The 1195 $cm^{-1}$ $\pi$ band of IPS is not observed in the $\alpha$-deuterated derivatives but appears at the same frequency in I$\beta d_1$ and I$\beta$, $\beta d_2$, in the latter case a moderate decrease in relative intensity being accompanied by it. This fact may support the assumption assigning the band to the CH wagging.

**The Bands at near 1070 cm$^{-1}$.**—The 1070 $cm^{-1}$ band of atactic polystyrene (APS) splits into two $\sigma$ bands (1080 $cm^{-1}$ and 1040 $cm^{-1}$) in IPS at crystallized state. The similar splitting of of IPS has been observed even in a molten or dissolved sample in these cases the peaks become obtuser and are spaced more closely). Therefore, the band splitting is assumed to arise from an intramolecular interaction between neighboring groups. This assumption seems to be supported by the following experimental facts which have been detected by Tadokoro et al.[5],*; the 1048 $cm^{-1}$ band of IPS appears in a mixed sample of IPS and I$\alpha$, $\beta$, $\beta d_3$, while the crystallization sensitive band at 983 $cm^{-1}$ of IPS decreases in intensity in the mixed sample and, therefore, has been concluded to be associated with an intermolecular interaction of the neighboring molecules in the crystalline lattice.

Although it was expected that some information would be gained about this band splitting from the data of various kinds of deuterated derivatives, the changes in the bands on deuteration are so complicated that it seems difficult to make a precise assignment. The 1048 $cm^{-1}$ band of IPS disappears in the skeletal-deuterated samples regardless of the positions of the deuterium atoms in the molecules. The same facts have been observed[6] in the case of poly-*p*-deuterostyrene. The 1080 $cm^{-1}$ band of IPS appears in all of our samples and also in I$\alpha$, $\beta$, $\beta d_3$. The relative intensity decreases with the number of the hydrogen atoms of the $\beta$-position, while it is hardly affected by whether the $\alpha$-position is deuterated or not. In the deuterated samples having one or two hydrogen atoms at the $\beta$-position, such as I$\alpha d_1$, I$\beta d_1$ and I$\alpha$, $\beta d_2$, the $\sigma$ band appears at near 1070 $cm^{-1}$. The corresponding band is not observed in I$\beta$, $\beta d_2$ and I$\alpha$, $\beta$, $\beta d_3$. These results are shown in Fig. 4.

Although these facts may imply a contribution of the CH and the $CH_2$ groups to the band splitting in IPS, that of the phenyl group must be considered since the bands are also remakably affected by the deuteration of the phenyl nucleus. Referring to the spectroscopic data of many other vinyl polymers, it may be expected that a $\sigma$ band may be found due to the stretching vibration of the skeletal chain, $\nu$(CC)E, in this region.

These bands may be assumed to be associated with skeletal modes coupled with a CH in-plane-deformation of the phenyl group.

**The Bands at near 900 cm$^{-1}$.**—The 906 $cm^{-1}$ band of APS splits into three bands, 920 $cm^{-1}$ ($\sigma$), 906 $cm^{-1}$ (no-dichroism) and 898 $cm^{-1}$ ($\pi$), in the crystallized sample of IPS. The band

4) H. Tadokoro, N. Nishiyama, S. Nozakura and S. Murahashi, *J. Polymer Sci.*, **36**, 553 (1959).

5) H. Tadokoro, T. Kitazawa, S. Nozakura and S. Murahashi, *High Polymer Chem.* (*Kobunshi Kagaku*), **17**, 231 (1960).

* The authors did not discuss the 1048 $cm^{-1}$ band in their paper, but in the spectra shown in the Fig. 3 of the paper we can find out the fact pointed out here.

6) H. Tadokoro, S. Nozakura, T. Kitazawa, H. Yasuhara and S. Murahashi, This Bulletin, **32**, 313 (1959).

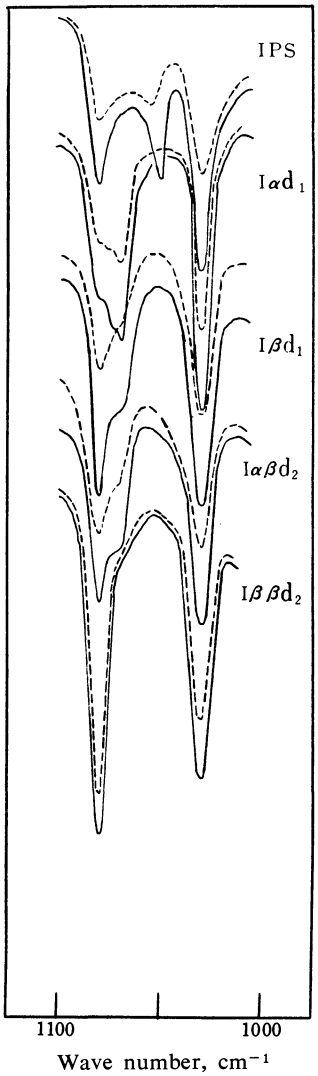



Fig. 4. Absorption bands at near 1070 $cm^{-1}$.
—— Electric vector perpendicular to elongation
---- Electric vector parallel to elongation

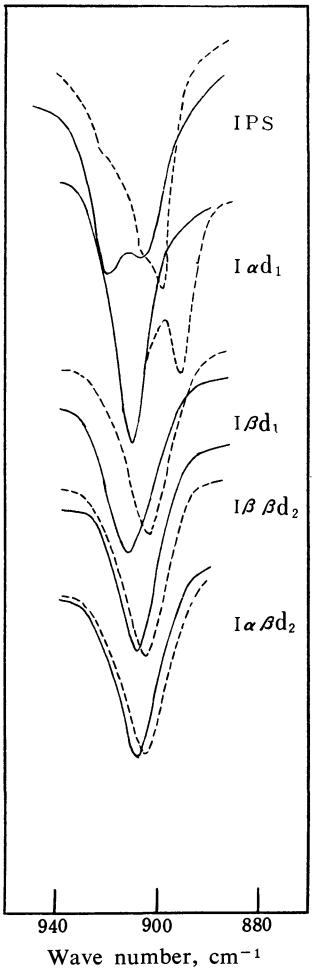



Fig. 5. Absorption bands at near 900 $cm^{-1}$.
—— Electric vector perpendicular to elongation
---- Electric vector parallel to elongation

splitting is sensitive to the degree of crystallinity of the sample and is not observed in the quenched or molten sample. Although it is expected that at this frequency the $\pi$ band assignable to Whiffen's i-mode of mono-substituted benzene (out-of-plane CH deformation) may be found, it was detected that the bands were affected by deuteration of the skeletal hydrogen atoms as shown in Fig. 5. In $I\beta d_1$, $I\alpha, \beta d_2$ and $I\beta, \beta d_2$, the closer spaced two bands of equal intensity appear at near 900 $cm^{-1}$ (912 $cm^{-1}$ and 903 $cm^{-1}$ in the case of $I\beta d_1$; 908 $cm^{-1}$ and 905 $cm^{-1}$ in $I\alpha, \beta d_2$ and $I\beta, \beta d^2$), the higher band showing $\sigma$ nature and the lower band $\pi$ nature. Similar bands were observed in $I\alpha, \beta, \beta d_3$. They may be assigned to i-mode and the difference in polarization property may correspond to the phase difference of the vibration of the neighboring phenyl groups in one molecule. The spectrum in this region of $I\alpha d_1$ is different not only from that of IPS but from that of the other deuterated samples; in this case the band exhibiting a remarkable $\sigma$ nature is not observed and the corresponding 910 $cm^{-1}$ band shows almost no dichroism. Further, the $\pi$ band of smaller intensity appears at the lower frequency, 891 $cm^{-1}$. From these facts it may be concluded that the $CH_2$ rocking vibration has an influence on the spectrum in this region.

Thus the effects of deuteration on the spectrum, especially that in the region of 1500~850 $cm^{-1}$ are very complicated. For the assignments of the bands in this region, one should

take into account some couplings of the deformations of the phenyl group with the skeletal modes or with the CH (or $CH_2$) deformational modes.

From this point of view the studies are in progress on the infrared spectra of some ring-deuterated derivatives of IPS.

*Osaka Industrial Research Institute*
*Oyodo-ku, Osaka*

# *The Scattering of Beams of Alkali Atoms in Various Gases. II. Sodium Atom Beam in Non-reactive and Reactive Gases*

By Kumasaburo KODERA and Teijiro TAMURA

(Received October 10, 1960)

In a previous paper[1], the scattering of atomic beams was discussed and the apparatus and the results obtained by scattering a sodium beam in argon were described. In this paper, rather simple molecules such as He, Ne, Ar, $H_2$, $N_2$ and CO, and molecules which might react with sodium atoms, such as NO, $O_2$ and $CO_2$ were used as scattering gases.

## Experimental

**Apparatus and Procedure.**—The apparatus was the same as described in detail in the previous paper except the McLeod gauge. The gauge had not sufficient accuracy for the purpose so that it was replaced by a new one which had frosted capillary tubes to avoid sticking of mercury thread; it also had larger bulb volume (250 cc. instead of 120 cc. of the former gauge). To measure the pressure of scattering gases, the same Pirani gauge was used but its calibration was done during every experiment in the pressure range of $10^{-4}\sim10^{-5}$ mmHg and not in a high pressure range as before. Procedure of measurements was also the same as before, but more precaution was taken in the measurement of pressures of scattering gases in the detector and the oven chambers, because effusion rates of the gases and pumping speed for them vary with their molecular weights and, for reactive gases, reaction with sodium also affects the stationary pressure.

**Materials.** — Sodium used for the beam was purified by repeated vacuum distillation as described before.

*Helium, Neon and Argon.* Gases labeled extra pure or 99.9% were purchased on the market and used without further purification. They were examined by CEC type 401 mass-spectrometer and proved that they contained no detectable impurity.

*Hydrogen* was made by electrolysis of sodium hydroxide solution with nickel electrodes and passed through soda-lime, heated reduced copper, concentrated sulfuric acid, phosphorus pentoxide and a liquid oxygen trap.

*Nitrogen* was made by heating ammonium nitrite solution made by dropping sodium nitrite solution into ammonium sulfate solution in a flask. The gas evolved was passed through a mixture of concentrated sulfuric acid and potassium dichromate and over soda-lime, heated reduced copper, soda-lime and a liquid oxygen trap, successively. The gas was examined by the mass-spectrometer and proved to contain no detectable impurity.

*Oxygen* was made by electrolysis of sodium hydroxide solution and purified in a way similar to that of the hydrogen, except for the fact that heated reduced copper was replaced by heated cupric oxide.

*Nitric oxide* was made by dropping concentrated sodium nitrite solution into a heated mixture of concentrated ferrous sulfate solution and hydrochloric acid. The gas evolved was passed over solid potassium hydroxide and silica gel and then condensed by a liquid nitrogen trap. The solidified gas was distilled into another trap, and the procedure was repeated several times.

*Carbon monoxide.* Concentrated sulfuric acid was dropped on heated sodium formate. The evolved gas was passed over fused potassium hydroxide, silica gel and through a liquid nitrogen trap.

*Carbon dioxide.* Solid carbon dioxide was evaporated and passed through concentrated sulfuric acid, then over calcium chloride and phosphorus pentoxide. The gas was condensed by a liquid oxygen trap and distilled several times as in the case of nitric oxide.

## Results

Weakening of sodium beams scattered in various gases are shown in Figs. 1 to 9. Calculated results are shown in Table I with other experimental data. In the table, $p$, $p_1$, $p_3$ represent relative pressures of scattering gas in the scattering-, the oven- and the detector-chambers, respectively. Mean free paths ($\lambda$)

* Present address, Chemistry, Institute, Faculty of Science, Kyoto University, Sakyo-ku, Kyoto.

1) K. Kodera and T. Tamura, This Bulletin, **31**, 206 (1958).

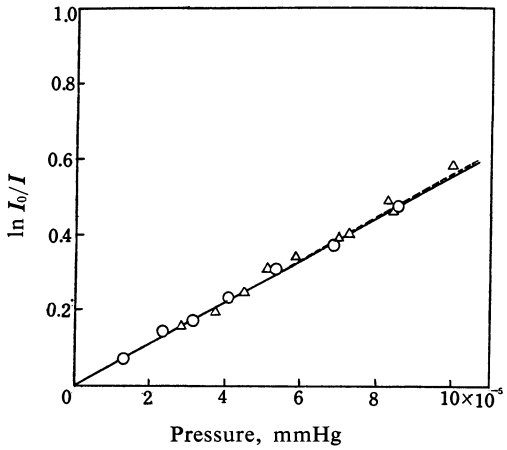



Fig. 1. Sodium beam in helium.

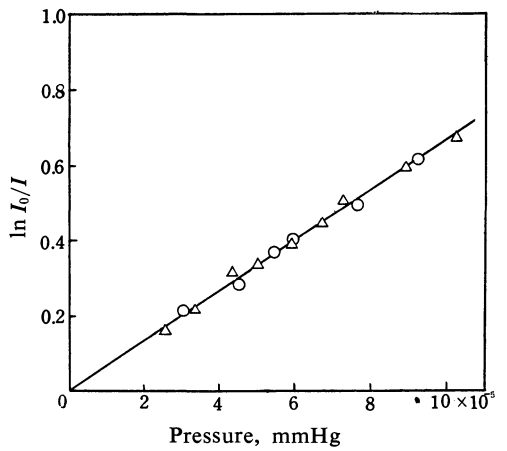



Fig. 2. Sodium beam in neon.

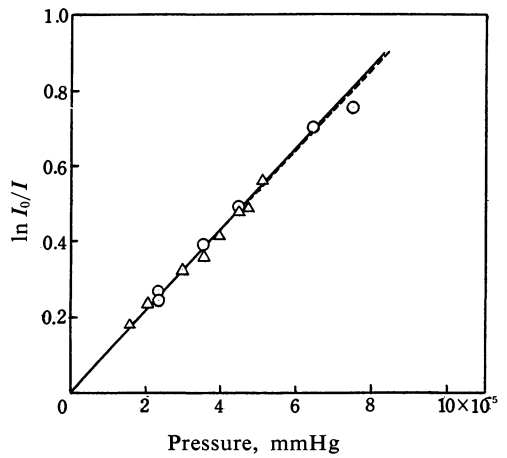



Fig. 3. Sodium beam in hydrogen.

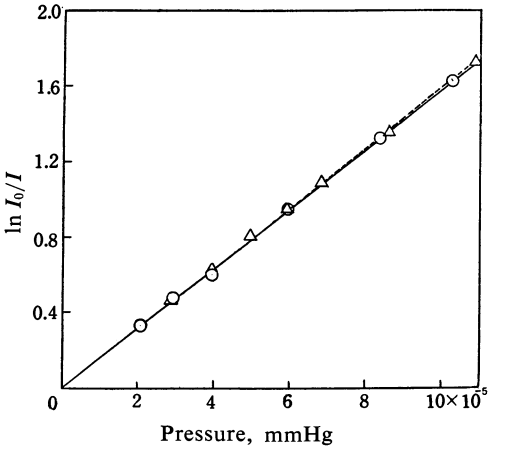



Fig. 4. Sodium beam in nitrogen.

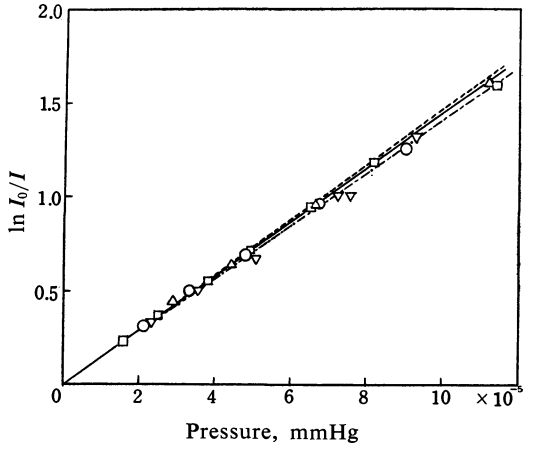



Fig. 5. Sodium beam in argon.

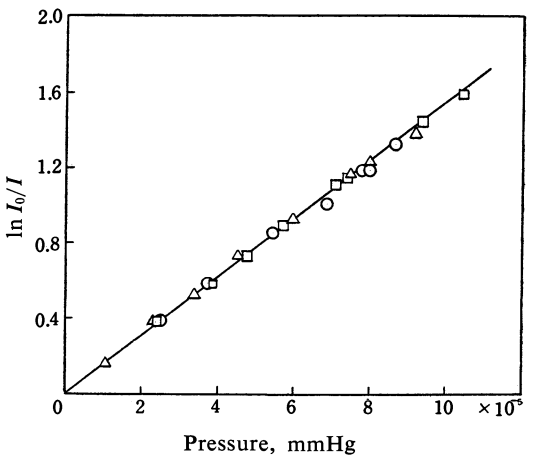



Fig. 6. Sodium beam in carbon monoxide.

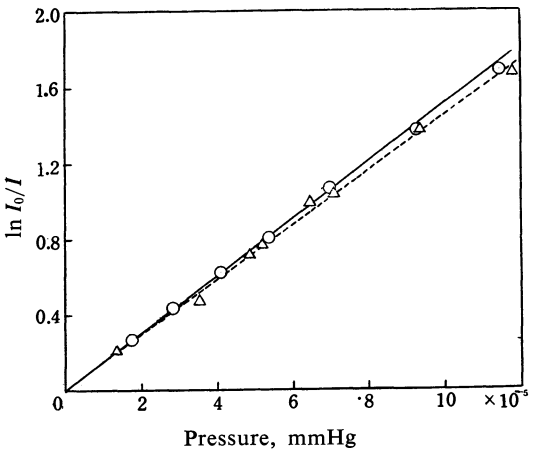



Fig. 7. Sodium beam in nitric oxide.

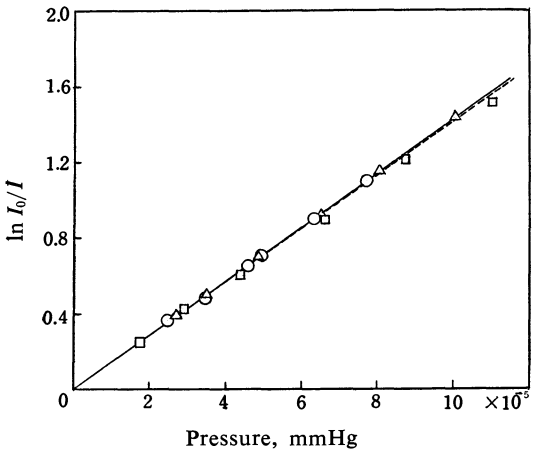



Fig. 8. Sodium beam in oxygen.

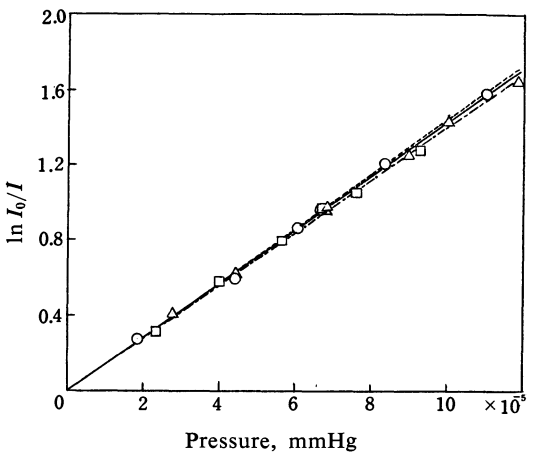



Fig. 9. Sodium beam in cabon dioxide.

are those of beam atoms in scattering gases at $10^{-4}$ mmHg. From these values, effective collision radii ($\sigma$) were calculated by Tait's equation using Rosenberg's table[2]. A detailed account of the calculation has been given in the previous paper. In Table II, average values of collision radii in Table I and collision cross sections are shown together with classical kinetic values ($\sigma_K$) for comparison. To evaluate these values, the radius of a sodium atom was assumed to be $3.0\times10^{-8}$ cm. as in the previous paper, and for the radii of the scattering gas molecules, values obtained from the viscosity measurements[3] were used.

## Discussion

The distributions of the scattering gases differ somewhat for each measurement. This fact may be attributable to the difference of pumping speeds as they were rather sensitive to the heating currents. For the detector chamber, the pressures were extremely low so that errors in the measurements were rather large but their contributions to $l_e$ were small. For reacting gases, pressures in the oven chamber were extremely low, because the gases effused into the chamber reacted with sodium deposited on its wall or in the gas phase. In these cases the pressures might also be changed by the surface state of the deposit. Therefore, calculated $l_e$ varied somewhat in some cases, but the values of collision radii which were obtained agreed satisfactorily.

Among scattering gases, rare gases, nitrogen and carbon monoxide will not react with sodium atoms. For hydrogen, there is a possibility of reaction with sodium atoms producing sodium hydride, but the pressure in the oven chamber indicates that, even if it is the case, the amount is negligible. On the other hand, pressures of oxygen, nitric oxide and carbon dioxide in the oven chamber were extremely low, indicating that the gases were consumed by the reactions with sodium deposited on the wall or in the gas phase. In the cases of oxygen and nitric oxide, the pressures were the same whether the oven was heated or not, so that the consumption of the gases should be considered to occur almost solely by the surface reaction. For carbon dioxide, when the oven was at room temperature, the pressure was intermediate between those of non-reactive gases and reactive gases. To see whether the reaction in the gas phase affects the stationary pressure of the scattering gas in this case,

2) P. Rosenberg, *Phys. Rev.*, **61**, 528 (1942).
3) E. H. Kennard, "Kinetic Theory of Gases", McGraw-Hill, New York (1938), p. 149; L. B. Loeb, "Kinetic Theory of Gases", McGraw-Hill, New York (1927), p. 529.

TABLE I. MEAN FREE PATHS AND EFFECTIVE COLLISION RADII

| Exp. No. | Gas | Press. dist. $p$ | $p_1$ | $p_3$ | Effective path $l_e$ cm. | Mean free path $\lambda$ cm. | Collision radius $\sigma$ $\times 10^{-8}$ cm. | Temp. of Na °K | Temp. of Gas °K |
|---|---|---|---|---|---|---|---|---|---|
| 1 | He | 1 | 0.28 | 0.017 | 5.04 | 9.16 | 6.69 | 569 | 106 |
| 2 | He | 1 | 0.30 | 0.014 | 5.01 | 8.93 | 6.83 | 577 | 109 |
| 3 | Ne | 1 | 0.28 | 0.012 | 4.99 | 7.45 | 8.35 | 599 | 108 |
| 4 | Ne | 1 | 0.27 | 0.016 | 5.01 | 7.49 | 8.34 | 596 | 109 |
| 5 | Ar | 1 | 0.36 | 0.013 | 5.06 | 3.50 | 12.46 | 567 | 109 |
| 6 | Ar | 1 | 0.30 | 0.014 | 5.04 | 3.47 | 12.36 | 553 | 104 |
| 7 | Ar | 1 | 0.30 | 0.025 | 5.10 | 3.49 | 12.46 | 592 | 109 |
| 8 | $H_2$ | 1 | 0.30 | 0.038 | 5.21 | 4.79 | 8.46 | 576 | 101 |
| 9 | $H_2$ | 1 | 0.33 | 0.021 | 5.08 | 4.72 | 8.52 | 576 | 103 |
| 10 | $N_2$ | 1 | 0.36 | 0.016* | 5.08 | 3.21 | 12.88 | 567 | 110 |
| 11 | $N_2$ | 〃 | 〃 | 〃 * | 〃 | 3.18 | 12.79 | 549 | 104 |
| 12 | CO | 1 | 0.36 | 0.014* | 5.05 | 3.25 | 12.76 | 554 | 108 |
| 13 | CO | 〃 | 〃 | 〃 | 〃 | 3.19 | 12.97 | 567 | 112 |
| 14 | CO | 1 | 0.26 | 0.003 | 5.01 | 3.23 | 12.81 | 595 | 108 |
| 15 | $O_2$ | 1 | 0.008 | 0.015* | 4.88 | 3.41 | 12.55 | 572 | 110 |
| 16 | $O_2$ | 〃 | 〃 | 〃 * | 〃 | 3.37 | 12.47 | 550 | 105 |
| 17 | $O_2$ | 1 | 0.001 | 0.003 | 4.77 | 3.39 | 12.59 | 593 | 110 |
| 18 | NO | 1 | 0.034 | 0.014 | 4.88 | 3.23 | 12.75 | 567 | 105 |
| 19 | NO | 1 | 0.054 | 0.012 | 4.88 | 3.35 | 12.77 | 592 | 114 |
| 20 | $CO_2$ | 1 | 0.003 | 0.014 | 5.07 | 3.51 | 14.37 | 606 | 206 |
| 21 | $CO_2$ | 1 | 0.006 | 0 * | 4.96 | 3.49 | 14.39 | 556 | 201 |
| 22 | $CO_2$ | 〃 | 〃 | 〃 * | 〃 | 3.54 | 14.18 | 550 | 201 |

* These values are average values of several observations before the experiments.

TABLE II. EFFECTIVE COLLISION RADII AND CROSS SECTIONS

| Gas | Temp. of Gas, °K | $\sigma$ $\times 10^{-8}$ cm. | $\pi\sigma^2$ $\times 10^{-16}$ cm$^2$ | Classical kinetic value $r_G$ $\times 10^{-8}$ cm. | $\sigma_K$ $\times 10^{-8}$ cm. | $\sigma/\sigma_K$ |
|---|---|---|---|---|---|---|
| He | 108 | 6.76 | 144 | 1.1 | 4.1 | 1.65 |
| Ne | 108 | 8.35 | 219 | 1.2 | 4.2 | 1.99 |
| Ar | 107 | 12.4 | 483 | 1.8 | 4.8 | 2.58 |
| $H_2$ | 102 | 8.51 | 227 | 1.4 | 4.4 | 1.94 |
| $N_2$ | 107 | 12.8 | 515 | 1.9 | 4.9 | 2.62 |
| CO | 109 | 12.8 | 515 | 1.8 | 4.8 | 2.67 |
| $O_2$ | 108 | 12.5 | 491 | 1.8 | 4.8 | 2.62 |
| NO | 109 | 12.8 | 515 | 1.7 | 4.7 | 2.72 |
| $CO_2$ | 201 | 14.3 | 642 | 2.3 | 5.3 | 2.70 |

number of carbon dioxide molecules which react with sodium atoms in the gas phase has been roughly calculated. The calculation revealed that, assuming reaction probability on collision to be unity, and assuming collision cross-section to be equal to the classical kinetic value, less than 4% of effusing molecules react with sodium atoms in the gas phase under the present experimental condition. Reaction probabilities of colliding molecules are in general far smaller than unity, so that the reaction cannot produce any detectable change upon the stationary pressure in the oven chamber. Thus, rather large pressure observed when the oven was at room temperature should be explained by the contamination of the deposit surface which retards the surface reaction. For the same reason, in the cases of oxygen and nitric oxide, the equal stationary pressures observed with or without sodium beams do not exclude the existence of the reaction in the gas phase.

As for reaction between these gases and sodium atoms in the gas phase no detailed investigations have been found in literatures, but Holt and Sims[4] found that sodium could be distilled in the atmosphere of completely dried oxygen without being oxidized. Therefore, it is reasonable to assume that the probability of reaction on collision is extremely small for oxygen and also for other gases, and the scattering can be treated as elastic, as in

4) W. Holt and W. E. Sims, *J. Chem. Soc.*, **65**, 432 (1894).

the case of the non-reactive gases.

In Table II, it is seen that ratios of measured collision radii to those of classical kinetic values, i. e., $\sigma/\sigma_K$, for molecules of rather small molecular weight, such as hydrogen, helium and neon, are less than two, whereas for other gases they are about 2.7. Similar large collision radii have also been found in the scattering experiments of alkali beams carried out by Mais[5], Rosin and Rabi[6], Sasaki and Kodera[7] and others[8]. As values of $\sigma/\sigma_K$, Sasaki and Kodera obtained 1.6 for hydrogen and 2.2 for oxygen, argon and chlorine with potassium beams. These values are smaller than the present ones. Measurements of Rosin and Rabi for sodium beams shown in Table III

TABLE III. COLLISION RADII AND CROSS SECTIONS (Rosin and Rabi)

| | $\sigma$ $\times 10^{-8}$ cm. | $\pi\sigma^2$ $\times 10^{-16}$ cm$^2$ | $\sigma/\sigma_K$ |
|---|---|---|---|
| He | 6.44 | 130 | 1.57 |
| Ne | 8.24 | 213 | 1.96 |
| Ar | 11.3 | 401 | 2.36 |
| $H_2$ | 7.01 | 154 | 1.59 |

gave $\sigma/\sigma_K$ for hydrogen, helium and neon smaller than 2 and for argon 2.4. The main difference in experimental conditions in these works are the geometric resolution, i. e., atoms deflected more than 25′ in average* in case of Sasaki and Kodera, 1.7′ in Rosin and Rabi, 41″ in present experiments fail to hit the detector filament and, therefore, measured as scattered. Estermann, Foner and Stern measured $\sigma$ for cesium and helium by an apparatus with 5″ resolution and obtained more than 50% larger value than that which Rosin and Rabi obtained with the same pair. As an example of measurement with an apparatus of similar resolving power as in the present case, i. e., 45″, there are Rosenberg's results with a potassium beam. From his data collision radii with gases which were commonly used in both cases have been calculated and listed in Table IV. To estimate values for sodium a factor 0.9, which is an average ratio of $\sigma$ for sodium and for potassium by Rosin and Rabi, was multiplied to these values and shown in the table. For argon and nitrogen, these values agree to ours fairly well, showing that measured radii increase with increasing resolving power, but will take same values by the same resolution. As described in the previous paper, the

TABLE IV. COLLISION RADII FOR POTASSIUM BY ROSENBERG AND CALCULATED VALUES FOR SODIUM

| | K $\times 10^{-8}$ cm. | Na(calcd.) $\times 10^{-8}$ cm. |
|---|---|---|
| He | 7.39 | 6.65 |
| Ar | 13.7 | 12.3 |
| $H_2$ | 7.94 | 7.15 |
| $N_2$ | 14.0 | 12.7 |

simplified quantum mechanical treatment of the colliding particles as hard spheres shows that the scattering intensity for small angles increase markedly below a certain angle $\theta_0$. For the present work, the largest value for $\theta_0$ is about 12° for hydrogen and the smallest value is about 1°40′ for carbon dioxide. The angles of resolution in the above-mentioned measurements are all far smaller than these values, therefore, contribution of the small angle scattering to the collision radius might be included almost completely in these experiments. Moreover, by this contribution the collision radius increases to the value only $\sqrt{2}$ times that of the classical one. Therefore, the change in collision radius with the resolving power and observed large values in the present experiment should be explained by the existence of considerable interaction between colliding particles. For molecules of rather small molecular weights such as hydrogen, helium and neon, values of $\sigma/\sigma_K$ are smaller than 2 both in the present and in the other experiments cited above. However, while the value of helium in the present work is reasonable compared with the others', that of neon is rather small and that of hydrogen is considerably large. The difference in the experimental conditions other than the resolving power are temperatures of beams and gases, i. e., in the work of Rosin and Rabi the beam was at 700°K and though the temperature of gases was not described, it is considered to be at room temperatures, and in the work of Rosenberg, the beams and the gases were at 500°K and 300°K, while in the present work they were at 570°K and 110°K (except carbon dioxide), respectively. Therefore the temperature of gases was very low in the latter. The theoretical collision radius of $\sqrt{2}$ times that of classical value mentioned above is that for particles colliding with infinite relative velocity, but it increases with decreasing relative velocity until at the limit it becomes 2 times that of the classical value. Thus, lowering of the temperature of gas should cause increase of the collision radius, however, in the temperature range in these experiments the effect is too small for the molecules of large molecular weights. For hydrogen it may be possible to detect this effect, but the discrepancy observed

5) W. H. Mais, *Phys. Rev.*, **45**, 773 (1933).
6) S. Rosin and I. I. Rabi, ibid., **48**, 373 (1935).
7) N. Sasaki and K. Kodera, *Mem. Col. Sci., Univ. Kyoto*, **25**, 84 (1949).
8) P. Rosenberg, *Phys. Rev.*, **55**, 1267 (1939); I. Estermann, S. N. Foner and O. Sterm, ibid., **71**, 250 (1947).
* In this experiment, a detector filament was placed in the scattering gas, therefore, the angle of resolution differed from place to place.

is too large to be explained by this cause.

In Table II, it is seen that nitrogen and carbon monoxide have equal radii, this is reasonable that these molecules have nearly equal molecular weights and identical electronic structures. Oxygen has a slightly smaller radius than nitrogen; this slight difference in radii is also seen in the results of Sasaki and Kodera with sodium and potassium beams, and also in classical kinetic values. In the present work, since pressure distributions of nitrogen and oxygen differ considerably because of the reactivity of oxygen with sodium, it is difficult to decide whether this slight difference in the radii has any significance, but the measurements of Sasaki and Kodera were carried out under the same condition for the two gases; therefore, it is possible that the quantity of oxygen is smaller than that of nitrogen.

## Summary

Collision radii considerably larger than those of classical kinetic values have been obtained. Among the measured values of collision radii, that for neon is rather smaller and that for hydrogen is considerably larger than those obtained by the other investigators. For molecules of rather large molecular weight, relative sizes among them are reasonable but they increase with the resolving power of the apparatus used. These large values of radii and their increase with the resolving power may be explained by the existence of considerable mutual interaction such as Van der Waals' force between colliding particles.

The authors wish to express their appreciation to Dr. T. Makita who examined the purities of gases with the mass-spectrometer. This work was partly supported by a grant from the Ministry of Education, to which the authors' thanks are also due.

*Department of Chemistry*
*Faculty of Industrial Arts*
*Kyoto Technical University*
*Sakyo-ku, Kyoto*

# *Diffusion in Glassy Polymers. I. Effects of Initial Concentration upon the Sorption of Organic Vapors in Polymers*

By Hisashi ODANI, Shigeru KIDA, Michio KURATA and Mikio TAMURA

(Received October 17, 1960)

Kishimoto et al.[1] have recently shown for a number of glassy polymer-organic vapor systems that when such a system is studied by the differential absorption technique, the sorption kinetics exhibits three types of non-Fickian anomalies as the initial concentration for each differential step increases. These non-Fickian anomalies are sigmoid type, pseudo-Fickian type and two-stage type. They also found that for amorphous systems the differential absorption process changes to the normal Fickian type in the vicinity of a penetrant concentration at which the given polymer-vapor mixture undergoes glass transition at the temperature of the experiment. The study reported in the present paper is concerned with integral absorption experiments in which the initial concentrations are taken in the regions corresponding to these four different types of differential absorption processes. It is expected that such a study will provide us with information about how small the concentration increment of each step should be in order that the absorption process may exhibit the behavior regarded as being characteristic of the initial concentration of the experiment. We have from existing literatures a vast amount of available experimental data for the integral absorption of vapors in polymeric solids[2-16].

1) A. Kishimoto, H. Fujita, H. Odani, M. Kurata and M. Tamura, *J. Phys. Chem.*, **64**, 594 (1960).

2) J. Crank and G. S. Park, *Trans. Faraday Soc.*, **45**, 240 (1949).
3) G. S. Park, ibid., **46**, 684 (1950).
4) L. Mandelkern and F. A. Long, *J. Polymer Sci.*, **6**, 457 (1951).
5) S. Prager and F. A. Long, *J. Am. Chem. Soc.*, **73**, 4072 (1951).
6) G. S. Park, *Trans. Faraday Soc.*, **47**, 1007 (1951).
7) A. T. Hutcheon, R. J. Kokes, J. L. Hoard and F. A. Long, *J. Chem. Phys.*, **20**, 1232 (1952).
8) R. J. Kokes, F. A. Long and J. L. Hoard, ibid., **20**, 1711 (1952).
9) G. S. Park, *J. Polymer Sci.*, **11**, 97 (1953).
10) S. Prager, E. Bagley and F. A. Long, *J. Am. Chem. Soc.*, **75**, 1255 (1953).
11) F. A. Long and R. J. Kokes, ibid., **75**, 2232 (1953).
12) R. J. Kokes and F. A. Long, ibid., **75**, 6124 (1953).
13) F. A. Long and L. J. Thompson, *J. Polymer Sci.*, **15**, 413 (1955).
14) M. J. Hayes and G. S. Park, *Trans. Faraday Soc.*, **51**, 1134 (1955).
15) A. Kishimoto and K. Matsumoto, *J. Phys. Chem.*, **63**, 1529 (1959).
16) H. Fujita, A. Kishimoto and K. Matsumoto, *Trans. Faraday Soc.*, **56**, 424 (1960).

However, the majority of them deal with experiments started from zero initial concentration, and data from non-zero concentrations are yet limited to a very few systems.

The systems chosen in this work are atactic polystyrene+benzene and cellulose nitrate+acetone, both at 25°C. Successive differential absorptions of these systems have been described in detail in Ref. 1. In the following pages we present data from experiments with the polystyrene system in greater detail, and only partial data are given for the cellulose nitrate system.

## Experimental

**Materials.**—The atactic polystyrene used was a commercial product "Lustrex hi-flow 77-234" and had a viscosity-average molecular weight of $2.2\times10^5$. The cellulose nitrate was a sample obtained from Fuji Photo Co. The intrinsic viscosity in acetone at 20°C and the nitrogen content (determined by the Lunge method) were 2.51 dl./g. and 11.95%, respectively. The polymer films used for sorption experiments were obtained by the same procedure reported elsewhere[1]. The penetrants were of A. R. grade.

**Apparatus and Procedure.**—The sorption apparatus used was practically the same as that reported elsewhere[1]. For absorption experiments the integral absorption technique was employed; i. e. a given polymer film was suspended from a sensitive quartz spring in a sorption tube and was equilibrated with the vapor of a given penetrant at a desired pressure $p_i$ (including zero). Then the pressure was suddenly increased to a higher pressure $p_f$ and the absorption process was followed by measuring the extention of the spring as a function of time. Although the term "integral" was previously referred to experiments with pressure differences ($\Delta p=p_f-p_i$) of relatively large magnitudes[1], results reported in this paper also include those obtained from "differential" absorptions in which $\Delta p$ is sufficiently small. All the measurements were conducted at 25°C. This temperature is well below the glass transition temperatures of the respective polymers in their dry state[17].

## Results and Discussion

**Atactic Polystyrene—Benzene System.**—As described in the previous paper[1], the successive differential absorptions for this system changed with the initial concentration according to the following scheme.

Sigmoid type → pseudo-Fickian type → two-stage type → Fickian type.

We studied integral absorptions for this system by choosing the initial concentrations in the regions corresponding to these four types of differential absorption.

17) H. Mark and A. V. Tobolsky, "Physical Chemistry of High Polymeric Systems", Interscience Pub. Inc., New York (1950), p. 347.

*Integral Sorptions from Initial Concentrations Corresponding to Differential Absorptions of Sigmoid Type.* — Figure 1 gives data of integral absorptions from zero pressure, and also includes partial results from the desorption runs; the solid lines refer to absorption and the dashed lines to desorption. These data were taken on films $2.40\times10^{-3}$ cm. thick.

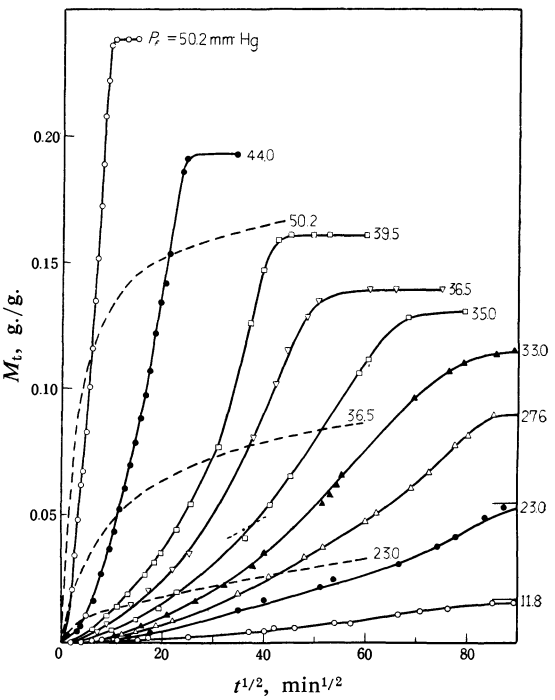



Fig. 1. Integral absorptions from and desorptions to zero pressure for atactic polystyrene at 25°C. $p_f$ is the final pressure of a particular run. $M_t$ is the weight of vapor absorbed or desorbed by mass of the polymer at time $t$. Solid lines, absorption; Dashed lines, desorption. Film thickness=$2.40\times10^{-3}$ cm.

The integral absorption processes are all non-Fickian over the entire range of vapor pressures studied. It is seen that even for the largest pressure interval the shape of the absorption curve is sigmoid. In all cases, the initial rate of desorption is greater than that of the corresponding absorption.

Long and Kokes[11] found that the integral absorptions from zero pressure were Fickian type when the final pressures were above the value corresponding to the equilibrium concentration at which the given polymer-penetrant mixture undergoes glass transition at the temperature of the experiment. However, it is seen from Fig. 1 that this is not the case with our atactic polystyrene—benzene system. The equilibrium concentration for $p_f=50.2$ mmHg is well above the critical concentration, 0.191

g./g., for this system to undergo glass transition at 25°C[1]. Nevertheless, the absorption for this pressure is evidently non-Fickian.

In Fig. 1 it is also noted that the absorption curves show a pronounced dependence upon the pressure difference. Many experimental results[1,4,8,9,11,13,18] show that when a given polymer-penetrant mixture is in the glassy state, the absorption processes depend not only upon the concentration of penetrant but also upon other factors, probably the time. Under such circumstances we are not able to evaluate the mutual diffusion coefficient of a given system by using the method which uses measurements of the initial rate of absorption[15,19]. We here choose the value of $1/(t/l^2)_{1/2}$ to measure the overall rate of each absorption curve, where $l$ is the thickness of the film, $t$ is time, and $(t/l^2)_{1/2}$ is the value of $t/l^2$ when the amount of vapor in the film reaches one half of the final equilibrium value.

The values of $1/(t/l^2)_{1/2}$ determined from the data of Fig. 1 are plotted semi-logarithmically against $C_f$, the concentration of benzene at absorption equilibrium, in Fig. 2. For

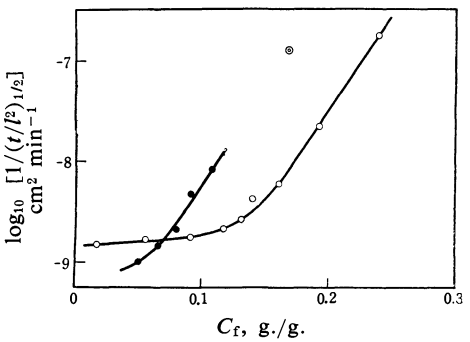



Fig. 2. Logarithmic correlation plots of $1/(t/l^2)_{1/2}$ and final equilibrium concentration $C_f$ for atactic polystyrene–benzene at 25°C. $(t/l^2)_{1/2}$ is the values of $t/l^2$ when the amount of vapor in polymer reaches one half of the final equilibrium value; $l$ is the thickness of film and $t$ is time. $C_i=0$. ○, $l=2.40\times10^{-3}$ cm.; ◎, $l=1.61\times10^{-2}$ cm.: ●, Park's data. $l=1.80\times10^{-2}$ cm. (These values have been calculated from the results given in Table I of Park's paper.[6]).

comparison the values calculated from the data of Park for the same kind of system[6] are included. It is seen that above 0.12 g./g. of $C_f$ our data for $\log[1/(t/l^2)_{1/2}]$ increase almost linearly with increasing $C_f$ and the shape of this plot is similar to that obtained from Park's data. However, the relative positions of the two curves are different from each other. This discrepancy may be attributed to the difference in thickness of the films used in the two studies*.

Integral absorptions from the initial concentration $C_i=0.095$ g./g. to several higher $C_f$ were also investigated by using films of $2.40\times10^{-3}$ cm. thick. Although the results are not given here, the absorption processes were of sigmoid type and the dependence of $1/(t/l^2)_{1/2}$ upon the difference between the initial and final concentrations, $\Delta C(=C_f-C_i)$, was similar to that obtained for the series with $C_i=0$.

In a summary it is concluded that in the region of initial concentrations $C_i$ where differential absorptions are of sigmoid type, absorption rates depend markedly upon the final concentration, $C_f$, or the concentration increment, $C_f-C_i$, and this dependence is not affected so appreciably by the value of $C_i$.

*Integral Absorptions from Initial Concentrations Corresponding to Differential Absorptions of Pseudo-Fickian Type.*—Integral absorptions from $C_i=0.118$ and 0.132 g./g. were investigated by using films of $2.40\times10^{-3}$ cm. thick. Although the results are not given here, the curves are very similar to those from zero initial concentration reported by Park for the polystyrene–methylene chloride system at 25°C[9] and also those by Long and Kokes for the same system at 30°C[11]. That is, for so small values of $\Delta p$ as to give only 0.010~0.015 g./g. concentration increment, the shape of absorption curves was of pseudo-Fickian type, but for larger values of $\Delta p$ the absorption curves changed to the sigmoid type and this feature persisted up to the largest of the $\Delta p$ investigated.

The values of $1/(t/l^2)_{1/2}$ increase with $\Delta C$, but to a less extent than in the case of integral absorptions from initial concentrations corresponding to differential absorption of sigmoid type.

*Integral Absorptions from Initial Concentrations Corresponding to Differential Absorptions of Two-stage Type.*—Integral absorptions from $C_i=$ 0.160, 0.169 and 0.181 g./g. were studied with films of $2.40\times10^{-3}$ cm. thick. Figure 3 gives data from a series of absorption experiments from $C_i=0.160$ g./g. For small $\Delta p$ the curves are similar in shape and show distinctly the two-stage characteristics, but as $\Delta p$ increases the two-stage character becomes less apparent and the inflection point on the second stage portion shifts markedly to the short time region. These

18) P. Drechsel, J. L. Hoard and F. A. Long, *J. Polymer Sci.*, **10**, 241 (1953).
19) R. M. Barrer, *J. Phys. Chem.*, **61**, 178 (1957); R. M. Barrer and R. R. Ferguson, *Trans. Faraday Soc.*, **54**, 989 (1958).

* As seen in Fig. 2, the point obtained from an experiment with a film of $1.61\times10^{-2}$ cm. thick appears at a smaller value of $C_f$ than do the plots obtained with a film of $2.40\times10^{-3}$ cm. thick.

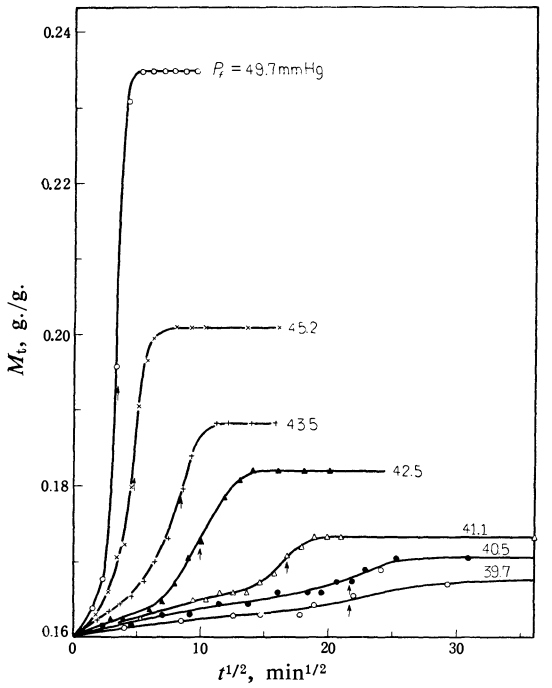



Fig. 3. Integral absorptions from a fixed non-zero initial pressure to different final pressures for atactic polystyrene–benzene at 25°C. Initial pressure $p_1$=39.3 mmHg. Film thickness=$2.40\times10^{-3}$ cm.

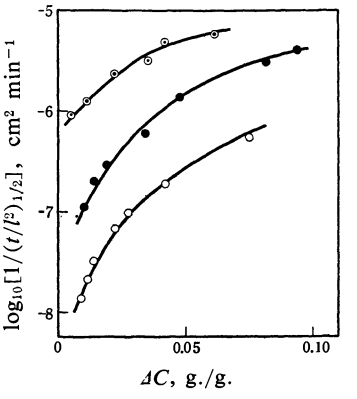



Fig. 4. Logarithmic correlation plots of $1/(t/l^2)_{1/2}$ and concentration difference $\Delta C$ for absorption of benzene in atactic polystyrene at 25°C. ○, $C_1$=0.160 g./g.; ●, $C_1$=0.169 g./g.; $C_1$=0.181 g./g. Film thickness=$2.40\times10^{-3}$ cm.

results are similar to those published by Long and Richman for the cellulose acetate–methyl iodide system at 40°C[20]. The data with $C_1$=0.169 and 0.181 g./g. showed the general trend similar to that obtained for $C_1$=0.160 g./g. Thus we see that the integral absorptions also depend strongly on $\Delta p$ when the experiments start from initial concentrations where differential absorption curves exhibit the two-stage behavior.

For small values of $\Delta p$ the contribution of the first stage absorptions to the total concentration increment is significant, but the time taken to attain the quasi-equilibrium of the first stage is much shorter than that taken for the total absorption process. Therefore, for this type of absorption curve we may use the quantity $1/(t/l^2)_{1/2}$ as an approximate measure of the overall rate of absorption. The values of this quantity determined from the data of Fig. 3 and the similar data at $C_1$=0.169 and 0.181 g./g. are plotted semi-logarithmically against $\Delta C$ in Fig. 4. It is seen that the dependences of $1/(t/l^2)_{1/2}$ on $\Delta C$ for the three $C_1$ values are hardly different from one another and that they are all so marked that an extremely small pressure increment must be used in this region of $C_1$ in order to obtain an absorption curve characteristic of a given initial concentration.

*Integral Absorptions from Initial Concentrations Corresponding to Differential Absorptions of Fickian Type.*—According to our previous investigation[1], the critical concentration of benzene in polystyrene at which the system undergoes glass transition at 25°C is 0.191 g./g. Choosing this concentration as $C_1$ we carried out integral absorption experiments for sample films which covered a five-hold range of thickness. We also performed similar experiments with $C_1$=0.235 g./g. for two films of different thicknesses. The results of these measurements are as follows:

a) Both absorption and desorption curves are initially linear; for absorption this linearity holds over about 70% of the total concentration increment and for desorption this is limited to about 50% of the total concentration increment.

b) Above the linear regions both absorption and desorption curves are concave against the time axis.

c) Desorption is always slower than absorption irrespective of the magnitude of $\Delta C$.

d) With the increase of $\Delta C$ absorption becomes faster and this is also the case for desorption.

These are the features of the true Fickian diffusion in which the diffusion coefficient increases with increasing concentration[21]. However, it was found that;

e) Data from varying thickness experiments could not be reduced to a single curve when plotted against the variable $t/l^2$; for the same

20) F. A. Long and D. Richman, *J. Am. Chem. Soc.*, **82**, 513 (1960).

21) H. Fujita, A. Kishimoto and H. Odani, *Suppl. Progr. Theor. Phys.*, **10**, 210 (1959).

value of $\Delta C$ thicker films gave curves which are located to the left of the curve obtained for thinner films, the behavior very similar to that exhibited by integral absorption curves started with zero initial concentration.

Because of this last feature it is concluded that even in the region of benzene concentrations where the given mixture is considered to be in the rubbery state the absorption process of benzene in atactic polystyrene is not altogether controlled by the purely Fickian mechanism.

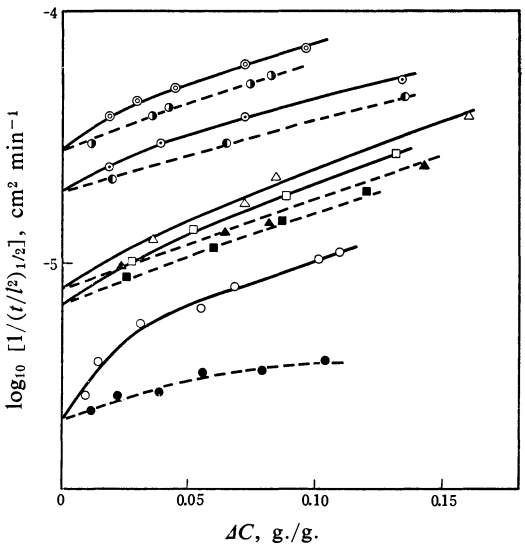



Fig. 5. Logarithmic correlation plots of $1/(t/l^2)_{1/2}$ and $\Delta C$ for atactic polystyrene –benzene at 25°C.

| | $l$, cm. | Absorptions | Desorptions |
|---|---|---|---|
| (a) $C_1$=0.191 g./g. | $2.40\times10^{-3}$ | ○ | ● |
| | $7.67\times10^{-3}$ | □ | ■ |
| | $1.12\times10^{-2}$ | △ | ▲ |
| (b) $C_1$=0.235 g./g. | $1.15\times10^{-2}$ | ⊙ | ◐ |
| | $1.70\times10^{-2}$ | ◎ | ◑ |

In Fig. 5 are plotted the values of $1/(t/l^2)_{1/2}$ determined from these measurements as a function of $\Delta C$, with $l$ and $C_1$ as parameters. It is seen that for both $C_1$ the thicker films give higher values of $1/(t/l^2)_{1/2}$ when compared at the same values of $\Delta C$. This is substantially equivalent to the feature (e) stated above. Finally, one may remark that the dependence of $1/(t/l^2)_{1/2}$ on $\Delta C$ in this region of $C_1$ is much milder than those obtained in the regions of $C_1$ where differential absorptions are non-Fickian.

It is generally conceived that when the system is in the glassy state there must be a time delay in the establishment of the equilibrium value of the diffusion coefficient and/or of the concentration on the sample surface. This may cause the absorption process of the system not to obey the purely Fickian diffusion mechanism. In the case treated above it is considered that the polymer-vapor mixtures were in the rubbery state at the start of the absorption experiments. Nevertheless, the absorption processes measured exhibited a non-Fickian feature (the film thickness effect). This appears to indicate that even when the mixture is in the rubbery state the diffusion of penetrant does not follow the Fickian mechanism if the penetrant concentration is not sufficiently above the critical concentration corresponding to the temperature of the experiment. Kishimoto and Matsumoto[22] have recently shown with polyvinyl acetate and polymethyl acrylate that integral absorptions of organic vapors into these amorphous polymers cannot be interpreted in terms of the purely Fickian mechanism when the temperatures of the systems are only 10 to 20°C above the glass transition temperatures of respective polymers. Although the effect of rising temperature may not exactly be equivalent to that of increasing diluent concentration, our observations of the non-Fickian feature at concentrations above the critical concentration appear to have a close correlation to those of Kishimoto and Matsumoto. A more detailed study of the sorption behavior in the region of initial concentrations above the critical concentration is now in progress in this laboratory and will be reported in a forthcoming article.

In a summary, it may be concluded as follows: The sorption rate of benzene into atactic polystyrene depends strongly on the concentration of benzene in the region of low $C_1$, the dependence becomes milder with increasing concentration of benzene and almost vanishes in the concentration region somewhat above the critical concentration for this system. Just above the critical concentration, the effect of sample thickness still exists, though the differential absorption curves in this region appear to have the shape expected from the purely Fickian mechanism.

**Cellulose Nitrate — Acetone System.**—The successive differential absorption curves for this system change their shape according to the following scheme[1]:

Sigmoid type → pseudo-Fickian type → two-stage type → sigmoid type.

We studied the integral sorptions from zero initial concentration and also from a non-zero initial concenration corresponding to a differential absorption of two-stage type.

22) A. Kishimoto and K. Matsumoto, private communication.

*Integral Absorptions and Desorptions from and to Zero Initial Concentration.*—Integral absorptions and desorptions from and to zero pressure were studied in the range of acetone pressure from 8.5 to 147 mmHg. The features of the curves obtained exactly resemble those for the atactic polystyrene–benzene system. That is, the integral absorption processes are all non-Fickian of sigmoid type over the entire range of vapor pressures studied and the initial rate of desorption is greater than that of the corresponding absorption for all cases. The absorption curves show a pronounced dependence on the pressure difference and the general feature of this dependence is very similar to that observed for the atactic polystyrene–benzene system.

In accordance with the atactic polystyrene–benzene system, we choose the quantity $1/(t/l^2)_{1/2}$ as a measure of absorption rate. Figure 6 gives the plots of $\log[1/(t/l^2)_{1/2}]$ against $C_f$, and the corresponding data for the atactic polystyrene–benzene system are also indicated for the sake of comparison. It is seen that the values of $1/(t/l^2)_{1/2}$ increase rapidly in the region of medium $C_f$ and the shape of the curve in this region is quite similar to that for atactic polystyrene–benzene system. Also it will be seen that in the region of high $C_f$ the plots approach a constant value. These observations suggest that there is no close correlation between the dependence of integral absorption rates upon the concentration of penetrant and the molecular features of the polymer, such as crystallinity and chain stiffness.

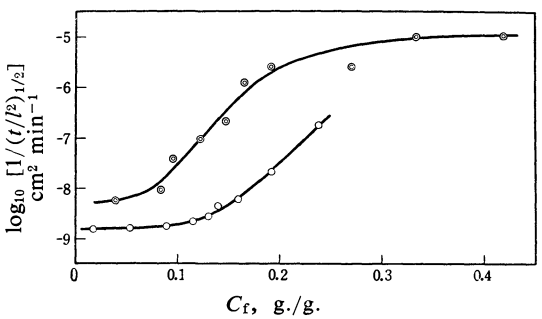



Fig. 6. Logarithmic correlation plots of $1/(t/l^2)_{1/2}$ and $C_f$ for cellulose nitrate–acetone and for atactic polystyrene–benzene at 25°C. $C_1=0$. Film thickness= $2.40\times10^{-3}$ cm. ◎, cellulose nitrate–acetone; ○, atactic polystyrene–benzene.

*Integral Absorptions from a Non-zero Initial Concentration Corresponding to a Differential Absorption of Two-stage Type.*—Figure 7 gives data from integral absorption experiments obtained with $C_1=0.192$ g./g. It is observed that the general feature of these curves is very similar to that for the atactic polystyrene–benzene system shown in Fig. 3. However, we may notice some differences between the two. First, absorption rates of the first stage of the two-stage sorption process for the cellulose nitrate–acetone system are much faster than those for the atactic polystyrene–benzene system. Second, in the former system the two-stage character first becomes increasingly apparent as $\Delta p$ increases, accompanied with a marked shift of the inflection point to the short time region and a rapid enhancement of the second stage rate.

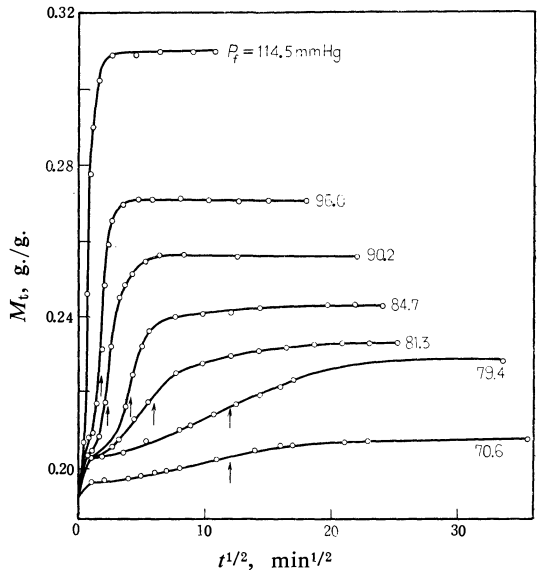



Fig. 7. Integral absorptions from a fixed non-zero initial pressure to different final pressures for cellulose nitrate–acetone at 25°C. $p_1=63$ mmHg. Film thickness= $2.40\times10^{-3}$ cm.

In a summary, it may be concluded that in the glassy state the dependence of integral absorption rates upon penetrant concentration for the cellulose nitrate–acetone system does not differ markedly from that for the atactic polystyrene–benzene system.

We wish to thank Professor H. Fujita and Dr. A. Kishimoto of this University for advice given during the course of this investigation. The study reported in this paper was supported in part by the Ministry of Education to which grateful acknowledgment is made.

*Department of Industrial Chemistry*
*Faculty of Engineering*
*Kyoto University*
*Sakyo-ku, Kyoto*

# *The Structure of 4-(α-Ethylenedioxy)ethyltropolone Methyl Ether*[1]

By Ichiro MURATA

(Received August 1, 1960)

4-Acetyltropolone[2] obtained by oxidation of β-dolabrin (4-isopropenyltropolone)[2] reacts with ethylene glycol in dehydrated benzene, in the presence of *p*-toluenesulfonic acid, and easily forms 4-(α-ethylenedioxy)ethyltropolone (I) as colorless prisms of m. p. 98°C. I easily reverts to 4-acetyltropolone on being heated with dilute mineral acid.

Methylation of I with an ether solution of diazomethane affords two kinds of methyl ethers in approximately 1 : 1 ratio, one a colorless needle (II), m. p. 110°C, and the other a colorless prism (III), m. p. 111°C. Admixture of II and III clearly indicates depression of the melting point. The ultraviolet spectra of II and III, shown in Fig. 1, clearly indicate the characteristic absorption of tropolone methyl ethers[3].

In order to establish the structure of these

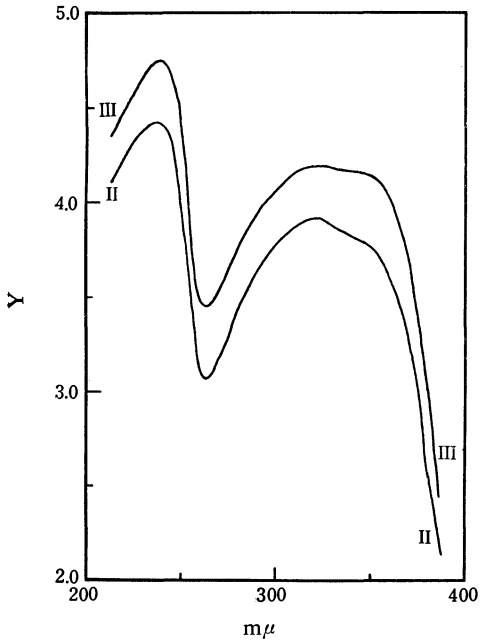



Fig. 1. Ultraviolet absorption spectra of II and III in methanol.
II: $Y=\log\varepsilon$; III: $Y=\log\varepsilon+0.3$

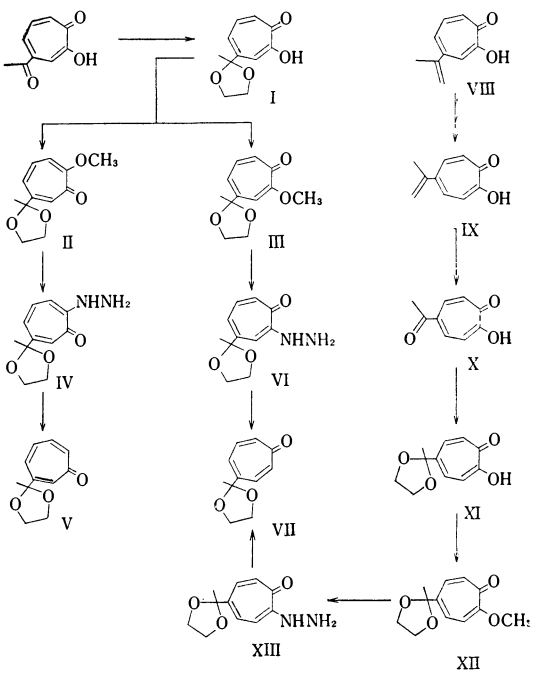



Fig. 2.

methyl ethers, the following reactions were examined.

When II is heated with hydrazine hydrate in ethanol, a hydrazino derivative IV is obtained in a good yield as orange needles, m. p. 99°C. The cyclohexylidene compound of IV comes as yellow needles of m. p. 95~96°C. Decomposition of IV with aqueous solution of copper sulfate in dilute acetic acid affords *x*-(α-ethylenedioxy)ethyltropone (V) as colorless prisms, m. p. 72°C.

On the other hand, a similar derivation of the methyl ether III of m. p. 111°C to the hydrazinotropone derivative VI, m. p. 124°C, and its subsequent decomposition with copper sulfate gives *x'*-(α-ethylenedioxy)ethyltropone (VII) as colorless scales, m. p. 81.5°C.

The two kinds of tropone derivatives V and VII so obtained show infrared absorption spectra[4] (region of out-of-plane vibrations) indicated in Fig. 3.

1) Paper presented at the 12th Annual Meeting of the Chemical Society of Japan, Kyoto, April, 1959.
2) T. Nozoe, K. Takase and M. Ogata, *Chem. and Ind.*, 1957, 1070.
3) M. Tsuboi, This Bulletin, 25, 369 (1952).
4) Infrared spectra were measured with a Perkin-Elmer model-21 spectrophotometer provided with a sodium chloride prism.

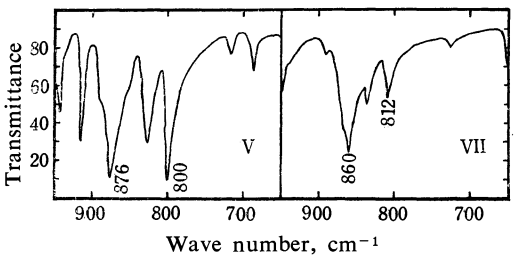



Fig. 3. Infrared absorption spectra of V and VII.

As had already been pointed out by Kitahara[5], the out-of-plane absorption of hydrogens in the seven-membered ring in the troponoid compounds is approximately in regularity with the number of adjacent hydrogen, as was found in benzenoid compounds.

The $\alpha$-ethylenedioxyethyl group in the tropone derivatives obtained by the removal of methoxyl group from the methyl ethers II and III should be present in the 3- or 4-position. If it is in the 3-position, the number of adjacent hydrogen atoms would be one and four, and their absorptions should appear at 760~810 $cm^{-1}$ (s) and at 860~900 $cm^{-1}$ (m). If in the 4-position, the number of adjacent hydrogen atoms would be two and three, and their absorptions should appear at 770~820 $cm^{-1}$ (s) and 820~860 $cm^{-1}$ (s).

It is clearly seen in Fig. 3 that V shows marked absorptions at 800 and 876 $cm^{-1}$, while VII has absorptions at 812 and 860 $cm^{-1}$. Consequently, it would seem possible to conclude that V is a 3-substituted tropone and VII is a 4-substituted tropone.

In order to prove the above assumptions by organic chemical means, the following reactions were carried out.

$\beta$-Dolabrin (VIII) was converted by the known process[6] into $\gamma$-dolabrin (IX) and oxidized with hydrogen peroxide and then with periodic acid into 5-acetyltropolone (X)[6]. Reaction of ethylene glycol on X in benzene, in the presence of *p*-toluenesulfonic acid, as in the case of 4-acetyltropolone, afforded 5-($\alpha$-ethylenedioxy)ethyltropolone (XI) as colorless needles, m. p. 104°C. Methylation of XI with an ether solution of diazomethane produced almost quantitatively the methyl ether (XII) of XI as colorless prisms, m. p. 115°C. Since XI is a 5-substituted tropolone, the structure of its methyl ether XII should be 2-methoxy-5-($\alpha$-ethylenedioxy)ethyltropone. XII forms a hydrazinotropone derivative XIII of m. p. 164°C (decomp.) with hydrazine hydrate.

5) Y. Kitahara, *Sci. Repts. Tohoku Univ.*, [I] **39**, 275 (1956).

6) T. Nozoe, T. Mukai, K. Yamane, T. Asao and I. Murata, Paper presented at the 11th Annual Meeting of the Chemical Society of Japan, Tokyo, April, 1958.

Decomposition of XIII with copper sulfate in dilute acetic acid affords a tropone derivative of m. p. 81.5°C, whose structure would clearly be 4-($\alpha$-ethylenedioxy)ethyltropone considering the route of its synthesis.

Of the two kinds of tropone derivatives V and VII obtained in the present series of work and described above, the one with m. p. 81.5°C (VII) agreed with the product obtained by decomposition of XIII in mixed melting point, and in ultraviolet and infrared absorption spectra, indicating them to be the same substance. Consequently, it becomes clear that the structure of V is 3-($\alpha$-ethylenedioxy)ethyltropone. This fact agrees well with the results of infrared spectral analysis mentioned above.

From the foregoing experimental facts, it is concluded that the structure of II is 2-methoxy-6-($\alpha$-ethylenedioxy)ethyltropone and that of III is 2-methoxy-4-($\alpha$-ethylenedioxy)ethyltropone.

## Experimental[7]

**4-($\alpha$-Ethylenedioxy)ethyltropolone (I).**—A mixture of 4-acetyltropolone (2.9 g.), dehydrated benzene (100 ml.), ethylene glycol (30 ml.), and *p*-toluenesulfonic acid (0.3 g.) was refluxed with stirring and the water was removed by azeotropic distillation with benzene through a column 20 cm. in length. During this time, 50 ml. of benzene was supplemented twice and the whole reaction was carried out over 20 hr. The reaction mixture was then diluted with water and extracted with benzene. The benzene layer was extracted with 2 N sodium hydroxide, the aqueous layer was acidified with hydrochloric acid and the crystals that formed were collected. Low-pressure sublimation of this product afforded 3.25 g. of I, m. p. 95~97°C. Recrystallization of I from a mixed solvent of benzene and cyclohexane gave colorless prisms, m. p. 97.5~98°C.

Found: C, 63.00; H, 6.05. Calcd. for $C_{11}H_{12}O_4$: C, 63.45; H, 5.81%.

**Methylation of I.**—To a suspension of I (3.2 g.) in ether (20 ml.), ether solution of diazomethane was added dropwise with ice-cooling, by which I gradually dissolved and needle crystals began to precipitate out. When the solution no longer colored with ferric chloride solution, the crystals were collected. Yield 1.45 g. M. p. 105~107°C.

The ethereal mother liquor was concentrated and a further crop (1.85 g.) of crystals, m. p. 95~106°C was obtained. Repeated fractional recrystallization from a mixed solvent of cyclohexane and benzene finally afforded II (1.1 g.) from the former as colorless needles, m. p. 109~110°C, and III (1.49 g.) chiefly from the latter as colorless prisms, m. p. 110~111°C. Admixture of II and III melting at 85~87°C.

Found (for II): C, 65.10; H, 6.29. Calcd. for $C_{12}H_{14}O_4$: C, 64.85; H, 6.35%. Ultraviolet $\lambda_{max}^{MeOH}$ m$\mu$ (log $\varepsilon$): 236 (4.44), 322 (3.92).

7) All melting points are not corrected.

Found (for III): C, 65.01; H, 6.24. Calcd. for $C_{12}H_{14}O_4$: C, 64.85; H, 6.35%. Ultraviolet $\lambda_{max}^{MeOH}$ mμ (log ε): 238 (4.48), 322 (3.91).

**2-Hydrazino-6-(α-ethylenedioxy)ethyltropone (IV).** —80% hydrazine hydrate (0.2 g.) was added to the solution on II (0.2 g.) dissolved in ethanol (0.5 ml.) and the mixture was heated at 90°C for 5 min. Evaporation of ethanol afforded crystals (0.2 g.) of m. p. 68~79°C which recrystallized from dilute ethanol to IV as orange needles, m. p. 98~99°C.

Found: C, 57.52; H, 6.35; N, 12.48. Calcd. for $C_{11}H_{14}O_3N_2$: C, 57.45; H, 6.35; N, 12.60%. Ultraviolet $\lambda_{max}^{MeOH}$ mμ (log ε): 250 (4.41), 340 (4.07), 402 (4.03).

**Cyclohexylidene Compound of IV.** — Cyclohexanone (0.06 g.) was added to the solution of IV (0.12 g.) dissolved in ethanol (1 ml.) and the mixture was boiled for 5 min. Removal of ethanol afforded 0.11 g. of crystals, m. p. 93~95°C, which recrystallized from ethanol to yellow prisms, m. p. 95~96°C.

Found: C, 67.33; H, 7.22; N, 9.19. Calcd. for $C_{17}H_{22}O_3N_2$: C, 67.52; H, 7.33; N, 9.27%.

**3-(α-Ethylenedioxy)ethyltropone (V).** — A solution of IV (0.5 g.) dissolved in a mixture of acetic acid (3 ml.) and water (10 ml.) was boiled. A 10% aqueous solution of copper sulfate (30 ml.), preliminarily boiled, was added to the foregoing solution in one portion, by which a vigorous evolution of nitrogen gas occurred. The mixture was boiled for 15 min., the precipitate was filtered off, and the filtrate was extracted with chloroform. The reddish oil left after evaporation of chloroform was sublimed at a reduced pressure and gave 0.03 g. of crystals, m. p. 70~72°C. Recrystallization from a mixed solvent of benzene and cyclohexane gave V as colorless prisms, m. p. 71~72°C.

Found: C, 68.76; H, 6.32. Calcd. for $C_{11}H_{12}O_3$: C, 68.73; H, 6.29%. Ultraviolet $\lambda_{max}^{MeOH}$ mμ (log ε): 227 (4.34), 305 (3.89).

**2-Hydrazino-4-(α-ethylenedioxy)ethyltropone (VI).** —To a solution of III (0.2 g.) dissolved in ethanol (0.5 ml.), 80% hydrazine hydrate (0.2 g.) was added and the mixture was heated at 90°C for 5 min. Removal of ethanol left 0.21 g. of crystals of m. p. 119~121°C which recrystallized from dilute ethanol to VI as yellow prisms, m. p. 123~124°C.

Found: C, 59.72; H, 6.36; N, 12.67. Calcd. for $C_{11}H_{14}O_3N_2$: C, 59.45; H, 6.35; N, 12.60%. Ultraviolet $\lambda_{max}^{MeOH}$ mμ (log ε): 252 (4.37), 338 (4.02), 408 (4.00).

**Cyclohexylidene Compound of VI.** — Cyclohexanone (0.06 g.) was added to the solution of VI (0.12 g.) dissolved in ethanol (1 ml.) and the mixture was boiled for 5 min. Evaporation of ethanol afforded crystals (0.12 g.) of m. p. 122~124°C which were recrystallized from a mixed solvent of cyclohexane and benzene to yellow needles, m. p. 124~125°C.

Found: C, 67.72; H, 7.03; N, 9.29. Calcd. for $C_{17}H_{22}O_3N_2$: C, 67.52; H, 7.33; N, 9.27%.

**4-(α-Ethylenedioxy)ethyltropone (VII).**—A solution of VI (0.5 g.) dissolved in a mixture of acetic acid (3 ml.) and water (10 ml.) was boiled, and a boiled 10% aqueous solution (30 ml.) of copper sulfate was added to it in one portion. The mixture was further boiled for 2 min., the precipitate was filtered off, and the filtrate was extracted with chloroform. The oil obtained by the evaporation of the chloroform was extracted with petroleum ether and crystals (0.13 g.) of m. p. 78~80°C were obtained. Sublimation under reduced pressure and recrystallization of the sublimate from a mixed solvent of benzene and cyclohexane afforded VII as colorless scales, m. p. 80.5~81.5°C. This substance contained 1 mol. of crystal cyclohexane.

Found: C, 73.18; H, 8.62. Calcd. for $C_{11}H_{12}O_3 \cdot C_6H_{12}$: C, 73.88; H, 8.75%. Ultraviolet $\lambda_{max}^{MeOH}$ mμ (log ε): 236 (4.54), 313 (3.97).

**5-Acetyltropolone (X).**—Prepared from β-dolabrin (VIII) by the method already described in the literature[7].

**5-(α-Ethylenedioxy)ethyltropolone (XI).**—A mixture of X (0.5 g.), dehydrated benzene (15 ml.), ethylene glycol (5 ml.), and *p*-toluenesulfonic acid (0.05 g.) was heated and the water which formed was removed azeotropically with benzene. After heating for 25 hr., the mixture was diluted with water and extracted with chloroform. The chloroform layer was extracted with 2 N sodium hydroxide and the alkali solution was acidified with hydrochloric acid. The crystals that precipitated out were collected and sublimed under reduced pressure to form crystals (0.51 g.) of m. p. 98~102°C. Recrystallization from a mixed solvent of cyclohexane and benzene afforded XI as colorless needles, m. p. 103~104°C.

Found: C, 63.20; H, 5.46. Calcd. for $C_{11}H_{11}O_4$: C, 63.45; H, 5.81%. Ultraviolet $\lambda_{max}^{MeOH}$ mμ (log ε): 237 (4.41), 327 (4.02), 367 (3.86).

**2-Methoxy-5-(α-ethylenedioxy)ethyltropone (XII).** —Ether solution of diazomethane was added to XI (0.4 g.) suspended in ether (10 ml.) to effect methylation. When the solution no longer colored with ferric chloride, the crystals that precipitated out and those obtained by concentration of the filtrate were combined and recrystallized from benzene to XII as colorless prisms, m. p. 114~115°C.

Found: C, 65.31; H, 5.98. Calcd. for $C_{12}H_{14}O_4$: C, 64.85; H, 6.35%. Ultraviolet $\lambda_{max}^{MeOH}$ mμ (log ε): 235 (4.45), 320 (4.08).

**2-Hydrazino-5-(α-ethylenedioxy)ethyltropone (XIII).**—To a solution of XII (0.5 g.) dissolved in ethanol (2 ml.), 80% hydrazine hydrate (0.3 g.) was added and the mixture was boiled for 5 min. The crystals that precipitated out on cooling the mixture were collected and the crude crystals (0.45 g.) of m. p. 160°C (decomp.) were recrystallized from ethanol to XIII as yellow scales, m. p. 164°C (decomp.).

Found: C, 59.80; H, 5.80; N, 12.56. Calcd. for $C_{11}H_{14}O_3N_2$: C, 59.45; H, 6.35; N, 12.60%. Ultraviolet $\lambda_{max}^{MeOH}$ mμ (log ε): 248 (4.38), 345 (4.18), 408 (4.06).

**Synthesis of VII from XIII.**—XIII (0.45 g.) was decomposed with aqueous solution of copper sulfate as in the case of IV and VI and the crystals (0.03 g.) of m. p. 78~79.5°C thereby obtained were recrystallized from a mixed solvent of cyclohexane and benzene to VII of m. p. 80~81.5°C, undepressed

on admixture with VII obtained from VI, but mixed melting point of 46~52°C was indicated on admixture with V.

The author expresses his gratitude to Professor Yoshio Kitahara for his unfailling guidance during the course of the present work. The author is indebted to Ogawa Perfumery Co., Ltd., for the kind supply of β-dolabrin used in this work and to Mr. S. Aono of this Research Institute for infrared spectral measurement.

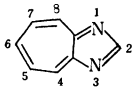
*The Chemical Research Institute*
*of Non-Aqueous Solutions*
*Tohoku University*
*Sendai*

# *5- and 2, 5-Substituted 1, 3-Diazaazulenes*[1]

By Ichiro MURATA

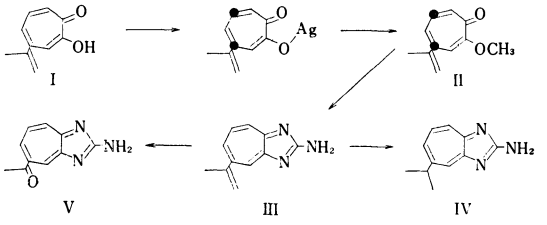
(Received August 1, 1960)

Compounds with various functional groups substituted in the 1, 3-diazaazulene ring known to date are (1) 2-substituted derivatives obtained by the reaction of tropolone methyl ether and guanidine or thiourea[2], (2) 2, 4-disubstituted derivatives obtained by the reaction of 2-bromo-7-methoxytropone and guanidine[3], (3) 2, 6-disubstituted derivatives obtained from 5-halo- or 5-nitrotropolone methyl ether and guanidine[4], and (4) 6-substituted derivatives obtained from 2, 5-diaminotropoimine and formic and acetic acids[5]. The chemical properties of these synthesized compounds have also been examined. However, 5-substituted and 2, 5-disubstituted derivatives are still not known, due to the difficulty of obtaining 4-halotropolones[6] which are their direct starting material.



In the present series of work, some of these compounds were newly prepared and are described herein.

β-Dolabrin (4-isopropenyltropolone) (I)[7] is transformed to its sodium salt in ethanol and then converted to its silver salt by silver nitrate. Reaction of methyl iodide with this silver salt suspended in benzene affords a mixture of two kinds of methyl ether in the form of a yellow oil (II). Condensation of II, without separation[8], with guanidine in the presence of potassium hydroxide gives 2-amino-5-isopropenyl-1, 3-diazaazulene (III) as yellow prisms, m. p. 230°C (decomp.) in a good yield. Catalytic reduction of III over palladium-carbon results in absorption of 1 mol. of hydrogen to form the known 2-amino-5-isopropyl-1, 3-diazaazulene (IV)[2], by which the structure of III is confirmed.




Consecutive oxidation of III first with hydrogen peroxide and then with periodic acid affords 2-amino-5-acetyl-1, 3-diazaazulene (V) as crystals melting at above 300°C but its yield is extremely poor.

The attempted conversion of 4-acetyltropolone (VI)[7], obtained by oxidation of I, to a mixture of methyl ethers VII with diazomethane and condensation of VII with guanidine to obtain V ended in failure, forming only a resinous substance. In order to protect

1) Paper read at the 12th Annual Meeting of the Chemical Society of Japan, Kyoto, April, 1959.

2) T. Nozoe, T. Mukai, K. Takase, I. Murata and K. Matsumoto, *Proc. Japan Acad.*, **29**, 452 (1953); T. Nozoe, T. Mukai and I. Murata, *J. Am. Chem. Soc.*, **76**, 3352 (1954).

3) T. Nozoe, T. Mukai, I. Murata, M. Ishii and K. Matsumoto, unpublished data.

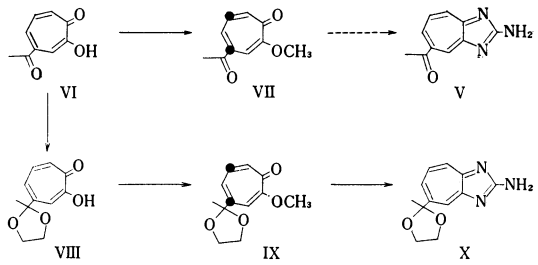
4) T. Nozoe, T. Mukai, I. Murata and T. Asao, unpublished data. Cf. T. Nozoe, *Croatica Chem. Acta*, **29**, 215 (1957).

5) T. Nozoe, M. Sato, S. Ito, K. Matsui and T. Matsuda, *Proc. Japan Acad.*, **29**, 565 (1953).

6) T. Sato, *J. Chem. Soc. Japan, Pure Chem. Sec.* (*Nippon Kagaku Zasshi*), **80**, 1171 (1959).

7) T. Nozoe, K. Takase and M. Ogata, *Chem. and Ind.*, **1957**, 1070.

8) 2-Amino-1, 3-diazaazulene hereby formed is symmetric and the same product is obtained from either of the two methyl ethers. Cf. Ref. 2.




the acetyl group, VI was reacted with ethylene glycol in dehydrated benzene to give 4-(α-ethylenedioxy)ethyltropolone (VIII)[9]. Treatment of VIII with diazomethane afforded a mixture of methyl ethers IX and condensation with guanidine gave 2-amino-5-(α-etylenedioxy)-ethyl-1, 3-diazaazulene (X) as pale yellow needles, m. p. 297°C (decomp.). Treatment of X with dilute hydrochloric acid easily converted it to V. Ultraviolet absorption spectra of III, V and X are shown in Fig. 1.

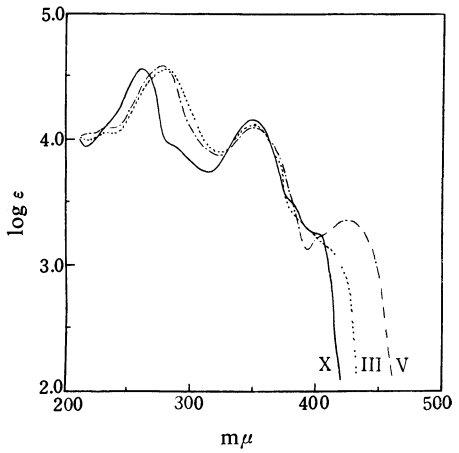
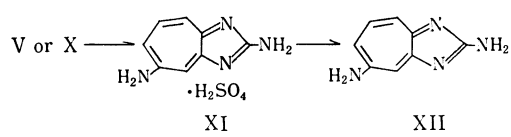



Fig. 1. Ultraviolet absorption spectra of III, V and X in methanol.

The application of the Schmidt reaction[10], already carried out with VI, to V gives yellow needles XI, m. p. above 300°C, which are also obtained by direct reaction of hydrazoic acid on X.

The estimation of sulfur in XI is positive and the treatment of XI with sodium hydrogen carbonate or ammonia water affords yellow prisms XII, m. p. 289°C (decomp.). From the analytical values of XII and the formation of a picrate of m. p. above 300°C, a diacetate of m. p. 285°C (decomp.), and a dibenzoate of m. p. 157°C, it is considered that XII is




2, 5-diamino-1, 3-diazaazulene[11]. Consequently, XI would be the sulfate of XII.

On the other hand, the reaction of thiourea on IX in the presence of sodium ethoxide affords 2-mercapto-5-(α-ethylenedioxy)ethyl-1,3-diazaazulene (XIII) as orange prisms, m. p. 246°C. The oxidative desulfurization of the mercapto group in XIII with hydrogen peroxide gives 5-(α-ethylenedioxy)ethyl-1, 3-diazaazulene (XIV) as yellow prisms, m. p. 153°C. The idea of the structure of these compounds is supported by the similarity of their ultraviolet absorption spectra with those of comoupnds lacking a side chain in the 5-position[2] and

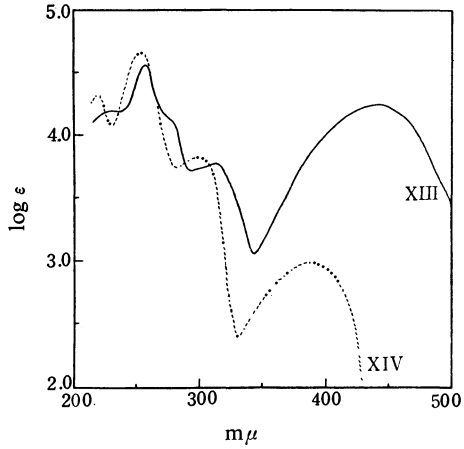



Fig. 2. Ultraviolet absorption spectra of XIII and XIV in methanol.

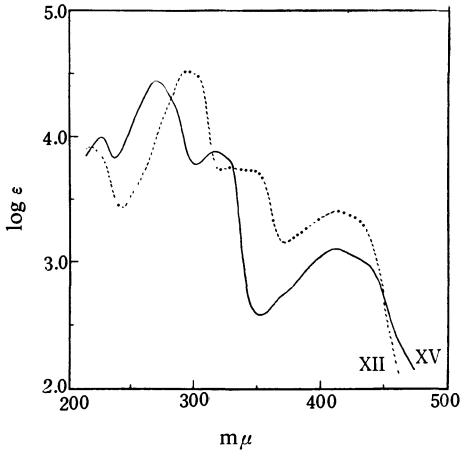


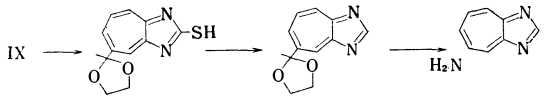

Fig. 3. Ultraviolet absorption spectra of XII and XV in methanol.

9) I. Murata, This Bulletin, 34, 577 (1961).
10) K. Doi, unpublished data.
11) In the Schmidt reaction of 4-acetyltropolone, the product is 4-aminotropolone and the acetylamino group is considered to have undergone hydrolysis in the intermediate stage. Cf. Ref. 10.

compounds possessing a methyl group in the 5-position[12].

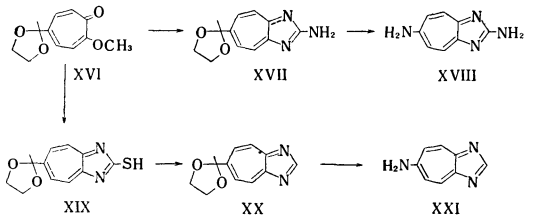
The Schmidt reaction of XIV affords yellow prisms, m. p. 214°C, though in a very poor yield. This substance forms a picrate of m. p. 244°C and its analytical values clearly indicate that it is the anticipated 5-amino-1, 3-diazaazulene (XV).

The ultraviolet spectra of 5-amino (XV) and 2, 5-diamino (XII) compounds are indicated in Fig. 3. These two compounds show corresponding absorptions but the spectrum of XII shows a fair amount of bathochromic and hyperchromic shifts from that of XV.



XIII XIV XV

The acetylamino group formed by the Schmidt reaction of $\alpha$-ethylenedioxyethyl group in both XII and XV undergoes hydrolysis and is found as the free amino group in the product. In order to prove this fact in other analogous compounds, the following experiments were carried out.



Condensation of 5-($\alpha$-ethylenedioxy)ethyltropolone methyl ether (XVI)[9] with guanidine afforded XVII, m. p. 200°C, the Schmidt reaction of which gave the known 2, 6-diamino-1, 3-diazaazulene[4] (XVIII), via its sulfate of m. p. above 300°C. The condensation of XVI with thiourea to form the 2-mercapto compound XIX and the Schmidt reaction of its desulfurized product XX afforded the known 6-amino-1, 3-diazaazulene[5] (XXI). These reaction results are entirely analogous to the case of 5-substituted derivative described above.

The amino group in 2-position of XVIII submits to the diazo reaction and undergoes coupling with phenols or the Sandmeyer reaction[4]. The amino group in 2-position of 2, 5-diamino-1, 3-diazaazulene (XII) is expected to undergo diazotisation[13] but, actually, the reaction is negative.

When XII is heated with concentrated hydrochloric acid or hydrobromic acid for several hours, one of the amino groups is hydrolysed and an amino-hydroxy compound XXIII is obtained. Acid hydrolysis of XII and XXIII in a sealed tube results in the formation of 2, 5-dihydroxy-1, 3-diazaazulene (XXIV). There is no reliable proof as to which of 2- or 5-position in XXIII is a hydroxyl group but, since similar hydrolysis of XVIII affords 2-amino-6-hydroxy compound[4], it seems natural to assume that XXIII is 2-amino-5-hydroxy-1, 3-diazaazulene. The ultraviolet absorption spectra of XXIII and XXIV are shown in Fig. 4.

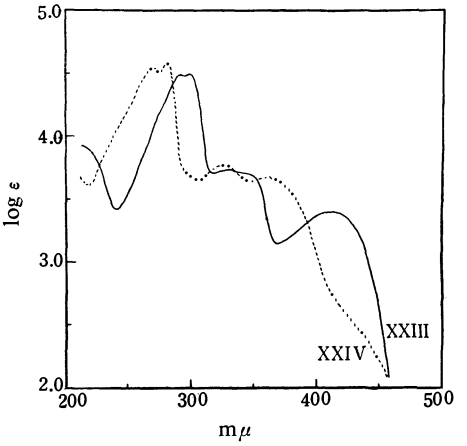
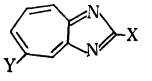



Fig. 4. Ultraviolet absorption spectra of XXIII and XXIV in methanol.

In order to obtain 2-hydroxy-5-amino-1, 3-diazaazulene (XXV), XIII was converted to XXVI with methyl iodide and the reaction of hydrazoic acid afforded 2-methylthio-5-amino-1, 3-diazaazulene (XXVII) as yellow silky needles, m. p. above 300°C. Formation of XXV by hydrolysis of the methylthio group[14] in XXVIII was not effected.



XXIII X=$NH_2$, Y=OH
XXIV X=Y=OH
XXV X=OH, Y=$NH_2$
XXVI X=$SCH_3$, Y=$C(OCH_2CH_2O)CH_3$
XXVII X=$SCH_3$, Y=$NH_2$

## Experimental[15]

**4-Isopropenyltropolone Methyl Ether (II).**—A solution of I (1.62 g.) dissolved in ethanol (7 ml.)

12) H. Akino, K. Sato and Y. Suzuki, *Sci. Repts. Tohoku Univ.*, [1] **40**, 92 (1956).
13) In 1, 3-diazaazulene, there is a large contribution of the polar form in which the 7-membered ring is positively charged and the 5-membered ring is negatively charged. Consequently, the 5-membered ring, i. e. 2-position, is considered to be preferentially diazotized. Cf. H. Kon, *Sci. Repts. Tohoku Univ.*, [1] **38**, 67 (1954).
14) I. Murata, This Bulletin, **33**, 1367 (1960).
15) All melting points are uncorrected.

was added to the solution of sodium hydroxide (0.4 g.) in water (40 ml.) to form the sodium salt. A solution of silver nitrate (1.7 g.) in water (50 ml.) was added to the solution of the sodium salt while stirring with ice-cooling. The precipitate thereby formed was collected by filtration, washed thoroughly with water and ethanol, and dried over phosphorous pentoxide. Yield, 2.45 g.

This silver salt was suspended in dehydrated benzene (50 ml.) and methyl iodide (1.5 g.) was added with stirring at room temperature. After stirring the mixture for 30 min., the reaction mixture was allowed to stand over night, the silver iodide formed was filtered off, and the filtrate was concentrated under a reduced pressure from which II was obtained as an orange oil (2.3 g.).

**2-Amino-5-isopropenyl-1, 3-diazaazulene (III).**—II (2.3 g.) was added to the solution of potassium hydroxide (505 mg.) dissolved in ethanol (30 ml.) and added with guanidine hydrochloride (870 mg.) and the mixture was refluxed on a water bath for 1.5 hr. The crystals that precipitated out when the reaction mixture cooled and the crystals obtained by concentration of the filtrate were combined and washed with water. Crude III (1.15 g.), obtained as yellow prisms, m. p. 229~230°C (decomp.), was recrystallized from ethanol but the melting point remained unchanged.

Found: C, 71.54; H, 5.53; N, 23.08. Calcd. for $C_{11}H_{11}N_3$: C, 71.33; H, 5.99; N, 22.69%. Ultraviolet $\lambda_{max}^{MeOH}$ m$\mu$ (log $\varepsilon$) : 235 (4.06), 283 (4.55), 348 (4.12).

*Acetate*: Colorless prisms (from ethanol and dioxane), m. p. 216°C (decomp.).

Found: C, 68.71; H, 5.55; N, 18.36. Calcd. for $C_{13}H_{13}ON_3$: C, 68.70; H, 5.77; N, 18.49%.

*Picrate*: Yellow needles (from ethanol and dioxane), m. p. 231°C (decomp.).

Found: C, 49.16; H, 3.57; N, 20.47. Calcd. for $C_{17}H_{14}O_7N_6$: C, 49.28; H, 3.41; N, 20.29%.

**Catalytic Reduction of III.** — A solution of III (50 mg.) in methanol (10 ml.), added with palladium-carbon (50 mg.) was submitted to catalytic reduction at atomospheric temperature and pressure, and ca. 7 cc. of hydrogen was absorbed in 2 hr. Palladium-carbon was filtered off, the filtrate was concentrated, and the residual crystals were recrystallized from ethanol to IV (30 mg.), m. p. 293°C (decomp.). The ultraviolet and infrared spectra of IV agreed with those of the known 2-amino-5-isopropyl-1,3-diazaazulene.

**2-Amino-5-(α-ethylenedioxy)ethyl-1,3-diazaazulene (X).**—A solution of potassium hydroxide (720 mg.), ethanol (30 ml.), and guanidine hydrochloride (1.21 g.), added with IX (2.65 g.), was refluxed for 2 hr. and cooled. The crystals that precipitated out and those obtained after concentration of the filtrate were combined, washed with water, and the pale yellow crystals (2.3 g.) of m. p. 297°C (decomp.) were recrystallized from ethanol to X as pale yellow needles, m. p. 297°C.

Found: C, 62.41; H, 5.71; N, 18.10. Calcd. for $C_{12}H_{13}O_2N_3$: C, 62.32; H, 5.67; N, 18.17%. Ultraviolet $\lambda_{max}^{MeOH}$ m$\mu$ (log $\varepsilon$) : 262 (4.58), 350 (4.17).

**2-Amino-5-acetyl-1, 3-diazaazulene (V).**—A solution of X (650 mg.) dissolved in 2 N hydrochloric acid (5 ml.) was heated on a water bath of 90°C for 20 min. The orange solution so formed was diluted with water and neutralized with sodium hydrogen carbonate by which an orange precipitate (550 mg.) of m. p. above 300°C, was obtained. Recrystallization from a mixed solvent of ethanol and dioxane afforded orange microprisms, V.

Found: C, 64.61; H, 5.18; N, 21.61. Calcd. for $C_{10}H_9ON_3$: C, 64.16; H, 4.85; N, 22.45%. Ultraviolet $\lambda_{max}^{MeOH}$ m$\mu$ (log $\varepsilon$) : 277 (4.60), 353 (4.11), 424 (3.36).

**2, 5-Diamino-1, 3-diazaazulene (XII).** — Sodium azide (0.65 g.) was added in small portions into a solution of X (2 g.) dissolved in concentrated sulfuric acid (6.5 ml.), while stirring at room temperature, and the mixture was further stirred for 2 hr. This was diluted with water (10 ml.), made slightly alkaline with 2 N sodium hydroxide, and allowed to stand in a cold place. The yellow crystals that precipitated out were collected by filtration to XI (1.7 g.) of m. p. above 300°C.

XI was dissolved in concentrated ammonia water (1.5 ml.), the solution was allowed to stand, and the pale yellow crystals (1.4 g.) that formed were recrystallized from water to XII as pale yellow prisms, m. p. 289°C (decomp.).

Found: C, 60.15; H, 4.57; N, 33.97. Calcd. for $C_8H_8N_4$: C, 59.98; H, 5.03; N, 34.98%. Ultraviolet $\lambda_{max}^{MeOH}$ m$\mu$ (log $\varepsilon$) : 292 (4.72), 343 (3.92), 415 (3.53); $\lambda_{max}^{0.1N\ HCl}$ : 290 (4.62), 325 (3.96), 335 (3.97), 377 (3.63); $\lambda_{max}^{0.1N\ NaOH}$ : 290 (4.75), 350 (3.97), 415 (3.48).

*Picrate*: Yellow needles (from ethanol), m. p. above 300°C.

Found: C, 42.46; H, 2.85; N, 24.21. Calcd. for $C_{14}H_{11}O_7N_7$: C, 43.19; H, 2.84; N, 24.26%.

*Benzoate*: Obtained as yellow crystals by application of benzoyl chloride in pyridine and recrystallized from dilute ethanol to yellow crystals, m. p. 157°C.

Found: C, 68.20; H, 4.80; N, 14.18. Calcd. for $C_{22}H_{16}O_2N_4 \cdot H_2O$: C, 68.38; H, 4.70; N, 14.50%. Ultraviolet $\lambda_{max}^{MeOH}$ m$\mu$ (log $\varepsilon$) : 230 (4.29), 305 (4.79), 346 (4.33), 395 (3.35).

*Acetate*: Obtained by refluxing in acetic anhydride for 20 min. Pale yellow needles (from dilute ethanol), m. p. 285°C (decomp.).

Found: C, 54.88; H, 5.28; N, 21.16. Calcd. for $C_{12}H_{12}O_2N_4 \cdot H_2O$: C, 54.95; H, 5.38; N, 21.37%. Ultraviolet $\lambda_{max}^{MeOH}$ m$\mu$ (log $\varepsilon$) : 224 (3.97), 288 (4.65), 344 (4.04), 395 (2.91).

**2-Mercapto-5-(α-ethylenedioxy)ethyl-1, 3-diazaazulene (XIII).** — A solution of sodium (120 mg.) dissolved in absolute ethanol (50 ml.), with thiourea (400 mg.) and IX (1.1 g.) added, was refluxed on a water bath for 3 hr., the ethanol was evaporated, and the residue was diluted with water (30 ml.). The precipitate formed by additional of acetic acid was collected and the orange crystals (950 mg.) of m. p. 235°C (decomp.) so obtained were recrystallized from ethanol to XIII as orange prisms, m. p. 246°C (decomp.).

Found: C, 57.88; H, 4.85; N, 11.68. Calcd. for $C_{12}H_{12}O_2N_2S$: C, 58.06; H, 4.84; N, 11.29%.

Ultraviolet $\lambda_{max}^{MeOH}$ mμ (log ε) : 227 (4.18), 253 (4.55), 310 (3.78), 440 (4.23).

**5-(α-Ethylenedioxy)ethyl-1, 3-diazaazulene (XIV).** —To a suspension of XIII (400 mg.) in water (4 ml.), 35% hydrogen peroxide (2 ml.) was added and the mixture was heated on a boiling water bath for a few minutes by which exothermic reaction occurred to form an orange solution. After cooling this mixture in ice, the mixture was made slightly alkaline with sodium hydrogen carbonate and extracted with chloroform. The chloroform residue was dissolved in benzene and passed through a column of alumina for purification by which yellow crystals (210 mg.), m. p. 152~153°C, were obtained. Recrystallization from a mixed solvent of benzene and cyclohexane afforded XIV as yellow prisms, m. p. 152~153°C.

Found: C, 66.56; H, 5.27; N, 12.87. Calcd. for $C_{12}H_{12}O_2N_2$: C, 66.65; H, 5.59; N, 12.96%. Ultraviolet $\lambda_{max}^{MeOH}$ mμ (log ε) : 219 (4.32), 255 (4.66), 300 (3.82), 386 (2.98).

*Picrate*: Yellow needles (from dilute ethanol), m. p. 181°C (decomp.).

Found: C, 48.56; H, 3.59; N, 15.80. Calcd. for $C_{18}H_{15}O_9N_5$: C, 48.54; H, 3.59; N, 15.73%.

**5-Amino-1, 3-diazaazulene (XV).** — Sodium azide (70 mg.) was added in small portions to a solution of XIV (220 mg.) dissolved in concentrated sulfuric acid (0.5 ml.) while stirring with cooling. After stirring for 2 hr., the mixture was diluted with water, made slightly alkaline with 2 N sodium hydroxide, and chilled. The crystalline precipitate (90 mg.) m. p. 209°C, so formed was recrystallized from water to XV as yellow prisms, m. p. 214°C.

Found: N, 28.81. Calcd. for $C_8H_7N_3$: N, 28.95%. Ultraviolet $\lambda_{max}^{MeOH}$ mμ (log ε) : 227 (4.00), 269 (4.45), 315 (3.89), 411 (3.11).

*Picrate*: Yellow prisms (from dilute ethanol), m. p. 244°C (decomp.).

Found: C, 44.94; H, 2.65; N, 21.89. Calcd. for $C_{14}H_{10}O_7N_6$: C, 44.92; H, 2.69; N, 22.46%.

**2-Amino-6-(α-ethylenedioxy)ethyl-1, 3-diazaazulene (XVII).**—A solution of potassium hydroxide (100 mg.) dissolved in ethanol (10 ml.), with guanidine hydrochloride (170 mg.) and XVI (400 mg.) added, was refluxed for 2 hr., the potassium chloride that precipitated out on cooling was removed by filtration, and the ethanol was evaporated. The crude crystals (290 mg.) of m. p. 190~191°C so obtained were recrystallized from water to XVII as yellow needles, m. p. 199~200°C.

Found: C, 59.74; H, 5.65; N, 17.41. Calcd. for $C_{12}H_{13}O_2N_3 \cdot 1/2H_2O$: C, 59.99; H, 5.87; N, 17.49%. Ultraviolet $\lambda_{max}^{MeOH}$ mμ (log ε) : 258 (4.54), 353 (4.25), 385 (infl.).

*Picrate*: Yellow scales (from dilute ethanol), m. p. 244°C (decomp.).

Found: C, 46.24; H, 2.93; N, 18.21. Calcd. for $C_{18}H_{16}O_9N_6$: C, 46.96; H, 3.50; N, 18.26%.

**2, 6-Diamino-1, 3-diazaazulene (XVIII).**—Sodium azide (25 mg.) was added in small portions to a solution of XVII (70 mg.) dissolved in concentrated sulfuric acid (0.3 ml.) while stirring at room temperature and the mixture was stirred for 2 hr. This was diluted with water, made slightly alkaline with 2 N sodium hydroxide, and the crystals (60 mg.) of m. p. above 300°C so obtained were treated with concentrated ammonia water. Recrystallization from water gave yellow silky needles, m. p. above 300°C, whose ultraviolet and infrared spectra were in complete agreement with those of the known 2,6-diamino-1,3-diazaazulene.

**2-Mercapto-6-(α-ethylenedioxy)ethyl-1, 3-diazaazulene (XIX).** — A solution of sodium (76 mg.) dissolved in absolute ethanol (30 ml.) and containing thiourea (255 mg.), with XVI (730 mg.) added, was refluxed for 3 hr., the ethanol was evaporated, and the residue was diluted with water. Acidification with acetic acid produced a precipitate which was recrystallized from dilute ethanol to 520 mg. of XIX as orange silky needles, m. p. 277°C (decomp.).

Found: C, 58.17; H, 5.04; N, 11.05. Calcd. for $C_{12}H_{12}O_2N_2S$: C, 58.06; H, 4.84; N, 11.29%. Ultraviolet $\lambda_{max}^{MeOH}$ mμ (log ε) : 230 (4.30), 251 (4.64), 305 (3.84), 440 (4.37).

**6-(α-Ethylenedioxy)ethyl-1, 3-diazaazulene (XX).** To a suspension of XIX (400 mg.) in water (6 ml.), 35% hydrogen peroxide (2 ml.) was added and the mixture was heated on a water bath for a few minutes, by which the reaction proceeded with effervescence and a clear solution was produced. The mixture was made slightly alkaline with sodium hydrogen carbonate and extracted with chloroform. The crude crystals (270 mg.) of m. p. 161~162°C (decomp.) so obtained were recrystallized from benzene to XX as yellow needles, m. p. 166.5~167.5°C (decomp.).

Found: C, 66.86; H, 5.07; N, 12.72. Calcd. for $C_{12}H_{12}O_2N_2$: C, 66.65; H, 5.59; N, 12.96%. Ultraviolet $\lambda_{max}^{MeOH}$ mμ (log ε) : 218 (4.16), 253 (4.56), 314 (3.88), 385 (2.99).

**6-Amino-1, 3-diazaazulene (XXI).**—Sodium azide (65 mg.) was added to a solution of XX (190 mg.) dissolved in concentrated sulfuric acid (0.5 ml.) while chilling in ice and the mixture was stirred for 2 hr. at room temperature. This was diluted with 2 ml. of water, neutralized to pH 5 with 2 N sodium hydroxide; an ethanol solution of picric acid was added. The precipitate formed was collected by filtration and a picrate (220 mg.) of m. p. 245°C (decomp.) was obtained. Repeated recrystallization from dilute ethanol afforded yellow needles, m. p. 282°C (decomp.), undepressed on admixture with the known 6-amino-1,3-diazaazulene picrate.

Found: C, 44.57; H, 2.79; N, 22.49. Calcd. for $C_{14}H_{10}O_7N_6$: C, 44.92; H, 2.69; N, 22.46%.

**2-Amino-5-hydroxy-1, 3-diazaazulene (XXIII).** — A mixture of XII (200 mg.) and 6 N hydrochloric acid (2 ml.) was refluxed in an oil bath for 6 hr. and hydrochloric acid was evaporated to dryness. The residue was neutrallized with a saturated solution of sodium hydrogen carbonate and the yellow crystals (120 mg.) of m. p. 226°C (decomp.) so obtained were recrystallized from water to XXIII as pale yellow prisms, m. p. 249°C (decomp.).

Found: N, 25.85. Calcd. for $C_8H_7ON_3$: N, 26.07%.

**2, 5-Dihydroxy-1, 3-diazaazulene (XXIV).**—A mixture of XII (200 mg.) and concentrated hydrochloric acid (2 ml.) was heated in a sealed tube at 170~180°C for 6 hr. Treatment as in the case of XXIII

afforded crystals (160 mg.) of m. p. above 290°C which were recrystallized from water to yellow microneedles, m. p. above 290°C.

Found: N, 17.56. Calcd. for $C_8H_6O_2N_2$: N, 17.28%. Ultraviolet $\lambda_{max}^{MeOH}$ m$\mu$ (log $\varepsilon$): 270 (4.54), 280 (4.57), 330 (3.76), 363 (3.67).

**2-Methylthio-5-(α-ethylenedioxy)ethyl-1, 3-diazaazule (XXVI).**—To a solution of potassium hydroxide (55 mg.) dissolved in absolute methanol (10 ml.), XIII (250 mg.) was added, followed by methyl iodide (170 mg.), and the mixture was refluxed gently on a water bath. After 45 min., methanol was evaporated and the residual crystals (250 mg.), m. p. 123~125°C, were recrystallized from cyclohexane to pale yellow needles, m. p. 128~129°C.

Found: C, 59.82; H, 5.16; N, 11.62. Calcd. for $C_{13}H_{14}O_2N_2S$: C, 59.53; H, 5.38; N, 10.68%. Ultraviolet $\lambda_{max}^{MeOH}$ m$\mu$ (log $\varepsilon$): 241 (4.42), 274 (4.35), 363 (4.25).

**2-Methylthio-5-amino-1, 3-diazaazulene (XXVII).**—Sodium azide (80 mg.) was added at room temperature to a solution of XXVI (260 mg.) dissolved in concentrated sulfuric acid, covered with chloroform, and the mixture was stirred for 3 hr. at room temperature. The mixture was diluted with water (2 ml.), neutrallized with 2 N sodium hydroxide, and the orange precipitate so produced was recrystallized from 50% ethanol, with treatment with activated carbon, to yellow silky needles, m. p. above 290°C.

Found: C, 47.98; H, 5.67; N, 18.40. Calcd. for $C_9H_9N_3S \cdot 2H_2O$: C, 47.57; H, 5.77; N, 18.40%. Ultraviolet $\lambda_{max}^{MeOH}$ m$\mu$ (log $\varepsilon$): 225 (4.08), 311 (4.68), 359 (4.05), 458 (3.50).

The author expresses his gratitude to Professor Yoshio Kitahara for his unfailing guidance during the course of the present work. He is indebted to Mr. S. Aono of this Research Institute for infrared spectral measurement and to Mr. S. Ohyama and Miss. Y. Endo for elementary analysis.

*The Chemical Research Institute of Non-Aqueous Solutions*
*Tohoku University*
*Sendai*

# SHORT COMMUNICATIONS

## *On the Optical Absorption Spectra of Semiquinone Ions*

By Yoshiya HARADA* and Yoshio MATSUNAGA

(Received December 16, 1960)

Although extensive experimental studies have been made of the electron spin resonance absorption spectra of semiquinone ions, the optical absorption spectra, especially of the semiquinone ions with simple molecular structure, have scarcely been investigated. As semiquinone ions are unstable intermediates in oxidation-reduction systems, the details of the optical spectra are usually obscured by overlapping with the spectra due to the other species. For instance, *p*-benzosemiquinone formed by photoöxidation of hydroquinone or by photoreduction of quinone in rigid solvents has been examined by Lewis and Bigeleisen[1] and by Linschitz et al.[2] The appearance of a single absorption peak at about 410 m$\mu$ has been reported. Therefore, it seemed valuable to seek for the experimental condition in which the desired semiquinone ion is well stabilized and exists practically as the sole species in the reaction system.

The semiquinone ions were prepared either by reduction of the quinones dissolved in a mixture of ethylene glycol and 2 M potassium hydroxide aqueous solution with a suitable reagent or by oxidation of the hydroquinones in ethylene glycol with atmospheric oxygen. By the latter method the formation of semiquinone ion occurs after the addition of a small amount of potassium hydroxide solution. Our viscous medium was found to be not only inert to most of the semiquinone ions but to be of great advantage to protect the free radicals from the rapid undesired reactions, namely over-oxidation or reduction and some side reactions. With our solvent system we could

* Present address: The Institute for Solid State Physics, The University of Tokyo, Azabu, Tokyo.

1) G. N. Lewis and J. Bigeleisen, *J. Am. Chem. Soc.*, **65**, 2424 (1943).
2) H. Linschitz, J. Rennert and T. M. Korn, ibid., **76**, 5839 (1954).

control the reaction to some extent and succeeded in observing the fine structure in the optical absorption spectra of several semiquinone ions. The measurements were carried out using a Cary model 14 spectrophotometer at room temperature.

The unsubstituted *p*-benzosemiquinone ion was found to be too unstable to be examined even in our solvent system. However, we could successfully prepare a yellow solution of stable 2, 5-di-*tert*-butyl-*p*-benzosemiquinone ion. This radical seems to be sterically stabilized by the bulky substitutents. It has been shown by the hyperfine structure in the electron spin resonance that unpaired electrons can migrate to the hydrogen atoms in tertialy butyl groups with a probability of $10^{-4}$ for a 1s orbit[3], but we may hope that the main feature of $\pi$-electronic structure of *p*-benzosemiquinone ion is not modified very much by this substituent. The spectral reponse curves obtained on oxidation of di-*tert*-butyl-*p*-hydroquinone dissolved in ethylene glycol are given in Fig. 1. Curve

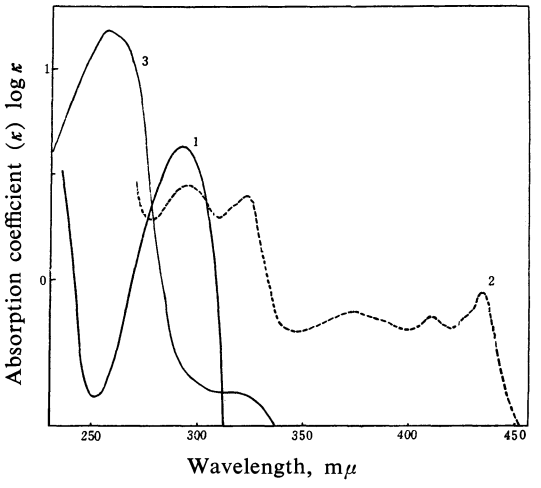



Fig. 1. Absorption spectra of 2,5-di-*tert*-butyl-*p*-benzohydroquinone: curve 1; semiquinone ion with some amount of hydroquinone, curve 2; and quinone; curve 3. The total concentration is $0.99\times 10^{-3}$ mol. per l.

1 shows the absorption spectrum of the original hydroquinone. When a small amount of potassium hydroxide solution was added to the sample solution, the hydroquinone was oxidized gently with atmospheric oxygen. Weak absorption peaks appeared at 436, 411 and 374 mμ, and a strong peak at 323 mμ, while the intensity of the 293 mμ peak was decreased considerably as shown by curve 2. The molar extinction coefficient for the peak of 323 mμ was estimated to be in the order of $10^4$. By further oxidation the spectrum of the quinone like curve 3 could be obtained. The original reduced form could be reproduced by the addition of a reducing reagent through the intermediate stage. Therefore, it is evident that the spectrum given by curve 2 is mostly ascribed to the semiquinone ion.

The absorption spectra of anthra- and phenanthra-semiquinone ions were also examined with success. The stabilities of these two semiquinone ions must be largely due to resonance. The reduction of the quinones was performed in the above-mentioned solvent with sodium dithionite or zinc dust. We should avoid the excessive use of dithionite because this reagent gives an absorption peak in the ultraviolet region studied for the semiquinone ions. In the anthrasemiquinone ion three peaks were observed at a wavelength of 480 mμ, at 400 mμ and at 297 mμ, and in the phenanthrasemiquinone ion two weak peaks at 507 and 475 mμ, two with medium intensity at 404 and 326 mμ and a strong peak at 270 mμ.

In order to analyse these optical absorption spectra we are attempting to study the $\pi$-electronic structure of these semiquinone ions by the aid of the semiempirical MO method developed by Pariser and Parr. The details of experiments and theoretical discussion will be submitted elsewhere.

The authors wish to thank Professor H. Akamatu of the Department of Chemistry and Professor H. Inokuchi and Professor S. Nagakura of the Institute for Solid State Physics for their kind direction and encouragement throughout the course of this work.

*Department of Chemistry*
*Faculty of Science*
*The University of Tokyo*
*Hongo, Tokyo*

3) G. K. Fraenkel, *Ann. N. Y. Acad. Sci.*, **67**, 546 (1957).

## *Electro-osmotic Permeability of Cation Exchange Membranes*

By V. Subrahmanyan and N. Lakshminarayanaiah

(Received December 26, 1960)

In a recent paper Mackay and Meares[1] have reported the measurements of rates of electro-osmotic flow of liquid through Permutit Zeo-Karb 315. By measuring its specific conductivity $k_{sp}$ ($ohm^{-1}\ cm^{-1}$), electro-osmotic permeability, $w$, ($cm^2\ V^{-1}\ sec^{-1}$), defined as the volume of solvent flowing per second through unit area of membrane for a potential gradient of one volt per cm., has been computed. $w$ is found to decrease with increasing external electrolyte concentration, and for any given concentration it is found to be independent of current in the range of 0.02 to 1.0 $mA \cdot cm^{-2}$.

Similar work is in progress in our laboratories. Rates of electro-osmotic flow of liquid through differently cross-linked polymethacrylate (PMA) membranes and cross-linked phenol sulphonate (PSA) membranes have been measured at 30°C employing a cell of the type described by Despic' and Hills[2].

The results of measurements of rates of electro-osmotic transport of liquid through 5, 10 and 15% cross-linked PMA membranes at one external electrolyte concentration (0.01 g. ions of $Na^+$ per litre) and at different currents in the range of 3 $mA \cdot cm^{-2}$ to 60 $mA \cdot cm^{-2}$ are collected in Table I. Measurements using PSA membranes in 0.01, 0.1, 0.5 and 1.0 N sodium chloride external electrolyte solutions at current densities ranging from 0.5 to 10.1 $mA \cdot cm^{-2}$ are presented in Table II.

The electro-osmotic permeability $w$, can be written as $w = \frac{V}{I} \times k_{sp}$, where $V$ is the rate of electro-osmotic flow of liquid in ml. per sec., $I$ is the constant current flowing through the system in amp. and $k_{sp}$ is the specific conductance of the membrane in reciprocal ohms per cm. At any given external electrolyte concentration in which the membrane is in equilibrium, $k_{sp}$ of the membrane is constant and is independent of current strength[3]. Therefore for the value of $w$ to remain constant over a range of current densities the ratio $V/I$ should be a constant. Mackay and Meares find this

Table I. Cross-linked PMA membranes

| $I$ | 5% | | 10% | | 15% | |
|---|---|---|---|---|---|---|
| | $V$ | $V/I$ | $V$ | $V/I$ | $V$ | $V/I$ |
| mA | (ml. $sec^{-1} \times 10^{-5}$) | (ml. $sec^{-1} \cdot amp^{-1} \times 10^{-2}$) | | | | |
| 2 | 0.57 | 0.285 | | | 0.54 | 0.270 |
| 3 | | | | | 0.67 | 0.223 |
| 5 | 1.31 | 0.262 | 1.73 | 0.346 | 0.96 | 0.192 |
| 10 | | | 3.07 | 0.307 | 1.88 | 0.188 |
| 15 | 3.52 | 0.235 | 4.30 | 0.287 | | |
| 20 | 4.39 | 0.220 | 5.63 | 0.282 | 3.83 | 0.192 |
| 25 | 5.19 | 0.208 | 6.90 | 0.276 | | |
| 30 | 6.00 | 0.200 | 8.25 | 0.275 | | |
| 35 | 7.01 | 0.200 | | | | |
| 40 | 8.20 | 0.205 | | | | |

Table II. PSA membranes

| $I$ | 0.01 N NaCl | | 0.1 N | | 0.5 N | | 1.0 N | |
|---|---|---|---|---|---|---|---|---|
| mA | $V$ | $V/I$ | $V$ | $V/I$ | $V$ | $V/I$ | $V$ | $V/I$ |
| 1 | 1.61 | 1.610 | 0.77 | 0.770 | 0.34 | 0.340 | 0.21 | 0.210 |
| 2 | 2.73 | 1.365 | 1.49 | 0.745 | 0.68 | 0.340 | 0.41 | 0.205 |
| 5 | 5.34 | 1.068 | 3.68 | 0.736 | 1.72 | 0.344 | 1.04 | 0.208 |
| 10 | 9.68 | 0.968 | 7.00 | 0.700 | 3.34 | 0.334 | 2.05 | 0.205 |
| 15 | 14.70 | 0.980 | 10.34 | 0.689 | 5.01 | 0.334 | 3.09 | 0.206 |
| 20 | 18.30 | 0.915 | 14.00 | 0.700 | 6.82 | 0.341 | 4.13 | 0.207 |

1) D. Mackay and P. Meares, *Trans. Faraday Soc.*, 55, 1221 (1959).

2) A. Despic' and G. J. Hills, *Discussions Faraday Soc.*, No. 21, 150 (1956).

3) N. Lakshminarayanaiah, *Current Sci.*, 28, 321 (1959).

to be so for their membranes. But the $V/I$ values given in columns 3, 5 and 7 of Table I and columns 3 and 5 of Table II contradict their findings. The values actually decrease with increasing currents and attain a limiting value. But $V/I$ values of PSA membranes in equilibrium with concentrated solutions (concentration$\geq$0.1 N) are constant over the current range studied and agree with their findings.

As the PSA membranes are chemically similar to Permutit Zeo-Karb 315, $V/I$ values for our membranes in equilibrium with 1.0, 0.5 and 0.1 N sodium chloride solution and those of Mackay and Meares for their membranes computed from the values of $w$ and $k_{sp}$ taken from their graphs are given in Table III.

TABLE III

| External electrolyte solution, NaCl | $V/I$ | $V/I$ Mackay & Meares |
|---|---|---|
| 1.0 N | $0.207\times10^{-2}$ | $0.159\times10^{-2}$ |
| 0.5 N | 0.339 〃 | 0.298 〃 |
| 0.1 N | 0.714 〃 | 0.639 〃 |

It is obvious from those values that our PSA membranes are more permeable electro-osmotically to liquid than Zeo-Karb 315.

Details including other aspects will be published elsewhere.

*Phsical Chemistry Laboratory*
*University of Madras*
*A. C. College of Technology*
*Guindy, Madras-25*
*India*

## *Absorption Isotherm for Sintered Palladium Black-Hydrogen System*

By Iwao YASUMORI, Takashi KOMORITA and Sadao SUZUKI

(Received February 2, 1961)

Below a critical temperature, the absorption isotherm for metallic palladium-hydrogen system has a plateau at constant pressure where two phases of absorbed hydrogen coexist[1]. The value of this pressure depends only on temperature for a bulk metal[2]. One of the authors, however, found recently that the pressure, for a palladium deposited on glass, is lower than that for bulk metal such as wire and foil and that it is increased by sintering[3]. Further information about this phenomenon is reported here.

The absorption of hydrogen was accordingly measured at 0 and 30°C by means of a gas pipette with a Bourdon manometer and an absorption cell connected to the former through a trap maintained at liquid nitrogen temperature. Hydrogen was purified by diffusing through a palladium thimble. Fresh palladium black which was obtained from palladium chloride by usual procedure of reduction[4], was put into the cell in a wet state and was then dried in vacuo, reduced with hydrogen of 50 mmHg and was evacuated for several hours at 120°C.

The results of successive measurements for a sample are shown in the figure. The absorbent was sintered between the respective measurements by heating in vacuo for 0.5~3.0 hr. at 200~400°C. The BET area of the surface was determined at each step by the use of nitrogen at −195°C, of which value varied as 13.6, 11.7, 9.4, 8.1 and 6.6 $m^2/g$. Pd corresponding to the isotherms, A, B, C, D and E. The pressure which corresponds to the plateau was appreciably lower than those for bulk metal, 25.2 (wire)[3], 22.6 (foil)[3], 19.4 (wire, bead, foil)[5], 18.7 (sufficiently sintered black)[6] mmHg (30° C) and 3.95 mmHg (0°C)[6] and increased with decreasing area of the surface. The mean size of the absorbent particles which was deduced from the line-width of X-ray diffraction increased from 90 Å, the initial value, to 250 Å after all the heat treatments. This change in particle size was also observed by electron-microscope; the particles smaller than 400 Å in size, of which the major part of the aggregations of the sample is consisted, were turned into those of smooth shape which were several times larger than the former. On the other hand, the mean radius which was estimated from the BET area by assuming the particles to be spherical, increased as 180, 210, 270, 310 and 380 Å corresponding to the respective isotherms. Moreover, the micro-pore distribution obtained by Inkley's procedure[7] showed that the initial distribution having a sharp maximum at 30 Å was transformed into a

1) F. Krüger and G. Gehm, *Ann. d. Physik*, **16**, 174 (1933).
2) J. R. Lacher, *Proc. Camb. Phil. Soc.*, **33**, 518 (1937).
3) S. Suzuki, *J. Chem. Soc. Jpaan, Pure Chem. Sec. (Nippon Kagaku Zasshi)*, to be published.
4) R. Willstätter and E. Waldschmidt-Leitz, *Ber.*, **54**, 122 (1921).
5) R. J. Ratchford and G. W. Castellan, *J. Phys. Chem.*, **62**, 1123 (1958).
6) L. J. Gillespie and F. P. Hall, *J. Am. Chem. Soc.*, **48**, 1207 (1926).
7) R. W. Cranston and F. A. Inkley, "Advances in Catalysis", Vol. 9, Academic Press Inc., New York (1957), p. 143.

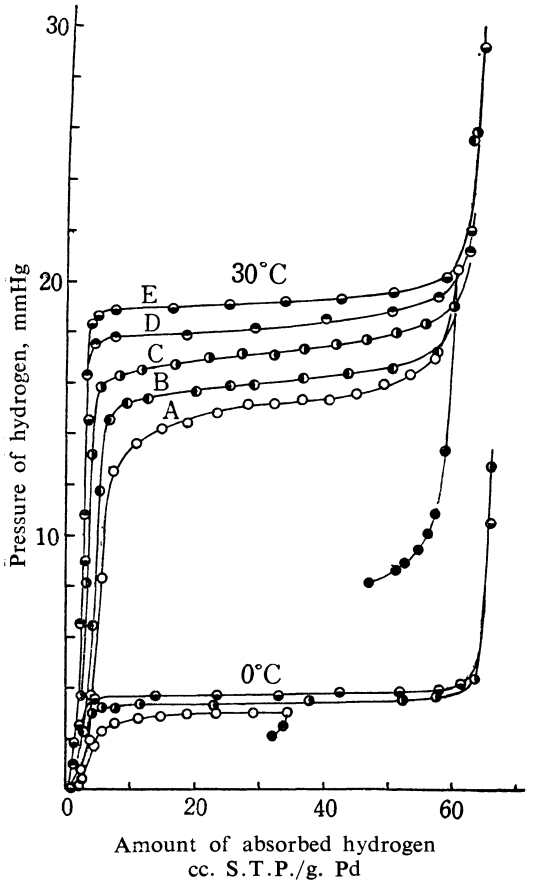



Fig. 1. Absorption isotherms for sintered Pd black-$H_2$ system. Every circles represent the values after standing for 20 min. Filled circles show desorption.

milder one with unchanged position of maximum.

The above information suggests that the pressure at the flat part depends on, even at the same temperature, the size and structure of particle of metallic palladium. The fact that the sigmoid isotherm is gradually deformed into that of folded-line type as the sintering proceeds, may be explained as that the particles distribute in various size and they grow by successive heating. The irregularities of structure, which may be the causes of this phenomenon, will disappear with the growth of particle and the equilibrium between gaseous and absorbed hydrogen may be sensitive to this change especially when the particle is sufficiently small. From the middle part of the isotherms the heat of absorption was estimated as 8.9 kcal./mol. which agrees well with those obtained hitherto[5].

It is to be suggested that this phenomenon will be available to elucidate the state of metallic palladium which is extremely dispersed on carriers.

*Laboratory of Physical Chemistry*
*(I. Y. & T. K.)*
*Research Laboratory of*
*Resources Utilization*
*(S. S.)*
*Tokyo Institute of Technology*
*Meguro-ku, Tokyo*

# *Fulvalmixene. I. Synthesis and Reaction of Fulvalmixene-1, 4-quinone*

By Yoshio KITAHARA, Ichiro MURATA and Takashi ASANO

(Received February 9, 1961)

Fulvalmixene[1] (I), one of the non-benzenoid aromatic compounds, is an interesting compound because of the possible contribution of ionic structures like Ia and for examination of its aromaticity. Its stability has been predicted to a certain extent from theoretical considerations[2].



I Ia

The synthesis of I has so far not been attained; only the tetrabenzo derivative[3] is known. The syntheses of 2, 3-benzofulvalmixene-1, 4-quinone and its parent compound, fulvalmixene-1, 4-quinone are described herein.

Reaction of indane-1, 3-dione (II) and 2 mol. equivalents of tropylium bromide (III) in aqueous solution afforded 2, 2-ditropylindane-1, 3-dione (IV), m. p. 167.5~168°C in 95%

1) The authors wish to use fulvalmixene as the name for cycloheptatrienylidene cyclopentadiene although mixed fulvalene[3] or sesquifulvalene* has been used. *W. von E. Doering, "Theoretical Organic Chemistry" (Kékule Symposium), Butterworth (1959), p. 35.

2) R. D. Brown, *Trans. Faraday Soc.*, **45**, 296 (1949); **46**, 146 (1950); J. F. Tinker, *J. Chem. Phys.*, **19**, 981 (1951); B. Pullman and A. Pullman, "Les Theories Electroniques de la Chimie Organique", Masson et Cie., Paris (1952).

3) B. Pullman, A. Pullman, E. D. Bergmann, H. Berthod, E. Fisher, Y. Hirshberg, D. Lavie and M. Mayot, *Bull. soc. chim. France*, **19**, 73 (1952).

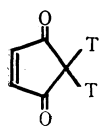
4) Heating of ditropylmalononitrile at 170~190°C results in formation of 8, 8-dicyanoheptafulvene (T. Nozoe, T. Mukai and K. Osaka, This Bulletin, in press).

5) C. H. DePuy and E. F. Zaweski, *J. Am. Chem. Soc.*, **81**, 4920 (1959).

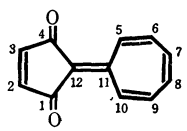
yeild (Found: C, 84.29; H, 5.41. Calcd. for $C_{23}H_{18}O_2$: C, 84.64; H, 5.56%. UV $\lambda_{max}^{MeOH}$ mμ (log ε): 227 (4.69), 252 (4.31), IR $\nu_{c=o}$ 1728, 1699 $cm^{-1}$) Heating of IV at 175~180°C for 30 min. under reduced pressure[4] left a red residue with liberation of cycloheptatriene. Recrystallization of this residue from benzene gave 2, 3-benzofulvalmixene-1, 4-quinone (V) as red needles, m. p. 244~245°C (Found: C, 81.71; H, 4.13. Calcd. for $C_{16}H_{10}O_2$: C, 82.04; H, 4.30%. UV $\lambda_{max}^{MeOH}$ mμ (log ε): 247 (4.43), 257 (4.40), 452 (4.57). IR $\nu_{c=o}$ 1645 $cm^{-1}$).

Reaction of cyclopentene-3, 5-dione[5] (VI) and 2 mol. equivalents of III in aqueous solution and adjustment of the reaction mixture to pH 6~7 with sodium hydrogen carbonate afforded in 93.5% yield, 4, 4-ditropylcyclopentene-3, 5-dione (VII) as yellow prisms, m. p. 121~122°C (Found: C, 82.45; H, 5.84. Calcd. for $C_{19}H_{16}O_2$: C, 82.58; H, 5.84%. IR $\nu_{c=o}$ 1735, 1696 $cm^{-1}$). Pyrolysis of VII did not give VIII.

Reaction of VI and 1 mol. equivalent of III in the presence of 1 mol. equivalent of hydrobromic acid and dehydrogenation of the resulting yellow oily product with chloranil in xylene gave fulvalmixene-1, 4-quinone (VIII) as red plates, m. p. 179~180°C (Found: C, 78.41; H, 4.26. Calcd. for $C_{12}H_8O_2$: C, 78.25; H, 4.38%. UV $\lambda_{max}^{MeOH}$ mμ (log ε): 222 (4.35), 253 (4.16), 420 (4.37). IR $\nu_{c=o}$ 1643 $cm^{-1}$).




T = Tropyl




VII VIII

The double bond at 2, 3 position in VIII is active and undergoes addition to give the following adducts:

*Dibromide (IX).*—Yellow scales, m. p. 148°C (decomp.) (Found: C, 42.51; H, 2.42. Calcd. for $C_{12}H_8O_2Br_2$: C, 41.89; H, 2.34%. UV $\lambda_{max}^{MeOH}$ mμ (log ε): 225 (4.30), 267 (4.21), 452 (4.43). IR $\nu_{c=o}$ 1627 $cm^{-1}$). V does not undergo the addition of bromine.

*Cyclopentadiene Adduct (X).*—Red prisms, m. p. 188~189°C (Found: C, 81.51; H, 5.25. Calcd. for $C_{17}H_{14}O_2$: C, 81.58; H, 5.64%. UV $\lambda_{max}^{MeOH}$ mμ (log ε): 235 (3.82), 289 (3.83), 450 (4.43). IR $\nu_{c=o}$ 1620 $cm^{-1}$).

*Diazomethane Adduct (XI).*—Orange needles, m. p. above 280°C (Found: C, 68.67; H, 4.33; N, 12.08. Calcd. for $C_{13}H_{10}O_2N_2$: C, 69.01; H, 4.46; N, 12.38%. UV $\lambda_{max}^{MeOH}$ mμ (log ε): 225 (4.33), 266 (4.23), 451 (4.42). IR $\nu_{c=o}$ 1618 $cm^{-1}$).

These 2, 3-adducts showed a red shift of ca. 30 mμ in the first absorption band in their ultraviolet spectra, compared to that of VIII, and the C=O stretching vibration in their infrared spectra also showed a shift of ca. 20 $cm^{-1}$ to lower frequencies[6]. These phenomena might be explained by assuming that conjugation within the O=C-C=C-C=O group hinders conjugation between the carbonyl group and the seven-membered ring.

Absence of hydroxyl band in the infrared spectra of adducts shows that they do not exist in the enol forms, 1, 4-dihydroxyfulvalmixenes.

*The Chemical Research Institute of Non-Aqueous Solutions*
*Tohoku University*
*Sendai*

6) The C=O stretching vibration in the dibromide IX is in smaller wave number region than in X and XI because it is an α-bromoketone (cf. L. J. Bellamy, "The Infra-red Spectra of Complex Molecules", Methuen Co., Ltd., London (1958), p. 139.

# *Thermal Annealing of Recoil Atoms in Neutron Irradiation of Inorganic Phosphorus Compounds*

By Hiroshi BABA, Kenji YOSHIHARA, Hiroshi AMANO, Kichizo TANAKA, and Nagao SHIBATA

(Received January 28, 1961)

The recoil effects in neutron-irradiated phosphorus compounds have been reported by several investigators. It was found that these phenomena were very complicated. The radiochemical distribution of phosphorus recoil atoms was remarkably effected by the condition of irradiation. The fact that the distribution of recoil atoms was changed by thermal annealing was pointed out by Lindner and Harbottle[1] and also by Yoshihara and Yokoshima[2]. The effect of thermal annealing, however, was not investigated systematically in these papers. The present authors studied these effects in a series of inorganic phosphorus

1) L. Lindner and G. Harbottle, CENT 70 (presented at the Symposium on Chemical Effects of Nuclear Transformations, Prague, October 1960).
2) K. Yoshihara and T. Yokoshima, This Bulletin, in press.

compounds in crystal and obtained the following results.

The samples which were irradiated in JRR-1 reactor (neutron flux $10^{11}$n./cm$^2$ sec., fast neutron was less than 5%) for 15 hr., were heated in an electric oven, dissolved in water, and separated by paper chromatography. The developing agent for this separation was a mixture of 2 N nitric acid and *n*-buthanol (1 : 1 ratio)[2].

On the isothermal annealing of irradiated sodium orthophosphate crystal (anhydrous, tribasic) at 167°C, the orthophosphate fraction increased remarkably, whereas the pyrophosphate fraction decreased appreciably, but the phosphite fraction* slightly decreased. This is presented in Fig. 1. The second order kinetics was applied to the rate of the decrease of the pyrophosphate or the polyphosphate fractions. On the other hand, the slight decrease of phosphite fraction followed approximately first order kinetics and the energy of activation in the phosphite annealing seemed to be higher than that of pyrophosphate or polyphosphate fractions.

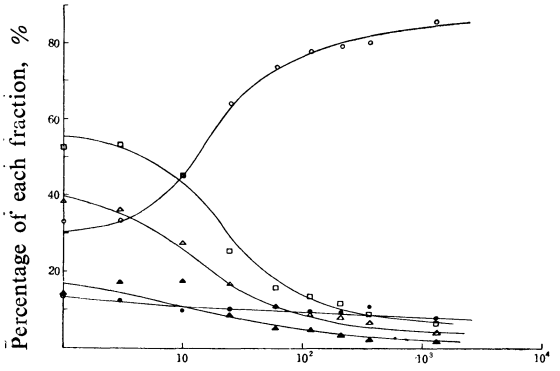



Fig. 1. Changes of distribution of recoil atoms in irradiated sodium phosphate crystals (tribasic) by thermal annealing at 167°C.
- ○ Phosphate
- ● Phosphite (+Hypophosphite)
- □ Pyrophosphate+polyphosphate
- △ Polyphosphate
- ▲ Pyrophosphate

* This fraction might include hypophosphite because hypophosphite was not separable from phosphite by the present method.

In the case of phosphate crystal (anhyrous, dibasic) the orthophosphate fraction first increased and then decreased, whereas the pyrophosphate fraction first decreased and then increased. The polyphosphate fraction decreased monotonously. The slight decrease of the phosphite fraction was observed. The data on each fraction are shown in Fig. 2 as a function of annealing time. The decrease of the orthophosphate fraction corresponded to the increase of the pyrophosphate fraction, and therefore, this is interpreted as the results of the thermal polymerization.

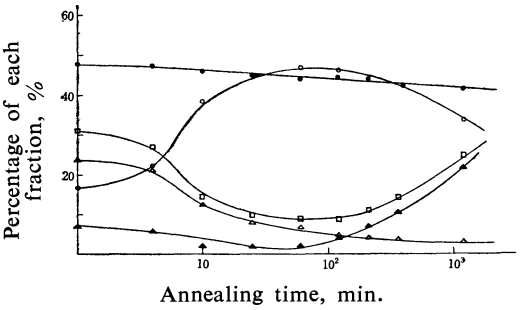



Fig. 2. Changes of distribution of recoil atoms in irradiated sodium phosphate crystals (dibasic) by thermal annealing at 166°C.
- ○ Phosphate
- ● Phosphite (+Hypophosphite)
- □ Pyrophosphate+polyphosphate
- △ Polyphosphate
- ▲ Pyrophosphate

The annealing effect of sodium pyrophosphate was also investigated. It was shown that the pyrophosphate fraction remarkably increased and the polyphosphate fraction decreased. However, both fractions of orthophosphate and phosphate only slightly decreased.

Further more delails are to be reported in full papers.

*Radioisotope Production Laboratory*
*Japan Atomic Energy Research Institute*
*Tokai, Ibaraki-ken*

# *Kinetics of the Reduction of Selenious Acid by Sulfur Dioxide. I. Reduction in Acidic Solution with Hydrochloric Acid**

By Keinosuke HAMADA

(Received February 17, 1960)

Raw materials for the production of selenium depend heavily on a sludge and a copper slime, which are obtained as a by-product of a sulfuric acid factory and a copper refinery, respectively. In order to investigate the behavior of selenium at the sulfuric acid production plant, to increase the yield of selenium recoverable from the sulfuric acid plant source and to establish a simple method for the refining of these raw materials, the following series of studies were undertaken.

Consideration will be given first to the kinetics of the reduction of selenious acid in hydrochloric acid by sulfur dioxide. The percentage completion of these reactions is calculated by weighing the selenium precipitated from a solution. Sulfur dioxide is passed into a solution continuously, so that the reaction is of zero order with respect to sulfur dioxide.

It has been proved that the reduction of selenious acid was of the second order with respect to selenious acid. Furthermore, a general equation was derived for the rate constant of the reaction by studying the effects of hydrogen ion concentration and temperature upon it.

## Experimental

**Materials.**—1.752, 0.736, 0.368 and 0.172 mol./l. aqueous solution of selenious acid were prepared by dissolving extra pure reagent selenious acid in distilled water. On the other hand, 12, 6, 4.5 and 3% (by volume) hydrochloric acid solutions were prepared by diluting the first grade reagent hydrochloric acid (s. g. 1.18~1.19) with distilled water. The pH*1 values of these acid solutions were 0.02, 0.31, 0.42 and 0.59, which corresponded to 0.96, 0.49, 0.38 and 0.26 g. ion/l. of hydrogen ion concentration*2, respectively. Liquid sulfur dioxide was purchased from Befu Chemical Industrial Co.

**Measurements.**—Experimental solutions were prepared as follows. Ten milliliters of the above aqueous solutions of selenious acid were placed in a 200 ml. measuring flask, which was filled with the above-mentioned dilute hydrochloric acid. The solution was poured into a 300 ml. Erlenmeyer's flask, and kept at a constant temperature within ±0.1°C by a thermostat, and then sulfur dioxide was passed into the solution. The sulfur dioxide was initially passed through a washing bottle filled with water kept at the same constant temperature. Each of the selenious acid solutions was reduced by sulfur dioxide in four kinds of hydrochloric acid solutions at various temperatures.

After a certain period, the contents in an Erlenmeyer's flask was poured into 600 ml. of distilled water. In this way the reaction could be prevented owing to the decrease of the hydrogen ion concentration as well as temperature[1]. Precipitated selenium was filtered with a previously weighed glass filter (1G-4), washed by water, dried at 105~110°C in an air bath and then weighed.

Percentage completion of reaction is expressed with (precipitated selenium/initial selenium in the solution) ×100.

## Results and Discussion

**Selenious Acid Concentration Dependence of the Reduction of Selenious Acid.**—Concentrations of the prepared selenious acid solutions in hydrochloric acid were 0.0876, 0.0368, 0.0184 and 0.0086 mol./l., respectively. At constant temperature (70°C) and constant hydrogen ion concentration (0.49 g. ion/l.), these selenious acid solutions were reduced by sulfur dioxide. The weight of precipitated selenium was converted into percentage completion according to the above expression. Fig. 1 shows the selenious acid concentration dependence of the reduction of selenious acid by plotting the percentage completion against the elapsed time.

The values of half time ($t_{1/2}$) can be obtained from Fig. 1, and these are 100, 260, 460 and 1200 sec., respectively. When $a$ is the initial concentration of selenious acid (mol./l.), $p$ the quantity of reduced selenious acid (equal to precipitated selenium) after time $t$ (in sec.), $k_1$*3 the rate constant (l. mol$^{-1}$ sec$^{-1}$), $t_{1/2}$ the half time (sec.), and the reaction is of the $n$th order with respect to selenious acid, this reaction can be expressed mathematically by

$$-\mathrm{d}(a-p)/\mathrm{d}t=\mathrm{d}p/\mathrm{d}t=k_1(a-p)^n \qquad (1)$$

The solution of Eq. 1 is as follows,

* Presented at the 13th Annual Meeting of the Chemical Society of Japan, Tokyo, April, 1960.

*1 Measured by a pH-meter with 0.01 pH accuracy.

*2 Calculated from pH value.

1) J. W. Mellor: "A Comprehensive Treatise on Inorg. and Theoret. Chem." Vol. X, S, Se, p. 699.

*3 $k_1$ does not mean the rate constant of first order reaction, but the rate constant of the reduction of selenious acid in hydrochloric acid.

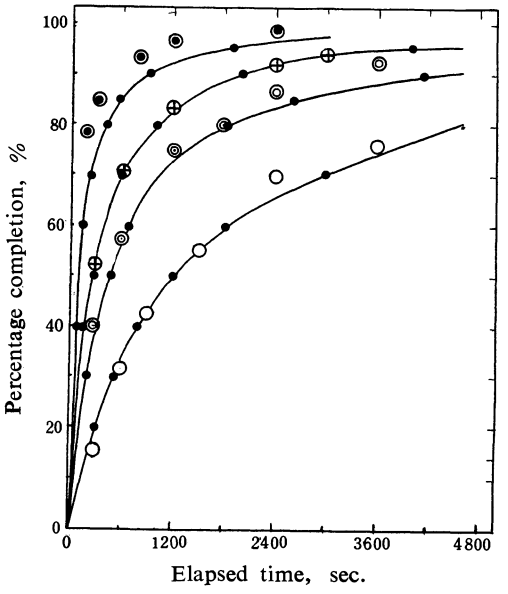



Fig. 1. $H_2SeO_3$ concn. dependence of the reduction of $H_2SeO_3$ in HCl at const. $[H^+]$ (0.49 g. ion/l.) and const. temp. (70°C).

◉ 0.0876 mol./l.
⊕ 0.0368 〃
◎ 0.0184 〃
○ 0.0086 〃
• Calculated by Eq. 2, with $n$ equal to 2.

$$t=\{a^{n-1}-(a-p)^{n-1}\}/\{k_1(n-1)\times(a-p)^{n-1}a^{n-1}\} \quad (2)$$

If $t$ is equal to $t_{1/2}$, $p$ is equal to $a/2$. Making these substitutions for $t$ and $p$ in Eq. 2, the result is

$$t_{1/2}=(2^{n-1}-1)/\{k_1(n-1)a^{n-1}\} \quad (3)$$

When the values of the initial concentration of selenious acid and the experimentally determined half time ($t_{1/2}$) are substituted for $a$ and $t_{1/2}$ in Eq. 3, four equations are obtained;

$$1200=(2^{n-1}-1)/\{k_1(n-1)\times 0.0086^{n-1}\} \quad (i)$$
$$460=(2^{n-1}-1)/\{k_1(n-1)\times 0.0184^{n-1}\} \quad (ii)$$
$$260=(2^{n-1}-1)/\{k_1(n-1)\times 0.0368^{n-1}\} \quad (iii)$$
$$100=(2^{n-1}-1)/\{k_1(n-1)\times 0.0876^{n-1}\} \quad (iv)$$

Combining these equations, one can obtain the values of $n$ which are 2.27, 1.82, 2.10, 2.05, 2.07 and 1.98. The mean value of $n$ is 2.05, and from this it can be established that this reaction is one of second order with respect to selenious acid. As $n$ is equal to 2, the values of $k_1$ can be calculated from the above four equations.

**Temperature Dependence of the Reduction of Selenious Acid.**—At constant initial concentration of selenious acid (0.0184 mol./l.) and constant hydrogen ion concentration (0.49 g. ion/l.), selenious acid in hydrochloric acid is reduced by sulfur dioxide, when the temperature is at 70, 60, 55 and 50°C. Fig. 2 shows the plot of the percentage completion against the elapsed time based upon the experimental data. As $n$ is equal to 2, and the values of the initial concentration of selenious acid are known and the values of half time can be obtained from Fig. 2, upon making these substitutions for the values for $n$, $a$ and $t_{1/2}$ in Eq. 3, the rate constants at 70, 60, 55 and 50°C are 0.118, 0.042, 0.020 and 0.012 l. $mol^{-1}$ $sec^{-1}$, respectively.

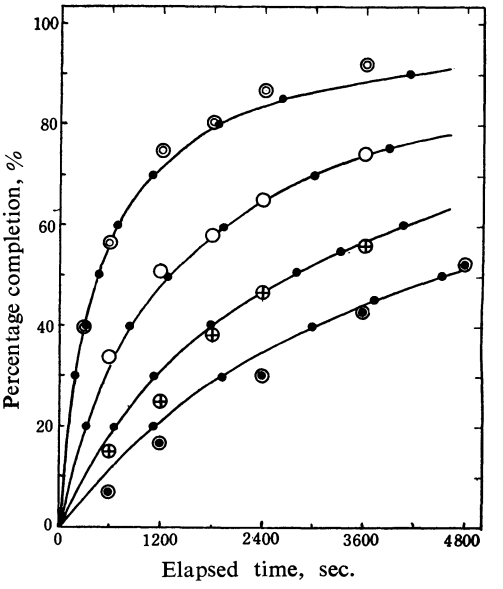



Fig. 2. Temperature dependence of the reduction of $H_2SeO_3$ at const. $[H_2SeO_3]$ (0.0184 mol./l.) and const. $[H^+]$ (0.49 g. ion/l.).

◎ 70°C
○ 60°C
⊕ 55°C
◉ 50°C
• Calculated by Eq. 2, with $n$ equal to 2.

The influence of temperature on reaction velocity can be derived by plotting the logarithm of the rate constant, $\log k_1$, against the reciprocal of the absolute temperature, $1/T$ (Fig. 3). As Fig. 3 shows that the experimental points fall on a straight line, the energy of activation $E$ can be calculated from the value of the slope in Fig. 3.

The slope is equal to $-E/2.303R$[2]. The slope of the straight line in Fig. 3 is equal to $-5.35\times10^3$, and as $R$ is taken as 1.987 cal. $deg^{-1}$ $mol^{-1}$, it follows that for the reduction of selenious acid $E$ is 24.5 kcal./mol. Moreover,

2) S. Glasstone, "Elements of Physical Chemistry", Maruzen, Tokyo (1958), p. 607.

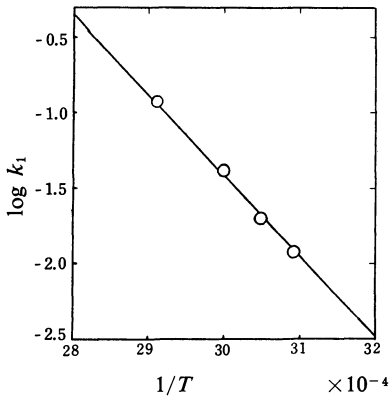



Fig. 3. Arrhenius' plot of the reduction of $H_2SeO_3$ by $SO_2$.

the rate constant $k_1$ is proportional to exp $(-E/RT)$.

**Hydrogen Ion Concentration Dependence of the Reduction of Selenious Acid.**—At a constant initial concentration of selenious acid (0.0184 mol./l.), the constant temperature (60°C) and various hydrogen ion concentrations (0.26, 0.38, 0.49 and 0.96 g. ion/l.), the selenious acid in hydrochloric acid were reduced by sulfur dioxide. These results are shown in Fig. 4.

Rate constant $k_1$ can be obtained from Eq. 3. Plotting the rate constant against the square of hydrogen ion concentration, it is seen in Fig. 5 that the experimental points fall on a straight line.

It is evident from Fig. 5 that rate constant $k_1$ is proportional to $[H^+]^2$.

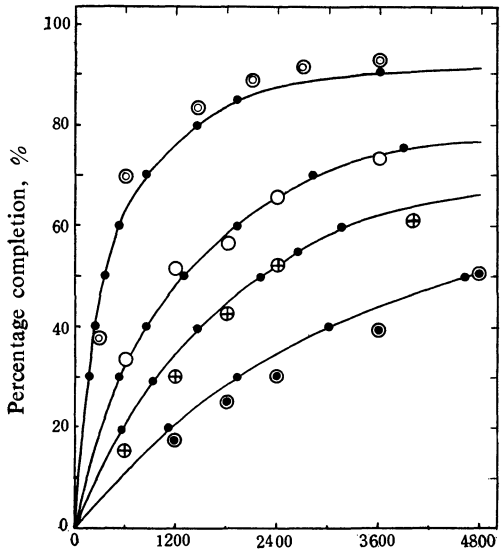



Fig. 4. $[H^+]$ dependence of the reduction of $H_2SeO_3$ at const. $[H_2SeO_3]$ (0.0184 mol./l.) and const. temp. (60°C).
◎ 0.96 g. ion/l.
○ 0.49 〃
⊕ 0.38 〃
◉ 0.26 〃
• Calculated by Eq. 2, with $n$ equal to 2.

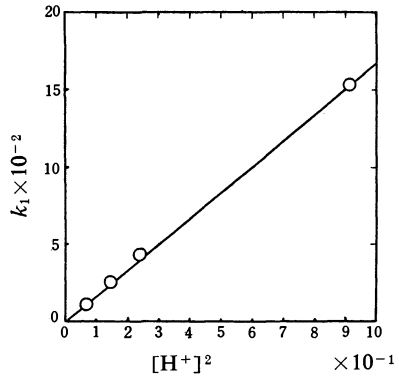



Fig. 5. Plot of $k_1$ against $[H^+]^2$.

When the temperature is equal to 60°C, hydrogen ion concentration is equal to 0.49 g. ion/l. and the initial concentration of selenious acid is equal to 0.0184 mol./l., the rate constant $k_1$ is evaluated to be 0.042 l. $mol^{-1}$ $sec^{-1}$. When these values*4 are adopted, the general Eq. 4 for rate constant can be derived, according to the above-mentioned temperature and hydrogen ion concentration dependence, that is,

$$k_1 = 2.054 \times 10^{15} \times [H^+]^2 \exp(-E/RT) \quad (4)$$

where $E$ is the energy of activation (24.5 kcal./mol.), $R$ the gas constant (1.987 cal. $deg^{-1}$ $mol^{-1}$) and $T$ the absolute temperature.

## Summary

(1) The reduction of selenious acid in hydrochloric acid by sulfur dioxide is a typical second order reaction with respect to selenious acid, while the reaction is of zero order with respect to sulfur dioxide because of the continuous passage of sulfur dioxide through a solution.

(2) The results obtained at 70, 60, 55 and 50°C ($a$=0.0184 mol./l., $[H^+]$ =0.49 g. ion/l.) give a good Arrhenius plot, leading to the value of 24.5 kcal. $mol^{-1}$ for the energy of activation.

(3) The rate constant of this reaction under a certain condition can be evaluated by the general equation,

$$k_1 = 2.054 \times 10^{15} \times [H^+]^2 \exp(-E/RT)$$

where $[H^+]$ is hydrogen ion concentration, $E$, the energy of activation and $T$ absolute temperature.

*4 These experimental data are in good accordance with theoretical values (denoted by •) obtained from Eq. 2.

(4) The reduction of selenious acid in sulfuric acid, which will be published in a subsequent paper, is a reversible reaction. The above equation for the rate constant is utilized as a basic equation, in order to determine the rate constant in the forward direction of the reversible reaction.

The author wishes to express his sincere thanks to Dr. H. Negita of the Department of Chemistry, Hiroshima University, for his discussion and advice, and also he wishes to thank Mr. M. Kodama for his assistance.

*Department of Chemistry*
*Faculty of Science*
*Hiroshima University*
*Hiroshima*

# *Kinetics of the Reduction of Selenious Acid by Sulfur Dioxide. II. Reduction in Acidic Solution with Sulfuric Acid**

By Keinosuke HAMADA

(Received Feburary 17, 1960)

This paper deals with the kinetics of the reduction of selenious acid in sulfuric acid by sulfur dioxide. Amelin and Yashke[1] investigated the reduction of selenious acid in concentrated sulfuric acid (60~80% by weight), and reported that the reaction was of first order with respect to selenious acid and to sulfur dioxide. The present author has studied the reduction of selenious acid by sulfur dioxide in dilute sulfuric acid, and has obtained different results from that obtained when concentrated sulfuric acid is utilized. The same method as that described in Part I[2] of this series was used. However, since it was found that the reaction in sulfuric acid was reversible, the method of measurements was improved by taking account of the equilibrium in the reversible reaction. The influences of temperature, initial concentration of selenious acid and hydrogen ion concentration on the reaction were investigated, and also general equations were derived for $k_2$*1 and $k_2'$ which were rate constants of the forward and reverse reactions.

## Experimental

**Materials.** — 0.736, 0.368 and 0.184 mol./l. aqueous solutions of selenious acid were prepared by dissolving extra pure reagent selenious acid in distilled water. Also prepared were 6.0, 4.5, 3.0 and 1.5% (by volume) sulfuric acid by diluting the first grade reagent sulfuric acid (s. g. about 1.84) with distilled water. pH*2 values were 0.08, 0.22, 0.38 and 0.62, and their hydrogen ion concentrations were evaluated to be 0.83, 0.60, 0.42 and 0.24 g. ion/l., respectively. The liquid sulfur dioxide was purchased.

**Measurements.** — This experiment was performed by means of the same procedures as those reported in Part I[2] of this series except that sulfuric acid was used in place of hydrochloric acid. However, since it was discovered that the reaction in sulfuric acid was reversible, the procedure suitable to this factor was adopted. That is, after the expected time for the reaction had elapsed, the precipitated selenium was filtered with a glass filter (1G-4)*3. Then the selenium was washed with dilute hydrochloric acid and water. Hereafter, the experimental procedures are the same as those in Part I[2] of this series.

## Results and Discussion

**Selenious Acid Concentration Dependence of the Reduction of Selenious Acid.** — Ten milliliters of the three selenious acid solutions were diluted to 200 ml. with 4.5% (by volume) sulfuric acid ($[H^+]=0.60$), the concentrations of the experimental solutions of selenious acid being 0.0092, 0.0184 and 0.0368 mol./l., respectively. These solutions were reduced by sulfur dioxide at constant temperature (60°C). Weights of precipitated selenium were converted into percentage completion, and the plot of the percentage completion against elapsed time (sec.) is shown in Fig. 1.

* Presented at the 13th Annual Meeting of the Chemical Society of Japan, Tokyo, April, 1960.

1) A. G. Amelin and E. V. Yashke, *Proc. Acad. Sci. U. S. S. R. Sec. Chem.*, **108**, 313 (1956); *Chem. Abstr.*, **51**, 54g (1957); *Chem. Zentr.*, **128**, 6688 (1957).

2) Part I: This Bulletin, **34**, 593 (1961).

*1 $k_2$ does not mean the rate constant of the second order reaction, but the rate constant of reaction in sulfuric acid.

*2 Measured by a pH-meter with 0.01 pH accuracy.

*3 Since the present reaction is reversible, diluting reactants with water can not be adopted to stop the process of the reaction. The effects of a reverse reaction appear conspicuously.

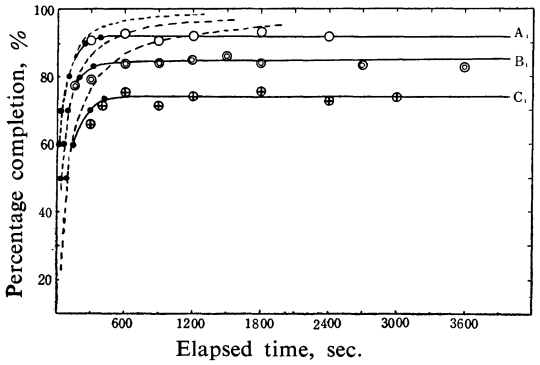



Fig. 1. $H_2SeO_3$ concn. dependence of the reduction of $H_2SeO_3$ at const. temp. (60°C) and const. $[H^+]$ (0.60 g. ion/l.).
○ 0.0368 mol./l. ◎ 0.0184 mol./l.
⊕ 0.0092 mol./l. • calculated by Eq. 4.
Dotted lines: forward reaction with rate constant obtained from Eq. 1, when reverse reaction does not occur.

Each curve of Fig. 1 reaches an equilibrium, which is very different from the results in hydrochloric acid[2]. It is certain that the present reaction which comes to equilibrium is reversible[3].

The lines estimated from the experiment in the region below 60% completion of reaction are in good accordance with those obtained from Eqs. 1 and 2 based on only the forward reaction[2] (dotted lines).

Accordingly, the effect of the reverse reaction can be neglected in the region below 60% completion, where the reaction appears to be similar to the simple reaction in hydrochloric acid.

Provided that the reaction in sulfuric acid is of the second order with respect to selenious acid as it was in the case of hydrochloric acid, the rate constant $k_2$ for the forward reaction can be calculated by $t_{1/2}=1/(k_2a)$*4.

In the region below 60% completion, the author could not obtain any experimental data which could discriminate between curves $A_1$, $B_1$ and $C_1$. However, the value of $k_2$ in the reaction for curve $C_1$ is calculated to be 1.278 l. $mol^{-1}$ $sec^{-1}$ from $t_{1/2}=1/(k_2a)$, since the half time ($t_{1/2}$) is evaluated to be 85 sec. from the curve $C_1$ of Fig. 1, which is estimated from the experiment ($a=0.0092$ mol./l.).

The general equation for the rate constant of the reaction in hydrochloric acid was obtained as follows[2];

$$k_1=2.054\times10^{15}\times[H^+]^2\times\exp(-E/\boldsymbol{RT})$$
$$(E=24.5 \text{ kcal./mol.})$$

When the experimental conditions for curve $C_1$, 60°C and 0.60 g. ion/l., are substituted for $T$ and $[H^+]$ in the above equation, the rate constant can be calculated to be 0.0629 l. $mol^{-1}$ $sec^{-1}$. This value is far below the above-mentioned value (1.278 l. $mol^{-1}$ $sec^{-1}$), so it has to be multiplied by 20 in order to be in good accordance with the latter value. In this way, the general equation for rate constant $k_2$ of the forward reaction in sulfuric acid is expressed tentatively as follows:

$$k_2=20\times k_1$$
$$k_2=4.108\times10^{16}\times[H^+]\times\exp(-E/\boldsymbol{RT})$$
$$(E=24.5 \text{ kcal./mol.}) \qquad (1)$$

The values of $k_2$ estimated from the experiment in the reaction for curves $A_1$ and $B_1$ of Fig. 1 are in accordance with the ones calculated from Eq. 1.

The reverse rate constant $k_2'$ can be obtained by substituting the value of forward rate constant $k_2$, which is calculated from Eq. 1 in Eq. 3. When $k_2$ and $k_2'$ are substituted in Eq. 4, the parts of the curves in Fig. 1 are drawn theoretically. The curvatures obtained from the experiment are in good accordance with those drawn by the calculated values from Eq. 4.

From these facts it is concluded that the values of $k_2$ based on Eq. 1 are correct.

Eq. 1 is derived by assuming that the activation energy $E$ of the reaction in sulfuric acid is equal to the one in hydrochloric acid ($E=24.5$ kcal./mol.). However, the coefficient of 20 may be due to the difference of the activation energy in each case. Although the energy of activation could not be obtained experimentally, it will be possible for it to be obtained by calculation. The values of $k_2$ at 60, 50, 40 and 30°C are calculated with Eq. 1 to be 1.258, 0.400, 0.118 and 0.032 l. $mol^{-1}$ $sec^{-1}$, respectively. The line A of Fig. 3 shows the plotting of the logarithm of $k_2$ against the reciprocal of the absolute temperature. Each point falls upon a straight line. It follows from the slope of the straight line that the energy of activation is 22.5 kcal./mol. So, Eq. 1 is rewritten as follows:

$$k_2=2.054\times10^{15}\times[H^+]^2\times\exp(-E/\boldsymbol{RT})$$
$$(E=22.5 \text{ kcal./mol.}) \qquad (1')*5$$

The dotted lines in each figure are obtained from Eqs. 1 and 2,

$$t=p/\{k_2a(a-p)\}=x/\{k_2a(1-x)\}$$
$$(p=ax) \qquad (2)*6$$

3) S. Glasstone, "Elements of Physical Chemistry", Maruzen, Tokyo (1958), p. 600.

*4 Eq. 3 in Part I[2] of this series (as $n=2$).

*5 Eq. 1′ is the same equation as Eq. 1. But, for the general equation of rate constant, the expression of Eq. 1′ seems to be better than the one of Eq. 1.

*6 Eq. 2 in Part I[2] of this series (as $n=2$).

where $t$ is the elapsed time (sec.) of reaction, $p$ the reduced quantity of selenious acid (mol./l.) when time $t$ has elapsed, $x$ percentage completion (%) when time $t$ has elapsed, $k_2$ rate constant (l. mol$^{-1}$ sec$^{-1}$), and $a$ initial concentration of selenious acid (mol./l.).

The reversible reaction which is of the second order with respect to selenious acid can be expressed mathematically[3] by

$$-\mathrm{d}(a-p)/\mathrm{d}t=\mathrm{d}p/\mathrm{d}t=k_2(a-p)^2-k_2'p^2 \qquad (3)^{4)*7}$$

The solution of Eq. 3 is as follows, ($p=ax$)

$$t=\frac{2.303}{2a\sqrt{k_2k_2'}}\times\log\left|\frac{\{(k_2-k_2')x-k_2-\sqrt{k_2k_2'}\}/(k_2-k_2')x-k_2+\sqrt{k_2k_2'}}{(-\sqrt{k_2k_2'}-k_2)/(\sqrt{k_2k_2'}-k_2)}\right| \qquad (4)$$

The curvatures of the practical lines are drawn according to Eq. 4. Values of $k_2'$ in Eq. 4 can be obtained from Eq. 5.

As the reverse reaction occurs, selenium must be dissolved in dilute sulfuric acid. However, the purchased selenium is not dissolved in dilute sulfuric acid or in basic solution ($NH_4OH$)*8. This is inconsistent with the fact that the reduction of selenious acid in dilute sulfuric acid is a reversible reaction. This discrepancy can be solved by assuming that $\alpha$ selenium is dissolved in dilute sulfuric acid or in a basic solution, whereas $\beta$ selenium is not dissolved*8. The purchased selenium is dried at 100~105°C, and is of the $\beta$ form.

On the contrary, the selenium produced by reducing selenious acid below 99°C is of the $\alpha$ form, because the allotropic transition temperature of selenium from $\alpha$ to $\beta$ is 99°C[5].

At equilibrium of the reversible reaction, it is evident that $\mathrm{d}p_m/\mathrm{d}t=0$ in Eq. 3 where $p_m$ is the value of $p$ at equilibrium (the value of $p$ at equilibrium is equal to the maximum value of $p$). When $p$ is equal to $p_m(ax=ax_m)$, Eq. 5 can be derived from Eq. 3 as follows,

$$\mathrm{d}p/\mathrm{d}t=k_2(a-p_m)^2-k_2'p_m^2$$
$$=k_2a^2(1-x_m)^2-k_2'a^2x_m^2=0 \qquad (5)$$

where $x_m$ is the maximum percentage completion at equilibrium. The values of $x_m$ obtained from Fig. 1 are 92, 85 and 74%, respectively. When the values of $x_m$ and $k_2$ (1.258 l. mol$^{-1}$ sec$^{-1}$) obtained from Eq. 1 are substituted in Eq. 5, then the values of $k_2'$ can be calculated to be 0.009, 0.039 and 0.155 l. mol$^{-1}$ sec$^{-1}$ for curves $A_1$, $B_1$ and $C_1$ in Fig. 1.

Table I shows the relation between the initial concentration of selenious acid, $a$, and the reverse rate constant, $k_2'$.
It is evident from Table I that $k_2'$ is inversely proportional to $a^2$.

TABLE I. RELATION BETWEEN $a^2$ AND $k_2'$

| $a$, mol./l. | $x_m$, % | $k_2$ | $k_2'$ | $a^2k^{2\prime}\times10^{-5}$ |
|---|---|---|---|---|
| 0.0368 | 92 | 1.258 | 0.009 | 1.30 |
| 0.0184 | 85 | 1.258 | 0.039 | 1.33 |
| 0.0092 | 74 | 1.258 | 0.155 | 1.24 |

**Temperature Dependence of the Reduction of Selenious Acid.** — At constant initial concentration of selenious acid (0.0184 mol./l.) and hydrogen ion concentration (0.60 g. ion/l), selenious acid in sulfuric acid is reduced by sulfur dioxide at different temperatures, 60, 50, 40 and 30°C.

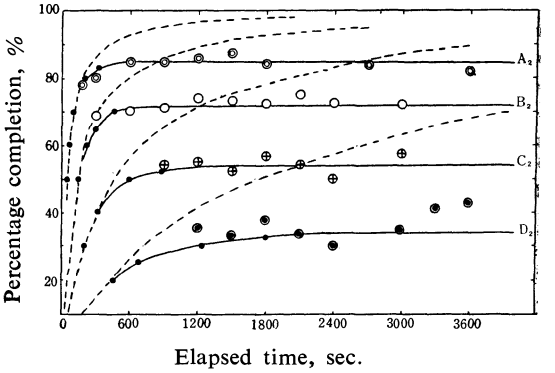



Fig. 2. Temp. dependence of the reduction of $H_2SeO_3$ at const. [$H_2SeO_3$] (0.0184 mol./l.) and const. [$H^+$] (0.60 g. ion/l.).
◎ 60°C ○ 50°C ⊕ 40°C ⊙ 30°C
• Calculated by Eq. 4.
Dotted lines: Ref. 2, Fig. 1

4) A. Wattilon and F. Grunderbeck, *Bull. soc. chim. Belges*, **65**, 657 (1956); *Chem. Abstr.*, **51**, 7103 (1957).

*7 Although the precipitated selenium coagulates gradually at a temperature above about 40°C in this experiment, the size of selenium particles prepared at the outset of the reaction is ultramicroscopic or electronmicroscopic. The very fine particles of selenium are dispersed by the passage of sulfur dioxide at the onset of the reaction. The reaction in the reverse direction is one where the dissolving of the precipitated selenium on its surface takes place. When $k_s$ is a rate constant for dissolving the solid and $S$ is the constant dependent on the surface of the solid, $k_sSp^2$ expresses a rate of the reverse reaction. If $S$ is constant under the present experimental conditions, $k_sSp^2$ can be expressed by $k_2'p^2$ in Eq. 3. From Figs. 1, 2 and 4, it is seen that the higher the temperature, greater hydrogen ion concentration and initial concentration of selenious acid are, the better are the experimental data in accordance with Eq. 3. If $S$ is variable under all experimental conditions, Eq. 3 can not be derived.

*8 Eq. 6 shows that the lower the hydrogen ion concentration, the higher is the value of $k'_2$ (rate constant of reverse reaction), i.e., selenium is dissolved in basic solution more easily than in acidic solution. In fact, selenium produced by reducing selenious acid at 60°C disappears by adding basic solution[2] ($NH_4OH$), but selenium dried over 100°C does not dissolve in basic solution.

5) Roger Dolique et al., *Bull. soc. chim. France, Mém.* [5], **10**, 231 (1943); *Chem. Abstr.*, **38**, 6156–8 (1944).

The results are shown in Fig. 2, where the precipitated selenium is converted into percentage completion. The values of $k_2$ at 60, 50, 40 and 30°C are calculated with Eq. 1 to be 1.258, 0.400, 0.118 and 0.032 l. $mol^{-1}$ $sec^{-1}$, respectively. The values of $x_m$ at the above temperature can be obtained from Fig. 2, and they are 85, 72, 54 and 34%, respectively. Making these substitutions for $k_2$ and $x_m$ in Eq. 5, the values of $k_2'$ at each temperature can be calculated to be 0.039, 0.060, 0.086 and 0.121 l. $mol^{-1}$ $sec^{-1}$.

Line B of Fig. 3 shows the plotting of the logarithm of $k_2'$ against the reciprocal of the absolute temperature ($1/T$). It is evident that experimental points fall upon a straight line. The relation between the rate constant of reverse direction and the temperature can be derived from the straight line B in Fig. 3 as follows.

$$k_2' \propto \exp(-E/RT)$$

The energy of activation $E$ can be calculated to be −8.06 kcal./mol. from the slope of the line B in Fig. 3.

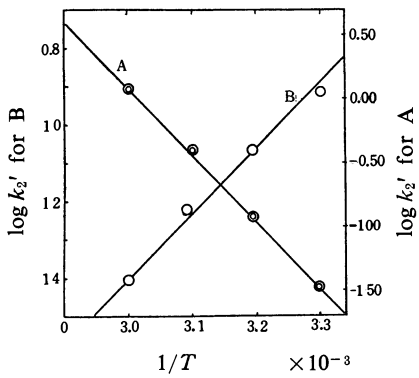



Fig. 3. Arrhenius' plot of the forward and reverse reaction.

**Hydrogen Ion Concentration Dependence of the Reduction of Selenious Acid.** — At constant initial concentration of selenious acid (0.0184 mol./l.), constant temperature (60°C) and various hydrogen ion concentrations (0.83, 0.60 and 0.042 g. ion/l.), selenious acid in sulfuric acid was reduced by sulfur dioxide.

The results are shown in Fig. 4, where precipitated selenium is converted into a percentage completion. The values of $k_2$ and $k_2'$ can be calculated from Eqs. 1 and 5, (see Table II).

From Table II, the rate constant of reverse direction, $k_2'$, is inversely proportional to the square of hydrogen ion concentration, $[H^+]^2$. According to the above-mentioned selenious acid concentration, temperature and hydrogen ion concentration dependence of the reverse

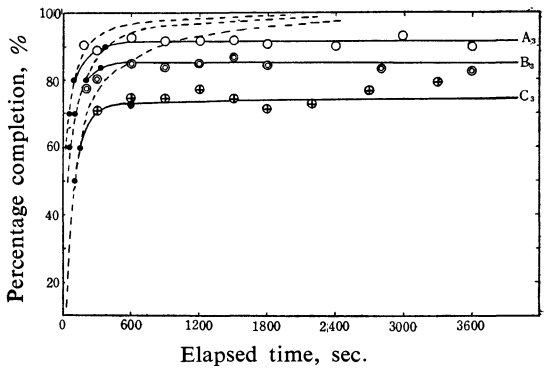



Fig. 4. $[H^+]$ dependence of the reduction of $H_2SeO_3$ at const. $[H_2SeO_3]$ (0.0184 mol./l.) and const. temp. (60°C).
○ 0.83 g. ion/l. ◎ 0.60 g. ion/l.
⊕ 0.42 g. ion/l. • Calculated by Eq. 4.
Dotted lines: Ref. Fig. 1

TABLE II. RELATION BETWEEN $k_2'$ AND $[H^+]$

| $[H^+]$ | $k_2$ | $x_m$, % | $k_2'$ | $[H^+]^2$ | $k_2' \times [H^+]^2$ ($\times 10^{-3}$) |
|---|---|---|---|---|---|
| 0.83 | 2.408 | 91.5 | 0.021 | 0.689 | 14.33 |
| 0.60 | 1.258 | 85.0 | 0.039 | 0.369 | 14.04 |
| 0.42 | 0.617 | 74.0 | 0.076 | 0.176 | 13.37 |

reaction, the general equation for the reverse rate constant $k_2'$ can be derived as follows:

$$k_2' = 2.413 \times 10^{-11} \times \{1/(a^2[H^+]^2)\} \times \exp(-E/RT) \quad (6)$$

where $a$ is the initial concentration of selenious acid, $[H^+]$ hydrogen ion concentration, $E$ activation energy ($-8.06 \times 10^3$ kcal./mol.), $R$ the gas constant and $T$ the absolute temperature.

Also, the data of curve $B_1$ in Fig. 1, curve $A_2$ in Fig. 2 and curve $B_3$ in Fig. 3 are adopted for the above Eq. 6.

**Relation among Rate Constant, Maximum Percentage Completion and Initial Concentration of Selenious Acid.**—Fig. 5 shows the plotting maximum percentage completion $x_m$ against

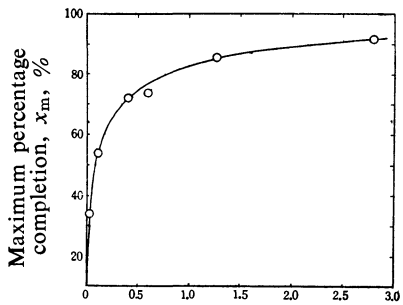



Fig. 5. Plot of maximum percentage ($x_m$) against forward rate constant ($k_2$).

forward rate constant $k_2$ at the constant initial concentration of selenious acid (0.0184 mol./l.). The experimental equation which expresses the relation between $x_m$ and $k_2$ can be derived from Fig. 5 by

$$x_m = 0.828 \times k_2^{0.114} \quad (\text{at } a = 0.0184 \text{ mol./l.}) \quad (7)$$

When the consideration of initial concentration of selenious acid $a$ is taken into Eq. 7, the relationship between $k_2$, $x_m$ and $a$ can derived as follows,

$$x_m = 1.306 \times (k_2 \cdot a)^{0.114} \quad (8)$$

## Summary

(1) The reduction of selenious acid in sulfuric acid by sulfur dioxide is a reversible reaction, because the reaction has an equilibrium and the process of the reaction is in good accordance with the equation which expressed mathematically the reversible reaction, that is,

$$-\mathrm{d}(a-p)/\mathrm{d}t = \mathrm{d}p/\mathrm{d}t = k_2(a-p)^2 - k_2' p^2$$

(2) Up to the present time the rate constant $k_2$ of the forward reaction was derived by substitution of the experimental data for $x_m$ in the following equation,

$$k_2 = \{2.303 x_m / 2a(x_m - 1)t\} \times \log[(x - x_m)/\{(2x_m - 1)x - x_m\}]$$

The general equation for $k_2$, which does not depend on $x_m$, has been obtained as follows,

$$k_2 = 2.054 \times 10^{15} \times [\mathrm{H}^+]^2 \times \exp(-E/RT)$$
$$(E = 22.5 \text{ kcal./mol.})$$

The rate constant $k_2'$ of the reverse reaction can be calculated by

$$k_2' = 2.413 \times 10^{-11} \times \{1/(a^2[\mathrm{H}^+]^2)\} \times \exp(-E/RT) \quad (E = -8.06 \text{ kcal./mol.})$$

(3) It has not previously been reported that $\alpha$ selenium is dissolved in dilute sulfuric acid (below 85% by weight), as shown by the present experimental procedure.

(4) The results obtained from this study are useful in the recovery and refinining of selenium. Then application to the recovery and refining of selenium will be expressed in another succeeding paper.

The author wishes to express his thanks to Dr. H. Negita of the Department of Chemistry, Hiroshima University for helpful discussion, and also he wishes to thank Mr. M. Kodama for his assistance.

*Department of Chemistry*
*Faculty of Science*
*Hiroshima University*
*Hiroshima*

# *Kinetics of the Reduction of Selenious Acid by Sulfur Dioxide. III. Application to Recovery and Purification of Selenium in Sulfuric Acid Works*

By Keinosuke HAMADA

(Received March 30, 1960)

The greater part of the starting materials for the productions of selenium consists of an anode-slime deposited in the electrolytic refining of copper and a sludge containing selenium recovered in the manufacturing process of sulfuric acid. The latter is called sulfuric acid sludge.

The reaction of selenious acid by sulfur dioxide was found to be a reversible reaction in sulfuric acid. The general equation for the rate constant of the forward reaction and the relation between the rate constant and the maximum percentage completion (maximum yield) were derived in the previous paper[1].

A great deal of sludge has recently been recovered from the mist acid which is a by-product of the manufacture of sulfuric acid, and a very simple and economical method of purification of selenium has been found by means of the application of the experimental results[1].

**Application to the Recovery of Selenium in the Mist Acid.**—A schematic diagram of the contact process for manufacturing sulfuric acid is shown in Fig. 1. Generally pyrites have about 12.6 parts of selenium per million[2] of pyrites. When pyrite is roasted, the selenium in the

1) Part II; This Bulletin, **34**, 596 (1961).
2) T. Tsuge et al., *J. Agr. Chem. Soc. Japan* (*Nippon Nogei-Kagaku Kaishi*), **23**, 421 (1950).

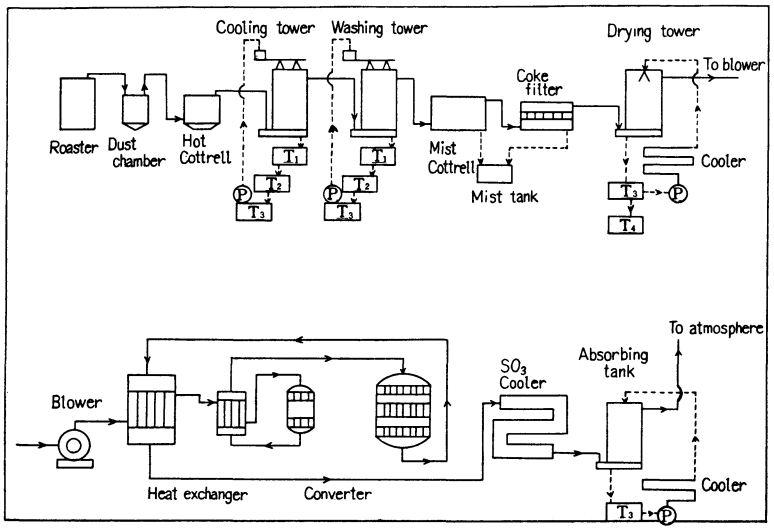



Fig. 1. Schematic diagram of contact process of sulfuric acid.

$T_1$: Cooling tank $T_4$: Storage tank →— Gas
$T_2$: Precipitating tank Ⓟ: Pump -→-- Acid
$T_3$: Pump tank

pyrite is oxidized to selenium dioxide. The part of the selenium dioxide is dissolved in the mist acid*, which is excluded from gas by a mist Cottrell and a coke filter, and is brought into a mist tank. The concentration of the mist acid is about 15° Bé (s. g. 1.115) while the acid is saturated with sulfur dioxide. Nevertheless, a large quantity of selenious acid exists in mist acid without being reduced to selenium. This fact can easily by explained according to the results of Part II[1] of this series, as follows. The reaction of selenious acid with sulfur dioxide in sulfuric acid is reversible, and the rate constant of the forward reaction, $k_2$, is expressed according to the following equation:

$$k_2 = 2.054 \times 10^{15} \times [H^+]^2 \times \exp(-E/RT) \quad (E = 22.5 \text{ kcal./mol.}) \qquad (1)$$

The equation which expresses the relation among rate constant, $k_2$, maximum percentage completion, $x_m$, and initial concentration of selenious acid, $a$, is as follows:

$$x_m = 1.306 \times (k_2 \cdot a)^{0.114} \qquad (2)$$

In these equations, $[H^+]$ is hydrogen ion concentration, $T$ absolute temperature of solution, $E$ the energy of activation, $R$ the gas constant and $a$ initial concentration of selenious acid. It is evident that maximum yield, $x_m$, depends heavily on temperature at the constant $[H^+]$ and $a$, according to Eqs. 1 and 2. When the mist acid is heated up to the boiling point, selenium can be precipitated. After heating the mist acid, the selenium content in the mist acid is found to be about 0.00015 mol./l. Ninety-five per cent of selenium in the mist acid can be recovered by only heating the mist acid. Selenium sludge gained from the mist acid has a high content of selenium (about 80%), and a great deal of sludge can be recovered each day, making sludge a useful and plentiful starting substance for the isolation of selenium.

**Application to the Purification of Selenium.** —Up to the present time, many studies[3-33]

* The mist acid has about 0.003 mol. selenious acid per liter.

3) Z. Littmann, *Z. angew. Chem.*, **19**, 1039 (1906).
4) N. Chikashige et al., Brit. Pat. 134536 (1919).
5) J. Sugie, *Osaka Ind. Lab.*, **1**, No. 1, 1 (1920).
6) T. Shimoi et al., Japan. Pat. 3629 (1920).
7) S. Sugie, *J. Japan Ceram. Assoc.*, **343**, 226 (1921).
8) W. Stahl, *Chemiker-Ztg.*, **50**, 280 (1926).
9) Z. Littmann, ibid., **50**, 704 (1926).
10) A. A. Borkovski et al., *Zavodskaya Lab.*, **3**, 306 (1934); *Chem. Abstr.*, **29**, 1739 (1935).
11) A. R. Lindblad, Brit. Pat. 423084 (1935); Fr. Pat. 777857 (1935); Ger. Pat. 641714 (1937).
12) O. C. Martin et al., U. S. Pat. 2039256 (1936).
13) F. W. Heberlein, Can. Pat. 364133 (1937).
14) C. W. Clark et al., *Am. Inst. Mining Met. Engrs., Tech. pub.*, **982**, 22 (1938).
15) H. C. Dudley, U. S. Pat. 2111112 (1938).
16) M. S. Belskaya, Russ. Pat. 58836 (1941).
17) N. R. Bierly, U. S. Pat. 2349697 (1944).
18) C. W. Clark, U. S. Pat. 2409835 (1946).
19) A. J. Philip et al., U. S. Pat. 2413374 (1946).
20) N. S. Artamonov, U. S. S. R. Pat. 66128 (1946).
21) D. Gardner, U. S. Pat. 2414295 (1947).
22) M. C. Bloom, U. S. Pat. 2414438 (1947).
23) N. V. Philips, Fr. Pat. 930184 (1948).
24) A. Voige et al., Ger. Pat. 800860 (1950).
25) T. Sawaya, Japan. Pat. 18 (1950).
26) K. Krebs, Brit. Pat. 644743 (1950).
27) Y. Terasaki, Japan. Pat. 2560 (1952).
28) N. A. Vaarro, Span. Pat. 207021 (1954).
29) T. Tamura, Japan. Pat. 7052 (1955).
30) K. Okamoto, Japan. Pat. 3508 (1955).
31) N. Imai et al., Japan. Pat. 3108 (1956).
32) Y. E. Lebedeff et al., U. S. Pat. 2775509 (1956).
33) S. Ato et al., *Repts. Sci. Research Inst. (Japan)*, **32**, 27 (1956).

have been performed concerning the purification of selenium, and each method of purification of selenium has had its own characteristics.

In the purification of sulfuric acid sludge, the Stahl[8] and Littmann[9] method was found to be the most suitable. However, the method has some difficulty, the yield is relatively lower (around 85%). The present author has noticed that the yield depended largely on the hydrogen ion concentration and temperature according to Eqs. 1 and 2. Therefore, these two factors were taken into account for their method[8,9] as described subsequently.

## Experimental

A great success has been attained in the purification of selenium on the industrial scale by enlarging the experimental procedures. Therefore, the process on an industrial scale will now be described in some detail. Figure 2 shows the schematic diagram of the plant for purification of sulfuric acid sludge according to the new method.

The dried sludge is brought into a reacting vessel, and 20 l. of fuming sulfuric acid (23%) per 1 kg. pure selenium in the sludge is added to the vessel.

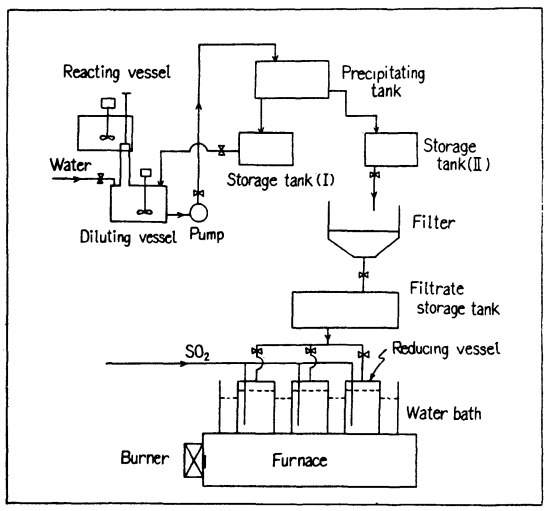



Fig. 2. Schematic diagram of purification plant of selenium.

These mixtures are agitated for two hours with a stirrer. The selenium in the sludge is changed to green selenium anhydro-sulphate ($SeSO_3$) according to the following reaction:

$$Se+H_2SO_4\cdot SO_3=SeSO_3+H_2SO_4$$

Then, 2 l. of nitric acid (62% by weight) per 1 kg. pure selenium in the sludge is added to this green solution, and agitation is continued for one additional hour.

The temperature is increased up to about 120°C, and a yellow solution of selenious acid results as follows.

$$SeSO_3+4HNO_3=H_2SeO_3+H_2SO_4+4NO_2$$

The mixture containing selenious acid is slowly dropped into a diluting vessel, to which 50 l. of water per 1 kg. pure selenium in the sludge has previously been added. The temperature of the solution is elevated up to approximately 140°C, by the heat of the dilution of the fuming sulfuric acid. The excess of nitric acid is released owing to the high temperature. Moreover, 20 l. of water per 1 kg. pure selenium is added to the above solution.

The mixtures in the diluting vessel are pumped up to a precipitating tank, and cooled to the chamber temperature. Solid materials in solution, of course, settle down in this tank. The supernatant is brought into a storage tank (I), and subsequently sent to a filter. The filtrate is introduced into reducing vessels via a filtrate storage tank, and reduced to selenium by some previously water-washed sulfur dioxide (about 6%) used in the manufacture of sulfuric acid. When the solution of selenious acid is reduced, it is kept at bout 70°C*1 in a water bath.

The selenium precipitated in the reducing vessel is removed, washed by water till all traces of sulfuric acid disappear and dried in an air bath at 110°C or lower. The waste solution is 35% (by weight) sulfuric acid, and this solution can be utilized elsewhere in industry.

## Results

The purpose of the present study is to find the most suitable method for manufacture of selenium that meets the minimum commercial requirements in the sulfuric acid works.

A 92% yield*2 has been secured and the purity of 99.9% has been obtained according to this new method. Table I shows a few

TABLE I. DATA OF ANALYSIS OF PURIFIED Se AND RAW MATERIALS

| | Se, % | Fe | Si | Te | Hg | As | Ag | Pb |
|---|---|---|---|---|---|---|---|---|
| Purified Se (A) | 99.94 | w | w | www | s | nil | ww | nil |
| Raw material (A) | 29.63 | ss | s | s | s | ww | s | ss |
| Purified Se (B) | 99.97 | w | w | www | w | nil | ww | nil |
| Raw material (B) | 88.99 | ss | s | s | w | ww | s | ss |

w, weak; ww, very weak; www, trace; s, strong; ss, very strong.

*1 It is evident according to Eqs. 1 and 2[1] that the higher the temperature of the solution is, the greater the yield is. However, the particles of selenium separated at high temperature (about 80°C) are very small. At about 70°C, most particles of the precipitated selenium can pass through a 80~100 mesh sieve, and so they meet commercial requirements. The difference of yield between those at 70°C and at 80°C can hardly be appreciated by the present experiments.

*2 Yield of conventional methods is between 80 and 90%.

examples of analysis*3 of selenium purified by the new method and raw materials.

Table I expresses the relative strength of the lines of emission spectra, except the data for selenium. A remarkable result is shown in Table I, namely, tellurium can be removed without any special effort, but on the contrary, most of the mercury remains in the purified selenium.

## Discussion

Selenium in mist acid can be recovered by heating the acid according to the results of Part II[1] of this series.

By improving the Stahl[8] and Littman[9] method according to the results of Part II[1], the simple method for purification of selenium has been found. It was already mentioned in the present paper that this method had many virtues. Especially, it is interesting to note that tellurium can be excluded from the purified selenium without any special steps. According to conventional methods, some special steps were necessary in order to exclude impurities; for example, tellurium. These special processes are: i) using hydrochloric acid[10], ii) ion-exchange resin[34], and iii) distillation[11,15,33,35-39,42]. But it is unnecessary to include any provisions for removal of tellurium in the present method*4[,40,41].

It is the defect of this method that the purity of four nine can not be secured, although that of three nine can be secured. This seems to be caused by the mercury as an impurity.

The author wishes to thank Dr. H. Negita of the Department of Chemistry, Hiroshima University, for the discussion, and also to express hearty thanks to the Factory Manager, E. Yamashita, for the K. Chemical Company of the application of the author's experimental results[1] to the purification of selenium on an industrial scale and the permission to publish the industrial method, also to the staffs of the Department of Sulfuric Acid and Laboratory in the company for their advice and help.

*Department of Chemistry*
*Faculty of Science*
*Hiroshima University*
*Hiroshima*

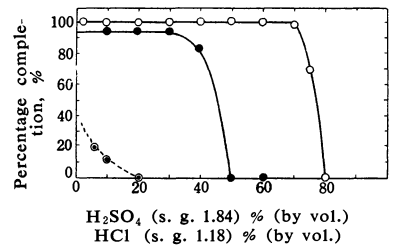



Fig. 3. Reduction of tellurous acid by $SO_2$.
◉ In acidic soln. with $H_2SO_4$
● In acidic soln. with {$H_2SO_4$+10cc. HCl(s. g. 1.18)}
○ In acidic soln. with HCl

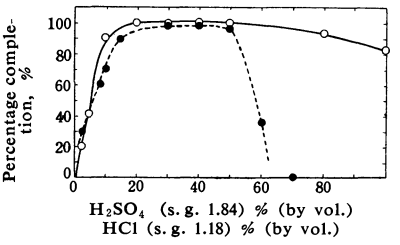



Fig. 4. Reduction of selenious acid by $SO_2$.
○ In acidic soln. with $H_2SO_4$
● In acidic soln. with HCl

*3 Selenium is determined by means of gravimetric analysis, while others were determined by spectrochemical analysis.

34) F. Aoi, This Bulletin, **26**, 480 (1953).
35) H. Bode, *Z. anal. Chem.*, **134**, 100 (1951).
36) A. I. Gaev, Russ. Pat. 51200 (1937).
37) N. S. Polvektov, *Microchemie*, **15**, 32 (1934).
38) S. T. Volkov, *Zavodskaya Lab.*, **5**, 1429 (1936); *Chem. Abstr.*, **31**, 6130 (1937).
39) V. K. Zemel, ibid., **5**, 1443 (1936).
40) E. M. Müller, *Z. physik. Chem.*, **100**, 346 (1922).
41) T. L. Pökrovskaya, *Zavodskaya Lab.*, **7**, 15 (1938); *Chem. Abstr.*, **32**, 4101 (1938).
42) T. Takei et al., *Repts. Sci. Research Inst. (Japan)*, **26**, 234 (1950).

*4 It is believed that, tellurium is excluded based on this fact, the higher the concentration of sulfuric acid, the smaller is the rate constant of reduction of tellurous acid in sulfuric acid. This can be guessed by the following simple, qualitative experiment. A solution of tellurous acid of 0.01 mol. per 200 ml. sulfuric acid of many kinds of concentrations were prepared, and left overnight at chamber temperature after being saturated with sulfur dioxide. Fig. 3 shows the plot of the tellurium precipitated (percentage completion) against each concentration of sulfuric acid. One can see that when the concentration of sulfuric acid is above 20% (by volume), tellurium can not be precipitated. Fig. 4 is the same plot as in the case of selenious acid for comparison with Fig. 3.

# *The Relation between Reactivity and Selectivity*

By Yoshiro OGATA and Iwao TABUSHI

(Received July 12, 1960)

Brown and his coworkers have pointed out the existence of the linear relation between the logarithm of the para partial rate factor of toluene, $\log p_f$, which they called a measure of activity of reagent and the selectivity factor which is expressed as the logarithm of ratio of para vs. meta partial rate factor, $\log(p_f/m_f)$[1]. As they have mentioned, the relation can be derived from the Hammett equation and is expressed as

$$\log p_f = \frac{\sigma_p}{\sigma_p - \sigma_m} \log(p_f/m_f) \qquad (1)$$

However, the term of $\log p_f$ is not the reactivity, but the distribution of a given reagent between benzene and toluene, or intermolecular selectivity and it is not surprising that the intermolecular selectivity is proportional to the intramolecular selectivity, $\log(p_f/m_f)$.

The reactivity of a reagent should be expressed as a value related to the rate constant for the reaction between a standard substance and the reagent at a standard condition or $k_0$. The value of $k_0$, however, depends on the reaction mechanism, the concentration of the actual attacking species, the environment and conditions. Hence it is difficult to compare the value of $k_0$ at a standared condition. Nevertheless, as shown in Table I, A-1 and A-2 the qualitative parallelism is sometimes observed between $k_0$ and the absolute value of $\rho$ or the sensitivity of the rate to the change of substituent in closely related reactions[1e].

If frequency factors are constant, the relative

TABLE I

(A) COMPARISON OF DIFFERENT ATTACKING REAGENTS

A-1) Aromatic alkylation

| Reaction | Solvent | $-\rho$ | $\log k_0$ l. mol$^{-1}$ sec$^{-1}$ | Ref. |
|---|---|---|---|---|
| ArH+MeBr, $AlCl_3$ | 1,2,4-$Cl_3C_6H_3$ | 3.64 | −2.444 | 6 |
| ArH+MeBr, $GaBr_3$ | ArH | 3.06 | −1.301 | 7 |
| ArH+EtBr, $GaBr_3$ | ArH | 2.66 | −0.799 | 7 |
| ArH+*i*-PrBr, $GaBr_3$ | ArH | 2.54 | +2.505 | 7 |

A-2) Electrophilic halogenation at 25°C (X; H or $CH_3$)

| Reaction | $-\rho$ | $\log k_0$, l. mol$^{-1}$ sec$^{-1}$ | Ref. |
|---|---|---|---|
| $C_6H_5X$+HClO | 7.77 | −3.380 | 8 |
| $C_6H_5X$+HBrO | 6.05 | −0.234 | 9 |

A-3) Electrophilic addition[10]

| Reaction | Products | |
|---|---|---|
| | 1-Halo-compound | 2-Halo-compound |
| $CH_2=CH-CH_3+HClO$ | $ClCH_2CHOHCH_3$ (90%) | $CH_2OHCHClCH_3$ (10%) |
| $CH_2=CH-CH_3+HCl$ | None | $CH_3CHClCH_3$ |
| $CH_2=CH-CH_2Cl+HClO$ | $ClCH_2CHOHCH_2Cl$ (30%) | $CH_2OHCHClCH_2Cl$ (70%) |
| $CH_2=CH-CH_2Cl+HCl$ | None | $CH_3CHClCH_2Cl$ |

(B) COMPARISON OF DIFFERENT SUBSTRATES

Second-order rate constants of chlorination[11], l. mol$^{-1}$ min$^{-1}$

| R | *p*-Me | H | *m*-$NO_2$ |
|---|---|---|---|
| 1. $R-C_6H_4CH=CHCOPh$ | 800 | 61 | 0.23 |
| 2. $R-C_6H_4CH=CH-CO_2H$ | 103 | 4.9 | 0.011 |
| $k_1/k_2$ | 7.76 | 12.4 | 20.9 |

1) a) H. C. Brown and K. L. Nelson, *J. Am. Chem. Soc.*, **75**, 6292 (1953).
b) H. C. Brown and W. H. Bonner, ibid., **76**, 605 (1954).
c) H. C. Brown and C. W. McGary, Jr., ibid., **77**, 2300 (1955).
d) H. C. Brown and C. R. Smoot, ibid., **78**, 6255 (1956).
e) L. M. Stock and H. C. Brown, ibid., **81**, 3233 (1959), **82**, 1942 (1960).

rate constant of substituted and unsubstituted reactants is expressed as

$$\ln(k/k_0) = -\frac{\Delta H^{\neq} - \Delta H_0^{\neq}}{RT} = \sigma\rho \qquad (2)$$

Hence it is rational that the absolute value of $\rho$ with constant $\sigma$ decreases with an increase of temperature[2] which accompanies an increase of the rate constant in the same reaction series. Furthermore, it is supposed from Eq. 2 that the absolute value of $\Delta H^{\neq} - \Delta H_0^{\neq}$ approaches zero, when both $\Delta H^{\neq}$ and $\Delta H_0^{\neq}$ approach zero or $k_0$ becomes very large. Therefore, the $\rho$ value with constant $\sigma$ tends to decrease with an increase of $k_0$ under this limitation. Thus the very fast reaction such as protonation have a constant value of rate constants ($3\times 10^{10}$ l. mol$^{-1}$ sec$^{-1}$ at 18~30°C) or the $\rho$ value of zero[3].

The selectivity may be expressed with either intramolecular selectivity, i. e., orientation, or intermolecular selectivity, i. e., relative rate. Since the former selectivity is proportional to the latter in aromatic compounds[4,5], as shown in Eq. 1, the reactivity-selectivity relation can be tested with any of these selectivities.

Table I shows A) comparison of different attacking reagents and B) comparison of some groups of substrates with different reactivities.

## Summary

The proportionality between $\log p_f$ and $\log(p_f/m_f)$ reported by Brown[1] seems to express the proportionality between inter- and intramolecular selectivities. The standard rate constant $k_0$ may be a measure for the reagent activity; the parallelism between $1/k_0$ and $|\rho|$ or selectivity is observed in very limited reactions.

*Department of Industrial Chemistry*
*Faculty of Engineering*
*Kyoto University*
*Sakyo-ku, Kyoto*

2) H. H. Jaffé, *Chem. Revs.*, **53**, 191 (1953); H. C. Brown and C. W. McGary, Jr., *J. Am. Chem. Soc.*, **77**, 2306 (1955).
3) R. P. Bell, *Quart. Revs.*, **13**, 169 (1959).
4) L. M. Stock and H. C. Brown, *J. Am. Chem. Soc.*, **81**, 2320 (1959).
5) The same is true with aliphatic compounds in which polar effect alone is important.
6) H. Jungk, C. R. Smoot and H. C. Brown, *J. Am. Chem. Soc.*, **78**, 2185 (1956).
7) H. C. Brown and H. Jungk, ibid., **77**, 5584 (1955).
8) P. B. D. de la Mare, J. T. Harvey, M. Hassan and S. Varma, *J. Chem. Soc.*, **1958**, 2756.
9) P. B. D. de la Mare and J. T. Harvey, ibid., **1956**, 36.
10) J. R. Shelton and L. Lee, *J. Org. Chem.*, **25**, 907 (1960). More reactive HClO adds less regularly to substituted ethylenes in comparison with less reactive HCl.
11) P. B. D. de la Mare, *Quart. Revs.*, **3**, 126 (1949).

# *Acid-Base Property and Metal Chelate Formation of 4-(2-Pyridylazo)-resorcinol**

By Toschitake IWAMOTO

(Received January 7, 1960)

4-(2-Pyridylazo)-resorcinol (PAR) has recently been suggested as a water-soluble metal indicator for the EDTA-titration of lead and other metal cations in place of 1-(2-pyridylazo)-2-naphthol (PAN)[1]. The latter forms a colloidal suspension when dissolved in water in the pH range 2 to 13[2], and this fact is one of the disadvantages of the reagent in aqueous systems. The use of PAR as a color reagent in colorimetric analysis[3] and as a metal indicator in precipitation titration[4] and in chelatometric titration[5] has been proposed, all of which is based on the formation of stable colored chelates of PAR with various heavy metals such as lead, cobalt and uranium.

The present paper concerns the acid dissociation of PAR, its chelate formation with some metal cations in aqueous solutions, the stability constant of copper(II)-PAR chelate and the comparison between PAR and PAN as analytical reagent.

The absorption spectra of PAR in aqueous

* Presented partly at the 13th Annual Meeting of the Chemical Society of Japan, Tokyo, April, 1960.

1) P. Wehber, *Z. anal. Chem.*, **158**, 10 (1957); **167**, 186 (1958).

2) B. F. Pease and W. B. Williams, *Anal. Chem.*, **31**, 1044 (1959).

3) F. H. Pollard, P. Hanson and W. J. Geary, *Anal. Chim. Acta*, **20**, 26 (1959).

4) R. Püschel, E. Lassner and R. Scharf, *Z. anal. Chem.*, **163**, 104, 344 (1958); **165**, 401 (1959).

5) E. J. Langmyhr and H. Kristiansen, *Anal. Chim. Acta*, **20**, 524 (1959).

solution at various pH values have been examined, the acid dissociation constants determined by pH-titration and colorimetric method. The composition of the metal chelates of PAR with tervalent iron, bivalent cobalt, nickel, copper, zinc, cadmium, mercury and lead has been determined with the aid of the continuous variation method[6] and the stability constant of copper(II)-PAR chelate determined potentiometrically by pH-titration; its utility in chelatometric analysis was discussed.

## Experimental

The PAR used in this study was a sample for test supplied by Dojin Pharmaceutical Laboratories, Kumamoto, Japan.

Found: C, 61.4; H, 4.5; N, 18.7; Calcd. for $C_{11}H_9O_2N_3$: C, 61.1; H, 4.2; N, 19.5[7].

PAR in free acid form is readily soluble in an aqueous alkaline solution. Solubility in water at 10°C was found to be only 5 mg./100 ml.

4-Benzeneazoresorcinol was kindly given by Dr. Yoshio Matsunaga in our laboratory.

A solution of $10^{-2}$ M potassium hydroxide was prepared by direct dissolution of metallic potassium (E. Merck) in deionized water in a current of nitrogen, and standardized against $1.007_4\times10^{-2}$ M hydrochloric acid. The standard solution of the

Fig. 1. Absorption spectra of PAR.
$5\times10^{-5}$ M: 1 cm. silica cell (Cary)

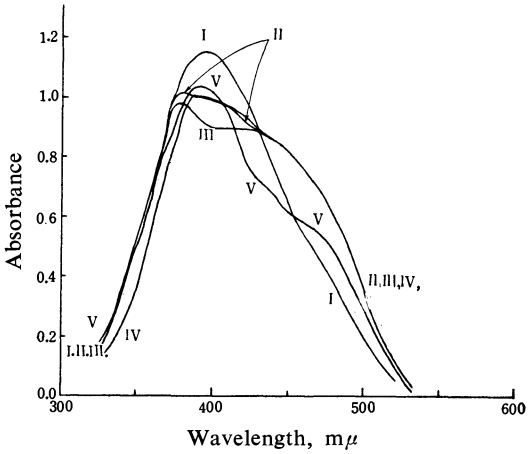



Fig. 1a. Absorption spectra of PAR in acid solutions.
I: 4.7 N $HNO_3$
II: 3.2 N $HNO_3$
III: 1.6 N $HNO_3$
IV: 0.1 N $HNO_3$
V: pH 3, acetate buffer (0.1 M $KNO_3$)

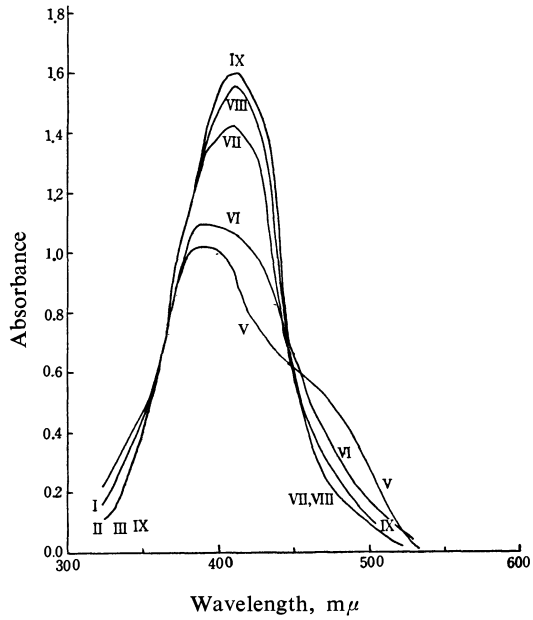



Fig. 1b. Absorption spectra of PAR in neutral solutions.
V: pH 3, acetate buffer
VI: pH 5, acetate buffer
VII: pH 7, phosphate buffer
VIII: pH 9, borax buffer
IX: pH 11, 0.001 N NaOH
(0.1 M $KNO_3$)

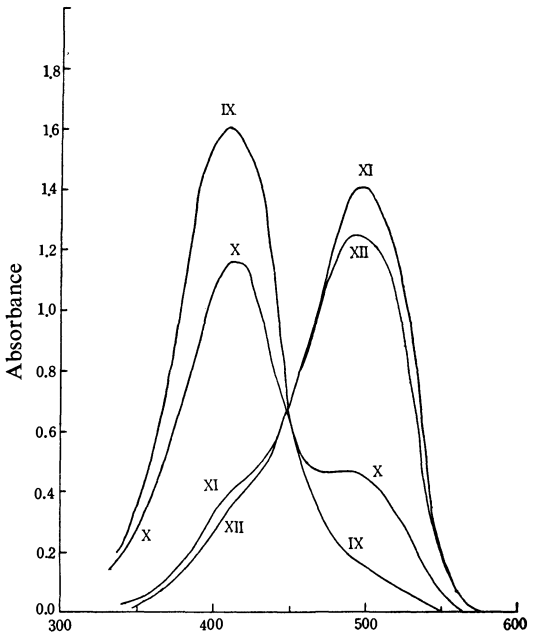



Fig. 1c. Absorption spectra of PAR in alkaline solutions.
IX: 0.001 N NaOH
X: 0.01 N NaOH
(0.1 M $KNO_3$)
XI: 0.1 N NaOH
XII: 1 N NaOH

6) Y. Shibata, T. Inouye and Y. Nakatsuka, *J. Chem. Soc. Japan (Nippon Kwagaku Kwaishi)*, **42**, 983 (1921); R. Tsuchida, This Bulletin, **10**, 27 (1933). Cf. P. Job, *Ann. chim.*, [10] **9**, 113 (1928).

7) Elementary analysis was performed by Mr. Shozo Masuda in our department. The PAR might contain some impurities (cf. Refs. 2 and 3). The purity of the PAR calculated from the content of nitrogen 18.7/19.5=0.96, agreed with that (0.94) determined by photometric titration with a copper nitrate solution.

acid was prepared by passing a known amount of potassium chloride solution through a column of cation-exchange resin in H-form (Diaion SK #1, analytical grade).

All the other chemicals were of reagent grade, and all metal salts were used as nitrates. Acetate, phosphate and borax buffer, nitric acid, potassium hydroxide and sodium hydroxide solution were used to control the pH. By photometric titrations[7a] with $1.00\times10^{-4}$ M copper nitrate solution, the PAR solutions were standardized after suitable dilution whenever necessary.

The absorption spectra were measured by a Cary Model 11 and a Shimadzu QB-50 spectrophotometer and the colorimetric measurements were done by a Hirama IIb filter electrophotometer. For pH-titrations and pH measurements a Denkishiki DG pH meter equipped with a glass and a calomel electrode was used; the measurements were carried out in a thermostat regulated at 25±0.2°C by circulating water from another large thermostat. During titration the solution was stirred magnetically and bubbled with nitrogen gas through a capillary.

## Results and Discussion

**Acid Dissociation of PAR.**—The absorption spectra of aqueous solutions of PAR depend on the pH values as shown in Fig. 1. The spectra in acid solutions have somewhat complicated aspects which may be caused by the presence of pyridinium form or azo-protonated forms as in case of PAN[2] and some azobenzene derivatives[8]. It can be suggested that an undissociated form a, two kinds of the dissociated forms b and c, and one-protonated form d exist in neutral and alkaline solutions. As the degree of acid dissociation of *o*-hydroxyl group may be lower than that of *p*-hydroxyl group through an intramolecular hydrogen bond formation, the absorption maxima at 390, 410 and 490 mμ can be assigned to a, b and c, respectively, and the broad shoulder from 400 to 470 mμ to d. The existence of these dissociation stages in neutral and alkaline solutions can be supported by similar study on 4-benzeneazoresorcinol. As shown in Fig. 2, in the neutral solution the spectrum has a doublet of 375 and 410 mμ (Curve I)[9]. In the weakly alkaline solutions the absorption maximum shifts to 430 mμ (Curves II and III) and in the more alkaline solution the maximum further shifts to 475 mμ and shows a shoulder at 390 mμ (Curve IV). These properties are analogous to those of PAR.

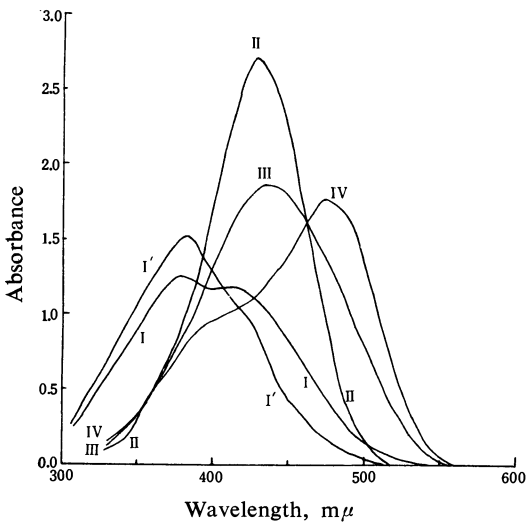
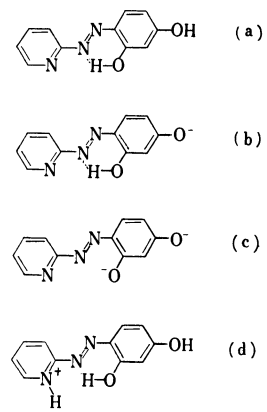



Fig. 2. Absorption spectra of benzeneazoresorcinol.
$7\times10^{-5}$ M: 1 cm. silica cell (Cary)
I: 8% ethanol
I′: 95% ethanol
II: $4\times10^{-4}$ M borax in 8% ethanol
III: $3\times10^{-2}$ M NaOH in 8% ethanol
IV: 0.7 M NaOH in 8% ethanol




**Determination of Acid Dissociation Constants of PAR.**—From the pH dependency of the spectra the acid dissociation constants of PAR $k_{a_1}$ and $k_{a_2}$ defined by Eqs. 1 and 2 are estimated as about $10^{-6}$ and $10^{-12}$, respectively.

$$k_{a_1}=\frac{[C_{11}H_8O_2N_3^-]\,[H^+]}{[C_{11}H_9O_2N_3]} \quad (1)$$

$$k_{a_2}=\frac{[C_{11}H_7O_2N_3^{2-}]\,[H^+]}{[C_{11}H_8O_2N_3^-]} \quad (2)$$

In order to obtain more accurate values 100 ml. of $4.72\times10^{-5}$ M PAR solution was titrated with $1.085\times10^{-2}$ M potassium hydroxide solution at 25°C (Fig. 3). One proton caused by the first dissociation was neutralized and $k_{a_1}$ was calculated as $1.48\times10^{-6}$ ($pk_{a_1}=-\log k_{a_1}=5.83$) according to the following equation:

7a) T. Iwamoto, *Japan Analyst (Bunseki Kagaku)*, **10**, 189 (1961).

8) M. T. Rogers, T. W. Campbell, R. W. Maatmann, *J. Am. Chem. Soc.*, **73**, 5122 (1951).

9) The absorption spectrum of 4-benzeneazoresorcinol in an ethanolic solution taken from the late Dr. F. Iimura's unpublished results shows also a singlet maximum at 375 mμ. The splitting may be elucidated in terms of solvent effect.

$$k_{a_1}=\frac{[H^+]\,(aC+[H^+]-[OH^-])}{C-(aC+[H^+]-[OH^-])} \qquad (3)$$

where $C$ stands for the total concentration of PAR and $a$ moles of base added per mole of the acid. Another proton caused by the second dissociation was not liberated under these conditions because of the low value of the second dissociation constant $k_{a_2}$, as foreseen by the absorption spectra measurements. Then it was approximately determined from absorption measurements of aqueous PAR solutions in the range of pH between 10 and 13.8 with a filter electrophotometer using the filters transparent in the vicinity of 420 and 485 mμ. From the curves in Fig. 4, $pk_{a_2}$ was estimated as 12.5 ($k_{a_2}=3.2\times10^{-13}$).

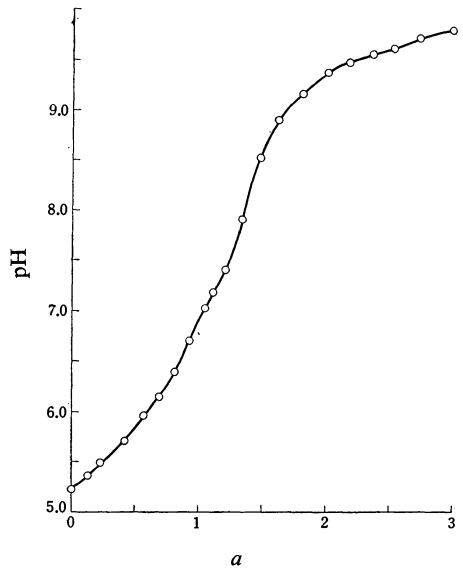



Fig. 3. pH-Titration of PAR free acid. 100 ml. of $5\times10^{-5}$ M PAR solution with 0.01 N KOH solution.
$a$: moles of base added per mole of acid

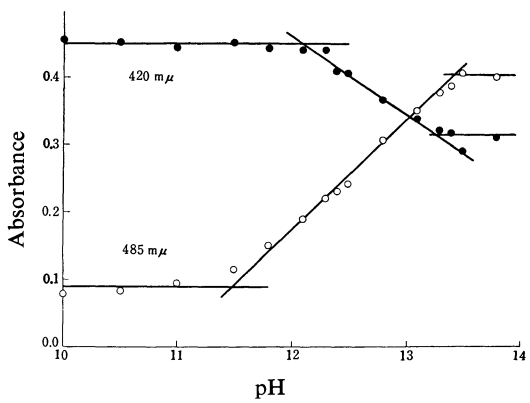



Fig. 4. Absorbance vs. pH of PAR solutions. $5\times10^{-6}$ M PAR, 2 cm glass cell.
Full circle, at 420 mμ; open circle, at 485 mμ

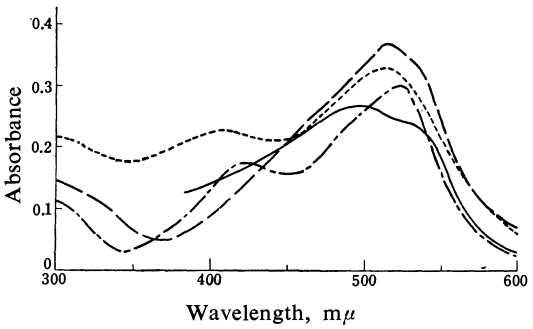



Fig. 5. Absorption spectra of metal-PAR chelates.

—— $Fe(PAR)_2$: $0.6\times10^{-5}$ M pH 4
—— $Co(PAR)_2$: $0.8\times10^{-5}$ M pH 4
—·— Cu(PAR): $1.0\times10^{-5}$ M pH 4
---- Pb(PAR): $1.0\times10^{-5}$ M pH 10
1 cm. silica cell (Shimadzu)

TABLE I. COMPOSITIONS AND MOLAR EXTINCTION COEFFICIENTS OF METAL-PAR CHELATES

| Metal | Composition | pH | ε at 517 mμ |
|---|---|---|---|
| Fe(III) | 1 : 2 | 4.0 | $4.2\times10^4$ |
| Co(II) | 1 : 2 | 4.0 | $4.2\times10^4$ |
| Ni(II) | 1 : 2 | 4.0 | $2.2\times10^4$ |
| Cu(II) | 1 : 1 | 4.0 | $3.0\times10^4$ |
| | 1 : 1 | 10.0 | $3.2\times10^4$ |
| Zn(II) | 1 : 1 | 10.0 | — |
| Cd(II) | 1 : 1 | 10.0 | — |
| Hg(II) | 1 : 1 | 10.0 | — |
| Pb(II) | 1 : 1 | 10.0 | $3.8\times10^4$ |

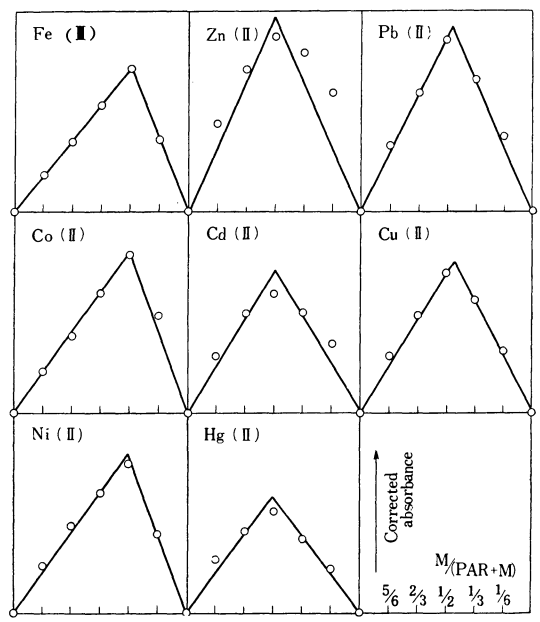
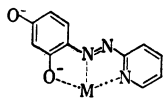



Fig. 6. Graphical determination of the composition of metal-PAR chelates.

**Compositions of PAR Chelates of Fe(III), Co(II), Ni(II), Cu(II), Zn(II), Cd(II), Hg(II) and Pb(II).**—Wehber[1] and Pollard et al.[3] reported the coloration of the chelates of PAR with various kinds of metals in aqueous solutions. In Fig. 5 are shown a few examples of absorption spectra measured by the present author. The composition of these chelates in aqueous solutions was determined by means of the continuous variation method using the filter photometer with a 517 mμ filter. The results and the molar extinction coefficients of the chelates are given in Table I. In Fig. 6, data are shown graphically. From these data PAR may be considered to act as terdentate ligand having three donor atoms in a plane [10]:



The details of the structure of metal-PAR chelare are now under investigation.

**Stability Constant of Copper(II)-PAR Chelate.**—In the presence of copper(II)-EDTA chelate, PAR may be applied as a metal indicator to the titration of metal cations which neither form colored chelates with PAR nor react with PAR rapidly and reversibly. To compare the function of the Cu-PAR indicator system with that of Cu-PAN[11], the stability constant of copper(II)-PAR chelate was determined by pH-titration. One hundred ml. of solution containing $4.72\times10^{-6}$ mol. of PAR and the equimolar amount of copper nitrate was titrated with the above-mentioned potassium hydroxide solution. The titration curve shown in Fig. 7 exhibits a marked inflection at $a\simeq2$. Acid dissociation and chelate formation of PAR are as follows:

$$H_2D = H^+ + HD^- \qquad (pk_{a_1}=5.83) \tag{4}$$

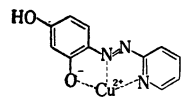
$$HD^- = H^+ + D^{2-} \qquad (pk_{a_2}=12.5) \tag{5}$$

$$Cu^{2+} + D^{2-} = CuD \text{ [12]} \tag{6}$$

$$Cu^{2+} + H_2D = 2H^+ + CuD \tag{6'}$$

$$CuD + H^+ = HCuD^+ \tag{7}$$

where $H_2D$ is PAR in undissociated form, $HD^-$ in b form (p. 607) and $HCuD^+$ is one-protonated form of Cu-PAR chelate that may exist in considerably low pH region:



The equilibrium constant for Eq. 6, $k=[CuD]/[Cu^{2+}][D^{2-}]$, gives the stability constant of copper(II)-PAR chelate provided that the activity coefficient of each species is maintained constant. If $k_a' = [H^+][CuD]/[HCuD^+]$ is postulated as the acid dissociation constant for the process reverse to Eq. 7, Eq. 8 gives the relation between $k$, $k_{a_1}$, $k_{a_2}$ and the concentration of $D^{2-}$ throughout the titration under the experimental conditions:

$$k[D^{2-}]^2([H^+]^2/k_{a_1}k_{a_2} + [H^+]/k_{a_2}) - [D^{2-}][H^+]^2/k_{a_1}k_{a_2} = (a-1) + [H^+] - [OH^-] \tag{8}$$

where $C$ stands for the total concentration of PAR (=that of $Cu^{2+}$) and $a$ the moles of base added per mole of PAR.

With the assumption that at adjacent plots of the measurements in the buffer region of the titration curve the value of $[D^{2-}]$ is the same, $k$ was calculated to be $5\times10^{11}$ as the mean value from thirty sets of simultaneous equations derived from Eq. 8. $k_a'$, which can be considered as the second dissociation constant of a hypothetical dibasic acid $H_2CuD^{2+}$,

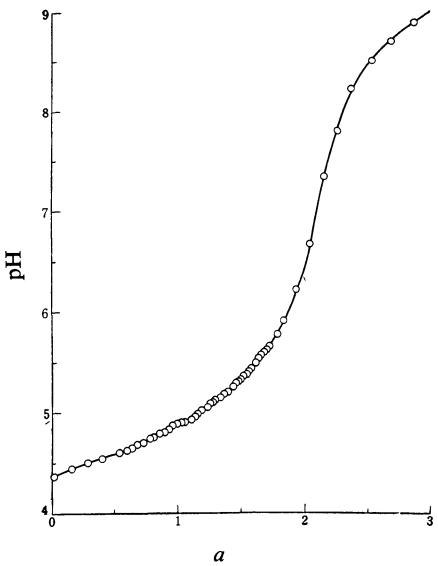



Fig. 7. Titration curve of copper(II)-PAR chelate.
$5\times10^{-5}$ M Cu-PAR solution 100 ml. with 0.01 M KOH solution
$\mu=0.1$ M $KNO_3$, 25°C
$a$: moles of base added per mole of chelate

10) Y. Muto, This Bulletin, **31**, 1017 (1958); F. Lions and K. V. Martin, *J. Am. Chem. Soc.*, **79**, 2733 (1957); F. Lions and H. A. Goodwin, ibid., **81**, 6415 (1959).

11) H. Flaschka and H. Abdine, *Z. anal. Chem.*, **152**, 77 (1956); *Chemist-Analyst*, **45**, 2 (1956).

12) It is not necessary for CuD to be neutral in charge, for PAR is considered as a terdentate ligand and the coordination requirement of copper(II) atom will be fulfilled by another unidentate anion (e. g. nitrate ion) in the solution.

was determined graphically[13] to be $5\times10^{-6}$ from the titration data.

## Analytical Aspects of PAR

**Cu-PAR Indicator in EDTA-Titrations.**—Pease and Williams[2] have determined the stability constant of copper(II)-PAN chelate to be approximately $10^{16}$. This value is considerably greater than that of PAR chelate, $5\times10^{11}$. Comparing the value for PAN chelate with that for copper(II)-EDTA chelate, $2\times10^{18}$, they have concluded "this is one reason that the copper(II)-PAN indicator may be successfully used in complexometric titrations of metals with EDTA".

According to Flaschka-Khalafallah's error-equation in visual end-point determination in chelatometric titration, Eq. 9[14], however, it may be concluded that $\Delta p$, the deviation of end-point (metal-combined indicator/free indicator=1/9) from equivalence-point, for the above-mentioned copper(II)-EDTA-PAN system is to be +0.04, i. e., the theoretical error is +4% when $C_M$ and $C_I$ were put as $10^{-3}$ and $10^{-6}$, respectively.

$$\Delta p=(9rC_M-0.01C_I-1/9k)/C_M \qquad (9)$$

where $C_M$: total concentration of metal,
$C_I$: total concentration of indicator,
$k$: stability constant of metal-indicator complex,
$K$: stability constant of metal-complexan, and $r=k/K$.

The error obtained here is contrary to Cheng's observation[15]. To make the error below 0.5%, the stability constant of metal-indicator complex must be below $10^{15}$. The value for Cu-PAR satisfies such a requirement. In regards to the relationship of the stability of copper(II)-indicator to that of copper(II)-EDTA, it may be concluded that PAR is a more accurate indicator than PAN provided that the stability constant of Cu-PAN is reliable. Nevertheless, for the practical applications as a titration indicator no remarkable difference between them, except the higher solubility of PAR in water, has yet been found out.

**PAR as a Detection Reagent for Heavy Metals.**—It must be mentioned that the high absorbancy in the visible region and the water-solubility of PAR chelates favor the detection of heavy metals and very high sensitivity can be achieved. For example, the identification limit of copper(II) in ordinary spot test was found to be 0.01 $\mu$g in 0.04 ml. test solution, i. e., limit of dilution is $1:2.5\times10^{-7}$, and that in resin spot test using a few grains of cation-exchange resin Dowex 50W-X8 in H-form as a collector of copper(II)-PAR chelate to be 0.0005 $\mu$g ($1:1.3\times10^{-8}$)[16].

## Summary

Acid dissociation stages of analytical reagent 4-(2-pyridylazo)-resorcinol (PAR) and metal chelate formation of PAR were investigated by absorption measurements and pH-titrations. The first acid dissociation constant was determined as $1.48\times10^{-6}$ ($pk_{a_1}=5.83$) and the second as $3.2\times10^{-13}$ ($pk_{a_2}=12.5$) at 25°C. PAR forms 1:2 chelate with Fe(III), Co(II) and Ni(II), and forms 1:1 chelate with Cu(II), Zn(II), Cd(II), Hg(II) and Pb(II). The stability constant of copper(II)-PAR chelate was determined as $5\times10^{11}$ at 25°C. Some analytical aspects of PAR were also discussed.

The author wishes to thank Dr. Eiiti Minami, Professor Emeritus, for his interst in this work and Mr. Kunihiko Mizumachi, Lecturer in Rikkio University, for his ardent encouragement and advice in the calculation of the chelate stability constant. He also thanks Dojin Pharmaceutical Laboratories for the gift of the sample of PAR.

*Department of Chemistry*
*Faculty of Science*
*The University of Tokyo*
*Hongo, Tokyo*

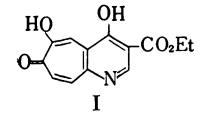
13) S. Glasstone, "An Introduction to Electrochemistry", Van Nostrand Co., New York (1956), p. 401.
14) H. Flaschka and S. Khalafallah, *Z. anal. Chem.*, **156**, 401 (1957).
15) K. L. Cheng, *Anal. Chem.*, **30**, 243 (1958).
16) M. Fujimoto and T. Iwamoto, unpublished results to be reported in detail together with the data for PAN.

# *A Ring-Chain Tautomerism in the Reaction Products of 3-Aminotropolone and Some Ethoxymethyleneacetates*[1]

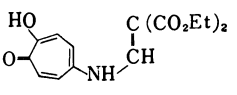
By Tetsuo Nozoe, Kozo Doi* and Kazuo Kitahara**

(Received April 11, 1960)

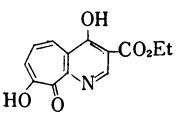
Slack and Attridge[2] reported the synthesis of a pyridotropolone (I) by application of the Gould-Jacobs' quinoline synthetic method[3] involving a process of pyrolysis of 5-(β, β-diethoxycarbonylvinylamino)tropolone (II), a condensation product of 5-aminotropolone and ethyl ethoxymethylenemalonate. This kind of synthetic method of pyridotropolones has also been applied to the other 5-aminotropolone derivatives[4] and 4-aminotropolone[5].



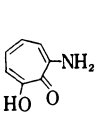
I



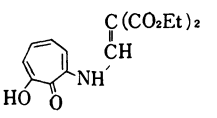
II



III



IV



V

In the present series of experiment an attempt was made to prepare a pyridotropolone (III) by application of the similar synthetic method to 3-aminotropolone (IV). Although this objective was not accomplished unfortunately, other interesting observations were made, which are described in this paper.

When 3-aminotropolone (IV) and ethyl ethoxymethylenemalonate were heated, a yellow condensation product of m.p. 138°C was formed in a good yield. Its analytical data agreed with those calculated for the anticipated diethoxycarbonylvinylaminotropolone (V). The ultraviolet absorption spectrum (Fig. 1) of the condensation product seemed to be fairly reasonable for the expected structure V, if the tropolone nucleus and the α, β-unsaturated ester system were to interact through the intermediate nitrogen atom.

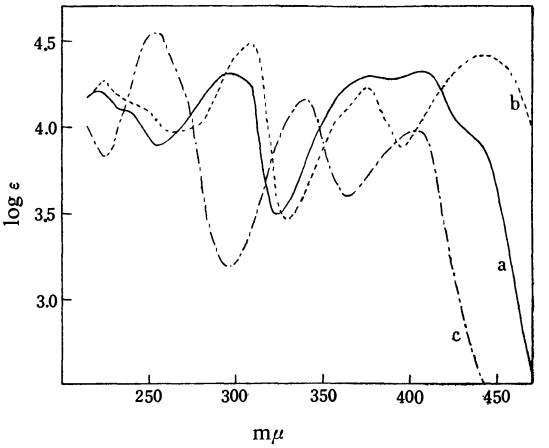



Fig. 1. Ultraviolet absorption spectra.
a) VIII in methanol
b) VIII in 0.01 N sodium hydroxide
c) IV in methanol

However, it has been found that pyrolysis of the above condensation product resulted in formation of not the anticipated pyridotropolone (III) but of another curious substances. Thus, on being heated at 250°C without a solvent, the condensation product afforded oxazolo[5 : 4-b]tropone*(VI) and ethyl malonate. The structure of the former VI was supported from its analytical values, determination of the molecular weight, and the close resemblance of its ultraviolet absorption curve (Fig. 2) to that of the known 2-methyloxazolo [5 : 4-b]-tropone[6] (VII). Ethyl malonate was identified as its dianilide[7].

The foregoing finding makes doubtful the assumption that the condensation product of the aminotropolone and ethoxymethylene-malonate may possess a structure like V. Virtually, the condensation product did not show any coloration with alcoholic ferric chloride and was inert to the action of diazomethane, the facts of which do not give

* Present address: The Chemical Research Institute of Non-Aqueous Solutions, Tohoku University, Sendai.
** Present address: The Research Laboratory, Tokyo Tanabe Pharmaceutical Co., Tokyo.

1) This work in part was presented at the Local Meeting of the Chemical Society of Japan, Yonezawa, June, 1956.
2) R. Slack and C. F. Attridge, *Chem. & Ind.*, **1952**, 471.
3) R. G. Gould and W. A. Jacobs, *J. Am. Chem. Soc.*, **61**, 2890 (1939).
4) K. Yamane, *J. Chem. Soc. Japan, Pure Chem. Sec. (Nippon Kagaku Zasshi)*, **80**, 75 (1959).
5) K. Doi, *Bull. Chem. Research Inst. Non-Aqueous Solns., Tohoku Univ.*, **9**, 19 (1959).
6) Y. Kitahara, *Science Repts. Tohoku Univ., Ser. I*, **40**, 83 (1956).
* Very recently the same authors have reported the another syntheses and some reactions of the oxazolotropone (VI). [This Bulletin, **34**, 312 (1961)].
7) M. Freund, *Ber.*, **17**, 134 (1884).

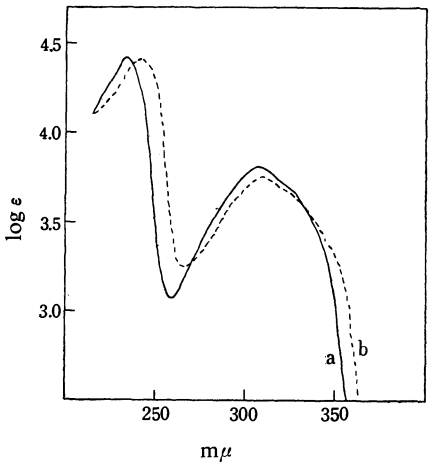
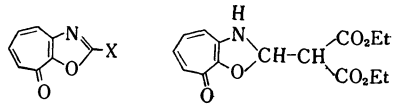



Fig. 2. Ultraviolet absorption spectra.
a) VI in methanol
b) VII in methanol

enough explanation for the condensation product to be a diethoxycarbonylvinylaminotropolone (V).

From the above facts it seems more reasonable to consider that the condensation product has a dihydro-oxazolotropone structure VIII.



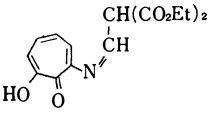
VI: X=H
VII: X=$CH_3$

VIII

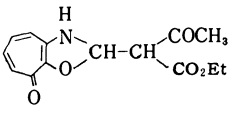
The ultraviolet absorption spectrum of VIII in an alkaline solution shows a red-shift in comparison to that in neutral solution, and this suggests that VIII results in ring-opening to V or IX in an alkaline solution (Fig. 1).

With aid to isolate the chain-isomer V or IX, the condensation product VIII was treated with ethanolic potassium hydroxide, neutralized carefully with dilute mineral acid, and subsequently extracted with chloroform. The fresh extract showed clearly a red coloration with ferric chloride, but the vacuum evaporation of the solvent resulted not in formation of the expected chain-isomer but in recovering of the raw material.

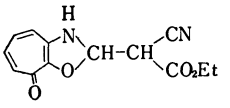
In the condensation reaction of 3-aminotropolone and ethoxymethylenemalonate, it is considered that the anticipated diethoxycarbonylvinylaminotropolone (V) or its isomeric azomethine derivative IX produces at first and spontaneously isomerizes to the ring-isomer VIII. It seems to leave no room for doubt, at any rate, that the condensation product of the aminotropolone and ethoxymethylenemalonate exists in the ring-form of VIII in a neutral state and that it exists in the chain-form of V or IX in an alkaline medium. That the ultraviolet absorption of VIII in methanol solution has maxima in the comparatively longer wavelength regions indicates probably, though not any evidences have been obtained, that VIII is ring-opening to V or IX at least in the condition of the spectral measurement.



IX



X



XI

On being heated with ethyl ethoxymethyleneacetoacetate and ethoxymethylenecyanoacetate in place of ethoxymethylenemalonate, 3-aminotropolone (IV) gave readily a condensation product, 2-(ω-acetyl-ω-ethoxy-carbonylmethyl)-2, 3-dihydroöxazolo[5 : 4-b]-tropone[8] (X) and 2-(ω-ethoxycarbonyl-ω-cyanomethyl)-2, 3-dihydroöxazolo[5 : 4-b]tropone (XI), respectively. The structures of these compounds were reasonably supported by the similarities of their ultraviolet absorptions (Fig. 3) to that of VIII and by the formation of the oxazolotropone (VI) by their pyrolysis.

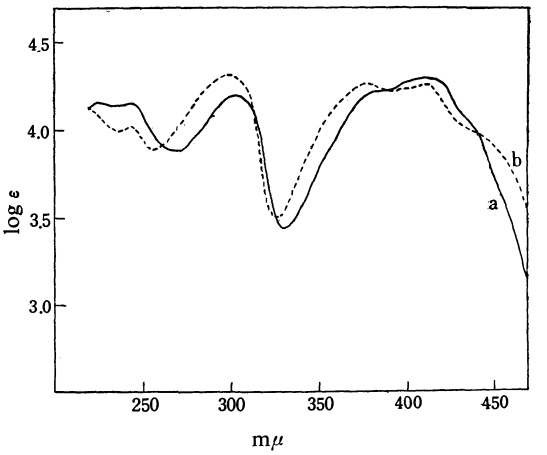



Fig. 3. Ultraviolet absorption spectra.
a) X in methanol
b) XI in methanol

The authors have found that the condensation products of o-aminophenol and the above three ethoxymethyleneacetates are also of the

8) Since the description of this work was completed, K. Yamane, *J. Chem. Soc. Japan, Pure Chem. Sec.* (*Nippon Kagaku Zasshi*), **81**, 509 (1960), have reported the synthesis of X by the same sequence.

cyclic structures of the corresponding benzoxazolines, the results of which will be described in the following paper.

## Experimental

The ultraviolet absorptions were determined in methanol solution, unless otherwise stated, with a Beckman model DU spectrophotometer.

**2-(ω, ω-Diethoxycarbonylmethyl)-2, 3-dihydrooxazolo[5 : 4-b]tropone (VIII).** — A mixture of 3-aminotropolone (IV, 1.0 g.) and ethyl ethoxymethylenemalonate (1.7 g.) was heated on an oil bath at 130°C for 30 min. After being cooled at room temperature, the residual solid was recrystallized from ethanol to give the dihydroöxazolotropone (VIII) as yellow leaflets, m. p. 138°C, in nearly quantitative yield.

Found: C, 58.60; H, 5.67; N, 5.05. Calcd. for $C_{15}H_{17}O_6N$: C, 58.63; H, 5.58; N, 4.56%. $\lambda_{max}$ mμ (log ε): in methanol, 220 (4.33), 295 (4.44), 381 (4.45), 408 (4.45); in 0.01 N sodium hydroxide, 225 (4.34), 310 (4.56), 377 (4.31), 442 (4.49).

The condensation product VIII did not show any coloration with alcoholic ferric chloride and remained inert to the action of diazomethane.

A mixture of VIII (0.3 g.), methanol (10 ml.), sodium hydroxide (0.4 g.) and water (5 ml.) was heated on a water bath at 50°C for 30 min. The orange solution so formed was cooled, neutralized cautiously with dilute hydrochloric acid, and then extracted with chloroform. The extract showed red coloration with ferric chloride, but its evaporation of the solvent under reduced pressure left only starting material VIII.

**Oxazolo[5 : 4-b]tropone (VI).**—VIII (1.45 g.) was placed in a Claisen flask of small capacity and heated on an oil bath at 230°C for 30 min. Colorless liquid (0.1 g.), which distilled out at 197~199°C and smelled like ethyl malonate, was collected. On being heated at 150°C with excess of aniline, it gave malonic dianilide, m. p. 275°C, undepressed on admixture with an authentic specimen[7]. The distilled residue, after extraction with warm benzene and subsequent evaporation of the solvent, crystallized from cyclohexane to give oxazolotropone (VI, 0.6 g.) as pale yellow prisms, m. p. 151~152°C.

Found: C, 65.60; H, 3.90; N, 9.40; mol. wt. (Rast), 146. Calcd. for $C_8H_5O_2N$: C, 65.30; H, 3.43; N, 9.52%; mol. wt., 147. $\lambda_{max}^{MeOH}$ mμ (log ε): 235 (4.42), 305 (3.80).

**2-(ω-Acetyl-ω-ethoxycarbonylmethyl)-2,3-dihydrooxazolo[5 : 4-b]tropone (X).** — A mixture of the aminotropolone (0.7 g.) and ethyl ethoxymethyleneacetoacetate[9] (0.9 g.) was heated at 130°C for 30 min. and the residual solid was crystallized from ethanol to give dihydroöxazolotropone (X) as yellow prisms, m. p. 136°C, in a nearly quantitative yield.

Found: C, 60.69; H, 5.42; N, 5.34. Calcd. for $C_{13}H_{15}O_5N$: C, 60.64; H, 5.45; N, 5.05%. $\lambda_{max}^{MeOH}$ mμ (log ε): 245 (4.30), 303 (4.35), 415 (4.45).

Pyrolysis of the product (X, 0.54 g.) at 250°C for 30 min. afforded the oxazolotropone (VI, 0.15 g.) and ethyl acetoacetate (50 mg.), identified as its anilide[10].

**2-(ω-Ethoxycarbonyl-ω-cyanomethyl)-2,3-dihydrooxazolo[5 : 4-b]tropone (XI).** — A mixture of the aminotropolone (140 mg.) and ethyl ethoxymethylenecyanoacetate[11] (170 mg.) was heated at 130°C for 30 min. and the residual solid was crystallized from methanol to give the condensation product (XI) as yellow needles, m. p. 182°C, in nearly quantitative yield.

Found: C, 60.06; H, 4.87; N, 10.86. Calcd. for $C_{13}H_{12}O_4N_2$: C, 59.99; H, 4.64; N, 10.77%. $\lambda_{max}^{MeOH}$ mμ (log ε): 245 (4.11), 300 (4.41), 378 (4.35), 410 (4.35).

Pyrolysis of XI (0.54 g.) as above described afforded also the oxazolotropone (VI, 0.2 g.) and ethyl cyanoacetate (50 mg.), identified as its amide[12].

The authors express their gratitude to Messrs. S. Ohyama, K. Kato, A. Iwanaga and S. Azumi for microanalyses.

*Department of Chemistry*
*Faculty of Science*
*Tohoku University*
*Katahira-cho, Sendai*

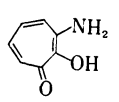
9) L. Claisen, *Ann.*, **297**, 16 (1897).
10) L. Knorr, ibid., **236**, 75 (1886).
11) M. E. G. deBollemont, *Bull. soc. chim. France*, [3] **25**, 20 (1901).
12) B. B. Corson, R. W. Scott and C. E. Vose, "Organic Syntheses," Coll. Vol. I, 173 (1932).

# *A Note on the Ring-Chain Tautomerism in the Reaction Products of o-Aminophenol and Some Ethoxymethyleneacetates*

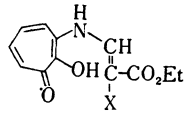
By Tetsuo Nozoe and Kozo Doi*

(Received August 25, 1960)

In the preceding paper[1], it was shown that the condensation reaction of 3-aminotropolone (I) and ethyl ethoxymethylenemalonate or some ethoxymethyleneacetates afforded, not the anticipated vinylaminotropolone (II), but its ring-tautomer, dihydro-oxazolotropone (III). This conclusion was drawn from the facts that the above condensation products did not show any coloration with ferric chloride test and were inert to the action of diazomethane, and that their pyrolyses resulted in a fragmentation to oxazolo[5:4-b]tropone (IV) and respective acetic acid derivatives. The authors stated, moreover, that the condensation products III probably exist in the chain-forms of II (or their possible azomethine type of isomers) in an alkaline medium.

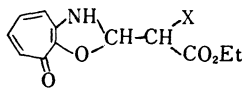


I



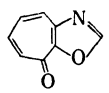
(X=$CO_2Et$, CN, $COCH_3$)

II



(X=$CO_2Et$, CN, $COCH_3$)

III



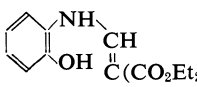
IV

There are not many systematic studies on the ring-chain tautomerism involving a nitrogen atom. Holly and Cope[2] elucidated this problem in the condensation products of *o*-aminobenzyl alcohol or *o*-hydroxybenzylamine with aldehydes or ketones through ultraviolet spectra and molecular refractions. Witkop and Beiler[3] also discussed this tautomerism in the arylidene Schiff bases derived from *o*-aminobenzyl alcohol through the spectral measurements.

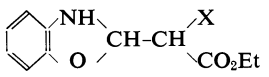
From the above point of view, the present authors have felt interest in a possible ring-chain tautomerism between the condensation products of *o*-aminophenol, analogous to 3-aminotropolone (I), and ethoxymethyleneacetates. In this series of experiments, the authors have obtained information similar to that in the case of the aminotropolone; these will be described below in brief.

Condensations of anilines and ethoxymethyleneacetates have been often carried out for many syntheses of quinolines[4] and for identifications of anilines[5], but no report seems to have been made on the condensation of *o*-aminophenol and ethoxymethyleneacetates.

On being heated with ethyl ethoxymethylenemalonate, *o*-aminophenol afforded a condensation product of colorless crystals, m. p. 140~141°C, in a good yield. It did not show any coloration with alcoholic ferric chloride and was inert to the action of diazomethane. As might have been expected from the conclusions in the case of 3-aminotropolone (I), the above experimental results show that the condensation product is not the anticipated vinylaminophenol (V) or its possible isomer of the Schiff base type but is presumably 2-($\omega$, $\omega$-diethoxycarbonylmethyl)benzoxazoline (VI). The reaction product, moreover, resulted in fission to form benzoxazole and ethyl malonate on pyrolysis, and this fact probably affords a more powerful proof for the assignment of structure VI to the condensation product.



V



VI: X=$CO_2Et$
VII: X=$COCH_3$
VIII: X=CN

The ultraviolet absorption of the compound VI in an alkaline solution has maxima at longer wavelength region than in a neutral solution (Fig. 1). This fact indicates probably that the compound VI may exist in the chain-form of V (or its isomeric Schiff base) in an alkaline medium, the conclusion of which is analogous to that of the case in the condensation products of 3-aminotropolone[1].

The use of ethoxymethyleneacetoacetate and ethoxymethylenecyanoacetate, in place of

* Present address: The Chemical Research Institute of Non-Aqueous Solutions, Tohoku University, Sendai.

1) T. Nozoe, K. Doi and K. Kitahara, This Bulletin, **34**, 611 (1961).

2) F. W. Holly and A. C. Cope, *J. Am. Chem. Soc.*, **66**, 1875 (1944).

3) B. Witkop and T. W. Beiler, ibid., **76**, 5589 (1954).

4) R. H. Reitsma, *Chem. Revs.*, **43**, 43 (1948).

5) G. R. Lappin, *J. Chem. Educ.* **28**, 126 (1951).

ethoxymethylenemalonate, in this condensation reaction afforded the respective benzoxazoline VII and VIII in a good yield. These structures were presumed from the facts that their ultraviolet absorptions were similar to that of the compound VI and that their pyrolyses yielded benzoxazole.

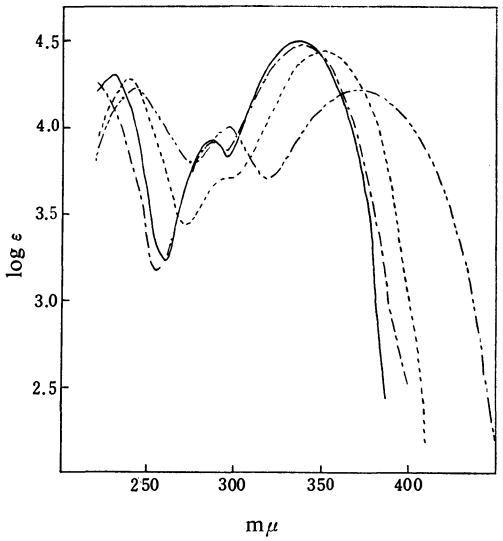



Fig. 1. Ultraviolet absorption spectra in methanol: curve —— VI; curve ---- VII; curve —— VIII; curve —— VI in 0.1 N sodium hydroxide solution.

## Experimental

The ultraviolet absorptions were measured in methanol, unless otherwise stated, with a Beckman model DU spectrophotometer.

**2-(ω, ω-Diethoxycarbonylmethyl)benzoxazoline (VI).** — A mixture of *o*-aminophenol (1.1 g.) and ethyl ethoxymethylenemalonate (2.2 g.) was heated on an oil bath at 130°C for 30 min., and then the residual solid was recrystallized from ethanol to form the benzoxazoline VI as colorless prisms, m. p. 140~141°C, in a nearly quantitative yield.

Found: C, 60.11; H, 5.72; N, 5.04. Calcd. for $C_{14}H_{17}O_5N$: C, 60.20; H, 6.14; N, 5.02%.

$\lambda_{max}$ mμ (log ε): in methanol, 230 (4.30), 286 (3.92), 335 (4.49); in 0.1 N sodium hydroxide, 243 (4.23), 295 (4.00), 370 (4.23).

**Pyrolysis of the Compound VI.** — The above benzoxazoline VI (5.6 g.) was placed in a Claisen flask with a small capacity and heated on an oil bath at 250°C. Vigorous boiling occurred and colorless liquid distilled out, which was separated into the two fractions by their boiling points at ordinary pressure: a) b. p. 175~185°C, 1.6 g., and b) b. p. 195~199°C, 2.7 g. Fraction (a) was distilled once again and the portion boiled at 180~182°C was collected. The cooled distillate crystallized to give benzoxazole (0.97 g.), alone and mixed m. p. 30~31°C[6]. The fraction (b), with an odor like that of ethyl malonate, afforded malonic dianilide, alone and mixed m. p. 275°C[7], on being heated with excess of aniline at 150°C.

**2-(ω-Acetyl-ω-ethoxycarbonylmethyl)benzoxazoline (VII).**—A mixture of *o*-aminophenol (1.1 g.) and ethyl ethoxymethyleneacetoacetate (1.9 g.) was heated at 130°C for 20 min. and the residual solid was recrystallized from methanol to give the benzoxazoline (VII) as colorless prisms, m. p. 146~147°C, in a good yield.

Found: C, 62.66; H, 5.98; N, 5.61. Calcd. for $C_{13}H_{15}O_4N$: C, 62.64; H, 6.07; N, 5.62%.

$\lambda_{max}^{MeOH}$ mμ (log ε): 238 (4.28), 350 (4.45).

VII resulted in the formation of benzoxazole and ethyl acetoacetate, identified as its anilide[8], on pyrolysis at 250°C.

**2-(ω-Ethoxycarbonyl-ω-cyanomethyl)benzoxazoline (VIII).** — An equimolar mixture of *o*-aminophenol and ethyl ethoxymethylenecyanoacetate was heated at 100°C for 30 min. and the residual solid crystallized from methanol to form the benzoxazoline (VIII) as colorless needles, m. p. 191~192°C, in a good yield.

Found: C, 62.04; H, 5.04; N, 11.90. Calcd. for $C_{12}H_{13}O_3N_2$: C, 62.06; H, 5.21; N, 12.06%.

$\lambda_{max}^{MeOH}$ mμ (log ε): 287 (3.91), 340 (4.47).

Pyrolysis of the compound VIII at 250°C gave also benzoxazole and ethyl cyanoacetate, identified as its amide[9].

The authors express their gratitude to Professor Yoshio Kitahara, the Chemical Research Institute of Non-Aqueous Solutions of Tohoku University, for his kind advice, to Mr. S. Ohyama and Miss Y. Endo for microanalyses.

*Department of Chemistry*
*Faculty of Science*
*Tohoku University*
*Katahira-cho, Sendai*

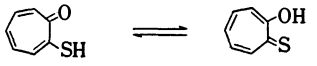
6) A. Ladenburg, *Ber.*, **10**, 1124 (1877).
7) M. Freund, ibid., **17**, 134 (1884).
8) L. Knorr, *Ann.*, **236**, 75 (1886).
9) B. B. Corson, R. W. Scott and C. E. Vose, "Organic Syntheses", Coll. Vol. I (1932), p. 173.

# *On the Structure of 2-Mercaptotropones*

By Tetsuo Nozoe and Kazuo Matsui

(Received August 16, 1960)

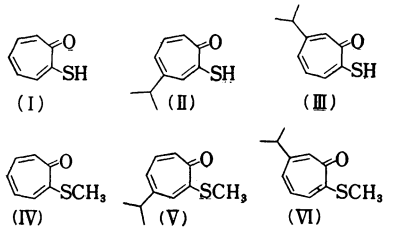
2-Mercaptotropone (I) was synthesized in 1953 by Nozoe and his collaborators[1,2]. It comes as reddish orange crystals of m. p. 55°C and the compound was assumed to be present in two tautomeric forms, A and B. Alkylation



(A) (B)

and acylation of I afford only sulfur-substituted derivatives, while reaction with hydrazine gives 2-hydrazinotropone. Bromine easily effects an oxidation to 2,2'-ditroponyl disulfide. These facts suggest a structure A of this compound and this was named 2-mercaptotropone. But further examination on its physicochemical properties as well as those of its homologs suggested that this should rather be a 2-hydroxyl derivative of tropothione, structure B, and details of this work are described herein.

Physical measurements were carried out with 4-isopropyl-2-mercaptotropone (II), 6-isopropyl-2-mercaptotropone (III), 2-methylthiotropone (IV), 4-isopropyl-2-methylthiotropone (V), and 6-isopropyl-2-methylthiotropone (VI)[3], besides the 2-mercaptotropone (I).



(I) (II) (III)

(IV) (V) (VI)

**Ultraviolet Absorption Spectra**[4].—The ultraviolet absorption spectra of I, II and III are indicated in Fig. 1 and those of IV, V and VI in Fig. 2. As will be seen from these, the spectral curve of 2-mercaptotropones in Fig. 1 shows a fair shift to the longer wavelength side than that of 2-methylthiotropones in Fig. 2, indicating that there is an essential difference in the structure of these two kinds of compounds. This relationship is the same as

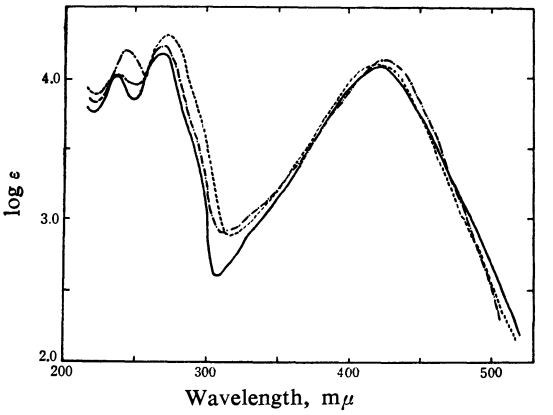



Fig. 1. Ultraviolet absorption spectra in cyclohexane.
——— I ------ II —·—· III

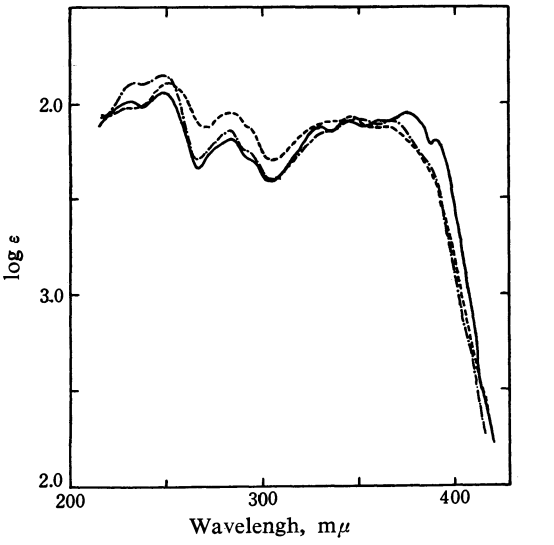



Fig. 2. Ultraviolet absorption spectra in cyclohexane.
——— IV ------ V —·—· VI

that between 2-thiopyridone and its *S*-methyl derivative[5], and if the B type of the structure is assigned to 2-mercaptotropones, the difference in ultraviolet absorptions could be explained as a bathochromic shift due to the C=S group.

1) T. Nozoe, M. Sato and K. Matsui, *Proc. Japan Acad.*, 29, 22 (1953).
2) Idem, *Sci. Repts. Tohoku Univ., I*, 37, 211 (1953).
3) K. Matsui, This Bulletin, 33, 1448 (1960).
4) Measured by a Beckman Model DU spectrophotometer.
5) A. Albert and B. Barlin, "Current Trends in Heterocyclic Chemistry", Butterworths Scientific Publications, London (1958), p. 51.

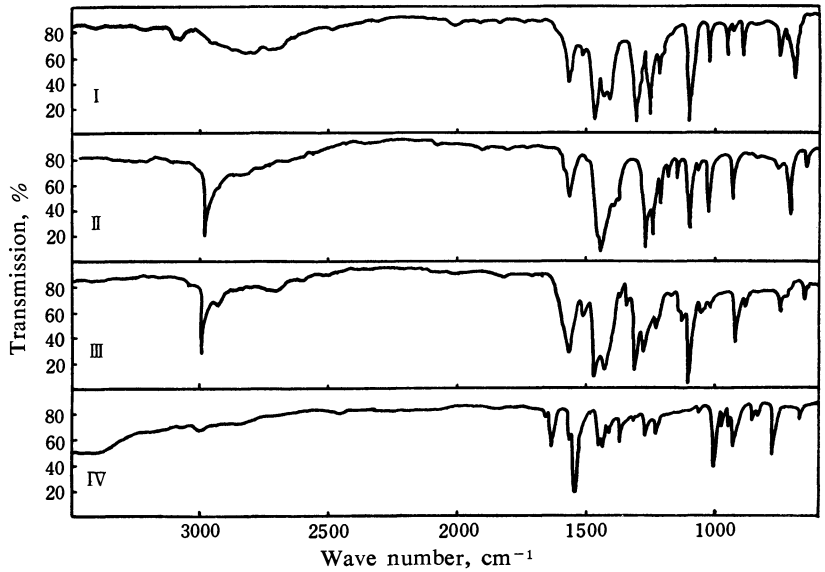



Fig. 3. Infrared absorption spectra.
I in 0.5% $CCl_4$ soln. II in 0.5% $CCl_4$ soln.
III in 0.5% $CCl_4$ soln. IV in KBr-pellet

**Infrared Absorption Spectra**[2,6]. — Infrared absorption spectra of I, II, III and IV are shown in Fig. 3. The absoprtion of IV in the double-bond region is similar to those observed in tropone, 2-methoxytropone, and 2-halotropone[7], but the spectra of I, II and III are quite different from those seen in tropones and tropolones in general. Furthermore, examination of the spectra of I in the 3000 $cm^{-1}$ region indicates the presence of a broad and weak absorption in the region of 3000~2600 $cm^{-1}$. It is rather appropriate to consider that I takes the structure B and the $\nu_{OH}$ absorption has been shifted to lower wave-numbers by chelation, than a shift of $\nu_{SH}$ absorption to higher wave-numbers side from the usual absorption at 2600~2550 $cm^{-1}$.

The absence of a strong absorption assignable to the C=O group in a higher wave-numbers side than 1500 $cm^{-1}$ in the double-bond region also agrees with the structure B and considering Mecke's law[8] the absorption at 1100 $cm^{-1}$ is assumed to correspond to $\nu_{C=S}$.

The same thing may be said of II and III, and 2-mercaptotropones are therefore assumed to take the B of the type structure from infrared absorption spectral examinations.

**Nuclear Magnetic Resonance Spectra**[9]. — The NMR spectra of I, II, III and IV were measured in carbon tetrachloride solution at 40 Mc./sec. at room temperature, with cyclohexane as the internal reference. The results are indicated in Fig. 4. It should be noted here that in I, II and III, the resonance line of the ring proton appears as two signals, at 280 and 230 c. p. s. Since the ring proton appears as one signal at ca. 240 c. p. s. in tropone and tropolone[10], the small signal at 280 c. p. s. in the considerably lower magnetic field side should be assigned to the ring proton

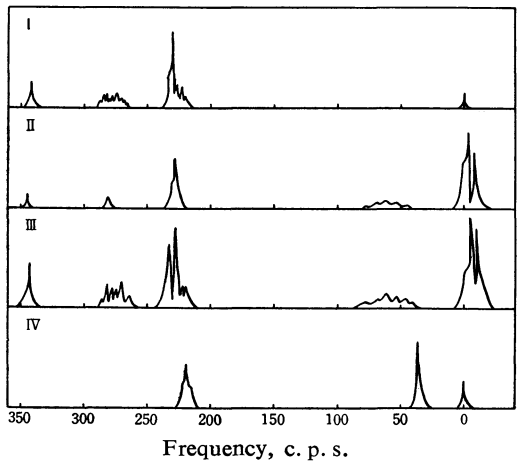



Fig. 4. NMR spectra of I, II, III and IV.

6) Measured by a Perkin-Elmer Model 21 double beam spectrophotometer.
7) S. Kinumaki, K. Aida and Y. Ikegami, *Sci. Repts. Reseach Inst. Tohoku Univ.*, A-8, 264 (1956).
8) R. Mecke, R. Mecke and A. Lüttringhaus, *Chem. Ber.*, **90**, 975 (1957).
9) Measured by a Varian V 4300 B spectrometer.
10) D. Ginsberg, "Chemistry of Non-benzenoid Aromatic Compounds", Interscience Publishers, New York (1959), p. 380.

next to sulfur group. Further, the fact that this is absent in IV suggests that, I, II and III take the B type of the structure, and the signal of proton attached to the carbon next to the C=S group appears in the lower magnetic field side because is it in a different magnetic surrounding from other protons.

The resonance line at ca. 340 c. p. s. in I, II, and III may be assignable to SH group, but the OH line in tropolone appears at ca. 280 c. p. s.[10] This is in reverse of the general observation that the resonance line of SH compounds appears in a higher magnetic field than the corresponding OH compounds[11,12]. This fact also denies the A type of the structure.

**p$K_a$ value.**—The fact that p$K_a$ value of I (5.89)[13] is smaller than that of tropolone (6.92)[14], is in agreement with the general observation that thiophenols show smaller p$K_a$ value than the corresponding phenols. The difference of I and tropolone is, however, only 1 p$K_a$ unit, and this rather small difference compared with that, ca. 3 p$K_a$ unit[15,16], between thiophenols and phenols might be explained by the assignment of the structure B rather than A to I as follows.

2-Thiopyridones[17] show smaller p$K_a$ values than the corresponding 2-pyridones[18] by ca. 2 p$K_a$ unit, which is presumably due to the difference in inductive and mesomeric effect between the C=S and the C=O group. Similarly, it might be expected that in the case of I, structure B, and the tropolone, the C=S group in I should activate the OH group, more than the C=O group in tropolone does. But spacious and electron-rich sulfur atom induced by these electronic effects of the C=S group, conversely tend to control the liberation of proton in the OH group located close by*, more than does the oxygen atom in tropolone.

As a result of these opposing effects of the C=S group in I, the small p$K_a$ difference between I and tropolone is understandable without inconsistency.

**Solubility.** — Mercaptans in general are practically insoluble in water, but the solubility of I in water is 0.846 g./l.[13] Such a large degree of solubility also supports the structure B.

The results of the foregoing ultraviolet, infrared, and NMR spectral measurements, p$K_a$ value, and solubility, all indicate the appropriateness of the B type of the structure for 2-mercaptotropones. It has therefore been clarified that, although the compounds behave as A type of the structure during various reactions, they take the B type of the structure in a static state.

Consequently, the conventional structure A for 2-mercaptotropone (I) should be corrected and the structure B, i. e. 2-hydroxytropothione, is forwarded.

The authors are grateful to Tanabe Seiyaku Co., Ltd. for allowing one (Matsui) of the authors to take part in this research at Sendai. The authors' deepest gratitudes are expressed to Dr. T. Isobe and his colleagues, Chemical Institute of Non-Aqueous Solutions, Tohoku University, for their technical cooperation and keen discussion on NMR spectra, and to Mr. Y. Ikegami, the same Institute, for his helpful advices in infrared analyses.

*Department of Chemistry*
*Faculty of Science*
*Tohoku University*
*Katahira-cho, Sendai*

11) B. P. Dailey and J. N. Shoolery, *J. Am. Chem. Soc.*, **77**, 3977 (1955).
12) L. H. Meyer, A. Saika and H. S. Gutowsky, ibid., **75**, 4567 (1953).
13) N. Yui, *Sci. Repts. Tohoku Univ., I*, **40**, 114 (1956).
14) Idem., ibid., **40**, 50 (1956).
15) G. Schwarzenbach and H. Egli, *Helv. Chim. Acta*, **17**, 1176 (1934).
16) W. H. Fletcher, *J. Am. Chem. Soc.*, **75**, 3784 (1953).
17) R. A. Jones and A. R. Katritzky, *J. Chem. Soc.*, **1958**, 3610.
18) A. Albert and J. N. Phillips, ibid., **1956**, 1294.

* It should be noted here that tropone and tropolone derivatives with the SH group are extremely unstable and undergo dehydrogenative condensation to yield disulfides, unless the SH group is situated at the carbon next to the C=O group and a hydrogen bond between these groups is formed[2].

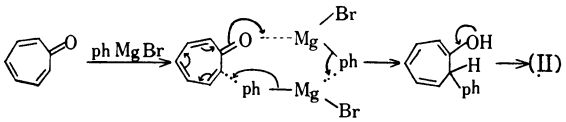
# *Reaction of Troponoids and Organometallic Compounds. VI*. Reaction of Tropone with Grignard Reagents***

By Tetsuo NOZOE, Toshio MUKAI and Takahiro TEZUKA

(Received August 29, 1960)

It has been known that tropolone methyl ethers undergo reaction with Grignard reagents to give tropone derivatives substituted in the 2-position[1,2]. Considering that tropone, the parent compound of tropolone, possesses some degree of ketonic properties[3], its Grignard reaction is considered to be of interest, but no report has been published on this subject. The present paper describes the reaction of methyl-, isopropyl- and phenylmagnesium halide on tropone and the preparation of tropone derivatives via the products thereby formed.

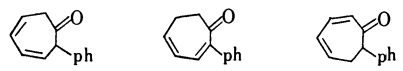
Applications of two molar equivalents of phenylmagnesium bromide on tropone (I) and subsequent decomposition of the magnesium complex with dilute hydrochloric acid gives an oil II, $C_{13}H_{12}O$; 2,4-dinitrophenylhydrazone, m. p. 135°C, maleic anhydride adduct, m. p. 147°C. Catalytic reduction of II results in absorption of 2 molar equivalents of hydrogen to form 2-phenylcycloheptanone. The NMR spectrum of II at 40 Mc. (Fig. 1)*** exhibits three sorts of signals due to phenyl (a), vinyl (b) and methylene (c) protons respectively. These observations indicate that II is one of the 2-phenylcycloheptadienone such as A, B or C, formed by ketonization of enolic intermediate III which was produced by 1,8-addition of the Grignard reagent to the conjugated system in I.




(I) (III)

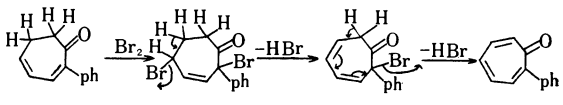
As in the reaction of Grignard reagents with tropolone methyl ethers, two molar equivalents of the reagent are also necessary in this reaction in order to obtain II in fair yield. This implies that the reaction proceeds through a complex formation between tropone and two molecules of the Grignard reagent, analogous to the cyclic intermediate suggested by Swain and others[4].

The infrared spectrum of II shows a carbonyl band at 1660 $cm^{-1}$ characteristic of the conjugated dienone system[5], implying that II is represented by B or C. The maxima in the ultraviolet spectrum of II, 235 and 315 m$\mu$ (log $\varepsilon$ : 3.98 and 3.85), also supports this view, and moreover, the bathochromic shift of 23 and 13 m$\mu$ compared with cyclohepta-2,4-dien-1-one[6], 292 m$\mu$ (log $\varepsilon$ : 3.97) and eucarvone[7], 302 m$\mu$ (log $\varepsilon$ : 3.82) respectively, indicates that II can be best represented by B rather than C.




(A) (B) (C)

II absorbs one molar equivalent of bromine in acetic acid to form an oily dibromide e. g. IV, which lacks the intensive maxima above 220 m$\mu$ in the ultraviolet spectrum. When IV is heated under reduced pressure, hydrogen bromide is liberated to form the hydrobromide of 2-phenyltropone, m. p. 145~147°C (30%), from which 2-phenyltropone (V)[1] is formed.




(II) (IV) (V)

Oxidation of II with selenium dioxide or chromium trioxide gives also 2-phenyltropone in 75 and 10% yield respectively.

In an earlier work[8] in this laboratory, it

* Part V: K. Kikuchi, This Bulletin 33, 628 (1960). This report is also Part VI of Tropones.

** Presented before the Local Meeting of the Chemical Society of Japan, Sendai, December, 1958.

1) (a) T. Nozoe, T. Mukai and J. Minegishi, *Proc. Japan Acad.*, **27**, 419 (1951); (b) T. Nozoe, T. Mukai and I. Murata, ibid., **28**, 142 (1952); (c) T. Nozoe, T. Mukai, J. Minegishi and T. Fujisawa, *Sci. Repts. Tohoku Univ., I*, **37**, 388 (1953).

2) (a) K. Kikuchi, *J. Chem. Soc. Japan, Pure Chem. Sec. (Nippon Kagaku Zasshi)*, **77**, 1439 (1956); (b) K. Kikuchi, ibid., **81**, 505 (1960); (c) K. Kikuchi, This Bulletin, **33**, 628 (1960).

3) T. Nozoe, T. Mukai and K. Takase, *Sci. Repts. Tohoku Univ., I*, **39**, 164 (1956).

*** All NMR spectra were measured with a Varian V-4300B spectrometer.

4) C. G. Swain and H. B. Boyles, *J. Am. Chem. Soc.*, **73**, 871 (1951).

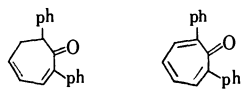
5) Eucarvon shows carbonyl band at 1661 $cm^{-1}$.

6) E. E. van Tamelen and G. T. H. Hildahl, *J. Am. Chem. Soc.*, **75**, 5451 (1953).

7) E. J. Corey and H. J. Burke, ibid., **76**, 5257 (1954).

8) (a) T. Nozoe, T. Mukai, M. Ishii and Y. Ikegami, unpublished work; (b) T. Mukai, This Bulletin, **31**, 852 (1958).

had been shown that the reaction of phenylmagnesium bromide on 2-phenyltropone afforded colorless plates (VII) $C_{19}H_{16}O$, m. p. 87°C, accompanied by 2,7-diphenyltropone (VIII), both of which gave 2,7-diphenylcycloheptanone on catalytic hydrogenation, but the structure of compound VII remained unestablished. It is likely now that VII has the structure as shown below.




(VII) (VIII)

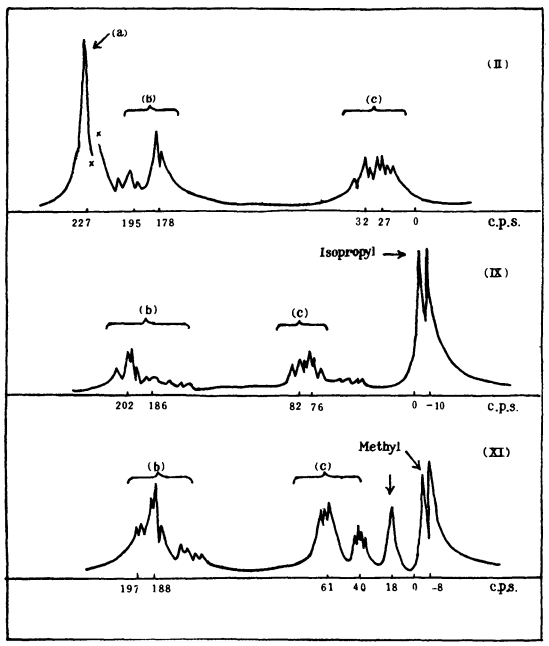
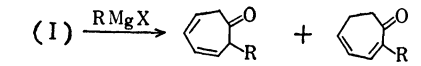



Fig. 1. NMR spectra of 2-phenyl-(II), 2-isopropyl-(IX) and 2-methylcycloheptadienone-(XI) at 40 Mc., relative to cyclohexane as inner reference.

The reaction of tropone with isopropylmagnesium bromide affords a liquid (IX), $C_{10}H_{14}O$, $\lambda_{max}$ 302 m$\mu$ (log $\varepsilon$: 3.31), which absorbs 2 molar equivalents of hydrogen on catalytic hydrogenation to give 2-isopropylcycloheptanone. The NMR spectrum of IX (Fig. 1) also suggests the cycloheptadienone type. Since the infrared spectrum indicates two carbonyl absorption bands at 1705 and 1658 $cm^{-1}$, it is assumed that IX is a mixture of IXa and IXb (R=*i*-$C_3H_7$). From the comparison of the absorption intensity in the ultraviolet spectrum of IX at 302 m$\mu$ with that of eucarvon (mentioned above), the proportion of IXa to IXb is assumed to be about 2 to 1.




(IXa) R=*i*-$C_3H_7$ (IXb) R=*i*-$C_3H_7$
(XIa) R=$CH_3$ (XIb) R=$CH_3$

IX adds one molar equivalent of bromine, but the dibromide thereby formed easily loses hydrogen bromide during removal of the solvent to afford an oily product (X) which gives the known 2-amino-7-isopyropyltropone[9] on being treated with hydrazine hydrate, indicating that X is 2-isopropyltropone.

Although the ultraviolet spectrum and the infrared diagram of X are analogous to those of known 2-methyl- and 2-ethyltropone[10], X does not form a picrate, an oxime or a 2,4-dinitrophenylhydrazone by the usual process and this may be due to the steric hindrance of the isopropyl group.

Similarly, the reaction of tropone with methylmagnesium iodide gives an oil (XI), $\lambda_{max}$ 235 and 298 m$\mu$ (log $\varepsilon$: 3.54 and 3.53), whose catalytic hydrogenation produces 2-methylcycloheptanone. Treatment of XI with bromine easily effects bromination-dehydrobromination to give the known 2-methyltropone.

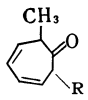
The infrared spectrum of XI exhibits carbonyl bands at 1710 and 1665 $cm^{-1}$ as in the case of IX, and XI is considered to be a mixture of XIa and XIb (R=$CH_3$). This is also supported by its NMR spectrum (Fig. 1) in which two kinds of signals due to the methyl group appear at +18 c. p. s. (singlet) and −8 c. p. s. (doublet). The former is assumed to come from the methyl group in XIb, whereas the latter is due to the methyl group in XIa. Moreover, the calculation of the areas of two signals due to methyl groups in NMR spectrum and the intensity in the ultraviolet spectrum of XI shows that XIa is more prominent than XIb in that mixture.

Both IX and XI are easily dehydrogenated by the treatment with selenium dioxide to give 2-isopropyl- or 2-methyltropone in 55 and 60% yields, respectively.

It follows, therefore, that the Grignard reaction of tropone is also useful as a general method for the preparation of tropone derivatives.

After the present work had been completed, it was learned very recently that Closs and Closs[11] had obtained a compound XII (R=H or $CH_3$) from the reaction of methyllithium on tropone or 2-methyltropone. They also

9) T. Nozoe et al., unpublished work.
10) T. Mukai, *J. Chem. Soc. Japan, Pure Chem. Sec.* (*Nippon Kagaku Zasshi*), **79**, 1547 (1958).
11) G. L. Closs and L. E. Closs, Abstracts of Papers, National Meeting of the American Chemical Society, Cleveland, April, 1960.



(XII)

obtained similar compounds by the application of methylene chloride and methyllithium on phenol or cresol, but details are not available. Our results in which the conjugated dienones with the double bond in position different from that in XII (R=H) has been obtained, would be due to a migration of the double bond during the decomposition of the magnesium complex with dilute hydrochloric acid.

## Experimental[12]

**2-Phenylcycloheptadienone (II).**—A solution of 3.0 g. of tropone in 40 ml. of absolute ether was added dropwise at 0°C with stirring to 2.2 mol. equiv. of Grignard reagent prepared from 10.3 g. of bromobenzene and 1.5 g. of magnesium in 40 ml. of absolute ether. After additional stirring for half an hour, the reaction mixture was decomposed with 1 N hydrochloric acid, extracted with ether, washed with water and dried over anhydrous sodium sulfate. Removal of the solvent afforded 7.5 g. of crude oil, whose distillation in vacuo gave 4.35 g. (84%) of pale yellow oil (II), b. p. 139~145°C (3 mmHg), $n_D^{16}$ 1.4890, $\lambda_{max}^{MeOH}$ 235 mμ (log ε: 3.98), 315 mμ (log ε: 3.85). For analysis, this oil was redistilled to give b. p. 143~145°C (3 mmHg).

Found: C, 84.31; H, 6.38. Calcd. for $C_{13}H_{12}O$: C, 84.75; H, 6.57%.

Application of 1.0 and 1.5 molar equivalents of the Grignard reagent on tropone afforded II in 30% and 75% yields with the recovery of tropone (35 and 3% respectively).

2,4-Dinitrophenylhydrazone, m. p. 134~135°C, $\lambda_{max}^{MeOH}$ 375 mμ (log ε: 4.15).

Found: C, 62.54; H, 4.31; N, 15.08. Calcd. for $C_{19}H_{16}O_2N_4$: C, 62.63; H, 4.43; N, 15.38%.

**Catalytic Reduction of 2-Phenylcycloheptadienone (II).**—A solution of 300 mg. of II in 4.5 ml. of ethanol was hydrogenated at 1 atm. and 18°C with prereduced palladium-carbon catalyst. After 125 min., 87 ml. (2.4 mol. equiv.) of hydrogen was absorbed. Removal of the catalyst and evaporation of the solvent afforded 300 mg. of an oil, which gave semicarbazone m. p. 150~151.5°C, undepressed on admixture with an authentic sample of 2-phenylcycloheptanone semicarbazone[1a].

**Bromination of 2-Phenylcycloheptadienone (II).**—A solution of bromine in acetic acid (88 mg./0.5 ml.) was added dropwise at 0°C to a solution of 100 mg. of II in 5 ml. of acetic acid, by which 1.2 mol. equiv. of bromine was absorbed. After stirring for one hour, the reaction mixture was diluted with water, extracted with benzene, washed with water and dried over anhydrous sodium sulfate. Removal of the solvent at room temperature under reduced pressure gave 200 mg. of brown oil, a chromatographic purification of which on alumina afforded dibromide IV as a viscous oil.

Found: C, 44.76; H, 3.34. Calcd. for $C_{13}H_{12}OBr_2$: C, 45.36; H, 3.51%.

**2-Phenyltropone.** — a) The dibromide (200 mg.) obtained above was heated at 80°C under reduced pressure (20 mmHg) overnight. The resultant residue was extracted with benzene, washed with water and dried. Evaporation of the solvent and chromatographic purification on alumina yielded 2-phenyltropone (70 mg.) as a reddish oil. On treatment of this oil (70 mg.) with hydrazine hydrate, crystals (20 mg.), m. p. 200~202°C were obtained. Recrystallization from benzene gave yellow needles, m. p. 203~204°C, identical with authentic 2-amino-7-phenyltropone[1].

b) II (1 g.) was brominated in acetic acid and the reaction mixture was treated as described above. On removal of the solvent at 80°C, 400 mg. of 2-phenyl tropone as colorless needles, m. p. 145~147°C*, which showed almost identical ultraviolet absorption maximum with that of 2-phenyltropone. This hydrobromide (200 mg.) was heated at 100°C under reduced pressure (20 mmHg) for 2 hr. and subsequently sublimed to afford 90 mg. of yellow needles, m. p. 82~83°C, undepressed on admixture with authentic 2-phenyltropone.

**Dehydrogenation of II with Selenium Dioxide.**—A solution of 200 mg. of II in 2 ml. of dioxane was heated under reflux with selenium dioxide (140 mg.) for 7 hr. The deposited selenium (30 mg.) was filtered off and the filtrate was concentrated. The resultant residue was dissolved in benzene, washed successively with saturated sodium bicarbonate solution and water, and dried. On removal of the solvent, 150 mg. (75%) of crystals, m. p. 70~75°C was obtained. Recrystallization from benzene and chromatographic purification on alumina gave yellow prisms, m. p. 83~84°C, identical with 2-phenyltropone.

**Oxidation of II with Chromium Trioxide.** — A solution of 1.9 g. of II in 6 ml. of pyridine was added to pyridine-chromic acid complex (1 g. $CrO_3$/10 ml. pyridine) at 15~20°C. After stirring for 10 hr. and standing for another 12 hr. at room temperature, the reaction mixture was treated with methanol to decompose excess of chromium trioxide, neutralized with concentrated hydrochloric acid, extracted with chloroform, washed with water and dried. Removal of the solvent and subsequent purification on alumina gave 70 mg. of an oil. Treatment of this oil (70 mg.) with hydrazine hydrate by usual way afforded 20 mg. of crystals, m. p. 198~202°C. Recrystallization from benzene gave yellow prisms, m. p. 206~207°C, identical with 2-amino-7-phenyltropone[1].

**Diels-Alder Reaction of II.** — A mixture of 200 mg. of II and 130 mg. (1.2 mol. equiv.) of maleic anhydride in 2 ml. of dry benzene was heated under reflux for 11 hr. On removal of the solvent 200 mg. of an oil was obtained which on standing for 10 days, gave 70 mg. of crystals, m. p. 145~170°C. Recrystallization from benzene gave white needles, m. p. 186~187°C.

Found: C, 71.88; H, 4.53. Calcd. for $C_{17}H_{14}O_4$: C, 70.33; H, 4.86%. $\lambda_{max}^{MeOH}$ 295 mμ (log ε: 2.43).

12) All the melting points are not crroected.

* On exposure in the air it decomposed to an oil.

**2-Isopropylcycloheptadienone (IX).**—A solution of 5 g. of tropone in 50 ml. of absolute ether was added at 0°C to a 2.2 mol. equiv. of Grignard reagent prepared from 13.36 g. of isopropyl bromide and 2.50 g. of magnesium in 40 ml. of absolute ether. The reaction mixture was treated as in the case of II. The resultant residue was distilled in vacuo to give three fractions: i) b. p. below 70°C (4 mmHg) $n_D^{15}$ 1.4870, 0.5 g.; ii) b. p. 70~75°C (4 mmHg), $n_D^{15}$ 1.4850, 4.4 g. (62%); iii) b. p. above 75°C (4 mmHg), small amount.

Found [for fraction (ii)]: C, 79.51; H, 9.05. Calcd. for $C_{10}H_{14}O$: C, 79.95; H, 9.39%.

**Hydrogenation of IX.**—2-Isopropylcycloheptadienone (IX) (300 mg.) was hydrogenated in 5 ml. of acetic acid at 1 atm. and 18°C with 10 mg. of prereduced platinum oxide catalyst. Ninty-five milliliters of hydrogen (2.0 mol. equv.) was taken up within 80 min. After removal of the catalyst, the mother liquor was diluted with water, extracted with petroleum ether, washed and dried. On evaporation of the solvent, 250 mg. of an oil was remained, which afforded semicarbazone, m. p. 170.5 ~171.5°C, undepressed on admixture with that of 2-isopropylcycloheptanone[13].

**Formation of 2-Isopropyltropone (X) by Bromination of IX.**—Bromine in carbon tetrachloride was added to a solution of 650 mg. of IX in 6.5 ml. of carbon tetrachloride by which 1.0 mol. equiv. bromine was absorbed. The reaction mixture was treated as in the case of II. Residual oil thus obtained was purified through its hydrochloride and then chromatographed on alumina, by which 160 mg. of brown oil was obtained. An ethanolic solution of this oil (160 mg.) was heated under reflux with 0.23 ml. of 80% hydrazine hydrate for 1 hr. Removal of the solvent followed by chromatography on alumina gave 100 mg. of crystals m. p. 40~50°C, $\lambda_{max}^{MeOH}$ 242, 336, 399 mμ, identical with that of 2-amino-7-isopropyltropone[9]. Hydrolysis of this crystals (100 mg.) with potassium hydroxide in aqueous ethanol afforded 60 mg. of an oil, having identical $R_f$ value with that of α-thujaplicin.

**Formation of 2-Isopropyltropone (X) by Dehydrogenation of IX with Selenium Dioxide.**—A solution of 1 g. of IX in 10 ml. of dioxane was heated under reflux with 440 mg. (1.2 mol. equiv.) of selenium dioxide for 1 hr. The reaction mixture was filtered to remove deposited selenium (150 mg.) which contains tarry matter and the mother liquor was concentrated. The resultant residue was dissolved in ether, washed with dilute silver nitrate solution and water, and dried. Removal of the solvent and subsequent distillation gave 550 mg. of an oil, b. p. ca. 80°C (2 mmHg), $\lambda_{max}^{MeOH}$ 233 mμ (log ε: 4.37), 312 mμ (log ε: 3.90). Heating of this oil (100 mg.) with 80% hydrazine hydrate (0.25 ml.) for 2 hr. under reflux afforded 90 mg. of yellow crystals, m. p. 40~60°C. Recrystallization from a mixture of benzene and petroleum ether gave yellow prisms, m. p. 88°C, undepressed on admixture with 2-amino-7-isopropyltropone[9].

**2-Methylcycloheptadienone (XI).**—A solution of 2.4 g. of tropone in 30 ml. of absolute ether was added to 2.2 mol. equiv. of Grignard reagent prepared from 7.5 g. of methyl iodide and 1.2 g. of magnesium, at 0°C and the reaction mixture was treated as in the case of II. On evaporation of the solvent, 1.7 g. of pale yellow oil was obtained. Distillation in vacuo gave three fractions: i) b. p. below 60°C (2 mmHg), trace; ii) b. p. 60~65°C (2 mmHg), 1.0 g. (38%), $n_D^{14}$ 1.480; iii) b. p. above 65°C (2 mmHg), trace.

Found [for fraction (ii)]: C, 77.42; H, 8.04. Calcd. for $C_8H_{10}O$: C, 78.65; H, 8.25%.

**Hydrogenation of XI.** — XI (500 mg.) in 10 ml. of acetic acid was hydrogenated at 1 atm. and 18°C with prereduced platinum oxide. After 100 min., 122 ml. (2.2 mol. equiv.) of hydrogen was absorbed. The catalyst was removed by filtration and the filtrate was diluted with water, extracted with petroleum ether, washed and dried. Removal of the solvent gave a volatile oil, which gave semicarbazone, m. p. 118°C on allowing to stand with semicarbazide for 20 days at room temperature, undepressed 2-methylcycloheptanone[14].

**2-Methyltropone by Bromination of XI.** — To a solution of 500 mg. of XI in 10 ml. of carbon tetrachloride was added with stirring a solution of bromine into carbon tetrachloride, by which 1.4 mol. equiv. of bromine was easily absorbed. Treatment of the reaction mixture as in the case of IX afforded 500 mg. (60%) of crystals, decomp. 135°C, $\lambda_{max}^{MeOH}$ 232, 315 mμ, similar with that of 2-methyltropone hydrochloride. Neutralization of these crystals (100 mg.) with saturated sodium bicarbonate solution gave an oil, which afforded picrate, m. p. 126~127°C (60 mg.). Recrystallization from ethanol gave yellow crystals, m. p. 127~128°C, undepressed on admixture with those of 2-methyltropone[10].

**Formation of 2-Methyltropone by Dehydrogenation of XI with Selenium Dioxide.**—A solution of 300 mg. of XI in 3 ml. of dioxane was refluxed with 163 mg. (1.2 mol. equiv.) of selenium dioxide for half an hour. Deposited selenium contaminated with tar (80 mg.) was filtered off and similar treatment of the mother liquor as in the case of X afforded 180 mg. of an oil (60%) which gave picrate m. p. 127~128°C, identical with that of 2-methyltropone[10].

The authors thank to Professor T. Isobe for NMR spectra measurement and his kind discussions thereof. Expenses for the present series of experiments were defrayed by a Grant in Aid for Scientific Research from the Ministry of Education.

*Department of Chemistry*
*Faculty of Science*
*Tohoku University*
*Katahira-cho, Sendai*

13) S. Seto, *Sci. Repts. Tohoku Univ.*, I, 37, 292 (1953).

14) D. N. Adamson and J. Kenner, *J. Chem. Soc.*, **1939**, 181.

# *Reaction of Hydrogen Peroxide on Fatty Acid Esters under Pressure. III. Oxidation of Methyl 9, 10-Dihydroxystearate*

By Hiromu KAMEOKA

(Received June 4, 1960)

The reaction of hydrogen peroxide on methyl oleate[1] and on saturated fatty acid methyl esters[2] under pressure has already been reported in detail. The present research was carried out with the intention of finding the kinds of compounds formed by the action of hydrogen peroxide on methyl 9, 10-dihydroxystearate produced by the oxidation of methyl oleate with potassium permanganate and of following up the course of the reaction in the oxidation with hydrogen peroxide as mentioned above.

When methyl oleate is oxidized under pressure by the use of hydrogen peroxide, the position between 9 and 10 having a double bond is oxidized. In this case, however, the formation of 9, 10-dihydroxystearic acid is not observed, but substances coming from cutting off the carbon chain of methyl oleate at the position between 9 and 10 are formed. Moreover, various lower homologues of monobasic and dibasic fatty acid are formed. These are presumably produced by the oxidation at the other position of the carbon chain.

Expecting that the position between 9 and 10 where a double bond exists initially in methyl oleate is most liable to be oxidized in the oxidation of methyl 9, 10-dihydroxystearate and consequently $C_9$-aldehyde and $C_9$-fatty acid may be formed with relatively good yields. Methyl 9, 10-dihydroxystearate was subjected to the action of a 30% hydrogen peroxide solution under pressure.

The results obtained in this reaction were like those in the oxidation of saturated fatty acid methyl esters under a similar condition, excepting that the position between 9 and 10 was oxidized.

## Experimental

**Methyl 9, 10-Dihydroxystearate.** — Commercial oleic acid was separated into solid acid and liquid acid through the lead-salt-ethanol process. The liquid acid was converted into lithium salt. This

1) H. Kameoka, *J. Chem. Soc. Japan, Ind. Chem. Sec.* (*Kogyo Kagaku Zasshi*), **63**, 741 (1960).
2) H. Kameoka, ibid., **63**, 744 (1960).

lithium salt, insoluble in a 50% ethanol solution, was filtered out and then changed to free fatty acid. The free fatty acid was subjected to the fractional distillation in a current of carbon dioxide gas three times. The distillate at the distillation temperature of 163~165°C/1 mmHg was oxidized in an aqueous alkaline solution of potassium permanganate, and sulfur dioxide gas was passed into the solution. After filtrating the aqueous solution, the remaining white substance was thoroughly washed with petroleum ether. This substance was recrystallized from a solution of 80% ethanol several times. The resulting crystalline substance having its melting point at 131~132°C and its neutralization value at 177.0 was esterified with methanol and sulfuric acid. The ester was recrystallized from an 80% ethanol solution once more. The ester thus prepared had an acid value 0.0, a saponification value 167.2, a hydroxyl value 334.5 and a melting point 104~105°C, and it was used as the sample of this research.

**Hydrogen Peroxide.**—A 30% solution was used.

**Reaction under Pressure.**—The sample (methyl 9, 10-dihydroxystearate) and a 30% hydrogen peroxide solution were enclosed in an autoclave (a capacity of 100 cc.) made of stainless steel, having an electromagnetic stirrer. The initial pressure in each test was maintained at 0 kg./cm². By heating the autoclave, the inside temperature and pressure of it were raised. In this case, heating was controlled in such a way that it may take about 1.5 hr. to reach the temperature shown in Table I, and the pressure was also raised up to the values given in Table I. The reaction time indicates the length of time held within the range of these temperatures and pressures. The conditions of reaction are shown in Table I.

**Treatment of the Reaction Products.** — Having been allowed to stand overnight after the completion of the reaction, the autoclave was opened. The reaction mixture was taken into a separating funnel. The interior of the autoclave was then thoroughly washed with distilled water and petroleum ether. The washing solutions used were also taken into the separating funnel. The content in the separating funnel was extracted with petroleum ether. In this way the content was separated into the soluble portion [A] and the insoluble portion [B].

As the petroleum ether soluble portion [A], a rather viscous oily substance was obtained after entirely removing the petroleum ether by distillation. This substance, after its constants were measured,

Table I. Conditions of reaction

| Reaction No. | Sample wt., g. | 30% $H_2O_2$ g. | Initial press. kg./cm² | Press. kg./cm² | Temp. °C | Final press. kg./cm² | Reaction time min. | Stir. r. p. m. |
|---|---|---|---|---|---|---|---|---|
| 1 | 5.0 | 50 | 0 | 65~ 80 | 100~110 | 40 | 90 | 60 |
| 2 | 5.0 | 50 | 0 | 110~120 | 130~140 | 75 | 120 | 60 |
| 3 | 5.0 | 60 | 0 | 130~145 | 138~146 | 65 | 120 | 60 |
| 4 | 5.0 | 50 | 0 | 115~120 | 145~155 | 70 | 180 | 60 |
| 5 | 6.8 | 50 | 0 | 110~125 | 145~155 | 65 | 180 | 60 |
| 6 | 10.2 | 50 | 0 | 100~110 | 125~140 | 60 | 120 | 60 |
| 7 | 10.2 | 50 | 0 | 120~135 | 140~150 | 60 | 180 | 60 |

Table II. Table of the systematic separation of the reaction products

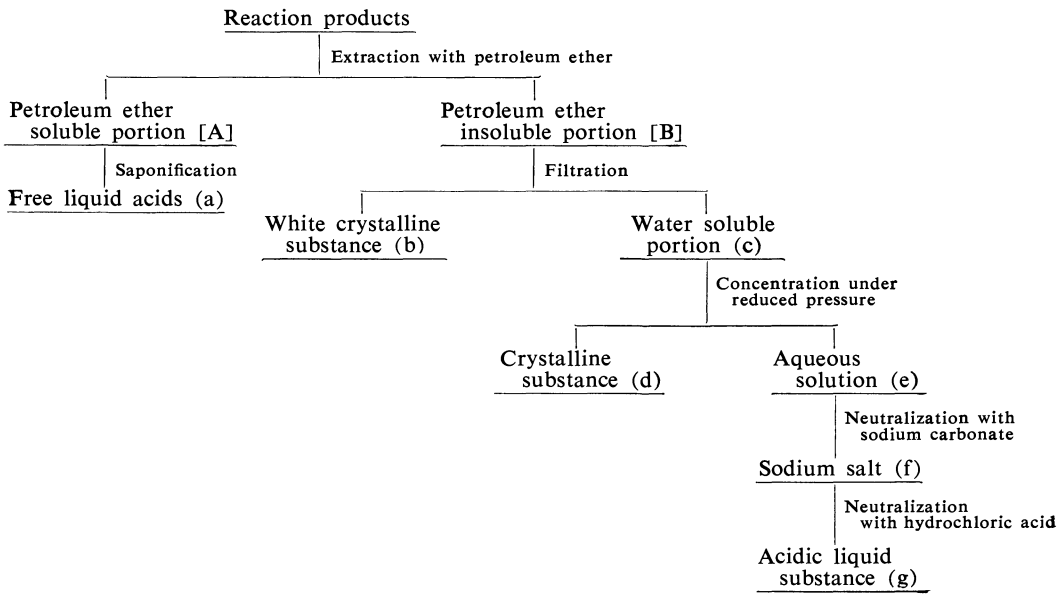


TABLE III. FRACTION (a). FREE ACID (Reaction No. 7, sample of fractional dist. 1.8 g.)

| Fraction No. | Temp. of dist., °C/mmHg | Yield g. | N. v. | $R_f$ value | Fatty acids detected |
|---|---|---|---|---|---|
| 1 | ~170 | 0.2 | 605.3 | * 0.69, 0.82 | $C_3$, $C_4$-monobasic |
| 2 | 170~210 | 0.3 | 461.9 | * 0.82, 0.90, 0.96 | $C_4$, $C_6$, $C_8$-monobasic |
| 3 | 120~140/15 | 0.6 | 365.6 | * 0.90, 0.95<br>△ 0.59 | $C_6$, $C_8$-monobasic<br>$C_9$-monobasic |
| 4 | 140~160/15 | 0.4 | 305.3 | △ 0.66, 0.59, 0.54 | $C_8$, $C_9$, $C_{10}$-monobasic |
| 5 | 160~170/15 | 0.2 | 279.6 | △ 0.54, 0.44 | $C_{10}$, $C_{12}$-monobasic |
| 6 | Residue | 0.1 | — | △ 0.44 | $C_{12}$-monobasic |

Paper chromatography: * Monobasic $C_2$~$C_8$-fatty acid, through the hydroxamic acid process[3]. —One-dimensional ascending method; development solvent, butanol saturated with water; filter paper, Toyo. No. 2; development temperature, 30°C; coloring matter, 10% ferric chloride-ethanol solution. △ Members above monobasic $C_8$-fatty acid, through the 2,4-dinitrophenylhydrazide process[4]. —One-dimensional ascending method; development solvent, methanol-acetic acid-tetraline; stationary phase, tetraline; filter paper, Toyo. No. 2; development temperature, 30°C; coloring matter, 0.5 N potassium hydroxide ethanol solution.

TABLE IV. FRACTION (d). CRYSTALLINE SUBSTANCE
(through fractional crystallization, sample 2.5 g.)

| Cryst., No. | Yield, g. | N. v. | M. p., °C | $R_f$ value | Fatty acids detected |
|---|---|---|---|---|---|
| 1 | 0.8 | 943.9 | 180~183 | □ 0.67 | $C_4$-dibasic |
| 2 | 1.2 | 763.5 | 150~153 | □ 0.88 | $C_6$-dibasic |
| 3 | 0.4 | 651.0 | 110~131 | □ 0.88<br>○ 0.48 | $C_6$-dibasic<br>$C_9$-dibasic |
| 4 | 0.1 | — | — | □ 0.89<br>○ 0.48 | $C_6$-dibasic<br>$C_9$-dibasic |

Paper chromatography: □ Dibasic $C_2$~$C_6$-fatty acid, through the chloroform-acetic acid-water process[5]. —One-dimensional ascending method; development solvent, chloroform-acetic acid-water; filter paper, Toyo. No. 2; development temperature, 20°C; coloring matter, 0.1% bromocresol-green-ethanol solution. ○ Members above dibasic $C_6$-fatty acid, through the petroleum ether-chloroform-acetic acid process[6]. —One-dimensional ascending method; development solvent, petroleum ether-chloroform-acetic acid; filter paper, Toyo. No. 2; development temperature, 20°C; coloring matter, 0.1% bromocresolgreen-ethanol solution.

was saponified to convert it into free fatty acids (a).

The petroleum ether insoluble portion [B] was spontaneously separated to a white crystalline substance (b) and a water-soluble portion (c). The crystalline substance b, which was filtered out from c, was washed with distilled water several times and the washing water used was added to c. The whole of c was concentrated under 20 mmHg pressure. In this case c was separated into an aqueous solution (e) and the crystalline substance (d). The aqueous solution (e) showing itself to be acidic was neutralized by the use of a 1% aqueous solution of sodium carbonate. By concentrating this solution, a solid sodium salt (f) was obtained. The salt f was acidified with hydrochloric acid, and then extracted with a large amount of ether. After removing the ether by distillation, an acidic liquid substance (g) was obtained. Examination was made about the substances separated through the process mentioned above respectively. In Table II, the treating procedure of the reaction products are represented.

**Petroleum Ether Soluble Portion** [A]. — This portion is a rather viscous oily substance and is fragrant. It being presumable that pelargonic aldehyde produced by the breakage between the positions of 9 and 10 may exist in the portion A, this portion was tested to see whether it may form an adduct of sodium bisulfite by the ordinary process or not. However, this test did not give any positive result. Then, a 2 N hydrochloric acid solution of 2,4-dinitrophenylhydrazine was added to the portion A. In this case, a very small amount of yellowish orange precipitates was obtained, the amount of which was not sufficient for identification.

This portion A was next converted to the free acid by saponification with a 5% alcoholic potassium hydroxide solution. The free acid thus obtained was subjected to fractional distillation and the constants of the distillates were measured. The result of Reaction No. 7 is given in Table III.

Each of the portion A obtained in Reactions No. 1—No. 6 was similarly subjected to fractional distillation. Almost the same result as that of Reaction No. 7 was obtained. Moreover, as the hydroxyl value of the portion A was all zero, this portion has no hydroxy compound.

3) Y. Inoue and M. Noda, *J. Japan Oil Chemist's Soc.* (*Yukagaku*), **1**, 136 (1952).
4) Y. Inoue and M. Noda, *Bull. Agr. Chem. Soc. Japan*, **19**, 214 (1955).
5) M. Kobayashi, *J. Japan Oil Chemist's Soc.* (*Yukagaku*), **4**, 53 (1955).
6) M. Kobayashi, ibid., **5**, 85 (1956).

Table V. Fraction (g). Acidic liquid substance
(sample of the fractional distillation, 1.5 g.)

| Fraction No. | Temp. of dist., °C | Yield g. | N. v. | $R_f$ value | Fatty acids detected |
|---|---|---|---|---|---|
| 1 | ~120 | 0.5 | 930.6 | * 0.50 | $C_2$-monobasic |
| 2 | 120~145 | 0.4 | 759.6 | * 0.50, 0.68 | $C_2$, $C_3$-monobasic |
| 3 | 145~165 | 0.4 | 633.0 | * 0.68, 0.82 | $C_3$, $C_4$-monobasic |
| 4 | Residue | 0.2 | 595.1 | * 0.82 | $C_4$-monobasic |

Paper chromatography: * Hydroxamic acid process[3].

**Petroleum Ether Insoluble Portion [B].**—*Crystalline Substance (d) Contained in the Water Soluble Portion (c).*—The substance is assumed to be dibasic acid from its good solubility in water, and good crystallizable property. This crystalline substance was fractionally crystallized from a 10% ethanol solution, and the crystals shown in Table IV were obtained in the case of Reaction No. 7.

The fraction d obtained in Reactions No. 1—No. 6 was similarly subjected to the fractional crystallization with almost the same result as that mentioned above. In cases of the oxidizing conditions as in Reactions No. 1, No. 3 and No. 6, the formation of low members of dibasic acid such as $C_2$ and $C_3$ was observed.

Each acid thus separated has nearly an equal neutralization value to the corresponding pure acid. Furthermore, no depression of the melting point was observed when each acid was subjected to the mixed melting point determination.

*The Sodium Salt (f) and the Acidic Liquid Substance (g).* — The substance g obtained from the salt f was fractionally distilled, and inquiries were made about the respective fractions. The result of Reaction No. 7 is shown in Table V.

In the result shown above, the neutralization values of fractions No. 1, No. 2 and No. 3 were nearly equal to those of acetic, propionic and butyric acids, 934.5, 757.4 and 637.1, respectively. Accordingly it may be confirmed that the main components of these fractions are acetic, propionic and butyric acids. The results of the fractional distillation of g obtained in Reactions No. 1—No. 6 were almost the same as the above. Furthermore, from the result of paper chromatography[3] (hydroxamic acid process: $R_f$ value 0.90) it was observed that small quantities of monobasic $C_6$ fatty acid were contained in g obtained in Reactions No. 1—No. 3.

*White Crystalline Substance (b).*—This substance is insoluble in water and petroleum ether. From its saponification value, hydroxyl value and melting point in addition to the insolubility nature mentioned above, this substance seemed to be non-oxidized methyl 9,10-dihydroxy stearate (Table VI). Furthermore, because of its slightly higher acid value and the considerably wide range of its melting point, the formation of free 9,10-dihydroxystearic acid due to the partial hydrolysis of the ester is presumable. Accordingly, this was saponified, and the melting point of 130~132°C and the neutralization value of 175~176 were obtained for the resulting acid. No depression of the melting point was observed when mixed with 9,10-dihydroxystearic acid. Moreover, the substance b was subjected to paper chromatography[5,6]. No existence of dibasic acid in it, however, was observed.

## Results

The yields and constants of the separated substances, and the results concerning them in paper chromatography are summarized in Table VI.

As shown in Table VI, lower members of monobasic acid were mainly detected in the portion A. Water soluble lower members of monobasic and dibasic acid and unchanged methyl 9, 10-dihydroxystearate were detected in the portion B. Further, it was found that under the reaction conditions as in Reactions No. 3, No. 4 and No. 5, more than 80% of the methyl 9, 10-dihydroxystearate used was oxidized.

## Discussion

In the present experiments, the reaction products, except the nonoxidized substance, had no hydroxyl value. This fact indicates that the hydroxyl group of the initial sample was removed during the oxidation with hydrogen peroxide.

Furthermore, from the fact that monobasic $C_9$-acid and dibasic $C_9$-acid were present in the portion A and also in the fraction d, it is clear that the positions of 9 and 10 where the hydroxyl group was initially located are oxidized. The production of the only small quantity of $C_9$-compounds by breakage at this position is probably explained by the consideration that this position is first attacked by oxygen and $C_9$-compounds are produced, but the resulting substances are immediately oxidized, and the compounds of smaller carbon numbers are formed. It is evident that lower monobasic acids than $C_{10}$ are liable to be oxidized with hydrogen peroxide[7]. Alternatively, it is considered that other positions of the carbon chain are simultaneously split by the oxidation. This fact is clearly found from the formation of $C_{12}$, $C_{10}$-acids and/or lower acids. In case

7) H. Kameoka, ibid., 9, 351 (1960).

TABLE VI. REACTION PRODUCTS

| Reaction No. | Petroleum ether soluble portion [A] | | | Petroleum ether insoluble portion [B] | | | | | | | | | | | |
|---|---|---|---|---|---|---|---|---|---|---|---|---|---|---|---|
| | | | | Water soluble portion (c) | | | | | | | White crystalline substance (b) | | | | |
| | | | | Crystalline substance (d) | | | Aqueous solution (e) | | | | | | | | |
| | | | | | | | | Acidic liquid substance, g. | | | | | | | |
| | Yield g. | N. v. | Fatty acids detected *, △ | Yield g. | N. v. | Acids detected □, ○ | Na-salt (f) g. | Yield g. | N. v. | Acids detected, * | Weight g. | A. v. | S. v. | M. p., °C | Acids detected |
| 1 | 1.5 | 235.7 | $C_{18}$, $C_{12}$, $C_{10}$, $C_9$, $C_8$, $C_6$, $C_4$-monobasic | 0.6 | 589.3 | $C_2$, $C_3$, $C_4$, $C_6$, $C_9$-dibasic | 1.3 | 0.3 | 320.9 | $C_2$, $C_3$, $C_4$, $C_6$-monobasic | 2.5 | 72.1 | 177.6 | 110～119 | Methyl 9,10-dihydroxy-stearate |
| 2 | 1.0 | 307.1 | $C_{18}$, $C_{12}$, $C_{10}$, $C_9$, $C_8$, $C_6$, $C_4$-monobasic | 1.1 | 659.9 | $C_4$, $C_6$, $C_9$-dibasic | 1.9 | 1.0 | 559.7 | $C_2$, $C_3$, $C_4$, $C_6$-monobasic | 1.7 | 55.8 | 188.4 | 89～ 96 | 〃 |
| 3 | 1.2 | 346.1 | $C_{12}$, $C_{10}$, $C_9$, $C_8$, $C_4$, $C_3$, $C_2$-monobasic | 1.8 | 603.2 | $C_2$, $C_3$, $C_4$, $C_6$, $C_9$-dibasic | 2.8 | 1.4 | 735.2 | $C_2$, $C_3$, $C_4$, $C_6$-monobasic | 0.5 | 43.0 | 186.8 | 94～104 | 〃 |
| 4 | 1.2 | 306.6 | $C_{12}$, $C_{10}$, $C_9$, $C_8$, $C_4$, $C_3$, $C_2$-monobasic | 1.7 | 594.8 | $C_4$, $C_6$, $C_9$-dibasic | 1.9 | 0.9 | 783.6 | $C_2$, $C_3$, $C_4$-monobasic | 1.0 | 47.1 | 180.6 | 88～104 | 〃 |
| 5 | 1.7 | 321.5 | $C_{12}$, $C_{10}$, $C_9$, $C_8$, $C_6$, $C_4$, $C_3$-monobasic | 2.1 | 615.0 | $C_4$, $C_6$, $C_9$-dibasic | 2.8 | 1.4 | 755.0 | $C_2$, $C_3$, $C_4$-monobasic | 1.4 | 39.8 | 176.5 | 92～104 | 〃 |
| 6 | 1.9 | 331.2 | $C_{12}$, $C_{10}$, $C_9$, $C_8$, $C_6$, $C_4$-monobasic | 2.0 | 605.1 | $C_3$, $C_4$, $C_6$, $C_9$-dibasic | 3.4 | 1.7 | 743.0 | $C_2$, $C_3$, $C_4$-monobasic | 4.3 | 40.5 | 179.8 | 93～104 | 〃 |
| 7 | 2.3 | 332.4 | $C_{12}$, $C_{10}$, $C_9$, $C_8$, $C_6$, $C_4$, $C_3$-monobasic | 3.2 | 590.6 | $C_4$, $C_6$, $C_9$-dibasic | 3.8 | 1.8 | 780.6 | $C_2$, $C_3$, $C_4$-monobasic | 2.5 | 43.6 | 181.5 | 89～104 | 〃 |

Paper chromatography: * hydroxamic acid process[3]; △ 2,4-dinitrophenylhydrazide process[4]; □ chloroform-acetic acid-water process[5]; ○ petroleum ether-chloroform-acetic acid process[6].

of the formation of $C_{12}$, $C_{10}$-acids, hydroxy acids were not obtained. The mechanism concerning no formation of hydroxy acid has not yet been available.

The formation of considerably large amount of $C_4$- and $C_6$-dibasic acids was observed. These products should result from (i) the further oxidation of the substances produced by the breakage of the bond between 9 and 10, and (ii) the secondary oxidation of monobasic $C_{12}$- and $C_{10}$-acids which are produced by the direct oxidation of methyl 9, 10-dihydroxystearate. The formation of considerably quantities of dibasic acids will be ascribed to the oxidation of the methyl group of the lower monobasic acids produced by the direct oxidation mentioned above. Moreover, in case of the oxidizing conditions as in Reactions No. 1, No. 3 and No. 6, the formation of lower members of dibasic acid such as $C_2$ and $C_3$ was recognized. These $C_2$- and $C_3$-dibasic acids may probably be formed under other conditions of reaction. Because of the easy decomposition of these dibasic acids, however, they will be decomposed when the reaction conditions are intense. Furthermore, it is considered that the formation of various lower homologues of fatty acid is due to the same oxidation course as that of the saturated fatty acid methyl ester[2] irrespective of the hydroxyl groups present in the sample molecule.

In short, in the oxidation of methyl 9, 10-dihydroxystearate with hydrogen peroxide, the following reactions will be presumed. That is, the positions 9, 10 containing hydroxyl groups are first oxidized, and the products of such oxidation are subjected to the secondary oxidation, and also there occurs the other reaction following the course of the oxidation similar to that of the saturated acid.

## Summary

Methyl 9, 10-dihydroxystearate is oxidized with a 30% hydrogen peroxide solution, under such conditions as the mole ratio of methyl 9, 10-dihydroxystearate to hydrogen peroxide is one to fifteen or more, the reaction time 2 hr., the temperature 138~155°C, and the pressure 110~145 kg./cm$^2$. Also, it was recognized that 80% or more of methyl 9, 10-dihydroxystearate was oxidized.

As the oxidation products, acetic, propionic, butyric, caproic, caprilic, pelargonic, caprinic and lauric acids were obtained as monobasic acids, and oxalic, malonic, succinic, adipic and azelaic acids were also produced as dibasic acids. Especially, succinic and adipic acids were obtained with good yield.

The author wishes to express his hearty thanks to Professor N. Hirao for his kind guidance and encouragement for the present work.

*Faculty of Science and Engineering*
*Kinki University*
*Fuse-shi, Osaka*

# *Polymerization of Allyl Chloride by Ziegler's Catalyst**

By Shunsuke MURAHASHI, Shun'ichi NOZAKURA and Kōichi HATADA

(Received July 11, 1960)

In recent years many papers have been published on the stereospecific polymerization of $\alpha$-olefins by Ziegler's catalyst. However it is well known that the catalyst, by itself, has little effect on the stereospecific polymerization of monomers containing any heteroatom, such as oxygen, nitrogen, sulfur or halogen, except only vinyl butyl ether, a stereospecific polymerization of which was found by Natta[1].

An attempt was made on the polymerization by Ziegler's type catalysts with allyl chloride as a monomer containing heteroatom. Since allyl chloride was first polymerized by Staudinger[2] to a syrupy low polymer, many investigations were done on the polymerization of this monomer, but no solid polymer has been obtained due to the "degradative chain transfer"[3] in its radical polymerization.

By Ziegler's type catalysts allyl chloride

* Presented at the 5th Meeting on High Polymer Chemistry, Kōbe, June, 1959.

1) G. Natta et al., *Angew. Chem.*, **71**, 205 (1959).

2) H. Staudinger and Th. Tleitmann, *Ann.*, **480**, 92 (1930).

3) P. D. Bartlett and R. Alschul, *J. Am. Chem. Soc.*, **67**, 812, 816 (1945). F. M. Lewis and F. R. Mayo, *J. Am. Chem. Soc.*, **76**, 457 (1954).

reacted rather rapidly at low temperatures with evolution of hydrogen chloride and gave a solid polymeric material. In the polymer produced the chlorine content was very much reduced for polyallyl chloride $[C_3H_5Cl]_n$ and indications of some unsaturation were observed. It was found that the polymerization took place only with catalysts having Al-Cl bond. Furthermore, the polymerization was accelerated by the presence of a small amount of benzene, which incorporated in the polymer.

On the basis of these results it was concluded that the polymerization of allyl chloride with Ziegler's type catalysts does not proceed by an anionic mechanism which is characteristic of these catalysts, but occurs with a some Friedel-Crafts type reaction caused by compounds such as $Et_2AlCl$, $EtAlCl_2$ or $AlCl_3$ formed in the reaction mixture. Also a cationic mechanism is likely to contribute simultaneously to the polymerization.

Similar results were obtained with the polymerization using allyl fluoride, allyl bromide, and 3, 3, 3-trichloropropene-1 as the monomer, respectivey.

## Experimental

**Materials.** — *Allyl Chloride.* — Commercial allyl chloride was purified by distillation and a fraction of b. p. 44.0~45.0°C was used.

*Allyl Bromide.* — Synthesized according to Kamm and Marvel[4]. B. p. 70°C.

*Allyl Iodide.* — Prepared from allyl chloride and sodium iodide as described by Letsinger and Traynham[5]. B. p. 48°C/108 mmHg.

*Allyl Fluoride.*—Prepared from silver fluoride and allyl iodide[6], and collected in a trap cooled in a dry ice-acetone bath. An infrared absorption spectrum of the gaseous sample was shown in Fig. 2.

*3,3,3-Trichloro-1-propene.* (*Nippon Soda Co.*). — Distilled and a fraction of b. p. 50~53°C/80 mmHg was used.

*n-Hexane.* — Purified in the usual manner and stored over metallic sodium.

*Triethylaluminum.* — Supplied by Mitsui Chem. Ind. Co. and was used as a solution in *n*-heptane.

*Titanium Tetrachloride.*—Supplied by Osaka Titanium Co. and was used as a solution in *n*-heptane.

**Apparatus.** — A 50 ml. five-necked flask[7] fitted with a thermometer, a stirrer, a nitrogen gas inlet tube and two silicone rubber caps was used as the polymerization vessel. Catalyst components, monomer, and solvent were introduced into the vessel through rubber caps with a hypodermic syringe.

**Preparation of Catalysts.**—After the vessel was flushed by dry nitrogen, 20 ml. of *n*-hexane and 0.25 g. of titanium tetrachloride were introduced. With boiling the mixture gently, 0.15 g. of $AlEt_3$ was slowly added dropwise, and heating was continued for further 5 min. and cooled. After precipitating the solid catalyst complex the supernatant liquid was removed by a syringe under dry nitrogen. The catalyst was washed three times with 20 ml. of *n*-hexane, and then 20 ml. of *n*-hexane and 0.15 g. of $AlEt_3$ was added.

Other catalysts of Ziegler's type were prepared in the same manner but the wash procedure was omitted.

**Polymerization.** — The catalyst was cooled to the polymerization temperature in a dry ice-acetone bath and with stirring the monomer was slowly added dropwise. The reaction was exothermic and the heat evolved spontaneously at or after the addition of the monomer, when deep cooling was required to keep the temperature constant. After three to five hours the reaction was stopped by adding 10 ml. of methanol containing a small amount of hydrochloric acid and the polymer was precipitated by pouring the mixture into about 300 ml. of methanol. After standing overnight the polymer was collected and washed with methanol, and dried in vacuo. The polymer was reprecipitated from its benzene solution by methanol.

Allyl fluoride was polymerized as follows. The monomer gas was introduced by a gas inlet tube bubbling through the catalyst suspension and the unreacted monomer was recycled through a trap cooled in dry ice-acetone bath.

**Double Bond Titration of Polymer.** — A known amount of polymer (about 0.05 g.) was dissolved in 8 ml. of carbon tetrachloride in a 100 ml. glass stoppered flask and 2 ml. of 0.5 N bromate-bromide solution and 1.3 ml. of 10% sulfuric acid were added. After shaking the mixture vigorously for three minutes 2 ml. of 20% aqueous potassium iodide solution were added and again the mixture was shaken vigorously for a minute. The liberated iodine was titrated by 0.1 N sodium thiosulfate solution with starch as an indicator.

**Reduction of Polymer with $LiAlH_4$.**—A polymer of allyl chloride (0.25 g.) polymerized by $AlEt_3$–$TiCl_4$ catalyst and containing 20.81% by weight of chlorine was reacted with 0.4 g. of $LiAlH_4$ in 30 ml. tetrahydrofuran. The reaction was carried out under dry nitrogen in a sealed tube with shaking for 150 hr. at 60°C. After cooling, the reaction mixture was poured into methanol containing nitric acid to decompose excess $LiAlH_4$. The precipitated polymer was collected, washed with methanol and dried in vacuo. The chlorine content of the product was 7.50% (by wt.).

## Results

The results were summarized in Tables I, II and III.

During the polymerization, especially in its initial stage, usually a sudden increase in temperature of the reaction mixture and a evolution of hydrogen chloride were observed, while the color of the catalyst turned to reddish brown gradually.

4) O. Kamm and C. S. Marvel, "Organic Syntheses", Coll. Vol. 1, (1956), p. 27.
5) R. L. Letsinger and J. G. Traynham, *J. Am. Chem. Soc.*, **70**, 2818 (1948).
6) M. H. Meslans, *Compt. rend.*, **111**, 882 (1890).
7) S. Murahashi, S. Nozakura, M. Sumi and K. Hatada, This Bulletin, **32**, 1094 (1959).

TABLE I. POLYMERIZATION OF ALLYL CHLORIDE WITH ZIEGLER'S CATALYST

Monomer: 5 ml. (4.70 g.), Catalyst: $AlEt_3$ 0.30 g. + $TiCl_4$ 0.25 g. ($AlEt_3/TiCl_4$=2 mol./mol.), Solvent: *n*-Hexane.

| Polymerization | | | Polymer | | | | |
|---|---|---|---|---|---|---|---|
| Temp. °C | Time hr. | Solvent ml. | Yield % | Cl-content*1 % | M. p. °C | $\eta_{sp}/C$*5 dl./g. | Double bond mol./$C_3$-unit |
| 20 | 3 | 15 | 29.3 | 12.53*2 | 73~ 75 | 0.043 | 0.16 |
| 0 | 5 | 20 | 9.9 | 20.61 | 80~ 81 | 0.035 | — |
| −10 | 5 | 20 | 9.1 | 19.55 | 85~ 86 | 0.040 | — |
| −20 | 5 | 20 | 9.6 | 21.40*3 | 89~ 91 | — | 0.17 |
| −30 | 5 | 45 | 7.1 | 18.26*4 | 105~108 | 0.081 | 0.13 |
| −70 | 170 | 20 | 1.5 | 22.25 | 73~ 75 | — | — |

*1 Theoretical value for poly(allyl chloride) $[-CH_2-CH(CH_2Cl)-]_n$: 46.33%.
*2 C, 74.64%; H, 9.20%; corresponding to $C_3H_{4.4}Cl_{0.17}$.
*3 C, 69.30%; H, 8.71%; corresponding to $C_3H_{4.5}Cl_{0.32}$.
*4 C, 73.21%; H, 8.66%; corresponding to $C_3H_{4.3}Cl_{0.25}$.
*5 Benzene solution (C=0.5 g./dl.) at 30°C.

TABLE II. POLYMERIZATION OF ALLYLHALIDES WITH ZIEGLER'S CATALYST

Catalyst: $AlEt_3$ 0.30 g. + $TiCl_4$ 0.25 g. ($AlEt_3/TiCl_4$=2 mol./mol.)
Solvent: *n*-Hexane.

| Monomer ml. | Polymerization | | Solvent ml. | Polymer | | | | |
|---|---|---|---|---|---|---|---|---|
| | Temp. °C | Time hr. | | Yield g. | Halogen content, % Found | Halogen content, % Theoretical | M. p. °C | $\eta_{sp}/C$(30°C) dl./g. |
| $CH_2$=CH-$CH_2F$ 1.0*1 | 50 | 45 | 20 | 0.030 | — | 31.63 | — | — |
| 3.2*1 | 25 | 7 | 25 | 0.050 | 3.2 | | 97~ 98 | — |
| 1.2*1 | −20 | 2.5 | 25 | 0.030 | 1.5 | | 75~ 77 | — |
| $CH_2$=CH-$CH_2Br$ 3.5 | −20 | 5 | 20 | 0.255 | 30.00*2 | 66.05 | 85~ 87 | 0.025 |
| $CH_2$=CH-$CH_2I$ 3.0 | −20 | 5 | 20 | trace | — | 75.55 | — | — |
| $CH_2$=CH-$CCl_3$ 2.0 | 20 | 5 | 20 | 0.180 | 35.28 | 73.14 | 135~140 | — |

*1 The quantities were shown as volumes at −80°C.
*2 C, 61.14%; H, 7.49%; corresponding to $C_3H_{4.4}Br_{0.22}$. Double bond 0.12 mol./$C_3$-unit.

The polymer obtained was a powder colored in faint yellow, having a melting point between 70~110°C and soluble in benzene, toluene, and tetrahydrofuran. Generally the chlorine content of the polymer was less than a half of the theoretical value (46.33%) for polyallyl chloride $[-CH_2-CH(CH_2Cl)-]_n$. The low viscosity of the polymer solution is indicative of the fairly low molecular weight of the polymer.

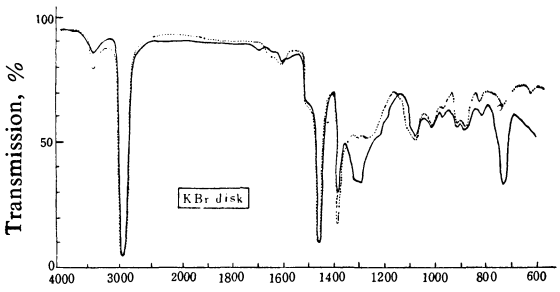



Fig. 1. Infrared absorption spectra of the polymer of allyl chloride (——) and its reduction product with $LiAlH_4$ (……).

Infrared spectra of a typical sample of the polymer and of its reduction product by lithium aluminum hydride were shown in Fig. 1. The absorption bands arising from C-Cl linkage appeared at 730 $cm^{-1}$ and about 1300 $cm^{-1}$, and the intensities were decreased with the reduced polymer. At 1378 $cm^{-1}$ and 1460 $cm^{-1}$ are located the absorption bands due to the presence of methyl and methylene groups, respectively. The former increased its intensity relatively to the latter by the reduction of the polymer, indicating the presence of $-CH_2Cl$ groups in the polymer. The bands in a region between 800 $cm^{-1}$ and 1000 $cm^{-1}$ seems to be characteristic of various types of double bonds. In addition to this spectral data the double bond titration of the polymer showed about 0.15 mol. unsaturations per monomer unit in general (Tabel I).

These polymers were shown to be amorphous by their X-ray diffractions.

The chlorine content of the polymer was independent of the polymerization temperature in the range between 0°C and −70°C, while the conversion was strongly depressed at −70°C. The melting point of the polymer and its solution viscosity in benzene decreased slightly with raising the polymerization temperature (Table I).

The polymerizations of allyl fluoride, allyl bromide and 3, 3, 3-trichloro-1-propene by $AlEt_3$-$TiCl_4$ catalyst gave similar solid polymers as obtained from allyl chloride and their halogen contents were also much less than the theoretical values calculated for the monomeric units (Table II). The polymers of allyl fluoride and allyl bromide gave the similar infrared absorption spectra as that given by the polymer of allyl chloride, but the very weak band at 1070 $cm^{-1}$ was considered to be of the C-F linkage in the former polymer (Fig 2). The band appeared to arise from the C-Br linkage was located at 569 $cm^{-1}$ in the polymer of allyl bromide.

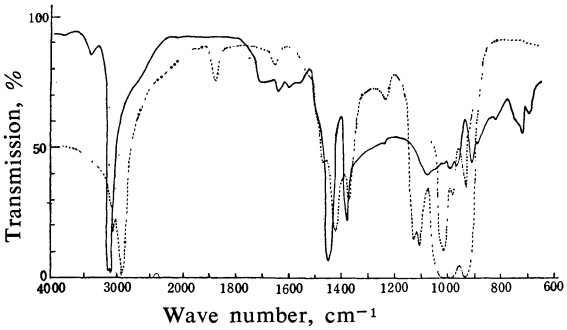



Fig. 2. Infrared absorption spectra of gaseous allyl fluoride (·····) and its polymer (—— KBr disk).

Allyl iodide gave no polymer by $AlEt_3$-$TiCl_4$ catalyst under the same condition as in the polymerization of allyl chloride.

Various types of catalysts were examined for the polymerization of allyl chloride (Table III). Among the Ziegler's type catalysts used, all the compounds having Al–Cl linkage, either the linkage was original or formed from the catalyst components, were capable of polymerizing allyl chloride. However, the catalysts such as $AlEt_3$-$Ti(OBu)_4$, LiBu-$TiCl_4$ and $ZnEt_2$ (ether solution)-$TiCl_4$ gave no polymer under similar or even more drastic conditions. It should be noted, however, that the catalyst prepared from $AlEt_3 \cdot Et_2O$ and $TiCl_4$ hardly polymerized allyl chloride, although the catalyst might have possibly Al–Cl linkage in it.

Of the catalyst for cationic polymerization, what possessed Al–Cl linkage also functioned as catalyst for the polymerization of allyl chloride, while no polymer was obtained with $TiCl_4$ and $BF_3 \cdot Et_2O$. On the other hand, all the basic catalysts examined, such as LiBu, $ZnEt_2$(ether solution) and $AlEt_3$, had no catalytic activity for the polymerization.

It was found that an addition of benzene to the reaction mixture caused remarkable increase in the polymer yield (Table III) and also in the evolution of hydrogen chloride during the polymerization. An infrared absorption spectrum of the yielded polymer (Fig. 3) showed absorption bands due to skeletal vibrations of a benzene ring at 1605

TABLE III. POLYMERIZATION OF ALLYL CHLORIDE WITH VARIOUS CATALYSTS

Monomer: 3.5 ml., Solvent: *n*-Hexane 25 ml., Polymerization temperature: −20°C, Polymerization time: 5 hr.

| Catalyst*6 | Benzene g. | Polymer: Yield % | Cl-content % | M. p. °C | $\eta_{sp}/C$*5 dl./g. | Double bond (mol./$C_3$-unit) |
|---|---|---|---|---|---|---|
| $AlEt_3$-$TiCl_3$ | 0 | 5.0*1 | 14.79 | 94～ 95 | 0.050 | — |
| $AlEt_3$-$VOCl_3$ | 0 | 6.4 | 18.71 | 86～ 89 | 0.043 | — |
| $AlEt_3 \cdot Et_2O$-$TiCl_4$ | 0 | 0.8 | — | — | — | — |
| $Et_2AlCl$-$TiCl_4$ | 0 | 10.8 | 19.20 | 83～ 85 | 0.050 | — |
| $Et_2AlCl$-$TiCl_4$ | 1.0 | 31.6*2 | 16.77 | 116～118 | 0.093 | 0.08 |
| $Et_2AlCl$ | 0 | 4.4 | 23.87 | 84～ 85 | 0.036 | — |
| $Et_2AlCl$ | 1.3 | 29.6*3 | 15.05 | 99～102 | 0.072 | 0.06 |
| $AlCl_3$ | 0 | 9.9 | 23.60 | 79～ 80 | 0.033 | — |
| $AlCl_3$ | 1.0 | 44.7*4 | 17.66 | — | — | — |

*1 Reaction time: 4 hr.

*2, *3, *4 Benzene-insoluble fractions were 31.7, 11.5, and 16.8%, based on the total amounts of polymers, respectively. The following data described above were obtained on the soluble fractions.

*5 Benzene solution (C=0.5 g./dl.) at 30°C.

*6 The ratios of the two components were unity, except 0.2 of $AlEt_3/TiCl_3$.

$cm^{-1}$ and 1498 $cm^{-1}$, indicating an existence of a benzene ring in the polymer chain. Furthermore, a part of this polymer was not soluble in any usual organic solvents and had no melting point even above 300°C, and was assumed to be a cross-linked polymer through benzene nuclei. The soluble fraction of this polymer had a higher melting point, a higher solution viscosity and a lower chlorine content, compared with the polymer formed under the same condition but without benzene.

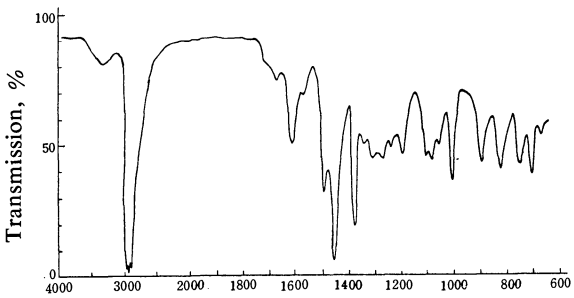



Fig. 3. Infrared absorption spectrum of the polymer of allyl chloride polymerized in the presence of benzene. KBr disk.

## Discussion

The results mentioned above reveals that the following features are involved in the polymerization of allyl chloride with Ziegler's type catalyst: a) An evolution of hydrogen chloride during the polymerization and a strongly reduced chlorine content of the resulting polymer. b) Only compounds containing Al-Cl bond such as $Et_2AlCl$, $EtAlCl_2$ and $AlCl_3$ function to polymerize allyl chloride. These compounds are powerful catalysts of Friedel-Crafts reaction. c) A marked increase in conversion with an addition of benzene to the system and an incorporation of benzene to the resulting polymer. d) An existence of double bonds in the polymer.

On the basis of these facts it is proposed that the Friedel-Crafts type reactions 1, 2 and 3 caused by a compound containing Al-Cl bond is essential in the polymerization of allyl chloride by Ziegler's type catalyst. It seems to be possible that a minor contribution of ordinary cationic processes 1 and 4 is involved and causes some complication in the reaction.

$$CH_2=CH-CH_2Cl + \dot{A}l\text{-}Cl$$

$$\longrightarrow CH_2=CH-\overset{+}{C}H_2\left[Cl\text{-}\dot{A}l\text{-}Cl\right]^- \quad (1)$$

$$CH_2=CH-\overset{+}{C}H_2\left[Cl\text{-}\dot{A}l\text{-}Cl\right]^- + CH_2=CH-CH_2Cl$$

$$\longrightarrow CH_2=CH-CH_2-CH=CH-\overset{+}{C}H_2\left[Cl\text{-}\dot{A}l\text{-}Cl\right]^- + HCl \quad (2)$$

or

$$CH_2=CH-CH_2-C(=CH_2)-\overset{+}{C}H_2\left[Cl\text{-}\dot{A}l\text{-}Cl\right]^- + HCl \quad (3)$$

$$CH_2=CH-\overset{+}{C}H_2\left[Cl\text{-}\dot{A}l\text{-}Cl\right]^- + CH_2=CH-CH_2Cl$$

$$\longrightarrow CH_2=CH-CH_2-CH_2-\overset{+}{C}H(CH_2Cl)\left[Cl\text{-}\dot{A}l\text{-}Cl\right]^- \quad (4)$$

The reaction may proceed in such a manner as follows: a slow first stage of the reaction catalyzed by a small amount of original species having Al-Cl linkage, such as $Et_2AlCl$, $EtAlCl_2$ or $AlCl_3$, is followed by a faster reaction owing to a gradual accumulation of these catalyst compound generated by a reaction between $AlEt_3$ and hydrogen chloride liberated during the polymerization, and this finally leads to a violent rise of temperature of the reaction mixture.

The fact that the polymerization is strongly accelerated by adding a small amount of benzene to the system is a further evidence for the Friedel-Crafts type mechanism of the polymerization reaction. The benzene may undergo a variety of reaction, thus forming cross-linkages in some extent between polymer chains and giving a rather large amount of insoluble fraction of the polymer.

Methyl groups in the polymer may be produced by the reactions as following scheme.

$$\sim\!\!C(=CH_2)\!\sim \xrightarrow{HCl} \sim\!\!C(Cl)(CH_3)\!\sim$$

$$\sim\!\!CH(CH_2Cl)\!\sim \xrightarrow{Et_3Al\ etc.} \sim\!\!CH(CH_3)\!\sim \text{ or } \sim\!\!CH(C_3H_7)\!\sim$$

In the case of $AlEt_3 \cdot Et_2O\text{-}TiCl_4$ catalyst, these components may also produce any compound such as $Et_2AlCl$, $EtAlCl_2$ or $AlCl_3$, but etherated. It is considered that the coordinated ether reduces the ionic character of the Al-Cl bond so strongly that the compound can not function as a catalyst for the Friedel-Crafts type reaction.

The authors wish to thank Mitsui Chem. Ind. Co. for the generous supply of triethylaluminum and Osaka Titanium Co. for titanium tetrachloride.

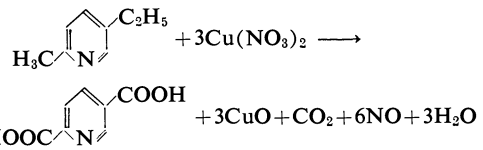
*Department of Chemistry*
*Faculty of Science*
*Osaka University*
*Nakanoshima, Osaka*

# *Oxidation of 2-Methyl 5-Ethyl Pyridine to Isocinchomeronic Acid*

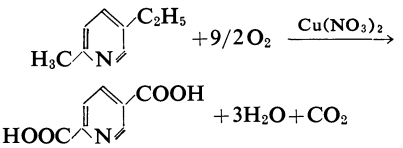
By Tokio KATO

(Received August 26, 1960)

In the preparation of isocinchomeronic acid (ICA) from 2-methyl 5-ethyl pyridine (MEP), several kinds of oxidizing reagents, such as sulfuric acid[1], selenium peroxide[2], nitric acid[3] and cupric nitrate[4] have been used. Cupric nitrate (with or without nitric acid) is said to give the highest yield of ICA among them, where this process consumes a large quantity of nitrate or nitric acid (more than 10 mol. as $NO_3$ to 1 mol. MEP oxidized).



MEP can not be oxidized with molecular oxygen as in the case of *p*-xylene with catalysts such as cobalt or manganese acetates. But the combined use of oxygen (a little more than theoretical moles for the oxidation of MEP) with cupric nitrate was found to be effective to obtain ICA (through its cupric salt) with a yield higher than 85 ml.% to MEP consumed, where the used cupric nitrate was easily recovered and reused.



## Experimental

**Materials.**—MEP of more than 98% purity was purchased from Carbide and Carbon Chem. Co. Ltd., and used without purification. Its specifications are as following; specific gravity (20°/20°), 0.918~0.922; b. p., 171~181°C (760 mmHg); water content, less than 0.2% by weight. Reaction vessel was 1 l. auto-clave (18:8 stainless steel) with magnetic stirrer.

**Oxidation.** — MEP, cupric nitrate (as 200 cc. aqueous solution) and oxygen were charged in the

TABLE I. REACTION VARIABLE IN THE OXIDATION OF MEP.

| Exp. No. | MEP mol. | $Cu(NO_3)_2$[a] mol. | Charged mol. ratio $Cu(NO_3)_2$/MEP | $N_2$[d]+$O_2$ atm. | $O_2$% by vol. | Duration min.[b] 180~200°C | 200~230°C |
|---|---|---|---|---|---|---|---|
| 1 | 0.149 | 0.79 | 5.30 | Not charged | | 10 | 200 |
| 2 | 〃 | 0.476 | 3.20 | 〃 | | 〃 | 〃 |
| 3 | 〃 | 0.155 | 1.04 | | | | |
| 4 | 0.197 | 0.203 | 〃 | 〃 | | 〃 | 〃 |
| 5 | 0.149 | 0.103 | 0.69 | 50 | 54 | 〃 | 130 |
| 6 | 〃 | 0.155 | 1.04 | 〃 | 55 | 3 | 100 |
| 7 | 〃 | 0.103[c5] | 0.69 | 〃 | 53 | 10 | 180 |
| 8 | 0.198 | 0.155 | 0.77 | 58 | 56 | 5 | 85 |
| 9 | 〃 | 〃 [c8] | 〃 | 〃 | 48 | 3 | 90 |
| 10 | 〃 | 〃 [c9] | 〃 | 〃 | 42 | 〃 | 120 |
| 11 | 0.197 | 0.203 | 1.04 | 〃 | 45 | 5 | 130 |
| 12 | 〃 | 〃 | 〃 | 〃 | 40 | 5 | 120 |
| 13 | 〃 | 〃 | 〃 | 50 | 44 | 〃 | 160 |
| 14 | 〃 | 〃 | 〃 | 53 | 50 | 30 | 95 |
| 15 | 〃 | 〃 | 〃 | 60 | 54 | 240 | 0 |
| 16 | 0.296 | 〃 | 0.69 | 90 | 48 | 30 | 180 |
| 17 | 〃 | 〃 [c16] | 〃 | 80 | 53 | 20 | 150 |

a) Used as 200 cc. aqueous solution in each experiments.
b) See Figs. 1, 2 and 3.
c) Recovered $Cu(NO_3)_2$ charged c5), c8), c9) and c16) mean recovered ones in Exps. No. 5, 8, 9 and 16 respectively.
d) Measured at 20°C before heating the vessel.

1) T. E. Jordan, *Ind. Eng. Chem.*, **44**, 332 (1952).
2) D. Jercher, *Chem. Ber.*, **88**, 156 (1955).
3) U. S. Pat. 2524957 (1950).
4) U. S. Pat. 2552268 (1951).

Table II. Results of experiments in Table I

| Exp. No. | $O_2$ Consumed moles mol. ratio $O_2$/MEP | | $CO_2$ Produced moles mol. ratio $CO_2$/MEP | | Cupric Isocinchomronate moles×2[a], % | yield[b] % | ICA Yield[b] % |
|---|---|---|---|---|---|---|---|
| 1 | Not charged | | 0.18 | 1.2 | Not charged | | 87 |
| 2 | 〃 | | 0.17 | 1.1 | 〃 | | 40 |
| 3 | 〃 | | 0.19 | 1.3 | 〃 | | 7 |
| 4 | 〃 | | 0.20 | 1.0 | 〃 | | 0 |
| 5 | 0.70 | 4.7 | 0.13 | 0.9 | 0.133 | 89 | 84 |
| 6 | 0.76 | 5.1 | 0.12 | 0.8 | 0.127 | 85 | 80 |
| 7 | 0·68 | 4.6 | 0.20 | 1.3 | 0.138 | 92 | 87 |
| 8 | 0.83 | 4.2 | 0.18 | 0·9 | 0.179 | 90 | 85 |
| 9 | 0.75 | 3.8 | 0.22 | 1.1 | 0.174 | 88 | 83 |
| 10 | 0.76 | 〃 | 0.24 | 1.2 | 0.179 | 90 | 85 |
| 11 | 0.87 | 4.4 | 0.20 | 1.0 | 0.180 | 91 | 86 |
| 12 | 0.80 | 3.9 | 0.16 | 0.8 | 〃 | 〃 | 〃 |
| 13 | 0.74 | 3.8 | 0.25 | 1.3 | 0.177 | 90 | 85 |
| 14 | 0.82 | 4.2 | 0.24 | 1.2 | 0.182 | 92 | 87 |
| 15 | 0.84 | 4.3 | 0.23 | 〃 | 0.181 | 〃 | 〃 |
| 16 | 1.27 | 〃 | 0.36 | 〃 | 0.278 | 94 | 88 |
| 17 | 1.25 | 4.2 | 0.33 | 1.1 | 0.279 | 〃 | 〃 |

a) 1 mol. of cupric salt is prepared from 2 mol. of MEP
b) Based upon consumed moles of MEP

Table III. Formation of ICA from its cupric salt

| Exp. No. | Aqueous soln. of NaOH Concn. of NaOH % by wt. | gr. | Mol. ratio NaOH/ICA | Conditions Temp. °C | Duration hr. | Moles | ICA Yield[a] % by wt. |
|---|---|---|---|---|---|---|---|
| 1 | 10 | 300 | 4.9 | 95 | 1.0 | 0.141 | 93 |
| 2 | 〃 | 200 | 3.3 | 〃 | 〃 | 0.143 | 94 |
| 3 | 〃 | 100 | 1.6 | 〃 | 〃 | 0.064 | 42 |
| 4 | 〃 | 〃 | 〃 | 〃 | 3.0 | 0.053 | 35 |
| 5 | 5 | 400 | 3.3 | 〃 | 1.0 | 0.145 | 95 |
| 6 | 〃 | 300 | 2.5 | 〃 | 〃 | 0.143 | 94 |
| 7 | 〃 | 〃 | 〃 | 75 | 〃 | 0.144 | 95 |

a) Based upon the cupric salt consumed, and in each Exp. 0.076 mol. (30.0 g.) of the cupric salt was used.

autoclave, where oxygen was diluted to less than 60% by volume with nitrogen. In some experiment, oxygen was not charged, in order to compare their results with that of other experiments, in which oxygen was used. The vessel was heated and its temperature was kept at 180~230°C, until oxygen was sufficiently absorbed to the oxidate and its pressure stopped dropping.

After the vessel was cooled to room temperature, the content of oxygen and carbon dioxide in the blowing gas was measured. The reaction product was filtered, where the deposit obtained was submitted to elementary analysis after being washed with water and dried in an air oven.

A certain quantity of the deposit was mixed and stirred with hot alkali aqueous solution, and copper was filtered off as cupric oxide from the solution.

Sodium salt of ICA (very soluble in water) formed in the filtrate was neutralized with concentrated aqueous hydrochloric acid, and white deposit liberated at pH 1.8~2.0, was also submitted to elementary analysis after being washed with water and dried in the air oven.

## Results and Discussion

Reaction variables in the oxidation of MEP and their results were shown in Tables I and II respectively.

With no oxygen charged as in Exps. 1—4, the cupric salt of I. C. A. in the reaction product was not pure, being mixed with other cupric salts such cupric oxide, cupric hydroxide, and cupric nitrite.

Furthermore the yield of ICA fell markedly with decrease of cupric nitrate charged.

In Exps. 5—17 with oxygen used, the deposits obtained were uniformly found to be pure cupric isocinchomeronate (2 mol. of isocinchomeronate combined with 1 mol. of $Cu^{2+}$).

Found: C, 42.09; H, 2.22; N, 7.02; Cu, 16.25. Calcd. for $(C_7H_4O_4N)_2Cu$: C, 42.49; H, 2.04; N, 7.08; Cu 16.05%.

With decrease of cupric nitrate charged, the yield was not lowerd (always not less than

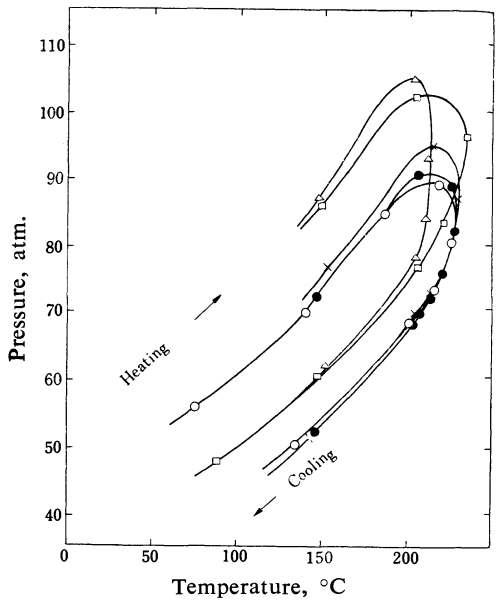



Fig. 1. Absorption of oxygen in the oxidation of MEP.
(Exp. Nos. 5—9) plotted per 30 min.
—○— No. 5 —△— No. 8
—×— 〃 6 —□— 〃 9
—●— 〃 7

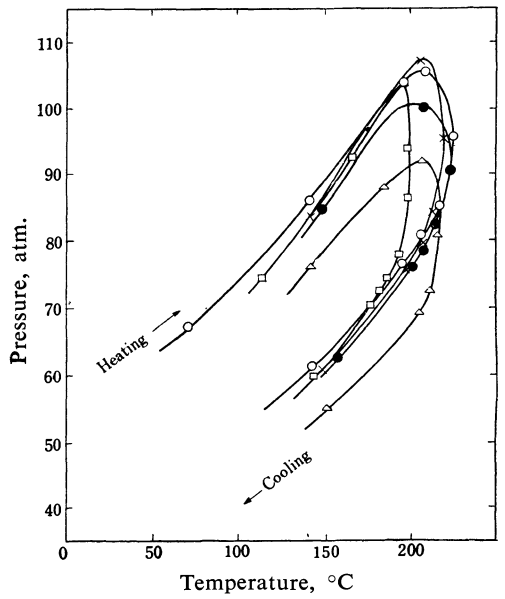



Fig. 2. Absorption of oxygen in the oxidation of MEP.
(Exp. Nos. 10—15) plotted per 30 min.
—○— No. 10 —△— No. 14
—×— 〃 11, 12 —□— 〃 15
—●— 〃 13

85 mol.% to MEP consumed), and any trace of nitrogen oxide or nitrogen dioxide was not detected in the reaction product and blowing gas. Cupric nitrate used was easily

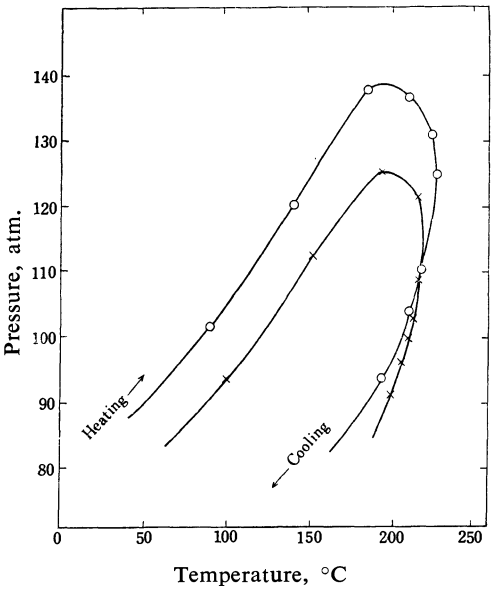



Fig. 3. Absorption of oxygen in the oxidation of MEP.
(Exp. 16 and 17) plotted per 30 min.
—○— No. 16 —×— No. 17

recovered by cupric oxide or cupric hydroxide being dissolved in the recovered filtrate and it was reused as in Exps. 7, 9, 10 and 17.

As shown in Figs. 1, 2 and 3, oxygen was absorbed at 180~230°C, where overheating was found to cause violent explosion. Molar ratio of oxygen consumed and carbon dioxide formed to that of MEP oxidized were approximately consistent to the theoretical values, 4.5 and 1.0 respectively. Based upon the results in Tables I, II and Figs. 1—3, the oxidation of MEP to cupric isocinchomeronate is considered to proceed as following;

$$C_2H_5(C_5NH_3)CH_3+9/2\,O_2+1/2\,Cu(NO_3)_2 \rightarrow$$
$$1/2(HOOC_5NH_3COO)_2Cu+3H_2O+CO_2+HNO_3$$

and oxygen only is consumed to oxidize MEP.

ICA prepared from its cupric salt, as shown in Table III, and its dimethyl ester melted at 237 and 164°C respectively, both of which agree with the values in the literature[5].

Isocinchomeronic acid in Table II.

Found: C, 49.98; H, 2.96; N, 8.34. Calcd. for $C_7H_5O_4N$: C, 50.34; H, 3.01; N, 8.38%.

The author is grateful to Dr. H. Sobue, Professor of Tokyo University, Dr. A. Tomita, Chief of the Laboratory Institute, and Dr. Y. Tsunoda for their valuable advice.

*Laboratory Institute*
*Tokai Electrode Mfg. Co.*
*Fujisawa, Kanagawa-ken*

5) Beilstein, Band 12, p. 154, 155.

# *The Crystal Structure of p-Aminobenzenearsonic Acid**

By Akira SHIMADA

(Received August 6, 1960)

The crystal structure of benzenearsonic acid has recently been reported by the present author[1] to reveal the molecular configuration of an organoarsenic compound and the hydrogen-bond formation in this crystal. In connection with the above work, the crystal structure of *p*-aminobenzenearsonic acid, $H_2N \cdot C_6H_4AsO(OH)_2$, was undertaken as a part of a program concerned with the crystal chemistry of organoarsenic compounds.

This study has another interest, since the sodium salt of this acid has always proved of great value in medicine under the name of "Atoxyl".

## Experimental

Suitable crystals for X-ray work were selected from the specimens kindly prepared and supplied by Professor H. Nakata of Konan University. They were colorless, transparent needles with a long dimension in the *b* direction. Oscillation and Weissenberg photographs were taken with Cu $K_\alpha$ radiation, and they showed that the unit cell is monoclinic with the following dimensions:

a=7.35 Å, b=6.35 Å, c=8.81 Å, and $\beta=101°$

It was already shown by Gilta[2] that this crystal belongs to the monoclinic system with the axial ratios, $a:b:c=1.162276:1:1.393499$, and the monoclinic angle, $\beta=101°20'$. The axial ratios given above by the morphological method can be compared with, 1.157 : 1 : 1.387, the values derived by the X-ray measurement. Two formula units per unit cell results in a calculated density 1.786 g. cm$^{-3}$**.

The only extinction rule was found for $(0k0)$ with $k$ odd, which indicates the probable space group $P2_1$ with the fact that a symmetry plane is not permissible, and this was confirmed in the course of the structure analysis. All the intensities were estimated visually with a calibrated scale, by making use of the mutiple-film technique. The data were recorded from small crystals [cross sections with rectangular dimensions; 0.18×0.11 mm. for $(h0l)$, and 0.09×0.21 mm. for $(0kl)$], and

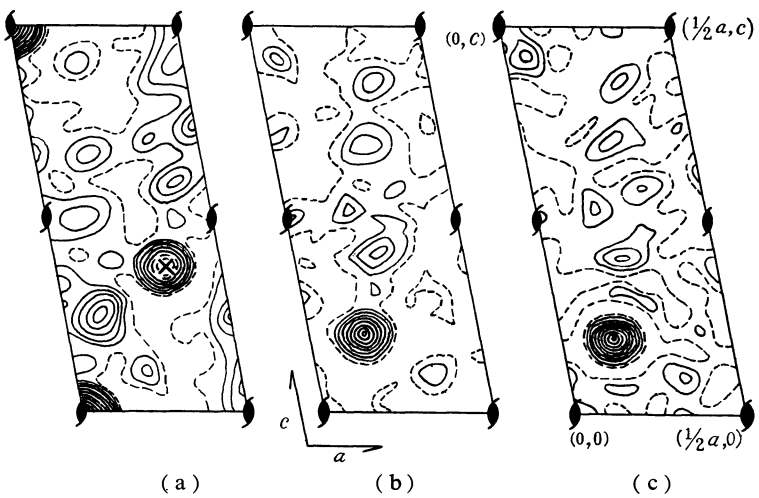



Fig. 1. (a) The Patterson projection, P($UW$), along the *b* axis, the rotation peak due to arsenic atoms being marked by a cross. Contours at arbitrary scale. (b) The minimum function, $M_2(XZ)$, derived from the rotation peak in Fig. 1a. (c) The electron-density projection, $\rho_1(XZ)$, for comparison with $M_2(XZ)$ in Fig. 1b. Contours at arbitrary scale.

* The major part of this paper was read at the 13th Annual Meeting of the Chemical Society of Japan, Tokyo, April, 1960.

1) A. Shimada, This Bulletin, 32, 309 (1959); A. Shimada, ibid., 33, 301 (1960).

2) G. Gilta, *Bull. soc. chim. Belges*, 32, 19 (1923).

** The density was measured to be 1.9571 g. cm$^{-3}$ by Lorenz and Schmidt (*Z. anorg. u. allgem. Chem.* 112, 269 (1920)), and the author obtained the value of 1.85 g. cm$^{-3}$ by floatation in bromoform and carbon tetrachloride mixture. These observed values are higher than the calculated value, but it seems certain that the unit cell contains two formula units.

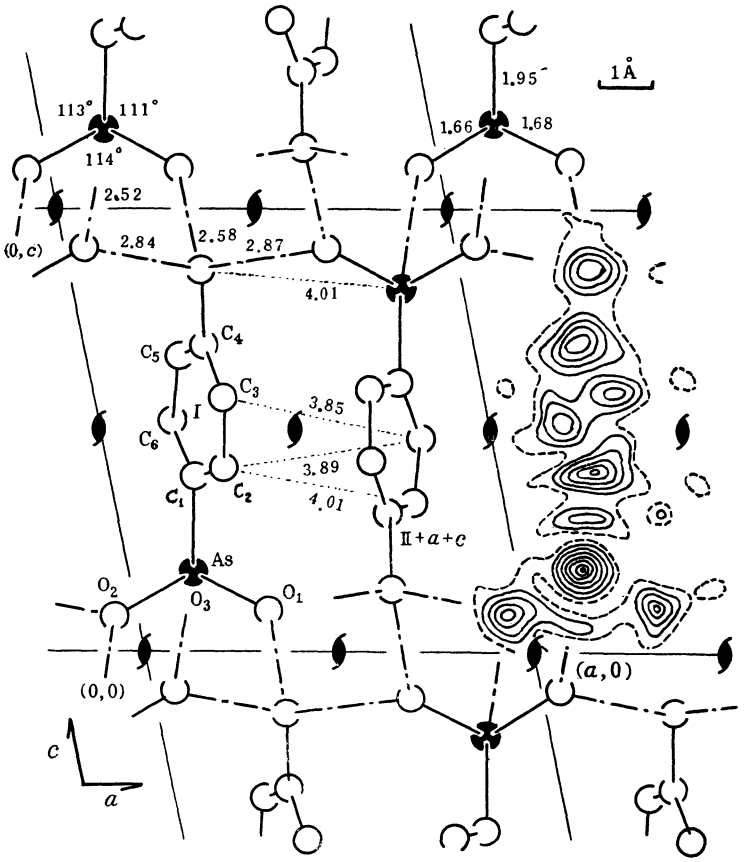



Fig. 2. The structure and the electron-density projection along the *b* axis, with bond angles, intra- and intermolecular distances (Å). Contours at intervals of $2\,e\text{Å}^{-2}$, starting at $2\,e\text{Å}^{-2}$ (broken lines), except the arsenic atom, where contours are at intervals of $10\,e\text{Å}^{-2}$. Dot-dash lines indicate hydrogen bonds.

no absorption corrections were applied. The corrections for polarization and Lorentz factors were made in the usual way.

## Structure Determination

The structure has been determined by making use of the heavy atome technique. The Patterson projection P(*UW*) onto the (010) plane was first synthesized, because the b axis is the shortest and the projection of the structure has a center of symmetry. This Patterson projection P(*UW*), as shown in Fig. 1a, seemed to give some clues to the outline of molecules due to vectors from the heavy arsenic atom to the lighter atoms in addition to the location of the arsenic atom due to the large rotation peak near the origin. Consequently, we set up the minimum function $M_2(XZ)$ based upon this rotation peak. At the same time, the electron-density projection $\rho_1(XZ)$ was synthesized, the Fourier terms being the observed structure amplitudes whose signs were determined only by the coordinates of an arsenic atom. It will be seen that there is a good correspondence between $M_2(XZ)$ and $\rho_1(XZ)$ as shown in Figs. 1b and 1c, and they are sufficient to give the approximate coordinates of lighter atoms. With these maps as a start, a sequence of electron-density projections were synthesized to make clear all of the atomic positions except hydrogen atoms.

Although the projection onto (100) plane has no center of symmetry, the electron-density projections were constructed by the successive refining, referring to the Patterson projection onto (100) plane and the refined electron-density projection onto (010) plane. The final electron-density projections are shown in Figs. 2 and 3, and the final coordinates are listed in Table I, being refined by the difference syntheses at later stages.

In the calculation of structure factors, McWeeny's scattering curves[3] for nitrogen

3) R. McWeeny, *Acta Cryst.*, **4**, 513 (1951).

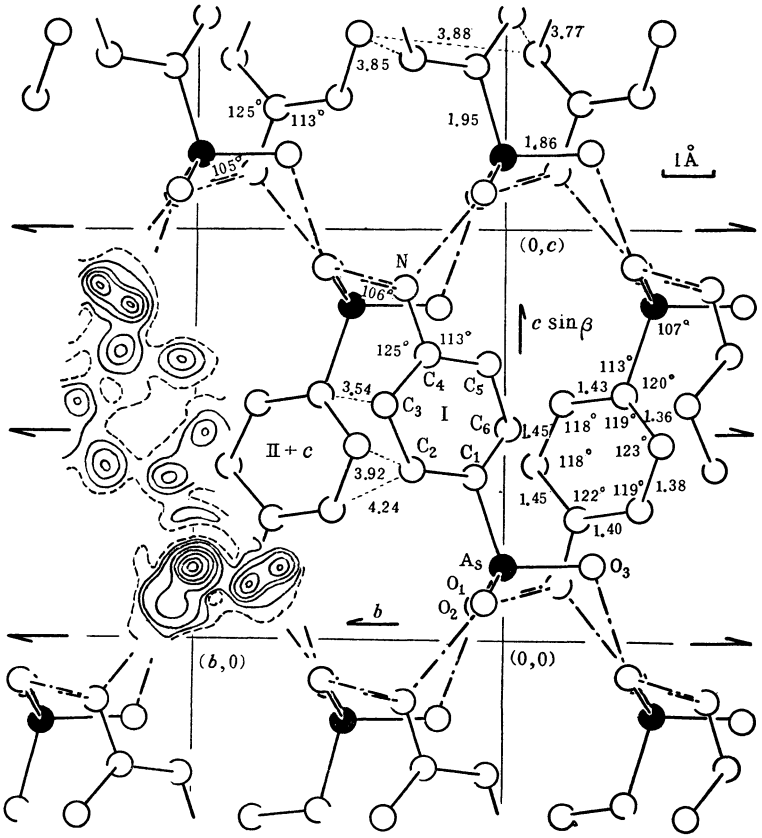



Fig. 3. The structure and the electron-density projection along the a axis, with bond angles, intra- and intermolecular distances (Å). Contours at intervals of $2\,e\text{Å}^{-2}$, starting at $2\,e\text{Å}^{-2}$ (broken lines), except the vicinity of the arsenic atom, where contours above $6\,e\text{Å}^{-2}$ are at intervals of $10\,e\text{Å}^{-2}$. Dot-dash lines indicate hydrogen bonds.

Table I. Atomic coordinates

| Atom | $x/a$ | $y/b$ | $z/c$ |
|---|---|---|---|
| As | $0.163_2$ | 0 | $0.183_1$ |
| $O_1$ | 0.338 | 0.063 | 0.093 |
| $O_2$ | −0.041 | 0.078 | 0.086 |
| $O_3$ | 0.156 | −0.293 | 0.185 |
| $C_1$ | 0.213 | 0.093 | 0.398 |
| $C_2$ | 0.299 | 0.295 | 0.418 |
| $C_3$ | 0.331 | 0.386 | 0.572 |
| $C_4$ | 0.298 | 0.254 | 0.698 |
| $C_5$ | 0.234 | 0.047 | 0.675 |
| $C_6$ | 0.184 | −0.028 | 0.523 |
| N | 0.327 | 0.318 | 0.863 |

atom, of "valence states" for carbon atom and of $1/3(f^{\parallel}+2f^{\perp})$ for oxygen atom were used, while the scattering curve given by Berghuis et al.[4] was used for arsenic atom. An isotropic temperature factor was estimated to be $2.7\,\text{Å}^2$ for all atoms. $R$ indicates for the final coordinates were 13.0 and 14.9% for $(h0l)$ and $(0kl)$ respectively, excluding terms too weak to be observed. The comparison of observed structure factors with calculated ones is shown in Fig. 4.

4) J. Berghuis, I. M. Haanappel, M. Poters, B. O. Loopstra, C. H. MacGillavry and A. L. Veenendaal, ibid., 8, 478 (1955).

## Description of the Structure

The general nature of the structure is shown in Figs. 2 and 3, which are b and a axis projections for this crystal. The arsenic atom is surrounded by a group consisting of three oxygen atoms, $O_1$, $O_2$ and $O_3$ of the arsonic acid and one carbon atom $C_1$ of the benzene ring. The average As-O distance is 1.73 Å, and the As-C distance is 1.95 Å. The disposition of bonds from the arsenic atom appears to be nearly tetrahedral, the angles between the bonds being abnut 109°. The benzene ring is planar and the average distance between adjacent carbon atoms is 1.41 Å, individual values ranging from 1.36 to 1.45 Å. The N-C distance is 1.49 Å and the nitrogen atom is found to lie on the plane of a benzene ring

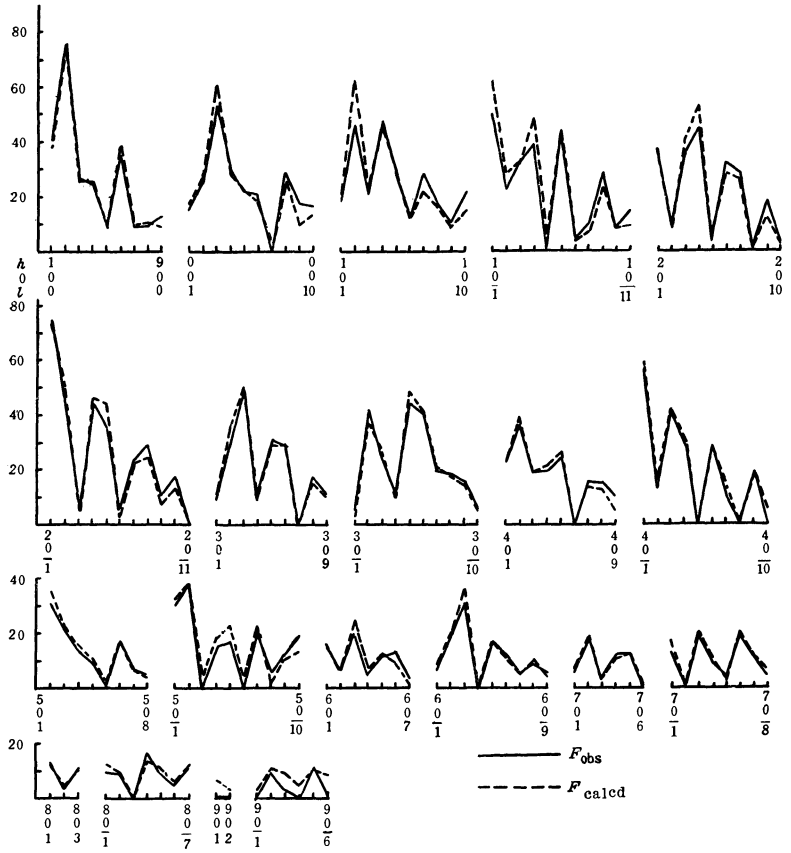



Fig. 4. (a) Comparison of observed and calculated structure factors, F($h0l$).

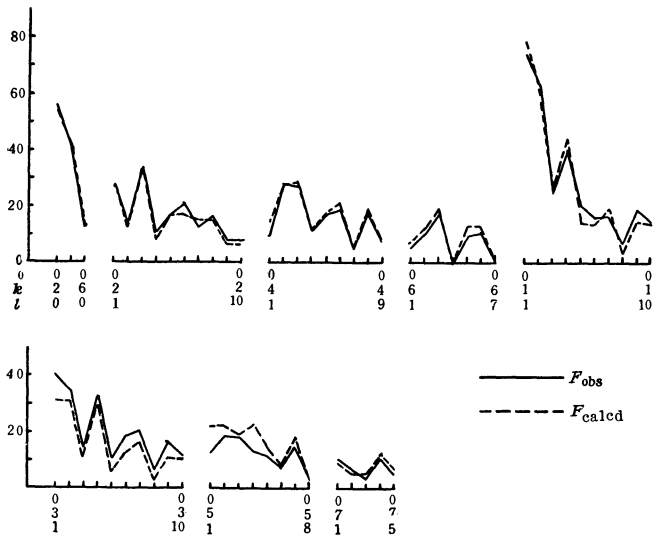



Fig. 4. (b) Comparison of observed and calculated structure factors, F($0kl$).

within the limit of experimental error.

The molecules are held together by a beautiful network of hydrogen bonds. These are four hydrogen atoms available for hydrogen bonding in an asymmetric unit. Two of them come from the *p*-amino group, two come from the arsonic group. There is one hydrogen bond between oxygen atoms and there are three hydrogen bonds between oxygen and nitrogen atoms. The hydrogen bond, with a length 2.52 Å from the atom $O_2$ of molecule I to the atom $O_3$ of molecule II, links molecules with each other to form endless chains along the screw axis perpendicular to the (010) plane. The nitrogen atom in the *p*-amino group of the molecule I forms three hydrogen bonds, the first with a length 2.84 Å to the atom $O_2$ of the molecule II$+c$ (molecule displaced by the unit vector $c$), the second with a length 2.58 Å to the atom $O_1$ of the molecule I$+c$, and the third with a length 2.87 Å to the atom $O_1$ of the molecule II$+a+c$. These three hydrogen bonds connect the endless chains through benzene rings to form a three dimensional net work. This triple hydrogen-bond formation of a nitrogen atom will suggest that one of hydrogen atoms is transferred from an arsonic acid group to the *p*-amino group. On this basis, the formula of the molecule should be written as $NH_3^+ \cdot C_6H_4 \cdot AsO_2(OH)^-$, which indicates that the molecule is in the zwitterion form in the crystal. This conclusion will be supported by the fact that this acid is strictly monobasic[5].

There is no seriously short van der Waals contact in this structure. The shortest distance between nighboring molecules, 3.51 Å, is found between the atom $O_2$ of the molecule I and the arsenic atom of the molecule II. There is also a contact at 3.54 Å between the atom $O_1$ of the molecule I and the atom $C_4$ of the molecule II$+a+c-b$. The shortest contact between adjacent benzene rings occurs at 3.54 Å between the atom $C_1$ of the molecule I and the atom $C_3$ of the molecule II$+a+c-b$. Other intermolecular distances exceed 3.55 Å. A comparison of this structure with that of the benzenearsonic acid is interesting. They are closely similar in having endless chains formed by the hydrogen bonds between arsonic acid groups, while in *p*-aminobenzenearsonic acid there are additional hydrogen bonds to connect these chains. This difference in mode of packing will explain why the crystal of *p*-aminobenzenearsonic acid has no cleavage, in contrast to that of benzenearsonic acid which shows cleavages along endless chains.

The author wishs to express his sincere thanks to Professor I. Nitta and Professor T. Watanabé of Osaka University for their helpful advice, and to Professor H. Nakata of Konan University for supplying the specimens.

*Department of Chemistry*
*Faculty of Science*
*Osaka City University*
*Kita-ku, Osaka*

5) A. E. Goddard, "A Text-book of Inorganic Chemistry", Vol. XI., Part II, Charles Griffin and Co., London (1930), p. 179.

# *Mass Spectrometric Study on Adsorption of Water Vapor on a Graphite Surface*

By Hokotomo INOUYE

(Received September 17, 1959)

Although it is of interest in connection with the study of the adsorption of gas on a solid surface to know what sorts of ions are formed by electron bombardment at the surface, there are few mass spectrometric studies on the subject.

By electron bombardment at surface, ions are formed both on the surface and in the gas phase. Therefore, it is important to distinguish the ions which are formed from adsorbed molecules on the surface from those formed simultaneously in the space adjacent to the surface. For this purpose the author has devised a method to know places of formation of ions by analyzing their peak shapes obtained by means of a single focusing mass spectrometer with a modified ionization chamber.

Plumlee and Smith[1] found that $O^+$ was

1) R. H. Plumlee and L. P. Smith, *J. Appl. Phys.*, **21**, 811 (1950).

emitted from an electron-bombarded molybdenum surface by means of a mass spectrometer with the ionization chamber of special structure. However, the author's method may be simpler and give more precise results than Plumlee's method.

The results obtained by application of the author's method to the ions formed by electron bombardment at a graphite surface covered with adsorbed water vapor are described below.

## Experimental

In Fig. 1 is shown the schematic diagram of the mass spectrometer used in the present work. The

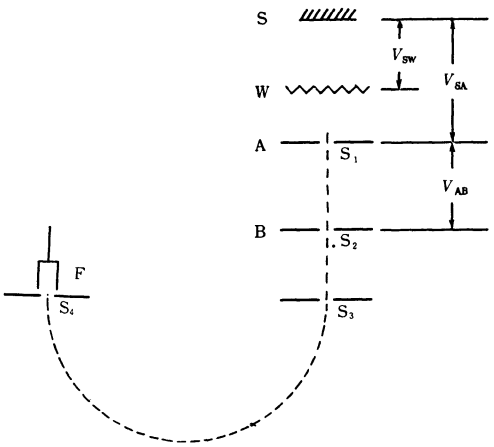



Fig. 1. Schematic diagram of the mass spectrometer.

repeller is replaced by a solid surface, S, to be studied. A hot filament, W, for an electron source is placed between S and the drawing-out electrode, A. Thermoelectrons emitted from W are accelerated by a potential difference $V_{SW}$ and strike S, forming ions on the surface and also in the space between the surface and the place where the potential corresponds to the ionization potential of a gas molecule. A part of these ions is drawn out of the slit $S_1$ of A by a definite potential difference $V_{SA}$ and is accelerated by the variable potential difference $V_{AB}$ for voltage scanning. Ions formed at different places in the ionization chamber, even if they have the same $m/e$, acquire different energies from $V_{SA}$, and hence, for scanning all of them, $V_{AB}$ should be varied over a certain range. Thus the peak shape of the ions will be determined by their distribution in the ionization chamber.

**Peak Shape of the Ions Formed on the Surface.**—If all the ions of one kind are emitted from the surface with zero initial kinetic energy, the only value, ${}_sV_{AB}$, of $V_{AB}$ will be sufficient to bring the ions to the exit slit, $S_4$, of the analyzer. The peak shape will be a symmetrical one characteristic of the instrument (Peak 1). Now, let $V_s$ be the total accelerating potential ($V_{SA}+{}_sV_{AB}$) for the apex of this peak.

If the ion has a certain initial kinetic energy $V_0$ and the angle between its direction and the normal to the surface is $\theta$, $V_{AB}$ bringing the ion to $S_4$ is ${}_sV_{AB}-V_0\cos\theta$, since it has the energy of $V_{SA}+V_0\cos\theta$ at $S_1$. As the directional divergency of the ion beam at $S_3$ is small owing to the geometry of the instrument, the position of the peak apex can be determined only by the energy divergency, or the distribution of $\theta$, among the ions passing through $S_3$. Some ions formed even with great values of $\theta$ are able to enter the analyzer through $S_3$. The value of $\theta$ of the most abundant ions in this distribution is assumed to be $\theta_m$. Then the peak apex will move from $V_s$ by $V_0\cos\theta_m$ towards the lower potential side on the potential axis representing $V_{SA}+V_{AB}$. The peak shape also depends on the directional distribution of the ions at formation and on the geometry of the instrument. Generally, the peak width is broader than that of the ions with zero initial kinetic energy (Peak 2).

If the magnitude of the initial kinetic energy extends over a certain range, this distribution will also affect the position and shape of the peak.

**Peak Shape of the Ions Formed in the Gas Phase.**—If the energy of an electron emitted from W becomes equal to the ionization potential $J$ of a gas molecule at P on the way to S, the molecule in the space between P and S will be ionized by a collision with the electron. The number of ions formed per unit volume, the unit electronic current and the unit time is given by the product of the ionization probability and the density of the gas molecules. Ionization probability increases with the increasing energy of the incident electron and decreases after reaching the maximum. Therefore, the number of the ions formed along the electron path increases from zero at P up to the maximum at S, provided that the applied accelerating potential $V_{SW}$ of the electron is higher than $J$ and lower than the value corresponding to the maximum probability.

Even if the ions thus formed are supposed to have zero initial kinetic energy, they acquire different energies from $V_{SA}$ according to the places of their formation; thus, a wide range of $V_{AB}$ is necessary for scanning all of them. When $V_{AB}$ is equal to ${}_sV_{AB}$ the ions formed just before S can arrive at $S_4$, and at greater values of $V_{AB}$ those formed at places distant from S arrive at $S_4$. The amount of the ions formed just before S is maximum, and it decreases as the distance of the place of the

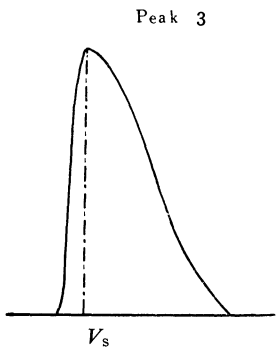



Fig. 2. Peak of the ions formed in the gas phase.

ion formation from S increases. Therefore, the peak has its apex at $V_S$, and its slope at the higher potential side is more gentle than that at the lower potential side as shown in Fig. 2 (Peak 3).

If $V_{SW}$ is higher than the value corresponding to the maximum probability, the place of the maximum ion formation moves from the surface toward P. So the apex moves from $V_S$ toward the higher potential side (Peak 4 in Fig. 3).

If the ions have some initial energies, the peak will be broadened also toward the lower potential side similarly to Peak 2, provided that any ion striking upon the surface underwent an elastic reflection. It may, however, be difficult to distinguish this peak from Peak 3.

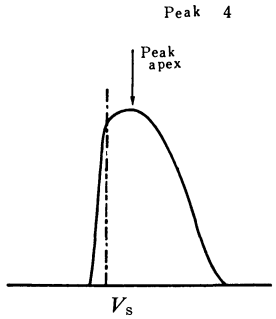



Fig. 3. Peak of the ions formed in the gas phase at $V_{SW}$ exceeding the value corresponding to the maximum ionization probability.

**Peaks of the Ions Formed Both on the Surface and in the Gas Phase.**—If an adsorbed gas is ionized in the gas phase after desorption as neutral molecules or atoms, the peak of the ions will have a shape quite similar to Peak 3. However, it is able to be distimguished from the peak of the ions due to the molecules originally present in the gas phase, because for the former peak the height is proportional to the square of the electronic current but for the latter it is directly proportional to the electronic current[2].

If the adsorbed gas is removed not only directly as ions from the surface but also as neutral molecules or atoms giving the ions of the same *m/e* afterwards, two kinds of peaks will result either from superposition of Peaks 1 and 3, or from that of Peaks 2 and 3.

(A) All the ions of the same *m/e* formed on the surface and in the gas phase are supposed to have no initial kinetic energy. Since Peak 1 is obtained for the former and Peak 3 for the latter, the observed peak will be one that results from superposition of both peaks as shown in Fig. 4 (Peak 5).

If $V_{SW}$ higher than the value corresponding to the maximum ionization probability is applied, the observed peak has a shape such as is shown in Fig. 5 (Peak 6), since Peak 4 takes the place of Peak 3 in Fig. 4. Thus, detection of the ions formed on the surface will become easier.

2) Y. Ohta, *J. Chem. Soc. Japan, (Nippon Kwagaku Kwaisi)*, **64**, 849, 986 (1943).

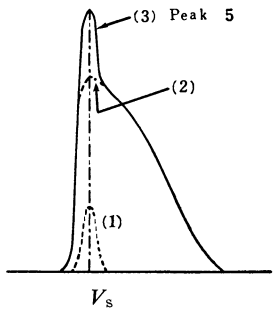



Fig. 4. Peaks of the ions of the same *m/e* formed simultaneously on the surface and in the gas phase with no initial kinetic energy. (1): peak of the ions formed on the surface, (2): peak of the ions formed in the gas phase, (3): the compounded peak of 1 and 2.

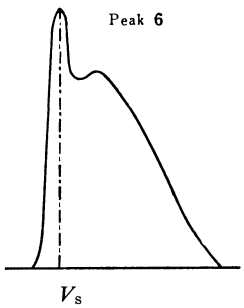



Fig. 5. Peak of the ions of the same *m/e* formed simultaneously on the surface and in the gas phase by application of $V_{SW}$ higher than the value corresponding to the maximum ionization probability.

(B) If the ions formed on the surface have a fairly high initial kinetic energy but those formed in the gas phase have little, Peak 2 is obtained for the former and Peak 3 for the latter. The compounded peak is such as is shown in Fig. 6 (Peak 7). However, in some cases this peak may be indistinguishable from Peak 2 or Peak 5.

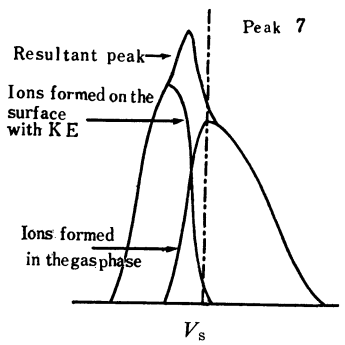



Fig. 6. Peak of the ions formed simultaneously on the surface with an initial kinetic energy and in the gas phase without initial kinetic energy

As described above, the shapes of ion peaks are different from one another according to the places of their formation and to the presence of the initial kinetic energy. From the shape of the peak one may be able to know the place of formation of the ions and also, though not so exactly, to estimate their initial kinetic energy.

## Experimental Results

Ions found in the present work have $m/e$ of $1(H^+)$, $2(H_2^+)$, $17(HO^+)$, $18(H_2O^+)$, $28(CO^+)$, and 183~186. The peaks of these ions are shown in Figs. 7—12. Besides them a group of ions which is supposed to be formed from grease vapor is found.

1) **$H_2O^+$ and $HO^+$.**—As the peak of $H_2O^+$ has a similar shape to Peak 3 in Fig. 2, this ion is supposed to be formed in the gas phase. The peak shape of $HO^+$ appears to be similar to Peak 7 rather than to Peak 3. Thus, some of them may be formed on the surface with kinetic energy. However, for the present, $HO^+$ is supposed to be formed only from water molecules in the gas phase, owing to the fact that the observed relative intensity of $HO^+$ to $H_2O^+$ is not greatly different from the result, i. e., 1 : 4 which Tate and others[3] have obtained on water vapor by voltage scanning, and that it is difficult because of their low intensity to judge certainly whether the peak is similar to Peak 7 or not.

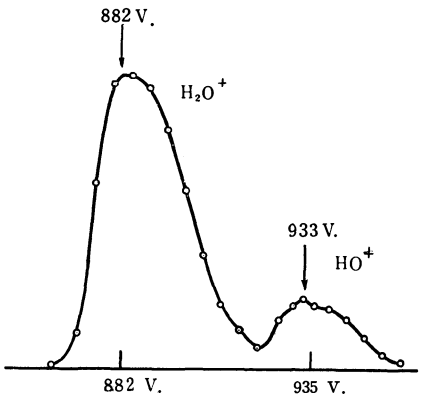



Fig. 7. $H_2O^+$ and $HO^+$. Figures on the potential axis indicate the normal position of the peak apex of the ion.

No measurement has yet been carried out to certify whether these ions are due to residual water vapor or due to the molecules desorbed by electron bombardment.

2) **$H_2^+$.**—As shown in Figs. 8 and 9, the peak shape is similar to Peak 5 in Fig. 4 when $V_{SW}$ is 50 V. and to Peak 6 in Fig. 5 when it is 100 V. The ions are supposed to be formed both on the surface and in the gas phase and neither of them is supposed to have any initial kinetic energy.

3) **$H^+$.**—As the peak has a similar shape, as shown in Fig. 10, to that of Peak 7, the ions are formed both on the surface and in the gas phase, and, at least, those formed on the surface seem to have a certain initial kinetic energy.

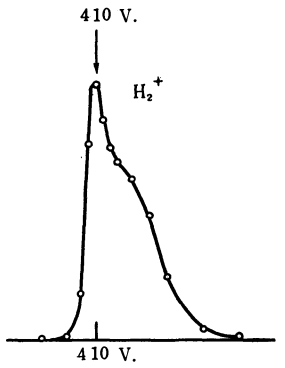



Fig. 8. $H_2^+$ when $V_{SW}$ is 50 V.

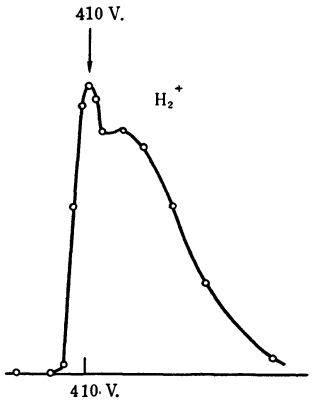



Fig. 9. $H_2^+$ when $V_{SW}$ is 100 V.

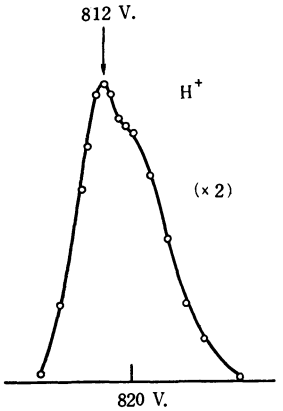



Fig. 10. $H^+$.

3) M. M. Mann, A. Hustrulid and J. T. Tate, *Phys. Rev.*, 58, 340 (1940).

The position of the peak apex of Fig. 8 corresponds to the total accelerating potential of $H_2^+$ leaving the surface without initial kinetic energy. From the value, 410 V., for the apex of $H_2^+$, the position of the apex of $H^+$, peak is calculated to be 820 V., whereas the observed value is 812. Hence, it is shifted by 8 V. towards the lower potential side. This shift will be due to the initial kinetic energy of $H^+$ from the surface.

Now, if the peak of the ions formed in the gas phase is assumed to be curve 1*1 of Fig. 11 and is deducted from the observed curve 3, then curve 2 will result. This curve corresponds to the peak of the ions leaving the surface with initial kinetic energy, the value of which is calculated*2 from the position of the apex to be 10 V.*3

**4) $CO^+$.**—Ions of *m/e* 28 correspond to $CO^+$ or $N_2^+$, but they are concluded to be $CO^+$ and not $N_2^+$, since $N^+$ (*m/e* 14) has not been found.

From the peak shape these ions are considered to consist of those formed in the gas phase and of those leaving the surface with kinetic energy, the value of which, however, would be small.

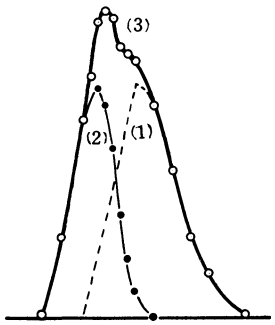



Fig. 11. $H^+$ peak divided into the component peaks.

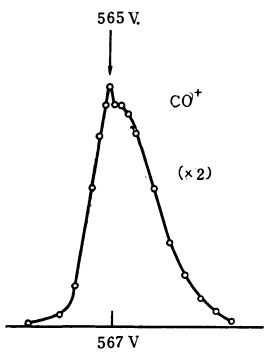



Fig. 12. $CO^+$.

**5) Ions of *m/e* 183~186.**—The behavior of this group of ions is very different from that of any other ion, and hence they are not supposed to be grease vapor ions but possibly $W^+$ which is produced by electron impact on tungsten vapor evaporating from the heated tungsten filament for the electron source. However, they have not yet been confirmed as such, because the resolving power of the instrument is not sufficient to determine exactly of what *m/e* of ions they consist.

## Consideration

Despite the fact that hydrogen and carbon monoxide were not introduced into the apparatus on purpose, it was found that $H_2^+$, $H^+$ and $CO^+$ were formed both on the surface and in the gas phase. Therefore, these ions must be formed from the water vapor adsorbed on graphite.

According to the results obtained by the thermal method on adsorption of water vapor on a carbon surface[4,5], $H_2$ will be desorbed from the surface even at room temperatures, and the gas removed from the surface at lower temperatures containing $CO_2$ and a smaller quantity of CO. At higher temperatures CO is increased. These facts are considered to suggest that the reaction of water with carbon gives adsorbed $H_2$ and two types of surface oxides of carbon; one that readily decomposes even by evacuation at room temperatures to give $CO_2$ and the other that is more stable and decomposes at higher temperatures with evolution of CO.

Thus, formation of $H_2^+$ and other ions both on the surface and in the gas phase may be interpreted as follows:

By electron bombardment upon the graphite surface covered with adsorbed water vapor, some of the adsorbed $H_2$ molecules may leave the surface directly as $H_2^+$, and others give $H_2^+$ in the gas phase by successive electron impact after desorption as neutral gaseous molecules. $H_2^+$ formed in the gas phase does not possess initial kinetic energy. Also $H_2^+$ directly leaving the surface will not have initial kinetic energy if the potential curves of the adsorbed $H_2$ molecules are not very different from those of gaseous $H_2$ molecules.

If the more stable surface oxide is assumed to take a configuration such that CO rather

*1 In the curve (1) the peak width due to the instrument is taken into consideration.

*2 As the $\theta$ distribution of the amount of the ions passing through $S_3$ is unknown, the amount of the ions emitted along the axis of the slit system is assumed to be maximum ($\theta_m=0$).

*3 Several possible peaks were tried as curve (1), but always 10 V. was obtained.

4) R. N. Smith, C. Pierce and C. D. Joel, *J. Phys. Chem.*, **58**, 298 (1954).

5) P. H. Emmett, *Chem. Revs.*, **43**, 69 (1948).

than O is adsorbed on the surface after the apparatus is sufficiently evacuated, it can be removed as CO or $CO^+$ by electron bombardment.

$H^+$ formed in the gas phase may originate from $H_2$ or H leaving the surface by electron bombardment and, in addition, from gaseous water molecules and grease vapor. However, most of them are probably due to dissociative ionization of $H_2$ or ionization of H, since the contribution of $H^+$ from the last two origins to the total $H^+$ current is small.

$H^+$ from the surface may also be due to the adsorbed $H_2$ which resulted from water adsorbed on the graphite surface.

According to the potential curves of higher energy states of $H_2$ molecules, there is the state of unstable $H_2^{2+}$ at 46 V. higher than the normal state, and this $H_2^{2+}$ gives two $H^+$'s, each with kinetic energy of about 7 V., after spontaneous dissociation. Also at 28 V. higher, there is the unstable $^2\Sigma_u$ state of $H_2^+$. It is dissociated into H and $H^+$, each with kinetic energy of about 5 V. Increased energy of the incident electrons can increase this energy up to about 7 V.[6].

If the electronic states of the adsorbed $H_2$ are not greatly different from those of the gaseous molecule, there is sufficient possibility of transition of the adsorbed $H_2$ to unstable $H_2^+$ or $H_2^{2+}$, because the energy $V_{SW}$ of the incident electrons is at least 50 V. When these unstable molecular ions are dissociated, if it is assumed that only one $H^+$ leaves the surface and the other $H^+$ or H is bound to the surface, the leaving $H^+$ will carry all of the initial energy of 10~15 V. for two particles.

Such being the case, and taking into consideration the presence of the directional distribution at formation, the presence of $H^+$ leaving the surface with kinetic energy of about 10 V. will, at least qualitatively, be explainable.

It has also been supposed that some of surface oxides formed from adsorbed water on a graphite surface might have OH-radicals[4]. If that is the case, formation of $HO^+$ on the surface will be possible. However, it was not confirmed in this work as mentioned in Experimental Results 1).

6) H. S. W. Massey and E. H. S. Burhop, "Electronic and Ionic Impact Phenomena", Oxford University Press (1952), p. 231.

## Summary

Peak shapes in mass spectra obtained by voltage scanning using a mass spectrometer with such a modified ionization chamber as that described above are characterized by the places of formation and the initial kinetic energy of the ions. Thus, from the shape of the peak, one may be able to decide the place of formation of the ions and, though not so precisely, to estimate their initial kinetic energy.

When the method was applied to the ions formed by electron bombardment at a graphite surface covered with adsorbed water vapor, it was found that (1) $H_2O^+$ and $HO^+$ were formed from residual or desorbed $H_2O$ only in the gas phase, (2) $H_2^+$, $H^+$ and $CO^+$ were formed both on the surface and in the gas phase, and (3) $H^+$ which formed on the surface had the initial kinetic energy of about 10 V. These results will confirm the fact that the adsorbed water molecule is dissociated into adsorbed $H_2$ and surface oxide of carbon that probably takes a configuration such that CO is adsorbed on the surface.

The author wishes to express his hearty thanks to Professor Nobuji Sasaki of Kyoto University for his guidance throughout the course of this work.

*Department of Chemistry*
*Faculty of Literature and Sciences*
*Kochi University*
*Kochi*

# *Kolbe's Reaction of Higher Fatty Acids. II. Electrolysis of Lauric Acid by a Pulsating Current with an Artificial Graphite Anode**

By Ryoichi MATSUDA, Takeo HISANO and Daishiro KUBOTA

(Received August 27, 1960)

In the previous paper[1] a study of electrolysis of lauric acid was reported with respect to the relation between the current efficiency of Kolbe's reaction and the anodic current density as well as the alkalinity of the electrolyte, and it was thereby conculded that nickel anode behaved almost similarly to platinum one towards Kolbe's reaction of lauric acid. In connection with the above mentioned result it was undertaken to study behaviors of other anode materials concerning the electrolysis of lauric acid in the present paper.

In Exp. 1 artificial graphite, lead, tantalum, molybdenum, tungsten and iron anodes were employed for electrolysis by direct current, but none of these anodes gave rise to Kolbe's reaction of lauric acid. Accordingly a pulsating current was applied instead of a direct current with the same anodes as those mentioned above, and it was found that only the artificial graphite anode was suitable for Kolbe's reaction. The other anodes were not desirable, being either unable to get the current flow or dissolved partly or entirely in the electrolyte solution. In Exp. 2 the effect of the anodic current density of the pulsating current upon the current efficiency of Kolbe's reaction in the electrolysis with an artificial graphite anode was studied, and comparison was made with the corresponding case employing direct current reported in the previous paper. Exp. 3 dealt with the effect of alkalinity of the electrolyte on the current efficiency of Kolbe's reaction and the result was compared with the corresponding case of the previous paper to discuss the mechanism of Kolbe's reaction.

## Experimental

The electrolytic vessel was the same as described in the previous paper. Four electrolytic solutions were prepared, each of them containing 1 mol. lauric acid and different portion of potassium hydroxide in a mixture of 800 cc. ethanol and 550 cc. water: thus solutions A, B, C and D contained 0.25, 0.5, 0.75 and 1.00 mol. potassium hydroxide respectively and 1 mol. lauric acid. Each electrolysis was conducted with 40 cc. electrolyte at 40°C. In each case 2200 coulombs of either direct or pulsating current were supplied, this quantity of electricity being nearly 90% of that electrochemically equivalent to the lauric acid present in the solution. The pulsating current was generated by a mercury filled Tunger rectifier, and consisted of half-waves of an approximately perfect sinnusoidal curve. The frequency was 60 cycles per second.

## Results and Discussion

**Experiment 1.**—Artificial graphite, lead, tantalum, molybdenum, tungsten and iron were used as anode to investigate the influence of anode material on Kolbe's reaction. The anode was a square plate 1×1 cm. except that of tungsten having a spiral form made of a wire 0.5 mm. of diameter and 15 cm. long. The cathode in each case was a square plate with the effective surface area ten times as large as the anode, and stood face to face with the latter. The anodic current density was 0.4~1.0 amp./cm$^2$. The result is summarised in Tables I and II.

TABLE I. BEHAVIORS OF VARIOUS ANODES IN THE ELECTROLYSIS WITH DIRECT CURRENT

| Anode | C | Pb | Ta | Mo | W | Fe |
|---|---|---|---|---|---|---|
| Cathode | C | Pb | Ni | Ni | Ni | Fe |
| Current | none | none | none | flow | flow | flow |
| Kolbe's reaction | none | none | none | none | none | none |

TABLE II. BEHAVIORS OF VARIOUS ANODES IN THE ELECTROLYSIS WITH PULSATING CURRENT

| Anode | C | Pb | Ta | Mo | W | Fe |
|---|---|---|---|---|---|---|
| Cathode | C | Pb | Ni | Ni | Ni | Fe |
| Current | flow | flow | none | — | flow | flow |
| Kolbe's reaction | partly occurred | none | none | — | none | none |

*Graphite Anode.*—The artificial graphite anode was coupled with a cathode of the same material. When direct current was applied through the circuit, its intensity decreased with unexpected rapidity, e. g., the initial amperage of 80 m amp. decaying to 5 m amp. in ten minutes. No appreciable change of the anode surface was observed during this period. When pulsating current was applied in place of direct current through the electrolyte which had just been treated with the latter, a stationary current was observed at 3 V. A fresh solution was then electrolyzed with pulsating current, and 0.87 g. docosane was obtained with a small amount of alcohol. The content of the vessel after electrolysis was heated with potassium carbonate and filtered. The precipitate was made alkaline with potassium carbonate solution and extracted with ether. The ethereal extract was concentrated and distilled under

* D. Kubota's graduation thesis at Tokushima University.

1) T. Mizuta, T. Hisano and R. Matsuda, This Bulletin, 33, 700 (1960).

reduced pressure, and the resulted 0.75 g. of the fraction with $K_7$=110~130°C was tested by diazo and Bittre color reactions. By both reactions the alcohol was detected. The anode surface was not changed in its appearance by either current. According to Kunugi[2] the use of the artificial graphite anode brought about 11~12% current efficiency of Kolbe's reaction when acetic acid was electrolyzed with direct current.

*Lead Anode.*—Direct current did not flow through the lead anode coupled with a lead cathode, neither changed the surface of the former electrode. However, by applying the pulsating current at 20~23 V., the current of 0.6 amp. was observed to pass, and the anode was entirely dissolved in the electrolyte solution after some thirty minutes.

*Tantalum Anode.*—The tantalum anode was coupled with a nickel cathode. Neither direct nor pulsating current flowed and no apparent change of the anode occurred.

*Molybdenum Anode.*—The molybdenum anode was entirely dissolved in the solution by direct current at 12~13.5 V.

*Tungsten Anode.*—The tungsten anode was coupled with a nickel cathode, and direct current flowed through it, but neither Kolbe's reaction nor any change of the anode occurred. Pulsating current flowed too, but it did not give rise to Kolbe's reaction.

*Iron Anode.*—Both direct and pulsating currents flowed through the iron anode which was coupled with an iron cathode. The anode was partly dissolved in the solution, but no Kolbe's reaction occurred. The reaction is, however, reported[2] to take place to a small extent when acetic acid is electrolyzed with the same anode as above mentioned by direct current.

**Experiment 2.** As the electrolysis by pulsating current with the artificial graphite anode was the only case which was found to be suitable for Kolbe's reaction in Exp. 1, the influence of current density upon the current efficiency was investigated under such condition as mentioned above. As shown in Fig. 1 the increase of current density of the pulsating current favored the current efficiency of Kolbe's reaction. Exp. 2 of the previous paper which dealt with the influenceof current density of direct current upon the current efficiency of Kolbe's reaction showed that there was a similar tendency. In comparing these two cases of electrolysis, however, it is to be born in mind that the solution of the present experiment is more concentrated with respect to potassium hydroxide than the other, and also that higher concentration with respect to the alkali is disadvantageous to the current efficiency of Kolbe's reaction irrespective of the nature of the current. In dealing with the current density of the artificial graphite anode itsporosity has to be taken into consideration.

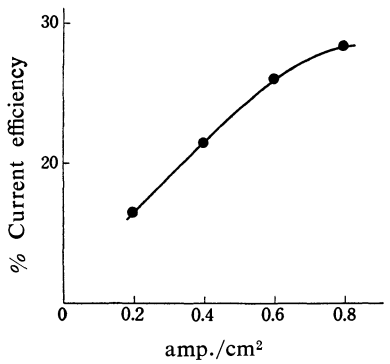



Fig. 1. Influence of anodic current density of pulsating current on docosane production.

**Experiment 3.** The influence of alkalinity of the electrolyte solutions upon Kolbe's reaction with the artificial graphite anode by pulsating current was studied and the result is shown in Fig. 2.

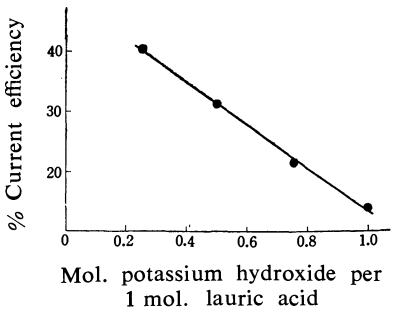



Fig. 2. Influence of alkalinity of solution on docosane production.

Corresponding cases with platinum and nickel anodes by direct current were described in the previous paper. When these two electrolyses are compared with the present case, it is seen that there is a common tendency between them that the current efficiency of Kolbe's reaction decreases linearly with increasing alkalinity. When the alkalinity is the highest one, the current efficiencies of the three cases are close to each other. With the decrease of alkalinity the current efficiency with the artificial graphite anode increases more slowly than the other two. At any rate it is evident that Kolbe's reaction of lauric acid has a close relationship with the alkalinity or the hydrogen ion concentration of the electrolyte solution. Matsuda[3] pointed out that there is an important relationship between Kolbe's reaction and hydrogen ion concentration when the aqueous solution of acetic acid is electrolyzed.

The authors wish to express their thanks to Nippon Oils and Fats Co., Ltd. who kindly offered them the lauric acid.

*Department of Applied Chemistry*
*Faculty of Engineering*
*Tokushima University*
*Tokushima*

2) T. Kunugi, *J. Electrochem. Soc. Japan (Denkikagaku)*, **20**, 208 (1952).

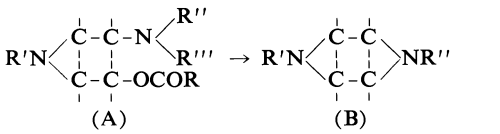
3) B. Matsuda, This Bulletin, **7**, 18, 297 (1932).

# *A New Method for the Preparation of Piperazines. I. Preparation of N-Mono-alkyl(-aryl)-piperazines*

By Kazuo NAKAJIMA

(Received October 8, 1960)

For the preparation of piperazine and its derivatives a number of methods have been proposed up to the present by several investigators[1]. Because of the complexity and the poor yield, these methods still leave much to be desired. Many trials, therefore, have been made by the present author to find out a new convenient route to these compounds. And, after all, it was found that a compound of the general formula A gives a piperazine derivative B under the elimination of an ester C, when it is heated at 200~300°C, according to the following Eq. 1.



(A) (B)

$$+ \mathrm{RCOOR'''} \quad (1)$$

(C)

In this equation, R′ and R″ represent alkyl, aralkyl, cycloalkyl, aryl or acyl groups which are destined to remain in the molecule of B after the fission. R‴ also may be an alkyl, aralkyl or cycloalkyl group (equal to or lower than R″), but neither aryl nor acyl group, for these groups are incapable of being removed as a part of the ester C. RCO– in A and in C is an acyl group, but, in fact, it is restricted to the easily available acetyl.

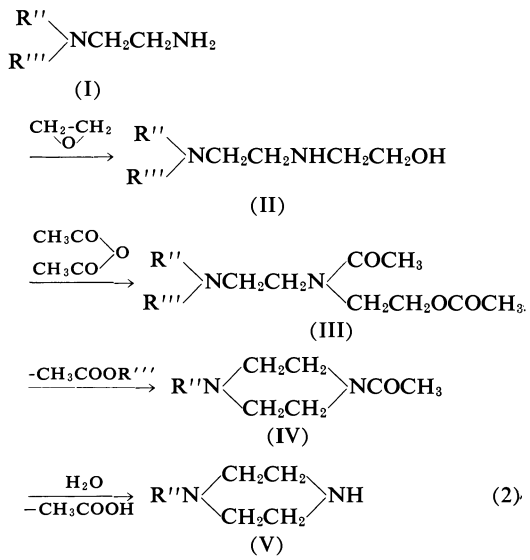
As can be seen from Eq. 1, this reaction seems to be quite a new type of reaction, i. e. the cyclization under the elimination of an ester*.

The actual procedure of this reaction consists in heating the compound A above 200°C, the conditions being arranged so that the ester C can be distilled over as it is formed during the heating, and in fractionating the resulting piperazine B under reduced pressure. Generally speaking from the data of the series of the experiments, the yields are fairly good.

The adequate selections of R′, R″ and R‴ in A make it possible to synthesize various compounds of piperazine-ring system.

As a part of synthetical works in the field of piperazines by the new route, synthesis of *N*-mono-alkyl(-aryl)-piperazines is dealt with in the present paper.

**Synthesis of *N*-Mono-alkyl(-aryl)-piperazines.**— The full course of synthesis of *N*-mono-alkyl-(-aryl)-piperazines (V) from *N*, *N*-disubstituted ethylenediamines (I) is represented by the following Eq. 2.



(I)

(II)

(III)

(IV)

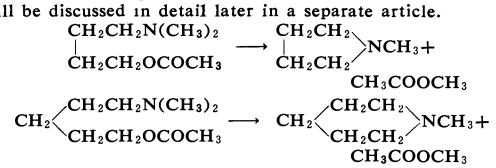
(V)

(2)

*N*, *N*-Disubstituted ethylenediamines (I)[2] are converted into *N*, *N*-disubstituted aminoethyl ethanolamines (II) by the action of ethylene oxide or ethylene chlorohydrin. In this reaction considerable quantities of *N*, *N*-disubstituted aminoethyl diethanolamines are formed, from which II can be isolated by fractionation under

1) D. S. Pratt and C. O. Young, *J. Am. Chem. Soc.*, **40**, 1428 (1918); W. B. Martin and A. E. Martell, ibid., **70**, 1817 (1948); T. S. Moore, H. Boyle and V. M. Thorne, *J. Chem. Soc.*, **1929**, 39; R. Baltzly, J. S. Buck, E. Lorz and W. Schön, *J. Am. Chem. Soc.*, **66**, 263 (1944), K. E. Hamlin et al., ibid., **71**, 2731 (1949); R. Baltzly, ibid., **76**, 1164 (1954); T. Ishiguro, E. Kitamura and M. Matsumura, *J. Pharm. Soc. Japan* (*Yakugaku Zasshi*), **73**, 1110 (1953); **74**, 1162 (1954); **75**, 1370 (1955).

* A similar type of reaction has also been found and will be discussed in detail later in a separate article.



2) K. Nakajima, *J. Chem. Soc. Japan, Pure Chem. Sec.* (*Nippon Kagaku Zasshi*), **81**, 499, 961, 1131, 1477 (1960).

TABLE I. PROPERTIES OF $HN\langle^{CH_2CH_2N(R'')R'''}_{CH_2CH_2OH}$

| Comp. No. | R'' | R''' | Phys. form (color) | M. p. °C | B. p., °C/mmHg† 10 | 20 | 50 | 100 | 760 | N, % Found | Calcd. | Picrate M. p. °C | Platinichloride Dec. p., °C | Pt, % Found | Calcd. |
|---|---|---|---|---|---|---|---|---|---|---|---|---|---|---|---|
| 1 | $CH_3$ | $CH_3$ | Mob. 1. (colorless) | | 80 | 97 | 118 | 135 | 205 | 21.02 | 21.19 | 200 (dec.) | 214 | 35.67 | 35.99 |
| 2 | $C_2H_5$ | $C_2H_5$ | 〃 | | 113 | 132 | 152 | 170 | 235 | 17.51 | 17.48 | 90 | * | | |
| 3 | $n$-$C_3H_7$ | $n$-$C_3H_7$ | 〃 | | 134 | 153 | 178 | 199 | 266 | 14.86 | 14.88 | 140 | * | | |
| 4 | $i$-$C_3H_7$ | $i$-$C_3H_7$ | 〃 | | 116 | 135 | 160 | 181 | 248 | 14.77 | 14.88 | 175 | * | | |
| 5 | $n$-$C_4H_9$ | $n$-$C_4H_9$ | Oily 1. (colorless) | | 150 | 164 | 188 | 208 | 280 | 13.01 | 12.95 | * | * | | |
| 6 | C$_6$H$_5$ | $CH_3$ | 〃 | | 168 | 186 | 210 | 230 | 302 | 14.14 | 13.98 | * | * | | |
| 7 | C$_6$H$_5$ | C$_6$H$_5$ | 〃 | | 220 | 236 | 264 | 286 (dec.) | | 10.32 | 10.44 | 193 | 212 | 28.78 | 28.76 |
| 8 | C$_6$H$_5$ | $CH_3$ | 〃 | | 182 | 199 | 222 | 244 | 317 | 14.33 | 14.42 | 153 | * | | |
| 9 | C$_6$H$_5$ | $C_2H_5$ | Wh. sld. (colorless) | 42 | 192 | 208 | 231 | 252 | 323 | 13.30 | 13.45 | 120 | 195 | 37.40 | 31.56 |

† uncorrected
* not obtained in crystalline form.
Key to abbreviation: Phys.=physical; mob. 1.=mobile liquid; wh. sld.=white solid; dec. p.=decomposition point.

TABLE II. PROPERTIES OF $CH_3CON\langle^{CH_2CH_2N(R'')R'''}_{CH_2CH_2OCOCH_3}$

| Comp. No. | R'' | R''' | Phys. form (color) | B. p., °C/mmHg† 6 | 8 | 10 | 20 | 50 | 100 | 760 | N, % Found | Calcd. | Picrate M. p. °C | Platinichloride Dec. p., °C | Pt, % Found | Calcd. |
|---|---|---|---|---|---|---|---|---|---|---|---|---|---|---|---|---|
| 1 | $CH_3$ | $CH_3$ | Oily 1. (colorless) | 140 | 147 | 152 | 170 | 188 | 205 | | 13.05 | 12.95 | 185 | 167 (melt) | 31.01 | 31.17 |
| 2 | $C_2H_5$ | $C_2H_5$ | 〃 | 164 | 174 | 180 | 192 | 212 (dec.) | | | 11.52 | 11.47 | * | * | | |
| 3 | $n$-$C_3H_7$ | $n$-$C_3H_7$ | 〃 | 182 | 189 | 194 | 210 (dec.) | | | | 10.27 | 10.28 | 195 | 198 | | |
| 4 | $i$-$C_3H_7$ | $i$-$C_3H_7$ | 〃 | 170 | 176 | 182 | 194 (dec.) | | | | 10.12 | 10.28 | 220 | * | | |
| 5 | $n$-$C_4H_9$ | $n$-$C_4H_9$ | 〃 | 189 | 296 | 202 | 216 (dec.) | | | | 9.30 | 9.33 | * | 209 | 19.50 | 19.30 |
| 6 | C$_6$H$_5$ | $CH_3$ | 〃 | 192 | 203 | 210 | 227 (dec.) | | | | 9.89 | 9.90 | * | * | | |
| 7 | C$_6$H$_5$ | C$_6$H$_5$ | 〃 | 240 (dec.) | 250 (dec.) | | | | | | 7.75 | 7.95 | * | * | | |
| 8 | C$_6$H$_5$ | $CH_3$ | 〃 | 211 | 218 | 224 | 243 | 270 | 291 (dec.) | | 10.21 | 10.06 | * | * | | |
| 9 | C$_6$H$_5$ | $C_2H_5$ | 〃 | 216 | 224 | 232 | 251 | 274 | 295 (dec.) | | 9.51 | 9.58 | * | * | | |

reduced pressure. Some physical properties of II are summarized in Table I.

The second stage is the acetylation of the secondary amino and hydroxyl group in II, which can be effected by two equivalent amounts of acetic anhydride. The reaction proceeds spontaneously with the evolution of heat, and the subsequent distillation under reduced pressure gives III almost in a quantitative yield.

Some physical properties of III are shown in Table II.

On the third stage, III is submitted to the thermal decomposition, which leads to IV and the ester. As outlined in the introduction, distillation of the ester formed during the heating, and subsequent vacuum-fractionation of IV remaining in the flask are the procedures sufficient to give a pure product for the present synthetic purpose.

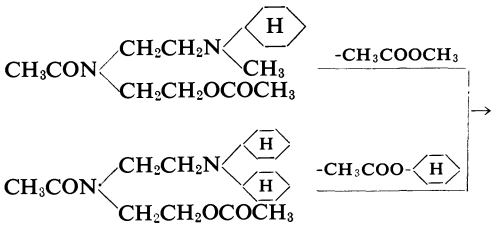
TABLE III. PROPERTIES OF $CH_3CON\langle^{CH_2CH_2}_{CH_2CH_2}\rangle NR''$

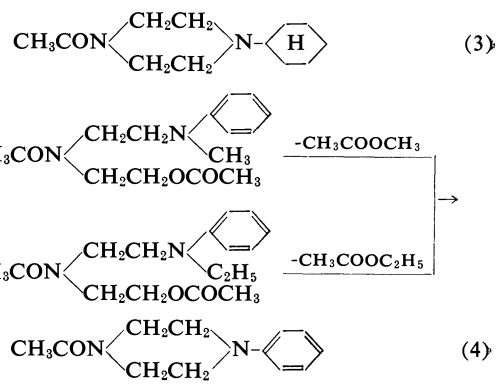
| Comp. No. | R'' | Phys. form (color) | M. p. °C | B. p., °C/mmHg† 10 | 20 | 50 | 100 | 760 | N, % Found | Calcd. | Picrate M. p. °C | Platinichloride Dec. p., °C | Pt, % Found | Calcd. |
|---|---|---|---|---|---|---|---|---|---|---|---|---|---|---|
| 1 | $CH_3$ | Mob. 1. (colorless) | | | | | | 168 | 19.50 | 19.70 | 280 (dec.) | 270 | 28.02 | 28.10 |
| 2 | $C_2H_5$ | 〃 | | 118 | 138 | 160 | 182 | 254 | 17.93 | 17.93 | 115 | 227 | 27.44 | 27.01 |
| 3 | $n$-$C_3H_7$ | 〃 | | 133 | 151 | 175 | 194 | 265 | 16.30 | 16.45 | 212 (dec.) | * | | |
| 4 | $i$-$C_3H_7$ | 〃 | | 124 | 146 | 171 | 193 | 263 | 16.27 | 16.45 | * | * | | |
| 5 | $n$-$C_4H_9$ | 〃 | | 146 | 165 | 190 | 210 | 280 | 15.11 | 15.20 | 190 (dec.) | * | | |
| 6,7 |  | Oily 1. (colorless) | | 186 | 202 | 226 | 248 | 320 | 13.09 | 13.31 | * | * | | |
| 8,9 |  | Cryst. (colorless) | 75 | 206 | 225 | 251 | 270 | 347 | 13.67 | 13.71 | * | 230 | 23.93 | 23.83 |

TABLE IV. PROPERTIES OF $HN\langle^{CH_2CH_2}_{CH_2CH_2}\rangle NR''$

| Comp. No. | R'' | Phys. form (color) | B. p., °C/mmHg† 10 | 20 | 50 | 100 | 760 | N, % Found | Calcd. | Picrate M. p. °C | Platinichloride Dec. p., °C | Pt, % Found | Calcd. |
|---|---|---|---|---|---|---|---|---|---|---|---|---|---|
| 1 | $CH_3$ | Mob. 1. (colorless) | | | 44 | 66 | 137 | 28.02 | 27.97 | 270 (dec.) | 275 | 28.11 | 28.25 |
| 2 | $C_2H_5$ | 〃 | | 40 | 64 | 84 | 157 | 24.42 | 24.53 | 250 (dec.) | 280 | 37.34 | 37.23 |
| 3 | $n$-$C_3H_7$ | 〃 | 47 | 65 | 89 | 110 | 180 | 22.00 | 21.85 | 228 | 260 | 36.18 | 36.23 |
| 4 | $i$-$C_3H_7$ | 〃 | 44 | 63 | 87 | 103 | 173 | 21.78 | 21.85 | 240 (dec.) | 266 | 36.24 | 36.23 |
| 5 | $n$-$C_4H_9$ | 〃 | 84 | 101 | 123 | 141 | 208 | 19.43 | 19.70 | 250 (dec.) | 250 | 35.22 | 35.34 |
| 6,7 |  | Oily 1. (colorless) | 116 | 135 | 158 | 177 | 248 | 16.45 | 16.65 | 225 (dec.) | 260 | 33.40 | 33.76 |
| 8,9 |  | Oily 1. (yellowish) | 139 | 154 | 178 | 180 | 272 | 17.30 | 17.27 | 150 | 259 | 33.99 | 34.10 |

As would be anticipated, β-(*N*-methyl-*N*-cyclohexylaminoethyl)-acetaminoethyl acetate (Table II, No. 6) and β-(*N*, *N*-dicyclohexylaminoethyl)-acetaminoethyl acetate (Table II, No. 7) give the same product, *N*-cyclohexyl-*N'*-acetyl-piperazine (Table III, No. 6, 7) under elimination of methyl acetate or cyclohexyl acetate respectively (Eq. 3). The same applies to the case of β-(*N*-methyl-*N*-phenylaminoethyl)-acetaminoethyl acetate (Table II, No. 8) and β-(*N*-ethyl-*N*-phenylaminoethyl)-acetaminoethyl acetate (Table II, No. 9), *N*-phenyl-*N*-acetyl-piperazine (Table III, No. 8, 9) being equally formed (Eq. 4).




Some physical properties of IV are shown in Table III.

The last stage is the de-acetylation of IV. It may be effected easily by heating the acetyl piperazines with an equal volume of 6 N hydrochloric acid under reflux for 2 hr. The *N*-mono-substituted piperazines thus prepared are a colorless liquid, readily soluble in water

with an exception of *N*-phenyl-piperazine.

Some physical properties of V are cited in Table IV.

The reaction mixture of II and acetic anhydride can conveniently be submitted to the thermal decomposition without isolation of the acetylated compounds.

## Experimental

***N*-(β-Diethylaminoethanol)-aminoethanol (Table I. No. 2).**—Ethylene oxide, generated by dropping 150 g. of 33% sodium hydroxide solution from a pressure-compensated dropping funnel upon a boiling mixture of 100 g. of ethylene chlorohydrin and 50 g. of water under reflux, is passed in a solution of 116 g. (1 mol.) of *N*,*N*-diethylethylenediamine in about 80 g. of methyl alcohol. Contineous shaking and cooling by cold water facilitate the absorption of ethylene oxide in the reaction mixture.

The gain of weight of the reaction mixture will be 44~50 g., and indicates that about one mole of ethylene oxide thereby can be brought into the reaction.

By distillation under atmospheric pressure, about 60 g. of *N*,*N*-diethylethylenediamine (b. p. 150~165°C) is recovered, and by fractionation under reduced pressure, about 50 g. of *N*-β-diethylaminoethylethanolamine, b. p. 113°C/10 mmHg, or 130°C/20 mmHg, and about 40 g. of *N*-β-diethylaminoethyldiethanolamine, b. p. 165°C/10mmHg, or 184°C/20 mmHg are obtained.

Ethylene chlorohydrin may be used instead of ethylene oxide as follows. Forty grams of ethylene chlorohydrin (0.5 mol.) is gradually added from a dropping funnel onto 116 g. (1 mol.) of *N*,*N*-diethylethylenediamine heated under reflux, thereby the reaction proceeds immediately at the rate of addition of the ethylene chlorohydrin. When the addition is complete, the reaction mixture is heated up to 200°C and maintained at this temperature for a while. Owing to the separation of hydrochloride of *N*,*N*-diethylethylenediamine, the reaction mixture is solidified. A hot solution of 30 g. (approx. 0.5 mol.) of potassium hydroxide in 80 cc. of methyl alcohol is gradually added to the reaction mixture with stirring. The precipitate of potassium chloride is removed by filtration and washed with a small quantity of methyl alcohol. After methyl alcohol has been removed from the filtrate and washings, 75 g. of *N*,*N*-diethylethylenediamine is recovered. The residual liquid is submitted to distillation under reduced pressure, whereby 45~50 g. of *N*-β-diethylaminoethylethanolamine and 25~30 g. of *N*-β-diethylaminoethyldiethanolamine are obtained.

***N*-(β-Diethylaminoethyl)-acetaminoethyl Acetate (Table II, No. 2).**—This compound can be obtained by addition of 23 g. (0.22 mol.) of acetic anhydride to 13 g. of *N*-β-diethylaminoethylethanolamine. Acetic acid and an excess of acetic anhydride are distilled off and the residue is distilled under reduced pressure, the expected acetate is collected at 175~177°C/10 mmHg, as a colorless oily liquid —yield 20~21 g. (about 90%).

The practical procedure in this piperazine-synthesis can be carried out so that the reaction mixture of *N*-β-disubstituted-aminoethylethanolamine and acetic anhydride is directly submitted to the thermal decomposition, the isolation of the acetylated compounds being omitted. The techniques here required are quite the same as in use of pure acetates isolated.

***N*-Ethyl-*N'*-acetyl-piperazine (Table III, No. 2).** — Twenty grams of *N*-β-diethylaminoethylacetaminoethyl acetate is heated in a Claisen flask, with a thermometer inserted through the straight neck so deep in the liquid as to read the internal reaction temperature and another thermometer fixed in the side neck of the flask. When the internal temperature reaches up above 250°C, the liquid turns brown in color and the boiling begins with the decomposition into *N*-ethyl-*N'*-acetyl-piperazine and ethyl acetate, which distills over as it is formed.

When the thermal decomposition is complete, the internal temperature is practically settled to a constant, i. e. 250~260°C.

On distillation, pure *N*-ethyl-*N'*-acetyl-piperazine comes over at 252~256°C as a colorless liquid—yield about 7 g. (Ca. 80%).

***N*-Ethyl-piperazine (Table IV, No. 2).**—*N*-Ethyl-*N'*-acetyl-piperazine (5 g.) is heated with 5 cc. of 20% hydrochloric acid under reflux for 2 hr. After the excess of hydrochloric acid has been distilled off, the resulting solution is made alkaline with a sodium hydroxide solution, and extracted with ether in a continuous extractor. The ether layer is dried over anhydrous sodium sulfate, the ether is removed, and the residue is distilled. About 3 g. of pure *N*-ethyl-piperazine is obtained as a colorless liquid b. p. 155~157°C—yield about 90%.

The author wishes to express his sincere gratitude to Professor Ryozo Goto (Kyoto University) for his kind guidance throughout the course of this work.

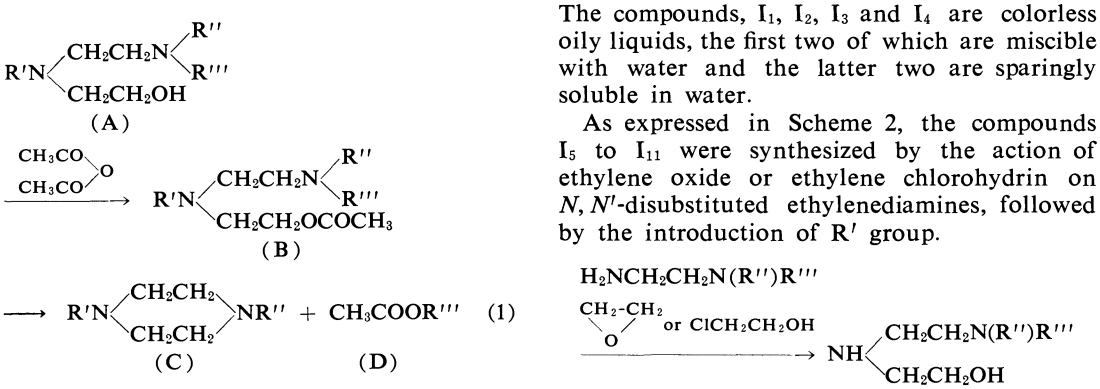
*Kyoto Works*
*Teikoku Chemical Industry Co., Ltd.*
*Nakagyo-ku, Kyoto*

# *A New Method for the Preparation of Piperazines. II. Preparation of N, N'-Disubstituted Piperazines*

By Kazuo NAKAJIMA

(Received September 20, 1960)

A new method for preparing piperazine derivatives has been proposed by the author in the preceding paper[1]. The present paper deals with the preparation of some *N*, *N'*-disubstituted piperazines by this method. The procedure consists in treating an *N*, *N'*, *N'*-trisubstituted *N*-*β*-aminoethylethanolamine of the general formula A with acetic anhydride to yield an *O*-acetyl derivative B, followed by heating at 200~300°C to split into the desired *N*, *N'*-disubstituted piperazine C, and an acetic ester D, as is seen in the following Scheme 1;



In the scheme, R' and R'' are alkyl, aralkyl, cycloalkyl or aryl group, whereas R''' is the same group as R'' or a lower alkyl, aralkyl or cycloalkyl group.

If R', R'' and R''' are chosen appropriately, it is possible to synthesize a variety of *N*, *N'*-disubstituted piperazines.

The properties of *N*, *N'*, *N'*-trisubstituted *N*-*β*-aminoethylethanolamines, which are used as the starting material, of their *O*-acetyl derivatives and of the end-products, *N*, *N'*-disubstituted piperazines are summarized in Tables I, II and III respectively.

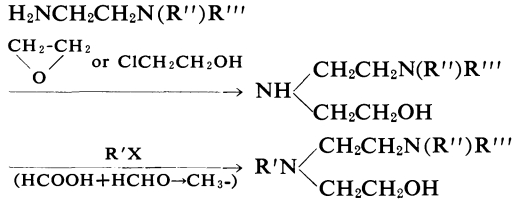
Many proposals have been made hitherto for the preparation of *N*, *N'*-disubstituted piperazines. Among the compounds of this series listed in Table III, *N*, *N'*-dimethyl-, *N*, *N'*-diethyl-, *N*, *N'*-di-*n*-propyl-, *N*-methyl-*N'*-phenyl, *N*-ethyl-*N'*-phenyl- and *N*, *N'*-diphenyl-piperazine are known.

The compounds $I_1$*, $I_2$, $I_3$ and $I_4$, where R', R'' and R''' are the same, are easily prepared through alkylation of *N*-*β*-aminoethylethanolamine.

The alkylation can be achieved by using alkyl halide, but the methylation is also readily accomplished with formic acid and formalin by the Eschweiler-Clarke procedure.

In the Experimental Part, the synthesis of *N*, *N'*, *N'*-trimethyl-*N*-*β*-aminoethylethanolamine ($I_1$) by the latter procedure and that of *N*, *N'*, *N'*-tri-*n*-butyl-*N*-*β*-aminoethylethanolamine ($I_4$) by the use of *n*-butyl bromide were examplified. The compounds, $I_1$, $I_2$, $I_3$ and $I_4$ are colorless oily liquids, the first two of which are miscible with water and the latter two are sparingly soluble in water.

As expressed in Scheme 2, the compounds $I_5$ to $I_{11}$ were synthesized by the action of ethylene oxide or ethylene chlorohydrin on *N*, *N'*-disubstituted ethylenediamines, followed by the introduction of R' group.



(2)

The preparation and properties of some of *N*-*β*-disubstituted aminoethylethanolamines have been shown in the preceding paper.

In the Experimental Part, the synthesis of ($I_5$) by the Eschweiler-Clarke procedure and that of ($I_{10}$) by the use of an alkyl halide have been illustrated.

The products thus obtained are colorless or yellowish oily liquids, sparingly soluble in water, with the exception of $I_5$ and $I_6$ which are freely soluble.

In compounds $I_{12}$ and $I_{13}$, group R' is cyclohexyl. An attempt was made to introduce this by cyclohexyl bromide, but the formation of a considerable quantity of cyclohexene resulted in a low yield of $I_{12}$ or $I_{13}$. In $I_{14}$ and $I_{15}$, R' is a phenyl group.

$I_{14}$ and $I_{15}$ were therefore prepared from *N*-phenyl-*N*-*β*-aminoethylethanolamine.

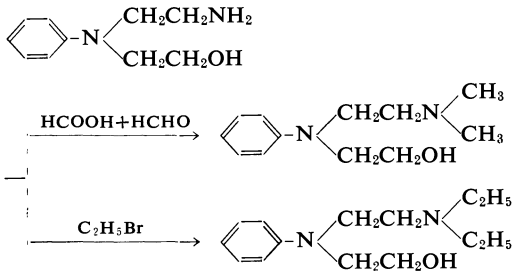
1) K. Nakajima, This Bulletin, **34**, 651 (1961).
* $I_1$ indicates compound 1 in Table I.

TABLE I. PROPERTIES OF $R'N\langle^{CH_2CH_2N(R'')R'''}_{CH_2CH_2OH}$

| Comp. No. | R' | R'' | R''' | Phys. form (color) | B. p., °C/mmHg 10 | 20 | 50 | 100 | 760 | N, % Found | Calcd. | Picrate M. p. °C | Platinichloride Dec. p. °C | Pt, % Found | Calcd. |
|---|---|---|---|---|---|---|---|---|---|---|---|---|---|---|---|
| 1 | $CH_3$ | $CH_3$ | $CH_3$ | Oily liq. (colorless) | 84 | 100 | 122 | 142 | 206 | 19.15 | 19.16 | 229 (dec.) | 215 | 34.75 | 35.08 |
| 2 | $C_2H_5$ | $C_2H_5$ | $C_2H_5$ | 〃 | 115 | 130 | 154 | 174 | 237 | 15.09 | 14.88 | * | 227 | 32.75 | 32.61 |
| 3 | $n$-$C_3H_7$ | $n$-$C_3H_7$ | $n$-$C_3H_7$ | 〃 | 142 | 157 | 180 | 199 | 266 | 12.30 | 12.16 | 164 | 227 | 30.39 | 30.47 |
| 4 | $n$-$C_4H_9$ | $n$-$C_4H_9$ | $n$-$C_4H_9$ | 〃 | 162 | 180 | 204 | 225 | 295 | 10.31 | 10.28 | * | 220 | 28.35 | 28.59 |
| 5 | $CH_3$ | $C_2H_5$ | $C_2H_5$ | 〃 | 90 | 110 | 134 | 155 | 225～226 | 15.98 | 16.08 | 218 | 215 | 33.39 | 33.40 |
| 6 | $n$-$C_3H_7$ | $C_2H_5$ | $C_2H_5$ | 〃 | 117 | 135 | 159 | 180 | 250 | 13.70 | 13.85 | 163 | 225 | 31.80 | 31.87 |
| 7 | $n$-$C_4H_9$ | $C_2H_5$ | $C_2H_5$ | 〃 | 129 | 158 | 170 | 192 | 262～263 | 12.63 | 12.95 | 66 | 215 | 31.26 | 31.15 |
| 8 |  | $C_2H_5$ | $C_2H_5$ | 〃 | 176 | 195 | 220 | 241 | 308 | 11.08 | 11.19 | 98 | 210 | 29.14 | 29.55 |
| 9 | $CH_3$ | $n$-$C_4H_9$ | $n$-$C_4H_9$ | 〃 | 127 | 145 | 169 | 190 | 260 | 12.10 | 12.16 | * | 228 | 30.60 | 30.63 |
| 10 | $C_2H_5$ |  | $CH_3$ | Syrupy (colorless) | 179 | 190 | 216 | 235 | 305 | 12.54 | 12.60 | 130 | red. | | |
| 11 | $CH_3$ |  | $C_2H_5$ | 〃 | 182 | 200 | 225 | 244 | 315 | 12.60 | 12.60 | * | * | | |
| 12 |  | $CH_3$ | $CH_3$ | 〃 | 150 | 165 | 189 | 210 | 280 | 12.97 | 13.07 | 158 | * | | |
| 13 |  | $C_2H_5$ | $C_2H_5$ | 〃 | 167 | 185 | 209 | 230 | Ca. 290 (dec.) | 11.21 | 11.56 | * | 190 | 30.10 | 29.91 |
| 14 |  | $CH_3$ | $CH_3$ | 〃 | 170 | 195 | 219 | 240 | 310 (dec.) | 13.36 | 13.45 | * | red. | | |
| 15 |  | $C_2H_5$ | $C_2H_5$ | 〃 | 180 | 197 | 222 | 242 | 313 (dec.) | 11.60 | 11.85 | 115 | red. | | |
| 16 |  |  | $-CH_2-CH_2-OH$ | Viscous (colorless) | 264 | 282 | 311 | 330 (dec.) | | 9.24 | 9.33 | 141 | 147 | 27.45 | 27.47 |

* Not obtained in crystalline form.

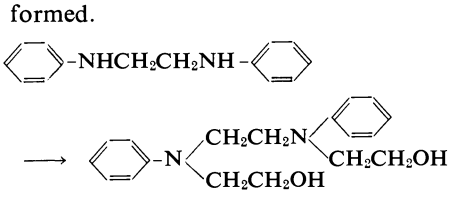
Key to abbreviation: Phys. form=physical form; liq.=liquid; dec. p.=decomposition point; red.=Platinichloride was reduced; mob. liq.=mobile liquid.




In the Experimental Part, synthesis of *N*-(β-diethylaminoethyl)-*N*-cyclohexylethanolamine ($I_{13}$) is cited.

The next step of this piperazine-synthesis is the formation of *O*-acetyl compounds from the *N*, *N'*, *N'*-trisubstituted *N*-β-aminoethylethanolamines with acetic anhydride. By the careful fractional distillation of the reaction mixture under reduced pressure the *O*-acetyl derivatives are obtained in an almost theoretical yield. However, the distillation must be carried out under fairly low pressure, say 10 mmHg, in order to obtain the *O*-acetyl compounds in a pure form, because they have a tendency to undergo decomposition over 200°C to piperazine derivatives. For any practical purpose. the *O*-acetyl compounds need not be isolated. The yields of piperazines are 70 to 95 per cent.

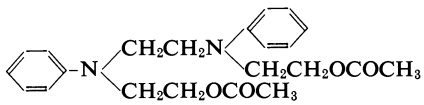
In the preparation of the compounds $III_1$ to $III_{15}$ from the corresponding *O*-acetyl compounds, methyl acetate or ethyl acetate is formed. From $II_{16}$, however, ethylene diacetate is formed.



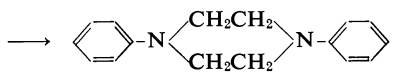

($I_{16}$)

TABLE II. PROPERTIES OF $R'N\langle^{CH_2CH_2N(R'')R'''}_{CH_2CH_2OCOCH_3}$

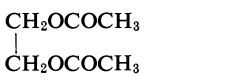
| Comp. No. | R′ | R″ | R‴ | Phys. form (color) | M.p. °C | B.p., °C/mmHg 10 | 20 | 50 | 100 | 760 | N, % Found | Calcd. | Picrate M.p. °C | Platinichloride Dec. p. °C | Pt, % Found | Calcd. |
|---|---|---|---|---|---|---|---|---|---|---|---|---|---|---|---|---|
| 1 | $CH_3$ | $CH_3$ | $CH_3$ | Oily liq. (colorless) | | 102 | 119 | 140 | 159 | Ca. 220 (dec.) | 14.58 | 14.88 | 263 | 222 | 32.49 | 32.62 |
| 2 | $C_2H_5$ | $C_2H_5$ | $C_2H_5$ | 〃 | | 125 | 142 | 166 | 186 | Ca. 230 (dec.) | 12.11 | 12.16 | 141 | 224 | 30.35 | 30.47 |
| 3 | $n$-$C_3H_7$ | $n$-$C_3H_7$ | $n$-$C_3H_7$ | 〃 | | 148 | 167 | 191 | 210 | Ca. 256 (dec.) | 10.22 | 10.28 | 134 | 222 | 28.35 | 28.59 |
| 4 | $n$-$C_4H_9$ | $n$-$C_4H_9$ | $n$-$C_4H_9$ | 〃 | | 167 | 185 | 209 | 230 | 229 (dec.) | 8.80 | 8.91 | 125 | 223 | 26.90 | 26.93 |
| 5 | $CH_3$ | $C_2H_5$ | $C_2H_5$ | 〃 | | 104 | 124 | 148 | 170 | 240 (dec.) | 13.10 | 12.95 | 163 | 166 | 31.23 | 31.16 |
| 6 | $n$-$C_3H_7$ | $C_2H_5$ | $C_2H_5$ | 〃 | | 127 | 146 | 169 | 190 (dec.) | | 11.50 | 11.46 | 105 | 208 | 29.70 | 29.82 |
| 7 | $n$-$C_4H_9$ | $C_2H_5$ | $C_2H_5$ | 〃 | | 128 | 157 | 180 | 202 (dec.) | | 10.71 | 10.89 | 125 | 222 | 29.40 | 29.19 |
| 8 |  | $C_2H_5$ | $C_2H_5$ | 〃 | | 180 | 200 | 225 | (dec.) | | 9.32 | 9.58 | 132 | 220 | 27.80 | 27.78 |
| 9 | $CH_3$ | $n$-$C_4H_9$ | $n$-$C_4H_9$ | 〃 | | 156 | 172 | 195 | 216 | (dec.) | 10.11 | 10.23 | 149 | 233 | 28.70 | 28.59 |
| 10 | $C_2H_5$ |  | $CH_3$ | Viscous (colorless) | | 196 | 215 (dec.) | | | | 10.59 | 10.60 | 98 | red. | | |
| 11 | $CH_3$ |  | $C_2H_5$ | 〃 | | 190 | 210 (dec.) | | | | 11.09 | 10.60 | 132 | 221 | 28.96 | 28.94 |
| 12 |  | $CH_3$ | $CH_3$ | 〃 | | 142 | 160 | 184 | 205 | (dec.) | 10.72 | 10.93 | Ca. 290 | 215 | 29.20 | 29.28 |
| 13 |  | $C_2H_5$ | $C_2H_5$ | 〃 | | 170 | 190 | 214 | 235 (dec.) | | 9.77 | 9.85 | 185 | 210 | 28.01 | 28.11 |
| 14 |  | $CH_3$ | $CH_3$ | 〃 | | 195 | 219 | 240 (dec.) | | | 11.36 | 11.19 | * | red. | | |
| 15 |  | $C_2H_5$ | $C_2H_5$ | 〃 | | 240 | 250 (dec.) | | | | 10.12 | 10.06 | 160 | 232 | | |
| 16 |  |  | $-CH_2CH_2OCOCH_3$ | Cryst. 76 (colorless) | | (243/3 mmHg dec.) | | | | | 7.20 | 7.29 | 140 | 202 | 24.80 | 24.56 |

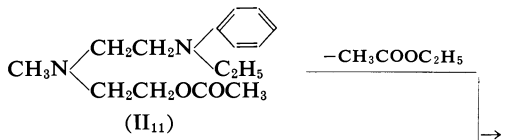


($II_{16}$)

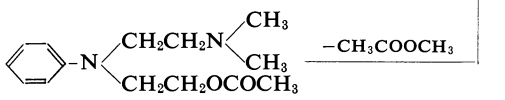


($III_{16}$)

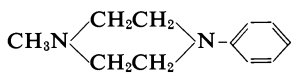




($II_{11}$)



($II_{14}$)



($III_{11}$, $III_{14}$)

$II_{11}$ and $II_{14}$ give the same product with liberation of ethyl acetate and methyl acetate respectively. This is also the case with $II_{10}$ and $II_{15}$.

In the Experimental Part, preparations of *N*, *N*′-dimethylpiperazine ($III_1$), *N*-methyl-*N*′-phenylpiperazine ($III_{14}$), and *N*, *N*′-diphenylpiperazine ($III_{16}$) have been cited.

TABLE III. PROPERTIES OF R'N<$CH_2CH_2$ / $CH_2CH_2$>NR''

| Comp. No. | R' | R'' | Phys. form (color) | M. p. °C | B. p., °C/mmHg 10 | 20 | 50 | 100 | 760 | N, % Found | Calcd. | Picrate M. p. °C | Platinichloride Dec. p. °C | Pt, % Found | Calcd. |
|---|---|---|---|---|---|---|---|---|---|---|---|---|---|---|---|
| 1 | $CH_3$ | $CH_3$ | Mob. liq. (colorless) | | | | 40 | 62 | 132 | 29.51 | 24.53 | 280 (dec.) | Ca. 270 | 37.25 | 37.23 |
| 5 | $CH_3$ | $C_2H_5$ | 〃 | | | 36 | 61 | 82 | 151～153 | 21.70 | 21.85 | 255 (dec.) | 248 | 36.35 | 36.26 |
| 9 | $CH_3$ | $n$-$C_4H_9$ | 〃 | | 62 | 81 | 105 | 126 | 196 | 18.03 | 17.93 | Ca. 240 (dec.) | 280 | 38.45 | 34.46 |
| 12 | $CH_3$ |  | Oily liq. (colorless) | | 111 | 131 | 155 | 196 | 246 | 15.42 | 15.37 | 224 (dec.) | 257 | 33.00 | 32.95 |
| 11, 14 | $CH_3$ |  | Viscous (yellowish) | 35 | 133 | 150 | 175 | 196 | 266 | 15.80 | 15.90 | Ca. 210 | 245 | 32.99, 33.10 | 33.29 |
| 2 | $C_2H_5$ | $C_2H_5$ | Oily liq. (colorless) | | 37 | 56 | 80 | 101 | 171～173 | 19.77 | 19.70 | Ca. 250 (dec.) | 263 | 35.32 | 35.34 |
| 6 | $C_2H_5$ | $n$-$C_3H_7$ | 〃 | | 52 | 76 | 94 | 115 | 188 | 19.82 | 19.93 | 235 | 225 | 34.45 | 34.46 |
| 7 | $C_2H_5$ | $n$-$C_4H_9$ | 〃 | | 76 | 95 | 119 | 140 | 210 | 16.24 | 16.45 | 230 | 260 | 33.50 | 33.63 |
| 8 | $C_2H_5$ |  | 〃 | | 150 | 170 | 194 | 208 | 278 | 13.40 | 13.71 | 147 | 260 | 31.63 | 31.77 |
| 13 | $C_2H_5$ |  | 〃 | | 134 | 152 | 177 | 197 | 268 | 14.12 | 14.27 | 220 | 258 | 32.03 | 32.18 |
| 10, 15 | $C_2H_5$ |  | Viscous (yellowish) | | 150 | 170 | 144 | 215 | 285 | 14.62 | 14.72 | 164 | 245 | 32.52, 32.57 | 32.51 |
| 3 | $n$-$C_3H_7$ | $n$-$C_3H_7$ | Oily liq. (colorless) | | 74 | 93 | 117 | 138 | 207～209 | 16.47 | 16.45 | 258 (dec.) | 275 | 33.70 | 33.63 |
| 4 | $n$-$C_4H_9$ | $n$-$C_4H_9$ | 〃 | | 99 | 127 | 152 | 173 | 243 | 14.17 | 14.12 | 245 (dec.) | Ca. 280 | 32.05 | 32.08 |
| 16 |  |  | Cryst. (colorless) | 163 | 226 | 242 | 266 | 288 | (dec.) | 11.75 | 11.76 | 192 | 245 | 30.09 | 30.10 |

## Experimental

***N*,*N'*,*N'*-Trimethyl-*N*-β-aminoethylethanolamine** ($I_1$).—To a mixture of 52 g. (0.5 mol.) of *N*-β-aminoethylethanolamine and 350 g. of 80% formic acid, heated under reflux, was added 175 g. of formalin (30%) dropwise from a dropping funnel.

A vigorous reaction set in with the evolution of carbon dioxide.

When the addition of formalin was complete, the reaction mixture was boiled under reflux until no more gas was evolved (about 6 hr.). After an addition of 150 ml. of hydrochloric acid (approx. 6 N), the solution was evaporated to dryness under reduced pressure on a steam bath.

To the resulting solid, was added 200 g. of 30% sodium hydroxide solution.

The solution was extracted with ether using a continuous extraction apparatus, until no more volume diminution of the aqueous layer was observed. After the removal of the ether, the residue was distilled fractionally. From the etherial solution there was obtained by the fractinal distillation 58～64 g. of $I_1$, a colorless oily liquid, b. p. 206°C, in an 80% yield.

This compound is readily miscible with water, alcohol, acetone and benzene; $d_4^{20}$ 0.9044. The hydrochloride is colorless crystals, m. p. 187°C.

***N*,*N'*,*N'*,-Tri-*n*-butyl-*N*-β-aminoethylethanolamine** ($I_4$).—In a three-necked flask equipped with a reflux condenser, a thermometer and a dropping funnel, was placed 52 g. (0.5 mol.) of *N*-β-aminoethylethanolamine, and heating was commenced.

When the temperature rose to about 100°C, 37 g. (0.25 mol.) of *n*-butyl bromide was carefully added from the dropping funnel.

When the addition was complete, the temperature of the reaction mixture was raised to about 180°C, and then the mixture was allowed to stand to cool. A hot solution of 14 g. of potassium hydroxide in 30 ml. of methyl alcohol was poured in, shaking well. The crystals of potassium bromide were separated by filtration, and washed with a small amount of methyl alcohol.

From the filtrate methyl alcohol and water were distilled off. The distillation was discontinued when the temperature of the residue in the flask reached 150°C.

This procedure was repeated twice, using 18.5 g. (0.125 mol.) of *n*-butyl bromide and 7 g. (0.125 mol.) of potassium hydroxide in 30 ml. of methyl alcohol the first time, and 10 g. of *n*-butyl bromide and 8 g.

of potassium hydroxide in 20 ml. of methyl alcohol in the second. $I_4$ was purified by distillation under reduced pressure. There was obtained about 110 g. of $I_4$ (approx. 80%) as a colorless oily liquid, b. p. 162°C/10 mmHg or 180°C/20 mmHg.

Almost the same yields were obtained with $I_2$ and $I_3$ in a manner similiar to that described above.

***N*-Methyl-*N*-(β-diethylaminoethyl) ethanolamine** ($I_5$). — Forty grams (0.25 mol.) of *N*-(β-diethylamino-ethyl)ethanolamine was mixed with 40 g. of formic acid (80%). With boiling under reflux, 25 g. of formalin was added dropwise.

The reaction was carried out in the same manner as in $I_1$. The yield of $I_5$, b. p. 225~226°C, was 35 g. (80%).

Similarly, *N*-methyl-*N*-(β-di-*n*-butylaminoethyl)-ethanolamine ($I_9$) could be prepared from *N*-(β-di-*n*-butylaminoethyl)ethanolamine.

***N*-Ethyl-*N*-(β-methylamino-ethyl) ethanolamine** ($I_{10}$). —In a pressure vessel, 22 g. (0.5 mol.) of ethylene oxide dissolved in 50 ml. of methyl alcohol was added to 76 g. (0.5 mol.) of *N*-methyl-*N*-phenyl-ethylenediamine and the mixture was allowed to stand until an exothermal but not violent reaction was complete.

Fractional distillation of this reaction mixture under reduced pressure gave about 30 g. of *N*-(β-methylanilinoethyl)ethanolamine, boiling at 182°C/10 mmHg, 199°C/20 mmHg, or 317°C/760 mmHg. From the fore-run of the distillation, about 20 g. of unchanged starting material, *N*-methyl-*N*-phenyl-ethylenediamine, was recovered (b. p. 124°C/10 mmHg, 142°C/20 mmHg, 257°C/760 mmHg). From the after-run, about 40 g. of *N*-(β-methylanilino-ethyl)-diethanolamine was obtained in the form of colorless oily liquid boiling at 208°C/10 mmHg or 231°C/20 mmHg.

For the purpose of preparing $I_{10}$, a mixture of 19.5 g. (0.1 mol.) of *N*-(β-methylanilino-ethyl)-ethanolamine and 11 g. (0.1 mol.) of ethyl bromide was heated under reflux.

After completion of the vigorous reaction, the reaction mixture was neutralized by adding a sodium hydroxide solution using phenolphthalein as the indicator. The oily layer was separated and distilled under reduced pressure.

There was obtained about 18 g. of $I_{10}$, as a colorless oily liquid boiling at 179°C/10 mmHg or 190°C/20 mmHg in an 80% yield.

***N*-(β-Diethylamino-ethyl)-*N*-cyclohexylethanolamine** ($I_{13}$). — A mixture of 18 g. (0.1 mol.) of *N*-(β-aminoethyl)-*N*-cyclohexylethanolamine (a colorless oily liquid, b. p. 162°C/10 mmHg, 181°C/20 mmHg, or 295°C/760 mmHg), and 11 g. (0.1 mol.) of ethyl bromide was heated under reflux. After a vigorous reaction had subsided, the cooled reaction mixture was made alkaline with 30% sodium hydroxide solution using phenolphthalein as the indicator.

The oily product that separated was shaken with an equal volume of water**, and distilled fractionally.

About 18 g. of $I_{13}$ was obtained as acolorless oily liquid, boiling at 167°C/10 mmHg or 185°C/20 mmHg.

** There is no appreciable difference between the boiling point of the starting material and that of $I_{13}$. But the former is miscible with water at any proportion, and the latter is sparingly soluble in it. The separation depends upon this difference of solubility.

***N*, *N'*-(Bis-β-hydroxxethyl)-*N*, *N'*-diphenyl-ethylenediamine** ($I_{16}$).—To 42 g. (0.2 mol.) of *N*,*N'*-diphenylethylenediamine was added 18 g. (0.4 mol.) of ethyleneoxide dissolved in 50 ml. of methyl alcohol. After being stored in a refrigerator for two days, the mixture was distilled. At 264°C/10 mmHg or 282°C/20 mmHg. $I_{16}$ was distilled off quantitatively as a colorless and strongly viscous liquid. The melting point of its picrate was 141°C, and that of its platinichloride 147°C.

***N*-Methyl-*N*-(β-dimethylamino-ethyl) aminoethyl Acetate** ($II_1$).—Acetic anhydride (12.5 g.) was added to 14.5 g. (0.1 mol.) of $I_1$. By fractional distillation of the mixture, $II_1$ was obtained at 119°C/20 mmHg, or 140°C/50 mmHg as a colorless oily liquid. The yield was 17 g. (approx. 90%).

***N*,*N'*-Dimethylpiperazine** ($III_1$).—$II_1$ was placed in a Claisen flask equipped with a thermometer inserted through the straight neck to indicate the internal temperature and another thermometer fixed in the side neck to detect the distilling temperature.

Distillation was carefully carried out. At the beginning, the temperature of the content remained at about 206°C, the boiling point of $II_1$. As the decomposition of $II_1$ proceeded, the internal temperature gradually fell, and the distillation of the methyl acetate began. After the theoretical amount of methyl acetate had distilled over, *N*,*N'*-dimethyl-piperazine was collected at 110~140°C.

Redistillation gave the pure product boiling at 130~132°C. The yield was 90% or greater.

***N*-Ethyl-*N'*-phenylpiperazine** ($III_{15}$).—A reaction mixture of 25 g. (0.1 mol.) of *N*-(β-diethylamino-ethyl)-*N*-phenylethanolamine ($I_{15}$) and 12 g. (0.12 mol.) of acetic anhydride was distilled in the same manner as in the preceding example.

After acetic acid formed and the excess acetic anhydride had distilled out, the temperature of the content increased gradually, reaching 300°C at one time. But as the decomposition proceeded, the internal temperature fell somewhat and ethyl acetate began to distill off at 80~100°C. After completion of the decomposition, the resulting brown liquid was purified by vacuum distillation. This purification furnished about 15 g. of $III_{15}$ in an 80% yield as a yellowish viscous liquid.

***N*, *N'*-Diphenylpiperazine** ($III_{16}$). — Acetic anhydride (25 g.; ca. 0.24 mol.) was added to 30 g. (0.1 mol.) of $I_{16}$. The reaction mixture was submitted to distillation in the same manner as in the preceding example with the object of decomposing it into $III_{16}$ and ethylenediacetate, which distilled out 180~190°C. The residual material was further distilled under reduced pressure. Recrystallization of the solidified distillate from methyl alcohol afforded about 18 g. of $III_{16}$ in colorless crystals, m. p. 163°C. The yield was about 80% of the theory.

The author is deeply grateful to Professor Ryozo Goto, Kyoto University, for giving much helpful advice and encouragement during the course of this work.

*Kyoto Works*
*Teikoku Chemical Industry Co., Ltd.*
*Nakagyo-ku, Kyoto*

# *Radiation-induced Reaction in an Aqueous Benzoic Acid Solution. I. Dose and Dose Rate Dependencies of Salicylic Acid, and of Biphenyldicarboxylic Acids*

By Akihisa SAKUMOTO and Gen-ichi TSUCHIHASHI

(Received July 28, 1960)

Reactive species such as hydrogen atoms and hydroxyl radicals, and so-called "molecular" products hydrogen and hydrogen peroxide from water are yielded by the actions of ionizing radiation on aqueous solutions. Hydrogen atoms and hydroxyl radicals in these species react rapidly with many solutes dissolved in solutions. The reaction of many organic compounds with these reactive species has been studied by a number of workers.

The radiation-induced reaction of an aqueous benzoic acid solution was studied first by Weiss[1] using X-rays, and recently by Downes[2] using very weak Co-60 gamma rays source. Little attention had been paid by earlier workers to the effect of dissolving oxygen occurring in the reactions when solutions of organic compounds were irradiated by ionizing radiations. The presence of molecular oxygen during irradiation, however, would lead not only to the quantitative differences in the efficiency of the oxidative process but also to some qualitative differences in the reaction products.

In the present work, the radiation-induced reaction of an aqueous benzoic acid solution with, and without, molecular oxygen has been studied and does and dose rate dependencies of the yield of salicylic acid, and of biphenyldicarboxylic acids produced have been examined at high dose and high dose rate, using 10 kc. Co-60 source of the Japan Atomic Energy Research Institute[3].

## Experimental

**Materials.** — Benzoic acid used in this work, obtained from a commercial source, was purified by recrystallization four times from ethanol, m. p. 122°C (uncorrected). Demineralized water was used to prepare a benzoic acid solution. Nitrogen to remove the oxygen contained in sample solutions was purified by letting it bubble through slightly acidified vanadyl sulfate solution[4]. Bomb oxygen was used without further purification.

**Preparation of Solutions.**—Solutions were 0.300% with regard to benzoic acid, and the pH was not specially adjusted. In order to prepare an oxygen free solution, oxygen contained in the solution was driven off by letting purified nitrogen bubble through for two hours. After this treatment, the concentration of oxygen in the solution is estimated to be lower than $1.9\times10^{-5}$ mol./l.[5] Solutions were charged in 30 ml. test tubes, fitted with glass stoppers. The irradiation vessels were cleaned with cleaning solution, rinsed several times, and then washed with distilled water.

Saturation of oxygen during the irradiation was held by continuous bubbling of bomb oxygen in the sample solution. ($[O_2]$ was measured to be $1.2\times10^{-3}$ mol./l.)[5]

**Irradiation.** — Both solutions with and without molecular oxygen were irradiated with gamma rays from 10 kc. Co-60 source with absorbed dose from $6.2\times10^5$ to $1.1\times10^7$ r and with dose rate from $2.7\times10^4$ to $3.9\times10^5$ r/hr. at room temperature. Dose rates were measured by means of both ferrous—ferric[6] and ceric-cerous[7] dosimeters, and the amount of energy absorbed in the solutions was calculated using $G$-values of $Fe^{2+}$ oxidized to $Fe^{3+}$ being 15.5 and of $Ce^{4+}$ reduced to $Ce^{3+}$ being 2.45.

**Determination of Salicylic Acid.** — The determination of salicylic acid was carried out by colourimetry. After adjusting the pH of the irradiation solution which, if necessary, was filtered off, between 2.5 and 2.8 by means of 50% acetic acid—3% ammonium acetate buffer, an adequate of 1% ferric chloride solution was added to give salicylic acid complex. The absorbance of salicylic acid complex was measured spectrophotometrically at 530 m$\mu$.

**Determination of Biphenyldicarboxylic Acids.**— Irradiation in the absence of oxygen gave biphenyldicarboxylic acids as precipitate. The precipitate including three isomers of biphenyldicarboxylic acids was separated from the solution using the ultracentrifuge. The collected precipitate was dried for five hours at 80~85°C. Yields of biphenyldicarboxylic acids were determined gravimetrically. Biphenyldicarboxylic acids did not precipitate in the case of irradiation with oxygen.

1) J. Weiss, H. Leobl and G. Stein, *J. Chem. Soc.*, **1951**, 405.
2) A. M. Downes, *Auster. J. Chem.*, **2**, 155 (1958).
3) A. Danno et al., The 7th Hot Laboratories and Equipment Conference, Cleveland (1959), pp. 349~360.
4) L. Meites and J. Meites, *Anal. Chem.*, **20**, 984 (1948).
5) H. Hotta, A. Terakawa and S. Ōno, This Bulletin, **33**, 442 (1960).
6) G. R. A. Johnson and J. Weiss, *Proc. Roy. Soc.*, **A240**, 189 (1957).
7) For example, T. Rigg, G. Stein and J. Weiss, ibid., **A211**, 375 (1952).

## Results and Discussion

Aqueous solutions of benzoic acid were irradiated with Co-60 gamma rays at a fixed absorbed dose of $3.8\times10^5$ r by varying dose rate from $2.7\times10^4$ to $3.9\times10^5$ r/hr. The yield of salcylic acid produced is plotted against the dose rate in Figs. 1 and 2, in which Fig. 1 shows the case of oxygen saturated solutions and Fig. 2 the case of oxygen free solutions. As is shown in these figures, the yield of salicylic acid is decreasing with increasing dose rate in both systems. The yield of salicylic acid in the presence of oxygen was about ten times greater than that in the absence of oxygen.

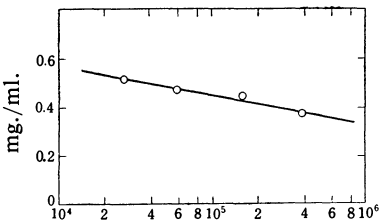



Fig. 1. Yields of salicylic acid produced in oxygen saturated solutions against dose rate. Dose is constant, $3.8\times10^6$ r.

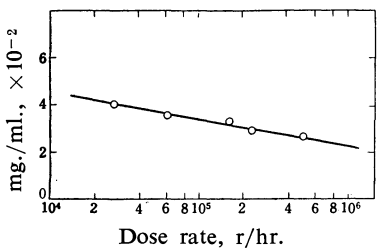



Fig. 2. Yields of salicylic acid produced in oxygen free solutions against dose rate. Dose is constant, $3.8\times10^6$ r.

Dose dependence of the yield of salicylic acid by a varying absorbed dose from $6.2\times10^5$ to $1.1\times10^7$ r at a fixed dose rate of $1.6\times10^5$ r/hr. is shown in Figs. 3 and 4, where Fig. 3 shows the system of oxygen saturated and Fig. 4 shows the system of oxygen free solution. Two curves show the same trend that the yield of salicylic acid at high dose is not linearly increasing with the absorbed dose, but gradually increases to approach some constant value. Salicylic acid was produced in both with, and without, molecular oxygen solutions, but biphenyldicarboxylic acids were not observed in the oxygen saturated solutions.

Absorbed dose and dose rate dependencies of yields of biphenyldicarboxylic acids were also studied. Figure 5 shows the plot of yields of biphenyldicarboxylic acids against dose rate.

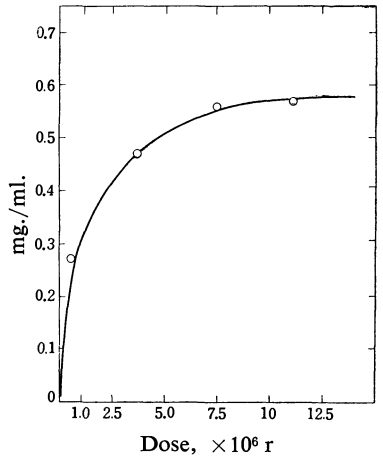



Fig. 3. Yields of salicylic acid produced in oxygen saturated solutions against dose. Dose rate is constant, $1.6\times10^5$ r/hr.

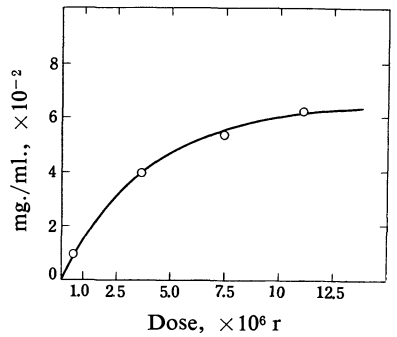



Fig. 4. Yields of salicylic acid produced in oxygen free solutions against dose. Dose rate is constant, $1.6\times10^5$ r/hr.

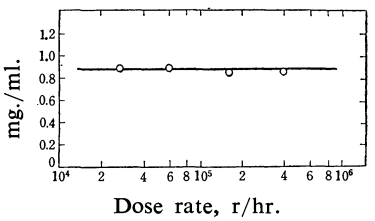



Fig. 5. Yields of biphenyldicarboxylic acid produced in oxygen free solutions against dose rate. Dose is constant, $3.8\times10^6$ r.

In this case, the absorbed dose was constant at $3.8\times10^6$ r. The yield of the dimer was constant independently of dose rates and $G=0.94$ was obtained. Figure 6 shows yields of biphenyldicarboxylic acids against the absorbed dose, which were produced when irradiation was carried out at a fixed dose rate of $1.6\times10^5$ r/hr. As is shown in this figure, yields of biphenyldicarboxylic acids have a linear relationship with the absorbed dose. This relationship is quite different from that of the

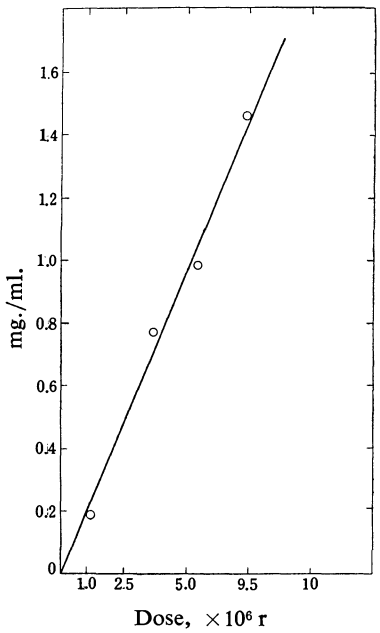



Fig. 6. Yields of biphenyldicarboxylic acid produced in oxygen free solutions against dose. Dose rate is constant, $1.6\times10^5$ r/hr.

yield of salicylic acid as is shown in Figs. 3 and 4.

Basing on the above results, the mechanism of the radiation-induced reaction in an aqueous solution of benzoic acid is assumed as follows.

In the present experiment, the concentration of benzoic acid was 3.0 mg./ml. of solution. At this relatively low concentration, the direct-hit effects of benzoic acid by gamma rays can be neglected. Water is decomposed by ionizing radiation into hydrogen atom, hydroxyl radical, hydrogen peroxide and hydrogen[8].

$$H_2O \rightsquigarrow H\cdot,\ HO\cdot,\ H_2O_2,\ H_2 \qquad (1)$$

Accordingly, the radiation-induced reaction in a dilute aqueous solution is assumed to be initiated by reactive species such as the hydrogen atom and/or the hydroxyl radical produced from the radiolytic decomposition of water.

When water containing molecular oxygen was irradiated, the hydrogen atom produced according to Eq. 1 reacts rapidly with dissolving oxygen giving the hydroperoxy radical[9].

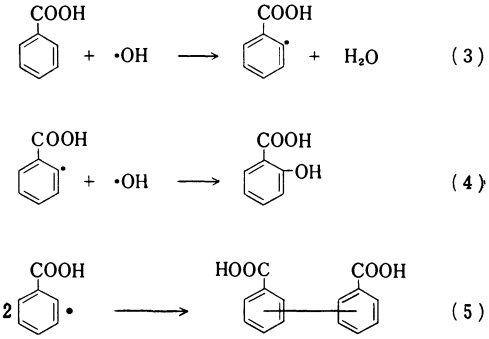
$$H\cdot + O_2 \rightarrow HO_2\cdot \qquad (2)$$

Owing to this reaction, the concentration of hydrogen atom in the presence of oxygen may be considerably lower than that in the absence of oxygen.

If this fact is taken into consideration, radiation-induced reaction in an aqueous solution containing molecular oxygen must be initiated by the hydroxyl radical and/or the hydroperoxy radical formed according to Eq. 2. However, it should be noticed that the hydroperoxy radical is assumed to have less oxidizing power than the hydroxyl radical on thermodynamic grounds because the bond dissociation energy of hydrogen peroxide, $D(H\text{-}O_2H)$, calculated to be 90 kcal./mol., is smaller than that of water, $D(H\text{-}OH)$, calculated to be 118 kcal./mol.[10]

Therefore, the hydroperoxy radical appears to be unreactive directly towards benzoic acid. From these reasons, it would be reasonable to consider that the disappearance of benzoic acid in an aqueous solution is initiated by hydrogen-abstraction with the hydroxyl radical produced from radiolytic decomposition of water.

Dehydrogenation of ring hydrogen of benzoic acid, giving hydroxycarbonylphenyl radical as an intermediate, can be followed by a two reaction process: first, the reaction of this radical with hydroxyl radical to form salicylic acid which shows the hydroxylation of ortho-position of benzoic acid, and second, the dimerization of these radicals to produce biphenyldicarboxylic acid as follows.




Biphenyldicarboxylic acids including all kinds of their isomers are insoluble in water giving a pale yellow precipitate and consequently do not suffer from further reaction. The yield of these acids is independent on the dose rate as is shown in Fig. 5, and has a first order relationship with the absorbed dose in the range of the present work (up to $1.1\times10^7$ r) as is shown in Fig. 6. These results signify that the formation of hydroxycarbonylphenyl radical produced as an intermediate according to Eq. 3 is linearly dependent on the absorbed dose.

8) A. O. Allen and H. A. Schwarz, Proceedings of the Second United Nations International Conference on the Peaceful Uses of Atomic Energy, **29**, 30 (1958).

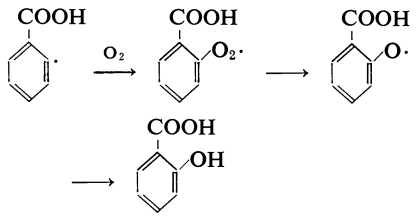
9) P. Riesz and E. J. Hart, *J. Phys. Chem.*, **63**, 858 (1959).

10) J. Weiss, *Internat. J. Appl. Radiation Isotopes*, **6**, 52 (1959).

Hydroxylation of benzoic acid takes place in all possible positions. Accordingly, three isomers of hydroxybenzoic acid may be formed. In the present work, the yield of only isomer, *o*-hydroxybenzoic acid, i. e. salicylic acid, was determined. The yield of salicylic acid at high dose does not show a linear relationship with absorbed dose, but increases gradually with increasing absorbed dose as is shown in Figs. 3 and 4. On the other hand, it is evident from the experimental results of Weiss[1] that the yield of the acid at the low dose (up to $5\times10^4$ E. U. in his work) has a linear relationship with the absorbed dose. It would seem, therefore, that the trend of the dose-yield curve of salicylic acid at the high dose in the present work may suggest further hydroxylation of salicylic acid to give di-hydroxybenzoic acids and the formation of these acids being more and more remarkable with increasing absorbed dose.

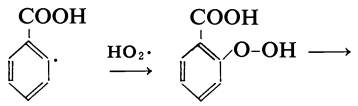
When irradiation of an aqueous solution containing molecular oxygen was carried out, hydroxylation of benzoic acid increased remarkably in comparison with that of the molecular oxygen free solution and the dimerization of hydrocarbonylphenyl radical did not occur. Therefore, the mechanism in this case must be mentioned compared to the different mechanism described above.

If a sufficient amount of molecular oxygen exists in an aqueous solution, it reacts easily with the hydroxycarbonylphenyl radical, as well as the hydrogen, and this reaction results finally in the formation of salicylic acid.




(6)

Consequently, the dimerization of the hydroxycarbonylphenyl radical was suppressed. Concerning the formation of salicylic acid in the presence of molecular oxygen, there is the possibility also of the reaction,




(7)

which can also lead to the eventual formation of salicylic acid. The contribution of this reaction is assumed to be small, because the concentration of oxygen is greater than that of hydroperoxy radical, provided that the reaction rate of the reaction 6 is of the same order as that of 7.

The authors wish to express hearty thanks to Professor Kenjiro Kimura, a director of the Institute, and Dr. A. Danno for their kind encouragement and discussion throughout the entire course of this study.

*Division of Radiation Applications*
*Japan Atomic Energy Research Institute*
*Tokai, Ibaraki-ken*

# *Radiation-induced Reaction in an Aqueous Benzoic Acid Solution. II. Determination of Products by Isotope Dilution Method*

By Akihisa SAKUMOTO and Gen-ichi TSUCHIHASHI

(Received August 3, 1960)

In the preceding paper*, dose and dose rate dependencies of the yield of salicylic acid, and of biphenyldicarboxylic acids were studied in the presence or the absence of molecular oxygen when aqueous solutions of benzoic acid were irradiated with Co-60 gamma rays. In the presence of molecular oxygen, the yield of salicylic acid was greater than that in the absence of molecular oxygen and biphenyldicarboxylic acids was not produced, whereas in the absence of melecular oxygen the main products were biphenyldicarboxylic acids. In the preceding paper, the isomers of hydroxybenzoic and biphenyldicarboxylic acids produced in the solution could not be identified.

The determination of 2-, 3- and 4-hydroxybenzoic acid and biphenyl as reaction products was carried out by Weiss and his collaborators

* Part I: A. Sakumoto and G. Tsuchihashi, This Bulletin, 34, 660 (1961).

using paper chromatography[1]. Recently, Downes separated the isomers of monohydroxybenzoic acids from benzoic acid, and the isomers of dihydroxybenzoic acids from salicylic acid as reaction products by radioactive assay and radiochromatography[2].

In the present work, an isotope dilution method was applied in order to determine the reaction products in the radiolysis of aqueous solutions of benzoic acid (carboxyl-$^{14}$C) in the presence or the absence of molecular oxygen. From the results obtained, a mechanism of the radiation-induced reaction will be discussed.

## Experimental

**Materials.**—Benzoic acid (carboxyl-$^{14}$C) was synthesized from phenylmagnesium bromide and $^{14}CO_2$ by Grignard reaction[3]. This acid was purified by recrystallization from ethanol-water to give a constant specific activity. The specific activity of the acid was $2.289\times10^{-2}$ mc./mol.

Each isomer of biphenyldicarboxylic acid used for the carrier of the isotope dilution method was synthesized according to the method cited in the literatures[4,5]. Each compound was purified by recrystallization except 4,4'-biphenyldicarboxylic acid which was purified by precipitation four times from dilute alkaline solution of it. The melting points** of the isomers were as follows: 2,2'-, 228.0~228.5°C; 3,3'-, 356~357°C. 4,4'-Biphenyldicarboxylic acid did not melt.

Commercial grade 2-, 3-, 4-hydroxybenzoic acid and 2,3-, 2,4-, 2,5-, 2,6-dihydroxybenzoic acid were also purified by recrystallization. The melting points** of the isomers were as follows; 2-, 157~158.5°C; 3-, 200~200.5°C; 4-, 213~213.5°C; 2,3-, 205~206°C; 2,4-, 212.5~213°C; 2,5-, 199~200°C; 2,6-, 149~151°C.

**Preparation of Solution.**—The preparation of 0.300% aqueous benzoic acid (carboxyl-$^{14}$C) solution was carried out by dissolving it in demineralized water. The pH of the solution was not specially adjusted. The irradiation samples of both oxygen free and saturated solution were prepared as described in the preceding paper.

**Irradiations.**—The irradiation vessels and method have been described in the preceding paper. In the present work, irradiations were carried out at the dose rate of $1.6\times10^5$ r/hr. and the absorbed dose of $4.0\times10^6$ r in the presence of molecular oxygen and at the dose rate of $1.7\times10^5$ r/hr. and the absorbed dose of $4.3\times10^6$ r in the absence of molecular oxygen at room temperature. The measurement of the absorbed dose was carried out according to the method as described in Part I.

**Radioactive Assay of Irradiation Products.**—Determination of the yield of irradiation products was carried out as follows. An adequate of analyzing carrier which was weighed accurately was added to an aliquot of irradiated solution, and then dissolved. After the solution was cooled to precipitate the added carrier, the precipitate was filtered off and purified several times by recrystallization to offer a constant counting rate after oxidation to barium carbonate.

Purification of 4,4'-biphenyldicarboxylic acid, being insoluble in ordinary organic solvents, was carried out by dissolving it in dilute sodium hydroxide and reprecipitating it by adding dilute hydrochloric acid.

The isotope dilution method was also applied in order to determine unreacted benzoic acid (carboxyl-$^{14}$C) left in the solution after irradiation. After the addition of non-active benzoic acid, the purification of the acid was carried out by recrystallization six time from ethanol-water and then by sublimation three or five times.

Each sample purified was oxidized according to the Van Slyke-Folch oxidation method[6]. Carbon dioxide liberated after oxidation of a purified sample was absorbed by 0.74 N sodium hydroxide solution and then precipitated as barium carbonate by adding 17.6% barium chloride-2.5% ammonium chloride solution.

The resulting barium carbonate was filtered off, washed with ethanol and dried. The specific activity of barium carbonate was measured at infinite thickness by a Tracerlab. T. G. C.-14 counter.

## Results

Isomers of hydroxybenzoic acid and biphenyldicarboxylic acid were assayed as products when

TABLE I. YIELDS OF PRODUCTS IN OXYGEN FREE SOLUTION OF BENZOIC ACID (CARBOXYL-$^{14}$C) IRRADIATED WITH Co-60 GAMMA RAYS

| Product | Weight mg./ml. | Yield % | *G*-Value |
|---|---|---|---|
| 2-Hydroxybenzoic acid | 0.040 | 1.3 | 0.066 |
| 3-Hydroxybenzoic acid | 0.047 | 1.6 | 0.077 |
| 4-Hydroxybenzoic acid | 0.056 | 1.9 | 0.092 |
| 2,2'-Biphenyldicarboxylic acid | 0.41 | 14 | 0.38 |
| 3,3'-Biphenyldicarboxylic acid | 0.072 | 2.4 | 0.068 |
| 4,4'-Biphenyldicarboxylic acid | 0.30 | 10 | 0.28 |
| Benzoic acid* | 1.86 | 62 | |
| −Benzoic acid** | 1.14 | 38 | 1.88 |

Dose, $4.3\times10^6$ r, dose rate, $1.7\times10^5$ r/hr.

* Unchanged benzoic acid (carboxyl-$^{14}$C) in the irradiated solution.

** The disappearance of benzoic acid (carboxyl-$^{14}$C), calculated from the amount of unchanged benzoic acid (carboxyl-$^{14}$C).

1) J. Weiss, H. Loeble and G. Stein, *J. Chem. Soc.*, **1951**, 405.
2) A. M. Downes, *Austr. J. Chem.*, **2**, 154 (1951).
3) W. G. Dauben and P. E. Yankwich, *Anal. Chem.*, **19**, 828 (1947).
4) "Organic Syntheses", Coll. Vol. I (1948), p. 222.
5) F. Ullman and O. Löwenthal, *Ann.*, **332**, 72 (1904).
** The melting point of each compound is uncorrected.
6) D. D. Van Slyke and H. Folch, *J. Biol. Chem.*, **136**, 509 (1940).

an aqueous solution of benzoic acid (carboxyl-$^{14}$C) irradiated in oxygen free solution. Results obtained are summarized in Table I shown as the yield and *G*-value of each reaction product. In Table I, benzoic acid indicates unchanged benzoic acid (carboxyl-$^{14}$C) which is left in the irradiated solution. *G*-Value of the disappearance of benzoic acid (carboxyl-$^{14}$C) shown as (-benzoic acid) in Table I, calculated from the amount of unchanged benzoic acid (carboxyl-$^{14}$C), is 1.88. The ratio of produced hydroxybenzoic acids and biphenyldicarboxylic acids is approximately 1:3. The *G*-value ratio of each hydroxybenzoic acid and each biphenyldicarboxylic acid will be discussed in the following section.

When irradiation was carried out in the presence of oxygen, the yield of products was quantitatively and qualitatively different from those in the absence of oxygen. 2,3-, 2,4-, 2,5- and 2,6-Dihydroxy benzoic acid are produced in place of isomers of biphenyldicarboxylic acid. The total amount of dihydroxy benzoic acids is 0.31 as *G*-value, being about one fifth of mono-hydroxybenzoic acids. Table II shows the yield and *G*-value of products in the oxygen saturated solution. In this case, *G*-value of 2,2'-biphenyldicarboxylic acid, the most abundant isomer in the irradiation of oxygen free solution, was estimated to be lower than 0.0003. Therefore, a noticeable amount of isomers of biphenyldicarboxylic acid was not observed in an oxygen saturated solution.

TABLE II. YIELDS OF PRODUCTS IN OXYGEN SATURATED SOLUTION OF BENZOIC ACID (CARBOXYL-$^{14}$C) IRRADIATED WITH Co-60 GAMMA RAYS

| Product | Weight mg./ml. | Yield % | *G*-value |
|---|---|---|---|
| 2-Hydroxybenzoic acid | 0.45 | 15 | 0.79 |
| 3-Hydroxybenzoic acid | 0.16 | 5.4 | 0.29 |
| 4-Hydroxybenzoic acid | 0.37 | 12 | 0.65 |
| 2,3-Dihydroxy-benzoic acid | 0.072 | 2.4 | 0.12 |
| 2,4-Dihydroxy-benzoic acid | 0.056 | 1.9 | 0.088 |
| 2,5-Dihydroxy-benzoic acid | 0.060 | 2.0 | 0.096 |
| 2,6-Dihydroxy-benzoic acid | 0.0036 | 0.12 | 0.0057 |
| Benzoic acid* | 1.31 | 61 | |
| −Benzoic acid** | 1.19 | 39 | 2.12 |
| 2,2'-Biphenyl-dicarboxylic acid | $2.9\times10^{-4}$ | | 0.0003 |

Dose, $4.0\times10^{6}$ r, dose rate, $1.6\times10^{5}$ r/hr.

* Unchanged benzoic acid (carboxyl-$^{14}$C) in the irradiated solution.

** The disappearance of benzoic acid (carboxyl-$^{14}$C) calculated from the amount of unchanged benzoic acid (carboxyl-$^{14}$C).

## Discussion

The mechanism of radiation-induced reaction of an aqueous solution of organic compound has been studied by a number of workers. The primary process of the reaction is assumed to be radiolytic decomposition of water. Recently, Burton and his collaborators proposed the following *G*-values for the species[7].

$$H_2O \rightsquigarrow H\cdot,\ HO\cdot,\ H_2,\ H_2O_2 \qquad (1)$$
$$G = 3.70\quad 2.93\quad 0.39\quad 0.78$$

These values will be used in the following discussion.

From the present results of radioactive assay, some information about the initial step of the radiation-induced reaction is obtained. As is shown in Tables I and II, *G*-values of the disappearence of benzoic acid were 2.12 in the presence of molecular oxygen and 1.88 in the absence of molecular oxygen. These values agree fairly well with each other in spite of irradiation conditions being different.

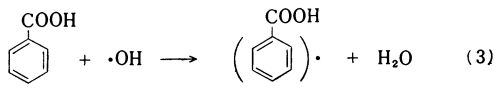
This agreement signifies that dissolving oxygen does not affect the initial step of the decomposition of benzoic acid. It would be, therefore, reasonable to consider that in both cases the initial stage of the reaction is initiated by the attack of the same radical on the benzoic acid molecule.

Hydrogen atom in the reactive species produced from water reacts easily with dissolving oxygen forming hydroperoxy radical in the presence of oxygen.

$$H\cdot + O_2 \rightarrow HO_2\cdot \qquad (2)$$

If the decomposition of benzoic acid is initiated by the hydrogen atom, it is impossible to explain the *G*-value of the decomposition of benzoic acid being almost of the same value regardless of the dissolving of oxygen. Consequently, a hydroxyl radical must be considered to be the only radical which can attack benzoic acid.

Based on the above reasons, the disappearence of benzoic acid in an aqueous solution is considered to be initiated by hydrogen-abstraction of hydroxyl radical as is proposed in the previous paper:



(3)

The concentration of hydroxycarbonylphenyl radical as an intermediate in the reaction must

7) K. C. Kurien, P. V. Phung and M. Burton, *Radiation Research*, 11, 283 (1959).

TABLE III. *G*-VALUE OF INTERMEDIATE RADICAL

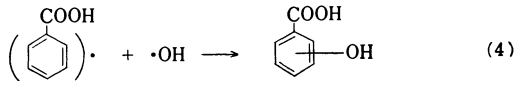
| Condition | Hydroxyl radical: Used for hydrogen-abstraction | Hydroxyl radical: Used for combination with H. C. P. radical | Total | H. C. P. radical*1 |
|---|---|---|---|---|
| Oxygen free | $G(H)$*2$+2G(B)$*3$=1.7$ | $G(H)=0.24$ | 1.94 | $G(H)+2G(B)=1.7$ |
| Oxygen saturated | $G(H)+2G(D)$*4$=2.3$ | zero | 2.3 | $G(H)+G(D)=2.0$ |

*1 H. C. P. radical is hydroxycarbonylphenyl radical
*2 The total *G*-value of hydroxybenzoic acids
*3 The total *G*-value of biphenyldicarboxylic acids
*4 The total *G*-value of dihydroxybenzoic acids
The *G*-value of hydroxyl radical produced in the primary process is 2.92[7].

be of the same value in both cases, because the *G*-value of hydroxyl radical produced primarily from radiolytic decomposition of water is constant of 2.93 regardless of whether with or without oxygen.

In spite of the constant *G*-value of the disappearance of benzoic acid, the products of the reaction in the presence of oxygen were quite different from those in the absence of oxygen. In the former case hydroxybenzoic acids were the predominant products, whereas biphenyldicarboxylic acids were the main products in the latter case.

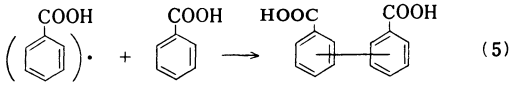
In the absence of oxygen, the total *G*-value of biphenyldicarboxylic acid as main product was 0.73, whereas that of hydroxybenzoic acid was 0.24. Hydroxybenzoic acid may be produced by the combination reaction of hydroxyl radical with hydroxycarbonylphenyl radical:



(4)

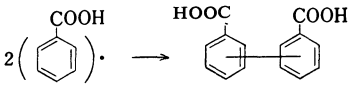
In this case, the amount of hydroxyl radical concerned in the hydroxylation of benzoic acid might be two fold of the amount of hydroxybenzoic acid, and so the *G*-value of this radical participating in the reaction will be calculated to be 0.48, and subsequently, the *G*-value of hydroxycarbonylphenyl radical produced in the reaction as an intermediate might be 0.24.

On the other hand, there are two possibilities of the formation of biphenyldicarboxylic acids from hydroxycarbonylphenyl radical. If biphenyldicarboxylic acids are produced by the substitution reaction of hydroxycarbonylphenyl radical as in the following,



(5)

the disappearance of benzoic acid in this case would be considerably greater than that in the presence of oxygen as mentioned below. It is because the same yield of hydroxycarbonylphenyl radical is proposed in both cases. Accordingly, the formation of biphenyldicarboxylic acids can be attributed to the dimerization of hydroxycarbonylphenyl radical.

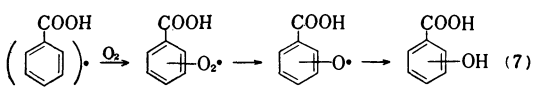


(6)

In this case, the amount of hydroxycarbonylphenyl radical converted into biphenyldicarboxylic acids is two times as much as that of biphenyldicarboxylic acid. If the predominant process of the reaction is the dimerization of hydroxycarbonylphenyl radicals, the total amount of hydroxycarbonylphenyl radical is 1.70 as calculated in Table III.

In the presence of molecular oxygen, hydroxybenzoic acids were predominant products. Noticeable amount of biphenyldicarboxylic acid was not observed. The *G*-value of 2,2′-biphenyldicarboxylic acid, the most abundant isomer in the absence of molecular oxygen, was reduced to the value of 0.0003. Therefore, it would be unlikely that hydroxybenzoic acid in the presence of molecular oxygen is produced by the combination reaction of hydroxycarbonylphenyl radical with a hydroxyl radical, because the formation of hydroxybenzoic acid by this type of the reaction would be, without fail, accompanying the formation of biphenyldicarboxylic acid as in the case of oxygen free solution.

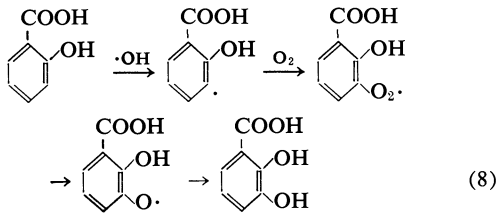
Hydroxycarbonylphenyl radical produced according to Eq. 3 reacts easily with dissolving oxygen to give a hydroxycarbonylphenylperoxy radical. It is, in general, considered that aromatic peroxide is very unstable. Consequently, the peroxy radical would decompose spontaneously into the phenoxy radical and then the reaction results finally in the formation of monohydroxybenzoic acid as is shown in the following:



(7)

The formation of dihydroxybenzoic acids as minor products may be also explained by the

same sequence starting from mono-hydroxybenzoic acid instead of benzoic acid. For example, the following sequence is given for 2, 3-dihydroxybenzoic acid:



(8)

The above mechanism is supported by the radiation-induced reaction of an aqueous ethanol solution by Weiss and collaborators[8]. They found butane-2, 3-diol as main products in the irradiation of an oxygen free solution,

$$CH_3\cdot CH_2OH \xrightarrow{HO\cdot} CH_3\cdot \dot{C}HOH$$

$$\rightarrow CH_3\cdot \underset{OH}{CH}\cdot \underset{OH}{CH}\cdot CH_3$$

but, in the presence of oxygen, the dimerization of these radicals was completely suppressed, and acetaldehyde was formed as a predominant product. In this case, they proposed the formation of the peroxy radical ($CH_3\cdot \underset{O_2\cdot}{CHOH}$) as an intermediate in the reaction.

$$CH_3\cdot \dot{C}HOH \xrightarrow{O_2} CH_3\cdot \underset{O_2\cdot}{CHOH} \rightarrow CH_3CHO$$

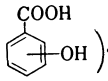
Table III shows the *G*-value of intermediate radicals produced in systems both with and without molecular oxygen. Based on the mechanism given by Eqs. 3, 7 and 8, the *G*-values of hydroxyl and hydroxycarbonylphenyl radicals as an intermediate in the presence of oxygen are calculated to be 2.3 and 2.0, respectively, as is shown in the Table III. The total *G*-value of reacting hydroxyl radical is close to that of hydroxyl radical produced in the primary process (1). Accordingly, it is likely that the most of the hydroxyl radicals formed in the primary process of the reaction react with benzoic acid giving the reaction products. The *G*-value of both hydroxyl and hydroxycarbonylphenyl radicals estimated here are greater in the presence of oxygen than in its absence.

There remain, therefore, some possibilities of the formation of hydroxyl radicals from hydroperoxy radicals produced according to Eq. 2 as follows:

$$2HO_2\cdot \rightarrow H_2O_2 + O_2 \quad (9)$$

$$H_2O_2 \rightarrow 2HO\cdot \quad (10)$$

Some information for the orientation of the hydroxycarbonylphenyl radical is obtained from the experimental values. *G*-Value of 2-, 3- and 4-hydroxycarbonylphenyl radical produced in the absence of oxygen are calculated to be 0.83, 0.21 and 0.65, respectively, basing on the yields of products summerized in Table I. Thus, the *G*-value ratio of 2-: 3-: 4-hyroxycarbonylphenyl radical is 1 : 0.26 : 0.79.

On the other hand, *G*-values of hydroxybenzoic acid, in the presence of oxygen, were 0.79, 0.29 and 0.65 for 2-, 3-, 4-isomer, respectively. In this case, the present authors can not predict any *G*-values of intermediate hydroxy, hydroxycarbonylphenyl radical isomers (  ). produced from mono-hydroxybenzoic acids. If the formation of dihydroxybenzoic acid, being much smaller than that of mono-hydroxybenzoic acid, might be neglected, the *G*-value ratio calculated as 1 : 0.37 : 0.82 for 2-: 3-: 4-hydroxycarbonylphenyl radical in the presence of molecular oxygen agrees fairly well with that in the absence of molecular oxygen. The easiness of the abstraction of ring hydrogen of benzoic acid by hydroxyl radical is shown, basing on the *G*-value ratio of 2-, 3- and 4-hydroxycarbonylphenyl radical, in the following.

ortho > para > meta

It seems also likely that this agreement supports the above postulate that the reaction is initiated by hydrogen-abstraction reaction of hydroxyl radical without regard to dissolving oxygen.

The ratio of hydroxybenzoic acids obtained by Weiss and his collaborators was approximately 5 : 2 : 10 for 2-: 3-: 4-hydroxybenzoic acid in the solution containing molecular oxygen, whereas the ratio was 6 : 4 : 10 under the condition of with insufficient quantity of available oxygen. In their results, the para-isomer was major component[1]. On the other hand, the ratio of mono-hydroxybenzoic acids obtained by Downes was approximately 9 : 5 : 4 for 2-: 3-: 4-hydroxybenzoic acid[2]. In this case, the ortho-isomer was a major component as well as in the present results, although a different ratio was obtained. These different ratios of products may be attributed rather to the different analytical method, the radiation energies or the experimental conditions such as temperature or concentration than to the different dose rate.

We wish to express our thanks to Professor K. Kimura for his kind guidance and Dr. A. Danno for his many helpful discussions.

*Division of Radiation Applications*
*Japan Atomic Energy Research Institute*
*Tokai, Ibaraki-ken*

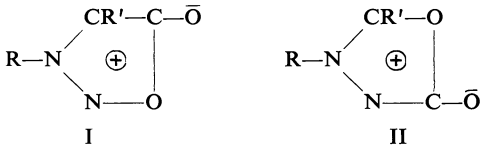
8) G. G. Jayson, G. Scholes and J. Weiss, *J. Chem. Soc.*, 1957, 1358.

# *Studies on Meso-ionic Compounds. XIII*[1]. *ψ-2, 4-Dihydro-4, 5-diphenyl-2-keto-1-oxa-3, 4-diazole**

By Mutsuko HASHIMOTO and Masaki OHTA

(Received October 20, 1960)

Since Earl et al.[2] synthesized in 1935 3-phenylsydnone (I; R=Ph, R'=H), many studies on meso-ionic compounds have been carried out especially with sydnones I, whereas not any meso-ionic compound of type II which differs from the sydnones in the reversal of the -CO-O- grouping is yet known, and we have therefore undertaken a general study of this new meso-ionic system.

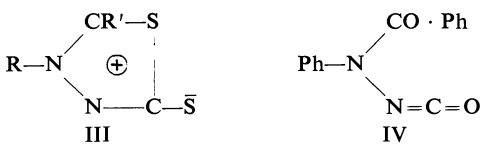


I II

VI; R=R'=$C_6H_5$
IX; R=$CH_3$, R'=$C_6H_5$

Fig. 1

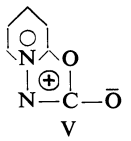
Attempts to prepare the compound II were already made by Baker et al.[3] in 1950. Their attempts were mainly based on methods by which the dithio-analogues III had been prepared[4], and the failure of their syntheses was due in several cases to the instability of carbamic acids. On the assumption that iso-cyanate IV might cyclise to the compound II, the reaction of the hydrochloride of *N*-benzoyl-*N*-phenylhydrazine with carbonyl chloride in boiling toluene was also tried, but they obtained *N*, *N'*-di(benzanilido)urea alone.



III IV

Fig. 2

On the other hand, Hoegerle[5] reported that *N*-aminopyridone-(2) was subjected to the action of carbonyl chloride in chloroform in the presence of potassium carbonate to give the compound V in which the meso-ionic ring in question forms part of a polycyclic system.



V

Fig. 3

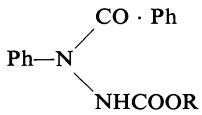
Now we treated *N*-benzoyl-*N*-phenylhydrazine with carbonyl chloride under the same conditions as Hoegerle used and recrystallized the product from dry benzene obtaining a crystalline solid $C_{48}H_{36}O_6N_6$, m. p. 161~162°C. This, if formulated as $3 \cdot C_{14}H_{10}O_2N_2$, $C_6H_6$, would correspond to the required meso-ionic compound VI incorporating benzene. Heating the crystalline solid at 100°C under reduced pressure for four days removed benzene from it to afford white crystals, m. p. 165~166°C, which gave analytical figures indicative of the formula $C_{14}H_{10}O_2N_2$.

A comparison of the infrared spectrum of the compound with that of its precursor, *N*-benzoyl-*N*-phenylhydrazine, led us to assign it the structure VI. That is: (1) the disappearance of bands at 3338 and 3278 $cm^{-1}$ in the precursor, arising from NH stretching, (2) the lack of the characteristic band for iso-cyanate group, and (3) the shift of Amide I band in the precursor at 1625 $cm^{-1}$ towards a band at 1755 $cm^{-1}$, which corresponds closely with the ester-carbonyl bands in sydnones listed by Earl et al.[6] and Fugger et al.[7] We therefore designated the compound VI as *ψ*-2, 4-dihydro-4, 5-diphenyl-2-keto-1-oxa-3, 4-diazole following the systematic nomenclature proposed by Baker et al.[8]

The *ψ*-oxadiazole VI is insoluble in absolute ethanol at room temperature, but on heating it converts into ethyl *N*-benzoyl-*N*-phenylhydrazinoformate (VII). When refluxed with cyclohexanol in dry benzene for 6 hr. VI gives

1) Part XII: M. Hashimoto and M. Ohta, This Bulletin, 33, 1394 (1960).
* Presented at the Local Meeting of the Chemical Society of Japan, Hokkaido, July, 1960.
2) J. C. Earl and A. W. Mackney, *J. Chem. Soc.*, **1935**, 899.
3) W. Baker, W. D. Ollis and V. D. Poole, ibid., **1950**, 1547.
4) M. Busch et al., *Ber.*, **28**, 2635 (1895); *J. pr. Chem.*, **60**, 218, 228, 231, 236 (1899); **67**, 201, 202, 246, 250, 257 (1903); W. Baker et al., *J. Chem. Soc.*, **1951**, 289.
5) K. Hoegerle, *Helv. Chim. Acta*, **41**, 548 (1958).
6) J. C. Earl et al., *J. Chem. Soc.*, **1951**, 2207.
7) J. Fugger et al., *J. Am. Chem. Soc.*, **77**, 1845 (1955).
8) W. Baker, W. D. Ollis and V. D. Poole, *J. Chem. Soc.*, **1949**, 311.

cyclohexyl *N*-benzoyl-*N*-phenylhydrazinoformate (VIII). Heating VI with *N*-benzoyl-*N*-phenylhydrazine at 100°C for 20 min. affords



VII; $R=C_2H_5$
VIII; $R=C_6H_{11}$

Fig. 4

*N*, *N'*-di(benzanilido)urea, which has a lower melting point by 10°C than that reported by Baker et al., but gives the correct analytical values. The same product is also obtained on treatment of VI with boiling water for 3 hr. When heated with aniline at 100°C for 15 min., VI gives 1-benzoyl-1, 4-diphenylsemicarbazide. On treatment with concentrated aqueous ammonia or aqueous dimethylamine, VI gives not the corresponding semicarbazides, but benzamide or *N*-benzoyl-*N*-phenylhydrazine, respectively.

These reactions which suggest the presence of a iso-cyanate group in a molecule were also observed in the polycyclic analogue V[5]. However, the fact that V can be recrystallized from ethanol but VI suffers a ring fission from hot ethanol indicates that VI is less stable than V.

By acid hydrolysis, VI regenerates *N*-benzoyl-*N*-phenylhydrazine. The probable mechanism of the above described hydrolysis is shown in

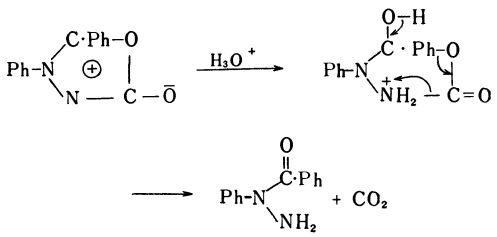


Fig. 5

Fig. 5 after that of acid hydrolysis of sydnones proposed by Baker et al.[9] Unlike sydnones**, *N*-benzoyl-*N*-phenylhydrazine obtained here is unaffected by acid and therefore no further degradation towards phenylhydrazine and benzoic acid might occur.

By alkaline hydrolysis, VI affords phenylhydrazine and benzoic acid. This observation could best be accounted for, if it is considered that the hydrolysis of lactonic group of VI produces unstable intermediate *N'*-carboxy-*N*-benzoyl-*N*-phenylhydrazine and this immediately decomposes to phenylhydrazine and benzoic acid.

Besides the above diphenyl derivative VI, attempts to prepare some analogues were frustrated except *ψ*-2, 4-dihydro-4-methyl-5-phenyl-2-keto-1-oxa-3, 4-diazole (IX) by the inaccessibility of *α*-acylhydrazines. The compound IX was prepared, in very poor yield, by the same treatment of *N*-benzoyl-*N*-methylhydrazine as that used for VI. Recrystallization from dry benzene afforded colorless needles, m. p. 150°C, which gave analytical figures indicative of the formula $C_9H_8O_2N_2$ (IX). Owing to the poor yield both of *N*-benzoyl-*N*-methylhydrazine and of IX, we obtained too small a quantity of IX to examine its infrared spectrum or to perform various reactions similar to those to which diphenyl derivative VI was subjected.

## Experimental

***N*-Benzoyl-*N*-phenylhydrazine.**—A mixture of *N'*-acetyl-*N*-benzoyl-*N*-phenylhydrazine (5 g.), concentrated sulfuric acid (5 ml.), water (25 ml.) and ethanol (35 ml.) was refluxed for 2 hr. Silky needles which separated on cooling were filtered off, suspended in plenty of water and neutralized with sodium carbonate affording colorless prisms (3.1 g.), m. p. 66°C. Recrystallization from dilute ethanol raised m. p. to 78°C (the reported melting point is 69~70°C.[10]).

Found: N, 13.03. Calcd. for $C_{13}H_{12}ON_2$: N, 13.20%.

***ψ*-2, 4-Dihydro-4, 5-diphenyl-2-keto-1-oxa-3, 4-diazole (VI).**—To a solution of *N*-benzoyl-*N*-phenylhydrazine (2 g.) in chloroform (200 ml.) was added finely powdered, anhydrous potassium carbonate (20 g.) and then a violent stream of carbonyl chloride was introduced with vigorous stirring at −7°C for 10 min. After it has been kept standing overnight, reaction mixture was allowed to reflux for 30 min. and sediments were removed. The filtrate was evaporated and the residue was recrystallized from dry benzene to give colorless lancets (1.71 g.), m. p. 161~162°C, which incorporate benzene.

Found: C, 72.16; H, 4.80; N, 10.98. Calcd. for $C_{48}H_{36}O_6N_6$ ($3\cdot C_{14}H_{10}O_2N_2$, $C_6H_6$): C, 72.72; H, 4.53; N, 10.66%.

When this compound was heated at 100°C under reduced pressure, benzene was removed affording white crystals, m. p. 165~166°C.

Found: C, 70.72; H, 4.52; N, 11.62. Calcd. for $C_{14}H_{10}O_2N_2$: C, 70.58; H, 4.23; N, 11.76%.

**Ethyl *N*-Benzoyl-*N*-phenylhydrazinoformate (VII).**—(a) A solution of VI (0.35 g.) in absolute ethanol (10 ml.) was warmed on a water bath and after 3 hr. evaporated under reduced pressure to give white powder (0.37 g.), m. p. 132°C. Recrystallization from dilute ethanol gave colorless

9) W. Baker and W. D. Ollis, *Quart. Rev.*, **11**, 22 (1957).

** When heated with aqueous acid, the sydnones give *N*-substituted hydrazine, carboxylic acid and carbon dioxide. The interesting production of *α*-acylhydrazine is observed only when 3-phenylsydnone is treated with one molecular proportion of water and hydrogen bromide.

10) O. Widman, *Ber.*, **26**, 947 (1893).

needles, m. p. 135~136°C, undepressed by admixture with the authentic sample prepared by route (b).

Found: C, 67.18; H, 5.92; N, 10.03. Calcd. for $C_{16}H_{16}O_3N_2$: C, 67.59; H, 5.67; N, 9.85%.

(b) To a solution of *N*-benzoyl-*N*-phenylhydrazine in ether was added equimolar ethyl chloroformate and the solid which separated was filtered off and recrystallized from dilute ethanol affording colorless needles, m. p. 136°C (Found: N, 9.95%).

**Cyclohexyl *N*-Benzoyl-*N*-phenylhydrazinoformate (VIII).**—A mixture of VI (0.5 g.), cyclohexanol (1 ml.) and dry benzene (20 ml.) was refluxed for 6 hr., evaporated under reduced pressure and the residue washed with ether and recrystallized twice from dilute dioxane to give colorless needles, m. p. 138~139°C.

Found: N, 8.05. Calcd. for $C_{20}H_{22}O_3N_2$: N, 8.28%.

***N*, *N'*-Di(benzanilido)urea.**—(a) *N*-Benzoyl-*N*-phenylhydrazine (1 g.) and VI (0.5 g.) were finely powdered, mixed up and kept at 100°C for 20 min. The cooled, hard solid was washed thoroughly with ether and further twice with hot chloroform (yield, 0.82 g.). Recrystallization from pyridine gave a white powder, m. p. 263°C (decomp.) (the reported melting point is 274°C[3]).

Found: C, 72.21; H, 5.33; N, 12.81. Calcd. for $C_{27}H_{22}O_3N_4$: C, 72.00; H, 4.89; N, 12.44%.

(b) VI (0.5 g.) was refluxed with water (20 ml.) with stirring for 3 hr. The precipitate was filtered off, washed with chloroform, dried (0.25 g.) and recrystallized from pyridine giving a white powder, m. p. 263.5°C (decomp.) (Found: C, 71.89; H, 4.93; N, 12.76%).

**1-Benzoyl-1, 4-diphenylsemicarbazide.**—VI (0.5 g.) was dissolved in purified aniline (1 ml.), heated at 100°C for 15 min. and then the solid which deposited was collected, washed with ether (yield, 0.6 g.) and recrystallized from dilute ethanol affording colorless needles, m. p. 210~211°C.

Found: C, 72.27; H, 5.37; N, 12.82. Calcd. for $C_{20}H_{17}O_2N_3$: C, 72.49; H, 5.17; N, 12.68%.

**Reaction of VI with Aqueous Ammonia.**—VI (1 g.) was added to concentrated aqueous ammonia (40 ml.) and stirred vigorously. After 3~4 hr. complete dissolution occurred, a pale orange color developing. After it has been kept standing at room temperature for 2 days, the reaction mixture was evaporated under reduced pressure and the residue with a smell of phenylhydrazine was collected, washed with ether, dried (yield, 0.14 g.) and recrystallized from a little water giving colorless needles, m. p. 126~127°C, undepressed by admixture with authentic benzamide.

Found: N, 11.64. Calcd. for $C_7H_7ON$: N, 11.57%.

**Reaction of VI with Aqueous Dimethylamine.**—VI (0.5 g.) was added to 40% aqueous dimethylamine (10 ml.) and stirred vigorously. After 15 min. complete dissolution occurred, an orange color developing. After it has been kept standing at room temperature for 5 days, the reaction mixture was evaporated under reduced pressure to give the residual oil which solidified on addition of concentrated hydrochloric acid. Recrystallization from ethanol-ether yielded colorless needles, m. p. 192~193°C (decomp.), which showed the positive Beilstein test.

Found: N, 11.46. Calcd. for $C_{13}H_{13}ON_2Cl$: N, 11.27%.

The authentic sample prepared by the action of concentrated hydrochloric acid on *N*-benzoyl-*N*-phenylhydrazine had m. p. 191~193°C (decomp.) (Found: N, 11.12%).

**Acid Hydrolysis.**—When VI (1 g.) was warmed with 10% aqueous hydrochloric acid on a water bath, complete dissolution did not occur but the form of crystallization gradually changed. The precipitate was filtered off, dried (0.66 g.) and recrystallized from water affording colorless needles, m. p. 199°C (decomp.), which showed the positive Beilstein test.

Found: C, 62.60; H, 5.49; N, 10.89. Calcd. for $C_{13}H_{13}ON_2Cl$: C, 62.78; H, 5.23; N, 11.3%.

**Alkaline Hydrolysis.**—VI (1 g.) was readily dissolved in 10% aqueous sodium hydroxide. After 45 min. the solution was acidified to give colorless leaflets (0.39 g.), m. p. 122°C, undepressed by admixture with authentic benzoic acid. The acidic filtrate was neutralized and extracted with ether. The extract was dried with sodium sulfate and evaporated to give an oily product, from which on addition of aqueous oxalic acid the oxalate of phenylhydrazine was obtained.

***φ*-2, 4-Dihydro-4-methyl-5-phenyl-2-keto-1-oxa-3,4-diazole (IX).**—To a solution of *N*-benzoyl-*N*-methylhydrazine (3.5 g.), prepared by Michaelis' method[11], in chloroform (600 ml.) was added finely powdered, anhydrous potassium carbonate (60 g.) and then a violent stream of carbonyl chloride was introduced with vigorous stirring at −5~−8°C for 10 min. After it has been kept standing overnight, the reaction mixture was refluxed for 30 min. and sediments were removed. The filtrate was evaporated to give very viscous oil with a strong smell of benzoyl chloride. Addition of ether afforded a small amount of crystalline solid, which was collected and recrystallized from dry benzene giving colorless needles, m. p. 150°C.

Found: C, 61.55; H, 4.88; N, 16.15. Calcd. for $C_9H_8O_2N_2$: C, 61.36; H, 4.58; N, 15.90%.

We are indebted to Dr. Asaji Kondo for microanalyses and to Dr. Tadashi Sato for infrared spectroscopic work.

*Laboratory of Organic Chemistry*
*Tokyo Institute of Technology*
*Meguro-ku, Tokyo*

11) A. Michaelis and E. Hadanck, ibid., **41**, 3288 (1908).

# *Bile Acids and Steroids. XXI*[1]. *Studies on the Hog Bile Acids (Part 5)*[1]. *On the Oxidation of Epimeric 3,6-Dihydroxycholanoic Acids with N-Bromosuccinimide*[*1]

By Jun'ichi KAWANAMI

(Received September 30, 1960)

Previously, it was described that $\alpha$-hyodeoxycholic acid is selectively oxidized at C-3 with *N*-bromosuccinimide (NBS) to give 3-oxo-6$\alpha$-hydroxy-5$\beta$-cholanoic acid[2], whereas it has been reported earlier by Wieland[3] that it was preferentially oxidized at C-6 with chromic acid. From this reverse result, it was of interest to investigate the oxidation of epimeric 3,6-dihydroxy-5$\beta$-cholanoic acids with NBS. Oxidation was carried out in both dioxane-water (9:1) and acetone-water (7:3) in order to obtain information depending on polarity of the solvent and with 1 and 2 molar equivalents of NBS respectively in order to obtain information depending on selectivity. As seen in Table I, the order of susceptibility to oxidation obtained from the results was as follows:

$$6\beta > 3\beta \ \& \ 3\alpha > 6\alpha \quad (\text{A/B: cis})$$

The 6$\beta$-hydroxyl group was most rapidly oxidized, the 6$\alpha$-hydroxyl group was not attacked and the ease of oxidation of both the 3$\beta$- and the 3$\alpha$-hydroxyl groups were in between. However, the difference between 3$\beta$- and 3$\alpha$-hydroxyl group was not definable in such an experiment. Although there is a method in which the reagent such as NBS is volumetrically titrated, it is presumed to complicate the results on account of two factors, both a consumption by the substrates and a decomposition by the solvent. Therefore, the author examined the oxidation using the absorption band at 1720 $cm^{-1}$ corresponding to the carbonyl group of the six-membered ketone in the infrared spectrum. This band is so strong that it is useful for determination. Since the reaction itself was assumed to be very complicated as mentioned above, it was most reliable to use the optical densities of the six-membered carbonyl band in the infrared spectrum for this purpose. In this case, as methyl 3-oxo-6$\alpha$-hydroxy-5$\beta$-cholanoate was oily, it was unsuitable for preparing the calibration curve. Consequently, methyl lithocholate[7] and methyl 3$\beta$-hydroxy-5$\beta$-cholanoate[8] were used as starting materials. Ester is also suitable to avoid the overlap of the acid carbonyl band with the six-membered ketone band in the infrared spectrum. As the six-membered carbonyl band was further somewhat overlapped with that of

TABLE I. THE POSITION ATTACKED AND THE YIELD IN EACH EPIMER

| Solvent | Dioxane-Water (9:1) | | Acetone-Water (7:3) | |
|---|---|---|---|---|
| Mol. equiv. of NBS | 1 | 2 | 1 | 2 |
| Reaction time at room temperature (20±2°C) | 1.5 hr. | 1.5 hr. | Overnight | 4 days |
| 3$\alpha$, 6$\alpha$ | 3(27.2%) | 3(30.1%) | 3(41.7%) | 3(61.8%) |
| 3$\beta$, 6$\alpha$[4] | 3(21.3%) | 3(45.7%) | 3(31%) | 3(62.5%) |
| 3$\beta$, 6$\beta$[5] | 6(77%) | 6(56.6%) | 6(77.5%) | 6(55%) |
| | | 3,6(14.3%) | | 3,6(19.3%) |
| 3$\alpha$, 6$\beta$[6] | 6(70%) | 6(60%) | 6(70%) | 6(59.4%) |
| | | 3,6(7.5%) | | 3,6(16%) |

*1 The rest is abbreviated as NBS.

1) Part XX: J. Kawanami, This Bulletin, **34**, 509 (1961).

2) K. Takeda and J. Kawanami, *J. Biochem. (Japan)*, **40**, 477 (1953).

3) H. Wieland and E. Dane, *Z. Physiol. Chem.*, **212**, 41 (1932).

4) $\beta$-Hyodeoxycholic acid was prepared from 3-oxo-6$\alpha$-hydroxy-5$\beta$-cholanoic acid according to Moffett method. (R. B. Moffett and W. Hoehn, *J. Am. Chem. Soc.*, **69**, 1995 (1947)).

5) Synthesis of 3$\beta$, 6$\beta$-dihydroxy-5$\beta$-cholanoic acid was described in the preceding part XX.

6) 3$\alpha$, 6$\beta$-Dihydroxy-5$\beta$-cholanoic acid was prepared from methyl 3$\alpha$-acetoxy-6-oxo-5$\beta$-cholanoate according to Moffett method. (R. B. Moffett and W. Hoehn, *J. Am. Chem. Soc.*, **68**, 1855 (1946)). This compound was also prepared in good yield by using sodium borohyride in place of Raney nickel.

7) Methyl lithocholate was prepared from cholic acid according to the usual method. (S. Sarel and Y. Yanuka, *J. Org. Chem.*, **24**, 2018 (1959)).

8) Methyl 3$\beta$-hydroxy-5$\beta$-cholanoate was prepared from both Methyl 3-oxo-cholanoate and Methyl 3$\alpha$-tosyloxy-5$\beta$-cholanoate according to Fieser's and Reindel's method respectively. (F. Reindel and K. Niederlandre, *Ber.*, **68**, 1243 (1935); L. F. Fieser and J. C. Babcock, *J. Am. Chem. Soc.*, **74**, 5474 (1952)).

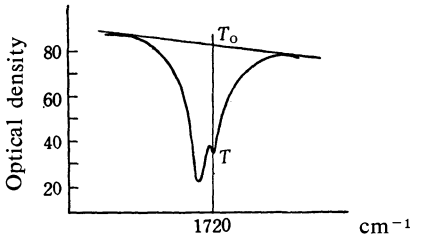



Fig. 1. Baseline method.

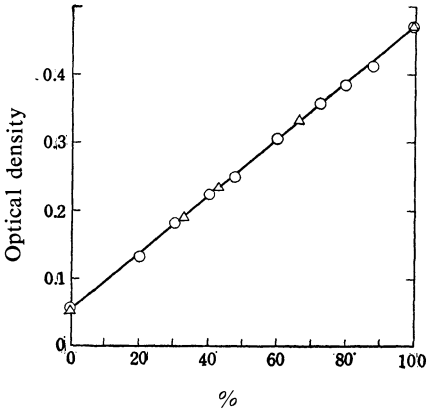



Fig. 2. Calibration curve.
—○— 3$\alpha$-epimer; —△— 3$\beta$-epimer

the ester group, $T_0$ was estimated according to the baseline method (Fig. 1).

The calibration curve was made by using a variety of mixtures consisting of each methyl 3$\beta$- or 3$\alpha$-hydroxy-5$\beta$-cholanoate and methyl 3-oxo-5$\beta$-cholanoate. As shown in Fig. 2, the calibration curve plotting the relationship between the optical density and the concentration ($W/W$%) of the oxidation product, 3-oxo-5$\beta$-cholanoate to each of methyl 3$\beta$- or 3$\alpha$-hydroxy-5$\beta$-cholanoate, formed a straight line which indicated its usefulness for a quantitative analysis. The values thus obtained are shown in Tables II and III. Then, the

TABLE II. RELATIONSHIP BETWEEN OPTICAL DENSITY AND RATIO ($W/W$%) OF THE 3-OXO DERIVATIVE TO THE 3$\alpha$-EPIMER

| Percentage of 3-oxo deriv. | 3-Oxo mg. | 3$\alpha$-OH mg. | $CCl_4$+ Sample mg. | $W$ % | $\overline{T}_0$ | $\overline{T}$ |
|---|---|---|---|---|---|---|
| 0 | 0 | 5.0 | 589.0 | 0.850 | 88.3 | 79.4 |
| 20 | 0.8 | 3.2 | 472.0 | 0.848 | 87.8 | 67.7 |
| 30 | 1.8 | 4.2 | 717.2 | 0.838 | 87.6 | 61.7 |
| 40 | 2.0 | 3.0 | 604.0 | 0.828 | 88.0 | 57.9 |
| 48 | 4.5 | 4.9 | 1163.1 | 0.807 | 87.7 | 55.2 |
| 60 | 3.0 | 2.0 | 594.0 | 0.842 | 87.7 | 48.5 |
| 72 | 4.3 | 1.7 | 704.5 | 0.852 | 87.3 | 43.5 |
| 80 | 4.0 | 1.0 | 588.0 | 0.850 | 87.3 | 41.3 |
| 87.4 | 6.9 | 1.0 | 942.9 | 0.837 | 87.1 | 39.6 |
| 100 | 6.3 | 0 | 792.4 | 0.795 | 87.2 | 36.6 |

TABLE III. RELATIONSHIP BETWEEN OPTICAL DENSITY AND RATIO ($W/W$%) OF THE 3-OXO DERIVATIVE TO THE 3$\beta$-EPIMER

| Percentage of 3-oxo deriv. | 3-Oxo mg. | 3$\beta$-OH mg. | Sample +$CCl_4$ mg. | $W$ % | $\overline{T}_0$ | $\overline{T}$ |
|---|---|---|---|---|---|---|
| 0 | 0 | 7.2 | 897.3 | 0.801 | 87.8 | 80.0 |
| 33.3 | 2.7 | 5.4 | 924.9 | 0.875 | 87.7 | 60.0 |
| 43.4 | 3.7 | 4.9 | 948.9 | 0.908 | 87.4 | 53.6 |
| 66.7 | 6.2 | 3.1 | 1081.8 | 0.859 | 87.1 | 45.5 |
| 100 | 6.3 | 0 | 792.4 | 0.795 | 87.2 | 36.6 |

TABLE IV. RELATIONSHIP BETWEEN THE YIELD OF OXIDATION PRODUCTS AND TIME AT 25°C

| No.* | $t$ min. | Sample mg. | Sample +$CCl_4$ mg. | $W$ % | $D$ | Yield |
|---|---|---|---|---|---|---|
| 1 | 30 | 45.5 | 5342.3 | 0.851 | — | — |
| 2 | 30 | 46.2 | 5490.0 | 0.841 | — | — |
| 3 | 50 | 41.2 | 4850.6 | 0.850 | 0.122 | 20 |
| 4 | 50 | 45.0 | 5305.0 | 0.848 | 0.105 | 15 |
| 5 | 70 | 35.0 | 4099.5 | 0.854 | 0.183 | 38 |
| 6 | 70 | 44.3 | 5215.3 | 0.851 | 0.144 | 27 |
| 7 | 90 | 44.6 | 5232.6 | 0.852 | 0.257 | 60 |
| 8 | 90 | 44.0 | 5171.0 | 0.850 | 0.227 | 51.5 |

* Odd numbers are from the 3$\beta$-epimer and even numbers from the 3$\alpha$-epimer.

TABLE V. THE OXIDATION OF BOTH EPIMERS FOR 60 min. AT 25°C

| Starting material | Sample mg. | Sample +$CCl_4$ mg. | $W$ % | $D$ | Yield of 3-oxo deriv. % |
|---|---|---|---|---|---|
| 3$\beta$ | 41 | 4.919 | 0.831 | 0.262 | 63.8 |
| 3$\alpha$ | 43.5 | 5.050 | 0.862 | 0.219 | 48.3 |

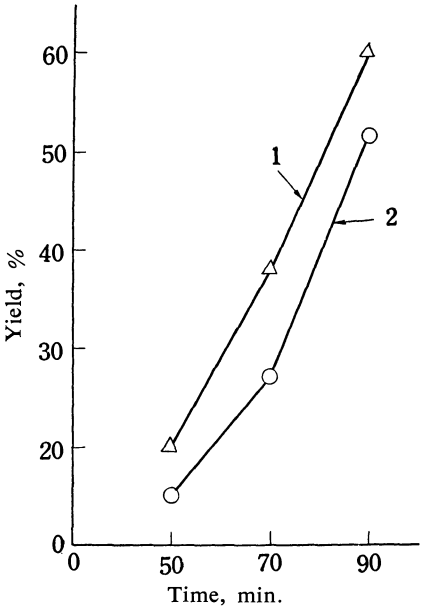



Fig. 3. Relationship between time and yield in each epimer.
(1) 3$\beta$-epimer; (2) 3$\alpha$-epimer

oxidation of epimeric methyl 3-hydroxy-5$\beta$-cholanoates was carried out with 1.3 molar equivalents of NBS in dioxane-water (9 : 1) solution at 25°C. There is a marked difference in the yield between 3$\beta$- and 3$\alpha$-hydroxyl derivatives (Fig. 3). The values obtained are shown in Tables IV and V. Accordingly, the order of susceptibility to oxidation obtained from the results described above was as follows:

$$6\beta(a) > 3\beta(a) > 3\alpha(e) > 6\alpha(e) \quad (A/B: \text{cis})$$

In order to obtain the further support on the influence of steric factors in this reaction, the oxidation of two 3,6-dihydroxy-5$\alpha$-cholanoic acid (3$\beta$,6$\beta$-dihydroxy-5$\alpha$-cholanoic acid and 3$\beta$,6$\alpha$-dihydroxy-5$\alpha$-cholanoic acid) was examined. The oxidation was carried out as in the previous case. While the oxidation of the former gave a 6-oxo derivative, the oxidation of the latter gave a 3-oxo derivative. From these results in A/B-trans series, the 6$\beta$-hydroxy group was also rapidly oxidized but the 6$\alpha$-hydroxyl group was not affected under such a condition and the ease of oxidation of the 3$\beta$-hydroxyl group was in between. Accordingly, the order of the susceptibility to the oxidation of hydroxyl groups in A/B-trans series was also as follows:

$$6\beta(a) > 3\beta(e) > 6\alpha(e) \quad (A/B: \text{trans})$$

**Discussion on the Reaction Mechanism**

Prior to considering the reaction mechanism of oxidation with NBS from the above result, the outline of reports on the reaction mechanism of chromic acid oxidation should be described. Westheimer and Nicolaides[9] minutely studied the reaction mechanism of chromic acid oxidation and they found that the rate-determining step is not the formation of a chromate ester but the cleavage of the carbon hydrogen bond.

(A) $R_2CHOH + HCrO_4^- + H^+ \overset{\text{fast}}{\rightleftarrows} R_2CHOCrO_3H + H_2O$

(B) $R_2C(H)\text{-}O\text{-}CrO_3H + H_2O \overset{\text{slow}}{\longrightarrow} R_2C{=}O + [HCrO_3^-] + H_3O^+$

Barton[10] found that the conformational factor determined nearly always the order of reactivity in oxidation among several hydroxyl groups and established a general rule that an axial alcohol is ordinarily more susceptible than the corresponding equatorial alcohol. There are, however, some cases in which an equatorial alcohol having a less accessible axial carbon hydrogen bond is faster oxidized than an axial alcohol (e. g. compare equatorial 11$\alpha$-hydroxyl with 3-axial hydroxyl group). Schreiber and Eschenmoser[11] measuring the reaction rates of oxidation of a number of hydroxy-5$\alpha$-cholestanes, confirmed again a general rule proposed by Barton and further defined a second factor determining reaction rates. That is, the transformation of the tetrahedral carbon of an alcoholic (or chromate ester) group to a trigonal carbonyl carbon often eliminates some or all of the repulsive interactions leading to instability. The reaction rates are thus dependent upon the extent of decrease in such interactions. A example in A/B-trans series is as follows:

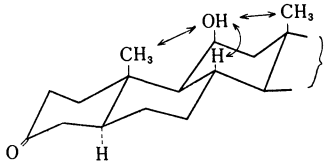



Fig. 4

As seen in Fig. 4, the 11$\beta$-hydroxyl group is under steric strain from the repulsions between the four groups, 11$\beta$-hydroxyl, C-10-methyl, C-13-methyl and 8$\beta$-hydrogen. Relief of this strain provides a driving force sufficient to promote the oxidation.

On the other hand, oxidation with reagents such as *N*-bromosuccinimide or *N*-bromoacetamide has been less clear from both mechanistic and conformational view points[12]. On the basis of the studies described above, the reaction mechanism of oxidation with NBS could be considered. The order of susceptibility to oxidation of the epimeric 3,6-dihydroxycholanoic acids with NBS was as follows:

(C) $6\beta(a) > 3\beta(a) > 3\alpha(e) > 6\alpha(e)$ (A/B: cis)

(D) $6\beta(a) > 3\beta(e) > 6\alpha(e)$ (A/B: trans)

On the other hand, the order in chromic acid oxidation of hydroxy-5$\alpha$-cholestanes by Schreiber at the corresponding position was as follows:

(E) $6\beta(a) > 3\alpha(a) > 6\alpha(e) > 3\beta(e)$
[36]* [3.0]* [2.0]* [1.0]*
(A/B: trans)

* Relative rates to 3$\beta$-hydroxy-5$\alpha$-cholestane.

From the results on the oxidation of $\alpha$-hyodeoxycholic acid with chromic acid, there are also the following positions.

9) F. H. Westheimer and N. Nicolaides, ibid., 71, 25 (1949).
10) D. H. R. Barton, *Experientia*, 6, 316 (1950); *J. Chem. Soc.*, 1953, 1027.
11) J. Schreiber and A. Eschenmoser, *Helv. Chim. Acta*, 38, 1929 (1955).
12) H. J. E. Loenthal, *Tetrahedron*, 6, 269 (1959).

(F) $6\alpha$(e)$>3\alpha$(e) (A/B: cis)

Compared with the above cited four expressions C, D, E and F, it is analogous in conformational view in accord with the Barton rule. In other words, an axial alcohol is more susceptible to oxidation than the corresponding equatorial epimer ($6\beta>6\alpha$, $3\beta>3\alpha$: A/B cis). Accordingly, in the case of the axial hydroxyl group, it is clear that the oxidation with NBS proceeds likewise to chromic acid oxidation, because both intermediates similarly have a more accessible C–H bond (equatorial) and a repulsive intermediate ester (axial). The concept described above will be also supported by the following examples.

cholestane-$3\beta$, $5\alpha$, $6\beta$-triol—
6-oxo derivative[13]

$3\beta$, $6\beta$-dihydroxy-$5\alpha$-cholanoic acid—
6-oxo derivative*2

$5\alpha$-cholestane-$3\beta$, $7\alpha$-diol—
7-oxo derivative[14]

$11\beta$-hydroxytigogenine—11-oxo derivative[15]

$11\beta$-hydroxyprogesterone—
11-oxo derivative[16]

($11\alpha$-hydroxyprogesterone was not affected under same condition).

On the other hand, in the series of the generally less reactive equatorial hydroxyl group, e.g. in the case of $\alpha$-hyodeoxycholic acid, the order with NBS was the reverse of that with chromic acid as seen in expressions C and F. This difference is supposed to depend on a driving force in the intermediate, because it is clear that the conformation of C–H bond (e.g. the $6\beta$-H in Figs. 5 and 6) is equivalent in each case. In the chromic acid oxidation, the intermediate ester has a strong driving force which is derived from both a large space-claim (" Raumbeanspruchung ") and an inductive factor (Fig. 5). On the other hand, in the oxidation with NBS, it is assumed that the intermediate ester has a little driving force which resulted from a smaller space-claim and from almost no inductive factor. (Fig. 6). The further explanation was as follows: in the chromic acid oxidation, since the $6\beta$-hydrogen suffers the driving force sufficient to promote the reaction as mentioned above, it can be more easily eliminated than the $3\beta$-hydrogen, whereas in the case of NBS, the driving force of the intermediate hypohalite is very insufficient. For this reason, an attack of the base on a hydrogen atom attached to the hydroxyl carbon is indispensable for the promotion of the reaction as well as the elimination of this hydrogen. Consequently, it may be deduced that the most important factor in the oxidation of the less reactive equatorial alcohol with NBS depends upon the extent of easiness of the proximity of base to the C–H bond of the alcoholic carbon being oxidized. Therefore, in the oxidation of $\alpha$-hyodeoxycholic acid with NBS, the $3\alpha$-hydroxyl group is more easily oxidized than the $6\alpha$-hydroxyl group owing to the vulnerability of the $3\beta$-hydrogen. This concept may be further supported by the fact that the less accessible C–H bonds such as in the $6\alpha$- or $11\alpha$-alcohol are not affected.

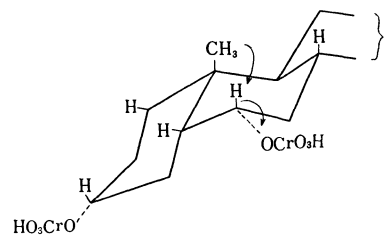



Fig. 5

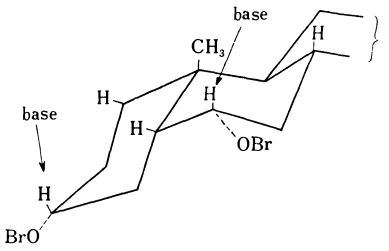



Fig. 6

Examples which show the concept described above are as follows:

$3\beta$, $6\alpha$-dihydroxy-$5\alpha$-cholanoic acid—
3-oxo derivative*2

$5\beta$-androstane-$3\alpha$, $11\alpha$, $17\beta$-triol—
3, 17-dioxo derivative[17]

$11\alpha$-hydroxypregnane-3, 20-dione is recovered unchanged after treatment with *t*-butylhypochlorite.

$3\beta$, $11\alpha$-dihydroxy-$5\alpha$-pregnan-20-one—
3, 20-dioxo derivative[18]

That desoxycholic acid was not affected with

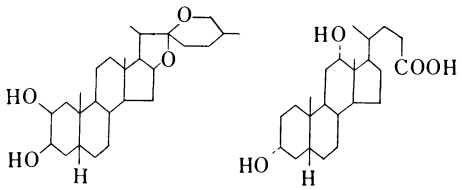
13) L. F. Fieser and S. Rajagopalan, *J. Am. Chem. Soc.*, **71**, 3938 (1949).
*2 See experimental part.
14) L. F. Fieser and S. Rajagopalan, ibid., **74**, 3309 (1952).
15) S. G. Brooks, J. S. Hunt, A. G. Long and B. Mooney, *J. Chem. Soc.*, **1957**, 1175.
16) A. R. Hanze, G. S. Fonken, A. V. McIntosch, A. M. Searcy and R. H. Levin, *J. Am. Chem. Soc.*, **76**, 3179 (1954).
17) H. L. Herzog, M. Jevnik. and E. B Hershberg, ibid., 75, 269 (1953).
18) O. Mancera, J. Romo, F. Sondheimer, G. Rosenkranz and C. Djerassi, *J. Org. Chem.*, **17**, 1066 (1952).

NBS in aqueous acetone or in aqueous sodium hydrogen carbonate[19] but with NBA in aqueous *t*-butanol[20], certainly appears to be governed principally by steric effects coupled with size of the reagent and solvating power of the solvent. Thereupon, all hydroxyl groups in which $\alpha$-hydrogen permits the approach of the base, should be oxidized and this theory was also supported by the following examples.

Ethyl 3$\beta$, 5$\beta$, 19-trihydroxyetianate—3-oxo derivative[21]

Methyl 3$\alpha$-hydroxy-9$\alpha$, 11$\alpha$-epoxy-5$\beta$-cholanoate—3-oxo derivative[22]

The hydroxyl group at $C_3$ in samogenine[23] (I) and in desoxycholic acid[19] (II), however, was not affected with NBS The reason is not clear in details but it perhaps depends upon the intermediate permitting no release of $\alpha$-hydrogen on account of vicinal effect or another interactions.




(I) (II)

## Experimental[24]

**Oxidation of Epimeric 3, 6-Dihydroxy-5$\beta$-cholanoic Acids with NBS** — General procedure of oxidation was performed by almost the same means as the method previous described[2].

**1) The Case of $\alpha$-Hydroxycholic Acid.** — *1.1) With 1 Molar Equivalent of NBS in Dioxane-Water.* —A mixture consisting of $\alpha$-hyodeoxycholic acid (761 mg.), dioxane-water (9 : 1) (15 ml.) and NBS. (380 mg.; 1.1 mol. equiv.) was allowed to stand for 1.5 hr. at room temperature (18°C). The mixture was changed from colorless to yellow and to orange successively in coloration. To the solution, 10% of aqueous sodium bisulfite was added. The ether extract was washed well with water and evaporated to dryness to afford oil (920 mg.) which was followed by esterification with methanol (4 ml.) and 10% of methanolic hydrochloric acid (0.5 ml.) overnight at room temperature. The ether extract, after isolation in the usual way, gave a yellow oil (777 mg.) which was chromatographed on alumina to afford methyl 3-oxo-6$\alpha$-hydroxy-5$\beta$-cholanoate 3-acetal, 237 mg. (27.2%), m. p. 153~154°C. Identity was established by a mixed melting point and the infrared spectrum with the authentic sample. Infrared spectrum: $\nu_{max}$ 3564 (OH); 1724 $cm^{-1}$ (C=O).

Found: C, 72.10; H, 10.30. Calcd. for $C_{27}H_{46}O_5$: C, 71.96; H, 10.29%.

*1.2) With 2 Molar Equivalents of NBS in Dioxane-Water.*—A mixture consisting of $\alpha$-hyodeoxycholic acid (605 mg.), dioxane-water (9 : 1) (10 ml.) and NBS (600 mg.; 2.2 mol. equiv.) was treated as in the previous case. The mixture gave methyl 3-oxo-6$\alpha$-hydroxy-5$\beta$-cholanoate 3-acetal, m. p. 152~153°C, 209 mg. (30.1%). This compound was identified by a mixed melting point and the infrared spectrum with the authentic sample.

*1.3) With 1 Molar Equivalent of NBS in Acetone-Water.*—A mixture consisting of $\alpha$-hyodeoxycholic acid (579 mg.), acetone-water (7 : 3) (13 ml.) and NBS (290 mg.; 1.1 mol. equiv.) was treated as in the previous case after being allowed to stand overnight at room temperature to furnish crystals, 224 mg., m. p. 146~151°C. The residue from the filtrate was chromatographed on alumina in the usual manner to afford the acetal with m. p. 149~151°C (53 mg.). Total yield were 41.7%. This sample was also identical in a mixed melting point and the infrared spectrum.

*1.4) With 2 Molar Equivalents of NBS in Acetone-Water.* — The mixture consisting of $\alpha$-hyodeoxycholic acid (929 mg.), pyridine (500 mg.), acetone-water (7 : 3) (20 ml.) and NBS (926 mg.; 2.2 mol. equiv.) was treated in a way similar to that of the case in the preceding section after being kept for four days at room temperature (20°C) to give the acetal with m. p. 150~152°C (660 mg.; 61.8%). Identity was established by a mixed melting point and the infrared spectrum. Found: C, 72.16; H, 10.26%.

**2) The Case of $\beta$-Hyodeoxycholic Acid.** — *2.1) With 1 Molar Equivalent of NBS in Dioxane-Water.* — After treatment as in the case of section 1.1 the above acetal with m. p. 152~153°C was obtained in 21.3% yield. This compound was identical with the authentic methyl 3-oxo-6$\alpha$-hydroxy-5$\beta$-cholanoate 3-acetal in a mixed melting point and the infrared spectrum.

*2.2) With 2 Molar Equivalents of NBS in Dioxane-Water.*—Treatment as in the case of section 1.2 afforded the acetal with m. p. 150~152°C in 45.7% yield. Identification was carried out by a mixed melting point and the infrared spectrum.

*2.3) With 1 Molar Equivalent of NBS in Acetone-Water.* — Treatment similar to that in the case of section 1.3 gave the acetal with m. p. 150~152°C in 31% yield. This compound was also identified

19) L. F. Fieser and S. Rajagopalan, *J. Am. Chem. Soc.*, **71**, 3535 (1949).
20) H. Reich and T. Reichstein, *Helv. Chim. Acta*, **26**, 562 (1943).
21) P. Herzig and M. Ehrenstein, *J. Org. Chem.*, **17**, 713 (1952).
22) L. F. Fieser and S. Rajagopalan, *J. Am. Chem. Soc.*, **73**, 118, 5252 (1951).
23) H. Ôsaka, private communication.
24) All melting points are uncorrected. Infrared spectra were recorded in Nujol Mulls with a "Koken DS 301" double beam infrared spectrophotometer, unless otherwise noted, and the ultraviolet spectra were taken in 95% ethanol solution using a "Hitachi EPS 2" spectrophotometer. Optical rotations were determined in a 1-dm. tube for chloroform solutions, unless otherwise specified. Alumina used for chromatography in this experiment was Merk's reagent grade standardized according to Brockmann and the chromatography was usually performed according to the method described by T. Reichstein. (T. Reichstein and W. Schoppee, *Diss. Faraday Soc.*, **1949**, 305) Extracts were dried over anhydrous sodium sulfate before evaporation unless stated otherwise.

by a mixed melting point and the infrared spectrum.

*2.4) With 2 Molar Equivalents of NBS in Acetone-Water.* — Isolation similar to that in the case of section 1.4 furnished the acetal with m. p. 148~150°C in 62.5% yield. Identity was established by a mixed melting point and the infrared spectrum.

**3) The Case of 3β, 6β-Dihydroxy-5β-cholanoic Acid.**—In this experiment, methyl 3β, 6β-dihydroxy-5β-cholanoate was used on account of insolubility of its acid in acetone-water (7 : 3).

*3.1) With 1 Molar Equivalent of NBS in Dioxane-Water.*—A mixture consisting of methyl 3β, 6β-dihydroxy-5β-cholanoate (350 mg.), dioxane-water (9 : 1) (10 ml.) and NBS (169 mg.; 1.1 mol. equiv.) was allowed to stand for 1.5 hr. at room temperature (22°C). To the solution, 10% of aqueous sodium bisulfite was added to decolorize it. The extract with ether was washed well with water and evaporated to dryness to yield orange oil (494 mg.) which was acetylated with pyridine (4 ml.) and acetic anhydride (4 ml.) under reflux for 2 hr. After cooling, the mixture was carefully diluted with water to afford crystals which were collected, washed throughly with water and recrystallized from methanol to methyl 3β-acetoxy-6-oxo-5α-cholanoate, 235 mg., scales, m. p. 156~158°C. Ether extraction from the above aqueous and methanolic filtrate afforded a yellow oil (156 mg.) which was followed by chromatography on alumina. The eluate with petroleum ether-benzene (2 : 8 and 1 : 1) and benzene gave the above 6-oxo derivative with m. p. 157.5~158°C (61 mg.). Total yield was 77%. This compound was identified by a mixed melting point and the infrared spectrum with the authentic methyl 3β-acetoxy-6-oxo-5α-cholanoate. $[\alpha]_D^{24} = -14 \pm 2°$ (*c* 1.038). Infrared spectrum: $\nu_{max}$ 1730, 1710 (C=O); 1252, 1239, 1169, 1039 $cm^{-1}$ (C-O).

Found: C, 72.65; H, 9.48. Calcd. for $C_{27}H_{42}O_5$: C, 72.61; H, 9.48%.

*3.2) With 2 Molar Equivalents of NBS in Dioxane-Water.*—A mixture consisting of methyl 3β, 6β-dihydroxy-5β-cholanoate (347 mg.) dioxane-water (9 : 1) (10 ml.) and NBS (320 mg.; 2.1 mol. equiv.) was treated as in the previous subsection to give an orange oil (413 mg.) which was followed by chromatography on alumina. The eluate with benzene-petroleum ether (1 : 1), benzene and benzene-chloroform (9 : 1) furnished methyl 3β-acetoxy-6-oxo-5α-cholanoate, 216 mg. (56.6%), scales, m. p. 158~159°C. This was identical with the above specimen in a mixed melting point and the infrared spectrum. The benzene-chloroform (8 : 2 and 1 : 1) elution afforded methyl 3, 6-dioxo-5α-cholanoate, 49 mg. (14.3%), m. p. 146~148°C. Zimmermann test gave cherry-red coloration. Infrared spectrum: $\nu_{max}$ 1745, 1711 $cm^{-1}$ (C=O).

Found: C, 74.19; H, 9.58. Calcd. for $C_{25}H_{38}O_4$: C, 74.59; H, 9.52%.

*3.3) With 1 Molar Equivalent of NBS in Acetone-Water.* — Isolation as in the section 3.1 after being kept overnight at room temperature (18°C) gave methyl 3β-acetoxy-6-oxo-5α-cholanoate, m. p. 157~158°C in 77.5% yield. Zimmermann test was negative. This compound was also identical with the above specimen by a mixed melting point and the infrared spectrum.

*3.4) With 2 Molar Equivalents of NBS in Acetone-Water.*—Treatment as in the previous case furnished methyl 3β-acetoxy-6-oxo-5α-cholanoate, m. p. 157~158°C in 55% yield from the elution with benzene-petroleum ether (1 : 1) and benzene, and methyl 3, 6-dioxo-5α-cholanoate, m. p. 148°C in 19.3% yield from the benzene-chloroform (9 : 1) eluate. These samples were also identified by a mixed melting point and the infrared spectrum.

**4) The Case of 3α, 6β-Dihydroxy-5β-cholanoic Acid.** — *4.1) With 1 Molar Equivalent of NBS in Dioxane-Water.*—To a solution of 3α, 6β-dihydroxy-5β-cholanoic acid (377 mg.) in dioxane-water (9 : 1) (10 ml.), NBS (188 mg.; 1.1 mol. equiv.) was added and kept for 1.5 hr. at room temperature (20±2°C). Isolation, esterification with ethereal diazomethane and acetylation in the usual way gave methyl 3α-acetoxy-6-oxo-5β-cholanoate as prisms, m. p. 150~153°C, 260 mg. $[\alpha]_D^{17} = -21 \pm 2°$ (*c* 1.052, dioxane). Infrared spectrum: $\nu_{max}$ 1703 (C=O); 1241, 1230, 1164, 1036, 1026 $cm^{-1}$ (C-O).

Found: C, 72.62; H, 9.59. Calcd. for $C_{27}H_{42}O_5$: C, 72.61; H, 9.48%.

By chromatography on alumina, the filtrate from the above crystals gave further 6-oxo derivative, 40 mg., m. p. 155~165°C (from methanol), a mixture of 5α- and 5β-series.

Found: C, 72.71; H, 9.53%. Total yield was 70%.

*4.2) With 2 Molar Equivalents of NBS in Dioxane-Water.* — Isolation in the usual way gave a mixture of 6-oxo derivative in 5α- and 5β-series with m. p. 143~147°C in 60% yield from the eluate with benzene-petroleum ether (1 : 1), benzene and benzene-chloroform (9 : 1). Infrared spectrum: $\nu_{max}$ 1741, 1712 (C=O); 1249, 1175, 1025 $cm^{-1}$ (C-O).

Found: C, 72.75; H, 9.43. Calcd. for $C_{27}H_{42}O_5$: C, 72.61; H, 9.48%.

The benzene-chloroform (8 : 2 and 1 : 1) eluate gave methyl 3, 6-dioxo-5α-cholanoate, m. p. 146~148°C, in 7.5% yield. Infrared spectrum: $\nu_{max}$ 1740, 1710 (C=O); 1171 $cm^{-1}$ (C-O).

Found: C, 74.19; H, 9.64. Calcd. for $C_{25}H_{38}O_4$: C, 74.59; H, 9.52%.

*4.3) With 1.Molar Equivalent of NBS in Acetone-Water.* — The methyl ester was used in this case because the acid was not dissolved in acetone-water (7 : 3). Treatment as in section 3.3 gave 6-oxo derivative, m. p. 150~155°C, in 70% yield. The identification was carried out by a mixed melting point and the infrared spectrum.

Found: C, 72.55; H, 9.64%.

*4.4) With 2 Molar Equivalents of NBS in Acetone-Water.* — Reaction and isolation as in section 3.4 afforded 6-oxo derivatives in 5α- and 5β-series with m. p. 155~160°C and m. p. 169~170°C, respectively in 59.4% yield from the eluate with benzene and benzene-chloroform (9 : 1). Zimmermann test was negative. Identity was established by a mixed melting point and the infrared spectrum.

Found: C, 72.92; H, 9.57%.

Benzene-chloroform (9 : 1) elution gave methyl 3, 6-dioxo-5β-cholanoate, m. p. 128~129°C, in 16% yield. Infrared spectrum: $\nu_{max}$ 1739, 1712 (C=O), 1171 $cm^{-1}$ (C-O).

Found: C, 74.07; H, 9.44%.

**Oxidation of 3β, 6α-Dihydroxy-5α-cholanoic Acid**[*3]. — To a solution of 3β,6α-dihydroxy-5α-cholanoic acid (140 mg.) and pyridine (37.3 mg.) in acetone (1.96 ml.) and water (0.84 ml.) was added NBS (82.5 mg.; 1.3 mol. equiv.). The resulting mixture was refluxed for 4.5 hr., and then the solvent was removed under reduced pressure to the point of distinct turbidity. After a large volume of water was added, the precipitate was collected and dried. This crude keto acid (46 mg.) was recrystallized from acetone to afford 3-oxo-6α-hydroxy-5α-cholanoic acid, fine needles, m.p. 195~197°C (20 mg.). Zimmermann test was positive. $[\alpha]_D^{32}=+4\pm2°$ (*c* 1.059, pyridine).

Found: C, 73.21; H, 9.85. Calcd. for $C_{24}H_{35}O_4$: C, 73.80; H, 9.81%.

The above crude acid was esterified with ethereal diazomethane to yield its methyl ester, melting at 90~97°C undefinitely. Zimmermann test was positive. $[\alpha]_D^{27}=+55\pm2°$ (*c* 1.038). Infrared spectrum: $\nu_{max}^{CHCl_3}$ 3524 (OH); 1731, 1711 $cm^{-1}$ (C=O).

Found: C, 72.86; H, 10.04. Calcd. for $C_{25}H_{40}O_4\cdot 1/2H_2O$: C, 72.61; H, 9.91%.

Acetylation of this methyl ester gave methyl 3-oxo-6α-acetoxy-5α-cholanoate, plates, m.p. 115~116°C (from ether-petroleum ether). Zimmermann test was positive. $[\alpha]_D^{33}=+48\pm4°$ (*c* 0.608)[*4]. Infrared spectrum: $\nu_{max}^{CHCl_3}$ 1729, 1712 (C=O); 1249, 1175, 1024 $cm^{-1}$ (C-O).

Found: C, 72.92; H, 9.81. Calcd. for $C_{27}H_{42}O_5$: C, 72.61; H, 9.48%.

**Oxidation of 3β, 6β-Dihydroxy-5α-cholanoic Acid**[*5]. — To a solution of 3β,6β-dihydroxy-5α-cholanoic acid (73 mg.) in acetone (6 ml.), water (1 ml.) and methanol (1.5 ml.), was added NBS (75 mg.; 2.3 mol. equiv.). After the resulting mixture was kept for 3 hr. at room temperature, aqueous sodium bisulfite was added, and the extract with ether was washed with water and evaporated to furnish needles with m.p. 235~237°C. This crude acid was recrystallized from acetone to methyl 3β-hydroxy-6-oxo-5α-cholanoic acid, m.p. 244~245°C, 23 mg. Zimmermann test was negative. Ultraviolet spectrum: $\lambda_{max}^{EtOH}$ 287 mμ (ε=45). Infrared spectrum: $\nu_{max}$ 1727, 1689 $cm^{-1}$ (C=O).

Found: C, 73.61; H, 9.68. Calcd. for $C_{24}H_{38}O_4$: C, 73.80; H, 9.81%.

Its methyl ester was obtained as scales from methanol, melting at 93~95°C. Acetylation of this methyl ester furnished methyl 3β-acetoxy-6-oxo-5α-cholanoate, m.p. 155~157°C, scales. A mixed melting point with methyl 3α-acetoxy-6-oxo-5β-cholanoate with m.p. 156~157°C was melted at 130~135°C. $[\alpha]_D^{32}=-9\pm2°$ (*c* 0.91, methanol).

Found: C, 72.62; H, 9.45. Calcd. for $C_{27}H_{42}O_5$: C, 72.61; H, 9.48%.

*3 Synthesis of this compound was described in preceding part XX.

*4 Optical rotation of methyl 3-oxo-6α-acetoxy-5β-cholanoate was as follows: $[\alpha]_D^{31}=-29\pm2°$ (*c* 1.057).

*5 As optical rotation of this compound had not been reported, it was measured by the author and its value was found to be as follows: $[\alpha]_D^{33}=-0.1\pm2°$ (*c* 1.057, pyridine).

**Spectroscopic Determination of the Order of Reactivity in the Oxidation of Methyl 3β- and 3α-Hydroxy-5β-cholanoate with NBS.** — *Measurement.*—For the measurement of the optical densities, a "Koken DS 301" (double beam) was used. Infrared spectra were measured by used of a 0.25 mm. cell and at the concentration of about 37% transmission of carbonyl stretching absorption band of the ester group which was controlled by dilution. The speed in the measurements was adjusted to 50 $cm^{-1}$ per 36 sec. at about 1700 $cm^{-1}$ for the purpose of a quantitative analysis. The optical densities of carbonyl band at 1720 $cm^{-1}$ in carbon tetrachloride solution was calculated by the base line method (Fig. 1). $T_0$ and $T$ were a mean value of three measurements.

*Procedure.* — A mixture consisting of 3-hydroxy compounds (210 mg.), NBS (126 mg.; 1.3 mol. equiv.) and dioxane-water (9:1) (22 ml.) in a 50 ml. reaction flask with stopper was allowed to stand at 25°C with use of thermostat. Each 5 ml. of the reaction mixture was pipetted at various times and the reaction in each aliquot was stopped with aqueous sodium bisulfite, extracted with ether and successively washed with water, soda and water (ten times). The ethereal layers were evaporated and finally dried in vacuo for 12 hr. at 60°C. The obtained residue (about 45 mg.) was dissolved in so much carbon tetrachloride as to make an adequate concentration giving optical density of the carbonyl band in the ester group at about 37% transmission. The yield of the oxidation product was estimated from the calibration curve prepared above (Fig. 2). These values are shown in Tables IV and V (Fig. 3).

## Summary

(1) The order of susceptibility of the hydroxyl groups in epimeric 3,6-dihydroxy-cholanoic acids to the oxidation with NBS was determined and the results were as follows:

6β(a) > 3β(a) > 3α(e) > 6α(e) (A/B: cis)

6β(a) > 3β(e) > 6α(e) (A/B: trans)

(2) Reaction mechanism of the oxidation with NBS was discussed.

The author is particularly indebted to Dr. K. Takeda, Director of this Laboratory, for his discussions and encouragement during this work. The author gratefully acknowledges many helpful discussions with Dr. W. Nagata. Thanks are also due to Mr. Y. Matsui for infrared spectral measurements, to Messers T. Ieki, K. Miyahara, K. Daikatsu, T. Takaoka and Miss. U. Kasugai for elementary analyses and to Mr. T. Iwata for measurements of optical rotation.

*Research Laboratory*
*Shionogi & Co., Ltd.*
*Imafuku, Amagasaki, Hyogo*

# *Mineral Content of Mixed Fertilizer*

By Jumpei ANDO and Seiichi MATSUNO

(Received September 28, 1960)

Recently in Japan nearly 1200000 tons of mixed fertilizer has been produced yearly by the following process:—calcium superphosphate, ammonium sulfate and potassium chloride are mixed, ammoniated so as to neutralize the free phosphoric acid in superphosfate, granulated between 3 and 20 meshes with sprayed water, dried in a rotary drier so as to have 2~3% free water, cooled to 40~60°C by rotary cooler, kept in storage pile for days or weeks and then packed. Ikeno[1] reported that ammonium syngenite and monoammonium phosphate were formed in 8-8-7 mixed fertilizer. No other report is found concerning the fertilizer.

In the present work the mineral content of the products having various $N : P_2O_5 : K_2O$ ratios and reactions during the production process were investigated so as to clarify the cause of caking of products which often takes place in the storage pile, the action of water in the products which must be known for calculation of material balance, and other problems concerning the fertilizer have been studied.

## Experimental and Results

**Mineral Content of Products.**—It was clarified by X-ray diffraction that commercial mixed fertilizers (Table I) were mainly composed of potassium ammonium syngenite (crystalline solution of potassium syngenite $K_2SO_4 \cdot CaSO_4 \cdot H_2O$ and ammonium syngenite $[(NH_4)_2SO_4 \cdot CaSO_4 \cdot H_2O]$, monoammoniumpotassium phosphate (crystalline solution of monoammonium phosphate $NH_4H_2PO_4$ and monopotassium phosphate $KH_2PO_4$), ammonium chloride and calcium sulfate anhydride. The minerals used as raw materials such as monocalcium phosphate monohydrate, ammonium sulfate and potassium chloride were not at all or were only slightly detected in the products. The amount of these minerals in the products was determined by X-ray diffractometer using spinel $MgO \cdot Al_2O_3$ as inner standard.

**Synthesis of Standard Samples.** — a) *Inner Standard.*—By preliminary tests it was found that spinel $MgO \cdot Al_2O_3$ was suitable as inner standard. A mixture of equal mole of refined magnesia and alumina was heated for 30 min. at 1600~1670°C. Spinel was formed almost completely. The product contained very few other minerals.

b) *Calcium Sulfate Anhydride.*—Calcium carbonate was treated with concentrated sulfuric acid.

c) *Syngenite.*—Ammonium sulfate or potassium sulfate or various mixtures of both of these was mixed with a theoretical amount of calcium sulfate anhydride and excess of water, heated at 45°C on a water bath and dried. Addition of water and drying were repeated until the single salts disappeared and syngenite or a homogeneous crystalline solution of syngenite was formed.

d) *Monoammoniumpotassium Phosphate.* — Monoammonium phosphate and monopotassium phosphate were mixed at various ratios, the mixture being wet with water, heated at 45°C on water bath

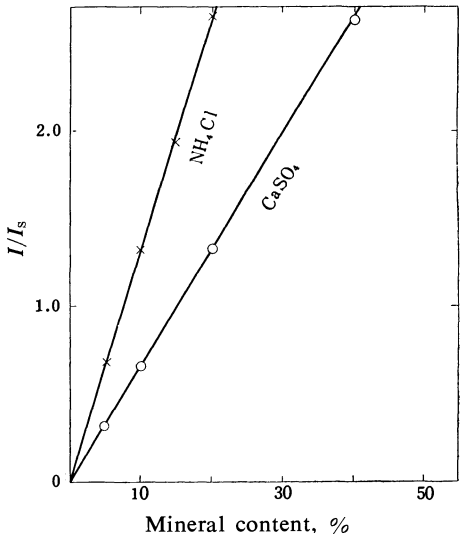



Fig. 1. Calibration curves of ammonium chloride and calcium sulfate anhydride.

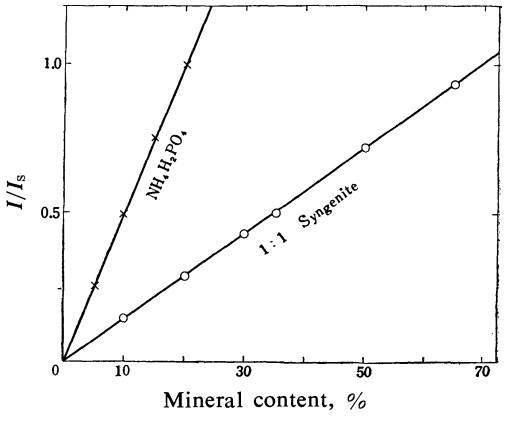



Fig. 2. Calibration curves of monoammonium phosphate and 1 : 1 syngenite.

1) R. Ikeno and Y. Shimomura, *J. Chem. Soc. Japan, Ind. Chem. Sec.* (*Kogyo Kagaku Zasshi*), **63**, 78 (1960).

and dried. A homogeneous crystalline solution was formed easily.

**Method of Determination.**—The Amount of each salt was determined measuring the diffraction peaks of the following angle ($2\theta$ by Cu ray): spinel 36.8°, crystalline solution of syngenite around 9°, monoammoniumpotassium phosphate around 16.6°, ammonium chloride 32.6°, calcium sulfate anhydride 25.4°, ammonium sulfate 20.4° and potassium chloride 28.3°. One handred parts of a mixture of 1 : 1 syngenite (crystalline solution of ammonium and potassium syngenite 1 : 1 by weight), monoammonium phosphate, ammonium chloride and calcium sulfate anhydride were mixed with 25 parts

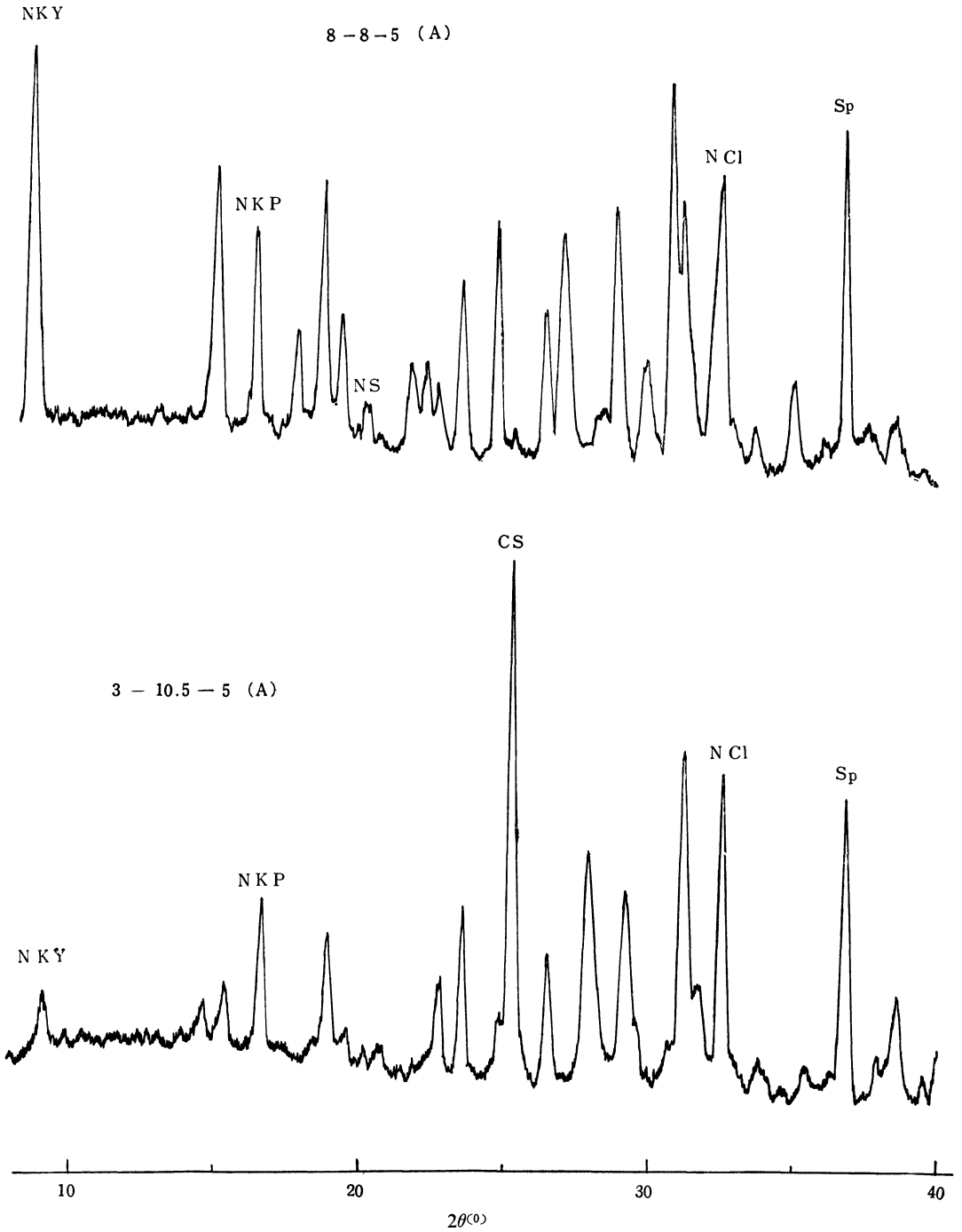



Fig. 3. X-ray diffraction patterns of mixtures of commercial fertilizers, 100 parts, and spinel, 25 parts (Cu ray, Ni filter).

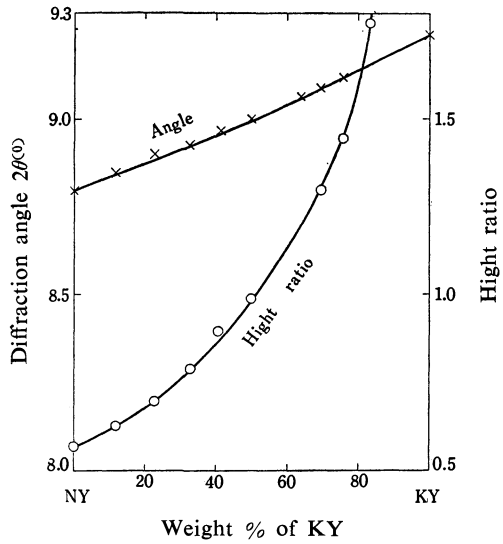



Fig. 4. Relation between weight ratio of ammonium syngenite (NY) component and potassium syngenite (KY) component in their crystalline solution and diffraction angle of center of the peak and also the ratio of height of the peak of 1 : 1 syngenite and that of other syngenite.

of spinel and were recorded by X-ray diffractometer. Calibration curves thus obtained are illustrated in Figs. 1 and 2.

One handred parts of mixed fertilizer and 25 parts of spinel were mixed and recorded by X-ray diffractometer (Fig. 3). The content of ammonium chloride and of calcium sulfate anhydride were determined by Fig. 1.

Figure 4 or 6 was plotted by measurement of various crystalline solution of syngenite or phosphate. The $NH_4/K$ ratio and amount of syngenite or phosphate in commercial fertilizer were determined using the relations of Figs. 2 and 4 or 6.

Results of determination of commercial fertilizer are shown in Table I. These samples contained 1~3% free water measured by weight loss on heating for 3 hr. at 100°C (Table II). A small part of salt was dissolved in the water and was not determined by X-ray. A sample 3-10-10 (C) contained a considerable amount of potassium chloride which was not detected in other samples. The samples contained less than 3% ammonium sulfate. No monocalcium phosphate monohydrate was detected in any sample. Considering these facts together with the results of Table II it is known that the quantitative analysis by X-ray was performed fairly accurately.

**Reactions during Production Process.**—Mixed fertilizer 8-8-6 was prepared in the laboratory under conditions similar to that of a large scale plant.

TABLE I. MINERAL CONTENT (%) OF COMMERCIAL MIXED FERTILIZER PRODUCED IN THREE PLANTS (A, B and C)

| Sample | $CaSO_4$ | $NH_4Cl$ | NKP | | | NKY | | | Total |
|---|---|---|---|---|---|---|---|---|---|
| | | | Sum | NP | KP | Sum | NY | KY | |
| 8-8-5 (A) | 1.7 | 6.5 | 12.5 | 11.9 | 0.6 | 58.8 | 41.2 | 17.6 | 81.0 |
| 6-9.5-5 (A) | 12.3 | 6.7 | 14.8 | 14.1 | 0.7 | 44.8 | 28.0 | 16.8 | 78.6 |
| 3-10.5-5 (A) | 27.5 | 8.5 | 15.6 | 11.2 | 4.4 | 24.6 | 5.7 | 18.9 | 76.2 |
| 8-8-5 (B) | 6.7 | 6.5 | 14.1 | 14.1 | 0 | 51.8 | 36.2 | 15.6 | 80.7 |
| 8-8-6 (C) | 3.4 | 7.2 | 14.7 | 14.3 | 0.4 | 66.4 | 41.5 | 24.9 | 91.7 |
| 8-7-8 (C) | 3.3 | 10.5 | 12.2 | 12.0 | 0.2 | 65.8 | 33.2 | 32.6 | 91.8 |
| 6-9-6 (C) | 20.1 | 7.5 | 14.8 | 13.8 | 1.0 | 47.7 | 25.3 | 22.4 | 90.1 |
| 8-7-8 (C) | 3.4 | 11.5 | 13.1 | 12.9 | 0.2 | 57.3 | 30.4 | 26.9 | 85.3 |
| 3-10-10 (C) | 31.6 | 5.7 | 21.6 | 15.0 | 6.6 | 25.3 | 4.8 | 20.5 | 84.2 |

NP=monoammonium phosphate, KP=monopotassium phosphate,
NKP=crystalline solution of NP and KP, NY=ammonium syngenite, KY=potassium syngenite,
NKY=crystalline solution of NY and KY

TABLE II. COMPARISON OF N, $P_2O_5$ AND $K_2O$ CONTENT DETERMINED BY CHEMICAL ANALYSIS (G) AND BY X-RAY ANALYSIS (X) OF TABLE I

| Sample | N | | $P_2O_5$ | | $K_2O$ | | Free water |
|---|---|---|---|---|---|---|---|
| | X | G | X | G | X | G | |
| 8-8-5 (A) | 6.88 | 8.76 | 7.65 | 8.79 | 5.55 | 5.56 | 3.0 |
| 6-9.5-5 (A) | 5.92 | 6.96 | 9.07 | 10.34 | 5.35 | 5.53 | 3.1 |
| 3-10.5-5 (A) | 4.07 | 4.05 | 9.21 | 10.61 | 7.26 | 7.68 | 5.5 |
| 8-8-5 (B) | 6.46 | 8.50 | 8.70 | 9.10 | 4.74 | 5.31 | 1.4 |
| 8-8-6 (C) | 7.11 | 8.33 | 9.04 | 9.10 | 7.70 | 6.25 | 0.8 |
| 8-7-8 (C) | 7.00 | 8.01 | 7.54 | 7.53 | 9.98 | 10.01 | 1.9 |
| 6-9-6 (C) | 5.78 | 6.02 | 9.03 | 9.10 | 7.16 | 7.20 | 2.2 |
| 8-7-8 (C) | 7.13 | 8.70 | 8.10 | 8.12 | 8.25 | 8.60 | 0.9 |
| 3-10-10 (C) | 3.72 | 3.80 | 12.70 | 11.46 | 6.47 | 10.70 | 2.5 |

The mineral content of samples during the course of preparation was determined by X-ray. Samples of each process in a large scale plant were investigated, too.

Superphosphate (−20 mesh, $P_2O_5$ 17.56%, free water 12.02%) 356 g., potassium chloride (red colored, −42 mesh) 73.5 g. and ammonium sulfate (−42 mesh) 266 g. were mixed and put in a porcelain rotary drum (26×26 cm.). After 74 cc. of 4.75% aqueous ammonia and 15 cc. of water were sprayed the mixture was granulated between 4 and 10 mesh and dried in an air oven at 130°C for 15, 30, 45 and 60 min. Fifty grams of the sample dried for 60 min. (containing 2.91% free water) was put in a 50 cc. stoppered bottle and kept at 50°C for 5 days and then at room temperature for 10 days. The mineral content of samples just after mixing, granulation, drying and keeping for each time were determined by X-ray. The free water of samples was measured by weight loss on drying powdered samples for 3 hr. at 100°C.

It was known by preliminary tests that when the sample containing much water was powdered finely and recorded by X-ray a remarkable change took place in the sample during this procedure. In order to determine the mineral content of samples without the change during analytical procedure the samples were washed with pure ethyl alcohol, filtered, dried at room temperature in vacuum desiccator in several minutes and tested by X-ray diffractometer. In this case the free water of samples was eliminated and the salts dissolved in the water were crystallized. The mineral content of the original sample was calculated multiplying the value of X-ray analysis by (100-free water %)/100. The results are shown in Fig. 7.

Figure 7 illustrates that the following chemical reactions take place partly soon after the mixing of raw materials and extensively by the addition of ammonia and water.

$$Ca(H_2PO_4)_2 \cdot H_2O + (NH_4)_2SO_4 = 2NH_4H_2PO_4 + CaSO_4 + H_2O \quad \text{.....(1)}$$

$$(NH_4)_2SO_4 + CaSO_4 + H_2O + (NH_4)_2SO_4 \cdot CaSO_4 \cdot H_2O \quad \text{.....(2)}$$

$$CaSO_4 \cdot 1/2H_2O + (NH_4)_2SO_4 + 1/2H_2O = (NH_4)_2SO_4 \cdot CaSO_4 \cdot H_2O \quad \text{.....(3)}$$

$$H_3PO_4 + NH_4OH = NH_4H_2PO_4 + H_2O \quad \text{.....(4)}$$

$$2KCl + (NH_4)_2SO_4 = K_2SO_4 + 2NH_4Cl \quad \text{.....(5)}$$

$$K_2SO_4 + Ca(H_2PO_4)_2 \cdot H_2O = 2KH_2PO_4 + CaSO_4 + H_2O \quad \text{.....(6)}$$

$$K_2SO_4 + CaSO_4 + H_2O = K_2SO_4 \cdot CaSO_4 \cdot H_2O \quad (7)$$

$$mKH_2PO_4 + nNH_4H_2PO_4 \rightarrow \text{crystalline solution} \quad \text{.....(8)}$$

$$r[(NH_4)_2SO_4 \cdot CaSO_4 \cdot H_2O] + s(K_2SO_4 \cdot CaSO_4 \cdot H_2O) \rightarrow \text{crystalline solution} \quad \text{.....(9)}$$

$$2KH_2PO_4 + (NH_4)_2SO_4 \cdot CaSO_4 \cdot H_2O = 2NH_4H_2PO_4 + K_2SO_4 \cdot CaSO_4 \cdot H_2O \quad (10)$$

Potassium sulfate formed by reaction 5 reacts

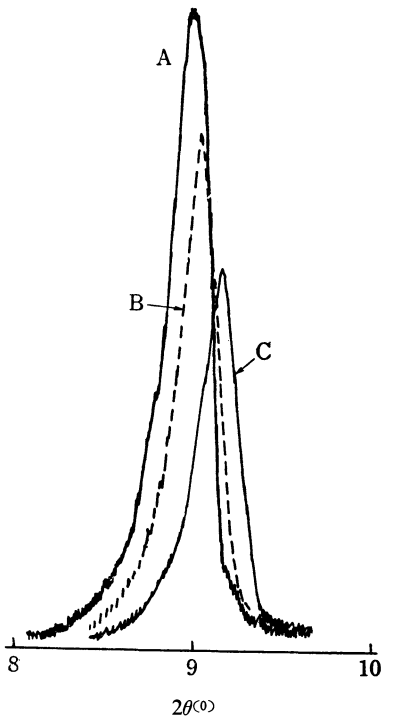



Fig. 5. Change of diffraction peak of crystalline solution of syngenite.
Weight ratios of ammonium and potassium syngenite are: A 66 : 34; B 50 : 50; C 24 : 76.

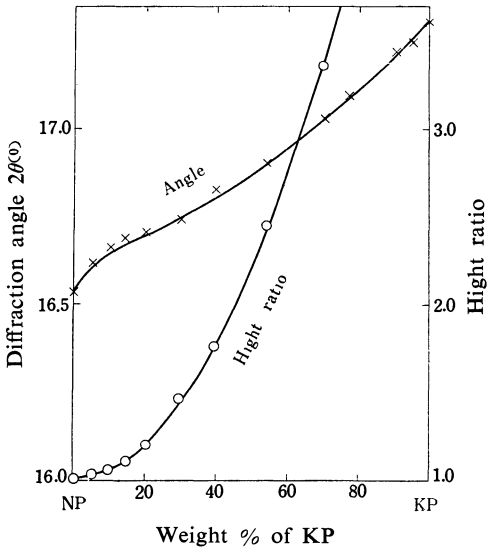



Fig. 6. Relation between weight ratio of monoammonium phosphate (NP) component and monopotassium phosphate (KP) component in their crystalline solution and diffraction angle of center of the peak and also the ratio of height of the peak of NP and that of the crystalline solution.

immediately to form potassium syngenite (7) and monopotassium phosphate(6) and does not actually exist in samples. Reactions 1-9 were almost completed when the granules were dried for 15 min. in a 130°C oven. At this time the free water of the sample was 8.52%.

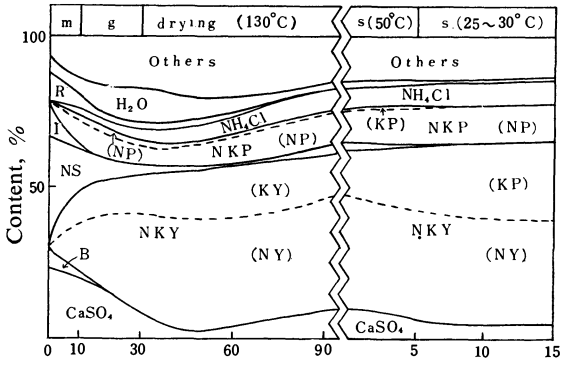



Fig. 7. Change of mineral content of samples in the midst of production process. m=mixing, g=granulation, s=storing in sealed bottles, R=KCl, I=$Ca(H_2PO_4)_2 \cdot H_2O$, NP=$NH_4H_2PO_4$, KP=$KH_2PO_4$, NKP=crystalline solution of NP and KP, NS=$(NH_4)_2SO_4$, KY=$K_2SO_4 \cdot CaSO_4 \cdot H_2O$, NY=$(NH_4)_2SO_4 \cdot CaSO_4 \cdot H_2O$, NKY=crystalline solution of NY and KY, B=$CaSO_4 \cdot 1/2H_2O$.

It was clarified that by further drying a part of syngenite was decomposed to form calcium sulfate anhydride and ammonium sulfate. When dried for 60 min. the free water of the sample was 2.91% and the content of ammonium sulfate and calcium sulfate anhydride increased to a fair extent (Fig. 7). After being stored for days in a sealed bottle at 50°C the free water and those minerals decreased to form syngenite and the grains of the sample slightly adhered to each other forming a cake. When the granulated sample was dried at 120°C for 60 min. the free water content of the sample was 4.32%. Decomposition of syngenite took place similarly. After being stored for days at 50°C the grains adhered to each other more firmly than they did in the above sample.

The reaction 10 took place gradually and continued even in storing at room temperature. By this reaction $NH_4/K$ ratio of crystalline solution of syngenite decreased and that of monophosphate increased.

Samples of 8-8-5 mixed fertilizer in the midst of each process of large scale production were tested in the same way. It was clarified that the above reactions took place similarly but often more slowly than in the laboratory test, perhaps because the raw materials were not mixed so well as in the laboratory. A greater amount of calcium sulfate anhydride and ammonium sulfate and less syngenite were contained in the sample before piling. The sample after being piled and caked contained a very small amount of free water and these salts.

**Thermal Decomposition of Syngenite.**—Figure 8 illustrates the weight loss of synthetic ammonium and potassium syngenite and crystalline solution of equal weight of the two when heated at a rate of 3~4°C/min. Ammonium syngenite was decomposed over 110°C. Over 160°C ammonium sulfate was volatilized. 1 : 1 syngenite or potassium syngenite was decomposed over 120°C or 240°C respectively. The syngenite contained in commercial fertilizer 8-8-6 or 8-8-5 resembled 1 : 1 syngenite and was not decomposed by heating for hours at 120°C. Ammonium syngenite was not decomposed by heating for hours at 100°C. However, it was clarified that the syngenite just after its formation in mixed fertilizer e. g. just after the granulation or at the begining of drying was partly decomposed

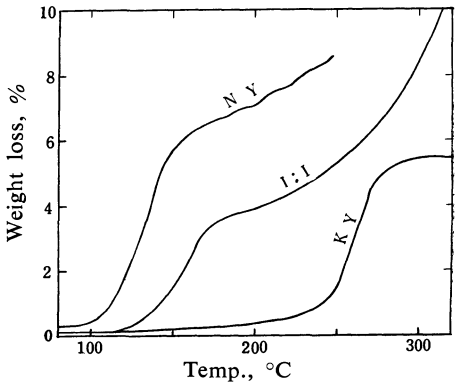



Fig. 8. Thermal decomposition of syngenite. NY=ammonium syngenite, KY=potassium syngenite, 1 : 1=crystalline solution of the two 1 : 1 by weight.

even by heating at 100°C, perhaps because syngenite crystals had not grown well and a small amount of impurities such as $HPO_4^{2-}$ instead of $SO_4^{2-}$ was contained in the crystal.

To determine exactly the free water content of such samples by heating at 100°C, the amount of crystallization water lost by the heating must also be measured determining the amount of syngenite decomposed.

## Discussion

It seems that syngenite, especially ammonium-rich syngenite plays an important role concerning the caking of products in a storage pile. In the preparation of standard samples it was observed that potassium rich syngenite was formed quickly and had little tendency of hardening and that ammonium-rich syngenite was formed slowly and hardened. Moreover, ammonium-rich syngenite is apt to decompose on drying and recrystallize during piling.

It has been known that mixed fertilizers such as 8-7-8, 8-8-6 and 8-8-5 are apt to form a hard cake and that the fertilizers such as 3-10-10, 3-10.5-5 etc. have little tendency of caking in a storage pile. This is attributable to the fact that the latter contain less and the former much ammonium syngenite component.

In large scale plants the granules are often dried in shorter time at a higher temperature than was done in the laboratory experiment. Thermal decomposition of syngenite must take place remarkably on the surface of grains which are dried enough and reach a high temperature. Free water remains in the inner part of the grains and gradually disperses to the surface to cause the recrystallization of syngenite and the caking of products. By the crystallization of syngenite the free water content of the products is reduced and a part of the salts dissolved in the water is crystallized promoting the formation of a hard cake.

The reaction 10 takes place successively in a storage pile. When the raw materials were not powdered finely or mixed well, reactions 1-9 are not completed before piling but occur continuously in the storage pile. All of these reactions are promoted by free water in the granules.

In order to prevent the caking of products (1) free water of the granules must be reduced as far as possible by drying, (2) drying at high temperature must be avoided so as to depress the thermal decomposition of syngenite, (3) the raw materials had better be powdered and mixed well so that the reactions 1-9 are almost finished before piling, and (4) the dried sample had better be cooled to a lower temperature. Of course it is desirable not to pile the products too high.

It was observed that ammonium chloride was volatilized slightly by heating at 130°C. In the drier of the large scale plant a small amount of ammonium chloride must be volatilized. Also for this reason the granules must not be dried at a high temperature.

Measurement of the amount of free and crystallization water of the products is nesessary for calculation of material balance. It was clarified that water of crystallization was contained only in syngenite and that its amount could be measured by X-ray determination of syngenite. The free water content of products stored for more than a week after granulation could be measured almost exactly by drying the samples for 3 hr. at 100°C. To measure the free water content of samples soon after production by the above method the loss of crystallization water by the drying must also be measured, determining the amount of syngenite before and after the drying. By such a method the material balance of mixed fertilizer could be calculated exactly.

## Summary

The mineral content of mixed fertilizer produced with calcium superphosphate, ammonium sulfate and potassium chloride and also the reactions during the production process were investigated by X-ray diffraction.

It was observed that remarkable reactions took place between monocalcium phosphate, calcium sulfate, ammonium sulfate and potassium chloride by the addition of water for granulation. At the beginning of drying of the wet granules these minerals almost disappeared to form ammonium chloride and crystalline solutions of ammonium and potassium syngenite and those of monoammonium and monopotassium phosphate.

The syngenite thus formed decomposed partly by further drying and again formed while the product was placed in a storage pile. It seems that the caking of the product which often occurs in a storage pile is caused mainly by the crystallization of syngenite which decreases the amount of free water in the product and makes other salts crystallize at the same time.

Thanks are extended to Kurehakagakukogyo Co., Ltd., Nihonsuisokogyo Co., Ltd. and Nissankagakukogyo Co., Ltd. for samples of mixed fertilizer, and to Mr. T. Noguchi of Kurehakagakukogyo Co., Ltd. for assistance with chemical analyses.

*Department of Industrial Chemistry*
*Faculty of Engineering*
*Chuo University*
*Bunkyo-ku, Tokyo*

# *An Empirical Method for Estimating Normal Boiling Point and other Physical Properties of Alkene Hydrocarbons*

By Mikio TAMURA, Michio KURATA, Koichiro NAKANISHI*1 and Isamu NAGATA*2

(Received October 20, 1960)

The structural variation in the physical properties of alkene hydrocarbons is determined by the number and relative position of double bonds and side chains in the molecule. Owing to the presence and mutual influence of two different kinds of chemical bonds and side chains, correlation between properties and molecular structure is far more complicated than that in the case of isoparaffins, for which an elaborate set of structural parameters can be successfully used[1,2]. Although a few attempts were made to correlate the boiling point[3,4] or critical constants[5,6] with the molecular structure of alkenes, no extensive method has been established at the present stage.

In this paper, an empirical relation between the physical properties of linear and branched alkenes and their molecular structure is proposed. The "effective carbon number" method which has been used for isoparaffins in the previous report[2] is again adopted. As will be shown later, a characteristic constant called "effective carbon number" can be defined for all the alkene hydrocarbons. Thus, this effective carbon number is first calculated by the proposed equation and then, by the use of a previously presented nomogram[2], the normal boiling point and other physical properties of the alkenes can be estimated from the knowledge of the structural formula alone.

## Effective Carbon Number

When the boiling points of normal paraffins are plotted against the number of carbon atoms, a family of curves for different pressures is obtained. Then, reading the boiling points of a given alkene on these curves, one can obtain a set of values of an "effective number" of carbon atoms, each corresponding to every different pressure. These sets of values for several alkenes obtained by this procedure are listed in Table I together with the used values of the boiling point[7,8], where a reasonable constancy of the values is observed over a considerably wide range of pressure. This effective number of carbon atoms depending on the structural feature of each compound but not on the external condition is called the "effective carbon number" and hereafter denoted by $n^*$. It is shown that the proper assignment of the $n^*$ value is advantageous not only for the estimation of the boiling point of the alkenes at various external pressures but also for that of other physical properties such as the critical constants, as in the case of isoparaffins[2].

TABLE I. CONSTANCY OF EFFECTIVE CARBON NUMBER OF ALKENES AT VARIOUS EXTERNAL PRESSURES

| Compound | Pressure, mmHg | 10 | 20 | 60 | 200 | 400 | 760 |
|---|---|---|---|---|---|---|---|
| 1-Butene | $T_b$[7] (°C) | −81.5 | −72.89 | −57.15 | −36.10 | −21.62 | −6.26 |
| | $n^*$ | 3.88 | 3.87 | 3.86 | 3.86 | 3.86 | 3.85 |
| 2-Methylpropene | $T_b$[7] (°C) | −81.95 | −73.37 | −57.664 | −36.666 | −22.227 | −6.900 |
| | $n^*$ | 3.87 | 3.85 | 3.84 | 3.85 | 3.84 | 3.84 |
| 1,3-Butadiene | $T_b$[8] (°C) | −79.7 | −71.0 | −55.1 | −33.9 | −19.3 | −4.5 |
| | $n^*$ | 3.92 | 3.93 | 3.93 | 3.90 | 3.89 | 3.86 |

*1 Present address: Department of Industrial Chemistry, Faculty of Engineering, Shinshu University, Nagano.
*2 Present address: Department of Chemical Engineering, Kyoto University, Kyoto.

1) H. Wiener, *J. Am. Chem. Soc.*, **69**, 17 (1947).
2) K. Nakanishi, M. Kurata and M. Tamura, *J. Chem. & Eng. Data*, 5, No. 2, 210 (1960).
3) W. J. Taylor, J. M. Pignocco and F. D. Rossini, *J. Research Natl. Bur. Standards*, **34**, 413 (1945).
4) C. W. Beck and L. Y. Beck, *Ind. Eng. Chem.*, **51**, 223 (1959).
5) G. V. Michael and G. Thodos, *Chem. Eng. Progr. Symposium Series* No. 7, **49**, 131 (1953).
6) G. Thodos, *A. I. Ch. E. Journal*, **1**, 165 (1955).
7) F. D. Rossini, K. S. Pitzer, R. L. Arnett and G. C. Pimentel, "Selected Values of Physical and Thermodynamic Properties of Hydrocarbons and Related Compounds", American Petroleum Institute Research Project 44, Carnegie Press, Pittsburgh, Pa. (1953).
8) D. R. Stull, *Ind. Eng. Chem.*, **39**, 517 (1947).

### Structural Units

The molecular structure of alkenes can be specified by the number and the relative position of double bonds and those of branching units. Therefore, if the mutual influence among these units is properly estimated, the deviation of the effective carbon number from the real one may be expressed as a linear combination of several factors, each corresponding to a double bond or a branching unit. Although various kinds of methods for such factorization would be possible, only the linear factorization is used here because of its simplicity for practical purposes.

The following four groups of carbon atoms are adopted as the structural units of alkenes: i. e. (I) double bond existing in the linear portion of the molecule, (II) double bond attached to branching atoms, (III) trifunctional branching and (IV) tetrafunctional branching. Schematically, these are

(I) -C=C-, (II) -C=C(-C)-C- or -C-C(-C)=C(-C)-C-,

(III) -C(-C)-C-C- and (IV) -C-C(-C)(-C)-C-

For each of the four structural units, the following equation is obtained after some troublesome analysis of available boiling point data:

$$\Delta n_{\mathrm{I}} = 0.24 - 0.12b_1 + 0.05b_2 \quad (1)$$

$$\Delta n_{\mathrm{II}} = 0.24 - 0.08b_1 + 0.07b_2 \quad (2)$$

$$\Delta n_{\mathrm{III}} = 0.28 - 0.06c_2 + 0.06c_3 \quad (3)$$

$$\Delta n_{\mathrm{IV}} = 0.73 - 0.14c_2 + 0.05c_3 \quad (4)$$

The difference of the effective carbon number $n^*$ from the real carbon number $n$ is then given by the sum of these contributions,

$$\Delta n = n - n^* = \sum_{\mathrm{I}} \Delta n_{\mathrm{I}} + \sum_{\mathrm{II}} \Delta n_{\mathrm{II}} + \sum_{\mathrm{III}} \Delta n_{\mathrm{III}} + \sum_{\mathrm{IV}} \Delta n_{\mathrm{IV}} \quad (5)$$

where the summation extends over all structural units of each type. The four parameters, $b_1$, $b_2$, $c_2$ and $c_3$, in Eqs. 1 to 4 are defined as follows:

- $b_1$—the number of carbon-carbon bonds adjacent to the double bond.
- $b_2$—the number of carbon-carbon bonds (single and double) next but one to the double bond.
- $c_2$—the number of the second neighbor carbon atoms of the branching point (tertiary or quaternary carbon atom).
- $c_3$—the number of the third neighbor carbon atoms of the branching point (tertiary or quaternary carbon atom).

As is easily seen, the intrinsic contribution of the structural unit I, III and IV is represented by the first term of Eqs. 1, 3 and 4, respectively, while two other terms which represent the contribution of adjacent carbon atoms to each structural unit are introduced to take the mutual correlation of the structural units into account. The choice of type II as an independent structural unit is also due to the fact that the correlation of the double bond with the branching is so strong that it can not be treated separately.

It is obvious from the definition that the effective carbon number of isoparaffins is given by

$$n^* = n - \sum_{\mathrm{III}} (0.28 - 0.06c_2 + 0.06c_3) - \sum_{\mathrm{IV}} (0.73 - 0.14c_2 + 0.05c_3) \quad (6)$$

The accuracy of this equation is of the same degree as that of Eq. 41 in the previous paper[2], which is expressed in terms of the Wiener parameters[1].

### Example of Calculation

The present method consists of the following two procedures:

(1) Effective carbon number $n^*$ is calculated by Eq. 5. Only the structural formula of alkene in question is required.

(2) The vapor pressure-temperature relationship, the critical constants and the heat of vaporization at normal boiling point can be read on nomogram[2] by using the value of $n^*$ just obtained.

For clear understanding of the method, calculation of the normal boiling point of 3, 5, 5-trimethyl-1-hexene is presented as an example.

3, 5, 5-Trimethyl-1-hexene

$$C^1=C^2-C^3(-C^7)-C^4-C^5(-C^8)(-C^9)-C^6$$

This compound contains the aforementioned structural units of I, III and IV types. The unit of type I is attached to one carbon-carbon bond to be counted as $b_1$, say $C^2$-$C^3$, and to two bonds to be counted as $b_2$, say $C^3$-$C^4$ and $C^3$-$C^7$; hence

$$\Delta n_{\mathrm{I}} = 0.24 - 0.12 \times 1 + 0.05 \times 2 = 0.22$$

The structural unit of type III or tertiary carbon atom $C^3$ has two second neighbors, say $C^1$ and $C^5$, and three third neighbors, say $C^6$, $C^8$ and $C^9$, hence

$$\Delta n_{\mathrm{III}} = 0.28 - 0.06 \times 2 + 0.06 \times 3 = 0.34$$

Quaternary carbon atom $C^5$ has one second neighbor, $C^3$, and two third neighbors, $C^2$ and $C^7$, and so

$$\Delta n_{\mathrm{IV}} = 0.73 - 0.14 \times 1 + 0.05 \times 2 = 0.69$$

TABLE II. NORMAL BOILING POINT OF MONOALKENES

| Compound | Normal boiling point $T^0_b$, °C | | Effective carbon number, $n^*$ | |
|---|---|---|---|---|
| | Obs.[9] | Calcd. | Obs. | Calcd. |
| Ethylene | −103.7 | −104.0 | 1.76 | 1.76 |
| Propylene | −47.7 | −47.0 | 2.86 | 2.88 |
| 1-Butene | −6.3 | −6.0 | 3.85 | 3.83 |
| 2-Butene | 1. | 2.0 | 4.04 | 4.00 |
| 2-Methylpropene | −6.9 | −2.0 | 3.84 | 3.92 |
| 1-Pentene | 29.9 | 30.0 | 4.83 | 4.83 |
| 2-Pentene | 36.1 | 34.0 | 5.00 | 4.95 |
| 2-Methyl-2-butene | 38.6 | 36.0 | 5.07 | 5.00 |
| 2-Methyl-1-butene | 31.2 | 31.0 | 4.86 | 4.85 |
| 3-Methyl-1-butene | 20.1 | 20.0 | 4.55 | 4.56 |
| 1-Hexene | 63.5 | 63.0 | 5.83 | 5.83 |
| 2-Hexene | 68.2 | 67.0 | 5.98 | 5.95 |
| 3-Hexene(*trans*) | 67.1 | 65.0 | 5.93 | 5.90 |
| 2-Methyl-1-pentene | 62.2 | 63.0 | 5.80 | 5.85 |
| 3-Methyl-1-pentene | 54.2 | 56.0 | 5.54 | 5.62 |
| 4-Methyl-1-pentene | 53.9 | 54.0 | 5.53 | 5.55 |
| 2-Methyl-2-pentene | 65.0 | 66.0 | 5.88 | 5.93 |
| 3-Methyl-2-pentene | 68.0 | 66.0 | 5.97 | 5.93 |
| 4-Methyl-2-pentene | 57.0 | 56.0 | 5.60 | 5.62 |
| 2-Ethyl-1-butene | 64.7 | 62.0 | 5.76 | 5.78 |
| 2,3-Dimethyl-1-butene | 55.6 | 51.0 | 5.58 | 5.46 |
| 3,3-Dimethyl-1-butene | 41.2 | 41.0 | 5.14 | 5.14 |
| 2,3-Dimethyl-2-butene | 73. | 71.0 | 6.1 | 6.08 |
| 1-Heptene | 93.6 | 93.0 | 6.83 | 6.83 |
| 2-Heptene | 98.5 | 97.0 | 7.00 | 6.95 |
| 3-Heptene | 95.6 | 95.0 | 6.90 | 6.90 |
| 2,3,3-Trimethyl-1-butene | 77.9 | 77.0 | 6.30 | 6.26 |
| 1-Octene | 121.3 | 120.0 | 7.83 | 7.83 |
| 2-Isopropyl-3-methyl-1-butene | 113.6 | 100.0 | 7.55 | 7.08 |
| 1-Nonene | 146.9 | 147.0 | 8.84 | 8.83 |
| 2,3,3,4-Tetramethyl-1-pentene | 133.2 | 133.0 | 8.30 | 8.32 |
| 1-Decene | 170.6 | 170.0 | 9.84 | 9.83 |
| 2,3,3,4,4-Pentamethyl-1-pentene | 158.8 | 157.0 | 9.33 | 9.27 |

$n^*_{obs}$=Effective carbon number at normal boiling point (cf. Table I)
$n^*_{calcd}$=Calculated value by Eq. 5

Thus, the summing up of the above three $\Delta n_j$'s gives,

$$\Delta n = 0.22 + 0.34 + 0.69 = 1.25$$

$$\text{or} \quad n^* = 9 - 1.25 = 7.75$$

Then, using the nomogram[2], 118°C is obtained for the normal boiling point which is to be compared with the observed value 119.4°C[9].

### Comparison with Experimental Data

A test of the present method by the procedure described in the last section was carried out for 188 monoalkenes and 46 dialkenes.

The average deviation of the calculated values of normal boiling point of the monoalkenes from the literature values[9,10] was as small as 2.5°C, with the maximum deviation −17°C for 2-*tert*-butyl-3, 3-dimethyl-1-butene. Only ten percent of the tested compounds showed an error higher than 5°C. Table II shows about 30 examples of this test.

In the case of dialkenes with no "conjugated double bond", the average deviation of the normal boiling point was found to be about 2.4°C, the maximum deviation was −11°C for 1, 4-heptadiene, and the deviation was less than 5°C for 87 percent of the tested compounds. Table III shows the results for typical examples.

In the presence of the conjugated double

9) G. Egloff, "Physical Constants of Hydrocarbons" Vol. V, Reinhold Publishing Corporation, New York, (1953).

10) S. W. Ferris, "Handbook of Hydrocarbons", Academic Press Inc., New York (1955).

Table III. Normal boiling point of dialkenes

| Compound | Normal boiling point $T^0_b$, °C | | Effective carbon number, $n^*$ | |
|---|---|---|---|---|
| | Obs.[10] | Calcd. | Obs. | Calcd. |
| 1,4-Hexadiene | 65. | 61.0 | 5.88 | 5.78 |
| 1,5-Hexadiene | 59.5 | 58.0 | 5.70 | 5.66 |
| 2-Methyl-1,4-pentadiene | 56. | 59.0 | 5.60 | 5.70 |
| 3-Methyl-1,4-pentadiene | 55. | 49.0 | 5.57 | 5.40 |
| 1,4-Heptadiene | 100.8 | 90.0 | 7.10 | 6.73 |
| 1,5-Heptadiene | 94.3 | 91.0 | 6.85 | 6.78 |
| 2-Methyl-1,5-hexadiene | 92.1 | 89.0 | 6.78 | 6.68 |
| 3-Methyl-1,5-hexadiene | 80.5 | 82.0 | 6.39 | 6.46 |
| 5-Methyl-1,4-hexadiene | 91.8 | 91.0 | 6.77 | 6.76 |
| 2,4-Dimethyl-1,4-pentadiene | 81.3 | 89.0 | 6.41 | 6.70 |
| 1,7-Octadiene | 117.5 | 116.0 | 7.69 | 7.66 |
| 3-Methyl-1,5-heptadiene | 110.5 | 112.0 | 7.44 | 7.51 |
| 2-Methyl-1,6-heptadiene | 115.6 | 116.0 | 7.65 | 7.68 |
| 2,4-Dimethyl-1,5-heptadiene | 132.1 | 134.0 | 8.29 | 8.41 |
| 2,6-Dimethyl-2,6-octadiene | 166.9 | 169.0 | 9.67 | 9.86 |

$n^*_{obs}$=Effective carbon number at normal boiling point (cf. Table I)
$n^*_{calcd}$=Calculated value by Eq. 5

Table IV. Comparison of calculated critical constants and heat of vaporization with literature values

| Compound | Effective carbon number, $n^*$ | Critical temperature °K | | | Critical pressure atm. | | | Heat of vaporization (kcal./mol.) at $T^0_b$ | | at 25°C | |
|---|---|---|---|---|---|---|---|---|---|---|---|
| | Calcd. | Obs.[7] | Calcd. | Thodos[5] | Obs.[7] | Calcd. | Thodos[5] | Obs.[7] | Calcd. | Obs.[7] | Calcd. |
| Ethylene | 1.76 | 282.4 | — | 290.3 | 50.0 | — | 50.7 | 3.24 | — | — | — |
| Propylene | 2.88 | 365.0 | 363.0 | 367.3 | 45.6 | 43.0 | 45.7 | 4.40 | 4.36 | — | 3.27 |
| 1-Butene | 3.83 | 419.6 | 415.0 | 425.3 | 39.7 | 37.0 | 39.8 | 5.24 | 5.14 | 4.87 | 4.70 |
| 2-Butene (*cis*) | 4.00 | 430.2 | 424.0 | 429.3 | 41. | 38.0 | 37.4 | 5.58 | 5.27 | 5.30 | 4.95 |
| (*trans*) | | | | 426.3 | | | 37.3 | 5.44 | | 5.15 | |
| 2-Methylpropene | 3.92 | 417.9 | 422.0 | 425.2 | 39.5 | 36.0 | 40.4 | 5.29 | 5.22 | 4.92 | 4.84 |
| 1-Pentene | 4.83 | 474.2 | 461.0 | 471.4 | 40. | 34.0 | 35.2 | — | 5.95 | — | 6.02 |
| 2-Pentene | 4.95 | 475.6 | 466.0 | 471.5 | 40.4 | 34.0 | 32.9 | — | 6.05 | — | 6.19 |
| 2-Methyl-2-butene | 5.00 | 470.2 | 468.0 | 471.2 | 34. | 33.0 | 33.2 | — | 6.09 | — | 6.06 |
| 2-Methyl-1-butene | 4.85 | — | 462.0 | 471.6 | — | 34.0 | 35.6 | — | 5.97 | — | 6.25 |
| 3-Methyl-1-butene | 4.56 | 464.8 | 450.0 | — | 33.9 | 35.0 | — | — | 5.75 | — | 5.69 |

bond, Eq. 5 fails to express the difference of the effective carbon number of compounds from the real carbon number. However, the effective carbon number itself can also be defined for this type of compound (see Table I), and a conventional procedure is possible. That is, if one boiling point datum is available, $n^*$ can be obtained on nomogram without the aid of Eq. 5.

Table IV shows the comparison of the estimated values of critical temperature, critical pressure and heat of vaporization with the observed values[7], where the critical constants estimated by the Thodos' method[5,6] are also given for comparison.

The application of Eq. 6 to isoparaffins is also satisfactory, though the results are not given here*3. It is especially favorable for the estimation of the heat of vaporization at normal boiling point and the critical temperature.

## Summary

A method of estimating the structural variation in the boiling point and other physical properties of alkenes is developed. By this method, all properties are expressed in terms of a structural constant called the "effective carbon number" which depends on the number and relative position of double bonds and those of side chains but not on external variables such as the temperature. An empirical equation is presented to correlate the effective carbon number with molecular structure. By combining the use with the previously presented nomogram*4, it is proved to be quite

*3 Details of the results will be published elsewhere.

*4 Copies of original drawing of the nomogram will be sent upon request.

useful for rapid evaluation of various properties including the temperature-vapor pressure relationship and the critical constants.

*Department of Industrial Chemistry*
*Faculty of Engineering*
*Kyoto University*
*Sakyo-ku, Kyoto*

# *Studies on Organophosphorus Compounds. I. The Reaction of O,O-Dimethyl Phosphonate with p-Benzoquinone*

By Yoshihiko NISHIZAWA

(Received September 1, 1960)

It is well known that phosphonates* having phosphorus-hydrogen linkage react with the carbonyl groups as aldol-condensation to produce $\alpha$-hydroxy phosphonate[1]:

$$C_6H_5CHO+HP(O)(OH)_2 \rightarrow C_6H_5CH(OH)P(O)(OH)_2$$

Ville[2] and Marie[3] studied this reaction with various ketones and aldehydes from 1889 to 1904.

Recently, it has been well known that Dipterex[4] was prepared by this reaction of *O,O*-dimethyl phosphonate with chloral, which proved to be very useful as an insecticide.

$$(CH_3O)_2P(O)H+OHC\cdot CCl_3 \rightarrow (CH_3O)_2P(O)\underset{\displaystyle OH}{\underset{|}{C}}HCCl_3$$

Furthermore, Sallman et al.[5] have reported that *O,O*-dialkyl phosphonates react with $\alpha,\alpha'$-dihalo-ketones to produce $\alpha$-hydroxy-$\beta,\beta'$-dihalo phosphonates which are also useful as an insecticide.

The products of this reaction, $\alpha$-hydroxy-$\beta$-halo phosphonates, have not only the agricultural usefulness but also a very interesting property which is that the phosphonates are changed to vinyl phosphorates under the presence of alkaline[6-8].

$$(CH_3O)_2P(O)\underset{\displaystyle OH}{\underset{|}{C}}H\cdot CCl_3 \xrightarrow{NaOH} (CH_3O)_2P(O)CCH=CCl_2$$

Thus, the reaction of phosphonate having the phosphorus-hydrogen linkage with carbonyl groups of aldehydes or ketones were studied widely, but the reaction with the carbonyl group of benzoquinone has not been reported yet.

During the course of an investigation of organophosphorus compounds, the present author found that the reaction of *O,O*-dimethyl phosphonate with carbonyl group of *p*-benzoquinone did not produce the usual $\alpha$-hydroxy phosphonate but the phosphorate having *p*-hydroxy-phenyl group.

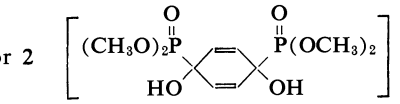
The reaction of two moles ratio of *O,O*-dimethyl phosphonate with one mole ratio of *p*-benzoquinone produced undistillable pale yellow oil. This product was purified by acetone and ligroin. The refractive index and the infrared absorption spectrum of this product was not changed by the purification using silica-gel column-chromatography. So, it was considered that this product was a pure substance. The microanalytical data of this product showed that this product was composed of one mole ratio of *O,O*-dimethyl phosphonate and one mole ratio of *p*-benzoquinone. Moreover, the reaction product of one mole ratio of *O,O*-dimethyl phosphonate and one mole ratio of *p*-benzoquinone showed the same refractive index, infrared absorption spectrum and microanalytical data as the above product.

$$n(CH_3O)_2P(O)H+O=\langle\rangle=O \rightarrow (CH_3O)_2P(O)O-\langle\rangle-OH$$

(I) (II) (III)

* Phosphorus compounds in this paper were named according to the Drake Comittee's Report (*Chem. Eng. News*, **30**, 4515 (1952)).

1) G. N. Kosolapoff, "Organophosphorus Compounds", Jhon Wiley & Sons. (1950), p. 129.
2) J. Ville, *Compt. rend.*, **107**, 659 (1888); **109**, 71 (1890); **110**, 384 (1890).
3) C. Marie, ibid., **133**, 219, 818 (1901); **134**, 286, 847 (1902); **135**, 106, 1118 (1902); **136**, 48, 234, 508 (1903); **137**, 124 (1903); **138**, 1707 (1904).
4) W. Lovenz, U. S. Pat. 2701225.
5) R. Sallman, D. R. Pat. 1000364.
6) W. F. Barthel, *J. Am. Chem. Soc.*, **77**, 2424 (1955).
7) W. Lorenz, ibid., **77**, 2554 (1955).
8) W. Perkow, D. R. Pat. 1024945.

$n$ is 1 or 2 

The infrared absorption spectrum of this product III did not show the absorption bands of the carbonyl group of *p*-benzoquinone, but strong absorption bands of phenyl group (1450, 1510 $cm^{-1}$)[9], P=O (1265 $cm^{-1}$)[9] and P-O-C (Arom) linkages (1205 $cm^{-1}$)[9] were observed. (see Fig. 1).

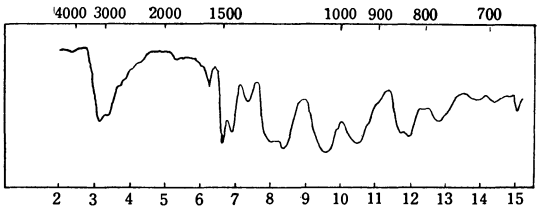



Fig. 1 The infrared spectrum of *O, O*-dimethyl-*O*-(*p*-hydroxy-phenyl)phosphorate (III) (liquid).

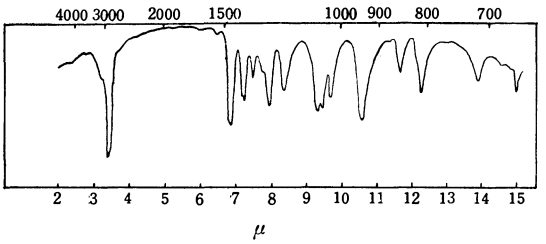



Fig. 2 The infrared spectrum of *O, O*-dimethyl-*O*-(4-hydroxy-2, 3, 5, 6-tetrachloro-phenyl)phosphorate (IV) (in Nujol).

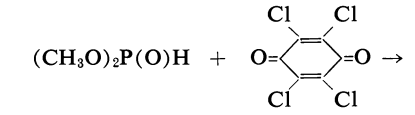
Moreover, the product showed the color reaction of phenol by ferric chloride and a hydrolysis of the product produced hydroquinone.

From the above results, it was presumed that the reaction of *O, O*-dimethyl phosphonate with the carbonyl group of *p*-benzoquinone did not produce the usual $\alpha$-hydroxy phosphonate but 4-hydroxy-phenyl phosphorate (III).

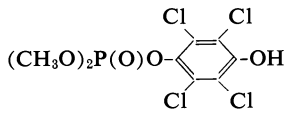
In the above experiments, there remained uncertainty whether the product is the pure material or not, because the product is an undistillable oil. However, the above presumption against the above experimental results was confirmed by the reaction of *O, O*-dimethyl phosphonate with chloranil. The reaction of one or two moles ratio of *O, O*-dimethyl phosphonate with one mole ratio of chloranil produced the same crystals which melt at 237~239°C.

9) L. J. Bellamy, "The Infrared Spectra of Complex Molecules"; Jhon Wiley & Sons. (1958).

The melting point of these crystals coincided with that of *O, O*-dimethyl-*O*-(4-hydroxy-2, 3, 5, 6-tetrachlorophenyl) phosphorate (IV) which was prepared by Ramirez's method[10] and the mixed melting point did not decrease.



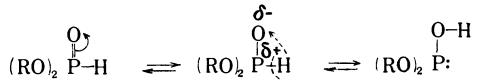
(I)



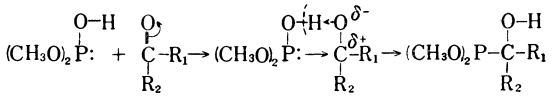
(IV)

It seems that the above reactions have different mechanism from the usual reactions of phosphonate with carbonyl groups of aldehydes and ketones.

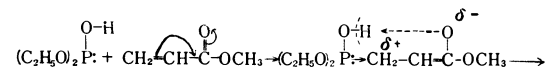
It is considered that *O, O*-dialkyl phosphonate have polymerized form of two or three molecules by hydrogen bonding at the free state[11-13], but in aldol type reactions, the hydrogen atom is released easily as proton and the phosphonate becomes the phosphite-form[14]:

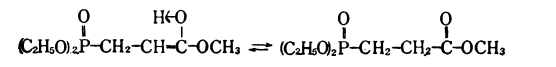


Therefore, when the phosphonate reacts with the aldehydes or ketones, this hydrogen atom cuts itself off as proton from phosphite molecule and the phosphite group reacts with the electrophilic carbon atom of carbonyl group just as the aldehyde group in aldol condensation does.



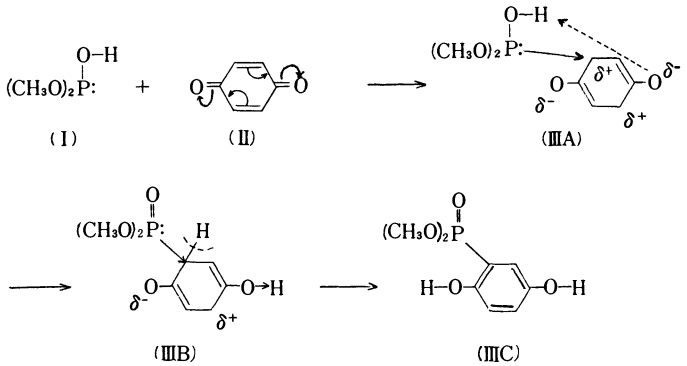
When the phosphonate reacts with the carbonyl group which has an ethylenic double bond in conjugated system, the phosphorus atom links the $\beta$-carbon atom of carbonyl group[15]. This reaction might be explained by the same mechanism as above.





10) F. Ramirez, *J. Am. Chem. Soc.*, **81**, 587 (1959).
11) B. A. Arbuzov, *Doklady Akad. Nauk S. S. S. R.*, **54**, 599 (1946).
12) B. A. Arbuzov, ibid., **54**, 787 (1946).
13) B. A. Arbuzov, ibid., **55**, 31 (1947).
14) M. Murakami, "Hanno-Yuukikagaku", Asakura-Syoten (1949), p. 316.
15) E. C. Ladd, Can. Pat. 509034.

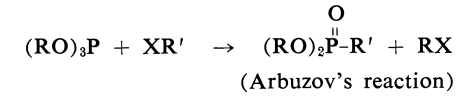
If the reaction of the phosphonate with the quinone has the same ionic mechanism, it may be considered that the quinone have the formula IIIA as excited resonance form[16]. According to this mechanism, it is normal that the phosphorus atom attacks the carbon atom of the quinone nucleus.



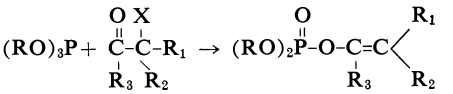
(I) (II) (IIIA) (IIIB) (IIIC)

In fact, hydrogen halides, benzene sulfonic acids or xanthic acids react with quinone and link the carbon atom of quinone nucleus according to the above mechanism[16]. But the reaction of phosphonate can not be explained by the above mechanism, since the experimental facts show the production of the phosphorate.

On the other hand, it is well known that the reaction of trialkyl phosphites with $\alpha$-halocarbonyl compounds does not produce the phosphonates as in Arbuzov's reaction but phosphorates as in Perkow's reaction[17].

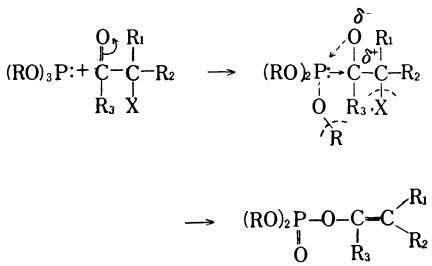


(Arbuzov's reaction)



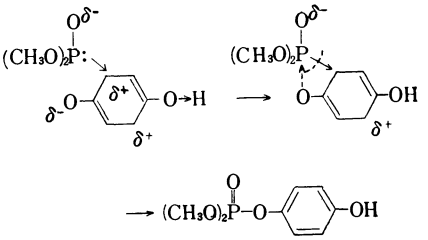
(Perkow's reaction)

On the above reaction mechanism, Allen[18] and Pudovik[19] have reported that the trialkyl phosphites attack the electrophilic carbon atom of carbonyl group and then the phosphorus atom forms the oxide ring as the intermediate:



In the reaction of *O*, *O*-dimethyl phosphonate with *p*-benzoquinone, it is considered that the reaction mechanism is the same as above, namely, phosphite group attacks the nucleophilic carbon atom of quinone nucleus and then the phosphorus atom forms the oxide ring as intermediate because there is a carbonyl group at $\alpha$-position.

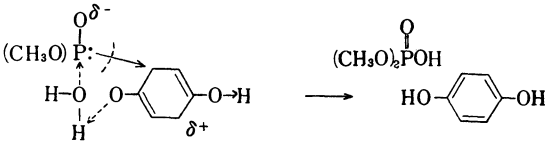
Accordingly, the phosphorus atom cuts itself off from the quinone nucleus instead of eliminating the hydrogen atom and then the phosphorate is produced.



(III)

It is well explained by this mechanism that the phosphonate reacts with *p*-benzoquinone by 1 : 1 mole ratio and does not produce the $\alpha$-hydroxy phosphonate but produces phosphorate and, moreover, when the water is presented in this reaction, hydroquinone is produced.

Namely, in the presence of water, the phosphorus atom forms the oxide ring between the oxygen atom of water instead of the oxygen atom of quinone. So, Perkow's rearrangement occurs between the phosphonate and the water.



16) M. Murakami, "Hanno-Yuukikagaku", Asakura-Syoten. (1949), p. 351.
17) W. Perkow, *Chem. Ber.*, **88**, 662 (1955).
18) J. Allen, *J. Am. Chem. Soc.*, **77**, 2871 (1955).
19) A. N. Pudovik, *J. Gen. Chem., USSR*, **26**, 2503 (1956).

## Experimental

**Reaction of *O*, *O*-Dimethyl Phosphonate with *p*-Benzoquinone.**—To a solution of 15 g. of *p*-benzoquinone and 0.5 g. of triethylamine in 45 ml. of dioxane was gradually added under cooling by water 32.0 g. of *O*, *O*-dimethyl phosphonate. After the addition, the reaction mixture was stirred for 7 hr. at 70°C and then allowed to stand over night at room temperature. The reaction mixture was condensed in vacuo (0.3 mmHg) at 60°C, 30.0 g. of the pale yellow oil was obtained.

This oil was dissolved in acetone and then ligroin was added gradually. The upper layer was separated by decantation, and the lower layer was concentrated in vacuo. The viscous oil was obtained and yielded 25.0 g. (83%) $n_D^{26}$ 1.5205.

Found : P, 14.3. Calcd. for $C_8H_{11}O_5P$ : P, 14.2%.

The same reaction using 16.5 g. of *O*, *O*-dimethyl phosphonate instead of 32.0 g. of *O*, *O*-dimethyl phosphonate, produced 23.8 g. of same oil.

**Hydrolysis of *O*, *O*-Dimethyl-*O*-(4-hydroxyphenyl)phosphorate (III).**—The mixture of 10.0 g. of *O*, *O*-dimethyl-*O*-(4-hydroxy-phenyl)phosphorate (III) and 30 ml. of 8% hydrochloric acid was heated at 80°C for 50 hr. The water layer was extracted continuously with ether and then the ether layer was dried over anhydrous sodium sulfate. After removal of the ether, the residue was recrystallized from benzene.

Four grams of *p*-hydroquinone was obtained and melted at 170~171°C. The melting point of a mixture of the hydroquinone and the authentic specimen did not decrease.

**Reaction of *O*, *O*-Dimethyl Phosphonate with Chloranil.**—To a solution of 24.6 g. of chloranil in 250 ml. of dioxane was added by drop-wise 11.0 g. of *O*, *O*-dimethyl phosphonate under cooling with ice water. After the addition, the reaction mixture was stirred for 5 hr. at 80°C and then cooled. The reaction mixture was concentrated under a reduced pressure and the crude crystals were precipitated. The crystals were recrystallized from methanol, melted at 237~239°C. and yielded 22.0 g. (61%). A mixture of these crystals and the authentic *O*, *O*-dimethyl-*O*-(4-hydroxy-2, 3, 5, 6-tetrachloro-phenyl)-phosphorate which was prepared by Ramirez's method[10] melted at 238~239°C.

Found : P, 9.2 ; Cl, 39.73. Calcd. for $C_8H_7Cl_4O_5P$ : P, 8.7 ; Cl, 39.88%.

**Reaction of *O*, *O*-Dimethyl Phosphonate with *p*-Benzoquinone under the Presence of Water.**—The solution of 15 g. of *p*-benzoquinone in 100 ml. of methanol which contained 5% water was added to the solution of 16.5 g. of *O*, *O*-dimethyl phosphonate in 50 ml. of benzene. After the reaction mixture was stirred, benzene, water and alcohol were removed and then the residue was extracted continuously with ether. The ether layer was dried over anhydrous sodium sulfate. After removal of the ether, the residue was recrystallized from benzene and 10.8 g. of the hydroquinone was obtained and melted at 171~172°C.

The author wishes to express his thanks to Professor Shinichirou Fujise and Professor Tarou Yamazaki of Tohoku University for helpful suggestions in the preparation of this manuscript. He also wishes to thank to the Sumitomo Chem. Co. Ltd., for permission to publish this work. He is indebted to his co-workers in the microanalytical section in this laboratory. He also wishes to express his thanks to Mr. M. Nakagawa for his earnest assistance.

*Sumitomo Chemical Co., Ltd.*
*Osaka Works*
*Konohana-ku, Osaka*

# *Internal Rotation and Low Frequency Spectra of Esters, Monosubstituted Amides and Polyglycine*

By Tatsuo MIYAZAWA*

(Received September 20, 1960)

Monosubstituted amides, polypeptides and proteins have been known to exhibit several prominent bands characteristic to the -CONH- group. The bands at about 3300 $cm^{-1}$ and 3100 $cm^{-1}$ are now considered to be due to the Fermi resonance between the fundamental N-H stretching vibration and the first overtone of the amide II vibration[1]. The amide I (1650 $cm^{-1}$), the amide II (1550 $cm^{-1}$), and the amide III (1250 $cm^{-1}$) vibrations involve the C=O stretching, the C-N stretching and the N-H in-plane bending modes. These vibrations have long been subjects of controversy; however, their nature has finally been elucidated

* Present address: Institute for Protein Research, Osaka University, Kita-ku, Osaka.

1) R. M. Badger and A. D. E. Pullin, *J. Chem. Phys.*, 22, 1142 (1954); T. Miyazawa, *J. Mol. Spectroscopy*, 4, 168 (1960).

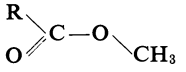
by a normal coordinate treatment of *N*-methylacetamide[2]. The amide IV (650 $cm^{-1}$), the amide V (750 $cm^{-1}$), and the amide VI (600 $cm^{-1}$) bands have been found to be due primarily to the O=C–N bending[3], the N–H out-of-plane bending[4], and the C=O out-of-plane bending modes[3], respectively. The torsional vibration (the amide VII) around the C–N bond is directly related to the potential barrier hindering internal rotation about the C–N bond. For the molecule of *N*-methylformamide the band at 356 $cm^{-1}$ has been assigned to this torsional mode[5].

Internal rotation around the C–N bond of the peptide group is one of the most important factors in determining the conformation or the secondary structure of polypeptides and proteins. Since biological activities of proteins are closely related to their secondary structures an extended spectroscopic study of the hindering potential was undertaken. The torsional vibrations in the low frequency region were assigned and normal coordinate treatments were made of the out-of-plane vibrations for the purpose of determining the potential barrier.

Monosubstituted amides exhibit infrared spectra analogous to those of esters and the analyses of the spectra of esters provide useful information in studying amide spectra. It may be remarked that esters and monosubstituted amides are isoelectronic with each other and, in addition, the mass of NH is not very different from the mass of the oxygen atom. Therefore spectroscopic studies were made of esters as well as of the monosubstituted amides in question.

## Internal Rotation around the C–O Bond of Esters

Electron diffration studies of the molecular structures of methyl formate and methyl acetate were made by O'Gorman et al.[6] and the molecule was found to be in the cis form




(R=H or $CH_3$)

The observed diffraction haloes were in accord with a structure slightly twisted from the planar structure by an internal rotation angle of about 25°. More recently the structure of methyl formate, however, was precisely determined by a microwave absorption measurement and the molecule was established to be in the planar cis form[7]. In the present study, therefore, the infrared spectra of esters will be discussed in terms of the planar cis structure.

Infrared spectra of methyl formate and methyl acetate in the gaseous state and in nonpolar solutions have been measured by Wilmshurst[8] in the region above 300 $cm^{-1}$. In the present work the measurements were extended out to 190 $cm^{-1}$ so that the torsional frequencies might be observed.

**Infrared Absorption Measurements.**—For the measurements in the region 400~190 $cm^{-1}$ a Perkin Elmer Model 12C spectrometer equipped with a cesium iodide prism[9] was used. Infrared spectra of methyl formate were measured in the gaseous state, in the solid nitrogen matrix, and in the crystalline state. The vapor spectra were obtained at room temperature with a 10 cm. gas cell and the gas pressure was 30 or 156 mmHg. The observed spectra are shown in Figs. 1 and 2A. A strong band was observed at 325 $cm^{-1}$ with shoulders at about 305 $cm^{-1}$ and at 340 $cm^{-1}$, in agreement with a previous result[8]. No other strong band, however, was observed below 300 $cm^{-1}$. The matrix spectra were recorded at 20°K for the molar ratio ($N_2$: ester) of 32 or 100, where 140 micromoles of the ester sample was dispersed in the matrix over an area of about 2 $cm^2$. The nitrogen gas used as the matrix material was purified by passing over copper at 600°C and then through a liquid nitrogen bath. The experimental technique of the matrix isolation method was described before[10]. The observed matrix spectra are shown in Fig. 2B. Two prominent bands were observed at

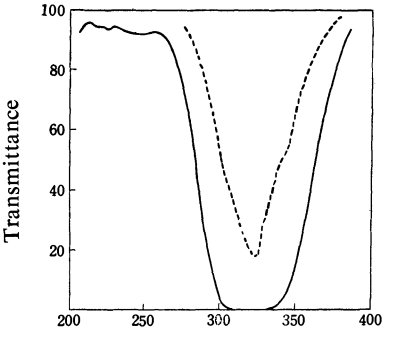



Fig. 1. Infrared spectra of methyl formate vapor, solid line : $p$=156 mmHg, broken line : $p$=30 mmHg.

2) T. Miyazawa, T. Shimanouchi and S. Mizushima, *J. Chem. Phys.*, **29**, 611 (1958).
3) T. Miyazawa, T. Shimanouchi and S. Mizushima, ibid., **24**, 408 (1956); T. Miyazawa, *J. Chem. Soc. Japan, Pure Chem. Sec.* (*Nippon Kagaku Zasshi*), **77**, 171, 321, 526 (1956).
4) H. K. Kessler and G. B. B. M. Sutherland, *J. Chem. Phys.*, **21**, 570 (1953).
5) D. E. DeGraaf and G. B. B. M. Sutherland, ibid., **26**, 716 (1957).
6) J. M. O'Gorman, Wm. Shand and V. Schomaker, *J. Am. Chem. Soc.*, **72**, 4222 (1950).
7) R. F. Curl, *J. Chem. Phys.*, **30**, 1529 (1959).
8) J. K. Wilmshurst, *J. Mol. Spectroscopy*, **1**, 201 (1957).
9) T. Miyazawa, *J. Chem. Phys.*, **29**, 421 (1958).
10) E. D. Becker and G. C. Pimentel, ibid., **25**, 224 (1956).

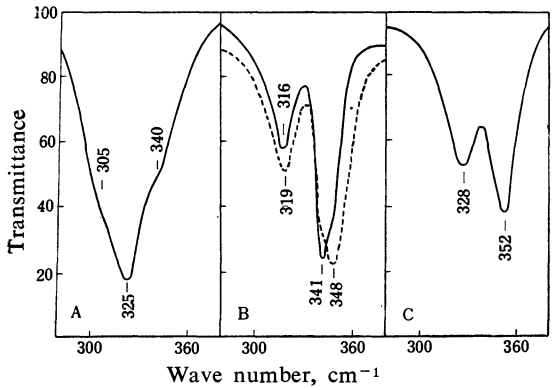



Fig. 2. Infrared spectra of methyl formate. A: vapor, B: matrix (solid line: molar ratio=100, broken line: ratio=32), C: crystal.

316 and 341 $cm^{-1}$ for the molar ratio of 100 and these peaks shifted to 319 and 348 $cm^{-1}$ for a lower ratio of 32. In preparing the crystalline specimen the ester gas was sprayed on a cesium bromide window kept at 140°K and the frozen sample was once slowly warmed up to a temperature slightly below the sublimation point allowing enough time for annealing and then cooled to 150°K for the absorption measurement. The observed crystalline spectrum is shown in Fig. 2C. Two bands were observed at 328 and 352 $cm^{-1}$, corresponding to the matrix bands at 319 and 348 $cm^{-1}$, respectively.

Infrared measurements in the vapor phase at room temperature were also made in the region 250~170 $cm^{-1}$ by the use of the grating spectrometer described by Bohn et al.[11] The path length of the vapor cell was 70 cm.; however, no band of methyl formate vapor was observed at a gas pressure of 50~100mmHg. On the other hand a fairly strong band of methyl acetate was observed at 213 $cm^{-1}$ with a gas pressure of 53 mmHg as shown in Fig. 3.

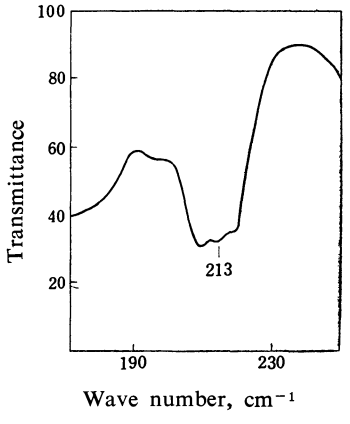



Fig. 3. Infrared spectrum of methyl acetate vapor.

**Vibrational Assignment of Methyl Formate.** —The vibrational modes of methyl formate expected in the region below 400 $cm^{-1}$ are the C-O-methyl bending mode and the twisting modes around the ester C-O bond and around the O-methyl bond. The strong vapor band at 325 $cm^{-1}$ corresponds to the fairly strong polarized Raman line at 332 $cm^{-1}$ in the liquid state and may be assigned to the C-O-methyl bending mode. The twisting frequencies depend of course upon the potential barrier hindering internal rotation. The three-fold potential barrier of the O-methyl bond has been determined to be 1150±100 cal./mol.[7] and the corresponding twisting frequency will be of the order of 150 $cm^{-1}$. On the other hand the potential barrier of the ester C-O bond may be of the same order of height as the barrier, 10 kcal./mol., of formic acid monomer[12] and the corresponding twisting frequency may well be in the region 400~200 $cm^{-1}$. Excepting the 325 $cm^{-1}$ band assigned to the C-O-methyl bending mode, however, no other band with more than 5% absorption was observed with the cell length of 10 cm. and with the gas pressure of 150 mmHg. It may be noted that the 325 $cm^{-1}$ band has a rather peculiar contour, suggesting the possibility of the overlapping of the bands due to the C-O-methyl bending mode and due to the C-O torsional mode.

In the solid matrix the complications arising from rotational fine structures are absent. In the case of formic acid[12] the O=C-O bending mode and the C-O twisting mode exhibit a vibration-rotation band with complicated contour in the vapor phase, whereas in the matrix the two frequencies were resolved. Therefore the matrix isolation technique was used in the present case of methyl formate and the vapor band at 325 $cm^{-1}$ was resolved into two distinct peaks in the nitrogen matrix. In order to establish the fact that these peaks are due to the two vibrational modes, C-O-methyl bending and C-O twisting of a single species, the effect of the molar ratio was observed (see Fig. 2B). On decreasing the molar ratio from 100 to 32, however, the relative intensities of the two peaks did not change appreciably, and these two peaks may now be assigned to the two modes mentioned above. It was not possible to decide which of the two peaks in the matrix was due to the twisting mode. Nevertheless the frequency of 325 $cm^{-1}$ may be taken to be the twisting frequency in the vapor phase.

11) C. R. Bohn, N. K. Freeman, W. D. Gwinn, J. L. Hollenberg and K. S. Pitzer, ibid., **21**, 719 (1953).

12) T. Miyazawa and K. S. Pitzer, ibid., **30**, 1076 (1959).

**Vibrational Assignment of Methyl Acetate.**— The molecule of methyl acetate has three skeletal in-plane bending modes and one skeletal out-of-plane bending mode. The Raman lines or the infrared bands at 640, 433, 303 and 610 $cm^{-1}$ have been assigned to these skeletal modes[8,13]. In the region below 400 $cm^{-1}$ three torsional frequencies are expected, one around the ester C-O bond, one around the O-methyl bond, and the last one around the C-methyl bond. As in the case of methyl formate the torsional frequency around the O-methyl bond will be of the order of 150 $cm^{-1}$. The potential barrier around the C-methyl bond of methyl acetate has not been determined as yet; however, it will not be too different from the value of 483±25 cal./mol. as found for acetic acid monomer[14]. The corresponding torsional frequency will be of the order of 100 $cm^{-1}$. The observed infrared band of methyl acetate at 213 $cm^{-1}$ is most reasonably assigned to the torsional mode around the ester C-O bond. The reduced moment of inertia for the internal rotation is greater for methyl acetate than for methyl formate and thus a torsional frequency somewhat lower than 325 $cm^{-1}$ of methyl formate may be expected for methyl acetate.

**Normal Coordinate Treatment of Out-of-plane Vibrations.** — In order to estimate the twofold potential barrier of the ester C-O bond the normal coordinate treatments were made of the out-of-plane vibrations of methyl formate and methyl acetate. The methyl groups of these esters were treated as single dynamic units. The symmetry coordinates and the inverse kinetic energy matrix were derived previously[12]. The bond lengths used in the calculation were $r$(C=O) = 1.22 Å, $r$(C-O) = 1.36 Å, $r$(O-methyl) = 1.46 Å, $r$(C-H) = 1.07 Å and $r$(C-methyl) = 1.52 Å, and all the valence angles were taken to be 120° for simplicity.

The out-of-plane potential function was expressed in terms of the out-of-plane bending constant for the three bonds of the carbonyl carbon atom, $H_\Omega$, the torsional potential constant for the ester C-O bond, $H_\theta$, and the interaction constant, $H_{\Omega\theta}'$. In the case of formic acid monomer[12] the interaction constant $H_{\Omega\theta}' = -0.00_5$ has been found to be negligible as compared to the potential constants, $H_\Omega = 0.58_3$ and $H_\theta = 0.13_1$. In the present treatments of esters the interaction constant was neglected. In calculating the torsional potential constant the correction for the anharmonicity of the two-fold torsional potential function, $V = V_2 \cdot (1-\cos 2\theta)/2$ was made to the observed torsional frequency. The correction $\nu_0 - \nu$ is equal to $h/8\pi^2 cI_r$ where $h$ is Planck's constant, $c$ the light velocity, and $I_r$ the reduced moment of inertia for intramolecular rotation[12]. The values of the correction were calculated to be 6 and 3 $cm^{-1}$ for the cis form and the trans form of methyl formate and 2 $cm^{-1}$ for both the cis form and trans form of methyl acetate. The CH out-of-plane bending frequency of 1019 $cm^{-1}$ and the corrected torsional frequency of 331 $cm^{-1}$ were used for the calculation of the potential constants of $H_\Omega = 0.55_8$ and $H_\theta = 0.18_2$ (in unit of $10^{-11}$ erg). Then the two-fold potential barrier of methyl formate was found to be 13.1 kcal./mol. The potential constants of methyl acetate were calculated to be $H_\Omega = 0.533$ and $H_\theta = 0.221$ from the skeletal out-of-plane bending frequency of 607 $cm^{-1}$ and the corrected torsional frequency of 215 $cm^{-1}$. The two-fold potential barrier of methyl acetate was found to be 15.9 kcal./mol. It may be noted that the potential barriers of esters are higher than those of formic acid (10 kcal./mol.) and of acetic acid (10 kcal./mol.)[15].

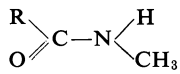
**Trans Form of Esters.**—The trans isomer of formic acid monomer has been found by the infrared spectra in the vapor phase, and the energy of the trans isomer has been found to be 2 kcal./mol. higher than the more abundant cis isomer[12]. The normal coordinate treatment of the out-of-plane vibrations was also made of the trans form of methyl formate as an aid in assigning the bands due to the trans form. Since the torsional potential constant of the trans isomer has been found to be the same as that of the cis isomer in the case of formic acid, the potential function of the cis form of methyl formate was also used for the treatment of the trans form. The C-H out-of-plane bending frequency and the torsional frequency were calculated to be 1053 and 233 $cm^{-1}$, respectively. As shown in Fig. 1, however, no band with more than 5% absorption has been observed in the vicinity of 233 $cm^{-1}$. From the intensity of the 325 $cm^{-1}$ band, the abundance ratio trans/cis was estimated to be less than 1% and the energy difference between the two forms is considered to be greater than 2.7 kcal./mol.

The relaxation absorption of sound in liquid ethyl formate has been ascribed to the rotational isomerism around the ester C-O bond[16]. Actually, however, there is also the rotational isomerism around the O-$CH_2$ bond of ethyl formate, and the hindering potential previously estimated from the ultrasonic studies may not be compared with the present results.

13) T. Miyazawa, *J. Chem. Soc. Japan, Pure Chem. Sec.* (*Nippon Kagaku Zasshi*), **77**, 619 (1956).
14) W. J. Tabor, *J. Chem. Phys.*, **27**, 974 (1957).
15) T. Miyazawa, unpublished.
16) J. Karpovich, *J. Chem. Phys.*, **22**, 1767 (1954); D. Tabuchi, ibid., **28**, 1014 (1958).

### Internal Rotation around the C–N Bond of the Peptide Group

The stable conformation of the peptide group has been established to be the planar trans form by Mizushima et al.[17] The vibrational analysis of *N*-methyl acetamide and *N*-methyl formamide will therefore be made with the planar trans structure,



***N*-Methylacetamide.**—The vibrational assignment as well as the normal coordinate treatment of the in-plane vibrations have been made[2,3,13] and the nature of the skeletal bending vibrations at 436 and 289 $cm^{-1}$ have already been elucidated. The Raman spectrum of liquid *N*-methylacetamide has been carefully measured by Sugita[18] and a new weak line has been observed at 206 $cm^{-1}$. Since the methyl torsional frequencies around the C–methyl bond and around the N–methyl bond will be lower than 150 $cm^{-1}$ as in the case of methyl acetate, the Raman line at 206 $cm^{-1}$ is most reasonably assigned to the torsional frequency around the C–N bond of the peptide group. It may be noted that this frequency is not very different from the corresponding frequency 213 $cm^{-1}$ of methyl acetate.

In the present study an approximate normal coordinate treatment of the out-of-plane vibrations was made, treating the methyl groups and the NH group as single dynamic units. The bond lengths used were the same as those used in the treatment of the in-plane vibrations[2]. Because of the approximate nature of the present treatment, the correction for the anharmonicity of the torsional frequency was not made. From the observed skeletal out-of-plane bending frequency of 600 $cm^{-1}$ (the amide VI band) and the torsional frequency of 206 $cm^{-1}$ the potential constants were calculated to be $H_\Omega=0.50_8$ and $H_\theta=0.19_5$, and then the two-fold potential barrier was estimated to be 14 kcal./mol. The bond order of the C–N bond of the peptide group may be estimated to be 0.3∼0.4 from the torsional potential constant as in the case of formic acid. This value agrees with the bond order 0.3∼0.4 derived from the bond distances.

***N*-Methylformamide.** — Infrared and Raman spectra of liquid *N*-methylformamide have been measured by DeGraaf and Sutherland[5]. The polarized Raman line at 302 $cm^{-1}$ has been assigned to the C–N–methyl skeletal bending vibration and the depolarized line at 356 $cm^{-1}$ to the torsional vibration around the peptide C–N bond. These frequencies correspond to the frequency of 325 $cm^{-1}$ observed for methyl formate.

The normal coordinate treatment of the out-of-plane vibrations of *N*-methylformamide was made as in the case of *N*-methylacetamide. The C–H bond length was taken as 1.07 Å and the other lengths were the same as those of *N*-methylacetamide. From the C–H out-of-plane bending frequency[3] of 1015 $cm^{-1}$ and the torsional frequency of 356 $cm^{-1}$ the potential constants were calculated to be $H_\Omega=0.53_2$ and $H_\theta=0.20_2$. This torsional potential constant corresponds to the potential barrier of 14 kcal./mol.

The two-fold potential barrier of the C–N bond of the peptide group has been estimated by Pauling and Corey[19] to be about 30 kcal./mol. As the results of the present spectroscopic studies, however, the values of the potential barrier of *N*-methylacetamide and *N*-methylformamide were both found to be about 14 kcal./mol., and this lower value is to be used in discussing the relative stabilities of the various conformations of a polypeptide chain.

### Low Frequency Infrared Spectra of Polyglycine I and II

Infrared absorption spectra have been widely used in studying the conformations of polymer chains. In the case of polypeptide chains the correlations between the chain conformations and the amide I and II frequencies were first noticed by Elliott and Ambrose[20]; that is to say the folded conformation exhibits the amide I and II bands at about 1650 and 1540 $cm^{-1}$ whereas the extended conformation exhibits the bands at 1630 and 1520 $cm^{-1}$. Recently these correlations were given theoretical interpretations and were refined and extended to cover the random coil conformation, the $\alpha$ helix, the antiparallel-chain extended conformation, and the parallel-chain extended conformation as well as Nylon 66[21]. These refined correlations, although useful for synthetic polypeptides and certain fibrous proteins, may not be too dependable in proteins exhibiting ill-defined amide I and II bands[22]. Therefore it should be worthwhile to find out other characteristic bands whose frequencies change more sensitively than do the amide I and II bands.

17) S. Mizushima, T. Shimanouchi, S. Nagakura, K. Kuratani, T. Tsuboi, H. Baba and O. Fujioka, *J. Am. Chem. Soc.*, **72**, 3490 (1950).
18) T. Sugita, unpublished.
19) L. Pauling and R. B. Corey, *Proc. Nat. Acad. Sci.*, **37**, 251 (1951).
20) A. Elliott and E. J. Ambrose, *Nature*, **165**, 921 (1950).
21) T. Miyazawa, *J. Chem. Phys.* **32**, 1647 (1960); T. Miyazawa and E. R. Blout, *J. Am. Chem. Soc.*, **83**, 712 (1961).
22) M. Beer, G. B. B. M. Sutherland, K. N. Tanner and D. L. Wood, *Proc. Royal Soc.*, **A249**, 147 (1959).

The N–H stretching vibration is localized in the N–H bond and involves only the nitrogen in the main chain of polypeptides. Its frequency, then, will not change appreciably with the chain conformation. On the other hand the torsional mode around the peptide C–N bond involves the $C_\alpha$–C–N–$C_\alpha$ atoms in the main chain and its frequency is expected to be most sensitive to the conformational change of the chain. In this connection normal coordinate treatments of the skeletal vibrations of the polymers of the type, $(-CH_2-)_n$ and $(-CH_2-O-)_n$, have been made, and in fact the low frequencies primarily due to the torsional modes have been found to change most sensitively with the chain conformation[23].

Polyglycine has been known to exist in two forms[24]; polyglycine I is in the antiparallel-chain extended conformation and polyglycine II is in the helical conformation with threefold screw axis[21,24,25]. In the present study the infrared spectra of these two forms of polyglycine were measured as Nujol paste in the region 400~190 $cm^{-1}$. The samples used were kindly given by Mr. Tsuchiya of the University of Tokyo. As shown in Fig. 4 polyglycine I exhibits a band at 217 $cm^{-1}$. This frequency appears to correspond to the frequency of 206 $cm^{-1}$ observed for *N*-methylacetamide and is most reasonably assigned to the torsional mode around the C–N bond of the antiparallel-chain extended conformation. On the other hand polyglycine II* exhibits the corresponding band at 365 $cm^{-1}$. It is remarkable to note that the torsional frequency of

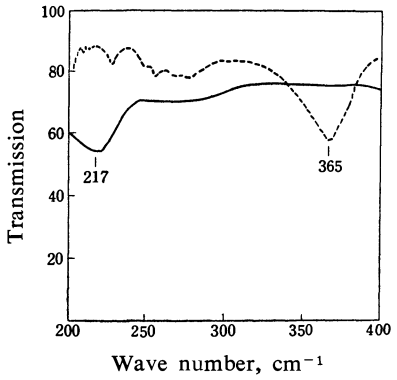



Fig. 4. Infrared spectra of polyglycine I (solid line) and polyglycine II (broken line).

polyglycine I is almost doubled by the transformation to polyglycine II. The amide VII band is thus found to be most sensitive to the conformation of polypeptide chains. It would be worth while to find out more extensive correlations between the various conformations and the infrared spectra in the low frequency region.

The author wishes to thank Professor K. S. Pitzer of the University of California for his interest and encouragement and to Mr. Shoji Tsuchiya of the University of Tokyo for generously supplying the samples of polyglycine. The present work was partly supported by the American Petroleum Institute Research Project 50.

*Department of Chemistry*
*University of California*
*Berkeley, California, U. S. A.*

*Institute for Protein Research*
*Osaka University*
*Kita-ku, Osaka*

23) T. Miyazawa, *Spectrochim. Acta*, **16**, 1231, 1233 (1960); *J. Chem. Phys.*, in press.
24) C. H. Bamford, L. Brown, E. M. Cant, A. Elliott, W. E. Hanby and B. R. Malcolm, *Nature*, **176**, 396 (1955).
25) F. H. C. Crick and A. Rich, ibid., **176**, 780 (1955).
* The weak peaks observed in the region 200~280 $cm^{-1}$ are presumably due to water vapor.

# *The Behavior of Fission Products Captured in Graphite Powder by Nuclear Recoil. IV. Further Studies on the Diffusion of Xenon-133 in Graphite*

By Seishi YAJIMA, Sumio ICHIBA, Yuichiro KAMEMOTO, Koreyuki SHIBA and Masaharu KORI

(Received September 3, 1960)

Several papers have been published on the diffusion of fission products in graphite[1-7]. Only artificial graphite in a form similar to a fuel element, a disk or a pellet, was used in those experiments. On the other hand, the authors have studied the diffusion of fission products in many kinds of graphite such as amorphous carbon, artificial graphite, and natural graphite. The diffusion of xenon[6], iodine[7], and tellurium[7] in graphite was previously reported. However, more recent study by the authors suggests that in the determination of activation energy of diffusion in such a complicated material as graphite the use of Fick's law is not entirely satisfactory and that fission products in graphite have many energy states. Consequently, this experiment has been undertaken to determine the diffusion rate of fission product xenon-133 in graphite and the distribution of xenon-133 among such energy states as mentioned above.

## Theoretical Consideration

In general, the escape rate $v$ of fission products captured in imperfections with energy $E$ is given by

$$v=-\frac{dn}{dt}=-\int\frac{n(x,y,t)}{a(x,y)}dxdy\,\nu \times\exp[-(E_D+E)/kT] \qquad (1)$$

where

$n(x,y,t)$ : number of fission products captured in a small region between $x$ and $x+dx$, and $y$ and $y+dy$.

$a(x,y)$ : number of jumps of fission products required to escape from the graphite.

$E_D$ : activation energy of diffusion of fission products.

$T$ : temperature in °K.

$\nu$ : frequency of vibration of a fission product in the graphite.

$k$ : Boltzmann constant.

If an isothermal escape rate of a fission product in a sample is determined at $T_1$,

$$v_1=-\int\frac{n_1(x,y,t)}{a(x,y)}dxdy\,\nu \times\exp[-(E_D+E)/kT_1] \qquad (2)$$

After time $t$, if $T_1$ is instantly increased to $T_2$ and an isothermal escape rate is determined at the temperature,

$$v_2=-\int\frac{n_2(x,y,t)}{a(x,y)}dxdy\,\nu \times\exp[-(E_D+E)/kT_2] \qquad (3)$$

When being extrapolated to $t$, $n_1$ is equal to $n_2$. Then,

$$\ln(v_2/v_1)=\frac{E_D+E}{k}\frac{T_2-T_1}{T_1T_2} \qquad (4)$$

or

$$E_D+E=\frac{2.303\,kT_1T_2}{T_2-T_1}\log(v_2/v_1) \qquad (4')$$

When the fission products are caught in imperfection distributed over various energy states of graphite, Eq. 4 must be carefully applied to the calculation of activation energies. As Mugnuson et al.[8] discussed, however, if the difference of temperature $T_1$ and $T_2$ is taken as small as possible, the most important activation energy of the diffusion of fission products within the range of $T_1$ and $T_2$ is calculated according to Eq. 4.

## Experimental

**Preparation of Samples.**—A mixture of 1 g. of graphite powder and 60 mg. of uranium dioxide was irradiated with thermal neutrons (thermal

1) D. Schulz, "Summary Report for January, February, and March, 1947", ANL-4006, Sec. 1. 6, 62 (Oct. 3, 1947).
2) C. A. Smith and C. T. Young, "Diffusion of Fission Fragments from Uranium-Impregnated Graphite", NAA-SR-72 (May 4, 1951).
3) D. Cubicciotti, "The Diffusion of Xenon from Uranium Carbide-Impregnated Graphite", NAA-SR-194 (Oct. 13, 1952).
4) C. T. Young and C. A. Smith, "Preliminary Experiments on Fission Product Diffusion from Uranium-Impregnated Graphite in the Range 1800~2200°C", NAA-SR-232 (March 25, 1953).
5) L. B. Doyle, "High-Temperature Diffusion of Individual Fission Element from Uranium Carbide-Impregnated Graphite", NAA-SR-255 (Sept. 11, 1953).
6) T. Nakai, S. Yajima, K. Shiba, J. Osugi and D. Shinoda, This Bulletin 33, 497 (1960).
7) S. Yajima, S. Ichiba, Y. Kamemoto and K. Shiba, ibid., 34, 493 (1961).
8) G. D. Mugnuson, W. Palmer and J. S. Koehler, *Phys. Rev.*, **109**, 1990 (1958).

neutron flux, about $5\times10^{11}$ neutrons/cm$^2$/sec.) for five hours in an experimental hole of JRR-1 reactor. After irradiation the mixture was treated with a hot 4 N nitric acid solution to dissolve uranium dioxide and neptunium-239 produced. In order to measure the activity of xenon-133 without any influence of other fission xenon nuclides and iodine-133, the irradiated graphite samples were cooled for four days before use.

Particle sizes of graphite samples used in this experiment and the analytical data on impurities are shown in Table I.

TABLE I. PARTICLE SIZES OF GRAPHITE SAMPLES AND ANALYTICAL DATA OF IMPURITIES

| | Sample | | |
|---|---|---|---|
| | AG (Artificial graphite) | NG-1 (Natural graphie-1) | NG-2 (Natural graphite-2) |
| Particle size (micron) | 30 | 1 | 50 |
| Impurity | | | |
| Ash (total) | 0.07% | 0.3% | 0.8% |
| $SiO_2$ | 250 p.p.m. | 220 p.p.m. | 3700 p.p.m. |
| $Al_2O_3$ | 210 | 60 | 3500 |
| $Fe_2O_3$ | 130 | 24 | 300 |
| MgO | 15 | 24 | 100 |
| CaO | 70 | 36 | 300 |
| $V_2O_5$ | — | 0.12 | 0.5 |
| MnO | — | — | — |
| $Na_2O$ | 20 | 12 | 25 |
| $K_2O$ | 15 | 12 | 20 |
| NiO | — | 0.06 | — |
| $ThO_2$ | — | 2.4 | — |
| CuO | — | — | — |
| $B_2O_5$ | 0.1 | 0.02 | 0.5 |

**Determination of Activation Energy.**—A flow system is illustrated in Fig. 1. Furnace-$C_1$ and Furnace-$C_2$ consisted of an alundum tube with a nichrome winding. The temperature of the furnaces could be increased to 1150°C and kept constant at a temperature with a transformer. The temperature was measured with a platinum-platinum rhodium thermocouple. The temperature of Furnace-$C_2$ was always kept about 50°C higher than that of Furnace-$C_1$.

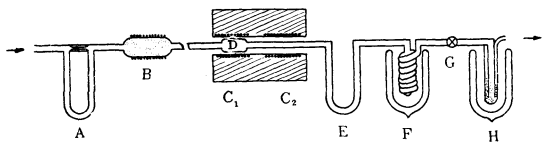



Fig. 1. Flow system.

A Flow meter B Sponge titanium
$C_1$, $C_2$ Furnace D Diffusion cell
E Phosphorus pentoxide
F Dry ice trap G Stopcock
H Charcoal trap cooled with dry ice

Each part of the system was made of hard glass except a silica tube in the furnace in which samples were heated, and each part was connected with a polyethylene tube.

Helium gas at a constant flow rate (100 ml./min.) was purified with sponge titanium heated at 800°C to eliminate a trace amount of oxygen. Phosphorus pentoxide was used to remove water in the gas which had swept over a sample. A dry ice trap was set to remove volatile fission products other than rare gases. Xenon-133, which was released, was adsorbed on charcoal cooled with dry ice which was set next to the trap without charcoal. When the charcoal trap was exchanged for a new one at appropriate intervals, a change-over cock was serviceable for the continuous catch of xenon-133 on charcoal.

A typical experiment was as follows. The graphite powder described above was placed in a silica boat which was slid into the silica tube. Then, helium gas was introduced into the system. After confirming that helium gas took the place of air, the tube was slid into Furnace-$C_1$. The graphite sample was heated at a constant temperature for 30 min. During this period the charcoal trap was exchanged every 5 min. Just 30 min. after the beginning of the heating, the sample together with the tube was slid into Furnace-$C_2$ whose temperature had been about 50°C higher than that of Furnace-$C_1$. The trap was exchanged every 2 min. and the sample was heated at a constant temperature for 12 min. The temperature was measured with a platinum-platinum rhodium thermocouple adjacent to the sample. Such a procedure was repeated at a set of increased temperatures.

**Making of Heating Curve.**—In order to make a heating curve, a graphite sample was heated with a constant increment of temperature and xenon-133 released during a constant period of time was adsorbed on charcoal.

The amount of the released nuclide was plotted versus temperature. The flow system is the same as that shown in Fig. 1 except a furnace and a tube in which a sample was heated. Because the temperature of samples must be continuously increased to temperatures as high as possible, silicon carbide was used as the heater of the furnace.

The sample described above was placed in an alundum boat which was slid into the alundum

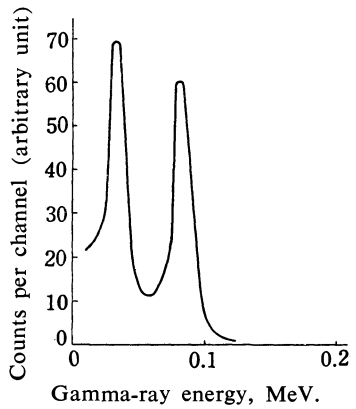



Fig. 2. Gamma-ray spectrum of xenon-133 in a charcoal trap.

tube. Then, helium gas was introduced into the system. After confirming that helium gas took the place of air, the tube was slid into the furnace. The sample was heated with a contsant increment of temperature, 3°C/min. Xenon-133 released was adsorbed charcoal in a trap cooled with dry ice, the trap being exchanged every 10 min.

**Activity Measurement.**—Activity of xenon-133 adsorbed on charcoal was measured with a RCL 256 channel gamma-ray spectrometer with a well type NaI scintillator (2 inch diameter×1.75). The charcoal was placed in the well, with its trap made of glass, and the activity was measured. The gamma-ray spectrum of xenon-133 is illustrated in Fig. 2.

## Results

The absolute value of $v_1$ and $v_2$ is not always necessary but the ratio of $v_2/v_1$ is necessary for determining the activation energy according to Eq. 4. Therefore, when amounts of xenon-133 remaining in graphite are plotted versus diffusion time, the ratio $v_2/v_1$ is equivalent to a ratio of tangential slopes at a discontinuous point of temperature. A typical plot is shown in Fig. 3. The values obtained from these plots are given in Table II, and the apparent activation energy versus absolute temperature is illustrated in Fig. 4.

Heating curves obtained by another experiment are illustrated in Figs. 5—7. The axis

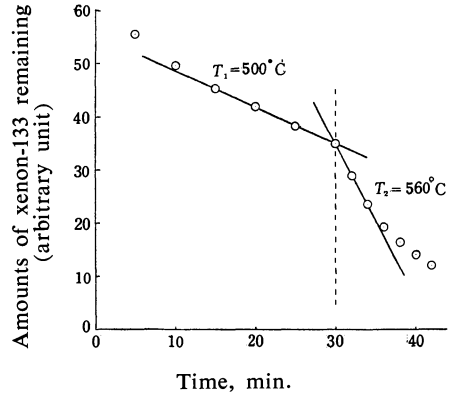



Fig. 3. Isothermal escape rates of xenon-133 in natural graphite-1 at 500 and 560°C.

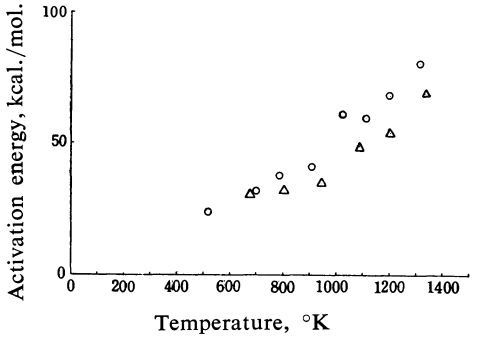



Fig. 4. Apparent activation energy versus temperature.
○ AG △ NG-1

TABLE II. ACTIVATION ENERGIES OF DIFFUSION OF XENON-133 IN GRAPHITE

AG (Artificial graphite)

| $T_1$ °C | $T_2$ °C | $v_2/v_1$ | $E+E_D$ kcal./mol. |
|---|---|---|---|
| 228 | 269 | 5.48 | 23.8 |
| 400 | 447 | 4.72 | 31.8 |
| 490 | 539 | 4.48 | 37.4 |
| 606 | 675 | 6.37 | 40.6 |
| 725 | 780 | 4.94 | 60.7 |
| 815 | 870 | 3.74 | 59.2 |
| 910 | 950 | 2.55 | 67.7 |
| 1023 | 1082 | 3.88 | 80.2 |

NG-1 (Natural graphite-1)

| $T_1$ °C | $T_2$ °C | $v_2/v_1$ | $E+E_D$ kcal./mol. |
|---|---|---|---|
| 380 | 418 | 3.58 | 30.3 |
| 500 | 560 | 4.28 | 32.0 |
| 656 | 696 | 2.17 | 34.6 |
| 786 | 840 | 3.06 | 48.6 |
| 915 | 956 | 2.12 | 53.3 |
| 1041 | 1090 | 1.81 | 68.4 |

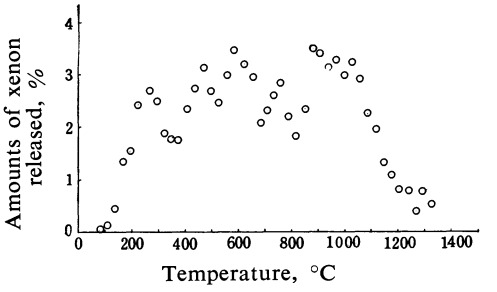



Fig. 5. Heating curve (3°C/min.) of natural graphite-1.

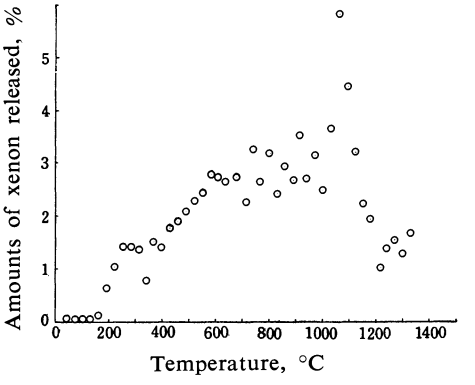



Fig. 6. Heating curve (3°C/min.) of natural graphite-2.

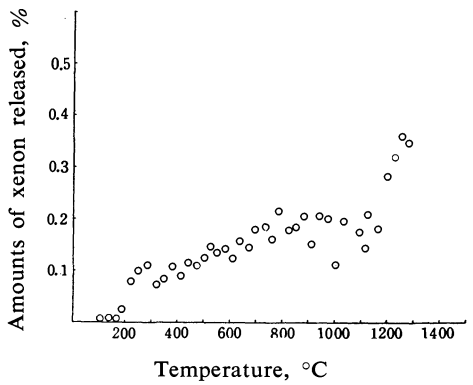



Fig. 7. Heating curve (3°C/min.) of artificial graphite.

of abscissa is temperature and the axis of ordinate is percent xenon-133 released from graphite every 10 min.

## Discussion

In the previous experiment[6], it was observed that the diffusion of xenon consisted of a rapid diffusion and a slow diffusion, and from the latter, the activation energy of the interstitial diffusion was calculated. But it is inadquate to treat the diffusion of xenon in graphite from the slow diffusion alone.

The tendency of the diffusion was observed by Argonne workers[1] and Cubicciotti[3]. The Argonne workers interpreted that there were two mechanisms for the diffusion, a rapid "pore" diffusion and a slow "crystallite" diffusion. However, as pointed out by Cubicciotti, if the above interpretation were correct, there would be a truly rapid diffusion which would eventually give way to a slow diffusion at one temperature; that is, all the rapidly diffusing material would have been gone in a short time and then, an increase in temperature would result in the simple diffusion of the slowly diffusing material. Experimentally, however, it is found that with each increase in temperature there is a rapid escape of xenon. Cubicciotti explains that the initial rapid escape is attributed to a rapid temperature increase of the sample. On the other hand, our experiment on natural graphite-2 showed no striking effect of the rate of temperature increase: the amount (46.3%) of xenon-133 released when the temperature of a graphite sample was increased from room temperature to 800°C in 3 min. and kept constant at 800°C for 90 min. was nearly equal to the amount (41.7%) of xenon-133 released when the temperature of another sample was increased from room temperature to 800°C at a rate of 3°C/min. This fact suggests that the amount of xenon-133 released is mainly determined by a final temperature.

Circles and triangles in Fig. 4 are not on a straight line parallel to the axis of abscissa but on ascending lines, respectively. In other words, the activation energy of the diffusion is not simple but consists of various values, say, 20~40 kcal. at 500 to 1000°K and higher at temperatures over 1000°K. This tendency is the same both in artificial and natural graphite except the fact that the activation energy of diffusion in artificial graphite is a little higher than that in natural graphite.

Heating curves in Figs. 5—7 show the distribution of the amount of released xenon over a wide range of temperature. These figures also indicate the distribution of the energy of xenon in graphite, when the relation shown in Fig. 3 is taken into account. The energy is considered to correspond to $E$ in Eq. 4 because $E_D$ is far smaller than $E$. From these observations, the fact that the diffusion rate of xenon in natural graphite was greater than that in artificial graphite will be explained as follows. Xenon atoms in natural graphite are distributed more in sites of a low activation energy while xenon atoms in artificial graphite are more in sites of a high activation energy. Therefore, the amount of xenon diffusing out at a temperature is greater in natural graphite than in artificial graphite. Although not studied thoroughly, it is supposed that xenon atoms exist on vacant sites of graphite lattice and that the above mentioned activation energies are determined according to the position of such xenon atoms, because the activation energy of the interlaminar diffusion in graphite is known to be very low. It is obvious by the X-ray diffraction and the electron diffraction methods that artificial graphite is more imperfect than natural graphite. This means that the number of vacancies is larger in artificial graphite than in natural graphite. In this sense, a heating curve is considered to show also the distribution of the vacancies among sites of various energies.

On the basis of discussion described above, a rapid diffusion and a slow diffusion in an isothermal curve are easily interpreted. When a graphite sample is rapidly heated to a certain temperature, a xenon atom existing in a site with an activation energy which corresponds to the temperature diffuses out through the interlaminar space: this is a rapid diffusion. During the maintenance of the temperature, xenon existing in a site with a larger activation energy escapes out with a certain probability: this is a slow diffusion. It is evident that Fick's law can not be applied

to such a system, because the law deals with diffusion only in terms of concentration gradient.

The authors wish to thank Dr. H. Suzuki of Solid State Physics Laboratory of JAERI for helpful discussions.

*Division of Chemistry*
*Japan Atomic Energy Research Institute*
*Tokai, Ibaraki-ken*
*(S. Y., S. I., Y. K. & K. S.)*

*Mitsubishi Atomic Power Industries*
*Inc. Laboratory*
*Omiya-shi Saitama-ken*
*(M. K.)*

# *Determination of Lanthanum, Samarium and Europium in Manganese Nodules by Neutron Activation**

By Toshi KAWASHIMA, Masumi OSAWA, Yoko MOCHIZUKI and Hiroshi HAMAGUCHI

(Received September 26, 1960)

So far the determination of a trace amount of rare earth elements have primarily been carried out by X-ray fluorometric, emission spectrometric or absorption spectrometric methods; but none of these methods have given satisfactory results. After the atomic pile has become available for wide use, ever growing attention has been paid to the application of radioactivation technique to the determination of many trace elements. A number of reports have proved the validity of the same technique for the determination of a trace amount of rare earth elements because of its selectivity and the high sensitivity.

Brooksbank and Leddicotte[1] determined a number of rare earth elements in biological materials (bones), by making use of the chromatographic separation and successive countings of the eluates after neutron irradiation of the sample. Likewise, Cornish[2] reported the ion exchange separation method. Jakovlev[3] discussed an approach for the determination of the total content of rare earth elements in high purity materials (graphite, beryllium, bismuth and germanium) on the basis of the activity of samarium and europium estimated by analyzing the decay curves, without resorting to chromatographic separation. Nakai et al.[4] reported the determination of dysprosium samarium, and lanthanum in thorium metal and oxide, based on gamma-ray counting of the rare earth fraction obtained by anion exchange separation from the sample irradiated in JRR-1.

Various nuclides are formed when a minute amount of rare earth elements in rocks and meteorites are irradiated with thermal neutrons.

TABLE I. NUCLEAR DATA

| Element | Clarke number | Radionuclide | Half life | Activity* dis./sec. |
|---|---|---|---|---|
| Sc | 0.0005 | $^{46}$Sc | 85 days | $2.65 \cdot 10^{2}$ |
| Y | 0.0028 | $^{90}$Y | 64 hr. | $2.3 \cdot 10^{3}$ |
| La | 0.0018 | $^{140}$La | 40 hr. | $9.0 \cdot 10^{3}$ |
| Ce | 0.0046 | $^{141}$Ce | 33 days | $3.6 \cdot 10$ |
| | | $^{143}$Ce | 33 hr. | $4.1 \cdot 10^{2}$ |
| Pr | 0.00055 | $^{142}$Pr | 19 hr. | $5.8 \cdot 10^{3}$ |
| Nd | 0.0024 | $^{147}$Nd | 11.3 days | $6.0 \cdot 10$ |
| | | $^{149}$Nd | 2 hr. | $1.9 \cdot 10^{3}$ |
| Sm | 0.00065 | $^{153}$Sm | 47 hr. | $1.2 \cdot 10^{4}$ |
| Eu | 0.00010 | $^{152}$Eu | 9.3 hr. | $1.5 \cdot 10^{5}$ |
| Gd | 0.00064 | $^{159}$Gd | 18 hr. | $7.6 \cdot 10^{2}$ |
| Tb | 0.00009 | $^{160}$Tb | 73 days | $2.5 \cdot 10$ |
| Dy | 0.00045 | $^{165}$Dy | 2.3 hr. | $4.7 \cdot 10^{5}$ |
| Ho | 0.00011 | $^{166}$Ho | 27 hr. | $5.7 \cdot 10^{3}$ |
| Er | 0.00025 | $^{177}$Er | 7.5 hr. | $6.6 \cdot 10^{2}$ |
| Tm | 0.00002 | $^{170}$Tm | 120 days | $2.2 \cdot 10$ |
| Yb | 0.00027 | $^{175}$Yb | 4.2 days | $1.2 \cdot 10^{3}$ |
| | | $^{177}$Yb | 1.8 hr. | $6.3 \cdot 10^{3}$ |
| Lu | 0.000075 | $^{177m}$Lu | 3.7 hr. | $8.3 \cdot 10^{3}$ |
| | | $^{177}$Lu | 6.9 days | $8 \cdot 10^{2}$ |

* $A$ (dps) = Clarke number $\cdot 10^{-2} \cdot Ab.(1/M)6.03 \cdot 10^{23} \cdot \sigma \cdot S$

$A$: Activity at the end of bombardment
$M$: Mass number $Ab$: Isotopic abundance
$S$: Saturation factor: $(1-e^{-\lambda t})$, $t=10$ hr.
$\sigma$: Neutron capture cross section.

* Presented at the 12th Annual Meeting of the Chemical Society of Japan, Kyoto, April, 1959.

1) W. A. Brooksbank and G. W. Leddicotte, *J. Phys. Chem.*, **57**, 819 (1953).
2) F. W. Cornish, *Brit. Atomic Energy Research Establishment Rept.*, AERE C/R-1224 (1953).
3) J. V. Jakovlev, *Proceedings of International Conference on Peaceful Uses of Atomic Energy, Geneva*, 1955, Paper 632 (USSR), Vol. 15, pp. 54—59; *Anal. Abstr.*, **4**, 1112 (1957).
4) T. Nakai et al., Presented at the 2nd symposium on radiochemistry, Kyoto, Nov., 1958.

Then, the nature and activity of the induced radionuclides which come into question when 1 g. of sample containing rare earth elements in its normal natural abundance ratio is irradiated for 10 hr. with thermal neutrons of its intensity of $10^{11}$n/cm$^2$/sec., are shown in Table I. These radionuclides would decay according to Fig. 1. It is clear that the nuclides which should be considered are lanthanum-140, samarium-153, europium-152 and yttrium-90 when as long as 20 hr. are needed for chemical processing after the end of irradiation.

The gamma ray spectrum of the rare earth fraction would then be considered to be the sum of photopeaks produced by X-rays which are induced by K electron capture, and compton continuums, and photopeaks produced by complete gamma ray absorption and bremsstrahlungs induced by $\beta$-rays which are emitted by lanthanum, samarium, europium and long lived nuclides. Therefore, the decay curve obtained by measuring the activity at a fixed base bias under the same counting conditions is expected to be analyzed into a few components. The present paper reports the determination of lanthanum, samarium, and europium in manganese nodules by means of a comparison method based on the counting rate of the respective components analyzed as above.

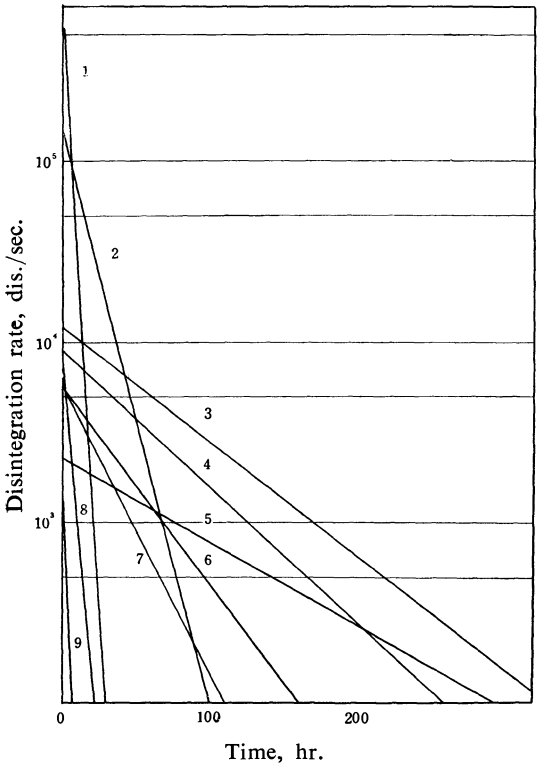



Fig. 1. Relative activities of rare earth radionuclides.

1: 2.3 hr. Dysprosium-165
2: 9.3 hr. Europium-152
3: 47 hr. Samarium-153
4: 40 hr. Lanthanum-140
5: 64 hr. Yttrium-90
6: 27 hr. Holmium-166
7: 19 hr. Praseodymium-142
8: 3.7 hr. Lutetium-177m
9: 1.8 hr. Ytterbium-177

## Experimental

**Reagents and Samples.** — Standard solutions of lanthanum, samarium and europium were prepared by dissolving respective metal oxides in nitric acid. The purity of these oxides listed by Johnson Mathey, was 99.99% for samarium oxide and 99.9% for europium and lanthanum oxides. These reagents were proved to be radiochemically pure by the activation analysis. Uranyl acetate (Merck) solution was used for the standard of uranium. All other chemicals used in this work were of c. p. or reagent grade.

Manganese nodule samples were offered by Professor E. D. Goldberg, Scripps Institution of Oceanography, La Jolla, California, to whom our thanks are due.

**Irradition.**—Manganese nodule samples of from 200 to 500 mg. were sealed in a silica tube and irradiated along with neutron monitors in the Japan Research Reactor-1 (JRR-1). The reactor was homogeneous, enriched uranium, water moderated and cooled type, and had a neutron flux of around $2\sim3\times10^{11}$ n/cm$^2$/sec. The flux monitors were prepared by evaporating a known amount (102, 3.5 and 0.35 $\mu$g) of lanthanum, samarium and europium in a silica tube or impregnating it into a filter paper wrapped in a vinyl bag. The irradiation lasted intermittently for 2~3 days, 5 hr. each day.

**Chemical Separation.**—After neutron irradiation and a suitable decay time (about one day), the manganese nodule was dissolved in aqua regia. Any residue was fused with sodium peroxide, dissolved in hydrochloric acid, and added to the main solution. An aliquot of the solution (1/10 of the total volume) was used for the determination of the rare earth elements, and the remainder of the solution was reserved for the determination of elements other than the rare earths. Twenty milligrams of lanthanum carrier was added to the pipetted aliquot and the rare earth activity was carried down with lanthanum fluoride precipitate by adding hydrofluoric acid to the solution. Further purification was achieved by going through the standard lanthanum fluoride cycle[5] three times. The final lanthanum hydroxide precipitate which was decontaminated from any activities other than those of the rare earth elements was then dissolved in hydrochloric acid and diluted to a known volume. An aliquot of this solution was used for $\gamma$-ray counting and the remainder for the determination of the

5) N. E. Ballou, "National Nuclear Energy Series, Radiochemical Studies: The Fission Products, Book 3", McGraw-Hill Book Co., Inc., New York (1953), p. 1673.

chemical yield by a conventional gravimetric method[6].

**Counting.** — The $\gamma$-rays and X-rays from the induced radioactive rare earth nuclides were detected and analyzed with the manual sweep scintillation spectrometer (Atomic Instrument Co., Model 510) equipped with a well type*, 1 3/4 in. by 2 in., sodium iodide (Tl) scintillation crystal. The quantitative analysis for each rare earth element was made by comparing the lanthanum-140, samarium-153 and europium-152 activities of rare earth fraction which is separated from the irradiated manganese nodules with the correspondingly irradiated monitor of the respective element, after measuring the activity of each of the nuclides as mentioned later. Decay measurements of the rare earth activities from the manganese nodule samples and the flux monitors gave the same half-life for each nuclide.

## Results and Discussion

The $\gamma$-ray spectrum of the rare earth fraction chemically separated and purified is shown in Fig. 2. Individual $\gamma$-ray spectra of lanthanum, samarium and europium obtained by the separate irradiation of the respective elements are shown in Fig. 3. These were measured at a channel width of 1 V. with the well type single channel scintillation spectrometer mentioned above. In this work, the counting rate at the peaks of 0.02, 0.09 and 0.5 MeV. for each sample were measured under exactly the same conditions.

**Determination of the Lanthanum, Samarium and Europium Activities.** — The activity of the rare earth fraction at the peak of 0.5 MeV. is attributed to 40 hr. lanthanum-140 plus long-lived components (Figs. 2 and 3). Therefore, the activity of lanthanum-140 at a given time can be determined by graphical analysis of the

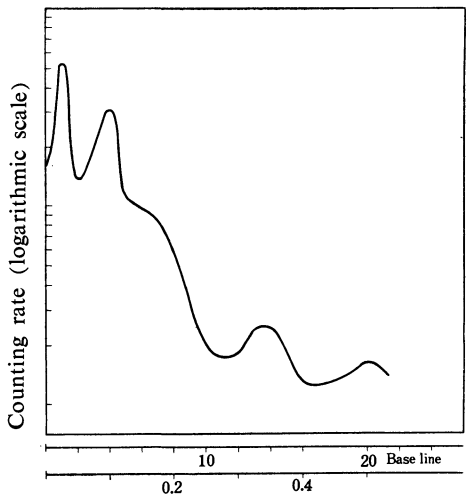



Fig. 2. Gamma-spectrum due to rare earth activities separated from neutron irradiated manganese nodule.

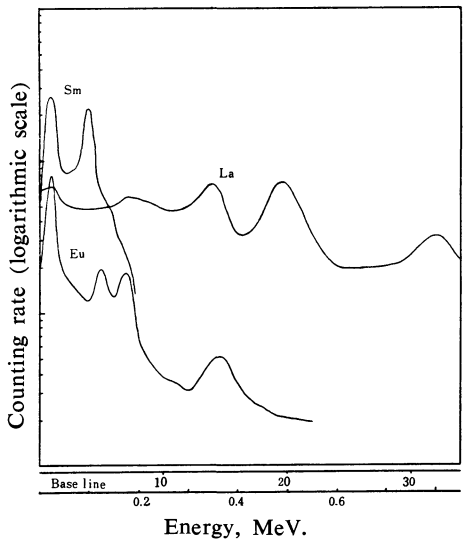



Fig. 3. Gamma-spectra of lanthanum-140, samarium-153 and europium-152.

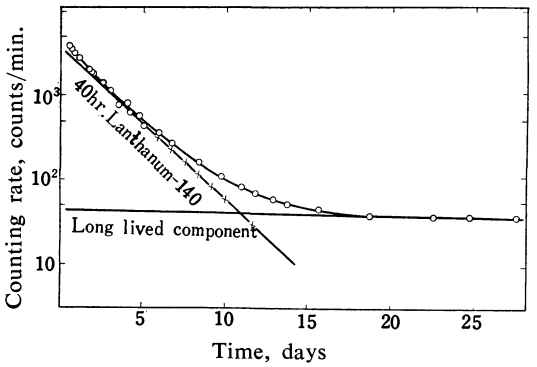



Fig. 4. Analysis of decay curve for the determination of lanthanum.

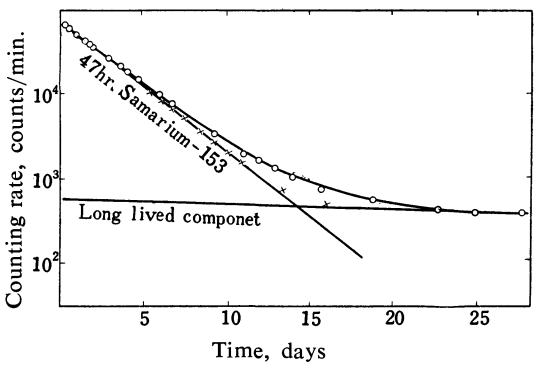



Fig. 5. Analysis of decay curve for the determination of samarium.

6) W. F. Hillebrand, E. F. Lundell, H. A. Bright and J. I. Hoffman, "Applied Inorganic Analysis", 2nd ed. John Wiley & Sons, Inc., New York (1953), p. 550.

* Hole 17mm$\phi$×80mm, covered with aluminium can.

TABLE II. LANTHANUM, SAMARIUM AND EUROPIUM CONTENT OF MANGANESE NODULES (p. p. m.)

| Sample | Location | Depth, m. | La | Sm | Eu |
|---|---|---|---|---|---|
| Horizon Guyot MP 26 A-3 | 19°N 169°W | 1440~1540 | 234 | 33 | 9.6 |
| | | | 201 | 24 | 7.7 |
| | | | 270 | 35 | 9.4 |
| | | | av. 235 | av. 31 | av. 8.9 |
| Horizon Guyot MP 25 F-2 | 19°N 170°W | 1870~1920 | 250 | 40 | 11.0 |
| | | | 378 | 60 | 19.6 |
| | | | av. 314 | av. 50 | av. 15.3 |
| Horizon Nodule | 40°N 155°W | 5500 | 357 | 108 | 19.6 |
| | | | 250 | 62 | 16.6 |
| | | | av. 303 | av. 85 | av. 18.1 |

decay curve, a typical one of which is given in Fig. 4.

Just as in the case of lanthanum mentioned above, the activity of 47 hr. samarium-153 is estimated based on the decay curve at the 0.09 MeV. peak, as shown in Fig. 5.

The activity of around 0.025 MeV. peak is the sum of activities due to europium-152, lanthanum-140, samarium-153 and longer-lived nuclides (Figs. 2 and 3). Therefore, the activity of the 9.3 hr. europium-152 component can be analyzed by the graphical analysis of the decay curve at the peak, an example of which is shown in Fig. 6. If the activity of long-lived component (curve B) plus 40 hr. lanthanum-140 component (curve C) is deducted from the gross decay curve A, we obtain the curve D which corresponds to the composite of the activity of europium and samarium. Here the contribution of lanthanum-140 component (curve C) is calculated by the experimentally determined ratio of the counting rate at the peak of around 0.025 MeV. to that of 0.5 MeV. (the ratio is around 1, see Fig. 3). By analyzing the curve D, the decay curve of 9.3 hr. europium-152, curve E, is obtained.

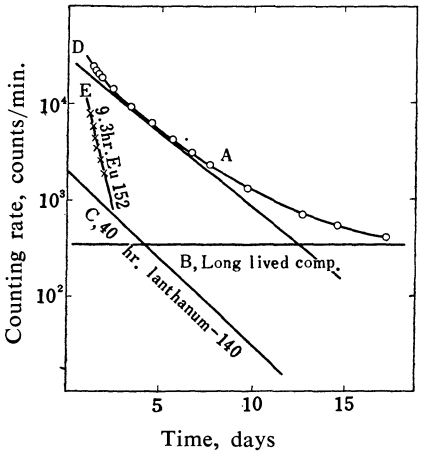



Fig. 6. Analysis of decay curve for determination of europium.

**Determination of Lanthanum, Samarium and Europium in Manganese Nodules.**—The amounts of lanthanum, samarium and europium in the sample are estimated by comparing the activities of each of the nuclides of the sample determined as above with that of the respective monitor. The results are summarized in Table II.

A possible interference of fission products of uranium in the manganese nodules should be taken into consideration, since lanthanum-140, samarium-153, and many other rare earth nuclides are produced by slow neutron fission of uranium. The interference should not be disregarded particularly in the case of lanthanum-140, because of the high fission yield of mass 140 chain. An experiment to examine this interference was performed by separating and measuring the fission product rare earths from an irradiated known amount of uranium. The uranium assay was carried out by utilizing the activity of fission product barium-140, on an aliquot of the reserved solution mentioned earlier. It was found that the interference with fission product rare earths from the uranium in the samples was negligibly small*.

The overall reproducibility of the method for manganese nodule samples is shown to be about 10~20%. Additional runs would probably increase the reproducibility of the method. As for the sensitivities of the method, as little as 1, 0.02 and 0.01 $\mu$g of lanthanum, samarium and europium respectively, could be detemined under the present experimental conditions.

Goldberg and Arrhenius[7], and also Young[8] gave 140 and 220 p.p.m. lanthanum respectively as the average for Pacific pelagic sediments by spectroscopic method. Our data indicate a

* The result of uranium assay will be reported in a later paper. Tatsumoto and Goldberg (*Geochim. et Cosmochim. Acta*, 17, 201 (1959)) gave 3.9, 3.6, 3.6 p. p. m. in Horizon Nodule by a spectrophotometric method.

7) E. D. Goldberg and G. O. S. Arrhenius, *Geochim. et Cosmochim. Acta*, 13, 153 (1958).

8) E. J. Young, *Bull. Geol. Soc. Amer.*, 65, 1329 (1954).

somewhat higher lanthanum content of the manganese nodules than pelagic sediments.

The relative abundance of the three elements was calculated for the three manganese nodules, which are tabulated in Table III. For reference,

TABLE III. RELATIVE ABUNDANCE OF LANTHANUM, SAMARIUM AND EUROPIUM

| | Sample | Relative abundance | | |
|---|---|---|---|---|
| | | La | Sm | Eu |
| 1a | Horizon Guyot MP 26 A-3 | 1 | 0.13 | 0.038 |
| 1b | Horizon Guyot MP 25 F-2 | 1 | 0.16 | 0.049 |
| 1c | Horizon Nodule | 1 | 0.28 | 0.060 |
| 2 | Crustal rocks (Clarke No.) | 1 | 0.33 | 0.056 |
| 3 | Cosmic* (Suess, Urey) | 1 | 0.332 | 0.093 |

* Atomic abundance ratio

the abundance ratio of the three elements for crustal rocks, and the cosmic abundance ratio as given by Suess and Urey[9] are also included in Table III. It is seen that no essential differences in the relative abundance of the three rare earth elements are observed among the three different types of materials.

9) H. E. Suess and H. C. Urey, *Revs. Mod. Phys.*, **28**, 53 (1956).

**Summary**

The gamma spectrometric method has been developed for simultaneous determination of microgram amounts of lanthanum, samarium and europium without chemical separation of each other. The method was based on the chemical separation of rare earth mixtures from neutron irradiated samples and subsequent $\gamma$-ray scintillation counting of the isolated rare earth fractions. The sample was irradiated for 2~3 days, 5 hr. each day, in the nuclear reactor JRR-1 at a flux of the order of $10^{11}$n/cm$^2$/sec. The rare earth mixture purified by lanthanum fluoride cycles was used for $\gamma$-ray counting at a given pulse height peak. The activity of each component could be evaluated by resolving the decay curves obtained, and the amount calculated by comparing the activity with that of each monitor.

We wish to express our hearty thanks to the staff of the Radiochemistry Group, Japan Atomic Energy Research Institute, for their help in making the irradiation. A part of the expense was defrayed from the Ministry of Education, to which our thanks are due.

*Department of Chemistry*
*Tokyo University of Education*
*Koishikawa, Tokyo*

# *Photoconductivity of Zinc Oxide under Different Ambient Conditions*

By Hiroshi KOKADO, Eiichi INOUE, Takashi YAMAGUCHI and Kenji TAKAHASHI

(Received October 28, 1960)

The existence of a close relationship between photoconduction and oxygen desorption process of zinc oxide has been made clear in some details since Bevan and Anderson's work[1]. The oxygen adsorbed on the surface of zinc oxide seems to produce an acceptor level for conduction electrons and to make a depletion layer under the surface. Destruction of the depletion layer or further formation of the space change layer[2] takes place accompanied by absorption of light, its wavelength is shorter than 4000 Å, and it yields a number of conduction electrons. This model well interprets the peculiarities of the photoconductive process of zinc oxide. Then, one can anticipate that the adsorption of other molecules than oxygen on a surface of zinc oxide too may give a similar or to some extent different effect on the dark- and photo-conduction of the material, depending upon the character of the adsorbant[3].

We have studied the effects of several kinds of ambient molecules on the surface conductivity of zinc oxide at room temperature. The

1) D. J. W. Bevan and J. S. Anderson, *Discussions Faraday Soc.*, No. 8, 238 (1950); D. B. Medved, *J. Chem. Phys.*, **28**, 870 (1958); D. A. Melnick, ibid., **26**, 1136 (1957); W. Ruppel, H. J. Gerritsen and A. Rose, *Helv. Phys. Acta*, **30**, 495 (1957).

2) R. J. Collins and D. G. Thomas, *Phys. Rev.*, **112**, 388 (1958).

3) V. I. Lyahenko and O. V. Snitko, *Trudy Inst. Fiz., Akad. Nauk, Ukr. USSR*, **91**, 1071 (1953); E. K. Putseiko and A. N. Terenin, *Doklady Akad. Nauk SSSR*, **101**, 645 (1955), *Problemy Kinetiki i Kataliza, Akad. Nauk SSSR*, **8**, 53 (1955).

specimens (ca. 20 $\mu$ in thickness) were made by depositing zinc oxide powder (Merck's reagent) from an ethanolic suspension on glass plates of 18×18 mm. in size. They possess parallel electrodes that are separated from each other by a gap of 5 mm. Silver paste was used as the electrode material. These specimens showed the values of $10^5 \sim 10^6$ times the initial conductivities measured in air ($10^{-11} \sim 10^{-13}$ ohm$^{-1}$ for 20 V. of applied voltage) when they were kept in vacuum to remove the oxygen adsorbed on the zinc oxide layer. After this treatment, the gases or vapors were introduced onto the specimens and the dark currents were observed after 10 min.

The curves in Fig. 1 show the typical effect of an acceptor ($O_2$), a donor ($NH_3$) and a neutral ($CO_2$) type molecule on the dark

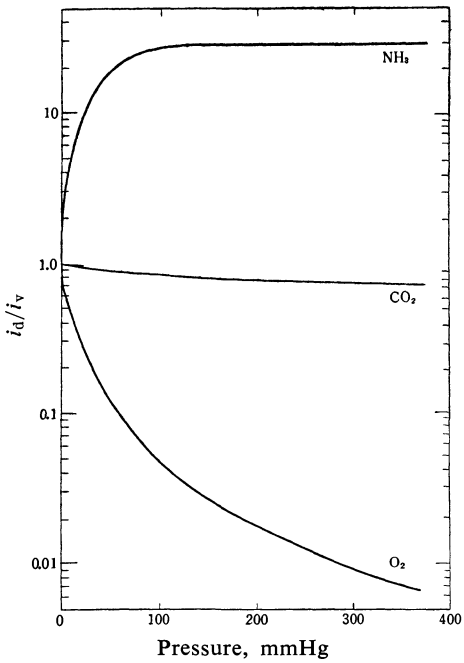



Fig. 1. Influence of the ambient gas on the dark conductivity of zinc oxide.
$i_d$ : Dark current in the gas
$i_v$ : Dark current in vacuum

conductivity. Ammonia was found to be effective on the electronic properties not only in vacuum but in atmospheric air. By pumping the ambient molecules off, the conductivity was unchanged in the case of oxygen, but in the case of ammonia, it returned to the initial value approximately. The behavior of nitrogen was quite similar to that of carbon dioxide and also methylamine to ammonia; otherwise the following three gases behaved as an acceptor type molecules; nitrogen oxide, nitrogen dioxide and methyl ethyl ketone (MEK). However, in the case of MEK, the conductivity was increased partly by taking it off. This seems to suggest that the nature of the adsorption was of somewhat different. Vapors of water, diethyl ether and ethyl alcohol did not change or slightly changed the conductivity of the zinc oxide cell.

As to the photoconductive sensitivity ($i_p/i_d$ in Table I), a remarkable increase was found by adsorption of the electronegative gases such

TABLE I

| Gas or vapor | Pressure mmHg | $i_d/i_v$ | $i_p/i_d$ | Decay |
|---|---|---|---|---|
| $O_2$ | 44 | $\sim 10^{-2}$ | $\sim 10^2$ | rapid |
| NO | 45 | $3\times 10^{-5}$ | $10^3 \sim 10^4$ | rapid |
| $NO_2$ | 0.3 | $<3\times 10^{-5}$ | $\sim 10^2$ | very rapid |
| MEK | 47 | $10^{-2} \sim 10^{-3}$ | $2\times 10^2$ | slow |
| Vacuum | — | — | 2～ 3 | very slow |
| $CO_2$ | 114 | 1 | 2～ 3 | very slow |
| $NH_3$ | 42 | ～10 | 2～ 3 | slow |
| Pyridine | 7.5 | $10^{-2} \sim 10^{-4}$ | — | — |

$i_v$ : Dark current in vacuum
$i_d$ : Dark current in gas or vapor
$i_p$ : Photocurrent in gas or vapor for $10^{12}$ photons/cm$^2$ sec. of 3650 Å light from an ultra-high pressure mercury lamp

as oxygen, nitrogen oxide and nitrogen dioxide, while no change was observed by adsorption of carbon dioxide or ammonia type molecules. In Table I, the results of qualitative observations on the rate of current decay after ceasing an irradiation on the cell were also tabulated. It is noteworthy that there exists a parallelism between the chemical activity of the ambient molecules and the rate of the decay process. The active electrons of these molecules may play an important role in the adsorption

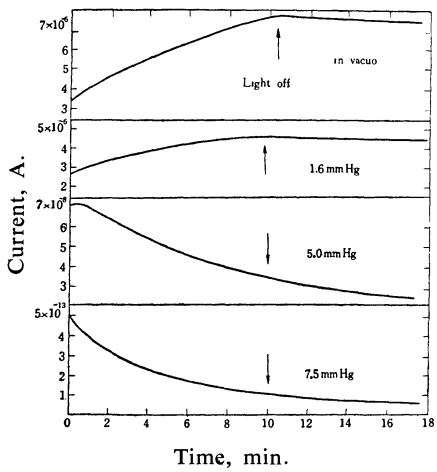



Fig. 2. Photoresponses of the conductivity of zinc oxide in pyridine vapor.

mechanism. MEK having no such active electrons, has only a weak effect to accelerate the decay[4].

The effect of aromatic and aliphatic hydrocarbons and also pyridine on the conductivity of zinc oxide were found to be rather obscure; the conductivity decreased by adsorption of these organic compounds. However, the irradiation on this system did not change the value of its conductivity; it monotonically decreased when an electric field was applied for measurement. This effect was more noticeable if the vapor pressure was increased, as shown in Fig. 2. The nature of this strange phenomenon is not yet clear.

4) By adsorbing ammonia or another donor type molecule too, a little higher decay rate is observed, associated with a greater density of recombination centers, with a greater capture cross section for the recombination, or with both (R. H. Bube, *Phys. Rev.*, **101**, 1668 (1956)).

*Graphic Engineering Laboratory*
*Tokyo Institute of Technology*
*Meguro-ku, Tokyo*

# *On the Fluorine Shift of Aromatic Fluorine Compounds**

By Teijiro YONEZAWA, Kenichi FUKUI, Hiroshi KATO, Hisao KITANO, Shuzo HATTORI and Shinichiro MATSUOKA

(Received October 24, 1960)

Numerous experimental data on fluorine chemical shifts of various organic compounds have been presented[1-5]. To explain the general trend of these shifts, some empirical interpretations based upon the electronegativity of the atom to which the fluorine is bonded[2], and upon the Hammett constant of a substituent in fluorobenzene have been proposed[3]. These interpretations, however, rest upon no clear basis of electronic configuration around the nucleus.

Ramsey[6] has derived a general expression of nuclear magnetic shielding constant, $\sigma$, in a molecule which has no orbital or spin angular momentum and contains only one nucleus of non-zero magnetic moment. The nuclear magnetic shielding is written by his expression

$$A_{v_\lambda}\sigma=\left(\frac{e^2}{3mc^2}\right)\left(0\left|\sum_k\frac{1}{r_k}\right|0\right)-2A_{v_\lambda}\left[\sum_{n_\lambda'}\frac{1}{E_n-E_0}\left\{(0_\lambda|\sum\mathbf{m}^0{}_{kz}|n_\lambda')\times\left(n_\lambda'\left|\sum_k\frac{\mathbf{m}^0{}_{kz}}{r_k{}^3}\right|0_\lambda\right)+\left(0_\lambda\left|\sum_k\frac{\mathbf{m}^0{}_{kz}}{r_k{}^3}\right|n_\lambda'\right)(n_\lambda'|\sum_k\mathbf{m}^0{}_{kz}|0_\lambda)\right\}\right] \quad (1)$$

where $r_k$ is the distance between the $k$th electron and the nucleus in question, $A_{v_\lambda}$ implies an average over all molecular orientations, each of which is specified by the subscript $\lambda$; and $\mathbf{m}^0{}_{kz}$ is the z component of the operator for the $k$th electron

$$\mathbf{m}^0{}_k=\left(\frac{ieh}{4\pi mc}\right)(\mathbf{r}_k\times\nabla_k) \quad (2)$$

The application of this formula to calculate the nuclear magnetic shielding of the nucleus in a complex molecule has been considered to be almost impossible due to the lack of our knowledge of the energies and wave functions of all excited states. Furthermore, as Ramsey[6] pointed out, the formula contains many terms which cancel each other, and this might bring about a considerable error in the numerical calculation.

An important contribution to develop the procedure of obtaining shielding constants was proposed by Saika and Slichter[7]. According to them the screening was divided into three terms.

1. The diamagnetic correction for the atom in question.

* This study was presented at the Symposium on Electronic Structures of Molecules, Tokyo, September, 1959.

1) L. H. Meyer and H. S. Gutowsky, *J. Phys. Chem.*, **57**, 481 (1953).

2) H. S. Gutowsky and C. J. Hoffman, *J. Chem. Phys.*, **19**, 114 (1951).

3) H. S. Gutowsky, D. W. McCall, B. R. McGarvey and L. H. Meyer, *J. Am. Chem. Soc.*, **74**, 4509 (1952).

4) T. Isobe, K. Inukai and K. Ito, *J. Chem. Phys.*, **27**, 1215 (1957); This Bulletin, **33**, 315 (1960).

5) K. Fukui, S. Hattori, T. Yonezawa, R. Kusaka and H. Kitano, *J. Chem. Soc. Japan, Pure Chem. Sec.* (*Nippon Kagaku Zasshi*), **80**, 541 (1959).

6) N. F. Ramsey, *Phys. Rev.*, **78**, 699 (1950).

7) A. Saika and C. P. Slichter, *J. Chem. Phys.*, **22**, 26 (1954).

2. The paramagnetic term for the atom in question.

3. The contribution from other atoms.

Based upon these divisions, they concluded that the $F^{19}$ nuclear magnetic shielding is mainly determined by the paramagnetic contribution of the electrons belonging to the fluorine atom in question. This conclusion was shown to be successful in calculating the chemical shift between HF and $F_2$. The equation developed by them remained, however, only available for evaluating fluorine shifts in some aliphatic compounds. Further application of their procedure to fluorine shifts in aromatic compounds seems never to have been attempted.

In the present paper, an extension of their analysis to more complex conjugated compounds is presented by using a molecular orbital treatment.

## Theoretical

The second order paramagnetic term of Ramsey[6] is approximated referring to the treatment by Saika and Slichter[7]. In the present paper, we have chosen the coordinate system of Fig. 1 whose origin is set at the

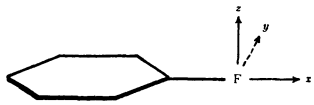



Fig. 1. The coordinate system adopted in the present treatment.

fluorine atom in question. Considering the paramagnetic contribution of electrons belonging to the fluorine, the paramagnetic shielding term, $\sigma_p$, in a conjugated molecule can be given by the mean of three principal components as

$$\sigma_p=\frac{1}{3}(\sigma_{l-\pi}+\sigma_{l-\sigma}+\sigma_{\sigma-\pi}) \tag{3}$$

These three components are obtained as

$$\left.\begin{aligned}
\sigma_{l-\pi}&=-\left(\frac{eh}{2\pi mc}\right)^2\left\langle\frac{1}{r^3}\right\rangle\sum^{\text{unocc}}\frac{2}{\varepsilon_i-\varepsilon_l}(c_F^i)^2\\
\sigma_{l-\sigma}&=-\left(\frac{eh}{2\pi mc}\right)^2\left\langle\frac{1}{r^3}\right\rangle\frac{2}{\varepsilon_\sigma^*-\varepsilon_l}(a^*)^2\\
\sigma_{\sigma-\pi}&=-\left(\frac{eh}{2\pi mc}\right)^2\left\langle\frac{1}{r^3}\right\rangle\left[\sum_i^{\text{unocc}}\frac{2}{\varepsilon_i-\varepsilon_\sigma}\right.\\
&\quad\times\left\{a^2(c_F^i)^2+\sqrt{\frac{2}{3}}abc_1^ic_F^i\right\}\\
&\quad\left.+\sum_j^{\text{occ}}\frac{2}{\varepsilon_\sigma^*-\varepsilon_j}\left\{(a^*)^2(c_F^j)^2+\sqrt{\frac{2}{3}}a^*b^*c_F^jc_1^j\right\}\right]
\end{aligned}\right\} \tag{4}$$

respectively, where $\langle 1/r^3\rangle$ is the average of $1/r^3$ for 2p electron of fluorine, $\varepsilon_i$ and $\varepsilon_l$ are the energies of the $i$ th $\pi$ molecular orbital and of the lone pair electrons of the fluorine atom, $c_F^i$ and $c_1^i$ are the coefficients of the $i$ th $\pi$ electronic LCAO MO, whose energy is $\alpha+\lambda_i\beta$, at the fluorine atom and its adjacent carbon atom, and $\sum^{\text{occ}}$, $\sum^{\text{unocc}}$ indicate summation over all occupied and unoccupied orbitals, respectively. The wave functions of bonding and antibonding C–F $\sigma$ orbitals, $\varphi_\sigma$ and $\varphi_\sigma^*$, whose energies are denoted by $\varepsilon_\sigma$ and $\varepsilon_\sigma^*$ in Eq. 4, respectively, may be expressed by the following linear combinations of two atomic orbitals, $\chi_F$ and $\chi_C$, which are the 2p $\sigma$ AO of fluorine and the $sp^2$ hybridized orbital of the adjacent carbon atom*.

$$\left.\begin{aligned}
\varphi_\sigma&=a\chi_F+b\chi_C\\
\varphi_\sigma^*&=a^*\chi_F+b^*\chi_C
\end{aligned}\right\} \tag{5}$$

The coefficients $a$, $b$, $a^*$ and $b^*$ are those appearing in Eq. 4. Three components in the right side of Eq. 3, $\sigma_{l-\pi}$, $\sigma_{l-\sigma}$ and $\sigma_{\sigma-\pi}$, can be obtained, as is shown by Eq. 4, by calculating the matrix elements in Eq. 1 between the ground state and the various singlet excited states resulting from one electron transition between MO's designated by each subscript, $l$, $\sigma$ and $\pi$, denoting the orbital of fluorine lone pairs, C–F $\sigma$ orbitals and $\pi$ molecular orbitals, respectively. In the last component $\sigma_{\sigma-\pi}$ which appears only when the $\pi$ conjugation takes place, the cross term arises from the circumstances that we take account of matrix elements of $\chi_C$ and $\pi$ AO on the adjacent carbon atom in $(0|\mathbf{m}^0_{ky}|n)$ and neglect $(0|\mathbf{m}^0_{ky}/r_k^3|n)$ terms on that carbon, as was done in Ref. 7. Equation 3 is easily shown to coincide with the equation given by Saika and Slichter[7] when one considers that no conjugation takes place. It can be shown also, that Eq. 3 in the present paper is also derivable by an alternative procedure proposed by Pople[8], in which attention was paid to the paramagnetic shielding resulting from the local paramagnetic current of the fluorine.

In the present paper, a chemical shift parameter, $\delta$, is defined as

$$\delta=\frac{H_r-H_c}{H_r} \tag{6}$$

where $H_r$ and $H_c$ are the resonance field for the reference compound and the sample compound, respectively.

The chemical shift, $\delta$, can be represented in terms of the paramagnetic shielding constant obtained by Eq. 3 whenever $\sigma$ is small and the change of diamagnetic shielding constant can be neglected. Thus the shift between the

* $\chi_c$ is written as $\sqrt{1/3}\chi_s+\sqrt{2/3}\chi_{2p\sigma}$, where $\chi_s$ and $\chi_{2p\sigma}$ are $2_s$ and $2_{p\sigma}$ AO's of carbon atom, respectively.

8) J. A. Pople, *Proc. Roy. Soc.*, **A239**, 541, 550 (1957).

compound in question and the reference one can be expressed as*1

$$\delta=\delta_p(\text{reference})-\sigma_p(\text{sample}) \tag{7}$$

## Numerical Calculation

In order to carry out calculation, the information on the energies of the molecular orbitals and the coefficients involved in Eq. 4 is indispensable. The $\pi$ molecular orbital energies and the coefficients are settled by the simple LCAO MO method. The values of the Coulomb integrals and the resonance integral representing the characteristics of a fluorine atom and a carbon atom adjacent thereto are taken as

$$\left.\begin{aligned}\alpha_F&=\alpha+1.8\beta\\ \alpha_{adj}&=\alpha+0.18\beta\\ \beta_{C-F}&=0.8\beta\end{aligned}\right\} \tag{8}$$

where $\alpha$ is the Coulomb integral of a carbon atom and $\beta$ is the resonance integral for a C–C bond in a benzene molecule. The values of $\alpha$ and $\beta$ are taken to be $-7.25$ eV. and $-2.3$ eV., respectively, in numerical calculation*2. Other Coulomb and resonance integrals used for amino and nitro groups in the present calculation are as follows:

$$\alpha_{-NH_2}=\alpha+0.4\beta$$
$$\beta_{C-NH_2}=0.4\beta$$
$$\alpha_N=\alpha+\beta$$
$$\alpha_O=\alpha+\beta$$

Since the simple LCAO MO studies for a $\sigma$ electron system have not been sufficiently copious for providing reliable numerical values of various parameters, an attempt to estimate these parameters is necessary for our calculation. Hereupon, the values of Coulomb and resonance integrals are determined on the basis of some experimental data in the following way. At first, the energies of $\sigma$-bonding and antibonding orbitals for the reference compound are put to $-14$ eV. and $-4$ eV., respectively. The energy of bonding orbital is equal to the absolute value of ionization potential of an electron localized in a C–F bond in methyl fluoride assigned by McDowell[9]. The energy of the antibonding orbital is estimated by the spectroscopic data on other methyl halides. The molecular orbital coefficients, $a$ and $b$, are determined from the magnitude of the bond moment, $\mu$, with the aid of simplified formulas*3

$$\left.\begin{aligned}\mu&=\frac{\lambda^2-1}{1+\lambda^2}eR\\ a&=\frac{-\lambda}{(1+\lambda^2)^{1/2}}\\ b&=\frac{1}{(1+\lambda^2)^{1/2}}\end{aligned}\right\} \tag{9}$$

where $R$ is a C–F bond distance, $e$ is the charge of an electron, and $\lambda(\lambda>0)$ is a coefficient representing the polarity of the molecular orbital. The bond moment, $\mu$, is adopted as 1.51 D and C–F distance as 1.39 Å. Inserting these values into Eq. 9, we obtain: $a=-0.783$ and $b=0.622$*4. The coefficients $a^*$ and $b^*$ are then obtained as 0.622 and $-0.783$, respectively.

Coulomb and resonance integrals in a C–F $\sigma$ electron system might be determined in such a way that in solving the secular determinant these integrals give the values of energies and orbital coefficients estimated above. It may be more reasonable, then, to consider that, as the character of the C–F $\sigma$ bond alters according to the change of molecular structure, the values adopted for the integrals may change. In this connection it may be recollected that in $\pi$ electron approximation a $\pi$ electron is considered to move in a resultant electric field from all other $\pi$ electrons and the $\sigma$ skeleton. Hence, in the treatment of $\sigma$ electrons, the electronic structure is naturally recognized to be affected by $\pi$ electronic distribution conversely.

Referring to the facts stated above, the Coulomb and resonance integrals available for a C–F $\sigma$ electron system are expressed as*5

$$\left.\begin{aligned}h_{FF}&=-10.16-\gamma_F(q_F^0-q_F)\\ h_{CC}&=-7.84-\gamma_C(q_C^0-q_C)\\ h_{CF}&=+4.84\text{*6}\end{aligned}\right\} \tag{10}$$

*1 The shielding constant $\sigma$ is represented by the sum of diamagnetic and paramagnetic shielding constant $\sigma_d$, $\sigma_p$ as $\sigma=\sigma_d+\sigma_p$. Then the shift becomes $\delta=\{\sigma_d(\text{reference})-\sigma_d(\text{sample})\}+\{\sigma_p(\text{reference})-\sigma_p(\text{sample})\}$. Neglecting the first term, we obtain Eq. 7.

*2 These values are determined so that the calculated highest occupied orbital energy of fluorobenzene ($\alpha+0.8441\beta$) becomes equal to the negative value of ionization potential of the compound, 9.19 eV. (V. J. Hammond, W. C. Price, J. P. Teeganand and A. D. Walsh, *Faraday Soc. Discuss.*, **9**, 53 (1950)). The value of $\alpha$ is not so unreasonable compared with the value $-7.18$ eV. adopted by Mulliken (*Phys. Rev.*, **74**, 736 (1948)). The value of $\beta$ is equal to that determined by Pariser and Parr (*J. Chem. Phys.* **21**, 767 (1953)).

9) C. A. McDowell and B. A. Cox, *Proc. Roy. Soc.*, **A241**, 194 (1957).

*3 Cf. C. A. Coulson, "Valence", Oxford Univ. (1952), p. 103; In the present formulas, the overlap integral is neglected.

*4 The minus sign of $a$ is determined so as to correspond with the coefficient of bonding $\sigma$ MO in the present coordinate system (see Fig. 1).

*5 These equations resemble those used in a semi-empirical SCF treatment carried out in a $\pi$ electron system. (Cf. e. g., R. S. Mulliken et al., *J. Am. Chem. Soc.*, **76**, 4770 (1954)). The present procedure, however, represents a reciprocal interaction of $\sigma$ electrons with $\pi$ electrons in a bond.

*6 The exchange integral is taken to be positive since the overlap integral between carbon and fluorine AO's in a C–F $\sigma$ bond is found to be negative in the present coordinate system (see Fig. 1).

TABLE I. TOTAL $\pi$ ELECTRON DENSITY, $\sigma$-ELECTRONIC ENERGY AND MOLECULAR ORBITAL COEFFICIENT

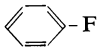
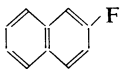
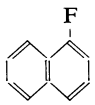
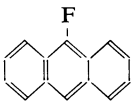
| | $q_F$ | $q_C$ | $\varepsilon_\sigma$ | $\varepsilon_\sigma$* | $\varepsilon_l$ | $a^2$ | $b^2$ |
|---|---|---|---|---|---|---|---|
|  | 1.9330 | 1.0204 | −13.977 | −4.023 | −10.000 | 0.6166 | 0.3834 |
|  | 1.9318 | 1.0196 | −13.993 | −4.033 | −10.024 | 0.6176 | 0.3824 |
|  | 1.9306 | 1.0216 | −14.008 | −4.043 | −10.048 | 0.6187 | 0.3813 |
|  | 1.9268 | 1.0162 | −14.057 | −4.075 | −10.124 | 0.6220 | 0.3780 |
|  | 1.9198 | 1.0128 | −14.147 | −4.132 | −10.264 | 0.6283 | 0.3717 |

TABLE II. TOTAL $\pi$ ELECTRON DENSITY, $\sigma$-ELECTRONIC ENERGY AND MOLECULAR ORBITAL COEFFICIENT

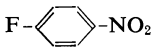
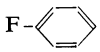
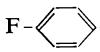
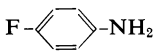
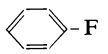
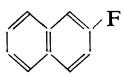
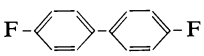
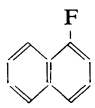
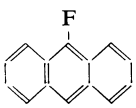
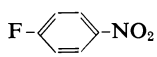
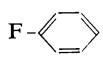
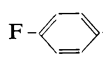
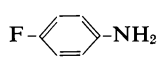
| | $q_F$ | $q_C$ | $\varepsilon_\sigma$ | $\varepsilon_\sigma$* | $\varepsilon_l$ | $a^2$ | $b^2$ |
|---|---|---|---|---|---|---|---|
|  | 1.9204 | 0.9686 | −14.173 | −4.183 | −10.252 | 0.6235 | 0.3765 |
|  | 1.9330 | 1.0204 | −13.977 | −4.023 | −10.000 | 0.6166 | 0.3834 |
|  | 1.9344 | 1.0342 | −13.949 | −3.995 | − 9.972 | 0.6165 | 0.3835 |
|  | 1.9352 | 1.0410 | −13.934 | −3.987 | − 9.956 | 0.6164 | 0.3836 |

TABLE III. CALCULATED SHIELDING CONSTANTS AND CHEMICAL SHIFTS

| | $-\sigma_{l-\sigma}$ | $-\sigma_{l-\pi}$ | $-\sigma_{\sigma-\pi}$ | $-\sigma_p$ | $\delta_{calcd}$ | $\delta_{obs}$ [a] |
|---|---|---|---|---|---|---|
|  | 165.398 | 15.761 | 146.921 | 1/3×328.080 | 0 | 0 |
|  | 164.590 | 16.400 | 146.914 | 1/3×327.904 | −0.06 | −0.18 |
|  | 163.731 | 16.632 | 146.875 | 1/3×327.238 | −0.28 | −0.26 |
|  | 161.144 | 18.462 | 147.262 | 1/3×326.868 | −0.40 | −1.02 |
|  | 156.305 | 22.273 | 147.623 | 1/3×326.201 | −0.63 | − |

(a) Ref. 5; in units of 10 p. p. m.

TABLE IV. CALCULATED SHIELDING CONSTANTS AND CHEMICAL SHIFTS

| | $-\sigma_{l-\sigma}$ | $-\sigma_{l-\pi}$ | $-\sigma_{\sigma-\pi}$ | $-\sigma_p$ | $\delta_{calcd}$ | $\delta_{obs}$ [b] |
|---|---|---|---|---|---|---|
|  | 159.962 | 20.738 | 152.238 | 1/3×332.938 | +1.62 | +1.08 |
|  | 165.398 | 15.761 | 146.921 | 1/3×328.080 | 0 | 0 |
|  | 165.453 | 15.505 | 145.714 | 1/3×326.672 | −0.47 | −0.64 |
|  | 165.537 | 15.214 | 144.889 | 1/3×325.640 | −0.78 | −1.46 |

(b) Ref. 3; in units of 10 p. p. m.

where these matrix elements are represented in units of eV., $q_F^0$ and $q_C^0$ denote the total $\pi$ electron densities at the fluorine and the adjacent carbon atom in the reference, respectively, and $q_F$ and $q_C$ are those in the sample compound. Parameters $\gamma_F$ and $\gamma_C$ are tentatively put at 20 and 2, respectively, in the present treatment. Using the integrals in Eq. 10, the energies of bonding and antibonding orbitals as well as the coefficients are calculated.

Finally the energy of lone pair electrons of fluorine, $\varepsilon_l$, is assumed to be*

$$\varepsilon_l = -10 - \gamma_F(q_F^0 - q_F) \qquad (11)$$

in which the second term has a similar meaning in Eq. 10. The value of $\langle 1/r^3 \rangle$ is put at $8.89/a_H^3$, where $a_H$ is the Bohr radius[7].

## Result and Discussion

It was discussed qualitatively by the present authors[5] that the two factors, the polarity of C–F bond and the $\pi$ electron density on fluorine, had a dominant role in determining a paramagnetic term in a conjugated molecule. The two empirical rules were proposed[5], whereby a qualitative analysis of magnetic shielding parameter $\delta$ was made. Further we pointed out that in polycondensed aromatics the magnitude of total $\pi$ electron more density decreases with the decrease of fluorine chemical shifts, while in some fluorobenzene derivatives this correlation is reversed. More precisely, the fluorine chemical shift seems to be governed by the polarity of a C–F $\sigma$ bond in fluorobenzene derivatives.

In the present paper an investigation on fluorine chemical shifts in these compounds is made quantitatively by making use of Eqs. 3 and 4.

In Tables I and II, the total densities at the fluorine and the adjacent carbon atom, the energies of bonding and antibonding orbitals, and the values of $a^2$ and $b^2$ for benzene derivatives and condensed aromatics are cited. One should note that the polarity of a C–F bond which is measured by the magnitude of $a^2$ seems to increase with the decrease of $q_F$ in Table I, while in Table II the polarity seems to increase with the increase of $q_F$.

In Tables III and IV, there are listed three principal components of the paramagnetic shielding constant, the mean of the constants and the calculated values of chemical shift together with observed ones.[3,5] With regard to 9-fluoroanthracene, there are unfortunately no data to be compared with the theoretical result. Though there remain many points to be modified in future, the good agreement observed between the present results and experimental data may be sufficiently valuable to be stressed.

## Summary

In order to make a quantitative analysis of the $F^{19}$ magnetic shielding parameters in conjugated molecules, an extension of the idea previously proposed by Saika and Slichter is made. Calculations are carried out with respect to several fluorobenzene derivatives and fluorinated polycondensed aromatic compounds by using the molecular orbital method. The agreement of our calculated shifts with observed shielding data is almost satisfactory.

*Faculty of Engineering*
*Kyoto University*
*Sakyo-ku, Kyoto*
*(T. Y., K. F., H. K. & H. K.)*

*Faculty of Science*
*Kanazawa University*
*Kanazawa*
*(S. H. & S. M.)*

* In a rough estimation, it may be assumed that this energy can be obtained by the equation, $\varepsilon_l = -I_F + 1/2(I_F - A_F)$, where $I_F$ and $A_F$ are the ionization potential and the electron affinity of the fluorine in its valence state. Using the published data, $I_F = 17.481$ eV., $A_F = 3.78$ eV., we can obtain $\varepsilon_l = -10.5$ eV. Therefore the value of $-10$ in Eq. 11 seems not to be so unreasonable.

# *An LCUAO Treatment of Reactivity in Aromatic Hydrocarbons*

By Kenichi FUKUI, Teijiro YONEZAWA, Chikayoshi NAGATA and Yoshimichi KONAKA

(Recieved October 28, 1960)

Several theoretical treatments of reactivity of conjugated molecules have achieved a brilliant develompent in accordance with the progress of the LCAO MO method. In this procedure, the molecular orbital is represented by the linear combination of $2\pi$ atomic orbitals. By the use of these coefficients useful indices of reactivity such as electron density[1], bond order[1], and frontier electron density[2] are derived.

On the other hand, a method, the so-called LCUAO MO, in which the molecular orbital is represented by the linear combination of united-atomic orbitals in each bond of a conjugated molecule has been developed by Brown and Matsen[3]. This method is an extension of united-atom approach[4] in hydrogen molecule to conjugated compounds.

This procedure may be considered to supply us more easily with information on the nature of a conjugated double bond if we introduce the frontier electron concept in LCAO MO treatment.

## Theoretical

By an ordinary procedure of LCUAO MO method[3], a molecular orbital is written as

$$\psi=\sum_i a_i\phi_i \qquad (1)$$

where $\phi_i$ is the UAO of the $i$th bond. The secular equation for the system can be obtained from this molecular orbital putting the matrix elements as following.

$$h_{ii}=\int\phi_i^* h\phi_i \mathrm{d}\tau=\alpha$$

$$h_{ij}=\int\phi_i^* h\phi_j \mathrm{d}\tau=\beta \text{ for adjacent bond} \qquad (2)$$

$$0 \text{ for non-adjacent bond}$$

where $h$ is the effective one electron hamiltonian, and $\alpha$ and $\beta$ are the standard Coulomb and resonance integrals in benzene, respectively. Then all the molecular orbital coefficients are determined from the roots of the secular equation by using normalizing condition

$$\sum_i (a_i)^2=1 \qquad (3)$$

Brown and Matsen[3] has proposed that bond order, $P_r$, for the $r$th bond can be obtained by

$$P_r=\sum_j \nu_j (a_r^j)^2 \qquad (4)$$

where $\nu_j$ is the occupation number for the $j$th molecular orbital. Then they showed that a good parallelism can be obtained between the bond orders obtained by simple LCAO MO treatment and by the present method.

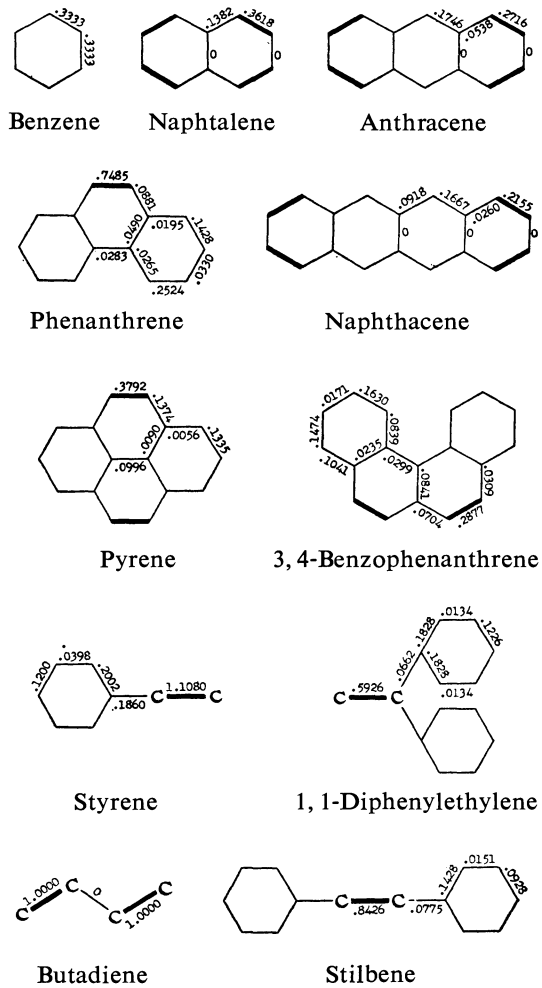



Fig. 1. Electron densities of the highest occupied orbital.

1) H. C. Longuet-Higgins and C. A. Coulson, *Proc. Roy. Soc.*, **A192**, 16 (1947).
2) K. Fukui, T. Yonezawa and H. Shingu, *J. Chem. Phys.*, **20**, 722 (1952); K. Fukui, T. Yonezawa, C. Nagata and H. Shingu, ibid., **22**, 1433 (1954).
3) R. D. Brown and F. A. Matsen, ibid., **21**, 1298 (1953).
4) R. D. Brown, *J. Chem. Soc.*, **1953**, 2615.

TABLE I. REACTIVE BOND IN AROMATIC HYDROCARBONS

| Compound | Experimentally most reactive bond* | Bond of largest frontier density | Bond of minimum ortho localization energy** |
|---|---|---|---|
| Benzene | 1 : 2 | 1 : 2 | 1 : 2 |
| Naphthalene | 1 : 2 | 1 : 2 | 1 : 2 |
| Anthracene | 1 : 2 | 1 : 2 | 1 : 2 |
| Phenanthrene | 9 : 10 | 9 : 10 | 9 : 10 |
| Pyrene | 4 : 5 | 4 : 5 | 4 : 5 |
| Naphthacene | 1 : 2 | 1 : 2 | 1 : 2 |
| 3,4-Benzophenanthrene (Benzo[*c*]phenanthrene) | 5 : 6 | 5 : 6 | 5 : 6 |

* Estimated from the addition reaction of $OsO_4$, which is considered to be an electrophilic addition taking place simultaneously at the two adjacent carbon atoms.
** Ref. 7.

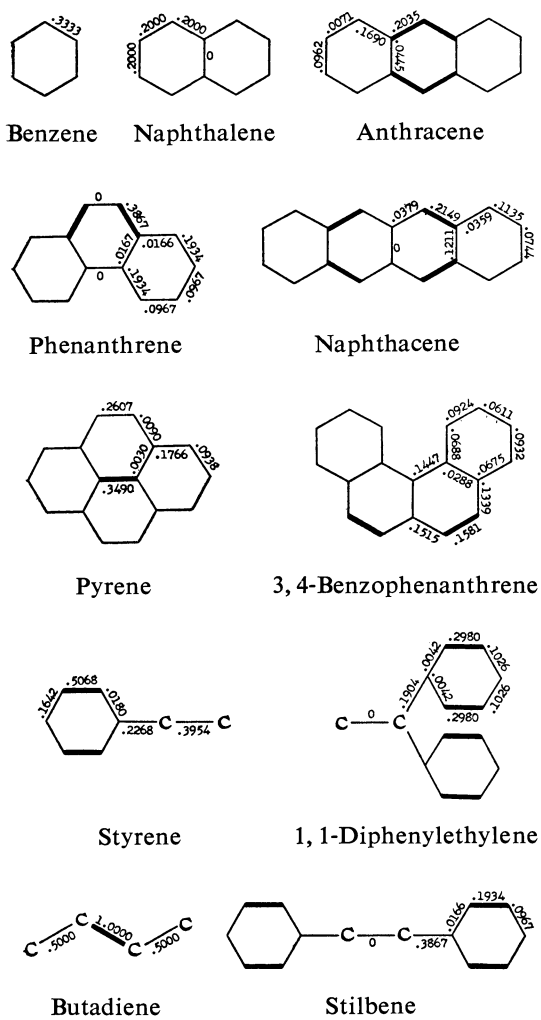



Fig. 2. Electron densities of the lowest vacant orbital.

In these circumstances the investigation is made to elucidate whether or not the frontier electron concept by which the chemical reactivity in conjugated molecules is successfully interpreted may be applicable in LCUAO MO method. The calculation is carried out with respect to benzene, naphthalene, anthracene, naphthacene, pyrene, 3,4-benzophenanthrene (benzo[*c*]phenanthrene), styrene, stilbene and 1,1-diphenylethylene. The electronic distributions of the highest occupied and the lowest vacant orbitals are calculated and indicated in Figs. 1 and 2.

## Results and Discussion

The bond of the largest frontier electron density for electrophilic reaction in polycondensed aromatics are indicated in the third column of the Table I. These results may give some information concerning the bond which will play a dominant role in the complex formation of aromatic hydrocarbons with $Ag^+$ ion[5] or $H^+$ ion. Furthermore the bond of the largest electron density of the highest occupied orbital in 1,1-diphenylethylene coincides with the position pointed out by Evans and his coworkers[6] in the complex formation of this compound with $H^+$. In regard to styrene, butadiene and stilbene, calculated results are considered to be reasonable.

On the other hand, the electronic distribution of the lowest vacant orbital shown in Fig. 2 seems to correspond to none of the chemical reactions ever known. But since there exist no experimental data available, we must refrain here from deciding whether the results thus obtained are essentially meaningless or not. But one thing attracts our attention. That is, the most reactive position does not coincide with what is predicted from the electronic distribution of the highest occupied orbital,

5) S. Winstein and H. J. Lucas, *J. Am. Chem. Soc.*, **60**, 836 (1938); R. E. Kofahl and H. J. Lucas, ibid., **76**, 3933 (1954).
6) A. G. Evans, D. M. S. Jones and J. H. Thomas, *J. Chem. Soc.*, **1957**, 104.

while the existing theories of these compounds predict the same position to be most reactive in both electrophilic and nucleophilic additions. A typical one of these theories is the localization theory[7]. This point should be investigated in future.

*Faculty of Engineering*
*Kyoto University*
*Sakyo-ku, Kyoto*

7) E. C. Kooyman and J. A. A. Ketelaar, *Rec. trav. chim.*, **65**, 859 (1946); R. D. Brown, *J. Chem. Soc.*, **1950**, 3249.

# *Application of RADME to the Chelatometric Determination of Metals Employing the Alternating Current Polarographic Method*

By Mutsuo KODAMA

(Received October 6, 1960)

Cadmium- and lead-nitrilotriacetate complexes give rise to two polarographic waves in acetate buffer solution (pH 4.5). The first one is a kinetic wave due to the elecrodeposition of metal ions formed by the dissociation of the complex, and the second is the one due to the direct reduction of complex[1,2]. In ammonia-ammonium nitrate buffer solution, the kinetic currents which originate from the dissociation can also be observed. Owing to the presence of the kinetic current, cadmium and lead can not be titrated with nitrilotriacetic acid (NTA) by employing the usual polarographic method.

In the previous paper, the concentration of copper in an acetate buffer solution of pH 6.0 was determined with NTA by the use of the alternating current polarographic method. In the titration, equivalence points were determined by plotting the peak currents of the alternating current polarograms of copper against the volume of NTA solution added.

The present investigation was directed to the application of rapidly dropping mercury electrode (RADME) to the chelatometric determination of copper, cadmium and lead, using the alternating current polarographic method. At RADME, peak currents due to the electrodeposition of these metal ions which were produced by the dissociation of complexes could not be observed. When RADME is used as an indicator electrode, experimental equivalence points agreed with the stoichiometric equivalence points.

## Experimental

**Apparatus.**—A Yanagimoto Model GA-103 galvarecorder equipped with an automatically scanning potentiometer was employed for the measurements of all current-voltage curves and also for the titrations. The current was determined point by point by manual operation.

Dropping mercury electode (DME) and RADME had the chracteristic features indicated in Table I, the measurements being conducted in air-free 0.1 M potassium chloride solutions with open circuit at $25\pm0.1$°C.

TABLE I. CHARACTERISTICS OF THE ELECTRODES MEASURED IN AIR-FREE 0.1 M POTASSIUM CHLORIDE SOLUTION WITH OPEN CIRCUIT AT $25\pm0.1$°C

| | Height of mercury head, cm. | $t$, sec. | $m$ mg./sec. |
|---|---|---|---|
| DME | 70.0 | 4.02 | $1.23_7$ |
| RADME | 60.0 | $0.35_3$ | 15.54 |

A simple beaker type cell was used for all measurements. A cell was connected to a saturated calomel electrode (S. C. E.) through a potassium nitrate agar bridge (1.5 kΩ). Semimicroburets of 5 ml. and 10 ml. capacity were used for titrations. During the titrations purified nitrogen gas was passed through the solution to remove dissolved oxygen, prior to the measurements of current-voltage curves and titration curves, which also were conducted after every addition of titrant. All polarographic measurements and titrations were carried out at $25\pm0.1$°C. The cell construction which was used fo rthe alternating current polarographic measurements is shown in Fig. 1. A large platinum electrode was inserted into the solution as the third electrode and this was connected to the anode through a condenser of 100 $\mu$F in order to keep the impedance of the electrolysis cell as low as possible.

**Reagent.** — Nitrilotriacetic acid (NTA) of analytical reagent grade (Wakō Pure Chemical Industries, Ltd.) was used without further purification. The stock solution of NTA was standardized with

1) J. Koryta and I. Kossler, *Collection Czechoslov. Chem. Communs. Suppl.*, **15**, 241 (1950).
2) K. Morinaga and T. Nomura, *J. Chem. Soc. Japan, Pure Chem. Sec.* (*Nippon Kagaku Zasshi*), **79**, 200 (1958).

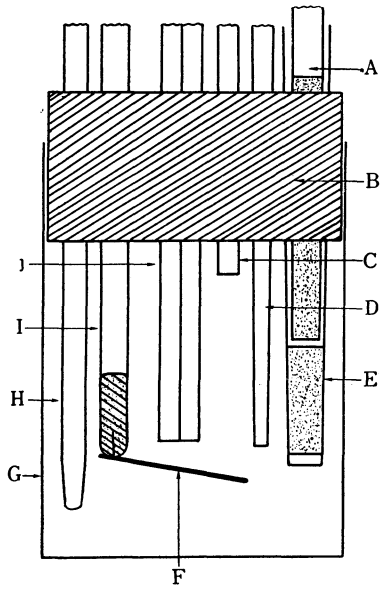



Fig. 1. Cell construction.

| | | | |
|---|---|---|---|
| A | S. C. E. | F | platinum plate |
| B | rubber | G | beaker type cell |
| C | gas outlet | H | gas inlet |
| D | buret | I | platinum electrode |
| E | sintered glass | J | DME or RADME |

standardized nickel solution[3,4]. Standard solutions of copper, lead and cadmium were prepared from chemicals of analytical reagent grade. The concentration of stock solution was determined gravimetrically[5]. The concentrations of copper and of cadmium were determined by amperometric titration[6,7], using the DME as an indicator electrode. Other chemicals used were all analytical reagent grade. The buffer solutions were prepared by the method described in the previous paper[4].

## Results and Discussion

**Direct Current (D. C.) Polarography.** —Current-voltage curves of cadium-nitrilotriacetate complex were obtained with DME at different heights of mercury column in de-aerated ammonia-ammonium nitrate buffer solution of pH 9.2 containing 0.005% gelatine. The ionic strength was adjusted to 0.7 with potassium nitrate.

As seen from current-voltage curve A (Fig. 2), the mixture of cadmium and nitrilotriacetic acid at the ratio of exactly 1 to 1, gives a polarogram with a small reduction wave of

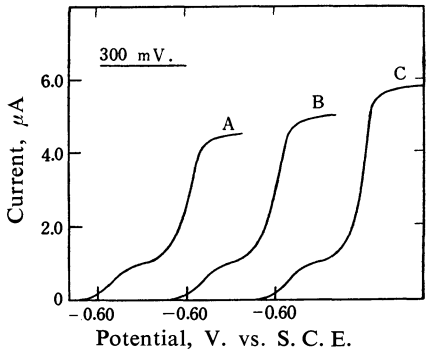



Fig. 2. Current-voltage curves of $1.09_8 \times 10^{-3}$ M cadmium nitrilotriacetate in an ammonia-ammonium nitrate buffer of pH 9.2 ($\mu$=0.7).

A Height of mercury column, 50 cm.
B Height of mercury column, 70 cm.
C Height of mercury column, 90 cm.

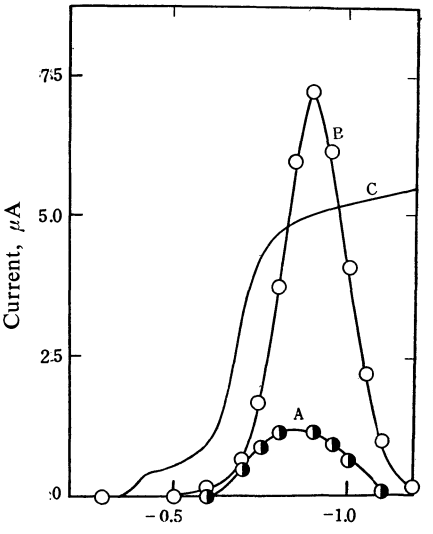



Fig. 3. Current-voltage curves of $1.18_6 \times 10^{-3}$ M lead-nitrilotriacetate in an ammonia-ammonium nitrate buffer of pH 8.2 ($\mu$=0.7) containig 50 mM tartarate.

A A. C. polarogram at DME
B A. C. polarogram at RADME
C D. C. polarogram at DME

cadmium (-amine complex) ion. Viewed from the experimental results obtained at different heights of mercury column (curves B and C in Fig. 2), the author's explanation that this small prewave must be kinetic in nature, may be justified. Lead-nitrilotriacetate complex in an ammonia-ammonium nitrate buffer solution of pH 8.2 containing 0.005% gelatin (50 mM sodium tartarate was added to avoid the undesirable hydrolysis of lead) also gave the kinetic current (curve C in Fig. 3). The ionic strength was also adjusted to 0.7 with potassium nitrate.

3) M. Kodama, A. Shimizu and H. Terakado, ibid. **81**, 1545 (1960).
4) G. Numaziri, M. Kodama and A. Shimizu, ibid., **81**, 454 (1960).
5) F. P. Treadwell and W. T. Hall, "Analytical Chemistry", Vol. 2 (1953), p. 58.
6) N. Tanaka, I. T. Oiwa and M. Kodama, *Anal. Chem.*, **28**, 1555 (1956).
7) N. Tanaka, M. Kodama, M. Sasaki and M. Sugino, *Japan Analyst* (*Bunseki Kagaku*), **6**, 86 (1957).

**Alternating Current (A. C.) Polalography.**— Alternating current polarograms of cadmium, lead and copper were recorded, using DME or RADME, under the same conditions as those used for direct current polarographic measurements. It was found for lead-nitrilotriacetate complex that the reduction wave of lead ion due to the dissociation of complex entirely disappeared at DME or RADME as shown in Fig. 3 (curves A and B). This phenomenon was also obtained in the reduction of cadmium-nitrilotriacetate complex, when RADME was employed as an indicator electrode (Fig. 4).

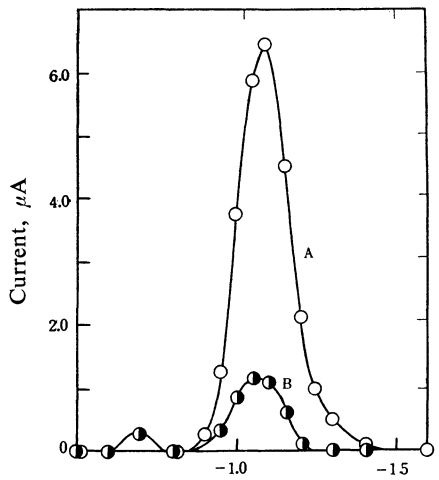



Fig. 4. Alternating current polarograms of $1.09_8\times10^{-3}$ M cadmium-nitrilotriacetate in an ammonia-ammonium nitrate buffer of pH 9.2 ($\mu$=0.7).

A at RADME B at DME

These results may indicate that the rate of the dissociation reaction of metal-nitrilotriacetate complex on the electrode surface is not sufficiently rapid to supply the requisite amount of metal ion to give the kinetic current during the short interval (0.02 sec.) of each alternating current voltage sweep at DME or RADME.

The value of the peak current of metal-nitrilotriacetate conmplex observed at RADME is higher than that observed at DME. In the potential range at which experiments were conducted, the surface-active substance, gelatine, is adsorped on the electrode surface to cover it. The extent of coverage of the rapidly dropping mercury electrode surface differs from that of the ordinary dropping mercury electrode surface, because the drop time of RADME is quite different from that of DME. This difference is related to the extent of inhibition of the electro-oxidation-reduction reaction of complex ion, which may be the reason why the peak current at RADME is higher than that at DME. The adsorption of gelatine on the mercury drop occurs over the entire range of potentials (about +0.4 to −2.0 V. vs. S.C.E.), and the tensammetric peaks due to the adsorption and the desorption of gelatine can not be observed under ordinary experimental conditions. In the case of camphor, however, two tensammetric peaks can be observed at about −0.25 and −1.15 V. vs. S.C.E. The peak in the positive potential region results from the adsorption of camphor, and the peak

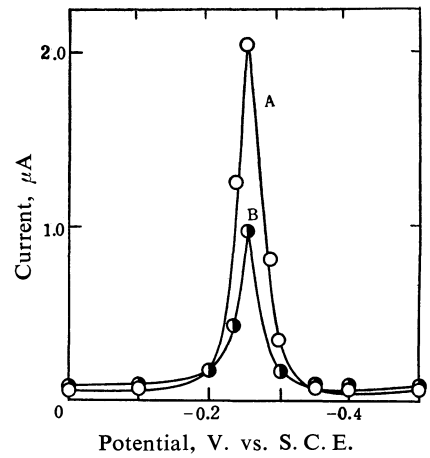



Fig. 5. Alternating current polarograms of 0.5 M $KNO_3$ solution containing $1.5\times10^{-3}$ M camphor.

A at RADME B at DME

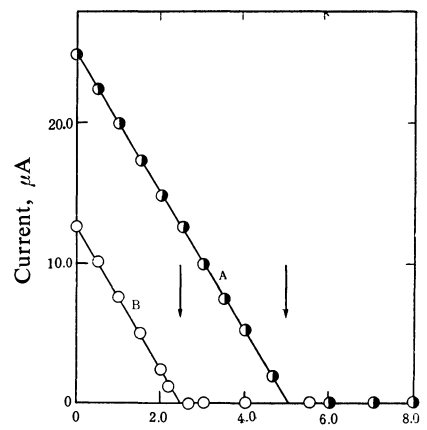


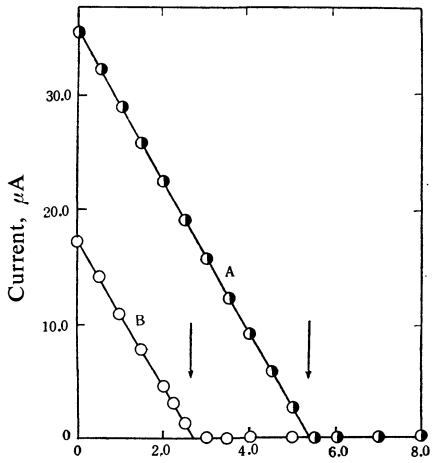

Fig. 6. Titration curves of cadmium with NTA in an ammonia-ammonium nitrate buffer of pH 9.2 ($\mu$=0.7).

A 50 ml. of $1.09_5\times10^{-3}$ M cadmium
B 50 ml. of $5.47_5\times10^{-4}$ M cadmium
Stoichiometric equivalence points are indicated by arrows.

in the negative potential region from the desorption of camphor. The peak currents of positive tensammetric wave of camphor obtained at DME and RADME in the nitrate media are shown in Fig. 5. The value of the peak current observed at RADME differs from that observed at DME. This fact also implies that the extent of coverage of the rapidly dropping mercury electrode surface by the surface-active substance is quite different from that of the dropping mercury electrode surface.

**A. C. Poralographic Titrations.** — From the above results and the well-known facts[8] that in the reversible case, the A. C. polarographic method is advantageous in the resolution of two component systems and in the determination of low concentration; it seems desirable to employ the A. C. polarographic method to determine the concentration of cadmium or lead with NTA at RADME in an ammnia-ammonium nitrate buffer solution.

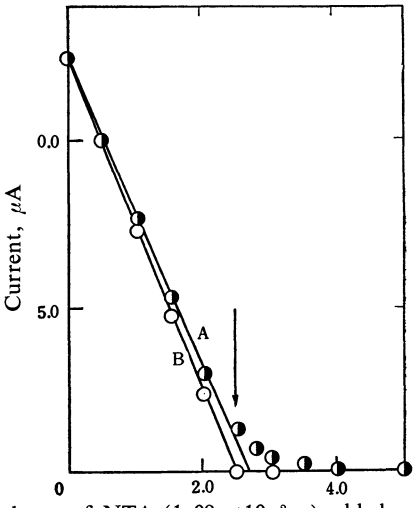
Polarographic titration employing the A. C. polarographic method (A. C. polarographic titration) was carried out, under the same conditions as that used for the polarographic measurements, in the concentration range from $1\times10^{-3}$ M to $1\times10^{-5}$ M. Titration curves were obtained by plotting the peak currents due to the electro-reduction of metal ions against the volume of NTA solution added. Typical examples of the titration curves are given in Figs. 6 and 7. These curves were corrected for dilution effect by the addition of titrant. The potential at which the peak currents are given were held constant during the titration. The results of the titration obtained are listed in Tables II and III. Experimental equivalence points agreed with calculated equivalence points satisfactorily. The results of the titration obtained for copper are also listed in Table IV.




Volume of NTA ($1.09_6\times10^{-2}$ M) added, ml.

Fig. 7. Titration curves of lead with NTA in an ammonia-ammonium nitrate buffer of pH 9.2 ($\mu$=0.7).

A 50 ml. of $1.18_8\times10^{-3}$ M lead.
B 50 ml. of $5.93_0\times10^{-4}$ M lead.
Stoichiometric equivalence points are indicated by arrows.




Volume of NTA ($1.09_8\times10^{-2}$ M) added, ml.

Fig. 8. Titration curves of cadmium with NTA in an ammonia-ammonium nitrate buffer of pH 9.2 ($\mu$=0.77); 50 ml. of $5.47_5\times10^{-4}$ M cadmium.

A 0.4 M ammonia B 0.1 M ammonia

TABLE II. A. C. POLAROGRAPHIC TITRATION OF CADMIUM WITH NTA USING RADME (INITIAL VOLUME 50 ml.)

| Concentration of cadmium, M | Concentration of NTA used for titration, M | NTA required, ml. | | Error, % |
|---|---|---|---|---|
| | | Stoichiometric | Experimental | |
| $1.09_5\times10^{-3}$ | $1.09_8\times10^{-2}$ | $4.98_7$ | 5.00 | +0.1 |
| $5.47_5\times10^{-4}$ | $1.09_8\times10^{-2}$ | $2.49_4$ | 2.48 | −0.6 |
| $2.73_8\times10^{-4}$ | $1.09_8\times10^{-2}$ | $1.24_7$ | 1.24 | −0.6 |
| $1.09_5\times10^{-4}$ | $1.09_3\times10^{-3}$ | $4.98_7$ | 4.96 | −0.6 |
| $5.47_5\times10^{-5}$ | $1.09_8\times10^{-3}$ | $2.49_4$ | 2.50 | +0.3 |
| $3.28_5\times10^{-5}$ | $1.09_8\times10^{-3}$ | $1.24_7$ | 1.45 | −3.0 |

8) P. Delahay, "New Instrumental Method in Electrochemistry" (1954), p. 176.

TABLE III. A. C. POLAROGRAPHIC TITRATION OF LEAD WITH NTA USING RADME (INITIAL VOLUME 50 ml.)

| Concentration of lead, M | Concentration of NTA used for titration, M | NTA required, ml. | | Error, % |
|---|---|---|---|---|
| | | Stoichiometric | Experimental | |
| $1.18_6\times10^{-3}$ | $1.09_8\times10^{-2}$ | $5.40_0$ | 5.40 | 0 |
| $5.93_0\times10^{-4}$ | $1.09_8\times10^{-2}$ | $2.70_0$ | 2.69 | −0.6 |
| $2.37_4\times10^{-4}$ | $1.09_8\times10^{-2}$ | $1.08_0$ | 1.07 | −1.0 |
| $1.18_6\times10^{-4}$ | $1.09_8\times10^{-3}$ | $5.40_0$ | 5.42 | +0.4 |
| $5.93_0\times10^{-5}$ | $1.09_8\times10^{-3}$ | $2.70_0$ | 2.72 | +0.8 |
| $2.37_4\times10^{-5}$ | $1.09_8\times10^{-3}$ | $1.08_0$ | 1.05 | −3.0 |

TABLE IV. A. C. POLAROGRAPHIC TITRATION OF COPPER WITH NTA USING RADME (INITIAL VOLUME 50 ml.)

| Concentration of copper, M | Concentration of NTA used for titration, M | NTA required, ml. | | Error, % |
|---|---|---|---|---|
| | | Stoichiometric | Experimental | |
| $1.13_0\times10^{-3}$ | $1.09_8\times10^{-2}$ | $5.15_0$ | 5.15 | 0 |
| $5.65_0\times10^{-4}$ | $1.09_8\times10^{-2}$ | $2.57_5$ | 2.58 | +0.2 |
| $2.26_5\times10^{-4}$ | $1.09_8\times10^{-2}$ | $1.03_0$ | 1.02 | −1.0 |
| $1.13_0\times10^{-4}$ | $1.09_8\times10^{-3}$ | $5.15_0$ | 5.16 | +0.2 |
| $5.65_0\times10^{-5}$ | $1.09_8\times10^{-3}$ | $2.57_5$ | 2.57 | −0.2 |

When a great excess of ammonia is presented in the solution, experimental equivalence points were somewhat greater than the stoichiometrical ones. This fact reveals that the presence of excess ammonia favors the dissociation reaction of the metal-nitrilotriacetate complex (Fig. 8).

## Summary

RADME was applied to the chelatometric determination of copper, cadmium and lead with NTA by employing the A. C. polarographic method. At RADME practically no kinetic effects due to the dissociation of metal-nitrilotriacetate complex were observed and the concentration of metal ions could be determined accurately in the concentration range from $1\times10^{-3}$ M to $1\times10^{-5}$ M.

The author thanks Dr. T. Takeshima for reading the manuscript and for advice.

*Department of Chemistry*
*Faculty of Arts and Sciences*
*Ibaraki University*
*Watari-machi, Mito*

# *Synthesis of α-Maltosides. I*

By Shoji MATSUBARA

(Received October 10, 1960)

Although a large number of glycoside derivatives[1,2] have been synthesized, many attempts to prepare various α-maltoside derivatives have not been promising[3]. At present, non-crystalline phenyl-α-maltoside and methyl-α-maltoside synthesized by Fischer and Bergmann[4], and also by Helferich and Peterson[5] have only been reported. After many trials, the author has succeeded in the synthesis of various α-maltosides.

1) G. Wagner, *Arch. Pharm.*, **290**, 625 (1957).
2) G. Wagner, ibid., **291**, 278 (1958).
3) G. Zemplén, *Ber.*, **60**, 1555 (1935).
4) E. Fischer, M. Bergmann and A. Rabe, ibid., **53**, 2362 (1920).
5) B. Helferich and S. R. Peterson, ibid., **68**, 790 (1935).

The purpose of this study is to obtain some fundamental information concerning the substrate specificity[6-8]; namely, it is to investigate the influence of substituents in the phenyl group on the enzymatic hydrolysis of phenyl-α-maltoside by taka-amylase A[9], and also the mode of interaction of the enzyme activity with structural changes in their substrates. From this point of view, the detailed descriptions of the synthesis are briefly described in this paper.

## Experimental

**Octaacetylmaltose**[3]. — To a solution of 20 g. of anhydrous maltose dissolved in 100 cc. of acetic anhydride, 20 g. of fused sodium acetate was added and the mixture was gently heated. The color of the solution changed from yellow through brown to dark brown. When the violent initial reaction ceased, the solution was heated under stirring for two hours at 100°C in a water bath, poured onto crushed ice, and then diluted with water. The separated yellowish brown oil was allowed to stand overnight in a refrigerator. The crystals which separated out were collected by filtration, dissolved in chloroform, and washed well with water, and dried over anhydrous calcium chloride. The solvent was then evaporated under reduced pressure. The solid was dissolved in hot methanol, filtrated, and the crystalline residue which was obtained from the mother liquor was recrystallized from methanol, giving 14 g. of octaacetylmaltose in the form of colorless crystals, m. p. 158~159°C, $[\alpha]_D^{19}=+124°$ (*c* 1.0, in chloroform).

**Heptaacetylphenyl-α-maltoside**[4,5]. — The mixture of 68 g. (1 mol.) of octaacetylmaltose, 57 g. (6 mol.) of phenol and 10 g. of fused zinc chloride was heated under violent stirring for two and a half hours at 100°C in a water bath. After cooling, the dark brown oily substance was diluted with water, to remove the zinc chloride. To the solution mixture, benzene was added and the benzene extract was well washed successively with water, with 1 N aqueous sodium hydroxide, with water until it became colorless, and finally dried over anhydrous calcium chloride. The solvent was then evaporated under reduced pressure, leaving a yellowish brown oil. The oily residue was crystallized from 100 cc. of ethanol to give colorless crystals. The crude crystals were combined and recrystallized from ethanol-dioxane mixture (contained 10% dioxane), m. p. 184~184.5°C, $[\alpha]_D^{20}=+170.2°$ (*c* 1.0, in chloroform).

Found: C, 53.92; H, 5.63. Calcd. for $C_{32}H_{40}O_{18}$: C, 53.91; H, 5.66%.

**Phenyl-α-maltoside.** — A solution of 10 g. of heptaacetylphenyl-α-maltoside dissolved in 100 cc. of a mixture of absolute methanol and chloroform (1 : 1, by volume) was saturated with ammonia gas under cooling. After being kept more than four hours at room temperature, the methanol and ammonia were removed under reduced pressure. The syrupy residue was dissolved in a small quantity of absolute ethanol, and the precipitate was obtained by adding ether. After removing the supernatant solvents, the residue was then successively treated in the same manner as described above to afford pure crystals. The precipitate obtained was combined and washed with ether. This crude crystalline phenyl-α-maltoside was crystallized from absolute ethanol. The yield was 4.75 g., m. p. 202~204°C, $[\alpha]_D^{14.5}=+211°$ (*c* 1.3, in water).

Found: C, 51.57; H, 6.25. Calcd. for $C_{18}H_{26}O_{11}$: C, 51.65; H, 6.27%.

The ultraviolet absorption of the product showed maxima at 266 mμ in water.

**Heptaacetyl-*p*-nitrophenyl-α-maltoside.** — To a mixture of 20 cc. of glacial acetic acid and 10 cc. of acetic anhydride, 5 g. of heptaacetylphenyl-α-maltoside was added. A mixture of 25 g. of concentrated sulfuric acid (95%) and 25 g. of glacial acetic acid was added under cooling and stirring. Then to this solution, a mixture of 5 g. of nitric acid (sp. gr. 1.38) and 10 cc. of glacial acetic acid was added dropwise, while stirring vigorously. The mixture was kept for four hours at room temperature, and poured into a large amount of ice and water. Within a few minutes a powdery white precipitate was separated, collected, washed completely with water, and dried over anhydrous calcium chloride. The yield of the crude substance was 4.83 g. The crude crystals were recrystallized from absolute ethanol, and the yield of heptaacetyl-*p*-nitrophenyl-α-maltoside was 4.75 g., m. p. 176~178°C, $[\alpha]_D^{14.5}=+223°$ (*c* 1.2, in chloroform).

Found: C, 50.71; H, 5.21; N, 1.83. Calcd. for $C_{32}H_{39}O_{20}N$: C, 50.74; H, 5.19; N, 1.85%.

***p*-Nitrophenyl-α-maltoside.** — The heptaacetyl-*p*-nitrophenyl-α-maltoside was deacetylated by dissolving in absolute methanol (200~300 cc. for 25 g.) and adding a freshly prepared solution of sodium methoxide (from sodium, 10~20 mg., and methanol, 10 cc.). The mixture was kept at room temperature overnight. The methanol was then removed under reduced pressure, and the oily substance was dissolved in 10 cc. of ethanol. The solid was obtained by adding ether, and was then successively treated in the same manner as described above to give pure maltoside crystals which were crystallized to constant melting point using, when possible, a mixture of ethanol-dioxane containing 10% of dioxane. The crude crystals were combined and recrystallized from absolute ethanol/petroleum ether, m. p. 145~146°C, $[\alpha]_D^{14.5}=+265°$ (*c* 1.0, in water).

Found: C, 46.72; H, 5.40; N, 3.04. Calcd. for $C_{18}H_{25}O_{13}N$: C, 46.63; H, 5.44; N, 3.02%.

The ultraviolet absorption of the product showed maxima at 310 mμ in water.

**Other Substituted Heptaacetylphenyl-α-maltosides.** — The corresponding phenols (0.3~0.4 mol.) and octaacetylmaltose (0.1 mol.) were heated with fused zinc chloride (0.5~2.0 g.) under violent stirring at 110~115°C for 1.5 to 2 hr. The cooled oily product was diluted with water and extracted with

6) R. L. Nath and H. N. Rydon, *Biochem. J.*, **57**, 1 (1954).
7) S. Matsubara, *J. Biochem.*, **49**, 226 (1961).
8) S. Matsubara, ibid., **49**, 232 (1961).
9) S. Matsubara, T. Ikenaka and S. Akabori, ibid., **46**, 425 (1959).

benzene to remove zinc chloride. The benzene solution was washed with water, and then repeatedly with 5% aqueous sodium hydroxide until the washings were colorless. The solution was again washed with water and dried over anhydrous calcium chloride. The solvent was then evaporated under reduced pressure, leaving a dark yellowish brown oil. The oily residue was crystallized from suitable solvents to give colorless crystals. The crude crystals were recrystallized from one more suitable solvent.

**Other Substituted Phenyl-α-maltosides.** — The other substituted phenyl-α-maltoside was prepared by the same method as with phenyl-α-maltoside. The obtained crude product was recrystallized from suitable solvents.

***o*-Cresyl-α-maltoside.** — Recrystallized from ethanol/ether, m. p. 182~183°C, $[\alpha]_D^{14.5}=+218°$ (*c* 1.0, in water).

Found: C, 52.50; H, 6.45. Calcd. for $C_{19}H_{26}O_{11}$: C, 52.75; H, 6.53%.

The heptaacetyl derivative recrystallized from ethanol, m. p. 175~176°C $[\alpha]_D^{18}=+182°$ (*c* 1.5, in chloroform).

Found: C, 54.60; H, 5.89. Calcd. for $C_{33}H_{42}O_{18}$: C, 54.56; H, 5.83%.

***m*-Cresyl-α-maltoside.**—This was very hydroscopic and resisted all attempts at recrystallization; the product, dried at 100°C in vacuo over $P_2O_5$, had m. p. 93~98°C, $[\alpha]_D^{17}=+235°$ (*c* 0.5, in water).

Found: C, 51.95; H, 6.42. Calcd. for $C_{19}H_{28}O_{11}$: C, 52.75; H, 6.53%.

The heptaacetyl derivative recrystallized from ethanol, m. p. 135~140°C, $[\alpha]_D^{18}=+185°$ (*c* 1.5, in chloroform).

Found: C, 54.53; H, 5.84. Calcd. for $C_{33}H_{42}O_{18}$: C, 54.56; H, 5.83%.

***p*-Cresyl-α-maltoside.** — Recrystallized from ethanol/ether, m. p. 192~194°C, $[\alpha]_D^{18}=+204°$ (*c* 0.5, in water).

Found: C, 53.02; H, 6.49. Calcd. for $C_{19}H_{28}O_{11}$: C, 52.75; H, 6.53%.

The heptaacetyl derivative recrystallized from ethanol, m. p. 180~181°C, $[\alpha]_D^{18}=+201°$ (*c* 1.0, in chloroform).

Found: C, 54.55; H, 5.81. Calcd. for $C_{33}H_{42}O_{18}$: C, 54.56; H, 5.83%.

***o*-Isopropylphenyl-α-maltoside.** — Recrystallized from ethanol/petroleum ether, m. p. 163~165°C, $[\alpha]_D^{18}=+222°$ (*c* 1.0, in water).

Found: C, 54.57; H, 7.10. Calcd. for $C_{21}H_{32}O_{11}$: C, 54.75; H, 7.01%.

The heptaacetyl derivative recrystallized from ethanol/petroleum ether, m. p. 110~111°C, $[\alpha]_D^{18}=+205°$ (*c* 1.0, in chloroform).

Found: C, 55.67; H, 6.08. Calcd. for $C_{35}H_{46}O_{18}$: C, 55.71; H, 6.15%.

***p*-Isopropylphenyl-α-maltoside.** — Recrystallized from ethanol/petroleum ether, m. p. 175~176°C, $[\alpha]_D^{14.5}=+216°$ (*c* 1.0, in water).

Found: C, 54.71; H, 6.98. Calcd. for $C_{21}H_{32}O_{11}$: C, 54.75; H, 7.01%.

The heptaacetyl derivative recrystallized from ethanol/petroleum ether, m. p. 145~147°C, $[\alpha]_D^{14.5}=+192°$ (*c* 1.0, in chloroform).

Found: C, 55.61; H, 6.21. Calcd. for $C_{35}H_{46}O_{18}$: C, 55.71; H, 6.15%.

***o*-*tert*-Butylphenyl-α-maltoside.** — This was very hydroscopic and resisted all attempts at recrystallization; the product, dried at 100°C in vacuo over $P_2O_5$, had m. p. 60~65°C, $[\alpha]_D^{18}=+232°$ (*c* 0.5, in water).

Found: C, 54.89; H, 7.18. Calcd. for $C_{22}H_{36}O_{11}$: C, 55.66; H, 7.23%.

The heptaacetyl derivative recrystallized from ethanol/petroleum ether, m. p. 212~214°C, $[\alpha]_D^{18}=+202°$ (*c* 1.15, in chloroform).

Found: C, 56.26; H, 6.28. Calcd. for $C_{36}H_{48}O_{18}$: C, 56.22; H, 6.30%.

***p*-*tert*-Butylphenyl-α-maltoside.** — Recrystallized from ethanol, m. p. 170~172°C, $[\alpha]_D^{18}=+228°$ (*c* 0.62, in water).

Found: C, 55.61; H, 7.20. Calcd. for $C_{22}H_{34}O_{11}$: C, 55.66; H, 7.23%.

The heptaacetyl derivative recrystallized from ethanol/petroleum ether, m. p. 78~80°C, $[\alpha]_D^{18}=+211°$ (*c* 1.32, in chloroform).

Found: C, 56.21; H, 6.26. Calcd. for $C_{36}H_{48}O_{18}$: C, 56.22; H, 6.30%.

***p*-Isoamylphenyl-α-maltoside.** — Recrystallized from ethanol, m. p. 160~163°C, $[\alpha]_D^{18}=+242°$ (*c* 0.65, in water).

Found: C, 56.48; H, 7.47. Calcd. for $C_{23}H_{36}O_{11}$: C, 56.52; H, 7.43%.

The heptaacetyl derivative recrystallized from ethanol/petroleum ether, m. p. 185~187°C, $[\alpha]_D^{18}=+213°$ (*c* 1.2, in chloroform).

Found: C, 56.80; H, 6.44. Calcd. for $C_{37}H_{50}O_{18}$: C, 56.80: H, 6.44%.

***o*-Methoxyphenyl-α-maltoside.** — Recrystallized from ethanol, m. p. 165~166°C, $[\alpha]_D^{14.5}=+184°$ (*c* 0.1, in water).

Found: C, 50.78; H, 6.27. Calcd. for $C_{19}H_{28}O_{12}$: C, 50.87; H, 6.30%.

The heptaacetyl derivative recrystallized from ethanol, m. p. 140~141°C, $[\alpha]_D^{14.5}=+162°$ (*c* 0.1, in chloroform).

Found: C, 53.36; H, 5.65. Calcd. for $C_{33}H_{42}O_{19}$: C, 53.38; H, 5.70%.

***m*-Methoxyphenyl-α-maltoside.** — Recrystallized from ethanol, m. p. 172~175°C, $[\alpha]_D^{14.5}=+193°$ (*c* 0.95, in water).

Found: C, 50.79; H, 6.26. Calcd. for $C_{19}H_{28}O_{12}$: C, 50.87; H, 6.30%.

The heptaacetyl derivative recrystallized from ethanol, m. p. 163~165°C, $[\alpha]_D^{14.5}=+165°$ (*c* 0.95, in chloroform).

Found: C, 52.90; H, 5.59. Calcd. for $C_{33}H_{42}O_{19}$: C, 53.38; H, 5.70%.

***p*-Methoxyphenyl-α-maltoside.** — Recrystallized from ethanol, m. p. 187~189°C, $[\alpha]_D^{14.5}=+201°$ (*c* 0.85, in water).

Found: C, 50.80; H, 6.28. Calcd. for $C_{19}H_{28}O_{12}$: C, 50.87; H, 6.30%.

The heptaacetyl derivative recrystallized from ethanol, m. p. 206~208°C, $[\alpha]_D^{14.5}=+195°$ (*c* 3.1, in chloroform).

Found: C, 53.31; H, 5.78. Calcd. for $C_{33}H_{42}O_{19}$: C, 53.38; H, 5.70%.

***o*-Chlorophenyl-α-maltoside.**—Recrystallized from ethanol, m. p. 193~196°C, $[\alpha]_D^{18}=+165°$ (*c* 0.5, in water).

Found: C, 47.68; H, 5.60; Cl, 7.84. Calcd. for $C_{18}H_{25}O_{11}Cl$: C, 47.72; H, 5.57; Cl, 7.83%.

The heptaacetyl derivative recrystallized from ethanol/petroleum ether, m. p. 195~197°C, $[\alpha]_D^{18}$ = +154° (*c* 2.3, in chloroform).

Found: C, 51.38; H, 5.23; Cl, 4.68. Calcd. for $C_{32}H_{39}O_{18}Cl$: C, 51.44; H, 5.27; Cl, 4.75%.

***p*-Chlorophenyl-α-maltoside.**—Recrystallized from ethanol, m. p. 205~206°C, $[\alpha]_D^{19}$ = +213° (*c* 1.13, in water).

Found: C, 47.70; H, 5.59; Cl, 7.81. Calcd. for $C_{18}H_{25}O_{11}Cl$: C, 47.72; H, 5.57; Cl, 7.83%.

The heptaacetyl derivative recrystallized from ethanol/petroleum ether, m. p. 197~199°C, $[\alpha]_D^{19}$ = +177° (*c* 1.5, in chloroform).

Found: C, 51.43; H, 5.25; Cl, 4.75. Calcd. for $C_{32}H_{39}O_{18}Cl$: C, 51.44; H, 5.27; Cl, 4.75%.

***o*-Nitrophenyl-α-maltoside.** — Recrystallized from ethanol/ether, m. p. 153~155°C, $[\alpha]_D^{14.5}$ = +245° (*c* 1.2, in water).

Found: C, 46.75; H, 5.48; N, 2.95. Calcd. for $C_{18}H_{25}O_{13}N$: C, 46.63; H, 5.44; N, 3.02%.

The heptaacetyl derivative recrystallized from ethanol, m. p. 185~187°C, $[\alpha]_D^{14.5}$ = +222° (*c* 1.5, in chloroform).

Found: C, 50.68; H, 5.15; N, 1.84. Calcd. for $C_{32}H_{39}O_{20}N$: C, 50.74; H, 5.19; N, 1.85%.

***m*-Nitrophenyl-α-maltoside.**—Recrystallized from ethanol/petroleum ether, m. p. 132~136°C, $[\alpha]_D^{14.5}$ = +261° (*c* 2.1, in water).

Found: C, 46.78; H, 5.39; N, 2.95. Calcd. for $C_{18}H_{25}O_{13}N$: C, 46.63; H, 5.44; N, 3.02%.

The heptaacetyl derivative recrystallized from ethanol, m. p. 170~171°C, $[\alpha]_D^{14.5}$ = +234° (*c* 1.8, in chloroform).

Found: C, 50.65; H, 5.11; N, 1.87. Calcd. for $C_{32}H_{39}O_{20}N$: C, 50.74; H, 5.19; N, 1.85%.

**α-Naphthyl-, cyclohexyl- and *o*-, *m*-, *p*-Nitrophenyl-α-maltosides.** — The mixture of α-naphthol, cyclohexanol, *o*-, *m*-, or *p*-nitrophenol (0.3~0.4 mol.) and octaacetyl-β-maltose (0.1 mol.) were heated with fused zinc chloride (0.5~2.0 g.) and titanic chloride[10] (10 g.) under violent stirring at 110~115°C for 1.5 to 2 hr. by the same method as that described above.

**α-Naphthyl - α - maltoside.** — Recrystallized from ethanol/ether, m. p. 156~158°C, $[\alpha]_D^{16}$ = +192° (*c* 1.5, in water).

Found: C, 56.41; H, 6.07. Calcd. for $C_{22}H_{28}O_{11}$: C, 56.39; H, 6.03%.

The heptaacetyl derivative recrystallized from ethanol/ether, m. p. 192~194°C, $[\alpha]_D^{16}$ = +185° (*c* 1.5, in chloroform).

Found: C, 56.71; H, 5.53. Calcd. for $C_{36}H_{42}O_{18}$: C, 56.67; H, 5.56%.

**Cyclohexyl - α - maltoside.** — Recrystallized from ethanol/ether, m. p. 112~115°C, $[\alpha]_D^{16}$ = +211° (*c* 1.5, in water).

Found: C, 50.85; H, 7.63. Calcd. for $C_{18}H_{32}O_{11}$: C, 50.91; H, 7.60%.

The heptaacetyl derivative recrystallized from ethanol, m. p. 152~155°C, $[\alpha]_D^{16}$ = +202° (*c* 1.5, in chloroform).

Found: C, 53.42; H, 6.50. Calcd. for $C_{32}H_{46}O_{18}$: C, 53.46; H, 6.46%.

**Alkyl-α-maltosides.**—Alkyl-α-maltosides could be prepared by warming maltose with an alcoholic solution of hydrochloric acid. Dry hydrogen chloride was passed into 200 g. of absolute alcohol, with ice cooling and exclusion of moisture, until the increase in weight amounted to 10 g. This solution 20 cc. was then diluted with 980 g. of alcohol, a 0.1% solution of hydrogen chloride being thus obtained. To this solution 50 g. of finely powdered anhydrous maltose was added, and the mixture was warmed at 50°C for forty-two hours, a clear solution being obtained after the first fifteen minutes' warming. It was well to attach a soda-lime tube to the upper end of the condenser, in order to exclude moisture. The clear pale yellow solution was cooled to 0°C, and crystallization was induced by scratching. After standing for two days at 0°C, the first crop was filtered by suction and was washed twice with 100 cc. portions of cold alcohol. The mother liquor and washings were returned to the flask and again warmed for forty-two hours under reflux at 50°C. The liquid was concentrated to 800 cc. and again chilled to 0°C, incubated and allowed to stand at 0°C for two days. The second crop of maltoside so obtained was filtered by suction and washed three times with each 100 cc. portion of cold alcohol. The mother liquor and washings were combined and concentrated to about 300 cc., chilled to 0°C, and again incubated and allowed to stand for two days. The resulting mush of crystals was dissolved in twice its weight of absolute ethanol, and, after standing for two days at 0°C, the third crop of maltoside was filtered. This was recrystallized from 2.5 parts of ethanol. The product was contaminated by slight traces of maltose and possessed a very faint reducing power towards Fehling's solution. For complete purification it was recrystallized (practically with neither loss nor change in melting point) from five parts of absolute ethanol with the use, if necessary, of decolorizing carbon.

**Methyl-α-maltoside.**—Recrystallized from ethanol, m. p. 201~202°C, $[\alpha]_D^{16}$ = +183° (*c* 1.0, in water).

Found: C, 43.77; H, 6.75. Calcd. for $C_{13}H_{24}O_{11}$: C, 43.80; H, 6.79%.

**Isopropyl - α - maltoside.** — Recrystallized from ethanol, m. p. 177~179°C, $[\alpha]_D^{16}$ = +166° (*c* 1.0, in water).

Found: C, 46.81; H, 7.32. Calcd. for $C_{15}H_{28}O_{11}$: C, 46.85; H, 7.35%.

***tert* - Butyl - α - maltoside.** — Recrystallized from ethanol, m. p. 188~190°C, $[\alpha]_D^{16}$ = +153° (*c* 1.0, in water).

Found: C, 48.18; H, 7.62. Calcd. for $C_{16}H_{30}O_{11}$: C, 48.21; H, 7.59%.

**Isoamyl-α-maltoside.** — Recrystallized from ethanol, m. p. 152~155°C, $[\alpha]_D^{16}$ = +143° (*c* 1.5, in water).

Found: C, 49.52; H, 7.80. Calcd. for $C_{17}H_{32}O_{11}$: C, 49.48; H, 7.82%.

## Summary

Substituted phenyl-, α-naphthyl-, and cyclohexyl-α-maltosides were prepared from octaacetyl-β-maltose and the corresponding phenols. *p*-Nitrophenyl-α-maltoside was also prepared by

10) A. P. Jansen and P. G. A. B. Wydeveld, *Nature*, **182**, 525 (1958).

another method from the nitration of hepta-acetylphenyl-$\alpha$-maltoside. Alkyl-$\alpha$-maltosides were prepared from maltose and corresponding alcohol.

The authors wishes to express his gratitude to Professor Shiro Akabori (Institute for Protein Research, Osaka University) for his helpful advice throughout this work.

*Department of Chemistry*
*Faculty of Science*
*Osaka University*
*Nakanoshima, Osaka*

# *Absorption Spectra of Nitrobenzene Derivatives. II. Effect of Solvent on Intramolecular Charge Transfer Spectra of Nitrobenzene Derivatives*

By Kimio SEMBA*

(Received September 7, 1960)

In a previous paper[1] intramolecular charge transfer spectra of nitrobenzene derivatives were studied from the viewpoint of Nagakura and Tanaka's theory[2]. These absorption spectra are strongly influenced by solvents and shift toward longer wavelengths for solvents of higher dielectric constant.

Several papers treating of the effect of solvent on the electronic spectra of organic compounds have been published[3]. Recently, Bayliss and McRae[4] discussed the effects in terms of the dipole-, polarization-, and hydrogen bonding forces between solute and solvent molecules. It is not always easy to interpret the solvent effects correctly because these often arise from the resultant of several individual effects reinforcing as well as cancelling each other. It seems certain that hydrogen bonding plays a very important role in the frequency shift, while effects from other origins are no less important, since frequency shifts are observed even in systems containing no hydrogen bonds.

In this paper the role of the electrostatic interaction between solute and solvent molecules in the intramolecular charge transfer spectra of *o*-, *m*- and *p*-nitrophenol, -nitroanisole, -nitroaniline and -nitron-*N*-dimethylaniline was examined on the basis of the general expression proposed by McRae[5] for the solvent effect on absorption spectra. The contribution of hydrogen bonding between solute and solvent molecules was also taken into consideration for some cases.

## Experimental

Absorption spectra in the wavelength region 250~400 m$\mu$ were obtained by a Hitachi automatic recording spectrophotometer, type EPS-2. Fused quartz cells of 1 cm. path length were used.

Samples of nitrobenzene derivatives were the same ones used in a previous work[1]. Solvents, *n*-hexane, dioxane, cyclohexane, carbon tetrachloride, toluene, benzene, ethyl ether, nitromethane, acetonitrile, methanol, and ethanol, were purified by the method recommended by Weissberger and Proskauer[6], special care having been taken to remove contaminating water.

## Result and Discussion

**Theoretical Expression for the Solvent Effect.** —In current discussions of the solvent effects on electronic absorption spectra the frequency shifts are mainly attributed to dipole, polarization and hydrogen bonding effects. The general formula* derived from the perturbation theory by McRae[5] for solvent-induced spectral shifts can be simplified for the discussion of present results in the following form[7]

* Present address: Research Laboratory, Kurosaki Firebrick Mfg. Co., Ltd., Fujita, Yawata.

1) K. Semba, This Bulletin, **33**, 1640 (1960).

2) S. Nagakura and J. Tanaka, *J. Chem. Phys.*, **22**, 236 (1954); S. Nagakura, ibid., **23**, 1441 (1955).

3) For example: N. D. Coggeshell and E. M. Lang, *J. Am. Chem. Soc.*, **70**, 3282 (1948); M. Kasha, *Discussions Faraday Soc.*, **9**, 14 (1950); H. McConnell, *J. Chem. Phys.*, **20**, 700 (1952); S. Nagakura and H. Baba, *J. Am. Chem. Soc.*, **74**, 5693 (1952).

4) N. Bayliss and E. G. McRae, *J. Phys. Chem.*, **58**, 1002, 1006 (1954).

5) E. G. McRae, ibid., **61**, 562 (1957).

6) A. Weissberger and E. S. Proskauer, "Organic Solvent", Interscience Publishers, Inc., New York (1955).

* Y. Ooshika has also given a similar formula: *J. Phys, Soc. Japan*, **9**, 542 (1954).

7) M. Ito, K. Inuzuka and S. Imanishi, *J. Am. Chem. Soc.*, **82**, 1317 (1960).

$$\Delta\nu = \text{dispersion term} + B\left[\frac{n_D^2-1}{2n_D^2+1}\right] + C\left[\frac{D-1}{D+2}-\frac{n_D^2-1}{n_D^2+2}\right] + E\left[\frac{D-1}{D+2}-\frac{n_D^2-1}{n_D^2+2}\right]^2 \quad (1)$$

where $B$, $C$ and $E$ are constants characteristic of the solute molecule,

$$B=\frac{1}{hc}\frac{(\mathbf{M}_{oo}^u)-(\mathbf{M}_{ii}^u)^2}{a^3} \quad (2)$$

$$C=\frac{2}{hc}\frac{(\mathbf{M}_{oo}^u)\,(\mathbf{M}_{oo}^u-\mathbf{M}_{ii}^u)}{a^3} \quad (3)$$

$$E=\frac{6}{hc}\frac{(\mathbf{M}_{oo}^u)\,(\alpha_o^u-\alpha_i^u)}{a^6} \quad (4)$$

$\mathbf{M}_{oo}^u$ and $\mathbf{M}_{ii}^u$ represent the vector dipole moments of the solute molecule in its electronic ground and excited states, respectively, and $a$ is Onsagar's reaction radius of the solute molecule. For the meaning of the various other quantities appearing in these equations McRae's original paper[5] is referred to.

**Effect of Electrostatic Interactions.**—Absorption maxima ($\nu_{max}$) of *o*-, *m*- and *p*-nitrobenzene derivatives in various solvents are given in Table I, in which refractive indices and dielectric constants are also given. The *p*-derivative shows only one absorption band which is in the near ultraviolet region due to the intramolecular charge transfer transition. On the other hand, the *o*- and *m*-derivatives show two intramolecular charge transfer bands due to the transitions $H_{x1}\rightarrow V_s$ and $H_{x2}\rightarrow V_s$, as observed in a previous paper[1]. The bands of *o*- and *m*-derivatives at shorter wavelengths in both toluene and benzene solutions can not be observed, because they are covered by solvent absorption bands, hence only the longer-wavelength bands due to the $H_{x1}\rightarrow V_s$ transition are considered.

We shall first consider the effect of non-polar solvents, *n*-hexane, dioxane, carbon tetrachloride, toluene and benzene, in the order of increasing refractive index. It is seen from the table that $\nu_{max}$ decreases with the increase in the refractive index of the solvent, with the exception of dioxane. Plots of $\nu_{max}$ against $(n_D^2-1)/(2n_D^2+1)$ for these derivatives are shown in Figs. 1—3. For each of these molecules the points for various solvents are approximately on a straight line, with the exception of the point for dioxane.

For non-polar solvents the third and the fourth terms in Eq. 1 may be neglected since $n_D^2 \approx D$, and only the first and the second terms have to be considered. Then, if the first term is much smaller than the second,

Table I. Absorption maxima of *o*-, *m*- and *p*-nitrobenzene derivatives in various solvents ($cm^{-1}$)

| Solvent | $n_D$ | $D$ | *o*-Nitrophenol | *o*-Nitroanisole | *o*-Nitroaniline | *m*-Nitrophenol | *m*-Nitroanisole |
|---|---|---|---|---|---|---|---|
| *n*-Hexane | 1.375 | 1.890 | 36400<br>28810 | 39800<br>32510 | 37160<br>26870 | 37850<br>32040 | 38200<br>31200 |
| Dioxane | 1.422 | 2.209 | 36420<br>28560 | 38690<br>31240 | 36160<br>25020 | 37090<br>30390 | 37160<br>30620 |
| Cyclohexane | 1.426 | 2.023 | 36700<br>28650 | 39670<br>32350 | 36390<br>26270 | 38160<br>31440 | 38080<br>31440 |
| Carbon tetrachloride | 1.460 | 2.238 | 36410<br>28420 | —<br>31740 | 36750<br>25900 | 38010<br>31440 | 37560<br>30900 |
| Toluene | 1.497 | 2.379 | —<br>28120 | —<br>31290 | —<br>25310 | —<br>30390 | —<br>30390 |
| Benzene | 1.501 | 2.284 | —<br>28040 | —<br>31100 | —<br>25310 | —<br>30690 | —<br>30370 |

| Solvent | *m*-Nitroaniline | *m*-Nitro-*N*-dimethylaniline | *p*-Nitrophenol | *p*-Nitroanisole | *p*-Nitroaniline | *p*-Nitro-*N*-dimethylaniline |
|---|---|---|---|---|---|---|
| *n*-Hexane | 38450*<br>29060 | 40310<br>26120 | —<br>35200 | —<br>34120 | —<br>31240 | —<br>28730 |
| Dioxane | 35700*<br>26800 | 40020<br>24840 | —<br>32780 | —<br>32720 | —<br>28080 | —<br>26140 |
| Cyclohexane | 37030*<br>28730 | 40180<br>26030 | —<br>35020 | —<br>22890 | —<br>30840 | —<br>28160 |
| Carbon tetrachloride | 36620<br>28240 | —<br>25440 | —<br>34060 | —<br>33380 | —<br>30040 | —<br>27430 |
| Toluene | —<br>27370 | —<br>24810 | —<br>33210 | —<br>32720 | —<br>28940 | —<br>26170 |
| Benzene | —<br>27390 | —<br>24560 | —<br>33100 | —<br>32560 | —<br>28890 | —<br>26030 |

* Absorption shoulder

or if the first term is nearly the equal of these solvents, an approximately linear relation between $\nu_{max}$ and $(n_D^2-1)/(2n_D^2+1)$ should hold. Although the frequency shift of absorption caused by non-polar solvents results from the effects of both the first and the second terms in Eq. 1, the second term mainly determines the amount of the shifts, if the first term is small.

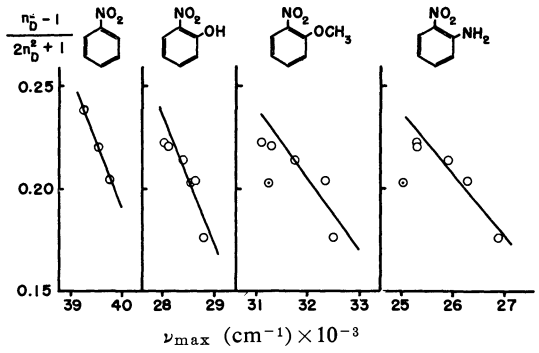



Fig. 1. Relation between $\frac{n_D^2-1}{2n_D^2+1}$ and $\nu_{max}$ (longer-wavelength bands) for nitrobenzene and *o*-nitrobenzene derivatives. (⊙: dioxane, the value $n_D$ for nitrobenzene was used for 250 m$\mu$)

For these nitrobenzene derivatives *B* in Eq. 2 is negative, indicating that $(\mathbf{M}_{oo}^{u})^2$ is smaller than $(\mathbf{M}_{ii}^{u})^2$, or that the dipole moment values of these derivatives increase in their electronically excited states reached by the absorption transition. The values of *B* can be evaluated from slopes of the straight lines as apparent in Figs. 1—3 and Table II. The *B* value for nitrobenzene is evaluated from the data of Bayliss and McRae[4] obtained for *n*-heptane, cyclohexane and carbon tetrachloride. For *p*-nitrobenzene derivatives the *B* values decrease with the increasing permanent dipole moments of the solute molecules, but for *o*- and *m*-derivatives these relations are not clearly observed. Spectral shifts are also much greater in nitrobenzene derivatives than nitrobenzene.

The present case of a polar solute dissolved in a non-polar solvent corresponds to the case

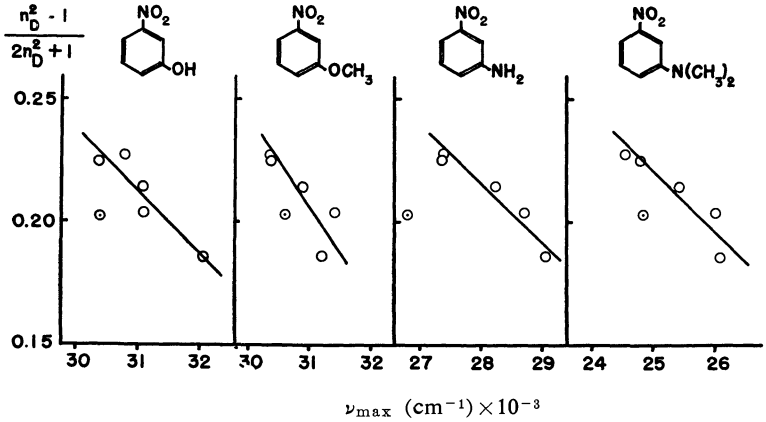



Fig. 2. Ralation between $\frac{n_D^2-1}{2n_D^2+1}$ and $\nu_{max}$ (longer-wavelength bands) for *m*-nitrobenzene derivatives. (⊙: dioxane)

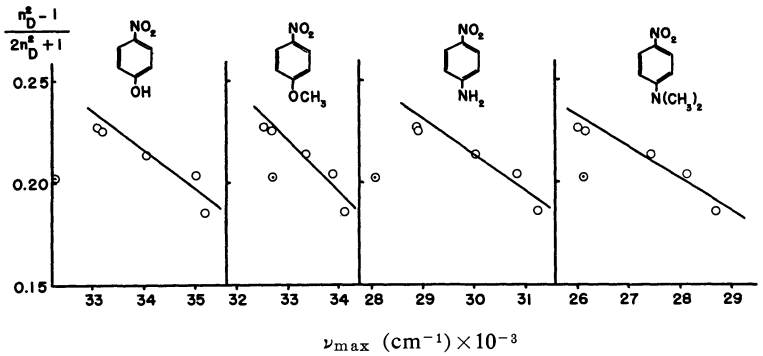



Fig. 3. Relation between $\frac{n_D^2-1}{2n_D^2+1}$ and $\nu_{max}$ for *p*-nitrobenzene derivatives. (⊙: dioxane)

TABLE II. EVALUATION OF $B$ VALUES ($cm^{-1}$)

| Molecule | $B$ | Ground state dipole moment* (Debye units) |
|---|---|---|
| Nitrobenzene | −32000** | 3.82~4.00 |
| *o*-Nitrophenol | −16000 | 4.10 |
| *o*-Nitroanisole | −30000 | 4.83 |
| *o*-Nitroaniline | −34000 | 4.26 |
| *m*-Nitrophenol | −40000 | 3.90 |
| *m*-Nitroanisole | −26000 | 3.86 |
| *m*-Nitroaniline | −40000 | 4.72 |
| *m*-Nitro-*N*-dimethylaniline | −40000 | 5.06 |
| *p*-Nitrophenol | −52000 | 5.05 |
| *p*-Nitroanisole | −40000 | 4.75 |
| *p*-Nitroaniline | −58000 | 6.32 |
| *p*-Nitro-*N*-dimethylaniline | −64000 | 6.87 |

* See Ref. 10.
** Evaluated from Bayliss and MaRae's data[4].

III b of Bayliss and McRae's paper[4], in which the solute dipole moment increases during the transition. According to their theory, the forces contributing to the solvation energy are dispersion and dipole-polarization forces (polarization of solvent molecules by the solute dipoles) and the latter is probably greater than the former. When the solute dipole moment increases as the result of the transition, the solvation energy becomes greater in the excited state than in the ground state, and hence absorption maxima are shifted to the red.

It is well known that dioxane behaves differently from other solvents and it can not be regarded as a non-polar solvent here[5,7,8]. Nitrophenol and nitroaniline probably from hydrogen bonds with dioxane and in these systems red shifts due to the hydrogen bonding effect may be expected. However, the anomalous shifts are also observed for nitroanisole and nitro-*N*-dimethylaniline in dioxane solutions, where no hydrogen bonding between solute and solvent molecules can be expected.

Absorption frequency shifts $\Delta\nu_{max}$ due to non-hydrogen bonding polar solvents can be simply expressed in a following form[7]

$$\nu_a-\nu_b=C\left[\frac{D_a-1}{D_a+2}-\frac{D_b-1}{D_b+2}\right]+E\left[\frac{D_a-1}{D_a+2}-\frac{D_b-1}{D_b+2}\right]^2 \quad (5)$$

where $\nu_a$ and $\nu_b$ are the $\nu_{max}$'s of the solutions in solvents a and b, and $D_a$ and $D_b$ are their respective dielectric constant values. To check this relation we chose ethyl ether with $n_D$= 1.356 and acetonitrile with $n_D$=1.344 for a and b. Their refractive indices are about the same. Moreover, the absorption spectra of these solvents are similar to each other in the point that they have no strong absorption above 200 m$\mu$, and the dispersion-term contributions from them are expected to be nearly equal[5]. On the other hand, the two solvents have quite different values of dielectric constant, 4.34 for ethyl ether and 37.50 for acetonitrile. Also ethyl ether and nitromethane ($n_D$=1.382, $D$=35.87) were used as solvents for *p*-nitro-*N*-dimethylaniline.

Absorption maxima of nitrobenzene, *o*-, *m*- and *p*-nitroanisole and *m*- and *p*-nitro-*N*-dimethylaniline were measured in solvents consisting of ethyl ether and acetonitrile mixed in various proportions*, in which no hydrogen bonding is expected to arise. The results are shown in Figs. 4—9, where for each solute molecule $\Delta\nu_{max}$ for ethyl ether and for the mixed solvents are plotted againt $(D-1)/(D+2)$ of the solvents.

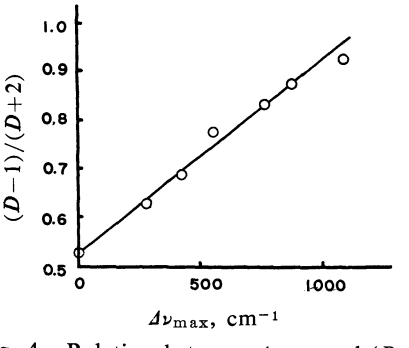



Fig. 4. Relation between $\Delta\nu_{max}$ and $(D-1)/(D+2)$ for nitrobenzene.

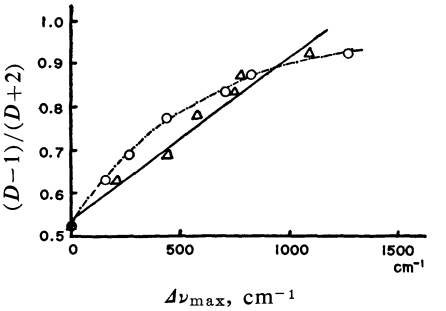



Fig. 5. Relation between $\Delta\nu_{max}$ and $(D-1)/(D+2)$ for *o*-nitroanisole. (○: $H_{x1}\rightarrow V_s$ transiton; △: $H_{x2}\rightarrow V_s$ transition)

* The dielectric constant of a mixed solvent was calculated according to Hoigne and Gaumann[9] by $D=D_0+bW$, where $D_0$ is the value of dielectric constant of ethyl ether, $b$ the difference of dielectric constant values of ethyl ether and acetonitrile, and $W$ the weight fraction of acetonitrile in the solution.

8) E. Lippert, *Z. Naturforsch.*, **10a**, 541 (1955).

9) J. Hoigne and T. Gaumann, *Helv. Chim. Acta*, **41**, 1933 (1958).

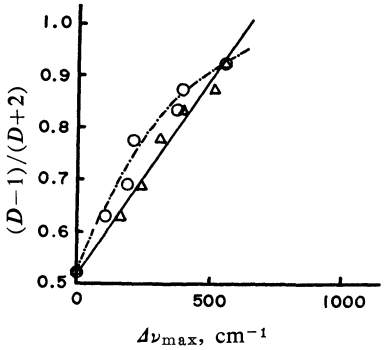



Fig. 6. Relation between $\Delta\nu_{max}$ and $(D-1)/(D+2)$ for *m*-nitroanisole. (○ : $H_{x1}\rightarrow V_s$ transition ; △ : $H_{x2}\rightarrow V_s$ transition)

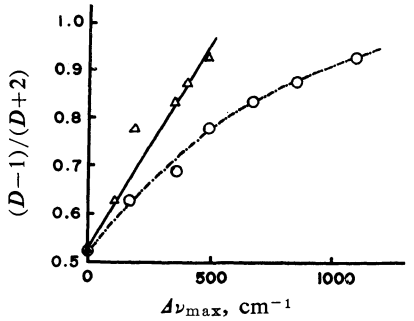



Fig. 7. Relation between $\Delta\nu_{max}$ and $(D-1)/(D+2)$ for *m*-nitro-*N*-dimethylaniline. (○ : $H_{x1}\rightarrow V_s$ transition ; △ : $H_{x2}\rightarrow V_s$ transition)

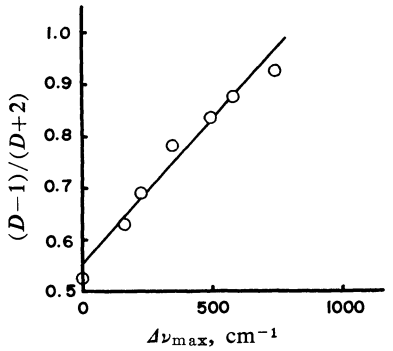



Fig. 8. Relation between $\Delta\nu_{max}$ and $(D-1)/(D+2)$ for *p*-nitroanisole.

For the shorter-wavelength bands of *o*- and *m*-nitrobenzene derivatives which arise from the $H_{x2}\rightarrow V_s$ transition, and also for the intramolecular charge transfer bands of nitrobenzene and *p*-nitrobenzene derivatives, the linear relation holds approximately. However, for all of the longer-wavelength bands of *o*- and *m*-nitrobenzene derivatives arising from $H_{x1}\rightarrow V_s$ transition the plots show obvious curvatures.

These facts indicate that while for the shorter-wavelength bands the shifts are determined only

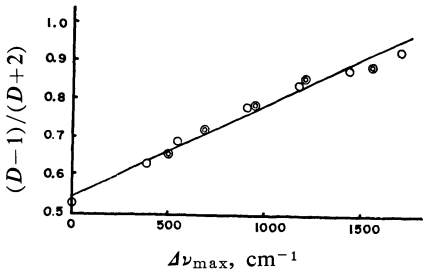



Fig. 9. Relation between $\Delta\nu_{max}$ and $(D-1)/(D+2)$ for *p*-nitro-*N*-dimethylaniline. (○ : in ethyl ether and acetonitrile ; ◎ : in ethyl ether and nitromethane)

by the first term in Eq. 5, for the longer-wavelength bands both the first and the second terms would be responsible. In other words, only the interaction between the permanent dipoles of solute and solvent molecules essentially contribute to the spectral shift for the first case, but for the latter case the interaction between the dipole of the solvent molecules and that induced in the solute molecule also makes possibly an important contribution to the shift.

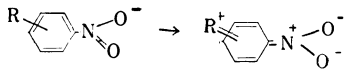
The values of $C$ in Eq. 5 are easily obtained from the slopes of the straight lines for the shorter-wavelength bands, from which we may calculate* the excited state dipole moment $\mathbf{M}_{11}^{u}$, if the values of $a$ are known. Similarly, for the longer-wavelength bands $\mathbf{M}_{11}^{u}$ as well as he polarizability differerence $(\alpha_0^{u}-\alpha_1^{u})$ of the solute in its ground and excited states may be estimated from $C$ and $E$ values.

The polarization effect on the spectral shift is apparent only in the $H_{x1}\rightarrow V_s$ transitions of *o*- and *m*-nitrobenzene derivatives. It could not be observed in all other absorption bands investigated. In all cases $C$ and $E$ in Eq. 5 are negative, showing that dipole moment and polarizability are greater in the excited state than in the ground state. This indicates that the stabilization energies arising from the electrostatic interactions between the solute and solvent molecules are much greater in the excited state than in the ground state. Thus, the main factor causing the red shift of these absorption band in polar solvents is the great stabilization in the excited state owing to the electrostatic interaction between the solute and solvent molecules. On the other hand, from the consideration of the obviously important resonance forms of these molecules

* For example, if we assume that $a$ is 4Å for *p*-nitroanisole, the excited state dipole moment $\mathbf{M}_{11}^{u}$ can be calculated to be 6.89 D. As its ground state dipole moment is 4.78 D[10], the dipole moment increases by 2.11 D in the excited state.

10) L. G. Wesson, "Tables of Electric Dipole Moments", The Technology Press, M. I. T. (1948).

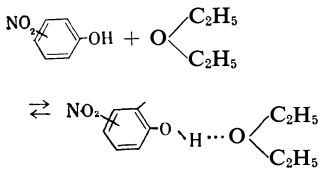
shown below, the optical absorption may well be accompanied by the excitation of the molecule according to the scheme



which would contribute largely to the moment of the excited state.

**Effect of Hydrogen Bonding.**—The hydrogen bonding plays a very important role in the spectral shift of a solution. The hydrogen bonding effect on the absorption spectra of *m*- and *p*-nitrophenol was observed in mixed solvents consisting of *n*-hexane and ethyl ether.

Figs. 10 and 11 show that the absorption maxima are shifted toward the red with an increasing proportion of ethyl ether in the solvent. In each case an isosbestic point is observed. The following hydrogen bonding reaction may be suggested



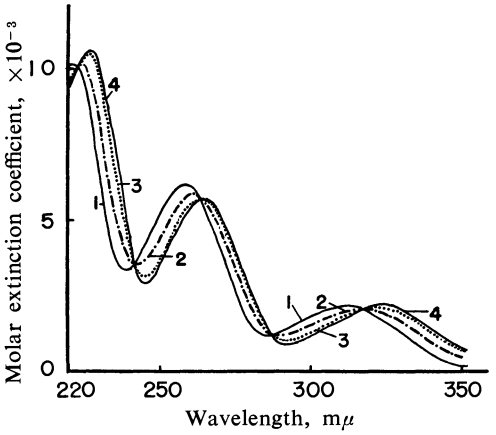



Fig. 10. Absorption curves of *m*-nitrophenol ($7.63\times10^{-5}$ mol./l.) in *n*-hexane solution containing ethyl ether at 12°C.
curve 1: *n*-hexane solution (free *m*-nitrophenol)
curve 2: ethyl ether $3.91\times10^{-3}$ mol./l.
curve 3: ethyl ether $7.81\times10^{-3}$ mol./l.
curve 4: calculated curve for bound *m*-nitrophenol

* The equilibrium constant $K$ is calculated as

$$K=\frac{\varepsilon-\varepsilon_A}{\varepsilon'-\varepsilon}\cdot\frac{1}{C_B}-\frac{\varepsilon'-\varepsilon_A}{\varepsilon'-\varepsilon}\cdot\frac{1}{C_B'}$$

where $\varepsilon_A$ is the molar extinction coefficient of free *p*-nitrophenol (curve 1), $\varepsilon$ and $\varepsilon'$ are those of the mixed solvents for curves 2 and 3, and $C_B$ and $C_B'$ are the concentrations of ethyl ether corresponding to the curves 2 and 3.

** The free energy difference $\Delta F$ is calculated as $\Delta F=-RT\ln K$.

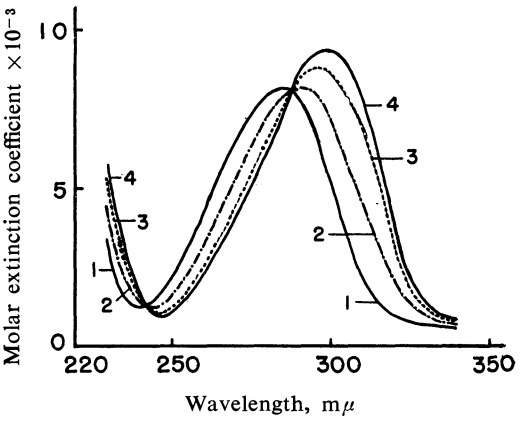



Fig. 11. Absorption curves of *p*-nitrophenol ($7.18\times10^{-5}$ mol./l.) in *n*-hexane solution containing ethyl ether at 20°C.
curve 1: *n*-hexane solution (free *p*-nitrophenol)
curve 2: ethyl ether $3.85\times10^{-2}$ mol./l.
curve 3: ethyl ether $1.93\times10^{-1}$ mol./l.
curve 4: calculated curve for bound *p*-nitrophenol

TABLE III. EQUILIBRIUM CONSTANTS AND FREE ENERGY DIFFERENCES FOR *m*- AND *p*-NITROPHENOL

| Molecule | Equilibrium constant | Free energy difference (kcal./mol.) |
|---|---|---|
| *m*-Nitrophenol | 113.1 | −2.6 (12°C) |
| *p*-Nitrophenol | 24.6 | −1.9 (20°C) |

From these curves the equilibrium constants* and the free energy differences** are obtained as given in Table III. The equilibrium constant for *m*-nitrophenol is much greater than that for *p*-nitrophenol, indicating that the former requires a very small amount of ethyl ether to reach equilibrium. This may be due to the meta-directing property of the nitro group[1].

For *m*- and *p*-nitroaniline no isosbestic point is clearly observed. This indicates that there is no simple equilibrium relation in the hydrogen bonding reaction. However, their absorption maxima are shifted toward the red with an increasing amount of ethyl ether in the solvents.

Next we shall consider the cases of *p*-nitroanisole and *p*-nitro-*N*-dimethylaniline dissolved in methanol and ethanol. In these systems hydrogen bonds may be expected to be formed between the nitro and the hydroxyl groups, the alcohol molecule playing the role of a proton donor according to the scheme

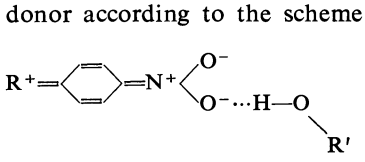


TABLE IV. CALCULATED BLUE-SHIFTS DUE TO $NO_2 \cdots H—O$ ($cm^{-1}$)

| Solvent (proton donor) | Nitro-benzene | *o*-Nitro-anisole | *m*-Nitro-anisole | *m*-Nitro-*N*-dimethyl-aniline | *p*-Nitro-anisole | *p*-Nitro-*N*-dimethyl-aniline |
|---|---|---|---|---|---|---|
| Methanol | — | 230 | 150 | 260 | — | — |
| | 130 | 290 | 200 | 330 | 150 | 370 |
| Ethanol | — | 320 | 220 | 250 | — | — |
| | 210 | 270 | 150 | 370 | 280 | 410 |

Absorption maxima of *p*-nitroanisole and *p*-nitro-*N*-dimethylaniline are at 32510 and 25540 $cm^{-1}$ in methanol and 32700 and 25700 $cm^{-1}$ in ethanol, respectively. The contribution of electrostatic interactions to the frequency shifts can be evaluated from Eq. 5 as the refractive indices of these alcohols are close to that of ethyl ether or acetonitrile. From the values of $C$ and the dielectric constant for alcohol solutions, the frequency shifts of *p*-nitroanisole relative to the ethyl ether solution can be evaluated as 960 $cm^{-1}$ and as 900 $cm^{-1}$, and the shifts of *p*-nitro-*N*-dimethylaniline as 1630 and 1520 $cm^{-1}$ for methanol and ethanol, respectively. The experimentally observed shifts for *p*-nitroanisole are 810 and 620 $cm^{-1}$, and for *p*-nitro-*N*-dimethylaniline 1260 and 1100 $cm^{-1}$, respectively, for methanol and ethanol. Thus the absorption maximum appears at a shorter wavelength than that expected from only the electrostatic origin in each case. The difference between experimentally observed and calculated frequency shifts may probably be accounted for on the basis of hydrogen bonding between the solute and alcohol molecules. Such differences are observed also for nitrobenzene, *o*- and *m*-nitroanisole, and *m*-nitro-*N*-dimethylaniline as shown in Table IV.

Baba[11] has shown that, if an alcohol molecule plays the role of the proton donor, a blue shift is expected in a $\pi \rightarrow \pi^*$ type transition. The present observed shifts are in good agreement with his theory. Shifts due to hydrogen bonding between the nitro and the hydroxyl groups are estimated as given in Table IV.

11) H. Baba, *Bull. Research Institute of Applied Electricity, Hokkaido University*, **9**, 84 (1957).

## Summary

Intramolecular charge transfer spectra of *o*-, *m*- and *p*-nitrobenzene derivatives were measured in solutions with various solvents. Frequency shifts induced by solvents were analyzed on the basis of current theories of solvent effects on absorption spectra. Results show that the frequency shifts in the absorption bands of nitrobenzene derivatives can be interpreted as arising from both the electrostatic and hydrogen bonding interactions.

The author wishes to thank Professor S. Imanishi and Dr. Y. Kanda of Kyushu University for their kind advice and encouragement throughout this investigations and to Dr. M. Ito for his helpful and valuable discussions. The author's thanks are also due to Drs. Y. Kora and T. Ikenoue of Kurosaki Firebrick Mfg. Co. for their kind encouragement.

*Department of Chemistry*
*Faculty of Science*
*Kyushu University*
*Hakozaki, Fukuoka*

# *Electronic and Vibrational States of Acrolein*

By Kōzō Inuzuka

(Received November 1, 1960)

Eastwood and Snow[1] carried out a vibrational and rotational analysis of the near ultraviolet spetrum of acrolein. Walsh[2] also studied the electronic spectrum of this compound in the vacuum ultraviolet region. Interest in this compound lies partly in the fact that it has a simple skeletal structure containing a system of conjugated double bonds, and that its electronic states can easily be discussed in terms of the MO theory[3]. In a previous paper[4] we studied the $n$-$\pi^*$ absorption bands of acrolein as measured with a photoelectric spectrometer. This time the absorption spectrum was measured photographically. In this paper is reported the results of our continued study on the electronic and vibrational states of the molecule. For aiding vibrational analysis, infrared and Raman spectra were also observed, although they have already been measured[5]. Using our new results, more detailed vibrational assignments for the excited state could be made.

## Experimental

Acrolein supplied by Tokyo Kasei Kogyo Co. was used. The sample was distilled before measurement. An absorption tube of 40 cm. length provided with quartz windows was used. The spectrum was photographed at various vapor pressures corresponding to temperatures between $-25$ and 180°C of the tube. The tube with the windows was always kept at temperature about 10°C higher than that of the sample site for purpose of avoiding condensation. A hydrogen or a tungsten lamp was used as the source of the continuum. A Shimadzu type QL-170 spectrograph was used throughout the work. Exposure time from 1 to 20 min. for the tungsten lamp and from 2 to 3 hr. for the hydrogen lamp with a slit width of 20 $\mu$. Fuji process plates were used. Wavelengths were determinined relative to those of iron lines, using a Shimadzu type SR-2 comparator.

For infrared and Raman measurements carbon tetrachloride or ethyl alcohol solution was used. Solvents were purified by Weissberger and Proskauer methods[6]. The Raman spectrograph used was of two dense flint prisms, having the linear dispersion of 24 Å/mm. at 4500 Å. Raman spectrum of acrolein was obtained with ethyl alcohol solution, as acrolein is very unstable chemically under strong irradiation and it was difficult to work with the liquid state. Renewing the sample at about one hour intervals a 12 hr. exposure was made with a slit width of 100 $\mu$. During the exposure filter solution of sodium nitrous oxide was circulated. The infrared absorption was measured with a Hitachi EPI double beam spectrometer with sodium chloride or potassium bromide prism. For acrolein vapor in the sodium chloride region a 10 cm. gas cell was used.

## Electronic Transition

Acrolein is a simple aliphatic aldehyde having a system of conjugated double bonds. Electron diffraction study[7] shows that the molecule has a planar *trans*-butadiene-like structure. The molecule thus belongs to the point group Cs and the electronic transitions are all symmetry-allowed. The molecule has four $\pi$-electrons and a pair of nonbonding electrons localized on the oxygen atom. Therefore $n$-$\pi^*$ and $\pi$-$\pi^*$ transitions are expected to occur. The absorption spectrum of acrolein solution in carbon tetrachloride in the 24993$\sim$ 33324 $cm^{-1}$ region shows a blue shift on addition of ethanol. In ethanol solution the acrolein absorption maximum shifts toward the blue by 400 $cm^{-1}$ relative to carbon tetrachloride solution[4]. The above result suggests the $n$-$\pi^*$ nature of this electronic transition. Walsh attributed this transition to a one-electon promotion from the n orbital to the first excited $\pi$ orbital. His assignment agrees with our calculation[3].

According to the MO theory this first excited state has A′ symmetry, and the lowest state is triplet. Consequently, the vapor absorption begining at 25851 $cm^{-1}$ is assigned to the transition of a nonbonding electron to the first excited singlet state ($^1A'' - {}^1A'$).

## Vibrational Analysis

On account of the low Cs symmetry of the molecule, the transition can be of an allowed type. So the 0, 0 band will probably be one

1) E. Eastwood and C. P. Snow, *Proc. Roy. Soc.*, **149A**, 446 (1935).
2) A. D. Walsh, *Trans. Faraday Soc.*, **41**, 498 (1945).
3) K. Inuzuka, This Bulletin, **34**, 6 (1961).
4) K. Inuzuka, ibid., **33**, 678 (1960).
5) M. Aime Cotton, *Compt. rend.*, **208**, 740 (1939).
6) A. Weissberger and E. S. Proskauer, "Organic Solvents", Interscience Publishers, Inc., New York, N. Y. (1955).
7) H. Mackle and L. E. Sutton, *Trans. Faraday Soc.*, **47**, 691 (1951).

of the stronger bands. The development of the spectrum with increasing temperature suggests that the 0, 0 band is surely the strong band at 25851 $cm^{-1}$. In an earlier work of Eastwood and Snow a band at 25860 $cm^{-1}$ was chosen as the 0, 0 band from rotational analysis, and two progressions of bands with mean separations of 1260 and 500 $cm^{-1}$ respectively were observed. Since our measurement was limited to about 30294 $cm^{-1}$, the progression corresponding to 1260 $cm^{-1}$ could not be followed further than the second overtone. These bands are accompanied each by a strong subsidary band with the separation of 499 $cm^{-1}$. In our analysis 1270 $cm^{-1}$ was taken as the interval of the progression. Among the observed bands, nearly 130 in number, some show rotational structures but many are not well defined. It is difficult to interpret correctly all of these observed bands on account of the low symmetry of the molecule, so we give in Table I the position and interpretations only

Table I. Vibrational analysis of ultraviolet absorption spectrum of acrolein vapor

| In. | Å | $cm^{-1}$ | Freq. distance from the 0, 0 band | Assignment |
|---|---|---|---|---|
| vs | 3867.2 | 25851 | 0 | 0, 0 |
| vs | 3794.0 | 26350 | 499 | 0+499 |
| m | 3705.7 | 26978 | 1127 | 0+1127 |
| vs | 3686.2 | 27121 | 1270 | 0+1270 |
| vs | 3666.6 | 27265 | 1414 | 0+1414 |
| bm | 3638.5 | 27476 | 1625 | 499+1127=1626 |
| s | 3620.0 | 27616 | 1765 | 1270+499=1769 |
| bs | 3601.6 | 27758 | 1907 | 499+1414=1913 |
| m | 3538.3 | 28254 | 2403 | 1270+1127=2397 |
| s | 3521.3 | 28391 | 2540 | 2(1270) |
| bm | 3502.2 | 28545 | 2694 | 1270+1414=2684 |
| m | 3484.1 | 28693 | 2842 | 2(1414) |
| m | 3461.6 | 28880 | 3029 | 2(1270)+499=3039 |
| w | 3387.4 | 29513 | 3662 | 2(1270)+1127=3667 |
| w | 3369.0 | 29674 | 3823 | 3(1270) |
| w | 3354.1 | 29806 | 3955 | 2(1270)+1414=3954 |
| w | 3324.5 | 30071 | 4220 | 3(1414) |

vs : very strong, s : strong, bm : broad medium, m : medium, w : weak

for stronger bands. The frequencies of 1270 and 499 $cm^{-1}$ are assigned definitely to two totally symmetric vibrations of type A′ of the lower electronic state. The very weak bands on the longer wavelength side of the 0, 0 band decrease their intensity with decreasing temperature, and the vicinity of 70°C is favorable for their observation. The number of moderately strong bands is small on this side of the 0, 0 band. A sharp band is separated from the 0, 0 band by 145 $cm^{-1}$, and three fine bands by about 313 $cm^{-1}$. The latter bands are the ones called by Eastwood and Snow a, b and c bands, although our wavelengths are slightly different from that of Eastwood and Snow.

In addition, there is a series of four bands 24636, 24611, 24577 and 24552 $cm^{-1}$ on the further long wavelength side. Among these bands the second one which is separated from the 0, 0 band by 1240 $cm^{-1}$ is the strongest. On the whole our observation agrees well with that of Eastwood and Snow. Besides these bands, two weak but sharp bands are observed at 24259 and 24240 $cm^{-1}$. There are no further bands on the red side of these two bands. The bands on the red side of the 0, 0 band having appreciable intencities usually represent fundamental vibrational frequencies of the ground state. From this viewpoint we may assign the two bands separated from the 0, 0 band by 1274 and 1611 $cm^{-1}$, respectively, to the two frequencies 1270 and 1623 $cm^{-1}$ found in infrared and Raman spectra. Bands other than those described above are tentatively interpreted as combination bands. A band with moderate intensity separated by 1127 $cm^{-1}$ from the 0, 0 band on its shorter wavelength side form a satellite accompanying the stronger 1270 $cm^{-1}$ band. The 1127 $cm^{-1}$ frequency appears also in other combination bands, so that it is reasonable to assume this frequency as a fundamental. There is a very strong band at 27265 $cm^{-1}$ separated by 1414 $cm^{-1}$ from the 0, 0 band. Starting from this band a progression containing two more bands with 1414 $cm^{-1}$ interval is observed. The 1414 $cm^{-1}$ frequency also appears in other combination bands, so that we may assume this to be another fundamental.

### Fundamental Vibrational Frequencies

The acrolein molecule, $CH_2CHCHO$, may belong, at the most, to the point group Cs. As it contains eight atoms, eighteen normal modes of vibration are possible, of which thirteen are of the totally symmetrical A′ type, and the remaining five are of the anti-symmetrical A″ type. Both types are active in infrared and Raman spectra. There will be seven essentially valency type vibrations of the four C–H, one C=C, one C–C and one C=O bonds. Analogously to 1, 3-butadiene[8,9] there will also be an A″ type torsional oscillation about the C–C bond. Another important mode of A′ is the planar deformation of the C=C–C=O skeleton.

8) C. M. Richards and J. R. Nielsen, *J. Opt. Soc., Am.* **40**, 438 (1950).
9) R. S. Rasmussen and R. R. Brattain, *J. Chem. Phys.*, **15**, 131 (1947).

TABLE II. INFRARED AND RAMAN FREQUENCIES OF ACROLEIN MOLECULE ($cm^{-1}$)

| Infrared | | | | Raman | | Assignment |
|---|---|---|---|---|---|---|
| $CCl_4$ solution | | vapor | | EtOH solution | | |
| w | 570 | | | w | 340 | Skeletal bending |
| | | | | m | 574 | Skeletal bending |
| s | 910 | m | 906 | | | |
| s | 959 | s | 917 | | | |
| s | 982 | s | 960 | w | 980 | CH and $CH_2$ wagging |
| | | s | 990 | | | |
| | | | 1147 | | | |
| s | 1152 | s | 1156 | w | 1170 | $CH_2$ rocking |
| | | | 1163 | | | |
| w | 1270 | w | 1262 | m | 1272 | C–C stretching |
| | | | 1280 | | | |
| m | 1360 | m | 1348 | s | 1360 | CH rocking |
| | | | 1366 | | | |
| m | 1420 | m | 1410 | w | 1426 | $CH_2$ deformation |
| | | | 1427 | | | |
| m | 1617 | m | 1613 | s | 1620 | C=C stretching |
| | | | 1632 | | | |
| vs | 1708 | vs | 1713 | vs | 1701 | C=O stretching |
| | | | 1727 | | | |
| m | 2700 | m | 2710 | | | |
| m | 2755 | m | 2790 | | | |
| m | 2805 | m | 2810 | | | C–H stretching |
| w | 2990 | w | 3000 | | | |
| w | 3100 | w | 3100 | | | |
| w | 3375 | w | 3388 | | | C=O overtone |

The infrared spectrum was measured in the 460~4000 $cm^{-1}$ region, but a weak band at 340 $cm^{-1}$ was found in the Raman spectrum. An analogous band was found in 1, 3-butadiene at 320 $cm^{-1}$ and has been assigned to a skeletal deformation vibration. Therefore we have assigned the Raman band of acrolein at 340 $cm^{-1}$ to an A'' type skeletal deformation vibration. We found a weak band at 570 $cm^{-1}$ in the infrared potassium bromide region, and in the Raman spectrum at 574 $cm^{-1}$. It may be assigned to an A' type skeletal deformation vibration. In 1, 3-butadiene the corresponding Raman band is at 513 $cm^{-1}$. Corresponding to the infrared bands in the 900 $cm^{-1}$ region only one Raman band at 980 $cm^{-1}$ was found with very small intensity. This band system may be due to the CH and $CH_2$ wagging vibrations. The infrared band at 1150 $cm^{-1}$ is strong and sharp, and the corresponding Raman band has exactly the same frequency shift.

This band may be assigned to the rocking vibration of the methylene radical. The Raman band at 1272 $cm^{-1}$ has medium intensity. In infrared two bands appear at 1235 and 1270 $cm^{-1}$, the former being very weak, and the latter medium strong. We may assign the latter frequency 1270 $cm^{-1}$ to the C-C stretching vibration, in analogy to the 1205 $cm^{-1}$ of 1, 3-butadiene and 1284 $cm^{-1}$ of biacetyl[10]. The value of 1270 $cm^{-1}$ for acrolein might appear too high for the C–C stretching frequency, but it is probably due to the partial double bond character of the bond in this molecule, whose length is 1.46 Å[7], considerably shorter than the normal C–C single bond length 1.53~1.54 Å. The band at 1360 $cm^{-1}$ was observed in both the Raman and infrared spectra with considerable intensity. This frequency may be assigned to the CH rocking vibration. The weak band at 1420 $cm^{-1}$ in infrared and at 1426 $cm^{-1}$ in Raman spectra may be assigned to the $CH_2$ deformation vibration in analogy to the Raman 1442 $cm^{-1}$ band in 1, 3-butadiene. The C=C stretching frequency is observed as the 1617 $cm^{-1}$ infrared band for solution, as the 1620 $cm^{-1}$ Raman medium strong band. The C=O stretching frequency is observed at 1695~1725 $cm^{-1}$ in solution with two peaks in the infrared and at 1700 $cm^{-1}$ in the Raman spectrum. It is the strongest band in both the spectra, but the Raman frequency seems to have been affected by the solvent. C–H valence vibration bands lying in the 2700~3000 $cm^{-1}$ region were not observed in the Raman spectrum as they may be hidden under excited Hg lines. Result of the vibrational analysis is given in Table II.

In a symmetry-allowed molecular electronic

10) J. W. Sidman and D. S. McClure, *J. Am. Chem. Soc.*, 77, 6471 (1955).

Table II. Fundamental vibrational frequencies ($cm^{-1}$)

| Raman (solution) | Infrared (vapor) | Lower state | Upper state | Assignment |
|---|---|---|---|---|
| 1701 | 1713}<br>1727} | 1720 | 1270 | C=O valence (A′) |
| 1620 | 1613}<br>1632} | 1623 | 1414 | C=C valence (A′) |
| 1272 | 1259}<br>1280} | 1270 | 1127 | C-C valence (A′) |
| 570 | | 570 | 499 | C=C-C=O bending (A′) |

transition, totally symmetric vibrational frequencies appear generally with large intensities in absorption. In the acrolein spectrum as analyzed above, all of the interval frequencies contained in prominent progressions can be assigned either to fundamental, or to combination frequencies of A′ type vibrational modes of the excited electonic state. In Table III correlations among upper and lower state vibrational frequencies are given. Of these fundamental frequencies those of the upper state of 1270 $cm^{-1}$ and 499 $cm^{-1}$ are the most important in the vapor absorption. The former is observed up to the second overtone ($3\times1270$ $cm^{-1}$) and is assigned to the C=O stretching mode. The latter frequency is assigned to a skeletal bending mode, as its corresponding lower state frequency is very probably 570 $cm^{-1}$ observed in both Raman and infrared spectra. The very strong band separated from the 0, 0 band by 1414 $cm^{-1}$ may be associated with another fundamental vibration, since we could not analyze so strong a band as a combination or overtone and since, moreover, its frequency separation 1414 $cm^{-1}$ is repeated twice more in forming a prominent progression. In our previous paper[4] this frequency was assigned to the C=C vibration, although a slightly different value was then reported. The 1127 $cm^{-1}$ frequency is observed as satellite bands accompanying each of the 1270 $cm^{-1}$ progression bands. This frequency was not reported in the above cited paper[4]. It can be assigned to the C-C vibration of the excited electronic state in analogy to the biacetyl 1136 $cm^{-1}$ (excited state) and 1284 $cm^{-1}$ (ground state). In acrolein the corresponding lower state frequency is 1270 $cm^{-1}$.

## Summary

The position, blue-shift and theoretical calculation[3] of the state energy of the electronic transition of acrolein in 24241～30294 $cm^{-1}$ region suggest that the transition is of the $n-\pi^*$ type. From the vibrational analysis of acrolein vapor spectrum, it is known that the vapor spectum of acrolein has four progressions corresponding to the C=O, C=C and C-C stretching, and skeletal bending frequency in the lower state.

The author expresses his sincere thanks to Professor S. Imanishi and Dr. Y. Kanda for their kind encouragements throughout this work. He is also indebted to Dr. M. Ito and Mr. R. Shimada for their helpful advice and discussions.

*Department of Chemistry*
*Facutly of Science*
*Kyushu University*
*Hakozaki, Fukuoka*

# *Electron Diffraction Investigations on the Molecular Structures of sec-Butyl Chloride and Alcohol*

By Mashio YAMAHA and Masato IGARASHI

(Received October 12, 1960)

The molecular structures of propane[1], butane[2] and their chlorine derivatives, such as *n*- and isopropyl chloride[3,4], 1,2-dichloropropane[5] and *tert*-butyl chloride[6,7] have already been studied by electron diffraction, using the visual method or the sector-microphotometer method. It appears that only a few studies have been done on the molecular structures of alcohols[4,8-10].

In this paper the results of electron diffraction investigation about *sec*-butyl chloride and alcohol using the sector-microphotometer method are described and compared with those of the related compounds.

## Experimental

*sec*-Butyl chloride and alcohol were kindly furnished by Dr. T. Miyazawa, the University of Tokyo. They were the same samples which were used in the spectroscopic studies.

The diffraction patterns were taken at room temperature of about 20°C using an apparatus[11] having an $r^2$-sector which was rotated rapidly during exposure. The exposures of each set were regulated to be about 2 : 1 in order to apply Karle's method[12]. The camera length was 11.82 cm. and the wavelength of electron was about 0.0567 Å, which was determined by measuring the transmission patterns of gold foil.

The optical densities of the photographic plates were measured by a microphotometer. The plates were rotated rapidly about their centers during scanning. The optical densities were converted to relative intensities by Karle's procedure[12]. A smooth background line was drawn through the intensity curve multiplied by $q$ and the molecular intensity curve $M(q)$ was obtained using the following formula,

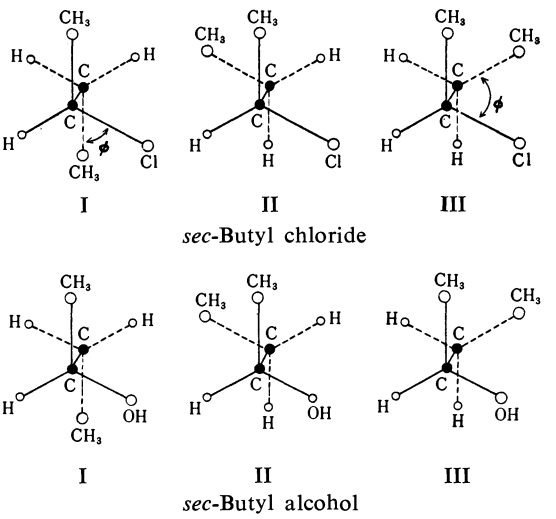



Fig. 1. Rotational isomers of *sec*-butyl chloride and alcohol.

TABLE I. LIST OF MOLECULAR CONSTANTS OF PROPANE, BUTANE AND THIR CHLORINE DERIVATIVES

| Molecule | C-C, Å | C-Cl, Å | Angle CCC | Angle CCCl | Reference |
|---|---|---|---|---|---|
| Propane | 1.54 ±0.02 | — | 111.5°±3° | — | 1 |
| *n*-Butane | 1.539±0.003 | — | 112°9′ ±9′ | — | 2 |
| *n*-Propyl chloride | 1.535±0.02 | 1.775±0.02 | 109.5°±2.5° | 111°±2° | 3 |
| Isopropyl chloride | 1.55 ±0.02 | 1.76 ±0.02 | 109.5°±1.5° | 111°±1.5° | 4 |
| 1, 2-Dichloropropane | 1.56 ±0.05 | 1.79 ±0.035 | 109.5°(ass.) | 108°±4° | 5 |
| *tert*-Butyl chloride | 1.54 ±0.01 | 1.80 ±0.01 | 111.5°±1° | — | 6 |
| *tert*-Butyl chloride | 1.54 ±0.03 | 1.80 ±0.04 | 111.5°±1.5° | — | 7 |

1) L. Pauling and L. O. Brockway, *J. Am. Chem. Soc.*, **59**, 1223 (1939).
2) K. Kuchitsu, This Bulletin, **32**, 748 (1959).
3) Y. Morino and K. Kuchitsu, *J. Chem. Phys.*, **28**, 175 (1958).
4) Y. Yamaha, This Bulletin, **27**, 170 (1954).
5) W. Wood and V. Schomaker, *J. Chem. Phys.*, **20**, 555 (1952).
6) O. Bastiansen and L. Smedvik, *Acta Chem. Scand.*, **7**, 653 (1953).
7) J. W. Coutts and R. L. Livingston, *J. Am. Chem. Soc.*, **75**, 1542 (1953).
8) K. Kimura and K. Kubo, *J. Chem. Phys.*, **30**, 151 (1959).
9) M. Kimura, *J. Chem. Soc. Japan, Pure Chem. Sec. (Nippon Kagaku Zasshi)*, **71**, 18 (1950).
10) V. Schomaker, *Acta Cryst.*, **3**, 46 (1950).
11) K. Kuchitsu, This Bulletin, **30**, 391 (1956).
12) J. Karle and I. L. Karle, *J. Chem. Phys.*, **18**, 957 (1950).

TABLE II. LIST OF MOLECULAR CONSTANTS OF ALCOHOLS

| Molecule | C-C, Å | C-O, Å | Reference |
|---|---|---|---|
| Methyl alcohol | — | 1.428±0.003 | 8 |
| Ethyl alcohol | 1.54(ass.) | 1.48 ±0.04 | 9 |
| Ethyl alcohol | 1.55±0.02 | 1.43 ±0.02 | 10 |
| Isopropyl alcohol | 1.54±0.02 | 1.45 ±0.03 | 4 |

$$M(q)=(I_T/I_B)-1 \quad (1)$$

where $I_T$ is the total intensity and $I_B$ is the background intensity.

## Analysis

The radial distribution curves were calculated by the following equation,

$$f(r)=\sum_{q=0}^{q=85} qM(q)\exp(-aq^2)\sin(\pi qr/10) \quad (2)$$

where $M(q)$ is the experimental molecular intensity obtained from Eq. 1. Here the correction for the non-nuclear scatterings was not made. The artificial damping factor $a$ was chosen so that $\exp(-aq^2)=0.1$ at $q=85$, and $q=(40/\lambda)\sin(\theta/2)$, where $\theta$ is the angle of scattering and $\lambda$ is the wavelength of the electron beam.

In the calculation of the radial distribution curve, the intensity curve below $q=15$ was spliced by the theoretical intensity curve with a constant coefficient. The intensity curve in such a region is hardly affected at all by the bond distance changes of the order 0.01 Å, but considerably affected by the internal rotation around the middle C-C bond (Fig. 1). Several steps of successive approximations were taken in order to make the assumed model practically selfconsistent with the final radial distribution curve.

The theoretical intensity curves were calculated using the following equation,

$$qM_c(q)=\sum_{i,j}(Z_iZ_j/r_{ij})\exp(-b_{ij}q^2)\sin(\pi qr_{ij}/10) \quad (3)$$

where $r_{ij}$ is the interatomic distance between the $i$th and $j$th atoms, $b_{ij}$ is its temperature factor which is calculated from the mean amplitude, $Z_i$ is the $i$th atomic number, except hydrogen, where the effective value 1.25 was used. The mean amplitudes used for the factors $b_{ij}$ are shown in Table III. The theoretical intensity curves of the mixed rotational isomers were considered.

***sec*-Butyl Chloride.**—The radial distribution curve (Fig. 3) has peaks at 1.085, 1.54, 1.80, 2.17, 2.715, 3.23 and 4.15 Å. The first peak is assigned to bonded C-H distances, the second to bonded C-C distances, the third to bonded C-Cl distance with some contributions of nonbonded H···H distances, the fourth to nonbonded C···H distances. The peak of the nonbonded C···H distances, when the fourth peak is resolved into its components, shows that the angles CCH are about 109.5°, if the C-H bond distances are assumed to be 1.09 Å. The fifth peak is mainly resolved into those of nonbonded C···C and C···Cl distances, although it involves some components of the others. If the C-Cl bond distance is assumed to be 1.80 Å, the peak of C···Cl distances shows that the angles CCCl are equal to 109.5°.

In the same way, the peak of C···C distances, although the height is less than that of C···Cl and its position is somewhat uncertain, shows that the angles CCC are about 110~112°. The peak at about 3.23 Å is characteristic of the gauche C···Cl and shows the existence of I or III or both the forms (Fig. 1). The peak shows also that the azimuthal angle $\phi$ is about 70°C. The peak at 4.15 Å is characteristic of the trans C···Cl and shows the existence of the form II. The peak of gauche C···C overlaps heavily with the other more predominant peaks and the peak of trans C···C is very low, so these two peaks are not so suitable to estimate the amount of forms I and III. As the area under the peak is approximately proportional to $Z_iZ_j/r_{ij}$, the amount of each form can be found from the area of the characteristic peak and since the areas of trans C···Cl and gauche C···Cl are

TABLE III. MEAN AMPLITUDES USED FOR THE ANALYSIS

| Atomic pair | Mean amplitude Å | Atomic pair | Mean amplitude Å |
|---|---|---|---|
| C-C | 0.050 | O···H | 0.114 |
| C-Cl | 0.050 | H···H | 0.135 |
| C-O | 0.050 | *trans*-C···C | 0.070 |
| C-H | 0.077 | *trans*-C···Cl | 0.068 |
| C···C | 0.079 | *trans*-C···O | 0.070 |
| C···Cl | 0.073 | *gauche*-C···C | 0.160 |
| C···O | 0.073 | *gauche*-C···Cl | 0.140 |
| C···H | 0.120 | *gauche*-C···O | 0.140 |
| Cl···H | 0.114 | | |

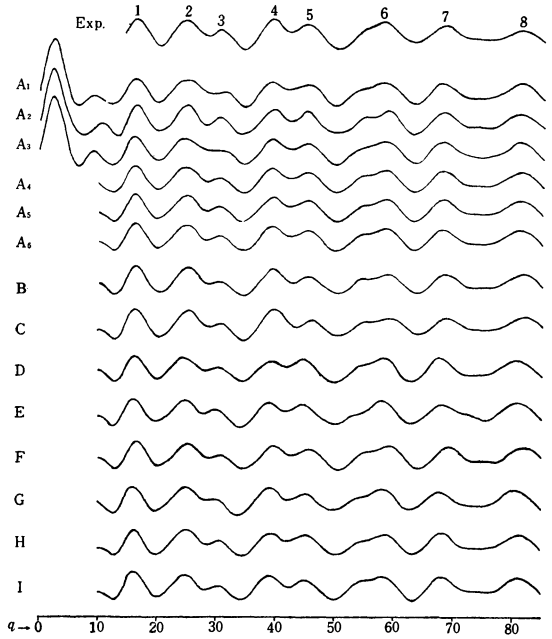



Fig. 2. Intensity curves of *sec*-butyl chloride.

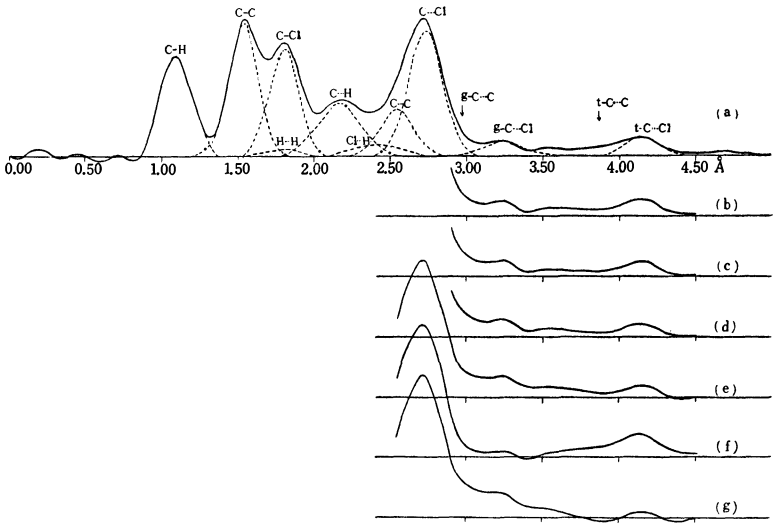



Fig. 3. Radial distribution curves of *sec*-butyl chloride. Spliced theoretical intensity curves below $q=15$ are as follows;

(a) I 50%, II 50%, (b) I 25%, II 50%, III 25%, (c) II 50%, III 50%, (d) I 33%, II 33%, III 33%, (e) I 100%, (f) II 100%, (g) III 100%

affected by the spliced theoretical intensity curves below $q=15$, various ratios of the three forms were tried so that the peaks became almost self consistent with the assumed ratio. The theoretical intensity curves of the forms I and II below $q=15$ are not so different from each other, so the radial distribution curve is not affected very much by the ratio of these two kinds of spliced portions. The ratio of the amounts of the forms I and III could not be obtained unambiguously. Only the ratio of the form II and the sum of the forms I and III was obtained rather definitely.

Its reasonable ratio was about 50% : 50%. The radial distribution curves a, b and c are almost selfconsistent with the assumed amounts of the rotational isomers, but d, e, f and g are not selfconsistent (Fig. 3).

Making reference to the results of the radial distribution curve, the theoretical intensity curves of various models were drawn in order to find the best model. The theoretical intensity curves of the three rotational isomers show some different features respectively at about $q=25\sim50$ and among the three, the forms I and III which have gauche C··· Cl resemble each other rather than the form II which has trans C···Cl. However the theoretical intensity curve of any one rotational isomer does not fit better with the experimental than that of the mixed one, so for one model of assumed bond distances and bond angles, some mixtures of the rotational isomers I, II and III were examined, but for the most part the ratio, form I : form II = 50% : 50% was assumed (Table IV). The intensity curves $A_5$ and $A_6$ fit with the experimental better than any other (Fig. 2). Next to them B fits well. Both curves C and D in which the C-Cl bond distance is 1.76 and 1.82 Å, respectively, show very different intensities at maxima 4 and 5 compared with the experimental. So the C-Cl bond distance can be determined to be 1.79±0.015 Å.

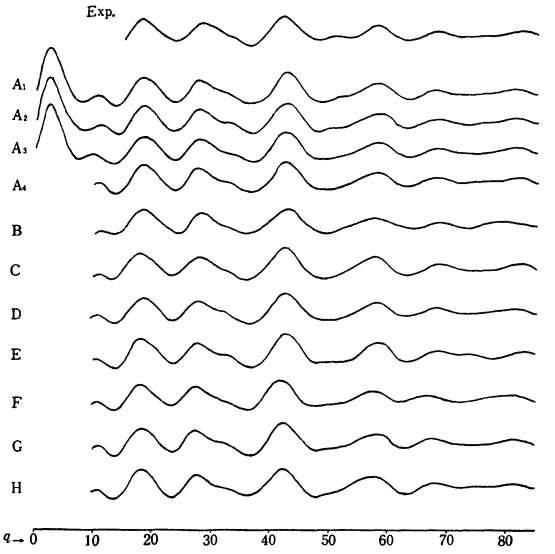



Fig. 4. Intensity curves of *sec*-butyl alcohol.

The intensity curves F and G in which C-C bond distances are 1.52 and 1.56 Å, respectively, have not very different appearances from the experimental, but the $q_{calcd}/q_{obs}$ values are not so good as that of 1.54 Å. The C-C bond distances can be considered to be 1.54±0.01 Å. The intensity curves H and I in which C-H bond distances are 1.07 and 1.11 Å, respectively, have different intensity ratios at maxima 4 and 5 compared with the experimental. The C-H bond distances seem to be 1.09±0.015 Å.

***sec*-Butyl Alcohol.**—The radial distribution curve has peaks at 1.06, 1.515, 2.16, 2.485, 2.93 and 3.73 Å (Fig. 5). The first peak is considered to be the resultant of bonded C-H and O-H peaks, the second to be that of bonded C-C and C-O peaks,

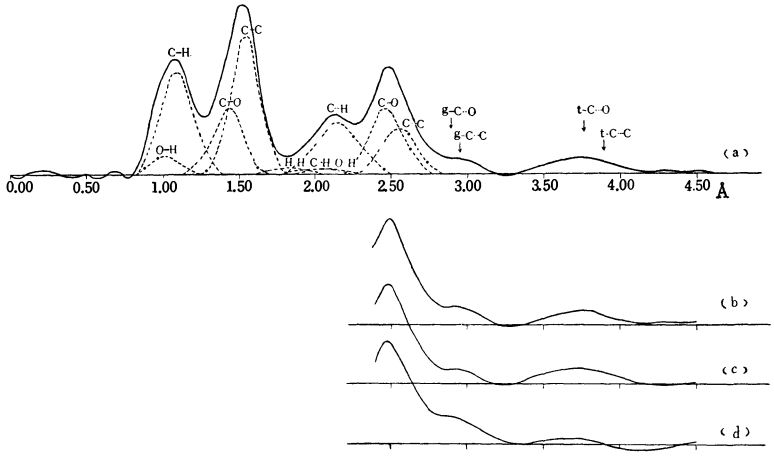



Fig. 5. Radial distribution curves of *sec*-butyl alcohol. Spliced theoretical intensity curves below $q=15$ are as follows;
(a) I 50%, II 50% (b) I 100%, (c) II 100%, (d) III 100%

TABLE IV. MOLECULAR MODELS OF *sec*-BUTYL CHLORIDE AND $q_{calcd}/q_{obs}$ VALUES

| Model | C-C Å | C-H Å | C-Cl Å | Angle CCC | Angle CCCl | Percent of rotational isomers I | II | III | Mean value of $q_{calcd}/q_{obs}$ | Average deviation |
|---|---|---|---|---|---|---|---|---|---|---|
| $A_1$ | 1.54 | 1.09 | 1.80 | 109.5° | 109.5° | 100 | 0 | 0 | 1.004 | 0.012 |
| $A_2$ | 1.54 | 1.09 | 1.80 | 109.5° | 109.5° | 0 | 100 | 0 | 0.997 | 0.007 |
| $A_3$ | 1.54 | 1.09 | 1.80 | 109.5° | 109.5° | 0 | 0 | 100 | — | — |
| $A_4$ | 1.54 | 1.09 | 1.80 | 109.5° | 109.5° | 33 | 33 | 33 | 0.997 | 0.006 |
| $A_5$ | 1.54 | 1.09 | 1.80 | 109.5° | 109.5° | 25 | 50 | 25 | 0.999 | 0.004 |
| $A_6$ | 1.54 | 1.09 | 1.80 | 109.5° | 109.5° | 50 | 50 | 0 | 0.999 | 0.005 |
| B | 1.54 | 1.09 | 1.78 | 109.5° | 109.5° | 50 | 50 | 0 | 1.006 | 0.005 |
| C | 1.54 | 1.09 | 1.76 | 109.5° | 109.5° | 50 | 50 | 0 | — | — |
| D | 1.54 | 1.09 | 1.82 | 109.5° | 109.5° | 50 | 50 | 0 | 0.991 | 0.005 |
| E | 1.54 | 1.09 | 1.80 | 112° | 112° | 50 | 50 | 0 | 0.989 | 0.007 |
| F | 1.52 | 1.09 | 1.78 | 109.5° | 109.5° | 50 | 50 | 0 | 1.014 | 0.008 |
| G | 1.56 | 1.09 | 1.80 | 109.5° | 109.5° | 50 | 50 | 0 | 0.991 | 0.008 |
| H | 1.54 | 1.07 | 1.80 | 109.5° | 109.5° | 50 | 50 | 0 | 0.999 | 0.006 |
| I | 1.54 | 1.11 | 1.80 | 109.5° | 109.5° | 50 | 50 | 0 | 0.997 | 0.005 |

TABLE V. MOLECULER MODELS OF *sec*-BUTYL ALCOHOL AND $q_{calcd}/q_{obs}$ VALUES

| Model | C-C Å | C-H Å | C-O Å | Angle CCC | Angle CCO | Percent of rotational isomers I | II | III | Mean value of $q_{calcd}/q_{obs}$ | Average deviation |
|---|---|---|---|---|---|---|---|---|---|---|
| $A_1$ | 1.54 | 1.09 | 1.43 | 109.5° | 109.5° | 100 | 0 | 0 | 1.000 | 0.009 |
| $A_2$ | 1.54 | 1.09 | 1.43 | 109.5° | 109.5° | 0 | 100 | 0 | 1.005 | 0.008 |
| $A_3$ | 1.54 | 1.09 | 1.43 | 109.5° | 109.5° | 0 | 0 | 100 | 1.004 | 0.009 |
| $A_4$ | 1.54 | 1.09 | 1.43 | 109.5° | 109.5° | 50 | 50 | 0 | 1.004 | 0.013 |
| B | 1.54 | 1.09 | 1.40 | 109.5° | 109.5° | 50 | 50 | 0 | 1.010 | 0.013 |
| C | 1.54 | 1.09 | 1.46 | 109.5° | 109.5° | 50 | 50 | 0 | 0.996 | 0.012 |
| D | 1.54 | 1.09 | 1.43 | 112° | 109.5° | 50 | 50 | 0 | 1.001 | 0.008 |
| E | 1.52 | 1.09 | 1.43 | 109.5° | 109.5° | 50 | 50 | 0 | 1.008 | 0.006 |
| F | 1.56 | 1.09 | 1.43 | 109.5° | 109.5° | 50 | 50 | 0 | 0.989 | 0.008 |
| G | 1.54 | 1.07 | 1.43 | 109.5° | 109.5° | 50 | 50 | 0 | 1.004 | 0.009 |
| H | 1.54 | 1.11 | 1.43 | 109.5° | 109.5° | 50 | 50 | 0 | 1.004 | 0.008 |

the third to be that of nonbonded C···cH, C···oH and O···cH peaks, the fourth to be that of nonbonded C···O and C···C peaks. Each of the above peaks consists of two or more components, so it is resolved into its components somewhat arbitrarily. Assuming the mean amplitudes listed in Table III, these peaks were resolved as in Fig. 5. The resolved peaks show that the angles CCH are about 109.5° and the angles CCC and CCO are both slightly greater than 109.5°.

The fifth peak at about 2.93 Å is characteristic of gauche C···O or C···C and the sixth peak at about 3.73 Å is characteristic of trans C···O or C···C. From both the peaks the amount of the rotational isomers are to be obtained. But these peaks are almost entirely controlled by the spliced intensity curves below $q=15$. They can be seen from the fact that the theoretical intensity curves of the rotational isomers above $q=15$ are not very different from each other. Moreover each peak may be constructed respectively from two adjacent components, C···O and C···C, and the resolution into its components is somewhat arbitrary. So it is difficult to determine the amounts of the rotational isomers unambiguously at the present step. It seems, however, that all the three rotational isomers may be present and the form II is predominant among them.

The theoretical intensity curves of various models listed in Table V are drawn in Fig. 4. As the intensity curves of models A, E and F do not show a greatly different appearance compared with the experimental, the C-C bond distances were estimated by the $q_{calcd}/q_{obs}$ values as $1.54\pm0.015$ Å (Table V). The intensity curves B and C have slightly different appearances from the experimental at the vicinity $q=50$ and unappropriate $q_{calcd}/q_{obs}$ values, so the C-O bond distance is considered to be $1.43\pm0.02$ Å. The intensity curves G and H have not greatly different features and $q_{calcd}/q_{obs}$ values compared with A, that the C-H bond distances cannot be determined within small limits of uncertainty. They seem to be $1.09\pm0.03$ Å.

## Summary and Discussion

The molecular structures of *sec*-butyl chloride and alcohol have been investigated by the sector and microphotometer method of electron diffraction. The structural information was derived from the radial distribution curves and correlation with the theoretical intensity curves. The results were as follows:

*sec*-Butyl chloride; C-C $=1.54\pm0.01$ Å, C-Cl $=1.79\pm0.015$ Å, angles CCC $=111\pm1.5°$, angles CCH $\approx 10.95°$, angle CCCl $\approx 109.5°$, the abundance ratio of the rotational isomer in which C···Cl is trans and that in which C···Cl are gauche is about 50% : 50%.

*sec*-Butyl alcohol; C-C $=1.54\pm0.015$ Å, C-O $=1.43\pm0.02$ Å, C-H $=1.09\pm0.03$ Å, angles CCC and CCO are slightly greater than 109.5°, angles CCH $\approx 109.5°$. The abundance ratio of the rotational isomers could not be determined unambiguously at present.

When the above results are compared with Tables I and II, the C-C bond distances, the angles CCC and CCCl coincide with each other, although the accuracies are somewhat different. The C-Cl bond distance of *sec*-butyl chloride coincides with the results on *n*-propyl chloride[3], 1,2-dichloropropane[5] and *tert*-butyl chloride[6,7], but it is about 0.03 Å longer than that of isopropyl chloride[4].

The C-O bond distance of *sec*-butyl alcohol coincides with most cases of alcohols.

As for the rotational isomers, the abundance ratio was obtained to some extent about *sec*-butyl chloride, but not obtained unambiguously about *sec*-butyl alcohol at the present step.

By the measurement of specific rotation of *D-sec*-butyl alcohol, Bernstein and Pedersen[13] have found the amounts of the three rotational isomers to be 42%(form I), 42%(form II), 15.3%(form III), assuming that forms I and II have the same energy and that the form III is less stable (Fig.1).

The amounts of rotational isomers will be obtained more accurately by the use of a long camera-length of electron diffraction apparatus.

The authors wish to express their hearty thanks to Professor A. Kotera for his kind guidance throughout this work, to Professor Y. Morino, the University of Tokyo, for the use of diffraction apparatus, to Dr. K. Kuchitsu and Dr. E. Hirota, the University of Tokyo, for their kind aid during the experiment and for their calculation by the Punched Card Machine; also to Dr. S. Shibata and Dr. H. Morimoto, Nagoya University, for the microphotometer-tracing.

*Department of Chemistry*
*Faculty of Science*
*Tokyo University of Education*
*Koishikawa, Tokyo*

13) H. Bernstein and E. E. Pedersen, ibid., **17**, 885 (1949).

# SHORT COMMUNICATIONS

## *On the Electromigration in Ion-exchange Papers*

By Takeo YAMABE, Manabu SENŌ and Nobuharu TAKAI

(Received March 6, 1961)

In electromigration of ions in ion-exchange papers, which are filter papers impregnated with pulverized ion-exchange resins, we may expect the contribution of ion-exchange adsorption to the electromigration behavior of ions. This behavior of alkaline earth metal ions and amino acid ions will be presented in this communication. This may be the first report dealing with the electrophoretic method using these papers, although some chromatographic experiments have been carried out[1].

The usual apparatus for paper electrophoresis (Toyo Roshi Type C) were used and the ionic mobilities under constant voltages were measured. Ion-exchange papers (Rohm and Haas Co.) were Amberlite SA-2 (sulfonic) and WA-2 (carboxylic), which were used after conditioning with acid, alkali and methanol. For comparison, Toyo Roshi No. 50 was used as an ordinary paper. Systems examined are $Mg^{2+}$, $Ca^{2+}$, $Sr^{2+}$ and $Ba^{2+}$ (chloride) supported in 0.05 N hydrochloric acid, sodium chloride or sodium hydroxide, and glycine, glutamic acid and lysine monohydrochloride supported in acetic acid-sodium acetate. For detection of spots of ions, coloration of alkaline earth metal with alizarin-ammonia and that of amino acid with ninhidrin were adopted.

TABLE I. MOBILITIES OF ALKALINE EARTH METAL IONS
10 V./cm., supporting media 0.05 N HCl

| | Mobilities, $cm^2/V.\ sec. \times 10^4$ | | | |
|---|---|---|---|---|
| | $Mg^{2+}$ | $Ca^{2+}$ | $Sr^{2+}$ | $Ba^{2+}$ |
| Toyo Roshi No. 50 | 3.1 | 3.6 | 3.6 | 3.9 |
| Amberlite SA-2 | 0.22 | 0.33 | 0.33 | 0.03 |
| Amberlite WA-2 | 2.6 | 3.0 | 3.0 | 3.3 |

1) M. M. Tuckerman, *Anal. Chem.*, **30**, 231 (1958); H. R. Roberts and M. G. Kolor, ibid., **31**, 565 (1959); H. T. Peterson, Jr., ibid., **31**, 1279 (1959).

TABLE II. MOBILITIES OF AMINO ACID IONS
25 V./cm., supporting media 1 M $CH_3COOH$

| | Mobilities, $cm^2/V.\ sec. \times 10^4$ | | |
|---|---|---|---|
| | Glycine | Glutamic acid | Lysine |
| Toyo Roshi No. 50 | 0.71 | 0.53 | 1.27 |
| Amberlite SA-2 | 0.11 | 0.09 | 0.01 |
| Amberlite WA-2 | 0.66 | 0.45 | 0.81 |

A part of the experimental results is shown in Tables I and II. The ionic electromigration in ion-exchange papers possesses the diminished velocity and tailing, in comparison with the case where the ordinary paper is used. This is remarkable on SA-2 paper which exhibits strong exchange adsorption for cations. It must be noticed that the ionic mobilities decrease in the same order, $Ba^{2+} > Sr^{2+}$, $Ca^{2+} > Mg^{2+}$, on the paper No. 50 as in free solution, but $Sr^{2+}$, $Ca^{2+} > Mg^{2+} > Ba^{2+}$ on sulfonic SA-2 paper in acidic medium*. This might be ascribed to especially strong affinity of sulfonic acid resin for barium ion, being in accordance with observation in the permselectivity of the ion-selective membrane[2]. On carboxylic WA-2 paper, there is scarecely adsorption effect in acidic medium, where the paper is not in dissociated state. In neutral and alkaline medium, the ionic mobilities have the order, $Ba^{2+} > Sr^{2+} > Mg^{2+} > Ca^{2+}$, e. g., calcium ion is retarded to a great extent. Amino acid ions in acidic medium decrease in migrating velocity on SA-2 (lysine most remarkable), but do not decrease largely on WA-2 which does not dissociate so that the adsorption effect is small.

From the above observation, it was confirmed that the synergetic effect of electromigration and ion-exchange adsorption exerts, and this method offers the practical application to separation of ions and is interesting in connection with the ionic transport behavior across the ion-exchange membranes.

*The Institute of Industrial Science*
*The University of Tokyo*
*Yayoi-cho, Chiba*

* In neutral and alkaline medium the similar results are obtained but calcium ion is retarded to some extent.

2) T. Yamabe, M. Senō, T. Tanaka and I. Kamii., This Bulletin, **33**, 1740 (1960).

## *Protection of Amide-Nitrogen for Peptide Synthesis. A Novel Synthesis of Peptides Containing C-Terminal Glutamine*

By Shiro AKABORI, Shumpei SAKAKIBARA and Yasutsugu SHIMONISHI

(Received January 11, 1961)

It is known that troublesome side reactions[1] occur in the synthesis of asparagine- or glutaminepeptides due to the instability of the $\beta$- or $\gamma$-amide groups. Therefore, a suitable protection of amide nitrogen is desirable, in which the protecting group should be easily removable after formation of the peptide bonds. Frankel et al.[2] reported that removal of the benzyl group from $N^{\beta}$-benzyl-asparagine was very difficult because of the unexpected stability of the group.

In the present work, glycyl-L-glutamine and L-alanyl-L-glutamine ware prepared using xanthydrol[3] (I) as a protective agent by the following procedures. $N^{\alpha}$-Cbzo*-$N^{\gamma}$-xanthyl-L-glutamine (II) was prepared from $N^{\alpha}$-cbzo-L-glutamine (III) in glacial acetic acid containing an equimolar amount of I. Yield 80%; m. p. 182~183°C, $[\alpha]_D^{17}-5.7°$ (*c* 5.7, dimethylformamide). Found: C, 66.36; H, 5.55; N, 6.13. Calcd. for $C_{26}H_{24}O_6N_2 \cdot 1/2H_2O$: C, 66.52; H, 5.37; N, 5.97%.

When II was treated with hydrogen bromide in glacial acetic acid, L-glutamine (IV) was recovered in 55% yield. IV had the same optical activity with the glutamine which was obtained directly from the starting material III, m. p. 187°C, $[\alpha]_D^{32.5}+6.4°$ (*c* 2.8, $H_2O$). It is interesting that $N^{\gamma}$-xanthyl-L-glutamine (V) was not obtained from IV and I in acetic acid. The substance V was first obtained by selective hydrogenation of II in ethanol using palladium-charcoal as catalyst; m. p. 222°C (dicomp.). Found: C, 65.71; H, 5.60; N, 8.97. Calcd. for $C_{18}H_{18}O_4N_2$: C, 66.24; H, 5.56; N, 8.58%.

**Synthesis of Glycyl-L-glutamine.** — $N^{\alpha}$-Cbzo-$N^{\gamma}$-xanthyl-L-glutamine methylester (VI) was prepared from II in dioxane by treatment with diazomethane. Recrystallization of VI from dioxane gave fine colorless needles (80~85%); m. p. 235~235.5°C. Found: C, 68.21; H, 5.58; N, 5.94. Calcd. for $C_{27}H_{26}O_6N_2$: C, 68.34; H, 5.52; N, 5.90%. The cbzo-group was removed by catalytic hydrogenation, and $N^{\gamma}$-xanthyl-L-glutamine methylester acetate (VII) was obtained as colorless needles (67%); m. p. 148~148.5°C. Fuond: C, 62.72; H, 6.07; N, 6.90. Calcd. for $C_{21}H_{24}O_6N_2$: C, 62.99; H, 6.04; N, 7.00%. Substance VII was coupled with cbzo-glycine *p*-nitrophenylester (VIII) in anhydrous chloroform[4,5], and cbzo-glycyl-$N^{\gamma}$-xanthyl-L-glutamine methylester (IX) was obtained as fine colorless needles after recrystallization from dioxane (70%); m. p. 184°C. Found: C, 65.49; H, 5.64; N, 7.89. Calcd. for $C_{29}H_{29}O_7N_3$: C, 65.52; H, 5.50; N, 7.91%. The product IX was carefully saponified in dioxane using *N*-sodium hydroxide, and cbzo-glycyl-$N^{\gamma}$-xanthyl-L-glutamine (X) was obtained. It was recrystallized from methanol-toluene (4 : 1) and water (77%) : m. p. 198°C. Found: C, 65.17; H, 5.39; N, 8.04; eq. wt.: Na, 516. Calcd. for $C_{28}H_{27}O_7N_3$: C, 64.98; H, 5.26; N, 8.12%; mol. wt. 517.5. Treatment of X with hydrogen bromide, foffowed by purification by Amberlite IR-4B, gave glycyl-L-glutamine monohydrate (XI) in 70% yield; m. p. 206°C (decomp.). Found: C, 38.02; H, 7.02; N, 19.12. Calcd. for $C_7H_{13}O_4N_3 \cdot H_2O$: C, 38.00; H, 6.84; N, 19.00%. $[\alpha]_D^{15}=-1.8°$ (*c* 3.8, water). Thierfelder[6] reported; m. p. 199~200°C, $[\alpha]_D^{15}-2.47°$ (*c* 4.20, water).

**Synthesis of L-Alanyl-L-glutamine.** — Cbzo-L-alanyl-$N^{\gamma}$-xanthyl-L-glutamine methyl ester (XII) was prepared by coupling cbzo-L-alanine *p*-nitrophenyl ester with VII in the same manner, and was recrystallized from ethanol (90%); m. p. 208°C (decomp.). Found: C, 65.17; H, 5.69; N, 7.79. Calcd. for $C_{30}H_{31}O_7N_3$: C, 66.04; H, 5.73; N, 7.70%. L-Alanyl-L-glutamine monohydrate was obtained from XII by the similar procedure to that of XI, m. p. 214~215°C (decomp.). Found: C, 40.42; H, 7.52; N, 17.82. Calcd. for $C_8H_{15}O_4N_3 \cdot H_2O$: C, 40.84; H, 7.28; N, 17.86%. $[\alpha]_D^{14}=+11.4°$ (*c* 3.70, water).

Detailed results will be published elsewhere.

*Institute for Protein Research*
*Osaka University*
*Kita-ku, Osaka*

1) J. Rudinger, *Angew. Chem.*, **71**, 742 (1959).
2) M. Frankel, Y. Liwschitz and A. Zilkha, *J. Am. Chem. Soc.*, **75**, 3270 (1953).
3) R. F. Phillips et al., *J. Org. Chem.*, **8**, 1355 (1943).
* Cbzo.....carbobenzoxy.
4) R. Schwyzer and P. Sieber, *Angew. Chem.*, **68**, 518 (1956).
5) M. Bodanszky and V. du Vigneaud, *J. Am. Chem. Soc.*, **81**, 5688 (1959).
6) H. Thierfelder et al., *Z. Physiol. Chem.*, **105**, 58 (1919).

## *Steric Configuration of the α, β-Diaminobutyric Acid Isolated from the Antibiotic Glumamycin*

By Masahiko FUJINO, Michitaka INOUE, Jisaburo UEYANAGI and Akira MIYAKE

(Recived February 20, 1961)

Inoue[1] previously isolated α, β-diaminobutyric acid from the acid hydrolysate of glumamycin, an acidic peptide antibiotic. Martin et al.[2] also reported the separation of α, β-diaminobutyric acid from Aspartocin, an antibiotic resembling glumamycin. Although both products seem to have the same configuration from their optical rotation, this has so far not been studied. Inoue has shown[3] that only one β-amino group of the two α, β-diaminobutyric acids* of glumamycin is free.

The configuration of the α-amino group has been studied by conversion of free amino group of glumamycin into a hydroxyl group and subsequent hydrolysis to α-amino-β-hydroxybutyric acid, and that of the β-amino group by oxidation of α, β-diaminobutyric acid to alanine.

Glumamycin was treated with sodium nitrite in 80% acetic acid to convert the free amino group into hydroxyl and the resulting hydroxy-glumamycin was hydrolyzed with hydrochloric acid. The reaction mixture was developed on a column of Dowex 50x4 (200 ~ 400 mesh) with ammonium formate buffer (pH 3.4)[4] and the crystals obtained from the threonine fraction of the eluate were recrystallized from aqueous ethanol (Found: C, 40.06; H, 7.81; N, 11.90. Calcd. for $C_4H_9O_3N$: C, 40.33; H, 7.62; 11.76%). The product was found to be a mixture of threonine and allothreonine by paper chromatography with *n*-butalnol·acetone·ammonia·water (50 : 6.25 : 6.25 : 37.5)[5]. However, since the β-position of α, β-diaminobutyric acid of glumamycin may undergo partial Walden inversion under the conditions, it is impossible to decide the configuration of the α-carbon atom directly from the optical rotation of the product. But DNP-L-threonine and DNP-L-allothreonine exhibit the same optical rotation, $[M]_D^{25} = +305°$ (4% sodium bicarbonate)[6]. The above product was converted into its DNP-derivative by the method of Levy[7] and then subjected to chromatography on Amberlite IRC-50 according to the method of Seki[8] to remove the DNP-OH which formed as a by-product. DNP-derivative showed an optical rotation of $[M]_D^{24} = -294° \pm 14$ (*c* 0.48, 4% sodium bicarbonate) and its yield was 92%. This fact shows that above product is a mixture of D-threonine and D-allothreonine, therefore α-carbon atom of α, β-diaminobutyric acid has the D-configuration. Further, as α, β-diaminobutyric acid obtained from the hydrolysate of hydroxy-glumamycin, and that obtained from the hydrolysate of glumamycin have the same optical rotation and physical properties, the two moles of α, β-diaminobutyric acid in glumamycin evidently have the same steric configuration.

Oxidation of α, β-diaminobutyric acid with hydrogen peroxide was conducted by the method of Dakin[9]. Namely, the compound was allowed to react with 2 mol. of 3% hydrogen peroxide at 50°C for one hour. The reaction mixture was passed through a column of Amberlite IR-120, the column was eluted with N-ammonium hydroxide, and the effluent was concentrated to give D-alanine (Found: C, 40.51; H, 7.88; N, 15.44%), $[\alpha]_D^{20} = -16$, (*c* 1, 6 N hydrochloric acid) which was confirmed by infrared spectrum and paper chromatography.

Thus, it was found that the β-carbon atom of α, β-diaminobutyric acid belongs to the D-series, and consequently α, β-diaminobutyric acid takes D-erythro-configuration.

The authors wish to express their sincere thanks to Dr. Satoru Kuwada, the Director of Research Laboratories, Dr. Sueo Tasuoka, Vice Director of Research Laboratories, Dr. Kuniyoshi Tanaka, the Head of 2nd Division of Research Laboratories for their guidance and encouragement.

*Research Laboratories*
*Takeda Chemical Industries, Ltd.*
*Higashiyodogawa-ku, Osaka*

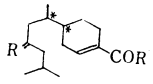
1) M. Inoue et al., This Bulletin, **33**, 1014 (1960).
2) J. H. Martin and W. K. Hausmann, *J. Am. Chem. Soc.*, **60**, 2079 (1960).
3) M. Inoue, in press.
* It is already recognized that glumamycin contains two moles of α, β-diaminobutyric acid and both amino groups of one mole are not free.
4) C. H. W. Hirs, S. Moore and W. H. Stein, *J. Biol. Chem.*, **195**, 669 (1952).
5) K. N. F. Shaw and S. W. Fox, *J. Am. Chem. Soc.*, **75**, 3421 (1953).
6) K. R. Rao and H. A. Sober, ibid., **76**, 1328 (1954).
7) A. L. Levy, *Nature*, **174**, 126 (1954).
8) T. Seki, *Chemistry of Proteins (Tokyo)*, **4**, 209 (1956).
9) H. D. Dakin, *J. Biol. Chem.*, **1**, 171 (1905); **4**, 63 (1908).

## *The Structure of Todomatuic Acid. Synthesis of (±)-Dihydro-desoxo-todomatuic Acid*

By Masao NAKAZAKI and Sachihiko ISOE

(Received March 6, 1961)

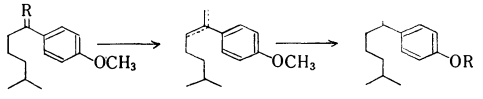
Todomatuic acid, $C_{15}H_{24}O_3$, monocyclic unsaturated keto-acid (m. p. 58.5°C, b. p. 200~215°C/3 mmHg, $[\alpha]_D^{32.5}+85.84°$; semicarbazone, m. p. 193.2~193.7°C), was first isolated by Tuchihashi and Hanzawa[1] on hydrolysis of the high boiling fraction of an oil, obtained as a by-product when *Abies sachalinensis* Mast. (to do matu) was digested with sulfite in pulp industry.



Ia R=O R'=OH
b R=$H_2$ R'=OH
c R=$H_2$ R'=$OCH_3$

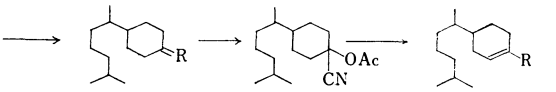
The structure Ia was advanced by Momose[2], mainly by the results of oxidative degradation of Ia with potassium permanganate which gave oxalic acid and an acyclic saturated keto-dicarboxylic acid (II), $C_{13}H_{22}O_5$ (semicarbazone, decomp. p. 185~186°C). Further oxidation of II with nitric acid gave isovaleric acid and $\beta$-($\alpha$-carboxyethyl)glutaric acid. Among various possible structures which satisfy the results of the degradation, Ia was favored because Ia is compatible with the isoprene rule.

In this communication, the synthesis of (±)-dihydro-desoxo-todomatuic acid (Xb) is reported.



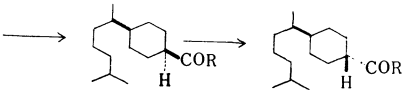
IIIa R=O IV Va R=$CH_3$
b R=OH, $CH_3$ b R=H

(4-Anisyl)-isohexyl ketone (IIIa) (b. p. 131~133°C/1 mmHg; semicarbazone, m. p. 124~125°C) obtained by Friedel-Crafts reaction of anisole with isocaproyl chloride, was converted into IIIb by Grignard reaction with methylmagnesium bromide, and then IIIb was dehydrated by boiling with acetic anhydride to the unsaturated phenol ether IV (b. p. 109~115°C/1 mmHg).



VIa R=OH, H VII VIIIa R=CN
b R=O b R=COOH

Catalytic hydrogenation of IV gave Va (b. p. 107~113°C/1 mmHg), which was hydrolyzed by boiling with hydroiodic acid in acetic acid to afford the phenol Vb (b. p. 127~128°C/1 mmHg). High pressure catalytic hydrogenation of Vb (Raney nickel, 130 atms., 30°C) yielded the alcohol VIa (b. p. 120~121°C/1 mmHg), which was oxidized with potassium dichromate in sulfuric acid to the ketone VIb (b. p. 113~114°C/1 mmHg; semicarbazone, m. p. 149~150°C). The cyanohydrin acetate VII (b. p. 145~147°C/1 mmHg) prepared from VIb with potassium cyanide and acetic anhydride, was pyrolyzed by passing through a heated Pyrex tube(600°C) packed with ceramic Raschig rings to give unsaturated cyanide VIIIa, which was then hydrolyzed to the unsaturated acid VIIIb (b. p. 163~165°C/1 mmHg).



IXa R=OH Xa R=$OCH_3$
b R=$OCH_3$ b R=OH
c R=$NHC_6H_5$
(or its antipode) (or its antipode)

Although two racemic forms are expected for the structure VIIIb, the infrared absorption spectrum of synthetic VIIIb was found superimposable on that of (+)-desoxo-todomatuic acid(Ib) (m. p. 59~60°C, $[\alpha]_D^{27}+94.3°$ in ethanol; anilide, m. p. 78~79°C) obtained by Wolff-Kishner reduction of Ia. Catalytic hydrogenation of the methyl ester Ic of natural Ib gave saturated methyl ester IXb in which only one asymmetric center remains.

Heating with sodium methoxide converted IXb into more stable methyl ester Xa, which was hydrolyzed to give (+)-dihydro-desoxo-todomatuic acid (Xb) (b. p. 150~153°C/1 mmHg, $n_D^{18}$ 1.4723, $[\alpha]_D^{27}+14.1°$ in ethanol; anilide Xc, m. p. 115~116°C). Following the same procedure, racemic IXb gave (±)-dihydro-desoxo-todomatuic acid (Xb) (b. p. 152~155°C/1 mmHg, $n_D^{18}$ 1.4723; anilide, Xc

1) R. Tuchihashi and T. Hanzawa, *J. Chem. Soc. Japan, Pure Chem. Sec.* (*Nippon Kagaku Zasshi*), **61**, 1041 (1940).
2) T. Momose, *J. Pharm. Soc. Japan* (*Yakugaku Zasshi*), **61**, 288 (1941).

m. p. 105~106°C). The infrared absorption spectra of racemic Xb, Xc and natural Xb, Xc were found superimposable in every detail.

These findings firmly establish the structure of todomatuic acid.

*Department of Chemistry*
*Institute of Polytechnics*
*Osaka City University*
*Kita-ku, Osaka*

# *Spectrophotometric Determination of Nitrite in Nitrate and Sulfate*

By Yukiteru KATSUBE, Katsuya UESUGI and John H. YOE

(Received November 17, 1960)

The purpose of this paper is to develop a rapid and sensitive method for the spectrophotometric determination of trace amounts of nitrite in the presence of large amounts of nitrate and sulfate. The method is based on the colored compound formed by the reaction between disodium 1-(4′-aminobenzeneazo)-2-amino-8-hydroxynaphthalene-2′, 6-disulfonate and nitrous acid. Details of this compound have been described in our previous paper[1].

For the determination of trace amounts of nitrite useing this compound, seventeen kinds of ions were found to cause the interference ($As^{3+}$, $Fe^{3+}$, $Ce^{3+,4+}$ *, $Hg^{+,2+}$, $Mn^{2+}$, $Sn^{2+,4+}$, $Ti^{4+}$, $Zr^{4+}$, $Br^-$, $F^-$, $I^-$, $MnO_4^-$, $MoO_4^{2-}$, $SeO_3^{2-}$**). The study of the effect of other ions in the previous paper suggested the possibility that they could be used for the determination of nitrite in nitrate and sulfate without any special procedure.

## Experimental

The apparatus and reagents were the same as those used in our previous work.

**Procedure.**—Transfer to a 25 ml. volumetric flask 1 ml. of the sample solution adjusted so as to contain 5 to 60 p.p.m. of nitrous acid. Add 20 ml. of distilled water, and 2.5 ml. of 0.05% reagent solution. Add 0.3 ml. of 6 N hydrochloric acid and shake well. Bring up to the mark with distilled water, thoroughly mix and, after ten minutes, measure the absorbance at 625 mμ, using a reagent blank solution*** as a reference.

## Results

The determination of nitrite in the presence of nitrate and sulfate was made. The results are given in Table I.

## Summary

A simple procedure has been developed for the determination of trace amounts of nitrite in large amounts of nitrate and sulfate, with disodium 1-(4′-aminobenzeneazo)-2-amino-8-hydroxy-naphthalene-2′, 6-disulfonate. The method is accurate and precise.

TABLE I. DETERMINATION OF NITROUS ACID

| Taken $HNO_2$ p. p. m. | Added $NO_3^-$ mg./25 ml. | Added $SO_4^{2-}$ mg./25 ml. | Absorbance* at 625 mμ | Standard deviation in absorbance unit |
|---|---|---|---|---|
| 0.20 | | | 0.080 | 0.002 |
| | 0.5 | | 0.082 | 0.003 |
| | 50.0 | | 0.076 | 0.003 |
| | 5000.0 | | 0.082 | 0.003 |
| | | 0.5 | 0.079 | 0.002 |
| | | 50.0 | 0.079 | 0.003 |
| | | 5000.0 | 0.082 | 0.004 |
| | 500.0 | 500.0 | 0.079 | 0.004 |
| 0.75 | | | 0.307 | 0.002 |
| | 500.0 | 500.0 | 0.304 | 0.004 |

$KNO_3$ and $K_2SO_4$ were used to make up the solution.

* These values were the averages of six replicate determinations.

1) Y. Katsube and J. H. Yoe, This Bulletin, 33. 190 (1960).

* In the previous paper, the reagent was tested with 67 kinds of ions not including $Ce^{4+}$.

** In the previous paper, $SeO_3^{2-}$ was mistyped as $CeO_3^{2-}$.

*** Use the sample solution as the reference when the sample contains $Cu^{2+}$ or $Ni^{2+}$.

*Himeji Technical Institute*
*(Y. K. & K. U.)*

*John Lee Pratt Trace Analysis Laboratory*
*University of Virginia*
*Charlottesville, Va., U. S. A.*
*(J. H. Y.)*

# *Nuclear Magnetic Resonance Study of the Steric Effect in Dimethylphenols*

By Ichiro YAMAGUCHI

(Received November 9, 1960)

In their various physicochemical properties, six isomers of dimethylphenol (xylenol) were observed to be slightly different from each other[1-5]. These differences have been ascribed mainly to the difference in the steric effect of the methyl group on the formation of an intermolecular hydrogen bond. The present author observed obvious differences among the nuclear magnetic resonance spectra of dimethylphenols. The difference could be closely correlated with the position of the methyl groups in the benzene ring relative to the hydroxyl group.

## Experimental

NMR measurements were carried out at 20°C with a Varian High Resolution NMR spectrometer operated at 56.4 Mc. The dimethylphenols measured were guaranteed grade reagents. The solvents used were carbon tetrachloride and acetone. These were purified with a Podobielniak fractional distillator. The values of the chemical shift were obtained referring to an external reference of water in a capillary, and the correction for bulk diamagnetic susceptibility was made. The solubility of dimethylphenols in carbon tetrachloride was poor except for 2,4-dimethylphenol. Therefore the measurements were made up to their saturated solutions at 20°C.

## Results and Discussion

Figure 1 shows the chemical shift-concentration diagrams for dimethylphenols in carbon tetrachloride solution. The curves with the highest chemical shift are due to methyl protons, and the ones with lower chemical shift are due to benzene ring protons and hydroxyl proton (thick line). The resonance fields for the methyl protons and the ring protons decrease on dilution. This is a characteristic feature of aromatic systems and is ascribed to the effect of the ring current in the neighboring solute molecules. The detailed results and discussions for each proton group are described as follows.

**Methyl Proton Resonance.**—The methyl protons in 3,4- and 3,5-dimethylphenols give only one resonance line. This means that the difference between the screening constants for *m*- and *p*-Me protons is so small that it can not be observed. In contrast to this, the

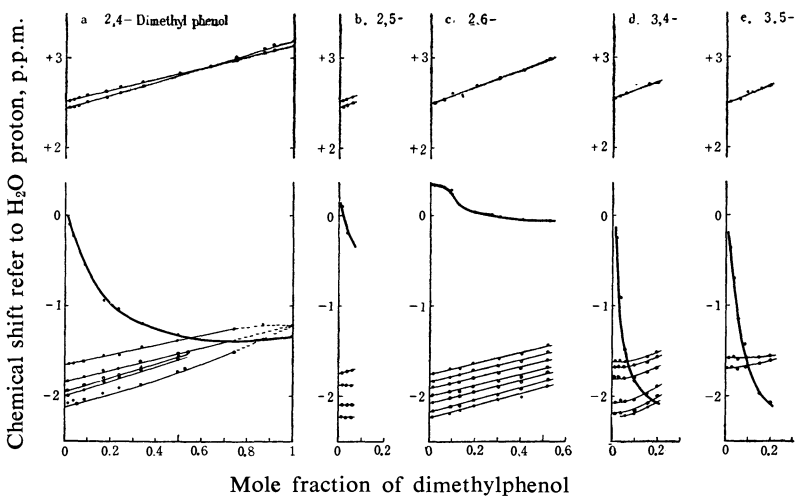



Fig. 1. Concentration dependence of chemical shift for $CCl_4$ solutions of dimethylphenols.

1) W. C. Sears and L. J. Kitchem, *J. Am. Chem. Soc.*, **71**, 4110 (1949).
2) A. Burawoy and J. T. Chamberlain, *J. Chem. Soc.*, **1952**, 2310.
3) M. Neuilly, *Compt. rend.*, **238**, 781 (1954).
4) W. Suetaka and M. Sanesi, *Ann. chim. (Rome)*, **46**, 1133 (1956).
5) D. Bono, *Bull. soc. chim. France*, **1956**, 1368; *Compt. rend.*, **242**, 375, 637 (1956).

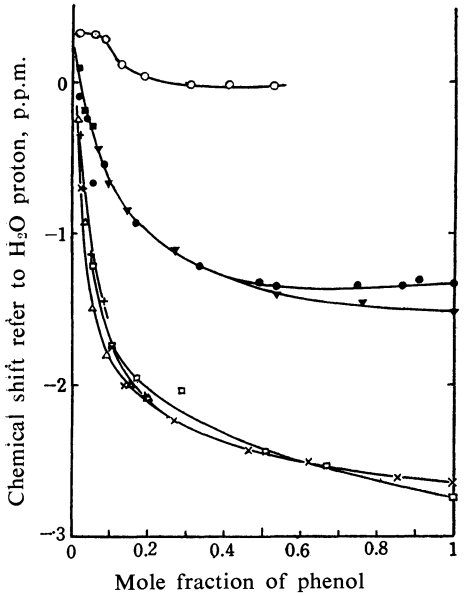



Fig. 2a. Concentration dependence of chemical shift of OH proton in various methyl phenols in $CCl_4$ solution.

—●— 2,4-Dimethylphenol
—■— 2,5- 〃
—○— 2,6- 〃
—△— 3,4- 〃
—+— 3,5- 〃
—▼— *o*-Cresol[a)]
—□— *m*- 〃 [a)]
—×— *p*- 〃 [a)]

a) I. Yamaguchi, unpublished work.

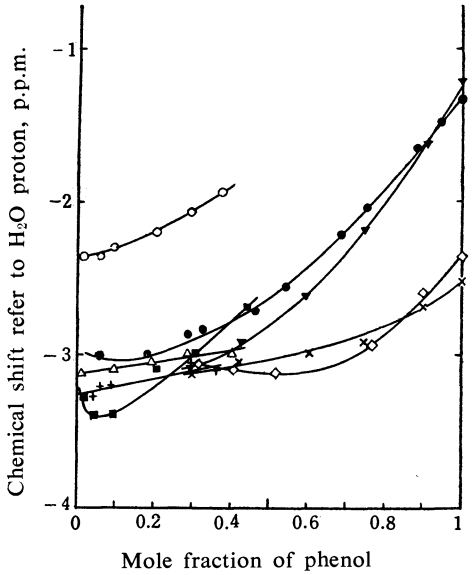



Fig. 2b. Concentration dependence of chemical shift of OH proton in various methylphenols in acetone solution.

—●— 2,4-Dimethylphenol
—■— 2,5- 〃
—○— 2,6- 〃
—△— 3,4- 〃
—+— 3,5- 〃
—▼— *o*-Cresol[b)]
—×— *p*- 〃 [b)]
—◇— Phenol[b)]

b) R. L. Batdort, Ph. D. Thesis, Univ. of Minnesota, 1955.

methyl protons in both 2,4- and 2,5-dimethylphenols give two resonance lines caused by the difference between the screening constants of the protons in 2(*o*)-Me group and that in 5(*m*)- or 4(*p*)-Me group. Furthermore, the two resonance curves for 2,4-dimethylphenol intersect each other at an intermediate concentration of carbon tetrachloride solution. Thus the concentration dependence of the resonance in 2(*o*)-Me protons is clearly different from that in 4(*p*)-Me protons. This suggests that the 2(*o*)-Me protons interact strongly with the OH group owing to the proximity of the two groups to each other.

Several effects are considered to induce the specific interaction between the groups. They might be the inductive and mesomeric effects of the OH group, effect of the electrostatic field[6)] originating from the bond moment of the OH group, or the effect of the dispersion force. The interaction caused by each effect should be greater with the *o*-Me protons than with the *m*- or *p*-Me protons. The magnitude of these effects would be affected by the change in the hydrogen bonding situations of the OH group. Therefore, the resonance line for the *o*-Me protons might be displaced by the change in the concentration of the solution in a way different from that for the *m*- or *p*-Me protons. However, it is unfortunately impossible to treat the resultant effect quantitatively. And at the present stage, we can not decide which curve should be assigned to *o*-Me protons.

**Hydroxyl Proton Resonance.**—Fig. 2 shows the concentration dependence of the chemical shift of the OH proton in dimethylphenols and cresols. Fig. 2a is of carbon tetrachloride solutions and Fig. 2b is of acetone solutions. Three types of the curves with distinctly different concentration dependence from one another are observed in the figures. The first group (a) at the highest field includes 2,6-dimethylphenol, the second (b) at the middle 2,4- and 2,5- dimethylphenols and *o*-cresol, and the third (c) at the lowest 3,4- and 3,5-dimethylphenols and *m*- and *p*-cresols. At the concetration of 1 mol. fraction (pure phenol), the values of the chemical shift are

6) A. D. Buckingham, *Can. J. Chem.*, **38**, 300 (1960).

about (a) +0.1 p.p.m., (b) −1.3 p.p.m. and (c) −2.5 p.p.m. This classification clearly correlates with the location of the methyl groups in the molecule: The phenol in (a) has two methyl groups at both the ortho positions to the OH group, and those in (b) and (c) have one and no methyl group ortho to the OH respectively. The methyl groups at the meta and para positions do not take part in this classification. In carbon tetrachloride solutions, all of the curves approach about +0.3 p.p.m. at the concentration of infinite dilution (extrapolated). Therefore, it would be reasonable to consider that in a free single molecule the effect of the *o*-Me group on the screening constant of a non-hydrogen bonded OH proton is very small.

These results that the difference in the resonance field of the OH proton among the isomers may primarily be ascribed to the steric hindrance of the *o*-Me group to form the intermolecular hydrogen bond. The values of the chemical shift for pure phenols may correlate with the extent of the steric effect of the methyl group on the hydrogen bond formation.

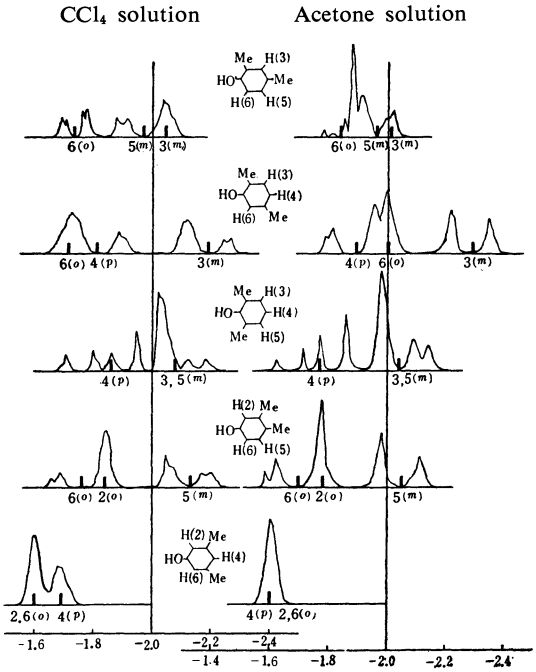
A flat range was observed for 2,6-dimethylphenol below the concentration of 0.05 mol. fractions. This implies the complete dissociation of the intermolecular hydrogen bond at the concentration range. This is an evidence that the two methyl groups at the 2(*o*)- and 6(*o*)-positions sterically inhibit the formation of the intermolecular hydrogen bond appreciably.

The concentration dependence of the chemical shift of the OH proton for the acetone solution is somewhat different from that for the carbon tetrachloride solution. For carbon tetrachloride solutions, the OH curve suggests a simple dissociation process of the intermolecular hydrogen bond on dilution. In contrast to this, for acetone solutions the curve shows a process to form a new hydrogen bond with acetone.

**Ring Proton Resonance.**—The dimethylphenol molecule has only three ring protons giving a rather simple spectrum. Therefore, the assignment of each spectral line to one of the protons can be made without any strict mathematical treatment of the spectrum. Fig. 3 shows the spectra for the ring protons in dimethylphenols in carbon tetrachloride and in acetone solutions with a concentration of about 0.1 mol. fractions. The position of the resonance field for each proton is indicated with a thick line with the figure of the location in the ring referring to the OH group.

The width of the ring proton resonance spectrum decreases generally with the increasing concentration as shown in Fig. 1. From detailed examinations of these spectra, it appears that the *o*- and *p*-proton resonance lines are at a higher field than that for the *m*-proton, and the slope of the curves for *o*- and *p*-protons is gentle compared with that for *m*-proton. Thus the curves for these protons approach each other as the concentration increases. This is the cause of the decrease of the width. The different concentration dependences of *o*- and *p*-protons from that of *m*-proton may be ascribed to the change in the magnitude of the mesomeric effect of the OH group on the ring protons with the change in the hydrogen bonding situation.

The differences between the ring proton spectra for carbon tetrachloride solution and that for acetone solution are observed as shown in Fig. 3. These arose from the different situations of the molecule in different mediums; one is a nearly free, non-hydrogen bonded molecule in carbon tetrachloride solution and another a hydrogen bonded molecule with the solvent in acetone solution. A noticeably different point is the displacement of the *o*-proton resonance lines to a lower field for 2, X-dimethylphenols (X=4 or 5) in acetone solution. It seems very probable that the displacement is caused by the formation of a hydrogen bond between the *o*-proton and the C=O group in an acetone molecule[7]: An




Chemical shift refer to $H_2O$ proton, p.p.m.

Fig. 3. Ring proton resonance spectra of dimethylphenols in $CCl_4$ and acetone solutions with concentration of about 0.1 mol. fraction.

7) T. Schaefer and W. G. Schneider, *J. Chem. Phys.*, **32**, 1218 (1960).

acetone molecule forms a strong hydrogen bond with the OH group. Therefore this O–H bond would be orientated inevitably to the side of the *o*-proton because of the steric hindrance of the *o*-Me group, and a weak hydrogen bond would be formed between the *o*-proton and the C=O group because of the proximity of these groups. Thus the decreased electron density in *o*-proton caused by the formation of the hydrogen bond would displace the resonance field of the *o*-proton to a lower field.

In 2,6-dimethylphenol, two methyl groups would inhibit the formation of a hydrogen bond with any proton donor or acceptor. Therefore, merely a minute change is observed in the ring proton spectrum with the change is observed in the ring proton spectrum with the change in solvent and concentration. 3,X-dimethylphenols (X=4 or 5) also show minute changes in their ring proton spectra. These molecules have no *o*-Me group, and the OH group may be able to rotate freely about the C–O axis. Therefore, there is no specific steric effect on the *o*-protons. This would be a reason why the changes in solvent and concentration do not displace the *o*-proton resonance lines appreciably.

**Summary**

The nuclear magnetic resonance in dimethylphenols were observed. The dependences of the chemical shifts for the methyl, hydroxyl and ring protons on solvent and concentration were measured and several clear differences were observed among the spectra of the isomers. The phenols with one or two ortho methyl groups showed peculiar behaviors which may be ascribed to the interaction between the hydroxyl group and the ortho proton or ortho methyl protons. The evidience of the steric hindrance of the ortho methyl group to form an intermolecular hydrogen bond is also shown in the present measurements.

The author wishes to express his sincere thanks to Professor S. Fujiwara and Dr. A. Danno for their kind guidance and encouragement throughout the present work. His thanks are also due to Drs. N. Nakagawa, H. Shimizu and N. Hayakawa who discussed the problem and gave their valuable suggestions.

*Radiation Application Division*
*Japan Atomic Energy*
*Research Institute*
*Tokai, Ibaragki-ken*

# *A UAO Treatment of the van der Waals Force*

By Teijiro YONEZAWA, Hiroshi KATO, Keiji MOROKUMA and Kenichi FUKUI

(Received November 17, 1960)

Dispersion forces for numerous molecules and atoms have been estimated by London's[1] and Slater-Kirkwood's[2] dispersion formula. However, the exact theoretical evaluation is nearly impossible to achieve except for the simplest molecules and atoms. Approximate formulas are usually used to estimate the magnitude of this force between them.

London's one-term approximation formula is written as:

$$\langle \Delta E \rangle_{AV} = -\frac{3}{2R^6} \frac{\Delta_1 \Delta_2}{\Delta_1 + \Delta_2} \alpha_1^0 \alpha_2^0 \qquad (1)$$

Here the subscripts refer to the two different molecules, $\alpha^0$ is the polarizability, and $\Delta$ is taken to be equal to the ionization energies of the molecules.

In the present paper, non-empirical calculation is made on the dipole-dipole interaction term of dispersion force between two $CH_4$, $NH_4^+$ and $H_2O$ molecules and two neon atoms by the perturbation theory. In the course of calculation, we make use of the UAO[3,4] (united atom approach or central field approximation) which was used to obtain ionization potential, dissociation energy and so on in simple molecules with nearly spherical configuration. By the UAO method, the total wave function for $CH_4$, $NH_4^+$ and $H_2O$ which involves only three parameters is a ten-electron Slater determinant $\Phi$ with configuration $(1s)^2\ (2s)^2\ (2p)^6\ {}^1S$ as same as neon atom. The one electron wave function of each molecule and atom is as follows:

1) F. London, *Trans. Faraday Soc.*, **33**, 8 (1937).
2) J. C. Slater and J. G. Kirkwood, *Phys. Rev.*, **37**, 682 (1931).
3) K. Funabashi and J. L. Magee, *J. Chem. Phys.*, **26**, 407 (1957).
4) M. J. M. Bernal, *Proc. Phys. Soc.*, **A66**, 514 (1953).

TABLE I. DISPERSION FORCE. THE VALUES OF THE COEFFICIENT OF $R^{-6}$ TERM (IN UNITS OF $10^{-60}$ erg. cm$^6$)

| | Ne | $NH_4^+$ | $CH_4$ | | $H_2O$ | |
|---|---|---|---|---|---|---|
| | | | 1 | 2 | 1 | 2 |
| $\alpha$ | 9.7 | 6.71 | 5.01 | 5.18 | 7.1648 | 7.3551 |
| $\beta$ | 5.86 | 2.17 | 5.01 | 5.18 | 7.1648 | 7.3551 |
| $\gamma$ | 5.86 | 1.62 | 3.00 | 2.59 | 3.5824 | 2.9420 |
| Our results | 5.75 | 153.9 | 181.5 | 375.4 | 112.7 | 278.4 |
| In Margenau's table[5] | 7.97<br>7.48<br>4.67 | (107.9) | 112 | | 47 | |
| Estimated by second virial coefficient[6] | 8.32 | — | 240 | | — | |
| $E_{AV}$* | 51.4 | 25** | 28.2 | | 25.6 | |

* The values of $E_{AV}$ adopted in this paper are the same as those in Margenau's paper[5].
** The value of ionization potential is roughly estimated from those of $NH_3$ and $CH_4$, and $\alpha^0$ is $2.68\times10^{-24}$ cm$^3$ estimated from atomic refractive indexes.

For $CH_4$ and $H_2O$ molecules[3]

$$\varphi_{1s}=\left(\frac{\alpha^3}{\pi}\right)^{1/2}e^{-\alpha r}$$

$$\varphi_{2s}=\frac{1}{4}\left(\frac{\beta^3}{2\pi}\right)^{1/2}(2-\beta r)e^{-(\beta/2)r}$$

$$\left.\begin{matrix}\varphi_{2px}\\ \varphi_{2py}\\ \varphi_{2pz}\end{matrix}\right\}=\left(\frac{\gamma^5}{32\pi}\right)^{1/2}r\,e^{-(\gamma/2)r}\left\{\begin{matrix}\sin\theta\cos\varphi\\ \sin\theta\sin\varphi\\ \cos\theta\end{matrix}\right.$$

For $NH_4^+$ ion, the radial factors are[4]

$$R_{1s}=(2\alpha)^{3/2}e^{-\alpha r}$$

$$R_{2s}=\left\{\frac{12\beta^5}{\alpha^2-\alpha\beta+\beta^2}\right\}^{1/2}\left\{1-\frac{1}{3}(\alpha+\beta)r\right\}e^{-\beta r}$$

$$R_{2p}=\left(\frac{4\gamma^5}{3}\right)^{1/2}r\,e^{-\gamma r}$$

As to the neon atom, we use the Slater orbitals, and the effective nuclear charge in each orbital is calculated by Slater's rule.

The values of the three parameters adopted are the same as in the quoted papers, and they aer listed in Table I.

The unperturbed total wave function $\Phi$ can be written as $\Phi=\Phi_1\cdot\Phi_2$, since the exchange of electrons does not occur in the range where the intermolecular distance between molecules (or atoms) 1 and 2 is very great.

The potential due to the dipole-dipole interaction between to molecules (or atoms) is given as follows:

$$V=\frac{e^2}{R^3}\sum_{i,j}(x_{1i}x_{2j}+y_{1i}y_{2j}-2z_{1i}z_{2j}) \qquad (2)$$

where $R$ is the distance between molecules or atoms, and $x_{1i}$, $y_{2j}$ are the $x$ and $y$ coordinates for $i$th and $j$th electrons belonging to molecules (or atoms) 1 and 2, respectively. The z-axes are taken along the intermolecular distance $R$.

Taking the interaction $V$ as a perturbation, the perturbation energy between the same molecules (or atoms) is given by

$$\Delta E=(00\,|\,V\,|\,00)+\sum_{k_1,k_2}\frac{|(00\,|\,V\,|\,k_1k_2)|^2}{2E(0)-E(k_1)-E(k_2)} \qquad (3)$$

where index 0 refers to the state function of the ground state, $k$ referring to all possible excited states.

In the above equation, it can be shown that $(00\,|\,V\,|\,00)$ is zero in the present treatment. In the second term, if one replaces the dominator of Eq. 3 by a mean $E_{AV}$, the second order perturbation energy can be

$$\Delta E=\frac{1}{E_{AV}}\sum_{k_1,k_2}|(00\,|\,V\,|\,k_1k_2)|^2=\frac{(00\,|\,V^2\,|\,00)}{E_{AV}} \qquad (4)$$

$E_{AV}$ is put equal to twice the ionization potential according to the treatment of Margenau[5].

Thus, $\Delta E$ is calculated as follows:

$$\Delta E=-\frac{24e^4}{R^6E_{AV}}\left[\frac{1}{3}(1s\,|\,r^2\,|\,1s)+\frac{1}{3}(2s\,|\,r^2\,|\,2s)+(2p_\sigma\,|\,z^2\,|\,2p_\sigma)+2(2p_\pi\,|\,z^2\,|\,2p_\pi)-2(1s\,|\,z\,|\,2p_\sigma)^2-2(2s\,|\,z\,|\,2p_\sigma)^2\right]^2 \qquad (5)$$

where $2p_\pi$ refers to $\varphi_{2px}$ or $\varphi_{2py}$ and $2p_\sigma$ is to $\varphi_{2pz}$, and

$$(1s\,|\,r^2\,|\,1s)=\int\varphi_{1s}^*r^2\varphi_{1s}\,d\tau$$

$$(2p_\sigma\,|\,z^2\,|\,2p_\sigma)=\int\varphi_{2pz}^*z^2\varphi_{2pz}\,d\tau$$

The numerical values of the coefficient of

5) H. Margenau, *Rev. Modern Phys.*, **11**, 1 (1939).

$R^{-6}$ term in $\Delta E$ of the present molecules and atoms are listed in Table I.

As to methane and neon with uniformly charged spherical configuration, the values of the coefficient of $R^{-6}$ term in $\Delta E$ almost agree with those calculated by London's approximate formula and also with those estimated by the second virial coefficient[6]. But, for $H_2O$, the value of the coefficient of $R^{-6}$ term in $\Delta E$ is greater than the one obtained by London's formula, since the $H_2O$ molecule belongs to $C_{2v}$ and its UAO treatment may be inadequate.

Two kinds of calculations referring respectively to case 1 and case 2, are made, in which three different parameters are adopted for wave functions. The results indicate that the values of the coefficient of $\Delta E$ depend greatly on the values of parameters, in particular, on those of the outermost shell orbital. For example, the calculated values in $H_2O$ in case 1 is three times as great as those in case 2. However, it may be remarked that the modification of these parameters in cases 1 and 2 causes a change of only less than 1% in the total electronic energy[3].

In regard to $NH_4^+$, $R^{-6}$ term in interaction energy is of minor importance, since this molecule is an ion. However, in a rough estimation of this term by Eq. 1, the coefficient of $R^{-6}$ term becomes 107.9. Hence, the calculated values seem to be reasonable.

The UAO procedure will also be applicable to $SiH_4$[7], $PH_3$ and other molecules which have at least a nearly spherical symmetry. This point will be investigated in future.

Our conclusion is as follows:

1) The UAO calculation of intermolecular interaction energy due to dipole-dipole is rather simple and easy, while the agreement is comparatively good.

2) Care must be taken, however, when one treats the molecule which deviates to a great extent from spherical symmetry.

3) The parameter dependence of the interaction energy is greater than that of the electronic energy of a molecule.

4) Therefore, to adopt better parameters is most important in carrying out the calculation by the UAO method. For this purpose, attention should be paid to the polarization which may take place when two molecules come near each other.

*Faculty of Engineering*
*Kyoto University*
*Sakyo-ku, Kyoto*

6) M. Mizushima, "Bunshiron", Kyoritu, Tokyo (1950), p. 270.

7) C. Carter, *Proc. Roy. Soc.* (*London*), **A235**, 321 (1956).

# *On the Electrical Conductivity of the Organic Thin Films: Perylene, Coronene and Violanthrene*

By Hiroo INOKUCHI, Haruo KURODA and Hideo AKAMATU

(Received November 1, 1960)

In recent years, the electronic conduction in organic compounds has aroused interest and a number of reports on their related behaviors have been accumulated[1,2]. The early works in this field were of the preliminary survey type, but recent articles tend to concentrate on the physico-chemical properties of the specific compounds under more carefully controlled conditions. However, some substantial discrepancies are still found in the results observed by different investigators. Some of the discrepancies may be due to the difference in the preparation or the formation of the specimens. For instance, thin evaporated films of aromatic hydrocarbons are frequently applied to the investigation of the semi- and photo-electrical conductivity. However, relatively little attention has been given to the structure of these films.

The present paper deals with the electrical conductivity and structural survey of thin organic films prepared in vacuo upon various substrates.

## Experimental

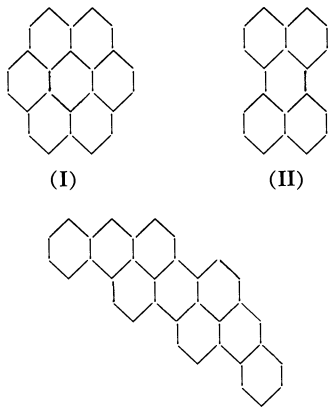
**Materials.**—*Coronene (I).*—This aromatic compound, including a small amount (nearly 5%) of higher condensed aromatic compounds, was provided

1) H. Akamatu and H. Inokuchi, "Proceedings of the Third Conference on Carbon", Pergamon Press, London (1959), p. 51.

2) C. G. B. Garrett, "Semiconductors", (N. B. Hannay, ed.), Reinhold, New York (1959), p. 634.

by Badische Anilin and Soda Fabrik A. G. in Germany[3]. First, the crude hydrocarbon was purified carefully by means of the recrystallization method from its benzene solution. In addition, through the repeated high vacuum sublimations, pure coronene, for which the melting point was 438°C, was separated as a beautiful yellow hydrocarbon[4].

*Perylene (II) and Violanthrene (III).*—These two polycyclic aromatic hydrocarbons were synthesized by Drs. T. Handa and J. Aoki. The purified hydrocarbons were obtained by evaporation in vacuo in a manner similar to that reported in the previous article[5].




**Procedures.**—The following three types of conductivity cells were employed to measure the electrical resistivity of the organic compounds.

*The Sandwich-type Cell.*—The aromatic hydrocarbons having approximately one or two microns in thickness was deposited by vacuum evaporation on a pyrex glass plate, which had been coated in advance with aluminium film to provide one electrode. A second electrode, thereafter, was formed by evaporation of aluminum film under a high vacuum as shown in Fig. 1. The electrical resistivity of this cell was measured in an atmosphere of argon. The estimation of specific resistivity was not so accurate, because of large errors incurred in the observation of the dimensions of the specimens.

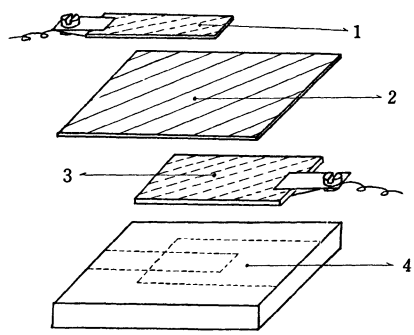



Fig. 1. The sandwich-type of cell. 1 and 3 are metal films which serve as electrodes. 2 is an organic film and 4 is a glass substrate.

*The Surface-type Cell.* — This type of cell was prepared by evaporation of an organic film on a pyrex glass plate which has parallel electrodes that are separated from each other by a gap of 2 mm. This cell was placed in a glass chamber as shown schematically in Fig. 2. These electrodes were

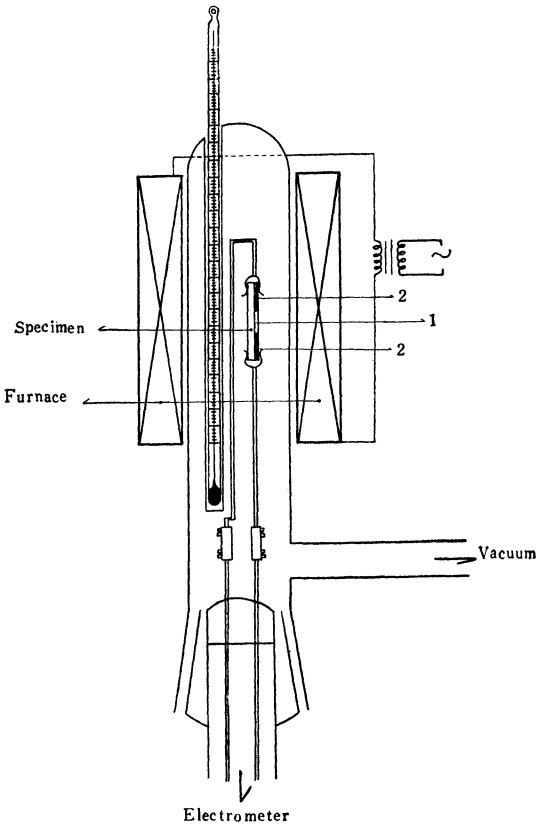



Fig. 2. The surface-type of conductivity cell placed in a glass chamber.
1, Organic thin layer
2, Terminal electrode

connected through two metal-to-glass seals to the vibration-reed electrometer. Throughout all the experiments, this chamber was maintained in a vacuum of $10^{-5}$ mmHg or less, to preclude an effect of air and/or of humidity on the films*.

*The Bulk Specimen.*—The crystalline powders were packed into a quartz cylinder, area 0.5 $cm^2$, between two platinum-plated brass electrodes. The specimens were compressed in the cylinder up to 116 kg./$cm^2$ by a lever system.

**Technique.**—*Electric Conduction.*—The resistances of the above specimens, at room temperature, were from $10^9$ to $10^{14}$ Ω. The measurements of high resistance were carried out, therefore, with the

3) L. Boente, *Brennstoff-Chem.*, **36**, 210 (1955).
4) E. Clar and W. Kelley, *J. Chem. Soc.*, **1956**, 3875.
5) H. Inokuchi, *J. Org. Synth. Japan*, **13**, 486 (1955).

* From a preliminary experiment, an introduction of air into the chamber is one of the most important reasons for the instability of the conductivity of thin films and also one of the interesting aspects of their studies.

association of the vibration-reed electrometer apparatus.

*X-Ray Diffraction.*—The transparent organic films evaporated on several substrates—glass, potassium chloride crystal, copper plate and also the cleavage surface of graphite—were examined as to their textured structures by means of a Geiger counter X-ray diffractometer.

*Electron Micrograph.*—The electron micrographs were made with association of the Hitachi electron-microscope, HU-10. The structural analysis of the small individual crystals ($1\,\mu \times 1\,\mu$) in the thin organic films could be carried out easily by means of the electron microdiffraction combined with the electron micrograph. As a specimen for the above two methods, the transparent organic films on glass substrates were stripped off from the substrates and in addition the carbon-replica technique was applied on them.

## Results and Discussions

Through all the experiments, the results of the electrical resistivity of various types of conductivity cells can be expressed by a semi-conductive equation[1] (Fig. 3):

$$\rho = \rho_0 \exp(\Delta\varepsilon/2kT)$$

where $\Delta\varepsilon$ is an apparent energy gap. The various forms of specimens with regard to the type of cells are thus compared with each other conveniently in terms of $\Delta\varepsilon$ and the electrical resistivity $\rho$ at 15°C in Table I.

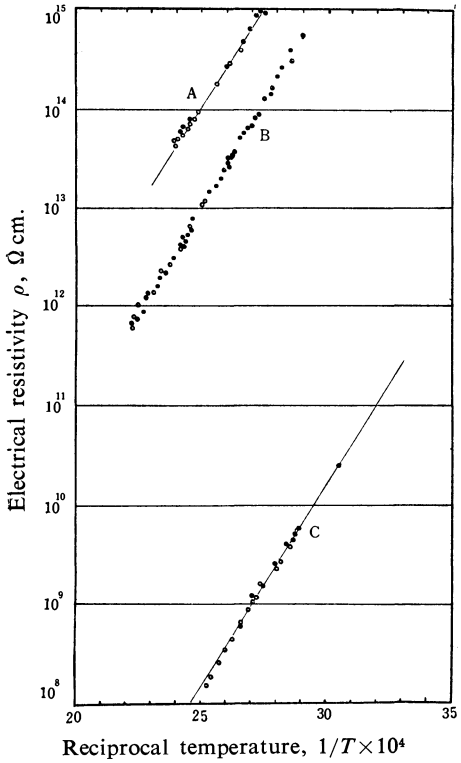



Fig. 3. The electrical resistivity versus temperature of various types of violanthrene conductivity cells.
A. Sandwich-type B. Bulk C. Surface-type

Table I. The electrical resistivity of polycyclic aromatics, observed from the various types of cell

| Compound | Perylene | Coronene | Violanthrene |
|---|---|---|---|
| From bulk specimen | | | |
| $\rho_{15}$(Ω cm.) | $4\times10^{18}$ | $1.7\times10^{17}$ | $2.1\times10^{14}$ |
| $\Delta\varepsilon$(eV.) | 2.0 | 1.7 | 0.85 |
| From surface-type cell | | | |
| $\rho_{15}$(Ω cm.) | $\sim10^{13}$ | $10^{12}\sim10^{13}$ | $\sim10^{9}$ |
| $\Delta\varepsilon$(eV.) | 2.2 | 1.65 | 0.9 |
| From sandwich-type cell | | | |
| $\rho_{15}$(Ω cm.) | $10^{18}\sim10^{19}$ | $10^{17}\sim10^{18}$ | $\sim10^{14}$ |
| $\Delta\varepsilon$(eV.) | 2.0 | 1.6 | 0.9 |

In this table, it is found that the electrical resistivity observed with the sandwich-type cell is in quite good agreement with that of the bulk specimen. However, a great difference is found between the resistivities of the sandwich-type cell and the surface-type one. The resistivity of the sandwich-type cell is much less than that of the surface-type by a factor of $10^4\sim10^5$. The electric field is applied along the surface of the film in the surface-type cell, while it is applied perpendicularly to the film for the sandwich-type cell. Therefore, the difference implies that there is an anisotropy of resistivity in the thin film.

It is well known that when a substance is deposited onto a substrate from solution or vapor phase to produce a thin film, a textured

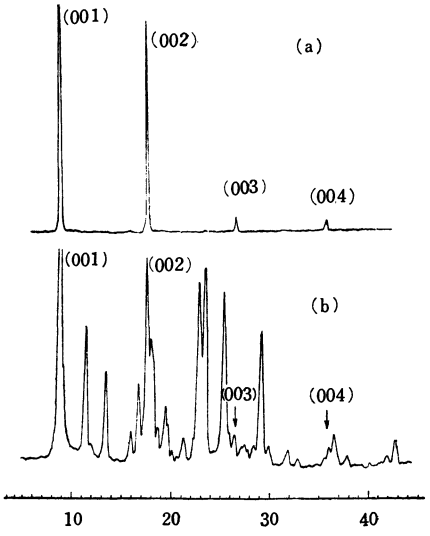
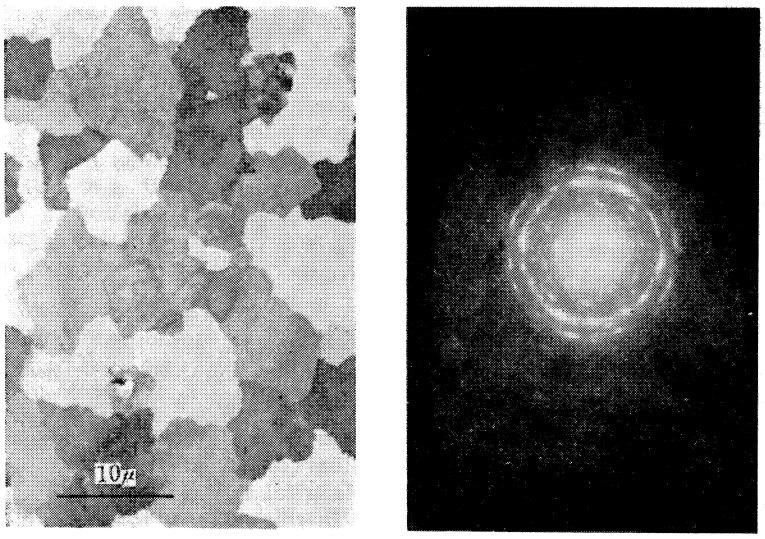



Fig. 4. The X-ray diffractometer records of (a) powder and (b) evaporated film of coronene.




(a) (b)

Fig. 5. (a) The electron micrograph and (b) the electron microdiffraction pattern of an evaporated film of coronene.

structure in which crystallites are arranged with a preferred orientation usually occurs. This was proved for the evaporated film of the aromatic compounds by means of X-ray diffraction. When the X-ray diffraction pattern of these organic thin films was examined with the diffractometer, it was found that diffraction lines were composed only of (00*l*) reflection and other reflections were missing completely (Fig. 4). This is the evidence for the fact that the crystallites of aromatic hydrocarbons were in alignment with their a·b planes parallel with the film surface. The mode of arrangement of crystallites is quite independent on the substrate materials which were described in the above section.

The electron microscopic observation and the application of electron microdiffraction verified the foregoing conclusion: From the electron micrographs (Fig. 5), it is found that the films consist of a number of single crystals which are arranged in closed packing with each other on the substrate, and the electron microdiffraction reveals that the crystallites are in alignment with their a·b planes parallel with the film surface.

Therefore, the discrepancy in resistivity between the surface-type and the sandwich-type cells could be attributed to the substantial anisotropy of resistivity of the crystals. Thus, the resistivity along the a·b plane of crystal should be much smaller than that perpendicular to the same plane for these compounds.

This conclusion is consistent with the results observed with anthracene single crystal. Mette and Pick have reported the anisotropy of electrical resistivity in anthracene[6], that is to say, the conductivity in a·b plane was a few times higher than that in a·c plane. Compton, Schneider and Waddington observed that the photocurrent along the b-axis direction is about one hundred times higher than that in the c-axis direction and several times larger than that along the a-axis direction[7].

The a·b plane is the cleavage plane of the crystal, and the molecules are so arranged that the molecular planes are nearly perpendicular to this plane. The nearest approach of neighboring molecules is found in the a·b plane. If there could be overlapping of molecular orbitals of $\pi$-electrons between neighboring molecules, it should take place along the direction parallel to this a·b plane. On the other hand, there is no reason to expect a stronger interaction between molecules in the direction along the c-axis. Therefore, it is reasonable to find the least value of resistivity along the a·b plane.

From Table I, it is seen that the anisotropy is found in the value of resistivity but not in the value of energy gap. Hence, there is no reason to expect a difference in the number of charge carriers which are in excited state. There should, however, be a large difference in the mobility of carriers depending on the direction of drift.

6) H. Mett and H. Pick, *Z. Physik*, **134**, 566 (1953).
7) D. M. J. Compton, W. G. Schneider and T. C. Waddington, *J. Chem. Phys.*, **27**, 160 (1957).

**Summary**

It was found that the various types of conductivity cells of aromatic hydrocarbons possess great discrepancies of their electrical resistivity. The resistivity observed with the sandwich-type cell, perylene; $10^{18\sim19}\,\Omega$cm., coronene; $10^{17\sim18}\,\Omega$cm., and violanthrene; $10^{14}\,\Omega$cm., is in quite good agreement with that of the bulk specimen. However, a great difference was found between the resistivities of the sandwich-type and the surface-type cells, perylene; $10^{13}\,\Omega$cm., coronene; $10^{12\sim13}\,\Omega$cm., and violanthrene; $10^{9}\,\Omega$cm. This discrepancy in resistivity can be assumed to be introduced from the textured structure of the evaporated films and the substantial anisotropy of crystals; the crystals are in alignment with their a·b plane with the film surface. This orientation was found from the X-ray diffraction results, combined with the electron microscopic observation and the electron microdiffraction results.

The authors express hearty thanks to Drs. T. Handa and J. Aoki who prepared the samples of this work. The cost of research has been defrayed from the Scientific Research Encouragement Grant from the Minstry of Education, to which the authors' thanks are due.

*Department of Chemistry*
*Faculty of Science*
*The University of Tokyo*
*Hongo, Tokyo*

# *Studies on the Chemical Decomposition of Simple Sugars. X. Acetol Formation from $^{14}C$-Labeled Hexoses**

By Ryozo GOTO, Jun'ichi HAYAMI, Kenichi KUDO and Sinichi OTANI

(Received November 17, 1960)

As is well known, carbohydrates, especially monosaccharides, have many reactive functional groups, and these compounds show various kinds of reactions. In an aqueous solution, monosaccharides show the following fourma in types of reactions, which depend upon the pH of the reaction medium.

These are a) the "Lobry de Bruyn-Alberda Van Eckenstein reaction[1], b) the formation of furfural derivatives[2a] in acid medium, c) the reverse aldolization[3] which gives rise to the formation of smaller fragments, a possible recombination reaction of these fragments which may occur, and d) an acid formation in an alkaline medium to yield lactic and saccharinic acids[4a].

Each of these reactions has been well-examined for a long time, and detailed mechanisms for these reactions were proposed. Recently, some of them have been confirmed chemically and also radiochemically[1,2b,4b].

Besides these reactions, there is another decomposition reaction, for example, when an aqueous solution of hexoses (pH 3~11) is heated, sugars are decomposed and some steam volatile products are formed. From the decomposition mixture Dakin[5], Nef[6], and Evans[7,8] have obtained methylglyoxal phenylosazone, and they concluded that the reaction product might be methylglyoxal. However, it is easily understood that methylglyoxal phenylosazone can be derived from either acetol or lactic aldehyde as well as from methyl glyoxal. Therefore methylglyoxal cannot be (concluded to be) a sole product. But with the use of semicarbazide, it is possible to distinguish methylglyoxal from acetol.

* Presented at the 11th Annual Meeting of the Chemical Society of Japan, Tokyo, April, 1958 and the 12th Annual Meeting of the Chemical Society, Kyoto, April 1959.

1) J. C. Speck, Jr., "Advances in Carbohydrate Chem.", Vol. 13 (1958), p. 63.

2) a) F. H. Newth, ibid.. Vol. 6. (1951), p. 83, and references cited therein; J. Kennerand G. N. Richards, *J. Chem. Soc.*, **1956**. 2921.

b) W. A. Bonner and M. R. Roth, *J. Am. Chem. Soc.*, **81**. 5454 (1959).

3) W. L. Evans, *Chem. Revs.*. **31**, 537 (1942).

4) a) J. C. Sowden, "Advances in Carbohydrate Chem.", Vol. 12, (1957), p. 36; R. L. Whistler and J. N. BeMiller, ibid., Vol. 13, (1958), p. 289; G. Machell and G. N. Richards, *J. Chem. Soc.*, **1960**, 1924, 1932, 1938.

b) J. C. Sowden et al.. *J. Am. Chem. Soc.*, **79**, 6450 (1957); J. C. Sowden and E. K. Pohlen, ibid., **80**. 242 (1958).

5) H. J. Dakin and H. W. Duddley, *J. Biol. Chem.*, **15**, 127 (1913).

6) J. U. Nef, *Ann.*, **357**, 214 (1907); **376**, 1 (1910); **403**, 204 (1914).

7) W. L. Evans, *J. Org. Chem.*, 1, 1 (1937) and references cited therein.

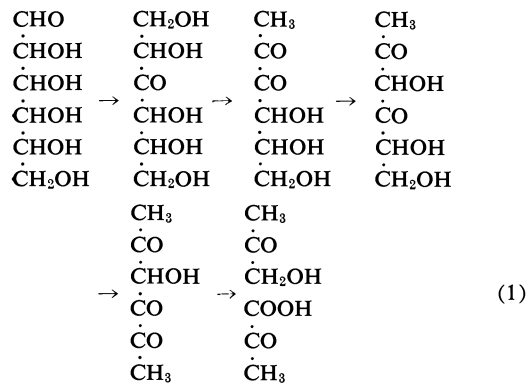
8) C. Enders et al., *Naturwiss.*, **29**, 46 (1941); *Biochem. Z.*, **312**, 349 (1942).

Nodzu[9] and Goto[10] have examined the decomposition products of glucose in a weakly acid and a weakly alkaline solution and isolated acetol semicarbazone instead of methylglyoxal bissemicarbazone. In a series of extensive experiments, they confirmed the fact that a) hexose[11a,b], methylpentose[10], and pentose[10] gave acetol accompanied by small amounts of diacetyl and of lactic aldehyde[11c] and these sugars gave substantially no methylglyoxal, b) tetrose[10] gave only diacetyl and did not produce acetol and c) triose[11d] gave methylglyoxal and diacetyl.

Recently, Sattler[12] observed the formation of acetol by the decomposition of simple sugars in a weakly alkaline aqueous solution. Prey[13], also, thoroughly examined the alkaline degradation of simple sugars and observed the formation of acetol.

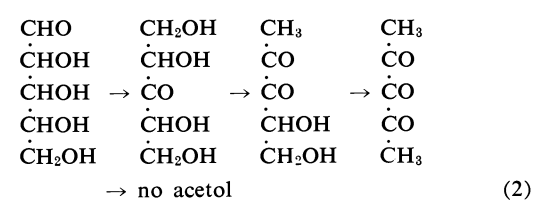
As it has been reasonably accepted that hexose and pentose can yield trioses through a reverse-aldolization[3], and that trioses in turn are easily dehydrated to methylglyoxal, the supposition of the formation of methylglyoxal which was claimed by early workers would be rather natural. Therefore, the formation of acetol, instead of methylglyoxal, seemed to be a novel reaction of a sugar. But little has been known regarding the mechanism of acetol formation from simple sugars.

Nodzu et al.[11d] noticed the formation of acetol accompanied by pyruvic acid and under the supposition of their simultaneous formation, the following mechanism (Scheme 1) which included acetylformoin[14] as a direct precursor of acetol was proposed. Acetylformoin is an acyloin formed from methylglyoxal.



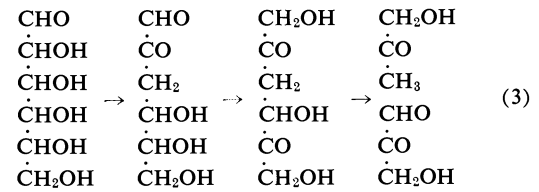
(1)

Later on, Goto inferred from Nodzu's mechanisms, that if it was applied to a pentose, it would lead to the formation of triketopentane as is shown in the following scheme:



(2)

Since no acetol is derived from this triketopentane, he propounded an alternative mechanism for the formation of acetol. His mechanism for this reaction is illustrated in Scheme 3:



(3)

These mechanisms, however, lack any positive evidence. For the better understanding of the mechanism of acetol formation, more detailed knowledge is required. To establish the nature and to confirm the precise mechanism for the acetol formation, the authors undertook the syntheses of $^{14}C$-labeled monosaccharides and examined the decomposition of these $^{14}C$-labeled monosaccharides.

In the present study, glucose-1-$^{14}C$, glucose-3,4-$^{14}C$, and glucose-6-$^{14}C$ were decomposed in a concentrated phosphate buffer to yield acetol, and the relative distribution of a label in the acetol was determined.

## Experimental

**Radioactive Sugars and Assay Method.** — D-Glucose-1-$^{14}C$ was prepared from D-arabinose by a cyanohydrin synthesis[15]. D-Glucose-3,4-$^{14}C$ was prepared from rat liver glycogen injected with $NaH^{14}CO_3$, according to Wood's method[16] with minor modifications. D-Glucose-6-$^{14}C$ was prepared from 1,2-*O*-isopropylidene-D-*xylo*-dialdopentofuranose[17]. In the course of synthesis, deionization at an ice temperature was undertaken with Amberlite type I IRCG-120, instead of ordinary IR-120, to secure a satisfactory exchange.

For an assay, except for specified ones, all sample were converted into barium carbonate by Van Slyke-Folch wet conbustion. Barium carbonate was collected on a filterpaper and counted in an infinite

9) R. Nodzu, This Bulletin, **10**, 122 (1935). (weakly acid region.)
10) R. Goto, ibid., **15**, 209 (1940); *J. Chem. Soc. Japan, Pure Chem. Sec.* (*Nippon Kwagaku Kwaisi*), **64**, 999, 1054, 1183 (1943). (weakly alkaline region.)
11) a) R. Nodzu and K. Matsui, This Bulletin, **10**, 467 (1935); b) R. Nodzu and R. Goto, ibid., **11**, 381 (1936); c) R. Goto, ibid., **15**, 103 (1940); d) R. Nodzu, et al., *Mem. Coll. Sci. Kyoto Imp. Univ.*, **A20**, 197 (1937).
12) L. Sattler and F. W. Zerban, *J. Am. Chem. Soc.*, **70**, 1975 (1948).
13) V. Prey and E. Waldman, *Monatsh.*, **83**, 55 (1952).
14) R. Nodzu and S. Kunichika, This Bulletin, **15**, 211 (1940).
15) H. S. Isbell et al., *J. Research N. B. S.*, **48**, 163 (1952).
16) H. G. Wood et al., *J. Biol. Chem.*, **159**, 475 (1945).
17) R. Schaffer and H. S. Isbell, *J. Research N. B. S.*, **56**, 191 (1956).

thickness under an end-window type G. M. counter. Probable errors of the counting were within 3% except for specified ones.

**Decomposition of Labeled Sugars.**—A solution of 5 g. of D-glucose in 200 ml. of concentrated potassium acid phosphate buffer (40%, pH 6.7) was heated and distilled, fresh water was added to maintain a constant volume. Two hundred and fifty mililiters of distillate was collected every 90 min., and distillation was continued until the distillate showed only a faint iodoform reaction, (total volume of distillate 5 l., 284 mg. as acetol). The amount of acetol contained in the distillate was determined by iodometric titration according to Nodzu[9] (1 ml. of 0.1 N $I_2$ solution corresponds to 0.73 mg. of acetol).

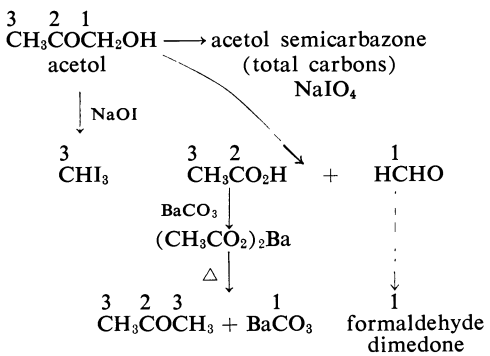
By the above titration, the methyl carbon of acetol was converted into iodoform. This compound was collected and assayed for activity.

**Acetol Semicarbazone.**—The combined distillate cited above was treated with semicarbazide hydrochloride and with sodium acetate (5 fold equivalents of acetol). The mixture was heated over a boiling water bath for 30 min., cooled and concentrated to a small volume under reduced pressure. Semicarbazone was separated and fractionally recrystallized from hot water. Successive recrystallizations gave 70 mg. of acetol semicarbazone as colorless needles, m. p. 199~200°C. The melting point showed no depression when mixed with an authentic sample.

**Degradation of Acetol.**—*Formaldehyde Dimedone from Acetol.*—An aqueous solution of acetol was treated with 50% excess of sodium metaperiodate in sodium bicarbonate buffer, and stood overnight at room temperature. The aqueous solution was concentrated under reduced pressure, and from the distillate, formaldehyde was precipitated as formaldehyde dimedone. It was recrystallized from an aqueous ethanol to give colorless needles, m. p. and mixed m. p. 190~191°C.

*Separation and Degradation of Barium Acetate.*—The residue from the periodate oxidation was treated with a carrier acetate, acidified, and was steam distilled. The iodic and periodic acid in the distillate were removed by silver carbonate[18], and formic acid was removed by oxidation with mercuric oxide*, according to Osburn's method[19]. The acetic acid was refluxed for a further 15 min. After cooling and filtration, acetic acid was distilled out with steam.

Scheme 4




Note: Numbers correspond to the one in the present acetol.

Table I. Radioassay data for $^{14}C$-labeled glucose (radioacetol from glucose-1-$^{14}C$)

| | Sample | Carbon atom(s) | Radioactivity μc./mol. |
|---|---|---|---|
| Glucose-1-$^{14}C$ | | | 435 |
| Acetol | Acetol semicarbazone | all | 203 |
| | Formaldehyde dimedone | $CH_2OH$ | 0 |
| | $BaCO_3$ from Ba acetate | CO | —*1 |
| | Iodoform | $CH_3$ | +*2 |

Table II. Radioassay data for $^{14}C$-labeled glucose (radioacetol from glucose-3,4-$^{14}C$)

| | Sample | Carbon atom(s) | Radioactivity μc./mol. |
|---|---|---|---|
| Glucose-3,4-$^{14}C$ | | | 31.7 |
| Acetol | Acetol semicarbazone | all | 32.6 |
| | Formaldehyde dimedone | $CH_2OH$ | 33*3 |
| | $BaCO_3$ from Ba acetate | CO | —*1 |
| | Iodoform | $CH_3$ | —*4 |

*1 Free from radioactivity, a carrier was used.
*2 Radioactivity was present.
*3 Probable error was less than 10%.
*4 Free from radioactivity.

Table III. Radioassay data for $^{14}C$-labeled glucose (radioacetol from glucose-6-$^{14}C$)

| | Sample | Carbon atom(s) | Radioactivity μc./mol. |
|---|---|---|---|
| Glucose-6-$^{14}C$ | | | 616 |
| Acetol | Acetol semicarbazone | all | 141 |
| | Formaldehyde dimedone | $CH_2OH$ | 35 |
| | —*1 | CO | —*1 |
| | Iodoform | $CH_3$ | 106*2 |

Table IV. Radioassay data for $^{14}C$-labeled glucose (radioacetol from glucose-1-$^{14}C$, pH 11)

| | Sample | Carbon atom(s) | Radioactivity μc./mol. |
|---|---|---|---|
| Glucose-1-$^{14}C$ | | | 435 |
| Acetol | Acetol semicarbazone | all | 173 |
| | Formaldehyde dimedone | $CH_2OH$ | 73 |
| | $BaCO_3$ from Ba acetate | CO | —*3 |
| | Iodoform | $CH_3$ | 108 |

*1 Not determined.
*2 Indirectly calculated.
*3 Almost free from radioactivity, a carrier was used.

* About 250 mg. of crude sodium acetate (with carrier), was dissolved in 50 ml. of water, 3 drops of sulfuric acid and 5 g. of mercuric oxide were added, and the mixture was refluxed. After 20 min., 3.5 ml. of phosphoric acid (85%) and 2 ml. of water were added, and the mixture

18) P. W. Clutterbuck and F. Reuter, *J. Chem. Soc.*, 1935, 1467.
19) O. L. Osburn et al., *Anal. Chem.*, 5, 247 (1933).

thus purified, was converted into barium salt, and recrystallized from water for an assay and a degradation. Barium acetate was degraded to acetone and barium carbonate by pyrolysis[20] in the usual way. Acetone was converted into 2, 4-dinitrophenylhydrazone and assayed directly.

The course of the degradation of acetol is summarized in Scheme 4, and radioactivity assay data are given in Tables I—IV respectively.

## Results and Discussion

The contents of assay data which are shown in Tables I—IV can be summarized as follows:

1) In the case of D-glucose-1-$^{14}$C, radioactive acetol of about a half molar activity of the original glucose was formed. Periodate oxidation of the acetol provided formaldehyde (corresponding to carbinol carbon of the acetol), which was almost free from activity. The other carbons—methyl and carbonyl carbon—were converted, at the same time, into acetic acid. The acetic acid was degraded by the usual method of pyrolysis and afforded radioactive acetone and nonactive barium carbonate. These facts show that acetol-3-$^{14}$C was formed from glucose-1-$^{14}$C.

2) In the case of D-glucose-3, 4-$^{14}$C, radioactive acetol was obtained which preserved the original molar activity of the reactant glucose. The acetol was degraded to radioactive formaldehyde and nonactive acetic acid. This means that radioactivity was present at the primary carbinol carbon of the acetol. From these facts, it is quite possible that acetol-1-$^{14}$C is produced from D-glucose-3, 4-$^{14}$C.

3) D-Glucose-6-$^{14}$C, as was expected from the results of Tables I and II, afforded acetol, labeled mainly at the methyl carbon. But it should be noted that between the methyl and the carbinol carbon an appreciable randomization of a label is observed. This randomization was confirmed by another repeated run. But, as the label was found mainly at the methyl carbon, it might be possible to say that D-glucose-6-$^{14}$C produces acetol-3-$^{14}$C.

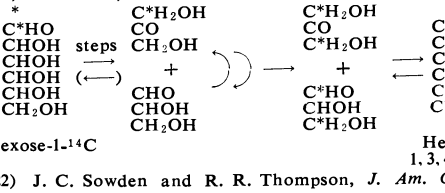
The patterns of the label cited above would reveal that, in the formation of acetol from glucose (hexose), C-1 and C-6 of the original glucose are converted into the methyl carbon of an acetol, while C-3 and C-4 of the original glucose are converted into the carbinol carbon of an acetol.

It is also remarkable that the acetol-1-$^{14}$C, which was produced from D-glucose-3, 4-$^{14}$C, preserves the molar radioactivity of the original glucose. This, coupled with the pattern of the label cited above, implies that, in the formation of acetol, C-1, 2, 3 and C-4, 5, 6 of the original glucose behave as a unit, and that no skeletal rearrangement in these $C_3$ units is involved. These facts further exclude the possibility of a random scission of the carbon-chain of a glucose in this reaction. This is because according to the mechanism of a random scission, universally labeled acetol might be produced, but it is not the case.

The randomization of a label might be attributed to the reverse-aldolization[3,21] and the recombination reaction of a hexose. This is because, as Sowden[22] pointed out, glucose-1-$^{14}$C and/or glucose-6-$^{14}$C could be converted into a hexose-1, 3, 4, 6-$^{14}$C through a reverse-aldolization and a recombination reaction of a hexose*. These reverse-aldolization and recombination reactions are shown to prevail in a high pH region, and in the present instance, radiactive acetol formed from glucose-1-$^{14}$C at pH 11 shows an appreciable randomization of a label (Table IV), where the carbinol carbon shows about 2/3 activity of the methyl carbon.

On the other hand, in a neutral or a weakly acid medium, the reverse aldolization and the recombination of a hexose have been believed not to occur[24,25]. And also, the lower half of a hexose was suspected to behave somewhat differently from the upper half of a hexose[21]. Therefore, at this stage, it is better not to attribute the randomization of a label in the case of glucose-6-$^{14}$C (pH 6.7, Table III) to the reverse aldolization (and recombination) of a hexose.

The pattern and the relative distribution of the label found in the present investion, would give the contribution ratio of the upper and the lower half of a hexose molecule[26]. For example Table III shows that 77% of the acetol would come from the nonactive upper half and 23% would come from the active lower half of the glucose-6-$^{14}$C. But, as the substantial nature of the randomization of the label remains unresolved, the validity of these figures of contribution ratio contains much ambiguity, and will require further examination.




Hexose-1-$^{14}$C — Hexose-1, 3, 4, 6-$^{14}$C

20) S. Aronoff et al., *Science*, **110**, 476 (1949).

21) M. Gibbs, *J. Am. Chem. Soc.*, **72**, 3964 (1950).

22) J. C. Sowden and R. R. Thompson, *J. Am. Chem. Soc.*, **80**. 1435 (1958).

23) V. Prey et al., *Monatsh.*, **85**, 1186 (1954).

24) A. A. Bothner-By and M. Gibbs, *J. Am. Chem. Soc.*, **72**, 4805 (1950).

25) H. G. Hers et al., ibid., **76**, 5160 (1954).

26) H. F. Bauer and C. Teed, *Can. J. Chem.*. **33**, 1824 (1955); F. Weygand and G. Billek, *Z. Naturforsch.*. **12b**, 601 (1957).

The authors wish to express their sincere thanks to Professor Teruaki Simamoto of the Pharmaceutical Institute of Kyoto University who offered much convenience and suggestions for the the use of animals for experiments.

*Institute of Chemistry*
*Faculty of Science*
*Kyoto University*
*Sakyo-ku, Kyoto*

# *Proton Magnetic Resonance Studies on the Thermally Dehydrated Products of Alumina Trihydrate*

By Tatsuo SAITO

(Received November 19, 1960)

In the previous communications[1-2], the proton magnetic resonance absorption spectra of thermally dehydrated products have been studied to obtain information about the mechanism of the thermal decomposition of bayerite. In the present paper, the author has tried to investigate the rehydration of the thermally dehydrated product of alumina trihydrate by means of the proton magnetic resonance absorption spectra.

The rehydration of the thermal decomposition product of alumina trihydrate has recently been studied by many investigators[3-6]. The present author has examined the rehydration of the hydrous alumina dehydrated at various temperatures in high vacuum system. The rehydration was carried out under the vapor pressure of saturated water vapor at room temperature in the vacuum system.

## Experimental

**Starting Material.**—The alumina trihydrate, bayerite, was prepared by a chemical reaction of 1 N aluminum chloride solution with a small excess of 1 N ammonium hydroxide solution at room temperature. The resulting precipitate was washed by decantation for about 10 days till it was free from chloride and was then dried at 50°C for 24 hr. This starting material was checked by X-ray diffraction study and it was found that the resulting diffraction diagram was the same as that of bayerite, as shown in Fig. 1.

**Apparatus and Procedure.**—The NMR measurements were performed using the modulation technique described by Bloembergen, Purcell and Pound[7].

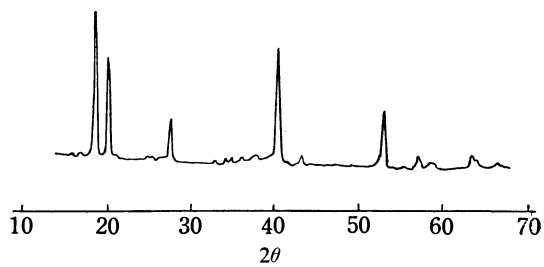



Fig. 1. X-Ray diffraction diagram of the starting material.

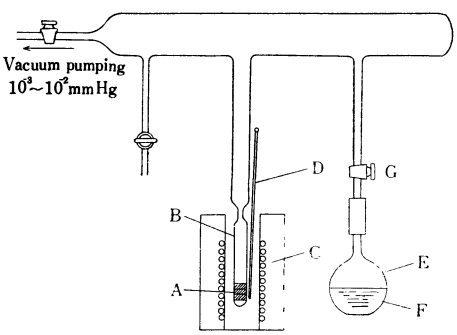



Fig. 2. Apparatus used to prepare the specimen for the NMR measurement.
A; Sample cake (dia. 8mm.)
B; Resonance sample tube
C; Electric furnace
D; Thermometer or thermocouple
E; Flask (100 cc.)
F; Distilled water in evacuated flask
G; Cock

The detecting apparatus has the ordinary constitution, which is composed of an r-f oscillator, an r-f amplifier, a detector, an audio-frequency amplifier, a lock-in amplifier and a recorder. More detailed reviews of this apparatus may be found in the article by Yano[8].

1) T. Hagiwara and T. Saito, This Bulletin, **33**, 1463 (1960).
2) T. Saito, ibid., **33**, 1626 (1960).
3) M. K. B. Day and V. J. Hill, *Nature*, **170**, 539 (1952); *J. Phys. Chem.*, **57**, 946 (1953).
4) R. Tertian and D. Papée, *Compt. rend.*, **236**, 1565 (1953); **238**, 98 (1954); **241**, 1575 (1955).
5) B. Imelik, ibid., **233**, 1284 (1951).
6) H. Thibon and E. Calvet, ibid., **239**, 1133 (1954).
7) N. Bloembergen, E. M. Purcell and R. V. Pound, *Phys. Rev.*, **73**, 679 (1948).
8) S. Yano, *J. Phys. Soc. Japan*, **14**, 942 (1959).

Each specimen used for the NMR measurement was prepared by the device of vacuum system illustrated in Fig. 2.

For the preparation of each specimen of thermally dehydrated product in vacuo, about 2 g. of the starting material was pressed into small cakes and they were put into the resonance sample tube which was connected to the high vacuum system. Then, each resonance sample tube was evacuated and heated from outside by the electric furnace for 3 hr. and it was then sealed off. The dehydration temperature was 100, 150, 200, 250, 300, 400 and 500°C, respectively.

For the preparation of rehydration-specimens, each sample after the treatment of the thermal dehydration in vacuo was immediately exposed at room temperature for 15 hr. to the saturated water vapor which entered through the cock (G) from the flask (E) (shown in Fig. 2).

Then, each sample tube containing this rehydrated specimen was pumped out to a high vacuum, either at room temperature during 12 hr. or at 110°C during 6 hr. and it was then sealed off.

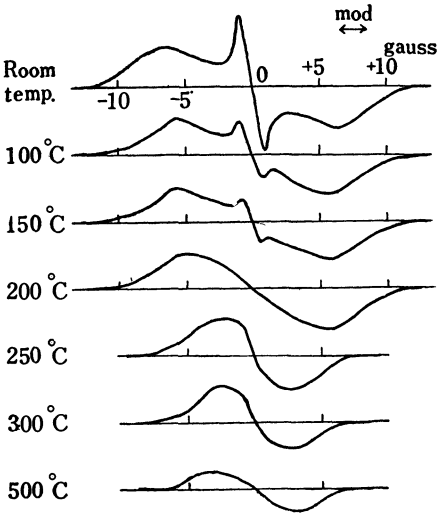



Fig. 3. Recorded derivatives of proton resonance in the thermal dehydration products in vacuo.

## Results and Discussion

**Thermal Dehydration in Vacuo.**—The derivative curves of the proton resonance absorption taken on the thermally dehydrated products in vacuo are shown in Fig. 3. The line shapes obtained from the specimens dehydrated at 100 and 150°C are both similar to that of the starting material, but the intensity of center peaks observed for these line shapes somewhat decreases with the rise of temperature. The line shape obtained from the specimen at 200°C has no central component though its line width is almost equal to that obtained from the specimen at 150°C.

This means that at the thermal dehydration till the temperature reaches 200°C, the structure water is not released but the adsorbed water

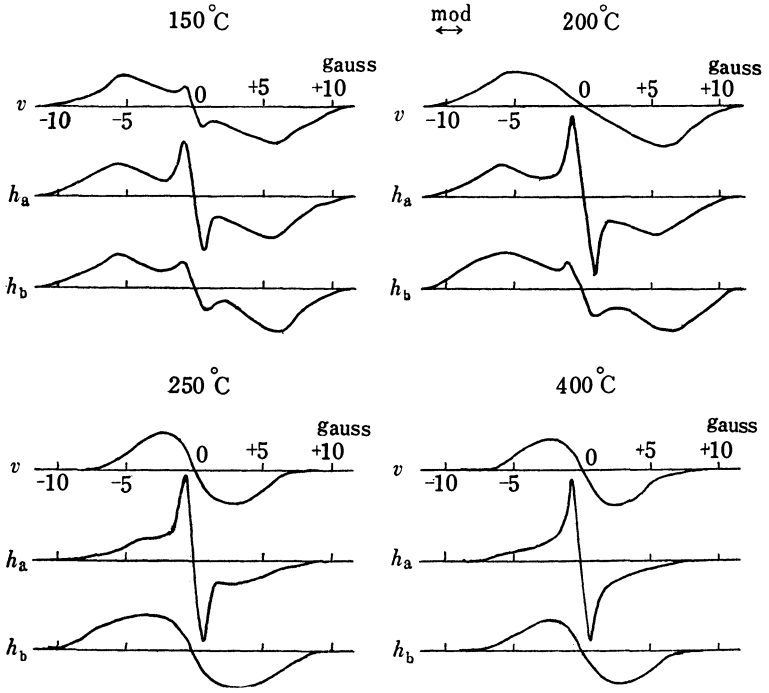



Fig. 4. Recorded derivatives of proton resonance in the thermal dehydration products in vacuo and their rehydrated samples.

vaporizes from the compound with the rise of temperature.

However, as shown in Fig. 3, the line width obtained from the specimen at 250°C suddenly becomes narrow and then the specimens at 300 and 500°C have also the same narrow width. This means that the starting material directly decomposes to the hydrous alumina at 200～250°C.

**Rehydration of Thermally Dehydrated Products in Vacuo.**—The NMR measurements were carried out on the specimens prepared by the rehydration of the thermally dehydrated products of bayerite in vacuo. The experimental derivative curves obtained from these measurements are shown in Fig. 4.

In Fig. 4, "$v$" is the recorded derivative of dehydrated product in vacuo at each temperature, and both "$h_a$" and "$h_b$" are the recorded derivatives of the rehydrated sample of the above dehydration-product. In this case, "$h_a$" shows the rehydrated sample having the after-treatment of a high vacuum pumping at room temperature during 12 hr. and "$h_b$" shows one having the after-treatment of a high vacuum pumping at 110°C during 6 hr.

As is seen in Fig. 4, the line shape of "$h_a$-series" has a sharp and intensive central component, but in the line shape of "$h_b$-series", the center peak observed for this line shape remarkably reduces in its intensity as compared with that of "$h_a$-series" or disappears. At 150°C, the line shape of the derivative "$h_b$" is the same as that of "$v$", but at 200°C, the line shape of the derivative "$h_b$" shows the difference from that of "$v$". This means that on the dehydration in vacuo at 200°C, the starting material partially decomposes to hydrous alumina and then this decomposed product is rehydrated by water vapor to aluminum hydroxide. At 250°C, the line width of the derivative "$h_b$" becomes larger than that of "$v$" and at 400°C, the line width of the derivative "$h_b$" is the same as that of "$v$".

The second moments calculated from these experimental derivative curves of "$v$-series" and "$h_b$-series" are shown in Table I and the variation of these values of second moments plotted as the function of the temperature are shown in Fig. 5.

Table I. The values of the second moments calculated from the experimental derivative curves

| Dehydration temp., °C | Thermally vacuum dehydration series, gauss² | Rehydration series "$h_b$-series" gauss² |
|---|---|---|
| room temp. | 13.6 | |
| 100 | 13.4 | |
| 150 | 13.3 | 14.0 |
| 200 | 12.1 | 13.9 |
| 250 | 4.8±0.5 | 8.2±0.3 |
| 300 | 4.3±0.2 | 5.8±0.3 |
| 400 | 4.5 | 4.6±0.2 |
| 500 | 4.1 | 4.4 |

As is seen in Fig. 5, the second moments of the thermal dehydration series in vacuo decrease from the value of 13～14 gauss² to that of 4～5 gauss² suddenly at 250°C and this value of 4～5 gauss² constantly continues till 500°C. In the variation curve of the second moments of the rehydration series—"$h_b$-series", the values of second moments below 200°C

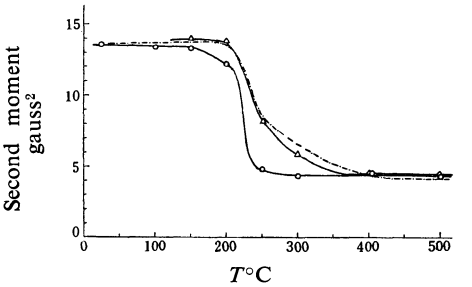



Fig. 5. Variation of the second moments with the temperature in the thermally vacuum-dehydration series and the rehydration series—"$h_b$-series"
○—○; Thermally vacuum-dehydration series
△—△; Rehydration series—"$h_b$-series"
·—·—; Thermal dehydration series in the air

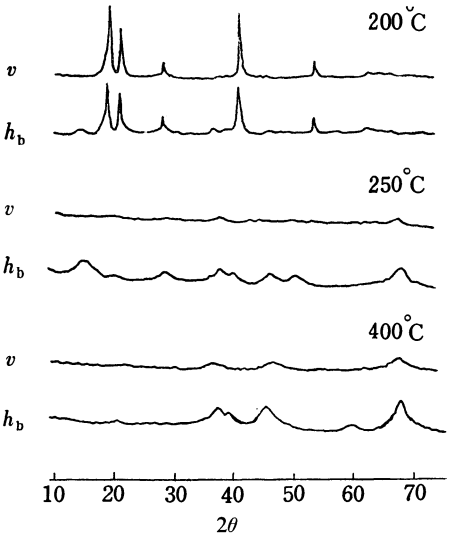



Fig. 6. X-Ray diffraction diagrams of the samples in the thermally vacuum-dehydration series and in the rehydration series—"$h_b$-series".
$v$; Thermally vacuum-dehydration series
$h_b$; Rehydration series—"$h_b$-series"

are about 13～14 gauss$^2$ and in the range from 200 to 400°C, the values gradually decrease with the rise of temperature. Then, in the range from 400 to 500°C, the second moments become stationary values of 4～5 gauss$^2$.

The above difference of the variation curve of second moments in the range from 200 to 400°C between "$v$-series" and "$h_b$-series" is interpreted as a result due to the formation of aluminum hydroxide by the rehydration of the thermally dehydrated product in vacuo.

This interpretation of the rehydration was ascertained by the X-ray diffraction study of the products. The diffraction diagrams of several specimens obtained in this study are shown in Fig. 6. From these diagrams, it is ascertained that, while the specimen of the thermal dehydration in vacuo at 250°C is crystallographically amorphous, the specimen obtained by the rehydration for the above sample shows a mixed phase of böhmite and $\eta$-alumina.

## Conclusion

1) The center peak observed for the line shape of the experimental derivative curve of proton resonance in the starting material decreases in its intensity during the thermal dehydration in vacuo at the temperature below 200°C, but it does not disappear till 150°C. The author assumes that this center peak shows the existence of the movable water which entered into the crevice of the lump of fine particles or entered into the space of the layer lattice of crystal.

2) On the thermal dehydration series in vacuo, the starting material directly decomposes to the hydrous alumina at the temperature of 200～250°C and the intermediary product, böhmite, is not found in the specimens at 250 and 300°C. This is ascertained in present NMR experiments.

3) The water which was adsorbed by the rehydration of the thermally dehydrated products in vacuo at 150°C is wholly removed by the treatment of a high vacuum pumping at 110°C.

4) In the rehydrated product of the thermally dehydrated sample in vacuo at 250°C, the adsorbed water of the product changes partially into the structure water and the formation of aluminum hydroxide occurs partially. This is ascertained by the NMR measurements.

5) In the rehydration specimen of the dehydration-product in vacuo at 400°C, the formation of aluminum hydroxide is not observed.

6) It is noteworthy that the variation curve of second moments for the rehydration series—"$h_b$-series" shows the same figure as the variation curve of second moments for the thermal dehydration series in the air[2].

The author wishes to express his sincere thanks to Dr. Y. Kotera of this Institute for his kind advice. The author also wishes to express his hearty thanks to Professor T. Hagiwara of Hiroshima University for his kind direction and also wishes to express his sincere thanks to Professor T. Sidei and Dr. S. Yano of Kyoto University for their continual guidance and encouragement throughout this study.

*Government Chemical Industrial Research Institute, Tokyo*
*Shibuya-ku, Tokyo*

# *Infrared Spectra of Water of Crystallization in Some Inorganic Chlorides and Sulfates*

By Itaru GAMO

(Received September 3, 1960)

The infrared investigation of water of crystallization provides much information on its binding state in the crystal[1,2]. The frequency shifts of its characteristic bands from those of the water vapor seem to be caused mainly by the coördination of water oxygen with metal and by the hydrogen bonding with outer ions. In the present paper, the absorption bands are investigated from this standpoint.

## Experimental

**Preparation.**—The samples were of commercial guaranteed grade. Most of them were recrystallized from water.

1) J. Lecomte, *J. Chim. Phys.*, **50**, C53 (1953).
2) J. Fujita, K. Nakamoto and M. Kobayashi, *J. Am. Chem. Soc.*, **78**, 3963 (1956).

**Measurements.**—The spectra were obtained by a Perkin-Elmer Infracord double beam spectrophotometer using a rock salt prism. The potassium bromide disk and the Nujol and H. C. B. mull techniques were employed.

## Results and Discussion

The results are shown in Table I together with those hitherto obtained. In general our values are in good agreement with them within experimental error. As examples, absorption bands of nickel chloride hexahydrate and zinc sulfate heptahydrate are shown in Figs. 1 and 2, respectively. The error is estimated to be about 2.5 $cm^{-1}$ in the 14 $\mu$ region, whereas it is 14 $cm^{-1}$ and 57 $cm^{-1}$, respectively, in the 6 $\mu$ and the 3 $\mu$ region. As will be shown later, the 14 $\mu$ band is very sensitive to coördination and hydrogen bonding. The 6 $\mu$ and the 3 $\mu$ band are less sensitive. Furthermore the error is very small in the 14 $\mu$ band. For these two reasons attention shall be focussed on the 14 $\mu$ region in the following discussion, though they are less prominent.

The author may consider the M—$OH_2$ and the O—H···X(X=Cl or O) distance as a measure

TABLE I[a]. OBSERVED WAVE NUMBERS, $cm^{-1}$ [b]

| Substance | This research Region | | | | | Other researches | Lit. |
|---|---|---|---|---|---|---|---|
| | 3 $\mu$ | 5 $\mu$ | 6 $\mu$ | 14 $\mu$ | others | | |
| $CaCl_2 \cdot 6H_2O$ | 3440 s | 2170w | 1630 s | 719m | | 3432, 3417, 3387, 1663 | 1 |
| | | | | | | 3440, 3298, 3250 | 2 |
| $SrCl_2 \cdot 6H_2O$ | 3470 s | 2130w | 1640m | 690w | | 3438, 3418, 3383, 1663 | 1 |
| | | | | | | 3611, 3436, 3391, 3221 | 3 |
| | | | | | | 3437, 2915, 1629 | 4 |
| $BaCl_2 \cdot 2H_2O$ | 3380 s | 2060w | 1620m | 709w | | 3455, 3324, 3237 | 5 |
| | | | | | | 3456, 3376, 3345, 3285, 717 | 6 |
| | | | | | | 3466, 3385, 3327, 3228 | 7 |
| | | | | | | 3568, 3300, 3230 | 8 |
| | | | | | | 3370, 1645, 1615, 700 | 9 |
| $MgCl_2 \cdot 6H_2O$ | 3430 s | 2250w | 1630 s | 714w | | 3387, 3227 | 5 |
| | | | | | | 3497, 3352 | 10 |
| $AlCl_3 \cdot 6H_2O$ | 3030s, b | 2420m | 1640m | 844m | 1950w | 3312, 3044 | 11 |
| | | | | | 1160w, v.b | 3272, 3057 | 10 |
| | | | | | | 3410, 2915, 1625 | 4 |
| $CoCl_2 \cdot 6H_2O$ | 3440 s | | 1620m | 781w | | 3513, 3393, 3151 | 5 |
| $NiCl_2 \cdot 6H_2O$ | 3370 s | | 1610m | 763w | | 3513, 3424, 3163 | 5 |
| | | | | | | 1481, 1089, 1018, 803 | 12 |
| $Na_2SO_4 \cdot 10H_2O$ | 3550 s | 2080w | 1650m | 719m | | 3513, 3431, 3372, 3276 | 3 |
| $MgSO_4 \cdot 7H_2O$ | 3290 s | | 1650w | 749w | | 3300, 3214, 3078, 2125, 2044 | 5 |
| | | | | | | 3393～3506, 3179～3346 | 10 |
| $ZnSO_4 \cdot 7H_2O$ | 3230 s | 2170w | 1590w | 758w | | 3407, 3292～3353 | 10 |
| $Al_2(SO_4)_3 \cdot 18H_2O$ | 3330 s | 2460w | 1640w | 704w | 2940 s | 2957～3528 | 10 |
| $FeSO_4 \cdot 7H_2O$ | 3360 s | | 1630m | 712w | | 3330, 1625, 611 | 9 |
| $CoSO_4 \cdot 7H_2O$ | 3230 s | | 1620w | 755w | | | |
| $NiSO_4 \cdot 7H_2O$ | 3280 s | | 1630w | 760w | | 3279, 3208, 3091, 2078 | 5 |

a) Abbreviations: s, strong; m, medium; w, weak; b, broad; v. b, very broad
b) Observed frequencies attributable to $SO_4^{2-}$ modes are omitted.


1) A. W. Marchand, *Compt. rend.*, **242**, 1791 (1956). R
2) G. P. Nayar, *Proc. Ind. Acad. Sci.*, **A8**, 419 (1938). R
3) E. Canals and Peyrot, *Compt. rend.* **207**, 224 (1938). R
4) P. J. Lucchesi and W. A. Glasson, *J. Am. Chem. Soc.*, **78**, 1347 (1956). IR
5) J. Lecomte, *J. Chim. Phys.*, **50**, C53 (1953). IR
6) A. Galy, *Compt. rend.*, **235**, 1504 (1952). R
7) O. Salvetti and D. Nobili, *Chem. Abstr.*, **51**, 12656b (1957). IR
8) C. Duval, *Anal. Chim. Acta*, **13**, 32 (1955). IR
9) F. A. Miller and C. H. Wilkins, *Anal. Chem.*, **24**, 1253 (1952). IR
10) O. Theimer, *Mh. Chem.*, **81**, 301 (1950). R
11) G. P. Nayar, *Proc. Ind. Acad. Sci.*, **A28**, 469 (1948). R
12) C. Duval, R. Duval and J. Lecomte, *Bull. soc. chim. France*, (V) **14**, 1048 (1947). IR


IR: observed in infrared spectra; R: observed in Raman spectra.

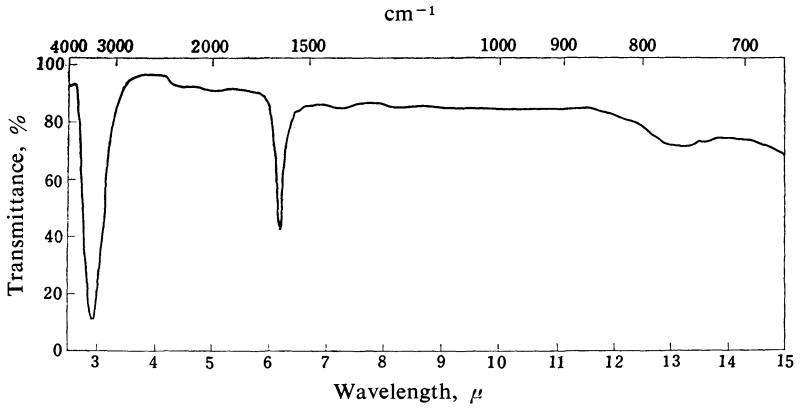



Fig. 1. Absorption bands of $NiCl_2 \cdot 6H_2O$.

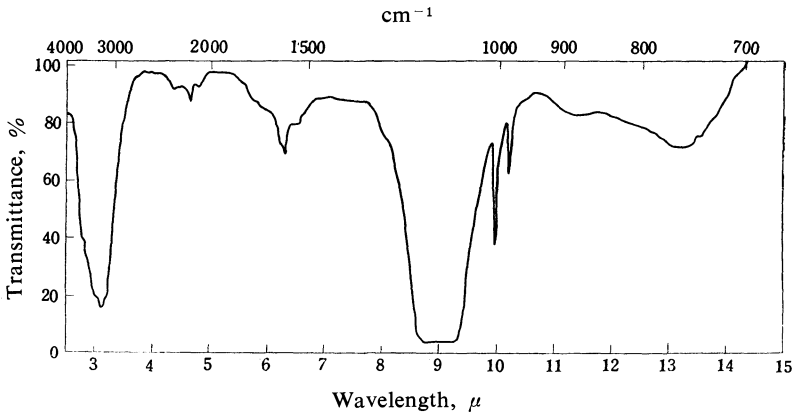



Fig. 2. Absorption bands of $ZnSO_4 \cdot 7H_2O$.

for the strength of coördination and that of hydrogen bonding respectively. The 14 $\mu$ band is attributable to either one of the wagging, twisting and rocking modes[2]. In the case of metal ammine complexes the rocking frequency of ammonia[3] seems to increase with increasing coördination and hydrogen bonding[4]. Assuming the additivity for these two effects in the case of water of crystallization also[2], and attributing tentatively our 14 $\mu$ band to the rocking mode, the wave number will decrease with increasing distance O—H···X, if the hydrogen bonding effect is predominant. Fig. 3 shows this to be inverse for strontium chloride hexahydrate and magnesium chloride hexahydrate. (The straight hydrogen bondings were assumed throughout, and in case there are more than two kinds of equivalent positions of water in one crystal, the nearest approaches were adopted for O—H···X and for M—$OH_2$, assuming that the observed band peaks correspond to them.). Therefore the coördination effect is larger in the magnesium-water bond than in that of the strontium-water. Correspondingly the former distance is considerably smaller than the latter.

The frequency of the rocking mode increases in the order, strontium chloride hexahydrate, cobaltous chloride hexahydrate and aluminum chloride hexahydrate. These three substances have a nearly equal O—H···Cl distance (3.10 Å), and the metal-water distance decreases in this order. Plotting the observed frequency against the metal-water distance, we obtain a straight line in Fig. 4. In the next place, magnesium chloride hexahydrate and nickel sulfate heptahydrate each occupies a position in the left side of this line corresponding to their metal-water distance. Also, the perpendicular distance between this point and the line is greater in the former than in the latter. This is understandable, since the weaker hydrogen bonding results in the lower frequency and O—H···Cl distances of the former and the latter are 3.21

3) S. Mizushima, I. Nakagawa and J. V. Quagliano, *J. Chem. Phys.*, **23**, 1367 (1955).
4) J. Fujita, K. Nakamoto and M. Kobayashi, *J. Am. Chem. Soc.*, **78**, 3295 (1956).

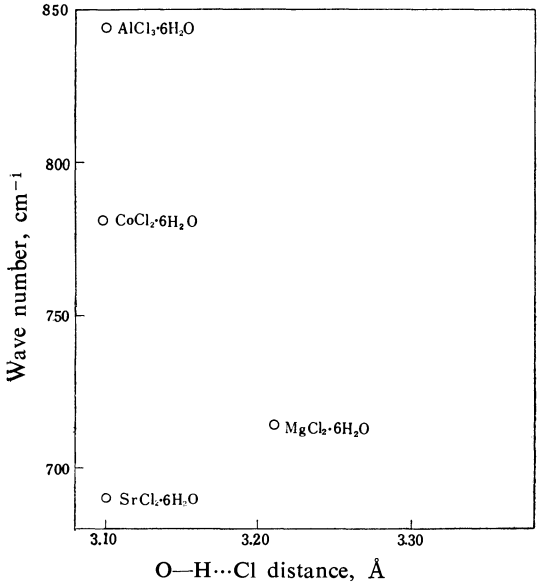



Fig. 3. Rocking frequency versus O—H···Cl distance. References for the interatomic distances :
$SrCl_2 \cdot 6H_2O$, A. T. Jensen, *Kgl. Danske. Videnskab. Selskab. Math-fys. Medd.*, **17**, No. 9 (1940).
$MgCl_2 \cdot 6H_2O$, K. R. Andress and J. Gundermann, *Z. Krist.*, **A87**, 345 (1934).
$CoCl_2 \cdot 6H_2O$, J. Mizuno, K. Ukei and T. Sugawara, *J. Phys. Soc. Japan*, **14**, 383 (1959).
$AlCl_3 \cdot 6H_2O$, K. R. Andress and C. Carpenter, *Z. Krist.*, **A87**, 446 (1934).

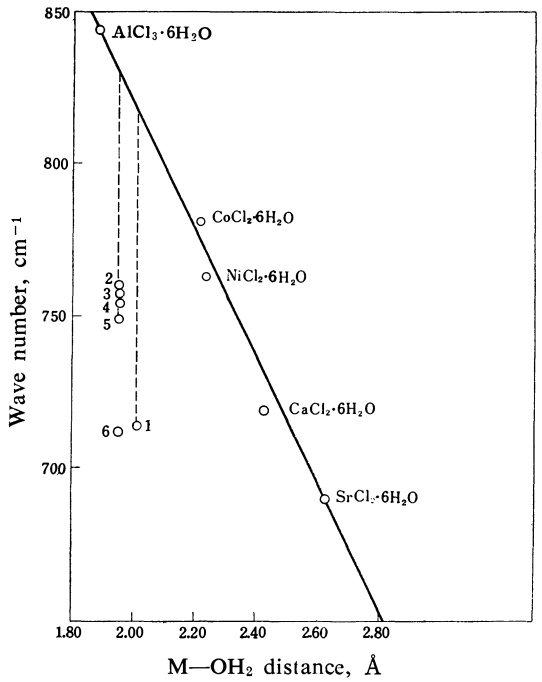



Fig. 4. Rocking frequency versus M—$OH_2$ distance.

1, $MgCl_2 \cdot 6H_2O$
2, $NiSO_4 \cdot 7H_2O$
3, $ZnSO_4 \cdot 7H_2O$
4, $CoSO_4 \cdot 7H_2O$
5, $MgSO_4 \cdot 7H_2O$
6, $FeSO_4 \cdot 7H_2O$

and 3.13Å*, respectively. The structures of the other crystals are not yet completely determined. Among them, however, nickel chloride hexahydrate is completely isomorphous with cobaltous chloride hexahydrate[6]. Therefore the periodic table suggests that nickel-water bond has nearly the same distance as cobalt-water. The position of nickel chloride hexahydrate in Fig. 4 seems to be valid on this assumption.

A similar consideration leads to the determination of other points. (Zinc sulfate heptahydrate and magnesium sulfate heptahydrate are isomorphous with nickel sulfate heptahydrate[5], and calcium chloride hexahydrate with strontium chloride hexahydrate[7]. Cobaltous sulfate heptahydrate and ferrous sulfate heptahydrate are mutually isomorphous[8].)

As a whole, the coördination seems to have a considerably greater effect upon this mode than the hydrogen bonding.

These relationships are less definite for the 6 $\mu$ (bending[1]) and the 3 $\mu$ (stretching[1]) mode. A more exact measurement will permit an analogous treatment.

The 5 $\mu$ band of the chlorides seems to be attributable to the combination of the bending and the rocking mode, as in the case of 2222 $cm^{-1}$ band in ice[1,9], although there remains a possibility of assigning it to the stretching mode strongly affected by the two effects, as Fujita et al. did for the weak band at 2270 $cm^{-1}$ in nickel glycinate dihydrate[2]. For the sulfates, this combination band may probably be overlapped with that of the totally symmetric and the triply degenerate stretching mode of sulfate ion.

## Summary

The characteristic bands of water of crystallization in various chlorides and sulfates were determined in the rock salt region. The results were classified and explained inclusively

* This 3.13 Å is obtained by subtracting the radius of oxygen atom 1.32 Å from the observed O—H···O distance[5], and adding the radius of chlorine atom 1.81 Å.

5) C. A. Beevers and C. M. Schwartz, *Z. Krist.*, **A91**, 157 (1935).

6) J. Mizuno, K. Ukei and T. Sugawara, *J. Phys. Soc. Japan*, **14**, 383 (1959).

7) A. T. Jensen, *Kgl. Danske Videnskab. Selskab. Math.-fys. Medd.*, **17**, No. 9 (1940).

8) I. Ness, *Naturwiss.*, **28**, 78 (1940).

9) J. J. Fox and A. E. Martin, *Proc. Roy. Soc.*, **A174**, 234 (1940).

by the effects of coödination and hydrogen bonding.

The author wishes to express his thanks to Professor Takehiko Shimanouchi of the University of Tokyo for his guidance throughout the course of this study.

*Chemical Laboratory*
*Department of General Education*
*Faculty of Science and Engineering*
*Waseda University*
*Shinjuku-ku, Tokyo*

# *Infrared Absorption Spectra of Water of Crystallization in Copper Sulfate Penta- and Monohydrate Crystals*

By Itaru GAMO

(Received September 20, 1960)

Infrared spectra of copper sulfate penta- and monohydrate have been separately subject to several investigations[1-3]. However, there has been no comparative study of these spectra in relation to their structural difference.

In the present paper, observed spectra were examined in relation to this difference, mainly to that of the binding state of the water molecules in them.

## Experimental

**Preparation.** — Copper sulfate pentahydrate of commercial first grade was made free from iron according to Gmelin's handbook[4]. The sample was then twice recrystallized from water. Copper sulfate monohydrate was obtained by keeping this purified pentahydrate at 110°C for 3 hr. under reduced pressure in an Abderhalden apparatus[5].

**Measurements.**—Spectra were obtained by means of a Perkin-Elmer Infracord spectrophotometer with a rock salt prism. The Nujol mull technique was employed throughout. The potassium bromide disk technique was unsuitable for the pentahydrate, because the prepared disk became dark brown. A similar phenomenon was observed in the case of cupric chloride dihydrate.

## Results

The spectra are given in Fig. 1. In the 3 $\mu$ region one peak is observed for the pentahydrate at 3420 $cm^{-1}$, and two peaks for the monohydrate at 3340 and 3190 $cm^{-1}$. These compare with the peak of various inorganic hydrated sulfates[6] in this region, and can be assigned to O-H stretching vibrations of water. Overlapping of the symmetric and the antisymmetric mode together with their splitting is probably responsible for the broadness of these three bands. In the 5 $\mu$ region the spectrum of the pentahydrate shows a weak band at 2120 $cm^{-1}$, attributable to a combination of the bending and the rocking mode of water or that of the totally symmetric and the triply degenerate stretching mode of sulfate ion. Of course there is a possibility of their overlapping. In the 6 $\mu$ region a band of medium intensity is observed at 1640 $cm^{-1}$ for the pentahydrate. At the same position a broad weak band is observed for the monohydrate, with an additional band of medium intensity at 1510 $cm^{-1}$. These three can be assigned to the bending modes of water, the latter two resulting from splitting.

In the 8 $\mu$ region, characteristic bands of inorganic sulfates[7] are observed for the pentahydrate at 1200 and 1170 $cm^{-1}$ and for the monohydrate at 1200 and 1120 $cm^{-1}$, attributable to the triply degenerate stretching vibrations of sulfate ion. The sharp 1000 and 966 $cm^{-1}$ bands of the former and the 1020 $cm^{-1}$ band of the latter can be assigned to the totally symmetric stretching vibrations that have become active in infrared by some perturbations. In this connection it is to be noticed that the intensities of the former two bands are considerably greater than in the usual cases of sulfates. The 875 $cm^{-1}$ band of

1) J. Lecomte, *Compt. rend.*, **226**, 1088 (1948); *J. chim. Phys.*, **50**, C53 (1953).
2) O. Matsumura. *Mem. Fac. Sci., Kyushu Univ., B*, I, 1 (1951).
3) J. Fujita, K. Nakamoto and M. Kobayashi, *J. Am. Chem. Soc.*, **78**, 3963 (1956).
4) "Gmelins Handbuch der anorganischen Chemie", part 60, Cu B1 (1958), p. 508.
5) ibid., p. 523.
6) I. Gamo, This Bulletin, **34**, 760 (1961).
7) L. J. Bellamy, "Infrared Spectra of Complex Molecules", Methuen and Co., Ltd., London (1958), p. 345.

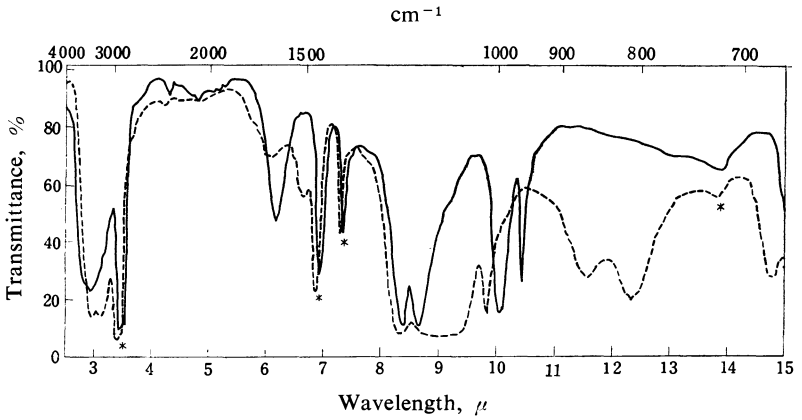



Fig. 1. Observed bands of $CuSO_4 \cdot 5H_2O$ and $CuSO_4 \cdot H_2O$.
———, $CuSO_4 \cdot 5H_2O$; ----, $CuSO_4 \cdot H_2O$
* Nujol bonds

the pentahydrate found by Fujita et al.[3] was observed in our study only when the spectrum in this region was recorded immediately after the mull preparation. In the 12$\mu$ region of the monohydrate spectrum, strong but broad peaks are observed at 866 and 813 $cm^{-1}$, in rough accord with Lecomte's values[1], 850 and 796 $cm^{-1}$, respectively. They are tentatively assigned to the rocking modes of water. The 676 $cm^{-1}$ band of the monohydrate are assigned to the triply degenerate bending vibration of sulfate ion.

Tables I and II summarize these results.

TABLE I. OBSERVED FREQUENCIES OF $CuSO_4 \cdot 5H_2O$

| Wave number, $cm^{-1}$ | Assignment |
|---|---|
| 3420 s | $\nu$ ($H_2O$) stretch. |
| 2120 w | $\nu_3+\nu_1$ ($SO_4$) and/or $\nu_R+\nu_2$ ($H_2O$) |
| 1640 m | $\nu_2$ ($H_2O$) bend. |
| 1200 s | $\nu_3$ ($SO_4$) stretch. |
| 1170 s | $\nu_3$ ($SO_4$) stretch. |
| 1000 s | $\nu_1$ ($SO_4$) stretch. |
| 966 s | $\nu_1$ ($SO_4$) stretch. |
| 875 s [a] | $\nu_R$ ($H_2O$) rock. |

a, Observed by Fujita et al. (See Ref. 3.)

TABLE II. OBSERVED FREQUENCIES OF $CuSO_4 \cdot H_2O$

| Wave number, $cm^{-1}$ | Assignment |
|---|---|
| 3340 s | $\nu$ ($H_2O$) stretch. |
| 3190 s | $\nu$ ($H_2O$) stretch. |
| 1640 w | $\nu_2$ ($H_2O$) bend. |
| 1510 w | $\nu_2$ ($H_2O$) bend. |
| 1200 s | $\nu_3$ ($SO_4$) stretch. |
| 1120 s | $\nu_3$ ($SO_4$) stretch. |
| 1020 s | $\nu_1$ ($SO_4$) stretch. |
| 866 m | $\nu_R$ ($H_2O$) rock. |
| 813 m | $\nu_R$ ($H_2O$) rock. |
| 676 m | $\nu_4$ ($SO_4$) bend. |

## Discussion

According to X-ray analysis[8], four of the water molecules in copper sulfate pentahydrate crystal are closely coördinated with a copper atom by fairly covalent bonds, making a square with the copper atom at the center. The fifth occupies a hole in the structure, and hardly differs from the free water molecule.

Although the interatomic distances in copper sulfate pentahydrate crystal are determined well by the X-ray analysis, those in the monohydrate crystal are completely unknown. Nevertheless comparison of the unit cell parameters (see Table III) shows that the structure of the latter is quite different from that of the former, corresponding to a considerable rearrangement of atoms upon partial dehydration. In the following, we shall confine our discussion mainly to water bands.

Since copper sulfate pentahydrate belongs to the symmetry class $C_1^1$ [8], we can expect theoretically many water bands, due mainly to the splitting of the bands of the free molecule. Actually, only two peaks were observed in our study that are attributable to water. The resolving power of the instrument, which becomes rapidly small with increasing wave number, seems to be partly responsible for this poor observation. Nevertheless some interesting results are obtained.

The author assume tentatively the 3420 $cm^{-1}$ band to be due to the antisymmetric stretching vibration affected by the coördination of copper-water and by the hydrogen bonding between the water molecule and the outer oxygen atom of sulfate ion. Its deviation from the vapor

8) C. A. Beevers and H. Lipson, *Proc. Roy. Soc.*, **A146**, 570 (1934).
9) F. Hammel, *Ann. Chim.*, (11) **11**, 247 (1939).

TABLE III. COMPARISON OF UNIT CELL PARAMETERS

| | Type | Symmetry | a | b | c | β | M | Lit. |
|---|---|---|---|---|---|---|---|---|
| $CuSO_4 \cdot 5H_2O$ | $H_{4_1}$ | $C_1^1$ | 6.12 Å | 10.70 Å | 5.97 Å | 107.4° | 2 | 8 |
| $CuSO_4 \cdot H_2O$ | — | m k l | 6.80 | 7.90 | 12.6 | ~90 | — | 9 |

frequency (3756.5 $cm^{-1}$) is reasonable as compared with those of other hydrated salts. The fairly large covalent character of the copper-water bond (distance 1.98 Å), together with the strong hydrogen bond of 2.75 Å, is sufficient to explain this order of magnitude. In the next place, both the 3340 and the 3190 $cm^{-1}$ band of the monohydrate can be reasonably assigned either to antisymmetric or to symmetric vibration. The observed doublings of the bending and the rocking vibration (see later) together with the nearly equal intensity of the two bands, seem to support this assignment strongly. The main cause of this doubling is probably a rather strong coupling of two neighboring water molecules through hydrogen bonding to the same oxygen atom of sulfate ion. The values of the two frequencies suggest that in this crystal, the binding strength between one water molecule and the neighboring sulfate ion is considerably greater than in the pentahydrate crystal. The magnitude of the change in the bending frequency of the pentahydrate is reasonable as compared with the values of other salts. In the monohydrate one of the two frequencies is reasonably higher than that in the vapor state (1595.5 $cm^{-1}$). The other is lower and therefore rather exceptional for this mode. Both bands are broader than in the usual cases of sulfates. This suggests stronger interaction. In these two respects, the bending modes of the water molecule in this crystal deserve to be noticed.

The shapes and the frequency values of the two rocking bands of the monohydrate are the same as usual. The great value of the splitting (53 $cm^{-1}$) as well as the value in the case of the bending mode (130 $cm^{-1}$) seems to support the above assumption of hydrogen bonding. An intensity consideration in the two modes (see Fig. 1) suggests that the two hydrogen bonds are not completely equivalent. This is understandable, since the numerical ratio of water molecules to sulfate ions in the crystal is 1 : 1, preventing the two water molecules from occupying a position equivalent to the same oxygen atom. We can roughly estimate the mean value of the two O–H···O distances by using the relation obtained in the preceding paper. The two water molecules are assumed to make covalent bonds of equal length (1.98 Å, value in the ligand water molecule of the pentahydrate) with two different copper atoms respectively. In Fig. 4 of that paper the O–H···O distance is thus estimated to be somewhat smaller than 2.61 Å using the mean value of the two rocking frequencies and the covalent bond length 1.98 Å.

The author could not observe the band peaks expected from the fifth almost free water molecule in the pentahydrate crystal. Probably they are weak and hidden in other bands.

The author shall now proceed to a brief discussion of the sulfate ion bands. For the pentahydrate, the observed two frequencies of $\nu_3$ are higher than that in solution (1104 $cm^{-1}$ [10]). For $\nu_1$, however, one component is higher and the other, lower than $\nu_1$ in solution (981 $cm^{-1}$ [10]). According to X-ray analysis[8], the four sulfate oxygen atoms in this crystal are all making different contacts with other atoms or molecules. Probably this is responsible for these splittings. For the monohydrate, the bands are fairly broader than in the pentahydrate. It is very interesting that one component of the doublet band $\nu_1$ (966 $cm^{-1}$ of the pentahydrate) disappears upon the partial dehydration.

## Summary

The observed spectra of water in the penta- and monohydrate crystals were interpreted by the effects of coördination copper-water and hydrogen bonding O–H···O. The whole difference in the spectra of the two crystals were explained in relation to the escape of the four ligand water molecules and the resulting rearrangement of atoms. The stretching, bending and rocking modes, which are single in the case of the pentahydrate, split into doublets in the monohydrate. This result was explained by a single assumption of strong coupling of two neighboring water molecules in the latter.

The author is indebted to Professor Takehiko Shimanouchi of the University of Tokyo for his helpful guidance.

*Chemical Laboratory*
*Department of General Education*
*Faculty of Science and Engineering*
*Waseda University*
*Shinjuku-ku, Tokyo*

10) K. W. F. Kohlrausch, "Ramanspektren. Hand- und Jahrbuch der chemischen Physik", 9, part 6 (1943), p. 399.

# *Polymerization of Propylene with Tin Tetraalkyl-Titanium Tetrachloride Catalyst*

By Nobuyuki ASHIKARI and Masakazu HONDA

(Received November 19, 1960)

Many studies[1] on the catalyst for preparing polypropylene have been performed, since Natta obtained the polypropylene having high molecular weight and high stereoregularity. On the polymerization of propylene using tin tetraalkyl as a catalyst component, only a Du Pont patent[2] has been known. However, the description is so brief that the details are not explained. From our preliminary experiments of the polymerization of propylene using tin tetraalkyl in combination with titanium tetrachloride, titanium trichloride, dichlorodialkyl titanate, or tetraalkyl titanate, it was found that the effective catalyst was only the complex comprising titanium tetrachloride as a component. Moreover, when the catalyst was used as soon as the two components were mixed, the polymer produced thereby contained a greater part of low polymer. Accordingly, the polymerization in this study was performed considering the adequate times for the production of the complex.

## Experimental and Results

**Reaction between Tin Tetraalkyl and Titanium Tetrachloride.**—The reaction between tin tetraalkyl and titanium tetrachloride does not proceed very fast, and so prolonged reaction times are required for the completion of the complex. The reaction rate depends, of course, upon the reaction temperature, the length of alkyl chain in the tin tetraalkyl, and the ratio of the catalyst components. Besides, the presence of a solvent will affect the reaction rate. However, the catalyst preparation in this study was performed without solvent, because the presence of the solvent makes the end-point of reaction obscure.

When the catalyst is prepared in a solvent without vigorous stirring, the product precipitates at the bottom of the vessel as an adhesive mass which can not be easily dispersed into the solvent. Generally, if the ratio of the two components deviates greatly from unity, both components still remain in liquid form after the reaction is over. Therefore, in this case, the end-point of reaction is not clear. On the other hand, when the ratio is about 1.0, the whole becomes solid exhibiting a comparatively apparent end-point. Therefore, the experiments for observing the times required for the production of the complex were carried out without any solvent at about equimolar composition of tin tetraalkyl and titanium tetrachloride. In Fig. 1, the effects of the alkyl radical in the tin tetraalkyl molecule and the reaction temperature upon the rate of the production of the complex are represented.

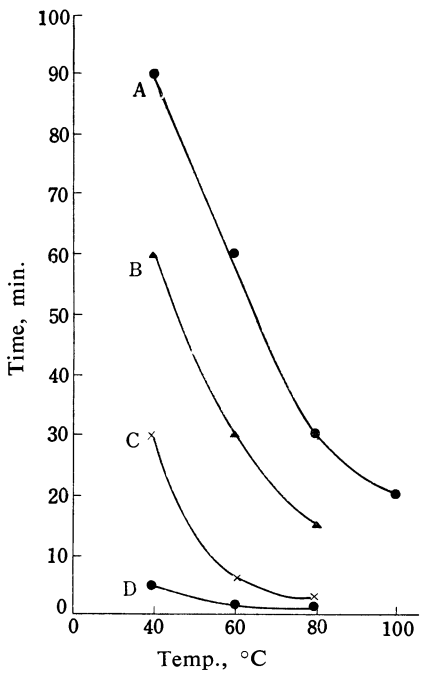



Fig. 1. Time required for the complex production.

A; *n*-Butyl C; Isopropyl
B; *n*-Propyl D; Ethyl

The vertical axis in Fig. 1 represents the times required for the solidifying of the two components which were mixed at a given temperature. The preparation of catalyst complex in the following experiments was performed referring to this condition; also analogously in the case where the ratio of the two component deviates passably from unity.

**Polymerization Procedure.** — In a cooled polymerization tube containing the complex which had been prepared by mixing the two components, a definite amount of monomer was introduced. The complex was shattered in a high speed shaker. In the case of polymerization in solution, the shattering of the complex was taken before the monomer

1) For example, G. Natta, I. Pasquon and E. Giachetti, *Angew. Chem.*, **69**, 213 (1957).
2) E. I. Du Pont de Nemours & Co., Brit. Pat. 777538 (June 26, 1957).

was introduced. The tube was immersed in a constant temperature bath. After the reaction proceeded for definite reaction times, the tube was cooled by dry ice-methanol, and vented. Then, the contents of the tube were treated with methanol acidified by hydrochloric acid to decompose the catalyst, washed with methanol several times, and dried under reduced pressure.

**Measurement of Viscosity.**—The viscosity of the polymer solution was measured using tetralin, as a solvent, which had been purified by distillation after being dried over sodium, using an improved Ubbelohde viscometer of dilution type, at 135± 0.05°C. The viscometer was filled with nitrogen during the measurement.

The molecular weight of the polymer was calculated using Ciampa's equation[3] shown below.

$$[\eta] = 0.25 \times 10^{-4} M$$

**Dependence of Conversion and Insoluble Part of Polymer in Boiling *n*-Hexane on the Composition of Catalyst.** — The influence of the ratio of catalyst components upon the conversion and the insoluble part of polymer in boiling *n*-hexane was investigated by the polymerization using a catalyst complex of tin tetraethyl-titanium tetrachloride. In each experiment, 5 g. of monomer was polymerized with a catalyst containing $9.26 \times 10^{-2}$ mol. of titanium tetrachloride and a definite amount of tin tetraethyl (which is represented in Table I), in 5 cc. of *n*-hexane at 30°C for 25 hr. The Results are shown in Table I.

TABLE I. EFFECT OF THE RATIO OF COMPONENTS IN THE COMPLEX UPON THE CONVERSION AND THE INSOLUBLE PART IN BOILING *n*-HEXANE

| No. | $SnR_4/TiCl_4$ | Convertion % | Insoluble part in *n*-hexane, % |
|---|---|---|---|
| 1 | 0.54 | 4.01 | 8.61 |
| 2 | 0.82 | 2.72 | 11.52 |
| 3 | 1.09 | 0.71 | 12.21 |
| 4 | 1.36 | 2.11 | 15.14 |
| 5 | 1.64 | 15.75 | 18.32 |
| 6 | 1.91 | 8.73 | 17.26 |

$TiCl_4$; $9.26 \times 10^{-2}$ mol., Monomer; 5 g. *n*-Hexane; 5 cc., Temp.; 30°C.

It is seen that a minimum for the rate of polymerization exists where the ratio of tin tetraethyl to titanium tetrachloride is about unity. This respect is discussed afterward.

**Effects of Alkyl Radical in $SnR_4$ and the Temperature of Complex Preparation upon the Conversion and the Molecular Weight of Polymer.**—In each experiment, 15 g. of monomer was polymerized with the catalyst which was prepared by mixing the two components, i.e., $2.024 \times 10^{-2}$ mol. of tin tetraalkyl and $1.852 \times 10^{-2}$ mol. of titanium tetrachloride, in a sealed tube at 40°C for 15 hr. Each polymer was then extracted by boiling *n*-hexane. This procedure was made to find the percentage of so-called isotactic polymer which had been defined by Natta as an isoluble part in boiling *n*-heptane. In this sence, the extraction has to be made, if possible, by *n*-heptane. However, the greater part of the polymer which would be extracted by boiling *n*-heptane is also extracted by boiling *n*-hexane, as is shown in Table III. Accordingly, the solvent, *n*-hexane was used. These results are shown in Table II.

The effect of the temperature of catalyst preparation upon the conversion is represented in Fig. 2.

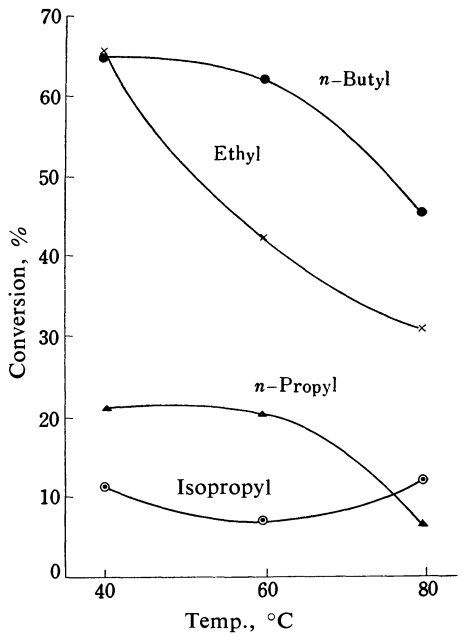



Fig. 2. Effect of the temperature of the catalyst preparation upon the conversion.

The polymerization with the catalyst prepared at lower temperature resulted in higher conversion, which gave lower molecular weight and further lower percentage of polymer insoluble in boiling *n*-hexane (except for the case of tin tetraethyl).

**Extraction of the Polymer with Various Solvents.** — To find the percentage of atactic and isotactic parts which are contained in the polymer prepared with the tin tetraethyl-titanium tetrachloride catalyst, 55.774 g. of the polymer was successively extracted by such series of solvents as acetone, diethyl ether, *n*-hexane, and *n*-heptane. The sample employed in this extraction was prepared by polymerizing 75 g. of monomer with the catalyst which had been prepared at 20°C by the reaction between 1.012 mol. of tin tetraethyl and 0.926 mol. of titanium tetrachloride. In this polymerization reaction (at 40°C, for about 15 hr.), 57.428 g. of the polymer was obtained (conversion; 76.6%). The viscosity of each fraction was measured by means of the aforementioned method. These results are shown in Table III.

It[4] has already been known that an organo

3) G. Ciampa, *Chim. e ind.* (*Milan*), **38**. 298 (1956).

4) N. G. Gaylord and H. F. Mark, "Linear and Stereoregular Addition Polymers" Interscience Publishers, Inc., New York (1959), p. 129.

TABLE II. POLYMERIZATIONS AT VARIOUS TEMPERATURES USING VARIOUS TIN TETRAALKYLS

| R in $SnR_4$ | Cat. preparation temp., °C | Conversion % | Insoluble part (%) in boiling hexane | $[\eta]\times10$ | $M\times10^{-3}$ |
|---|---|---|---|---|---|
| Ethyl | 40 | 65.7 | 18 | 2.4 | 9.7 |
| 〃 | 60 | 42.5 | 12 | 1.5 | 6.2 |
| 〃 | 80 | 31.6 | 14 | 1.9 | 5.1 |
| *n*-Butyl | 40 | 65.4 | 4 | 0.8 | 3.2 |
| 〃 | 60 | 62.4 | 3 | 1.0 | 4.1 |
| 〃 | 80 | 45.7 | 5 | 1.4 | 5.6 |
| Isopropyl | 40 | 11.5 | — | 0.4 | 1.4 |
| 〃 | 60 | 7.4 | — | 0.4 | 1.7 |
| 〃 | 80 | 12.1 | — | 0.3 | 1.1 |
| *n*-Propyl | 40 | 21.1 | 2.6 | 0.8 | 3.2 |
| 〃 | 60 | 20.4 | 4.2 | 1.1 | 4.0 |
| 〃 | 80 | 6.4 | 4.0 | 1.3 | 5.1 |

The viscosity was measured for the original polymer.
Monomer; 15 g., Temp.; 40°C, Time; 15 hr.
$SnR_4$; $2.024\times10^{-2}$ mol., $TiCl_4$; $1.852\times10^{-2}$ mol.
The polymers prepared with $Sn(i\text{-}C_3H_7)_4$-$TiCl_4$ were grease-like, and so, the extractions were not carried out.

TABLE III. EXTRACTION WITH VARIOUS SOLVENTS

| Solvent | Polymer, g. | Fraction, % | $[\eta]$ | $M\times10^{-3}$ | M. p., °C |
|---|---|---|---|---|---|
| Acetone | 2.584 | 4.6 | — | — | |
| Ether | 22.370 | 40.1 | 0.11 | 4.4 | |
| *n*-Hexane | 20.363 | 40.4 | 0.13 | 5.2 | |
| *n*-Heptane | 2.036 | 3.7 | 0.26 | 10.4 | 120 |
| (Residue) | 6.255 | 11.2 | 1.02 | 40.8 | 155～160 |

metallic compound containing the metal with smaller ionic radius, results in a higher yield of isotactic polymer. Accordingly, it is natural that the polymerization using a compound of tin as a catalyst component results in a lower yield of isotactic polymer.

**Rate of Polymerization.**—In order to find the rate of polymerization, the following experiment was performed. Each polymerization was carried out in a sealed tube with tin tetraethyl-titanium tetrachloride catalyst consisting of $2.024\times10^{-2}$ mol. of the former and $1.852\times10^{-2}$ mol. of the latter. The catalyst was shattered finely by a high speed shaker in 15 cc. of *n*-hexane before the monomer (10 g.) was introduced. The polymers were treated by means of the aforementioned method. The relation between the conversion and the reaction time is represented in Fig. 3.

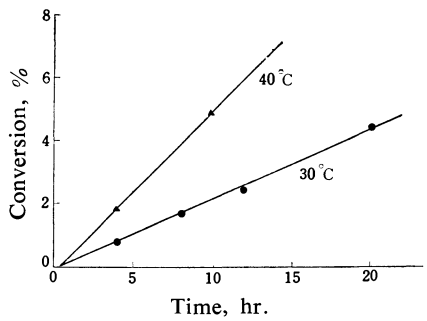



Fig. 3. Polymerization rate in *n*-hexane.

The rates at 30 and 40°C were calculated from Fig. 3 as 0.22%-conversion/hr. and 0.5%-conversion/hr., respectively. The values indicate that the polymerization of propylene with tin tetraalkyl-titanium tetrachloride catalyst proceeds very slowly in the solution system.

**Infrared Spectra.** — In order to compare the microstructure of the polymer prepared by the tin tetraethyl-titanium tetrachloride catalyst with that

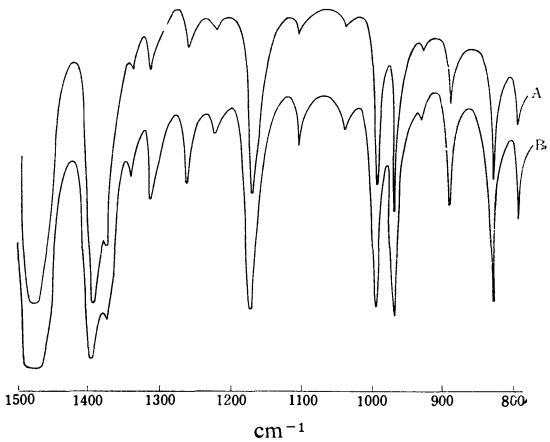



Fig. 4. Infrared spectra of in boiling heptane insoluble polymers.
A; Polymer prepared with $SnR_4$-$TiCl_4$
B; Moplen

of ' Moplen ', the polymer prepared by aluminium-trialkyl-titanium trichloride catalyst, the infrared spectrum of the insoluble part in boiling *n*-heptane was observed. B is a spectrum of *n*-heptane insoluble part of Moplen. From the comparison of A with B, it is obvious that these polymers are strikingly similar in their microstructures.

## Discussion

Generally, the Ziegler catalyst consists of Lewis acid and Lewis base. Therefore, a cationic or an anionic reaction will predominantly occur according to the catalyst composition in which Lewis acid or base is contained in excess, respectively.

The double bond of propylene, of course, is easily attacked by a cationic catalyst, owing to the effect of the methyl group. Moreover, it is also well known that, in the case of cationic polymerization, the growth of the chain easily terminates by a chain transfer. Thus, the rate of cationic polymerization is steady, but the polymer produced has usually a low molecular weight and further low stereoregularity. On the other hand, in the case of anionic polymerization, a polymer having a high molecular weight and further high stereoregularity is usually obtained, while the rate of reaction becomes smaller than that of cationic reaction.

From the facts mentioned above, it may be said that the decrease of conversion (from No. 1 to No. 3) with an increase in the amount of tin tetraethyl will mean that the cationic character is replaced gradually by the anionic character. It is also considered that, in Nos. 3—6, the effective anionic catalyst increases with the increase of the amount of tin tetraethyl.

Next we discuss the effects of temperature of catalyst preparation upon the convertion, the insoluble part in boiling *n*-hexane and stereospecificity. As is apparent from Fig. 1, the reducing power is the strongest in the case of tin tetraethyl, so that the effective anionic catalyst will be produced even at a lower temperature, in such a case. The fact that both the conversion and the stereospecificity decrease with an increase in the temperature will mean a decreasing of the active center which is in suitable valence state.

In the case of the propyl or butyl radical, the reducing power is so much weaker than that of the ethyl radical, that a temperature which is suitable for preparing the effective complex containing the latter, is unsuitable for producing the effective one containing the former. At such a lower temperature, the somewhat cationic character will still remain in the complex. When the temperature becomes higher, the cationic character will decrease, and so the conversion decreases while the stereospecificity increases, as is seen in Table II.

In regard to the effects of the length of the alkyl radical upon the conversion and the stereospecificity, no distinct relations between them were obtained.

*Electrical Communication Laboratory*
*Nippon Telegraph and*
*Telephone Public Corporation*
*Musashino-shi, Tokyo*

# *Neutron and γ-Irradiation of Propionamide*

By Enzō TACHIKAWA and Gen-ichi TSUCHIHASHI

(Received August 12, 1960)

When molecules containing nitrogen atoms are irradiated with neutron, the nuclear transformation

$$^{14}N + n \rightarrow (^{15}N)^* \rightarrow {}^{14}C + p$$

takes place. A carbon-14 atom thus produced immediately ruptures the bond which holds it due to its tremendous recoil energy and becomes a hot atom. Therefore, an unusual reaction is expected to occur as the hot atom loses its energy by collision. As an example of neutron irradiation of nitrogenous organic compound, ammonium nitrate was first studied with a view of the production of carbon-14 activity by Ruben and Kamen[1] in 1940. Recently, several researchers have attempted the neutron irradiation of many compounds[2]. But these results were not completely accounted for either by the simple random substitution of carbon atom or, of course, by ordinary thermal reaction.

1) S. Ruben and M. D. Kamen, *Phys. Rev.*, **57**, 549 (1940).
2) R. C. Extermann, "Radioisotopes in Scientific Research". Vol. II, Pergamon Press, London (1958), p. 114.

In order to examine the mechanism of hot atom reaction in detail, the present authors carried out the neutron irradiation of propionamide and found that the methylation of the amide was the main results and the authors determined the activity distributions in the products: $^{14}$C-propionamide, $^{14}$C-butyramide, $^{14}$C-isobutyramide, $^{14}$C-ethyl methyl ketone. Methyl radicals produced by γ-irradiation are less energetic than the hot atoms produced from the nuclear transformation. In order to compare the reactivity of the carbon-14 hot atoms with those of methyl radicals from carbon-carbon bond fissions by γ-ray irradiation, the γ-ray irradiation of propionamide-(carbonyl-$^{14}$C) was studied also in the present work and the yields of butyramide and isobutyramide were determined by the isotope dilution method.

Moreover, the reaction of propionic acid with thermal methyl radicals produced by the decomposition of acetyl peroxide was studied and the abnormality in the distribution of products in the above cases is discussed in comparison with the result of the thermal reaction.

## Experimental

**Neutron Irradiation.**—*Irradiation of Sample.*—Propionamide was synthesized from propionic acid and ammonium carbonate by Coleman-Alvarado's method[3] and recrystallized from methanol-ether solution. The butyramide and isobutyramide used as carriers were synthesized by the same method as propionamide. Commercial ethyl methyl ketone was purified by fractionation with a Podbielniak high temperature distillation apparatus (60-plates heli-grid packing column). Fifteen grams of the propionamide were covered with a polyethylene sheet and then packed in a polyethylene capsule. The assembled mass was iraadiated in the J. R. R.-1 reactor at an approximate flux of $10^{11}$ neutron/cm$^2$/sec. for about 120 hr. After irradiation, about a month was allowed for the decay of short-lived species in the capsule. As soon as it was opened, the irradiated sample was separated into several portions for the subsequent experiments.

*Separation of Products.*—To separate butyramide and isobutyramide a carrier was added to the irradiated sample. In the case of propionamide, some more non-active carrier was added. The mixture was hydrolyzed by refluxing for 2 hr. with 50% hydrochloric acid and the resulting substance was purified by distillation and by a Podbielniak gas chromatography on a 1/4″×4ft. column containing fire brick celite (30~80 mesh): 50% D. C. 710 silicone plus 10% stearic acid constituted the liquid phase. The column temperature was kept at 100°C and helium was used as the carrier gas.

*Separation of Ethyl Methyl Ketone.*—Ethyl methyl ketone was separated as 2,4-dinitrophenyl hydrazone by addition of 2,4-dinitrophenylhydrazine and this was recrystallized from ethanol several times to give a constant specific activity.

Table I. The quantities of irradiated sample and carriers

| Separated sample | Irradiated sample, g. | Carrier, g. |
|---|---|---|
| Propionic acid | 4.133 | — |
| Butyric acid | 3.465 | 4.809 |
| Isobutyric acid | 3.465 | 4.581 |
| Ethyl methyl ketone | 0.243 | 1.193 |

**γ-Irradiation.**—*Irradiation of Sample.*—About 5 g. of propionic acid purified with the distillation apparatus was added to sodium propionate (carbonyl-$^{14}$C) (0.1 mg., 0.1 mc./mg.). Propionyl chloride-(carbonyl-$^{14}$C) was synthesized from the mixture and benzoyl chloride by the method that is cited in the literature[4]. The distillate up to 81°C was dissolved in benzene and converted to propionamide-(carbonyl-$^{14}$C) with ammonia. It was recrystallized from methanol-ether several times to give a constant specific activity of $4.7\times10^2$ μc./mol. Three grams of the propionamide-(carbonyl-$^{14}$C) were irradiated by the 10000-curie $^{60}$Co γ-source[4] with a dose rate of $1.2\times10^5$ r./hr. at room temperature. The dose rate was determined by both cerous-ceric[6] and ferric-ferrous[7] dosimeter. The absorbed dose was $2\times10^8$ r.

After irradiation the sample was separated into several portions for the subsequent experiments.

*Separation of Products.*—In this case, propionamide was added as a hold back carrier, also. Acids were separated by the same procedure as that described above. The acids were converted again to amide by benzoyl chloride and ammonia and then were recrystallized.

Table II. The quantities of irradiated sample and carriers

| Separated sample | Irradiated sample, g. | Carrier g. | Hold back carrier, g. |
|---|---|---|---|
| Butyric acid | 1.00 | 1.50 | 2.00 |
| Isobutyric acid | 1.00 | 1.50 | 2.00 |

**3. Decomposition of Acetyl Peroxide in Propionic Acid-(Carboxyl-$^{14}$C).** — *Preparation and Purity of Acetyl Peroxide.*—Acetyl peroxide was synthesized by the Gambarjan method[8] modified by Kharasch[9].

Its purity was 99.86%.

3) G. H. Coleman and A. M. Alvarado, "Organic Syntheses", Coll. Vol. I, (1948), p. 3.

4) N. D. Cheronis, "Technique of Organic Chemistry", Vol. VI, "Micro and Semimicro Method", Interscience Publishers, Inc., New York (1954), p. 284.

5) A. Danno et al., Abstract of the 7th Hot Laboratories and Equipment Conference, Cleveland (1959), p. 349~360.

6) For example, T. Rigg, G. Stein and J. Weiss, *Proc. Roy. Soc.*, **A211**, 375 (1952).

7) G. R. A. Johnson and J. Weiss, ibid., **A240**, 189 (1952).

8) S. Gambarjan, *Ber.*, **42**, 4010 (1909).

9) M. S. Kharasch, H. C. Mckay and W. H. Urry, *J. Org. Chem.*, **10**, 394 (1945).

*Propionic Acid-(Carboxyl-$^{14}C$).*—Non-active propionic acid which was purified by the Podbielniak high temperature distillation apparatus was added to the sodium propionate-(carboxyl-$^{14}C$) (0.1 mc./mg.).

The mixture was purified by several distillations in the distillation apparatus. The specific activity of the purified propionic acid-(carboxyl-$^{14}C$) was 4.25 mc./mol.

*Decomposition of Acetyl Peroxide.*—Acetyl peroxide (507.8 mg.) was dissolved in 4.00 ml. of propionic acid-(carboxyl-$^{14}C$). The mixture was heated at 95~100°C for five hours.

*Separation of Acids.*—Acids were separated and purified by the same procedure as in the case of $\gamma$-irradiation.

TABLE III. THE QUANTITIES OF SOLUTION AND CARRIERS

| Separated sample | Reaction mixture, ml. | Carrier ml. | Hold back carrier, ml. |
|---|---|---|---|
| Isobutyric acid | 1.00 | 2.00 | 2.00 |
| Butyric acid | 1.00 | 2.00 | 2.00 |

*Oxidation and Counting.*—The purified compounds were converted to carbon dioxide by the Van Slyke-Folch oxidation method[10].

The resulting carbon dioxide was absorbed by 0.74 N sodium hydroxide solution and then precipitated as barium carbonate by the addition of barium chloride-ammonium chloride solution. The specific activity of the barium carbonate was measured at infinite thickness by a Tracerlab T. G. C-14 counter.

## Result and Discussion

The obtained results about the neutron irradiation of propionamide are shown on Table IV. The approximate relative ratio of the yields of ethyl methyl ketone, butyric acid, isobutyric acid, propionic acid were 1 : 2 : 3 : 4. $^{14}C$-Propionamide would be produced by the replacement of a carbon atom in the parent molecule with the recoiling carbon-14.

$$CH_3CH_2CONH_2 \xrightarrow{^{14}N\,(n,\,p)\,^{14}C} \text{recoil } ^{14}C + \text{molecular fragments} \quad (1)$$

$$\text{recoil } ^{14}C + CH_3CH_2CONH_2 \longrightarrow {}^{14}CH_3CH_2CONH_2 \;/\; CH_3{}^{14}CH_2CONH_2 \;/\; CH_3CH_2{}^{14}CONH_2 + \text{knockon-}^{12}C + \text{etc.} \quad (2)$$

Ethyl methyl ketone was produced by a "knockon" reaction by $^{14}C$ at nitrogen in the parent compound. Butyramide and isobutyramide were formed by the replacement of hydrogen in propionamide with $^{14}C$-radicals, respectively.

$$(^{14}CH_3\cdot)^* \text{ or } (^{14}CH_2{:})^* + CH_3CH_2CONH_2 \longrightarrow {}^{14}\text{C-butyramide or } {}^{14}\text{C-isobutyramide} + \text{etc.} \quad (3)$$

It is known that in ordinary free radical reactions, the hydrogen attached to a secondary carbon atom is more reactive with a free radical than that attached to a primary carbon atom. If butyramide and isobutyramide were formed by the thermal reaction of free methyl or methylene radical, the yield of isobutyramide which would be produced by the substitution of the hydrogen atom attached on the secondary carbon of propionamide would be much larger than that of butyramide. However, the ratio of the yields of butyr- and isobutyramide in the present study was about 3 : 2 as is shown in Table IV. The value agrees with the ratio of the number of hydrogen atoms available for substitution in the propionamide to give butyr- or isobutyramide. Accordingly, another mechanism should be considered instead of the ordinary free radical mechanism. Here the present authors propose the following mechanism:

(1) $^{14}C$-Propionamide is produced by a "knockon" reaction of the carbon in the compound by the carbon-14 having high kinetic energy. (Eq. 2). (2) Most of the recoil carbon-14 are cooled by collisions with atoms or molecules to some extent so that its energy would be in the order of 25~50 eV.[11] However the recoil carbon-14 is extremely active and reacts with its surroundings, and its predominant tendency will be to gain hydrogens as follows.

$$\text{recoil carbon-14} + \text{organic matrix} \longrightarrow {}^{14}CH_3\cdot,\ {}^{14}CH_2{:},\ {}^{14}CH_3{}^{+},\ \text{etc.} \quad (4)$$

The energy of these radicals will be so high that, at random, substitution reaction will occur. Assuming the above mechanism, the distribution of activity in butyric and isobutyric acid would be 3 : 2.

**$\gamma$-Irradiation.**—When the organic compounds are irradiated by $\gamma$-rays, the C-H, and C-C bonds are broken to yield $CH_3$ and other radicals. To compare the reactivity of the radicals produced by $\gamma$-irradiation with that of $^{14}C$-hot atom, the $^{60}Co$ $\gamma$-ray irradiation of propionamide-(carbonyl-$^{14}C$) was performed. Methyl radical, ethyl radical, carbon monoxide and so on are formed from propionamide by $\gamma$-rays irradiation. Methyl radical attacks the propionamide to produce butyramide or isobutyramide. The ratio of the yield of butyramide- and isobutyramide was determined by the

10) D. D. Van Slyke and H. Folch, *J. Biol. Chem.*, **136**, 509 (1940).

11) A. P. Wolf, C. S. Redvanly and C. Anderson, *J. Am. Chem. Soc.*, **79**, 3717 (1959).

TABLE IV. THE NEUTRON IRRADIATION OF PROPIONAMIDE

| Product | Activity, $\mu$c. 1. | 2. | Average | % to the total activity | Relative ratio |
|---|---|---|---|---|---|
| Propionamide | 1.40 | 1.30 | 1.35 | 3.3 | 4.2 |
| Butyramide | 0.86 | 0.90 | 0.88 | 2.1 | 2.7 |
| Isobutyramide | 0.69 | 0.71 | 0.70 | 1.7 | 2.1 |
| Ethyl methyl ketone | 0.31 | 0.33 | 0.32 | 0.8 | 1.0 |
| Total activity | 42.0 | 40.0 | 41.0 | | |

TABLE V. $\gamma$-IRRADIATION OF PROPIONAMIDE (CARBONYL-$^{14}$C)

| Product | Activity, $\times 10^{-1}$ $\mu$c. 1. | 2. | Average, $\times 10^{-1}$ $\mu$c. | Relative ratio | $G$-Value |
|---|---|---|---|---|---|
| Butyramide | 2.49 | 2.68 | 2.59 | 3.1 | 0.83 |
| Isobutyramide | 1.65 | 1.61 | 1.63 | 2.0 | 0.53 |

isotope dilution method using propionamide-(carbonyl-$^{14}$C.).

As it is shown in Table V, the ratio of the yield of butyric acid to that of isobutyric acid from the corresponding amides was 3 : 2. This ratio shows a good agreement with that in the case of the neutron irradiation.

These results can not be explained by thermal free radical reactions, but by the following mechanism: Propionamide decomposes to methyl and other radicals by the action of $\gamma$-rays as indicated by Eq. 5.

$$CH_3CH_2CONH_2 \xrightarrow{\gamma\text{-rays}} CH_3\cdot, \quad CH_3CH_2\cdot, \ CONH_2\cdot, \text{ etc.} \qquad (5)$$

The energy of methyl radicals will be so high that random substitutions will take place. Its energy, perhaps, is in the order of 5$\sim$10 eV.[12], so that the so-called "high energy reaction" should be considered to take place in this case and, by this mechanism, the present experimental results can be sufficiently explained.

**Thermal Free Radical Reaction in Solution.**— In order to compare such a high energy reaction as that indicated above with thermal free radical reaction, decomposition of acetyl peroxide in propionic acid-(carboxyl-$^{14}$C) was carried out.

Acetyl peroxide is decomposed in solution by heat as follows.

$$(CH_3COO)_2 \xrightarrow{\text{heat}} CH_3\cdot + CO_2\cdot + CH_3COO\cdot \qquad (6)$$

Most of the methyl radicals would carry out hydrogen abstraction reaction on the analogy of the reaction of acetyl peroxide with acetic acid[13].

However some of the methyl radicals formed combine with propionic acid-(carboxyl-$^{14}$C) to give butyric acid-(carboxyl-$^{14}$C) or isobutyric acid-(carboxyl-$^{14}$C). The isotope dilution method was applied to the determination of the ratio of butyric and isobutyric acid. The results are summarized in Table VI and the ratio of the yields of butyric and isobutyric acid is 1 : 2. The number of hydrogen atoms available for the substitution being taken into account, the result of the above ratio is that the hydrogen atom at the 2-position is three times more reactive with methyl radical compared with that at the 3-position, in the case of the substitution reaction of propionic acid. This result is quite different from those in the cases of neutron and $\gamma$-ray irradiation. The reaction of methyl radical from acetyl peroxide with propionic acid must be classified as a typical thermal free radical reaction in solution.

TABLE VI. THE DECOMPOSITION OF ACETYL PEROXIDE IN PROPIONIC ACID (CARBOXYL-$^{14}$C)

| Product | Activity, $\times 10^{-1}$ $\mu$c. | Relative ratio |
|---|---|---|
| Butyric acid | 2.31 | 1.0 |
| Isobutyric acid | 5.14 | 2.2 |

## Summary

Two methylation reactions of propionamide by $^{14}$C-hot atom, and of methyl radical from $^{60}$Co $\gamma$-ray irradiation and methylation reaction of propionic acid by methyl radical from thermal decomposition of acetyl peroxide were carried out and the reactivities of these species were studied. The methyl radical produced by $^{60}$Co $\gamma$-ray irradiation of propionamide gave the 3 : 2 mixture of butyr- and isobutyramide. This ratio agrees with the activity distribution of butyr- and isobutyramide in the neutron irradiation of propionamide. On the other hand the methyl radical produced by the

12) T. Watanabe, private communication.
13) A. Fry, B. M. Tolbert and M. Calvin, *Trans. Faraday. Soc.*, **49**, 1444 (1953).

thermal decomposition of acetyl peroxide in propionic acid gave 1:2 mixture of butyric and isobutyric acid. From the above results the reactions in the neutron irradiation and in the $\gamma$-ray irradiation are considered to be high energy reactions, whereas the methylation reaction of acetyl peroxide in propionic acid is considered to be a free radical reaction.

The authors wish to express sincere thanks to Professor K. Kimura and Dr. A. Danno for their kind encouragement and helpful discussions throughout the present work.

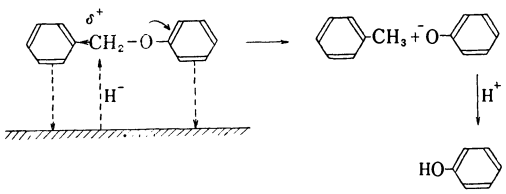
*Division of Radiation Applications*
*Japan Atomic Energy Research Institute*
*Tokai, Ibaraki-ken*

# *Stereochemistry and Mechanisms of Catalytic Hydrogenolysis and Hydrogenation. I. Catalytic Hydrogenolysis of Optically Active Compounds with Raney Nickel*

By Sekio MITSUI and Shin IMAIZUMI

(Received August 15, 1960)

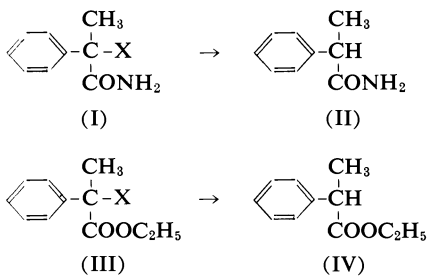
There have been only a few investigations on the mechanisms of catalytic hydrogenolysis taking the action of catalysis into consideration. Brenner and Keeys[1] presumed that the furyl carbonium ion was produced at an intermediate stage of the course of catalytic hydrogenolysis reaction of furfuryl alcohol, which yielded methylfuran, and this concept was supported by Lukes[2]. Pines et al.[3] presumed that the dehydroxylation reaction of alcohols at high temperature and pressure takes place via the carbonium ion. On the other hand, Mitsui et al.[4] presented papers reporting as follows: in the case of catalytic hydrogenolysis of phenyl benzyl ethers, these substances are adsorbed on the catalyst surface and the electron density between C-O bond decreases, and also the carbon of benzyl group becomes $\delta^+$, and the hydrogen adsorbed on the catalyst surface dissociates into $H^-$ and $H^+$. This hydride is presumed to attack $\delta^+$ carbon.




The above mentioned mechanism elucidates clearly the cases of various benzyl ether and benzylamine derivatives[5]. The question as to the mechanism by which the reaction takes place, may be clearly elucidated upon catalytic hydrogenolysis of optically active compounds with tertiary carbon. That is, if carbonium ion is formed, optically inactive compounds would be produced and if attacking reaction of hydride ion occurs, optically active compounds must be produced. Ott et al.[6], already reported that (+)-$\alpha$-phenylpropionic acid was obtained when (−)-$\alpha$-phenyl-$\alpha$-chloropropionic acid was subjected to catalytic hydrogenolysis using palladium-charcoal as a catalyst and that (−)-$\alpha$-phenylpropionic acid was obtained when (−)-$\alpha$-phenyl-$\alpha$-chloropropionic acid was reduced with zinc and acetic acid. Bonner[7,8] performed catalytic hydrogenolysis of several atrolactic acid derivatives I and III with excess of Raney nickel in boiling alcohol. The results were as follows: in cases of phenyl thioether (I, $X=SC_6H_5$) and of $\alpha$-phenyl-$\alpha$-benzenesulfinylpropionamide (I, $X=SOC_6H_5$), racemic $\alpha$-phenylpropionamide (II) was produced. However, in cases of $\alpha$-phenyl-$\alpha$-benzenesulfonylpropionamide (I, $X=SO_2C_6H_5$) and of ethyl $\alpha$-phenyl-$\alpha$-benzenesulfonylpropionate (III, $X=SO_2C_6H_5$), II or

1) J. G. M. Brenner and R. K. F. Keeys, *J. Chem. Soc.*, **1947**, 1067.
2) R. M. Lukes and C. L. Wilson, *J. Am. Chem. Soc.*, **73**, 4792 (1951).
3) H. Pines, M. Shamarieger and W. S. Postl, ibid., **77**, 5099 (1955); H. Pines, J. Marechal and W. S. Postl, ibid., **77**, 6390 (1955).
4) S. Mitsui, N. Inoue and A. Kasahara, *J. Chem. Soc. Japan, Pure Chem. Sec.* (*Nippon Kagaku Zasshi*), **71**, 203 (1951); *Chem. Abstr.*, **46**. 8102 i (1952).
5) S. Mitsui and N. Kiseki, ibid., **70**, 203 (1950); *Chem. Abstr.* **45**, 6631 g (1951); S. Mitsui, A. Kasahara and N. Endo, ibid., **75**, 234 (1954); *Chem. Abstr.*, **49**, 10210 d (1955); S. Mitsui and S. Imaizumi, ibid., **75**, 974 (1954); *Chem. Abstr.*, **51**, 14608 i (1957); S. Mitsui, S. Imaizumi and J. Kusume, ibid., **75**, 1065 (1954); *Chem. Abstr.*, **51**, 14609 c (1957).
6) E. Ott and K. Krömer, *Ber.*, **68**, 1655 (1935).
7) W. A. Bonner, *J. Am. Chem. Soc.*, **74**, 1034 (1952).
8) W. A. Bonner, ibid., **74**, 5089 (1952).

ethyl $\alpha$-phenylpropionate (IV), with only 10% recemization, was obtained, and it was definitely evidenced that Walden inversion accompanied this occasion. Thus he presented the mechanisms of these reactions. Developing this investigation, Bonner et al.[9,10] obtained ethyl D(+)-$\alpha$-phenylpropionate (IV) with 79% of retention of configuration from ethyl D(−)-atrolactate (III, X=OH) and methyl D(+)-$\alpha$-phenylpropionate with 72% of retention of configuration from methyl D(+)-$\alpha$-phenyl-$\alpha$-methoxypropionate, respectively. Cram et al.[11] obtained (+)-2-phenylbutane with 64% retention of optical activity from (+)-2-hydroxy-2-



(I) (II)



(III) (IV)

phenylbutane over excess of Raney nickel by means of boiling in alcohol. Barnes et al.[12] conducted catalytic hydrogenation of L(−)-1,2-diphenyl-1,2-propanediol over copper-chromium oxide catalyst at 200°C with hydrogen at 1400 p. s. i. and obtained L(+)-1,2-diphenylpropane with 22.3% retention of optical activity (61.2% retention of configuration).

The results indicate that optically active hydrogenolyzed products are obtained exclusive of poisonous compounds such as thioether and sulfinyl compounds. This fact seems to support the present author's concept described earlier.

The author et al. have conducted many investigations on catalytic hydrogenolysis of optically active derivatives of atrolactic acid in order to elucidate more clearly the mechanism of catalytic hydrogenolysis by which the mechanism of catalytic hydrogenation may be explained. One of the present authors, Imaizumi[13], already performed catalytic hydrogenation of ethyl L(+)-atrolactate (III, X=OH), $[\alpha]_D^8$ +25.30° (92.4% optical purity), over Raney nickel catalyst at ordinary temperature and pressure and obtained ethyl L(−)-$\alpha$-phenylpropionate (IV)*, $[\alpha]_D^9$ −54.82°, which upon hydrolysis gave L(−)-$\alpha$-phenylpropionic acid (V), $[\alpha]_D^7$ −73.2° (82.2% optical purity), with 89% retention of optical activity. Upon catalytic hydrogenation of ethyl L(+)-$\alpha$-phenyl-$\alpha$-chloropropionate (III, X=Cl), $[\alpha]_D^{21}$ +2.36° (42.1% optical purity), over 7.7% palladium-charcoal, L(−)-IV, $[\alpha]_D^{19}$ −4.97° (L(−)-V, $[\alpha]_D^{18}$ −7.20°, 7.6% optical purity), was obtained with 18% of optical activity. However, ethyl L(−)-$\alpha$-phenyl-$\alpha$-phenoxypropionate (III, X=$OC_6H_5$), $[\alpha]_D^{15}$ −2.10° (35.9% optical purity), gave D(+)-IV, $[\alpha]_D^{14}$ +23.3° (D(+)-V, $[\alpha]_D^{13}$ +30.5°, 34.2% optical purity), and ethyl D(+)-$\alpha$-phenyl-$\alpha$-phenoxypropionate, $[\alpha]_D^{15}$ +1.02° (18.4% optical purity), gave L(−)-IV, $[\alpha]_D^{16}$ −11.61° (L(−)-V, $[\alpha]_D^{15}$ −16.10°, 17.1% optical purity), with 95% and 93% retention of optical activity. It was evident that the Walden inversion accompanied this process simultaneously. An optically inactive product IV resulted from the hydrogenolysis of ethyl D(+)-$\alpha$-phenyl-$\alpha$-ethylmercaptopropionate (III, X=$SC_2H_5$), $[\alpha]_D^{20}$ +4.11°, and ethyl D(−)-$\alpha$-phenyl-$\alpha$-phenylmercaptopropionate (III, X=$SC_6H_5$), $[\alpha]_D^{29}$ −31.3°[14]. Accordingly, in the case of thioethers, nearly perfect racemization is observed to occur, which is in accord with the result of Bonner's experiments.

Considering the results of catalytic hydrogenolysis of these optically active ethylatrolactate derivatives, the authors[15] proposed to classify them into the following four kinds (or six kinds) of mechanisms of catalytic hydrogenolysis, according to both chemical constitution of compounds and stereochemical constitution of compounds. Explained in detail, in the case of strong catalytic poisonous compounds like thioether (III, X=$SC_2H_5$, $SC_6H_5$), the carbon-sulfur bond cleaves to radicals because three groups, carboethoxy, phenyl and sulfur atom, of the molecules may be adsorbed and chemisorption of the sulfur atom occurs strongly, and then hydrogen is incorporated with the radicals (radical cleavage reaction 1). Accordingly racemization ensues. If groups, incorporated into the asymmetric carbon atom, are not chemisorption groups such as carboethoxy or phenyl but are like alkyl groups, which do not cause chemisorption —if they cause any, it is an extremely weak one—, these groups probably act as electron releasing groups, and accordingly they cleave both to carbonium ion and to sulfide anion and then hydrogen is incorporated, ensuing on this occasion racemization too ($S_N1$ reaction,

9) W. A. Bonner, J. A. Zderic and G. A. Casaletto, ibid., **74**, 5086 (1952).
10) W. A. Bonner and J. A. Zderic, ibid., **78**, 3218 (1956).
11) D. J. Cram and J. Allinger, ibid., **76**, 4516 (1954).
12) R. A. Barnes and B. R. Juriano, ibid., **81**, 6462 (1959).
13) S. Imaizumi, *J. Chem. Soc. Japan, Pure Chem. Sec.* (*Nippon Kagaku Zasshi*), **77**, 1511 (1956); *Chem. Abstr.*, **53**, 5179 g. (1959).
* D(−) Atrolactic acid has been correlated in two independent ways with D(+) $\alpha$-phenylpropionic acid by E. L. Eliel and J. P. Freeman [*J. Am. Chem. Soc.*, **74**, 923 (1952)] and Bonner[9]. Rotations of the acid and its ethyl ester have the same sign.
14) S. Imaizumi, *J. Chem. Soc. Japan, Pure Chem. Sec.* (*Nippon Kagaku Zasshi*), **78**, 1396 (1957); *Chem. Abstr.*, **54**, 1403 h (1960).
15) S. Mitsui and S. Imaizumi, ibid., **77**, 1516 (1956); *Chem. Abstr.*, **53**, 5180 e (1959).

reaction 2). However, in the case of oxygen compounds like ethyl atrolactate (III, X=OH) and its phenyl ether (III, $X=OC_6H_5$), cleavage does not occur by the adsorption on the catalyst surface because chemisorption of the oxygen atom proceeds comparatively weakly. By the chemisorption of phenyl, carboethoxy and OR groups, the asymmetric carbon atom bears a positive charge ($\delta^+$), to which electron and proton or electrons and proton are transferred from the catalyst to produce ·OR radical or :OR anion and thereupon the reaction completes itself with the incorporation of electron and proton or proton to hold optical activity. On this occasion, if carboethoxy, phenyl and OR groups are adsorbed on the same catalyst surface, and the electron is transferred from the same catalyst surface, the reaction is the retention of configuration which we have designated as $S_Ni$ type reaction on catalyst (reactions 3 and 4). In the case of ethyl atrolactate, since carboethoxy, phenyl and hydroxy groups can be easily adsorbed on the same surface of the catalyst without any steric hindrance, the $S_Ni$ type reaction with retention of configuration occurs (Fig. 1). In the case of phenoxy compound (III, $X=OC_6H_5$), owing to the plane structure of the phenoxy group, when this plane is adsorbed on a catalyst surface, three groups, carboethoxy, phenyl and phenoxy, of the compound can not be so easily adsorbed on the same catalyst surface because of steric hindrance among these groups. However, when the phenoxy group is adsorbed on one catalyst surface and carboethoxy and phenyl groups are adsorbed on another catalyst surface, adsorption proceeds easily on the catalyst surfaces as there occurs no steric hindrance (Fig. 2). Then the asymmetric carbon atom is drawn near to the latter surface and the electron or electrons are transferred from the latter surface pushing out the phenoxy group to another catalyst surface and thereupon Walden inversion occurs. We have designated this reaction as $S_N2$ type reaction on catalyst (reactions 5 and 6).

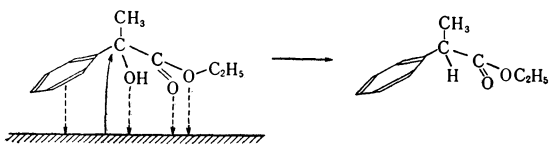


Fig. 1

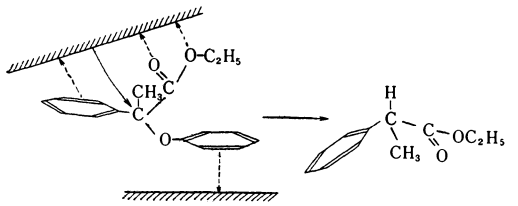
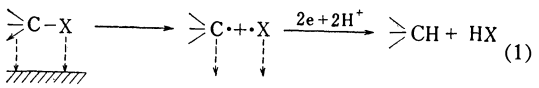


Fig. 2

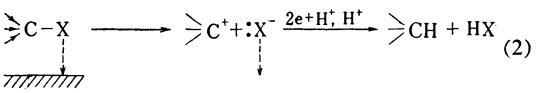
In the case of ethyl α-phenyl-α-chloropropionate (III, X=Cl), palladium-charcoal was used as the catalyst and because of comparatively strong chemisorption of chlorine, radical cleavage reaction 1 occurred predominantly. Besides this reaction, $S_Ni$ type

i) Radical cleavage reaction on catalyst



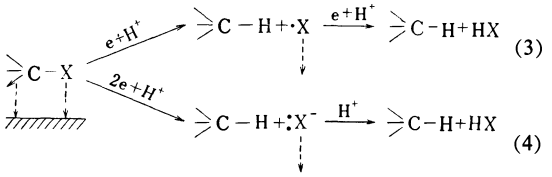
(1)

ii) $S_N1$ type reaction on catalyst



(2)

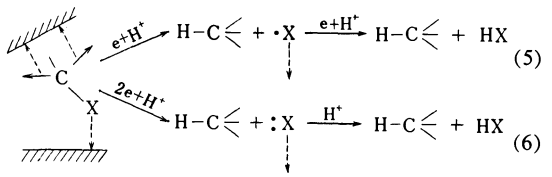
iii) $S_Ni$ type reaction on catalyst



(3)

(4)

iv) $S_N2$ type reaction on catalyst



(5)

(6)

reactions 3 and 4 proceeded as well, which led us to consider that retention of optical activity seemed to be scanty.

To verify the previously presented mechanisms of catalytic hydrogenolysis, investigations on catalytic hydrogenolysis of various optically active derivatives of ethyl atrolactate over Raney niekel were conducted, First, from ethyl L(−)-α-phenyl-α-ethoxypropionate (III, $X=OC_2H_5$), $[\alpha]_D^{17}-31.93°$ (82.4% optical purity), which is presumed to undergo chemisorption in a similar manner as that of ethyl atrolactate, ethyl (−)L-α-phenylpropionate (IV), $[\alpha]_D^{18}-53.4°$ (74.1% optical purity), was obtained with retention of configurations, as was expected, and the retention of optical activity was 90%. As for methyl α-phenyl-α-methoxypropionate, Bonner et al.[10] reported as mentioned before and the present authors investigated the matter also to obtain D(+)-IV, $[\alpha]_D^{16}+53.7°$ (74.4% optical purity), from ethyl D(+)-α-phenyl-α-methoxypropionate (III,

X=$OCH_3$), $[\alpha]_D^{15}$ +47.96° (88.6% optical purity), with 83% retention of optical activity. Secondly, from several aryloxy compounds (III, X=OAr) which are presumed to undergo chemisorption over Raney nickel in a similar manner as that of phenoxy compound (III, X=$OC_6H_5$), IV with Walden inversion was obtained with more than 90% retention of optical activity.

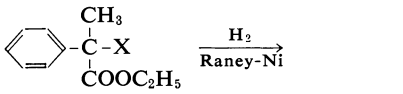
These facts can be explained as follows: ethyl α-phenyl-α-aryloxypropionate is adsorbed on both sides of the surface of Raney nickel catalyst to react readily and react with difficulty when adsorbed on one side of the surface. In the case of ethyl α-phenyl-α-alkyloxypropionate, as there exists no steric hindrance, it is adsorbed on one side of the surface to react. Thus, the previously presented conception is verified as correct and also indicates that Raney nickel catalyst has such a surface structure that ethyl α-phenyl-α-aryloxypropionate is easily adsorbed on both sides of its surface. This fact elucidates the fact that when palladium-charcoal or palladium-alumina is used as catalyst, ethyl α-phenylpropionate produced in the catalytic hydrogenolysis of optically active ethyl α-phenyl-α-phenoxypropionate accompanies retention of configuration if palladium concentration is dilute against carrier, and Walden inversion if palladium concentration is dense. According to the structure of catalyst surface, either retention of configuration or Walden inversion occurs, the fact concerning which will be reported in the next paper.

In Table I are shown the results of investigations of catalytic hydrogenolysis of optically active ethyl atrolactate derivatives over Raney nickel, which have been carried out so far.

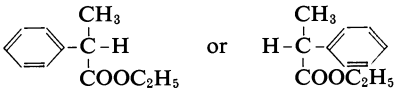
Ethyl α-phenylpropionate was produced with Walden inversion from acyloxy compounds (III, X=OCOR) which is prevented from being adsorbed on one side of the surface because of steric hindrance as in the case of aryloxy compounds. However, in the case of benzoyloxy compound (III, X=$OCOC_6H_5$) retention of optical activity is as small as 34%. These results lead us to presume that these phenomena occur because radical cleavage reaction and/or $S_N1$ type reaction and/or $S_Ni$ type reaction partially occur with $S_N2$ type reaction in the case of benzoyloxy compound owing to their benzoyloxy group's strong power of adsorption. We will report about this mechanism at a later date.

The above-mentioned mechanism may clarify not only catalytic hydrogenolysis of benzyl-, aralkyl-, and allyl-compounds but also hydrogenolysis of compounds of aromatic ring, hetero-aromatic ring and unsaturated bond to which are combined halogens, OR, SR, CN etc., directly. In these cases, however, there exists Y=C-X on the same plane and it is scarcely possible for adsorption on both sides to occur. Accordingly $S_N2$ type reaction is not supposed to occur. If adsorption of double bond occurs, production of carbonium ion is least probable. But when this adsorption of X is strong, 2′ reaction might occur. In the case of strong adsorption of X (catalytic poisonous compounds), mainly 1′ reaction would proceed. When adsorption of X is comparatively weak and temperature is comparatively low, mainly 3′ or 4′ reaction proceeds. If temperature is high, 1′ reaction proceeds. Also the dehydroxylation reaction

TABLE I



(III)



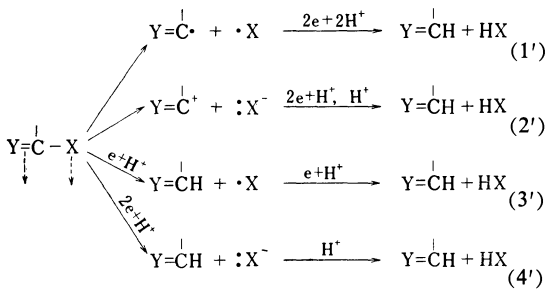
(IV)

| | X | Maintained optical activity %[a] | | Configuration |
|---|---|---|---|---|
| 1 | O-H | 89[13] | 79[9,10] | rentention |
| 2 | O-$CH_3$ | 83 | 72[b,10] | 〃 |
| 3 | O-$C_2H_5$ | 90 | | 〃 |
| 4 | O-$CH_2$-$C_6H_5$ | 87[16] | | 〃 |
| 5 | O-$C_6H_5$ | 95[13] | | inversion |
| 6 | O-$C_6H_4$-$CH_3$(*o*) | 96 | | 〃 |
| 7 | 〃 (*p*) | 92 | | 〃 |
| 8 | O-$C_6H_4$-$OCH_3$(*o*) | 94 | | 〃 |
| 9 | 〃 (*p*) | 92 | | 〃 |
| 10 | O-$C_{10}H_7$(β) | 91 | | 〃 |
| 11 | $SO_2$-$C_6H_5$ | 81[16] | 90[7] | 〃 |
| 12 | $SO_2$-$C_6H_4$-$CH_3$(*p*) | 75[16] | | 〃 |
| 13 | S-$C_2H_5$ | 0[14] | | racemization |
| 14 | S-$C_6H_5$ | 0[14] | | 〃 |
| 15 | S-$C_6H_4$-$CH_3$(*p*) | 0[16] | | 〃 |
| 16 | Cl | 0[c] | | 〃 |
| 17 | O-$COCH_3$ | 67[16] | | inversion |
| 18 | O-$COC_2H_5$ | 82[16] | | 〃 |
| 19 | O-$COC_6H_5$ | 34[16] | | 〃 |

a) Author's %=(optical activity of IV/optical activity of III)×100=2×Bonner's %−100. Bonner's %=50+author's %/2.
b) Methyl ester.
c) In case of 7.7% palladium charcoal catalyst, which maintained optical activity of resulting IV was 18% with retention of configuration[13]. However, in case of Raney nickel catalyst, the resulting IV was almost completely racemic (cf. Experimental).

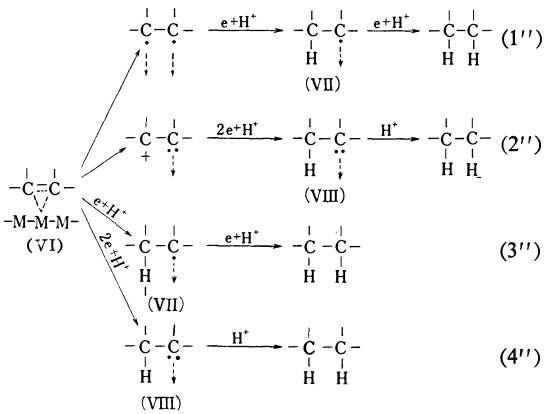
16) S. Imaizumi, ibid., **81**, 625, 631, 633 (1960).

of saturated alcohol at high temperature is presumed to be the type of 2′.



The hydrogenolysis of such bonds as $\ddot{N}$–$\ddot{N}$ and $\ddot{N}$–$\ddot{O}$ which have lone pairs is presumed to undergo exactly the same mechanism[17].

On the basis of this mechanism of catalytic hydrogenolysis, when the mechanism of catalytic hydrogenation is speculated upon, the following may be indicated. $\pi$-Electrons of unsaturated linkage transfer into d-band vacancy of the catalyst metal surface to form $\pi$-complex VI. Then, according to the kinds of catalyst and to the reaction condition, the unsaturated linkage cleaves to radicals or to carbonium ion and to anion to which $e+H^+$ or $2e+H^+$ transfers to become the half-hydrogenated state[18], VII or VIII. To this $e+H^+$ or $H^+$ transfers and the reaction is completed (1″, 2″ reactions). Otherwise by forming $\pi$-complex, carbon becomes $\delta^+$, to which transfers $e+H^+$ or $2e+H^+$ from catalyst and the reaction is completed via half-hydrogenated state VII or VIII (3″ and 4″ reactions). At comparatively low temperature, the reaction is of mainly 3″ or 4″ type, and at high temperature, 1″ or 2″ type reaction may occur.



17) S. Mitsui and S. Imaizumi, ibid., **78**, 812 (1957).
18) J. Horiuchi and M. Polanyi, *Trans. Faraday Soc.*, **30**, 1164 (1934).
19) L. Smith, *J. Prakt. Chem.*, [2] **84**, 738 (1911).
20) A. McKenzie and G. W. Clough, *J. Chem. Soc.*, **97**, 2564 (1910).

## Experimental

**Optically Active Ethyl Atrolactate ($III_1$).**—Atrolactic acid was resolved according to the procedure of Smith[19] and converted to the ethyl ester $III_1$[20]. The value for the rotation of optically pure ester $III_1$ is 27.38° (neat)[13].

**Optically Active Ethyl α-Phenyl-α-chloropropionate ($III_{16}$).**—This chloride was prepared from the above optically active ester $III_1$ and thionyl chloride by the method of McKenzie and Clough[20]. This reaction has been demonstrated to occur with the retention of configuration[20]. For the rotation of optically pure chloride $III_{16}$, we adopted the greatest value, $[\alpha]_D+5.6°$ (neat)[20], reported hitherto for the chloride.

**Optically Active Ethyl α-Phenyl-α-aryloxypropionate ($III_{6-10}$).**—Related phenol (0.05 mol.) was dissolved in a solution of sodium (0.05 mol.) in absolute ethanol (50 ml.). The above optically active chloride $III_{16}$ (0.05 mol.) was added to the alcoholic solution, and the mixture was boiled under reflux for 15 hr. The reaction mixture was freed of solvent by distillation, and after being cooled poured into water. The mixture was extracted twice with ether, and the extract was washed twice with 5% sodium hydroxide solution, and twice with water. The extract was then dried over anhydrous sodium sulfate, and the solvent was distilled. The residual oil was distilled thrice at reduced pressure to give 20~40% yield of arylethers $III_{6-10}$. This reaction has been demonstrated to occur with inversion of configuration in other systems[21]. Considering the stereochemical results of catalytic hydrogenolysis of these arylethers, the reaction of these arylethers formation took place with almost complete retention of optical activity. Therefore, optical activities of these arylethers were taken from the optical activity of chloride $III_{16}$.

*Ethyl* D(−)-*α-Phenyl-α-(o-cresoxy)propionate*($III_6$). — B. p. 145~146°C/3 mmHg, $[\alpha]_D^7-7.3°$ (*c* 5.6, absolute ethanol), 45.2% optical purity.

Found: C, 75.85; H, 7.23. Calcd. for $C_{18}H_{20}O_3$: C, 76.03; H, 7.09%.

*Ethyl* L(+)-*α-Phenyl-α-(p-cresoxy)propionate*($III_7$). — B. p. 143~145°C/0.5 mmHg, $[\alpha]_D^3+3.5°$ (*c* 5.4, absolute ethanol), 37.5% optical purity.

Found: C, 76.16; H, 7.36. Calcd. for $C_{18}H_{20}O_3$: C, 76.03; H, 7.09%.

*Ethyl* L(+)-*α-Phenyl-α-(o-anisoxy)propionate*($III_8$). — B. p. 158~160°C/2 mmHg, $[\alpha]_D^5+13.6°$ (*c* 4.2, absolute ethanol), 52.5% optical purity.

Found: C, 72.21; H, 6.99. Calcd. for $C_{18}H_{20}O_4$: C, 71.98; H, 6.71%.

*Ethyl* D(−)-*α-Phenyl-α-(p-anisoxy)propionate*($III_9$). — B. p. 170~172°C/3 mmHg, $[\alpha]_D^4-8.4°$ (*c* 5.3, absolute ethanol), 45.2% optical purity.

Found: C, 71.95; H, 6.64. Calcd. for $C_{18}H_{20}O_4$: C, 71.98; H, 6.71%.

*Ethyl* D(+)-*α-Phenyl-α-(β-naphthoxy)propionate* ($III_{10}$).—B. p. 190~191°C/1 mmHg, m. p. 65~66°C, $[\alpha]_D^8+4.8°$ (*c* 7.3, absolute ethanol), 45.2% optical purity.

21) H. Hart and H. S. Eluterio, *J. Am. Chem. Soc.*, **76**, 519 (1954).

Found: C, 78.74; H, 6.56. Calcd. for $C_{21}H_{20}O_3$: C, 78.72; H, 6.29%.

**Optically Active Ethyl α-Phenyl-α-alkyloxypropionate ($III_{2-3}$).**—The following preparation is an adaptation of the methods of Freudenberg[22] and Bonner[10]. A mixture of alkyl halide (6 ml.), silver oxide (6 g.) and optically active ethyl atrolactate (6 g.) was stirred at room temperature for 5 days, whereupon it was treated with ether and filtered. The filter cake was washed thrice with ether, and the filtrate and washings were freed of solvent. The residual oil was distilled at reduced pressure, and the specific rotation of the oil was examined, and then the oil was retreated in the above manner six additional times. The specific rotation and boiling point of the six treated materials were compared with seven treated ones. The final oil was distilled at reduced pressure to give optically active alkylether $III_{2-3}$. It is clear that the reaction proceeds without modification of configuration.

*Ethyl* D(+)-*α-Phenyl-α-methoxypropionate* ($III_2$).—B. p. 128~129°C/14 mmHg, $d_4^{15}$ 1.047, $[\alpha]_D^5$ +47.96° (neat). On the basis of the ethyl D(−)-atrolactate ($III_1$) ($[\alpha]_D^{21}$ −24.27° (neat)) used, the methyl ether appears to be 88.6% optically pure.

Found: C, 69.54; H, 7.82. Calcd. for $C_{12}H_{16}O_3$: C, 69.21; H, 7.74%.

*Ethyl* L(−)-*α-Phenyl-α-ethoxypropionate* ($III_3$).—B. p. 130~131°C/13 mmHg, $d_4^{17}$ 1.041, $[\alpha]_D^{17}$ −31.93° (neat). On the basis of the ethyl L(+)-atrolactate ($III_1$) ($[\alpha]_D^9$ +22.56° (neat)) used, the ethyl ether appears to be 82.4% optically pure.

Found: C, 70.33; H, 8.15. Calcd. for $C_{13}H_{18}O_3$: C, 70.24; H, 8.16%.

**Catalytic Hydrogenation of Optically Active Ethyl α-Phenyl-α-aryloxypropionate ($III_{6-10}$).**—A mixture of 1.5 g. of optically active arylether $III_{6-10}$, 50 ml. of absolute ethanol and 1.5 g. of W-5 Raney nickel was shaken under hydrogen at ordinary temperature and pressure for 5 hr. The catalyst was filtered and rinsed with ethanol, and the solvent was distilled. The residual oil was taken up in ether, and extracted with 5% sodium hydroxide solution. The alkali-insoluble material was dried over anhydrous sodium sulfate, and the solvent was removed. The residual oil was distilled at reduced pressure to give ethyl α-phenylpropionate (IV). The specific rotation of optically pure IV is 67.5° (neat) and 72.2° (absolute ethanol)[14].

The alkaline extract was acidified with hydrochloric acid, and the resulting oil was taken up in ether, dried, and the solvent was removed by distillation and the residue was converted into a solid derivative. These results were as follows.

D(−)-$III_6$ (45.2% optical purity) gave L(−)-IV (b. p. 101~102°C/10 mmHg, $[\alpha]_D^7$ −31.2° (*c* 6.4, absolute ethanol), 43.2% optical purity) and *o*-cresol (its tosylate, m. p. 54~55°C[23]).

L(+)-$III_7$ (37.5% optical purity) gave D(+)-IV (b. p. 103~104°C/12 mmHg, $[\alpha]_D^7$ +23.3° (*c* 8.6, absolute ethanol), 34.5% optical purity) and *p*-cresol (its tosylate, m. p. 69~70°C[23]).

L(+)-$III_8$ (52.5% optical purity) gave D(+)-IV (b. p. 101~102°C/10 mmHg, $[\alpha]_D^3$ +34.2° (*c* 8.1, absolute ethanol), 47.4% optical purity) and guaiacol (*o*-anisoxyacetic acid, m. p. 126~127°C[24]).

D(−)-$III_9$ (45.2% optical purity) gave L(−)-IV (b. p. 103~104°C/12 mmHg, $[\alpha]_D^7$ −28.20° (neat), $[\alpha]_D^4$ −30.1° (*c* 7.0, absolute ethanol), 41.7% optical purity) and *p*-methoxyphenol (m. p. 52~53°C).

D(+)-$III_{10}$ (45.2% optical purity) gave L(−)-IV (b. p. 103°C/11 mmHg, $[\alpha]_D^{12}$ −29.6° (*c* 9.1, absolute ethanol), 41.0% optical purity), 1,2,3,4-tetrahydro-β-naphthol (its phenylurethane, m. p. 98~99°C[25]) and 5,6,7,8-tetrahydro-β-naphthol (m. p. 57~59°C).

It is calculated from the above results that the percentages of retention of optical activity in the catalytic hydrogenolysis of $III_{6-10}$ to IV on Raney nickel, accompanied by inversion of configuration, are 96, 92, 94, 92 and 91%, respectively.

**Catalytic Hydrogenation of Ethyl D(+)-α-Phenyl-α-methoxypropionate ($III_2$).**—A mixture of 1 g. of D(+)-$III_2$ (88.6% optical purity), 30 ml. of absolute ethanol and 10 g. of W-5 Raney nickel was shaken under hydrogen at ordinary temperature and pressure for 3 days. The catalyst was filtered and rinsed with ethanol, and then the solvent was removed. The residual oil was distilled at 110~112°C (17 mmHg) to give 0.4 g. of D(+)-IV, $[\alpha]_D^{16}$ +53.6° (*c* 6.7, absolute ethanol), 74.4% optical purity. The percentage of retention of optical activity in IV is calculated to be 83% with retention of configuration.

The above mixture was shaken for 6 days in the same condition. The usual processing yielded 0.6 g. of D(+)-IV, $[\alpha]_D^{18}$ +34.5° (*c* 7.0, absolute ethanol), 47.8% optical purity. In this case, partial racemization of the IV produced appears to take place in the prolonged reaction time.

**Catalytic Hydrogenation of Ethyl L(−)-α-Phenyl-α-ethoxypropionate ($III_3$).**—A mixture of 1 g. of L(−)-$III_3$ (82.4% optical purity), 30 ml. of absolute ethanol and 10 g. of W-5 Raney nickel was shaken under hydrogen at ordinary temperature and pressure for 3 days. The catalyst was filtered and rinsed with ethanol, and then the solvent was removed. The residual oil was distilled at 110~111°C (16 mmHg) to give 0.3 g. of L(−)-IV, $[\alpha]_D^{18}$ −53.4° (*c* 5.2, absolute ethanol), 74.1% optical purity. The percentage of retension of optical activity in IV is calculated to be 90% with retention of configuration.

The above mixture was shaken under hydrogen at about 70°C for 20 hr. The customary work-up gave 0.5 g. of oil, b. p. 110~120°C/17 mmHg, $[\alpha]_D^{17}$ +13.5° (*c* 5.0, absolute ethanol). The product could not be identified, but seems to be a mixture of IV and cyclohexyl derivatives of $III_3$ and/or IV.

**Catalytic Hydrogenation of Ethyl L(+)-α-Phenyl-α-chloropropionate ($III_{16}$).**—A mixture of 2.1 g. of L(+)-$III_{16}$ ($[\alpha]_D^{12}$ +3.40° (neat), 60.7% optical purity), 50 ml. of absolute ethanol and 6 g. of W-5 Raney nickel was shaken under hydrogen at ordinary themperature and pressure for 2 hr. The catalyst was filtered and rinsed with ethanol and the solvent was distilled. The residual oil was taken up in ether, and extracted with 5% sodium

22) K. Freudenberg, J. Todd and R. Seidler, *Ann.*, **501**, 199 (1933).
23) F. Beverdin and P. Crépieux, *Ber.*, **35**, 1439 (1902).
24) O. Behaghel, *J. prakt. Chem.*, **114**, 296 (1926).
25) F. Straus and A. Rohrbacher, *Ber.*, **54**, 55 (1921).

carbonate solution. The alkali-insoluble material was dried over anhydrous sodium sulfate, and the solvent was removed. The residual oil was distilled at 108~110°C (14 mmHg) to give 1.2 g. of IV, $[\alpha]_D^{18}+0.49^\circ$ (neat), 0.7% optical purity. The percentage of retention of optical activity in IV is calculated to be 1% with inversion of configuration. Therefore, in the hydrogenolysis, almost complete racemization occurred.

*Department of Applied Science*
*Faculty of Engineering*
*Tohoku University, Sendai*

# *Fischer-Tropsch Synthesis with Tubular Reactor of 18.1 l. Catalyst Bed. I. Reactor with Constant Temperature Wall*

By Michio KURAISHI*, Minoru KURITA, Tadasuke HOSOYA, Hideo ICHINOKAWA, Kiyoshi OGAWA and Hiroshi UCHIDA

(Received September 13, 1960)

In our previous paper[1] dealing with the Fischer-Tropsch synthesis in a tubular reactor, a procedure for calculating temperature profiles from experimental concentration gradients of components along the reactor was proposed. The procedure was developed by making use of experimental data available with the reactor which contained a catalyst bed of 2 l., and which was held in a circulating oil bath at a constant temperature. Under the assumption that situations in the synthesis are similarly realized independently of the sizes of the reactor, the procedure promises that we may foresee performances of reactors of a larger size. Along this line of expectation, precalculations of temperature profiles are made for the synthesis with any reactor of similar construction but about ten times as large as the previous one. The applicability of the procedure may then be checked by comparing the results of precalculation with the experimental temperature profile in the synthesis with the present reactor of the larger size. Moreover, the same procedure is followed to give the temperature profiles from the experimental concentration gradients along the present reactor.

## Experimental

Raw water-gas for the synthesis is produced from coke and steam by the usual procedure. Hydrogen sulfide and carbon dioxide in the gas are removed in a gas purification train consisting of a sodium carbonate solution washer, an iron oxide box, and finally a caustic soda solution washer. The gas is then compressed at about 100 kg./cm$^2$ into a high pressure gas storage of 2000 l. (B), from which the compressed gas is introduced into a synthesis unit through a vessel (C) containing active charcoal for removal of organic sulfur. As shown in Fig. 1, the synthesis unit consists of a reactor (D), two hot separators (E), two cold separators (G) with

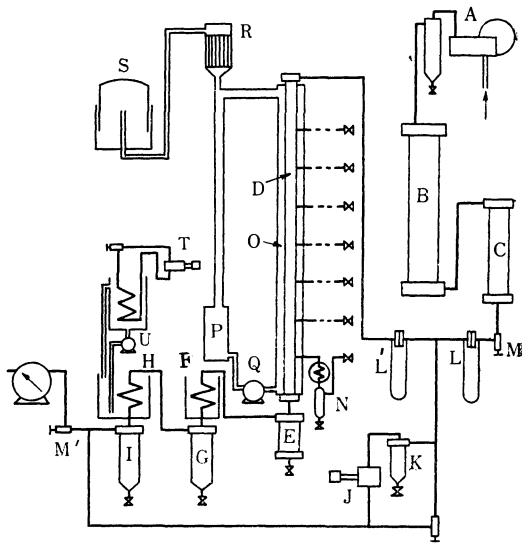



Fig. 1. Flow diagram of synthesis.

| | |
|---|---|
| A, Gas compresser | B, Pressure reservoir |
| C, Desulfrizer | D, Reactor |
| E, Hot separator | F, Water cooler |
| G, Cold separator | H, Brine cooler |
| I, Cold separator | J, Gas circulating pump |
| K, Oil separator | L, L', Flow meter |
| M, M', Reducing valves | N, Cold separator |
| O, Oil bath | P, Hot oil reservoir |
| Q, Hot oil pump | R, Condenser |
| S, $N_2$ gas holder | T, Refrigerator |
| U, Brine pump | |

* Present address : Japan Gas Chemical Co., Enoki-cho, Niigata.

1) M. Kuraishi, H. Ichinokawa, K. Ogawa, M. Kurita, T. Hosoya and H. Uchida, *J. Chem. Soc. Japan, Ind. Chem., Sec.* (*Kogyo Kagaku Zasshi*), **63**, 1588 (1960).

coolers (F), a low temperature separator (I) with a cooler (H), and a gas circulating pump (J) equipped with an oil separator (K), every one of which is of a design similar to, but about ten times as large as the corresponding equipment in the previous plant[1]. Having been mixed with part of the end-gas from the low temperature separator, an amount of the fresh gas is fed through a flow meter (L) into the reactor top where it flows in a downward direction through the catalyst bed. The volume of the fresh gas thus introduced is estimated from the degree of pressure decrease in the pressure gas storage and the flow rate is controlled by means of are ducing valve (M) and a flow meter (L). The volume of the fresh gas having been once estimated, one can easily calculate the flow rate of the circulating gas from carbon dioxide balance between the gases after and just before the reactor. Part of the gas after being separated at the low temperature separator is purged through a reducing valve (M'). In the above estimation, the volume of the gas thus purged is to be taken into account.

The reactor is 70 mm. in outer diameter and 50 mm. in inner diameter by 10 m. high[2], and is a simple reactor type with a constant temperature wall, being placed coaxially in a cylinder of oil (Dowtherm) bath (O). Into the bottom of the cylinder hot oil is fed at the flow rate of 2.5 $m^3$/hr., and flows upwards through an annular space between the cylinder wall and the reactor to the top, where the oil is allowed to flow down to a hot oil reservoir (P) which is being kept at a definite temperature. The recycling system of hot oil is always enclosed in an atmosphere of nitrogen which is supplied from a nitrogen gas holder (S) through an oil condenser (R).

The reactor contains a bed of 18.1 l. reduced catalyst (37.06 kg.). Two coaxial thermocouple wells 5 m. in length, 10 mm. in outer diameter, and 5 mm. in inner diameter, either one of which is fixed at the top or the bottom cover, go through the catalyst bed, and scanning of the temperature profile along the whole length of the reactor is made by moving the thermocouples in the wells. From seven successive ports at different heights along the catalyst bed, all of which are 1.2 m. apart from each other, a small portion of the fluid is withdrawn through a small cold separator (N) to be freed of water and oil, and the residual gaseous mixture is analyzed for the compositions. From the results of the analyses together with weighed amounts of the water, concentration gradients of the individual components along the catalyst bed are determined.

A sintered catalyst has been employed in the present synthesis. It was prepared, according to the procedure reported in our previous paper[4], from powders of a fused iron oxide catalyst containing in parts by weight 93.25 $Fe_3O_4$, 3 $Al_2O_3$, 1 CaO, 1 MgO, 1 $WO_3$, 0.25 CuO and 0.5 $K_2O$. The catalyst powders less than 100 mesh in size were pressed into tablets of 4×4 mm., which were sintered at 1000°C for one hour. Before use in the synthesis, the finished catalysts were completely reduced in a separate oven in a current of hydrogen at 500°C, and were removed from the oven to be packed into the synthesis reactor in carbon dioxide atmosphere.

## Prediction of Temperature Profile

Among the synthesis experiments with the reactor of 2 l. catalyst bed (25 mm. I. D.)[1], Exp. No. 6 showed that a temperature difference of 24°C appeared between the oil bath and the center across the bed during the synthesis where by using a sintered catalyst[5] a product (oil plus wax) yield of 2.72 kg./day was obtained under the following synthesis conditions: the pressure was 25 kg./$cm^2$, and the space velocities based on the recycle and the fresh gases were 1975 and 763, respectively. This makes us feel uncertain whether a smooth operation of the synthesis can be made with the present reactor, since the temperature in the present synthesis may be liable to rise too high. In this connection, a preliminary calculation is made to predict the temperature rise. The precalculation is made by the aid of the procedure proposed by us[1], being combined with reasonable assumptions on the synthesis for the scaled-up reactor.

Heat transfer in a catalyst bed packed in a single tubular reactor is generally given by the following equation,

$$C_p G\frac{\partial t}{\partial x}=\frac{1}{r}\left\{\frac{\partial}{\partial r}\left(\lambda_r\cdot r\,\frac{\partial t}{\partial x}\right)+\frac{\partial}{\partial x}\left(\lambda_x\cdot r\frac{\partial t}{\partial x}\right)\right\}+\sum v_i q_i \qquad (1)$$

with the following boundary conditions,

$$\left.\begin{aligned}&[t]_{x=0}=t_0\\&\left[\lambda_r\frac{\partial t}{\partial r}+Ut\right]_{r=r_2}=0\\&\left[\frac{\partial t}{\partial r}\right]_{r=r_1}=0\end{aligned}\right\} \qquad (2)$$

where $C_p$ is the heat capacity per unit mass of fluid, $G$ is the mass velocity, $t$ is the temperature difference between a catalyst bed and an oil bath, $x$ is the distance from the top of the bed, $r$ is the distance in lateral direction, $\lambda$ is the effective thermal conductivity of the catalyst bed fluid system, $v$ is the reaction rate, $q$ is the reaction heat, $U$ is the overall heat transfer coefficient, $r_1$ and $r_2$ are the inner and the outer radii of the catalyst bed, respectively.

2) According to the paper by Tramm[3], a great number of the reactors of this size are placed in an oven for the Industrial synthesis.

3) H. Tramm, a paper presented at the Fifth World Petroleum Congress, Section III (1959).

4) H. Uchida and H. Ichinokawa, *J. Chem. Soc. Japan, Ind. Chem. Sec. (Kogyo Kagaku Zasshi)*, **58**, 563 (1955).

5) The sintered catalyst used in the previous study was prepared from powders of a fused iron oxide catalyst containing in parts by weight 94 $Fe_3O_4$, 4 $Al_2O_3$, 1 CaO and 1 $K_2O$.

The last term in the right side of Eq. 1 concerns heat quantities of the reaction. It is usually determined according to a rate equation of the synthesis, and is a function of temperature and concentration. However, our previous work[1] pointed out that the term could be approximated to the following formula[6].

$$\sum v_i q_i = Q(\text{kcal./m}^3\text{ hr.}) = c_1 e^{-Mx} - c_2 e^{-Nx} \quad (3)$$

where $Q$ stands for the heat evolved per hour in unit volume of the catalyst bed at a distance $x$ from the top, and $c_1$, $c_2$, $M$ and $N$ are constants. Numerical values of the constants could then be determined from the distribution curve of the reaction heat given as a function of $x$. In this respect our previous paper[1] stated details of drawing the curve on the basis of experimental concentration gradients along the reactor.

Substitution of Eq. 3 into Eq. 1 and subsequent solution of the resulting equation result in the following formula,

$$t = t_0 \sum_1^{\infty} \frac{2U_1(a_n)\,U_0(a_n r/r_2)\,\exp(-\alpha_n^2 y)}{\left(a_n[\{1+(a_n^2/b^2)\}U_1^2(a_n) - (r_1/r_2)^2 U_0^2(a_n r_1/r_2)]\right)} + \sum_1^{\infty} \frac{2U_1(a_n)\,U_0(a_n r/r_2)}{\left(a_n[\{1+(a_n^2/b^2)\}U_1^2(a_n) - (r_1/r_2)^2 U_0^2(a_n r_1/r_2)]\right)} \times \left\{ \frac{[c_1(\exp(-my) - \exp(-\alpha_n^2 y))]}{[\lambda_r(a_n^2/r_2^2 - m - \lambda_x M^2/\lambda_r)]} - \frac{[c_2(\exp(-ny) - \exp(-\alpha_n^2 y))]}{[\lambda_r(a_n^2/r_2^2 - n - \lambda_x N^2/\lambda_r)]} \right\} \quad (4)$$

$$U_0(a_n r/r_2) \equiv J_0(a_n r/r_2) - cY_0(a_n r/r_2)$$

$$U_1(a_n r/r_2) \equiv J_1(a_n r/r_2) - cY_1(a_n r/r_2)$$

$$C \equiv J_1(a_n r_1/r_2)/Y_1(a_n r_1/r_2) = [a_n J_1(a_n) - bJ_0(a_n)]/[a_n Y_1(a_n) - bY_0(a_n)]$$

In Eq. 4 $a_n$ and $\alpha_n$ stand for roots of equations $a_n U_1(a_n) = aU_0(a_n)$ and $A\alpha_n^4 + \alpha_n^2 - a_n^2/r_2^2 = 0$, respectively. In addition, there are following relations,

$$A \equiv \lambda_x \lambda_r/(C_p G)^2,\ b \equiv Ur^2/\lambda_r,\ y \equiv \lambda_r x/C_p G,$$

$$m \equiv MC_p G/\lambda_r \text{ and } n \equiv NC_p G/\lambda_r.$$

$J_0$ and $J_1$ are Bessel functions of first kind, zeroth and first order, respectively, and $Y_0$ and $Y_1$ are the same functions of second kind, zeroth and second order, respectively.

Let us calculate $t$ with the present reactor by the aid of Eq. 4. Before proceeding to the calculation, it is assumed that the same synthesis conditions as these for Exp. No. 6 with the previous reactor hold again for the predicted synthesis, and that the same situations are realized in the predicted synthesis as were realized in the previous Exp. No. 6. Under these assumptions, the flow rate of the gaseous components and the yield of the product (oil plus wax) are 18.1/2 times as great as they were in Exp. No. 6. Hence the product yield attains 24.6 kg./day, and the flow rate of the gaseous components is 30 kg./hr.. Modified Reynolds number ($R_{ep} = d_p G/\mu$) takes a value of $7.22 \times 10^2$, where $d_p$ is 4 mm. Characteristic constants, such as the specific heat ($C_p$), the viscosity ($\mu$), and the thermal conductivity ($k$) of the fluid are determined in the following manner where compromise averages are taken between these based on the inlet and the exit gases. This results in the following values of $C_p = 0.42$ kcal./kg.°C, $\mu = 0.088$ kg./m. hr. and $k = 0.088$ kcal./m. hr.°C, respectively.

Moreover, the following values of the heat transfer constants are obtained as regards the predicted synthesis: $\lambda = 5.65$ kcal./m. hr.°C (2.61), $h = 866$ kcal./m² hr. °C (1086), and $h_L = 174$ kcal./m² hr. °C (120)[10], where $h$ and $h_L$ are the tube wall coefficients of heat transfer based on the inner and the outer surfaces of the reactor, respectively. Numericals in the brackets give the corresponding values for Exp. No. 6 with the previous reactor. As a consequence, a higher value of the overall heat transfer coefficient ($U$), which is 184 kcal./m² hr. °C as compared with 160 kcal./m²·hr. °C in Exp. No. 6, is obtained. Anyhow, the increase in the value of $U$ is mainly due to the higher value of $h_L$ in the predicted synthesis.

The constants in Eq. 3 have remained undetermined as yet. In interpretation of the data of Exp. No. 6, they were evaluated to be

$$Q(\text{kcal./m}^3\text{ hr.}) = 6.12 \times 10^5 e^{-0.18x} - 4.99 \times 10^5 e^{-1.01x} \quad (5)$$

The length of the reactor being denoted by $L$, the equation can be rewritten

$$Q(\text{kcal./m}^3\text{ hr.}) = 6.12 \times 10^5 e^{-0.82x/L} - 4.99 \times 10^5 e^{-4.60x/L} \quad (6)$$

since $L$ for the previous reactor was 4.55 m. Eq. 6 can represent the distribution of the reaction heat independently of the dimensions of the reactor, provided that the synthesis proceeds with the same tendency as that which took place in Exp. No. 6, namely that the

6) Kodama et al.[7], Shindo[8], and Maeda[9] had already given the exprssion of $\sum v_i q_i = ce^{-kx}$.
7) S. Kodama and K. Fukui, *Kagaku Kikai*, **12**, (1948).
8) M. Shindo, *Memoir Muroran Univ. Eng.*, **1**, 51 (1950).
9) S. Maeda, *Kagaku Kikai*, **15**, 5 (1951).
10) $\lambda$ and $h$ have been evaluated by using the formula by Hatta et al.[11], while $h_L$ has been evaluated by using the formula recommended by McAdams[12].
11) S. Hatta and S. Maeda, *Kagaku Kikai*, **13**, 79 (1949).
12) W. H. McAdams, "Heat Transmission", McGraw Hill Co. New York (1954).

heat evolving within unit volume of the catalyst bed at a value of $x/L$ is equal to the corresponding one in Exp. No. 6. The constants for the predicted synthesis are then given by putting $L=9.6$ m. in Eq. 6, which follows

$$Q(\text{kcal./m}^3\text{ hr.}) = 6.12\times10^5 e^{-0.085x} - 4.99\times10^5 e^{-0.48x} \quad (7)$$

For the sake of convenience, a graphical representation of the results is given in Fig. 2 (curve A) as a plot of $q$ (kcal./m. hr.), which is defined by $q=Q/\pi(r_2^2-r_1^2)$, against $x$. According to the definition, $q$ stands for the reaction heat evolved in an hour within the catalyst bed occupying the unit length of the reactor.

By putting the above numerical values of the constants into Eq. 4, the temperature profile either along or across the catalyst bed can be drawn, as shown in Fig. 2 (curves B and B'). The curves indicate that in the predicted synthesis with the present reactor the temperature difference between the oil bath and the center cross the catalyst bed attains only 31.5°C at the highest. Considering that the temperature difference in Exp. No. 6 was 24°C, and that the reaction heat evolving within a volume occupying the unit length of the present reactor becomes about fourtimes[13] as great as the heat with the previous reactor, the difference appears rather small.

We experienced the fact that with the previous reactor the synthesis could be carried out without serious difficulties, even when the temperature difference between the oil bath and the catalyst bed attained as high as 49°C (refer to Exp. No. 5 in our previous paper[1]). Based on the magnitude of predicted temperature rise, an operation of the synthesis with the present reactor may be expected to be probable.

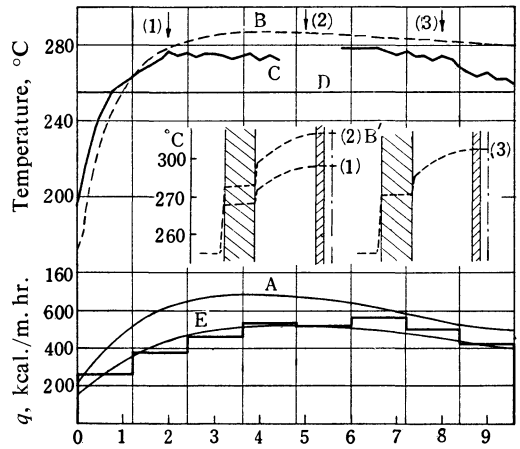



Fig. 2. Above, predicted and experimental temperature profiles. Below, distribution of $q$.
A, Predicted distribution of $q$
B, B', Predicted temperature profile (B, axial, B', radical)
C, Experimental temperature profile
D, Oil bath temperature
E, Experimental distribution of $q$

In the drawing of curves B', the magnitude of temperature rise from the oil bath to the outer wall-surface of the reactor ($t_{wo}$) and that to the inner wall-surface ($t_{w1}$) are given by the respective following formulae of the heat balance,

$$t_{wo}=t_{r=r_2}r_2U/r_3h_L, \quad t_{w1}=t_{r=r2}(1-U/h)$$

where $r_3$ is the outer radius of the reactor.

## Results and Discussion

**Experimental Results.** — The synthesis was made under the operating conditions as cited in Table I. The table also includes the operating conditions, product yield, and other points

Table I. Synthesis conditions, conversion, product yield, and other matters with those of predicted synthesis

| | Pressure kg./cm² | Oil bath temperature °C | Space velocity, hr⁻¹ Base on fresh gas | Space velocity, hr⁻¹ Based on recycle gas | Volume contract % |
|---|---|---|---|---|---|
| Exp. | 30 | 255 | 620 | 2070 | 42.2 |
| Predicted | 25 | 255* | 763 | 1975 | 43.1 |
| | Oil plus wax kg./day | Water kg./day | Oil plus wax per ($H_2$+CO) m³ | Use ratio ($H_2$/CO) | Recycle ratio |
| Exp. | 14.42 | 22.65 | 99.4 | 1.074 | 2.35 |
| Predicted | 24.62 | 19.10 | 130.5 | 0.819 | 1.59 |

* In the prediction of the temperature profile, wit as needless to consider the oil bath temperature, while for a convenient comparison of the predicted profile with the actual one curve A in Fig. 2 is drawn on the basis of the oil bath temperature of 255°C.

13) Strictly speaking, the heat is $(25^2-5^2)/(12.5^2-4^2)$ times in amount, where the numerals 5 and 4 are radii (mm.) of the thermocouple wells in the present and the previous reactors, respectively.

for the predicted synthesis. In the synthesis a much lower yield of oil plus wax[14] has been obtained with a greater amount of water than was predicted. As naturally expected from the lower yield, the actual temperature profile lies lower than the predicted profile (refer to Fig. 2). It may be noted, however, that the shape of the predicted profile is very similar to the actual profile except that the actual one is higher by 20°C at the topzone of the catalyst bed.

**Calculation of Temperature Profile from Concentration Gradient.**—Figure 3 shows the determined concentration gradients of reactants

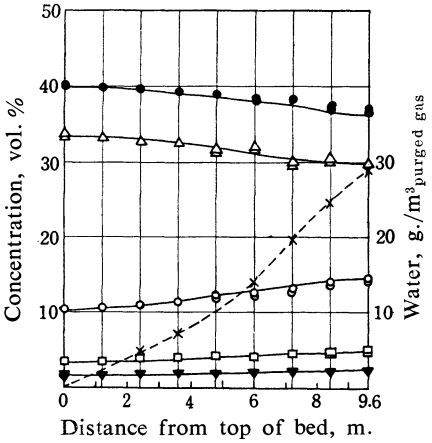



Fig. 3. Concentration gradients and amounts of water produced as a function of $x$.

—●— Hydrogen
—△— Carbon monoxide
—○— Carbon dioxide
—□— Gaseous paraffin
—▼— Gaseous olefin
--×-- Water

($H_2$, CO) and products ($H_2O$, $CO_2$, et al.) as a function of distance from the top along the catalyst bed. Our previous paper[1,15] reported that amounts of carbon monoxide consumed either by the hydrocarbon synthesis according to consecutive reactions of $H_2+CO\rightarrow >CHOH$ and $>CHOH+H_2\rightarrow -CH_2-+H_2O$ or by the water-gas shift[17,18] could be estimated from the concentration gradients, and the same procedure is now followed to result in Fig. 4. As soon as the carbon monoxide consumptions

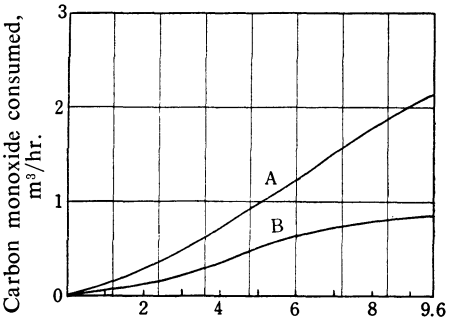



Fig. 4. Carbon monoxide consumptions.

A, By the hydrocarbon synthesis
B, By the water-gas shift reaction

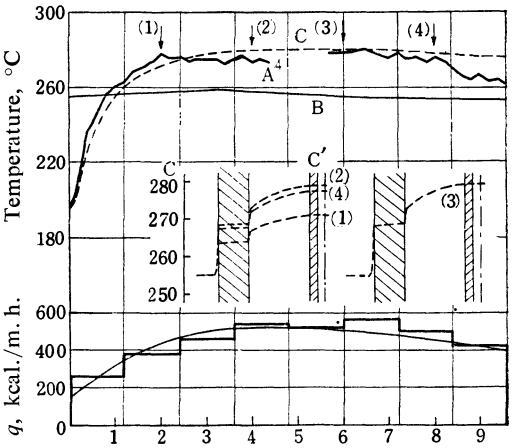



Fig. 5. Above, predicted and experimental temperature profiles. Below, distribution of $q$.

A, Experimental temperature profile
B, Oil bath temperature
C, C', Temperature profiles calculated from experimental concentration gradients
D, Experimental distribution of $q$

have been determined, magnitudes of the reaction heat can easily be calculated by taking theoretical quantities of the reaction heat into consideration. The quantities are 1.86 kcal./l. $CO_{consumed}$ and 0.41 kcal./l. $CO_{consumed}$ for the reaction heats with the hydrocarbon synthesis and the water-gas shift, respectively. The results are given in Fig. 5 as a stepwise plot (steplength, 1.2 m.) of the heat evolved per volume occupying unit length of the catalyst bed against the bed length. From the plot one can evaluate the constants in Eq. 3 to give $c_1=5.84\times10^5$, $c_2=5.05\times10^5$, $M=0.095$, and $N=0.35$. On the other hand, the other constants included in Eq. 4 have been evaluated on the basis of the actual synthesis conditions, which

14) The lower yield may have been partly owing to the poisoning of the catalyst with organic sulfur in the raw gas, since the capacity of active charcoal was insufficient to maintain the sulfur content less than 1~2 mg./m³ throughout the period of the synthesis.
15) Refer to the paper by Anderson et al.[16] also.
16) R. B. Anderson, A. Krieg et al., *Ind. Eng. Chem.*, **41**, 2189 (1949).
17) H. Koelbel and F. Engelhartdt, *Chem. Ing. Tech.*, **22**. 27 (1950).
18) R. B. Anderson et al., *Ind. Eng. Chem.*, **44**, 391 (1952).

appear to be: $C_p=0.41$ kcal./kg.°C, $\mu=0.090$ kg./m.hr., $k=0.085$ kcal./m. hr. °C, $G=1.682\times10^4$ kg./m² hr., $R_{ep}=7.48\times10^2$ ($d_p=0.004$ m.), $\lambda=5.62$ kcal./m. hr.°C, $h=836$ kcal./m² hr. °C, $h_L=174$ kcal./m² hr. °C, and $U=183$ kcal./m² hr. °C.

The problem is to draw the temperature profiles. This can be done by putting the above numerical values into Eq. 4. The results are shown in Fig. 5 as the temperature profiles along and across the catalyst bed, of which the former profile agrees well with the actually determined one. We have thus been able to obtain the temperature profile from the experimental concentration gradient with the present reactor.

However, the reactor suffered from the following limitation, that temperature in the catalyst bed was liable to fluctuate, even though the output remained less than had been expected. This may have been brought about by a slight change in either the composition or the flow rate of the feed gas, fine control of which was difficult. As it is, temperature may rise so high until the catalyst bed beomes ignited with the increasing output, unless greater amount of the reaction heat is carried away from the catalyst bed. As expected from a higher value of $h$ than that of $h_L$, the heat transfer encounters more difficulty at the outer surface area than at the inner surface area of the reactor. This is shown more substantially with the radial temperature profile in Fig. 5 (refer to 3 in the figure): namely, the temperature difference within the bed remains only 6.3°C at a reactor cross section which is 6 m. apart from the top, while the difference between the center and the oil bath attains as high a point as 24.1°C. For the more satisfactory operation of the synthesis it, therefore, is desired to improve the heat transfer referred to the outer surface area by any chosen device. The result with the reactor improved along this line will be reported in the next paper.

## Summary

By the aid of the calculating procedure developed by us on the basis of experimental data available in the synthesis with the reactor of 2 l. catalyst bed, prediction of the temperature profile as regards the synthesis with the reactor of 18.1 l. catalyst bed has been made. The predicted temperature profile expresses the tendencies observed in the actual synthesis with the latter reactor, though a complete agreement has not yet been obtained because of a lower output than was expected.

The calculating procedure has been applied to draw the temperature profile on the basis of the present experimental concentration gradients along the reactor. The profile thus drawn agrees well with the measured one.

The authors are particularly indebted to Messrs. M. Oba, A. Matsuda and H. Imai for their assistance in the synthesis experiment.

*Governments Chemical Industrial Research Institute, Tokyo*
*Shibuya-ku, Tokyo*

# *On the pd Hybridization of the Sulfur Atom in Thiothiophten. I. The Calculations of the Overlap Integrals Involving d Orbitals*

By Kôgorô Maeda

(Received October 6, 1960)

The structure of a molecule named "thiothiophten" was recently clarified through the X-ray analysis study by Bezzi, Mammi and Garbuglio[1], who proposed for this compound a condensed ring system similar to that of thiophten[2] (see Fig. 1), and characterized it by no-bond resonance structure. Giacometti and Rigatti[3], following the deduction to this peculiar structure, have made simple LCAO treatment on the superimposed $\sigma$ and $\pi$ systems of non-localized electrons in thiothiophten, by using only p type orbitals for bonding with respect to sulfur atoms. However, since the system involving no-bond resonance structure is somewhat unlikely to occur, an alternative

1) S. Bezzi, M. Mammi and C. Garbuglio, *Nature*, **182**, 247 (1958).
2) H. C. Louguet-Higgins, *Acta. Cryst.*, **3**, 76 (1950).
3) G. Giacometti and G. Rigatti, *J. Chem. Phys.*, **30**, 1633 (1959).

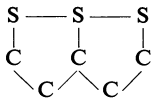


Fig. 1. Molecular structure of thiothiophten.

interpretation on the electronic structure of thiothiophten was given in the previous paper of this series[4], where the explicit participation of d orbitals on the sulfur atoms in bonding was attempted through pd hybridization. Adopting the hybridization for the central sulfur atom, the electronic structure of thiothiophten was treated according to the usual LCAO $\pi$ approximation without considering the $\sigma$ skeleton of the molecule. The results obtained there were appropriate in any case, although they were not necessarily the best.

In the present report, further discussions will be conducted on the pd hybridization of the central sulfur atom in thiothiophten, and the possibility of participation of the d orbital will be examined on the standpoint of overlap criterion, giving the values of the overlap integrals.

**pd Hybridization.**—In considering the valency state of the central sulfur atom in thiothiophten it is convenient to define its coordinates with the sulfur atom as origin so that straight bond S-S-S may go along the coordinate axis and the second axis may be perpendicular to the molecular plane. In this case, the central C-S bond lies on the remaining one, because S-S-C bond with respect to the central sulfur atom has its valency angle of 90°.

It is possible that a 3p electron of the sulfur atom is promoted to a 3d orbital and interacts with other 3p electrons through pd hybridization[5]. The pd configuration of electrons is used in the formation of $\sigma$ orbitals and the linear arrangement of bonds is obtained from this electron configuration[6]. Then, as pointed out in the previous paper, it may be reasonable to consider that the central sulfur atom in the straight bond S-S-S is not in the normal electron configuration but in a valency state capable of forming a $\sigma$ skeleton of the bond through the pd hybridization. The central sulfur atom is no longer in the bivalent state, but as the result of the hybridization, is in a tetra-valent state as in the case of the carbon atom. The expected valency state of the central sulfur atom would be in the electron configuration $3s^23p^33d$; two orbitals of 3p's are adopted to form a C-S $\sigma$ bond with one of the $sp^2$ orbitals of the neighboring central carbon atom and to participate in the $\pi$ electron conjugation system of thiothiophten. The remaining 3p orbital would hybridize with a 3d orbital, and would be going to make up the $\sigma$ bonds of S-S-S in the linear arrangement. These configurations can account for both the right angle of S-S-C with respect to the central sulfur atom and the so-called abnormal length of the bond between two sulfur atoms[5,7,8].

Now a problem still remains, the discussion as to which of the d orbitals of the sulfur atom may hybridize with the 3p orbital to form the $\sigma$ skeleton of the S-S-S bond. On the sulfur atom there are five d orbitals available for bonding. Of these, two orbitals would be ready to participate in the hybridization, namely $3d_z$ and $3d_{xy}$ orbitals (notation of Pauling and Wilson[9]), both of which have their maximum densities of electron distributions along the respective coordinate axes. In general, the bond-forming power should be a maximum along the direction with maximum electron distributions of the orbitals concerned[10]. The hybrid orbitals may be written as the linear combination of the 3p and the 3d orbitals. The approximate forms of the orbitals after the hybridization are shown in Fig. 2. Either set of the hybrid orbitals may go to form the $\sigma$ bonds with 3p orbitals of neighboring sulfur atoms.

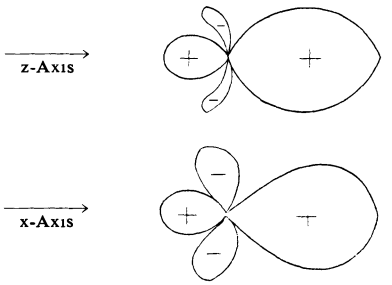



Fig. 2. Approximate forms of hybrid orbitals.

**Overlap Integral.**—It is, in general, impracticable to calculate accurately the energy of formation of a bond between two atoms. Instead of this, the overlap criterion may be used conveniently in discussing the bond formation[7,8]. The value of the overlap integral may give some measure of the strength of a

4) K. Maeda, This Bulletin, 33, 1466 (1960).
5) K. Maeda, ibid., 33, 303 (1960).
6) H. Eyring, J. Walter and G. E. Kimball, "Quantum Chemistry", John Wiley & Sons, Inc., New York (1944), p. 230.
7) D. P. Craig, A. MacColl, R. S. Nyholm, L. E. Orgel and L. E. Sutton, *J. Chem. Soc.*, **1954**, 332.
8) D. P. Craig and E. A. Magnusson, ibid., **1956**, 4895.
9) L. Pauling and E. B. Wilson, "Introduction to Quantum Mechanics", McGraw-Hill, New York (1935), p. 138.
10) C. A. Coulson, "Valence", Oxford University Press, London (1952), p. 195.

TABLE I. OVERLAP INTEGRALS: $S(3p_\sigma - 3d_{xy})$

| $p/t$ | −0.5 | −0.4 | −0.3 | −0.2 | −0.1 | 0.0 | 0.1 | 0.2 | 0.3 | 0.4 | 0.5 |
|---|---|---|---|---|---|---|---|---|---|---|---|
| 0 | 0 | 0 | 0 | 0 | 0 | 0 | 0 | 0 | 0 | 0 | 0 |
| 0.5 | | | | | | −0.145 | −0.161 | −0.163 | −0.151 | −0.126 | −0.093 |
| 1.0 | −0.028 | −0.063 | −0.110 | −0.165 | −0.220 | −0.265 | −0.293 | −0.298 | −0.276 | −0.232 | −0.173 |
| 1.5 | | | | | | −0.342 | −0.377 | −0.383 | −0.358 | −0.304 | −0.229 |
| 2.0 | −0.055 | −0.106 | −0.171 | −0.242 | −0.310 | −0.366 | −0.402 | −0.410 | −0.387 | −0.334 | −0.257 |
| 2.5 | | | | | | −0.341 | −0.372 | −0.382 | −0.367 | −0.324 | −0.258 |
| 3.0 | −0.063 | −0.107 | −0.154 | −0.200 | −0.242 | −0.275 | −0.301 | −0.312 | −0.307 | −0.283 | −0.236 |
| 3.5 | | | | | | −0.187 | −0.203 | −0.217 | −0.224 | −0.220 | −0.197 |
| 4.0 | −0.052 | −0.071 | −0.083 | −0.087 | −0.088 | −0.091 | −0.099 | −0.113 | −0.132 | −0.147 | −0.148 |
| 4.5 | | | | | | −0.000 | −0.000 | −0.015 | −0.042 | −0.079 | −0.096 |
| 5.0 | −0.029 | −0.022 | −0.002 | 0.026 | 0.055 | 0.076 | 0.082 | 0.069 | 0.038 | −0.004 | −0.046 |
| 5.5 | | | | | | 0.134 | 0.145 | 0.135 | 0.101 | 0.053 | −0.001 |
| 6.0 | −0.003 | 0.021 | 0.057 | 0.100 | 0.141 | 0.172 | 0.186 | 0.178 | 0.148 | 0.098 | 0.038 |
| 6.5 | | | | | | 0.192 | 0.208 | 0.204 | 0.178 | 0.130 | 0.069 |
| 7.0 | 0.016 | 0.047 | 0.087 | 0.129 | 0.168 | 0.197 | 0.215 | 0.214 | 0.193 | 0.151 | 0.092 |
| 7.5 | | | | | | 0.192 | 0.208 | 0.211 | 0.196 | 0.161 | 0.107 |
| 8.0 | 0.027 | 0.057 | 0.092 | 0.125 | 0.154 | 0.178 | 0.194 | 0.199 | 0.191 | 0.163 | 0.116 |
| 8.5 | | | | | | 0.160 | 0.175 | 0.182 | 0.178 | 0.159 | 0.120 |
| 9.0 | 0.031 | 0.056 | 0.081 | 0.104 | 0.123 | 0.139 | 0.152 | 0.162 | 0.163 | 0.151 | 0.120 |
| 9.5 | | | | | | 0.119 | 0.131 | 0.140 | 0.146 | 0.139 | 0.117 |
| 10.0 | 0.031 | 0.049 | 0.065 | 0.078 | 0.089 | 0.099 | 0.110 | 0.120 | 0.126 | 0.126 | 0.111 |

bond. In practice, it was used successfully in discussing the possibility of participation of d orbital in the $\pi$ conjugation system with respect to the sulfur atom in thiophene. In this paper, as in the case of thiophene, with the aid of the overlap criterion, the contribution of the d orbital to the hybridization will be examined on the central sulfur atom in thiothiophten. Comparison is made between the values of overlap integral of the 3p and the 3d orbitals with $3p_\sigma$ of the neighboring sulfur atom. A larger amount of the value about the 3d orbital will be associated by a greater extent of the contribution, to the hybridization because the integral of the hybrid orbital may be written as the sum of those of the participating orbitals. The values of the integral of $3p_z - 3d_z$ were already given by Craig et al.[7], while those of $3p_\sigma - 3d_{xy}$ have not been published yet. In this paper, therefore, the values for $3p_\sigma - 3d_{xy}$ were calculated, together with those of $B_n(\alpha)$ necessary to evaluate the overlap integral. In Tables I and II are given the results.

In calculating the integral $S(3p_\sigma - 3d_{xy})$, one must pay some attention to the orientation of the $3d_{xy}$ orbital, because the internuclear axis is usually taken as the z-axis of the coordinate system of integration. The orbital should be rotated by 90° about the y-axis. After the rotation, the angular part of the orbital, $\sin^2\vartheta\cos^2\varphi$, turns into $(\cos^2\vartheta - \sin^2\vartheta\sin^2\varphi)$. The explicit expressions for the overlap integral are as follows:

for $t \neq 0$,

$$S(3p_\sigma - 3d_{xy}) = (1/2^7 \times 3\sqrt{5})(1-t^2)^{7/2} \times p^7 \times \{-A_0(3B_3 - B_5) - A_1(3B_2 - 2B_4 - B_6) + A_2(3B_1 + B_3 + 2B_5) + A_3(3B_0 - B_2 + B_4 - 3B_6) - A_4(2B_1 + B_3 + 3B_5) - A_5(B_0 + 2B_2 - 3B_4) - A_6(B_1 - 3B_3)\}$$

for $t = 0$,

$$S(3p_\sigma - 3d_{xy}) = (1/2^6 \times 315\sqrt{5}) \times p^7 \times (-48A_1 + 256A_3 - 112A_5)$$

for $p = 0$, $\quad S(3p_\sigma - 3d_{xy}) = 0$

where the method of evaluation described by Mulliken et al. and their notations[11] were used. The values of the function $A_n(\alpha)$'s which appear in the above expressions were taken from the table given by Kotani and his collaborators[12]. Those of $B_n(\alpha)$'s were evaluated by them for a wide range of the parameter $\alpha$ and also by Craig et al. for the small values of $\alpha$ [7]. However, some of the values necessary in the calculations of Table I were not available. Therefore, in this paper, a number of $B_n(\alpha)$ were calculated and the results are shown in Table II, together with those obtained by Craig et al.[7] In calculating the values of $B_n(\alpha)$, the recursion formula for $B_n(\alpha)$,

11) R. S. Mulliken, C. A. Rieke, D. Orloff and H. Orloff, *J. Chem. Phys.*, **17**, 1248 (1949).

12) M. Kotani, A. Amemiya, E. Ishiguro and T. Kimura, "Table of Molecular Integrals", Maruzen Co., Tokyo (1955), p. 146.

TABLE II. $B_n(\alpha)=\int_{-1}^{+1}x^n e^{-\alpha x}dx$

| $\alpha$ | $B_0(\alpha)$ | $-B_1(\alpha)$ | $B_2(\alpha)$ | $-B_3(\alpha)$ | $B_4(\alpha)$ | $-B_5(\alpha)$ | $B_6(\alpha)$ |
|---|---|---|---|---|---|---|---|
| 0 | 2 | 0 | 0.666667 | 0 | 0.400000 | 0 | 0.285714 |
| 0.05 | 2.00083 | 0.033342 | 0.667167 | 0.020006 | 0.400357 | 0.014290 | 0.286055 |
| 0.10 | 2.00334 | 0.066733 | 0.668668 | 0.040048 | 0.401429 | 0.028609 | 0.286824 |
| 0.15 | 2.00751 | 0.100225 | 0.671173 | 0.060161 | 0.403219 | 0.042982 | 0.288218 |
| 0.20 | 2.01336 | 0.133867 | 0.674686 | 0.080382 | 0.405729 | 0.057440 | 0.290171 |
| 0.25 | 2.02090 | 0.167711 | 0.679213 | 0.100746 | 0.408965 | 0.072009 | 0.292688 |
| 0.30 | 2.03014 | 0.201806 | 0.684763 | 0.121290 | 0.412932 | 0.086718 | 0.295776 |
| 0.35 | 2.04108 | 0.236204 | 0.691346 | 0.142051 | 0.417639 | 0.101596 | 0.299439 |
| 0.40 | 2.05376 | 0.270958 | 0.698973 | 0.163067 | 0.423095 | 0.116672 | 0.303687 |
| 0.45 | 2.06819 | 0.306119 | 0.707657 | 0.184374 | 0.429310 | 0.131975 | 0.308527 |
| 0.50 | 2.08438 | 0.341741 | 0.717416 | 0.206011 | 0.436297 | 0.147534 | 0.313969 |
| 0.55 | 2.10237 | 0.377879 | 0.728265 | 0.228016 | 0.444069 | 0.163382 | 0.320025 |
| 0.60 | 2.12218 | 0.414586 | 0.740224 | 0.250431 | 0.452640 | 0.179547 | 0.326706 |
| 0.65 | 2.14384 | 0.451920 | 0.753315 | 0.273294 | 0.462029 | 0.196063 | 0.334027 |
| 0.70 | 2.16738 | 0.489937 | 0.767562 | 0.296648 | 0.472253 | 0.212961 | 0.342003 |
| 0.75 | 2.19284 | 0.528696 | 0.782989 | 0.320534 | 0.483332 | 0.230274 | 0.350650 |
| 0.80 | 2.22026 | 0.568256 | 0.799625 | 0.344995 | 0.495288 | 0.248037 | 0.359985 |
| 0.85 | 2.24968 | 0.608679 | 0.817499 | 0.370077 | 0.508144 | 0.266285 | 0.370028 |
| 0.90 | 2.28115 | 0.650027 | 0.836643 | 0.395825 | 0.521925 | 0.285052 | 0.380800 |
| 0.95 | 2.31470 | 0.692365 | 0.857093 | 0.422286 | 0.536658 | 0.304377 | 0.392322 |
| 1.00 | 2.35040 | 0.735759 | 0.878885 | 0.449507 | 0.552373 | 0.324297 | 0.404618 |
| 1.05 | 2.38830 | 0.780277 | 0.902057 | 0.477540 | 0.569099 | 0.344852 | 0.477714 |
| 1.10 | 2.42845 | 0.825988 | 0.926653 | 0.506435 | 0.586869 | 0.366083 | 0.431636 |
| 1.20 | 2.51577 | 0.921285 | 0.980294 | 0.567025 | 0.625685 | 0.410739 | 0.462076 |
| 1.25 | 2.56307 | 0.971022 | 1.00944 | 0.598833 | 0.646806 | 0.434253 | 0.478656 |
| 1.30 | 2.61290 | 1.02226 | 1.04019 | 0.631726 | 0.669124 | 0.458620 | 0.496188 |
| 1.35 | 2.66532 | 1.07507 | 1.07263 | 0.665766 | 0.692683 | 0.483888 | 0.514708 |
| 1.40 | 2.72043 | 1.12955 | 1.10679 | 0.701106 | 0.717529 | 0.510108 | 0.534254 |
| 1.50 | 2.83904 | 1.24385 | 1.18057 | 0.775410 | 0.771280 | 0.565613 | 0.576587 |
| 1.60 | 2.96946 | 1.36592 | 1.26206 | 0.855464 | 0.830800 | 0.625579 | 0.623538 |
| 1.65 | 3.03935 | 1.43011 | 1.30589 | 0.897799 | 0.862869 | 0.657384 | 0.648864 |
| 1.70 | 3.11251 | 1.49654 | 1.35187 | 0.941778 | 0.896560 | 0.690487 | 0.675494 |
| 1.75 | 3.18904 | 1.56533 | 1.40009 | 0.987483 | 0.931941 | 0.724956 | 0.703482 |
| 1.80 | 3.26908 | 1.63659 | 1.45065 | 1.03500 | 0.971858 | 0.753143 | 0.758606 |
| 1.90 | 3.44017 | 1.78700 | 1.55912 | 1.13584 | 1.04893 | 0.837261 | 0.796188 |
| 1.95 | 3.53149 | 1.86639 | 1.61724 | 1.18935 | 1.09181 | 0.877915 | 0.830218 |
| 2.00 | 3.62686 | 1.94877 | 1.67809 | 1.24505 | 1.13675 | 0.920311 | 0.865927 |
| 2.20 | 4.05191 | 2.31086 | 1.95113 | 1.49202 | 1.33916 | 1.10910 | 1.02709 |
| 2.25 | 4.16993 | 2.41031 | 2.02743 | 1.56038 | 1.39592 | 1.16158 | 1.07238 |
| 2.30 | 4.29301 | 2.51367 | 2.10721 | 1.63165 | 1.45535 | 1.21638 | 1.11985 |
| 2.50 | 4.84016 | 2.96977 | 2.46435 | 1.94861 | 1.72239 | 1.46106 | 1.33362 |
| 2.55 | 4.99177 | 3.09546 | 2.56396 | 2.03658 | 1.79713 | 1.52923 | 1.39359 |
| 2.60 | 5.14979 | 3.22624 | 2.66807 | 2.12838 | 1.87536 | 1.60047 | 1.45641 |
| 2.70 | 5.48612 | 3.50401 | 2.89056 | 2.32417 | 2.04291 | 1.75274 | 1.59114 |
| 2.80 | 5.85137 | 3.80503 | 3.13349 | 2.53749 | 2.22638 | 1.91913 | 1.73895 |
| 2.85 | 6.04559 | 3.96492 | 3.26319 | 2.65125 | 2.32454 | 2.00804 | 1.81814 |
| 2.90 | 6.24797 | 4.13145 | 3.39870 | 2.77002 | 2.42725 | 2.10101 | 1.90106 |
| 3.00 | 6.67858 | 4.48558 | 3.68820 | 3.02358 | 2.64715 | 2.29987 | 2.07885 |
| 3.20 | 7.65368 | 5.28738 | 4.34907 | 3.60191 | 3.15130 | 2.75525 | 2.48758 |
| 3.40 | 8.80315 | 6.23362 | 5.13632 | 4.29074 | 3.75522 | 3.30040 | 2.97892 |
| 3.50 | 9.45293 | 6.76935 | 5.58473 | 4.68327 | 4.10062 | 3.61216 | 3.26065 |
| 3.60 | 10.15859 | 7.35194 | 6.07418 | 5.11195 | 4.47864 | 3.95343 | 3.56953 |
| 3.80 | 11.75758 | 8.67526 | 7.19166 | 6.09173 | 5.34523 | 4.73615 | 4.27944 |
| 4.00 | 13.64496 | 10.24288 | 8.52352 | 7.26148 | 6.38348 | 5.67476 | 5.13281 |

TABLE III. OVERLAP INTEGRALS: $S(3p_z-3d_z)$

| $p/t$ | −0.5 | −0.4 | −0.3 | −0.2 | −0.1 | 0.0 | 0.1 | 0.2 | 0.3 | 0.4 | 0.5 |
|---|---|---|---|---|---|---|---|---|---|---|---|
| 0 | 0 | 0 | 0 | 0 | 0 | 0 | 0 | 0 | 0 | 0 | 0 |
| 0.5 | | | | | | −0.167 | −0.185 | −0.188 | −0.174 | −0.146 | −0.107 |
| 1.0 | −0.033 | −0.072 | −0.127 | −0.190 | −0.254 | −0.306 | −0.339 | −0.344 | −0.319 | −0.268 | −0.199 |
| 1.5 | | | | | | −0.395 | −0.435 | −0.443 | −0.413 | −0.351 | −0.265 |
| 2.0 | −0.063 | −0.122 | −0.197 | −0.279 | −0.358 | −0.423 | −0.464 | −0.473 | −0.447 | −0.386 | −0.297 |
| 2.5 | | | | | | −0.393 | −0.430 | −0.441 | −0.423 | −0.375 | −0.298 |
| 3.0 | −0.073 | −0.123 | −0.178 | −0.231 | −0.279 | −0.318 | −0.347 | −0.360 | −0.355 | −0.327 | −0.272 |
| 3.5 | | | | | | −0.216 | −0.235 | −0.251 | −0.259 | −0.254 | −0.228 |
| 4.0 | −0.060 | −0.082 | −0.096 | −0.101 | −0.102 | −0.105 | −0.114 | −0.131 | −0.152 | −0.170 | −0.171 |
| 4.5 | | | | | | −0.000 | −0.001 | −0.017 | −0.048 | −0.092 | −0.111 |
| 5.0 | −0.033 | −0.025 | −0.002 | 0.030 | 0.063 | 0.088 | 0.095 | 0.080 | 0.044 | −0.005 | −0.053 |
| 5.5 | | | | | | 0.155 | 0.167 | 0.156 | 0.117 | 0.061 | 0.001 |
| 6.0 | −0.004 | 0.024 | 0.066 | 0.116 | 0.163 | 0.199 | 0.215 | 0.206 | 0.171 | 0.113 | 0.044 |
| 6.5 | | | | | | 0.222 | 0.240 | 0.236 | 0.205 | 0.150 | 0.079 |
| 7.0 | 0.018 | 0.054 | 0.100 | 0.149 | 0.194 | 0.228 | 0.248 | 0.247 | 0.223 | 0.174 | 0.106 |
| 7.5 | | | | | | 0.221 | 0.241 | 0.244 | 0.226 | 0.186 | 0.124 |
| 8.0 | 0.031 | 0.066 | 0.106 | 0.144 | 0.178 | 0.205 | 0.224 | 0.230 | 0.220 | 0.188 | 0.134 |
| 8.5 | | | | | | 0.184 | 0.202 | 0.210 | 0.206 | 0.184 | 0.139 |
| 9.0 | 0.036 | 0.065 | 0.094 | 0.120 | 0.142 | 0.161 | 0.176 | 0.187 | 0.188 | 0.174 | 0.138 |
| 9.5 | | | | | | 0.137 | 0.151 | 0.162 | 0.169 | 0.161 | 0.135 |
| 10.0 | 0.036 | 0.057 | 0.075 | 0.090 | 0.103 | 0.114 | 0.127 | 0.138 | 0.146 | 0.145 | 0.128 |

$$B_n(\alpha)=(1/\alpha)\{(-1)^n e^{\alpha}-e^{-\alpha}+nB_{n-1}(\alpha)\}$$

was used, and the values of $e^{\alpha}$ and $e^{-\alpha}$ were taken from the table published by the Computation Laboratory of NBS[13]. Some of the exponential functions were derived by using the table of hyperboric functions[14]. According to Mulliken's convention concerning the sign of $t$ [11], the values of $S(3p_{\sigma}-3d_{xy})$ for $t<0$ were also evaluated. These are given in Table I. These values can easily be derived by replacing $B_n(\alpha)$ with $B_n(-\alpha)$ of the above expression and $B_n(-\alpha)$ is obtained from $B_n(\alpha)$ through the relation $B_n(-\alpha)=(-1)^n\times B_n(\alpha)$. These integrals are corresponding to the values obtained when $3d_{xy}$ orbital has its greater effective nuclear charge than that of $3p_x$. Further, in Table III, the overlap integrals $S(3p_z-3d_z)$ with the parameter $p$ at intervals of 0.5 and of 1.0 are shown for $t>0$ and $t<0$ respectively. Some of the values were already given, as mentioned above, by Craig et al.[7], who evaluated the values with $p$ at intervals of 1.0.

In order to estimate the values of overlap integrals using the above tables, it is necessary to know the effective nuclear charges of the orbitals concerning the atoms. The respective charges found in accordance with Slater's formula[15] are as follows: 5.80 and 1.00 for 3p and 3d orbitals on the central sulfur atom and 5.45 for 3p orbital on the neighboring sulfur atom. Since the bond distance S-S is 2.36 Å, the values about 3p−3d give 0.7 and 5 for $t$ and $p$ (see Ref. 11) respectively. From Tables I and III it is inferred that negative values of overlap integrals result from these $t$ and $p$ values. With this result, one might not expect any participations of the d orbitals in bonding to occur through the hybridization. This may be due to the straightforward application of Slater's rule to the estimation of the effective nuclear charges of the atoms. As already mentioned[5], since the maximum of the radial function of the d orbital with its effective nuclear charge 1 lies at 9 atomic units, the orbital may be regarded as including the full $\sigma$ skeleton of thiothiophten, so that it would be impossible to avoid the influence of the neighboring atoms in the molecule. The charges of the atoms may contract the d orbital and enlarge its nuclear charge, leading to a comparable value of the overlap integral to that of 3p orbital. Then it might be expected that the participation of the d orbital in the hybridization would take place to an extent not much smaller than that of 3p orbital. It is necessary, therefore, to examine the influence of the nuclear charges of the neighboring atoms of thiothiophten upon the d orbital of the central sulfur atom. Further discussions, however, will be given in subsequent publications.

It is of interest to notice the following

13) Computation Laboratory, "Tables of the Exponential Function $e^x$", Natl. Bur. Standards, Washington (1951).
14) Committee for the Calculation of Mathematical Tables, "British Association Mathematical Tables", 1, 30 (1951).
15) J. C. Slater, *Phys. Rev.*, 36, 57 (1930).

points with respect to the values of overlap integral given in Tables I and III; the value $S(3p_z-3d_z)$ is greater than that of $S(3p_\sigma-3d_{xy})$. This may predict a greater possibility of the participation of $3p_z$ orbital than that of $3d_{xy}$. In both tables, the value for $t<0$ is small, as a whole, compared with that for $t>0$. This may imply that it is not easy to form a bond between 3d with a greater effective nuclear charge and 3p with a smaller one.

The author wishes to express his sincere thanks to Dr. S. Nagakura, The University of Tokyo, for his kind advice and helpful discussions.

*Electrochemical Laboratory*
*Tanashi, Tokyo*

# *The Effects of pH on the Flocculation of Quartz Aqueous Suspensions*

By Tadashi OHYAMA, Junzo SHIMOIIZAKA and Shinnosuke USUI

(Received November 2, 1960)

Control of the state of dispersion or flocculation of mineral suspension is widely required for proper operation of many chemical engineering processes. It is well known that, especially in the case where metal ions are dissolved, the pH of the solution is closely related to the stability of suspensions. From this point of view, the effects of pH on the flocculation of quartz aqueous suspensions containing a cation, such as $Ba^{2+}$, $Fe^{3+}$ or $Cu^{2+}$, respectively, are investigated by means of electrokinetic measurements.

## Experimental

Quartz suspensions, 6% by weight, were provided for the flocculation experiments. A monocrystalline quartz was ground by a laboratory roll crusher, and it was washed with hydrochloric acid; the washing was followed by successive decantation with distilled water until no $Cl^-$ could be detected, and the quartz powder under 150 mesh was well reground in an agate mortar after drying. $Ba^{2+}$, $Fe^{3+}$ or $Cu^{2+}$ was supplied by $BaCl_2$, $FeCl_3$ or $CuSO_4 \cdot 5H_2O$ in reagent grade, respectively. The pH of solution was adjusted with hydrochloric acid or sodium hydroxide and measured by a glass electrode pH meter. The degree of flocculation was evaluated by measuring the transparency of suspensions, a Hitachi EPO-B photoelectric photometer was available for transparency measurements. The $\zeta$ potential of quartz in the solution containing $Fe^{3+}$ or $Cu^{2+}$ was measured by a microscopic electrophoresis cell, considering the fact that, for the system in which insoluble hydroxide is formed, the condition of streaming potentential method made on relatively coarse particles may differ from that of flocculation experiment carried out on the suspensions containing fine particles. For the solution of $Ba^{2+}$, on the other hand, the streaming potential method was adopted.

The quartz in the streaming potential measurements is the 48/65 mesh fraction, and the apparatus is the same as that used by Gaudin and Fuerstenau[1].

**The Effects of pH on the Flocculation of Quartz Suspensions Containing $Ba^{2+}$.** — Fig. 1 shows transparency-time curves under various pH of the suspension containing $Ba^{2+}$ of 1 mmol./l. in concentration. The abscissa is the elapsed time after shaking the suspension, the ordinate being

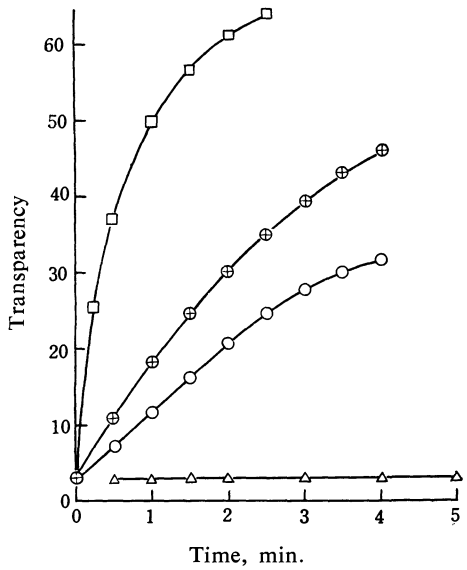
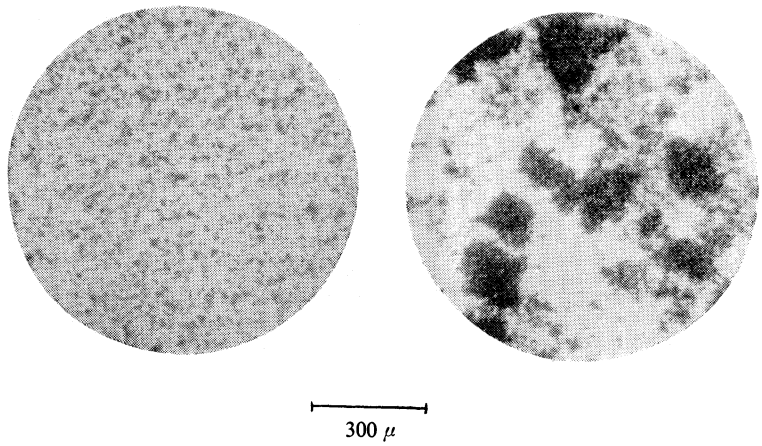



Fig. 1. Transparency-time curves of quartz suspension under various pH at the concentration of $BaCl_2$ 1.0 mmol./l.

△ pH=3.0, 6.8, 8.8
○ pH=10.8
⊕ pH=11.0
□ pH=12 or more

1) A. M. Gaudin and D. W. Fuerstenau, *Min. Eng.*, 7, 66 (1955).




(a) $BaCl_2$ 10 mmol./l., pH 5.0

(b) $BaCl_2$ 10 mmol./l., pH 11.5

Fig. 2. Photomicrographs of flocs.

the degree of flocculation. From this figure it can be seen that the degree of flocculation becomes stronger with increasing pH in alkaline solutions. The flocculation in high pH is characterized by the formation of gel-like flocs. When the concentration of $Ba^{2+}$ is increased to more than 3 mmol./l., which is the flocculation value of $Ba^{2+}$ for the quartz suspension adopted at pH 7, the flocculation of the suspension is also observed in the acidic side. The flocculation in acidic solution, however, is relatively weak and no gel-like floc formation is observed. Fig. 2 shows the photomicrographs of flocs formed at the concentration of $Ba^{2+}$ 10 mmol./l.; Figs. 2a and 2b show flocs at pH 5.0 and pH 11.5, respectively. The flocculation of the quartz suspension disappears with decrease of the $Ba^{2+}$ concentration even in the solution of high pH, and the critical $Ba^{2+}$ concentration for flocculation is found to be 0.6 mmol./l. at pH 11.0. The critical $Ba^{2+}$ concentration decreases with increasing pH of the solution. When the pH is lowered to that of the acidic side the critical $Ba^{2+}$ concentration is also decreased, and at pH about 2 flocculation occurs without the addition of $Ba^{2+}$.

**The Effects of pH on the Flocculation of Suspensions Containing $Fe^{3+}$ or $Cu^{2+}$.** — In the suspensions containing $Fe^{3+}$, no visible flocculation takes place in the range of low pH even though the $Fe^{3+}$ concentration reaches 0.4 mmol./l. However, the addition of sodium hydroxide to the above suspension produces a violent flocculation at about neutral pH. This flocculation is weakened, however, by the increase of pH and dissappears at the pH region higher than 10. Fig. 3 gives the relation between the transparency at 5 min. after shaking the suspension and pH of the solution containing $Fe^{3+}$ of 0.4 mmol./l. in concentration. For the suspension containing $Cu^{2+}$, 4 mmol./l., a remarkable flocculation takes place in the pH range of 6~12. This is also illustrated in Fig. 3. It is always observed in the above experiments that the upper solution appearing after sedimentation of flocs is colorless and transparent, and the sediment with

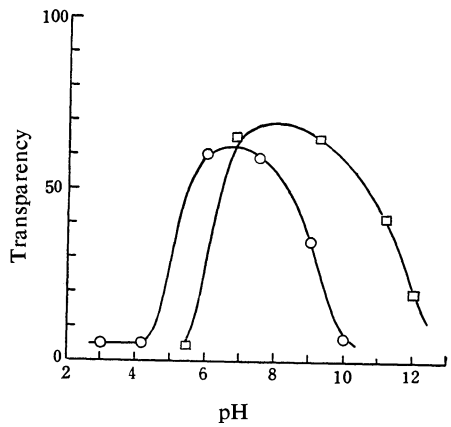



Fig. 3. Transparency at 5 min. after preparation of suspensions containing $Fe^{3+}$ or $Cu^{2+}$ as a function of pH.

○ $Fe^{3+}$ 0.4 mmol./l.
□ $Cu^{2+}$ 4.0 mmol./l.

color of the hydroxide of the respective ion is formed, such as light brown for $Fe^{3+}$ and light blue for $Cu^{2+}$. The deflocculation of the suspensions occurs when the pH exceeds 10 for $Fe^{3+}$ and 12 for $Cu^{2+}$. On the other hand, in the suspension containing $Ba^{2+}$ the violent flocculation still takes place even in the pH region higher than 12.

These observations seem to indicate that the pH range in which the violent flocculation occurs is related to the solubility of the hydroxide of the ion involved; the larger the solubility of the hydroxide, the higher pH range where the flocculation is maintained is expected.

**ζ Potential.**—ζ Potential of quartz in the solutions of various concentrations of $Ba^{2+}$, i.e. 0.1, 0.2 and 1.0 mmol./l., as a function of pH is given in Fig. 4. The ζ potential at pH 11 in the presence of $Ba^{2+}$ of 0.6 mmol./l., the critical concentration for the flocculation, is also plotted in the same figure. Fig. 5 represents the ζ poten-

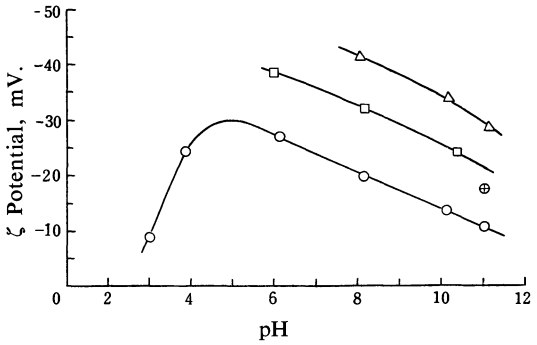



Fig. 4. Influence of pH on ζ potential of quartz in $BaCl_2$ solutions.

△ $BaCl_2$ 0.1 mmol./l.
□ $BaCl_2$ 0.2 mmol./l.
⊕ $BaCl_2$ 0.6 mmol./l.
○ $BaCl_2$ 1.0 mmol./l.

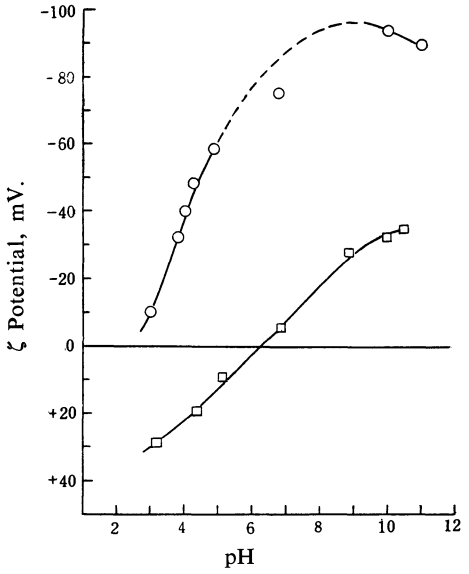



Fig. 5. ζ Potential of quartz in the absence or presence of $Fe^{3+}$ as a function of pH.

○ Absence of $Fe^{3+}$
□ $Fe^{3+}$ 0.4 mmol./l.

tial of quartz in the solutions containing only hydrochloric acid or sodium hydroxide and $Fe^{3+}$, 0.4 mmol./l., as a function of pH. From these figures it can be seen that the ζ potential decreases with increasing pH in alkaline solution at the respective $Ba^{2+}$ concentration, on the other hand, its value is considered to be determined mainly by $H^+$ in acidic solution. Gaudin and Fuerstenau[1] have shown that, in the streaming potential study made on 48/65 mesh quartz, the reliable values of the ζ potential were obtainable in the solution over $10^{-4}$ in ionic strength, below which it was necessary to consider the effect of surface conductivity. In the present investigation, the effect of surface conductivity was not appreciated, so that in Fig. 5 the region of lower ionic strength was expressed by a dotted line; if the correction is made, higher negative potential values would be expected. In the absence of $Fe^{3+}$, the isoelectric point of quartz seems to be in the neighbourhood of pH 2.5. On the other hand, the isoelectric point shifts to higher value of pH, i.e. about pH 6, in the presence of $Fe^{3+}$.

## Discussion

The stability of lyophobic colloids or suspensions depends upon the energy of interaction between two approaching particles. According to Verwey and Overbeek[2] the energy is composed of electrical repulsion and long range van der Waals attraction. For a given suspension the attraction is assumed to be constant while the repulsion changes with the electrolyte content of the system. These concepts will lead us to the prediction that the violent flocculation of the quartz suspension containing $Ba^{2+}$ in alkaline solution is due to the decrease of electrical repulsion. Verwey and Overbeek have calculated the repulsive potential of interaction between two flat double layers in the solution containing a species of binary electrolyte, and Eq. 1 has been obtained as the repulsive potential per unit area if the interaction is not so strong;

$$\left.\begin{aligned} V_R &= (64nkT/\kappa)\gamma^2 \exp(-2\kappa d) \\ \kappa &= (8\pi ne^2v^2/\varepsilon kT)^{1/2} \\ \gamma &= \{\exp(z/2)-1\}/\{\exp(z/2)+1\} \\ z &= ve\psi_0/kT \end{aligned}\right\} \quad (1)$$

where $n$ is the number of ions per $cm^3$ far from the surface, $k$ the Boltzmann constant, $T$ the absolute temperature, $e$ the elementary charge, $v$ the valency of counter ion, $\varepsilon$ the dielectric constant, $\psi_0$ the surface potential and $d$ the half-distance of separation.

Eq. 1, however, cannot be applied to the system in which more than two species of counter ions of different valency is involved. It is difficult to obtain a general formula representing the repulsive potential energy, but the repulsive potential can be expressed as Eq. 2[3] if ζ potential is not so high;*

$$\left.\begin{aligned} V_R &= (\varepsilon/2\pi)\kappa\zeta^2 \exp(-2\kappa d) \\ \kappa &= (4\pi e^2 \Sigma n_i v_i^2/\varepsilon kT)^{1/2} \end{aligned}\right\} \quad (2)$$

Thus, the repulsive potential is directly related to $\kappa$ and ζ. As indicated in Fig. 1, a remarkable flocculation takes place at pH 11 (NaOH,

2) E. J. W. Verwey and J. Th. G. Overbeek, "Theory of the Stability of Lyophobic Colloids", Elsevier, Amsterdam, (1948).
3) S. Usui, *J. Mining and Metallurgical Inst. Japan*, (*Nippon Kogio Kaishi*), 75, 1025 (1959).
* On the system containing a binary electrolyte, it is calculated that Eq. 2 gives the value of 1.0~1.1 times the one evaluated from Eq. 1 in the range of $Z(=ve\zeta/kT$ for Eq. 2) = 0~1.5.

1 mmol./l.), while no flocculation appears at pH 3 (HCl, 1 mmol./l.) despite of the same concentration of $Ba^{2+}$, i.e. 1 mmol./l. The values of $\kappa$ at pH 11 and pH 3 may be almost equal since it is evaluated by analogy with the experimental results by Gaudin and Chang[4] that the decrease of $Ba^{2+}$ concentration in bulk solution resulting from the adsorption of $Ba^{2+}$ is of the order of 10%, which corresponds to the decrease of $\kappa$ of about 3% under the adopted condition. As illustrated in Fig. 4, the $\zeta$ potential of quartz in the solution containing $Ba^{2+}$ of 1 mmol./l. is $-11$ mV. at pH 11 and $-9$ mV. at pH 3; the value of $\zeta$ at the former where the remarkable flocculation is exhibited is somewhat higher than that at the latter where no visible flocculation is observed. From the inspection of $\kappa$ and $\zeta$, it is difficult to explain the singular flocculation in alkaline solution in terms of the decrease of repulsion in alkaline solution. These considerations will lead to the conclusion that such a flocculation in alkaline solution is not due to the decrease of the repulsion but to the incease of attraction.

The attractive potential energy should be known in addition to the repulsive potential energy in order to obtain the total potential energy of interaction between approaching particles. London-van der Waals attractive potential for two approaching flat plates has been expressed as Eq. 3[5], when $d$ is small compared with the thickness of the plates;

$$V_A = -A/48\pi d^2 \qquad (3)$$

where $A$ is called "Hamaker constant". It is necessary to determine the value of $A$ in calculating $V_A$ according to Eq. 3. However, since the proper evaluation of $A$ has not yet been established, the examination by which $A$ is determined empirically has been undertaken by using Eq. 4,

$$\left.\begin{aligned} C_{floc.} &= 3.1\times10^{-24} z^4/A^2 v^6 \text{ mmol./l.} \\ &\text{at } 25^\circ\text{C} \\ z &= ve\zeta/kT \end{aligned}\right\} \qquad (4)$$

which is derived as a flocculation value from Eqs. 2 and 3 on the basis of the Verwey-Overbeek theory. Thus, $A$ was determined to be $3.4\times10^{-13}$ *, where the empirical value of $C_{floc.}$ of $Ba^{2+}$ and $\zeta$ potential were 3 mmol./l. and $-20$ mV. respectively. In Fig. 6, the total potential energy curves at pH 11 under various

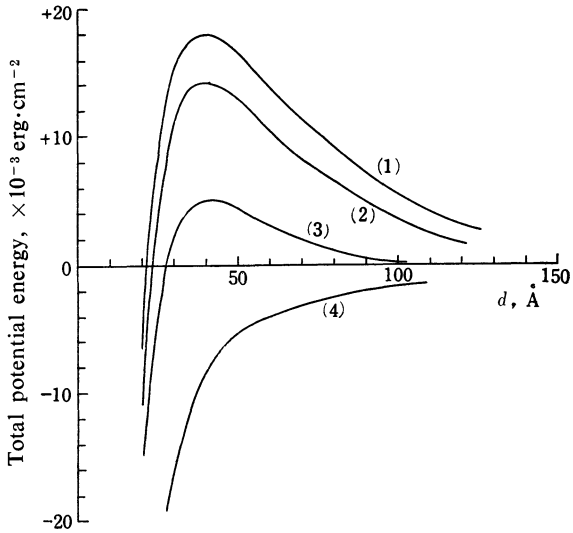



Fig. 6. Total potential energy between approaching quartz particles in solutions containing $Ba^{2+}$ at pH 11.0 as a function of half-distance of separation.

(1) $Ba^{2+}$ 0.1 mmol./l.
(2) $Ba^{2+}$ 0.2 mmol./l.
(3) $Ba^{2+}$ 0.6 mmol./l.
(4) $Ba^{2+}$ 1.0 mmol./l.

concentrations of $Ba^{2+}$, i.e. 0.1, 0.2, 0.6 and 1.0 mmol./l., are illustrated as a function of half-distance of approaching particles. It can be seen from this figure that there is a potential barrier of about $5\times10^{-3}$ erg./cm$^2$ at $Ba^{2+}$ concentration of 0.6 mmol./l. which is the flocculation value at pH 11. The barrier corresponds to 7500 $kT$ per particle if a stably suspended quartz particle is assumed to be a cube of 1 $\mu$ edge length, or to 75 $kT$ if 0.1 $\mu$ edge length is assumed*; This will be an insurmountable obstacle to flocculation.

Now, the discrepancy between the flocculation experiment and the potential energy consideration may well be explained by assuming a certain attractive force by which the potential barrier is lowered. Mattson[7] has suggested that the strong flocculation of quartz particles in alkaline solution is due to the formation of particle-paricle linkage action through polyvalent cation, see Fig. 7. These linkage actions may well be supported by the consideration of energy described above. At first sight, it seems possible to explain the remarkable flocculasion of the suspention containing $Fe^{3+}$ in the range of neutral pH in terms of the

4) A. M. Gaudin and C. S. Chang, *Min. Eng.*, **4**, 193 (1952).
5) E. J. W. Verwey and J. Th. G. Overbeek, "Theory of the Stability of Lyophobic Colloids", Elsevier, Amsterdam, (1948), p. 101.
* $A$ is taken as $1\sim2\times10^{-12}$ by Verwey and Overbeek. and $\ll5\times10^{-14}$ by Derjaguin[6].
6) B. V. Derjaguin, *Discussions Faraday Soc.*, **18**, 36 (1954).

* A sphere of 1.0 $\mu$ in diameter and of specific gravity 2.7 falling in water under the influence of gravity aquires a kinetic energy of only $6\times10^{-21}$ erg or of $1.5\times10^{-7}$ in unit of $kT$.
7) S. E. Mattson, *Kolloidchem. Beihefte*, **14**, 227 (1922).

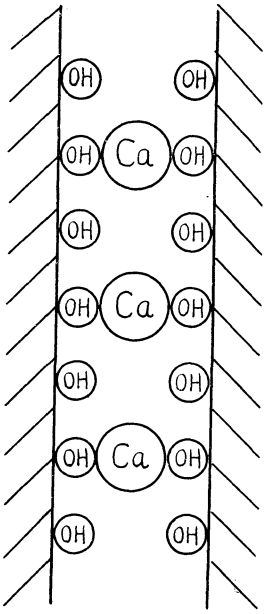



Fig. 7. Schematic illustration of linkage action of $Ca^{2+}$.

lowering of $\zeta$ potential (see Figs. 3 and 5); the value of $\zeta$ lies in zero or in its vicinity at about neutral pH. However, there is no visible flocculation of quartz particles in a solution containing $Fe^{3+}$ 0.14 mmol./l. at pH 3.5 despite the fact that the $\zeta$ potential is zero. In the case of the suspension containing $Cu^{2+}$, it is understood by the inspection of $\zeta$ potential data that the repulsive potential between particles in the pH range of 9~11, wherein a violent flocculation takes place, is higher than that at pH 5.2 wherein no visible flocculation is observed.

Thus, the flocculation depending upon the pH of the solution containing $Fe^{3+}$ or $Cu^{2+}$, as well as the case where $Ba^{2+}$ is contained, can not be interpreted only in terms of the decrease of repulsion caused by the decrease of $\zeta$ potential. An uncertainty still remains whether these flocculation characteristics are due to the bridging action by metal ion and $OH^-$ as in the case of $Ba^{2+}$ and $OH^-$ or to the so-called "heteroflocculation"[8], between metal hydroxide and quartz perticles. The flocculation mechanism of macromolecular flocculants for suspensions has been interpreted by the concept of molecular bridging action caused by its fibrous structure[9]. It is now worthwhile to point out that, in the case where a simple metallic ion is involved, not only London-van der Waals attractive force but also a certain attractive force by which a special linkage action is brought about must be taken into account.

## Summary

The effects of pH on the flocculation of quartz aqueous suspensions containing $Ba^{2+}$, $Fe^{3+}$ or $Cu^{2+}$, respectively, were investigated by means of electrokinetic measurements. The violent flocculation takes place in the characteristic range of pH with respective cation involved. The calculation of the potential energy between approaching quartz particles indicates that the violent flocculation is readily explained, not by the decrease of electrical repulsion, but by the consideration of an attractive force other than van der Waals attraction.

*Department of Mining*
*Faculty of Engineering*
*Tohoku University*
*Sakurakoji, Sendai*

8) B. V. Derjaguin, *Discussions Faraday Soc.*, **18**, 85 (1954).
9) R. A. Ruehrwein and D. W. Ward, *Soil Sci.*, **73**, 485 (1952).

# *Dehydrogenation of Secondary Alcohols with Reduced Copper. IV*[1]. *Catalytic Dehydrogenation of Isopropyl Alcohol (Part 2)**

By Kazuaki KAWAMOTO**

(Received October 24, 1960)

As has already been pointed out in the preceding paper[1], the activity and the selectivity of various copper catalysts depend not only upon the reaction temperature at which the catalysts are employed, but also on the precipitants in the preparation of the copper catalysts. For instance, the catalyst prepared with potassium bicarbonate shows the greatest activity for dehydrogenating isopropyl alcohol to acetone with no side reaction, while the copper catalyst prepared with sodium hydroxide under the same condition shows the smallest dehydrogenating activity, producing condensation products.

Earlier, Audibert and Raineau[2] reported that a highly active catalyst for the decomposition of methanol was obtained by adding a solution of alkali hydroxide to a boiling solution of copper nitrate, and reducing the black precipitate with hydrogen, and that the catalyst prepared from the oxide precipitated with ammonia from a cold copper nitrate solution was totally inactive for the same reaction. On the other hand, Frolich et al.[3] prepared copper catalysts from the precipitates obtained by adding ammonia to a solution of copper nitrate at various temperatures (0, 10, 22, 55, 85 and 100°C), and found that the greatest activity for the decomposition of methanol was achieved with the precipitate at 22°C. Thus there is non-conformity in the results obtained by various workers.

The present author found that dehydrogenation of isopropyl alcohol at 220~250°C with the copper catalysts prepared with alkali hydroxide gives oily products (isobutyl methyl ketone and diisobutyl ketone) in addition to acetone, and that the copper catalyst prepared with potassium hydroxide gives a smaller yield of the oily products than that prepared with sodium hydroxide under the same condition[1]. The present investigation was undertaken to confirm this unexpected behavior of the copper catalyst prepared with sodium hydroxide, and to study the effect of the precipitation temperature on the amounts of acetone and the oily products to find a preparation procedure of the most suitable copper catalyst for the production of acetone, precipitation being carried out at 5, 22, 55 and 90°C[4].

It was presumed in the preceding paper that the formation of isobutyl methyl ketone is due to the condensation of the isopropyl alcohol and acetone produced. In order to confirm this formation process, and to determine whether a large quantity of the oily products could be formed from a mixture of isopropyl alcohol and acetone, various mixtures of the alcohol and acetone were passed over the copper catalyst prepared with sodium hydroxide at 22°C.

## Experimental

**Purification of Isopropyl Alcohol and Acetone.** —Isopropyl alcohol and acetone were purified as in the preceding paper. Isopropyl alcohol: b. p. 82~82.5°C, $n_D^{25}$ 1.3753, $d_4^{25}$ 0.7811. Acetone: b. p. 56.2~56.3°C, $n_D^{25}$ 1.3564, $d_4^{25}$ 0.7844.

TABLE I. PREPARATION OF PRECIPITATES

| Catalyst | Temperature of precipitation °C | Time of drying hr. | Color |
|---|---|---|---|
| Cu VI | 5 | 24 | dark gray |
| Cu VII | 22 | 20 | dark gray |
| Cu VIII | 55 | 20 | black |

TABLE II. PREPARATION OF PRECIPITATES

| Catalyst | Precipitant and amount g. | Distilled water ml. | Time of drying hr. | Color |
|---|---|---|---|---|
| Cu IX | $K_2CO_3$, 25 | 500 | 10 | green |
| Cu X | $KHCO_3$, 40 | 400 | 10 | green |
| Cu XI | $Ba(OH)_2$, 57 | 1000 | 20 | dark gray |

TABLE III. PREPARATION OF PRECIPITATES

| Catalyst | Precipitant and amount g. | Distilled water ml. | Time of drying hr. | Color |
|---|---|---|---|---|
| Cu XII | NaOH, 15 | 300 | 20 | dark gray |
| Cu XIII | $K_2CO_3$, 25 | 500 | 10 | green |
| Cu XIV | $KHCO_3$, 40 | 400 | 10 | green |

1) Part III. This Bulletin, **34**, 161 (1961).

* Presented at the Chugoku Shikoku Local Meeting of the Chemical Society of Japan, Kochi, November, 1959.

** Present address: Institute of Commodities, Faculty of Economics, Kagawa University, Takamatsu.

2) E. Audibert and A. Raineau, *Ind. Eng. Chem.*, **20**, 1105 (1928).

3) P. K. Frolich, M. R. Fenske and D. Quiggle, *J. Am. Chem. Soc.*, **51**, 61 (1929).

4) The case of 90°C was described in the preceding paper[1].

**Preparation of Catalysts.**—Cupric nitrate hexahydrate was prepared from electrolytic copper and nitric acid, and was purified by recrystallization. The catalysts were prepared as shown in Tables I, II and III. Precipitates for catalysts Cu VI~Cu VIII (Table I) were prepared as follows: A solution of 30 g. of cupric nitrate hexahydrate in 900 ml. of distilled water was heated or cooled to the temperature chosen for precipitation. A sodium hydroxide solution, prepared from 15 g. of sodium hydroxide and 300 ml. of distilled water, was brought to the same temperature and added rapidly to the copper nitrate solution with stirring. After the mixture was stirred at the same temperature for 30 min., the precipitate was washed well by decantation with distilled water at the same temperature, collected on a glass filter, dried in an electric oven at 105°C for the time given in the table, powdered in an agate mortar, and stored in a stoppered bottle. Precipitates for Cu IX~Cu XI (Table II) were prepared by the same method as for Cu VII except for the precipitants and the volume of distilled water to dissolve them. Precipitates for Cu XII~Cu XIV (Table III) were prepared by the following method: Thirty grams of cupric nitrate hexahydrate was dissolved in 600 ml. of distilled water, and 300 ml. of ethyl alcohol was then added. To the solution kept at 22°C a solution of the precipitant dissolved in distilled water as shown in Table III was added, and the precipitate was treated similarly.

**Apparatus and Procedure.** — The apparatus was exactly the same as that described in the preceding paper. A definite amount (10 g.) of the precipitate was placed in the reaction tube and reduced by passing hydrogen (750~900 ml./hr.) at a temperature below 185°C. The resulting catalyst was then heated to the operating temperature. Experiments were usually performed at 185, 220, 250, 305 and 325°C under the ordinary pressure, and isopropyl alcohol and the various mixtures of isopropyl alcohol and acetone were passed through the tube, respectively, at a constant rate of flow. The liquid product was collected by the method similar to that described in the preceding paper. The volume of the non-condensable gas evolved by the reaction was measured at intervals of 15~30 min., and the change in catalytic activity was denoted by the volume. All values given in the present research are averages of three to four measurements under a constant operating condition.

**Analysis of the Products.** — The reaction mixture was treated with water to remove the acetone and unchanged isopropyl alcohol. The content of acetone in the aqueous solution was determined by the hydroxylamine method. The oily products obtained in some of the experiments were dried with anhydrous sodium sulfate and fractionally distilled, and the constituents of the cuts were identified by boiling points, densities, refractive indices, 2,4-dinitrophenylhydrazones and semicarbazones. The oily products were found to consist mainly of isobutyl methyl ketone and diisobutyl ketone.

5) Those from the reducing condition of precipitates with hydrogen and the velocity of passing the substance over reduced copper.

## Results

**Influences of the Temperature of Precipitation and That of Reaction on the Dehydrogenating Activity of Reduced Copper.**—The influences of the temperature of precipitation and that of reaction on the activity of copper catalysts are shown in Table IV. The amounts of reaction products given in Tables IV~VII are reproducible within 1%. Experiments were carried out under controlled conditions in order to eliminate so far as possible effects[5] other than that of the temperature of precipitation or reaction. Table IV indicates that the dehydrogenating activity to give acetone and the condensing activity to give isobutyl methyl ketone and diisobutyl ketone depend on the temperatures of precipitation and of the reaction. As the catalytic activity for the dehydrogenation of isopropyl alcohol varied irregularly with the precipitation temperature, it is impossible to find any simple relation between them. The highest dehydrogenation activity is obtained with the catalyst (Cu VIII) precipitated at 55°C. On the other hand, the yield of the oily products is the highest with the catalyst (Cu VII) precipitated at 22°C. As the dehydrogenating activity of reduced copper varies with the precipitation temperature, it is necessary to fix the precipitation temperature to get the constant activity.

In Fig. 1, the yield of acetone with various specimens of reduced copper is plotted against the reaction temperature. The yield of acetone

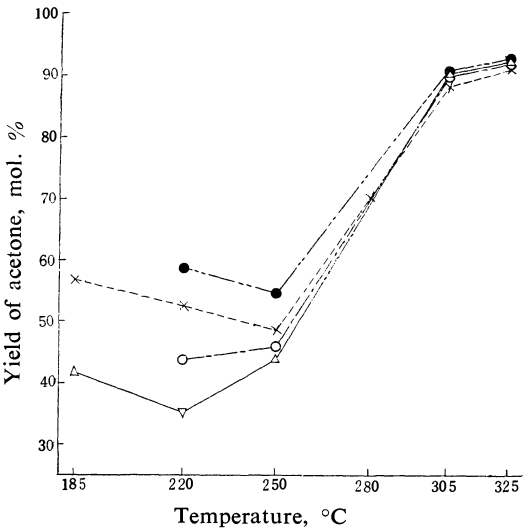



Fig. 1. The effect of temperature on the dehydrogenation of isopropyl alcohol with various copper catalysts.

○ Cu VI, △ Cu VII, ● Cu VIII, × Cu I (described in the preceding paper).

Table IV. Influences of the temperature of precipitation and that of reaction on the dehydrogenating activity of copper catalysts

| Catalyst | Temp. °C | Isopropyl alcohol g. | Velocity g./hr. | Acetone g. | Oily products g. | Gases collected l. | Percentage of conversion % |
|---|---|---|---|---|---|---|---|
| Cu VI | 220 | 39.38 | 11.53 | 16.66 | 11.58 | 8.85 | 60.2 |
| | 250 | 39.28 | 13.46 | 17.42 | 12.31 | 9.42 | 64.3 |
| | 305 | 39.36 | 11.52 | 34.31 | 0 | 13.69 | 93.2 |
| | 325 | 39.31 | 11.79 | 35.12 | 0 | 14.08 | 96.0 |
| Cu VII | 185 | 38.96 | 11.69 | 15.72 | 5.47 | 7.35 | 50.5 |
| | 220 | 38.93 | 11.39 | 13.24 | 15.29 | 8.19 | 56.4 |
| | 250 | 38.83 | 11.65 | 16.48 | 13.40 | 9.11 | 62.9 |
| | 280 | 39.19 | 11.47 | 32.22 | 0.67 | 13.01 | 89.0 |
| | 305 | 39.02 | 11.15 | 34.21 | 0 | 13.78 | 94.7 |
| | 325 | 38.95 | 11.40 | 34.94 | 0 | 14.04 | 96.6 |
| Cu VIII | 220 | 38.70 | 12.55 | 21.98 | 4.14 | 9.79 | 67.8 |
| | 250 | 39.21 | 11.48 | 20.72 | 9.69 | 10.28 | 70.3 |
| | 305 | 38.72 | 12.56 | 34.14 | 0 | 13.60 | 94.2 |
| | 325 | 38.90 | 11.67 | 35.04 | 0 | 13.95 | 96.2 |

Table V. Influence of precipitants on the dehydrogenating activity of reduced copper

| Catalyst | Temp. °C | Isopropyl alcohol g. | Velocity g./hr. | Acetone g. | Oily products g. | Gases collected l. | Percentage of conversion % |
|---|---|---|---|---|---|---|---|
| Cu IX | 185 | 39.36 | 10.99 | 19.86 | 0 | 7.90 | 53.8 |
| | 220 | 39.24 | 11.48 | 27.67 | 0 | 10.99 | 75.1 |
| | 250 | 39.24 | 11.48 | 32.36 | 0 | 12.80 | 87.5 |
| | 280 | 39.32 | 11.51 | 34.24 | 0 | 13.55 | 92.4 |
| | 305 | 39.36 | 11.81 | 35.54 | 0 | 14.05 | 95.7 |
| | 325 | 39.34 | 11.80 | 36.00 | 0 | 14.11 | 96.2 |
| Cu X | 185 | 39.21 | 11.20 | 19.80 | 0 | 7.88 | 53.9 |
| | 220 | 39.26 | 11.49 | 27.43 | 0 | 10.85 | 74.1 |
| | 250 | 39.30 | 10.97 | 31.41 | 0 | 12.38 | 84.5 |
| | 305 | 39.24 | 11.21 | 35.17 | 0 | 13.77 | 94.1 |
| | 325 | 39.40 | 11.53 | 35.96 | 0 | 14.19 | 96.6 |
| Cu XI | 220 | 38.77 | 13.29 | 16.35 | 12.59 | 9.00 | 62.2 |
| | 250 | 38.68 | 11.16 | 15.72 | 13.58 | 8.90 | 61.7 |

increases rapidly with the rising reaction temperature, becoming almost quantitative at 325°C, but is reduced by the formation of considerable amounts of the oily products at lower temperatures.

**Influence of Precipitants on the Dehydrogenating Activity of Reduced Copper.** — Comparison of Tables IV and V shows that Cu IX and Cu X, obtained by using potassium carbonate and potassium bicarbonate respectively as precipitants, gave the highest yield of acetone at the highest temperature as far as the experiments were performed. These copper catalysts act only to dehydrogenate isopropyl alcohol to acetone at all temperatures, while the catalysts prepared with sodium hydroxide act similarly at the higher temperatures but act on isopropyl alcohol at the lower temperatures not only to dehydrogenate it to acetone but also to produce isobutyl methyl ketone and diisobutyl ketone. The catalyst prepared with barium hydroxide behaves at the lower temperatures similarly to those prepared with sodium hydroxide.

The precipitate prepared with potassium carbonate at 90°C was dark brown, and the catalyst prepared from it gave isobutyl methyl ketone and diisobutyl ketone together with acetone[1].

**Use of Isopropyl Alcohol and Acetone as Starting Materials.**—Investigation was made as to whether or not the amount of the oily products is changed by adding acetone to isopropyl alcohol in the charge. The results summarized in Table IV show that acetone mixed beforehand does not essentially participate in the production of isobutyl methyl ketone and diisobutyl ketone.

**Influence of the Addition of Ethyl Alcohol to Copper Nitrate Solution.** — Investigation was made as to whether or not the dehydrogenating activity of reduced copper could be

TABLE VI. THE EFFECT OF THE RATIOS OF ISOPROPYL ALCOHOL TO ACETONE ON THE YIELD OF OILY PRODUCTS

| Acetone g. | Isopropyl alcohol g. | Temp. °C | Velocity g./hr. | Acetone in reaction product g. | Oily products g. | Gases collected l. | Percentage of conversion % |
|---|---|---|---|---|---|---|---|
| 38.82 | 0 | 220 | 12.59 | 37.54 | 0 | 0.17 | — |
| 38.98 | 0 | 250 | 12.64 | 37.72 | 0 | 0.17 | — |
| 31.93 | 7.71 | 220 | 12.52 | 34.26 | — | 1.63 | 56.6 |
| 19.50 | 19.70 | 220 | 12.71 | 25.44 | 5.06 | 3.87 | 52.7 |
| 7.68 | 31.45 | 220 | 11.45 | 21.04 | 8.08 | 7.04 | 60.0 |
| 0 | 38.93 | 220 | 11.39 | 13.24 | 15.29 | 8.19 | 56.4 |
| 0 | 38.83 | 250 | 11.65 | 16.48 | 13.40 | 9.11 | 62.9 |

TABLE VII. INFLUENCE OF THE ADDITION OF ETHYL ALCOHOL TO COPPER NITRATE SOLUTION

| Catalyst | Temp. °C | Isopropyl alcohol g. | Velocity g./hr. | Acetone g. | Oily products g. | Gases collected l. | Percentage of conversion % |
|---|---|---|---|---|---|---|---|
| Cu XII | 220 | 39.07 | 10.90 | 13.91 | 15.10 | 8.38 | 57.5 |
| | 250 | 38.95 | 11.68 | 16.73 | 13.42 | 9.20 | 63.3 |
| | 305 | 39.06 | 11.72 | 34.89 | 0 | 13.83 | 94.9 |
| | 325 | 39.03 | 11.71 | 35.57 | 0 | 14.08 | 96.7 |
| Cu XIII | 220 | 39.30 | 10.97 | 25.92 | 0 | 10.21 | 69.6 |
| | 250 | 39.33 | 10.98 | 31.37 | 0 | 12.35 | 84.2 |
| | 305 | 39.33 | 11.80 | 35.76 | 0 | 13.96 | 95.1 |
| | 325 | 39.19 | 10.94 | 36.35 | 0 | 14.23 | 97.3 |
| Cu XIV | 220 | 38.97 | 12.64 | 16.28 | 0 | 6.56 | 45.1 |
| | 250 | 39.05 | 12.33 | 26.57 | 0 | 10.39 | 71.3 |
| | 305 | 39.08 | 11.44 | 33.70 | 0 | 13.35 | 91.6 |
| | 325 | 39.06 | 11.43 | 35.59 | 0 | 14.03 | 96.3 |

increased by the addition of ethyl alcohol in the preparation of the precipitate. The results are shown in Table VII. Comparison of Table VII with Table IV (Cu VII) and with Table V (Cu IX and Cu X) shows that the catalytic activity of reduced copper is not significantly affected by the addition of ethyl alcohol except that the catalyst (Cu XIV), prepared with potassium bicarbonate and used at the lower temperatures, is less active.

**Catalysts.** — Frolich et al.[3] reported that the gels precipitated at 85°C or higher temperatures consist essentially of copper oxide and only a small amount of copper hydroxide, and that lowering of the temperature of precipitation increases the amount of copper hydroxide. Further, it was found by Milligan[6] that the pure blue gel is hydrous cupric hydroxide and the black gel is hydrous cupric oxide. As shown in Table I, the precipitates obtained at various temperatures differ from each other in color. Thus the precipitates prepared at 5 and 22°C are blue, and these precipitates change gradually to dark gray in color. On the other hand, the precipitates prepared at 55 and 90°C are black. The precipitates resulting from lower precipitation temperatures are much more hydrated and bulky than those obtained at higher precipitation temperatures.

Orito and Kawachi[7] found that the activity of the mixed Cu-Cr basic carbonate catalyst for the liquid-phase hydrogenation of acetone is high when it is calcined previously at about 350°C and reduced before use in a stream of hydrogen. However, it seems that the copper prepared by direct reduction of basic copper carbonate possesses a higher dehydrogenation activity than that resulting from copper oxide.

## Discussion

**Cause of Condensation.** — It was reported[8] that the copper catalyst, containing an alkaline oxide such as zinc oxide or magnesium oxide and composed of oxides having dehydrogenating and dehydrating properties, converts isopropyl

6) W. O. Milligan, *J. Phys. & Colloid Chem.*, **55**, 497 (1951).

7) Y. Orito and S. Kawachi, *J. Chem. Soc. Japan, Ind. Chem. Sec.* (*Kogyo Kagaku Zasshi*), **60**, 703 (1957).

8) V. N. Ipatieff and V. Haensel, *J. Org. Chem.*, **7**, 189 (1942); L. L. Gershbein, H. Pines and V. N. Ipatieff, *J. Am. Chem. Soc.*, **69**, 2888 (1947); F. W. Major and F. E. Salt, Brit. Pat. 656405 (1951); *Chem. Abstr.*, **46**, 8147 (1952); S. Kudo, *J. Chem. Soc. Japan, Ind. Chem. Sec.* (*Kogyo Kagaku Zasshi*), **58**, 785 (1955). T. Kanamori, ibid., **61**, 1576 (1958).

alcohol to isobutyl methyl ketone and diisobutyl ketone along with others. As described in the preceding paper, similar condensation products were obtained by employing copper catalysts prepared with alkali hydroxides as precipitants. Such a condensation has not yet been reported to occur with a copper catalyst alone.

The present author first assumed that this condensation was caused by traces of alkali in the catalyst, but the copper catalyst prepared with an excess of potassium bicarbonate did not cause this condensation. Takayasu[9] determined the amounts of the residual oxide in various specimens of reduced copper, and observed that hydrogen might be incapable of reducing copper oxide completely into metallic copper. Further, he showed that the precipitates prepared by adding aqueous sodium hydroxide to aqueous copper nitrate at 100°C and at 30°C consist of $5CuO \cdot H_2O$ and $3CuO \cdot H_2O$, respectively. Audibert and Raineau[2] found that the precipitate prepared by adding an alkali hydroxide to a boiling solution of copper nitrate consists of $4CuO \cdot H_2O$. Ipatieff and Haensel[8] reported that an infinitesimal amount of water is required to start the condensation reaction. Considered from these items of information in the literature, the formation of the higher ketones in the present research seems also to be attributed to the effect either of traces of water or of a lower oxide of copper in the catalysts.

9) M. Takayasu, *J. Chem. Soc. Japan (Nippon Kwagaku Kwaisi)*, **64**, 675 (1943), **65**, 46 (1944).

## Summary

The present work is to determine whether the yields of acetone and of the oily products (isobutyl methyl ketone and diisobutyl ketone) to be obtained from isopropyl alcohol by the catalytic action of reduced copper are affected by the precipitation temperature in the preparation of the catalysts, and to find a catalyst efficient for the production of oily products. Isopropyl alcohol was changed to acetone in 91~95% yield with no side reaction, by being passed over various copper catalysts at 325°C. The maximum yield of the oily products was obtained with the catalyst prepared with sodium hydroxide as a precipitant and at 22°C as the precipitation temperature, and at the reaction temperature of 220°C, amounting to 39.28% based on isopropyl alcohol used.

The author wishes to express his hearty thanks to Professor Tamon Matsuura for his kind guidance throughout this work.

*Department of Chemistry*
*Faculty of Science*
*Hiroshima University*
*Hiroshima*

# *Dehydrogenation of Secondary Alcohols with Reduced Copper. V*[1]. *Catalytic Dehydrogenation of sec-Butyl Alcohol**

By Kazuaki KAWAMOTO

(Received November 18, 1960)

The preparation of copper catalysts, and the production of acetone and oily products (isobutyl methyl ketone and diisobutyl ketone) from isopropyl alcohol were described in detail in the previous papers[1,2], and it has been found that two distinct types of copper catalysts are obtained according to the precipitants. One type catalyses the decomposition of isopropyl alcohol to acetone and hydrogen. The other type catalyses the conversion of isopropyl alcohol into isobutyl methyl ketone and diisobutyl ketone together with acetone and hydrogen. That is to say, the copper catalysts prepared by reducing precipitates obtained by adding a solution of potassium bicarbonate or potassium carbonate to a solution of copper nitrate at 22°C gave the highest yield of acetone when used at the highest reaction temperature (325°C). On the other hand, the copper catalyst prepared by the reduction of the precipitate obtained from sodium hydroxide and copper nitrate at 22°C showed the greatest activity for the condensation of isopropyl alcohol. The

1) K. Kawamoto, This Bulletin, **34**, 795 (1961).

* The major part of this research was presented at the 13th Annual Meeting of the Chemical Society of Japan, Tokyo, April, 1960.

2) K. Kawamoto, This Bulletin, **34**, 161 (1961).

TABLE I. INFLUENCE OF PRECIPITANTS AND THE REACTION TEMPERATURE ON THE DEHYDROGENATION OF *sec*-BUTYL ALCOHOL

| Expt. No. | Precipitant | Temp. °C | *sec*-Butyl alcohol g. | Velocity g./hr. | Reaction product | | | | | Ketone in aq. soln. g. | Gas collected l. | Yield of ketone* mol. % | Percentage of conversion** % |
|---|---|---|---|---|---|---|---|---|---|---|---|---|---|
| | | | | | Yield g. | $n_D^{25}$ | $d_4^{25}$ | Ketone g. | Unchanged alcohol, g. | | | | |
| 1 | NaOH | 185 | 40.03 | 9.61 | 38.58 | 1.3862 | 0.8077 | 19.99 | 16.29 | 0.37 | 6.60 | 52.3 | 54.5 |
| 2 | $K_2CO_3$ | 185 | 40.22 | 10.49 | 39.24 | 1.3840 | 0.8061 | 23.77 | 13.60 | 0.58 | 7.86 | 62.2 | 64.6 |
| 3 | NaOH | 220 | 40.08 | 10.02 | 38.76 | 1.3862 | 0.8105 | 26.15 | 7.67 | 0.52 | 8.61 | 68.4 | 71.0 |
| 4 | $K_2CO_3$ | 220 | 40.03 | 11.72 | 38.59 | 1.3807 | 0.8057 | 28.90 | 8.22 | 0.82 | 9.45 | 76.3 | 78.1 |
| 5 | NaOH | 250 | 39.99 | 10.00 | 38.58 | 1.3802 | 0.8100 | 31.49 | 4.38 | 0.83 | 10.32 | 83.1 | 85.3 |
| 6 | $K_2CO_3$ | 250 | 39.45 | 10.76 | 38.86 | 1.3793 | 0.8073 | 32.13 | 5.21 | 0.92 | 10.58 | 86.1 | 88.7 |
| 7 | NaOH | 280 | 40.07 | 10.23 | 38.41 | 1.3781 | 0.8077 | 33.40 | 3.44 | 0.91 | 10.95 | 88.0 | 90.3 |
| 8 | $K_2CO_3$ | 280 | 40.22 | 10.06 | 38.38 | 1.3775 | 0.8060 | 34.68 | 2.70 | 0.98 | 11.33 | 91.2 | 93.2 |
| 9 | NaOH | 305 | 40.03 | 11.44 | 38.20 | 1.3777 | 0.8076 | 34.82 | 1.60 | 1.06 | 11.41 | 92.1 | 94.2 |
| 10 | $K_2CO_3$ | 305 | 40.26 | 11.24 | 38.29 | 1.3774 | 0.8044 | 36.13 | 0.94 | 1.03 | 11.77 | 94.9 | 96.7 |
| 11 | NaOH | 325 | 40.06 | 10.23 | 38.40 | 1.3775 | 0.8081 | 35.42 | 1.43 | 1.10 | 11.63 | 93.7 | 96.0 |
| 12 | $K_2CO_3$ | 325 | 40.22 | 10.63 | 38.46 | 1.3779 | 0.8081 | 36.20 | 0.55 | 1.17 | 11.86 | 95.5 | 97.5 |

* This value was an average of three determinations under the constant operating condition, but the fluctuation in the yield of ethyl methyl ketone obtained by the repeated experiments was less than 1%.

** The percentage of the volume of the gaseous product to the theoretical calculated on the assumption that original *sec*-butyl alcohol were transformed completely either into the ketone and hydrogen or into butylenes and water.

TABLE II. THE PROPERTIES OF DISTILLED FRACTIONS OF EXPERIMENT No. 3

| Fraction | B. p. °C | Yield % | $n_D^{25}$ | $d_4^{25}$ | Ketone % | Unchanged alcohol % |
|---|---|---|---|---|---|---|
| 1 | 72.5～ 80 | 40.31 | 1.3788 | 0.8221 | 81.14 | 8.52 |
| 2 | 80 ～ 85 | 19.58 | 1.3799 | 0.8050 | 77.99 | 19.71 |
| 3 | 85 ～ 90 | 14.14 | 1.3818 | 0.7990 | 66.82 | 32.16 |
| 4 | 90 ～100 | 10.11 | 1.3897 | 0.8007 | 25.77 | 73.01 |
| 5 | 100 ～155 | 1.51 | 1.4016 | 0.8060 | — | — |
| 6 | 155 ～158 | 12.53 | 1.4129 | 0.8162 | — | — |
| 7 | residue | 0.34 | 1.4194 | — | — | — |

TABLE III. THE PROPERTIES OF DISTILLED FRACTIONS OF EXPERIMENT No. 4

| Fraction | B. p. °C | Yield % | $n_D^{25}$ | $d_4^{25}$ | Ketone % | Unchanged alcohol % |
|---|---|---|---|---|---|---|
| 1 | 71.5～80 | 36.45 | 1.3782 | 0.8170 | 86.84 | 6.09 |
| 2 | 80 ～85 | 41.15 | 1.3782 | 0.8016 | 83.45 | 16.09 |
| 3 | 85 ～90 | 7.29 | 1.3814 | 0.7999 | 69.12 | 30.78 |
| 4 | 90 ～98 | 11.45 | 1.3907 | 0.8022 | 19.32 | 79.12 |
| 5 | residue | 1.68 | 1.4032 | — | — | — |

Table IV. The properties of distilled fractions of Experiment No. 11

| Fraction | B. p. °C | Yield % | $n_D^{25}$ | $d_4^{25}$ | Ketone % | Unchanged alcohol % |
|---|---|---|---|---|---|---|
| 1 | 71.5~80 | 66.84 | 1.3770 | 0.8136 | 93.07 | 1.48 |
| 2 | 80 ~81 | 29.36 | 1.3770 | 0.8006 | 94.71 | 4.50 |
| 3 | residue | 1.17 | 1.3852 | — | — | — |

Table V. The properties of distilled fractions of Experiment No. 12

| Fraction | B. p. °C | Yield % | $n_D^{25}$ | $d_4^{25}$ | Ketone % | Unchanged alcohol % |
|---|---|---|---|---|---|---|
| 1 | 71.5~80 | 67.00 | 1.3772 | 0.8100 | 94.12 | 0.66 |
| 2 | 80 ~80.8 | 28.50 | 1.3772 | 0.8000 | 96.32 | 3.06 |
| 3 | residue | 1.24 | 1.4085 | — | — | — |

highest yield of the condensation products was obtained with the catalyst at the reaction temperature of 220°C.

The present paper describes the results of similar experiments with *sec*-butyl alcohol and the two types of catalysts. In the present research, one type was prepared with potassium carbonate, and the other type with sodium hydroxide. The vapor phase dehydrogenation of *sec*-butyl alcohol was carried out with these two types of catalysts at several temperatures between 185 and 325°C.

Up to the present, there have been a large number of patents and a few reports about the vapor phase dehydrogenation of *sec*-butyl alcohol to ethyl methyl ketone, and the majority deal with the use of copper mixed with other metals. Dunbar and Arnold[3] found that in the presence of a copper-chromium-oxide catalyst, the dehydrogenation of *sec*-butyl alcohol at 300~325°C furnishes 68% of ethyl methyl ketone.

## Experimental

**Purification of *sec*-Butyl Alcohol.**—Commercial extra pure *sec*-butyl alcohol was purified by being dried with quick lime, followed by fractional distillation. B. p. 98.7~99.2°C, $n_D^{25}$ 1.3950, $d_4^{25}$ 0.8029.

**Preparation of Catalysts.** — The two specimens of copper catalysts used in the present research are identical with Cu VII and Cu IX which were described in the preceding paper[1].

**Apparatus and Procedure.** — The apparatus for the dehydrogenation was exactly the same as that previously described[2]. The precipitate (10 g.) to be reduced was placed in the reaction tube. After the tube was filled with hydrogen, the furnace was heated to the reduction temperature below 185°C. Hydrogen was passed through the tube at the rate of 750~900 ml. per hour, and *sec*-butyl alcohol was passed under the ordinary pressure over the catalyst heated to 185, 220, 250, 280, 305 and 325°C, respectively. The vapor coming out from the reaction tube was condensed by passing it through a condenser cooled with ice water and the gas escaping from the condenser was scrubbed with ice-cooled distilled water (50 ml.) to remove the ethyl methyl ketone and the unchanged alcohol from the hydrogen stream. The volume of the non-condensable gas was measured at intervals of 15~30 min. At the end of a run, the weight of liquid products and of that absorbed by the distilled water were measured.

**Analysis of the Products.**—The relative content of ethyl methyl ketone and unchanged *sec*-butyl alcohol in the liquid product was determined by the hydroxylamine method[4] and the acetic anhydride-pyridine method[5], respectively. The product in the aqueous solution was recognized to be ethyl methyl ketone by the preparation of its 2,4-dinitrophenylhydrazone (m. p. 118°C) and semicarbazone (m. p. 144°C), and further its content was determined by the hydroxylamine method. The reliability of these analytical methods was checked by titrating the known samples of ethyl methyl ketone and *sec*-butyl alcohol, respectively. The result was found to be correct within experimental errors. The liquid product was dried with anhydrous sodium sulfate in every case, and then fractionally distilled through an electrically heated Widmer column. As examples, the properties of distilled fractions of Experiments No. 3, 4, 11 and 12 in Table I are shown in Tables II, III, IV and V.

Fractions 1, 2 and 3 in Table II correspond in physical constants to ethyl methyl ketone. The 2,4-dinitrophenylhydrazone and semicarbazone melted at 118 and 144°C, respectively, both alone and in admixture with the corresponding derivatives of authentic ethyl methyl ketone. From Fraction 4 a phenylurethan was obtained, which was identified as that of *sec*-butyl alcohol by mixing with an authentic specimen. Fraction 6 gave a crystalline

3) R. E. Dunbar and M. R. Arnold, *J. Org. Chem.*, **10**, 501 (1945).

4) M. Katsuno, *J. Soc. Chem. Ind., Japan* (*Kōgyō Kagaku Zassi*), **46**, 112 (1943).

5) C. L. Ogg, W. L. Porter and C. O. Willits, *Ind. Eng. Chem. Anal. Ed.*, **17**, 394 (1945).

semicarbazone melting at 95~96°C which was identified with the semicarbazone of 5-methyl-3-heptanone[6]. Judging from the physical constants of this fraction, the semicarbazone and the formation of isobutyl methyl ketone from isopropyl alcohol as described previously, it seems that Fraction 6 (b. p. 155~158°C) consists mainly of 5-methyl-3-heptanone. The formation of unsaturated and hydroxy ketones such as 5-methyl-4-hepten-3-one and 5-methyl-5-hydroxy-3-heptanone was not detected in the reaction product. As shown in Table III, no fraction corresponding in the boiling point to 5-methyl-3-heptanone was found in the reaction product obtained by employing the copper catalyst prepared with potassium carbonate.

## Results and Discussion

The results are summarized in Table I. In the range of 185 to 325°C *sec*-butyl alcohol does not decompose in the absence of catalysts. Consequently the changes observed in the present research do not involve the simple pyrolysis of *sec*-butyl alcohol. The yield of ethyl methyl ketone and the percentage of conversion recorded in Table I do not necessarily represent the maximum values. The difference between the yield of ethyl methyl ketone and the percentage of conversion was a few per cent. Therefore, the dehydration of *sec*-butyl alcohol to butylenes seems to occur little at temperatures below 325°C, and the yield of total ethyl methyl ketone agrees closely with the value calculated from the amount of the escaping gas in each experiment.

**Influence of the Reaction Temperature on the Dehydrogenating Activity of Reduced Copper.**— In Fig. 1 the yield of ethyl methyl ketone is plotted against the reaction temperature. As seen from Tables I—V and Fig. 1, the rates of the dehydrogenation of *sec*-butyl alcohol to ethyl methyl ketone and that of the conversion of *sec*-butyl alcohol to 5-methyl-3-heptanone depend upon the reaction temperature. The reaction products obtained at the higher temperatures contained more ethyl methyl ketone than those obtained at the lower temperatures, and the conversion of *sec*-butyl alcohol to ethyl methyl ketone was very high at the highest reaction temperature (325°C) so that unchanged *sec*-butyl alcohol was scarcely found in the reaction products. The higher ketone was not obtained at all or only a little was obtained except in Experiment No. 3, where 5-methyl-3-heptanone was produced along with ethyl methyl ketone.

6) 5-Methyl-3-heptanone was prepared according to Powell and Secoy's method: Ethyl methyl ketone was first condensed in the presence of powdered barium oxide, and the 5-methyl-4-hepten-3-one thus formed was reduced selectively over platinum catalyst to give 5-methyl-3-heptanone, and its semicarbazone melted at 95~96°C. S. G. Powell and C. H. Secoy, *J. Am. Chem. Soc.*, 53, 765 (1931).

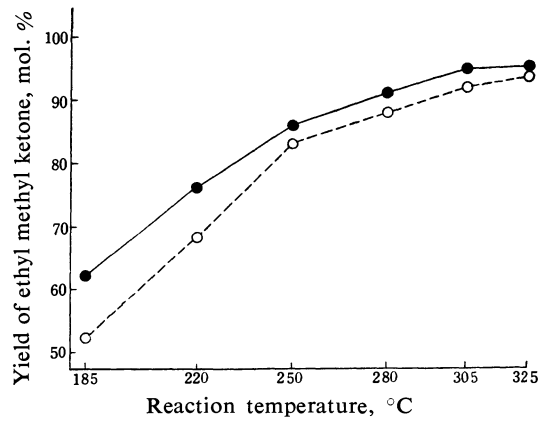



Fig. 1. The effect of temperature on the dehydrogenation of *sec*-butyl alcohol with two types of copper catalysts.
●: Catalyst prepared with potassium carbonate.
○: Catalyst prepared with sodium hydroxide.

The volume of the evolved gas, mainly consisting of hydrogen, is plotted against the reaction time in Figs. 2 and 3, which show that the activity of the catalysts holds over the period of the operation. Further, a parallelism exists between the amount of gas evolved and the temperature.

**Two Types of Reduced Copper.** — As in the case of isopropyl alcohol, the copper catalyst prepared with potassium carbonate promotes dehydrogenation alone, but that prepared with sodium hydroxide catalyses not only dehydrogenation but also condensation reactions.

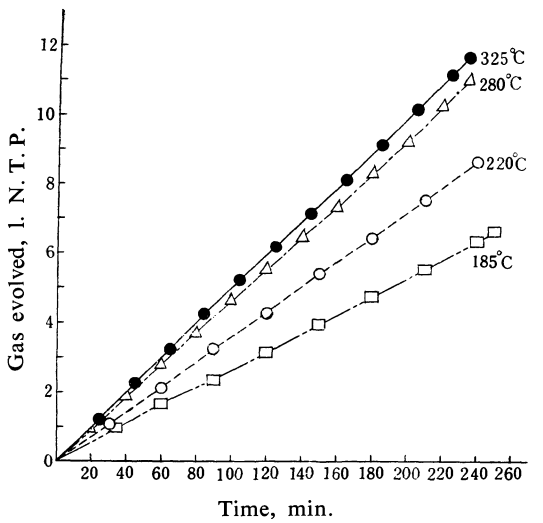



Fig. 2. Relation between volume of gas evolved and time of reaction at various temperatures (Precipitant in the preparation of catalyst; NaOH).

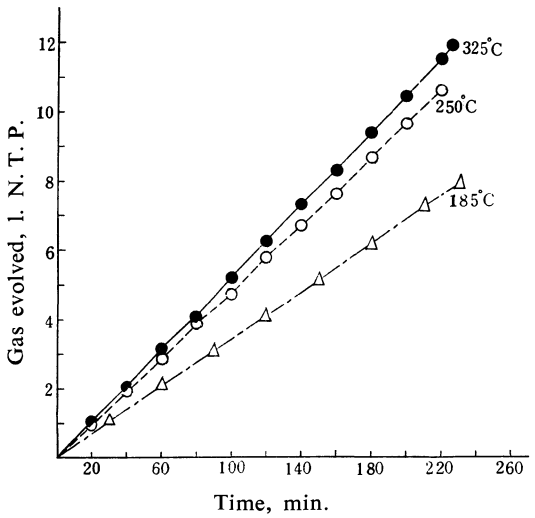



Fig. 3. Relation between volume of gas evolved and time of reaction at various temperatures (Precipitant in the preparation of catalyst; $K_2CO_3$).

**The Activity of Dehydrogenating Various Secondary Alcohols to the Corresponding Ketones.** — The copper catalyst prepared by reduction of the precipitate obtained by adding an excess of a dilute sodium hydroxide solution to an aqueous solution of cupric nitrate changed isoborneol[7] to camphor (yield 96%) at 220°C, *l*-menthol[8] to menthones (*d*-isomenthone and *l*-menthone) (yield 74%) and a small amount of thymol under similar conditions, and cyclohexanol[8] to cyclohexanone (yield 63%) and a trace of phenol. In the case of isopropyl alcohol[1], the yield of acetone amounted to about 93% at 325°C, while at 220°C the yield of acetone decreased to 35% with the formation of the condensation products, isobutyl methyl ketone and diisobutyl ketone. *sec*-Butyl alcohol behaved similarly, giving a condensation product (5-methyl-3-heptanone) along with ethyl methyl ketone at 220°C but the latter alone did so at higher temperatures with greater ease than isopropyl alcohol.

Thus the copper catalyst is suitable for dehydrogenating secondary alcohols to the corresponding ketones, but the dehydrogenating and the condensing abilities of the copper catalyst vary with the species of alcohols, and it seemed that the alcohols which possess a methyl group adjacent to the hydroxylated carbon atom give rise to the condensation reaction.

7) T. Matsuura and K. Kawamoto, *J. Chem. Soc. Japan, Pure Chem. Sec.* (*Nippon Kagaku Zasshi*), **80**, 94 (1959).
8) K. Kawamoto, ibid., **80**, 681 (1959).

**5-Methyl-3-heptanone.** — Up to the present, 5-methyl-3-heptanone has been prepared by the following methods: (1)[6,9] *sec*-Butyl alcohol is first dehydrogenated to ethyl methyl ketone, and the latter is condensed in the presence of alkali or calcium carbide to give 5-methyl-4-hepten-3-one and then the unsaturated ketone thus formed is hydrogenated to 5-methyl-3-heptanone. (2)[10] It is prepared by treating *sec*-butyl alcohol with ethyl methyl ketone in the vapor phase under pressure in the presence of a mixed catalyst with dehydrogenating and dehydrating properties. A new synthetic process for 5-methyl-3-heptanone, consisting in passing *sec*-butyl alcohol over reduced copper under the atmospheric pressure at 220°C, is now proposed.

## Summary

It was confirmed that ethyl methyl ketone and 5-methyl-3-heptanone are produced from *sec*-butyl alcohol with reduced copper alone. Two distinct types of reduced copper were prepared by precipitation with sodium hydroxide and with potassium carbonate. They differ somewhat in their ability to promote dehydrogenation of *sec*-butyl alcohol and differ greatly in their power to bring about condensation. The copper catalyst prepared with potassium carbonate acts to dehydrogenate *sec*-butyl alcohol at all the temperatures examined (185~325°C), giving ethyl methyl ketone, but the catalyst prepared with sodium hydroxide acts to dehydrogenate and to condense simultaneously at a certain temperature (220°C), giving 5-methyl-3-heptanone along with ethyl methyl ketone, and this affords a new synthetic method for 5-methyl-3-heptanone. *sec*-Butyl alcohol was converted into ethyl methyl ketone in 94~96% yield with no side reaction by passing it over these catalysts at 325°C.

The author wishes to express his hearty thanks to Professor Tamon Matsuura of Hiroshima University for his kind guidance and valuable suggestions throughout this work, and also to Mr. T. Hiraki for his able assistance of this work.

*Institute of Commodities*
*Faculty of Economics*
*Kagawa University, Takamatsu*

9) V. I. Esafov, V. M. Gulyakov, V. V. Kargopol'tseva, A. P. Kulakova, G. V. Razmyslov and N. D. Toporov, *Chem. Abstr.*, **35**, 3958 (1941); C. Weizmann, Brit. Pat. 573724 (1945); *Chem. Abstr.*, **43**, 4287 (1949); R. Ya. Levina and N. P. Shusherina, ibid., **44**, 9336 (1950); A. N. Pudovik, R. D. Sabirova and T. A. Tener, ibid., **49**, 8790 (1955).
10) J. W. Mecorney and Geo. W. Gaertner, Jr., U. S. Pat. 2725400 (1955); *Chem. Abstr.*, **50**, 10762 (1956); N. V. de Bataafsche Petroleum Maatschappij, Dutch Pat. 83028 (1956); *Chem. Abstr.*, **52**, 2890 (1958).

# *Differential Thermal Analysis of Aluminum Soaps*

By Sukekuni SHIBA

(Received November 19, 1960)

It has been known that the metal soaps show complex thermal behaviors due to their polymorphism when they are heated. Lawrence[1] pointed out the temperature at which the soaps become plastic, before they reach the melting points, and the soaps show swelling and gellation in hydrocarbon media. The application of the differential thermal analysis, which has been used in metallography and in the study of clay minerals, to these phenomena, was attempted first by Vold[2], and the phase state of the metal soaps and soap-hydrocarbon systems were investigated successfully. Later, many authors reported the differential thermal analysis of metal soaps and the experimental apparatus applicable to such substances[3-5].

The thermal behaviors of aluminum soaps have not yet been fully clarified, and conflicting data were reported due to their relatively low heat of transition and the difficulty of obtaining pure soaps[6]. It is generally believed from various experiments, that the aluminum soaps, prepared by the usual metathetic process from aqueous solution of alkali soaps and aluminum salt, consist mainly of aluminum hydroxydisoaps, $Al(OH)A_2$, and they are the only definite compounds as aluminum soaps[7-9]. Recently, it was found that the aluminum trisoaps can be obtaind through interaction of aluminum trialkoxide or trialkyl aluminum with fatty acids in anhydrous organic media, and they are decomposed to disoaps in the presence of water[10-12].

The present investigation was carried out to examine the thermal behaviors of aluminum soaps by differential thermal analysis, and to obtain some information on the structure of aluminum soaps from thermal data.

## Experimental

**Preparation of Soaps.** — The aluminum soaps used in this work were prepared from purified fatty acids by an aqueous metathetic process. The fatty acids which were solid at room temperatures (stearic-lauric) were purified by repeated recrystallization from 80 vol. % ethanol. Capric and caprylic acids were purified by distillation under reduced pressure. The purity of the acids was examined by melting points and neutralization equivalent through titration, as is shown in Table I.

TABLE I. PHYSICAL CONSTANTS OF FATTY ACIDS

| Fatty acid | M. p., °C | | Neut. equiv. | |
|---|---|---|---|---|
| | Found | Lit.[13] | Found | Calcd. |
| Stearic | 69.5 | 69.6 | 282 | 284.5 |
| Palmitic | 62.2 | 62.9 | 258 | 256.4 |
| Myristic | 54.5 | 54.4 | 229 | 228.4 |
| Lauric | 43.3 | 44.0 | 201 | 200.3 |
| Capric | 30.1 | 31.3 | 173 | 172.3 |
| Caprylic | 14.3 | 16.3 | 144 | 144.2 |

Fatty acid was treated with an excess of sodium hydroxide solution and distilled water to yield an approximately 5% solution of sodium soap. The mixture was heated to dissolve the soap and the solution was kept completely transparent at 70~80°C for soaps from stearate to laurate, at 50°C for caprate and caprylate. A hot solution of aluminum sulfate was added slowly while being stirred vigorously, until a slight excess was present and the precipitation was complete. The precipitated aluminum soap was filtered off and washed with distilled water, until the filtrate was free from sulfate when tested with barium chloride solution under slightly acidic medium. The soap was then dried to constant weight at 110°C, and stored in a desiccator over phosphorus pentoxide. Dried soaps were analyzed for aluminum by ignition to oxide.

The reaction between sodium soap and aluminum salt solution in the presence of excess of sodium hydroxide is expressed generally by,

$$2n\mathrm{NaA}+\mathrm{Al_2(SO_4)_3}+2(3-n)\mathrm{NaOH} \rightarrow 2\mathrm{Al(OH)_{3-n}A_n}+3\mathrm{Na_2SO_4} \quad (1)$$

$$n=0\sim3 \quad (2)$$

1) A. S. C. Lawrence, *Trans. Faraday Soc.*, **34**, 660 (1938).
2) R. D. Vold, *J. Phys. Chem.*, **49**, 315 (1945).
3) C. J. Penter, S. T. Abrams and F. H. Stross, *Anal. Chem.*, **23**, 1459 (1951).
4) D. Evans, J. F. Hutton and J. B. Matthews, *J. Applied Chem.*, **2**, 252 (1952).
5) D. B. Cox and J. F. McGlynn, *Anal. Chem.*, **29**, 960 (1957).
6) G. S. Hattiangdi, M. J. Vold and R. D. Vold, *Ind. Eng. Chem.*, **41**, 2320 (1949).
7) V. R. Gray and A. E. Alexander, *J. Phys. Colloid Chem.*, **53**, 23 (1949).
8) W. W. Harple, S. E. Wiberley and W. H. Bauer, *Anal. Chem.*, **24**, 635 (1952).
9) W. H. Bauer, J. Fisher, F. A. Scott and S. E. Wiberley, *J. Phys. Chem.*, **59**, 30 (1955).
10) J. Glazer, T. S. McRoberts and J. H. Schulman, *J. Chem. Soc.*, **1950**, 2082.
11) A. Gilmour, A. A. Jobling and S. M. Nelson, ibid., **1956**, 1972.
12) A. E. Leger, R. L. Haines, C. E. Hubley, J. C. Hyde and H. Sheffer, *Can. J. Chem.*, **35**, 799 (1957).
13) A. W. Ralston, "Fatty Acids and their Derivatives", John Wiley and Sons Inc., New York (1948), p. 23.

where, A is the acid radical, and it is assumed that the soaps containing continuously 0~3 mol. of fatty acids per 1 mol. of aluminum are obtainable. It is possible by this relation to control the composition of the aluminum soap changing the excess of the sodium hydroxide in the aqueous medium. The composition of the soaps is shown in Table II.

TABLE II. COMPOSITION OF ALUMINUM SOAPS

| Al soap | No. of C atoms in acid | Excess of NaOH % | Al wt.% analyzed | Mol. acid per mol. Al |
|---|---|---|---|---|
| Stearate-3.22 | 18 | −25 | 2.91 | 3.22 |
| 〃-2.29 | 〃 | 0 | 3.92 | 2.29 |
| 〃-2.12 | 〃 | 10 | 4.25 | 2.12 |
| 〃-1.89 | 〃 | 25 | 4.68 | 1.89 |
| 〃-1.71 | 〃 | 40 | 5.10 | 1.71 |
| 〃-0.95 | 〃 | 100 | 8.23 | 0.95 |
| Palmitate | 16 | 45 | 5.80 | 1.62 |
| Myristate | 14 | 〃 | 5.96 | 1.77 |
| Laurate | 12 | 〃 | 6.38 | 1.87 |
| Caprate | 10 | 〃 | 7.36 | 1.87 |
| Caprylate | 8 | 〃 | 9.17 | 1.72 |

**Apparatus.** — An apparatus adequate to analyze the soaps or soap-oil systems, which are liable to be oxidized below their melting points, was constructed. The apparatus is able to control and record the temperatures automatically, in the temperature range up to 300°C, with a small amount of sample.

The apparatus consists of four basic parts; the sample and reference cells, electric furnace, temperature control mechanism, and recorder. The sample cells used are similar to those of Vold[14]. They are made of 18-8 stainless steel, machined to a wall thickness less than 0.4 mm., and have a sample capacity of 2 cc. The cells are closed by screw caps; a protection tube for the thermocouple is fitted in the center of the cap. The furnace is heated by a two-element heater, and the cells are set through a teflon collar and sleeve in a hole of a copper block which is placed in the center of the furnace.

The temperature of the block is detected by a chromel-alumel thermocouple, and is regulated by a potentiometer type controller. The controller detects the difference in the electromotive force of the couple and the settled potential which varies linearly with time, and regulates the temperature. The rate of heating or cooling is adjusted by changing the gear ratio of the controller. For the detection of the differential temperature of the sample and the reference cells, a chromel-alumel thermocouple was used, because of its sensitivity, stability, and linearity of the emf against temperature. The thermoelements were insulated with glass fiber tubing and impregnated with silicone varnish. The potential difference obtained from two cells is amplified by a chopper type DC amplifier, and recorded on a strip chart multipoint electronic recorder with the temperature of the reference cell. By a proper selection of the rang of amplifier and recorder, it is possible to record the temperature difference of ±0.3~±25°C on the full scale of the recorder.

**Analysis of Thermogram.** — The thermogram is analyzed for temperature and latent heat of transition. When the thermal transition does not occur, the temperature difference between the sample and the reference cells, $y$, is expressed by a curve which approaches $y_\infty$ at time infinity; i. e.,

$$y = y_\infty + (y_0 - y_\infty)\exp(-a(t-t_0)) \tag{3}$$

$$y_\infty = (C_s/\alpha_s - C_r/\alpha_r)\frac{dT_r}{dt} \tag{4}$$

$$a = \alpha_s/C_s \tag{5}$$

where, $T$ is the temperature; $C$, the heat capacity, $\alpha$, a constant including the coefficient of the overall heat transfer to the cell and dimensions of the thermal path as a whole: the subscripts $s$ and $r$ mean that the quantities refer to sample cell and to the reference cell. The interaction of the two cells are neglected. The temperature difference between the center ($T_s$) and wall ($T_f$) of the cell is expressed approximately by,

$$T_f - T_s = \frac{C_s}{\alpha_s} \cdot \frac{dT_s}{dt} \tag{6}$$

The actual temperature, at which the sample near the wall of the cell begins to undergo transition, is determined by the breaking point of the thermogram corrected by this relation.

When a transition of the sample is observed, enthalpy change of the sample cell, $\Delta H$, is expressed as follows;

$$\Delta H = \alpha_s \int_{t_1}^{t_2} (y - y')\, dt = \alpha_s A \tag{7}$$

where $t_1$ and $t_2$ are the optional time before and after the transition, $y'$ is the temperature difference when the transition does not occur, and $A$ is the area of the peak of the thermogram.

The apparatus was calibrated with stearic acid (m.p. 69.3°C, heat of melting, 47.6 cal./g.) and benzoic acid (m. p. 122°C, heat of melting, 33.9 cal./g.). It was shown that the determination of the transition temperature could be made accurately by adopting the temperature at the apex of the peak in the thermogram, after being corrected to the temperature difference between the sample and reference cells. A conversion factor, 0.370 cal. per unit area of the peak (in deg. min.), was obtained from both acids, when 0.5~1.0 g. of the sample was used.

**Procedure.**—The soap was weighed in the sample cell, and alumina or Nujol as a reference material was also filled in the reference cell. The cells were placed in the furnace, and heating and cooling at a constant rate were repeated. Experimental conditions were;

| | |
|---|---|
| Temperature, | up to 300°C |
| Rate of heating, | 0.5~1.2 deg./min. |
| Weight of the specimen, | 0.5~1.0 g. |

14) M. J. Vold, *Anal. Chem.*, **21**, 683 (1949).

15) S. Shiba, *Railway Technical Research Report*, No. **162** (1960).

Details of the apparatus, analysis, and procedure were described in the previous paper[15].

## Results and Discussion

**Thermogram of Aluminum Stearate.** — For most of the aluminum soaps, transition points are observed between room temperature and their melting points. Typical examples of the heating and cooling thermograms of an aluminum stearate are shown in Figs. 1 and 2.

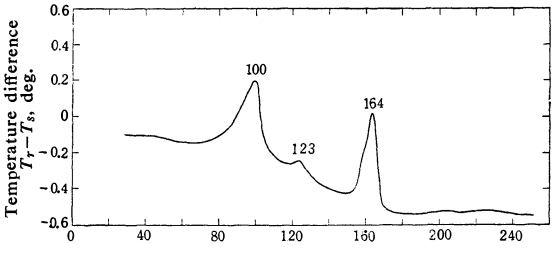



Fig. 1. Heating thermogram of aluminum stearate. (Ste−1.71).

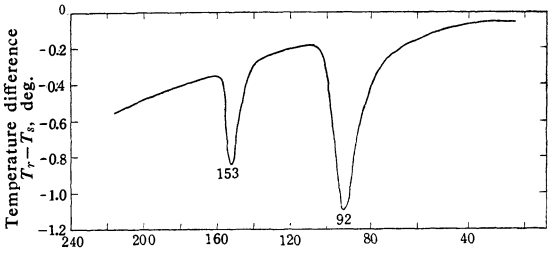



Fig. 2. Cooling thermogram of aluminum stearate. (Ste−1.71).

Three distinct peaks of transition are found in the heating thermogram, and two peaks are found in the cooling thermogram. Numbers in the thermograms show the temperature of the sample cell at the apex of the peaks. The cooling thermograms show a lower transition temperature and less repeatability due to the super-cooling of the soaps.

When heating and cooling are repeated for one specimen, the thermal behaviors are repeatable in general. However, the initial heating sometimes gives a little different thermogram from that obtained by the following runs; e. g., two indistinct peaks are observed in the initial run instead of one peak near 100°C in the following runs. These facts were reported by Vold[16], and they may be ascribed partly to the condition of the specimen packed in the cell before it is melted. In fact, the aluminum soap powders, when once melted, give a transparent glue-like mass, and show different bulk physical properties. No appreciable chemical changes of the specimen during the thermal analysis, oxidation, dehydration etc., were ascertained by the infrared absorptions before and after the analysis. In this report, discussions are held on the definite transitions which are obtained repeatably, and the small peaks which are obscure as found occasionally near 82°C are neglected.

**Aluminum Stearates of Different Compositions.** —The transition temperatures and heats of transition of aluminum stearates are summarized

TABLE III. TRANSITION TEMPERATURES AND HEATS OF TRANSITION OF ALUMINUM STEARATES

| Sample | Heating | | Cooling | |
|---|---|---|---|---|
| | Tr. temp. °C | Heat of tr. cal./g. | Tr. temp. °C | Heat of tr. cal./g. |
| Ste-3.22 | 69 | 16.0 | 58 | 14.2 |
| | 104 | 7.0 | 79 | 7.0 |
| Ste-2.29 | 65 | 8.0 | 59 | 2.4 |
| | 104 | 8.1 | 87 | 6.8 |
| Ste-2.12 | 66 | 3.0 | 85 | 7.4 |
| | 99 | 5.8 | 134 | 0.9 |
| | 150 | 0.9 | | |
| Ste-1.89 | 101 | 7.8 | 88 | 9.2 |
| | 157 | 3.2 | 137 | 2.1 |
| Ste-1.71 | 99 | 5.8 | 89 | 10.6 |
| | 119 | 0.4 | 144 | 2.5 |
| | 162 | 2.1 | | |
| Ste-0.95 | 97 | 2.8 | 95 | 7.8 |
| | 124 | 0.8 | 145 | 1.1 |
| | 162 | 1.3 | | |

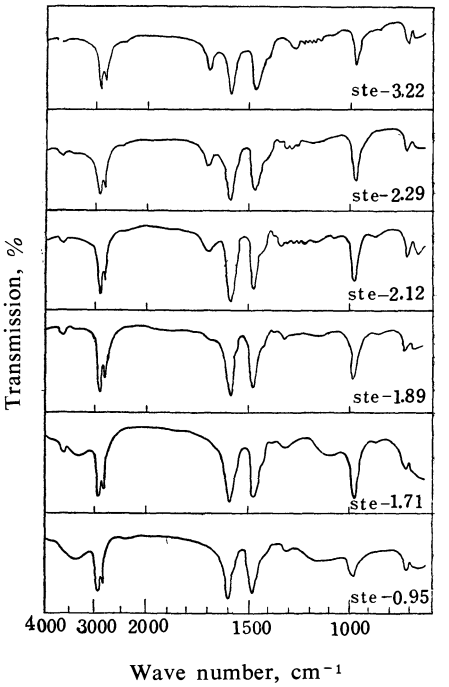



Fig. 3. Infrared spectra of aluminum stearates.

16) M. J. Vold, G. S. Hattiangdi and R. D. Vold, *Ind. Eng. Chem.*, **41**, 2539 (1949).

in Table III. Infrared absorption spectra of the same soaps, obtained by the potassium bromide disk method using a double beam spectrometer (Perkin-Elmer IR-21), are also shown in Fig. 3.

The thermograms of these soaps are somewhat different from those of examples shown in Figs. 1 and 2. The soaps containing more than 2 mol. of fatty acid per mole of aluminum, exhibit transitions near 70°C which are not found in Fig. 1. This transition point corresponds to the melting point of stearic acid. The heat of transition of this peak increases with an excess of the fatty acid over 2 mol. per aluminum. The infrared absorption at 1720 $cm^{-1}$, which is due to the presence of the carbonyl group, shows the same tendency. These facts confirm the fact that these soaps contain free fatty acids, and that the peaks are due to the melting of the acids. The results also indicate that the preparation of aluminum trisoaps by metathetic processes is impossible. Even though trisoaps exist, they will be decomposed to hydroxydisoaps and fatty acids by the effect of water. The soaps containing more than 2 mol. of fatty acids per aluminum, show weak transition peaks or lack of them at higher temperatures. This is attributed to the co-existence of fatty acids which melt at lower temperatures. When the fatty acids in the soap are extracted off by heptane, the transition at 160°C is found for the residual soap.

The soaps containing less than 2 mol. of acid per aluminum show no additional peaks, and they show less heat of transition, probably due to the presence of aluminum hydroxide in the soap. Infrared absorptions at 3720 $cm^{-1}$ which are assigned to free OH stretching, are found for most of the soaps; while in the soap Ste-0.95, a broad absorption is found near 3400 $cm^{-1}$ corresponding to bonded OH, and both absorptions are found for Ste-1.71. The infrared data retain the possibility of the existence of dihydroxymonosoaps as a discrete compound; however, the thermal data offer no positive evidence for the existence of the monosoaps.

The heat of transition obtained, show rather disjoined results, presumably because of the difference in heat transfer between specimen and cell, and in the specimen. Total heat of transition per mole of Ste-1.89 is about 6.4 kcal./mol., considerably less than that of alkali soaps (e. g., NaSte, 14.6 kcal./mol.).

**Aluminum Soaps from Various Fatty Acids.** —Transition temperatures and heats of transition of various aluminum soaps are summarized in Table IV. The structure and composition of these soaps are essentially the same,

TABLE IV. TRANSITION TEMPERATURES AND HEATS OF TRANSITION OF ALUMINUM SOAPS FROM VARIOUS FATTY ACIDS

| Sample | Heating | | Cooling | |
|---|---|---|---|---|
| | Tr. temp. °C | Heat of tr. cal./g. | Tr. temp. °C | Heat of tr. cal./g. |
| Palmitate | 90 | 4.0 | 80 | 4.5 |
| | 128 | 1.0 | 152 | 2.0 |
| | 170 | 2.1 | | |
| Myristate | 92 | 3.0 | 84 | 2.1 |
| | 136 | 1.4 | 156 | 2.7 |
| | 179 | 2.5 | | |
| Laurate | 86 | 1.4 | 78 | 1.2 |
| | 149 | 1.2 | 152 | 3.0 |
| | 185 | 3.2 | | |
| Caprate | 196 | 4.8 | 160 | 4.2 |
| Capylate | 216 | 6.4 | 176 | 4.1 |

and no free fatty acids are incorporated in the soaps, as are ascertained by the infrared spectra.

The thermograms of palmitate, myristate, and laurate show three distinct transition points similar to stearate; whereas, caprate and caprylate show only one transition point corresponding to the highest one of the soaps from higher fatty acids. The transition heat of the lowest transition decreases with the decrease in number of carbon atoms in the fatty acid, and disappears for caprate and caprylate. On the other hand, the heat of the highest transition increases with the decrease in number of carbon atoms, resulting in a similar total heat of transition per gram. The lack of these characteristic transitions of the aluminum soaps in the lower soaps, is consistent with the change of may other properties of the soaps with the change in the length of the constituent fatty acids; e. g., the thickening and gelling

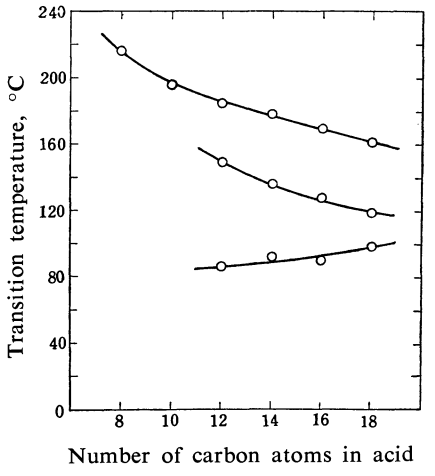



Fig. 4. Transition temperatures of aluminum soaps.

properties of aluminum soaps in organic media[17], etc.

Changes in corresponding transition temperatures with the carbon number of the fatty acids are shown in Fig. 4. Each transition temperature changes regularly, and it seems that the temperatures approach constant values as the chain length increases.

**Assignment of Transition Points.** — It is an inherent characteristic of the differential thermal analysis that it enables some thermal change in the specimen to be caught, but gives no information on the nature of the transition. Some other data are necessary for this purpose.

The additional peaks which are obtained for the soaps containing more than 2 mol. of fatty acids in a soap molecule, are assigned to the fatty acid, and the disappearance of the higher transitions is also due to the presence of the fatty acid, as shown previously.

An observation was made on the visual change of the soaps under a hot stage microscope. The apparent melting points are summarized in Table V. It is apparent that these melting points correspond to the highest transition points, excluding some exceptions; i. e., the highest transition is due to melting.

TABLE V. APPARENT MELTING POINTS AND THE HIGHEST TRANSITION TEMPERATURES OF ALUMINUM SOAPS

| Sample | M.p., °C | Tr. temp., °C |
|---|---|---|
| Ste-3.22 | 111 | 104 |
| Ste-2.29 | 122 | 104 |
| Ste-2.12 | 133 | 150 |
| Ste-1.89 | 157 | 157 |
| Ste-1.71 | 163 | 162 |
| Ste-0.95 | — | 162 |
| Palmitate | 171 | 170 |
| Myristate | 183 | 178 |
| Laurate | 188 | 185 |
| Caprate | 196 | 196 |
| Caprylate | 209 | 216 |

Many disagreements have been reported on the melting points of aluminum soaps. Licata reported the melting point of aluminum monostearate as 158~163°C; Lawrence, as 280°C for stearate[1,18]. The disagreement comes probably from the difference in the composition of the samples and in the experimental techniques used. Recently, Wagner reported the softening points of industrial aluminum soaps; 109~118°C for tristearate, 121~133°C for distearate, and 165~170°C for monostearate[19]. It is interesting that these points correspond nearly to the three major transition points, or to the melting point of Ste-3.22, Ste-2.12 and Ste-1.71 in this experiment; however, in his report, one of the three transition points might be observed as melting points due to the impurities contained in the soaps.

The soap at room temperature is in crystalline phase, as found by X-ray diffraction measurement, although the crystallinity of the soap is not so good. The transition below their melting temperature, will be ascribed to some change in crystal structure of the soaps, and the soap passes into a plastic phase with less degree of crystallinity, presumably owing to the disordering of the lateral arrangement. It will be possible to consider that the degree of the loss in the crystallinity by a transition is proportional to the heat of the transition. In this consideration, the stearate shows the most plastic phase at temperatures between the lower and higher transition points. A less degree of crystallinity is found for the soap cooled from the liquid state, in X-ray diffraction measurement, which supports the fact that phase change in the initial heating is irreversible.

**Mechanism of Formation of Aluminum Soaps.** —The mechanism of soap formation in the aqueous metathetic process is examined. Alexander stated that the precipitate, formed by addition of aluminum salt solution into alkali soap solution, is fatty acid adsorbed on the precipitated aluminum hydroxide, and that the soaps are formed in the drying process. In fact, the fatty acids which are heated at 160°C with aluminum hydroxide give infrared absorption at 980 $cm^{-1}$, which shows the formation of the aluminum soap polymer skeleton, Al-O-Al. Similarly, the soaps containing more than 2 mol. of acid per aluminum and dried by heating to 110°C, show more intense absorption at 980 $cm^{-1}$ and less absorption at 1720 $cm^{-1}$ than the same soap dried in vacuum at room temperature; these facts suggest that the formation of the soap proceeds by heating, from the fatty acids and aluminum hydroxide in the precipitate. However, the soaps containing less than 2 mol. of acid per aluminum dried by the two methods, give quite identical spectra, which shows that in these conditions, the soaps are formed when precipitated from aqueous solutions.

## Summary

Differential thermal analysis of two series of aluminum soaps—aluminum stearates of different compositions, and aluminum soaps from various parent fatty acids—are carried out, and

17) S. Shiba, This Bulletin, 34, 198 (1961).
18) F. J. Licata, "Metallic Soaps", Metasap Chemical Co., Harrison, New Jersey (1940).
19) E. S. Pattison (Editor), "Industrial Fatty Acids and their Applications", Reinhold Publishing Corp., New York (1959), p. 104.

transition temperatures and the heats of transition are obtained. Each transition point is assigned to a certain change in the structure of the soap or to the soap composition. The structure of the the soaps and the mechanism of soap formation are also discussed, based on the differential thermal analysis and infrared data.

The author wishes to express his sincere thanks to Professor H. Akamatu and Dr. H. Takahashi, both of the University of Tokyo, for their interest and kind discussions throughout this investigation; thanks are also due to Dr. M. Kawano, of the Railway Technical Research Institute, for the infrared measurements.

*Railway Technical Research Institute*
*Kunitachi, Tokyo*

# *Differential Thermal Analysis of the Systems Aluminum Soap-Hydrocarbon*

By Sukekuni SHIBA

(Received November 19, 1960)

Studies on the metal soap-hydrocarbon systems have been carried out in order to obtain basic knowledge on the industrial applications of the metal soaps, especially for the manufacture of lubricating greases. Visual observation and optical methods have been used to establish the relation of the phase state on temperature and composition. Recently, differential thermal analysis offered a powerful means for obtaining such diagrams precisely.

Disagreements in the results have been observed due to the complex behaviors of the systems and the differences in the experimental techniques used: Doscher and Vold[1], and also, Stross and Abrams[2] reported quite different types of phase diagrams on the system sodium stearate-cetane; Vold[3] and Cox[4], on the system lithium stearate in cetane and in mineral oils.

Phase behaviors of the aluminum soaps were discussed in the preceding paper with the aid of differential thermal analysis[5]. In this paper, the thermal behaviors of aluminum soap-hydrocarbon systems are studied by the same method to obtain the phase behaviors of the systems and to have some information on the structure of the systems and the aluminum soaps themselves.

## Experimental

The aluminum soaps used in this study were prepared by an aqueous metathetic process. Details of the preparation were described in the preceding paper[5]. Nujol, a liquid paraffin of commercial grade, was used as a model of the mineral oils. The purity of the Nujol was checked by infrared absorption measurement, which proved that it is a paraffin-rich hydrocarbon, and showed the absence of aromatic components or impurities. The physical properties were, $d_4^{25}=0.8429$, $n_D^{20}=1.467$, $\eta_{25}=0.217$ poise.

The apparatus and procedure were also described previously.

## Results and Discussion

**The System Aluminum Stearate-Nujol.**—The transition temperatures and heats of transition, obtained from the heating and cooling thermograms on the aluminum stearate-Nujol, are summarized in Table I. The aluminum soaps have three transition points in general. They are named for convenience the transitions I, II and III, from low to high temperatures. Thermograms for repeated heating and cooling show that the phase changes are practically reversible. In the initial heating, however, slightly different transition temperatures and appearance of peaks, for instance, that of the soap itself, are obtained incidentally, and they are not found in the following runs. This may be due to the difference in heat transfer in the specimens and incomplete mixing of the soaps in oil.

An equilibrium phase diagram for the

1) T. M. Doscher and R. D. Vold, *J. Colloid Sci.*, **1**, 299 (1946).
2) F. H. Stross and S. T. Abrams, *J. Am. Chem. Soc.*, **73**, 2825 (1951).
3) M. J. Vold and R. D. Vold, *J. Colloid Sci.*, **5**, 1 (1950).
4) D. B. Cox, *J. Phys. Chem.*, **62**, 1254 (1958).
5) S. Shiba, This Bulletin, **34**, 2611 (1961).

TABLE I. TRANSITION TEMPERATURES AND HEATS OF TRANSITION OF THE SYSTEM ALUMINUM STEARATE-NUJOL

| Soap conc. | Heating | | Cooling | |
|---|---|---|---|---|
| | Tr. temp. | Heat of tr. | Tr. temp. | Heat of tr. |
| wt. % | °C | cal./g. | °C | cal./g. |
| 100 | 99 | 5.8 | 89 | 10.6 |
| | 119 | 0.4 | 144 | 2.5 |
| | 162 | 2.1 | | |
| 90 | 94 | 5.0 | 85 | 12.8 |
| | 114 | 1.1 | 140 | 1.9 |
| | 159 | 0.7 | | |
| 70 | 96 | 14.4 | 81 | 12.4 |
| | 109 | | 95 | |
| 50 | 101 | 11.8 | 87 | 14.7 |
| 30 | 99 | 13.4 | 80 | 14.1 |
| 10 | 98 | 12.6 | 71 | 15.4 |
| 5 | 100 | 13.3 | 71 | 11.5 |

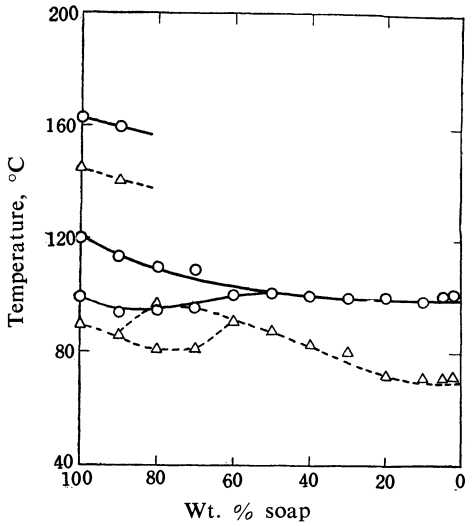



Fig. 1. Phase diagram of the system aluminum stearate-Nujal.

system, obtained from the transition temperatures, is shown in Fig. 1. The full lines represent the phase transitions on heating, and the dotted lines, on cooling. The transition temperatures when they are heated, undergo changes by the addition of Nujol. The heat of transition at high temperatures decreases conspicuously, and the transition III disappears when more than 10 wt.% of Nujol is contained. The transition II coincides with the transition I, when more than 30 wt.% is contained. In the system containing more than 30 wt.% of Nujol, the soap dissolves in Nujol at the transition I, and shows no transition above this temperature. Concerning the transition I, when a small amount of Nujol is added, the peak is broadened, showing sometimes 2 or 3 apexes. In this diagram, the most intense apexes are adopted as the transition temperatures. By further addition of Nujol, the peak of the transition I becomes sharp again, and the temperature reaches a constant value.

The phase diagram obtained by cooling shows only two transition temperatures which are lower than the temperatures obtained by heating, and in this case, both a change in transition temperatures and disappearance of the transition points are observed.

The disappearance of the transition points, which was also found in the case of the contaminant free fatty acids in the soaps[5], shows an entirely different behavior of aluminum soaps compared with other metal soaps. Most of the systems, metal soaps-hydrocarbon, undergo phase transitions on heating, which are either related to the transitions on heating, which are either related to the transitions of the oil-free soaps or are more complicated; and the transition temperatures are reduced in general by the addition of hydrocarbon[6].

The phase diagram is obtained concerning one vehicle, Nujol; however, essentially the same or at least similar results are expected for other hydrocarbons, e. g., petroleum oils, as were found for lithium soaps in various petroleum oils[4].

**Systems of Aluminum Palmitate and Laurate-Nujol.**—The phase diagrams for the systems of aluminum palmitate-Nujol and aluminum laurate-Nujol are shown in Figs. 2 and 3. Aluminum palmitate shows similar results to stearate: although slightly different transition temperatures are obtained. Aluminum laurate shows different behaviors. The transition

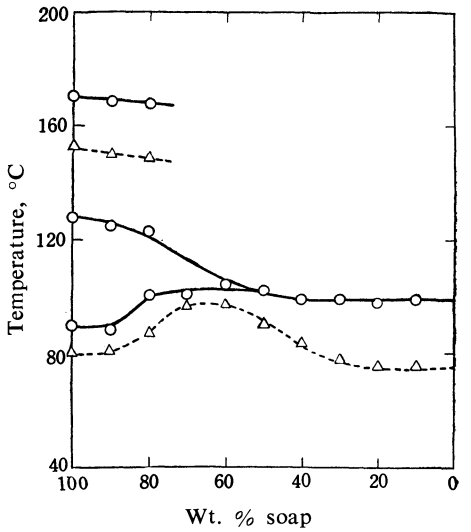



Fig. 2. Phase diagram of the system aluminum palmitate-Nujol.

6) M. J. Vold, G. S. Hattiangdi and R. D. Vold, *Ind. Eng. Chem.*, **41**, 2539 (1949).

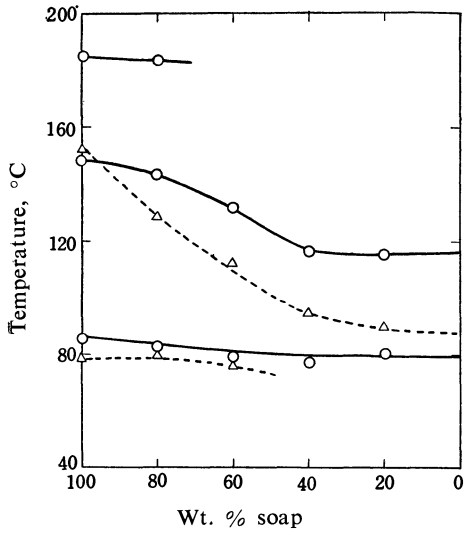



Fig. 3. Phase diagram of the system aluminum laurate-Nujol.

temperature varies definitely with the concentration of the soap, in both heating and cooling thermograms. The transition II shows marked absorption of heat, as the Nujol is added; on the contrary, the heat of the transition III decreases and disappears at the concentration of Nujol above 20 wt. %; and the heat of transition I remains unchanged. For instance, the heats of transitions I, II and III, of the system containing 40% of Nujol are 1.2, 6.3 and 0 cal./g., whereas the soap itself shows 1.4, 1.2 and 3.2 cal./g., respectively. In the system containing more than 20% of Nujol, the soap dissolves in hydrocarbon at temperatures above the transition II.

The phase transition of the system aluminum laurate-Nujol on cooling, shows tendencies similar to the transition on heating. In this case, the lower transition disappears and only the higher transition remains in dilute systems.

**Colloidal Structures of the Aluminum Soaps in Hydrocarbon.**—The aluminum soaps, which are composed mainly of aluminum hydroxy disoaps, and a small amount of contaminant aluminum hydroxide, free fatty acid, and a trace of water, make the stable skeletons of Al-O-Al with adjacent soap molecules through the hydroxyl group, which shows the polymeric nature of the soaps. These skeletons form fibrous soap polymer, and are maintained even when the soaps are dispersed in hydrocarbon media, and result in the extraordinarily strong gelling or thickening properties.

The dispersed systems, aluminum soap gels in hydrocarbon, are essentially a dispersion of aluminum soap particles combined weakly with secondary bonding, as found from X-ray diffraction, electron microscope techniques, and rheological measurements[7-9]. The results of differential thermal analysis, which show that the systems are thermally reversible, suggest that the structure of the soap particles at room temperatures, dispersed by heating in hydrocarbon media, are almost identical with the original solid phase of the soaps; i. e., the isotropic solution becomes a jelly by cooling, and the soap micelles in the jelly convert rapidly to soap crystallites.

At higher temperatures above their transition points, the soap crystallites are dissolved in the hydrocarbon media, and the system becomes a transparent viscous solution. It is supposed that the soaps retain their polymeric nature even in the solutions, because of their typical visco-elastic properties.

In the practical applications of the aluminum soaps, the soaps are used generally at concentrations of a few per cent. In such cases, the phase behavior is very simple as is expected from the phase diagrams as shown in Figs. 1—3, and the transition points correspond to the temperatures at which the systems become transparent viscous solution on heating, and turbid gel on cooling. The phase changes of the dilute systems obtained in this experiment are consistent with the results from the sudden change in dynamic rheological properties with temperature[10].

## Summary

The phase behaviors of the system aluminum stearate, palmitate, and laurate-Nujol are studied by differential thermal analysis. Phase diagrams are obtained, and it is found for stearate and palmitate that soaps dissolve in hydrocarbon at the lower transition points of the soaps, and that the higher transition points disappear by addition of hydrocarbon. Differences in phase behaviors are found between laurate and other soaps. Some discussions are made on the colloidal structures of the dispersed systems aluminum soaps-hydrocarbon.

The author wishes to express his sincere thanks to Professor H. Akamatu and Dr. H. Takahashi, both of the University of Tokyo, for their interest and kind discussions throughout this work.

*Railway Technical Research Institute*
*Kunitachi, Tokyo*

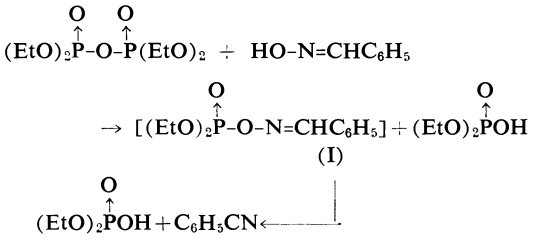
7) S. S. Marsden, Jr., K. J. Mysels and G. H. Smith, *J. Colloid Sci.*, 2, 265 (1947).
8) D. Evans and J. B. Matthews, ibid., 9, 60 (1954).
9) W. H. Bauer, N. Weber and S. E. Wiberley, *J. Phys. Chem.*, 62, 106 (1958).
10) S. Shiba, This Bulletin, 34, 194 (1961).

# *The Preparation of Diethyl Phosphate*

By Teruaki MUKAIYAMA and Tamotsu FUJISAWA

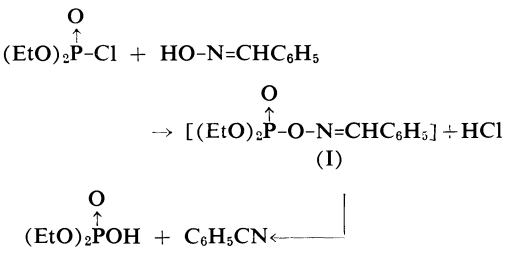
(Received November 7, 1960)

Intramolecular dehydration reactions of primary nitroparaffins[1,2], aldoximes[3,4] and hydroxamic acids[5] into nitrile oxides, nitriles and isocyanates, respectively, by means of organic reagents have been described in preceding papers. It was shown in them[4] that benzaldoxime is dehydrated by means of esters of phosphoric acid and it was demonstrated that the dehydration proceeds through an intermediate, diethyl benzaldimino phosphate (I), formed by the bond fission of pyrophosphate linkage by an attack of benzaldoxime.



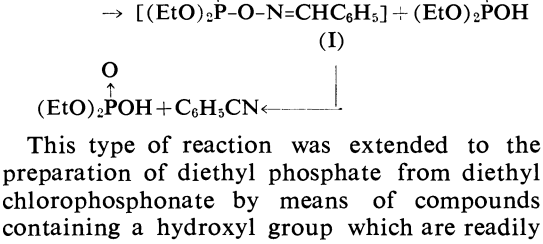
This type of reaction was extended to the preparation of diethyl phosphate from diethyl chlorophosphonate by means of compounds containing a hydroxyl group which are readily dehydrated to give unsaturated compounds, such as benzaldoxime and *tert*-butyl alcohol.

The reaction of benzaldoxime with diethyl chlorophosphonate initially yields diethyl benzaldimino phosphate (I), which in turn decomposes to give diethyl phosphate and benzonitrile in good yields.



When diethyl chlorophosphonate and benzaldoxime are allowed to react in dry benzene at room temperature, a violent reaction takes place and a large amount of benzaldoxime hydrochloride, which retards the formation of I, precipitates. Since the hydrochloride decomposes into benzaldoxime and hydrogen chloride on gentle heating, the reaction is best effected when two reactants are mixed at one time and heated at about 70°C.

On the other hand, the reaction of *tert*-butyl alcohol with diethyl chlorophosphonate does not take place at room temperature, but it is effected well by refluxing them in carbon tetrachloride for 3 hr. Isobutylene, hydrogen chloride and *tert*-butyl chloride formed by the addition of hydrogen chloride to isobutylene are obtained along with diethyl phosphate.



As described in the experimental part, *tert*-butyl alcohol is dehydrated in a nearly quantitative yield; however, the yield of diethyl phosphate is comparatively low. This may be attributed to a useless dehydration of *tert*-butyl alcohol catalyzed by the phosphate formed. The use of 2 mol. of *tert*-butyl alcohol did not lead to a good result though the yields of isobutylene and *tert*-butyl chloride were increased.

These methods for the preparation of diethyl phosphate from diethyl chlorophosphonate are a simpler procedure than that reported by Toy[6] which involves 2 steps of hydrolysis.

Moreover, an attempt to prepare diethyl chlorophosphonate in a better yield by the reaction of phosphorus oxychloride with 2 mol. of ethyl alcohol gave a successful result. Several methods[7-10] are reported in the literature for this reaction; however, the yield is less than 25% even when a basic medium

1) T. Mukaiyama and T. Hoshino, *J. Am. Chem. Soc.*, **82**, 5339 (1960).
2) T. Mukaiyama and T. Hata, This Bulletin, **33**, 1382 (1960).
3) T. Mukaiyama and T. Hata, ibid., **33**, 1712 (1960).
4) T. Mukaiyama and T. Hata, ibid., **34**, 99 (1961).
5) T. Mukaiyama and H. Nohira, *J. Org. Chem.*, **26**, 782 (1961).
6) A. D. F. Toy, *J. Am. Chem. Soc.*, **70**, 3882 (1948).
7) P. Nylén, Dissertation, Uppsala, 1930.
8) J. Walczynska, *Roczniki Chem.*, **6**, 110 (1926).
9) H. Wichelhaus, *Ann. Suppl.*, **6**, 257 (1868).
10) T. W. Mastin, G. R. Norman and E. A. Weilmuenster, *J. Am. Chem. Soc.*, **67**, 1662 (1945).

such as pyridine is used. In the present experiment, in order to avoid unnecessary heating, the reaction was carried out in petroleum ether under 0°C over a period of 4.5 hr. After the completion of the reaction, the solvent was removed at room temperature under reduced pressure and distilled. By this method, a 76% yield of diethyl chlorophosphonate was obtained.

As shown in Table II, the yield of diethyl chlorophosphonate became higher when the amount of reactants was smaller, and also it can be noted that the elevation of reaction temperature over 0°C resulted in a decrease of the yield.

## Experimental

**Diethyl Phosphate.**—*By Means of Benzaldoxime.*—To 17.2 g. (1/10 mol.) of diethyl chlorophosphonate dissolved in 10 ml. of carbon tetrachloride was added at one time with vigorous stirring a solution of 12.1 g. (1/10 mol.) of benzaldoxime in 10 ml. of carbon tetrachloride. Then the reaction mixture was refluxed on a water bath for an hour. After the evolution of hydrogen chloride, the carbon tetrachloride was removed and 9 g. (87% yield) of benzonitrile (b. p. 78°C/16 mmHg) and 11 g. (71% yield) of diethyl phosphate (b. p. 112~127°C/0.02 mmHg) were obtained.

If a solution of the aldoxime was added more slowly at room temperature, a white precipitate melting at about 80°C was obtained. This substance generated hydrogen chloride on heating and gave benzaldoxime by means of distillation. Besides that, from the filtrate were obtained benzonitrile and diethyl phosphate in 51% and 35% yields, respectively.

*By Means of tert-Butyl Alcohol.*—A mixture of 17.2 g. (1/10 mol.) of diethyl chlorophosphonate and 7.5 g. (1/10 mol.) of *tert*-butyl alcohol dissolved in 10 ml. of carbon tetrachloride was refluxed on a water bath for 3 hr. During this period, isobutylene and hydrogen chloride were generated from the mixture. Distillation gave *tert*-butyl chloride and diethyl phosphate. The yields and boiling points are listed in Table I.

Table I

| Product | Yield | B. p. |
|---|---|---|
| Isobutylene | 1.5 l. 67% | |
| *tert*-Butyl chloride | 3.5 g. 38% | 49~50°C/760 mmHg |
| Diethyl phosphate | 7.5 g. 48% | 111~114°C/0.005 mmHg |

**Diethyl Chlorophosphonate.**—The preparation of diethyl chlorophosphonate from phosphorus oxychloride was tried under several conditions as listed in Table II. In the case of 1 mol. of phosphorus oxychloride, the best procedure was found to be as follows: To 153.5 g. (1 mol.) of phosphorus oxychloride dissolved in 80 ml. of petroleum ether cooled by an ice-salt bath was added with vigorous stirring a solution of 105 g. (2.28 mol.) of 99% ethyl alcohol in 50 ml. of petroleum ether at a rate such that the addition was completed in about 3.5 hr. The stirring was continued for an hour after all the solution of ethyl alcohol had been added. During this period, the temperature was maintained under 0°C and then the stirring was further continued without the ice-salt bath until the mixture was warmed to room temperature. After the hydrogen chloride dissolved in the reaction mixture and the petroleum ether were removed under reduced pressure at room temperature, diethyl chlorophosphonate was obtained by distillation, b. p. 72°C/6 mmHg, yield 130 g. (76%).

Table II

| Solvent | Rate of addition hr. | Reacn. time hr. | Moles of $POCl_3$ | Yield % | Reacn. temp. °C |
|---|---|---|---|---|---|
| $CCl_4$ | 1 | 1.5 | 0.2 | 80 | 0 |
| $CCl_4$ | 1 | 1.5 | 0.2 | 43 | room temp. |
| PE | 1 | 2 | 0.2 | 85 | 0 |
| PE | 3.5 | 5 | 1 | 76 | 0 |
| $CCl_4$ | 2 | 4.5 | 1.65 | 50 | 0 |

PE = petroleum ether

*Department of Chemistry*
*Tokyo Institute of Technology*
*Meguro-ku, Tokyo*

# *Non-benzenoid Aromatic Heterocycles. V*,[1]. An Attempted Synthesis of 4,7-Dihydro-4,7-phenanthroline Derivatives*

By Hiroshi KATO and Masaki OHTA

(Received November 15, 1960)

Heptalene (I) was first proposed by Baker[2] in 1945 as a possible aromatic, wholly conjugated compound. Many synthetic trials of its derivatives have since been carried out[3], and yet their synthesis has not been successful with only one exception of condensed heptalene derivative II[4], while this compound should rather be regarded as an azulene derivative. The results of a few theoretical treatments[5] on this compound I also do not coincide with one another in the stability of this hydrocarbon.

In connection with this problem, the authors attempted the synthesis of 4,7-dihydro-4,7-phenanthroline derivatives III. These compounds are planar without undue strain and are wholly conjugated, and they have seven $\pi$-electrons in each hetero-ring. In this respect, these compounds are similar in their electronic structure to the supposed hydrocarbon heptalene (I).

As a possible route to III, the hydrogenation of 4,7-phenanthroline dimethiodide (IV) was first attempted. The reduction of 4,7-phenanthroline 4,7-dimethiodide was reported by Karrer et al.[6] They used sodium hyposulfite and obtained a red substance, to which the formula V was suggested. The present authors attempted the reduction of IV by catalytic hydrogenation or by zinc powder. In neither case was the expected III (R, R''=Me, R', R'''=H) obtained, but instead an intense red solution, presumably the same substance as reported by Karrer, was formed.

Next, the dehydrogenation of tetrahydro-4,7-phenanthroline was attempted. It has been found[7] with quinoline that the methiodide reacts with Grignard reagents to form 1,2-dihydroquinoline derivative, and the present authors expected a reaction of the same type in 4,7-phenathroline dimethiodide. 4,7-Phenanthroline 4,7-dimethiodide reacted with methylmagnesium iodide as expected, to give the desired 3,4,7,8-tetrahydro-3,4,7,8-tetramethyl-4,7-phenanthroline (VI). It is markedly unstable to air and quickly combines with oxygen on being kept in air and an intensely green substance was formed. When VI was treated with chloranil, a dark precipitate (presumably an addition complex) was rapidly formed, and even after four hours' reflux in xylene, no tetrachlorohydroquinone was formed, which showed that no dehydrogenation had occurred in tetrahydrophenanthroline (VI). When VI was treated with concentrated sulfuric acid, the starting material was recovered accompanied by an intensely green substance.

Finally, an addition of organometallic compounds to 4,7-phenanthroline (VII) was attempted. It has been reported that phenazines give *N,N'*-disubstituted *N,N'*-dihydrophenazines by the action of Grignard reagents or organolithium compounds, followed by alkyl halides[8]. Hence, if the structure III is sufficiently stable, the organometallic compounds should add to VII to form 4,7-disubstituted 4,7-dihydro-4,7-phenanthrolines (III). Although phenanthroline was recovered unchanged by the action of phenylmagnesium bromide, when it was treated with phenyllithium followed by methyl iodide, a yellow compound of a formula $C_{19}H_{16}N_2$ with strong green fluorescence (VIII) was obtained. Evidently, the addition of phenyllithium took place, but structures VIIIa and VIIIb would be possible to this substance because the addition of phenyllithium to 1,2-position of pyridines and quinolines has been reported[9]. The yellow color of this substance suggests that it is not the expected 4,7-dihydro-4,7-phenanthroline derivatives. Further, the hydrochloride and the picrate of VIII are red, while Karrer et al.[6] reported that *N*-methyl-1,2,3,4-tetrahydro-4,7-phenanthroline hydrochloride also is red. This fact also throws doubt on the supposed structure VIIIa. The

* Presented at the Meeeting of the Chemical Society of Japan, Tokyo, October, 1960.

1) Part IV. H. Kato and M. Ohta, This Bulletin, **34**, 357 (1961).

2) W. Baker, *J. Chem. Soc.*, **1945**, 258.

3) Cf. for example, W. Baker and J. F. W. McOmie, "Non-benzenoid Aromatic Compounds", in "Progress in Organic Chemistry", Vol. 3, Butterworths Scientific Publications, London (1955), p. 44.

4) K. Hafner and J. Schneider, *Ann.*, **624**, 37 (1959).

5) R. B. Brown, *Trans. Faraday Soc.*, **45**, 296 (1949); **46**, 146 (1950); D. P. Craig, *J. Chem. Soc.*, **1951**, 3175, etc.

6) P. Karrer, A. Pletscher and W. Manz, *Helv. Chim. Acta*, **30**, 1146 (1947).

7) W. Bradly and F. Jeffrey, *J. Chem. Soc.*, **1954**, 2770.

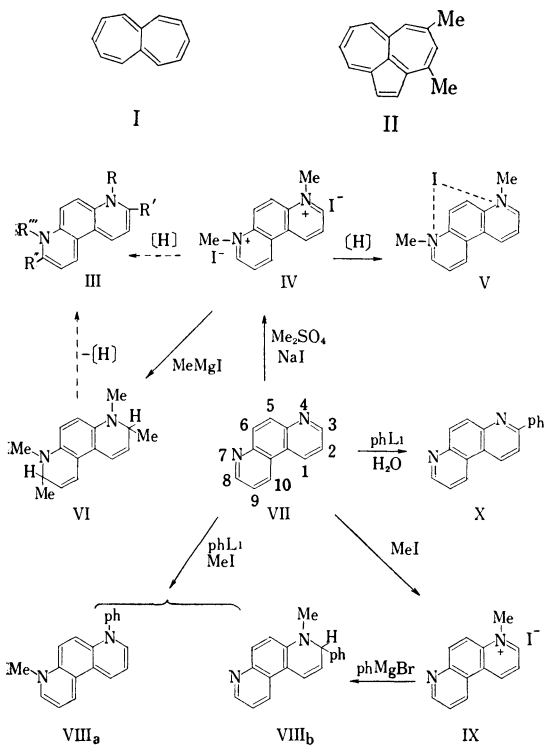
8) H. Gilman and Dietrich, *J. Am. Chem. Soc.*, **79**, 6178 (1957).

9) K. Ziegler and H. Zeiser, *Ber.*, **63**, 1847 (1930); *Ann.*, **485**, 174 (1931).

structure of VIII was proved to be VIIIb by treating 4,7-phenanthroline monomethiodide (IX) with phenylmagnesium bromide to give the indentical product with VIII.

In connection with this reaction, the reaction of phenyllithium to 4,7-phenanthroline was studied in more detail. When two or more molar equivalents of phenyllithium was used, no disubstituted tetrahydrophenanthroline derivative was formed, and the dihydro-derivative VIIIb was the sole product. When the addition product of phenyllithium was hydrolyzed with water, 3-phenyl-4,7-phenanthroline (X) was formed, probably via the dihydro compound.

From these facts, one may reasonably assume that the compound of the type III, although planar and wholly conjugated, are not stable and of which no aromaticity can be expected.




## Experimental

**4,7-Phenanthroline (VII).**—a) To a mixture of 6-aminoquinoline (12 g.), orthoarsenic acid (13 g.) and glycerol (36 g.), there was added dropwise concentrated sulfuric acid (32 g.) with stirring and heating at 130~140°C. The mixture was heated and stirred for four hours and then poured into a solution of potassium hydroxide in ice-water. The black resinous residue and the aqueous layer were extracted continuously for fifteen hours with benzene, and the benzene extract was treated with a large quantity of charcoal. On evaporation of benzene, practically pure 4,7-phenanthroline was obtained (11 g.), m. p. 170~173°C[10]. This substance was used directly for the following reactions.

b) To a mixture of *p*-phenylenediamine (60 g.), orthoarsenic acid (150 g.) and glycerol (300 g.), there was added dropwise concentrated sulfuric acid (150 g.), with stirring and heating at 130~140°C. The mixture was heated and stirred for six hours; then the mixture was diluted with ice-water and neutralized with ammonia. The black resinous product was extracted several times with hot benzene, and the benzene extract was treated with charcoal. On evaporation of benzene, crude 4,7-phenanthroline (48 g.) was obtained, m. p. 165~169°C. Recrystallization from benzene afforded pale yellow needles, m. p. 173°C.

**4,7-Phenanthroline Monomethiodide (IX).** — A benzene solution of 4,7-phenanthroline (2 g.) and methyl iodide was gently refluxed for thirty minutes; then methyl iodide was added further and reflux was continued for another half an hour. The yellow crystals which separated out (3 g.) were collected and recrystallized from water to give bright yellow needles (2 g.), m. p. 270°C[12].

**4,7-Phenanthroline Dimethiodide (IV).** — A mixture of 4,7-phenanthroline (20 g.) and dimethyl sulfate (40 g.) was heated at 160°C for two hours and then diluted with water, and sodium iodide (50 g.) was added. The brown precipitate which separated out was collected and recrystallized from water to give pale brown plates (18 g.), m.p. 264°C[13].

**Reduction of 4,7-Phenanthroline Dimethiodide.** —To a solution of 4,7-phenanthroline dimethiodide (2.3 g.) in water (50 ml.), there was added zinc powder (0.7 g.) in small portions with stirring and warming. The solution quickly turned to an intense wine-red color. The colored substance could not be extracted with ether, benzene, chloroform, etc.

When this reaction was carried out in cold water, or in aqueous or absolute ethanol, the same result was observed. When 4,7-phenanthroline dimethiodide was hydrogenated with Pd-C (5%) or Pd-$CaCO_3$ (2%) in water, ethanol or acetone, the same coloration took place accompanied by the starting material.

**3,4,7,8-Tetrahydro-3,4,7,8-tetramethyl-4,7-phenanthroline (VI).**—To an ether solution (25 ml.) of methylmagnesium iodide (prepared from 1 g. of magnesium and 5.7 g. of methyl iodide), there was added portionwise fine powdered 4,7-phenanthroline dimethiodide (2.3 g.) with stirring and under an atmosphere of nitrogen. Stirring was continued for an additional two hours after the addition was complete, while heat was evolved slightly and the dimethiodide gradually dissolved. The solution was decomposed with aqueous ammonium chloride and extracted with ether. The ether extract was dried over potassium carbonate, the ether was evaporated under nitrogen and the residue was washed with methanol and ether to give a dark

10) Reported m. p.[11] 173°C.
11) I. Heilbron, "Dictionary of Organic Compounds", Vol. IV, Oxford University Press, New York (1953), p. 87.
12) Reported m. p.[11] 268~269°C.
13) Reported m. p.[11] 265°C.

yellow powder (0.7 g.), m. p. 113~117°C. Recrystallization from ether afforded yellow prisms (0.2 g.), m. p. 147°C. This compound is very sensitive to air and rapidly turns intense green on standing.

Found: C, 79.80; H, 8.68; N, 11.76. Calcd. for $C_{16}H_{20}N_2$ (VI): C, 79.95; H, 8.39; N, 11.66%.

**Air Oxidation of VI.** — A current of air was bubbled into an ethanolic solution of VI (0.1 g.) for two days. The resultant intensely green substance (0.07 g.) was purified by chromatography (alumina-benzene) to give a dark green amorphous powder. This compound does not show a definite m. p. but melts at about 230°C.

Found: C, 65.68; H, 6.92%.

When it was allowed to stand in air for a long time, it became practically insoluble in most solvents.

**Attempted Dehydrogenation of VI with Chloranil.** — Chloranil (0.2 g.) and VI (0.2 g.) were refluxed for four hours in xylene (10 ml.). A black precipitate was rapidly formed. This precipitate (0.4 g.) was scarcely soluble in most organic solvents and is positive to Beilstein's halogen test. On treatment of the filtrate with aqueous potassium hydroxide, no tetrachlorohydroquinone was obtained.

**Treatment of VI with Concentrated Sulfuric Acid.** — A solution of VI (0.2 g.) in concentrated sulfuric acid (10 ml.) was warmed at 60~70°C for an hour and was kept standing overnight at room temperature. The starting material was recovered unchanged accompanied by a small amount of green insoluble substance.

**3,4-Dihydro-4-methyl-3-phenyl-4,7-phenanthroline (VIIIb).**—a) An ether solution (20 ml.) of phenyllithium (prepared from 3.14 g. of bromobenzene and 0.3 g. of lithium) was added dropwise under an atmosphere of nitrogen into a tetrahydrofuran solution (30 ml.) of 4,7-phenanthroline (3 g.) with cooling and stirring. The solution turned wine-red. After half an hour, a tetrahydrofuran solution (10 ml.) of methyl iodide (3 g.) was added to the solution with cooling and stirring. The solution turned greenish yellow after the addition was complete. After two hours, the solution was decomposed by addition of an aqueous solution of ammonium chloride and the resultant solution was extracted with ether followed by chloroform and each extract was dried over calcium chloride.

The ether extract was concentrated to give a yellow residue (2.8 g.). Recrystallization from acetone afforded yellow fine needles with strong green fluorescence, m. p. 155°C.

Found: C, 83.50; H, 6.08; N, 10.53. Calcd. for $C_{19}H_{16}N_2$ (VIIIb): C, 83.79; H, 5.92; N, 10.27%.

The same compound was obtained when two or more molar equivalents of phenyllithium were reacted with 4,7-phenanthroline.

This compound turns red-colored on addition of hydrochloric acid.

Picrate: red needles (from aqueous dimethylformamide), m. p. 173°C.

Found: N, 13.85. Calcd. for $C_{25}H_{19}N_5O_7$: N, 13.97%.

The chloroform extract in the above experiment was concentrated and the residue (0.5 g.) was recrystallized from benzene to give white needles, m. p. 171~172°C, undepressed on admixture with an authentic specimen of 4,7-phenanthroline.

When 4,7-phenanthroline was treated with phenylmagnesium bromide followed by methyl iodide, the starting material was recovered.

b) To an ether solution (30 ml.) of phenylmagnesium bromide (prepared from 3.2 g. of bromobenzene and 0.5 g. of magnesium), there was added fine powdered 4,7-phenanthroline monomethiodide with stirring. After an hour, this solution was poured into aqueous ammonium chloride, extracted with ether and benzene and the extract was dried over calcium chloride. The solvent was removed and the residue (1.2 g., m. p. 152~154°C) was recrystallized from acetone to give yellow fine needles with strong green fluorescence, m. p. 155°C. Picrate, red needles, m. p. 173°C. Neither melting point was depressed on admixture with the specimens prepared by procedure a).

**3-Phenyl-4,7-phenanthroline (X).** — An ether solution (40 ml.) of phenyllithium (prepared from 6.3 g. of bromobenzene and 0.6 g. of lithium) was added dropwise under an atmosphere of nitrogen into a tetrahydrofuran solution (30 ml.) of 4,7-phenanthroline (3 g.) with stirring and cooling. After thirty minutes, the reaction mixture was decomposed by addition of aqueous ammonium chloride and extracted with ether, the ether extract was dried over calcium chloride, and the solvent was removed. Recrystallization of the residue from acetone afforded yellow fine needles with green fluorescence (1 g.), m. p. 187°C[14].

Found: C, 83.85; H, 4.92; N, 10.81; Mol. wt. (Rast) 260. Calcd. for $C_{18}H_{12}N_2$ (X): C, 84.35; H, 4.72; N, 10.85%; Mol. wt. 255.

The authors are indebted to Dr. Asaji Kondo for performing the microanalyses.

*Laboratory of Organic Chemistry*
*Tokyo Institute of Technology*
*Meguro-ku, Tokyo*

14) Reported m. p.[11] 183°C.
15) C. Willgerodt and S. Jabolinsky, *Ber.*, 33, 2918 (1900).

# *Diffusion in Glassy Polymers. II. Effects of Polymer-penetrant Interaction; Diffusion of Ethyl Methyl Ketone in Atactic Polystyrene*

By Hisashi ODANI, Jun HAYASHI and Mikio TAMURA

(Received November 21, 1960)

Sorption processes of organic vapors in glassy polymers exhibit a variety of anomalous or "non-Fickian" features[1]. In the hope of obtaining information about how the polymer-penetrant interaction affects these feature, we have measured in the present work the rates of absorption of ethyl methyl ketone by atactic polystyrene, using both the integral and differential absorption techniques and have compared the data obtained with those reported previously for the system benzene-atactic polystyrene[1,2]. Ethyl methyl ketone and benzene have about the same molecular volumes, but their solvent powers for polystyrene are different; ethyl methyl ketone is less soluble in polystyrene than benzene is. Thus it is expected that the comparison of the present data with the previous ones for benzene will provide us with some useful information pertaining to the purpose mentioned above.

## Experimental

The atactic polystyrene (A-PS) used was the same as that described previously[1]. Its viscosity-average molecular weight was $2.2\times10^5$. Films $2.40\times10^{-3}$ cm. thick were used. Ethyl methyl ketone was purified by fractional distillation after drying over anhydrous potassium carbonate. Both integral and differential sorptions were studied under a variety of conditions at 25°C. This temperature is well below the glass transition temperature of the polymer[3].

## Results and Discussion

**Absorption Isotherms.**—Absorption isotherm data for this system at 25°C are given in Fig. 1. Here the ordinate represents the mass of absorbed penetrant in grams per gram of dry polymer and the abscissa the relative pressure of ambient vapor. The data from integral absorption experiments and those from differential ones fall satisfactorily on a single curve. The corresponding data for the system A-PS-benzene at the same temperature are included in the figure for comparison. We see that the solubility of ethyl methyl ketone in A-PS is lower than that of benzene over the entire range of vapor pressure investigated.

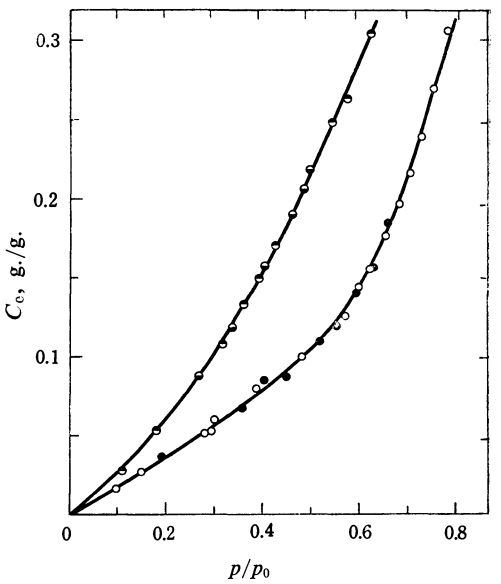



Fig. 1. Absorption isotherms of A-PS-ethyl methyl ketone and A-PS-benzene at 25°C.

| | Integral absorption | Differential absorption |
|---|---|---|
| A-PS-ethyl methyl ketone | ○ | ● |
| A-PS-benzene | ◓ | ◒ |

**Successive Differential Absorptions.**—The data of successive differential absorptions for the A-PS-ethyl methyl ketone system at 25°C are given in Fig. 2. The increments of ethyl methyl ketone concentration in successive steps were kept approximately constant, about 0.01 g. of penetrant per gram of dry polymer, which is almost the same as those used in the previous experiments for benzene at the same temperature. The successive differential absorption curves shown in Fig. 2 change their type with the initial concentration according to the following scheme;

sigmoid type → pseudo-Fickian type
→ two-stage type → pseudo-Fickian type
→ Fickian type.

1) A. Kishimoto, H. Fujita, H. Odani, M. Kurata and M. Tamura, *J. Phys. Chem.*, **64**, 594 (1960).
2) H. Odani, S. Kida, M. Kurata and M. Tamura, This Bulletin, **34**, 571 (1961).
3) H. Mark and A. V. Tobolsky, "Physical Chemistry of High Polymeric Systems", Interscience Pub. Inc., New York (1950), p. 347.

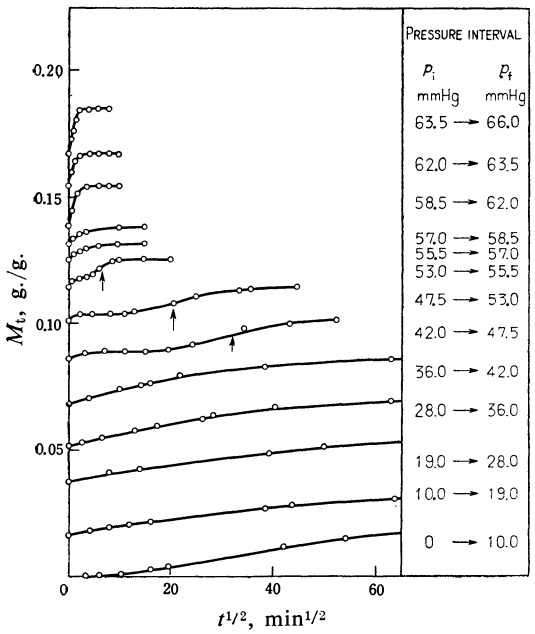



Fig. 2. Successive differential absorptions. Initial and final pressures, $p_i$ and $p_f$, of each step are given in the right columns.

Though the general character of the family of curves for the present system is similar to that obtained for the benzene system[1], we may point out some significant and interesting differences between the two systems.

First, in the region of fairly low initial concentrations, only the first step is sigmoid and the second step already exhibits the pseudo-Fickian character. On the other hand, for benzene the shift from the sigmoid type to the pseudo-Fickian type began at a much higher concentration than for the present system. This relation is also the case with the initial concentration at which the transition from the pseudo-Fickian type to the two-stage type occurs. Secondly, the ninth and the tenth steps in Fig. 2 exhibit the typical pseudo-Fickian character, differing from the data for benzene where the transition from two-stage to the normal Fickian process occurred without the intervention of any pseudo-Fickian process.

It was demonstrated in the previous paper[1] that the successive differential absorption curves changed their type from pseudo-Fickian to Fickian when the penetrant concentration passed the point at which the polymer-penetrant mixture underwent glass transition at the temperature of the experiment. From the data shown in Fig. 2 and also from other differential absorption data obtained with concentration intervals of nearly the same magnitude, we may estimate such a critical concentration for the present system to be 0.139 g. ethyl methyl ketone per gram of dry A-PS. This value is lower than that for benzene at the same temperature. In that case the critical concentration of benzene was 0.191 g./g. As noted above, the solubility of ethyl methyl ketone in A-PS is lower than that of benzene, and the molar volumes of the two penetrants do not differ appreciably from each other. It appears, therefore, that for a given polymer at a given temperature a penetrant of poorer solubility gives a lower critical concentration if comparison is made for penetrants of about the same molar volumes. This implies that a penetrant molecule of less solvent-ability for the polymer will cause a greater decrease in the activation energy required for the segmental motion of polymer chains. In this connection it is of interest to note that Jenckel and Heusch[4] demonstrated that with solvents of about the same molar volumes the weaker the thermodynamic interaction with the polymer molecule the lower was the solvent concentration at which the mixture underwent the glass transition at a given temperature.

**Concentration Dependence of the Second-stage Mechanism.** — As mentioned in the previous paper[1], it is generally accepted that the second stage portion of a two-stage absorption is governed by the rate at which the network of polymer chains changes configuration under swelling pressure, while the first stage involves the ordinary diffusion mechanism. In accordance with the treatment presented in the previous investigation[1], we have chosen the quantity $t_*$ to characterize the position of the second stage portion on the time axis, where $t_*$ is the time corresponding to the inflection point on the second stage of the two-stage curve. In general, the value of $t_*$ for the given initial concentration, $C_1$, increases with the decrease of the pressure interval $\Delta p$ of each experiment and converges to the limit characteristic of the given $C_1$. This is also true in the case of the present system.

The values of $t_*$ determined from the data of Fig. 2 and from other differential absorption data with about the same magnitude of $\Delta p$ are plotted semi-logarithmically against $C_1$ in Fig. 3*. For the sake of comparison, the corresponding data for other systems reported in the previous paper[1] are included in the figure. It is seen that the data for the present system are approximately linear and that the slope of this line is as steep as those for the other amorphous polymer-organic vapor systems indicated. It is of special interest that the plot for the A-PS-ethyl methyl ketone system is nearly

4) E. Jenckel and R. Heusch, *Kolloid-Z.*, **130**, 89 (1953).

* The magnitudes of $\Delta p$ used in these differential absorption experiments are sufficiently small to give the values of $t_*$ characteristic of a given $C_1$. This will be seen later in Fig. 6.

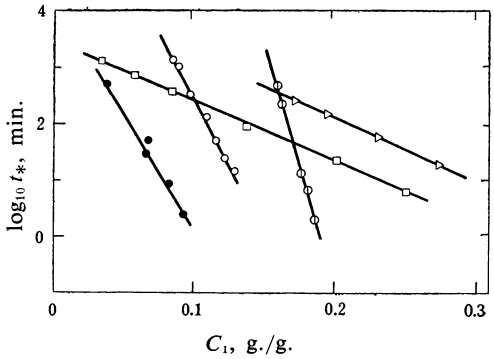



Fig. 3. Logarithmic correlation plots of $t_*$ and initial concentration $C_1$ for some polymer-vapor systems. $t_*$ is the time corresponding to the inflection point of the second stage of the two-stage process;

- ○ A-PS-ethyl methyl ketone at 25°C;
- ◑ A-PS-benzene at 25°C;
- ● Polymethyl methacrylate-methyl acetate at 30°C;
- □ Cellulose acetate-methyl acetate at 20°C;
- △ Cellulose nitrate-acetone at 25°C.

parallel with that for the A–PS-benzene system at the same temperature. This suggests that for a given polymer the slope of $\log t_*$ vs. $C_1$ plot is approximately independent of penetrant species. As noted above, it is generally conceived that the rate-determining factor for the second stage absorption process is the rate of relaxation of the polymer chains. Thus it appears reasonable that the second stage absorption process primarily reflects the characteristic relaxation-motion of the network chains of a given polymer, irrespective of any difference in penetrant species. This may explain the independence of the slope of $\log t_*$ vs. $C_1$ plot upon penetrant species. The position of the $\log t_*$ vs. $C_1$ plot for methyl ethyl ketone is in the region of values of $C_1$ lower than that for benzene. This is the reflection of the fact that the value of $C_1$ at which absorption curves change their shape from pseudo-Fickian to two-stage type is lower for the former system than for the latter.

**Integral Absorptions.** — We have studied integral absorptions by choosing the initial concentrations in the regions corresponding to the four types of differential absorption, i. e., sigmoid type, pseudo-Fickian type, two-stage type and Fickian type.

Fig. 4 gives data of integral absorptions from zero concentration, and this initial concentration corresponds to a differential absorption of sigmoid type. The integral absorption processes are sigmoid for all pressure intervals studied and the initial rate of desorption is greater than that of the corresponding absorption. The absorption curves show a pronounced dependence on the final concentration, $C_f$.

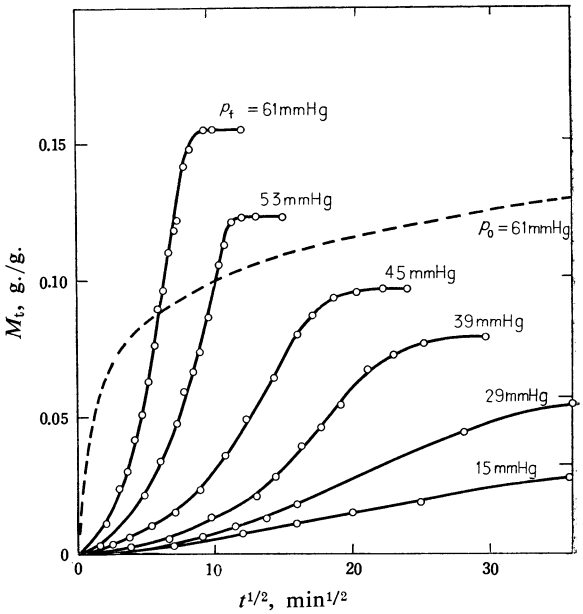



Fig. 4. Integral absorption and desorption curves from and to zero concentration. $p_f$ is the final pressure of a particular run. Solid line, absorption; Dashed line, desorption.

In accordance with the treatment of the A–PS-benzene system[2], we chose the value of $1/(t/l^2)_{1/2}$ as a measure of the absorption rate of each curve, where $l$ is the thickness of the film, $t$ is time and $(t/l^2)_{1/2}$ is the value of $t/l^2$:

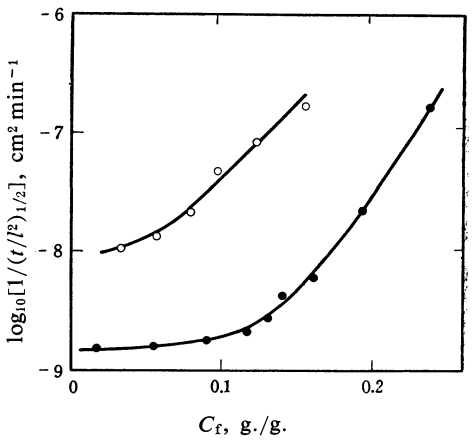



Fig. 5. Logarithmic correlation plots of $1/(t/l^2)_{1/2}$ and final equilibrium concentration $C_f$ for A–PS-ethyl methyl ketone and for A–PS-benzene at 25°C. $(t/l^2)_{1/2}$ is the value of $t/l^2$ when the amount of vapor in polymer reaches one half of the final equilibrium value; $l$ is the thickness of film and $t$ is time. ○, A–PS-ethyl methyl ketone. ●, A–PS-benzene.

when the amount of vapor in the film reaches one half of the final equilibrium value. The values of $1/(t/l^2)_{1/2}$ determined from Fig. 4 are plotted semi-logarithmically against $C_f$ in Fig. 5, where the corresponding data for benzene system are also included for the sake of comparison. We see that the values of $1/(t/l^2)_{1/2}$ for ethyl methyl ketone increase with increasing $C_f$ and, though the slope of the curve is quite similar to that for benzene they are always higher than those for benzene when compared at fixed values of $C_f$. This fact implies that the rate of diffusion of ethyl methyl ketone into A-PS is faster than that for benzene in the region of $C_f$ studied.

Integral absorptions from an initial concentration corresponding to a differential absorption of pseudo-Fickian type were investigated at $C_1=0.055$ g./g. Although the results are not given here, the shape of absorption curves for small values of $\Delta p$ was of pseudo-Fickian type, and with further increase in $\Delta p$ the absorption curves changed to the sigmoid type and this feature persisted up to the largest of the $\Delta p$ investigated. The values of $1/(t/l^2)_{1/2}$ increased with the difference between the initial and final concentrations, $\Delta C(=C_f-C_1)$, and the dependence of $1/(t/l^2)_{1/2}$ upon $\Delta C$ was about the same as that obtained for the series of absorption curves from $C_1=0$.

Fig. 6 shows integral absorption curves from $C_1=0.100$ g./g. This $C_1$ was in the region where differential absorption curves exhibited two-stage behavior. It is seen that for small $\Delta p$ the curves are similar in shape and the values of $t_*$ are practically the same. With further increase in $\Delta p$ the inflection point on the second stage portion shifts markedly to the short time region. The two-stage behavior is still apparent at $p_f=62$ mmHg, but the absorption curve for $p_f=80$ mmHg exhibits a sigmoid character. For this $C_1$ the absorption rates changed more mildly with $\Delta C$ than in the regions of $C_1$ corresponding to differential absorptions of sigmoid and pseudo-Fickian types.

Integral absorptions and desorptions from an initial concentration corresponding to a differential absorption of Fickian type were studied at the critical concentration at which the A-PS-ethyl methyl ketone mixture undergoes the glass transition at the temperature of the experiment. The features of the curves obtained were those of the true Fickian diffusion in which the diffusion coefficient increases with increasing concentration. However, the results from experiments with films of various thicknesses revealed a thickness anomaly as in the case of the corresponding experiments with the A-PS-benzene system[2]. A detailed study of the sorption behavior in this region of $C_1$ is now in progress in this laboratory and will be reported in near future. The dependence of $1/(t/l^2)_{1/2}$ on $\Delta C$ in this region of $C_1$ was much milder than those in the regions of lower $C_1$ corresponding to non-Fickian differential absorptions.

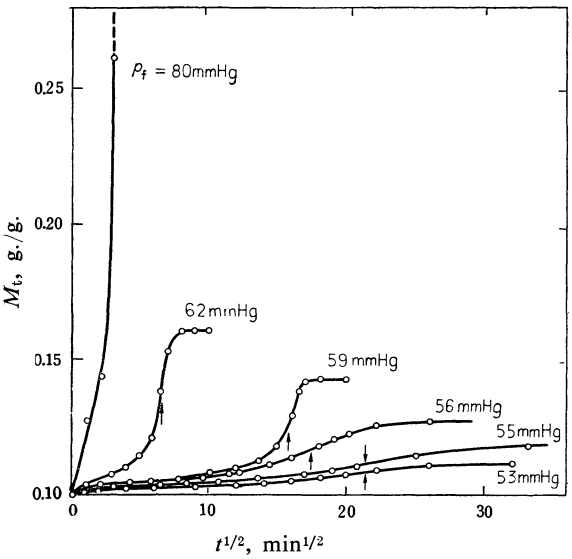



Fig. 6. Absorptions from a fixed non-zero initial concentration to different final pressures. $p_f$ is the final pressure of a particular run. Initial pressure $p_1=47.5$ mmHg. The arrows indicate the positions of the inflection points of the second stage curves.

**Summary**

The successive differential absorptions for the A-PS-ethyl methyl ketone system change with the initial concentration according to the same scheme as that presented previously as typical systems of amorphous polymer-organic vapor; that is,

sigmoid type → pseudo-Fickian type
→ two-stage type → pseudo-Fickian type
→ Fickian type

The last transition, from pseudo-Fickian to Fickian types, for ethyl methyl ketone occurs at lower concentration than that for benzene. The second stage portion of the two-stage process shifts rapidly to the short time regions as the initial concentration of each step increases. The rate of this shift depends upon initial concentration in nearly the same manner as in the A-PS-benzene system. The general features of integral absorptions for the present system are very similar to those for benzene system, irrespective of the difference in the penetrant-polymer interaction between the two systems. The dependence of absorption rate

upon $\Delta C$ is also similar in general character to that for benzene system.

We wish to thank Professors H. Fujita, M. Kurata and Dr. A. Kishimoto of this University for their helpful advice during the course of this invesigation. The study reported in this paper was partly supported by the Ministry of Education, to which grateful acknowledgement is made.

*Department of Industrial Chemistry*
*Faculty of Engineering*
*Kyoto University*
*Sakyo-ku, Kyoto*

# *Infrared Spectra of Acyclic Imides. III. Infrared Dichroism of Dipropionamide and N-Acetylpropionamide Crystals*

By Toyozo UNO and Katsunosuke MACHIDA

(Received November 10, 1960)

In order to obtain information on the molecular structure of acyclic imides in the form B, infrared dichroic measurement has been made for dipropionamide and *N*-acetylpropionamide. These compounds were chosen as examples of the simplest acyclic imides being stable in the form B. Their oriented crystals were easily prepared on sodium chloride plates. Further evidences for the trans-trans planar structure[1] could be given to these molecules from the dichroic properties of the imide characteristic bands and some other bands. With the aid of these evidences, the splitting of the N-H stretching bands which is one of the important features in the infrared spectra of the form B, will be discussed in terms of the Fermi resonance.

## Results and Discussion

**Configurations of Imide Group and Molecular Symmetries.**—Since the dichroic property of an infrared absorption band, if the molecule in question has any symmetry at all, depends on the symmetry of the vibrational mode from which the band arises, the interpretation of infrared dichroism should be closely related to molecular symmetry. In this connection, a brief survey of the relationship of molecular symmetry to the configurations of the -CONHCO- group will be presented here. In the trans-trans or the cis-cis configuration of this group, both the C=O bonds take an equivalent position with respect to the N-H bond. Consequently, as long as we are concerned with an isolated molecule, symmetrically substituted acyclic imides in the trans-trans configuration, as well as cyclic imides with polymethylene chains can be regarded to have the molecular symmetry $C_{2v}$. However, for actual molecules in the crystalline state, this is not always true exactly. For instance, although succinimide clearly takes the cis-cis configuration, those two C=O bonds in this molecule are not equivalent to each other regarding their nature in the crystalline state. The X-ray diffraction study[2] has shown that only one C=O bond for each molecule is involved in hydrogen bond, the other C=O bond not being so. Thus, just as in the case of diacetamide in the form A[3], every two molecules of succinimide form a ring dimer in the crystalline state. Furthermore, the five-membered ring of this molecule forms an oblique pentagon in which no two-fold axis exists. Speaking thus more strictly, the molecular symmetry of succinimide is not $C_{2v}$ but $C_s$, in which only the plane of symmetry coinciding with the molecular plane remains. A similar situation may be seen for symmetrically substituted acyclic imides in the trans-trans configuration since they can exactly have the symmetry $C_{2v}$ only if those two C=O bonds in the -CONHCO- group are equivalent to each other in their nature as well as in their configuration. Although we have shown that the infrared spectra of acyclic imides in the form B are reasonably interpreted in terms of the symmetry $C_{2v}$[1], it is not yet determined whether they exactly have the symmetry $C_{2v}$ or whether the deviations from $C_{2v}$ are too small to affect their infrared spectra. Under these situations,

1) T. Uno and K. Machida, This Bulletin, 34, 545, 551 (1961).

2) R. Mason, *Acta Cryst.*, 9, 405 (1956).

3) T. Watanabé and K. Osaki, unpulished.

the results of infrared dichroic measurements in the present study will be discussed on the basis of the approximation in which symmetri-

TABLE I. INFRARED DICHROISM OF DIPROPIONAMIDE

| Frequency, $cm^{-1}$ | Intensity*1 // | Intensity ⊥ | Assignments (species) |
|---|---|---|---|
| 3500 | w | — | 1736×2 ($A_1$) |
| 3280 | vs | — | N-H stretch. ($A_1$) |
| 3200 | vs | — | 1690+1504 ($A_1$) |
| 3005 | sh | — | 1504×2 ($A_1$) |
| 2992 | s | s | C-H stretch. |
| 2948 | — | sh | |
| 2923*2 | — | m | |
| 2875 | — | w | |
| 2693 | w | — | 1504+1180 ($A_1$) |
| 1860 | vw | — | ? |
| 1736 | vs | vw | sym. imide I ($A_1$) |
| 1690 | sh | w | antisym. imide I ($B_1$) |
| 1504 | — | vs | imide II ($B_1$) |
| 1459 | m | m | $CH_3$ asym. def. (//: $A_1$, ⊥: $B_1$ and $B_2$) |
| 1420 | s | w | $CH_2$ bend. (//: $A_1$, ⊥: $B_1$) |
| 1384 | m | sh | $CH_3$ sym. def. (//: $A_1$, ⊥: $B_1$) |
| 1367 | — | s | $CH_2$ wag., imide II and imide III ($B_1$) |
| 1263 | w | w | //: C-N-C sym. stretch., $CH_2$ wag. ($A_1$); ⊥: $CH_2$ twist. ($B_2$) |
| 1180 | w | vs | imide III ($B_1$) |
| 1080 | — | w | |
| 1075 | m | — | C-C stretch. |
| 1009 | — | w | (//: $A_1$, ⊥: $B_1$) |
| 994 | m | — | $CH_3$ rock. |
| 955 | w | w | (//: $A_1$, ⊥: $B_1$ or $B_2$) |
| 843 | — | w | $CH_2$ rock. (⊥: $B_2$) |
| 806 | — | w | |
| 732 | — | w | imide V ($B_2$) |

*1 vs : very strong, s : strong, m : medium, w : weak, vw : very weak, sh : shoulder.
*2 Probably due to the $CH_2$ out-of-phase stretch. ($B_2$) mode.

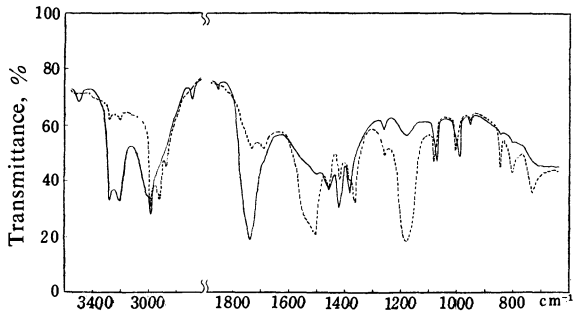



Fig. 1. Infrared dichroism of dipropionamide ($CH_3CH_2CONHCOCH_2CH_3$)
solid line : //, broken line : ⊥

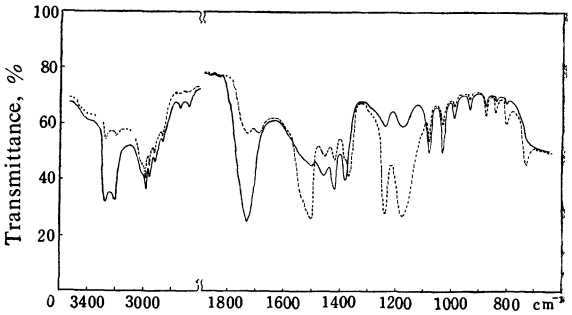



Fig. 2. Infrared dichroism of *N*-acetylpropionamide ($CH_3CH_2CONHCOCH_3$)
solid line : //, broken line : ⊥

TABLE II. INFRARED DICHROISM OF *N*-ACETYLPROPIONAMIDE

| Frequency, $cm^{-1}$ | Intensity // | Intensity ⊥ | Assignments (species) |
|---|---|---|---|
| 3280 | vs | w | N-H stretch. (A′) |
| 3200 | vs | w | 1690+1504 (A′) |
| 3000 | sh | sh | 1504×2 (A′) |
| 2978 | m | m | C-H stretch. |
| 2960 | m | m | |
| 2920 | w | w | |
| 2875 | w | w | |
| 2750 | w | — | 1504+1240 (A′) |
| 2690 | w | — | 1504+1180 (A′) |
| 1734 | vs | w | sym. imide I (A′) |
| 1690 | — | w | antisym. imide I (A′) |
| 1504 | vw | vs | imide II (A′) |
| 1458 | m | w | $CH_3$ ($\beta$) asym. def. (A′ or A″) |
| 1419 | m | w | $CH_3$ ($\alpha$) asym. def. (A′ or A″), $CH_2$ bend. (A′) |
| 1380 | m | sh | $CH_3$ ($\alpha$ or $\beta$) sym. def. (A′) |
| 1370 | — | s | $CH_2$ wag., imide II and imide III (A′) |
| 1240 | w | vs | imide III (A′) |
| 1180 | w | vs | imide III (A′) |
| 1081 | m | w | |
| 1035 | m | w | |
| 994 | w | vw | C-C stretch. (A′) |
| 938 | w | vw | $CH_3$ rock. (A′ or A″) |
| 879 | w | w | $CH_2$ rock. (A″) |
| 845 | vw | w | |
| 808 | vw | w | |
| 733 | — | w | imide V (A″) |

cally substituted acyclic imides in the trans-trans configuration are regarded to have the symmetry $C_{2v}$. Discussions will also be made on the nature of the hydrogen bond in the form B which is closely related to whether those two C=O bonds in the -CONHCO- group are equivalent or not.

As shown in Figs. 1 and 2, dipropionamide

and *N*-acetylpropionamide show marked infrared dichroism. Tables I and II show the dichroic properties of the absorption bands of these acyclic imides together with the assignments given to these bands. The symbols // and $\perp$ are used for the polarized light with the electric vector parallel and perpendicular, respectively, to the elongation direction of the crystal. Since the molecular symmetry of dipropionamide ($C_{2v}$) and that of *N*-acetylpropionamide ($C_s$) are different from each other with respect to their alkyl groups, discussions will be made separately for these two compounds.

**Dipropionamide.**—As shown in Table I, the dichroic properties of the characteristic bands of dipropionamide in the sodium chloride region, previously assigned on the basis of the trans-trans configuration of the -CONHCO- group, are closely related to the symmetry species of these bands. That is to say, the bands belonging to $A_1$ species show parallel dichroism while the bands belonging to $B_1$ or $B_2$ species show perpendicular dichroism. In order to explain these facts, the following structure may be proposed for the crystal preparations. In this structure, the two-fold axis of each molecule is parallel to the elongation direction of crystal while there are molecules whose molecular planes are not perpendicular to the incident light. The latter situation may be realized by the uniaxial orientation of the crystallites even in a case where the unit cell consists only from molecules whose molecular planes are parallel to one another. It will now be shown that the consistency between the dichroic properties of individual characteristic bands and the proposed structure is quite sufficient. The marked parallel dichroism of the bands at 3280 and 3200 $cm^{-1}$, whose origin will be discussed later, may be taken as indicating that the direction of the N-H bond involved in hydrogen bond (i. e. the direction of the two-fold axis) is parallel to the elongation direction of the crystal. The strong band at 1736 $cm^{-1}$ also shows marked parallel dichroism supporting the assignment to the C=O symmetric stretching mode ($A_1$) as well as the trans-trans configuration of the -CONHCO- group, in which all the N-H and the C=O bonds are nearly parallel to one another. The weak band at 1690 $cm^{-1}$, which has been assigned to the C=O antisymmetric stretching mode ($B_1$), seems to show perpendicular dichroism although this is not so obvious owing to the broadness of the adjacent strong band at 1736 $cm^{-1}$. On the other hand, the marked perpendicular dichroism of the imide II (1504 $cm^{-1}$) and the imide III (1180 $cm^{-1}$) band is consistent with the assignment to $B_1$ fundamentals whose vibrational transition moments are perpendicular to the plane of symmetry bisecting the angle C-N-C. The imide V band at 732 $cm^{-1}$, to which the N-H out-of-plane deformation vibration mainly contributes, shows perpendicular dichroism. If all the molecular planes in the crystal are perpendicular to the incident radiation, the band due to an out-of-plane vibration will not be observed, regardless of polarization. The proposed structure, however, may afford reasonable elucidation to the dichroic property of this band. The weak band at 1263 $cm^{-1}$ shows no dichroism. This fact may be taken as indicating that the band showing parallel dichroism resulting from the C-N-C symmetric stretching vibration ($A_1$) is overlapped by a band due to $B_1$ or $B_2$ vibration. This is probable since the $B_2$ $CH_2$ twisting band may occur in this region.

Further evidences for the proposed structure are obtained from the dichroic properties of the bands due to the vibrations of the C-H bonds. In the region where the C-H stretching bands occur, no band shows appreciable dichroism except for the band at 2923 $cm^{-1}$, which shows perpendicular dichroism and may be assigned to the $CH_2$ out-of-phase stretching mode. If the $C_{2v}$ trans-trans configuration is assumed for dipropionamide, each of the C-H stretching vibrations will belong to the following symmetry species shown in parentheses: the $CH_3$ symmetric ($A_1$, $B_1$), the $CH_3$ asymmetric ($A_1$, $B_1$, $A_2$, $B_2$), the $CH_2$ in-phase ($A_1$, $B_1$) and the $CH_2$ out-of-phase ($A_2$, $B_2$). Thus, the dichroic properties of the C-H stretching bands are consistent with the proposed structure. A similar situation is seen for the C-H deformation bands at 1459, 1420 and 1384 $cm^{-1}$, each of which occurs for the polarized light with the electric vector along the elongation direction of the crystal as well as for the light polarized perpendicular to this direction. However, the dichroic ratio $I_{//}/I_{\perp}$ of the band at 1420 $cm^{-1}$, which is due to the $CH_2$ bending vibrations, is appreciably greater than unity, indicating that the magnitude of the vibrational transition moment of the $A_1$ mode is greater than that of the $B_1$ mode. This fact is consistent with the proposed structure where a molecule of dipropionamide has two equivalent $CH_2$ groups. With respect to the bending vibration of the $CH_2$ group at either side of the N-H bond, the component of the vibrational transition moment parallel to the N-H bond (the two-fold axis) is greater than the perpendicular component. Thus, the interaction between this vibration and the same vibration of the other $CH_2$ group results in a greater change of dipole moment for the

in-phase ($A_1$) vibration than for the out-of-phase ($B_1$) vibration. The band at 1367 $cm^{-1}$, which disappears on deuteration, shows marked perpendicular dichroism. Possible vibrations which contribute to this band may be the $B_1$ $CH_2$ wagging, the N-H in-plane deformation, and the C-N-C antisymmetric stretching mode. Thus, we may notice that the coupling between the imide characteristic vibrations (the imide II and the imide III mode) and the C-H deformation vibrations takes place to some extent.

Generally speaking, for the bands which exhibit distinguished dichroism in the region 1800 to 900 $cm^{-1}$, there is a simple relation between the dichroic property and the behavior on deuteration. In other words, the bands showing perpendicular dichroism (1504, 1367, 1180, 1080 and 1009 $cm^{-1}$) shift, while the bands showing parallel dichroism (1736, 1075 and 994 $cm^{-1}$) do not shift on deuteration. This fact means that two propionyl groups in a molecule take an equivalent configuration with respect to the central N-H bond. There are three cases which satisfy this condition, namely, the symmetry $C_2$ with the two-fold axis coinciding with the N-H bond, the symmetry $C_s$ with the plane of symmetry bisecting the angle C-N-C, and the symmetry $C_{2v}$ with both of these symmetry elements. However, the first two are not likely since an appreciable angle between two C=O bonds in the -CONHCO- group is inconsistent with the weakness of the C=O antisymmetric stretching band at 1690 $cm^{-1}$.

As discussed in the previous section, the study only on the infrared spectra seems to be insufficient to estimate the deviation from the exact equivalence of these two C=O bonds. Furthermore, since the imide hydrogen atom is clearly involved in the hydrogen bond, the exact equivalence of the proton acceptors can not be attained without the presence of the so-called bifurcated hydrogen bond, whose existence, however, has been reported for few molecules[4]. Although more detailed investigations such as the X-ray diffraction study must be carried out to decide the exact feature of this hydrogen bond, it is here pointed out that molecular structures where both the bonded and the free C=O bond exist can hardly elucidate the experimental results up to the present study; for instance, the occurrence of only one strong C=O stretching band with comparatively high frequency (1736 $cm^{-1}$) and its parallel dichroism. The bands in the 3 $\mu$ region observed for these acyclic imides are very sharp in contrast with other cases where the bonded N-H stretching bands are very broad. Furthermore, the imide II band, which is partly due to the N-H in-plane deformation mode, is remarkably broad. It is suggested that these features may be closely related to the nature of hydrogen bonds in these acyclic imides in the form B.

***N*-Acetylpropionamide.** — The dichroic properties of the imide characteristic bands of *N*-acetylpropionamide are quite similar to those of the corresponding bands of dipropionamide. It is noticed here that both of the two imide III bands (1240 and 1180 $cm^{-1}$) of *N*-acetylpropionamide show the same perpendicular dichroism. Although this molecule has no two-fold axis, the vibrational transition moments of these bands are considered to be almost perpendicular to the N-H bond owing to the large amplitude of the N-H in-plane deformation vibration contributing to the vibrational modes of these bands. The weak antisymmetric imide I band, which has not been resolved from the strong symmetric imide I band at 1734 $cm^{-1}$ in the spectrum of non-oriented sample, appears at 1690 $cm^{-1}$ with the light with electric vector perpendicular to the elongation direction of the crystal. On the other hand, the clear-cut relation between the behavior on deuteration and the dichroic property which is seen for all the bands showing remarkable dichroism in the region 1800 to 900 $cm^{-1}$ of dipropionamide, does not hold well for the bands in the region 1100 to 900 $cm^{-1}$ of *N*-acetylpropionamide. That is to say, all the bands showing parallel dichroism (1081, 1035, 994 and 938 $cm^{-1}$), which may be due to the vibrations of alkyl groups, shift or split on deuteration. These results are consistent with the trans-trans configuration of the -CONHCO- group since *N*-acetylpropionamide in this configuration can be regarded to have the symmetry $C_{2v}$ only in the approximation where the difference between the $CH_3$ and the $CH_3CH_2$ groups is neglected.

**Fermi Resonance in the 3 $\mu$ Region.**—On the basis of the planar trans-trans configuration, the origin of the splitting of the N-H stretching bands of these acyclic imides in the form B will now be discussed. From the spectral features of the *N*-deuterated species in the region 2500 to 2300 $cm^{-1}$, where no more than one strong band appears, it is obvious that the situation giving rise to this splitting must be what vanishes on deuteration. From this point of view, the band near 3280 $cm^{-1}$ is assigned to the N-H stretching mode and the band near 3200 $cm^{-1}$ to a combination band of some lower fundamentals enhanced by Fermi resonance with the N-H stretching mode. Other possible reasons for the splitting of the band

4) For instance, see R. Marsh, *Acta Cryst.*, 11, 662 (1958).

Table III. The combination frequencies of the *N*-deuterated species of saturated acyclic imides near 2300 $cm^{-1}$

| Compound | Frequency $cm^{-1}$ | Intensity | Imide II′ frequency $cm^{-1}$ | Imide III′ frequency $cm^{-1}$ |
|---|---|---|---|---|
| Diacetamide-*d* | 2295 | w | 1348 | 951 |
| *N*-Acetylpropionamide-*d* | 2300 | w | 1329 | 961 |
| Dipropionamide-*d* | 2283 | m | 1304 | 986 |
| *N*-Propionyl-*n*-butyramide-*d* | 2290 | w | 1307 | 987 |
| Di-*n*-butyramide-*d* | 2300 | w | 1332 | 985 |
| Di-*n*-butyramide-*d* | 2283 | w | 1314 | 985 |

in the 3 $\mu$ region, such as the intermolecular interaction in the unit cell, or the presence of two species of hydrogen bonds, must hold equally well for the undeuterated and the *N*-deuterated species to give rise to the splitting of the N-D stretching band of the latter. It is also difficult to explain the same parallel dichroism of these two bands near 3280 and 3200 $cm^{-1}$ from these reasons. On the other hand, regarding whether appropriate fundamentals giving rise to an overtone or a combination tone in the regions in question exist or not, the situation for the undeuterated species is obviously different from that for the *N*-deuterated species. As the fundamentals which combine to give rise to the band near 3200 $cm^{-1}$, the antisymmetric imide I band (near 1700 $cm^{-1}$) and the imide II band (near 1500 $cm^{-1}$) are the most reasonable ones. In the $C_{2v}$ approximation for the planar trans-trans configuration, these two bands belong to the $B_1$ species. Thus, it may be expected that the N-H stretching vibration ($A_1$) is involved in Fermi resonance with the combination tone of these two frequencies to give rise to two bands showing parallel dichroism in the 3 $\mu$ region just as has been observed. The constant frequencies of these lower fundamentals (near 1700 and 1500 $cm^{-1}$) throughout all of these acyclic imides result in a practically identical feature of the bands near 3280 and 3200 $cm^{-1}$. Similar Fermi resonance has already been reported for both the trans and the cis configuration of monosubstituted amides[5,6]. For the *N*-deuterated species of these acyclic imides in the form B, one or two weak bands sometimes appear near 2300 $cm^{-1}$. In contrast with the band near 3200 $cm^{-1}$ for the undeuterated species, appreciable differences in frequencies and intensities of these weak bands are observed among the *N*-deuterated species of these acyclic imides. These bands may be assigned to the combination tones of the imide II′ and the imide III′ bands which also belong to the $B_1$ species. The imide II′ and the imide III′ frequencies of the *N*-deuterated species of these acyclic imides in the form B are appreciably different from one another and give rise to their combination bands in a somewhat different manner regarding both the frequencies and the intensities. These combination frequencies are shown in Table III, where good correspondences of these frequencies to the sums of the imide II′ and the imide III′ frequencies are observed.

5) R. M. Badger and A. D. E. Pullin, *J. Chem. Phys.*, **22**, 1142 (1954); M. Beer, H. B. Kessler and G. B. B. M. Sutherland, ibid., **29**, 1097 (1958).

6) T. Miyazawa, *J. Mol. Spectroscopy*, **4**, 168 (1960).

## Conclusion

By the examination of infrared dichroism of dipropionamide and *N*-acetylpropionamide, not only the assignments previously given to the characteristic and the C-H deformation bands have been confirmed, but further information concerning some other bands has also been obtained on the basis of the trans-trans configuration of the -CONHCO- group. Although some of the assignments proposed in the present study may be tentative, it seems significant that nearly all the infrared active vibrations in the sodium chloride region for the structure in question could have been attributed to the bands observed in this region.

The origin of the splitting of the N-H stretching band has been made clear in terms of Fermi resonance from the dichroic properties and the behavior on deuteration of these bands although there remains an interesting problem in regard to the nature of the hydrogen bond in which the N-H and the C=O bonds may be involved.

## Experimental

**Materials.**—Oriented crystallites of *N*-acetylpropionamide and those of dipropionamide from molten liquid were prepared on sodium chloride plates with the application of temperature gradient. Their infrared spectra were confirmed to be identical with those of the crystals from petroleum ether in the paste method.

**Dichroic Measurement.**—The Hitachi EPI-2 infrared spectrophotometer with the sodium chloride prism, the IM-2P infrared microilluminator and the silver chloride transmission polarizer were used.

The measurements were carried out in the region 4000 to 650 $cm^{-1}$. The 1 m. gas cell was inserted in the path of the reference beam. The application of the radiations polarized parallel and perpendicular to the elongation direction of the crystal was attained with the rotation of the polarizer by 90°. The 100% line was adjusted by the attenuator for each radiation. Other conditions were similar to those described in the preceding papers[1].

The authors express their thanks to Dr. T. Miyazawa of Osaka University and to Dr. K. Nakamura of the Research Laboratory, Dainihon & Co. Ltd., for their frequent kind advice. Thanks are also due to Dr. H. Tadokoro of Osaka University and to Mr. K. Tatsuka of Osaka Custom House for infrared dichroic measurements.

*Faculty of Pharmacy*
*Kyoto University*
*Sakyo-ku, Kyoto*

# *Spectrophotometric Determination of Uranium with Sodium 2'', 6''-dichloro-4'-hydroxy-3, 3'-dimethylfuchsone-5, 5'-dicarboxylate*

By Yukiteru KATSUBE, Katsuya UESUGI and John H. YOE

(Received November 24, 1960)

For the colorimetric determination of uranium, various organic reagents have been used : sodium salicylate[1], tannic acid[2], thioglycollic acid[3], oxine[4-6], chromotropic acid[7-9], dimethyldithiocarbamate[10], dibenzoylmethane[11-15], morin[16], acetylacetone[17], thorin[18], neothorin[19] and arsenazo[20-21].

In this paper, a new method is described for the colorimetric determination of small amounts of uranium. It is based on the colored complex formation between uranyl ions and sodium 2'', 6''-dichloro-4'-hydroxy-3,3'-dimethylfuchsone-5, 5'-dicarboxylate. This compound has recently been used for the determination of beryllium, iron and copper and observations suggested a possibility that it could also be used for uranium[22].

## Experimental

The spectrophotometer and photoelectric photometer were the same as those used in our previous work[22].

**Ion Exchange Resin.**—Tube, 10 mm. in diameter, with a high-porosity glass filter disk fused to the lower end was used. The resin was a quaternary ammonium anion exchange type, a modification of Amberlite IRA-410. Before use, the resin was converted into the sulfate form by treating it with 10% sulfuric acid. The treated resin was washed with distilled water until the effluent solution was neutral. The resin was added to the tube with distilled water to give a column height of 15 cm.

**Uranium Standard Solution.**—A standard stock solution of uranium was prepared by dissolving uranyl nitrate in distilled water. The solution contained 100 $\gamma$ of uranyl ions per milliliter.

**Reagent Solution.**—A 0.2% reagent solution was prepared by dissolving sodium 2'', 6''-dichloro-4'-hydroxy-3, 3'-dimethylfuchsone-5, 5'-dicarboxylate in 99% ethanol.

***p*-Nitrophenol Indicator.**—A 0.4% solution was prepared by dissolving *p*-nitrophenol in distilled water.

All other chemicals were of analytical reagent grade.

1) H. Muller, *Chemiker Ztg.*, **43**, 739 (1919).
2) P. N. Das Gupta, *Analyst*, **55**, 154 (1930).
3) W. H. Davenport and P. F. Thomason, *Anal. Chem.*, **21**, 1093 (1949).
4) A. A. Smales and H. N. Wilson, *U. S. Atomic Energy Comm. Report*, BR-150, Feb. 22 (1943).
5) E. F. Orelemann, ibid., CD-2228, Feb. 26 (1945).
6) C. L. Rulfs, A. K. De. J. Lakritz and P. L. Elving, *Anal. Chem.*, **27**, 1802 (1955).
7) W. B. Mason and N. H. Furman, *U. S. Atomic Energy Comm. Report*, A-1057, Sec. 2E, Sept. 30 (1944).
8) E. Ware, ibid., MDDC-1432, Aug. 20 (1945).
9) A. K. Mukerjee, *J. Indian Chem. Soc.*, **35**, 113 (1958).
10) R. J. Lacoste, M. H. Earing and S. E. Wiberly, *Anal. Chem.*, **23**, 871 (1951).
11) J. H. Yoe, F. Will and R. A. Black, *Anal. Chem.*, **25**, 1200 (1953).
12) R. Přibil and M. Jelinek, *Chem. listy*, **47**, 512 (1953).
13) P. Blanquet, *Anal. Chim. Acta*, **16**, 44 (1957).
14) C. A. Francois, *Anal. Chem.*, **30**, 50 (1958).
15) C. A. Horton and J. C. White, *Anal. Chem.*, **30**, 1779 (1958).
16) M. T. Beck and E. Hantos, *Acta. Chim. Acad. Sci. Hung.*, **8**, 233 (1955).
17) A. Kirshen and H. Freiser, *Anal. Chem.*, **29**, 288 (1957).
18) J. K. Foreman, C. J. Riley and T. D. Smith, *Analyst*, **82**, 89 (1957).
19) S. Shibata and T. Matsumae, This Bulletin, **31**, 377 (1958).
20) J. S. Fritz and M. J. Richard, *Anal. Chim. Acta.*, **20**, 164 (1955).
21) H. P. Holcomb and J. H. Yoe, *Anal. Chem.* **32**, 616 (1960).
22) Y. Katsube, K. Uesugi and J. H. Yoe, This Bulletin, **34**, 72 (1961).

**Separation of Interfering Ions.**—Uranium was separated from other ions according to Fisher's procedure[23].

**Procedure for Determination of Uranium.**—Pipet 23 ml. of a slightly acidified sample solution, which has been adjusted so as to contain 1 to 10 $\gamma$ uranium per milliliter, and one drop of *p*-nitrophenol indicator solution to a 25 ml. volumetric flask. Add 0.05 N sodium hydroxide solution dropwise until the indicator just turns yellow, then discharge yellow color by careful addition of 0.05 N hydrochloric acid dropwise. The resultant solution should be adjusted to pH 5.2±0.4. Add one milliliter of the reagent solution, shake well, make up to the mark with distilled water and mix thoroughly. Measure the absorbance at 610 m$\mu$, after ten minutes, using distilled water as reference. Determine the weight or the concentration of uranium in the sample from a calibration curve prepared by the same procedure used for the sample.

## Results and Discussion

**Absorption Spectra.**—Color reactions between many ions and sodium 2'',6''-dichloro-4'-hydroxy-3, 3'-dimethylfuchsone-5, 5'-dicarboxylate were recorded in our previous paper[22]. Uranyl ions react with the compound to give a blue complex in dilute acid solution. Absorption spectra of the compound in a solution and of its uranyl complex are shown in Fig. 1.

The maximum absorption of the uranyl complex solution occurs at 610 m$\mu$. The reagent solution has little or no absorption at this wavelength. A large excess of the reagent must be avoided because its solution has a slight absorption at 610 m$\mu$ when the concentration is greater than about 80 p.p.m. It is not necessary, however, to use the same concentration of the reagent for standards and unknowns, when the concentration of unreacted reagent is in range of 80 to 40 p.p.m.

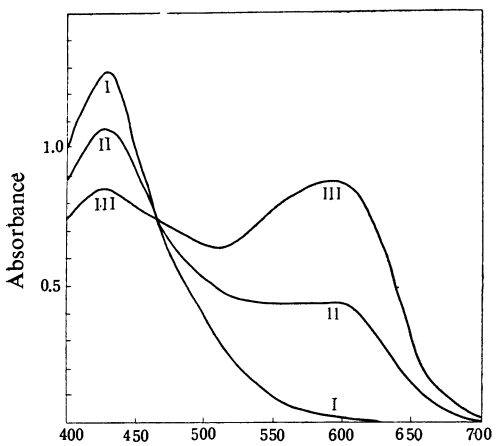



Fig. 1. Absorption spectra of the reagent solution and of its uranyl complex. pH 5.2.
I : Reagent 80 p.p.m.
II : Reagent (80 p.p.m.)+U(4.0$\gamma$/ml.)
III: Reagent (80 p.p.m.)+U(8.0$\gamma$/ml.)

**Molar Ratio.**—The colored complex in solution was found to have a molar ratio of 2 to 1, reagent to uranyl ions. The mole ratio method[24] and the continuous variation method[25-26] were used to establish the molar ratio. The continuous variation method was applied by mixing $X$ ml. of $3.7\times10^{-3}$ M reagent solution and $(1.00-X)$ ml. of uranyl solution of $3.7\times10^{-3}$ M and diluting to 25 ml. after adjusting to pH 5.2. The results are shown in Figs. 2 and 3.

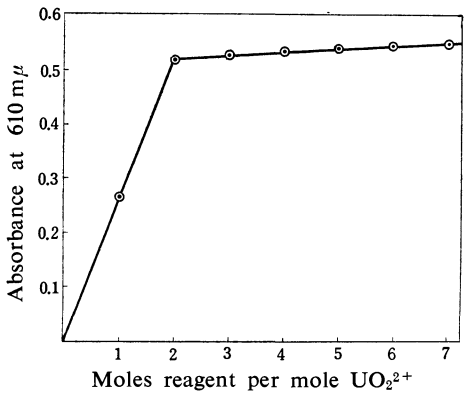



Fig. 2. Mole ratio method showing a ratio of 2 to 1, reagent to $UO_2^{2+}$, in the colored complex. pH 5.2.

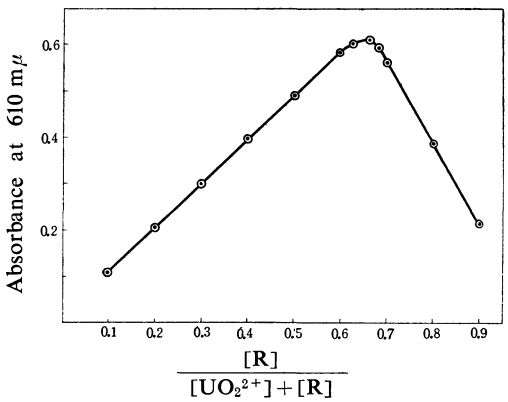



Fig. 3. Continuous variation method showing a ratio of 2 to 1, reagent to $UO_2^{2+}$, in the colored complex. pH 5.2.

23) S. Fisher, U. S. Atomic Energy Comm., Document RMO-2530 (1954).

24) J. H. Yoe and A. L. Jones, *Ind. Eng. Chem., Anal. Ed.*, **16**, 111 (1944).

25) P. Job, *Ann. chim.*, (10), **9**, 113 (1928).

26) W. C. Vosburgh and G. R. Cooper, *J. Am. Chem. Soc.*, **63**, 437 (1941).

**Effect of pH.**—The effect of pH on the color reaction was examined by measuring the absorbance of a colored solution, at 610 mμ, containing 3.52 p.p.m. of uranium and 80 p.p.m. of the reagent, the pH being adjusted by adding dilute hydrochloric acid or dilute sodium hydroxide solution. The uranyl complex has a maximum intensity in the pH range 4.8 to 5.8 as shown in Fig. 4.

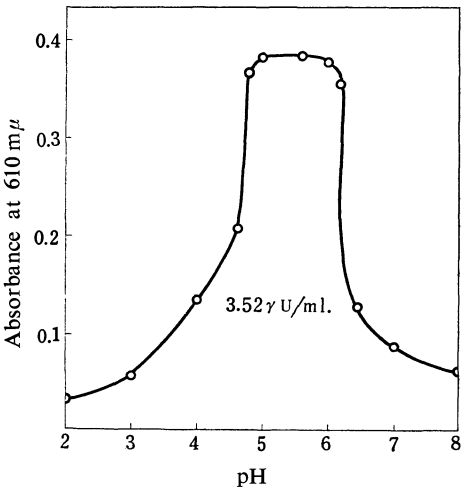



Fig. 4. Effect of pH on the uranyl complex.

A pH of 5.2±0.4 should be used when making absorbance measurements of the complex.

Several buffer solutions were tried: borax-succinic acid, acetate-acetic acid, phthalate, and phosphate buffers were unsatisfactory. All lowered the color intensity of the complex. Dilute hydrochloric acid and sodium hydroxide solution were satisfactory for pH adjustment with *p*-nitrophenol as indicator.

**Rate of Color Formation.**—Within the optimum pH range (5.2±0.4), the color intensity reaches a maximum in ten minutes and remains unchanged for about an hour. It is necessary, therefore, to allow the colored solution to stand at least ten minutes and then to measure the absorbance within an hour.

**Effect of Temperature.**—There is no variation in the absorbance of the colored complex over a temperature range 15 to 30°C.

**Interfering Ions.**—The reagent was tested on a spot plate[22]. Twelve ions were found to interfere: $Al^{3+}$, $Be^{2+}$, $Cu^{2+}$, $Fe^{2+}$, $Fe^{3+}$, $Ga^{3+}$, $Gd^{3+}$, $Nd^{3+}$, $Ni^{2+}$, $Pr^{3+}$, $Sc^{2+}$ and $Y^{3+}$. The effect of some common ions on the determination of uranium is shown in Table I. The limiting concentration was taken to be one that causes a deviation of more than 0.01 unit in the absorbance of a solution containing 5.28 γ uranium per milliliter.

TABLE I. EFFECT OF DIVERSE IONS

| Ion | Added as | Limiting concentration, γ ions per milliliter |
|---|---|---|
| $Al^{3+}$ | sulfate | 0.02 |
| $Be^{2+}$ | chloride | 0.02 |
| $Ca^{2+}$ | chloride | >1500 |
| $Cu^{2+}$ | sulfate | 1 |
| $Cr^{3+}$ | sulfate | 150 |
| $Fe^{2+}$ | Mohr's salt | 2 |
| $Fe^{3+}$ | iron alum | 0.8 |
| $Ni^{2+}$ | nitrate | 80 |
| $Mg^{2+}$ | chloride | >1500 |
| $Zn^{2+}$ | chloride | >1000 |

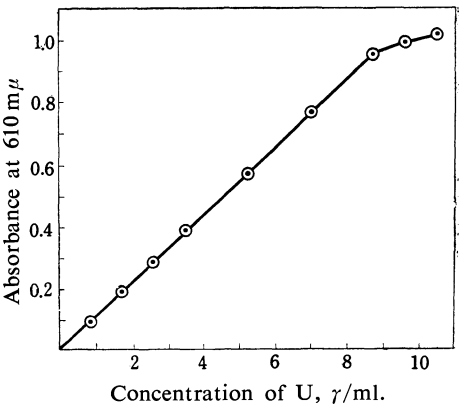



Fig. 5. Beer's law curve. pH 5.2.

TABLE II. DETERMINATION OF URANIUM

| Solution analyzed | | Added γ/50 ml. | Found U* γ | Error % |
|---|---|---|---|---|
| 1 | $Al^{3+}$ | 200 | | |
| | $Be^{2+}$ | 50 | | |
| | $Fe^{2+}$ | 200 | | |
| | $Fe^{3+}$ | 200 | | |
| | U | 132.0 | 130.0 | −0.2 |
| 2 | $Al^{3+}$ | 1000 | | |
| | $Be^{2+}$ | 200 | | |
| | $Fe^{3+}$ | 500 | | |
| | U | 176.0 | 169.6 | −3.6 |
| 3 | $Al^{3+}$ | 1000 | | |
| | $Be^{2+}$ | 500 | | |
| | $Cu^{2+}$ | 1000 | | |
| | $Cr^{3+}$ | 1000 | | |
| | $Fe^{2+}$ | 1000 | | |
| | $Ni^{2+}$ | 1000 | | |
| | U | 44.0 | 45.8 | +4.1 |

* These values are the averages of 5 replicate determinations.

Several methods were tried to eliminate interfering ions. The method proposed by Fisher[23] was adopted. It makes use of an anion exchange resin as mentioned in this paper. Ferric ions are reduced to ferrous

ions with sulfurous acid before passing the sample solution through the resin column.

**Beer's Law.**—Beer's law is obeyed up to about 8.8 $\gamma$ of uranium per milliliter (See Fig. 5).

**Determination of Uranium in Synthetic Solutions Containing Other Ions.**—The determination of uranium in the presence of certain other ions was made. The results are given in Table II.

## Summary

A procedure has been developed for the spectrophotometric determination of small amounts of uranium with sodium 2'',6''-dichloro-4'-hydroxy-3, 3'-dimethylfuchsone-5,5'-dicarboxylate. Beer's law is obeyed up to about 9 $\gamma$ of uranium per milliliter. The accuracy and precision are satisfactory. Interference of foreign ions is eliminated by using an anion exchange resin.

*Himeji Technical Institute*
*Idei-600, Himeji*
*(Y. K & K. U.)*

*John Lee Pratt Trace Analysis Laboratory*
*University of Virginia*
*Charlottevill Va.*
*U. S. A.*
*(J. H. Y.)*

# *Studies on Metal Complex Species Using an Anion Exchange Resin. I. Derivation of Equations and Application to Mercury(II)-Nitrate Complex*

By Hirohiko WAKI

(Received October 10, 1960)

An equation and a method for determining the composition of metal complex species using an anion exchange resin have been developed by Kraus et al.[1,2] These are mostly applicable[3] in the case where a stable negatively-charged complex ion of a metallic element is formed even in a dilute solution and adsorbed in the same form as that in the solution when it is in contact with the resin. On the other hand, it is also often observed that a metallic element may be significantly adsorbed on an anion exchange resin even from a solution in which the presence of any complex anion seems hardly to be considered. In this case it is likely enough that a metal ion or a low complex ion of the metallic element enters the resin phase and then converts itself there into a complex anion or a higher complex ion respectively, because the resin phase may be regarded as a kind of extremely concentrated solution of electrolytes. Accordingly, the complex formation in such a case should rather depend directly on the concentration of an anion as a ligand and on the ionic strength in the resin phase. In this paper an equation for determining the composition of metal complex species, including the cases mentioned above, will be derived by introducing the complex formation equilibrium in the resin phase and applied to mercury-nitrate complex taken up by anion exchange resin.

1) K. A. Kraus and G. E. Moore, *J. Am. Chem. Soc.*, 73, 9 (1951).
2) K. A. Kraus and F. Nelson, "Anion Exchange Studies of the Fission Products" in "Peaceful Uses of Atomic Energy", Proceedings of the International Conference in Geneva, Vol. 7, p. 113 (1955) (United Nations).
3) S. Misumi and T. Taketatsu, This Bulletin, 32, 876 (1959).

## Derivation of Equations

Since the ion exchange can be theoretically treated as a Donnan equilibrium, the following relationship holds between the ion concentrations in the resin phase [ ] and in the external solution ( ) in the equilibrium state:

$$[M^{a+}]\,[X^{b-}]^{a/b}\gamma_{[M]}\gamma_{[M]}^{a/b} = (M^{a+})\,(X^{b-})^{a/b}\gamma_{(M)}\gamma_{(X)}^{a/b} \quad (1)$$

where $M^{a+}$ and $X^{b-}$ represent a metal ion and an anion respectively, and $\gamma$ stands for the activity coefficient of the ion given as subscript. When a complex ion $MX_m^{(bm-a)-}$ is formed in the external solution, the formation constant is defined by

$$K_m = \frac{(MX_m^{(bm-a)-})}{(M^{a+})\,(X^{b-})^m} \cdot \frac{\gamma_{(MX_m^{(bm-a)-})}}{\gamma_{(M)}\gamma_{(X)}^m} \quad (2)$$

Since the resin phase may be regarded as a concentrated aqueous solution of electrolytes, the formation constant may also be defined by

$$K_n=\frac{[MX_n^{(bn-a)-}]}{[M^{a+}]\,[X^{b-}]^n}\cdot\frac{\gamma_{[MX_n^{(bn-a)-}]}}{\gamma_{[M]}\gamma_{[X]}^n} \quad (3)$$

for a complex ion $MX_n^{(bn-a)-}$ in the resin phase, in analogy to Eq. 2. For the purpose of the determination of the complex form, the formation equilibria in both phases should be taken into account.

The distribution coefficient may be defined at

$$D=\sum[M]/\sum(M) \quad (4)$$

where $\sum[M]$ and $\sum[M]$ are the total stoichiometric concentrations of the metallic element in the resin and the solution phase (irrespective of species). If it is assumed for simplicity that the greater part of the metallic element in the resin exists in the form $MX_n^{(bn-a)-}$ and in the solution in the form $MX_m^{(bm-a)-}$ (generally $n$ is not equal to $m$), the coefficient may be written as

$$D\doteqdot\frac{[MX_n^{(an-a)-}]}{(MX_m^{(bm-a)-})} \quad (5)$$

From Eqs. 1, 2, 3 and 5 the following equation is derived:

$$D=\frac{[X^{b-}]^{n-a/b}}{(X^{b-})^{m-a/b}}\cdot\frac{K_n}{K_m}\cdot\frac{\gamma_{(MX_m^{(bm-a)-})}\gamma_{[X]}^{n-a/b}}{\gamma_{[MX_n^{(bn-a)-}]}\gamma_{(X)}^{m-a/b}} \quad (6)$$

or

$$\log D=(n-\frac{a}{b})\log[X^{b-}]-(m-\frac{a}{b})\log(X^{b-})+K+G \quad (7)$$

where

$$K=\log\{K_n/K_m\}$$

$$G=\log\frac{\gamma_{(MX_m^{(bm-a)-})}\gamma_{[X]}^{n-a/b}}{\gamma_{[MX_n^{(bn-a)-}]}\gamma_{(X)}^{m-a/b}}$$

And

$$\frac{d\{\log D+(m-a/b)\log(X^{b-})\}}{d\log[X^{b-}]}=n-\frac{a}{b} \quad (8)$$

$$\frac{d\{\log D-(n-a/b)\log[X^{b-}]\}}{d\log(X^{b-})}=-(m-\frac{a}{b}) \quad (9)$$

when $K$ and $G$ are constant. When $m$ is known and $D$, $(X^{b-})$ and $[X^{b-}]$ are measurable, $n$ can be determined graphically, and $m$ is also obtained when $n$ is known. Even if both are unknown, one of them can be determined in a case where either $(X^{b-})$ or $(X^{b-})$ can be kept constant.

Although it is practically impossible to set a condition in which the activity coefficient term is strictly constant, this condition may be realized roughly when a small quantity of the metallic element is used and the ionic strengths in the two phases are each kept constant by the addition of an indifferent anion, and therefore the complex form may be determined through measurements in the range where the greater part of the anion given is $X^{b-}$.

In the case of the mercury(II)-nitrate complex in the presence of sodium nitrate and perchlorate, where $Hg^{2+}$ is taken as $M^{a+}$, $NO_3^-$ as $X^{b-}$ and $ClO_4^-$ as an additional anion, Eq. 7 may become as follows:

$$\log D=(n-2)\log[NO_3^-]-(m-2)\log(NO_3^-)+K+G \quad (10)$$

Assuming that a mercuric ion does not form any metal-nitrate complex species in a moderately concentrated aqueous solution of nitrates, the following equations may be applicable,

$$\log D-2\log(NO_3^-)=(n-2)\log[NO_3^-]+K+G \quad (11)$$

and

$$\frac{d\{\log D-2\log(NO_3^-)\}}{d\log[NO_3^-]}=n-2 \quad (12)$$

where $K$ and $G$ are constant. From the slope of the curve $\log D-2\log(NO_3^-)$ vs. $\log[NO_3^-]$, $n$ can be determined. When $n$ is not in the vicinity of an integer, the coexistence of two complexes may be presumed.

## Experimental

Sodium nitrate solution and sodium perchlorate solution were prepared from the guaranteed and the first class reagent, respectively. Mercuric nitrate solution was prepared by dissolving the guaranteed reagent $Hg(NO_3)_2\cdot 1/2\sim 1\ H_2O$ in dilute nitric acid. These solutions were added to the resin so that the mixture of solutions had a volume of 10 ml., and contained 0.1 mmol. of mercury, 0.5 mmol. of nitric acid and a series of $NaNO_3+NaClO_4$ of various mixing ratios, providing that its total concentration was constant at individual series.

An anion exchanger Dowex 1-X8 of nitrate form was swollen in water and then filtered under suction, followed by the removal of the attached water by pressing between filter papers. Two or three grams of this resin was at once put in a stoppered small glass vessel. At the same time another 0.5 g. of this resin was converted into

chloride form in a small column and its exchange capacity was determined by the elution of the chloride ion with a sodium nitrate solution and by Mohr's titration of the effluent. The resin set in this way have a relatively constant exchange capacity and does not suffer an appreciable change in volume when it comes in contact with nitrate solution.

The batch experiment was carried out at total concentrations of the solution of 0.5, 1, 2, 3 and 5 M, and each series consisted of 4—6 batches of various nitrate concentrations. The resin and the solution were equilibrated at room temperature by being allowed to stand for an hour with frequent shaking.

After the supernatant liquid was directly taken for the dilute solution or the resin was separated from the solution by filtering with a glass filter under suction without further washing for the concentrated solution, the mercury in the solution was titrated as follows: mercury in 5 ml. of the supernatant or the filtrate was titrated with 0.0100 M EDTA solution after 1 ml. of 0.05 M Mg-EDTA, 1 ml. of $NH_4OH$-$NH_4Cl$ buffer (pH=10) and a few drops of Eriochrome Black T indicator were added. The amount of mercury in the resin was estimated by subtraction of that in the solution from the total amount. The distribution coefficient was calculated as

$$D=\frac{\left(\begin{array}{c}\text{millimole of Hg adsorbed per}\\ \text{milliequivalent of the resin}\end{array}\right)}{\left(\begin{array}{c}\text{millimole of Hg per milliliter}\\ \text{of the solution}\end{array}\right)}$$

On the other hand, the nitrate in the resin was determined spectrophotometrically as follows: the resin separated from the solution in the way described above was wrapped in a filter paper and pressed to remove the solution attached to the surface. About 1 g. of this resin was transferred into a short column, and then the nitrate ions were desorbed by 25 ml. of 2 M perchloric acid. The effluent was diluted to 50 ml. and its absorbance was measured at 300 mμ using the Shimadzu spectrophotometer QB-50. As shown by the calibration curve in Fig. 1, it may be recognized that the absorption of nitrate ion in the region $\sim 10^{-1}$ M in the presence of 1 M perchloric acid obeys Beer's law. The presence of mercuric, sodium and perchlorate ions has no effect. The exchange capacity of resin in the column was determined in the same way as was done before, for the purpose of estimating the total amount of nitrate in the resin. The amount of nitrate in the solution was estimated by subtraction. The nitrate concentration in the resin phase was represented as millimole of the ion per milliequivalent of the resin as in the calculation of $D$, because the quantity of an ion adsorbed per apparent weight of the resin is not suitable for a representation of concentration in a mixed solution system, since the density of resin varies with the nitrate-perchlorate exchange.

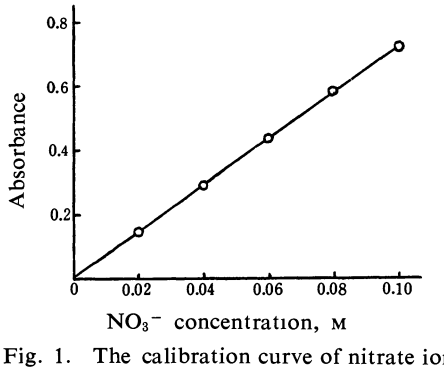



Fig. 1. The calibration curve of nitrate ion in the 1 M perchloric acid by spectrophotometric measurement at 300 mμ.

## Results and Discussion

Data of the measurement and the calculation are tabulated in Table I. $[NO_3]^*$ from spectrophotometric measurement means the total nitrate concentration in the resin phase i. e., the sum of concentrations of the free nitrate ion and the nitrate ion bound to the mercuric ion. Accordingly, the free nitrate ion concentration is represented by

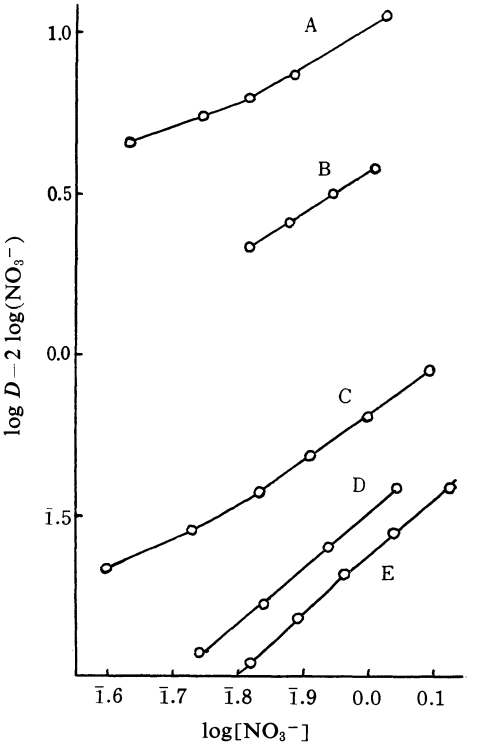



Fig. 2. Determination of $n$ at various total concentrations of the external solution in the nitrate-rich range. The rightest point in each curve is one in the absence of perchlorate.
Total external concentration: A: 0.5 M, B: 1 M, C: 2 M, D: 3 M and E: 5 M.

$$[NO_3^-] = [NO_3]^* - n[Hg]$$

assuming that almost all mercury in the resin exists as $Hg(NO_3)_n^{(n-2)-}$. Since $n$ is still unknown, $[NO_3^-]$ is practically estimated by

$$[NO_3^-] = [NO_3]^* - n^*[Hg]$$

where $n^*$ represents an approximate value of $n$, which may be obtained by $\log D - 2\log(NO_3^-)$ vs. $\log[NO_3]^*$ plot. A little deviation of $n^*$ from $n$ may hardly affect $[NO_3^-]$ and therefore the value of $n$.

In Fig. 2, $\log D - 2\log(NO_3^-)$ is plotted

TABLE I

A. 0.5 M series — Resin: 4.68 meq. Solution: 10 ml.

| Batch No. | 1 | 2 | 3 | 4 | 5 |
|---|---|---|---|---|---|
| $NaNO_3$ given, mmol. | 1.80 | 2.40 | 3.00 | 3.60 | 4.80 |
| $NaClO_4$ 〃, 〃 | 3.00 | 2.40 | 1.80 | 1.20 | 0.00 |
| $HNO_3$ 〃, 〃 | 0.50 | 0.50 | 0.50 | 0.50 | 0.50 |
| $Hg(NO_3)_2$ 〃, 〃 | 0.105 | 0.105 | 0.105 | 0.105 | 0.105 |
| (Hg), mmol./ml. | 0.00678 | 0.00632 | 0.00584 | 0.00538 | 0.00448 |
| [Hg], mmol./meq. | 0.00795 | 0.00893 | 0.00996 | 0.01094 | 0.01286 |
| $D$, ml./meq. | 1.17 | 1.41 | 1.71 | 2.04 | 2.87 |
| $[NO_3]^*$, mmol./meq. | 0.452 | 0.582 | 0.686 | 0.804 | 1.107 |
| $(NO_3^-)$, mmol./ml. | 0.507 | 0.507 | 0.518 | 0.523 | 0.500 |
| $\log D - 2\log(NO_3^-)$ | 0.659 | 0.740 | 0.803 | 0.872 | 1.060 |
| $n^*$[Hg], mmol./meq. ($n^*=3.2$) | 0.026 | 0.029 | 0.032 | 0.036 | 0.041 |
| $[NO_3^-]$, mmol./meq. | 0.426 | 0.553 | 0.654 | 0.767 | 1.065 |
| $\log[NO_3^-]$ | $\bar{1}.629$ | $\bar{1}.743$ | $\bar{1}.815$ | $\bar{1}.885$ | 0.027 |

B. 1 M series — Resin: 4.72 meq. Solution: 10 ml.

| Batch No. | 1 | 2 | 3 | 4 |
|---|---|---|---|---|
| $NaNO_3$ given | 7.60 | 8.40 | 9.20 | 10.00 |
| $NaClO_4$ 〃 | 2.40 | 1.60 | 0.80 | 0.00 |
| $HNO_3$ 〃 | 0.50 | 0.50 | 0.50 | 0.50 |
| $Hg(NO_3)_2$ 〃 | 0.105 | 0.105 | 0.105 | 0.105 |
| (Hg) | 0.00544 | 0.00484 | 0.00418 | 0.00370 |
| [Hg] | 0.01072 | 0.01199 | 0.01338 | 0.01440 |
| $D$ | 1.97 | 2.48 | 3.20 | 3.89 |
| $[NO_3]^*$ | 0.687 | 0.794 | 0.922 | 1.068 |
| $(NO_3^-)$ | 0.954 | 0.983 | 1.003 | 1.014 |
| $\log D - 2\log(NO_3^-)$ | 0.336 | 0.409 | 0.502 | 0.578 |
| $n^*$[Hg] ($n^*=3.3$) | 0.035 | 0.039 | 0.043 | 0.047 |
| $[NO_3^-]$ | 0.652 | 0.755 | 0.879 | 1.021 |
| $\log[NO_3^-]$ | $\bar{1}.814$ | $\bar{1}.878$ | $\bar{1}.944$ | 0.009 |

C. 2 M series — Resin: 6.90 meq. Solution: 10 ml.

| Batch No. | 1 | 2 | 3 | 4 | 5 | 6 |
|---|---|---|---|---|---|---|
| $NaNO_3$ given | 14.0 | 15.2 | 16.4 | 17.6 | 18.8 | 20.0 |
| $NaClO_4$ 〃 | 6.0 | 4.8 | 3.6 | 2.4 | 1.2 | 0.0 |
| $HNO_3$ 〃 | 0.50 | 0.50 | 0.50 | 0.50 | 0.50 | 0.50 |
| $Hg(NO_3)_2$ 〃 | 0.102 | 0.102 | 0.102 | 0.102 | 0.102 | 0.102 |
| (Hg) | 0.00670 | 0.00598 | 0.00524 | 0.00450 | 0.00384 | 0.00320 |
| [Hg] | 0.00507 | 0.00612 | 0.00719 | 0.00826 | 0.00922 | 0.01014 |
| $D$ | 0.76 | 1.02 | 1.37 | 1.84 | 2.40 | 3.17 |
| $[NO_3]^*$ | 0.414 | 0.555 | 0.706 | 0.841 | 1.030 | 1.287 |
| $(NO_3^-)$ | 1.88 | 1.90 | 1.91 | 1.94 | 1.93 | 1.87 |
| $\log D - 2\log(NO_3^-)$ | $\bar{1}.333$ | $\bar{1}.454$ | $\bar{1}.574$ | $\bar{1}.688$ | $\bar{1}.810$ | $\bar{1}.957$ |
| $n^*$[Hg] ($n^*=3.5$) | 0.018 | 0.021 | 0.025 | 0.029 | 0.032 | 0.035 |
| $[NO_3^-]$ | 0.396 | 0.534 | 0.681 | 0.812 | 0.998 | 1.252 |
| $\log[NO_3^-]$ | $\bar{1}.598$ | $\bar{1}.728$ | $\bar{1}.833$ | $\bar{1}.910$ | $\bar{1}.999$ | 0.097 |

TABLE I (Continued)

D. 3 M series — Resin: 4.96 meq. Solution: 10 ml.

| Batch No. | 1 | 2 | 3 | 4 |
|---|---|---|---|---|
| $NaNO_3$ given | 26.4 | 27.6 | 28.8 | 30.0 |
| $NaClO_4$ 〃 | 3.6 | 2.4 | 1.2 | 0.0 |
| $HNO_3$ 〃 | 0.50 | 0.50 | 0.50 | 0.50 |
| $Hg(NO_3)_2$ 〃 | 0.104 | 0.104 | 0.104 | 0.104 |
| (Hg) | 0.00688 | 0.00596 | 0.00484 | 0.00380 |
| [Hg] | 0.00701 | 0.00887 | 0.01112 | 0.01322 |
| $D$ | 1.02 | 1.49 | 2.30 | 3.48 |
| $[NO_3]^*$ | 0.579 | 0.728 | 0.912 | 1.156 |
| $(NO_3^-)$ | 2.92 | 2.97 | 3.00 | 3.00 |
| $\log D - 2\log(NO_3^-)$ | $\bar{1}.073$ | $\bar{1}.227$ | $\bar{1}.407$ | 1.588 |
| $n^*[Hg]$ ($n^*=3.8$) | 0.027 | 0.034 | 0.042 | 0.051 |
| $[NO_3^-]$ | 0.552 | 0.694 | 0.869 | 1.105 |
| $\log[NO_3^-]$ | $\bar{1}.742$ | $\bar{1}.841$ | $\bar{1}.939$ | 0.043 |

E. 5 M series — Resin: 4.84 meq. Solution: 10 ml.

| Batch No. | 1 | 2 | 3 | 4 | 5 |
|---|---|---|---|---|---|
| $NaNO_3$ given | 45.2 | 46.4 | 47.6 | 48.8 | 50.0 |
| $NaClO_4$ 〃 | 4.8 | 3.6 | 2.4 | 1.2 | 0.0 |
| $HNO_3$ 〃 | 0.50 | 0.50 | 0.50 | 0.50 | 0.50 |
| $Hg(NO_3)_2$ 〃 | 0.103 | 0.103 | 0.103 | 0.103 | 0.103 |
| (Hg) | 0.00470 | 0.00382 | 0.00304 | 0.00242 | 0.00190 |
| [Hg] | 0.01161 | 0.01342 | 0.01504 | 0.01632 | 0.01740 |
| $D$ | 2.47 | 3.51 | 4.94 | 6.74 | 9.16 |
| $[NO_3]^*$ | 0.706 | 0.829 | 0.981 | 1.155 | 1.429 |
| $(NO_3^-)$ | 4.73 | 4.79 | 4.84 | 4.87 | 4.86 |
| $\log D - 2\log(NO_3^-)$ | $\bar{1}.043$ | $\bar{1}.185$ | $\bar{1}.326$ | $\bar{1}.454$ | $\bar{1}.588$ |
| $n^*[Hg]$ ($n^*=3.8$) | 0.045 | 0.052 | 0.058 | 0.063 | 0.079 |
| $[NO_3^-]$ | 0.661 | 0.777 | 0.923 | 1.092 | 1.350 |
| $\log[NO_3^-]$ | $\bar{1}.820$ | $\bar{1}.890$ | $\bar{1}.965$ | 0.038 | 0.130 |

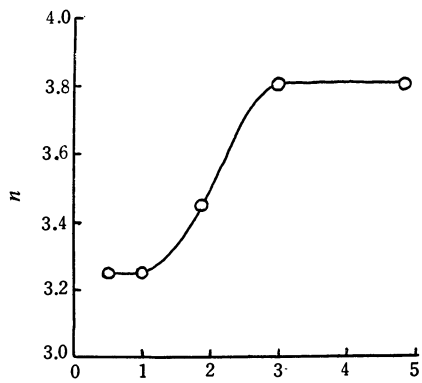



Fig. 3. $n$-Value of the mercury (II)-nitrate complex adsorbed from sodium nitrate solution of various concentrations.

against log $[NO_3^-]$. Each curve is approximately linear in the range where nitrate is rich compared with perchlorate in the resin. The gradient increases with the external total concentration from 1 M to 3 M, and scarcely varies in a region less than 1 M and from 3 to 5 M.

In Fig. 3, $n$ obtained from the slope is plotted against the concentration of the external solution.

From this curve, it will be recognized that mercury is taken up from a sodium nitrate solution as $Hg(NO_3)_3^-$ in the region from 0.5 to 1 M of the external concentration, as $Hg(NO_3)_4^{2-}$ in the region from 3 to 5 M, and as a mixture of $Hg(NO_3)_3^-$ and $Hg(NO_3)_4^{2-}$ in the region from 1 to 3 M. One might presume that some portions are adsorbed as $Hg(NO_3)_3^-$ in the region from 3 to 5 M solution, since $n=3.8$. However, this possibility may be weakened by considering the fact that $n$ does not rise with an increase of the external nitrate concentration in this region. Furthermore, it may be reasonable to consider that the complex contains no hydrogen ion because the concentration of nitric acid is low.

Although it was assumed that mercury exists only as $Hg^{2+}$ in the solution phase, it may

also be possible that a lower complex, such as $Hg(NO_3)^+$ or $Hg(NO_3)_2^0$, exists there when the nitrate concentration is as high as 3 or 5 M. When the presence of these species is assumed in the solution phase, $n$-value may somewhat deviate from that in the case when the presence of $Hg^{2+}$ only is assumed, through the change of $m$ in Eq. 10. However, these deviations are so small at 3 and 5 M, as estimated from data in Table I, that this uncertainty may hardly affect the conclusion as a whole. The reason why $n$ at the plateau does not take an integer is not clear enough at present.

A number of sources of error are considered. First, failure in realizing the condition where the activity coefficient term is constant for lack of knowledge on activity in a resin and a concentrated solution, must be mentioned. The ideal condition could not be established even by keeping the external ionic strength constant. Besides, there are experimental errors; namely, poor reproducibility of dryness of the resin on weighing, the change in volume on mixing of the resin and the solution, and imperfect removal of the attached solution from the resin. In spite of these difficulties, the present method appears to give some conclusion on a metal complex form.

Though the changes of pH and temperature may have some appreciable effect, they were not studied in this work.

**Summary**

1) The equations for determining the composition of a metal complex using an anion exchange resin have been derived by considering the complex formation equilibria in both the resin phase and the solution phase.

2) The method based on these equations was successfully applied to the investigation of mercury(II)-nitrate complex at various external nitrate concentrations by means of the sodium nitrate-sodium perchlorate mixed solution.

3) Mercury(II) adsorbed from a sodium nitrate solution exists in the form of $Hg(NO_3)_3^-$ at the external nitrate concentration of 0.5～1 M, $Hg(NO_3)_4^{2-}$ at 3～5 M and a mixture of $Hg(NO_3)_3^-$ and $Hg(NO_3)_4^{2-}$ at the middle of these concentrations, though no anionic complex appears to be present in an ordinary nitrate solution.

The author wishes to express his sincere thanks to Professor J. Yoshimura of Kyushu University for his suggestions and encouragement.

*Department of Chemistry*
*Faculty of Science*
*Kyushu University*
*Hakozaki, Fukuoka*

# *Theory on the Light Scattering of High Polymer Solutions Considering the Anisotropy of Segments**

By Masayuki NAKAGAKI

(Received November 21, 1960)

To discuss the physico-chemical properties of high polymer solutions, the so-called pearl necklace model is often used. In the theory of light scattering, too, the segments are usually assumed to be small spheres which scatter light according to Rayleigh's theory, and the interference between scatterd light from these Rayleigh spheres is considered[1,2]. In some cases, however, the segments of high polymer are not spherical but optically anisotropic.

In the present paper, the angular distribution of the intensity of light scattered by the high polymer solution is calculated theoretically, taking the anisotropy of the segments into account, and the theory is applied for the analysis of the Zimm plot.

## Theoretical

**Scattering at Infinite Dilution.**—In the studies of light scattering of high polymer solutions, the Zimm plot method is often used. Curves on the Zimm plot are usually formulated by the following equation for the polymers of spherical segments and for infinite dilution ($c \to 0$):

* Presented at the 9th Annual Meeting of the Society of Polymer Science, Osaka, May, 1960.

1) B. H. Zimm, R. S. Stein and P. Doty, *Polymer Bull.*, **1**, 90 (1945).

2) P. Debye, *J. Phys. & Colloid Chem.*, **51**, 18 (1947).

$$Kc/R_u(\theta) = 1/MP_1(\theta) \quad (1)$$

where $K$ is the well-known constant, $c$ is the concentration, $M$ is the molecular weight, and $P_1(\theta)$ is the intramolecular (intersegmental) interference factor given by[1,2]

$$P_1(\theta) = (2/\sigma^2)\,[\exp(-\sigma) - (1-\sigma)] \quad (2)$$

In this equation,

$$\sigma = (8\pi^2/3)\,(\overline{R^2}/\lambda^2)\sin^2(\theta/2) \quad (3)$$

where $\overline{R^2}$ is the mean square end-to-end distance, $\lambda$ is the wavelength of light in the medium, and $\theta$ is the scattering angle. The wavelength in the medium $\lambda$ is related to the the wavelength in vacuum $\lambda_0$ by the equation,

$$\lambda = \lambda_0/\mu_1 \quad (4)$$

where $\mu_1$ is the refractive index of the medium.

The quantity $R_u(\theta)$ is defined by

$$R_u(\theta) = \frac{J_u(\theta)/I_0}{1+\cos^2\theta} \quad (5)$$

where $J_u(\theta)$ is the intensity of scattered light per unit solid angle at the scattering angle $\theta$ when unpolarized incident light is used, and $I_0$ is the intensity of incident light (per unit area). The factor $(1+\cos^2\theta)$ in Eq. 5 expresses the angular dependency of the scattered light from a Rayleigh sphere or a spherical segment, and because of this factor, the quantity $R_u(\theta)$ is called reduced scattering intensity. It is, however, obvious that the angular dependency of scattered intensity can not be reduced by the factor $(1+\cos^2\theta)$ if the segments are not spherical. In the latter case, another factor $P_u(\theta)$ must be introduced, and Eq. 1 must be rewritten to

$$Kc/R_u(\theta) = 1/M^*P_1(\theta)P_u(\theta) \quad (6)$$

where $M^*$ is the apparent molecular weight of the high polymer, and

$$P_u(\theta) = \frac{2}{1+\cos^2\theta} \cdot \frac{\langle i_u(\theta)\rangle}{\langle i_u(0)\rangle} \quad (7)$$

The quantity $\langle i_u(\theta)\rangle$ is defined by the equation:

$$J_u'(\theta)/I_0 = (\lambda^2/4\pi^2)\langle i_u(\theta)\rangle \quad (8)$$

where $J_u'(\theta)$ is the intensity of light scattered by one segment.

**Scattering from an Anisotropic Segment.**—A segment or a particle may have two kinds of optical anisotropy: the one is "intrinsic" anisotropy and the other is "form" anisotropy. The intrinsic anisotropy occurs when the dispersed phase (that is the material composing the particle) itself has optical anisotropy because of, e. g., the orientation of valence bonds in the phase. In this case, the "excess" polarizability[3] of the dispersed phase can be expressed by an ellipsoid (a tensor in a more mathematical terminology) or a spheroid. For the sake of simplicity, a spheroid of the excess polarizability with principal axes $(\alpha_a, \alpha_b, \alpha_b)$ will be considered here. Then, the optical anisotropy is expressed by the ratio $p_\alpha$,

$$p_\alpha = (\alpha_b/\alpha_a) \quad (9)$$

The form anisotropy, on the other hand, is the optical anisotropy due to the anisometry. In other words it is due to the anisotropic shape of the particle made of isotropic phase. If the shape of the particle is assumed to be a spheroid (it may of course be an ellipsoid in more general cases) and its semi-axes are $(a, b, b)$, the anisometry is expressed by the axial ratio:

$$p = a/b \quad (10)$$

If the particle is sufficiently small compared to the wavelength of light, it may be assumed that one dipole is induced in a particle and the oscillation of the dipole radiates the scattered light. In this case, too, a spheroid of excess polarizability can be considered for each spheroidal particle, although the axial ratio of the polarizability spheroid $p_\alpha$ is not necessarily equal to the axial ratio $p$ of the particle. Therefore, it can be expected that both kinds of anisotropy give the same type of expression for the angular dependency of the scattered light intensity.

The intensity of scattered light can easily be calculated for a particle having a spheroid of excess polarizability $(\alpha_a, \alpha_b, \alpha_b)$ by assuming that the electric vector of the scattered light is parallel and proportional to the induced dipole, the proportionality constant being set at $k$. On the other hand, the intensity of scattered light by an anisometric particle has already been calculated by Rayleigh[4] and Gans[5], if the particle is sufficiently small compared to the wavelength of light. These two theories give equations of the same form as expected above:

$$\left.\begin{aligned}
i_{//\to//} &= \left[A\cos\theta + B\left(\sin^2\Theta\cos^2\varphi\cos\theta + \frac{1}{2}\sin 2\Theta\cos\varphi\sin\theta\right)\right]^2 \\
i_{//\to\perp} &= \left[\frac{1}{2}B\sin^2\Theta\sin 2\varphi\right]^2 \\
i_{\perp\to//} &= \left[\frac{1}{2}B(\sin^2\Theta\sin 2\varphi\cos\theta + \sin 2\Theta\sin\varphi\sin\theta)\right]^2 \\
i_{\perp\to\perp} &= [A + B\sin^2\Theta\sin^2\varphi]^2
\end{aligned}\right\} \quad (11)$$

3) It is the difference between the polarizabilities of particle and medium as already used, for example, by A. Peterlin, W. Heller and M. Nakagaki [*J. Chem. Phys.*, **28**, 470 (1958).].

4) L. Rayleigh, *Phil. Mag.*, **44**, 28 (1897).

5) R. Gans, *Ann. Phys.*, (4), **37**, 881 (1912), **62**, 33 1(1920).

where $\theta$ is the scattering angle and $(\Theta, \varphi)$ are the spherical coordinates of the direction of the symmetry axis of the spheroid ($\alpha_a$-axis or a-axis). The suffixes $i_{//\to\perp}$ and so forth mean that the incident light is oscillating parallel to the observation plane and the component of scattered light oscillating prependicularly to the observation plane is observed and so forth. The constants $A$ and $B$ are, in the case where the spheroid of excess polarizability is considered

$$\left.\begin{aligned} A&=k\alpha_b \\ B&=k(\alpha_a-\alpha_b) \end{aligned}\right\} \quad (12)$$

and in the case of anisometric particle

$$\left.\begin{aligned} A&=p^2\alpha^3(m^2-1)/[3+(m^2-1)(3/4\pi)P'] \\ B&=p^2\alpha^3(m^2-1)/[3+(m^2-1)(3/4\pi)P]-A \end{aligned}\right\} \quad (13)$$

Here

$$\alpha = 2\pi a/\lambda \quad (14)$$

and

$$m = \mu_2/\mu_1 \quad (15)$$

where $\mu_2$ and $\mu_1$ are refractive indices of the particle and the medium, respectively. As shown by Gans[5]

$$P+2P'=4\pi \quad (16)$$

For a prolate spheroid ($p\leqslant 1$),

$$P=4\pi[(1-e^2)/e^2] \times\{(1/2e)\ln[(1+e)/(1-e)]-1\} \quad (17)$$

where $e$ is the eccentricity given by

$$e=\sqrt{1-p^2} \quad (18)$$

and for an oblate spheroid ($p\geqslant 1$),

$$P=(4\pi/\varepsilon^2)[1-(\sqrt{1-\varepsilon^2}/\varepsilon^2)\sin^{-1}\varepsilon] \quad (19)$$

where $\varepsilon$ is the eccentricity given by

$$\varepsilon=\sqrt{1-1/p^2} \quad (20)$$

**Optical Anisotropy of Anisometrical Segments.** —As already stated, a spheroid of excess polarizability can be considered for each spheroidal particle (segment in the present paper) if the size of the spheroid is small compared to the wavelength of light used, but the axial ratio of these spheroids, $p_\alpha$ and $p$, are not necessarily equal. Now, on the basis of Eq. 12,

$$p_\alpha=1/(B/A+1) \quad (21)$$

and according to Eq. 13,

$$p_\alpha=[1+(m^2-1)(P/4\pi)]/[1+(m^2-1)(P'/4\pi)] \quad (22)$$

For spherical particles ($p=1$), the relation $P=P'=4\pi/3$ is obtained from Eq. 17 and also from Eq. 19, which gives

$$p_\alpha=1 \qquad \text{for } p=1 \quad (23)$$

In this case, and only in this case, $p_\alpha=p$. On the other hand, if the particle is an infinitesimally thin rod ($p=0$), the relations $P=0$ and $P'=2\pi$ are obtained from Eqs. 16 and 17, which give

$$p_\alpha=2/(m^2+1) \qquad \text{for } p=0 \quad (24)$$

while if the particle is an infinitesimally thin disk ($p=\infty$), the relations $P=4\pi$ and $P'=0$ are obtained from Eqs. 16 and 19, which give

$$p_\alpha=m^2 \qquad \text{for } p=\infty \quad (25)$$

Referring to these extreme cases, it can be concluded that the value of $p$ and $p_\alpha$ are not equal for anisometric particles. Moreover, the value of $p_\alpha$ must be in the range,

$$2/(m^2+1) < p_\alpha < m^2 \quad (26)$$

for anisometrical particles and, if the value of $p_\alpha$ is out of this range, particles must have the intrinsic anisotropy.

**Scattering from Randomly Oriented Segments.** —If the orientation of segments in a flexible high polymer molecule is assumed to be completely random, the value of $\langle i\rangle$ can be calculated by averaging Eq. 11 over all ranges of $\Theta$ and $\varphi$. The results are:

$$\left.\begin{aligned} \langle i_{//\to//}\rangle &= (1/15)B^2+[A^2+(2/3)AB \\ &\quad +(2/15)B^2]\cos^2\theta \\ \langle i_{//\to\perp}\rangle &= \langle i_{\perp\to//}\rangle=(1/15)B^2 \\ \langle i_{\perp\to\perp}\rangle &= A^2+(2/3)AB+(1/5)B^2 \end{aligned}\right\} \quad (27)$$

Therefore, the quantity $\langle i_u(\theta)\rangle$ for unpolarized light:

$$\langle i_u(\theta)\rangle=(1/2)\langle i_{//\to//}+i_{//\to\perp}+i_{\perp\to//}+i_{\perp\to\perp}\rangle \quad (28)$$

can be expressed as follows:

$$\langle i_u(\theta)\rangle=(1/2)\{[A^2+(2/3)AB+(2/5)B^2 +[A^2+(2/3)AB+(2/15)B^2]\cos^2\theta\} \quad (28a)$$

This gives the following value of $P_u(\theta)$ of Eq. 7.

$$\left.\begin{aligned} P_u(\theta)&=1+Q_u(1-\cos^2\theta)/(1+\cos^2\theta) \\ Q_u&=(2/15)(B/A)^2/[1+(2/3)(B/A) \\ &\quad +(4/15)(B/A)^2] \end{aligned}\right\} \quad (29)$$

The value of $P_u(\theta)$ reduces to unity for spherical segments, because $B=0$ and $Q_u=0$ if $p=1$.

In an actual high polymer molecule, the mutual orientation of segments in a molecule might not be completely random, and this might require us to recalculate $P_1(\theta)$ of Eq. 6, but it is not easy to know the mutual orientation of segments in a polymer molecule. However, one may, at first, average the intensity of light scattered from each segment over all

possible orientations of the segment, and then consider the interference of these scattered beams, because the segments are originally defined as dynamically independent units. In this method of approximation, one can use Eq. 6 together with Eq. 29 for $P_u(\theta)$ and Eq. 2 for $P_1(\theta)$. Of course, the extension of the high polymer chain might be different according to whether the segments are isotropic or anisotropic. This affects the value of $P_1(\theta)$. This effect, however, had already been taken care of by $\overline{R^2}$ in Eq. 3.

**Apparent Molecular Weight.**—In the case of $\theta=0$, Eq. 6 reduces to

$$Kc/R_u(0)=1/M^* \tag{30}$$

but the apparent molecular weight $M^*$ thus obtained does not coincide with the true molecular weight $M$ except when the segments are spherical.

Debye's theory[6] of light scattering based upon the fluctuation theory is originally derived for the turbidity $\tau$, but not for the reduced scattering intensity $R_u(\theta)$. Therefore,

$$Hc/\tau=1/M \tag{31}$$

is always correct for infinitely dilute solutions irrespective of whether the particles (segments in the present paper) are spherical or not, but Eq. 30 is not always correct because the relation used in order to convert $\tau$ to $R_u(\theta)$:

$$R_u(\theta)/\tau=3/16\pi \qquad \text{for } p=1 \tag{32}$$

is correct only for spherical particles. Therefore, the relation

$$K=(3/16\pi)H \tag{33}$$

must not be used for anisometric particles to obtain the correct values of the molecular weight, or, if the Eq. 33 is still used for anisometric particles, the apparent molecular weight $M^*$ thus obtained must be reduced to the true molecular weight $M$, by using a correction factor to be obtained from the true relationship between $R_u(\theta)$ and $\tau$.

The reduced scattering intensity $R_u(\theta)$ is given by

$$R_u(\theta)=(\lambda^2N/4\pi^2)\,[\langle i_u(\theta)\rangle/(1+\cos^2\theta)]\,P_1(\theta) \tag{34}$$

where $N$ is the number of segments per unit volume, while the turbidity $\tau$ is given by

$$\tau=(\lambda^2N/2\pi)\int_0^\pi \langle i_u(\theta)\rangle \sin\theta\, d\theta \tag{35}$$

By using Eq. 28a,

$$\tau=(2\lambda^2N/3\pi)\,[A^2+(2/3)AB+(1/3)B^2] \tag{35a}$$

is obtained. Then referring to Eq. 29 and to the equation:

$$R_u(\theta)/\tau=(3/16\pi)P_1(\theta)P_u(\theta)M^*/M \tag{36}$$

the relation:

$$M/M^*=1+(1/15)(B/A)^2/[1+(2/3)(B/A)+(4/15)(B/A)^2] \tag{37}$$

is obtained, keeping the relation between $K$ and $H$ as it is in Eq. 33.

### Comparison with Experimental Data

Serious anomalies in the Zimm plots have been found by Ehrlich and Doty[7] for aqueous solutions of copolymers of methacrylic acid and 2-dimethylaminoethyl methacrylate. Their data for isoionic P-7 (a fractionated sample) in 0.10 M sodium chloride and in distilled water are read off from their figures and plotted in Figs. 1 and 2 for the values extrapolated

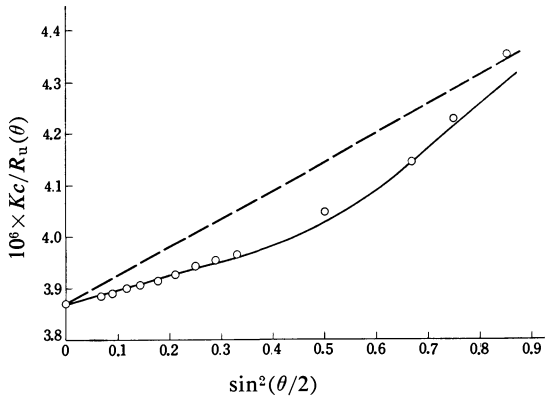



Fig. 1. Isoionic P-7 in 0.10 M sodium chloride.

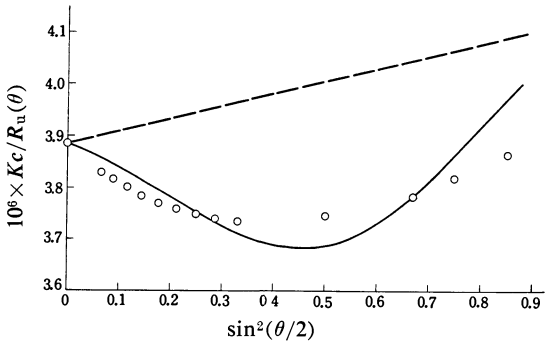



Fig. 2. Isoionic P-7 in distilled water.

to the infinite dilution. They also stated in their paper that the molecular weight of the sample P-7 obtained from light scattering measurement by the dissymmetry method was 270000 and that the square root of the mean

6) P. Debye, *J. Appl. Phys.*, **15**, 338 (1944).

7) G. Ehrlich and P. Doty, *J. Am. Chem. Soc.*, **76**, 3764 (1954).

square end-to-end distance $\sqrt{\overline{R^2}}$ obtained from viscosity data on the basis of the Flory-Fox theory with the correction for polydispersity was 410 Å in 0.10 M sodium chloride and 270 Å in distilled water. The wavelength used was $\lambda_0=4360$ Å in vacuum, so that $\lambda=3254$ Å in water since $\mu_1=1.33986$ at 25°C. By using these values in Eqs. 2 and 3, the value of $P_1(\theta)$ can be calculated. If the segments are assumed to be spherical and $P_u(\theta)=1$, the value of $Kc/R_u(\theta)$ can be calculated from Eq. 6 by using the experimental values of $Kc/R_u(0)$, which is equal to $1/M^*$. The results of calculations are shown in Figs. 1 and 2 with broken lines. Experimental values shown by open circles are definitely lower than broken lines especially at about $\sin^2(\theta/2)=0.5$ or $\theta=90°$. If these discrepancies are due to the anisotropy of segments, the deviation of $P_u(\theta)$ from unity must be expressed by Eq. 29. Using the values of $Q_u$ determined to obtain the best fit with the experimental plots and cited in Table I, solid curves in Figs. 1 and 2 are obtained.

TABLE I. CONSTANTS FOR ISOIONIC P-7

| | In 0.10 M NaCl (Fig. 1) | In water (Fig. 2) |
|---|---|---|
| $Q_u$ | 0.0291 | 0.0870 |
| $B/A$ | 0.565 | 1.190 |
| $p_\alpha$ | 0.639 | 0.457 |
| $\rho_2$ | 3.26 | 5.93 |
| $M^*$ | 258000 | 257000 |
| $M/M^*$ | 1.0146 | 1.0448 |
| $M$ | 262000 | 269000 |

In the case of 0.10 M sodium chloride as the solvent (Fig. 1), the initial slope of the Zimm plot is smaller than that of the broken curve, although its sign is still positive. In the case of distilled water as the solvent (Fig. 2), the initial slope is negative. The anomalous negative slope could not be expected from any theory presented so far. On the basis of the present aspect, however, the anomalous negative value can be explained by the great value of $Q_u$, the value being about three times greater for Fig. 2 than for Fig. 1. The value of $B/A$ calculated from Eq. 29 is about twice as great for Fig. 2 as for Fig. 1. However, the axial ratio $p_\alpha$ of the spheroid of polarizability to give the anisotropy of segments is only 30% smaller for Fig. 2 than for Fig. 1. This demonstrates that only the small difference in the anisotropy of segments results in any very great difference in the initial slope of the Zimm plot.

The value of $p_\alpha$ for either case is smaller than unity. This means that the spheroid of the excess polarizability is prolate in both cases. To discuss whether this anisotropy is due to intrinsic anisotropy or anisometry, the value of the relative refractive index $m$ must be known. On the basis of the mixture rule,

$$d\mu_{12}/dc=(m-1)\mu_1/\rho_2 \qquad (38)$$

By using $d\mu_{12}/dc=0.188$ as reported by the original authors, the value of $m$ is obtained if the value of the density of the polymer $\rho_2$ is known. If the value of $\rho_2$ is 1.4, the value of $m$ is 1.20. These values seem to be reasonable. Then, according to Eq. 26,

$$0.82<p_\alpha<1.44 \qquad \text{for } m=1.20 \qquad (39)$$

if the anisotropy is due to the anisometry. Since the values cited in Table I are smaller than the limiting value, the anisotropy in these cases must be intrinsic. Putting it the other way around, the value of $\rho_2$, which is necessary to explain the anisotropy as the form anisotropy, may be estimated according to Eq. 24 for infinitesimally thin rods. The values of $\rho_2$ must be greater than 3~6 as shown in Table I, which is too great for polymers. Therefore, the anisotropy seems to be intrinsic.

On the molecular weight of the polymer, the value of the apparent molecular weight $M^*$ obtained from the value of $Kc/R_u(0)$ and cited in Table I is a little too small compared to the value $M=270000$ reported by the original authors. The correction factor $M/M^*$ given by Eq. 37 is calculated and cited in Table I. The molecular weight corrected by this factor ($M$ in Table I) is closer to 270000 than $M^*$ is.

Thus the essential feature of the anomalous $\theta$ dependency of the Zimm plot of isoionic P-7 could be explained by assuming that the segments are anisotropic. However, the agreement between the experimental plots and the theoretical curves in Figs. 1 and 2 is not perfect yet. For the discrepancy, several reasons may be pointed out: Some errors might have been made in the double extrapolation in the Zimm-plot to obtain the value of $Kc/R_u(0)$; the estimation of $\overline{R}^2$ used to calculate $P_1(\theta)$ might not be correct; the effect of the molecular weight distribution was neglected; the mutual orientation of segments in a polymer chain is not completely random, but this effect was neglected. Some of these points, especially the last one, will be discussed in a later paper.

### Proposal for the Direct Measurement of $Q_u$

If the value of $Q_u$ can be measured directly, it will give a good criterion to see whether the phenomenon is actually due to the anisotropy of segments or not. This will be done by measuring the scattering ratio, $S$, that is

the ratio of scattered intensities from parallelly and perpendicularly polarized incident beams.

$$S(\theta)=J_{//}(\theta)/J_{\perp}(\theta)=\langle i_{//}(\theta)\rangle/\langle i_{\perp}(\theta)\rangle \quad (40)$$

According to the relations:

$$\left.\begin{aligned}\langle i_{//}\rangle&=\langle i_{//\to//}+i_{//\to\perp}\rangle=(2/15)B^2\\&\quad+[A^2+(2/3)AB+(2/15)B^2]\cos^2\theta\\\langle i_{\perp}\rangle&=\langle i_{\perp\to//}+i_{\perp\to\perp}\rangle=A^2\\&\quad+(2/3)AB+(4/15)B^2\end{aligned}\right\} \quad (41)$$

the value of $S(\theta)$ theoretically obtained is

$$S(\theta)=Q_u+(1-Q_u)\cos^2\theta \quad (42)$$

At $\theta=90°$,

$$S(90)=Q_u \quad (43)$$

Therefore, the scattering ratio at 90° is the value of $Q_u$.

## Summary

The anomaly of the angular dependency of the reduced scattering intensity in the Zimm plot for infinitely dilute solution was discussed for the solutions of high polymer molecules having anisotropical segments, and the theoretical relationship between $Kc/R_u(\theta)$ and $\theta$ was derived. The equation had the same form for both intrinsic anisotropy and form anisotropy. In the latter case, the axial ratio of the spheroid of excess polarizability was concluded to be not equal to the axial ratio of the segment. Moreover, the correction factor for the molecular weight was derived.

Applying these theoretical equations to the experimental data by Ehrlich and Doty on the solution of copolymer of methacrylic acid and 2-dimethylaminoethyl methacrylate, it was shown that the anomalies of the Zimm plot could be explained by assuming that the segments have intrinsic anisotropy.

It was also suggested that the scattering ratio is a good criterion to see whether the anomaly is actually due to the anisotropy of segments or not.

*Faculty of Pharmacy*
*Kyoto University*
*Sakyo-ku, Kyoto*

# *The Mannich Base of Troponoid and its Application. V. On the Mannich Base of 3-Isopropyltropolone (α-Thujaplicin)*

By Kyozo OGURA

(Received December 2, 1960)

Seto and the present author applied the Mannich reaction to 3, 7-dibromotropolone and prepared various 5-substituted derivatives of tropolone[1-3]. In order to make further extension of the Mannich reaction to tropolones, examinations were made on the Mannich reaction of 3-isopropyltropolone. The present paper describes the syntheses of a few Mannich bases of 3-isopropyltropolone and some of their properties.

Treatment of 3-isopropyltropolone (I) with folmaldehyde solution and morpholine, in the presence of acetic acid, affords 3-isopropyl-5, 7-dimorpholinomethyltropolone (II) as colorless crystals,, m. p. 76°C. The use of piperidine in place of morpholine gives 3-isopropyl-5, 7-dipiperidinomethyltropolone (III) as yellow crystals, m. p. 79.5°C. The morpholinomethyl group in II and the piperidinomethyl group in III are easily substituted by cationoid reagents. Reaction of II and III with *p*-tolyldiazonium salt respectively gives 3-isopropyl-5-tolylazo-7-morpholinomethyl- (IV), m. p. 134°C, and 3-isopropyl-5-tolylazo-7-piperidinomethyltropolone (V), m. p. 192°C. Both II and III give the known 3-isopropyl-5, 7-dibromotropolone[4] (VI) by the action of two molar equivalents of bromine. Treatment of II with excess of piperidine and formaldehyde solution gives III. In this case, no reaction occurs if formaldehyde is not used so that the above reaction is not a simple amine exchange but the substitution of the morpholinomethyl group with piperidinomethyl group.

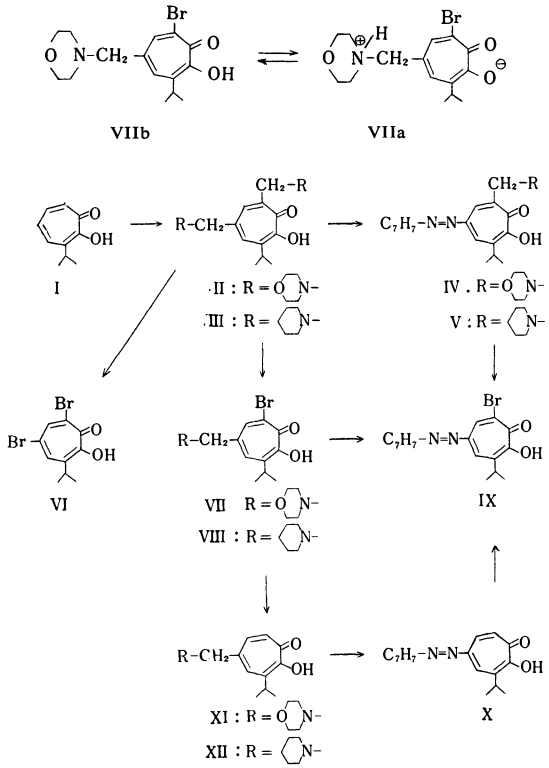
Addition of one molar equivalent of bromine to II and III affords the respective monobromo compounds of m. p. 93°C and of m. p. 137°C.

1) S. Seto and K. Ogura, This Bulletin, 32, 493 (1959).
2) S. Seto and K. Ogura, ibid., 32, 1118 (1959).
3) S. Seto and K. Ogura, ibid., 33, 1084 (1960).

These were identified from experimental facts described below as 3-isopropyl-5-morpholinomethyl-7-bromotropolone(VII) and 3-isopropyl-5-piperidinomethyl-7-bromotropolone (VIII). Addition of formaldehyde solution and morpholine to 3-isopropyl-7-bromotropolone[4] affords the same monobromo compounds as that derived from II. However, this fact alone is not sufficient to conclude that the structure of this substance is represented by VII since the bromine in the 7-position might have undergone rearrangement to 5-position during the Mannich reaction of 3-isopropyl-7-bromotropolone*1.

The reaction of VII and VIII with *p*-tolyldiazonium salt results in the formation of 3-isopropyl-5-tolylazo-7-bromotropolone (IX), m. p. 145°C from both compounds and IX is also obtained by the application of bromine to IV, V or 3-isopropyl-5-tolylazotropolone[4] (X). Hydrogenolysis of VII and VIII over palladium-carbon catalyst results in absorption of one molar equivalent of hydrogen and a monomorpholinomethyl- (m. p. 78°C) and a monopiperidinomethyl derivative (m. p. 113°C) are obtained respectively. Since these substances form 3-isopropyl-5-tolylazotropolone (X) by the reaction with *p*-tolyldiazonium salt, these are known to be 3-isopropyl-5-morpholinomethyl- (XI) and 3-isopropyl-5-piperidinomethyltropolone (XII). These facts prove that the above-mentioned monobromo compounds are VII and VIII.

Recrystallization of VII from methanol produces yellow granular crystals (VIIa) of m. p. 93°C which, upon further recrystallization from petroleum ether, change into colorless rods (VIIb), m. p. 64°C. The mixed melting point of these substances gives an intermediate value and when VIIb is left in air, it gradually acquires a yellowish tint and changes into VIIa. From elemental analytical values and comparison of infrared absorption spectra in the solid state, the former VIIa was found to have one mole of water of crystallization and to take the zwitter-ion structure. The infrared spectrum of VIIa lacked the absorption band due to the OH stretching vibration of tropolone and exhibited an intense absorption of $N^+H$ stretching mode at 2530 $cm^{-1}$. There were absorption bands at 3470 and 3400 $cm^{-1}$ due to crystal water. On the other hand, the infrared spectrum of VIIb lacked the absorption corresponding to $N^+H$ stretching mode but exhibited a strong absorption band of OH stretching mode at 3180 $cm^{-1}$. Similarly, examination of the infrared spectra showed that the yellow crystalline III, VIII and XII took the zwitter-ion structure and that the colorless crystalline II and XI did not take such a structure.




## Experimental*2

**3-Isopropyl-5,7-dimorpholinomethyltropolone(II).** — A mixture of 1 g. of 3-isopropyltropolone, 4 ml. of 37% formalin, 4 ml. of morpholine and 0.8 ml. of acetic acid was stirred mechanically at 60°C for 1 hr., 10 ml. of water was added, and wall of the vessel was scratched with a glass rod while being cooled with ice, by which crystals gradually precipitated. After allowing the mixture to stand overnight in an ice chamber, the crystals were collected by filtration, washed with water, and recrystallized from methanol to colorless needles (II), m. p. 74~76°C. Yield, 1.8 g.

Found: C, 66.22; H, 7.74; N, 7.83. Calcd. for $C_{20}H_{30}O_4N_2$: C, 66.27; H, 8.34; N, 7.73%.

UV $\lambda_{max}^{MeOH}$ m$\mu$ (log $\varepsilon$): 246 (4.47), 326 (3.92), 370 (3.74).

**3-Isopropyl-5,7-dipiperidinomethyltropolone(III).** — A mixture of 0.6 g. of 3-isopropyltropolone, 2 ml. of 37% formalin, 2 ml. of piperidine, and 0.4 ml. of acetic acid was stirred mechanically at 60°C for 1 hr., 5 ml. of water was added, and wall of the vessel was scratched with a glass rod while being cooled in ice, by which yellow crystals gradually

4) T. Nozoe, Y. Kitahara and T. Ikemi, *Proc. Japan Acad.*, **27**, 193 (1951).

*1 S. Seto and T. Sato found that application of the Mannich reaction to 4-isopropyl-7-bromotropolone afforded 3-bromo-4-isopropyl-7-morpholinomethyltropolone.

*2 All melting points are uncorrected. The microanalyses were carried out by Mr. S. Oyama and Miss Y. Endo of this Institute, to whom the author is indebted.

precipitated out. After standing in an ice chamber overnight, the crystals were collected by filtration, washed with water, and recrystallized from methanol. M. p. 78~79.5°C. Yield, 0.9 g.

Found: C, 73.41; H, 9.22; N, 7.43. Calcd. for $C_{22}H_{34}O_2N_2$: C, 73.70; H, 9.56; N, 7.81%.

UV $\lambda_{max}^{MeOH}$ mμ (log ε): 250 (4.36), 346 (3.88), 400 (3.58).

IR ν $N^+$-H 2220 and 2480 $cm^{-1}$ (broad) (KBr disk).

**3-Isopropyl-5-tolylazo-7-morpholinomethyltropolone (IV).** — To a solution of 180 mg. of II in 1 ml. of pyridine, a diazonium salt prepared from *p*-toluidine, 40 mg. of sodium nitrite, and 0.2 ml. of concentrated hydrochloric acid was added under cooling with ice by which a red precipitate separated out immediately. The precipitate was collected and recrystallized from methanol to reddish orange crystals (IV), m. p. 133~134°C. Yield, 150 mg.

Found: C, 69.03; H, 7.02; N, 10.87. Calcd. for $C_{22}H_{27}O_3N_3$: C, 69.27; H, 7.13; N, 11.02%.

UV $\lambda_{max}^{MeOH}$ mμ (log ε): 237 (4.26), 290 (4.07), 400 (4.36), 460 (4.08).

**3-Isopropyl-5-tolylazo-7-piperidinomethyltropolone (V).** — A diazonium salt, prepared from 30 mg. of *p*-toluidine, 20 mg. of sodium nitrite, and 0.1 ml. of concentrated hydrochloric acid, was added to pyridine solution (ca. 1 ml.) of 100 mg. of III and a red precipitate formed immediately. V was obtained as orange crystals of m. p. 191~192°C by the same procedure as for IV. Yield, 50 mg.

Found: C, 72.68; H, 7.48; N, 11.18. Calcd. for $C_{23}H_{29}O_2N_3$: C, 72.79; H, 7.70; N, 11.07%.

UV $\lambda_{max}^{MeOH}$ mμ (log ε): 237 (4.05), 252 (4.16), 296 (4.04), 412 (4.35), 462 (4.37).

**Reaction of II with Bromine.** — A solution of 280 mg. of bromine in 0.5 ml. of methanol was added dropwise into a solution of II dissolved in 0.5 ml. of methanol, while being stirred under ice cooling. After completion of the addition, the solvent was evaporated under a reduced pressure and colorless needles, m. p. 75~77°C, precipitated out. This substance showed no depression of melting point on admixture with an authentic sample of 3-isopropyl-5, 7-dibromotropolone[4] and its analytical values and ultraviolet absorption spectra showed satisfactory agreement.

**Reaction of II with Formaldehyde and Piperidine.** — A mixture of 100 mg. of II, 0.5 ml. of 37% formalin, 0.5 ml. of piperidine, and 0.1 ml. of acetic acid was stirred mechanically at 70°C for 4 h., 1 ml. of water was added, and the wall of the vessel was scratched with a glass rod under ice-cooling by which III was obtained as yellow crystals.

**3-Isopropyl-5-morpholinomethyl-7-bromotropolone (VII).** — A solution of 1.76 g. of bromine dissolved in 12 ml. of methanol was added dropwise into 4 g. of II suspended in 30 ml. of methanol, while being stirred under ice cooling. The reaction mixture gradually aquired yellow tint as bromine was added. After completion of the addition, the solvent was evaporated to dryness under a reduced pressure and left a mixture of colorless crystals, m. p. 208~209°C (decomp.), and a yellow viscous residue. The crystals were the hydrobromide of VII.

Addition of hydrochloric acid to this residual mixture resulted in solidification of the viscous residue to colorless crystals, which were collected by filtration. Addition of 15 ml. of 2 N sodium acetate solution to these crystals, changed them to a yellow viscous substance which, when heated for ca. 10 min. at 60°C, formed a yellow solid. The precipitate so formed was collected, washed with water, and recrystallized from methanol to yellow granular crystals (VIIa), m. p. 91~93°C. Yield, 3.3 g.

Recrystallization of VIIa from petroleum ether produced colorless rods (VIIb), m. p. 64~65°C.

Found (for VIIa): C, 49.10; H, 5.65; N, 3.55. Calcd. for $C_{15}H_{20}O_3NBr \cdot H_2O$: C, 50.00; H, 6.11; N, 3.89%.

Found (for VIIb): C, 52.77; H, 5.79; N, 4.47. Calcd. for $C_{15}H_{20}O_3NBr$: C, 52.63; H, 5.85; N, 4.09%.

UV $\lambda_{max}^{MeOH}$ mμ (log ε): 259 (4.44), 338 (3.78), 380 (3.67).

IR (VIIa): 3470 and 3400 $cm^{-1}$ (water of crystallization), 2660 (sh.), 2530, and 2370 $cm^{-1}$ (sh.) (ν $N^+$-H).

IR (VIIb): 3200 $cm^{-1}$ (ν O-H).

**3-Isopropyl-5-piperidinomethyl-7-bromotropolone (VIII).** — A solution of 1.4 g. of bromine, dissolved in 12 ml. of methanol, was added dropwise into a suspension of 3.1 g. of III in 60 ml. of methanol, while being stirred under ice cooling, and the solvent was evaporated under a reduced pressure after completion of the addition. About 15 ml. of water was added to the residue and the yellow solid that formed was recrystallized from methanol. M. p. 135~137°C (decomp.). Yield, 2.6 g.

Found: C, 56.14; H, 6.41; N, 4.17. Calcd. for $C_{16}H_{22}O_2NBr$: C, 56.46; H, 6.46; N, 4.10%.

UV $\lambda_{max}^{MeOH}$ mμ (log ε): 260 (4.47), 340 (3.91), 390 (3.59).

IR 2540 $cm^{-1}$ (broad) (ν $N^+$-H)

**3-Isopropyl-5-tolylazo-7-bromotropolone (IX).** — a) To a solution of 100 mg. of VII or VIII dissolved in ca. 0.2 ml. of pyridine, diazonium salt solution prepared from 40 mg. of *p*-toluidine, 30 mg. of sodium nitrite, and 0.1 ml. of concentrated hydrochloric acid was added while being stirred under ice cooling and red crystals precipitated out immediately. The crystals were collected and recrystallized from methanol to orange crystals (IX), m. p. 142~145°C. Yield, 120 mg.

b) To a suspension of 50 mg. of IV or V in ca. 0.2 ml. of methanol, a solution of 20 mg. of bromine dissolved in 0.5 ml. of methanol was added with stirring and the crystals that formed were collected by filtration. Recrystallization from methanol gave a product, m. p. 143~145°C which showed no depression of the melting point on admixture with the product obtained by the method (a). Yield, 30 mg.

c) A solution of 20 mg. of bromine dissolved in ca. 0.5 ml. of methanol was added to 40 mg. of 3-isopropyl-5-tolylazotropolone suspended in ca. 0.2 ml. of methanol and the crystals formed were collected by filtration. Recrystallization from methanol afforded a product which showed no depression in the melting point on admixture with

the products obtained by the methods (a) and (b). Yield, 50 mg.

Found : C, 56.58 ; H, 4.23 ; N, 7.85. Calcd. for $C_{17}H_{17}O_2N_2Br$ : C, 56.52 ; H, 4.74 ; N, 7.85%.

UV $\lambda_{max}^{MeOH}$ m$\mu$ (log $\varepsilon$): 256 (4.20), 299 (4.15), 415 (4.38), 477 (4.39).

**3-Isopropyl-5-morpholinomethyltropolone (XI).**— A solution of 1 g. of VII dissolved in ca. 20 ml. of ethanol and added with 220 mg. of sodium hydroxide and 200 mg. of palladium-carbon was shaken in a hydrogen stream. Absorption of hydrogen stopped after an equivalent mole was absorbed. The solvent was evaporated under a reduced pressure and addition of hydrochloric acid to the residue to neutralization precipitated crystals. The crystals were collected and recrystallized from petroleum ether to colorless prisms (XI), m. p. 77~78°C. Yield, 500 mg.

Found : C, 68.17 ; H, 7.64 ; N, 5.14. Calcd. for $C_{15}H_{21}O_3N$ : C, 68.41 ; H, 8.04 ; N, 5.32%.

UV $\lambda_{max}^{MeOH}$ m$\mu$ (log $\varepsilon$): 242 (4.41), 326 (3.92).

Treatment of XI with 3 N hydrochloric acid afforded colorless crystals, m. p. 124~129°C, the hydrochloride of XI.

Found : C, 56.23 ; H, 7.05 ; N, 4.08. Calcd. for $C_{15}H_{22}O_3NCl \cdot H_2O$ : C, 56.69 ; H, 7.61 ; N, 4.41%.

**3-Isopropyl-5-piperidinomethyltropolone (XII).**— A suspension of 0.9 g. of VIII in 20 ml. of ethanol with 0.3 g. of potassium hydroxide and 0.1 g. of palladium-carbon added was shaken in a hydrogen stream. After absorption of an equivalent mole of hydrogen the solvent was evaporated under a reduced pressure and addition of hydrochloric acid to the yellow viscous residue to neutralization precipitated slight yellow crystals. The crystals were collected and recrystallized from methanol or benzene. M. p. 110~113°C. Yield, 0.6 g.

Found : C, 72.91 ; H, 8.78 ; N, 5.11. Calcd. for $C_{16}H_{23}O_2N$ : C, 73.53 ; H, 8.87 ; N, 5.36%.

UV $\lambda_{max}^{MeOH}$ m$\mu$ (log $\varepsilon$): 242 (4.41), 326 (3.89).

IR $\nu$ $N^+$-H, 2500 $cm^{-1}$ (broad) (KBr disk).

**Reaction of XI with *p*-Tolyldiazonium Salt.**— To a solution of 160 mg. of XI dissolved in ca. 0.2 ml. of pyridine, a diazonium salt prepared from 30 mg. of *p*-toluidine, 20 mg. of sodium nitrite, and ca. 0.1 ml. of concentrated hydrochloric acid was added while being stirred under ice cooling, by which orange crystals separated out. The crystals were collected and recrystallized from methanol to orange prisms, m. p. 129~130°C, undepressed on admixture with an authentic sample of 3-isopropyl-5-tolylazotropolone.

## Summary

The Mannich reaction was applied to 3-isopropyltropolone and 3-isopropyl-5, 7-dimorpholinomethyl, and 3-isopropyl-5, 7-dipiperidinomethyltropolone were obtained. These substituents were easily substituted by diazonium salt or bromine. Some of the Mannich bases obtained were found to retain the zwitter-ion structure in the solid state.

The author expresses his deep gratitude to Professor Shuichi Seto for his kind guidance. He is indebted to Mr. S. Aono for infrared spectral measurements and to Mr. F. Sato for ultraviolet spectral measurements. A part of the expense for the present research was defrayed by Sankyo Co., Ltd., to whom the author wishes to express his sincere gratitude.

*The Chemical Research Institute of Non-Aqueous Solutions*
*Tohoku University*
*Katahira-cho, Sendai*

# *Iodine-catalyzed Thermal cis-trans Isomerization of Azobenzene*

By Shigeru YAMASHITA

(Received November 2, 1960)

Since Hartley[1] showed the existence of cis-form azobenzene, cis-trans conversion of azobenzene has been studied thermally or photochemically by Le Fevre[2], Zimmerman[3] and also by Birnbaum and Style[4]. However, all of these studies were carried out in the absence of any catalyst. In the present work, the effect of iodine catalyst on the thermal cis → trans conversion of azobenzene has been studied kinetically in *n*-hexane solution. Since azobenzene forms a molecular complex with iodine, the equilibrium constant for its formation and its bearing on the isomerization reaction have also been studied.

1) G. S. Hartley, *J. Chem. Soc.*, **1938**, 633.
2) R. J. W. Le Fevre and J. Northcott, ibid., **1953**, 867.
3) G. Zimmerman et al., *J. Am. Chem. Soc.*, **80**, 3528 (1958).
4) P. P. Birnbaum and D. W. G. Style, *Trans. Faraday Soc.*, **50**, 1191 (1954).

## Experimental

**Materials.**—*cis-Azobenzene.*—The method of preparation presented by Hartley[1] was followed.

*trans-Azobenzene.*—The commercial reagent was used after repeated recrystallization. The absorption curves of these two isomers of azobenzene were in good agreement with those in the literature[1,3].

*Iodine and n-Hexane.*—The purification of these compounds has already been described in the previous paper[5].

**Procedure.**—The equilibrium of complex formation between azobenzene and iodine in *n*-hexane was studied spectrophotometerically in a manner similar to that described previously for the iodine-stilbene complex[5].

The rate of iodine-catalyzed cis → trans conversion of azobenzene was determined also spectrophotometrically by the same procedure as that described for the case of iondine-catalyzed cis → trans conversion of stilbene[6]. Since *cis*-azobenzene was found to isomerize far more easily than stilbene, the measurement of reaction rate was carried out at a lower temperature range than in the case of stilbene. The *cis*- and *trans*-azobenzene concentrations were determined spectrophotometrically in a manner similar to that described by Zimmerman[3] in his photoequilibrium study of azobenzene.

## Results and Discussion

**The Molecular Complex formed between Azobenzene and Iodine.**—As seen in Fig. 1, the visible absorption band maximum of free iodine at 520 mμ shifts to one at a shorter wavelength of 435 mμ when combined with *cis*-azobenzene to form a complex, and at the same time a new strong absorption band maximum appears at 305 mμ. This is probably a charge-transfer band. A rather large molar extinction coefficient of $6.7\times10^3$ found for the latter peak (Table I) supports such an interpretation.

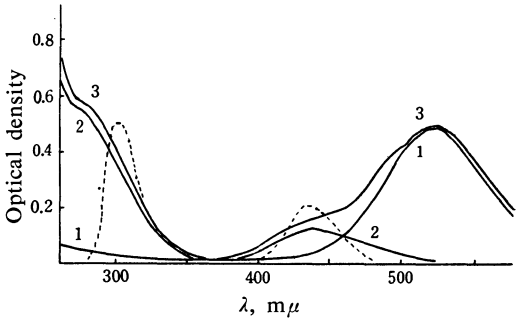



Fig. 1. Optical density increment in the mixture of *cis*-azobenzene and iodine in *n*-hexane solution. Temperature, 25°C. Curve 1: $(I_2)=5.0\times10^{-4}$(mol./l.). Curve 2: $(C)=1.0\times10^{-4}$(mol./l.), C denoting *cis*-azobenzene. Curve 3: $(C)=1.0\times10^{-4}$(mol./l.); $(I_2)=5.0\times10^{-4}$(mol./l.). Dotted line indicates the optical density increment due to the molecular complex, $CI_2$ (in 10 times enlarged scale of ordinate).

5) S. Yamashita, This Bulletin, 32, 1212 (1959).
6) S. Yamashita, ibid., 34, 487 (1961).

TABLE I. EQUILIBRIUM CONSTANTS OF *cis*-AZOBENZENE-IODINE COMPLEX AND RELATING QUANTITIES. CHARGE-TRANSFER BAND; $\lambda_{max}=305$ mμ, $\varepsilon_{max}=6.7\times10^3$. BLUE SHIFT OF IODINE ABSORPTION; $\lambda_{max}=435$ mμ

| Temperature, °C | $K_C$, l./mol. |
|---|---|
| 25.0 | 97 |
| 20.0 | 121 |
| 15.0 | 150 |
| 10.0 | 192 |

The equilibrium constant for the complex formation was obtained by the Benesi-Hildebrand type relations[7] represented as follows[8]:

$$1/(\varepsilon_A-\varepsilon_F)=1/(\varepsilon_C-\varepsilon_F)\,(1/K_C)\,(1/C_A)+1/(\varepsilon_C-\varepsilon_F) \quad (1)$$

Here, $\varepsilon_F$ and $\varepsilon_C$ are, respectively, the molar extinction coefficients for free *cis*-azobenzene and the complex in the mixture, and $\varepsilon_A=d/((Az)\cdot l)$, where $d$ is the measured optical density of the solution containing the complex, $(Az)$ is the total concentration of *cis*-azobenzene (free and complexed) and $l$ is the path length of the absorption cell (1 cm.). The term $C_A$ is actually the concentration of iodine left free in the mixture but can be equated to its total concentration when the concentration of the complex is considerably smaller than that of free iodine as it is in the present case.

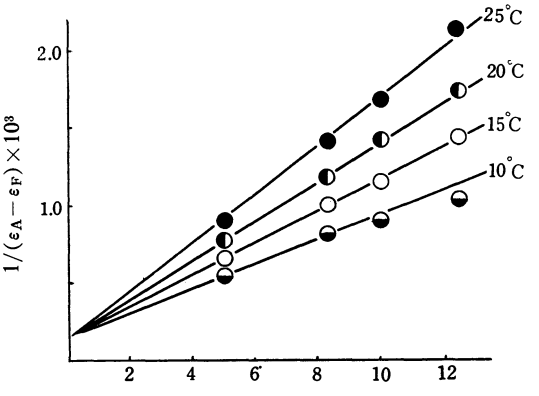



Fig. 2. $1/(\varepsilon_A-\varepsilon_F)\sim1/C_A$ diagram for the *cis*-azobenzene-iodine system in *n*-hexane.

7) a) H. A. Benesi and J. H. Hildebrand, *J. Am. Chem. Soc.*, 71, 2703 (1949); b) L. J. Andrews and R. M. Keefer, ibid., 77, 4202 (1955).
8) M. Chowdhury and S. Basu, *J. Chem. Phys.*, 32, 1450 (1960).

Eq. 1 was applied to the change-transfer absorption maximum at 305 mμ, absorption of free iodine at this wavelength being taken into account[8]. The results are shown in Fig. 2. The equilibrium constants of complex formation obtained from these plots are listed in Table I. From the Arrhenius plot of these values of $K_C$, the heat of complex formation $-\Delta H$ was found to be 7.5±0.2 kcal./mol. This value of $-\Delta H$ and the absorption maximum of the complexed iodine, 435 mμ, satisfy the empirical relation found by Ham[9] between the heat of complex formation and the magnitude of blue shift in the absorption band of iodine caused by complex formation (Fig. 3). In the case of *trans*-azobenzene-iodine system, no appreciable spectral change was observed.

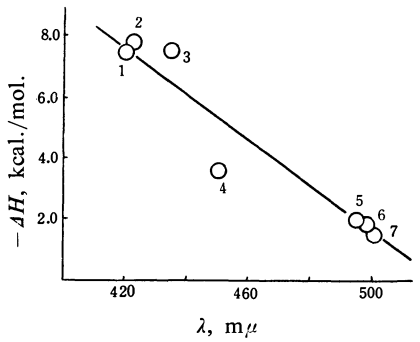



Fig. 3. Correlation between heat of formation of complex and blue shift of iodine. 1, *cis*-stilbene[5]; 2, pyridine; 3, *cis*-azobenzene; 4, dioxane; 5, xylene; 6, toluene; 7, benzene

**Isomerization Reaction.**—As in the previous study[6] of the iodine-catalyzed thermal cis → trans conversion of stilbene, only the initial rates of isomerization were determined. Since *cis*-azobenzene is more labile than *cis*-stilbene, reaction rate measurements could be carried out at lower temperatures than with stilbene.

In Figs. 4 and 5 the dependence of the rate of isomerization on the concentration of *cis*-azobenzene and of iodine are shown respectively. These results conform to the rate expression

$$-\mathrm{d(C)}/\mathrm{d}t = k\,\mathrm{(C)\,(I_2)} + k'\,\mathrm{(C)} \qquad (2)$$

where (C) and ($I_2$) are the concentration of *cis*-azobenzene and iodine, respectively. The second term in Eq. 2 represents the spontaneous isomerization of *cis*-azobenzene which can not be neglected as is evidently seen in Fig. 5[10].

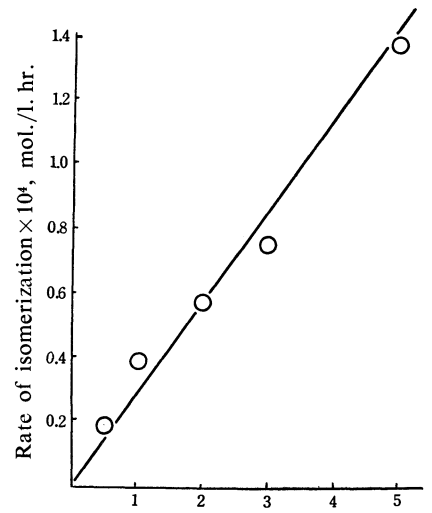



Fig. 4. Dependence of the reaction rate on the concentration of *cis*-azobenzene. Concentration of iodine, $5\times10^{-4}$ mol./l.; temperature, 30°C.

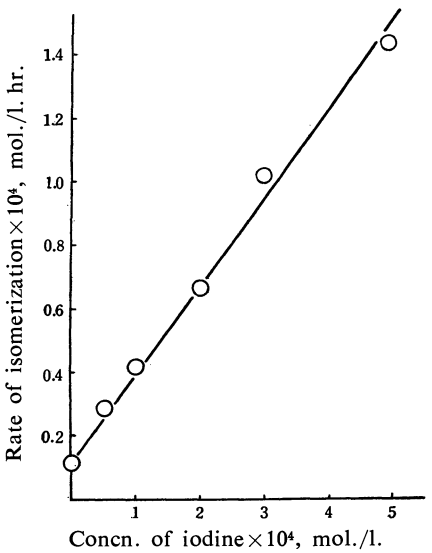



Fig. 5. Dependence of the rate on the concentration of iodine. Concentration of *cis*-azobenzene, $5\times10^{-4}$ mol./l.; temperature, 30°C.

In Table II the values of the rate constants $k$ and $k'$ at varied temperatures are shown and the Arrhenius constants obtained from these values of $k$'s are listed in Table III. Both the $A$-factor and activation energy for the spontaneous isomerization are in fairly good agreement with those previously reported[2]. These results suggest that the spontaneous isomerization of *cis*-azobenzene probably takes place via the "singlet mechanism" of Magee, Shand and

9) J. Ham, *J. Am. Chem. Soc.*, **76**, 3875 (1954); see also T. Kubota, *J. Chem. Soc. Japan (Nippon Kagaku Zasshi)*, **78**, 196 (1957); J. H. Hildebrand et al., *J. Chem. Phys.* **33**, 621 (1960).

10) That the spontaneous isomerization of *cis*-azobenzene is of first order has previously been shown by Hartley and Le Fevre[1,2].

Table II. Values of the rate constants $k$ and $k'$

| Temperature °C | $k \times 10^{-2}$ cc. $mol^{-1}$ $sec^{-1}$ | $k' \times 10^{6}$ $sec^{-1}$ |
|---|---|---|
| 30 | 1.84 | 3.75 |
| 40 | 2.50 | 11.3 |
| 50 | 3.50 | 31.4 |

Table III. Arrhenius constants of the rate constants $k$ and $k'$

| Rate constant | $A$-factor | Activation energy |
|---|---|---|
| $k$ | $6.44\times10^{6}$ cc. $mol^{-1}$ $sec^{-1}$ | 6.3 kcal./mol. |
| $k'$ | $5.20\times10^{9}$ $sec^{-1}$ | 21.0 kcal./mol. |

Eyring[11], though the activation energy is considerably lower than those for some reactions quoted by them as examples for the singlet mechanism.

A simple way to explain the conversion catalyzed by iodine might be to assume a collisional catalysis by iodine molecules which enables *cis*-azobenzene to isomerize through a "triplet mechanism" similar to that proposed by Harman and Eyring[12]. The activation energy of 6.3 kcal./mol., however, seems too small to make such a simple collisional mechanism acceptable. An alternative explanation, which seems much more probable, is given by the isomerization of the molecular complex, the existence of which was shown above:

$$C + I_2 \rightleftarrows CI_2 \qquad \text{(fast)}$$

$$CI_2 \rightarrow TI_2 \text{ or } T + I_2 \qquad \text{(slow)}$$

where C and T represent *cis*- and *trans*-azobenzene, respectively.

According to this interpretation, the rate of iodine-catalyzed isomerization is given by

$$-d(C)/dt = k''(CI_2)$$

where

$$k'' = 2.10\times10^{10}\exp(-13.8 \text{ kcal. } mol^{-1}/\boldsymbol{RT}) \quad (sec^{-1})$$

Here the activation energy of 13.8 kcal./mol. results from the sum of 6.3 kcal./mol. and the heat of formation of the molecular complex, 7.5 kcal./mol.

Further study seems necessary before it can be clarified whether this lowering of activation energy is accompanied by the change in mechanism from that of "singlet" to that of "triplet".

## Summary

The equilibrium of 1 : 1 molecular complex formation between *cis*-azobenzene and iodine in *n*-hexane has been studied spectrophotometrically in the temperature range 10~25°C. The heat of formation of the complex has been found to be $-\Delta H = 7.5$ kcal./mol. The rate of iodine-catalyzed isomerization of *cis*-azobenzene determined spectrophotometrically in *n*-hexane solution has been found to be proportional to the concentration of *cis*-azobenzene as well as to that of iodine, with an activation energy of 6.3 kcal./mol. over the temperature range 30~50°C. The most probable interpretation of the rate measurements is that the complex of *cis*-azobenzene with iodine isomerizes with an activation energy of 13.8 kcal./mol. under the experimental conditions of the present work.

The present author is particularly indebted to Professor O. Toyama of the College of Engineering and to Dr. T. Hayakawa for their discussions and encouragement during this investigation. The author wishes to thank Mr. J. Mukunoki for his assistance.

*Department of Chemistry*
*College of General Education*
*The University of Osaka Prefecture*
*Sakai, Osaka*

11) J. L. Magee, W. Shand and H. Eyring, *J. Am. Chem. Soc.*, **63**, 677 (1941).
12) R. A. Harman and H. Eyring, *J. Chem. Phys.*, **10**, 557 (1942).

# $n$-$\pi^*$ Absorption Spectra of Some Aliphatic Aldehydes

By Hiroko OSHIMA

(Received October 3, 1960)

Whenever a carbonyl group is in a molecule, a weak absorption appears in a relatively long-wave region. With saturated aldehydes, this absorption appears near 2900 Å and possesses a low intensity which is about the same for all these molecules. The unfailing appearance of this absorption in molecules having a carbonyl group shows that it is due to the CO group and the constancy of its intensity in all these molecules suggests that the corresponding transitions can be given by a common interpretation. The interpretation was first made by Mulliken[1] and McMurry[2]. They say that an electron was thought to be excited from a non-bonding orbital localized on the O atom into an anti-bonding orbital. Such a transition involving the excitation of a non-bonding electron to an anti-bonding $\pi$ orbital was designated an $n$-$\pi^*$ transition by Kasha[3].

In this paper the effects of substituents and of solvents on the 0-0 band frequency of the $n$-$\pi^*$ absorption spectra of some aliphatic aldehydes, together with their $f$-values, are investigated.

## Experimental

A Hitachi automatic recording spectrophotometer EPS-2 was used for the measurement of the spectra. A 10 cm. cell was used for vapor, and a 1 cm. cell for solution. The temperature effect was investigated using a 2 cm. cell designed by Ito[4]. The optical density at various concentrations was measured and Beer's law was found to hold for all cases. For the infrared region a Hitachi double-beam recording infrared spectrophotometer EPI-2 was used.

Propionaldehyde, $n$-butyraldehyde and isobutyraldehyde were supplied by Tokyo Kasei Co. Samples were distilled just before the absorption measurement. $n$-Hexane was vigorously shaken with concentrated sulfuric acid, fuming sulfuric acid and nitric acid, then shaken with water, concentrated aqueous solutions of sodium hydroxide and potassium permanganate, dried over calcium chloride, refluxed over phosphorus pentoxide, distilled, passed through a column of freshly activated silica gel and finally distillled. Ethyl alcohol was shaken with ordinary silica gel, refluxed over sodium hydroxide, then finally distilled. Purifications of other solvents were essentially the same as those described in literature*.

## Results and Discussion

**Position of the $n$-$\pi^*$ Absorption.**—The $n$-$\pi^*$ absorption spectra of aliphatic aldehydes generally appear near 2900 Å. The frequencies of absorption maxima for propionaldehyde, $n$-butyraldehyde and isobutyraldehyde are given in Table I together with values taken from literature for other aliphatic aldehydes. The maxima of the $n$-$\pi^*$ absorption of corresponding carboxylic acids are cited in Table II from literature.

TABLE I. $\nu_{max}$ OF $n$-$\pi^*$ ABSORPTION OF SOME ALDEHYDES IN $n$-HEXANE SOLUTION AND IN VAPOR STATE

| Molecule | $\nu_{max}$, cm$^{-1}$ | |
|---|---|---|
| | $n$-hexane | vapor |
| Formaldehyde | 34010[5] | |
| Acetaldehyde | 34500[6] | 34591[7] |
| Propionaldehyde | 34119 | 34143 |
| $n$-Butyraldehyde | 33980 | 34003 |
| Isobutyraldehyde | 33865 | 33888 |

TABLE II. $\nu_{max}$ OF $n$-$\pi^*$ ABSORPTION OF SOME CARBOXYLIC ACIDS IN LIQUID STATE

| Molecule | $\nu_{max}$, cm$^{-1}$ liquid[8] |
|---|---|
| Formic acid | 48410 |
| Acetic acid | 49003 |
| $n$-Butyric acid | 48764 |
| Palmitic aic | 47831 |

Baba and Nagakura[9] observed for carboxylic acids and ketones that the smaller the ionization potential of the substituent adjacent to the C=O group is, the greater the $n$-$\pi^*$ band shifts toward the blue, interpreting the trend in the following way on the basis of the electron migration idea. In the ground state,

1) R. S. Mulliken, *J. Chem. Phys.*, 3, 564 (1935).
2) H. L. McMurry, ibid., 9, 231, 241 (1941).
3) M. Kasha, *Discussions Faraday Soc.*, No. 9, 14 (1950).
4) M. Ito, *J. Mol. Spectroscopy*, 4, 106 (1960).

* A. Weissberger, E. S. Proskauer, J. A. Riddick and E. E. Toops, Jr., "Organic Solvents", Interscience Publishers, Inc., New York (1955).
5) V. Henri and S. A. Schou, *Z. Physik.*, 49, 774 (1928).
6) W. Herold, *Z. physik. Chem.*, B18, 265 (1932).
7) P. A. Leighton and F. E. Blacet, *J. Am. Chem. Soc.*, 55, 1766 (1933).
8) H. Ley and B. Arends, *Z. physik. Chem.*, B17, 177 (1932).
9) H. Baba and S. Nagakura, *J. Chem. Soc. Japan, Pure Chem. Sec.* (*Nippon Kagaku Zasshi*), 72, 72, 74, 277, 341 (1951).

electron migration from the substituent to the excited $\pi^*$ orbitals of the C=O group occurs easily, but in the $n$-$\pi^*$ excited state, this electron migration becomes difficult since the non-bonding electron then occupies the part of the $\pi^*$ orbitals. As a result the stabilization energy gained by the molecule due to this electron migration is greater for the ground state than for the $n$-$\pi^*$ excited state. So a substituent causes a blue shift for the $n$-$\pi^*$ absorption of the unsubstituted compound. Moreover the smaller the ionization potential of the substituent adjacent to the C=O group is, the more easily the electron migration occurs. In other words, the smaller the ionization potential of the substituent is, the larger is the blue shift. The above general view was testified for the case of some aldehydes. No ionization potential data of methyl, ethyl, $n$-propyl and isopropyl radicals were available, but their order could be estimated from the values for paraffines given in Table III. From

Table III. Ionization potential of paraffines

| Molecule | Ionization potential, eV.[10] |
|---|---|
| Methane | 13.04 |
| Ethane | 11.76 |
| Propane | 11.21 |
| $n$-Butane | 10.80 |

these data it can be assumed that the ionization potential decreases in the order of methyl, ethyl, $n$-propyl and isopropyl radicals. From Baba and Nagakura's theory it is then expected that the $n$-$\pi^*$ absorption band of aldehydes would show increasing blue shifts in the order of formaldehyde, acetaldehyde, propionaldehyde, $n$-butyraldehyde and isobutyraldehyde. However, the actual observation is that while the absorption maxima of acetaldehyde and propionaldehyde lie on the blue side of the formaldehyde maximum, $n$-butylardehyde and isobytyraldehyde lie on its red side. The situation is about the same as that of the corresponding carboxylic acids, where, acetic and $n$-butyric acids show blue shifts with respect to formic acid, but palmitic acid shows a red shift of about 580 $cm^{-1}$. From these observations it seems to be difficult to interpret the effect of the substituent on the absorption frequency solely by the magnitude of ionization potential and to consider only the phenomenon of blue shift as characteristic of the $n$-$\pi^*$ transition. In addition to the blue shift caused by the ionizing tendency of the substituent, there seem to be other factors which may counteract the effect causing the blue shift. For such factors hyperconjugation, greater complexity of the molecule and hence steric effects of the alkyl radical may be considered and the general theoretical view of the spectral shift[9] due to the introduction of a substituent must be supplemented by the consideration of these additional factors.

**Positions of the 0-0 Band.** — Absorption spectra were measured at various temperatures

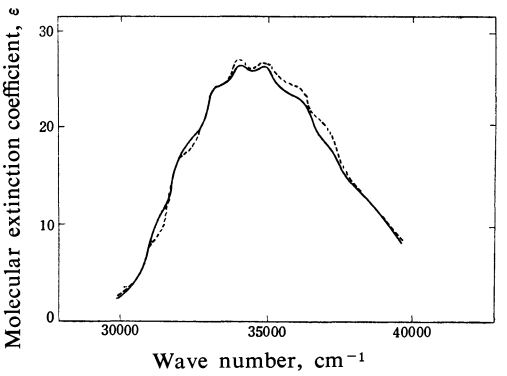



Fig. 1. Effect of temperature on the $n$-$\pi^*$ absorption spectrum of propionaldehyde.
——, 9°C; ----, −78°C

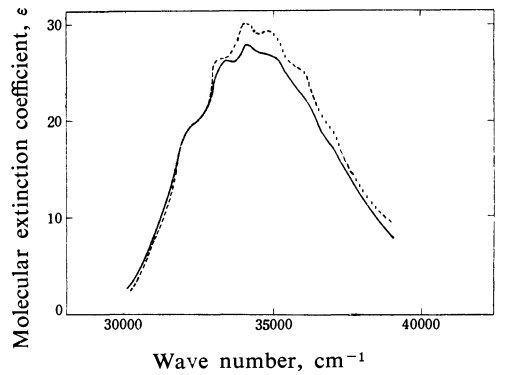



Fig. 2. Fffect of temperature on the $n$-$\pi^*$ absorption spectrum of $n$-butyraldehyde.
——, 9°C; ----, 78°C

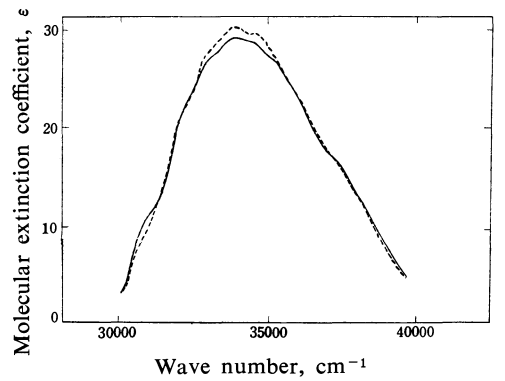



Fig. 3. Effect of temperature on the $n$-$\pi^*$ absorption spectrum of isobutyraldehyde.
——, 9°C; ----, −78°C

10) R. E. Honig, *J. Chem. Phys.*, **16**, 105 (1948).

to facilitate the location of the 0-0 band. The $n$-$\pi^*$ absorption spectra of aldehydes in $n$-hexane solution at 9 and $-78°C$ are shown in Figs. 1, 2 and 3.

Absorptions on the longer wave side of the 0-0 band arise from vibrational levels in the ground state and it is expected that the absorption intensity on the red side of the 0-0 band will increase and that on the shorter wave side it will decrease with increasing temperature. If we plot the absorption curves for various temperatures, an intersection point will be obtained near the position of the 0-0 band[13]. The positions of the 0-0 bands determined in this way are given in Table IV. As shown in

TABLE IV. POSITION OF 0-0 BAND AND $f$-VALUE OF $n$-$\pi^*$ ABSORPTION OF SOME ALDEHYDES

| Molecule | 0-0 Band, $cm^{-1}$ | $f$-Value (29400~43200 $cm^{-1}$) |
|---|---|---|
| Propionaldehyde | 32250 | $5.56\times10^{-4}$ |
| $n$-Butyraldehyde | 32100 | $5.82\times10^{-4}$ |
| Isobutyraldehyde | 32000 | $5.58\times10^{-4}$ |

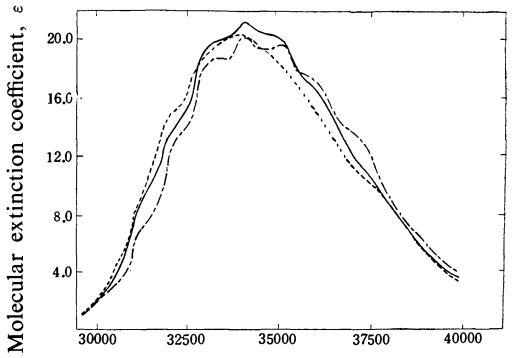



Fig. 4. $n$-$\pi^*$ Absorption spectra of propionaldehyde (-·--), $n$-butyraldehyde (——) and isobutyraldehyde (-----).

Fig. 4 the $n$-$\pi^*$ absorption spectra of propionaldehyde, $n$-butyraldehyde and isobutyraldehyde show the progressions of about 940 $cm^{-1}$ interval and $\nu_{max}$'s appear at the respective 0-2 band. The fact that the 0-0 band is weak and the 0-2 band is strong means that the minima of potential curves for the ground and excited states do not lie on top of each other but the minimum of the excited state is shifted so as to correspond to a greater equilibrium C-O distance, or that the force constant of the C=O stretching vibration decreases in the exited state.

**Oscillator Strength.**—As the $n$ and $\pi^*$ orbitals are both formed of the 2p orbitals of different symmetry an $n$-$\pi^*$ transition between them is forbidden by local symmetry ("U-A" transition)[14], giving a weak absorption with the $f$-value of the order of $10^{-4}$. $f$-Values calculated for aldehydes are given in Table IV. They are all of the order of $10^{-4}$.

**Solvent Effect.**—Next we shall discuss the solvent effect on the $n$-$\pi^*$ absorption spectra of aldehydes investigated on the basis of a theoretical equation proposed by McRae[15]. We employ McRae's equation in a simplified form after Ito et al.[16] as applied for ketone spectra,

$$\Delta\nu = \text{dispersion term} + B\frac{n_D^2-1}{2n_D^2+1} + C\left[\frac{D-1}{D+2} - \frac{n_D^2-1}{n_D^2+2}\right]$$

$$B = \frac{1}{hc}\,\frac{(M^u_{oo})^2-(M^u_{11})^2}{a^3}$$

$$C = \frac{2}{hc}\,\frac{M^u_{oo}\{(M^u_{oo})-(M^u_{11})\}}{a^3} \qquad (1)$$

TABLE V. PROPERTIES OF VARIOUS SOLVENTS

| Solvent | Refractive index $n_D$ | Dielectric constant $D$ | $\frac{n_D^2-1}{2n_D^2+1}$ | $\frac{D-1}{D+1}$ |
|---|---|---|---|---|
| $n$-Hexane | 1.375 | 1.89 | 0.186 | |
| Carbon tetrachloride | 1.460 | 2.238 | 0.215 | |
| Benzene | 1.501 | 2.284 | 0.227 | |
| Toluene | 1.498 | | 0.226 | |
| Dioxane | 1.422 | 2.209 | 0.202 | |
| Ethyl ether | 1.356 | 4.335 | | 0.526 |
| Methyl acetate | 1.362 | 6.68 | | 0.654 |
| Acetonitrile | 1.344 | 37.5 | | 0.924 |
| Chloroform | 1.449 | 4.806 | | 0.559 |
| Ethyl alcohol | 1.361 | 24.3 | | 0.809 |
| Isobutyl-alcohol | 1.398 | 17.7 | | |

TABLE VI. $\nu_{max}$ OF $n$-$\pi^*$ ABSORPTION OF SOME ALDEHYDES IN VARIOUS SOLVENTS

| Solvent | $\nu_{max}$, $cm^{-1}$ | | |
|---|---|---|---|
| | Propion-aldehyde | Isobutyr-aldehyde | $n$-Butyr-aldehyde |
| (Vapor) | 34140 | 33980 | 34000 |
| $n$-Hexane | 34120 | 33870 | 33980 |
| Carbon tetra-chloride | 34150 | 33910 | 34050 |
| Benzene | 34330 | 34040 | 34150 |
| Toluene | 34340 | 33970 | 34150 |
| Dioxane | 34470 | 34070 | 34240 |
| Ethyl ether | 34310 | 33910 | 34170 |
| Methyl acetate | 34470 | 34040 | 34270 |
| Acetonitrile | 34760 | 34330 | 34450 |
| Chloroform | 34630 | 34120 | 34300 |
| Ethyl alcohol | 35050 | 34260 | 34470 |
| Isobutyl alcohol | 35080 | | 34470 |

13) S. Broderson and A. Langseth, *Danske Mat. Fys. Medd.*, 26, No. 3 (1951).

14) J. R. Platt, *J. Chem. Phys.*, **18**, 1168 (1950).

15) E. G. McRae, *J. Phys. Chem.*, **61**, 562 (1957).

16) M. Ito, K. Inuzuka and S. Imanishi, *J. Am. Chem. Soc.*, **82**, 1317 (1960).

For the meaning of the symbols appearing in Eq. 1 the paper by Ito et al. is referred to.

Properties of various solvents used are given in Table V and $\nu_{max}$ in Table VI.

**Solvent Effect of Non-polar Solvents, *n*-Hexane, Carbon Tetrachloride, Benzene, Toluene and Dioxane.**—A vibrational fine structure was fairly well observed in the *n*-hexane solution, but in other solvents the stfucture is partially blurred and in dioxane hardly observable at all. This is probably due to the slightly polar nature (0.4 D) of dioxane.

The frequency shift of the solution in non-polar solvents is given as the sum of contributions represented by the first and the second terms of Eq. 1. The contribution from the first term usually gives a red shift, while the contribution from the second term depends on the dipole-polarization force. As the dipole moment of the C=O group in aldehydes decreases during the $n$-$\pi^*$ transition, the stabilization by this force is greater in the ground than in the excited state, so that the effect of this force gives a blue shift. If the effect due to the first term is very small compared with that of the second term, a linear relation between $\nu_{max}$ and $(n_D^2-1)/(2n_D^2+1)$ should be obtained. However, from the plots of $\nu_{max}$ against $(n_D^2-1)/(2n_D^2+1)$ shown in Fig. 5, the

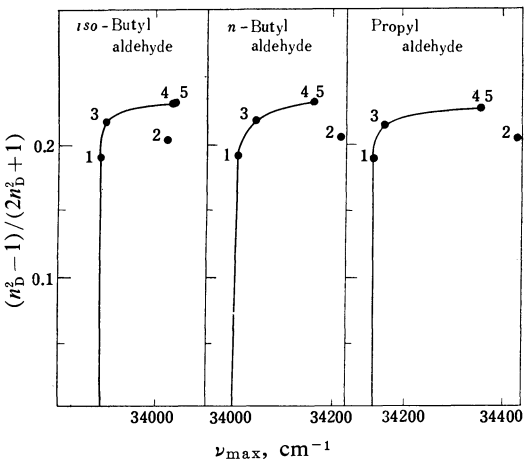



Fig. 5. Relations between $\nu_{max}$ and $(n_D^2-1)/(2n_D^2+1.)$
1, *n*-Hexane 2, dioxane 3, carbon tetrachloride 4, toluene 5, benzene.

linear relation is not observed. It is felt that the contribution from the dipole-polarization effect is greater than the dispersion effect for $\pi$-electron containing solvents such as benzene and toluene. For other solvents fairly large red shifts presumably caused by the dispersion effect are observed. The unusually large blue shift in the case of dioxane may be due to the dipole moment of the molecule as mentioned above.

**Solvent Effect of Non-Hydrogen Bonding Polar Solvents, Ethyl Ether, Methyl Acetate and Acetonitrile.**—The stabilization energy due to the dipole-dipole force between the solute and solvent molecules becomes smaller after the $n$-$\pi^*$ transition. In consequence of the Franck-Condon principle, excited solute molecules will be momentarily surrounded by solvent molecules with sizes and orientations appropriate to their ground state, and as the result of this the excited state energy will become higher, leading to a blue shift. For the case of polar solvents the contribution from the third term in Eq. 1 will be the greatest and the shift depends on $D$. We assume here that for any of the three polar solvents 1, 2 and 3 the refractive index as well as the dispersion effect of each of them is nearly equal. Then Eqs. 2 and 3 follow from Eq. 1,

$$\nu_1-\nu_2=C\left[\frac{D_1-1}{D_1+2}-\frac{D_2-1}{D_2+2}\right] \quad (2)$$

$$\nu_1-\nu_3=C\left[\frac{D_1-1}{D_1+2}-\frac{D_3-1}{D_3+2}\right] \quad (3)$$

The plots of $\Delta\nu(\nu_{max}-\nu_{max,\,vapor})$ against $(D-1)/(D+2)$ are shown in Fig. 6. A linear

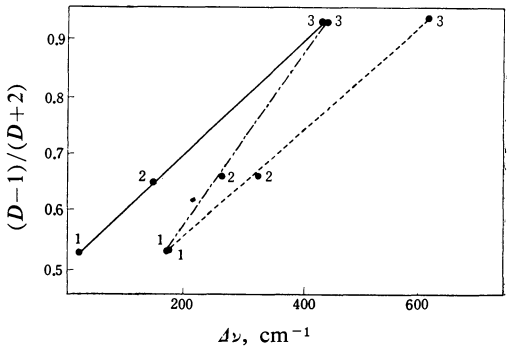



Fig. 6. Relations between frequency difference of $n$-$\pi^*$ bands of propionaldehyde (----) *n*-butyraldehyde (-·-·) and isobutyraldehyde (——) and $(D-1)/(D+2)$ of various solvents.
Solvent: 1, ethyl ether 2, methyl acetate 3, acetonitrile.

relationship is seen for propionaldehydehyde, *n*-butyraldehyde and isobutyraldehyde. From the slopes of the straight lines the values of $C$ in Eq. 1 are obtained. If we know the magnitude of the quantity of $a$, $M^u_{oo}(M^u_{oo}-M^u_{II})$ can be calculated, and if moreover the values of $M^u_{oo}$ are known, $M^u_{II}$ can be obtained. Diple moment value for the ground state taken from literature and that of the excited state calculated following the above are given in Table VII. If we consider two

TABLE VII. DIPOLE MOMENT AND CONTRIBUTION OF THE $C^+-O^-$ STRUCTURE OF SOME ALDEHYDES CALCULATED FOR $a=3$ Å IN EQUATION 1

| Molecule | Dipole moment $D$ | | Contribution of the $C^+-O^-$ structure, % | |
|---|---|---|---|---|
| | Ground state | Excited state | Ground state | Excited state |
| Propionaldehyde | 2.54 | 1.33 | 43.3 | 22.9 |
| *n*-Butyraldehyde | 2.57 | 1.82 | 43.8 | 31.1 |
| Isobutyraldehyde | 2.58 | 1.48 | 43.9 | 25.2 |

resonating structures C=O and $C^+-O^-$ the wave function is given by

$$\Psi = a\psi(C{=}O) + b\psi(C^+{-}O^-)$$

and the dipole moment $D$ can be calculated as

$$D = a^2D'(C{=}O) + b^2D'(C^+{-}O^-)$$

where we take the moments of C=O and $C^+-O^-$ as 0 and $er$, respectively, $r$ being the C–O distance. The calculated results are given in Table VII, showing that the contribution from the structure $C^+-O^-$ is small in the excited state. From this it, is obvious that the electronic configuration of the C=O group is modified greatly in consequence of the $n$-$\pi^*$ transition.

**Effect of Solvents Forming Hydrogen Bonds with Solute Molecules, Chloroform, Ethyl Alcohol and Isobutyl Alcohol.** — Frequency shifts are great and $\nu_{max}$'s appear at longer wavelengths than the respective 0-2 band. The reason for these shifts may be attributed to the hydrogen bond formation. As the non-bonding electron localized on the O atom can form hydrogen bonds with solvent molecules the stabilization energy in the ground state will be great. On the other hand, in the excited state one electron is removed from the $n$-orbital and the remaining one electron is not sufficient to form a strong hydrogen bond. Therefore the stabilization energy will be small. In this case a large blue shift will be expected. New bands arise at shorter wavelengths than that of the 0-2 band. The hydrogen bond formation is confirmed by infrared absorption spectra of aldehydes in carbon tetrachloride, ethyl alcohol and isobutyl alcohol solutions. The new bands are distinguished from the C=O stretching vibration bands and are clearly attributable to the hydrogen bond formation.

## Summary

The $n$-$\pi^*$ absorption spectra of propionaldehyde, $n$-butyraldehyde and isobutyraldehyde were measured in various solvents and the effects of substituents and solvents on the $n$-$\pi^*$ absorption spectra were investigated. For the former effect red shifts instead of blue shifts reported as the characteristic of $n$-$\pi^*$ transitions were observed. The latter effect was studied using McRae's equation. Hydrogen bonding between solute and solvent molecules is also considered.

The author wishes to express her hearty thanks to Professor S. Imanishi, Drs. Y. Kanda and M. Ito for their guidance and valuable discussions throughout this investigation. She is also indebted to Messrs. H. Tsukioka and S. Aziki for providing purified solvents.

*Department of Chemistry*
*Faculty of Science*
*Kyushu University*
*Hakozaki, Fukuoka*

# *A Molecular Orbital Treatment of Triallyl Isocyanurates and Related Allyl Esters*

By Kenichi FUKUI, Hiroshi KATO, Teijiro YONEZAWA, Fumio TANIMOTO and Hisao KITANO

(Received November 29, 1960)

Triallyl cyanurate is known to be synthesized by the Schotten-Baumann reaction of allyl alcohol with cyanuric chloride[1,2]. Poly(triallyl cyanurate)[2] and triallyl cyanurate copolymer[2,3] with unsaturated polyester or other vinyl monomers have an excellent acid, alkali and heat-resistance. On the other hand, triallyl isocyanurate was prepared by the reaction of allyl chloride with potassium cyanate in acetonitrile[4] as the solvent under superatomospheric pressure, but it was not obtained in the pure crystalline form. Accordingly its melting point had not been known until triallyl isocyanurate was efficiently synthesized in our laboratory by a new method. It was carefully purified to polymerization[5]. Triallyl isocyanurate[5] which boils at 146°C/6 mmHg and melts at 23~25°C, polymerizes alone or copolymerizes with a number of vinyl monomers. The polymerization is catalyzed by peroxide to form a hard clear polymer[5].

As a preliminary consideration in connection with the experiments stated above, we are going to investigate theoretically their chemical reactivity, stability and other physical properties of some isocyanurates by the simple LCAO treatment.

The theoretically predicted properties have been found to agree well with those of the compounds which were synthesized, polymerized and treated with some reagents in our laboratory[6]. In the early stage of investigation of cyanurates and isocyanurates, Hantzsch and Bauer[7] reported the formation of mixed esters having alkyl groups on both the N and the O atom in one and the same triazine ring, and some additional, indirect evidences[8] were obtained which stood for the existence of *O, O, N*-ester (Drittel-pseudo-Cyanursäure-ester and *O, N, N*-ester (Zweidrittel-pseudo-Cyanursäure-ester). However subsequent attempts by Slotta and Tschesche[9] to prepare the mixed esters by methods diffenent from the above resulted in failure to lead them to the "Principle of Symmetry".

**$\pi$-Electron Distribution in Cyanate Group.**— Metal cyanates are hydrolyzed by water to liberate the active cyanate anion[10]. The isocyanate group of organic isocyanates is characterized by the polymerization or self-condensation and the condensation with various reagents containing active hydrogen atom[11]. Hence, in the first stage of LCAO molecular orbital investigation on the physical properties of isocyanurates, we calculate the $\pi$-electron distribution of NCO anion which is considered as a structural component of isocyanurates. The calculated values of total $\pi$-electron density, net charge and frontier electron density in each atom of NCO anion are listed in Table I.

TABLE I. THE ELECTRON DENSITY IN $(NCO)^-$ ANION

| | N | C | O |
|---|---|---|---|
| Total $\pi$-electron density | 1.7204 | 0.6507 | 1.6290 |
| Net charge | −0.7204 | +0.3493 | −0.6290 |
| Frontier electron density | 1.4627 | 0.0315 | 0.5048 |

TABLE II. THE VALUES OF FRONTIER ELECTRON DENSITY AND ONE TERM APPROXIMATION OF SUPERDELOCALIZABILITY OF THE ACTIVE METHYLENE AND THE $\gamma$-CARBON IN ALLYL GROUP IN FOUR ESTERS

| Ester | $f_{=H_2}$ | $S'_{=H_2}$ | $f_{=CH_2}$ | $S'_{=CH_2}$ |
|---|---|---|---|---|
| *N, N, N*- | 0.0794 | 0.1145 | 0.1049 | 0.1513 |
| *N, N, O*- | 0.1581 | 0.2692 | 0.1089 | 0.1855 |
| *N, O, O*- | 0.1393 | 0.2306 | 0.1053 | 0.1743 |
| *O, O, O*- | 0.0847 | 0.1398 | 0.0646 | 0.1066 |

1) J. R. Dudley, J. T. Thurston, F. C. Schaefer, D. Holm-Hansen, C. J. Hull and P. Adams, *J. Am. Chem., Soc.*, **73**, 2986 (1951).
2) H. M. Day and D. G. Patterson, *Modern Plastics*, **29**, July, 116 (1951).
3) P. M. Elliott, ibid., **29**, July, 113 (1951); H. W. Starkweather, Jr., A. Adicoff and F. R. Eirich, *Ind. Eng. Chem.*, **47**, 302 (1955); W. Cummings and M. Botwick, ibid., **47**, 1317 (1955).
4) D. W. Kaiser, U. S. Pat. 2536849 (1951).
5) K. Fukui and H. Kitano, Japanese Pat. 7835 (1960).
6) K. Fukui, H. Kitano and F. Tanimoto, unpublished work (1958).
7) A. Hantzsch and H. Bauer, *Ber.*, **38**, 1005 (1905).
8) A. Hantzch, *Z. anorg. Chem.*, **209**, 213 (1932).
9) K. Slotta and R. Tschesche, *Ber.*, **60**, 301 (1927).
10) O. Masson and I. Masson, *Z. physik. Chem.*, **70**, 290 (1910).
11) R. G. Arnold, J. A. Nelson and J. J. Verbanc, *Chem. Revs.*, **57**, 47 (1957).

TABLE III. THE VALUES OF TOTAL $\pi$-ELECTRONIC ENERGIES AND CONJUGATION ENERGIES OF FOUR ESTERS

| Ester | $\varepsilon$ | $\Delta E_\pi$ |
|---|---|---|
| *N,N,N-* | $24\alpha+44.5572\beta$ | $1.5293\ (-\beta)$ |
| *N,N,O-* | $24\alpha+42.3475\beta$ | $1.5451\ (-\beta)$ |
| *N,O,O-* | $24\alpha+40.1390\beta$ | $1.5620\ (-\beta)$ |
| *O,O,O-* | $24\alpha+37.9162\beta$ | $1.5647\ (-\beta)$ |

TABLE IV. THE VALUES OF PARAMETERS USED IN OUR CALCULATION

| Coulomb integrals | Resonance integrals |
|---|---|
| $\alpha_{=H_2}=\alpha-0.5\beta$ | |
| $\alpha_N=\alpha+\beta$ | $\beta_{C=H_2}=2\beta$ |
| $\alpha_{=O}=\alpha+2\beta$ | $\beta_{C=O}=\sqrt{2}\beta$ |
| $\alpha_{-O-}=\alpha+\beta$ | $\beta_{C-O-}=\beta$ |
| $\alpha_{O^-}=\alpha+1.5\beta$ | $\beta_{N-C}=\beta$ |

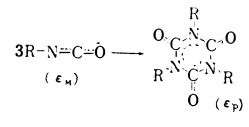
The results show that a polarization occurs through the transfer of an electron from the carbon atom to the nitrogen and the oxygen atoms in NCO anion. It is calculated that the nitrogen atom is the reaction position in its nucleophilic attack, referring to the values of reactivity indexes, in particular to the magnitude of the frontier electron density of this anion as a nucleophilic reagent. The values of parameters used in the calculation throughout the present paper are listed in Table IV.

**The Stability of the Isocyanuric Ring.** — To investigate the stability of the isocyanuric ring, we calculated the conjugation energy ($\Delta E_\pi$) and the resonance energy ($E_R$) of isocyanuric acid triester. The results obtained are compared with values of benzene.

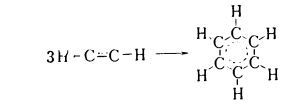
*Conjugation Energy.*—The conjugation energy ($\Delta E_\pi$) is defined as follows:

$$\Delta E_\pi = 3\varepsilon_M - \varepsilon_P$$

where $\varepsilon_P$ is the total $\pi$ electron energy of an isocyanurate, and $\varepsilon_M$ is that of the isocyanate. Since the group R is not a conjugative one, it is left out of account in the calculation. An isocyanurate ring consists of three isocyanate molecules as follows:



Then the conjugation energy, $\Delta E_\pi$, defined above becomes 1.4888 $(-\beta)$, while with regard to benzene,



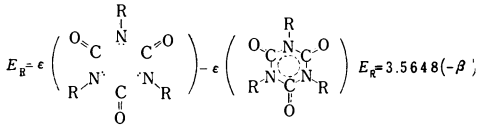
we obtain $\Delta E_\pi = 2(-\beta)$.

*Resonance Energy.*—The resonance energy $E_R$ is defined

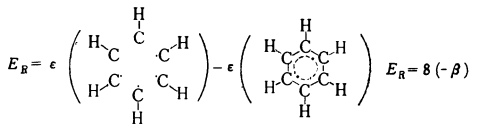
$$E_R = \varepsilon_L - \varepsilon_P$$

where $\varepsilon_L$ is the total $\pi$ electronic energy of an extreme structure in which each two $\pi$ electrons are localized in each bond.

Therefore, on an isocyanurate, the resonance energy is defined as



In a similar way, we calculate the resonance energy of benzene by the following equation.



Thus we know that the conjugation energy of an isocyanurate molecule is equal to ca. 75% of that of benzene, the resonance energy of the former being 44% of benzene.

These results will account for the remarkable heat stability of the isocyanuric ring[12].

**The Stability and Reactivity of Triallyl Cyanurate and Isocyanurate.** — Four structural isomers of triallyl ester are indicated as *O,O,O-*, *O,O,N-*, *O,N,N-* and *N,N,N-*esters. In these are included the isomeric esters of Hantzsch and Bauer[7]. Their structure and the electrophilic frontier electron densities ($f_r$) are indicated in Fig. 1. We calculate further the one term approximation of superdelocalizability ($S'_r$)[13], the total $\pi$-elecronic energy ($\varepsilon$), the conjugation energy ($\Delta E_\pi$)*, and the energy of the highest occupied orbital ($\varepsilon_f$).

The calculated results enable us to derive the following conclusions.

*Reactivity of Double Bond in Polymerization and Radical Reactivity.*—The values of electrophilic frontier electron density ($f_r$) and one term approximation of superdelocalizability ($S'_r$) of the methylene radical in allyl group

12) P. Lemoult, *Ann. chim. phys.*, (7) **16**, 338 (1848); A. Hofmann, *Ber.*, **3**, 264 (1879).

* In the present calculation, allyl group is taken into consideration.

13) K. Fukui, T. Yonezawa and C. Nagata, *J. Chem. Phys.*, **27**, 1247 (1957).

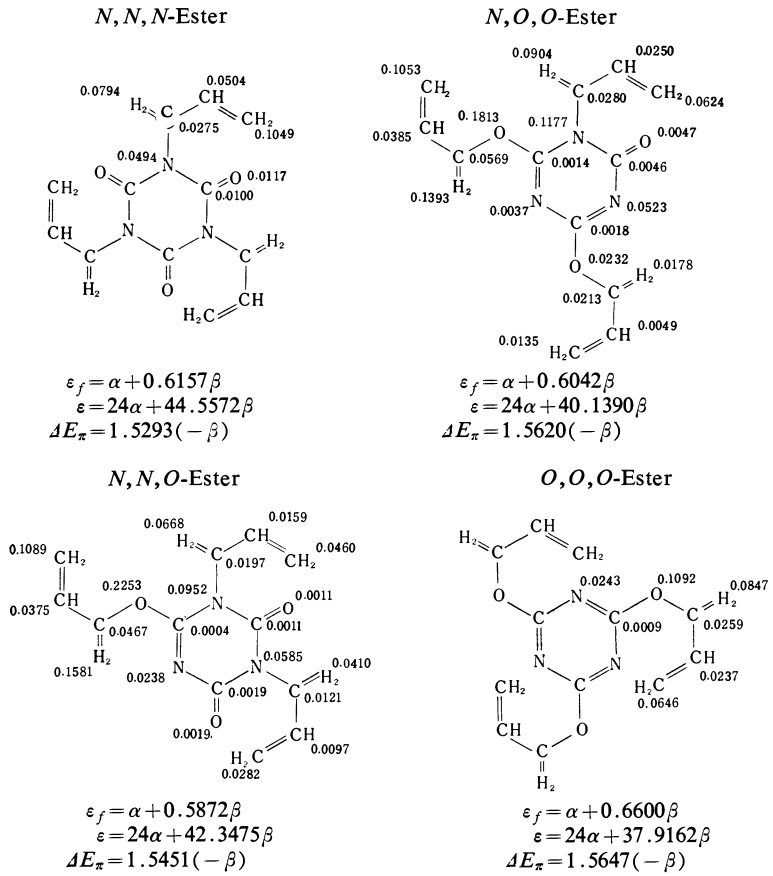



Fig. 1. Frontier electron densities, frontier orbital energy, total $\pi$-electronic energy and conjugation energy of four triallyl esters.

and the $\gamma$-carbon atom in allyl group of the isomeric esters are listed in Table II, in which are indicated the maximum values among three allyl groups of each monomer. It is found in the table that the reactivity of the methylene radical in allyl group decreases in the order *N, N, O-* ; *N, O, O-* > *O, O, O-* > *N, N, N*-ester. It is worthy of note that the methylene radical in asymmetric esters should be more reactive than those in symmetric esters.

Pure triallyl isocyanurate was easily polymerized in the presence of benzoyl peroxide to give clear resin. The activation energies of the radical polymerization were observed 20.6 kcal./mol. for the *N, N, N*-ester and 43.2 kcal./mol. for the *O, O, O*-ester[6]. Further, the order of electrophilic reactivity of double bond in isomeric esters is shown to be *N, N, O-* ; *N, N, N-* ; *N, O, O-* $\gg$ *O, O, O*-ester. This result is important, because it gives us a certain of information on the reactivities of these esters in cationic polymerization.

*Reaction and Heat-stability of Triallyl-cyanurate and Isocyanurate.*—The values of total $\pi$-electronic energy ($\varepsilon$) and conjugation energy ($\Delta E_\pi$) of the isomeric esters are listed in Table III. As far as $\pi$-electronic energies in these esters are concerned, the values of $\Delta E_\pi$ seem to indicate that the ease of hydrolysis and transesterification of allyl groups decreases in the order *O, O, O-* > *N, O, O-* > *N, N, O-* > *N, N, N*-ester, if we consider the fact that a change in activation energy parallels closely to a change of $\Delta E_\pi$. Furthermore, referring to the values of $\varepsilon$, esters formed may have a tendency to isomerize to the *N, N, N*-ester and through this isomerization these esters beome stabilized.

In our experiments[6], however, the *N, N, N*-ester could not be prepared from the *O, O, O*-ester by thermal isomerization, because the *O, O, O*-ester decomposes and polymerizes during distillation at atmospheric pressure. On the other hand, the *N, N, N*-ester could be distilled at 289°C/760m mHg in nitrogen current. Further, the infrared spectroscopic results[6,14] for the polymer of the *O, O, O*-ester showed

14) B. H. Clampitt, D. German and J. R. Galli, *J. Polymer Sci.*, **27**, 515 (1958).

that a sort of *N, N, N*-ester structure had been formed by an isomerization during the polymerization process.

On the other hand, the weight loss on 1 hr. exposure to 300°C of the resin which was prepared by polymerization initiated by benzoyl peroxide was below 5% for the *N, N, N*-ester polymer and above 7% for the *O, O, O*-ester polymer[6]. These results indicate that the two polymers stated above are not completely identical and the *N, N, N*-ester polymer possesses a better heat stable property and a larger resistance for air oxidation than *O, O, O*-ester polymer.

*Faculty of Engineeering*
*Kyoto University*
*Sakyo-ku, Kyoto*

# *Studies on the Chemical Equilibrium Lag during the Rapid Expansion through the Rocket Nozzle*

By Soji TSUCHIYA

(Received on December 2, 1960)

The expansion process causes chemical reactions in the gas flowing through a rocket nozzle, since unstable molecules and atoms involved in the combustion product reassociate in the course of the temperature drop due to the expansion. However, when the gas expands through a nozzle in very short duration as in the case of a rocket engine, the rates of chemical reactions cannot maintain the chemical equilibrium of the system, and a relaxational phenomenon occurs; in other words, the composition of the gas reaches the chemical non-equilibrium state by way of the expansion process. The observation of such a relaxational process will give information concerning the fast chemical reaction kinetics at high temperature, and also give the descriptions of hypersonic flow with chemical reactions, since great energy changes due to chemical reactions affect the velocity of flowing gas or other parameters.

These problems occur in hypersonic flows or shock waves. First, Penner pointed out this problem in the case of a rocket engine[1], and Wegener determined the rate constant of $N_2O_4 \rightleftarrows 2NO_2$ using the hypersonic nozzle flow[2], but few experimental results have been available in a nozzle flow of a rocket engine.

The present author has constructed the automatic recording pyrometer having a short response time to observe the temperature of the nozzle exhaust gas of the JP4-nitric acid rocket, and has considered the chemical equilibrium during the rapid expansion through the *de Laval* nozzle.

## Pyrometer*

In the case of the pyrometry of hypersonic gas flows, optical methods are more suitable than the methods using a thermocouple or pneumatic probe to avoid a inserting material's aerodynamic heating. The automatic recording pyrometer constructed here is a modified type of the Na D line reversal method and is similar to Heidmann or Millar's technique[3], which has been improved in regard to the accuracy of measurement in this apparatus.

The Na D line reversal method is based on the fact that the flame temperature and the brightness temperature of the source lamp are the same, when the flame containing sodium atoms has neither emission nor absorption of Na D line in reference to the background spectrum of the source lamp. In the present method, the intensity of absorption or emission of the gas was measured when the source lamp had a fixed brightness temperature, and the difference between the temperature of the gas and the source lamp was determined. The accuracy obtained in the pyrometer was $\pm 10°K$ at 2000°K of the flame temperature, when the difference between the flame temperature and the brightness temperature of the lamp was 100°K. The temperature range observable by the pyrometer was from about 1500 to 3300°K,

1) D. Altman and S. S. Penner, *J. Chem. Phys.*, **17**, 56 (1949); S. S. Penner, ibid., **19**, 877 (1951).
2) P. P. Wegener, ibid., **28**, 724 (1958); *Phys. Fluid*, **2**, 264 (1959).

* Presented at the 13th Annual Meeting of the Chemical Society of Japan, Tokyo, April, 1960.
3) M. F. Heidmann and R. J. Priem, *J. Am. Rocket Soc.*, **23**, 248 (1953); G. H. Millar, J. G. Winans, O. A. Uyehara and P. S. Myers, *J. Opt. Soc. Am.*, **43**, 609 (1953).

and the response time was 0.1 sec. More detailed descriptions on the pyrometer will be given in the other paper[4].

## Results

The rocket test equipment was described in the other paper[5]. The temperature measurement of the exhaust gas was performed using the following propellant:

Oxidant: White fumic nitric acid with 0.3 wt.% of sodium nitrate

Fuel: JP4 70 vol.%; *n*-Butyl vinyl ether 30 vol.%

The above propellant reacted in the combustion chamber at 20 atm., and the gas produced in the chamber expanded to atmospheric pressure through the nozzle.

The exhaust gas emitted Na D line by the contamination of sodium nitrate in the oxidant, and this contamination scarcely affected the rocket performance or the flame temperature. The results are shown in Table I.

Table I. Experimental results

| Exp. No. | 14 | 19 | 21 | |
|---|---|---|---|---|
| Chamber pressure | 20.2 | 20.0 | 21.4 | atm. |
| Thrust | 101 | 100 | 100 | kg. |
| Oxidant flow rate | 406 | 405 | 404 | g./sec. |
| Fuel flow rate | 81 | 80 | 82 | g./sec. |
| O/F* | 5.0 | 5.1 | 4.9 | |
| Specific impulse | 207 | 206 | 206 | sec. |
| Exhaust temperature | 1870 | 1830 | 1829 | °K |

* Oxidant to Fuel wt. ratio

The pyrometry by the Na D line reversal method should be applied in the case of a non-luminous flame, and the exhaust gas of a rocket engine using a hydrocarbon fuel contains carbon particles, which may cause the observed reversal temperature to be different from the real temperature of the gas. The effective emissivity due to carbon particles involved in the gas was measured without contamination of sodium nitrate by the monochromator used here and was about 0.01~0.02, which was much less than the emissivity due to sodium atoms (=0.1~0.2). Therefore, the observed exhaust temperature has nearly the same value as the real exhaust temperature.

## Discussion

**Calculation of Theoretical Temperatures.**— First, the temperature $T_c$ and the composition of the gas in the combustion chamber are calculated by the assumption that the chemical equilibrium is attained in the combustion chamber at pressure $P_c$, and that the following enthalpy relation is held:

$$\sum_i (N_i^c/\overline{M}_c)\{H^0(T_c) - H_0^0 + H_f\}_i = l\{H^0(298.16) - H_0^0 + H_f\}_{fuel} + m\{H^0(298.16) - H_0^0 + H_f\}_{oxid} - \Delta q_c \quad (1)$$

where $N_i^c$ is the mole fraction of component i of the product, and $\overline{M}_c$ is the mean molecular weight of the gas in the combustion chamber, and $\{H^0(T) - H_0^0 + H_f\}_i$ is the total enthalpy of component i per mole[6], and $l$ and $m$ are the mole number of fuel and oxidant resoectively per unit mass of propellant, and $\Delta q_c$ is heat loss in the combustion chamber per unit mass of the gas. $\Delta q_c$ is assumed to be the same as Zucrow's experimental value[7]. The chemical equilibria considered here are the following seven equations:

$$\left.\begin{aligned} &H_2O \rightleftarrows OH + 1/2\,H_2 \\ &H_2O \rightleftarrows H_2 + 1/2\,O_2 \\ &CO_2 \rightleftarrows CO + 1/2\,O_2 \\ &1/2\,O_2 \rightleftarrows O \\ &1/2\,H_2 \rightleftarrows H \\ &NO \rightleftarrows 1/2\,N_2 + 1/2\,O_2 \\ &1/2\,N_2 \rightleftarrows N \end{aligned}\right\} \quad (2)$$

The calculation is carried out by the trial and error method using Huff et al.'s thermodynamic tables[8].

The expansion process through the rocket nozzle is assumed to be adiabatic, and the flow of the expanding gas is considered as a one-dimentional flow ignoring the diffusion or friction. Since the entropy of the gas per unit mass is constant during the expansion;

$$(1/\overline{M}_c)\sum_i\{N_i^c S_i(T_c) - \boldsymbol{R}\ln N_i^c P_c\} = (1/\overline{M}_e)\sum_i\{N_i^e S_i(T_e) - \boldsymbol{R}\ln N_i^e P_e\} \quad (3)$$

where the suffixes c and e show the quantities of the gas in the combustion chamber and exhaust jet, respectively, and $S_i$ is entropy per mole of i component of the gas. By this entropy relation, the temperature of the exhaust gas $T_e$ can be calculated in the cases of both the frozen and shifting chemical equilibria during the nozzle expansion. In the former

4) S. Tsuchiya, *Aero. Res. Inst. Univ. Tokyo. Report*, No. 366 (1961).

5) K. Kuratani, G. Onoue and S. Tsuchiya, *Collected Pap. Aero. Res. Inst. Univ. Tokyo*, (*Kôkû Kenkyûjo Shûhô*), 2, 11 (1960).

6) Heats of formation used here are the following: $H_f$(JP4) = −0.419 kcal./g., $H_f$(*n*-Butyl vinyl ether) = −48 kcal./mol., estimated by Pauling's method, $H_f$(Nitric acid) = −41.10 kcal./mol., at 298.16°K.

7) M. J. Zucrow and C. M. Beighley, *J. Am. Rocket Soc.*, 22, 323 (1952).

8) V. N. Huff, S. Gordon and V. E. Morell, *NACA Rep.*, 1037 (1951).

case, the exhaust temperature $T_e^{frozen}$ is calculated by the condition $N_i^c = N_i^e$, that is, the mole fractions of components of the gas are constant during the nozzle flow. In the latter case, however, the mole fractions vary according to the chemical equilibria in Eq. 2, which are shifting as the temperature of the gas is lowered during the expansion process; therefore $N_i^c \neq N_i^e$. The exhaust temperature $T_e^{equil}$ has generally a higher value than $T_e^{frozen}$ because the heat of reactions due to the shifting of the chemical equilibria is partly given to the expanded gas.

Since the nozzle expansion process is not strictly adiabatic, the entropy change $\Delta s$ produced by heat loss at the nozzle should be considered;

$$\Delta s = \int dq_n/T \fallingdotseq q_n/T_t \qquad (4)$$

where $q_n$ is heat loss at the nozzle per unit mass of the flowing gas, and $T_t$ is the temperature of the gas at the throat of the nozzle. This approximation is based on the fact that the heat loss at the nozzle occurs mostly in the throat, and the value used here is Zucrow's data[7].

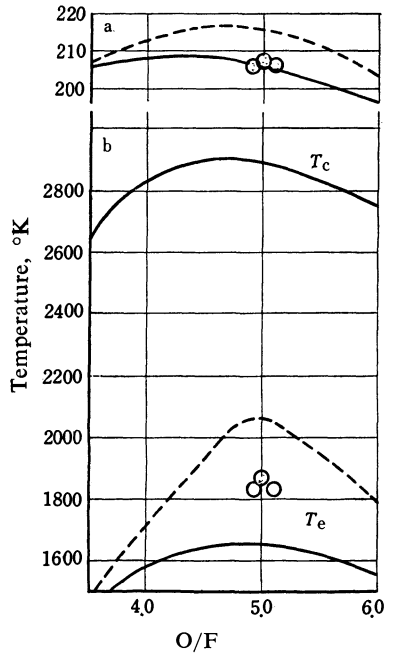



Fig. 1. Specific impulse (a) and temperature in the chamber and the exhaust (b), with correction due to heat loss in the chamber 0.05 kcal./cm²·sec., and in the nozzle 0.084 kcal./cm²·sec.;

○ : experimental value,
—— and ----: with chemical equilibria frozen and shifting, respectively.

The velocity of the exhaust gas or specific impulse $I_{sp}$ is obtained from the enthalpy decrease of the gas due to the expansion.

$$(1/2)v_e^2 = (1/\bar{M}_c)\sum_i N_i^c\{H^0(T_c) - H_0^0 + H_f\}_i - (1/\bar{M}_e)\sum_i N_i^e\{H^0(T_e) - H_0^0 + H_f\}_i \qquad (5)$$

$$I_{sp} = v_e/g \qquad (6)$$

The results of calculations are given in Fig. 1 by the method above mentioned, and the equilibrium compositions of the gas in the chamber and exhaust are also given in Table II.

Table II. Equilibrium mole fractions (O/F=5.0)

| | in chamber $T_c$=2890°K $P_c$=20 atm. | in exhaust $T_e$=2070°K $P_e$=1 atm. |
|---|---|---|
| $CO_2$ | 0.23546 | 0.30655 |
| CO | 0.06743 | 0.01062 |
| $H_2O$ | 0.43881 | 0.48706 |
| $H_2$ | 0.01750 | 0.00338 |
| $O_2$ | 0.03096 | 0.00492 |
| NO | 0.00772 | 0.00072 |
| $N_2$ | 0.17260 | 0.18441 |
| OH | 0.02296 | 0.00211 |
| H | 0.00328 | 0.00015 |
| N | 0.00008 | 0.00000 |
| O | 0.00320 | 0.00009 |

**Relaxation of Chemical Equilibrium.**—By comparison of the observed exhaust temperatures $T_e^{obs}$ with the calculated values, $T_e^{obs}$ is lower than $T_e^{equil}$ and higher than $T_e^{frozen}$. This fact shows that the chemical equilibria may be neither shifting nor frozen during the actual expansion through the nozzle, and that the relaxation of the chemical equilibrium occurs during the expansion process. Since the velocity of the gas reaches $1\times10^5$ cm./sec. at the nozzle throat and the length of the divergent part of the nozzle used here is 7 cm., the time for the gas to pass the nozzle is of the order of $10^{-5}$ sec. It is considered, therefore, that the rates of the chemical reactions can not maintain the equilibrium in this short time. To analyze the situations of the chemical equilibrium during the expansion, it must be necessary that the hypersonic flow through the *de Laval* nozzle be treated taking the chemical reactions into account besides the flow descriptions[9]. This treatment is very difficult in the

9) The relaxational phenomenon on the internal energy states as well as the chemical equilibria must be considered here, but the relaxation time of internal energy may be much smaller than that of the chemical reaction, and the internal energy states scarcely deviate from equilibrium in the nozzle flow discussed here.

present nozzle flow, since the chemical reactions Eq. 2, which should occur during the expansion, are very complicated. Therefore, the approximate analysis is adopted here.

**Approximate Treatment of Chemically Relaxed Flow.**—Here, $-(\mathrm{d}t/\mathrm{d}T)$ is considered as the parameter showing whether the composition of the expanding gas has chemical equilibrium or non-equilibrium; $-(\mathrm{d}t/\mathrm{d}T)$ equals a time to change the temperature of the gas 1°K, and when $-(\mathrm{d}t/\mathrm{d}T)$ has a smaller value, the chemical equilibrium tends to be relaxed[1]. To derive the value of $-(\mathrm{d}t/\mathrm{d}T)$, the temperature, pressure and velocity of the expanding gas are calculated in relation to the coordinate taken in the direction of the nozzle axis. The calculation is based on the following fundamental equations:

$$\left.\begin{aligned} &(\mathrm{d}\rho/\rho)+(\mathrm{d}v/v)+(\mathrm{d}A/A)=0 && \text{conservation of mass}\\ &v\mathrm{d}v+\mathrm{d}h=0 && \text{conservation of energy}\\ &\mathrm{d}s=0 && \text{isentropic relation}\\ &P=(R/\bar{M})\rho T && \text{equation of state} \end{aligned}\right\} \quad (7)$$

where $\rho$ is the density of the gas, $v$ velocity of the gas, $A$ area of the nozzle section, $h$ enthalpy per unit mass of the gas. In the case of chemical equilibrium flow, the equations of chemical equilibria must be added to the above fundamental equations. The results are shown in Fig. 2, where the section of the *de Laval* nozzle used in this experiment is also shown. From the calculated temperature and velocity profile through the nozzle, $-(\mathrm{d}t/\mathrm{d}T)$ can be easily derived, and relations of $-(\mathrm{d}t/\mathrm{d}T)$ and the temperature of the gas are given in Fig. 3 in the cases of both frozen and equilibrium flow. At the divergent part of the nozzle, the order of $-(\mathrm{d}t/\mathrm{d}T)$ is $10^{-8}$ sec./deg., and is of much greater value near the combustion chamber. It is, therefore, probable that the nozzle flow of the gas may have chemical equilibrium near the throat of the nozzle and the relaxational phenomenon may occur after the gas passes the throat.

Then, the chemically relaxed flow of the gas can be treated by the following approximation: the combustion product in the chamber at pressure $P_c$ expands to a pressure $P^*$ and a

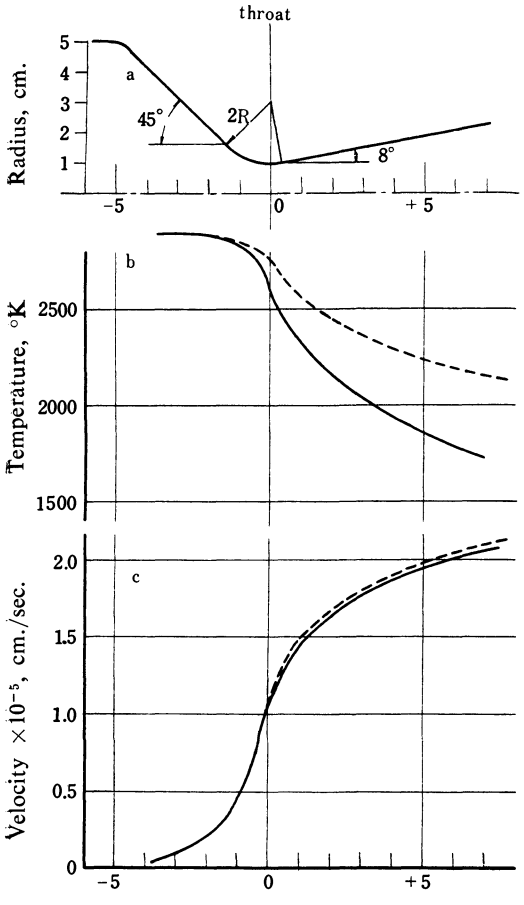



Fig. 2. Section of the nozzle parallel to the nozzle axis (a), and temperature (b) and velocity (c) profiles during the expansion process at O/F=5.0, without correction due to heat loss in the nozzle;
—— and ----: with chemical equilibria frozen and shifting, respectively.

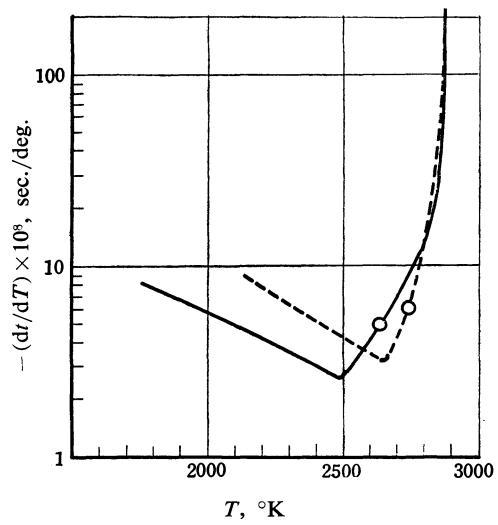



Fig. 3. Calculated curve of $-(\mathrm{d}t/\mathrm{d}T)$ during expansion through the nozzle in relation to the temperature of the gas at O/F=5.0, without correction due to heat loss in the nozzle;
○ : value of $-(\mathrm{d}t/\mathrm{d}T)$ at the throat,
—— and ----: with chemical equilibria frozen and shifting, respectively.

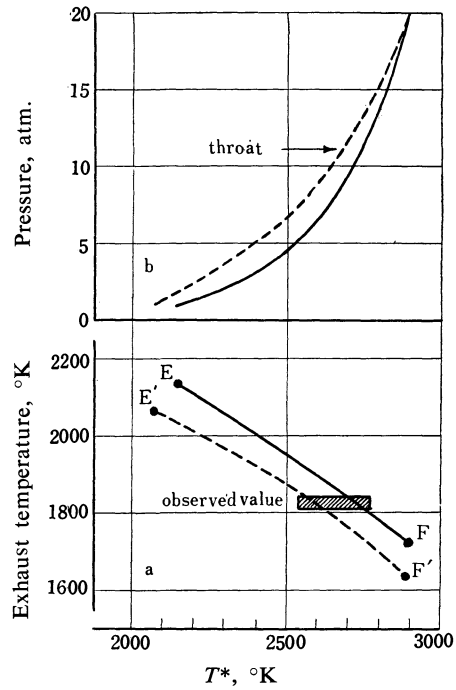



Fig. 4. Calculated exhaust temperature by 'suddenly frozen' approximation (a) and pressure of the gas (b) against $T^*$ at O/F= 5.0;
—— and ----: without and with correction due to heat loss in the nozzle, respectively. Points F and E in curve (a) correspond to the exhaust temperatures with chemical equilibria frozen and shifting, respectively.

temperature $T^*$ with the chemical equilibria shifting, and from a pressure $P^*$ to the exhaust pressure $P_e$ with the chemical equilibria frozen. This approximation means:

$$\text{at } T>T^* \text{ and } P>P^*, \quad -(dt/dT)=\infty,$$

$$\text{at } T<T^* \text{ and } P<P^*, \quad -(dt/dT)=0,$$

in other words, the expansion through the nozzle proceeds from $P_c$ to $P^*$ at infinitely low speed and from $P^*$ to $P_e$ at infinitely high speed. Recently, the author has treated the expansion process of hydrogen gas with recombining reaction of hydrogen atoms more strictly, and ascertained that the above approximation gives nearly the right illustration of the flow through the *de Laval* nozzle[10]. The foundation of this approximation is that the relaxational process ends in a very short time after the composition of the gas deviates from an equilibrium state, and that the chemical equilibria of the system are instantly frozen. In general, the relaxation of the chemical equilibrium increases the entropy of the system[11]. However, this entropy increase may be small owing to the shortness of the relaxational process, and the isentropic condition may be assumed. The same situations about the flow of diatomic gases through the *de Laval* nozzle have been considered also by Bray and by Hall and Russo[12].

The calculated results by this 'suddenly frozen' approximation are shown in Fig. 4. The pressure $P^*$ and the temperature $T^*$ at which the relaxation of chemical equilibrium occurs in the present nozzle flow, can be determined by a comparison of the observed exhaust temperature $T_e^{obs}$ and the exhaust temperature $T_e^{sf}$ calculated by the 'suddenly frozen' approximation. $T_e^{obs}$ agrees $T_e^{sf}$ at $T^* \fallingdotseq 2600°K$ and $P^* \fallingdotseq 10$ atm. This means that the chemical equilibrium may be relaxed near about 2600°K and 10 atm. during the expansion. The position, where the temperature and pressure of the gas reach the obtained $T^*$ and $P^*$, is slightly outside the throat of the nozzle. The $-(dt/dT)$ at this position is about $5\times10^{-8}$ sec./deg., and the relaxation is estimated to occur at $-(dt/dT)^*=3\sim8\times10^{-8}$ sec./deg.

The obtained limiting value of $-(dt/dT)$ for keeping the chemical equilibrium of the system can be related to the chemical reaction rate, but the kinetic mechanism is too complicated to analyze the present expansion through the nozzle, in which the recombination of atoms and the oxidation of carbon monoxide or hydrogen may be the main reactions, as Table II shows. Altman and Carter say that $-(dt/dT)$ ranges from about 7 to $3\times10^{-7}$ sec./deg. at a divergent part of a nozzle in a rocket having a large thrust like the V-2, since $-(dt/dT)$ is approximately proportional to a square root of thrust. Considering the atomic recombining reaction rate, they estimate that the expansion through such a nozzle proceeds with the chemical equilibria shifting[13]. This estimation is consistent with the present experiment.

If a more simple system is treated, the rapid expansion through the *de Laval* nozzle can be used as a new technique for the measurement of fast reaction rate at high temperature.

## Summary

The pyrometer fitted for the temperature measurement of exhaust gas of the rocket, was constructed, and the exhaust temperature of

10) S. Tsuchiya, to be published.

11) W. W. Wood and J. G. Kirkwood, *J. Applied Phys.*, **28**, 395 (1957).

12) K. N. C. Bray, *J. Fluid Mech.*, **6**, 1 (1959); J. G. Hall and A. L. Russo, *Cornell Aero. Lab. AFOSR TN* 59-1090 (1959).

13) D. Altman and J. M. Carter, "Combustion Process", Ed. by B. Lewis, R. N. Pease and H. S. Taylor, Princeton Univ. Press, Princeton (1956), p. 51.

the JP4-nitric acid rocket having 100 kg. of thrust, was observed. From the obtained exhaust temperature, it has been ascertained that the expansion of the gas through the present nozzle proceeds with chemical equilibria neither shifting nor frozen, and that relaxation occurs. From the approximate analysis of chemically relaxed flow, the relaxational process is assumed to occur at $-(dt/dT)^*=3\sim8\times10^{-8}$ sec./deg., $T^*\fallingdotseq2600°K$ and $P^*\fallingdotseq10$ atm.

The author wishes to express his sincere thanks to Assistant Professor K. Kuratani for his kind encouragement throughout this work. His thanks are also expressed to Mr. G. Onoue for his help in constructing the apparatus.

*Aeronautical Research Institute*
*The University of Tokyo*
*Meguro-ku, Tokyo*

# *Solvent Extraction of Inorganic Nitrates with Diphosphonate Ester. I. Zirconium, Yttrium and Lanthanide Nitrates*

By Hideo SAISHO

(Received December 8, 1960)

Various extracting agents have been investigated on the solvent extraction of many elements. Much attention has been paid to such extracting agents as organophosphorus compounds (tri-*n*-butyl phosphate and others) and β-diketones (thenoyltrifluoroacetone and others).

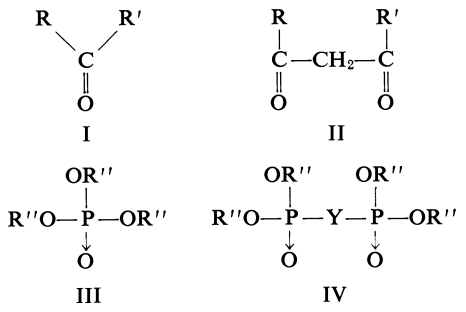



Fig. 1. The structural formulae of ketone (I), β-diketone (II), tri-*n*-alkyl phosphate (III) and diphosphonate ester (IV).

The extractability of various metal ions with β-diketone (Fig. 1-II) is much higher than that with ketone (Fig. 1-I), though both ketone and β-diketone are used for the solvent extraction. From the similarity of structural formulae as shown in Fig. 1, it is expected that diphosphonate ester (Fig. 1-IV) may show better extractability than tri-*n*-alkyl phosphate (Fig. 1-III). Thus, in the present paper tetra-*n*-butyl ethylenediphosphonate* (TBEDP), $(BuO)_2P(O)(CH_2)_2(O)P(BuO)_2$, was chosen, and the extractability of zirconium, yttrium and several lanthanide elements (cerium, promethium, europium and lutetium) was studied on the system between TBEDP-kerosene and various nitric acid concentrations.

Although Kennedy et al.[1] reported the solvent extraction of uranium with diphosphonate esters, the extracting behavior was not studied in detail. Since then, no investigations on the diphosphonate esters extraction of some elements other than uranium have been reported.

## Experimental

**Solvent.**—TBEDP purchased from the Tama Chem. Co., Tokyo, Japan, was used without any further purification. TBEDP was diluted with kerosene to 0.1 or 0.2 M according to the experimental requirements. Kerosene used here had flash point above 60°C and was not specially purified. Nitric acid solutions were prepared by diluting concentrated nitric acid, special grade. The acidity range of the solution covered from 0.01 to 13 M. The acidity was determined volumetrically, whenever necessary.

**Determination of Distribution Ratios.** — The distribution ratio of a given nuclide, defined as the concentration of the nuclide in the organic phase divided by that in the aqueous phase, was determined radiochemically.

Five millilitres of nitric acid solution containing the radioactive tracer and the equal volume of TBEDP diluted with kerosene were placed together in a 30 ml. glass-stoppered cylinder, and shaken vigorously in a thermostat kept at 25±0.5°C. Shaking was continued for 30 min. Preliminary

* Tetra-*n*-butyl ethylenediphosphonate is abbreviated as TBEDP.

1) T. V. Healy and J. Kennedy, *J. Inorg. & Nucl. Chem.*, **10**, 128 (1959).

tests showed that the equilibrium was attained in less than 10 min. Then, the two phases were separated by the use of a separating funnel.

Aliquots from organic or aqueous phases were taken into small stainless steel dishes and carefully dried under an infrared lamp.

Radioactivity of Y-91, Ce-144, Pm-147, Eu-152-154 and Lu-177 was measured with a G.-M. counter having a window of 3.10 mg./cm$^2$ thick. As it took at least about four hours to evaporate aliquots to dryness, Ce-144 and its daughter, Pr-144 reached the radioactive equilibrium completely when the activities were counted. Amounts of Zr-95 were measured at the Zr-95 (0.754 and 0.722 MeV.) photopeaks by an Argonne Type 256 Channel Pulse Height Analyzer with a 3'' diameter ×3'' NaI(Tl) crystal.

**Radioisotopes Used.**—The radioisotopes used in this experiment were Zr-95, Y-91, Ce-144, Pm-147, Eu-152-154 and Lu-177. These tracers were imported from Oak Ridge National Laboratory, U.S.A. or Radiochemical Centre, U. K.

Ce-144 and Eu-152-154 received as nitrates were used without further treatments. However, Y-91, Pm-147 and Lu-177 were converted into nitrates by a cation exchange technique**, because they were imported as chlorides. The cerium tracer was always kept in the trivalent state.

Zr-95 tracer[2] was freed from Nb-95 as follows: Zr-95 was first extracted into a 0.5 M TTA (thenoyltrifluoroacetone)-xylene solution from 2 M nitric acid solution containing Zr-Nb-95. The Zr-95 tracer was stripped into 8 M nitric acid solution from the organic phase diluted with xylene by a factor of 10 or more. The solution was used immediately after the separation.

## Results and Discussion

**Effect of Nitric Acid Concentration.**— The results obtained are plotted in Figs. 2-4, where other authors' results[3-6] for each element in the extraction with TBP (tri-*n*-butyl phosphate) from nitric acid are added for comparison.

Fig. 2 shows the variation of distribution ratio, $K_d$, of zirconium in the range of nitric acid concentration from 0.01 to 13 M, keeping the TBEDP concentration 0.1 M. As Fig. 2 shows, the acid-dependence curves for TBP and TBEDP have a similar tendency concerning the fact that the distribution ratios increase with increasing acidity in both cases.

Fig. 3 also shows the variation of $K_d$ of yttrium and lutetium in the same acidity range

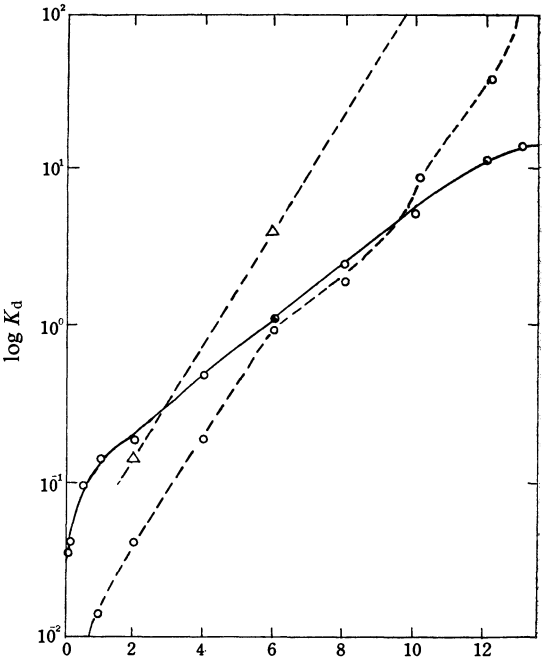



Fig. 2. The $K_d$ values of zirconium.
—○—: 0.1 M TBEDP in kerosene
--○--: McKay et al.[3], 19% TBP in kerosene
--△--: Peppard et al.[4], 100% TBP

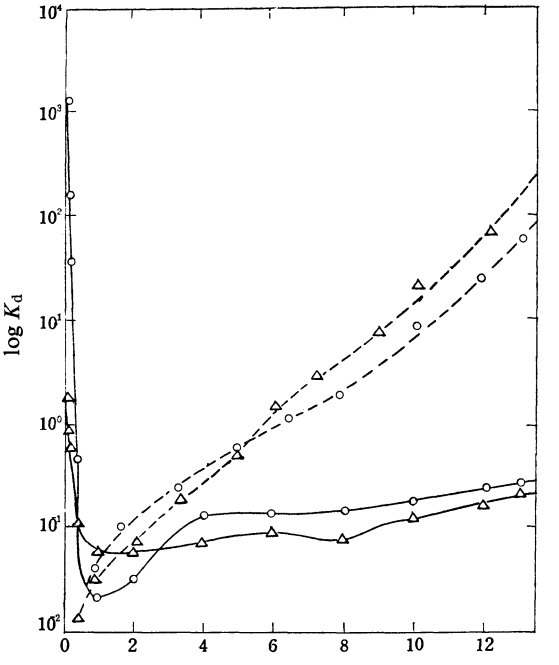



Fig. 3. The $K_d$ values of yttrium and lutetium.
——: 0.2 M TBEDP in kerosene
----: McKay et al.[5,6], 100% TBP
○ : Yttrium △ : Lutetium

** The radioactive tracer was adsorbed on the resin Dowex 50-X8, H form column and then eluted with nitric acid solution.

2) F. L. Moore, *Anal. Chem.*, **28**, 997 (1956).
3) K. Alcock, F. C. Bedford, W. H. Hardwich and H. A. C. McKay, *J. Inorg. & Nucl. Chem.*, **4**, 100 (1957).
4) K. F. Peppard, G. W. Mason and J. L. Maier, ibid., **3**, 215 (1956).
5) D. Scargill, K. Alcock, J. M. Fletcher, E. Hesford and H. A. C. McKay, ibid., **4**, 304 (1957).
6) E. Hesford, E. E. Jackson and H. A. C. McKay, ibid., **9**, 279 (1959).

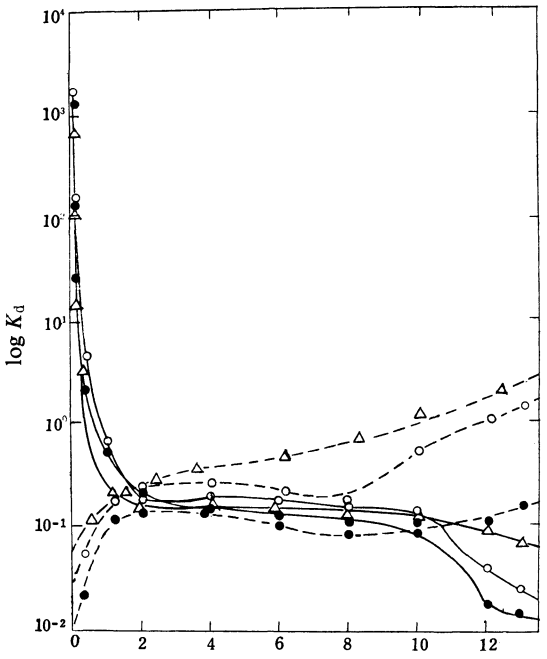



Fig. 4. The $K_d$ values of cerium, promethium and europium.
——: 0.2 M TBEDP in kerosene
----: McKay et al.[5,6], 100% TBP
● : Cerium ○ : Promethium
△ : Europium

as in the case of zirconium, keeping the TBEDP concentration 0.2 M. As shown in Fig. 3, there is a remarkable difference between TBP and TBEDP in the very low acidity range below about 0.5 M nitric acid. In TBEDP extraction the $K_d$ values are very high at 0.01 M nitric acid and decrease sharply with increasing acidity up to about 1 M nitric acid. In the higher acidity range the $K_d$ values by TBEDP tend to increase gradually, while those by TBP increase rapidly. Similarity in the extraction of yttrium and lutetium with TBEDP appears to be in accordance with the fact that they belong to the yttrium group.

Fig. 4 indicates the results for cerium, promethium and europium under the same experimental conditions as the case for yttrium and lutetium. In the low acidity region the extracting behavior of cerium, promethium and europium is very similar to that of yttrium and lutetium; the $K_d$ values of these three elements decrease sharply with increasing acidity. On the contrary in the higher acidity the $K_d$ values have decreasing tendency, though those by TBP increase in this region. It is interesting for the author that the sequence of the $K_d$ values by TBEDP in the region agrees with that by TBP.

From the above-mentioned facts, it may be said that this extracting agent is very excellent for the extraction of trivalent elements such as lanthanide elements especially in the low acidity region. The difference between $K_d$ values for a lanthanide element and zirconium is so great in the low acidity region that a lanthanide element may be separated from zirconium very easily.

**Effect of Nitrate Concentration on Extraction of Zirconium.**—The results obtained with 0.1 M TBEDP concentration are given in Table I. This table shows that the distribution ratios

Table I. Effect of nitrate concentration on extraction of zirconium (0.1 M TBEDP in kerosene)

| Molarity | | | | | Distribution |
|---|---|---|---|---|---|
| $HNO_3$ | $NH_4NO_3$ | $Ca(NO_3)_2$ | $Al(NO_3)_3$ | Total $NO_3$ | ratio |
| 4 | — | — | — | 4 | 0.50 |
| 8 | — | — | — | 8 | 2.85 |
| 4 | 4 | — | — | 8 | 1.43 |
| 4 | — | 2 | — | 8 | 2.81 |
| 4 | — | — | 1.33 | 8 | 3.45 |
| 10 | — | — | — | 10 | 5.40 |
| 4 | 6 | — | — | 10 | 1.93 |
| 4 | — | 3 | — | 10 | 3.49 |
| 4 | — | — | 2 | 10 | 6.53 |
| 12 | — | — | — | 12 | 10.75 |
| 4 | 8 | — | — | 12 | 3.45 |
| 4 | — | 4 | — | 12 | 8.09 |
| 4 | — | — | 2.66 | 12 | 11.10 |

can increase when other nitrates are added to nitric acid. This fact suggests that the extraction of zirconium by TBEDP depends on nitrate ion concentration to some extent. The results also indicate that zirconium is extracted much more readily from nitric acid solution containing aluminum nitrate, than from pure nitric acid solution of the same total nitrate ion concentration.

The author wishes to express his sincere thanks to Dr. Hiroshi Ohinouye, Director of the Laboratory of Mitsubishi Atomic Power Industries, Inc., and Mr. Kazumu Sugimoto, Chief of Chemistry Section of the Laboratory for their support and permission to present this work.

Thanks are also due to Professor Nobufusa Saito and Assistant Professor Yuji Yokoyama of the University of Tokyo for their suggestions and guidance, and Mr. Ryoichi Uehara for his effort in the synthesis of tetra-*n*-butyl ethylenediphosphonate.

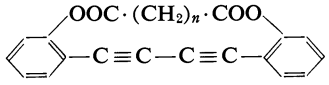
*Engineering & Research Laboratory*
*Mitsubishi Atomic Power Industries, Inc.*
*Ohmiya, Saitama*

# *Cyclic Acetylenes. V. Syntheses and Properties of Strained Cyclic Ethers of o, o'-Dihydroxydiphenyldiacetylene*

By Fumio TODA and Masazumi NAKAGAWA

(Received December 9, 1960)

In the previous paper of this series[1], the present authors reported the syntheses and the ultraviolet spectroscopic properties of a series of diacetylenic macrolides (I, $n=3$, 4, 5 and 7). In the course of the synthesis of the compound I, it was found that the ester linkages are

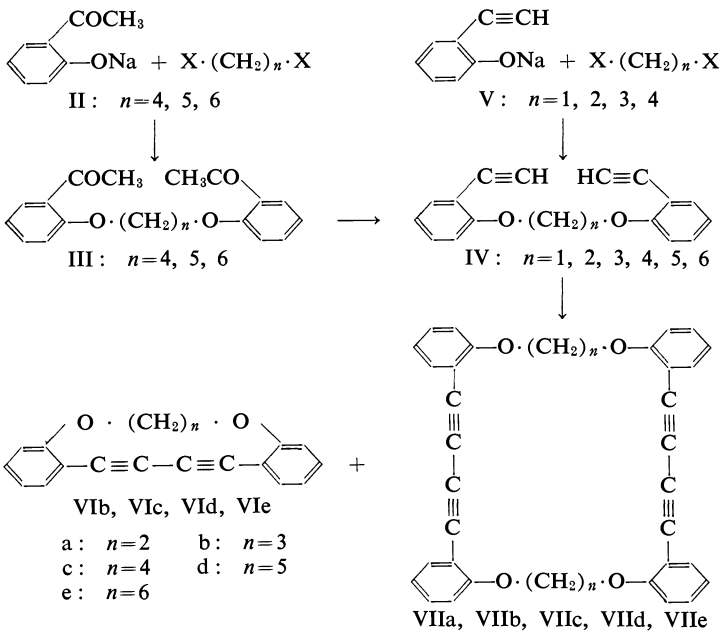


I

cleft when the number of methylene groups is 2 or 3 yielding 2,2'-dibenzofuranyl and other related compound, and the cleavage of the ester linkage was attributed to the large ring strain involved in I. The present paper deals with the syntheses of a series of analogous cyclic diacetylenes in which the ester linkage is replaced by the ether linkage to avoid the cleavage reaction in the course of the ring closure. The synthesis was carried out according to the following series of reactions.

The diketone III which was obtained by the reaction of polymethylene dihalide ($n=4$, 5 and 6) with sodium salt of *o*-hydroxyacetophenone (II) was treated with phosphorus pentachloride to yield the chloro-derivative. The chloro-derivative was dehydrochlorinated with sodamide in liquid ammonia to yield the terminal diacetylene IV, ($n=4$, 5 and 6).

The terminal diacetylene IV, ($n=1$, 2, 3 and 4) was also prepared by the reaction of sodium *o*-ethynylphenoxide (V) with polymethylene dihalide ($n=1$, 2, 3 and 4). The terminal diacetylene IV thus obtained was submitted to the oxidative coupling reaction according to Eglinton's procedure[2]. The yields of the cyclic diacetylenes $VI_b$, $VI_c$, $VI_d$ and $VI_e$ formed by the intramolecular oxidative coupling were found to be 3, 40, 40 and 40%, respectively. In the case of $n=2$, the cyclic diacetylene could not be isolated from the reaction mixture. This is probably attributable to the high strain which may arise from the ring formation. The cyclic tetraacetylenes $VII_a$, $VII_b$, $VII_c$ and $VII_e$ which are the products of the bimolecular




1) F. Toda and M. Nakagawa, This Bulletin, 33, 223 (1960).

2) G. Eglinton and A. R. Galbraith, *Chem. & Ind.*, 1956, 737; *J. Chem. Soc.*, 1959, 889.

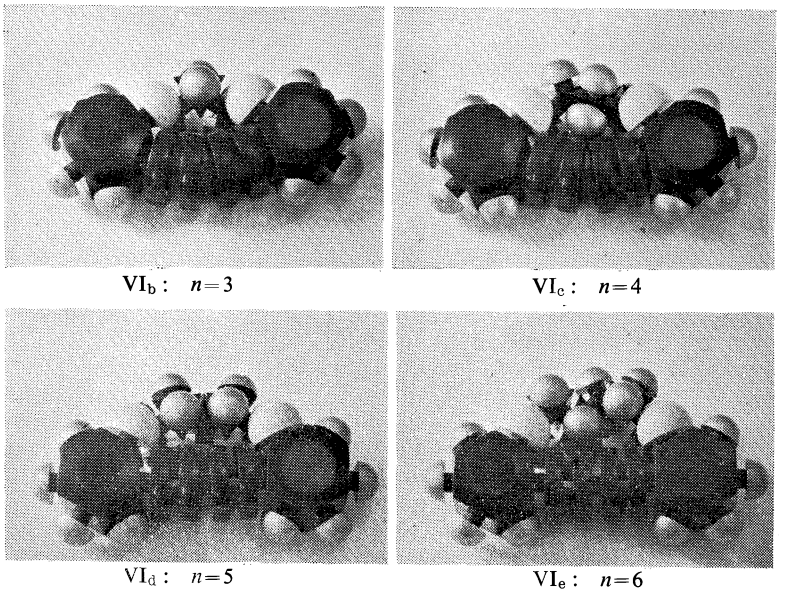



Fig. 1. The molecular models of VI (Courtauld model).

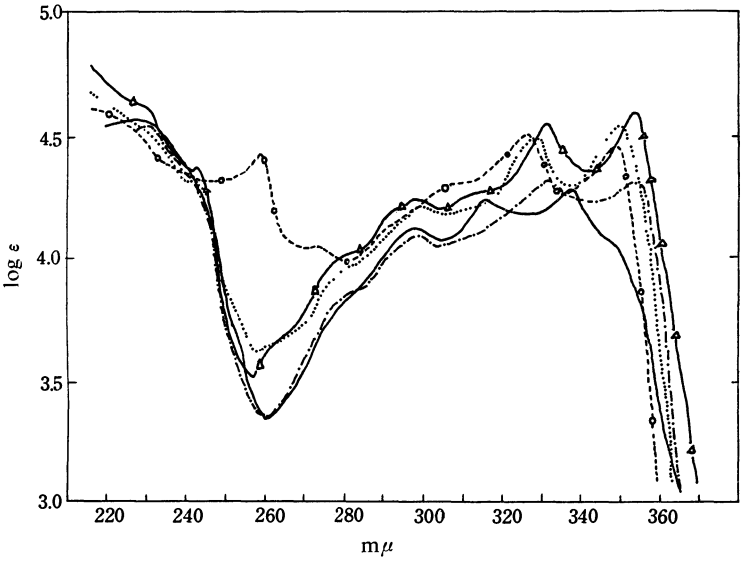



Fig. 2. The ultraviolet spectra of the cyclic diacetylenes (VI) and $VIII_a$.
———: $VI_b$ in 99.5% ethanol
—·—·: $VI_c$ in 95% ethanol
—△—△: $VI_d$ in 95% ethanol
·····: $VI_e$ in 95% ethanol
--○--○: $VIII_a$ in 95% ethanol

coupling reaction were isolated from the reaction mixture in the yield of 2.5, 1, 2, trace and 10%, respectively. The formation of a cyclic dimer is an interesting contrast to the fact that the oxidative coupling of di-*o*-ethynylphenyl polymethylene dioate gave only the monomeric cycle I and the formation of the dimeric tetraacetylene was not observed[1].

The structures of VI and VII were determined by the analytical data, molecular weight determination and ultraviolet and infrared spectroscopic evidences. VI is a fairly stable compound, except in the case of $VI_b$ which is found to be unstable to heat. The molecular weight of $VI_b$ could not be determined by the Rast method due to its thermal instability; therefore the molecular weight was estimated by the X-ray method*.

* The determination of molecular weight by the X-ray method was kindly performed by Dr. Y. Tomiie of the Laboratory of Physical Chemistry of this Department to whom the authors express their sincere gratitude.

TABLE I

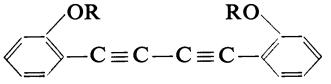
| Compound | Solvent | Absorption | | | | | |
|---|---|---|---|---|---|---|---|
| $VI_b$ | E | 231 (300) | 298 (111) | 316 (144) | 337 (159) | | |
| $VI_c$ | E* | 230 (345) | 299 (122) | 331 (201) | 353 (199) | | |
| $VI_d$ | E* | 243 (218) | 299 (161) | 331 (317) | 353 (365) | | |
| $VI_e$ | E* | 242 (203) | 299 (158) | 328.5 (297) | 349 (336) | | |
| $VII_a$ | D | 260 (285) | **272** (112) | 310 (186) | 324 (240) | | 344 (174) |
| $VII_b$ | D | 259.5 (100) | **276** (76) | 310 (135) | 324 (232) | | 351 (216) |
| $VII_c$ | D | 261 (350) | **275** (105) | 310 (185) | 321 (196) | | 349 (115) |
| $VII_d$ | D | 260 (148) | 276 (97) | 313 (197) | 331 (324) | | 353 (331) |
| $VII_e$ | D | 261 (269) | 274 (100) | 313 (188) | 329 (257) | | 351.5 (212) |
| $VIII_a$ | E* | 259.5 (265) | 274.5 (111) | **309** (203) | 326 (321) | | 349 (286) |
| $VIII_a$ | E | 259 (260) | 273 (107) | **310** (199) | 326 (327) | | 348 (293) |
| $VIII_b$ | E | 259.5 (282) | 274 (108) | **310** (194) | 326 (297) | | 349 (253) |
| $IX_a$ | D | | **280** (91) | 299 (199) | 320 (333) | | 343 (390) |
| $IX_a$ | E | **230** (377) | **280** (98) | 298 (205) | 319 (338) | | 341 (392) |
| $IX_b$ | E | **230** (395) | **280** (100) | 298 (182) | 322.5 (241) | | 341 (248) |
| XII | E | **230** (399) | **280** (93) | 298 (172) | 319 (226) | | 341 (247) |
| XIII | D | 261 (222) | **275** (104) | 309 (184) | 328 (251) | | 350 (202) |
| XV | D | 261 (287) | **275** (130) | 310 (212) | 328 (323) | | 351 (285) |
| XV | E | 260 (289) | 273 (110) | 310 (215) | 326 (346) | | 348 (300) |
| XVII | E | 232 (288) | **278** (75) | 296 (168) | 317 (269) | | 338.5 (291) |
| XVIII | E | 258 (204) | 273 (76) | 307 (168) | 323.5 (278) | | 346 (239) |
| XIX | E* | 260 (213) | 275 (85) | 305 (168) | 323 (270) | | 345 (236) |
| DDD | E | 258 (262) | 273 (100) | 291 (127) | 326 (300) | | 348.5 (277) |
| DDD | NaOH aq. | 218 (616) | **261** (228) | 278 (97) | 296 (99) | 317 (110) | 359 (226) |

The figures indicate the $\lambda_{max}$ in m$\mu$.
The figures in parentheses are $\varepsilon_{max} \times 10^{-2}$.
The bold figures indicate shoulders.
E, E* and D denote 99.5% ethanol, 95% ethanol and dioxane, respectively.
DDD means *o*, *o'*-dihydroxydiphenyldiacetylene.

It is to be noted that $VI_c$ and $VII_e$ exist in dimorphic forms and the melting points of the former substance were found to be 96 and 112°C, and those of the latter were 184~185°C (stable form) and 207~208°C. The analytical data and the measurement of solvent of crystallization revealed that $VII_b$ contains 2 mol. of benzene.

An examination of the scale model of VI reveals that the polymethylene bridge in $VI_d$ is slightly short and that of $VI_e$ is slightly long to hold the molecule in a uniplanar, strain free conformation, but the ring strain involved in $VI_d$ and $VI_e$ seems to be very small and these molecules may have an almost planar and rigid structure. On the other hand, the diacetylenic linkage in $VI_c$ is forced to bend owing to the length of its bridging chain, the

degree of bending of the diacetylenic bond being much larger in $VI_b$ in accordance with the shorter methylene bridge as illustrated in Fig. 1. *o*, *o'*-Dimethoxydiphenyldiacetylene ($VIII_a$) and *o*, *o'*-diethoxydiphenyldiacetylene ($VIII_b$) were prepared and the ultraviolet spectra of these open chain analogues were compared with those of VI. As indicated in Fig. 2 and Table I, the location of the absorption maxima in the spectra of $VI_d$ and $VI_e$ at the long wavelength region were found to be almost identical with those of the open chain models $VIII_a$ and $VIII_b$. But the absorption intensities ($\varepsilon_{max}$) of $VI_d$ and $VI_e$ are found to be larger than those of $VIII_a$ and $VIII_b$ indicating the rigid and planar structure of these cyclic diacetylenes. The sequence of



VIIIa: R=$CH_3$ VIIIb: R=$C_2H_5$

decrease of the $\varepsilon_{max}$-values are found to be $VI_e > VI_d > VI_c > VI_b$. This sequence of the $\varepsilon_{max}$ indicates that the planarity of the molecule increases the transition probability and the increase in the bending of diacetylenic linkage causes the decrease of the probability. It is remarkable that the $\lambda_{max}$ of $VI_b$ shifted about 12 m$\mu$ to shorter wavelength as compared with $VI_d$, $VI_e$ and the open chain models. It has been already known in numerous examples, especially in substituted biphenyls[4] or substituted acetophenones[5], that relatively weak steric hindrance in the excited state of these molecules diminishes the transition probability resulting in the decrease of absorption intensity, and the presence of a strong steric hindrance in the excited state causes a hypsochromic shift of the absorption maxima as the result of the increased transition energy. As the two phenyl groups in the molecule of $VI_b$ are held in a coplanar position owing to the short methylene bridge, the hypsochromic shift and the hyperchromic effect observed in $VI_b$ may be attributed to the bending of the diacetylenic linkage. This may be the first example in which the bending of acetylenic linkage results in a hypsochromic shift of the characteristic K-band. The methylene chain in VI is held closely parallel with the diacetylenic unit and the ultraviolet spectra of these cycles show a sharp and intense $\lambda_{min}$ at ca. 260 m$\mu$ making a sharp contrast with those of VIII and VII in which a $\lambda_{max}$ exists at the same wavelength. This absorption minimum was also observed in the spectra of I ($n=3$ and 4). As pointed out in the previous paper[1], the disappearance of $\lambda_{max}$ at this position may be ascribed to the presence of a proximity effect of the methylene group to the acetylenic linkage (Figs. 3 and 4, Table I). Also the appearance of a new $\lambda_{max}$ in the spectra of VI near 230~240 m$\mu$ is the same trend as observed in I. These results are also confirmed with $X_a$, $X_b$, XIII and XV, which will be discussed in the following section.

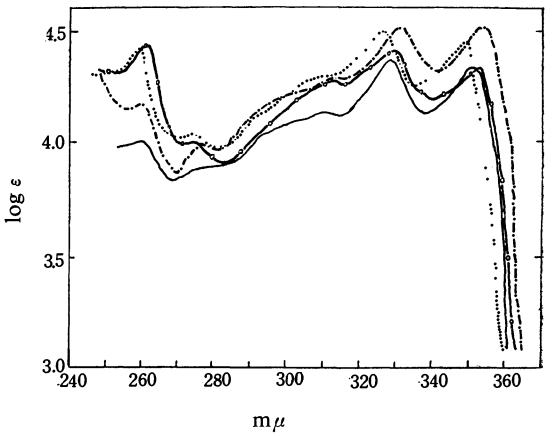



Fig. 3. The ultraviolet spectra of the cyclic dimers (VII) and $VIII_a$.
———: $VII_b$ in dioxane
·-·-·-: $VII_d$ in dioxane
—o—o: $VII_e$ in dioxane
·····: $VIII_a$ in 95% ethanol
The curve of VII was drawn using the reduced ε values corresponding to a diyne-unit.

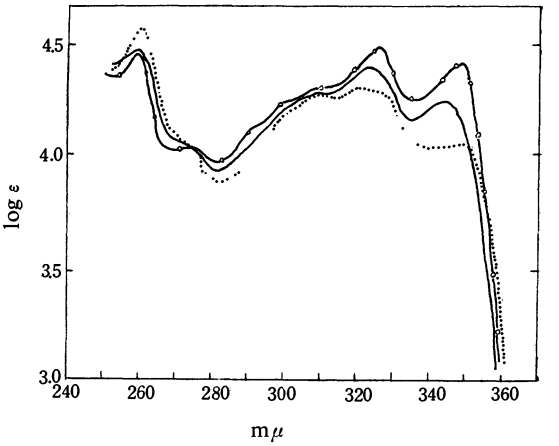
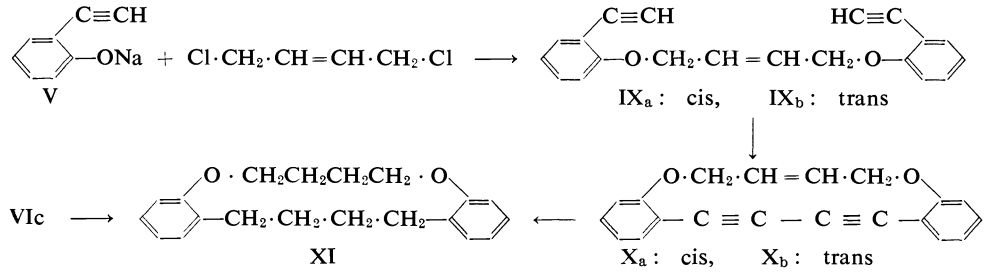


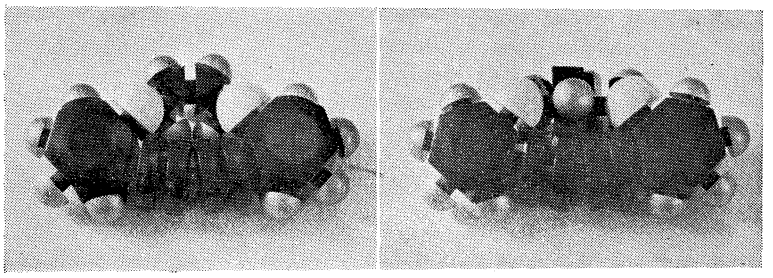

Fig. 4. The ultraviolet spectra of the cyclic dimers (VII) and $VIII_b$.
·····: $VII_c$ in dioxane
———: $VII_a$ in dioxane
—o—o: $VIII_b$ in 99.5% ethanol
The curve of VII was drawn using the reduced ε values corresponding to a diyne-unit.

4) E. A. Braude and E. A. Evans, *J. Chem. Soc.*, **1954**, 607; M. T. O. Shaughnessy and W. H. Rodebush, *J. Am. Chem. Soc.*, **62**, 2906 (1940).
5) E. A. Braude, F. Sondheimer and W. F. Forbes, *Nature*, **173**, 117 (1954).

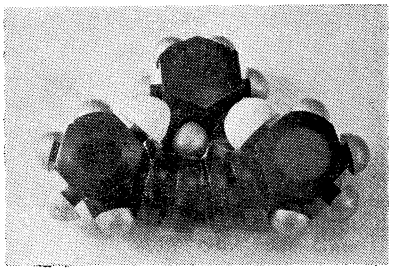
The ultraviolet spectra of $VII_b$, $VII_d$ and $VII_e$ do not depart from those of the open chain analogues as illustrated in Fig. 3 (cf. Table I). On the other hand, abnormal absorption spectra were observed in the case of $VII_a$ and $VII_c$ (Fig. 4 and Table I). An examination of the scale models of these cyclic dimers reveals that the molecule bearing a short methylene bridge of an even number of carbon atoms can not take uniplanar structure, and the abovementioned anomalous ultraviolet spectra of $VII_a$ and $VII_c$ may be attributed to the non-planar geometry of these molecules.

The reaction of sodium *o*-ethynylphenoxide (V) with *cis*- or *trans*-1,4-dichloro-2-butene yielded the terminal diacetylene, $IX_a$ and $IX_b$, respectively. The oxidative coupling of IX by means of cupric acetate in pyridine[2] resulted in the cyclic diacetylenes, $X_a$ and $X_b$ in a 33 and 30% yield, respectively. These diacetylenic cycles were found to be unstable to heat. It was observed that $X_a$ (m. p. 154°C (decomp.)) is completely decomposed when heated to a temperature of 145°C for 30 min. The structure of $X_a$ and $X_b$ were inferred from its analytical data and its ultraviolet and infrared spectroscopic evidences. The molecular weight of $X_a$ and $X_b$ could not be determined by Rast's method on account of its thermal instability, therefore the molecular weight of the decahydroderivatives XI were determined by Rast's method in camphor. Also the structure of XI was confirmed by the identity with the reduction product of $VI_c$. Inspection of the scale models of $X_a$ and $X_b$ indicates that the molecules involve large ring strain due to the bending of the diacetylenic linkage as shown in Fig. 5. The ultraviolet spectra of $X_a$ and $X_b$ showed a shift to shorter wavelength about 8 m$\mu$ as illustrated in Fig. 6 (Table I). This fact may be ascribed to the increase of the transition energy on account of the strong ring strain. Interestingly, enough, the ultraviolet spectrum of $X_b$ has broad absorption peaks as compared with those of $X_a$ (Fig. 6). The scale models of $X_a$ and $X_b$ indicate that the ethylenic bond in the former is held apart from the diacetylenic unit in the cycle; on the other hand, the double bond in the bridging chain in the latter molecule is held closely to



$X_a$ $X_b$



XII

Fig. 5. The molecular models of X and XII (Courtauld).

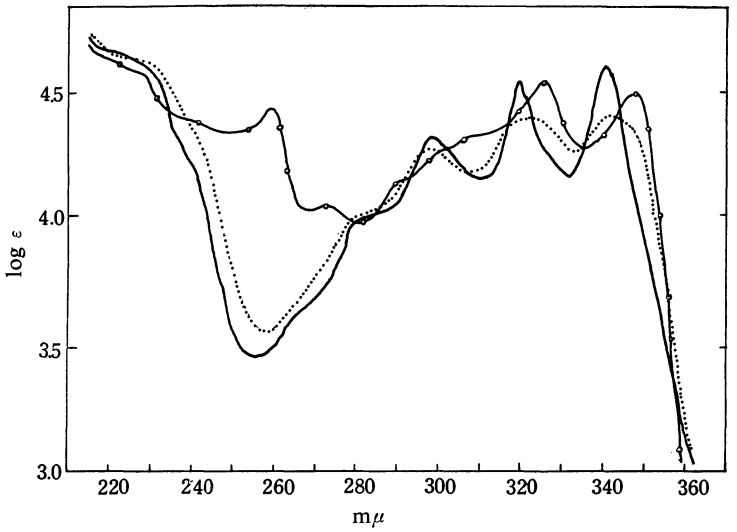



Fig. 6. The ultraviolet spectra of X and $VIII_a$ (in 99.5% ethanol).
———: $X_a$ ·····: $X_b$ —○—○: $VIII_a$

the diacetylenic linkage (Fig. 5). Therefore the above-mentioned anomalousness of the absorption peaks of $X_b$ seem to be associated with a transannular interaction between the $\pi$-electrons of the double bond in the bridging chain and those of the diacetylenic unit. Another example of the same type of transannular phenomenon will be discussed in the following paper[6].

The oxidative coupling of the terminal diacetylene obtained by the reaction of *o*-xylylene dibromide with V afforded the cyclic diacetylene XII and the cyclic dimer XIII in a yield of 8 and 3%, respectively. XII was found to be a heat sensitive substance, and the molecular weight was determined with the reduction product, XIV. The ultraviolet spectrum of XII does not depart from that of $X_a$ indicating that the ring strain in XII is almost equal to that of $X_a$. Also the similarity of the ultraviolet spectra of XII and $X_a$ exclude the possibility of the presence of a transannular interaction between the phenylene group in the bridging chain and the diyne unit. In the most probable geometry of the molecule of XII which was inferred from the inspection of the scale model; the *o*-phenylene group seems to hold too far apart from the diacetylenic linkage for interstitial effects to operate (Figs. 5 and 7). The fact that the cyclic dimer XIII crystallized with two moles of benzene is the same as in the case of $VII_b$. The configuration of XIII seem to be almost strain free, since the ultraviolet absorption spectrum of XIII is similar to those of VIII and XV as recorded in Fig. 8 and Table I.

6) F. Toda and M. Nakagawa, This Bulletin, 32, 514 (1959).

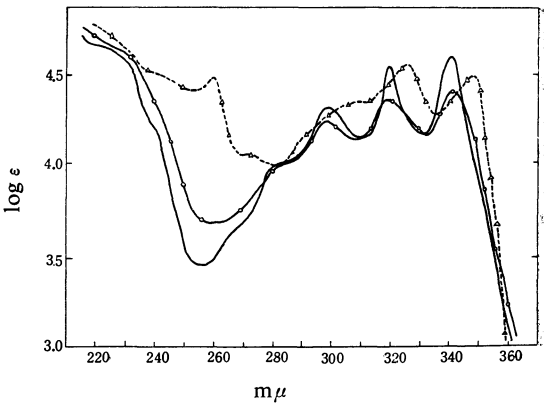
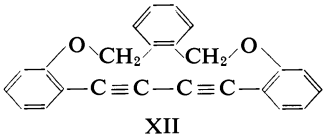
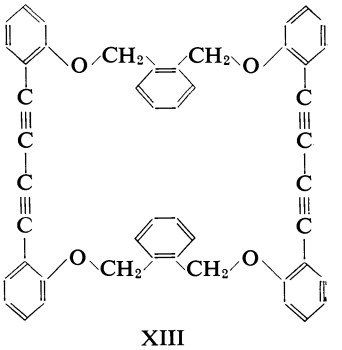


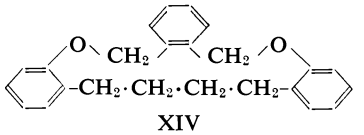

Fig. 7. The ultraviolet spectra of $X_a$, XII and XV (in 99.5% ethanol).
———: $X_a$ —○—○: XII ···△···△: XV



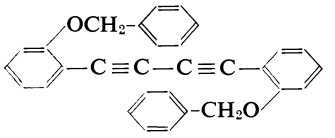

XII




XIII



XIV



XV

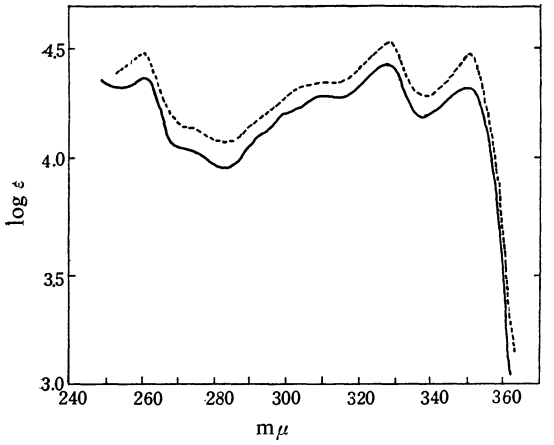



Fig. 8. The ultraviolet spectra of the cyclic tetraacetylene (XIII) and the open chain analogue (XV) (in dioxane).
——: XIII ·····: XV
The curve of XIII was drawn using the reduced ε values corresponding to a diyne-unit.

The diethynyl compound XVI which was prepared by the reaction of 1,4-dichloro-2-butyne and V was oxidized according to the procedure of Eglinton. The cyclic triacetylene XVII was obtained in a yield of 3.5% as heat sensitive crystals together with a large amount of sparingly soluble amorphous solid with high melting point. The monomeric structure of XVII was inferred from the ultraviolet and infrared spectroscopic evidences. It was observed that the ultraviolet absorption maxima in the spectrum of XVII shifts to shorter wavelength (ca. 8 mμ) as compared with those of the open chain analogue (XVIII). (Fig. 9 and Table I). Substitution of a hydrogen atom in the methyl group of

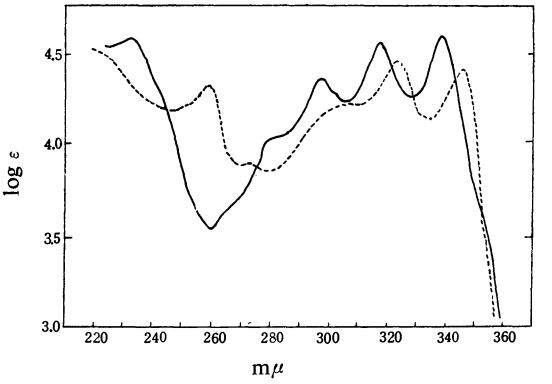
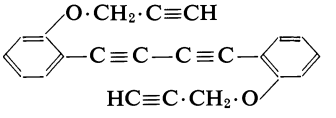
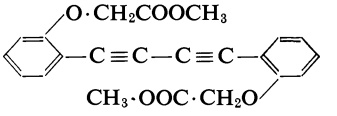



Fig. 9. The ultraviolet spectra of the cyclic triacetylene (XVII) and the open chain analogue (XVIII) (in 99.5% ethanol).
——: XVII ------: XVIII

the phenoxy ether by an electron attracting group such as ethynyl or carboxymethyl group result in a slight hypsochromic shift of the ultraviolet spectra as illustrated in Fig. 10, therefore XVIII was chosen as a linear model of XVII. Conversly the ultraviolet spectrum of *o*, *o'*-dihydroxydiphenyldiacetylene in an

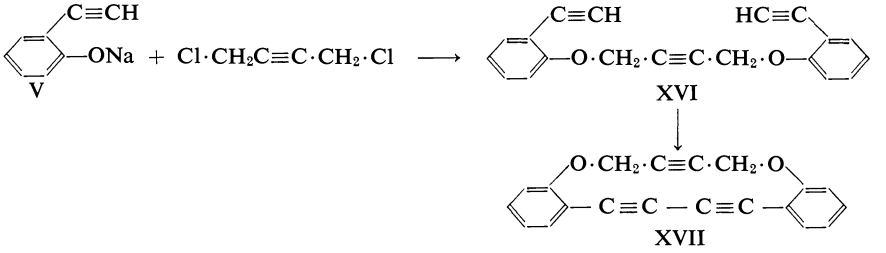


XVIII



XIX

aqueous alkali showed a red-shift with a change in the absorption curve as compared with that of in a neutral solution (Fig. 11). The ultraviolet spectroscopic behavior of the derivatives of *o*, *o'*-dihydroxydiphenyldiacetylene indicates that the availability of electrons on the oxygen atoms in the conjugated position to the chromophor system of *o*, *o'*-dihydroxydiphenyldiacetylene is responsible for the abovementioned blue- or red-shift of the spectrum. The heat sensitivity and the hypsochromic shift of the spectrum of XVII may be associated with the deformation of diacetylenic linkage due to the large ring strain.



V XVI XVII

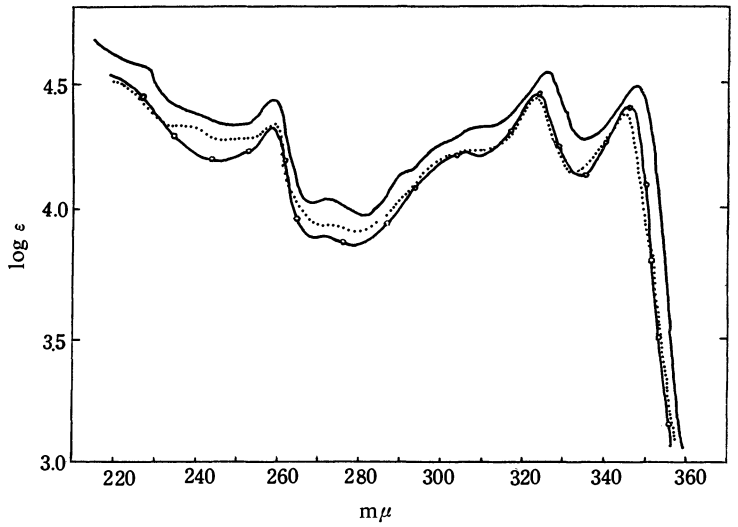



Fig. 10. The ultraviolet spectra of XVIII, XIX and $VIII_a$.
———: $VIII_a$ in 99.5% ethanol —○—○: XVIII in 99.5% ethanol
·····: XIX in 95% ethanol

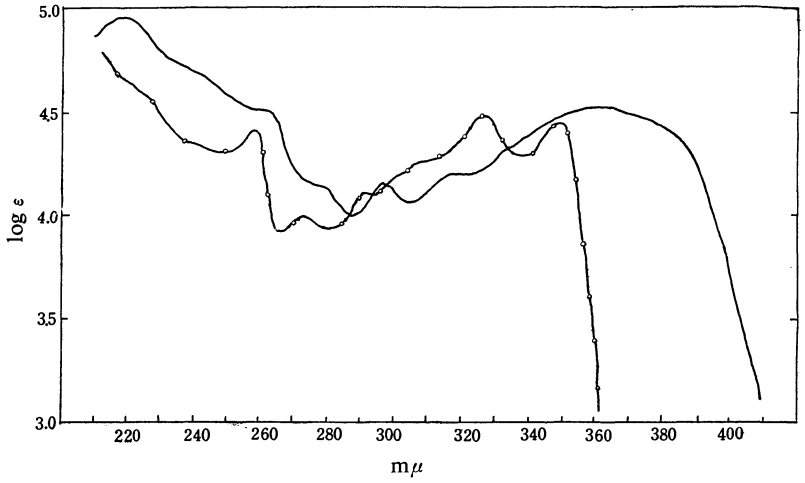



Fig. 11. The ultraviolet spectra of *o,o'*-dihydroxydiphenyldiacetylene in a neutral and an alkaline solution.
—○—○: in 99.5% ethanol ———: in an aqueous sodium hydroxide

It was revealed from the above-mentioned observations that the bending of the diyne in the diphenyldiacetylene system in which the two phenyl groups are held in a uniplanar or in a near uniplanar position exerts a minor effect on the ultraviolet spectrum. It was well-known that the twist of single bond in a conjugate system such as *o,o'*-disubstituted acetophenones[4] or 2,2'-disubstituted biphenyls[5] results in a remarkable change in their ultraviolet spectra. An insulation of conjugation at the position of the twisted single bond was assumed from the change of the ultraviolet spectra of *o,o'*-disubstituted acetophenones and 2,2'-disubstituted biphenyls bearing substituents with large steric requirement. The maximal shift among the abovementioned strained cyclic diacetylenes was found to be 12 mμ. The

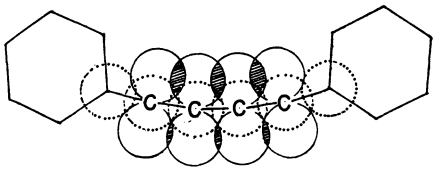



Fig. 12. A schematic illustration of p-orbital overlapping in a bent diphenyldiacetylene system.

minor effect on the bending of the diyne unit on the spectrum is quite understandable if we consider the shape of p-orbitals of conjugated acetylenic linkage. As schematically illustrated in Fig. 12, the bending of the diacetylenic linkage causes only a minor change in the overlapping of its p-orbitals. This may be the cause of the slight hypsochromic shift of the strained diacetylenic cycles.

As reported in the previous paper[1], the smallest macrolide I, ($n=3$) was a very photosensitive substance, and the sensitivity was attributed to the bending of the diacetylenic linkage. But the highly strained ether analogues such as $VI_b$, $X_a$, $X_b$, XII and XVII were found to be fairly stable to light, but sensitive to heat. These findings indicate that the photosensitivity of I ($n=3$) may possibly be attributable to a photochemical reaction of the carbonyl function with the acetylenic bond which is held in the proximity of the ester linkage or the creavage of the strained ester linkage by the photoexcitation on the molecule. To confirm this point, it appeared desirable to examine the photosensitivity of another cyclic diacetylene containing carbonyl function in the bridging chain. The present authors have attempted the synthesis of a keto-ether derivative of *o*, *o'*-dihydroxydiphenyldiacetylene. The high dilution Dieckmann condensation of carbomethoxymethyl ether of *o*,*o'*-dihydroxydiphenyldiacetylene (XIX)[1] to yield a cyclic ketocarboxylate resulted in the formation of a brown red resinous material, and the expected ketoester could not be isolated.

## Experimental**

**1, 5-Bis-(*o*-acetylphenoxy)-pentane (III, $n=5$).**—*o*-Hydroxyacetophenone (10.9 g., 0.08 mol.) was added to an ethanolic solution of sodium ethoxide (sodium, 2.0 g. and absolute ethanol, 25 ml.), and the solvent was removed under reduced pressure. The sodium phenoxide thus obtained II was mixed with 1,5-diiodopentane (13.6 g., 0.042 mol.) and the mixture was heated to 160~170°C for 4 hr. The cooled reaction mixture was filtered and the solid was washed with ethanol, hot water and ethanol, successively. The dried material was recrystallized from benzene or ethanol yielding III ($n=5$), colorless needles, m. p. 104~105°C. 5.5 g. (40%).

Found: C, 74.14; H, 7.16. Calcd. for $C_{21}H_{24}O_4$: C, 74.09; H, 7.11%.

IR max., 1665 (C=O), 1245 (=C-O-) $cm^{-1}$.

**1, 6-Bis-(*o*-acetylphenoxy)-hexane (III, $n=6$).**—The reaction of 1,6-diiodohexane and II according to the method similar to that described above resulted in III ($n=6$), colorless plates or needles, m. p. 121°C in a yield of 42%.

Found: C, 74.80; H, 7.47. Calcd. for $C_{22}H_{26}O_4$: C, 74.55; H, 7.39%.

IR max., 1667 (C=O), 1250 (=C-O-) $cm^{-1}$.

**1, 4-Bis-(*o*-acetylphenoxy)-butane (III, $n=4$).**—The reaction of II with 1,4-diiodobutane was carried out according to the above-mentioned procedure yielding III ($n=4$), colorless needles, m. p. 147°C in a yield of 34%.

Found: C, 73.18; H, 6.88. Calcd. for $C_{20}H_{22}O_4$: C, 73.60; H, 6.79%.

IR max., 1665 (C=O), 1242, 1231 (=C-O-) $cm^{-1}$.

**Syntheses of IV ($n=4$, 5 and 6) from III.**—The mixture of phosphorus pentachloride (12.0 g., 0.058 mol.), $III_{n=6}$ (9.0 g., 0.025 mol.) and phosphorus oxychloride (15 ml.) was heated to 80~85°C for 45 min. The phosphorus oxychloride was removed under reduced pressure. The crude chloride thus obtained was dissolved in anhydrous ether (50 ml.). The ethereal solution was added into the solution of sodamide in liquid ammonia (prepared from sodium, 5 g., 0.23 mol. and ammonia, 200 ml.) during a period of 20 min. under mechanical stirring. Stirring was continued for a further 1.5 hr., and the ammonia was allowed to evaporate. The residual solid was mixed with water (200 ml.) and extracted with ether (350 ml.). The extract was washed with water and dried over magnesium sulfate. The solvent was distilled, resulting in a crystalline solid. The solid was recrystallized repeatedly from ethanol using active charcoal to yield $IV_{n=6}$, colorless needles, m. p. 89~90°C, 3.8 g. (47%).

Found: C, 82.49; H, 7.22. Calcd. for $C_{22}H_{22}O_2$: C, 82.98; H, 6.96%.

IR max., 3270 (-C≡CH), 1245 (=C-O-) $cm^{-1}$.

The reaction of $III_{n=5}$ with phosphorus pentachloride followed by dehydrochlorination yielded $IV_{n=5}$, colorless needles, m. p. 91.5~92°C, (38%).

Found: C, 82.65; H, 6.85. Calcd. for $C_{21}H_{20}O_2$: C, 82.86; H, 6.62%.

IR max., 3280 (-C≡CH), 2110 (-C≡C-), 1252 (=C-O-) $cm^{-1}$.

Similar treatment of $III_{n=4}$ afforded $IV_{n=4}$, colorless prisms, m. p. 82°C, (40%).

Found: C, 82.43; H, 6.24. Calcd. for $C_{20}H_{18}O_2$: C, 82.73; H, 6.25%.

IR max., 3250 (-C≡C-), 1250 (=C-O-) $cm^{-1}$.

**Syntheses of IV ($n=1$, 2, 3 and 4) from V.**—*o*-Hydroxyphenylacetylene (2.3 g., 0.02 mol.) was added to a solution of sodium ethoxide in ethanol (sodium, 0.5 g. and absolute ethanol, 5 ml.). The solvent was removed under reduced pressure at room temperature to yield V. A solution of 1,4-diiodobutane (3.1 g., 0.01 mol.) in dimethylformamide (20 ml.) was added to V, and the mixture was refluxed for 2.5 hr. The cooled reaction mixture was poured into ice-water (200 ml.). The crude crystals deposited were filtered, then washed with water and ethanol, successively. The crude $IV_{n=4}$ thus obtained was recrystallized from ethanol using active charcoal to give pure $IV_{n=4}$, colorless prisms, m. p. 82°C, 1.7 g. (59%), undepressed on admixture with $IV_{n=4}$ which was derived from $III_{n=4}$.

The reaction of *o*-hydroxyphenylacetylene (1.5 g.)

** No melting points were corrected. Infrared spectra were measured by the Nujol mull method and molecular weights were obtained by the Rast method (in camphor). Otherwise some special indication was given.

with 1,3-dibromopropane according to the above-mentioned procedure yielded crude $IV_{n=3}$ as a viscous oil, (1.7 g.), IR max., 3400 (-C≡CH), 2160 (-C≡C-), 1260 (=C-O-) $cm^{-1}$. The crude oil was used without further purification for the oxidative coupling.

A similar reaction of *o*-hydroxyphenylacetylene (1.5 g.) with ethylene dibromide gave $IV_{n=2}$, colorless prisms, m. p. 150°C, 250 mg., (15%).

Found: C, 82.27; H, 5.29. Calcd. for $C_{18}H_{14}O_2$: C, 82.42; H, 5.38%.

IR max., 3280 (-C≡CH), 2130 (-C≡C-), 1252 (=C-O-) $cm^{-1}$.

Similarily the reaction of *o*-hydroxyphenylacetylene (1.5 g.) with dibromomethane yielded $IV_{n=1}$, viscous oil, (1.9 g.), IR max., 3370 (-C≡CH), 2160 (-C≡C-) and 1230 (=C-O-) $cm^{-1}$.

**Oxidative Coupling of $IV_{n=6}$.** — The mixture of cupric acetate monohydrate (15 g.), pyridine (150 g.) and $IV_{n=6}$ (1.5 g.) was stirred for 4 hr. at 55~60°C. The solvent was distilled under reduced pressure at a temperature below 40°C. Water was added to the residue, and extracted with ether (300 ml.). The extract was washed with an aqueous solution of cupric acetate and water, successively. The ether solution was dried over anhydrous magnesium sulfate. The residue obtained by evaporating the solvent was dissolved in benzene (20 ml.) and treated with active charcoal. The crude crystals obtained by concentrating benzene were fractionally recrystallized from ethyl acetate. The crystals from the more soluble portions were recrystallized from aqueous acetic acid to yield pure $VI_e$, colorless needles, m. p. 130°C, 0.6 g. (40%).

Found: C, 83.43; H, 6.59. Mol. wt., 322. Calcd. for $C_{22}H_{20}O_2$: C, 83.51; H, 6.37%. Mol. wt., 316.

IR max., 2150 (-C≡C-), 1272, 1243 (=C-O-) $cm^{-1}$.

The crystals obtained from the less soluble portions were recrystallized from ethyl acetate yielding $VII_e$, colorless needles, m. p. 207~208°C, 0.15 g. (10%). The melting point of this substance changed to 184~185°C on standing at room temperature for several days.

Found: C, 83.13; H, 6.49. Mol. wt., 630. Calcd. for $C_{44}H_{40}O_4$: C, 83.51; H, 6.37%. Mol. wt., 632.

IR max., 2137 (-C≡C-), 1250 (=C-O-) $cm^{-1}$.

**Oxidative Coupling of $IV_{n=5}$.**—$IV_{n=5}$ (1.0 g.) was added to the mixture of pyridine (150 g.) and cupric acetate monohydrate (10 g.), and the mixture was stirred for 3 hr. at 55°C. The crude crystals obtained by the treatment of the reaction mixture were recrystallized repeatedly from aqueous acetone yielding needles mixed with a small amount of crystalline grains. The crystalline mixture was digested with ethyl acetate to dissolve the needles. The insoluble crystalline grains were filtered and the filtrate was concentrated to dryness. Repeated recrystallization of the residual solid from aqueous acetone yielded pure $VI_d$, colorless needles, m. p. 132~132.5°C, 0.4 g. (40%).

Found: C, 83.27; H, 5.93. Mol. wt., 312. Calcd. for $C_{21}H_{18}O_2$: C, 83.42; H, 6.00%. Mol. wt., 302.

IR max., 2200 (-C≡C-), 1250 (=C-O-) $cm^{-1}$.

The elementary analysis of the crystalline grains (m. p. 180~181°C) could not be performed owing to its small amount, but the molecular weight determination (Found: 514) indicates that the grains should be the cyclic dimer ($VII_d$, $C_{42}H_{36}O_4$: Mol. wt., 604) of $IV_{n=5}$. IR max., 2200, 2137 (-C≡C-), 1250 (=C-O-) $cm^{-1}$.

**Oxidative Coupling of $IV_{n=4}$.** — A solution of $IV_{n=4}$ (1.0 g.) and cupric acetate monohydrate (10.0 g.) in pyridine (100 g.) was stirred for 4 hr. at 50°C. The crude crystals isolated from the reaction mixture were digested with hot ethanol. The insoluble material was filtered, and the filtrate was cooled to deposite crystals. The crystals, on recrystallization from ethanol, gave pure $VI_c$, colorless needles or plates, m. p. 96 or 112°C, 0.4 g. (40%). It was observed that $VI_c$ melts at 112°C when the temperature of a heating bath is gradually raised from room temperature. But $VI_c$ melts at 96°C when the bath was heated previously to 80°C. The solid obtained by cooling the molten crystals melts at 112°C by the ordinary method of measurement, but it melts also at 96°C in a preheated bath.

Found: C, 83.01; H, 5.42. Mol. wt., 271. Calcd. for $C_{20}H_{16}O_2$: C, 83.31; H, 5.59%. Mol. wt., 288.

IR max., 2210 (-C≡C-), 1240 (=C-O-) $cm^{-1}$.

The above-mentioned insoluble solid was recrystallized from ethyl acetate yielding $VII_c$, colorless needles, m. p. 237~238°C, 20 mg. (2%).

Found: C, 82.52; H, 5.45. Mol. wt., 533. Calcd. for $C_{40}H_{32}O_4$: C, 83.31; H, 5.59%. Mol. wt., 576.

IR max., 2210, 2150 (-C≡C-), 1240 (=C-O-) $cm^{-1}$.

**Hydrogenation of $VI_c$.**—$VI_c$ (100 mg.) in benzene (15 ml.) was reduced over 5% palladium-on-charcoal (20 mg.). After removal of the solvent in a vacuum, the residue was recrystallized from aqueous ethanol yielding XI, colorless plates, m. p. 63.5°C, 100 mg.

Found: C, 80.48; H, 8.09. Mol. wt., 303. Calcd. for $C_{20}H_{24}O_2$: C, 81.04; H, 8.16%. Mol. wt., 296.

XI showed no depression of the mixed melting point on admixture with the hydrogenation products of $X_a$ and $X_b$. Also the infrared spectra of these saturated macrocycles are found to be identical over the entire region of wavelength.

**Oxidative Coupling of $IV_{n=3}$.** — Treatment of $IV_{n=3}$ (1.7 g.) with Eglinton's reagent (cupric acetate monohydrate, 10 g. and pyridine, 100 g.) at 47°C for 4 hr. gave crude crystals. The crude material was digested with hot ethanol (30 ml.) to remove the insoluble material. The crystals obtained by diluting the ethanolic solution with water was recrystallized repeatedly from aqueous ethanol to give pure $VI_b$, colorless needles, m. p. 115°C, (decomp.), 50 mg. (3%).

Found: C, 83.31; H, 5.34. Calcd. for $C_{19}H_{14}O_2$: C, 83.20; H, 5.15%.

IR max., 2210 (-C≡C-), 1227 (=C-O-) $cm^{-1}$.

The monomeric nature of $VI_b$ was deduced from the X-ray crystallographic data (space group, $C_{2h}^6$–$C^2/c$, dimension of unit cell, a=22.22 Å, b=13.04 Å, c=11.20 Å, Z=8).

The abovementioned ethanol insoluble material was dissolved in benzene and treated with active charcoal. The crystals deposited from the benzene solution were recrystallized from benzene resulting in $VII_b$, colorless needles, m. p. 228~229°C (decomp.), 20 mg. (1%). It was observed that the transparent crystals on the hot stage of a Kofler

block became turbid at about 100°C. This phenomenon could be ascribed to the loss of the solvent of crystallization (benzene).

Found: C, 85.13; H, 5.76, benzene of crystallization, 22.47%. Calcd. for $C_{38}H_{28}O_4 \cdot 2C_6H_6$: C, 85.20; H, 5.72, benzene of crystallization, 22.03%.

The analytical data of the solvent-free material was found to be as follows:

Found: C, 83.83; H, 5.11. Mol. wt., 534. Calcd. for $C_{38}H_{28}O_4$: C, 83.20; H, 5.15%. Mol. wt., 548.

IR max., 2160 (-C≡C-), 1250 (=C-O-) $cm^{-1}$.

**Oxidative Coupling of $IV_{n=2}$.** — A mixture of $IV_{n=2}$ (200 mg.), cupric acetate monohydrate (3.0 g.) and pyridine (30 g.) was kept for 4.5 hr. at 40°C under mechanical stirring. The reaction mixture was treated according to the usual manner. The crude crystals thus obtained were recrystallized from ethyl acetate or ethyl acetate-methanol yielding $VII_a$, colorless needles, m. p. 250~252°C (decomp.), 5 mg. (2.5%), Mol. wt., 505. Calcd. for $C_{36}H_{24}O_4$: Mol. wt., 520. IR max., 1245 (=C-O-) $cm^{-1}$.

***o, o'*-Dimethoxydiphenyldiacetylene ($VIII_a$).**—*o, o'*-Dihydroxydiphenyldiacetylene (1.0 g., 0.043 mol.) was dissolved in an ethanolic solution of sodium ethoxide (sodium, 0.23 g. and absolute ethanol, 30 ml.). Methyl iodide (14.2 g., 0.1 mol.) was added to the solution. The mixture changed to neutral after heating at 50~60°C for 0.5 hr. and at 95°C for 1 hr. The crystals obtained by cooling the reaction mixture were filtered, then washed with water and ethanol, successively. The crude material was recrystallized from ethanol giving $VIII_a$, colorless prisms, m. p. 138°C, 1.0 g. (90%).

Found: C, 82.13; H, 5.57. Calcd. for $C_{18}H_{14}O_2$: C, 82.42; H, 5.38%.

IR max., 2146 (-C≡C-), 1246 (=C-O-) $cm^{-1}$. (measured by KBr-disk method).

***o, o'*-Diethoxydiphenyldiacetylene ($VIII_b$).** — A mixture of *o, o'*-dihydroxydiphenyldiacetylene (1.0 g., 0.0043 mol.), sodium ethoxide in ethanol (sodium, 0.46 g. and absolute ethanol, 20 ml.) and ethyl bromide (10 g., 0.1 mol.) was heated to 55~60°C for 30 min. and to 95°C for 2 hr. The neutral reaction mixture was filtered to remove the inorganic salt. Water was added to the filtrate and extracted with ether (50 ml.). The extract was washed with aqueous potassium hydroxide and water, successively, and dried over anhydrous magnesium sulfate. The oily material obtained by evaporating the solvent changed gradually to a crystalline mass. $VIII_a$ was obtained as colorless needles, m. p. 72°C, 1.1 g. (91%) on the recrystallization of the mass from ethanol.

Found: C, 82.59; H, 6.27. Calcd. for $C_{20}H_{18}O_2$: C, 82.73; H, 6.25%.

IR max., 2180 (-C≡C-), 1250 (=C-O-) $cm^{-1}$.

**Synthesis of $IX_b$.**—*o*-Hydroxyphenylacetylene (2.1 g., 0.018 mol.) was dissolved in a solution of sodium ethoxide in ethanol (sodium, 0.4 g. and absolute ethanol, 5 ml.). After removal of the alcohol in a vacuum at room temperature, the residue was mixed with *trans*-1,4-dichloro-2-butene (1.2 g., 0.009 mol.), a catalytic amount of potassium iodide and dimethylformamide (20 ml.) and the mixture was refluxed for 1 hr. The neutral reaction mixture was poured into ice-water. The crystals deposited were filtered, then washed with water and ethanol, successively. The crude crystals were recrystallized from ethanol yielding $IX_b$, colorless leaflets, m. p. 118~119°C, 1.5 g. (60%).

Found: C, 82.72; H, 5.66. Calcd. for $C_{20}H_{16}O_2$: C, 83.31; H, 5.59%.

IR max., 3255 (-C≡CH), 2105 (-C≡C-), 1240 (=C-O-), 975 (*trans*-ethylene) $cm^{-1}$.

**Synthesis of $IX_a$.** — The reaction of *cis*-1,4-dichloro-2-butene (1.2 g., 0.009 mol.) with *o*-hydroxyphenylacetylene (2.1 g., 0.018 mol.) according to the same procedure as that described above yielded $IX_a$, red oil, 2.3 g. (85%).

IR max., 3400 (-C≡CH), 2160 (-C≡C-), 1250 (=C-O-) $cm^{-1}$.

The crude $IX_a$ was employed without further purification to the subsequent reaction.

**Oxidative Coupling of $IX_a$.** — $IX_a$ (2.3 g.) was oxidized with cupric acetate monohydrate (15 g.) in pyridine (110 g.). After stirring for 4 hr. at 50~52°C, the solvent was removed under reduced pressure at a temperature below 30°C. The residue was extracted with ether (250 ml.), washed with aqueous cupric acetate and water, successively, and dried over anhydrous sodium sulfate. The crude crystals from the ether extract, on repeated recrystallization from benzene, gave $X_a$, colorless prisms, m. p. 154°C (decomp.), 0.7 g. (33%). Complete decomposition was observed when the crystals were heated to 140°C for 30 min.

Found: C, 83.73; H, 4.94. Calcd. for $C_{20}H_{14}O_2$: C, 83.90; H, 4.93%.

IR max., 2230, 2165 (-C≡C-), 1257, 1215 (=C-O-), 742, 720 (*cis*-ethylene) $cm^{-1}$.

The monomeric nature of $X_a$ was inferred from the molecular weight of the reduction product XI.

**Hydrogenation of $X_a$.**—$X_a$ (200 mg.) in benzene (20 ml.) was hydrogenated over 5% palladium-on-charcoal (20 mg.). The reduction product was recrystallized from aqueous ethanol yielding XI, colorless plates, m. p. 63.5°C, 200 mg. (96%). This substance showed no depression of the melting point on admixture with the reduction product of $VI_c$ and $X_b$. Also the infrared spectra of these reduction products were found to be identical over the entire region of wavelength.

**Oxidative Coupling of $IX_b$.**—A solution of $IX_b$ (1.3 g.) and cupric acetate monohydrate (15 g.) in pyridine (120 g.) was heated to 50°C for 3 hr. Treatment of the reaction mixture according to the usual method afforded crude crystals. The crude material was repeatedly recrystallized from ethyl acetate containing a small amount of ethanol yielding $X_b$, colorless plates, m. p. 130°C (decomp.), 0.4 g. (30%).

Found: C, 83.80; H, 5.02. Calcd. for $C_{20}H_{14}O_2$: C, 83.90; H, 4.93%.

IR max., 2205 (-C≡C-), 1237 (=C-O-), 960 (*trans*-ethylene) $cm^{-1}$.

**Hydrogenation of $X_b$.**—Hydrogenation of $X_b$ in benzene over 5% palladium-on-charcoal gave XI, colorless plates, m. p. 63.5°C in a yield of 96%.

**Syntheses of XII and XIII.** — *o*-Hydroxyphenylacetylene (2.4 g., 0.02 mol.) was dissolved in a solution of sodium methoxide in methanol (sodium, 0.5 g. and absolute methanol, 7 ml.). After removal of the solvent under reduced pressure at room

temperature, the residue was mixed with *o*-xylylene dibromide (2.7 g., 0.01 mol.), a trace of potassium iodide and dimethylformamide (20 ml.), and the mixture was refluxed for 1.5 hr. The cooled neutral reaction mixture was poured into ice-water, and extracted with ether. The ether layer was washed with water and dried over magnesium sulfate. The viscous oil (3.5 g., IR max., 3360 (-C≡CH), 2160 (-C≡C-), 1250 (=C-O) $cm^{-1}$) from the ether layer, was mixed with a solution of cupric acetate monohydrate (15 g.) in pyridine (150 g.). The mixture was stirred for 4 hr. at 50°C. Isolation with ether as before yielded crude crystals. The crude substance was washed with a small amount of cold benzene and digested with hot ethanol. The insoluble material was removed by filtration. The crystals from the filtrate were recrystallized from ethanol to yield XII, colorless needles, m. p. 148.5°C, (decomp.), 250 mg. (8%).

Found: C, 85.37; H, 4.83. Calcd. for $C_{24}H_{16}O_2$: C, 85.69; H, 4.79%.

IR max., 2220 (-C≡C-), 1222, 1208 (=C-O-), 1375 ($\delta$ CH) $cm^{-1}$. (measured by KBr-disk method).

It is to be noted that the infrared spectrum of XII lacks the absorption peak arising from the stretching of methyl group.

Owing to the thermal instability, the molecular weight of XII was inferred from that of the reduction product XIV.

The abovementioned insoluble solid was recrystallized from benzene yielding XIII, colorless plates, m. p. 230~231°C, 100 mg. (3%). It was observed that the transparent crystals turn to opaque at about 100°C. This phenomenon is attributable to the loss of benzene of crystallization. The amount of benzene of crystallization was found to be 19.06%. (Calcd. for $C_{48}H_{32}O_4 \cdot 2C_6H_6$: 18.84%).

Found: C, 85.29; H, 4.82. Mol. wt., 667. Calcd. for $C_{48}H_{32}O_4$: C, 85.69; H, 4.79%. Mol. wt., 672.

IR max., 1240 (=C-O-) $cm^{-1}$.

**Hydrogenation of XII.**—XII (130 mg.) in benzene (15 ml.) was reduced over 5% palladium-on-charcoal (20 mg.). After removal of the catalyst, the solvent was distilled and the residual solid was recrystallized from ethyl acetate-ethanol resulting in XIV, colorless needles, m. p. 180°C, 125 mg.

Found: C, 83.55; H, 7.06. Mol. wt., 346. Calcd. for $C_{24}H_{24}O_2$: C, 83.69; H, 7.02, Mol. wt., 344.

IR max., 2930, 2865 ($\nu$ CH), 1383 ($\delta$ CH), 1230 (=C-O-) $cm^{-1}$ (KBr-disk).

***o,o'*-Dibenzyloxydiphenyldiacetylene (XV).**—*o,o'*-Dihydroxydiphenyldiacetylene (1.0 g., 0.0086 mol.) and a trace of potassium iodide were added to a solution of sodium ethoxide in ethanol (sodium, 0.2 g., and absolute ethanol, 20 ml.). After refluxing for 1 hr., the reaction mixture was cooled. The crystals deposited were filtered, then washed with water and ethanol, successively. The crude material was recrystallized from benzene or ethyl acetate to give XV, colorless needles, m. p. 152~152.5°C, 0.9 g. (53%).

Found: C, 86.91; H, 5.23. Calcd. for $C_{30}H_{22}O_2$: C, 86.93; H, 5.35%.

**Synthesis of XVI.** — *o*-Hydroxyphenylacetylene (1.5 g., 0.013 mol.) was dissolved in a solution of sodium ethoxide in ethanol (sodium, 0.3 g. and absolute ethanol, 5 ml.). After the removal of the ethanol at room temperature in a vacuum, the residue was mixed with 1,4-dichloro-2-butyne (0.8 g., 0.0065 mol.), dimethylformamide (13 ml.) and a catalytic amount of potassium iodide, and refluxed for 1.5 hr. The cooled reaction mixture was poured into ice-water and extracted with ether (100 ml.). The extract was washed with aqueous potassium hydroxide and water, successively, and dried over sodium sulfate. The crude crystals obtained by evaporating the ethereal solution were purified by repeated recrystallization from aqueous ethanol resulting in XVI, colorless needles, m. p. 75°C, 0.5 g. (35%).

Found: C, 83.48; H, 5.01. Calcd. for $C_{20}H_{14}O_2$: C, 83.90; H, 4.93%.

IR max., 3370 (-C≡CH), 1240 (=C-O-) $cm^{-1}$.

**Oxidative Coupling of XVI.** — The mixture of XVI (420 mg.), cupric acetate monohydrate (4.5 g.) and pyridine (45 g.) was stirred at 40°C for 4 hr. and then at 50°C for 1 hr. The solvent was removed under reduced pressure at a temperature below 35°C. The residue thus obtained was extracted with ether (100 ml.). An amorphous solid with high melting point suspended in ethereal solution was removed by filtration (300 mg.). No investigation on the nature of the amorphous solid was carried out. The ethereal solution was treated according to the usual procedure yielding crude XVI. This was recrystallized from benzene-light petroleum (b. p. 60~70°C) to give pure XVI, colorless needles, m. p. 167°C (decomp.), 15 mg. (3.5%).

Found: C, 84.48; H, 4.06. Calcd. for $C_{20}H_{12}O_2$: C, 84.49; H, 4.25%.

IR max., 2230 (-C≡C-), 1267 (=C-O-) $cm^{-1}$.

XVI was found to be a heat sensitive substance. The crystals of XVI changed to pink, then to red when heated to 120°C and melted at 167°C, forming a reddish brown liquid.

**Synthesis of XVIII.** — *o,o'*-Dihydroxydiphenyldiacetylene (1.1 g., 0.047 mol.) was dissolved in a solution of sodium ethoxide in ethanol (sodium, 0.2 g. and absolute ethanol, 20 ml.). Propargyl bromide (1.1 g., 0.094 mol.) and a small amount of potassium iodide were added to the ethanolic solution and refluxed for 1.5 hr. The crude crystals obtained by chilling the reaction mixture were washed with ethanol, hot water and ethanol, successively. The crude substance thus obtained was recrystallized from benzene-light petroleum (b. p. 60~70°C). It was observed that the crystals were contaminated with a small amount of 2,2'-dibenzofuranyl[6]. The last mentioned substance was removed by digesting the crude crystals with benzene. The crystals remained were recrystallized from benzene resulting in XVIII, colorless needles, m. p. 151~152°C (decomp.), 200 mg., (14%).

Found: C, 84.89: H, 4.64. Calcd. for $C_{22}H_{14}O_2$: C, 85.14; H, 4.55%.

IR max., 3270 (-C≡CH), 2160, 2130 (-C≡C-), 1225 (=C-O-) $cm^{-1}$.

The attempt of the intramolecular oxidative coupling of XVIII resulted in the formation of a resinous material.

The authors are grateful to Professor Yasuhide Yukawa for his valuable discussions.

They are also indebted to Mr. M. Okumiya for the microanalyses. A part of the expenses of this research was defrayed from the Grant-in-Aid of the Ministry of Education, to which the authors thanks are also due.

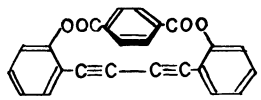
*Department of Chemistry*
*Faculty of Science*
*Osaka University*
*Nakanoshima, Osaka*

# *Cyclic Acetylenes. VI. Transannular and Proximity Effects in the Cyclic Derivatives of o, o'-Dihydroxydiphenyldiacetylene*

By Fumio TODA and Masazumi NAKAGAWA

(Received December 9, 1960)

It was pointed out in Part II[1] of this series that the cyclic terephthalate of *o, o'*-dihydroxydiphenyldiacetylene (I) may be a suitable substance for the study of the transannular effect between the benzene ring of the bridging chain and the diacetylenic function. But the



I

attempts to prepare I by the intramolecular oxidative coupling of 2-ethynylphenyl terephthalate gave unsatisfactory results. It was observed that the ester linkage is easily cleft during the course of oxidative coupling giving benzofurane derivatives. Therefore the authors have carried out the synthesis of an analogous substance of I in which the ester linkage is replaced by ether linkage.

Sodium *o*-ethynylphenoxide (II) was treated with *p*-xylylene dibromide to yield the terminal diacetylene III. Oxidative coupling of III, according to Eglinton's procedure[2], gave the cyclic diacetylene IV in 25% yield. The monomeric nature of IV was inferred from the molecular weight of the octahydroderivative V, since IV itself was found to have a poor solubility in camphor.

As illustrated in Fig. 1, the scale model of IV indicates that the molecule is almost strain

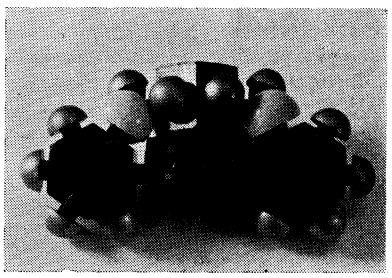
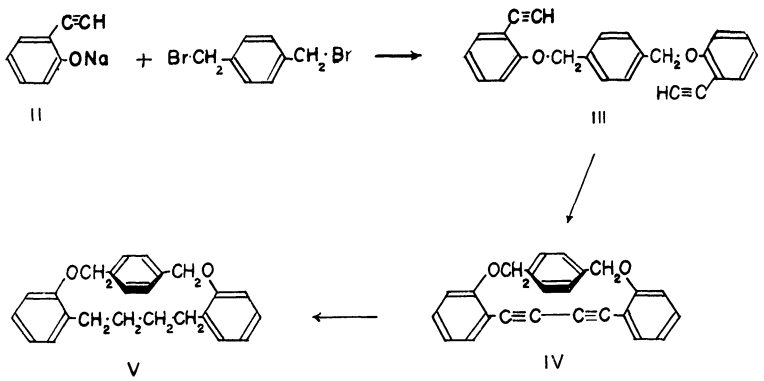


Fig. 1. The molecular model of IV (Courtauld model).



II III IV V

1) F. Toda and M. Nakagawa, This Bulletin, **33**, 230 (1960).

2) G. Eglinton and A. R. Galbraith, *Chem. & Ind.*, **1956**, 737; *J. Chem. Soc.*, **1959**, 889.

free and the benzene nucleus in the bridging chain is held closely parallel to the diacetylenic linkage. A part of the infrared spectra of III, IV and V are recorded in Fig. 2. The absorption bands arising from the out-of-plane deformation of the adjecent two hydrogen atoms

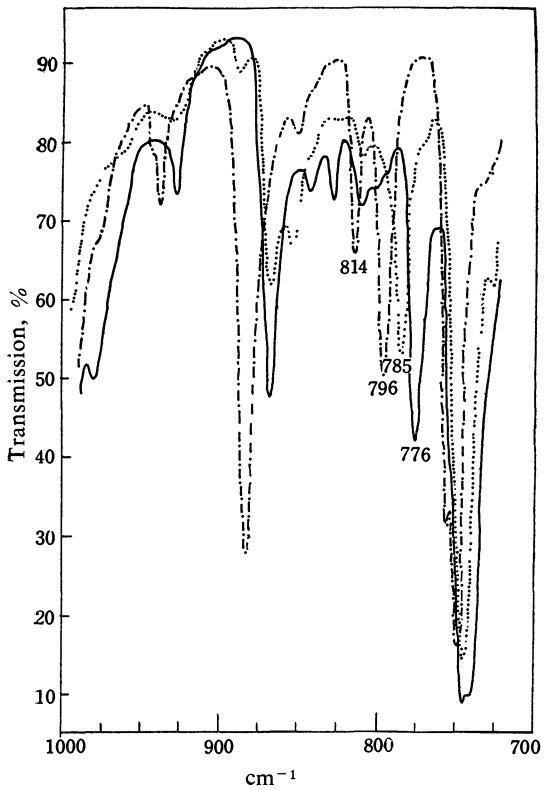



Fig. 2. The infrared spectra of III, IV and V.
·-·-·: III ——: IV ·····: V

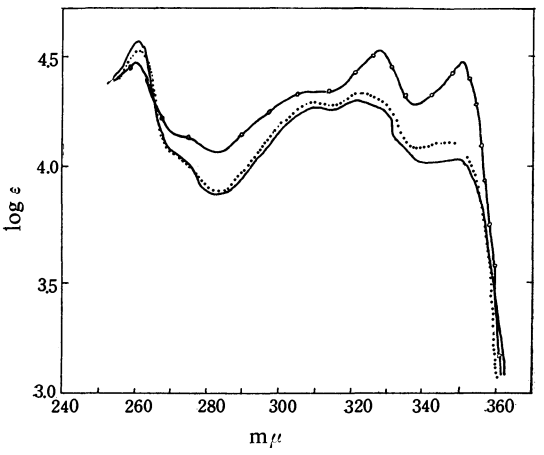



Fig. 3. The ultraviolet spectra of the cyclic diacetylene (IV), the cyclic tetraacetylene (IX) and the open chain analogue (VI) (in dioxane).
·····: IV ——: IX -○-○-: VI

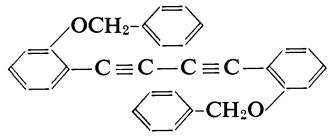
in the *p*-disubstituted benzene nucleus appeared at 814 $cm^{-1}$ and 796 $cm^{-1}$ in the case of III, whereas the corresponding absorption band shifted to 776 $cm^{-1}$ and 785 $cm^{-1}$ in IV and V, respectively. The infrared spectroscopic anomalousness of IV and V can be explained on the basis of a non-bonded interaction of hydrogen atoms in the benzene nucleus of the bridging chain with the diacetylenic linkage or with the $-(CH_2)_4-$ chain which is held in a proximate position to the hydrogen atoms. As indicated in Fig. 3 and Table I, the ultraviolet spectrum

Table I

| Compound | Absorption | | | | |
|---|---|---|---|---|---|
| IV | 261 (322) | **275** (105) | 310 (189) | 322 (208) | 346 (127) |
| VI | 261 (287) | **275** (130) | 310 (212) | 328 (323) | 351 (285) |
| IX | 261 (350) | **275** (105) | 310 (185) | 321 (196) | 349 (115) |

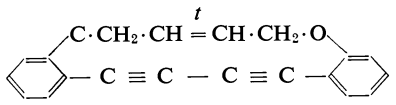
All spectra were measured in dioxane.
The figures indicate the $\lambda_{max}$ in mμ.
The figures in parentheses are $\varepsilon_{max} \times 10^{-2}$.
The bold figures indicate shoulders.

of IV also shows an anomalous feature. Loss of the sharpness and the marked decrease of the absorption intensities of the peaks at the longer wavelength region were observed in the spectrum of IV as compared with that of the open chain analogue, *o*, *o'*-dibenzyloxydiphenyldiacetylene (VI)[3].



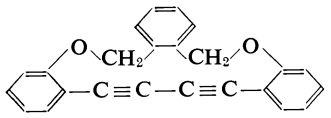

VI

It is to be noted that the ultraviolet spectrum of VII[3] also showed broad absorption peaks. On the other hand, the *ortho*-isomer of IV (VIII)[3] has a well defined, fine structure in




VII

the ultraviolet spectrum, in spite of the shifts in the absorption peaks. As already discussed in the preceding paper, the *trans*-ethylenic

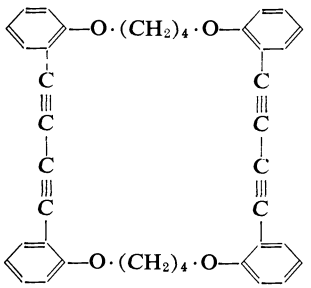



VIII

3) F. Toda and M. Nakagawa, This Bulletin, 34, 862 (1961).

bond in VII is held closely to the diacetylenic function; on the contrary, the *o*-xylylene group in VIII is fixed fairly far apart from the diacetylenic linkage. Therefore the anomalousness in the ultraviolet spectra of IV and VII is probably associated with a transannular interaction of $\pi$-electrons in the bridging chain with those of the diyne function.

As already pointed out in the previous papers[3,4], the strained cyclic derivatives of *o*, *o'*-dihydroxydiphenyldiacetylene have a sharp and intense $\lambda_{min}$ at ca. 260 m$\mu$ in their ultraviolet spectra, and the presence of this $\lambda_{min}$ was attributed to a proximity effect of *o*, *o'*-bridging chain to the diacetylenic linkage. The ultraviolet spectrum of IV lacks the $\lambda_{min}$, but has a $\lambda_{max}$ at the same wavelength. An examination of the scale model of IV reveals that the methylene groups in the benzyl position of the bridging chain are fixed fairly far apart from the diacetylenic function owing to the presence of the rigid benzene nucleus. As the result of the above-mentioned spatial position of the methylene groups, there might be no proximity effect to operate in IV, in spite of the fact that the cycle has a short bridging chain.



IX

The ultraviolet spectrum of the cyclic tetraacetylene IX which was reported in the preceding paper[3] was found to be quite similar to that of IV (Fig. 3). The spectroscopic similarity suggests the possibility that the molecule of IX can assume the geometry of a puckered ring in which two of the four benzene rings are faced to the diacetylenic functions making it possible for some transannular effect to operate (Fig. 4).

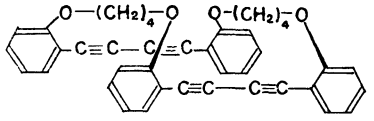


Fig. 4. A puckered structure of IX.

4) F. Toda and M. Nakagawa, 33, 223 (1960).

## Experimental*

**Synthesis of 1, 4-Bis-(*o*-ethynylphenoxymethyl)-benzene (III).**—*o*-Hydroxyphenylacetylene (3.54 g., 0.03 mol.) was dissolved in a solution of sodium ethoxide in ethanol (sodium, 0.69 g., 0.03 mol. and absolute ethanol, 10 ml.) and the solvent was removed in vacuo. The sodium phenoxide thus obtained was mixed with *p*-xylylene dibromide (3.96 g., 0.015 mol.), a catalytic amount of potassium iodide and dimethylformamide (25 ml.). After being refluxed for 2.5 hr., the mixture was cooled and poured into ice-water. The solid deposited was filtered and then washed with water and ethanol. The dried material was repeatedly recrystallized from ethanol giving III, colorless prisms or needles, m. p. 93~94°C, 3.90 g. (78%).

Found: C, 84.91; H, 5.40. Calcd. for $C_{24}H_{18}O_2$: C, 85.18; H, 5.36%.

IR max., 3280 (-C≡CH), 2940, 2880 ($\nu$ CH), 2110 (-C≡C-), 1470, 1386 ($\delta$ CH), 1242 (=C-O-), 814, 796 (*p*-disubst. benzene), 740 (*o*-disubst. benzene) $cm^{-1}$.

**Oxidative Coupling of III.**—The mixture of III (1.5 g.), cupric acetate monohydrate (15 g.) and pyridine (150 g.) was stirred for 4 hr. at 50°C. The reaction mixture was cooled and the crystals deposited were filtered and then washed with water and ethanol. The filtrate was concentrated under reduced pressure yielding crystals. The crystals were washed with water and ethanol, and combined with the first crop. Repeated recrystallization of the combined material from benzene afforded cyclic diacetylene IV, colorless needles, m. p. 274~275°C (decomp.), 370 mg. (25%).

Found: C, 85.34; H, 4.99, Mol. wt., 354. Calcd. for $C_{24}H_{16}O_2$: C, 85.69; H, 4.79%, Mol. wt., 336.

IR max., 2920, 2870 ($\nu$ CH), 2220, 2150 (-C≡C-), 1380 ($\delta$ CH), 1245, 1220 (=C-O-), 776 (*p*-disubst. benzene), 746 (*o*-disubst. benzene) $cm^{-1}$.

**Hydrogenation of IV.**—IV (210 mg.) was hydrogenated in benzene (100 ml.) over 5% palladium-on-charcoal (20 mg.). After removal of the catalyst, the solvent was distilled, resulting in crystals. On recrystallization from ethyl acetate-ethanol or benzene-petroleum ether (b. p. 60~70°C) the crystals afforded V in quantitative yield, colorless needles, m. p. 195~197°C.

Found: C, 83.67; H, 6.83, Mol. wt., 381. Calcd. for $C_{24}H_{24}O_2$: C, 83.69; H, 7.02%, Mol. wt., 344.

IR max., 2930, 2860 ($\nu$ CH), 1380 ($\delta$ CH), 1230 (=C-O-), 785 (*p*-disubst. benzene), 745 (*o*-disubst. benzene) $cm^{-1}$.

The authors are grateful to the Ministry of Education for the Grant-in-Aid for fundamental scientific research.

*Department of Chemistry*
*Faculty of Science*
*Osaka University*
*Nakanoshima, Osaka*

* All melting points were not corrected. The infrared spectra were measured by KBr-disk method. The microanalyses were performed by Mr. M. Okumiya of the microanalytical laboratory of this Department.

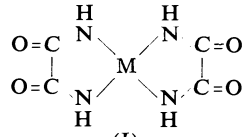
# *Infrared Spectra and the Structure of Some Metal-oxamide Complexes*

By Yoko KURODA, Michinobu KATO* and Kôzô SONE**

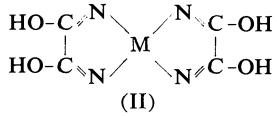
(Received December 4, 1960)

Many kinds of proteins, polypeptides and biuret-like compounds react with $Cu^{2+}$ ions in basic solutions, forming chelate complexes with characteristic red or violet colors ("biuret reaction")[1-4]. Oxamide is known to be the simplest one among molecules that exhibit this reaction, and the composition of the red product can be formulated as $A_2[Cu(C_2H_2N_2O_2)_2]$, where A represents a univalent ion (e. g. alkali metal ion). It is also known that $Ni^{2+}$ ions form a yellow complex of analogous composition[5,6].

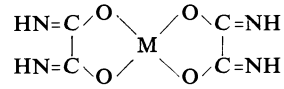
Although the formula of these complexes and the reported diamagnetism of the nickel complex[7] afford some evidence in favor of the presumption that these complexes are tetra-coordinated chelates, their structure has not yet been established definitely***. The reason is as follows: An oxamide molecule contains two nitrogen and two oxygen atoms capable of forming coordinate bonds with a metal, while the constitution of a tetra-coordinated complex with a bivalent central ion does not permit all these atoms to be involved in metal-ligand linkages. This situation makes a number of structures conceivable, e. g.,



(I)



(II)



(III)

etc., among which the formula I seems to be more probable than the others, because of the analogy of the color and general mode of formation of these complexes with those of biuret complexes of the corresponding metals[1-4].

In connection with this problem, it can be expected that infrared spectroscopy will provide a powerful means for the determination of the kind of donor atoms in these complexes, and the elucidation of their geometric structure. In this paper, the infrared absorption spectra of $K_2[Ni(C_2H_2N_2O_2)_2]$ and $K_2[Cu(C_2H_2N_2O_2)_2]$ are reported and discussed from this point of view.

## Experimental Procedure and Results

**Materials.** — Potassium bis(oxamido)niccolate-(II) and potassium bis(oxamido)cuprate(II) were prepared by the method of Hofmann and Ehrhardt[6]. and dried over potassium hydroxide.

Found: Ni, 18.1; N, 16.8. Calcd. for $K_2[Ni(C_2H_2N_2O_2)_2]$: Ni, 19.0; N, 18.1%.

Found: Cu, 18.5; N, 17.4. Calcd. for $K_2[Cu(C_2H_2N_2O_2)_2]$: Cu, 20.2; N, 17.9%.

A specimen of oxamide, $C_2H_4N_2O_2$, was obtained from L. Light & Co. Ltd.

**Measurements.** — The infrared spectra were recorded by means of a Hilger H-800 spectrophotometer. The absorption measurements were made at room temperature using pressed potassium bromide disk technique in the wave number range from 700 to 4000 $cm^{-1}$ with a rock-salt prism. A fluorite prism was also used for a range above 1200 $cm^{-1}$, but no additional information was obtained. The results were checked using Nujol mulls. The spectra obtained are shown in Fig. 1, and the observed frequencies of the absorption bands are listed in Table I. The present data on oxamide are in good agreement with those reported by Miyazawa[8] and by Scott and Wagner[9].

## Discussion

A close resemblance exists between the absorption patterns of the metal complexes, indicating that they have a similar structure. On

* Chemical Laboratory, Aichi Prefectural University for Women, Mizuho-ku, Nagoya.

** Chemical Laboratory, Aichi Gakugei University, Higashi-ku, Nagoya.

1) G. Wiedemann, *Ann.*, **68**, 323 (1848).

2) M. M. Rising, J. S. Hicks and G. A. Moerke, *J. Biol. Chem.*, **89**, 1 (1930).

3) M. Kato, *Z. anorg. u. allgem. Chem.*, **300**, 84 (1959).

4) K. Sone and M. Kato, Proc. Symposium on the Chemistry of Co-ordination Compounds, Agra (India), Part III, 16 (1960).

5) H. Schiff, *Ann.*, **299**, 236 (1898).

6) K. A. Hofmann and U. Ehrhardt, *Ber.*, **46**, 1457 (1913).

7) L. Cambi and E. Tremolada, *Gazz. chim. ital.*, **65**, 322 (1935).

*** The recent X-ray studies by Freeman et al. (H. C. Freeman, J. E. W. L. Smith and J. C. Taylor, *Nature*, **184**, 707 (1959).) on the structure of bis(biureto)cuprate(II) is of interest in connection with this study.

8) T. Miyazawa, *J. Chem. Soc. Japan, Pure Chem. Sec.* (*Nippon Kagaku Zasshi*), **75**, 86 (1954).

9) T. A. Scott, Jr. and E. L. Wagner, *J. Chem. Phys.*, **30**, 465 (1959).

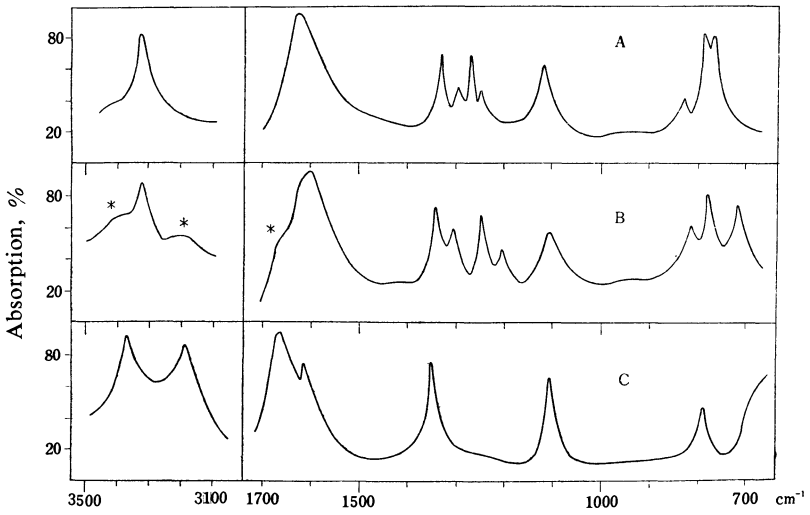



Fig. 1. The infrared spectra of (A): potassium bis(oxamido)niccolate(II), (B): potassium bis-(oxamido)cuprate(II), and (C): pure oxamide. The peaks marked with an asterisk seem to be due to the contamination of oxamide[2] produced by the decomposition of the easily hydrolyzable copper complex, because their positions coincided with those of the strong absorption bands of oxamide and their intensity increased considerably after the complex was exposed to atmospheric moisture.

TABLE I. OBSERVED INFRARED ABSORPTION FREQUENCIES IN $cm^{-1}$

| $K_2[Ni(C_2H_2 \cdot N_2O_2)_2]$ | $K_2[Cu(C_2H_2 \cdot N_2O_2)_2]$ | Assignment |
|---|---|---|
| 3320 (s) | 3313 (s) | $\nu_{N-H}$ |
| 1628 (vs) | 1600 (vs) | $\nu_{C=O}$ |
| 1325 (m) | 1343 (m) | $\nu_{C-N}$ |
| 1285 (w) | 1305 (w) | |
| 1268 (m) | 1253 (m) | |
| 1250 (w) | 1215 (w) | |
| 1124 (m) | 1120 (m) | $\rho_{N-H}$ |
| 831 (w) | 815 (w) | $\nu_{C-C}$ |
| 786 (s) | 788 (s) | $\omega_{N-H}$ |
| 765 (s) | 722 (s) | $\rho_{C=O}$ |

Absorption intensities are shown by letters in parentheses, i.e., vs: very strong, s: strong, m: medium, w: weak.

Vibrational types are expressed by greek letters, i.e., $\nu$: stretching, $\rho$: in-plane deformation, $\omega$: out-of-plane deformation.

the other hand, the feature of these spectra is much different from that of an oxamide molecule. It has revealed that heavy atoms in an oxamide molecule are arranged in a trans ($C_{2h}$) form in solid state[8,9]. However, it is unbelievable that an oxamide molecule having the trans form can act as a bidental ligand, provided that the coordination takes place through one kind of donor atoms. A more complicated spectral feature of the metal complexes probably reflects a less symmetrical structure of the ligand. The complication of the spectra should partly be caused by vibrational couplings between two ligands through coordination linkages. This effect is expected to be more appreciable for the vibrational modes of groups directly attached to the metal than for those of end groups.

In the first place, a remarkable difference between the spectra of an oxamide molecule and those of the metal complexes was found in the region from 3100 to 3400 $cm^{-1}$. The former show two strong bands arising from the N-H stretching vibrations of primary amide groups, O=C-$NH_2$, while the latter show only one peak. This fact means that the primary amide structure is absent in these metal complexes. Another evidence in favor of the absence of an $NH_2$ group in metal complexes is provided by a spectral feature in the wave number range near 1600 $cm^{-1}$. For an oxamide molecule, the $NH_2$ bending frequency was found at 1610 $cm^{-1}$, whereas the corresponding band is absent in the spectra of the metal complexes. The values of 3320 $cm^{-1}$ for the nickel complex and of 3313 $cm^{-1}$ for the copper complex are reasonable for the N-H stretching frequencies of secondary amides in solid state[10], although there still remains a possibility of assigning them to the frequency of hydrogen-bonded OH groups. This ambiguity of assignment for these frequencies can be removed by examining the C=O stretching

10) L. J. Bellamy, "The Infrared Spectra of Complex Molecules", 2nd Ed., Methuen, London (1958), p. 205.

band. If the metal complexes take a structure having OH groups, such as II, an intense absorption at about 1600 $cm^{-1}$ characteristic of C=O bonds should be replaced by a C=N stretching band which is generally less intense than a C=O band. But this was not the case. In this region, both of the metal complexes show a band of nearly the same intensity as the C=O stretching band of an oxamide molecule. Therefore, the band at about 3320 $cm^{-1}$ of the metal complexes was assigned unequivocally to the N-H stretching vibration.

Also the characteristic C=O band above 1600 $cm^{-1}$ is expected to disappear from the spectra of metal complexes, if the ligands were coordinated to the metal through oxygen atoms (structure III), since it can be reasonably presumed that the formation of metal-oxygen bonds will cause a shift in the C=O stretching band to a much lower frequency owing to the decreasing double bond character of the C=O group. Moreover the CO bonds incorporated in a five-membered chelate ring will have no longer the character of end groupswhich display a simple absorption band, so that the appearance of the absorptions is expected to be greatly complicated because of coupling with other skeletal vibrations. Therefore, the presence of a simple C=O band in the spectra of metal complexes may be taken as sufficient evidence for the fact that these complexes have metal-nitrogen bonds rather than metal-oxygen bonds.

The value of 1628 $cm^{-1}$ for the nickel complex and that of 1600 $cm^{-1}$ for the copper complex are slightly lower than the value of 1660 $cm^{-1}$ for the C=O frequency of an oxamide molecule, indicating the decreased double bond character of the C=O bonds in the coordinated ligands. This effect is certainly due to the increased ionic character of such ligands, because the metal-nitrogen bonds are expected to have only a partial covalent character. It is of interest to note that the infrared spectra of the oxalate complexes of bivalent metals, $[M^{II}(C_2O_4)_2]^{2-}$, bear a close resemblance to this case[11]. The carboxylate frequencies of these complexes are intermediate between those of the oxalates of alkali metals and those of dimethyl oxalate, suggesting a partial covalent character of their metal-oxygen bonds. The fact that the observed frequency of the C=O stretching vibration of the nickel complex is higher than that of the copper complex indicates that the metal-nitrogen bonds of the former have a greater covalent character than those of the latter.

The spectral changes caused by the formation of the metal complexes are most apparent in the wave number range from 1350 to 1200 $cm^{-1}$. An oxamide molecule has a strong absorption band at 1355 $cm^{-1}$ arising from the C-N stretching vibration, while the metal complexes exhibit four peaks, two of which are of medium intensity and others are weak. It can be expected that the C-N stretching frequencies of the metal complexes will also appear in this region, since the double bond character of these bonds should not be affected so much on substitution of the hydrogen atoms of the $NH_2$ groups with a metal atom. However, the absorption feature will be complicated by vibrational coupling through the metal-nitrogen linkages. The spectral pattern in this region must therefore depend on the geometric structures of these complexes.

Conceivable models for these complexes are as follows. (1) A planar structure in which four metal-nitrogen bonds as well as all the heavy atoms of the two ligands lie on a plane ($D_{2h}$). (2) Structures in which the coordination type is planar and each ligand takes a non-planar form, owing to a rotation about a C-C single bond from the cis configuration. Depending on the relative orientation of two ligands, two forms are conceivable, one of which has a center of symmetry ($C_{2h}$) while the other has not ($D_2$). (3) One form of tetrahedral chelation of two planar ligands ($D_{2d}$). (4) Two forms of tetrahedral chelation of two non-planar ligand ($D_2$ and $C_2$).

Selection rules operating on these models are summarized in Table II. These rules should hold rather strictly in the skeletal vibrations such as C-C and C-N vibration, while the end groups are presumed to be free from these. Actually, no splitting was observed for the N-H and C=O stretching bands of the metal complexes.

For the C-N stretching vibration, $D_{2h}$ and $C_{2h}$ models have two infrared active modes and two inactive ones. A $D_{2d}$ model has two active modes, one of which is degenerate, and an inactive one. A $D_2$ model has three active ones and an inactive one. With a model having $C_2$ symmetry, all four modes are active. The four bands observed in this wave number region readily permit one to exclude the $D_{2d}$ and $D_2$ models. However, it is difficult for other models ($D_{2h}$, $C_{2h}$ and $C_2$) to decide which is the closest one to the actual structure, because these selection rules are valid only for a free molecule and the removal of prohibition can be expected to some extent in the solid state, for which intermolecular or interlattice effects should not be ignored. Therefore, there is a possibility of assigning these two weak bands to the inactive modes of the $D_{2h}$ or $C_{2h}$ model.

11) M. J. Schmelz, T. Miyazawa, S. Mizushima, T. J. Lane and J. V. Qaugliano, *Spectrochim. Acta*, **9**, 51 (1957).

TABLE II. CLASSIFICATION OF VIBRATIONAL TYPES FOR CONCEIVABLE MODELS OF $[M^{II}(C_2H_2N_2O_2)_2]^{2-}$

| | $D_{2h}$ | $C_{2h}$ | $D_{2d}$ | $D_2$ | $C_2$ |
|---|---|---|---|---|---|
| $\nu_{N-H}$, $\nu_{C=O}$, $\nu_{C-N}$, $\rho_{N-H}$, $\rho_{C=O}$ | $A_{1g}(R)$ | $A_g(R)$ | $A_1(R)$ | $A_1(R)$ | 2A(R, I) |
| | $B_{1u}(I)$ | $A_u(I)$ | $B_2(R, I)$ | $B_1(R, I)$ | |
| | $B_{2g}(R)$ | $B_g(R)$ | E(R, I) | $B_2(R, I)$ | 2B(R, I) |
| | $B_{3u}(I)$ | $B_u(I)$ | | $B_3(R, I)$ | |
| $\nu_{C-C}$ | $A_{1g}(R)$ | $A_g(R)$ | $A_1(R)$ | $A_1(R)$ | 2A(R, I) |
| | $B_{1u}(I)$ | $B_u(I)$ | $B_2(R, I)$ | $B_1(R, I)$ | |
| $\omega_{N-H}$ | $A_{1u}$(ia) | $A_u(I)$ | $B_1(R)$ | $A_1(R)$ | 2A(R, I) |
| | $B_{1g}(R)$ | $A_g(R)$ | $A_2$(ia) | $B_1(R, I)$ | |
| | $B_{2u}(I)$ | $B_u(I)$ | E(R, I) | $B_2(R, I)$ | 2B(R, I) |
| | $B_{3g}(R)$ | $B_g(R)$ | | $B_3(R, I)$ | |

The meaning of letters in parentheses are as follows; R : Raman active, I : Infrared active, ia : inactive in both.

On the other hand, it has been revealed from a magnetic study[7] that the nickel complex is diamagnetic and hence tetrahedrally chelated structures are unlikely. Furthermore, it is possible that the $\pi$ electron systems of the four amide groups give rise to some extent of conjugation effects through the $d_\pi$ orbitals of the central metal, and if such effects are taken into account, the planar form ($D_{2h}$) seems to be the most probable among the possible models. The whole spectra of these complexes are satisfactorily interpreted in terms of the structure I with a $D_{2h}$ symmetry, although there is an alternative possibility that the symmetry may be of $C_{2h}$.

Bands of the nickel complex at 831 $cm^{-1}$ and of the copper complex at 815 $cm^{-1}$ have no counterpart in the spectra of oxamide, but the frequencies are very close to a Raman frequency 800 $cm^{-1}$ ascribed to the C-C stretching vibration of oxamide[8]. The position and the weak intensity of these bands give a good evidence for assigning them to the C-C stretching mode.

Other frequencies expected to appear in the rock-salt region are the in-plane N-H deformation, the out-of-plane N-H deformation and the in-plane C=O deformation. According to general knowledge, the first has the highest frequency among them. Therefore, a band of the nickel complex at 1124 $cm^{-1}$ and a band of the copper complex at 1120 $cm^{-1}$ were assigned to this vibration. Two other bands of the nickel complex at 786 and 765 $cm^{-1}$ as well as those of copper complex at 788 and 722 $cm^{-1}$ were tentatively assigned to the out-of-plane N-H deformation and the in-plane C=O deformation, respectively. These assignments seem to be adequate, because in *N*-monosubstituted amides, it was found that the frequency of the former vibration is higher and its intensity is larger than those of the latter[12]; for example, the former is assigned to 778 $cm^{-1}$ and the latter to 765 $cm^{-1}$ in the case of *N*, *N'*-dimethyloxamide, which was examined by studying the deuteration effect[13].

These assignments are also listed in Table I.

## Summary

The infrared absorption spectra of potassium bis(oxamido)niccolate(II) and potassium bis-(oxamido)cuprate(II) were recorded in the wave number region from 700 to 4000 $cm^{-1}$ and compared with those of pure oxamide. These spectra revealed that metal-nitrogen bonds are formed in these complexes. The observed frequencies were interpreted in terms of a planar structure having the symmetry $D_{2h}$.

The authors wish to express their appreciation to Professor Masaji Kubo of Nagoya University for helpful discussions.

*Chemistry Department*
*Nagoya University*
*Chikusa, Nagoya*

12) T. Miyazawa, *J. Chem. Soc. Japan, Pure Chem. Sec.* (*Nippon Kagaku Zasshi*), **77**, 526 (1956).
13) T. Miyazawa, ibid., **76**, 1018 (1955).

# SHORT COMMUNICATIONS

## *Nuclear Magnetic Resonance of Tar Products. II**

By Shizuo FUJIWARA and Tohru WAINAI

(Received December 14, 1960)

Tar products consist of chemically similar components of high boiling points, which are very difficult to be distinguished from each other. As the means of analyses of these products, measurements of infrared spectra are usually made, but, other methods seem necessary to be explored. Nuclear Magnetic Resonance (NMR) technique has the advantage that we can analyze the functional groups in any liquid samples under nondestructive condition. Thus, Williams[1] made NMR measurements for saturated aromatic and olefinic components in distilled fractions of petroleum, Richards[2] for the aromatic compounds in various kinds of coals, and Schoolery[3] tried to determine the hydrogen contents of naphthalene derivatives.

The present authors performed the analysis of $\alpha$- and $\beta$-methyl-naphthalenes and reported elsewhere*. This paper will present the preliminary results of NMR measurements for distilled fractions of tar products.

*Samples.*—Samples used in this experiments are shown in Table I, which were collected from the plant of Yokohama Factory of Tokyo Gas Co., Ltd. at the working condition.

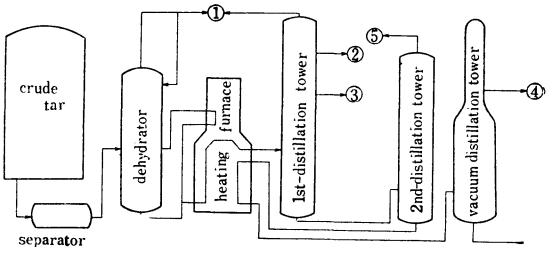
*NMR Measurements.*—Measurements of the NMR absorption spectra were caried out at 27 Mc./sec., and 40 Mc./sec. by the apparatus constructed by one of the authors (S. F.) and by the Japan Electron Optics Laboratory Co., Ltd., respectively. The concentration of sample is 50% (wt.) in carbon tetrachloride which contains a small amount of cyclohexane as the internal reference. Sample was spun rapidly during measurements.

*Results.*—The characteristic features of NMR spectra at 27 Mc./sec. were complicated and found to be insufficient for the analyses of functional groups. Even so, we could easily identify the paraffinic, alpha-alkyl and aromatic protons in the spectra. As the preliminary investigations, the results of measurements at 40 Mc./sec. seem satisfactory, which are shown in Fig. 1. Light oil has four absorptions in the aromatic region as well as the absorptions of aromatic hydroxyls of phenol and cresol at 6.3 and 8.6 P./10 M. (benzene=0), respectively. The absorption at 39.1 P./10 M. results from pyridine or picoline. The absorption in paraffinic region is stronger in light oil than in carbolic oil. The absorption of light oil in alpha-alkyl region overlaps those of methyl hydrogens of toluene and xylene. Four absorption bands at 2.4~7.5 P./10 M. observed in carbolic oil were assigned to hydroxyl groups of phenol and of cresol. Carbolic oil is also characterized by three strong absorptions at naphthalene region and a weak one at alpha-methyl region, which is weaker than that in light oil. According to the results of Fig. 1, we can see that naphthalene oil and top oil of the second tower are close to each other in the compositions. Heavy oil showed a broad absorption at aromatic region and other spectra at 37.1, 39.9 P./10 M. which are attributed to $\beta$-alkyl hydrogen.

We also examined the fractions obtained by rectifying distillation. The fractions of the

TABLE I

| No. | Sample | B.p., °C | S.g. | Tar acid % | Naphthalene % |
|---|---|---|---|---|---|
| 1 | Light oil | 85~190 | 0.919 | 14 | — |
| 2 | Carbolic oil | 180~200 | 1.025 | 46 | 16.8 |
| 3 | Naphthalene oil | 200~250 | | 9 | 58.0 |
| 4 | Heavy oil | 225~295 | 1.079 | 6 | 2.5 |
| 5 | Top oil (2nd tower) | 195~270 | | 9 | 29.6 |




1) R. B. Williams, A. S. T. M. Special Technical Publication, No. 224, p. 168 (1958).
2) R. E. Richards and R. W. Yorke, *J. Chem. Soc.*, **1960**, 2489.
3) J. N. Schoolery, Lectured at the Chemical Society of Japan, Tokyo, Oct. 1960.
* Report I: *Anal. Chem.*, in press.

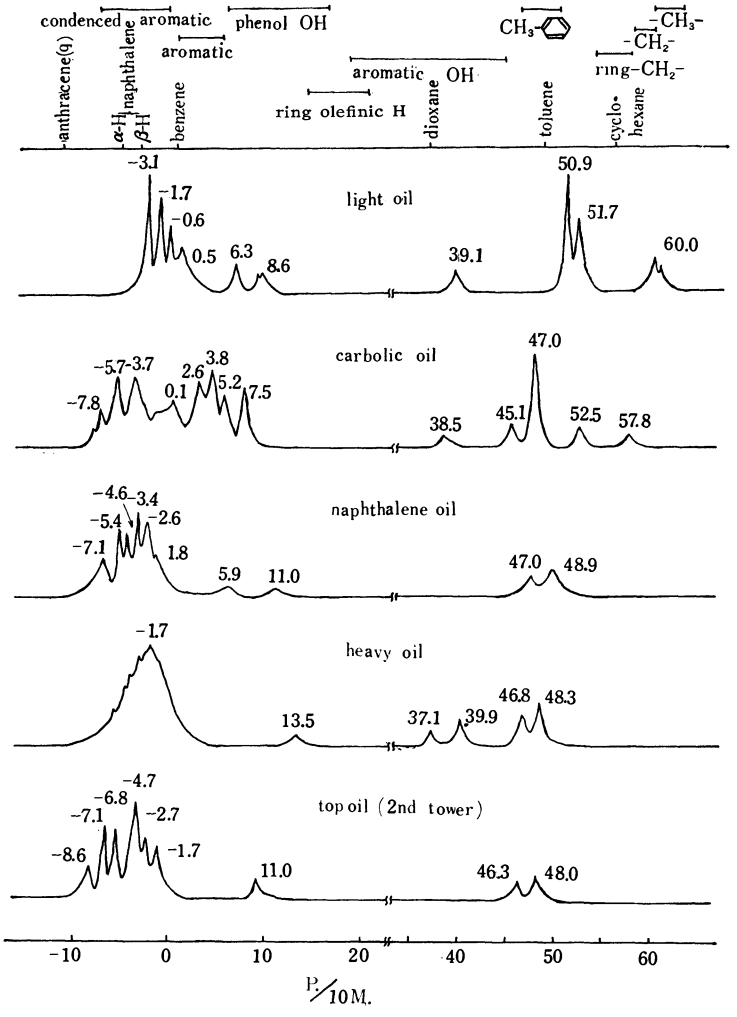



Fig. 1

factory distills which were rectified through the rectifying column were measured by NMR. According to the results of these measurements (not shown here) as well as those shown above, we conclude that the NMR method is quite useful for the analysis of tar products, and useful to figure out the efficiencies of the fractionation processes.

The authors are grateful to Mr. M. Takeuchi of the Japan Electron Optics Laboratory Co., Ltd. for measurement of the spectra at 40 Mc./sec. and to the Tokyo Gas Co., Ltd. for the supply of samples.

*Department of Chemistry*
*Faculty of Science*
*The University of Tokyo*
*Hongo, Tokyo*
(*S. F.*)

*Department of Industrial Chemistry*
*Faculty of Science and Engineering*
*Nihon University*
*Surugadai, Tokyo*
(*T. W.*)

## *The Crystallinity of Polyaldehydes*

By Hiroshi SOBUE and Hideo KUBOTA

(Received February 27, 1961)

Recently a few reports[1-3] on the stereospecific polymerization of aliphatic aldehydes were published, but the properties of these polymers remain hardly known[3]. As the crystalline property of the polymer is very interesting from practical point of view, we have examined the crystalline properties of some aldehyde polymers, i. e. the polymers of propionaldehyde, *n*-butyraldehyde, isobutyraldehyde, *n*-caproaldehyde, *n*-enauthaldehyde. The polymerization was carried out in hydrocarbon solvent such as heptane or toluene, with triethylaluminum as catalyst, at the temperature −80 or −40°C. In usual procedure we used 20 ml. of solvent, 0.0014 mol. of catalyst and 10 ml. of monomer.

All of the polymers obtained are crystalline. The X-ray diffraction patterns of powders of these polymers treated under various conditions are shown in Figs. 1—5. When treated with boiling chloroform or benzene for several hours, all of these polymers give sharper X-ray diagram than the untreated. As shown in Figs. 1, 3, 4 and 5, the samples swelled in some

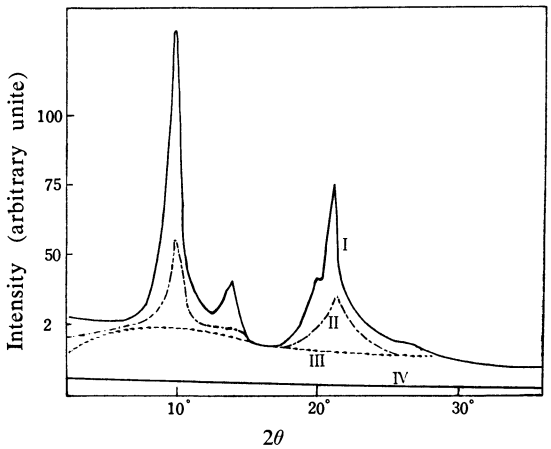



Fig. 1. The X-ray diffraction patterns of poly-propionaldehydes.
- I Sample treated with boiling chloroform for 8 hr. (polymerization at −78°C).
- II Sample swelled in chloroform. Amorphous part assumed.
- III Amorphous parts assumed.
- IV Pattern by air.

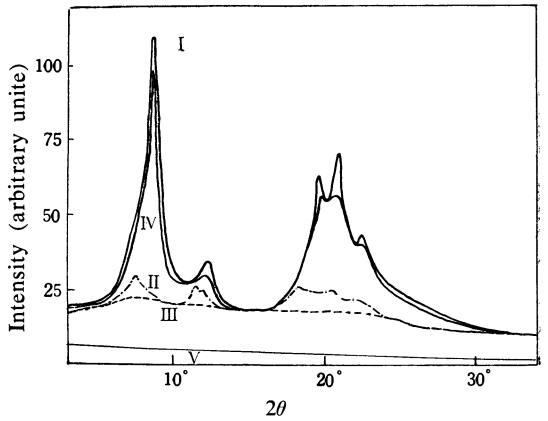



Fig. 2. The X-ray diffraction patterns of poly-*n*-butyraldehydes.
- I Sample treated with boiling chloroform for 6 hr. (polymerization at −80°C).
- II Sample partially depolymerized (gel-form).
- III Amorphous parts assumed.
- IV Untreated sample (polymerization at −40°C).
- V Pattern by air.

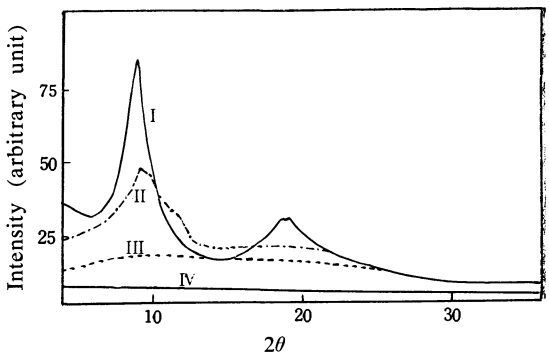



Fig. 3. The X-ray diffraction patterns of poly-isobutyraldehydes.
- I Sample treated with boiling chloroform for 6 hr. (polymerization at −78°C).
- II Sample swelled in chloroform.
- III Amorphous parts assumed.
- IV Pattern by air.

organic solvents were also examined by X-ray diffractometer. The untreated polymers of *n*-butyraldehyde depolymerize in certain condition to give gel-substances, whose patterns are shown in Fig. 2. Generally, the polymer which was kept at higher temperature than 170°C, partially depolymerized to give more diffused patterns.

Assuming the amorphous parts are given by dotted lines in each diagram, (the pattern of amorphous parts will be discussed in detail later,) we calculated the crystallinity of the polymers by integral intensity; as following

1) G. Natta et al., *Makromol. Chem.*, 37, 156 (1960).
2) J. Furukawa et al., ibid., 37, 149 (1960).
3) O. Vogl, *J. polymer Sci.* 46, 261 (1960).

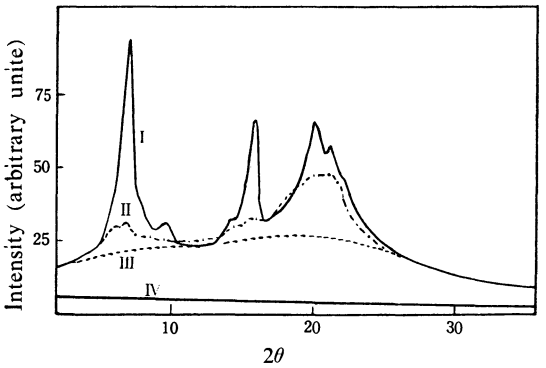



Fig. 4. The X-ray diffraction patterns of poly-*n*-caproaldehyde.
I Sample treated with boiling benzene for 6 hr. (polymerization at −78°C).
II Sample swelled in benzene.
III Amorphous parts assumed.
IV Pattern by air.

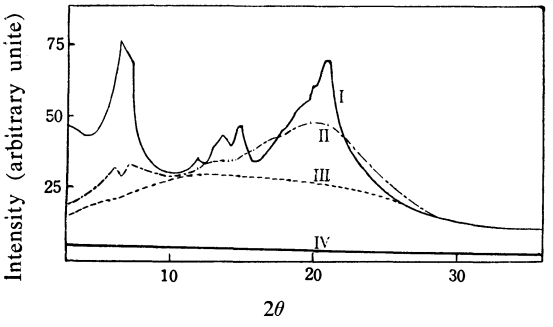



Fig. 5. The X-ray diffraction patterns of poly-*n*-enauthaldehydes.
I Sample treated with benzene.
II Sample swelled in benzene-chloroform.
III Amorphous parts assumed.
IV Pattern by air.

about 40% for poly-propion-, 45% for poly-butyr-, 49% for poly-isobutyr-, 37% for poly-*n*-capro-, 32% for poly-*n*-enauth-aldehyde. These polymers are crystalline even in untreated state and can not be dissolved in usual organic solvents, but are capable to be made a film by calendering at higher temperature than 100°C. The essential difference between the polymers obtained at −80 and −40°C, and the difference between the polymers prepared in heptane and toluene could not be found in the case of poly-*n*-butyraldehyde. At higher temperature than −35°C, the polymers could not be obtained. The kinetics of the polymerization will be reported later.

*Department of Applied Chemistry*
*Faculty of Engineering*
*The University of Tokyo*
*Hongo, Tokyo*

# *Syntheses of Two Kinds of Metal-free Tetra-azaporphines by the Urea-melt Method**

By Naomi FUKADA

(Received November 15, 1960)

In previous papers, it was shown that various metallo-derivatives (metal chelates) of ammonium phthalocyaninetetra-(4)-sulfonate[1] and of tetra-2, 3-pyridinoporphyrazine[1] were synthesized by the so-called urea-melt method in good yields and that the metal-free macrocycles of these metallo-derivatives, namely the parent substances, were prepared from the derivative of magnesium[2], of manganese[1], or of zinc[1]. In the present paper, it is reported that the metal-free macrocycles were obtained directly by the urea process.

No blue product was obtained from the mixtures of triammonium 4-sulfophthalate (10 g.) and urea (50～75 g.), or of quinolinic acid (10 g.) and urea (50～75 g.) by heating to 230°C. However, boric acid (0.5～1.5 g.) and ammonium molybdate (1.0～2.5 g.) were added to them as catalysts and heated together at 170～250°C for 0.5～1.5 hr., ammonium phthalocyaninetetra-(4)-sulfonate or tetra-2, 3-pyridinoporphyrazine was synthesized in fairly well yields (8～18%). It was further found that the metal-free macrocycles were prepared in high yields (26～42%), when a powdered metal (1.0～2.5 g.), such as chromium, molybdenum, or manganese, was used with boric acid and ammonium molybdate and that while in the absence of both boric acid and ammonium molybdate only very small amounts of the macrocycles were formed. When molybdenum was used, no metal chelate of the macrocycle was mixed, but when chromium or manganese was used, a small amount of the metal chelate was mingled. In the case of ammonium phthalocyaninetetra-(4)-sulfonate, a mixture of the metal-free macrocycle and the chromium chelate (about 9 : 1) was obtained. The chromium chelate was removed by extracting with a mixture of water, methanol and acetone (4 : 5 : 1). In the case of tetra-2, 3-pyridinoporphyrazine, a mixture of the free base and the

* Presented partly at the 10th Symposium on Coordination Compounds held by the Chemical Society of Japan, Sendai, September, 1960, and at the Takada Local Meeting of the Chemical Society of Japan, Takada, October, 1960.

1) N. Fukada, *J. Chem. Soc. Japan, Pure Chem. Sec.* (*Nippon Kagaku Zasshi*), **75**, 378, 380, 586, 1141 (1954); **76**, 1378 (1955); **77**, 1421 (1956); **78**, 1378 (1957); **79**, 396, 980 (1958).

2) R. P. Linstead et al., *J. Chem. Soc.*, **1937**, 911.

chromium chelate (about 2 : 1), or of the free base and the manganese chelate (about 4 : 1) was obtained. The manganese chelate was converted into the free base by the action of 98% sulfuric acid. On the contrary, the chromium chelate, as its coordinated chromium could not be eliminated by dissolving in strong mineral acids, was separated from the free base by treating with aqueous solution (50~75%) of benzenesulfonic acid because of the greater solubility of the free base.

The purification of crude ammonium phthalocyaninetetra-(4)-sulfonate was carried out as follows. The reaction mixture was powdered and extracted with water. The extract was evaporated to dryness. The residue was again extracted with water and the extract evaporated to dryness. This treatment was repeated about 10 times. The residue was thoroughly washed with 70% ethanol and added into an ammoniac saturated solution of ammonium carbonate and the solution was warmed. The macrocycle was salted out to give ammonium sulfonate. The crude ammonium salt was thoroughly washed with 70% ethanol and then boiled in 95% ethanol. Its chemical formula was $(C_8H_3N_2 \cdot SO_3NH_4)_4H_2$ (Found: S, 14.0; N, 18.3; $NH_3$, 7.2%).

The tetraammonium sulfonate was converted into the corresponding tetrasulfonic acid by treating with 6 N or more concentrated hydrochloric acid. The blue crystalline product formed was collected by filtration, washed with 6 N hydrochloric acid and dissolved in a small amount of ethanol. The ethanol solution was evaporated to dryness. The sulfonic acid was recrystallized from 8 N hydrochloric acid to give long thready crystals. The chemical formula of the acid was $(C_8H_3N_2SO_3H)_4H_2$ (Found: S, 15.1; N, 13.0%). The tetrasulfonic acid in solid form had an intense purple reflex and was hygroscopic. The tetrasulfonic acid was found to be identical with the one reported previously[1].

The purification of crude tetra-2, 3-pyridinoporphyrazine was carried out as follows. The reaction mixture was powdered, mixed with a large amount of 1 N hydrochloric acid, allowed to stand overnight at room temperature and filtered off. The residue was boiled with water, heated several times with 0.2 N hydrochloric acid at 80~90°C for 0.5 hr. and heated further several times with 0.1 N sodium hydroxide solution at 80~90°C for 0.5 hr., each time filtered off, and washed with dilute hydrochloric acid and with water. The bluish-black residue was dried at 100°C. The dried solid was dissolved in a small quantity of 98% sulfuric acid and the solution after being filtered was poured into a large excess of water. The blue crystalline product thereby deposited was collected, washed with hot dilute aqueous sodium hydroxide and with hot water, and dried at 100°C. The dried solid was powdered, heated under reflux (Soxhlet) with 95% ethanol, acetone and ether, successively, and filtered off. The purified product was dried at 185°C for 1 hr. Its chemical formula was $(C_7H_3N_3)_4H_2$ (Found: N, 31.5%). The metal-free macrocyclic pigment was found to be identical with the one reported previously by Linstead et al.[2] from its coincidence in physical and chemical properties as well as in elementary composition.

*Department of Chemistry*
*Faculty of Science*
*Niigata University*
*Niigata*

## *Constituents of the Antibiotic, Glumamycin*

By Michitaka INOUE

(Received February 20, 1961)

In the previous paper[1] it was reported that glumamycin, an acidic peptide antibiotic, consists of six amino acids and an unsaturated fatty acid.

Subsequently another acidic amino acid was detected by paper chromatography in the acidic amino acid portion of the glumamycin hydrolyzate; this acidic portion was submitted to partition column chromatography and colorless needle-like crystals, m. p. 254~256°C, $[\alpha]_D^{20} = +13°$ (*c* 1, 5 N HCl) were obtained (Found: C, 40.54; H, 6.18; N, 9.27; C-$CH_3$, 10.33. Calcd. for $C_5H_9NO_4$: C, 40.82; H, 6.12; N, 9.52; C-$CH_3$, 10.20%). The infrared spectrum of this compound was in good agreement with that* of $\alpha$(L), $\beta$-methylaspartic acid ($\beta$-Me-L-Asp), separated by Baker et al.[2]

Also in the previous paper[1] the basic amino acid component of glumamycin was presumed to be $\alpha, \beta$-diaminobutyric acid ($\alpha, \beta$-Dab). In the present work, the basic amino acid was converted with one mole of sodium nitrite

1) M. Inoue et al., This Bulletin, 33, 1014 (1960).

* The author wishes to express his thanks to Dr. N. Bohonos and Dr. J. H. Martin, Lederle Laboratories Division American Cyanamid Co., for their kind information on infrared spectrum of $\beta$-Me-L-Asp.

2) H. A. Baker et al., *Arch. Biochem. Biophys.*, **78**, 468 (1958).

into α-hydroxy-β-aminobutyric acid monohydrate, m. p. 223°C (Found: C, 35.08; H, 7.98; N, 9.81; $H_2O$, 13.98%), and oxidation of the amino acid with periodic acid gave acetaldehyde. Thus, the structure of the basic amio acid was established to be α, β-diamino-*n*-butyric acid.

For further confirmation of this structure, an attempt** was made to synthesize α, β-diamino-*n*-butyric acid from ethyl α, β-dibromobutyrate via the azide compound II by the method used for the synthesis of β-alanine by Horner et al.[3] Hydrolysis with hydrobromic acid of the phosphin imine compound, obtained by the reaction between II and triphenyl phosphin, produced α, β-Dab, m. p. 178°C (decomp.) (IIIa), and reduction of II under high pressure yielded IIIa and hydrochloride of its isomer (IIIb), m. p. 199~201°C (decomp.). Benzoylation of IIIa by Schotten-Baumann's method gave IV, m. p. 216~218°C (Found: C, 66.14; H, 5.41; N, 8.73%). The ethyl α, β-dibenzoylaminobutyrate (V) from IV and from glumamycin exhibited the same infrared spectrum in chloroform.

The DNP-glumamycin obtained by Sanger's[4] method was hydrolyzed with 6 N hydrochloric acid and the hydrolyzate was extracted with ether, but no DNP-amino acid was found in the ether-soluble portion. Therefore the free amino group of glumamycin was assumed to be the α- or β-amino group of the α, β-Dab of glumamycin. The water soluble portion of the hydrolyzate was spotted on paper in the *n*-butanol, acetic acid, water (4 : 1 : 5) system, and gave a spot at $R_f$ 0.68. On the other hand, in this system the β-mono-DNP-α, β-diaminobutyric acid had a $R_f$ of 0.68 and α-mono-DNP-α, β-diaminobutyric acid had a $R_f$ of 0.75. These two DNP-derivatives were prepared by partial dinitrophenylation of α, β-Dab from glumamycin hydrolyzate. Therefore the fact that a DNP-amino acid with $R_f$ 0.68 was obtained from the DNP-glumamycin hydrolyzate shows that, in glumamycin, the β-amino group of α, β-Dab was dinitrophenylated. Consequently the β-amino group of the α, β-Dab is free, and the α-amino group takes part in the peptide linkage in glumamycin.

The amino acid components of glumamycin were determined quantitatively. Four moles of Asp, 2 mol. of Gly, 1 mol. of Pro, and 1 mol. of Val were detected by the method of Moore and Stein[5], but in this method, β-Me-L-Asp had the same elution curve with that of Asp, pipecolic acid gave an anomalous ninhydrin coloration, and α, β-Dab was not eluted respectively. For the determination of these three abnormal amino acids, the method of Levy[6] which comprises subjecting DNP-amino acids to paper chromatography was used. To obtain the analytical values, the determination was conducted after ascertaing that the dinitrophenylation rate and elution rate of each amino acid can be measured with an error within ±4%. Even with two dimensional paper chromatography (the first solvent; *n*-butanol saturated with 2 N aqueous ammonia, the second solvent; 1.5 M phosphate buffer)[7], Asp could not be separated from β-Me-L-Asp, but the analytical values of 4 mol. of Asp (including β-Me-L-Asp), 2 mol. of Gly, 1 mol. each of Pro, Val, and 2 mol. of α, β-Dab were in good agreement with the results by the method of Moore, Stein.

In the previous paper[1] the molecular weight of glumamycin was supposed to be about 1800 from its titration value, and about 1500 from the yield of unsaturated fatty acid. However, the molecular weight is calculated to be about 1300 from the result of the above amino acid determination; therefore about 1300 seems to represent the correct minimum molecular weight*** of glumamycin.

Aspartocin[8] in an antibiotic closely resembling glumamycin, but it is clearly different from the latter in the behavior in paper chromatography.

*Research Laboratories*
*Takeda Chemical Industries, Ltd.*
*Higashiyodogawa-ku, Osaka*

** Synthesis of α, β-Dab was carried out by Neuberg (*Biochem. Z.*, **1**, 282 (1906)), but since it could not be isolated in crystalline form, it was converted to the phenylisocyanate and picrate. Recently, Martin[8] attempted the synthesis but did not report the results in detail.

3) L. Horner and A. Gross, *Ann.*, **591**, 117 (1955).
4) F. Sanger, *Biochem. J.*, **39**, 507 (1945); **45**, 563 (1949).
5) S. Moore and W. H. Stein, *J. Biol. Chem.*, **192**, 663 (1951); **176**, 367 (1948).
6) A. L. Levy, ibid., **213**, 187 (1955); **213**, 487 (1955); *Nature*, **174**, 126 (1954).
7) K. Satake et al., Kagaku no Ryoiki Supplementum, **34**, 77 (1959).
*** The molecular weight of glumamycin is calculated to be 1350 from the adsorbance of DNP-glumamycin (M. Fujino, M. Inoue and A. Miyake; unpublished).
8) J. H. Martin et al., *J. Am. Chem. Soc.*, **60**, 2079 (1960).

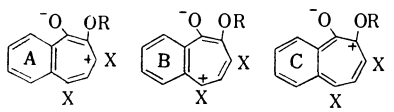
## *Anionoid Substitution of Bromo-3, 4-benzotropolones**

By Seizi EBINE

(Received April 15, 1961)

It was recently reported that 3, 4- and 4, 5-benzotropolones failed to react with thionyl chloride[1]. The present author has studied on anionoid substitution of bromo-3, 4-benzotropolones in detail and the results are summarized herein.

7-Bromo-3, 4-benzotropolone (I) reacts with thionyl chloride to yield an adduct, m. p. 147°C (Found: C, 35.77; H, 1.80. Calcd. for $C_{11}H_7O_2Br \cdot SOCl_2$: C, 35.69; H, 1.91%), which, on recrystallization from ethanol, gives 5, 7-dichloro-3, 4-benzotropolone, m. p. 137°C (Found: C, 54.97; H, 2.40. Calcd. for $C_{11}H_6O_2Cl_2$: C, 54.80; H, 2.51%). 5, 7-Dibromo-3, 4-benzotropolone (II) with thionyl chloride affords the same dichlorobenzotropolone. The methyl ethers of I and II react with dilute hydrochloric acid in methanol at reflux temperature to give 7-chloro-3, 4-benzotropolone methyl ether, m. p. 97°C (Found: C, 65.30; H, 4.06. Calcd. for $C_{12}H_9O_2Cl$: C, 65.31; H, 4.11%) and 5, 7-dichloro-3, 4-benzotropolone methyl ether, m. p. 106°C (Found: C, 56.46; H, 3.11. Calcd. for $C_{12}H_8O_2Cl_2$: C, 56.49; H, 3.16%), respectively. The methyl ether of I, on treatment with dilute alkali in methanol at room temperature, affords 6-hydroxy-7-methoxy-2, 3-benzotropone, m. p. 115~116°C (Found: C, 71.56; H, 5.06. Calcd. for $C_{12}H_{10}O_3$: C, 71.28; H, 4.99%). In these reactions, the hydroxyl groups of bromobenzotropolones and the methoxyl groups of their methyl ethers remained unaffected, whereas the bromine atoms at 5- and 7-positions of these compounds were replaced with ease.




These behaviors of bromobenzotropolones and their methyl ethers are different from those of monocyclic bromotropolones and their methyl ethers; bromotropolones react with thionyl chloride to yield chlorotropones[2] and their methyl ethers, on treatment with dilute alkali are hydrolyzed or further rearranged into aromatic compounds, bromines remaining unreplaced[3]. Such a difference in behavior may be ascribed to the resonance structures of bromobenzotropolones and their methyl ethers. The contribution of the formulas A and B are great but that of the formula C is to a limited extent because its benzene ring is not aromatic but quinonoid, hence the bromines at 5- and 7-positions are highly susceptible to but the 1-hydroxyl and 1-methoxyl groups are almost inert towards the anionoid substitution.

II is reduced with hydriodic acid at 100°C to 5-bromo-3, 4-benzotropolone, m. p. 140°C (Found: C, 52.86; H, 2.67. Calcd. for $C_{11}H_7O_2Br$: C, 52.61; H, 2.81%). The methyl ether of II reacts with hydriodic acid in methanol under reflux to afford 5-bromo-7-iodo-3, 4-benzotropolone methyl ether, m. p. 130~131°C (Found: C, 36.69; H, 2.07. Calcd. for $C_{12}H_8O_2BrI$: C, 36.86; H, 2.06%) and rearranges with dilute alkali in methanol under reflux into 1-hydroxy-4-bromo-2-naphthoic acid, m. p. and mixed m. p. 237°C (decomp.). Coupling of II with diazotized *p*-toluidine produces 2-(*p*-tolylazo)-4-bromo-1-naphthol, m. p. and mixed m. p. 183~184°C. In these reactions, the bromine at 5-position of II or its methyl ether remained unreplaced, presumably because the action of iodide, hydroxide and diazonium ions on the 5-position is sterically hindered due to being the *peri* position of the condensed benzene ring. This fact seems to be another characteristic of bromobenzotropolones.

*Department of Chemistry*
*Saitama University*
*Urawa, Saitama-ken*

* Presented at the 14th Annual Meeting of the Chemical Society of Japan, Tokyo, April, 1961.

1) W. E. Parham, D. A. Bolon and E. E. Schweizer, *J. Am. Chem. Soc.*, **83**, 603 (1961).

2) W. von E. Doering and L. H. Knox, ibid., **74**, 5683 (1952); B. J. Abadir, J. W. Cook, J. D. Loudon and D. K. V. Steel, *J. Chem. Soc.*, **1952**, 2350.

3) T. Nozoe, Y. Kitahara and S. Masamune, *Proc. Japan Acad.*, **27**, 649 (1951).

## *The Synthesis of 3-α-Carboxyethylcyclopentanol Lactone**

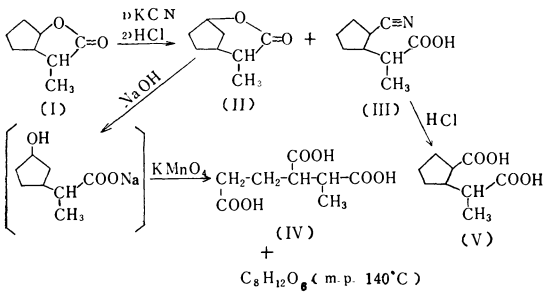
By Tsuguo TANAKA

(Received April 15, 1961)

The synthesis of *cis*- and *trans*-lactones of 2-α-carboxyethylcyclopentanol was previously reported[1].

Now, *cis*-3-α-carboxyethylcyclopentanol lactone was obtained as one of the reaction products of *cis*-2-α-carboxyethylcyclopentanol lactone with potassium cyanide. The formation of this lactone indicates a possibility of a new rearrangement[2] reaction.

*cis*-2-α-Carboxyethylcyclopentanol lactone (I) was heated with potassium cyanide[3] in a sealed tube at 250~260°C for 24 hr., and the products were isolated and fractionally distilled. These were lactone $C_8H_{12}O_2$ (II) [b. p. 85~86°C/3.5 mmHg; $\lambda_{max}^{EtOH}$ 211 mμ, $\nu_{max}$ 5.83 μ[4] (C=O), 8.24 μ (C-O); Found: C, 68.05; H, 8.80. Calcd. for $C_8H_{12}O_2$: C, 68.54; H, 8.63%] and a cyanoacid $C_9H_{13}O_2N$ (III) [b. p. 126~127°C/0.6 mmHg; $\lambda_{max}^{EtOH}$ 212.5 mμ, $\nu_{max}$ 5.84 μ (C=O), 4.42 μ (C≡N); Found: C, 64.12; H, 8.22; N, 6.99. Calcd. for $C_9H_{13}O_2N$: C, 64.65; H, 7.84; N, 8.38%].



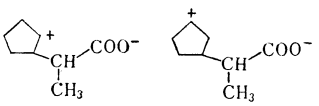

The lactone (II) was hydrolyzed with 10% aqueous sodium hydroxide solution and the sodium salt solution of hydroxyacid was oxidized with potassium permanganate.

Tricarboxylic acids $C_8H_{12}O_6$ (IV) (m. p. 180 °C.; Found: C, 47.05; H, 6.28. Calcd. for $C_8H_{12}O_6$: C, 47.06; H, 5.92%), which was identified as α-methyl-β-carboxyadipic acid[5] both by mixed melting point and infrared spectra, and $C_8H_{12}O_6$ (m. p. 140°C.; Found: C, 47.26; H, 6.21. Calcd. for $C_8H_{12}O_6$: C, 47.06; H, 5.92%), which was not identified[6], were obtained as the oxidation products.

The formation of α-methyl-β-carboxyadipic acid suggested the structure (II) of *cis*-3-α-carboxyethylcyclopentanol lactone.

Hydrolysis of cyanoacid (III) with hydrochloric acid yielded a dicarboxylic acid $C_9H_{14}O_4$ (V) (m. p. 130°C; Found: C, 57.77; H, 7.62. Calcd. for $C_9H_{14}O_4$: C, 58.05; H, 7.58%) in agreement with the structure III of cyanoacid.

The conversion from *cis*-2-α-carboxyethylcyclopentanol lactone into *cis*-3-α-carboxyethylcyclopentanol lactone, would involve intermediates such as anion of III, and carbonium ions VI and VII.



*Department of Chemistry*
*Faculty of Liberal Arts*
*Saga University*
*Honjo, Saga-shi*

* Presented at the 13th Annual Meeting of the Chemical Society of Japan, Tokyo, April, 1960.

1) T. Tanaka, This Bulletin, **32**, 1320 (1959).

2) C. C. Price and W. Kaplan, *J. Am. Chem. Soc.*, **66**, 477 (1944).

3) G. Komppa, *Ber.*, **41**, 4472 (1908); M. A. Haller, *Compt. rend.*, **112**, 446 (1896).

4) R. N. Jones, P. Humphries and K. Dobriner *J. Am. Chem. Soc.*, **72**, 956 (1950); G. Stork and R. Breslow, ibid., **75**, 3291 (1953); A. Lardon, O. Schindler and T. Reichstein, *Helv. Chim. Acta*, **40**, 666 (1957).

5) W. N. Haworth and W. H. Perkin, *J. Chem. Soc.*, **93**, 581 (1908).

6) This acid showed melting point depression by mixed melting with authentic β-(α-carboxyethyl)-glutaric acid reported by Z. H. Skraup, *Monatsh.*, **21**, 907 (1900).

## *The Crystal Structure of Phenazine-5, 10-dioxides*

By Yoshiyuki NAMBA, Tsutomu ODA
and Tokunosuké WATANABÉ

(Received May 4, 1961)

The authors have carried out an investigation of the crystal structure of phenazine-5, 10-dioxide in order to amplify the knowledge of the dative bond, N–O. In the course of the present investigation, the crystal structure of phenazine-*N*-oxide has been published[1].

Phenazine-5, 10-dioxide was prepared by oxidizing phenazine-*N*-oxide. It crystallizes out in needle-like crystals, deep red in color. They decompose at about 190°C. Oscillation and Weissenberg photographs taken with copper $K_\alpha$ radiation, showed that the crystal is monoclinic with the unit cell having the dimensions:

$$a=7.83,\quad b=3.95,\quad c=15.50\,\text{Å},\quad \beta=104°48'$$

and the space group $P2_1/c$. From the observed density, the unit cell was found to contain two molecules, implying that the molecules must be placed at special positions having centers of symmetry. The intensities of reflections, $(h0l)$ and $(0kl)$, obtained by the multiple-film technique were measured by the visual method, using standard scales, and no correction was made for absorption.

Since the dimension of the b-axis is short (3.95 Å), it was expected that there is no overlap of atoms in the projection to the b-plane. The optical transform methods[2] were employed to determine the orientation of the molecule in the unit cell, as well as to determine the signs of the structure factors of strong reflections[3]. The $h0l$ Fourier projection was refined in the usual way and the electron density map, $\rho(xz)$, is shown in Fig. 1. To determine the $z$-coordinates of atoms, we employed usual trial and error methods taking into account the plane structure of this molecule, followed by the least square methods. The atomic arrangement projected along the b and a axes are given in Figs. 2 and 3, respectively. This arrangement of molecules is quite similar to that reported for anthraquinone[4], whose unit cell dimensions are also similar to those of phenazine-5,10-dioxide. The configuration of this molecule is found to be

1) R. Curti et al., *Acta Cryst.*, **14**, 133 (1961).
2) C. A. Taylor, et al., ibid., **4**, 261 (1951).
3) C. A. Taylor and H. Lipson, *Nature*, **167**, 809 (1951); T. Watanabé and M. Otsuka, *Acta Cryst.*, **10**, 377 (1957).
4) S. N. Sen, *Indian J. Phys.*, **22**, 347 (1948).

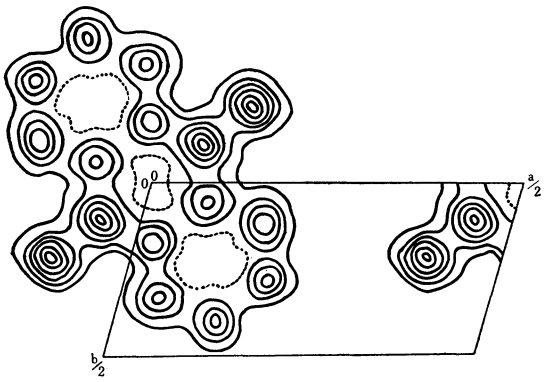



Fig. 1. Electron density map projected on the b plane.

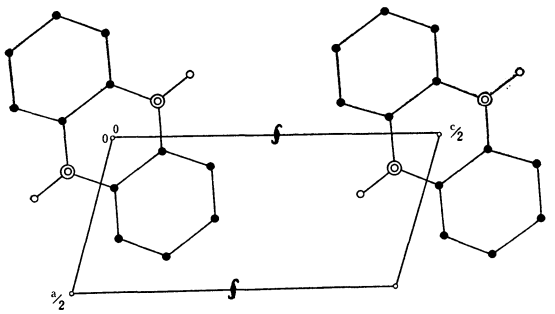



Fig. 2. Projection of the structure, on the b plane.
○ Oxygen, ◎ Nitrogen, ● Carbon.

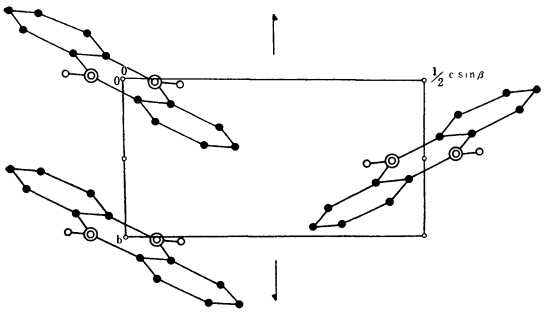



Fig. 3. The view of the structure along the a-axis.

almost planer with reasonable interatomic distances. In phenazine-*N*-oxide, a statistical arrangement of the oxygen atoms has been reported[1]. It is interesting to note that the average structure of phenazine-*N*-oxide is similar to the present structure.

The authors wish to thank Professor E. Matsumura and Mr. H. Takeda for their kind helps for the preparation of this crystal. Part of the cost of this study has been defrayed by a Grant of the Ministry of Education, to which the authors' thanks are due.

*Laboratory of Physical Chemistry*
*Osaka University of Liberal Arts and Education*
*Tennoji, Osaka*
*(Y. N. & T. O.)*

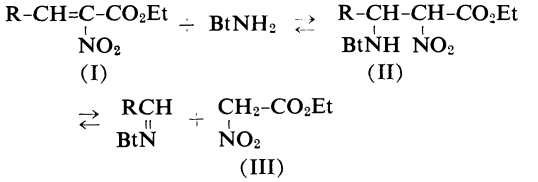
*Department of Physics*
*Osaka University, Osaka*
*(T. W.)*

## *Synthesis of Isoxazolecarboxylic Acids from Schiff Bases and Nitroacetate*[1]

By Shonosuke ZEN and Sumio UMEZAWA

(Received May 9, 1961)

The authors wish to report a new and general method for the synthesis of 4-substituted isoxazole-3, 5-dicarboxylic acids. We have previously reported[2] that dibutylamides of 4-substituted isoxazole-3,5-dicarboxylic acids were obtained when $\alpha, \beta$-unsaturated $\alpha$-nitroesters were treated with *n*-butylamine in an anhydrous solvent, and assumed that the reaction proceeds through a key intermediate IV which is formed by the addition of nitroacetate to $\alpha, \beta$-unsaturated $\alpha$-nitroester. Subsequently, the authors could isolate benzylidene-*n*-butylamine (a Schiff base) from the mother liquor of 4-phenyl-3, 5-bis(*n*-butylcarbamoyl)isoxazole which is obtained from ethyl $\alpha$-nitrocinnamate by refluxing with *n*-butylamine in absolute ethanol. Therefore, it is suggested that the initial reaction may involve the addition of butylamine to $\alpha, \beta$-unsaturated $\alpha$-nitroester I and the adduct II generates nitroacetate III, which adds to $\alpha, \beta$-unsaturated system of I in the presence of a basic catalyst (*n*-butylamine) by the mechanism of the Michael reaction to give the key intermediate IV, as outlined in the following scheme:



(I) (II) (III)

1) Presented in part at the Division of Organic Chemistry of the 14th Annual Meeting of the Chemical Society of Japan, Tokyo, April, 1961.

2) S. Umezawa and S. Zen, This Bulletin, 33, 1016 (1960).

$$\mathrm{I} + \mathrm{III} \rightarrow \mathrm{EtO_2C\text{-}\underset{\underset{\mathrm{NO_2}}{|}}{\overset{\overset{\mathrm{R\text{-}CH\text{-}CH\text{-}CO_2Et}}{|}}{CH}}\text{-}CH\ NO_2}$$

(IV)

As regards the sequel of the path from IV to bis(*n*-butylcarbamoyl) derivatives of isoxazole, the authors had already mentioned in a previous paper[2].

If the above mechanism is valid, one should be able to obtain the derivatives of isoxazole-3, 5-dicarboxylic acid by the reaction of Schiff bases with nitroacetate in the presence of basic catalysts. The expectation has now been realized. When an excess of *n*-butylamine was added to a mixture of Schiff base (1 mol.) and ethyl nitroacetate (2 mol.) in absolute ethanol, an exothermic reaction occurred. After refluxing for several hours, the mixture was concentrated to give a crystalline solid of bis(*n*-butylcarbamoyl) derivative of isoxazole.

The following compounds were prepared by the general procedure: 4-methyl-3, 5-bis(*n*-butylcarbamoyl)isoxazole*; 4-(*n*-propyl)-3, 5-bis(*n*-butylcarbamoyl)isoxazole (V), m. p. 112.5 ~115.5°C; 4-phenyl-3, 5-bis(*n*-butylcarbamoyl)-isoxazole*, 4-(*p*-nitrophenyl)-3, 5-bis(*n*-butylcarbamoyl)isoxazole (VI), m. p. 133~135°C; 4-(*m*-nitrophenyl)-3, 5-bis(*n*-butylcarbamoyl)-isoxazole (VII), m. p. 168~169°C; 4-(*p*-chlorophenyl)-3, 5-bis(*n*-butylcarbamoyl)isoxazole (VIII), m. p. 126~127°C; 4-(2, 4-dichlorophenyl)-3, 5-bis(*n*-butylcarbamoyl)isoxazole (IX), m. p. 139~140.5°C; 4-(*p*-acetamidophenyl)-3,5-bis(*n*-butylcarbamoyl)isoxazole (X), m. p. 159~160°C; 4-(*p*-dimethylaminophenyl)-3,5-bis(*n*-butylcarbamoyl)isoxazole (XI), m. p. 117~118.5°C.

These derivatives were hydrolyzed with 10% sodium hydroxide in 50% aqueous ethanol at about 60°C to give 4-substituted isoxazole-3, 5-dicarboxylic acids. V, VI, VIII and IX were converted, respectively, to 4-(*n*-propyl)isoxazole-3,5-dicarboxylic acid, m. p. 176~177°C (decomp.), 4-(*p*-nitrophenyl)isoxazole-3, 5-dicarboxylic acid, m. p. 172~174°C (decomp.), 4-(*p*-chlorophenyl)isoxazole-3, 5-dicarboxylic acid, m. p. 187~187.5°C (decomp.), and 4-(2, 4-dichlorophenyl)isoxazole-3, 5-dicarboxylic acid, m. p. 183~186°C (decomp.). The product from X was led to methyl 4-(*p*-aminophenyl)isoxazole-3,5-dicarboxylate, m. p. 163~166°C.

The authors are indebted to Mr. S. Nakada for microanalyses.

*Department of Applied Chemistry*
*Faculty of Engineering*
*Keio University, Tokyo*

* Compounds marked with an asterisk were already prepared by another procedure and reported. S. Umezawa, S. Zen, loc. cit.

# *Polarographic Studies of Metallic Complexes. VI*[1]. *Tetracyanocobaltate(III) Complex*[2]

By Nobufumi MAKI and Ryutaro TSUCHIDA

(Received May 2, 1961)

In the earlier papers[3,4] it was reported that the pentacyanocobaltate(III) complexes are all reduced in one or two steps to cobalt(I) complexes at the dropping mercury electrode (DME)[5].

A similar polarographic behaviour was found in the case of tetracyanocobaltate(III) complex, $Na_5[Co(CN)_4(SO_3)_2]$[6].

Namely, disulphono-tetracyanocobaltate(III) ion[7] gave a well-defined wave of one step at the DME in 0.5 F sodium sulphite supporting electrolyte (Fig. 1). The current is controlled only by diffusion. The diffusion current and the concentration of the depolarizer are linearly related in the concentration range from $5\times10^{-4}$ to $10^{-2}$ F.

The wave, corresponding to an acceptance of two electrons, represents the reduction to a univalent cobalt complex, whose formula is presumed analogously in the cases of cyanocobalt(I) complexes[4,8,9] to be the same as that of the oxidized form. Hence, the process of the electrode reaction is considered as follows:

$$[Co^{III}(CN)_4(SO_3)_2]^{5-} + 2e^- \longrightarrow [Co^{I}(CN)_4(SO_3)_2]^{7-}$$

The above electrode process belongs to the quasi-reversible reaction polarographically. For further detail on this point, an oscillographic-polarographic study will be reported later.

The mechanism of the electron transfer and the change of the electronic configuration for the above reaction are explained by the atomic orbital method[10] as follows.

1) Part V of this series; N. Maki, Y. Shimura and R. Tsuchida, This Bulletin, **32**, 833 (1959).
2) Presented at the Symposium on Polarography, Kyoto, October, 1959.
3) N. Maki, J. Fujita and R. Tsuchida, *Nature*, **183**, 458 (1959).
4) N. Maki, ibid., **185**, 682 (1960).
5) D. N. Hume and I. M. Kolthoff, *J. Am. Chem. Soc.*, **71**, 867 (1949).
6) P. R. Rây and S. C. Chackrabarty, *Z. anorg. u. allgem. Chem.*, **211**, 173 (1933).
7) The "sulphono-group", which is $SO_3^{2-}$ radical bound to the central metal ion by the sulphur atom, is distinguished from the "sulphito-group", $OSO_2^{2-}$ bound by the oxygen.
8) N. Maki, *Nature*, **188**, 227 (1960).
9) W. P. Griffith and G. Wilkinson, *J. Chem. Soc.*, **1959**, 2757.
10) A. A. Vlček, *Collection Czechoslov. Chem. Communs.*, **20**, 894 (1955).

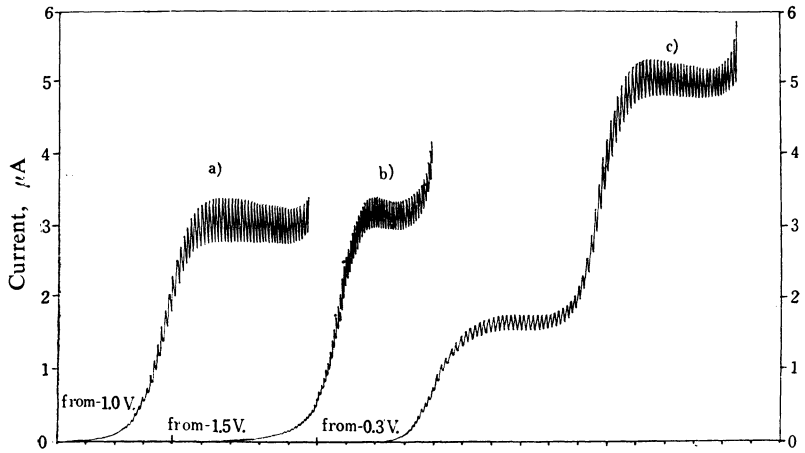



Fig. 1. Polarograms of sulphono- and sulphito-cobalt(III) complexes obtained at the concentration of 0.001 F complex ion in sodium sulphite supporting electrolyte (25°C). Each the height of the waves is seen to be proportional to the electron numbers of reduction process.

a) $Na_5[Co(CN)_4(SO_3)_2]$
Supporting salt: 0.5 F $Na_2SO_3$
Sensitivity: 0.04 μA/mm., Damping: 100, from −1.0 V. vs. S. C. E.
$E_{1/2} = -1.36$ V.

b) $K_4[Co(CN)_5SO_3]\cdot 2H_2O$
Supporting salt 1F $Na_2SO_3$
Sensitivity: 0.04 μA/mm., Damping: 200, from −1.5 V. vs. S. C. E.
$E_{1/2} = -1.54$

c) $[Co(NH_3)_5SO_3]Cl$
Supporting salt: 1F $Na_2SO_3$
Sensitivity: 0.04 μA/mm, Damping: 100, from −0.30 V. vs. S. C. E.
$E_{1/2}$ (1st wave) = −0.74 V., $E_{1/2}$ (2nd wave) = −1.30 V.
Voltage unit: vs. the saturated calomel electrode (S. C. E.), 100 mV./absc.

The acceptance of the electrons occurs in two stages.

$$d^2d^2d^2[D^2SP^3] \xrightarrow{e^-} d^2d^2d^2[D^2SP^3]d^1$$

$$\longrightarrow d^2d^2d^2d^1[DSP^2][PD]$$

$$\xrightarrow{e^-} d^2d^2d^2d^2[DSP^2][PD]$$

First, the electron is accepted into the 4d peripheral orbitals temporarily, where it is held loosely, since the 3d atomic orbitals of Co(III) are fully occupied. After that the consecutive change of the electronic configuration and the placement of the electron in the stable 3d orbitals occur gradually. Thus, the electronic configuration of cobalt(I) complex is considered to consist of a coplanar structure through $3d4s4p^2$ hybrid orbital and a linear structure through 4p4d hybrid orbital separately, so the resulting cobalt(I) ion, $[Co^I(CN)_4\cdot(SO_3)_2]^{7-}$, may probably have a trans-configuration rather than that of cis-one.

*Department of Chemistry*
*Osaka University*
*Kita-ku Osaka*

## *Catalytic Dimerization of Monoalkyl Acetylenes*

By Nobue HAGIHARA, Masuhiko TAMURA, Hiroshi YAMAZAKI and Magosaburo FUJIWARA

(Received May 4, 1961)

It has been described by some investigators[1] that acetylene and substituted acetylenes were polymerized with Ziegler type catalysts forming linear high molecular weight polymer or benzene derivatives.

We observed that with a catalyst obtained in the reaction of chromium tetra-*tert*-butoxide[2] with diethylzinc, monoalkyl acetylenes could be dimerized to the compound I in a good yield.

$$RC{\equiv}C{-}CR{=}CH_2 \qquad (1)$$

1) G. Natta, P. Pino and G. Mazzanti, Belg. Pat. 546151 (1956); W. R. Smith, Brit. Pat. 820510 (1958); B. Franzus, P. J. Canterino and R. A. Wickliffe, *J. Am. Chem. Soc.*, **81**, 1514 (1959).

2) N. Hagihara and H. Yamazaki, ibid., **81**, 3160 (1959); *J. Chem. Soc. Japan, Pure Chem. Sec.* (*Nippon Kagaku Zasshi*), **81**, 821 (1960).

On the other hand, the reaction of monoalkyl acetylenes resulted only in the polymerization to trialkyl benzenes with a catalyst obtained from the reaction of chromium tetra-*tert*-butoxide with triethylaluminum.

*n*-Propylacetylene dimerizes to 2,4-di-*n*-propyl-1-buten-3-yne (II) in almost quantitative yield at 30°C for 10 hr. at $Et_2Zn/(tert\text{-}BuO)_4Cr$ ratio of 3. II is colorless liquid and boils at 88~89°C (40 mmHg) ($n_D^{20}=1.455$, Found: C, 87.80; H, 11.76. Calcd. for $C_{10}H_{16}$: C, 88.16; H, 11.84%). Fifteen moles of dimer per mole chromium compound were obtained.

The structure of the dimer was estimated as I by molecular weight determination and the presence of infrared absorption corresponding $-C\equiv C-$ and $>C=CH_2$ at 2230 and 890 $cm^{-1}$. Identity was established by comparison of the infrared spectrum with that of authentic sample (b. p. 87~88°C (40 mmHg), $n_D^{20}=1.457$, Found: C, 87.77; H, 11.97. Calcd. for $C_{10}H_{16}$: C, 88.16; H, 11.84%) which was prepared from 4-nonyen-6-one ($C_3H_7C\equiv C-COC_3H_7$) and methylene triphenyl phosphorane ($Ph_3P=CH_2$) according to the Wittig reaction.

Optimum ratio of diethylzinc to chromium tetra-*tert*-butoxide was 3 to 1. Although rate of the reaction is fast at high temperature, the formation of tri-*n*-propyl-benzene and high polymer is often considerable in this case.

This type of dimerization is not limited to *n*-propyl-acetylene. *n*-Butylacetylene was dimerized to 2,4-di-*n*-butyl-1-buten-3-yne (b. p. 64.5~65.0°C (5 mmHg), $n_D^{20}=1.459$, Found: C, 87.38; H, 12.31. Calcd. for $C_{12}H_{20}$: C, 87.73; H, 12.27%) and *tert*-butylacetylene to 2,4-di-*tert*-butyl-1-buten-3-yne (b. p. 92~93°C (90 mmHg), $n_D^{20}=1.438$, Found: C, 87.45; H, 11.90. Calcd. for $C_{12}H_{20}$: C, 87.73; H, 12.27%).

It is interesting that the catalytic dimerization of monoalkyl acetylenes with the catalyst in the present work gives exclusively I without the formation of 1,4-dialkylbutenyne ($RC\equiv C-CH=CHR$).

*Osaka University*
*The Institute of Scientific and Industrial Research*
*Sakai, Osaka*

# *Electron Spin Resonance of Tetracene-Antimony Pentachloride*

By Yoshio MATSUNAGA*

(Received April 7, 1961)

It has been known that aromatic hydrocarbons give deeply colored unstable molecular compounds with antimony pentachloride[1]. Brass and his coworkers have reported the isolation of some compounds consisting of two molecules of hydrocarbon and one of antimony pentachloride[2,3]. Recently Weissman and his coworkers have observed the ESR of some of these molecular compounds both in the solid and in the dissolved states. They have suggested that singly charged hydrocarbon positive ions, which are formed by oxidation with antimony pentachloride, are responsible for, at least, part of the observed paramagnetism[4]. Hoijtink and Weijland have also pointed out the fact that the electronic absorption spectrum of perylene with antimony pentachloride in chloroform is closely similar to that of perylene monopositive ion produced in concentrated sulfuric acid[5]. Here we wish to report our preliminary ESR experiments on the products given by the reaction of antimony pentachloride with tetracene and also some other aromatic hydrocarbons.

Small amount of powdered hydrocarbon was put into a sample tube for the ESR measurements, then a dried chloroform solution of antimony pentachloride was added. After the solvent and excess of the reagent were quickly removed by evacuation, the ESR of the product in vacuum was recorded at room temperature and at a frequency of 9 kMc./sec. The rapid decrease of intensity of ESR was observed in many cases. The line width was given by the distance between the points of maximum slope. All of $g$-values were found to be near 2.004.

A sharp resonance absorption peak was detected from the products prepared with the following hydrocarbons; 1, 2-benzanthracene, width 2.0 gauss, perylene 1.2, 1, 12-benzperylene 0.6, mesonaphthodianthrence 1.5, bianthryl 1.2, pyranthrene 1.6, and violanthrene 1.7. In

* Present address: Cyanamid European Research Institute, Cologny, Geneva, Switzerland.

1) S. Hilpert and L. Wolf, *Ber.*, **46**, 2215 (1913).
2) K. Brass and E. Tengler, ibid., **64**, 1650 (1931).
3) K. Brass and K. Fanta, ibid., **69**, 1 (1936).
4) S. I. Weissman, E. de Boer and J. J. Conradi, *J. Chem. Phys.*, **26**, 963 (1957).
5) G. J. Hoijtink and W. P. Weijland, *Rec. trav. chim.*, **76**, 836 (1957).

the other case the spectrum was found to consist of two or three absorption peaks. The product from anthracene gives two peaks. The widths of the two may be in the range from 3.5 to 5.5 gauss. Three peaks were observed from the mixture of chrysene and antimony pentachloride. The peak in the highest magnetic field has a width of 0.9 gauss, the central one about 2.5 gauss, and the last 2.5 gauss. The separation between the first and the last is about 5.5 gauss. The estimation of these widths can not be accurate because of overlapping of the peaks. It is not yet clear whether the appearance of two or three peaks in the present cases is due to the coexistence of two or three kinds of paramagnetic species or due to the anisotropy of *g*-value in one species. However, the formation of two kinds of compounds could be definitely shown in the case of tetracene.

The spectrum obtained from the mixture of tetracene and antimony pentachloride consists of one sharp peak with a *g*-value of 2.0045 and one broad one with a *g*-value of 2.0056.

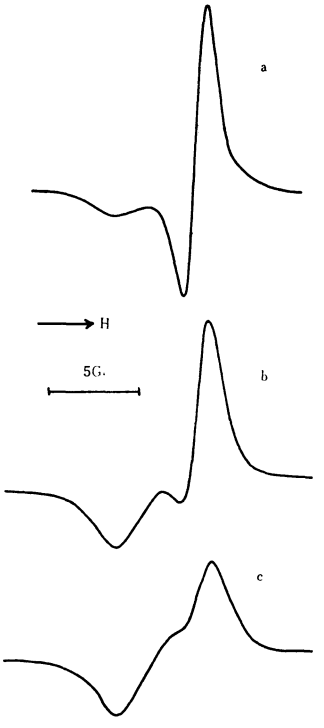



Fig. 1. Derivatives of ESR from tetracene and antimony pentachloride. a ; tetracene with excess of antimony pentachloride, b and c ; after removal of some amount of the reagent.

Their intensities were found to depend on the ratio of antimony pentachloride to the hydrocarbon. As shown in Fig. 1a, a sharp peak appeared in the presence of an excess of antimony pentachloride. On the removal of some amount of the reagent this peak with a width of 1.1 gauss decreases its intensity and the broad peak with a width of 5.3 gauss becomes stronger as seen in Figs. 1b and c. The reverse change could be observed on addition of antimony pentachloride. We observed also that the intensities of two peaks with *g*-values of 2.0039 and 2.0048 respectively from the mixture of triphenylene and antimony pentachloride depend similarly on the condition of preparation.

One of the two peaks, probably the broad one, appeared on addition of antimony pentachloride to tetracene may arise from the fairly stable molecular compound $2C_{18}H_{12}\cdot SbCl_5$ described by Brass and Fanta[3]. It is apparent that the species, which gives the peak with a *g*-value of 2.0045, is formed by the further addition of the complex-forming agent to the species which gives the broad peak with a *g*-value of 2.0056. The shift of *g*-value found here seems to be consistent with Wahler and Thon's observation that the magnitude of *g*-value of diarylnitrogen oxide in solution shows a marked decrease by the addition of *m*-dinitro- or *s*-trinitrobenzene[6]. The *g*-value of hydrocarbon monopositive ions in sulfuric acid has been reported to be 2.0028[7] and that of perylene perchlorate 2.0025[8]. It is unlikely that the *g*-value of paramagnetic tetracene ion becomes as high as 2.0056 by the interaction with antimony compound. Therefore, the species observed here may be not the salts of tetracene monopositive ion but the molecular compounds between the hydrocarbon and antimony pentachloride as reported by Brass[2,3]. The paramagnetic molecular compounds where the ground-state is supposed to be chiefly of non-bonding have been found in the case of aromatic hydrocarbons with halogens[9,10].

*Department of Chemistry*
*Faculty of Science*
*The University of Tokyo*
*Hongo, Tokyo*

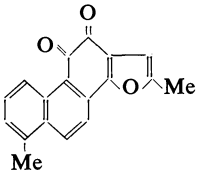
6) B. E. Wahler and H. G. Thon, *Arch. Sci. (Geneva)*, **11**, 165 (1958).
7) A. Carrington, F. Dravnieks and M. C. R. Symons, *J. Chem. Soc.*, **1959**, 947.
8) Y. Matsunaga, This Bulletin, to be published.
9) Y. Matsunaga, ibid., **28**, 475 (1955).
10) Y. Matsunaga, *J. Chem. Phys.*, **30**, 855 (1959).

# *The Structure of Tanshinone-II**

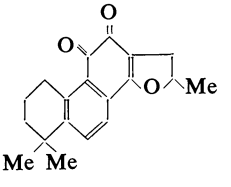
By Yasuaki OKUMURA, Hiroshi KAKISAWA, Mitsuko KATO and Yoshimasa HIRATA

(Received December 12, 1960)

Nakano and Fukushima isolated[1] three pigments, tanshinone-I, tanshinone-II and tanshinone-III, from the root of *Salvia miltorrhiza* Bge. (Chinese drug, Tan-shen). Among these pigments, tanshinone-III was shown afterwards by Takiura[2] to be a mixture of tanshinone-II and a new pigment, cryptotanshinone. Von Wessely et al.[3] proved that tanshinone-I was a condensed phenanthrenequinone of the structure I, and cryptotanshinone was proved by Takiura[4] to have the diterpenoid naphthoquinone structure II.



I



II

Von Wessely and Lauterbach[5] worked on the chromophore of tanshinone-II but the whole structure of this pigment was not clarified. Thomson assigned a structure to tanshinone-II in his book[6], but it has no experimental basis.

Tanshinone-II is an orange-red substance of molecular formula $C_{19}H_{18}O_3$. It is shown to be an *o*-quinone by formation of a quinoxaline derivative on condensation with *o*-phenylenediamine[2] and from infrared absorption maxima at 1701 and 1650 $cm^{-1}$ attributed to quinone carbonyl absorptions. The ultraviolet absorption spectrum of this substance has four absorption maxima at 223, 268, 344 and 457 m$\mu$ and is obviously different from those of tanshinone-I and cryptotanshinone (Fig. 1). Leucotanshinone-II-diacetate and leucotanshinone-II-dimethyl ether (VI) derived from tanshinone-II by reductive acetylation and reductive methylation, respectively, show ultra-

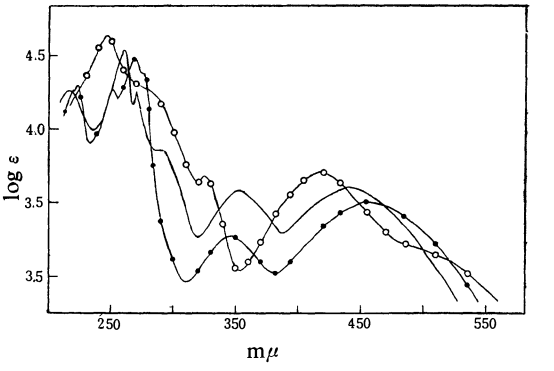



Fig. 1. Ultraviolet absorption spectra of tanshinones;
—○— Tanshinone-I, —•— Tanshinone-II,
—— Cryptotanshinone in ethyl alcohol.

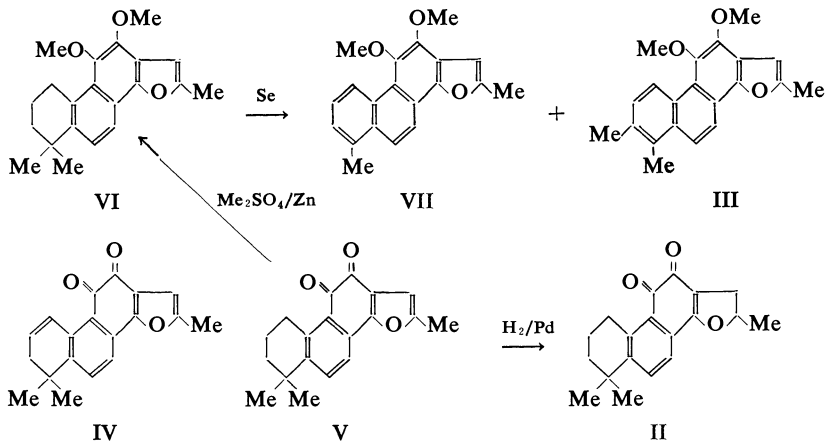
violet absorption maxia at 250, 257, 326 and 342 m$\mu$, and their spectra are distinctly different from those of leucotanshinone-I-dimethyl ether ($\lambda_{max}$: 270, 316 and 347 m$\mu$) and of 1-ethoxy-3, 4-diacetoxy-naphthalene ($\lambda_{max}$: 295, 323 m$\mu$), synthesized as a model compound. The characteristics in the ultraviolet absorption show that tanshinone-II is neither a furanophenanthrenequinone, like tanshinone-I, nor merely an *o*-naphthoquinone derivative, like cryptotanshinone.

Of the three oxygen atoms of tanshinone-II, $C_{19}H_{18}O_3$, two are attributable to quinone carbonyls, while the third must be in an ether structure, since tanshinone-II and leucotanshinone-II-diacetate show no O–H stretching absorption and leucotanshinone-II-dimethyl ether shows no C=O stretching absorption in their infrared spectra.

The ultraviolet absorption spectrum of the semicrystalline solid which was obtained from leucotanshinone-II-dimethyl ether (VI) by Se-dehydrogenation under a mild condition is almost identical with that of leucotanshinone-I-dimethyl ether (VII), so it is conceivable that tanshinone-II has the same carbon skeleton as tanshinone-I. But this dehydrogenation product is not identical with leucotanshinone-I-dimethyl ether in its infrared spectrum, and it shows two fluorescent spots on paper in chromatography, one of which coincides with leucotanshinone-I-dimethyl ether. Thus, the

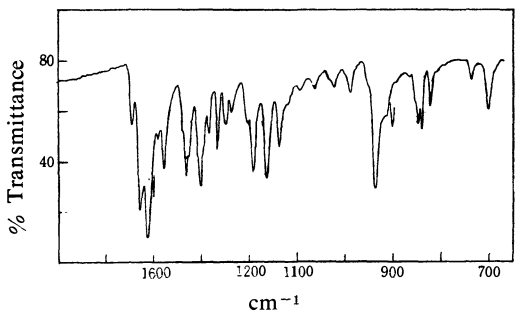
* Presented at the 12th Annual Meeting of the Chemical Society of Japan, Kyoto, April, 1959.

1) M. Nakano and T. Fukushima, *J. Pharm. Soc. Japan* (*Yakugaku Zassi*), **54**, 154 (1934).
2) K. Takiura, ibid., **61**, 475 (1941).
3) F. von Wessely and S. Wang, *Ber.*, **73**, 19 (1940).
4) K. Takiura, *J. Pharm. Soc. Japan* (*Yakuguku Zassi*), **61**, 482 (1941).
5) F. von Wessely and T. Lauterbach, *Ber.*, **75**, 958 (1942).
6) R. H. Thomson, "Naturally Occurring Quinones", Butterworths Sci. Pub. (1957), p. 263.

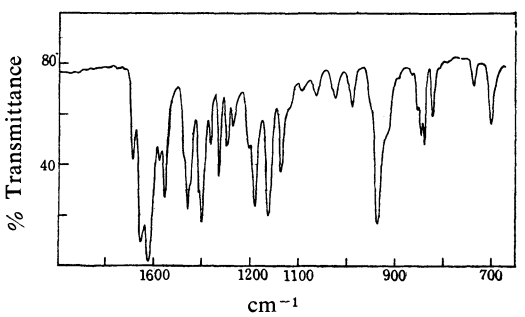



dehydrogenation product is a mixture. Tanshinone-II and its derivatives show absorptions ascribed to a gemdimethyl group at 1381 and 1361 $cm^{-1}$ in their infrared spectra; therefore the second fluorescent spot may be due to the substance III, which can be produced by the migration of one methyl group during the Se-dehydrogenation process[7].

On catalytic hydrogenation with Pd-charcoal in methanol, tanshinone-II absorbs two moles of hydrogen and becomes colorless, but this colorless substance is readily autoxidized to an orange substance. When this hydrogenation product is treated with ferric chloride-acetic acid solution and the separated ferric chloride-complex is decomposed with water, orange needles of melting point 187°C are obtained. The infrared spectrum of this orange substance is identical with that of cryptotanshinone (Fig. 2). Since tanshinone-I, tanshinone-II, and their leuco-derivatives show absorptions characteristic of the furan ring[8] at 3155 and 860 $cm^{-1}$ in their infrared spectra, tanshinone-II must be represented by structure V. If tanshinone-II has structure IV, it must be converted into an alkali-soluble substance by cleavage of the dihydrofuran ring with alkali in the same fashion as cryptotanshinone[4] and β-lapachone[9]. But tanshinone-II does not undergo this transformation, and this fact also supports the structure V[10].




Infrared Spectrum of the hydrogenated tanshinone-II (KBr).




Infrared spectrum of the cryptotanshinone (KBr).

Fig. 2.

## Experimental

All melting points are uncorrected. Infrared spectra were obtained with a Hilger H-800 double beam spectrophotometer and ultraviolet absorption spectra were obtained with Beckman DK-2 spectrophotometer.

**Tanshinone-II.**—The ether extract of roots of *Salvia miltorrhiza* was fractionated according to the method of Takiura, and it gave tanshinone-I (m.p. 231~232°C), cryptotanshinone (m. p. 191°C), and tanshinone-II, (m. p. 211°C).

Ultraviolet absorption maxima in ethanol, log in parentheses: 457 (3.45), 344 (3.23), 268 (4.37), 250 (4.24) and 223 mμ (4.31). Infrared absorptions (KBr): 3157, 1701, 1650, 1584, 1539 and 1505 $cm^{-1}$.

7) H. H. Zeiss and F. W. Grant, Jr., *J. Am. Chem. Soc.*, **79**, 1201 (1957); E. Lederer, F. Marx, D. Mercier and G. Perot, *Helv. Chim. Acta*, **29**, 1354 (1946).

8) "Kagaku no Ryoiki (IR Tokushiu)", 3, Nankodo (1954), p. 101.

9) S. C. Hooker, *J. Chem. Soc.*, **61**, 611 (1892); **69**, 1355 (1896).

10) A private communication from K. Takiura told us that he had reached the same conclusion as ours by other methods.

Found: C, 77.58, 77.71; H, 6.000, 6.033. Calcd for $C_{19}H_{18}O_3$: C, 77.55; H, 6.12%.

**Leucotanshinone-II-diacetate.**—One hundred milligrams of tanshinone-II was heated for five minutes with 0.6 ml. acetic anhydride, 20 mg. fused sodium acetate, and 200 mg. zinc dust. Following removal of the zinc dust, the filtrate was concentrated under reduced pressure in a stream of nitrogen. The residue gave purple-fluorescent white crystals melting at 174~175°C on recrystallization from ethanol.

Ultraviolet absorption maxima in ethanol: 340 (4.23), 324 (3.24), 310 (3.08), 285 (3.72), 257 (shoulder 3.81), 254 (4.81) and 240 mμ (4.74).

Found: C, 72.70, 72.40; H, 6.30, 6.27. Calcd. for $C_{23}H_{24}O_3$: C, 72.61; H, 6.36%.

**Leucotanshinone-II-dimethyl Ether.**—Tanshinone-II (100 mg.) was dissolved in 10 ml. ethanol, and 15 ml. of 10% sodium hydroxide solution was added. On boiling gently in the atmosphere of nitrogen, the mixture turned pale yellow. Then, 6 ml. of dimethyl sulfate was dropped gradually into this boiling mixture. After cooling, the reaction mixture was extracted with ether, and the ether layer was washed with 1 N sodium hydroxide, then with water, and dried with anhydrous sodium sulfate. A pale yellow resinous substance was obtained on evaporation of the solvent under reduced pressure. This was dissolved in hexane and submitted to chromatography on a column of alumina. The fraction eluted by hexane gave white crystals, m. p. 103~104°C, on recrystallization from ethanol.

Ultraviolet absorption maxima in ethanol 343 (3.28), 327 (3.35), 258 (4.95) and 250 mμ (4.84).

Infrared spectrum (KBr), 3157, 1635, 1567, 1520 and 1508 $cm^{-1}$.

Found: C, 77.60, 77.86; H, 7.47, 7.40. Calcd. for $C_{21}H_{22}O_3$: C, 77.75; H, 7.46%.

**Dehydrogenation of Leucotanshinone-II-dimethyl Ether.**—A mixture of 100 mg. leucotanshinone-II-dimethyl ether and 100 mg. selenium powder was heated in a metal bath at 230°C for 24 hr. After cooling, the mixture was extracted three times with 20 ml. ether, and the extracts were combined and washed with dilute sodium hydroxide solution and then with water. On evaporation of ether after drying with anhydrous sodium sulfate, a yellow viscous oil was obtained. This oil was dissolved in hexane and submitted to chromatography on a column of alumina. The fraction eluted by a (9 : 1)-mixture of hexane and benzene gave a semi-crystalline substance, which on crystallization from ethanol melted at 131~140°C.

Ultraviolet absorption maxima in ethanol: 315, 295 and 272 mμ.

**Catalytic Hydrogenation of Tanshinone-II.**—Tanshinone-II (100 mg.) dissolved in 50 ml. of methanol was stirred with 100 mg. of 10% Pd-charcoal in the atmosphere of hydrogen at room temperature. After absorption of 26 ml. of hydrogen the solution became colorless. The catalyst was filtered off, and the filtrate was concentrated under reduced pressure in a stream of nitrogen. The residue was dissolved in 3 ml. of acetic acid, and then treated with ferric chloride-acetic acid solution. Black crystals of ferric chloride-complex were separated on the funnel, washed with glacial acetic acid, and then dried in a vacuum dessicator. This complex was decomposed with water and extracted with ether. The ether extract gave an orange solid on evaporation. This was recrystallized from methanol as orange crystals, m. p. 187°C, the infrared spectra was identical with that of cryptotanshinone (Fig. 2).

**1-Ethoxy-3, 4-diacetoxynaphthalene.**—A mixture of 500 mg. 4-ethoxy-β-naphtoquinone, 1 g. zinc dust, 6 ml. acetic anhydride, and one drop of triethylamine was boiled for 5 min. The cooled mixture was filtered, and the filtrate was evaporated under reduced pressure and resulted in a pale yellow viscous oil. This was recrystallized from ethanol-water.

White prisms, m. p. 106°C. Ultraviolet maxima in ethanol: 323 (3.43) and 295 mμ (3.83).

Found: C, 66.72, 66.54; H, 5.64, 5.71. Calcd. for $C_{16}H_{16}O_5$: C, 66.66; H, 5.59%.

We sincerely acknowledge our debt to Dr. M. Ohara and Mr. S. Ohta at the Research Laboratory of Fujisawa Pharmaceutical Company for providing us with extraction materials and for elemental analyses, respectively.

*Chemical Institute*
*Faculty of Science,*
*Nagoya University*
*Chikusa-ku, Nagoya*

# *The Aconite Alkaloids. XXXV*[1]*. On Lucidusculine. V*[2]

By Takashi AMIYA

(Received December 12, 1960)

Lucidusculine (I) ($C_{24}H_{35}O_4N$) is a monoacetate, and gives on hydrolysis[5,6], a trihydric amino alcohol, luciculine (II) ($C_{22}H_{33}O_3N \cdot H_2O$). In contact with Pd-carbon in the presence of hydrogen and methanol, compound II isomerized to a ketone base, isoluciculine (III) ($C_{22}H_{33}O_3N \cdot 1/2H_2O$), m. p. 131~136°C. The infrared spectrum of compound III shows a band at 1716 $cm^{-1}$ due to a ketone carbonyl group in a six-membered ring, but lacks the bands characteristic of a terminal methylene group, corresponding to the bands (1642 and 907 $cm^{-1}$) of compound II[6,7]. It has already been shown that a terminal methylene group exists in compound II[5]. The ultraviolet absorption spectrum of compound III has a maximum ($\lambda_{max}$ 302 m$\mu$, log $\varepsilon$ 1.4), indicating the presence of a ketone carbonyl group and, therefore, is apparently distinguishable from the ultraviolet spectra[6] of compounds I and II, which show only end absorption (Fig. 1). From these considerations regarding the spectra it may be reasonably concluded that in this isomerization a ketone carbonyl group is newly formed with simultaneous disappearance of a terminal methylene group. Therefore, this reaction seems to proceed similarly to those of Shimoburo base I[8], hypognavine[9], kobusine[10] and napellonine[11,*] as follows:

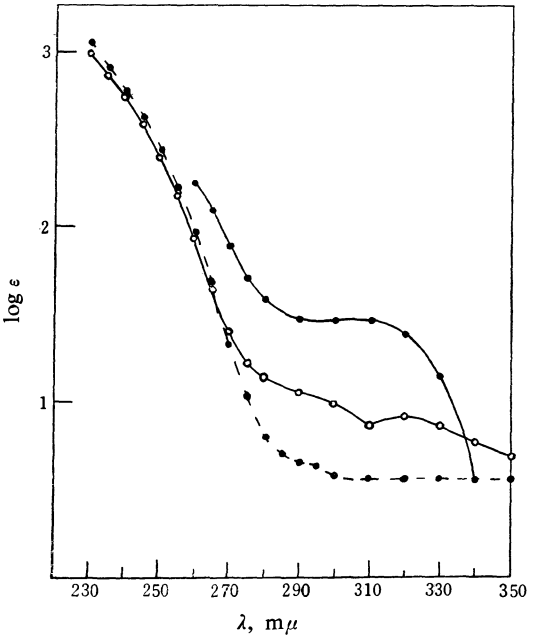
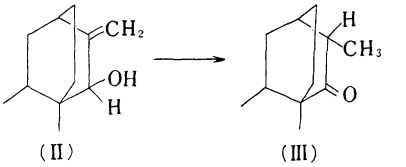



Fig. 1

—○—○— Lucidusculine (I)
--●--●-- Luciculine (II)
—●—●— Isoluciculine (III)




(II) (III)

Fig. 2

On the basis of the observation of this process, the presence of an allyl alcohol moiety constituting a six-membered ring may be claimed in the structure of compound II as shown in Fig. 2.

A report regarding bromoanhydrolucidusculine hydrobromide (IV) has been published[7]. Recently, it has been found that compound IV decomposed spontaneously on standing for about two years. Hence, a freshly prepared sample, m. p. 195°C (decomp.)**, was analyzed once more, and found to have composition $C_{24}H_{37}O_8NBr_2$. The infrared spectrum is nearly identical with that previously described[7]. The detailed data of this compound may be reported latter. The determinations of bromine and

1) The present paper constitutes Part XXXV of the series entitled "The Aconite Alkaloids" by H. Suginome and Part XXXIV[3] corresponds to "On Lucidusculine. IV".

2) A preliminary note partly describing the matter of the present paper appeared in this Bulletin[4].

3) T. Amiya, This Bulletin, 33, 1175 (1960).

4) T. Amiya, ibid., 32, 421 (1959).

5) H. Suginome, T. Amiya and T. Shima, ibid., 32, 824 (1959).

6) T. Amiya, ibid., 32, 1133 (1959).

7) T. Amiya, ibid., 33, 644 (1960).

8) T. Sugasawa, *Pharm. Bull.*, 4, 6 (1956).

9) S. Sakai, ibid., 5, 1 (1957).

10) T. Okamoto, ibid., 7, 44 (1959).

11) K. Wiesner, Z. Valenta, J. F. King, R. K. Maudgal, L. G. Hamber and S. Itô, *Chemistry & Industry*, 1957, 173.

* It has been shown that napellonine is identical with Shimoburo base I[12].

12) K. Wiesner, S. Itô and Z. Valenta, *Experientia*, 14, 167 (1958).

** The melting point given in the previous paper[7] should be revised to this.

specific rotation reported in the previous paper[7] were made by using a sample, freshly prepared then, and the ultraviolet absorption spectrum was measured with the same material once dried at 110°C in vacuo.

## Experimental

**Isoluciculine (III).**—To luciculine (300 mg.) dissolved in 15 cc. of methanol, 10% Pd-C (200 mg.) was added. The mixture was shaken under $H_2$-atmosphere for 2.5 hr. The absorption of $H_2$ proceeded rapidly and practically stopped within 15 min.; in total about 30 cc. of $H_2$ was absorbed. After elimination of the catalyst the solvent was removed, and the residue was crystallized from methanol. The substance melted at 131~136°C. The ultraviolet absorption spectrum of the base in methanol showed $\lambda_{max}$ 302 m$\mu$, log $\varepsilon$ 1.4 (Fig. 1). The infrared absorption spectrum in Nujol had no peak attributable to a terminal methylene group but showed the presence of hydroxyl groups (3375 $cm^{-1}$) and a ketone carbonyl group (1716 $cm^{-1}$).

Found: C, 71.22; H, 9.33; N, 3.32; $H_2O$, 2.33. Calcd. for $C_{22}H_{33}O_3N \cdot 1/2H_2O$: C, 71.72; H, 9.30; N, 3.80; $H_2O$, 2.44%.

**Bromoanhydrolucidusculine Hydrobromide (IV).**—A freshly prepared sample showed m. p. 195°C (decomp.). The infrared absorption spectrum in Nujol showed the presence of hydroxyl groups (3410~3360 $cm^{-1}$), and acetoxyl group (1724 and 1235 $cm^{-1}$) and water (1628 $cm^{-1}$). It showed no peak attributable to a terminal methylene group.

Found: C, 45.57, 45.57; H, 5.85, 6.08. Calcd. for $C_{24}H_{37}O_8NBr$: C, 45.92; H, 5.94%.

## Summary

Luciculine (II) was isomerized to a ketone base, isoluciculine (III), and this fact shows the presence of an allyl alcohol system in the structure of compound II. The previous report concerning bromoanhydrolucidusculine hydrobromide (IV) was in part revised.

The author wishes to express his sincere thanks to Professor Harusada Suginome, President of Hokkaido University, for his unfailing kindness in encouraging this work.

*Department of Chemistry*
*Faculty of Science*
*Hokkaido University*

# *Out-of-Plane Hydrogen Vibrations of ortho-, meta- and para-Deuterated Mono-substituted Benzenes*

By Yuzo KAKIUTI and Jiro OGURA

(Received December 19, 1960)

The authors have recently reported a theoretical explanation of the out-of-plane CH vibrations of benzene derivatives for both the fundamentals and their combination tones which appear in the regions of 650 to 1000 $cm^{-1}$ and of 1650 to 2000 $cm^{-1}$, respectively[1,2]. The results of the calculations were in good agreement with those observed[1-3]. This enabled us to calculate frequencies and absorption intensities of the out-of-plane hydrogen vibration bands for some deuterium homologs of benzene derivatives.

In the present paper, normal coordinate treatments have been made on the out-of-plane hydrogen vibrations for *ortho-*, *meta-* and *para-*deuterated compounds of mono-substituted benzenes. This treatment seems to be applicable for the identification of each molecule as well as for the purpose of confirming the validity of our earlier theories[1,2].

## Calculated Frequencies

The normal coordinate treatment was carried out according to the method using $\boldsymbol{G}$ and $\boldsymbol{F}$ matrices, as introduced by Wilson[4]. The procedures of the calculations were the same as those given in the preceding papers[1,2], except for some minor modifications in the form of the $\boldsymbol{G}$ matrix.

Fig. 1 shows the molecular model used, where X is a substituent atom or group and

1) T. Shimanouchi, Y. Kakiuti and I. Gamo, *J. Chem. Phys.*, **25**, 1245 (1956); Y. Kakiuti, *J. Chem. Soc. Japan, Pure Chem. Sec.* (*Nippon Kagaku Zasshi*), **77**, 1572, 1591 (1956).

2) Y. Kakiuti, *J. Chem. Phys.*, **25**, 777 (1956); *J. Chem. Soc. Japan, Pure Chem. Sec.* (*Nippon Kagaku Zasshi*), **77**, 1839 (1956).

3) Y. Kakiuchi, ibid., **80**, 28 (1959).

4) E. B. Wilson, Jr., *J. Chem. Phys.*, **7**, 1047 (1939); **9**, 76 (1941).

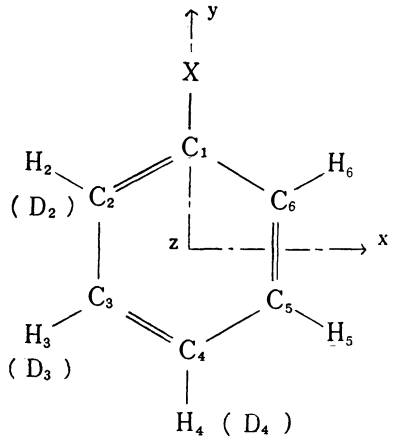



Fig. 1. *o*-, *m*- and *p*-Deuterated mono-substituted benzene.

| | $r_2\gamma_2$ | $r_3\gamma_3$ | $r_4\gamma_4$ | $r_5\gamma_5$ | $r_6\gamma_6$ | $\sigma_2$ | $\sigma_3$ | $\sigma_4$ |
|---|---|---|---|---|---|---|---|---|
| $r_2\gamma_2$ | $H$ | $J$ | $K$ | 0 | $K$ | $u$ | $-v$ | $w$ |
| $r_3\gamma_3$ | | $H$ | $J$ | $K$ | 0 | $-u$ | $v$ | $w$ |
| $r_4\gamma_4$ | | | $H$ | $J$ | $K$ | $u$ | 0 | $-2w$ |
| $r_5\gamma_5$ | | | | $H$ | $J$ | $-u$ | $-v$ | $w$ |
| $r_6\gamma_6$ | (Symmetric) | | | | $H$ | $u$ | $v$ | $w$ |
| $\sigma_2$ | | | | | | $P$ | 0 | 0 |
| $\sigma_3$ | | | | | | | $Q$ | 0 |
| $\sigma_4$ | | | | | | | | $Q$ |

Fig. 2. $\boldsymbol{G}$ or $\boldsymbol{F}$ matrix.

H(D) denotes H or D atom; that is, *ortho*-, *meta*- and *para*-deuterated molecules are designated as 1-X-benzene-2-*d* -3-*d* and -4-*d*, respectively. The $\boldsymbol{G}$ and $\boldsymbol{F}$ matrices are expressed as shown in Fig. 2, where the meanings of the notations are as given in the preceding papers[1]; that is, $r_0$ is the equilibrium length of C–H or D bond, $\gamma_i$ and $\sigma_i$ are the internal coordinates referring to bending of the $C_i$–$H_i$ or $D_i$ bond and twisting of the C–C bond, respectively.

The approximation according to Crawford, Edsall and Wilson[4,5] has been applied, and the first row and column corresponding to the low-frequency coordinate of the substituent (X), $r_1\gamma_1$ are omitted. As shown in Table I, the values of the elements of the $\boldsymbol{G}$ matrix are nearly the same as those presented in our earlier papers[1], and those of the $\boldsymbol{F}$ matrix are exactly the same, because the same force constants obtained by the analysis of out-of-plane vibrations of benzene and its deuterium homologs[6] were also applied in this case.

5) B. L. Crawford, Jr. and J. T. Edsall, ibid., 7, 223 (1939).

6) Y. Kakiuti and T. Shimanouchi, ibid., 25, 1252 (1956); Y. Kakiuti, *J. Chem. Soc. Japan, Pure Chem. Sec.* (*Nippon Kagaku Zasshi*), 80, 21 (1959).

TABLE I. ELEMENTS OF $\boldsymbol{G}$ AND $\boldsymbol{F}$ MATRICES SHOWN IN FIG. 2 (FORCE CONSTANT IN mdyn./Å, LENGTH IN Å, AND MASS IN amu)

| | in $\boldsymbol{G}$ | in $\boldsymbol{F}$ |
|---|---|---|
| $H$ | 1.635888 (1.140309)[a] | 0.402 |
| $J$ | −0.330622 | −0.073 |
| $K$ | 0.050292 | 0 |
| $P$ | 3.998719 | 0.205 |
| $Q$ | 1.332906 | 0.193 |
| $u$ | 0.967934 | −0.106961 |
| $v$ | 0.554978 | −0.113449 |
| $w$ | 0.320417 | −0.0655 |

a) When a hydrogen atom is replaced by deuterium, the $H$-value in parenthesis must be used (See text).

Exchanging the H atom for the D affects only the value of the corresponding diagonal term, $H$, in the $\boldsymbol{G}$ matrix. When the hydrogen atom of the $i$-th $C_i$–$H_i$ bond shown in Fig. 1 is replaced by deuterium, the $H$-value in parenthesis shown in Table I must be used for the diagonal term corresponding to the coordinate $r_i\gamma_i$ in the $\boldsymbol{G}$ matrix.

The secular equation to be solved is expressed as

$$| \boldsymbol{GF}-\boldsymbol{E}\lambda | =0 \qquad (1)$$

where $\boldsymbol{E}$ is the unit matrix, $\lambda$ is $4\pi^2\boldsymbol{c}^2\nu^2$, $\boldsymbol{c}$ is the light velocity, and $\nu$ is the wave number. In the case of the *para*-deuterated molecule, the secular Eq. 1 is further split due to the symmetry of the molecule by using suitable symmetry coordinates which are shown in Table II, where the $s_1$, $s_2$ and $\sigma_3$ belong to the species $A_2$ and the $s_3$, $s_4$, $s_5$, $\sigma_2$ and $\sigma_4$ to the species $B_2$. The roots of the secular equation of each molecule are shown in Table III and illustrated in Fig. 3. The Latin and Greek notations denote the fundamentals and binary combinations, respectively.

TABLE II. SYMMETRY COORDINATES USED FOR *p*-DEUTERATED MONO-SUBSTITUTED BENZENE

| | $r_2\gamma_2$ | $r_3\gamma_3$ | $r_4\gamma_4$ | $r_5\gamma_5$ | $r_6\gamma_6$ |
|---|---|---|---|---|---|
| $s_1$[a] | 1/2 | −1/2 | 0 | 1/2 | −1/2 |
| $s_2$ | 1/2 | 1/2 | 0 | −1/2 | −1/2 |
| $s_3$ | 1/2 | 1/2 | 0 | 1/2 | 1/2 |
| $s_4$ | 1/2 | −1/2 | 0 | −1/2 | 1/2 |
| $s_5$ | 0 | 0 | 1 | 0 | 0 |

a) For example, $s_1=(r_2\gamma_2-r_3\gamma_3+r_5\gamma_5-r_6\gamma_6)/2$.

## Normal Coordinates

When the relation between the normal coordinates and the intensity in infrared absorption is discussed, it is necessary to express normal coordinates, $Q$, in terms of Cartesian displacement coordinates, $Z$, as discussed

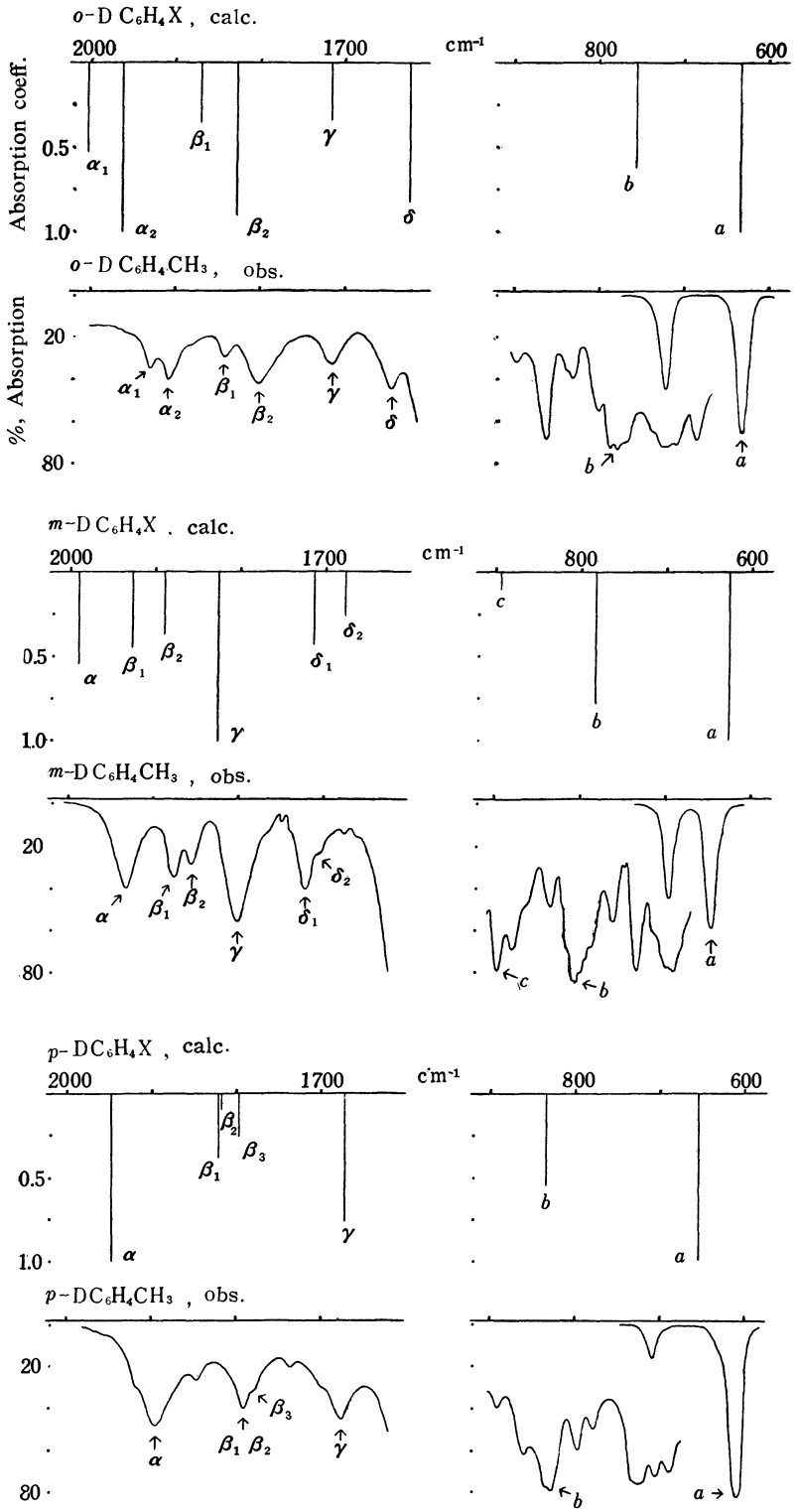



Fig. 3. Illustration of calculated frequencies, absorption intensities, and observed absorption spectra[9,10] (See Table III.).

TABLE III-A. FUNDAMENTALS OUT-OF-PLANE HYDROGEN VIBRATIONS

| Freq. calc., $cm^{-1}$ | | $\kappa_i$[a] calcd. | For $DC_6H_4CH_3$ Freq. anal. $cm^{-1}$ | For $DC_6H_4CH_3$[9,10] freq. obs. $cm^{-1}$ | For $DC_6H_4CH_3$[9,10] %, absorption obs. |
|---|---|---|---|---|---|
| *o*-$DC_6H_4X(C_s)$ | | | | | |
| $A''$(IR,R) | *a* 634 | 1.000 | 631 | 631 | very strong |
| | *b* 756 | 0.621 | 779 | 775 | 75, broad |
| | *c* 868 | 0.000 | 867 | | |
| | *d* 960 | 0.036 | 937 | | |
| | *e* 1002 | 0.000 | 968 | | |
| *m*-$DC_6H_4X(C_s)$ | | | | | |
| $A''$(IR,R) | *a* 626 | 1.000 | 645 | 645 | very strong |
| | *b* 782 | 0.776 | 813 | 806 | 90, broad |
| | *c* 894 | 0.101 | 891 | 894 | 80 |
| | *d* 931 | 0.055 | 909 | | |
| | *e* 995 | 0.000 | 965 | | |
| *p*-$DC_6H_4X(C_{2v})$ | | | | | |
| $B_2$(IR,R) | *a* 630 | 1.000 | 607 | 607 | very strong |
| | *b* 835 | 0.551 | 838 | 838 | 80, broad |
| | *c* 963 | 0.007 | 942 | | |
| $A_2$(R) | *d* 837 | 0 | 837 | | |
| | *e* 984 | 0 | 952 | | |

a) Relative values for each molecule.

TABLE III-B. BINARY COMBINATIONS OF OUT-OF-PLANE HYDROGEN VIBRATIONS

| Freq. calc., $cm^{-1}$ | | | $\kappa_{ij}$ calcd.[a] | For $DC_6H_4CH_3$ freq. anal. $cm^{-1}$ | For $DC_6H_4CH_3$[9,10] freq. obs. $cm^{-1}$ | For $DC_6H_4CH_3$[9,10] %, absorption obs. |
|---|---|---|---|---|---|---|
| | *o*-$DC_6H_4X$ ($C_s$) | | | | | |
| $\alpha_1$ | 2*e* | 2004 | 0.534 | 1936 | 1930 | 35 |
| $\alpha_2$ | *d*+*e* | 1962 | 1.000 | 1905 | 1908 | 40 |
| $\beta_1$ | *c*+*e* | 1870 | 0.359 | 1835 | 1842 | 30 |
| $\beta_2$ | *c*+*d* | 1828 | 0.904 | 1804 | 1800 | 40 |
| $\gamma$ | *b*+*d* | 1716 | 0.346 | 1716 | 1718 | 30 |
| $\delta$ | *b*+*c* | 1624 | 0.821 | 1646 | 1645 | 45 |
| | 2*b* | 1512 | 0.234 | 1558 | | |
| | *a*+*c* | 1502 | 0.464 | 1498 | | |
| | *a*+*b* | 1390 | 0.295 | 1410 | | |
| | 2*a* | 1268 | 0.274 | 1262 | | |
| | *m*-$DC_6H_4X$ ($C_s$) | | | | | |
| $\alpha$ | 2*e* | 1990 | 0.550 | 1930 | 1931 | 40 |
| $\beta_1$ | *d*+*e* | 1926 | 0.462 | 1874 | 1875 | 35 |
| $\beta_2$ | *c*+*e* | 1889 | 0.376 | 1856 | 1855 | 30 |
| $\gamma$ | *c*+*d* | 1825 | 1.000 | 1800 | 1800 | 55 |
| $\delta_1$ | *b*+*d* | 1713 | 0.443 | 1722 | 1721 | 40 |
| $\delta_2$ | *b*+*c* | 1676 | 0.270 | 1704 | 1705 | 20 |
| | 2*b* | 1564 | 0.190 | 1626 | | |
| | *a*+*c* | 1520 | 0.341 | 1536 | | |
| | *a*+*b* | 1408 | 0.155 | 1458 | | |
| | 2*a* | 1252 | 0.286 | 1290 | | |
| | *p*-$DC_6H_4X$ ($C_{2v}$) | | | | | |
| $\alpha$ | *c*+*e* | 1947 | 1.000 | 1894 | 1894 | 50 |
| $\beta_1$ | *d*+*e* | 1821 | 0.391 | 1789 | 1789 | 40 |
| $\beta_2$ | *b*+*e* | 1819 | 0.104 | 1790 | | |
| $\beta_3$ | *b*+*c* | 1798 | 0.261 | 1780 | ~1780 | ~30 |
| $\gamma$ | *b*+*d* | 1672 | 0.773 | 1675 | 1675 | 45 |
| | *a*+*d* | 1467 | 0.418 | 1444 | | |
| | *a*+*b* | 1465 | 0.107 | 1445 | | |
| | 2*a* | 1260 | 0.192 | 1214 | | |

a) Relative values for each molecule. The combinations whose $\kappa_{ij}$-values are very small, are omitted in this Table.

TABLE IV. ELEMENTS OF $L$-MATRICES[a] (FOR THE UNITS USED, SEE TABLE I)

*o*-$DC_6H_4X$ ($C_s$)

| Freq. calcd.[b] cm$^{-1}$ | 388 | 459 | 634† | 756† | 802 | 868† | 960† | 1002† |
|---|---|---|---|---|---|---|---|---|
| | $A''$(IR,R) | | | | | | | |
| $Z(C_1)$ | 0.0170 | −0.1409 | −0.0213 | 0.0974 | −0.1281 | 0.0109 | 0.0070 | 0.0003 |
| $Z(C_2)$ | −0.1064 | 0.0300 | −0.1094 | −0.0011 | 0.1512 | −0.0388 | −0.0389 | −0.0059 |
| $Z(C_3)$ | 0.1297 | 0.1409 | −0.0394 | 0.0237 | −0.0585 | 0.0816 | 0.0828 | 0.0497 |
| $Z(C_4)$ | 0.0015 | −0.1637 | 0.0074 | −0.0917 | 0.0307 | 0.0543 | −0.0423 | −0.0824 |
| $Z(C_5)$ | −0.1341 | 0.0927 | −0.0406 | −0.0083 | −0.1057 | −0.0236 | −0.0577 | 0.0783 |
| $Z(C_6)$ | 0.1193 | 0.0538 | 0.0364 | −0.1031 | 0.0684 | −0.0891 | 0.0658 | −0.0401 |
| $Z(D_2)$ | −0.2555 | 0.0686 | 0.5262 | −0.2107 | −0.0929 | 0.0975 | 0.0960 | 0.0202 |
| $Z(H_3)$ | 0.2113 | 0.1834 | 0.2906 | 0.2944 | −0.1451 | −0.4863 | −0.5369 | −0.3386 |
| $Z(H_4)$ | 0.0216 | −0.2873 | 0.2727 | 0.3458 | 0.2892 | −0.4030 | 0.2517 | 0.5625 |
| $Z(H_5)$ | −0.2421 | 0.1567 | 0.1252 | 0.5482 | 0.1828 | 0.2061 | 0.3963 | −0.5324 |
| $Z(H_6)$ | 0.1981 | 0.0862 | 0.2481 | 0.2231 | 0.3577 | 0.5449 | −0.5011 | 0.2713 |

*m*-$DC_6H_4X$ ($C_s$)

| Freq. calcd.[b] cm$^{-1}$ | 385 | 453 | 626† | 782† | 801 | 894† | 931† | 995† |
|---|---|---|---|---|---|---|---|---|
| | $A''$(IR,R) | | | | | | | |
| $Z(C_1)$ | 0.0096 | −0.1299 | 0.0645 | −0.1010 | 0.1132 | 0.0001 | 0.0103 | 0.0004 |
| $Z(C_2)$ | 0.1285 | 0.0561 | −0.0374 | 0.0809 | −0.0654 | −0.0952 | −0.0799 | 0.0173 |
| $Z(C_3)$ | −0.1125 | 0.0615 | −0.1256 | −0.0033 | 0.1194 | 0.0228 | 0.0624 | 0.0094 |
| $Z(C_4)$ | 0.0288 | −0.1682 | −0.0276 | 0.0085 | −0.0687 | 0.0610 | −0.0771 | −0.0669 |
| $Z(C_5)$ | 0.1087 | 0.1201 | 0.0080 | −0.1112 | 0.0035 | 0.0271 | 0.0057 | 0.0942 |
| $Z(C_6)$ | −0.1330 | 0.0254 | −0.0398 | 0.0331 | −0.1274 | −0.0494 | 0.0641 | −0.0588 |
| $Z(H_2)$ | 0.2091 | 0.1071 | 0.2444 | 0.1774 | −0.2117 | 0.6817 | 0.4862 | −0.1124 |
| $Z(D_3)$ | −0.2699 | 0.1669 | 0.4916 | −0.1643 | −0.1329 | −0.0590 | −0.1757 | −0.0303 |
| $Z(H_4)$ | 0.0306 | −0.2789 | 0.3069 | 0.3654 | 0.0646 | −0.3919 | 0.4873 | 0.4571 |
| $Z(H_5)$ | 0.1826 | 0.2134 | 0.2508 | 0.3649 | 0.4811 | −0.1544 | 0.0112 | −0.6337 |
| $Z(H_6)$ | −0.2423 | 0.0404 | 0.0966 | 0.5273 | 0.2343 | 0.3822 | −0.4611 | 0.4026 |

*p*-$DC_6H_4X$ ($C_{2v}$)

| Freq. calcd.[b] cm$^{-1}$ | 436 | 630† | 784 | 835† | 963† | 398 | 837† | 984† |
|---|---|---|---|---|---|---|---|---|
| | $B_2$(I,RR) | | | | | $A_2$(R) | | |
| $Z(C_1)$ | −0.1372 | −0.0257 | 0.1572 | 0.0468 | 0.0008 | 0 | 0 | 0 |
| $Z(C_2)$ | 0.0361 | 0.0167 | −0.1320 | 0.0170 | −0.0546 | 0.1284 | 0.0661 | 0.0659 |
| $Z(C_3)$ | 0.1077 | −0.0174 | 0.0590 | 0.0566 | 0.0755 | −0.1284 | 0.0661 | −0.0659 |
| $Z(C_4)$ | −0.1221 | −0.1417 | −0.0382 | −0.1106 | −0.0417 | 0 | 0 | 0 |
| $Z(C_5)$ | 0.1077 | −0.0174 | 0.0590 | 0.0566 | 0.0755 | 0.1284 | −0.0661 | 0.0659 |
| $Z(C_6)$ | 0.0361 | 0.0167 | −0.1320 | 0.0170 | −0.0546 | −0.1284 | −0.0661 | −0.0659 |
| $Z(H_2)$ | 0.0332 | 0.2321 | 0.0051 | −0.5317 | 0.3553 | 0.2273 | −0.4427 | −0.4431 |
| $Z(H_3)$ | 0.1435 | 0.3088 | 0.2764 | −0.1891 | −0.4893 | −0.2273 | −0.4427 | 0.4431 |
| $Z(D_4)$ | −0.3459 | 0.4652 | −0.1211 | 0.2237 | 0.1291 | 0 | 0 | 0 |
| $Z(H_5)$ | 0.1435 | 0.3088 | 0.2764 | −0.1891 | −0.4893 | 0.2273 | 0.4427 | −0.4431 |
| $Z(H_6)$ | 0.0332 | 0.2321 | 0.0051 | −0.5317 | 0.3553 | −0.2273 | 0.4427 | 0.4431 |

a) $Z$(X) is always zero, because of the approximation used in calculations (See text).

b) †-Marks denote out-of-plane hydrogen vibrations. The residues are skeletal vibrations, which can be expected to be weak in infrared absorption and are omitted in Table III and Fig. 3.

already in the preceding papers[1,2]. To do this, the $L$ matrix must be calculated. It is defined as

$$Z=LQ \tag{2}$$

which can also be expressed as

$$L=M^{-1}B'_JG^{-1}L_J \text{[7]} \tag{3}$$

where $M$ is the diagonal matrix, the elements of which are the masses of atoms associated with the Cartesian coordinates. The $B_J$ matrix relates the internal coordinates, $J$, to the Cartesian coordinates,

$$J=B_JZ \tag{4}$$

The elements of the $B_J$ matrix are the same

7) B. L. Crawford, Jr. and W. H. Fletcher, *J. Chem. Phys.*, **19**, 141 (1951); D. A. Long, *Proc. Roy. Soc.* **A217**, 203 (1953).

TABLE V. ASSIGNMENTS OF OUT-OF-PLANE HYDROGEN VIBRATIONS FOR SEVERAL *p*-$DC_6H_4X$ TYPE MOLECULES ($cm^{-1}$)

| | | | *p*-$DC_6H_4Br$ | | *p*-$DC_6H_4CHCH_2$ | | $[p\text{-}DC_6H_4CHCH_2]_n$ | |
|---|---|---|---|---|---|---|---|---|
| | | | Anal. | Obs.[11] | Anal. | Obs.[11] | Anal. | Obs.[11] |
| Fundamentals | | *b* | 840 | 841 s | 850 | 856 s | 850 | 852 s |
| | | *c* | 940 | | 950 | 957 w | 950 | 952 w |
| | | *d* | 830 | | 850 | | 845 | |
| | | *e* | 955 | | 965 | | 960 | |
| Combinations | $\alpha$ | $c+e$ | 1895 | 1899 | 1915 | 1910 | 1910 | 1914 |
| | $\beta_1$ | $d+e$ | 1785 | | 1815 | 1820 | 1805 | |
| | $\beta_2$ | $b+e$ | 1795 | 1783 | 1815 | | 1810 | 1803 |
| | $\beta_3$ | $b+c$ | 1780 | | 1800 | 1806 | 1800 | |
| | $\gamma$ | $b+d$ | 1670 | 1670 | 1700 | 1693 | 1695 | 1696 |

as those given in the preceding papers[1]. The $\boldsymbol{L}_J$ matrix relates the internal coordinates to the normal coordinates,

$$J=\boldsymbol{L}_J Q \tag{5}$$

and it is obtained when the secular Eq. 1 is solved.

The calculated reoults of $\boldsymbol{L}$ matrices are shown in Table IV, where the normalization of the $\boldsymbol{L}$ matrix is made by the following equation

$$\boldsymbol{L}'\boldsymbol{M}\boldsymbol{L}=\boldsymbol{E} \tag{6}$$

### Absorption Intensities

The in-plane or out-of-plane component of the molecular dipole moment, $\mu_x$, $\mu_y$ or $\mu_z$ may be expanded in an even or odd power series of the normal coordinates as follows, respectively, neglecting the higher terms:

$$\left.\begin{aligned}\mu_x&=\mu_{x0}+\sum_{i,j} a_{ij}Q_iQ_j,\\ \mu_y&=\mu_{y0}+\sum_{i,j} b_{ij}Q_iQ_j,\\ \mu_z&=\sum_i c_iQ_j,\end{aligned}\right\} \tag{7}$$

where $\mu_{x0}$ and $\mu_{y0}$ are the constant terms for every molecule. When the vibration is mechanically harmonic, the integrated absorption coefficient of the fundamental band produced by $Q_i-(\kappa_i)-$ and that of the combination band produced by $Q_i$ and $Q_j-(\kappa_{ij})-$ are expressed as follows:

$$\kappa_i=\pi/3c\cdot c_i^2$$
$$\kappa_{ij}=\boldsymbol{h}/12c^2\pi\cdot(\nu_i+\nu_{ij})(a_{ij}^2+b_{ij}^2)/\nu_i\nu_j\text{*1} \tag{8}$$

respectively, where $\boldsymbol{h}$ is Planck's constant, and $\nu_i$ or $\nu_j$ is the wave number of the fundamental referring to $Q_j$ or $Q_i$. Eq. 8 are the same those presented by Wilson et al.[8] and in our earlier papers[2].

When the formal electric charge associated with each atom or atomic group does not change by small vibrational displacement, and some further assumptions referred to in the preceding papers[1,2] are applied, the coefficients of Eq. 7, $a_{ij}$, $b_{ij}$, and $c_i$ can be shown to have simple relationships to the elements of $\boldsymbol{L}$ matrices. This enables us to calculate the values of $\kappa_i$ and $\kappa_{ij}$. The results of calculations as relative values of $\kappa_i$ and $\kappa_{ij}$ are shown in Table III and illustrated in Fig. 3, where it is assumed that all the C-H bond moments are equal, and the contribution of the motion of the C-X bond is neglected in the total molecular dipole moment*2.

### Comparison with the Experimental Data

The infrared spectra of *ortho*-, *meta*- and *para*-deuterated toluene have been presented by Turkevich et al.[9] and Tiers et al.[10] These experimental data are shown in Table III and Fig. 3.

Each molecule shows a strong absorption band in the region of 600 to 650 $cm^{-1}$, which can be assigned with certainty to the first fundamental band of the out-of-plane hydrogen vibrations. The binary combination bands of the out-of-plane hydrogen vibrations can be readily identified in the region of 1600 to 2000 $cm^{-1}$. These bands can be easily assigned by comparison with the results of calculations for every molecule, as shown in Fig. 3. The "analyzed values" of the fundamental and combination frequencies are determined so as to give the best fit with the above assigned

*1 The practical value of $\kappa_{ij}$ in Eq. 8 must be given as $2\kappa_{ij}=\kappa_{ij}+\kappa_{ji}$ $(i\neq j)$ corresponding to the two terms, $a_{ij}Q_iQ_j$ or $b_{ij}Q_iQ_j$ and $a_{ji}Q_jQ_i$ or $b_{ji}Q_jQ_i$ appearing in Eq. 7.

8) E. B. Wilson, Jr., J. C. Decius and P. C. Cross, "Molecular Vibrations", McGraw-Hill, New York (1955), § 7-9.

*2 The motion of the carbon atom of the C-X bond takes place with small amplitude for the vibrations under consideration, and the X atom does not move at all according to the approximation used in low-frequency splitting.

9) J. Turkevich, H. A. McKenzie, L. Friedman and R. Spurr, *J. Am. Chem. Soc.*, **71**, 4045 (1949).

10) G. V. D. Tiers, *J. Chem. Phys.*, **19**, 1072 (1951). G.V.D. Tiers and J. H. Tiers, ibid., **20**, 761 (1952).

frequencies of fundamentals and their combination bands. As shown in Table III and Fig. 3, the analyzed frequencies are in good agreement with the assigned values.

Recently, Murahashi et al.[11] observed the spectra of *para*-deuterated derivatives of bromobenzene, styrene and polystyrene (atactic) in the region of 700 to 3000 $cm^{-1}$. Table V shows that our assignments are valid and our theories are applicable also in these cases.

11) S. Murahashi, S. Nozakura and H. Tadokoro, to be published shortly.

The authors wish to express their sincere thanks to Professor Takehiko Shimanouchi at the University of Tokyo and to Dr. Hiroyuki Tadokoro at Osaka University for their useful comments and interest in this work.

*Department of Chemistry*
*College of Science*
*St. Paul's University*
*Ikebukuro, Tokyo*

# *Polarographic and Spectrophotometric Studies on Trimethylpyruvic Acid*

By Masanosuke TAKAGI

(Received December 20, 1960)

Recent studies on pH-dependence of the limiting current of $\alpha$-keto acids[1] have revealed that the theory given by Brdicka et al.[2-4] for pyruvic acid and phenylglyoxylic acid, based on the kinetic character of the current due to the recombination of the dissociated acid anion with proton, does not fully explain the behavior of $\alpha$-keto acids, including the above two acids. In order to interpret the decrease of the limiting current with decreasing pH in acid media, the roles of hydration of the keto form and also enolization in some cases have been suggested, compared with the spectrophotometric measurements[1]. However, the contributions of these factors to the limiting current are in most cases difficult to analyze separately, consequently the interpretation of the phenomenon has remained qualitative.

Although the polarographic and spectrophotometric behavior of trimethylpyruvic acid has already been briefly described with other $\alpha$-keto acids[1], more detailed investigations on this acid seem to be interesting, since the acid has at least no possibility of enolization and would be therefore expected to give some quantitative knowledge concerning the relation between the polarographic behavior and the spectrophotometric.

## Experimental

**Materials.**—Trimethylpyruvic acid was prepared according to Richard[5] by oxidizing pinacolone with alkaline potassium permanganate. B. p. 75°C at 10 mmHg. Freshly prepared trimethylpyruvic acid was dissolved into distilled water to be $5\times10^{-3}$ M aqueous solution, which was used as stock solution for polarographic measurements.

**Buffer Solutions.**—McIlvain's buffer for pH 2.2 to 8.0 and Walpole's buffer for pH 0.65 to 5.20 were used. For pH below 1, hydrochloric acid or sulfuric acid solutions of various concentrations were used.

**Apparatus and Procedure.**—A Heyrovsky-Shikata type polarograph was used with a Yanagimoto Galvarecorder. The characteristics of the capillary used were $m=2.45$ mg./sec., $t=2.92$ sec. at the applied potential of $-1.40$ (vs. N.C.E.) in a buffer solution of pH 4.35, when the height of mercury reservoir was 60 cm. A normal calomel electrode was used as an outer reference electrode. The reference electrode was connected with the electrolytic cell by an agar bridge saturated with potassium nitrate, which was attached to the cell through sintered glass. The total cell resistance was any time less than 500 ohm. The dissolved oxygen in electrolytic solution was removed by bubbling nitrogen gas. The concentration of trimethylpyruvic acid in final electrolytic solutions was $5\times10^{-4}$ M and the ionic strength was adjusted to be 0.5 by adding sodium chloride, except for the strong acid range. Polarograms were taken at $25\pm0.05$°C. No maximum suppressor was used throughout the experiments. For spectrophotometric measurements, Shimadzu Type QB-50 spectrophotometer with a 1.0 cm. quartz cell was employed. Temperature control was made within $\pm0.05$°C by circulating water of constant temperatures through the jacket attached to the cell. pH Measurements for the electrolytic solutions and also for the determination of p$K$ value of trimethylpyruvic acid were carried out with Horiba Model-P pH meter with a glass electrode.

In order to determine the hydration constant of

1) S. Ono, M. Takagi and T. Wasa, *Collection Czechoslov. Chem. Communs.*, **26**, 141 (1961).
2) R. Brdicka and K. Wiesner, ibid., **12**, 39 (1947).
3) R. Brdicka, ibid., **12**, 212 (1947).
4) J. Koutecky and R. Brdicka, ibid., **12**, 337 (1947).
5) A. Richard, *Ann. chim.* (Paris), [8], **21**, 360 (1910).

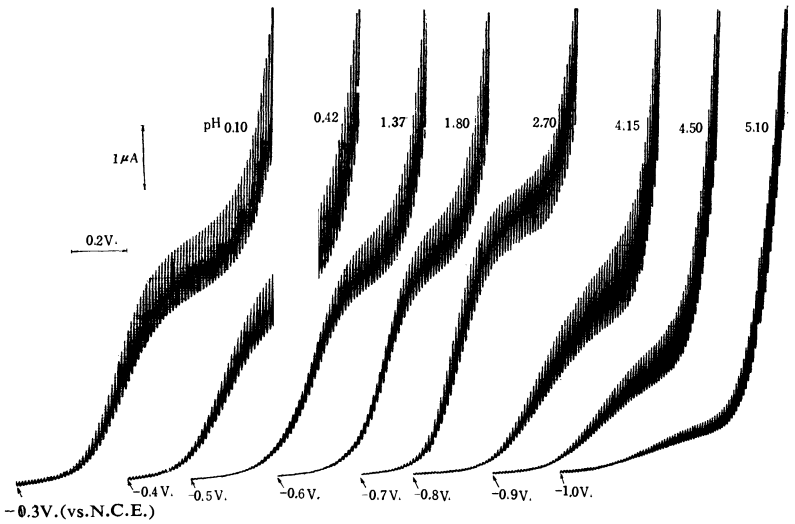
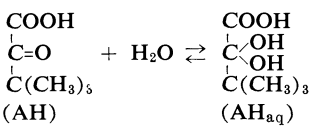



Fig. 1. Polarograms of trimethylpyruvic acid in various pH's, Concn.: $5\times10^{-4}$ M, Temp.: 25°C, Ionic strength: 0.5.

trimethylpyruvic acid in undissociated state, the following kinetic measurments were carried out: about 0.3 ml. of 0.25 M trimethylpyruvic acid aqueous solution containing 1 N hydrochloric acid, which had been kept at 25°C, was rapidly mixed with about 2.7 ml. of McIlvain's buffer of pH 8, which had been taken in the spectrophotometric cell and also kept at 25°C. The change of the optical density at 310 m$\mu$ was followed with time.

## Results and Discussion

Polarograms of trimethylpyruvic acid in various pH's are presented in Fig. 1. From Fig. 1 it can be seen that the limiting current of trimethylpyruvic acid has a minimum value in a rather acid pH as it has been known with other $\alpha$-keto acids[1]. The decrease of the current with increasing pH in pH above 3, coincides with the observation by Clair and Wiesner[6] and can be attributed to the decrease of the rate of recombination of the dissociated acid anion with proton. Since trimethylpyruvic acid has no possibility of enolization, the decrease of the current in acid pH has been accounted for by the hydration of carbonyl group in undissociated state[1]. The hydration of carbonyl group is also considered from the absorption spectra as shown in Fig. 2. The fact that the optical density at 310 m$\mu$ due to C=O group, in 1.8 N hydrochloric acid, is smaller than those in alcohol or in acetate buffer of pH 5.09, can be interpreted by the formation of the hydrated form as



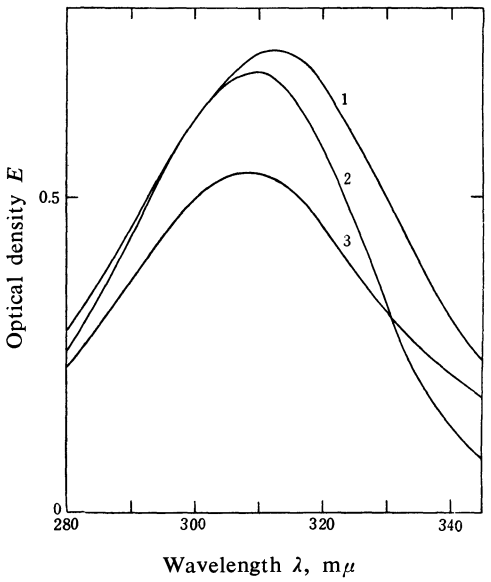




Fig. 2. Absorption spectra of trimethylpyruvic acid. Concn.: 0.025 M, Temp.: 25°C, 1 in alcohol, 2 in acetate buffer of pH 5.09, 3 in 1.8 N HCl aqueous solution.

Utilizing the difference in optical density at 310 m$\mu$ of the two states, the dissociated and undissociated, the apparent dissociation constant of trimethylpyruvic acid can be determined by measuring the change in optical density with pH as shown in Fig. 3. pH was changed by adding sodium acetate or hydrochloric acid and the concentration of trimethylpyruvic acid was kept constant. The p$K_a$ value has been found to be 1.52 at 25°C at the ionic strength of 0.04, which is in agreement with the value of 1.47 cited in "International Critical Tables" but which

6) E. G. Clair and K. Wiesner, *Nature*, 165, 202 (1950).

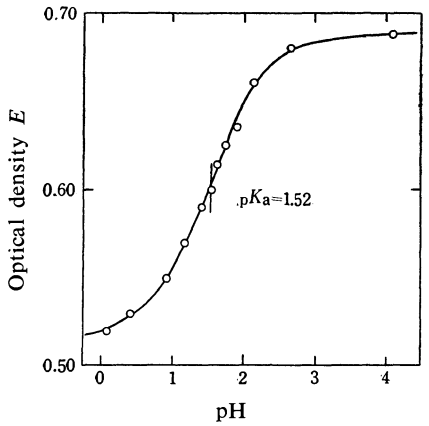



Fig. 3. Change of the optical density of trimethylpyruvic acid. At 310 mμ with pH. Concn.: 0.025 M, Temp.: 25°C. pH was changed by adding either HCl or sodium acetate.

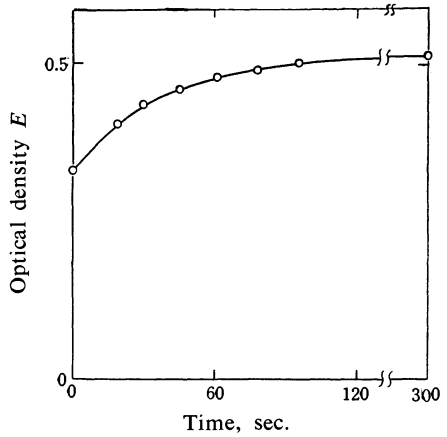



Fig. 4. Measurement of the rate of dehydration of hydrated trimethylpyruvate in pH about 5.
Change of the optical density at 310 mμ was followed with time. The optical density at zero time ($E_0$) was obtained by extrapolation of the log plot of Fig. 5.

considerably differs from the value of 2.3 used by Clair and Wiesner[6].

From the above change in optical density with pH and also from the observation that the optical density in undissociated state changed with temperature, while that in the dissociated remained constant, it has been assumed that trimethylpyruvic acid is appreciably hydrated in undissociated state, while its anion ($A^-$) is almost free from the hydration. This assumption may be allowed, referred to the same kind of property of phenylglyoxylic acid, for which the same assumption was deduced, comparing the ultraviolet absorption areas of the free acid anion with those of benzoic acid and cinnamic acid[1]. As in the present experiments, molecular extinction coefficients of AH and $A^-$ can not be taken to be equal as in the case of phenylglyoxylic acid, the direct comparison of the optical densities between the dissociated and undissociated states has little significance for obtaining the quantitative knowledge on the hydration in undissociated state. A more direct attempt was therefore made kinetically, under the assumption that, when the undissociated acid, which exists in an equilibrium between AH and $AH_{aq}$, is mixed with a sufficiently larger volume of basic buffer solution, the dissociation of the acid occurs instantly to attain its equilibrium, while the dehydration reaction of the hydrated anion ($A^-_{aq}$) takes place so slowly that it can be followed photometrically as the change of the optical density at 310 mμ. An example of the experimental results is presented in Figs. 4 and 5. Since the dehydration is a first order reaction, the hydration constant of the undissociated acid can be obtained as

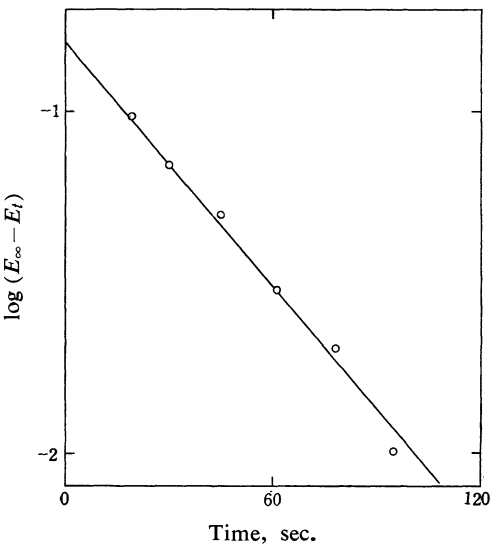



Fig. 5. Log plot of $(E_\infty - E_t)$ of Fig. 4 against time.

$$K_h = [AH_{aq}]/[AH] = (E_\infty - E_0)/E_0 \qquad (1)$$

where $E_\infty$ and $E_0$ are the optical densities of the anion at the reaction times, $t=\infty$ and 0, respectively, the latter of which can be obtained from the extrapolation of the log plot in Fig. 5. The average hydration constant from three runs was 0.46 at 25°C. From the same log plot the average rate constant of dehydration in pH about 5 at 25°C has been obtained to be $2.8\times10^{-2}\,sec^{-1}$. The hydration constants of different temperatures were calculated from

TABLE I. TEMPERATURE DEPENDENCE OF THE OPTICAL DENSITY AND HYDRATION CONSTANT OF TRIMETHYLPYRUVIC ACID IN 1 N HYDROCHLORIC ACID AQUEOUS SOLUTIONS

| Temp., °C | $E$ at 310 mμ | $K_h=(E^*-E)/E$ |
|---|---|---|
| 13.0 | 0.467 | 0.814 |
| 19.5 | 0.530 | 0.598 |
| 25.0 | 0.580 | 0.460 |
| 31.5 | 0.630 | 0·344 |
| 37.0 | 0.670 | 0.264 |

Concn. of trimethylpyruvic acid: 0.0274 M.
$E^*=0.847$ is the value corresponding to the optical density when no hydration occurs, which was evaluated from $E$ at 25°C with the corresponding $K_h$ 0.460 as obtained above.

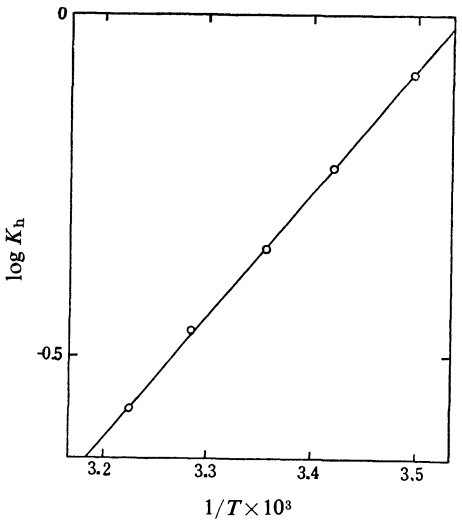



Fig. 6. Log plot of the hydration constant of trimethylpyruvic acid against reciprocal absolute temperature.

the corresponding optical densities versus the above obtained value at 25°C (Table I). The log plot of these constants against the reciprocal absolute temperatures gives a straight line, from whose slope the heat of hydration has been obtained to be −8.2 kcal. (Fig. 6).

The pH-dependence of the polarographic limiting current of trimethylpyruvic acid can be considered with the following scheme

$$AH_{aq} \underset{}{\overset{K_h}{\rightleftarrows}} AH \underset{k_r}{\overset{k_d}{\rightleftarrows}} A^-$$

(Electroactive)

↓ Electrode reaction

Reduced form

where $k_d$ and $k_r$ are the rate constants of dissociation and recombination of AH, respectively, and AH is only the electroactive form for the reduction at the dropping mercury electrode. $A^-_{aq}$ and also the transformation between $AH_{aq}$ and $A^-$ via $A^-_{aq}$ are neglected, since the equilibrium between $A^-$ and $A^-_{aq}$ has been known to be much shifted toward $A^-$ from the above experimental results and consequently the concentration of $A^-_{aq}$ in equilibrium is negligible in any pH.

Under the assumption that the rate of dehydration from $AH_{aq}$ is so slow that it causes no kinetic current, while the recombination of $A^-$ with proton causes the kinetic current, the equation for the limiting current of trimethylpyruvic acid as a function of hydrogen ion concentration can be derived as follows.

Writing the apparent dissociation constant $K_a$ in the form

$$K_a=[A^-][H^+]/([AH]+[AH_{aq}]) \quad (2)$$

the dissociation constant for free acid $K_0$ can be expressed as

$$K_0=k_d/k_r=[A^-][H^+]/[AH]=K_a(K_h+1) \quad (3)$$

As the analytical concentration of the acid [a] is

$$[a]=[AH]+[AH_{aq}]+[A^-] \quad (4)$$

to a first approximation, the limiting current can be written as being proportional to the concentration of AH at the electrode surface, which is supplied by diffusion from AH in bulk or by the recombination reaction of $A^-$ with proton, involving the kinetic current, for which Koutecky's equation[4] can be valid. The limiting current is then prexessed as

$$i_l=i_d\frac{[AH]}{[a]}+i_d\frac{[A^-]}{[a]}\times\frac{0.87[H^+](k_rt/K_0)^{1/2}}{1+0.87[H^+](k_rt/K_0)^{1/2}} \quad (5)$$

where $i_d$ is the diffusion current corresponding to [a] and $t$ is the drop time.

Substituting relations 1 to 4 into Eq. 5 and rearranging the resulting equation, the following equation for the limiting current as a function of $[H^+]$ can be obtained.

$$i_l=\frac{i_d[H^+]}{K_a+[H^+]}\left(\frac{1}{K_h+1}+\frac{0.87K_a[k_rt/K_a(K_h+1)]^{1/2}}{1+0.87[H^+][k_rt/K_a(K_h+1)]^{1/2}}\right) \quad (6)$$

The use of this equation may be allowed for the limited case where the diffusion current due to AH in bulk is not appreciable as far as the recombination reaction of $A^-$ with proton causes the kinetic current and when the recombination reaction is no longer the rate-determining, the limiting current is the diffusion current due to AH corresponding to the concentration $[A^-]+[AH]$.

In Fig. 7 the pH-dependence of the limiting current of trimethylpyruvic acid is presented. The theoretical curve was drawn according to

Eq. 6, substituting, as $K_a$, $K_h$ and $t$, the above experimentally obtained values into the equation and choosing other values i. e. $k_r$ and $i_d$ so as to fit the curve to the experimental points. The agreement of the theoretical curve with the experimental results is good except for the strong acid range, where the deviation of the experimental results from the theoretical may be qualitatively interpreted by the acid catalyzed dehydration of $AH_{aq}$, whose contribution is not considered in the equation. The experimental conditions as ionic strength, viscosity etc. in this range, can not be the same because of increasing acid concentration and moreover the measurements of the limiting current may have considerable error because of the deformation of the wave; consequently, no further analysis was attempted.

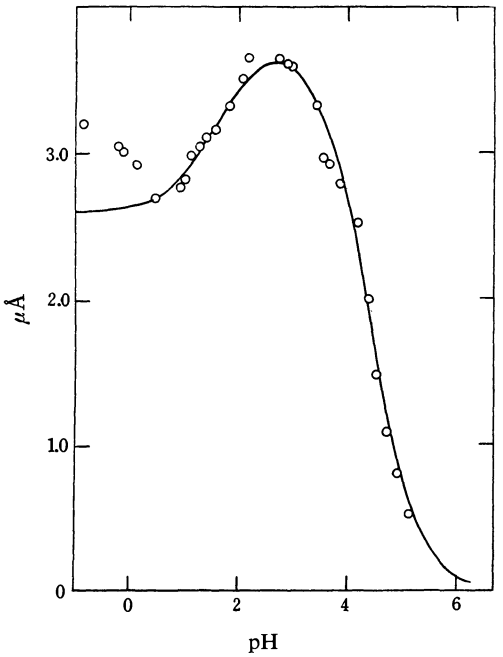



Fig. 7. pH-Dependence of the limiting current of trimethylpyruvic acid. Concn.: $5\times10^{-4}$ M, Temp.: 25°C, ionic strength: 0.5. Solid line represents the theoretical curve according to Eq. 6. ○ experimental points.

The rate constants of dissociation and recombination of trimethylpyruvic acid obtained from the above treatment are $k_r=1.4\times10^7$ l. $mol^{-1}\,sec^{-1}$ and $k_d=6.0\times10^5\,sec^{-1}$, respectively. Although considerably larger values were obtained than those by Clair and Wiesner, $k_r$ is still small, compared with those for other acids. Since $k_r$ should not be very different of usual acids, for which $10^{10}\sim10^{11}$ l. $mol^{-1}\,sec^{-1}$ have been reported by different authors with different methods[7-9] of determination, indicating the diffusion velocity of hydronium ion, this relatively small value of $k_r$ of trimethylpyruvic acid may partly attributed to the steric factor of the methyl groups against the recombination reaction. This kind of steric factor may be excluded in the case of pyruvic acid, for which larger values of $k_r$ than that of trimethylpyruvic acid have been known[10].

As for pyruvic acid, Becker and Strehlow[11] have recently reported the revised values of $k_r$ and $k_d$ by using their equation, involving the contribution of hydration and the hydration constant estimated on the basis of their spectrophotometric measurements. However, as it was pointed out in the previous paper[1], pyruvic acid is not free from the possibility of enolization. The spectrophotometric behavior of pyruvic acid differs from that of trimethylpyruvic acid, especially in alcoholic solution; the optical density of pyruvic acid in alcohol at the wave length of the maximum absorption is considerably lower than that of pyruvate in buffer solution (pH 6), while the reverse tendency is seen with trimethylpyruvic acid as in Fig. 2. Also the fact that $pK_a$ value of pyruvic acid (2.50) is larger than that of trimethylpyruvic acid, is difficult to understand only with the difference in the hydration and the steric hindrance, when considered with the reverse order of $pK$ values between acetic acid and trimethylacetic acid, though such an interpretation was attempted in the previous paper. As far as the question whether the enolization participates in the polarographic and spectrophotometric behavior of pyruvic acid, remains unsolved, the present results on trimethylpyruvic acid may be said to be more significant for the quantitative approach in the studies of this kind.

## Summary

Polarographic and spectrophotometric behavior of trimethylpyruvic acid has been investigated.

The limiting current of trimethylpyruvic acid shows a minimum value in pH about 0.5. The absorption spectra show the absorption maximum at about 310 mμ in aqueous solutions, indicating the decrease of the optical density in strongly acid pH. These facts have been accounted for by the hydration of carbonyl group of undissociated acid.

7) M. Eigen, *Z. physik. Chem. N. F.*, **1**, 176 (1954).
8) M. Eigen and J. Schoen, ibid., **3**, 126 (1955).
9) A. Weller, ibid., **3**, 238 (1955).
10) R. Brdicka, *Collection Czechoslov. Chem. Communs.*, **19**, 41 (1954).
11) M. Becker and H. Strehlow, *Z. Elektrochem.*, **64**, 129 (1960).

p$K_a$ for apparent dissociation constant of trimethylpyruvic acid has been spectrophotometrically obtained to be 1.52 at 25°C.

Hydration constant of the undissociated acid ($K_h = [AH_{aq}]/[AH]$) has been kinetically obtained to be 0.46 at 25°C. The rate constant of dehydration of hydrated trimethylpyruvate in buffer solution of pH about 5 was $2.8 \times 10^{-2}$ $sec^{-1}$ at 25°C. From the temperature dependence of the hydration constant, the heat of hydration of unhydrated acid has been found to be $-8.2$ kcal.

A quantitative interpretation of the pH-dependence of the limiting current has been attempted by deriving the equation, involving the hydration and dissociation factors. The agreement of the theoretical curve with the experimental is good, except for the pH range below 0.5, where acid catalyzed dehydration of hydrated acid should be taken into consideration.

Rate constants of the dissociation and recombination of trimethylpyruvic acid have been found to be $k_d = 6.0 \times 10^5$ $sec^{-1}$ and $k_r = 1.4 \times 10^7$ l. $mol^{-1}$ $sec^{-1}$, respectively.

The author wishes to express his sincere thanks to Professor Sôzaburo Ono for his kind guidance and encouragement throughout this work. He also thanks Mr. Shigeo Sawada for technical assistance.

*Laboratory of Biophysical Chemistry*
*College of Agriculture*
*University of Osaka Prefecture*
*Sakai*

# *Electron Paramagnetic Resonance Study of Diphenyl Nitric Oxide in Single Crystals**

By Yasuo DEGUCHI

(Received December 27, 1960)

The study of organic free radicals by electron paramagnetic resonance has been developed during the last several years. Most of these studies were done in liquid states[1]. However, Kittel et al.[2], Weissman et al.[3], Cohen and Kikuchi[4], Gordy et al.[5], McConnel et al.[6] and Whiffen et al.[7], reported the study of organic free radicals in solid state.

Cohen and Kikuchi[4] measured the angular variation of $g$-value and half-power width of single crystals of pure diphenylpicrylhydrazyl. Weissman et al., observed the maximum hyperfine splitting of crystals of peroxylamine disulfonate ion ($(SO_3)_2NO^{2-}$) diluted with $K_2(SO_3)_2NOH$.

We investigated the angular variation of the line width and the hyperfine splitting in EPR spectra of single crystals of pure diphenyl nitric oxide and of the ones diluted with benzophenone which is diamagnetic.

## Preparation of the Single Crystals

Following the method of Wieland and Roth[8], we synthesized diphenyl nitric oxide. From saturated ether solutions of diphenyl nitric oxide, we obtained single crystals of pure diphenyl nitric oxide as large as $6\times1.5\times0.5$mm.

In order to make magnetically diluted single crystals, the saturated ether solutions with various mixing ratios of diphenyl nitric oxide to benzophenone were made. The concentration** of mixed crystals were pure, 4.4, 3.3, 2.9, 1.9, 0.84, 0.51, 0.41, 0.35, 0.1, 0.01, 0.001 and 0.0005 mol./l., most of which crystallized in prismatic form. The largest crystal thus obtained was $8\times4\times3$ mm.

* This work was supported by the U. S. Air Force through the Air Force Office of Scientific Research of the Air Research and Development Command under contract. Reproduction in whole or in part is permitted for any purpose of the U. S. Government.

1) D. J. E. Ingram, "Free Radicals as Studied by Electron Spin Resonance", Academic Press (1958), p. 168.
2) A. N. Holden, C. Kittel, F. R. Merritt and W. A. Yager, *Phys. Rev.*, **77**, 147 (1950).
3) S. I. Weissman and D. Banfill, *J. Am. Chem. Soc.*, **75**, 2534 (1953).
4) C. Kikuchi and V. W. Cohen, *Phys. Rev.*, **93**, 394 (1954).
5) A. Roggen, L. Roggen and W. Gordy, ibid., **105**, 50 (1957).
6) H. M. McConnel, C. Heller, T. Cole and R. S. Fessenden, *J. Am. Chem. Soc.*, **82**, 766 (1960).
7) N. M. Atherton and D. H. Whiffen, *Mol. Phys.*, 3, 1 (1960).
8) H. Wieland and K. Roth, *Ber.*, **53**, 216 (1920).

** These concentrations were calculated from the values of weight mixing ratio regarding benzophenone as solvent.

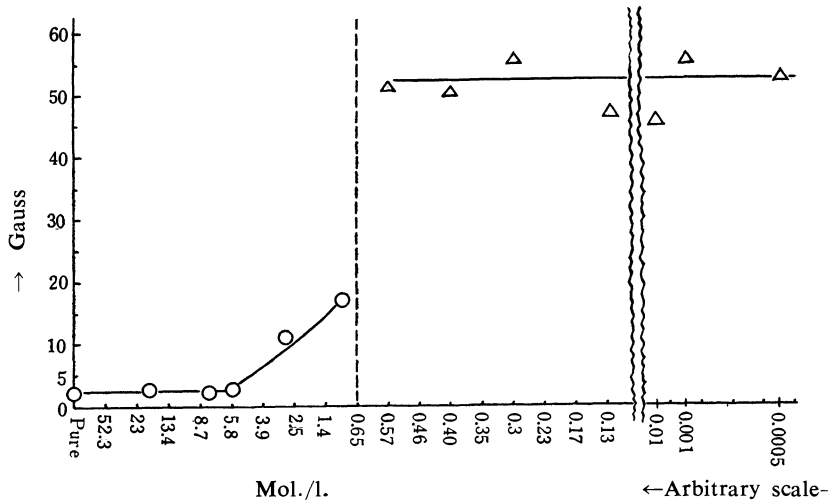



Fig. 1. The variation of half-widths and hyperfine splitting with changing concentrations. The left hand-side region of the broken line is the single line region and the right-hand-side region is the hyperfine splitting region. In the right hand-side region of the wavy line, the concentration scale is taken arbitrarily.

## Experimental

The EPR spectrometer employed in this work was constructed by Professor J. Townsend, Washington University, St. Louis. The details of this spectrometer will be described elsewhere.

The crystal structure of diphenyl nitric oxide has not been determined yet, but the crystal structure of benzophenone has been investigated by Banrajee and Haque[9]. According to their result, it is orthorhombic with $a=10.30$ Å, $b=12.11$ Å and $c=8.04$ Å. Its unit cell contains 4 molecules and its space group belongs to $D^4{}_2-P_{2_12_12_1}$. But, as Lonsdale pointed out[10] the above crystal symmetry description is not the definite one but the possible one guessed from the static magnetic susceptibility measurement results.

As each single crystal forms with a broad face and a long edge, an axis normal to the broad face was designated as the c-axis, the one parallel to the long edge, a-axis, and the one perpendicular to both a and c, the b-axis. To rotate the crystal about these mutually perpendicular axes in the cavity, the crystal was mounted at the end of a quartz rod with oil clay.

In each measurement one of these axes was set parallel to the applied static magnetic field. Then we obtained the absorption spectra at every 15 degrees of rotation from 0 to 180°. The $g$-value was determined comparing the spectra thus obtained with the one of peroxylamine disulfonate in dilute aqueous solution. The $g$-value and separation between the outside lines and the center line of the peroxylamine disulfonate were well confirmed by Weissman et al.[11] as $g=2.0054$ and the separation is 13 gauss.

The concentration of mixed crystal was determined by comparing the optical absorption intensities of the cyclohexane solutions of mixed crystals in various mixing ratios with those of solutions containing a known amount of pure diphenyl nitric oxide which show the absorption peaks at 3680 and 3030 Å respectively.

## Results and Discussion

The relation between half-width of the absorption line and the concentration is shown in Fig. 1 where $\Delta H_{1/2}$ is the width between the steepest deflection points of the resonance absorption line and is measured at the orientation of crystal with respect to the static magnetic field; that is, the long axis a is perpendicular and the c-axis is parallel to the static magnetic field.

But the attempt to maintain the same orientation of the crystals at all concentrations may not have been successful because of the uncertainty over the structure of the concentrated crystals. When the mixing ratio of diphenyl nitric oxide to benzophenone becomes less than 0.1, the spectra no longer show a single line, but instead show hyperfine structures due to the interaction of the unpaired electron with the nuclear moment of nitrogen ($^{14}N$). In Fig. 1, within the single line region where the exchange narrowing effect is dominant, the more the content of benzophenone increases i. e. the less the mixing ratio becomes, the wider the line becomes.

After passing over the single line region, the hyperfine lines are not well resolved but overlap each other. This overlapping structure, however, turns out to be well resolved by decreasing

9) K. Banrajee and A. Haque, *Indian J. Phys.*, **12**, 87 (1938).
10) K. Lonsdale, *Proc. Roy. Soc.*, **A171**, 562 (1939).
11) G. E. Pake, J. Townsend and S. I. Weissman, *Phys. Rev.*, **85**, 682 (1952).

the mixing ratio $((C_6H_5)_2NO)/((C_6H_5)_2CO)$. Finally well-resolved hyperfine lines can be obtained. And the half-width of each component line does not change by varying the mixing ratio.

In the concentration region where the hyperfine lines appear, not only three but also four or five lines appear at certain rotation angles as shown in Fig. 2.

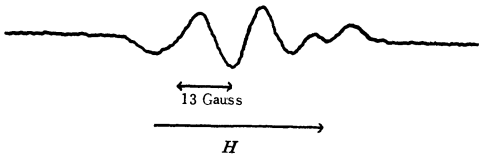



Fig. 2. The spectrum of the intermediate concentration region where four or five lines appear. The concentration of crystal is 0.1 mol./l.

The remarkable feature of the extra lines is that they never appear symmetrically with respect to the three main lines and their relative intenstities compared with the main lines are one third or one fourth and they do not change with varying concentrations of crystal.

The analysis of the spectrum in terms of the hyperfine interaction Hamiltonian

$$H=a\vec{I}\cdot\vec{S}+b\Big[S_zI_z(1-3\cos^2\theta)-\frac{3}{2}(S_+I_z+S_zI_+)\sin\theta\cos\theta e^{-i\varphi}-\frac{3}{2}(S_-I_z+S_zI_-)\sin\theta\cos\theta e^{i\varphi}\Big]$$

reveals that the weak lines which accompany simultaneous electron and nuclear spins transitions should be about 4% of the strong allowed lines. So this is not the case.

Another possible explanation for the appearance of extra lines may be as follows.

In the very concentrated region where the strong exchange interaction is dominant, the crystal structure of single crystals will be exclusively the one of diphenyl nitric oxide. On the other hand, the crystal structure of the very diluted single crystals will be the one of benzophenone. But in the intermediate concentration region, diphenyl nitric oxide and benzophenone may not be completely miscible. Then the crystals will no longer be perfect but rather contain misoriented crystallites in them. Thus these misoriented crystallites will show those extra lines in spectra.

In case of 0.0005 mol./l. mixed crysal, there appear three lines at certain rotation angles but still they do not show any hyperfine lines because of the protons adjacent to the ring carbon atoms. On the other hand well-resolved proton hyperfine splittings are obtained in oxygen-free solutions with low viscosity[12].

The higher the viscosity of the solutions are raised, the broader the proton hyperfine lines become and finally all proton hyperfine lines are broadened out and only three broad lines due to the nitrogen nuclear moment hyperfine interaction remain.

Thus we could not expect well-resolved proton hyperfine lines in diluted crystals.

**Exchange Narrowing Effect in the Concentrated Crystals.** — Many authors[13-19] have studied the theory of the line shape in the magnetic resonance. Kubo and Tomita[19] have developed the general theory of the line shape rigorously based on the quantum mechanics. Yokota and Koide[16] applied their theory to the absorption spectra of paramagnetic inorganic crystals, and Kivelson[20,21] extended it to the calculation of the line shape of organic free radicals.

In this paper we shall follow Kivelson's calculation.[21] According to his calculations, in case of strong exchange $J\gg A^2$ where $J$ and $A$ are defined below, the frequency of the resonance line is equal to

$$\omega_0-\Delta$$

where

$$\omega_0=\Big[\gamma+\frac{\Delta\gamma}{3}(3\cos^2\beta-1)-\delta\gamma\sin^2\beta\cos^2\gamma\Big]B_0$$

$$\Delta=T_1'^{-1}(IS)\int_0^{\omega_0/\omega_e}\exp(u^2/2)\,du$$

$\Delta$: non-secular shift due to the electron and nuclear spin interaction

$B_0$: static magnetic field

$\gamma$: gyromagnetic ratio tensor i.e. $(1/3)T_r\vec{\gamma}$

$\Delta\gamma=\gamma_s-\frac{1}{2}(\gamma_r+\gamma_s)$, $\delta\gamma=\frac{1}{2}(\gamma_p-\gamma_r)$ } where $p, r, s$: x, y, z coordinates in the molecule fixed frame

$\beta$: the angle between the molecular s-axis and the crystal b-axis

$\gamma$: the angle of rotation about the molecular s-axis

12) Y. Deguchi, to be published; Y. Deguchi, *J. Chem. Phys.*, **32**, 1584 (1960).
13) M. H. L. Pryce, *Nature*, **162**, 538 (1948).
14) J. H. Van Vleck, *Phys, Rev.*, **74**, 1168 (1948).
15) N. Bloembergent, E. M. Purcell and R. V. Pound, ibid., **73**, 679 (1948).
16) M. Yokota and S. Koide, *J. Phys. Soc. Japan*, **9**, 953 (1954).
17) P. W. Anderson and P. R. Weisse, *Rev. Mod. Phys.*, **25**, 269 (1953).
18) P. W. Anderson, *J. Phys. Soc. Japan*, **9**, 316 (1954).
19) R. Kubo and K. Tomita, ibid., **9**, 884 (1954).
20) D. Kivelson, *J. Chem. Phys.*, **27**, 1087 (1957).
21) D. Kivelson, ibid., **33**, 1094 (1960).

$\alpha$: the angle of rotation about the crystal b-axis

$\omega_e^2=(2/3)S(S+1)J^2$, $J$: exchange integral

$A_\lambda^2=\{(\Phi_{zz}^{(\lambda)}-a_\lambda)^2+4|\Phi_{z+}^{(\lambda)}|^2\}$ (see Appendix)

And the total line width $2T_2^{-1}$ is equal to the sum of the secular line width $2T_2'^{-1}$ and the non-secular line width $2T_1'^{-1}$

$$2T_2^{-1}=2T_2'^{-1}+2T_1'^{-1}$$

where

$$T_2'^{-1}(IS)=\frac{\pi^{1/2}}{2[3S(S+1)]^{1/2}J}\sum_\lambda n_\lambda I_\lambda(I_\lambda+1)\times[(\Phi_{zz}^{(\lambda)}-a_\lambda)^2+4|\Phi_{z+}^{(\lambda)}|^2]$$

$$T_1'^{-1}(IS)=\frac{\pi^{1/2}}{2[3S(S+1)]^{1/2}J}\sum_\lambda n_\lambda I_\lambda(I_\lambda+1)\times\left[\left(\frac{1}{2}\Phi_{zz}^{(\lambda)}+a_\lambda\right)^2+2|\Phi_{z+}^{(\lambda)}|^2+4|\Phi_{++}^{(\lambda)}|^2\right]\times\exp(-\omega_0^2/2\omega_e^2)$$

For the extreme exchange case which is analogous to the extreme motional narrowing, $(J^2\gg\gamma^2B_0^2\gg A^2)$

$$T_2^{-1}(IS)=\frac{\pi^{1/2}}{2[3S(S+1)]^{1/2}J}\sum_\lambda n_\lambda I_\lambda(I_\lambda+1)\times\left[\frac{4}{5}|\Phi_{zz}^{(\lambda)}|^2-a_\lambda\Phi_{zz}^{(\lambda)}+2a_\lambda^2+6|\Phi_{z+}^{(\lambda)}|^2+4|\Phi_{++}^{(\lambda)}|^2\right]$$

In organic free radicals, we can assume

$$\delta\gamma=0$$

$$c_\lambda=d_\lambda=0$$

Then for the strong exchange case $(J^2\gg A^2)$

$$\omega=\gamma+\frac{\Delta\gamma}{3}(3\cos^2\beta-1)-\Delta$$

$$T_2'^{-1}(IS)=\frac{\pi^{1/2}}{2[3S(S+1)]^{1/2}J}\sum_\lambda n_\lambda I_\lambda(I_\lambda+1)\times\left\{[(3\cos^2\beta-1)(b_\lambda^2/4-b_\lambda a_\lambda)+b_\lambda^2/2+a_\lambda^2]+\left[(1-3\cos^2\beta)\left(\frac{1}{3}b^2-\frac{1}{2}a_\lambda b_\lambda\right)+b_\lambda^2/2+a_\lambda^2\right]\right\}\exp(-\omega_0^2/2\omega_e^2)$$

and for the extreme exchange case

$$T_2'^{-1}(IS)=\frac{\pi^{1/2}}{2[3S(S+1)]^{1/2}J}\sum_\lambda n_\lambda I_\lambda(I_\lambda+1)\times\left[(3\cos^2\beta-1)\left(\frac{1}{8}b^2-\frac{1}{2}b_\lambda a_\lambda\right)+b_\lambda^2+2a_\lambda^2\right]$$

In case of diphenyl nitric oxide, we have three different equivalent groups of nuclei, that is, one nitrogen, six protons at para- and ortho-positions and four protons at meta-positions in two benzene rings.

As shown in the Appendix, we obtain the following isotropic and anisotropic hyperfine splitting factors, that is,

Nitrogen isotropic hyperfine splitting factor

$$a_N=-9.5 \text{ gauss}$$

Nitrogen anisotropic hyperfine splitting factor

$$b_N=-13.92 \text{ gauss}$$

Para- and ortho-proton isotropic splitting factor

$$a_{p,o}=+1.96 \text{ gauss}$$

Para- and ortho-proton anisotropic splitting factor

$$b_{p,o}=-1.564 \text{ gauss}$$

Meta-proton isotropic splitting factor

$$a_m=-0.98 \text{ gauss}$$

Meta-proton anisotropic hyperfine splitting factor

$$b_m=-0.782 \text{ gauss}$$

and the total electron spin $S=1/2$.

Then

$$T_2^{-1}(IS)=\frac{\pi^{1/2}}{3J}\left[2\left\{(3\cos^2\beta-1)\left(\frac{1}{8}b_N^2-\frac{1}{2}b_Na_N\right)+b_N^2+2a_N^2\right\}-\frac{9}{2}\left\{(3\cos^2\beta-1)\left(\frac{1}{8}b_{p,o}^2-\frac{1}{2}b_{p,o}a_{p,o}\right)+b_{p,o}^2+2a_{p,o}^2\right\}-3\left\{(3\cos^2\beta-1)\left(\frac{1}{8}b_m^2-\frac{1}{2}b_ma_m\right)+b_m^2+2a_m^2\right\}\right]$$

At $\beta=0°$, $\Delta H_{1/2}$ at the maximum slope is equal to 2.3 gauss from the measurement. Then assuming the Gaussian line shape for the spectra, we have

$$J=284.96 \text{ gauss } (0.0262 \text{ cm}^{-1})$$

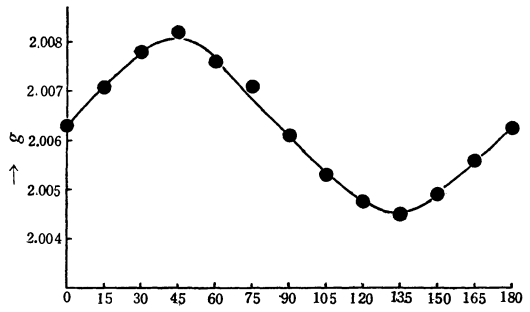
that is, if we consider $J$ as an adjustable parameter[16] and choose the above value for $J$, a good agreement with the experiment will be obtained.

This exchange integral value is about ten times smaller than the one obtained in inorganic paramagnetic salts[17,18].

The angular variations of $g$-value and half-width are shown in Figs. 3 and 4.

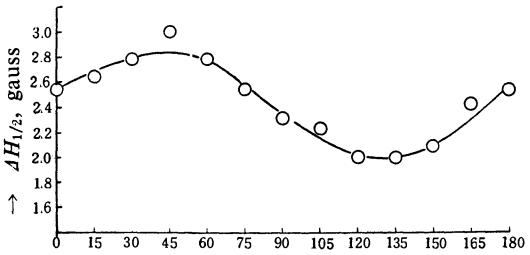
As mentioned before, things are rather complicated in the intermediate concentration region.

According to Kubo and Tomita's theory[19] EPR spectra in this region should show a




→ Rotation angle, degree

Fig. 3. The angular variation of $g$-values rotated around the a-axis for the pure crystal.




→ Rotation angle, degree

Fig. 4. The angular variation of half-widths rotated around the a-axis for the pure crystal.

microwave frequency dependence. Unfortunately, the apparatus we employed is a fixed microwave frequency one. Thus we shall not discuss it here.

**The Weak Exchange Interaction Case in Single Crystals Diluted with Benzophenone.**— As stated at the beginning of this section, the hyperfine spectra consist of the three broad but well-separated lines at a certain orientation of crystal. Since the exchange interaction in diluted crystals is reduced to small magnitude, the main contribution to the line broadening comes from the magnetic dipolar interaction due to an electron spin and protons in molecules in the crystal.

As shown in Appendix, the resonance frequency is given as follows:

$$\left[\gamma+\frac{\Delta\gamma}{3}(3\cos^2\beta-1)\right]B_0+\sum_\lambda A_\lambda M_\lambda-\frac{S(S+1)}{3}K$$

where

$$A_\lambda^2=\left[-a_\lambda+\frac{b}{2}(1-3\cos^2\beta)\right]^2+\frac{9}{4}b_\lambda^2\sin^2\beta\cos^2\beta$$

$$K=J^2\sum_\lambda g_{M'}\left[\sum_{M_\lambda'\neq M_\lambda}A_\lambda(M_\lambda-M_\lambda')\right]^{-1}$$

$$NJ^2=\sum_j\sum_{i\neq j}J^2{}_{ij}$$

$$g_M=\Pi W(n_\lambda,M_\lambda,I_\lambda)(2I_\lambda+I)^{-n_\lambda}$$

Using the above formula, we can obtain the expression for the separation between the center line and the outside one, i. e.

$$\Delta H_{ab}=\Delta H_{bc}=A_N$$

where $K$ term is neglected, since it is actually a very small quantity. Comparing with the experimental results.

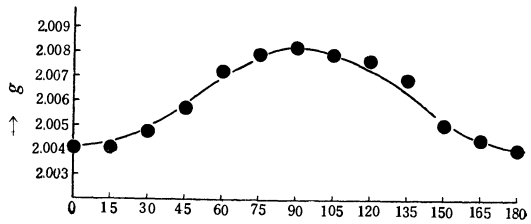
$$-(a_N+b_N)=23.42 \text{ (gauss) at } \beta=0°$$

$$-a_N+b_N/2=2.54 \text{ (gauss) at } \beta=90°$$

Then one obtains

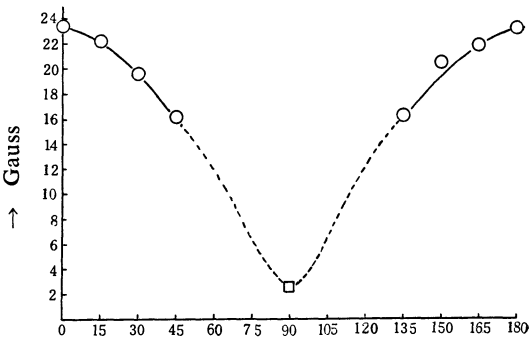
$a_N=-9.5$ gauss (isotropic splitting coeff.)

$b_N=-13.92$ gauss (anisotropic splitting coeff.)



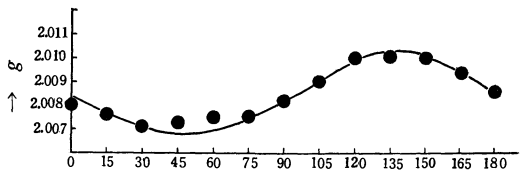

→ Rotation angle, degree

Fig. 5. The angular variation of $g$-values rotated around the a-axis for the 0.0005 mol./l. crystal.




→ Rotation angle, degree

Fig. 6. The angular variation of the hyperfine splittings rotated around the a-axis for the 0.0005 mol./l. crystal where the open circles are the measured widths and the square is the graphically obtained one.




→ Rotation angle, degree

Fig. 7. The angular variation of $g$-values rotated around the b-axis for the 0.0005 mol./l. crystal.

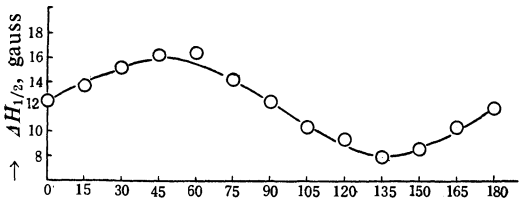



Fig. 8. The angular variation of half-widths rotated around the b-axis for the 0.0005 mol./l. crystal. In this direction there appear only single lines.

The angular variations of the separation between the two successive lines are shown in Figs. 5—8.

From Fig. 6, above 60° rotation of the crystal, the spectrum collapses into a single line. Then we can not measure the separations directly. In order to avoid this difficulty we employed the graphical method, that is, assuming a Gaussian shape for each line, we tried the graphical composition to obtain a composed single line changing the relative distance between the centered line and the outside ones. Thus 2.5 gauss was obtained for the separation at 90° rotation of the crystal.

The anisotropic splitting coefficient $b_N$ will be exressed as

$$b_N = -(4/5)\gamma\gamma_N\hbar(0|r^{-3}|0)$$

where

$\gamma, \gamma_N$: the gyromagnetic ratio for an electron and a nitrogen respectively.

$\hbar$: Planck's constant divided by $2\pi$

$(0|r^{-3}|0)$: the expectation value of the enclosed operator between $2p\pi$ wave functions.

Hence one can obtain

$$(0|r^{-3}|0) = 8.54\times10^{24}\ \mathrm{cm}^{-3}$$

Accoeding to Dousmanis' calculation[20], the "best" theoretical value is

$$(0|r^{-3}|0) = 22.5\times10^{24}\ \mathrm{cm}^{-3}$$

Then the ratio of our result to the Dousmanis' will be

$$(0|r^{-3}|0)/(0|r^{-3}|0) = 0.38$$

This ratio means that in diphenyl nitric oxide the electron distribution amplitude of $2p\pi$ wave function expanded in the series of an orthonormal set of A. O. functions may be 0.38. In other words, this value is the probability of finding an unpaired electron on the nitrogen atom. As mentioned before, the spectra of very diluted single crystals do not give well-resolved proton hyperfine lines but show nitrogen hyperfine lines. Thus we can not apply the results of the weak exchange case in Kivelson's theory.

From Figs. 5—8, the angular variation of $g$-values about a certain axis is larger than the one about another axis perpendicular to the former. Furthermore, in the former case, there appear three well-resolved hyperfine lines and these collapse into a single line by 90° rotation, but in the latter case, the hyperfine line is single and stays in a single line during a rotation.

From these results and the crystallographic orientation of the benzophenone molecules, we might conclude that the p-orbital of a nitrogen atom in diphenyl nitric oxide molecule would be almost parallel to one crystal axis of the bulk crystal.

## Summary

Electron paramagnetic resonance experiments of diphenyl nitric oxide single crystals were performed. Variation of exchange narrowed line were measured by changing the magnitude of magnetic dilution in crystals. Angular variations of $g$-value and of hyperfine spectra were investigated. The value of the exchange integral in pure crystal and the spin density on $^{14}N$ atom in the molecule were determined.

The author wishes to thank Professor S. I. Weissman for his helpful discussions and suggestions; special thanks are due to Professor J. Townsend for offering the chance to used the EPR apparatus which was constructed by him.

*Department of Chemistry*
*Washington University*
*St. Louis, Mo., U. S. A.****

*** On leave from Kyoto University; Fulbright Scholar 1958-1959. Present address: Department of Chemistry, Faculty of Science, Kyoto University, Sakyo-ku, Kyoto.

## Appendix

**Determination of the Isotropic and Anisotropic Hyperfine Splitting Factors for Nitrogen, para-, ortho- and meta-Protons in Benzene Rings of Diphenyl Nitric Oxide.**

Kivelson[20,21] applied the Kubo and Tomita's theory[19] to the organic free radicals in both cases of liquid and solid. We shall summarize the results of his calculation briefly.

In case of weak exchange (i. e. in case of diluted mixed crystals) the resonance frequency of each hyperfine line is

$$\omega = [\gamma + (1/3)\Delta\gamma(3\cos^2\beta - 1) - \delta\gamma\sin^2\beta\cos^2\gamma]B_0$$

$$+\sum_{\lambda} A_\lambda M_\lambda - \frac{S(S+1)K}{3} \tag{1}$$

where

$$A_\lambda^2 = \{(\Phi_{zz}^{(\lambda)} - a_\lambda)^2 + 4 \mid \Phi_{z+}^{(\lambda)} \mid^2\} \tag{2}$$

$$K = J^2 \sum_{M' \neq M} g_{M'} [\sum_{\lambda} A_\lambda (M_\lambda - M_\lambda')]^{-1} \tag{3}$$

$$NJ^2 = \sum_{j} \sum_{i \neq j} J^2_{ij} \tag{4}$$

$$g_M = \prod_{\lambda} W(n_\lambda, M_\lambda, I_\lambda)(2I_\lambda + 1)^{-n_\lambda} \tag{5}$$

$$\Phi_{zz}^{(\lambda)} = \frac{b_\lambda}{2}(3\cos^2\beta - 1) - \sin^2\beta(c_\lambda e^{-2i\tau} + c_\lambda^* e^{2i\tau}) + \sin 2\beta(id_\lambda e^{-i\tau} - id_\lambda^* e^{i\tau}) \tag{6}$$

$$\Phi_{z+}^{(\lambda)} = \{(3/8)b_\lambda i \sin 2\beta - (1/2)i \sin\beta \times [c_\lambda(1+\cos\beta)e^{-2i\tau} - c_\lambda^*(1-\cos\beta)e^{2i\tau}] - (1/2)[d_\lambda(2\cos^2\beta + \cos\beta - 1)e^{-i\tau} + d_\lambda^*(-2\cos^2\beta + \cos\beta + 1)e^{i\tau}]\}e^{-i\alpha} \tag{7}$$

where $J_\lambda$ and $M_\lambda$ are the total and the z-component of angular momentum, respectively, for the $\lambda$'th group of equivalent nuclei in a molecule. There are one nitrogen, 6 para- and ortho-protons and 4 meta-protons in case of diphenyl nitric oxide. $W(n_\lambda, M_\lambda, I_\lambda)$ is the degeneracy of an $M_\lambda$ spin state which is composed of $n_\lambda$ equivalent nuclei with spin $I_\lambda$. In our case we have 3 different $W(n_\lambda, M_\lambda, I_\lambda)$'s, i.e. $W(n_N, M_N, I_N)$, $W(n_{p,o}, M_{p,o}, I_{p,o})$ and $W(n_m, M_m, I_m)$. And $N_N=1$, $M_N=0, \pm 1$, $I_N=1$; $n_{p,o}=6$, $M_{p,o}=0, \pm 1, \pm 2, \pm 3$, $I_{p,o}=1/2$; $n_m=4$, $M_m=0, \pm 1, \pm 2$, $I_m=1/2$. $\gamma$, $\Delta\gamma$, $\delta\gamma$, $\beta$, $\gamma$ and $B_0$ have been explained in the preceding section. Then we shall obtain 105 absorption lines corresponding to the combinations of $M_N$, $M_{p,o}$ and $M_m$. However, in the crystal of diphenyl nitric oxide case only three rather broad absorption lines wese observed.

In order to determine the anisotropic hyperfine splitting coefficients, one inserts the experimental results into the Eq. 1 and calculates the $A_\lambda$'s. The isotropic hyperfine splitting coefficients were determined by direct measurements from the spectra of degassed and vacuum sealed ether solution of diphenyl nitric oxide.

Since a detailed explanation will be given in the forthcoming paper, a brief description of the calculation method of the isotropic and anisotropic hyperfine splitting factors of proton in diphenyl nitric oxide will be presented below.

From the direct measurement of diphenyl nitric oxide spectra, one can obtain the isotropic hyperfine splitting coefficients for para-, ortho- and meta-position protons respectively, i. e.

$$a_{p,o} = +1.96 \text{ gauss}$$

$$a_m = -0.98 \text{ gauss}$$

where we assumed that the spin density at ortho- and para-position ($\rho_{p,o}$) is about twice as large as the one at meta-position ($\rho_m$) and $\rho_{p,o}$ is negative and $\rho_m$ is positive.

The anisotropic hyperfine splitting coefficients will be evaluated as follows[21]

$$b_{p,o} = -\gamma\gamma_H\hbar\langle 0.6\rangle \times 10^{24}\rho_{p,o}$$

$$b_m = -\gamma\gamma_H\hbar\langle 0.6\rangle \times 10^{24}\rho_m$$

where $\gamma$ and $\gamma_H$ are the gyromagnetic ratios of an electron and a proton, respectively.

# *Chemical Studies on Wood Hemicelluloses. III. On the Hemicellulose of Ganpi Bast Fibers. II**

By Seishi MACHIDA and Sadanori NISHIKORI**

(Received September 28, 1960)

In the previous paper, the hemicellulose from the Ganpi plant (*Wichstroemia sikokiana* Franch. et Sav.) was studied in connection with Japanese paper making[1]. It was concluded that a complete picture of the chemical nature of hemicellulose is essential to explain the excellent characteristics of the hand-made paper of Japan.

The present investigation is an attempt in this direction, and the results reported here relate mainly to uronic acid which is the most important component of the hemicellulose. The chemical structure of the hemicellulose was also investigated.

The hemicellulose obtained from holocellulose of Ganpi bast fibers by alkaline extraction gave upon hydrolysis a mixture of an aldobiouronic acid, 4-*O*-methyl-D-glucuronic acid and D-xylose together with small amounts of D-galacturonic acid, D-mannose, D-galactose, L-arabinose and L-rhamnose.

The acidic components were separated from

* The principal part of this paper was presented at the Local Meeting of the Chemical Society of Japan (Chugoku and Shikoku Branch), Matsue, July, 1960.

** Present address: Industrial Experimental Station of Shimane Prefecture, Matsue.

1) S. Machida and S. Nishikori, This Bulletin, 31, 1021 (1958).

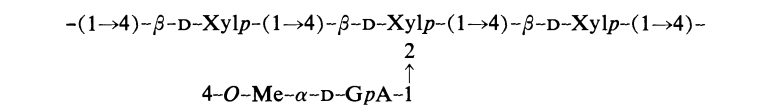



Fig. 1. Structure of Ganpi Hemicellulose.

the hydrolyzate by the use of an anion-exchange resin. By means of chromatography on a column of cellulose[2], 4-*O*-methyl-D-glucuronic acid, D-galacturonic acid and an aldobiouronic acid were isolated from the acidic components.

The 4-*O*-methyl-D-glucuronic acid was characterized after reduction of its ester glycoside with lithium aluminum hydride followed by hydrolysis, as 4-*O*-methyl-D-glucose[3].

The aldobiouronic acid was designated as 2-*O*-(4-*O*-methyl-α-D-glucopyranosyluronic acid)-D-xylopyranose by the following evidences: a paper chromatographic study proved that the $R_X$ value and color reaction of the acid were the same as for 2-*O*-(4-*O*-methyl-D-glucopyranosyluronic acid)-D-xylopyranose[4], and the methoxyl group content and average equivalent weight corresponded to the calculated value of the acid. A high positive specific optical rotation presumed the presumed of an α-glycosidic linkage in the molecule[5]. The aldobiouronic acid hydrolyzed with considerable difficulty and concomitant destruction.

After conversion to the methyl ester methyl glycoside by methanolysis, however, it was comparatively easily hydrolyzed and afforded 4-*O*-methyl-D-glucuronic acid and D-xylose in equal amounts. Reduction of the ester glycoside of the aldobiouronic acid with lithium aluminum hydride followed by hydrolysis readily yielded 4-*O*-methyl-D-glucose and D-xylose. The aldobiouronic acid isolated here is identical with that obtained by partial hydrolysis of a large number of wood hemicelluloses[6].

The D-galacturonic acid was identified chromatographically after being conversed into D-galactose. But the D-galacturonic acid is believed to originate in pectic substances in the bast fibers. As has previously been reported, pectic substances are contained in the bast fibers of the Ganpi plant, and the hemicellulose isolated from the fibers is unavoidably contaminated more or less with the pectic substances[7]. The D-galacturonic acid is not a component of the hemicellulose molecule.

By oxidation of the Ganpi hemicellulose with 0.27 M sodium periodate[8], it was shown that the periodate uptake was about one mole per pentose unit. The reaction, however, was not and it was found that a small amount of D-xylose unid in the hemicellulose remained unoxidized. It is believed that the D-xylose unit had been attached by a 4-*O*-methyl-D-glucuronic acid side chain in the main chain of the molecule.

From the above consideration, it seems justifiable to assign the main chain of the Ganpi hemicellulose to the structure as Fig. 1. As was reported in the previous paper, the Ganpi hemicellulose has basically a linear structure built up from about 160 xylose residues with, on the average, every sixth xylose units carrying a uronic acid residue[1].

The xylopyranose residues are jointed together with 1, 4-β-linkages. The side chain is formed from single 4-*O*-methyl-D-glucuronic acid residue which is linked to the main chain by a 1, 2-α-linkage.

The constitution of the hemicellulose of the Ganpi bast fibers is similar, albeit not identical, to that of other sorts of wood hemicelluloses[6]. But it is noticeable that this hemicellulose molecule has a comparatively longer chain and has more uronic acid groups along the chain than other wood hemicelluloses.

The studies on the methylation of the hemicellulose will be reported in the next paper.

## Experimental

All evaporation were carried out under reduced pressure at a bath temperature not exceeding 40°C. Optical rotations were determined at 16°C and in water unless otherwise stated. In paper chromatographic studies, the sugar and uronic acid mixtures were separated on a sheet of Toyo Roshi No. 50 filter paper by the ascending method, using one of the following solvents in the volume ratios as indicated: (A) ethyl acetate-acetic acid-formic acid-water (18 : 3 : 1 : 4), (B) *n*-butanol-ethanol-water (40 : 11 : 19), (C) ethyl acetate-pyridine-water

2) L. Hough, J. K. N. Jones and W. H. Wadman, *J. Chem. Soc.*, **1950**, 1702.
3) B. Lythgoe and S. Trippett, ibid., **1950**, 1983; F. Smith, ibid., **1951**, 2646.
4) G. G. S. Dutton and F. Smith, *J. Am. Chem. Soc.*, **78**, 2505 (1956); C. P. J. Glaudemans and T. E. Timell, ibid., **80**, 941 (1958).
5) J. K. N. Jones and L. E. Wise, *J. Chem. Soc.*, **1952**, 3380; R. L. Whistler, H. E. Conrad and L. Hough, *J. Am. Chem. Soc.*, **76**, 1668 (1954).
6) G. O. Aspinall, "Advances in Carbohydrate Chemistry", Vol. 14, Academic Press, New York (1959), p. 429; W. J. Polglase., ibid., Vol. 10 (1959), p. 283; R. L. Whistler, ibid., Vol. 5 (1950), p. 269.
7) S. Machida and S. Nishikori, *Bull. Fac. Text. Fibers, Kyoto Univ. Ind. Arts & Text. Fibers*, **3**, 94 (1960).
8) S. K. Chanda, E. L. Hirst, J. K. N. Jones and G. V. Percival, *J. Chem. Soc.*, **1950**, 1289.

TABLE I. FRACTION OF ACID COMPONENT OF HEMICELLULOSE

| Fraction | Yield (%) from Hemicellulose | $[\alpha]_D^{16}$ | Average equivalent weight | $R_x$[a] | Coloration[b] after five min. | Coloration[b] after a few days |
|---|---|---|---|---|---|---|
| A | 1.9 | 75.6 | 202 | 1.60 | Red | Yellowish brown |
| B | 5.2 | 94.7 | 332 | 0.74 | Red | Red |
| C | 1.2 | 69.8 | 200 | 0.48 | Red | Brown |

a) Solvent A.
b) 3% Butanol solution of *p*-anisidine hydrochloride.

(2 : 1 : 2). All sugars and uronic acids were located by spraying the paper with an aqueous solution of *p*-anisidine hydrochloride unless otherwise stated. $R_x$ represents the rate of movement on the paper relative to D-xylose.

**Separation of the Acid Component of Ganpi Hemicellulose.**—The hemicellulose was prepared by the extraction of holocellulose of bast fibers of the Ganpi plant with 5% sodium hydroxide solution in the manner described in the previous paper[1].

The hemicellulose (10 g.) was dissolved in 1 N sulfuric acid (500 ml.) and heated on a water bath for 8 hr. The cooled solution was neutralized with barium hydroxide solution to a pH of 3, and barium sulfate was removed by filtration. The filtrate was passed through a column of Amberlite IR-120 resin to remove barium ions. The acid eluate was passed through a column of Amberite IR-4B resin and the column was washed until the washings gave a negative Molish test. The acid component was eluted from the resin with 1 N sodium hydroxide solution (25 ml.), the alkaline solution passed through Amberlite IR-120 and the eluate therefrom concentrated to dryness, giving a glassy solid (1.1 g.). On analysis, the average equivalent weight by titration was 314 and the methoxyl group content was 6.2%; theoretical values calculated for $C_{12}H_{20}O_{11}$ are 340 and 9.1% respectively. Paper chromatography using solvent A showed the fraction to be a mixture of 4-*O*-methyl-D-glucuronic acid ($R_x$ 1.60), an aldobiouronic acid ($R_x$ 0.72) and D-galacturonic acid ($R_x$ 0.48).

**Fractionation of the Acid Component of Ganpi Hemicellulose.**—The mixture (1 g.) was fractionated on a column of cellulose[2] (3 cm. diameter, 25 cm. long) with, as eluant, ethyl acetate-acetic acid-water (9 : 2 : 2).

The normal rate at which the eluant passed through the column was about 0.25 ml. per min. The effluent was collected on an automatic fraction collector and, after examination of paper chromatograms, was grouped into three separated fractions. Each fraction was extracted with an equal volume of water, the aqueous phase separated and the organic phase discarded. The aqueous solution was extracted four times with an equal volume of ether to remove acetic acid-ethyl acetate, and then evaporated to dryness. Table I shows the yields and properties of the three fractions.

**Characterization of the Fractions.** — *Fraction A*: Paper chromatography showed the fraction to be mainly 4-*O*-methyl-D-glucuronic acid[3]. To confirm this, a portion of the glassy matter (110 mg.) was refluxed with 1.8% methanolic hydrogen chloride (50 ml.) for 6 hr. After neutralization with silver carbonate, filtration, and evaporation, the methyl ester methyl glycoside was obtained. It was dissolved in tetrahydrofuran (150 ml.) and reduced with a solution of lithium aluminum hydride (200 mg.) in the same solvent (50 ml.). After half an hour the excess of lithium aluminum hydride was decomposed by the addition of ethyl acetate and the mixture was diluted with water. The organic solvents were evaporated, the solution filtered and the filtrate was deionized with Amberlite resins IR-4B and IR-120. The neutral solution was evaporated to syrup. On paper chromatograms, as is shown in Table II, it gave three spots corresponding to 4-*O*-methyl-D-glucose, D-xylose and D-galactose. The spots of the last two sugars were very faint. From the data shown in Tables I and II, the Fraction A was found to be

TABLE II. PAPER CHROMATOGRAPHY OF THE REDUCING SUGARS FROM REDUCTION OF THE FRACTION A

| Sugar detected | $R_x$ value Solvent A | Solvent B | Solvent C |
|---|---|---|---|
| 4-*O*-Methyl-D-glucose | 1.30 | 1.20 | 1.14 |
| D-Xylose | 1.00 | 1.00 | 1.00 |
| D-Galactose | 1.41 | 0.76 | 0.61 |

4-*O*-methyl-D-glucuronic acid accompanying traces of D-xylose and D-galacturonic acid. D-Galactose was probably derived from D-galacturonic acid[7].

When the fraction A was preserved in a desiccator for a long time, a part of the 4-*O*-methyl-D-glucuronic acid was found to change to its lactone, which gave a pink spot ($R_x$ 1.60) on a paper chromatogram in solvent A.

*Fraction B*; Paper chromatography showed the fraction to be an aldobiouronic acid. As is shown in Table I, $R_x$ value in solvent A, average equivalent weight and optical rotation corresponded to those of 2-*O*-(4-*O*-methyl-D-glucopyranosyluronic acid)-D-xylopyranose[4,5].

A portion of the aldobiouronic acid (500 mg.) was converted to its ester methyl glycoside by methanolysis with 5% methanolic hydrogen chloride (25 ml.). After removing the solvent, a syrup was yielded. The syrup was dissolved in 1 N hydrochloric acid, and the solution was heated on a boiling water bath for 25 hr., the course of hydrolysis being followed by iodometric titrations. The solution was neutralized with silver carbonate, filtered and removed from silver ion with hydrogen sulfide. Filtration and evaporation of the solution yielded a syrup (300 mg.) which, by paper

chromatographic examination, was found to consist mainly of 4-*O*-methyl-D-glucuronic acid and D-xylose in equal amounts. A trace of aldobiouronic acid unreacted was also detected as a faint pink spot in the chromatogram. The syrup of the hydrolyzate was fractionated by chromatography on ten sheets of Toyo Roshi No. 50 filter paper (30×60 cm.) using solvent A. The fraction corresponding to 4-*O*-methyl-D-glucuronic acid was extracted from the appropriate strips of paper with methanol in a Soxhlet apparatus and syrup (70 mg.) was yielded by evaporating the extract. The fraction corresponding to D-xylose was extracted with water. The extract was deionized by passing down a column of Amberlite IR-4B resin and evaporated to a syrup (190 mg.) which on cooling gave crystalline D-xylose. After recrystallisation from methanol the pure D-xylose had m. p. 142~143°C, $[\alpha]_D^{16}$ +17.6°.

Another portion of the aldobiouronic acid (100 mg.) was converted to its methyl ester glycoside by refluxing with 1.8% methanolic hydrogen chloride (50 mg.) for 8 hr. Neutralization with silver carbonate and evaporation yielded a syrup which was dissolved in tetrahydrofuran (50 ml.) and reduced with lithium aluminum hydride (200 mg.). Hydrolysis of the neutral disaccharide with 1 N sulfuric acid, neutralization with barium carbonate, and concentration yielded a clear syrup which yielded two spots of equal intensity on the paper chromatogram in solvent A, corresponding in color reaction and position to 4-*O*-methyl-D-glucose and D-xylose.

*Fraction C.* Paper chromatography showed the fraction to be D-galacturonic acid[7]. A portion of the fraction was converted to its ester methyl glycoside by methanolysis and reduced with lithium aluminum hydride in the manner described above. Only D-galactose was obtained. This was confirmed by paper chromatography.

**Periodate Oxidation of Ganpi Hemicellulose.**— The hemicellulose (160 mg.) was shaken with water (25 ml.), and to it was added 0.27 M sodium metaperiodate solution (25 ml.) at room temperature in the dark. At intervals portions (5 ml.) were withdrawn and the periodate contents were determined by the arsenite method. The results obtained are shown in Table III. After the oxidation, the excess of periodate was destroyed by adding ethylene glycol. The solution was dialyzed against tap water to remove inorganic ions, evaporated to a syrup, and hydrolyzed with 1 N sulfuric acid for 6 hr. Neutralization with barium hydroxide solution, filtration and then evaporation of the filtrate, yielded a syrup. Examination by paper chromatography indicated the presence of D-xylose only.

Table III. Periodate uptake of Ganpi hemicellulose

| Time, hr. | 17 | 65 | 141.5 | 232.5 |
|---|---|---|---|---|
| $NaIO_4/C_5H_8O_4$ | 0.98 | 1.02 | 1.18 | 1.17 |

## Summary

The hemicellulose of Ganpi bast fibers (*Wickstroemia sikokiana* Franch. et Sav.) gave upon hydrolysis a mixture of an aldobiouronic acid, 4-*O*-methyl-D-glucuronic acid and D-xylose together with small amounts of D-galacturonic acid, D-mannose, D-galactose, L-arabinose and L-rhamnose.

The acidic components were separated, and by means of chromatography on a column of cellulose, 4-*O*-methyl-D-glucuronic acid, D-galacturonic acid and 2-*O*-(4-*O*-methyl-D-glucopyranosyluronic acid)-D-xylopyranose were isolated and characterized.

A structure was proposed for the hemicellulose which has a straight chain of about 160 1,4-linked-β-D-xylopyranose residues with, on the average, every sixth residue carrying a terminal 4-*O*-methyl-α-D-glucopyranosyluronic acid residue linked through position 2.

The D-galacturonic acid is believed to originate in pectic substance and not a component of the hemicellulose.

A part of the expense for this work was defrayed by the Grant-in-Aid for Scientific Research from the Ministry of Education. This is gratefully acknowledged.

*Chemical Laboratory of Textile Fibers*
*Kyoto University of Industrial Arts*
*and Textile Fibers*
*Kita-Ku, Kyoto*

# *Polarographic Studies of Some Organo-sulfur Compounds. I. A. C. and D. C. Polarography of Potassium Thiobenzoate*

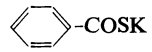
By Koichi OKAMOTO

(Received August 31, 1960)

A number of the polarographic investigations of various organo-sulfur compounds have been reported. Especially thiol-type compounds such as cysteine[1] and glutathion[2] have been studied in detail, related to their reduction-oxidation systems.

Thiobenzoyl type sulfur compounds, however, have not been studied polarographically.

In this paper, the polarographic behaviors of potassium thiobenzoate (I), will be reported.




(I)

## Experiments and Results

The polarograph used was the Yanagimoto model PA-102 [D.C. & A.C. (superimposed with sinusoidal A.C. of 50 c.p.s. in frequency and of 15 mV. r.m.s. in amplitude)]. The characteristics of the dropping mercury electrode used were: $m=0.986$ mg. $sec^{-1}$, $t=4.74$ sec. (open circuit).

Synthesized pure potassium thiobenzoate (PTB) was used and its purity was tested by iodometric titration and microanalysis. All other reagents were of reagent grade.

Experiments were carried out 2 or 3 times on the same kind of sample at 25°C and the values obtained were averaged in general. The values of potentials were expressed in V. vs. S. C. E. and of currents in $\mu$ぅ or in $\mu$A.

**The Influences of pH to the Limiting Currents $i_l$, the Peak Currents $i_s$ and to the Half-wave Potentials $E_{1/2}$, the Summit Potentials $E_s$.**—In the buffer solutions of pH 1.5~12.0, PTB showed three oxidation waves; some of them are shown in Fig. 1.

The relationships of pH to $i_l$, $i_s$ and $E_{1/2}$, $E_s$ are shown in Table I, Figs. 2 and 3.

The first wave had a half-wave potential very close to the second, while the third occurred at more negative potentials.

The D. C. wave heights of the 1st and the 2nd waves were both independent of pH, but the 3rd

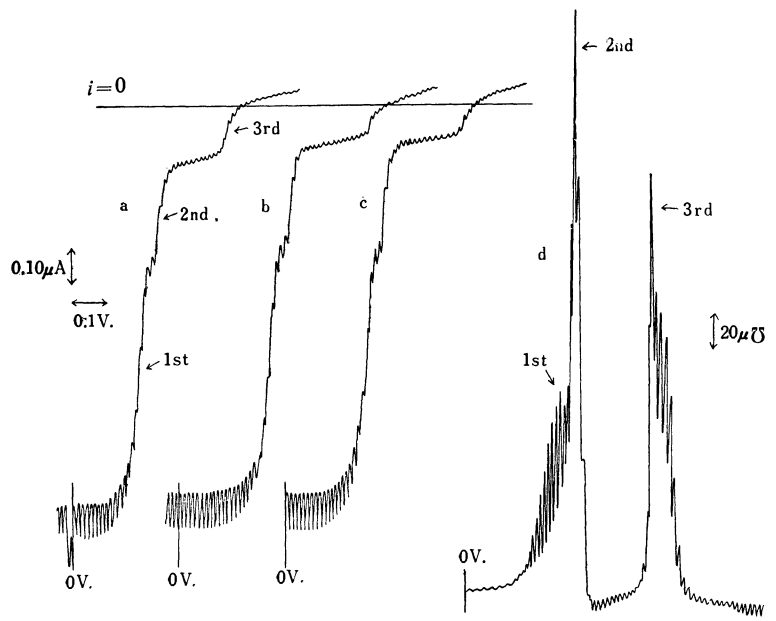



Fig. 1. Typical polarograms of PTB. a: D.C. pH=1.5, b: D.C. pH=5.0, c: D.C. pH=10.0, d: A.C. pH=10.0, [PTB]=$0.5\times10^{-3}$ mol./l., at 25°C. The solutions were air-free. Damping (D.C.)=50$\mu$F, capacitance (A.C.)=0$\mu$F.

1) I. M. Kolthoff and J. J. Lingane, "Polarography", Interscience Publishers, New York (1952), p. 779.

2) I. Tachi et al., *J. Agr. Chem. Soc. Japan* (*Nippon Nogei-Kagaku Kaishi*), 25, 278, 281, 325 (1952).

TABLE I. THE VARIATION OF $i_1$, $i_s$ and $E_s$, $E_{1/2}$ WITH pH
[PTB] $=0.5\times10^{-3}$ mol./l., measured at 25°C

| pH | Buffer | $i_1$, μA | | | $i_s$, μʊ | | | $-E_{1/2}$, V. vs. S.C.E. | | | $-E_s$, V. vs. S.C.E. | | |
|---|---|---|---|---|---|---|---|---|---|---|---|---|---|
| | | $i_1^1$ | $i_1^2$ | $i_1^3$ | $i_s^1$ | $i_s^2$ | $i_s^3$ | $E_{1/2}^1$ | $E_{1/2}^2$ | $E_{1/2}^3$ | $E_s^1$ | $E_s^2$ | $E_s^3$ |
| 1.5 | A | 0.730 | 0.283 | 0.139 | 128 | 313 | 309 | 0.188 | 0.256 | 0.435 | 0.215 | 0.260 | 0.434 |
| 2.5 | A | 0.725 | 0.285 | 0.113 | 112 | 298 | 283 | 0.219 | 0.291 | 0.487 | 0.241 | 0.291 | 0.489 |
| 3.2 | B | 0.723 | 0.289 | 0.100 | 106 | 285 | 266 | 0.235 | 0.300 | 0.520 | 0.255 | 0.310 | 0.526 |
| 4.0 | B | 0.730 | 0.291 | 0.090 | 109 | 295 | 266 | 0.243 | 0.308 | 0.534 | 0.257 | 0.309 | 0.526 |
| 5.0 | B | 0.728 | 0.290 | 0.085 | 114 | 310 | 261 | 0.250 | 0.320 | 0.542 | 0.258 | 0.305 | 0.525 |
| 6.0 | C | 0.727 | 0.298 | 0.090 | 114 | 305 | 247 | 0.250 | 0.314 | 0.536 | 0.258 | 0.305 | 0.526 |
| 7.5 | C | 0.737 | 0.291 | 0.090 | 113 | 303 | 260 | 0.250 | 0.314 | 0.533 | 0.258 | 0.307 | 0.526 |
| 9.0 | D | 0.738 | 0.290 | 0.098 | 114 | 292 | 237 | 0.250 | 0.312 | 0.524 | 0.259 | 0.308 | 0.529 |
| 10.0 | E | 0.741 | 0.291 | 0.100 | 113 | 290 | 244 | 0.250 | 0.310 | 0.516 | 0.258 | 0.310 | 0.529 |
| 12.0 | E | 0.735 | 0.299 | 0.100 | 111 | 295 | 240 | 0.250 | 0.309 | 0.519 | 0.258 | 0.312 | 0.528 |

A: 0.1 M $CH_3COOH$-HCl, B: 0.1 M $CH_3COOH$-$CH_3COONa$, C: 0.1 M $KH_2PO_4$-$Na_2HPO_4$,
D: 0.1 M $Na_2B_4O_7$-HCl, E: 0.1 M $Na_2B_4O_7$-NaOH.

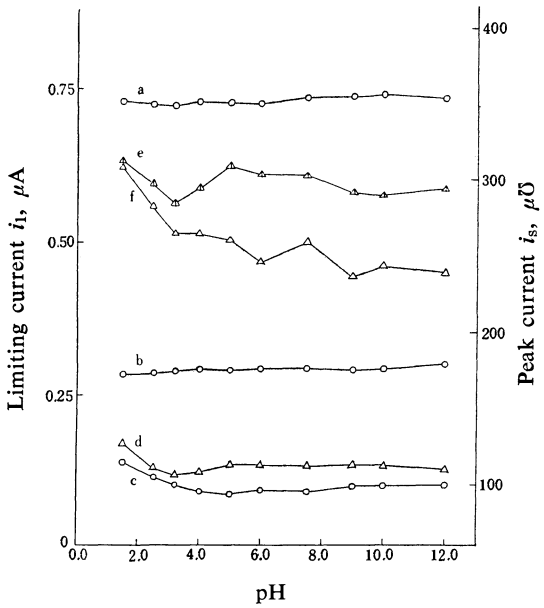



Fig. 2. The relation of $i_s$ and $i_1$ to pH.
a: D.C. 1st wave d: A.C. 1st wave
b: D.C. 2nd wave e: A.C. 2nd wave
c: D.C. 3rd wave f: A.C. 3rd wave
[PTB] $=0.5\times10^{-3}$ mol./l., at 25°C

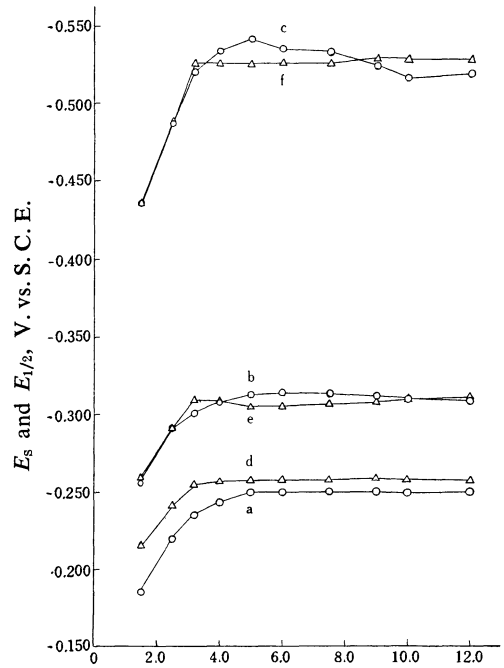



Fig. 3. The relation of $E_s$ and $E_{1/2}$ to pH.
a, b, c: D.C. 1st, 2nd and 3rd wave respectively
d, e, f: A.C. 1st, 2nd and 3rd wave respectively
[PTB] $=0.5\times10^{-3}$ mol./l., at 25°C.

seemed to be fairly affected with pH in very acidic solutions.

In A.C. polarography, the 2nd and the 3rd waves showed very large peak current in comparison with the 1st; the pH-dependence of them, however, was almost the same as that of the D.C. waves.

As shown in Fig. 3, the negative shift of $E_{1/2}$ and $E_s$ of 1st and 2nd waves with pH increase was observed in more acidic conditions than pH 3.5 and in the more basic region they were both independent of pH.

A theoretical equation[2] of the reversible oxidation wave of sulfhydryl compounds to the corresponding disulfides was expressed in Eq. 1;

$$E=E_0+(\boldsymbol{RT}/\boldsymbol{F})\ln[H^+]-(\boldsymbol{RT}/2\boldsymbol{F})\ln(i_d-i)^2/i + (\boldsymbol{RT}/2\boldsymbol{F})\ln(K\mathrm{D}_{red}/2\mathrm{D}_{ox}^{1/2}) \quad (1)$$

then half-wave potential $E_{1/2}$ was in Eq. 2;

$$E_{1/2}=E_0+(\boldsymbol{RT}/\boldsymbol{F})\ln[H^+]-(\boldsymbol{RT}/2\boldsymbol{F})\ln(i_d/2 + (\boldsymbol{RT}/2\boldsymbol{F})\ln(K\mathrm{D}_{red}/2\mathrm{D}_{ox}^{1/2}) \quad (2)$$

where $K$ is a dissociation constant.

According to Eq. 2, under the conditions of constant concentration and moreover of $[H^+] \gg K$, the half-wave potential may shift to more negative potentials, but of $[H^+] \ll K$, it may be independent of pH values.

It was found that the relations shown in Fig. 3 almost completely followed Eq. 2. $K$ of PTB obtained from Fig. 3 was approximately 3.5.

In neutral buffer solutions, the solutions of PTB often came to be turbid and in acidic solutions (pH<4), A. C. polarograms had complicated forms, therefore the following experiments were carried out in basic buffer solution of pH 10.0 (0.1 M borate buffer).

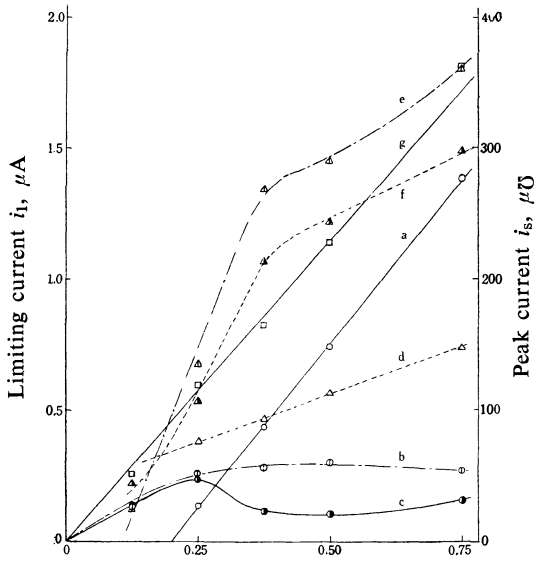



Fig. 4. The relation of $i_s$ and $i_l$ to the concentration.
a, b, c: D. C. 1st, 2nd and 3rd wave respectively
d, e, f: A. C. 1st, 2nd and 3rd wave respectively
g: D. C. total wave (1st+2nd+3rd)
Supporting electrolyte is 0.1 M borate buffer pH 10.0.

**The Relations of the Concentrations of PTB to $i_l$, $i_s$ and $E_{1/2}$, $E_s$.**—In the cases where there was diffusion or kinetic currents, good linearity was generally found between concentrations and wave heights. A linear relation was observed for the 1st wave, but it did not pass the zero point. Better linearity was found for the total wave as shown in Fig. 4.

Saturation phenomena were found for the 2nd and the 3rd waves of both D. C. and A. C. polarograms.

The relations between $E_{1/2}$, $E_s$ and $C$ were shown in Fig. 5. A negative shift of $E_{1/2}$ and $E_s$ of the 1st and 2nd waves was observed, while the 3rd seemed to be independent of the concentrations.

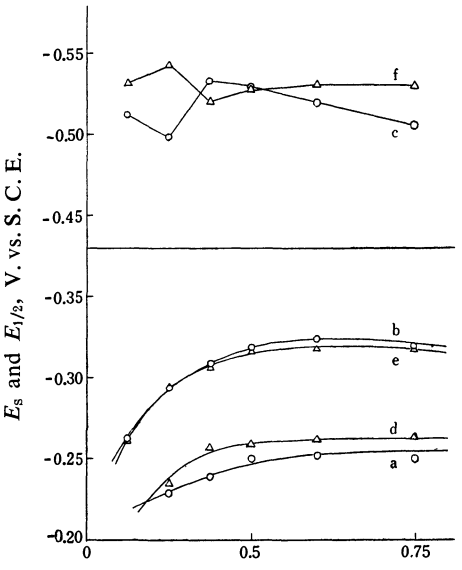



Fig. 5. The relation of $E_{1/2}$ and $E_s$ to the concentrations.
a, b, c: D. C. 1st, 2nd and 3rd wave respectively
d, e, f: A. C. 1st, 2nd and 3rd wave respectively
Supporting electrolyte is 0.1 M borate buffer pH 10.0.

In Eq. 2, it was shown that at constant pH, the half-wave potentials may shift to more negative potentials with concentration increase. The behaviors of the 1st and the 2nd waves seemed to coincide approximately with the theory.

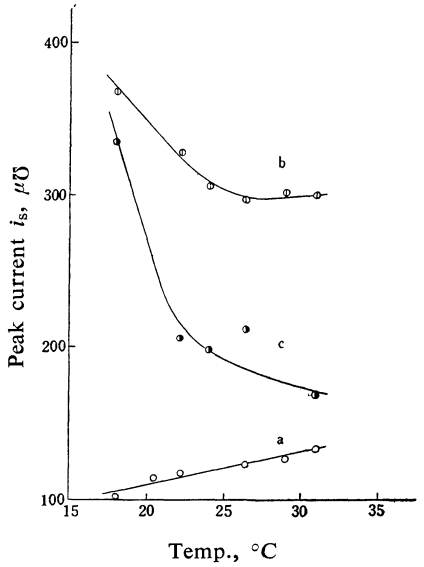



Fig. 6. The relation of $i_s$ to temperature.
a: 1st, b: 2nd, c: 3rd wave.
[PTB] $= 0.5 \times 10^{-3}$ mol./l. in 0.1 M borate buffer pH 10.0.

**The Influences of Temperature upon $i_1$, $i_s$ and $E_{1/2}$, $E_s$.**—Very different results were obtained in D. C. and A. C. polarograms. In D. C., all temperature coefficients of the first, the 2nd and the 3rd were 2.15, 0.74 and 3.51% respectively, but in A. C., only the 1st had the positive coefficient of 1.94% and the others showed negative values as shown in Fig. 6.

It could be known that the 2nd and the 3rd waves were tensammetric and the 1st was considered to contain partly the kinetics current.

As shown in Table II, both the A. C. and D. C. waves shifted to more positive potentials according to the rise of temperature.

TABLE II. THE VARIATIONS OF $E_{1/2}$ AND $E_s$ WITH TEMPERATURE
[PTB] $=0.5\times10^{-3}$ mol./l. in 0.1 M borate buffer pH 10.0

| Temp. °C | $-E_{1/2}$* | | | $-E_{1/2}$* | | |
|---|---|---|---|---|---|---|
| | $-E^1_{1/2}$ | $-E^2_{1/2}$ | $-E^3_{1/2}$ | $-E^1_s$ | $-E^2_s$ | $-E^3_s$ |
| 18.0 | 0.250 | 0.323 | 0.540 | 0.267 | 0.317 | 0.540 |
| 20.5 | — | — | — | 0.265 | 0.313 | 0.529 |
| 22.2 | 0.250 | 0.322 | 0.532 | 0.269 | 0.312 | 0.525 |
| 24.0 | 0.250 | 0.315 | 0.521 | 0.267 | 0.312 | 0.526 |
| 26.4 | 0.250 | 0.311 | 0.516 | 0.260 | 0.300 | 0.517 |
| 29.0 | 0.240 | 0.308 | 0.510 | 0.255 | 0.301 | 0.511 |
| 31.0 | 0.240 | 0.300 | 0.496 | 0.256 | 0.297 | 0.510 |

* V. vs. S. C. E.

**The Relation between the Mercury Reservoir Height $H$ and the Wave Height $i_1$ in D. C. Polarograms.** — Good linearities were obtained between $\log H$ (corrected with the reverse pressure, $3.1/(mt)^{1/3}$) and $\log i_1$. They could be written as follows:

$$\text{1st wave:} \quad i_1 = H^{0.18} + K_1 \qquad \text{(I)}$$

$$\text{2nd wave:} \quad i_1 = H^{0.64} + K_2 \qquad \text{(II)}$$

$$\text{3rd wave:} \quad i_1 = H^{0.61} + K_3 \qquad \text{(III)}$$

$$\text{Total wave:} \quad i_1 = H^{0.33} + K_4 \qquad \text{(IV)}$$

where $K_1, \cdots, K_4$ were constants.

It seemed that the 1st consisted of the two components; kinetic and diffusion currents and the two others, of diffusion and adsorption currents.

In the case of the complicated systems, the usual analysis of the relationship between $H$ and $i_1$, such as the plotting of $H^{1/2}$ against $i_1$ or $H$ against $i_1$, was considered to be less accurate than the method of the plotting of $\log H$ against $\log i_1$. In fact, the relation between $H$ or $H^{1/2}$ and $i_1$ both showed appearent linearities, so that no definite results could be obtained.

**Logarithmic Plotting.** — The relations between the applied potentials $E$ and $\log\{i/(i_d-i)\}$ and $\log\{i/(i_d-i)^2\}$ were investigated. Only the 1st wave showed good linearity of $RT/nF=28$ mV., if $E$ was plotted against $\log\{i/(i_d-i)^2\}$, the two others showed S-shaped curves, and the relations of $E$ to $\log\{i/(i_d-i)\}$ of each three waves were S-shaped too.

The 1st wave was considered to be two electrons oxidation producing one mole of the oxidation form from two moles of the reduced form.

**Electrocapillary Curve.**—When the adsorption or desorption of depolarizers takes place on the surface of D. M. E., some irregularities may be found in the electrocapillary curves.

As shown in Fig. 7, a remarkable irregularity was found from −0.65 up to 0 V. having a sharp minimum at −0.27 V.; this minimum corresponded to the 2nd wave approximately.

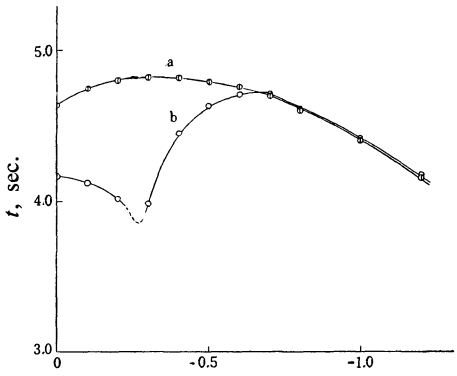



Fig. 7. Electrocapillary curves.
a: Reference pH 10.0, 0.1 M borate buffer.
b: 1 mM PTB in a.

**Polarograms Obtained with a Rotating Platinum Microelectrode.**—In order to know the real oxidation potential of PTB to the disulfide form, benzoyl disulfide, a platinum electrode was employed. The polarograms obtained are shown in Fig. 8. The

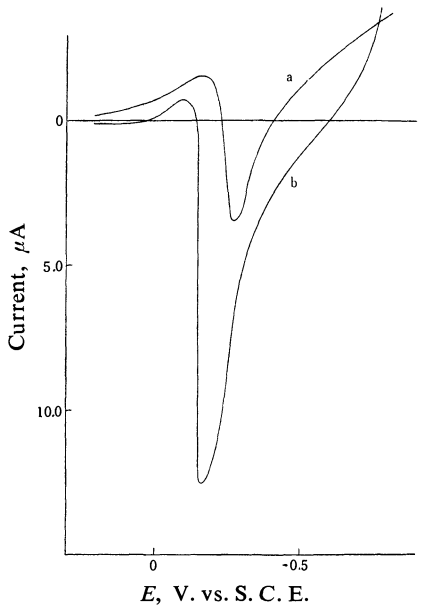



Fig. 8. Polarograms with a rotating platinum electrode. (1400 r. p. m., $\phi=0.8$ mm., $l=6$ mm. horizontal)
a: 0.5 mM, b: 1 mM PTB in a 0.1 M borate buffer (pH 10.0).

reproducibility and the reversibility of the waves, however, were inferior to those of D. M. E., but a notable peak at the potential of $-0.1\sim-0.3$ V. was recognized in every experiment.

This irreversible peak current was considered to be the oxidation wave of PTB to its disulfide, because the formations of mercury salts of PTB do not occur in the case of the oxidation reaction with Pt-electrode. It coincided with the oxidation waves obtained at D. M. E., therefore the oxidation which occurred at D. M. E. was thought to be the formation of disulfide.

## Discussion

The characteristics of the three oxidation waves of PTB are summarized as follows:

(1) The 1st wave is considered to be the diffusion current having the slight kinetic properties and to be two-electrons oxidation forming its disulfide.

(2) The 2nd and the 3rd waves are so-called tensammetric waves, owing to the adsorption or the desorption at the surface of D. M. E. and this adsorption is thought to continue during the applied potentials which change from $-0.65$ V. to more positive potentials beyond 0 V.

The oxidation of PTB takes place at $-0.5$ V. approximatly; then the adsorption of PTB to the surface of D.M.E. occurs continuously. The adsorbed PTB might be electro-inactive, so that the rise of the oxidation current is suppressed during the adsorption continuing down to $-0.3$ V. At the potential $-0.3$ V. PTB is desorbed and becomes electro-active again, therefore the oxidation current begins to increase.

The oxidation product of PTB also seems to be adsorptive to D. M. E., because the abnormal decrease of $t$ is observed at more positive potentials than $-0.3$ V. (Fig. 7).

Slight kinetic properties, described in previous sections, of the 1st wave are attributed to the continuous adsorption, desorption and oxidation of PTB and to the secondary adsorption of the oxidation product.

The whole oxidation process is expressed as follows:

$$2C_6H_5COS^- \rightleftarrows (C_6H_5COS)_2+2e$$

## Summary

The polarographically new sulfur compound, potassium thiobenzoate, was investigated, using A. C. and D. C. polarographs. Comparatively complicated three oxidation waves were observed in both polarograms.

According to the various investigations about the properties of these waves, it was found that the whole reaction was the oxidation of PTB to its disulfide, benzoyl disulfide. The 1st wave was mainly due to this oxidation reaction and the two others were mainly due to the adsorption and the desorption of PTB at the surface of D. M. E.

The reversible oxidation-reduction system consisting of PTB and benzoyl disulfide would not be expected owing to the adsorption and desorption processes that interfered with the normal oxidation of PTB to benzoyl disulfide, if the studies were done with a dropping mercury electrode.

The author is very much indebted to Director M. Matsui for affording facilities for this investigation.

*Physicochemistry Section*
*Research Department*
*Sankyo Co., Ltd.*
*Shinagawa-ku, Tokyo*

# *Studies on the Chemical Decomposition of Simple Sugars. XI. Acetol Formation from $^{14}C$-Labeled Pentoses**

By Jun'ichi HAYAMI

(Received December 16, 1960)

In the preceding report[1], formation of acetol from labeled hexoses was examined, and the examination of the activity distribution revealed the origins of every carbon atom of acetol produced. The terminal carbons of hexoses were found to be converted into methyl carbon of acetol.

Moreover, some characteristic properties of

* Presented at the 13th Annual Meeting of the Chemical Society of Japan, Tokyo, April, 1960.

1) R. Goto, J. Hayami, K. Kudo and S. Otani, This Bulletin, 34, 753 (1961).

the reaction suggested that on one of the steps of the reaction, a cleavage in the carbon chain of an intermediate occured between the C-3 and the C-4 of the original hexose, and that no skeletal rearrangement in the $C_3$-group was involved before and after the splitting of the chain.

In a series of papers of the same title, two different mechanisms of acetol formation were proposed[1], the one—Nodzu's mechanism[2a]—assumed an intermediate formation of acetylformoin from a hexose, and the other—Goto's mechanism—assumed an intramolecular oxidation reduction of 3-deoxyhexosone. Goto's challenge for Nodzu's mechanism[2b], had its starting point in the need of a general interpretation for the acetol formation from pentose and hexose. He inferred from Nodzu's mechanism that if it was applied to a pentose, it could not lead to the formation of acetol. However, a pentose as well as a hexose gives acetol. Therefore, for the establishment of a general mechanism of acetol formation, it is important to decide whether there is a common mode of reaction between the mode of acetol formation from pentose and that from hexose.

In the present work, D-xylose-1-$^{14}$C and D-arabinose-5-$^{14}$C were synthesized and these were decomposed in concentrated buffer solution of potassium hydrogen phosphate and acetol was isolated. The distribution of labeled positions was, then, determined.

## Experimental

**Labeled Sugars and Assay Method.**—*D-Xylose-1-$^{14}$C.*—D-Xylose-1-$^{14}$C was synthesized from D-glucose-1-$^{14}$C by Sowden's method[3] with an improvement in the reduction procedure*1; that is, instead of the catalytic hydrogenation of 1,2-*O*-isopropylidene-D-*xylo*-dialdopentofuranose (I)*2, reduction with lithium aluminum hydride was adopted as was the case with the synthesis of 3-*O*-methyl-D-xylose by Corbett[4].

I was prepared from 2.5 g. of D-glucose-1-$^{14}$C according to Sowden's method. Ethereal solution (70 ml.) of I was placed in a two-necked flask equipped with a dropping funnel and a reflux condenser. Lithium aluminum hydride (0.75 g.) in ether (75 ml.) was added dropwise in 30 min.; the mixture was refluxed for 30 min. Excess of lithium aluminum hydride was decomposed with ethyl acetate (2.5 ml.) and water (45 ml.); ether on the upper layer was removed by air current. Residual aqueous solution was neutralized with dilute sulfuric acid and filtered. The filtrate was concentrated under reduced pressure. The residual light syrup was dissolved in 60 ml. of 0.1 N sulfuric acid and heated in a boiling water bath for an hour. After cooling, the hydrolyzate was passed through an ion-exchange resin (10 ml. of Amberlite IR-120 and 25 ml. of Amberlite IR-45). The effluent and the washing were combined and concentrated under reduced pressure. D-Xylose-1-$^{14}$C often crystallized on concentration. However, if necessary, the solution was lyophilized after concentration to an appropriate volume, and the residue was crystallized from methanol-isopropanol in the usual way[5]. Yield; 1.5 g. or 72% (in typical run).

*D-Arabinose-5-$^{14}$C.* — D-Arabinose-5-$^{14}$C was synthesized by Ruff degradation according to Isbell[6].

*Radioassay.* — Every sample was converted into barium carbonate by Van Slyke-Folch wet combustion. Barium carbonate was collected on filter paper, and counted in an infinite thickness in a $2\pi$-gas flow counter*3. Only iodoform was counted in a medium thickness and corrected for an infinite thickness by parallel counting of the parent sugar of about an equal thickness. Probable errors of the counting were all within 5%.

**Decomposition of Labeled Pentose.**—Ten grams of arabinose or xylose was dissolved into 200 ml. of concentrated solution of potassium hydrogen phosphate (40%, pH 6.7); the mixture was heated and distilled in the way described earlier[1,7].

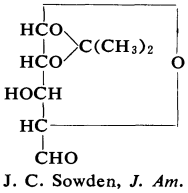
TABLE I. RADIOASSAY DATA FOR $^{14}$C-LABELED PENTOSES

| | Sample | Carbon atom (s) | Radioactivity μc/mol. |
|---|---|---|---|
| | Radioacetol from D-xylose-1-$^{14}$C | | |
| | Xylose-1-$^{14}$C | | 19.6 |
| Acetol | Acetol semicarbazone | all | 9.7 |
| Acetol | Iodoform | $CH_3$ | 9.5 |
| Acetol | Indirectly determined | CO | —* |
| Acetol | Formaldehyde dimedone | $CH_2OH$ | almost 0 |
| | Radioacetol from D-arabinose-5-$^{14}$C | | |
| | Arabinose-5-$^{14}$C | | 257 |
| Acetol | Acetol semicarbazone | all | 136 |
| Acetol | Iodoform | $CH_3$ | 125 |
| Acetol | Indirectly determined | CO | —* |
| Acetol | Formaldehyde dimedone | $CH_2OH$ | 14 |

* Substantially free from radioactivity.

2) a) R. Nodzu et al., *Mem. Coll. Sci. Kyoto Imp. Univ.*, **A20**, 197 (1937).
b) R. Goto, *J. Chem. Soc. Japan* (*Nippon Kwagaku Kwaisi*), **64**, 999, 1054 (1943).

*1 Isbell et al. also proposed an excellent method of reduction with $LiBH_4$ in tetrahydrofuran. (H. S. Isbell et al., *J. Research NBS*, **64A**, 359 (1960)).

*2  (I) or its dimeric form.

3) J. C. Sowden, *J. Am. Chem. Soc.*, **73**, 5496 (1951).
4) W. M. Corbett, G. N. Richards and R. L. Whistler, *J. Chem. Soc.*, **1957**, 11.
5) Cf. H. S. Isbell et al., *J. Research NBS*, **48**, 163 (1952).
6) H. S. Isbell, N. B. Holt and H. L. Frush, ibid., **57**, 95 (1956).
*3 A product of Metro Electronic Institute, Kyoto.
7) R. Nodzu, This Bulletin, **10**, 122 (1935).

Degradation was carried out in the same way as reported earlier[1], but degradation of the acetic acid was not undertaken. Radioactivity of the carbonyl carbon of acetol was determined indirectly from the total activity of acetol deducting the activities of methyl and carbinol carbon. These data are summarized in Table I.

## Results and Discussion

The results from radioassay may be expressed in the following way.

1) In the case of D-xylose-1-$^{14}$C, radioacetol of about a half specific radioactivity of the parent xylose was obtained.

On the degradation, the methyl carbon of acetol was converted into iodoform which contains substantially all the activity of the acetol. The carbinol carbon of acetol was converted into formaldehyde by periodate oxidation and was captured as formaldehyde dimedone which was found almost free from activity. In consequence, xylose-1-$^{14}$C was proved to produce acetol-3-$^{14}$C (methyl-$^{14}$C).

2) D-Arabinose-5-$^{14}$C similarly yielded radioacetol of about a half specific activity of the original arabinose.

The degradation gave iodoform which containes almost all the radioactivity of parent acetol, however a slight degree of activity was observed for formaldehyde which was derived from carbinol carbon of acetol.

Therefore, it may be concluded that arbinose-5-$^{14}$C produces acetol-3-$^{14}$C.

The above results are in accord with the expectation from a tracer experiment of hexoses, that is, the terminal carbon of a pentose —C-1 and C-5— are converted into methyl carbon of acetol.

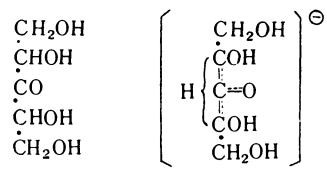
These facts suggest that a common mechanism operates in the formation of acetol from simple sugars.

From Table I, a similar behavior of D-arabinose-5-$^{14}$C and D-xylose-1-$^{14}$C in the formation of acetol is perceived. These facts constitute the characteristics of the acetol formation from a pentose.

Ignoring the effect of a difference in configuration between arabinose and xylose, also ignoring the slight randomization of a label, the contribution ratio of the upper $C_3$ and the lower $C_3$ of a pentose may be postulated as about 1 : 1[8]. Almost an equal contribution of upper and lower $C_3$ part of a pentose for formation of acetol, suggests participation of an intermediate of a good symmetrical structure. This means destruction of the configurational difference between arabinose and xylose to yield an intermediate of common or analogous nature through some transformation reaction of a pentose*4.

In such a reaction an isomerization of a sugar plays an important role on the essential pathway of the reaction, an effect of symmetrical natures of an intermediate may be often visualized[9].

An examination of the mechanism of acetol formation, which will be discussed in detail in a succeeding paper[10], suggests the above intermediate to be 3-ketopentose (II) or its enediolate*5,11,12 (III), in which, the configurational difference between arabinose and xylose is destroyed.



(II) (III)

The author wishes to express his sincere thanks to Professor Ryozo Goto for his constant guidance and encouragement throughout the course of this work. The author also thanks Mr. Shinichi Otani and Mr. Yo Takeda for their generous assistance in carrying out the tracer experiments with labeled xylose.

*Institute of Chemistry*
*Faculty of Science*
*Kyoto University*
*Sakyo-ku, Kyoto*

*4 In addition, there is no essential difference between the acetol formation and a configuration of a monosaccharide. Also refer to R. Goto (loc. cit.)

8) H. F. Bauer and C. Teed, *Can. J. Chem.*, 33, 1824 (1955). Also refer to M. Gibbs, *J. Am. Chem. Soc.*, 72, 3964 (1950).

*5 Or their equivalent compounds.

9) J. C. Sowden, M. G. Blair and D. J. Kuenne, *J. Am. Chem. Soc.*, 79, 6450 (1957).

10) J. Hayami, This Bulletin, 34, 927 (1961).

11) R. L. Whistler and J. N. BeMiller, "Advances in Carbohydrate Chem.", Vol. 13, (1957), p. 289.

12) J. C. Sowden, ibid., Vol. 12, (1957) p., 36. J. C. Speck, Jr., ibid., Vol. 13, (1958), p. 63.

# *Studies on the Chemical Decomposition of Simple Sugars. XII. Mechanism of the Acetol Formation**

By Jun'ichi HAYAMI

(Received December 19, 1960)

Decomposition of partially $^{14}C$-labeled hexoses and of pentoses, which was reported in preceding papers[1,2] revealed the origin of every carbon atom of a resulting acetol, and the terminal carbons of a hexose and of a pentose (C-1 and C-6 of a hexose, C-1 and C-5 of a pentose) were found to be converted into the methyl carbon of acetol.

The next step is to elucidate the mechanism through which the methyl or acetyl group of acetol is formed.

As was already pointed out[2,3], triose can not be an essential intermediate in the formation of acetol from a monosaccharide. Accordingly, a direct transformation of a $C_5$ and of a $C_6$ compound is expected to take place. Generally speaking, except for hydrogenolysis and catalytic hydrogenation, examples of a direct reduction of an aldehydic or a primary carbinol group into a methyl group are scarce, especially in an aqueous reaction medium. In the present instance of acetol formation, aldose may be transformed into a ketose, and the C-1 (and C-5 or C-6) of a ketose may be converted into methyl through one of the following three possible mechanisms.

a) $CH_2OH \cdot CHOH \cdot (CHOH) \rightarrow CH_2 \cdot C(=O) \cdot CHOH \cdot (CHOH) \rightarrow CH_3 \cdot CO \cdot (CHOH)$

b) $CH_2OH \cdot CO \cdot (CHOH) \xrightarrow{RCHO} CH_3 \cdot CO \cdot (CHOH) + (RCOOH)$

c) $CH_2OR \cdot CHOH \cdot CO \rightarrow CH_2 \cdot C(=O) \cdot CO + OR^{\ominus} \rightarrow CH_3 \cdot CO \cdot CO$

(R: alkyl or hydrogen)

They are: **a)** Simple dehydration of vic-diol, which is similar to the thermal decomposition of glycerol[4].

**b)** Mutual oxidation and reduction between $\alpha$-ketol and aldehyde, a reaction which is analogous to the levulinic acid formation from 5-hydroxylevulinic aldehyde[5].

**c)** $\beta$-Hydroxy-carbonyl elimination from 3-ketose or its equivalent compound, a reaction which prevails in the reaction of carbohydrates[6,7].

Among these reactions, the possibility of **a)** can be ruled out, because sugar alcohol such as mannitol yields no acetol by the action of phosphate under decomposition condition[8].

As for **b)**, though this mechanism has been believed to operate in the formation of levulinic acid from hydroxymethylfurfural, there is opposition to this view[9], and in some cases, even an intermediate formation of 5-hydroxylevulinic aldehyde is accepted with doubt[10]. In the Teunissen's mechanism[11], 5-hydroxylevulinic aldehyde is to be converted into levulinic acid through (an intramolecular) acetal formation. This mechanism requires a specific arrangement of a hydroxyl group and an aldehydic group and, in an aqueous medium, an example of acetalformation between separated alcohols and aldehydes is yet unknown. When the above-mentioned acetal formation is to be regarded as proceeding if at all, it can be inhibited through *O*-alkylation at C-1 and/or C-6 of a hexose (C-1 and/or C-5 of a pentose), because no acetal can be produced by action of ether upon an aldehyde. Therefore, acetol formation from 1-*O*-alkylated sugars must be retarded.

As for **c)**, on the other hand, the introduction of an *O*-alkyl group on C-1 (or C-5, C-6)

* Presented at the 13th Annual Meeting of the Chemical Society of Japan, Tokyo, April, 1960.

Part XI, the preceding paper.

1) R. Goto, J. Hayami, K. Kudo and S. Otani, This Bulletin, **34**, 753 (1961).
2) J. Hayami, ibid., **34**, 924 (1961).
3) R. Goto, *J. Chem. Soc. Japan, (Nippon Kwagaku Kwaisi)* **64**, 999, 1054, 1183 (1943); *Mem. Coll. Sci. Kyoto Imp. Univ.*, **A20**, 197 (1937).
4) J. U. Nef, *Ann.*, **335**, 247 (1904).
5) F. H. Newth, "Advances in Carbohydrate Chemistry", **6**, 83 (1951), and references cited therein.
6) J. C. Sowden, ibid., **12**, 36 (1957).
7) R. L. Whistler and J. N. BeMiller, ibid., **13**, 289 (1958).
8) R. Goto, unpublished work.
9) A. P. Dunlop and F. N. Peters, "Furans", Reinhold, New York (1953), p. 648.
10) F. Leger and H. Hibbert, *Can. J. Research*, **16B**, 68 (1938).
11) H. P. Teunissen, *Rec. trav. chim.*, **50**, 1 (1930); R. Pummerer and W. Gump, *Ber.*, **56**, 999 (1923); R. Pummerer, O. Guyot and L. Birkofer, ibid., **68**, 480 (1935).

may facilitate the β-hydroxy-carbonyl elimination from 3-ketose to convert the C-1 into methyl group; thus the formation of acetol from the sugar may be accelerated.

In the present work, 1-*O*-methyl-D-fructose (I), 3-*O*-methyl-D-glucose (II), and 6-*O*-methyl-D-glucose (III) were decomposed to decide which of these two cases actully occurs, and combining the results with those of tracer experiments reported earlier, a general mechanism of acetol formation was made clear.

## Experimental

**Methylated Sugars.**—1-*O*-Methyl-D-fructose[12] was synthesized from sucrose through di-*O*-isopropylidene fructose, and 3-*O*-metyl-D-glucose[12] was synthesized from glucose through di-*O*-isopropylidene-D-glucose in the usual way. 6-*O*-Methyl-D-glucose was synthesized through 1,2-*O*-isopropylidene-6-*O*-tosyl-D-glucose and 1,2-*O*-isopropylidene-5,6-epoxy-D-glucose according to the combination of Reist's method[13] with Ohle's method[14].

**Decomposition of Methylated Sugars.**—A solution of 5.4 g. of 1-*O*-methyl-D-fructose or 6-*O*-methyl-D-glucose in 200 ml. of concentrated potassium hydrogen phosphate buffer (40%, pH 6.7), was heated and distilled in the usual way which was described earlier in a paper[1] (Part X) of this series. In the case of 3-*O*-methyl-glucose, 10.8 g. of the sugar was decomposed in the same way. In the reference experiment, each 5 g. or 10 g. of parent sugar was decomposed.

**Estimation of Acetol in a Distillate**[15].—To 10 ml. of the distillate were added 10 ml. of N/10 KI-$I_2$ solution and 10 ml. of 10% potassium hydroxide solution. After 30 min., the mixture was acidified with 8 ml. of 15% hydrochloric acid, and liberated iodine was titrated with N/10 $Na_2S_2O_3$ standard solution. One milliliter of N/10 KI-$I_2$ solution corresponds to 0.73 mg. of acetol. The amount of acetol was plotted against time, thus distillation curves were given for each sugar and derivative respectively (Figs. 1—3).

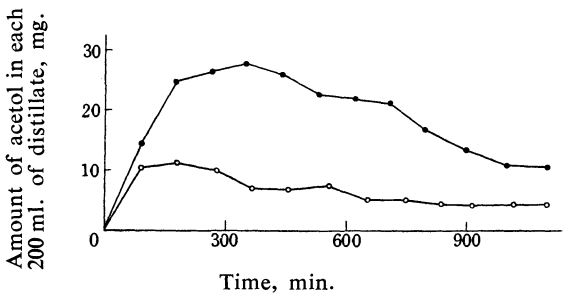



Fig. 1. Acetol formation from 3-*O*-methyl-D-glucose (—○—) (10.8 g.) and from D-glucose (—●—) (10.0 g.) in 200 ml. of potassium hydrogen phosphate buffer solution (ca. 40%, pH 6.7); 200 ml. of distillate was collected for each 90 min. The amount of acetol was determined by iodometric titration, though 3-*O*-methyl-D-glucose actually gave no acetol (also refer to Table I).

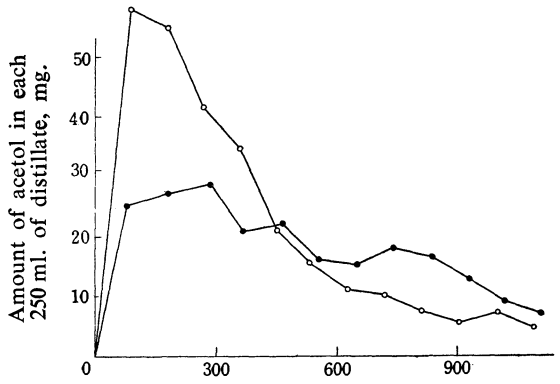



Fig. 2. Acetol formation from 1-*O*-methyl-D-fructose (—○—) (5.4 g.) and from D-fructose (—●—) (5.0 g.) in 200 ml. of potassium hydrogen phosphate buffer solution (ca. 40%, pH 6.7); 250 ml. of distillate was collected for each 90 min. The amount of acetol was determined by iodometric titration.

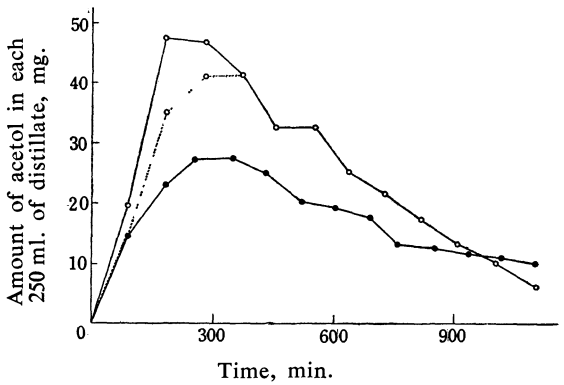



Fig. 3. Acetol formation from 6-*O*-methyl-D-glucose (—○—) (5.4 g.) and from D-glucose (—●—) (5.0 g.) in 200 ml. of potassium hydrogen phosphate buffer solution (ca. 40%, pH 6.7); 250 ml. of distillate was collected for each 90 min. The amount of acetol was determined by iodometric titration (solid line) and corrected by UV. absorption measurement (dotted line).

Every distillate was collected, and acetol in the distillate was treated with 5-fold equivalents of semicarbazide hydrochloride and of sodium acetate. The mixture was heated over a boiling water bath for 30 min., cooled and concentrated under reduced pressure. Acetol semicarbazone was separated and repeatedly recrystallized from hot water to give colorless needles. Melting point and mixed melting point 199~200°C.

12) W. L. Glen, *J. Chem. Soc.*, **1951**, 2568.
13) E. J. Reist et al., *J. Org. Chem.*, **23**, 1753 (1958).
14) H. Ohle and L. Vargha, *Ber.*, **62**, 2435 (1929).
15) R. Nodzu, This Bulletin, **10**, 122 (1935).

TABLE I. ACETOL FORMATION FROM PARTIALLY *O*-METHYLATED HEXOSES

| Sample | | Distillate ml. | Acetol* mg. | Acetol semicarbazone mg. |
|---|---|---|---|---|
| | 3-*O*-Methyl-D-glucose | | | |
| 3-*O*-Methyl-D-glucose | 10.8 g. | 2400 | 79.3 | 0 |
| Glucose | 10.0 g. | 2400 | 251.6 | 70 |
| | 1-*O*-Methyl-D-fructose | | | |
| 1-*O*-Methyl-D-fructose | 5.4 g. | 3000 | 269.8 | 83 |
| Fructose | 5.0 g. | 3000 | 218.2 | 65 |
| | 6-*O*-Methyl-D-glucose | | | |
| 6-*O*-Methyl-D-glucose | 5.4 g. | 3000 | 322.6 (288.9)** | 100 |
| Glucose | 5.0 g. | 3000 | 223.7 | 60 |

* Calculated from the titration of iodine consuming substances (assuming only acetol was present).
** Corrected value from the peak hight of UV absorption spectrum.

## Results and Discussion

The results which are shown in the above table and figures can be expressed as follows.

i) In the case of 3-*O*-methyl-D-glucose(II), the formation of iodine-consuming substances were depressed in a marked degree. Acetol semicarbazone could not be isolated, and the ultraviolet absorption spectrum of the distillate did not show the characteristics[16] of acetol. Thus, the introduction of 3-*O*-methyl group was shown to hinder the formation of acetol from glucose.

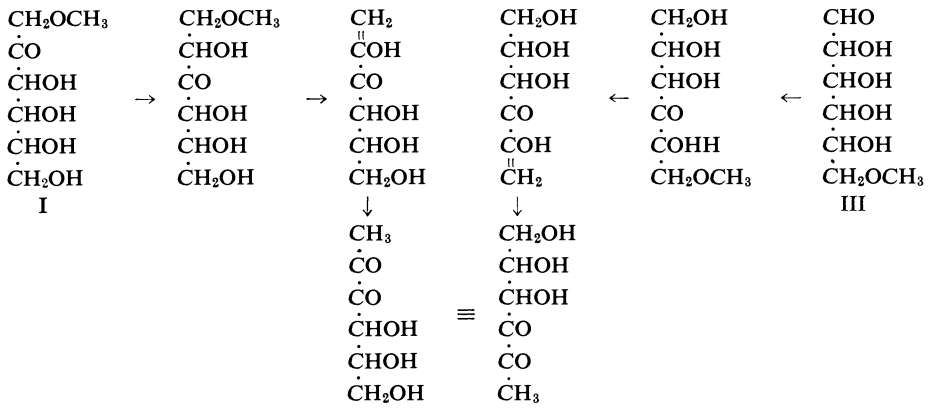
ii) On the other hand, remarkably rapid formation of acetol from 1-*O*-methyl-D-fructose (I) was observed; the rate of formation was about twice that from the parent fructose. Acetol semicarbazone was actually isolated from the decomposition distillate of 1-*O*-methyl-D-fructose as well as from that of D-fructose.

iii) 6-*O*-Methyl-D-glucose(III) also showed enhanced rate of acetol formation, and the amount of acetol was even greater than that of glucose. The amount of acetol estimated by iodometric titration was corrected by the peak height of ultraviolet absorption spectrum and was shown in Fig. 3 (dotted line). These facts might mean that the introduction of 6-*O*-methyl group would raise the amount of acetol formation but not the rate of formation.

It is well known[6,7] that *O*-alkylation of the hydroxyl group located at the $\beta$-position to the carbonyl group always facilitates an elimination of alkoxyl anion more (compared with that of hydroxyl anion from parent compound).

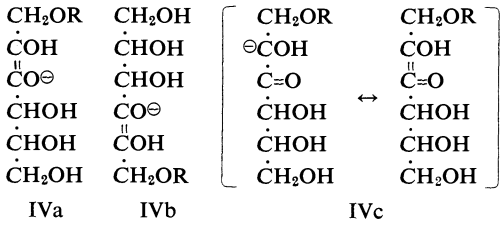
In the present instance, the formation of acetol was accelerated by introduction of 1-*O*-methyl (and 6-*O*-metyl) group into hexose. These facts mean that $\beta$-hydroxy-carbonyl elimination from 3- (and/or 4-) ketohexose is operating on an essential pathway of this reaction, and that oxidation-reduction mechanism (the pathway b cited above) do not play an important role.

These processes may be written as follows:



16) R. Nodzu and R. Goto, ibid. **11**, 281 (1936).

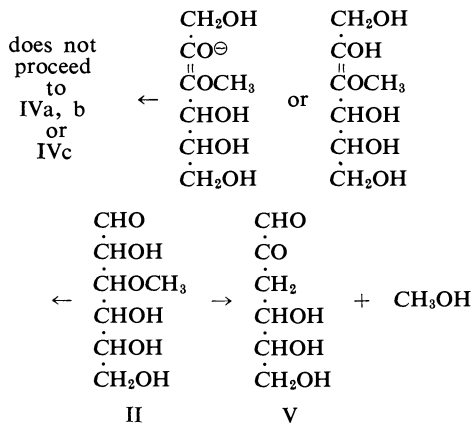
3- or 4-ketohexose in the above scheme may actually be a hexose-2, 3- or 3, 4-enediol. According to Isbell[17] (IVa, b) and to Whistler[7] (IVc), a direct intermediate from which alkoxyl anion is eliminated may be an enediolate anion.



IVa IVb IVc

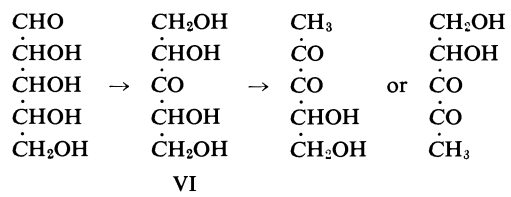
These enediol or enediolate are quite probable intermediates in the transformation of sugars[18], in fact Sowden[19] offered a solid experimental evidence of the existence and of the important role of the hexose-3, 4-enediols in the isomerization of hexose.

With above illustrations, the behavior of 3-*O*-methyl-D-glucose (II) can be well understood in the following way.



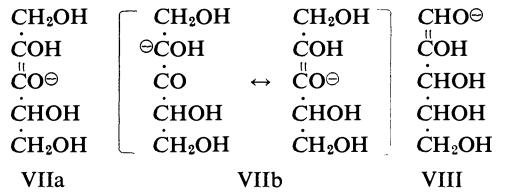
First, under the influence of carbonyl group located at C-1, the elimination of $OR^{\ominus}$ ($OCH_3^{\ominus}$) anion from 3-position ($\beta$- to the carbonyl group) is facilitated. Thus, 3-deoxyosone (V) (or its enol form) may be formed, and make it difficult to transform the C-1 into methyl group. Second, 3-*O*-alkyl group hinders the enol traverse down the carbon chain to form IVa, b or IVc, which is required for formation of acetol.

When the above illustrations are applied to a pentose, $\beta$-hydroxy-carbonyl elimination from a 3-ketose will proceed as follows:



VI

The actual intermediates from which hydroxyl anion is eliminated may be an enediolate anion VIIa or VIIb. These endiolate anions would be derived either directly from VI or from VIII by prototropy.

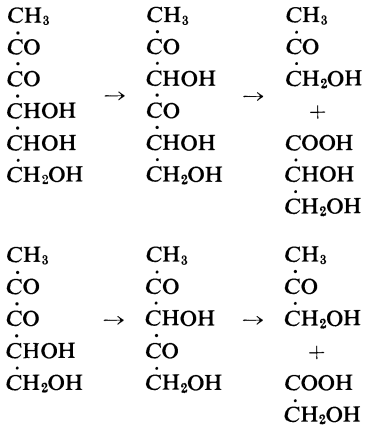


VIIa VIIb VIII

Examination of these formulae of the intermediate shows that $\beta$-hydroxy-carbonyl elimination may take place either at C-1 or at C-5 with equal chance. Or strictly speaking, contribution of the lower $C_3$ part of the pentose may be greater than that of the hexose. In other words, the intermediate for formation of acetol from a pentose might have a high degree of symmetry. This was proved to be the case as was described in Part XI of this series of papers[2].

From the above discussion, it should be clearly evident that $\beta$-hydroxy-carbonyl elimination from 3-ketose (and/or from 4-ketose in the case of hexose) takes place as an essential part of the general mechanism of the acetol formation.

Fate of the $\alpha$-diketones, formed by $\beta$-hydroxy-carbonyl elimination, is supposed as follows:



i) In the pH region where formation of acetol is to be observed (pH 3~11), these

17) H. S. Isbell, *J. Research NBS.*, **32**, 45 (1944); and also refer to the excellent reviews by Sowden (loc. cit.).
18) J. C. Speck, Jr., "Advances in Carbohydrate Chemistry", Vol. 13, 63 (1958).
19) J. C. Sowden, and R. R. Thompson, *J. Am. Chem. Soc.*, **80**, 1435 (1958).

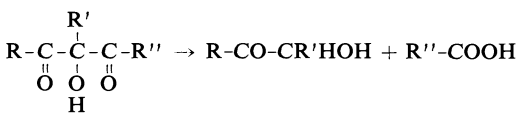
$\alpha$-diketones do not rearrange*1 by a benzilic acid type of reaction to yield saccharinic acids.

ii) These $\alpha$-diketones would be isomerized into $\beta$-diketones*2 (diacylcarbinols), and then hydrolytically cleft into $\alpha$-ketol and acid.

iii) Among these processes, no skeletal rearrangement of the $C_6$ and of the $C_5$ chain would take place, and this third supposition had its evidence as already described in the Part X of this series of the paper[1].

Isomerization of the $\alpha$-diketone into $\beta$-diketone (diacylcarbinol), is one of the general transformations of ketol, and an example by Hesse and Stahl[20] illustrates a quite similar reaction of the isomerization of pentane-2, 3-dione-4-ol to diacetyl carbinol.

The resulting diacylcarbinol is quite reactive and is facile to be cleft hydrolytically according to the following general formula[21-24].



and R''-CO-CR'HOH + R-COOH

R=R''=Et, R'=Me (House[21])

R=R'=R''=Me (Juni and Heym[22])

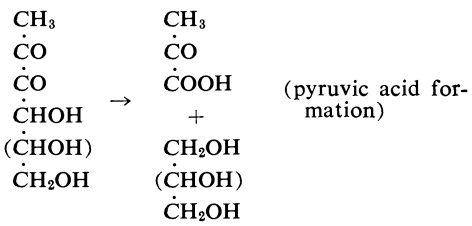
R=R''=Me, R'=H (Combes[23])

R=R''=Ph, R'=H (Karrer[24])

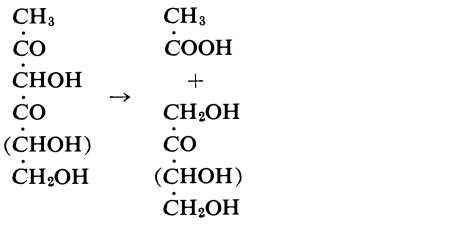
This hydrolytic cleavage can be taken as an extreme case of an acyloin cleavage[25] which is shown as follows:



These hydrolytic cleavages may take part in constituting the side reactions in the following way:



(pyruvic acid formation)



The accompanying formation of pyruvic acid with acetol is already referred to[26]. But the origins and the mode of the formation of the other minor products still remain to be resolved.

As for the role of hydrogen phosphate in the formation of acetol, the following inferences seem to be possible: a) acting as an effective buffer solution keeping the pH of the solution nearly constant. Without these buffers, the pH of the solution decreases remarkably to about 3*3, b) acting as a base as well as acting as an acid, thus promoting the transformation of sugars[18] and promoting elimination of $OH^{\ominus}$ anion and of a proton from some intermediates, c) raising the reaction temperature and raising the dielectric constant of the solution to facilitate the ionic processes. These inferences will be examined in detail in future studies.

Essential features of the formation of acetol can be summarized in the following sequences and are expressed in the scheme shown below.

I) Isomerization of monosaccharides to produce 3-ketoses (and/or 4-ketose in the case of hexose) or their equivalent intermediates.

II) $\beta$-Hydroxy-carbonyl elimination from the 3-ketose to yield methyl-$\alpha$-diketones.

III) Hydrolytic cleavage of $\beta$-diketone (diacylcarbinol) produced by the isomerization of methyl-$\alpha$-diketone.

*1 A benzilic acid type of rearrangement proceeds with a rate proportional to concentration of $OH^-$ ion. In addition, in one of the most simple examples of the rearrangement, methylglyoxal produces lactic acid (cf. J. C. Sowden and E. K. Pohlen, *J. Am. Chem. Soc.*, **80**, 242 (1958).) only in alkaline solution that is stronger than N/100 NaOH (about pH 12) (cf. V. Prey et al., *Monatsh.*, **85**, 1186 (1954)).

*2 Further $\beta$-hydroxy-carbonyl elimination from this $\beta$-diketone might result. In the case of hexose, $CH_3COCO \cdot CHOHCOCH_3$ (Nodzu's acetylformoin) may result by elimination reaction. As was reported earlier, Nodzu confirmed the formation of acetol and of pyruvic acid by a (hydrolytic) cleavage of this compound.

In a sense, the present work appears to offer a theoretical and experimental evidence for part of Nodzu's mechanism, and the present author will not exclude the possibility that in the case of hexose Nodzu's mechanism operates as a minor pathway of the acetol formation.

20) G. Hesse and H. Stahl, *Ber.*, **88**, 2414 (1956).

21) H. O. House and W. F. Ganon, *J. Org. Chem.*, **23**, 879 (1958).

22) E. Juni and G. A. Heym, *Arch. Biochem. Biophys.*, **67**, 410 (1957).

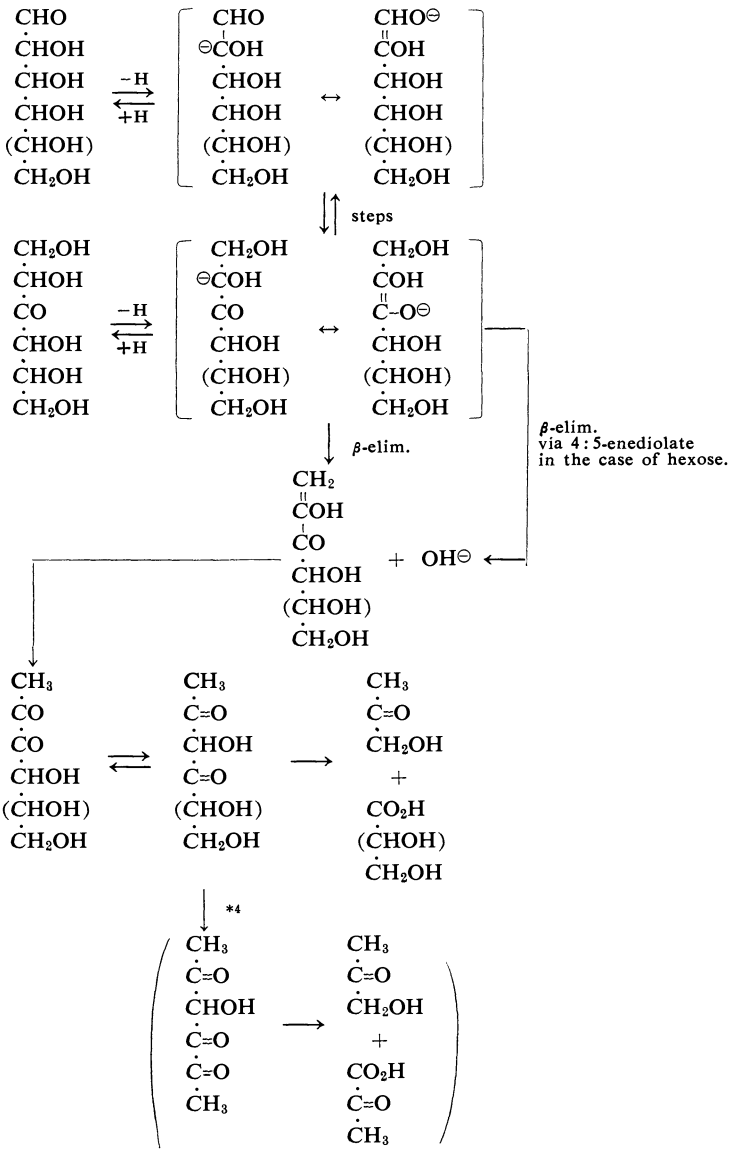
23) A. Combes, *Compt. rend.*, **111**, 421 (1890).

24) P. Karrer et al., *Helv. Chim. Acta*, **33**, 1711 (1950); **34**, 1014, 1498 (1952).

25) D. B. Sharp and E. L. Miller, *J. Am. Chem. Soc.*, **74**, 5643 (1952).

26) R. Nodzu et al., *Mem. Coll. Sci. Kyoto Imp. Univ.*, **A20**, 197 (1937).

*3 Formation of acetol is to be seen at pH 3~11 with an increased yield with the increase in pH. Also refer to R. Montgomery and L. F. Wiggins, *J. Soc. Chem. Ind.*, **66**, 31 (1947); M. L. Wolfrom and W. L. Shilling, *J. Am. Chem. Soc.*, **73**, 3557 (1951).




The formation of acetol constitutes one example of a new combination of the two basic reactions of carbohydrate chemistry—the transformation (van Eckenstein reaction) and the benzilic acid type of rearrangement. While no transformation and no rearrangement occur in the furfural formation, saccharinic acid formation requires both the transformation and the rearrangement, and metasaccharinic acid formation requires no transformation but requires rearrangement. In the present case, the transformation is not followed by any rearrangement.

In the present instance, needless to add, much possibility of another pathway which competes with the acetol formation is expected though the nature of such a competing reaction is entirely unknown.

Study on the individual reactions involved in the present instances is in progress and will be reported later.

The author wishes to express his sincere thanks to Professor Ryozo Goto for his kind guidance and encouragement throughout the course of the present work.

*Institute of Chemistry*
*Faculty of Science*
*Kyoto University*
*Sakyo-ku, Kyoto*

*4 in the case of hexose.

# *A Simple Reactivity Index for Alternant Hydrocarbons*

By Kenichi FUKUI, Hiroshi KATO, Chikayoshi NAGATA and Teijiro YONEZAWA

(Received September 1, 1960)

Several quantum-chemical reactivity indexes for the conjugated system have been proposed in LCAO MO treatment and each of these quantities has been found to explain well the experimental results. One of these indexes is the superdelocalizability, $S_r$. This is derived from the frontier electron theory[1] and has been proved to be an excellent guide to explain various experimental results of conjugated molecules. In the larger molecules, however, a laborious calculation is required to obtain its value. Therefore, a method to be a good appoximation to $S_r$, which would make computation considerably easier, may be looked forward to. In this view the authors derive a new reactivity index, $\bar{S}_r$ for alternant hydrocarbons. That is, $\bar{S}_r$ is the ratio of $b_{r,m-1}$ to $a_m$, where $a_m$ and $b_{r,m-1}$ are the constant terms of expanded secular determinants given by Eq. 4. In this paper, values of $\bar{S}_r$ are compared with exact values of $S_r$, and also with experiments together with the localization energy.

In spite of its extreme simplicity, $\bar{S}_r$ is a good reactivity index of the alternant hydrocarbon. Accordingly, it is suggested to use this index widely for the purpose of concise explanation of reactivity of large alternant hydrocarbon molecules.

## Theoretical

Superdelocalizability, $S_r$, is given by the following formula[1]

$$S_r=\sum_{j=1}^{N}\frac{(\nu_j-\nu)(c_r^j)^2}{\lambda_j} \tag{1}$$

where $c_r^j$ is the coefficient of the $r$th atomic $\pi$-orbital in the $j$th molecular orbital, and $\lambda_j$ is the energy of the $j$th molecular orbital in unit of $\beta$ (the resonance integral of benzene), respectively; $\nu_j$ is the number of electrons in the $j$th molecular orbital, $\nu$ is the number of electrons at the pseudo-$\pi$ orbital in the transition state and stands for 0, 1 and 2, for an electrophilic, radical and nucleophilic reaction, respectively. Also $N$ represents the total number of molecular orbitals.

In our previous paper[2] a function $G_r(y)$ is defined as

$$G_r(y)=\Delta_{rr}(iy)/iy\Delta(iy) \tag{2}$$

where $\Delta(\lambda)$ is the secular determinant for the isolated molecule, and $\Delta_{rr}(\lambda)$ is the $(rr)$ minor of $\Delta(\lambda)$. In Eq. 2 the argument $\lambda$ is replaced by $iy$. In alternant hydrocarbons, Eq. 1 is represented, using the function $G_r(y)$, by an integral formula as

$$S_r=\frac{(-\beta)}{\pi}\int_{-\infty}^{\infty}G_r(y)\mathrm{d}y \tag{3}$$

The determinants $\Delta(iy)$ and $\Delta_{rr}(iy)$ are expanded in the forms;

$$\left.\begin{aligned}(-1)^m\Delta(iy)&=y^{2m}+a_1\beta^2y^{2m-2}\\&\quad+a_2\beta^4y^{2m-4}+\cdots\cdots+a_m\beta^{2m}\\(-1)^m\frac{\Delta_{rr}(iy)}{iy}&=y^{2m-2}+b_{r,1}\beta^2y^{2m-4}\\&\quad+b_{r,2}\beta^4y^{2m-6}+\cdots\cdots+b_{r,m-1}\beta^{2m-2}\end{aligned}\right\} \tag{4}$$

It is proved algebraically that

$$\left.\begin{aligned}&a_i>0\quad(i=1,2,\cdots\cdots,m)\\&b_{r,i}>0\quad(i=1,2,\cdots\cdots,m-1)\\&\frac{b_{r,j}}{a_j}\geqq\frac{b_{r,j+1}}{a_{j+1}}\quad(j=0,1,2,\cdots\cdots,m-1)\\&\frac{b_{r,j-1}}{a_j}\leqq\frac{b_{r,j}}{a_{j+1}}\quad(j=0,1,2,\cdots\cdots,m-1)\\&\qquad(b_{r,-1}=0,\ a_0=b_{r,0}=1,\ b_{r,m}=0)\end{aligned}\right\} \tag{5}$$

Considering the conditions of Eq. 5, one can easily show that $G_r(y)$ is positive with respect to all the real values of $y$. Further, it is clearly seen that $G_r(0)$ is equal to $b_{r,m-1}/a_m\cdot\beta^{-2}$, and that $G_r(y)$ is an even function of $y$ and converges to zero according as $y$ tends to infinite, and $\frac{\mathrm{d}}{\mathrm{d}y}G_r(y)$ is negative with respect to all the positive values of $y$. The curve of $G_r(y)$ plotted against $y$ can be qualitatively shown in Fig. 1. The integration of curve I in the range $-\infty<y<+\infty$ gives the value of $S_r$ exactly. Here, we adopt an approximation. In place of curve I, the integration of curve II is carried out. Its value is equal to $G_r(0)$ between $-\pi(-\beta)/2$ and $+\pi(-\beta)/2$ and is zero for $|y|>\pi(-\beta)/2$. If we designate the

1) K. Fukui, T. Yonezawa and C. Nagata, *J. Chem. Phys.*, **27**, 1247 (1957).
2) K. Fukui, T. Yonezawa and C. Nagata, ibid. **26**, 831 (1957).

TABLE I. THE VALUES OF $S_r$ AND $\bar{S}_r$ IN SEVERAL ALTERNANT HYDROCARBONS IN COMPARISON WITH EXPERIMENT

| Compound | Position | $S_r$ | $\bar{S}_r$ |
|---|---|---|---|
| Benzene | | 0.833 | 0.750 |
| Naphthalene | 1* | 0.994 | 1.222 |
| | 2 | 0.873 | 0.889 |
| | 9 | 0.703 | 0.555 |
| Anthracene | 9* | 1.314 | 2.500 |
| | 1 | 1.073 | 1.625 |
| | 2 | 0.921 | 1.125 |
| Naphthacene | 12* | 1.505 | 3.800 |
| | 1 | 1.121 | 2.000 |
| | 2 | 0.961 | 1.400 |
| Pentacene | 13* | 1.794 | 6.250 |
| | 14 | 1.634 | 5.111 |
| | 1 | 1.154 | 2.361 |
| | 2 | 0.991 | 1.694 |
| Phenanthrene | 10* | 0.997 | 1.240 |
| | 1 | 0.978 | 1.160 |
| | 4 | 0.940 | 1.140 |
| | 3 | 0.892 | 0.960 |
| | 2 | 0.859 | 0.840 |
| Pyrene | 3* | 1.150 | 1.444 |
| | 2 | 1.026 | 1.417 |
| | 4 | 0.829 | 0.750 |
| 1,2-Benzanthracene | 9 | 1.250 | 2.184 |
| | 10 | 1.186 | 1.939 |
| | 5 | 1.060 | 1.510 |
| | 8 | 1.039 | 1.449 |
| 3,4-Benzpyrene** | 5* | — | 3.000 |
| | 6 | — | 1.667 |
| | 7 | — | 1.667 |
| 1,2,5,6-Dibenzanthracene | 9* | 1.146 | 1.750 |
| | 3 | 1.040 | 1.444 |
| | 4 | 1.021 | 1.361 |

* Experimentally most reactive position in the molecule.

** $S_r$ of this componud has not yet been obtained.

TABLE II. THE VALUES OF $\bar{S}_r+\bar{S}_s$ AND PARA-LOCALIZATION ENERGY IN COMPARISON WITH EXPERIMENTAL DATA OF DIELS-ALDER REACTION

| Compound | Position | $\bar{S}_r+\bar{S}_s$ | Para-localization energy | Experiment |
|---|---|---|---|---|
| Hexacene | (6, 15) | 17.713 | 3.16 | reactive |
| | (5, 16) | 12.857 | 3.23 | |
| | (1, 4) | 4.772 | 3.61 | |
| Pentacene | (6, 13) | 12.500 | 3.18 | reactive |
| | (5, 14) | 10.222 | 3.23 | |
| | (1, 4) | 4.772 | 3.61 | |
| Naphthacene | (5, 12) | 7.600 | 3.25 | reactive |
| | (1, 4) | 4.000 | 3.62 | |
| 1,2-Benznaphthacene | (6, 11) | 6.543 | 3.28 | reactive |
| | (5, 12) | 5.889 | 3.36 | |
| Anthracene | (9, 10) | 5.000 | 3.31 | reactive |
| | (1, 4) | 3.250 | 3.63 | |
| 1,2-Benzanthracene | (9, 10) | 4.163 | 3.41 | less reactive |
| | (1', 4') | 2.204 | 3.78 | than anthracene |
| 1,2,3,4-Dibenzanthracene | (9, 10) | 3.539 | 3.49 | less reactive |
| | (5, 8) | 2.769 | — | than anthracene |
| 1,2,5,6-Dibenzanthracene | (9, 10) | 3.500 | 3.59 | less reactive |
| | (1', 4') | 2.222 | 3.79 | than anthracene |
| Naphthalene | (1, 4) | 2.444 | 3.68 | not reactive |
| Phenanthrene | (1, 4) | 2.300 | 3.77 | not reactive |
| Benzene | (1, 4) | 1.504 | 4.00 | not reactive |

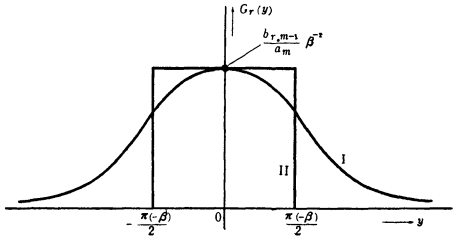



Fig. 1. The curve of the function $G_r(y)$.

integration of curve II by $\bar{S}_r$, it follows that

$$\bar{S}_r=\frac{(-\beta)}{\pi}\int_{-\frac{\pi(-\beta)}{2}}^{\frac{\pi(-\beta)}{2}}G_r(0)\mathrm{d}y$$

$$=\frac{(-\beta)}{\pi}\int_{-\frac{\pi(-\beta)}{2}}^{\frac{\pi(-\beta)}{2}}\frac{b_{r,m-1}}{a_m}\beta^{-2}\,\mathrm{d}y=\frac{b_{r,m-1}}{a_m} \qquad (6)$$

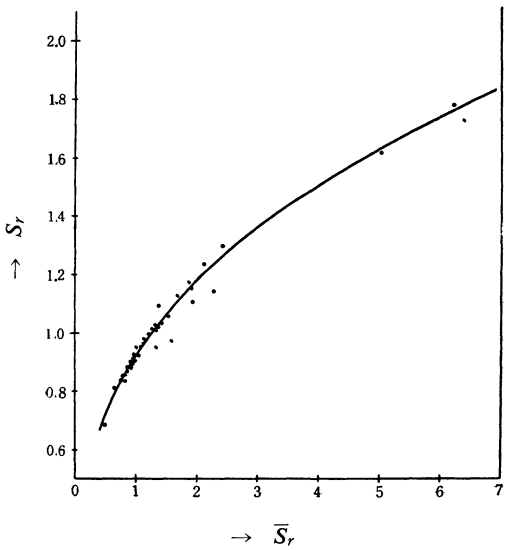
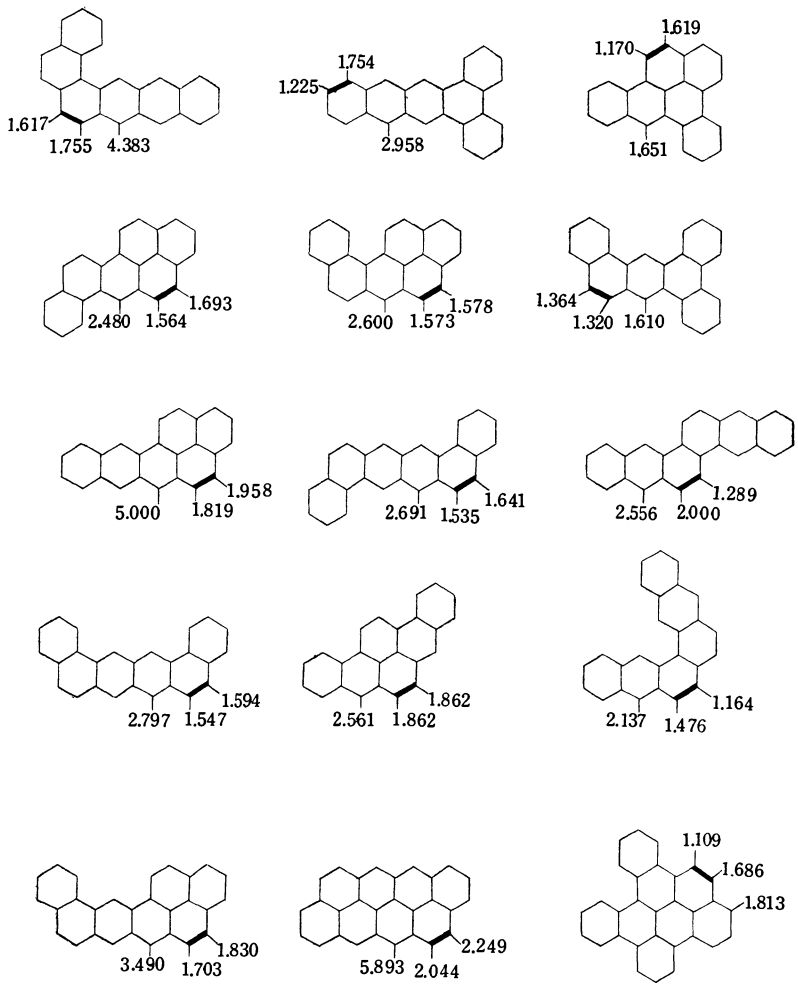



Fig. 2. The relation between $S_r$ and $\bar{S}_r$.




(A thick line in the diagram designates the most reactive bond in the molecule.)

Fig. 3. Prediction of the most reactive position and bond of some condensed aromatic hydrocarbons by the values of $\bar{S}_r$.

Accordingly, it can be calculated very easily even in larger conjugated hydrocarbons. In Appendix I, a simple way of obtaining the values of $a_m$ and $b_{r,m-1}$ is given by using the expansion formulas of secular determinant, wich have already been treated in our previous paper[3].

Bearing in mind the result of our previous paper[2], we obtain an equation which can relate $\bar{S}_r$ with Dewar's approximate localization energy, $l_r$. That is,

$$l_r = -\frac{2}{(-\beta)(G_r(0))^{1/2}} = \frac{2}{(\bar{S}_r)^{1/2}} \cdot \beta \qquad (7)$$

## Results and Discussion

The calculated values of $\bar{S}_r$ in different positions of some aromatic hydrocarbons are shown in the following tables in comparison with experimental data together with other reactivity indexes.

In Table I, the calculated values of $S_r$ and $\bar{S}_r$ in several hydrocarbons are indicated. The experimentally most reactive positions are shown by an asterisk and the figures corresponding to the predicted most reactive position are shown by heavy asterisks. The larger the value of $\bar{S}_r$ is, the more easily that position is to be attacked. The parallelism between the values of $S_r$ and $\bar{S}_r$ is very intimate, indicating that the latter can be a good approximation to the former. It is seen that $\bar{S}_r$ is also a good index for explaining the relative reactivity between different molecules. For instance, the order of susceptibility of three hydrocarbons to a substituting agent—methylformanilide—is: anthracene > 1, 2-benzanthracene > 1, 2, 5, 6-dibenzanthracene[4]. Furthermore, through the experiment of Fieser and Hershberg[5] 3, 4-benzpyrene was found to react more readily with lead tetraacetate than 1, 2, 5, 6-dibenzanthracene. This order of reactivity in heterolytic reaction is in agreement with the order in homolytic reaction; that is, Szwarc showed that the order of methyl affinity of some polycondensed aromatic hydrocarbons was: naphthacene > anthracene > 1, 2-benzanthracene > phenanthrene > naphthalene > benzene[6]. These experimental data are expected from the values of $\bar{S}_r$ in Table I.

Thus, $\bar{S}_r$ itself can be a good reactivity index. But, if one would desire to obtain an approximate value of $S_r$ from the value of $\bar{S}_r$, we can do that by the use of Fig. 2, which

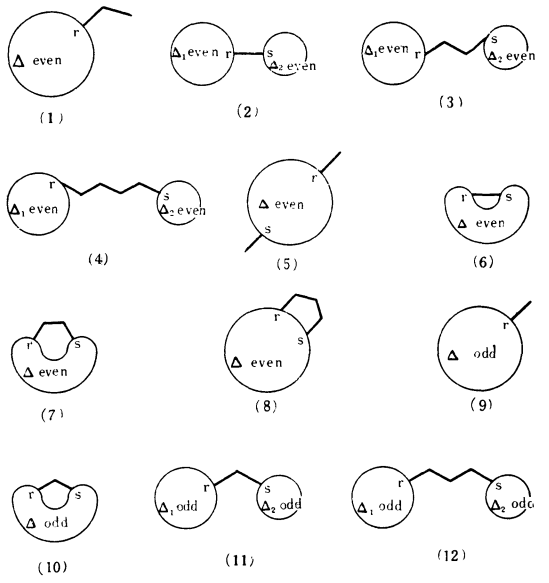



Fig. 4. General formulas for evaluating the value of $a_m$.

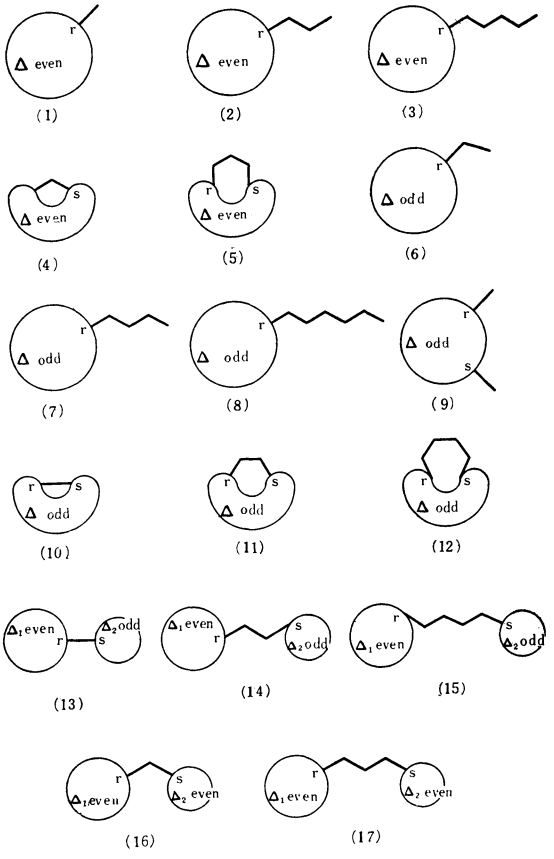



Fig. 5. General formulas for evaluating the value of $b_{r,m-1}$.

3) K. Fukui, C. Nagata, T. Yonezawa and A. Imamura, This Bulletin, 32, 450 (1959).
4) L. F. Fieser and J. L. Hartwell, *J. Am. Chem. Soc.*, 60, 2559 (1938).
5) L. F. Fieser and E. B. Hershberg, ibid., 60, 2542 (1938).
6) M. Szwarc, *J. Polymer Sci.*, 16, 367 (1955).

provides the numerical relation between $S_r$ and $\bar{S}_r$.

In Table II, the values of $\bar{S}_r+\bar{S}_s$ are compared with the values of Brown's para localization energy for some polycyclic hydrocarbons. In the simultaneous addition reaction the sum of superdelocalizability at the attacked positions was found to be a good index in our previous study[7], accordingly, $\bar{S}_r+\bar{S}_s$ also is expected to be a good index of addition reaction. In Table II a coincidence between the values of $\bar{S}_r+\bar{S}_s$ and para localization energy is observed and both of these indexes explain well the observed data in the Diels-Alder reaction.

In Fig. 3, predictions of the reactivity of some hexa-cyclic and larger condensed hydrocarbons are made. In this figure the molecules treated by Gore[8] using Dewar's approximate localization energy method were omitted, and the values of $\bar{S}_r$ at the most reactive position and of the most reactive bond in the molecule are shown. Comparison of these predictions with actual reactivity is hoped to be carried out by future experiments. Calculation of $\bar{S}_r$ of the molecules having as many as eight or more benzene nulei is not tedious. The simple method of calculation proposed in this paper will find its applicability in a discussion of reactivity of larger molecules.

*Faculty of Engineering*
*Kyoto University*
*Sakyo-ku, Kyoto*

7) K. Fukui, T. Yonezawa and C. Nagata, This Bulletin, to be published.
8) P. H. Gore, *J. Chem. Soc.*, **1954**, 3166.

## Appendix I

We derive several formulas which are useful for calculating the values of $a_m$ and $b_{r,m-1}$. By using these formulas, $a_m$ and $b_{r,m-1}$ in larger molecules can be obtained by utilizing those of smaller molecules. Some of these formulas correspond to the expansion formulas of secular determinant previously derived by the present authors[3] and the number of each formula corresponds to the number of the type in Figs. 4 and 5.

(A) General formulas for evaluating the value of $a_m$.

(1) $D(0)=-\Delta(0)$

(2) $D(0)=\Delta_1(0)\Delta_2(0)$

(3) $D(0)=-\Delta_1(0)\Delta_2(0)$

(4) $D(0)=\Delta_1(0)\Delta_2(0)$

(5) $D(0)=\Delta_{rrss}(0)$

(6) $D(0)=\Delta(0)-\Delta_{rrss}(0)-2(-1)^{r+s+1}\Delta_{rs}(0)$

(7) $D(0)=-\Delta(0)+\Delta_{rrss}(0)-2(-1)^{r+s+1}\Delta_{rs}(0)$

(8) $D(0)=\Delta(0)-\Delta_{rrss}(0)-2(-1)^{r+s+1}\Delta_{rs}(0)$
$(\Delta^2_{rs}(0)=-\Delta(0)\Delta_{rrss}(0))$

(9) $D(0)=-\Delta_{rr}(0)$

(10) $D(0)=-\Delta_{rr}(0)-\Delta_{ss}(0)+2(-1)^{r+s+1}\Delta_{rs}(0)$

(11) $D(0)=-\Delta_1(0)\Delta_{2ss}(0)$

(12) $D(0)=\Delta_1(0)\Delta_{2ss}(0)$

The values of $a_m$ in polycondensed aromatic hydrocarbons are easily obtained by classifying these compounds into the following several types.

(B) General formulas for evaluating the value of $b_{r,m-1}$.

(1) $\left(\frac{D(\lambda)}{-\lambda}\right)_{\lambda=0}=\Delta(0)-\left(\frac{\Delta_{rr}(\lambda)}{-\lambda}\right)_{\lambda=0}$

(2) $\left(\frac{D(\lambda)}{-\lambda}\right)_{\lambda=0}=-2\Delta(0)+\left(\frac{\Delta_{rr}(\lambda)}{-\lambda}\right)_{\lambda=0}$

(3) $\left(\frac{D(\lambda)}{-\lambda}\right)_{\lambda=0}=3\Delta(0)-\left(\frac{\Delta_{rr}(\lambda)}{-\lambda}\right)_{\lambda=0}$

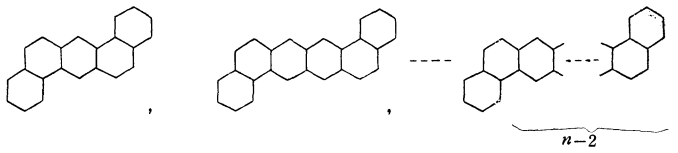
(4) $\left(\frac{D(\lambda)}{-\lambda}\right)_{\lambda=0}=\Delta(0)-\left\{\left(\frac{\Delta_{rr}(\lambda)}{-\lambda}\right)_{\lambda=0}+\left(\frac{\Delta_{ss}(\lambda)}{-\lambda}\right)_{\lambda=0}\right\}+2(-1)^{r+s+1}\left(\frac{\Delta_{rs}(\lambda)}{-\lambda}\right)_{\lambda=0}$

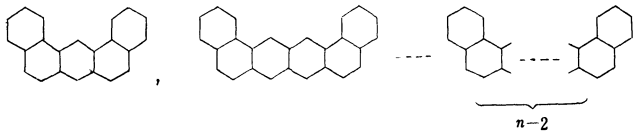
(5) $\left(\frac{D(\lambda)}{-\lambda}\right)_{\lambda=0}=-2\Delta(0)+\left\{\left(\frac{\Delta_{rr}(\lambda)}{-\lambda}\right)_{\lambda=0}+\left(\frac{\Delta_{ss}(\lambda)}{-\lambda}\right)_{\lambda=0}\right\}+\Delta_{rrss}(0)+2(-1)^{r+s+1}\left(\frac{\Delta_{rs}(\lambda)}{-\lambda}\right)_{\lambda=0}$

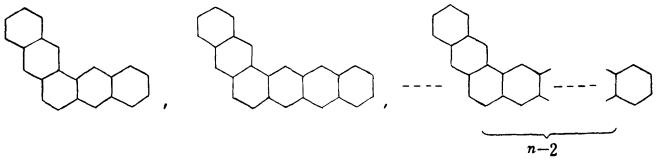
(a) $\Delta(0)=-(n+1)^2$

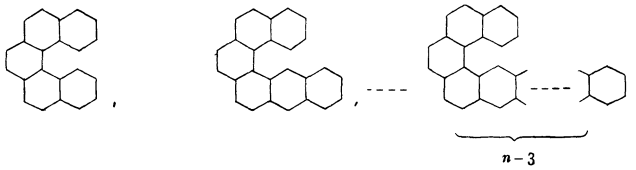
(b) $\Delta(0)=-(2n-1)^2$

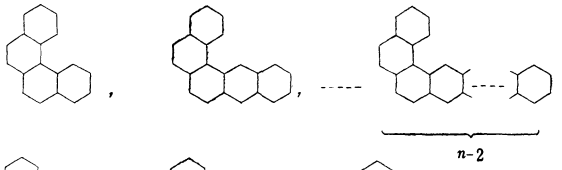
(c) $\Delta(0)=-\frac{1}{5}\left\{\left(\frac{1+\sqrt{5}}{2}\right)^{n+2}-\left(\frac{1-\sqrt{5}}{2}\right)^{n+2}\right\}^2$

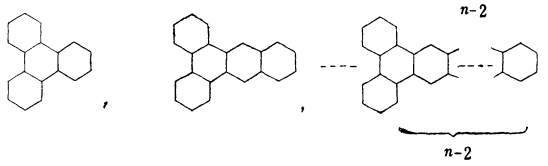
(d)  $\Delta(0) = -(4n-8)^2$

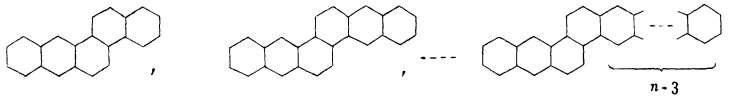
(e)  $\Delta(0) = -(4n-8)^2$

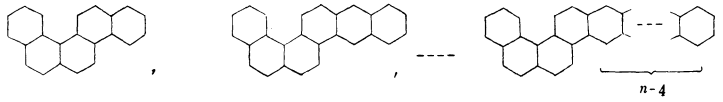
(f)  $\Delta(0) = -(3n-5)^2$

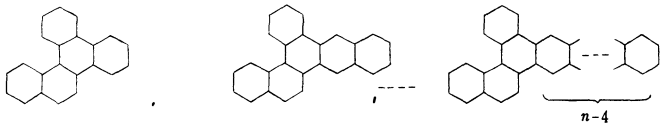
(g)  $\Delta(0) = -(5n-12)^2$

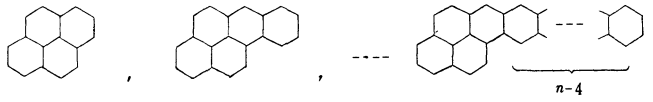
(h)  $\Delta(0) = -(3n-4)^2$

(i)  $\Delta(0) = -(4n-7)^2$

(j)  $\Delta(0) = -(4n-9)^2$

(k)  $\Delta(0) = -(5n-12)^2$

(l)  $\Delta(0) = -(6n-16)^2$

(m)  $\Delta(0) = -(3n-6)^2$

$$(6)\quad \left(\frac{D(\lambda)}{-\lambda}\right)_{\lambda=0}=-\Delta_{rr}(0)-\left(\frac{\Delta(\lambda)}{-\lambda}\right)_{\lambda=0}$$

$$(7)\quad \left(\frac{D(\lambda)}{-\lambda}\right)_{\lambda=0}=2\Delta_{rr}(0)+\left(\frac{\Delta(\lambda)}{-\lambda}\right)_{\lambda=0}$$

$$(8)\quad \left(\frac{D(\lambda)}{-\lambda}\right)_{\lambda=0}=-3\Delta_{rr}(0)-\left(\frac{\Delta(\lambda)}{-\lambda}\right)_{\lambda=0}$$

$$(9)\quad \left(\frac{D(\lambda)}{-\lambda}\right)_{\lambda=0}=-\{\Delta_{rr}(0)+\Delta_{ss}(0)\}+\left(\frac{\Delta_{rrss}(\lambda)}{-\lambda}\right)_{\lambda=0}$$

$$(10)\quad \left(\frac{D(\lambda)}{-\lambda}\right)_{\lambda=0}=\left(\frac{\Delta(\lambda)}{-\lambda}\right)_{\lambda=0}-\left(\frac{\Delta_{rrss}(\lambda)}{-\lambda}\right)_{\lambda=0}-2(-1)^{r+s+1}\left(\frac{\Delta_{rs}(\lambda)}{-\lambda}\right)_{\lambda=0}$$

$$(11)\quad \left(\frac{D(\lambda)}{-\lambda}\right)_{\lambda=0}=-\left(\frac{\Delta(\lambda)}{-\lambda}\right)_{\lambda=0}-\{\Delta_{rr}(0)+\Delta_{ss}(0)\}+\left(\frac{\Delta_{rrss}(\lambda)}{-\lambda}\right)_{\lambda=0}-2(-1)^{r+s+1}\left(\frac{\Delta_{rs}(\lambda)}{-\lambda}\right)_{\lambda=0}$$

$$(12)\quad \left(\frac{D(\lambda)}{-\lambda}\right)_{\lambda=0}=\left(\frac{\Delta(\lambda)}{-\lambda}\right)_{\lambda=0}+2\{\Delta_{rr}(0)+\Delta_{ss}(0)\}-\left(\frac{\Delta_{rrss}(\lambda)}{-\lambda}\right)_{\lambda=0}-2(-1)^{r+s+1}\left(\frac{\Delta_{rs}(\lambda)}{-\lambda}\right)_{\lambda=0}$$

$$(13)\quad \left(\frac{D(\lambda)}{-\lambda}\right)_{\lambda=0}=\Delta_1(0)\left(\frac{\Delta_2(\lambda)}{-\lambda}\right)_{\lambda=0}-\Delta_{2ss}(0)\left(\frac{\Delta_{1rr}(\lambda)}{-\lambda}\right)_{\lambda=0}$$

$$(14)\quad \left(\frac{D(\lambda)}{-\lambda}\right)_{\lambda=0}=-\Delta_1(0)\left(\frac{\Delta_2(\lambda)}{-\lambda}\right)_{\lambda=0}-\Delta_1(0)\Delta_{2ss}(0)+\Delta_{2ss}(0)\left(\frac{\Delta_{1rr}(\lambda)}{-\lambda}\right)_{\lambda=0}$$

$$(15)\quad \left(\frac{D(\lambda)}{-\lambda}\right)_{\lambda=0}=\Delta_1(0)\left(\frac{\Delta_2(\lambda)}{-\lambda}\right)_{\lambda=0}+2\Delta_1(0)\Delta_{2ss}(0)-\Delta_{2ss}(0)\left(\frac{\Delta_{1rr}(\lambda)}{-\lambda}\right)_{\lambda=0}$$

$$(16)\quad \left(\frac{D(\lambda)}{-\lambda}\right)_{\lambda=0}=\Delta_1(0)\Delta_2(0)-\left\{\Delta_2(0)\left(\frac{\Delta_{1rr}(\lambda)}{-\lambda}\right)_{\lambda=0}+\Delta_1(0)\left(\frac{\Delta_{2ss}(\lambda)}{-\lambda}\right)_{\lambda=0}\right\}$$

$$(17)\quad \left(\frac{D(\lambda)}{-\lambda}\right)_{\lambda=0}=-2\Delta_1(0)\Delta_2(0)+\left\{\Delta_2(0)\left(\frac{\Delta_{1rr}(\lambda)}{-\lambda}\right)_{\lambda=0}+\Delta_1(0)\left(\frac{\Delta_{2ss}(\lambda)}{-\lambda}\right)_{\lambda=0}\right\}$$

where $\Delta(\lambda)$ and $D(\lambda)$ is the secular determinants of a molecule before and after the growth and $\Delta_{rs}(\lambda)$ and $\Delta_{rrss}(\lambda)$ are the $(rs)$ and $(rrss)$ minors of $\Delta(\lambda)$, respectively.

# *Stereoregular Polymers. VIII. Effects of Various Organic Compounds on the Polymerization of Styrene with Ziegler Catalyst. Part I**

By Shunsuke MURAHASHI, Shun'ichi NOZAKURA and Kōichi HATADA

(Received October 1, 1960)

Much literature has been published in regard to the polymerization of olefins with Ziegler type catalyst. However, only a few of them have given the information as to the polymerization of monomer containing any heteroatom such as oxygen, nitrogen, sulfur or halogen[1].

It is considered that the electron-donating character of these atoms causes strong complex formation between the compound and the catalyst leading to the inhibition of anionic coordination of the double bond of the monomer to the catalyst.

The authors have previously investigated the polymerization of allylchloride[2] with Ziegler catalyst and found that the Friedel-Crafts type reaction caused by compounds containing Al–Cl bond such as $Et_2AlCl$, $EtAlCl_2$ or $AlCl_3$ formed in the system is essential in the polymerization.

It should be interesting to investigate the effect of the usual organic compound containing heteroatom on the polymerization by Ziegler catalyst using styrene as a monomer. From such experiments any information would be

* This work was presented at the 13th Meeting of the Chemical Society of Japan, Tokyo, April, 1960.

1) J. Lal, *J. Polymer Sci.*, **31**, 179 (1958); E. J. Vandenberg et al., ibid., **41**, 519 (1959); R. F. Heck and D. S. Breslow, ibid., **41**, 520 (1959); G. Natta et al., *Angew. Chem.*, **71**, 205 (1959); W. S. Etlis et al., *Visokomolek. Soed.*, **1**, 1403 (1959); E. J. Vandenberg, Ital. Pat. 571741 (1959); Ger. Pat. 1030562; 1031515 (1958).

2) S. Murahashi, S. Nozakura and K. Hatada, This Bulletin, **34**, 631 (1961).

expected to be drawn in correlation to the polymerization of any monomer containing heteroatom by this catalyst.

From this point of view, about forty compounds including halides, oxides, carbonyl compounds, amines, nitro compounds, nitriles, sulfides and phosphines, were examined. The stereospecificity of the Ziegler catalyst for the polymerization of styrene was lost by all of them excepting halobenzenes, di-*n*-hexyl ether, triphenylphosphine, thiophene and furan. These exceptions did not destroy the stereospecificity but modified the catalyst system in various extents.

The effects of thiophene and furan were studied in detail. The results indicated that thiophene may not be attacked so strongly by the Ziegler catalyst predicting the possibility of forming stereospecific polymers of vinylthiophenes by this catalyst. However, only amorphous polymers resulted from these monomers.

## Experimental

**Materials.**—*Styrene.*—Commercial styrene was washed with 5% aqueous sodium hydroxide and water, dried over calcium chloride and distilled under reduced nitrogen pressure before use.

*2-Vinylthiophene.*-This was synthesized according to Emerson[3], b. p. 59.0°C (46 mmHg), $n_D^{25}$ 1.5707. Found: C, 65.15; H, 5.54; S, 28.84. Calcd. for $C_6H_6S$: C, 65.41; H, 5.49; S, 29.10%.

*3-Vinylthiophene.*—This was synthesized according to Troyanowsky[4], b.p. 50.5°C (20 mmHg), $n_D^{15}$ 1.5683. Found: C, 66.06; H, 5.73; S, 28.78. Calcd. for $C_6H_6S$: C, 65.41; H, 5.49; S, 29.10%.

*n-Hexane.*—A commercial material was shaken with fuming sulfuric acid, washed with 5% aqueous sodium hydroxide and water, dried over calcium chloride, distilled and stored over metallic sodium.

*Various Organic Compounds used as Additives.*—Most of the compounds were obtained commercially, but ethylene glycol dimethyl ether, di-*n*-butyl sulfide, triethylphosphine and triphenylphosphine were synthesized. All were purified by the usual methods and distilled under dry nitrogen before use.

*Triethylaluminum and Titanium Tetrachloride.*—Triethylaluminum and titanium tetrachloride were supplied by Mitsui Chem. Ind. Co. and by Osaka Titanium Co., respectively, and both were used as solutions in *n*-heptane.

**Polymerization of Styrene.**—A 50 ml. five-necked flask[5] was fitted with a thermometer, a nitrogen gas inlet tube and rubber caps, and was flushed by dry nitrogen. Then 20 ml. of *n*-hexane and 0.25 g. (0.00132 mol.) of titanium tetrachloride were charged. While boiling the mixture gently, 0.15 g. (0.00132 mol.) of triethylaluminum was added slowly, and heating was continued for further five minutes and cooled. After precipitating the solid catalyst complex the supernatant liquid was removed by a hypodermic syringe equipped with a long needle under dry nitrogen. The catalyst was washed three times in the flask with 20 ml. of *n*-hexane and then 20 ml. of *n*-hexane and 0.15 g. of triethylaluminum was added. The catalyst mixture was heated to about 60°C and 0.01 mol. of additive compound was added. After the mixture was kept at 60°C for fifteen minutes with occasional shaking, 5 ml. (4.54 g.) of styrene were charged. The polymerization was performed at 60°C for 4 hr. All the procedures were carried out under a stream of dry nitrogen. The polymerization was stopped by adding 10 ml. of methanol and 1 ml. of concentrated hydrochloric acid. The polymer was precipitated by pouring the mixture into about 300 ml. of methanol. After standing overnight, the polymer was collected and washed throughly with methanol and dried in vacuo. The polymer obtained was extracted with a hundred times amounts of methyl ethyl ketone under reflux for three hours. After standing overnight at room temperature the isotactic polymer remained insoluble was collected and washed with methyl ethyl ketone and dried in vacuo at 100°C. The stereospecificity (%) of the polymer was determined as 100×(weight of isotactic part)/(weight of total polymer).

Because of the poor reproducibility of Ziegler type polymerization the conditions and procedures were kept carefully as constant as possible for all over the runs.

## Results

Styrene was polymerized by Ziegler catalyst under the same conditions described in the experimental part but without additive compound. The results of the four runs were shown in Table I. The stereospecificity of this catalyst

TABLE I. STEREOSPECIFICITY OF POLYSTYRENE POLYMERIZED BY ZIEGLER CATALYST

| | Polymer yield, % | | Stereospecificity, % |
|---|---|---|---|
| | Total | Isotactic part | |
| | 12.3 | 4.3 | 34.8 |
| | 13.4 | 4.5 | 33.5 |
| | 13.1 | 5.1 | 38.9 |
| | 11.6 | 5.6 | 48.0 |
| Average | 12.6 | 4.9 | 38.8 |

was lower than that of the catalyst[5] prepared in boiling *n*-heptane in a similar manner. This is probably due to the lower temperature at the catalyst formation and also the ageing of the catalyst caused by fifteen minutes time interval before the introduction of monomer.

The results obtained from the experiments with additive compounds were summarized in Table II.

**Halides.**—When *n*-butyl chloride was added, the catalyst solid was completely dissolved with a violent evolution of hydrogen chloride.

3) W. E. Emerson and T. M. Patrick, "Organic Synthesis" Vol. 38, (1958), p. 86.

4) C. Troyanowsky, *Bull. soc. chim. France*, 1955, 424.

5) S. Murahashi, S. Nozakura, M. Sumi and K. Hatada, This Bulletin 32, 1094 (1959).

TABLE II. EFFECTS OF VARIOUS ORGANIC COMPOUNDS ON THE STEREOSPECIFIC POLYMERIZATION OF STYRENE BY ZIEGLER CATALYST

| Type of compound | Compound | Conversion, % | Stereospecificity % | Change of catalyst |
|---|---|---|---|---|
| | None | 12.6 | 38.8 | |
| Halide | $n$-$C_4H_9Cl$ | 82.6 | 0 | Dissolved, HCl evolved |
| | $C_6H_5Cl$ | 9.7 | 45.4 | Unchanged |
| | $C_6H_5Br$ | 8.5 | 39.5 | Unchanged |
| | $CCl_4$ | 79.2 | 0 | Dissolved, HCl evolved |
| Ether | $CH_3OCH_2CH_2OCH_3$ | 2.0 | 0 | Unchanged |
| | $(n\text{-}C_4H_9)_2O$ | 7.1 | 0 | Unchanged |
| | $(n\text{-}C_6H_{13})_2O$ | 5.0 | 33.9 | Unchanged |
| | Tetrahydrofuran | 2.3 | 0 | Unchanged |
| | Dioxane | 2.8 | 0 | Unchanged |
| | $(CH_3CHO)_3$ | 0.5 | 0 | Unchanged |
| Acetal | $CH_2(OCH_3)_2$ | 24.8 | 0 | Unchanged |
| | $CH_3CH(OC_2H_5)_2$ | 11.4 | 0 | Unchanged |
| Ketone and aldehyde | $CH_3COCH_3$ | 0.3 | 0 | Dissolved |
| | $CH_3COC_2H_5$ | 0.7 | 0 | Dissolved |
| | $C_6H_5COCH_3$ | 0.2 | 0 | Dissolved |
| | $C_6H_5CHO$ | 0.2 | 0 | Dissolved |
| Ester and acid anhydride | $CH_3COOC_2H_5$ | 4.3 | 0 | Gradually dissolved |
| | $CH_3COOC_4H_9(n)$ | 5.2 | 0 | Gradually dissolved |
| | $(CH_3CO)_2O$ | 5.7 | 0 | Unchanged |
| Amine | $C_6H_5NH_2$ | 2.6 | 0 | Dissolved, gas evolved |
| | $C_5H_5N$ | 0.3 | 0 | Gradually dissolved |
| | $(C_2H_5)_3N$ | 1.3 | 0 | Unchanged |
| Acid amide | $CH_3CONH_2$ | 1.4 | 0 | Partly dissolved, gas evolved |
| | $HCON(CH_3)_2$ | 1.0 | 0 | Dissolved |
| Nitro compound | $CH_3CH(NO_2)CH_3$ | 0.7 | 0 | Dissolved |
| | $C_6H_5NO_2$ | 0.2 | 0 | Color changed[a] |
| Nitrile and azobenzene | $C_6H_5CN$ | 1.5 | 0 | Dissolved |
| | $C_6H_5N{=}NC_6H_5$ | 0.2 | 0 | Color changed[b] |
| Sulfur compound | $n$-$C_3H_7SH$ | 0.1 | 0 | Dissolved, gas evolved |
| | $(n\text{-}C_4H_9)_2S$ | 6.7 | 0 | Dissolved |
| | $CS_2$ | 5.3 | 0 | Unchanged |
| | S | 2.0 | 0 | Gradually dissolved |
| | $(CH_3)_2SO$ | 16.8 | 0 | Dissolved |
| | Thiophene | 5.7 | 67.3 | Unchanged |
| Furan | Furan | 8.2 | 85.7 | Unchanged |
| Phosphorus compound | $(C_2H_5)_3P$ | 1.0 | 0 | Dissolved |
| | $(C_6H_5)_3P$ | 4.4 | 35.0 | Unchanged |

a) The brownish black color of the solid catalyst almost disappeared.
b) The color of the solid catalyst was slightly faded.

Styrene was polymerized by the dissolved catalyst to give polystyrene in high yield. At the addition of the monomer, however, a red coloration and a remarkable temperature rising of the reaction mixture were observed. These signified cationic polymerization of styrene by aluminum chloride, and the resulted polymer was shown to be completely amorphous. The behavior of carbon tetrachloride was similar to that of *n*-butyl chloride.

**Ethers and Acetals.**—By the addition of di-*n*-hexyl ether the catalytic activity was fairly decreased, but the stereospecificity was retained invariably. The isotactic part of the polymer obtained was swollen in methyl ethyl ketone and showed rather lower melting point (215～217°) than ordinary isotactic polystyrene (m. p. 230～233°).

By the additions of the other ethers and acetals the appearance of the catalyst solid

remained unchanged but the stereospecificity was completely lost.

**Ketones, Aldehydes, Esters, Acid Anhydride, Amides and Amines.**—Triethylamine did not affect the catalyst in appearance, but completely diminished the stereospecificity of the polymerization. The catalyst solid was dissolved by the addition of each of all the other compounds listed. The dissolved catalyst showed low activity and gave no stereospecific polymer.

**Nitro Compounds, Nitrile and Azobenzene.**—Upon adding 2-nitropropane the catalyst was dissolved immediately. Nitrobenzene and azobenzene changed the color of the catalyst solid, but did not dissolved it, while cyanobenzene dissolved the catalyst. These four compounds strongly lowered the catalytic activity, and no stereospecificity resulted.

**Sulfur Compounds and Furan.**—Sulfur, mercaptane, thioether and sulfone, all these sulfur compounds examined dissolved the catalyst and destroyed the stereospecificity.

Contrary to most of the compounds of this group thiophene and furan did remarkably improve the stereospecificity of the catalyst for the polymerization of styrene. A number of additional polymerizations were carried out by varying the amount of these additives, where the catalyst was prepared as mentioned in the experimental part but without washing. The results were given in Figs. 1 and 2, both of which showed the same trend. The yield of atactic polystyrene decreased rapidly by the addition up to one-fourth molar ratio of the additive compound to titanium tetrachloride and remained almost constant at the higher ratios. On the other hand, the yield of isotactic polymer was unchanged almost constant.

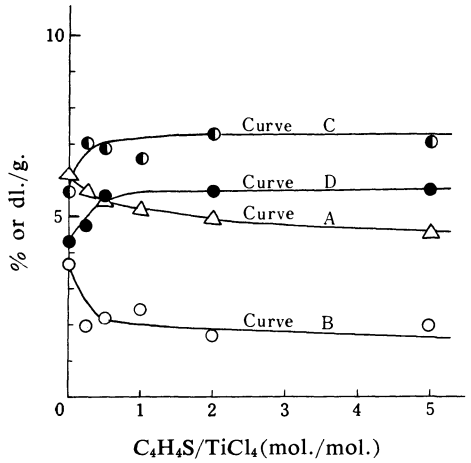



Fig. 1. Effect of thiophene on the polymerization of styrene with Ziegler catalyst.
Curve A: yield of isotactic polystyrene
Curve B: yield of atactic polystyrene
Curve C: stereospecificity $\times 10^{-1}$
Curve D: intrinsic viscosity of the isotactic polystyrene in toluene at 30.0°C

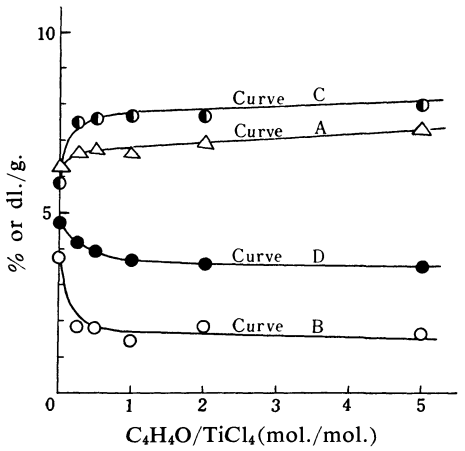



Fig. 2 Effect of furan on the polymerization of styrene with Ziegler catalyst.
Curve A: yield of isotactic polystyrene
Curve B: yield of atactic polystyrene
Curve C: stereospecificity $\times 10^{-1}$
Curve D: intrinsic viscosity of the isotactic polystyrene in toluene at 30.0°C

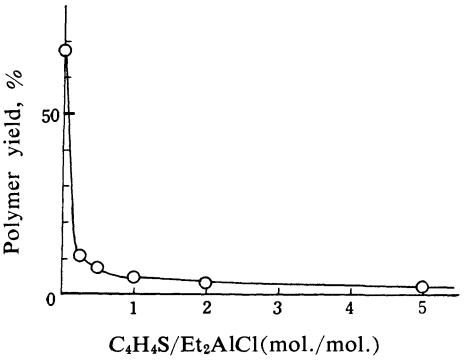



Fig. 3. Effect of thiophene on the polymerization of styrene by $Et_2AlCl$.
Polymerization temperature: 60°C, polymerization time: 4 hr., styrene; 5 ml., *n*-heptane: 20ml., $Et_2AlCl$: $1.32\times10^{-3}$ mol.

In an attempt to elucidate the action of these compounds the polymerizations of styrene catalyzed by $Et_2AlCl$ were similarly carried out using thiophene as an additive. The results were shown in Fig. 3. The curve in Fig. 3 closely resembled that of the atactic yield in Fig. 1.

Carbon disulfide did not change the appearance of the catalyst but destroyed the stereospecificity at all.

**Phosphorus Compounds.**—Triethylphosphine dissolved the catalyst to lose the activity and the stereospecificity, while triphenylphosphine behaved similarly as di-*n*-hexyl ether did and gave isotactic polystyrene having a lower

melting point (219~221°C) but not being swollen in methyl ethyl ketone.

**Polymerization of Vinylthiophenes.**—2-Vinylthiophene and 3-vinylthiophene were synthesized and polymerized with several catalysts of the Ziegler type. All of the polymers obtained were shown to be amorphous by their X-ray diffractions.

## Discussion

The additive compounds examined were found to fall into four groups according to their behavior to the Ziegler catalyst.

**Group I.**—This group includes alkyl halides and carbon tetrachloride. The compounds dissolve the catalyst solid with a violent evolution of hydrogen chloride. In this case the polymerization shows a sign of cationic process and givesan atactic polystyrene in high yield.

In the case of *n*-butyl chloride the evolution of hydrogen chloride takes place analogously to the reaction between butyl bromide and aluminum bromide[6], as follows:

$$CH_3CH_2CH_2CH_2Cl \xrightarrow{Et_2AlCl\ etc.} CH_3CH_2CH=CH_2+HCl$$

In the first stage, this reaction proceeds very slowly by a catalytic action of small amounts of original species having Al-Cl linkage such as $Et_2AlCl$, $EtAlCl_2$ or aluminum chloride, then becomes faster owing to a gradual accumulation of these compounds generated by the reaction between triethylaluminum and hydrogen chloride liberated, and is finally led to the violent reaction. These compounds containing Al-Cl linkage may catalyze the polymerization of styrene in a cationic mechanism.

**Group II.**—The compounds belonging to this group are ketones, aldehydes, esters, amides, primary and secondary amines, pyridine, aliphatic nitro compounds, nitriles, mercaptanes, thioethers and so on. Every compound of this group leads the catalyst to dissolution and destroys its stereospecificity as well as the catalytic activity for the polymerization of styrene. Each of these compounds has a strong electron donor group, an active hydrogen atom or any of the other functional groups, all of which seem to react with organometallic compounds and could probably destroy the activity of the Ziegler catalyst.

**Group III.**—By the compounds of this group the catalyst is not changed in appearance, but the stereospecificity is destroyed. The compounds may include ethers, acetals, acid anhydride and tertiary amines. All of these have a electron-donor group and may be capable of forming a Lewis acid-Lewis base type complexes with triethylaluminum and/or with titanium trichloride in the catalyst. This complex formation must destroy the suitable site for the isotactic polymerization of styrene in the catalyst.

It should be noted, however, that the stereospecificity of the catalyst is not destroyed by a compound having bulky substituent groups around the hetero atom, such as di-*n*-hexyl ether. Triethylamine causes no dissolution of the catalyst, although it has stronger electronegativity than pyridine, a member of Group II. This may be attributed to the steric hindrance around the nitrogen atom[7].

**Group IV.**—The stereospecificity of the catalyst is not destroyed by the compounds of this group. These includes halobenzenes, di-*n*-hexyl ether, thiophene, furan and triphenylphosphine.

By the additions of thiophene and furan the stereospecificity is remarkably increased, while the total polymer yield is relatively reduced. This means that the action of these additives is related to an inhibition of the atactic polymerization of styrene by the catalyst. The feature is demonstrated in detail by Figs. 1 and 2, which were obtained from the experiments with varying the amounts of the additives.

When the catalyst is formed by the preparative method used in these experiments, it is considered that more than ninety percent of titanium tetrachloride are reduced to titanium trichloride and triethylaluminum is converted to diethylaluminum chloride, ethylaluminum dichloride and aluminum chloride, all of which are responsible for the formation of atactic polystyrene by this catalyst[5,8].

$$Et_3Al+TiCl_4 \rightarrow Et_2AlCl+TiCl_3+Et\cdot \quad (1)$$

$$Et_2AlCl+TiCl_4 \rightarrow EtAlCl_2+TiCl_3+Et\cdot \quad (2)$$

$$EtAlCl_2+TiCl_4 \rightarrow AlCl_3+TiCl_3+Et\cdot \quad (3)$$

The plots in Figs. 1 and 2 were obtained from the experiments without washing the catalyst. As the molar ratio of triethylaluminum to titanium tetrachloride was higher than unity, diethylaluminum chloride must be the main product among the three aluminum chlorides, and may be present in an approximately equimolar amount to that of titanium trichloride or, accordingly, of titanium tetrachloride used. The similarity of the two curves, Curve B in Fig. 1 and the curve in Fig. 3, indicates evidently the interaction between thiophene and diethylaluminum chloride being

6) J. J. Burbage, *J. Phys. Chem.*, **56**, 730 (1952).

7) W. Gordy et al., *J. Chem. Phys.*, **8**, 170 (1940).

8) W. M. Saltman, W. E. Gibbs and J. Lal, *J. Am. Chem. Soc.*, **80**, 5615 (1958).

the substantial cause in the inhibition of the atactic polymerization of styrene. Probably diethylaluminum chloride may form an acid-base type complex with thiophene or furan and lose the catalytic activity for the cationic polymerization of styrene. It is remarkable that only one-fourth molar amount of thiophene or furan against diethylaluminum chloride sufficiently inhibits the polymerization. On the other hand, the electronegativities weakened by the conjugate system of these compound are supposed to be not sufficient to affect the active site of the solid catalyst for the isotactic polymerization of styrene.

Between the actions of thiophene and furan some differences are found. The isotactic yield decreased slightly and the molecular weight of the isotactic polymer increased gradually with the increasing amount of thiophene, while the increasing amount of furan gave the reverse tendencies. The explanation of these facts has still not been obtained.

Vinylthiophene gave no isotactic polymer by the Ziegler catalyst. This suggests that the active species of the catalyst for the isotactic polymerization of styrene does not always function as an active site for the isotactic polymerization of any other monomers.

Triphenylphosphine and di-*n*-hexyl ether, which have rather strong electronegativities, do not destroy the activity of the catalyst for the isotactic polymerization of styrene because of the steric effects of the bulky substituent groups on the phosphor and the oxygen atoms. The lower melting point of the isotactic polymer produced in the presences of these additives suggests that the polymer may be constructed by isotactic stereoblocks. This is probably caused by the modification of active center of the catalyst with these compounds.

We wish to thank Mitsui Chem. Ind. Co. and Osaka Titanium Co. for the generous supply of triethylaluminum and titanium tetrachloride, respectively. We are also grateful to Mr. T. Niki for his preparation of 3-vinylthiophene.

*Department of Polymer Science*
*Faculty of Science*
*Osaka University*
*Nakanoshima, Osaka*

# *Analysis of Variation of Coil Character by Aqueous Solution with Q-Meter*

By Sadaharu TOYODA

(Received September 7, 1960)

It is interesting in many respects to notice how the character of a circuit is changed by inserting a substance into its condenser-type electrode or its coil. Several papers[1-10] have been reported already, and especially the effect of an aqueous solution, for high frequency titration, has been studied by many investigators[11-27]. In Ref. 25, a description was given, showing that the resistance of aqueous solution was used as an important factor for explaining the effect caused by the aqueous solution. It was based on an experiment using the resistance-type instrument shown in Ref. 26.

Recently the relationship between the variable

1) P. W. West et al., *Anal. Chem.*, **23**, 1625 (1951).
2) B. W. Thomas et al., ibid., **23**, 1750 (1951).
3) F. W. Jensen et al., ibid., **23**, 1770 (1951).
4) P. H. Monaghan et al., ibid., **24**, 193 (1952).
5) P. W. West et al., ibid., **24**, 1250 (1952).
6) M. Honda, *J. Chem. Soc. Japan, Pure Chem. Sec.* (*Nippon Kagaku Zasshi*), **73**, 529 (1952); **74**, 371 (1953).
7) D. G. Flom et al., *Anal. Chem.*, **25**, 541 (1953).
8) T. Yano, S. Musya, T. Wada and T. Hino, *Chem. Eng.* (*Kagaku Kōgaku*), **20**, 339 (1956).
9) F. J. Schmidt, *Anal. Chem.*, **29**, 1060 (1957).
10) P. F. Knewstubb et al., *Trans. Faraday Soc.*, **54**, 372 (1958).
11) F. W. Jensen et al., *Ind. Eng. Chem., Anal. Ed.*, **18**, 595 (1946).
12) W. J. Blaedel et al., *Anal. Chem.*, **22**, 734 (1950).
13) K. Anderson et al., ibid., **22**, 743, 1272 (1950).
14) W. J. Blaedel et al., ibid., **22**, 1410 (1950).
15) J. L. Hall et al., ibid., **23**, 966 (1951).
16) F. W. Jensen et al., ibid., **23**, 1327 (1951).
17) J. L. Hall, ibid., **24**, 1236, 1244 (1952).
18) O. I. Milner, ibid., **24**, 1247 (1952).
19) S. Musya, M. Itō and M. Takeda, *J. Chem. Soc. Japan, Pure Chem. Sec.* (*Nippon Kagaku Zasshi*), **73**, 482 (1952).
20) S. Fujiwara and S. Hayashi, ibid., **74**, 171 (1953).
21) K. Nakano, ibid., **74**, 172 (1953).
22) C. N. Reilley et al., *Anal. Chem.*, **25**, 86 (1953).
23) S. Fujiwara and S. Hayashi, ibid., **26**, 239 (1954).
24) K. Nakano, *J. Chem. Soc. Japan, Pure Chem. Sec.* (*Nippon Kagaku Zasshi*), **75**, 494, 773 (1954); **76**, 1096 (1955); **77**, 551 (1956).
25) K. Nakano, ibid., **75**, 776 (1954).
26) K. Nakano, ibid., **74**, 227 (1953); K. Nakano, R. Hara and K. Yashiro, *Anal. Chem.*, **26**, 636 (1954).
27) K. Nakano and S. Shibata, *J. Chem. Soc. Japan, Pure Chem. Sec.* (*Nippon Kagaku Zasshi*), **76**, 223 (1955).

resistance and the resistance of aqueous solution at high frequency was clarified to some extent[28]. In that calculation, the equivalent circuit containing the variable resistance and the other factors was used. However, the value of the distributed capacity of coil, $C_0$, could not be obtained by the equation for the coil-type instrument. Then, the value shown in Ref. 25 was used. In the present paper both the method, measuring the distributed capacity of coil, and the results of calculation for the variations of $Q$ and $C$, which are based on the previous papers[28-30], will be described for the case of coil using the Q-meter.

## Experimental

The Q-meter system used in this experiment is shown in Fig. 1. A voltage stabilizer is employed for the Q-meter. The curve of $V/V_0$ vs. $C$, as shown in Fig. 2, is obtained at a constant frequency, $f$, when the capacity of the variable condenser is changed. When an aqueous solution is inserted into the coil, this curve shifts to the dotted line, as is also shown in Ref. 29. The variation of coil character is visualized by these curves. Then the quality of a coil ($Q$) is defined by the maximum value of $V/V_0$. In the present paper, assuming that these curves are symmetric, the capacity of condenser at tuning point (or the tuning capacity) is calculated by taking an average of two values ($C'$, $C''$ in Fig. 2), at which the values of $V/V_0$ are equal to each other. This method is convenient since the precise value can be easily obtained in comparison with another method.

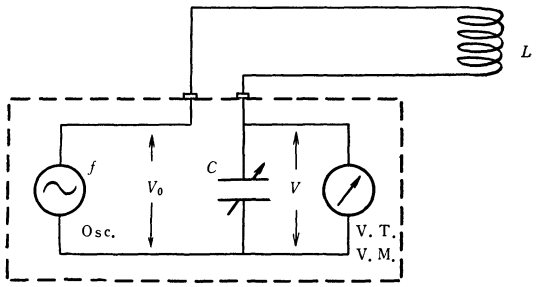



Fig. 1. Q-Meter and coil.

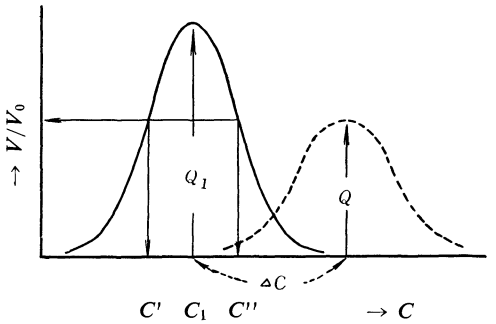



Fig. 2. These curves show the variation of coil character.

The coil shown in Fig. 3 is wound on the quartz bobbin (diameter 31 mm.) which has another quartz tube serving as a guide for the vessel containing the sample solution. The number of turns of the coil, which consists of a copper wire (diameter 1.3 mm.), is 17.5 and the height of the coil is 26 mm. The vessel for sample solution is also made of the quartz tube, of which the inner diameter is 17.1~3 mm. The length of the sample solution in the vessel is 65 mm. and its temperature is kept in the range of 25±0.5°C.

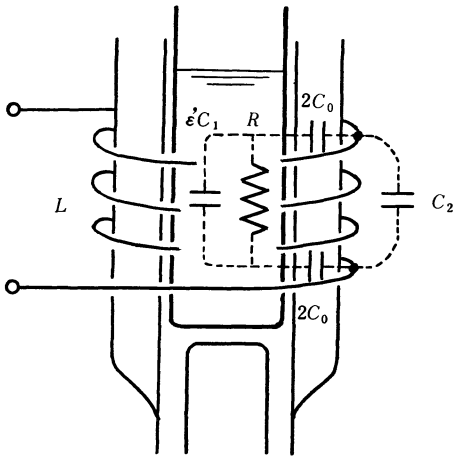



Fig. 3. Relationship between sample solution and coil, connected by equivalent circuit.

## Calculation by Equivalent Circuit

The equivalent circuit of the coil containing the sample solution is considered as Fig. 3 (except the effect of eddy current), where $\varepsilon'$ and $R$ show the real part of the dielectric constant and the resistance of sample solution at high frequency (3 Mc.), respectively. The distributed capacity of the coil consists of capacities, $C_0$, $C_1$ and $C_2$. The notations of $R$ and $C_0$ have the same physical meaning as that in Refs. 25, 29 and 28. The sample solution in the coil has the capacitance, which is omitted in Refs. 25 and 29, under the assumption that the effect of capacitance is negligible when the value of the resistance ($R$) is not so great. However, at the end of Ref. 29 "the dielectric constant of sample solution may be a significant factor" has been suggested. In the present paper the capacitance is expressed by the notation $\varepsilon' C_1$ in Fig. 3, since $\varepsilon' C_1$ as well as $C_2$ has been described in Ref. 28. Then the equivalent circuit of the total system is

28) S. Toyoda, This Bulletin, 33, 504 (1960).
29) M. Honda, K. Nakano and A. Satsuka, *J. Chem. Soc. Japan, Pure Chem. Sec.* (*Nippon Kagaku Zasshi*), 75, 1299 (1954).
30) W. J. Blaedel et al., *Anal. Chem.*, 24, 198 (1952).

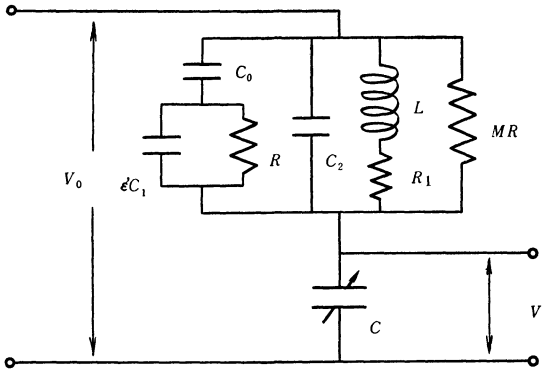



Fig. 4. Equivalent circuit of total system.

illustrated in Fig. 4, taking account of the eddy current in the sample solution and the loss of coil without sample solution ($R_1$). The resistance factor, $MR$, displays the effect of eddy current and has the same significance as $KLR$ in Refs. 25, 29 and 28. The low resistance, $R_1$, will be calculated from the $Q$-value of the coil without sample solution. The position of $R_1$ in Fig. 4 is based on Fig. 8 in Ref. 28.

Thus the equations about $Q$ and $C$ at the tuning point are obtained by the following calculation. If $Z_2$ is the impedance of condenser $C$ and $Z_1$ is the impedance of the rest in Fig. 4, $Q$ and $Z_1$ are written as follows:

$$Q=\left|\frac{Z_2}{Z_1+Z_2}\right| \tag{1}$$

$$\frac{1}{Z_1}=\frac{(\omega C_0)^2R}{1+\omega^2(\varepsilon' C_1+C_0)^2R^2}+\frac{R_1}{R_1^2+(\omega L)^2}+\frac{1}{MR}+j\left[\frac{\omega C_0\{1+\omega^2\varepsilon' C_1(\varepsilon' C_1+C_0)R^2\}}{1+\omega^2(\varepsilon' C_1+C_0)^2R^2}+\omega C_2-\frac{\omega L}{R_1^2+(\omega L)^2}\right]\equiv A+jB \tag{2}$$

On the other hand, the variable condenser is adjusted at the tuning point under the constant frequency of oscillation. This means the following relation, as shown in Ref. 29.

$$(Z_1+Z_2)_{\text{imag}}=0 \tag{3}$$

After rearrangement, it is written as

$$-B\omega C=A^2+B^2 \tag{4}$$

Substituting the above equations into Eq. 1, the following relation is easily obtained.

$$Q=-\frac{B}{A} \tag{5}$$

If the $Q$ of the coil without sample solution is denoted by $Q_1$, one obtains the following expression, substituting the condition ($\varepsilon'=1$, $R=\infty$) into Eq. 5:

$$Q_1=\frac{\omega L}{R_1}\left[1-\omega^2L\left(C_2+\frac{C_0C_1}{C_1+C_0}\right)\left\{1+\left(\frac{R_1}{\omega L}\right)^2\right\}\right] \tag{6}$$

## Calculation of Distributed Capacity

The tuning capacity is shown by Eq. 4. After rearrangement, Eq. 4 is written as

$$\left[1-\omega^2L\left(C_2+C_0\frac{1+qx^2}{1+x^2}\right)\left\{1+\left(\frac{R_1}{\omega L}\right)^2\right\}\right]\omega^2LC$$
$$=1-2\omega^2L\left(C_2+C_0\frac{1+qx^2}{1+x^2}\right)+\left\{\omega^2L\left(C_2+C_0\frac{1+qx^2}{1+x^2}\right)\right\}^2\left\{1+\left(\frac{R_1}{\omega L}\right)^2\right\}+\alpha^2\left\{\left(\frac{px}{1+x^2}\right)^2+\frac{1}{(Mpx)^2}\right\}\left\{1+\left(\frac{R_1}{\omega L}\right)^2\right\}+\frac{2\alpha px}{1+x^2}\frac{R_1}{\omega L}+\frac{2\alpha^2}{M(1+x^2)}\left\{1+\left(\frac{R_1}{\omega L}\right)^2\right\}+\frac{2\alpha}{pMx}\frac{R_1}{\omega L} \tag{7}$$

where

$$x\equiv\omega(\varepsilon' C_1+C_0)R,\qquad \alpha\equiv\omega^2LC_0$$
$$p\equiv\frac{C_0}{\varepsilon' C_1+C_0},\qquad q\equiv\frac{\varepsilon' C_1}{\varepsilon' C_1+C_0}$$

Let us take the special case when the vessel in the coil has no sample solution, so that the tuning capacity for the coil without sample solution, $C_l$, is written as the following expression, substituting the condition ($\varepsilon'=1$, $x=\infty$) into the above equation.

$$\left[1-\omega^2L\left(C_2+\frac{C_0C_1}{C_1+C_0}\right)\left\{1+\left(\frac{R_1}{\omega L}\right)^2\right\}\right]\omega^2LC_l$$
$$=1-2\omega^2L\left(C_2+\frac{C_0C_1}{C_1+C_0}\right)+\left\{\omega^2L\left(C_2+\frac{C_0C_1}{C_1+C_0}\right)\right\}^2\left\{1+\left(\frac{R_1}{\omega L}\right)^2\right\} \tag{8}$$

On the other hand, $C_0$, $C_1$ are the order of magnitude $10^{-12}$ Farad or less and $C_2$ seems to be probably the same order, though $C_2$ may be larger than $C_0$ or $C_1$, and $M\approx10^3$, as being deduced from Refs. 25 and 28. As these capacities are much smaller in value than $C_l$ ($346\times10^{-12}$ Farad), one obtains the following relation from Eq. 6.

$$Q_1\fallingdotseq\frac{\omega L}{R_1} \tag{9}$$

Thus, taking account of $Q_1\gg1$ (refer to Table II), Eq. 8 is written as follows:

$$C_l=\frac{1}{\omega^2L}-C_2-\frac{C_0C_1}{C_1+C_0} \tag{10}$$

Neglecting the second and the third terms, the inductance of the coil at 3 Mc. can be calculated ($L=8.1_4\times10^{-6}$ Henry), so that the loss of the coil is $0.80_3\,\Omega$ by Eq. 9 using $Q_1=191$ (mean value in Table II). If the resistance of the

TABLE I

| Sample solution | | 25°C $10^6$ | 25°C $10^7$ | 25°C $3\times10^6$ | Calcd. $\Delta C$ | Exp. (mean value) $\Delta C$ | Exp. (mean value) $\Delta C'$ | $f_1$ | $f_2$ |
|---|---|---|---|---|---|---|---|---|---|
| Carbon tetrachloride | $\varepsilon'$ | 2.17 | 2.17 | 2.17 | −0.026 | −0.03 | −0.08 | *810 | *37000 |
| | $r$ | $>2\times10^{10}$ | $>4\times10^8$ | $>4\times10^8$ | | | | | |
| *n*-Butyl alcohol | $\varepsilon'$ | 17.4 | 17.4 | 17.4 | −0.215 | −0.23 | −0.28 | 3895 | — |
| | $r$ | $1.1\times10^7$ | $4.3\times10^5$ | $>4\times10^5$ | | | | | |
| Ethyl alcohol | $\varepsilon'$ | 24.5 | 24.1 | 24.3 | −0.258 | −0.26 | −0.31 | 4760 | 178000 |
| | $r$ | $8.2\times10^5$ | $2.3\times10^5$ | $5\times10^5$ | | | | | |
| Methyl alcohol | $\varepsilon'$ | 31 | 31 | 31 | — | −0.29 | −0.34 | 5560 | 189000 |
| | $r$ | $2.9\times10^5$ | $2.2\times10^5$ | $2.5\times10^5$ | | | | | |
| Nitrobenzene | $\varepsilon'$ | 35.6 | 34.4 | 35.2 | −0.305 | −0.31 | −0.36 | 5720 | 192000 |
| | $r$ | $6.3\times10^6$ | $5.8\times10^5$ | $6\times10^5$ | | | | | |
| Distilled water | $\varepsilon'$ | 78.2 | 78.2 | 78.2 | — | −0.39 | −0.44 | 7880 | 210000 |
| | $r$ | $5.8\times10^5$ | $5.0\times10^5$ | $5.5\times10^5$ | | | | | |

* Benzene.
Specific resistance unit, Ω·cm.; capacity unit, $10^{-12}$ Farad; frequency unit, cycle.

sample solution at high frequency is very great, in other words $x\gg1$, all terms following the third term in the right-hand side of Eq. 7 can be neglected in comparison with the rest. Thus, one obtains

$$C=\frac{1}{\omega^2L}-C_2-C_0\frac{1+qx^2}{1+x^2} \tag{11}$$

In Fig. 2, the curve of $V/V_0$ vs. $C$ changes as shown by the dotted line, after the sample solution is inserted into the coil. Then the following equation shows the difference, $\Delta C$, between the tuning capacity of the two cases ($x=\infty$ and $x\gg1$).

$$C-C_l=\frac{C_0C_1}{C_1+C_0}-C_0\frac{1+qx^2}{1+x^2} \tag{12}$$

In Table I, the values of specific resistance of organic solutions and distilled water at $10^6$-, $10^7$-cycles are calculated by the following relation,

$$\frac{1}{\rho}=\frac{f(\varepsilon'/\varepsilon_0)\tan\delta}{1.8\times10^{12}}\ [\text{mho-cm.}]\quad (f \text{ in c.p.s.})$$

as described in the literature[31], and the value of their dielectric constants is also detailed in Ref. 31. The values of dielectric constant and specific resistance at $3\times10^6$-cycle are deduced from the respective values at $10^6$-, $10^7$-cycles. The specific resistance of sample solution, $r$, is proportional to $R$.

$$R=kr \tag{13}$$

On the other hand, the experimental values of $\Delta C$ and $\Delta C'$ in Table I are obtained by the following manipulation at 3 Mc. In the first place, one measures the tuning capacity for the coil, into which the quartz vessel containing the sample solution is inserted, by the method which was detailed previously. Again, the tuning capacity for the coil without the quartz vessel is measured by the same method. Thus the change of the tuning capacity, $\Delta C'$, which is caused by the vessel containing the sample solution, is obtained by subtracting the latter from the former. Similarly $\Delta C''(=-0.05\,\mu\mu$ Farad), which is caused by the quartz vessel without sample solution, is also obtained. Finally, $\Delta C$ is computed by subtracting $\Delta C''$ from $\Delta C'$.

Now, let us calculate the values of $C_0$ and $C_1$ using the methyl alcohol and the distilled water as sample solutions. The following equation can be introduced from Eq. 12,

$$C-C_l=\frac{C_1C_0}{C_1+C_0}-\frac{\varepsilon'C_1C_0}{\varepsilon'C_1+C_0} \tag{14}$$

assuming the relations, $\omega^2\varepsilon'C_1(\varepsilon'C_1+C_0)R^2\gg1$, $\omega^2(\varepsilon'C_1+C_0)^2R^2\gg1$ which may be considered to be correct since the value of their specific resistance is very large in Table I. Accordingly the simultaneous equation for two samples is obtained and one can find the results $C_0=0.52_3\times10^{-12}$, $C_1=0.025_3\times10^{-12}$ Farad. The capacity $C_2$ is neglected in the following discussions since the value can not be obtained by this method, to one's regret.

## Calculation of $Q$-change and $M$ Using Aqueous Solution

It has been described in Ref. 29 that the $Q$ of coil containing the aqueous solution of hydrogen chloride changes with the concentration. The same results as this are obtained as shown in Table II and Fig. 5, when the quartz vessel containing the aqueous solution of potassium chloride or hydrogen chloride is placed in the coil. The values of $Q_1$ in Table II are the $Q$ of coil without the quartz vessel. They are used instead of the $Q$-value of coil with only the quartz vessel, since the variation

31) Arthur R. von Hippel, "Dielectric Materials and Applications", The Technology Press of M. I. T. and J. Wiley & Sons, Inc., New York, Chapman & Hall, Ltd., London (1954), pp. 294, 361, 362, 364.

TABLE II

| Aq. soln., N KCl | Aq. soln., N HCl | $r$(Ω·cm., 25±0.5°C) cycle $3\times10^6$ | cycle $10^3$ | $Q_1$ | $Q$ | $Q/Q_1\times100$ | Mean value $Q/Q_1\times100$ | Mean value $\Delta C'$(pF) |
|---|---|---|---|---|---|---|---|---|
| (Dist. water) | | *5.5×10⁵ | ~10⁶ | 190.5 | 190 | 99.7 | 99.7 | −0.44 |
| | | 1 〃 | | 190 | 190.5 | 〃 | | |
| $10^{-5}$ | | 3.3×10⁴ | 2 ×10⁵ | 190.5 | 190 | 99.7 | 99.7 | −0.43 |
| | $10^{-5}$ | 1.3 〃 | 10⁵ | 191 | 189 | 99.0 | 99.0 | −0.43 |
| | | | | 〃 | 〃 | 〃 | | |
| $10^{-4}$ | | 1.2 〃 | 4.2×10⁴ | 192.5 | 189.5 | 98.4 | 98.5 | −0.44 |
| | | | | 〃 | 190 | 98.7 | | |
| | $10^{-4}$ | 6500 | 2.9 〃 | 192 | 189 | 98.4 | 98.3 | −0.44 |
| | | | | 192.5 | 〃 | 98.2 | | |
| $3\times10^{-4}$ | | 5070 | 2.2 〃 | 191 | 187 | 97.9 | 97.8 | −0.46 |
| | | | | 191.5 | 〃 | 97.7 | | |
| $10^{-3}$ | | 3630 | 6600 | 192.5 | 186 | 96.6 | 96.5 | −0.49 |
| | | | | 192 | 185 | 96.3 | | |
| | $10^{-3}$ | 1680 | 2140 | 192 | 186.5 | 97.1 | 97.0 | −0.52 |
| | | | | 192.5 | 〃 | 96.9 | | |
| $3\times10^{-3}$ | | 1620 | 2280 | 192 | 186.5 | 97.1 | 97.3 | −0.54 |
| | | | | 〃 | 187 | 97.4 | | |
| 0.01 | | 454 | **707 | 193 | 188 | 97.4 | 97.7 | −0.54 |
| | | | | 194 | 190 | 97.9 | | |
| 0.03 | | 220 | 244 | 188 | 185 | 98.4 | 98.1 | −0.56 |
| | | | | 189 | 〃 | 97.8 | | |
| | 0.01 | 187 | 205 | 191 | 186 | 97.4 | 97.5 | −0.55 |
| | | | | 191.5 | 187 | 97.7 | | |
| 0.1 | | 31.3 | **77.6 | 192.5 | 183.5 | 95.3 | 95.2 | −0.55 |
| | | | | 〃 | 183 | 95.1 | | |
| 0.3 | | 17.5 | 27.8 | 192.5 | 176 | 91.4 | 91.2 | −0.61 |
| | | | | 193 | 175.5 | 90.9 | | |
| | 0.1 | 14.0 | 21.6 | 192 | 172.5 | 89.8 | 89.7 | −0.61 |
| | | | | 192.5 | 〃 | 89.6 | | |
| 1 | | 8.06 | **8.94 | 192.5 | 159 | 82.6 | 82.6 | −0.76 |
| | | | | 〃 | 〃 | 〃 | | |
| 3 | | 3.34 | 3.40 | 190 | 132 | 69.5 | 69.5 | −0.94 |
| | 1 | 2.75 | 2.62 | 190 | 127 | 66.8 | 66.9 | −0.97 |
| | | | | 189 | 126.5 | 67.0 | | |

* Table I.
** Ref. 32.

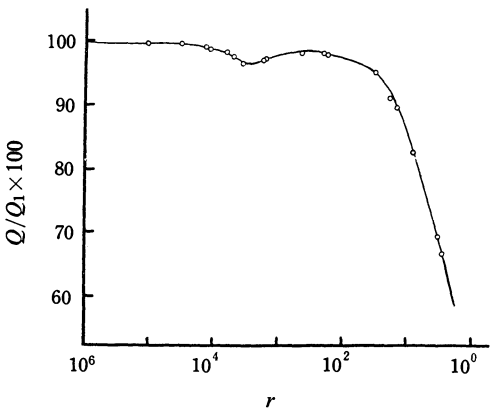



Fig. 5. Relationship between $Q/Q_1$ and specific resistance of aqueous solution.

32) Compiled by Chem. Soc. Japan, "Handbook on Chemistry (Kagaku Benran)", Maruzen, Tokyo (1953), p. 603.

of $Q$ caused by the vessel is so small that one can not detect it. The value of $Q_1$ in Table II changes slightly in spite of an experiment made with the voltage stabilizer. And so the factor, $Q/Q_1$, will be picked up in the following discussion instead of considering the variation of $Q$. After rearrangement of Eq. 5, one obtains

$$\frac{Q}{Q_1}=\frac{1-\omega^2L\left\{C_2+\frac{C_0(1+qx^2)}{1+x^2}\right\}\left\{1+\left(\frac{R_1}{\omega L}\right)^2\right\}}{1-\omega^2L\left(C_2+\frac{C_0C_1}{C_1+C_0}\right)\left\{1+\left(\frac{R_1}{\omega L}\right)^2\right\}}\times\frac{1}{1+\alpha\left(\frac{px}{1+x^2}+\frac{1}{pMx}\right)\frac{\omega L}{R_1}\left\{1+\left(\frac{R_1}{\omega L}\right)^2\right\}} \tag{15}$$

The first term in the right-hand side is approximately equal to unity, taking account of the facts that the distributed capacity is much

TABLE III

| $r$ | $\left(\frac{Q_1}{Q}-1\right)\frac{R_1}{\omega^2L^2}$ | $R$ | $\frac{(\omega C_0)^2R}{1+\omega^2(\varepsilon'C_1+C_0)^2R^2}$ | $MR$ | $M$ | $M'$ |
|---|---|---|---|---|---|---|
| 2.75 | $1.69\times10^{-5}$ | 16.0 | $1.6\times10^{-9}$ | $5.92\times10^{4}$ | $3.70\times10^{3}$ | $7.01\times10^{3}$ |
| 3.34 | $1.50$ 〃 | 19.5 | $1.9$ 〃 | $6.67$ 〃 | $3.42$ 〃 | $6.12$ 〃 |
| 8.06 | $7.19\times10^{-6}$ | 47.1 | $4.6$ 〃 | $1.39\times10^{5}$ | $2.95$ 〃 | $4.83$ 〃 |
| 14.0 | $3.92$ 〃 | 81.7 | $7.9$ 〃 | $2.56$ 〃 | $3.13$ 〃 | $3.73$ 〃 |
| 17.5 | $3.29$ 〃 | 102 | $9.9$ 〃 | $3.05$ 〃 | $2.99$ 〃 | $3.49$ 〃 |
| 31.3 | $1.72$ 〃 | 183 | $1.8\times10^{-8}$ | $5.88$ 〃 | $3.21$ 〃 | $2.42$ 〃 |
| | | | | | $M_{\text{mean}}=3.2\times10^{3}$ | |

smaller than $C_l$ and $(R_1/\omega L)^2\ll1$. Therefore, the behavior of the curve of $Q/Q_1$ is chiefly ruled by the following function of $\varepsilon'$, $R$ or $x$

$$f(x)=\alpha\left(\frac{px}{1+x^2}+\frac{1}{pMx}\right)\frac{\omega L}{R_1} \tag{16}$$

Taking it into account that the dielectric constant of aqueous solution does not change greatly with concentration, since it has been shown in Refs. 30 and 33, one differentiates the function with respect to $x$ and puts the differential coefficient equal to zero, so that the following conditions, which give the minimum and the maximum points of $Q/Q_1$ curve, are obtained:

$$x=\sqrt{\frac{p^2M-2\pm\sqrt{(p^2M-2)^2-4(p^2M+1)}}{2(p^2M+1)}} \tag{17}$$

where positive and negative signs show minimum and maximum, respectively.

On the other hand, the specific resistance, $r$, at $3\times10^6$-cycle shown in Table II is obtained by the following method. One connects the sample solution, which is contained in the proper glass pipe having the electrode of wire, parallel to the variable condenser of Q-meter and measures the $Q$-value, so that the next relation can be used:

$$r=\frac{1}{\omega C}\frac{QQ_1}{Q_1-Q}\frac{\sigma}{h} \tag{18}$$

where $\sigma$ is the section area of sample solution and $h$ the length of the one between two electrodes.

Let us consider the minimum point of $Q/Q_1$ curve. Assuming $p^2M\gg1$, the condition giving the minimum value is written as follows:

$$\omega(\varepsilon'C_1+C_0)R=1 \tag{19}$$

The concentration of aqueous solution giving minimum point seems to be $10^{-3}$ N of potassium chloride in Table II. The resistance of aqueous solution is proportional to the specific resistance of the one. Then one finds $K=5.84$, $(Q/Q_1)_{\min}=97.1\%$ by some calculations. The value of $(Q/Q_1)_{\min}$ is approximately in accordance with the experimental value. However, one should be contented with such consistency taking account of the fluctuation in the cases when measuring capacity, $Q$-value and so forth. The value of $M$ can be calculated by the following expression.

$$\frac{1}{MR}=\left(\frac{Q_1}{Q}-1\right)\frac{R_1}{(\omega L)^2}-\frac{(\omega C_0)^2R}{1+\omega^2(\varepsilon'C_1+C_0)^2R^2} \tag{20}$$

In Table III, $M'$ means the $M$-value obtained by calculation with the specific resistance of aqueous solution at $10^3$-cycle instead of $3\times10^6$-cycle, so that the values of $M'$ are rather scattered.

As a result of calculation about maximum point, one obtains $(Q/Q_1)_{\max}=99.0\%$, with the following equation taking account of $p^2M\approx100$.

$$\left(\frac{Q}{Q_1}\right)_{\max}\fallingdotseq\frac{1}{1+\dfrac{2\alpha Q_1\{1-(1/2p^2M)\}}{\sqrt{M}}} \tag{21}$$

This value seems to be near the value of $Q/Q_1$ for the aqueous solution of $3\times10^{-2}$ N potassium chloride, though the correct experimental value of $(Q/Q_1)_{\max}$ is not evident. Now let us calculate the specific resistance of aqueous solution at maximum point, which is obtained by Eq. 17. Then, one finds it to be 307 Ω cm., which is located between the values for $10^{-2}$ N and $3\times10^{-2}$ N of potassium chloride solutions. It may be considered that the maximum point is located in this interval. Though there are many assumptions on the process of calculation, they seem to become valid by some calculations using the value of $\varepsilon'$, $r$, $k$ and so forth.

In Ref. 28, some of the calculated values of depth at minimum point are considerably great or small in comparison with the experimental one in the case of the coil-type instrument and can not be obtained in the case of the condenser-type instrument. As a result of calculation taking another factor into account, it has been found that the consideration of the factor, $\varepsilon'C_1$, seems to be helpful for the solution of the problem. Similarly, the factor, $\varepsilon'C_1$, is

33) W. J. Blaedel et al., *Anal. Chem.*, **24**, 1240 (1952).

also contained in the condition for the minimum point (Eq. 19). This factor has the same significant meaning as the one in Ref. 28, setting apart the point that a different value will be given to the proportional constant ($k$) in Eq. 13 due to $\varepsilon' C_1$, since Eq. 17 is slightly different from Eq. 20 in Ref. 29. When the dielectric constant of sample solution, $\varepsilon'$, is very large as in the case of water, the term, $\varepsilon' C_1$, becomes greater than $C_0$. Therefore, the former can not be neglected in comparison with the latter, though $C_1$ is fairly small in omparison with $C_0$ in the present paper. The function $f(x)$, which determines the value of $Q/Q_1$ at minimum point, contains the factor $p$. Furthermore the value of this factor becomes somewhat smaller than unity and it depends upon the ratio of $C_0$ to $\varepsilon' C_1$, so that $(Q/Q_1)_{min}$ is ruled to a great extent by this ratio. Then this result seems to support the previous view in Ref. 28.

It has been reported in Ref. 34 that "for high frequency titrations, changes of dielectric constant during the titration will be a factor in the determination of curve form only if there is an appreciable change in the composition of the solvent during the course of the titration". In the present paper, one considers that the dielectric constant of aqueous solution does not change greatly with the concentration. The value of $(Q/Q_1)_{min}$ obtained by Eq. 15, however, seems to become smaller when $C_0$ becomes larger or $\varepsilon'$, $C_1$ smaller. Therefore, it is very significant to consider how the curve of $Q/Q_1$ vs. $x$ changes when a sample solution has another constant value $\varepsilon'$. From Eq. 17 the value of $x$ in the case when $Q/Q_1$ has a minimum value, is independent upon $\varepsilon'$,

TABLE IV

| $\varepsilon'$ | $p$ | $x$ at min. | $x$ at max. | $(Q/Q_1)_{min}$ | $p^2M$ |
|---|---|---|---|---|---|
| 1 | 0.954 | 0.999 | 0.0185 | 87.9 | 2911 |
| 2 | 0.912 | 〃 | 0.0194 | 88.3 | 2660 |
| 3 | 0.873 | 〃 | 0.0202 | 88.8 | 2440 |
| 4 | 0.838 | 〃 | 0.0211 | 89.2 | 2246 |
| 5 | 0.805 | 〃 | 0.0219 | 89.6 | 2075 |
| 6 | 0.775 | 〃 | 0.0227 | 89.9 | 1940 |
| 7 | 0.747 | 〃 | 0.0236 | 90.3 | 1786 |
| 8 | 0.721 | 〃 | 0.0245 | 90.6 | 1663 |
| 9 | 0.697 | 〃 | 0.0254 | 90.9 | 1553 |
| 10 | 0.674 | 〃 | 0.0262 | 91.2 | 1453 |
| 20 | 0.508 | 0.998 | 0.0346 | 93.2 | 826.9 |
| 30 | 0.408 | 0.996 | 0.0432 | 94.5 | 532.8 |
| 40 | 0.341 | 0.994 | 0.0518 | 95.4 | 371.5 |
| 50 | 0.293 | 0.992 | 0.0603 | 95.9 | 273.8 |
| 60 | 0.256 | 0.990 | 0.0690 | 96.6 | 210.0 |
| 70 | 0.228 | 0.988 | 0.0775 | 96.8 | 166.2 |
| 80 | 0.205 | 0.985 | 0.0860 | 97.1 | 134.9 |
| 90 | 0.187 | 0.982 | 0.0946 | 97.3 | 111.5 |
| 100 | 0.171 | 0.980 | 0.103 | 97.5 | 93.88 |

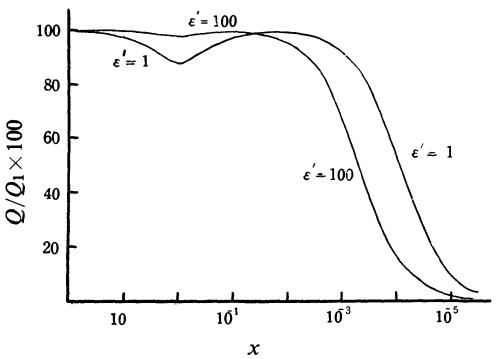



Fig. 6. Relation between values of $Q/Q_1$ for different dielectric constant.

TABLE V. VALUES OF $Q/Q_1$

| $\varepsilon'$ | $x$ = 100 | 30 | 10 | 3 | 1 | 0.3 | 0.1 | $3\times10^{-2}$ |
|---|---|---|---|---|---|---|---|---|
| 1 | 99.7 | 99.1 | 97.4 | 92.3 | 87.9 | 92.9 | 97.2 | 98.6 |
| 4 | 99.8 | 99.2 | 97.7 | 93.1 | 89.2 | 93.8 | 97.5 | 98.9 |
| 10 | 〃 | 99.4 | 98.1 | 94.5 | 91.2 | 94.8 | 97.9 | 〃 |
| 40 | 99.9 | 99.7 | 99.0 | 97.1 | 95.4 | 97.3 | 98.7 | 98.8 |
| 80 | 〃 | 99.8 | 99.4 | 98.2 | 97.1 | 98.2 | 98.9 | 98.4 |
| 100 | 〃 | 〃 | 99.5 | 98.5 | 97.5 | 98.5 | 99.0 | 98.1 |

| $\varepsilon'$ | $x$ = $10^{-2}$ | $3\times10^{-3}$ | $10^{-3}$ | $3\times10^{-4}$ | $10^{-4}$ | $3\times10^{-5}$ | $10^{-5}$ | $3\times10^{-6}$ |
|---|---|---|---|---|---|---|---|---|
| 1 | 98.8 | 96.9 | 91.2 | 76.1 | 51.4 | 24.1 | 9.6 | 3.1 |
| 4 | 98.7 | 96.4 | 90.3 | 73.5 | 48.1 | 21.7 | 8.5 | 2.7 |
| 10 | 98.4 | 95.7 | 88.2 | 69.2 | 42.7 | 18.3 | 7.0 | 2.2 |
| 40 | 97.3 | 91.9 | 79.1 | 53.2 | 32.6 | 10.1 | 3.6 | 1.1 |
| 80 | 95.8 | 87.2 | 69.7 | 40.7 | 18.7 | 6.4 | 2.2 | 0.7 |
| 100 | 94.9 | 85.1 | 65.5 | 36.4 | 15.9 | 5.4 | 1.9 | 0.6 |

34) J. L. Hall et al., ibid., 26, 1539 (1954).

whereas the minimum value of $Q/Q_1$ depends on it, since Eq. 16 has the factor $p$ and $p^2M \gg 1$, as shown in Table IV. On the contrary, in the case of the maximum, the value of $x$ depends upon $\varepsilon'$, whereas the maximum value of $Q/Q_1$ is independent on it (refer to Eq. 21). The values of $Q/Q_1$ for various dielectric constants are listed in Table V, and the relation between some of them is illustrated by Fig. 6.

## Calculation of Capacity Change for Various Solutions

The change of tuning capacity, $\Delta C$, is caused by inserting the sample solution into the coil. When the dielectric loss of sample solution is fairly small in value, in other words, the specific resistance is very large in value, $\Delta C$ can easily be calculated by Eq. 14. Then it seems to be found that the result of calculations for some organic solutions is consistent with the experimental value in Table I. On the other hand, the significant result[35] has been obtained using the heterodyne type instrument, which is based upon the principle that the frequency of an oscillator changes with a change of composition of the core material of the tank circuit coil. The beat frequency changes induced by a number of organic compounds at 4 Mc. have been measured. Therefore, some of them ($f_1$) are shown in Table I. As compared with $\Delta C$, the beat frequency change increases with the decrease of $\Delta C$. Consequently, this beat frequency change seems to be owing to the dielectric constant of core material ($\varepsilon'$), because the change of the tuning capacity due to core material means the change of the reasonance frequency of coil. Furthermore, significant results[36] have been obtained by the instrument with some modification of tank circuit. The beat frequency change has been observed, which is caused by the sample in the capacitor cell. Then some of them $f_2$ are listed in Table I as well as $f_1$. The meaning of the variation of $\Delta C$ seems to become more obvious, taking account of the similarity of the equivalent circuits for the condenser-type electrode and the coil in Ref. 28, and considering the following matter in Ref. 30. The response of many organic solutions is inherently simpler than that of conducting systems, for all changes are essentially capacitive.

Finally, let us consider the change of tuning capacity for the aqueous solution. In Table II the value of $\Delta C'$, monotonously decreases with the decrease of resistance of aqueous solution. On the other hand, investigating each term in Eq. 7, the value of the last term in the right-hand side becomes $7.9\times10^{-5}$ when $x=3\times10^{-4}$ ($r=1.09\,\Omega\cdot$cm.). The minimum observable capacity with Q-meter is 0.01 $\mu\mu$ Farad, and $C_l=346$ $\mu\mu$ Farad, so that $(\Delta C)_{\min}/C_l=2.9\times10^{-5}$. This result seems to suggest that the value of the last term in Eq. 7 can reach sufficient value to be measured, when $x$ approaches $3\times10^{-4}$. All terms following the third term in the right-hand side of Eq. 7 have smaller values than $7.9\times10^{-5}$. Thus they seem to be out of the question in the range of $x$ more than $3\times10^{-4}$. Then, Eq. 11 can be used instead of Eq. 7, for the tuning capacity of coil containing aqueous solution, and so Eq. 12 will be discussed. The change of tuning capacity, $\Delta C$, by Eq. 12 monotonously decreases with the decreasing of $x$, assuming that $\varepsilon'$ is constant. Therefore, the behavior of the curve of $\Delta C$ vs. $x$ obtained by Eq. 12 corresponds with the behavior of the curve of $\Delta C$ vs. $r$. But the value of $\Delta C$ calculated by Eq. 12 is greater than the experimental value in the range of the thick solution. The coil, perhaps, has some floating capacity which is not shown in Fig. 4 since it has been connected with the Q-meter by a rather long lead. This capacity may be one of the causes of discrepancy.

## Conclusion

In the present paper, a method was proposed for the calculation of the distributed capacity of a coil, and the capacity was calculated by using two liquids, though $C_2$ can not be obtained. With these values and the equations as mentioned above, the $Q$-value for the aqueous solution of various concentrations could be calculated. In the case of an organic solution having a large specific resistance, the calculated values of the changes of tuning capacity ($\Delta C$) agree with the experimental values, and the dielectric constant, $\varepsilon'$, seems to be the predominant cause of the effect for a coil. In Ref. 28 "the consideration of the factor, $\varepsilon' C_1$, is significant in order to solve the problem" was found only by calculation. In the present paper, similarly, as a result of some calculations including the factor, $\varepsilon' C_1$, as well as $C_0$, it is shown that the dielectric constant, $\varepsilon'$, is likely to be a significant factor for the variation of $Q$, though the dielectric loss (or the specific resistance) is also important.

The author desires to thank Dr. K. Nakano for his kind discussion.

*Shigengijutsu-Shikenjo*
*Resources Research Institute*
*Kawaguchi-shi, Saitama*

35) P. W. West et al., ibid., **22**, 469 (1950).
36) O. A. Nance et al., ibid., **24**, 214 (1952).

# *Distribution of Various Elements between Nitric Acid and Anion Exchange Resin*

By Fujio ICHIKAWA, Shinobu URUNO and Hisashi IMAI

(Received November 9, 1960)

Previous studies showed that successful separation of plutonium[1] or neptunium[2,3] from fission products was carried out using anion exchange techniques in nitric acid solution. In these cases, plutonium or neptunium(IV) was strongly adsorbed on anion exchange resin from 7.5 M nitric acid while the bulk of fission products were eluted. The anion exchange of thorium[4], lead and bismuth[5] in nitric acid solution has been studied by other researchers. Authors previously reported the anion exchange behaviors of neptunium[3], thorium, uranium, protactinium[6] and rare earth elements[7] in nitric acid.

In the present paper, the distribution of some metallic elements between anion exchange resin and nitric acid is studied and results are shown in a periodic table as is shown in Kraus and Nelson's work[8].

## Experimental

**Resin.** — A strongly basic anion exchange resin Dowex 1, X8 100~200 mesh, was used as an exchanger. The resin was treated with 10% sodium hydroxide solution, washed with water and then converted into nitrate form with nitric acid. The used resin was dried in a desiccator with silica gel at room temperature.

Half a gram of dried resin was used for each experiment.

**Radioactive Tracers.** — For the measurement of distribution coefficient, the radioactive isotopes were used as nitric acid solution of desirable concentration. Some of these isotopes were imported from U. S. A. or the United Kingdom. The others were prepared by neutron irradiation of each element in J. R. R.-1 Reactor. The radiochemical purity of these isotopes was determined by $\gamma$-ray spectrum, $\gamma$-ray decay or absorption curve of $\beta$-ray with aluminum plates. The used nuclides and the method of their preparation are shown in Table I.

**Nitric Acid.**—Reagent grade nitric acid was diluted with distilled water to a desirable concentration varying from 0.1 to 14.5 M.

**Determination of Distribution Coefficient ($K_d$).** —Half a gram of the dried resin was immersed in 5 ml. of the nitric acid solution of the given element for 24 hr. at room temperature. The solution was filtered and the radioactivity of 1 ml. of the filtrate was compared with that of the reference solution which contains no resin. $K_d$ was calculated by the following equation,

$$K_d = \frac{C_1}{C_2}$$

where $C_1$ means the adsorbed radioactivity on 1 g. of resin and $C_2$ means the radioactivity of 1 ml. of the filtrate.

**Experimental Error.**—Polyethylene beakers were used for equilibrium experiments in order to avoid the adsorption of radioactive element on a glass wall. In all cases, a slight increase in the concentration of radioactive element in the supernatant solution occurred. This would be due to the absorption of swelling water by dried resin. But this effect was so small that the $K_d$ value was not corrected.

After the resin was treated with concentrated nitric acid for 24 hr., the color of resin changed from light yellow to dark yellow, but it was found from the results of titration that the decrease of exchange capacity was very small.

## Results and Disscusion

Results are shown in Fig. 1. $K_d$ values were plotted against the concentration of nitric acid both in logarithmic scale. The oxidation state of each element is considered to be the most stable one in nitric acid and is noted in the figure. Based on the periodic table, the feature of $K_d$ curves for each group is described as follows.

**Alkali Metals.** — The adsorption of alkali metals did not occur practically from any concentration of nitric acid.

Because of the absence of available radioisotopes, lithium and francium were not examined, but it was suggested that the resin did not adsorb these elements from nitric acid. $K_d$ value increased slowly with increasing concentration of nitric acid for sodium, potassium, rubidium and cesium and decreased again at a concentration above 8~10 M nitric acid. This trend is one of the typical features of $K_d$ curve.

**Beryllium, Magnesium and Alkaline Earths.** —Beryllium and magnesium were not examined

1) C. Philips and E. N. Jenkins, *J. Inorg. Nucl. Chem.*, 4, 220 (1957).
2) J. S. Nairn et al., A/Conf. 15/p/1458 (1958).
3) F. Ichikawa, This Bulletin, 31, 778 (1958).
4) J. Danon, *J. Am. Chem. Soc.*, 78, 5935 (1956).
5) F. Nelson and K. A. Kraus, ibid., 76, 5916 (1954).
6) F. Ichikawa and S. Uruno, This Bulletin, 33, 569 (1960).
7) F. Ichikawa, ibid., 34, 183 (1961).
8) K. A. Kraus and F. Nelson, A/Conf. 8/p/837.

TABLE I. THE PREPARATION AND COUNTING METHOD OF USED RADIOISOTOPES

| Atomic number | Nuclide | Half life | Preparation | Counting method |
|---|---|---|---|---|
| 11 | $^{24}Na$ | 15.0 h. | Irradiation of $Na_2CO_3$ | $\gamma$ |
| 19 | $^{42}K$ | 12.7 h. | Irradiation of $K_2CO_3$ | $\gamma$ |
| 20 | $^{45}Ca$ | 164 d. | Imported | $\beta$ |
| 21 | $^{46}Sc$ | 85 d. | Irradiation of $Sc_2O_3$ | $\gamma$ |
| 24 | $^{51}Cr$ | 27.8 d. | Imported | $\gamma$ |
| 25 | $^{56}Mn$ | 2.58 h. | Irradiation of $MnO_2$ | $\gamma$ |
| 26 | $^{55}Fe+^{59}Fe$ | 30 y., 45.1 d. | Imported | $\gamma$ |
| 27 | $^{60}Co$ | 5.2 y. | Imported | $\gamma$ |
| 28 | $^{63}Ni$ | 85 y. | Imported | $\gamma$ |
| 29 | $^{64}Cu$ | 12.8 h. | Irradiation of Cu metal | $\gamma$ |
| 30 | $^{65}Zn$ | 245 d. | Imported | $\gamma$ |
| 31 | $^{72}Ga$ | 14.2 h. | Irradiation of $Ga_2O_3$ | $\gamma$ |
| 32 | $^{71}Ge$ | 11.4 d. | Irradiation of Ge metal | $\gamma$ |
| 34 | $^{75}Se$ | 119.9 d. | Imported | $\gamma$ |
| 37 | $^{86}Rb$ | 19 d. | Imported | $\gamma$ |
| 38 | $^{90}Sr$ | 28 y. | Imported | $\beta$ |
| 39 | $^{90}Y$ | 64 h. | Milking from $^{90}Sr$ | $\beta$ |
| 41 | $^{94}Nb$ | 35 d. | Separation from $^{95}Zr$ | $\gamma$ |
| 42 | $^{99}Mo$ | 67 h. | Irradiation of molybdic acid | $\gamma$ |
| 43 | $^{99m}Tc$ | 6.04 h. | Separation from irradiated $HMoO_4$ | $\gamma$ |
| 44 | $^{106}Ru+^{106}Rh$ | 1.0 y., 30 s. | Imported | $\gamma$ of $^{106}Rh$ |
| 46 | $^{109}Pd$ | 13.6 h. | Irradiation of Pd metal | $\gamma$ |
| 47 | $^{110m}Ag$ | 233 d. | Irradiation of Ag metal | $\gamma$ |
| 48 | $^{115}Cd$ | 53 d. | Irradiation of Cd metal | $\gamma$ |
| 49 | $^{114m}In$ | 49 d. | Imported | $\gamma$ |
| 50 | $^{113}Sn$ | 112 d. | Irradiatton of Sn meial | $\gamma$ |
| 51 | $^{124}Sb$ | 60 d. | Imported | $\gamma$ |
| 55 | $^{137}Cs$ | 30 y. | Imported | $\gamma$ |
| 56 | $^{140}Ba$ | 12.8 d. | Imported | $\gamma$ |
| 57 | $^{140}La$ | 40.2 d. | Milking from $^{140}Ba$ | $\gamma$ |
| 58 | $^{141}Ce$ | 33 d. | Irradiation of $Ce_2O_3$ | $\gamma$ |
| 59 | $^{143}Pr$ | 13.7 d. | Irradiation of $Pr_2O_3$ | $\gamma$ |
| 60 | $^{147}Nd$ | 11.3 d. | Irradiation of $Nd_2O_3$ | $\gamma$ at 0.092 MeV. |
| 61 | $^{147}Pm$ | 2.6 y. | Imported | $\beta$ |
| 62 | $^{153}Sm$ | 47 h. | Irradiation of $Sm_2O_3$ | $\gamma$ |
| 63 | $^{152}Eu$ | 13 y. | Irradiation of $Eu_2O_3$ | $\gamma$ |
| 64 | $^{159}Gd$ | 18.0 h. | Irradiation of $Gd_2O_3$ | $\gamma$ at 0.364 MeV. |
| 65 | $^{160}Tb$ | 73 d. | Irradiation of $Tb_2O_3$ | $\gamma$ |
| 66 | $^{165}Dy$ | 2.3 h. | Irradiation of $Dy_2O_3$ | $\gamma$ |
| 67 | $^{166}Ho$ | 27.3 h. | Irradiation of $Ho_2O_3$ | $\gamma$ |
| 68 | $^{165}Er$ | 10.0 h. | Irradiation of $Er_2O_3$ | $\gamma$ |
| 69 | $^{170}Tm$ | 129 d. | Irradiation of $Tm_2O_3$ | $\gamma$ |
| 70 | $^{175}Yb$ | 4.2 d. | Irradiation of $Yb_2O_3$ | $\gamma$ at 0.394 MeV. |
| 71 | $^{176}Lu+^{177}Lu$ | 6.8 d. | Irradiation of $Lu_2O_3$ | $\gamma$ |
| 75 | $^{186}Re$ | 3.87 d. | Irradiation of Re metal | $\gamma$ |
| 76 | $^{191}Os$ | 15 d. | Imported | $\gamma$ |
| 77 | $^{192}Ir+^{194}Ir$ | 74.4 d., 19 h. | Irradiation of Ir metal | $\gamma$ |
| 78 | $^{193m}Pt+^{197}Pt$ | 3.5 d., 18 h. | Irradiation of Pt metal | $\gamma$ |
| 79 | $^{198}Au$ | 2.72 d. | Irradiation of Au metal | $\gamma$ |
| 80 | $^{203}Hg$ | 4.54 d. | Imported | $\gamma$ |
| 81 | $^{204}Tl$ | 4.0 y. | Imported | $\beta$ |
| 82 | $^{212}Pb$ | 10.6 h. | Separation from imported $^{228}Th$ | $\gamma$ |
| 84 | $^{210}Po$ | 138.4 d. | Separation from irradiated Bi | $\alpha$ |
| 90 | $^{234}Th$ | 24.1 d. | Separation from natural U | $\gamma$ |
| 91 | $^{233}Pa$ | 27.4 d. | Separation from irradiated Th | $\gamma$ |
| 92 | nat. U | | | Colorimetric |
| 93 | $^{239}Np$ | 2.33 d. | Separation from irradiated U | $\gamma$ |

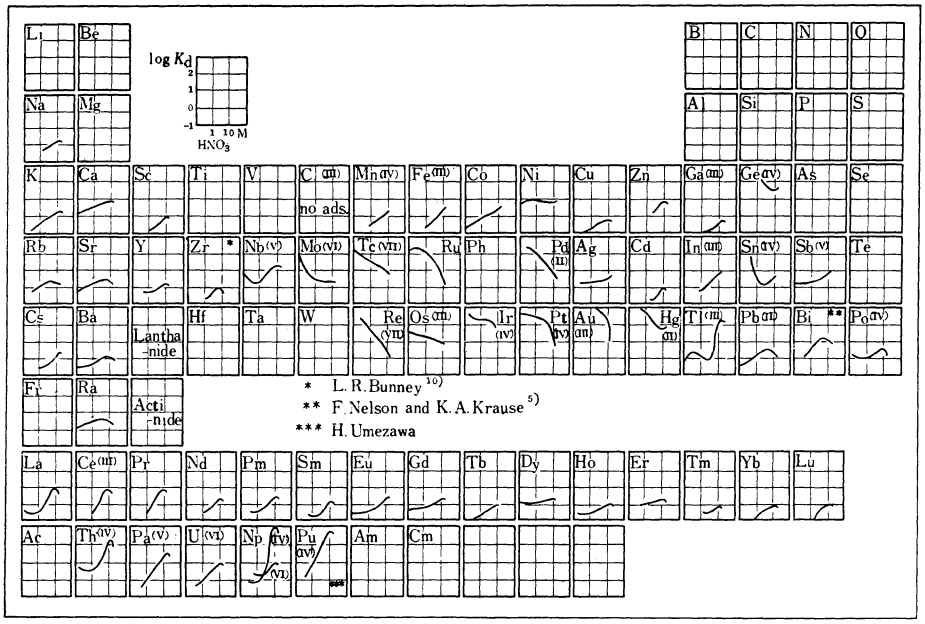



Fig. 1. Distribution coefficients between anion exchange resin and nitric acid.

for the same reason as lithium. Alkaline earths were not adsorbed practically at lower concentration of nitric acid, but they were slightly adsorbed at a concentration above 4 M nitric acid.

**Scandium, Yttrium and Lanthanide Elements.** —In every case, there was a maximum $K_d$ value at 8 M nitric acid. Scandium and yttrium were scarcely adsorbed at all. As was shown in the previous paper[7], there is an interesting trend in the $K_d$ values of lanthanide elements. The $K_d$ values of lanthanide elements at 8 M nitric acid decrease with increasing atomic number.

**Actinide Elements.**—Of the actinide elements thorium(IV), protactinium(V), uranium(VI), neptunium(IV) and neptunium(VI) were examined. The data on plutonium(IV), which was reported by Umezawa[9], is also shown. As in the case of neptunium, the high adsorbability in tetravalence state was already reported, and was applied to the separation of neptunium from fission products and uranium. Thorium and protactinium were strongly adsorbed on the resin from 8 M nitric acid solution. Uranium was slightly adsorbed under the same condition. From these facts this method may be applied to the separation of uranium-233 from irradiated thorium.

**Zirconium and Niobium.** — The data of zirconium were cited from the report[10] of Bunney et al., who used Dowex 2 as an anion exchanger. Both zirconium and niobium were slightly adsorbed on the resin and therefore, a long column will be needed for the separation.

**Molybdenum, Technetium and Rhenium.** — These elements showed similar $K_d$ curves. From a very dilute nitric acid, these elements were adsorbed strongly on the resin and the adsorbability decreased with increasing concentration of nitric acid. This is probably due to the decrease of the dissociation of these oxy acids. For instance, rhenium is present in water as $ReO_4^-$ and is adsorbed on the resin as an anion, but when the acidity of nitric acid increases the dissociation of $HReO_4$ becomes small, resulting in desorption from anion exchanger.

**Chromium(III), Manganese, Iron(III), Cobalt and Nickel.**—Only nickel was slightly adsorbed and the others were not practically adsorbed. If a more detailed discussion is permitted, $K_d$ values of manganese and iron(III) increase with a slope of 1 and this means the formation of anionic species which has one negative charge.

**Ruthenium, Paradium, Osmium, Iridium, Platinum and Gold.** — These elements were strongly adsorbed from nitiric acid of lower concentration and desorbed from nitric acid of higher concentration. The metals of these elements were dissolved in aqua regia, evaporated to dryness and redissolved in nitric acid. Therefore it is likely that these elements exist as chloro metallic acid in nitric acid, and that the anionic chloro complexes are adsorbed on

9) H. Umezawa, *J. Atomic Energy Soc. Japan*, **2**, 478 (1960).
10) L. R. Bunney et al., *Anal. Chem.*, **31**, 325 (1959).

the resin from nitric acid of low concentration.

**Silver, Copper, Zinc, Cadmium and Mercury.** — Copper and cadmium were not adsorbed. Zinc and silver were slightly adsorbed at higher concentration of nitric acid. Mercury was strongly adsorbed from dilute nitric acid and $K_d$ value decreases at concentrated nitric acid.

**Gallium, Indium, Germanium and Tin(IV).** — Gallium and indium were not adsorbed from nitric acid of any concentration. Germanium and tin(IV) were strongly adsorbed in dilute nitric acid and the $K_d$ value showed a negative slope with increasing concentration of nitric acid.

**Thallium, Lead, Bismuth and Polonium.** — These elements exist as daughter products of natural radioactive decay series. The data on bismuth is cited from Kraus-Nelson's report[5]. Lead and polonium were slightly adsorbed on the resin from 8 M nitric acid. Thallium was strongly adsorbed at a concentration above 10 M nitric acid, but it was scarcely adsorbed at lower concentration of nitric acid.

## Summary

Distribution coefficient of some metallic elements between nitric acid and anion exchange resin were measured. From the results described above, the fundamental data on the separation of each element in nitric acid were obtained.

Authors wish to express sincere thanks to Dr. T. Nakai for his encouragement.

*Japan Atomic Energy Research Institute*
*Tokai, Ibaraki-ken*

# *A Simplified Model for the Structure of Water*

By Goro WADA

(Received October 6, 1960)

Water is very special in its physical properties as well as very familiar to us in its occurrence on the earth. Its peculiarity has been considered to be caused mainly by the hydrogen bonds formed between water molecules. Bernal and Fowler[1] studied for the first time the quasi-crystalline structure of water by X-rays and found it to be composed of the intermediate of trydimite, crystobalite and the closest packing. Eucken[2] described the peculiar properties of water, especially from the points of view of the density and the compressibility, assuming that water is an equilibrating mixture of four species: $H_2O$, $(H_2O)_2$, $(H_2O)_4$ and $(H_2O)_8$. Recently, the structure of water was discussed variously on the bases of bending in the hydrogen bonds by Pople[3], of the covalency in the hydrogen bonds by Frank[4] and of the radial distribution function of water by X-rays by van Panthaleon van Eck et al.[5,6] and by Brady et al.[7-9] These works seem to be too complicated and rigorous to explain the simple observed facts, and often involve too many assumptive parameters. Hall[10] tried to simplify Eucken's model and regarded water as existing in two different energy states to account for the excess ultrasonic absorption of water. Using this model, the pressure effects of the ultrasonic absorption[11,12] and of the thermal conductivity[13] of water were also treated. In the present paper, various properties of water will be explained by a simple two-state model that water is equilibrated between the so-called "iceberg" having locally the ice structure and the structure more closely packed than the iceberg.

1) J. D. Bernal and R. H. Fowler, *J. Chem. Phys.*, **1**, 515 (1933).
2) A. Eucken, *Nachricht. Akad. Wiss. Göttingen, Math.-Phys. Klasse*, 38 (1946).
3) J. A. Pople, *Proc. Roy. Soc.*, **A205**, 163 (1951).
4) H. S. Frank, ibid., **A247**, 481 (1958).
5) C. L. van Panthaleon van Eck, H. Mendel and W. Boog, *Discussions Faraday Soc.*, **24**, 200 (1957).
6) C. L. van Panthaleon van Eck, H. Mendel and J. Fahrenfort, *Proc. Roy. Soc.*, **A247**, 471 (1958).
7) G. W. Brady and J. T. Krause, *J. Chem. Phys.*, **27**, 304 (1957).
8) G. W. Brady, ibid., **28**, 464 (1958).
9) G. W. Brady, ibid., **29**, 1371 (1958).
10) L. Hall, *Phys. Rev.*, **73**, 775 (1948).
11) A. H. Smith and A. W. Lawson, *J. Chem. Phys.*, **22**, 351 (1954).
12) T. A. Litovitz and E. H. Carnevale, *J. Appl. Phys.*, **26**, 816 (1955).
13) A. W. Lawson, R. Lowell and A. L. Jain, *J. Chem. Phys.*, **30**, 643 (1959).

### Equilibrium between Icy State and Packed State

Ice melts at 0°C, accompanied by an abrupt decrease in volume, and water yet continues a gradual contraction as the temperature is raised after melting, until it arrives at a minimum volume at 3.98°C, over which it begins to expand, under an atmospheric pressure. This fact would be recognized by a new model relating to the structure of water, proposed by the author that liquid water consists of two states of aggregation, namely icy state $(H_2O)_{icy}$, with lower density and packed state $(H_2O)_{packed}$, with higher density and that these two states hold a chemical equilibrium

$$(H_2O)_{icy} \rightleftarrows (H_2O)_{packed} \qquad (1)$$

The volume of liquid water is the sum of those of the two states, and the equilibrium trends to the right-hand side of the equation when the temperature is raised, each of the states showing the respective thermal expansions. Water molecules of the icy state correspond to the molecular associates with local and temporary quasi-crystalline ice structure, which have hitherto been called "iceberg", "cluster" or "icelikeness" drifting in liquid water, by several workers[14].

Then, the equilibrium constant $K$ of Eq. 1 is expressed by the following equation, $x$ being the mole fraction of $(H_2O)_{icy}$ at $t$°C, and $\Delta G$ the free energy.

$$K=\frac{1-x}{x}=\exp(-\Delta G/RT) \qquad (2)$$

When the volumes of the icy and the packed states at 0°C and at $t$°C are represented by $v_i^0$ and $v_p^0$, and $v_i$ and $v_p$ in cc. g$^{-1}$ respectively, and the coefficients of thermal expansion $\alpha_i$ and $\alpha_p$ respectively, the volume of liquid water $v$ is given by

$$v=xv_i+(1-x)v_p$$
$$=xv_i^0(1+\alpha_i t)+(1-x)v_p^0(1+\alpha_p t) \qquad (3)$$

where, for the values of $v_i^0$ and $\alpha_i$, can be used those for the pure ice. From the observed values of $v$ at various temperatures[15], $x$'s can be known at the respective temperatures, only assuming that $x$ is just equal to 0.2 at 100°C. This assumption is introduced by the method of trial and error, so as to be consistent with other properties of water most satisfactorily, as will be mentioned in the next chapter.

Although, in Eucken's model[2], the total mole fraction of associating molecules at 100°C was also 0.2, there were introduced some other numerical assumptions which were ambiguous in physical meanings, while the present model involves no other assumptions than that of $x=0.2$ at 100°C. Thus, $x$'s at various temperatures are computed as shown in Table I, $\alpha_p$ being determined from this assumption.

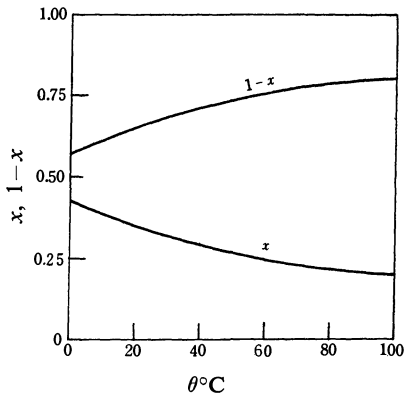



Fig. 1. Temperature dependence of $x$ and $1-x$.

TABLE I. MOLE FRACTIONS OF THE ICY STATE $x$ AND OF THE PACKED STATE $1-x$ AT VARIOUS TEMPERATURES

| $t$°C | $v$, cc.g$^{-1}$ | $v_i$, cc.g$^{-1}$ | $v_p$, cc.g$^{-1}$ | $x$ | $1-x$ | $K$ |
|---|---|---|---|---|---|---|
| 0 | 1.0001 | 1.0905 | 0.9334 | 0.4246 | 0.5754 | 1.355 |
| 1 | 1.0001 | 1.0907 | 0.9343 | 0.4207 | 0.5793 | 1.377 |
| 2 | 1.0000 | 1.0908 | 0.9353 | 0.4161 | 0.5839 | 1.403 |
| 3 | 1.0000 | 1.0910 | 0.9362 | 0.4121 | 0.5879 | 1.427 |
| 4 | 1.0000 | 1.0911 | 0.9372 | 0.4081 | 0.5919 | 1.450 |
| 5 | 1.0000 | 1.0913 | 0.9381 | 0.4040 | 0.5960 | 1.475 |
| 6 | 1.0000 | 1.0914 | 0.9391 | 0.3999 | 0.6001 | 1.501 |
| 7 | 1.0001 | 1.0916 | 0.9400 | 0.3964 | 0.6036 | 1.523 |
| 8 | 1.0001 | 1.0917 | 0.9410 | 0.3922 | 0.6078 | 1.550 |
| 9 | 1.0002 | 1.0919 | 0.9419 | 0.3887 | 0.6113 | 1.573 |
| 10 | 1.0003 | 1.0920 | 0.9429 | 0.3850 | 0.6150 | 1.597 |
| 15 | 1.0009 | 1.0930 | 0.9476 | 0.3665 | 0.6335 | 1.729 |
| 20 | 1.0018 | 1.0938 | 0.9523 | 0.3495 | 0.6505 | 1.861 |

14) H. S. Frank and W. Y. Wen, *Discussions Faraday Soc.*, 24, 133 (1957).

15) "Chemical Handbook", Ed. by Chem. Soc. Japan, Maruzen, Tokyo (1952), p. 287.

The basic values for calculations are as follows.

$$v_i^0 = 1.0905 \qquad v_p^0 = 0.9334 \text{ cc. g}^{-1} \quad (4)$$

$$\alpha_i = 1.52 \times 10^{-4} \qquad \alpha_p = 1.013 \times 10^{-3} \text{ deg}^{-1} \quad (5)$$

The variation of the mole fraction of the icy state, $x$, and that of the packed state, $1-x$, over the temperature range 0~100°C are depicted in Fig. 1. The icy state is found to remain unmelted as much as 40% of the whole liquid water at 0°C.

## Properties of Water Explained by the Model

**Heat of Fusion of Ice.**—As is shown in Fig. 2, one obtains a fine straight line by plotting $\log K$ against $1/T$, from which the intrinsic heat of fusion of ice, $\Delta H_f$, i. e. the enthalpy of the transition $(H_2O)_{icy} \rightarrow (H_2O)_{packed}$ at 0°C is calculated.

$$\Delta H_f = 2.51 \text{ kcal. mol}^{-1} \text{ at } 0°C \quad (6)$$

The commonly known value as the heat of fusion of ice, 1.43 kcal. $mol^{-1}$, is not per mole in reality but per $1-x=0.5754$ mol. at 0°C. The true corrected value per mol. is $1.43 \div 0.5754 = 2.49$ kcal. $mol^{-1}$, which agrees very well with Eq. 6.

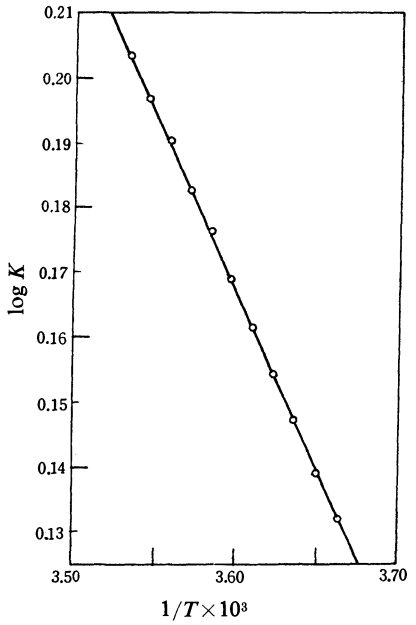



Fig. 2. The intrinsic heat of fusion of ice.

**Free Energy and Entropy of Fusion of Ice.**—Free energy and entropy of fusion of ice at 0°C, $\Delta G$ and $\Delta S_f$, are easily calculated from $K$'s in Table I and $\Delta H_f$ in Eq. 6, as follows.

$$\Delta G = -165.1 \text{ cal. mol}^{-1} \text{ at } 0°C \quad (7)$$

$$\Delta S_f = 9.79 \text{ cal. deg}^{-1} \text{ mol}^{-1} \text{ at } 0°C \quad (8)$$

Entropy of fusion of ice obtained from the observed heat of fusion is $1.43 \div (0.5754 \times 273.1) = 9.10$ cal. $deg^{-1} mol^{-1}$, which does not greatly differ from Eq. 8. In general, entropies of fusion for normal triatomic molecules should have nearly equal values: those for carbon disulfide and nitrous oxide are, for instance, 8.4 and 8.6 cal. $deg^{-1}$ $mol^{-1}$, respectively[16], to which the value of Eq. 8 is fairly approximate*.

**Specific Heat.**—Using the observed results of specific heats of ice[17], one obtains the following empirical formula for ice at the temperature range of −60~0°C.

$$c_i = 0.48986 + 1.357 \times 10^{-3} t - 2.625 \times 10^{-7} t^2 + 3.708 \times 10^{-7} t^3 \text{ cal. deg}^{-1}\text{g}^{-1} \quad (9)$$

If Eq. 9 is applicable to an imaginary piece of ice above 0°C, namely the icy state in liquid water, an equation for the specific heat of water can be given, the partial fusion of the icy state with rise of temperature being taken into account.

$$C = xC_i + (1-x)C_p - \Delta H_f \frac{dx}{dT} \quad (10)$$

where $C$, $C_i$ and $C_p$ are the molecular heats of the liquid water, the icy state and the packed state, respectively. Then, from Eqs. 2 and 10, the molecular heat of the packed state is given by

$$C_p = \frac{C - xC_i}{1-x} - \frac{x(\Delta H_f)^2}{RT^2} \quad (11)$$

In Table II, the values of $C_p$ at various temperatures are listed. The molecular heat

Table II. Molecular heat of the packed state of water

| $t$ °C | $c$[13] cal.deg$^{-1}$g$^{-1}$ | $c_i$ cal.deg$^{-1}$g$^{-1}$ | $c_p$ cal.deg$^{-1}$g$^{-1}$ | $C_p$ cal.deg$^{-1}$mol$^{-1}$ |
|---|---|---|---|---|
| 0 | 1.0092 | 0.48986 | 0.3928 | 7.071 |
| 5 | 1.0051 | 0.49669 | 0.4325 | 7.784 |
| 10 | 1.0021 | 0.50377 | 0.4705 | 8.469 |
| 15 | 1.0001 | 0.51141 | 0.5076 | 9.136 |
| 20 | 0.9988 | 0.51986 | 0.5418 | 9.752 |

16) J. O. Hirschfelder, C. F. Curtiss and R. B. Bird, "Molecular Theory of Gases and Liquids", John-Wiley, New York (1954), p. 285.

17) "International Critical Tables", Vol. V (1929), p. 95.

* For comparison, the calculated thermodynamic values at 0°C together with those of the previous investigators are shown as follows.

| | $\Delta G$ cal.· mol$^{-1}$ | $\Delta S_f$ cal. deg$^{-1}$· mol$^{-1}$ | $\Delta H_f$ cal.· mol$^{-1}$ | $x$ |
|---|---|---|---|---|
| Present author | −165.1 | 9.79 | 2510 | 0.4246 |
| Lawson et al.[13] | −150 | 11.5 | 3000 | 0.42 |
| Litovitz et al. [12] | −500 | 5 | 870 | 0.32 |
| Smith et al.[11] | 0 | 9.5 | 2600 | 0.50 |
| Hall[10] | +500 | — | — | 0.70 |

Hall assumed a possibility of a two-state representation, one state of larger volume and lower energy and the other state of smaller volume and higher energy, which is quite different from the models of the present author and other investigators except Hall.

of liquid water is ordinarily known to be 18 cal. deg$^{-1}$mol$^{-1}$, but $C_p$'s of the packed state over the temperature range of 0~20°C lie between 7 and 10 cal. deg$^{-1}$ mol$^{-1}$, which seems to be appropriate compared with the values of the molecular heat for methyl alcohol (18.7 cal. deg$^{-1}$mol$^{-1}$ at 12°C) or for ethyl alcohol (26.6 cal. deg$^{-1}$mol$^{-1}$ at 20°C).

**Vapor-pressure and Heat of Vaporization.** — The ratios of the vapor-pressure of liquid water, $p$, to that of ice, $p_i$, are expressed empirically as a function of temperature as follows[18].

$$\log\frac{p}{p_i}=\frac{-1.1489\,t}{273.1+t}-1.330\times10^{-5}t^2+9.084\times10^{-8}t^3 \qquad (12)$$

Admitting that water is an ideal mixture of the icy and the packed states, the vapor-pressure of the liquid water can be shown, according to Raoult's rule.

$$p=xp_i+(1-x)p_p \qquad (13)$$

Then, the partial pressures of the packed state, $p_p$'s, are calculated at various temperatures by the following equation derived from Eqs. 12 and 13 and are listed in Table III, where $p$'s are known empirically[19].

$$p_p=\frac{1-x\frac{p_i}{p}}{1-x}p \qquad (14)$$

TABLE III. VAPOR-PRESSURE OF WATER

| $t$, °C | $p/p_i$ | $p$[19], mmHg | $p_p$, mmHg |
|---|---|---|---|
| 0 | 1.00000 | 4.579 | 4.579 |
| 1 | 0.99048 | 4.926 | 4.892 |
| 2 | 0.98093 | 5.294 | 5.221 |
| 3 | 0.97140 | 5.685 | 5.542 |
| 4 | 0.96207 | 6.101 | 5.935 |
| 5 | 0.95284 | 6.543 | 6.323 |
| 6 | 0.94372 | 7.013 | 6.735 |
| 7 | 0.93469 | 7.513 | 7.168 |
| 8 | 0.92576 | 8.045 | 7.628 |
| 9 | 0.91693 | 8.609 | 8.113 |
| 10 | 0.90819 | 9.209 | 8.627 |

As is pictured in Fig. 3, the plot of $\log p_p$ against $1/T$ gives a straight line, from the slope of which is obtained the heat of vaporization of the packed state $\Delta H_{v(p)}$.

$$\Delta H_{v(p)}=9.70 \text{ kcal. mol}^{-1} \text{ at } 0°C \qquad (15)$$

Since the heat of vaporization of water, $\Delta H_v$, is represented by

$$\Delta H_v=x\Delta H_s+(1-x)\Delta H_{v(p)} \qquad (16)$$

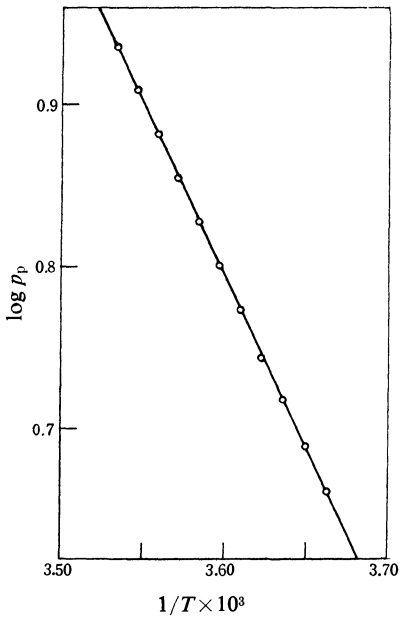



Fig. 3. Heat of vaporization of water.

and since the heat of sublimation of ice, $\Delta H_s$, is expressed by an equation $\Delta H_s=\Delta H_f+\Delta H_{v(p)}$, $\Delta H_v$ is expected to be composed of the heat of fusion of the icy state and of vaporization of the packed state by the following relation:

$$\Delta H_v=x\Delta H_f+\Delta H_{v(p)} \qquad (17)$$

Therefore,

$$\Delta H_v=10.77 \text{ kcal. mol}^{-1} \text{ at } 0°C \qquad (18)$$

$$\Delta H_s=12.21 \text{ kcal. mol}^{-1} \text{ at } 0°C \qquad (19)$$

The heat of vaporization of liquid water and the heat of sublimation of ice directly observed by experiments at 0°C are 10.73 kcal. mol$^{-1}$ and 12.16 kcal. mol$^{-1}$ respectively, both of which agree with Eqs. 18 and 19 quite satisfactorily.

**Molar Volume and Molecular Distance.**— According to the additivity rule that molar volume of a normal liquid is predicted by the algebraic sum of the individual atomic volumes of composing atoms of the molecules, the calculated molar volume of the packed state may be 14.8 cc. mol$^{-1}$, which approximates 16.8 cc. mol$^{-1}$ computed from Eq. 4.

From the works of van Panthaleon van Eck et al.[5,6], the radial distribution curve of water measured by X-rays is reproduced in Fig. 4, which reveals two peaks in the curve at the molecular distances 3.1 and 4.5 Å. Van Panthaleon van Eck et al. concluded that the nearest molecular distance 3.1 Å coincides with the theoretical value of the molecular distance between the first neighbors, calculated from the density of liquid water, when liquid water

18) J. H. Perry, "Chemical Engineers' Handbook" McGraw-Hill, New York (1950).
19) "Chemical Handbook", Ed. by Chem. Soc. Japan, Maruzen, Tokyo (1952), p. 382.

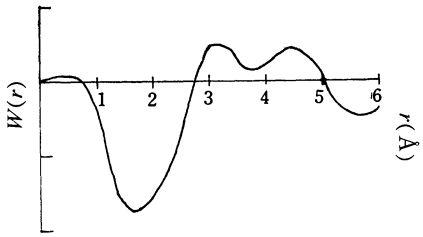



Fig. 4. Radial distribution curve of water at 2.6°C (quoted from C. L. van Panthaleon van Eck et al.[5,6]).

is assumed to be octahedrally coordinated, and that, therefore, water has a uniform structure of octahedron in liquid state, instead of that of the tetrahedron which is popularly believed to exist in ordinary ice.

But, on the contrary, the present new model concerning liquid water can describe more naturally the results of Fig. 4 as follows. Since the icy state has, of course, the ice-structure, water molecules in the icy state takes a tetrahedral arrangement, and the O-O distance of hydrogen bond must be 2.76Å as usual. And it is reasonable to consider that the packed state of water has lost the icelike structure with hydrogen bondings between O-O atoms and is rather more densely packed in closest packing, as is often seen in case of general ideal liquids, such as argon or molten metals. From the molar volumes of the icy and the packed states (Eq. 4), the molecular distances at 0°C are calculated, and listed in Table IV.

TABLE IV. MOLECULAR DISTANCE AND COORDINATION NUMBER OF THE TWO STATES

| | Icy state (Tetrahedral) | | Packed state (Closest packing) | |
|---|---|---|---|---|
| | Distance Å | Coordination number | Distance Å | Coordination number |
| First neighbor | 2.76 | 4 | 3.46 | 12 |
| Second neighbor | 4.51 | 12 | 4.89 | 6 |

According to this model, the peak at 3.1Å can be explained as the result of the overlapping of two curves, each corresponding to the icy and the packed states, with the weights of the mole fraction and the coordination number, respectively. If the two curves, which exhibit peaks at 2.76 and 3.46Å by the first neighbors, respectively, are gently sloping near the maximum points, the resultant curve of the two may have a single peak between the two individual peaks, at 3.1Å.

In addition, the observed fact that the number of the first neighbors increases gradually as the temperature is raised[20] seems to be caused by the successive transition of the icy state with smaller coordination number to the packed state with larger coordination number. If liquid water were uniformly octahedral, the number of the first neighbors would rather decrease, since the number of holes caused by thermal agitation should increase with temperature. The fact that both the peak at 4.5Å and the bottom at 5.6Å of the radial distribution curve at 2.6°C shown in Fig. 4 almost diminish at 60°C[5] may be due to the results of only existence of the short range order of liquid.

**Surface Tension.**—Regarding water of the packed state as a normal liquid, the molecular parachor is found to be $P=50.8$ from the summation of the individual atomic parachor[21],*. Thence, the surface tension of the packed state $\gamma_p$ can be derived by use of the relation between the parachor and the surface tension,

$$P=M\gamma_p^{1/4}/(\rho-\rho_0) \tag{20}$$

where $M$ is the molecular weight of water, and $\rho$ and $\rho_0$ are the density of water of the packed state and of vapor upon the packed state, respectively, which are known from Eq. 4 and Table III.

$$\gamma_p=83.58 \text{ dyn. cm}^{-1} \text{ at } 0°C \tag{21}$$

This value of $\gamma_p$ is slightly larger than that observed for liquid water at 0°C, 75.64 dyn. $cm^{-1}$.

The surface tension of a mixed liquid is expressed as follows, the heat of mixing being taken as zero[22].

$$\gamma=\gamma_1+\frac{RT}{A_1}\ln\frac{x'}{x}=\gamma_p+\frac{RT}{A_p}\ln\frac{1-x'}{1-x} \tag{22}$$

where $A_1$ and $A_p$ are the molar area of water in the icy and the packed states respectively, and $x'$ is the mole fraction of the icy state on the surface of liquid water. As $A_p=6.043\times10^8$ $cm^2$, $x'$ is calculated from the following equation.

$$\frac{1-x'}{1-x}=\exp[(\gamma-\gamma_p)A_p/RT] \tag{23}$$

$$x'=0.819 \text{ at } 0°C \tag{24}$$

From the value of Eq. 24, it is found that the icy state is positively adsorbed on the surface of liquid water; in other words, it behaves like a so-called "surface active substance".

20) J. Morgan and B. E. Warren, *J. Chem. Phys.*, 6, 666 (1938).

21) R. C. Reid and T. K. Sherwood, "The Properties of Gases and Liquids", McGraw-Hill, New York (1958), p. 21.

* Since the hydrogen atom in the packed state does not form any hydrogen bond, the atomic parachor of hydrogen must be not 10.0 but 15.5, the former being the value for hydrogen in OH and the latter for ordinary hydrogen as in hydrocarbons[21].

22) J. A. V. Butler, *Proc. Roy. Soc.*, A135, 348 (1932); J. H. Hildebrand and R. L. Scott, "The Solubility of Nonelectrolytes", Reinhold (1950), p. 406; T. P. Hoar and D. A. Melford, *Trans. Faraday Soc.*, 53, 315 (1957).

**Energy State of Water.**—The various energy relations of water mentioned above are illustrated all together in Fig. 5. An assumed state of energy of water that only the hydrogen bondings in ice are broken but that the geometrical molecular configuration is still maintained to be tetrahedral, is drawn as T-state in the figure, and it is 6.5 kcal. $mol^{-1}$ higher in energy than the packed state, the latter state being realized by the cohesion force between the dipoles of water molecules from the former state, since the energy of a hydrogen bond O-H···O in ice is 4.50 kcal. $bond^{-1}$. The phenomenon of premelting of ice would be demonstrated as the local occurrence of the T-state in ice structure.

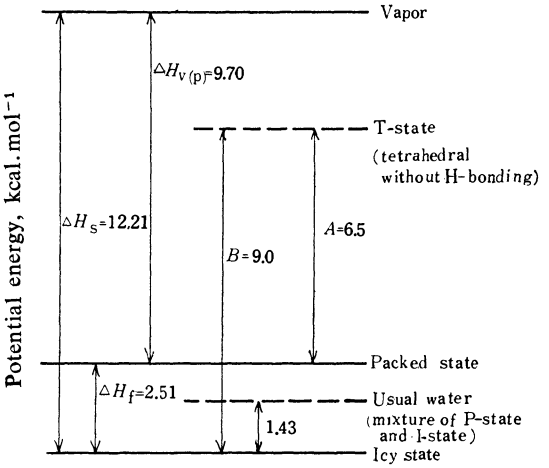
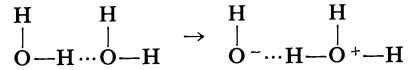



Fig. 5. Energy state of water at 0°C.

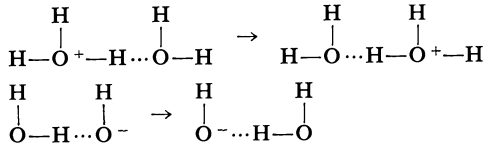
**Activation Energy of Self-diffusion.** — The observed value of the activation energy of self-diffusion of liquid water is 5.3 kcal. $mol^{-1}$ [23]. Since water molecules of the icy state may be compared to "macromolecules" although unstable, it might be rather single molecules of the packed state that take a greater part in self-diffusion in liquid water. And, since the intermediate state in the process of self-diffusion must necessarily be of an open structure with many holes, similar to the T-state shown in Fig. 5, the activation energy of self-diffusion must be approximately equal to $A$ (=6.5 kcal. $mol^{-1}$), which agrees with the observed value without serious error.

**Heat of Ionization.**—In order to dissociate a water molecule into a hydrogen ion and a hydroxyl ion, three steps must take place: (a) a proton jump between adjacent two water molecules through a hydrogen bonding,



23) N. Morita and T. Titani, This Bulletin, 13, 543 (1938).

(b) successive proton transfers along the chains combined by hydrogen bondings,



and (c) rotation of either of $H_3O^+$ ion, $OH^-$ ion and $H_2O$. Steps a and b means separation of the charge or ionization in a narrow sense, but the separated ions have yet a large probability of recombination or association via the reverse paths of steps b and a. Step b is a proton jump between two symmetrical structures, and therefore proceeds athermally, while step a is an asymmetrical charge separation, thus being endothermic, and the activation energy of step a might be about 4 kcal. $mol^{-1}$, somewhat larger than that of step b, according to Conway et al.[24],* For the completion of ionization of a water molecule, it is needed that the chain of hydrogen bonds through which proton transfers occur must be broken down in order to interfere with an easy recombination of the two ions once separated. This breakdown of the chain can be carried out through step c by an insertion of chain imperfection, such as a doubly occupied hydrogen bond O-H···H-O or a vacant bond O···O. Since the rotation of $H_3O^+$, $OH^-$ or $H_2O$ can take place only when the rotating particle overcomes the attractive force between the dipoles and destroys the hydrogen bond, it requires energies near to the heat of sublimation of ice 12.2 kcal. $mol^{-1}$. After all, it is concluded that the apparent activation energy for protonic dissociation of water may be $12.2+4\approx16$ kcal. $mol^{-1}$ and the heat of dissociation a certain value between 16 and 12.2 kcal. $mol^{-1}$. The observed values of the activation energy and the heat for dissociation of water are 15.5~16.5 kcal. $mol^{-1}$ and 13.5 kcal. $mol^{-1}$ respectively[25], both of which agree with the above considered expectation very well.

**Activation Energy of Electric Conduction.**—The measured values of d. c. electric conductance of the sufficiently carefully prepared ice[26],* and liquid water[28] at near 0°C, $\kappa_1$ and $\kappa$, are

24) B. E. Conway, J. O'M. Bockris and H. Linton, *J. Chem. Phys.*, **24**, 834 (1956).
* The activation energy of symmetric proton jump is 3.85 kcal. $mol^{-1}$ [24].
25) M. Eigen and L. de Maeyer, *Proc. Roy. Soc.*, **A247**, 505 (1958).
26) R. S. Bradley, *Trans. Faraday Soc.*, 53, 687 (1957).
* According to the results of Gränicher et al.[27], the apparent activation energy of electric conduction of ice is 13.8 kcal. $mol^{-1}$, being slightly larger than Eq. 25.
27) H. Gränicher, C. Jaccard, P. Sherrer and A. Steinemann, *Discussions Faraday Soc.*, **23**, 50 (1957).
28) "Chemical Handbook", Ed. by Chem. Soc. Japan, Maruzen, Tokyo (1952), p. 601.

represented by the following empirical formulas.

$$\kappa_l = 23.4 \exp(-12300/RT)\ \Omega^{-1}\mathrm{cm}^{-1} \quad (25)$$

$$\kappa = 0.119 \exp(-8570/RT)\ \Omega^{-1}\mathrm{cm}^{-1} \quad (26)$$

Since ice and liquid water were nearly equally electroconductive at near 0°C, it was thought that the mechanisms of the electric conduction in both media must also resemble each other. But recently, it was found that the mobility of a proton in ice is twice faster than that in liquid water, while the concentration of dissociated ions in ice is half as much as that in water[25]. These facts are convinced by a statement that, since the chains connected by hydrogen bondings in ice are longer and in better order than those in water, the proton jump is easier, the lattice imperfection arises with less probability, and, therefore, the occurrence of ionic recombination is more probable in ice. The fact that both the activation energy and the pre-exponential factor in water are lower than in ice as is seen in Eqs. 25 and 26, is thus qualitatively acknowledged on this reason as well.

When the proton jumps have once propagated successively along a chain of hydrogen bonds in the direction of electric field, all the molecules that proton jumps have taken place between the neighboring molecules must rotate in order to conduct electricity in the same direction once more. The rate-determining step of electric conduction of ice and water in a static field is, therefore, the process of molecular rotation, as in the case of ionization of water described in the last section, and the apparent activation energy during the overall process of electric conduction must be much higher than the height of the energy barrier for proton jumps.

Especially in case of liquid water, the matter is more complicated than in the case of ice, because, even if the electric conduction is mostly owing to the proton jumps in the icy state, rather than to the migration or diffusion of ions themselves, the fraction of the icy state decreases as the temperature rises, and this fact makes the apparent activation energy somewhat lower than in ice*.

**Temperature of Maximum Density.**—From Eq. 3, next relation can be derived,

$$\frac{dv}{dT} = (v_i - v_p)\frac{dx}{dT} + x\alpha_i v_i^0 + (1-x)\alpha_p v_p^0 \quad (27)$$

where, at the temperature of the maximum density $T_m$, $dv/dT$ is equal to zero. Since the second and the third terms in the right-hand side of Eq. 27 are both positive, and $dx/dT$ in the first term is negative, one of the necessary conditions that an equilibrating liquid mixture of multicomponent system like liquid water has a maximum density at a certain temperature is generally $v_i > v_p$. Among many associating liquids, some might satisfy this condition, but unfortunately they can not be observed in practice, unless $T_m$ is above the freezing points. Thus $T_m$ can be known from Eq. 27 theoretically, inserting the relation $dx/dT = -x(1-x)\Delta H_f/RT^2$. But, for instance, an error of ±0.05 kcal. mol$^{-1}$ in $\Delta H_f$ corresponds to that of about ±1°C in $T_m$ in case of water, which is not so adequate as to predict $T_m$ correctly.

When a small amount of a different substance is dissolved in water, the temperature of the maximum density of the solution is either raised or lowered from 3.98°C. This is because the balance of Eq. 1 fluctuates by either the hydration or the dehydration of water molecules surrounding the added molecules, according to the polarity of the latter. In the right-hand side of Eq. 27, ignoring the contribution of the second term compared with those of the first and the third terms, and admitting $v_i - v_p \approx v_i^0 - v_p^0$ approximately, the following equation is obtained,

$$\frac{\Delta H_f}{RT_m^2}\Big/\left[1+\exp\left(-\frac{\Delta G}{RT_m}\right)\right] \approx \frac{\alpha_p v_p^0}{v_i^0 - v_p^0} \quad (28)$$

according to which, $T_m$ is found to vary mainly as a function of $\Delta H_f$ and $\Delta S_f$, if the density of the added substance does not affect seriously,

$$\left(\frac{\partial T_m}{\partial \Delta H_f}\right)_{\Delta S_f} = \frac{\dfrac{RT_m^2}{(\Delta H_f)^2}\left[1+\exp\left(-\dfrac{\Delta G}{RT_m}\right)\right] + \dfrac{T_m}{\Delta H_f}\exp\left(-\dfrac{\Delta G}{RT_m}\right)}{\dfrac{2RT_m}{\Delta H_f}\left[1+\exp\left(-\dfrac{\Delta G}{RT_m}\right)\right] + \exp\left(-\dfrac{\Delta G}{RT_m}\right)} > 0 \quad (29)$$

$$\left(\frac{\partial T_m}{\partial \Delta S_f}\right)_{\Delta H_f} = \frac{-\dfrac{T_m^2}{\Delta H_f}\exp\left(-\dfrac{\Delta G}{RT_m}\right)}{\dfrac{2RT_m}{\Delta H_f}\left[1+\exp\left(-\dfrac{\Delta G}{RT_m}\right)\right] + \exp\left(-\dfrac{\Delta G}{RT_m}\right)} < 0 \quad (30)$$

After all, $T_m$ will be lowered by the dissolution of a substance which makes $\Delta H_f$ decrease or $\Delta S_f$ increase; namely, which inclines the

* The electric conductance of ice and liquid water may be represented in another formula: $\kappa = en\mu$, where $e$ is a protonic charge, and $n$ and $\mu$ are the number and the mobility of charge carriers, respectively. $n$ is closely related to the degree of ionization of water, which is affected by the energy of rotation of water molecules, while the factor which determines $\mu$ is the activation energy of a proton jump, or the height of the energy barrier in the potential curve of hydrogen bond.

equilibrium of Eq. 1 towards the right-hand side, and vice versa. In short, a part of the icy state is fused and the depression of $T_m$ occurs. So far as observed experimentally, all the electrolytes[29] and general hydrophilic non-electrolytes lower $T_m$, while some alcohols such as *tert*-butyl alcohol raise $T_m$ exceptionally[30]. The structure of water around ions or dissolved strange molecules will be discussed elsewhere.

## Summary

Various characteristic properties of liquid water can be explained fairly well by a simple structural model proposing that water consists of an equilibrating mixture between two states: the icy state which possesses ice structure and appears and disappears locally and temporarily, and the packed state in which water molecules are closely packed without hydrogen bondings. Only assuming that the fraction of the icy state at 100°C is 0.2, the fractions and the equilibrium constants at various temperatures are calculated, and therefrom the heat and the entropy of fusion of ice, the specific heat and the heat of vaporization of liquid water are derived, which are all in good agreement with the observed values. The radial distribution function of water obtained by X-rays reveals the packed state to have a structure similar to the closest packing, and the surface tension of water tells that the surface of water is more abundant in the icy state than the bulk water is, positively adsorbed as if it were a kind of surfactants. The heat of ionization and the activation energy of electric conduction are qualitatively described by the rotation mechanism of water molecules in the icy state. A reasonable explanation concerning the existence of the temperature of the maximum density and the effects of different substances upon it are also offered.

*Department of Chemistry*
*Faculty of Science*
*Kobe University*
*Higashinada, Kobe*

29) R. Wright, *J. Chem. Soc.*, **115**, 119 (1919); "International Critical Tables," Vol. III, p. 107.
30) G. Wada and S. Umeda, unpublished.

# *Investigation on Mixed Complexes. VI*[1]*. General Discussion on the Formation of Mixed Complexes*

By Sigeo KIDA

(Received November 1, 1960)

The main purpose of this series of investigations has been to ascertain the stability of mixed complexes, as compared with that of their parent complexes*. It seems to the present author that there have been few investigations of this problem. Bjerrum[2] has made a careful study of the factors which influence the ratios between the consecutive formation constants by sub-dividing these factors into the "statistical effect" and the "ligand effect". The former effect can be evaluated by calculation, and this principle can also be applied to the present investigation. The latter is further classified into the "electrostatic effect" and the "rest effect"; that is, if we regard metal-ligand bonds as purely ionic, the ligand effect should be an electrostatic one, while the rest effect may be mainly attributed to the covalency of the coordination bond. Bjerrum's considerations were ingenious and comprehensive. However, his efforts were mainly devoted to obtaining the values of consecutive formation constants of various complexes, and much importance was not paid to the stability of mixed complexes.

In this paper, factors which influence the relative stability of a mixed complex are pointed out and discussed on the basis of the experimental data previously obtained by various investigators.

**Electrostatic Effect.**—It is assumed here, for convenience, that a complex species consists of point charges representing a central metal ion and its ligands. For instance, in the following complexes it is assumed: that M, X and Y are point electrical charges, $+e$, $-e'$ and $-e''$,

1) Part V of this series: S. Kida, This Bulletin, 33, 2269 (1960).

* Throughout this series, $[MA_n]$ and $[MB_n]$ have been defined as denoting the parent complexes of the mixed complex, $[MA_iB_j]$, where A and B and M stand for the ligands, and the central metal ion, respectively, under the condition of $n=i+j$.

2) J. Bjerrum, "Metal Ammine Formation in Aqueous Solution", Haase and Son, Copenhagen (1941).

TABLE I. CALCULATED FORMATION ENERGIES OF COMPLEXES OF VARIOUS TYPES, ON THE ASSUMPTION THAT THEY CONSIST OF POINT CHARGES

4-Coordinated planar type

$$E(MX_3Y)-\frac{1}{4}\{3E(MX_4)+E(MY_4)\}=(e'-e'')^2(2\sqrt{2}+1)/4r=0.957(e'-e'')^2/r$$

$$E(cis\text{-}MX_2Y_2)-\frac{1}{2}\{E(MX_4)+E(MY_4)\}=(e'-e'')^2(\sqrt{2}+1)/2r=1.207(e'-e'')^2/r$$

$$E(trans\text{-}MX_2Y_2)-\frac{1}{2}\{E(MX_4)+E(MY_4)\}=(e'-e'')^2\cdot\sqrt{2}/r=1.414(e'-e'')^2/r$$

4-Coordinated tetrahedral type

$$E(MX_3Y)-\frac{1}{4}\{3E(MX_4)+E(MY_4)\}=(e'-e'')^2\cdot 3\sqrt{6}/8r=0.917(e'-e'')^2/r$$

$$E(MX_2Y_2)-\frac{1}{2}\{E(MX_4)+E(MY_4)\}=(e'-e'')^2\cdot\sqrt{6}/2r=1.225(e'-e'')^2/r$$

6-Coordinated octahedral type

$$E(MX_5Y)-\frac{1}{6}\{5E(MX_6)+E(MY_6)\}=(e'-e'')^2(4\sqrt{2}+1)4r=1.664(e'-e'')^2/r$$

$$E(cis\text{-}MX_4Y_2)-\frac{1}{6}\{4E(MX_6)+2E(MY_6)\}=(e'-e'')^2(3\sqrt{2}+1)/2r=2.621(e'-e'')^2/r$$

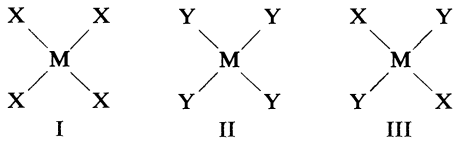
$$E(trans\text{-}MX_4Y_2)-\frac{1}{6}\{4E(MX_6)+2E(MY_6)\}=(e'-e'')^2\cdot 2\sqrt{2}/r=2.828(e'-e'')^2/r$$

$$E(cis\text{-}cis\text{-}MX_3Y_3)-\frac{1}{2}\{E(MX_6)+E(MY_6)\}=(e'-e'')^2(6\sqrt{2}+3)/4r=2.871(e'-e'')^2/r$$

$$E(cis\text{-}trans\text{-}MX_3Y_3)-\frac{1}{2}\{E(MX_6)+E(MY_6)\}=(e'-e'')^2(8\sqrt{2}+1)/4r=3.078(e'-e'')^2/r$$

$E(MX_6)$ or $E(MY_6)$ denotes the formation energy of the complex, $[MX_6]$ or $[MY_6]$, respectively.

respectively; that both the distances of M-X and M-Y are maintained constant at distance $r$; and that X and Y occupy corners of a regular square with M at its center.




If we denote the formation energies of the complexes, I, II and III, by $E(MX_4)$, $E(MY_4)$ and $E(trans\text{-}MX_2Y_2)$, respectively, they can be represented as follows:

$$E(MX_4)=\frac{ee'}{r}\times 4-\frac{(e')^2}{\sqrt{2}r}\times 4-\frac{(e')^2}{2r}\times 2$$

$$E(MY_4)=\frac{ee''}{r}\times 4-\frac{(e'')^2}{\sqrt{2}r}\times 4-\frac{(e'')^2}{2r}\times 2$$

$$E(trans\text{-}MX_2Y_2)=\frac{ee'}{r}\times 2+\frac{ee''}{r}\times 2-\frac{e'e''}{\sqrt{2}r}\times 4-\frac{(e')^2}{2r}-\frac{(e'')^2}{2r}$$

Hence, we obtain:

$$E(trans\text{-}MX_2Y_2)-\frac{1}{2}\{E(MX_4)+E(MY_4)\}=\frac{\sqrt{2}}{r}(e'-e'')^2\geqq 0$$

From the equation we can conclude that the mixed complex has more formation energy than the average energies of the parent complexes. In other words, a mixed complex is easily formed from its respective parent complexes. Similar calculations can also be made for other types of complexes, as indicated in Table I.

Some investigators[2,3] have taken the electrostatic repulsion into consideration as a factor which greatly influences the stability of mixed complexes, but their considerations were limited to an electrostatic effect of ionic ligands, e. g., $Cl^-$ or $C_2O_4^{2-}$, the neutral ligand being neglected in most cases. It is now generally believed that in the so-called normal complexes, the electrostatic force plays an important role even in the case of a neutral ligand, since the ligand field theory has succeeded in explaining the absorption spectra and stabilities of these complexes, by regarding a neutral ligand as a point dipole[4]. In the present study, neutral ligands are also taken into account; in plactice, however, they are replaced by appropriate negative point charges.

Before this conclusion is applied to actual problems, it is necessary to discuss in more detail the meaning of the term " negative point

3) For instance, N. Bjerrum, *Z. Phys. Chem.*, **106**, 238 (1923); G. Schwarzenbach, *Helv. Chim. Acta*, **16**, 522 (1933).
4) For instance, Y. Tanabe and S. Sugano, *J. Phys. Soc. (Japan)*, **9**, 753, 766 (1954).

charges" which were located around the central ion, in the above discussion.

The electric dipole moment is defined as the magnitude of the charge at one center of the molecule times the distance between centers. This distance, for practical purposes, may be considered equivalent to the internuclear distance for a diatomic molecule. In the case of metal complexes, one may consider that the centers of negative charges are closer to the metal ion than the nuclei of the donor atoms of the complex, for the following reasons: (1)

TABLE II. RELATIVE STABILITIES OF MIXED COMPLEXES OF VARIOUS TYPES

Type 1. $[MA_2] + [MB_2] \rightleftarrows 2[MAB]$

| M | A | B | $\log K_m$ | $\log K_{stat}$ | $\log K_{stab}$ | Reference |
|---|---|---|---|---|---|---|
| Cu(II) | $(dig\text{-}H)^-$ | $aca^-$ | −0.04 | 0.60 | −0.64 | a) |
| 〃 | en | 〃 | 0.42 | 〃 | −0.18 | 〃 |
| 〃 | 〃 | $C_2O_4^{2-}$ | 1.10 | 〃 | 0.50 | 〃 |
| 〃 | 〃 | $P_2O_7^{4-}$ | 1.70 | 〃 | 1.10 | b) |
| Hg(II) | $Cl^-$ | $Br^-$ | 2.0 | 〃 | 1.4 | c) |
| 〃 | 〃 | $I^-$ | 1.75 | 〃 | 1.15 | 〃 |
| 〃 | $Br^-$ | 〃 | 1.10 | 〃 | 0.50 | 〃 |

Type 2. $[MA_2] + [M(OH_2)_4] \rightleftarrows 2[MA(OH_2)_2]$

| M | A | $\log K_m \left(=\log \frac{k_1}{k_2}\right)$ | $\log K_{stat}$ | $\log K_{stab}$ | $\frac{1}{4}\log K$ | Reference |
|---|---|---|---|---|---|---|
| Cu(II) | en | 1.40 | 0.60 | 0.80 | 5.01 | d) |
| Zn(II) | 〃 | 0.77 | 〃 | 0.17 | 2.77 | 〃 |
| Cd(II) | 〃 | 0.92 | 〃 | 0.32 | 2.50 | 〃 |
| Zn(II) | $C_2O_4^{2-}$ | 2.32 | 〃 | 1.72 | 2.59 | 〃 |
| Co(II) | $(salcylaldehyde)^-$ | 1.04 | 〃 | 0.44 | 2.08 | 〃 |
| Ni(II) | 〃 | 1.2 | 〃 | 0.60 | 2.3 | 〃 |
| Cu(II) | 〃 | 1.5 | 〃 | 0.90 | 3.3 | 〃 |
| Zn(II) | 〃 | 0.9 | 〃 | 0.70 | 2.01 | 〃 |
| Pb(II) | 〃 | 3.4 | 〃 | 2.8 | 3.7 | 〃 |
| Mg(II) | $aca^-$ | 1.46 | 〃 | 0.86 | 2.28 | 〃 |
| Mn(II) | 〃 | 1.06 | 〃 | 0.46 | 2.49 | 〃 |
| Fe(II) | 〃 | 0.98 | 〃 | 0.38 | 3.25 | 〃 |
| Co(II) | 〃 | 1.32 | 〃 | 0.72 | 3.18 | 〃 |
| Ni(II) | 〃 | 1.30 | 〃 | 0.70 | 3.03 | 〃 |
| Cu(II) | 〃 | 1.26 | 〃 | 0.64 | 4.55 | 〃 |

Type 3. $[MA_4] + [M(OH_2)_4] \rightleftarrows 2[MA_2(OH_2)_2]$

| M | A | $\log K_m \left(=\log \frac{k_1k_2}{k_3k_4}\right)$ | $\log K_{stat}$ | $\log K_{stab}$ | $\frac{1}{4}\log K$ | Reference |
|---|---|---|---|---|---|---|
| Cu(II) | $NH_3$ | 2.63 | 1.56 | 1.07 | 3.17 | e) |
| Zn(II) | 〃 | 0.16 | 〃 | 1.40 | 2.37 | 〃 |
| Cd(II) | 〃 | 2.38 | 〃 | 0.82 | 1.78 | 〃 |
| Cu(II) | $Cl^-$ | 2.8 | 〃 | 1.2 | 1.15 | f) |
| Cd(II) | $CN^-$ | 2.36 | 〃 | 0.80 | 4.71 | 〃 |
| 〃 | $I^-$ | −0.68 | 〃 | −2.34 | 1.62 | 〃 |
| Sn(II) | $Cl^-$ | 2.98 | 〃 | 1.42 | 0.38 | 〃 |

Type 4. $[MA_3] + 2[M(OH_2)_6] \rightleftarrows 3[MA(OH_2)_4]$

| M | A | $\log K_m \left(=\log \frac{k_1^2}{k_2k_3}\right)$ | $\log K_{stat}$ | $\log K_{stab}$ | $\frac{1}{6}\log K$ | Reference |
|---|---|---|---|---|---|---|
| Mn(II) | en | 2.53 | 1.43 | 1.10 | 0.94 | e) |
| Fe(II) | 〃 | 3.32 | 〃 | 1.89 | 1.59 | 〃 |
| Co(II) | 〃 | 3.85 | 〃 | 2.42 | 2.30 | 〃 |
| Ni(II) | 〃 | 4.37 | 〃 | 2.94 | 3.10 | 〃 |
| Fe(II) | dip | −5.0 | 〃 | −6.43 | 2.93 | d) |
| Mn(III) | $C_2O_4^{2-}$ | 10.52 | 〃 | 9.09 | 3.24 | 〃 |
| Fe(III) | $(salicylate)^-$ | 17.7 | 〃 | 16.3 | 5.74 | 〃 |

(Table II Countinued)

Type 5. $[MA_6] + [M(OH_2)_6] \rightleftarrows 2[MA_3(OH_2)_3]$

| M | A | $\log K_m \left(=\log \frac{k_1k_2k_3}{k_4k_5k_6}\right)$ | $\log K_{stat}$ | $\log K_{stab}$ | $\frac{1}{6}\log K$ | Reference |
|---|---|---|---|---|---|---|
| Co(II) | $NH_3$ | 4.77 | 2.60 | 1.87 | 0.85 | e) |
| Ni(II) | 〃 | 4.80 | 〃 | 2.20 | 1.46 | 〃 |
| Al(III) | $F^-$ | 10.16 | 〃 | 7.56 | 3.31 | f) |
| Cr(III) | $NCS^-$ | 7.8 | 〃 | 5.20 | 0.63 | 〃 |
| Co(III) | $NH_3$ | 5.04 | 〃 | 2.44 | 5.87 | e) |

$K_m$: Disproportionation constant of a mixed complex.
$K_{stab}$: Stabilization constant of a mixed complex, defined as following; $\log K_{stab} = \log K_m - \log K_{stat}$ (according to Marcus[c]) (see foot note p. 965*[1]).
$K_{stat}$: Statistical value of $K_m$, i. e., the calculated value of $K_m$ on the assumption that formation of a mixed complex proceeds statistically (see also foot note p. 965*[1]).
$k_1, k_2, k_3 \cdots\cdots$: Consecutive formation constants of a complex in aqueous solution.
$K$: The gross formation constant (according to Bjerrum[e]), $K = k_1 \cdot k_2 \cdot k_3 \cdots\cdots k_n$.

a) S. Kida, This Bulletin, **29**, 805 (1956).
b) R. De Witt and J. Watters, *J. Am. Chem. Soc.*, **76**, 3810 (1954).
c) Y. Marcus, *Acta Chem. Scand.*, **11**, 610 (1957).
d) A. E. Martelle and M. Calvin, "Chemistry of the Metal Chelate Compounds", Prentice-Hall, Inc., New York (1952).
e) J. Bjerrum, "Metal Ammine Formation in Aqueous Solution", Haase and Son, Copenhagen (1957).
f) J. Bjerrum, *Chem. Revs.*, **46**, 381 (1950).
dig-H=dimethyl glyoxime
en=ethylenediamine
aca=acetylacetone

the orbitals of a donor atom will suffer considerable deformation by the electric field of the central ion, which makes the center of negative charge (or "point negative charge") closer to the center of the complex; (2) when a metal complex is in solution, the outer part of the ligands is surrounded by molecules of the solvent, and its mutual electrostatic repulsion between ligands in a complex is reduced, since the dielectric constant of the solvent is generally large. Accordingly, the only important effect in the mutual electrostatic repulsion between ligands is that of the inner part of ligands, i. e., "point negative charge" which is situated close to the central ion.

Since the ionic radius of a certain metal ion is approximately constant regardless of its surroundings, the assumption that the distance between a negative point charge and the central ion is approximately constant regardless of the species of ligands can be applied to practical problems.

It is evident from Table I that the electrostatic ligand effect, as described above, always promotes the formation of a mixed complex. Table II shows that $\log K_{stab}$*[1] is generally positive, indicating that mixed complexes are more stable than statistically expected.

**The Effect of ($\sigma-$) Covalent Bond***[2]. — Although the above discussion is based on the assumption that the bond between a metal ion and a ligand is purely ionic, it always contains some covalent character.

It has been shown by the above calculation, that although the mutual electrostatic repulsion between ligands in a complex reduces its stability, such an effect is smaller in a mixed complex than in parent ones, and consequently the formation of the mixed complex is favored. If pure covalent bonds are formed by coordination, the central metal ion accepts electrons from the ligands, and its electronegativity is decreased. In this case Pauling's electroneutrality principle should be satisfied. This principle may be expressed in the following way; if electrons of donor atoms are closely concentrated around the central atom, mutual repulsion of these electrons acts so as to keep

*[1] For example, in case of an equilibrium of the form, $MX_4 + MF_4 \rightleftarrows 2MX_2Y_2$, by definition,

$$K_m = \frac{[MX_2Y_2]}{[MX_4]\,[MY_4]}$$

If one assumes that there is no energy difference between the species on both sides of this equilibrium, one can calculate the value of $K_m$ statistically. This calculated value is defined as $K_{stat}$ in the present paper. Therefore, ($K_m$-$K_{stat}$) is useful as a measure of a stabilizing or unstabilizing effect in the formation of a mixed complex. In this paper, ($K_m$-$K_{stat}$) is designated as the stabilization constant of a mixed complex, and denoted by $K_{stab}$, i. e., it is the ratio of the observed equilibrium constants to the statistically calculated ones. Accordingly, if $\log K_{stab}$ has a positive value, the mixed complex is easily formed from its parent complexes, and vice versa in the case of the negative value.

*[2] In this section, the $\pi$-bond is not taken into consideration, and the "covalent" or the "covalency" is referred to the bond of $\sigma$-type only.

the ligands away from each other, just like the repulsion between the negative charges of ligands in the case of ionic complexes. Therefore, it seems to the present author that the electrostatic and the ($\sigma$-) covalent-bond effects work in the same direction.

From the above discussion, it is expected that the covalent bond effect is inclined to promote the formation of a mixed complex, quite analogously to the electrostatic effect, and accordingly, mixed-complex formation might also be favored in penetration complexes, such as those of cobalt(III) and chromium(III). The fact that this expectation is fulfilled is seen in Table II (though examples of this kind are rare). Furthermore, the stabilization constant of a mixed complex, $K_{stab}$*1, appears to have a tendency to become larger as the stabilities of the parent complex become larger. For instance, in the case of ethylenediamine complexes the increasing order of the value of the log $K_{stab}$*1 of Mn(II), Fe(II), Co(II) and Ni(II) complexes is in accord with that of the stabilities of these complexes (log $K$), as seen in Table II. Thus, since the log $K_{stab}$'s*1 are neither random nor show an increase in value followed by a decrease, we may conclude from these results, that the covalent-bond effect has no tendency to depress the formation of a mixed complex.

**Cases where Mixed Complexes are not Observed.** — In the preceding papers[1,5,6] some special cases were reported in which mixed complexes could not be detected. These are divided into two groups; 1) those similar to some nickel(II) complexes, and 2) those which may be exemplified with some platinum(II) complexes.

It is well known that nickel(II) forms two types of complexes; one having paramagnetic octahedral configuration, such as $[Ni(OH_2)_6]^{2+}$, $[Ni(NH_3)_6]^{2+}$ and [Ni en$_3$]$^{2+}$ etc., and the other which has a diamagnetic square planar configuration, such as $[Ni(CN)_4]^{2-}$ and $[Ni(C_2O_2S_2)_2]^{2-}$*3 etc. It was verified, in the preceding paper[5], that in both of the mixed solutions of $[Ni(OH_2)_6]^{2+}$ and $[Ni(C_2O_2S_2)_2]^{2-}$, and [Ni en$_3$]$^{2+}$ and $[Ni(CN)_4]^{2-}$, no mixed complexes were formed. It was also reported by Kato[7] that an ammine-biuret nickel(II) complex could not be detected in solution, whereas an ammine-biuret copper(II) complex was easily formed in solution. This was attributed to the fact that the biuret nickel(II) complex has a planar configration, while the amine nickel(II) complex has an octahedral one. From these observations it appears that, in general, no mixed complex can be formed when the reacting species (parent complexes) are different in geometrical configuration.

It is to be noted that no mixed cyano platinum(II) complexes have been found; for instance, as was reported in the preceding papers[1,6], each of the complex ions, e. g., $[Pt\ Cl_4]^{2-}$, $[Pt\ Br_4]^{2-}$ [6] and [Pt en$_2$]$^{2+}$, reacts with cyanide ions in solution forming the complex ion, $[Pt(CN)_4]^{2-}$, only, regardless of the fact that mixed cyano complexes of other metal ions, such as [Pd(CN)$_2$ en], $[Ni(CN)_2 \cdot (C_2O_2S_2)]^{2-}$ and [Cd(CN)$_2$ en] are easily formed[1,8]. This example illustrates that mixed-complex formation does not always occur between complexes of the same configuration, since platinum(II) complexes are known to posses a diamagnetic square planar configuration.

TABLE III. FORCE CONSTANTS OF THE METAL-CARBON AND THE METAL-NITROGEN BONDS IN THE CYANO- AND THE AMMINE COMPLEXES[1,2] (md./Å)

| | | | |
|---|---|---|---|
| $[Pt(CN)_4]^{2-}$ | 3.43 | $[Au(CN)_2]^-$ | 1.83 |
| $[Pt(NH_3)_4]^{2+}$ | 2.80 | $[Hg(CN)_2]^-$ | 2.61 |
| $[Co(CN)_6]^{3-}$ | 2.33 | $[Ag(CN)_2]^-$ | 1.83 |
| $[Fe(CN)_6]^{4-}$ | 2.33 | $[Hg\ NH_3]_2^{2+}$ | 1.70 |

1) S. Mizushima and T. Shimanouchi, "Infrared Spectra and Raman Effect", Kyoritsu Co., Tokyo (1958).
2) F. A. Cotton, "The Infrared Spectra of Transitional Metal Complexes", Ch. 5 in J. Lewis and D. G. Wilkins ed., "Modern Coordination Chemistry", Interscience Publ. Inc., New York (1960), p. 335.

In order to clarify the above fact, attention was first directed towards the platinum-cyanide bond, to which the strong covalency should be attributed on the basis of the infrared absorption studies as indicated in Table III. The behavior of the platinum(II) complexes mentioned above is paradioxical, if one considers only the $\sigma$-covalent-effect since $\sigma$-covalence of the coordination bond promotes the formation of a mixed complex, as discussed before. Therefore, there must be another factor which is greately responsible for this paradox....., the formation of $\pi$-bonds between platinum and carbon, a distinctive feature of the cyano complex.

The existence of $\pi$-bonding in cyano complexes has been discussed by many authors[9]. It is now believed that $\pi$-bonds plays an important role in regard to the remarkable stability of cyano complexes.

5) S. Kida, This Bulletin, 32, 982 (1959).
6) S. Kida, ibid., 33, 587 (1960).
7) M. Kato, *Z. anorg. Chem.*, 300, 84 (1959).
*3 $C_2O_2S_2$=dithiooxalate.
8) S. Kida, This Bulletin, 33, 1204 (1960).
9) For instance, D. P. Craig, A. Maccoll, R. S. Nyholm, L. E. Orgel and L. E. Sutton, *J. Chem. Soc.*, 1954, 332.

Assuming that the ligand which is capable of forming a $\pi$-bond with a central metal ion has a tendency to exclude the ligand which is not able to undergo $\pi$-bonding, one may expect that the ligand which has such a donor atom, containing an unsaturated $\pi$-oribital, could form a mixed cyano complex to a greater or less extent. A suitable example can be found in complexes of the type, $[Co(CN)_5X]^{n-}$ [10]; the pentacyano cobalt(III) complexes, $[Co(CN)_5 \cdot X]^{n-}$, can be synthesized, when $X=NO_2^-$, $N_3^-$, $S_2O_3^{2-}$, $SCN^-$, $Cl^-$, $Br^-$ and $I^-$, while in the cases when $X=NH_3$ and $F^-$, which are considered to have no tendency to form $\pi$-bonds, the pentacyano complexes have not been synthesized. Furthermore, it is interesting to note that the stability of the pentacyano complex, $[Co(CN)_5X]^{n-}$, seems to increase in the order of $X=Cl^-$, $Br^-$ and $I^-$ [11], but on the other hand the reverse order is observed in the halogeno-pentammine cobalt(III) complexes[12].

Although the complex ion, $[Co(CN)_4\ dip]^-$, (dip=dipyridyl) can be prepared[13], the complex ion, $[Co(CN)_4\ en]^-$, is unknown. This fact may be due to the same reason as in the above case, since the dipyridyl molecule has an unsaturated $\pi$-orbital in its donor atom, whereas the ethylenediamine molecule has no such orbital. According to this assumption, it is expected that the ligand which has unsaturated $\pi$-orbitals in its donor atom, such as dipyridyl, forms the complex where $\log K_{stab}$*1 is negative, as seen in Table II; it is a remarkable exception to the general rule discussed above.

Now, we must consider the reason why the ligand which has the unsaturated $\pi$-orbital tends to exclude from the complex the ligand having no such orbital. As discussed before, electrons of donor atoms are concentrated on the central atom as the result of coordination, and thus, the repulsion of these electrons depresses the stability of the complex. This effect was considered analogous to the electrostatic one, and accordingly, it was expected to exert a similar influence on the formation of a mixed complex. On the other hand, the formation of $\pi$-bonds between the central metal ion and its donor atom allows electrons from the saturated $d_\pi$-orbitals of the central metal ion to be donated into unsaturated $\pi$-orbitals of ligand atom, lowering the electron concentration on the central metal atom. Thus, very strong coordination bonds can be formed in cyano complexes (especially in the case of platinum(II)), without decreasing the electronegativity of the central atom. Therefore the "$\sigma$-bond effect", which is considered to promote mixed-complex formation, can be weakened by this "$\pi$-bond effect" to a greater or less degree.

Since the "$\sigma$-bond effect" discussed above is the only strong effect of many factors caused by $\sigma$-bond formation, when it is eliminated or weakened by $\pi$-bonding, some other effects, in turn, may possibly play an important role in determining the relative stability of mixed complexes, perhaps acting to depress mixed complex formation. For these new effects the present author has made some considerations; for instance, in the case of platinum(II) complexes $dsp^2$- and $d^3p$- hybridization of the orbitals can best be formed when all the ligands coordinated are the same species*4. This would make the mixed complex less stable than the parent ones.

In order to achieve a final conclusion, however, further studies are needed.

## Summary

The stability of a mixed complex, $[MA_iB_j]$, was discussed and compared with the complexes, $[MA_n]$ and $[MB_n]$, (where A, B and M represent ligands and central ion, respectively, and $i+j=n$).

It was verified by calculation that the electrostatic effect exerts an influence so as to promote the formation of a mixed complex. The effect of $\sigma$-covalency of the coordination bond can be considered analogously to the electrostatic one, and is expected to have a similar influence upon mixed-complex formation. The above discussion is supported by experimental data, showing that the mixed complex is formed, in general, more often than can be expected statistically.

However, there are some exceptions to the above-mentioned rule, for instance, in the cases of cyano platinum(II) complexes or dipyridyl complexes. They are attributed to $\pi$-bonding between the ligands and the central ion. Discussion has been made concerning the reason why $\pi$-bonds depress the formation of mixed complexes.

The author wishes to express his sincere thanks to Professor R. Tsuchida of Osaka

10) J. Fujita, Reported at the Symposium on Coordination Compounds, Tokyo, November, 1958.
11) J. Fujita, Private communication.
12) S. Ahrland, *Acta Chem. Scand.*, 10, 723 (1956).
13) L. Cambi and E. Paglia, "Chemistry of Coordination Compounds", (A Symposium) Vol. 1, Pergamon Press (1958), p. 249.

*4 It was verified by Pauling that (L. Pauling, "Nature of the Chemical Bond", Cornell University Press, New York (1940).) $dsp^2$-hybridization brings about the larger overlapping of the $\sigma$-orbitals between the ligands and the central atom in planar complexes, such as those of platinum(II). Although not verified, the present author believes that it is very probable that in planar complexes $\pi$-bonding is most favorably achieved by $d^3p$-hybridization.

University for his kind advice and encouragement throughout this work. His appreciation is also due to Dr. H. Yoneda for his helpful discussions.

*Department of Chemistry*
*Wakayama University*
*Masagocho, Wakayama*

# *Oxidation of Terpene Compounds with tert-Butyl Chromate. VII*[1]. *Oxidation of d-p-Menthene-3*

By Kozo Fujita

(Received November 18, 1960)

On the oxidation of monocyclic terpene compounds of *p*-menthane type, such as *d*-carvomenthene[2], *dl*-$\alpha$-terpineol[3], *dl*-$\alpha$-terpinyl acetate[4], *d*-limonene[5] and terpinolene[1], with *tert*-butyl chromate, it has been previously stated in this series that, in general, an active methylene adjacent to an endocyclic double bond was preferentially oxidized to an $\alpha, \beta$-unsaturated carbonyl. This fact has also been reported by Dupont et al.[6] on the oxidation of carvomenthene by this oxidant. All these communications concerned the oxidation of the terpene compounds which have an endocyclic double bond between $C_{(1)}$ and $C_{(2)}$ in the skeleton of *p*-menthane type.

The present investigation deals with the oxidation of *d-p*-menthene-3 (I), which has an endocyclic double bond between $C_{(3)}$ and $C_{(4)}$, on purpose to compare the oxidative action of *tert*-butyl chromate with that in the previous experiments.

## Results

*d-p*-Menthene-3 employed was prepared by pyrolysis of *l*-menthyl xanthate[7], but it was accompanied by a by-product, *d-p*-menthene-2, in the yield of 30%.

The oxidant, of type C presented by Oppenauer et al.[8], was prepared in the manner similar to that in the previous reports[1-4] from chromic anhydride and *tert*-butyl alcohol; also glacial acetic acid and acetic anhydride were added. The mole ratio of the sample to *tert*-butyl chromate was 1 to 3.

The oxidation reaction was carried out at 50°C during 36 hr. After the reaction was over, an excess of the oxidant was decomposed and then the reaction mixture was separated into an aqueous solution and a benzene solution.

In the aqueous solution, a trace of the unchanged starting material and a small quantity of acetone were found. From the benzene solution was obtained a crude neutral oil, which was fractionally distilled, whereas no acidic product was isolated. The fractions thus obtained were separated into their constituents by elution-chromatography. The constituent in the low-boiling fractions (b. $p._{40}$ 51~77°C) was identified with the starting material, which accounted for 7.9% of the initial quantity, while those in the high-boiling fractions (b. $p._{7}$ 75~150°C) consisted of *d*-carvenone (II), *dl-p*-menthen-3-one-5 (III) and an unidentified carbonyl compound in the yields of 49.6, 15.6 and 4.2%, respectively.

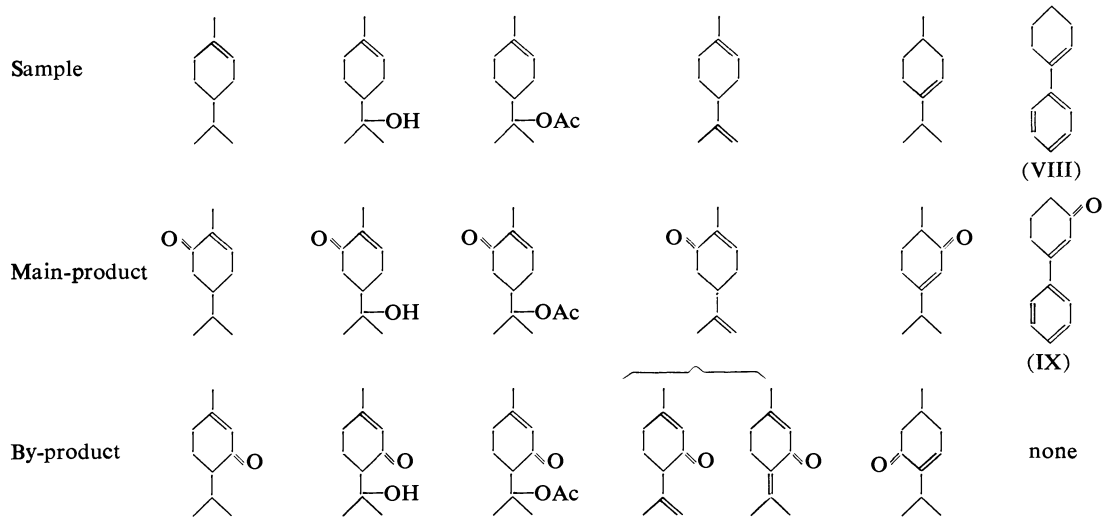
Besides, there was no identification of any compound which seemed to come from the oxidation of *d-p*-menthene-2 admixed in the starting sample.

## Discussion

On the above oxidation of *d-p*-menthene-3 with *tert*-butyl chromate, it was clarified that an active methylene adjacent to the double bond is selectively oxidized to a carbonyl without an oxidative cleavage of the double bond or an attack at the side chains. Between *d*-carvenone and *dl-p*-menthen-3-one-5 obtained by this oxidation, it would be considered that *d*-carvenone is also produced from *d-p*-menthene-2 admixed in the starting sample. Now, on the assumption that *d-p*-menthene-2

1) Part VI: T. Matsuura, K. Saito and Y. Shimakawa, This Bulletin, 33, 1151 (1960).
2) K. Fujita and T. Matsuura, *J. Sci. Hiroshima Univ.*, **A18**, 455 (1955).
3) T. Matsuura and T. Suga, *J. Chem. Soc. Japan, Pure Chem. Sec. (Nippon Kagaku Zasshi)*, **78**, 1117 (1957).
4) T. Matsuura, T. Suga and K. Suga, ibid., **78**, 1122 (1957).
5) K. Fujita, ibid., **78**, 1112 (1957).
6) G. Dupont, R. Dulou and O. Mondou, *Bull. soc. chim. France*, **1953**, 60.
7) L. Tschugaeff, *Ber.*, **32**, 3332 (1899).
8) R. V. Oppenauer and H. Oberrauch, *Anales asoc. quim. Argentina*, **37**, 246 (1949).

TABLE I




is oxidized entirely to *d*-carvenone, the amount of *d*-carvenone calculated from *d*-*p*-menthene-2 is subtracted from the total amount of *d*-carvenone. Even in this case, the remaining amount of *d*-carvenone is larger than the yield of *dl*-*p*-menthen-3-one-5. Therefore, it may be said that, between the two active methylenes in the molecule of *d*-*p*-menthene-3, the oxidation of the $C_{(2)}$ active methylene to a carbonyl (to give II) proceeds predominantly in comparison with that of the $C_{(5)}$ active methylene (to III). On the other hand, it has been previously made clear on the oxidation of *d*-carvomenthene (*d*-*p*-menthene-1, IV)[2,6],*1 with the same oxidant under conditions similar to those of the present work that the $C_{(6)}$ methylene activated by the vicinal double bond between $C_{(1)}$ and $C_{(2)}$ is predominantly oxidized

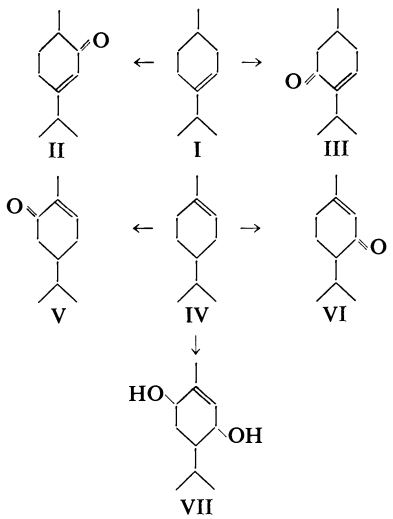



Fig. 1

*1 Kozo Fujita, to be published.

to a carbonyl (to give V as a main product) accompanying the oxidation at the $C_{(3)}$ active methylene (with the formation of small amounts of VI and VII). These are shown in Fig. 1.

It is interesting to consider why one of the two characteristic methylenes is predominantly oxidized by this oxidant. On the oxidation of *d*-carvomenthene, an active methylene adjacent to $\overset{*}{C}$-position in $-\overset{*}{C}(R)=CH-$ linkage is predominantly oxidized to a carbonyl, yielding *dl*-carvotanacetone (V). If the oxidation reaction of *d*-*p*-menthene-3 proceeds in a manner analogous to that in the case of *d*-carvomenthene, the $C_{(5)}$ methylene should be preferentially attacked. But this is not the case; the result of the present work shows, contrary to expectation, that the $C_{(2)}$ methylene remote from the $\overset{*}{C}$-position in $-\overset{*}{C}(R)=CH-$ linkage is oxidized preferentially to a carbonyl yielding *d*-carvenone (II). It may therefore be considered that an active methylene which is predominantly attacked is not always located at the position adjacent to the $\overset{*}{C}$-atom in $-\overset{*}{C}(R)=CH-$ linkage.

However, there is an analogy between the oxidation of the two isomers, when attention is paid to the distance from an easily oxidizable methylene to the two side chains. That is, whether a double bond may be located between $C_{(3)}$ and $C_{(4)}$ or between $C_{(1)}$ and $C_{(2)}$, the active methylene remote from the isopropyl group is predominantly attacked. This may be tentatively explained on the assumption that the steric inhibition of the isopropyl group to the oxidizability of an active methylene is reduced with the increase of the distance between the two groups, isopropyl and active methylene, while the effect of the methyl group is small.

This assumption may be supported by the results obtained from the oxidations of the *p*-menthane-type terpene compounds with *tert*-butyl chromate[3-5], which are shown in Table I, omitting the oxidative fission product, homoterpenyl methyl ketone. Moreover, it has been reported that 1-phenylcyclohexene (VIII) yields exclusively 3-phenylcyclohex-2-enone (IX)[9] by this oxidant. There is also a predominance of oxidizability of an active methylene remote from the phenyl group in the molecule.

In the present work, when the *p*-menthene-3 (I) employed was dextrorotatory, among the reaction products, carvenone (II) showed the dextrorotation, whereas *p*-menthen-3-one-5 (III) was optically inactive. Similarly among the oxidation products of *d*-carvomenthene (IV)[2],*1, carvotanacetone V was optically inactive, whereas piperitone VI was dextrorotatory.

In these cases, such optically inactive products as *p*-menthen-3-one-5 and carvotanacetone result from the oxidation of an active methylene adjacent to the $\overset{*}{C}$-atom in $-\overset{*}{C}(R)=CH-$ linkage ($C_{(4)}$ in I or $C_{(1)}$ in IV). It may be assumed that, on the oxidation of *d-p*-menthene-3 with *tert*-butyl chromate as well as in the case of *d*-carvomenthene, an optically inactive product is given by the formation of a *dl*-form via tautomeric intermediate radicals. This is also confirmed by the fact that, on the oxidation of *d*-limonene[5], *dl*-carvone is given as the result of the attack on an active methylene at the similar relative position.

It may be furthermore considered that acetone found in the aqueous solution is formed by the oxidation of surviving *tert*-butyl alcohol in the concentrated oxidant[10].

## Experimental

**Oxidation of *d-p*-Menthene-3.**—*d-p-Menthene-3.*—The material (b. p. 164.5~165°C, $n_D^{25}$ 1.4498, $d_4^{25}$ 0.8116, $[\alpha]_D^{20}$ +111.9°, nitrosochloride m. p. 127~127.5°C) was prepared by the method of Tschugaeff[7], which consists in treating *l*-menthol (m. p. 42.5~43.5°C) with metallic sodium and carbon disulfide in toluene successively, methylating the resulting sodium menthylxanthate with methyl iodide on dilution with ether, pyrolyzing the methyl menthylxanthate thus obtained (m. p. 39~40°C) at 210°C, and rectifying the crude product.

The hydrocarbon obtained as above was analyzed according to the racemization procedure of Hückel et al.[11,12] by refluxing with toluene-*p*-sulfonic acid in ethanol solution, and it was shown that this contained 70.1% of *d-p*-menthene-3 and 29.9% of *d-p*-menthene-2. Because of the difficulty of isolating the two components, this material was used as the sample without further separation.

*Oxidant.*—*tert*-Butyl chromate used as an oxidant was prepared by adding 120 g. of chromic anhydride in small portions to 266 g. of *tert*-butyl alcohol under ice-cooling, diluting the resultant with 600 cc. of benzene, drying the resulting benzene solution over anhydrous sodium sulfate, and concentrating it to 75 vol. % under reduced pressure. To the concentrated solution were added 80 g. of glacial acetic acid and 110 g. of acetic anhydride just prior to the oxidation.

*Oxidation Process.*—The acidified oxidant was added dropwise with stirring at 50±1°C to 55 g. of the starting material during 2 hr., and continuously stirred at the same temperature for a further 34 hr., under an atmosphere of carbon dioxide.

The reaction mixture was then left to stand at room temperature for 12 hr. and treated with water and oxalic acid to decompose the excess of the oxidant. The resulting mixture was separated into two layers, an aqueous solution and a benzene solution, and the former was repeatedly extracted with benzene. The benzene extract was then combined with the benzene solution.

**Identification of Oxidation Products.**—*Benzene Solution.*—The combined benzene solution mentioned above was washed with water and was treated with a saturated aqueous solution of sodium bicarbonate to extract acidic products. After further washing with water, drying over anhydrous sodium sulfate and removing the solvent, the resulting benzene solution gave a neutral brown oil which amounted to 56.8 g.

*Neutral Oil.*—The crude neutral oil obtained above was fractionated to 13 fractions and left a resinous residue in an amount of 7.67 g. The yield and physical properties of these fractions were given as in Fig. 2.

(1) Low-boiling Fractions (b. $p._{40}$ 51~77°C).—The total yield of fractions 1 and 2 amounted to 10.3% of the neutral oil*2 or to 7.9% of the starting material. On the strip-chromatogram[13], sprayed

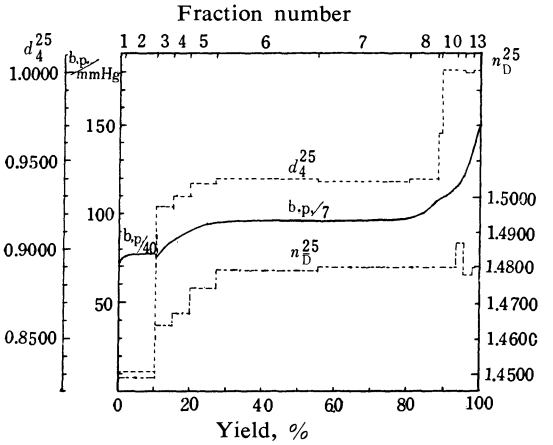


Fig. 2

9) D. Ginsburg and R. Pappo, *J. Chem. Soc.*, **1951**, 516.
10) T. Suga, *J. Chem. Soc. Japan, Pure Chem. Sec.* (*Nippon Kagaku Zasshi*), **80**, 948 (1959).
11) W. Hückel and W. Tappe, *Ann.*, **537**, 113 (1939).
12) W. Hückel, W. Tappe and G. Legutke, ibid., **543**, 197 (1940).

*2 It shows hereafter the neutral oil free from distillation residue.
13) J. G. Kirchner, J. M. Miller and G. J. Keller, *Anal. Chem.*, **23**, 420 (1951); J. M. Miller and J. G. Kirchner, ibid., **25**, 1107 (1953); T. Furukawa, *J. Sci. Hiroshima Univ.*, **A21**, 285 (1958).

with 5 vol.% concentrated nitric acid in concentrated sulfuric acid, these two fractions showed only one spot of $R_f$*3 value 0.89 agreeing with that of the starting material. Furthermore, these fractions gave *d*-*p*-menthene-3 nitrosochloride, m. p. 127~128°C, showing no depression by mixing with the known sample. From the estimation by the racemization procedure mentioned above[11,12], it was found that the combined low-boiling fraction consisted of 98% of *p*-menthene-3 and 2% of *p*-menthene-2.

It was thus confirmed that the low-boiling fractions were virtually unchanged *p*-menthene-3.

(2) High-boiling Fractions (b. p.$_{.7}$ 75~150°C).—The total yield of high-boiling fractions, from fraction 3 to fraction 13, amounted to 89.7% of the neutral oil or to 69.3% of the starting material. The strip-chromatograms of these fractions, sprayed with 2,4-dinitrophenylhydrazine-hydrochloric acid, gave two notable spots, $R_f$ values of which were 0.47 and 0.35, respectively, and a faint spot of $R_f$ value 0.20. Every fraction was then eluted through a silica gel column with 15~20 vol.% ethyl acetate in *n*-hexane, giving the following constituents.

(a) *dl*-*p*-Menthen-3-one-5.—The component which gave a spot of $R_f$ value 0.47 (yield: 20.1% to the neutral oil or 15.6% to the starting material) showed the optical rotation $[\alpha]_D^{17}$ 0° (*c* 8.73 in ethanol, *l* 0.947). An absorption maximum $\lambda_{max}^{alc}$ 235 mμ ($a$*4=56.2) in the ultraviolet spectrum and an absorption band at 1675 cm$^{-1}$ (liquid film) in the infrared spectrum indicated the presence of an $\alpha,\beta$-unsaturated carbonyl group. In the infrared absorption spectrum, two special wave numbers 1360 and 809 cm$^{-1}$, characteristic of the isopropyl group and of the linkage of type $R_1R_2C{=}CHR_3$, respectively, were also observed.

The component gave the following derivatives, agreeing with those of *dl*-*p*-menthen-3-one-5, respectively.

Semicarbazone, m. p. 142~142.5°C (lit., 142°C[14], 141~142°C[15]).

Oxime, m. p., 66°C (lit., 66°C[14,15]).

2,4-Dinitrophenylhydrazone, m. p. 143~143.5°C (lit., 145~146°C[16]).

These showed that this component consisted of *dl*-*p*-menthen-3-one-5.

(b) *d*-Carvenone.—The component which gave a spot of $R_f$ 0.35 (yield: 71.5% to the neutral oil or 49.6% to the starting material) exhibited the optical rotation $[\alpha]_D^{21}$ +45.4° (*c* 10.16 in ethanol, *l* 0.947). The ultraviolet spectrum of the component showed the absorption maximum $\lambda_{max}^{alc}$ 234 mμ ($a$= 96.5), which corresponded to that of $\alpha,\beta$-unsaturated ketone.

The following derivatives, prepared from the component, agreed well with those of *d*-carvenone respectively.

Semicarbazone, m. p. 200~201°C (lit., 199~201°C[17]).

2,4-Dinitrophenylhydrazone, m. p. 165°C (lit., 164°C[18]).

Thus, it was established that this component consisted of *d*-carvenone.

(c) Unidentified Carbonyl Compound.—The component gave a spot of $R_f$ value 0.20. Its yield amounted to 5.5% of the neutral oil or 4.2% of the starting material. The component was considered to be a carbonyl compound because of its positive reaction to the carbonyl reagents, sodium nitroprusside and 2,4-dinitrophenylhydrazine. But, owing to its small quantity, further investigation was given up.

*The Extract with Sodium Bicarbonate Solution.*—Acidified with 10% sulfuric acid and extracted with ether, the sodium bicarbonate extract gave a dark-brown viscous oil in the amount of 2.5 g., from which no reaction product was distilled out but the resinous residue remained behind.

*Aqueous Solution.*—The aqueous solution mentioned above was neutralized with sodium carbonate and extracted with chloroform and ether, successively, and the residual solution was distilled out. From both of the extracts and from the aqueous distillate, a trace of the starting sample was found on the strip-chromatogram and a small amount of acetone was isolated as its 2,4-dinitrophenylhydrazone, m. p. and mixed m. p. 125~126°C.

## Summary

On oxidation with *tert*-butyl chromate, *d*-*p*-menthene-3 gave *d*-carvenone as a main product and *dl*-*p*-menthen-3-one-5 as a by-product.

In this oxidation, it is found that, when an endocyclic double bond is in the position between $C_{(3)}$ and $C_{(4)}$ in monocyclic terpenes of *p*-menthane type, two active methylenes adjacent to the endocyclic double bond are selectively oxidized to carbonyls as in the case of the terpenes containing an endocyclic double bond in the position between $C_{(1)}$ and $C_{(2)}$, and that, between the two active methylenes, the one remote from the isopropyl group attached to $C_{(4)}$ is preferentially attacked rather than the other which is close to the same group.

The author wishes to express his hearty thanks to Professor Dr. Tamon Matsuura of the Faculty of Science of this University for his guidance and encouragement, and to Mr. K. Nigota for his assistance in the experiment. This research was aided by a grant from the Ministry of Education.

*Chemical Laboratory*
*Shinonome Branch of*
*Hiroshima University*
*Hiroshima*

*3 $R_f$ shows hereafter the value on chromatogram which was developed with 15 vol.% ethyl acetate in *n*-hexane on a silica-plaster of Paris (4:1) strip.

*4 Absorptivity, using the concentration in g./l. and the cell length in cm.

14) Q. Wallach, *Ann.*, **397**, 213 (1913); A. Kötz and H. Steinhorst, "Beilstein", VII$_1$-66 (*Ann.*, **379**, 23 (1911)).

15) W. Treibs, G. Lucius, H. Kögler and H. Breslauer, *Ann.*, **581**, 59 (1953).

16) H. E. Eschinazi and H. Pines, *J. Am. Chem. Soc.*, **78**, 1176 (1956).

17) G. Büchi and R. E. Erickson, ibid., **76**, 3493 (1954).

18) J. K. Roy, *Chem. Abstr.*, **48**, 13660 (1954).

# *Iodine-photocatalyzed cis-trans Isomerization of Stilbene*

By Shigeru YAMASHITA

(Received November 2, 1960)

The light absorption of a solution of *cis*- or *trans*-stilbene in an inert solvent such as *n*-hexane and carbon tetrachloride covers a range of wavelength shorter than about 350 mμ[1]. Stilbene in such a solvent undergoes isomerization when irradiated by the light of wavelength shorter than 350 mμ whereas the light of longer wavelength is ineffective. In the presence of iodine, however, it may be possible that the light of longer wavelength becomes effective. Iodine which is known to catalyze the cis-trans isomerization of a number of organic compounds[2] has an absorption maximum at about 520 mμ in the above solvents; in addition, *cis*- or *trans*-stilbene and iodine form a 1:1 molecular complex whose absorption maximum is situated in the neighborhood of 400 mμ in these solvents[3].

In this paper a spectrophotometric study is reported about the kinetics of isomerization of stilbene in *n*-hexane solution with added iodine under the irradiation of light. The range of light wavelength was adjusted by filters in order to investigate the effect of light absorption by iodine and the iodine-stilbene complex.

## Experimental

**Procedure.**—In Fig. 1 the absorption curves of *cis*- and *trans*-stilbene, their iodine-complexes, and free iodine in *n*-hexane solution are shown. The absorption curves of iodine-complexes appear in the shorter wavelength than that of free iodine absorption, indicating the blue shift of the visible band of iodine caused by complex formation. The Mazda SHL-100UV mercury lamp was used for the light source. Taking the above absorption curves into account, the mercury lines to be used for irradiation were filtered out as follows: the use of the Mazda V-03 filter gave the light beam in the range of wavelength 530~600 mμ which was absorbed practically solely by iodine; by use of the combination of Walz UV and Mazda V-P1.5 filter, the reaction system was irradiated by the light in the range 360~430 mμ which was absorbed almost solely by the iodine-*cis*-stilbene complex. For the trans→cis isomerization of stilbene the combination of Mazda UV-D2 and an aqueous solution of copper nitrate was used as a filter. This allowed the light in the range of 310~400 mμ to enter the reaction vessel. The absorbing species in this case are *trans*-stilbene and its iodine-complex. Although there was a little overlap of absorption of the exciting light by the iodine-*cis*-stilbene and iodine-*trans*-stilbene complex on account of some imperfections in the monochromatism of exciting light, the contribution of the reverse process was negligible since the measurements of isomerization rate were confined to the initial low conversion stage. Because of the low concentration of the absorbing species, the rate of absorption of light by the reaction system was taken as proportional to the incident light intensity and to the concentration of the light absorbing entity as in the previous work[4]. Quantum yields were also obtained by the same procedure as that given in the work[4].

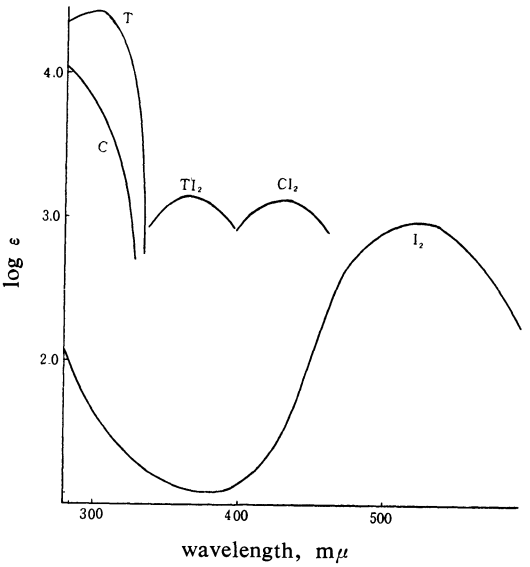



Fig. 1. Molar extinction coefficients. C and T are *cis*- and *trans*-stilbene; $CI_2$ and $TI_2$ are respective molecular complexes with iodine.

## Results and Discussion

**Conversion of *cis*-Stilbene in the Range of Wavelength 530~600 mμ.**—As shown in Figs. 2

1) G. N. Lewis, T. T. Magel and D. Lipkin, *J. Am. Chem. Soc.*, **62**, 2973 (1940).

2) a) G. M. Wyman, *Chem. Revs.*, **55**, 625 (1955). b) B. Tamamushi, This Bulletin, **19**, 147 (1944). c) R. E. Wood and R. G. Dickinson, *J. Am. Chem. Soc.*, **61**, 3259 (1939). d) R. G. Dickinson et al., ibid., **71**, 1239 (1949). e) Y. Urushibara and O. Simamura, This Bulletin, **12**, 507 (1937).

3) S. Yamashita, ibid., **32**, 1212 (1959).

4) S. Yamashita, ibid., **34**, 487, 490 (1961).

and 3, the rate of isomerization is proportional to the square root of light intensity, to the *cis*-stilbene concentration and to the square root of iodine concentration. Accordingly, when $I_0$ represents the intensity of the incident light, (C) the initial concentration of *cis*- stilbene, and $(I_2)$ the initial concentration of iodine, the rate of conversion is given by

$$-d(C)/dt = kI_0^{1/2}(C)(I_2)^{1/2} \qquad (a)$$

Fig. 4 shows the Arrhenius plot of the values of $k$ obtained at 10, 15, 20, 25 and 30°C which yields the activation energy of 7.6±0.1

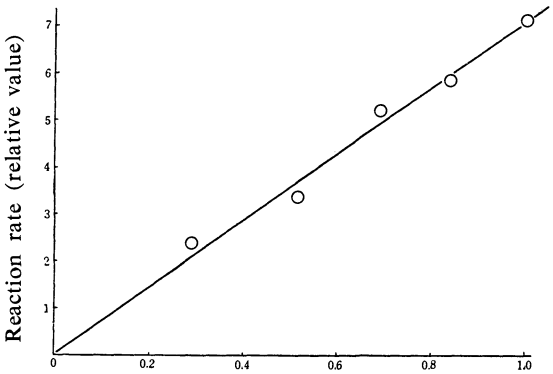



Fig. 2. Dependence of the rate of cis→trans isomerization on light intensity. Wavelength, 530~600 mμ; temperature, 25°C; (C), $5.0\times10^{-5}$ (mol./l.); $(I_2)$, $5.0\times10^{-5}$ (mol./l.).

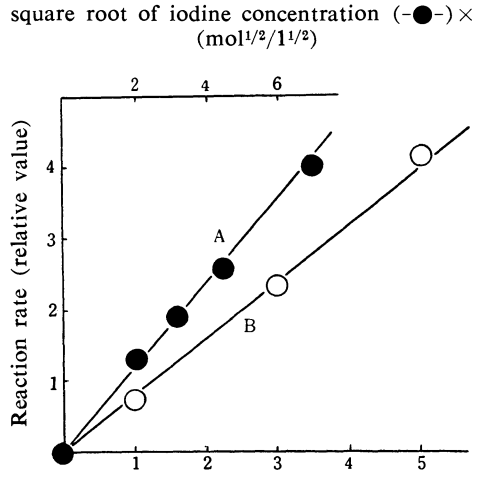



Fig 3. Dependence of the rate of cis→trans isomerization on the concentration of *cis*-stilbene and iodine.
Wavelength, 530~600 mμ; temperature, 25°C
Curve A is for $(C)=5.0\times10^{-5}$(mol./l.)
Curve B is for $(I_2)=5.0\times10^{-5}$(mol./l.)

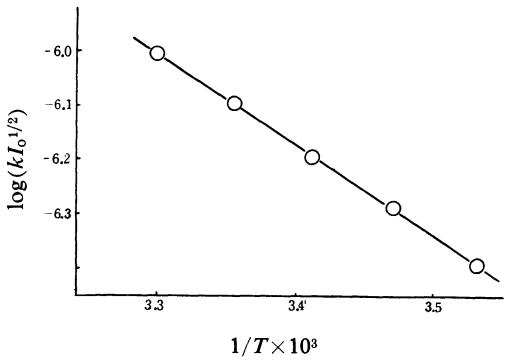



Fig. 4. Temperature dependence of the rate constant. Wavelength, 530~600 mμ; $I_0$, $6.6\times10^{-9}$ Einstein/sec.

kcal./mol. The quantum yield referred to free iodine as the absorbing entity was found to be about 0.08 at 25°C under the condition that $(C)=5.0\times10^{-5}$ mol./l., $(I_2)=5.0\times10^{-5}$ mol./l., $I_0=2.2_3\times10^{-8}$ Einstein/sec.

The rate expression (a) is identical with that obtained for the iodine-catalyzed thermal cis→trans conversion of stilbene in the previous work[4] except for the light intensity term. It seems therefore most probable that the iodine atoms produced by photodissociation of iodine molecules catalyze the conversion reaction with the same mechanism as in the case of thermal reaction, since in the wavelength range concerned here iodine is the only light-absorbing entity. The reaction is thus represented by the following scheme:

$$I_2 + h\nu \rightarrow I + I \qquad (1)$$
$$C + I \rightarrow CI \qquad (2)$$
$$CI \rightarrow C + I \qquad (3)$$
$$CI \rightarrow TI \qquad (4)$$
$$TI \rightarrow T + I \qquad (5)$$
$$I + I \rightarrow I_2 \qquad (6)$$

Here, C and T represent *cis*- and *trans*-stilbene respectively. Provided that the concentration of transient complexes CI and TI are sufficiently small, this scheme leads to the following expression for the reaction rate in the steady state:

$$-d(C)/dt = \{\alpha_i^{1/2}k_2k_4/(k_3+k_4)k_6^{1/2}\} \times I_0^{1/2}(C)(I_2)^{1/2} \qquad (b)$$

where $\alpha_i$ is equal to $\phi_i a_i l$; $\phi_i$, $a_i$ and $l$ denoting the quantum yield of the photodissociation of iodine, its molar absorption coefficient and the light path length, respectively.

Eq. b is consistent with the experimental rate expression (a) and hence

$$k = \alpha_i^{1/2}k_2k_4/(k_3+k_4)k_6^{1/2}$$

or

$$k \cdot k_6^{1/2}/\alpha_i^{1/2} = k_2k_4/(k_3+k_4) \qquad (c)$$

It has previously been found that the term $k_2k_4/(k_3+k_4)$ has a temperature dependence corresponding to an activation energy of 7 kcal./mol. in the iodine-catalyzed thermal cis→trans isomerization of stilbene in *n*-hexane[4]. Since the temperature dependence of $\alpha_i$ and $k_6$ are reasonably supposed to be small, the fact[5] that the rate constant $k$ in Eq. c has an almost identical activation energy of 7.6 kcal./mol. may be taken as evidence in favor of the reaction scheme given above. The relatively low value of the quantum yield obtained here may be ascribed to the recombination of iodine atoms in reaction 6 and to the small quantum yield of iodine photodissociation $\phi_i$[6]. According to the results reported by Meadows and Noyes[7], the values of $\phi_i$ observed under irradiation of 546 and 577~579 m$\mu$ mercury lines are respectively 0.46 and 0.36 in *n*-hexane solution at 25°C.

It has been suggested by the present author that the photoisomerization of *cis*-stilbene may involve a triplet state[4]. It is generally accepted from the studies of phosphorescence phenomena that the internal conversion between the singlet and triplet state is facilitated in the presence of heavy atoms such as lead or iodine[8]. Eyring and Harman[9] explained the catalytic activity of paramagnetic substances observed in cis-trans isomerization reactions by such an internal conversion mechanism. Hence, as described in the previous study of the iodine-catalyzed thermal cis-trans conversion of *cis*-stilbene[4], it is likely that a triplet state plays a role in the process 4 although the present work provides no definite evidence for such an interpretation[10].

**Conversion of *cis*-Stilbene in the Range of Wavelength 360~430 m$\mu$.**—Effect of concentrations and light intensity on the conversion velocity are shown in Figs. 5 and 6. The rate of

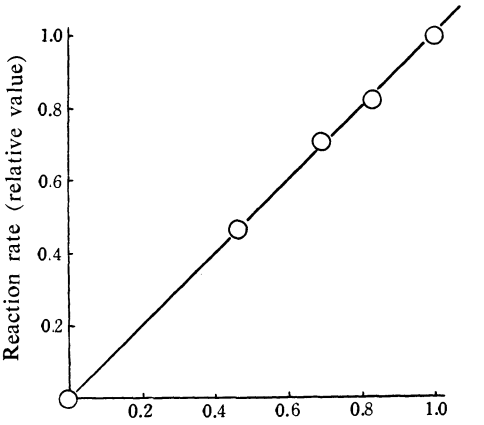



Fig. 5. Dependence of the rate of cis→trans isomerization on light intensity.
Wavelength, 360~430 m$\mu$; temperature, 25°C; (C), $5.0\times10^{-5}$(mol./l.); ($I_2$), $5.0\times10^{-5}$(mol./l.)

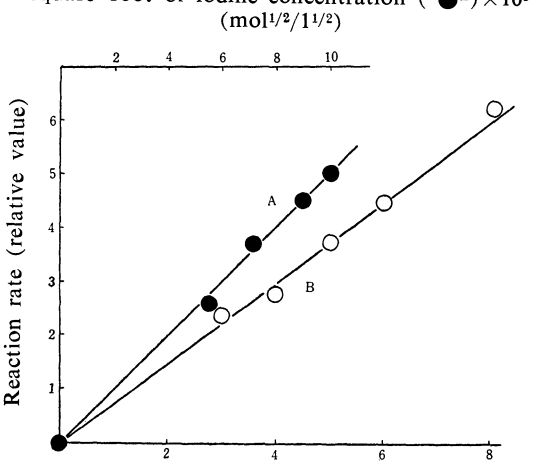



Fig. 6. Dependence of the rate of cis→trans isomerization on the concentration of *cis*-stilbene and indine.
Wavelength, 360~430 m$\mu$; temperature, 25°C
Curve A is for (C)=$5.0\times10^{-5}$ (mol./l.)
Curve B is for ($I_2$)=$5.0\times10^{-5}$ (mol./l.)

reaction is therefore represented by an equation of the same form as Eq. a.

$$-d(C)/dt = k'I_0^{1/2}(C)(I_2)^{1/2} \qquad (d)$$

The reaction mechanism, however, can not be supposed to be identical with that given above for the reaction under irradiation of light 530~600 m$\mu$: the quantum yield of conversion obtained by assuming the absorbing species again to be free iodine proves to be almost

5) This fact implies that the activation energy for the iodine-catalyzed isomerization of *cis*-stilbene under irradiation of light in this range of wavelength is lower than that for the iodine-catalyzed thermal isomerization by half the dissociation energy of molecular iodine as it should be (see Ref. 4).

6) a) R. L. Strong and J. E. Willard, *J. Am. Chem. Soc.*, **79**, 2098 (1957). b) E. Rabinowitch and W. C. Wood, *Trans. Faraday Soc.*, **31**, 547 (1935).

7) a) L. F. Meadows and R. M. Noyes, *J. Am. Chem. Soc.*, **82**, 1872 (1960). b) R. M. Noyes, *Z. Elektrochem.*, **64**, 153 (1960).

8) a) D. S. McClure, *J. Chem. Phys.*, **17**, 905 (1949). b) E. Clement and M. Kasha, ibid., **26**, 956 (1957).

9) R. A. Harman and H. Eyring, ibid., **10**, 557 (1942).

10) In the course of the present work phosphorescence was studied with a phosphoroscope similar to that described by Kasha[8]. The results obtained with *cis*-stilbene in isopentane - methylcyclohexane rigid solvent at liquid nitrogen temperature showed that the lifetime of the phosphorescent state was remarkably shortened by the presence of iodine.

100 times[11] as great as that found in the range 530~600 mμ, and such a large variation can not be explained merely by the difference between the quantum yields of iodine dissociation in the two ranges of wavelength. The only absorbing species, which explains reasonably the conversion in the range 360~430 mμ, is therefore the iodine-complex of *cis*-stilbene[12]. The quantum yield of conversion referred to this complex was found to be about 1.2 at 25°C under the condition that $(C)=5.0\times10^{-5}$ mol./l., $(I_2)=5.0\times10^{-5}$ mol./l., $I_o=1.99\times10^{-9}$ Einstein/sec. In Fig. 7 the Arrhenius plot of

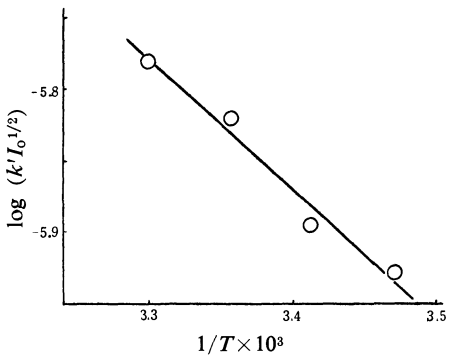



Fig. 7. Temperature dependence of the rate constant. Wavelength, 360~430 mμ; $I_o$, $1.9\times10^{-9}$ Einstein/sec.

the values of the rate constant $k'$ obtained at 15, 20, 25 and 30°C, is shown which yields an activation energy of 4.1±0.2 kcal./mol. Such a lower activation energy, compared to 7.6 kcal./mol. as found for the conversion in the range 530~600 mμ, also seems to indicate that the mechanism of conversion is not the same in the two ranges of wavelength.

The primary process is therefore assumed to be

$$CI_2+h\nu \rightarrow CI_2^* \qquad (1')$$

followed by

$$CI_2^*+C \rightarrow CI+CI \qquad (1'')$$

Subsequent steps may again be represented by the above-mentioned reactions 2—6. As for the elimination of unstable species, however, Eqs. 7 and 8 will have to be taken into account in addition to Eq. 6 because of the higher concentration of CI compared to the conversion in the range 530~600 mμ.

$$CI+I \rightarrow CI_2 \text{ or } C+I_2 \qquad (7)$$

$$CI+CI \rightarrow C+CI_2 \text{ or } 2C+I_2 \qquad (8)$$

Rand and Strong[13] have recently found that a transient complex $C_6H_6\cdot I$, supposed to be a charge-transfer complex, is formed by flashing the benzene solution of iodine, and that it disappears with second order kinetics just as represented by reaction 8. It is well-known that a 1 : 1 molecular complex $C_6H_6\cdot I_2$ is formed between iodine and benzene as in the case of the iodine-stilbene system. Hence, on flashing the benzene solution of iodine, the transient complex $C_6H_6\cdot I$ would have been formed by processes similar to 1′ and 1″ as well as to 1 and 2.

If $k_7=2(k_6k_8)^{1/2}$, as is frequently assumed for radical elimination[14], the following rate expression is derived from reaction 1′, 1″ and 2—8 for the steady state

$$-d(C)/dt=\kappa I_o^{1/2}(C)(I_2)^{1/2} \qquad (e)$$

where

$$\kappa=[\alpha_c^{1/2}k_4K^{1/2}\{2(\alpha_cKI_o(I_2))^{1/2}+k_2k_6^{-1/2}(C)^{1/2}\}]\div[k_3+k_4+k_8^{1/2}(C)^{1/2}\{2(\alpha_cKI_o(I_2))^{1/2}+k_2k_6^{-1/2}(C)^{1/2}\}] \qquad (f)$$

$K$ is the equilibrium constant of the process $C+I_2\rightleftarrows CI_2$, and $\alpha_c$ is equal to $a_cl$, $a_c$ representing the molar absorption coefficient of $CI_2$ complex and $l$ the light path length. If under the experimental conditions of the present work, the quantity represented by $\kappa$ depends only slightly on the variation of $I_o$, (C) and $(I_2)$, Eq. e explains the experimental rate Eq. d. When all the molecules of the transient complex CI produced in the process 1″ are converted into isomeric molecules, the quantum yield of reaction would be equal to 2. The result obtained therefore implies that about a half of CI molecules produced primarily isomerize, if the primary process is Eq. 1′ followed by 1″.

An alternative primary process may be supposed as

$$CI_2+h\nu \rightarrow CI+I \qquad (1''')$$

However, replacing 1′ and 1″ by reaction 1‴ produces no substantial alteration in the rate expression e except that a numerical factor of 2 in the numerator and denominator of Eq. f is now eliminated. The quantum yield of 1.2 seems to favor reactions 1′ and 1″.

**Conversion of *trans*-Stilbene.**—The conversion of *trans*-stilbene was measured in the presence of iodine under irradiation of mercury lines in the range 310~400 mμ. The rate of

11) Such an apparently large quantum yield arises from the very weak absorption of free iodine in this range of wavelength (see Fig. 1).

12) It has been confirmed that *cis*-stilbene, having negligible absorption in the range of wavelength longer than 350 mμ, is not converted to the trans-form by irradiation of light in the range 360~430 mμ.

13) S. J. Rand and R. L. Strong, *J. Am. Chem. Soc.*, **82**, 5 (1960).

14) A factor of 2 is the symmetry number for the collision frequency.

conversion was found to be the same as that obtained in the absence of iodine as shown in Table I. It may therefore be concluded that

TABLE I. EFFECT OF IODINE ADDITION ON THE RATE OF TRANS→CIS PHOTOISOMERIZATION OF STILBENE: INCIDENT LIGHT INTENSITY, $6.6\times10^{-9}$ EINSTEIN/sec.; LIGHT WAVELENGTH, 310～400 mμ; REACTION TEMPERATURE, 25.0±0.1°C.

| Run | Initial concn. of *trans*-stilbene mol./l.×10⁵ | Concn. of iodine mol./l.×10⁵ | Reaction time, min. | Concn. *cis*-stilbene produced mol./l.×10⁵ |
|---|---|---|---|---|
| 1 | 2.0 | 4.0 | 60 | 0.27 |
| 2 | 2.0 | 2.0 | 60 | 0.26 |
| 3 | 2.0 | 20.0 | 60 | 0.27 |
| 4 | 2.0 | 0.4 | 60 | 0.26 |
| 5 | 2.0 | 0 | 60 | 0.27 |

the trans→cis conversion here observed is solely caused by the direct absorption of light by *trans*-stilbene and that iodine makes no contribution to the conversion process.

The thermal equilibrium between cis- and trans-isomer is in general shifted to the trans side, and the thermal isomerization of trans-form can not be observed at low temperatures. Under irradiation of light, however, a photostationary state is brought about. Since in this photostationary state the composition is usually intermediate between 100% cis and 100% trans, conversion occurs on irradiating the trans-form with the light of suitable wavelength. Iodine as a catalyst can not shift the thermal equilibrium between cis- and trans-isomer; even under irradiation, the atomic iodine or TI complex formed from molecular iodine or $TI_2$ complex by light absorption can not shift the equilibrium. Only direct absorption of light by *trans*-stilbene enables it to isomerize. In fact, no conversion was observed in the presence of iodine under irradiation of 546 and 577～579 mμ mercury lines which are strongly absorbed by iodine but not by *trans*-stilbene.

**Summary**

The rate of isomerization of *cis*- and *trans*-stilbene in *n*-hexane solution has been studied spectrophotometrically over the temperature range 10～30°C in the presence of iodine under irradiation of light. The conversion rate of *cis*-stilbene has been found to be proportional to the square root of light intensity, to the concentration of *cis*-stilbene and to the square root of the iodine concentration in both wavelength ranges 360～430 and 530～600 mμ. The activation energies and quantum yields of conversion are however different in these ranges of wavelength. These results, combined with absorption curves of various components present in solution, show that the primary process in the range 530～600 mμ is $I_2+h\nu\rightarrow 2I$ and that in the range 360～430 mμ it is probably $CI_2+h\nu\rightarrow CI_2^*$ followed by $CI_2^*+C\rightarrow 2CI$, where $CI_2$ represents a molecular complex formed between iodine and *cis*-stilbene. Secondary reactions, suggested from the kinetics, are $C+I\rightleftarrows CI$ and $CI\rightarrow TI\rightarrow T+I$ with one or more elimination steps for unstable species, T representing *trans*-stilbene. Rate of isomerization of *trans*-stilbene in the presence of iodine under irradiation of light in the range of wavelength 310～400 mμ has been found to be identical with the rate observed in the absence of iodine under the same condition, excepting the absence of iodine. An explanation for this finding has been given.

The present research was conducted under the kind direction of Professor O. Toyama of the College of Engineering. The author is also deeply indebted to Dr. T. Hayakawa for his invaluable advice and unfailing encouragement throughout this work.

*Department of Chemistry*
*College of General Education*
*The University of Osaka Prefecture*
*Sakai, Osaka*

# *A Study of Dehydration and Hydration of Oxalic Acid by Means of the Deuterium Exchange Reaction*

By Nobukazu OKAZAKI and Eiko TAKEMURA

(Received November 11, 1960)

The dehydration of hydrated salts has been studied by various method, but the use of isotopic tracer in the study of the dehydration process has seldom been reported[1,2]. The process is generally considered to involve the following three steps[3]: (1) the decomposition of the hydrate to give an amorphous intermediate, which then crystallizes, (2) diffusion of the liberated water molecules through the product, and (3) evaporation of the water molecules from the surface of the product. The hydration process would follow the above steps in reverse. In the course of these events, there may occur interchange of protons between water and anhydrous substance. The study of such proton exchange reaction by the use of deuterium tracer may give some information as to the behavior of protons and water molecules in the process of dehydration, and possibly also as to the nature of the dehydration product.

In this work, the following facts have been noted; (1) relation of the deuterium exchange reaction to the surface area of the dehydrated product, and the amorphous character of the product formed on dehydration in vacuo at low temperatures, (2) recrystallization of the amorphous anhydrous acid in the presence of the adsorbed water vapor, (3) deuterium exchange reaction in partially hydrated oxalic acid, and (4) the effect of water vapor upon the rehydration rate of the amorphous anhydrous oxalic acid.

## Experimental

**Procedures.** — A known amount of anhydrous oxalic acid was hydrated in a vacuum system with a known amount of heavy water vapor. The pressure of the vapor was chosen to be lower than the vapor pressure of the saturated solution of oxalic acid, and higher than the dissociation pressure of oxalic acid dihydrate, at the temperature of the experiment. After the completion of the hydration, which was checked manometrically, the oxalic acid dihydrate formed was dehydrated in vacuo by condensing the water vapor from the dihydrate into a receiver cooled by solid carbon dioxide. The water was then distilled into a glass tube, purified thoroughly, and its deuterium content was determined by the floatation method. The deuterium content of heavy water used was ca. 1%.

**Materials.**—Anhydrous oxalic acid was prepared from commercial oxalic acid dihydrate (special grade), by the following two methods.

Sample I. Oxalic acid dihydrate was dehydrated at 100°C in a drying oven, until its loss in weight exceeded the theoretical value[4]. It was weighed in a glass vessel, attached to the vacuum system, pumped for a while to remove a small quantity of water which might have been absorbed during the manipulations, and then hydrated with heavy water vapor.

Sample II. A known amount of dihydrate was placed in the vacuum system, and dehydrated in vacuo at ordinary temperatures (usually at 25°C), as mentioned above. The anhydrous acid so prepared was used directly for exchange reaction without taking it out of the vacuum system.

It has been observed that, especially at lower temperatures (ca. 10°C or below), a small amount of water remaining at the final stage of dehydration is difficult to remove, and, as will be shown later, it plays an important role in the recrystallization of metastable anhydrous acid formed on dehydration in vacuo (Sample II). But the amount of this water is estimated to be so small that it can not affect the deuterium content to any serious extent.

**The Relation between the Degree of Deuterium Exchange and the Molar Ratio of the Reactants.** —The exchange reaction in question may be expressed by the following equation:

$$(COOH)_2 + HDO(vapor) \xrightarrow{\text{hydration}} \text{Oxalic acid dihydrate} + \text{Anhydrous oxalic acid} \xrightarrow{\text{dehydration}} COOH\cdot COOD + H_2O\ (vapor)$$

It should be mentioned that the anhydrous acid was always used in excess, and a part of it was left unhydrated even after the completion of the hydration process.

With regard to the balance of deuterium atoms, the reaction may be written simply as,

$$(COOH)_2 + HDO \rightleftarrows COOH\cdot COOD + H_2O$$

1) A. W. C. Menzies and F. T. Miles, *J. Am. Chem. Soc.*, **56**, 3502 (1934).

2) J. S. Anderson, R. H. Purcell, J. G. Pearson, A. King, F. W. Jones, H. J. Emeleus and H. V. A. Briscoe, *J. Chem. Soc.*, 1937, 1492.

3) W. E. Garner, "The Chemistry of the Solid State", Butterworths, London, (1955), Chap. 8, p. 213.

4) This sort of anhydrous acid may be of the β-form (Dr. H. Chihara, private communication).

The equilibrium condition for this reaction is

$$k=M_w(D_i-D_f)/(M_oD_f)=M_w\cdot\Delta D/(M_oD_f) \quad (1)$$

where, $M_o$ and $M_w$ are the numbers of moles of anhydrous oxalic acid and heavy water vapor, $D_i$ and $D_f$ are the initial and final deuterium contents of heavy water, respectively, and $k$ is the deuterium partition coefficient between oxalic acid and water, or the ratio of the equilibrium atomic fraction of deuterium in oxalic acid to that in water. From a study of the deuterium exchange reaction between oxalic acid and water in solution, $k$ was determined to be $0.94\pm0.01$.

Since the anhydrous oxalic acid is always used in excess, the total amount used does not take part in the exchange reaction. If, of the $M_o$ moles of anhydrous acid used, $M_o'$ moles take part in the exchange reaction, Eq. 1 must be rewritten as,

$$k=M_w\cdot\Delta D/(M_o'D_f) \quad (2)$$

A probable assumption is involved in this equation; namely that those parts of anhydrous oxalic acid which take part in the reaction, or more precisely, which are brought into contact with adsorbed water, are brought into exchange equilibrium with water rapidly relative to the time required for hydration or dehydration.

Eq. 2 may be written as,

$$\Delta D/D_f=(kM_o'/M_o)(M_o/M_w) \quad (3)$$

where $M_o'/M_o$ is the molar ratio of oxalic acid which takes part in the exchange reaction to the total amount of oxalic acid used. According to this equation, if we plot the result of the exchange reaction, taking $\Delta D/D_f$ as ordinate, and $M_o/M_w$ as abscissa, the slope of the line passing through the plotted point and the origin gives the value of $kM_o'/M_o$, and hence of $M_o'/M_o$.

In a particular case, where heavy water exchanges its deuterium atoms with anhydrous acid in equivalent proportion, the value of $M_w/M_o'$ in Eq. 2 is 2, as can be readily seen from the formula $(COOH)_2\cdot2H_2O$. In this case, according to Eq. 2, the value of $\Delta D/D_f$ should be 0.5 ($k\fallingdotseq1$) irrespective of the value of $M_o/M_w$.

## Results and Discussion

**Deuterium Exchange Reaction in Relation to the Nature of the Dehydration Product.**—The dependence of the degree of deuterium exchange ($\Delta D/D_f$) on the molar ratio of the reactants ($M_o/M_w$) is shown in Fig. 1. These results were obtained at 25°C and with the use of heavy water vapor of 4.6 mmHg for the hydration process. Other data were obtained under various conditions of temperature (0~28°C) and relative pressure (0.17~0.85) of heavy water vapor. But the temperature and the relative pressure were found to have little effect upon the exchange reaction.

It will be seen from the figure that there exists between Sample I and Sample II a remarkable difference in the dependence of deuterium exchange reaction on $M_o/M_w$. The

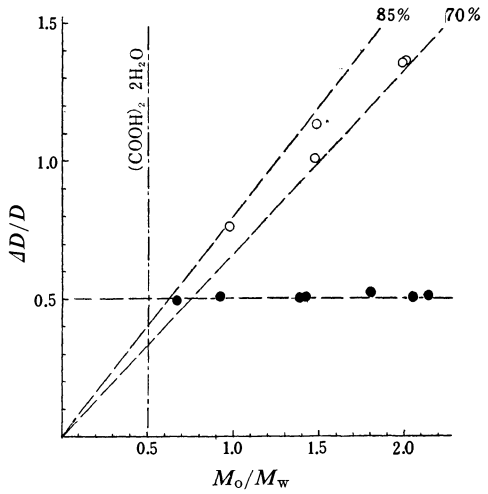



Fig. 1. Difference of the degree of deuterium exchange with the method of preparation of anhydrous oxalic acid. Solid circles: Sample I, prepared at 100°C. Open circles: Sample II, prepared in vacuo at room temperature.

difference appears to be qualitative rather than quantitative, and it seems to suggest the existence of a qualitative difference between the natures of the two sorts of anhydrous oxalic acid.

In the case of Sample I, which is prepared from the dihydrate at 100°C (probably $\beta$-form), the value of $\Delta D/D_f$ is always about 0.5, irrespective of the value of $M_o/M_w$. From the reasoning mentioned in the experimental part, it may be concluded that, in this case, heavy water exchanges its deuterium atoms with anhydrous acid always in equivalent proportion.

On the other hand, the $\Delta D/D_f$ value of Sample II, which is prepared by dehydration in vacuo at room temperature, increases with increasing $M_o/M_w$. That is, the amount of anhydrous oxalic acid which takes part in the exchange reaction increases with the increasing excess of the anhydrous oxalic acid.

To visualize the ratio of oxalic acid which takes part in the exchange reaction to the total amount of oxalic acid used, the lines having the slopes ($kM_o'/M_o$) of 0.8 and 0.67 respectively, are drawn in Fig. 1. Taking $k=0.94$, these values correspond to the values of $M_o'/M_o$ of 0.85 and 0.71, respectively. It will be seen that 70 to 85% of the anhydrous acid takes part in the exchange reaction, the percentage decreasing from 85 to 70 with increasing $M_o/M_w$.

The results obtained with Sample II show considerable scatter. This is probably due to the persistence in the dehydrated product of a small uncontrollable quantity of water, which

accelerates the recrystallization and consequently reduces the exchange reaction of the anhydrous acid (see later).

From the mechanism of the processes of the dehydration and the hydration of crystal hydrate, mentioned in the introduction of this paper, it may be inferred that, in the exchange reaction in question, the places where the reaction occurs, or the sites of the reaction, are, (1) the surfaces of the dehydration product, and (2) the reaction zone and the crystal lattice of the hydrate.

If the exchange reaction occurs exclusively in (2), where heavy water and anhydrous acid react always in equivalent proportion, $\Delta D/D_f$ should be 0.5, irrespective of the value of $M_o/M_w$. This is the case with the exchange reaction of Sample I (oxalic acid prepared at 100°C).

On the other hand, if the exchange reaction takes place in the surfaces of anhydrous acid, the increasing amount of anhydrous acid implies an increase in the number or the area of the site of the exchange reaction, and $\Delta D/D_f$ should increase with increasing $M_o/M_w$. This type of exchange reaction is observed with Sample II (anhydrous oxalic acid prepared in vacuo at low temperatures).

Consequently, it may be concluded that, in the case of Sample I, the exchange reaction occurs mainly in the crystal lattice of the dihydrate, and/or in the reaction zone on the occasion of the formation and the decomposition of the hydrate lattice. In the crystal lattice of the oxalic acid dihydrate[5], the water molecules are linked to the oxygen atoms of the carboxyl groups by hydrogen bonds. In such a structure, there may occur ready exchange of protons between carboxyl groups and water molecules by mere shifts of protons. It is well-known that, in aqueous solution, the hydrogen atoms linked to electronegative atoms are easily replaced by the deuterium atoms of heavy water. The exchange reaction in aqueous solution of oxalic acid would be quite analogous to that in the solid oxalic acid and would proceed through such a hydrogen-bonded intermediate.

As to the exchange reaction in the surfaces of anhydrous acid, a possible mechanism would be the one which involves capillary condensation of water vapor and the subsequent dissolution of oxalic acid in the condensed phase. But, as it has been observed that 70 to 85% of anhydrous acid used takes part in the exchange reaction, the above mechanism requires the dissolution of most of the anhydrous acid used. This seems to be incompatible with the observations during the experiments. Moreover, if capillary condensation and solution played an important role in the reaction, the degree of exchange would probably depend upon the relative pressure and the temperature. But, as mentioned above, such dependence has not been observed.

Therefore, in the case of Sample II, it is necessary to consider that the increase in the degree of exchange relative to that of Sample I is due to direct exchange of deuterium between adsorbed water molecules and solid anhydrous acid. The oxalic acid molecules involved in such a direct exchange mechanism would be restricted within a few outermost molecular layers of the solid anhydrous acid, and except in the case of a highly dispersed solid, the surface exchange mechanism could not contribute any appreciable portion to the total exchange reaction.

From the results of deuterium exchange reaction, the molar ratio of oxalic acid in the surface to that of the bulk may be estimated as follows: The amount of oxalic acid which takes part in the exchange reaction is given by Eq. 2.

$$M_o' = M_w \cdot \Delta D/(k \cdot D)$$

Of this amount, a part which is equivalent to the amount of water vapor used for the hydration takes part in the reaction through hydrate formation. The remainder $M_o' - (M_w/2)$ is the number of moles of oxalic acid which contributes to the surface exchange. The total number of moles of anhydrous oxalic acid which is left unhydrated at the completion of the hydration process is given by $M_o - (M_w/2)$. Thus the desired ratio $\beta$ is,

$$\begin{aligned}\beta &= [M_o' - (M_w/2)] / [M_o - (M_w/2)] \\ &= [(1/k)(\Delta D/D) - 0.5] / [(M_o/M_w) - 0.5]\end{aligned} \quad (4)$$

The values of $\beta$ are calculated to be 0.59~0.71 for five specimens of anhydrous oxalic acid dehydrated in vacuo at 25°C. That is, 60 to 70% of the molecules of the anhydrous acid are in the surface.

If it is assumed that only the outermost molecular layer is involved in the exchange reaction during the hydration and the redehydration, the exchange of inner layers being associated with a slow diffusion process, then, on the average, 60 to 70% of the molecules in a crystallite of the anhydrous oxalic acid are in the outermost molecular layer. A substance composed of such crystallites may be termed amorphous.

It is well known that amorphous intermediates result from the dehydration of some

5) J. M. Robertson and I. Woodward, *J. Chem. Soc.*, **1936**, 1817; J. D. Dunitz and J. M. Robertson, ibid., **1947**, 142.

hydrated salts in vacuo at low temperatures[3]. In the present case, the X-ray diffraction method has failed to detect the amorphous character of the anhydrous oxalic acid. But it has been observed that the electron micro-diffraction patterns of oxalic acid dihydrate change from spots or sharp rings to diffuse halos characteristic of an amorphous substance in the course of dehydration in the vacuum of electron microscope. Yet the electron microscopic image remains unaltered. This fact ensures that it is the dehydration process and not the decomposition by electron beams which is responsible for the change in diffraction patterns. The failure of the X-ray diffraction method is probably due to the recrystallization by the catalytic action of a small amount of residual water.

**Recrystallization of Amorphous Anhydrous Oxalic Acid in the Presence of Adsorbed Water Vapor.** — Anhydrous oxalic acid prepared by dehydration in vacuo at 25°C (Sample I) was exposed to heavy water vapor of 2 mmHg pressure for 15 min. Then the anhydrous acid was isolated from the source of water vapor, and kept in contact with adsorbed water at 25°C for definite times. During this period of contact, the pressure of water vapor above the anhydrous acid increased from 2 to 2.7 mmHg (dissociation pressure of the dihydrate at 25°C). This is probably due to the contraction of the surface area of the anhydrous acid and the consequent desorption of water vapor. This fact may be regarded as an evidence of the recrystallization process. In the experiments with longer times of contact, the recrystallized crystals having the form of a six-sided plate became visible even to the naked eye. It was identified with $\alpha$-form by X-ray diffraction method.

After a given time of contact, the anhydrous acid was hydrated with heavy water vapor and subsequently redehydrated in vacuo at 25°C, and the water obtained on dehydration was analysed for deuterium content.

In Fig. 2, per cent $\alpha(=M_o'/M_o\times 100)$ of oxalic acid which takes part in the exchange reaction is plotted against the time of contact of anhydrous acid with adsorbed water. As controls, deuterium exchange of the anhydrous acid kept for definite times in the absence of water vapor was also studied. The results are given by the upper curve in Fig. 2.

Fig. 2 shows that, whereas in the control experiments percentage exchangeability $\alpha$ of anhydrous oxalic acid decreases only slightly with time, that of anhydrous acid treated preliminarily with water vapor decreases definitely with time.

As discussed above, the increase in the exchangeability of highly dispersed anhydrous

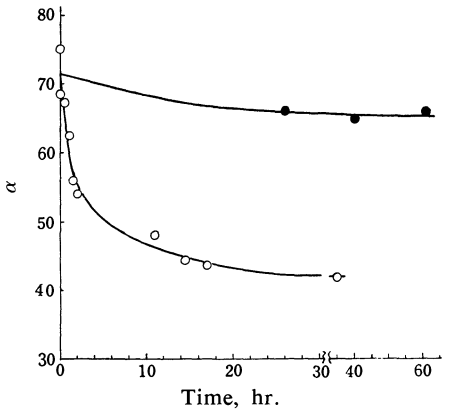



Fig. 2. Decrease in the degree of deuterium exchange due to the recrystallization of highly dispersed oxalic acid at 25°C. $M_o/M_w=1.5$. Upper curve: in the absence of water vapor. Lower curve: in the presence of water vapor.

acid relative to that of crystalline anhydrous acid is due to the exchange reaction in the surface, and this surplus exchangeability may be considered to be a measure of the surface area of the anhydrous acid. Consequently, the decrease in the value of $\alpha$ means the progress of recrystallization, and the completion of it is characterized by the value of $\alpha$ which is characteristic of the crystalline anhydrous acid (in the present case, $\alpha=0.354$).

The comparison of two curves in Fig. 2 shows that adsorbed water exerts considerable effect on the recrystallization of amorphous oxalic acid. Recrystallization in the presence of water vapor (2 mmHg initially) at 25°C proceeds rather rapidly for the first few hours and goes almost to completion within about 10 hr.

The catalytic effect of water on the recrystallization of amorphous intermediates in the dehydration of salt hydrates has been studied by several authors. Volmer and Seydel[6] have found by the X-ray diffraction method that, whereas the anhydrous manganous oxalate formed on dehydration in vacuo is amorphous, the dehydration in the presence of water vapor yields crystalline manganous oxalate, and attributed its formation to the recrystallization of amorphous product by the catalytic action of water vapor. Frost, Moon and Tompkins[7] have deduced from thermal measurements the fractional amounts of amorphous intermediate in the dehydration products of copper sulfate pentahydrate prepared under

6) M. Volmer and G. Seydel, *Z. physik. Chem.* (*Leipzig*), **A179**, 153 (1937).
7) G. B. Frost, K. A. Moon and E. H. Tompkins, *Can. J. Chem.*, **29**, 604 (1951).

various pressures of water vapor, and found that the fractional amount decreases with increasing water vapor pressure.

Oxalic acid offers a new example of the formation of amorphous intermediate and of the catalytic effect of water on its recrystallization. In this example, the two processes were studied separately and the course of the latter was followed by deuterium exchange reaction.

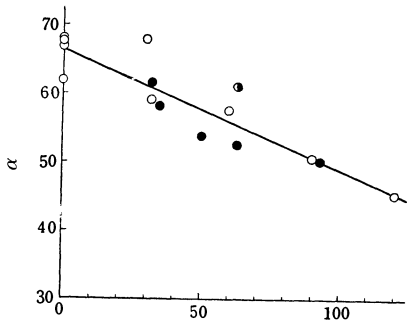



Fig. 3. The effect of temperature on the recrystallization rate of highly dispersed oxalic acid. $M_0/M_w=2.0$.
●: 35.1°C, ◑: 30.0°C, ○: 25.0°C

In order to gain further information as to the nature of the recrystallization process, the effect of temperature has been studied at 25 and 35°C.

Fig. 3 shows that the recrystallization rates are scarcely affected by the change of temperature. It appears that oxalic acid molecules are almost free to move on the surface of the highly dispersed oxalic acid.

**Deuterium Exchange Reaction in Partially Hydrated Oxalic Acid.** — When amorphous oxalic acid is partially hydrated with heavy water vapor and left for a time, the oxalic acid molecules which are left undeuterated in the process of hydration, become progressively deuterated,

Oxalic acid + Oxalic acid dihydrate-*d*

$\rightleftarrows$ Oxalic acid-*d* + Oxalic acid dihydrate

As a consequence, the deuterium content of water obtained upon dehydration of oxalic acid partially hydrated with heavy water vapor decreases with the time during which oxalic acid is kept in the partially hydrated state.

The results are shown in Fig. 4, in which per cent of oxalic acid which takes part in the exchange reaction is plotted against time. Within experimental errors, the percentage increases almost linearly with time, and the curves for the two temperatures are almost parallel to each other. This seems to suggest that the rate of this exchange is almost independent of temperature.

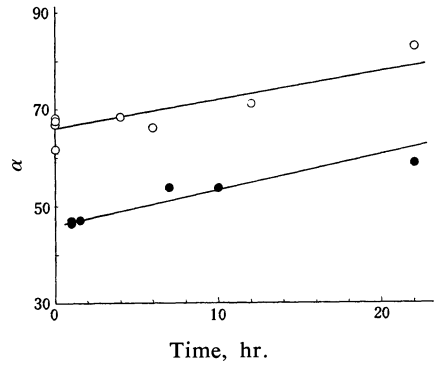



Fig. 4. Deuterium exchange reaction within partially hydrated oxalic acid.
○: 25°C, ●: 15°C

It is probable that this increase in the degree of exchange is caused by the propagation of deuterium exchange into the inner layers of anhydrous oxalic acid, since the surface layer would be completely deuterated during the hydration process.

A possible mechanism of this process consistent with the fact that the process is associated with small or zero activation energy would be the following: During the recrystallization by the action of adsorbed water, oxalic acid molecules leave the original lattices and migrate to the new crystals. Thus the adsorbed water molecules are brought into contact successively with the fresh layer of anhydrous acid, and exchange deuterium atoms with these fresh surface molecules. The deuterium atoms of the adsorbed water are supplied by the surface migration of protons or water molecules, or from the vapor phase by adsorption and desorption.

**The Effect of Water Vapor on the Rehydration Rate of Amorphous Oxalic Acid.**—In the course of this investigation, it has been observed that treatment of amorphous anhydrous oxalic acid with a small amount of water vapor gives rise to a characteristic change in the rehydration rate according to the amount of water vapor.

A known amount of water vapor was introduced from a gas burette into a vessel containing amorphous oxalic acid prepared in vacuo at 25°C. The pressure of water vapor in the vessel, as measured by an oil manometer and a traveling microscope, changed with time as a result of the progress of adsorption and recrystallization. It was lower than 0.01 mmHg in most of the runs. After the treatment with water vapor for 1.5 hr. at 25°C, the anhydrous acid was hydrated with water vapor of 4.6 mmHg pressure, liquid water maintained at 0°C being used as the source of the vapor.

The results are given in Fig. 5, in which rehydration rates are plotted against the amounts of water vapor initially introduced into the reaction vessel. As a measure of the rehydration rate, the reciprocal of time required for a definite amount of oxalic acid (0.11 mol.) to absorb 1 g. of water vapor was taken. This measure, though giving only an integrated rate would serve for qualitative discussions.

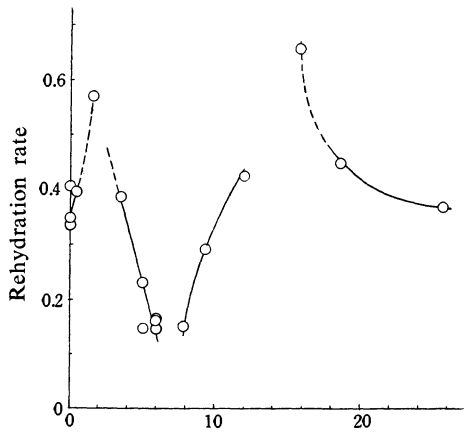



Fig. 5. Effect of preliminary water vapor treatment on the rehydration rate of amorphous anhydrous oxalic acid.

It will be seen that there is a minimum of rehydration rate in the region of $6\sim8\times10^{-5}$ mol. $H_2O$ per mol. of oxalic acid, with a maximum on each side of the minimum. This effect bears an apparent resemblance to the effect of water vapor on the nucleation rate of chrome alum observed by Garner and Jennings[8]. They have found that water vapor causes nucleation of the dehydration product in a slightly dehydrated surface of chrome alum, and that it has an optimum effect for a particular value of its pressure. The results have been interpreted by them as due to the conversion of collapsed lattice into product lattice under the loosening action of water.

In the present case, it seems probable that a high rate of nucleation or a high rate of recrystallization would retard the rehydration rate by decreasing the surface area of anhydrous acid. Or, it seems also possible that formation of anhydrous acid nuclei at a high rate would consume those parts of the collapsed lattice which are responsible for the formation of dihydrate nuclei. At present, it is not possible to give any reasonable interpretation to this phenomenon. It will be studied further.

8) W. E. Garner and T. J. Jennings, *Proc. Roy. Soc.*, **224A**, 460 (1954).

**Summary**

The deuterium exchange reaction in the course of the hydration of anhydrous oxalic acid with heavy water vapor and subsequent dehydration of the product has been studied.

Two exchange mechanism have been suggested to be operative; the hydrate formation mechanism and the surface exchange mechanism. A distinction may be made between the two by the dependence of exchange reaction on the molar ratio of the reactants.

Anhydrous oxalic acid prepared by dehydration at 100°C takes part in the exchange reaction through hydrate formation; while, with the anhydrous acid prepared by dehydration in vacuo at ordinary temperatures, the surface exchange mechanism comes into play.

For the specimens of anhydrous acid prepared in vacuo, the molar ratio of oxalic acid in the surface to that of the bulk is estimated to be 0.6~0.7 from the results of the deuterium exchange reaction. Dehydration of oxalic acid dihydrate in the vacuum of electron microscope yields amorphous anhydrous acid.

The recrystallization of amorphous anhydrous oxalic acid was studied by the use of deuterium exchange reaction as a measure of surface area. It has been shown that adsorbed water exerts catalytic effect on the recrystallization. The process is associated with small or zero activation energy. Anhydrous oxalic acid recrystallized in the presence of water has been identified with $\alpha$-form.

Deuterium exchange reaction between unhydrated oxalic acid and hydrate water occurs in anhydrous oxalic acid partially hydrated with heavy water vapor. The rate of this exchange is practically independent of temperature. The reaction probably consists in the deuteration of the molecules in the interior of the anhydrate lattice.

Treatment of amorphous anhydrous acid with a small amount of water vapor causes a peculiar change in the rate of subsequent rehydration. There is a considerable retarding effect on the rehydration rate for a particular range of the amount of water vapor.

The authors wish to express their thanks to Professor T. Titani, Tokyo Metropolitan University, for his encouragement and advice, and to Professor I. Nitta and Dr. H. Chihara, Osaka University, for X-ray analyses. They are also indebted to Miss A. Sakai and Mrs. Y. Kubo for their assistance in electron microscopic works.

*Department of Chemistry*
*Nara Women's University*
*Nara*

# *Deuterium and Oxygen-18 Tracer Study of the Dehydration and the Hydration of Copper Sulfate*

By Nobukazu OKAZAKI, Akiko OKUMURA and Keiko NAKAGAWA

(Received November 11, 1960)

In a tracer study of dehydration and hydration of oxalic acid[1], it has been shown that amorphous anhydrous acid results from the dehydration of dihydrate in vacuo at low temperatures. The highly dispersed character of the dehydration product reveals itself in its increased degrees of deuterium exchange with heavy water vapor as compared with the crystalline anhydrous acid. It seems desirable to check this relation between the degree of deuterium exchange and surface area of the dehydration product with the hydrate whose dehydration product in vacuo at low temperatures is definitely known to be amorphous. As a hydrate of this kind, copper sulfate[2] was chosen as the subject of the present study.

There are a few reports of deuterium tracer study on the hydrate water of copper sulfate. Menzies and Miles[3] have found complete exchange of deuterium between water vapour and monohydrate in the course of its hydration and the subsequent dehydration of the product. In a work by Briscoe et al.[4], anhydrous copper sulfate was hydrated with heavy water to give monohydrate, and then with ordinary water to pentahydrate. On dehydrating the pentahydrate, they have found an interchange of deuterium between the fifth and the remaining four molecules of the hydrate water.

Since, as is well-known, the fifth water molecule is firmly held by copper sulfate, it seems interesting to see whether there is ready interchange of water molecules between monohydrate and water vapor. But, as it has been shown[1] that the interchange of proton occurs between anhydrous oxalic acid and water vapor, it seems possible that, in the above experiments with copper sulfate, the interchange of proton might occur independently of the interchange of water molecules as a whole between monohydrate and water. Therefore, the oxygen exchange between copper sulfate monohydrate and water vapor enriched in heavy oxygen has been studied at the same time.

## Experimental

Experimental procedures were almost the same as those described in the previous paper[1]. The water enriched in heavy oxygen used in the earlier part of this study was kindly supplied by Professor N. Morita of Nagoya University. Later, it was obtained from a fractionating column of this laboratory, and had excess density due to heavy oxygen of about 600 $\gamma$. The deuterium content of the heavy water was normalized by repeated exchange with ammonium chloride. Copper sulfate monohydrate was prepared by dehydration of pentahydrate (special grade). Two kinds of samples of monohydrate were used; (1) amorphous monohydrate which was prepared by dehydration in vacuo at 35°C, and (2) crystalline monohydrate prepared by dehydration at 105±5°C under atmospheric pressure to constant weight[2]. The monohydrate was hydrated with about 1 g. of heavy water vapor, whose pressure was kept higher than the dissociation pressure of pentahydrate at the temperatures of the experiments. Various conditions of the temperature of the monohydrate and the pressure of water vapor were tried. The time required for the completion of hydration varied from a few hours to several days according to the condition chosen, but it did not affect the result of the exchange reaction. After the completion of the hydration, the hydrated product was redehydrated in vacuo at 35°C, and the water obtained was analyzed for its isotopic content by the floatation method. The time required for redehydration ranged from a few to several days. In general, the hydrate from the amorphous monohydrate decomposed more slowly than that from the crystalline monohydrate.

## Results and Discussion

The results are shown in Fig. 1, in which the degree of exchange $\Delta D/D$ is plotted against the molar ratio of the reactants $M/M_w$ ($\Delta D$ is the decrease of deuterium content of water in the course of hydration of monohydrate and subsequent redehydration of the product, $D$ is the deuterium content of heavy water obtained on redehydration, and $M$ and $M_w$ are the numbers of moles of copper sulfate and heavy water used for the reaction).

In the region for which the values of the

1) N. Okazaki and E. Takemura, This Bulletin, **34**, 977 (1961).
2) V. Kohlschütter and H. Nitschmann, *Z. physik. Chem.*, Bodensteinfestband, 494 (1931).
3) A. W. C. Menzies and F. T. Miles, *J. Am. Chem. Soc.*, **56**, 3502 (1934).
4) J. S. Anderson, R. H. Purcell, J. G. Pearson, A. King, F. W. Jones, H. J. Emeleus and H. V. A. Briscoe, *J. Chem. Soc.*, **1937**, 1492.

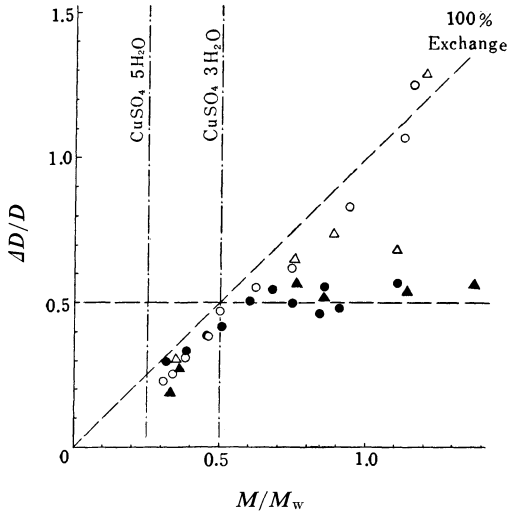



Fig. 1. Deuterium and oxygen-18 exchange reaction between amorphous and crystalline copper sulfate monohydrate and water. Deuterium exchange: ● ; crystalline, ○ ; amorphous. Oxygen exchange: ▲ ; crystalline, △ ; amorphous

molar ratio $M/M_w$ are greater than 0.5, increased exchangeability of amorphous monohydrate over that of crystalline monohydrate may be seen from the figure. The effect is similar to that observed with oxalic acid, and supports the suggestion of the previous report concerning the formation of highly dispersed anhydrous acid in the dehydration of oxalic acid dihydrate in vacuo and the relation of the deuterium exchange reaction to the surface area of the dehydration product.

In this molar ratio region, the values of $\Delta D/D$ for the crystalline monohydrate are almost constant ($\fallingdotseq 0.5$) independently of the value of the molar ratio. This implies that the monohydrate and heavy water vapor react in a constant proportion irrespective of the presence of the excess of the former, and it leads to the conclusion that the exchange reaction is associated with hydrate formation[1]. The value of the molar ratio $M'/M_w$ is given by the relation,

$$M'/M_w = (1/k)(\Delta D/D)$$

as 0.5, which corresponds to the composition $CuSO_4 \cdot 3H_2O$ ($CuSO_4 \cdot H_2O : 2H_2O$). That is, exchange reaction of crystalline monohydrate under the given condition proceeds through the formation of trihydrate.

In the molar ratio region corresponding to the compositions between pentahydrate and trihydrate, the two sorts of samples of monohydrate behave similarly toward the deuterium exchange reaction. The values of $\Delta D/D$ in this region correspond to the almost complete equilibration of the monohydrate with heavy water vapor.

In this region, pentahydrate and trihydrate may be expected as the hydration product of the crystalline monohydrate, the deuterium content of the trihydrate being lower than that of the pentahydrate. As an extreme case, if the hydrate water of pentahydrate and that of trihydrate equilibrate with each other in the course of the experiment, the result is the complete equilibration of deuterium between the monohydrate and water vapor. In the case of the other extreme where pentahydrate and trihydrate are dehydrated independently without exchanging their deuterium atoms with each other, it may be easily shown by calculation that, though the value of $\Delta D/D$ is slightly lower than that of the complete equilibration, the difference is well within the range of experimental errors. Thus, if pentahydrate and trihydrate are formed as the product of hydration, the results are always the nearly complete equilibration of monohydrate with the water vapor, which may also be expected for amorphous monohydrate.

If, on the other hand, the pentahydrate alone was formed in this molar ratio region, the values of $\Delta D/D$ should be 0.25, irrespective of the values of the molar ratio, which is contrary to the results. Thus, the exchange reaction may be used to determine the composition of the hydrate formed on hydrating an anhydrate or a lower hydrate, provided that the anhydrate has an exchangeable hydrogen atom.

The increased exchangeability of amorphous monohydrate as compared with crystalline monohydrate is due to the exchange reaction between surface molecules and adsorbed water, as in the case of oxalic acid. The fractions of the amorphous monohydrate which takes part in the exchange reaction to the total amount used are calculated by the relation[1],

$$M'/M = (1/k)(\Delta D/D)/(M/M_w)$$

to be 0.75～1.08. The corresponding values obtained with oxalic acid are 0.71～0.85.

The molar ratio of the monohydrate in the surface as defined by the deuterium exchange reaction to the monohydrate of the bulk may be calculated by the relation[1],

$$\beta = [(1/k)(\Delta D/D) - x]/[(M/M_w) - x]$$

where $x$ is a constant, which has the value of 0.5 if trihydrate is formed on hydrating the amorphous monohydrate, and of 0.25 if pentahydrate is formed.

Above the value of the molar ratio corresponding to the composition of trihydrate, the dissociation pressure of the partially hydrated amorphous monohydrate is of the order of

that of monohydrate in the case of fast hydration, owing probably to the strong adsorptive power of the amorphous monohydrate, and is in the neighborhood of that of trihydrate in the case of slow hydration. It is probable that, in this region, amorphous monohydrate at first absorbs water vapor and subsequently combines with it rather slowly to form trihydrate as hydration product.

The surface to bulk ratios as given by the above relation are now calculated for the five specimens of the amorphous monohydrate whose exchange results are plotted in Fig. 1. The results are 0.44, 0.48, 0.75, 0.91 and 1.10. The values of the ratio obtained with amorphous oxalic acid are 0.60~0.70[1]. These values may compare nearly with each other. This result, together with the similarity of the results of the exchange reaction between oxalic acid and copper sulfate, confirms the view mentioned in the previous report[1] concerning the nature of the dehydration product and the relation between the degree of deuterium exchange and surface area of the product.

The results of oxygen exchange reaction are the same in essentials as those of deuterium exchange reaction. It may be concluded that interchange of water molecules as well as of protons occurs in the course of the hydration of monohydrate with heavy water vapor and subsequent dehydration of the product. Accordingly, in the dehydration of copper sulfate pentahydrate, the fifth water molecule is interchangeable with the remaining four. The discussions of the previous[1] and the present papers, concerning the nature of the dehydration products, the relation of the exchange reaction to the surface area of the dehydration products, and the mechanisms of the exchange reaction, are applicable with necessary change to the oxygen exchange reaction.

## Summary

The deuterium and oxygen-18 exchange reaction of amorphous and crystalline copper sulfate monohydrate with water in the course of the hydration of the monohydrate with heavy water vapor and the subsequent dehydration of the product has been studied.

The exchange reaction of crystalline monohydrate is associated with the formation of hydrate. Amorphous monohydrate shows an increased degree of exchange over crystalline monohydrate. This increased exchangeability of amorphous monohydrate is due to the exchange reaction between surface molecules and adsorbed water. The similarity of the results of deuterium exchange reaction between oxalic acid and copper sulfate confirms the suggestion of the previous report that anhydrous oxalic acid prepared by dehydration in vacuo at low temperatures is amorphous and the degree of deuterium exchange reaction is related to the surface area of the dehydration product.

The results of the oxygen-18 exchange reaction of copper sulfate monohydrate with water vapor are almost identical in essentials with those of the deuterium exchange reaction. The fifth water molecule of copper sulfate is interchangeable with the other four in the process of dehydration of pentahydrate and the hydration of monohydrate.

*Department of Chemistry*
*Nara Women's University*
*Nara*

# *A Study of Dehydration and Hydration of Sodium Dihydrogen Phosphate and Racemic Acid by Means of the Deuterium Exchange Reaction*

By Nobukazu OKAZAKI and Akiko OKUMURA

(Received November 11, 1960)

In a study of dehydration and hydration of oxalic acid by means of the deuterium exchange reaction[1], the following facts have been observed; (1) the difference of exchange behavior of the anhydrate with the method of its preparation, and the amorphous character of the anhydrate prepared by dehydration in vacuo at low temperatures, (2) recrystallization of the amorphous anhydrate under the catalytic action of water vapor, and (3) deuterium

1) N. Okazaki and E. Takemura, This Bulletin, **34**, 977 (1961).

exchange reaction in anhydrate-hydrate mixture. It is the purpose of the present work to examine with other salt hydrates whether or not the phenomena are of general occurrence.

The experimental procedures were almost the same as those used in the previous work[1].

**Difference of Exchange Behavior of Anhydrate with the Method of Dehydration.** — *Sodium Dihydrogen Phosphate.* — Commercial sodium dihydrogen phosphate dihydrate (special grade reagent) was used without further purification. Two sorts of samples of the anhydrate were used; one was prepared by dehydration of dihydrate to constant weight at 130°C in a drying oven, and the other by dehydration in vacuo at ordinary temperatures. The procedures for the deuterium exchange experiment were the same as those used previously.

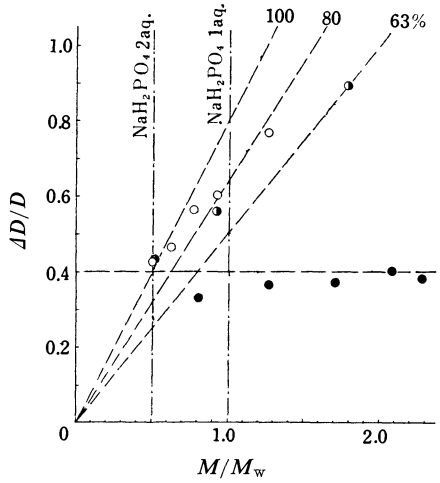



Fig. 1. Difference of the deuterium exchange reaction between anhydrous sodium dihydrogen phosphate prepared by dehydration in vacuo at ordinary temperatures (○; 20°C, ◑; 11°C) and that prepared at 130°C (●).

The results are shown in Fig. 1, in which the degree of exchange $\Delta D/D_f$ is plotted against the molar ratio of the reactants $M/M_w$ (for notations and formulas, see the previous work). As in the case of oxalic acid[1], there is a qualitative difference of exchange behavior between the two sorts of anhydrous sodium dihydrogen phosphate.

The exchange reaction of the anhydrous phosphate prepared at 130°C was studied at 11°C. In these experiments, the values of $\Delta D/D_f$ are about 0.4 for the values of the molar ratio ranging from 1.0 to 2.5. This fact means that, in these cases, the amount of the anhydrous phosphate which takes part in the exchange reaction is always in a definite ratio to the amount of water used, irrespective of the presence of the excess anhydrous phosphate. This ratio $M'/M_w$ may be calculated by the relation,

$$M'/M_w = (2/kn)(\Delta D/D_f)$$

where, $k$ is the partition coefficient of deuterium between anhydrous phosphate and water, and $n$ is the number of exchangeable hydrogen atoms in sodium dihydrogen phosphate.

The value of $k$ has been determined from the exchange reaction in solution to be 0.806 $\pm$0.008 (mean of four determinations), which is somewhat smaller than the value commonly accepted for the partition coefficient of hydroxyl hydrogen[2].

By using the above value of $k$ and taking $n=2$, the values of $M'/M_w$ are calculated to be 0.5 or 1 : 2, which corresponds to the composition $NaH_2PO_4 \cdot 2H_2O$. It may be concluded that the exchange reaction of the anhydrate prepared at 130°C proceeds through the formation of dihydrate.

The existence of monohydrate of sodium dihydrogen phosphate is known, but the formation of monohydrate was not observed under the condition of the experiments. In correspondence with this, the dehydration of dihydrate yielded anhydrate directly; dehydration curves were constructed at 11.0, 20.0 and 28.0°C, but no sign of the formation of monohydrate has been observed. The values of the dissociation pressure obtained from the dehydration curves are 3.84 mmHg at 11.0°C, 7.98 mmHg at 20.0°C, and 14.77 mmHg at 28.0°C. Each of these values is the mean of seven to ten measurements obtained at various stages of dehydration. These values gave a good linear plot of $\log p$ against $1/T$, from which the heat of dissociation of sodium dihydrogen phosphate dihydrate into anhydrate has been calculated to be 13.5 kcal. per mol. $H_2O$. In these experiments, the dissociation pressure was measured by a mercury U-tube manometer (1.8 cm. bore). The temperature was measured by a mercury thermometer graduated in 0.1°C (uncalibrated).

As exemplified by the above results, the exchange reaction in question may be used to determine the composition of the hydrate formed on hydrating an anhydrate or a lower hydrate. Another example may be found in the previous paper[3], where the hydration product of copper sulfate monohydrate was identified by this method with trihydrate or with a mixture of tri- and pentahydrate according to the condition of hydration.

The exchange reaction of the anhydrous phosphate prepared in vacuo was studied at

2) See, for example, V. Gold and D. P. N. Satchell, *Quart. Rev.*, **9**, 51 (1955).

3) N. Okazaki, A. Okumura, and K. Nakagawa, This Bulletin, **45**, 983 (1961).

two temperatures, 11 and 20°C. The increased exchangeability of the phosphate prepared in vacuo as compared with the phosphate prepared at 130°C may be seen in Fig. 1. As in the cases of oxalic acid and copper sulfate, it should be attributed to the exchange reaction between adsorbed water and the phosphate occurring in the extended surface of the latter.

The values of the degree of exchange obtained at 11°C are considerably lower than those obtained at 20°C. It is probably due to the increased adsorption of water in the reaction zone during the preliminary dehydration and the consequent increase in the degree of recrystallization of the dehydration product at the lower temperature.

The values of the ratio of the amount of the anhydrous phosphate which takes part in the exchange reaction to the total amount used, as calculated by the relation,

$$M'/M=(1/k)(\Delta D/D_f)/(M/M_w)$$

are 0.77~1.06 for the specimens of anhydrous phosphate prepared in vacuo at 20°C and 0.63~1.03 for those prepared at 11°C. The values obtained for oxalic acid and copper sulfate[1,3] are 0.71~0.85 and 0.75~1.08, respectively.

The surface to bulk ratio $\beta$ as defined by the deuterium exchange reaction may be calculated by the relation[1],

$$\beta=[(1/k)(\Delta D/D_f)-0.5]/[(M/M_w)-0.5]$$

The values obtained are 0.59~0.71 for the specimens of anhydrous phosphate prepared in vacuo at 20°C, and 0.48 for two specimens prepared at 11°C.

*Racemic Acid Monohydrate.* — Racemic acid monohydrate was prepared from *d*-tartaric acid by the usual method, and purified by repeated crystallization from aqueous solution. The specimens of anhydrous racemic acid were prepared partly by dehydration of monohydrate in vacuo at 20°C, and partly by dehydration at 100°C under atmospheric pressure.

The results are shown in Table I.

Table I. Exchange reaction of anhydrous racemic acid at 20°C

| Specimen | $M/M_w$ | $\Delta D/D_f$ | $M'/M$ | $\beta$ |
|---|---|---|---|---|
| Anhydrous racemic acid prepared in vacuo at 20°C | 1.383 | 2.34 | 0.94 | 0.71 |
| | 1.438 | 2.61 | 0.91 | 0.70 |
| | 1.851 | 3.20 | 0.86 | 0.69 |
| Anhydrous racemic acid prepared at 100°C | 1.120 | 2.22 | | |
| | 1.495 | 2.03 | — | — |
| | 1.591 | 2.27 | | |

As with the other hydrates previously studied, the degree of exchange is independent of the molar ratio in the case of the anhydrous acid prepared at 100°C, and increases with the value of the molar ratio in the case of the anhydrous acid prepared in vacuo at 20°C. The number of exchangeable hydrogen atoms is calculated to be 4, that is, two carboxyl hydrogen and two hydroxyl hydrogen atoms, from the results of the exchange reaction of anhydrous acid prepared at 100°C.

The values of the surface to bulk ratio $\beta$ as defined by the deuterium exchange reaction are calculated by[1],

$$\beta=[(1/2k)(\Delta D/D_f)-1]/[(M/M_w)-1]$$

The values obtained are compared with those of the other hydrates in Table II.

Table II

| Specimen | $\beta$ | Temp. of Dehydration °C |
|---|---|---|
| Anhydrous oxalic acid | 0.60~0.70 | 25 |
| Copper sulfate monohydrate | 0.44~1.10 | 35 |
| Anhydrous sodium dihydrogen phosphate | 0.59~0.71 | 20 |
| | 0.48 | 11 |
| Anhydrous racemic acid | 0.70 | 20 |

It will be seen that the values for four substances are comparable with each other. The copper sulfate monohydrate prepared by dehydration in vacuo at low temperature is known to be amorphous[4], and the dehydration product of oxalic acid dihydrate in the vacuum of electron microscope has also been shown to be amorphous[1]. Though the above ratio does not bear a definite physical significance, yet it would be useful for semi-quantitative discussion. Thus, the similarity of the values of the ratio suggests that the dehydration products of racemic acid, sodium dihydrogen phosphate as well as oxalic acid in vacuo at ordinary temperatures are amorphous, and adds new evidence to the postulate that dehydration of salt hydrates proceeds through the intermediate formation of an amorphous product.

**Effect of Adsorbed Water on the Recrystallization of Amorphous Anhydrous Sodium Dihydrogen Phosphate.**—The anhydrous phosphate prepared in vacuo at 20°C was exposed to water vapor of 2 mmHg in a vacuum system at 11°C for twenty minutes, liquid water maintained at −10°C being used as the source of the vapor. Then, the anhydrous phosphate was isolated from the vapor source, and kept in contact with the adsorbed water at 11°C for definite times. After a given time of contact, the anhydrous phosphate was hydrated with a known amount of water vapor of a definite pressure, and subsequently redehydrated. The water obtained on redehydration was analyzed for its deuterium content.

4) V. Kohlschütter and H. Nitschmann, *Z. physik. Chem.*, Bodensteinfestband, 494 (1931).

As in the case of the oxalic acid, the pressure of the water vapor above the anhydrous phosphate increases during the time of contact of the phosphate with adsorbed water vapor. It may be attributed to the recrystallization of the amorphous phosphate and the consequent desorption of the water vapor. The pressure begins to increase after the induction period of 30 to 40 min., and within a few hours it reaches a maximum value of about 4.8 mmHg which is well above the dissociation pressure of dihydrate (3.8 mmHg at 11°C). The pressure increase begins to decline at about 4 mmHg, which is probably due to the beginning of hydrate formation. After the maximum has been attained, the pressure decreases at first rather rapidly to about 4 mmHg, and then very slowly toward 3.8 mmHg. The amount of water liberated by the phosphate during the period of pressure increase is estimated to be $3\times10^{-4}$ mol. per mol. of the phosphate.

The results of the exchange reaction are shown in Fig. 2. The exchangeability $M'/M$ of the amorphous phosphate decreases with the time of contact of the phosphate with water vapor, while in the absence of water vapor the exchangeability decreases only slightly.

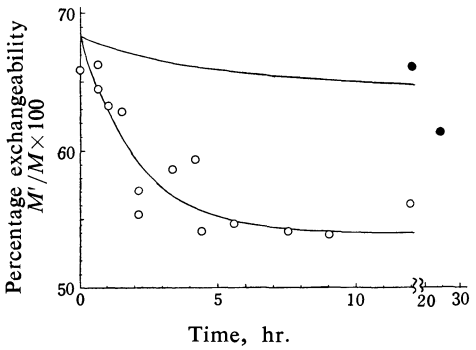



Fig. 2. Decrease in the exchangeability of amorphous anhydrous sodium dihydrogen phosphate due to recrystallization under the catalytic action of water vapor. $M/M_w=1.25$. Solid circle; in the absence of water vapor. Open circle; in the presence of water vapor.

It appears that catalysis of the recrystallization of highly dispersed dehydration intermediate by adsorbed water is of general occurrence.

The process of recrystallization may be visualized as dissolution of the energy-rich anhydrate into adsorbed water; that is, the formation of two-dimensional solution and recrystallization from it of crystalline anhydrate. Below a particular concentration of this two-dimensional solution, it comes to be in equilibrium with hydrate instead of anhydrate, that is, nucleation of hydrate begins. Thus, according to this view, the relation of recrystallization to nucleation of hydrate would be analogous to the relation of anhydrate to hydrate, each in equilibrium with its saturated solution.

**Deuterium Exchange Reaction between Unhydrated and Hydrated Phosphate in Partially Hydrated Amorphous Sodium Dihydrogen Phosphate.** — Anhydrous phosphate prepared by dehydration in vacuo at 20°C was hydrated with heavy water vapor of 9 mmHg pressure and left for a given time at 15°C. Then, it was dehydrated in vacuo at 20°C, and the water obtained was analyzed for its deuterium content.

The results are shown in Fig. 3. As in the case of oxalic acid, the degree of exchange $M'/M$ of the phosphate increases with the time

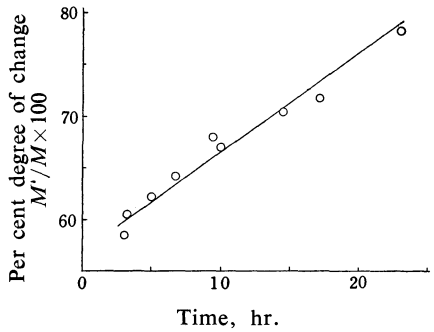



Fig. 3. Progress of deuteration of sodium dihydrogen phosphate in partially hydrated state.

during which the phosphate has been kept in the partially hydrated state. The increase is probably due to the deuteration of the primary phosphate ions in the interior of the crystallites. A possible mechanism of this process has been suggested with reference to the exchange reaction of oxalic acid[1].

## Summary

In order to examine the generality of the results obtained with oxalic acid, the following questions were studied with sodium dihydrogen phosphate and in part with racemic acid: (1) the relation between the deuterium exchange reaction and the surface area of the anhydrate, and the amorphous character of the anhydrate prepared by dehydration in vacuo at low temperatures, (2) recrystallization of the amorphous anhydrate under the catalytic action of adsorbed water, and (3) deuterium exchange reaction in anhydrate-hydrate mixture.

The results obtained with sodium dihydrogen phosphate and racemic acid are similar to those obtained with oxalic acid. It appears that formation of amorphous anhydrate in the dehydration of crystal hydrate in vacuo at low

temperatures and its recrystallization under the catalytic action of adsorbed water are phenomena of general occurrence.

The deuterium exchange reaction of crystalline anhydrate may be used to determine the composition of the hydrate formed on hydrating an anhydrate under a given condition.

The authors wish to thank Mrs. M. Kitora and Mrs. Y. Sawanobori for their assistance in part of this work.

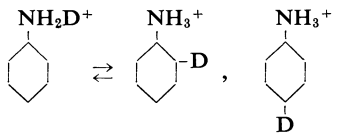
*Department of Chemistry*
*Nara Women's University*
*Nara*

# *The Rearrangement of N-Deuterated Aromatic Amine Hydrochloride into its Ring-deuterated Analogue in the Solid Phase: The Rearrangements of o- and m-Toluidine Hydrochlorides and the Effect of Anions on the Rate of Rearrangement of Anilinium Salts*

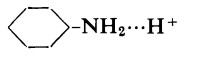
By Nobukazu Okazaki and Akiko Okumura

(Received November 18, 1960)

When aniline hydrochloride-*N*-*d* is heated at about 150°C or above, it rearranges into its ring-deuterated analogues[1]



The reaction may as well be regarded as the deuterium exchange reaction between the $NH_3^+$ group and the benzene nucleus in aniline hydrochloride. The rearrangement occurs well below the melting point of the hydrochloride. The deuterated positions of the benzene nucleus have been determined by the reverse rearrangement of *o*,*p*-trideuterio-aniline hydrochloride to be the ortho and the para positions[1b]. It has been suggested that the mechanism of this rearrangement is an electrophilic substitution as in the case of the liquid phase deuteration of aromatic nucleus by acidic deuterating agents[2], and that anilinium ion acts as proton acceptor at least in the state of partial dissociation in the solid phase,



Further study of this rearrangement with *p*-toluidine hydrochloride[3] has shown that the number of nuclear hydrogen atoms which take part in the rearrangement is 2, probably ortho positions, when the rearrangement takes place in the solid phase, and 4, probably ortho and meta positions, when the rearrangement takes place in the molten phase. This qualitative difference in exchange equilibria suggests that different mechnisms are responsible for the exchange reaction in the solid and for that in the molten phase, and serves to exclude the possibility that the exchange reaction in the solid phase might be caused by local melting due to the presence of a small amount of moisture or other contaminations.

The purpose of the present work is to supplement the earlier results with the study of the exchange reaction of *o*- and *m*- toluidine hydrochloride and with the comparative study of the rate of rearrangement of aniline hydrochloride and hydrobromide, in the hope of approaching the elucidation of the mechanism of this rearrangement.

## Experimental

**Materials.**—Commercial *o*-toluidine (extra pure reagent) was first treated with oxalic acid in order to exclude the possible contamination with para isomer. After repeated distillations, it was neutralized with hydrochloric acid (special grade reagent), and recrystallized twice from water.

*m*-Toluidine was synthesized partly from *p*-toluidine and partly from benzaldehyde by the usual methods. It was acetylated, and the aceto-toluidide obtained was purified by repeated recrystallization from water. Then the amine was again set free, distilled repeatedly and neutralized with hydrochloric acid. The hydrochloride was recrystallized from water twice (m. p. 215.5~216.0°C, corrected).

1) a) M. Harada and T. Titani, This Bulletin, **11**, 554 (1936). b) N. Okazaki, *J. Chem. Soc. Japan*, **62**, 52 (1941); N. Okazaki and M. Koizumi, This Bulletin, **16**, 371 (1941).

2) C. K. Ingold, C. G. Raisin and C. L. Wilson, *J. Chem. Soc.*, **1936**, 1637.

3) N. Okazaki and J. Kuroda, *J. Chem. Soc. Japan, Pure Chem. Sec.* (*Nippon Kwagaku Kwaisi*), **62**, 57 (1941); This Bulletin, **11**, 417 (1941).

Commercial aniline (special grade) was neutralized with hydrochloric acid, and the salt solution was treated with steam to remove the possible contamination with nonbasic compounds. Then the amine was again set free, distilled repeatedly, and neutralized with hydrochloric acid (special grade) or redistilled hydrobromic acid (first grade). The salts were recrystallized three times from alcohol.

**Procedure.** — The experimental procedures are almost the same as those described in the earlier paper[1b]. A known amount of *N*-deuterated anilinium or toluidinium salt which was prepared by the exchange reaction with heavy water (ca. 1%) and dried in a vacuum desiccator over phosphorus pentoxide, was sealed in vacuo in a glass tube, and heated for a definite time in a vapor bath of organic liquid.

The relation between the initial and equilibrium deuterium contents, $D_i$ and $D_e$, of the $NH_3^+$ group of the salt is given by

$$nk=3(D_i-D_e)/D_e$$

where $k$ is the deuterium partition coefficient between the $NH_3^+$ group and the benzene nucleus, $n$ is the number of the nuclear hydrogen atoms which take part in the exchange reaction.

As the value of $k$ may be taken to be nearly unity, the number $n$ of exchangeable hydrogen atoms of the benzene nucleus may be judged readily from the value of $nk$.

The value of $\alpha$ defined by an analogous relation,

$$\alpha=3(D_i-D_t)/D_t$$

may be used to follow the exchange reaction, where $D_t$ is the deuterium content of $NH_3^+$ group at time $t$. At equilibrium $\alpha$ is equal to $nk$.

The deuterium content of the $NH_3^+$ group was determined by equilibrating the salt with water of known amount and known deuterium content at low temperature (ca. 60°C or below). The deuterium content of the equilibrated water was measured by the floatation method, the proportionality of the deuterium atom fraction of heavy water to its excess density being assumed.

**Kinetic Formula.**—If it is assumed that the rate of the deuteration of ortho and para positions of anilinium salt may be described by one and the same rate constant, the reaction may be treated as a first order reversible reaction with respect to the deuterium content. The appropriate rate equation is

$$k_1=(kD_e/tD_i)\ln((D_i-D_e)/(D_t-D_e))$$

where, $k_1$ is the first order rate constant of the deuterium exchange reaction between $NH_3^+$ and aromatic nucleus, or the rate of the corresponding hydrogen exchange in undeuterated salts.

In terms of $\alpha$, defined above, the rate equation becomes,

$$k_1=(2.303/t)(k/k+1)\log((\alpha+3)/(3-(\alpha/k)))$$

## Results and Discussion

**I. The Rearrangements of *o*- and *m*-Toluidine Hydrochlorides.**—Fig. 1 shows the rates of the exchange reactions, expressed by the value of $\alpha$ after one hour from the start of the exchange reaction, of *o*- and *m*-toluidine hydrochlorides at various temperatures. For comparison, the rate-temperature curves of aniline and *p*-toluidine hydrochlorides are also shown. In the latter salt, the rate is expressed by the value of $\alpha$, after 3.5 hr. from the start of the reaction.

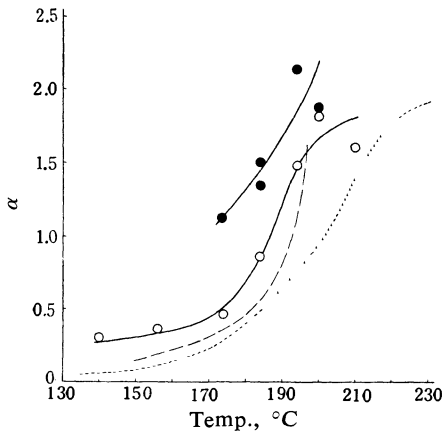



Fig. 1. Rearrangement of aniline and toluidine hydrochlorides at various temperatures. ●, *m*-Toluidine hydrochloride; ○, *o*-Toluidine hydrochloride; – – –, Aniline hydrochloride; ------, *p*-Toluidine hydrochloride

The exchange reaction of *o*-toluidine hydrochloride is measurable even at 140°C (ca. 75°C below its melting point). Apart from the exchange reaction of *m*-toluidine hydrochloride in which the methyl group cooperates with the amino group to facilitate the deuteration of the ortho and the para positions to the amino group, the ease of the exchange reactions of the hydrochlorides is in the order,

*o*-toluidine hydrochloride
> aniline hydrochloride
> *p*-toluidine hydrochloride

This corresponds to the reverse of the order of the basic dissociation constants of the amines at ordinary temperature (the values of $K_B$ are $3\times10^{-10}$, $5\times10^{-10}$ and $2\times10^{-9}$ at 25°C, respectively[4]), or to the order of the acid strengths of their conjugate acids, *o*-toluidinium, anilinium and *p*-toluidinium ions. This order of the acid strengths of the conjugate acids would probably hold even at the temperatures of the rearrangement. Thus, the ease of the exchange reaction increases with the increasing proton releasing power of the $NH_3^+$ group for the aromatic nuclei of comparative reactivities.

This fact serves to confirm the earlier view that the mechanism of this exchange reaction is an electrophilic substitution, and that anili-

4) Landolt, "Physikalisch-chemische Tabellen", Bd. II, 5te Auflage, P. 1160.

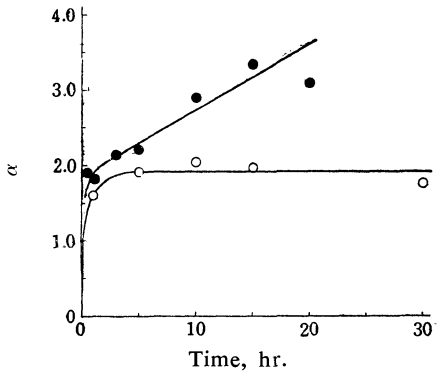



Fig. 2. Difference of equilibria between the exchange reactions of *o*-toluidine hydrochloride in the solid phase and in the liquid phase. ○, 210°C (solid phase), ●, 224°C (liquid phase)

nium or toluidinium ion acts as a proton acceptor at least in the state of partial dissociation. This is also a necessary condition for the $NH_3^+$ group to act as a proton donator.

Figure 2 shows the variation of the value of $\alpha$ with time for *o*-toluidine hydrochloride. At 210°C (below the melting point of the hydrochloride), the value of $\alpha$ reaches the equilibrium value of about 2 in less than five hours, but does not exceed 2 even after thirty hours. On the other hand, at 224°C (above the melting point of the hydrochloride) the value of $\alpha$ definitely exceeds 2 after three hours, and increases steadily towards the equilibrium value of probably 4.

The equilibrium values of $\alpha$ for the exchange reaction of *m*-toluidine hydrochloride at 200 and 218°C are shown in Table I, the melting point of the hydrochloride being 216°C.

Table I. The equilibrium values of $\alpha$ for the exchange reaction of *m*-toluidine hydrochloride at 200 and 218°C

| Temp. °C | Time hr. | *nk* | Temp. °C | Time hr. | *nk* |
|---|---|---|---|---|---|
| 200 | 5 | 2.54 | 218 | 10 | 4.20 |
| 200 | 7 | 2.82 | 218 | 15 | 4.32 |
| 200 | 10 | 2.59 | 218 | 20 | 4.07 |

Table I shows that three hydrogen atoms are exchangeable in the solid phase exchange reaction, and four hydrogen atoms take part in the liquid phase exchange.

If it were assumed that these differences in the *nk* values are due to the effect of temperature on the rate of exchange of the third or the fourth nuclear hydrogen atoms, then it should follow that, for the rearrangement of *o*-toluidine hydrochloride, the rate of this exchange at 224°C is at least ten times as fast as the rate at 210°C, and the exchange reaction is associated with an improbably large activation energy of 80 kcal. or more. The difference can not of course be attributed to the ordinary effect of temperature on the exchange equilibria. Therefore, these differences in the values of *nk* should be due to the difference of the mechanism between the solid phase and the liquid phase exchanges.

The values of *nk* found with hydrochlorides of aniline and toluidines are as follows;

| | Below the m.p. | Above the m.p. |
|---|---|---|
| Aniline hydrochloride | 3(ortho, para) | — |
| *o*-Toluidine 〃 | 2 | — |
| *m*-Toluidine 〃 | 3 | 4 |
| *p*-Toluidine 〃 | 2 | 4 |

The results are reasonably interpreted in terms of the assumption that only the ortho and the para positions of the benzene nucleus are reactive in the solid phase exchange reaction, and in the liquid phase meta positions are deuterated slowly. This lends support to the view that the mechanism of this reaction is an electrophilic substitution. The deuteration of meta positions in the liquid phase exchange may be due to toluidinium ions acting as proton acceptors. The fact that in the solid phase deuteration occurs exclusively at ortho and para positions, requires that the proton acceptor in this exchange reaction should be the molecules of toluidine or the toluidinium ions at least in the state of partial dissociation.

The crystals of toluidine hydrochlorides are probably composed of toluidinium ions and chlorine ions, by analogy with the crystals of aniline hydrochloride[5] and hydrobromide[6]. In view of this fact, it is rather surprising that meta positions are not deuterated in the solid phase exchange. Two mechanisms are possible for the exchange reaction; intermolecular and intramolecular mechanisms.

If the exchange reaction in the solid state occurs intermolecularly, probably through the intervention of lattice imperfections, for example, between two toluidinium ions, the absence of meta deuteration requires that, whenever two toluidinium ions react, the proton-accepting toluidinium ion as well as the donating one should be at least in the state of partial dissociation. This is equivalent to the requirement that almost all of the toluidinium ions in the crystal should be at least in the state of partial dissociation at the temperatures of the rearrangement, which seems improbable. The presence of an appreciable amount of toluidinium ions would make

5) J. C. Brown, *Acta Cryst.*, **2**, 228 (1949).
6) I. Nitta, T. Watanabe and I. Taguchi, *X-rays* (*Japan*), **5**, 31 (1948).

the meta deuteration observable. Moreover, if the toluidinium ions in the crystal were in the state of partial dissociation to any extent which makes the meta deuteration unobservable, they would at least remain so in the liquid phase, and the meta deuteration should be unobservable even in the liquid phase.

An alternative mechanism is an intramolecular shift of proton from the $NH_3^+$ group along the $\pi$-electron cloud of the benzene nucleus (formation of $\pi$-complex or the like) to the positions of the attack. In this case, the toluidinium ions react necessarily in the dissociated state, and the exclusive deuteration of ortho and para positions may be readily explained.

In the liquid phase, increased degrees of freedom of molecular motion would allow the toluidinium ions to collide with the proton donating species, and deuteration of meta positions takes place.

**II. The Rates of Rearrangement of Aniline Hydrochloride and Hydrobromide.** — The intramolecular character of the rearrangement of aromatic amine hydrochlorides being accepted, it is interesting to see whether the rate of rearrangement differs with the nature of the anion. As the rearrangement in the solid phase occurs in the nearly ordered arrangement of ions on which information is available from X-ray crystal analyzes[5,6], it would be suited for the study of the role of anions.

Figure 3 shows the variations of $\alpha$ with time for various temperatures for the rearrangement of aniline hydrochloride. Figure 4 is the corresponding figure for aniline hydrobromide. It will be seen that the rearrangement of the hydrochloride is considerably faster than that of the hydrobromide.

The equilibrium values of $\alpha$ are 2.72 and 2.37 for the hydrochloride and the hydrobromide respectively, the effect of temperature on the

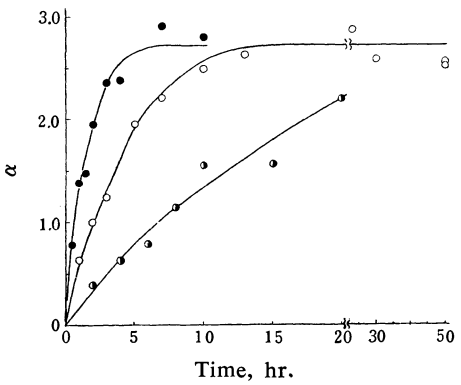



Fig. 3. Variation of $\alpha$ with time for the rearrangement of *N*-deuterio-aniline hydrochloride. ●, 194°C ○, 184°C ◑, 173°C

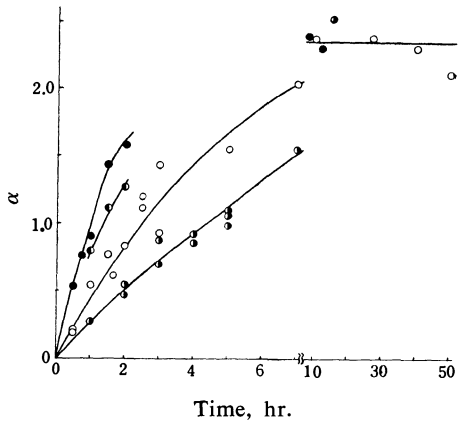



Fig. 4. Variation of $\alpha$ with time for the rearrangement of *N*-deuterio-aniline hydrobromide. ●, 225°C ◐, 222°C ○, 218°C ◑, 211°C

exchange equilibria being neglected. From this value, the number of the nuclear hydrogen atoms of the hydrobromide which take part in the exchange reaction may be determined as 3. The positions of these hydrogen atoms are probably ortho and para by analogy with the result obtained with the hydrochloride[1b]. The values of the partition coefficients $k$ are $0.90_1$ and $0.79_0$ for the hydrochloride and the hydrobromide. It cannot be decided whether the difference is real or due to some experimental errors.

The first order plots of the rearrangement of the hydrochloride and the hydrobromide are shown in Figs. 5 and 6.

The linearity of the plots is not quite satisfactory. This is at least partly due to the

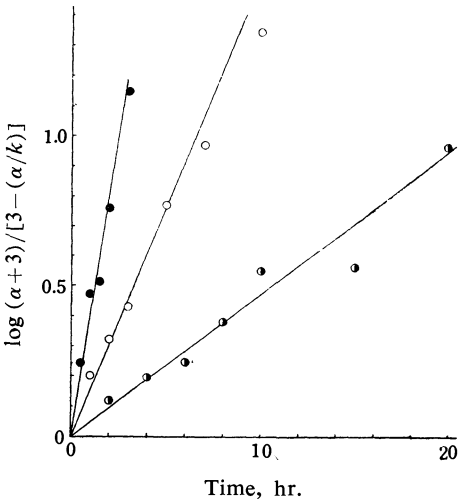



Fig. 5. First order linear plot for the rearrangement of *N*-deuterio-aniline hydrochloride. ●, 194°C ○, 184°C ◑, 173°C

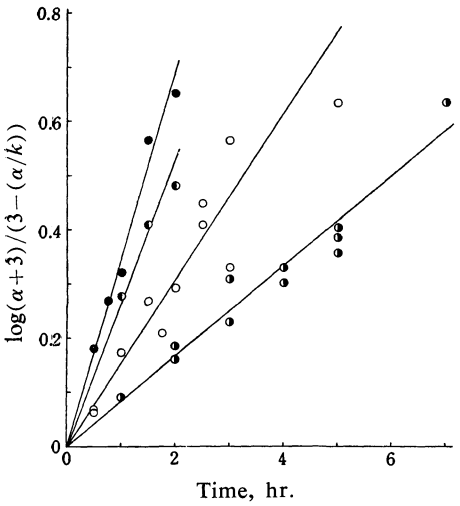



Fig. 6. Fist order linear plot for the rearrangement of *N*-deuterio-aniline hydrobromide.
●, 225°C ◐, 222°C ○, 218°C ◑, 211°C

indirect nature of the deuterium analysis (equilibration with water), and to the complicated sequence of operations. It is possible that the departure of the plots from linearity is partly caused by the failure of the assumption that the deuteration of the ortho and the para positions is characterized by the same rate constant.

Figures 7 and 8 are the Arrhenius plots. The Arrhenius parameters were determined by the method of least squares. The results are;

$$k_1^{Cl}(sec^{-1}) = 10^{16.7}\exp((44000\pm1200)cal./\boldsymbol{RT})$$

and

$$k_1^{Br}(sec^{-1}) = 10^{16.3}\exp((46000\pm2000)cal./\boldsymbol{RT})$$

for aniline hydrochloride and hydrobromide, respectively.

The entropies of activation were calculated by the equation, $A = e\cdot(kT/h)\cdot\exp(\Delta S/R)$, to be 15 and 13 cal./deg. for the hydrochloride and the hydrobromide.

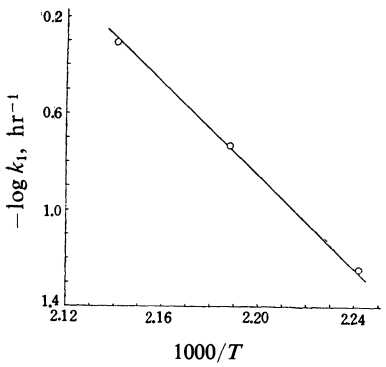



Fig. 7. Arrhenius plot for the rearrangement of *N*-deuterio-aniline hydrochloride.

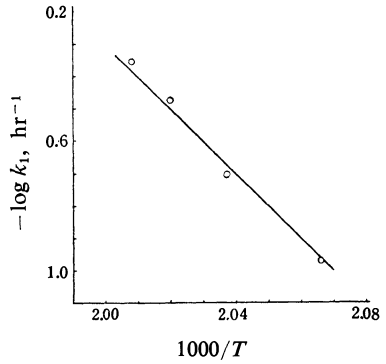



Fig. 8. Arrhenius plot for the rearrangement of *N*-deuterio-aniline hydrobromide.

Owing to the errors in the determinations of the rate constants, the accuracy of the absolute magnitudes of the energies and the entropies might not be claimed, but the order of magnitude of these values is probably correct, and they would be sufficient for the purpose of comparison.

These is no other example of the deuterium exchange reaction in the solid state to be compared with the present results. In pure liquid phase, the deuterium exchange reactions of phenol[7] and of *o*-cresol[8] have been studied. The reactions proceed through bimolecular mechanism. The values of activation energies are 34.8 kcal. for the exchange reaction of phenol and 23 kcal. for that of cresol. The value of the frequency factor for the exchange reaction of phenol is $10^{9.49}$. Comparison of these results with the present ones suggests that there is a difference in the mechanisms of nuclear deuteration between the two cases. As suggested above, the rearrangement probably proceeds through the intramolecular shift of protons from $NH_3^+$ groups to aromatic nuclei, where they attack the carbon atoms with higher electron densities. The protons leaving the $NH_3^+$ groups will move along the $\pi$-electron clouds to the nuclei, or they will combine with the halide ions to form transient molecules of hydrogen halide. The latter process is the necessary preliminary to the sublimation of the amine hydrochloride, which becomes marked side by side with the rearrangement with increasing temperature. Thus, the protons of the anilinium ions would be in a relatively free to-and-fro movement between $NH_3^+$ groups, $Cl^-$ ions, and aromatic nuclei, at high temperatures. In the course of these movements, they will come across the ortho and the para

7) A. I. Brodskii and I. I. Kukhtenko, *Zhur. Fiz. Khim.*, **25**, 920 (1951); *Chem. Abstr.*, **47**, 3814f.
8) I. I. Kukhtenko, *Doklady Akad. Nauk, S. S. S. R.*, **93**, 487 (1953); *Chem. Abstr.*, **49**, 3054.

positions and happen to attack the nuclear carbon atoms. The reaction may be formulated as,

$$C_6H_5NH_2D^+ \overset{K}{\rightleftarrows} C_6H_5NH_2+D^+(\cdots X)$$

$$C_6H_5NH_2+D^+(\cdots X) \overset{k_0}{\rightarrow} C_6H_4D\cdot NH_2+H^+(\cdots X)$$

where, $H^+(\cdots X)$ may be the proton attached to the aromatic nucleus (formation of $\pi$-complex), or it may be the transient molecule of hydrogen halide, or some form of proton which is in a relatively free state.

According to the above scheme, the first order rate constant $k_1$ of the deuterium exchange, or the rate of hydrogen exchange between $NH_3^+$ and aromatic nucleus of undeuterated salt, may be expressed as,

$$k_1=k_0(H^+)(C_6H_5NH_2)=k_0K(C_6H_5NH_3^+)$$

Therefore, the Arrhenius parameters obtained from the temperature dependence of $k_1$ contain, besides those of the rate-controlling step, the contributions from the energy and the entropy of the dissociation of the preequilibrium step, which by the nature of the reaction should have rather large positive values. Thus the large activation energies and large positive entropies of the rearrangement of anilinium halide may be interpreted qualitatively in terms of the above scheme.

The similarity of the Arrhenius parameters between the rearrangement of the two salts suggests that the role of anion in this reaction should be only subsidiary and the mechanism of the rearrangement involves primarily the anilinium ion alone, which is consistent with the intramolecular mechanism.

The difference of the rate of rearrangement between the two salts seems to be chiefly due to the difference in the activation energies, and it should be attributed to the effect of anions.

The results of X-ray crystal analysis[5,6] show that the $NH_3^+$ group is coordinated by four bromine ions, two at a distance of 3.48 Å and the other two at 3.65 Å, in the crystal lattice of the hydrobromide, and by three chlorine ions at a distance of 3.16 Å in that of the hydrochloride. The difference in the N–X distances is greater than that of the ionic radii of the halide ions, and it is expected that the chlorine ion exerts a more powerful polarizing effect upon the N–H bond. Thus, the protons of the $NH_3^+$ groups would be more loosened in the hydrochloride than in the hydrobromide in the initial state of the reaction, and this difference would contribute to the lowering of the energy of activation.

The distances between the halide ions and the ortho and the para carbon atoms may be calculated from the data of the X-ray crystal analyzes. The shortest distances are 3.87 Å for ortho and 3.98 Å for para carbon atoms in the crystal lattice of the hydrobromide, and 3.53 and 3.85 Å for ortho and para carbon atoms in that of the hydrochloride, the sum of van der Waals radii being 3.80 and 3.65 Å for hydrobromide and hydrochloride, respectively. It might be expected that the presence of the negatively charged anions in the neighborhood of the reaction centre would stabilize the positively charged activated complex. And, if it is the case, the extent of stabilization would also be in favor of the chlorine ions.

## Summary

The rearrangement of *N*-deuterated aromatic amine hydrochloride into its ring-deuterated analogues has been studied in the solid and the liquid phases with *o*- and *m*-toluidines, and studied kinetically with anilinium chloride and bromide at 173~194°C and at 210~225°C, respectively.

The ease of the rearrangement of the hydrochlorides in the solid phase is in the order,

*o*-toluidine hydrochloride
> aniline hydrochloride
> *p*-toluidine hydrochloride

which is the reverse of the order of the basic dissociation constants of the amines at 25°C. *m*-Toluidine hydrochloride is more reactive than *o*-toluidine hydrochloride.

The numbers of nuclear hydrogen atoms which take part in the rearrangement are, 2 in the solid phase and >3 in the liquid phase rearrangement of *o*-toluidine hydrochloride, and for *m*-toluidine hydrochloride 3 and 4 in the solid and the liquid phases respectively. This result, taken in conjunction with the earlier ones with aniline and *p*-toluidine hydrochlorides, confirms the view that in the solid phase rearrangement the ortho and the para positions are exclusively deuterated, and in the liquid phase deuteration of the meta positions takes place.

The rearrangement of the anilinium salts is characterized by high activation energy (ca. 45 kcal.) and large positive entropy of activation (ca. 15 cal./deg.).

These results are reasonably interpreted by the intramolecular electrophilic mechanism.

A small difference of the activation energies between the rearrangement of the two anilinium salts (ca. 2 kcal.) may be explained in terms of the different polarizing effects of the halide ions on the initial state and possibly also on the activated complex.

The authors wish to thank Professor T. Titani, Tokyo Metropolitan University, for his interest and advice.

*Department of Chemistry*
*Nara Women's University*
*Nara*

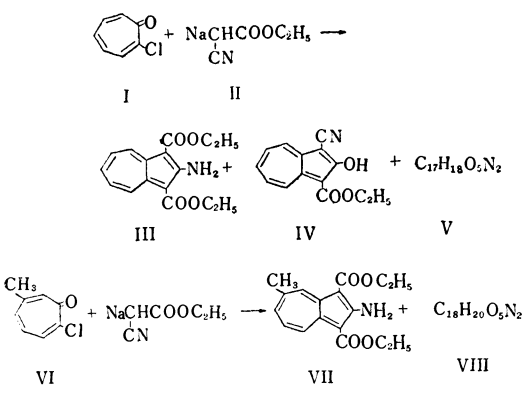
# *The Structure of the Condensation Products of Troponoids and Ethyl Cyanoacetate*

By Shingo MATSUMURA

(Received December 2, 1960)

Nozoe and his co-workers have already reported that the condensation of 2-chlorotropone (I) and ethyl sodiocyanoacetate (II) formed 2-amino-1, 3-diethoxycarbonylazulene (III), 1-cyano-2-hydroxy-3-ethoxycarbonylazulene (IV), and a structurally unknown compound (V) of m. p. 137°C, whose analytical values correspond to the molecular formula of $C_{17}H_{18}O_5N_2$[1].

Similar condensation was carried out by Akino[2] on 2-chloro-6-methyltropone (VI) and he observed the formation of 2-amino-1, 3-diethoxycarbonyl-5-methylazulene (VII) and a compound (VIII) of m. p. 103°C, whose analytical values agree with $C_{18}H_{20}O_5N_2$.




Examinations were made on the structure of V and VIII.

The ultraviolet absorption spectra[3] of V and VIII, shown in Fig. 1, are very similar to each other and the two compounds are assumed to have a common skeletal structure.

V and VIII easily form picrates melting at 215 and 196°C, respectively. The infrared ab-

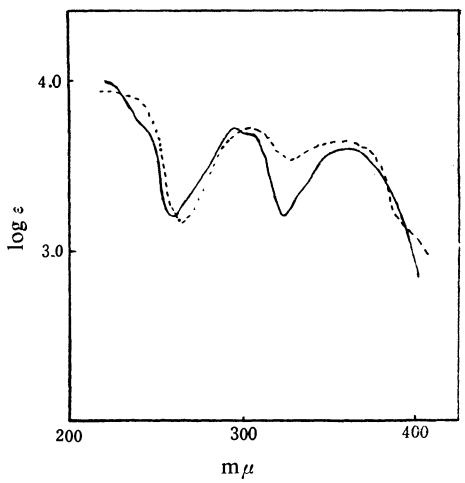



Fig. 1. Ultraviolet absorption spectra in methanol.
—— V, ---- VIII

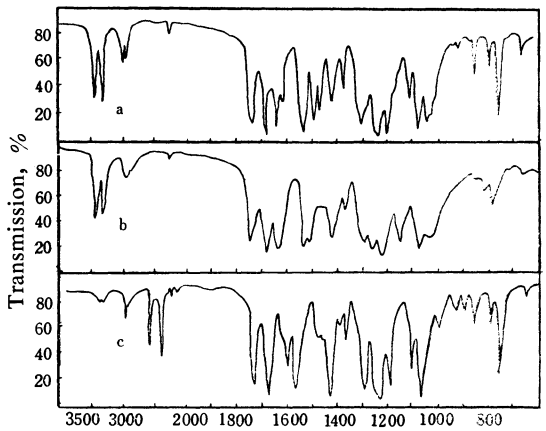



Fig. 2. Infrared absorption spectra in KBr disk.
a V, b VIII, c XIII

1) T. Nozoe, S. Seto, S. Matsumura and T. Asano, *Proc. Japan Acad.*, 32, 339 (1956).
2) H. Akino, to be published.
3) Ultraviolet spectra were measured with a Hitachi EPU-2A spectrophotometer by Mr. F. Sato of this Institute, to whom the author is deeply indebted.

sorption spectra[4] of V and VIII are shown in Fig. 2, a and b.

The infrared spectrum of V exhibits absorption bands at 3455 and 3323 $cm^{-1}$ for the primary amino or hydroxyl and imino group, at 2260 $cm^{-1}$ for cyano group, at 1735 $cm^{-1}$ for ester carbonyl, at 1678 $cm^{-1}$ for ester carbonyl conjugated with unsaturated bond, and at 1635 $cm^{-1}$ for absorption due to the deformation vibration of N-H group. Similar bands are found in the spectrum of VIII.

When V is warmed with dilute hydrochloric acid in ethanol for a short period, colorless crystals (IX), m. p. 93°C, are obtained. IX is also obtained on decomposition of the picrate of V with sodium hydrogencarbonate solution. Analytical values of IX agree with $C_{12}H_{10}O_4$.

The reaction of V with dilute acid for 4 hr. affords colorless crystals (X), m. p. 188°C, which are also formed on treatment of IX with dilute acid. X is an acid substance since it dissolves in sodium hydrogen carbonate solution. Analytical values of X correspond to the molecular formula of $C_{10}H_6O_4$. The ultraviolet absorption spectra of IX and X, shown in Fig. 3, are similar to the absorption curves of coumarin derivatives. Thermal decomposition of X produces colorless crystals (XI), m. p. 68°C, with an aroma. The ultraviolet absorption spectrum of XI (Fig. 3) and its melting point is identical

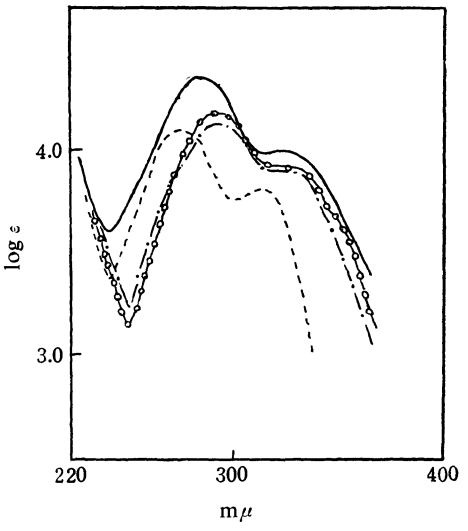
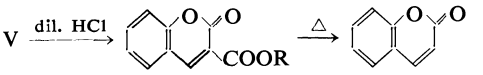



Fig. 3. Ultraviolet absorption spectra in methanol.

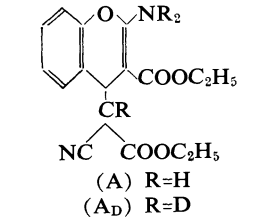
-o-o IX, -·-· X, ---- XI, —— XV

with that of coumarin and on admixture it is confirmed that XI is coumarin.

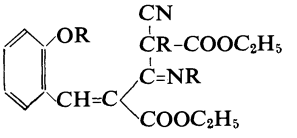
Consequently, IX is 3-ethoxycarbonylcoumarin and X is 3-carboxycoumarin. The melting points of IX and X are in good agreement with those reported in the literature.



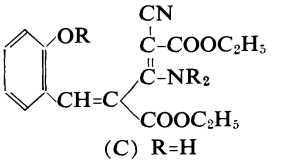

From these experimental results, formulae A, B, C and D are taken into consideration for the structure of V.



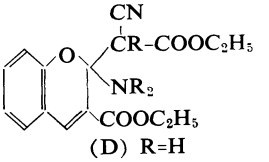

(A) R=H
($A_D$) R=D




(B) R=H
($B_D$) R=D




(C) R=H
($C_D$) R=D




(D) R=H
($D_D$) R=D

If formula A is correct, its ultraviolet absorption should be similar to that of *o*-alkylphenol[5]. However, V has absorption maxima at 296 and 365 mμ, differing from those of *o*-alkylphenols, so that the structure of V is not A.

The formulae B, C and D are tautomeric.

Baron[6] prepared a dimer (XII) by condensation of two molecules of ethyl cyanoacetate and gave the ketimine-type structure alone for XII, but it should also take a tautomeric amino-type structure. The infrared spectrum

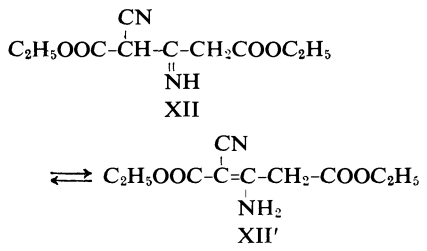
4) Infrared spectra were measured with a Perkin-Elmer Model 21 double beam spectrophotometer by Mr. S. Aono of this Institute, to whom the author is deeply indebted.

5) H. F. Hunter, R. A. Morton and A. T. Carpenter, *J. Chem. Soc.*, **1950**, 441.

6) H. Baron, ibid., **85**, 1736 (1904).

of XII exhibits absorption bands at 3420 and 3300 $cm^{-1}$ for the primary amino group, at 2215 $cm^{-1}$ for the cyano group conjugated with unsaturated bond, at 1710 $cm^{-1}$ for ester carbonyl, and at 1680 $cm^{-1}$ for ester carbonyl conjugated with unsaturated bond.

These facts indicate that the dimer XII takes the amino form XII′ in crystalline state.



XII



XII′

In analogy with the above, it is more likely that V takes the amino-type C structure rather than the imino-type B. However, the infrared spectrum of V has an absorption for cyano group at 2260 $cm^{-1}$, but not of a cyano group conjugated with unsaturated bond. Moreover there is an absorption due to ester carbonyl not conjugated with unsaturated bond at 1735 $cm^{-1}$. It follows, therefore, that V has the structure of D, i.e. 2-amino-2-(cyano-ethoxycarbonyl-methyl)-3-ethoxycarbonyl-$\alpha$-benzopyrane.

VIII is a methyl derivative of V and the position of the methyl is assumed to be at 7-position, since there is absorption of C–H out-of-plane vibration at 820 $cm^{-1}$ [7].

In order to confirm the formula D for V, the deuterated compound XIII of V was prepared and its infrared absorption spectrum was examined. XIII is obtained by recrystallization of V from 50% dioxane-deuterium oxide mixture. Admixture of XIII and V shows no depression in the melting point and the ultraviolet spectra of two compounds are identical.

The infrared spectrum of XIII (Fig. 2c) shows that the absorption bands at 3455, 3323, 2937, 1635, 1528, 1490, 1418, 1280, 1175, 1037 and 1025 $cm^{-1}$ in V disappear in XIII, and new bands at 2576, 2418, 2160, 1565, 1430 and 1000 $cm^{-1}$ appear in XIII. The absorption bands at 940 and 915 $cm^{-1}$ in V shift to 934 and 900 $cm^{-1}$ with slightly increasing intensity in XIII. The fact that no ring-substitution has occurred by deuteration is proved by the absence of any change in the C–H out-of-plane deformation vibration absorption in V and XIII. If all the deuterable functional groups in B, C and D structures assumed for V have been completely deuterated, the structures $B_D$, $C_D$ or $D_D$ would be possible for XIII. The wave number ratio of 3455 $cm^{-1}$ in V and 2576 $cm^{-1}$ in XIII is 1.34, and that of 3323 $cm^{-1}$ in V and 2418 $cm^{-1}$ in XIII is 1.38. These ratios agree with the usual values of $\nu(N-H)/\nu(N-D)$.

The disappearance of the absorption band at 2937 $cm^{-1}$ and appearance of a new absorption band at 2160 $cm^{-1}$ gives a wave number ratio of 1.36, which agrees with the usual value of $\nu(C-H)/\nu(C-D)$.

The absorption band at 2937 $cm^{-1}$ in V is not due to the stretching absorption of C–H in aromatic ring or that in unsaturated double bond. This indicates that the deuterable hydrogen in the methine group of V has undergone an exchange reaction with deuetrium. Consequently, there should be no absorption band of $\nu(C-D)$ in formula $C_D$ and this formula is excluded.

Mecke et al.[8] examined infrared absorption spectra of phenol and deuterated phenol, and assigned the bands at 1399～1332 and 1230～1180 $cm^{-1}$ for characteristic absorption of $\nu(C-O)$ and $\delta(O-H)$ in phenol. They showed that new absorption bands appeared at 1300 and 980～920 $cm^{-1}$ in deuterated phenol.

There are absorption band at 1370 and 1175 $cm^{-1}$ in V.

The band at 1175 $cm^{-1}$ is active to deuteration but that at 1370 $cm^{-1}$ is inactive. There is no absorption band due to $\delta(O-D)$ at 980～920 $cm^{-1}$ in XIII. The absorption band at 1635 $cm^{-1}$ in V is active to deuteration and this band may be assigned to $\delta(N-H)$. These facts suggest that V takes the formula D and not B.

Bechert[9] obtained a compound XIV of m. p. 140°C by condensation of salicylaldehyde and ethyl cyanoacetate with alkoxide.

Knoevenagel et al.[10] obtained XIV by the use of piperidine in place of alkoxide. Both workers gave the molecular formula of $C_{17}H_{18}O_5N_2$ for XIV.

Since the melting point of XIV is close to that of V and the molecular formula of the two compounds are identical, XIV was prepared by the method of Knoevenagel and its admixture with V showed no depression of the melting point. Further the ultraviolet absorption spectra of the two compounds were found to be identical.

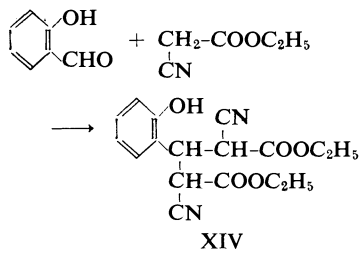
Bechert and Knoevenagel et al. assigned the structure of diethyl-$\alpha,\gamma$-dicyano-$\beta$-(2-hydroxyphenyl)-glutarate as XIV, i.e. V, but this structure cannot explain the ultraviolet and infrared spectral data obtained with V.

7) L. J. Bellamy, "The Infrared Spectra of Complex Molecules", Methuen, London, (1958), p. 65.

8) R. Mecke and G. Rossmy, *Z. Elektrochem.*, **58**, 866 (1955).

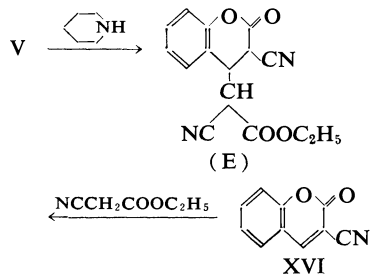
9) C. Bechert, *J. prakt. Chem.*, [2] **50**, 1 (1894).

10) E. Knoevenagel and R. Ornot, *Ber.*, **37**, 4496 (1904).



XIV

Seshadri et al.[11] found that on refluxing XIV in ethanol containing piperidine, a compound XV of m. p. 248°C, was obtained. From the identity of XV with the condensation product of 3-cyanocoumarin (XVI) and ethyl cyanoacetate, they gave the structure of ethyl 3-cyano-3, 4-dihydrocoumarin-4-cyanoacetate (E) for XV.



If Seshadri's assumption is correct, formation of XV from the proposed structure of $\alpha$-benzopyrane derivative for V cannot be explained. Therefore, re-examination was made on the structure of XV. The ultraviolet spectrum of XV, shown in Fig. 3, is similar to that of coumarin derivatives. The infrared spectrum of XV, as indicated in Fig. 4, exhibits absorption at 3410 and 3280 $cm^{-1}$ for the primary amino group, at 2210 $cm^{-1}$ for the cyano group conjugated to unsaturated bond, and at 1710 and 1680 $cm^{-1}$ for lactonic carbonyl and ester carbonyl conjugated with unsaturated bond.

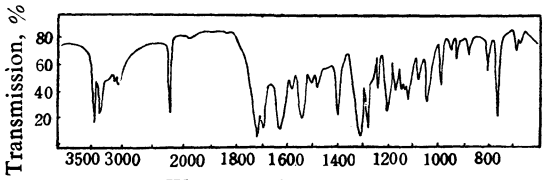
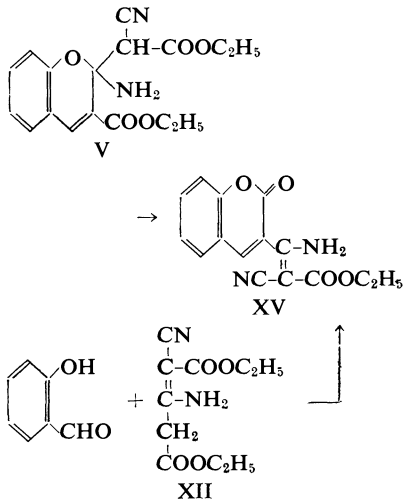



Fig. 4. Infrared absorption spectrum of XV in KBr disk.

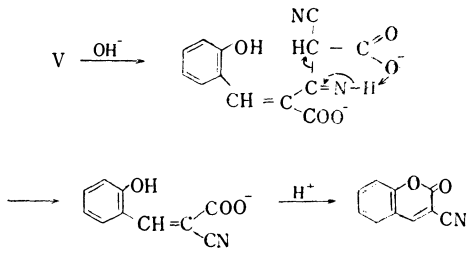
These data suggest that the structure of XV is not E as proposed by Seshadri but must be $\alpha$-amino-$\alpha$-(3-coumarinyl)-$\beta$-cyano-$\beta$-ethoxycarbonylethylene.

Condensation of salicylaldehyde and XII, in the presence of potassium hydroxide or piperidine, affords a compound corresponding to XV.



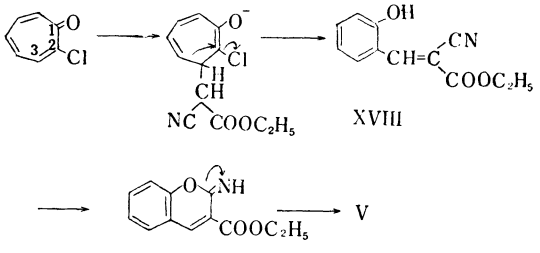
Knoevenagel et al.[10] reported the formation of 2-oxo-$\beta$-phenylpropane-$\alpha$, $\alpha$, $\gamma$-tricarboxylic anhydride (XVII) from V but re-examination of this reaction showed the formation of IX alone and not the compound corresponding to XVII.

It has been found that hydrolysis of V with ethanolic solution of potassium hydroxide produces XVI[9]. This reaction mechanism must be such as is indicated in Scheme 1.



Scheme 1.

This reaction is similar to the mechanism of formation of aromatic nitrile by alkaline hydrolysis of trichloro-aryl-ketimine[12].



XIX

Scheme 2.

11) V. D. N. Sastry and T. R. Seshadri, *Proc. Indian Acad. Sci.*, 16A, 29 (1942); *Chem. Abstr.*, 37, 880 (1943).

12) J. Houben and W. Fisher, *J. prakt. Chem.*, 123, 313 (1929); D. T. Mowry, *Chem. Revs.*, 42, 221 (1948).

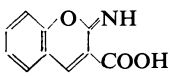
The mechanism for formation of V by the condensation of I and II is illustrated in Scheme 2.

Formation of salicylaldehyde derivatives by nucleophilic attack against tropone derivatives has already been witnessed in the reaction of 2, 7-dihalotropone with alkali[13] or ammonia[14], of 2-halo-7-phenyltropone and 2, 4, 7-tribromotropone[15,16].

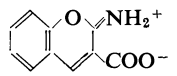
Kitahara[17] assumed a reaction mechanism for this kind of rearrangement reaction in which the nucleophilic reagent attacks the 3-position of the tropone ring.

Formation of V from I is assumed to follow similar rearrangement reaction mechanism.

Formation of an intermediate XIX is supported by the following evidence. Baker et al.[18] found that heating of salicylidenecyanoacetic acid (XX) in ethanol changed it into a substance XXI sparingly soluble in ethanol, and XXI was easily soluble in water and neutralization of its aqueous solution resulted in the formation of X. They therefore assumed for XXI an imino compound like XXIa or an intramolecular salt of imino compound like XXIb.




XXIa




XXIb

## Experimental[19]

**Picrate of V.**—A saturated ethanolic solution of picric acid was added to a solution of 100 mg. of V dissolved in 3 ml. of ethanol and 150 mg. of yellow needles, m. p. 215°C (decomp.), separated out immediately. This picrate undergoes decomposition when heated in ethanol and changes into an easily soluble substance.

Found: C, 49.52; H, 3.91; N, 12.63. Calcd. for $C_{23}H_{21}O_{12}N_5$: C, 49.37; H, 3.75; N, 12.52%.

**Picrate of VIII.**—Yellow needles, m. p. 195~196°C.

Found: N, 12.53. Calcd. for $C_{24}H_{23}O_{12}N_5$: N, 12.21%.

**Reaction of V with Dilute Acids.** — a) A solution of 500 mg. of V dissolved in 10 ml. of ethanol, added with 0.2 ml. of 6 N hydrochloric acid, was boiled for 3 min. and evaporation of ethanol left prismatic crystals. The addition of water to this crystalline residue resulted in the melting of the crystals to form an oily substance which crystallized on standing. Recrystallization from ethanol afforded 250 mg. of colorless prisms (IX), m. p. 92~93°C which showed no depression on admixture with 3-ethoxycarbonylcoumarin.

Found: C, 66.38; H, 4.95. Calcd. for $C_{12}H_{10}O_4$: C, 66.05; H, 4.62%.

b) A mixture of 100 mg. of V in 3 ml. of 2 N hydrochloric acid was refluxed at 100~110°C for 1 hr., by which V dissolved gradually. Water was added to the reaction mixture under cooling and colorless crystals precipitated out. Recrystallization from ethanol afforded 40 mg. of IX.

c) A mixture of 100 mg. of V in 1 ml. of 6 N hydrochloric acid was heated on a water bath for 4 hr., water was evaporated, and the precipitate thereby formed was recrystallized from ethanol, affording 20 mg. of X, m. p. 186~188°C, which showed no depression on admixture with 3-carboxycoumarin.

Found: C, 63.02; H, 3.61. Calcd. for $C_{10}H_6O_4$: C, 63.16; H, 3.18%.

**Formation of Coumarin (X).**—Low-pressure sublimation of 50 mg. of X by heating at 200~230°C produced some crystals with an aroma. Reccystallization of the sublimate from cyclohexane gave colorless plates (X), m. p. 67~68°C, undepressed on admixture with coumarin.

**Deuteration of V.** — V was recrystallized from 50% mixture of dehydrated dioxane and deuterium oxide.

**Formation of α-Amino-α-(3-coumarinyl)-β-cyano-β-ethoxycarbonylethylene (XV).**—A suspension of 100 mg. of V in 1 ml. of ethanol, with 3 drops of piperidine added, was refluxed for 4 hr., by which V dissolved once, and colorless needle crystals began to precipitate out as the reaction proceeded. Recrystallization of these crystals from a large volume of ethanol gave 60 mg. of XV, m. p. 245~246°C.

Found: C, 63.12; H, 4.34; N, 9.85. Calcd. for $C_{15}H_{12}O_4N_2$: C, 63.38; H, 4.26; N, 9.86%.

UV. $\lambda_{max}^{MeOH}$ mμ (log ε): 280 (4.36), 318 (4.0).

**Synthesis of XV.**—A solution of 50 mg. of salicylaldehyde and 100 mg. of XII dissolved in 0.5 ml. of absolute ethanol with 1 drop of piperidine added was allowed to stand at room temperature. The crystals that precipitated out were recrystallized from ethanol and 120 mg. of XV was obtained.

The author takes this opportunity to express his deep gratitude to Professor Tetsuo Nozoe and Professor Shuichi Seto for their unfailing guidance and to Mr. Yusaku Ikegami and Mr. Kyozo Ogura for much helpful advice. Also the author expresses his thanks to Mr. S. Ohyama and Miss A. Iwanaga for the microanalyses.

*The Chemical Research Institute of Non-Aqueous Solutions*
*Tohoku University*
*Katahira-cho, Sendai*

13) S. Seto, *Sci. Repts. Tohoku Univ.*, (I), **37**, 275 (1953).
14) T. Nozoe. S. Seto and T. Sato, *Proc. Japan Acad.*, **30**, 473 (1954).
15) T. Mukai, This Bulletin, **32**, 272 (1959).
16) T. Nozoe, K. Doi and S. Endo, This Bulletin, **33**, 1285 (1960).
17) Y. Kitahara, *Sci. Repts. Tohoku Univ.*, (I), **39**, 250 (1956).
18) W. Baker and A. Lapworth, *J. Chem. Soc.*, **127**, 560 (1925).
19) All melting points are uncorrected.

# *Oxidation of o-Hydroxyphenylacetylene and o, o'-Dihydroxydiphenyldiacetylene by Copper Ion*

By Fumio TODA and Masazumi NAKAGAWA

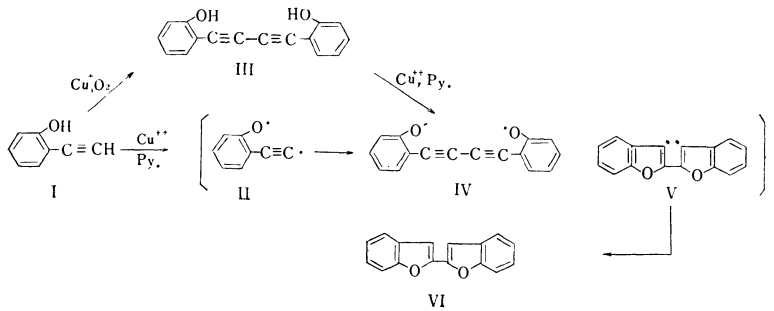
(Received December 9, 1960)

Previously the present authors have reported the quantitative formation of 2, 2'-dibenzofuranyl (VI) by the intramolecular cyclization of *o*, *o'*-dihydroxydiphenyldiacetylene (III) on treatment with basic reagents[1]. It has been found that VI is also formed quantitatively by the photodecomposition of the silver salt of III[2]. It is apparent that the former reaction involves an intramolecular nucleophilic addition of a phenoxide anion to the triple bond and the latter reaction proceeds through a radical intermediate.

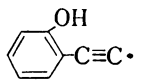
The present paper deals with the formation of VI from *o*-hydroxyphenylacetylene (I) or III by the action of cupric acetate in pyridine. The treatment of I with the conventional cuprous chloride-ammonium chloride coupling reagent in an atmosphere of oxygen yielded the expected product III in a reasonable yield[1]. Unexpectedly, however, an evolution of heat was observed when I was added to a solution of cupric acetate in pyridine which is an excellent reagent of oxidative coupling of ethynyl compound proposed by Eglinton[3], and VI was isolated in a yield of 30% from the reaction mixture together with fairly large amount of an unidentified neutral oily material. A similar treatment of III with the Eglinton's reagent gave VI in quantitative yield. No change was observed when III was treated with pyridine without cupric acetate, in spite of the intramolecular cyclization of III could be caused by a weak base such as sodium carbonate or sodium hydrogen carbonate. Therefore, the presence of cupric ion is essential for the cyclization of III to VI.

Transitory formation of ethynyl radical during the course of oxidation of terminal acetylene by aqueous solution of cupric salt was postulated by Klebanski et al[4]. One electron oxidation of an ethynyl anion by cupric ion results in a transitory radical. Rapid combination of two of the ethynyl radicals forms diacetylenic product. The formation of the ethynyl radical VII seems to be probable in the course of the photochemical transformation of silver acetylide of I into coumarone[5]. Also the appearance of the phenoxyl radical IV seems to be highly probable in an intermediate stage of transformation of the silver salt of III into VI by irradiation[2]. More recently the appearance of phenoxyl radical was confirmed in several instances[6].

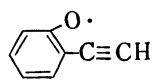
From the above-mentioned consideration, it appears likely that we may conclude that the reaction of I with cupric ion proceeds through the formation of free radical II. The coupling of two of II results in the new radical IV which is the same with the intermediate of the photochemical formation of VI from the silver salt of III. The oxidation of I with cupric ion may produce other radicals such as VII




1) F. Toda and M. Nakagawa, This Bulletin, 32, 514 (1959).
2) F. Toda and M. Nakagawa, ibid., 33, 1287 (1960).
3) G. Eglinton and A. R. Galbraith, *Chem. & Ind.*, **1956**, 737; *J. Chem. Soc.*, **1959**, 889.
4) A. L. Klebanski, I. V. Grachev and O. M. Kustretsova, *Zhur. Obshchei Khim.*, **27**, 2977 (1957).
5) V. Prey and G. Pieh, *Monath. Chem.*, **80**, 790 (1949).
6) A. S. Hay, H. S. Blanchard, G. F. Endres and J. W. Enstance, *J. Am. Chem. Soc.*, **81**, 6335 (1959); G. D. Staffin and C. C. Price, ibid., **82**, 3632 (1960).



VII



VIII

and VIII. Coupling two of VII and subsequent oxidation of the hydroxyl groups may be another route leading I to IV. Cyclization or other side reactions of II, VII and VIII which occur prior to the coupling reaction leading to IV may be responsible for the low yield of VI and the formation of a neutral oily by-product in the reaction of I with Eglinton's reagent.

The great difference between the mode of oxidation of I by the conventional coupling technique employing cuprous salt and that of the one by the Eglinton's procedure is remarkable, because cupric ion produced by the aerial oxidation of cuprous ion is regarded as the oxidizing agent in the former reaction[3] and also the oxidizing agent in the latter process is undoubtedly the same cupric ion. Quite recently, Hay[7] has reported that phenylacetylene and diethynylbenzenes can be coupled rapidly at room temperature with oxygen or air in a pyridine solution containing catalytic amount of cuprous chloride. He pointed out also that cupric carboxylates are catalysts for the reaction but they have far inferior catalytic activity as compared with cuprous salts. The copper ion in these coupling reagents must exist in some form of complex and it seems to be highly possible that the ethynyl compound takes the part of the ligand of the copper complex. Therefore, the marked difference of the oxidizing power of these coupling reagents is associated with the difference of the structure of copper complex formed in the particular reaction mixture.

## Experimental

**Oxidative Coupling of *o*-Hyroxyphenylacetylene by the Eglinton's Method.**—A solution of *o*-hydroxyphenylacetylene (I, 5.0 g.) in ethanol (10 ml.) was added to a deep blue solution of cupric acetate monohydrate (30 g.) in pyridine (65 g.). An appreciable elevation of the temperature of the mixture was observed and the color of the mixture rapidly changed to green. The reaction mixture was stirred for 2 hr. under cooling with running water. Stirring was continued for further 2 hr. at 50°C. After removal of the solvent under reduced pressure the residue was mixed with water and extracted with ether. The ether extract was washed with aqueous solution of cupric acetate and water, successively and dried over sodium sulfate. Tiny colorless needles suspended in an oily liquid were obtained after evaporating the solvent. The crystals were filtered, washed with ethanol and recrystallized from benzene using active charcoal giving colorless needles, m.p. 194.5~195.5°C, 1.5 g. (30%). The substance showed no depression of the melting point on admixture with a genuine sample of 2,2'-dibenzofuranyl (VI)[1].

**Oxidation of *o*, *o'*-Dihydroxydiphenyldiacetylene with the Eglinton's Reagent.**—A mixture of *o*, *o'*-dihydroxydiphenyldiacetylene (III, 0.50 g.), cupric acetate monohydrate (3.0 g.) and pyridine (20 g.) was stirred for 3 hr. at 60°C. The solvent was distilled in vacuo. The residue was mixed with water and extracted with ether. The extract was washed with aqueous cupric acetate and water, successively. The dried solution (over magnesium sulfate) was concentrated, yielding crude crystals, m. p. 194.5~195.5°C, 0.5 g. The crude material was recrystallized from benzene employing active charcoal to give colorless needles, m. p. 194.5~195.5°C, 0.45 g. (90%). This was identified as 2,2'-dibenzofuranyl (VI) by the mixed melting point determination with an authentic specimen of VI[1].

The authors are indebted to the Ministry of Education for a Research Grant. Thanks are also offered to Mr. M. Okumiya for the microanalyses.

*Department of Chemistry*
*Faculty of Science*
*Osaka University*
*Nakanoshima, Osaka*

7) A. S. Hay, *J. Org. Chem.*, 25, 1276 (1960).

# *Aggregation of Ion-exchange Resin Particles*

By Manabu SENŌ and Takeo YAMABE

(Received December 20, 1960)

An ion-exchange resin is a crosslinked polyelectrolyte gel, which dissociates to produce cations or anions. Polystyrenesulfonic acid-divinylbenzene and polyvinylbenzyltrimethylammonium hydroxide-divinylbenzene are a typical cation-exchange resin and a typical anion-exchange resin used now, respectively. These resins exhibit a remarkable swelling behavior when the degree of crosslinking, e. g., the content of divinylbenzene is small[1]. Resins with a high degree of crosslinking scarcely swell at all and, using these resins, researches not on the swelling behavior of resins but on the aggregation behavior are able to be carried out.

The cation- and the anion-exchange resins have negative and positive charges, respectively, in the dissociated states and, therefore, it is expected that the interparticlar interaction exerts itself between two kinds of these resin particles. In practice, it is often observed that such an aggregation takes place in a mixed bed water purification apparatus. In this paper, some observation on the aggregation behavior will be presented. Independently of this investigation, Grubhofer described recently a similar observation[2]. It is believed that this behavior is of interest colloid-chemically and the ion-exchange resins are interesting samples to investigate colloid-chemical phenomena in this respect. Recently, Schenkel and Kitchener used similar particles to test the Derjaguin-Verwey-Overbeek theory[3].

## Experimental

Ion-exchage resins used primarily in this experiment are commercially-available ones, Dowex 50W and Dowex 1, which are strongly acidic and strongly basic polystyrene-based resins with sulfonic acid group or quarternary ammonium group, respectively. In addition, the following resins were used; Amberlite IR-120 (strongly acidic), Amberlite IRA-400 (strongly basic), Amberlite IRC-50 (weakly acidic) and Amberlite IR-4B (weakly basic). The former two are polystyrene-type resins and the later two are polyalkene-type ones with carboxyl acid group and secondary or tertiary amino group, respectively. The $H^+$-form cation exchanger or the $OH^-$-form anion-exchanger is prepared by treating them with hydrochloric acid or sodium hydroxide solution, respectively, after conditioning them several times and washing them thoroughly with deionized water.

The aggregation behavior was observed directly with the naked eye or by microphotography and, as a measure of the degree of aggregation, the sedimentation volumes were measured. About 1 g. of air-dried resins was taken into 20 ml. of suspending media in the sedimentation tube, which is 15 cm. in height and 1.5 cm. in inner diameter. The suspending media were deionized water except when stated otherwise. After being stirred vigorously, the sedimentation tube was settled in the quiescent state overnight at room temperature, 20~25°C, and the sedimentation volume was read. By correcting for the moisture content of resins, the specific sedimentation volume was gained. The moisture content was measured gravimetrically by drying them on phosphorus pentoxide in vacuo.

## Results and Discussion

**Formation of Aggregation.**—Dowex 50W resins of hydrogen-form or Dowex 1 resins of hydroxyl-form, individually, form dense sediments in water, the specific sedimentation volume being 2.6 ml./g., respectively. When both kinds of resins are mixed, remarkable aggregation takes place; very bulky sediment is formed and the specific sedimentation volume is 21 ml./g. (volume fraction of particles in the sediment is 0.04). By observing the microscopic photograph of these systems shown in Fig. 1, it is clear that, although each kind of resins, individually, disperses uniformly, in the mixture of them both resins combine with each other to form agglomerates with large voids.

It is well-known that, the stronger is the attracting interaction between the particles, the larger is the sedimentation volume of the particles. Recently, Vold[4] calculated the sedimentation volume of the colloidal particles whose attracting range extends over a distance $r$ times larger than the particle radius from their surface. According to her calculation, the ion-exchange particles under study now have a range of attraction nearly equal to the particle radius ($r \approx 1$).

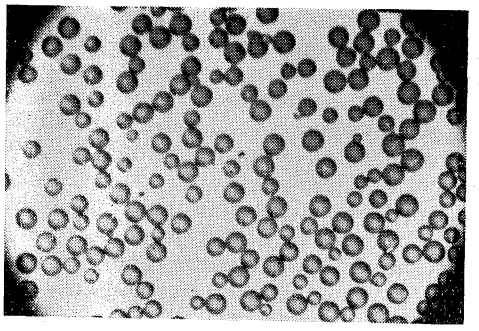
These agglomerates are formed in the systems of weakly dissociated resins, e. g., between

1) M. Senō and T. Yamabe, presented at the 9th Annual Meeting of the Society of Polymer Science, Osaka, May, 1960.

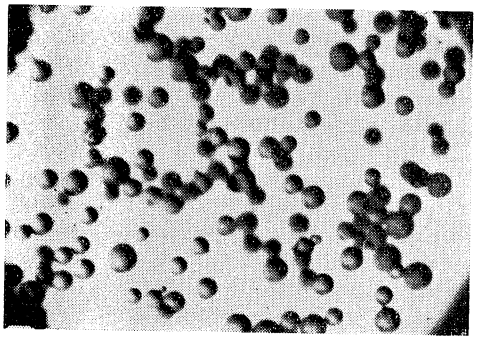
2) N. Grubhofer, *Angew. Chem.*, **71**, 215 (1959).

3) J. H. Schenkel and J. A, Kitchener, *Trans. Faraday Soc.*, **56**, 161 (1960).

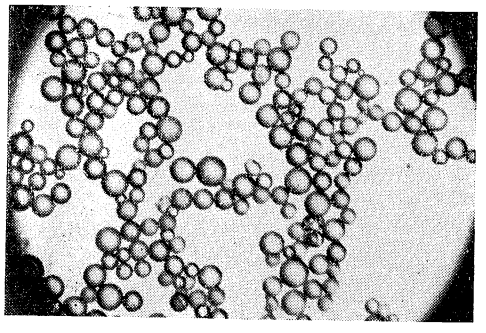
4) M. J. Vold, *J. Colloid Sci.*, **14**, 168 (1959).



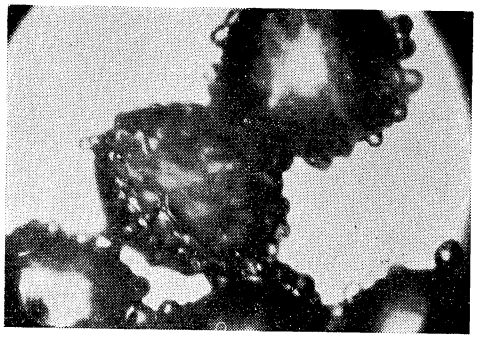
a



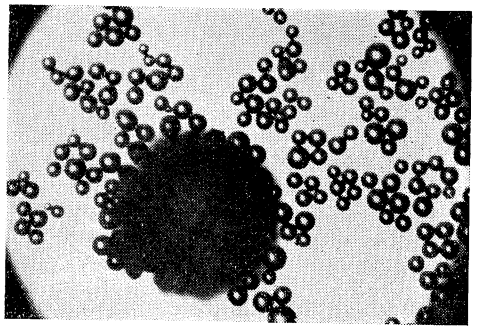
b



c



d



e

Fig. 1. Microphotographs of various ion-exchange systems (×60).

a. Dowex 50W-X8, 200 mesh. (Particles disperse uniformly.)
b. Dowex 50W-X8, 200 mesh-Dowex 1-X8, 200 mesh, 10 : 1 by wt. ratio. (Small agglomerates are formed.)
c. Dowex 50W-X8, 200 mesh-Dowex 1-X8, 200 mesh, 1 : 1 by wt. ratio. (Large agglomerates are formed over a whole system.)
d. Dowex 50W-X8, 20 mesh-Dowex 1-X8, 200 mesh, 10 : 1 by wt. ratio. (Larger particles combine each other through the medium of smaller particles.)
e. Dowex 50W-X8, 20 mesh-Dowex 1-X8, 200 mesh, 1 : 1 by wt. ratio. (Larger particles are covered with smaller particles and stabilized.)

Amberlite IR-120 and Amberlite IRA-400, Amberlite IR-120 and Amberlite IR-4B, Amberlite IRC-50 and Amberlite IRA-400, and Amberlite IRC-50 and Amberlite IR-4B. But the last system, e. g., the weakly acidic and the weakly basic resins, do aggregate only to less extent. The degree of aggregation of these systems is given in Table I.

Table I. Degree of aggregation of various particle systems

| System* | Degree of aggregation** |
|---|---|
| IR-120-IRA-400 | 2.8 |
| IR-120-IR-4B | 1.9 |
| IRC-50-IRA-400 | 2.5 |
| IRC-50-IR-4B | 1.3 |

* All the particles are Amberlite ion-exchange resins, 20 mesh of particle size and 1 : 1 mixture by weight.
** Degree of aggregation are defined as the ratio of sedimentation volume (aggregate) in pure water to the volume (non-aggregate) in 1 N sodium chloride.

**Effect of Addition of Salts.**—The aggregates are destroyed by addition of salts. The specific sedimentation volumes diminish on addition of salts such as sodium chloride as shown in Fig. 2. As for the breaking-down of aggregates by

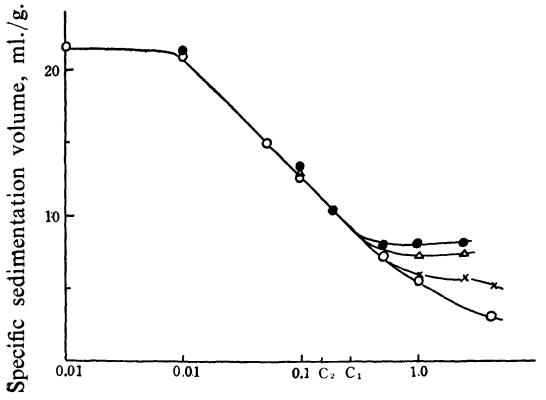



Fig. 2. Effects of addition of salts on sedimentation volume. System; Dowex 50W (200 mesh)-Dowex 1 (200 mesh), 1 : 1 by weight. -○- NaCl, -×- $MgCl_2$, -△- $Na_2SO_4$, -●- $MgSO_4$. $C_1$ and $C_2$ are saturation concentrations of Dowex 50W and Dowex 1, calculated from the total exchange capacities of resins.

addition of salts the following results are to be pointed out;

(1) The effect of destruction of agglomerates is primarily governed by equivalent concentration of salt solution, independently of variation of the kind of salts.

(2) In high concentration range of salts, in which the aggregates are completely broken down, the specific sedimentation volume changes with the variation of salts. But this difference is primarily due to the difference in the density of the salt solution, and it is finally observed that the anion-exchange resin, the lighter one, is separated from the cation-exchange resin, the heavier one, and floats up.

(3) When the saturation concentration which is calculated from the total exchange capacity of resins is reached, the hydrogen ions or the hydroxyl ions may be largely replaced for, say, the sodium ions or the chloride ions and at this concentration the aggregate is completely broken down. In the far lower concentration range than this saturation concentration, the aggregate is destroyed considerably and there is a linear relationship between the specific sedimentation volume and the logarithm of the concentration of the added salt solution.

(4) The aggregates are broken down by the addition of acids or alkaline solutions. The strongly acidic resin-the weakly basic resin (Amberlite IR-120-Amberlite IR-4B) destroyed with hydrochloric acid, and the weakly acidic resin-the strongly basic resin (Amberlite IRC-50-Amberliet IRA-400) destroyed with sodium hydroxide become to form aggregation again, on washing them with deionized water. It may be due to hydrolysis of weakly dissociated resins.

**Aggregation in Non-aqueous Media.**—As it appears that the interparticlar force is electrostatic in nature, it seems to be interesting to investigate the aggregation behavior in non-aqueous media, the dielectric constant of which is small. It is well-known that the minute amount of water influences greatly the electrostatic coagulation and the air-dried ion-exchange resins contain the considerable amount of water, for these are very lyophilic gels, and hence the air-dried resins must be dried on phosphorus pentoxide in vacuo to remove moisture from them completely. The sedimentation volume of these dried resins in dried benzene was measured and was shown in Fig. 3. As seen

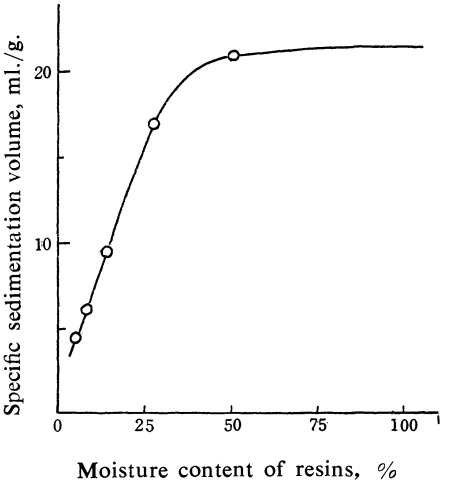



Fig. 3 Effect of moisture on sedimentation volumes of resins in benzene. Dowex 50W (200 mesh)-Dowex 1 (200 mesh)

in this figure, in which the specific sedimentation volume is plotted against the moisture content of resins, the resins do not form an aggregate in the complete absence of water.

**Mechanism of Aggregation.**—It is supported by the above-mentioned results that the interparticlar force which causes aggregation is electrostatic in nature. The agglomeration takes place between the hydrogen-form cation-exchange resins and the hydroxyl-form anion-exchange resins. A kind of neutralization reaction occurs between the particles of hydrogen-form resin and the hydroxyl-form resin and results in producing the negatively charged and the positively charged resin particles and Coulombic interaction is exerted between these charged particles. Such a coagulation behavior

was observed also between a polymeric acid and a polymeric base by Deuel et al.[5]

The presence of small additional ions such as sodium or chloride ions screens the charges on the particles and the interparticlar Coulombic attraction decreases. In benzene free from water the degree of dissociation of counterions is so small that the neutralization does not proceed between hydrogen- and hydroxyl-form particles. Hence the aggregates are not formed in such a system.

**Steric Factor on Aggregation.**—It is well-known that the steric factors such as the size and shape of particles affect greatly the aggregation behavior of colloidal particles. The ion-exchange particles used in this investigation are very large in size and spherical in shape. Therefore, it seems that the effect of size ratio of both particles participated with aggregation is more interesting than that of the size and shape itself. In Fig. 4, the aggregation behavior of the ion-exchange resin particles, Dowex 50W and Dowex 1, with different sizes is shown. As seen in this figure, the particles with the same sizes show a maximum aggregation on mixing at the equal amounts of both resins and the particles with the different sizes show a maximum aggregation on mixing at a larger amount of the larger particle and a smaller amount of the smaller particle. The weight fraction of the cation-exchange resin, Dowex 50W, that gives the maximum aggregation is shown against the ratio of radii between both of the resin particles in Fig. 5. It is clearly noticed that the difference in size between both particles influences markedly the aggregation behavior.

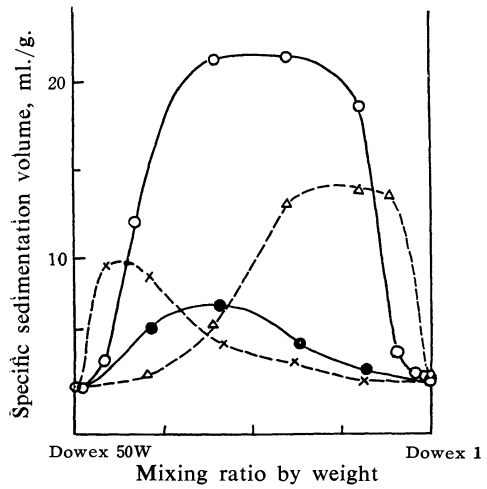



Fig. 4 Sedimentation volumes of mixtures of resins of various particle sizes.

| Mesh size; | Dowex 50 W | Dowex 1 |
|---|---|---|
| —○— | 200(0.043 mm.) | 200(0.055 mm.) |
| --×-- | 20(0.375 mm.) | 200 |
| --△-- | 200 | 40(0.190 mm.) |
| —●— | 20 | 40 |

Average radii of resin particles are given in parentheses.

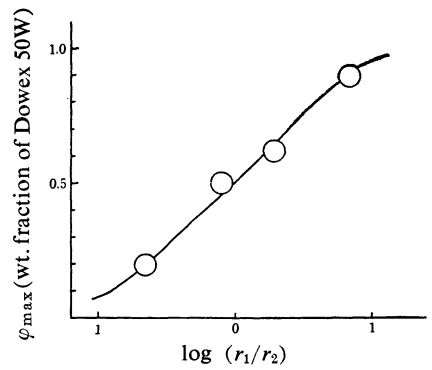



Fig. 5. Relation of the mixing ratio of maximum aggregation and the particle size ratio.

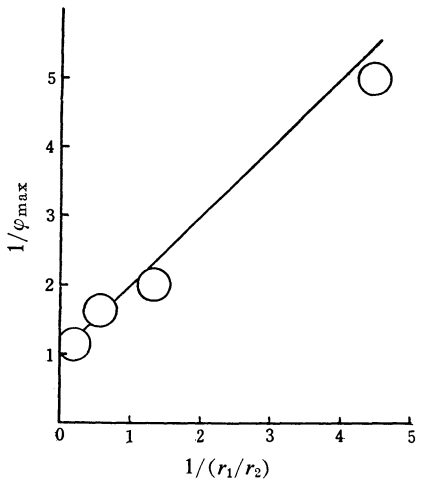



Fig. 6. Plots of $1/\varphi_{max}$ against $r_2/r_1$. Full line is the theoretical.

Now, it is assumed that the maximum aggregation takes place in the case where the total surface areas of the two kinds of particles are equal. The following formula is derived from this assumption.

$$\varphi_{max}=\frac{r_1}{r_1+r_2}$$

where $\varphi_{max}$ is the weight fraction of Dowex 50W giving maximum aggregation, and $r_1$ and $r_2$ are radii of Dowex 50W and Dowex 1 particles, respectively. In Fig. 6, the reciprocal of $\varphi_{max}$ is plotted against the reciprocal of $r_1/r_2$. If the above-mentioned assumption is valid, this plot should be a straight line

5) H. Deuel, J. Solms and A. Denzler, *Helv. Chim. Acta*, 36, 1671 (1953).

intersecting the ordinate at unity. As shown in Fig. 6, it is confirmed that this is the case in the present systems.

**Summary**

Some observations are presented on the aggregation behavior of the ion-exchange resin particles. On mixing the hydrogen-form cation-exchange resin particles with the hydroxyl-form anion-exchange resin particles, remarkable aggregation takes place. It seems that this aggregation is due to the electrostatic attraction force exerted between resin particles. This is supported by the results that the aggregation is destroyed by addition of salts and that the agglomerates are not formed in non-polar medium in the complete absence of water. Moreover, it was demonstrated that the variation of the size ratio of particles influences markedly the aggregation behavior. A simple explanation is given for such a coagulation phenomena.

*The Institute of Industrial Science*
*The University of Tokyo*
*Yayoi-cho, Chiba*

*Added in proof:*

It was shown by further observations done after contribution of this paper that salt-form ion-exchange resin particles, for example, sodium-form cation-exchange resin and chloride-form anion-exchange resin aggregate in pure water where no additional salt is completely absent and also red color due to the formation of ferric thiocyanate complex does not appear when ferric-form cation-exchange resin and thiocyanate-form anion-exchange resin are mixed in pure water. From these observations it is clear that no chemical reaction takes place practically between these particles and some modifications should be applied to the coagulation mechanism proposed in the present paper. A portion of counterions distributes outside of the resin particle, so that the fixed charges of the resin are not completely neutralized by the counterions in the volume occupied by the particle. Therefore, the cation-exchange resin particles carry negative charges and the anion-exchange resin particles carry positive charges in their suspension. Electrostatic interaction is exerted between these particles. Distribution of counterions would be largely affected by the salt concentration, the dielectric constant of medium and the degree of dissociation of fixed ionized groups. The details will be reported later.

# *Hydrogen Peroxide Oxidation. V. Selenium Dioxide Catalyzed Oxidative Rearrangement Reaction of Desoxybenzoin*[1]

By Noboru SONODA and Shigeru TSUTSUMI

(Received December 14, 1960)

The previous papers[2-4] in this series described the fact that the selenium dioxide catalyzed hydrogen peroxide oxidation of enolizable ketones produces carboxylic acids by the intramolecular migration of alkyl or aryl group to the $\alpha$-carbon atom of the carbonyl group. The present study was undertaken to provide additional informations pertinent to active species of these reactions and the reaction processes.

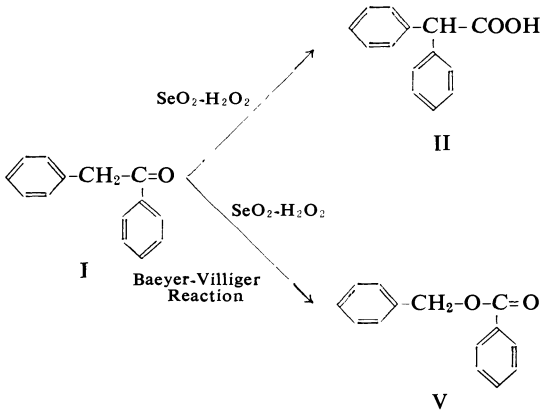
For this purpose, desoxybenzoin was selected as a starting material. According to the procedure[4] previously employed for phenyl alkyl ketones, desoxybenzoin (I) was oxidized with hydrogen peroxide in the presence of a catalytic amount of selenium dioxide in tertiary butyl alcohol at 82°C. The formation of diphenyl acetic acid (II) was observed and benzoic acid was also isolated as a acidic product.

After unreacted desoxybenzoin was removed, small amounts of benzil (III) and benzoin (IV) were isolated from the neutral part of the reaction products, and an oily substance was also isolated as the residue. The strong infrared absorption bands at 1110 (sym. C-O-C), 1270 (asym. C-O-C) and 1710 $cm^{-1}$ (C=O) of the residue indicated the presence of an ester group, and it was confirmed to be benzyl benzoate (V) by gaschromatographic analysis.

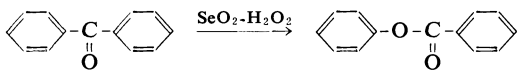
Diphenyl acetic acid (II) should be produced by the migration of phenyl group to the $\alpha$-carbon atom of the benzyl group in conformity

1) Reported at the Autumn Meeting of Chemical Society of Japan, Tokyo, October, 1959.
2) N. Sonoda and S. Tsutsumi, This Bulletin, 32, 505 (1959).
3) N. Sonoda, T. Yamaguchi and S. Tsutsumi, *J. Chem. Soc. Japan, Ind. Chem. Sec.* (*Kogyo Kagaku Zasshi*), 63, 737 (1960).
4) N. Sonoda and S. Tsutsumi, This Bulletin, 33, 1440 (1960).

with the reaction aptitude observed in the previous paper[4], whereas the formation of benzyl benzoate (V) may be apparently due to Baeyer-Villiger oxidative rearrangement reaction[5,6].

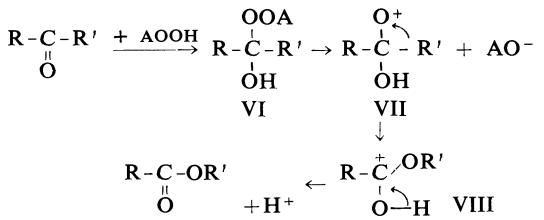



It was confirmed experimentally that benzyl benzoate is not an intermediate in the reaction path of the production of diphenyl acetic acid. Therefore, both the rearrangement reactions described above may proceed competitively in the same reaction system. This is also supported by the fact that the Baeyer-Villiger reaction is generally applicable to the non enolizable ketones which can not produce the rearranged carboxylic acids. For example, benzophenone was oxidized by the selenium dioxide catalyzed hydrogen peroxide yielding phenyl benzoate or its hydrolyzed products.




Baeyer-Villiger reaction is interpreted as one of the reactions of ketones with peroxyacids. The favored reaction mechanism was first proposed by Criegee[7], who assumed that the addition of peroxyacid to the carbonyl group produced a hydroxyperoxide VI (referred to as "Criegee Intermediate"), which dissociated to give an electron-deficient ion VII, and then was rearranged to form carbonium ion VIII with cleavage of a carbon-carbon bond, and VIII decomposed to the ester.

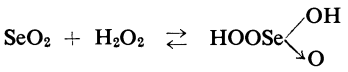
Accordingly, the formation of benzyl benzoate from desoxybenzoin may be due to some kind of peroxyacid as the active oxidizing species in the selenium dioxide-hydrogen

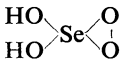



AOOH: peroxyacid

peroxide system, and this fact is also consistent with our previous assumption[2] that peroxyselenious acid is the most probable catalyst.

The formation of peroxyselenious acid was first assumed by Hughes and Martin[8] from the kinetic study of the oxidation of selenium dioxide with hydrogen peroxide to selenic acid.



Recently, Ogata and Tabushi[9] have reported in the kinetic study of the oxidation of dimethylaniline that a kind of peroxide such as peroxyselenious acid or  is assumed to be produced as the active oxidizing species.

Although the formation of selenic acid would be possible in this reaction system, the selenic acid might not be the active species, because desoxybenzoin was oxidized with selenic acid to yield benzil as well as in the case of the selenious acid oxidation, and no rearrangement reaction was observed. In addition, Ogata and Tabushi[9] have shown in the kinetic study that peroxyselenic acid[10] may not be an active oxidizing species.

Hawthorne and his co-workers[11] reported that the Baeyer-Villiger rearrangement of desoxybenzoin with trifluoroperoxyacetic acid gave benzyl benzoate and phenyl phenylacetate in the ratio of 51 : 39. In contrast to this result, only benzyl benzoate was isolated as ester in the selenium dioxide catalyzed hydrogen peroxide oxidation, and phenyl phenylacetate was not detected by the gas chromatography which was capable of analyzing both the esters. It is interesting to note that the rearrangement aptituds of the two possible

5) For a review of the Baeyer-Villiger reaction, see C. H. Hassall, "Organic Reactions", Vol. IX. John Wiley & Sons, Inc., New York, N. Y. (1957), pp. 73—106.

6) Recently, Hellman and Rosegay have also reported the occurrence of the Baeyer-Villiger reation from the isolation of 6-hydroxycaproic acid in the oxidation products of cyclohexanone with selenic acid-hydrogen peroxide reagent; H. M. Hellman and A. Rosegay, *Tetrahedron Letters*, 1959, No. 13, 1~3; *Chem. Abstr.*, 54, 4345 (1960).

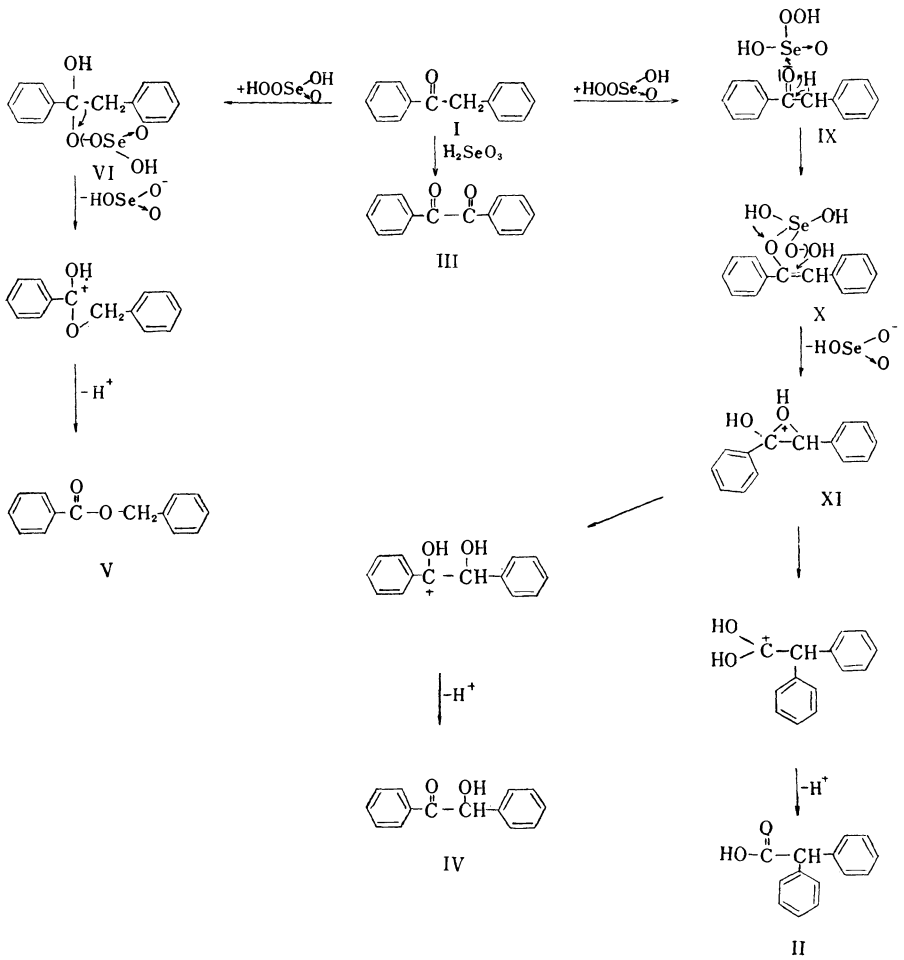
7) R. Criegee, *Ann*, 560, 127 (1948).

8) F. J. Hughes and D. S. Martin Jr., *J. Phys. Chem.*, 59, 410 (1955).

9) Y. Ogata and I. Tabushi, This Bulletin, 32, 215 (1959).

10) The formation of peroxyselenic acid ($H_2SeO_5$) was assumed by several workers; (a) R. R. Worsley and H. B. Baker, *J. Chem. Soc.*, 123, 2870 (1923). (b) C. W. Smith and R. T. Holm, *J. Org. Chem.*, 22, 746 (1957). But the evidence and the other information of the peroxyselenic acid were not obtainable. See (c) W. C. Schumb et al., "Hydrogen Peroxide", Reinhold Pub., New York, N. Y (1955), p. 477.

11) M. F. Hawthorne, W. D. Emmons and K. S. McCallum, *J. Am. Chem. Soc.*, 80, 6393 (1958).



migrating groups, phenyl and benzyl groups, are largely dependent on the kind of the oxidative reagent in the Baeyer-Villiger reaction. Such a difference in the migrating aptitude was also reported by Howthorne and the co-workers[11], who showed that the greater selectivity between migrating groups was observed in the cleavage of phenyl cyclohexyl ketone with peroxyacetic acid as compared with the similar reaction with trifluoroperoxyacetic acid.

The simplest interpretation of the reaction mechanism of the diphenyl acetic acid formation may involve the electrophilic attack of the peroxyacid to a double bond formed between the carbonyl carbon and the methylene carbon atoms. The formation of this double bond was assumed from the observation[2,3,12] that the orientation of the migration of alkyl groups in the selenium dioxide catalyzed rearrangement reaction of aliphatic unsymmetrical ketones with hydrogen peroxide was comparable to the orientation of the enol form or of diketone formation with selenious acid. Accordingly, it is reasonable to say that the initial state of the attack of peroxyselenious acid to the ketone will be analogous to that of selenious acid. Although we have proposed the inferential mechanism[2] which comprises the enol formation followed by the attack of the peroxyselenious acid, the other possible reaction path will be suggested from the recent study on the mechanism of selenium dioxide oxidation of ketones, in which Corey and Schaefer[13] have pointed out that the electrophilic character to the carbonyl group may be served by 4d-orbitals of selenium in the first step of the reaction. In the present case the formation of the double bond may be induced by the electrophilic addition of the peroxyselenious acid to the carbonyl oxygen (IX), and then electrophilic attack by hydroperoxy group occurs intramolecularly (X) as shown below.

12) The detailed results were presented at the 13th Annual Meeting of the Chemical Society of Japan, Tokyo, April, 1960.

13) E. J. Corey and J. P. Schaefer, *J. Am. Chem. Soc.*, **82**, 918 (1960).

Elimination of selenious acid from X may yield hydronium ion (XI) which will be rearranged to produce the carboxylic acid (II).

Our results are not sufficient to allow a choice between the two proposed reaction paths; however, the latter may be more favorable because of the distinctive character of the peroxyselenious acid as compared with the other peroxyacids.

Since no products other than benzil have been found[13] in the oxidation of desoxybenzoin with selenious acid, the formation of benzoin might be illustrated in the path via hydronium ion intermediate (XI).

## Experimental[14]

**Materials.**—Desoxybenzoin was prepared from phenyl acetic acid, phosphorus trichloride and benzene according to the procedure of Allen and Barker[15]; b. p. 158°C (4 mmHg). A sample, m. p. 57°C, was obtained by the recrystallization from methanol.

**Reagent for Oxidation.** — A solution containing 20 ml. of 30% hydrogen peroxide and 80 ml. of tertiary butyl alcohol was dried over 60 g. of anhydrous sodium sulfate for two days. After filtration of sodium sulfate, 0.2 g. of selenium dioxide was dissolved in 25 ml. of this solution. The solution prepared was used as a reagent for oxidation.

**Oxidation of Desoxybenzoin.**—In a 15 ml. of tertiary butyl alcohol, was dissolved 4.9 g, (0.025 mol.) of desoxybenzoin by slight heating, and 25 ml. of hydrogen peroxide-selenium dioxide reagent (0.05 mol. of hydrogen peroxide and 0.2 g. of selenium dioxide) was added. The reaction mixture was refluxed for 17 hr., and was distilled under reduced pressure to remove the solvent and water. The residue was diluted with 100 ml. of ether and was filtered to remove a small amount of metallic selenium deposited. The ethereal solution was extracted with 10% potassium carbonate solution.

*Acidic Products.*—The potassium carbonate solution was acidified with 4 N hydrochloric acid and extracted with ether. The ether extract was dried over anhydrous sodium sulfate and removal of the ether left 1.3 g. of mixture of acids. Benzoic acid (0.6 g.) was separated as the soluble part of the mixture in warm water, m. p. 121°C (lit.[16] 121°C), mixed melting point with an authentic sample was not depressed.

The insoluble part (0.5 g.) was recrystallized from a small amount of benzene to remove the brown impurities and was further recrystallized from hot water. This yielded white crystals, 0.2 g. of diphenyl acetic acid (6% yield based on the unrecovered desoxybenzoin); m. p. 145°C (lit.[16] 145°C), mixed melting point with an authentic sample showed no depression.

Found: C, 79.00; H, 5.52. Calcd. for $C_{14}H_{12}O_2$: C, 79.22; H, 5.70%.

*Neutral Products.* — The ethereal solution, from which the acidic products were removed was dried over anhydrous sodium sulfate, and the ether was evaporated. On distillation of the residual brown oily liquid under reduced pressure, 3.0 g. of yellow oily products were obtained, b. p. 140~166°C (4 mmHg). After cooling overnight, crystals deposited were filtered and recrystallized from methanol giving 1.6 g. of recovered desoxybenzoin, m. p. 55°C. The filtrate was further cooled at 0°C for two days, and crystals deposited were filtered and recrystallized from ethanol giving a small amount of recovered desoxybenzoin and 35 mg. of benzil; faint yellow crystalline solid, m. p. 94~95°C (lit.[16] 95°C), undepressed when mixed with an authentic sample.

Found: C, 80.15; H, 5.11. Calcd. for $C_{14}H_{10}O_2$: C, 79.98; H, 4.79%.

The filtrate was cooled further at 0°C for 3 weeks and isolated crystalline solid was recrystallized from ethanol; 25 mg. of white crystals were obtained, m. p. 130~132°C; the infrared spectrum[17] exhibited strong absorption bands at 3320 (OH) and 1680 $cm^{-1}$ (conjugated C=O), and was identical with an authentic benzoin; vicinal hydroxy ketone test[18] by periodic acid reagent gave positive result. In the above respects this sample was confirmed to be mainly benzoin (lit.[16] m. p. 133°C).

Found: C, 79.23; H, 5.78. Calcd. for $C_{14}H_{12}O_2$: C, 79.22; H, 5.70%.

The residual liquid was redistilled under reduced pressure, and 0.9 g. of oily product, benzyl benzoate, was obtained. The infrared spectrum[17] of analytical sample, b. p. 156~157°C (3 mmHg), showed strong bands at 1710 (C=O), 1270 (asym. C-O-C) and 1110 $cm^{-1}$ (sym. C-O-C), and was identical with an authentic sample.

Found: C, 79.50; H, 5.54. Calcd. for $C_{14}H_{12}O_2$: C, 79.22; H, 5.70%.

Presence of phenyl phenylacetate was not detected by the gaschromatography which was capable of separating phenyl phenylacetate and benzyl benzoate: column, Silicone-550; column temperature, 205°C; carrier gas, $H_2$.

**Oxidation of Benzophenone.**—To a 25 ml. of selenium dioxide-hydrogen peroxide reagent (0.05 mol. of hydrogen peroxide and 0.2 g. of selenium dioxide) was added 50 ml. of tertiary butyl alcohol and 9.1 g. (0.05 mol.) of benzophenone, and the mixture was refluxed for 24 hr. After removal of the solvent from the reaction mixture, the residual products was separated into acidic and neutral parts according to the usual procedure. From the acidic part was isolated 0.2 g. of benzoic acid. For the purpose of saponification of the ester contained, the neutral product was treated with 5 g. of sodium hydroxide in 90% aqueous methanol solution at 65°C for 2 hr. After removal of the methanol, 20 ml. of water was added and the neutral substance was extracted with ether. The ether extract gave 6.8 g. of unreacted benzophenone, b. p. 124~129°C

14) The boiling and the melting points are uncorrected.
15) C. F. H. Allen and W. E. Barker, "Organic Syntheses", Coll. Vol. II (1948), p. 156.
16) R. R. L. Shriner, R. C. Fuson and D. Y. Curtin, "The Systematic Identification of Organic Compounds", 4th Ed., John Wiley & Sons, Inc., New York, N. Y. (1956).
17) The infrared spectra were obtained on a Shimadzu Model IR-27A instrument.
18) Ref. 16, p. 129.

(3 mmHg). Acidification of the water soluble part yielded 0.4 g. of benzoic acid, and small amount of phenol was also isolated; the tribromide was prepared which melted at 94°C (lit.[16] m. p. 95°C), mixed melting point with an authentic sample showed no depression. The formation of phenyl benzoate was confirmed from the above experiments.

**Oxidation of Desoxybenzoin with Selenic Acid.** —To a mixed solution of 50 ml. of tertiary butyl alcohol and 50 ml. of methanol was added 9.8 g. (0.05 mol.) of desoxybenzoin. The solution was heated to 70°C, and 18 g. of 40% aqueous selenic acid (0.05 mol.) was added dropwise to the solution. After the solution was maintained at 70°C for 24 hr., metallic selenium deposited was filtered off. The filtrate was distilled to remove the solvent, and the residue was separated into acidic and neutral parts according to the usual procedure. From the acidic part was isolated 0.15 g. of benzoic acid. The neutral part gave 7.6 g. of benzil, m. p. 94~95°C, and 1.8 g. of unidentified substance (probably, some organo selenium compound).

## Summary

1) Selenium dioxide catalyzed oxidation of desoxybenzoin with hydrogen peroxide in tertiary butyl alcohol gave diphenyl acetic acid which was produced by the rearrangement of phenyl group to the methylene carbon atom.

2) Baeyer-Villiger reaction was also occurred competitively in this reaction system, and benzyl benzoate was isolated as ester from the neutral products. Such an observation shows that the active oxidizing species may be some kind of peroxyacid. This fact is consistent with our previous assumption that peroxyselenious acid is the most probable catalytic form.

3) It is assumed in the reaction path of the formation of the rearranged carboxylic acid that the initial state of the attack of the peroxyselenious acid to the ketone may be analogous to that of selenious acid. From this point of view, a possible reaction path was proposed.

The authors wish to thank Dr. Y. Odaira for his helpful suggestions and encouragement.

*Department of Chemical Technology*
*Faculty of Engineering*
*Osaka University*
*Miyakojima-ku, Osaka*

# *Kerr Effect in Liquid State*

By Hideo OKABAYASHI

(Received December 23, 1960)

In the calculation of a physical property of liquid on the basis of a molecular theory, a form of local (or internal)[1] field may play an important role.

A theoretical formula for the dielctric constant of liquid has been derived, in which the local field is assumed to have the following expression[2].

$$F_i=\left(1-\frac{\varphi_i\alpha_j}{v}\right)^{-1}\left(E_1+\frac{\varphi_i\mu_{0i}}{v}\right)=\gamma_i\left(E_1+\frac{\varphi_i\mu_{0i}}{v}\right)$$

$$\varphi_i=2\pi a_1a_2a_3\int_0^\infty \frac{du}{(a_i^2+u)\sqrt{(a_1^2+u)(a_2^2+u)(a_3^2+u)}} \quad (1)$$

The liquid is considered as consisting of molecules, each of which has a permanent dipole and an anisotropic polarizability. Each component of the dipole moment is denoted as $\mu_{01}$, $\mu_{02}$ and $\mu_{03}$. The component of the polarizability tensor along the principal axis is represented as $\alpha_1$, $\alpha_2$ and $\alpha_3$, respectively. The molecular shape is assumed to be ellipsoid. $2a_1$, $2a_2$ and $2a_3$ are the lengths of the principal axes. The molecular volume is $v$. Further it is assumed that the direction of each principal axis is coincident with that of each principal axis of the polarizability.

In the present paper, Eq. 1 is applied to the derivation of a theoretical formula of Kerr constant in liquid state. The numerical calculation of the Kerr constant is also made and compared with the experimental value.

**The Formula of the Kerr Constant in Liquid State.**—Generally, a liquid may be birefringent

1) M. Born used the term "das wirkende Feld"; M. Born, "Optik", Verlag von J. Springer. (1933); P. Debye used the term "das (wirksame) innere Feld"; P. Debye, "Polare Molekeln", Verlag von S. Hirzel, Leipzig (1929). J. H. Van Vleck used the term "local field", and used the term "internal field" instead of the term "self-field" in the previous paper[2]; J. H. Van Vleck, "The Theory of Electric and Magnetic Susceptibilities", Oxford Press (1932). The terminology "local field" or "internal field" is according to H. Fröhlich; H. Fröhlich, "Theory of Dielectrics", Oxford Press (1950).

2) M. Yasumi, H. Okabayashi and H. Komooka, This Bulletin, 31, 402, 673 (1958).

when an electric field is applied. The magnitude of the artificial birefringence is represented quantitatively by Kerr constant $B$ [3].

$$B=\frac{n_{\parallel}-n_{\perp}}{\lambda E^2}$$

where $n_{\parallel}$ and $n_{\perp}$ denote the refractive indices of the liquid parallel to and perpendicular to the applied field, respectively. $\lambda$ is the wavelength of light in vacuo. $E$ is the magnitude of the applied static electric field.

The theory of the Kerr effect was derived by Born[4]. According to his theory, the Kerr constant has the following expression.

$$B=\frac{\pi N_c}{3n\lambda}(n^2+2)^2\left(\frac{\varepsilon+2}{3}\right)^2(\Theta_1+\Theta_2)$$

$$\Theta_1=\frac{1}{45kT}\sum_{1,2,3}\{\alpha_i(\omega)-\alpha_j(\omega)\}\{\alpha_i(0)-\alpha_j(0)\}$$

$$\Theta_2=\frac{1}{45k^2T^2}\sum_{1,2,3}\{\alpha_i(\omega)-\alpha_j(\omega)\}\{\mu_{0i}^2-\mu_{0j}^2\} \quad (2)$$

$\varepsilon$ is the static dielectric constant of the liquid and $n$ is the ordinary refractive index. $N_c$ is the number of molecules in a unit volume. $\alpha_i(\omega)$ is the polarizability at the angular frequency of $\omega$. This formula has been successfully applied to the case of gases. A molecule of the gas may either be polar or non-polar. However, as yet no theory of Kerr effect in liquid state could explain experimental facts sufficiently[5]. The discrepancy between theory and experiment may lie in the inappropriate assumption of the local field. In the following, on the basis of the formula 1 for the local field, the Kerr constant of liquid is calculated.

The strength of the total electric field in the medium is denoted by $\vec{E}_t$, and

$$\vec{E}_t=\vec{E}+\vec{e}\cdot\exp(-i\omega t) \quad (3)$$

$\vec{E}$ is the static part and $\vec{e}\cdot\exp(-i\omega t)$ is the oscillating part. The static part of the local field is expressed as before:

$$F_i=\left\{1-\frac{\varphi_i\alpha_i(0)}{v}\right\}^{-1}\left(E_i+\frac{\varphi_i\mu_{0i}}{v}\right)$$
$$=\gamma_i(0)\left(E_i+\frac{\varphi_i\mu_{0i}}{v}\right) \quad (1)'$$

$\alpha_i(0)$ is used instead of $\alpha_i$, in order to indicate that it concerns the static field.

The oscillating part of the local filed $\vec{f}\cdot\exp(-i\omega t)$ is represented as,

$$f_ie^{-i\omega t}=\left\{1-\frac{\varphi_i\alpha_i(\omega)}{v}\right\}^{-1}e_ie^{-i\omega t}=\gamma_i(\omega)e_ie^{-i\omega t} \quad (4)$$

The expression 4 is obtained from the assumption that the liquid molecule can not follow the oscillating field.

To obtain the formula of the Kerr constant, the value of the electric moment due to the oscillating field must be known.

It is denoted by $\vec{\mu}_e\cdot\exp(-i\omega t)$, and

$$\mu_e=\frac{\vec{\mu}_e\cdot\vec{e}}{e}=\frac{\sum\alpha_i(\omega)f_ie_i}{e} \quad (5)$$

The refractive index $n_e$ along the $\vec{e}$ is related to the mean value of $\mu_e$ as follows;

$$(n_e^2-1)e=4\pi N_c\langle\mu_e\rangle \quad (6)$$

$\langle\mu_e\rangle$ is obtained according to the Boltzmann statistics.

$$\langle\mu_e\rangle=\frac{\int\mu_e\exp(-U/kT)d\Omega}{\int\exp(-U/kT)d\Omega} \quad (7)$$

$d\Omega$ represents elementary solid angle. $U$ is the potential energy under the influence of the field.

$$U=-\left\{\frac{1}{2}\sum\alpha_i(0)F_i^2+\sum\mu_{0i}F_i\right\} \quad (8)$$

Here an assumption is made that,

$$E_1,\ E_2,\ E_3\gg e_1,\ e_2,\ e_3 \quad (9)$$

In the calculation of $\langle\mu_e\rangle$, $\exp(-U/kT)$ is expressed in the power series of $E$, and only the terms proportional to $E$ and $E^2$ are retained. Two distinct cases must be considered.

(1) If the direction of the electric vector of the incident light is coincident with that of the static electric field, and $\langle\mu_e\rangle$ is denoted as $\langle\mu_{\parallel}\rangle$, then

$$\langle\mu_{\parallel}\rangle=e\left[\frac{1}{3}\sum\alpha_i(\omega)\gamma_i(\omega)\right.$$
$$+\frac{E^2}{45kT}\sum_{1,2,3}\{\alpha_i(\omega)\gamma_i(\omega)-\alpha_j(\omega)\gamma_j(\omega)\}$$
$$\times\{\alpha_i(0)\gamma_i^2(0)-\alpha_j(0)\gamma_j^2(0)\}$$
$$+\frac{E^2}{45k^2T^2}\sum_{1,2,3}\{\alpha_i(\omega)\gamma_i(\omega)-\alpha_j(\omega)\gamma_j(\omega)\}$$
$$\left.\times\{\mu_{0i}^2\gamma_i^4(0)-\mu_{0j}^2\gamma_j^4(0)\}\right] \quad (10)$$

$\langle\mu_{\parallel}\rangle$ is related to $n_{\parallel}$ as follows.

$$(n_{\parallel}^2-1)e=4\pi N_c\langle\mu_{\parallel}\rangle \quad (11)$$

3) This definition is based on the experimental method. From the theoretical standpoint, it is more convenient to define $K=B\lambda$ as the Kerr constant than $B$. However, in the present paper the quantity of $B$ is dealt with according to the traditional custom.

4) M. Born, *Ann. Physik*, **55**, 177 (1918).

5) c. g. A. Peterlin and H. A. Stuart, *Z. Physik*, **113**, 663 (1937); H. A. Stuart, "Die Physik der Hochpolymeren", Bd. I., Springer-Verlag, Berlin (1952), p. 426.

(2) If the electric vector of the light is perpendicular to the direction of the static electric field and $\langle\mu_e\rangle$ is denoted as $\langle\mu_\perp\rangle$, then

$$\langle\mu_\perp\rangle=e\Big[\frac{1}{3}\sum\alpha_i(\omega)\gamma_i(\omega) - \frac{E^2}{90kT}\sum_{1,2,3}\{\alpha_i(\omega)\gamma_i(\omega)-\alpha_j(\omega)\gamma_j(\omega)\} \times\{\alpha_i(0)\gamma_i^2(0)-\alpha_j(0)\gamma_j^2(0)\} - \frac{E^2}{90k^2T^2}\sum_{1,2,3}\{\alpha_i(\omega)\gamma_i(\omega)-\alpha_j(\omega)\gamma_j(\omega)\} \times\{\mu_{0i}^2\gamma_i^4(0)-\mu_{0j}^2\gamma_j^4(0)\}\Big] \quad (12)$$

and

$$(n_\perp^2-1)e=4\pi N_c\langle\mu_\perp\rangle \quad (13)$$

The Kerr constant $B$ is expressed as:

$$B=\frac{\pi N_c}{n\lambda}\Big[\frac{1}{15kT}\sum_{1,2,3}\{\alpha_i(\omega)\gamma_i(\omega)-\alpha_j(\omega)\gamma_j(\omega)\} \times\{\alpha_i(0)\gamma_i^2(0)-\alpha_j(0)\gamma_j^2(0)\} + \frac{1}{15k^2T^2}\sum_{1,2,3}\{\alpha_i(\omega)\gamma_i(\omega)-\alpha_j(\omega)\gamma_j(\omega) \times\{\mu_{0i}^2\gamma_i^4(0)-\mu_{0j}^2\gamma_j^4(0)\}\Big] \quad (14)$$

Because of small magnitude of $(n_\parallel-n_\perp)$, $(n_\parallel+n_\perp)$ is replaced by $2n$.

In the case when the direction of the permanent dipole moment is coincident with the direction of one of the principal axes of the molecular ellipsoid (i.e. $a_1$ axis), Eq. 14 is simplified as,

$$B=\frac{\pi N_c}{n\lambda}\Big[\frac{1}{15kT}\sum_{1,2,3}\{\alpha_i(\omega)\gamma_i(\omega)-\alpha_j(\omega)\gamma_j(\omega)\} \times\{\alpha_i(0)\gamma_i^2(0)-\alpha_j(0)\gamma_j^2(0)\} + \frac{1}{15k^2T^2}\{3\alpha_1(\omega)\gamma_1(\omega)-\sum\alpha_i(\omega)\gamma_i(\omega)\} \times\mu_0^2\gamma_1^4(0)\Big] \quad (15)$$

**Comparison of Eq. 15 with Experiments.**— In the calculation of the Kerr constant with Eq. 15, the value of permanent dipole moment, that of the component of polarizability and that of the molecular dimension must be known. Values of these quantities are taken

TABLE I. THE VALUES OF $\mu_0$, $\alpha_i(\omega)$, $(P_E+P_A)$ AND THE AXIAL RATIO OF THE MOLECULAR ELLIPSOID[a)]

| Substance | $\mu_0\times10^{18}$ | $\alpha_1\times10^{25}$ | $\alpha_2\times10^{25}$ | $\alpha_3\times10^{25}$ | $(P_E+P_A)$ | Axial ratio |
|---|---|---|---|---|---|---|
| Carbon disulfide | 0 | 151.4 | 55.4 | 55.4 | 22.7[4)] | 1 : 0.54 : 0.54 |
| Chloroform | 1.05 | 66.8 | 90.1 | 90.1 | 25.3[4)] | 1 : 1.54 : 1.54 |
| Methylene dichloride | 1.62 | 59.6 | 84.7 | 50.2 | 20.0[4)] | 1 : 1.50 : 0.91 |
| Methyl iodide | 1.65 | 87.2 | 65.7 | 65.7 | 21.9[5)] | 1 : 0.64 : 0.64 |
| Nitromethane | 3.46 | 51.8 | 71.7 | 18.3 | 18.3[5)] | 1 : 0.94 : 0.73 |
| Diethyl ether | 1.17 | 78.7 | 112.6 | 70.7 | 23.2[4)] | 1 : 1.80 : 0.82 |
| Benzene | 0 | 123.1 | 123.1 | 63.5 | 27[4)] | 1 : 1 : 0.52 |
| Toluene | 0.37 | 156.4 | 136.6 | 74.8 | 32.3[4)] | 1 : 0.76 : 0.47 |
| *m*-Xylene | 0.34[1)] | 161.6[1)] | 178.3[1)] | 83.5 | | 1 : 1.30 : 0.57 |
| Fluorobenzene | 1.57 | 112.6 | 110.6 | 71.1 | 31.3[5)] | 1 : 0.85 : 0.49 |
| Chlorobenzene | 1.70 | 155.1 | 138.2 | 74.2 | 34.9[4)] | 1 : 0.76 : 0.44 |
| Bromobenzene | 1.64 | 168.4 | 121.3 | 95.6 | 35.6[5)] | 1 : 0.74 : 0.44 |
| Iodobenzene | 1.70 | 198.4 | 140.7 | 113.6 | 41.4[5)] | 1 : 0.71 : 0.47 |
| *p*-Dichlorobenzene | 0 | 212.9 | 124.8 | 88.3 | 37.9[4)] | 1 : 0.66 : 0.38 |
| *m*-Dichlorobenzene | 1.72 | 158.2 | 178.4 | 90.4 | 39.0[4)] | 1 : 1.28 : 0.52 |
| *o*-Dichlorobenzene | 2.50 | 176.8 | 158.5 | 89.7 | 40.2[4)] | 1 : 0.92 : 0.55 |
| $\alpha$-Bromonaphthalene | 1.45[2)] | 239[3)] | 214.5[3)] | 128[3)] | | 1 : 1.01 : 0.44 |
| Nitrobenzene | 4.19 | 171.6 | 141.9 | 74.1 | 36.2[4)] | 1 : 0.76 : 0.44 |
| Acetone | 2.87 | 69.6 | 72.2 | 48.2 | 16.7[4)] | 1 : 1.24 : 0.47 |
| Ethyl-methyl ketone | 2.87 | 85.5 | 98.3 | 60.2 | | 1 : 1.50 : 0.74 |
| Pyridine | 2.15 | 108.4 | 118.8 | 57.8 | | 1 : 0.98 : 0.56 |

a) The values of $\mu_0$, $\alpha_i(\omega)$ and the axial ratio of the molecular ellipsoid are the same as values in the previous paper except for *m*-xylene and $\alpha$-bromonaphthalene (This Bulletin, **31**, 402, 673 (1958)).

1) H. A. Stuart and H. Volkmann, *Z. Physik*, **80**, 107 (1933).
2) C. G. Le Fèvre and R. J. W. Le Fèvre, *J. Chem. Soc.*, **1955**, 1641.
3) C. G. Le Fèvre and R. J. W. Le Fèvre, *Rev. Pure Appl. Chem.*, **5**, 26 (1955). They have assumed that $(P_E+P_A)=1.1\ P_E$.
4) Landolt-Börnstein Tabellen, 6. Aufl., Bd. I., Teil 3 (1951). p. 514. The value of $\alpha_i(0)$ is obtained on the assumption that $R_\lambda=(4\pi/3)N_A\{\sum\alpha_i(\omega)/3\}$ and $\alpha_i(0)/\alpha_i(\omega)=(P_E+P_A)/R_\lambda$. $N_A$ is Avogadro's number.
5) C. G. Le Fèvre and R. J. W. Le Fèvre, *J. Chem. Soc.*, **1954**, 1577. The value of $\alpha_i(0)$ is obtained on the assumption that $P_E=(4\pi/3)N_A\{\sum\alpha_i(\omega)/3\}$ and $\alpha_i(0)/\alpha_i(\omega)=(P_E+P_A)/P_E$.

TABLE II. THE CALCULATED AND OBSERVED VALUES OF THE KERR CONSTANT[a)]

| Substance | Temp. °C | Wavelength mμ | $B_{calcd}\times10^{7}$ [b,c)] (Eq. 15) | $B_{calcd}\times10^{7}$ (Eq. 15) | $B_{calcd}\times10^{7}$ [c)] (Eq. 2) | $B_{obs}\times10^{7}$ | ε |
|---|---|---|---|---|---|---|---|
| Carbron disulfide | 20 | 589.3 | 4.44 (1 : 0.54 : 0.54)<br>3.64 (1 : 0.50 : 0.50)<br>3.14 (1 : 0.48 : 0.48) | 4.74<br>3.87<br>3.34 | 8.56 | 3.226[1)] | 2.632[2)] |
| Chloroform | 25 | 589.3 | −2.13 (1 : 1.54 : 1.54)<br>−1.80 (1 : 1.82 : 1.82) | −3.08<br>−2.58 | −4.74 | −2.56[3)] | 4.724[3)] |
| | 20 | 546 | −2.41 (1 : 1.54 : 1.54)<br>−2.04 (1 : 1.82 : 1.82) | −3.49<br>−3.14 | −5.46 | −3.08[1)] | 4.81[2a)] |
| Methylene dichloride | 18 | white | −1.51 (1 : 1.50 : 0.91) | −2.09 | −12.4 | −1.16[1)] | 9.14[2a)] |
| Methyl iodide | — | red | 4.26 (1 : 0.64 : 0.64)<br>5.29 (1 : 0.68 : 0.68) | 5.32<br>6.83 | 31.1 | 6.74[1)] | 7.00[2a)] |
| Nitromethane | — | white | 4.60 (1 : 0.94 : 0.73) | 11.7 | 846 | 10.65[1)] | 38.57[2a)] |
| Diethyl ether | 25 | 589.3 | −0.69 (1 : 1.80 : 0.82) | −0.74 | −1.42 | −0.614[3)] | 4.265[3)] |
| Benzene | 25 | 589.3 | 0.59 (1 : 1 : 0.52)<br>0.40 (1 : 1 : 0.44) | 0.62<br>0.42 | 1.12 | 0.41[4)] | 2.2725[4)] |
| Toluene | 20 | 546 | 1.22 (1 : 0.78 : 0.47) | 1.27 | 6.24 | 0.835[1)] | 2.379[2a)] |
| *m*-Xylene | 20 | 546 | 1.22 (1 : 1.30 : 0.57) | | 2.16 | 0.809[1)] | 2.386[5)] |
| Fluorobenzene | 16.5 | red | 2.36 (1 : 0.86 : 0.50) | 3.04 | 14.3 | 6.16[1)] | 5.54[6)] |
| Chlorobenzene | 23.5 | 589.3 | 6.95 (1 : 0.77 : 0.43) | 8.11 | 39.1 | 11.4[3)] | 5.634[3)] |
| | 20 | 546 | 7.78 (1 : 0.77 : 0.43) | 9.08 | 40.6 | 10.5[1)] | 5.612[2b)] |
| Bromobenzene | 24.9 | 560 | 9.15 (1 : 0.75 : 0.45) | 10.2 | 38.1 | 9.9[1)] | 5.39[2b)] |
| Iodobenzene | 17.1 | red | 11.2 (1 : 0.69 : 0.45) | 12.1 | 39.3 | 9.29[1)] | 4.625[2a)] |
| *p*-Dichlorobenzene | 75 | 546 | 1.11 (1 : 0.65 : 0.37) | 1.20 | 2.77 | 2.63[1)] | |
| *m*-Dichlorobenzene | 19 | 546 | 6.45 (1 : 1.28 : 0.52) | 7.31 | 18.6 | $8.9_3$[1)] | 5.039[2b)] |
| *o*-Dichlorobenzene | 21 | 546 | 29.6 (1 : 0.93 : 0.55) | 36.2 | 201 | ca. 44.0[1)] | 9.930[2b)] |
| α-Bromonaphthalene | 21.5 | 580 | 8.43 (1 : 1.01 : 0.44) | 9.85 | 27.4 | 10.5[1)] | 4.83[7)] |
| Nitrobenzene | 23 | 546 | 68.7 (1 : 0.77 : 0.43) | 78.5 | 6407 | 354[8)] | 34.5[3)] |
| Acetone | 20 | 589.3 | 11.0 (1 : 1.24 : 0.74) | 11.6 | 178 | 16.3[3)] | 19.6[3)] |
| Ethyl methyl ketone | — | white | 7.86 (1 : 1.53 : 0.74) | | 93.8 | 13.6[1)] | 18.51[2a)] |
| Pyridine | — | red | 8.50 (1 : 1 : 0.57) | | 112 | 20.4[1)] | 13.55[2a)] |

a) In the case in which the temperature $t$ or the wavelength $\lambda$ of light is not specified, it is assumed that $t=20°C$ or $\lambda=589$ mμ.
b) Figures in parentheses are the assumed values of axial ratios.
c) Calculated on the assumption that $\alpha_1(0)=\alpha_1(\omega)$.

1) H. A. Stuart, "Hand- und Jahrbuch über Chemischen Physik," Bd. I/III, Leipzig (1939). p. 49.
2) Quoted from the table in the previous paper (This Bulletin, **31**, 673 (1958)). a) Observed value at 20°C. b) Observed value at 25°C.
3) C. G. Le Fèvre and R. J. W. Le Fèvre, *J. Chem. Soc.*, **1953**, 4041.
4) C. G. Le Fèvre and R. J. W. Le Fèvre, *Rev. Pure Appl. Chem.*, Chem., **5**, 261 (1955).
5) L. M. Heil, *Phys. Rev.*, **39**, 666 (1932).
6) R. Mecke and K. Rosswog, *Z. Elektrochem.*, **60**, 47 (1956).
7) The observed value at 25°C. W. M. Heston, E. J. Hennelly and C. P. Smith, *J. Am. Chem. Soc.*, **72**, 2071 (1950).
8) H. Friedrich, *Physik. Z.*, **38**, 318 (1937).

from the literatures by the method similar to that written in the previous paper[2].

Contrary to the case of the calculation of the static dielectric constant, in the case of the calculation of the Kerr constant, both the values of $\alpha_i(0)$ and $\alpha_i(\omega)$ are needed. However, as yet the value of $\alpha_i(0)$ is not known. Stuart[6] and Le Fèvre[7] have assumed that $\alpha_i(0)/\alpha_i(\omega)=(P_E+P_A)/R_\lambda$. $P_E$ is electronic polarisation and $P_A$ is atomic polarization. $R_\lambda$ is molecular refraction for the wavelength of $\lambda$.

In Table I the values of the following quantities are tabulated; the value of permanent dipole moment $\mu_0$, the value of the component of polarizability $\alpha_i(\omega)$, the value of $(P_E+P_A)$ and the values of the ratios of axial lengths of the molecular ellipsoid.

The Kerr constant of about twenty substances is calculated with Eq. 15 and compared with the experimental value.

The value calculated with Eq. 2 is also compared with experimental one.

Generally speaking, the considerable discrepancy between the theoretical value and the experimental one is observed if we apply Eq. 2, and moreover, the greater the value of the dielectric constant of liquid, the greater becomes the discrepancy[8].

On the contrary, the calculated value with Eq. 15 is not very far from the experimental one.

When atomic polarization is taken in account, the coincidence is not unsatisfactory.

In Table II, the calculated and the experimental values of $B$ are tabulated. In the fourth column, the calculated values with Eq. 15 are tabulated, in which $\alpha_i(0)$ is replaced by $\alpha_i(\omega)$. In the fifth, the value of $\alpha_i(0)$ is taken in account.

In the sixth, the values of $B$ calculated with Eq. 2 are represented. The experimental values of $B$ are also represented in the seventh column. In addition, the values of $\varepsilon$ are tabulated in the eighth.

For a symmetrical top molecule the calculation which is to be described in the following is also made.

A symmetrical top molecule can be approximated as a spheroid. The shape of a spheroid can be determined by only one axial ratio. In this case, the value of the axial ratio is chosen as to fit the experimental value of the Kerr constant, and is compared with the geometrical one.

In the case of a general ellipsoidal molecule, the Kerr constant is calculated with Eq. 15, in which the value of axial ratio is taken as the value of the geometrical one.

In the following, some remarks are made on special cases.

**Spheroide Molecules.** — a) *Carbon Disulfide* —For liquid carbon disulfide the calculated value of the Kerr constant is sensitive to the assumed axial ratio. The value of axial ratio 0.48 is fitted best to the observed value of the Kerr constant. In the case of dielectric constant the value of axial ratio 0.50 is the fittest value. The geometrical value is 0.54.

b) *Benzene.* — The obtained value of the axial ratio 0.44 is smaller than the geometrical one 0.52.

c) *Chloroform.* — The value of axial ratio 1.82 is the fittest value if atomic polarization is taken in account. The geometrical value is 1.54.

**General Ellipsoid Molecules.** — a) *Benzene Derivatives.*—The calculated value of the Kerr constant gives the right magnitude, but the values for fluorobenzene[10], *p*-dichlorobenzene and nitrobenzene are excepted. As the only one exceptional case, the value for *p*-dichlorobenzene obtained with Eq. 2 is better than the value obtained with Eq. 15. The calculated value of the Kerr constant of liquid fluorobenzene is lower than the experimental one. The theoretical value for nitrobenzene is much lower than the experimental one.

b) *Pyridine.*—The calculated value is lower than the experimental one.

c) *Nitromethane.*—The value of electronic polarization and that of atomic polarization are evaluated by Le Fèvre[7] as 12.0 cc. and 6.3 cc., respectively. The calculated value of the Kerr constant coincides fairly with the observed one if atomic polarization is taken in account. However, whether the coincidence is fortuitous or not is not determined as yet.

d) *Diethyl Ether.*—For diethyl ether planer zigzag form is assumed. The value of axial ratio calculated from the molecular model is fairly consistent with the value which is fittest for the value of the Kerr constant.

e) *Ethyl Methyl Ketone.*—Also the model of planer zigzag form is adopted. The calculated value is lower than the experimental one.

6) H. A. Stuart and H. Volkmann, *Ann. Physik*, 18, 121 (1933).

7) C. G. Le Fèvre and R. J. W. Le Fèvre, *J. Chem. Soc.*, 1953, 4041. Further they have used $P_E=R_\infty$ (molecular refraction for light of infinite wavelength) instead of $R_\lambda$.

8) However, the so-called $4\pi/3$ catastrophe[9] does not arise in the Kerr effect.

9) J. H. Van Vleck, *Ann. N. Y. Acad. Sci.*, 40, 295 (1940).

10) It is interesting to note that the value of the component of the molecular polarizability of fluorobenzene is almost the same as that of benzene. Le Fèvre[7] has obtained the following values.

| | $\alpha_1\times10^{25}$ | $\alpha_2\times10^{25}$ | $\alpha_3\times10^{25}$ |
|---|---|---|---|
| Benzene | 111.4 | 111.4 | 73.6 |
| Fluorobenzene | 112.6 | 110.6 | 71.1 |

**Summary**

A formula for the Kerr constant in liquid state has been derived, in which the form of the local field is assumed to be the same as that derived previously[2]. The formnla is able to explain experimental data to some extent, although there are some exceptions.

The author is grateful to Professor Masasi Yasumi for his kind guidance and encouragement throughout this work, and to Mr. Hitoshi Komooka for his advice. Thanks are also due to the Ministry of Education for a grant in aid of this research.

*Aeronautical Research Institute*
*The University of Tokyo*
*Meguro-ku, Tokyo*

# *Organic Semiconductors with High Conductivity. III. Perylene-Iodine Complex*

By Tokiko UCHIDA and Hideo AKAMATU

(Received December 24, 1960)

Polycyclic aromatic hydrocarbons with halogens form molecular complexes in solid state and those complexes of the charge transfer type possess relatively high electrical conductivity. The preliminary survey for the semiconductive properties of these complexes has been given in the first paper[1] of this series of investigations. Concerning the mechanism of electronic conduction in organic solids, the charge transfer complexes are so suggestive that their structures with their physical properties are specially interesting. In the preceding paper[2], the violanthrene-iodine system was investigated in connection with its structure. In this paper, the investigation of the perylene-iodine system, another typical example for this series of complexes, is presented.

**Preparation and Composition of Perylene-Iodine Complex.**—The formation of a solid molecular compound between perylene and iodine has been known for many years since the investigations of Clar and Brass[3], and also, by Zinke et al.[4] However, concerning the composition of this complex, these investigators did not come to agreement with each other.

When perylene is added to the benzene solution of iodine, the molecular complex is obtained as a black precipitate which consists of needle-shaped minute crystals. This complex is somewhat unstable in the atmosphere and has tendency to liberate iodine. The following procedure was employed for the determination of the composition. Perylene (100~130 mg.) and iodine (appropriate amount) were dissolved in 50 ml. of benzene. By heating this solution under reflux condenser, both components were homogeneously dissolved. Then the container was transferred into a thermostat of 20°C, and the complex was precipitated from the solution. For the purpose of keeping the equilibrium between the precipitated complex and the solution, the container was held at this temperature for more than 15 hr. being continuously vibrated. Then by a suction through a glass filter, the precipitate was separated from the solution as quickly as possible, and was kept in a desiccator. The iodine content in the solution was determined by the titration with sodium thiosulfate solution. The iodine content of the precipitate was also determined by the same method after dissolving it into benzene.

In Fig. 1, the iodine content of the benzene solution which is in equilibrium with the precipitate is plotted against the composition of the precipitate. The composition is expressed with the number of iodine molecules added to one molecule of perylene (mole ratio).

On this curve, the isotherm for the heterogeneous equilibrium of the perylene-iodine system, the horizontal part AB indicates that the precipitate should consist of two sorts of solid phase, one is perylene and the other is the complex which has the composition of

1) H. Akamatu, H. Inokuchi and Y. Matsunaga, This Bulletin, **29**, 213 (1956).
2) H. Akamatu, Y. Matsunaga and H. Kuroda, ibid., **30**, 618 (1957).
3) E. Clar and K. Brass, *Ber.*, **65**, 1660 (1932); **72**, 604 (1939).
4) A. Zinke and A. Pongratz, ibid., **70**, 214 (1937); A. Zinke and H. Troger, ibid., **74**, 107 (1941); M. Pestemer and E. Treiber, ibid., **74**, 964 (1941).

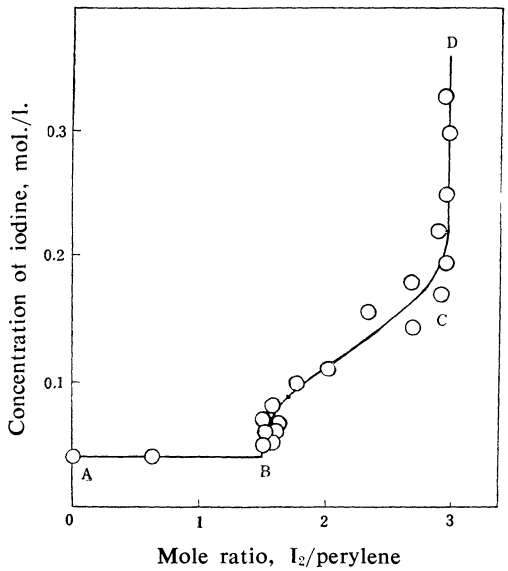



Fig. 1. The isotherm of perylene-iodine system. The concentration of iodine in benzene solution is plotted against the composition of precipitate.

Perylene·1.5 $I_2$. It can be seen directly or under a microscope that the precipitate is a mixture of yellow crystals (perylene) and black needles (complex). As will be shown in the latter section, the magnetic susceptibility measurement also verifies the existence of Perylene·1.5 $I_2$. At the vertical part CD, the precipitate is made of one phase which has the composition of Perylene·3$I_2$. Thus, there are two kinds of complexes which have different compositions. The precipitate at the intermediate part BC should be made of a solid solution of these two kinds of complexes. The shape of the curve BC is similar to that of the violanthrene-iodine system, which was discussed in the previous paper[2].

The spectrophotometric measurement was made for the mixed solution of perylene and iodine in benzene and also in chloroform, but the absorption band due to the complex formation could not be found over 3000~7000 Å range. This result implies that the molecular complex has poor solubility or it might be stable only in the solid state. Thus the equilibrium between perylene and iodine, for instance when the concentration of iodine is high enough, can be expressed as

$$\text{Perylene(soln.)} + 3I_2\text{(soln.)} \rightleftarrows [\text{Perylene}\cdot 3I_2]$$

The equilibrium constant in benzene solution has been found to be $K_c = 2.1 \times 10^5$ (in mol./l. unit, 20°C). This leads to the free energy of the complex formation, $-RT \ln K_c = -7.1$ kcal./mol.

**Electrical Properties.**—The electrical resistivity of perylene-bromine complex is not stable because of the substitution reaction of bromine as reported in the previous paper[1]. This is not the case, however, for the perylene-iodine complex; the substitution reaction does not take place between iodine and hydrogen, and the complex can be kept stable if it is sealed in the dry atmosphere.

The precipitate from the benzene solution was applied to the resistivity measurement. The specimen powder was compressed between the metal electrodes in an ebonite tube having inside diameter of 8.0 mm. The electrode surfaces were coated with platinum plates. The electrical field applied to the specimen was about 20 V./cm. and the resistance was read with an ohmmeter.

The observed resistivity was dependent on the applied pressure and it decreased with the reciprocal of pressure in a linear way when the applied pressure was above 50 kg./cm$^2$. This might be due to the presence of contact resistance between particles. Thus, the limiting value was read by the extrapolation to the infinite pressure. This value, $\rho(p=\infty)$, is assumed as the intrinsic resistivity of the sample and is shown in Table I, where the observed

TABLE I. SEMICONDUCTIVE DATA OF PERYLENE-IODINE COMPLEX

| Composition in mole ratio, $I_2$/perylene | Electrical resistivity at 15°C, ohm.cm. $p=116$ | $p=\infty$ | $\varepsilon$ eV. | Temperature range |
|---|---|---|---|---|
| Perylene | $4.0\times10^{18}$ | | $2.0_1$ | 108~−170°C |
| 0.23 | $6.8\times10^{3}$ | 500 | 0.09 | Room temp.~− 80°C |
| 0.86 | 74 | 30 | 0.06 | Room temp.~−170°C |
| 1.08 | 27 | 15 | 0.06 | 〃 |
| 1.56 | 16 | 9 | 0.06 | 〃 |
| 1.80 | 19 | 9 | 0.06 | 〃 |
| 2.42 | 19 | 10 | 0.05 | 〃 |
| 2.96 | 20 | 10 | 0.06 | 〃 |
| 5.8 | 22 | 15 | 0.07 | Room temp.~−150°C |
| Iodine* | $5.8_6\times10^{6}$ | | $4.5_1$ | 25~113°C |

* M. Rabinowitsch, *Z. Physik. Chem.*, **119**, 82 (1926).

resistivity at the pressure of 116 kg./cm$^2$ is also shown for comparison.

The voltage dependence for the current was examined with the complex having the composition of Perylene·2.53 $I_2$. The linear relationship was observed between the current and the applied voltage when the voltage was not higher than 25 V./cm. In this region where the Ohm's law holds, the current was stable and quite reversible. This indicates that the conduction is the electronic one. However, when a higher voltage than this value was applied, the larger current deviating from the linear relationship was observed instantaneously and then it decreased gradually. After the external field was removed, the cell was still polarized slightly for a while.

The temperature dependence for the resistivity was observed in the range from room temperature down to −170°C. No higher temperature can be applied to the sample for it decomposes and liberates iodine.

It was observed that the resistivity increases with decreasing temperature, and a good linear relationship was found between the logarithm of resistivity and the reciprocal of temperature. This linear relation was found even in a case of which the sample consisted of two solid phases (perylene and complex) or of the solid solution, similarly as in the case of a pure simple compound (for instance perylene).

Assuming the formula $\rho=\rho_0\exp(\varepsilon/2kT)$, where $\rho$ is the resistivity and $\rho_0$ is a constant, the value of $\varepsilon$, the "energy gap" for the generation of charge carriers was estimated. This value is shown in Table I.

In Table I, it is seen that the $\varepsilon$-value is nearly constant (about 0.06 eV.) over a very wide range of the mole ratio. This might be due to the fact that the observed value was the one having the narrowest energy gap which participated predominantly in the generation of charge carriers at the low temperature range where the experiment was carried out.

There are two kinds of intermolecular compounds, as mentioned in the preceeding section, Perylene·1.5 $I_2$ and Perylene·3$I_2$. It is noticeable, however, that no important distinction can be found for the values of the energy gap between those complexes, similarly for the values of resistivity. Therefore, it can be concluded that both complexes, Perylene·1.5 $I_2$ and Perylene·3 $I_2$, possess resistivity of 9～10 ohm.cm. and an energy gap of 0.06 eV. In consequence the solid solution of these complexes possesses the same values regardless of its composition.

For the purpose of knowing the principal charge carriers, whether electrons or positive holes, the preliminary examination of the thermoelectric power of the cell was made. Both leads of the cell were connected to a galvanometer. When the one side of the cell was heated to a higher temperature than the other side, the flow of a minute current was observed. The direction of the current indicated that the warm side electrode was negative against the cold side electrode of the cell. The amount of the thermoelectric power was roughly estimated as a few micro volts per degree. This indicates that positive holes contribute to the current more predominantly than electrons.

**Magnetic Susceptibility.**—Both perylene and iodine are diamagnetic substances. In the case of the formation of the charge transfer complex, however, the magnetic susceptibility of the system shows a large deviation from the additive property of diamagnetism[5]. This offers a method to examine the composition of the intermolecular compound formed in the system. The Gouy method was employed for the susceptibility measurement at the room temperature. The observed values are summarized in Table II and illustrated in Fig. 2 as the function of iodine content.

The remarkable depression of diamagnetism from the value given by the additivity rule

Table II. The diamagnetic susceptibility of perylene-iodine system

| Wt. percentage of $I_2$ | Mole ratio $I_2$/perylene | Specific susceptibility $\chi\times10^6$ |
|---|---|---|
| 0 | 0 | −0.632±0.007 |
| 22.6 | 0.29 | −0.517±0.004 |
| 44.0 | 0.78 | −0.418±0.007 |
| 62.2 | 1.63 | −0.343±0.009 |
| 65.7 | 1.90 | −0.324±0.006 |
| 68.8 | 2.20 | −0.338±0.007 |
| 75.1 | 3.00 | −0.337±0.009 |
| 100 | | −0.36* |

* International Critical Table VI, p. 355.

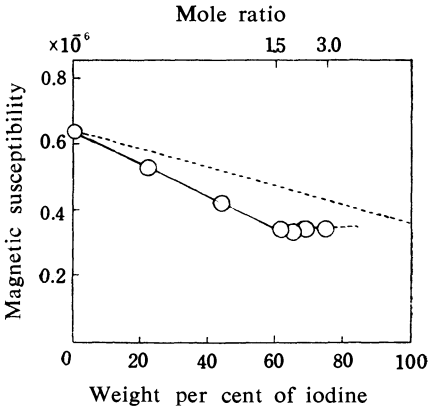



Fig. 2. The plot of the diamagnetic susceptibility of perylene-iodine system as the function of iodine content.

(the dotted line) is seen in Fig. 2. The depression proceeds in a linear way as the iodine content increases up to 60 per cent. Then, from 60 per cent up the susceptibility appears almost constant; but probably it proceeds toward the value of iodine. Thus a sharp break is found at the iodine content of 60 per cent (the mole ratio is 1.5). The linear part of susceptibility below this iodine content follows the additivity rule in regard to the mixture of pure perylene and the complex of this composition. This proves the complex formation of Perylene·1.5 $I_2$. Its molar susceptibility is $-217\times10^{-6}$, which implies that the depression from the diamagnetic additivity is $80\times10^{-6}$ per mole of perylene. However, the recognition of the formation of Perylene·3 $I_2$ is difficult from the magnetic susceptibility measurement, as its value is almost the same as the value of Perylene·1.5 $I_2$ and also is not far from the value of iodine. This suggests that in the formation of Perylene·3 $I_2$ from Perylene·1.5 $I_2$ by further addition of iodine, the electronic state of the system is not greatly influenced. The molar susceptibility of Perylene·3 $I_2$ is $-342\times10^{-6}$ and the diamagnetic depression is $92\times10^{-6}$. This is comparable to that of Perylene·1.5 $I_2$.

**ESR Absorption.**—The diamagnetic depression from the additivity rule should be attributed to the paramagnetic contribution of the unpaired electrons which are generated in association with the formation of charge transfer complex, as Matsunaga[5,6] has pointed out previously. The electron spin resonance absorption was examined for the perylene-iodine system as the function of iodine content. An x-band microwave spectrometer, Hitachi MPS-1 was employed. The measurement was carried out at room temperature. The spin concentration and the *g*-value were determined referring to the values of DPPH. The results are summarized in Table III.

TABLE III. THE ELECTRON SPIN RESONANCE ABSORPTION OF PERYLENE-IODINE SYSTEM (AT ROOM TEMPERATURE)

| Mole ratio $I_2$/perylene | Line width at half maximum gauss | Number of spins per g. | Number of spins per one molecule of perylene ESR | Static* |
|---|---|---|---|---|
| 0.29 | 8 | $1.8\times10^{19}$ | 0.01 | 0.01 |
| 0.78 | 8 | $2.3\times$ 〃 | 0.02 | 0.03 |
| 1.52 | 8 | $5.5\times$ 〃 | 0.06 | 0.06 |
| 1.84 | 11 | $5.2\times$ 〃 | 0.06 | 0.06 |
| 2.22 | 11 | $5.2\times$ 〃 | 0.06 | 0.06 |
| 2.53 | 13 | $3.3\times$ 〃 | 0.05 | 0.06 |
| 3.00 | 13 | $3.0\times$ 〃 | 0.05 | 0.07 |

* These values were calculated with the deviation from the additivity rule for molar susceptibility, dividing by $1270\times10^{-6}$.

The *g*-value was observed to be constant, 2.0043, regardless of the composition of the complex. The spin concentration varies with the iodine content, but the number of spins assigned to one molecule of perylene becomes nearly constant in any system whose mole ratio is more than 1.5. In the last column of the table, the number of unpaired electrons calculated from the diamagnetic depression in molar susceptibility is shown. These values are in good agreement with those observed by ESR absorption. The most interesting point in this result is that the number of unpaired electrons assigned to one perylene molecule is essentially constant for both Perylene·1.5 $I_2$ and Perylene·3 $I_2$. This suggests again, with the electrical property, that the electronic states are not greatly different from each other in those two complexes.

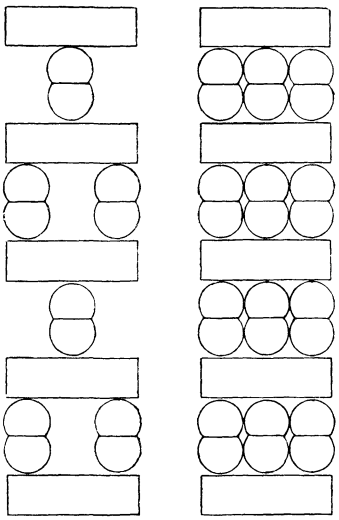
**On the Structure of Perylene-Iodine Complex.**—The X-ray diffraction patterns have been examined with the association of the "Geigerflex" diffractometer for the complexes which have the compositions of Perylene·1.5 $I_2$ and Perylene·3 $I_2$ respectively. Both complexes give sharp crystalline patterns which are quite different from that of perylene. This is in marked contrast to the violanthrene-iodine complex, which gives an amorphous pattern[2]. The main diffraction lines of Perylene·1.5 $I_2$ and Perylene·3 $I_2$ are in common with each other regarding the position as well as the intensity ratio. This indicates that these two complexes have structures very similar to each other.

Concerning the crystal system, no information could be obtained from the observed values of spacing alone, because it possesses low symmetry. However, three series of diffraction lines could be found in the observed principal lines. The first series consists of lines whose spacing is 13.5Å and possesses the largest intensity compared to the other series. The second and the third series consist of lines which have the spacing of 11.5 and 10.7Å respectively. In all of these series, the first order diffraction lines are weak in intensity, but the second order diffraction lines possess enough intensity and are well resolved.

Hassel and Strømme[7] have made investigation on the crystal structure of the benzene-bromine complex. It was concluded that in this solid complex the molecules of bromine and benzene are arranged alternately with each other, directing the molecular axis of bromine

5) Y. Matsunaga, This Bulletin, **28**, 475 (1955).
6) Y. Matsunaga, *J. Chem. Phys.*, **30**, 855 (1959).
7) O. Hassel and K. O. Stromme, *Acta Chem. Scand.*, **12**, 1146 (1958).

nearly perpendicular to the molecular plane of benzene. A similar structure could be assumed for the perylene-iodine complex. If an iodine molecule is sandwiched between two perylene molecules, directing its molecular axis perpendicularly to the plane of the perylene molecule, the distance between the two perylene molecules would be 10.7 Å (the thickness of aromatic molecular plane = 3.7 Å and the length of iodine molecule = 7.0 Å). This value is in coincidence with the observed spacing of 10.7 Å The molecular plane of perylene possesses enough area to accommodate three iodine molecules. Thus, it is likely that the complex is made of a structural unit such as is shown in Fig. 3. The reflection planes which have the spacing of 13.5 Å and give the strongest diffraction lines should be the planes which contain iodine molecules in the highest density, and could be constructed by stacking such structural units. However, no further information can be derived from the powder diffraction diagram alone.



(a) Perylene·1.5 $I_2$ (b) Perylene·3 $I_2$

Fig. 3. The proposed structure of perylene-iodine complex. (a) Perylene·1.5 $I_2$ (b) Perylene·3 $I_2$

The density of the perylene-iodine system has been examined. The pycnometer was employed in association with an aqueous medium containing a small amount of surfactant. In Fig. 4, the specific volume is plotted against the iodine content. The specific volume of perylene is 0.741 cc./g. and that of iodine is 0.202 cc./g. The broken line indicates the specific volume of the binary system assuming the additivity of volume. The observed values are situated above this line. This indicates that complex has the structure with interstices where water molecules can not penetrate. However, when the iodine content increases up to the composition of Perylene·3 $I_2$, the observed specific volume is 0.340 cc./g.; this value is in good agreement with the calculated value assuming the additivity law. This indicates that this complex has the most closed packing structure.

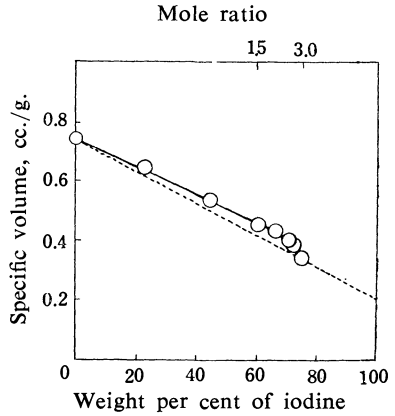



Fig. 4. The specific volume of perylene-iodine system.

## Discussion

Most organic compounds are electrical insulators, because the intermolecular coupling is so poor that electrons can hardly transfer from molecule to molecule, even in the electronic excited state. In organic semiconductors, the activation energy for generating charge carriers possesses relatively low values (1 eV. or less), whereas the resistivity possesses high values ($10^7 \sim 10^{14}$ ohm. cm.). However, if, in the formation of crystal, the condensation of molecules is caused by an interaction such as that which is associated with the exchange of electrons between molecules, it could be expected that those electrons can move throughout the crystal lattice. This could result in the drift mobility under the applied electrical field. This is the case of charge transfer complex in the solid state.

In the solid complex, in order to expect the conductance, the donor molecules (D) and the acceptor molecules (A) should be arranged alternately with each other in such a way as D·A·D·A···, thus the charge transfer interaction could be conjugated between neighboring molecules throughout the crystal lattice. The proposed model for the perylene-iodine complex illustrated in Fig. 3 is likely to be reasonable.

In the case of simple semiconductive compounds (polycyclic aromatic hydrocarbons), the resistivity and also the activation energy for generating charge carriers are depending markedly on the size of the aromatic molecule.

However, in the case of the charge transfer complex, their semiconductive property is quite independent of the size of the hydrocarbon molecule, as is seen in Table IV. This implies that the charge transfer interaction itself, between donors and acceptors, is the principal cause for generating mobile electrons which can contribute to the electrical conduction. The ESR absorption is observed commonly in charge transfer complexes and a close connection between the unpaired electrons and the charge carriers be presumed[8].

TABLE IV. THE SEMICONDUCTIVE DATA OF AROMATIC HYDROCARBONS AND IODINE COMPLEXES

| Complex | Mole ratio | $\rho_{15°C}$ ohm.cm. | $\varepsilon$ eV. |
|---|---|---|---|
| Perylene-iodine | 1 : 1.5 | 9 | 0.06 |
| Perylene-iodine | 1 : 3 | 10 | 0.06 |
| Pyranthrene-iodine | 1 : 2 | 20 | 0.09 |
| Violanthrene-iodine | 1 : 2 | 13 | 0.15 |
| Pure hydrocarbon | | | |
| Perylene | | $4.0\times10^{18}$ | 2.0 |
| Pyranthrene | | $4.5\times10^{16}$ | 1.07 |
| Violanthrene | | $2.0\times10^{14}$ | 0.94 |

The isotherm for the phase equilibrium of perylene-iodine system indicates the formation of two sorts of intermolecular compounds which have the composition of Perylene·1.5 $I_2$ and Perylene·3$I_2$ respectively. The investigation of the magnetic susceptibility also suggests the existence of the compound of Perylene·1.5$I_2$. However, concerning the electrical property almost no difference could be found between those two sorts of compounds. These two compounds possess not only the same semiconductive property but also the similar structure and almost the same number of unpaired electrons. These facts lead to the assumption that when three iodine molecules combine with two perylene molecules, not only the framework of the crystal structure but also the electronic state (for the charge transfer type of combination) are completed, and almost no further improvement takes place by adding the three more iodine molecules. Those added iodine molecules can occupy the interstices in the framework to complete the closed packed structure (mainly with non-bonding type of combination), but result in no further important change in the electronic state for the complex formation.

8) J. Kommandeur and L. S. Singer, Conference on Electronic Conductivity in Organic Solids, Duke University, April, 1960; D. R. Kearns, G. Tollin and M. Calvin, *J. Chem. Phys.*, 32, 1020 (1960).

## Summary

Concerning the solid complex of perylene-iodine system, it has been clarified that two sorts of molecular addition compounds are formed. One has the composition of Perylene·1.5 $I_2$ (or 2 Perylene·3 $I_2$) and the other is Perylene·3$I_2$. Both complexes are semiconductive with low resistivity; the resistivity at the room temperature is 9～10 ohm.cm. and the energy gap is 0.06 eV. Concerning those values, both complexes possess almost the same values. Not only the elecrical properties and the magnetic properties, but also, both complexes possess similar crystal structures. To explain those facts, the structural units for those complexes have been proposed. These consist of the conjugation between perylene molecules and iodine molecules with the charge tranfer type of interaction.

The authors desire to express their thanks to Dr. Yoshio Matsunaga for his cooperation and advice. The cost of this study was defrayed from the grant of the Ministry of Education to which the authors' thanks are due.

*Department of Chemistry*
*Faculty of Science*
*The University of Tokyo*
*Hongo, Tokyo*

# *Ion-exchange Behavior of Acidic and Basic Amino Acids*

By Manabu SENŌ and Takeo YAMABE

(Received December 20, 1960)

In the preceding paper[1] the ion-exchange behavior of some neutral amino acids was described and it was pointed out that amino acids are absorbed most predominantly on ion-exchange resins in the pH range near the isoelectric points of the amino acids. In this paper, some experimental results concerning the ion-exchange behavior of the acidic and the basic amino acid are presented and discussed.

## Experimental

Glutamic acid was used as an acidic amino acid and lysine monohydrochloride as a basic amino acid. These dissociation constants p$K$ and isoelectric points pI are as follows.

| | p$K_1$ | p$K_1'$ | p$K_2$ | p$K_2'$ | pI |
|---|---|---|---|---|---|
| Glutamic acid | 2.19 | 4.25 | 9.67 | — | 3.22 |
| Lysine | 2.18 | — | 8.95 | 10.76 | 9.70 |

p$K$'s are defined by equations given later. The ion-exchange resins used were Amberlite resins, IR-120, IRC-50, IRA-400 and IR-4B, the exchange capacities of which are 4.24, 10.0, 2.15 and 8.0 meq./g. dry resin, respectively.

The experimental procedures were the same as those in the preceding paper[1]. All measurements were carried out batchwise; a constant volume (50 ml.) of a solution containing a constant amount (about 2 mmol.) of an amino acid and being adjusted to a desired pH by adding hydrochloric acid or sodium hydroxide, was added onto a constant quantity (about 1 meq.) of the ion-exchange resin. The details are as follows.

| Amino acid | Total amounts $a$ mmol. | H- or OH-form resins $w$ g. (dried) IR-120 | IRC-50 | IRA-400 | IR-4B |
|---|---|---|---|---|---|
| Glutamic acid | 2.09 | 0.180 | 0.091 | 0.344 | 0.110 |
| Lysine | 2.13 | 0.170 | 0.097 | 0.336 | 0.109 |

After being allowed to stand for a few days, which were long enough for the attaining of the exchange equilibrium, the pH and the remaining amount of the amino acid in the solution phase were measured and the adsorbed amount of the amino acid was estimated. All the experiments were made at room temperature, 5~15°C.

## Results and Discussion

Experimental results were shown in Figs. 1 and 2, in which the adsorbed amounts of amino acids were plotted against the pH of the equilibrium external solution. Like the neutral amino acids, the acidic and the basic amino acid are adsorbed most intensively at pH values close to the isoelectric point and, in the lower and the higher pH range, the adsorbed amounts of the amino acids decrease sharply owing to the competitive adsorption of hydrogen or hydroxyl ions. The amounts of uptake of amino acids by sodium- or chloride-form strongly dissociated resins are less than those by hydrogen-form or hydroxyl-form resins, especially in the pH range near the isoelectric point.

The pH dependence of adsorption of amino acids is more remarkable and more characteristic, compared to the case of neutral amino acids. As shown already by several investigators[2,3], glutamic acid is adsorbed predominantly on the anion-exchange resins and lysine on the cation-exchange resins. Glutamic acid is adsorbed very intensively in the limited pH range, 3~5, on a weakly basic ion-exchanger, IR-4B, while it is well adsorbed in a wider, namely, higher pH range in the case of a strongly basic ion-exchanger, IRA-400. This is owing to the strong affinity of IR-4B to the hydroxyl ion. Lysine shows a peculiar behavior, probably because it was used in the monohydrochloride form. The resulting solution from it is acidic, and sodium hydroxide must be added to bring the solution pH to the isoelectric point of lysine. The maximum adsorption of lysine takes place in pH 2~3 on IR-120, and in pH 7~9 on IRC-50. In other words, the addition of sodium ions decreases the amount of uptake of lysine on IR-120 and increases the amount adsorbed on IRC-50. This behavior is owing to the strong affinity of IRC-50 to the hydrogen ion and that of IR-120 to the sodium ion.

The adsorption mechanism of amino acids on the ion-exchange resins was described in the preceding paper. That is to say, when the amino acid cations are adsorbed on the hydrogen-form cation-exchanger, the hydrogen ions

1) M. Senō and T. Yamabe, This Bulletin, 33, 1532 (1960).

2) P. B. Hamilton, "Ion Exchangers in Organic and Biochemistry", Ed. by C. Calmon and T. R. K. Kressman, Interscience Pub., New York (1957), p. 255.

3) O. Samuelson, "Ion Exchangers in Analytical Chemistry", John Wiley & Sons, Inc., New York (1953), p. 210.

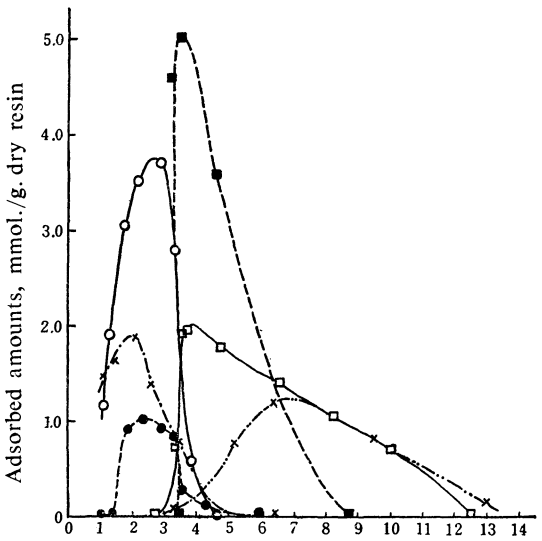



Fig. 1. Adsorption of glutamic acid on ion-exchange resins.

—○— IR-120, $H^+$-form
--●-- IRC-50, $H^+$-form
—□— IRA-400, $OH^-$-form
--■-- IR-4B, $OH^-$-form
-·×·- IR-120, $Na^+$-form
-··×··- IRA-400, $Cl^-$-form

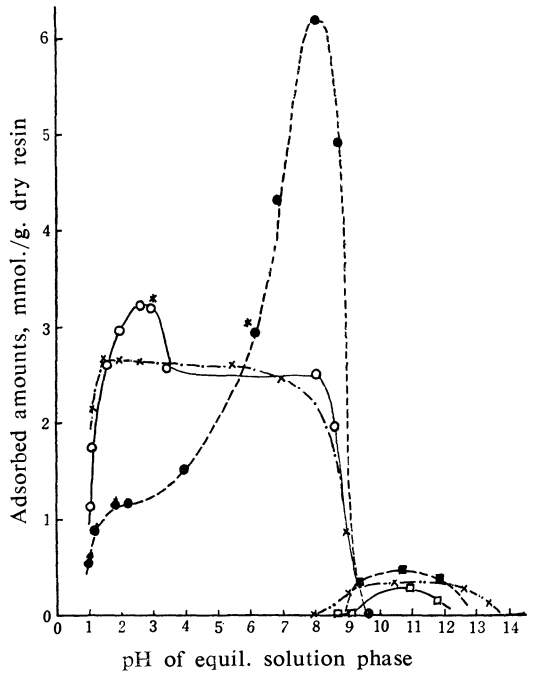



Fig. 2. Adsorption of lysine monohydrochloride on ion-exchange resins (Symbols are the same as those in Fig. 1).
A mark * represents for no addition of acid or base.

are liberated from resins and promote the association of the amino acid to produce the amino acid cations. These result in further exchange of the amino acid cations for the hydrogen ions. The exchange reaction attains equilibrium through such a repeating process. Similar reactions take place in other systems.

**Relations between the Adsorbed Amount of Amino Acids and the pH of the External Solution.**—The dissociation constants of the acidic amino acid are given as

$$\left.\begin{aligned} &AH^+ \rightleftarrows A^\pm + H^+ \quad K_1=\frac{[A^\pm]_s[H^+]_s}{[AH^+]_s} \\ &A^\pm \rightleftarrows A^- + H^+ \quad K_1'=\frac{[A^-]_s[H^+]_s}{[A^\pm]_s} \\ &A^- \rightleftarrows A^{2-} + H^+ \quad K_3=\frac{[A^{2-}]_s[H^+]_s}{2[A^-]_s} \end{aligned}\right\} \quad (1)$$

where the term arising from activity coefficients is neglected. In a case when the acidic amino acid is exchanged for hydrogen ions on the cation-exchanger, the selectivity coefficient is defined as

$$\left.\begin{aligned} &RH + AH^+ \rightleftarrows RAH + H^+ \\ &K_H=\frac{[AH^+]_r[H^+]_s}{[AH^+]_s[H^+]_r} \end{aligned}\right\} \quad (2)$$

where $[A]_s$ is the concentration of ion A in the equilibrium external solution in the unit, meq./ml., and $[A]_r$ is that in the resin phase in the unit, meq./g. dry resin.

Under the present experimental condition, that is; (1) the total amount of the amino acid in the system is constant, $a$ mmol., (2) the amount of the exchangeable ions in the ion-exchanger is constant, $c$ meq., $c=Cw$, where $C$ is the exchange capacity (meq./g. dry resin) of the resin and $w$ is the weight of the resin used, and (3) the volume of the external solution is constant, $v$ ml., the following relationship holds between the adsorbed amount of the amino acid, $[AH^+]_r=y$, and the hydrogen ion concentration in the external solution, $[H^+]_s=x$,

$$\left.\begin{aligned} &\frac{(a-wy)(c-wy)}{y}=\frac{vw}{K_H}f(x) \\ &f(x)=\frac{x^3+K_1x^2+K_1K_1'x+K_1K_1'K_2}{x^2} \end{aligned}\right\} \quad (3)$$

This formula is similar to that derived on the system of neutral amino acids[1].

When the acidic amino acid is adsorbed on the hydroxyl-form anion-exchanger, two species of the amino acid anions participate in the exchange reaction as follows,

$$\left.\begin{aligned} &ROH + A^- \rightleftarrows RA + OH^- \\ &K_{OH} = \frac{[A^-]_r [OH^-]_s}{[A^-]_s [OH^-]_r} \\ &2ROH + A^{2-} \rightleftarrows R_2A + 2OH^- \\ &K'_{OH} = \frac{[A^{2-}]_r [OH^-]_s^2}{[A^{2-}]_s [OH^-]_r^2} \end{aligned}\right\} \quad (4)$$

and the following formulas are derived between quantities, $[A^-]_r = y_1$, $[A^{2-}]_r = 2y_2$ and $[OH^-]_s = x'$,

$$\left.\begin{aligned} &\frac{[a - w(y_1 + y_2)]\,[c - w(y_1 + 2y_2)]}{y_1} = \frac{vw}{K_{OH}} f(x') \\ &\frac{[a - w(y_1 + y_2)]\,[c - w(y_1 + 2y_2)]^2}{y_2} \\ &\quad = \frac{vw^2}{K'_{OH}} \frac{K_w}{K_2} f(x') \\ &f(x') = \frac{K_1 K_1' K_2 x'^3 + K_1 K_1' K_w x'^2 + K_1 K_w^2 x' + K_w^3}{K_1 K_1' K_w x'} \end{aligned}\right\} \quad (5)$$

Similar formulas are obtained on the exchange reaction of a basic amino acid such as lysine, which dissociates as follows,

$$\left.\begin{aligned} &AH_2^{2+} \rightleftarrows AH^+ + H^+ \\ &K_1 = \frac{2[AH^+]_s [H^+]_s}{[AH_2^{2+}]_s} \\ &AH^+ \rightleftarrows A^\pm + H^+ \\ &K_2 = \frac{[A^\pm]_s [H^+]_s}{[AH^+]_s} \\ &A^\pm \rightleftarrows A^- + H^+ \\ &K_2' = \frac{[A^-]_s [H^+]_s}{[A^\pm]_s} \end{aligned}\right\} \quad (6)$$

where the selectivity coefficients are defined as

$$\left.\begin{aligned} &RH + AH^+ \rightleftarrows RAH + H^+ \\ &K_H = \frac{[AH^+]_r [H^+]_s}{[AH^+]_s [H^+]_r} \\ &2RH + AH_2^{2+} \rightleftarrows R_2AH_2 + 2H^+ \\ &K'_H = \frac{[AH_2^{2+}]_r [H^+]_s^2}{[AH_2^{2+}]_s [H^+]_r^2} \end{aligned}\right\} \quad (7)$$

The relationship between the quantities, $[AH^+]_r = y_1$, $[AH_2^{2+}]_r = 2y_2$ and $[H^+]_s = x$, is

$$\left.\begin{aligned} &\frac{[a - w(y_1 + y_2)]\,[c - w(y_1 + 2y_2)]}{y_1} = \frac{vw}{K_H} f(x) \\ &\frac{[a - w(y_1 + y_2)]\,[c - w(y_1 + 2y_2)]^2}{y_2} = \frac{vw^2}{K'_H} K_1 f(x) \\ &f(x) = \frac{x^3 + K_1 x^2 + K_1 K_2 x + K_1 K_2 K_2'}{K_1 x} \end{aligned}\right\} \quad (8)$$

While, in a case when the basic amino acid is adsorbed on the hydroxyl-form anion-exchanger, the simpler relation is derived between $[A^-]_r = y$ and $[OH^-]_s = x'$,

$$\left.\begin{aligned} &\frac{(a - wy)(c - wy)}{y} = \frac{vw}{K_{OH}} f(x') \\ &f(x') = \frac{K_1 K_2 K_2' x'^3 + K_1 K_2 K_w x'^2 + K_1 K_w^2 x' + K_w^3}{K_1 K_2 K_2' x'^2} \end{aligned}\right\} \quad (9)$$

It must be noted that these relationships hold for the two-component systems that contain hydrogen or hydroxyl ions besides amino acid ions.

**$f(x)$ or $f(x')$ Functions.**—As described in the preceding paper, functions $f(x)$ or $f(x')$, which appear to the right of the above equations,

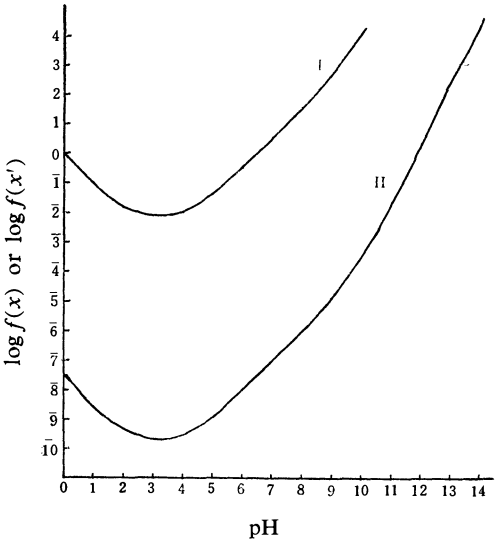



Fig. 3. $f(x)$ and $f(x')$ of glutamic acid.
I $f(x)$, II $f(x')$

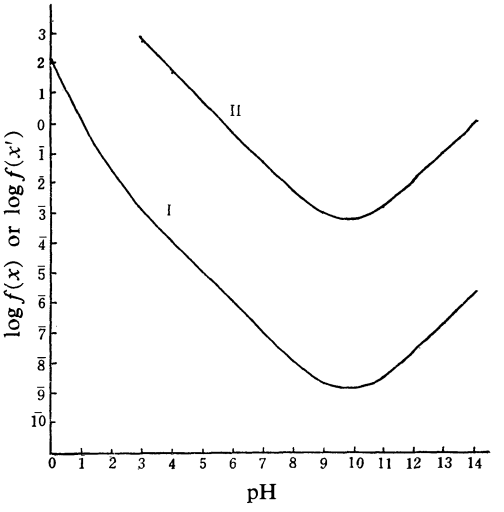



Fig. 4. $f(x)$ and $f(x')$ of lysine.
I $f(x)$, II $f(x')$

contain only a variable, the solution pH, and give the characteristic exchange behavior of amino acids. These functions have minimum values at the isoelectric points of amino acids as shown in Figs. 3 and 4, in which these are plotted against pH. At the minimum of these functions, the adsorbed amount of amino acids is the maximum. This can be shown directly by differentiating the above equations.

The amounts of adsorbed amino acids are related inversely to $f(x)$ or $f(x')$. For example, the relation derived from Eq. 3 is

$$y=\frac{ac}{w\left(a+c+\frac{v}{K_H}f(x)\right)}+\frac{a^2c^2}{w\left(a+c+\frac{v}{K_H}f(x)\right)^3}+\cdots \quad (10)$$

and the similar equation is obtained from Eq. 9. In the system where two ionic species of amino acids participate in the exchange reaction, such a simple relation can not be derived and, however, when $K'$ is not much larger than $K$ in Eqs. 7 or 8, $y_2$ is very small compared to $y_1$ in the pH range near the isoelectric point and the similar relations to Eq. 10 are derived in these cases.

This is closely related to the fact that $f(x)$ and $f(x')$ of the acidic and the basic amino acid are more strongly dependent on pH than those of neutral amino acids[1], that the ion-exchange behavior of the former has more remarkable pH effect than that of the latter. In passing, it is noticed that the exchange reaction takes place in a wider pH range in the cases where two ionic species praticipate.

**Ion Species Exchanged.**—In order to estimate the selectivity coefficients $K$ and $K'$, the ionic species exchanged for hydrogen or hydroxyl ions must be discriminated. This requires a complicated procedure experimentally[4]. Hence, it is assumed that the same dissociation equilibrium is attained in the resin phase as in the solution phase. Then, in the case of an acidic amino acid,

$$\frac{K_2}{K_w}=\frac{[A^{2-}]_r}{2[A^-]_r[OH^-]_r} \quad (11)$$

and under the present condition the following relation is obtained between $y_1$ and $y_2$,

$$y_2=\frac{K_2(c-wy_1)y_1}{w(2K_2y_1+K_w)} \quad (12)$$

Putting Ep. 12 into Eq. 5, $K_H$ and $K_{II}'$ are estimated at least in principle, if the amount (in mole) of adsorbed amino acids is known.

A similar relation is derived as that for a basic amino acid. The relation

$$K_1=\frac{2[AH^+]_r[H^+]_r}{[AH_2^{2+}]_r} \quad (13)$$

is assumed and the following formula is obtained.

$$y_2=\frac{(c-wy_1)y_1}{w(K_1+2y_1)} \quad (14)$$

It might be reasonably expected that these relations are valid for strongly dissociated ion-exchangers. In the case of weakly dissociated ion-exchangers, these relations are not always satisfied, because all the ions exchanged are not in the dissociated state[5].

From Eq. 12 or 14 and the known quantities, the numerical relation between $y_1$ and $y_2$ can estimated and the mole ratio of monovalent amino acid ion to all the exchanged amino acid ions in the resin phase, $y_1/(y_1+y_2)$, is shown against the total amino acid ions exchanges in mole in Fig. 5. Using this diagram

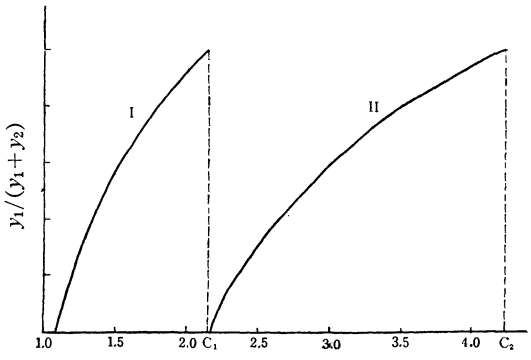



Fig. 5. Fraction of ionic species of amino acids in ion-exchange resins.
I Glutamic acid-IRA-400, II lysine-IR-120, $c_1$ and $c_2$ are the exchange capacities of IRA-400 and IR-120, respectively.

and the experimental data shown in Figs. 1 and 2, the adsorbed amino acids can be discriminated into two ionic species, mono- and di-valent ions. The result is given in Fig. 6.

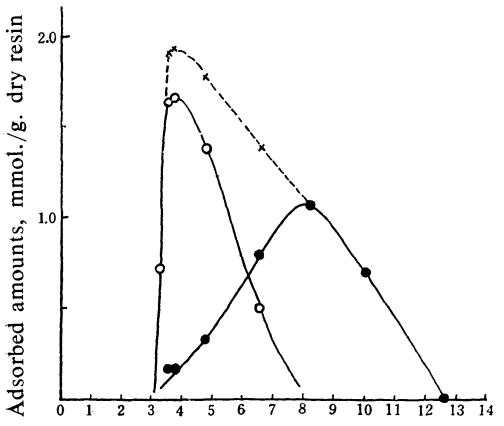
It is shown by differentiating Eq. 12 that, when $y_1$ has the following value

$$y_1=\frac{1}{2}\left(\sqrt{\left(\frac{K_w}{K_2}\right)^2+2C\frac{K_w}{K_2}}-\frac{K_w}{K_2}\right) \quad (15)$$

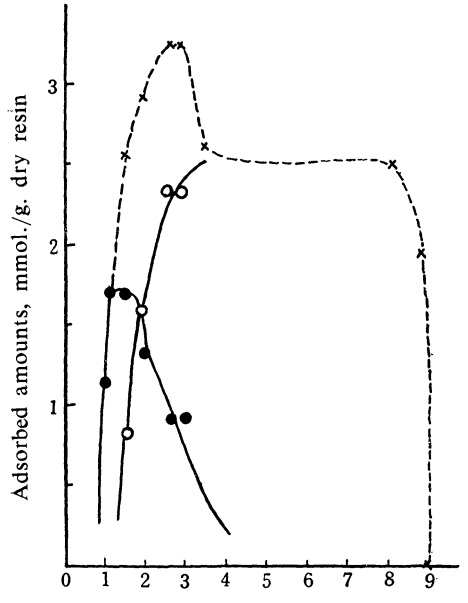
$y_2$ has a maximum value

4) In order to discriminate ionic species of adsorbed amino acids experimentally, the adsorbed amount must be measured in the two units, mole and equivalent number. The molar quantity was measured in this experiment and the equivalent quantity will be obtained by knowing the contents of hydrogen or hydroxyl ions in the ion-exchange resin in equilibrium in an appropriate way.

5) These relations can be extended to this case by assuming that the exchange capacity $C$ is a variable which depends on the dissociation constants of the exchange sites combined with various ions adsorbed on the resins.




Glutamic acid-IRA-400, —○— $A^-$, —●— $A^{2-}$, --×-- total ($A^- + A^{2-}$)




Lysine-IR-120, —○— $AH^+$, —●— $AH_2^{2+}$, --×-- total ($AH^+ + AH_2^{2+}$)

Fig. 6. Ionic species of amino acids adsorbed on ion-exchange resins.

$$y_{2,\max} = \frac{1}{2}\left(C + \frac{K_w}{K_2} - \sqrt{\left(\frac{K_w}{K_2}\right)^2 + 2C\frac{K_w}{K_2}}\right) \tag{16}$$

Putting these values into the second equation of Eq. 5, it is shown that $y_2$ has a maximum value when

$$f(x') = K'_{OH}\frac{\left(a - \frac{1}{2}c\right)}{v} \tag{17}$$

In the case of glutamic acid-Amberlite IRA-400, using the known values and the value of $K'_{OH}$ obtained in the next section, Eq. 17 becomes

$$f(x') = 2.27 \times 10^{-7}$$

This value corresponds to pH=7.4.

A similar relation is derived in the case of lysine-Amberlite IR-120. The value of $y_2$ is maximum when

$$f(x) = K_H'\frac{\left(a - \frac{1}{2}c\right)}{v} \tag{18}$$
$$= 1.48 \times 10^{-2}$$

This corresponds to pH 2.0. All the values explain well the experimental results presented in this paper.

**Selectivity Coefficient.**—The selectivity coefficients were estimated from the above-mentioned experimental data, using Eqs. 3, 5, 8 and 9, with Eqs. 12 and 14[6]. The latter equations can not be successfully applied to the cases of weakly dissociated resins. On this account, the selectivity coefficients in the systems, glutamic acid-IR-4B and lysine-IRC-50, can be obtained immediately. However, as revealed in the systems, glutamic acid-IRA-400 and lysine-IR-120, monovalent amino acid ions play the predominant role in the pH range close to the isoelectric point and divalent amino acid ions contribute predominantly to the ion-exchange in the pH-range for from the isoelectric point[7]. It may be safely assumed that similar reactions take place also in systems of weakly dissociated ion exchangers. The selectivity coefficients thus obtained are given in Table I.

Table I. Selectivity coefficients

| | Glutamic acid | | Lysine | |
|---|---|---|---|---|
| | $\log K_H$ | $\log K'_H$ | $\log K_{OH}$ | $\log K'_{OH}$ |
| IR-120 | 0.23 | — | 1.81 | $\bar{1}$.62 |
| IRC-50 | $\bar{2}$.43 | — | $\bar{5}$.83 | $\bar{3}$.14 |
| | $\log K_{OH}$ | $\log K'_{OH}$ | $\log K_{OH}$ | $\log K'_{OH}$ |
| IRA-400 | $\bar{3}$.32 | $\bar{6}$.82 | $\bar{3}$.75 | — |
| IR-4B | $\bar{8}$.08 | — | $\bar{3}$.38 | — |

6) In this calculation, it happens that $c - w(y_1 + 2y_2)$ equals nearly zero. Then, the following formulas derived from Eqs. 12 and 14 are used.

$$c - w(y_1 + 2y_2) = \frac{K_w(c - wy_1)}{2K_2y_1 + K_w} \quad \text{(glutamic acid-IRA-400)}$$
$$= \frac{K_1(c - wy_1)}{K_1 + 2y_1} \quad \text{(lysine-IR-120)}$$

7) This situation is verified by the variation of the ionic species of amino acids due to the pH change. The predominant ionic species in solutions with various pH's are as follows.

| pH | | 2.2 | | 4.3 | | 9.7 | |
|---|---|---|---|---|---|---|---|
| Glutamic acid | $AH^+$ | | $A^\pm$ | | $A^-$ | | $A^{2-}$ |
| pH | | 2.2 | | 9.0 | | 10.8 | |
| Lysine | $AH_2^{2+}$ | | $AH^+$ | | $A^\pm$ | | $A^-$ |

In general, $K_H$'s of the amino acids are larger than $K_{OH}$'s. $K_H$ or $K_{OH}$ in the case of the weakly dissociated resins is rather small. This is owing to their strong affinity to hydrogen or hydroxyl ions and it is clear from Figs. 1 and 2 that IRC-50 of sodium-form or IR-4B of chloride-form has a strong affinity to amino acids.

## Summary

The ion-exchange behavior of the acidic and the basic amino acids was described and discussed. The maximum uptake of amino acids takes place in the pH range close to the isoelectric points and the pH effect is more remarkable and more characteristic, in comparison with the case of neutral amino acids. Theoretical treatment on ion-exchange equilibria, which takes account of the dissociation equilibria of amino acids, explains well the experimental results and the selectivity coefficients were estimated herefrom.

*The Institute of Industrial Science*
*The University of Tokyo*
*Yayoi-cho, Chiba*

# *Photoreduction of Acridine in Deaerated and Aerated Ethanol Solutions*

By Shunji KATO, Shigekazu MINAGAWA and Masao KOIZUMI

(Received December 26, 1960)

Photochemical reaction of acridine was studied recently by several workers[1-6]. According to Zanker, the solution of acridine in ethanol when irradiated by ultraviolet light, yields diacridane in case when the concentration is above $10^{-3}$ M; this was confirmed by means of infrared spectrum and polarography. Zanker's result was reconfirmed by Kellman[4]. Zanker further found that when the concentration of acridine is below $10^{-3}$ M, the photoproduct consists mainly of acridane.

Zanker's remark that he studied the reaction under the presence of dissolved oxygen attracted much of our attention, because we formerly found that the photochemical reduction of eosine dissolved in ethanol is completely suppressed by the presence of a very small quantity of oxygen[7]. Nothing, however, is described in Zanker's paper about the effect of oxygen on the reaction. We made some preliminary investigations on this problem.

Although our experiments were done only under the limited condition, the results obtained are so specific that they seem to be very important for elucidating the mechanism of the reaction. At least the results must be taken into account in order to give a correct description of the photochemical behavior of acridine in ethanol. Therefore, it is worth while to report, as we believe, the results obtained and some deductions based on them.

## Experimental

**Sample.**—Tokyo Kasei's acridine was recrystallized twice from the water-ethanol mixture (3 : 2 in volume ratio). Wako Junyaku's ethanol (G. R.) was used without further purification.

**Procedure of Degassing.** — In order to exclude the air from the solution, the following procedure was employed. The sample solution was put into B (Fig. 1) and was evacuated by a diffusion pump through a trap A dipped in liquid air. Most of the dissolved air was eliminated during the distilla-

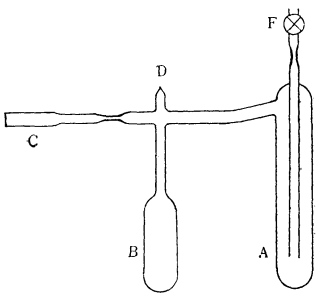



Fig. 1. The degassing apparatus.

1) V. Zanker and P. Schmid, *Z. physik. Chem.*, **17**, 11 (1958).
2) V. Zanker and P. Schmid, *Ber.* **92**, 2210 (1959).
3) A. Kellman, *J. de Chemie phys.*, **56**, 574 (1959).
4) A. Kellman, ibid., **57**, 1 (1960).
5) N. Ivanoff, ibid., **55**, 786 (1958).
6) V. Zanker and F. Mader, *Ber.*, **93**, 850 (1960).
7) M. Imamura and Koizumi, This Bulletin, **29**, 899 (1956).

tion of the solvent from B to A. When all the solvent went to A, tap F was closed and the solvent was distilled back from A to B, dipping B in liquid air. The above procedure was repeated.

In Fig. 1, C is the reaction cell ($1\times1\times4$ cm.) and D is the inlet of sample solution.

The above procedure is superior to repeated distillation in a closed system since it requires far less time for the satisfactory degassing. The loss of the solvent is negligible.

**Apparatus.** — The apparatus is shown in Fig. 2.

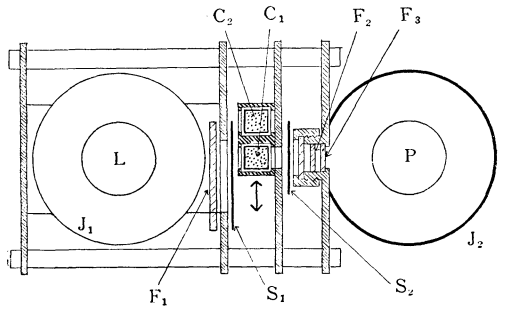



Fig. 2. Diagram of the apparatus of the reaction.

- L : Mazda super-high-press. Hg lamp SHL-100 UV
- $J_1$: Glass cylinder
- $J_2$: Brass cylinder which contains a photoelectric cell and an amplifier set up in a unit
- P : Photoelectric cell of Mazda #7211
- $F_1$, $F_3$: Filter of Hoya U-2, transmitting chiefly the light near 360 m$\mu$
- $F_2$: Frosted glass
- $C_1$: Reaction cell
- $C_2$: Cell containing pure solvent as a reference
- $S_1$, $S_2$: Shutter

The illuminating light is comparatively pure monochromatic light of 365 m$\mu$. The electric source is supplied from VOLCO-HT high-grade automatic voltage stabilizer.

The reaction is followed by the change of optical density at 365 m$\mu$, the reading of the meter being carried out during the course of the reaction.

**Quantum Yield.**—Quantum yield was determined by potassium ferri-oxalate actinometer.

## Results

**Comparison of Aerated and Deaerated Solutions.**—The experiments were done with the solution of acridine $1\times10^{-4}$ M in ethanol dissolving various amounts of oxygen from air-saturation to complete degassing. In order to check the effect of a small quantity of water contained in alcohol, the reaction was tried with the solution containing various amounts of water and it was established that a small amount of water does not affect essentially the rate of the reaction. Hence the alcohol employed was not particularly dehydrated by any chemical method.

In case the rate of the disappearance of acridine is proportional to the light absorption, the relation

$$-\frac{dc}{dt}=\frac{kI_0}{d}(1-e^{-E})\times1000 \qquad (a)$$

must hold, where $E=\alpha cd$, $c$ is the concentration of acridine, $\alpha$ the absorption coefficient at 365 m$\mu$. Integrating, one obtains

$$\ln(e^{-E}-1)=\ln(e^{E_0}-1)-1000\,k\alpha I_0 t \qquad (b)$$

Hence $\ln(e^{E}-1)$, when plotted against $t$, must give a straight line with the inclination of $1000k\alpha I_0$, which gives the relative rate of the reaction. The experimental results satisfy the above relation very satisfactorily as shown in Fig. 3, for both the air-saturated and the deaerated solution. It is seen from these results that the rate in the aerated solution is about one-third of that in the deaerated solution.

The absorption spectra of the solution were

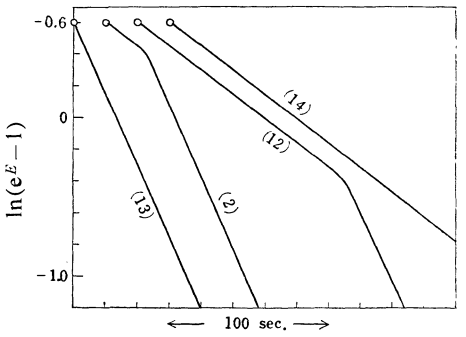



Fig. 3. Plots of $\ln(e^{E}-1)$ vs. time for typical decay. The numbers in the figure point out the experimental number in Table I.

examined immediately after the reaction, and it was found that there is no difference in the two cases, aerated and deaerated, and they are quite the same as the one reported by Zanker. Thus it can safely be concluded that the reductive photochemical reaction can occur even in the presence of oxygen. This is somewhat surprising and is in sharp contrast to the case of eosine in ethanol solution.

**The Effect of Oxygen Concentration.**—When the concentration of the dissolved oxygen is below a certain value, $\ln(e^{E}-1)\sim t$ relation shows quite a sharp breaking point at a certain point and the inclination of the line preceeding the breaking point is almost equal to that of the air-saturated solution, while the one after the breaking point is approximately equal to that for the evacuated solution. It was found that the length of the initial part with

smaller inclination becomes shortened with the decrease of oxygen concentration and yet the inclination itself remains practically constant irrespective of the oxygen concentration. Typical results are shown in Fig. 3 and the complete data are given in Table I.

TABLE I. THE EFFECT OF OXYGEN CONCENTRATION UPON THE RATE OF THE PHOTOCHEMICAL REACTION OF ACRIDINE
[Acridine] $=1\times10^{-4}$ M

| Exp. No. | $[O_2]$ $\times10^4$ M | Temp. °C | $k\alpha I_0\times10^5$ sec$^{-1}$ | |
|---|---|---|---|---|
| 13 | 0 | 13.3 | | 2.28 |
| 19 | 0 | 25.0 | | 2.16 |
| 20 | 0 | 25.0 | | 2.38 |
| 21 | 3.63 | 18.8 | 0.78 | |
| 22 | 7.75 | 14.5 | 0.86 | |
| 14 | air-saturation | 13.0 | 0.73 | |
| 18 | 〃 | 25.0 | 0.70 | |
| Average | | | 0.77 | 2.27 |
| | | | Before breaking point | After breaking point |
| 1 | 0.336 | 16.3 | 1.02 | 1.99 |
| 9 | 0.340 | 19.3 | 0.83 | 2.06 |
| 2 | 0.465 | 19.3 | 0.83 | 2.16 |
| 8 | 0.460 | 21.4 | 0.78 | 1.82 |
| 10 | 0.600 | 17.0 | 0.96 | 1.91 |
| 3 | 0.656 | 20.7 | 0.86 | 2.12 |
| 15 | 0.720 | 13.2 | 0.78 | 1.76 |
| 11 | 0.740 | 18.3 | 0.73 | 2.06 |
| 4 | 0.919 | 18.6 | 0.83 | 1.76 |
| 12 | 0.920 | 22.9 | 0.78 | 2.01 |
| 17 | 0.985 | 13.7 | 0.78 | 1.76 |
| Average | | | 0.85 | 1.95 |

Although the reproducibility is not so good, it is apparent that the rate before the breaking point is, on the average, about one third of that for the deaerated solution and that the rate after breaking point is approximately equal to that of the deaerated solution.

Further, the results in Table I seem to indicate that the rate of reaction is not so much dependent upon temperature, whether oxygen is present or not. To confirm this, the reaction rate of the evacuated solution was investigated in the wider range of temperature. The results shown in Table II establish quite definitely the temperature independence of the rate in the degassed solution.

TABLE II. THE EFFECT OF TEMPERATURE ON THE RATE FOR THE DEGASSED SOLUTION OF ACRIDINE
[Acridine] $=0.7\times10^{-4}$ M

| Temp., °C | $k\alpha I_0\times10^5$ sec$^{-1}$ | |
|---|---|---|
| 25 | 2.28 | Average |
| | 1.90 | 2.09 |
| 35 | 2.16 | |
| | 2.13 | 2.14 |
| 45 | 2.27 | |
| | 1.93 | 2.10 |

From the above results, it can be said that the rate is about one third of the deaerated solution as long as a very small amount of oxygen is present in the solution and that the oxygen is exhausted near the crossing point of the two linear parts, whence the rate gets the value of the degassed solution.

To confirm this further, the following experiment was performed using a special reaction cell. The volume of the upper part, i. e. the gaseous part of the cell was increased about three times to that of the liquid part. The area of the liquid surface was so small that the dissolution of oxygen during the course of the reaction, would be neglected in view of a rather rapid rate of the reaction. Now, if the solution of acridine in ethanol containing a proper amount of oxygen is irradiated in such a cell, one would expect the breaking point to appear after a certain time interval when the oxygen in the liquid phase is consumed. Furthermore one would expect that if one shakes the cell at this stage in order to bring on a new equilibrium of dissolution between gaseous and liquid phase, and then continue to irradiate the solution again, the rate would fall down to the original value and another breaking point would once more appear after a certain time. These expectations were in fact realized as shown in Fig. 4.

Thus one can conclude with much confidence that in the presence of oxygen the reduction of acridine and the consumption of oxygen takes place simultaneously and that the latter process is intimately connected with the recovery of acridine from a certain transient intermediate.

The decrease of acridine concentration during the consumption of dissolved oxygen can easily

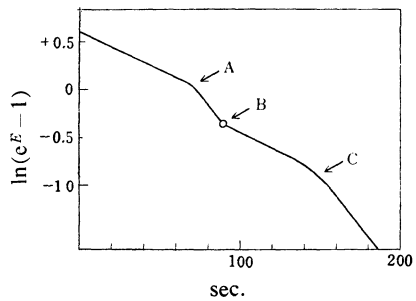



Fig. 4. A decay curve in the special cell. At the time A, dissolved oxygen would exhausted. At B, the cell was shaken and oxygen was introduced into the liquid phase, then at C it would be exhausted again.
$[O_2]=0.912\times10^{-4}$ M (35.0 mmHg), 18°C, $C_0=1\times10^{-4}$ M

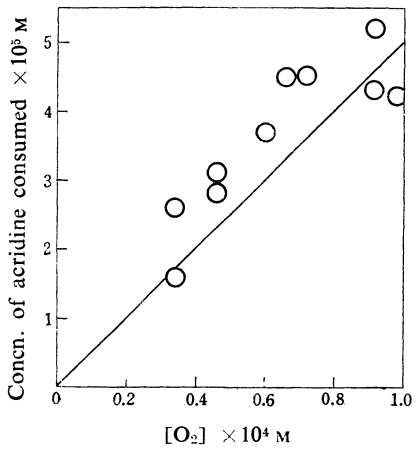



Fig. 5. Plots of the decrease of acridine concentration before the breaking point of the decay curve, vs. the initial concentration of dissolved oxygen.

be evaluated and this is plotted in Fig. 5 against the concentration of oxygen dissolved in the solution. Since the initial concentration of acridine obtained from the optical density is always a little less than $1\times10^{-4}$ M, the concentration of the prepared solution, the latter was used, though somewhat arbitarily, instead of the former.

There is an appreciable scattering of the points, but it is evident that the ratio (consumed oxygen): (reduced acridine) lies near 2 : 1.

**Quantum Yield.**—The light intensity entering into the solution was measured to be $0.156\times10^{-7}$ M $sec^{-1}cm^{-2}$. Since $\alpha$ is $1.14\times10^{4}$ at 365 m$\mu$, from the value of $k\alpha I_0$, the quantum yield for the deaerated solution was found to be about 0.13.

## Discussion

The plausible scheme for the deaerated solution may be pictured as follows

$$\left.\begin{aligned} &A+h\nu \rightarrow A^* \\ &A^*+RH_2 \rightarrow AH\cdot+RH\cdot \end{aligned}\right\} \quad (0)$$

$$AH\cdot+RH\cdot \rightarrow AH_2+R \quad (1)$$

$$AH\cdot+RH\cdot \rightarrow A+RH_2 \quad (2)$$

$$AH\cdot+AH\cdot \rightarrow AH_2+A \quad (3)$$

$$RH\cdot+RH\cdot \rightarrow HR\text{–}RH \text{ or } R+RH_2 \quad (4)$$

where A, $RH_2$, R are acridine, ethanol, acetaldehyde respectively and A* denotes the excited singlet or triplet state as the case may be.

The above scheme is essentially the same as that of Kellman[4] except that it involves the recovery of A and $RH_2$ (process 2).

At first, let us consider the molecular species X which oxygen attacks. Since the rate of the reaction is independent of the concentration of oxygen unless it is too low, the rate with which oxygen attacks X should be much faster than the rate with which X disappears in the deaerated solution. Supposing that the diffusion of oxygen is the rate-determining step of the reaction between $O_2$ and X, as is plausible, the experimental result that the rate is independent of oxygen concentration above $10^{-5}$ M leads to the conclusion that the life of X in the deaerated condition is $\sim10^{-5}$ sec. or more. Hence X can not be the singlet excited state. We have found that the fluorescence of acridine is not quenched appreciably by oxygen and this discovery also supports the above conclusion.

If X is triplet, then the formation of molecular associate $X\cdots O_2$ analogous to the intermediate of the Schenck's scheme[8] might be conceivable, but it is difficult to interpret the reductive reaction on this basis.

The possibility that T-state is quenched partially by oxygen depending on its concentration can of course be rejected on the ground that the rate is independent on the concentration of oxygen. Thus it is most plausible to assume that oxygen attacks the semi-reduced form of A produced by the process 0. In case of reductive photobleaching of eosine in ethanol, this process really takes place very rapidly*. In that case, however, the reaction was completely suppressed by a very small quantity of oxygen and the following scheme could account for the experimental results[7].

$$DH\cdot+O_2 \rightarrow D+HO_2\cdot$$

$$RH\cdot+O_2 \rightarrow RH\cdots O_2$$

$$HO_2\cdot+HO_2\cdot \rightarrow H_2O_2+O_2$$

$$RH\cdots O_2+RH\cdots O_2 \rightarrow 2\ \text{Acid}+H_2O_2$$

$$RH\cdots O_2+HO_2\cdot \rightarrow H_2O_2+\text{aldehyde}+O_2$$

But in the present case where acridine is reduced even in high oxygen concentration, one can not interpret the formation of acridan in any way by a single process in which oxygen attacks AH·. This leads to the assumption that some other intermediate such as $AH\cdots O_2$ be produced and some of them go back to A and the remainder turns into $AH_2$ through a bimolecular reaction. Perhaps $AH\cdots O_2$ may have its hydrogen attached to nitrogen, and the oxygen loosely combined with 9-carbon.

Now the scheme should further account for the following three experimental results.

8) G. O. Schenck, *Naturwissenschaften*, **40**, 212 (1953).

* From the results of the flash experiment, it is not proper to say that oxygen attacks only semiquinone. See Ref. 9.

9) S. Kato et al., This Bulletin, 33, 262 (1960).

[a] The rate of the reaction is proportional to the rate of light absorption for both the aerated and the deaerated condition.

[b] The rate in the aerated solution is about one third of that in the deaerated solution.

[c] The ratio of consumed oxygen to the reduced acridine ($=\gamma$) is about 2.

Now in the deareated condition one can easily derive the following equation by means of steady state method

$$-\frac{d[A]}{dt}=\frac{d[AH_2]}{dt}=\frac{\phi I_{abs}(k_1+\sqrt{k_3k_4})}{k_1+k_2+2\sqrt{k_3k_4}}=\phi\beta f_{abs} \quad (a)$$

$$\beta=\frac{k_1+\sqrt{k_3k_4}}{k_1+k_2+2\sqrt{k_3k_4}}$$

where $\phi$ is the quantum yield of the formation of AH· and RH·, and $k_1$, $k_2$, $k_3$ and $k_4$ are respectively the rate constants of the processes 1, 2, 3 and 4.

Assuming the formation of $AH\cdots O_2$ and $RH\cdots O_2$, the following processes may be conceivable for the aerated solution.

$$AH\cdot+O_2 \rightarrow AH\cdots O_2 \quad (5)$$

$$RH\cdot+O_2 \rightarrow RH\cdots O_2 \quad (5')$$

$$2AH\cdots O_2 \rightarrow AH_2+A+2O_2 \quad (6)$$

$$AH\cdots O_2 \rightarrow A+HO_2\cdot \quad (7a)$$

$$2RH\cdots O_2 \rightarrow 2\ Acid+H_2O_2 \quad (8)$$

$$AH\cdots O_2+RH\cdots O_2 \rightarrow AH_2+R+2O_2 \quad (9)$$

$$AH\cdots O_2+RH\cdots O_2 \rightarrow A+R+H_2O_2+O_2 \quad (10)$$

$$AH\cdots O_2+RH\cdots O_2 \rightarrow A+RH_2+2O_2 \quad (11)$$

In the presence of oxygen the reaction 5 is so fast that the reactions 1, 2 and 3 can be neglected.

To simplify the discussion, only the following two extreme cases will be considered.

**Case I.** — When $AH\cdots O_2$ disappears mainly through the reactions 6 and 7a, the reaction 8 must take place accompanied by them. If so, the formation of acridane would not be simply proportional to the rate of light absorption, because the process 7a is a first order reaction concerning $[AH\cdots O_2]$ while 6 is a second order one. This contradicts the experimental result [a]. Hence, the reaction 7a should be replaced

$$2AH\cdots O_2 \rightarrow 2A+H_2O_2+O_2 \quad (7)$$

by a bimolecular reaction and the steady state method leads to the following expression.

$$-\frac{d[A]}{dt}=\frac{d[AH_2]}{dt}=\frac{k_6\phi I_{abs}}{2(k_6+k_7)} \quad (b)$$

$$-\frac{d[O_2]}{dt}=\frac{\phi I_{abs}(2k_6+3k_7)}{2(k_6+k_7)} \quad (c)$$

Thus the result [b] requires

$$\frac{k_6}{2(k_6+k_7)}=\beta/3 \quad (d)$$

while $\gamma$ can be expressed as,

$$\gamma=\frac{d[O_2]/dt}{d[A]/dt}=\frac{(2k_6+3k_7)}{k_6}=2+3k_7/k_6 \quad (e)$$

From d and e the following relation holds,

$$\gamma=4.5/\beta-1$$

Since $\beta$ is smaller than unit, $\gamma$ should be greater than 3.5. Thus $\gamma$ does not satisfy the result [c] and we can safely reject this case.

**Case II.**—When 9, 10 and 11 are the main reactions, the steady state method leads to the following expression

$$-d[A]/dt=d[AH_2]/dt=\phi I_{abs}k_9/(k_9+k_{10}+k_{11})$$

$$-d[O_2]/dt=\phi I_{abs}k_{10}/(k_9+k_{10}+k_{11})$$

The result [b] requires that

$$k_9/(k_9+k_{10}+k_{11})=\beta/3 \quad (f)$$

and $\gamma$ is given as follows from the result [c]

$$\gamma=k_{10}/k_9=2 \quad (g)$$

From f and g

$$k_{11}/k_9=3/\beta-3 \quad (h)$$

Then, this ratio is shown for some values of $\beta$,

| $\beta$ | 1 | 0.8 | 0.6 | 0.5 | 0.4 | 0.3 |
|---|---|---|---|---|---|---|
| $k_{11}/k_9$ | 0 | 0.75 | 2 | 3 | 4.5 | 7 |

The independence of $\phi$ and $\beta$ on temperature in the deaerated solution strongly suggests that the process 1 or 3 only prevails and the process 2 does not occur appreciably. If one excludes 2, then the value of $\beta$ is limited from 1 to 1/2. The higher limit corresponds to the case in which reaction 1 prevails and the lower to the case in which reaction 3 is a chief one. In view of the fact that dimerization does not occur in diluted solution, reaction 1 seems to be more desirable than 3. Then the only possible case will be the Case II in which $\beta=1$, $k_{11}=0$. In connection with this scheme, it is to be added that there is another possibility in which a certain type of radical complex $AH\cdots RH$ with an appreciable life is formed and it is attacked by oxygen decomposing in three different ways;

1) $AH\cdots RH+O_2 \rightarrow A+RH_2+O_2$

2) $AH\cdots RH+O_2 \rightarrow A+R+H_2O_2$

3) $AH\cdots RH+O_2 \rightarrow AH_2+R+O_2$

This case is quite analogous to the above case at least kinetically.

Of course further investigations are needed to substantiate the above deduction and to

decide the scheme unequivocally. Perhaps the flash technique will be most helpfull.

## Summary

1. The deaerated solution of acridine $1 \times 10^{-4}$ M in ethanol, when irradiated by 365 mμ produces acridane with a quantum yield of about 0.13. This reductive reaction can proceed even in the air-saturated solution with the rate about one third of that of the deaerated solution. For both cases the rate is simply proportional to the absorption of light.

2. When the concentration of dissolved oxygen is more than about twice that of acridine concentration, the rate of the reaction is approximately equal to that of the air-saturated solution independent of the oxygen concentration, and at the same time oxygen is consumed at the rate about twice as great as that of the reduction of acridine. Hence, when the existent oxygen is exhausted, the rate gains the value of the deaerated solution.

3. All the above results are almost entirely independent of temperature.

4. A possible scheme was proposed in which a certain type of intermediate is formed between semireduced acridine and oxygen and, from this intermediate acridine is partially recovered accompanied with the consumption of oxygen and, in competition with this, acridane is poduced, both by a bimolecular process.

*Department of Chemistry*
*Faculty of Science*
*Tohoku University*
*Katahira-cho, Sendai*

# *Electronic Structure of Benzyl Radical*[1)]

By Yuji Mori

(Received December 12, 1960)

The electronic spectrum of benzyl radical[2,3)] has been investigated theoretically by the methods of MO[4-6)] and VB[6)]. However, there is no theoretical interpretation of the correlation between the electronic structures of benzyl radical and of benzene. The purpose of the present paper is to show the electronic structure of benzyl radical in correlation with that of benzene.

The singlet states of benzene correlate with the doublet states of benzyl radical and the triplet states of benzene correlate with the doublet and quartet states of benzyl radical. Therefore, it is expected that the lowest triplet level $^3B_{1u}$ of the benzene ring will be lowered by the interaction between $\pi$-electrons of the benzene ring and methylene radical and that this will give rise to the lowest excited state $^2B_2$ of benzyl radical.

In view of this, a simpie calculation is carried out by using an approximation that the wave function of benzyl radical can be expressed in terms of the $\pi$-electron wave function of the benzene ring and that of the methylene group ($CH_2$).

## Method of Caluculation

The method of calculation is similar to the method of composite systems presented by London[7)], by Longuet-Higgins and Murrell[8)] and by the present author[9)].

The molecular orbital of the benzene ring is

$$\varphi_l(\nu)=\sqrt{6}^{-1}\sum_{t=1}^{6}\exp[-2\pi il(t-1)/6]\,\chi_t(\nu)$$

where $l=0, \pm1, \pm2, 3$ and $\chi_t(\nu)$ is the $2P\pi$ AO of the $t$th carbon atom in the benzene ring. At the carbon atom 1 the hydrogen atom is substituted by $CH_2$ and the $2P\pi$ orbital of $CH_2$ is represented by $\chi_7(\nu)$.

The wave functions oe the benzene ring are, with an obvious abbreviation,

1) Y. Mori, *J. Chem. Phys.*, **24**, 1253 (1956).
2) H. Schüler, *Z. Naturforsch.*, **A10**, 559 (1955).
3) G. Porter and J. Norman, *Nature*, **174**, 508 (1954); J. Norman and G. Porter, *Proc. Roy. Soc.*, **A230**, 399 (1955); G. Porter and F. J. Wright, *Trans. Faraday Soc.*, **51**, 1469 (1955).
4) H. C. Longuet-Higgins and J. A. Pople, *Proc. Phys. Soc.*, **A68**, 591 (1955).
5) C. Komatsu, Y. Mori and I. Tanaka, *J. Chem. Soc. Japan, Pure Chem. Sec. (Nippon Kagaku Zasshi)*, **77**, 643 (1956).
6) W. Bingel, *Z. Naturforsch.*, **A10**, 462 (1955).
7) A. London, *J. Chem. Phys.*, **13**, 396 (1945).
8) H. C. Longuet-Higgins and J. N. Murrell, *Proc. Phys. Soc.*, **A68**, 601 (1955).
9) Y. Mori, This Bulletin, **28**, 291 (1955).

$^1A_{1g}$ ;

$$\psi_1=|\varphi_0(1)\overline{\varphi}_0(2)\varphi_{+1}(3)\overline{\varphi}_{+1}(4)\varphi_{-1}(5)\overline{\varphi}_{-1}(6)|$$
$$=|0\,\bar{0}\,+1\,+\bar{1}\,-1\,-\bar{1}|$$

$^1B_{1u}$ ;

$$\psi_2=1/2\{|0\,\bar{0}\,+1\,+\bar{1}\,-1\,+\bar{2}|$$
$$-|0\,\bar{0}\,+1\,+\bar{1}\,-\bar{1}\,+2|+|0\,\bar{0}\,-1\,-\bar{0}\,+1\,-2|$$
$$-|0\,\bar{0}\,-1\,-\bar{1}\,+\bar{1}\,-2|\}$$

$^3B_{1u}$ ;

$$\psi_3{}^a=1/2\{|0\,\bar{0}\,+1\,+\bar{1}\,-1\,+\bar{2}|$$
$$+|0\,\bar{0}\,+1\,+\bar{1}\,-\bar{1}\,+2|+|0\,\bar{0}\,-1\,-\bar{1}\,+1\,-\bar{2}|$$
$$+|0\,0\,-1\,-\bar{1}\,+\bar{1}\,-2|\}$$
$$\psi_3{}^b=1/\sqrt{2}\{|0\,\bar{0}\,+1\,+\bar{1}\,-1\,+2|$$
$$+|0\,\bar{0}\,-1\,-\bar{1}\,+1\,-2|\}$$

$^1E_{1u}$ ;

$$\psi_4=1/2\{|0\,\bar{0}\,+1\,+\bar{1}\,-1\,-\bar{2}|$$
$$-|0\,\bar{0}\,+1\,+\bar{1}\,-\bar{1}\,-2|+|0\,\bar{0}\,-1\,-\bar{1}\,+1\,+\bar{2}|$$
$$-|0\,\bar{0}\,-1\,-\bar{1}\,+\bar{1}\,+2|\}$$
$$\psi_8=1/2\{|0\,\bar{0}\,+1\,+\bar{1}\,-1\,-\bar{2}|$$
$$-|0\,\bar{0}\,+1\,+\bar{1}\,-\bar{1}\,-2|-|0\,\bar{0}\,-1\,-\bar{1}\,+1\,+2|$$
$$+|0\,\bar{0}\,-1\,-\bar{1}\,+\bar{1}\,+2|\}$$

$^3E_{1u}$ ;

$$\psi_5{}^a=1/2\{|0\,\bar{0}\,+1\,+\bar{1}\,-1\,-2|$$
$$+|0\,0\,+1\,+\bar{1}\,-\bar{1}\,-2|+|0\,\bar{0}\,-1\,-\bar{1}\,+1\,+\bar{2}|$$
$$+|0\,\bar{0}\,-1\,-\bar{1}\,+\bar{1}\,+2|\}$$
$$\psi_5{}^b=1/\sqrt{2}\{|0\,\bar{0}\,+1\,+\bar{1}\,-1\,-2|$$
$$+|0\,0\,-1\,-\bar{1}\,+1\,+2|\}$$
$$\psi_9{}^a=1/2\{|0\,\bar{0}\,+1\,+\bar{1}\,-1\,-\bar{2}|$$
$$+|0\,0\,+1\,+\bar{1}\,-\bar{1}\,-2|-|0\,\bar{0}\,-1\,-\bar{1}\,+1\,+\bar{2}|$$
$$-|0\,\bar{0}\,-1\,-\bar{1}\,+\bar{1}\,+2|\}$$
$$\psi_9{}^b=1/\sqrt{2}\{|0\,\bar{0}\,+1\,+\bar{1}\,-1\,-2|$$
$$-|0\,\bar{0}\,-1\,-\bar{1}\,+1\,+2|\}$$

$^1B_{2u}$ ;

$$\psi_6=1/2\{|0\,\bar{0}\,+1\,+\bar{1}\,-1\,+\bar{2}|$$
$$-|0\,\bar{0}\,+1\,+\bar{1}\,-\bar{1}\,+2|-|0\,\bar{0}\,-1\,-\bar{0}\,+1\,-\bar{2}|$$
$$+|0\,\bar{0}\,-1\,-\bar{1}\,+1\,-2|\}$$

$^3B_{2u}$ ;

$$\psi_7{}^a=1/2\{|0\,\bar{0}\,+1\,+\bar{1}\,-1\,+\bar{2}|$$
$$+|0\,\bar{0}\,+1\,+\bar{1}\,-\bar{1}\,+2|-|0\,\bar{0}\,-1\,-\bar{1}\,+1\,-2|$$
$$-|0\,\bar{0}\,-1\,-\bar{1}\,+\bar{1}\,-2|\}$$
$$\psi_7{}^b=1/\sqrt{2}\{|0\,0\,+1\,+\bar{1}\,-1\,+2|$$
$$-|0\,\bar{0}\,-1\,-\bar{1}\,+1\,-2|\}$$

The unperturbed wave functions of benzyl radical are given in Table I, where those are the eigenfunctions of the operators of spin component $S_z$ and total spin $S^2$.

TABLE I. THE UNPERTURBED WAVE FUNCTIONS OF BENZYL RADICAL

a) Doublet configurations ($M_S=+1/2$)

$^2B_2$ ;

$$\Psi_1=|\phi_1\cdot\chi_7|$$
$$\Psi_2=|\phi_2\cdot\chi_7|$$
$$\Psi_3=\sqrt{3}^{-1}[|\phi_3{}^a\cdot\chi_7|-\sqrt{2}\,|\phi_3{}^b\cdot\overline{\chi}_7|]$$
$$\Psi_4=|\phi_4\cdot\chi_7|$$
$$\Psi_5=\sqrt{3}^{-1}[|\phi_5{}^a\cdot\chi_7|-\sqrt{2}\,|\phi_5{}^b\cdot\overline{\chi}_7|]$$

$^2A_2$ ;

$$\Psi_6=|\phi_6\cdot\chi_7|$$
$$\Psi_7=\sqrt{3}^{-1}[|\phi_7{}^a\cdot\chi_7|-\sqrt{2}\,|\phi_7{}^b\cdot\overline{\chi}_7|]$$
$$\Psi_8=|\phi_6\cdot\chi_7|$$
$$\Psi_9=\sqrt{3}^{-1}[|\phi_9{}^a\cdot\chi_7|-\sqrt{2}\,|\phi_9{}^b\cdot\overline{\chi}_7|]$$

b) Quartet configurations ($M_S=+3/2$)

$^4B_2$ ;

$$\Psi_{10}=|\phi_3{}^b\cdot\chi_7|$$
$$\Psi_{11}=|\phi_5{}^b\cdot\chi_7|$$

$^4A_2$ ;

$$\Psi_{12}=|\phi_7{}^b\cdot\chi_7|$$
$$\Psi_{13}=|\phi_9{}^b\cdot\chi_7|$$

* $\chi_7$ is the $2P\pi$ orbital of $CH_2$.

In order to simplify the procedure of calculation, the following assumption will be used. Namely, all of the interactions between the benzene ring and the $CH_2$ group are ignored except only that by exchange of $\pi$-electrons.

Though this is very crude and theoretically insufficient, this will not be unacceptable because the perturbation by the odd electron in the $\pi$-orbital of the $CH_2$ group is not so large that this assumption causes serious error in the results.

Neglecting non-neighbors, the interaction by electron exchange can be written

$$\iint\varphi_l(\nu)\chi_7(\mu)H\chi_7(\nu)\varphi_m(\mu)d\tau_\nu d\tau_\mu$$
$$=[l\theta H\theta m]$$
$$=1/6\iint\chi_1(\nu)\chi_7(\mu)H\chi_7(\nu)\chi_1(\mu)d\tau_\nu d\tau_\mu$$
$$=\alpha/6 \qquad (1)$$

where $\alpha$ is the exchange energy in the VB theory and $H$ is the complete electronic Hamiltonian. The value of the interaction integral is evaluated to be $-0.32$ eV. taking the value of $\alpha$ as $-1.92$ eV. as suggested by Sklar[10] and Craig[11].

## Results

The numerical values of the matrix elements are shown in Table II. In evaluating the diagonal matrix elements the energy levels of

10) A. L. Sklar, *J. Chem. Phys.*, **5**, 669 (1937).
11) D. P. Craig, *Proc. Roy. Soc.*, **A200**, 399 (1950).

benzene which were given by Pariser[12] have been used. In Table III the calculated energy levels of the benzyl radical are shown as the roots of the secular determinants, relative to the energy of the ground state.

TABLE II. THE VALUES OF $H_{jk}$ (eV.)

| | |
|---|---|
| $H_{22}=H_{11}-5.9595$ | $H_{12}=0.32$ |
| $H_{33}=H_{11}-2.9495$ | $H_{13}=-0.5543$ |
| $H_{44}=H_{11}-6.7595$ | $H_{14}=0.32$ |
| $H_{55}=H_{11}-3.5095$ | $H_{15}=-0.5543$ |
| | $H_{23}=H_{45}=0$ |
| $H_{66}=H_{11}-4.7095$ | $H_{24}=0$ |
| $H_{77}=H_{11}+4.0695$ | $H_{25}=H_{34}=0$ |
| $H_{88}=H_{11}+6.7595$ | $H_{35}=-0.64$ |
| $H_{99}=H_{11}-3.5095$ | |
| | $H_{67}=H_{89}=0$ |
| $H_{10,10}=H_{11}+3.9095$ | $H_{68}=0.32$ |
| $H_{11,11}=H_{11}+4.4695$ | $H_{69}=-0.5543$ |
| | $H_{78}=-0.5543$ |
| $H_{12,12}=H_{11}+5.0295$ | $H_{79}=0.32$ |
| $H_{13,13}=H_{11}+4.4695$ | |
| | $H_{10,11}=0.32$ |
| | $H_{12,13}=0.32$ |

The calculated wave functions of the ground and lower excited states, $^2B_2$ (ground state), $^2B_2$ (2.99 eV.) and $^2A_2$ (3.42 eV.) are;

ground state ($^2B_2$)

$$\Phi_1=0.9612\Psi_1-0.0495\Psi_2+0.2018\Psi_3-0.0439\Psi_4+0.1761\Psi_5$$

excited states

($^2B_2$; 2.99 eV.)

$$\Phi_2=0.2625\Psi_1+0.0261\Psi_2-0.8259\Psi_3+0.0209\Psi_4-0.4978\Psi_5$$

($^2A_2$; 3.42 eV.)

$$\Phi_6=0.3297\Psi_6-0.3599\Psi_7-0.0849\Psi_8+0.8686\Psi_9 \qquad (2)$$

Since all of the dipole matrix elements

$$eq_{jk}=e\int\Psi_j^*\sum_\nu q(\nu)\Psi_k\mathrm{d}V$$

are zero except for $eq_{11}$ and $eq_{18}$[13], the moments of the transitions from the ground state to $\Phi_2$ and $\Phi_6$ are

$$eQ_{12}=e\int\Phi_1^*\sum_\nu q(\nu)\Phi_2\mathrm{d}V=0.00856eq_{14}$$

$$eQ_{16}=e\int\Phi_1^*\sum_\nu q(\nu)\Phi_6\mathrm{d}V=0.0816eq_{18} \qquad (3)$$

12) R. Pariser, *J. Chem. Phys.*, **24**, 250 (1956).

13) $eq_{14}$ and $eq_{18}$ are those of the transitions $^1A_{1g}$-$^1E_{1u}$ of benzene,
$|q_{14}|=|q_{18}|=R=1.39$ Å,
where $R$ is the C-C bond-length in benzene ring.

TABLE III. THE ENERGY LEVELS OF BENZYL RADICAL

| State | Energy, eV. | |
|---|---|---|
| | Calculated | Observed |
| $^2B_2$ | — | — |
| $^2B_2$ | 2.99 | 2.8 |
| $^2A_2$ | 3.42 | |
| $^4B_2$ | 4.01 | |
| $^2B_2$ | 4.18 | 4.0 |
| $^2A_2$ | 4.33 | |
| $^4A_2$ | 4.57 | |
| $^4B_2$ | 4.86 | |
| $^2A_2$ | 5.13 | |
| $^4A_2$ | 5.42 | |
| $^2B_2$ | 6.23 | |
| $^2B_2$ | 7.02 | |
| $^2A_2$ | 7.17 | |

By using the calculated wavelengths for these transitions, the oscillator strength are given

$$f_{12}=3.7\times10^{-5}$$
$$f_{16}=3.8\times10^{-3} \qquad (4)$$

## Discussion

The emission spectrum of benzyl radical has a band which was observed by Schüler[2] at about 4500 Å. This will arise from the transition between the ground state and the lowest excited state $^2B_2$(2.99 eV.). However, no absorption band which corresponds to this transition has been observed. The result that the bands arising from the lower excited states of benzyl radical will have very weak intensities will serve as an interpretation for this experimental result. By a similar consideration it will be explained that the band arising from the transition to $^2A_2$(3.42 eV.) has not been observed.

It is seen that the lower excited states of benzyl radical, $^2B_2$(2.99 eV.) and $^2A_2$(3.42 eV.), have the character of the triplet states of benzene. Then the oscillator strengths are due to the degrees of contributions from $\Psi_4$ or $\Psi_8$ which have the components of $^1E_{1u}$ of benzene. Therefore the transitions from the ground state to these excited states are almost forbidden though these are allowed by selection rule.

The small oscillator strengths to the lower excited levels were suggested by Longuet-Higgins[4] and Bingel[6] in terms of molecular orbital theory. The results of the present paper, however, differ from those by molecular orbital calculations in the order of the positions of energy levels. In the present paper, the lowest excited state is $^2B_2$(2.99 eV.). This is inconsistent with the prediction by the other calculations[4,6] that the lowest excited state of benzyl radical will be $^2A_2$. This discrepancy arises,

TABLE IV. THE ESTIMATED LOWEST EXCITED STATES OF RADICALS

| Radical | $\Delta E(T-N)$, eV. | $\lvert C_{mr}\rvert^2=\lvert C_{m'r}\rvert^2$ | $-2\lvert C_{mr}\rvert^2\cdot\alpha$, eV. | Excitation energy, eV. |
|---|---|---|---|---|
| Allyl | 5.78[a] | 0.5 | 1.92 | 3.86 |
| Pentadienyl | 3.92[b] | 0.3618[c] | 1.39 | 2.53 |
| Benzyl | 3.59 | 0.1667 | 0.64 | 2.95 |
| Triphenylmethyl | 3.59 | 0.1667[d] | 0.64[d] | 2.95[d] |
| $\alpha$-Naphthylmethyl | 2.16[e] | 0.1809[e] | 0.69 | 1.47 |
| $\beta$-Naphthylmethyl | 2.16 | 0.0691[e] | 0.27 | 1.89 |

a R. G. Parr and R. Pariser, *J. Chem. Phys.*, **23**, 711 (1955).
b R. Pariser and R. G. Parr, *J. Chem. Phys.*, **21**, 767 (1953).
c Calculated by the simple LCAO-MO method.
d See Appendix.
e R. Pariser, *J. Chem. Phys.*, **24**, 250 (1956).

in some degree, from the difference of configuration interactions included in the calculations. In the present treatment the first order configuration interaction is that between the locally excited configurations in the benzene ring. The first order configuration interaction in molecular orbital treatment has the character of interaction between the electron transfer configurations between the benzene ring and the methylene group.

The assignment of the excited state which will give rise to the absorption band[3] at 3100 Å is uncertain, since there are two excited levels in the vicinity of 4 eV., $^2B_2$(4.18 eV.) and $^2A_2$(4.33 eV.).

The intensities of the bands arising from the higher excited states will be more intense than those of the lower ones, because larger contributions from the configurations $\Psi_4$ and $\Psi_8$ are expected.

Though the present treatment showed satisfactory results, it is difficult to undertake a more precise quantitative discussion concerning the energy levels and the intensities of the bands, because of the assumption that the effect of interaction by electron transfer is completely neglected. Therefore, the treatment in this paper may be useful for the qualitative discussion of the correlation between the electronic structures of the radical and the parent molecule, for instance, between the benzene and benzyl radicals.

As the application of this treatment, simplified consideration can be made on the lowest excited levels of some conjugated free radicals, like benzyl radical. It will be possible that the lowest excited state of a radical can be approximated by the single configuration. The component is the lowest triplet state of the parent molecule.

By this approximation, the excitation energy from the ground state to the lowest excited state of the radical will be given

$$\Delta E=\Delta E(T-N)+3/2\,[m\theta H\theta m]+1/2\,[m'\theta H\theta m']$$

In the above, $\Delta E(T-N)$ is the excitation energy from the ground state to the lowest triplet state of the parent molecule in which one electron is excited to a vacant MO $\varphi_{m'}$ from an occupied MO $\varphi_m$, and $[m\theta H\theta m]$ is the integral of interaction by the exchange of $\pi$-electron in $\varphi_m$ and the methylene group.

By using the nearest neighbor approximation, the excitation energy of the radical can be written

$$\Delta E=\Delta E(T-N)+\{3/2\,|C_{mr}|^2+1/2\,|C_{m'r}|^2\}\alpha \tag{5}$$

where $C_{mr}$ is the coefficient of $\varphi_m$ at carbon atom $r$, where the hydrogen atom is substituted by a methylene radical. In Table IV, the lowest excitation energies of the conjugated free radicals calculated by Eq. 5 are shown.

It is interesting that the excitation energy of the lowest excited state of $\alpha$-naphthylmethyl radical is lower than that of $\beta$-naphthylmethyl radical and the lowest excited states of benzyl radical and triphenylmethyl radical have the same excitation energy. Although triphenylmethyl radical is not planar, the result of this paper shows qualitative agreement with the experimental result that this radical has the first absorption band at about 5000 Å[14] with weak intensity. The lowest excitation energy of allyl radical in Table IV may be compared with those by Moffit[15], by Higuchi[16] and by Longuet-Higgins and Pople[4].

By this treatment it can be said that the lowest excited levels of each free radical in Table IV will be lower than the lowest triplet levels of the parent molecule and will give rise to a weak absorption band.

## Summary

The electronic structure of benzyl radical was shown by the approximation of the composite system in which all of the interactions

14) T. L. Chu and S. I. Weissman, *J. Chem. Phys.*, **22**, 21 (1954).
15) W. Moffit, *Proc. Roy. Soc.*, **A218**, 486 (1953).
16) J. Higuchi, *J. Chem. Phys.*, **26**, 151 (1957).

are ignored except only the interaction by exchange between $\pi$-electrons of the benzene ring and the methylene group ($CH_2$). The results are qualitively in agreement with the experimental observations[2,3] and the results of the other calculations[4,6]. The discrepancy between the results of the present paper and the other calculations are discussed.

The lowest excited states of some conjugated free radicals are also discussed.

The author is greatly indebted to professor I. Tanaka for his continuous encouragement and discussion.

*Laboratory of Physical Chemistry*
*Tokyo Institute of Technology*
*Meguro-ku, Tokyo*

## Appendix

The wave function of the ground state of triphenylmethyl radical is

$$\Psi_1=\phi_1\phi_1'\phi_1''\theta$$

where $\phi_1$, $\phi_1'$ and $\phi_1''$ are the wave functions of the ground states of the benzene rings I, II and III respectively, and $\theta$ is the $2P\pi$ orbital of carbon atom at the center of the molecule.

For the excited states, the wave functions are

$$\Psi_2^{\pm}=\sqrt{3}^{-1/2}[(\phi_3\cdot\theta)\phi_1'\phi_1'' + \exp(\pm 2\pi i/3)\phi_1(\phi_3'\cdot\theta)\phi_1'' + \exp(\pm 4\pi i/3)\phi_1\phi_1'(\phi_3''\cdot\theta)]$$

$$\Psi_3=\sqrt{3}^{-1/2}[(\phi_3\cdot\theta)\phi_1'\phi_1''+\phi_1(\phi_3'\cdot\theta)\phi_1'' + \phi_1\phi_1'(\phi_3''\cdot\theta)]$$

where $(\phi_3\cdot\theta)$, $(\phi_3'\cdot\theta)$ and $(\phi_3''\cdot\theta)$ are similar to $\Psi_3$ in the case of benzyl radical.

Therefore, neglecting non-neighbors, the lowest excitation energy is given as

$$H_{22}-H_{11}=H_{33}-H_{11} =2.95\ \text{eV}.$$

# *The Effect of Electron Transfer in the Electronic Structure of Benzyl Radical*

By Yuji MORI

(Received December 12, 1960)

In the previous paper[1], the correlation between the energy levels of benzyl radical and those of benzene has been shown by the present author, though neglecting all of the interactions between benzene ring and $CH_2$ in benzyl radical except only the interaction by exchange of $\pi$-electrons. However, there is the question as to the different results which may be obtained if the assumption of the calculation is altered. In the present paper, the purpose is to show how the results may be affected by the change of the assumption in the treatment.

In the present paper, the assumption is used that the interaction between benzene ring and $CH_2$ arises from the transfer of the electron. This assumption is introduced in the calculation by the use of the approximation of integrals suggested by Pariser and Parr[2]. This treatment is the same as the method of composite systems[3].

1) Y. Mori, This Bulletin, **34**, 1031 (1961).
2) R. Pariser and R. G. Parr, *J. Chem. Phys.*, **21**, 767 (1953).
3) A. London, ibid., **13**, 396 (1945); H. C. Longuet-Higgins and J. N. Murrell, *Proc. Phys. Soc.*, **A68**, 101 (1955); Y. Mori, This Bulletin, **28**, 291 (1955).

## Calculation

The molecular orbitals of benzene ring are written in the real form as,

$$\begin{aligned}
\varphi_0(\nu) &= \sqrt{6}^{-1}\{\chi_1(\nu)+\chi_2(\nu)+\chi_3(\nu)\\
&\quad +\chi_4(\nu)+\chi_5(\nu)+\chi_6(\nu)\}\\
\varphi_1(\nu) &= \sqrt{12}^{-1}\{2\chi_1(\nu)+\chi_2(\nu)-\chi_3(\nu)\\
&\quad -2\chi_4(\nu)-\chi_5(\nu)+\chi_6(\nu)\}\\
\varphi_2(\nu) &= 2^{-1}\{\chi_2(\nu)+\chi_3(\nu)-\chi_5(\nu)\\
&\quad -\chi_6(\nu)\}\\
\varphi_3(\nu) &= \sqrt{12}^{-1}\{2\chi_1(\nu)-\chi_2(\nu)-\chi_3(\nu)\\
&\quad +2\chi_4(\nu)-\chi_5(\nu)-\chi_6(\nu)\}\\
\varphi_4(\nu) &= 2^{-1}\{\chi_2(\nu)-\chi_3(\nu)+\chi_5(\nu)\\
&\quad -\chi_6(\nu)\}\\
\varphi_5(\nu) &= \sqrt{6}^{-1}\{\chi_1(\nu)-\chi_2(\nu)+\chi_3(\nu)\\
&\quad -\chi_4(\nu)+\chi_5(\nu)-\chi_6(\nu)\}
\end{aligned} \qquad (1)$$

In the above $\chi_t(\nu)$ is the $2P\pi$ atomic orbital of $\nu$th electron at $t$th carbon atom, and $CH_2$ is attached to carbon atom 1 of benzene ring.

The unperturbed wave functions of benzyl

TABLE I. THE WAVE FUNCTIONS

Doublet configurations ($M_s=+1/2$)

Non-polar

$^2B_2$

$$\Psi_1=|\varphi_0(1)\alpha(1)\varphi_0(2)\beta(2)\varphi_1(3)\alpha(3)\varphi_1(4)\beta(4)\varphi_2(5)\alpha(5)\varphi_2(6)\beta(6)\chi_7(7)\alpha(7)|=|0\,\bar{0}\,1\,\bar{1}\,2\,\bar{2}\,7|$$

$$\Psi_2=1/2\{|0\,\bar{0}\,1\,\bar{3}\,2\,\bar{2}\,7|-|0\,\bar{0}\,\bar{1}\,3\,2\,\bar{2}\,7|+|0\,\bar{0}\,1\,\bar{1}\,2\,\bar{4}\,7|-|0\,\bar{0}\,1\,\bar{1}\,\bar{2}\,4\,7|\}$$

$$\Psi_3=\sqrt{12}^{-1}\{|0\,\bar{0}\,1\,\bar{3}\,2\,\bar{2}\,7|+|0\,\bar{0}\,\bar{1}\,3\,2\,\bar{2}\,7|-2|0\,\bar{0}\,1\,3\,2\,\bar{2}\,\bar{7}|+|0\,\bar{0}\,1\,\bar{1}\,2\,\bar{4}\,7|+|0\,\bar{0}\,1\,\bar{1}\,\bar{2}\,4\,7|-2|0\,\bar{0}\,1\,\bar{1}\,2\,4\,\bar{7}|\}$$

$$\Psi_4=1/2\{|0\,\bar{0}\,1\,\bar{3}\,2\,\bar{2}\,7|-|0\,\bar{0}\,\bar{1}\,3\,2\,\bar{2}\,7|-|0\,\bar{0}\,1\,\bar{1}\,2\,\bar{4}\,7|+|0\,\bar{0}\,1\,\bar{1}\,\bar{2}\,4\,7|\}$$

$$\Psi_5=\sqrt{12}^{-1}\{|0\,\bar{0}\,1\,\bar{3}\,2\,\bar{2}\,7|+|0\,\bar{0}\,\bar{1}\,3\,2\,\bar{2}\,7|-2|0\,\bar{0}\,1\,3\,2\,\bar{2}\,\bar{7}|-|0\,\bar{0}\,1\,\bar{1}\,2\,\bar{4}\,7|-|0\,\bar{0}\,1\,\bar{1}\,\bar{2}\,4\,7|+2|0\,\bar{0}\,1\,\bar{1}\,2\,4\,\bar{7}|\}$$

$^2A_2$

$$\Psi_6=1/2\{|0\,\bar{0}\,1\,\bar{4}\,2\,\bar{2}\,7|-|0\,\bar{0}\,\bar{1}\,4\,2\,\bar{2}\,7|-|0\,\bar{0}\,1\,\bar{1}\,2\,\bar{3}\,7|+|0\,\bar{0}\,1\,\bar{1}\,\bar{2}\,3\,7|\}$$

$$\Psi_7=\sqrt{12}^{-1}\{|0\,\bar{0}\,1\,\bar{4}\,2\,\bar{2}\,7|+|0\,\bar{0}\,\bar{1}\,4\,2\,\bar{2}\,7|-2|0\,\bar{0}\,1\,4\,2\,\bar{2}\,\bar{7}|+|0\,\bar{0}\,1\,\bar{1}\,2\,\bar{3}\,7|+|0\,\bar{0}\,1\,\bar{1}\,\bar{2}\,3\,7|-2|0\,\bar{0}\,1\,\bar{1}\,2\,3\,\bar{7}|\}$$

$$\Psi_8=1/2\{|0\,\bar{0}\,1\,\bar{4}\,2\,\bar{2}\,7|-|0\,\bar{0}\,\bar{1}\,4\,2\,\bar{2}\,7|-|0\,\bar{0}\,1\,\bar{1}\,2\,\bar{3}\,7|-|0\,\bar{0}\,1\,\bar{1}\,\bar{2}\,3\,7|\}$$

$$\Psi_9=\sqrt{12}^{-1}\{|0\,\bar{0}\,1\,\bar{4}\,2\,\bar{2}\,7|+|0\,\bar{0}\,\bar{1}\,4\,2\,\bar{2}\,7|-2|0\,\bar{0}\,1\,4\,2\,\bar{2}\,\bar{7}|-|0\,\bar{0}\,1\,\bar{1}\,2\,\bar{3}\,7|-|0\,\bar{0}\,1\,\bar{1}\,\bar{2}\,3\,7|+2|0\,\bar{0}\,1\,\bar{1}\,2\,3\,\bar{7}|\}$$

Electron transfer

$^2B_2$

$$\Psi_{10}=|0\,\bar{0}\,1\,2\,\bar{2}\,7\,\bar{7}|$$

$$\Psi_{11}=|0\,\bar{0}\,1\,\bar{1}\,2\,\bar{2}\,3|$$

$$\Psi_{12}=|0\,\bar{0}\,3\,2\,\bar{2}\,7\,\bar{7}|$$

$$\Psi_{13}=|0\,\bar{0}\,1\,3\,\bar{3}\,2\,\bar{2}|$$

$$\Psi_{14}=\sqrt{2}^{-1}\{|0\,\bar{0}\,1\,2\,\bar{4}\,7\,\bar{7}|-|0\,\bar{0}\,1\,\bar{2}\,4\,7\,\bar{7}|\}$$

$$\Psi_{15}=\sqrt{2}^{-1}\{|0\,\bar{0}\,1\,\bar{1}\,2\,\bar{4}\,3|-|0\,\bar{0}\,1\,\bar{1}\,\bar{2}\,4\,3|\}$$

$$\Psi_{16}=\sqrt{6}^{-1}\{|0\,\bar{0}\,1\,2\,\bar{4}\,7\,\bar{7}|-|0\,\bar{0}\,1\,\bar{2}\,4\,7\,\bar{7}|-2|0\,\bar{0}\,\bar{1}\,2\,4\,7\,\bar{7}|\}$$

$$\Psi_{17}=\sqrt{6}^{-1}\{|0\,\bar{0}\,1\,\bar{1}\,2\,\bar{4}\,3|+|0\,\bar{0}\,1\,\bar{1}\,\bar{2}\,4\,3|-2|0\,\bar{0}\,1\,\bar{1}\,2\,4\,\bar{3}|\}$$

$^2A_2$

$$\Psi_{18}=|0\,\bar{0}\,1\,\bar{1}\,2\,7\,\bar{7}|$$

$$\Psi_{19}=|0\,\bar{0}\,1\,\bar{1}\,4\,2\,\bar{2}|$$

$$\Psi_{20}=|0\,\bar{0}\,4\,2\,\bar{2}\,7\,\bar{7}|$$

$$\Psi_{21}=|0\,\bar{0}\,1\,\bar{1}\,2\,3\,\bar{3}|$$

$$\Psi_{22}=\sqrt{2}^{-1}\{|0\,\bar{0}\,1\,2\,\bar{3}\,7\,\bar{7}|-|0\,\bar{0}\,1\,\bar{2}\,3\,7\,\bar{7}|\}$$

$$\Psi_{23}=\sqrt{2}^{-1}\{|0\,\bar{0}\,1\,\bar{4}\,2\,\bar{2}\,3|-|0\,\bar{0}\,\bar{1}\,4\,2\,\bar{2}\,3|\}$$

$$\Psi_{24}=\sqrt{6}^{-1}\{|0\,\bar{0}\,1\,2\,\bar{3}\,7\,\bar{7}|+|0\,\bar{0}\,1\,\bar{2}\,3\,7\,\bar{7}|-2|0\,\bar{0}\,\bar{1}\,2\,3\,7\,\bar{7}|\}$$

$$\Psi_{25}=\sqrt{6}^{-1}\{|0\,\bar{0}\,1\,\bar{4}\,2\,\bar{2}\,3|+|0\,\bar{0}\,\bar{1}\,4\,2\,\bar{2}\,3|-2|0\,\bar{0}\,1\,4\,2\,\bar{2}\,\bar{3}|\}$$

Quartet configuration ($M_s=+3/2$)

Non-polar

$^4B_2$

$$\Psi_{26}=\sqrt{2}^{-1}\{|0\,\bar{0}\,1\,3\,2\,\bar{2}\,7|+|0\,\bar{0}\,1\,\bar{1}\,2\,4\,7|\}$$

$$\Psi_{27}=\sqrt{2}^{-1}\{|0\,\bar{0}\,1\,3\,2\,\bar{2}\,7|-|0\,\bar{0}\,1\,\bar{1}\,2\,4\,7|\}$$

$^4A_2$

$$\Psi_{28}=\sqrt{2}^{-1}\{|0\,\bar{0}\,1\,4\,2\,\bar{2}\,7|+|0\,\bar{0}\,1\,\bar{1}\,2\,3\,7|\}$$

$$\Psi_{29}=\sqrt{2}^{-1}\{|0\,\bar{0}\,1\,4\,2\,\bar{2}\,7|-|0\,\bar{0}\,1\,\bar{1}\,2\,3\,7|\}$$

Electron transfer

$^4B_2$

$$\Psi_{30}=|0\,\bar{0}\,1\,2\,4\,7\,\bar{7}|$$

$$\Psi_{31}=|0\,\bar{0}\,1\,\bar{1}\,2\,4\,3|$$

$^4A_2$

$$\Psi_{32}=|0\,\bar{0}\,1\,2\,3\,7\,\bar{7}|$$

$$\Psi_{33}=|0\,\bar{0}\,1\,4\,2\,\bar{2}\,3|$$

radical used in the present calculation are shown in Table I.

In Table I, $\chi_7(\nu)$ is the $2P\pi$ orbital of $CH_2$. The configurations from $\Psi_1$ to $\Psi_9$ are those of the previous paper[4] and these are the non-polar configuration. The electron transfer configurations from $\Psi_{10}$ to $\Psi_{25}$ (polar configurations) are neccessary to consider the effect of electron transfer.

By the use of Pariser-Parr approximation, with the neglect of penetration integral and all of the differential overlaps except resonance

4) The correlations between the electronic states of benzene and those of benzyl radical are

$\phi(^1A_{1g})-\Psi_1$; $\phi(^1E_{1u})-\Psi_2,\Psi_8$; $\phi(^1B_{1u})-\Psi_4$; $\phi(^1B_{2u})-\Psi_6$; $\phi(^3E_{1u})-\Psi_3$, $\Psi_9$, $\Psi_{29}$; $\phi(^3B_{1u})-\Psi_5$, $\Psi_{27}$; $\phi(^3B_{2u})-\phi_4$, $\phi_{28}$.

integral, the energies of the electron transfer configurations degenerate in pairs

$$H_{v,v}=H_{v+1,\,v+1}$$

where $v$ is an even number[5].

The matrix elements $H_{jk}$'s $(j\neq k)$ are not zero in the following two cases;
1) between an electron transfer configuration and a non-polar configuration of the same symmetry class both of which differ by the position of just one electron, and 2) between both electron transfer configurations of the same direction and of the same symmetry class. However, the interactions between excited electron transfer configurations are not considered, as these contribute very slightly to the energies and to the wave functions of the lower excited states of benzyl radical.

Then by taking the linear combinations

$$\left.\begin{aligned}\Psi_v^+&=\Psi_v+\Psi_{v+1}\\ \Psi_{v+1}^-&=\Psi_v-\Psi_{v+1}\end{aligned}\right\}\qquad(2)$$

each secular determinant is factored as shown in Table II. The values of the integrals are those by Pariser[6].

Then the wave functions of benzyl radical are classified into classes as follows:

The wave functions represented by the linear combinations of

a) $\Psi_1,\ \Psi_3,\ \Psi_5,\ \Psi_{11}^-,\ \Psi_{13}^-,\ \Psi_{14}^+,\ \Psi_{17}^-$
b) $\Psi_2,\ \Psi_4,\ \Psi_{10}^+,\ \Psi_{12}^+,\ \Psi_{15}^-,\ \Psi_{16}^+$
c) $\Psi_6,\ \Psi_9,\ \Psi_{18}^+,\ \Psi_{20}^+,\ \Psi_{23}^-,\ \Psi_{23}^+$
d) $\Psi_7,\ \Psi_8,\ \Psi_{19}^-,\ \Psi_{21}^-,\ \Psi_{22}^+,\ \Psi_{25}^-$
e) $\Psi_{26},\ \Psi_{27},\ \Psi_{31}^-$
f) $\Psi_{30}^+$
g) $\Psi_{28},\ \Psi_{33}^-$
h) $\Psi_{29},\ \Psi_{32}^+$

Since the non-vanishing dipole matrix elements,

$$eq_{jk}=e\int\Psi_j\sum_\nu q(\nu)\Psi_k\mathrm{d}V$$

TABLE II. THE MATRIX ELEMENTS. (The values are given in eV.)

(I) $^2B_2$

(a) $E_1=H_{11}$

| | (1) | (3) | (5) | (11⁻) | (13⁻) | (14⁺) | (17⁻) |
|---|---|---|---|---|---|---|---|
| (1) | $E_1$ | | | | | | |
| (3) | 0 | $E_1+4.1485$ | | | | | |
| (5) | 0 | 0 | $E_1+3.5895$ | | | | |
| (11⁻) | +1.9359 | +1.6766 | +1.6766 | $E_1+6.1602$ | | | |
| (13⁻) | 0 | −1.6766 | −1.6766 | +0.9470 | $E_1+11.2744$ | | |
| (14⁺) | 0 | 0 | 0 | +1.3888 | 0 | $E_1+12.7060$ | |
| (17⁻) | 0 | +1.3689 | −1.3689 | 0 | 0 | 0 | $E_1+11.1485$ |

(b) $E_4=H_{44}=E_1+5.9595$

| | (2) | (4) | (10⁺) | (12⁺) | (15⁻) | (16⁺) |
|---|---|---|---|---|---|---|
| (2) | $E_4+0.8000$ | | | | | |
| (4) | 0 | $E_4$ | | | | |
| (10⁺) | +0.9680 | +0.9680 | $E_4+0.2007$ | | | |
| (12⁺) | +0.9680 | +0.9680 | +0.9470 | $E_4+5.3152$ | | |
| (15⁻) | +1.3689 | −1.3689 | +1.3888 | 0 | $E_4+6.7465$ | |
| (16⁺) | 0 | 0 | 0 | 0 | 0 | $E_4+5.1889$ |

(II) $^2B_2$

(c) $E_9=H_{99}=E_1+4.1495$

| | (6) | (9) | (18⁺) | (20⁺) | (23⁻) | (24⁺) |
|---|---|---|---|---|---|---|
| (6) | $E_9+0.5600$ | | | | | |
| (9) | 0 | $E_9$ | | | | |
| (18⁺) | +0.9680 | −1.6766 | $E_9+2.3410$ | | | |
| (20⁺) | +0.9680 | −1.6766 | 0 | $E_9+7.3224$ | | |
| (23⁻) | +1.3689 | 0 | −0.6696 | 0 | $E_9+7.9980$ | |
| (24⁺) | 0 | −1.3689 | −1.1598 | 0 | 0 | $E_9+8.2180$ |

5) See Appendix. This relation is plausible in simple MO calculations.

6) R. Pariser, *J. Chem. Phys.*, **24**, 250 (1956).

TABLE II (Continued)

(d) $E_7=H_{77}=E_1+4.7095$

| | (7) | (8) | (19⁻) | (21⁻) | (22⁺) | (25⁻) |
|---|---|---|---|---|---|---|
| (7) | $E_7$ | | | | | |
| (8) | 0 | $E_7-2.0500$ | | | | |
| (19⁻) | +1.6766 | −0.9680 | $E_7+1.7810$ | | | |
| (21⁺) | −1.6766 | +0.9680 | 0 | $E_7+6.7624$ | | |
| (22⁺) | 0 | −1.3689 | −0.6696 | 0 | $E_7+7.4380$ | |
| (25⁻) | +1.3689 | 0 | −1.1598 | 0 | 0 | $E_7+7.6580$ |

(III) $^4B_2$

(e) $E_{27}=H_{27,27}=E_1+3.5895$

| | (26) | (27) | (31⁻) |
|---|---|---|---|
| (26) | $E_{27}+0.5600$ | | |
| (27) | 0 | $E_{27}$ | |
| (31⁻) | +1.3689 | −1.3689 | $E_{27}+6.1602$ |

(f) $E_{30^+}=H_{31^+,31^+}=E_1+9.7497$

(IV) $^4A_2$

(g) $E_{28}=H_{28,28}=E_1+4.7095$

| | (28) | (33⁻) |
|---|---|---|
| (28) | $E_{28}$ | |
| (33⁻) | +1.3689 | $E_{28}+5.705$ |

(h) $E_{29}=H_{29,29}=E_1+4.1495$

| | (29) | (32⁻) |
|---|---|---|
| (29) | $E_{29}$ | |
| (32⁺) | −1.3689 | $E_{29}+5.9305$ |

TABLE III. THE NON-VANISHING DIPOLE MATRIX ELEMENTS[a]

$q_{12}=[q:13]+[q:24]$
$q_{11^-,10^+}=1/2\{[q:77]-[q:33]\}$
$q_{11^-,12^+}=[q:13]$
$q_{11^-,15^-}=\sqrt{2}\,[q:24]$
$q_{13^-,12^+}=1/2\{[q:77]-[q:33]\}$
$q_{14^+,15^-}=1/2\{[q:77]-[q:33]\}$
$q_{17^-,16^+}=1/2\{[q:77]-[q:33]\}$
$q_{18}=[q:14]-[q:23]$
$q_{11^-,21^-}=[q:14]$
$q_{14^+,19^-}=-\sqrt{2}^{-1}[q:14]$
$q_{17^-,19^-}=-\sqrt{3/2}[q:14]$

a) $[q:lm]=\int\varphi_l(\nu)q(\nu)\varphi_m(\nu)d\tau_\nu$

$[q:77]=\int\chi_7(\nu)q(\nu)\chi_7(\nu)d\tau_\nu$

TABLE IV. THE LOWER ENERGY LEVELS OF BENZYL RADICAL

| State | Class | Energy, eV.[a] |
|---|---|---|
| $^2B_2$ | a | 0 |
| $^2B_2$ | a | 2.75 (2.99) |
| $^2A_2$ | c | 3.21 (3.42) |
| $^2A_2$ | d | 3.70 (4.33) |
| $^4B_2$ | e | 3.92 (4.01) |
| $^2B_2$ | a | 4.16 (4.18) |
| $^4A_2$ | h | 4.59 (4.57) |
| $^4B_2$ | e | 4.74 (4.86) |
| $^2A_2$ | c | 5.08 (5.13) |
| $^4A_2$ | g | 5.12 (5.42) |
| $^2B_2$ | b | 5.29 (6.23) |

a) The values in the parentheses are those in the previous paper.

where $q(\nu)$ is the position of the $\nu$th electron, are those shown in Table III, the transitions from the ground state to the excited states of classes a and c are almost forbidden but the transitions to the excited states of classes b and d are allowed, though these four transitions are allowed by selection rule.

The energy levels of benzyl radical by the present treatment are show in Table IV.

## Discussion

The lowest excitation energy from the ground state to the lowest excited state $^2B_2$ calculated by this treatment is 2.75 eV. and this value will be compared to the transition energy 2.8 eV. of the "V"-band[7] of benzyl radical which was observed by Schüler. From the consideration on the transition moments it was shown that the transition to the lowest $^2A_2$ (3.21 eV.) of class c is almost practically forbidden and the transition to $^2A_2$ (3.75 eV.) of class d is allowed. Therefore, the absorption band observed by Porter at about 3100 Å[8] will be assigned to the excitation from the ground state to the excited state $^2A_2$ (3.75 eV.; 3300 Å).

In the present treatment, the weak intensities of the lower absorption bands are predicted though the effect of electron transfers was taken into account. There are two directions of the electron transfers. One is the electron transfer from benzene ring to $CH_2$ and the other is the reverse. Further the effect of these two electron transfers are equal in magnitude and opposite in direction, and cancel each other on the transition moments of the excitation to the states of class a. On the other hand, in the transitions to the states of class b the effect of electron transfer may be considerable, because for these transitions the two electron transfers contribute to enhance the oscillator strengths.

The effect of electron transfer on the transitions to the states of classes c and d is indirect. The directions of these transition moments are orthogonal to the direction of electron transfer. In this case, the transition moments are given by the mixing with the configuration $\Psi_8$ where the mixing arises from the electron transfer interaction. Therefore, the intensity of the transition to $^2A_2$ (3.21 eV.) may be weak, as no mixing with $\Psi_8$ occurs and $^2A_2$ (3.75 eV.) will give rise to a strong absorption band by the mixing with $\Psi_8$.

Consideration may be given to the intensities of the lowest absorption bands of radicals in which the $CH_2$ group of benzyl radical is substituted by another atom or group. By the substitution, the electronegativity of the attached group or atom is changed from that of $CH_2$. By this change the difference is given between the weights of contributions from the two opposite electron transfer states. Then the intensities of the lowest bands of these radicals may be more intense than that of benzyl radical because the effects of the two electron transfers of opposite directions do not cancel completely in such radicals.

The results of the present paper are similar to those obtained by the treatment in the previous paper[1] and also the inconsistency with the results calculated by the method of MO[9,10] is seen. This inconsistency arises from the difference of the configuration interactions included in the calculations as shown in the previous paper. The results of the present paper may be more reliable than that in the previous paper because of the improved procedure of calculation.

## Summary

The method of composite system was applied to the calculation of the electronic spectra of benzyl radical. The results are very similar to those in the previous paper[1] and there is no important difference between these two results though the procedures of calculation are different.

The effect of electron transfer on the transition moments of lower bands of some radicals was discussed.

The author wishes to express his sincere thanks to Professor I. Tanaka for his kind advice and discussions.

*Laboratory of Physical Chemistry*
*Tokyo Institute of Technology*
*Meguro-ku, Tokyo*

## Appendix

The diagonal matrix elements of the electron transfer configurations are written in the form

$$H_{jj}=E_P(j)+U(j)$$

In the above, $E_P(j)$ represents the energies of charge components in the electron transfer $j$ and $U(j)$ is the Coulomb potential between charged components.

The molecular integral are abbreviated as

$$I_{mm}=\int\varphi_m(\nu)H_{core}(\nu)\varphi_m(\nu)d\tau_\nu$$

$$[ll:mm]=\iint|\varphi_l(\nu)|^2e^2/r_{\nu\mu}|\varphi_m(\mu)|^2d\tau_\nu d\tau_\mu$$

7) H. Schüler, *Z. Naturforsch.*, **A10**, 459 (1955).
8) G. Porter and J. Norman, *Nature*, **174**, 508 (1954).
9) H. C. Longuet-Higgins and J. A. Pople, *Proc. Phys. Soc.*, **A68**, 591 (1955).
10) W. Bingel, *Z. Naturforsch.*, **A10**, 462 (1955).

$$[lm : lm] = \iint \varphi_l(\nu)\varphi_m(\nu)e^2/r_{\nu\mu}\varphi_m(\mu)\varphi_l(\mu)\mathrm{d}\tau_\nu \mathrm{d}\tau_\mu$$

$$(tt : uu) = \iint |\chi_t(\nu)|^2 e^2/r_{\nu\mu}|\chi_u(\mu)|^2 \mathrm{d}\tau_\nu \mathrm{d}\tau_\mu$$

where $\varphi_l(\nu)$ and $\varphi_m(\nu)$ are the $\pi$-electron molecular orbitals of benzene.

Applying the following relations (the last three are Eqs. 28, 46 and 47 in Ref. 6),

$$[11 : mm] = [33 : mm], \quad [22 : mm] = [44 : mm]$$

$$[12 : 12] = [34 : 34], \quad [23 : 23] = [14 : 14]$$

$$\mathbf{I}_{mm} = \mathbf{W}_{2P} - \sum_t (C_{mt})^2 \sum_{u(\neq t)} (tt : uu) + k_m\beta$$

$$2\sum_{m=0}^{2} [ll : mm] = \sum_t (C_{lt})^2 \sum_u (tt : uu)$$

$$2\sum_{m=0}^{2} \{[1m : 1m] + [3m : 3m]\}$$

$$= 2\sum_{m=0}^{2} \{[2m : 2m] + [4m : 4m]\} = (11 : 11)$$

one has

$$\mathrm{E}_P(10) = E_P(11), \qquad \mathrm{E}_P(18) = \mathrm{E}_P(19)$$

By the above equations and by the relations

$$[11 : 33] = [22 : 44], \quad [01 : 01] = [02 : 02]$$

$$[03 : 03] = [04 : 04], \quad [13 : 13] = [24 : 24]$$

the following is given

$$\mathrm{E}_P(v) = \mathrm{E}_P(v+1)$$

where $v$ is an even number.

The Coulomb potential $\mathrm{U}(j)$ is given subject to the symmetry (except U(20) and U(21)),

$$^2\mathrm{B}_2 \text{ and } ^4\mathrm{B}_2 \quad \mathrm{U}(j) = -[11 : 77]$$

$$^2\mathrm{A}_2 \text{ and } ^4\mathrm{A}_2 \quad \mathrm{U}(j) = -[22 : 77]$$

The potentials U(20) and U(21) are

$$\mathrm{U}(20) = \mathrm{U}(21) = -2[11 : 77] + [22 : 77]$$

Thus the following is given

$$\mathrm{H}_{v,\,v} = \mathrm{H}_{v+1,\,v+1}$$

# *Polarographic Determination of the Formation Constant of Sulfatonickel(II) Complex*

By Nobuyuki TANAKA and Hiroshi OGINO

(Received December 24, 1960)

In the previous paper[1], a new method for the determination of the formation constants of metal acetato complexes and its application to acetatonickel(II) complexes were presented. The method is based on the polarographic measurement of the sum of the equilibrium concentrations of hydrated metal ions and metal acetato complexes in the presence of an appropriate auxiliary complex-forming substance. Although similar functions are derived, the method is essentially different from the DeFord and Hume's method[2] that is based on the displacements of the half-wave potential of metal ions in the presence of a complex-forming substance[3].

Because of the increasing interest in the determination of the formation constants of less stable complexes, especially those with two or more different ligands, it seems worth while to generalize the treatment of the method reported in the previous paper[1] and to increase its applicability.

In the present paper, the case where a co-existing ion, $Z^{z-}$, is added to the system of Ni(II)—auxiliary complex-forming substance—acetate is dealt with. A general procedure for the determination of the formation constants of $Ni(OAc)_i^{(2-i)+}$ and $Ni(Z)_j^{(2-zj)+}$ as well as $Ni(OAc)_i(Z)_j^{(2-i-zj)+}$ is presented, and the formation constants of monosulfatonickel(II) complex, which were determined with sulfate ions used as the co-existing ion, are reported.

## Theoretical

Let us consider the acetate buffer solution which contains nickel(II)[4], nitrilotriacetate (NTA)[4] and a co-existing ion. There exist the following equilibria:

$$Ni^{2+} + X^{3-} \rightleftarrows NiX^- \quad (1)$$

$$NiX^- + H^+ \rightleftarrows NiHX \quad (2)$$

$$Ni^{2+} + i\,OAc^- + j\,Z^{z-} \rightleftarrows Ni(OAc)_i(Z)_j^{(2-i-zj)+} \quad (3)$$

1) N. Tanaka and K. Kato, This Bulletin, 32, 516 (1959).
2) D. D. DeFord and D. N. Hume, *J. Am. Chem. Soc.*, 73, 5321 (1951).
3) D. N. Hume, *Anal. Chem.*, 32, 137R (1960).
4) Nickel(II) and nitrilotriacetate may be replaced by other appropriate metal ions and complex-forming substances, respectively.

where $X^{3-}$ denotes a tervalent NTA anion and $Z^{z-}$, a co-existing ion, e. g., sulfate.

The total concentration of nickel, $[Ni]_t$, and that of NTA, $[NTA]_t$, in the solution are given in terms of the ionic and the molecular species as follows:

$$[Ni]_t = \sum_{i=0}^{n}\sum_{j=0}^{p}[Ni(OAc)_i(Z)_j^{(2-i-zj)+}] + [NiX^-] + [NiHX] \quad (4)$$

$$[NTA]_t = [NTA]_f + [NiX^-] + [NiHX] \quad (5)$$

where $\sum_{i=0}^{n}\sum_{j=0}^{p}[Ni(OAc)_i(Z)_j^{(2-i-zj)+}]$ represents the sum of the concentrations of hydrated nickel ions and complexes of nickel(II) co-ordinating with acetate and/or $Z^{z-}$ ions, and $[NTA]_f$, the sum of the concentrations of the uncomplexed NTA.

The polarographic diffusion current of nickel ions obtained in the solution which contains acetate and $Z^{z-}$ ions corresponds to the sum of the diffusion current due to the hydrated nickel ions and of those due to the complexes of nickel(II) co-ordinating with acetate and/or $Z^{z-}$ ions[1]. If the hydrated ion and the complexes have nearly the same diffusion current constants, the sum of their concentrations can be determined from the polarographic diffusion current, if necessary, after correction. Then, we write the equation as,

$$[Ni^{2+}]_{app} = \sum_{i=0}^{n}\sum_{j=0}^{p}[Ni(OAc)_i(Z)_j^{(2-i-zj)+}] \quad (6)$$

where $[Ni^{2+}]_{app}$ is the concentration that can be determined polarographically. Eq. 4 is rewritten as,

$$[Ni]_t = [Ni^{2+}]_{app} + [NiX^-] + [NiHX] \quad (7)$$

The concentrations of $NiX^-$, $Ni^{2+}$ and $X^{3-}$ are given by

$$[NiX^-] = \frac{[Ni]_t - [Ni^{2+}]_{app}}{\beta} \quad (8)$$

$$[Ni^{2+}] = \frac{[Ni^{2+}]_{app}}{\sum_{i=0}^{n}\sum_{j=0}^{p}K_{Ni(OAc)_i(Z)_j}[OAc^-]^i[Z^{z-}]^j} \quad (9)$$

$$[X^{3-}] = \frac{[NTA]_f}{\alpha} \quad (10)$$

where

$$\alpha = 1 + \frac{[H^+]}{K_{HX}} + \frac{[H^+]^2}{K_{H_2X}K_{HX}} + \frac{[H^+]^3}{K_{H_3X}K_{H_2X}K_{HX}}$$

and

$$\beta = 1 + K^H_{NiHX}[H^+]$$

$K_{H_3X}$, $K_{H_2X}$ and $K_{HX}$ represent the first, the second and the third dissociation constant of nitrilotriacetic acid, respectively, $K^H_{NiHX}$, the equilibrium constant of the reaction given by Eq. 2 and $K_{Ni(OAc)_i(Z)_j}$, the overall formation constant of $Ni(OAc)_i(Z)_j^{(2-i-zj)+}$. It may be defined that when both $i$ and $j$ are zero, the value of $K_{Ni(OAc)_i(Z)_j}$ equals unity.

The formation constant of $NiX^-$, consequently, is given as

$$K_{NiX} = \frac{[NiX^-]}{[Ni^{2+}][X^{3-}]} = \alpha\{[Ni]_t - [Ni^{2+}]_{app}\} \times \frac{\sum_{i=0}^{n}\sum_{j=0}^{p}K_{Ni(OAc)_i(Z)_j}[OAc^-]^i[Z^{z-}]^j}{\beta[Ni^{2+}]_{app}[NTA]_f} \quad (11)$$

Introducing to Eq. 11 the expression for the concentration of uncomplexed NTA given as

$$[NTA]_f = [Ni^{2+}]_{app} - [Ni]_t + [NTA]_t \quad (12)$$

the relation

$$\frac{\{[Ni^{2+}]_{app} - [Ni]_t + [NTA]_t\}[Ni^{2+}]_{app}}{[Ni]_t - [Ni^{2+}]_{app}} = \frac{\alpha}{\beta K_{NiX}}\sum_{i=0}^{n}\sum_{j=0}^{p}K_{Ni(OAc)_i(Z)_j}[OAc^-]^i[Z^{z-}]^j \quad (13)$$

is obtained. It may be obvious that both $\alpha$ and $\beta$ in Eq. 13 are constant in the solution of the given pH and the given ionic strength.

First, the values of $[Ni^{2+}]_{app}$ are determined by the polarographic method at the given pH, the given ionic strength and the given concentration of acetate, but at varied concentrations of $Z^{z-}$, with which the values for the left-hand side of Eq. 13 are calculated. In this case it may be convenient to express Eq. 13 as,

$$F_0 = \frac{\alpha}{\beta K_{NiX}}\sum_{i=0}^{n}K_{Ni(OAc)_i}[OAc^-]^i + \frac{\alpha}{\beta K_{NiX}}\sum_{i=0}^{n}K_{Ni(OAc)_i(Z)}[OAc^-]^i[Z^{z-}] + \cdots\cdots + \frac{\alpha}{\beta K_{NiX}}\sum_{i=0}^{n}K_{Ni(OAc)_i(Z)_p}[OAc^-]^i[Z^{z-}]^p \quad (13')$$

where the left-hand side of Eq. 13 is replaced by $F_0$. Eq. 13′ shows clearly that the plot of $F_0$ against the concentration of $Z^{z-}$ gives a curves of $p$th degree with respect to $[Z^{z-}]$. From extrapolation of the $F_0$ plot to the zero concentration of $Z^{z-}$, the value of $\frac{\alpha}{\beta K_{NiX}}\sum_{i=0}^{n}K_{Ni(OAc)_i}[OAc^-]^i$ is obtained. Then, the function $F_j(Z)$ $(1 \leq j \leq p+1)$ is defined as

$$F_j(Z) \equiv \frac{F_{j-1}(Z) - \frac{\alpha}{\beta K_{NiX}} \sum_{i=0}^{n} K_{Ni(OAc)_i(Z)_{j-1}} [OAc^-]^i}{[Z^{z-}]}$$

$$= \frac{\alpha}{\beta K_{NiX}} \sum_{i=0}^{n} K_{Ni(OAc)_i(Z)_j} [OAc^-]^i + \frac{\alpha}{\beta K_{NiX}} \sum_{i=0}^{n} K_{Ni(OAc)_i(Z)_{j+1}} [OAc^-]^i [Z^{z-}] + \cdots\cdots \quad (14)$$

$F_j(Z)$ is plotted against the concentration of $Z^{z-}$ and the value of $\frac{\alpha}{\beta K_{NiX}} \sum_{i=0}^{n} K_{Ni(OAc)_i(Z)_j} [OAc^-]^i$ is determined by extrapolating the $F_j(Z)$ plot to zero concentration of $Z^{z-}$. Repeating the procedure until the relation,

$$F_{p+1}(Z) = 0$$

is obtained, the value of $p$ can be determined.

Secondly, the values of $[Ni^{2+}]_{app}$ are determined by the polarographic method at the given pH, the given ionic strength and the given concentration of $Z^{z-}$, but at varied concentrations of acetate. The left-hand side of Eq. 13 is calculated and plotted against the concentration of acetate. Eq. 13 is also written as a function of the concentration of acetate:

$$F_0 = \frac{\alpha}{\beta K_{NiX}} \sum_{j=0}^{p} K_{Ni(Z)_j} [Z^{z-}]^j + \frac{\alpha}{\beta K_{NiX}} \sum_{j=0}^{p} K_{Ni(OAc)(Z)_j} [Z^{z-}]^j [OAc^-] + \cdots\cdots + \frac{\alpha}{\beta K_{NiX}} \sum_{j=0}^{p} K_{Ni(OAc)_n(Z)_j} [Z^{z-}]^j [OAc^-]^n \quad (13'')$$

From extrapolation of the $F_0$ plot to zero acetate concentration, the value of $\frac{\alpha}{\beta K_{NiX}} \sum_{j=0}^{p} K_{Ni(Z)_j} [Z^{z-}]^j$ is obtained.

The function $F_i(OAc)$ $(1 \leq i \leq n+1)$ is also defined as,

$$F_i(OAc) \equiv \frac{F_{i-1}(OAc) - \frac{\alpha}{\beta K_{NiX}} \sum_{j=0}^{p} K_{Ni(OAc)_{i-1}(Z)_j} [Z^{z-}]^j}{[OAc^-]}$$

$$= \frac{\alpha}{\beta K_{NiX}} \sum_{j=0}^{p} K_{Ni(OAc)_i(Z)_j} [Z^{z-}]^j + \frac{\alpha}{\beta K_{NiX}} \sum_{j=0}^{p} K_{Ni(OAc)_{i+1}(Z)_j} [Z^{z-}]^j [OAc^-] + \cdots\cdots \quad (15)$$

$F_i(OAc)$ is plotted against the concentration of acetate and the value of $\frac{\alpha}{\beta K_{NiX}} \sum_{j=0}^{p} K_{Ni(OAc)_i(Z)_j} [Z^{z-}]^j$ is detremined. If the procedure concerning the $F_i(OAc)$ plot is repeated at $p+1$ different concentrations of $Z^{z-}$, $(n+1)(p+1)$ pieces of equations with $(n+1)(p+1)$ unknown quantities, which are $K_{Ni(OAc)_i(Z)_j}$ $(0 \leq i \leq n,\ 0 \leq j \leq p$ except $i=j=0)$ and $\frac{\alpha}{\beta K_{NiX}}$, are yielded. Solving these equations, all of $K_{Ni(OAc)_i(Z)_j}$ can, at least theoretically, be determined.

## Experimental

**Reagents.**—A standard solution of nickel nitrate was prepared by dissolving an appropriate amount of pure nickel metal in nitric acid. The concentration of nickel was determined by the conventional gravimetric method with dimethylglyoxime[5]. A solution of disodium nitrilotriacetate was prepared from the commercial nitrilotriacetic acid (DOTITE NTA), and standardized against the standard solution of nickel(II) nitrate by amperometric titration with a similar procedure for ethylenediaminetetraacetate[6,7]. A solution of potassium sulfate was prepared from the guaranteed grade reagent. The sulfate concentration was determined by the conventional gravimetric method[8]. All other chemicals used were of analytical reagent grade.

**Apparatus and Procedure.**—A Yanagimoto PB-4 pen-recording polarograph was used for the measurement of the current-voltage curves. The dropping mercury electrode used had an $m$ value of 2.13 mg./sec. and a drop time $t_d$ of 4.07 sec., being measured in an air-free 0.2 M potassium nitrate solution containing $2 \times 10^{-6}$ M polyoxyethylene lauryl ether (LEO) at 25°C and at −0.5 V vs. SCE. The sum of the diffusion currents of hydrated nickel ions, acetatonickel(II), sulfatonickel(II) and, if any, acetatosulfatoniccolate(II) complexes were determined in the acetate buffer of pH 3.66±0.02 containing sulfate, nickel(II) and a slight excess of NTA at 15, 25 and 35°C. The concentration of acetate in the buffer was varied from 0.025 to 0.100 M at the constant concentration of sulfate of 0.03 M, while that of sulfate was varied from 0.01 to 0.05 M at the constant concentration of acetate of 0.05 M. The ionic strength of the solution was adjusted to be 0.2 with potassium nitrate. LEO was added as a maximum suppressor by $1 \times 10^{-6}$ M (at 15°C) or $2 \times 10^{-6}$ M (at 25 and 35°C) in concentration. The pH of the solution was measured

5) F. P. Treadwell and W. T. Hall, "Analytical Chemistry", Vol. 2, John Wiley & Sons, Inc., New York (1951), p. 193.

6) N. Tanaka, M. Kodama, M. Sasaki and M. Sugino, *Japan Analyst (Bunseki Kagaku)*, **6**, 86 (1957).

7) N. Tanaka, I. T. Oiwa and M. Kodama, *Anal. Chem.*, **28**, 1555 (1956).

8) F. P. Treadwell and W. T. Hall, "Analytical Chemistry", Vol. 2, John Wiley & Sons, Inc., New York (1951), p. 393.

accurately, after the polarographic measurement, with a Hitachi Model EHP-1 pH meter with a glass electrode.

## Results and Discussion

The polarograms were recorded with the solution of pH 3.66 containing $1.00\times10^{-3}$ M nickel nitrate, $1.09\times10^{-3}$ M NTA and various concentrations of acetate and sulfate, unless otherwise stated. Nickel(II) gave an irreversible wave with the half-wave potential of about $-1.05$ V vs. SCE in the acetate-sulfate-nitrate media. This wave is considered to be due to the reductions of hydrated nickel(II) ions, acetatonickel(II), sulfatonickel(II) and, if any, acetatosulfatoniccolate(II) complexes. The limiting current of the wave was found to be proportional to the concentration of the electroactive species and also to the square root of the effective height of mercury column on the dropping mercury electrode. This clearly showed that the limiting current is diffusion-controlled.

The apparent diffusion current constants of nickel(II) were determined from the measurements of the diffusion current at various acetate and sulfate concentrations. The values of $[Ni^{2+}]_{app}$ of Eq. 6 were calculated, with the aid of those apparent diffusion current constants, from the limiting currents obtained with the reaction mixtures.

**Presence of Sulfato Complexes.**—The polarograms were recorded with the solutions containing 0.0500 M actate and various concentrations of sulfate at various temperatures. With the values of $[Ni^{2+}]_{app}$ obtained, the left-hand side of Eq. 13, $F_0$, was calculated and plotted against the sulfate concentration. The results are shown in Fig. 1, where it is clearly seen that the plots of $F_0$ vs. $[SO_4^{2-}]$ give straight lines. This fact indicates that $p$ is equal to 1 and no appreciable amount of complexes with two sulfates or more co-ordinated is present in the solution under the experimental conditions. From the plots in Fig. 1, the values of $\frac{\alpha}{\beta K_{NiX}}\sum_{i=0}^{n} K_{Ni(OAc)_i}[OAc^-]^i$ and $\frac{\alpha}{\beta K_{NiX}}\sum_{i=0}^{n} K_{Ni(OAc)_i(SO_4)}[OAc^-]^i$ in Eq. 13′ were determined, the former being given by the intercept at $[SO_4^{2-}]=0$ and the latter, by the slope.

**Absence of Acetatosulfato Complexes.**—The polarograms were recorded with the solutions containing 0.0297 M sulfate and various concentrations of acetate at 25°C, and the values of $[Ni^{2+}]_{app}$ were determined. The left-hand side of Eq. 13, $F_0$, was calculated and plotted against the acetate concentration. (A in Fig. 2).

A linear relation between $F_0$ and the concentration of acetate clearly indicates that $n$ is equal to 1 and no appreciable amount of complexes with two acetates or more co-ordinated is present in the solution under the experimental condition. The fact that $n$ and $p$ are equal to 1, respectively, suggests that $NiOAc^+$, $NiSO_4$ and $Ni(OAc)(SO_4)^-$ may exist in the solution under the experimental condition.

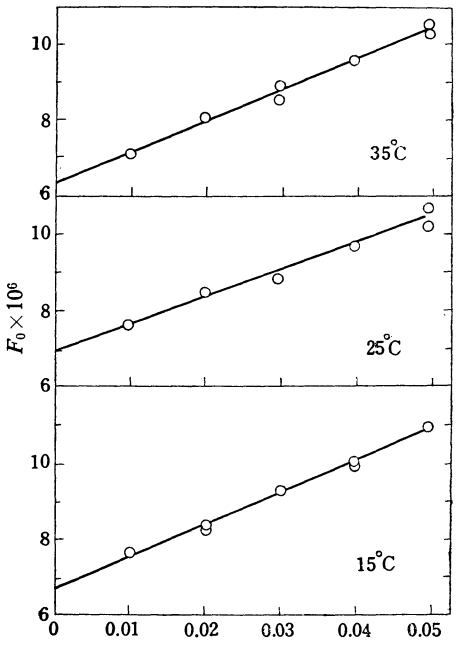



Fig. 1. Relation between the values of left-hand side of Eq. 13, $F_0$, and the concentration of sulfate at various temperatures. Acetate concentration is 0.0500 M.

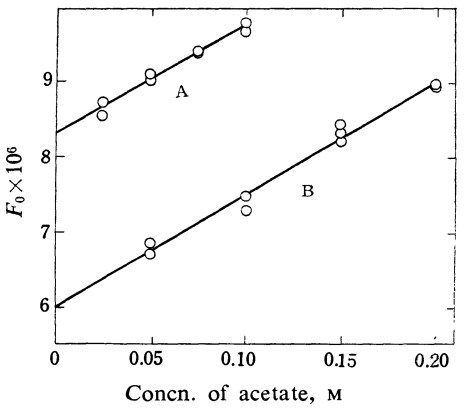



Fig. 2. Relations between the value of left-hand side of Eq. 13, $F_0$, and the concentration of acetate at 25°C, obtained in the presence of 0.0297 M sulfate (A) and in the absence of sulfate (B).

TABLE II. THE REPORTED VALUES OF FORMATION CONSTANTS OF SULFATONICKEL(II) COMPLEX

| Investigator | Method | Temp., °C | Ionic strength | $K_{NiSO_4}$ | Ref. |
|---|---|---|---|---|---|
| Money et al. | e. m. f. | 25 | 0 | 250 | 9 |
| | | | 0.2 | 22* | |
| Brown et al. | freezing point | 0 | 0 | 114～244 | 10 |
| | | | 0.2 | 8～16* | |
| Kenttämaa | freezing point | 0 | 0 | 220 | 11 |
| | | | 0.2 | 15* | |

* These are the formation constants which were calculated by the present authors with the values reported in the literature referred to.

From the following experiment, however, it is concluded that $Ni(OAc)(SO_4)^-$ is not present in an appreciable concentration: The polarograms were obtained with the solutions containing $1.00\times10^{-3}$ M nickel nitrate, $1.10\times10^{-3}$ M NTA and various concentrations of acetate but none of sulfate at 25°C and pH 3.68. The values of $F_0$ were calculated with the observed $[Ni^{2+}]_{app}$'s and plotted against the acetate concentration with a linear relation as shown by B in Fig. 2. The value of $\frac{\alpha}{\beta K_{NiX}}K_{NiOAc}$ which was determined from the slope of plot B in Fig. 2 is $1.48\times10^{-5}$, while that of $\frac{\alpha}{\beta K_{NiX}}(K_{NiOAc}+K_{Ni(OAc)(SO_4)}[SO_4^{2-}])$ obtained from the slope of plot A in Fig. 2 is $1.41\times10^{-5}$. The agreement of these two values indicates that the term $K_{Ni(OAc)(SO_4)}[SO_4^{2-}]$ is negligible and, therefore, no appreciable amount of $Ni(OAc)(SO_4)^-$ is present under the experimental condition.

**The Determination of the Formation Constant of Sulfatonickel(II) Complex.**—It has been known that nickel(II) forms only a monoacetato complex in the solution containing acetate up to 0.2 M in concentration at ionic strength 0.2 at temperature ranging from 15 to 35°C[1]. From this and the fact that $Ni(OAc)(SO_4)^-$ is considered not to be present under the experimental condition, Eq. 13′ is simplified as,

$$F_0=\frac{\alpha}{\beta K_{NiX}}+\frac{\alpha}{\beta K_{NiX}}K_{NiOAc}[OAc^-]+\frac{\alpha}{\beta K_{NiX}}K_{NiSO_4}[SO_4^{2-}]$$

The formation constant of acetatonickel(II) complex has been given as 2.6 and 2.4 at 15 and 35°C, respectively[1]. The value at 25°C was determined to be 2.5 from plot B in Fig. 2, and this value was in satisfactory agreement with that obtained previously[1]. With the aid of these values, the formation constants of sulfatonickel(II) complex at various temperatures were obtained from the intercepts and the slopes in Fig. 1. These are given in Table I.

TABLE I. FORMATION CONSTANTS OF SULFATONICKEL(II) COMPLEX AT VARIOUS TEMPERATURES

| Temp., °C | $K_{NiSO_4}$ |
|---|---|
| 15 | 14.3±0.4* |
| 25 | 11.6±0.9* |
| 35 | 14.6±0.7* |

* The accuracy of $K_{NiSO_4}$ was calculated with the standard deviations of the intercepts and the slopes of the $F_0$ plots.

The formation constants of the sulfatonickel(II) complex which have been reported by other researchers are given in Table II. The original values in their papers were corrected for ionic strength and also listed in Table II. In this calculation, the activity coefficients of nickel(II) and sulfate ions were estimated to be 0.33 and 0.27, respectively[12], at 25°C and ionic strength 0.2. At 0°C and ionic strength 0.2, they were estimated to be 0.29 and 0.23, respectively[12]. It is probably seen that the formation constants of monosulfatonickel(II) complex obtained in this study are in an essential agreement with those given in Table II.

Besides, Table I clearly indicates that the formation constants of monosulfatonickel(II) complex, $K_{NiSO_4}$, are almost independent of temperature at 15 to 35°C. The same tendency has been found for the formation constants of monoacetatonickel(II) complex reported previously[1].

## Summary

A method for the determination of the formation constants of less stable metal complexes has been developed. The method is based on the polarographic measurement of the sum of the equilibrium concentrations of

9) R. W. Money and C. W. Davies, *Trans. Faraday Soc.*, **28**, 609 (1932).
10) P. G. Brown and J. E. Prue, *Proc. Roy. Soc.*, A, **232**, 320 (1955).
11) J. Kenttämaa, *Suomen Kemistilehti*, **29B**, 59 (1956).
12) J. Kielland, *J. Am. Chem. Soc.*, **59**, 1675 (1937).

hydrated metal ions and the complexes coordinating with acetate and/or co-existing ions in the presence of an appropriate auxiliary complex-forming substance. Essential advantages of the method are those of the method that was previously reported and applied to the formation constants of acetatonickel(II) complex.

The procedure developed is applied to the study of the nickel(II) complexes present in the acetate buffer solution containing nitrilotriacetate as an auxiliary complex-forming substance and sulfate as co-existing ions. The results obtained reveal that, under the experimental condition, the monoacetatonickel(II) ions $NiOAc^+$ and the monosulfatonickel(II) $NiSO_4$ are present in the solution but not the acetatosulfatoniccolate(II) $Ni(OAc)(SO_4)^-$. The formation constants of monosulfato complex, $K_{NiSO_4}$, at ionic strength 0.2 are calculated to be 14.3±0.4 at 15°C, 11.6±0.9 at 25°C and 14.6±0.7 at 35°C.

The authors thank the Ministry of Education for the financial support granted for this research.

*Department of Chemistry*
*Faculty of Science*
*Tohoku University*
*Katahira-cho, Sendai*

# SHORT COMMUNICATIONS

## *Infrared Spectra of Some Deuterated Crystalline Polystyrenes. III. Characteristic Bands of Isotactic Polymer from Styrene-$d_5$*

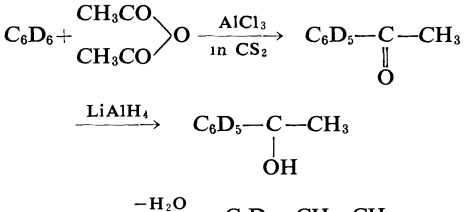
By Masamichi KOBAYASHI

(Received April 8, 1961)

In order to interpret the absorption bands characteristic of the helical conformation of isotactic polystyrene, several deuterated derivatives in which the hydrogen atoms of the skeletal chain are substituted with deuterium, such as crystalline poly-$\alpha d_1$-, poly-$\beta d_1$-, poly-$\alpha, \beta d_2$- and poly-$\beta, \beta d_2$-styrene, have been synthesized and their infrared spectra have been investigated[1,2]. It was found that the characteristic bands appearing (1) in the region of 1450~1180 $cm^{-1}$ ($1364\sigma$, $1314\sigma$, $1297\pi$ and $1195\pi$), (2) at near 1070 $cm^{-1}$ and (3) at near 900 $cm^{-1}$ were remarkably affected by the sites and the numbers of the substituted deuterium atoms. However, the frequency shifts of these bands on deuteration were not always so simple that it seemed difficult to assign them to simple vibrational modes. Although it seems reasonable to consider that the deformational vibrations of the skeletal CH and $CH_2$ groups and the stretching vibrations of the carbon chain in the helix contribute to the appearance of the characteristic bands, we could not disregard the effects of the coupling of these modes with the CH deformations of the side group, since it was known that[3] some of the characteristic bands were moderately affected by deuteration of the para position.

In order to throw some light on the problem, the infrared spectra of the polymers (both isotactic and atactic) of the monomer $C_6D_5CH=CH_2$ were investigated.

The monomer was prepared by the following scheme



$C_6D_6$ was prepared from benzene and deutero-sulfuric acid, $D_2SO_4$, by an exchange reaction, the product contained about 85 mol.% of deuterium. The monomer thus obtained was polymerized in *n*-heptane using Ziegler type catalyst, then isotactic polystrene-$d_5$ was obtained. The atactic polymer was prepared by bulk polymerization using B. P. O. as a catalyst.

In Fig. 1 the spectra of the atactic and isotactic (crystallized) polymers were compared with each other.

1) M. Kobayashi, This Bulletin, 33, 1416 (1960).
2) M. Kobayashi, ibid., in press.
3) H. Tadokoro et. al., ibid., 32, 313 (1959).

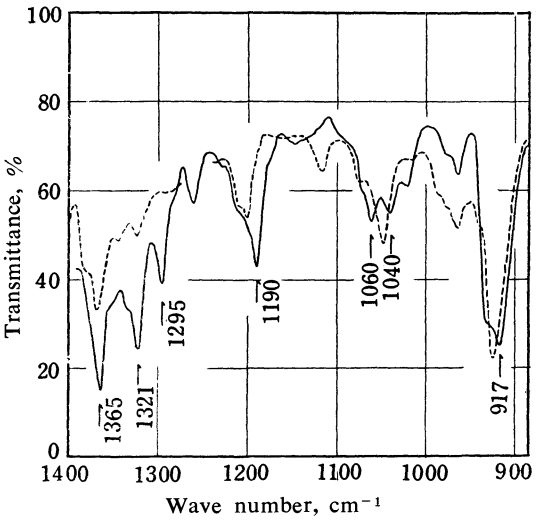



Fig. 1. Infrared spectra of polystyrene-$d_5$.
—— isotactic polymer at crystalline state
---- atactic polymer

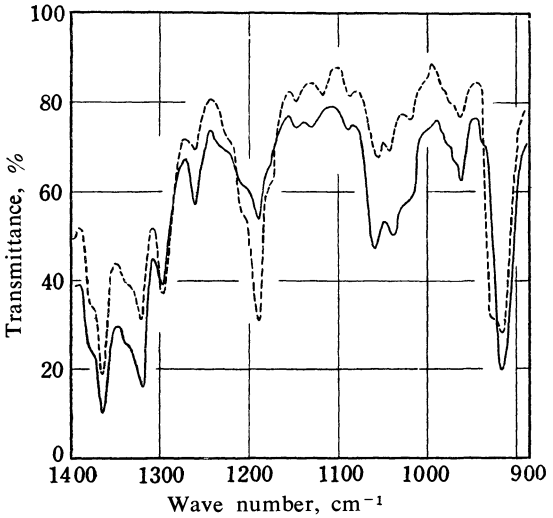



Fig. 2. Polarized infrared spectra of isotactic polystyrene-$d_5$.
—— electric vector perpendicular to elongation
---- electric vector parallel to elongation

A most noticeable feature is that the spectroscopic characters of isotactic polystyrene are observed also in our deuterated sample; the appearance of the bands at 1365, 1321, 1295 and 1190 $cm^{-1}$ and the splitting of the bands at near 1070 $cm^{-1}$ and at near 900 $cm^{-1}$ on crystallization. Especially, the bands in the region of 1450~1180 $cm^{-1}$ have almost the same frequencies and relative intensities as those of polystyrene. Moreover, as shown in Fig. 2, measurements of the polarization spectra of the oriented crystallized sample show that the polarization properties of the characteristic bands coincide with those of isotactic polystyrene.

These results may support the assumption that the CH deformations of the phenyl group have little effect upon the appearance of the characteristic bands of isotactic polystyrene, especially, those in the region of 1450~1180 $cm^{-1}$. Then, it may be concluded that the helical conformation of the isotactic polystyrene molecule reflects mainly on the absorption bands associated with the modes of the groups composing the skeletal chain.

The detail of this work will be reported in elsewhere.

*Osaka Industrial Research Institute*
*Oyodo-ku, Osaka*

## *Infrared Spectra of Polyacrylonitrile Polymerized by Gamma-irradiation at Low Temperatures*

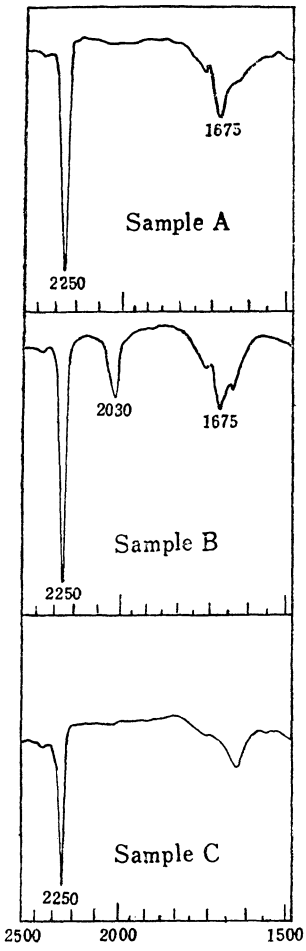
By Yoshizo TSUDA

(Received May 15, 1961)

In order to study the effect of polymerization condition on the infrared spectrum of polyacrylonitrile, acrylonitrile was polymerized in bulk and in various solutions by gamma-irradiation at low temperatures and it was found that the intensities of absorption bands at 1675 and 2030 $cm^{-1}$ vary according to the polymerization conditions, i. e., the solvent species and the irradiation temperatures. Figure 1 shows the infrared spectra in the 1500~2500 $cm^{-1}$ region obtained from the potassium bromide disks of some different polyacrylonitrile samples. Samples A, B and C were obtained by gamma-irradiation of pure acrylonitrile at 17, $-78.5$ and $-196$°C, respectively. Figure 2 shows that of sample D which was obtained by gamma-irradiation of acrylonitrile in triethylamine solution at $-78.5$°C. As may be seen in these figures, the absorption band at 1675 $cm^{-1}$ is much more intense in sample D than in samples A and B and this band is not observed at all in sample C. On the other hand, the band at 2030 $cm^{-1}$ which is not observed in samples A, C and D is intense in sample B. The band at 1675 $cm^{-1}$ was assigned by Liang and Krimm[1] to a vibration of an impurity. On the basis of the behavior of this band, it is sure that this band should be assigned to a vibration characteristic of a special structure of polyacrylonitrile itself.

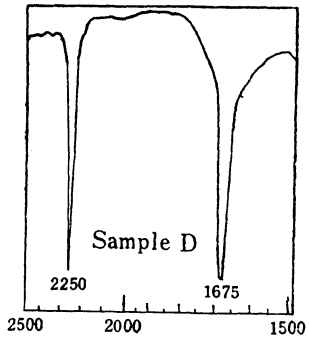
From the copolymerization studies of acrylonitrile and styrene by gamma-irradiation at

1) C. Y. Liang and S. Krimm, *J. Polymer Sci.*, **31**, 513 (1958).




Wave number, $cm^{-1}$

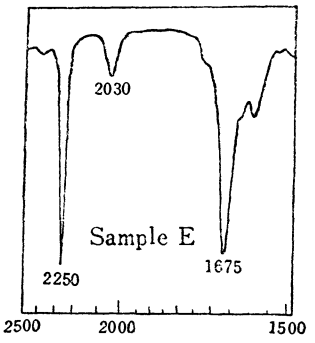
Fig. 1. Infrared spectra of polyacrylonitrile obtained by gamma-irradiation. Samples A, B and C were polymerized in bulk at 17, −78.5 and −196°C, respectively.




Wave number, $cm^{-1}$

Fig. 2. Infrared spectrum of polyacrylonitrile obtained by gamma-irradiation in triethylamine solution at −78.5°C.

−78.5°C[2], it was shown that the polymerization proceeds in bulk by a free-radical mechanism, on the other hand, in dilute organic solutions predominantly by an anionic mecha-



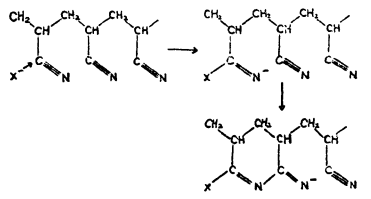

Wave number, $cm^{-1}$

Fig. 3. Infrared spectrum of polyacrylonitrile obtained by gamma-irradiation in *N*, *N*-dimethylformamide solution at −78.5°C.

nism. In view of these facts, it can be considered reasonably that the band at 2030 $cm^{-1}$ is due to the keteneimine linkage, as has been described previously[3], and the band at 1675 $cm^{-1}$ is due to the C=N linkage which comes from a reaction by an anionic mechanism. The latter band is also intense in the spectrum of polymer obtained in dimethylformamide solution as shown in Fig. 3.

In order to determine whether the C=N linkage is formed by the action of radiations on the polymer or is formed by the polymerization processes themselves, the polymer sample C which has no absorption at 1675 $cm^{-1}$ was dissolved in dimethyl formamide and then irradiated at −78.5°C. In the infrared spectrum of the irradiated polymer the band at 1675 $cm^{-1}$ was observed to be as intense as that of the sample D. When this polymer solution was irradiated at room temperature, any increase of the absorption at 1675 $cm^{-1}$ was not observed in the spectrum of the irradiated polymer. These facts indicate that the formation of C=N linkage is due to the action of radiations on the polymer in these solutions at low temperatures.

From the above consideration, the following reaction to give the conjugated C=N linkage to the polymer can be assumed to occur by gamma-irradiation at low temperatures,



where $X^-$ denotes an anion formed by the irradiation of solvent molecule at low temperatures. The formation of the same structure was also assumed recently in an anionic

2) Y. Tsuda, *J. Polymer Sci.*, in press.
3) C. S. H. Chen, N. Colthup, W. Deichert and R. L. Webb, *J. Polymer Sci.*, **45**, 247 (1960).

polymerization of acrylonitrile[4]. This reaction proceeds easily by an anionic mechanism as shown above, however, it seems that the similar reaction proceeds also by a free-radical mechanism, the rate of formation being very small, as shown by the presence of the weak absorption at 1675 $cm^{-1}$ in the spectrum of polymer obtained in bulk.

The infrared spectra of the polymer samples were obtained using Perkin-Elmer model 21 spectrophotometer. The gamma-rays of $^{60}Co$ were used for the gamma-irradiation at the dose rate of $4 \times 10^4$ r/hr.

The author wishes to thank Dr. H. Kobayashi for permitting the publication of this paper. He also thanks Mr. Y. Hayakawa for his help in experiments.

*Central Research Laboratories*
*Toyo Rayon Co., Ltd.*
*Otsu, Shiga*

4) P. Claes and G. Smets, *Makromol. Chem.*, **44**, 212 (1961).

## *Isolation of 6-O-Methyl-D-galactose from the Agar of Ceramium Boydenii*

By Susumu HIRASE and Choji ARAKI

(Received May 27, 1961)

The chemical structure of agar has been extensively investigated in this Institute[1]. One of the present writers has assigned the linear structure consisting of D-galactose and 3, 6-anhydro-L-galactose to agarose, which is the main polysaccharide of the agar of *Gelidium amansii*[2]. Besides these two sugars, there are also contained L-galactose, xylose, D-glucuronic acid, pyruvic acid and sulfuric acid in the agar[1]. The present communication reports the isolation of 6-*O*-methyl-D-galactose in 12% yield from the hydrolysis products of the agar of *Ceramium boydenii*. This is the first reported instance of 6-*O*-methyl-D-galactose as far as agar is concerned. The synthesis of the sugar has been reported on several occasions[3-5]. It has also been isolated from the non-gelling polysaccharide of the red seaweed *Porphyra capensis*[6].

### Experimental

**Preparation of Agar.**—Agar was extracted from dry *Ceramium boydenii* with hot water and purified by freezing and thawing in the usual way. It contains 2.81% of ash and 1.18% of sulfate on the dry basis.

**Hydrolysis of the Agar.**—The agar (15 g. on the dry basis) was hydrolyzed with N-sulfuric acid (200 ml.) in a boiling water bath for 15 hr. After filtration followed by neutralization with barium carbonate and subsequent refiltration, the solution was allowed to pass through columns of Amberlite IR-120 (100 ml.) and Amberlite IR-4B (100 ml.) in succession. The resins were then washed with water (1500 ml.). All the effluents were combined and evaporated under reduced pressure to a sirup (7.5 g.). Paper chromatographic examination using *n*-butanol-ethanol-water (4 : 1 : 2 v/v) as a developing solvent and aniline hydrogen phthalate as a sprayer indicated the prensence of galactose, xylose, 6-*O*-methyl-galactose and 5-hydroxymethylfuraldehyde. The last compound would arise from 3, 6-anhydrogalactose which would have been decomposed during the hydrolysis[7].

**Isolation of 6-*O*-Methyl-D-galactose.**—The sirup obtained above afforded D-galactose on crystallization from a mixture of methanol (25 ml.) and ethanol (35 ml.); yield 2.6 g., m. p. 160~165°C; $[\alpha]_D^{24}$ +78.0° (*c* 0.80 in water). The mother liquor (4.7 g.) was then chromatographed on a charcoal-Celite column, from which a mixture (2.9 g.) of galactose and xylose was eluted with first 2 l. of water. Further elution with additional 5 l. of the same solvent afforded chromatographically pure 6-*O*-methyl-D-galactose; yield 1.8 g. (12% of the agar). The sugar was purified by recrystallization twice from absolute ethanol; m. p. 122~124°C; $[\alpha]_D^{20}$ +135°→+77.0° (*c* 1.0 in water) (Found: C, 43.15; H, 7.11; $OCH_3$, 16.15. Calcd. for $C_7H_{14}O_6$: C, 43.29; H, 7.27; $OCH_3$, 15.98%). The melting point and optical rotation reported for 6-*O*-methyl-D-galactose are: m. p. 128°C, $[\alpha]_{578}^{20}$ +114°→+77°[3]; m. p. 118°C, $[\alpha]_D^{20}$ +120°→+70°[4]; m. p. 122~123°C, $[\alpha]_D^{18}$ +112°→+66°[4]; m. p. 113~114°C, $[\alpha]_D^{18}$ +137°→+77°[5]; m. p. 122~123°C, $[\alpha]_D^{17}$ +117°→+77.3°[6]. For comparison, 6-*O*-methyl-D-galactose was prepared by the method of Freudenberg and Smeykal[3] and purified on a charcoal-Celite column. It had the same melting point and mixed melting point as that isolated above.

The sugar was also identified as its phenylosazone[3-6]: m. p. and mixed m. p. 200~201°C; $[\alpha]_D^{20}$ +140° (*c* 0.40 in pyridine) (Found: N, 14.98; $OCH_3$, 8.19. Calcd. for $C_{19}H_{24}O_4N_4$: N, 15.05; $OCH_3$, 8.33%).

*Institute of Chemistry*
*Faculty of Industrial Arts*
*Kyoto Technical University*
*Matsugasaki, Kyoto*

1) See review: C. Araki, "Proc. 4th Intern. Congr. Biochem.", 1, Pergamon Press, London, New York & Paris (1959), p. 15; "Progress in Org. Chem." (Yūki-kagaku no Shinpo), Ed. by M. Murakami, Vol. 13, Kyōritsu Shuppan, Tokyo (1959), p. 221.
2) C. Araki, This Bulletin, **29**, 543 (1956), *Memoirs Fac. Ind. Arts, Kyoto Tech. Univ., Sci. & Tech.*, **5**, 21 (1956).
3) K. Freudenberg and K. Smeykal, *Ber.*, **59**, 100 (1926).
4) J. Munro and E. G. V. Percival, *J. Chem. Soc.*, 1936, 640.
5) E. Pacsu and S. M. Trister, *J. Am. Chem. Soc.*, **62**, 2301 (1940).
6) J. R. Nunn and M. M. von Holdt, *J. Chem. Soc.*, 1957, 1094.
7) C. Araki and K. Arai, *J. Chem. Soc. Japan (Nippon Kwagaku Kwaisi)*, **63**, 1522 (1942).

# *Photoreduction of Methylene Blue by Visible Light in the Aqueous Solution Containing Certain Kinds of Inorganic Salts. I. General Features of the Reaction*

By Yoshiharu Usui, Hiroshi Obata and Masao Koizumi

(Received January 10, 1961)

In connection with the study of photoreduction of methylene blue with aliphatic amines, we did some experiments on the irreversible photodecomposition of the dye in the aerated aqueous solution[1]. It was our plan at that time to investigate systematically, varying pH of the solution, about the effect of the oxygen concentration upon the rate of this irreversible photodecomposition. But it happens that we had found the reversible photobleaching to take place with an appreciable rate in the degassed solution containing certain kinds of inorganic salts commonly used for buffering. Here "reversible" means that the dye is recovered when the air is introduced into the solution and the colorless product was confirmed to be the leuco compound of the dye. This fact which we have found seems to be of foundamental importance for the chemistry of dye in general, since the buffered solution which was found to be effective in promoting this novel photoreduction, is usually used for the dye solution. The object of this paper is to report some reults of our experiments undertaken to clarify the general nature of this extraordinary photoreduction which proceeds without any addition of particular reducing agent.

## Experimental

**Sample.** — *Methylene Blue.* — Grübler's dye was recrystallized from *n*-butyl alcohol three times and was dried in vacuum.

$$\varepsilon_{\lambda=665\,m\mu}=6.0\times10^{4}$$

*Inorganic Reagents.*—Sodium borate, sodium monohydrogen phosphate, potassium dihydrogen phosphate, sodium sulfate, sodium chloride, sodium iodide, hydrochloric acid, sodium hydroxide. All of the salts were of special grade and they were recrystallized from the redistilled water 2 or 3 times. Hydrochloric acid of special grade was distilled twice at the azeotropic point. Sodium hydroxide of special grade was used without further purification.

**Apparatus and Procedure.** — Degassing of the solution was performed in a suitable ampule by repeating freezing and evacuation 5~7 times. The solution then was poured into a reaction cell which is a spectrophotometer cell $1\times1\times4$ cm., connected to the evacuation apparatus via the tube fused to the upper part of the cell. The reaction was performed in a thermostat of $30\pm0.5$°C. The light source was a 500 W-75 V. projection lamp. It was used at $55.0\pm0.5$ V. and the intensity was checked by a photocell (PT 17 V 2) during the course of the reaction. At various time intervals, the cell was taken out and the absorption spectrum was measured by a Hitachi or a Kotaki spectrophotometer.

## Results

**1. The Irreversible Bleaching by Oxygen and the Reversible One in the Evacuated Solution.**— The feature of the photobleaching of methylene blue in the borate buffer solution containing various amounts of oxygen was examined.

The composition of the solution was as follows; methylene blue $1.2\times10^{-5}$ M, borate, $7.8\times10^{-2}$ M, hydrochloric acid $1.4\times10^{-1}$M, pH=7.62.

In case of the dye solution saturated with air, the irradiation causes a gradual decrease of the absorption spectra of methylene blue without any noticeable change of the maximum position.

When the concentration of oxygen is decreased down to $1.41\times10^{-5}$ M, the bleaching caused by irradiation is still irreversible, the introduction of air not causing any recovery of dye. It was found that the absorption maximum shifts towards violet more and more, when the oxygen concentration is decreased.

When the solution is completely degassed, the bleaching still occurs and with a much greater rate than that of the oxygen-containing solution. However, the shift of the absorption maximum is somewhat less than in the case in which the oxygen concentration is small. The notable fact in this case is that the color appreciably recovers when the air is introduced after the irradiation. The position of the absorption maximum of the aerated solution exactly coincides with that of the partially bleached solution before aeration.

The rate of bleaching is proportional to the quantity of light absorption, that is

$$k't=-\ln(e^{acd}-1)+\text{const.} \qquad (1)$$

1) H. Obata, K. Kogasaka and M. Koizumi, This Bulletin, 32, 125 (1959).

except the two cases, i. e., the completely evacuated solution and the one dissolving the least amount of oxygen.

In evaluating the value of $k'$ from Eq. 1, $\alpha$-value was conventionally chosen as $\varepsilon$-value in order to compare the results with those of the pure aqueous solution[1], and the remaining quantity of methylene blue was obtained by use of Blaisdell's[2] method. The above equation does not hold for the two exceptional cases mentioned above, the rate in these cases decreasing more rapidly than calculated by Eq. 1. In Table I are given the values of $k'$ and the shift of maximum absorption ($\Delta\lambda$) after 50 min. $k'$ for the two exceptional cases were tentative as they were calculated from the initial slope of the curve drawn according to Eq. 1.

The concentration of oxygen was analyzed by a specially designed apparatus.

Table I

| Concn. of $O_2$, M | $k'$, $min^{-1}$ | $\Delta\lambda$, m$\mu$ |
|---|---|---|
| 0 | $(2.0 \times 10^{-1})$ | 5 |
| $3.2_0 \times 10^{-5}$ | $(1.4 \times 10^{-2})$ | 9 |
| $6.76 \times 10^{-5}$ | $1.14 \times 10^{-2}$ | 8 |
| $8.58 \times 10^{-5}$ | $1.08 \times 10^{-2}$ | 5 |
| $1.13 \times 10^{-4}$ | $1.14 \times 10^{-2}$ | 3 |
| $1.53 \times 10^{-4}$ | $1.32 \times 10^{-2}$ | 3 |
| $3.40 \times 10^{-4}$ | $1.66 \times 10^{-2}$ | 0 |

As seen from Table I the value of $k'$ is not affected so much by the concentration of oxygen. The results conform well with those of the pure aqueous solution, where it was found that the rate is almost constant down to about $4 \times 10^{-5}$ M of oxygen whence the rate begins to decrease. The order of the $k'$ value is also the same as that of the pure aqueous solution, in view of the difference of the light intensity[1].

**2. Bleached Product of Methylene Blue in the Deaerated Solution.**—In order to make clear the cause for photobleaching in the evacuated solution and the recovery of color by aeration, the absorption spectra of the solution irradiated for various times were examined from 200 to 700 m$\mu$. Figure 1 shows the results obtained when the phosphate buffer solution of methylene blue was irradiated.

It is evident that accompanied with a decline of the main absorption of methylene blue, a new absorption appears in the ultraviolet region with the maximum at 255 m$\mu$. Further it is observed that the change in ultraviolet region takes place with an isosbestic point at about 273 m$\mu$. The absorption at 255 m$\mu$ coincides essentially with that of the leuco methylene blue chemically prepared, and it was almost

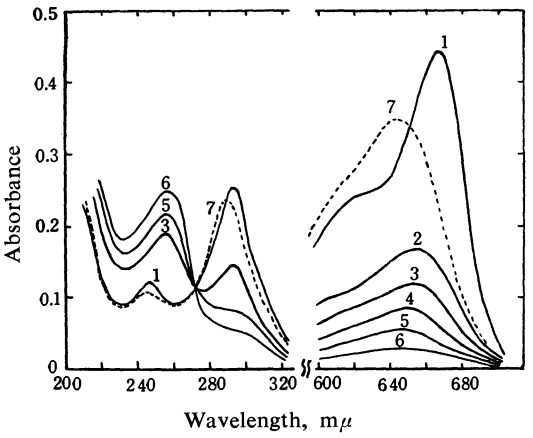



Fig. 1. The absorption spectra of the irradiated solution of methylene blue in deaerated phosphate buffer. $[Na_2HPO_4] = 1.2 \times 10^{-2}$ M, $[KH_2PO_4] = 2.8 \times 10^{-3}$ M, pH=7.57.

1. Initial
2. 5 min.-irradiation
3. 10 min.-irradiation
4. 20 min.-irradiation
5. 50 min.-irradiation
6. 80 min.-irradiation
7. Aeration

definitely established by Obata[3] that the bleached product is nothing but the leuco form of dye which is but partially demethylated. It is to be added here that the dotted line in Fig. 1 which represents the absorption spectra of the recovered dye after aeration, has exactly the same maximum position as that of the partially bleached solution (see Sec. 6).

In connection with the formation of leuco dye, it seems to be worthy of reconfirming and studying further what Lewis[4] et al. formerly observed. Thus they perceived a slight fall of the absorption at 660 m$\mu$ with the rise of temperature ($\Delta D/\Delta T = 0.03/40°C$) in the aqueous solution of methylene blue at three different concentrations, $9.0 \times 10^{-6}$, $1.9 \times 10^{-6}$, $6.3 \times 10^{-7}$ M, and they attributed this change to the formation of a colorless form according to the equilibrium; $D^+ + H_2O \rightleftarrows (DOH)H^+$. They, however, did not study about the change in the ultraviolet region. Hence we carefully examined the absorption spectra of the aqueous dye solution $6.3 \times 10^{-7}$ M, at various temperatures from 20 to 75°C in the region 200 ~700 m$\mu$, using a long path cell (10 cm.).

At first the aerated solution was examined at several temperatures, varying the temperature from low to high and then in the inverse direction. Three such independent experiments were done but no change beyond experimental

2) B. E. Blaisdell, *J. Soc. Dyers & Colorists*, 65, 619 (1949).
3) Part II of this series.
4) G. N. Lewis et al., *J. Am. Chem. Soc.*, 65, 1150 (1943).

error was observed. In some cases rather opposite changes were observed; thus $\varepsilon_{max}$ increased with the rise of temperature and decreased to its original value with the fall of the temperature. This would perhaps be due to the adsorption and desorption of dye on the cell wall. Thus the aerated solution did not show any sign of the phenomenon that Lewis et al. had claimed to perceive.

Next, the three analogous experiments were performed using the evacuated solution, and this time, a small depression beyond the experimental error was observed in the visible region with the rise of temperature. In addition to this change a clear reversible change was observed in the neighborhood of 250 m$\mu$. A typical result is shown in Fig. 2. It is seen that a new peak appears when the temperature is raised. Thus the formation of the colorless form that Lewis had postulated seems to be substantiated in the case of the degassed solution.

This colorless form might somehow be related to the formation of leuco dye, but there is no doubt that the change of spectra in the irradiated solution is not due to what Lewis et al. supposed to be, as was confirmed by Obata[3].

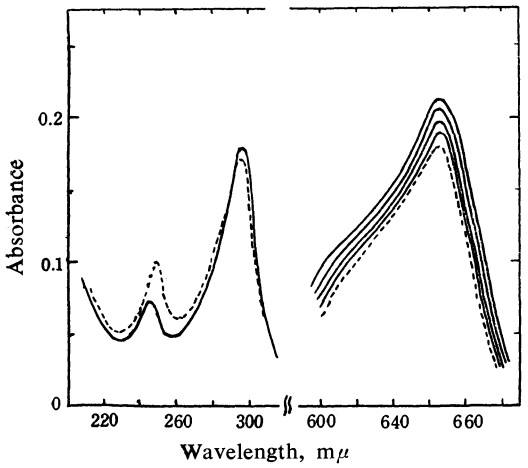



Fig. 2. Reversible temperature dependence of the absorption spectrum of methylene blue in aqueous solution degassed. ($6.3\times10^{-7}$ M)
Visible region; from upper to lower 20, 30, 40, 50 and 60°C (dotted line)
Ultraviolet region; 20, 60°C (dotted line)

**3. Studies about the Solution Containing Various Kinds of Salts.**—Since it has become established in Sec. 2 that methylene blue is photoreduced in the presence of certain salts, the next problem is to examine whether the similar phenomena be observed for other salts and how the rate will depend upon the type of salts, including the plain aqueous solution. The salts examined were sodium borate, sodium hydrogen phosphate, potassium dihydrogen phosphate, sodium sulfate, sodium chloride, sodium iodide, hydrochloric acid and sodium hydroxide.

The results obtained were quite similar at least qualitatively in all respects, thus in regards to the spectral change, recovery of color by aeration and the maintainance of the maximum position when recovered. But the rate depends very much upon the types of salts and a quite large difference is also observed in the magnitude of the spectral shift.

In Fig. 3 some typical cases are shown.

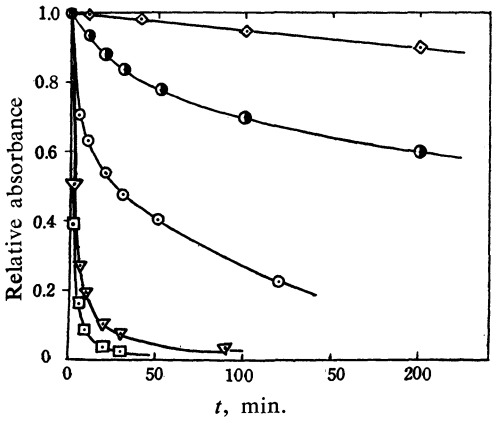



Fig. 3. Photobleaching of methylene blue in deaerated aqueous solutions containing various inorganic compounds at 30°C.

- ◈ HCl $1.0\times10^{-3}$ M (pH=3.0)
- ◑ $Na_2SO_4$ $1.0\times10^{-2}$ M (pH=6.1) (NaI, NaCl and the plain aqueous solution are similar to $Na_2SO_4$)
- ⊙ Borate buffer (pH=7.55)
- ▽ NaOH $1.0\times10^{-3}$ M (pH=10.9)
- ◙ Phosphate buffer (pH=7.57)

In the case of phosphate buffer and sodium hydroxide the rate is far greater in the order of magnitude, next comes the borate buffer and in the case of other salts and plain aqueous solution, the rate is less than one hundredth of the first class. The rate is still slower in the case of hydrochloric acid.

Experimental results are given in Table II in which $\Delta D$ and $\Delta\lambda_{max}$ are respectively the depression and the shift of the absorption maximum per twenty minutes. As for the shift, details will be described further in Sec. 6. All these solutions are of course stable in the dark.

It is well-known that methylene blue is very weak against alkali, and for caution's sake, the spectral change of methylene blue in

Table II

| Condition | $D_0$ | $\Delta D$ | $\Delta\lambda_{max}$ mμ |
|---|---|---|---|
| Phosphate buffer soln. | 0.550 | 0.515 | 17 |
| Borate buffer soln. | 0.621 | 0.304 | 2 |
| NaOH ($1\times10^{-3}$ M) aq. soln. | 0.619 | 0.543 | 8 |
| NaI ($1\times10^{-2}$ M) aq. soln. | 0.910 | 0.062 | 0 |
| NaCl ($1\times10^{-2}$ M) aq. soln. | 0.830 | 0.075 | 0 |
| $Na_2SO_4$ ($1\times10^{-2}$ M) aq. soln. | 0.580 | 0.070 | 0 |
| Plain aq. soln. | 0.986 | 0.088 | 1 |
| HCl ($1\times10^{-3}$ M) aq. soln. | 0.774 | 0.010 | 0 |

sodium hydroxide alkaline solution in the dark was examined.

In the case of 1 N solution, the absorption spectra in the visible region rapidly change into broader ones with a maximum near 590 mμ, whether the solution was degassed or not. When not deareated, this band remains constant after 41 hr. standing in the dark. But under the degassed condition the band gradually declines accompanied with a growth of a new peak at 250 mμ, and upon introduction of air it almost recovers its original height. When the concentration of sodium hydroxide is $10^{-3}$ N, there is no marked change observed in either aerated or deaerated solutions at room temperature. But when the temperature of the deaerated solution is raised to 60°C, a similar spectral change as in the case of 1 N sodium hydroxide (deaerated) takes place.

From the above observations it looks as if the spectral changes in the alkaline solutions are somewhat related to those in the neutral solutions caused by the temperature change. They may deserve further study but here it is enough to say that at $10^{-3}$ N sodium hydroxide scarcely any spectral changes occur in the dark at room temperature.

**4. Scrutiny about any Possible Effect of Impurity.**—In view of the rather unusual character of the present reductive reaction which proceeds without any reducing agent in the ordinary sense, it seems essential to scrutinize cautiously about the possible effect of any contaminating impurity which might act as a reducing agent, especially in cases of phosphate and borate where the rate is appreciably great. For this purpose the following experiment was performed.

Air was introduced to the nearly completely photobleached solution and the recovered dye was eliminated from the solution by adsorbing it on charcoal and filtering the solution through glass wool. Into the buffer solution thus pretreated, methylene blue was newly dissolved and the reaction was once more repeated. The rate proved to be almost the same as that of the preceeding experiment. From the above experiment any possible effect of impurity which might be contained in the buffer solution can be neglected.

Since it is very difficult to prepare a very pure sample of dye, the following special method was adopted in order to scrutinize the possible effect of any impurity contained in the dye.

According to Oster[5] the irradiation of the solution containing methylene blue, EDTA, *o*-phenanthroline and ferric salt, produces the complex between $Fe^{2+}$ and *o*-phenanthroline and the reaction persists as long as ferric salt exists in the solution. This is because the leuco form of methylene blue produced by the photochemical reaction between EDTA and dye, reduces the ferric salt, the dye being recovered by this reaction. The similar reaction should necessarily be expected in our case since the leuco dye is produced by the irradiation. Accordingly the solution containing methylene blue, borate buffer, $Fe^{3+}$ ($6.0\times10^{-4}$ M) and *o*-phenanthroline ($2.3\times10^{-3}$ M) was degassed and then irradiated. The result was that an absorption spectrum of $Fe^{2+}$-phenanthroline complex ($\lambda_{max}=510$ mμ) did appear and that the concentration of the complex produced, attained more than ten times than that of the dye. Hence it can safely be concluded that most part of the reaction is not due to any impurity contained in the dye sample. The details of this experiment will be described in Part III.

**5. Search for other Reaction Products.**—Since the dye is reduced to the leuco compound, it is naturally expected that some oxidizing substances be produced. Hence it was undertaken to detect hydrogen peroxide and oxygen.

After the reaction was performed using a cell with a breakable joint, the solvent was distilled in vacuum through the joint upon the mixed powder of ferric salt (12 mg.) and potassium ferricyanide (16 mg.). In case of borate buffer, the existence of hydrogen peroxide was in fact ascertained by a green tint, while in case of phosphate buffer no change was observed.

In case of phosphate buffer, a very small amount of gas collected (about 30% of the employed dye) after the irradiation was examined by a mass-spectrometer*. Oxygen was detected but it was interpreted to be due to the air since nitrogen and argon were also detected and the ratio of the three patterns practically coincided with that of the air. The

5) G. K. Oster and G. Oster, ibid., **81**, 5543 (1959).

* We are indebted to Professor T. Titani of Tokyo Metropolitan University for this analysis.

gas in question might have been due to the leak in the gas collection apparatus.

Thus according to this analysis no oxygen was detected. But this negative result does not necessarily deny the formation of oxygen. Because if oxygen be produced, there is no doubt that part of it must be consumed in the irreversible photo-decomposition of dye mentioned in Sec. 1. Moreover, when the phosphate buffer solution of dye partially bleached was kept in the dark for a long time, it recovered its color very gradually and this perhaps may be attributed to the existence of a very small quantity of oxygen produced during the irradiation.

**6. Relation between the Quantity of Demethylation and That of the Produced Leuco Dye.**— The shift of absorption spectra accompanied with the photobleaching can be attributed most certainly to the dimethyl amino groups[3]. Now to know the relation between these two quantities, the ratio $D/D_0$ ($D$ and $D_0$ are respectively, the optical density of maximum absorption at time $t$ and at $t=0$) is conventionally plotted against the position of maximum absorbance for all the results so far obtained. Figure 4 shows the plots for the phosphate buffer. In this case shift and bleaching apparently proceed in a parallel way and the position of absorption maximum in the final stage seems to tend toward the neighborhood of 640 m$\mu$. When the absorption spectra of a partially bleached solution is divided by Blaisdell's method into two parts, i.e. the part due to the remaining methylene blue and that of other compounds, then the absorption of the latter always has its maximum near 640~645 m$\mu$ as shown in Fig. 5.

This strongly suggests that throughout irradiation or in most periods of irradiation except

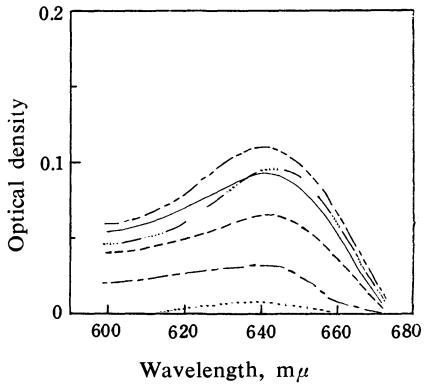



Fig. 5. The absorption spectra of the demethylated component separated by Blaisdell's treatment (in phosphate buffer pH=7.58).

| | | Irradiation time, min. | Opt. density remaining methylene blue at 665 m$\mu$ |
|---|---|---|---|
| a) | | 0 | 0.550 |
| b) | ·—· | 1 | 0.278 |
| c) | — | 2 | 0.173 |
| d) | — | 4 | 0.090 |
| e) | — | 6 | 0.065 |
| f) | — | 11 | 0.035 |
| g) | ····· | 20 | (0.028) |

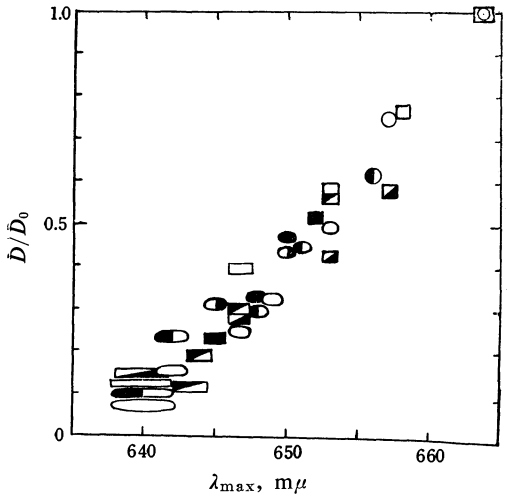



Fig. 4. Plot of $D/D_0$ against $\lambda_{max}$ for the various conditions in phosphate buffer.

| | | | |
|---|---|---|---|
| ● | [Dye] 4 ×10$^{-6}$ M | ■ | pH=8.81 |
| ◑ | 8 ×10$^{-6}$ | ◪ | 8.07 |
| ◐ | 1.2×10$^{-5}$ | ◪ | 7.71 |
| ○ | 1.6×10$^{-5}$ | □ | 6.94 |

all pH=constant all [Dye]=constant

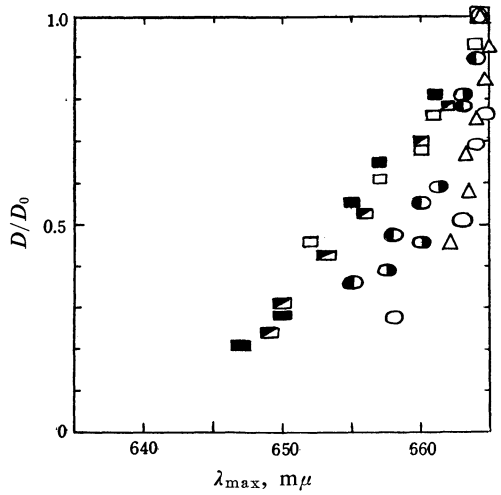



Fig. 6. Plot of $D/D_0$ against $\lambda_{max}$ for the various conditions in borate buffer.

| | | | |
|---|---|---|---|
| ● | [Dye] 4 ×10$^{-6}$ M | ■ | pH=9.14 |
| ◑ | 8 ×10$^{-6}$ | ◪ | 8.30 |
| ◐ | 1.2×10$^{-5}$ | □ | 7.85 |
| ○ | 1.6×10$^{-5}$ | | |

all pH=constant all [Dye]=constant

the last stage, a single molecular species is predominantly formed as a result of demethylation. In case of other salts, the relation between bleaching and shift is somewhat different from that of the phosphate buffer, as shown in Fig. 6.

There are many cases in which demethylation is appreciably delayed than bleaching. In case of borate buffer, demethylation seems to be accelerated by the increase of pH. Summarizing all the results, demethylation apparently takes place with a rate about equal to bleaching at most, or with a much smaller rate. But in all cases the band maximum of demethylated compound lies near 640~650 mμ as in the case of phosphate buffer, suggesting again the formation of a single molecular species through demethylation. An example of borate buffer is shown in Fig. 7.

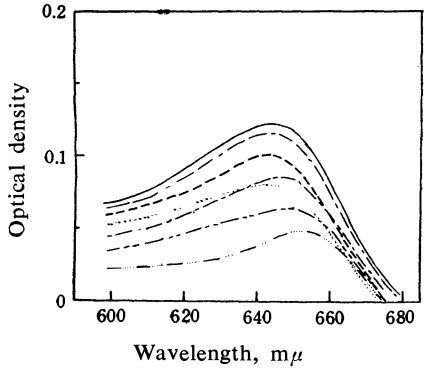



Fig. 7. The absorption spectra of the demetylated component separated by Blaisdell's treatment (in borate buffer pH=8.30).

| | | Irradiation time, min. | Opt. density remaining methylene blue at 665 mμ |
|---|---|---|---|
| a) | | 0 | 0.563 |
| b) | ·—· | 4 | 0.472 |
| c) | ——— | 10 | 0.409 |
| d) | — — | 20 | 0.340 |
| e) | — — | 50 | 0.209 |
| f) | —— | 80 | 0.153 |
| g) | ——— | 152 | 0.093 |
| h) | ····· | 212 | 0.078 |

Now correct data for the absorption maximum of mono-, di-*N*, *N'*-, di-*N*, *N*- and trimethylthionine can not be found in the literature, so that the number of demethylation can not be decided from Figs. 5 and 7, though the latter two seem rather plausible.

Suspecting the possibility that a small amount of hydrogen peroxide produced might cause demethylation to occur, the effect of the addition of hydrogen peroxide was examined. Such an investigation is also desirable from the standpoint of examining the effect of the reaction product upon the entire reaction.

The experiment was done using the aqueous solution of methylene blue and the intensity of the illuminating light was chosen so great that about 90% bleaching took place in about 10 hr. Plots of $D/D_0$ against $\lambda_{max}$ are given in Fig. 8.

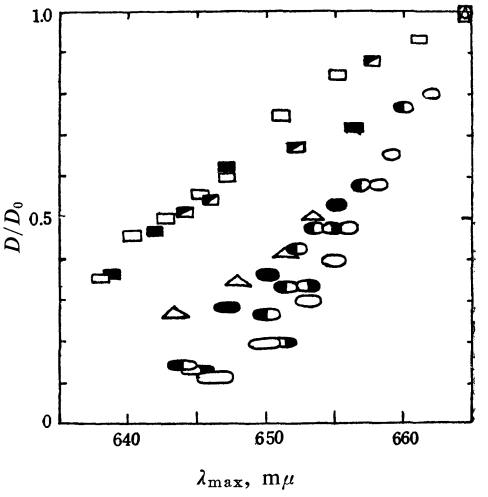



Fig. 8. Plot $D/D_0$ against $\lambda_{max}$ for the various concentrations of $H_2O_2$ in plain aqueous solution.

| | |
|---|---|
| ◩ $5.15\times10^{-4}$ M | △ $3.09\times10^{-5}$ M |
| ■ $1.03\times10^{-4}$ M | ◐ $2.58\times10^{-5}$ M |
| □ $1.03\times10^{-4}$ M | ◑ $2.06\times10^{-5}$ M |
| ● $7.20\times10^{-5}$ M | ○ 0 |

It is evident that demethylation is much accelerated when the added hydrogen peroxide exceeds $7.22\times10^{-5}$ M. But when the concentration of hydrogen peroxide is $3.9\times10^{-5}$ M or $2.5\times10^{-5}$ M, there is no noticeable effect observed. Accordingly, it is clear that demethylation occurring without added hydrogen peroxide is not due to hydrogen peroxide produced during the reaction. In the presence of a large quantity of hydrogen peroxide irreversible photodecomposition becomes marked and at $5.15\times10^{-4}$ M of the added hydrogen peroxide, the reaction consists only of the irreversible photodecomposition. But the contribution of such an irreversible decomposition is negligible when the concentration of hydrogen peroxide is $\sim10^{-5}$ M.

Of course, it was ascertained that the addition of hydrogen preoxide in the above order of magnitude does not cause any dark reaction. In connection with the above experiments, the effect of the addition of pyruvate was examined and it was found that the recovery of dye exceeds 85~90% of the original dye (measured by $D/D_0$) when it is added, as against 80% when it is not added.

## Discussion

The present reaction as a whole is very complicated and as to the dye, there occur simultaneously three types of reaction; demethylation, formation of leuco compound and the irreversible decomposition. The magnitude of the dye decomposed irreversibly is estimated at most to be about 20~30% of the entire dye disappearing (irreversible decomposition plus leuco formation), but the correct value can not be obtained since the extinction coefficient of the demethylated compound is unknown.

The fact that the magnitude of recovered dye when pyruvate is added to the plain aqueous solution (in this case no shift occurs) reaches about 90%, strongly supports the view that the greater part of the irreversible decomposition is due to some oxidative substance produced during the photoreduction. At the present stage it is not certain whether and how much the irreversible decomposition is essentially connected with the formation of leuco compound but 10% or less would be plausible from the above data.

As for the relation between demethylation and leuco formation, the following conclusions can be drawn from the experimental results. Thus the two reactions are not directly interrelated with each other but rather take place seemingly at least, as two independent simultaneous reactions; because the addition of pyruvate can almost completely suppress demethylation without essentially affecting the rate of leuco formation.

From the absorption spectra of the oxidized form of demethylated dye, the number of demethylation is perhaps one or two. The spectrum as seen in Figs. 5 and 7, rises at first and reaches a maximum when the optical density of the remaining methylene blue falls near one third of the original value and then declines gradually. The absorption spectra of the solutions which have been partially photobleached and then recolored by the introduction of air, have almost the same maximum position as that of the solution before aeration. The latter fact indicates that the ratio between methylene blue and demethylated dye in the oxidized form is quite similar to that in the reduced form. This conforms well with the fact that oxidation potential of the demethylated compound is almost the same as that of methylene blue[6]. The variation of the concentration of the oxidized form of demethylated dye, as judged from its absorption spectra, can well be interpreted, if one assumes that an equilibrium is rapidly attained between the oxidized and reduced form of methylene blue and the corresponding forms of the demethylated dye. If one further assumes that demethylation and leuco-formation have about the same rate (this situation perhaps corresponds to the case of phosphate buffer approximately) then the concentration of the oxidized form of demethylated dye will simply be given as follows.

Putting the mole fractions of the oxidized and reduced form of methylene blue as $y_1$ and $x_1$ respectively and the corresponding quantity for the demethylated dye as $y_2$ and $x_2$, then the total mole fraction of reduced form is $x=x_1+x_2$, and the total mole fraction of demethylated dye is $x_2+y_2$. From the assumption, $x_2+y_2=x_1+x_2$ or $y_2=x_1$.

If one assumes, to simplify the matter, that there is no irreversible decomposition, then $x_1+x_2+y_1+y_2=1$.

Since the percentage of the demethylated compound is the same in oxidized and reduced form, the following formula can easily be obtained, utilizing the above relations.

$$x_1/y_1=y_2/y_1=x_2/y_2=(1-y_1-y_2)/(y_1+y_2) \quad (2)$$

Hence

$$y_2=-y_1+\sqrt{y_1}$$

From the following figures calculated by Eq. 2 one can see how the changes in $y_1$ and $y_2$ are related with each other.

| | | | | | | | |
|---|---|---|---|---|---|---|---|
| $y_1$ | 0.81 | 0.49 | 0.25 | 0.16 | 0.09 | 0.04 | 0.01 |
| $y_2$ | 0.09 | 0.21 | 0.25 | 0.24 | 0.21 | 0.16 | 0.09 |

For the sake of completeness, the numerical figures will be given below when the rate of demethylation is 0.7 and 0.5 times that of bleaching, i. e. $x_2+y_2=0.7(x_1+x_2)$ and $x_2+y_2=0.5(x_1+x_2)$.

| $x_2+y_2=0.5(x_1+x_2)$ | | | | | | | |
|---|---|---|---|---|---|---|---|
| $y_1$ 0.8 | 0.6 | 0.5 | 0.4 | 0.3 | 0.2 | 0.1 | 0.04 |
| $y_2$ 0.06 | 0.104 | 0.118 | 0.125 | 0.122 | 0.106 | 0.070 | 0.034 |
| $x_2+y_2=0.7(x_1+x_2)$ | | | | | | | |
| $y_1$ 0.8 | 0.6 | 0.5 | 0.4 | 0.3 | 0.2 | 0.1 | 0.04 |
| $y_2$ 0.076 | 0.135 | 0.157 | 0.172 | 0.174 | 0.162 | 0.12 | 0.10 |

The real situation is that the irreversible decomposition always takes place more or less, but it is evident from the above data that the changes of absorption spectra of methylene blue and the demethylated dye in most cases (Figs. 5 and 7) correspond to the case that demethylation has roughly the same rate as that of bleaching.

The result that a small quantity of dissolved oxygen increases the degree of demethylation,

6) L. Rapkin, A. P. Struky and R. Wurmser, *J. Chim. Phys.*, **76**, 340 (1926); See also Part II of this series.

can be accounted for as due to the repeated reoxidation of leuco dye, since this process retards the leuco-formation, increasing the relative magnitude of demethylation.

In some cases demethylation is found to proceed noticeably at a later stage and this strongly suggests, as already mentioned, that the reduced dye is more susceptible to demethylation. Thus it is plausible that demethylation and bleaching are in this sense related with each other although they are in fact independent simultaneous reactions.

A brief structural discussion will be added at the end.

Since demethylation is related with the amino group of a side chain while the formation of leuco dye is connected with the ring nitrogen, it is natural that the two reactions take place independently. In general demethylation is considered to take place oxidatively so that it is plausible in the present case that the (transient) removal of the lone pair electrons participates in the course of demethylation. This view seems to account for the difference of salts in suppressing demethylation. Thus according to the results so far obtained less demethylation seems to occur in the presence of $SO_4^{2-}$, $Cl^-$, $I^-$, $OH^-$ when compared with borate and phosphate, and this might be due to the attachment of such simple anions to the amino group which hinders the removal of lone pair electrons. The anticipation that the leuco form is more susceptible to demethylation is compatible with the above view, since the leuco dye is electroneutral and can not combine with an anion. This might be the reason why demethylation becomes more pronounced at a later stage.

As for the formation of leuco dye, it is most plausible to consider that the primary process for the reaction consists in the acceptance of an electron by the excited dye, but it is not known at the present stage what kind of molecular species acts as an electron donor. It is conceivable that the amino group of the dye molecule plays this role, but there seems to be another possibility that hydroxide ion loosely attached to or existing in the neighborhood of ring nitrogen behaves as an electron donor. The latter possibility might be supported by the existence of a colorless form $(DOH)H^+$ which Lewis first postulated and which the present paper further supports.

At any rate there is scarcely any doubt that the ultimate fission of water by the visible light is taking place in this case. Such a possibility was formerly considered as a very unlikely event from the standpoint[7] of energy, but recently experimental evidence for such a process to occur, seems to be rather strengthened[8]; the present result, we believe, demonstrates unequivocally that it can really occur though the mechanism is still entirely unknown and is to be solved in future.

## Summary

It was discovered that the irradiation of the aqueous solution of methylene blue containing various kinds of salts, produces the leuco form of dye; accompanied with this reaction, irreversible photodecomposition of dye and demethylation occurs to some extent. Hydroxide, phosphate and borate were found to be most effective in promoting this photoreduction. Careful studies were performed to counteract the possible effect of impurity. Since the present reaction was considered most certainly to be due to the ultimate fission of water, the analysis for Oxygen and hydrogen peroxide was undertaken. The former was not detected by means of a mass-spectrograph in case of phosphate, but the latter was chemically detected in case of borate buffer. The connection between the quantity of demethylation and that of the formation of leuco dye was investigated and clarified to some extent.

*Department of Chemistry*
*Faculty of Science*
*Tohoku University*
*Katahira-cho, Sendai*

7) E. I. Rabinowitch, "Photosynthesis and Related Process", Vol. I, New York (1945), p. 78.

8) I. Fridovich and P. Handler, *J. Biol. Chem.*, **235**, 1835 (1960); W. J. Nickerson and G. Strauss, *J. Am. Chem. Soc.*, **82**, 5008 (1960).

# *Photoreduction of Methylene Blue by Visible Light in the Aqueous Solution Containing Certain Kinds of Inorganic Salts. II. Photobleached Product*

By Hiroshi OBATA

(Received January 10, 1961)

Koizumi, Usui and the present author have discovered[1] that the deaerated aqueous solution of methylene blue undergoes photobleaching by visible light, and they have clarified the general features of the phenomenon. The bleached solution has a well-defined absorption spectra with a new peak at 256 m$\mu$ and the color is recovered when air is introduced into the solution. It was further established that the absorption peak of the remaining oxidized form gradually shifts accompanied with the bleaching reaction. Also the recovered dye has its maximum at about 640 m$\mu$, which is essentially the same as the ultimate position of the remaining oxidized form before aeration.

As regards the photobleaching it seems most probable to attribute it to the formation of leuco dye, but if so, one has perhaps to assume the ultimate fission of water by visible light, which occurs with great difficulty for the energetic reason. If the photobleached product be some substance other than the leuco dye, this difficulty may be avoided. In connection with such a possibility it seems necessary to pay some attention to Lewis' suggestion[2] that a certain colorless form of methylene blue with the structure $(Mb^+\cdots OH^-)H^+$ ($OH^-$ is attached to ring nitrogen) exists in the aqueous solution. In case the photobleached product be such a substance or some others related with it instead of the leuco dye, then its chemical behavior would be expected to be quite different from that of the chemically prepared leuco dye which is believed to be MbH.

Secondly, as to the cause for the shift of the absorption maximum, Yoshida's work seems to be noteworthy[3]. He concludes that in the alcoholic solution methylene blue is demethylated by exposure to the visible light accompanied with the photoreduction. It seems natural to expect that the same reaction occurs in the aqueous solution, but as another possibility, the photo-hydrolysis of the dimethylamino group cannot be neglected a priori since it is well-known that in the alkaline aqueous solution, methylene blue is converted into methylene violet[4].

The present paper concerns the elucidation of the above two problems, and the investigation consists mainly of the comparison between the chemically prepared leuco dye and the photobleached product from the following three standpoints.

1) Comparison of the absorption spectra of the photobleached product with those of leucomethylene blue, benzoylleucomethylene blue and acetylleucomethylene blue. The latter two substances are considered to have a structure related with MbOH.

2) Comparison of the oxidative and reductive behavior of the photobleached product with that of leucomethylene blue.

3) Comparison of the pH dependence of the absorption spectrum of the photobleached product and that of leucomethylene blue.

The results lead to the conclusion that the photobleached product is most certainly a leuco dye partially demethylated.

## Experimental

**Materials.**—*Methylene Blue.*—Grübler's reagent was recrystallized twice from water and then once more from butanol. The molar extinction coefficient was 62000. Most experiments were done with the solution of $2\times10^{-5}$ mol./l.

*Leucomethylene Blue.*—The deaerated solution of methylene blue was reduced to the leuco form by warming the solution to about 60°C with a small amount of zinc powder. The maximum of the absorption spectrum of this solution is 256 m$\mu$ and the value agrees with that of the solution reduced by sodium hydrosulfite or hydrogen with palladium asbestos. This result ensures that the solution reduced by adding zinc powder is leucomethylene blue. The solution reduced by passing hydrogen in the presence of palladium asbestos was used for a few experiments.

**Benzoylleucomethylene Blue and Acetylleucomethylene Blue**[5].—*Leucomethylene Blue.*—A solution of 25 g. of methylene blue in 500 ml. of water was heated almost to boiling, 25 g. of zinc powder was

1) Y. Usui, H. Obata and M. Koizumi, This Bulletin, **34**, 1049 (1961).
2) G. N. Lewis, O. Goldschmid, T. T. Magel and J. Bigeleisen, *J. Am. Chem. Soc.*, **65**, 1150 (1943).
3) Z. Yoshida and S. Kazama, *J. Chem. Soc. Japan, Ind. Chem. Sec.* (*Kogyo Kagaku Zasshi*), **59**, 1418 (1956).
4) A. Bernthsen, *Anr.* **230**, 211 (1885).
5) G. Cohn, *Ber.*, **33**, 1567 (1900); L. Chalkley, *J. Am. Chem. Soc.*, **47**, 2057 (1925).

added and then, during vigorous stirring, 70 ml. of pure concentrated hydrochloric acid was added as quickly as possible. After a few minutes, the color of this solution changed to pale greenish yellow. The filtrate was allowed to stand in the nitrogen atmosphere overnight; it was then cooled in an ice-bath and filtered. The precipitate obtained was well dried in a vacum desiccator. This precipitate was greenish and stable in the air for several days; yield 30 g.

*Benzoylation.*—The 4.5 g. of dry zinc salt obtained was dissolved in 9 ml. of dry pyridine, previously deoxygenated by flashing with nitrogen gas, and the solution was treated with 5 ml. of benzoyl chloride, heated for one hour in the nitrogen gas, and then allowed to stand overnight. The reaction mixture was poured into a large volume of cold water, the tarry substance that separated off was washed with 10% sodium carbonate solution and with water until it became a white powder, and then it was extracted with 10% hydrochloric acid. The acidic solution was made alkaline with aqueous ammonia and the white precipitate was collected and dried. The dried substance was recrystallized twice from alcohol. The crystalline substance obtained was pale yellow and melted at 190.5~192°C. The molar extinction coefficient was 55000.

**Acetylation.**—Acetylation was done with acetic anhydride by the same method as benzoylation. The melting point was 180.3~180.5°C, pale green. The molar extinction coefficient was 51000.

$K_3Fe(CN)_6$, $K_4Fe(CN)_6$ — G. R. reagents were recrystalized from water three times.

$SnCl_4 \cdot 5H_2O$, $SnCl_2 \cdot 2H_2O$ — G. R. reagents were used without further purification.

**Apparatus for Photobleaching and Procedures.**—Figure 1 shows the main part of the apparatus for bleaching the aqueous solution of methylene blue. As a light source, two tungsten lamps for spot light (500 W) were employed and the range of wavelength was chosen by means of a filter (Mazda VR2) and any shorter wavelength than 600 m$\mu$ was cut off completely. The reaction cell was a glass rectangular type for Beckman spectrophotometer and could be degassed. Absorption spectra were measured by a Kotaki or Hitachi spectrophotometer according to the visible or ultraviolet region. The photobleaching reaction of methylene blue was carried out in the aqueous solution without any buffered reagents at 30°C.

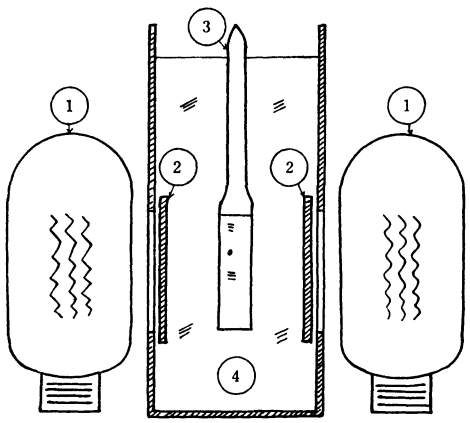



Fig. 1. Apparatus for photobleaching.
① Tungstene lamp for spot light (500 W)
② Filter
③ Reaction cell
④ Thermostatt

## Results

**Photobleaching of Aqueous Methylene Blue Solution in Vacuo.**—It required more than ten hours for the aqueous methylene blue solution to be bleached in vacuo. After the irradiation of 10 hr., there remained about ten per cent of the oxidized form and the wavelength of absorption maximum (667 m$\mu$) moved to about 640~650 m$\mu$. Further, when the bleached solution was exposed to the air, the solution regained the blue color and the position of the absorption peak was practically the same as in the case of the above value. The optical density of the recolorized solution was about 70 per cent that of the original methylene blue solution. Thus the general features of the spectral change is quite similar to that in the case of the buffered solution[1].

**Comparison of the Absorption Spectra of the Photobleached Product with Those of the Related Compounds.**—If there should exist any difference in the absorption spectra of leucomethylene blue (DH) and those of DOH, the photobleached product would easily be identified spectroscopically. But the fact is that nothing has been reported about DOH, except Lewis' proposal so far as the author knows and still less about its absorption spectra. For the purpose of getting knowledge about the absorption spectra of DOH, those of the synthesized benzoylleucomethylene blue and acetylleucomethylene blue were measured.

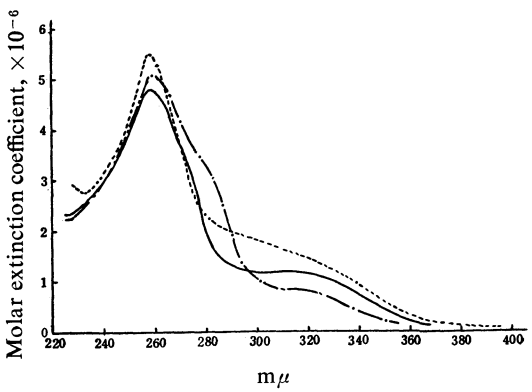



Fig. 2. Absorption spectra of leucomethylene blue and its derivatives.
—— Leucomethylene blue
----- Benzoylleucomethylene blue
—·— Acetylleucomethylene blue

These were fairly stable in the aerated condition and were expected to have the absorption band similar to that of DOH, because they are closely related with DOH in structure. The absorption spectra of benzoylleucomethylene blue and acetylleucomethylene blue were compared with that of leucomethylene blue in alcoholic solution. Figure 2 shows the absorption spectra of these three substances. They are similar in shape and the wavelengths of the maxima agree fairly completely. These results suggest that the absorption bands of DH and DOH resemble each other, hence one can not decide spectroscopically whether the photobleached product be DH or DOH.

**Comparison of the Oxidative and Reductive Behavior between Photobleached Product and Leucomethylene Blue.**—The reactivity of the photobleached product was compared with that of leucomethylene blue. The outline of the principle for this comparison is as follows. Two solutions containing respectively about equal amounts of leucomethylene blue and the photobleached product are added in vacuo, each to the same amount of solution containing a definite quantity of a suitable oxidation reduction system. Then the quantity of dye which has been oxidized is determined spectroscopically. The comparison of the ratio of the colored and colorless species in the equilibrium state for the two cases would be useful for the identification of the photobleached product. The reagents chosen are (1) $K_3Fe(CN)_6$–$K_4Fe(CN)_6$ system, (2) $SnCl_4$–$SnCl_2$ system and (3) thionine-leucothionine system.

(1) *The Reaction with $Fe(CN)_6^{3-}$—$Fe(CN)_6^{4-}$ System.*—The mixture of $K_3Fe(CN)_6$ and $K_4Fe(CN)_6$, each $1.6\times10^{-5}$ mol., was added in vacuo to 7 ml. of the solution containing the dye system (leucomethylene blue or the photobleached product). The calculated concentration of $K_3Fe(CN)_6$ and $K_4Fe(CN)_6$ in the solution thus prepared, being $2.3\times10^{-3}$ mol./l., was about 100 times that of the dye-system. As expected from the values of $E_0'$ at pH 7 (0.43 V. for $Fe(CN)_6^{3-}$-$Fe(CN)_6^{4-}$, 0.011 V. for methylene blue-leucomethylene blue)[6] the addition of $K_3Fe(CN)_6$–$K_4Fe(CN)_6$ system to the solution of methylene blue rapidly produced a blue color of the oxidized dye; but the solution gradually changed its color and turned to a green tint after a few minutes. As to the photobleached solution, a change quite similar to that above was observed.

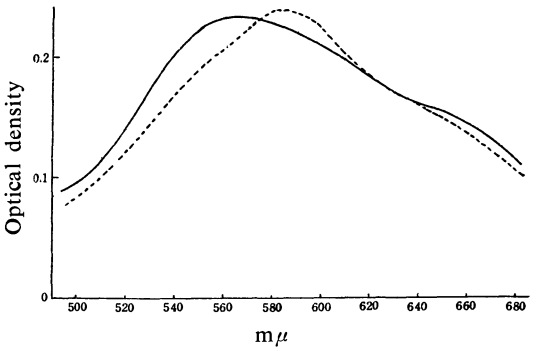



Fig. 3. Absorption spectra of the complex with $K_3Fe(CN)_6$.
—— Oxidized form of the photobleached product
---- Oxidized form of leucomethylene blue

In Fig. 3 the absorption spectra of these two solutions are shown and in addition, that of the aqueous methylene blue solution containing $K_3Fe(CN)_6$. A large shift of $\lambda_{max}$ of methylene blue suggests the formation of a certain complex between the dye and $K_3Fe(CN)_6$. A further shift for the photobleached product, ca. 15 mμ corresponds, without doubt, to that of the component dye.

(2) *The Reaction with $Sn^{4+}$—$Sn^{2+}$ System.*—In this case a more quantitative comparison can be done. Thus when a large quantity of the solution containing $SnCl_4$ and $SnCl_2$, 1 : 1 in mole ratio, is added to the solution of the reduced dye, the latter will be oxidized to such an extent that its potential attains the value of $Sn^{4+}$-$Sn^{2+}$ system, which on account of its great excess, maintains practically its original value. The concentration of oxidized form ($X_o$) and that of reduced form ($X_r$) of dye in the equilibrium state can easily be obtained spectroscopically by measuring the optical density of the above solutions in both deaerated and aerated conditions, the former providing the value of $X_o$ and the latter $X_o+X_r$. In this way the value of $X_o/X_r$ in two cases, leucomethylene blue and the photobleached product can be compared at a constant oxidation reduction potential determined by $Sn^{4+}/Sn^{2+}$ ratio.

In practice the experiment was done as follows. The stock solutions of stannic chloride and stannous chloride both in 1 N hydro chloric acid were neutralized by sodium acetate to adjust the pH value to 5. Two milliliters of 1 : 1 stannic chloride-stannous chloride solution was added to 5 ml. of reduced dye solution, the concentration of stannic chloride and stannous chloride having been suitably selected to make their ultimate concentration 0.02 mol./l. Upon mixing, the blue color immediately

6) M. Clark, "Oxidation Reduction Potential in Organic System", Williams & Wilkins Co., Balimore (1960), p. 132; L. F. Hewitt, "Oxidation-Reduction Potential in Bacteriology and Biochemistry", 6th Ed., Livingstone Ltd., Edinburgh (1950), p. 21.

appeared and its optical density was measured at 660 and 645 mμ respectively for the case of leucomethylene blue and the photobleached dye. Aerating the system the optical density was measured once more at the above wavelengths. Typical results are shown in Table I.

TABLE I. OPTICAL DENSITY OF LEUCOMETHYLENE BLUE AND THE PHOTOBLEACHED PRODUCT AFTER ADDING $SnCl_4$-$SuCl_2$ SYSTEM

| | Leucomethylene blue | Photobleached product |
|---|---|---|
| Deaerated state | 0.201 | 0.286 |
| Aerated state | 0.352 | 0.380 |
| $X_o/X_r$ | 1.331 | 3.04 |

$E_0'$ value of the photobleached product may be evaluated in the following way. The oxidation-reduction potential of the solution which is practically decided by the $Sn^{4+}/Sn^{2+}$ ratio is expressed as follows.

$$E_h = E'_{o_{Sn}} + \frac{RT}{2F} \ln \frac{[Sn^{4+}]}{[Sn^{2+}]}$$

$$= E'_{o_{Mb}} + \frac{RT}{2F} \ln \frac{X_{o_{Mb}}}{X_{r_{Mb}}}$$

$$E'_{o_{ph}} + \frac{RT}{2F} \ln \frac{X_{o_{ph}}}{X_{r_{ph}}}$$

where $E'_{o_{Sn}}$, $E'_{o_{Mb}}$ and $E'_{o_{ph}}$ are respectively the midpoint potential (the potential when the concentration of oxidant and reductant is the same) of $Sn^{4+}/Sn^{2+}$, methylene blue, and the photobleached system at pH 5. Using the value of $E'_{o_{Mb}}$ (0.101 V.)[6] in the literature and the value of $X_{o_{Mb}}/X_{r_{Mb}}$ in Table I, one can determine the $E_h$ value, which was found to be 0.1048 V. Since $E_h$ has the same value for the photobleached system, one can easily get $E'_{o_{ph}}$ from $X_{o_{ph}}/X_{r_{ph}}$. The value obtained is 0.090 V. which is close to the value of methylene blue.

(3) *The Reaction with Thionine-Leucothionine System.*—$E_0'$ of thionine is only a little higher than that of methylene blue and the light absorption by thionine is almost negligible in the concentration $10^{-5}$~$10^{-6}$ mol./l. at a wavelength of the absorption maximum of methylene blue. But, if the concentration of the thionine solution was chosen above $10^{-3}$ mol./l. in order to keep the value of $E_h$ approximately constant after mixing, then the absorption of thionine at 665 mμ would become so great that it would prevent a simple spectroscopic analysis of the methylene blue system. Moreover it is troublesome to prepare a solution containing a definite amount of thionine and leucothionine and to add it to the solution to be tested in vacuo. For this reason the analogous experiment as in the case of $Sn^{4+}$-$Sn^{2+}$ system was not undertaken in this case and the following procedure was adopted. A suitable amount of thionine solution ~$10^{-6}$ mol./l. in concentration is added to the solution to be examined in order to oxidize about a half of the existent leuco form. In case of leucomethylene blue, the concentration of oxidized form produced by the addition of thionine can easily be obtained spectroscopically. The total sum of oxidized and reduced form is also determined by measuring the optical density of the solution after aeration. From these two values the concentration of the oxidized and reduced forms of methylene blue as well as thionine in the equilibrium can easily be calculated. The use of $E_0'$ value of thionine[6] (0.068 V. at pH 6.8) enables one to decide the $E_0'$ value of methylene blue and vice versa. After having checked the above method by leucomethylene blue, it was applied to the photobleached product in order to estimate its $E_0'$ value. But in this case the exact value for the concentration of oxidized and reduced form can not be decided spectroscopically because of the lack of the molar absorbancy. As an approximation the value of the molar extinction coefficient of methylene blue at 665 mμ was provisionally used.

To illustrate by an example, the absorption spectra when 3 ml. of thionine solution was added to the solution of 5 ml. of photobleached product are shown in Fig. 4. Curves ② and

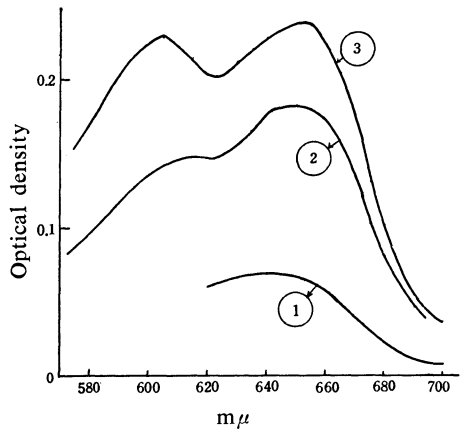



Fig. 4. Absorption spectra of the photobleached product when thionine solution added.

③ refer respectively to the deaerated and aerated solution and ① is the absorption spectrum due to the remaining oxidized form in the original photobleached solution (after having been corrected for dilution). From these data the concentration of each species in the equilibrium state was calculated and shown in Table II.

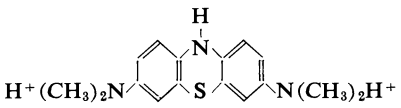
TABLE II. CONCENTRATION IN THE EQUILIBRIUM STATE BETWEEN THIONINE AND THE PHOTOBLEACHED PRODUCT

| | Oxidized form | Reduced form | $E_h$ |
|---|---|---|---|
| Thionine | $0.08\times10^{-6}$ | $2.04\times10^{-6}$ | 0.0257 |
| Photobleached product | $3.64\times10^{-6}$ | $1.10\times10^{-6}$ | |

(The oxidized form remaining in the original photobleached solution: $1.6\times10^{-6}$ mol./l.)

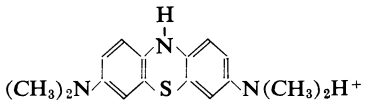
From the data in Table II $E_o'$ of the photobleached product was calculated to be 0.0101 V. Two other similar experiments gave the values, 0.0090 and −0.0122 V. The average is 0.0023 V. It is to be added that when 10% less value is used for the extinction coefficient of the photobleached product, $E_o'$ value in the above case varies from 0.0101 to 0.028 V.; thus the value itself is not so exact, but it is certain that it is close to that of methylene blue.

**Comparison of the pH Dependence of the Absorption Spectra between Methylene Blue and the Photobleached Product.**—Leucomethylene blue ionizes in two steps at pH 4.5 and 5.9, that is, there are three species of leucomethylene blue in respective pH regions as shown below.



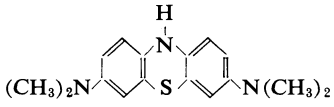
(a)

pH<4.5



(b)

4.5<pH<5.9



(c)

pH>5.9

Accordingly, the absorption spectra of leucomethylene blue in three pH regions may be different from each other. This was examined and the analogous experiment was done also for the photobleached product. Five milliliters of the solution of leucomethylene blue or the photobleached product was poured into 2 ml. of the acetate buffer solution in vacuo. The pH values chosen were 3.54, 4.02, 5.00, 6.62 and 8.25 each successively corresponding to the region where the species a, a, b, c, and c are predominant.

One could find, however, no differences between methylene blue and the photobleached product both in shape and in the position of the maximum wavelength at all pH values, the latter always being at 256 mμ. But some difference was found in the molar extinction coefficient at 256 mμ, with the highest value at pH 5 and decreasing both in larger and smaller pH regions. The results are shown in Table III and Fig. 5. In Table III the optical

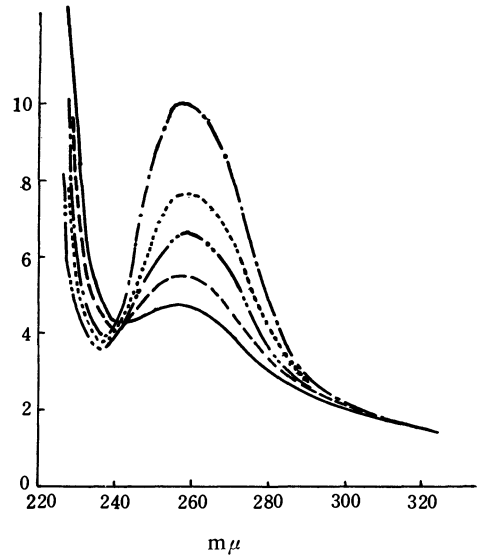



Fig. 5. Absorption spectra of the photobleached product in respective pH value.
(Absorption bands in shorter wavelength than 240 mμ are caused by acetic acid.)

——— pH 3.54 ····· pH 6.62
------- pH 4.02 —·—· pH 8.62
— · — pH 5.50

density of the leuco form at the maximum absorption (256 mμ) (denoted as B), that of the oxidized form produced by aeration of the respective solution of leuco form (at 665 mμ for methylene blue and 645 mμ for the photobleached product) (denoted as A), and the ratio B/A are tabulated. The value of B/A or its relative value standardized to that at pH 5 would be a measure of the molar extinction coefficient at 256 mμ of leuco dye, because the absorption spectrum of methylene blue is essentially the same in the above pH region and the same would perhaps apply to the photobleached product.

In evaluating the data in Table III it must be noted that a certain correction was made for a small amount of coexisting oxidized form in the solution of leuco dye, by making use

TABLE III. OPTICAL DENSITIES IN VARIOUS pH VALUES

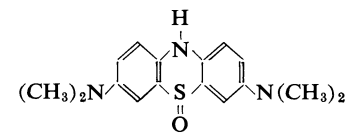
| | | pH | | | | |
|---|---|---|---|---|---|---|
| | | 3.54 | 4.02 | 5.00 | 6.62 | 8.25 |
| Photobleached product | A | 0.442 | 0.335 | 0.186 | 0.380 | 0.372 |
| | B | 0.610 | 0.561 | 0.405 | 0.463 | 0.384 |
| | B/A | 1.447 | 1.675 | 2.18 | 1.22 | 1.033 |
| | Relative value | 0.663 | 0.768 | 1 | 0.559 | 0.474 |
| Leucomethylene blue | A | 0.340 | 0.243 | 0.230 | 0.160 | 0.164 |
| | B | 0.284 | 0.367 | 0.254 | 0.168 | 0.161 |
| | B/A | 0.836 | 0.992 | 1.045 | 0.730 | 0.636 |
| | Relative value | 0.798 | 0.947 | 1 | 0.698 | 0.606 |

of the fact that the ratio of the optical density at 256 m$\mu$ to that of 665 m$\mu$ or 645 m$\mu$, as the case may be, in the oxidized form is approximately 1 : 3.

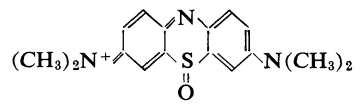
From the above results it is certain that as regards the pH dependence of the absorption spectrum there is no marked difference between leucomethylene blue and the photobleached product.

## Discussion

From the results obtained in the present paper which demonstrate clearly the marked resemblance between the photobleached product and leucomethylene blue both in oxidative and reductive behavior as well as acid base character, there scarcely remains any doubt that the photobleached product is a leuco form dye. Lewis' colorless species $(DOH)H^+$ [2], for which the oxidative and reductive behavior as observed would never be expected, can safely be rejected as a photoproduct. But here another conceivable substance which is speculative but somewhat fascinating will be mentioned in connection with this colorless form. This is a compound supposed to be formed, should $OH^-$ be photochemically split into $H^-$ and O (I). It may happen that this is oxidized to II by aeration. If such a compound as I were



(I)



(II)

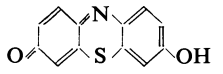
formed, there might be a possibility that the photofission becomes more feasible and that such a reaction is accompanied by the product of neither oxygen nor hydrogen peroxide. Although there are no such substances cited in the literature, but some *S*-oxides are really known in the derivatives of phenthiazines, which are hypsochromic than their mother compounds, for example, such compounds as 2, 7 - dinitrophenthiazine - *S* - oxide[7] (yellow against dark brown of 2, 7-dinitrophenthiazine) and benzothiazino tropone-*S*-oxide[8] (380 m$\mu$ against 440 m$\mu$ of benzothiazino-tropone). Hence the compound I does not contradict the present result so far as the shift of the absorption peak is concerned.

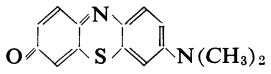
Apart from such a speculation one may conclude that the photobleached product is a leuco dye of a certain kind.

Next, there will be discussion as to whether the accompanying photoreaction is demethylation or hydrolysis of dimethylamino group. Substances to be taken up as possible photobleached products would be the following four; methylene azur A (*N*, *N*-dimethylthionine), methylene azur B (trimethylthionine), or thionol (III), methylene violet (*N*, *N*-dimethylthionolin) (IV). Unfortunately there are few reliable data available either for the absorption spectra or for the oxidation-reduction potential of such substances, and comparison with the present results are not always possible. According to Kehrmann[9] the absorption maximum of methylene azur A and methylene azur B are respectively 638 m$\mu$ and 656 m$\mu$ and the former is rather close to this observed value. As for the reduction potential on the other hand, Rapkin et al.[10] reported that $E_o'$ of methylene azur B is about the same as that of methylene blue but their data have seemingly

7) F. Kehrmann, *Ber.*, **46**, 2809 (1913); F. Kehrmann and H. Goldstein, *Helv. Chim. Acta.*, **4**, 27 (1921).
8) Unpublished result in Prof. Nozoe's Laboratory in our Faculty.
9) F. Kehrmann, *Ber.*, **46**, 2136 (1913).
10) L. Rapkin, A. P. Struky and R. Wurmser, *J. Chim. Phys.*, **26**, 340 (1926).

to be reexamined according to a recent investigation[11].


(III)


(IV)

Thionol was reported to have the absorption maximum at 590 or 595 mμ[4,12], which does not agree with the present value, while methylene violet has an absorption maximum at 635 mμ in the aqueous solution[4] (or 597.4 mμ in alcoholic solution[13]). As for the $E_0'$ value of the latter compounds there is evidence that it is much lower than that of methylene blue, although its reliable value is not found in the literature. Thus the $E_0'$ value of thionolin, the demethylated analogue of methylene violet, was reported to be −0.22 V. (at pH 7.11)[14], which is much lower than that of thionine (0.062 V. at pH 7.0), the demethylated analogue of methylene blue (0.011 V. at pH 7.0). From these data it would be natural to expect that the $E_0'$ value of methylene violet is smaller than −0.22 V. at pH 7. Thus the possibilities of photohydrolysis which lead to III or IV, can be denied altogether.

11) For example, as regards toluidin blue, compare Rapkin's data with B. P. Nikol'skü and V. V. Pal'chevskü, *Zhur. Fiz. Khim.*, **32**, 1280 (1958).
12) S. Granick and L. Michaelis, *J. Am. Chem. Soc.*, **69**, 2883 (1947).
13) M. Althausse und G. Krüss, *Ber.*, **22**, 2065 (1889).
14) S. Granick, L. Michaelis and M. Schubert, *J. Am. Chem. Soc.*, **62**, 1802 (1940).

To sum up the above discussion, a photobleached product is most certainly a partially demethylated methylene blue, which is perhaps methylene azur A.

## Summary

In order to identify the photobleached substances which are produced when the aqueous solution of methylene blue is irradiated with visible light, the following three kinds of experiments were carried out.

1) Comparison of the absorption spectra of the photobleached product with those of leucomethylene blue, benzoylleucomethylene blue and acetylleucomethylene blue.

2) Comparison of the oxidative and reductive behavior of the photobleached product with that of leucomethylene blue.

3) Comparison of the pH dependence of the absorption spectrum of the photobleached product and that of leucomethylene blue.

It was concluded that the photobleached product is the leuco form dye and its oxidized form is most certainly a partially demethylated methylene blue, perhaps methylene azur A.

The author wishes to express his thanks to Professor Masao Koizumi for his suggestions and criticism throughout this investigation.

*Department of Chemistry*
*Faculty of Science*
*Tohoku University*
*Katahira-cho, Sendai*

# *A. C. Polarography of Thiamine Hydrochloride in Weakly Acidic Buffer Solutions**

By Koichi OKAMOTO

(Received August 31, 1960)

A number of polarographic investigations on thiamine hydrochloride have been reported[2]. Most of these studies have been carried out in highly acidic or basic solutions or in unbuffered solutions, because their D. C. reduction waves were not well-defined in weakly acidic or in neutral buffer solutions owing to the overlapping of hydrogen discharging currents or pre-sodium waves.

The stability of thiamine under such extreme conditions was not sufficient to carry out the polarographic measurements and in unbuffered solutions the real pH-values at the surface of D. M. E. could not be defined experimentally. Therefore, the investigations have to be done in buffered solutions in order to know the real polarographic reduction waves of thiamine in weakly acidic solutions.

When the A. C. polarographic method was applied, thiamine hydrochloride was found to show one or two well-defined peak currents in weakly acidic and in neutral buffer solutions. Especially the behavior of the first wave

* Polarographic Studies of some Organo-sulfur Compounds, Part II[1].

1) Part I. K. Okamoto, This Bulletin, **34**, 920 (1961).

2) M. Brezina and P. Zuman, "Polarography in Medicine, Biochemistry and Pharmacy", Interscience Publishers, New York (1958), p. 382.

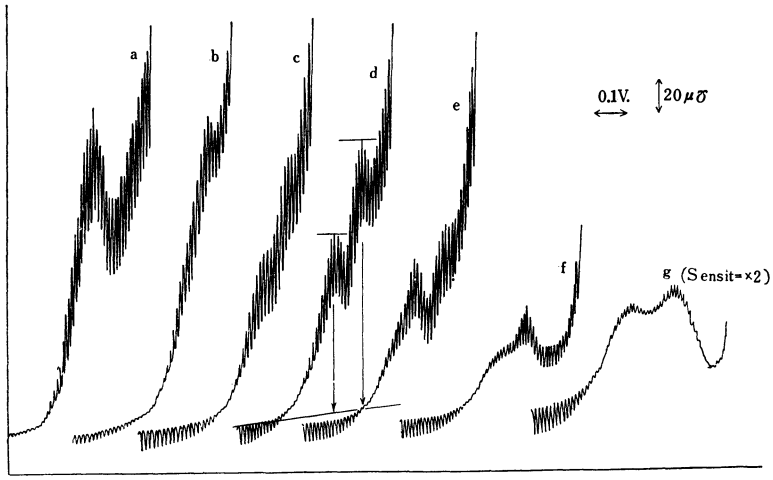



Fig. 1. Typical polarograms of $B_1$-HCl. a: pH 3.00, b: 4.75, c: 5.50, d: 6.00, e: 7.00, f: 7.90, g: 8.95. The applied voltage starts from −1.0 V. vs. S. C. E. [$B_1$-HCl] = $1\times10^{-3}$ mol./l. The solutions were air-free. Parallel capacitance is zero.

was distinctly observed in the solutions of pH 4.75~7.0. These two waves were considered to be attributed to the reduction of two species of thiamine hydrochloride in a solution.

In this paper, these A. C. polarographic behaviors of thiamine hydrochloride will be reported.

## Experiments and Results

The polarograph used was the same as that reported in the previous paper[1]. The characteristics of the dropping mercury electrode were: $m$=0.917 mg. $sec^{-1}$, $t$=4.68 sec. (open circuit), 3.92 sec. (at −1.30 V. vs. S. C. E.), 3.85 sec. (at −1.40 V.).

The thiamine hydrochloride and other reagents used were of reagent grade.

Experiments were carried out 2 or 3 times on the same kind of sample at 25°C and the values obtained were averaged in general. All potentials and peak currents were expressed in V. vs. S. C. E. and μA, respectively.

TABLE I. THE VARIATION OF THE SUMMIT POTENTIALS $E_S$ AND THE PEAK CURRENTS $i_S$ WITH pH
[$B_1$-HCl] = $1\times10^{-3}$ mol./l., 25°C

| pH | Buffer | $-E_S$, V. vs. S.C.E. | | $i_S$, μA | |
|---|---|---|---|---|---|
| | | $-E_S^1$ | $-E_S^2$ | $i_S^1$ | $i_S^2$ |
| 3.00 | A | N.W. | 1.273 | N.W. | 234.6 |
| 4.00 | A | N.W. | 1.275 | N.W. | 233.2 |
| 4.25 | A | N.W. | 1.299 | N.W. | 227.0 |
| 4.50 | A | N.W. | 1.316 | N.W. | 209.0 |
| 4.75 | A | N.W.* | 1.320 | N.W. | 199.2 |
| 5.00 | A | 1.275 | 1.335 | ca. 120 | 185.6 |
| 5.25 | A | 1.290 | 1.357 | 114.9 | 178.8 |
| 5.50 | A | 1.300 | 1.370 | 111.3 | 165.0 |
| 5.75 | A | 1.307 | 1.390 | 102.8 | 157.7 |
| 6.00 | B | 1.310 | 1.392 | 94.0 | 147.0 |
| 7.00 | B | 1.351 | 1.445 | 85.4 | 82.0 |
| 7.90 | B | 1.320 | 1.399 | 45.0 | 61.9 |
| 8.95 | C | 1.317 | 1.453 | 28.0 | 29.3 |
| 10.00 | D | N.W. | N.W. | N.W. | N.W. |

A: 0.5 M acetate buffer
B: 0.5 M phosphate buffer
C: 0.1 M borate buffer+$KH_2PO_4$
D: 0.1 M borate buffer+NaOH
N. W.: No wave * Shoulder

**The Influences of pH to $i_S$ and $E_S$.** — In the buffer solutions of pH 3.0~10.0, containing $1\times10^{-3}$ mol./l. thiamine hydrochloride ($B_1$-HCl), the variation of the wave forms with pH was observed, especially in the region of pH 4.00~6.00.

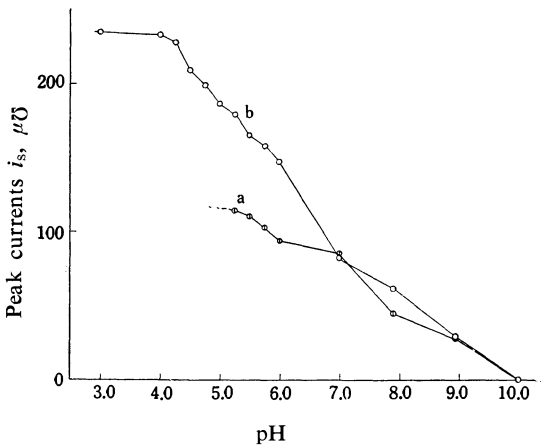



Fig. 2. The relation of the peak currents to pH.
a: 1st wave b: 2nd wave
[$B_1$-HCl] = $1\times10^{-3}$ mol./l., 25°C

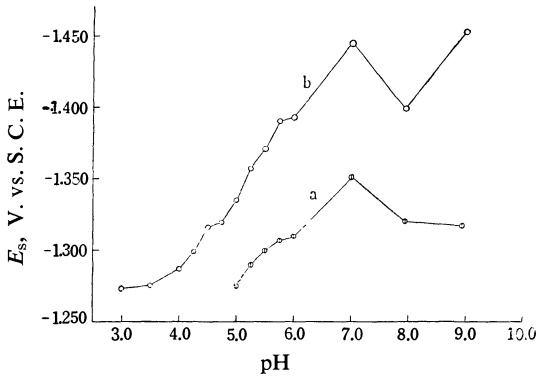



Fig. 3. The relation of $E_s$ to pH.
a: first wave b: second wave
$[B_1\text{-HCl}] = 1\times10^{-3}$ mol./l., 25°C

Some of the typical polarograms were shown in Fig. 1 and the relations of peak currents $i_s$ or of summit potentials $E_s$ to pH were summarized in Table I, Figs. 2 and 3.

Wave heights were measured following the method shown in Fig. 1.

Only one peak current was obtained in the region of pH 3.0~4.75, two peak currents were observed in the region of pH 4.75~9.0. They had the same wave heights at pH 7.0. In basic solutions of pH 7.0~10.0, these two waves changed irregularly and completely disappeared at pH 10.0.

As shown in Figs. 1 and 2, the 1st wave began to be separated at pH about 4.75 and decreased gradually with pH-increase in the same manner as the second.

Gradual negative shifts of $E_s$ of the first and the second waves with pH-increase were found, certain irregularities, however, being observed in basic solutions as shown in Fig. 3.

**The Relations of the Concentrations of $B_1$-HCl to $i_s$ and $E_s$.**—In order to know whether these two peak currents were both due to the reduction of $B_1$-HCl itself, the relation between the concentrations and $i_s$ was investigated in 0.5 M phosphate buffer of pH 6.00.

The results obtained were shown in Table II and Fig. 4. Good linearities were found for

Table II. The variations of $i_s$ and $E_s$ with the concentrations of $B_1$-HCl
Supporting electrolyte; 0.5 M phosphate buffer (pH 6.00), 25°C

| Concn. ($\times10^{-3}$ mol./l.) | $i_s$, μ⅁ | | $-E_s$, V. vs. S.C.E. | |
|---|---|---|---|---|
| | $i_s^1$ | $i_s^2$ | $-E_s^1$ | $-E_s^2$ |
| 0.20 | 16.2 | 33.6 | 1.295 | 1.361 |
| 0.40 | 41.5 | 74.7 | 1.300 | 1.369 |
| 0.60 | 68.2 | 105.2 | 1.307 | 1.386 |
| 0.80 | 93.2 | 137.0 | 1.307 | 1.384 |
| 1.00 | 119.0 | 174.5 | 1.309 | 1.390 |

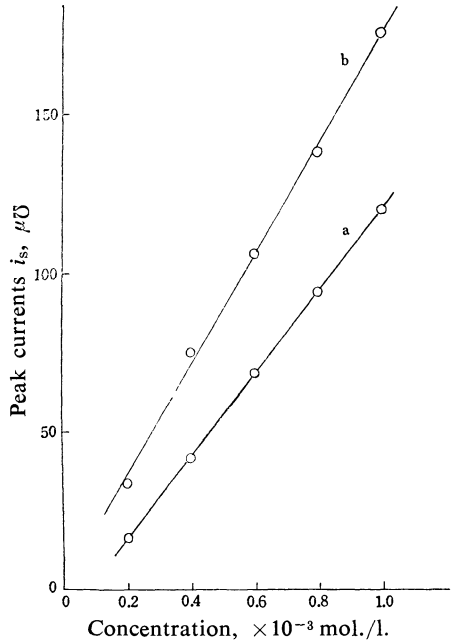



Fig. 4. The relation between the concentrations and the peak currents in 0.5 M-phosphate buffer of pH 6.00.
a: first wave b: second wave

two waves and the saturation tendencies occurred usually in cases where adsorption or desorption waves were not recognized at all.

Therefore, both of the waves seemed to be the real reduction waves of $B_1$-HCl itself.

The summit potential $E_s$ fairly shifted to negative potentials with the increase of the concentrations of $B_1$-HCl.

**Temperature Coefficients of $i_s$.**—Temperature coefficients of the first and the second wave heights were obtained as 1.64 and 1.56% respectively on 0.5 M phosphate buffer solutions of pH 6.0 containing $1\times10^{-3}$ mol./l. of $B_1$-HCl.

These coefficients coincided with the theoretical value of 1.6% of the diffusion currents.

**The Influence of Mercury Heights $H$ to $i_s$.**—The relationship of $H$ to $i_s$ was studied using the method of the plotting $\log H$ (corrected with the reverse pressure of mercury height) against $\log i_s$. The sample offered was $1\times10^{-3}$ mol./l. of $B_1$-HCl dissolved in 0.5 M phosphate buffer of pH 6.00.

The following equations were obtained:

$$\text{first wave;} \quad i_s^1 = H^{0.34} + K_1$$

$$\text{second wave;} \quad i_s^2 = H^{0.29} + K_2$$

where $K_1$ and $K_2$ are constants.

The peak currents were not proportional to the square root of $H$.

**Electrocapillary Curve.**—When strong adsorption-desorption phenomena occurred at the

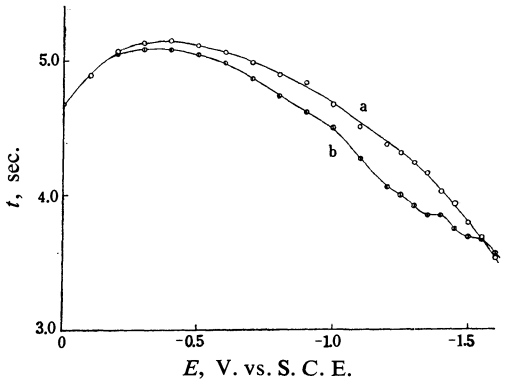



Fig. 5. Electrocapillary curves.
a: Reference; 0.5 M-phosphate buffer pH 6.00
b: 1 mmol $B_1$-HCl in reference soln. a.

surface of D. M. E., the electrocapillary curve was known to show certain irregularities.

The electrocapillary curve of $B_1$-HCl in pH 6.00 phosphate buffer solution was shown in Fig. 5.

In a very wide potential range $-0.20\sim-1.55$ V., the drop time $t$ was smaller in a solution of $B_1$-HCl than in a solution without it, and two small minima were observed at potentials $-1.35$ and $-1.50$ V. corresponding to the slightly negative potentials of each two peak current.

Weak adsorption seemed to take place at the surface of D. M. E., but it could have no remarkable effects upon A. C. polarographic waves; therefore, two A. C. waves were both considered to be not entirely so-called tensammetric waves.

## Discussion

As described in the above section, comparatively-well defined two A. C. polarographic waves of $B_1$-HCl observed in weakly acidic buffer solutions, were not the simple tensammetric, but the reduction waves with a few tensammetric properties.

When the aqueous solution of $B_1$-HCl was titrated with sodium hydroxide solution, two equivalent points were observed[3], the first point corresponding to 1 mol. equivalent of sodium hydroxide and to the process I→II (Fig. 6), another to 3 mol. equivalent of sodium hydroxide and to the process V→VI, while no point corresponding to 2 mol. of sodium hydroxide was detected. The values of $pK_1$ and $pK_2$ were 4.70~4.80 and 9.30~9.37, respectively at 25°C[2].

On the other hand, a new polarographic wave began to be observed at about pH 4.75;

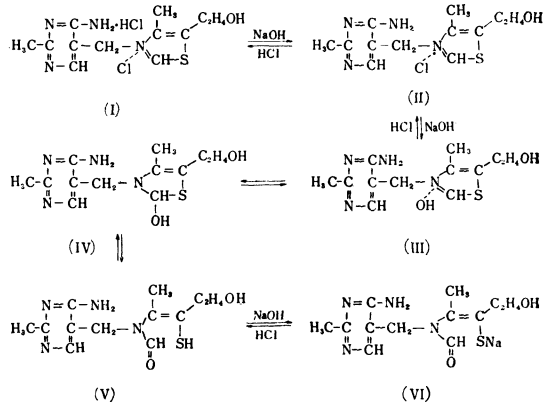



Fig. 6. The variation of $B_1$-HCl when titrated with HCl or NaOH solutions[3].

therefore, this (first wave) was considered to correspond to a reduction of species II that would increase from pH about 3.5 up to neutral range, then the second wave was to correspond to a reduction of species I that gradually decreased with pH-increase.

The first wave seemed to overlap with the second in the region of pH smaller than 4.75, but as the negative shift of the second was larger than of the first, it came to appear at pH 4.75.

At pH 4.70~4.80 the ratio of the polarographic wave heights of the first and the second should be 1 : 2 and at pH 7.0 should be 1 : 1 theoretically. Similar results were obtained experimentally as shown in Fig. 2.

The gradual decreasing of both wave heights with pH-increasing was explained as follows by the above dissociation processes (Fig. 6). If the polarographic reduction of thiamine took place at the double bond >N=C- in thiazole ring, IV, V and VI could not be reduced at D. M. E. Although these formes were not detected in the titration curve, they were considered to exist together in the solutions of pH about 5~9, so that the gradual decrease of wave heights were mainly due to this gradual increase of non-reductive IV or V.

The difference between the summit potentials of the first and second waves was up to about 100 mV., the influence of hydrochloric acid combining to pyrimidine ring or in other words to whole molecule of $B_1$, might produce this difference.

## Summary

Although in ordinary D. C. polarography no well-defined polarographic reduction waves of thiamine in weakly acidic or in neutral buffer solutions have been reported, it was found that A. C. polarographic methods would be suitable for these studies.

3) A. Watanabe and Y. Asahi, *J. Pharm. Soc. Japan* (*Yakugaku Zasshi*), 75, 1046 (1955).

A. C. polarographic waves of thiamine appeared at $-1.27\sim-1.35$ V. in buffer solutions of pH 3.0~4.75, and in the region of pH 4.75~7.0 a new wave began to be observed at more positive potentials than $-1.27\sim1.35$ V., while another wave was observed at $-1.32\sim-1.44$ V. in the same pH region. The heights of two waves decreased with the increase of pH.

In basic buffer solutions the wave forms varied irregularly and the waves disappeared completely at pH 10.0.

According to the relation of $i_s$ to temperature, mercury heights and concentrations, these two waves were both recognized as diffusion currents with a few tensammetric properties.

The nature of the first and second waves were attributed to the reductions of thiamine with $Cl^-$, and with hydrochloric acid and $Cl^-$ to each dihydrothiamine, respectively.

The author is very much indebted to Director M. Matsui of our Laboratory for affording facilities for this investigation.

*Physicochemistry Section*
*Research Department*
*Sankyo Co., Ltd.*
*Shinagawa-ku, Tokyo*

# Studies on the Silk-platinum Catalyst. I. Its Preparation and Activity

By Akira Akamatsu, Yoshiharu Izumi and Shiro Akabori

(Received January 19, 1961)

Recently, Izumi[1] reported on an entirely new type of palladium hydrogenation catalyst, which is unique in that its carrier is fibers of silk-fibroin. Parlladium chloride was easily coordinated with the silk-fibroin protein and then the resulting silk-palladium chelate was hydrogenated to give the catalyst. It is assumed that the metal in the catalyst is highly dispersed and tightly fixed to the micelle structure of silk-fibroin in a finely devided state, and consequently the active surface of the metal is considerably increased. Furthermore, the catalyst has a number of characteristics due to the nature of the carrier silk-fiibroin fibers.

In addition to these characteristics, other interesting properties were expected to be found, when palladium was replaced by platinum. A brown hair-like silk-platinum chelate was successfully formed, when silk-fibroin fibers were boiled with an aqueous solution of potassium tetrachloroplatinate ($K_2PtCl_4$). Activation of this chelate by hydrogenation gave the black-colored silk-platinum catalyst.

This catalyst was found to catalyze the hydrogenation of various compounds, as will be reported in the following papers of this series[2]. In general it showed the highest hydrogenation activity for aromatic nitro compounds. In the hydrogenation of nitrobenzene to aniline, its activity was about two hundred and fifty times as high as that of a platinic oxide catalyst containing the same amount of platinum metal. Further advantages of this catalyst, as of a silk-palladium catalyst, are the facility with which it can be mixed with reactants and separated from the reaction mixture without detachment of the metal from the carrier, and the fact that it can be stored for a long period in air-dried conditions without undergoing spontaneous combustion.

The present paper describes the conditions used for the preparation of this catalyst, and its activity and stability.

## Results and Discussion

**Conditions for Preparation of the Chelate.**— In order to obtain a catalyst with high activity, as well as to minimize expensive loss of platinum, the platinum content of the chelate preparation must be increased. In the previous paper[1] Izumi reported on an "easily detachable form" of metal in the silk-palladium catalyst, which did not contribute to the activity. It is probable that this "easily detachable form" is free metal which has been reduced without forming a chelate. Similarly, platinum in the chelate is assumed to consist of "coordinated" and "not coordinated" platinum. The latter is simply deposited on the silk-fiboin fibers as the free metal. It is possible that the former is readily soluble in concentrated hydrochloric acid while the latter is insoluble. Optimal conditions not only for "the

1) Y. Izumi, This Bulletin, 32, 932 (1959).
2) A. Akamatsu, Y. Izumi and S. Akabori, in preparation.

total platinum content", but also "the coordinated platinum content" were studied; the latter estimated as the concentrated hydrochloric acid soluble part. The results are shown in Fig. 1. (a) Four hundred milligrams of silk-fibroin fibers were boiled with an aqueous solution of potassium tetrachloro-platinate. The ratio of crystalline potassium tetrachloro-platinate to silk-fibroin in the solution, and the boiling time were constant. The concentration of the solution was varied by changing the volume of the solvent. Thus, the optimum concentration was found to be about 0.75%. (b) The boiling time was also kept constant and the volume of the 0.75% aqueous solution of potassium tetrachloro-platinate was varied. Comparatively high contents of platinum were obtained using more than 20 ml. of solution. (c) An adequate boiling time was found to be 14 to 20 min. Thus, the most desirable result was obtained when 400 mg. of silk-fibroin fibers were boiled with 20 ml. of a 0.75% aqueous solution of potassium tetrachloro-platinate for 14 to 20 min. This preparation was used for the work described in the following sections of this paper. Prolonged boiling of more than 20 min. only resulted in an increase in the "not coordinated part". Another good result was obtained, when a suspension of silk-fibroin in potassium tetrachloro-platinate solution was heated at 55°C in an air bath for 17 hr., instead being boiled.

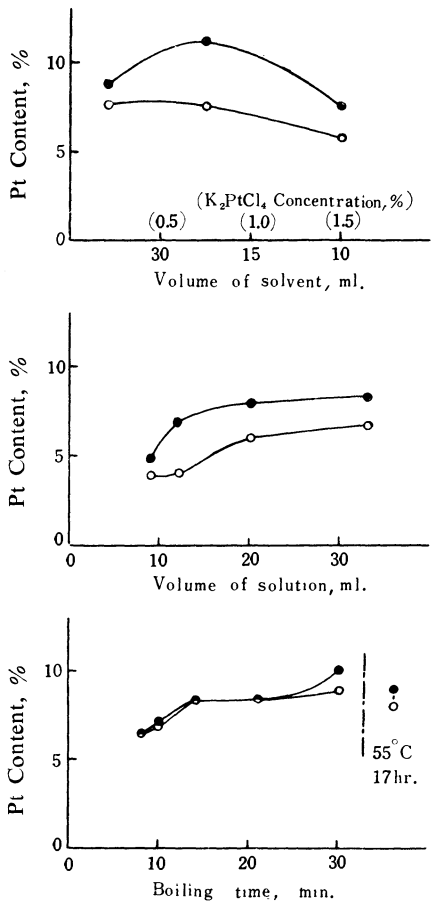



Fig. 1. Platinum content of chelate prepared under various conditions.

● Total platinum content, ○ Coordinated platinum

400 mg. of silk-fibroin was boiled (a) in an aq. solution containg 150 mg. of $K_4PtCl_4$ for 14 min., (b) in a 0.75% $K_2PtCl_4$ aq. solution for 14 min., and (c) in 20 ml. of a 0.75% $K_2PtCl_4$ aq. solution.

In the preparations described above, about 50% of the platinum in solution was used up in formation of the chelate. The remainder in the mother liquor was recovered and used for subsequent preparations.

**Conditions for Activation of the Chelate.**— The above chelate was converted to the active catalyst by reducing it with ca. 90 kg./cm$^2$ of hydrogen in an autoclave. To find the optimal conditions for activity, the hydrogenation reaction was carried out in various solvents at various temperatures for different periods. Representative experiments are summarized in Tables I to IV, in which the activity of the resulting catalysts are represented by their reaction velocity ($v$) during the hydrogenation of nitrobenzene to aniline using the same amount of catalyst in each case, and by their activity yield ($y \cdot v$.) which means their activity on the basis of the same amount of the metal in the catalyst. $v$ was calculated according to the equation; $v=100/t$, where $t$ is the time in minutes required for 70% hydrogen uptake. $y \cdot v$ was calculated as the product of the reacion velocity ($v$) and the gravity yield*[1] ($y$). The decrease in the gravity yield is due to destruction of the carrier fibroin fibers. In general, activation at high temperatures resulted in a high activity yield and low gravity yield. The former is not due only to an increase in the metal content resulting from destruction of the carrier.

When water was used as solvent during activation (Table I), carrier fibers were broken to pieces at above 150°C, and almost completely destroyed and dissolved in the solvent at 200°C. Activation for two hours gave a comparatively active catalyst. The most active catalyst was obtained at 160°C.

With diethyl succinate or methanol, less active catalysts were obtained with the silk-platinum catalyst (Table II), though in the

*[1] For example, when 100 mg. of the chelate is hydrogenated to give 50 mg. of the active catalyst, the gravity yield is 50%.

TABLE I. ACTIVATION OF THE CHELATE IN 50 ml. OF WATER

| Cat. No. | Precursor chelate, mg. | Temp. °C | Time hr. | Grav. yield $y$, % | React. vel. at 32°C, $v$ | Act. yield $y \cdot v$ |
|---|---|---|---|---|---|---|
| 1 | 250 | 80 | 1 | 88 | 2.1 | 1.8 |
| 2 | | | 2 | 91 | 2.5 | 2.3 |
| 3 | | 100 | 1 | 84 | 2.6 | 2.2 |
| 4 | | | 2 | 84 | 2.7 | 2.3 |
| 5 | 200 | 150 | 1 | 73 | 5.4 | 3.9 |
| 6 | | | 2 | 69 | 5.9 | 4.1 |
| 7 | | | 3 | 62 | 4.5 | 2.9 |
| 8 | | 178 | 2 | 44 | 11.5 | 5.0 |
| 9 | | 200 | 1 | — | — | — |
| 10 | 100 | 160 | 2 | 61 | 9.5 | 5.8 |

TABLE II. ACTIVATION OF THE CHELATE (200 mg.) FOR 2 hr. IN METHANOL AND DIETHYL SUCCINATE

| Cat. No. | Solvent 50 ml. | Temp. °C | Grav. yield $y$, % | React. vel. at 32°C, $v$ | Act. yield $y \cdot v$ |
|---|---|---|---|---|---|
| 11 | Methanol | 100 | 90 | 2.9 | 2.6 |
| 12 | | 150 | 83 | 3.4 | 2.8 |
| 13 | diEt. Succ. | 100 | 95 | 0.4 | 0.4 |
| 14 | | 150 | 94 | 1.8 | 1.7 |
| 15 | | 200 | 81 | 4.0 | 3.2 |

TABLE III. ACTIVATION OF THE CHELATE AT 160°C FOR 2 hr. IN DILUTE ACETIC ACID

| Cat. No. | Solvent 50 ml. | Precursor chelate, mg. | Grav. yield $v$, % | React. vel. at 32°C, $v$ | Act. yield $y \cdot v$ |
|---|---|---|---|---|---|
| 16 | 1% AcOH | 100 | 52 | 19.3 | 10.0 |
| 17 | 2.5% AcOH | | 55 | 11.8 | 6.5 |
| 18 | 5% AcOH | | 54 | 17.9 | 9.7 |
| 19 | 1% AcOH | 2000 | 56 | 3.6 | 2.0 |

TABLE IV. REPEATED ACTIVATION OF CATALYST No. 19 FOR 1 hr.

| Cat. No. | Method | Solvent ml. | Precursor catalyst, mg. | Grav. yield $y \cdot y'$ | React. vel. at 32°C, $v$ | Act. yield $y \cdot y' \cdot v$ |
|---|---|---|---|---|---|---|
| 20 | Reduction at 160°C | 1% AcOH (30) | 300 | 31 | 60.0 | 18.8 |
| 21 | Heating at 160°C | 1% AcOH (50) | 100 | 35 | 34.9 | 12.5 |
| 22 | Boiling in flask | 1% AcOH (50) | | 51 | 3.0 | 1.5 |
| 23 | Reduction at 160°C | 1% $NH_3$ (50) | | 25 | 7.5 | 1.9 |

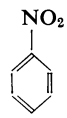
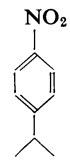
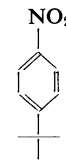
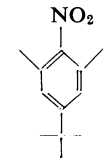
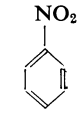
TABLE V. STABILITY OF CATALYST

| Storage time weeks | React. vel. at 32°C, $v$ |
|---|---|
| 0 | 60.7 |
| 2 | 50.5 |
| 5 | 89.0 |
| 12 | 85.8 |

case of the silk-palladium catalyst, an exceedingly active catalyst was obtained with diethyl succinate (Table VI).

However, the use of dilute acetic acid as a solvent (Table III), increased the activation. One per cent acetic acid was the most effective among the other solvents tested. But increasing the amount of the precursor chelate in proportion to that of the solvent, failed to give satisfactory results (Cat. No. 19). So, for the repeated activation of this catalyst, the various conditions shown in Table IV were tested. Repeated hydrogenation under the same conditions resulted in an extremely high activity. Heating in an autoclave without hydrogen also gave a very active catalyst though it was less

Table VI. Reaction velocity in hydrogenation of alkyl nitrobenzenes

| Substrate |  |  |  |  |  |
|---|---|---|---|---|---|
| | 4 g. | 5.4 g. | 5.9 g. | 6.3 g. | 4 g. |
| Solvent | Dioxane | | | | Methanol |
| Silk-Pt 40 mg. [Ratio] | 13.0 (52°C) [1.00] | 11.4 (52°C) [0.86] | 6.90 (55°C) [0.53] | 0.18 (50°C) [0.01] | 37.7 (23°C) |
| $PtO_2$ 15 mg. [Ratio] | 0.15 (50°C) [1.00] | 0.15 (50°C) [1.00] | 0.11† (50°C) [0.73] | 0.03† (100°C) [0.18] | 0.15 (17°C) |
| Silk-Pd 140 mg. [Ratio] | 3.30 (100°C) [1.00] | 0.90 (100°C) [0.27] | 0.65 (100°C) [0.20] | 0 [0.00] | 3.42 (18°C) |
| Silk-Pd-DES 54 mg. [Ratio] | 5.03 (52°C) [1.00] | 1.07 (50°C) [0.21] | — | — | 15.6 (18°C) |

† Calculated value

active than the former. However, boiling in a flask with 1% acetic acid was not effective. Repeated hydrogenation with 1% aqueous ammonia was not effective for increasing the total activity yield ($y \cdot y' \cdot v$), but it did increase the reaction velocity.

The present results show that the activity of the catalyst is influenced very much by the solvent used, and the temperature and time of activation. The destruction of the carrier and the increase in the metal content of the catalyst are evidently effected by these conditions, and indeed might contribute to some extent to the activity represented by the activity yied. But a low gravity yield was not always accompanied by a high actvity yield as shown by comparison of catalysts Nos. 9 and 16. It may be that these conditions directly and independently influence the activity. The solvent especially is an important factor in the activation, as Hartung et al.[3] reported concerning the effect of certain organic anions on the preparation of the palladium-charcoal catalysts. It was proved in this work that regardless of the extent of the gravity yield, use of acetic acid resulted in a very good activity, while methanol, diethyl succinate, and aqueous ammonia were not effective.

It does not seem unreasonable, as Hartung pointed out, to attribute these solvent effects on the arrangement of the crystalline structure or the spacing of the active centers on the catalyst. It should also be noted that the ratio of the volume of solvent to the amount of the precursor-chelate used influenced the activity to a large extent, though such a phenomenon was not seen in the case of the silk-palladium catalyst.

3) W. H. Hartung et al., *J. Org. Chem.*, **21**, 999 (1956).

**Stability of the Catalyst.** — In Table V are shown the reaction velocities observed in the hydrogenation of nitrobenzene to aniline, using the final catalyst*2 both immediately after its activation and after storage of the dry catalyst for several weeks in a stoppered bottle. The results clearly show the silk-platinum catalyst can be stored for a long period without loss and even with some increase of activity. No spontaneous combustion took place during the storage period.

**Activity with Aromatic Nitro Compounds.** — The activity of the silk-platinum catalyst*2 in the hydrogenation of various alkyl derivatives of nitrobenzene to the corresponding amines was compared with that of platinic oxide catalyst, silk-palladium catalyst (activated in methanol) and silk-palladium-DES catalyst (activated in diethyl succinate)*3. Table VI shows the reaction velocities for the hydrogenation of the same amount (1/30 mol.) of the various compounds, using catalysts, each of which contains the same amount (13 mg.) of metal. The silk-platinum catalyst showed the highest activity of all the catalysts with all the compounds tested. Notably in the hydrogenation of nitrobenzene in methanol, the reaction velocity was 254 times as fast as that with the platinic oxide catalyst. When methanol was used as a solvent, the reaction velocity for the silk-platinum and the silk-palladium-DES catalyst was faster than when dioxane was used, in spite of the low reaction temperature.

The ratios of the reaction velocity of alkyl nitrobenzenes to that of non-substituted nitrobenzene were calculated and are shown in

*2 This catalyst was prepared under the same conditions as that for catalyst No. 20 in Table IV. See Experimental.

*3 See Experimental.

brackets in Table VI. In the series of alkyl nitrobenzenes the ratios decreased as the alkyl groups increased in substituents and branching. This decrease is distinguishable with catalysts in which the carrier is silk-fibroin fibers. It is possible that, not only the bulkiness of the reactants, but also the characteristic structure of carrier silk-fibroin[4] exerts some steric hindrance retarding the hydrogenation.

## Experimental

**Determination of Platinum.** — Platinum was measured by the iodine method[5], after the chelated sample had been treated as follows;

*1) For Estimation of the Total Platinum Content.* —About 15 mg. of the chelated sample were accurately weighed in a crucible and heated with 0.5 ml. of concentrated nitric acid on a steam bath for 20 min. The mixture was evaporated to dryness and the residue was strongly heated to ash over a burner. After the ash had been dissolved in 0.5 ml. of aqua-regia, the soluion was evaporated to dryness. One milliliter of concentrated hydrochloric acid was added to the residue and evaporated off twice to remove the nitrate. The residue was then dissolved in water and the solution diluted to 50.0 ml. Exactly 5.00 ml. of the solution was used for each determination.

*2) For Estimation of Coordinated Platinum.* — About 15 mg. of the chelated sample were accurately weighed in a test tube and heated with 2.0 ml. of 30% hydrochloric acid on a steam bath for 30 min. The mixture was filtered through filter paper and the filter paper was washed with water. The combined filtrates were transferred to a crucible and ashed by evaporation and strong heat. Then the ash was treated in the same way as described above for the estimation of the total platinum content.

**Reaction Vessel.**—The same autoclave as described in the previous paper[1] was used for activation of the chelate and for hydrogenation reactions.

**Measurement of the Reaction Velocity.** — One thirtieth of a mole of the substrates (for nitrobenzene, 4 g.) dissolved in 50 ml. of methanol and the catalysts to be tested (for silk-platinum catalyst, 40 mg.) were placed in the autoclave, into which hydrogen was then introduced to a pressure of 90 kg./cm$^2$. The initial pressure was read after shaking to allow equilibration, and then the shaking was continued until 70% of the theoretical amount of hydrogen had been taken up.

**Preparation of Catlysts.**—*1) Silk-platinum Catalyst.*—The catalyst, used in investigations of stability and activity, was prepared by the following method; a) Twenty grams of sik-fibroin fibers previously washed with boilng water were mixed with 1 l. of an 0.75% aqueous solution of potassium tetrachloroplatinate and the mixture was boiled for 18 min. The silk-platinum chelate obtained was filtered off, washed with water, methanol and then ether, and finally dried in vacuo. b) Twenty grams of the chelate were suspended in 500 ml. of 1% acetic acid reduced with hydrogen (80 kg./cm$^2$) at 160°C for 2 hr. in a 1 l. autoclave. The catalyst obtained was filtered off, washed with water, methanol and ether, and dried in vacuo (12 g., 60%). The reaction velocity ($v$) with nitrobenzene at 16°C was 1.8. Repeated hydrogenation of 4 g. of this catalyst by the same method for 1 hr. gave the final catalyst (2.6 g., 66%). The reaction velocity ($v$) of this catalyst at 32°C was 60.7.

*2) Platinic Oxide Catalyst.*—This was prepared by the method of Ref. 6.

*3) Silk-palladium Catalyst.*—This was prepared as described in the previous paper[1].

*4) Silk-Palladium-DES Catalyst.* — Two hundred milligrams of the silk-palladium chelate[1] were suspended in 50 ml. of diethyl succinate and reduced with hydrogen (80 kg./cm$^2$) at 220°C for 2 hr. in a 100 ml. autoclave. The resulting catalyst was washed with methanol and dried in vacuo.

**Isolation of Products.** — The products on the hydrogenation of nitrobenzene and of its alkyl derivatives were isolated as follows:

*Aniline.* — This was isolated as described previously[1].

*p-Aminoisopropylbenzene, p-Amino-tert-butylbenzene.* —The reaction mixture was filtered and the filtrate distilled in vacuo. The amines obtained were acetylated and the crude acetyl derivatives were recrystallized from alcohol: *p*-Aminoisopropylbenzene; b. p. 112°C/19 mmHg (lit.[7] 225°C/760 mmHg). *p*-Amino-*tert*-butylbenzene; b. p. 117~119°C/15 mmHg (lit.[8] 120~132°C/15 mmHg). *p*-Acetaminoisopropylbenzene; m. p. 105°C (lit.[9] 105~106°C). *p*-Acetamino-*tert*-butylbenzene; m. p. 171°C (lit.[8] 171~172°C).

*3,5-Dimethyl-4-amino-tert-butylbenzene.*—The crude amine was converted to its 2-nitro derivative and this was recrystallized; m. p. 86°C (lit.[10] 88~89°C).

## Summary

1. A silk-platinum chelate, which had the highest platinum content, involving both the total platinum content and the coordinated platinum, was obtained when 400 mg. of silk-fibroin was boiled with 20 ml. of a 0.75% aqueous solution of potassium tetrachloroplatinate for 14 to 20 min.

2. The most active silk-platinum catalyst was obtained when reduction of the chelate was pepeated twice in 1% acetic acid with 90 kg./cm$^2$ of hydrogen at 160°C. The activity was much influenced by the solvent, temperature and time used for its activation.

3. The catalyst could be stored for a long

4) S. Akabori, S. Sakurai, Y. Izumi and Y. Fujii, *Nature*, **178**, 323 (1956); S. Akabori, Y. Izumi, Y. Fujii and S. Sakurai, *J. Chem. Soc. Japan, Pure Chem. Sec.* (*Nippon Kagaku Zasshi*), **77**, 1374 (1956); S. Akabori, Y. Izumi and Y. Fujii, ibid., **78**, 886 (1957); Y. Izumi, This Bulletin, **32**, 942 (1959).

5) E. B. Sandell, "Colorimetric Determination of Traces of Metals", Interscience Publishers, New York (1950), p. 493.

6) "Organic Synthesis", Coll. Vol. **1**, 463 (1948).

7) M. S. Carpenter et al., *J. Org. Chem.*, **16**, 586 (1951).

8) B. M. Wepster et al., *Rec. trav. chem.*, **71**, 321 (1952).

9) B. M. Wepster et al., ibid., **71**, 340 (1952).

10) M. S. Carpenter et al., *J. Org. Chem.*, **19**, 77 (1954).

period in the dry state and even showed some increase in activity during storage.

4. The most active catalyst had about two hundred and fifty times as much activity as that of a platinic oxide catalyst in the hydrogenation of nitrobenzene to aniline.

5. The characteristic structure of the carrier seems to exert some steric hindrance on the hydrogenation of highly branched aromatic nitro compounds.

The authors wish to express their gratitude to Dr. S. Yamada for his suggestion concerning the platinum complex, to Mr. S. Watarai for supplying various alkyl nitrobenzene derivatives and to Mr. T. Kojima for his technical assistance in this investigation. They are also greately indebted to the Gunze Seishi Co., Ltd. for supplying the silk fibers.

*Division of Organic Chemistry*
*Institute for Protein Research*
*Osaka University*
*Nishi-ku, Osaka*

# *Reduction of Organic Compounds with Urushibara Catalysts under High Pressure. VIII*[1]. *Reduction of Acetophenone, Especially with Urushibara Nickel Catalyst Prepared by Various Modified Methods*

By Shin-ichi TAIRA

(Received December 27, 1960)

In the preceding paper[1] of this series, catalytic reduction of benzophenone with various Urushibara catalysts under various conditions was reported, and activities of Urushibara nickel, Urushibara cobalt and Urushibara copper, prepared by various methods were compared with each other.

The procedure for preparing Urushibara nickel catalyst has been successively modified since its discovery and some varieties of this catalyst were reported. The preparation of the Urushibara nickel catalyst is divided into two steps; namely, the preparation of precipitated nickel and the digestion of the precipitated nickel with acid or alkali. Varieties of the Urushibara nickel catalyst originate in methods of preparing the precipitated nickel and succesive treatment with acid or alkali. The precipitated nickel, prepared from nickel chloride or nickel acetate solution with zinc dust, gives Urushibara nickel B (U-Ni-B)[1,2] or Urushibara nickel CB (U-Ni-CB)[1] by digestion with caustic alkali. The same precipitated nickel gives Urushibara nickel A (U-Ni-A)[1,3] or Urushibara nickel CA (U-Ni-CA)[1] by treatment with acetic acid in place of caustic alkali. The U-Ni-CB and U-Ni-CA are prepared from the precipitated nickel which was obtained from nickel chloride solution and zinc dust at a low temperature. The precipitated nickel, prepared from nickel chloride solution with aluminum grains, gives Urushibara nickel BA (U-Ni-BA)[4,5] by treatment with sodium hydroxide solution, and Urushibara nickel AA (U-Ni-AA)[6] by treatment with acetic acid and sodium chloride.

In the present paper, reduction of acetophenone with various Urushibara nickel catalysts is investigated. In this connection, the possibility of preservation of the precipitated nickel retaining the activity of the catalyst therefrom was examined. The renewal of used catalyst was also examined, and it was found that a highly active catalyst can be regenerated from a used catalyst by a simple procedure.

## Experimental

**Apparatus.**—Reduction was carried out in the same autoclave (Sakashita SE-20; electro-magnetically stirring type autoclave having a capacity of 200 ml.) used in the experiments reported in the preceding paper[1].

**Materials.**—Commercially available acetophenone was purified by repeated crystallization.

**General Procedure for Reduction.**—Any catalyst, prepared so as to contain 1 g. of nickel, was carefully transferred with ethanol into the autoclave. Then the air present in the autoclave was replaced

1) Part VII: S. Taira, This Bulletin, **34**, 261 (1961).
2) Y. Urushibara and S. Nishimura, ibid., **27**, 480 (1954).
3) Y. Urushibara, S. Nishimura and H. Uehara, ibid., **28**, 446 (1955).
4) K. Hata, S. Taira and I. Motoyama, ibid., **31**, 776 (1958).
5) I. Motoyama, ibid., **33**, 232 (1960).
6) K. Hata, K. Watanabe and H. Watanabe, ibid., **32**, 6 (1959).

by hydrogen gas four times. All operations were carried out under the following condition: (1) acetophenone: 30 g. (0.25 mol.), (2) ethanol: 60 ml., (3) pH: 9~11 (It has been recognized[1,7,8] that the catalytic reduction of carbonyl group with Urushibara catalyst was accelerated by a trace of alkali. When U-Ni-A or U-Ni-CA was used, 1 ml. of 10% sodium hydroxide solution was added.), (4) agitation: 40~45 strokes per minute, (5) reaction temperature: as a remarkable hydrogen uptake was found to begin at about 60°C in reduction of carbonyl group[7], agitation was started when the temperature in the autoclave reached about 60°C, and the temperature was kept between 60 and 70°C throughout the operation, (6) pressure: as it had been found that, in the case of the reduction of carbonyl group under high pressure, the velocity of reduction was only slightly affected by the initial pressure under 100 kg./cm$^2$ [1,7], the effect of the initial pressure was ignored and (7) when the pressure in the autoclave dropped to 20~30 kg./cm$^2$, supplementary hydrogen gas was charged two or three times in every course of the operation, and the reduction was continued until the hydrogen uptake ceased. Pressure was observed at intervals of five minutes.

After the reduction was finished, the catalyst was filtered off and washed with ethanol. From the combined filtrate, the major part of the ethanol was removed by distillation on a water bath, and the residual liquid was distilled under reduced pressure. The fraction, distilling at 89~91°C/15 mmHg, was collected. The yield of methylphenylcarbinol was 91~95 per cent of the theoretical amount.

**Preparation of Catalysts.** — The U-Ni-B[1,2], U-Ni-CB[1], U-Ni-BA[4,5], U-Ni-A[3] and U-Ni-CA[1] were prepared by the methods described in the references cited. Regenerated Urushibara nickel catalyst was prepared from any used catalyst by the following methods. The used catalyst was recovered by filtration after the previous reaction, and dried at about 100°C and stored.

(A) To well-mixed zinc dust (5 g.) and recovered U-Ni-A (1.3 g.) with water (3 ml.) was added 80 g. of 10% sodium hydroxide solution. The mixture was occasionally stirred for 20 min. at 50~55°C and then 5 min. at 75~80°C. At the end of this process, generation of hydrogen gas ceased and grayish white zinc compounds were deposited. The upper liquor was removed by decantation and the residual solid was washed with 200 ml. of hot water and then with two 50 ml. portions of ethanol. Every washing was decanted.

(B) Recovered U-Ni-A (1.3 g.), used in Exp. No. 113 and left standing for 55 days, was well mixed with zinc dust (10 g.) and water (5 ml.). The mixture was treated with 160 g. of 13% acetic acid for about 5 min. As hydrogen gas was vigorously generated at first, good agitation by hand was required to prevent the contents from running over. In this case the solid did not come up to the surface of the solution which was green in color. The solid was collected on a glass filter and washed with 200 ml. of water and then with 100 ml. of ethanol.

(C) To a mixture of the recovered U-Ni-A (1.1 g.) used in Exp. No. 32, zinc dust (5 g.) and water (3 ml.) was added 80 g. of 13% acetic acid. The following procedure was similar to that described in B, and a very fine catalyst was obtained.

(D) To a mixture of recovered U-Ni-A (1.4 g.), zinc dust (2.5 g.) and water (2.5 ml.) was added 40 g. of 13% acetic acid. The following procedure was similar to that described in B.

(E) The recovered U-Ni-B (7.3 g.) used in Exp. No. 11 was treated with 160 g. of 13% acetic acid until the solid came up to the surface of the solution which had turned green. Since the major part of the zinc dust had been removed in the previous preparation of the U-Ni-B, only a small quantity of hydrogen gas was evolved in this process. The solid was collected on a glass filter, and washed with 200 ml. of water and then with 100 ml. of ethanol.

(F) The recovered U-Ni-CB (7 g.) used in Exp. No. 19 was treated with 160 g. of 13% acetic acid. Generation of hydrogen gas was hardly observed, and the solution turned black owing to the suspension of fine solid. After about 8 min. the solid was separated by centrifuge from the solution which was green in color. The solid was washed with two 200 ml. portions of water and then two 50 ml. portions of ethanol in the centrifugal tube. The washings were decanted.

(G) To a mixture of recovered U-Ni-A (1.4 g.) and water (2 ml.) was added 50 g. of 20% acetic acid. The mixture was then digested at 70~75°C for one minute on a boiling water bath. The U-Ni-A reacted vigorously with acetic acid at this temperature. Then solid, adsorbing hydrogen gas, came up to the surface of the solution which was green in color. The solid was collected on a glass filter and washed with 200 ml. of water and then with 100 ml. of ethanol.

(H) The weight of recovered U-Ni-A, prepared so as to contain 1 g. of nickel, being ordinary 1.3 ~1.4 g., the recovered U-Ni-A (0.9 g.) used in Exp. No. 37 was supplemented by 0.5 g. of recovered and stored U-Ni-A. To this was added 2 ml. of water and the mixture was treated as is described in G.

(I) To a mixture of recovered U-Ni-A (1.4 g.) and water (2 ml.) was added 50 g. of 10% acetic acid. The mixture was digested at 75~80°C for one minute on a water bath. The following procedure was similar to that described in G.

In all procedures, distilled water was used for washing, and the obtained catalyst was protected from contact with air as far as possible.

## Results and Discussion

As reported in the preceding paper[1] on the reduction of benzophenone, the activity of various Urushibara nickel catalysts in the reduction of acetophenone was studied by comparing the time required for the completion

7) K. Hata, S. Taira and T. Higase, *J. Chem. Soc. Japan, Pure Chem. Sec.* (*Nippon Kagaku Zasshi*), **78**, 186 (1957).

8) S. Nishimura, ibid., **79**, 56 (1958).

TABLE I. REDUCTION OF ACETOPHENONE WITH VARIOUS URUSHIBARA NICKEL CATALYSTS

| Exp. No. | Catalyst[a] | pH | Total weight of catalyst g.[b] | Initial pressure kg./cm² | Total pressure depression kg./cm² [c] | Initial temp. °C | Reaction temp. °C | Time min. |
|---|---|---|---|---|---|---|---|---|
| 11 | U-Ni-B | 10 | 7.3 | 45 | 56.5 | 22 | 61～70 | 125 |
| 12 | U-Ni-B | 9.7 | 8.6 | 50 | 54.5 | 23 | 60～70 | 90 |
| 13 | U-Ni-B | 9.3 | 7.4 | 47 | 57 | 22 | 61～70 | 80 |
| 14 | U-Ni-B | 9 | 7.5 | 46 | 52 | 21 | 62～70 | 70 |
| 15 | U-Ni-B[d] | 10.6 | 10.5 | 42 | 59 | 25 | 62～70 | 105 |
| 16 | U-Ni-B[d] | 10.5 | 10.8 | 45 | 55 | 21 | 60～70 | 105 |
| 17 | U-Ni-BA | 9.4 | 1.2 | 40.5 | 51 | 25 | 61～70 | 120 |
| 18 | U-Ni-BA | 10.4 | 1.1 | 45 | 50 | 23 | 62～70 | 95 |
| 19 | U-Ni-CB | 9.7 | 7 | 49.5 | 56.5 | 22 | 63～66 | 65 |
| 110 | U-Ni-CB | 10.4 | 9.2 | 50 | 63 | 21 | 61～66 | 60 |
| 111 | U-Ni-CB | 10.7 | 8.4 | 49 | 71 | 30 | 64～69 | 50 |
| 112 | U-Ni-A | 9.5[e] | 1.3 | 47 | 54.5 | 24 | 60～68 | 40 |
| 113 | U-Ni-A | 10 [e] | 1.3[f] | 45 | 51.5 | 24 | 60～68 | 35 |
| 114 | U-Ni-A | 9.8[e] | 1.3 | 46 | 50 | 24 | 61～68 | 35 |
| 115 | U-Ni-A | 9.2[e] | 1.3[f] | 49 | 55.5 | 24 | 62～70 | 25 |
| 116 | U-Ni-CA | 9.5[e] | 0.9[g] | 42 | 49.5 | 20 | 62～69 | 50 |
| 117 | U-Ni-CA | 9.6[e] | 0.8[g] | 47.5 | 55.5 | 20 | 62～66 | 50 |
| 118 | U-Ni-CA | 9.4[e] | 0.6 | 49 | 51 | 17 | 65～70 | 40 |
| 119 | U-Ni-CA | 9.4[e] | 0.7 | 44 | 46.5 | 22 | 61～69 | 40 |

a) Each catalyst was prepared so as to contain 1 g. of nickel.
b) The figures were obtained by weighing the recovered and dried catalysts.
c) Supplementary hydrogen gas was charged two or three times in course of the operation. Every depression of the pressure was sumed up.
d) The catalyst was prepared from the precipitated nickel, obtained from nickel acetate solution and zinc dust.
e) 1 ml. of 10% sodium hydroxide solution was added.
f) About 0.83 g. of nickel was found to be contained by analysis.
g) About 0.57 g. of nickel was found to be contained by analysis.

TABLE II. REDUCTION OF ACETOPHENONE WITH URUSHIBARA NICKEL CATALYSTS PREPARED FROM PRESERVED PRECIPITATED NICKEL[a]

| Exp. No. | Catalyst[b] | pH | Total weight of catalyst g.[c] | Initial pressure kg./cm² | Total pressure depression kg./cm² [d] | Initial temp. °C | Reaction temp. °C | Time min. |
|---|---|---|---|---|---|---|---|---|
| 21 | U-Ni-B | 9.2 | 9 | 48 | 57 | 32 | 60～69 | 85 |
| 22 | U-Ni-B | 9.3 | 8.6 | 47 | 55 | 24 | 60～68 | 50 |
| 23 | U-Ni-A | 9.4[e] | 1.2 | 48 | 53.5 | 27 | 60～68 | 35 |
| 24 | U-Ni-A | 9.7[e] | 1.3 | 50 | 52.5 | 25 | 61～65 | 40 |

a) All catalysts were prepared from precipitated nickel, obtained from nickel chloride solution and zinc dust, washed with water, dried at about 100°C and left standing for a week in the air.
b) Each catalyst was prepared so as to contain 1 g. of nickel.
c) The figures were obtained by weighing the recovered and dried catalysts.
d) Supplementary hydrogen gas was charged twice in course of the operation. Every depression of the pressure was sumed up.
e) 1 ml. of 10% sodium hydroxide solution was added.

of reduction under nearly the same condition.

A series of experiments shown in Table I was carried out to confirm the activity of each catalyst and to offer the standard of reference for the subsequent experiments. The reduction of acetophenone was effectively achieved with U-Ni-B, U-Ni-BA, U-Ni-CB, U-Ni-A and U-Ni-CA, among which U-Ni-A proved to be the most useful. The U-Ni-B, prepared from nickel acetate and zinc dust, which had been found to be similarly active in the reduction of benzophenone, was also effective for the reduction of acetophenone though somewhat less active (Exp. Nos. 15 and 16). The U-Ni-BA, which had been proved to be specially useful for hydrogenation of aromatic nucleus[4,5], was not so particularly active (Exp. Nos. 17 and 18) as it was in the reduction of

TABLE III. REDUCTION OF ACETOPHENONE WITH REGENERATED URUSHIBARA NICKEL CATALYSTS

| Exp. No. | Catalyst (regenerated) | Original catalyst | Method of regeneration[a] | Total weight of catalyst g.[b] | Initial press. kg./cm² | Total press. depression kg./cm²[c] | Initial temp. °C | Reaction temp. °C | Time min. |
|---|---|---|---|---|---|---|---|---|---|
| 31 | U-Ni-B | U-Ni-A | A | 5.7 | 49.5 | 59 | 21 | 60~64 | 130 |
| 32 | U-Ni-A | U-Ni-A | B | 1.1 | 50.5 | 50 | 14 | 65~69 | 30 |
| 33 | U-Ni-A | U-Ni-A | C | 0.9[d] | 45.5 | 51.5 | 20 | 61~64 | 45 |
| 34 | U-Ni-A | U-Ni-A | D | 1.1 | 47 | 52 | 18 | 60~64 | 40 |
| 35 | U-Ni-A | U-Ni-B | E | 1.1[e] | 46 | 55.5 | 21 | 60~68 | 45 |
| 36 | U-Ni-A | U-Ni-CB | F | 0.8[d] | 46.5 | 52.5 | 26 | 63~69 | 60 |
| 37 | U-Ni-A | U-Ni-A | G | 0.9 | 47.5 | 55.5 | 26 | 60~64 | 40 |
| 38 | U-Ni-A | U-Ni-A | H | 0.9 | 48 | 55.5 | 22 | 61~63 | 40 |
| 39 | U-Ni-A | U-Ni-A | I | 0.8 | 48.5 | 54.5 | 20 | 60~65 | 45 |

In all operations excepting Exp. No. 31, 1 ml. of 10% sodium hydroxide solution was added.
a) The marks A, B, C and etc. indicate the paragraphs in Experimental part.
b) The figures were obtained by weighing the recovered and dried catalysts.
c) Supplementary hydrogen gas was charged twice in course of the operation. Every depression of the pressure was sumed up.
d) About 0.5 g. of nickel was found to be contained by analysis.
e) About 0.7 g. of nickel was found to be contained by analysis.

benzophenone[1]. The activities of U-Ni-CB and U-Ni-CA were found to be fairly high, though they were somewhat inferior to that of U-Ni-A.

The usual Urushibara nickel catalysts B and A can be prepared by a simple operation in only one hour or less. Supposing the relation of the precipitated nickel to Urushibara nickel catalyst is similar to that of Raney alloy to Raney nickel catalyst, the operation of preparing Urushibara nickel catalyst is certainly more simplified when precipitated nickel can be stored in the state ready to use. It has been claimed that precipitated nickel is inherently provided with active nickel surfaces and acid or alkali is not effective to create any active state on the surfaces, and that the rôle of acid or alkali is to remove the basic zinc chloride which has been formed by the reaction of zinc dust with nickel chloride solution[3]. It is presumable in this view that exposure of precipitated nickel to air for a long time may cause the deactivation or lowering of activity of the catalyst prepared from it. Some experiments on the preservation of precipitated nickel have already been reported in regard to the preparation of U-Ni-BA[5]. Precipitated nickel prepared from nickel chloride solution with aluminum grains was preserved in distilled water, 99% ethanol or dry state under reduced pressure. The U-Ni-BA, prepared from the preserved precipitated nickel, was unexpectedly shown to have practically the same activity as that which the catalyst prepared from freshly prepared precipitated nickel has.

The present author tried reduction of acetophenone with the U-Ni-B and U-Ni-A obtained from precipitated nickel, which was prepared from nickel chloride solution with zinc dust by the ordinary methods[2,3], dried at about 100°C, and left standing for a week in the air. The results are shown in Table II. These results do not differ from those obtained with the normally prepared U-Ni-B and U-Ni-A. Therefore, contact with air is safely permitted for precipitated nickel. It may not be necessary for the water for washing to be distilled in the preparation of precipitated nickel.

One of the features of the Urushibara nickel catalyst is that it is not self-inflammable by contact with air under ordinary conditions. Consequently, nickel can be recovered from such waste catalyst as nickel chloride which can be used again for the preparation of the Urushibara nickel catalyst. But the operation may be troublesome and expensive. If recovered Urushibara nickel can be repeatedly used in place of the precipitated nickel, the time for preparing the precipitated nickel and the cost of nickel chloride will be saved. For the purpose of attaining this request a series of experiments was carried out to regenerate the active catalyst directly from recovered catalyst (Table III).

First, the U-Ni-B was prepared from the mixture of recovered U-Ni-A and zinc dust by treatment with sodium hydroxide solution. The regenerated catalyst was found to be useful enough for the reduction of acetophenone though it was somewhat less active (Exp. No. 31). The cause of this reactivation was considered to result from the removal of adsorbed substances on the surfaces of nickel particles by hydrogen gas generated from zinc dust with caustic alkali. Then the catalyst prepared from recovered U-Ni-A and zinc dust by

treatment with acetic acid was also expected to have considerable activity. In fact, such a catalyst proved to be highly active and gave a better result than that obtained with the original U-Ni-A (Exp. No. 32). To save the amount of zinc dust, the next catalysts were prepared by using one half or one fourth the amount of zinc dust as the quantity used for preparing the catalyst in Exp. No. 32. They had also high activities (Exp. Nos. 33 and 34), and gave practically the same results as those obtained with the normally prepared U-Ni-A (cf. Exp. Nos. 112—115 in Table I). If the existence of a small amount of zinc is enough to reactivate the recovered catalyst, the recovered U-Ni-B and U-Ni-CB may become active by being treated with acetic acid. Actually, each of the catalysts prepared from the recovered U-Ni-B and U-Ni-CB used in Exp. Nos. 11 and 19, gave a better result than those obtained with the original catalysts (Exp. Nos. 35 and 36). As the recovered U-Ni-B and U-Ni-CB contain only a small quantity of zinc, only a little hydrogen gas is evolved by the digestion with acetic acid. Accordingly, zinc dust is supposed to be excluded from the reagents necessary for the renewal of the catalyst. Thus some catalysts were prepared from recovered U-Ni-A by being treated with acetic acid only, and these catalysts were also found to be highly active (Exp. Nos. 37, 38 and 39). In these cases, however, nickel itself reacted vigorously with hot acetic acid, and solid, adsorbing hydrogen gas, came up to the surface of the green solution. In consideration of the results described above, acetic acid must have, in case of preparing the U-Ni-A, some activating effect on the surfaces of nickel particles besides the chemical function of generating hydrogen gas and removing deactivating substances (basic zinc chloride and others). Probably one important function of acetic acid may consist in eroding the surfaces of nickel particles and creating new ones. This assumption accounts for the reactivation of recovered catalysts and also for the fact that the U-Ni-A has not high activity, when the digestion with acetic acid is interrupted before the solution turns green by the formation of nickel ion[1]. The discussion as to whether or not the precipitated nickel has inherently active nickel surfaces seems not to be important.

## Summary

Catalytic reduction of acetophenone with various Urushibara nickel catalysts was studied under high pressure. The U-Ni-A with a small amount of alkali was found to be the most useful. The U-Ni-CB and U-Ni-CA were also highly active as they were in case of the reduction of benzophenone. The activity of the U-Ni-A and U-Ni-B, prepared from preserved precipitated nickel, was the same as that of the catalysts obtained from the freshly prepared precipitated nickel. In addition, it was found that the recovered Urushibara nickel catalyst could be repeatedly used after a simple regeneration process especially in the form of U-Ni-A. Such a regenerated catalyst had practically the same activity as that of the normally prepared U-Ni-A.

The author wishes to express his thanks to Professor Kazuo Hata for his continuous encouragement throughout this work.

*Department of Chemistry*
*Faculty of Science*
*Tokyo Metropolitan University*
*Setagaya-ku, Tokyo*

# *A Theoretical Treatment of Molecular Complexes. I. Silver-Aromatic Hydrocarbon Complexes*

By Kenichi FUKUI, Akira IMAMURA, Teijiro YONEZAWA and Chikayoshi NAGATA

(Received January 11, 1961)

Theoretical researches of molecular complexes have become active since Mulliken combined the old concepts of molecular compound and established a new theory[1]. Prior to this research many qualitative discussions on molecular complexes had been presented. These are the covalent bond theory by Bennett and Willis[2], the polarization aggregate theory by Briegleb[3], the ionic complex theory by

1) R. S .Mulliken. *J. Am. Chem. Soc.*, **74**, 811 (1952).

2) G. M. Bennett and G. H. Willis, *J. Chem. Soc.*, **1929**, 256.

3) G. Briegleb, *Z. physik. Chem.*, **B16**, 249 (1932).

Weiss[4], and the complex resonance by Brackmann[5]. Weiss had pointed out that molecular complexes have an ionic structure $B^+A^-$, so that the lower the ionization potential for an electron donor is, and the higher the electron affinity for an electron accceptor is, the more easily the molecular complex is formed. Brackmann regarded the structure of complex as a resonance hybrid to which no-bond and dative structures contribute.

$$D:A \leftrightarrow D^+:A^-$$

Based upon these concepts, Mulliken presented a quantum mechanical theory on the charge transfer spectra of molecular complex[1]. Further, Mulliken predicted the configuration of benzene-iodine complex, benzene-silver complex and $BF_3$-$N(CH_3)_3$ complex, and his assumption was proved to be correct except in the case of benzene-iodine complex. With regard to benzene-iodine complex, Aono discussed Mulliken's model and presented a corrected one[6]. It may be true that in spite of these successes, Mulliken's procedure is not very useful to discuss the relative ease of complex formation among different molecules. There are often found some trials of discussing this problem by comparing the magnitude of ionization potentials of electron donors. For example, with respect to the silver-aromatic molecular complex, a correlation between the magnitude of ionization potential of methyl derivatives of 1,2-benzanthracene and their equilibrium constants in complex formation was pointed out by Nakajima[7]. However, this treatment has only a limited application since the ionization potential is not the sole factor relating to the ease of complex formation, and is hence not suitable in discussing the configuration of complex.

In the present paper we make use of the delocalization method in order to approach the conformation of molecular compound, finding a clear correlation between the equilibrium constant and the calculated value of the delocalization energy for silver-aromatic hydrocarbon complexes.

## Model and Formulation

In this paper the delocalization method was applied to silver-aromatic hydrocarbon complexes. Since it has been confirmed by X-ray diffraction that in silver-benzene complex silver cation is located above the middle of a carbon-carbon bond of benzene plane[8], we assume that silver cation approaches from above the molecular plane to the middle of a carbon-carbon bond of a benzene ring in aromatic hydrocarbons to form the molecular complex. The $\pi$ electronic stabilization energy due to delocalization from the occupied orbitals of the aromatic hydrocarbon to the lowest vacant orbital of the silver cation is calculated by the perturbation theory. This procedure is quite similar to the one which has been used in the frontier electron theory presented by some of the present authors[9]. When the aromatic molecule is confined to alternant hydrocarbons and their derivatives, and the silver cation is combined with the $r$th and the $s$th carbon atoms of the aromatic hydrocarbon by a weak bond, the secular equation of the $\pi$ part of the total system which includes the silver cation and the aromatic molecule is written in the simple LCAO MO treatment (overlap neglected) as follows:

$$D(\lambda)=\begin{vmatrix} h-\lambda & 0 & 0 \cdots\cdots 0 & \gamma & \gamma & 0 \cdots\cdots 0 \\ 0 & a_{11}-\lambda & a_{12}\cdots\cdots & a_{rr} & a_{1s} & \cdots\cdots a_{1n} \\ 0 & a_{21} & a_{22}-\lambda\cdots & a_{2r} & a_{2s} & \cdots\cdots a_{2n} \\ \vdots & & & & & \\ 0 & & & & & \\ \gamma & a_{r1} & a_{r2}\cdots\cdots & a_{rr}-\lambda & a_{rs} & \cdots\cdots a_{rn} \\ \gamma & a_{s1} & a_{s2}\cdots\cdots & a_{sr} & a_{ss}-\lambda & \cdots\cdots a_{sn} \\ 0 & & & & & \\ \vdots & & & & & \\ 0 & a_{n1} & a_{n2}\cdots\cdots & a_{nr} & a_{ns} & \cdots a_{nn}-\lambda \end{vmatrix}$$

$$=(h-\lambda)\Delta(\lambda) -\gamma^2\{\Delta_{rr}(\lambda)+\Delta_{ss}(\lambda)-2\Delta_{rs}(\lambda)\} \quad (1)$$

where

$$\Delta(\lambda)=\begin{vmatrix} a_{11}-\lambda & a_{12} & \cdots\cdots & a_{1n} \\ a_{21} & a_{22}-\lambda & \cdots\cdots & a_{2n} \\ \vdots & \vdots & & \vdots \\ a_{n1} & a_{n2} & \cdots\cdots & a_{nn}-\lambda \end{vmatrix} \quad (2)$$

is the secular determinant for the isolated aromatic molecule, and $\Delta_{rr}(\lambda)$, $\Delta_{ss}(\lambda)$, and $\Delta_{rs}(\lambda)$ are the minors of $\Delta(\lambda)$ corresponding to $(rr)$, $(ss)$ and $(rs)$ elements, respectively; $a_{ii}$ and $a_{ij}(i\neq j)$ are the Coulomb and the resonance integrals, respectively; and $h$ and $\gamma$ are the Coulomb integral of the silver cation and the resonance integral between the silver cation and the $r$th and the $s$th atoms of the aromatic molecule at which the delocalization of $\pi$ electron takes place, respectively. In presenting the value of energies, we make the zero point equal to the Coulomb integral of

4) J. Weiss, *J. Chem. Soc.*, **1942**, 245; **1943**, 462.
5) W. Brackmann, *Rec. trav. chim.*, **68**, 147 (1949).
6) S. Aono, *Progr. Theoret. Phys. Japan*, **22**, 313 (1959).
7) T. Nakajima, *The Science Reports of the Tôhoku Univ. Ser. I*, **41**, 171 (1957).
8) R. E. Rundle and J. H. Goring, *J. Am. Chem. Soc.*, **72**, 5337 (1950).
9) K. Fukui, T. Yonezawa and C. Nagata, This Bulletin, **27**, 423 (1954).

benzene carbon and express them in units of $(-\beta)$ which is the resonance integral of the benzene C-C bond. If we designate the roots of $\Delta(\lambda)=0$ and $D(\lambda)=0$ as

$$\lambda_1, \lambda_2, \cdots\cdots \lambda_n\ ;\ \lambda^{(1)}, \lambda^{(2)} \cdots\cdots^{(n)}, \lambda^{(h)}$$
$$(\lambda_1 > \lambda_2 > \cdots\cdots > \lambda_n)$$

respectively, among which $\lambda^{(h)}$ will be very close to the value of $h$ and $\lambda^{(j)}$ to $\lambda_j$ $(j=1,2 \cdots\cdots n)$ since $\gamma$ is small. Namely $\lambda^{(j)}$ and $\lambda^{(h)}$ can be written as $\lambda^{(j)}=\lambda_j+\delta_j$, $\lambda^{(h)}=h+\delta_h$ in which $|\delta_j|$ and $|\delta_h|$ are small. For simplicity, we exclusively treat the following two cases in which $\Delta(\lambda)$ has no multiple root.

Case 1: When $h$ is not equal to any $\lambda_j$, we can obtain $\delta_j$ as

$$\left.\begin{aligned}\delta_j &= 2\left\{\frac{\Delta_{rr}(\lambda_j)}{(h-\lambda_j)\Delta'(\lambda_j)}+\frac{\Delta_{ss}(\lambda_j)}{(h-\lambda_j)\Delta'(\lambda_j)}-\frac{2\Delta_{rs}(\lambda_j)}{(h-\lambda_j)\Delta'(\lambda_j)}\right\}\gamma^2+[\gamma^4] \\ &\qquad (j=1,2\cdots\cdots n) \\ \delta_h &= -\sum_{j=1}^{n}\left\{\frac{\Delta_{rr}(\lambda_j)}{(h-\lambda_j)\Delta'(\lambda_j)}+\frac{\Delta_{ss}(\lambda_j)}{(h-\lambda_j)\Delta'(\lambda_j)}-\frac{2\Delta_{rs}(\lambda_j)}{(h-\lambda_j)\Delta'(\lambda_j)}\right\}\gamma^2 \\ &\quad +[\gamma^4]\end{aligned}\right\} \quad (3)$$

where $[\gamma^4]$ denotes the higher terms. The delocalization energy, $\Delta E$, is defined as follows:

$$\Delta E = 2\sum_{j=1}^{m}(\lambda^{(j)}-\lambda_j) \quad (4)$$

$$=2\sum_{j=1}^{m}\left\{\frac{\Delta_{rr}(\lambda_j)+\Delta_{ss}(\lambda_j)-2\Delta_{rs}(\lambda_j)}{(h-\lambda_j)\Delta'(\lambda_j)}\right\}\gamma^2+[\gamma^4]$$

$$=-2\sum_{j=1}^{m}\frac{(C_r^j+C_s^j)^2}{h-\lambda_j}\gamma^2+[\gamma^4] \quad (5)$$

where $j=1,2\cdots\cdots m$ denote the occupied orbitals, and the $r$th and the $s$th carbon atoms are adjacent to each other. And $C_r^j$ is the coefficient of the $r$th atomic orbital in the $j$th molecular orbital of the isolated aromatic molecule. When $h$ is equal to zero, then the total delocalization energy becomes

$$\Delta E=\{S_r^{(E)}+S_s^{(E)}+2S_{rs}^{(E)}\}\gamma^2+[\gamma^4] \quad (6)$$

where $S_r^{(E)}$, $S_s^{(E)}$ are superdelocalizabilities at the $r$th and the $s$th carbon atoms for the electrophilic reaction[9], and $S_{rs}^{(E)}$ is given in Eq. 7 and may be named bond-delocalizability of the bond $rs$.

$$S_{rs}=\sum_{j=1}^{n}\frac{(\nu_j-\nu)C_r^jC_s^j}{\lambda_j} \quad (7)$$

where $\nu_j$ is the number of $\pi$ electrons in the $j$th molecular orbital and $\nu$ is the number of $\pi$ electrons in the approaching orbital to or from which the delocalization of electrons occurs. $S_{rs}^{(E)}$ designates $S_{rs}$ in which $\nu=0$.

The formula obtained by Eq. 5 indicates that the magnitude of delocalization energy depends sensitively upon the local symmetry of the molecular orbital; that is to say, when $C_r^j$ and $C_s^j$ have same signs, the magnitude of delocalization energy is large, while it is small in case of different signs. It may be stressed that a conclusion similar to that of Mulliken has thus been derived by the present treatment.

Case 2: When $h$ is equal to the energy of the highest occupied orbital of the isolated aromatic molecule $\lambda_f$,

$$\left.\begin{aligned}\delta_j &= 2\left\{\frac{\Delta_{rr}(\lambda_j)}{(h-\lambda_j)\Delta'(\lambda_j)}+\frac{\Delta_{ss}(\lambda_j)}{(h-\lambda_j)\Delta'(\lambda_j)}-\frac{2\Delta_{rs}(\lambda_j)}{(h-\lambda_j)\Delta'(\lambda_j)}\right\}\gamma^2+[\gamma^4] \\ &\qquad (j=1,2,\cdots\cdots n) \\ \left.\begin{matrix}\delta_h\\ \delta_f\end{matrix}\right\} &= \pm\sqrt{-\frac{\Delta_{rr}(h)+\Delta_{ss}(h)-2\Delta_{rs}(h)}{\Delta'(h)}} \\ &\quad \times\gamma+[\gamma^2]\end{aligned}\right\} \quad (8)$$

and the delocalization energy depends dominantly upon the term of first order. Hence, we obtain

$$\Delta E=2\sqrt{-\frac{\Delta_{rr}(h)+\Delta_{ss}(h)-2\Delta_{rs}(h)}{\Delta'(h)}}\gamma+[\gamma^2]$$
$$=2|C_r^f+C_s^f|\gamma+[\gamma^2] \quad (9)$$

It may be remarked that in case 2, the magnitude of $\Delta E$ depends upon the local symmetry of the highest occupied orbital, the frontier orbital at the bond to be attacked.

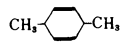
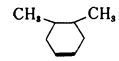
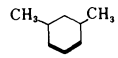
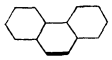
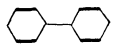
Then the following conclusion can be derived. When $h$ is not equal to any $\lambda_j$, the larger the value of $-\sum_j\frac{(C_r^j+C_s^j)^2}{h-\lambda_j}$ is, the easier the molecular complex formation is, and when $h$ is equal to $\lambda_f$, the reactivity is proportional to $|C_r^f+C_s^f|$.

## Results and Discussion

The easiness of the molecular complex formation depends upon many factors such as delocalization energy, dispersion energy, exchange repulsion energy and electrostatic energy. Therefore, the reactivity should be discussed under consideration of all these factors. In discussing the relative easiness of complex formation of a series of similar compounds, however, it is expected that the energies, other than delocalization energy, contributing to the activation energy, may be approximately constant or negligible. In such a case, the delocalization energy is considered to play a dominant role.

In the present paper, an attempt is made to

TABLE I. THE VALUES OF THE INDEX FOR COMPLEX FORMATION AND THE EQUILIBRIUM CONSTANT FOR THE COMPLEX BETWEEN SILVER CATION AND AROMATIC COMPOUNDS

| Aromatic compound | $K_1$ (mol./l.)$^{-1}$ | $S_r^{(E)}+S_s^{(E)}+2S_{rs}^{(E)}$ | Energy of the highest occupied orbital |
|---|---|---|---|
|  | 2.41 | 1.333 | −1.000 |
|  | 2.63 | 1.402 | −0.669 |
|  | 2.89 | 1.553 | −0.707 |
|  | 2.95 | 1.418 | −0.823 |
|  | 3.03 | 1.466 | −0.763 |
|  | 3.08 | 1.600 | −0.618 |
|  | 3.67 | 1.798 | −0.605 |
|  | 3.94 | 1.370 | −0.705 |
|  | 6.3 | 2.139 | −0.504 |
|  | 18.2 | 2.089 | −0.662 |

Thick lines in the figure of aromatic compounds indicate the bonds with maximum value of the index, which are assumed to be the positions of attack by silver cations.

With regard to toluene and xylene, and carbon-carbon bond adjacent to the methyl group is not taken into account for the sake of steric circumstances.

$K_1$ is the equilibrium constant for the following reaction

$$Ag^+ + Ar = AgAr^+ \qquad K_1 = (AgAr^+)/(Ag^+)(Ar)$$

explain the reactivity of complex formation of a series of similar compounds by the consideration of the delocalization energy only. The delocalization energies calculated by the formulas stated above are tabulated in Table I together with the equilibrium constants of the first step of the molecular complex formation between silver cation and aromatic compound[10]. A clear parallelism is seen between the index and the equilibrium constant. The parameters used in calculation for methyl group are as follows.

$\alpha_{CH_3}$ (Coulomb integral for methyl group in Eq. 1) = 3

$\beta_{C\text{-}CH_3}$ (resonance integral for $CH_3$-C bond in Eq. 1) = 1

The energies of the highest occupied levels thus obtained are compared with the observed ionization potentials in Table II. At a glance at this table, a good parallelism is observed between the ionization potential and the energy of the highest occupied level. This implies that the adopted parameters should be appropriate.

TABLE II. RELATION BETWEEN THE IONIZATION POTENTIAL AND THE HIGHEST OCCUPIED LEVEL IN AROMATIC COMPOUNDS

| Aromatic compound | Ionization potential eV. | Highest occupied level |
|---|---|---|
| Benzene | 9.24[a] | −1.000 |
| Toluene | 8.82[b] | −0.823 |
| *m*-Xylene | 8.58[a] | −0.763 |
| *o*-Xylene | 8.58[a] | −0.707 |
| *p*-Xylene | 8.48[a] | −0.669 |
| Naphthalene | 8.12[a] | −0.618 |

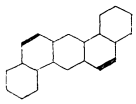
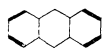
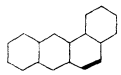
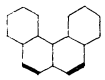
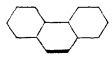
a; From F. H. Field and J. L. Franklin, "Electron Impact Phenomena", Academic Press, Inc., New York (1957).

b; K. Watanabe, *J. Chem. Phys.*, **26**, 542 (1957).

The value of index for *o*-xylene seems too large. This discrepancy may partly be ascribed to the neglect of the effect of the steric hindrance between two methyl groups. With regard to biphenyl, the calculation is carried out with

10) L. J. Andrews and R. R. M. Keefer, *J. Am. Chem. Soc.*, **71**, 3644 (1949); **72**, 5034 (1950).

TABLE III. THE VALUES OF THE INDEX FOR COMPLEX FORMATION AND THE EQUILIBRIUM CONSTANT FOR THE COMPLEX BETWEEN SILVER CATION AND POLYCONDENSED AROMATIC HYDROCARBONS

| Aromatic compound | $K_1$ | $S_r^{(E)}+S_s^{(E)}+2S_{rs}^{(E)}$ | Energy of the highest occupied orbital |
|---|---|---|---|
|  | 1.65 | 1.864 | −0.474 |
|  | 1.35 | 1.747 | −0.414 |
|  | 1.33 | 1.900 | −0.452 |
|  | 1.30 | 1.737 | −0.568 |
|  | 1.09 | 1.798 | −0.605 |

Thick lines in the figure of aromatic compounds indicate the bonds with maximum value of the index, which are assumed to be the positions of attack by silver cations.

$K_1$ is the equilibrium constant for the following reaction.

$$Ag^+ + Ar = AgAr^+ \qquad K_1 = (AgAr^+)/(Ag^+)(Ar)$$

the assumption that this compound has a plane structure. Experimental data show that this compound is not planar. If two benzene nuclei are but little conjugated with each other, the value of the equilibrium constant for this compound may reasonably be expected to be approximately twice as large as that of benzene as was pointed out by Andrews et al.[10] On the other hand, the index is scarcely affected by the degree of conjugation between two benzene nuclei. On the occasion of comparison with the value of the index, therefore, the observed value of equilibrium constant must be divided by a factor which is larger than unity and smaller than two. This is the reason why the observed value of the equilibrium constant seems too large in comparison with the magnitude of the index calculated.

It seems that also the value of energy of the highest occupied orbital can be a good measure for complex formation. This fact shows that the ionization potential is also useful as a rough index to discuss the easiness of complex formation, though it is impossible to predict the position of attack as stated above.

Furthermore, the complex formation in polycondensed aromatic hydrocarbons is treated in a similar manner and the results are shown in Table III. In this series the parallelism between the value of index and equilibrium constant[11] is not so good. In these polycondensed aromatic hydrocarbons their molecular size is not uniform. The coordination with silver cations may take place at more than one positions in a molecule which has more than one positions of equal or nearly equal reactivity. One silver cation which has already added to a position in a hydrocarbon molecule will not exert a substantial influence upon the later addition of another silver cation to another position in the same molecule, provided these two positions are sufficiently apart from each other. In such a case, in order to be compared with the calculated value of the theoretical index, the observed value of the equilibrium constant must be modified by considering the number of sites in one molecule as is stated above in the case of biphenyl.

Another factor influencing the easiness of the complex formation is the polarizability which may be different in various cases. This means that ion-induced dipole interactions are not uniform from molecule to molecule, and it is indispensable for the prediction of reactivity to take the ion-dipole interaction into account. This point will be discussed in future.

*Faculty of Engineering*
*Kyoto University*
*Sakyo-ku, Kyoto*

11) R. E. Kofahl and H. J. Lucas, *J. Am. Chem. Soc.*, 76, 3931 (1954).

# *Infrared Spectra of Cyclohexanoxime and Cyclohexanoxime-d*

By Masao KIMURA, Yoko KURODA, Osamu YAMAMOTO* and Masaji KUBO

(Received January 17, 1961)

Although several studies have been made on the infrared spectra of oximes, most of them have dealt with OH and C=N stretching vibration. Other vibrational frequencies of the functional group of oximes such as those of the NO stretching, the OH bending, etc. have attracted less attention. The infrared spectra of diacetyl monoxime and isonitrosoacetone have already been reported[1]. The study was undertaken in an attempt to inquire into the character of the absorption spectra of oximes. However, each molecule of these compounds has a carbonyl group in conjugation with a C=N bond. Moreover, the type of hydrogen bondings in these compounds could not be determined uniquely, because both a nitrogen atom and an oxygen atom in an oxime group as well as the oxygen atom of a carbonyl group may take part in hydrogen bonds as a proton acceptor. In the present study, it is attempted to assign the observed bands of cyclohexanoxime and cyclohexanoxime-*d* to various modes of the functional group. These compounds are devoid of conjugate systems. In addition, the crystal structure of cyclohexanoxime has already been determined by X-ray analysis[2]. It is reported that the crystal consists of trimers linked by O-H···N hydrogen bonds. Accordingly, all absorption bands, at least those observed in the spectra of the solid, can be interpreted as arising from the vibrations of assciated molecules linked by hydrogen bonding of this type.

The infrared spectrum of cyclohexanoxime has been recorded by Cross and Rolfe[3], Palm and Werbin[4], Califano and Lüttke[5], Matsui[6] and Bredereck et al.[7], but no complete assignment of bands has been carried out as yet.

## Experimental

A commercial preparation of cyclohexanoxime was purified by recrystallization from a solution in ligroin. A deuterated sample was prepared by exchanging hydrogen of OH groups with deuterium from heavy water. These samples were dried before use.

The spectra were taken with a Hilger H-800 spectrophotometer equipped with rock-salt and potassium bromide prisms, the region scanned covering 4000~500 $cm^{-1}$. Both potassium bromide disks and Nujol or hexachlorobutadiene mulls were employed for taking the spectra of solids. Solutions of various concentrations in carbon tetrachloride and carbon disulfide were also used in order to observe changes in absorption intensity with concentration. All the infrared spectra were recorded at room temperature.

## Assignment and Discussion

All absorptions associated with the functional group -C=N-OH of oximes except for the C=N stretching vibration are expected to show an appreciable concentration dependence, just as is observed in the spectra of diacetyl monoxime and isonitrosoacetone[1]. On deuteration, new bands arising from OD groups should appear in place of all bands attributable to OH groups. Therefore, attention was paid especially to the concentration dependence of absorption intensity as well as to the disappearance of certain bands on deuteration. Bands involving changes in intensity with concentration are listed in Table I. The C=N stretching frequency is also given in Table I, since it is considered to be a frequency characteristic of the functional group of oximes.

**OH and OD Stretching Frequencies, $\nu$(OH) and $\nu$(OD).**—For the OH stretching vibration, a single sharp band and a composite broad band consisting of two sub-maxima were observed in the range 3600~3000 $cm^{-1}$ (Fig. 1). The intensity of the latter band became strong with increasing concentration at the expense of that of the former. Only the broad band was present in the spectrum of the solid. These bands shifted towards much lower frequencies on deuteration (Table I). The band of the OD stretching vibration showed a general pattern and a concentration change almost identical with those of the OH stretching

* Present address: Kao Soap Company, Wakayamashi.

1) M. Kimura, Y. Kuroda, H. Takagi and M. Kubo, This Bulletin, 33, 1086 (1960).

2) Y. Okaya, A. Shimada and I. Nitta, ibid., 29, 210 (1956).

3) L. H. Cross and A. C. Rolfe, *Trans. Faraday Soc.*, 47, 354 (1951).

4) A. Palm and H. Werbin, *Canad. J. Chem.*, 31, 1004 (1953).

5) S. Califano and W. Lüttke, *Z. physik. Chem., N. F.* 5, 240 (1955).

6) Y. Matsui, Symposium on Infrared and Raman Spectroscopy, Tokyo, September, 1959.

7) H. Bredereck, A. Wagner, D. Hummel and H. Kreiselmeier, *Ber.*, 89, 1532 (1956).

TABLE I. FREQUENCIES OBSERVED FOR THE FUNCTIONAL GROUP OF CYCLOHEXANOXIME AND CYCLOHEXANOXIME-*d*

| Frequency, $cm^{-1}$ -CNOH | Frequency, $cm^{-1}$ -CNOD | Intensity change on dilution | Assignment |
|---|---|---|---|
| 3598* | | increase | $\nu$(OH), free |
| 3250, 3115 | | decrease | $\nu$(OH), assoc. |
| | 2670* | increase | $\nu$(OD), free |
| | 2400 | decrease | $\nu$(OD), assoc. |
| 1662 | 1652 | no change | $\nu$(C=N) |
| 1480 A** | | decrease | $\delta$(OH), assoc. |
| 1372* B | | increase | $\delta$(OH), free |
| 1237* C | | increase | $\delta$(OH), free |
| | 1080 A' | decrease | $\delta$(OD), assoc. |
| | 1015* B' | increase | $\delta$(OD), free |
| | 971* C' | increase | $\delta$(OD), free |
| 961 D | 955 D' | decrease | $\nu$(NO), assoc. |
| 948* E | 944* E' | increase | $\nu$(NO), free |
| 933* F | 930* F' | increase | $\nu$(NO), free |
| 795 | | | $\gamma$(OH), assoc. (solid) |
| 740* | | decrease | $\gamma$(OH), assoc. (soln.) |
| | 580 | | $\gamma$(OD), assoc. (solid) |
| | 535* | decrease | $\gamma$(OH), assoc. (soln.) |

* These bands were not found in the spectra of the solid.
** Some of the peaks in Figs. 2 and 3 are indicated by letters.

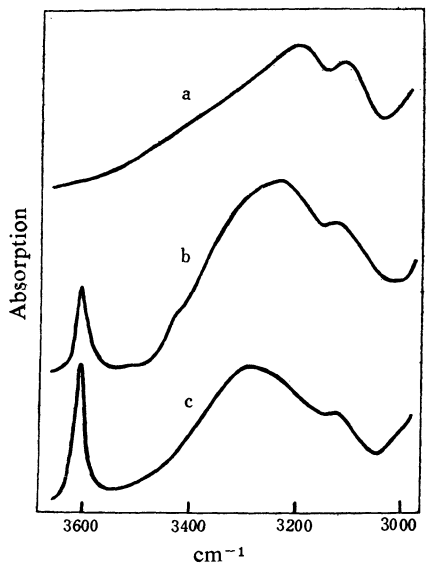



Fig. 1. Infrared absorption spectra of cyclohexanoxime. (a) Solid in a KBr disk, 2 mg./200 mg. KBr. (b) 0.24 mol./l. $CCl_4$ solution, 0.2 mm. cell. (c) 0.10 mol./l. $CCl_4$ solution, 0.53 mm. cell.

vibration. However they were masked by the absorption bands of carbon dioxide to such an extent that it was not feasible to locate them exactly. The single sharp band and the broad band were ascribed to the stretching vibrations of the OH or OD bond of free molecules and associated molecules, respectively.

The broad band of bonded OH groups at about 3200 $cm^{-1}$ showed nearly the same appearance regardless of the state of the samples (Fig. 1), indicating that the type of hydrogen bonding formed in solution was -OH···N=C<. The appearance of the band was almost independent of the concentration of solutions. Accordingly, the presence of two sub-maxima in the bonded OH stretching band observed in solutions is not attributable to different kinds of hydrogen bondings or to various polymeric molecules involving hydrogen bondings of various extents. In the spectra of diacetyl monoxime and isonitrosoacetone, similar composite absorptions having few sub-maxima were observed for the bonded OH stretching vibrations. In the previous paper, the form of hydrogen bonding was presumed for these compounds to be of the -OH···O=C< type. However, unlike the behavior of the stretching band of bonded OH groups in cyclohexanoxime, the shape of the bands and the position of the sub-maxima in the spectra of diacetyl monoxime and isonitrosoacetone changed to some extent with the state of aggregation and also with the concentration of solutions. The frequency shift of the OH stretching vibration caused by association was about 240 $cm^{-1}$ in diacetyl monoxime and isonitrosoacetone, whereas it was about 400 $cm^{-1}$ in cyclohexanoxime. This suggests that the

hydrogen bonds in cyclohexanoxime are different from and stronger than those in diacetyl monoxime and isonitrosoacetone.

**C=N Stretching Frequency, $\nu$(C=N).** — Only one absorption band of medium intensity could be observed in the range 1750～1500 $cm^{-1}$ (Table I). Accordingly, this absorption was assigned to the C=N stretching vibration. The band showed no change in its intensity with concentration and state, although deuteration caused a slight lowering of the frequency.

The value of 1662 $cm^{-1}$ for the C=N stretching vibration is in agreement with 1669 $cm^{-1}$ reported by Cross and Rolfe[3], 1662 $cm^{-1}$ by Palm and Werbin[4] and 1665 $cm^{-1}$ by Bredereck et al.[7] These values are characteristic of unconjugated oximes such as acetaldoxime and formaldoxime and are higher than those of conjugated oximes such as diacetyl monoxime (1630 $cm^{-1}$) and isonitrosoacetone (1613 $cm^{-1}$). Since in cyclohexanoxime, diacetyl monoxime and isonitrosoacetone, association caused no frequency shift of the C=N stretching band while deuteration was accompanied by a shift of only about 10 $cm^{-1}$, a separation between the C=N stretching frequencies of conjugated and

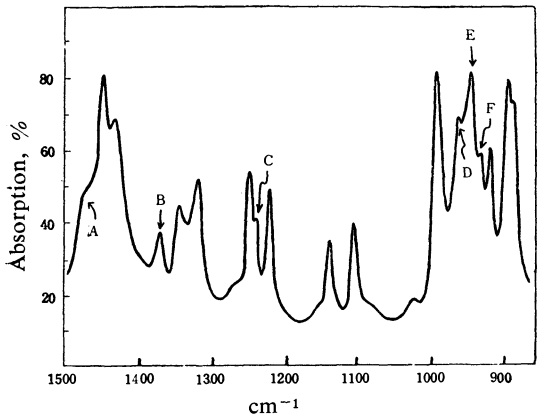



Fig. 2a.

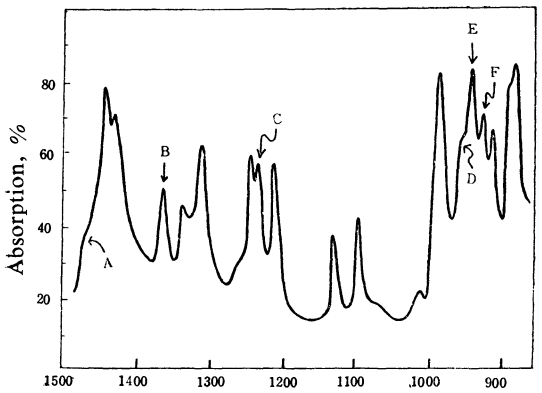



Fig. 2b.

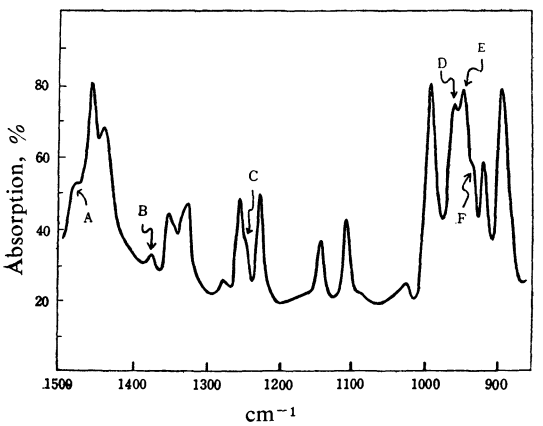



Fig. 2c.

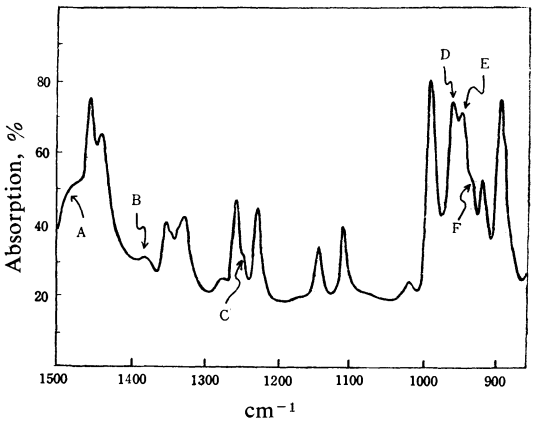



Fig. 2d.

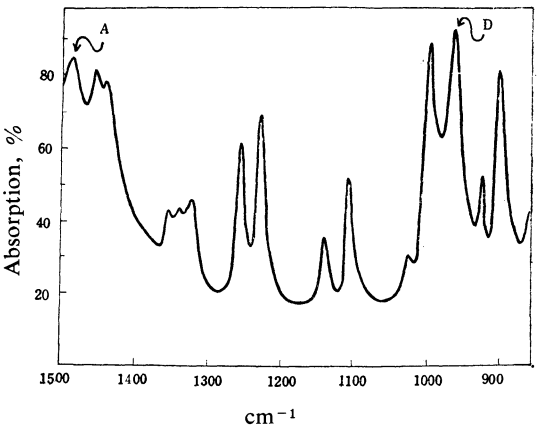



Fig. 2e.

Fig. 2. Infrared absorption spectra of cyclohexanoxime. (a) 0.055 mol./l. $CCl_4$ or $CS_2$ solution, 1.6 mm. cell. (b) 0.22 mol./l. $CCl_4$ or $CS_2$ solution, 0.4 mm. cell. (c) 0.88 mol./l. $CCl_4$ solution, 0.1 mm. cell. (d) 1.77 mol./l. $CCl_4$ solution, 0.05 mm. cell. (e) Solid in a KBr disk, 2 mg./200 mg. KBr.

unconjugated oximes is presumably due to the difference in the double bond character of the C=N bond. In fact, the C=N bond of *p*-benzoquinone monoxime involving a very strong conjugation absorbs at 1555 $cm^{-1}$, which is much lower than the corresponding wave number of diacetyl monoxime and isonitrosoacetone[8].

**OH and OD In-plane Bending Frequencies, $\delta$(OH) and $\delta$(OD), and Out-of-plane Bending Frequencies, $\gamma$(OH) and $\gamma$(OD).** — Bands disappearing on deuteration and the corresponding bands of the deuterated compound are associated with the absorptions by OH and OD groups, respectively (Table I). Such bands appearing below 1500 $cm^{-1}$ can be classified into two groups on the basis of their frequencies and the widths. One of them includes bands showing a distinct absorption peak in the higher frequency region except for a band at 1480 $cm^{-1}$, which was partly masked by a strong absorption due to the $CH_2$ bending. The other is comprised of relatively diffuse bands appearing in the lower frequency region. Bands at 1480, 1372 and 1237 $cm^{-1}$ and the corresponding bands of the deuterated compound at 1080, 1015 and 971 $cm^{-1}$ belong to the former group and must be ascribed to the in-plane bending vibration of the OH and OD groups, respectively, because they are in a wave number range, in which this kind of vibration is usually expected (Figs. 2 and 3). The band of cyclohexanoxime near 750 $cm^{-1}$ and that of the deuterated compound at about 550 $cm^{-1}$ belong to the latter group and were assigned to the out-of-plane bending vibration of the OH and OD groups, respectively (Figs. 4 and 5). No absorption band arising from the OH out-of-plane bending vibration of free molecules will be observed in the potassium

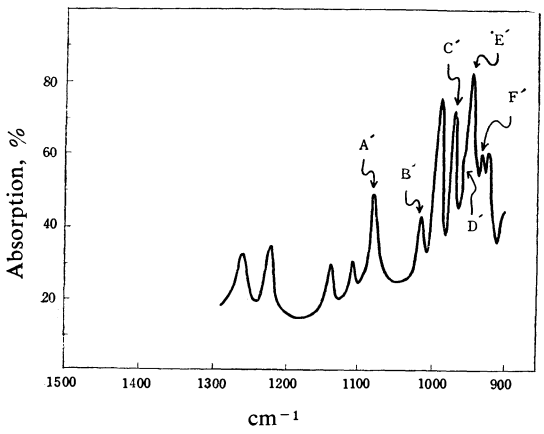



Fig. 3a.

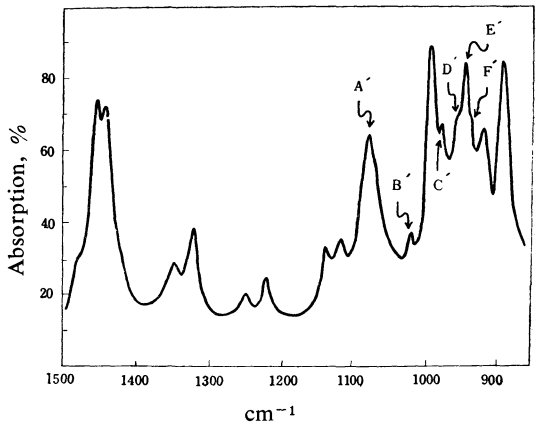



Fig. 3b.

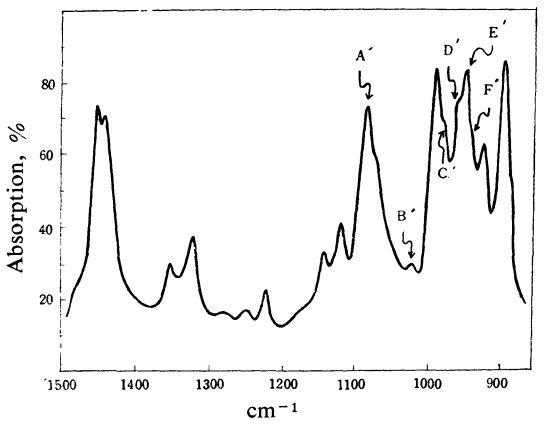



Fig. 3c.

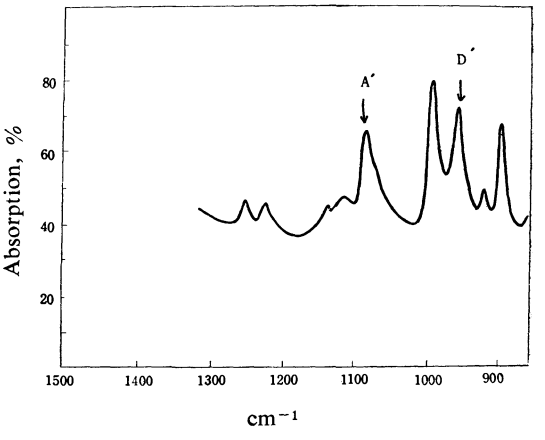



Fig. 3d.

Fig. 3. Infrared absorption spectra of cyclohexanoxime-*d*. (a) 0.035 mol./l. $CS_2$ solution, 1.5 mm. cell. (b) 0.22 mol./l. $CCl_4$ or $CS_2$ solution, 0.5 mm. cell. (c) 0.56 mol. $CCl_4$ solution, 0.2 mm. cell. (d) Solid in a Nujol mull.

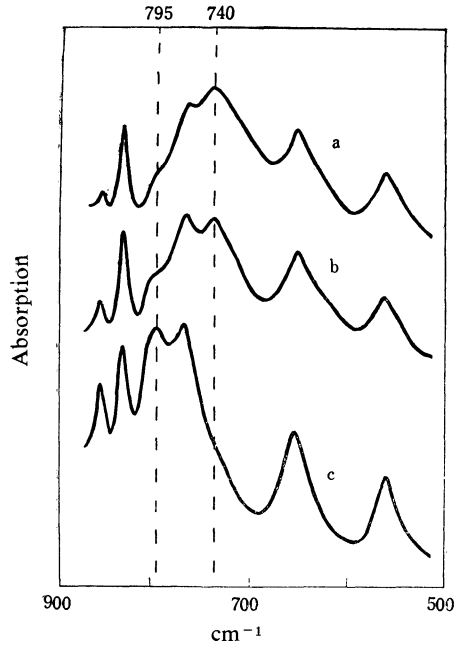



Fig. 4. Infrared absorption spectra of cyclohexanoxime. (a) 0.168 mol./l. $CS_2$ solution, 0.53 mm. cell. (b) 1.04 mol./l. $CS_2$ solution, 0.083 mm. cell. (c) Solid in a Nujol mull.

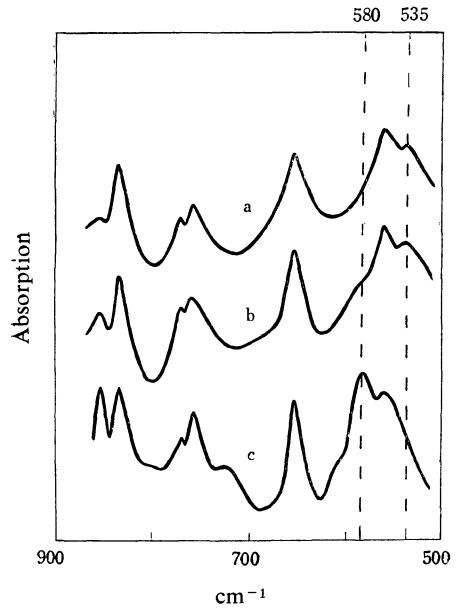



Fig. 5. Infrared absorption spectra of cyclohexanoxime-*d*. (a) 0.168 mol./l. $CS_2$ solution, 0.53 mm. cell. (b) 1.04 mol./l. $CS_2$ solution, 0.083 mm. cell. (c) Solid in a Nujol mull.

bromide region. Generally speaking, the OH or OD bending frequency of associated molecules of organic compounds is higher than that of free molecules. Bands arising from free molecules must be absent in the spectra of solids. Thus, the band of cyclohexanoxime at 1480 $cm^{-1}$ and that of the deuterated compound at 1080 $cm^{-1}$ were reasonably assigned to the vibration of associated molecules. This assignment is consistent with the change of intensity with concentration.

Two bands were found to be associated with the OH in-plane bending vibration of free molecules. A similar situation was observed in some alcohols by Tarte and Deponthière[9] and Maclou and Henry[10]. For instance, Tarte and Deponthière have reported two bands at 1243 and 1030 $cm^{-1}$ for ethanol vapor and assigned them to the OH in-plane bending vibration of free molecules, because these bands were replaced by two bands at 890 and 790 $cm^{-1}$ on deuteration. As was pointed out Tarte and Deponthière, two reasons are conceivable for the origin of the appearance of two bands: rotational isomerism about a C-O bond and some coupling such as Fermi resonance. Pritchard and Nelson[11] interpreted the bands of *tert*-butanol in solutions at 1329 and 1141 $cm^{-1}$ as the coupled bands of the $CH_3$ rocking and the OH in-plane bending of free molecules. However, such coupling seems unlikely to exist in cyclohexanoxime. The ratio of the product of two frequencies for the OH in-plane bending vibration and that for the OD in-plane bending vibration is 1.72 rather than $\sqrt{2}$ as expected from the product rule. The value seems to favor an interpretation of the double band in terms of rotational isomerism about an N-O bond. Such double OH bending frequency was not observed for diacetyl monoxime and isonitrosoacetone. In these compounds, a lower frequency band due to free OH groups might be masked by other strong absorption bands, although it is conceivable that these compounds have a single OH in-plane bending band. Califano and Lüttke did not mention the double character of the free OH bending vibration in their study on acetaldoxime and formaldoxime. Further examination is required in order to elucidate this problem.

Bands at 795 and 580 $cm^{-1}$ observed in the crystals of cyclohexanoxime and cyclohexanoxime-*d*, respectively, could not be observed even in concentrated solutions. However, new very broad bands appeared at 740 and 535 $cm^{-1}$. The frequency difference between crystals and solutions will be due to the different molecular environments.

8) D. Hadži, *J. Chem. Soc.*, **1956**, 2725.
9) P. Tarte and R. Deponthière, *J. Chem. Phys.*, **26**, 962 (1957).
10) M. Maclou and L. Henry, *Compt. rend.*, **244**, 1494 (1957).
11) J. G. Pritchard and H. M. Nelson, *J. Phys. Chem.*, **64**, 795 (1960).

**NO Stretching Frequeny, $\nu$(NO).**—Bands at 961, 948 and 933 $cm^{-1}$ and the corresponding bands of the deuterated compound at 955, 944 and 930 $cm^{-1}$ can be assigned unequivocally to the NO stretching vibrations (Figs. 2 and 3). From their concentration dependence, it is evident that the band of cyclohexanoxime at 961 $cm^{-1}$ and that of the deuterated compound at 955 $cm^{-1}$ are due to the NO stretching vibration of associated molecules.

Two bands were assigned to the NO stretching vibration of free molecules. They can possibly be ascribed to the respective NO stretching absorptions of two isomers. This fact provides an indirect but additional evidence in favor of the presence of rotational isomers. Deuteration gave rise to a slight shift of the NO stretching frequency to a lower frequency, while association caused a shift to a higher frequency by about 13 $cm^{-1}$, which is nearly equal to the amount of shift observed in diacetyl monoxime and isonitrosoacetone[1]. The NO stretching frequency observed in the present study is lower than those of *p*-benzoquinone monoxime and naphthoquinone monoximes[8] at about 1000 $cm^{-1}$, but is much higher than those of alkyl nitrites[12] covering a range 814 $\sim$751 $cm^{-1}$.

12) P. Tarte, *Bull. soc. chim. Belges*, **60**, 227 (1951); *J. Chem. Phys.*, **20**, 1570 (1952).

**Summary**

The infrared absorption bands due to the functional group of cyclohexanoxime and cyclohexanoxime-*d* were reasonably assigned by taking into account the concentration dependence of these bands in solutions. Cyclohexanoxime having no conjugate system showed a spectral feature different in many respects from that of diacetyl monoxime or isonitrosoacetone already studied. The type of hydrogen bonding is -OH···N=C< both in solutions and in the solid state. Consequently, the stretching frequency of bonded OH groups of cyclohexanoxime is different from those of diacetyl monoxime and isonitosoacetone. The doubling of absorption bands was observed for both the OH in-plane bending vibration and the NO stretching vibration of free molecules. This suggests the presence of rotational isomers. The wave numbers of the C=N stretching vibration is higher, while that of the NO stretching vibration is lower than those of the corresponding vibrations of diacetyl monoxime and isonitrosoacetone. This indicates that the double bond character of the C=N bond in cyclohexanoxime is greater than that in oximes having a conjugate system.

*Department of Chemistry*
*Nagoya University*
*Chikusa-ku, Nagoya*

# *Dye-sensitized Photopolymerization of Vinyl Compounds. Polymerization of Acrylonitrile by Stannous Chloride and Acriflavine. I**

By Ai WATANABE and Masao KOIZUMI

(Received January 17, 1961)

The photochemical polymerization of vinyl compounds in the presence of a dye and a suitable reducing agent has been found by Oster[1], and it has been proposed that the initiation step is due to a certain kind of radical produced by the action of the oxygen upon leuco dye, which has been formed by the reduction of the original dye. It seems that most of the reactions can be well interpreted by this scheme, and yet there are only a few cases in which detailed kinetic studies have established the above scheme.

For example, the photopolymerization of acrylonitrile in the presence of a dye and a metallic ion such as $Sn^{2+}$, has not yet fully investigated, though it has been established by Oster that such systems are excellent for the preparatory purpose[2].

In the course of the preliminary investigations upon such systems which include more than twenty dyes and various reducing agents such as potassium thiocyanate, thiourea (TU), ascorbic acid (AA), sodium thiosulfate, stannous chloride etc., it was felt that a different scheme may occur in certain cases, especially in cases

* Partly presented at the 12th Annual Meeting of the Chemical Society of Japan, Kyoto, April, 1959.

1) G. Oster, *Nature*, 173, 300 (1954).

2) G. Oster, *Chem. Abstr.*, 53, 12747 (1959).

TABLE I. SOME RESULTS OF THE PRELIMINARY EXPERIMENTS
[D] = $1.2\times10^{-4}$ M, [reducing agent] = 0.12 M

| | | KSCN | TU | AA | $SnCl_2$** | $Na_2S_2O_3$ | None |
|---|---|---|---|---|---|---|---|
| Thionine | P | + | + | − | + | − | − |
| | B | ++ | ++ | (+) | +++ | | |
| Methylene blue | P | + | + | − | ++ | − | − |
| | B | + | ++ | (+) | +++ | ++ | |
| Uranine | P | − | ± | − | ± | − | − |
| | B | | + | (+) | + | | |
| Eosine | P | ++ | ++ | − | − | + | − |
| | B | + | + | + | ++ | | |
| Erythrosine* | P | ++ | ++ | ++ | ± | + | − |
| | B | ++ | + | ++ | ++ | | |
| Acridine yellow | P | − | + | ± | +++ | − | − |
| | B | | | | | ++ | |
| Acriflavine | P | − | − | ± | +++ | − | − |
| | B | | | | | | |

* Concentration is less than $10^{-4}$ M.
** ca. $2.9\times10^{-2}$ N HCl solution
P: Polymerization, B: Bleaching
+ and − represent respectively the occurrence and non-occurrence of the reaction. The number of + signs roughly gives the magnitude of the reaction. (+) shows that the bleaching takes place completely or nearly completely when mixed.

where stannous chloride is used as a reducing agent. Hence using acriflavine which was found to be most efficient in combination with stannous chloride, we have examined kinetically the effect of various factors upon the rate of photopolymerization. This paper pertains to the results obtained when the system containing dimethylformamide (DMF), water, acrylonitrile (AN), acriflavine (Af or D) and stannous chloride was irradiated in the presence of oxygen.

## Preliminary Experiment

More than twenty dyes were tested preliminarily for examining their efficiency in promoting the polymerization, when they were added to the mixture of AN, water, methanol (2 : 1 : 1.2 in volume) containing potassium thiosulfate, TU, AA, sodium thiosulfate or stannous chloride as reducing agents. The samples in test tubes were irradiated by a 100 V.-500 W projection lamp (used at 80 V.) placed 10 cm. apart from the tubes for 1 hr. The magnitude of polymerization was visually judged from the quantity of the precipitate produced. The purpose of the experiments was to find extremely prominent cases, and the exact comparison of the result is of course impossible on account of crudeness in procedure, observation etc. In Table I are given the results obtained for the three types of dyes, about which the oxidative and reductive behavior have been examined to some extent. It is evident from the above table that there exists no parallelism between the magnitude of polymerization and the easiness in bleaching and recovery of color. For example, thiazine dyes which are easily reduced as well as rapidly reoxidized by oxygen, have rather a small power of initiating the polymerization. It is ture that the excess of oxygen will inhibit the polymerization since it has been confirmed by the suppression of polymerization by bubbling the air through the solution. But it is expected that the consumption of oxygen during the reoxidation of leuco dye will soon realize the situation in which the polymerization may take place rather smoothly. The above results in thiazine dyes contradict this expectation altogether. On the other hand xanthene dyes, of which the leuco form shows a great resistance against reoxidation by oxygen, can have some power of inducing polymerization when coupled with proper reducing agents. Acridine dyes, which lie between the above two classes as judged from our unpublished results which demonstrate that these dyes make reversible bleaching in the aqueous solution containing $Sn^{2+}$ whether oxygen exists or not, show a very pronounced efficiency for promoting polymerization when used with stannous chloride.

All these facts suggest that the photopolymerization induced by dyes would some in cases go via a different scheme from Oster's, especially in case of acriflavine and stannous chloride.

From such a viewpoint the quantitative investigation upon the system acriflavine-stannous chloride was undertaken.

## Experimental

**Materials.**—Acrylonitrile from American Cyanamide Co. was distilled after dehydrating with calcium chloride, b. p. 76.5°C. Dimethylformamide

(DMF) from Du Pont was dehydrated by potassium carbonate and then distilled, b. p. 151~151.5°C. $SnCl_2 \cdot 2H_2O$ (G. R) and $SnCl_4 \cdot 3H_2O$ (G. R) were used without further purification. Acriflavine from Merck was also used without purification.

**Procedure.**—As a light source a projection lamp 100 V.-500 W was used at 80 V. The distance between the light source and a reaction cell placed in a thermostat is 33 cm. Mazda Color Filter V-Y3C which cuts off $\lambda <$ ca. 420 m$\mu$ is set in front of the reaction cell. In the experiments for studying the effect of light intensity, neutral filters were used. A reaction cell is made of terex glass $1 \times 1 \times 4.5$ cm. and it is connected with a capillary utilized as a dilatometer. The drop of meniscus in the capillary due to polymerization was followed by use of a travelling microscope. All the experiments were done at 35°C except otherwise described.

To prepare the sample for reaction, (1) acrylonitrile, (2) the aqueous solution of dye and (3) DMF dissolving stannous chloride were mixed in a proper ratio. The concentration of dye and stannous chloride in the latter two solutions are adjusted to get a desired composition of the ultimate sample. In studying the effect of [AN], the ratio of 1 and 3 was changed keeping the quantity of 2 as constant, while for investigating the effect of [$H_2O$] the ratio of 2 and 3 was changed keeping the quantity of 1 as constant. It is to be noted that DMF solution of stannous chloride must be prepared prior to the experiment in order to get a good reproducibility.

In order to separate the polymer the sample, after the reaction, was poured into a large quantity of methanol and the precipitate was washed with methanol containing hydrochloric acid (concentrated hydrochloric acid : methanol = 0.0015 : 1 in volume) and after washing once more with methanol was dried at 40°C in vacuo. The molecular weight of the polymer thus obtained was determined by measuring the viscosity of the solution of DMF containing about 0.1% of polymer at 25°C. To calculate the intrinsic viscosity Schulz and Sing's formula[3] was employed.

$$[\eta] = \frac{\eta_{sp}/c}{1 + 0.28\eta_{sp}}$$

The average molecular weight was evaluated from the following relation[4].

$$[\eta] = 3.92 \times 10^{-4} \overline{M}^{0.75}$$

## Results

When the sample containing stannous chloride and acriflavine is irradiated, the polymerization usually commences at once, but when the sample contains only either of the two the polymerization does not occur in fact. There is no dark reaction perceived even when a large quantity of stannous chloride and acriflavine are added. In Fig. 1, curve 1 represents the rate for the sample, AN : $H_2O$ : DMF = 4 : 3 : 4.2 (in volume), [$SnCl_2$] = $2.73 \times 10^{-2}$ M, [Acriflavine] = $2.73 \times 10^{-4}$ M. Accompanied with the polymerization, the solution becomes turbid due to the precipitation of the polymer. When the concentration of stannous chloride is small a certain period of induction appears and after that the curve becomes linear (curve 2). As regards curve 3 mention will be made later. In case of a small concentration of dye the rate begins to decrease earlier than in other cases. In all cases the rate was evaluated from the initial linear portion of the curve. It is to be noted that when the same cell was used for a long period of time, the cell walls gradually became opaque and it had to be renewed occasionally. Therefore, it is not always possible to compare and to correlate the data of a different series of experiments described below.

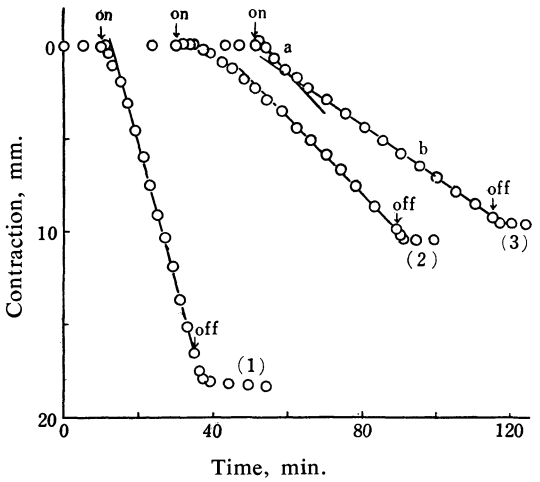



Fig. 1. The contraction-time curves.

| | [D] $10^{-4}$ M | [$SnCl_2$] $10^{-3}$ M | AN : $H_2O$ : DMF (in volume) |
|---|---|---|---|
| (1) | 2.73 | 27.3 | 4 : 3 : 4.2 |
| (2) | 2.73 | 1.71 | 4 : 3 : 4.2 |
| (3) | 3.00 | 11.0 | 3.6 : 0.51 : 5.89 |

**1. The Effect of Evacuation.** — The relative rates of the cautiously degassed samples were 1.02, 1.16 as compared with 1.49, 1.52, 1.46 of the aerated ones ([Acriflavine] = $1.0 \times 10^{-4}$ M, [$SnCl_2$] = $1.25 \times 10^{-2}$ M, AN : $H_2O$ : DMF = 3.3 : 2.0 : 4.7 (in volume)). It is evident that the polymerization does take place in the evacuated sample though the rate is somewhat smaller than the aerated solution. The ratio of the rates in two cases being about 1 : 1.4, it seems rather plausible to consider that the effect of oxygen is of the secondary importance (see Discussion). Tentatively assuming the above viewpoint and to orient the investigation, the effect of various factors upon the rate was examined in the first place using aerated solution. Another reason for this was to avoid

3) G. V. Schulz and G. Sing, *J. Prakt. Chem.*, **161**, 161 (1942).
4) P. F. Onyon, *J. Polymer Sci.*, **22**, 13 (1956).

the troublesome procedure for repeated evacuation. The results given below concern only with such aerated samples.

**2. The Effect of Dye Concentration.** — The variation of the rate when the concentration of acriflavine is changed from zero to $1.4\times10^{-4}$ M is shown in Fig. 2. It is apparent from the

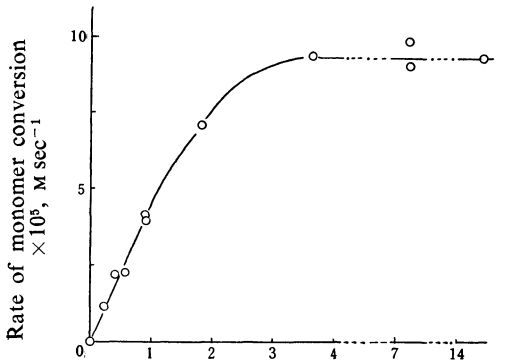



Fig. 2. Dependence of rate on acriflavine concentration.
$[SnCl_2]=1.8\times10^{-2}$ M; AN : $H_2O$ : DMF = 4 : 3 : 4.2 (in volume)

figure that in the region of $\sim10^{-6}$ M of dye, the rate linearly increases with the dye concentration. This was further confirmed by log (rate)$\sim$log[AF] curve, which gave the slop of 0.9. When the concentration of dye exceeds ca. $3.5\times10^{-5}$ M, the rate remains constant. From the above results it is concluded that, at a small concentration of dye, the rate is proportional to the dye concentration and it appears to be proportional also to the absorbed light but it will be shown below that it is not the fact (see Sect. 7).

**3. The Effect of the Concentration of Stannous Chloride.**—The effect of the concentration of stannous chloride on the rate is shown in Fig. 3. Although there exists some scattering of the experimental points, it is still evident that in the low concentration region ($<$ ca. $3.5\times10^{-3}$ M) the linearity holds between the rate and $[SnCl_2]$, and this fact was also confirmed by the slope of 0.9 for log (rate)$\sim$log $[SnCl_2]$ plot. Above ca. $10^{-2}$ M of stannous chloride the rate remains constant. It is to be added that in the case of a high concentration of $[SnCl_2]$ the polymer deposits throughout the entire cell while in case of low concentration, the polymer adheres to the lower half of the front wall of the vessel.

**4. The Effect of Monomer Concentration.**— In Fig. 4, the rate is plotted against the square of the monomer concentration. It is apparent that the rate $\propto[AN]^2$. Another series of experiments gave a similar result. log(rate)$\sim$log[AN] plot gave a straight line of slope 1.9$\sim$2.05.

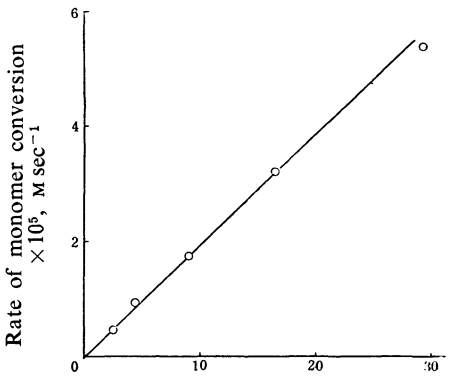



Fig. 4. Dependence of rate on acrylonitrile concentration.
$[D]=3.00\times10^{-4}$ M; $[SnCl_2]=1.37\times10^{-2}$ M; $[H_2O]=14.9$ M

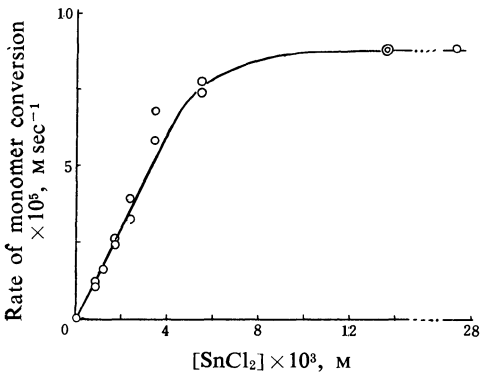



Fig. 3. Dependence of rate on stannous chloride concentration.
$[D]=2.73\times10^{-4}$ M; AN : $H_2O$ : DMF = 4 : 3 : 4.2 (in volume)

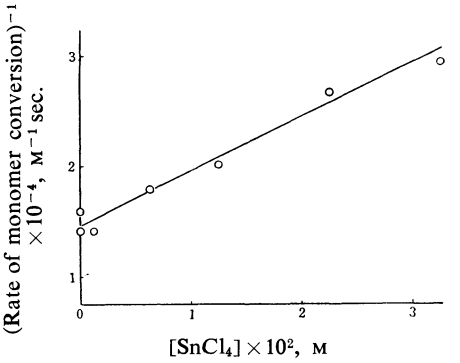



Fig. 5. Dependence of rate on stannic chloride concentration.
$[D]=2.00\times10^{-4}$ M; $[SnCl_2]=1.25\times10^{-2}$ M; AN : $H_2O$ : DMF = 3.6 : 2.5 : 4.0 (in volume)

**5. The Effect of the Concentration of Stannic Chloride.** — When $SnCl_4$ is added, the rate is decreased. As shown in Fig. 5, there exists an approximate linearity between the reciprocal of the rate and the concentration of stannic chloride.

**6. The Effect of Water Content.** — It was found that the polymerization can occur without any water being added, and the effect of water content on the rate was investigated in some detail. Time plots in the case of a large quantity of water were simple as shown in Fig. 1 (1), but they were curved as shown in Fig. 1 (3) when the content of water was low. Corresponding to this anomaly the polymer did not appear at first; the above phenomenon may perhaps be connected with the precipitation of the polymer. In Fig. 6 the rate is plotted against $[H_2O]/[DMF]$; × and ○ represent respectively the rates evaluated from parts a and b of the curve. It is apparent from

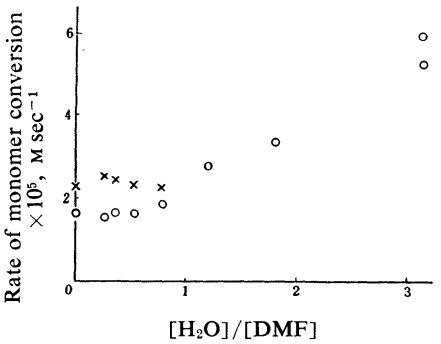



Fig. 6. Dependence of rate on $[H_2O]/[DMF]$.
$[AN]=5.4$ M; $[D]=3.0\times10^{-4}$ M; $[SnCl_2]=1.1\times10^{-2}$ M

the figure that the addition of water up to about $[H_2O]/[DMF]=1$ scarcely affects the rate but a larger quantity causes an increase to some extent. It is known that 1 : 1 complex is formed between DMF and water[5], and the above result might be correlated with this phenomenon.

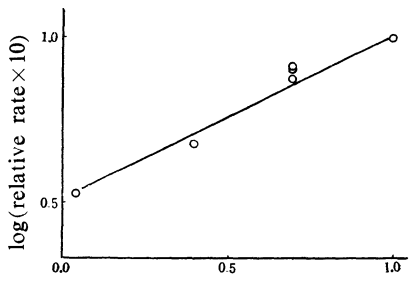



Fig. 7. The intensity exponent.
$[D]=2.00\times10^{-4}$ M; $[SnCl_2]=1.25\times10^{-2}$ M;
AN : $H_2O$ : DMF = 3.6 : 2.5 : 4.0 (in volume)

5) A. D. Jenkins and R. Johnston, ibid., 39, 81 (1959).

**7. The Effect of Light Intensity.** — The intensity of the exciting light was changed to 50, 25 and 11% of the standard light by use of neutral filters. As seen from Fig. 7 the rate is nearly proportional to the root of light intensity. Although these experiments were done only for the samples containing such a large quantity of dye as to absorb almost all the effective light, there is scarcely any doubt that this relation also holds for the case of a small concentration of dye.

**8. Average Degree of Polymerization.**—The effect of the monomer concentration on the degree of polymerization was examined. As shown in Fig. 8, linear relation holds approximately between $\bar{P}$ and [AN]. The effect of the addition of stannic chloride on $\bar{P}$ was also

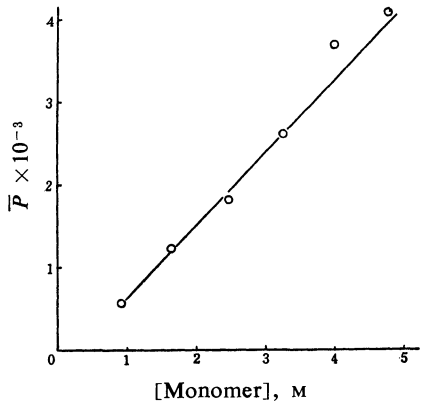



Fig. 8. Dependence of average degree of polymerization on acrylonitrile concentration.
$[D]=2.00\times10^{-4}$ M; $[SnCl_2]=1.25\times10^{-2}$ M; $[H_2O]=13.9$ M

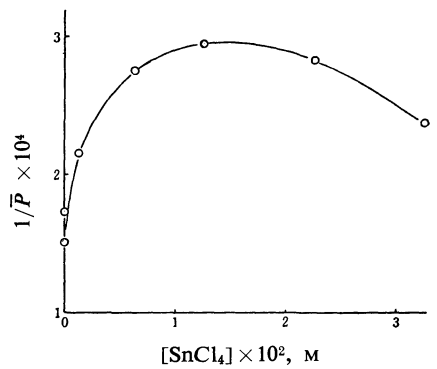



Fig. 9. Dependence of average degree of polymerization on stannic chloride concentration.
$[D]=2.00\times10^{-4}$ M; $[SnCl_2]=1.25\times10^{-2}$ M; AN : $H_2O$ : DMF = 3.6 : 2.5 : 3.9 (in volume)

examined. The result is shown in Fig. 9. If stannic chloride only takes part in the termination or chain transfer process, $1/\bar{P}$ should increase monotonously with $[SnCl_4]$, so that it is certain that stannic chloride interferes with other processes, particularly with the initiation step.

**9. Activation Energy.**—The temperature dependence of the rate was measured in the region from 16.5 to 40°C. The Arrhenius plot is shown in Fig. 10. The rate is almost independent of temperature between 25 and 40°C. But below about 25°C, the rate decreases with the fall of temperature. The apparent activation energy is evaluated to be 7±2 kcal./mol.

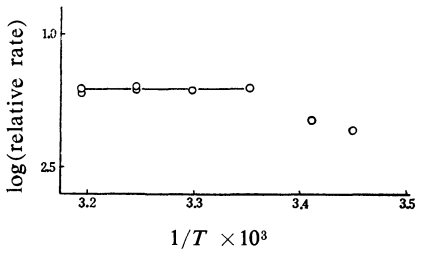



Fig. 10. Arrhenius plot.
$[D]=2.00\times10^{-4}$ M; $[SnCl_2]=1.25\times10^{-2}$ M; AN : $H_2O$ : DMF = 3.6 : 2.5 : 4.0 (in volume)

## Discussion

From the result that the polymerization takes place in the degassed solution and with the same order of rate as that of the aerated one, it is certain that the existence of oxygen is not of primary importance for the reaction to occur. Hence it is tentatively assumed that oxygen is not involved in the essential steps of the reaction, particularly in the early stages of the initiation. Then the molecular species which participate in the initiation step would be stannous chloride, acriflavine and AN, since both water and stannic chloride do not affect the rate so much. Thus the addition of stannic chloride as much as $3\times10^{-2}$ M only decrease the rate to about a half and 15 M of water increases the rate only 3~4 times, a small amount scarcely affecting the rate. It may be certain that stannous chloride employed contains a small amount of stannic chloride, but its effect may be neglected from the experimental results. Hence attention will be paid only on the dependence of the rate upon $[SnCl_2]$, [D], [AN] and intensity of light $I_0$.

Now the overall rate of polymerization is in general expressed by the following equation if the condition of steady state is satisfied.

$$v=k_p[R][M] \qquad (I)$$

where [R] and [M] are the concentrations of growing polymer and monomer. [R] can be expressed by II or III according as the termination process is the first order or the second order in regard to [R].

$$[R]=v_i/k_t \qquad (II)$$

$$[R]=(v_i/k_t)^{1/2} \qquad (III)$$

The experimental rate formula satisfies the following condition

$$v \propto [D][SnCl_2][M]^2$$

and

$$v \propto I_0^{1/2}$$

when [D] and $[SnCl_2]$ are small.

Hence $v_i$ in this case must be expressed as follows:

case II, $v_i \propto [D]^{1/2}[D^*]^{1/2}[SnCl_2][M]$

case III, $v_i \propto [D][D^*][SnCl_2]^2[M]^2$

where D* is the excited dye. Case III however can be rejected since it was found experimentally that the following relation holds,

$$\bar{P} \propto [M]$$

and in general $\bar{P}$ may be equated to $v/v_i$ at least approximately (unless the rate of chain transfer is quite appreciable). Thus the initiation processes must be those that satisfy the following relations.

When [D] and $[SnCl_2]$ are small

$$v_i \propto [D]^{1/2}[D^*]^{1/2}[SnCl_2][M] \qquad (IV)$$

When both [D] and $[SnCl_2]$ are large

$$v_i \propto [M]I_0^{1/2} \qquad (V)$$

The equations IV and V look rather unusual and these suggest the peculiar character of the reaction scheme.

Here we propose the following two schemes as plausible ones.

A. $D \xrightarrow[(1)]{h\nu} D^* \xrightarrow[(3)]{D} D^t \xrightarrow[(5)]{Sn^{2+}} (D^- \cdots\cdots Sn^{3+})$

$D^*$ —(2)→ D; $D^t$ —(4)→ D; $(D^- \cdots\cdots Sn^{3+})$ —(6′)→ $D+Sn^{2+}$; —(6)→ $Leuco+Sn^{4+}$

$\xrightarrow[(7)]{Sn^{2+}} D + Sn^+ + Sn^{3+} \xrightarrow{(8)} D + 2Sn^{2+}$

(or $D^- + Sn^{3+}$) (or $D + Sn^{2+}$)

$Sn^{3+} + M \xrightarrow[(9)]{k_1} R$

(or $Sn^+ + M \longrightarrow R$)

B. $D + Sn^{2+} \underset{(0)}{\overset{K_0}{\rightleftarrows}} (DSn^{2+}) \xrightarrow[(1)]{h\nu} (D^*Sn^{2+})$

$(D^*Sn^{2+})$ —(2)→ D

$\xrightarrow[(3)]{D} (D^tSn^{2+}) \xrightarrow[(5)]{} (D^- \cdots\cdots Sn^{3+})$

$(D^tSn^{2+})$ —(4)→ D; $(D^- \cdots\cdots Sn^{3+})$ —(6′)→ $D+Sn^{2+}$; —(6)→ $Leuco+Sn^{4+}$

$\xrightarrow[(7)]{Sn^{2+}}$ same as above

In scheme A, $Sn^{2+}$ participates in the steps 5 and 7 while in scheme B a complex is formed between $Sn^{2+}$ and D and the corresponding scheme to 5 in A is lacking. In both schemes it is assumed that the transition from singlet excited state (D*) to triplet ($D^t$) is induced by the ground state dye molecule. Although this is plausible and in fact such a process has also been accepted by Oster for the case of acridine dyes[6], it is noteworthy that there is another possibility that the excimer[7] be formed between D and D*. The discrimination may however be impossible only from the rate formula. ($D^- \cdots\cdots Sn^{3+}$) is supposed to be a charge transfer complex or the like.

For both schemes A and B the essential point is that two kinds of molecular species of radical nature produced by process 7, react almost exclusively in such a way as to produce stable molecular species and only a small fraction of them react with monomer to produce an initiator of polymerization 9. Thus when $D^-$ and $Sn^{3+}$ are produced by 7 electron transfer should rapidly occur between them, recovering D and $Sn^{2+}$, while when D, $Sn^+$ and $Sn^{3+}$ are produced, the analogous electron transfer should take place between $Sn^+$ and $Sn^{3+}$ (8), $Sn^+$, $Sn^{3+}$, $D^-$ (this is rather unplausible) or all of them may initiate the polymerization. In fact such schemes as above seem almost indispensable to interpret the following relations consistently.

$$v_1 \propto I_0^{1/2}, \qquad v \propto [M]^2, \qquad \bar{P} \propto [M]$$

From the above schemes, the following rate formulas can be derived.

Case A

$$v_1 = \left[\left\{\frac{k_1 I_0 k_3 [D]}{k_2 + k_3 [D]}\right\}\left\{\frac{k_5 [Sn^{2+}]}{k_4 + k_5 [Sn^{2+}]}\right\} \times \left\{\frac{k_7 [Sn^{2+}]}{k_6 + k_6' + k_7 [Sn^{2+}]}\right\}\right]^{1/2} \frac{k_9}{k_8^{1/2}} [M] \qquad (VI)$$

Case B

$$v_1 = \left[\left\{\frac{I_0 k_1 K_0 [Sn^{2+}]}{1 + K_0 [Sn^{2+}]}\right\}\left\{\frac{k_3 [D]}{k_2 + k_3 [D]}\right\}\left\{\frac{k_5}{k_4 + k_5}\right\} \times \left\{\frac{k_7 [Sn^{2+}]}{k_6 + k_6' + k_7 [Sn^{2+}]}\right\}\right]^{1/2} \frac{k_9}{k_8^{1/2}} [M] \qquad (VII)$$

Both VI and VII can express the experimental results satisfactorily as in the following way.

i) Large [D]: $v$ is independent of [D].

$$v \propto I_0^{1/2}$$

ii) Small [D]: $k_1 I_0$ may be put approximately proportional to [D]. Hence

$$v \propto [D]$$

iii) Large $[Sn^{2+}]$: $v$ is independent of $[Sn^{2+}]$.

iv) small $[Sn^{2+}]$: $v \propto [Sn^{2+}]$

v) In all cases, $v \propto [M]^2$

As for the effect of water, both hydration of D and the formation of a certain ion pair from $Sn^{2+}$ and $OH^-$ would favor the reaction. For example the formation of $(SnOH)^+$ would promote processes 5 and 7 in both case A and case B; moreover the hydration of D would also be favorable for these process and in addition, for 3 and 0 (in case B). All these effects together should cause the rate to increase with the content of water. But these effects are of secondary importance in the reaction scheme and to not affect the rate very much.

In connection with the above schemes, it may be worthy of adding here some discussions about the rate of dye bleaching in the absence of acrylonitrile. Provided that process 7 be neglected, the rate of bleaching of dye will be given as follows:

Case A

$$\frac{k_1 I_0 k_3 [D]}{k_2 + k_3 [D]} \cdot \frac{k_5 [Sn^{2+}]}{k_4 + k_5 [Sn^{2+}]} \cdot \frac{k_6}{k_6 + k_6'} \qquad (VIII)$$

Case B

$$\frac{k_1 I_0 K_0 [Sn^{2+}]}{1 + K_0 [Sn^{2+}]} \cdot \frac{k_3 [D]}{k_2 + k_3 [D]} \cdot \frac{k_5}{k_4 + k_5} \cdot \frac{k_6}{k_6 + k_6'} \qquad (IX)$$

Thus the similar relation in respect to [D] and $[Sn^{2+}]$ will hold for two cases. But when the process 7 participate in the reaction the rate would decrease when the concentration of $Sn^{2+}$ exceeds a certain value. It may be possible to examine this effect experimentally.

If Oster's mechanism holds in the present case, which postulates the formation of leuco dye prior to the initiation process, the rate formula of initiation would be similar to VIII and IX which contradicts the experimental results altogether. Thus three relations $v \propto I_0^{1/2}$, $v \propto [M]^2$ and $\bar{P} \propto [M]$ can not be interpreted satisfactorily on this basis. Analogous discussion may be extended to the effect of oxygen on the rate, the increase amounting to about 40% of that of the evacuated solution. If this increase is due to the participation of the process $D + SnCl_2 \rightarrow Leuco + SnCl_4$, $Leuco + O_2 \rightarrow$ active radical, then the kinetic order in respect to $[SnCl_2]$ and [D] would be the average of the two simultaneous reactions and

6) F. Millich and G. Oster, *J. Am. Chem. Soc.*, **81**, 1357 (1959).
7) B. Stevens and E. Hutton, *Nature*, **186**, 1045 (1960).

would not be the whole number as experimentally obtained. Hence it seems more plausible that oxygen interferes with the intermediate ($D^- \cdots\cdots Sn^{3+}$) rather than its attack on leuco dye. The discrimination between cases A and B may perhaps be made by spectroscopic investigation. Further investigations are now under way to confirm the above schemes more definitely and to select case A or case B.

## Summary

When the aerated solution of acrylonitrile, acriflavine and stannous chloride in the mixture of water and dimethylformamide is irradiated by the visible light, the polymerization of acrylonitrile immediately takes place. The presence of water and oxygen was found to be unnecessary for the reaction to occur. The dependence of rate on the concentration of each species and on the light intensity ($I_0$) can be summarized as follows.

| | |
|---|---|
| Acriflavine | $<$ca. $1\times10^{-5}$ M, 1st order; |
| | $>$ca. $3.5\times10^{-5}$ M, const. |
| Stannous chloride | $<$ca. $3.5\times10^{-3}$ M, 1st order; |
| | $>$ca. $1.2\times10^{-2}$ M, const. |
| Acrylonitrile, | 2nd order |
| $I_0$, | 1/2th order |

It was further found that the average degree of polymerization is proportional to the monomer concentration. The scheme involving the photoreduction of dye by stannous chloride and its recovery by the existent oxygen cannot explain the present result. It was proposed as a new mechanism that a transient metallic ion of tin with an odd valency is formed and this, interacting with acrylonitrile, initiates the polymerization.

The present research was mostly performed by Ai Watanabe at Osaka City University and was finished during her stay at Sendai as a visiting research fellow. The authors express their cordial thanks to Professor R. Fujishiro of Osaka City University for his interest and encouragement.

*Department of Chemistry*
*Faculty of Science*
*Tohoku University*
*Katahira-cho, Sendai*

# *The Photovoltaic Behavior in Organic Compounds*

By Hiroo INOKUCHI*, Yusei MARUYAMA* and Hideo AKAMATU

(Received January 17, 1961)

The study on the photo-electrical behavior in organic semiconductors produced by excitation accompanying absorption of light, especially the investigation of the photoconduction, has been carried out by several workers[1]. However, relatively little is known about the photovoltaic phenomena of these organic compounds[2].

In one of the few articles on this subject, Nelson[3] reported a photovoltaic behavior of junctions between organic compounds and cadmium sulfide in association with optical sensitization in photography. The author proposed that the induced photovoltage is related to the difference in energy between the conduction band of the organics (dye) and that of cadmium sulfide. On the other hand, Calvin and Kearns[4] reported interesting results on photovoltaic organic junctions: Mg-phthalocyanine || tetramethyl-*p*-phenylene diamine and coronene || chloranil junctions.

In this paper, we show that the photovoltaic behaviors have been observed with a simple cell, consisting of a junction between aromatic compounds and metal or stannic oxide. Further, in comparison with other semiconductive behaviors of polycyclic aromatic compounds, the produced electromotive force will be discussed.

## Experimental Procedures

For an observation of photo-electromotive force between organic semiconductor and metal or metal

* Present address: The Institute for Solid State Physics, The University of Tokyo, Azabu, Tokyo.

1) H. Inokuchi and H. Akamatu, "Solid State Physics", Vol. 12, Chapter 2, Academic Press. New York, (1961).

2) H. Baba, K. Chitoku and K. Nitta, *Nature*, **177**, 672 (1956).

3) R. C. Nelson, *J. Chem. Phys.*, **22**, 885, 890, 892 (1954), **29**, 388 (1958); *J. Opt. Soc. Am.*, **45**, 774 (1955); **46**, 13 (1956).

4) M. Calvin and D. Kearns, *J. Chem. Phys.*, **29**, 950 (1958).

oxide, a sandwich-type cell was applied. This cell was made by sandwiching aromatic compounds between two electrodes: The evaporated film of aromatic compounds was deposited onto a glass plate which had been coated in advance with a thin metal film or onto a stannic oxide conducting layer to provide a junction electrode. The specimen film was usually one or two microns in thickness. Further, the second electrode was evaporated onto the specimen film. The conducting path between these electrodes extended through the specimen film. The resulting construction of the cell was illustrated in Fig. 1 of the previous report[5].

For the preparation of alkali metal-aromatics junction, as shown in Fig. 1, the alkali metal, evaporated onto organic film as a second electrode under less than $10^{-5}$ mmHg, acted as a junction electrode. After the evaporation of alkali metal, all observations of their electromotive forces were carried out under a high vacuum to avoid a decomposition of the alkali metal by an action of moisture. However, a fluctuation was frequently introduced concerning the direction of electromotive force. For the elimination of this fluctuation, the construction of a more precise apparatus is in due course.

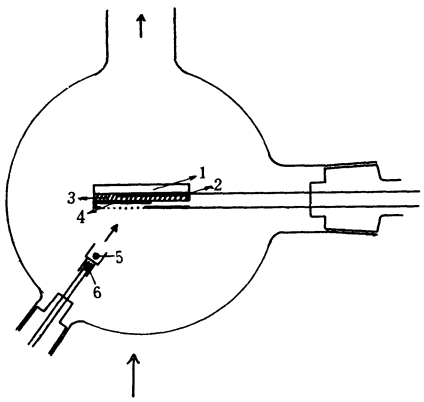



Fig. 1 The arrangement for preparation of alkali metal-aromatics junction. (1) Pyrex glass plate, (2) terminal electrode, (3) aromatic compound, (4) junction metal (alkali metal), (5) nickel dish, and (6) electric heater for evaporation.

The sandwich-type aromatics-aromatics junction was made by the successive evaporation of two sorts of aromatic compounds, kept in the vessel 5 of Fig. 1, onto a conducting glass plate without an intrusion of air into the contact area between these two compounds.

The illumination of white light was produced from a tungsten lamp onto the side of the junction metal. The measurement of induced photovoltage had to be associated with a vibration-reed electrometer because its produced electric power was extremely low. By means of a quartz-prism monochrometer and also of interference filters, a spectral response of photo-electromotive force in the range from 350 m$\mu$ to 1300 m$\mu$ was observed.

The applied aromatic compounds, perylene, violanthrene and violanthrone, were provided from Drs. T. Handa and also J. Aoki. Coronene, a seven membered aromatic hydrocarbon, was provided from Badisch Anilin und Soda Fabrik, Germany. These organic compounds were purified with a combination of three methods; recrystallization, sublimation and chromatography.

## Results and Discussions

When the contact between an organic semiconductor and a metal was illuminated with white light from a tungsten lamp, the induced electromotive force reached immediately a saturated value and this was kept quite steadily for a long period. However, in the alkali metal-aromatics junction it was found that its electromotive force decreased to a value smaller than the original one. This behavior would be introduced from a high reactivity of alkali metal with moisture and/or from a formation of charge transfer complex between the metal and the aromatic compound.

For the noble metal-aromatics junction, the observed photoelectromotive force varied from a few millivolts to 10 mV. depending on the sorts of metals applied to the junction and also on the condition of preparation technique as illustrated in Table I. In all of these photocells, the junction metal acted as a negative electrode against the terminal electrode; thereby, at the junction, electrons flowed from the hydrocarbons to the junction metals under the illumination.

On the other hand, a quite stable photovoltage was produced at the contact between perylene and stannic oxide, and its saturated value reached 80 mV. when a light was incident on it through the transparent stannic oxide electrode (electrical conducting glass electrode). The spectral response of this electromotive force was a curve which is in good coincidence with the optical absorbance curve and also with the response curve of photoconduction for solid perylene as illustrated in Fig. 2.

Similar behavior of the photovoltaic effect was found in the junction between coronene, violanthrene or violanthrone and stannic oxide, whose electromotive forces were 20, 450 and 80 mV. respectively. These four hydrocarbons acted as electron acceptors with respect to stannic oxide under illumination of panchromatic light. However, the spectral response of photovoltage of violanthrone junction was a quite peculiar one as shown in Fig. 3. Its threshold value was found to be around 0.9 eV., which is in agreement with that of the photoconduction of its aromatic compound.

5) H. Inokuchi, H. Kuroda and H. Akamatu, This Bulletin, 34, 749 (1961).

TABLE I. THE PHOTOVOLTAGE OF METAL-AROMATICS JUNCTIONS

| Photovoltaic junction | | Photo-emf | |
|---|---|---|---|
| Aromatics (sign) | Metal (sign) | Voltage, mV. | Wattage, W. |
| Violanthrene (+) | Pt (−) | 2∼ 3 | $\sim 10^{-17}$ |
| Violanthrene (+) | Au (−) | 6∼ 9* | $\sim 10^{-16}$ |
| Violanthrene (+) | Ag (−) | Detectable | |
| Violanthrene (+) | Sn (−) | 2∼ 8 | $\sim 10^{-16}$ |
| Violanthrene (+) | Pb (−) | 4∼14 | $\sim 10^{-16}$ |

* As a special case, emf reached to 50 mV.

TABLE II. THE PHOTO-ELECTROMOTIVE FORCE OF ALKALI METAL-AROMATICS JUNCTIONS

| Photovoltaic junction | | Photo-emf | | |
|---|---|---|---|---|
| Aromatics (sign) | Metal (sign) | Voltage, V. | Wattage, W. | $\Delta\varepsilon/2$, eV. |
| Perylene (−) | Li (+) | 0.3∼1.0 | $\sim 10^{-10}$ | 1.0 |
| Coronene (−) | Li (+) | 0.3 | $\sim 10^{-10}$ | 0.8 |
| Violanthrene (−) | Li (+) | 0.3∼0.8 | $\sim 10^{-9}$ | 0.43 |
| Violanthrone (−) | Li (+) | 0.2∼0.9 | $\sim 10^{-10}$ | 0.39 |
| Perylene (+) | Na (−) | 0.3∼1.0 | $\sim 10^{-11}$ | 1.0 |
| Violanthrene (+) | Na (−) | 0.3∼0.8 | $\sim 10^{-10}$ | 0.43 |
| Violanthrone (±) | Na (∓) | 0.1∼0.5 | $\sim 10^{-8}$ | 0.39 |
| Perylene (±) | K (∓) | 0.2∼0.9 | $\sim 10^{-10}$ | 1.0 |
| Violanthrene (+) | K (−) | 0.2∼0.8 | $\sim 10^{-10}$ | 0.43 |
| Violanthrone (−) | K (+) | 0.2∼0.5 | $\sim 10^{-9}$ | 0.39 |

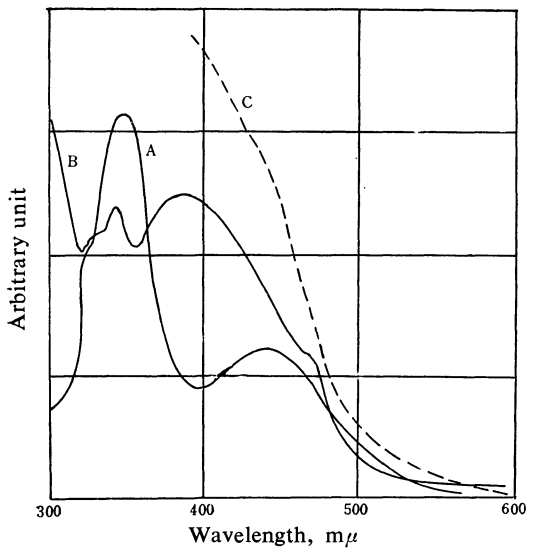



Fig. 2 The spectral response curves of photoconductivity (A), absorption spectrum (B) and photovoltage (C) for perylene in solid phase.

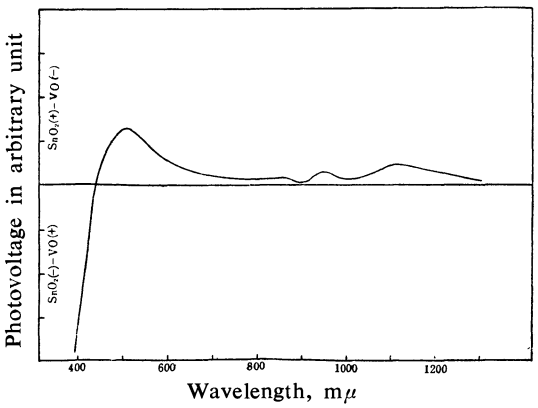



Fig. 3 The spectral response curve of photovoltage for the $SnO_2$-violanthrone ($SnO_2$-VO) junction.

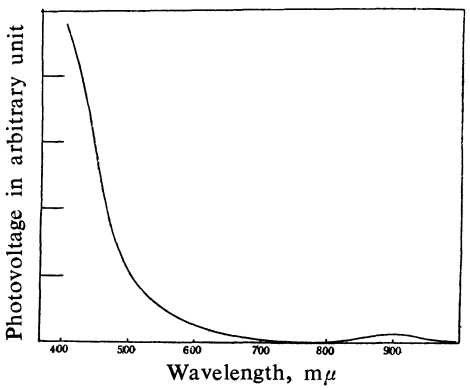



Fig. 4 The spectral response of photovoltage produced at the junction between sodium metal and violanthrene.

These results imply that the spectral responses of the photovoltage are predominated by the electronic structure of polycyclic aromatic compounds but not by that of stannic oxide. In this connection, no optical absorption in stannic oxide film was found in a visible region longer than 390 mμ.

In the alkali metal-aromatics junction, the induced photo-electromotive force reached to almost one volt as listed in Table II. Its

spectral response was a curve falling monotonously from short wavelength to long wavelength side. An extrapolation of this decrement found a tentative threshold value, which is sited in a range from 600 to 700 m$\mu$ as shown in Fig. 4.

A weak but definite response of photovoltage was found in a longer wavelength region than the extrapolation value. However, further investigations are restricted by fluctuation concerning the direction of electromotive force and also by the lack of stability of the force. In the lithium-aromatics junction, the metal acted as a positive electrode relative to the terminal electrode. Most of the aromatic compounds in the sodium-aromatics junction, however, acted as a positive electrode with respect to sodium; that is to say, electrons were transferred from the hydrocarbons to the junction metal at the junction and then the organic solids acted as electron donors. In the potassium-aromatics junction, the direction of photo-electromotive force was changed depending on the sorts of organic solids and also on the wavelength of incident light.

These values of photovoltage decreased to a small value in time. This decrease may be introduced from the complex formation between aromatic compound and alkali metal and/or may be produced by a decomposition of the junction. These fluctuations on the observed values may be eliminated by means of the application of ultra-high vacuum.

As a preliminary work of aromatics-aromatics junction, we have found that a fairly large electromotive force ($10\sim10^2$ mV.) was produced at the contact between two pure aromatic hydrocarbons; for instance, perylene and violanthrene, under illumination. The details of this work will appear elsewhere.

When a contact between semiconductive material (band gap : $\Delta\varepsilon$) and metal is made, it is believed that the flow of charge carrier, $I_o \exp[-\Delta\varepsilon/2kT]$, happended at the contact and a potential barrier occurs at the boundary layer. On illuminating the contact of junction, the flows of forward and backward currents, $I_f$ and $I_b$, are expressed as

$$I_f = I_o \exp[-(\Delta\varepsilon/2 - eV_{op})/kT] \quad (1)$$

$$I_b = I_o \exp[-(\Delta\varepsilon/2)/kT] + I_L \quad (2)$$

respectively, where $I_L$ is the excess flow of charge carrier under illumination and $V_{op}$ is photo-electromotive force, measured for an open circuit condition. At an equilibrium condition, $V_{op}$ is expressed as

$$V_{op} = \frac{kT}{e} \ln\left[1 + \frac{I_L}{I_o \exp[-(\Delta\varepsilon/2)/kT]}\right] \quad (3)$$

because of $I_f = I_b$.

When the induced current $I_L$ under illumination of light is large, Eq. 3 is rewritten as

$$V_{op} \fallingdotseq \frac{\Delta\varepsilon}{2e} + \frac{kT}{e} \ln\frac{I_L}{I_o} \approx \frac{\Delta\varepsilon}{2e} \quad (kT \ll e) \quad (4)$$

$$V_{op} \fallingdotseq \frac{kT}{e} \frac{I_L}{I_o} \exp[-(\Delta\varepsilon/2)/kT] \ll 1 \quad (5)$$

For the alkali metal-aromatics junction, it is expected the produced photovoltage, $V_{op}$, follows Eq. 4 because the excess flow of illuminated current is great. On the contrary, the minute photovoltage for the noble metal-aromatics junctions is explained by Eq. 5 tentatively.

## Summary

When a contact between a semiconductive material and a metal is made, it is expected that a potential barrier occurs at the boundary layer and the photovoltaic effect which is observed with illumination on this barrier. It has been found that this is the case for organic semiconductors. The photovoltaic cell was made with aromatic compounds sandwiched between two metal layers or metal and stannic oxide. One of them was a terminal electrode and the other, the junction electrode, was made with evaporated film of platinum, gold, silver, tin, lead or alkali metal. All observations of photovoltage were carried out in vacuo or in an atmosphere of inert gas.

With the illumination of white light from a tungsten lamp, the induced photovoltage varied from several millivolts to one volt, depending on the sorts of metals applied to the junctions. In most of these junctions, the organic solids acted as positive electrodes with respect to the junction metal.

In the alkali metal-aromatics system, a fluctuation was frequently observed concerning the direction of electromotive force, but the value of photovoltage was generally much higher than in the case of the other metals; thus the spectral response of the voltage was measurable. This response was less dependent on the sorts of organic solids but dependent on the sorts of metals. On the other hand, the spectral response in the junction between organic solid and stannic oxide, was a curve which is in good coincidence with the optical absorption curve for solid organics.

The cost of this research has been defrayed from the Grant in Aid for Fundamental Scientific Research from the Ministry of Education, to which the author's thanks are due.

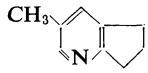
*Department of Chemistry*
*Faculty of Science*
*The University of Tokyo*
*Hongo, Tokyo*

# *Isolation of 2, 3-Cyclopenteno-5-methylpyridine from Coal Tar Bases*

By Hajime SUZUMURA

(Received January 24, 1961)

It was previously reported that 3, 4, 5-collidine and 2, 3-cyclopenteno-6-methylpyridine were isolated from the tertiary amine fraction boiling about 210°C in coal tar bases and their chemical structure were confirmed[1]. On further investigation, a $C_9H_{11}N$ base was isolated by solvent extraction and picrate formation from bases boiling about 220°C. This was identified as 2, 3-cyclopenteno-5-methylpyridine, comparing the physical properties of the isolated base and its derivatives with those of the synthesized base[2].



2, 3-Cyclopenteno-5-methylpyridine

The presence of this base in coal tar and petroleum distillates has not hitherto been reported. In Table I is shown the comparison of the isolated base with the synthesized compound.

## Experimental

**Original Material.** — The material used in the present investigation is a coal tar base fraction called "toluidine-xylidine fraction" ($TX_n$) furnished by Yawata Chemical Industry Co., Kyushu, Japan. The boiling point range of the material is shown in Table II. This sample contains 10% of neutral oil and 34% of primary amines determined as xylidines by diazotization-titration, therefore the content of the tertiary amines which constitute the rest of the sample is approximately 56%.

**Separation of the Tertiary Amines.**—A mixture of 6 kg. $TX_n$ and 1350 cc. of concentrated sulfuric acid was steam-distilled and neutral oil and a small amount of tar acids were respectively removed as a distillate. By addition of sodium hydroxide to the residual acidic solution, 4.84 kg. of the base was recovered. Then, 2.9 kg. of acetic anhydride was added and refluxed to remove the primary amines. The reaction mixture was distilled through a 30 cm. column and the distillate up to 250°C was collected and made alkaline with sodium hydroxide and steam-distilled. The disillate, after being dried over solid sodium hydroxide, was distilled in vacuo through a fractionating column[1] with a reflux ratio of 20 : 1 and divided into the fractions shown in Table III.

In the fractions Nos. 5 and 6, which were to be examined, the primary amines were still present to a minor extent and the acetylation procedure was repeated.

TABLE I. 2,3-CYCLOPENTENO-5-METHYLPYRIDINE

| Property | The isolated base | The synthesized base | |
|---|---|---|---|
| | | By the author | Literature[2] |
| M. p.*, °C | 38.5～41 | 38.7～41 | 39～41 |
| B. p.*, °C | 225 (756 mmHg) | 225 (756 mmHg) | 222 (752 mmHg) |
| M. p. of picrate, °C | 205.2～206.2 | 204.8～205.8 | 204～206 |
| D. p. of picrolonate, °C | 211.5～212.5 | 211.5～212.5 | 210～212 |
| Elementary analysis | | | (calcd.) |
| C, % | 80.75 | 81.12 | 81.16 |
| H, % | 8.39 | 8.44 | 8.33 |
| N, % | 10.41 | 10.31 | 10.52 |
| Neutralization equivalents | 134 | — | 133.2 |

* M. p. and b. p. (micro method) are corrected values.

TABLE II

| Distillate Vol. % | First drop | 5 | 10 | 50 | 90 | 95 | Dry point |
|---|---|---|---|---|---|---|---|
| B. p., °C | 200.5 | 204.0 | 206.0 | 210.0 | 222.5 | 225.0 | 228.0 |

1) S. Jifuku, S. Nakayama, H. Suzumura and M. Uemura, *Coal Tar (Tokyo)*, **10**, 126 (1958).

2) H. L. Lochte and A. G. Pittman, *J. Am. Chem. Soc.*, **82**, 469 (1960).

TABLE III. FRACTIONATION OF THE TERTIARY AMINES

| No. of fraction | B. p. (30 mmHg) °C | Distillate g. | $n_D^{25}$ | B. p. (micro) °C | Xylidine % |
|---|---|---|---|---|---|
| 1 | FD~102 | 277.7 | 1.5160 | | |
| 2 | 102~106 | 112.9 | 1.5207 | | |
| 3 | 106~111 | 163.7 | 1.5348 | | |
| 4 | 111~114 | 65.5 | 1.5319 | 213.1 | 12.1 |
| 5 | 114~117 | 135.3 | 1.5309 | 223.6 | 7.3 |
| 6 | 117~121 | 64.7 | 1.5387 | 227.6 | 3.6 |
| 7 | 121~125 | 109.1 | 1.5720 | 231.0 | |
| 8 | 125~ | 1941.0 | | | |
| | Total | 2869.9 | | | |

The properties of the fraction, after this treatment, are shown in Table IV.

TABLE IV

| No. of fraction | 4' | 5' | 6' |
|---|---|---|---|
| $n_D^{25}$ | 1.5277 | 1.5281 | 1.5345 |
| Yield, g. | 50 | 117 | 49 |

**Isolation of 2, 3-Cyclopenteno-5-methylpyridine.** —As the chromatographic separation using a column of cupric chloride-aluminum oxide and also the urea adduct method were ineffective, the separation by solvent extraction was carried out. As the solutes, the fractions Nos. 5' and 6' of Table IV were used. A countercurrent extraction apparatus of semiautomatic type equipped with one hundred distribution tubes was employed. The volume of each tube was 20 cc. Ligroin was introduced into the apparatus as the light phase and the acidic sodium phosphate buffer solution (pH 4.78) as the heavy phase. By a single withdrawal procedure, the ligroin layers were transferred successively, giving a series of fractions, and from those fractions the bases were collected as the picrates. Results of the extractions using Nos. 5' and 6' as the solutes are shown in Table V.

The melting points shown in the table were determined on the picrates once recrystallized from ethanol. From Table V, it was observed that the new component was, next to quinoline, not easily soluble in the buffer solution; the base had a relatively large distribution coefficient.

In order to obtain a large amount of the base to work with, the extraction whose scheme is shown in Table VI was carried out using a 300 cc. separating funnel. Twenty-five grams of the fraction No. 6' was diluted with ligroin to 100 cc., to which 100 cc. of the buffer solution was added, shaken for 3 min., then allowed to settle. The heavy phase

TABLE V. COUNTERCURRENT EXTRACTION

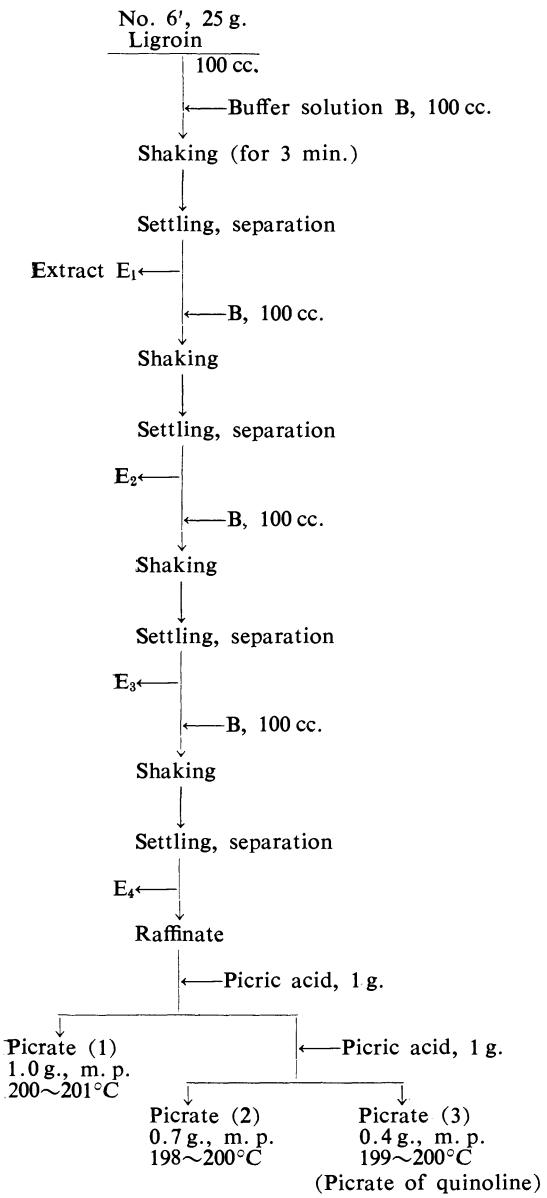
| Light phase No. | No. 5' (0.6 g.) M. p. of picrate °C | No. 5' (0.6 g.) Yield and appearance | No. 6' (1.0 g.) M. p. of picrate °C | No. 6' (1.0 g.) Yield and appearance |
|---|---|---|---|---|
| 1 | 187~189 | Yellow needles | 197 ~199 | Orange yellow plates, 0.2 g. |
| 2 | 160~167 | | 198 ~200 | |
| 3 | 164~178 | | 199 ~200 | |
| 4 | 189~194 | Pale yellow needles | 185 ~192 | Yellow needles, 0.1 g. |
| 5 | 191~194 | | 168 ~171 | |
| 6 | 195~198 | | 175 ~181 | |
| 7 | 192~198 | | 193 ~196 | |
| 8 | 192~196 | | 197 ~199 | |
| 9 | 191~195 | | 199.5~200.5 | |
| 10 | 189~192 | | 199 ~200 | |
| 11 | | | 199 ~200 | |
| 12 | | | 199.5~200 | |
| 13 | | | 198.5~199.5 | |
| 14 | | | 198 ~199 | |
| 15 | | | 197 ~198 | |
| 16 | | | 197 ~198 | |

Crude picrates from Nos. 5—9 were combined and after recrystallization from ethanol, 0.1 g. of picrate was obtained, m. p. 201~202°C.

Base from Nos. 1, 2 and 3 were identified as quinoline by their picrates and tartrates.

was drawn off and the new buffer solution was added; the extraction was repeated three more times in the same manner as described above. After the bulk of the solvent was removed by distillation, the raffinate was purified as a picrate. Recrystallization from ethanol yielded 1.7 g. of picrate, which melted at about 200°C. This picrate, when admixed with the picrate of quinoline, m. p. 198~200°C (uncorr.), showed a large melting point depression amounting to 20°C, hence it is obviously different from that of quinoline.

TABLE VI. EXTRACTION USING A SEPARATING FUNNEL




From 20 g. of fraction No. 5' by the same procedure, 0.9 g. of picrate, m. p. 196~198°C (uncorr.), was obtained. The picrate, recrystallized from ethanol melted at 201~202°C (uncorr.). This purified picrate was decomposed by addition of sodium hydroxide and the regenerated base was recovered by steam distillation followed by extraction with ether. The ether extract of the distillate was concentrated to give colorless plates, m. p. 38.5~41°C.

**Properties, Derivative and Absorption Spectra of the Isolated Base.**—*Neutralization Equivalents.*—The base (0.073 g.) was titrated by 0.1 N hydrochloric acid (F 0.999) using bromophenol blue as an indicator and measuring the pH of the solution. For the neutralization of the base, 5.45 cc. of 0.1 N hydrochloric acid was required.

Found: 134. Calcd. for $C_9H_{11}N$; 133.

*The Picrate.*—Several recrystallizations from ethanol yielded yellow needles, m. p. 205.2~206.2°C.

Found: N, 15.16. Calcd. for $C_{15}H_{14}N_4O_7$: N, 15.47%.

*The Picrolonate.*—It was prepared from equimolar quantities of picrolonic acid and the base in ethanol. Recrystallization from ethanol yielded yellow needles which decomposed at 211.5~212.5°C.

*The Ultraviolet Absorption Spectrum.*—The spectrum in cyclohexane is shown in Fig. 1.

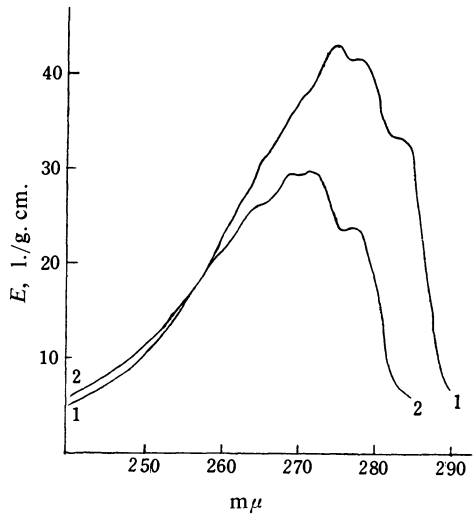



Fig. 1.
1, 2,3-Cyclopenteno-5-methylpyridine
2, 2,3,5-collidine

The ultraviolet spectrum of 2,3-cyclopenteno-5-methylpyridine ($\lambda_{max}$ 276 mμ) has the same similarity to that of 2,3,5-collidine ($\lambda_{max}$ 271 mμ) as the spectrum of 2,3-cyclopenteno-6-methylpyridine ($\lambda_{max}$ 275 mμ) has to that of 2,3,6-collidine ($\lambda_{max}$ 270 mμ)[1,2].

*The Infrared Absorption Spectrum.*—The spectrum in carbon disulfide is shown in Fig. 2.

Characteristic absorption bands at 13.7 μ and 14.1 μ are similar to those of 2,3,5-collidine. This similarity may well be explained by the relationship between absorption bands and the position of substituents of alkyl pyridines[3].

3) H. Shindo and N. Ikekawa, *Pharm. Bull.* (*Tokyo*), **4**, 192 (1956).

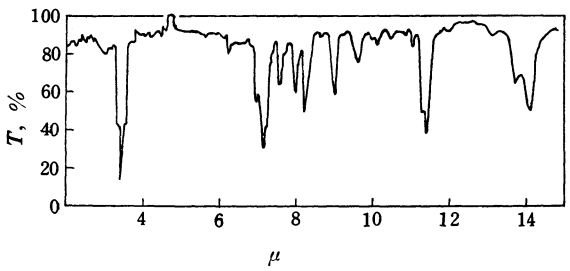



Fig. 2.

In Fig. 3 are shown the specific absorption bands appearing in the fingerprint region of cyclopenteno-pyridine, 2,3-dimethylpyridine, 2,3-cyclopenteno-6-methylpyridine and 2,3,6-collidine.

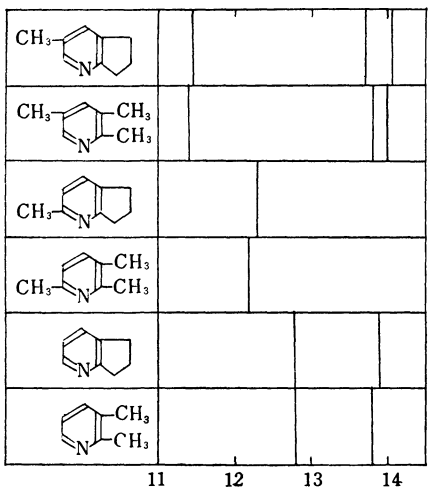
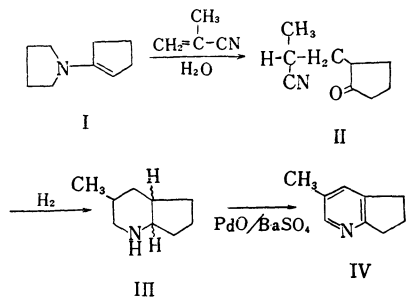



Fig. 3.

**The Synthesis of 2,3-Cyclopenteno-5-methylpyridine.**—In order to compare the isolated base from coal tar with the authentic sample of the base, a synthesis was carried out in the manner similar to that described by Lochte et al.[2]. The procedure is schematically shown below.




*Cyclopentano-pyrrolidine Enamine (I).*—A solution of 10 g. of cyclopentanone and 26 g. of pyrrolidine in 140 cc. of dry benzene was refluxed for 6 hr. in a flask fitted with an azeotropic water separator. The benzene and the excess of pyrrolidine were distilled off leaving a viscous liquid, 15.8 g., which was used without further purification in the subsequent reaciton.

*2-(2-Methyl-2-cyanoethyl)-cyclopentanone (II).*—Methacrylonitrile* (9.5 g.) was added to a solution of the enamine I in 100 cc. of dimethylformamide. The resulting solution was refluxed for 31 hr. in a flask fitted with a tower of calcium chloride. The bulk of the solvent was then removed by distillation and to the residue were added 57 cc. of water and 4 cc. of glacial acetic acid. This solution was refluxed for 2 hr. 40 min., cooled and extracted four times with benzene. The combined benzene extracts were washed three times with 10% hydrochloric acid, twice with 10% potassium carbonate solution, and once with water and dried over sodium sulfate. After removal of the benzene, the residue was distilled in vacuo giving 4.6 g. of a liquid boiling at 125~126°C (5 mmHg), $n_D^{25}$ 1.4580 and 1.1 g., $n_D^{25}$ 1.4709 (reported $n_D^{25.5}$ 1.4624). The semicarbazone prepared from the two fractions melted at 195.4°C and 189~190°C respectively (reported 195°C).

*Hexahydro-2,3-cyclopenteno-5-methylpyridine (III).*—Raney nickel** was added to a solution of II in absolute ethanol. This mixture was hydrogenated at an initial $H_2$ pressure of 34 kg./cm² and 120°C in a 100 cc. autoclave equipped with an elecromagnetic stirring device. The Raney nickel was filtered off and the solvent was removed by distillation in vacuo. The residual liquid was distilled in a Claisen flask yielding a corless liquid, b. p. 85°C (21 mmHg).

The experimental results are shown in Table VII.

*2,3-Cyclopenteno-5-methylpyridine (IV).*—In the present experiment, III was dehydrogenated in the liquid phase with palladium oxide/barium sulfate in place of palladium-carbon described in the literature cited. A mixture of equal amounts by weight of the base and the catalyst (palladium oxide/barium sulfate) was placed in a flask and refluxed in a nitrogen stream in an oil bath. The cooled mixture was extracted with ether and the ether extract was concentrated to give the crude base.

The experimental result was shown in Table VIII. The pure base was obtained by the decomposition of the recrystallized picrate as described above.

*Preparation of Palladium Oxide/Barium Sulfate*[5].—Palladium chloride (0.3 g.) was dissolved in a mixture of 15 cc. of 2 N sulfuric acid and 120 cc.

* Preparation of methacrylonitrile—commercial methacrylamide (17.0 g.) and 20 g. of $P_2O_5$ were thoroughly mixed and heated in a flask over free flame. The distillate, after treatment with a small amount of $K_2CO_3$, was distilled to give a fraction, 8 g., boiling at 89~89.5°C, $n_D^{22}$ 1.4001 (reported[4] $n_D^{20}$ 1.4007).

4) Rohm and Haas, G. m. b. H., U. S. Pat. 2210320 (1940).

** Raney nickel—one gram of commercial alloy (Ni : Al = 50 : 50) was gradually added with stirring to 10 cc. of 20% sodium hydroxide solution in a beaker placed in a water bath maintained at 50°C, over a period of about 50 min. After the addition was complete, the resulting Raney nickel was washed with water to the neutral pH, then with 95% ethanol and finally with absolute ethanol.

5) R. Kuhn and H. J. Haas, *Angew. Chem.*, 67, 785 (1955).

Table VII. Hydrogenation

| Sample g. | Conditions | | | | Product | | |
|---|---|---|---|---|---|---|---|
| | $H_0$ kg./cm² | $\Delta P$ kg./cm² | Temp. °C | Period | Wt. g. | $n_D^{25}$ | Yield % |
| 2.9 | 33.8 | 10.8 | 108～120 | 4 hr. 35 min. | 3.75 | 1.4820 | 63 |
| 3.4 | 34.1 | 15.7 | 108～118 | 5 hr. 30 min. | | | |

Table VIII. Dehydrogenation

| Hexahydro-base(III) g. | $PdO/BaSO_4$ g. | Conditions | | Product | |
|---|---|---|---|---|---|
| | | Temp., °C | Period | Yield, g. | M. p., °C |
| 0.37 | 0.37 | 180 | 6 hr. | 0.35 | below 20 |
| 0.52 | 0.52 | 200～210 | 8 hr. 15 min. | 0.35 | 35～37 |

of water which was kept at 80°C. After the solution was allowed to settle for 20 min., it was poured with vigorous stirring into 165 cc. of 0.2 N barium hydroxide yielding a precipitate. It was filtered off by suction, washed with 240 cc. of water and dried in vacuo. Pale brown powder was obtained; 3.7 g.

**Derivatives of the Synthesized Base.** — *The Picrate.* — Yellow needles, m. p. 204.8～205.8°C. From 900 mg. of the picrate, 250 mg. of the base, m. p. 38.7～41°C was regenerated by addition of sodium hydroxide followed by steamdistillation.

*The Picrolonate.*—It was prepared in the same manner as described in the case of the isolated base. Recrystallization from ethanol yielded yellow needles which decomposed at 211.5～212.5°C.

**Confirmation.** — The isolated 2,3-cyclopenteno-5-methylpyridine, the picrate and the picrolonate when admixed with the corresponding synthesized sample gave no melting point depression. The infrared absorption spectrum of the isolated base and that of the synthesized base were superimposable.

The author wishes to thank Professor Ryozo Goto, Kyoto University, for his helpful discussions and criticisms of this work.

*The Laboratory of Research Centre*
*Yawata Chemical Industry Co., Ltd.*
*Chuo-ku, Tokyo*

# *Fischer-Tropsch Synthesis with Tubular Reactor of 18.1 l. Catalyst Bed. II. Reactor with Temperature Gradient along Out-side Wall*

By Michio KURAISHI*, Minoru KURITA, Tadasuke HOSOYA, Hideo ICHINOKAWA, Kiyoshi OGAWA and Hiroshi UCHIDA

(Received January 18, 1961)

A previous paper[1] in this series described the Fischer-Tropsch synthesis with the reactor whose out-side wall temperature was kept constant along the whole length by means of a heat transfer medium of flowing oil. However, the catalyst bed temperature tended to rise very high, and the product yield remained below that to be expected from the synthesis results with the reactor of the same design but of a much smaller catalyst bed of 2 l. A closer investigation in this respect disclosed that the large magnitude of temperature rise was mainly due to a high heat transfer resistance across an oil film on the out-side wall of the reactor. For the better performance, therefore, the reactor ought to be modified in construction in order that the heat transfer efficiency across the oil film might be improved. By the use of the reactor which has been improved along this line, the present synthesis experiments are conducted.

The previous paper, in addition, dealt with

* Present address: Japan Gas Chemical Co., Enoki-cho, Niigata.

1) M. Kuraishi, M. Kurita, T. Hosoya, H. Ichinokawa, K. Ogawa and H. Uchida, This Bulletin, 34, 780 (1961).

the calculation of the temperature profile in the catalyst bed on the basis of the concentration gradient determined along the heights of the catalyst bed. Because of the temperature gradient already present in the oil surrounding the reactor, the method of the calculation, however, can be applied with difficulty to the result with the present reactor. In this paper the calculating method with the result is proposed.

## Experimental

In an effort to improve the heat transfer efficiency across the oil film on the out-side wall of the previous reactor, the previous reactor system was subjected to some modifications. Fig. 1 shows a

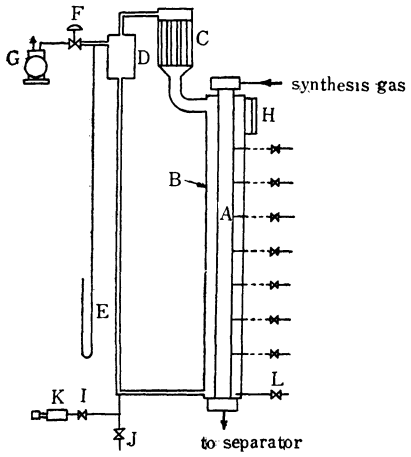



Fig. 1. Schematic diagram of reactor system.
A, Reactor
B, Cylinder for oil bath
C, Condenser
D, Reservoir
E, Contact manometer
F, Magnetic valve
G, Pump
H, Level indicator
I, J, L, Needle valves
K, Dowtherm feeder

schematic diagram of the system after the modifications. The main modification made was that the reactor (A, 10 m. high by 50 mm. I. D.) was placed in a cylinder (B) which was filled with oil (Dowthem) boiling under a reduced nitrogen pressure, whereas the previous reactor had been held in the oil under forced circulation at a fixed flow rate under an atmospheric pressure of nitrogen. A small amount (ca. 200 l./hr.) of nitrogen was always being introduced from a valve (L) into the oil bath by way of a number of openings (0.8 mm. diameter) perforated along two semi-circular tubes placed, opposite to each other, at the bottom of the cylinder. The nitrogen gas passed upwards through the oil, and could easily be controlled at a fixed pressure by means of a leak opened by a magnetic valve (F) which was coupled with a mercury contact manometer (E).

The top zone of the oil bath was equipped with a level indicator (H), by the aid of which the oil was maintained at a constant level by either introducing or withdrawing a small quantity of oil through a valve (I) or (J), respectively. A condenser (C) was placed directly above the top of the cylinder, in which the oil vapor accompanying the nitrogen stream was refluxed back into the oil bath. A reservoir (D) served to avoid a sudden change in the nitrogen pressure. After passing through C, D and F, the gas was finally drawn out by a pump (G).

In view of the kind of reactor type called rectification cooling type, which was originated by Dorschner[2], the present reactor may also be known as such, but it differs from Dorschner's reactor in some respects.

Besides the sintered catalyst (designated catalyst A hereafter) in the previous paper[1], a fused iron catalyst (designated catalyst B hereafter) of the same promoter-composition was employed in this study. Granules of the catalyst ranging from 5 to 2 mm. in size were used, and the catalyst bed of 18.1 l. contained 39.41 kg. of the granules after reduction. The technique of the catalyst pretreatment as well as of the synthesis was essentially the same as was described elsewhere[3] in detail.

## Results and Discussion

**Results.** — Table I shows, together with the synthesis variables, results from a series of five experiments, among which two experiments were carried out by using catalyst A while the other three ones by using catalyst B. Numerals listed in the column of nitrogen pressure serve as a measure to estimate roughly the oil bath temperature: the higher the pressure is, the higher the temperature rises. Further, the axial temperature profiles in the catalyst bed as well as in the oil bath are exemplified in Figs. 2A, B, C and D for experiments Nos. 1, 2, 6 and 7, respectively.

It was after the experiment described in the previous paper[1] (hereafter simply called experiment A) had been made that the bed of catalyst A was used in this study, and hence the bed had already undergone an activity decrease to some extent. In this connection, a much higher yield of the product (oil plus wax) may have not been produced in experiment No. 1 as compared with the yield (14.14 kg./day) in experiment A, in spite of the improvement made for the heat transfer efficiency[4]. Nevertheless, one can yet recognize the effects of the improvement clearly. One of the effects is the axial temperature gradient

2) O. Dorschner, *Chem. Ing. Tech.*, **25**, 277 (1953).
3) M. Kuraishi, H. Ichinokawa et al., *J. Chem. Soc. Japan, Ind. Chem. Sec.* (*Kogyo Kagaku Zasshi*), **63**, 1588 (1960).
4) It is to be noted that in experiment No. 1 the temperature at the axial middle point of the oil bath was essentially the same as the oil bath temperature in experiment A.

TABLE I. RESULTS OF SYNTHESIS EXPERIMENTS

| Exp. | Catalyst | Pressure kg./cm² (gauge) | Nitrogen pressure mmHg | Space velocity of inlet gas $hr^{-1}$ | Space velocity of raw gas $hr^{-1}$ | Volume contraction % | Oil plus wax kg./day | Aqueous product kg./day | Oil plus wax per $m^3$ $(CO+H_2)$ g. | Use ratio $H_2/CO$ |
|---|---|---|---|---|---|---|---|---|---|---|
| No. 1 | A | 30 | 580 | 2250 | 668 | 41.1 | 15.91 | 21.94 | 105 | 1.10 |
| No. 2 | A | 30 | 760 | 2270 | 816 | 44.6 | 21.21 | 27.45 | 106 | 1.11 |
| No. 5 | B | 25 | 440 | 2080 | 582 | 41.5 | 16.83 | 20.09 | 131 | 1.06 |
| No. 6 | B | 30 | 520 | 2125 | 790 | 48.1 | 24.39 | 32.82 | 118 | 1.06 |
| No. 7 | B | 30 | 480 | 1670 | 785 | 49.8 | 26.03 | 30.96 | 125 | 1.10 |

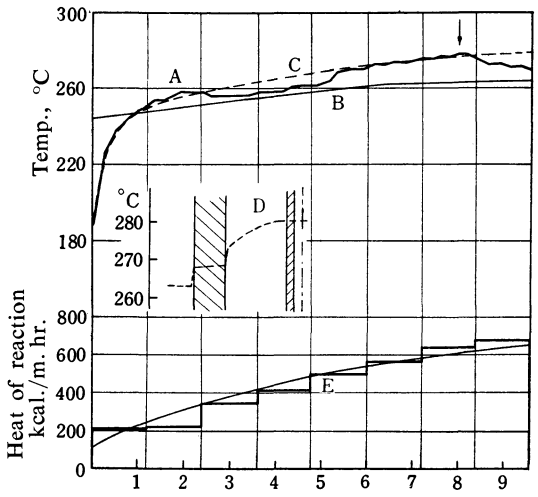



Fig. 2A. Experiment No. 1.

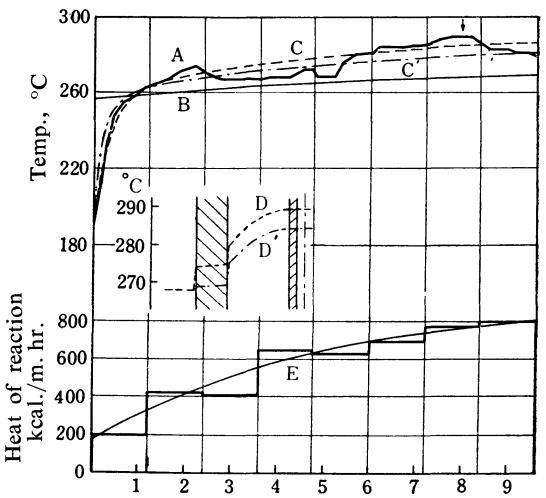



Fig. 2B. Experiment No. 1.
C, D, Temperature profile calculated by the use of $h'_L=600$ kcal./m² hr.°C
C', D', Temperature profile calculated by the use of $h'_L=4800$ kcal./m² hr.°C

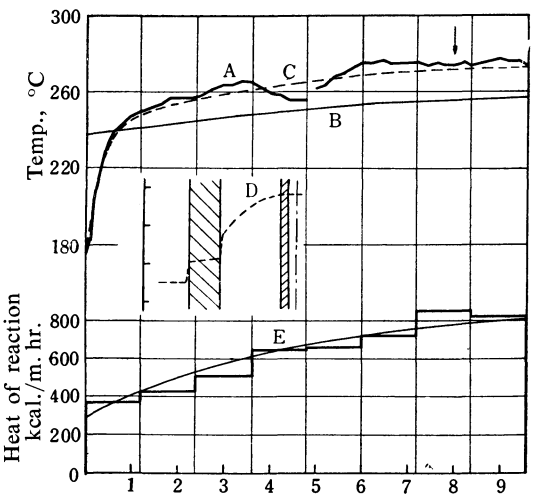



Fig. 2C. Experiment No. 6.

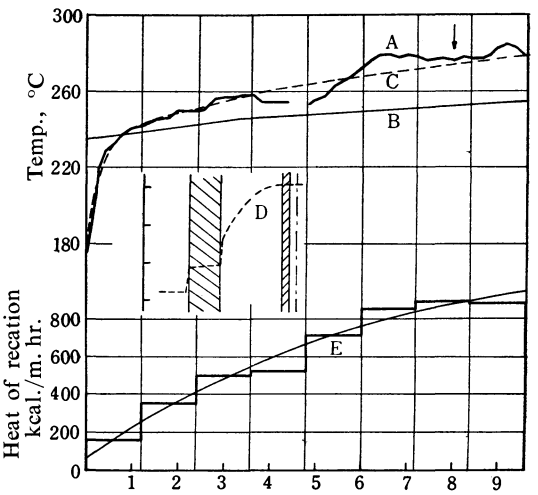



Fig. 2D. Experiment No. 7.

Figs. 2A-D. Experimental and calculated temperature profiles (above) and heat of reaction as function of $x$ (below, E).
A, Experimental temperature profile
B, Oil bath temperature
C, Calculated axial profile
D, Calculated radial profile

in the oil bath, increasing continuously from top to bottom. The appearance of the gradient arises from the fact that the boiling temperature of oil is continuously increased with gravity of increasing amounts of oil in the oil bath cylinder from top to bottom. The temperature gradient thus produced along the oil bath may have helped the catalyst bed temperature to rise with the distance ($x$) from the top of the bed. In contrast to the above, the temperature profile in the bed of experiment A showed a downward tendency along the lower half of the bed. Another effect is the smaller magnitude of temperature difference between the oil bath and the reactor axis, in other words, the smaller magnitude of the bed over-temperature (hereafter denoted by $(t-t_b)$, where $t$ and $t_b$ are the temperatures measured along the axis of catalyst bed and along the oil bath, respectively), which was 15°C at a maximum for experiment No. 1 while 25°C for experiment A.

By using a fresh bed of catalyst B in place of the deteriorated one of catalyst A, much higher yields of the product, attaining from 24 to 26 kg./day, were produced (refer to the results of experiments Nos. 6 and 7), even though the nitrogen pressure was kept below that of experiment Nos. 1 and 2. Moreover, the magnitude of $(t-t_b)$ remained comparatively small: at the region of a maximum $(t-t_b)$, 22 and 30°C for experiments Nos. 6 and 7, respectively. The somewhat larger magnitude of $(t-t_b)$ observed with the latter experiment may be accounted for by a lower

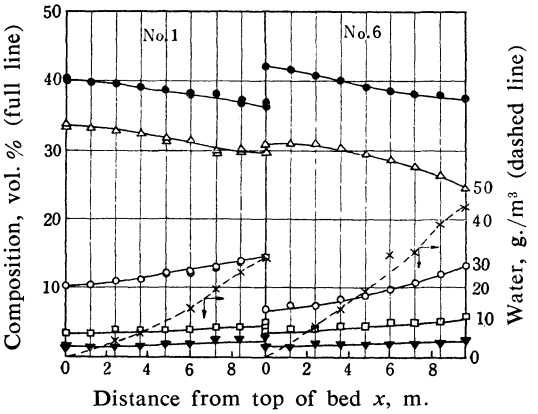



Fig. 3. Concentration gradient along catalyst bed.

—●— Hydrogen
—△— Carbon monoxide
—○— Carbon dioxide
—□— Gaseous paraffin
—▼— Gaseous olefin
—×— Water

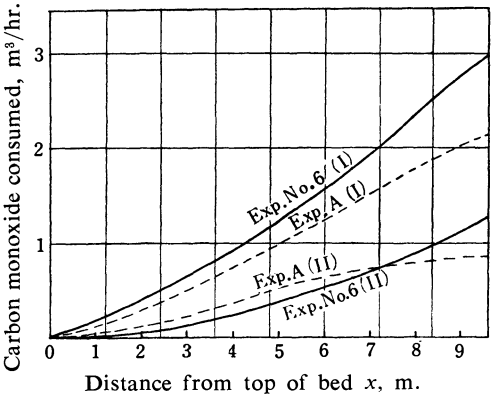



Fig. 4. Carbon monoxide consumed by either reaction (1) or (2) as a function of $x$.

space velocity of the inlet gas, details of which will be stated later.

The concentration gradient of the individual components along the reactor was determined in the same manner that was made in experiment A[1]. Among the results the gradient for experiment No. 6, for instance, is shown in the right half of Fig. 3, while the gradient for experiment A is given again in the other half. Starting with the results of Fig. 3 and following the procedure as reported in the previous paper[1], one can calculate amounts of carbon monoxide consumed with the progress of the synthesis either by $2H_2+CO \rightarrow >CH_2+H_2O\cdots$ (1) or by $CO+H_2O \rightarrow CO_2+H_2\cdots$(2). Fig. 4 illustrates plots of the amount vs. $x$, together with the recited ones for experiment A. The figure discloses that although the amounts of carbon monoxide consumed by the reaction 1 in the top zone of the catalyst beds differ slightly from each other the amount at the end of the bed in experiment No. 6 attains 3/2.1 times as large as the amount in experiment A. In view of the fact it can be seen that in experiment No. 6 better use was made of the lower half of the catalyst bed than that in experiment A.

**Method of Calculating Temperature Profiles in Catalyst Bed.**—Because of the presence of the temperature gradient along the oil bath, the solution to the heat balance equation, as cited in the previous paper[1], is to be made under the different boundary conditions from the previous ones. The equation is then given as follows.

$$C_pG\frac{\partial t}{\partial x}=\frac{1}{r}\left[\frac{\partial}{\partial r}\left(\lambda_r\cdot r\frac{\partial t}{\partial r}\right)+\frac{\partial}{\partial x}\left(\lambda_x\cdot r\frac{\partial t}{\partial x}\right)\right]+Q \quad (1)$$

with the following boundary conditions,

$$t=t_0 \quad \text{at} \quad x=0$$

$$\lambda_r\partial t/\partial r+U(t-t_b)=0 \quad \text{at} \quad r=r_2$$

and $\partial t/\partial r=0$ at $r=r_1$

where $C_p$ is the heat capacity per unit mass of fluid, $G$ is the mass velocity based on an empty tube, $r$ is the distance in lateral direction, $\lambda$ is the effective thermal conductivity of the catalyst bed system, $Q$ is the reaction heat, $U$ is the overall heat transfer coefficient, $r_1$ and $r_2$ are the inner and the outer radii of the catalyst bed, respectively.

A numerical solution of Eq. 1 may be possible. However, the calculation will be very time-consuming since $t_b$ varies with $x$. As a compromise, it would be rather convenient for the present purpose to start with a more simplified equation of the heat balance, in which the temperature is assumed to be radially uniform at every cross section of the bed that an average temperature[5] ($t_{av}$) over the bed cross section may simply be taken into account. The solution then gives the axial temperature profile. Once the axial temperature profile has been drawn, Eq. 1 can be solved more easily with respect to a cross section, in the neighborhood of which the axial temperature is kept essentially constant. The solution gives the radial temperature profile.

Under the assumption of uniform temperature across the bed, the following equation of the heat balance can be established,

$$G_pG\mathrm{d}t/\mathrm{d}x+2\pi r_2U'(t-t_b)/S=Q \qquad (2)$$

with the boundary condition that $t=t_0$ at $x=0$. The symbol $S$ in the equation is the cross sectional area of the bed, and the second term in the left-hand side of the equation concerns the heat transfer across the tube wall of the reactor held in the oil bath whose axial temperature gradient is assumed to be given by a linear function of $x$, namely $t_b=t_{bo}+ax$, where $t_{bo}$ is the oil bath temperature at $x=0$. The constant $a$ takes a value characteristic of the gradient in the oil bath. It should further be noted that $U'$ is to be distinguished from $U$ in Eq. 1. The calculation of $U'$ is made by taking the tube wall coefficient of the heat transfer based on $t_{av}$ (denoted by $h'$) into account whereas $U$ by taking the coefficient based on $t$ at $r=r_2$ (denoted by $h$) into account. In this paper, $h'$ with respect to the present annular shaped cylinderical bed was evaluated by making use of the formula[6] proposed by Maeda et al.[7] for $h'$ with a cylindrical bed, while $h$ by the aid of the formula[8] by the Hatta et al.[9] In the latter formula, $\lambda_r$ is taken into consideration.

In Eq. 2, $Q$ is again approximated to

$$Q=C_1\mathrm{e}^{-Mx}-C_2\mathrm{e}^{-Nx} \qquad (3)$$

where $C_1$, $C_2$, $M$ and $N$ are constants. Combination of 2 with 3, and subsequent rearrangement give

$$\mathrm{d}t/\mathrm{d}x+A(t-t_{bo}-ax)=G_1\mathrm{e}^{-Mx}-G_2\mathrm{e}^{-Nx} \qquad (4)$$

in which the following abbreviations are introduced.

$$A\equiv 2\pi r_2U'/C_pGS,\quad G_1\equiv C_1/C_pG$$
$$G_2\equiv C_2/C_pG \qquad (5)$$

The solution of Eq. 4 is given by

$$t=t_{bo}+\mathrm{e}^{-Ax}\left[t_0-t_{bo}+\frac{G_1}{A-M}\left\{\mathrm{e}^{(A+1)x}-1\right\}-\frac{G_2}{A-M}\left\{\mathrm{e}^{(A-N)x}-1\right\}\right]+a\left\{x-\frac{1}{A}(1-\mathrm{e}^{-Ax})\right\} \qquad (6)$$

On the other hand, under the assumption of $\mathrm{d}t/\mathrm{d}x=0$, Eq. 1 is reduced to a simpler form of

$$\lambda_r\{\mathrm{d}^2t/\mathrm{d}r^2+(1/r)(\mathrm{d}t/\mathrm{d}r\}+Q=0 \qquad (7)$$

with the boundary conditions that $\mathrm{d}t/\mathrm{d}r=0$ at $r=r_1$, and $\lambda_r\mathrm{d}t/\mathrm{d}r+U(t-t_b)=0$ at $r=r_2$. The solution results in Eq. 8.

$$t=t_b+\frac{Qr_2^2}{4\lambda_r}\left[\left\{1-\left(\frac{r}{r_2}\right)^2\right\}+2\left(\frac{r_1}{r_2}\right)^2\ln\frac{r}{r_2}+\frac{2\lambda_r}{Ur_2}\left\{1-\left(\frac{r_1}{r_2}\right)^2\right\}\right] \qquad (8)$$

By the aid of Eqs. 6 and 8 both the axial and the radial temperature profiles can be drawn.

Let us make an approximate check on the accuracy of the present calculation method by performing a profile calculation. The calculation is carried out on the basis of the experimental data of experiment A, and the resulting profiles are shown in Fig. 5 with the dotted and dashed lines, of which the radial one is given for the cross section at $x=6$ m. In the neighborhood of the cross section, the axial temperature has been found nearly constant. For the sake of comparison, the figure is included with the previous profiles (dashed lines) calculated by using the solution with no simplification of Eq. 1. The respective profiles calculated by either one of the two

5) The average temperature ($t_{av}$) is defined by

$$t_{av}=\int_{r_1}^{r_2}t\cdot 2\pi r\mathrm{d}r/\pi(r_2^2-r_1^2)$$

6) $h'D/k=4.90(R_{ep})^{0.60}\mathrm{e}^{-2.2d_p/D}$, where $D$ is the diameter of bed, $k$ is the thermal conductivity of fluid, $R_{ep}$ is the modified Reynolds number, and $d_p$ is the diameter of catalyst granules (4 and 3.4 mm. for catalysts A and B, respectively). In the evaluation of $h'$, $D_{eq}$ defined by $D_{eq}=D_2-D_1$ is used in place of $D$.

7) S. Maeda and K. Kawazoe, *Chem. Eng. Japan* (*Kagaku Kogaku*), **17**, 276 (1953).

8) $\lambda_r/k=0.209(R_{ep})^{0.87}$ and $hD_{eq}/\lambda_r=127(R_{ep}\cdot d_p/D_{eq})^{-0.87}$.

9) S. Hatta and S. Maeda, *Chem. Eng. Japan* (*Kagaku Kikai*), **13**, 79 (1949).

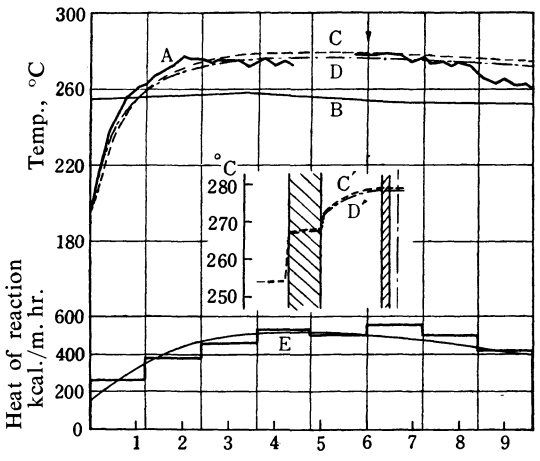



Fig. 5. Experimental and calculated temperature profiles (above) and reaction heat as a function of $x$ (below, E) for experiment A.

A, Experimental temperature profile
B, Oil bath temperature
C, C', Profiles as cited in previous paper
D, D', Profiles calculated by the aid of Eqs. 6 and 8

different methods show a good approximation with each other. However, it should be noted that the present method of calculating the axial temperature profile is available only when $\lambda$ is so high that the radial temperature gradient can be ignored. It otherwise may lead to errors, for instance, in such a case that the synthesis is made by the once-through operation where the mass velocity of the inlet gas, as a consequence, $\lambda$ is usually much lower.

**Calculation of Temperature Profile.** — Before proceeding to the profile calculation, the coefficient ($h_L$) of heat transfer referred to the out-side wall of present reactor, over which the oil film is kept under nucleated boiling, has to be evaluated. Although there have appeared a few papers[10] dealing with the heat transfer phenomenon considered, none of them except for the paper by Nishikawa[11] is available for the calculation. Accordingly, a rough estimation of $h_L$ is made for experiment No. 2 by means of Nishikawa's formula, which results in the value of 4800 kcal./m² hr. °C. By using this value the profile calculation is made[12]. The profiles thus drawn are shown in Fig. 2B with the dotted and dashed lines, which appear to be in a poor agreement with the experimental profiles: the calculated axial temperature profile rises more rapidly in the top zone while it lies below the experimental one in the lower half of the catalyst bed, and in addition the radial temperature profile at the cross section of $x=8$ m. shows a maximum temperature across the bed of 284.3°C, in contrast to the measured one of 289°C. The disagreement may probably be due to too high an estimated value of $h'_L$, consequently of $U'$.

The calculation is then repeated with other different values of $h'_L$ for a better agreement between the measured axis-temperature in the bed and the calculated one, and finally $h'_L=600$ kcal./m² hr. °C, consequently $U'=391$ kcal./m² hr. °C, is conveniently chosen, by the choice of which the temperature of 289.5°C is attained. The value of $h'_L$ has thus appeared only one eighth of the value afore-cited[13], but it is still 3.5 times as much as the value in the previous reactor. The axial profile calculations have then been made, and an improvement in the accordance between the calculated and the measured profiles is obtained (refer to the dashed line in Fig. 2B). The same calculations made on the basis of the data of the other experiments of Nos, 1, 6 and 7 results in the profiles as cited in Figs. 2A, C and D, respectively. The profiles are in a good agreement with measured ones, except for a small intermediate range where the measured profile lies somewhat below the calculated one. Moreover, the radial temperature profile is visualized by the calculation as shown in the figure, and a comparison of the profile with that in Fig. 5 is suggestive of the improving effect of the present procedure on the heat transfer efficiency across the out-side wall. In this study, however, no experimental evidence is available for the radial profile.

It should be noted that the present procedure of improving the heat transfer efficiency can effectively be applied only when the difficulty exists in the heat transfer resistance across the liquid film on the out-side wall of the reactor. In this respect, a comparison between the results of experiment Nos. 6 and 7 shows that the magnitude of $(t-t_b)$ is a

10) Y. Y. Hsu and J. W. Westwater, *Am. Inst. Chem. Engrs. J.*, **4**, 58 (1958); C. Corty and A. S. Foust, *Chem. Eng, Progr., Symposium Ser.* No. 17, **51**, 1 (1955). S. A. Guerrieri and R. D. Talty, ibid., No. 18, **52**, 69 (1956), et al.

11) K. Nishikawa, *Trans. Jap. Soc. Mech. Eng.*, No. 120, **22**, 551 (1956).

12) In fact, the temperature gradient in the oil bath is convex upwards instead of being a linear function of $x$, as shown in Figs. 2A, D. In the calculation of the profile, a few axial step lengths are chosen, and the solution is applied to each of the steps successively. Although the integration constant in the solution remains the same in the first step where the boundary condition is $t=t_0$ at $x=0$, it differs in value for the succeeding steps because the different boundary condition that $t$ at the end of the first step is equal to $t$ at the top of the second step, and so forth, are established.

13) We are not as yet certain of the accurate reason why the value of $h'_L$ thus chosen is far smaller than that obtainable from Nishikawa's formula.

little smaller for experiment No. 6 which was conducted under the essentially same operating conditions, except for the greater $G$, than those in experiment No. 7. As regards the present two experiments where $h'_L$ is as high as 600 kcal./m$^2$ hr. °C, the greater value of $\lambda$[14], which is necessarily accompanied by the increasing $G$, may therefore become rather responsible for the smaller magnitude of $(t-t_b)$. The effect of varying values of $G$ on $(t-t_b)$ can be seen more clearly when the results of the once-through operation is considered[15].

Dorschner[2] has already pointed out that the outside wall temperature gradient increasing from top to bottom exerts an advantageous effect on an efficient use of the catalyst bed. For the purpose of producing such a temperature gradient, he employed a bath of an oil mixture consisting of hydrocarbons of different boiling points, whereas in the present procedure one kind of oil, Dowtherm, is simply used. In addition, the procedure has another advantage of providing a better means of temperature control: the oil bath temperature has to be increased successively to follow the deterioration of the catalyst activity, which can be done by a simple regulation of the nitrogen pressure. However, it suffered from the following limitation that a considerable magnitude of the temperature difference (for example, ca. 20°C from top to bottom in the present reactor) can not be produced until the reactor reaches as high as 10 m.

14) The values of $\lambda$ for experiment Nos. 6 and 7 were 5.09 and 4.03 kcal./m.·hr. °C, respectively.
15) The results will be reported elsewhere.

**Summary**

The present experiments on the Fischer-Tropsch synthesis have been made with the reactor which was placed in a bath of oil boiling under a reduced nitrogen pressure. The heat transfer efficiency referred to the out-side wall of the reactor has been improved considerably, and, as a consequence, the magnitude of the bed over-temperature remains comparatively small, in spite of the high yield of the product attaining 24~26 kg./day.

The axial and the radial temperature profiles have been separately calculated on the basis of the concentration gradient determined along the heights of the reactor: first the calculation of the former profile under the assumption of uniform temperature across the bed, and secondly that of the latter profile at a cross section in the neighborhood of which the axial temperature is approximately constant. By the convenient choice of 600 kcal./m$^2$ hr. °C for the tube wall coefficient of heat transfer referred to the out-side wall of the present reactor, the calculated axial temperature profile is in good agreement with the experimental profile except for a small intermediate range.

The authors are grateful to Mr. M. Oba, Mr. A. Matsuda, Mr. H. Imai and Mr. K. Shimomura for their assistance in the synthesis experiments.

*Government Chemical Industrial Research Institute, Tokyo*
*Shibuya-ku, Tokyo*

# *Organoboron Compounds. I. On the Reaction of n-Butylboronic Acid with Polyvinylalcohol*

By Seiji KATO, Yojiro TSUZUKI and Shigenobu KITAJIMA

(Received October 17, 1960)

It is well-known that boric acid reacts with various diols and sugars, giving more acidic complexes, and thus boric acid can be titrated with standard sodium hydroxide in the presence of mannitol. One of the authors[1] previously studied the reactions polarimetrically and showed that the formation of the complexes is a reaction of ionic nature. Boric acid, reacting with polyvinylalcohol, also forms polyvinyl borate ester. Owing to this reaction a remarkable change is observed on the viscosity of aqueous polyvinylalcohol on the addition of boric acid, hence boric acid is available as a modification agent of the viscosity of aqueous polyvinylalcohol when filaments are spum from it. In a similar manner esters of boronic acid with polyols can be formed, which have been known as arneboronates. Kuivila[2] prepared

1) Y. Tsuzuki, This Bulletin, **16**, 23 (1941).

2) H. Kuivila, *J. Org. Chem.*, **19**, 780 (1954).

them by the reaction of some arylboronic acid with numerous diols and sugars.

The present paper deals with the reaction of *n*-butylboronic acid with polyvinylalcohol, and discusses the experimental method, esterification grade, and some properties of the products.

## Experimental

**Preparation of *n*-Butylboronic Acid.** — *n*-Butylboronic acid was prepared in an atmosphere of nitrogen, practically according to Johonson's method[3], in the following way:

$$n\text{-Bu-MgBr}+B(OCH_3)_3 \rightarrow n\text{-Bu-B}(OCH_3)_2+MgBrOCH_3$$

$$n\text{-Bu-B}(OCH_3)_2+H_2O \rightarrow n\text{-Bu-B}(OH)_2+CH_3OH$$

From 80.6 g. (0.50 mol.) of *n*-butylmagnesiumbromide and the equivalent quantity of methylborate (52 g.) was obtained *n*-butylboronic acid as fine crystals, m. p. 92~94°C, yield ca. 50 g. (ca. 50% of the theory).

**Esterification of Polyvinylalcohol with *n*-Butylboronic Acid.** — Purified polyvinylalcohol (PVA) which has the polymerization grade of about 1500 and was reprecipitated by the usual method is dissolved in water, the concentration of which is always kept constant (2.5%). The concentration of boronic acid solutions varied from experiment to experiment. The solution of boronic acid is placed in a 500 ml. four-necked flask with a reflux condenser, and a 2.5% solution of PVA is dropped from a separating funnel at a temperature from 40 to 70°C during one hour, and stirring is continued for one more hour. An insoluble product appears as a white emulsion. On salting out this emulsion, a gum-like material is produced. This product is dried in vacuo and reprecipitated from benzene solution into cold methanol for purification.

**Determination of Boron.**—Although a number of methods for the analysis of boron have been proposed, they are for the most part troublesome. The present authors have modified the method of Martin in the following way[4], which is proved to be easier and more practical.

The sample is refluxed with a sodium peroxide solution for several hours until it is dissolved. The solution is exactly neutralized to pH 6.9 with hydrochloric acid by the help of a pH-meter and on adding mannitol the solution is titrated back until the pH-meter exactly indicates the mark of 6.9. The content of boron can be estimated from the data*.

**Infrared Spectra.** — *n*-Butylboronate ester is dissolved in carbon tetrachloride and a thin film is made on a mercury dish. The thickness was about 0.03 mm. The apparatus used was a Hitachi spectrophotometer EPI-2.

## Results and Discussion

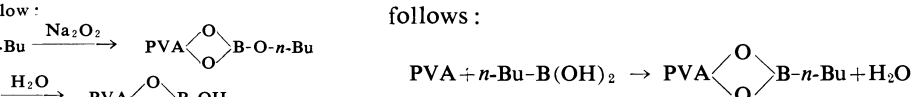
Polyvinylalcohol (PVA) reacts with *n*-butylboronic acid instantly in aqueous solution. The product is obtained in a state of emulsion, but after salting out, it can be obtained as a solid. If the concentration of *n*-butylboronic acid is varied against the constant concentration of PVA, the products are varied in form from gum-like to transparent white hard solids. The materials obtained are all insoluble in water, but dissolve in many organic solvents. These differences chiefly depend upon the boron content of the products. The solubility of the products increases with the increasing boron content. Table I shows the solubility in several organic solvents, of the product which contains the highest quantity of boron.

TABLE I. THE SOLUBILITY OF PVA-*n*-BUTYLBORONATE

| Solvent | Solubility | Solvent | Solubilty |
|---|---|---|---|
| Methanol (in hot) | s | Chloroform | ss |
| Ethanol | s | Benzene | ss |
| Buthanol | s | Toluene | ss |
| Ether | ss | Nitrobenzene | sw |
| Tetrahydrofuran | ss | Phenol | sw |
| Petroleum-ether | sw | Chlorobenzene | s |
| Acetone | sw | Aniline | is |
| Ethylacetate | s | Pyridine | s |
| Carbon disulfide | ss | Formic acid | is |
| Carbon tetrachloride | ss | Acetic acid | sw |

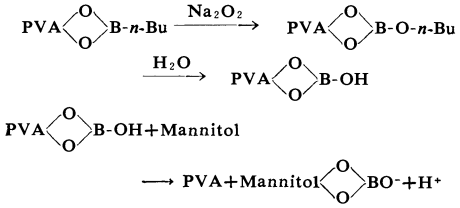
Note, s: soluble ss: very soluble
is: insoluble sw: swelling

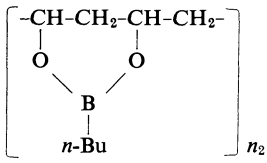
It has been known that in acetalization of PVA, the product acetalized dissolves in various organic solvents, and that the solubility increases with the acetalization grade. In view of these phenomena, the authors have estimated the esterification grade of PVA-boronates by determining the boron content of the products, the formation of which is formulated as follows:



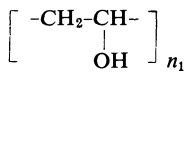
In the above reaction PVA is partially esterified with boronic acid; hence the product may be represented as consisting of the following two parts:

3) J. R. Johnson et al., *J. Am. Chem. Soc.*, **60**, 115 (1938).
4) J. R. Martin, *Anal. Chem.*, **24**, 182 (1952).
* While PVA-borate is produced as the result of oxidation and hydrolysis, it gives free PVA on adding mannitol as seen below:





Mol. wt. = 153.8



Mol. wt. = 44

Then,

$$N = 2n_2 + n_1$$

where $N$ is the polymerization grade of PVA, and

$$B\% = (10.8\, n_2)/(153.8\, n_2 + 44\, n_1) \times 100$$

$$E_g = 2n_2/N \times 100$$

where $E_g$ is the esterification grade.

From the above three equations, it follows that

$$E_g = (133.74 \times B\%)/(16.41 - B\%)$$

Flory[5] has shown from the statistical theory that the maximum grade of acetalization is 86.47%; that is to say, 13.53% of the hydroxyl groups in PVA remains unreacted. While Noma and his coworkers[6] obtained experimentally the maximum value of acetalization, they used the reaction of PVA with diethylchloroacetal, and by determining the chlorine content by the Carius method, they found that the acetalization grade is not affected by the concentration of diethylchloroacetal, and the maximum value is in reality less than 85%. As to the reaction of PVA with *n*-butylboronic acid, the esterification grade $E_g$ increases with concentration of the latter. Table II shows the relation between the concentration of *n*-butylboronic acid and $E_g$, where the concentration of PVA is fixed to be 2.5%.

Table II. Relation between concentration of reactant and $E_g$

| No. | *n*-Butylboronic acid | Molar ratio | B% | $E_g$, % |
|---|---|---|---|---|
| B-1 | 1.25 | 1/2 | —* | — |
| B-2 | 2.50 | 1 | 5.97 | 75.4 |
| B-3 | 5.00 | 2 | 6.17 | 80.6 |
| B-4 | 7.50 | 3 | 6.31 | 83.6 |
| B-5 | 10.00 | 4 | 6.39 | 85.6 |

* Not salted out.

As seen from Table II the molar ratio of PVA to *n*-butylboronic acid is varied from one half to four. Above this concentration *n*-butylboronic acid dissolves incompletely, and hence the reaction does not proceed normally.

It is, however, to be remarked that the maximum value of $E_g$ agrees with the values obtained by Flory[5] and Noma[6]. The structure of PVA has been studied by many authors[7] and is generally considered to be of 1, 3-glycol form, but in the above equations the forms of 1, 2- and 1, 4-glycol, are not effective in estimating the value of $E_g$, because the molecular weight of the unit is equal.

Observing the fact that these esters in benzene as well as carbon tetrachloride can be spun into poor solvents and that the esters are very soluble in various solvents it may be considered that PVA reacts with boronic acid to form no didiol complexes II of so-called network structure but yields a monodiol I. This presumption is supported by the investigations of PVA-borate by Irany[8] and by Deuel[9]. Sakurada and Okada[10] previously reported on the reaction of PVA with boric acid, showing the structure of the product by means of X-ray diffraction, that the trivalent hydroxyl groups in boric acid form a cyclic structure such as III and when the relative concentration of boric acid to PVA becomes higher, a didiol structure II should also be taken into consideration.

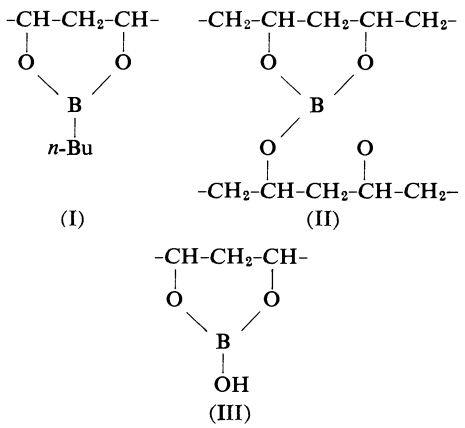


Fig. 1

In the case of *n*-butylboronic acid, however, a structure as II is not conceivable, for boronic acid is of divalent character and the boron atom is sterically hindered by the *n*-butyl group greater than the hydroxyl of boric acid.

**The Effect of Catalyst and Temerature.** — While in acetalization of PVA, an acid catalyst is fundamental for determining the reaction velocity[11], but the reaction of this esterification

5) P. J. Flory, *J. Am. Chem. Soc.*, **61**, 1518 (1939).
6) K. Noma et al., *High Polymer Chem.* (*Kobunshi Kagaku*), **6**, 439 (1939).
7) C. S. Marvell and C. E. Denoon, *J. Am. Chem. Soc.*, **60**, 1045 (1938).
8) E. P. Irany, *Ind. Eng. Chem.*, 35, 1290 (1943).
9) H. Deuel und H. Neukom, *Makromol. Chem.*, **3**, 13 (1949).
10) I. Sakurada and A. Okada, *High Polymer Chem.*, (*Kobunshi kagaku*), **15**, 491 (1958).
11) G. Smets and B. Pett, *Makromol. Chem.*, 33, 41 (1959). Y. Ogata et al., *J. Am. Chem. Soc.*, **78**, 2962 (1956).

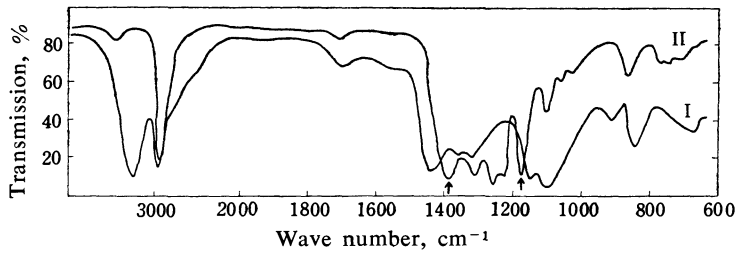



Fig. 2. Infrared spectra of polyvinylalcohol (I) and polyvinyl *n*-butylboronate (II).

proceeds instantly, and the determination of $E_g$ showed that the influence of $H^+$ on the reaction was not noticeable. Of course in alkaline solution, esterification does not proceed; the ester, if produced, may be saponified as soon as it is formed.

**The Effect of Temperature.** — The effect of temperature on $E_g$ is remarkable. In the range of 40 to 70°C, the values of $E_g$ rise as the temperature is raised, as shown in Table III.

TABLE III

| Temp., °C | 40 | 50 | 60 | 70 |
|---|---|---|---|---|
| $E_g$, % | 69.3 | 71.9 | 80.3 | 85.6 |

**Infrared Spectra.** — In order to study the structure of the esterification products, deeper infrared spectra were taken in the form of films prepared from carbon tetrachloride solutions of the esters on a mercury dish, the results of the observation being shown in Fig. 2.

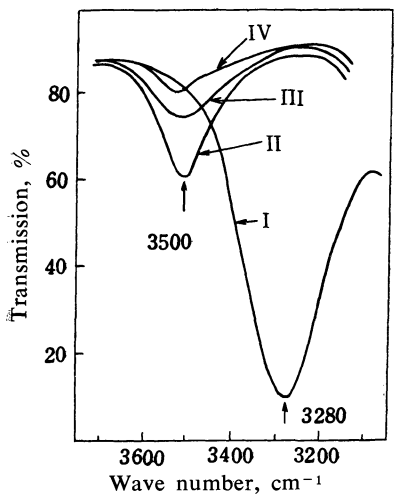



Fig. 3. Shifts of OH absorption band.
I: PVA II: B-2 III: B-4 IV: B-5

Curve I in Fig. 2 shows the spectrum of PVA unreacted. On treating with *n*-butylboronic acid it shows new absorption bands in the region of 1000 to 1500 $cm^{-1}$. In this region 1190 and 1390 $cm^{-1}$ can be assigned respectively to -B-C and -B-O bonds[12-14]. At the same time the OH stretching absorption band at 3280 $cm^{-1}$ of PVA shifts to a higher frequency by treatment with boronic acid and decreases in intensity with the increasing value of $E_g$ as shown in Fig. 3.

As seen in Fig. 3, it is observed that the decrease in intensity is related to $E_g$ qualitatively, and quantitative treatments will be reported in a later paper.

## Summary and Conclusion

It has been shown that PVA is partially esterified with *n*-butylboronic acid, giving products of the form of PVA  B-*n*-Bu.

The esterification grade, $E_g$, of the products is estimated from the boron content. $E_g$ increases with the increasing concentration of *n*-butylboronic acid used, the maximum $E_g$ being 85.6%. $E_g$ rises from 69.3 to 85.6% as the reaction temperature is elevated from 40 to 70°C.

On treating with *n*-butylboronic acid PVA shows new absorption bands 1190 and 1390 $cm^{-1}$ in deeper infrared spectra, which are assigned respectively to -B-C and -B-O bonds. At the same time the OH stretching absorption band at 3280 $cm^{-1}$ of PVA shifts to a higher frequency, and decreases in intensity with the increasing $E_g$.

*Tokyo College of Science*
*Shinjuku-ku, Tokyo*

12) W. J. Lehmann, *J. Chem. Phys.*, **28**, 777 (1958).
13) Jeo Cazes, *Compt. rend.*, **247**, 2019 (1958).
14) H. R. Snyder et al., *J. Am. Chem. Soc.*, **80**, 3612 (1958).

# *A New Quantum-mechanical Reactivity Index for Saturated Compounds*

By Kenichi FUKUI, Hiroshi KATO and Teijiro YONEZAWA

(Received January 24, 1961)

In our previous paper[1], the frontier electron density[2] was shown to become a good intramolecular index of the reactivity in a metathetical reaction of saturated compounds.

In the present paper, we treat several lower paraffins and halomethanes by using the same method as that used in the previous treatment[1], and attempt to derive a new intermolecular index of the reactivity, which is hereafter referred to as the delocalizability, $D_r$. This index is similar to the superdelocalizability[3] of conjugated molecules. It is found that the magnitude of $D_r$ in these compounds has an intimate correlation with the value of activation energy observed in metathetical reactions.

## Electronic Structure of *n*-Paraffins and Methyl Fluoride

The calculated values of orbital energies and electron distributions in methane, ethane, propane, *n*-butane and methyl fluoride are listed in Table I.

With regard to *n*-paraffins, we can point out the following characteristics:

(1) The bonding electrons tend to localize in the particular bonds in each molecular orbital. For example, the electrons in the highest occupied and the lowest vacant orbitals in these compounds except methane, have a general trend to localize in the central C-C bonds as shown in Fig. 1*.

(2) The electron distributions of occupied and unoccupied orbitals are almost symmetrical with respect to the energy equal to $\alpha$ (see below) as is seen in Fig. 1.

(3) The distances of levels of molecular orbital energy in these compounds are much larger than those of conjugated molecules. The excitation energy of the N-V transition in a simple LCAO MO sense is, therefore, estimated to be 9~10 eV. referring the presumed value

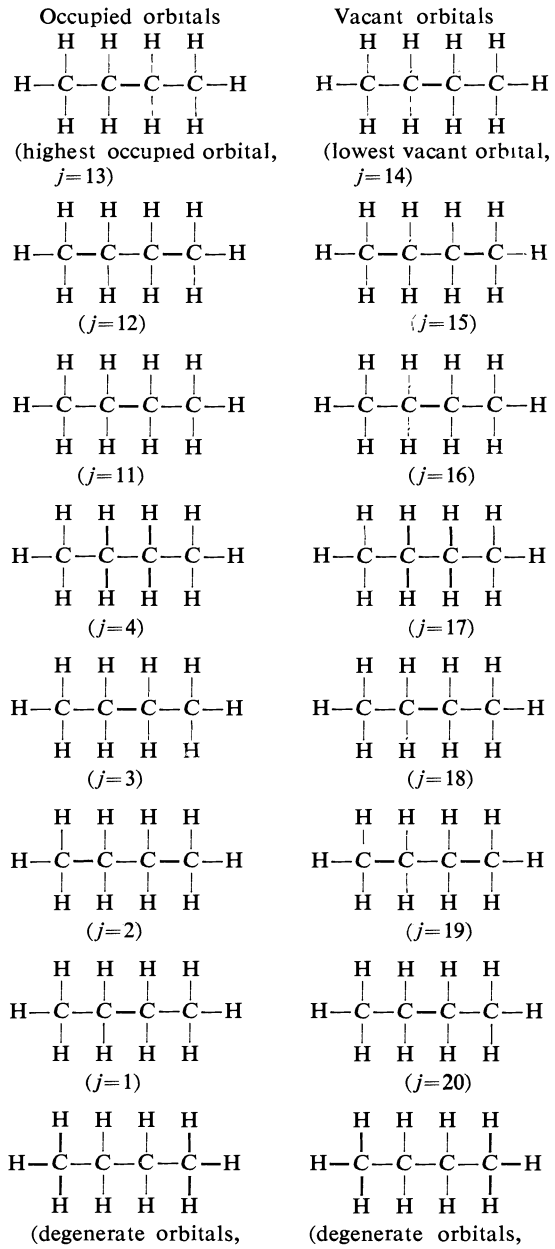
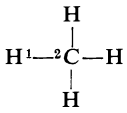



Fig. 1. The electron distributions of *n*-butane.
(Thick lines denote the most densely populated bonds of bonding electrons.)

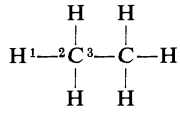
1) K. Fukui, H. Kato and T. Yonezawa, This Bulletin, 34, 442 (1961).
2) See e. g. K. Fukui, T. Yonezawa, C. Nagata and H. Shingu, *J. Chem. Phys.*, 22, 1432 (1954).
3) K. Fukui, T. Yonezawa and C. Nagata, This Bulletin, 27, 423 (1954).
* This result suggests that in lower *n*-paraffins their first ionization can be attributed to the removal of one electron localized in C-C bonds.

TABLE I. THE ORBITAL ENERGIES AND ELECTRON DISTRIBUTIONS IN SEVERAL SATURATED COMPOUNDS



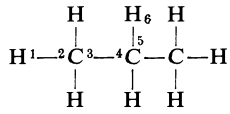
| Orbital energy | | Electron distribution |
|---|---|---|
| $j$ | $\varepsilon_j$ | $(C^j_{H1})^2$ $(C^j_{C2})^2$ |
| 6,7,8 | $\alpha-1.3722\beta$* | 0.1171 0.1329 |
| 5 | $\alpha-0.8478\beta$ | 0.1856 0.0644 |
| 2,3,4 | $\alpha+0.8322\beta$* | 0.1329 0.1171 |
| 1 | $\alpha+1.6678\beta$ | 0.0644 0.1856 |

* threefold degenerate



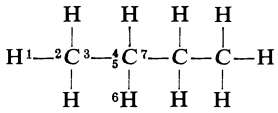
| Orbital energy | | Electron distribution | | |
|---|---|---|---|---|
| $j$ | $\varepsilon_j$ | $(C^j_{H1})^2$ | $(C^j_{C2})^2$ | $(C^j_{C3})^2$ |
| 11,12,13,14 | $\alpha-1.3722\beta$* | 0.0781 | 0.0886 | 0 |
| 10 | $\alpha-1.3527\beta$ | 0.0323 | 0.0355 | 0.2966 |
| 9 | $\alpha-1.0019\beta$ | 0.1057 | 0.0561 | 0.0145 |
| 8 | $\alpha-0.6881\beta$ | 0.0878 | 0.0173 | 0.1847 |
| 7 | $\alpha+0.7254\beta$ | 0.0336 | 0.0238 | 0.3278 |
| 3,4,5,6 | $\alpha+0.8322\beta$* | 0.0886 | 0.0781 | 0 |
| 2 | $\alpha+1.5208\beta$ | 0.0465 | 0.1139 | 0.0187 |
| 1 | $\alpha+1.7566\beta$ | 0.0274 | 0.0867 | 0.1575 |

* fourfold degenerate



| Orbital energy | | Electron distribution | | | | | |
|---|---|---|---|---|---|---|---|
| $j$ | $\varepsilon_j$ | $(C^j_{H1})^2$ | $(C^j_{C2})^2$ | $(C^j_{C3})^2$ | $(C^j_{C4})^2$ | $(C^j_{C5})^2$ | $(C^j_{H6})^2$ |
| 16,17,18,19,20 | $\alpha-1.3722\beta$* | 0.062 | 0.071 | 0 | 0 | 0.053 | 0.047 |
| 15 | $\alpha-1.3576\beta$ | 0.011 | 0.012 | 0.105 | 0.106 | 0.115 | 0.104 |
| 14 | $\alpha-1.3482\beta$ | 0.021 | 0.023 | 0.183 | 0.186 | 0 | 0 |
| 13 | $\alpha-1.0614\beta$ | 0.058 | 0.036 | 0.035 | 0 | 0.070 | 0.113 |
| 12 | $\alpha-0.8535\beta$ | 0.090 | 0.032 | 0.028 | 0.105 | 0 | 0 |
| 11 | $\alpha-0.6169\beta$ | 0.045 | 0.006 | 0.144 | 0.100 | 0.013 | 0.089 |
| 10 | $\alpha+0.6997\beta$ | 0.020 | 0.014 | 0.207 | 0.191 | 0 | 0 |
| 9 | $\alpha+0.7548\beta$ | 0.013 | 0.009 | 0.117 | 0.128 | 0.081 | 0.108 |
| 4,5,6,7,8 | $\alpha+0.8322\beta$* | 0.071 | 0.062 | 0 | 0 | 0.047 | 0.053 |
| 3 | $\alpha+1.4502\beta$ | 0.026 | 0.058 | 0.001 | 0.043 | 0.142 | 0.063 |
| 2 | $\alpha+1.6419\beta$ | 0.035 | 0.099 | 0.079 | 0.020 | 0 | 0 |
| 1 | $\alpha+1.7919\beta$ | 0.014 | 0.045 | 0.100 | 0.121 | 0.078 | 0.024 |

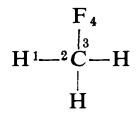
* fivefold degenerate



| Orbital energy | | Electron distribution | | | | | | |
|---|---|---|---|---|---|---|---|---|
| $j$ | $\varepsilon_j$ | $(C^j_{H1})^2$ | $(C^j_{C2})^2$ | $(C^j_{C3})^2$ | $(C^j_{C4})^2$ | $(C^j_{C5})^2$ | $(C^j_{H6})^2$ | $(C^j_{C7})^2$ |
| 21,22,23,24,25,26 | $\alpha-1.3722\beta$* | 0.052 | 0.059 | 0 | 0 | 0.044 | 0.039 | 0 |
| 20 | $\alpha-1.3612\beta$ | 0.005 | 0.006 | 0.047 | 0.048 | 0.074 | 0.066 | 0.092 |
| 19 | $\alpha-1.3546\beta$ | 0.014 | 0.016 | 0.133 | 0.134 | 0.037 | 0.034 | 0 |
| 18 | $\alpha-1.3436\beta$ | 0.012 | 0.013 | 0.104 | 0.101 | 0.005 | 0.005 | 0.200 |
| 17 | $\alpha-1.0870\beta$ | 0.035 | 0.022 | 0.032 | 0.002 | 0.057 | 0.087 | 0.007 |
| 16 | $\alpha-0.9473\beta$ | 0.070 | 0.032 | 0 | 0.032 | 0.012 | 0.027 | 0.083 |
| 15 | $\alpha-0.7567\beta$ | 0.064 | 0.016 | 0.077 | 0.116 | 0.006 | 0.023 | 0.009 |
| 14 | $\alpha-0.5822\beta$ | 0.026 | 0.003 | 0.099 | 0.058 | 0.008 | 0.063 | 0.114 |
| 13 | $\alpha+0.6971\beta$ | 0.012 | 0.008 | 0.128 | 0.113 | 0.001 | 0.002 | 0.192 |
| 12 | $\alpha+0.7339\beta$ | 0.016 | 0.011 | 0.151 | 0.155 | 0.024 | 0.033 | 0 |
| 11 | $\alpha+0.7627\beta$ | 0.005 | 0.004 | 0.047 | 0.053 | 0.055 | 0.072 | 0.119 |
| 5,6,7,8,9,10 | $\alpha+0.8322\beta$* | 0.059 | 0.052 | 0 | 0 | 0.039 | 0.044 | 0 |
| 4 | $\alpha+1.4135\beta$ | 0.014 | 0.031 | 0 | 0.037 | 0.107 | 0.050 | 0.014 |
| 3 | $\alpha+1.5585\beta$ | 0.029 | 0.074 | 0.024 | 0.002 | 0.036 | 0.014 | 0.065 |
| 2 | $\alpha+1.7073\beta$ | 0.023 | 0.070 | 0.094 | 0.064 | 0.022 | 0.007 | 0.004 |
| 1 | $\alpha+1.8098\beta$ | 0.008 | 0.026 | 0.063 | 0.084 | 0.057 | 0.017 | 0.103 |

* sixfold degenerate

TABLE I (Continued)



| | Orbital energy | Electron distribution | | | |
|---|---|---|---|---|---|
| $j$ | $\varepsilon_j$ | $(C^j_{H1})^2$ | $(C^j_{C2})^2$ | $(C^j_{C3})^2$ | $(C^j_{F4})^2$ |
| 7,8 | $\alpha-1.3722\beta$* | 0.1561 | 0.1773 | 0 | 0 |
| 6 | $\alpha-1.0729\beta$ | 0.1756 | 0.1112 | 0.1291 | 0.0083 |
| 5 | $\alpha-0.2183\beta$ | 0.0656 | 0 | 0.6691 | 0.1338 |
| 3,4 | $\alpha+0.8322\beta$* | 0.1773 | 0.1561 | 0 | 0 |
| 2 | $\alpha+1.0527\beta$ | 0.0188 | 0.0244 | 0.0724 | 0.7962 |
| 1 | $\alpha+1.6184\beta$ | 0.0723 | 0.1978 | 0.1285 | 0.0618 |

* doubly degenerate

of $-\beta$ (6~7 eV.). This excitation energy is consistent with the spectroscopic data[4].

The characteristics of orbital energies and of the electron distribution stated above agree with the properties observed experimentally in saturated compounds and also with calculated results obtained by Lennard-Jones and Hall's equivalent orbital method[5].

In the doubly degenerate highest occupied orbitals of methyl fluoride, the bonding electrons localize dominantly in the methyl group. In the next highest occupied orbital, an exceedingly large density is observed on the fluorine atom in accordance with the facts pointed out by Frost and McDowell[6], who measured the ionization potentials of methyl halides.

The Coulomb and resonance integrals used in the present paper are summarized in the following table.

| | |
|---|---|
| $\alpha_H=\alpha-0.2\beta$ | $\beta_{cc}=0.34\beta$* |
| $\alpha_F=\alpha+0.9\beta$ | $\beta_{CH}=1.1\beta$ |
| $\alpha_{Cl}=\alpha+0.5\beta$ | $\beta_{CF}=0.5\beta$ |
| $\alpha_{Br}=\alpha+0.45\beta$ | $\beta_{CCl}=0.65\beta$ |
| $\alpha_I=\alpha+0.40\alpha$ | $\beta_{CBr}=0.58\beta$ |
| $\alpha_C=\alpha$ | $\beta_{CI}=0.53\beta$ |

* $\beta_{cc}$ refers to the resonance integral between two $sp^3$ orbitals attached to one and the same carbon atom.

## A New Reactivity Index for Radical Reactions of Saturated Compounds, $D_r^{(R)}$

The radical reactions of alkyl compounds are covered by the general equation

$$R\text{-}X+Y\cdot\rightarrow[R\cdots X\cdots Y]\rightarrow R\cdot+X\text{-}Y \qquad (1)$$

where R is an alkyl group, X is the group to be extracted and Y is an attacking radical or atom. The bracket in the equation refers to the transition state.

The secular determinant for the activated complex, [R-X···Y], is written

$$\Delta_\sigma=\begin{vmatrix} \alpha_Y-\varepsilon & \gamma\beta & 0 & 0 & 0 & 0 & 0 \\ \gamma\beta & \alpha_X-\varepsilon & \beta_{CX} & 0 & 0 & 0 & 0 \\ 0 & \beta_{CX} & \alpha_C-\varepsilon & \beta_{CH} & \beta_{cc} & & \\ 0 & 0 & \beta_{CH} & \alpha_H-\varepsilon & 0 & & \\ 0 & 0 & \beta_{cc} & 0 & \alpha_C-\varepsilon & & \\ 0 & \multicolumn{6}{l}{\text{(The secular equation for the R-X molecule)}} \end{vmatrix}$$

where $\alpha_A$ refers to the Coulomb integrals of atom A, $\beta_{AB}$ is the resonance integral between bonding orbitals of atom A and B, and $\gamma$ is a parameter for the resonance integral of the X-Y incipient bond in the transition state.

By using the perturbation theory, we can derive a new reactivity index, named $D_r$, for metathetical radical reactions in saturated compounds, in place of the superdelocalizability ($S_r$) in our previous paper[3].

$$D_r^{(R)}=\sum_j^{occ}\frac{(C_r^j)^2}{\varepsilon_j-\alpha}\beta+\sum_j^{unocc}\frac{(C^j_r)^2}{\alpha-\varepsilon_j}\beta \qquad (3)$$

where $C_r^j$ is the coefficient of the $r$th atomic orbital in the $j$th molecular orbital, $\varepsilon_j$ is the $j$th molecular orbital energy, $\alpha$ is the Coulomb integral of a $sp^3$ orbital in a carbon atom, and $\beta$ is the resonance integral between two $sp^3$ orbitals in a C-C bond.

In the derivation of Eq. 3, we assume that $\alpha_X$ is equal to $\alpha$, and the values of $\alpha$ and $\beta$ in the activated complex are the same as those of the isolated molecule.

It may be worthy of notice that $D_r^{(R)}$ represents the stabilization energy due to $\sigma$ type interaction in a radical reaction, while $S_r^{(R)}$ denotes the stabilization energy which

4) P. G. Wilkinson and H. L. Jhonston, *J. Chem. Phys.*, **18**, 190 (1950); W. P. Potts, ibid., **20**, 809 (1952).
5) J. Lennard-Jones and G. G. Hall, *Disc. Faraday Soc.*, **10**, 18 (1951); *Trans. Faraday Soc.*, **47**, 581 (1952); K. Fueki and K. Hirota, *J. Chem. Soc. Japan, Pure Chem. Sec. (Nippon Kagaku Zasshi)*, **81**, 212 (1960).
6) D. C. Frost and C. A. McDowell, *Proc. Roy. Soc.*, **A241**, 194 (1957).

TABLE II (a). THE CALCULATED VALUES OF $D_r^{(R)}$ AND OBSERVED ACTIVATION ENERGIES IN SEVERAL *n*-PARAFFINS

$R\text{-}H+R'\cdot \rightarrow R\cdot+R'\text{-}H$

| Compound R-H | | $D_r^{(R)}(H)$ | $E$(kcal./mol.)[8] | | |
|---|---|---|---|---|---|
| | | | $CH_3\cdot$ | $CH_3CH_2\cdot$ | $CH_3CH_2CH_2\cdot$ |
| $CH_3$-H | | 0.9926 | 11.5 | 15.0 | 16.5 |
| $CH_3CH_2$-H | (prim-H) | 1.0029 | 10.0 | 14.8 | 16.2 |
| $CH_3CH_2CH_2$-H | (prim-H) | 1.0032 | 9.5 | 14.2 | 15.5 |
| $CH_3CH_2CH_2CH_2$-H | (prim-H) | 1.0043 | 9.3 | 13.9 | 15.3 |
| $(CH_3)_2CHCH_2$-H | (prim-H) | 1.0049 | — | — | — |
| $(CH_3)_2CH$-H | (sec-H) | 1.015 | 8.7 | 13.3 | 14.5 |
| $CH_3CH_2CH(CH_3)$-H | (sec-H) | 1.016 | 8.2 | 12.7 | 14.1 |
| $(CH_3)_3C$-H | (tert-H) | 1.027 | 7.7 | 11.6 | 13.4 |

TABLE II (b). THE AVERAGE VALUES OF $D_r^{(R)}$ (H) AND RATE CONSTANTS CHARACTERISTICS OF VARIOUS TYPES OF HYDROGEN ATOM IN ALKANES

| Type of hydrogen atom | $D_r^{(R)}(H)$ | $k_C\times10^{-6}$ at 182°C (mol$^{-1}$ cc. sec$^{-1}$*[7]) |
|---|---|---|
| H in methane | 0.993 | — |
| Primary H | 1.003 | 0.3 |
| Secondary H | 1.016 | 2.1 |
| Tertiary H | 1.027 | 15 |

* $k_C$ means the rate constant divided by the number of H atoms of the same kind.

arises from the hyperconjugation taking place between a reagent and a conjugated molecule.

## Results and Discussions

In our previous paper[1], the magnitudes of the frontier electron densities at hydrogen atoms in several saturated hydrocarbons ran parallel with the experimental reactivities[7] of hydrogen atoms in metathetical reactions. The frontier electron density for radical attack was shown to be a good intramolecular index of reactivity. This index, however, does not indicate the correct order of reactivity in different molecules. Therefore, we adopt $D_r^{(R)}$ which is useful not only as an intramolecular index but also as an intermolecular index. The calculated values of $D_r^{(R)}$ in several saturated compounds are listed together with the observed values of activation energy[8,9] in various metathetical reactions in Tables II and III.

TABLE III. THE VALUES OF $D_r^{(R)}(H)$ AND ACTIVATION ENERGIES OF HALOMETHANES IN METATHETICAL REACTIONS

(a) $CH_nCl_{4-n}+CH_3\cdot \rightarrow CH_{n-1}Cl_{4-n}\cdot+CH_4$

| Compound | $D^{(R)}(H)$ | $E$(kcal./mol.)[9] |
|---|---|---|
| $CHCl_3$ | 2.181 | 5.8 |
| $CH_2Cl_2$ | 1.237 | 7.2 |
| $CH_3Cl$ | 1.058 | 9.4 |

(b) $CH_nF_{4-n}+CH_3\cdot \rightarrow CH_{n-1}F_{4-n}\cdot+CH_4$

| Compound | $D_r^{(R)}(H)$ | $E$(kcal./mol.)[9] |
|---|---|---|
| $CH_3F$ | 1.181 | 8.7 |
| $CH_2F_2$ | 1.235 | 6.2 |

(c) $CH_nX_{4-n}+Br\cdot \rightarrow CH_{n-1}X_{4-n}\cdot+HBr$

| Compound | $D_r^{(R)}(H)$ | $E$(kcal./mol.)[9] |
|---|---|---|
| $CH_4$ | 0.993 | 17.8 |
| $CH_3Br$ | 1.071 | 15.6 |
| $CHCl_3$ | 2.181 | 10.0 |

**Hydrogen Extraction Reaction.**—In the case of reaction $RH+R'\cdot \rightarrow R\cdot+R'H$, results of calculation and experiments are cited in Table II (a) and (b), where R and R′ are two different alkyl groups. The values of $D_r^{(R)}$ at hydrogen atoms in several lower paraffins indicate a tendency that the larger the molecule RH is, the smaller is the magnitude of activation energy, this being in accord with experiments[8]. Furthermore, these values of $D_r^{(R)}$ agree with the activities of various kinds of hydrogen atoms estimated by Trotman-Dickenson[7] as shown in Table II (b).

In Table III (a), (b) and (c), the calculated values of $D_r^{(R)}$ at hydrogen atoms in various halomethanes are listed together with the observed activation energies[9]. In Table III (a), the radical reactions between methyl radical and chlorine-substituted methanes are indicated. The greater the number of chlorine atoms in methane is, the smaller is the activation energy, and also the magnitude of $D_r^{(R)}$ at hydrogen atoms increases with the number of chlorine atoms. The results on fluorine-substituted methanes are shown in Table III (b), and

7) A. F. Trotman-Dickenson, *Quart. Revs.*, **7**, 198 (1953).

8) N. N. Tikhomirova and V. V. Voevodskı, *Chem. Abstr.*, **45**, 9940 (1951).

9) E. W. R. Steacie, "Atomic and Free Radical Reactions", Reinhold Co., New York. (1946); ibid., Second Ed. Vol. II (1954).

the case where a bromine atom attacks methane derivatives is indicated in Table III (c). Also in the last two cases, although experimental data are few, a parallelism between the values of $D_r^{(R)}$ and the activation energies[9] is clearly observed.

**Halogen Abstraction Reaction.**—In Table IV (a), (b) and (c) are illustrated both the calculated values of $D_r^{(R)}$ at the halogen atom

TABLE IV. THE VALUES OF $D_r^{(R)}$(X) AND ACTIVATION ENERGIES IN HALOMETHANES IN METATHETICAL REACTIONS

(a) $CH_3X+H\cdot \rightarrow CH_3\cdot+HX$

| $CH_3X$ | $D_r^{(R)}$(X) | $E$(kcal./mol.)[9] |
|---|---|---|
| $CH_3I$ | 1.851 | 5 |
| $CH_3Br$ | 1.669 | — |
| $CH_3Cl$ | 1.496 | 7~9 |
| $CH_3F$ | 1.415 | 9 |

(b) $CH_nCl_{4-n}+H\cdot \rightarrow CH_nCl_{3-n}\cdot+HCl$

| Compound | $D_r^{(R)}$(Cl) | $E$(kcal./mol.)[9] |
|---|---|---|
| $CH_3Cl$ | 1.496 | 7~9 |
| $CH_2Cl_2$ | 1.756 | 6 |
| $CHCl_3$ | 3.200 | 4.3 |
| $CCl_4$ | 3.829 | 3.5 |

(c) $CH_nBr_{4-n}+Na\cdot \rightarrow CH_nBr_{3-n}\cdot+NaBr$

| Compound | $D_r^{(R)}$(Br) | $E$(kcal./mol.)[9] |
|---|---|---|
| $CH_3Br$ | 1.669 | 5.9 |
| $CH_2Br_2$ | 2.045 | 2.6 |
| $CHBr_3$ | 4.889 | 0.3 |

in various halomethanes and the observed values of activation energy in the halogen extraction reactions[9]. In Table IV (a), a good agreement is observed between the values of $D_r^{(R)}$ and the activation energies of various monosubstituted halomethanes. In Table IV (b), the values of $D_r^{(R)}$ at chlorine atoms in various chlorine-substituted methanes and the activation energies in the hydrogen-atom reactions are indicated. In Table IV (c), the values of $D_r^{(R)}$ at bromine atoms in several bromomethanes are compared with the activation energies in the sodium-atom reaction.

In spite of the fact that this is the first attempt of the quantum-mechanical investigation of the reactivity of saturated compounds, the agreement of the theory with experience is almost satisfactory, and hence the new quantum-mechanical quantity $D_r^{(R)}$ can be a useful index for predicting the reactivity of saturated compounds, equally with $S_r$ in conjugated molecules. There remain, however, some points to be checked in future. These are summarized as follows:

(1) We assume that $\alpha_x$ is equal to $\alpha$ to derive $D_r$. Meanwhile, a slight change in activation energy is experimentally observed according to the species of attacking reagents. Hence, if the values of $\alpha_x$ would be modified according to the change of the attacking reagent, this effect can be interpreted in the present procedure.

(2) In the present treatment, we do not take into account the stabilization energy due to the resonance in an attacking alkyl radical or the radical formed. It has been made clear that this resonance energy has a remarkable influence on the magnitude of the activation energy[10]. In this connection, the present treatment should be modified so as to involve the contribution of this kind of resonance to the activation energy.

(3) A disagreement between the values of $D_r^{(R)}$ in methyl halides and the experimental activation energies is observed. This is probaly because the energies of the vacant orbitals of some methyl halides are nearly equal to $\alpha$. Thus, the values of the $D_r^{(R)}$ become extremely large. If carefully selected values of parameters for halogen atoms should be adopted, these disagreements may be avoidable.

*Faculty of Engineering*
*Kyoto University*
*Sakyo-ku, Kyoto*

10) M. G. Evans, *Disc. Faraday Soc.*, **10**, 1 (1951); C. A. Coulson, ibid., **2**, 9 (1947).

# *Studies on the Diacylaminoanthraquinone Dyes*

By Takayuki HAYASHI and Reiko SHIBATA

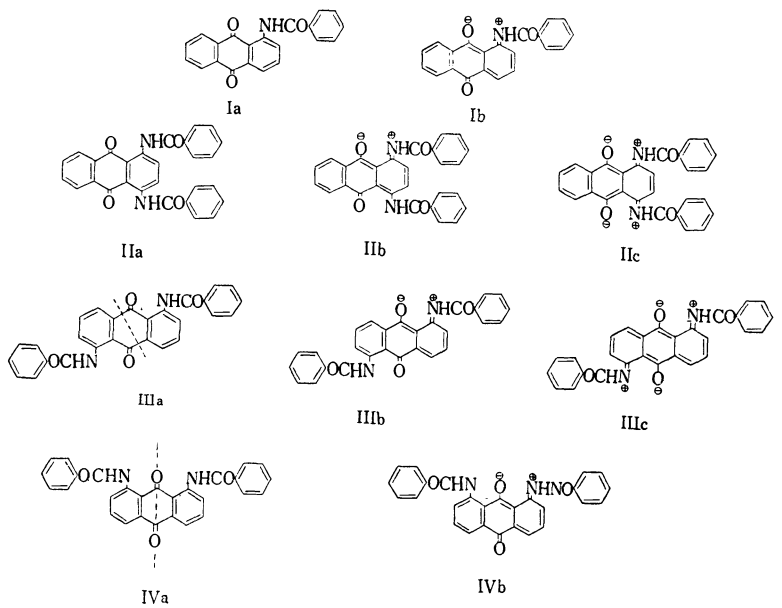
(Received September 20, 1960)

In our previous papers[1-5], 1-acylamino-, 1,4-, 1,5- and 1,8-diacylaminoanthraquinones having $NO_2$, Cl, OMe, $SO_2N(Me)_2$ or $NH_2$ (X or Y)* as a substituent in the acyl group were prepared. Visible and infrared absorption spectra of these dyes were measured in solution and in solid, respectively, and cotton was dyed with them, and their light fastness on cotton was tested. On the basis of these results, the effects of X and Y substituent groups were discussed with their various properties, such as wavelengths of absorption maxima, relative difficulties of vatting, color tones of vat solutions, shades of dyed cotton, and light fastness. In this paper, the above-mentioned properties have been discussed correlatively for all of these dyes.

## Results and Discussion

**Visible Absorption Spectra.**—Visible absorption spectra of 1-acylamino-, 1,4- and 1,5-diacylaminoanthraquinone series were observed and discussed by Peters and Sumner[6]. In this paper, from the results of visible absorption for 1-acylamino-, 1,4-, 1,5- and 1,8-diacylaminoanthraquinones, the relation between wavelengths or intensities of the absorption maximum and positions of acyl groups has been discussed. Furthermore, for each series of 1-acylamino-, 1,4-, 1,5- and 1,8-diacylaminoanthraquinones the effect of the substituent (X or Y) in the acyl group upon the wavelength and intensity of the absorption maximum has been considered.

The absorption maxima[1-4] of 1-benzoylamino-, 1,4-, 1,5- and 1,8-dibenzoylaminoanthraquinones appeared at 421, 502, 448 and 455 m$\mu$ in *o*-dichlorobenzene with the peak molar extinction coefficient of 5900, 7600, 12000 and 11000, respectively. Since the molecule of the 1,5-derivative is divided into two halves diagonally as in III, simple additivity is established between two chromophoric systems within it, and one to three benzene rings in




1) T. Hayashi and R. Shibata, *J. Chem. Soc. Japan, Ind. Chem Sec.* (*Kogyo Kagaku Zasshi*), **63**, 513 (1960).
2) T. Hayashi and R. Shibata, ibid., **63**, 840 (1960).
3) T. Hayashi, ibid., **63**, 1241 (1960).
4) T. Hayashi, ibid., **63**, 1395 (1960).
5) T. Hayashi, ibid., **63**, 1985 (1960).
* X or Y denotes a substituent in the acyl group of acylaminoanthraquinones.
6) R. H. Peters and H. H. Sumner, *J. Chem. Soc.*, **1953**, 2101.

the anthraquinone nucleus increase their quinonoid character, thereby reducing the aromaticity, but the extent of the contribution of a structure IIIc to the resonance is exceedingly small. For the 1-derivative, on the other hand, one to two benzene rings in the anthraquinone nucleus increase their quinonoid character as in I, thereby reducing the aromaticity, and only one carbonyl group of the anthraquinone nucleus takes part in conjugation, this being different from the 1, 5-derivative. The wavelength of the absorption maximum for the 1, 5-derivative should therefore be somewhat longer than for the 1-derivative, but the intensity of the former should be approximately twice that of the latter. Since the molecule of the 1, 8-derivative is divided into two halves vertically as in IV, simple additivity is established between two chromophoric systems within it as the 1, 5-derivative, but one to two benzene rings in the anthraquinone nucleus increase their quinonoid character, thereby reducing the aromaticity, this being different from the 1, 5-derivative. Though one carbonyl group is held by two chromophoric systems in common for the 1, 8-derivative, mesomeric shifts of electrons within the chromophoric systems are suppressed, owing to cross conjugation of two systems, in which case the extent of the contribution of a structure IVb to the resonance should be a little greater than for a structure IIIb. The effective area of $\pi$-electron systems[7,8] for IV is also slightly smaller than for III. The wavelength of the absorption maximum for the 1, 8-derivative should therefore be somewhat longer than for the 1, 5-derivative, and the intensity of the former should be a little lower than for the latter but approximately twice that of the 1-derivative. For the 1, 4-derivative one to two benzene rings in the anthraquinone nucleus increase their quinonoid character, thereby reducing the aromaticity, and the extent of the contribution of a structure IIc to the resonance is more marked. The 1, 4-derivative shows no such simple additivity as indicated in III owing to interaction between their two chromophoric systems, probably producing a new one, and an effective area of $\pi$-electron systems for II is smaller than for III or IV. The wavelength of the absorption maximum for the 1, 4-derivative should therefore be the longest among them and the intensity should lie between those of 1- and 1, 8-derivatives. Such relations should be established similarly among 1-acylamino-, 1, 4-, 1, 5- and 1, 8-diacylaminoanthraquinones with the same substituent in the acyl group.

From results[1-4] of the bands for each series, it was known that electron-attracting substituents mainly showed a +I effect and electron-donating substituents mainly a −T effect and the *p*-dimethylsulfamyl group showed a +I effect similar to a *p*-nitro group, this being different from the result of the *p*-sulfamyl group obtained by Zollinger[9]. For the bands of each series, it was shown that the shifts of the absorption maximum complied with Hammett's rule[10] and that the relationship between the wavelengths of the absorption maximum and Brown's $\sigma^+$ values[11,12] was

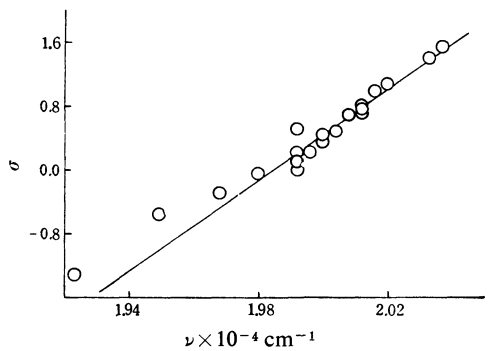



Fig. 1. The relationship between wave-number ($\nu$) of the maximum absorption and Hammett's $\sigma$ value on the 1,4-diacylaminoanthraquinone series.

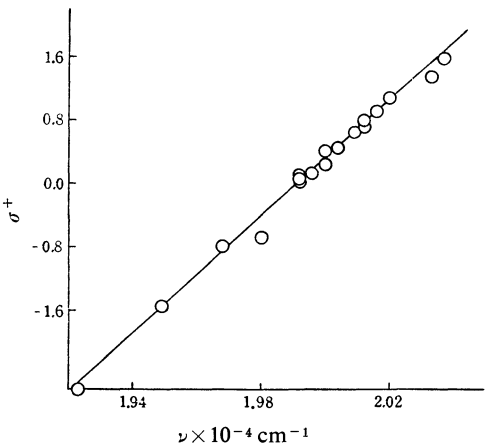



Fig. 2. The relationship between the wave-number ($\nu$) of the maximum absorption and Brown's $\sigma^+$ value on the 1,4-diacylaminoanthraquinone series.

7) E. A. Braude, ibid., **1950**, 379.
8) R. H. Peters and H. H. Sumner, *J. Soc. Dyers Colorists*, **71**, 130 (1955).
9) H. Zollinger and C. Wittwer, *Helv. Chim. Acta*, **39**, 347 (1956).
10) H. H. Jaffé, *Chem. Revs.*, **53**, 191 (1953).
11) H. C. Brown and Y. Okamoto, *J. Am. Chem. Soc.*, **80**, 4979 (1958).
12) G. W. Gray, "Steric Effects in Conjugated Systems", Butterworths Scientific Publications, London (1958), p. 100.

more linear than that between them and Hammett's $\sigma$ values[10] as indicated in Figs. 1 and 2 for the 1,4-diacylaminoanthraquinone series. Accordingly it is possible to estimate a shift from Brown's $\sigma^+$ value of a substituent in the acyl group and obtain an expected shift of the absorption maximum by introduction of an adequate substituent with known Brown's $\sigma^+$ value to the acyl group. Hammett's $\sigma$ value of *p*- and *m*-dimethylsulfamyl groups were 0.70 and 0.53, and Brown's $\sigma^+$ values of these were 0.86 and 0.68, respectivery, from Figs. 1 and 2.

For each series, dyes with *o*-chloro, *o*-methoxy or *o*-nitro groups, besides an *o*-amino group, as X and Y, showed a considerably hypsochromic shift and a decreasing intensity in their absorption maxima. Both the wavelengths and the intensities were almost independent of all combinations of substituents in two acyl groups for each series. As indicated in Table I, the absorption maximum of 1,5-diacetylaminoanthraquinone agreed with those of 1,5-di-*o*-substitutes. This fact was admitted on the other *o*-substitutes. The effect of the *o*-substituted phenyl group should therefore be much the same as that of the methyl group, and this fact shows that the benzene ring has been twisted around the C-C linkage between

Table I. Visible absorption bands of *o*-substituted benzoylamino- and acetylamino-anthraquinones[1-4]

| | *o*-Substitute | Acetylamino-anthraquinone |
|---|---|---|
| 1-Derivative | 407~411 (5300~6000)** | 415 (5300) |
| 1,4-Derivative | 483~486 (6950~7100) | 487 (7550) |
| 1,5-Derivative | 437~439 (10500~11500) | 438 (11000) |
| 1,8-Derivative | 438~441 (9700~10200) | 440 (10400) |

the *o*-substituted phenyl and the carbonyl group in the acyl group. The twisting may be attributed to the steric hindrance between the *o*-nitro and the carbonyl group or to the repulsion between the *o*-chloro or *o*-methoxy and the carbonyl group in the acyl group. The wavelengths of the absorption maximum of 1-*o*-amino-, 1,4-, 1,5- and 1,8-di-*o*-amino-substitutes were 436, 514, 460 and 463 m$\mu$ in *o*-dichlorobenzene, respectively. As these absorption peaks do not show a hypsochromic shift, they are different from the ones of the other *o*-substitutes, such the interesting twisting of the benzene ring as in *o*-substitutes may not arise.

** Wavelength, m$\mu$ (molar extinction coefficient).

**Infrared Absorption Spectra.**—Three and six $\mu$ bands of infrared absorption spectra for some acylaminoanthraquinones have been observed as powders suspended in Nujol on account of their limited solubility and were discussed by Flett[13]. In this work, infrared absorption spectra of 1-acylamino-, 1,4-, 1,5- and 1,8-dibenzoylaminoanthraquinones have also been observed as powders suspended in Nujol and information has been gained about their structures in the solid. This information may be, to some extent, similar to deduction for the structure of the dye molecule in cotton dyed with them.

As indicated in Table II, a C=O frequency in the peri-position of the benzoyl group for 1,4-dibenzoylaminoanthraquinone is lower than for the 1,5-isomer, and then the C=O bond of the former is more weakened than for the latter. This fact may generally suggest that the shade of the 1,4-diacylaminoanthraquinone series on cotton is more bathochromic than in the case of the 1,5-isomer. As 3 $\mu$ bands of 1,5-dibenzoylaminoanthraquinone almost agree with those of the 1,8-isomer, the effect of imino groups on the whole of the molecule is much the same in both cases. This fact may generally suggest that a shade of the 1,5-diacylaminoanthraquinone series on cotton is approximately the same with that of the 1,8-isomer.

Table II. 3 and 6 $\mu$ bands of solid benzoylaminoanthraquinones[5]

| | 3 $\mu$ bands $cm^{-1}$ | 6 $\mu$ bands $cm^{-1}$ (C=O frequencies) |
|---|---|---|
| 1-Derivative | 3175 | 1681, 1669, 1637 |
| 1,4-Derivative | 3125, 3086, 3058 | 1686, 1639 |
| 1,5-Derivative | 3226, 3195, 3125[a] | 1689, 1639 |
| 1,8-Derivative | 3226, 3185, 3125[a] | 1701, 1681, 1631 |

a) 3 $\mu$ bands obtained from KBr discs of 1,5- and 1,8-derivatives were all the same (3257, 3226, 3125 $cm^{-1}$).

Though it is known that the question, whether or not shifts of a C=O frequency comply with Hammett's rule, must be generally discussed in regard to the result obtained from the dilute solution of a nonpolar solvent, the results obtained from the solid of the 1-acylaminoanthraquinone series have been examined on account of its limited solubility in the present work. Shifts in the C=O frequency of the acyl groups were in harmony with Hammett's rule, as indicated in Fig. 3. Shifts in the C=O frequency of the peri-position of the acyl groups lay on the S-shaped curve against

13) M. S. C. Flett, *J. Chem. Soc.*, **1948**, 1441.

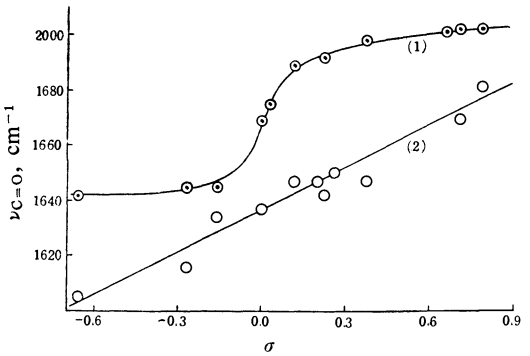



Fig. 3. The relationship between the C=O frequency ($\nu_{C=O}$) and Hammett's $\sigma$ value on the 1-acylaminoanthraquinone series.
(1) The quinone-type C=O frequency in the peri-position of the acylamino group.
(2) The C=O frequency in the acyl group.

Hammett's $\sigma$ value, as indicated in Fig. 3, and the latter C=O bond was therefore strengthened to much the same degree for the dyes with any of the electron-attracting substituents and the reverse was found to be true for the dyes with any of the electron-donating substituents. For the 1-derivative with a *p*- or *m*-dimethylsulfamyl group which is intensely electron-attracting, the C=O bonds of its molecule in solid have been strengthened to the extent indicated on the curve of Fig. 3.

As C=O frequencies[5] of (*o*-nitrobenzoyl)-aminoanthraquinone agree with those of 1-acetylaminoanthraquinone[13], the effect of the *o*-nitrophenyl group on them is thought to be of the same degree as that of the methyl group. This fact shows that the benzene ring of the former has been twisted around the C-C linkage between the *o*-substituted phenyl and the carbonyl group in the acyl group, and that the twisting may be attributed to steric hindrance between the *o*-nitro and the carbonyl group in the acyl group. For the *o*-nitro-substitute, this interpretation of its molecular structure in solid is the same as the deduction on that in solution on the basis of the results of the visible absorption. From shifts in the C=O frequency[5] of the acyl group for *o*-chloro- and *o*-methoxy-substitutes, however, it seems probable that such twisting of the benzene ring does not arise on the molecule in solid, this being different from the molecule in solution. Though the benzene ring of the *o*-chloro- or *o*-methoxy-substitute in solution has been twisted by repulsion between the *o*-chloro or *o*-methoxy and the carbonyl group in the acyl group, such twisting may be suppressed in a solid where the molecules are paked closely. From the result of infrared absorption, it seems likely that for the *o*-amino-substitute in solid the benzene ring also does not twist, this being identical with the deduction on its molecular structure in solution on the basis of the results of the visible absorption.

**Relative Difficulties of Vatting.**—It has been concluded that from the interpretation of visible absorption for the acylaminoanthraquinone series, an electron density of the quinone-type carbonyl group within the chromophoric system decreases in the order of 1, 4-, 1, 8- and 1, 5-isomers, and that it decreases in the order of 1, 4- and 1, 5-isomers from examinations of their infrared absorption. From both these bits of information and a reduction mechanism of anthraquinone[14], it is deduced that difficulty of reduction, namely difficulty of vatting, should naturally increase in the order of 1, 4-, 1, 8- and 1, 5-isomers. The result has also been obtained from our experiments[2-4] showing that difficulty of vatting increases in the order of 1, 4-, 1, 8- and 1, 5-isomers and vatting of the 1, 8-isomer is no more difficult than vatting of the 1, 4-isomer.

The result has been obtained from our experiments[2-4] that, for each seris of 1, 4-, 1, 5- and 1, 8-diacylaminoanthraquinones, the effect of X or Y on the difficulty of vatting increases in the order of *p*-$SO_2N(Me)_2$, *m*-$SO_2N(Me)_2$, *m*-OMe, *m*-Cl, *p*-OMe, *p*-Cl, *m*-$NO_2$, *p*-$NO_2$. But difficulties of vatting of *m*-methoxy-, *m*-chloro- and *p*-methoxy-substitutes have been of much the same degree as that of the non-substitute and those of dimethylsulfamyl-substitutes have been especially small[2-4]. It is known that the relative difficulty of vatting, namely the relative difficulty of reduction,

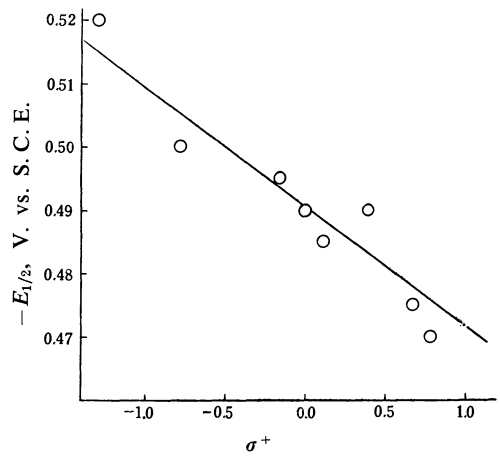



Fig. 4. The relationship between the first half-wave potential ($-E_{1/2}$) in ethanol and Brown's $\sigma^+$ value on the 1-acylaminoanthraquinone series.

14) T. Vickerstaff, "Physical Chemistry of Dyeing", Oliver & Boyd, London (1954), p. 282.

is dependent on both the magnitude of the reduction potential and the degree of the rate of reduction[14]. For the reduction potential, shifts of the reduction potential for 2-substitutes of 1, 4-naphthoquinone or for 3-substitutes of phenanthrenquinone were in harmony with Hammett's rule[2], and a relationship between the first half-wave potentials of 1-acylaminoanthraquinone series and Brown's $\sigma^+$ values were also in accordance with Hammett's rule, as indicated in Fig. 4. From these results, there seems likely to be a correlation between the magnitude of the reduction potential and Hammett's $\sigma$ or Brown's $\sigma^+$ value of the substituent for each series of acylaminoanthraquinones. On the contrary, from our results described above, it is evident that the effect of X or Y on the difficulty of vatting has been dependent not only on Hammett's $\sigma$ or Brown's $\sigma^+$ value but also on the hydrophilic or hydrophobic property of X or Y. Therefore, it seems likely that for each series the relative difficulty of vatting is dependent on both the magnitude of the reduction potential and the degree of the rate of reduction, and that the rate of reduction bears a relation to the hydrophilic or hydrophobic property of X or Y.

**Color Tones of Vat Solutions.** — For leuco salts of these dyes, as two electron-donating substituents ($O^-$) occupy 9- and 10-positions where they have the maximum conjugation with the anthracene nucleus, the effect of these substituents is considerably greater than that of such substituents as acyl groups occupying the other positions. Therefore, the entire visible absorption curve, that is, color tones of vat solution for all of 1,4-, 1,5- and 1,8-diacylaminoanthraquinone series should be similar to one another. Such deduction has been consistent with our results[2-4], that is, the color tones of vat solution for all of them, except for di-*o*-substitutes, were from reddish violet-blue to reddish violet. Waters[15] and Venkataraman[16] also reported that for the vat solutions of anthraquinone, aminoanthraquinone, acylaminoanthraquinone and others the visible absorption curves with maximum absorption bands at 425 and 515 m$\mu$ were given, being approximately similar to one another.

**Shades of Dyes.**—The 1, 4-diacylaminoanthraquinone series was a red dye, and 1, 5- and 1, 8-derivatives were yellow dyes but the shade of the latter on cotton was somewhat more bathochromic than that of the corresponding isomer of the former[2-4]. For all of the dyes with a nitro group as X or Y, the shades on cotton were from brown to intensly brownish on account of the amino group (reduction of the nitro group)[2-4]. The fact that the shade is hypsochromic in the order of 1, 4-, 1, 8- and 1, 5-isomers, is explained in the same way by electronic interpretations on shifts in visible absorption bands for these dyes in solution. It was admitted that for each series of diacylaminoanthraquinones a shade of the XY type*** was in the middle between shades of the corresponding XX type and of the YY type, and this fact has shown that the effects of X and Y on the shift of the shade are additive. An electron-donating substituent in the acyl group causes the bathochromic shift of the shade and the reverse is found for electron-attracting substituents. Though *p*- and *m*-dimethylsulfamyl groups were found to be intensly electron-attracting from examinations of the visible absorption, the shades of dyes with these groups as X or Y have merely shown a change from the weak hypsochromic to the weak bathochromic shift. For 1,4- and 1,5-diacylaminoanthraquinone series, an effect of X or Y on enhancement of brilliance of the shade has been shown to be greater in the *m*- than in the *p*-position within the acyl group, as described in the PB Report[17], but such a difference has not been found for the 1,8-derivative. Generally speaking, the degree of brilliance on the shade of the XY type for each series of diacylaminoanthraquinones was higher than that of the corresponding XX or YY type.

It is known that adsorption of leuco vat dyes on cellulose is dependent on both their affinity and rate of diffusion[18], but as the rate of diffusion may be independent of a kind of X or Y for the acylaminoanthraquinone series, it seems likely that adsorption of leuco acylaminoanthraquinones is dependent on their affinity, and, therefore, the greater the affinity is, the greater is the depth of the shade. From affinities of some acylaminoanthraquinones for cotton, it has been concluded that for any one of these series there is little difference in affinity between the *m*- and *p*-substitutes but their affinities are greater than that of a non-substitute and a great reduction in affinity is shown on the *o*-substitutes[8,18]. From these bits of information, the depth of the shade of the non-substitute should be less than those of *m*- and *p*-substitutes and those of the *o*-substitutes should be especially small for each series. Such deductions have been consistent with our results[2-4] obtained from comparison

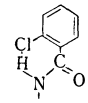
15) E. Waters, *J. Soc. Dyers Colorists*, **66**, 544 (1950).
16) M. R. Padhye, N. R. Rao and K. Venkataraman, *J. Sci. Ind. Research (India)*, **13B**, 759 (1954); *Chem. Abstr.*, **49**, 15836 (1955).

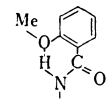
*** The XX or YY type denotes the diacylaminoanthraquinone with the same two acyl groups and the XY type that with two different acyl groups.
17) BIOS 987 (PB 75860) p. 185.
18) T. Vickerstaff, loc. cit., p. 299.

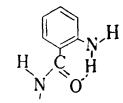
with the depth of the shade for many sets of the same shade. It is known that there is a definite correlation between affinity and molecular weight for these dyes, except for *o*-substitutes[8,18], but for dyes with a dimethylsulfamyl group as X or Y, the depth of the shade has been less in spite of the increase of molecular weight with the increasing surface area. This fact is due to a reduction of van der Waals force based on a decreasing coplanarity which is attributed to the bulky volume of the dimethylsulfamyl group.

***o*-Substitutes.**—It has been known from our experiments[2-4] that vatting of *o*-substitutes is more difficult than for *m*- and *p*-substitutes and the color tones of the vat solution for the former are more hypsochromic and pale than for the latter, and the former has dyed cotton with more difficulty.

From interpretations of visible absorption bands for *o*-substitutes, it has been concluded that mesomeric shifts of electrons within their chromophoric system are suppressed by the *o*-substituents, namely the *o*-substituents lower the electron density of the quinone-type carbonyl group. In consideration of both this fact and the vatting mechanism of *o*-substitutes, it is natural that these dyes have increasing difficulty in vatting, as described above. For leuco *o*-substitutes the hypsochromic shifts in the color tone of their vat solutions, described above, are attributed to the reduced conjugation between the anthracene nucleus and *o*-substituted benzoyl groups, and the palenen of vat solutions may be due to a decrease in an effective area of the $\pi$-electron system for *o*-substitutes. For *o*-chloro- and *o*-methoxybenzoylaminoanthraquinones, Valentin[19] has partially attributed their reduced affinities to internal chelation within acylamido groups, as indicated in Va and Vb, but the reduced affinity of *o*-methylbenzoylaminoanthraquinone[8,18] can not be explained satisfactorily from his suggestion, and the presence of the internal chelation is inconsistent with the information about the molecular structure obtained from their visible absorption. As *o*-substituents make it difficult for the *o*-substitutes to attain a planar configuration as indicated by this information, these dyes may dye cotton with diffiiculty, as described above, on account of the reduction of van der Waals force with the decreased affinity.


Va

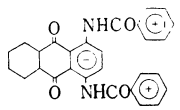

Vb

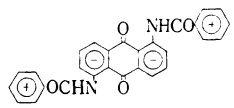

Vc

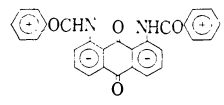
From interpretations on their visible absorption, it seems likely that *o*-amino-substitutes (reduction of the *o*-nitro-substitutes) have maintained coplanarity of the molecule, but the *o*-aminosubstitutes have also dyed cotton with difficulty. These results may be taken to show that the *o*-amino group prevents the hydrogen bond formation between the amido group and the cellulose hydroxyl group on account either of the steric hindrance of the *o*-amino group or the internal chelation as indicated in Vc.

**Light Fastness.** — Several relations between chemical constitutions of 1,4-, 1,5- and 1,8-diacylaminoanthraquinone series and their light fastness have been drawn from the results[2-4] of the light fastness test for them. In the first place, grades of light fastness on cotton for 1,4-, 1,5- and 1,8-dibenzoylaminoanthraquinones were 7, 6 and 5, respectively. The light fastness of the diacylaminoanthraquinone series on cotton has generally become lower in the order of 1,4-, 1,5- and 1,8-isomers. The shades of these dyes on cotton, except for *p*-substitutes of the 1,4-diacylaminoanthraquinone series, have not shown fading, but have shown a sign of turning brown under sunlight. For 1,5- and 1,8-diacylaminoanthraquinone series the light fastness of *p*-substitutes was generally higher than that of corresponding *m*-substitutes, which was higher than that of corresponding *o*-substitutes for each series of 1,4-, 1,5- and 1,8-diacylaminoanthraquinones. For each series of them, in comparison with the light fastness of a non-substitute, the dyes with a chloro group as X have shown almost no lowering, but the dyes with a methoxy or dimethylsulfamyl group have shown slight lowering, and all of the dyes with a nitro group (an amino group on cotton) evident lowering.

It is know that for a group of dyes of the


VIa


VIb


VIc

19) L. Valentin, *J. Soc. Dyers Colorists*, **72**, 286 (1956).

same type, for example simple azo dyes, in general, the greater the difference is of an electron density on two parts within a molecule of the dye, the higher the light fastness of the dye is. For dibenzoylaminoanthraquinones it seems likely that an electron density of the benzene ring in the benzoyl group is lower than that of the benzene ring within the anthraquinone nucleus, as indicated in VIa, VIb and VIc, from both pieces of information about mesomeric shifts of electrons within the chromophoric systems and examinations of some reactions of the dyes with reagents. For 1,4-dibenzoylaminoanthraquinone two chromophoric systems hold one benzene ring within the anthraquinone nucleus in common, but for 1,5- and 1,8-dibenzoylaminoanthraquinones two chromophoric systems bear relations with different benzene rings in the anthraquinone nucleus respectively. The difference between electron densities of the benzene ring in the benzoyl group and of the benzene ring in the anthraquinone nucleus for the 1,4-derivative should therefore be greater than for the 1,5- or 1,8-derivative. From interpretations of both visible and infrared absorption for 1,5- and 1,8-derivatives, it has been concluded that an electron density of the quinone-type carbonyl group on the peri-position of the benzoylamido group for the latter is somewhat higher than for the former. As two chromophoric systems of the 1,8-derivative holding one carbonyl group in common are cross conjugation, mesomeric shifts of electrons within them are suppressed by each other; but, on the other hand, two chromophoric systems of the 1,5-derivative bear almost no relation to each other. The extent of the mesomeric shift of electrons within one chromophoric system for the former is therefore less than for the latter, and then the difference between electron densities of the benzene ring in the benzoyl group and of the benzene ring in the anthraquinone nucleus for the former is less than for the latter. Finally, the difference between electron densities of two benzene rings decreases in the order of 1,4-, 1,5- and 1,8-isomers, and this order may be responsible for the lowering of light fastness in the order of 1,4-, 1,5- and 1,8-isomers, described above. An alternative possibility is that the 1,5-isomer being transform it probably packs more compactly than the 1,8-isomer which is in cis-form in the solid of the dye within the fiber, and also that the light fastness of the former may be higher than that of the latter.

The effects of Cl, OMe or $NH_2$ as X on light fastness, described above, were similar to the results[20] already known concerning many dyes. Though a dimethylsulfamyl group is intensely electron-attracting, shades of the dyes with this group as X or Y have only shown changes from weak bathochromic to weak hypsochromic shifts in comparison with the shade of the non-substitute, and further the dimethylsulfamyl group has an appearance of a weak electron-attracting or weak electron-donating group in these cases. This fact may bear some relation to the lowering of the light fastness of these dyes described above. The lowering of light fastness may be due to the fact that these dyes can not pack compactly in the solid of the dye within the fibre owing to the bulky volume of the dimethylsulfamyl group.

The authors wish to express their sincere thanks to Professor Yoshio Nagai and Dr. Shimpachiro Kato of Tokyo University for their helpful suggestions and encouragement in the course of this work. They also wish to thank the Tokuyama Research Laboratory of Idemitsu Kōsan Co. for infrared measurements.

*Department of Chemistry*
*Faculty of Literature and Science*
*Yamaguchi University*
*Ushirogawara, Yamaguchi-shi*

20) A. Gebhard. ibid., **25**, 305 (1909).

# *Polyterpenes. III*[1]. *The Structure of Thujopsene**

By Hiroshi KOBAYASHI, Shizuo NAGAHAMA and Saburo AKIYOSHI

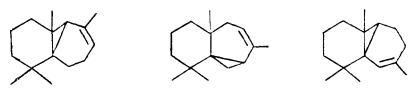
(Received November 19, 1960)

Thujopsene, the main component of Hiba wood oil, has attracted much attention in the last few years[2]. Hirose and Nakatsuka[3] pointed out that widdrene[4], which was later shown to be widely distributed in *Cupressaceae*[5], was identical with thujopsene. Erdtman and Norin[6] confirmed this identity and proposed structure Ia for this compound. Independently we also arrived at the same conclusion and proposed structure Ia and Ib[7], of which the former is preferred[5]. Subsequently Erdtman and Norin[9] presented further evidence and revised their structure to Ib. Sisido and Nozaki[10] proposed structure Ic for thujopsene, but later withdrew their suggestion[11] in favor of Erdtman and Norin's proposal. In view of the evidence presented[12] we also consider that the properties of thujopsene are best explained by the formula Ib.

We now wish to present our findings which have already been outlined in our short communication[8].

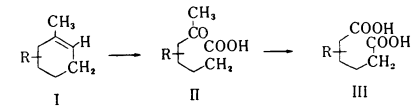
Thujopsene (I) possesses the molecular formula $C_{15}H_{24}$ and is a tricyclic hydrocarbon compound having an unsaturated bond. On the permanganate oxidation in acetone, it gives ketocarboxylic acid, $C_{15}H_{24}O_3$ (II), as a main product in addition to other by-products. Ozonolysis of thujopsene gives the same acid II. This acid II is therefore considered as the primary product to which thujopsene cleaves at the unsaturated bond without any other change. Thus, the purpose of the studies comes to determine the structure of acid II.

Hypobromite oxidation of II affords a dicarboxylic acid, $C_{14}H_{22}O_4$ (III), which shows the presence of the $CH_3$-CO- group in the keto acid II, and these results, when considered together with the preceding data, seem

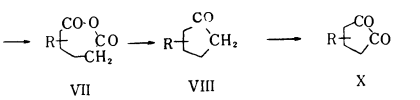


Ia Ib Ic

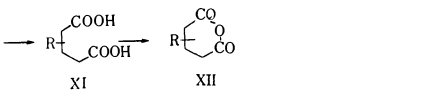
Fig. 1



I II III

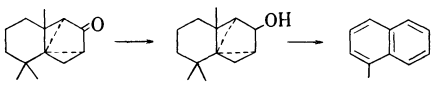


VII VIII X



XI XII

Fig. 2



VIII XV



XVI

Fig. 3. In VIII, a cyclopropane ring is fused to a cyclopropanone ring in either of the ways which are showed above by the two broken lines.

The broken lines in XV and XVI present the same meaning as in VIII.

---

* Contribution No. 16 from the Department of Organic Synthesis, Faculty of Engineering, Kyushu University.

1) Previous paper: S. Nagahama, H. Kobayashi and S. Akiyoshi, This Bulletin, **32**, 366 (1959).

2) For references to previous studies, see S. Akiyoshi and S. Nagahama, This Bulletin, **30**, 886 (1957).

3) Y. Hirose and T. Nakatsuka, *J. Jap. Wood Res. Soc.*, **4**, 26 (1958).

4) H. Erdtman and B. R. Thomas, *Acta Chem. Scand.*, **12**, 267 (1958).

5) H. Erdtman and Z. Pelchowicz, *Chem. Ber.*, **89**, 341 (1956); C. Enzell, *Acta Chem. Scand.*, **14**, 81 (1960); C. Pilo and J. Runeberg, ibid., **14**, 353 (1960); J. Runeberg, ibid., **14**, 797 (1960).

6) H. Erdtman and T. Norin, ibid., **13**, 1124 (1959).

7) S. Akiyoshi, H. Kobayashi and S. Nagahama, presented at the 2nd Symposium on Perfumary of Terpene and Essential Oil Chemistry, Hiroshima, October, 1958.

8) H. Kobayashi, S. Nagahama and S. Akiyoshi, This Bulletin, **32**, 203 (1959).

9) H. Erdtman and T. Norin, *Chem. & Ind.*, **1960**, 622.

10) K. Sisido and H. Nozaki, *J. Org. Chem.*, **25**, 875 (1960).

11) K. Sisido, H. Nozaki and Y. Imagawa, presented at the 4th Symposium on Natural Organic Compounds, Kyoto, October, 1960.

12) S. Forsén and T. Norin, *Acta Chem. Scand.*, in press. We thank Dr. Norin for the kind presentation of his manuscript of this paper.

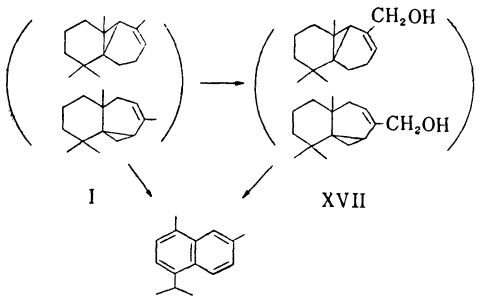



Fig. 4

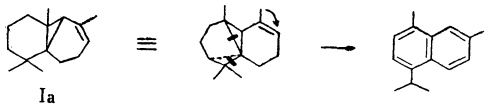



Fig. 5

to indicate the presence of the structure $CH_3-\underset{\underset{C-}{|}}{C}=C-$ in thujopsene.

The keto acid II is, when treated with mineral acid, easily isomerized to a ketolactone (carbonyl absorptions 1774 and 1724 $cm^{-1}$) accompanied with a cleavage of a ring in the keto acid II. It possibly indicates the presence of a small ring in the keto acid II.

The $C_{14}$-dicarboxylic acid (III) gives two different monomethyl esters, $C_{15}H_{24}O_4$, one (IV) of which is obtained by acid catalyzed esterification with methanol and the other (V) by hydrolysis of dimethyl ester (VI) with methanolic potassium hydroxide. The former (IV) is also obtained from the methyl ester of II, when treated with hypobromite in aqueous dioxane, and it seems therefore that one of the two carboxyl groups in III is much more hindered than the other and that the former results from $CH_3-CO-$ group in II.

The $C_{14}$-dicarboxylic acid (III) is dehydrated to an anhydride, $C_{14}H_{20}O_3$ (VII) (carbonyl adsorptions 1799 and 1752 $cm^{-1}$), which is easily pyrolyzed at about 300°C to a cycloketone, $C_{13}H_{20}O$ (VIII), accompanying decarboxylation[13].

Calcium and barium salt of dicarboxylic acid III also give cycloketone VIII by pyrolysis but they do so in poor yield.

Cycloketone VIII is condensed with ethyl formate in the presence of sodium metal to an enol, $C_{14}H_{20}O_2$ (IX), and is oxidized to a yellow 1,2-diketone, $C_{13}H_{18}O_2$ (X), with selenium dioxide in dioxane. Each of these two characteristic reactions results in the quantitative formation of the corresponding product and exclusively of only a single corresponding species. It seems therefore that the carbonyl group in VIII connects to a methylene group at one side and to a more substituted carbon atom at the other side. This presumption becomes more certain by the fact that 1,2-diketone (X) is converted into a dicarboxylic acid, $C_{13}H_{20}O_4$ (XI), without loss of the carbon atom when treated with alkaline hydrogen peroxide.

The $C_{13}$-dicarboxylic acid (XI) gives the corresponding anhydride, $C_{13}H_{18}O_3$ (XII), by heating. All attempts to get $C_{12}$-cycloketone from XI have failed.

XII shows infrared absorptions of the carbonyl group at 1799 and 1754 $cm^{-1}$. Therefore XII is considered to be of glutaric anhydride type, and the cycloketone to be of structure VIII, and further the ring containing an unsaturated bond in thujopsene is six-membered.

$C_{13}$-dicarboxylic acid (X), like acid III, also easily gives two different monomethyl esters, $C_{14}H_{20}O_4$, one (XIII) by esterification and the other (XIV) through hydrolysis of dimethyl ester.

Cycloketone VIII gives an alcohol, $C_{13}H_{22}O$ (XV), when reduced with lithium aluminum hydride. It is of interest that the reduction with lithium aluminum hydride proceeds stereospecifically and the epimer of XV does not occur[14].

Alcohol XV is dehydrogenated by selenium to 1-methylnaphthalene with loss of two carbon atoms. If the two carbon atoms eliminated on dehydrogenation are regarded as that of one methyl of the geminal dimethyl group and that of the angular methyl group, the skeleton of alcohol XV is considered as formula XV. The position of the hydroxyl group is determined as follows. By means of methyl magnesium iodide, a methyl group is introduced on the carbon atom of the carbonyl group in VIII, which leads to a corresponding alcohol, $C_{14}H_{24}O$ (XVI). Selenium dehydrogenation of alcohol XVI gives 1,6-dimethylnaphthalene. The methyl group introduced is on 6-position unless a migration of the methyl group occurs on dehydrogenation, and thus the groups in question are considered to be on the position indicated.

The enlarging of the five-membered ring in alcohol XV to the six-membered ring by aromatization, when considered together with the acid-catalyzed cleavage of a ring in the keto acid II, seems to indicate the presence of the

13) This ketone was first reported by T. Ozeki, S. Seto and T. Nozoe at the 10th Annual Meeting of the Chemical Society of Japan, Tokyo, 1957, and called "pyroketone" by them. On the preparation of this ketone by another route, see previous paper, Ref. 1.

14) The epimer of alcohol XV was obtained from lead tetraacetate oxidation product of thujopsene, see Ref. 1.

cyclopropane ring fused to the five-membered ring in XV. In addition, the infrared and ultraviolet spectral data of keto acid II, its methyl ester and cycloketone VIII are corroborative of the conjugation of the ketonic group with the cyclopropane ring[15].

Thus Ia or Ib is proposed for the structure of thujopsence. The fact that the dehydrogenation of thujopsene and its alcoholic derivative, $C_{15}H_{24}O$ (XVII), afford 1,7-dimethyl-4-isopropylnaphthalene is unfavorable for structure Ib which is less amenable to the rearrangement in regard to the naphthalene derivatives.

## Experimental

**Ester of Ketocarboxylic Acid II.**—Methylation with diazomethane gave a methyl ester which was purified by distillation under reduced pressure, b. p. 151~158°C/7 mmHg, m.p. 42~43°C. Infrared max. (Nujol) 1700 and 1735 $cm^{-1}$; ultraviolet max. 222 m$\mu$ ($\varepsilon$ 3160) and 284 m$\mu$ ($\varepsilon$ 40). $[\alpha]_D^{26}$ −94.0° (*c* 1.54).

Found: C, 71.96; H, 9.84. Calcd. for $C_{16}H_{26}O_3$: C, 72.14; H, 9.84%.

**Esters of Dicarboxylic Acid III.**—Dimethyl ester VI was prepared through methylation with diazomethane in ether. The solution was evaporated to dryness, and the residue was purified by recrystallization from methanol, m. p. 72~73°C. Infrared max. (carbon tetrachloride) 1737 $cm^{-1}$.

Monomethyl ester IV was prepared from dicarboxylic acid III by esterification with methanol. The details were presented in the previous paper. Melting point 59~60°C. Infrared max. (Nujol) 1700 and 1736 $cm^{-1}$. This monomethyl ester was also obtained by treating the methyl ester of the ketocarboxylic acid II (2.50 g.) with excess of sodium hypobromite solution (aqueous dioxane 1 : 1) for 2.5 hr. at room temperature. The reaction mixture was diluted with water, acidified and extracted with ether. The ethereal extract was washed twice with water, extracted with aqueous sodium bicarbonate (7%) and then with aqueous sodium hydroxide (5%). When the sodium bicarbonate extract acidified, dicarboxylic acid III was mainly obtained, m. p. 209~210°C, mixed melting point with dicarboxylic acid III undepressed. From the sodium hydroxide extract the monomethyl ester (1.30 g.) was obtained, m. p. 58~59°C and mixed melting point with that obtained by esterification of III undepressed.

**Monomethyl Ester V.**—The dimethyl ester prepared by methylation with diazomethane was refluxed in methanolic potassium hydroxide (5%) for 6 hr. The reaction mixture was diluted with water, washed with ether, acidified, and extracted with ether. The last ethereal extract was washed with water, and extracted with aqueous sodium bicarbonate (7%) and then with aqueous sodium hydroxide (5%). The sodium bicarbonate extract was acidified and extracted with ether. The extract was washed with water, evaporated to dryness, the residue being recrystallized from aqueous methanol, m. p. 208~209°C. Mixed melting point with dicarboxylic acid III (m.p. 209~210°C) was undepressed. The sodium hydroxide extract was acidified and then treated as above. The product obtained was a monomethyl ester of m. p. 114.5~115.5°C. Infrared max. (chloroform) 1693 and 1720 $cm^{-1}$.

Found: C, 67.02; H, 9.02. Calcd. for $C_{15}H_{24}O_4$: C, 67.13; H, 9.02%.

This monomethyl ester was reconverted to dimethyl ester VI by methylation with diazomethane in ether.

**Cycloketone VIII.**—The acid anhydride VII (5.0 g.) was pyrolyzed at 280~320°C for 40 min. under air-cooling reflux; distillation of the product gave 3.4 g. of a distillate, which was refluxed in methanolic potassium hydroxide (5%) for an hour. The reaction mixture was diluted with water, extracted with ether, and the ethereal extract was washed with water and then the solvent was removed to dryness. The residue was steam-distilled and ketone VIII separated as crystalline precipitates was dissolved in ether and dried over sodium sulfate. After the solvent was removed to dryness, the residue was recrystallized from petroleum ether, m.p. 117~118°C, and was further purified by sublimation under reduced pressure, m.p. 118~119.5°C, yield 1.7 g.. Infrared max. (Nujol) 1727 $cm^{-1}$. Ultraviolet max. (ethanol) 278 m$\mu$ ($\varepsilon$ 55.5). $[\alpha]_D^{26}$ +62.2° (*c* 0.602).

This ketone was also obtained by pyrolysis of calcium salt and of barium salt of III.

**Hydroxymethylation of VIII, Enol IX.**—The cycloketone VIII (600 mg.) and ethyl formate (700 mg.) were allowed to react in cold benzene solution (8 ml.) in the presence of sodium dust (200 mg.) for two days, when methanol was added to decompose the residual sodium metal. Water was added and the aqueous layer was acidified. The crude enol was collected (250 mg., m. p. 97~98°C) and decolorized with active charcoal. Recrystallization from aqueous ethanol gave white needles of m.p. 105~106°C, which gave purple color in the ferric chloride test. Infrared max. (chloroform) 1668 $cm^{-1}$, (Nujol) 1681 and 2680 $cm^{-1}$.

Found: C, 75.63; H, 9.22. Calcd. for $C_{14}H_{20}O_2$: C, 76.32; H, 9.15%.

From the benzene layer, the starting material (330 mg.) was recovered.

**Diketone X.**—Cycloketone VIII (130mg.), selenium dioxide (130 mg.) and dioxane (2.5 ml.) were heated in a sealed tube for 6 hr. at 200°C. Selenium was filtered off and washed with petroleum ether. The filtrate and washings were combined and water (30 ml.) was added to it; the yellow diketone was dissolved in ethereal layer. The aqueous layer was extracted with petroleum ether until the extract was no longer colored yellow. The combined extract was washed with water and dried over sodium sulfate. After the solvent was removed from the dried solution the residue solidified

15) E. N. Trachtenberg and G. Odian, *J. Am. Chem. Soc.*, **80**, 4018 (1958); R. J. Mohrbacher and N. H. Cromwell, ibid., **79**, 401 (1957).

immediately. Yield of crude product 130 mg., m.p. 170~171°C. Recrystallization from petroleum ether raised the melting point to 180~181°C. Infrared max. (Nujol) 1736 $cm^{-1}$.

Found: C, 75.78; H, 8.87. Calcd. for $C_{13}H_{18}O_2$: C, 75.69; H, 8.80%.

**Dicarboxylic Acid XI**[16].—To the mixture of diketone X (50 mg.), ethanol (6 ml.) and hydrogen peroxide (30%, 2 ml.) was dropwise added aqueous sodium hydroxide (10%, 2 ml.), and after being allowed to stand for half an hour, the reaction mixture was warmed at 80°C in a water bath for a few minutes and, after being cooled, was acidified and the crystalline precipitatates wese recrystallized from aqueous ethanol, m.p. 210~211°C. The dicarboxylic acid XI was dehydrated to the acid anhydride XII with acetic anhydride, and recrystallized from benzene-petroleum ether, m.p. 211~212°C.

No ketone formation was observed during the pyrolysis of the acid anhydride XII, which was also true in the cases of calcium- and barium dicarboxylate XI.

**Alcohol XV.**—An ethereal solution of lithium aluminum hydride (30 mg.) was added with swirling into an ethereal solution of cycloketone VIII (500 mg.). After being allowed to stand overnight, a small amount of water was added to decompose the residual lithium aluminum hydride. The resultant mixture was extracted with an additional amount of ether. The ethereal extract was washed with dilute sulfuric acid the then several times with saturated salt solution, and was dried over sodium sulfate. The solvent was evaporated to dryness and the residue was crystallized immediately, yield 450 mg., and recrystallized from petroleum ether, m.p. 132~133°C. Infrared max. (Nujol) 3280 $cm^{-1}$. $[\alpha]_D^{26}+19.2°$ (*c* 0.802).

Found: C, 80.30; H, 11.68. Calcd. for $C_{13}H_{22}O$: C, 80.35; H, 11.41%.

Alcohol XV (2.0 g.) was oxidized to cycloketone VIII by treatment with sodium bichromate (1.5 g.), water (2 ml.) and acetic acid (16 ml.) for 30 hr. at room temperature. The reaction mixture was diluted with water and was extracted with ether. The ethereal extract was washed several times with aqueous sodium bicarbonate (7%), with water and dried over sodium sulfate. After the solvent was removed to dryness the residue was crystallized immediately. Repeated recrystallization from petroleum ether gave m.p. 117~118°C. This substance was identified as being the original cycloketone VIII by mixed melting point test and infrared spectrum comparison.

**Dehydrogenation of Alcohol XV.**—The alcohol XV (2.0 g.) and selenium (3.0 g.) were heated under reflux at 400°C for 165 hr. The oily product was distilled and the main fraction (b.p. 230~240°C) was eluted from alumina (50×70 mm. column) with petroleum ether, yield 0.30 g., $n_D^{17}$ 1.5803. The picrate of the above hydrocarbon compound was orange needles and recrystallizations from ethanol afforded the material of m.p. 137~138°C. The pure hydrocarbon compound was regenerated from picrate by elution from alumina with petroleum ether. $n_D^{17}$ 1.6125.

Found: C, 92.86; H, 7.33. Calcd. for $C_{11}H_{10}$: C, 92.91; H, 7.09%.

Picrate of the purified material showed m.p. 138~139°C, and mixed melting point with the picrate of 1-methylnaphthalene[17] (m.p. 139~140°C) was undepressed.

Found: C, 54.89; H, 3.63; N, 11.39. Calcd. for $C_{17}H_{13}O_7N_3$: C, 54.99; H. 3.53; N, 11.32%.

**Methylcarbinol XVI.**—The ethereal solution of cycloketone (4.3 g.) was dropwise added to ethereal methyl magnesium iodide (from methyl iodide (3.6 g.), magnesium (0.6 g.) and ethyl ether (13 ml.)). The Grignard complex was decomposed by treatment with aqueous ammonium chloride. The methylcarbinol was extracted with an additional ether from the above reaction mixture, yield 4.2 g., and was purified by recrystallization from petroleum ether and sublimation under reduced pressure, m.p. 62~63°C. $[\alpha]_D^{20}+14.3°$ (*c* 1.87). Infrared max. 3245 $cm^{-1}$.

Found: C, 80.92; H, 11.76. Calcd. for $C_{14}H_{24}O$: C, 80.71; H, 11.61%.

**Dehydrogenation of Methyl Carbinol XVI.**—Methyl carbinol XVI (2.0 g.) and selenium (3.0 g.) were heated at 400°C for 104 hr. The same treatment as that of alcohol XV yielded an oily product (0.3 g.), the main fraction distilling at 240~250°C. The infrared spectrum of the hydrocarbon compound coincided with that of 1,6-dimethylnaphthalene and its picrate recrystallized from ethanol was of m.p. 111~112°C. The pure hydrocarbon compound was regenerated from picrate by means of elution from alumina with petroleum ether. $n_D^{12}$ 1.6047.

Found: C, 92.13; H, 8.02. Calcd. for $C_{12}H_{12}$: C, 92.26; H, 7.74%.

**Esters of the Dicarboxylic Acid XI.**—The dimethyl ester was prepared by methylation with diazomethane by a method similar to the case of the dicarboxylic acid III. M. p. 70~72°C.

**Monomethyl Ester XIII.**—Dicarboxylic acid anhydride XII (490 mg.) was refluxed in methanol (2 ml.) containing two drops of concentrated sulfuric acid for half an hour. The reaction mixture was diluted with water and extracted with ether. The ethereal extract was washed with water and extracted with aqueous sodium bicarbonate (7%). The aqueous extract was washed with ether, acidified and extracted again with ether. The last ethereal extract was evaporated to dryness and the solid residue was recrystallized from aqueous methanol to give a compound, m.p. 58~62°C, which decomposed at about 90°C and again solidified and melted at 208~209°C. The decomposed product was identical with the dicarboxylic acid anhydride XII (mixed melting point test and infrared spectrum comparison).

The monomethyl ester was converted to the dimethyl ester with diazomethane, and hydrolyzed

16) The same dicarboxylic acid had been obtained in the series of lead tetraacetate oxidation of thujopsene and the chemical data of acid XI and its anhydride XII had been presented in Ref. 1.

17) An authentic sample was synthesized according to the direction of O. Grummitt et al., *J. Am. Chem. Soc.*, 65, 295 (1943).

to the original dicarboxylic acid with aqueous potassium hydroxide.

**Monomethyl Ester XIV.**—Dimethyl ester (1.0 g.) prepared by methylation with diazomethane was refluxed in methanolic potassium hydroxide (10%, 25 ml.) for 5 hr. The reaction mixture was diluted with water, and the neutral oil which separated, on solidification, was filtered off. The aqueous portion was acidified and the crystalline precipitates collected, yield 300 mg., were recrystallized from petroleum ether, m.p. 145~145.5°C, which was reconverted to the starting material by the methylation.

**Dehydrogenation of Thujopsene.**—Thujopsene (5.0 g.) and selenium (10.0 g.) were heated at 330°C for 190 hr. The oily product obtained on distillation (b.p. above 120°/5 mmHg) was eluted from alumina (50×50 mm. column) by petroleum ether, yield 0.54 g., $n_D^{18}$ 1.5702; the product when chilled on dry ice gradually solidified. Repeated recrystallizations from methanol afforded colorless plates of m.p. 60~61°C. The infrared spectrum of the hydrocarbon compound agreed with that of 1,7-dimethyl-4-isopropylnaphthalene.

Found: C, 90.72; H, 9.41. Calcd. for $C_{15}H_{18}$: C, 90.85; H, 9.15%.

The picrate was recrystallized from ethanol and had m.p. 88~89°C.

Found: C, 58.96; H, 4.96; N, 9.85. Calcd. for $C_{21}H_{21}O_7N_3$: C, 59.01; H, 4.95; N, 9.83%.

**Aldehyde**[18].—Thujopsene (9.5 g.) was added to the ethanol solution of selenium dioxide (5.2 g. of selenium dioxide in 60 ml. of absolute ethanol). The mixture was gently refluxed for 20 hr. at boiling point. The reaction mixture, after the selenium (2.2 g.) was filtered off, was concentrated to about 20 ml. under reduced pressure and a large amount of water was added to the remainder, the organic portion of which was extracted by benzene. The benzene extract was washed twice with saturated salt solution, with saturated aqueous lead acetate and again with salt solution three times, and dried over sodium sulfate. After the solvent was removed the remainder was fractionated. The aldehyde was obtained from the fraction of b.p. 133~134.5°C/3.5 mmHg, yield of crude product 7.1 g.. Repetition of recrystsllization raised the melting point to 74~75°C. Infrared max. (Nujol) 1683 $cm^{-1}$.

**Alcohol XVII.**—The warm solution of aldehyde (5.54 g. of aldehyde in 26 ml. of methanol) was added to the solution of sodium borohydride (0.344 g. of the hydride in 3 ml. of methanol). After being heated for ten minutes, the mixture was left to cool at room temperature for two hours. Aqueous acetic acid was added to the reaction mixture to decompose the residual hydride. When the resulting mixture was diluted with water, the product was immediately solidified. The crystalline precipitates were collected and washed with water thoroughly. White needles of m.p. 102.5~103.5°C were obtained by recrystallization from petroleum ether. $[\alpha]_D^{20}-109°$ ($c$ 0.90). Infrared max. (Nujol) 3320 $cm^{-1}$.

Found: C, 81.84; H, 11.01. Calcd. for $C_{15}H_{24}O$: C, 81.76; H, 10.98%.

**Dehydrogenation of Alcohol XVII.**—Alcohol XVII (5.0 g.) and selenium (10.0 g.) were heated at 330°C for 30 hr. The oily product obtained (b.p. above 120°C/4.5 mmHg) was eluted from alumina (20×100 mm. column) with petroleum ether, yield 0.20 g., $n_D^{18}$ 1.5642. Though the picrate was prepared, its melting point could not be raised to that reported by Sörm[19]. The infrared spectrum of the hydrocarbon compound which was regenerated from the crude picrate coincided to a fair extent with that of 1,7-dimethyl-4-isopropylnaphthalene. The regenerated hydrocarbon compound was semi-solid, and rigid determination of its melting point was not conducted owing to the lack of a sample.

*Department of Organic Synthesis*
*Faculty of Engineering*
*Kyushu University*
*Hakozaki, Fukuoka*

18) This aldehyde is that reported by Erdtman and Norin, Ref. 6.

19) J. Príva, V. Herout, B. Schneider and F. Sörm, *Collection Czechoslov. Chem. Communs.*, **18**, 500 (1953).

# *Mercury Photosensitized Decomposition of Carbon Dioxide by 1849 Å ($Hg^*6^1P_1$)*

By Yuji MORI

(Received January 24, 1961)

Few studies[1,2] have been made of reactions induced by the 1849 Å mercury resonance line, because of the difficulty of eliminating the effect of the other resonance line of mercury at 2537 Å.

In the case of carbon dioxide most of the above difficulties may be reduced. The possibility of direct photolysis by 2537 Å is eliminated since carbon dioxide is transparent above 1850 Å. The excitation energy of $6^3P_1$ of mercury, 112.2 kcal., is insufficient to bring about the reaction

$$CO_2+Hg^*(6^3P_1) \rightarrow CO+O+Hg(^1S_0)$$

and the reaction

$$CO_2+Hg^*(^3P_1) \rightarrow CO+HgO$$

is slow and has no important effect[3] on the photosensitized decomposition by $6^1P_1$ of mercury. The excitation energy of $6^1P_1$ of mercury, 153.9 kcal., is sufficient to bring about the decomposition of carbon dioxide.

Therefore, it is possible to investigate the photosensitized decomposition and the direct photolysis of carbon dioxide induced by the resonance line at 1849 Å without any important interference caused by the resonance line at 2537 Å.

## Experimental

**Photosensitized Decomposition.**—Carbon dioxide obtained from sodium bicarbonate was dried by passing it over calsium chloride and magnesium perchlorate. Then the gas was stored after purification by bulb to bulb distillation, using dry ice and liquid nitrogen. Before each run, gases noncondensable in ilquid nitrogen were remonved by pumping in liquid nitrogen.

The reaction was carried out in a cylindrical fused quartz cell (5 cm. in diameter 10 cm. long) illuminated by the radiation from a low pressure mercury lamp operated at a constant current 90 ma. from a 2000 V. leakage transformer. The gas saturated with mercury vapor by passing it over a mercury surface in a heated U tube, was introduced into the reaction cell. To keep the gas saturated with mercury vapor throughout a run, liquid mercury was intoduced into the reaction cell. When no liquid mercury was introduced in the cell, the reduction of the rate of the reaction was observed by the depletion of mercury due to the formation of the oxide of mercury. The temperature of the reaction cell was kept at room temperature.

The gaseous products, noncondensable in liquid nitrogen, were analysed in a conventional analysis system. The amount of noncondensable gas was measured by compressing it into a constant volume burette using a small mercury diffusion pump backed by a Töepler pump. The volume of carbon monoxide in the noncondensable products was determined by means of copper oxide heated at around 300°C.

**Direct Photolysis.**—In the investigation of the direct photolysis, the carbon dioxide used was prepared in a system completely free from mercury vapor in order to eliminate the mercury photosensitization. The pressure of carbon dioxide in the reaction cell was measured by means of a Bourdon gauge. After the photolysis, the gaseous products noncondensable in liquid nitrogen, were analysed by connecting the reaction cell to an analysis system by means of a ground joint.

Since the absorption coefficient of carbon dioxide at 1849 Å is very small[4], the investigation was carried out in a higher pressure region than in the case of photosensitization. The reaction was carried out at room temperature.

## Results

**Photosensitization.**—Carbon monoxide was the only product which was noncondensable in liquid nitrogen, and no oxygen was detected. This means that the rate of formation of oxygen is at most a few percent of that of carbon monoxide. A colored substance, assumed to be an oxide of mercury, was found on the surface of the front window of the reaction cell. This was soluble in dilute sulfuric acid and was removed by flaming in vacuum.

The average rate of production of carbon monoxide, (amount of carbon monoxide produced)/(irrandiation time), depends on the time of irradiation and the pressure of carbon

1) C. C. McDonald, A, Kahn and H. E. Gunning, *J. Chem. Phys.*, **22**, 908 (1954).

2) J. D. McGilvery and C. A. Winkler, *Can. J. Chem.*, **30**, 194 (1952).

3) In fact, the formation of an oxide of mercury and carbon monoxide was observed in the experiment using a filter which cuts off the light below 2300 Å. But the rate of this reaction was very slow and showed that its effect would be negligible.

4) E. C. Y. Inn, K, Watanabe and M. Zelikoff, *J. Chem. Phys.*, **21**, 1648 (1953).

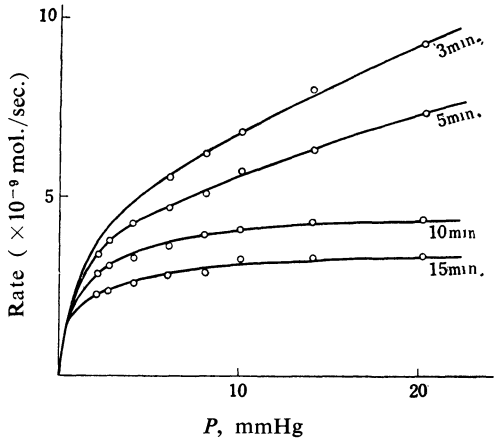



Fig. 1. The average rate of production of carbon monoxide in photosensitized decomposition of carbon dioxide.

TABLE I. THE AVERAGE RATE OF PRODUCTION OF CARBON MONOXIDE IN PHOTOSENSITIZED DECOMPOSITION OF CARBON DIOXIDE

| Pressure | Rate ($\times 10^{-9}$ mol./sec.) | | | | $r_0(t=0)$ |
|---|---|---|---|---|---|
| mmHg | 3 min. | 5 min. | 10 min. | 15 min. | |
| 2.0 | | 3.39 | 2.78 | 2.23 | 4.06 |
| 2.6 | | 3.79 | 3.00 | 2.30 | 5.27 |
| 4.0 | | 4.22 | 3.23 | 2.59 | 5.56 |
| 6.0 | 5.56 | 4.66 | 3.58 | 2.80 | 7.41 |
| 8.0 | 6.18 | 5.10 | 3.89 | 2.86 | 8.44 |
| 10.0 | 6.78 | 5.70 | 4.00 | 3.21 | 8.83 |
| 14.0 | 7.97 | 6.26 | 4.28 | 3.25 | 11.52 |
| 20.0 | 9.30 | 6.98 | 4.30 | 3.30 | 14.11 |
| 40.0 | 13.62 | 11.56 | 8.57 | | 17.64 |

dioxide as shown in Table I and in the plots in Fig. 1.

The gradual decrease of transparency of the front window of the reaction cell by the formation of the oxide of mercury, decreases the rate of production of carbon monoxide (i. e., the rate of decomposition of carbon dioxide) with the increase of irradiation time $t$. Therefore, the initial rate $r_0$ was obtained by extrapolation to $t=0$ assuming the formula

$$r = r_0 + at + bt^2$$

where the constants $a$ and $b$ depend on the pressure of carbon dioxide.

The initial rates for various pressures are given in Table I (last column) and the plots in Fig. 2.

**Direct Photolysis.** — The products, non-condensable in liquid nitrogen, were oxygen and carbon monoxide in a ratio around 1 : 5, which is far from the stoichiometric ratio of 1 : 2. No solid deposit was found on the front window of the reaction cell. The results are shown in Table II and in Fig. 3. It will be

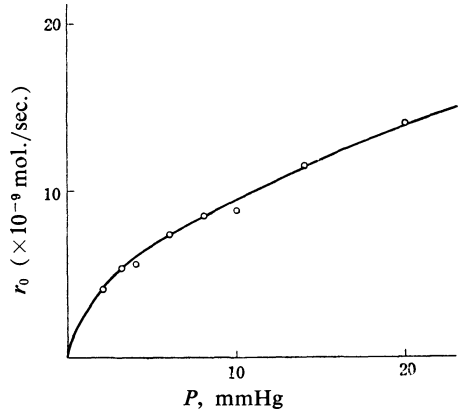



Fig. 2. The initial rate of carbon monoxide in photosensitisation.

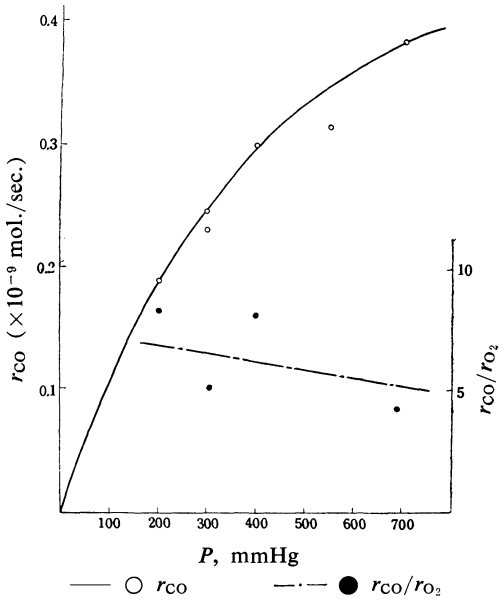



Fig. 3. The results of direct photolysis of carbon dioxide by 1849 Å.

TABLE II. THE RESULTS OF DIRECT PHOTOLYSIS OF CARBON DIOXIDE BY 1849 Å

| Pressure | Rate ($\times 10^{-9}$mol./sec.) | | |
|---|---|---|---|
| mmHg | $r_{CO}$ | $r_{O_2}$ | $r_{CO}/r_{O_2}$ |
| 200 | 0.189 | 0.027 | 7.0 |
| 300 | 0.229 | 0.044 | 5.2 |
| | 0.245 | 0.013 | 18.8* |
| 400 | 0.299 | 0.042 | 7.1 |
| 550 | 0.312 | 0.009 | 34.6* |
| 700 | 0.383 | 0.090 | 4.3 |

* The reaction cell was flamed and pumped before introduction of carbon dioxide.

seen from the data in Table II that the rate of oxygen formation was markedly reduced when the reaction cell was flamed in pumping before a run.

## Discussion

In the case of direct photolysis, the deficiency of oxygen produced is greatly affected by the flaming in pumping. Therefore this deficiency of oxygen could be explained by assuming the wall reaction

$$O+O+\text{Wall} \rightarrow O_2\ (\text{Wall})$$

In the investigation of photodecomposition of carbon dioxide by the resonance radiation from the xenon lamp, Wijnen[5] and Tanaka[6] observed that oxygen and carbon monoxide were obtained in the ratio 1 : 9 at room temperature and 1 : 3 at 300°C. This increase of oxygen production at a higher temperature can be explained by the decrease of oxygen adsorbed (or absorbed) on the wall of the reaction cell.

Some of the deficiency of oxygen may be the result of the formation of ozone by the reaction

$$O_2+O+M \rightarrow O_3+M$$

Mahan[7] observed that ozone was formed in his experiment of the photodecomposition of carbon dioxide by the xenon lamp. Since ozone absorbs the resonance line at 2537 Å and is then decomposed, the deficiency of oxygen can not be explained entirely by the formation of ozone.

In the photosensitized decomposition, no oxygen was detected and the oxide of mercury was deposited on the window of the cell. Therefore, the possible reactions which will form the oxide of mercury may be as follows:

a) $CO_2+Hg^*(6^1P_1) \rightarrow CO+HgO$

or

b) $CO_2+Hg^*(6^1P_1) \rightarrow CO_2^*+Hg(^1S_0)$

$CO_2^* \rightarrow CO_2+h\nu$

$CO_2^* \rightarrow CO+O$

$O+Hg+M \rightarrow HgO+M$

$O+O+\text{Wall} \rightarrow O_2\ (\text{Wall})$

Callear, Patrick and Robb[8] suggested that the oxide of mercury was formed in the mercury photosensitized reaction of oxygen by the following

$$O_3+Hg^* \rightarrow O_2+HgO$$

In the present investigation, however, it is unlikely that the oxide of mercury was formed by the above reaction, since the concentration of oxygen in the reaction cell was very low.

The approximate value of the quenching cross section ($\sigma^2$) of carbon dioxide for excited mercury atoms $Hg^*(6^1P_1)$ may be obtained by assuming that the rate of production of the carbon monoxide is equal to the rate of decomposition and to the rate of the quenching reaction of excited mercury atoms by carbon dioxide. From this view point, the mechanism is assumed to be the following:

$$Hg+h\nu \rightarrow Hg^*(6^1P_1) \qquad I_{abs}$$

$$Hg^*(6^1P_1) \rightarrow Hg+h\nu \qquad k_1$$

$$Hg^*(6^1P_1)+CO_2 \rightarrow CO+HgO \quad \text{or} \quad \rightarrow Hg+CO+O \qquad k_2$$

Thus the relation between the initial rate of production of carbon monoxide and the pressure of carbon dioxide will be written as

$$1/r_0 = 1/I_{abs} + k_1/I_{abs}k_2P \qquad (1)$$

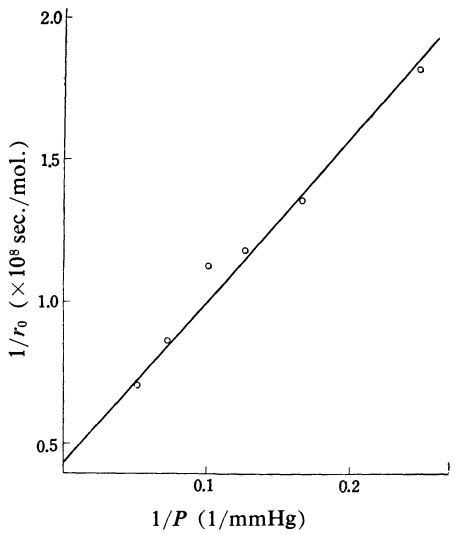



Fig. 4. The plots of $1/r_0$ against $1/P$.

where $r_0$ is the initial rate of production of carbon monoxide and $P$ is pressure of carbon dioxide. The plots of $1/r_0$ against $1/P$ is linear as shown in Fig. 4. Therefore, utilizing Eq. 1 and from the result shown in Fig. 4, it was found that $\sigma^2=320$ or 64 Å$^2$ according to whether the life time of excited mercury atom, $Hg^*(6^1P_1)$, is $0.3\times10^{-9}$ or $1.6\times10^{-9}$ sec.[9]

It will be difficult to determine the correct value of the quenching cross section even if the exact life time of the excited mercury atom is given. The value of the apparent quenching cross section calculated by Eq. 1 will be smaller than the correct one when other quenching reactions which do not form carbon monoxide are not negligible. Another

5) M. H. J. Wijnen, ibid., **24**, 851 (1956).
6) Unpublished data.
7) B. H. Mahan, *J. Chem. Phys.*, 33, 959 (1960).
8) A. B. Callear, C. R. Patrick and J. C. Robb, *Trans. Faraday Soc.*, 55, 280 (1959).
9) A. C. G. Mitchel and M. W. Zemansky, "Resonance Radiation and Excited Atoms", The McMillan Co., New York (1934).

difficulty will be in the uncertainty in the effective life time of excited mercury atom due to reabsorption of the resonance radiation of 1849 Å. The resonance radiation emitted by an excited mercury atom will be absorbed by another mercury atom in the ground state, with some probability. This leads to an increase of the effective life time of the excited mercury atom and to an increase in the apparent quenching cross section.

However, it is possible to think that the quenching cross section of carbon dioxide for $Hg^*(6^1P_1)$ is larger than 2.48 $Å^2$ for $Hg^*(6^3P_1)$[10].

This is supported by the consideration that the attractive interaction between the excited mercury atom $Hg^*(6^1P_1)$ and carbon dioxide is stronger than that between $Hg^*(^3P_1)$ and carbon dioxide. The lower excited singlet states of carbon dioxide have higher energies than $Hg^*(6^1P_1)$[11]. The lowering of the energies of the excited states of mercury atom due to the induced dipole-dipole interaction at large intermolecular distance is written

$$\Delta E_k = \sum_j W(\mu_k \cdot \mu_j)/E_k - E_j$$

where $E_k$ is the energy of the excited state $k$ of the mercury atom, $E_j$ is the energy of the excited state $j$ of carbon dioxide and $W(\mu_k \cdot \mu_j)$ is the interaction energy between transition moment of the mercury atom $\mu_k$ and that of carbon dioxide $\mu_j$. Therefore, this induced dipole-dipole interaction has a much stronger effect for $Hg^*(6^1P_1)$ than for $Hg^*(6^3P_1)$ because of their energies and transition moments. In a similar consideration the charge transfer interaction is more effective in $Hg^*(6^1P_1)$ since the energy difference between $Hg^*(6^1P_1)$ and the charge transfer state is smaller than in the case of $Hg^*(6^3P_1)$.

10) M. W. Zemansky, *Phys. Rev.*, **36**, 919 (1930).
11) R. S. Mulliken, *Can. J. Chem.*, **36**, 10 (1958).

## Summary

The photosensitized decomposition of carbon dioxide by $Hg^*(6^1P_1)$ and the direct photolysis by 1849 Å was investigated by the static method.

The product in photosensitization was carbon monoxide and no oxygen was detected. The deficiency of oxygen in the product may be due to the formation of an oxide of mercury which was deposited on the front window of the reaction cell.

In photolysis of carbon dioxide, carbon monoxide and oxygen were produced in the ratio around 5 : 1. The deficiency of oxygen may be due to the wall effect and partly due to the formation of ozone.

The apparent quenching cross section was obtained by assuming a simple mechanism. The large value of the apparent quanching cross section of $Hg^*(6^1P_1)$ is discussed from the point of view of intermolecular interaction between the excited mercury atom and carbon dioxide in the ground state.

The author is greatly indebted to Professor Ikuzo Tanaka for his continuous encouragement and discussions.

*Laboratory of Physical Chemistry*
*Tokyo Institute of Technology*
*Meguro-ku, Tokyo*

# *Kinetic Studies on Solvolysis. VI. Kinetic Evidence of the Distinct Rôle of the Hydrogen Atom of Hydroxylic Solvent Molecules as an Attacking Center at the First Ionization Stage*

By Kunio OKAMOTO and Haruo SHINGU

(Received October 22, 1960)

Acceleration by hydroxylic groups has been well known for solvolytic reactions of several secondary and tertiary halides[1], and it was previously pointed out[1a,2] that this kind of acceleration would be a specific driving force by hydrogen-bonding to the leaving halide ion and that it was superimposed on the acceleration by general solvent effect which was assumed to be proportional to the reciprocals of dielectric constants of the solvents[2]. However, previous investigations[1,2] have not given any evidence of the distinct rôle of the hydrogen atom as a reactive center in the

1) a) For the review see A. Streitwieser, Jr., *Chem. Revs.*, **56**, 622 (1956). b) Y. Pocker, *J. Chem. Soc.*, **1959**, 1179.

2) Part IV. H. Shingu and K. Okamoto, *J. Chem. Soc. Japan, Pure Chem. Sec.* (*Nippon Kagaku Zasshi*), **78**, 558 (1957).

hydroxyl group. In the present investigation linear catalysis by ortho- and para-substituted phenols, mono- and di-hydric alcohols and several polar molecules in acetolysis of *tert*-butyl bromide has been examined in order to see if the intramolecularly fixed, or chelated, hydrogen atom of the hydroxyl group would lose its accelerating function as a hydrogen-bonding center, and also to ascertain if there was co-operating acceleration by two adjacent hydroxylic groups in a molecule. Furthermore, the solvolysis rates of *tert*-butyl bromide in phenol-carbon tetrachloride mixtures have been quantitatively discussed from the point of view that the hydrogen atoms of the various species of "associated" phenol molecules would be operative as the key atoms at the first ionization stage of the solvolysis in these phenolic solvents.

When *tert*-butyl bromide was subjected to acetolysis in acetic acid-carbon tetrachloride mixture (1 : 3 by vol.) in the presence of sodium acetate, it was found that several phenols, glycols, and some other polar molecules showed linear catalysis, as has previously been known in the case of the unimolecular reaction in nitromethane[1b]. In Table I the catalytic constants of these hydroxylic molecules are compared. The catalytic constants of the ortho-substituted phenols in which the hydroxyl groups are intramolecularly fixed by a hydrogen bridge are smaller than those of corresponding para-derivatives, as evidenced by the data for nitro-, chloro-, hydroxy- and methyl derivatives of phenols. Among them the effect of the *o*-nitro group is particularly striking in that the catalytic constant of *o*-nitrophenol is the smallest and comparable to that of nitrobenzene, while that of *p*-nitrophenol is the largest one. These observations may lead to the conclusion that the hydrogen atom in the free, or non-chelated, hydroxyl group is the center of reaction in the first ionization stage of the $S_N1$-type solvolysis.

TABLE I. CATALYTIC CONSTANTS OF PHENOLS, ALCOHOLS AND SEVERAL POLAR AND NON-POLAR COMPOUNDS IN ACETOLYSIS OF *tert*-BUTYL BROMIDE IN ACETIC ACID-CARBON TETRACHLORIDE MIXTURE (1 : 3 BY VOL. AT 25.0°C) AT 70.0°C

| Accelerating substance | $10^5 \times$ Catalytic constants* $sec^{-1}M^{-1}$ |
|---|---|
| Phenol | 2.53 |
| *p*-Cresol | 4.44 |
| *o*-Cresol | 2.90 |
| *p*-Chlorophenol | 5.34 |
| *o*-Chlorophenol | 2.52 |
| *p*-Nitrophenol | 11.75 |
| *o*-Nitrophenol | 0.925 |
| Hydroquinone | 10.8 |
| Catechol | 8.34 |
| Carbon tetrachloride | −0.100 |
| Dioxane | −0.745 |
| Acetone | 1.38 |
| Acetic acid | 1.15 |
| Water | 5.41 |
| Methanol | 2.63 |
| Ethanol | 1.41 |
| Ethylene glycol | 7.69 |
| Cyclohexanol | 0.90 |
| *cis*-1,2-Cyclohexanediol | 3.04 |
| *trans*-1,2-Cyclohexanediol | 3.09 |
| Benzene | 0.440 |
| Toluene | 0.370 |
| Chlorobenzene | 0.810 |
| Nitrobenzene | 0.955 |

* Initial concentration of sodium acetate, 0.0500 N; standard rate constant $k_1°$, $6.72 \times 10^{-6}$ ($sec^{-1}$).

For this acetolysis the catalytic order of the substituted phenols is qualitatively, but not quantitatively, the same as the acidity order, while for the solvolysis in nitromethane[1b] this correlation was found to be quantitatively applicable. This inconsistency would probably be due to the complexity resulting from the hydrogen-bonding interaction between these phenols and acetic acid.

In this connection it is noteworthy that even non-hydroxylic polar molecules, e. g., toluene, chlorobenzene, nitrobenzene, and acetone, and also benzene could give small but definitely positive catalytic constants which were comparable to that of acetic acid per se. This may be explained on the basis that these molecules would modify the self-hydrogen-bonding interaction of the acetic acid molecules to the extent that a certain increase of their free hydrogen atoms and, therefore, relative enhancement of ionizing power of acetic acid would result.

The negative catalytic constant for dioxane can be explained on a basis similar to the above consideration by supression of the catalytic action of acetic acid due to the hydrogen-bonding, or hydrogen-accepting, nature of dioxane.

A further evidence of the necessity of free hydroxyl groups is revealed by the following fact: that in intramolecularly hydrogen-bonded methyl salicylate solvent, *tert*-butyl bromide did not show any hydrogen bromide evolution for 4.0 hr. at 70°C, while in phenolic solvent this bromide was easily solvolysed even at room temperature.

For dihydroxylic compounds, like 1,2-cyclohexanediols, ethylene glycol, catechol and water, the catalytic constants are greater than

TABLE II. VALUES* of $S_n$'s AND $k$'s IN EQUATION 1 : $k=\sum_1^n S_n k_n$

| Phenol concn. M | Phenolysis rate const. $k$, $sec^{-1}$ | $S_1$ | $S_2$ | $S_3$ | $S_4$ | $S_5$ | $S_6$ | $S_7$ | $S_8$ | $S_9$ | $S_{10}$ | $S_{>10}$** |
|---|---|---|---|---|---|---|---|---|---|---|---|---|
| 3.4 | $1.0\times10^{-4}$ | 31 | 22 | 15 | 10 | 7.1 | 5.1 | 3.7 | 2.5 | 1.7 | 1.2 | 3.4 |
| 3.0 | $6.6\times10^{-5}$ | 30 | 21 | 14 | 9.9 | 6.6 | 4.5 | 3.0 | 2.1 | 1.5 | 0.9 | 2.4 |
| 2.5 | $4.1\times10^{-5}$ | 28 | 19 | 13 | 8.2 | 5.5 | 3.8 | 2.3 | 1.6 | 1.1 | 0.8 | 1.7 |
| 2.25 | $3.3\times10^{-5}$ | 27 | 18 | 12 | 7.7 | 5.0 | 3.2 | 1.9 | 1.3 | 0.9 | 0.6 | 1.3 |
| 2.0 | $2.7\times10^{-5}$ | 27 | 17 | 11 | 7.4 | 4.4 | 2.6 | 1.7 | 1.0 | 0.7 | 0.4 | 1.0 |
| 1.75 | $2.2\times10^{-5}$ | 26 | 17 | 10 | 6.5 | 3.9 | 2.3 | 1.2 | 0.8 | 0.5 | 0.2 | 0.6 |
| 1.5 | $1.6\times10^{-5}$ | 26 | 17 | 9.0 | 5.6 | 3.0 | 1.8 | 1.1 | 0.6 | 0.3 | 0.2 | 0.4 |
| 1.25 | $1.1\times10^{-5}$ | 24 | 14 | 7.9 | 4.6 | 2.5 | 1.3 | 0.7 | 0.3 | 0.3 | 0.1 | 0.1 |
| 1.0 | $7.0\times10^{-6}$ | 23 | 12 | 6.3 | 3.3 | 1.6 | 0.8 | 0.4 | 0.3 | 0.1 | 0.1 | 0.1 |
| 0.75 | $4.2\times10^{-6}$ | 21 | 9.7 | 4.5 | 2.2 | 1.1 | 0.5 | 0.2 | 0.1 | — | — | — |
| 0.50 | $2.2\times10^{-6}$ | 18 | 7.0 | 2.8 | 1.2 | 0.5 | 0.2 | 0.1 | — | — | — | — |

* Calculated from interpolated values of $\alpha_n$'s using Eq. 2.
** For phenol polymer species with more than eleven phenol molecules. The average number of $n$ was assumed to be thirteen.

twice those of monohydroxylic compounds, like cyclohexanol, ethanol, phenol and methanol, respectively (cf. Table I). Although some electronic effect, especially in the dihydroxylic phenols, might be responsible for these results, the marked acceleration would be mostly attributed to the sterically co-operating attack of two adjacent hydroxyl groups in these molecules.

On the basis of the foregoing discussion, it appears to be reasonable to reconsider the solvent effect of hydroxylic compounds from the point of view that the ionization is controlled by the co-operating attack of hydroxyl groups of the various species of associated hydroxylic molecules. For a discussion of this problem the data for the association degree of those compounds are required. Fortunately the calculated results for the distribution of various associated phenol species in carbon tetrachloride at 20.0°C are available[3]. Therefore, the solvolysis rates of *tert*-butyl bromide in various phenol-carbon tetrachloride mixtures were measured in the presence of sodium phenolate at 20.0°C and after suitable correction for the initial concentrations of sodium phenolate (see Experimental) the data were tested by the following equations which were derived in order to correlate the observed solvolysis rates with the concentrations of the various species of associated phenol molecules.

Provided that reacting phenols are short-lived polyhydroxylic polymers with various degrees of association, the total rate of the solvolysis may be expressed in the Eq. 1,

$$\text{rate}=(\sum_1^n k_n[S_n])[\text{RX}]=k[\text{RX}] \qquad (1)$$

where $S_n$ represents the time-average concentration of a phenol polymer species $n$, and $k_n$ represents the rate constant for the phenol polymer species $n$. Furthermore, the $S_n$ in the Eq. 1 is expressed by Eq. 2,

$$S_n=(\text{Phenol conc.})\times\alpha_n/n\times100 \qquad (2)$$

where $\alpha_n$ represents the percentage of the number of the phenol molecules forming polymer species $n$ to the total number of the phenol molecules. Thus, using the values of $\alpha_n$'s given by Kempter and Mecke[3] and of the observed rate constants for the corresponding phenol-carbon tetrachloride mixtures, we can estimate the approximate values for $k_n$'s. In Table II the values for the coefficients of $k_n$'s, i. e., the values of $S_n$'s in Eq. 1, are shown along with the corresponding eleven interpolated values of observed total rate constants.

In examining the relation between the observed total rate constants and the $S_n$'s in eleven simultaneous equations obtained from the values in Table II, it is obvious that an increasing series of values for $k_n$'s is required for good agreement between the observed total rate constants and those calculated from the right side of Eq. 1, and one of such series for the $k_n$'s is shown in the following: $k_1, k_2=0.05\times10^{-4}$, $k_3, k_4=0.1\times10^{-4}$, $k_5, k_6=0.3\times10^{-4}$, $k_7, k_8=1\times10^{-4}$, $k_9, k_{10}=6\times10^{-4}$, $k_{>10}=18\times10^{-4}$ ($sec^{-1}$). Using these $k_n$'s the calculated values for the total rate constants are compared with the observed ones in Fig. 1.

Thus, on the basis of Mecke's polymer distribution values[3] for phenol polymer species in carbon tetrachloride, we may conclude that

3) H. Kempter and R. Mecke, *Z. physik. Chem. Abt. B*, **46**, 229 (1946).

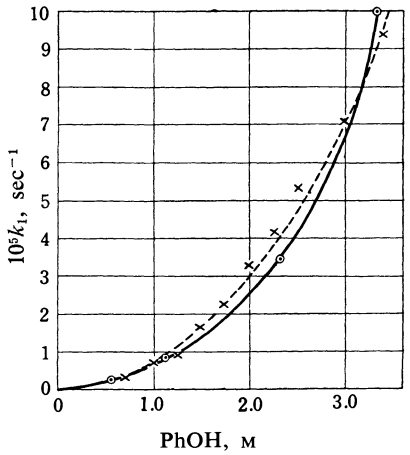



Fig. 1. Phenolysis rate of *tert*-butyl bromide in phenol-carbon tetrachloride mixtures at 20.0°C.
⊙ Observed × Calcd. from Eq. 1

the phenol polymer species with higher association degree should show more effective acceleration presumably because of their cooperative action as a kind of polyhydroxylic molecule. This would be a more detailed expression of the "polymolecular"[4] acceleration in solvolysis.

## Experimental[5]

**Materials.**—*tert*-Butyl bromide[6], *cis*-[7] and *trans*-[8] cyclohexanediol were prepared by published procedures. Sodium phenolate was previously prepared[9]. Sodium acetate[9], dioxane[9], phenol[9] and acetic acid[10] were purified by a previously reported method. All the reagents employed were of reagent grade quality, and purified by fractional distillation or by recrystallization. *o*-Cresol, m. p. 30.0~31.0 °C; *p*-cresol, m. p. 33.0~34.0°C; *p*-nitrophenol, m. p. 113.0~114.0°C; *o*-nitrophenol, m. p. 44.0~45.0°C; *p*-chlorophenol, m. p. 41.0~42.0°C; catechol, m. p. 104.0~105.0°C; hydroquinone, m.p. 172.0°C; *cis*-1,2-cyclohexanediol, m. p. 97.5~98.0 °C; *trans*-1,2-cyclohexanediol, m. p. 103.5~104.0 °C; *tert*-butyl bromide, b. p. 73.0°C; methanol, b. p. 64.0~65.0°C; ethanol, b. p. 78.0°C; phenol, b. p. 180.0~181.0°C; cyclohexanol, b. p. 161.0°C; ethylene glycol, b. p. 197.0~198.0°C; *o*-chlorophenol, b. p. 175.0~176.0°C; benzene, b. p. 80.0°C; toluene, b. p. 110.0°C; acetone, b. p. 56.0°C; dioxane, b. p. 101.0°C; carbon tetrachloride, b. p. 76.0°C; chlorobenzene, b. p. 132.0°C; nitrobenzene, b. p. 210.0~211.0°C; acetic acid, b. p. 117.0°C.

The solvent for the kinetic determinations of the acetolysis rates consisted of one volume of acetic acid and three volumes of carbon tetrachloride at 25.0°C. The solvents for the phenolysis were prepared at 25.0°C.

**Rate Measurements.**—A) *Acetolyses in Carbon Tetrachloride-Acetic Acid (3 : 1 by vol.).*—A sealed-ampoule technique was used. The reaction mixtures were prepared by mixing the weighed amounts of *tert*-butyl bromide and aliquots of solutions of known concentrations of sodium acetate and of hydroxylic compounds in carbon tetrachloride-acetic acid mixutre at 25.0°C. Each ampoule contained 1.000 cc. of aliquot of the reaction mixture. The thermostat was controlled to ±0.01° at 70.0°C. After reaction for appropriate lengths of time, the ampoules were cooled. Each sample was run into a flask and after being rinsed with about 5 cc. of acetic acid the unchanged sodium acetate was titrated with 0.050 N perchloric acid solution in acetic acid with crystal violet indicator. Rate constants were calculated graphically assuming that the reaction was of the first order. Decrease of sodium acetate associated with solvolysis of *tert*-butyl bromide in each run obeyed good first-order kinetics, this being illustrated graphically in Fig. 2 for several runs.

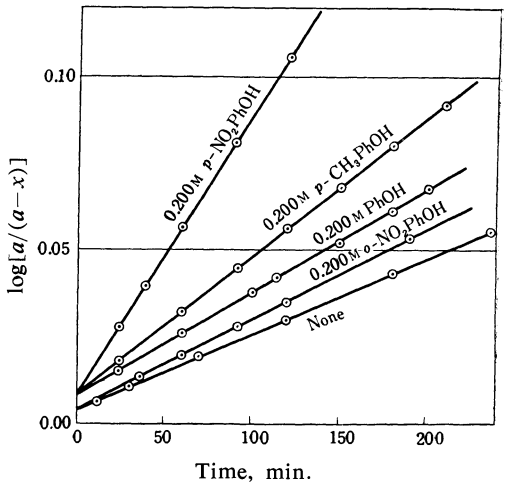



Fig. 2. Rates of acetolyses of *tert*-butyl bromide in acetic acid-carbon tetrachloride (1 : 3 by vol., at 25.0°C) in the presence of phenols at 70.0±0.01°C, 0.100 M *t*-BuBr, 0.0500 N NaOAc.

B) *Solvolyses in Phenol-Carbon Tetrachloride Mixtures.*—A weighed amount of *tert*-butyl bromide and an aliquot of the solution of a known concentration of sodium phenolate in an appropriate mixture of phenol and carbon tetrachloride were mixed in a measuring flask placed in a thermostat kept at 20.0±0.01°C. At appropriate time intervals, aliquot portions (1.000 cc.) were pipetted into 2 cc. of cold acetic acid at 15°C and the solutions were titrated according to the method described in section A. Rate constants were calculated from the first

4) L. P. Hammett, "Physical Organic Chemistry", McGraw-Hill Book Co., Inc., New York (1940), p. 169.
5) Melting points are not corrected.
6) K. A. Cooper and E. D. Hughes, *J. Chem. Soc.*, **1937**, 1185.
7) S. Winstein, H. V. Hess and R. E. Buckles, *J. Am. Chem. Soc.*, **64**, 2796 (1942).
8) A. Roebuck and H. Adkins, "Organic Syntheses", Coll. Vol. 3 (1955), p. 217.
9) H. Shingu and K. Okamoto, *J. Chem. Soc. Japan, Pure Chem. Sec.* (*Nippon Kagaku Zasshi*), **81**, 111 (1960).
10) H. Shingu, K. Okamoto and E. Ajisaka, ibid., **78**, 554 (1957).

TABLE III. SUMMARY OF RATE CONSTANTS FOR ACETOLYSIS OF *tert*-BUTYL BROMIDE IN ACETIC ACID-CARBON TETRACHLORIDE MIXTURE (1 : 3 BY VOL. AT 25.0°C) AT 70.0°C

| Exp. No. | Accelerating substance | Concn. M | $10^6 \times k_1$* $sec^{-1}$ | Exp. No. | Accelerating substance | Concn. M | $10^6 \times k_1$* $sec^{-1}$ |
|---|---|---|---|---|---|---|---|
| 40 | None | | 6.72 | 27 | Methanol | 0.200 | 11.5 |
| 29 | None | | 6.72 | 53 | Ethanol | 0.100 | 8.23 |
| 14 | None | | 6.72 | 24 | Ethanol | 0.200 | 9.32 |
| 58 | None | | 6.72 | 55 | Ethylene glycol | 0.100 | 14.4 |
| 39 | Phenol | 0.100 | 9.23 | 54 | Ethylene glycol | 0.200 | 22.3 |
| 13 | Phenol | 0.200 | 11.8 | 60 | Cyclohexanol | 0.100 | 7.60 |
| 19 | *p*-Cresol | 0.100 | 11.2 | 59 | Cyclohexanol | 0.200 | 8.52 |
| 12 | *p*-Cresol | 0.200 | 15.5 | 66 | *cis*-1, 2-Cyclohexanediol | 0.100 | 9.98 |
| 52 | *o*-Cresol | 0.100 | 9.67 | 65 | *cis*-1, 2-Cyclohexanediol | 0.200 | 12.4 |
| 51 | *o*-Cresol | 0.200 | 12.5 | 64 | *trans*-1, 2-Cyclohexanediol | 0.100 | 9.98 |
| 43 | *p*-Chlorophenol | 0.100 | 12.4 | 63 | *trans*-1, 2-Cyclohexanediol | 0.200 | 12.5 |
| 16 | *p*-Chlorophenol | 0.200 | 16.7 | 38 | Nitrobenzene | 0.100 | 7.68 |
| 47 | *o*-Chlorophenol | 0.100 | 9.25 | 15 | Nitrobenzene | 0.200 | 8.62 |
| 22 | *o*-Chlorophenol | 0.200 | 11.7 | 20 | Chlorobenzene | 0.200 | 8.34 |
| 18 | *p*-Nitrophenol | 0.100 | 18.5 | 42 | Toluene | 0.100 | 7.08 |
| 11 | *p*-Nitrophenol | 0.200 | 30.1 | 21 | Toluene | 0.200 | 7.47 |
| 56 | Hydroquinone | 0.050 | 12.1 | 28 | Acetone | 0.200 | 9.48 |
| 62 | Catechol | 0.100 | 14.0 | 23 | Benzene | 0.200 | 7.60 |
| 61 | Catechol | 0.200 | 25.5 | 32 | Dioxane | 0.200 | 6.23 |
| 49 | Water | 0.100 | 12.1 | 31 | Carbon tetrachloride | 0.200 | 6.52 |
| 26 | Water | 0.200 | 17.6 | 17 | Acetic acid | 0.200 | 7.87 |
| 50 | Methanol | 0.100 | 9.58 | | | | |

* Initial concentrations; *tert*-butyl bromide 0.100 M, sodium acetate 0.0500 N.

TABLE IV. SUMMARY OF RATE CONSTANTS FOR PHENOLYSIS OF *tert*-BUTYL BROMIDE IN PHENOL-CARBON TETRACHLORIDE MIXTURES AT 20.0°C

| Exp. No. | Phenol concn. vol. %* | Phenol concn. M | Concn. of sodium phenolate, N | $k_1$ $sec^{-1}$ | $k_1$ N=∞ |
|---|---|---|---|---|---|
| 8 | 50.0 | 5.68 | 0.0456 | $2.35\times10^{-4}$ | |
| 9 | 50.0 | 5.68 | 0.0225 | $2.12\times10^{-4}$ | |
| | | | | | $2.70\times10^{-4}$ |
| 14 | 40.0 | 4.45 | 0.0754 | $1.45\times10^{-4}$ | |
| 12 | 40.0 | 4.45 | 0.0505 | $1.26\times10^{-4}$ | |
| 13 | 40.0 | 4.45 | 0.0251 | $1.15\times10^{-4}$ | |
| | | | | | $1.64\times10^{-4}$ |
| 5 | 30.0 | 3.37 | 0.0995 | $8.37\times10^{-5}$ | |
| 6 | 30.0 | 3.37 | 0.0496 | $7.40\times10^{-5}$ | |
| 7 | 30.0 | 3.37 | 0.0245 | $6.75\times10^{-5}$ | |
| | | | | | $1.00\times10^{-4}$ |
| 17 | 20.0 | 2.33 | 0.0525 | $3.05\times10^{-5}$ | |
| 18 | 20.0 | 2.33 | 0.0257 | $2.80\times10^{-5}$ | |
| | | | | | $3.39\times10^{-5}$ |
| 16 | 10.0 | 1.11 | 0.0313 | $7.34\times10^{-6}$ | |
| 19 | 10.0 | 1.11 | 0.0157 | $6.71\times10^{-6}$ | |
| | | | | | $8.33\times10^{-6}$ |
| 20 | 5.00 | 0.559 | 0.0147 | $1.45\times10^{-6}$ | |
| 21 | 5.00 | 0.559 | 0.0104 | $1.21\times10^{-6}$ | |
| | | | | | $2.70\times10^{-6}$ |

* at 25.0°C

** Initial concentration of *tert*-butyl bromide, 0.100 M.

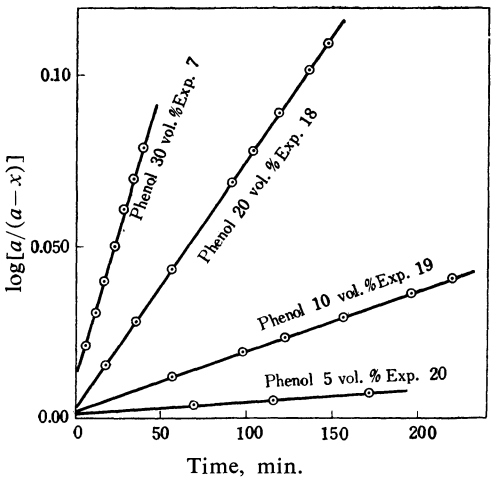



Fig. 3. Rates of phenolyses of *tert*-butyl bromide in phenol-carbon tetrachloride mixtures at 20.0°C, 0.100 M *t*-BuBr, 0.147 ~0.0245 N NaOPh.

order rate equation by a graphical method, and satisfactory first order behavior was observed for each run, this being shown graphically in Fig. 3.

## Results

The rate constants of acetolyses used for the calculation of catalytic constants of phenols, alcohols, and several polar and non-polar compounds are summarized in Table III. The catalytic constants were calculated by Eq. 3.

$$k_1(\text{obs.}) = k_1^\circ + k_2(\text{Conc. of the accelerating substance}) \quad (3)$$

where $k_1^\circ$ represents the standard rate constant and $k_2$ represents the catalytic constant.

The first order rate constants for the solvolyses of *tert*-butyl bromide in phenol-cardon tetrachloride mixtures depended on the initial concentrations of sodium phenolate and at high concentrations they increased reaching the maximum values which were previously concluded to be the rates of the first ionization step of *tert*-butyl bromide[9]. According to the total rate expression[9] for the phenolysis of this compound, these maximum values for the rate of ionization were estimated from the plots of the reciprocals of observed rate constants vs. those of the initial concentrations of sodium phenolate. In Table IV, the observed rate constants are summarized along with the estimated maximum values for the rate of ionization ($k_1$, N=∞).

## Summary

The catalytic constants of phenols, alcohols, and several polar and non-polar molecules in acetolysis of *tert*-butyl bromide were measured in acetic acid-carbon tetrachloride (1:3 by vol., at 25.0°C) in the presence of sodium acetate at 70.0°C. Ortho substituted ($NO_2$, Cl, $CH_3$, OH) phenols gave smaller constants than those of corresponding para derivatives, and among them *o*-nitrophenol gave the smallest one which was comparable to that of nitrobenzene. Dihydroxylic compounds, like 1,2-cyclohexanediols, ethylene glycol, catechol and water, gave constants greater than twice those of the corresponding monohydroxylic compounds, like cyclohexanol, ethanol, phenol and methanol, respectively. It was concluded that, in view of the lack of catalytic action of intramolecularly hydrogen-bridged hydroxylic compounds, the hydrogen atom of those hydroxylic molecules was distinctly the center of attack in the first ionization stage of the solvolysis and that two adjacent hydroxyl groups in dihydric compounds sterically co-operated in this stage. On these bases, similar accelerating action of various species of associated phenol molecules was suggested and illustrated by the analysis of the data of solvolysis rates of *tert*-butyl bromide in phenol-carbon tetrachloride mixtures at 20.0°C. It was shown that phenol polymer species with higher association degree exhibited more effective acceleration.

The authors are indebted to Mr. Ken-ichi Takeuchi who measured part of the phenolysis rates.

*Department of Fuel Chemistry*
*Faculty of Engineering*
*Kyoto University*
*Sakyo-ku, Kyoto*

# *Kinetic Studies on Solvolysis. VII. On the Kinetic Resolution at the First Stage of the $S_N1$-type Solvolysis of α-Phenethyl Chloride in Optically Active Carboxylic Acid Solvents*

By Kunio Okamoto, Ken-ichi Takeuchi and Haruo Shingu

(Received November 21, 1960)

In the previous paper[1] we have demonstrated that the acetolysis of *tert*-butyl bromide proceeds with some linear rate acceleration in the presence of *p*-nitrophenol and some other *p*-substituted phenols, while the presence of *o*-substituted phenols in which the hydroxyl groups are fixed by intramolecular hydrogen-bridge does not cause any catalytic acceleration. From this it was concluded that the free hydroxyl group was distinctly the center of the reaction in those hydroxylic molecules including alcohols, phenols, carboxylic acids and water. It is, therefore, clear that they play a rôle not only as a general solvent but also as a kind of reactant molecule in the first ionization stage of the $S_N1$-type solvolysis.

Thus it may be anticipated that, when the $S_N1$-type solvolysis of a racemic halide is carried out in an optically active solvent, there would be observed a kinetic resolution in the first stage of the solvolysis with the result that the unchanged asymmetric halide may have some optical activity. This possibility of asymmetric solvolysis of $S_N1$-type was examined in the case of the solvolysis of (±)-α-phenethyl chloride in (+)-α-methyl hydrogen camphorate and in (−)-pinonic acid. This paper presents evidence in support of the existence of such kinetic resolution in those optically active solvents.

**$S_N2$-type Kinetic Resolution of (±)-α-Phenethyl Chloride in Dioxane.**—The rate studies on the $S_N1$-type solvolysis in these optically active solvents in the presence of 0.1 M of triethylamine showed that both of the reactions were of the first order in α-phenethyl chloride and of zero order in the added base, this being illustrated in Figs. 1 and 2. Although these results indicate that the reactions proceed predominantly by $S_N1$ mechanism, they do not exclude a slight, presumably less than 1%, concurrency of $S_N2$ mechanism[2].

As a control experiment, thererfore, the extent and direction of the $S_N2$-type kinetic resolution of α-phenethyl chloride was examined under the reaction conditions comparable to those of the $S_N1$-type resolution. For this purpose the $S_N2$-reaction of α-phenethyl chloride and triethylammonium salt of the optically active carboxylic acid was carried out in dioxane, which is a favorable solvent for the

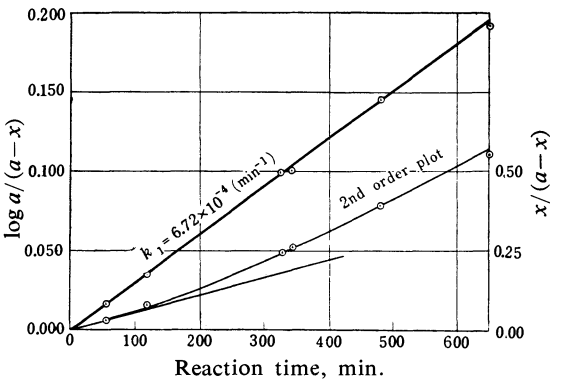



Fig. 1. Solvolysis rate of (±)-α-phenethyl chloride in (−)-pinonic acid, $[\alpha]_D^{20}$ −51.5°, in the presence of 0.116 M of triethylamine at 80.0±0.1°C. The initial concentration of the chloride, 0.116 M.

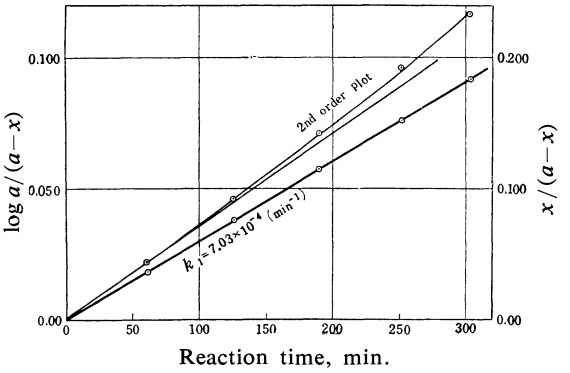



Fig. 2. Solvolysis rate of (±)-α-phenethyl chloride in α-methyl hydrogen camphorate, $[\alpha]_D^{15}$ 58.0°, in the presence of 0.123 M of triethylamine at 98.0±0.1°C. The initial concentration of the chloride, 0.123 M.

1) K. Okamoto and H. Shingu, This Bulletin, **34**, 1131 (1961).
2) H. Shingu and K. Okamoto, *J. Chem. Soc. Japan, Pure Chem. Sec.* (*Nippon Kagaku Zasshi*), **78**, 547 (1957).

Table I. Summary of optical purities of the recovered α-phenethyl chloride and of α-phenethyl alcohol in the $S_N1$-type solvolysis of (±)-α-phenethyl chloride

| Solvent | Nucleophile | Temp. °C | Time[a] hr. | Optical purity, % α-Phenethyl chloride (recovered) | Optical purity, % α-Phenethyl alcohol[b] |
|---|---|---|---|---|---|
| (+)-α-Methyl hydrogen camphorate $[\alpha]_D^{15}$ 58.0° | Triethyl-ammonium (+)-α-methyl camphorate | 98~100 | 7.5 | L[c] 0.54±0.13 | L 2.24±0.28 |
| | | 98 | | L 0.58±0.09 | L 2.95±0.74 |
| | | 100 | | (L 2.82±0.01[d]) | (D[c] 10.6 ±0.09) |
| (−)-Pinonic acid $[\alpha]_D^{18}$ −10.9° | Triethyl-ammonium | 70 | 15 | D 0.27±0.08 | D 0.57±0.07 |
| $[\alpha]_D^{20}$ −51.5° | | 70~80 | 15.5 | D 0.20±0.05 | D 1.04±0.25 |
| $[\alpha]_D^{18}$ −76.1° | | 70 | 15 | D 0.13±0.02 | L 1.56±0.39 |
| Acetonitrile | Anilinium (+)-α-methyl camphorate[e] | 85 | 4.85 | 0.00±0.02 | — |
| | Anilinium (−)-pinonate[f] | 85 | 4.35 | 0.00±0.03 | L 3.22±1.38 |
| Dioxane[g] | Triethyl-ammonium (+)-α-methyl camphorate[e] | 100 | 9[h] | L 0.08±0.01 | (L)[i] |
| | Triethyl-ammonium (−)-pinonate[f] | 70 | 16[h] | L 0.15±0.01 | (L)[i] |

a) Approximately the half life time for each reaction.
b) The alcohol obtained from α-phenethyl ester.
c) Configuration.
d) The run with L-(+)-α-phenethyl chloride; $[\alpha]_D^{15}$ 30.4°, optical purity 28.7%.
e) The acid, $[\alpha]_D^{15}$ 58.0°, chloroform.
f) The acid, $[\alpha]_D^{20}$ −75.0°, chloroform.
g) The reaction under $S_N2$ mechanism.
h) The reaction time for the stage of 5% conversion of the chloride.
i) Deduced from the principle that the inversion of configuration occurs in the $S_N2$-type reaction.

$S_N2$ mechanism. In the reaction with triethylammonium (−)-pinonate (the acid $[\alpha]_D^{20}$ −75°), about 5% of (±)-α-phenethyl chloride was consumed in 16 hr. at 70°C and the unchanged chloride of 0.15% optical purity (L configuration) was obtained (cf. Table I). A similar reaction was carried out with triethylammonium (+)-α-methyl camphorate (the acid $[\alpha]_D^{15}$ +58°) and the unchanged α-phenethyl chloride showed 0.08% of optical purity (L configuration) after 9 hr. at 100°C at the stage of about 5% conversion. These values would indicate the extent of the kinetic resolution caused by the supposedly co-existing $S_N2$ mechanism in the $S_N1$-type reactions in these optically active carboxylic acid solvents.

**Possibility of the Induced Resolution Caused by Kinetic Resolution at the Second Stage of $S_N1$-type Solvolysis.** — The slight resolution observed in the $S_N2$ condition would indicate another mechanism for interpretation of the results of the $S_N1$-type resolution. Since the intermediate in the $S_N1$-type solvolysis is converted to the product by a process quite similar to the $S_N2$ mechanism, the starting chloride which is in equilibrium with the intermediate may also become optically active, even if the intermediate was kinetically resolved by an optically active nucleophile at the second stage of solvolysis, instead of being resolved at the first ionizing stage.

In order to examine this possibility, another control experiment was carried out under conditions that should cause kinetic resolution only at the second stage, i.e., the product forming stage. For this purpose acetonitrile, which does not react with the intermediate, was used as a solvent for the solvolysis of α-phenethyl chloride. As is expected from the $S_N1$ mechanism, the solvolysis rates optically active nucleophiles (anilinium (−)-pinonate and (+)-α-methyl camphorate) were found to obey good first order kinetics at 85°C, this being shown in Figs. 3 and 4. Half way through the reactions the recovered α-phenethyl chloride did not give any optical activity for either

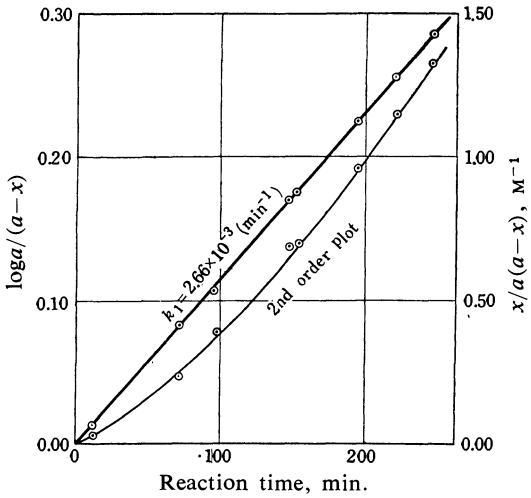



Fig. 3. Solvolysis rate of (±)-α-phenethyl chloride in acetonitrile in the presence of 0.675 N anilinium (−)-pinonate at 85.0±0.1°C. The initial concentration of the chloride, 0.675 M.

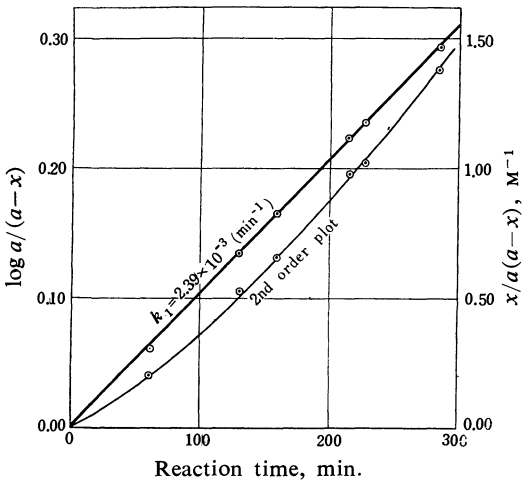



Fig. 4. Solvolysis rate of (±)-α-phenethyl chloride in acetonitrile in the presence of 0.682 N anilinium (+)-α-methyl camphorate at 85.0±0.1°C. The initial concentration of the chloride, 0.682 M.

of the nucleophiles within the experimental error, while the small amount of α-phenethyl alcohol obtained after hydrolysis of α-phenethyl pinonate showed about 5% of optical purity (D-configuration) (cf. Table I). This eliminates the possibility that the kinetic resolution at the second stage of the $S_N1$-type solvolysis can induce any preceptible resolution at the first ionization stage.

**Kinetic Resolution at the Ionization Stage of the $S_N1$-type Solvolysis.**—With these considerations in mind, we first carried out the $S_N1$-type solvolysis in (+)-α-methyl hydrogen camphorate in the presence of triethylamine at 98~100°C for 7.5 hr. until about 50% of α-phenethyl chloride was consumed, and the unchanged chloride had 0.54±0.13% of optical purity (L-configuration) (cf. Table I). In a similar experiment at 98°C for 9.5 hr., α-phenethyl chloride of 0.58±0.09% of optical purity (L-configuration) was recovered. Although the direction of the rotation of the recovered chlorides was the same as in the above mentioned reaction of the $S_N2$ mechanism in dioxane, the degree of optical purity, i. e., the extent of the kinetic resolution, is obviously greater than the one expected in the $S_N2$-type reaction under the corresponding reaction conditions, even after the correction of optical purity for the difference of the reaction percentage in both of the mechanisms. Hence it is evident that the optical rotation in the recovered chloride was predominantly caused by the kinetic resolution at the first ionization stage of the $S_N1$-type solvolysis in (+)-α-methyl hydrogen camphorate.

In a similar manner analogous experiments on the $S_N1$-type solvolysis of α-phenethyl chloride in the other optically active solvent was carried out in the presence of triethylamine in (−)-pinonic acids of various optical rotations for 15 hr. at about 70°C. In pinonic acid of optical rotations, $[\alpha]_D^{18}$ −10.9°, $[\alpha]_D^{20}$ −51.5° and $[\alpha]_D^{18}$ −76.1°, the unreacted chlorides showed 0.27±0.08, 0.20±0.05 and 0.13±0.02% of optical purity (D-configuration), respectively.

As above mentioned, in the resolution of the $S_N2$ mechanism with triethylammonium (−)-pinonate in dioxane the direction of rotation of the unreacted chloride was that of L-configuration, and this is just opposite to the one (D-configuration) observed in the reactions carried out in (−)-pinonic acid. This result clearly indicates that the kinetic resolution occurred at the first ionization stage of the $S_N1$-type solvolysis in this optically active solvent.

Finally, the kinetic resolution at the ionization stage of these $S_N1$-type solvolyses may be considered as a further evidence for the solvent molecule playing a rôle as a kind of reactant in this stage[1].

**Configuration of the Optically Active α-Phenethyl Alcohol Derived from α-Phenethyl Esters of Optically Active Carboxylic Acids.**—In the reactions in (+)-α-methyl hydrogen camphorate the isolated β-(α-phenethyl) α-methyl camphorate was hydrolysed with alcoholic sodium hydroxide or reduced with lithium aluminum hydride, and the optical purity of the recovered α-phenethyl alcohol

Table II. Relationship between configurations of recovered α-phenethyl chloride and α-phenethyl alcohol derived from α-phenethyl ester obtained in the $S_N1$-type solvolysis of (±)-α-phenethyl chloride in optically active carboxylic acids

| Configuration of recovered α-phenethyl chloride | Resolution controlling stage for α-phenethyl alcohol | Configuration for α-phenethyl alcohol derived from α-phenethyl esters | Optically active carboxylic acids as a solvolytic solvent |
|---|---|---|---|
| L | first | L | (+)-α-Methyl hydrogen camphorate |
| | second* | L | —— |
| D | first | D | (−)-Pinonic acid, $[\alpha]_D$ −10.9° and −51.5° |
| | second* | L | (−)-Pinonic acid, $[\alpha]_D$ −76.1° |

* It is assumed that the resolution at the second stage gives the alcohol with L-configuration by the $S_N2$ mechanism (see text).

amounted to 2.24±0.28 and 2.95±0.74% (L-configuration) for each run (cf. Table I), while α-phenethyl alcohols derived from α-phenethyl (−)-pinonate by alkaline hydrolyses showed optical purities of 0.57±0.07 (D-configuration), 1.04±0.25 (D-configuration) and 1.56± 0.39% (L-configuration) for the reactions in (−)-pinonic acid with optical rotations, $[\alpha]_D^{18}$ −10.9°, $[\alpha]_D^{20}$ −51.5° and $[\alpha]_D^{18}$ −76.1°, respectively (cf. Table I).

In these reactions the directions of rotation for the α-phenethyl alcohols derived from the ester of the optically active carboxylic acids doubtless controlled, generally, by two factors, namely, the kinetic resolution caused by the attack of the optically active nucleophile at the second stage of the solvolysis and the resolution in the intermediate determined by the electrophilic attack by optically active solvent molecules at the first ionization stage.

The resolution at the first ionization stage has already been discussed in the previous section. For the discussion of the results of the resolution at the second stage the knowledge about the steric behavior of α-phenethyl chloride at this stage is required, since it is uncertain whether the configuration of the chloride would invert at the second stage of the $S_N1$-type reaction in these optically active carboxylic acids. Thus, the solvolysis of originally optically active chloride, L-(+)-α-phenethyl chloride, was carried out in (+)-α-methyl hydrogen camphorate in the presence of triethylamine at 100°C. Half way through the reaction α-phenethyl alcohol of 37% inversion, 63% racemization of configuration was obtained after reductive hydrolysis of β-(α-phenethyl) α-methyl camphorate (cf. Table I)[3].

This indicates that at the second stage of this solvolysis the chloride reacted predominantly with inversion of the configuration. This is consistent with the results previously known in the reaction of this chloride in the other hydroxylic solvents[4].

Considering this inversion of configuration of α-phenethyl chloride at the second stage of the $S_N1$-type solvolysis, we may expect that the direction of the second stage resolution would be the same as that of the resolution by the $S_N2$-type mechanism. This is verified by the fact that the $S_N1$-type resolution of (±)-α-phenethyl chloride with anilinium (−)-pinonate in acetonitrile, used as a solvent in which the resolution occurs only at the second stage, gives alcohol with L-configuration which is the same type obtainable in the $S_N2$-type resolution, e. g., in dioxane (cf. Table I).

Assuming that the direction of second stage resolution in the $S_N1$-type solvolysis in the optically active carboxylic acids would be the same as in acetonitrile, we can determine the resolution controlling stage, first or second, for the α-phenethyl alcohol derived from the esters by comparing the direction of resolution for the recovered chloride with those of the alcohol obtained, this being indicated in Table II.

In Table II it is shown that in (−)-pinonic acids, $[\alpha]_D$ −10.9° and −51.5°, the configuration of the resolved α-phenethyl alcohol (cf. Table I) is predominantly determined at the first ionization stage, while in almost optically pure (−)-pinonic acid with $[\alpha]_D$ −76.1° it is determined at the second stage of the reaction. In α-methyl hydrogen camphorate it seems likely that the configuration of α-phenethyl alcohol (cf. Table I) is predominantly controlled at the first ionization stage, since the

3) The recovered α-phenethyl chloride was mostly racemic and retained only 10% of the original optical purity, as is expected from the reversibility of the ionization process at the first stage of the $S_N1$-type solvolysis.

4) E. D. Hughes, C. K. Ingold and A. D. Scott, *J. Chem. Soc.*, 1937, 1201.

resolution percentage of α-phenethyl chloride at the $S_N2$ condition, i. e., in dioxane, is considerably less than that observed at the $S_N1$-type reaction in this optically active solvent.

## Experimental[5]

**Specific Rotations in Chloroform for Optically Pure α-Phenethyl Alcohol and α-Phenethyl Chloride.**—Because of the lack of previously reported data, specific rotations in chloroform for α-phenethyl alcohol of the rotations $\alpha_D$, neat, −37.0° (at 15.0°C), +19.4° (at 24.4°C) and −40.1° (at 25.4°C), *l* 1 dm. for all, were measured, and the following results were obtained: $[\alpha]_D$ −47.5° (at 15.0°C, *c* 16.0), +24.8° (at 24.4°C, *c* 6.70) and −50.7° (at 25.4°C, *c* 6.70), respectively. From these values and the reported value[6] for neat rotation of optically pure α-phenethyl alcohol ($\alpha_D^{25}$ 43.7°, *l* 1 dm.), a specific rotation in chloroform for the optically pure alcohol was estimated to be 55.9° (at 15~25°C, *c* 6.70~16.0). In a similar manner, a specific rotation in chloroform for optically pure α-phenethyl chloride was estimated to be 105~107° (at 17~25°C, *c* 6.8~6.9) from the following data: reported value[7] for neat rotation of optically pure chloride, $\alpha_D^{25}$ 126~129°, *l* 1 dm.; observed specific rotations in chloroform for α-phenethyl chloride of neat rotations $\alpha_D$ −34.8° (at 17.0°C, *l* 1 dm.) and +17.8° (at 25.7°C, *l* 1 dm.): −28.9° (at 17.0°C, *c* 6.83) and +14.9° (at 25.7°C, *c* 6.90), respectively.

**Reaction of (±)-α-Phenethyl Chloride and Triethylammonium (−)-Pinonate in (−)-Pinonic Acid.**—(−)-Pinonic acid was prepared by potassium permanganate oxidation of α-pinene according to the previously reported method[8]. A mixture of pinonic acid (35.0 g., b. p. 152~156°C/4 mmHg, $[\alpha]_D^{18}$ −10.9°, *c* 10.9, chloroform), triethylamine (7.0 g., b. p. 88~89°C) and (±)-α-phenethyl chloride (10.45 g., b. p. 92.0°C/36 mmHg) was kept at 70°C for 15 hr. After addition of ether (50 cc.) the ethereal solution containing crystals of triethylammonium hydrochloride was washed successively with two 50 cc. portions of 10% aqueous sodium hydroxide and two 50 cc. portions of water, dried, and concentrated. The residue was fractionally distilled in vacuo, giving α-phenethyl chloride (6.9 g., b. p. 77.0~78.0°C/18 mmHg., $n_D^{20}$ 1.5265, $\alpha_D^{18}$ −0.180±0.005°, $[\alpha]_D^{18}$ −0.287°, *l* 2 dm., *c* 31.4, chloroform, Found: C, 68.18; H, 6.27. Calcd. for $C_8H_9Cl$: C, 68.33; H, 6.45%). The residual mass was refluxed with a mixture of 20% aqueous sodium hydroxide (15 cc.) and ethanol (10 cc.) for 4 hr. and distilled with steam. The distillate (about 100 cc.) was extracted with two 50 cc. portions of ether. Concentration of the combined ether solutions afforded an oily material which was distilled in vacuo to give α-phenethyl alcohol (2.2 g., b. p. 80.0~81.0°C/7 mmHg, $n_D^{20}$ 1.5245, $\alpha_D^{17}$ −0.040 ±0.005°, $[\alpha]_D^{17}$ −0.320°, *l* 2 dm., *c* 6.23, chloroform, Found: C, 78.62; H, 8.26. Calcd. for $C_8H_{10}O$: C, 78.65; H, 8.25%).

The second run carried out under similar conditions, 70~80°C, 15.5 hr., with pinonic acid (20.0 g., b. p. 152.0°C/7 mmHg, m. p. 70~80°C, $[\alpha]_D^{20}$ −51.5°, chloroform), triethylamine (5.0 g.) and (±)-α-phenethyl chloride (7.0 g.) afforded α-phenethyl chloride (3.3 g., b. p. 58.0°C/7.5 mmHg, $\alpha_D^{15}$ −0.100±0.025°, $[\alpha]_D^{15}$ −0.21°, *l* 2 dm., *c* 23.8, chloroform) and α-phenethyl alcohol (2.2 g., b. p. 80~82.0°C/9 mmHg, $\alpha_D^{18}$ −0.105±0.025°, $[\alpha]_D^{18}$ −0.58°, *l* 2 dm., *c* 9.1, chloroform, Found: C, 78.58; H, 8.06%).

Starting from pinonic acid (25.0 g., m. p. 65.0~75.0°C, $[\alpha]_D^{18}$ −76.1°, *c* 9.63, chloroform), triethylamine (5.0 g.) and α-phenethyl chloride (6.75 g.), the third run afforded at 70°C for 15 hr. α-phenethyl chloride (4.0 g., b. p. 58.0~59.0°C/9 mmHg, $n_D^{20}$ 1.5230, $\alpha_D^{18}$ −0.040±0.005°, $[\alpha]_D^{18}$ −0.141°, *l* 2 dm., *c* 14.2, chloroform, Found: C, 68.38; H, 6.59%) and α-phenethyl alcohol (0.50 g., b. p. 68.0~69.0°C/3 mmHg, $n_D^{20}$ 1.5210, $\alpha_D^{18}$ 0.020±0.005°, $[\alpha]_D^{18}$ 0.872°, *l* 2 dm., *c* 1.15, Found: C, 78.35; H, 8.44%).

**Reaction of (±)-α-Phenethyl Chloride and Triethylammonium (+)-α-Methyl Camphorate in (+)-α-Methyl Hydrogen Camphorate.**—α-Methyl hydrogen camphorate was obtained by esterification of camphoric acid according to the previously reported method[9]. To a mixture of α-methyl hydrogen camphorate (52.5 g., m. p. 56.0~57.0°C, $[\alpha]_D^{15}$ 58.0°, chloroform) and triethylamine (10.0 g.), (±)-α-phenethyl chloride (14.0 g.) was added. After being kept at 98~100°C for 7.5 hr., the reaction mixture was taken into ether (100 cc.), and washed successively with water (100 cc.), three 50 cc. portions of 10% aqueous sodium hydroxide, and two 50 cc. portions of water. The ethereal solution was dried with anhydrous sodium sulfate and concentrated. The oily material was fractionally distilled in vacuo, giving a fore-run (1.0 g.), containing styrene and a small amount of α-phenethyl chloride, α-phenethyl chloride (5.6 g., b. p. 53.0 ~ 55.0°C / 8.5 mmHg, $n_D^{20}$ 1.5274, $\alpha_D^{13}$ 0.020±0.005°, $[\alpha]_D^{13}$ 0.57°, *l* 2 dm., *c* 1.71, chloroform, Found: C, 68.14; H, 6.58%) and β-(α-phenethyl) α-methyl camphorate (10.4 g., b. p. 165~168°C/2 mmHg, $n_D^{20}$ 1.5052).

Found: C, 71.41; H, 8.11. Calcd. for $C_{19}H_{26}O_4$: C, 71.67; H, 8.23%.

β-(α-Phenethyl) α-methyl camphorate was reduced with lithium aluminum hydride. A mixture of lithium aluminum hydride (5.0 g.) and dry ether (250 cc.) was stirred for 1 hr. under a nitrogen atmosphere and treated with β-(α-phenethyl) α-methyl camphorate (10.0 g.) dissolved in ether (50 cc.) over a period of 5 min. After being stirred for 5 hr. and being kept overnight at 15°C, the mixture was treated with water (10 cc.) which was added over a period of half an hour. The precipitated material was filtered and washed with ether (100 cc.), and the combined ether solution was concentrated. The residue was distilled under reduced pressure to give α-phenethyl alcohol (2.6 g., b. p. 70.0~71.0°C/7 mmHg, $n_D^{20}$ 1.5260, $\alpha_D^{17}$

5) Microanalyses by Microanalytical Center, Kyoto University. Melting points are not corrected. For the measurement of optical rotations "Zeiss Winckel, Kreispolarimeter, 0.01°" was used.

6) E. Downer and J. Kenyon, *J. Chem. Soc.*, **1939**, 1156.

7) R. L. Burwell, Jr., A. D. Shields and H. Hart. *J. Am. Chem. Soc.*, **76**, 908 (1954).

8) G. Dupont and G. Brus, *Ann. Chim.*, **19**, 186 (1923).

9) J. Walker, *J. Chem. Soc.*, **61**, 1088 (1892).

0.400+0.005°, $[\alpha]_D^{17}$ 1.25°, *l* 2 dm., *c* 16.0, chloroform. Found: C, 78.75; H, 8.36%).

The second run carried out at 98°C for 9.5 hr. with α-methyl hydrogen camphorate (23.0 g.), triethylamine (5.0 g.), and (±)-α-phenethyl chloride (7.0 g.), afforded α-phenethyl chloride (1.9 g., b. p. 49.0~51.0°C/6 mmHg, $\alpha_D^{15}$ 0.13±0.02°, $[\alpha]_D^{15}$ 0.62°, *l* 2 dm., *c* 10.5, chloroform) and after alkaline hydrolysis of the ester α-phenethyl alcohol (0.15 g., b. p. 80.0°C/9 mmHg, $\alpha_D^{15}$ 0.04±0.01°, $[\alpha]_D^{15}$ 1.65°, *l* 2 dm., *c* 1.21, chloroform) was obtained.

**Reaction of (+)-α-Phenethyl Chloride and Triethylammonium α-Methyl Camphorate in (+)-α-Methyl Hydrogen Camphorate.**—(±)-α-Phenethyl alcohol was resolved according to the published method[6] and the first crop of brucine salt of α-phenethyl hydrogen phthalate gave (−)-α-phenethyl alcohol, $[\alpha]_D^{15}$ −47.5°, *c* 16.0, chloroform, From the first mother liquors (+)-α-phenethyl alcohol ($[\alpha]_D^{13}$ 37.0°, *c* 15.4, chloroform) was obtained. From this (+)-alcohol (+)-α-phenethyl chloride ($[\alpha]_D^{15}$ 30.4°, *c* 7.15, chloroform) was prepared by chlorination with thionyl chloride according to the previously reported method[3]. The reaction was carried out with (+)-α-methyl hydrogen camphorate (50.0 g.), triethylamine (4.5 g.) and (+)-α-phenenethyl chloride (5.6 g., $[\alpha]_D^{15}$ 30.4°) at 100°C for 8 hr. After treatment similar to the previous experiment with (±)-α-phenethyl chloride, α-phenethyl chloride (2.4 g., b. p. 51.0~52.0°C/6 mmHg, $n_D^{20}$ 1.5268, $\alpha_D^{15}$ 0.450±0.01°, $[\alpha]_D^{15}$ 2.98°, *l* 2 dm., *c* 7.55, chloroform, Found: C, 68.40; H, 6.37%) was recovered.

After reduction with lithium aluminum hydride, β-(α-phenethyl) α-methyl camphorate (4.6 g., b. p. 173°C/2 mmHg, $n_D^{20}$ 1.5034, Found: C, 71.88; H, 8.31%.) afforded α-phenethyl alcohol (0.9 g., b. p. 63.0~67.0°C/3 mmHg, $n_D^{20}$ 1.5169, $\alpha_D^{15}$ −0.580±0.005°, $[\alpha]_D^{15}$ −5.93°, *l* 2 dm., *c* 4.90, chloroform, Found: C, 78.48; H, 8.43%).

**Reaction of (±)-α-Phenethyl Chloride and Triethylammonium (+)-α-Methyl Camphorate in Dioxane.** — Triethylammonium (+)-α-methyl camphorate was prepared by mixing the equivalent amounts of triethylamine and (+)-α-methyl hydrogen camphorate in dioxane. A mixture of triethylamine (5.0 g.), (+)-α-methyl hydrogen camphorate (10.6 g.), dry dioxane (24.5 g.) and (±)-α-phenethyl chloride (7.0 g.) was kept at 100°C for 9 hr. The reaction percentage of the chloride was estimated to be about 5% from the aliquot titration of unchanged triethylammonium α-methyl camphorate with acetic acid solution of perchloric acid. After addition of ether (100 cc.) the mixture was washed with four 100 cc. portions of water, dried with anhydrous sodium sulfate, and concentrated. The residue was fractionally distilled under reduced pressure to give α-phenethyl chloride (5.8 g., b. p. 89.0°C/38 mmHg, $n_D^{20}$ 1.5264, $\alpha_D^{20}$ 0.055±0.005°, $[\alpha]_D^{20}$ 0.086°, *l* 2 dm., *c* 31.8, chloroform, Found: C, 68.58; H, 6.52%).

**Reaction of (±)-α-Phenethyl Chloride and Triethylammonium (−)-Pinonate in Dioxane.** — A mixture of triethylamine (5.0 g.), (−)-pinonic acid (9.2 g., $[\alpha]_D^{20}$ −75.0°, chloroform), dry dioxane (25 cc.) and (±)-α-phenethyl chloride (7.0 g.) was kept at 70°C for 16 hr. The reaction percentage of the chloride was estimated to be about 5% from the titration of unchanged triethylammonium pinonate. After addition of ether (100 cc.) the mixture was treated in a manner similar to the reaction with triethyl ammonium α-methyl camphorate. The recovered α-phenethyl chloride gave the following constants; b. p. 89.0°C/37 mmHg, $n_D^{20}$ 1.5272, $\alpha_D^{20}$ 0.09±0.005°, $[\alpha]_D^{20}$ 0.16°, *l* 2 dm., *c* 28.0, chloroform, Found: C, 68.58; H, 6.52%.

**Reaction of (±)-α-Phenethyl Chloride and Anilinium (+)-α-Methyl Camphorate in Acetonitrile.** — Anilinium α-methyl camphorate solution (0.750 N) was prepared from equivalent amounts of aniline and (+)-α-methyl hydrogen camphorate ($[\alpha]_D^{15}$ 58.0°) in acetonitrile. (±)-α-Phenethyl chloride (4.92 g.) was dissolved in the anilinium salt solution and diluted to a volume of 50 cc. with the solution. The mixture was kept in a sealed tube for 291 min. (half life time of the reaction) at 85.0°C. Ether (100 cc.) was added to the cooled reaction mixture, and the mixture washed with water (50 cc.). After evaporation of ether the residual oily mass gave α-phenethyl chloride (2.3 g., b. p. 55.0~56.0°C/6 mmHg, $n_D^{20}$ 1.5251, $\alpha_D^{21}$ 0.00± 0.02°, *l* 1 dm., neat). In the distillation residue no ester was found.

**Reaction (±)-α-Phenethyl Chloride and Anilinium (−)-Pinonate in Acetonitrile.**—In a manner similar to the reaction with anilinium (+)-α-methyl camphorate (±)-α-phenethyl chloride (5.81 g.) was kept with 0.750 N anilinium (−)-pinonate (the acid $[\alpha]_D^{20}$ −75.0) solution for 261 min. (half life time of the reaction) at 85.0°C. The recovered chloride (2.22 g.) gave the following constants; b. p. 53.0°C/ 2 mmHg, $n_D^{20}$ 1.5239, $\alpha_D^{21}$ 0.00±0.03°, *l* 1 dm., neat, Found: C, 68.63; H, 6.60%. The higher boiling fraction (5.24 g., 137~140°C/0.8 mmHg) was hydrolysed with 20% aqueous sodium hydroxide (15 cc.) and ethanol (10 cc.) for 4 hr., and distilled with steam. The recovered α-phenethyl alcohol (0.05 g.) gave slight optical activity ($\alpha_D^{20}$ 0.07±0.03°, $[\alpha]_D^{20}$ 1.8°, *l* 1 dm. *c* about 4, chloroform).

**Kinetic Measurement.**—The reactions in (+)-α-methyl hydrogen camphorate ($[\alpha]_D^{15}$ 58°) and (−)-pinonic acid ($[\alpha]_D^{20}$ −51.5°) were carried out in a 15 cc. measuring flask placed in a thermostat. To a weighed amount of α-phenethyl chloride in the flask the optically active carboxylic acid solution of triethylamine was added to the volume of 15 cc. at the reaction temperature. After various periods of time, aliquot portions (1.000 cc.) were pipetted into 5 cc. of cold acetic acid and the solutions were titrated with 0.0672 N perchloric acid in acetic acid with crystal violet indicator. The rates in acetonitlile were measured by a sealed-ampoule technique. Each sample (1.000 cc.) was titrated with 0.245 N perchloric acid in acetic acid. The rate constants were calculated from the first order rate equation by a graphical method.

## Summary

1) In $S_N2$ displacement reactions of (±)-α-phenethyl chloride with triethylammonium (+)-α-methyl camphorate and with triethylammonium (−)-pinonate in dioxane, α-phenethyl chloride of 0.08% of optical purity (L-

configuration) and of 0.15% of optical purity (L-configuration) were recovered at the stage of about 5% conversion, respectively.

2) In $S_N1$-type solvolysis of (±)-α-phenethyl chloride with anilinium (+)-α-methyl camphorate and (−)-pinonate in acetonitrile, the recovered α-phenethyl chlorides showed no perceptible optical activity on the half way for each of the reactions. From this, the possibility of the induced resolution caused at the first stage by kinetic resolution at the second stage of the $S_N1$-type solvolysis was eliminated.

3) In $S_N1$-type solvolysis of (±)-α-phenethyl chloride in (+)-α-methyl hydrogen camphorate and in (−)-pinonate, about half of the chloride was converted to the ester at the similar reaction conditions (temperature and time) to the $S_N2$ displacement reactions carried out in dioxane. The recovered chloride in the reaction in hydrogen camphorate showed optical purity of 0.54~0.58% (L-configuration). In pinonic acids with various optical activities the recovered chlorides possessed optical purity of 0.13~0.27% (D-configuration).

4) In comparing the configurations and optical purities in $S_N1$- and $S_N2$-conditions, it is concluded that optically active solvent molecules, like (+)-α-methyl hydrogen camphorate and (−)-pinonic acid, can cause kinetic resolution in the first ionization stage of the $S_N1$-type solvolysis and therefore they obviously play a rôle as a kind of reactant molecule which controls the steric course of the solvation reaction in the first stage of this solvolysis.

5) In the $S_N1$-type solvolysis of optically active α-phenethyl chloride in presence of triethylamine in (+)-α-methyl hydrogen camphorate, optically active β-(α-phenethyl)-α-methyl camphorate gave optically active α-phenethyl alcohol of 37% inversion, 63% racemization of configuration. From this it was concluded that $S_N2$-like spatial orientation predominates at the second stage of this solvolysis.

6) For each of the resolution results of α-phenethyl chloride under $S_N1$- and $S_N2$-conditions, the relationship between the configuration of the resolved alcohol and the resolution-controlling stage was predicted on the basis of the observed inversion at the second stage of the solvolysis. The configurations observed for the α-phenethyl alcohols were found to be consistent with the predictions.

The authors wish to thank Mr. Ryôichi Kanô for his assistance in preparation of (−)-pinonic acid.

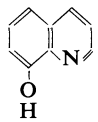
*Department of Fuel Chemistry*
*Faculty of Engineering*
*Kyoto University*
*Sakyo-ku, Kyoto*

# *Study on Metal Complexes of Analytical Importance. I. Vanadium Complexes of 8-Quinolinol and 2-Methyl-8-quinolinol*[1]

By Hiroji NAKAMURA, Yoichi SHIMURA and Ryutaro TSUCHIDA

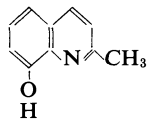
(Received November 24, 1960)

8-Quinolinol (A) is a popular analytical reagent, being used in the analysis of vanadium.



A

8-Quinolinol
(symbol: oxinH)



B

2-Methyl-8-quinolinol
(symbol: $CH_3$-oxinH)

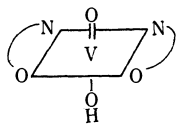
The reaction of vanadate with 8-quinolinol in aqueous solution at pH 4~5 produces a bluish-black complex. This complex dissolves in lower aliphatic alcohols to give red solutions, while in chloroform it gives a violet one[2]. From boiling alcohol solutions saturated with this complex is deposited a brownish black complex on cooling, which dissolves in chloroform to show red color instead of violet.

Bielig and Bayer[2] reported that these two complexes were geometrical isomers which had a molecular formula $[VO(OH)(oxin)_2]$, and they named the bluish-black complex "violet form" and the brownish black complex "red form" by the colors of the chloroform solutions of these complexes.

1) A part of this study was presented at the Symposium on Coordination Compounds of the Chemical Society of Japan, Sendai, September, 1960.

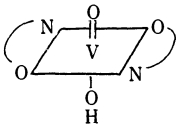
2) H.-J. Bielig and E. Bayer, *Ann.*, **584**, 96 (1953).

Based on rather weak experimental evidences, they reported that the violet form had the cis structure and that the red form had the trans structure which are shown in Fig. 1.



cis structure

Fig. 1 (a)



trans structure

Fig. 1 (b)

Contrary to their conclusion, Blair and Pantony[3] assumed that the red form had the molecular formula [VO(O-R)(oxin)$_2$] (R is an alkyl group), namely that the complex was an alkyl ester of [VO(OH)(oxin)$_2$]. As for the violet form, Blair and Pantony explained that it had the trans structure, but no experimental evidence was given.

In order to decide the configurations of the complexes, we have prepared new complexes of 2-methyl-8-quinolinol, and from experimental data of these complexes have discussed the problem.

## Results and Discussion

**Complexes of 2-Methyl-8-quinolinol with Vanadium(V).**—As will be seen in the experimental part, 2-methyl-8-quinolinol produces with vanadate a yellow complex, not a black one. In the case of 8-quinolinol a bluish-black complex (violet form) is separated under the same conditions. In this respect, the yellow complex resembles neither the violet nor the red form.

Recrystallization of the yellow complex from 98% methanol also produces a yellow complex. The complex thus obtained is yellow in crystalline state, but shows red color in absolute methanol giving an absorption band at 60.6 $\times 10^{13}$ sec$^{-1}$ (Fig. 2a). The solution in 98% methanol gives a weaker band at the same frequency (Fig. 2b). The higher the water content of the solvent is, the weaker is the absorption band (Fig. 2b-f). Thus, the color in 90% methanol solution is almost yellow.

Elementary analysis of the yellow complex shows that it has the formula of VO(OH)(CH$_3$-oxin)$_2$·2H$_2$O, and over phosphorus pentoxide in vacuo the complex gradually changes black with decrease of its weight. In three weeks the color changes completely to black, and the decrease of weight corresponds to two molecules of water. The black complex thus obtained has the empirical formula VO(OH)(CH$_3$-

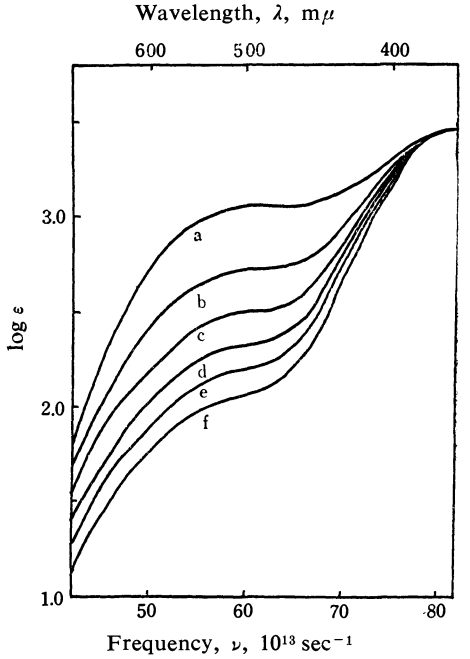



Fig. 2. Absorption spectra of [VO(OH)(CH$_3$-oxin)$_2$(OH$_2$)$_2$] in absolute methanol and in diluted methanol.
a, absolute; b, 98%; c, 96% d, 94%; e, 92%; f, 90%.

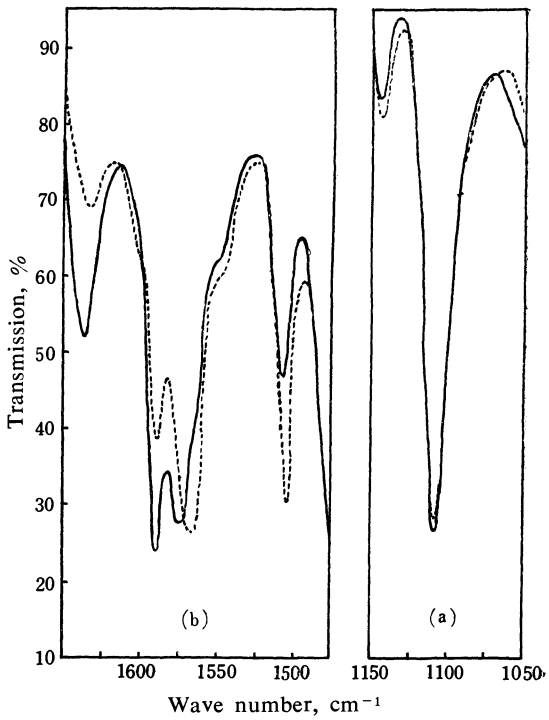



Fig. 3. Infrared absorption spectra of [VO(OH)(CH$_3$-oxin)$_2$(OH$_2$)$_2$] (——) and [VO(OH)(CH$_3$-oxin)$_2$] (----).
(a): C-O stretching band
(b): C=N or C=C stretching bands

3) A. J. Blair and D. A. Pantony, *J. Inorg. Nucl. Chem.*, 5, 316 (1958).

oxin)$_2$. Accordingly it is clear that the difference between the yellow and the black colors is due to the water molecules. Judging from the marked change of the color, the water molecules are not merely of crystallization character but are coordinated. The black complex cannot have the cis structure owing to the steric hindrance between the methyl groups of the ligands. It is considered to have the trans structure (Fig. 1).

Since the maximum coordination number of the quinquevalent vanadium is six, the yellow complex [VO(OH)(CH$_3$-oxin)$_2$(OH$_2$)$_2$] must have an octahedral configuration. Consequently the two 2-methyl-8-quinolinol ions are coordinated as unidentate ligands. The difference between 8-quinolinol and 2-methyl-8-quinolinol is only that the latter has a methyl group at the carbon atom adjacent to the nitrogen atom. Therefore, it seems that the nitrogen atoms are not bound to the vanadium ion. Infrared absorption spectra of these two complexes show that this consideration is correct.

Both the yellow and the black complexes exhibit a strong band of C–O stretching[4] at the same wave number 1108 cm$^{-1}$ (Fig. 3). This shows that in each complex, oxygen atoms are bound to the vanadium ion. If the bond V–O were broken in the yellow complex, the position of the C–O stretching band of the complex would differ from that of the black. Moreover, these complexes show four bands over the region between 1640 and 1500 cm$^{-1}$ which are considered to be C=N or C=C stretching vibrations[5] in the ligands. Considerable differences are recognized between the corresponding bands of the two complexes not only in their positions, but also in intensities (Fig. 3). These differences suggest that in the yellow complex the nitrogen atoms are not bound to the central vanadium ion.

Now we have been led to the conclusion that the yellow complex [VO(OH)(CH$_3$-oxin)$_2$(OH$_2$)$_2$] has an octahedral structure and that the 8-quinolinol ions are not bidentate but unidentate ligands which are bound to the central vanadium ion by their oxygen atoms.

**Structure of the Red Form.**—As was described in the preceding section, the black complex [VO(OH)(CH$_3$-oxin)$_2$] has the trans structure. Therefore, the comparison of the absorption spectrum of [VO(OH)(CH$_3$-oxin)$_2$] with those of the red and the violet forms may give us some suggestions about the structures of these complexes.

The absorption spectra of these three complexes in chloroform are shown in Fig. 4. [VO(OH)(CH$_3$-oxin)$_2$] shows two bands at $60.6\times10^{13}$ and $80.6\times10^{13}$ sec$^{-1}$. The positions

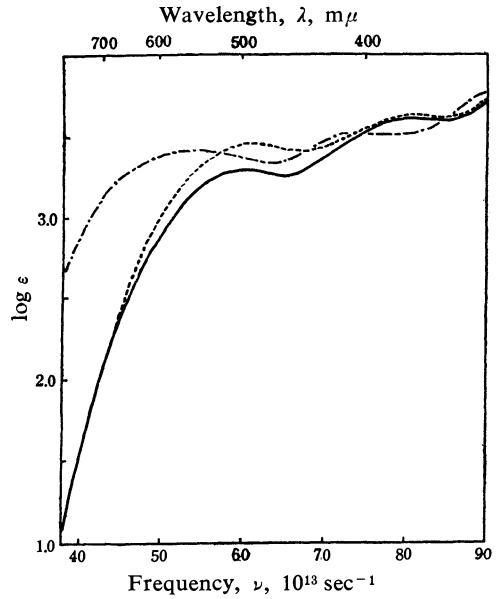



Fig. 4. Absorption spectra of 8-quinolinol-vanadium complexes and 2-methyl-8-quinolinol-vanadium complex in chloroform.
—·— violet form
---- red form
—— [VO(OH)(CH$_3$-oxin)$_2$] (trans)

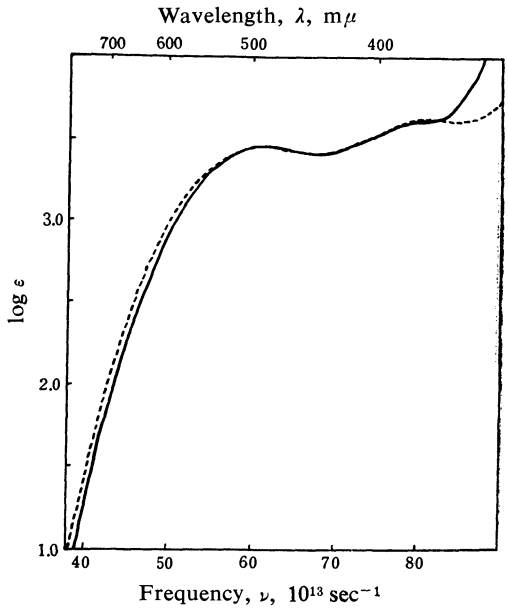



Fig. 5. Absorption spectra of [VO(OH)(oxin)$_2$] (red form) (——) and [VO(O-CH$_3$)(oxin)$_2$] (----) in benzene. The enhancement of the curve (——) at the shorter wavelength region is owing to the absorption of 8-quinolinol which is added in excess.

4) R. G. Charles, H. Freiser, R. Friedel, L. E. Hillard and W. D. Johnstone, *Spectrochim. Acta*, **8**, 1 (1956).
5) L. J. Bellamy, "The Infrared Spectra of Complex Molecules", 2nd ed. (1958), pp. 270-286.

of the bands coincide with those of the red form. Accordingly it seems that the red form has the trans and the violet form has the cis structure. In this respect, these results support Bielig's opinion. But as will be seen in the experimental part, Blair's opinion that the red form has a formula $[VO(O\text{–}R)(oxin)_2]$ is also correct. 8-Quinolinol complexes which are recrystallized from boiling methanol and isopropyl alcohol respectively have the empirical formulae corresponding to $[VO(O\text{–}CH_3)(oxin)_2]$ and $[VO(O\text{–}C_3H_7)(oxin)_2]$. To obtain a red 8-quinolinol complex without using alcohols, we examined many solvents. No solvent, however, was effective. Next, the reaction between vanadium(V) quinaldinate and 8-quinolinol in benzene was tried. Instantly the color changed to red and the absorption spectrum of the solution was quite like that of the red form which was obtained from boiling methanol solution (Fig. 5).

Now we can conclude that the violet form has the cis structure, while the red form has the trans structure, and further that the esterification of the red form does not induce any striking change of color.

**Yellow 8-Quinolinol Complex.** — Both the violet and the red forms are almost black in the crystalline state, as was described in the preceding section. But a yellow 8-quinolinol complex can also be obtained, which is prepared as a sodium salt at higher pH[2]. Bielig and Bayer gave the formula $Na[VO(O)(oxin)_2]\cdot H_2O$ to the yellow complex salt. They carried out the chemical analysis of the yellow complex after drying it over phosphorus pentoxide at 100°C in a high vacuum. The sodium salt which was dried in air has an empirical formula $NaVO(O)(oxin)_2\cdot 4H_2O$. The yellow color of this salt may be understandable on the assumption that it has the formula $Na[VO(O)(oxin)_2(OH_2)_2]\cdot 2H_2O$ corresponding to the yellow 2-methyl-8-quinolinol complex $[VO(OH)(CH_3\text{-}oxin)_2(OH_2)_2]$.

## Experimental

**Preparation of 2-Methyl-8-quinolinol Complexes of Vanadium.**—The yellow complex was prepared as follows: 3.2 g. of 2-methyl-8-quinolinol was dissolved in 60 ml. of 1 N acetic acid and was diluted to 250 ml. To the solution was added drop by drop 2.0 g. of sodium metavanadate tetrahydrate ($NaVO_3\cdot 4H_2O$) dissolved in 100 ml. of 0.2 N sodium hydroxide. A muddy yellow precipitate appeared. The pH of the mixture was adjusted to 5.0 by the use of 1 N acetic acid and it was digested for two hours at 70°C. The crude complex thus obtained was recrystallized three times from 98% methanol by evaporating the solvent at 40°C in vacuo. The yellow complex obtained as pure crystals was dried over calcium chloride. For analyzing the coordinated water of this complex, heating is not suitable, since the complex decomposes at a high temperature. Therefore, drying over phosphorus pentoxide was adopted for the analysis of the coordinated water.

Found: $H_2O$, 8.10; C, 54.96; H, 4.85; N, 6.40; V, 11.51. Calcd. for $C_{20}H_{17}O_4N_2V\cdot 2H_2O = [VO(OH)(CH_3\text{-oxin})(OH_2)_2]$: $H_2O$, 8.26; C, 55.04; H, 4.85; N, 6.42; V, 11.68%.

The complex is soluble in lower aliphatic alcohols, cyclohexanone, pyridine and diluted solution of alkali, and insoluble in ethyl ether, 2-butanone, cyclohexane, benzene, chloroform, carbon tetrachloride and water.

The black complex was prepared by expeling the water molecules of the yellow complex over phosphorus pentoxide in vacuo.

Found: C, 60.04; H, 4.18; N, 7.10; V, 12.65. Calcd. for $C_{20}H_{17}O_4N_2V = [VO(OH)(CH_3\text{-oxin})_2]$: C, 60.00; H, 4.28; N, 7.00; V, 12.73%.

The black complex is soluble in chloroform, benzene and whatever the yellow complex is soluble in, sparingly soluble in ethyl ether, insoluble in cyclohexane, carbon tetrachloride and in water, and soluble with decomposition in dioxane, acetone and 2-butanone.

**Violet Form of 8-Quinolinol-Vanadium Complex.** —This complex was prepared by the method of Bielig and Bayer[2] and also of Blair and Pantony[3].

**Red Forms of 8-Quinolinol-Vanadium Complex.** —The methyl ester was prepared as follows: 1.0 g. of violet form was refluxed for 90 min. with 400 ml. of methanol. After filtration, the solution was concentrated to about 40 ml. The brownish black crystals then separated were filtered and dried in air.

Found: C, 59.16; H, 4.20; N, 7.35; V, 13.01. Calcd. for $C_{19}H_{15}O_4N_2V = [VO(O\text{–}CH_3)(oxin)_2]$: C, 59.09; H, 3.91; N, 7.25; V, 13.19%.

The isopropyl ester was prepared in almost the same way as was the methyl ester.

Found: C, 61.61; H, 4.66; N, 6.81; V, 12.08. Calcd. for $C_{21}H_{19}O_4N_2V = [VO(O\text{–}C_3H_7)(oxin)_2]$: C, 60.80; H, 4.62; N, 6.80; V, 12.30%.

**Yellow 8-Quinolinol Complex of Vanadium.**— This complex was prepared by the method of Bielig and Bayer[2] and was analyzed after being dried in air.

Found: C, 45.52; H, 4.25; N, 5.91; V, 10.60. Calcd. for $C_{18}H_{20}O_8N_2NaV = Na[VO(O)(oxin)_2(OH_2)_2]\cdot 2H_2O$: C, 45.87; H, 4.27; N, 5.94; V, 10.81%.

**Preparation of Sodium Salt of 2-Methyl-8-quinolinol-Vanadium Complex.**—The same method as that used in the preparation of $Na[VO(O)(oxin)_2(OH_2)_2]\cdot 2H_2O$ was not effective for the preparation of this complex. So the desired complex was prepared as follows: 2.1 g. of $[VO(OH)(CH_3\text{-oxin})_2(OH_2)_2]$ was dissolved in 200 ml. of 0.2 N sodium hydroxide. After being filtered, the solution was concentrated at 50°C in vacuo to 20 ml. The complex salt thus obtained was recrystallized twice from 98% methanol.

Found: C, 48.59; H, 4.65; N, 5.42; V, 10.05. Calcd. for $C_{20}H_{24}O_8N_2NaV = Na[VO(O)(CH_3\text{-oxin})_2(OH_2)_2]\cdot 2H_2O$: C, 48.59; H, 4.89; N, 5.67; V, 10.30%.

**Absorption Spectrum of the Red Form which is Not Esterified.**—For the first time, vanadium quinaldinate was prepared as follows: 0.97 g. of $NaVO_3 \cdot 4H_2O$ was dissolved in 50 ml. of 2 N sodium hydroxide. To this solution was added 1.73 g. of quinaldinic acid dissolved in 50 ml. of 2 N sodium hydroxide. This mixture was acidified with 10 ml. of 2 N acetic acid. The white precipitate which appeared was separated by filtration after it had been digested for two hours at 60°C.

The benzene solution of this complex was colorless. To the solution was added a benzene solution of 8-quinolinol (almost colorless). The solution instantly became red, which was quite similar to the color of the solution of the red form prepared from the violet form by the use of methanol (Fig. 5). The same behavior was recognized in dioxane too.

**Measurements.**—Visible and ultraviolet absorption spectra were determined with a Beckman DU and a Hitachi EPU-2A spectrophotometers using the cells which have 1 and 10 cm. light paths.

Infrared absorption measurements were made by the pressed disk technique in a Hitachi EPI-2 infrared spectrophotometer, the disks being 200 mg. of dried potassium bromide containing 1.5 mg. of complexes.

## Summary

New complexes, $[VO(OH)(CH_3\text{-oxin})_2]$, $[VO(OH)(CH_3\text{-oxin})_2(OH_2)_2]$ and $Na[VO(O)(CH_3\text{-oxin})_2(OH_2)_2] \cdot 2H_2O$ have been prepared and discussed in relation to the structures.

From experimental evidences of these complexes and of 8-quinolinol-vanadium complexes, we have concluded that the violet form of 8-quinolinol-vanadium complex has a cis configuration and that the red form has a trans one.

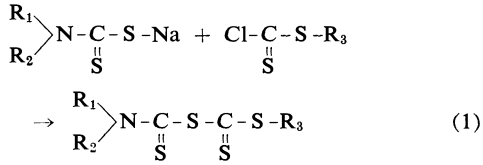
*Department of Chemistry*
*Faculty of Science*
*Osaka University*
*Kita-ku, Osaka*

# *Studies on the Thiocarbamoylthiocarbonates. II. Synthesis and Thermal Decomposition of Aryl Thiocarbamoyltrithiocarbonates*

By Aritsune KAJI

(Received November 24, 1960)

The syntheses and characteristics of *N, N*-disubstituted *O*-aryl *S*-thiocarbamoyldithiocarbonates have been reported previously[1]. Aryl esters of *N, N*-disubstituted thiocarbamoyltrithiocarbonic acid were also synthesized by the reaction of aryl chlorodithioformates with sodium or ammonium salts of *N, N*-disubstituted dithiocarbamic acid as shown in Eq. 1.

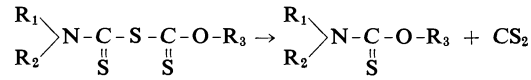


(1)

In this way, various compounds were obtained in good yields as shown in Tables I—IV.

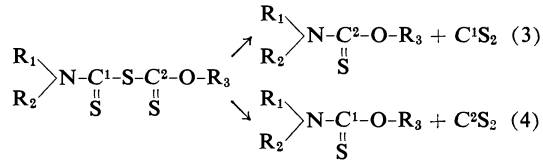
*N*-Monosubstituted aryl thiocarbamoyltrithiocarbonates could not be obtained, however, by this method, owing to their probable decomposition during the reaction.

As has been described in the previous paper[1], aryl ester of *N, N*-disubstituted *S*-thiocarbamoyldithiocarbonic acid, when kept at a temperature higher than its melting point, decomposes into *N, N*-disubstituted *O*-aryl thionocarbamate liberating carbon disulfide (Eq. 2).



(2)

It is easily seen that two ways are possible to eliminate carbon disulfide, which can be shown in Eqs. 3 and 4.



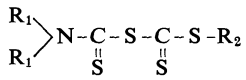
(3)

(4)

In order to decide the preferable course of the elimination reaction, the thermal decomposition of the compounds labeled with radioactive sulfur was studied. By the thermal decomposition of *O*-(4-tolyl) *S*-(*N, N*-dimethylthiocarbamoyl)dithiocarbonate (I), in which

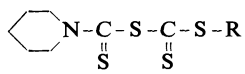
1) A. Kaji, This Bulletin, 34, 254 (1961).

TABLE I. ARYL *N,N*-DIALKYLTHIOCARBAMOYLTRITHIOCARBONATES



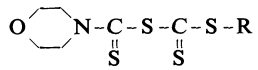
| $R_1$ | $R_2$ | Appearance | M. p., °C | Yield % | Formula | Anal. C, % Found (calcd.) | Anal. H, % Found (calcd.) |
|---|---|---|---|---|---|---|---|
| Methyl | Phenyl | Orange prisms | 134 ~134.5 | 87 | $C_{10}H_{11}NS_4$ | 44.50 (43.96) | 4.06 (4.03) |
| Methyl | 2-Tolyl | Orange prisms | 80 ~ 81 | 75 | $C_{11}H_{13}NS_4$ | 46.60 (45.99) | 4.35 (4.53) |
| Methyl | 4-Tolyl | Orange needles | 107 ~108 | 87 | $C_{11}H_{13}NS_4$ | 46.47 (45.99) | 4.99 (4.53) |
| Methyl | 2-Chlorophenyl | Orange pillars | 93 ~ 94 | 65 | $C_{10}H_{10}ClNS_4$ | 39.45 (39.02) | 3.35 (3.25) |
| Methyl | 4-Chlorophenyl | Orange prisms | 104 ~105 | 81 | $C_{10}H_{10}ClNS_4$ | 39.45 (39.02) | 3.21 (3.25) |
| Methyl | 2,4,5-Trichlorophenyl | Orange prisms | 112 ~112.5 | 94 | $C_{10}H_8Cl_3NS_4$ | 32.08 (31.87) | 2.18 (2.12) |
| Methyl | 1-Naphthyl | Orange prisms | 97 ~ 98 | 58 | $C_{14}H_{13}NS_4$ | 52.30 (52.01) | 4.05 (4.02) |
| Ethyl | Phenyl | Orange needles | 68.5~ 69.5 | 75 | $C_{11}H_{15}NS_4$ | 47.95 (47.84) | 5.05 (4.98) |
| Ethyl | 4-Chlorophenyl | Orange needles | 72 ~ 73 | 64 | $C_{12}H_{14}ClNS_4$ | 42.50 (42.92) | 4.21 (4.17) |
| Ethyl | 2,4,5-Trichlorophenyl | Orange needles | 129 ~130 | 70 | $C_{12}H_{12}Cl_3NS_4$ | 35.85 (35.60) | 2.94 (2.97) |
| Ethyl | Pentachlorophenyl | Orange prisms | 121 ~122 | 68 | $C_{12}H_{10}Cl_5NS_4$ | 30.93 (30.80) | 2.46 (2.14) |
| Ethyl | 4-Tolyl | Orange needles | 66 ~ 67 | 60 | $C_{13}H_{17}NS_4$ | 49.42 (49.52) | 5.64 (5.40) |

TABLE II. ARYL PIPERIDINOTHIOCARBONYLTRITHIOCARBONATES



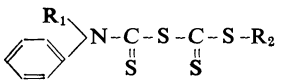
| R | Appearance | M. p., °C | Yield, % | Formular | Anal. C, % Found (calcd.) | Anal. H, % Found (calcd.) |
|---|---|---|---|---|---|---|
| Phenyl | Orange prisms | 76.5~ 77 | 60 | $C_{13}H_{15}NS_4$ | 49.75 (49.84) | 5.13 (4.79) |
| 4-Tolyl | Orange prisms | 108 ~110 | 71.5 | $C_{14}H_{17}NS_4$ | 51.62 (51.68) | 5.12 (5.20) |
| 4-Chlorophenyl | Orange prisms | 135 ~136 | 86 | $C_{13}H_{14}ClNS_4$ | 45.37 (44.92) | 4.10 (4.03) |

TABLE III. ARYL MORPHOLINOTHIOCARBONYLTRITHIOCARBONATES



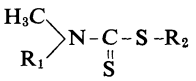
| R | Appearance | M. p., °C | Yield, % | Formular | Anal. C, % Found (calcd.) | Anal. H, % Found (calcd.) |
|---|---|---|---|---|---|---|
| 2-Tolyl | Yellow prisms | 104 ~105 | 63 | $C_{13}H_{15}NOS_4$ | 47.30 (47.42) | 4.48 (4.56) |
| 4-Tolyl | Orange prisms | 122 ~123 | 67.5 | $C_{13}H_{15}NOS_4$ | 47.57 (47.42) | 4.84 (4.56) |
| 2-Chlorophenyl | Orange prisms | 114.5~115.5 | 67 | $C_{12}H_{12}ClNOS_4$ | 41.45 (41.20) | 3.77 (3.43) |
| 2,4,5-Trichlorophenyl | Orange prisms | 142 ~143 | 86 | $C_{12}H_{10}Cl_3NOS_4$ | 34.85 (34.41) | 2.49 (2.39) |

TABLE IV. ARYL ARYLTHIOCARBAMOYLTRITHIOCARBONATES



| $R_1$ | $R_2$ | Appearance | M. p., °C | Yield % | Formula | Anal. C, % Found (calcd.) | Anal. H, % Found (calcd.) |
|---|---|---|---|---|---|---|---|
| Methyl | 4-Tolyl | Orange prisms | 98 ~ 99 | 86 | $C_{15}H_{15}NS_4$ | 54.88 (55.01) | 4.50 (4.30) |
| Methyl | 4-Chlorophenyl | Orange prisms | 87 ~ 88 | 74 | $C_{15}H_{12}ClNS_4$ | 48.90 (48.71) | 2.87 (3.25) |
| Phenyl | 4-Tolyl | Orange plates | 101 ~102 | 65 | $C_{21}H_{17}NS_4$ | 60.70 (61.31) | 4.22 (4.14) |
| Phenyl | 4-Chlorophenyl | Orange prisms | 125.5~126.5 | 54 | $C_{20}H_{14}ClNS_4$ | 55.95 (55.62) | 3.30 (3.24) |

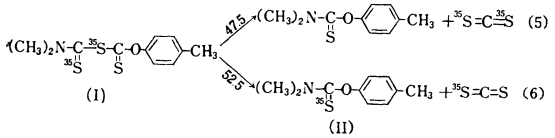
TABLE V. ARYL *N,N*-DISUBSTITUTED-DITHIOCARBAMATES



| $R_1$ | $R_2$ | Appearance | M. p., °C | Yield % | Formula | Anal. C, % Found (calcd.) | Anal. H, % Found (calcd.) |
|---|---|---|---|---|---|---|---|
| Methyl | 4-Tolyl | Colorless prisms | 112~113 | 77.5 | $C_{10}H_{13}NS_2$ | 56.71 (56.87) | 6.21 (6.16) |
| Methyl | 4-Chlorophenyl | Colorless needles | 101~103 | 82 | $C_9H_{10}ClNS_2$ | 47.15 (46.65) | 4.13 (4.32) |
| Phenyl | 4-Tolyl | Colorless needles | 132~133 | 76 | $C_{15}H_{15}NS_2$ | 66.25 (65.93) | 5.38 (5.49) |
| Phenyl | 4-Chlorophenyl | Colorless lozenges | 147~149 | 80.5 | $C_{14}H_{12}ClNS_2$ | 57.56 (57.24) | 4.12 (4.07) |

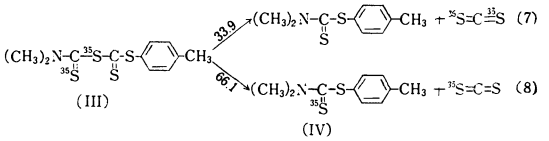
two S atoms in the thiocarbamoylthio group were labeled with $^{35}_{16}S$, radio-active *O*-(4-tolyl) *N,N*-dimethylthionocarbamate (II) was produced. The relative activity of II against I was found to be 0.2625, while the theoretical value, based on Eq. 5 should be zero, and based on Eq. 6, it should be 0.5000.

But this result may be explained if one postulates that the two courses of decomposition (Eqs. 5 and 6) occur simultaneously at the rate of 47.5 : 52.5.



*N,N*-Disubstituted aryl thiocarbamoyltrithiocarbonates were found to decompose, when kept at temperatures higher than their melting points, into *N,N*-disubstituted aryl dithiocarbamates liberating carbon disulfide. The crystalline decomposition products of some trithiocarbonates are listed in Table V.

By the thermal decomposition of *S*-(4-tolyl) *S*-(*N,N*-dimethylthiocarbamoyl) trithiocarbonate (III) in which the two S atoms were labeled with $^{35}_{16}S$ similarly as in the case of I, radio-active 4-tolyl *N,N*-dimethyldithiocarbamate (IV) was given. But the relative activity of IV against III was found to be 0.3305. Thus the proportion of the two courses was concluded to be 33.9 : 66.1 (Eqs. 7 and 8) in this case.

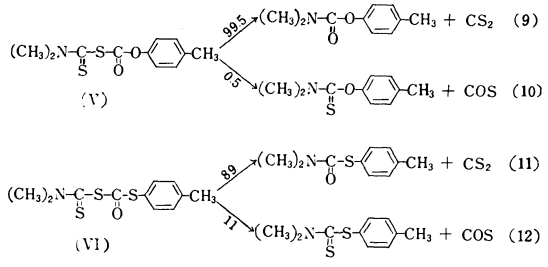


These facts show that the two courses of decomposition can occur simultaneously, but the rate of their occurrence is strongly influenced by substituting O atom with S atom.

To discover what influences would appear when another one of the S atoms was substituted with an O atom, the thermal decomposition of the compounds containing $>C^2=O$ in place of $>C^2=S$ (cf. Eqs. 3 and 4) was studied. This could produce carbon disulfide if the reaction occurred as Eq. 3, or carbon oxysulfide if the reaction followed Eq. 4. By the thermal decomposition of V and VI, both carbon disulfide

and carbon oxysulfide were evolved as decomposition fragments in each case (cf. Eqs. 9—12). Also, the volume rates of $CS_2$ : COS were found to be 99.5 : 0.5 and 89 : 11 respectively, by gas-chromatographic analyses of the above fragments.

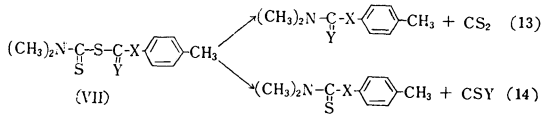
These results show that the proportions of the two courses in each case should be 99.5 : 0.5 (Eqs. 9 and 10), and 89 : 11 (Eqs. 11 and 12).




(9) (10) (11) (12)

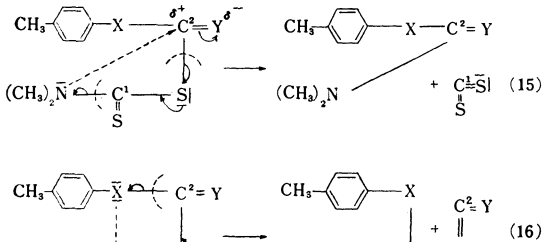
These results show that the proportion of the occurrence of reaction 13 against reaction 14 increases according to the variation of X and Y to S or O atom as follows.

$$X=Y=O>X=S,\ Y=O>X=O,\ Y=S>X=Y=S$$

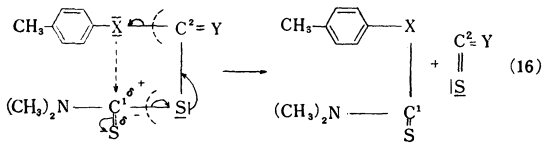



(13) (14)

Summarizing the decomposition reactions mentioned above, it may be concluded that there are two reaction mechanisms on the thermal decomposition reaction of *N*, *N*-disubstituted aryl thiocarbamoylthiocarbonates, which can be written as follows.



(15)



(16)

(X, Y : O and/or S)

Reaction 15 occurs by co-ordination of $(C^2)^+$ to $\overline{N}$, and reaction 16, by co-ordination of $(C^1)^+$ to $\overline{X}$. The electron density on $C^2$ and electro-negativity of -X-, which vary according to the variation of X and Y to S or O atom, may have some influence on the reaction courses.

By comparison of the electron densities on $C^1$ in $>N-\overset{1}{C}=S$ and $C^2$ in $-X-\overset{2}{C}=Y$, when both X and Y are O atoms, the electron density on $C^2$ is far smaller than that on $C^1$, owing to the greater polarization of $>C=O$ than that of $>C=S$ and greater electro-negativity of -O- than that of -S-. Thus reaction 15 may occur almost exclusively in this case. When X is an S atom, however, the electron density on $C^2$ increases, for the electro-negativity of -X- becomes smaller owing to replacement of O atom by S atom. This will make not only the co-ordination of $(C^2)^+$ to $\overline{N}$ unfavorable, but also the co-ordination of $(C^1)^+$ to $\overline{X}$ favorable. Thus reaction 16 may occur to some extent in this case. When Y is an S atom, the difference of the electron densities on $C^1$ and on $C^2$, due to the respective polarity of $>C=Y$ and $>C=S$, will disappear. Thus the two sorts of co-ordination become concurrent. When X is also an S atom, reaction 16 occurs most easily for the reasons mentioned above.

These situations may explain the relationships between the mechanisms of thermal decomposition of the compounds VII and their structures.

## Experimental

**Starting Materials.**—Sodium or ammonium salts of *N*, *N*-disubstituted-dithiocarbamic acid were synthesized by the known methods[1]. Aryl esters of chlorodithioformic acid were synthesized similarly to aryl chlorothionoformates which were previously reported[1], by the reaction of thiophosgen, thiophenol and sodium hydroxide.

**4-Tolyl *N*, *N*-Dimethylthiocarbamoyltrithiocarbonate.** — To a solution of 14.3 g. (0.1 mol.) of sodium dimethyldithiocarbamate in 100 cc. of water, was added gradually 20.3 g. (0.1 mol.) of 4-tolyl chlorodithioformate, keeping the temperature at 10～15°C during the reaction period of 2 hr. The reaction mixture produced 25 g. (yield, 87%) of orange crystals with m. p. 105～106°C. Recrystallization from acetone-ethanol gave orange needles of m. p. 107～108°C.

**4-Tolyl *N*-Methyl-*N*-phenylthiocarbamoyltrithiocarbonate.**—To a suspension of 20 g. (0.1 mol.) of ammonium *N*-methyl-*N*-phenyldithiocarbamate in 100 cc. of acetone, was added gradually 20.3 g. (0.1 mol.) of 4-tolyl chlorodithioformate, keeping the temperature at 5～10°C during the reaction period of 1 hr. The reaction mixture poured into 200 cc. of cold water produced 30 g. (yield, 86%) of orange crystals with m. p. 96～99°C. Recrystallization from acetone-ethanol gave orange prisms with m. p. 98～99°C.

The other esters shown in Tables I—IV were synthesized similarly to the synthesis of the above examples.

***S*-(4-Tolyl) *S*-(*N*, *N*-Dimethylthiocarbamoyl)dithiocarbonate (VI).**—This could also be synthesized in a similar way, by reacting 27.1 g. (0.1 mol.) of *S*-(4-tolyl) chlorothiolformate with 14.3 g. (0.1 mol.) of sodium dimethyldithiocarbamete in 150 cc. of acetone. Yield : 27.8% ; Yellow needles of m. p. 69～70°C.

Found: C, 48.66; H, 4.72; N, 5.33. Calcd. for $C_{11}H_{13}NOS_3$: C, 48.71; H, 4.80; N, 5.17%.

**Thermal Decomposition of V and VI.** — In a sealed flask (1000 cc. in volume) which was filled with nitrogen gas at 10 mmHg., 2 g. of V or VI was fused at 160°C for 1 hr. After the subsidence of evolution of gas, nitrogen gas was led into the flask until the pressure became 760 mmHg. Further, the ratio of carbon oxysulfied and carbon disulfide, in the gas obtained, was measured by gas-chromatography (column: tricresyl phosphate, at 42.5°C; carrier: $H_2$).

**Thermal Decomposition of Radio-active 4-Tolyl *N*, *N*-Dimethylthiocarbamoyltrithiocarbonate (III).** —In an oil bath, 0.575 g. of III (specific activity: 47.84 mc./mol.), synthesized by the reaction between 4-tolyl chlorodithioformate and radio-active sodium *N*,*N*-dimethyldithiocarbamate in which the two S atoms were labeled with $^{35}_{16}S$, was fused at 160°C for 1 hr. in nitrogen atmosphere of 10 mmHg. After the subsidence of evolution of radio-active carbon disulfide, the decomposition product was twice recrystallized from 2.4 cc. of ethanol and produced 0.327 g. (yield, 77.5%) of radio-active 4-tolyl *N*,*N*-dimethyldithiocarbamate (VI), of which the specific activity was 15.81 mc./mol. with m. p. 112~113°C. The relative specific activity of VI against III was 0.3305 (=15.81/47.84).

By the thermal decomposition of radio-active *O*-(4-tolyl) *S*-(*N*,*N*-dimethylthiocarbamoyl)dithiocarbonate (I) (specific activity: 23.85 mc./mol.), radio-active *O*-(4-tolyl) *N*,*N*-dimethylthionocarbamate (II) (specific activity: 6.26 mc./mol.) was produced in a similar way. Thus the relative activity of II against I was 0.2625.

The author wishes to express his sincere thanks to Professor Dr. Ryozo Goto, Kyoto University, for his guidance and encouragement throughout this work. The author also thanks Professor Dr. Hiroshi Watanabe, Konan University, for his helpful advice. He is also grateful to Dr. N. Oda, Mr. M. Kubo, Mr. K. Norishima, Mr. G. Tsuchihashi, Mr. S. Ono and Mr. A. Nomura for gas-chromatographic and elemental analyses, to Dr. K. Taniguchi for his guidance, and to Mr. K. Miyazaki, Mr. K. Hashimoto and Mr. Y. Aoki for their assistance with the experimental work.

*Takaoka Factory, Nippon Soda Co., Ltd.*
*Mukaino-honmachi, Takaoka, Toyama*

# *Benzylideneaniline. III. Anils of Substituted Benzaldehydes*

By Nozomu EBARA

(Received January 21, 1961)

In the first paper of this series[1] a non-planar structure was proposed for benzylideneaniline, where the benzene ring of aniline part is almost perpendicular to the rest of the molecule (Fig. 1). In such a case the ultraviolet absorption spectrum of this molecule would be closely allied to those of benzaldehyde type I and aniline type II molecular halves, and it was assumed that the absorption maxima at 263 m$\mu$ (A) and at 315 m$\mu$ (B) is due to I and II respectively. The effects of substituents upon these bands were examined and it was found that the substituents on II had little to do with band A, whereas marked shifts were experienced by band B.

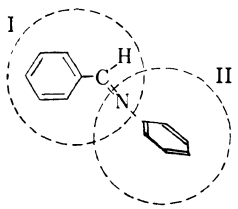



Fig. 1. Assumed structure of benzylideneaniline.

In the present paper, derivatives of benzylideneaniline of which the substituents are on aldehyde ring I, together with anils bearing aliphatic halves, were synthesized and their spectral features as well as other properties were examined.

**Ultraviolet Absorption Spectra.**—Ultraviolet absorption spectra of anils were measured in *n*-heptane, ethyl alcohol and 50% mixture of hydrochloric acid and ethyl alcohol. The spectra in *n*-heptane are illustrated in Fig. 2 and pertinent data are listed in Table I.

*Bands A.*—Bands A shift markedly as substituents vary, in contrast to the case where the substituents are on II. Moreover, they shift furthermore towards longer wavelengths when alcohol is used as solvent. In acidic

1) N. Ebara, This Bulletin, 33, 534 (1960).

Table I. Wavelengths of UV absorption maxima

(in Å)

| R | Solvent | | | Crystal state | in | in | in |
|---|---|---|---|---|---|---|---|
| | $C_7H_{16}$ | $C_2H_5OH$ | HCl+ $C_2H_5OH$ | | $C_2H_5OH$ (above 3000 Å) | $C_2H_5OH$ | $C_7H_{16}$ |
| *p*-OH | 2750<br>3150 | (2950)<br>3140 | | | — | 2815 | |
| *p*-$OCH_3$ | 2790<br>3150 | (2790)<br>3030 | | 2800<br>3250 | — | 2765 | 2680 |
| *o*-OH | 2680<br>3010<br>3180<br>3415 | 2700<br>2990<br>3160<br>3360 | 2570<br>3240 | 3100～3500 | 3280 | 2540<br>3244 | 2540<br>2590<br>3170 |
| *o*-$OCH_3$ | 2650<br>3220 | 2660<br>3280 | | | 3200? | 2528<br>3210 | |
| *p*-$NO_2$ | 2860<br>3130<br>3420 | 2910<br>3180 | 2340<br>(3500) | | — | | |
| *p*-$NMe_2$ | 3000<br>3100<br>3200<br>3270 | 3430 | 2430<br>2815<br>(3500) | | — | 3420 | 3390 |
| *p*-Cl | 2680<br>3180 | 2685<br>3150 | 2590<br>2900<br>(3480) | | — | | |
| *m*-$NO_2$ | 2550<br>3220 | 2580<br>3180 | 2340<br>(3480) | | — | | |
| *m*,*m*'-$(NO_2)_2$ | 2550<br>3160 | 2590<br>3200 | 2640<br>3180<br>(3670) | | | | |

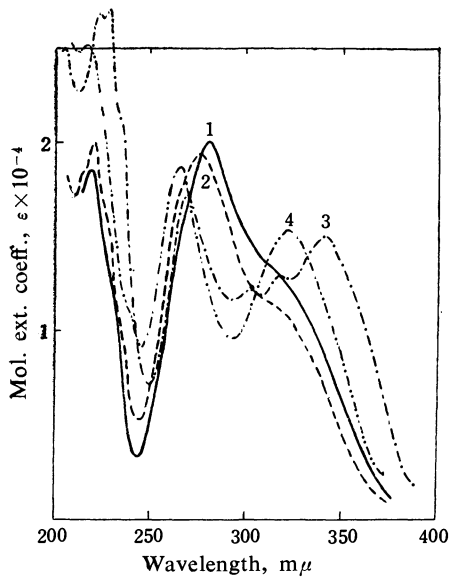



Fig. 2(A). Spectra of anils in *n*-heptane.

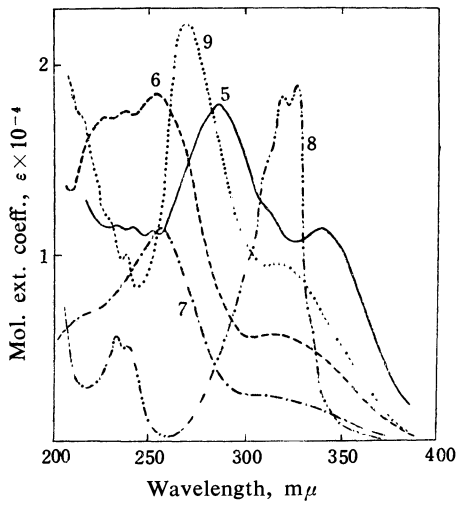
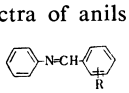



Fig. 2(B). Spectra of anils in *n*-heptane:



R= 1) *p*-OH; 2) *p*-$OCH_3$; 3) *o*-OH; 4) *o*-$OCH_3$; 5) *p*-$NO_2$; 6) *m*-$NO_2$; 7) *m*, *m*'-di$NO_2$; 8) *p*-$N(CH_3)_2$; 9) *p*-Cl; (Intensities of 3 and 7 are in arbitrary unit and that of 8 in half scale).

medium, the blue shift is again observed with these bands as in the former case[1], but their maxima are by no means at the same position, but vary in a manner similar to those of corresponding anils and aldehydes. These facts are in good accordance with the above proposal that band A is largely of the nature of CT band of I.

*Bands B.*—Unfortunately the behavior of bands B is not quite obvious as anils bearing the electron-donating groups at the ortho position of I exhibit the expected maxima of enhanced intensities at the longer wavelength region (presumably the second CT bands[2] from I) and the positions of bands B become obscure. But in cases where they are observable, they are in general almost at the same position. It is perplexing, however, that substitution at the para position of I by $NO_2$ group also gives rise to a new band at the longer wavelength region, of which the explanation is not yet deduced.

There remains another discrepancy as to the intensities of bands B, which are too much enhanced to be largely of the nature of $A_1-B_2$ transition of II.

**Comparison with the Anils Bearing Aliphatic Halves.** — Benzylidene-*n*-butylamine, anisylideneisopropylamine, *p*-dimethylaminobenzylideneisopropylamine, salicylideneisopropylamine and *n*-butylideneaniline were synthesized and their spectra were measured (Fig. 3).

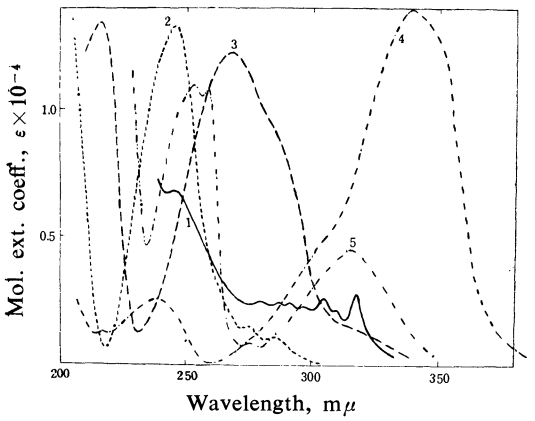
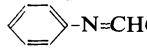
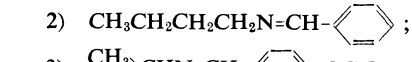
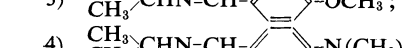
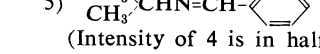



Fig. 3. Spectra of aliphatic anils in *n*-heptane:
1) 
2) 
3) 
4) 
5) 
(Intensity of 4 is in half scale).

Anils of aliphatic amines and aromatic aldehydes exhibit intense bands in the proximity of those of aldehydes, which may therefore be correlated to bands A of aromatic anils. Bands B vanish completely in these anils.

*n*-Butylideneaniline shows an intense band at 2470 Å and a weak one with a structure between 2820 and 3200 Å, which should correspond to those of aniline. The position of the latter band coincides almost exactly with band B of benzylideneaniline, although their intensities differ considerably. It is not certain whether *n*-butylideneaniline assumes benzaldehyde type or aniline type structure (presumably, the former), but apart from this, it may be concluded that $A_{1g}-B_{2u}$ transition of benzene at 2600 Å rises to this position in the presence of the perturbation of R–CH=N– and that this band shifts no more towards longer wavelengths when R turns from aliphatic to aromatic groups.

Therefore, no substantial difference seems to exist between the spectra of aliphatic and aromatic anils.

**Spectra of *N*-Methylated and Protonated Anils.**—Similar spectra are observed with *N*-methylated anils and with *N*-protonated anils. Bands B vanish completely, whereas bands A shift towards shorter wavelengths: the explanation of the latter phenomenon was given tentatively in terms of hybridization change in the previous paper[1].

No anils giving rise to second CT bands of I miss these bands when they are methylated or protonated.

***p*-Hydroxybenzylidene- and Anisylideneaniline.**—Striking are the features of the spectra of

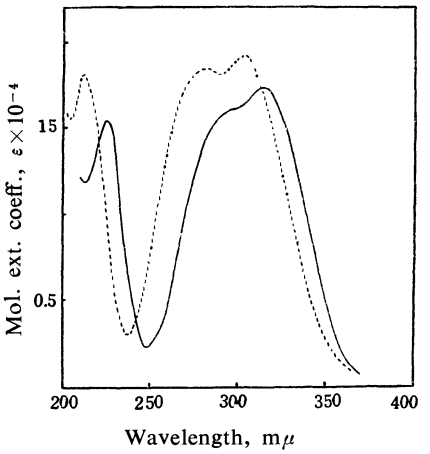
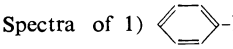
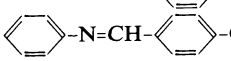


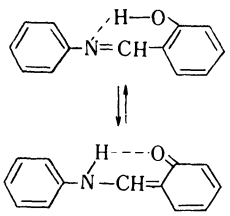

Fig. 4. Spectra of 1)  and 2)  in $C_2H_5OH$.

2) J. Tanaka and S. Nagakura, *J. Chem. Soc. Japan, Pure Chem. Sec. (Nippon Kagaku Zasshi)*, **78**, 1200 (1957).

*p*-hydroxybenzylidene- and anisylideneaniline, where the spectra are very greatly different in alcohol as compared with those in *n*-heptane, the latter exhibiting the ordinary shape of anils (Fig. 4). In contrast to this, the spectra of anils bearing these substituents on II are free from any remarkable solvent effect. It seems plausible to assume that the bands A at 2750 Å and at 2790 Å of these compounds in *n*-heptane, presumably the CT band of I, shift to 3140 and 3030 Å in alcohol, respectively, owing to the pronounced stabilization of the solvated excited states where there are large resonance polarizations due to strongly electron-donating substituents at the para positions. These molecules decompose very quickly in alcohol, as will be described in a following section, and the bands near 2800~2900 Å may be attributed to the inevitably present decomposition products.

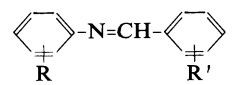
**Salicylidene- and *o*-Methoxybenzylideneaniline.** —Another peculiar feature is that of salicylideneaniline, where three bands are observed above 3010 Å, which are too conspicuous to be the vibrational structure. It had been reported that strong hydrogen bonding exists between hydroxyl hydrogen and azomethine nitrogen atoms[3], and that this would be responsible for the unusual spectrum of this molecule[4]. But it is highly improbable that a hydrogen bonding would cause such a large variation in the spectrum as the appearance of new bands.

In phenylazonaphthol a tautomerism is known to exist between azo and hydrazone forms[5], whereas *o*-hydroxyazobenzene does not exhibit this tautomerism[6]. To see whether this is the case or not with salicylideneaniline, and to examine whether or not some of these bands correspond to the tautomeric enamine form, the temperature dependence of the ultraviolet absorption spectrum was examined. The



spectrum was measured at several temperatures between −60 and 47°C, but no remarkable change was observed except for the ordinary sharpening and broadening of the peaks accompanying the temperature change. The infrared spectrum was also examined in carbon tetrachloride solution and in solid state, but there was observed no band attributable to C=O stretching vibrational mode. Moreover the spectra in the solution and in the solid state resemble each other very closely, indicating that the molecular structure is not so greatly different in these two states, and that there seemes to exist no tautomeric equilibrium between the above two structures. The shift of C=N stretching vibration from that of unsubstituted benzylideneaniline is considerably great as compared with other anils where the shifts are at most within a few $cm^{-1}$ (Table II). OH stretching vibration is hidden under the lower frequency side of CH stretching vibration. Deuterated salicylideneaniline was synthesized. This gives rise to a very broad band between 2020~2180 $cm^{-1}$, doubtless attributable to OD stretching vibration, from which the position of the original OH band is calculated to lie between 2800~3000 $cm^{-1}$, showing an unusual shift towards lower frequencies.

TABLE II. WAVE NUMBERS OF C=N STRETCHING VIBRATIONS



in $CCl_4$

| R | R′ | Wave number, $cm^{-1}$ |
|---|---|---|
| H | H | 1629 |
| *p*-$OCH_3$ | H | 1626 |
| *o*-Cl | H | 1630 |
| *m*-Cl | H | 1631 |
| *p*-Cl | H | 1628 |
| *m*-$NO_2$ | H | 1631 |
| H | *p*-$OCH_3$ | 1624 |
| H | *o*-$OCH_3$ | 1620 |
| H | *m*-$NO_2$ | 1629 |
| H | *p*-$NO_2$ | 1629 |
| H | *o*-OH | 1616 |

Presumably a large resonance coupling would exist between azomethine and enamine forms, the former still being predominant. The molecule may safely be referred to as existing almost exclusively in azomethine form rather than in enamine form in the solution as well as in the solid state, and the new ultraviolet absorption bands might not be ascribed to the tautomerism.

Ionization equilibrium might exist in this molecule between phenolic and phenolate structures, and some of the bands might be attributed to anion form. But this seems also not to be the case, as the change of solvent, as well as of temperature, proves no evidence of the noticeable variation in the ionization constant. Moreover, in alkaline solution, the

3) e. g., L. Kahovec and K. W. Kohlrausch, *Zeitschr. phys. Chem.*, (B) **38**, 119 (1938).
4) A. von Kiss and G. Auer, ibid., (A) **189**, 344 (1941).
5) e. g., A. Burawoy and I. Markowitsch, *Ann.*, **503**, 180 (1933).
6) e. g., D. Hadži, *J. Chem. Soc.*, **1956**, 2143.

bands above 3010 Å disappear and a new band comes out at 3800 Å, which is raised too much to be led back to any of the bands of salicylideneaniline.

It turns out that an intense band exists at 3220 Å in the spectrum of *o*-methoxybenzylideneaniline. This is all but congruent with that at 3210 Å of *o*-methoxybenzaldehyde and is presumably the second CT band of I. Salicylaldehyde, salicylaldoxime[7], salicylaldimine[7] and bis-salicylidene-ethylenediamine[8] as well as *N*-methyl-salicylideneanilinium ion exhibit similar bands. All of these bands may demand their replica in the spectrum of salicylideneaniline: the band at 3415 Å is the most adequate for this, though it is conflicting that this band experiences the blue shift when alcohol is used as solvent.

One of the other two bands at 3010 and 3180 Å, preferably the latter, may be assigned as band B, which comes from I of the molecule.

**Hydrolyzation Reaction of *p*-Hydroxybenzylidene-, Anisylidene- and *o*-Methoxybenzylideneaniline.**—These three compounds decompose very quickly in alcoholic solutions. The reaction rates were found to depend upon the water content of alcohol, and would conceivably be hydrolyzation reactions. The rates of these reactions were measured at several temperatures by tracking their spectral changes, and it was found that the reactions are first-order as to the concentrations of anils in the presence of excess water. The results are shown in Table III and in Figs. 5, 6 and 7.

Table III. Hydrolyzation reaction rates in $C_2H_5OH(2)+H_2O(1)$

| Temp., °C | $k\times10^2$ | $E$, kcal./mol. | A |
|---|---|---|---|
| *o*-Methoxybenzylideneaniline | | | |
| 31.6 | 9.90 | 7.72 | $1.6\times10^4$ |
| 26.0 | 7.92 | | |
| 20.6 | 6.40 | | |
| 12.0 | 4.40 | | |
| *p*-Hydroxybenzylideneaniline | | | |
| 45.6 | 5.87 | 6.56 | $2.5\times10^3$ |
| 40.1 | 4.95 | | |
| 25.85 | 2.97 | | |
| 13.95 | 1.89 | | |
| Anisylideneaniline | | | |
| 45.5 | 5.16 | 6.11 | $1.0\times10^3$ |
| 39.7 | 4.28 | | |
| 24.5 | 2.62 | | |
| 13.85 | 1.77 | | |

It is probable that owing to the strongly electron-donating properties of the substituents, the addition of proton at the nitrogen atom, or conceivably the heterolytic fission of OH bond of hydrogen-bonded water at the nitrogen atom, accompanied by the addition of $OH^-$ to the azomethine carbon atom, would proceed easily.

The activation energies are almost equal in these three cases, whereas the frequency factor is the largest in *o*-methoxybenzylideneaniline. One tentative explanation is that owing to the closely standing hydrogen-bonded *o*-methoxyl group, the chance of the reaction in which water participates is greater in this case.

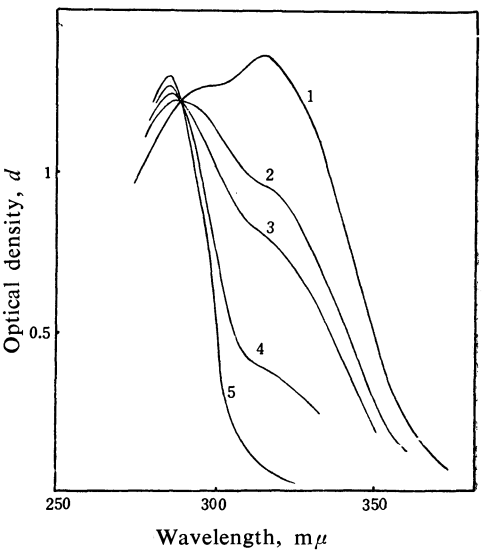
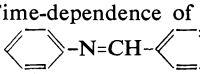



Fig. 5. Time-dependence of the spectrum of 
1) Immediately after dissolution;
2) After 7 min.; 3) After 10 min.;
4) After 24 min.; 5) After 4 hr.

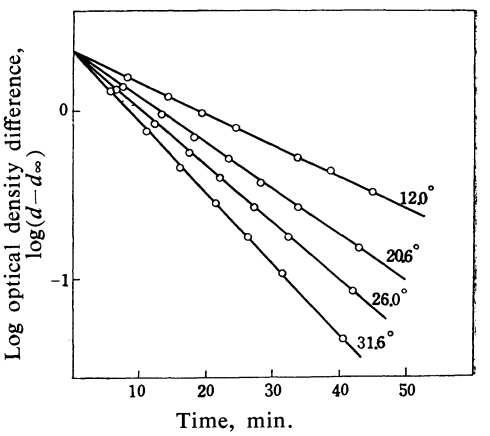
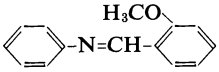



Fig. 6. Hydrolyzation reaction of  in $C_2H_5OH(2)+H_2O(1)$.

7) K. Sone, *J. Am. Chem. Soc.*, **75**, 5207 (1953).
8) L. N. Ferguson and I. Kelly, ibid., **73**, 3707 (1951).

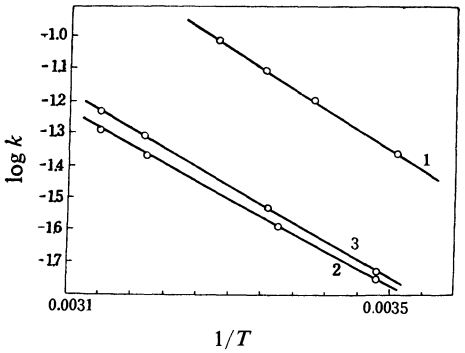
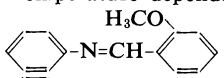
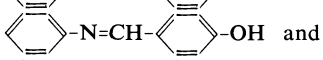
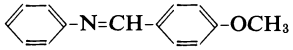



Fig. 7. Temperature dependences of

1) 

2) 

3) 

When the substituents are on II, hydrolyzation reaction does not take place, presumably because the substituents would only affect the C=N bond through the participation in the migration aptitude of nitrogen non-bonding electrons.

**Spectra in the Solid States.**—The spectra of benzylideneaniline, anisylideneaniline, salicylideneaniline, salicylidene-*p*-chloraniline and salicylidene-*p*-bromoaniline were measured in the solid states by means of either the potassium chloride disk method or the film method (Fig. 8). In the former three cases the spectra are very similar to those in *n*-heptane solutions, indicating that the molecular shapes are not greatly different in these two states, provided that the ignorance of the effect due to the orientation of the crystal axis may be permitted in the latter method. In the latter two cases, single peaks are always observed above 3000 Å instead of three, though their spectra in the solution are very similar to that of salicylideneaniline. It is not certain whether this is due to the variation in molecular shapes or due to the difference in crystal structures, or in turn due to the preferred orientation of crystal axis against the plates, which tends to favor the absorption band whose transition moment is perpendicular to it.

**Trial Interpretation of UV Spectrum on the Basis of Planar Model.** — Because of some discrepancies arising in the above consideration, the interpretation of the ultraviolet spectrum of benzylideneaniline is intended tentatively to be regarded on the basis of the planar model.

The symmetry $C_{2v}$ may be assigned to the molecule, so far as the $\pi$ electrons are concerned. In this approximation, the allowed

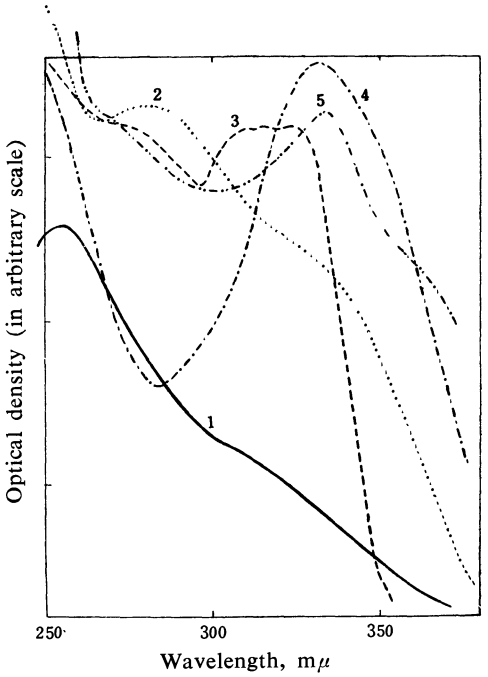
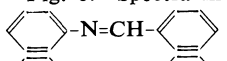
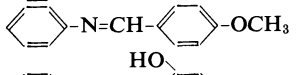
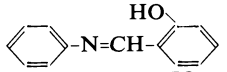
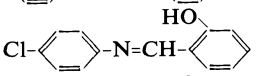


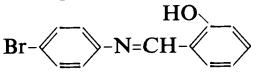

Fig. 8. Spectra in solid states,

1) 

2) 

3) 

4) 

5) 

electronic transitions are $A_1-A_1$ and $A_1-B_2$ ($A_1-B_1$ may be excluded, because the $\pi$ electronic levels are always constructed with atomic 2p orbitals).

Following the method of Nagakura and Tanaka[9], the perturbation diagram of this molecule is drawn, where the ionization potential and electron affinity of C=N group are assumed to lie between those of C=O and C=C, largely approaching the former (Fig. 9). Although the coefficients of atomic orbitals at N and C atoms in the MO of C=N group differ from each other, the resulting molecular energy level diagram might not be so far from those of stilbene and azobenzene at least in the lower region, and the lower excitations should be $\pi-\pi^*$ (or $A_1-A_1$) and $\pi-\phi^*$ (or $A_1-B_2$)[10]. The former should involve the charge transfer from two benzene rings to the

9) S. Nagakura and J. Tanaka, *J. Chem. Phys.*, **22**, 236 (1954).

10) The energy diagram is drawn by taking account of Jaffé's calculations (see Ref. 11).

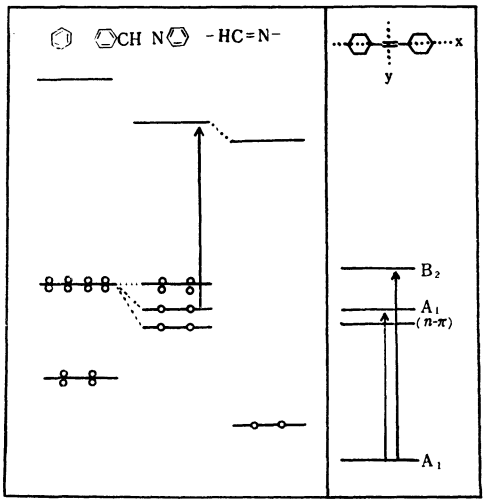



Fig. 9. Energy level diagrams of planar benzylideneaniline molecule.

central C=N part, although the mixing with other configurations would in part reduce it. The latter has much in common with benzene $A_{1g}-B_{2u}$ transition except that it becomes allowed by the perturbation. The intensity of the former should be reduced by the unsymmetrically situated central N atom and that of the latter would be much lower.

Two bands, A and B, arising in the spectrum of benzylideneaniline must be interpreted from the above standpoint. Jaffé[11] had assumed that they are $\pi-\phi^*$ and $\pi-\pi^*$, respectively.

In the present experiment, however, it was found that band A has the character of CT band, whereas band B does not, and that the nitrogen non-bonding electrons are responsible for the appearance of band B. Moreover this band is too intense to be $A_1-B_2$ transition. These findings go behind with Jaffé's interpretation.

An alternative interpretation in which band A is assigned as $\pi-\pi^*$ does not hold, as the energy of this transition might not be so great.

Thus, the planar model presents more discrepancies with regard to the ultraviolet spectrum of the molecule.

## Conclusion

The results obtained here can be explained adequately by the non-planar model proposed in the previous paper. In particular, the coincidence in the ultraviolet spectrum seems to be excellent. But the explanation is not unique and leaves many discrepancies. It remains in doubt whether or not the failure of explaining the spectrum of this molecule with the hitherto believed planar model might be ascribed to the misestimation or ignorance of some quantities which will arise in the calculation of molecular energies.

The molecule seems to assume the same conformation in the solid state as in the solution. The X-ray crystal analysis is now in progress. This will provide indisputable information with regard to the precise conformation of benzylideneaniline molecule.

## Experimental

**Materials.**—Benzylidene-, *p*-hydroxybenzylidene-, *p*-chlorobenzylidene-, *p*-nitrobenzylidene, *m*-nitrobenzylidene-, anisylidene-, *p*-dimethylaminobenzylidene- and salicylideneaniline were prepared by the direct condensation of aniline with corresponding aldehydes, without any dehydrating agent and were recrystallized from ethyl or isopropyl alcohol. M. p. 63, 193~194, 61~62, 90~90.5, 64.5~65, 51.5~52, 67~68 and 50~50.5°C, respectively.

*o*-Methoxybenzaldehyde was prepared from salicylaldehyde by methylating it with dimethyl sulfate. The distilled and crystallized aldehyde was readily submitted to condensation reaction with aniline, affording *o*-methoxybenzylideneaniline. The product was dehydrated and distilled and then recrystallized from isopropyl alcohol. M. p. 39~40°C.

Salicylidene-*p*-chloraniline and -*p*-bromaniline were synthesized by the condensation of salicylaldehyde with corresponding anilines and recrystallized from ethyl alcohol. M. p. 100 and 107°C, respectively.

*n*-Butylideneaniline, benzylidene-*n*-butylamine and anisylidene-, salicylidene- and *p*-dimethylaminobenzylideneisopropylamine were prepared by the following procedure. Equimolecular amounts of corresponding amines and aldehydes were put into a round-bottomed flask equipped with a good condenser. Vigorous reaction took place and water was separated out. The mixture was heated on a water bath for about one hour, then shaken with ether, dried over calcium chloride and distilled under reduced pressure. B. p. 118°C/13 mmHg, 111°C/17 mmHg, 119~120°C/14 mmHg., 155°C/25 mmHg, respectively.

**Deuterated Salicylideneaniline.** — Deuterated ethyl alcohol was prepared from sodium ethoxide and deuterium oxide, and this alcohol was again used for the preparation of sodium ethoxide. The procedure was repeated so as to reduce the hydrogen content of the resulting alcohol. Salicylideneaniline was dissolved in this alcohol and the solvent was evaporated at room temperature under reduced pressure. The moisture was carefully excluded throughout the whole process.

***N*-Methylated Anils.**—Excess amounts of methyl iodide were added in the solutions of anils and they were kept standing for several hours. The absorption spectra were measured at times in order to check the degree of completion of the reaction. The intense absorbancy due to methyl iodide was compensated for, but the spectra below 3000 Å could not be measured. Another method is

11) H. H. Jaffé, Si-Jung Yeh and R. W. Gardner, *J. Molecular Spectroscopy*, 2, 120 (1958).

employed as well, in which anils were dissolved in pure methyl iodide, kept standing for a night, desiccated to dryness, dissolved in alcohol and subjected to the measurements of absorption spectra.

**Measurements.**—Ultraviolet spectra were measured by means of a Cary 14-type self-recording spectrophotometer using 1 cm. quartz cell. To follow the reaction rate, the spectra were measured by the use of Hitachi EPU 2-type spectrophotometer.

**Hydrolyzation Reactions.**—The anils were dissolved in alcohol containing one-third the amount of water, and immersed in a thermostat. The absorbances of the solutions were measured at times in the vanishing band region. The final absorbances were also measured from which a rate equation could be derived. The plotted points fell on straight lines in very good coincidence.

Infrared spectra were measured by means of Nihon-bunko self-recording spectrophotometer model 301, using sodium chloride prism and sodium chloride cells of 0.1 mm. in thickness. Solid samples were prepared by allowing the melt to cool between sodium chloride plates pressed together.

Solid samples for the ultraviolet measurements were prepared either by allowing the melt to cool between quartz plates or by pressing the mixtures of finely powdered materials with specially prepared potassium chloride crystals[12].

The author wishes to express his sincere thanks to Professor Saburo Nagakura of the University of Tokyo for his kind guidance throughout this study.

*Department of Chemistry*
*College of General Education*
*The University of Tokyo*
*Meguro-ku, Tokyo*

12) J. L. Hales and W. Kynaston, *Analyst*, **79**, 702 (1954).

# *Abnormal Acceleration of the Rate of Bulk Polymerization of Styrene**

By Norio NISHIMURA

(Received November 21, 1960)

It is well known that an acceleration in rate can be observed during polymerization reactions. In the early stage of this investigation, Trommsdorff et al.[1] ascribed this phenomenon to the increase in viscosity of the reaction system. It is now currently accepted that the increase in both rate and degree of polymerization is brought about by a decrease in termination constant due to the gel effect (or Trommsdorff effect). In a viscous solution, the termination constant is affected first. Propagation and transfer reactions involving small monomer and catalyst molecules are less affected by viscosity.

There have been some investigations on the effect of viscosity on the reaction rate and the individual rate constants[1-4].

Recently, Tobolsky et al.[5] have shown that the limiting fractional conversion at infinite time of a radical initiated vinyl polymerization could be predicted from a knowledge of the kinetic rate constants under certain conditions where the gel effect does not invalidate the theory.

## Experimental

**Reagents.** — Commercial 2,2'-azobisisobutyronitrile was recrystallized twice from ether solution m. p. 103~103.5°C. Styrene monomer was washed with 10% sodium hydroxide and then with water. After drying over calcium chloride, the monomer was distilled and stored in the dark. Just before use, it was fractionated at 25 mmHg and the middle fraction was used. Benzene was washed in turn with concentrated sulfuric acid, dilute sodium hydroxide and water. Then it was dried over calcium chloride, then over metallic sodium wire and distilled. *n*-Butanol of reagent grade was used after distillation.

**Procedure.**—All polymerizations were carried out in glass dilatometers, the type of which was similar to that used before[6]. After being filled with the requisite amounts of catalyst and monomer, the tubes were connected to a vacuum line and sealed off. The tubes were then held in a thermostat at 60°C.

The volume contraction of the solution was

* Presented at the Local Meeting of the Chemical Society of Japan, Hiroshima, November, 1960.

1) E. Trommsdorff, H. Köhle and P. Lagally, *Makromol. Chem.*, **1**, 169 (1948).

2) S. W. Benson and A. M. North, *J. Am. Chem. Soc.*, **81**, 1339 (1959).

3) H. Miyama, *J. Chem. Soc. Japan, Pure Chem. Sec. (Nippon Kagaku Zasshi)*, **78**, 714 (1957).

4) M. F. Vaughan, *Trans. Faraday Soc.*, **48**, 576 (1952).

5) G. V. Tobolsky, C. E. Rogers and R. D. Brickman, *J. Am. Chem. Soc.*, **82**, 1277 (1960).

6) S. Hasegawa, N. Hirai, N. Nishimura and T. Kawano, This Bulletin, **31**, 696 (1958).

followed with a travelling microscope. At high conversion where dilatometric technique could not be applied because of high viscosity, the gravimetric method was used. In order to calculate the degree of conversion from the contraction of the solution, the densities of polystyrene in the monomer (solution polymer density) and styrene monomer at 60°C were taken as 1.0563 and 0.869[7], respectively. Hence, for bulk polymerization of styrene, 100% conversion corresponds to a 17.7% contraction in volume of the original monomer.

The induction period could not be observed in every experiment. At specified times, the contents of the tubes were properly dissolved in benzene and then poured dropwise into a much greater quantity of ice-methanol. The precipitate was filtered off and dried in vacuo.

The intrinsic viscosities of the benzene solutions of polystyrene were determined at 30±0.01°C using an Ostwald viscometer. The number average degree of polymerization was estimated from the following equation[8]

$$\bar{P}_n = 1770[\eta]^{1.40}$$

In order to obtain the distribution of the degrees of polymerization at high conversion, *n*-butanol was slowly added to the benzene solution of the polymer (about 1.5%). The addition of the *n*-butanol was stopped before precipitation of the polymer appeared. By slow evaporation of the relatively volatile benzene, the solution becomes richer in less volatile *n*-butanol, and the precipitation of polystyrene results. After temperature equilibrium was attained in a thermost at 30°C, the precipitate in a gel state was separated by decantation from the solution and the same procedure was repeated. The precipitate was then dissolved again in benzene and poured into ice-methanol followed by drying in vacuo. This method is almost the same as that adopted by Chitani et al.[9]

## Theoretical

Notation

$M$—Number of moles of monomer,
$P$ —Number of moles of polymer,
$I$ —Number of moles of catalyst,
$f$ —Catalyst efficiency,
$k_p$—Rate constant for propagation,
$k_t$—Rate constant for termination,
$k_d$—Rate constant for the first order decomposition of catalyst,
$\alpha$ —Total volume shrinkage for the complete conversion of monomer to polymer,
$\bar{P}_n$—Cumulative value for number average degree of polymerization,
$\bar{\bar{P}}_n$—Instantaneous value for number average degree of polymerization.

It is well known that the rate of radical polymerization initiated by a catalyst is expressed as

$$-\frac{d[M]}{dt} = K[I]^{1/2}[M] \tag{1}$$

where

$$K \equiv \frac{k_p}{k_t^{1/2}} k_d^{1/2} f^{1/2} \tag{2}$$

If the decomposition rate of the catalyst is of the first order with respect to its concentration, then the conversion $x$ at time $t$ may be expressed by

$$x = 1 - \exp\{A(e^{-(1/2)k_d t} - 1)\} \tag{3}$$

where

$$A \equiv \frac{2K}{k_d}[I]_0^{1/2} \tag{4}$$

The value of $K$ can easily be obtained from the slope of the initial rate of polymerization against the square root of the catalyst concentration. From Eq. 3 it may be seen that the fractional conversion $x$ reaches a limiting value $x_\infty$ when $t \to \infty$.

$$x_\infty = 1 - \exp(-A) \tag{5}$$

Tobolsky[10] showed this relationship and compared it with experimental results. In the previous paper[6], which describes the polymerization of vinyl acetate in the benzoyl peroxide-iron(II)-benzoin redox system, the same concept of the limiting conversion was proposed by us. Later Tobolsky et al.[5] proposed a modified form of the kinetic expressions. The equations derived above have not been corrected for a net volume shrinkage of the system. If the volume shrinkage is taken into account, then the effective monomer and catalyst concentrations are

$$[M] = \frac{[M]_0}{(1-\alpha x)}(1-x) \tag{6}$$

$$[I] = \frac{[I]_0}{(1-\alpha x)} e^{-k_d t} \tag{7}$$

respectively. From Eqs. 1, 6 and 7, one obtains

$$\frac{(1-\alpha x)^{3/2}}{(1-x)} dx = K[I]_0^{1/2} e^{-(1/2)k_d t} \cdot dt \tag{8}$$

Integration of Eq. 8 leads to

$$\frac{2}{3}y^3 + 2a^2 y + a^3 \ln\frac{(y-a)}{(y+a)} = Ae^{-(1/2)k_d t} + C \tag{9}$$

where

$$\left.\begin{aligned} C &\equiv \frac{2}{3} + 2a^2 + a^3 \ln\frac{(1-a)}{(1+a)} - A \\ y &\equiv (1-\alpha x)^{1/2}; \quad a \equiv (1-\alpha)^{1/2} \end{aligned}\right\} \tag{10}$$

7) M. S. Matheson, E. E. Auer, E. B. Bevilacqua and E. T. Hart, *J. Am. Chem. Soc.*, **73**, 1700 (1951).
8) D. H. Johnson and A. V. Tobolsky, ibid., **74**, 938 (1952).
9) T. Chitani, G. Meshitsuka and Y. Matsui, *High Polym. Chem.* (*Kobunshi Kagaku*), **10**, 175 (1953).
10) A. V. Tobolsky, *J. Am. Chem. Soc.*, **80**, 5927 (1958).

Eqs. 8 and 9 are somewhat different from the similar expressions derived by Tobolsky et al.[5]

It is rather complex to calculate the limiting conversion $x_\infty$ from Eq. 9. But if the corresponding value of $y$ is expressed by $y_\infty$, then from Eq. 9,

$$Z \equiv \frac{2}{3}(y^3-y_\infty^3)+2a^2(y-y_\infty) + a^3 \ln \frac{(y-a)(y_\infty+a)}{(y+a)(y_\infty-a)} = Ae^{-(1/2)k_d t} \quad (11)$$

or taking the logarithm,

$$\ln Z = \ln A - \frac{1}{2}k_d t \quad (12)$$

Therefore, if the values of $K$ and $k_d$ are accurately known, it is possible to draw an $x \sim t$ curve over the whole course of polymerization and compare it with the experimental curve. And if a deviation between them is seen, it might be explained as indicative of a change in circumstance such as gel formation. In a case where no such deviation occurs, one can obtain $K$ and $k_d$ directly by applying Eq. 12. In Eq. 12, if $\ln Z$ is plotted against time $t$, a straight line should be obtained and the slope and the intercept will give $(1/2)k_d$ and $\ln A$, respectively.

The number average degrees of polymerization of a polymer instantaneously formed and cumulatively formed are related to each other by Eq. 13.

$$\bar{\bar{P}}_n = \frac{\bar{P}_n}{1-\frac{x}{\bar{P}_n}\cdot\frac{d\bar{P}_n}{dx}} \quad (13)$$

Applying Eq. 13, one can calculate $\bar{\bar{P}}_n$ from the $\bar{P}_n \sim x$ curve which can be obtained experimentally. Eq. 13 was derived by Schulz et al.[11] and Wall et al.[12], independently.

It is of great interest to note that according to Eq. 13, the value of the instantaneous degree of polymerization will become infinitely large when the value of $(x/\bar{P}_n)\cdot(d\bar{P}_n/dx)$ approaches unity. So, one can tentatively refer $\bar{\bar{P}}_n \to \infty$ as a measure of gel formation.

In a bulk polymerization of vinyl monomer, if chain transfers to monomer and initiator are both neglected, $\bar{P}_n$ may be expressed as

$$\bar{P}_n = \frac{[M]_0-[M]}{f\{[I]_0-[I]\}} \quad (14)$$

for combination termination.

In a case where volume shrinkage can be neglected,

$$\bar{P}_n = \frac{[M]_0}{f[I]_0}\cdot\frac{x}{1-\exp(-k_d t)} \quad (15)$$

Taking the volume shrinkage into account, it follows that

$$\bar{P}_n = \frac{[M]_0}{f[I]_0}\cdot\frac{x}{1-\alpha x-\exp(-k_d t)} \quad (16)$$

It was pointed out by Robertson[13] that the catalyst efficiency $f$ started to decrease rapidly as bulk polymerization proceeded in the case of styrene and methyl methacrylate. In this case, remembering that $\bar{P}_n$ is a cumulative value for the number average degree of polymerization, the catalyst efficiency $f$ in Eq. 14 must also be a cumulative one. Then, rearranging Eq. 14 and inserting $\bar{f}$ instead of $f$,

$$\bar{f} = \frac{[M]_0-[M]}{\bar{P}_n([I]_0-[I])} \quad (17)$$

The true value of $f$ at conversion $x$ may be expressed by

$$f = \bar{f} + x\frac{d\bar{f}}{dx} \quad (18)$$

It is well known that an abnormal explosive reaction is followed by an increase in the degree of polymerization. Hence, the comparison of the experimental molecular weight distribution with the theoretical one will offer interesting information.

According to rigorous kinetics, the molecular distribution for combination termination is given by[14]

$$r[M_r] = \frac{1}{2}R_i\delta^2\left[\left(\frac{r}{[M]_0}+\frac{1}{R_i^{1/2}\delta}\right)\exp\left\{-\frac{R_i^{1/2}\delta}{[M]_0}(r-1)\right\} - \left(\frac{r}{[M]}+\frac{1}{R_i^{1/2}\delta}\right)\exp\left\{-\frac{R_i^{1/2}\delta}{[M]}(r-1)\right\}\right] \quad (19)$$

where $M_r$ is the number of moles of a polymer having $r$ monomer nuits, $\delta$ a quantity approximated to $k_t^{1/2}/k_p$ and $R_i$ the rate of initiation.

## Results and Discussion

The bulk polymerizations of styrene catalyzed by 2, 2′-azobisisobutyronitrile were carried out at 60°C, and the fractional conversion $x$ was

11) G. V. Schulz and G. Harborth, *Makromol. Chem.*, **1**, 106 (1947).
12) F. T. Wall and L. F. Beste, *J. Am. Chem., Soc.*, 69, 1761 (1947).
13) E. R. Robertson, *Tsans. Faraday Soc.*, **52**, 426 (1956).
14) E. F. Herrington and A. Robertson, ibid., **40**, 236 (1944); G. M. Burnett, "Mechanism of Polymer Reactions", Interscience Publishers, New York (1954), p. 106.

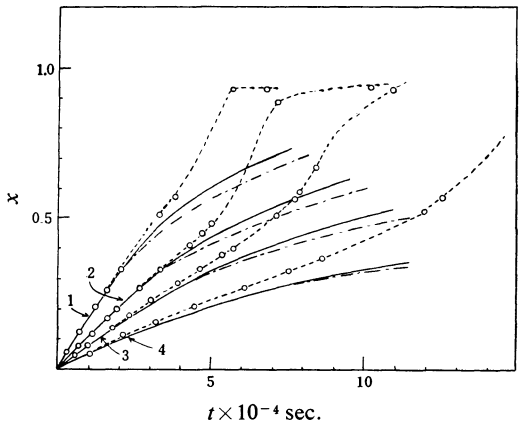



Fig. 1. Fractional conversion $x$ vs. $t$ for the bulk polymerization of styrene at 60°C, using 2,2'-azobisisobutyronitrile as initiator.
--○-- experimental ——— calcd. by Eq. 9
——— by Eq. 3 $[I]_0\times10^2$ mol./l.: 1, 5.00; 2, 2.00; 3, 1.00; 4, 0.36

plotted against time $t$ over the whole course of polymerization as shown in Fig. 1.

The initial rates of the reaction $R_0$ obtained from the figure were plotted against the square root of the initial concentrations of the catalyst, giving a straight line as expected from Eq. 1. This is shown in Fig. 2. From the slope, the value of $K$ was found to be $0.86\times10^{-4}$ $mol^{-(1/2)}\,l^{1/2}\,sec^{-1}$, which is in good agreement with the value obtained by Tobolsky et al.[8] The spontaneous decomposition of 2,2'-azobisisobutyronitrile has been widely studied and various values for the rate constant $k_d$ have been reported. Using the $^{14}C$ labelled initiator, Bevington[15] proposed the value of $1.20\times10^{-5}\,sec^{-1}$ as the best. Using this value together with the above-mentioned value of $K$, one can calculate the whole course of the

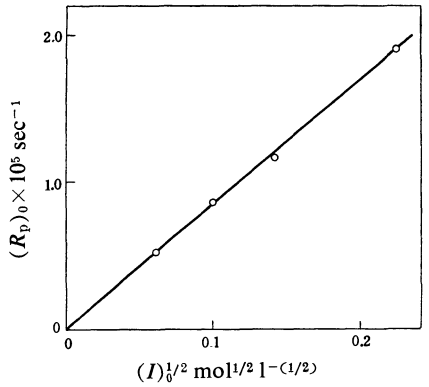



Fig. 2. Initial rate of conversion $(dx/dt)_0$ vs. $[I]_0^{1/2}$.

15) J. C. Bevington, *Trans. Faraday Soc.*, **51**, 1392 (1955).

Table I. Experimental values of $x$, $\bar{P}_n$ and $\bar{f}$

| $[I]_0$ mol./l. | $t\times10^{-4}$ sec. | $x$ | $\bar{P}_n$ | $\bar{f}$ (Eq. 15) | $\bar{f}$ (Eq. 16) |
|---|---|---|---|---|---|
| 0.05 | 0.72 | 0.130 | 375 | 0.70 | 0.79 |
| | 1.80 | 0.297 | 353 | 0.72 | 0.82 |
| | 3.96 | 0.595 | 579 | 0.45 | 0.52 |
| | 5.76 | 0.937 | 1920 | 0.16 | 0.20 |
| | 6.84 | 0.934 | 1879 | 0.15 | 0.17 |
| 0.02 | 1.26 | 0.141 | 608 | 0.69 | 0.69 |
| | 2.70 | 0.274 | 608 | 0.68 | 0.68 |
| | 4.32 | 0.420 | 739 | 0.59 | 0.59 |
| | 7.20 | 0.891 | 2835 | 0.23 | 0.26 |
| | 10.26 | 0.941 | 3123 | 0.18 | 0.19 |
| 0.01 | 1.80 | 0.150 | 890 | 0.72 | 0.69 |
| | 3.24 | 0.249 | 948 | 0.68 | 0.65 |
| | 5.76 | 0.405 | 1010 | 0.67 | 0.65 |
| | 8.46 | 0.674 | 2023 | 0.44 | 0.44 |
| | 10.98 | 0.931 | 4671 | 0.23 | 0.24 |
| 0.0036 | 2.16 | 0.120 | 1684 | 0.72 | 0.66 |
| | 6.12 | 0.277 | 1921 | 0.64 | 0.58 |
| | 8.82 | 0.380 | 2246 | 0.60 | 0.55 |
| | 12.54 | 0.577 | 3598 | 0.48 | 0.45 |
| | 17.28 | 0.903 | 6853 | 0.35 | 0.35 |

Table II. Calculated values of $x$ and $\bar{P}_n$ applying Eqs. 3 and 15*

| $t\times10^{-4}$ sec. | $[I]_0$ mol./l. | $x$ | $\bar{P}_n$ |
|---|---|---|---|
| 0 | 0.05 | 0.000 | 382 |
| 1 | | 0.170 | 359 |
| 2 | | 0.304 | 340 |
| 3 | | 0.411 | 324 |
| 4 | | 0.495 | 310 |
| 5 | | 0.564 | 298 |
| 7 | | 0.667 | 280 |
| 10 | | 0.765 | 261 |
| ∞ | | 0.960 | 229 |
| 0 | 0.02 | 0.000 | 605 |
| 1 | | 0.111 | 585 |
| 2 | | 0.203 | 568 |
| 3 | | 0.285 | 562 |
| 4 | | 0.351 | 549 |
| 5 | | 0.409 | 540 |
| 7 | | 0.501 | 525 |
| 10 | | 0.600 | 511 |
| ∞ | | 0.869 | 517 |
| 0 | 0.01 | 0.000 | 852 |
| 1 | | 0.080 | 843 |
| 2 | | 0.149 | 833 |
| 3 | | 0.210 | 828 |
| 4 | | 0.263 | 822 |
| 5 | | 0.309 | 816 |
| 7 | | 0.388 | 814 |
| 10 | | 0.475 | 810 |
| ∞ | | 0.761 | 906 |
| 0 | 0.0036 | 0.000 | 1423 |
| 1 | | 0.049 | 1435 |
| 2 | | 0.093 | 1445 |
| 3 | | 0.132 | 1447 |
| 4 | | 0.167 | 1451 |
| 5 | | 0.200 | 1468 |
| 7 | | 0.255 | 1486 |
| 10 | | 0.321 | 1520 |
| ∞ | | 0.577 | 1910 |

* $K=0.86\times10^{-4}\,mol^{-(1/2)}\,l^{1/2}\,sec^{-1}$, $k_d=1.20\times10^{-5}\,sec^{-1}$ and $\bar{f}=0.70$ was used.

polymerization by Eq. 3 or, exactly, by Eq. 9. Some experimental and calculated values of $x$ at various times are listed in Table I and Table II, and predicted $x\sim t$ curves are also shown in Fig. 1, $\alpha=0.177$ being used in Eq. 9.

As seen in the figure, these two calculated curves coincide with each other almost perfectly below 20% conversion, and above it, they separate gradually. At high convertion, the difference becomes fairly appreciable. Such a fact must be taken into account when polymerization, are followed by large valume shrinkage as seen in the bulk polymerization of vinyl acetate. Comparing the predicted and experimental values of $x$ in each catalyst concentration, it seems that, at very low conversion, these values agree fairly well. In the second step, however, there appears a clear deviation between them which seems to appear at lower conversion in lower initial catalyst concentration. The accelerated polymerizations proceed almost linearly with respect to time. Then, there is a third step where the rate of the polymerization becomes explosive, and at the beginning of the step, production of gas bubbles was always seen. It made the dilatometric analysis impossible. Above 90% conversion, the viscous solution changed into hard plastic and the reaction ceased few percent less than perfect conversion. Since this anomalous rate acceleration cannot be considered as associated with change in $k_d$, it must be owing to change in $K$. The values of $K$ at any fractional conversions can be calculated by Eq. 8, in which the slope $dx/dt$ at $x$ may be obtained from Fig. 1, the value of $k_d$ being taken again as $1.20\times10^{-5}\,\mathrm{sec}^{-1}$ and as constant at any conversions. It must be noted that in deriving the values of $K$ from Eq. 8, it was tacitly assumed that the steady state for radicals holds even at the explosive step.

Remembering that $K=k_pk_d^{1/2}f^{1/2}/kt^{1/2}$, the values of $f^{1/2}k_p/kt^{1/2}$ were plotted against $x$ as shown in Fig. 3. The form of the curves in the figure is quite similar to one which was reported by other investigators[5,13].

From Fig. 3, it is obvious that the values of $f^{1/2}k_p/k_t^{1/2}$ are almost constant up to 20~30% conversion in every initial catalyst concentration. They increase gradually and then rapidly as $x$ increases. It is clear that the increase in $f^{1/2}k_p/k_t^{1/2}$ occurs at lower fractional conversion the lower the initial catalyst concentration is. The reasonable explanation is as follows: As has been pointed out by some investigators, the termination constant $k_t$ including two large growing polymer chains is first diffusion-controlled. The lower the catalyst concentration, the greater becomes the degree of polmerization and hence the viscosity of solution. If $k_t$ is affected first, the increase in viscosity will result in the decrease in $k_t$.

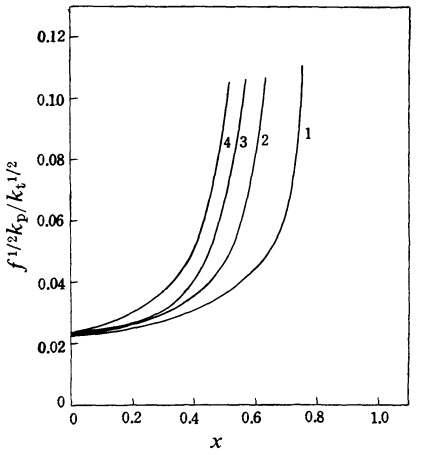



Fig. 3. $f^{1/2}k_p/k_t^{1/2}$ determined from the rate of polymerization data (Eq. 8) vs. $x$.
$[I]_0\times10^2$ mol./l.: 1, 5.00; 2, 2.00; 3, 1.00; 4, 0.36

The increase in $f^{1/2}k_p/k_t^{1/2}$ may also be reflected on the fact that the experimental conversions were higher than the predicted ones in each experiment with one exception. According to Eq. 5, as $A$ and hence $f^{1/2}k_p/k_t^{1/2}$ increase, the value of $x$ approaches unity.

The explosive polymerization is usually followed by an increase in the degree of polymerization. In the polymerization of styrene, the chain transfer to monomer is small and so, its contribution to the degree of polymerization may be neglected if catalyst concentration is properly chosen.

Since chain termination by combination is exclusive in the polymerization of styrene, the cumulative number average degree of polymerization $\bar{P}_n$ may be expressed approximately by Eq. 14. In Figs. 4 and 5, $\bar{P}_n$ is plotted against $x$.

Applying Eq. 14 ($f=0.7$ was used), the theoretical plots of $\bar{P}_n$ vs. $x$ are expressed by curves I and I′ in each figure, the volume shrinkage being neglected for simplicity. As seen in the figure, the predicted value of $\bar{P}_n$ is not so much affected by the fractional conversion unless the catalyst concentration is extremely small or very large. The experimental plots of $\bar{P}_n$ vs. $x$ which are denoted by curves II and II′, show that the values of $\bar{P}_n$ in each run agree fairly well with the predicted value up to 20~30% conversion. With $[I]_0=0.0036$ mol./l., the deviation is the greatest. However the value of $\bar{P}_n$ increases gradually thereafter, then more rapidly toward the last.

According to Eq. 14, $\bar{P}_n$ is a function of

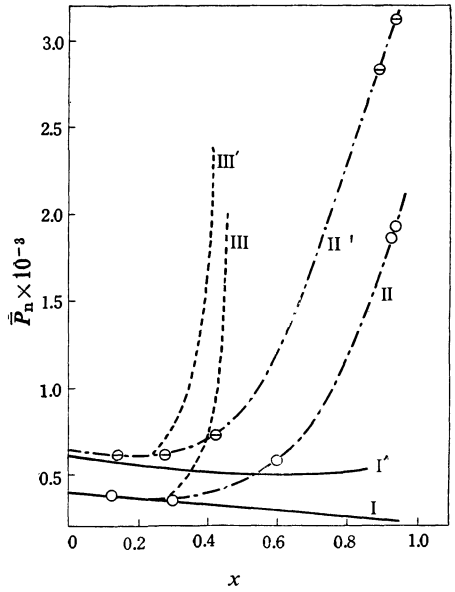



Fig. 4. Cumulative and instantaneous average degree of polymerization $\bar{P}_n$ and $\bar{\bar{P}}_n$ vs. $x$.
—— theoretical (Eq. 15) —·— experimental plots of $\bar{P}_n$; ---- experimental $\bar{\bar{P}}_n$ (Eq. 13)
I, II and III for $[I]_0=0.05$, I', II' and III' for $[I]_0=0.02$ mol./l., respectively

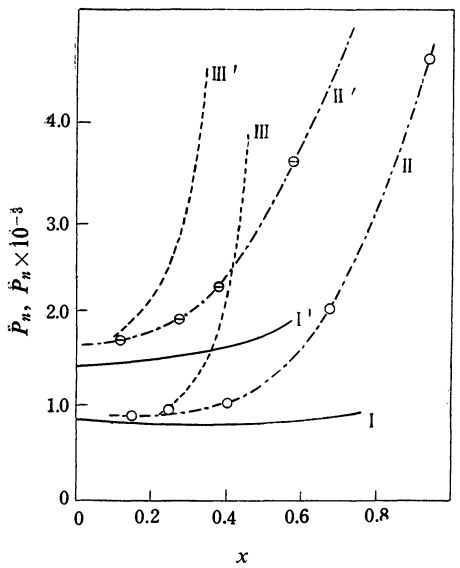



Fig. 5. Cumulative and instantaneous average degree of polymerization $\bar{P}_n$ and $\bar{\bar{P}}_n$ vs. $x$.
—— theoretical (Eq. 15) —·— experimental plots of $\bar{P}_n$; ---- experimental $\bar{\bar{P}}_n$ (Eq. 13)
I, II and III for $[I]_0=0.01$, I', II' and III' for $[I]_0=0.0036$ mol./l., respectively

monomer and catalyst concentrations and catalyst efficiency. Accordingly, the (cumulative) catalyst efficiency $\bar{f}$ can be obtained on inserting the experimental values of $\bar{P}_n$, $[M]$ and calculated values of $[I]$ into Eq. 17. In Table I are listed some values of $\bar{f}$ which were calculated by Eqs. 15 and 16, the volume shrinkage being taken into account in the latter equation. As may be seen in Fig. 6, the values of $\bar{f}$ are plotted against $x$. The average value of $\bar{f}$ at low conversion is about 0.7, which is very close to the value obtained by Tobolsky et al.[5] It is of interest to note that the catalyst efficiency $\bar{f}$ seems to depend only upon conversion and not upon the initial concentration of the catalyst. The instantaneous catalyst efficiency $f$ which was calculated by Eq. 23 may also be seen in Fig. 6.

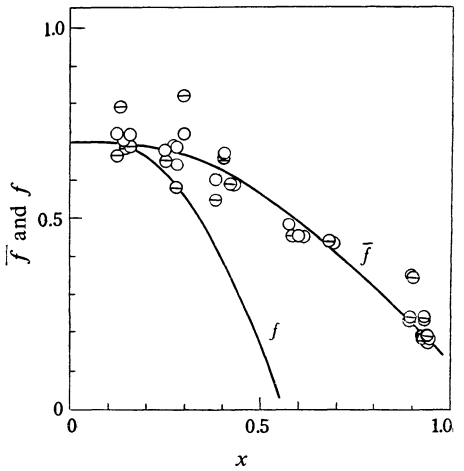



Fig. 6. Apparent dependence of cumulative and instantaneous catalyst efficiency $\bar{f}$ and $f$ upon $x$.
○ calcd. by Eq. 15; ⊖ calcd. by Eq. 16

The shape of the curves is similar to but somewhat different from that obtained by Robertson[13]. This true value of catalyst efficiciency at any $x$ decreases rapidly with increasing conversion. There is a doubt as to whether or not the catalyst efficiency is much affected by change in environment such as an increase in viscosity. Since the dimensions of the catalyst and the monomer are very small compared with the dimension of the polymer, it is unlikely that those molecules suffer an effect of diffusion in such a low conversion step. Hence it is very doubtful whether the catalyst efficiency is diffusion controlled. In deriving Eq. 16, it was tacitly assumed that the chain transfer to polymer does not take place and hence each polymer produced is a long chain molecule which has two catalyst fragments at its ends. If this is not so and the chain transfer to already dead polymers might occur

considerably Eq. 16 would no more be applied. If the chain transfers to polymers occur in such a manner as to cross-link together the polymers previously formed, a rapid increase in the average degree of polymerization will result. The apparent decrease in $f$ might be owing to this fact.

The instantaneous degree of polymerization $\overline{\overline{P}}_n$ at any conversion may be calculated by Eq. 15. In Figs. 4 and 5, $\overline{\overline{P}}_n$ is plotted against $x$ as shown in curves III and III'. As seen in these figures, each value of $\overline{\overline{P}}_n$ increases steeply toward infinity as $x$ increases. Above 40~50% conversion, the value of $\overline{\overline{P}}_n$ takes a negative value in each experiment.

This interesting phenomenon was first observed by Wall et al.[12] According to them, the formation of cross-linking of polymer molecules not only increases the average molecular weight, but simultaneously, diminishes the number of polymer molecules, thus accounting for the observed results. It is clear from the definition $\overline{\overline{P}}_n = -dM/dP$ that $\overline{\overline{P}}_n$ takes a negative sign when $dP$ is negative.

On account of the fact that any polymers produced by chain reactions must have a certain dispersion of molecular sizes, the study of size distribution in polymers is of great importance in connection with the kinetic mechanisms of polymerizations. Among several experimental techniques for the fractionation of polymers, those based on solubility are most generally used. However, the fractions obtained in any experimental techniques are always heterogeneous with respect to molecular weight and, so far, the problem of the overlapping of the polymer species has never been overcome.

The fractionations of two samples were carried out in order to obtain the distribution of molecular sizes at high conversion, and the results are listed in Table III. As an approximation, the degrees of polymerization in each fraction were calculated from the data of viscosity measurements, using the relation $\bar{P}_n = 1770 [\eta]^{1.40}$ which was applied for the unfractionated polymers.

TABLE III. FRACTIONATION RESULTS OF POLYMERS

| Fraction No. | Weight, g. | % | $\overline{DP}$ |
|---|---|---|---|
| Unfractionated | 6.000 | | 6853 |
| 1 | 1.347 | 22.7 | 26980 |
| 2 | 0.575 | 9.7 | 11480 |
| 3 | 1.174 | 19.7 | 9820 |
| 4 | 0.369 | 6.2 | 5681 |
| 5 | 0.745 | 12.5 | 4142 |
| 6 | 1.277 | 21.5 | 2258 |
| 7 | 0.455 | 7.7 | 818 |
| Unfractionated | 5.523 | | 3123 |
| 1 | 0.465 | 8.4 | 14090 |
| 2 | 0.788 | 14·3 | 8048 |
| 3 | 0.392 | 7.1 | 4508 |
| 4 | 1.279 | 23.2 | 2501 |
| 5 | 1.112 | 20.1 | 1183 |
| 6 | 1.140 | 20.7 | 652 |
| 7 | 0.344 | 6.2 | 242 |

The integral weight distribution curves were obtained by plotting the weight of each fraction as a function of the degree of polymerization, adding the weight of each fraction to the weight of the preceding fraction. The smooth lines drawn in Fig. 7 are the integral and differential weight distribution curves. The latter lines were obtained by taking the slope of the integral weight distribution curves as a function of the degree of polymerization.

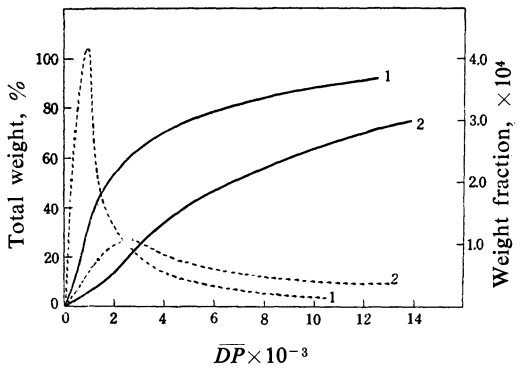



Fig. 7. Molecular weight distribution.
—— integral, ----- differental weight distributions
1: $[I]_0 = 0.02$ mol./l., $x = 0.941$, $\bar{P}_n = 3123$
2: $[I]_0 = 0.0036$ mol./l., $x = 0.903$, $\bar{P}_n = 6853$

It was pointed out by Guzmán[16] that this classical method of approaching the problem about molecular weight distribution is rather imperfect because there is an inevitable source of error such as the overlapping of polymer species. He compared the results obtained by the classical procedure with those obtained statistically, based on the same experimental data, and showed that there was a considerable difference between them. In spite of being more logical and reasonable, the statistical approach involves a great labor of mathematical computation and is not easy to handle.

Instead, the size distribution curves of the polymer at conversion $x = 4\%$ were drawn as shown in Fig. 8 in accordance with Eq. 21 which was derived from the kinetic mechanism of the initial polmerization step alone.

16) G. M. Guzmán, *J. Polymer Sci.*, **19**, 519 (1956),

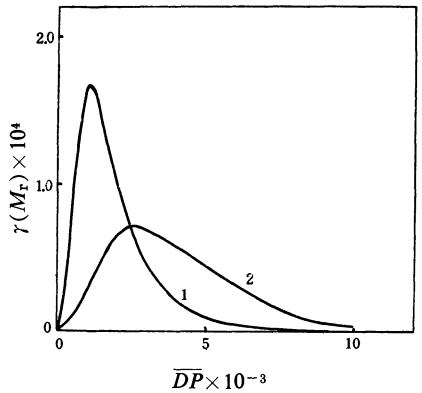



Fig. 8. Theoretical differential weight distributions (Eq. 19) at $x=0.04$.
1: $[I]_0=0.02$; 2: $[I]_0=0.0036$ mol./l.

It is clear from Figs. 7 and 8 that there is a considerable difference between experimental and calculated differential weight distributions. The shape of the corresponding curves up to the maximum weight fraction is very similar. However, beyond this, the experimental curves fall much less rapidly and unsymmetrically than do the calculated ones.

It may reasonably be assumed that the experimental molecular weight distribution consists of two parts, normal and abnormal distributions of molecular species. The part of the normal distribution may correspond to that which can be obtained from the initial stage of polymerization, while the part of the abnormal distribution may arise from the explosive polymerization. The kinetic treatment of such abnormal weight distribution may be complex. Nevertheless, it is of great interest that the result of explosive polymerization is reflected on such weight distribution.

From the study of the molecular weight distribution, it seems that the abnormal increase of the degree of polymerization at high conversion is not owing to the chain transfer to the already dead polymers, but is, probably, owing to the burying of the growing polymer radicals, because the produced polymer at high conversion involves a considerable part of low molecular weight.

## Summary

The bulk polymerization of styrene initiated by 2, 2′-azobisisobutyronitrile was carried out up to high conversion at 60°C. The comparison of the experimental conversion~time data with calculated ones showed that there was a considerable deviation between them. The rate of the polymerization became explosively great toward the last.

Assuming the combination termination, the cumulative degree of polymerization was calculated and the values were compared with those obtained experimentally. The deviation at high conversion might be owing to the decrease in the catalyst efficiency as suggested by Robertson. However, the assumption that the polymer molecules have been produced only by combination is very doubtful.

The study of the molecular weight distribution suggested that the abnormal increase in the rate and the degree of polymerization seemed to be owing to the burying of the growing polymer radicals in themselves in the highly viscous solution.

The author wishes to express his thanks to Professor Shigeo Hasegawa and Professor Nishio Hirai for helpful suggestions and encouragement.

*Department of Chemistry*
*Faculty of Science*
*Okayama University*
*Tsushima, Okayama*

# *On the pd Hybridization of the Sulfur Atom in Thiothiophten. II. The Contraction of the d Orbital*

By Kôgorô MAEDA

(Received December 27, 1960)

In the previous paper of this series[1], the pd hybridization was proposed on the central sulfur atom in thiothiophten to compose the full $\sigma$ skeleton of condensed ring system of the molecule. It was shown that the above configuration of electrons on the central sulfur atom is favored in accounting for both the so-called abnormal length of the bond between two sulfur atoms and the right angle of S-S-C, and that the electronic structure of thiothiophten can be treated according to the usual LCAO $\pi$ approximation without considering the $\sigma$ skeleton, unlike the procedure proposed by Giacometti and Rigatti[2]. Further, the possibility of participation of the d orbital in the hybridization was examined from the standpoint of overlap criterion, giving the values of the overlap integrals. As the result of the inspection, however, it turned out that one might not except any participation of the d orbitals in bonding to occur through the hybridization. It was pointed out there that this may be due to the straightforward application of Slater's rule[3] to the estimation of the effective nuclear charges for the d orbitals. As already mentioned, since the maximum of the radial function of the d orbital with its effective nuclear charge required by Slater's rule lies at 9 atomic units, the orbital may be regarded as including the full $\sigma$ skeleton of thiothiophten, so that it would be impossible to avoid the influence of the neighboring atoms in the molecule. The charges of the atoms may contract the d orbital and enlarge its nuclear charge, leading to a value of overlap integral comparable to that of 3p orbital. Contraction of this kind was once examined in the case of the d orbital in thiophene[4], where it might be expected that as the result of the contraction by the perturbation of neighboring carbon atoms, the participation of the d orbitals in bonding would take place to a greater extent than predicted by the direct application of free atom parameter by Slater's rule.

In the present paper, following the treatment about the d orbital of the sulfur atom in thiophene, the influence of neighboring atoms upon the d orbital will be examined on the central sulfur atom in thiothiophten and the possibility of the participation in the hybridization will be inquired into from the standpoint of overlap criterion, comparing the values of overlap integral.

**Orbital Contraction.**—A model is employed here, in which a single d electron on the central sulfur atom is supposed to move in the field of the nucleus of charge $Z_S$, and upon this hydrogen-like atom system a perturbation is superposed consisting of three positive charges of the neighboring atoms of thiothiophten. The positive charges come because the field of an atom capable of forming a covalent bond is substantially electron-attracting. The perturbing charges are composed of those of the two sulfur atoms of magnitude $Z_A(=Z_B)$ at the distance of S-S bond, 4.461 atomic units ($\sigma_A(=\sigma_B)$) and of the carbon atom of $Z_C$ at the distance of central C-S, 3.440 atomic units ($\sigma_C$). These charges will be treated, not as three hydrogen-like atoms, but just as point charges of respective magnitudes. The actual potential of the perturbation is very intricate because it involves many factors, the attraction of the surrounding nuclei, the coulomb repulsions of their electrons, exchange terms, and others; hence the dependence on distance of the potential will not follow the $r^{-1}$ law at all closely. The system being thus too complicated to be considered, the point charge model is employed as approximation in this paper. The magnitudes of the perturbing charges will be treated rather as parameters, values plausible in a wider range being involved.

Under this point charge approximation, the potential by the outlying charges may be expanded as a sum in the usual $1/r$ series[5] as follows:

For the two charges of sulfur atoms,

1) (a) K. Maeda, This Bulletin, 33, 1466 (1960); (b) K. Maeda, ibid., 34, 785 (1961).
2) G. Giacometti and G. Rigatti, *J. Chem. Phys.*, **30**, 1633 (1959).
3) J. C. Slater, *Phys. Rev.*, 36, 57 (1930).
4) K. Maeda, This Bulletin, 33, 303 (1960); The idea of orbital contraction was first given by D. P. Craig and E. A. Magnusson, *J. Chem., Soc.*, **1956**, 4895.
5) H. Eyring, J. Walter and G. E. Kimball, "Quantum Chemistry", John Wiley & Sons Inc., New York (1944), p. 369.

$$V_{A,B}(r>\sigma_A) = -(2Z_A/r)\{1+(1/2)(3\sin^2\vartheta \times\cos^2\varphi-1)(\sigma_A/r)^2+\cdots\cdots\}$$
$$V_{A,B}(r<\sigma_A) = -(2Z_A/\sigma_A)\{1+(1/2)(3\sin^2\vartheta \times\cos^2\varphi-1)(r/\sigma_A)^2+\cdots\cdots\}$$

and for the carbon atom,

$$V_C(r>\sigma_C) = -(Z_C/r)\{1+\sin\vartheta\sin\varphi\,(\sigma_C/r) +(1/2)(3\sin^2\vartheta\sin^2\varphi-1) \times(\sigma_C/r)^2+\cdots\cdots\}$$
$$V_C(r<\sigma_C) = -(Z_C/\sigma_C)\{1+\sin\vartheta\sin\varphi\,(r/\sigma_C) +(1/2)(3\sin^2\vartheta\sin^2\varphi-1) \times(r/\sigma_C)^2+\cdots\cdots\}$$

The perturbation energy due to the outlying potential is given by $\int\psi v\psi d\tau$, where $\psi$ is the d electron wave function of the usual Slater type. As the wave function, two for the d orbital are taken, $3d_z$ and $3d_{xy}$ (notation of Pauling and Wilson[6]), which were discussed in the previous paper[2]. In integrating the two orbitals, one must pay some attention to the orientation of the $3d_z$ orbital, because in the present consideration the Z-axis is taken to be normal to the molecular plane, and the Y-axis goes along the central C-S bond. The oribital should be rotated by 90° about the Y-axis. After the rotation, the angular part of the orbital, $(3\cos^2\vartheta-1)$, turns into $(3\sin^2\vartheta\times\cos^2\varphi-1)$. Hereafter, the orbital is described as $3d_{x(z)}$ in this paper.

The total perturbation energy is given as the sum of the energies by the above three positive charges, and the terms higher than the 2nd of the potential may be neglected because of their small contributions to the energy. Hence, after the integration, the respective energies of the two orbitals are given as follows:

For $3d_{x(z)}$

$$E = -(2Z_A/\sigma_A)\{\sigma_A R^0_{33}(\alpha\sigma_A) +(2/7)\sigma_A R^2_{33}(\alpha\sigma_A)\} -(Z_C/\sigma_C)\{\sigma_C R^0_{33}(\alpha\sigma_C) -(1/7)\sigma_C R^2_{33}(\alpha\sigma_C)\}$$

and for $3d_{xy}$

$$E = -(2Z_A/\sigma_A)\{\sigma_A R^0_{33}(\alpha\sigma_A) +(1/7)\sigma_A R^2_{33}(\alpha\sigma_A)\} -(Z_C/\sigma_C)\{\sigma_C R^0_{33}(\alpha\sigma_C) +(1/7)\sigma_C R^2_{33}(\alpha\sigma_C)\}$$

where $R^p_{nn}(\alpha\sigma)$ is the auxiliary function which was used in the case of thiophene[4], and its explicit form is

$$R^p_{nn}(\alpha\sigma) = (1/\sigma)(2\alpha\sigma/n)^{2n+1}\{1/(2n)!\} \times\{(2n+p)!\times(n/2\alpha\sigma)^{2n+p+1} -A_{2n+p}(2\alpha\sigma/n)+A_{2n-p-1}(2\alpha\sigma/n)\}$$

where

$$A_n(\omega) = \int_1^\infty r^n\exp(-\omega r)dr$$

In the above expressions, $\alpha$ is a parameter to be determined to minimize the total energy which is the sum of the perturbation energy and the unperturbed given by

$$W = (\alpha/3^2)(\alpha/2-Z_s)$$

for the hydrogen-like orbital of free atom parameter $Z_s$; that is, the procedure to be performed now is to find the new value of effective nuclear charge for which the total energy is a minimum for given magnitudes of $\sigma_A$, $\sigma_C$, $Z_A$ and $Z_C$. The new value of the charge will offer an appropriate basis for the discussion about the d orbital under the perturbation.

In conducting the procedure, it is necessary to set the values of $Z_s$, $Z_A$ and $Z_C$. As the value of $Z_s$, 1 and 2 are chosen, and for $Z_c$ three values are taken, 1, 2 and 3, which were used in the case of thiophene[4]. With respect to the value of $Z_A(=Z_B)$, four values are assigned, 1, 3, 5 and 6. All the above values are to be treated as tentative parameters. In the real system, it is difficult to determine the straightforward values of the parameters equivalent to the outlying potential, because, as mentioned above, the real field is not truly coulombic but much more complicated. Furthermore, there is, in general, a considerable difference between so-called potential- and field-determined nuclear charge on the same atom[7]. Hence, in this paper, some attention will be paid rather to a variation in $\alpha$ by adopting the values of the above parameters in wider range. In finding the minimum of the total energy, it is necessary to know the values of $\sigma R^p_{nn}(\alpha\sigma)$, which are taken from the table in the previous paper[4].

In Table I are given the results. From this table it is found that the new values of the effective charges under perturbation are considerably greater compared with those of free atom parameters, without exception, and furthermore that there are only small variations between these values despite the adoption of a wider range of the parameters. In the case of thiophene, it was shown that the magnitude of the new value is more sensitive to the bond distance $\sigma$ than to the parameters for the outlying potential, and that it is little altered

6) L. Pauling and E. B. Wilson, "Introduction to Quantum Mechanics", McGraw-Hill, New York (1935), p. 138.

7) For example, see: F. W. Brown, *Phys. Rev.*, **44**, 214 (1933).

TABLE I. EFFECTIVE NUCLEAR CHARGE $\alpha$ OF 3d ORBITAL UNDER THE PERTURBATION

I. $3d_{xy}$

| $Z_s$ | $Z_c$ | $Z_A(=Z_B)$ 1 | 3 | 5 | 6 |
|---|---|---|---|---|---|
| 1 | 1 | 2.34 | 2.66 | 2.80 | 2.92 |
| 1 | 2 | 2.55 | 2.78 | 2.90 | 2.96 |
| 1 | 3 | 2.73 | 2.90 | 3.00 | 3.04 |
| 2 | 1 | 2.75 | 3.05 | 3.05 | 3.10 |
| 2 | 2 | 2.90 | 3.10 | 3.15 | 3.20 |
| 2 | 3 | 3.05 | 3.10 | 3.25 | 3.30 |

II. $3d_{x(z)}$

| | | | | | |
|---|---|---|---|---|---|
| 1 | 1 | 2.34 | 2.63 | 2.75 | 2.82 |
| 1 | 2 | 2.50 | 2.70 | 2.83 | 2.88 |
| 1 | 3 | 2.63 | 2.80 | 2.86 | 2.94 |
| 2 | 1 | 2.68 | 2.88 | 2.96 | 3.00 |
| 2 | 2 | 2.90 | 3.02 | 3.02 | 3.05 |
| 2 | 3 | 3.05 | 3.12 | 3.15 | 3.10 |

by the charges of neighboring atoms in the range 2~3 when $\sigma=3$ and 4. In the present consideration, with respect to the bond distance $\sigma$, the fixed values are assigned, $\sigma_A(=\sigma_B)$ and $\sigma_C$, which are taken from the actual distances in thiothiophten, obtained from the X-ray analysis study by Bezzi, Mammi and Garbuglio[8]. Considering the above situation in thiophene, therefore, the present results may be convincing in regard to making fast the values of $\sigma$. This fact is worthy of notice, because to obtain the same results through the different starting points of $Z_s$ might indicate the existence of a self-consistent value of $\alpha$ appropriate for the perturbation in which the geometrical configuration of the outlying potential to the atom in question is settled. In fact, the values given in the Table would serve as the first steps of the procedure to the self-consistent value. The value would probably remain settled near 3~4. Of course, it must be emphasized that this discussion on the effective value for $\alpha$ is by all means of tentative character under the present point charge approximation. Furthermore, the value of $\alpha$ appropriate to the real system should be determined precisely with respect to the whole energy of the molecule. The values in the Table, however, may be used as useful clues to the studies about the behavior of the d orbital on the central sulfur atom in thiothiophten.

From these discussions, it might be inferred in any case that the effective nuclear charge for the d orbital on the central sulfur atom in thiothiophten would not bear the free atom parameter, but it should bear a greater value considering the influence by the surrounding nuclei, probably near 3~4. As suggested earlier in this paper, the value for the d orbital will furnish an appropriate basis of the discussion about the orbital.

**Overlap Integral.** — In the previous section, the influence of the surrounding nuclei upon the d orbital was examined, and the results were given in Table I. Using these results, the overlap integral with the 3p $\sigma$ orbital of the neighboring sulfur atom were estimated for the corresponding values of $Z_s$, $Z_A$ and $Z_C$. These are given in Table II. In calculating these values, the tables of the integrals given in the previous paper[1b] were used, and as the effective nuclear charge for the 3p orbital, the direct value through Slater's rule was assigned, because it was shown that the value for 3p is little affected by the outlying perturbing charges when $\sigma=3$ and 4, and moreover, because, although it was accurate in the case of thiophene[4], in general, the contraction of the orbital is great only when the orbital with high screened and loosely bound electrons lies under the perturbation.

TABLE II. OVERLAP INTEGRALS OF 3d ORBITALS WITH 3p ORBITALS OF NEIGHBORING S ATOM

I. $3d_{xy}$

| $Z_s$ | $Z_c$ | $Z_A(=Z_B)$ 1 | 3 | 5 | 6 |
|---|---|---|---|---|---|
| 1 | 1 | 0.082 | 0.129 | 0.148 | 0.163 |
| 1 | 2 | 0.113 | 0.145 | 0.161 | 0.166 |
| 1 | 3 | 0.138 | 0.161 | 0.170 | 0.172 |
| 2 | 1 | 0.141 | 0.173 | 0.173 | 0.178 |
| 2 | 2 | 0.161 | 0.178 | 0.181 | 0.185 |
| 2 | 3 | 0.173 | 0.178 | 0.189 | 0.192 |

II. $3d_{x(z)}$

| | | | | | |
|---|---|---|---|---|---|
| 1 | 1 | 0.092 | 0.143 | 0.162 | 0.173 |
| 1 | 2 | 0.121 | 0.154 | 0.175 | 0.181 |
| 1 | 3 | 0.143 | 0.170 | 0.178 | 0.190 |
| 2 | 1 | 0.151 | 0.181 | 0.192 | 0.195 |
| 2 | 2 | 0.183 | 0.197 | 0.197 | 0.200 |
| 2 | 3 | 0.200 | 0.206 | 0.210 | 0.204 |

The values in Table II are all positive and of the order of 0.1~0.2. Craig et al.[9] once proposed that for significantly strong binding a value of the overlap integral of about 0.1 or greater is necessary. According to this proposition, one might expect some significant binding to take place between the 3d and the 3p orbitals. The participation of the d orbital to bonding is performed through the pd hybridization in the present problem, and whether the d orbital is to be used or not depends, amongst other factors, upon whether the overlap integral involving the d orbital is comparable

8) S. Bezzi, M. Mammi and G. Garbuglio, *Nature*, **182**, 247 (1958).

9) D. P. Craig and E. A. Magnusson, *J. Chem. Soc.*, **1956**, 4895.

TABLE III. OVERLAP INTEGRALS: $S(3p\sigma-3p\sigma)$

| $p/t$ | 0.0 | 0.1 | 0.2 | 0.3 | 0.4 | 0.5 |
|---|---|---|---|---|---|---|
| 0.0 | −1.000 | −0.966 | −0.867 | −0.719 | −0.543 | −0.365 |
| 0.5 | −0.965 | −0.933 | −0.840 | −0.698 | −0.531 | −0.359 |
| 1.0 | −0.866 | −0.839 | −0.761 | −0.640 | −0.494 | −0.342 |
| 1.5 | −0.715 | −0.696 | −0.639 | −0.549 | −0.436 | −0.312 |
| 2.0 | −0.531 | −0.520 | −0.488 | −0.435 | −0.361 | −0.272 |
| 2.5 | −0.333 | −0.331 | −0.324 | −0.307 | −0.275 | −0.224 |
| 3.0 | −0.140 | −0.146 | −0.161 | −0.178 | −0.183 | −0.170 |
| 3.5 | 0.031 | 0.019 | −0.013 | −0.056 | −0.094 | −0.114 |
| 4.0 | 0.171 | 0.155 | 0.111 | 0.050 | −0.013 | −0.060 |
| 4.5 | 0.273 | 0.256 | 0.208 | 0.136 | 0.055 | −0.011 |
| 5.0 | 0.342 | 0.324 | 0.275 | 0.200 | 0.114 | 0.033 |
| 5.5 | 0.377 | 0.361 | 0.314 | 0.243 | 0.155 | 0.068 |
| 6.0 | 0.385 | 0.371 | 0.331 | 0.266 | 0.184 | 0.096 |
| 6.5 | 0.373 | 0.362 | 0.328 | 0.273 | 0.199 | 0.116 |
| 7.0 | 0.346 | 0.338 | 0.312 | 0.268 | 0.205 | 0.129 |
| 7.5 | 0.311 | 0.306 | 0.287 | 0.253 | 0.202 | 0.136 |
| 8.0 | 0.273 | 0.269 | 0.257 | 0.233 | 0.194 | 0.138 |
| 8.5 | 0.233 | 0.231 | 0.225 | 0.210 | 0.181 | 0.136 |
| 9.0 | 0.195 | 0.195 | 0.193 | 0.185 | 0.166 | 0.130 |
| 9.5 | 0.161 | 0.162 | 0.163 | 0.160 | 0.149 | 0.123 |
| 10.0 | 0.130 | 0.132 | 0.135 | 0.137 | 0.132 | 0.114 |

to that of 3p in terms of overlap approximation employed here. Therefore, the integral between $3p\sigma$ orbitals of S-S bond in thiothiophten was estimated, for the sake of comparison, using free atom parameters, and it was obtained as 0.243. In estimating this value, Table III given in the present paper was used. The overlap integral $S(3p\sigma-3p\sigma)$ was once given by Mulliken et al. for $t=0$[10], and also by Craig et al., who evaluated the values with parameters $p$ and $t$ in the ranges of 2∼10 and 0∼0.5 at the respective intervals of 1.0 and 0.1[11]. In the present paper, the values with $p$ in the wider range of 0∼10 at the intervals of 0.5 were calculated, and in Table III are given the results obtained.

From the above estimation of the overlap integrals, it is found that almost comarable values are obtained for both the integrals involving the 3p and the 3d orbitals. These values would become more close when the so-called self-consistent value above mentioned may be used as the effective nuclear charge for the d orbital. Then, it may be said that the participation of the d orbital in the hybridization is more favorable than predicted through the direct employment of free atom parameters by Slater's rule, and that the extent to which the d orbital participates in bonding through the hybridization will be of the order nearly the same as, or at least not much less than, that of the 3p orbital. These results may be somewhat deficient in precision under the present point charge and overlap approximations employed in this paper. However, they may be sufficiently valid for discussing semi-quantitatively how the d orbital behaves under the perturbation in the actual molecule.

It is of interest to notice that the values of the overlap integral for the 3d orbital lie very nearly at the corresponding maxima for the respective effective nuclear charges of the orbital (see Tables I and III in Ref. 2). These values approach more nearly to the maxima when the self-consistent values under the present perturbation, 3∼4, may be used, or when a larger value of the distance between the orbitals is adopted. This is because the parameter $p$ in the calculation of overlap integral involves the distance between the orbitals. Hence the so-called abnormal length of S-S bond in thiothiophten may be rather consistent to give the greater possibility of participation of the d orbital in the hybridization.

**Hybrid Orbitals.** — From the above considerations, it is found that the d orbitals on the central sulfur atom in thiothiophten might be able to participate in the hybridization to the same as, or at least to an extent comparable to that of the 3p orbital. Then the hybrid orbitals may be written with the same mixing coefficient for the two d orbitals in question as follows:

For $3d_{xy}$,

$$(1/\sqrt{2})\,(\psi_{3d_{xy}}\pm\psi_{3p})$$

10) R. S. Mulliken, C. A. Rieke, D. Orloff and H. Orloff, *J. Chem. Phys.*, **17**, 1248 (1949).
11) D. P. Craig, A. Macoll, R. S. Nyholm, L. E. Orgel and L. E. Sutton, *J. Chem. Soc.*, **1954**, 332.

and for $3d_{x(z)}$,

$$(1/\sqrt{2})(\psi_{3d_{x(z)}} \pm \psi_{3p})$$

The mixing coefficient is fortunately compatible with the conditions required from the linear bond of S-S-S in thiothiophten and the symmetrical skeleton of the molecule[12]. The approximate forms of the hybrid orbitals were already shown in Fig. 2 of the previous paper[1b].

Of the two sets of hybrid orbitals, those involving the $3d_{x(z)}$ orbital may be more probable for participating in the hybridization to form the S-S-S bond in thiothiophten, because the values of the overlap integral are greater for the $3d_{x(z)}$ than for the $3d_{xy}$ with corresponding $p$ and $t$ values.

All the above discussions are those under the point charge approximation and within the framework of the overlap criterion. Therefore it is more or less inevitable that the results obtained in this paper should not be so readily sufficient for an accurate discussion of the formation of the possibe bond in thiothiophten. Furthermore, in fact, the accurate discussion dealing with the final determining factor in bonding, that is, on balancing of energy should be taken up for consideration with respect to the whole molecule of thiothiophten. Nevertheless, the results obtained above will be valuable enough for approximate and semi-quantitative discussion about the possibility of participation of the d orbital in the central sulfur atom in thiothiophten. Therefore it can now be said that the structure of thiothiophten is not one involving the no-bond resonance structure proposed by Bezzi et al.[8], but rather it may be the condensed ring system of the full $\sigma$ skeleton involving the hybrid orbitals on the central sulfur atom of the molecule.

12) C. A. Coulson, "Valence", Oxford University Press, London (1952), p. 195.

*Electrotechnical Laboratory*
*Tanashi, Tokyo*

# *Studies on Organophosphorus Compounds. II. On Phosphite Cuprous Halide Complex Compounds*[*1]

By Yoshihiko NISHIZAWA

(Received November 26, 1960)

Although many workers have studied complex compounds having phosphorus atom, many of them reported on phosphine[*2] complex compounds such as phosphine platinum halides[1], phosphine cuprous iodides[2] and phosphine chromium halides[3], while phosphite complex compounds were reported on only by Arbuzov[4] and others.

Arbuzov has reported that phosphites give phosphite cuprous halide complex compounds which have two experimental formulae, $(RO)_3PCuX$(I) and $[(RO)_3P]_2CuX$ (II), and that *O,O*-dialkyl phosphonates give no complex compounds. Therefore, this reaction has been utilized as an identification of phosphite from phosphonate.

The present author separated two compounds having formulas I and II and measured their molecular weights in various organic solvents. It was made clear as a result, that these complex compounds showed an interesting behavior in organic solvents and reacted with pyridine, aniline and their analogues and produced new complex compounds having phosphites and amines.

**Preparation of Phosphite Cuprous Halide Complex Compounds.**—Phosphite cuprous halides were prepared by the reaction of phosphite with cuprous halide in a benzene solution. After cuprous halides were dissolved in benzene, the benzene was evaporated under reduced pressure, the complex compounds were obtained as white crystals or colorless oil.

Changing the mole ratio of phosphites to cuprous halides obtained two complex compounds, namely, phosphite cuprous halides I and bis-phosphite cuprous halides II. Triphosphite cuprous halide could not be prepared from three moles of phosphite and one mole

*1 Presented at the annual meeting of Chemistry of Coordination Compounds of Japan, Fukuoka, Oct., 1959.

*2 The phosphorus compounds in this paper were named according to the Drake Committee's Report (*Chem. Eng. News*, **30**, 4515 (1952).).

1) J. Chatt, *J. Chem. Soc.*, **1951**, 625.
2) F. G. Man, ibid., **1936**, 1503.
3) K. Issleib, *Z. anorg. u. allgem. Chem.*, **298**, 84 (1959).
4) A. Arbuzov, *Ber.*, **38**, 1171 (1905).

TABLE I. YIELDS, MELTING POINTS AND MICROANALYTICAL DATA OF PHOSPHITE CUPROUS HALIDES $(RO)_3PCuX$ (I)

| No. | R | X | Yield % | M.p. °C | M.p. (°C) by A. Arbuzov[4] | Halogen, % Found | Halogen, % Calcd. | Phosphorus, % Found | Phosphorus, % Calcd. | Copper, % Found | Copper, % Calcd. |
|---|---|---|---|---|---|---|---|---|---|---|---|
| Ia | *iso*-$C_3H_7$ | Cl | 95.1 | 117 | 112 ~114 | 11.63 | 11.60 | 10.3 | 10.1 | 20.5 | 20.8 |
| Ib | $C_6H_5$ | Cl | 98.1 | 88~ 89 | 95 ~ 96 | 8.55 | 8.68 | 7.7 | 7.6 | 15.2 | 15.5 |
| Ic | *iso*-$C_3H_7$ | Br | 96.2 | 146~147 | 149 ~150 | 22.61 | 22.82 | 9.0 | 8.8 | 18.3 | 18.1 |
| Id | $C_6H_5$ | Br | 97.7 | 91~ 92 | 90.5~ 91.5 | 17.51 | 17.64 | 6.8 | 6.8 | 14.3 | 14.0 |
| Ie | $C_2H_5$ | I | 88.6 | 110~111 | 109 ~110 | — | — | 8.9 | 8.7 | 17.8 | 17.8 |
| If | *n*-$C_3H_7$ | I | 90.2 | 61~ 63 | — | — | — | 7.7 | 7.8 | 16.4 | 16.0 |
| Ig | *iso*-$C_3H_7$ | I | 93.5 | 199~200 | 184 ~185 | — | — | 7.7 | 7.8 | 16.2 | 16.0 |

TABLE II. YIELDS, MELTING POINTS AND MICROANALYTICAL DATA OF BIS-PHOSPHITE CUPROUS HALIDES $(RO)_3PCuXP(OR')_3$ (II)

| No. | R | R' | X | Yield % | M.p. °C | M.p., °C by A. Arbuzov[4] | Halogen, % Found | Halogen, % Cald. | Phosphorus, % Found | Phosphorus, % Calcd. | Copper, % Found | Copper, % Calcd. |
|---|---|---|---|---|---|---|---|---|---|---|---|---|
| II a | *iso*-$C_3H_7$ | *iso*-$C_3H_7$ | Cl | 93.1 | 69~70 | — | 6.75 | 6.89 | 11.9 | 12.0 | 12.8 | 12.3 |
| II b | $C_6H_5$ | $C_6H_5$ | Cl | 95.9 | 98~99 | — | 4.71 | 4.94 | 8.4 | 8.6 | 9.1 | 8.8 |
| II c | *iso*-$C_3H_7$ | *iso*-$C_3H_7$ | Br | 91.9 | 58~59 | — | 14.22 | 14.30 | 10.9 | 11.1 | 10.6 | 11.3 |
| II d | $C_6H_5$ | $C_6H_5$ | Br | 93.2 | 67~68 | 73~77 | 10.34 | 10.48 | 8.0 | 8.1 | 8.6 | 8.3 |
| II e | *iso*-$C_3H_7$ | *iso*-$C_3H_7$ | I | 95.6 | 94~95 | — | — | — | 10.3 | 10.2 | 10.6 | 10.5 |
| II f | $C_6H_5$ | $C_6H_5$ | I | 94.8 | 70~72 | 73~75 | — | — | 7.8 | 7.6 | 8.1 | 7.8 |
| II g | $C_2H_5$ | $C_6H_5$ | Cl | 97.8 | 75~76 | — | 6.15 | 6.17 | 11.2 | 10.9 | 10.8 | 11.0 |

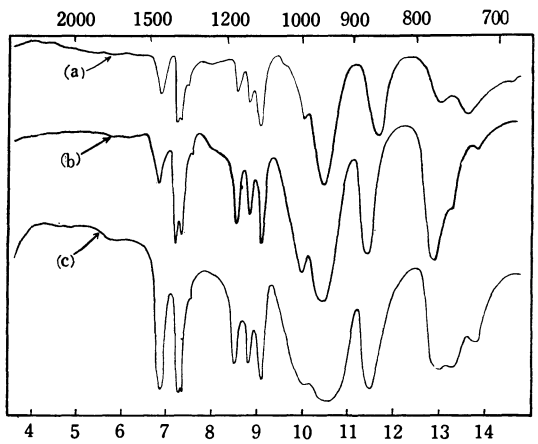



Fig. 1. Infrared absorption spectra (in Nujol) of (a) triisopropyl phosphite, (b) triisopropyl phosphite cuprous chloride (Ia) and (c) bis-(triisopropyl phosphite) cuprous chloride (IIa).

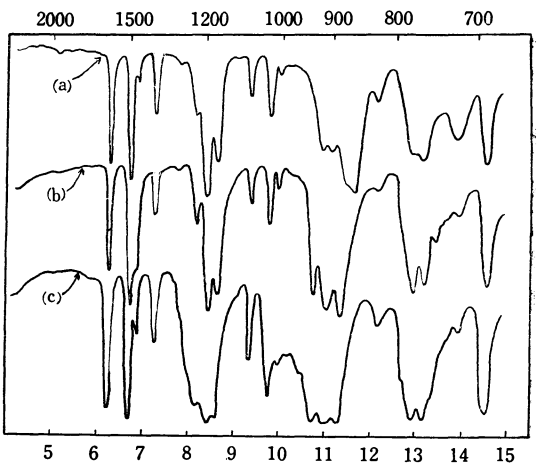



Fig. 2. Infrared absorption spectra (in Nujol) of (a) triphenyl phosphite, (b) triphenyl phosphite cuprous chloride (Ib) and (c) bis-(triphenyl phosphite) cuprous chloride (IIb).

of cuprous halides, but a product corresponding to one mole of bis-phosphite cuprous halides II and one mole of phosphite was obtained.

$$(RO)_3P + CuX \rightarrow \underset{(I)}{(RO)_3PCuX}$$

$$2(RO)_3P + CuX \rightarrow \underset{(II)}{[(RO)_3P]_2CuX}$$

Phosphite cuprous halides I gave bis-phosphite cuprous halides II by adding one mole ratio of phosphite and II gave also I by adding one mole ratio of cuprous halides.

Bis-phosphite cuprous halides II were converted to phosphite cuprous halides I by heating under reduced pressure.

$$\underset{(II)}{[(RO)_3P]_2CuX} \xrightarrow{heat} \underset{(I)}{(RO)_3PCuX} + (RO)_3P \uparrow$$

TABLE III. MOLECULAR WEIGHTS OF PHOSPHITE CUPROUS HALIDES $(RO)_3PCuX$ (I) IN VARIOUS SOLVENTS

| No. | R | X | Cryoscopic solvent (*K*) | Concn. g./G% | *ΔT* °C | Molecular Weight Experimental | Molecular Weight Calcd. (monomeric) | Degree of association |
|---|---|---|---|---|---|---|---|---|
| Ia | *iso*-$C_3H_7$ | Cl | Benzene (5120) | *0* | — | *1230* | 306 | 4.02 |
| | | | | 0.635 | 0.027 | 1204 | | |
| | | | | 1.172 | 0.050 | 1200 | | |
| | | | | 2.005 | 0.088 | 1167 | | |
| | | | Cyclohexane (20100) | *0* | — | *1265* | | 4.13 |
| | | | | 0.636 | 0.103 | 1241 | | |
| | | | | 1.201 | 0.200 | 1207 | | |
| | | | | 1.605 | 0.268 | 1204 | | |
| Ib | $C_6H_5$ | Cl | Benzene | *0* | — | *1555* | 409 | 3.80 |
| | | | | 0.639 | 0.021 | 1558 | | |
| | | | | 1.333 | 0.044 | 1551 | | |
| | | | | 1.901 | 0.062 | 1569 | | |
| | | | Bromoform (14050) | *0* | — | *1230* | | 3.01 |
| | | | | 0.532 | 0.061 | 1225 | | |
| | | | | 1.426 | 0.168 | 1193 | | |
| | | | | 2.106 | 0.249 | 1188 | | |
| | | | Cyclohexane | *0* | — | *1565* | | 3.83 |
| | | | | 0.775 | 0.099 | 1573 | | |
| | | | | 1.426 | 0.183 | 1566 | | |
| | | | | 2.221 | 0.283 | 1577 | | |
| Ic | *iso*-$C_3H_7$ | Br | Benzene | *0* | — | *1410* | 350.5 | 4.02 |
| | | | | 0.436 | 0.016 | 1395 | | |
| | | | | 1.326 | 0.049 | 1386 | | |
| | | | | 2.108 | 0.079 | 1366 | | |
| Id | $C_6H_5$ | Br | Benzene | *0* | — | *1730* | 453.5 | 3.81 |
| | | | | 0.476 | 0.014 | 1741 | | |
| | | | | 1.181 | 0.036 | 1680 | | |
| | | | | 2.700 | 0.081 | 1707 | | |
| | | | Bromoform | *0* | — | *780* | | 1.72 |
| | | | | 0.663 | 0.123 | 757 | | |
| | | | | 1.641 | 0.309 | 746 | | |
| | | | | 2.326 | 0.460 | 710 | | |
| Ie | $C_2H_5$ | I | Benzene | *0* | — | *1200* | 356.5 | 3.37 |
| | | | | 0.536 | 0.023 | 1193 | | |
| | | | | 1.487 | 0.070 | 1088 | | |
| | | | | 2.235 | 0.150 | 1090 | | |
| If | *n*-$C_3H_7$ | I | Benzene | *0* | — | *1135* | 397.5 | 2.86 |
| | | | | 0.500 | 0.023 | 1113 | | |
| | | | | 0.841 | 0.040 | 1076 | | |
| | | | | 2.011 | 0.100 | 1030 | | |
| Ig | *iso*-$C_3H_7$ | I | Benzene | *0* | — | *1160* | 397.5 | 2.92 |
| | | | | 0.638 | 0.028 | 1167 | | |
| | | | | 1.273 | 0.057 | 1143 | | |
| | | | | 2.081 | 0.092 | 1158 | | |

It is clear from the following experimental facts that these complex compounds I and II have the phosphite group in their molecules. These compounds reacted with acetyl chloride in benzene solution to give *O,O*-dialkyl-acetyl phosphonates (A) and cuprous halides. The melting point of *p*-nitrophenylhydrazone of the phosphonate A coincided with that of *p*-nitrophenylhydrazone of the product prepared from trialkyl phosphite and acetyl chloride by Arbuzov's reaction[5].

$$[(RO)_3P]_nCuX \xrightarrow{n\cdot CH_3COCl} n\cdot(RO)_2\overset{\overset{O}{\|}}{P}-COCH_3 + CuX + n\cdot RCl$$

(A) → *p*-Nitrophenylhydrazone

$$(RO)_3P + CH_3COCl \rightarrow (RO)_2\overset{\overset{O}{\|}}{P}-COCH_3 + RCl$$

(*n* is 1 or 2 and R is alkyl group).

The infrared absorption spectra*3 of these

5) M. I. Kabachnik, *Izvest. Akad. Nauk. SSSR.*, **1945**, 364.

*3 Perkin Elmer 21 Spectrophostometer was used.

TABLE IV. MOLECULAR WEIGHTS OF BIS-PHOSPHITE CUPROUS HALIDES $[(RO)_3P]_2CuX$ (II) IN VARIOUS SOLVENTS

| No. | R | X | Cryoscopic solvent (*K*) | Concn. (g./G%) | *ΔT* °C | Molecular Weight: Experimental | Molecular Weight: Calcd. (monomeric) | Degree of association |
|---|---|---|---|---|---|---|---|---|
| IIa | *iso*-$C_3H_7$ | Cl | Benzene (5120) | *0* | — | *498* | 515 | 0.97 |
| | | | | 0.431 | 0.045 | 490 | | |
| | | | | 1.231 | 0.130 | 485 | | |
| | | | | 2.260 | 0.250 | 463 | | |
| | | | Bromoform (14050) | *0* | — | *513* | | 1.00 |
| | | | | 0.251 | 0.070 | 504 | | |
| | | | | 1.449 | 0.400 | 509 | | |
| | | | | 2.396 | 0.685 | 491 | | |
| | | | Cyclohexane (20100) | *0* | — | *503* | | 0.98 |
| | | | | 0.509 | 0.205 | 499 | | |
| | | | | 1.581 | 0.640 | 497 | | |
| | | | | 2.561 | 1.050 | 490 | | |
| IIb | $C_6H_5$ | Cl | Benzene | *0* | — | *713* | 719 | 0.99 |
| | | | | 0.412 | 0.030 | 703 | | |
| | | | | 1.636 | 0.120 | 698 | | |
| | | | | 2.511 | 0.190 | 677 | | |
| IIc | *iso*-$C_3H_7$ | Br | Benzene | *0* | — | *553* | 559.5 | 0.99 |
| | | | | 0.565 | 0.053 | 546 | | |
| | | | | 1.401 | 0.130 | 552 | | |
| | | | | 2.611 | 0.250 | 535 | | |
| | | | Bromoform | *0* | — | *530* | | 0.95 |
| | | | | 0.395 | 0.105 | 529 | | |
| | | | | 1.405 | 0.390 | 506 | | |
| | | | | 2.793 | 0.770 | 510 | | |
| IId | $C_6H_5$ | Br | Benzene | *0* | — | *782* | 763.5 | 1.02 |
| | | | | 0.599 | 0.040 | 767 | | |
| | | | | 1.315 | 0.090 | 748 | | |
| | | | | 2.461 | 0.175 | 720 | | |
| IIe | *iso*-$C_3H_7$ | I | Benzene | *0* | — | *580* | 606.5 | 0.96 |
| | | | | 0.431 | 0.038 | 581 | | |
| | | | | 1.691 | 0.151 | 573 | | |
| | | | | 2.813 | 0.253 | 569 | | |
| | | | Bromoform | *0* | — | *598* | | 0.99 |
| | | | | 0.813 | 0.192 | 594 | | |
| | | | | 1.906 | 0.461 | 581 | | |
| | | | | 2.741 | 0.661 | 583 | | |
| IIf | $C_6H_5$ | I | Benzene | *0* | — | *802* | 810.5 | 0.99 |
| | | | | 0.685 | 0.044 | 797 | | |
| | | | | 1.801 | 0.117 | 788 | | |
| | | | | 2.589 | 0.170 | 780 | | |

compounds I and II showed the absorption band of *P-O*-isopropyl group at 1010 $cm^{-1}$ or *P-O*-phenyl group at 1200 $cm^{-1}$ according to the kinds of phosphites in complex compounds I and II. (see Figs. 1 and 2).

However, the absorption bands of P-O stretching vibration[6] of phosphite at 857 and 769 $cm^{-1}$ shift to 879 and 779 $cm^{-1}$ respectively. Form this shift, it is considered that P-O bonds are shortened by the formation of the complex, namely, the bonding strength of P-O in these complex compounds becomes stronger than that of phosphite (see Figs. 1 and 2).

In the ultraviolet absorption spectra*4 of these complex compounds, absorption maximum $\lambda_{max}$ of phosphite at 263.5 shifts to 265 and absorption bands became more broad by the formation of complex (see Fig. 3). This shift seems to show the usual correlation between the coordination compound and its donor[7].

**Molecular Weights of Phosphite Cuprous Halide Complex Compounds.**—The molecular weights of these complex compounds were measured by the cryoscopic method[8] in benzene, bromoform and cyclohexane, which are all prepared by purification of guaranteed reagents in the usual manner[9].

6) J. Bellamy, "The Infrared Spectra of Complex Molecules", John Wiley & Sons, New York (1958).

*4 Shimadzu QB-50 Spectrophotometer was used.

7) K. Sone, *J. Am. Chem. Soc.*, 75, 5207 (1953).

8) J. Sameshima, "Buturikagaku-Zikken-Hô", Syokabo, Tokyo, (1959).

9) T. Kuwata, "Yôzai", Maruzen Pub. Co., Tokyo (1951).

TABLE V. YIELDS, MELTING POINTS AND MICROANALYTICAL DATA OF DIISOPROPYL PHENYL PHOSPHONITE CUPROUS HALIDES $[(iso\text{-}PrO)_2PC_6H_5]_m$ CuX (III), (IV).

| No. | X | m | Yield % | M.p., °C | Halogen, % | | Phosphorus, % | | Copper, % | |
|---|---|---|---|---|---|---|---|---|---|---|
| | | | | | Found | Calcd. | Found | Calcd. | Found | Calcd. |
| IIIa | Cl | 1 | 98.5 | 141~142 | 10.88 | 10.92 | 9.4 | 9.5 | 19.8 | 19.5 |
| IIIb | Br | 1 | 97.9 | 143~144 | 21.91 | 21.64 | 8.1 | 8.4 | 17.3 | 17.2 |
| IIIc | I | 1 | 95.6 | 183~184 | — | — | 7.5 | 7.4 | 15.6 | 15.2 |
| IVa | Cl | 2 | 98.4 | 144~145 | 6.39 | 6.44 | 11.0 | 11.2 | 11.9 | 11.5 |
| IVb | Br | 2 | 99.0 | 148~149 | 13.18 | 13.43 | 10.3 | 10.4 | 10.5 | 10.7 |
| IVc | I | 2 | 98.0 | 187~189 | — | — | 9.8 | 9.6 | 9.6 | 9.9 |

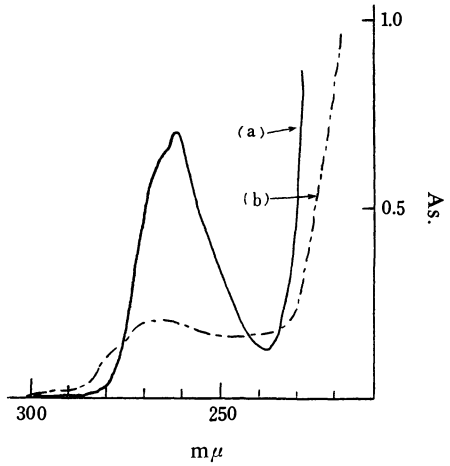



Fig. 3. Ultraviolet absorption spectra (in ethanol) of (a) triphenyl phosphite and (b) bis-(triphenyl phosphite) cuprous Chloride (IIb).

The results of these experiments are shown in Tables III and IV.

It is clear from Tables III and IV that the complex compounds I form associated molecules in organic solvents and that the degree of association are changed according to the kinds of halogens or solvents; on the contrary, the complex compounds II form simple molecules in organic solvents unconcerned with the kinds of halogens or solvents.

It seems to be possible that the apparent values of molecular weights will become smaller, if the associated molecules are dissociated in organic solvents. These possibilites are supported by the fact the degrees of association in nonpolar solvents are greater than that in polar solvent.

So, the present author prepared phenyl phosphonite, which is an analogue of phosphite but has the property of phosphine to a slight degree, and leads[10] to the complex compounds III and IV.

**Preparation and Molecular Weight of *O, O*-Diisopropylphenyl Phosphoniten Cuprous Halides (III) and (IV).**—Complex compounds III and IV were prepared from *O, O*-diisopropylphenyl phsophonite[11] and cuprous halide by the same method as phosphite I and II. The yield, the melting points and the microanalytical data of the complex compounds III and IV are shown in Table V.

As is clearly shown in Table VI, phenyl phosphonite cuprous halides (III) form tetramer and bis-(phenyl phosphonite) cuprous halides (IV) form dimer in organic solvents irrespectively of the kinds of halogens or solvents.

From the above results of Table VI and phosphine cuprous iodide which is reported as tetramer[2], it may be considered that complex compounds I will also be tetramer and complex compounds II dimer but these compounds I and II will be dissosiated in organic solvents.

But the real structures of these compounds must be determined by x-ray analysis.

**Phosphite Cuprous Halide Amine Complex Compounds.**—It was mentioned already that phosphite cuprous halides I reacted with more one mole ratio of phosphite and gave bis-phosphite cuprous halides II. In this reaction when aniline, pyridine and their derivatives are used instead of the phosphite, new complex compounds were prepared[12] on the contrary bis-phosphite cuprous halides II did not react with the above amines.

That is to say, to the acetone solution containing one mole of phosphite cuprous halides I, one mole of aniline, pyridine or their derivatives wasadded and thus, white crystals were obtained. These crystals had sharp melting points and showed the experimental formula of $(RO)_3PCuX\cdot$ Amine.

$$\underset{(I)}{(RO)_3PCuX} + \text{Amine} \rightarrow \underset{(V),\ (VI)}{(RO)_3PCuX\cdot\ \text{Amine}}$$

Changing the mole ratio of amines to phosphite cuprous halides I neither phosphite cuprous halide bis-amines $(RO)_3PCuX(Amine)_2$

10) Y. Nishizawa and Y. Suzuki, Japan. Pat. Applied No. 21678 (1959).

11) A. Arbuzov, *Chem. Abstr.*, **40**, 3411 (1946).

12) Y. Nishizawa and M. Nakagawa, Japan. Pat. Applied No. 21679 (1959).

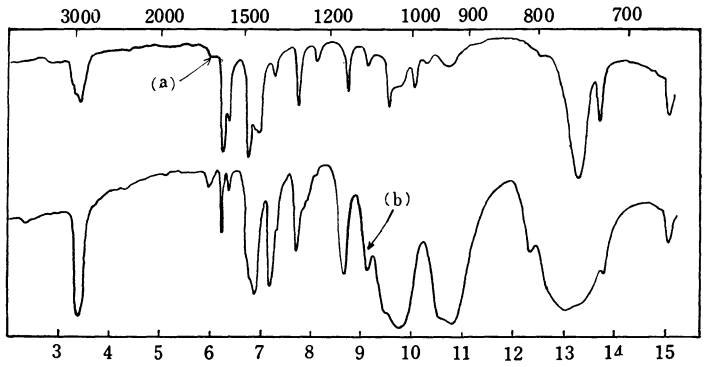



Fig. 4. Infrared absorption spectra of (a) α-picoline (liquid) and (b) triethyl phosphite cuprous iodide α-picoline complex compound (Ve) (in Nujol).

TABLE VI. MOLECULAR WEIGHTS OF PHENYL PHOSPHONITE CUPROUS HALIDES $[(iso\text{-}C_3H_7O)_2PC_6H_5]_mCuX$ (III) AND (IV) IN VARIOUS SOLVENTS

| No. | X | *m* | Cryoscopic solvent (*K*) | Concn. (g./G%) | *ΔT* °C | Molecular weight: Experimental | Molecular weight: Calcd. (monomeric) | Degree of association |
|---|---|---|---|---|---|---|---|---|
| IIIa | Cl | 1 | Benzene (5120) | *0* | — | *1280* | 325 | |
| | | | | 0.593 | 0.024 | 1265 | | 3.93 |
| | | | | 1.911 | 0.086 | 1138 | | |
| | | | | 2.730 | 0.127 | 1101 | | |
| | | | Bromoform (14050) | *0* | — | *1220* | | |
| | | | | 0.465 | 0.055 | 1188 | | 3.75 |
| | | | | 1.382 | 0.166 | 1170 | | |
| | | | | 2.655 | 0.322 | 1158 | | |
| | | | Cyclohexane (20100) | *0* | — | *1340* | | |
| | | | | 0.298 | 0.046 | 1302 | | 4.12 |
| | | | | 0.951 | 0.147 | 1300 | | |
| | | | | 2.411 | 0.389 | 1261 | | |
| IIIb | Br | 1 | Benzene | *0* | — | *1450* | 369.5 | |
| | | | | 0.675 | 0.025 | 1382 | | 3.92 |
| | | | | 1.715 | 0.069 | 1273 | | |
| | | | | 2.816 | 0.125 | 1153 | | |
| | | | Bromoform | *0* | — | *1425* | | |
| | | | | 0.593 | 0.059 | 1412 | | 3.86 |
| | | | | 1.491 | 0.151 | 1387 | | |
| | | | | 2.615 | 0.270 | 1361 | | |
| IIIc | I | 1 | Benzene | *0* | — | *1685* | 416.5 | |
| | | | | 0.427 | 0.013 | 1682 | | 4.05 |
| | | | | 1.793 | 0.054 | 1700 | | |
| | | | | 2.381 | 0.072 | 1693 | | |
| IVa | Cl | 2 | Benzene | *0* | — | *1100* | 551 | |
| | | | | 0.298 | 0.014 | 1090 | | 2.00 |
| | | | | 1.613 | 0.076 | 1087 | | |
| | | | | 2.803 | 0.135 | 1063 | | |
| | | | Bromoform | *0* | — | *1080* | | |
| | | | | 0.445 | 0.058 | 1077 | | 1.96 |
| | | | | 1.412 | 0.187 | 1061 | | |
| | | | | 2.561 | 0.342 | 1052 | | |
| IVb | Br | 2 | Benzene | *0* | — | *1265* | 595.5 | |
| | | | | 0.343 | 0.014 | 1254 | | 2.12 |
| | | | | 1.612 | 0.065 | 1270 | | |
| | | | | 2.635 | 0.108 | 1249 | | |
| IVc | I | 2 | Benzene | *0* | — | *1190* | 642.5 | |
| | | | | 0.441 | 0.019 | 1188 | | 1.85 |
| | | | | 1.391 | 0.061 | 1181 | | |
| | | | | 2.546 | 0.111 | 1172 | | |

TABLE VII. YIELDS, MELTING POINTS AND MICROANALYTICAL DATA OF PHOSPHITE CUPROUS HALIDE AMINE COMPLEX COMPOUNDS $(RO)_3PCuX \cdot Amine$ (V), (VI)

| No. | R | X | Amine | Yield % | M.p. °C | Nitrogen, % Found | Nitrogen, % Calcd. | Halogen, % Found | Halogen, % Calcd. | Phosphorus, % Found | Phosphorus, % Calcd. | Copper, % Found | Copper, % Calcd. |
|---|---|---|---|---|---|---|---|---|---|---|---|---|---|
| V a | $C_2H_5$ | Cl | Pyridine | 98.8 | 56~ 57 | 4.22 | 4.07 | 10.00 | 10.32 | 8.9 | 9.0 | 19.1 | 18.5 |
| V b | $C_2H_5$ | Br | Pyridine | 97.2 | 105~106 | 3.81 | 3.60 | 20.38 | 20.59 | 7.9 | 8.0 | 15.8 | 16.3 |
| V c | $C_2H_5$ | I | Pyridine | 97.9 | 72~ 73 | 3.50 | 3.21 | — | — | 6.8 | 7.1 | 14.6 | 14.6 |
| V d | $C_6H_5$ | Cl | Pyridine | 93.5 | 126~127 | 2.76 | 2.87 | 7.55 | 7.27 | 6.6 | 6.4 | 13.3 | 13.0 |
| V e | $C_2H_5$ | I | $\alpha$-Picoline | 90.4 | 59~ 60 | 3.35 | 3.11 | — | — | 7.2 | 7.1 | 14.6 | 14.1 |
| V f | $C_2H_5$ | I | $\beta$-Picoline | 96.2 | 84~ 85 | 3.08 | 3.11 | — | — | 6.9 | 7.1 | 14.0 | 14.1 |
| V g | $C_2H_5$ | I | $\gamma$-Picoline | 88.2 | 76~ 77 | 3.31 | 3.11 | — | — | 7.3 | 7.1 | 13.8 | 14.1 |
| V h | $C_2H_5$ | I | 2,4-Lutidine | 77.5 | 97~ 99 | 3.15 | 3.02 | — | — | 6.7 | 6.9 | 14.1 | 13.7 |
| V i | $C_2H_5$ | I | 2,6-Lutidine | 82.8 | 70~ 71 | 3.31 | 3.02 | — | — | 6.8 | 6.9 | 13.6 | 13.7 |
| V j | $C_2H_5$ | Cl | $\alpha,\alpha'$-Dipyridyl | 98.1 | 105~106 | 3.66 | 3.42 | — | — | 7.1 | 7.4 | 15.2 | 15.1 |
| VI a | $C_2H_5$ | I | Aniline | 71.5 | 80~ 81 | 3.50 | 3.11 | — | — | 6.8 | 6.9 | 14.3 | 14.1 |
| VI b | $C_2H_5$ | I | *p*-Toluidine | 97.2 | 60~ 61 | 3.15 | 3.01 | — | — | 6.5 | 6.7 | 13.9 | 13.7 |
| VI c | $C_2H_5$ | I | *p*-Anisidine | 96.5 | 66~ 67 | 2.65 | 2.91 | — | — | 6.3 | 6.4 | 12.9 | 13.2 |
| VI d | $C_2H_5$ | I | *p*-Chloroaniline | 95.5 | 72~ 73 | 2.65 | 2.83 | — | — | 6.5 | 6.3 | 12.6 | 12.8 |
| VI e | $C_2H_5$ | I | *m*-Chloroaniline | 98.3 | 60~ 62 | 2.91 | 2.83 | — | — | 6.3 | 6.3 | 13.1 | 12.8 |

TABLE VIII. YIELDS, PHYSICAL CONSTANTS AND MICROANALYTICAL DATA OF PHOSPHITES $(RO)_3P$

| R | Yield % | B. p. °C | B. p. mmHg | $n_D$ ($t$°C) | Phosphorus, % Found | Phosphorus, % Calcd. | Carbon, % Found | Carbon, % Calcd. | Hydrogen, % Found | Hydrogen, % Calcd. |
|---|---|---|---|---|---|---|---|---|---|---|
| $C_2H_5$ | 82 | 55~57 | 19 | 1.4135(20) | 19.8 | 19.9 | 46.31 | 46.15 | 9.25 | 9.04 |
| *n*-$C_3H_7$ | 85 | 82~83 | 10 | 1.4263(20) | 15.1 | 14.9 | 52.06 | 51.92 | 10.09 | 10.10 |
| *iso*-$C_3H_7$ | 80 | 60~61 | 9 | 1.4079(29) | 15.0 | 14.9 | 51.88 | 51.92 | 10.41 | 10.10 |
| $C_6H_5$ | 63 | 170 | 0.3 | m.p.25°C | 9.8 | 10.0 | 69.53 | 69.68 | 4.97 | 4.84 |

nor bis-amine cuprous halides $(Amine)_2CuX$ were obtained.

The yields, the melting points and the microanalytical data of these new complex compounds V and VI are shown in Table VII. The infrared absorption spectra of these complex compounds V and VI showed that these compounds V and VI have both the amine molecule and the phosphite molecule. Infrared absorption spectrum of triethyl phosphite cuprous iodide $\alpha$-picoline (Ve) is shown in Fig. 4 as a representation.

It was interesting to see that ortho-substituted anilines, *O*-chloroaniline, *O*-toluidine, *O*-anisidine etc., did not give these complex compounds VI. The cause may be considered from models of complex molecules to be a steric hindrance owing to the ortho-substituent in aniline.

In the pyridine series, all derivatives gave new complex compound, irrespective of the position of substituents.

It was also made clear by the present author that all of the above mentioned compounds I, II, III, IV, V and VI had strong fungicidal activities[13], and the data of their biological activities will be reported in other paper.

## Experimental

**Preparations of Phosphites.**—Trialkyl or triphenyl phosphites were prepared by Ford-Moore's methods[14] and their yields, physical constants and microanalytical data are shown in Table VIII.

**Preparation of Diisopropyl Phenyl Phosphonite.**—This phosphonite was prepared from phenyl dichlorophosphine and isopropyl alcohol by Arbuzov's method[11]. The boiling point is 110°C/0.5 mmHg, the refractive index is $n_D^{25}$ 1.5000 and the yield is 84%.

Found, P, 13.7; C, 63.59; H, 8.59. Calcd. for $C_{12}H_{19}O_2P$, P, 13.7; C, 63.72; H, 8.41%.

**Preparation of Phosphite or Phosphonite Cuprous Halides I or III.**—The following example illustrates the preparation of phosphite or phosphonite cuprous halides I or III. Other examples are shown in Tables I and V and their molecular weights are shown in Tables III and VI.

**Preparation of Diisopropyl Phenyl Phosphonite Cuprous Chloride (IIIa).**—To a solution of 14.3 g. (0.05 mol.) of diisopropyl phenyl phosphonite in 50 ml. of benzene was gradually added 4.95 g. (0.05 mol.) of cuprous chloride. The temperature rose gradually and cuprous chloride was dissolved in benzene. After one hour's stirring, the trace of insoluble matter was filtered off and concentrated under reduced pressure. White crystals (18.9 g,.

13) J. Hattori and Y. Nishizawa, Japan. Pat. Applied No. 36382 (1958), 3506, 22572, 22573 (1959).

14) A. H. Ford-Moore, "Organic Syntheses", Vol. 31, John Wiley & Sons, New York, (1951), p. 111.

98.5%) were obtained and recrystallized from petroleum ether, m. p. 141~142°C.

Found: Cl, 10.88; P, 9.4; Cu, 19.8. Calcd. for $C_{12}H_{19}O_2PCuCl$: Cl, 10.92; P, 9.5; Cu, 19.5%.

**Preparation of Bis-phosphite or Bis-phosphonite Cuprous Halides II or IV.**—The following example illustrates the preparation of bis-phosphite or bis-phosphonite cuprous halides II or IV. Other examples are shown in Tables II and V and their molecular weights are shown in Tables IV and VI.

**Preparation of Bis-(diisopropyl Phenyl Phosphonite) Cuprous Chloride (IVa).**—The compound was prepared from 28.5 g. (0.1 mol.) of diisopropyl phenyl phosphonite and 4.95 g. (0.05 mol.) of cuprous chloride in benzene solution as above mentioned. White crystals (32.9 g., 98.4%) were obtained and melted at 144~145°C (from ligroin).

Found: Cl, 6.39; P, 11.0; Cu, 11.9. Calcd. for $C_{24}H_{38}O_4P_2CuCl$: Cl, 6.44; P, 11.2; Cu, 11.5%.

**Reaction of Triisopropyl Phosphite Cuprous Chloride (Ia) with Triisopropyl Phosphite.**—To a solution of 15.3 g. (0.05 mol.) of triisopropyl phosphite cuprous chloride (Ia) in 50 ml. of benzene was added 10.4 g. (0.05 mol.) of triisopropyl phosphite. The temperature did not rise during this addition. The benzene was evaporated under reduced pressure, white crystals (23.8 g.) were obtained and melted at 69~70°C. A mixture of the crystals and the authentic bis-(triisopropyl phosphite) cuprous chloride which was prepared from two moles of triisopropyl phosphite and one mole of cuprous chloride, melted at 69~70°C.

**Reaction of Triethyl Phosphite Cuprous Chloride[4] with Triphenyl Phosphite.**—Triphenyl phosphite (15.5 g., 0.05 mol.) was added to a solution of 13.3 g. (0.05 mol.) of triethyl phosphite cuprous chloride in 50 ml. of benzene. After the benzene was evaporated off, white crystals of triethyl phosphite triphenyl phosphite cuprous chloride (IIg) (28.1 g, 97.8%) were obtained and melted at 75~76°C.

Found: Cl, 6.15; P, 11.2; Cu, 10.8. Calcd. for $C_{24}H_{30}O_6P_2CuCl$: Cl, 6.17; P, 10.9; Cu, 11.0%

**Reaction of Bis-(triisopropyl phosphite) Cuprous Chloride (IIa) with Cuprous Chloride.**—There was added 4.95 g. (0.05 mol.) of cuprous chloride to a solution of 25.7 g. (0.05 mol.) of bis-(triisopropyl phosphite) cuprous chloride (IIa) in 50 ml. of benzene. After cuprous chloride was dissolved in benzene, the reaction mixture was filtered off and concentrated. White crystals (29.6 g) were obtained and melted at 117°C.

This melting point coincides with that of the authentic triisopropyl phosphite cuprous chloride (Ia) prepared from one mole ratio of triisopropyl phosphite and one mole ratio of cuprous chloride, and the mixed melting point was not depressed.

**Reaction of Triethyl Phosphite Cuprous Iodide (Ie) with Acetyl Chloride.**—To a solution of 17.8 g. (0.05 mol.) of triethyl phosphite cuprous iodide (Ie) in 50 ml. of benzene, there was gradually added 3.9 g. of acetyl chloride. The temperature of the reaction mixture rose and white inorganic compounds were precipitated. After one hour's refluxing, the precipitates were filtered off and the filtrate was concentrated. The residual oil was fractionated under reduced pressure. The main product was distilled at 78~79°C/3 mmHg, and yielded 7.7 g.

$n_D^{20}$ 1.4209. Found: P, 17.1; C, 39.81; H, 7.34. Calcd. for $C_6H_{13}O_4P$: P, 17.2; C, 40.00; H, 7.22%. *p*-Nitrophenylhydrazone of the aforesaid main product was prepared from *p*-nitrophenylhydrazine in the usual manner.

This hydrazone melted at 131~132°C (recryst. from ethanol) and the mixed melting point with authentic *p*-nitrophenylhydrazone of *O,O*-diethyl-acetyl phosphonate prepared from triethyl phosphite and acetyl chloride was not depressed.

Found: P, 9.6; C, 45.59; H, 5.89; N, 13.31. Calcd. for $C_{12}H_{18}N_3O_5P$: P, 9.8; C, 45.71; H, 5.71; N, 13.33%

**Pyrolysis of Bis-(triisopropyl Phosphite) Cuprous Chloride (IIa).**—The compound IIa (25.8 g., 0.05 mol.) was set in a distillation flask (50 ml.) which was combined with a trap cooled at −50°C and heated at 100°C under 0.3 mmHg for 6 hr.

The crystals IIa melted and then crystallized again. The product was recrystallized from petroleum ether and melted at 116~117°C. This melting point coincides with that of the authentic triisopropyl phosphite cuprous halide (Ia) prepared from one mole ratio of triisopropyl phosphite and one mole ratio of cuprous chloride and the mixed melting point was not depressed.

On the other hand, colorless oil which was captured in a trap, was distilled at 60~62°/9mmHg and yielded 7.7 g, $n_D^{28}$ 1.4081.

Found: P, 14.6; C, 15.80; H, 10.35. Calcd. for $C_9H_{21}O_3P$: P, 14.9; C, 15.92; H, 10.10%

This oil was added to a benzene solution containing 5.3 g. of cuprous chloride and gave white crystals which melted at 116~117°C. The melting point of these crystals coincided with the authentic triisopropyl phosphite cuprous chloride (Ia) and the mixed melting point was not depressed.

**Reaction of Phosphite Cuprous Halides I with Amines.**—The following example illustrates the preparation of phosphite cuprous halide amine complex V or VI. Other examples are shown in Table VII.

**Reaction of Triethyl Phosphite Cuprous Chloride with Pyridine.**—To a solution of 26.5 g. (0.1 mol.) of triethyl phosphite cuprous chloride in 100 ml. of acetone was added 7.9 g. (0.1 mol.) of pyridine.

The acetone was evaporated off under reduced pressure and light green crystals (33.9 g.) were obtained. White needles were recrystallized from ligroin and melted at 56~57°C.

Found: N, 4.22; Cl, 10.00; P, 8.9; Cu, 19.1. Calcd. for $C_{11}H_{20}ClNO_3PCu$: N, 4.07; Cl, 10.32; P, 9.0; Cu, 18.5%

## Summary

Phosphites or phosphonites react with cuprous halides in one to one or two to one mole ratio to give phosphite, phosphonite, bis-phosphite or bis-phosphonite cuprous halides complex compounds. Their molecular weights

in various organic solvents showed that these compounds formed polymer.

Phosphite cuprous halides react with pyridine, aniline or their derivatives and gave new complex compounds having phosphite, cuprous chloride and amine.

The author wishes to express his thanks to Professor Shinichiro Fujise and Professor Taro Yamazaki of Tohoku University and Professor Ryutaro Tsuchida of Osaka University for their helpful suggestions in the preparation of this manuscript. He also wishes to thank the Sumitomo Chem. Co., Ltd. for permission to publish this work. He is indebted to co-workers in the analytical section of this laboratory. He also wishes to express his thanks to Messrs. M. Nakagawa and Y. Suzuki for their never failing assistance.

*Sumitomo Chem. Co., Ltd.*
*Osaka Works*
*Konohana-ku, Osaka*

# *An Attempt to Discuss Reactivities of Excited Molecules by the Molecular Orbital Method*

By Kenichi FUKUI, Keiji MOROKUMA and Teijiro YONEZAWA

(Received December 29, 1960)

In order to elucidate the mechanisms of reactions of conjugated or non-conjugated organic compounds which are in their ground state, a number of quantum mechanical, especially molecular orbital, studies have been performed and have achieved remarkable success in predicting theoretically their chemical reactivities[1-4]. In connection with the recent advance of techniques of photochemical investigation, chemical reactivities of electronically excited molecules have aroused our interest.

Because of the complicated characters and the multifariousness of reactions of excited molecules, only a few theoretical discussions have ever been made. As regards the problem of their self-dissociation, some qualitative discussions in terms of the potential energy curve have prevailed[5]. For discussing the energy transfer reaction between an excited molecule and an unexcited one, the collision theory has prevailed as a powerful tool[6]. On account of the lack in systematic experimental data and, in addition, because of the difficulties in the theoretical treatment, only a few quantum chemical studies have been presented on excited molecules involved in the addition reactions of large organic molecules. Photopolymerization of hydrocarbons has been discussed in terms of free valence of the molecules in their lowest excited state. The intramolecular orientation in the reaction of anthracene or naphthacene has been explained well[7]. But that of acenaphthylene has not been[8]; free valence of its lowest excited states is greatest at positions 5 and 6, and, on the contrary, the photodimer of the componud is produced through positions 1 and 2.

In the present paper, as was previously done with reference to the molecules in their ground state by the present authors[9,10] and by Brown[11], the reactivites of excited molecules are assumed to be parallel with the $\pi$ stabilization energy at the transition state due to the interaction of the molecule with the reagent (molecule, ion or radical) through the position of attack. Under this assumption the reactivity indexes are derived by the use of the molecular orbital method.

1) G. W. Wheland, *J. Am. Chem. Soc.*, **64**, 900 (1942).
2) C. A. Coulson and H. C. Longuet-Higgins, *Proc. Roy. Soc.*, **A191**, 39 (1947).
3) F. H. Burkitt, C. A. Coulson and H. C. Longuet-Higgins, *Trans. Faraday Soc.*, **47**, 553 (1951).
4) K. Fukui, T. Yonezawa and C. Nagata, This Bulletin, **27**, 423 (1954); *J. Chem. Phys.*, **27**, 1247 (1957),
5) K. Yagi, Z. Yoshida and T. Tabata, "Fluorescence", Nanko-do, Tokyo (1958); and references cited there.
6) M. Shimizu, "Symposium on Molecular Structure and Chemical Reaction", held in Nov. 1960, Tokyo, p. 149; and references cited there.
7) C. Sandorfy, *Compt. rend.*, **230**, 961 (1950).
8) V. A. Crawford and C. A. Coulson, *J. Chem. Soc.*, **1948**, 1990.
9) K. Fukui, K. Morokuma, T. Yonezawa and C. Nagata, *J. Chem. Phys.*, **32**, 1743 (1960).
10) T. Yonezawa, K. Hayashi, C. Nagata, S. Okamura and K. Fukui, *J. Polymer Sci.*, **14**, 312 (1954).
11) R. D. Brown, *J. Chem. Soc.*, **1959**, 2224.

## Formulation and Comparison with Experiments

Reactions of an excited molecule with an unexcited molecule are classified into several cases from the point of view of the spin multiplicity of reactants. The assumptions, the formulations and general considerations of the present molecular orbital treatments leading to the theoretical measures of reactivity will be described rather circumstantially in the first few cases, and in other cases only the indexes of reactivity derived will be given.

**Reaction of an Excited Triplet Molecule with an Unexcited Radical.**—First of all, attention is paid to the reaction of an excited triplet molecule ($^3$A) with an unexcited radical ($^2$B), where the numbers on the left shoulder refer to the multiplicity of the molecules. Here it would be rational for practical purposes in treating photochemical reactions to assume that the molecule $^3$A has only one excited electron. Then the wave functions of these molecules are written as follows:

$$\Psi(^3\mathrm{A}) = A\left[\cdots(\phi_1\alpha)^{m-3}(\phi_1\beta)^{m-2}(\phi_{01})^{m-1}(\phi_{02})^{m} \times \begin{Bmatrix} \alpha(m-1)\alpha(m) \\ \beta(m-1)\beta(m) \\ (1/\sqrt{2})\{\alpha(m-1)\beta(m)+\beta(m-1)\alpha(m)\} \end{Bmatrix}\right] \quad (1)$$

$$\Psi(^2\mathrm{B}) = A\left[\cdots(\phi_1\alpha)^{n-2}(\phi_1\beta)^{n-1}\begin{Bmatrix}(\phi_0\alpha)^n \\ (\phi_0\beta)^n\end{Bmatrix}\right]$$

where $\phi_i$ and $\phi_j$ are the molecular orbitals of molecules A and B, respectively, whose numbering is schematically shown in Fig. 1, 01 and 02 denoting the lower and the higher half-occupied levels, of A, respectively, and (0) denoting the half-occupied level of the radical B; $m$, an even integer, is the number of electrons of the molecule A and $n$, an odd number, is that of the radical B; $A$ is the antisymmetrizing operator including the normalization constant; and each line in braces may constitute one wave function.

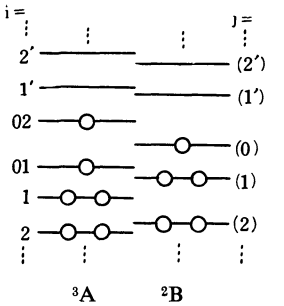



Fig. 1. Numbering of molecular orbitals.

The states of the total system consisting of the triplet A and the doublet B would be a quartet and a doublet. But the quartet, which would be proved later to be less significant in this discussion, is abandoned. The doublet wave function for $M_S=1/2$* is

$$^2\Psi_{1/2}[^2(\mathrm{AB})] \equiv \Psi[0] = A[\cdots(\phi_1\alpha)^{m-3}(\phi_1\beta)^{m-2} \cdots(\phi_1\alpha)^{m+n-2}(\phi_1\beta)^{m+n-1}(\phi_{01})^{m-1}(\phi_{02})^{m} \times(\phi_0)^{m+n}\{(\alpha\beta+\beta\alpha)\alpha-2(\alpha\alpha)\beta\}/\sqrt{6}] \quad (2)$$

where, for example, $\alpha\beta\alpha$ means $\alpha(m-1)\beta(m)\alpha(m+n)$. That for $M_S=-1/2$ is not written because the energetical argument is similar. Thus the state $\Psi[0]$ is assumed to correspond to the initial system of the reaction in question. If A and B are far separated from each other, the energy of the state is the same as that of the product function $\Psi(^3\mathrm{A})\cdot\Psi(^2\mathrm{B})$. The molecular orbitals may include all $\pi$ ones and $\sigma$ ones, but in this paper we consider the reactions in company with only the $\pi$ electron excitation, and hence $\sigma$ orbitals will rationally be omitted as making an invariant framework.

At the transition state of the reaction the two molecules, $^3$A and $^2$B, will stay at a distance, making a weak interaction through the atoms at which the reaction takes place. This interaction is assumed to be a kind of $\pi-\pi$ conjugation and in this simple LCAO MO approach it will be represented by a small resonance integral $\gamma\beta$ between the atomic $\pi$ orbitals $r$ and $s$ of the reactants, A and B, respectively, where $\beta$ is the resonance integral of the C-C $\pi$ bond in benzene. This perturbation makes the initial state $\Psi[0]$ come to the direct or indirect interaction with various electronic configurations of the combined system. Of these configurations only those, which have energy matrix elements with the initial state in scope of the simple LCAO MO approximation, are taken into account. This means that the configurations (of course, doublet and $M_S=1/2$) in which one electron transfers from $^3$A to $^2$B and vice versa have concern with the transition state of the reaction, whereas those which correspond to intramolecular one-electron transitions do not.

Under these assumptions the electron configurations to be taken into account are those corresponding to the following one-electron transfers, represented by $l\rightarrow m$, from an occupied or half-occupied orbital, $l$, to an unoccupied or half-occupied orbital, $m$:

$$\begin{aligned} &02\rightarrow(0),\ 02\rightarrow(j'),\ 01\rightarrow(0),\ 01\rightarrow(j') \\ &i\rightarrow(0),\ i\rightarrow(j'),\ (0)\rightarrow01,\ (0)\rightarrow02 \\ &(0)\rightarrow i',\ (j)\rightarrow01,\ (j)\rightarrow02,\ (j)\rightarrow i' \end{aligned} \quad (3)$$

* $M_S$ denotes the eigenvalue of $S_z$, the $z$ component of the spin momentum operator.

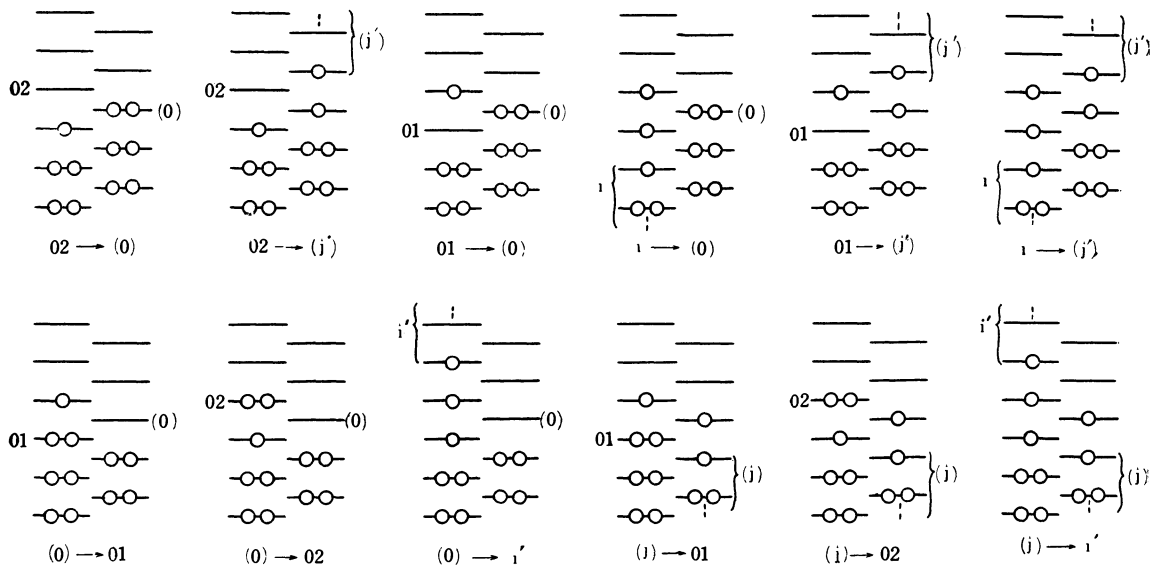



Fig. 2. Electronic configurations taken into account.

where

$i=1, 2, \cdots$ (occupied orbitals of $^3$A)

$i'=1', 2' \cdots$ (unoccupied orbitals of $^3$A)

$(j)=(1), (2), \cdots$ (occupied orbitals of $^2$B)

$(j')=(1'), (2'), \cdots$ (unoccupied orbitals of $^2$B)

They are schematically illustrated in Fig. 2. For an illustration, the configuration associated with the transfer 02→(0), will have the following wave function:

$$\Psi[02\rightarrow(0)] = \boldsymbol{A}[\cdots(\phi_0\alpha)^{m+n-2}(\phi_0\beta)^{m+n-1}(\phi_0\alpha)^{m+n}] \quad (4)$$

The energy matrix element between these configurations and the initial state can be expressed in terms of the integral $\gamma\beta$. For example,

$$\left|\int \Psi^*[02\rightarrow(0)]\, H\Psi(0)\mathrm{d}\tau\right| = |\, c_r^{02} d_s^{0} \gamma\beta\,| \quad (5)$$

where $c_r^k$ and $d_s^l$ are the coefficient of the atomic orbitals $r$ and $s$ in the molecular orbital $k$ and $l$ of the molecules A and B, respectively.

The transition state of the reaction is the lowest energy state resulting from the interaction mentioned above. The difference in $\pi$ electronic energy, i. e. the stabilization energy, between the initial state and the transition state, was assumed in the preceding section to parallel the activation energy, of the reaction, and accordingly the reactivity of the excited molecule. This stabilization energy would be expanded in powers of $\gamma$ by regarding it to be small. There arise three main subcases according to the mutual relation of the energy levels 01 and 02 of the molecule $^3$A and (0) of the molecule $^2$B*. In the following $Y_{k,l}$ denotes the energy in units of $(-\beta)$ turned out in one electron transfer from the molecular orbital $k$ of the one molecule to the molecular orbital $l$ of the other one. That is, $Y_{k,l}$ is positive if the level $k$ is higher than the level $l$ and vice veras. Thus we reach the final reactivity indexes of excited molecules.

(a) If $Y_{02,0}>Y_{0,01}>0$, that is, if the half-occupied level of the molecule $^2$B lies between the levels 01 and 02 of $^3$A and is nearer to 01 than to 02, as is shown in Fig. 3 (a), the stabilization energy to the second order of $\gamma$ is written in the following expression**:

$$\Delta E=\left[Y_{02,0}+\frac{(3/2)(c_r^{02})^2(d_s^0)^2}{Y_{02,0}}\gamma^2\right](-\beta) \quad (6)$$

From this formula some general conclusions on reactivities of excited molecules may be

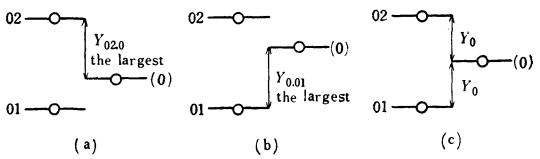



Fig. 3. Mutual relation of molecular levels.

* Some rare cases, for instance, $Y_{0.02}>0$ or $Y_{01.0}>0$, are not included for the sake of brevity.

** In general the stabilization energies for each $M_S$ component may differ from each other. In the surroundings of reaction no magnetic field being applied, no specialization of the component is possible and the mean of all components would be significant as a real stabilization energy. In this case the energy for $M_S=1/2$ is the same as that for $M_S=1/2$; also the mean energy becomes the same.

TABLE I. RATE CONSTANT AND $\pi$ STABILIZATION ENERGY OF POLYMERIZATION OF STYRENE

| Reaction[a] | Rate constant[b] $k$ (l. mol$^{-1}$ sec$^{-1}$) | $\pi$ Stabilization energy (in units of $-\beta$) |
|---|---|---|
| R·+$^3$A→RA· | $\sim 10^{11}$ | $0.414+0.801\gamma^2$ (position 9) |
| | | $0.414+0.400\gamma^2$ (position 1) |
| | | $0.414+0.200\gamma^2$ (position 2) |
| R·+A→RA· | $3.4\times 10^2$ | $0.926\gamma^2$ |
| R·+M→R· | $1.2\times 10^2$ | $0.932\gamma^2$ |
| RA·+M→R· | 0.8 | $0.739\gamma^2$ |

a) Abbreviations, R·: polymer radical of styrene; $^3$A: triplet anthracene; A: anthracene; M: styrene.
b) Taken from Ref. 10.

derived. In most reactions between unexcited molecules, terms first appear in the second order of $\gamma$, whereas in Eq. 6 the term in zero order exists. The appearance of the zero order term is universal in all the following cases and subcases, making clear the reason why the reactions including excited molecules proceed so fast. The difference in reactivity of several excited molecules would thus dominantly be decided by this term. The intramolecular orientation, on the other hand, depends on the term in the second order. More minutely, so far as attention is paid to the lowest excitation of the molecule A as is expected in real photochemical reactions of conjugated molecules, the atom where $(c_r^{02})^2$, the frontier electron density for a nucleophilic attack in the ground state, is the greatest is the most reactive in an excited molecule. The coefficient (3/2) is characteristic to the triplet A molecule. If the molecule A is excited in the singlet state it amounts to (1/2), as will be mentioned in the next section. The difference would not necessarily mean the difference in reactivity of these two states, since the approximation is too simple to discuss at this point, on which there will be some discussion in a later section.

To the transition state the electron configuration corresponding to the one-electron transfer 02→(0) has the greatest contribution, since the other configurations have the first contribution to $\Delta E$ in the fourth order. Therefore, the direction of charge transfer is from molecule A to molecule B.

(b) If $Y_{0,01}>Y_{02,0}>0$, i. e., if the half-occupied level of $^2$B lies between the levels 02 and 01, and nearer to 02 than to 01, as shown in Fig. 3 (b), then

$$\Delta E=\left[Y_{0,01}+\frac{(3/2)(c_r^{01})^2(d_s^0)^2}{Y_{0,01}}\gamma^2\right](-\beta) \quad (7)$$

In this subcase also the rate of reaction is great and the intramolecular orientation of the excited molecule is controlled by $(c_r^{01})^2$, the frontier electron density for an electrophilic attack in the ground state. The most contributive configuration in this subcase corresponds to the transition (0)→01, resulting in a charge transfer from B to A.

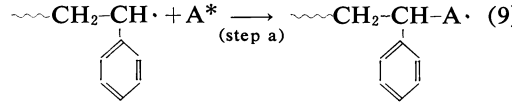
(c) If $Y_0\equiv Y_{02,0}=Y_{0,01}>0$, i. e., if the level (0) is just in the midst of the levels 01 and 02, as shown in Fig. 3 (c), then

$$\Delta E=\left[Y_0+\frac{(3/2)[(c_r^{01})^2+(c_r^{02})^2](d_s^0)^2}{Y_0}\gamma^2\right]\times(-\beta) \quad (8)$$

A large rate constant is confirmed also in this subcase, and $[(c_r^{01})^2+(c_r^{02})^2]$, the frontier electron density for a radical attack in the ground state, comes to the point.

So far as alternant hydrocarbons are concerned, however, the equality $(c_r^{01})^2=(c_r^{02})^2$ holds in the simple LCAO MO approximation, so that in all subcases and the following cases the most reactive position in a molecule in its lowest excited state is the same as that in the ground state. This explains the great reactivity of meso position of anthracene. Further experimental studies are anticipated with respect to the intramolecular orientation in nonalternant hydrocarbons and heterocyclic compounds where the equality mentioned above no more exists.

Here a comparison with experimental data may be given. Excited triplet anthracene was reported by Norrish et al.[12] to enter into the chain of polymerization of styrene in the following way:



(9)

Observed rate constant, $k_a$, and calculated $\pi$ stabilization energy $\Delta E$ are tabulated in Table I. The stabilization in the reaction a is calculated by using Eq. 8. Those of other reactions in which only molecules in their ground state participate are given by the usual formula for stabilization energy[10]:

12) V. S. Anderson and R. G. W. Norrish, *Proc. Roy. Soc.*, **A251**, 1 (1959); R. G. W. Norrish and J. P. Simons, ibid., **A251**, 4 (1959).

$$\Delta E=\left[\sum_{j}^{\text{unocc}}\sum_{i}^{\text{all}}\nu_i-\sum_{j}^{\text{occ}}\sum_{i}^{\text{all}}(2-\nu_i)\right]\times\frac{(c_r^i)^2(d_s^j)^2}{Y_{ji}}\gamma^2(-\beta) \qquad (10)$$

where $\nu_i$ is the number of electrons in the $i$th molecular orbital of A. The extraordinary great magnitude of rate constant of reaction a is well understood in connection with the presence of the zero order term. Further, the position 9 is the most active, at which anthracene would enter into the polymer chain. An appropriate choice of the value of $\gamma$ ($=0.7$) makes the $\log k_a-\Delta E$ plots practically linear.

The wave functions (Eq. 1) of $^3$A and $^2$B may be combined so as to construct a quartet instead of the doublet (Eq. 2). The quartet state has matrix elements with some configurations in Eq. 3, only to give the stabilization energy in the second order. Because of the lack of the zero order terms and, accordingly, because of the instability of the transition state, reactions would not be considered to proceed by way of the quartet transition state.

**Reaction of an Excited Singlet Molecule with an Unexcited Radical.**—The reaction of an excited singlet molecule ($^1$A) with an unexcited radical ($^2$B) can be discussed in a way similar to that of a triplet molecule ($^3$A) mentioned in the preceding reaction. The doublet wave function for $M_S=1/2$ of the combined system is, in place of Eq. 2 in the triplet case,

$$\Psi[0]=\mathcal{A}[\cdots(\phi_{01})^{m-1}(\phi_{02})^{m}(\phi_0)^{m+n}\times\{(\alpha\beta-\beta\alpha)\alpha\}/\sqrt{2}] \qquad (11)$$

Also, we are led to the same equations as Eqs. 3, 4 and 5, excepting that the numerical coefficient in the second term should be read (1/2) in this case, instead of (3/2). The meanings of the frontier electron density and the direction of charge transfer in each subcase are entirely the same as in the last case; and therefore discussions may be omitted for brevity.

**Reaction of an Excited Tripled Molecule with an Unexcited Molecule.**—The reaction of an excited triplet molecule ($^3$A) with an unexcited singlet molecule ($^1$B)* now comes to our attention. Discussions are almost alike, so that the only important formulas would be summarized in this case and in the following case. The numbering of molecular orbitals is illustrated in Fig. 4. The states of the combined system at the initial stage of reaction are represented by a set of three triplet wave functions, one with $M_S=1$, one with $M_S=0$ and the other with $M_S=-1$, as follows:

* The singlet molecule $^1$B may be an ion whose spin is singlet.

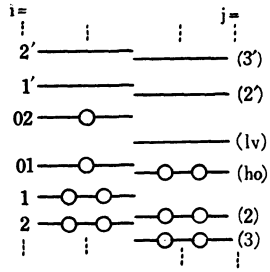



Fig. 4. Numbering of molecular orbitals. lv and ho mean the lowest unoccupied and the highest occupied orbitals, respectively.

$$\left.\begin{aligned}
{}^3\Psi_1&=\mathcal{A}[\cdots(\phi_{01})^{m+n-1}(\phi_{02})^{m+n}\times\alpha(m+n-1)\alpha(m+n)]\\
{}^3\Psi_0&=\mathcal{A}[\cdots(\phi_{01})^{m+n-1}(\phi_{02})^{m+n}\times(\alpha(m+n-1)\beta(m+n)+\beta(m+n-1)\alpha(m+n)\}/\sqrt{2}]\\
{}^3\Psi_{-1}&=\mathcal{A}[\cdots(\phi_{01})^{m+n-1}(\phi_{02})^{m+n}\times\beta(m+n-1)\beta(m+n)]
\end{aligned}\right\} \qquad (12)$$

Electronic configurations which are taken into account in the perturbation calculation are summarized in Fig. 5 with illustrations. Each $M_S$ component of the functions 12 will have matrix elements with the same $M_S$ component of the wave functions for the configurations

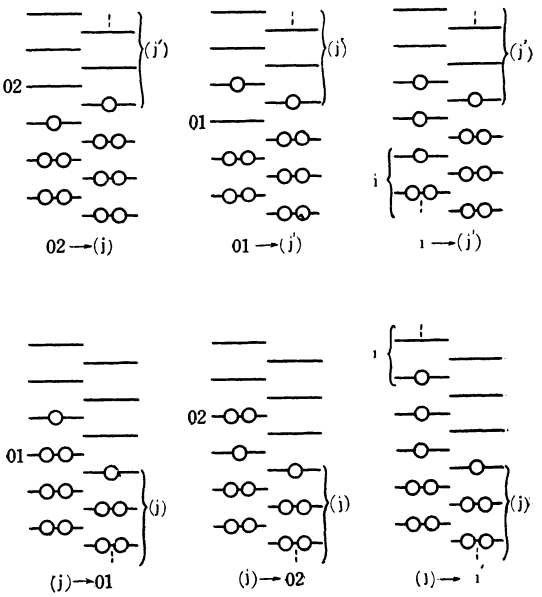



Fig. 5. Electronic configurations taken into account.
$i=1,2,\cdots$ (occupied orbitals of $^3$A); $i'=1',2',\cdots$ (unoccupied orbitals of $^3$A); $j=$ ho, 2, $\cdots$ (occupied orbitals of $^1$B); and $j'=$ lv, 2', $\cdots$ (unoccupied orbitals of $^1$B).

TABLE II. $\pi$ STABILIZATION ENERGY IN PHOTODIMERIZATION OF POLYACENES AND ACENAPHTHYLENE

| Compound | Pairs of positions to react with | $\pi$ Stabilization energy (in units of $-\beta$) |
|---|---|---|
| Anthracene | 9-9, 10-10 (central) | $0.547\gamma$ |
| | 1-1, 4-4 (end) | $0.273\gamma$ |
| Naphthacene | 5-5, 12-12 (central) | $0.417\gamma$ |
| | 1-1, 4-4 (end) | $0.159\gamma$ |
| Pentacene | 6-6, 13-13 (central) | $0.400\gamma$ |
| | 5-5, 14-14 | $0.299\gamma$ |
| | 1-1, 4-4 (end) | $0.100\gamma$ |
| Acenaphthylene | 1-1, 2-2 | $0.568\gamma$ |
| | 5-5, 6-6 | $0.375\gamma$ |

in Fig. 5. Then the stabilization energy* is obtained as follows, according to the mutual relation of energy levels:

(a) If $Y_{02,1v}$ is positive and the most positive of all $Y$'s, then

$$\Delta E=\left[Y_{02,1v}+\frac{(c_r^{02})^2(d_s^{1v})^2\gamma^2}{Y_{02,1v}}\right](-\beta) \qquad (13)$$

This is the case for most electrophilic reagents (cations) serving as $^1B$.

(b) If $Y_{ho,01}$ is positive and the most positive of all $Y$'s, then

$$\Delta E=\left[Y_{ho,01}+\frac{(c_r^{01})^2(d_s^{ho})^2\gamma^2}{Y_{ho,01}}\right](-\beta) \qquad (14)$$

Most nucleophilic reagents (anions) as $^1B$ are included in this subcase.

(c) If $Y_{02,1v}=Y_{ho,01}$, and they are positive (then of course the most positive), then, putting them equal to $Y_0$,

$$\Delta E=\left[Y_0+\frac{\{(c_r^{02})^2(d_s^{1v})^2+(c_r^{01})^2(d_s^{ho})^2\}\gamma^2}{Y_0}\right]\times(-\beta) \qquad (15)$$

Such a conjugated molecule as has its lowest excitation energy smaller than the excitation energy to the triplet of the molecule A would be classified in this subcase.

(d) If all $Y$'s are negative, then

$$\Delta E=\left[\sum_j^{unocc}\sum_i^{all}\nu_i-\sum_j^{occ}\sum_i^{all}(2-\nu_i)\right]\frac{(c_r^i)^2(d_s^j)^2\gamma^2}{Y_{ji}}\times(-\beta) \qquad (16)$$

In this subcase the stabilization energy begins in the second order terms, predicting a slow rate in the process of reaction.

(e) If $Y_{02,1v}=0$ and the others are negative, then

$$\Delta E=\left[\,|\,(c_r^{02})(d_s^{1v})\,|\,\gamma+\left\{\sum_j^{unocc}\sum_i^{all}\nu_i-\sum_j^{occ}\sum_i^{all}(2-\nu_i)\right\}'\frac{(c_r^i)^2(d_s^j)^2\gamma^2}{2Y_{ji}}\right](-\beta) \qquad (17)$$

* Each $M_S$ component gives the same stabilization energy, and the mean is, therefore, the same.

where the mark $'$ on the summation tells to omit the set ($j$=1v, $i$=02).

(f) If $Y_{ho,01}=0$ and others are negative, then, similarly

$$\Delta E=\left[\,|\,(c_r^{01})(d_s^{ho})\,|\,\gamma+\left\{\sum_j^{unocc}\sum_i^{all}\nu_i-\sum_j^{occ}\sum_i^{all}(2-\nu_i)\right\}'\frac{(c_r^i)^2(d_s^j)^2\gamma^2}{2Y_{ji}}\right] \qquad (18)$$

$'$ indicating the neglect of the set ($j$=ho, $i$=01).

(g) If $Y_{02,1v}=Y_{ho,01}=0$ and others are negative, we obtain

$$\Delta E=\left[\sqrt{(c_r^{02})^2(d_s^{1v})^2+(c_r^{01})^2(d_s^{ho})^2}\,\gamma+\left\{\sum_j^{unocc}\sum_i^{all}\nu_i-\sum_j^{occ}\sum_i^{all}(2-\nu_i)\right\}'\times\frac{(c_r^i)^2(d_s^j)^2\gamma^2}{2Y_{ji}}\right](-\beta) \qquad (19)$$

neglecting in the summation the sets ($j$=ho, $i$=01) and ($j$=1v, $i$=02) In the latter three subcases the stabilization is of the first order, and for the lowest excited molecule the frontier electron density controls a main part of the reactivity indexes. The subcase g includes reactions of an excited molecule with an unexcited molecule of the same kind.

The photodimerization of aromatic hydrocarbons has been considered to pass through the following mechanism:

$$A^*+A \underset{\text{(step b)}}{\longrightarrow} (AA^*) \underset{\text{(step c)}}{\longrightarrow} AA \qquad (20)$$

Though the detail of the intermediate (AA*) is not clear, assuming the present type of complex for the transition state of step b, one can discuss the reactivity of this reaction as belonging to the subcase g. In Table II calculated values of the $\pi$ stabilization energy are collected. In that table, reagents are assumed to make two weak bondings through two meso positions, as illustrated in Fig. 6; the assumption of one bonding would only need to divide the values by the factor 2.

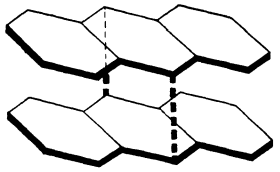
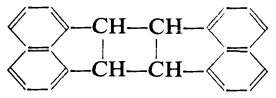


Fig. 6. Model of transition state of photodimerization of anthracene.

Anthracene is well known to make a photodimer at 9 and 10 positions, in accord with our calculation. Also in other polyacenes the most central meso-positions have the largest stabilization energy. This result is compatible with the experiment[13]. Bowen and Marsh[14] studied the photodimerization of acenaphthylene, finding that the structure of the photodimer was



This finding was first theoretically discussed by Crawford and Coulson[8]. They calculated the free valence of this molecule in its lowest excited state and found that the values of positions 5 and 6 (0.62) are greater than those of positions 1 and 2 (0.57), which conflicted with the above experimental results. Thus they stated that the free valence is not a sufficient guide to reactivity. Recently this experiment has been interpreted successfully by the present authors in terms of the frontier electron density for a radical reaction[15]. The frontier electron density of positions 1 and 2 is greater than that of positions 5 and 6. In that paper the excited acenaphthylene was regarded as an ordinary radical reagent attacking an acenaphthylene molecule in the ground state. At this time it would be interesting to apply the present theory which involves an explicit consideration of the excitation. This belongs to the subcase g. As is seen in Table II the stabilization energy of the reaction through pairs of positions 1-1 and 2-2 is greater than that through 5-5 and 6-6, in accordance with the experiment.

In intermolecular comparison it is said that the ease of photodimerization is greater in pentacene than in anthracene[13]. But this is not a direct comparison of the rate constant $k_b$ of the step b but a rough estimation from the amount of dimers produced. The total rate of dimer formation would be affected not only by the rate constant $k_b$ but also by various competitive reactions such as the collisional or spontaneous degradation of the excited A molecule, dissociation of (AA*), and so forth. To measure and compare the rate constant with calculated stabilization energy would be interesting.

**Reaction of an Excited Singlet Molecule with an Unexcited Molecule.**—The method and the results of the treatment for this kind of reaction is exactly the same as that in the last case if only the wave function, Eq. 12, is replaced by the following equation:

$$^1\Psi_0 = \boldsymbol{A}[\cdots(\psi_{01})^{m+n-1}(\psi_{02})^{m+n}\{\alpha(m+n-1) \times\beta(m+n)-\beta(m+n-1)\alpha(m+n)\}/\sqrt{2}] \quad (21)$$

Eqs. 13 to 20 are also valid in this case.

**Reaction of an Excited Molecule with Another Excited Molecule.**—We derived also the equations giving the stabilization energy in a reaction of an excited molecule (singlet or triplet) with another excited molecule (singlet or triplet) in a similar way. But as they are less meaningful for practical purposes and rather intricate, we do not give their explicit forms. It would be noteworthy that in this case also the frontier electron densities decide the intramolecular orientation.

## Discussion

We have derived formulas giving the $\pi$ stabilization energy and the reactivity index, discussing the rate of reactions of excited molecules. But we do not, at all, regard this theory as complete but merely as a simple pioneering attempt in the molecular orbital method; the assumptions included may have to be subjected to some improvements in future. For discussing the difference in rate constant caused by the difference in multiplicity of states, interactions of electrons should be explicitly taken into account. For discussing various dissociation reactions, attention would have to be paid to $\sigma$ electrons in the bond to be broken. Furthermore, in order to understand all the figures of reactions of an excited molecule, discussions on relations between various elementary steps involved in the reaction would be expected.

*Faculty of Engineering*
*Kyoto University*
*Sakyo-ku, Kyoto*

13) For example, M. Nakagawa, "Gendai Kagaku", III-D, Iwanami, Tokyo (1956); M. Koizumi and M. Shiba, ibid., I-E, (1956).
14) E. L. Bowen and J. D. F. Marsh, *J. Chem. Soc.*, **1947**, 109.
15) K. Fukui, T. Yonezawa and C. Nagata, This Bulletin, **34**, 37 (1961).

# *Polarography of Narcotine-N-oxide**

By Yutaka ASAHI

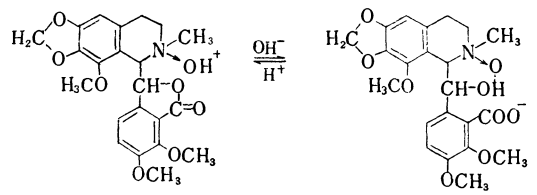
(Received January 7, 1961)

It has been reported by Kirkpatrick[1] that narcotine, an opium alkaloid, shows a catalytic hydrogen wave as do the other alkaloids, and according to Holubeck[2], narcotine and hydrastin can be determined quantitatively with the the reduction wave of their oxidation product, opianic acid. It is known that *N*-oxides such as pyridine-*N*-oxide[3] and nitrogen mustard *N*-oxide[4] are reduced polarographically to the corresponding amines, but the polarography of narcotine-*N*-oxide has not been reported yet.

In this paper the polarographic determination of narcotine-*N*-oxide in the oxidation products of narcotine is attempted and further-more, the electrode reaction and behaviors of narcotine-*N*-oxide in aqueous solutions are examined by means of DC- and AC-polarography, electrocapillarity, potentiometric titration and ultraviolet absorption spectrometry. Narcotine-*N*-oxide shows 2-electron reduction waves of *N*-oxide, which are complicated by the adsorption on the electrode, the kinetic current of protonation and the reversible cleavage of lactone.

## Experimental

The Yanagimoto pen-recording polarograph model PA 2, the Beckman pH meter model G and Beckman spectrophotometer model DU or DK 2 were used. The dropping mercury electrode has such characteristics as $m=0.817$ mg. $sec^{-1}$, $t=3.94$ sec., $m^{2/3}t^{1/6}=1.097$ and $h=70$ cm. Polarograms were taken in buffer solutions of acetate, phosphate,



(I) (II)

borate, hydrochloric acid and sodium hydroxide at 25±0.1°C after bubbling nitrogen gas, using N calomel electrode as the external reference electrode.

Narcotine hydrochloride and its *N*-oxide were given by Dr. H. Matsumaru of the Tokyo factory of our company.

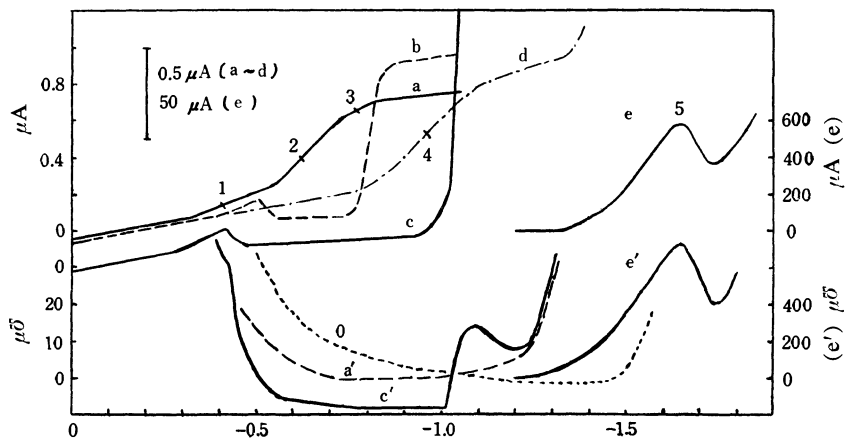



Fig. 1. D. C. (upper) and A. C. (lower) Polarograms of narcotine-*N*-oxide in pH 4. a, a, e, e', d: 0.2 mM, b: 0.3 mM, c, c': 1 mM, O: blank, d: hydroxycarboxylic acid form. 1~5: see Fig. 2.

* Polarographic studies of Pharmaceuticals. XXV. XXIV: *J. Pharm. Soc. Japan* (*Yakugaku Zasshi*), **80**, 1226 (1960).

1) H. F. W. Kirkpatrick, *Quart. J. Pharm. Pharmacol.*, **18**, 338 (1945).

2) J. Holubek, *Pharmazie*, **11**, 577 (1956).

3) A. Foffani and F. Fornasari, *Gazz. Chim. Ital.*, **83**, 1051, 1059 (1953).

4) I. Aiko, *Pharm. Bull.*, **1**, 335 (1953).

## Results

**Catalytic Hydrogen Wave.** — Narcotin-*N*-oxide shows a great increase of current from about −1.2 V. and generally a maximum wave in a buffer solution of pH 1～9. (Fig. 1e) The maximum wave height ($i_m$) is greatest at about pH 7 (Fig. 2 (5)) and tends to reach a limiting value at higher concentrations. The height ($i_m$) in a 0.2 mM solution of the *N*-oxide is supressed from 56 μamp. to 40 and 20 μamp. in the presence of 0.01 and 0.05% gelatin, respectively. The maximum potential ($E_m$), −1.4～−2 V., becomes more negative in higher wave heights and higher concentrations: $E_m$ −1.44 V., $i_m$ 0.09 μamp. $c$ 0.05 mM; $E_m$ −1.55 V., $i_m$ 7.6 μamp., $c$ 0.2 mM; $E_m$ −1.70 V., $i_m$ 38.2 μamp., $c$ 0.6 mM at pH 9.2. The temperature coefficient of $i_m$, 8% deg.$^{-1}$, is very high. The height decreases with the increase of mercury head ($h$) : $i_m$ in a 0.1 mM solution of pH 9.2 is 1.62, 1.19 and 0.89 μamp. at 48, 68 and 88 cm. of $h$ respectively.

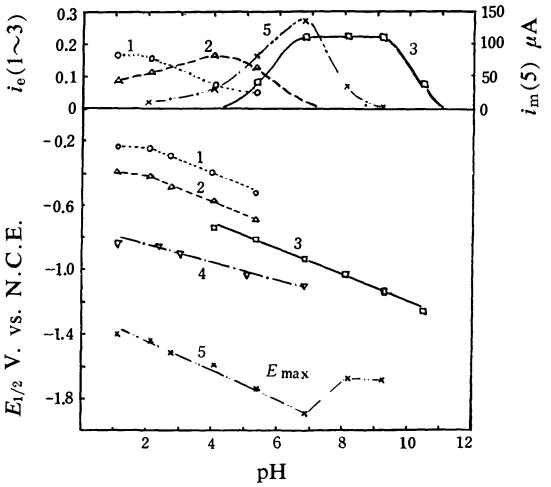



Fig. 2. $E_{1/2}$-pH curves (lower) and wave height-pH curves of narcotine-*N*-oxide (0.1 mM).
1) Absorption wave, 2) Reduction wave of cation, 3) Reduction wave of free base, 4) Reduction wave of hydroxy-carboxylic acid form, 5) Catalytic hydrogen wave.

**Reduction Wave of Lactone type Narcotine-*N*-oxide (I).**—0.1 mM narcotine-*N*-oxide hydrochloride in a buffer solution of pH 1～10 shows 1～3 steps of reduction waves at the potential more positive than that of the catalytic hydrogen wave (Fig. 1a). The total wave height is independent of pH in a range of 1～9, but decreases at above pH 9 (Fig. 2 (1～3)). In 0.1 N hydrochloric acid, the total wave height ($i_d$) of 3 steps is proportional to the concentration ($c$) in a range of 0.1～1 mM and the diffusion current constant ($k_D$) is calculated as 2.3 (μamp. mM$^{-1}$ mg$^{-2/3}$ sec$^{1/2}$).

Their 1st step is considered as an adsorption wave since the relationships between the wave height ($i_1$) and the concentration ($c$) fulfil the equation $i_1 = a \cdot b \cdot c/(1+b \cdot c)$ with $a$=1.25 $b$=2.67 mM$^{-1}$.

In acetate buffer of pH 4, 3 steps of reduction waves are also obtained in low concentration (0.05～0.23 mM), but in higher concentration (0.24～1 mM) an anomalous minimum wave in some potential range is obtained (Fig. 1, b, c). Thus the current is strongly suppressed in the potential range of −0.42～−1.04 V. at 1 mM and −0.6～−0.7 V. at 0.24 mM. The limiting current at −1.1 V. corrected for the residual current is, however, proportional to the concentration.

At pH 6.8～9.2, one reduction wave is observed near a catalytic hydrogen wave. Since the wave height tends to a limiting value (0.3 μamp.) at higher concentration (0.05～0.6 mM) and its temperature coefficient is small (0.4% deg$^{-1}$), this wave is assumed to be an adsorption wave.

When the pH value increases from 4 to 7, the wave heights of the 1st and the 2nd steps decrease and that of the 3rd step increases (Fig. 2). The apparent p$K$ of I is assumed to be 5.6 from the pH in which the 1st and 2nd wave height is equal to the 3rd one.

$E_{1/2}$-pH curves can be shown by the equation $E_{1/2} = E_0 + a$ pH, where $E_0$ are −0.08, −0.26 and −0.30 V. for 1st, 2nd and 3rd waves, respectively and $a$ is about −0.08 V. (Fig. 2).

The slope of the reduction wave of narcotine-*N*-oxide at −0.2～−0.9 V. in 0.25 mM solution of pH 3.7, becomes steep and the foot of the wave shifts toward the negative side in the presence of 0.1～2 mM narcotine. The potential range of the anomalous wave observed at −0.47～−0.89 V. in 0.5 mM at pH 4.1 becomes more negative and less wide (−0.63～−0.92V.) in the presence of 2 mM narcotine. In both cases the total wave height is also proportional to the concentration of the *N*-oxide and is not altered with narcotine. Similar phenomena are observed in the coexistence of 0.01～0.02% gelatin and 0.2～1 mM the *N*-oxide.

**Change of Polarograms of Narcotine-*N*-oxide by Alkali and Acid.**—The reduction wave of narcotine-*N*-oxide hydrochloride (I) disappears gradually in alkali. From the current-time curve at a fixed potential, the reaction is estimated to be of the 1st order. Its velocity constant ($k_1$) is proportional to [OH$^-$] ion concentration. The reaction product II gives no wave above pH 9 but a reduction wave at more negative potential than that of I at pH

1～7 (Fig. 1d) and reverse to the original one I by acid. The velocity constant ($k_2$) of the reverse reaction is proportional to [$H^+$] ion concentration (Fig. 3).

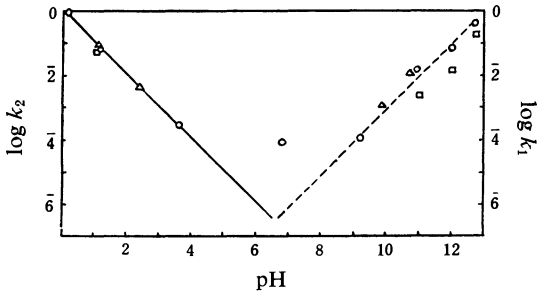



Fig. 3. Relationships between pH and reaction velocity constant of cleavage of the lactone ($k_1$) and of its formation ($k_2$) of narcotine (□) or its *N*-oxide (○, △) observed by reduction wave height (△) or $\varepsilon_{313m\mu}$ (○, □) at 25°C.

**Change of Ultraviolet Absorption Spectra of Narcotine and its *N*-oxide by Alkali and Acid.**—Narcotine hydrochloride gives a peak with $\lambda_{max}$ 313 m$\mu$ ($\varepsilon$ 4000) and a shoulder at 290 m$\mu$ in 20% ethanol solution (pH 5). The spectra change gradually to $\lambda_{max}$ 282 m$\mu$ ($\varepsilon$ 3200) in alkali.

Narcotine-*N*-oxide gives $\lambda_{max}$ 313 m$\mu$ ($\varepsilon$ 4000) and shoulders at 290 and 240 m$\mu$ in acid, and $\lambda_{max}$ 278 m$\mu$ ($\varepsilon$ 2800) in alkali. These changes occur reversibly and in measurable speed. The velocity constant of the 1st order reaction observed by absorbance at 313 m$\mu$ is proportional to [$OH^-$] in alkali and [$H^+$] in acid, and is in good agreement with that obtained by polarography (Fig. 3).

**A. C. Polarography.**—0.2 mM Narcotine-*N*-oxide in a buffer solution of pH 4 gives a large A. C. Polarogram ($i_p$ 710 $\mu\bar{v}$) at the potential $E_p$ −1.67 V. corresponding to the catalytic hydrogen wave but no wave at the potential of reduction of *N*-oxide. At higher concentration (1 mM) in the same buffer, the A. C. polarogram is suppressed in the potential range −0.5～−1 V. as D. C. polarogram.

**Electrocapillary Curve.**—The relationships between the applied potential and drop time of the mercury electrode in an acetate buffer of pH 4 is shown in the electrocapillary curve with a maximum at −0.6 V. (Fig. 4 ——). In the presence of 0.2 mM narcotine-*N*-oxide, the surface tension of the electrode is suppressed at −0.2～−1.4 V. and the curve extends to negative at −1.5～−1.7 V. because of the ohmic drop with the large catalytic current (Fig. 4------).

**Potentiometric Titration.**—Titration of 1 cc. of 10 mM narcotine-*N*-oxide·HCl with 0.1 cc. of

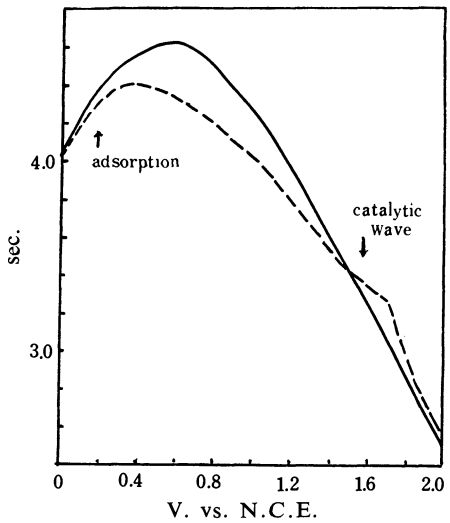



Fig. 4. Electrocapillary curves of acetate buffer (pH 4, ——) and with 0.2 mM narcotine-*N*-oxide (------).

0.1 N sodium hydroxide at 25°C reveals it to be an acid of p$K$ 3.75. After an alkaline (5 mM the *N*-oxide, 0.02 N sodium hydroxide, 10 cc.) is heated at 100°C for 5 min., two acid groups of p$K$ 6.0 and below 3 are observed by titration with 0.1 N hydrochloric acid or sodium hydroxide in nitrogen atmosphere and the product shows an absorption maximum at 280 m$\mu$. When the solution of pH 2.7 is heated at 100°C for 30 min., an acid group of p$K$ 3.7 and an absorption maximum at 313 m$\mu$ is obtained again. This alternation is ascribed to the reversible cleavage of the lactone. A similar phenomenon is also observed in narcotine, where the lactone type gives p$K$ 6.1 and the hydroxycarboxyl type gives p$K$ 9.4 and below 3.5 in 50% ethanol solution.

## Discussion

The maximum wave of narcotine-*N*-oxide at about −1.4～−2 V. is considered to be a catalytic hydrogen wave as narcotine and other alkaloids. This is useful for a microdetermination of pure alkaloid because of its high sensitivity, but can not be used for the specific determination of each alkaloid.

The reduction wave of narcotine-*N*-oxide must be due to the *N*-oxide group as this wave is not observed in narcotine. The total wave height of the *N*-oxide in acetate buffer solution of pH about 4 can be utilized for its determination in the mixture of alkaloids. Applying Ilkovič's equation, $k_D=607\ nD^{1/2}=i_d$. $c^{-1}m^{-2/3}t^{-1/6}$, with $k_D=2.3$ at pH 1～9 and $D=4.1\cdot10^{-6}$ ($cm^2\ sec^{-1}$) which is estimated from the molecular weight, $n=1.88\fallingdotseq2$ is obtained.

As the wave is very flat and no A. C. polarogram is obtained at the corresponding potential, the electrode process may be irreversible. In strong acid solutions, narcotine (p$K$ 6.1) and its $N$-oxide (p$K$ 3.75) exist as proton adducts with lactone moiety I. Then the 1st and 2nd steps at pH 1~5 are assumed to be due to the following reaction.

$$\left(\rangle N\rightarrow O\right)H^+ + 2e + 2H^+ \rightarrow \rangle NH^+ + H_2O$$

The fact that the apparent p$K$ 5.6 obtained from the wave height-pH curves is greater than p$K$ 3.75, is explained by the kinetic current due to the protonation of the base on the electrode. The 3rd wave at pH 5~10 may be ascribed to the reduction of the $N$-oxide base to narcotine.

$$\rangle N\rightarrow O + 2e + 2H^+ \rightarrow \rangle N + H_2O$$

It is clear from the hysteresis of potentiometric titration curve and ultraviolet absorption spectra in acid and alkali that narcotine and its $N$-oxide change reversibly from lactone types I in acid to hydroxy-carboxylate types II in alkali. Because of this reaction, the wave height of the 3rd step decreases at pH above 10. The $N$-oxide with a hydroxy-carboxylate group II give more negative $E_{1/2}$ than that of lactone type I, perhaps because the $N$-oxide is stabilized by the formation of hydrogen bond $\left(\rangle N\rightarrow O\cdots HO-\right)$.

The 1st step of the $N$-oxide with lactone ring has the character of an adsorption wave and disappears in the presence of narcotine or gelatin. Moreover the fact that the surface tension of the mercury electrode is suppressed in more negative potential than the 1st wave, confirms the adsorption of the reduction product, narcotine, on the electrode surface. Applying Brdička's equation[5], $z = i_a t / nF\Delta q$, with $i_a = 0.3\,\mu$ amp. (pH 9.2), $t = 3.94$ sec. and $\Delta q = 0.85\ (mt)^{2/3} = 0.0185\,cm^2$, the maximum number of adsorbed molecule ($z$) is estimated to be $3.3\times10^{-10}$ mol. $cm^{-2}$ and the cross-sectional area of a narcotine molecule on the electrode surface ($A$) is calculated as 50 Å$^2$. From $i_a = 1.25\,\mu$ amp. in 0.1 N hydrochloric acid, $A$ is estimated to be 12 Å$^2$. These values are comparable to the minimum cross-sectional area of a molecule packing closely on the mercury surface.

The curious polarograms in higher concentration at pH about 4 are ascribed to the inactivation of the mercury electrode by the adsorption layer.

5) R. Brdička: *Z. Elektrochem.*, **48**, 778 (1942).

## Summary

Narcotine-$N$-oxide shows a catalytic hydrogen wave as narcotine and other alkaloids. The reduction waves of narcotine-$N$-oxide are ascribed to the 2-electron reduction of the $N$-oxide to narcotine. Their 1st step is an adsorption wave of the reductant. The adsorped film disturbs the further electrode reaction, an anomalous minimum wave is observed in higher concentration. The 2nd step in pH 1~5 corresponds to the proton adduct of the $N$-oxide with lactone and the 3rd step in pH 5~10 to the base of the $N$-oxide.

Narcotine and its $N$-oxide change reversibly to hydroxycarboxylate type in alkali, which gives more negative reduction potential of the $N$-oxide and an absorption maximum in shorter wavelength. The velocity constants of cleavage of the lactone and of the reverse reaction are proportional to [$OH^-$] and [$H^+$], respectively.

The author express his sincre thanks to Dr. S. Kuwada, Dr. A. Watanabe and Dr. T. Kanzawa of this laboratory.

*Research Laboratories*
*Takeda Pharmaceutical*
*Industries, Ltd.*
*Higashiyodogawa-ku, Osaka*

# *A Novel Synthetic Route of 3,6-Dimethyl-2,3-dihydro-1H-cyclopent-[a]anthracene and 6-Methyl-2,3-dihydro-1H-cyclopent[a]anthracene*

By Masao NAKAZAKI, Kikuo YAMAGAMI and Sachihiko ISOE

(Received December 26, 1960)

Tsuda and coworkers[1] reported the isolation of a hydrocarbon ($C_{19}H_{18}$, oil, melting point of the picrate, 133~134°C) among the products of selenium dehydrogenation of the phenol II which they obtained by the dienone-phenol rearrangement of 7-keto-5,8(9)-cholestadien-3$\beta$-yl acetate. The same compound was isolated by them[2] from the selenium dehydrogenation products of the anthrasteroid III from 5,8(9)-cholestadien-3$\beta$-ol.

Starting from 1-methyl-2-naphthoic acid (IV) we[3] succeeded in preparing 3,6-dimethyl-2,3-dihydro-1*H*-cyclopent[*a*]anthracene (I). This structure I was assigned by Tsuda and coworkers to their dehydrogenation product, but the comparison of the ultraviolet absorption spectra of synthetic I and the dehydrogenation product indicated that the latter was considerably contaminated with non-anthranoid impurities. Having established the structure of anthracholestatetraene, proposed by Mosettig[4], by an excellent method[5], Burgstahler and Mosettig[6] prepared *dl*-5,7,9,14-anthratetraen-17-one (V) to study a possible general synthetic route to anthrasteroids as well as to examine their carcinogenic properties. Sodium borohydride reduction of ketone V afforded alcohol VI, but the dehydrogenation which was expected to be accompanied by the migration of the 18-methyl group to 17-position to give I was found fruitless[7].

Since 3,6-dimethyl-2,3-dihydro-1*H*-cyclopent-[*a*]anthracene (I) is an analog of Diel's hydrocarbon usually obtained by the dehydrogenation of steroids, and since we happened to need a considerable amount of it for biological experiments, we explored a simpler route to compound I. In the present paper a new synthetic route to compound I and its nor-compound XIIIb is described.

Our synthesis, shown in Fig. 1, employs the

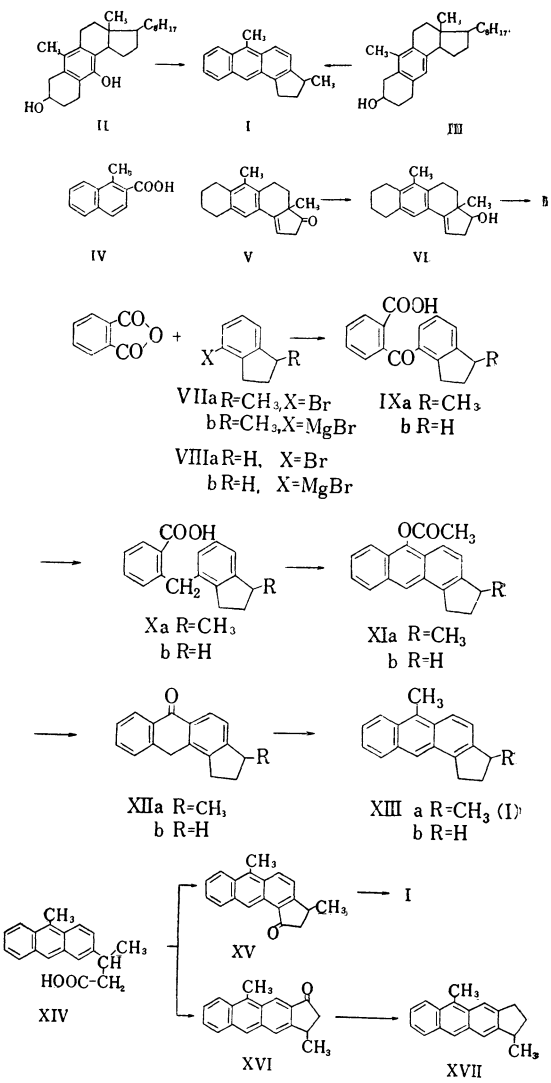



Fig. 1

method developed by Fieser and Hershberg[8] for the general synthesis of 9-alkylanthracene derivatives. Since the syntheses of I and XIIIb are similar, that of I is described at length. 4-Bromo-1-methylindan (VIIa), our starting substance, had been obtained by Hoyes[9] by

1) K. Tsuda, K. Arima and R. Hayatsu, *J. Am. Chem. Soc.*, **76**, 2933 (1954).
2) K. Tsuda and R. Hayatsu, ibid., **77**, 3089 (1955).
3) M. Nakazaki and S. Isoe., *Chem. & Ind.*, **1958**, 43; This Bulletin, **32**, 1202 (1959).
4) See Ref. 8 in our paper[3].
5) A. W. Burgstahler, *J. Am. Chem. Soc.*, **79**, 6047 (1957).
6) A. W. Burgstahler and E. Mosettig, ibid., **81**, 3697 (1959).
7) Private communication from Dr. Mosettig, National Institutes of Health, Bethesda, Maryland, U.S.A.
8) L. F. Fieser and E. B. Hershberg, *J. Am. Chem. Soc.*, **59**, 2331 (1937); **60**, 940 (1938).
9) H. Hoyes, *J. prakt. Chem.*, **139**, 242 (194).

reduction with hydriodic acid and phosphorus of 4-bromo-1-hydroxy-1-methylindan (b. p. 135~136°C/25 mmHg, m. p. 33~34°C), prepared from 4-bromo-1-indanone and methylmagnesium bromide. When we carried out the reaction of methylmagnesium bromide with the bromoketone, we obtained unsaturated 7-bromo-3-methylindene (b. p. 137~139°C/19 mmHg) which did not show an OH band in infrared spectrum but could be hydrogenated in a good yield to saturated 4-bromo-1-methylindan (VIIa) (b. p. 75~77°C/1.5 mmHg) in the presence of platinum oxide.

Although Kon and Woolman[10] observed that 4-bromoindan (VIIIa) could be converted with difficulty into a Grignard complex even under the condition elaborated by Fieser and Hershberg[8], bromide VIIa could be made to react smoothly with magnesium to afford Grignard compound VIIb, which gave 2-(1-methylindan-4-carbonyl)benzoic acid (IXa) (m. p. 123.5~124.4°C) with phthalic anhydride. The conversion into 2-(1-methylindan-4-ylmethyl)-benzoic acid (Xa) (m. p. 126~127°C) was effected by the high pressure catalytic hydrogenation with a copper chromite catalyst.

Heating with zinc chloride in acetic anhydride and acetic acid accomplished the ring closure of acid Xa to 6-acetoxy-3-methyl-2, 3-dihydro-1*H*-cyclopenta[*a*]anthracene (XIa) (m. p. 161~161.5°C), which, because of its instability toward acid and alkali, was hydrolyzed indirectly according to Fieser and Hershberg's method[8].

The reaction of methylmagnesium bromide with acetate XIa provided 3-methyl-6-oxo-2, 3, 6, 11-tetrahydro-1*H*-cyclopent[*a*]anthracene (XIIa) (m. p. 99~100°C), accompanied by a high melting compound (m. p. 221~223°C). The latter, in spite of its sparing solubility in benzene, always appeared in the mother liquor of recrystallization of even the purest sample of anthrone XIIa from benzene. From this behavior, together with other evidences (molecular weight, ultraviolet spectrum and infrared spectrum) it appears that the substance is a condensation product from two anthrone molecules, analogous to the high melting products obtained by Fieser and Hershberg[8] in their synthesis of 10-isopropyl-1', 2', 3', 4'-tetrahydro-1, 2-benzanthracene.

The product from the Grignard reaction of anthrone XIIa with methylmagnesium bromide was decomposed with an acid and extraction with ether gave a highly blue-green fluorescent oil, which was purified by chromatography on alumina to afford pale yellow needles, m. p. 80.5~81°C. The substance was identified with 3,6-dimethyl-2,3-dihydro-1*H*-cyclopent[*a*]anthracene (I) prepared previously[3] by mixed melting point determination, comparison of infrared and ultraviolet spectra and mixed melting point determination of the trinitrobenzene complex.

In our previous synthesis of I, there remained a question whether the ring closure of acid XIV took place at 1-position to give XV or at 3-position to give XVI. Then, structure XVI was ruled out mainly on account of two observations, i. e. the 1-position of the anthracene nucleus is much more reactive toward electrophilic substitution, and the keto compound (XV) (m. p. 142~143.5°C) obtained showed a markedly similar ultraviolet spectrum with 1-acetylanthracene and exhibited an absorption at 12.2 $\mu$ in infrared spectrum which could be attributed to the presence of two adjacent hydrogen atoms in the anthracene nucleus[11]. The present synthesis with no such ambiguity can be taken as a support to the above view.

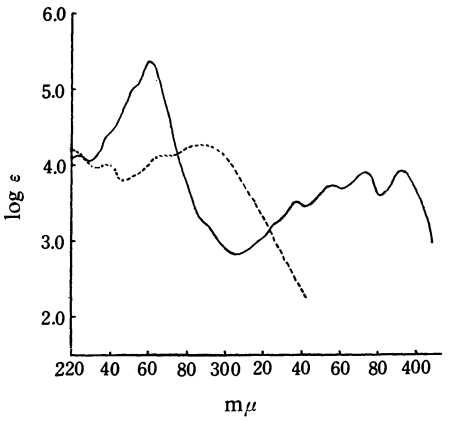
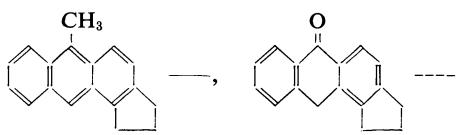



Fig. 2.




Solvent: 95% ethanol

TABLE I. ULTRAVIOLET ABSORPTION SPECTRA (in 95% ethanol)

| I | | XIIIb | | XIa | | XIb | |
|---|---|---|---|---|---|---|---|
| $\lambda_{max}$ | log ε | $\lambda_{max}$ | log ε | $\lambda_{max}$ | log ε | $\lambda_{max}$ | log ε |
| 261 | 5.33 | 261 | 5.22 | 259 | 5.30 | 259 | 5.29 |
| 338 | 3.46 | 338 | 3.53 | | | | |
| 354 | 3.73 | 354 | 3.79 | 353 | 3.81 | 356 | 3.40 |
| 372 | 3.90 | 372 | 3.95 | 371 | 3.95 | 375 | 3.55 |
| 392 | 3.89 | 392 | 3.95 | 391 | 3.94 | 396 | 3.55 |

10) G. A. Kon and A. M. Woolman *J. Chem. Soc.*, **1939**, 796.

11) H. Dannenberg and D. D. Dannenberg, *Ann.*, **585**, 1 (1954), see also W. West, "Chemical Applications of Spectroscopy", Interscience Pub. Inc., New York (1956), pp. 388—406.

The synthesis of 6-methyl-2,3-dihydro-1*H*-cyclopent[*a*]anthracene (XIIIb) was carried out in a way analogous to that described above, m. p. 127~128°C; melting point of the trinitrobenzene complex, 149.5~150.5°C; melting point of the picrate, 144~145°C, ultraviolet spectrum overlapping that of I (see Fig. 2 and Table I).

## Experimental*

**Ethyl *o*-Nitrocinnamate**[12]. — Cinnamic acid was nitrated to give a mixture of *o*- and *p*-nitrocinnamic acids, which were esterified with ethanol and hydrogen chloride gas. From the mixture of ethyl *o*- and *p*-nitrocinnamates, the *o*-isomer was separated by virtue of its facile solution in m. p. 42°C, yield, 21.4%.

**Hydrocarbostyril.**—Ethyl *o*-nitrocinnamate (30 g.) was dissolved in 300 cc. of ethanol and hydrogenated in the presence of 4~5 g. of Raney nickel W-6 at 55~60°C and 47 atms. for 5~7 hr. Hydrocarbostyril was obtained in a yield of 79%, m. p. 163°C, (literature[13]: m. p. 165~166°C).

**β-(2-Bromophenyl)propionic Acid (XVIII)**[14].—*a. From Hydrocarbostyril*[15]. — A mixture of 30 g. of hydrocarbostyril, 97 g. of crystalline barium hydroxide and 400 cc. of water was refluxed for 20 hr. in a stream of nitrogen. The solution was diluted with 500 cc. of water and a stream of carbon dioxide was passed through it to precipitate barium carbonate.

After being freed from barium carbonate, the solution was made just alkaline to phenolphthalein with 10% sodium carbonate solution. The precipitated sodium salt, after being dried and washed with acetone, weighed 64.7 g. (yield, 84%), m. p. 155°C. A solution of 18.7 g. of this sodium salt and 6.9 g. of sodium nitrite in 100 cc. of water was added dropwise into 42 cc. of 48% hydrobromic acid chilled at 0~5°C in an ice bath. Cuprous bromide was precipitated by adding 6.3 g. of sodium sulfite to a mixture of 25 g. of cupric sulfate, 14.6 g. of sodium bromide and 100 cc. of water, and was dissolved by adding 6 cc. of 48% hydrobromic acid, and the solution was kept boiling. Onto this boiling solution, the above-mentioned diazonium bromide solution was added in four portions and the whole was refluxed for 30 min. The precipitated bromo acid was taken into ether, and the ethereal solution was washed with water and dried with anhydrous sodium sulfate. After removal of the solvent, the residue was recrystallized from aqueous acetic acid, m. p. 91~93°C, 5.6 g. The mother liquor was distilled and the fraction which boiled at 127~128°C/1 mmHg solidified on standing, m. p. 90°C, 1.2 g.

*b. From o-Bromobenzyl Bromide.*—*o*-Bromotoluene was brominated according to the procedure of Weizman and Patai[16], affording *o*-bromobenzyl bromide, m. p. 30°C (yield, 78%). To ethanolic sodium ethoxide prepared from 9.25 g. of sodium and 300 cc. of absolute ethanol, was added 28.5 g. of ethyl malonate and the mixture was heated for 15 min. on a water bath. After a solution of *o*-bromobenzyl bromide in 100 cc. of ethanol was added with stirring during 1 hr., the solution was stirred and refluxed for 3 hr.

The solvent was removed and the residue was diluted with ice water, and then concentrated hydrochloric acid was added to make the solution acidic to Congo red. After extraction with ether, the ether extract was washed with water and dried with anhydrous sodium sulfate. Removal of the solvent afforded a residue which was distilled to give ethyl *o*-bromobenzylmalonate boiling at 165~170°C/3 mmHg, 64.7 g. (yield, 82%)[10,14]. This malonate (64.5 g.) was hydrolyzed by boiling with 150 g. of potassium hydroxide, 175 cc. of ethanol and 300 cc. of water for 1 hr. After the ethanol was removed 250 cc. of concentrated hydrochloric acid was added to precipitate *o*-bromobenzylmalonic acid, which was collected and dried, 87 g. The malonic acid (87 g.) was decarboxylated by boiling with 400 cc. of water for 5 hr.

A heavy red oil which separated was extracted with ether and the ethereal solution was washed with water. After drying with anhydrous sodium sulfate, the solvent was removed to give β-(2-bromophenyl) propionic acid, m. p. 90°C. The yield was about 80% from the malonic ester.

**4-Bromo-1-indanone (XIX).**—Although Miersch[17] reported the formation of the bromoindanone XIX in a yield of 10% by the cyclization with concentrated sulfuric acid, XVIII did not give XIX with polyphosphoric acid[18] either under a rather mild condition (130°C, 20 min., recovery) or under a drastic condition (250°C, 20 min., polymerization). A mixture of 8.9 g. of crude XVIII and 15.6 g. of thionyl chloride was refluxed for 3 hr. After the excess of the thionyl chloride was removed, the residue, β-(2-bromophenyl)propionyl chloride, b. p. 120~123°C/2 mmHg, was dissolved in 240 cc. of carbon disulfide, and the solution was chilled at 5°C. To the stirred solution, 7.6 g. of aluminum chloride was added during 1.5 hr. After being allowed to stand at room temperature for 1.5 hr., the reaction mixture was refluxed for 15 min., and then a mixture of 100 cc. of concentrated hydrochloric acid and 300 cc. of water was added to decompose the reaction complex. The bromindanone was steam-distilled and recrystallized from ethanol, colorless needles, m. p. 95~96°C, (literature[15], m.p. 98~99°C), 6.2 g. (yield, 85%).

* All melting points are uncorrected. All ultraviolet spectra were measured with an EPS-2 Hitachi autorecording spectrophotometer and infrared spectra with a Perkin Elmer Model 12C. The analyses were performed in the microanalytical laboratory of the Institute of Polytechnics, Osaka City University.

12) L. Müller, *Ann.*, **212**, 124 (1882); L. Vanino, "Handbuch der Präparativen Chemie", Band II, Ferdinand Enke, Stuttgart (1937), p. 599.

13) E. R. Blout and D. C. Silverman, *J. Am. Chem. Soc.*, **66**, 1442 (1944).

14) For detailed discussion on the preparation of XVIII, see L. F. Fieser and A. M. Seligman, ibid., **57**, 2175 (1935).

15) F. Mayer, H. Phillips, F. W. Ruppert and A. T. Schmidt, *Ber.*, **61**, 1966 (1928).

16) M. Weizman and S. Patai, *J. Am. Chem. Soc.*, **68**, 151 (1946).

17) W. Miersch, *Ber.*, **25**, 2109 (1892).

18) F. D. Popp and W. E. Ewen, *Chem. Revs.*, **58**, 321 (1958).

**4-Bromoindan (VIIIa)**[10,14].—To a solution of 11.0 g. of XIX and 110 cc. of ethanol, 99 g. of amalgamated zinc was added with 70 cc. of concentrated hydrochloric acid. While the mixture was refluxed for 3 hr., 60 cc. of concentrated hydrochloric acid was added in three portions, and refluxing was further continued for 2 hr. The reaction mixture was diluted with water and, after the excess of zinc was removed, was extracted with ether. After drying with anhydrous sodium sulfate, the solvent was removed to give a liquid, which was distilled in vacuo, b. p. 75~77°C/2 mmHg, 8.7 g. (yield 85%), (literature, b. p. 118°C/18 mmHg[14], 100°C/1.5 mmHg[10]).

**7-Bromo-3-methylindene (XX)**[9].—Methyl bromide gas was introduced into a stirred mixture of 6.1 g. of magnesium and 200 cc. of ether until the magnesium disappeared. To the Grignard reagent, a solution of 2.5 g. of XIX in 500 cc. of ether was added during 1 hr., and the mixture was refluxed for 2 hr. While the solution was cooled in an ice bath, a mixture of 100 cc. of concentrated hydrochloric acid and 500 cc. of ice water was added, and the solution was extracted with ether. After the extract was washed with water and dried with anhydrous sodium sulfate, the solvent was removed to give an oil, which was distilled in vacuo, b. p. 137~139°C/19 mmHg, 11.1 g. (yield, 45%).

**4-Bromo-1-methylindan (VIIa).**—To a solution of 11.1 g. of XX in 50 cc. of ethanol, 0.2 g. of platinum oxide was added and the mixture was shaken in an atmosphere of hydrogen. Hydrogen was absorbed rapidly, and after 2 hr. the solution was freed from the catalyst. Removal of the solvent gave an oil, which was distilled in vacuo, b. p. 75~77°C/1.5 mmHg, 9.4 g. (yield, 84%), (literature[9], b. p. 245°C).

**2-(1-Methylindan-4-carbonyl)benzoic Acid (IXa).**—When a mixture of 5 drops of ethyl iodide and 10 drops of VIIa was added to a stirred mixture of 2.16 g. of magnesium and 5 cc. of ether, ebullition of ether was observed to indicate the start of the Grignard reaction. With stirring and heating on a water bath, a solution of 9.4 g. of VIIa in 80 cc. of ether was added during 3 hr., and the mixture was refluxed for 15 hr. in an atmosphere of nitrogen.

The Grignard solution was transferred into a dropping funnel with the aid of the pressure of nitrogen from a tank; then the reaction flask was washed with 100 cc. of ether, and the washing was transferred again into the funnel.

To a solution of 11.4 g. of phthalic anhydride in 200 cc. of benzene, the above Grignard solution was added during 1.5 hr. with stirring and refluxing, and the mixture was stirred and refluxed for 2 hr. in an atmosphere of nitrogen. Dilute hydrochloric acid was added to decompose the Grignard complex, and the solution was steam-distilled. The precipitate which separated from the distillated was dissolved in 10% sodium carbonate solution, and the resulting solution was again steam-distille. The turbid solution was filtered through a layer of Hyflo and was made acidic with dilute hydrochloric acid to precipitate IXa, which was recrystallized from benzene, m. p. 114~120°C. Recrystallization from benzene-ligroin yielded pure carboxylic acid, m. p. 123.5~124.5°C, 4.5 g. (yield, 36%). IR spectrum: 5.95 and 6.0 $\mu$.

Found: C, 77.15; H, 5.89. Calcd. for $C_{18}H_{16}O_3$: C, 77.12; H, 5.75%.

**2-(1-Methylindan-4-ylmethyl)benzoic Acid (Xa).**—A mixture of 3.5 g. of IXa and 140 cc. of ethanol was refluxed with a small amount of Raney nickel. The Raney nickel was filtered off, and the solution was hydrogenated with 0.5 g. of a copper chromite catalyst in a steel bomb at 149~155 atms. and 210~220°C for 4 hr. After the bluish green solution was freed from the catalyst, hydrogen sulfide was introduced to remove copper and chromium ions, and precipitated sulfides were filtered off through a layer of Hyflo. Removal of the solvent from the filtrate gave crystals, which were recrystallized from ethanol, m. p. 126~127°C, 3.2 g. IR spectrum: 5.9 $\mu$

**6-Acetoxy-3-methyl-2,3-dihydro-1*H*-cyclopent[*a*]anthracene (XIa).**—To a mixture of 3.2 g. of Xa, 30 cc. of acetic anhydride and 20 cc. of acetic acid, was added 0.27 g. of fused zinc chloride. After the brown mixture was refluxed for 1 hr., 50 cc. of water was added and the precipitated crystals were recrystallized from ethanol, m. p. 137~138°C, 2.5 g. (yield, 72%). IR spectrum: 5.7 $\mu$. UV spectrum: see Table I.

Found: C, 82.87; H, 6.64. Calcd. for $C_{20}H_{18}O_2$: C, 82.73; H, 6.25%.

**3-Methyl-6-oxo-2,3,6,11-tetrahydro-1*H*-cyclopent[*a*]anthracene (XIIa).**—To a Grignard reagent, prepared from 0.755 g. of magnesium, 30 cc. of ether and methyl bromide gas, 2.3 g. of XIa was added with 90 cc. of benzene. After the ether was removed, 90 cc. of benzene was added and the mixture was refluxed for 30 min. To the yellow solution, 100 cc. of diluted hydrochloric acid was added and the product was extracted with ether. After the ether extract was washed with water and dried with anhydrous sodium sulfate, the solvent was removed and the crystals were recrystallized from ethanol-ligroin, m. p. 86~93°C. For the preparation of an analytical sample, the product was recrystallized from methanol, m. p. 99~100°C.

Found: C, 86.11; H, 6.26. Calcd. for $C_{18}H_{16}O$: C, 87.06; H, 6.50%.

The mother liquor gave sparingly soluble crystals which were recrystallized from benzene-ethanol, m. p. 221~223°C.

**3,6-Dimethyl-2,3-dihydro-1*H*-cyclopent[*a*]anthracene (I).**—To the Grignard reagent, prepared from 0.252 g. of magnesium, 30 cc. of ether and methyl bromide, 427 mg. of XIIa was added with 50 cc. of benzene. After the ether was removed, the reaction mixture was refluxed on a water bath for 30 min. While the solution was chilled in an ice bath, 50 cc. of 2 N hydrochloric acid was added and the product was extracted with ether. The greenish blue fluorescent ether extract was washed with water and dried with anhydrous sodium sulfate. Removal of the solvent gave an oil which was chromatographed on 10 g. of alumina. Elution with benzine-benzene gave crystals which were recrystallized from methanol, pale yellow crystals, m. p. 80.5~81°C, 177 mg. (yield, 42%). The substance was found identical with I previously

prepared[3] by the comparison of the infrared spectra and the mixed melting point determination. UV spectrum: see Table I.

Found: C, 92.14; H, 7.60. Calcd. for $C_{19}H_{18}$: C, 92.63; H, 7.37%.

The trinitrobenzene complex was prepared from 35 mg. of I and 30 mg. of trinitrobenzene in benzene, and recrystallized twice from ethanol, reddish scarlet needles, m. p. 141.5~142°C. The mixed melting point determination (m. p. 140.5~142.5°C) confirmed the identity with the trinitrobenzene complex previously prepared[3] (m. p. 142~142.5°C).

Found: C, 65.37; H, 4.60; N, 9.15. Calcd. for $C_{25}H_{21}O_6N_3$: C, 65.35; H, 4.61; N, 9.15%.

**2-(4-Indancarbonyl)benzoic Acid (IXb).** — To a suspension of 2.05 g. of magnesium in 5 cc. of ether, was added a mixture of 2 drops of ethyl iodide and 10 drops of VIIIa to start the Grignard reaction. When ebullition of ether was observed, a mixture of 8.7 g. of VIIIa and 60 cc. of ether was added dropwise during 4 hr. After the solution was refluxed and stirred for 20 hr., the solution was transferred into a dropping funnel by means of the pressure of nitrogen from a tank, then the flask was washed with 100 cc. of ether and the washing was also transferred into the dropping funnel. To a solution of 11.3 g. of phthalic anhydride in 120 cc. of benzene, was added the above Grignard solution during 1.5 hr., and the mixture was refluxed for 30 min. A mixture of concentrated hydrochloric acid and 300 cc. of ice water was added to the reaction mixture and the whole was steam-distilled to remove volatile by-products. Ketoacid IXb was separated and dissolved in 150 cc. of a 10% sodium carbonate solution and the solution was steam-distilled for 2 hr. Fifty cubic centimeters of concentrated hydrochloric acid was added to the solution to give IXb, which was collected and recrystallized from benzene, m. p. 174~175°C. For the preparation of an analytical sample, the substance was recrystallized from benzene, m. p. 175~176°C, 6.8 g. (yield, 58%). IR spectrum: 6.01 and 5.94 $\mu$.

Found: C, 76.29; H, 5.54. Calcd. for $C_{17}H_{14}O_3$: C, 76.67; H, 5.30%.

**2-(4-Indanylmethyl)benzoic Acid (Xb).**—A solution of 6.2 g. of IXb in 125 cc. of ethanol was refluxed with a small amount of Raney nickel. The solution, after the catalyst was filtered off, was hydrogenated in a steel bomb with 0.3 g. of a copper chromite catalyst at 199~202 atoms. and 215°C for 4 hr. The solution was separated from the catalyst and treated with hydrogen sulfide to remove copper and chromium ions as the sulfides. The solution was filtered through a layer of Hyflo and the filtrate was concentrated under reduced pressure to afford crystals, which were recrystallized from benzene, m. p. 146~146.5°C, 5.42 g. (yield, 72%). IR spectrum: 6.01 $\mu$.

Found: C, 81.00; H, 6.24. Calcd. for $C_{17}H_{16}O_2$: C, 80.92; H, 6.39%.

**6-Acetoxy-2, 3-dihydro-1*H*-cyclopent[*a*]anthracene (XIb).**—To a mixture of 4.2 g. of Xb, 30 cc. of acetic acid and 20 cc. of acetic anhydride, was added 0.35 g. of zinc chloride and the solution was refluxed for 1 hr. To the brown solution, 200 cc. of water was added to precipitate a dark brown solid mass, which was continuously extracted with benzene to remove a brown insoluble by-product. The benzene extract was concentrated to afford yellow crystals, which were recrystallized from benzene, yellow prisms, m. p. 161~161.5°C, 3.4 g. (yield, 74%). IR spectrum: 5.70 and 12.35 $\mu$. UV spectrum: see Fig. 1 and Table I.

Found: C, 82.69; H, 6.12. Calcd. for $C_{19}H_{16}O_2$: C, 82.58; H, 5.84%.

**6-Oxo-2,3,6,11-tetrahydro-1*H*-cyclopent[*a*]anthracene (XIIb).** — To the Grignard reagent, prepared from 1.15 g. of magnesium, 60 cc. of ether and methyl bromide, was added 3.4 g. of XIb in three portions, which was followed by 40 cc. of benzene and then the ether was distilled off. The yellow reaction complex was decomposed with 100 cc. of water, while the solution was chilled in an ice bath, and the product was extracted with ether. After the ether extract was washed with water and dried with anhydrous sodium sulfate, the solvent was removed to give crystals, m. p. 115~140°C, which were recrystallized from benzene, m. p. 160~163°C. For the preparation of an analytical sample, the substance was recrystallized from benzene, m. p. 165~166°C, 0.981 g. (yield, 34%). IR spectrum: 6.10 $\mu$. UV spectrum: see Fig. 1.

Found: C, 86.68; H, 6.25. Calcd. for $C_{17}H_{14}O$: C, 87.15; H, 6.02%.

The mother liquor gave pale yellow needles, which were sparingly soluble in benzene, m. p. 222~223.5°C.

Found: C, 86.40; H, 5.63%.

**6-Methyl-2,3-dihydro-1*H*-cyclopent[*a*]anthracene (XIIIb).**—To the Grignard solution, prepared from 0.488 g. of magnesium, 30 cc. of ether and methyl bromide, was added 0.98 g. of XIIb, which was followed by 50 cc. of benzene. After the ether was distilled off, the benzene solution was refluxed for 30 min. After diluted hydrochloric acid was added to decompose the Grignard complex, the solution was extracted with ether. The bluish green fluorescent ether extract was washed with water and dried with anhydrous sodium sulfate. Removal of the solvent gave orange yellow needles, which were recrystallized from benzene to give pale yellow needles, m. p. 127~128°C. The mother liquor was concentrated and the residue was chromatographed on 10 g. of alumina affording an additional crop, with made the total yield of XIIIb 434 mg. (yield, 56%). UV spectrum: see Fig. 1 and Table I.

Found: C, 92.83; H, 6.85. Calcd. for $C_{18}H_{16}$: C, 93.06; H, 6.94%.

The trinitrobenzene complex was prepared from 20 mg. of XIIIb and 20 mg. of trinitrobenzene, and was recrystallized from ethanol, reddish scarlet needles, m. p. 149.5~150.5°C.

Found: C, 64.92; H, 4.35; N, 9.59. Calcd. for $C_{24}H_{19}O_6N_3$: C, 64.71; H, 4.30; N, 9.34%.

The picrate was recrystallized from benzene, brownish black needles, m. p. 144~145°C.

Found: C, 62.87; H, 4.19; N, 8.88. Calcd. for $C_{24}H_{19}O_7N_3$: C, 62.47; H, 4.15; N, 9.11%.

The authors are indebted to Mr. Yoshio Ota for his technical assistance, and also to

Mr. Eiichi Togashi, the Vice President of Shiono Koryo Kaisha, for a generous gift of cinnamic acid and to Kotobukiya Distillery and Nitto Kasei Co. for financial support.

*Department of Chemistry*
*Institute of Polytechnics*
*Osaka City University*
*Kita-ku, Osaka*

# SHORT COMMUNICATIONS

## *Manganese(III) Complexes with Ethylenediaminetetraacetic Acid*

By Yukichi Yoshino, Yoshikazu Tsunoda and Akira Ouchi

(Received June 1, 1961)

Although there have been some papers[1-3] on the analytical use of maganese(III) complexes with ethylenediaminetetraacetic acid (EDTA), little is known of the nature of the complex compounds. The authors had studied the critical condition of their formation in solution and could isolate the crystalline solid.

Three methods of the preparation of Mn-(III)-EDTA complexes from compounds of manganese in higher valency states have been examined. (1) Manganese dioxide suspended in water was mixed with solid ethylenediaminetetraacetic acid ($H_4Y$) under vigorous stirring. (2) In place of the free acid, a mixture of disodium salt of EDTA ($Na_2H_2Y \cdot 2H_2O$) and acetic acid was added to manganese dioxide. (3) Mn(II)-EDTA complex solution and manganese dioxide were mixed. Of these methods, the first was found to be the most suitable.

The relation between the mole ratio of manganese dioxide to EDTA and that of manganese dioxide to the produced Mn(III)-EDTA was shown in Fig. 1. Through the reaction a little of EDTA was lost and this may be due to its oxidation by manganese dioxide. However the mole ratio of Mn(III) to EDTA in the complex was approximately 1 : 1. Of course permanganate can also be

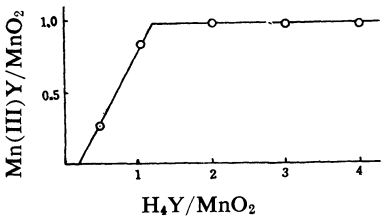



Fig. 1. Relation between the mole ratio of EDTA ($H_4Y$) : $MnO_2$ and the mole ratio of Mn(III)-EDTA : $MnO_2$ ($MnO_2$ : $2.69 \times 10^{-4}$ mol.).

used in place of manganese dioxide in all of these three methods.

The general method used to prepare the solid complex was as follows: to manganese dioxide precipitated by reducing potassium permanganate with ethanol, EDTA (in the acid form) was added in a ratio of little less than 1 : 1. On vigorous stirring reaction took place, evolving carbon dioxide, and a deep red solution was obtained. Filtering off the excess manganese dioxide, an equal volume of cold ethanol was added to the filtrate. The solution was allowed to stand for 1~2 hr. Deep red crystals thus obtained were washed with 90% ethanol and then with ethyl ether. Finally it was dried in the air in cold dark place; yield: 45~55%.

The crystal is deep red in color and decomposes easily in the light or on heating, giving carbon dioxide. The decomposition rate seems to be increased by the presence of Mn-(II) ion. The oxidation equivalent of the complex was evaluted as 435±3 by iodometric titration. It is very soluble in water but insoluble in most of organic solvents. When a sample was heated with gradual elevation of temperature, 12~13% of weight loss took place at 25~130°C. This value may correspond to the sum of the weight of the water of crystallization and of EDTA partially decomposed. The remaining EDTA was completely

1) R. Přibil and J. Horacek, *Collection Czechoslov. Chem. Communs.*, **14**, 626 (1949).
2) R. Přibil and V. Sumon, ibid., **14**, 454 (1949).
3) R. Přibil and E. Hornychova, *Chem. Listy*, **40**, 101 (1950).

decomposed at 260~300°C. The solid gave the analysis: K, 9.50; Mn, 12.52; C, 28.56; H, 3.57; N, 6.53%. From these results the formula $K[Mn(EDTA)(OH_2)_2]\cdot H_2O$ was tentatively given as in the case of Cr(III)-EDTA complex[4].

Visible absorption spectra of the complex in acetic acid-sodium acetate buffer solutions of various pH were illustrated in Fig. 2. In the solution of pH 2.5~4.0 the maximum absorption was observed at 500 mμ, while in the higher pH region the color turned yellow and the maximum shifted to 450 mμ. By plotting the extinction against pH of the solution, the p$K$ value between the red and the yellow species was evaluated as 5.3. It was also found that the red complex was strongly adsorbed on an anion-exchange resin in the chloride form. On titrating the complex with sodium hydroxide the curve in Fig. 3 was obtained. This curve has a single inflection at a neutralization point with approximately 1 mol. of sodium hydroxide per 1 mol. of the chelate. The pH of the half-neutralized solution is 5.5; which agrees fairly well with the p$K$ value obtained from spectral data.

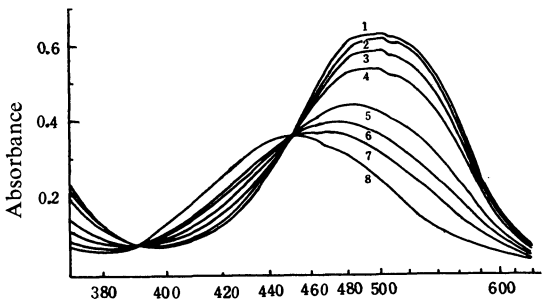



Fig. 2. The absorption spectra of Mn(III)-EDTA in $CH_3COOH$-$CH_3COONa$ buffer solutions of various pH ($\mu$=0.1) (Mn(III): $9.34\times10^{-4}$ mol./l.).

1: pH=2.50 2: pH=4.09 3: pH=4.54
4: pH=4.98 5: pH=5.40 6: pH=6.00
7: pH=6.28 8: pH=8.70

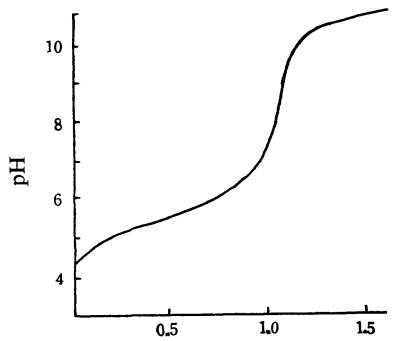



Fig. 3. Potentiometric titration of Mn(III)-EDTA with NaOH. (Concentration of Mn(III): $0.21\times10^{-2}$ mol./50 ml., NaOH: $9.89\times10^{-2}$ mol./l.).

4) C. Furlain, G. Morpurgo and C. Sartori, *Z. anorg. u. allgem. Chem.*, 303, 1 (1960).

The authors thank to Dr. Masuo Kojima for the spectral measurements, to Mr. Shozo Masuda for the elementary analysis and to their colleagues in the laboratory for their helpful discussions.

*College of General Education*
*The University of Tokyo*
*Meguro-ku, Tokyo*

## *The Electron Spin Resonance Absorption of Vanadium Pentoxide Catalysts*

By Kimio TARAMA, Shiichiro TERANISHI, Satohiro YOSHIDA and Hiroshi YOSHIDA

(Received June 2, 1961)

Kozyrev[1] and Pecherskaya et al.[2] studied the electron spin resonance (ESR) absorption of $VO^{2+}$ in organic solvents at room temperature and observed that its spectrum consisted of eight hyperfine components, while Sands[3] reported the ESR absorption of $V^{4+}$ ions in glass, and Faber et al.[4] observed the hyperfine structures of $VO^{2+}$ ions on the ion exchangers. But no one has ever reported the ESR absorption of vanadium pentoxide.

The ESR method was used in order to study the magnetic properties of vanadium pentoxide and the binary system of vanadium pentoxide-potassium pyrosulfate.

Vanandium pentoxide was prepared by calcining ammonium metavanadate at 450°C, and vanadium pentoxide-potassium pyrosulfate

1) B. M. Kozyrev, *Discussions Faraday Soc.*, **19**, 135 (1955).
2) Y. I. Pecherskaya et al., International Congress on Catalysis, Paris, 1960.
3) R. H. Sands, *Phys. Rev.*, **99**, 1222 (1955).
4) R. Faber and M. Rogers, *J. Am. Chem. Soc.*, **81**, 1849 (1959).

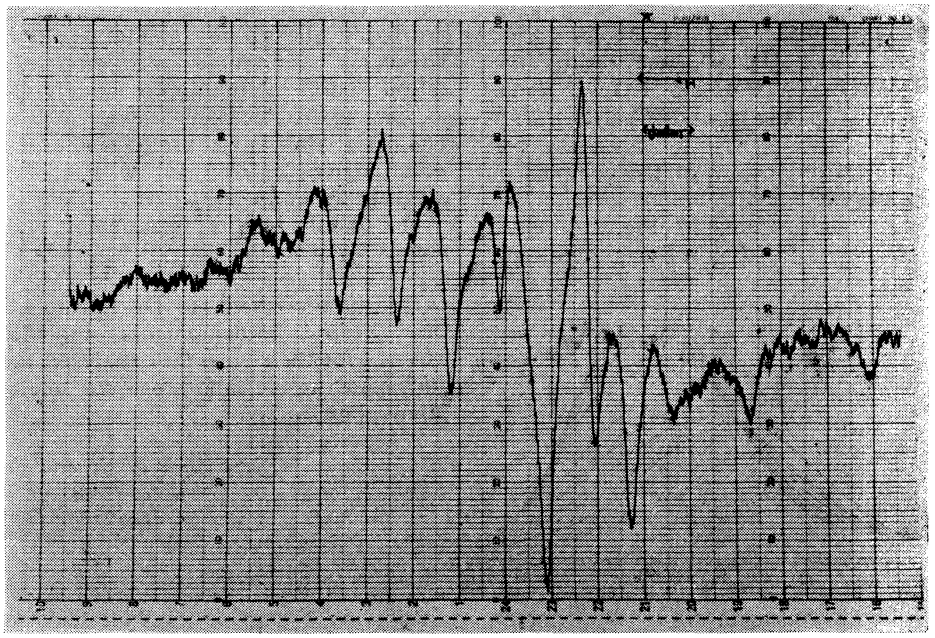


Fig. 1. ESR spectrum of the solid solution of vanadium pentoxide and potassium pyrosulfate.

samples were prepared by calcination of the mixture vanadium pentoxide and potassium pyrosulfate which contained vanadium pentoxide 10, 15, 25, 40, 50 and 70 mol. % respectively at 450°C, in closed glass vessels. Vanadium pentoxide-potassium pyrosulfate samples containing vanadium pentoxide less than 40 mol. % melted completely, and changed into amorphous substances of dark brownish color.

The spectrometer used in this research was of reflecting-type, and its resonance frequency was 9410 Mc. The observation were carried out at room temperature and also at liquid oxygen temperature.

In the case of vanadium pentoxide, an asymmetric ESR signal was observed and the $g$-value was 1.96. The line width ($\Delta Hmsl$) was 89 gauss at 16°C and 173 gauss at −183°C.

ESR signals of vanadium pentoxide-potassium pyrosulfate samples containing vanadium pentoxide less than 25 mol. %, showed the well-resolved hyperfine structures at room temperature. Fig. 1 shows the hyperfine structure of the sample consisting of vanadium pentoxide 15 mol. % and potassium pyrosulfate 85 mol. %. Eleven components are observed and its central eight components are stronger than the others.

In the case of the samples containing vanadium pentoxide more than 25 mol. %, the spectrum was not so well-resolved as Fig. 1.

The analysis of this spectrum according to Kozyrev's method shows that the $g$-value and the coupling constant for the central eight components are 1.98 and 98 gauss, and for the other three components are 1.92 and 320 gauss respectively.

The spectrum of vanadium pentoxide-potassium pyrosulfate is quite similar to that of $VO^{2+}$ ions on the ion exchangers observed by Faber et al.[4] and this fact shows that the observed paramagnetic absorption results from $VO^{2+}$ ions.

The authors wish to thank Professor Seizo Okamura, Kyoto University, for allowing one of the authors to use the ESR absorption apparatus.

*Faculty of Engineering*
*Kyoto University*
*Sakyo-ku, Kyoto*

## *Synthesis of* D-*Threosamine and* D-*Erythrosamine*[1]

By Juji YOSHIMURA, Yoshiaki OHGO and Tetsuo SATO

(Received June 27, 1961)

In the course of studies on the glycosylation of aminosugars[2], the requirement of a lower 2-aminosugar had arisen, so we attempted to synthesize 2-amino-D-tetroses. Recently, the synthesis of them was reported by Kuhn et al.[3], in which the hydrochlorides of D-threosamine and D-erythrosamine were obtained by catalytic half reduction of *N*-benzyl-D-tetrosaminonitriles ($III_b$ and $IV_b$) prepared by acidic hydrolysis of corresponding acetone derivatives ($I_b$ and $II_b$).

It prompts us to record further observations related to their work. To obtain *N*-substituted-D-tetrosaminonitriles (III and IV) two paths shown in Fig. 1 were examined. By treatment of D-glyceraldehyde[4] with amines (aniline, benzylamine and isopropylamine respectively) and hydrogen cyanide, *N*-phenyl-D-threosaminonitrile ($IV_a$), m. p. 114~116°C, $[\alpha]_D$ −247.2° (*c* 0.72, ethanol), Found: C, 62.38; H, 6.30; N, 14.5, Calcd. for $C_{10}H_{12}O_2N_2$: C, 62.48; H, 6.29; N, 14.58%, and *N*-isopropyl-D-erythrosaminonitrile ($III_c$), m. p. 103~104°C, $[\alpha]_D$ + 48.1° (*c* 0.21, methanol), Found: C, 53.43; H, 8.90; N, 17.48. Calcd. for $C_7H_{14}O_2N_2$: C, 53.14; H, 8.92; N, 17.71%, were obtained as colorless needles.

On the other hand, when acetone-D-glyceraldehyde[5] was treated in the same manner, two epimeric pairs of the corresponding acetone-aminonitriles ($I_a$, $II_a$, $I_b$ and $II_b$) were separated in crystalline forms (acetone-*N*-phenyl-D-erythrosaminonitrile ($I_a$), m. p. 124°C, $[\alpha]_D$ +157.9° (*c* 0.69, methanol), yield 7.4%, Found: C, 66.30, H, 6.85; N, 12.06, Calcd. for $C_{13}H_{16}O_2N_2$: C, 67.22; H, 6.94; N, 12.06%, acetone-*N*-phenyl-D-threosaminonitrile (IIa), m. p. 100~102°C, $[\alpha]_D$ −149.4° (*c* 0.86, methanol), yield 30%, Found: C, 67.40; H, 7.04; N, 11.94. Calcd. for $C_{13}H_{16}O_2N_2$: C, 67.22; H, 6.94; N, 12.06%. The physical properties of *N*-benzyl derivatives, $I_b$ and $II_b$, are entirely consistent with those of the substances reported by Kuhn et al.[3] respectively.

In addition to them, a trace of rhombic colorless crystal, m. p. 115~116°C, $[\alpha]_D$ +15° (*c* 0.77, methanol), having the same analytical values as the epimeric pair (Found: C, 67.06; H, 7.02; N, 11.92%) in the case of *N*-phenyl derivatives and a small amount of crystals corresponding to $C_{13}H_{18}O_4N_2$, m. p. 255~256°C, and $C_{16}H_{16}O_2N_2$, m. p. 216~218°C in the case of *N*-benzyl derivatives were obtained.

To prepare *N*-substituted D-tetrosaminonitriles the above acetone derivatives were subjected to hydrolysis in a mineral acid, to which *N*-benzyl derivatives ($I_b$ and $II_b$) showed such an extraordinary resistance that it was impracticable to obtain hydrolyzates of $I_b$ and $II_b$ even in 2 N hydrochloric acid solution of 80% ethanol at room temperature for 24 hr., although Kuhn et al. carried out successfully by exsiccating the 2 N hydrochloric acid solution of $I_b$ or $II_b$ on phosphorus pentoxide at room temperature. *N*-Phenyl derivatives ($I_a$ and $II_a$) changed gradually in their optical rotation in a 1 N mineral acid solution of 80% ethanol at room temperature [$I_a$: $[\alpha]_D$ +107° (5 min.)→ +156° (3 hr.)→+165° (22 hr. approximately const.), $II_a$: $[\alpha]_D$ −164° (3 min.)→−177° (1 hr.) →−220° (20 hr.)→−222° (41 hr.)→−228° (92 hr. const.)]. Colorless needles, m. p. 114~116°C, obtained from the reaction mixture of $II_a$, was agreed with $IV_a$ described above.

The presumption whether these aminonitrile derivatives belong to the threo-type or the erythro-type was deduced from the general survey on their yields and their optical rotational data. In general, an epimer in which -NHR group has trans configuration to the hydroxyl gronp attached to the adjacent carbon precedes the cis isomer in their yield[6]. Moreover, the one having -NHR group on the right hand in the Fischer projection shows generally more positive optical rotation than the other, when they are measured in an inert solvent. This relationship seems to be closely akin to the acid-amide rule[7] in the sugar series. Fortunately, Kuhn et al. established the configurations of $I_b$ and $II_b$ by converting them into the configurationally known α-amino-β, γ-dihydroxybutyric acid[8], and the result coincides with the above mentioned presumption.

To obtain pure epimeric pair of aminosugars,

1) This work was presented at the 14th Annual Meeting of the Chemical Society of Japan, Tokyo, April, 1961.
2) J. Yoshimura, N. Muramatsu and T. Sato, *J. Chem. Soc. Japan, Pure Chem. Sec.* (*Nippon Kagaku Zasshi*), **79**, 1503 (1958); ibid., **80**, 1472 (1959).
3) R. Kuhn and H. Fischer, *Ann.*, **641**, 152 (1961).
4) E. Baer and H. O. L. Fischer, *J. Am. Chem. Soc.*, **61**, 761 (1939).
5) E. Bear and H. O. L. Fischer, *J. Biol. Chem.*, **128**, 463 (1939).
6) R. Kuhn, W. Bister and H. Fischer, *Ann.*, **617**, 109 (1958); ibid., **628**, 193 (1959).
7) C. S. Hudson and S. Komatsu, *J. Am. Chem. Soc.*, **40**, 813 (1918); ibid., **41**, 1141 (1919).
8) E. E. Hamel and E. P. Painter, ibid., **75**, 1362 (1953).

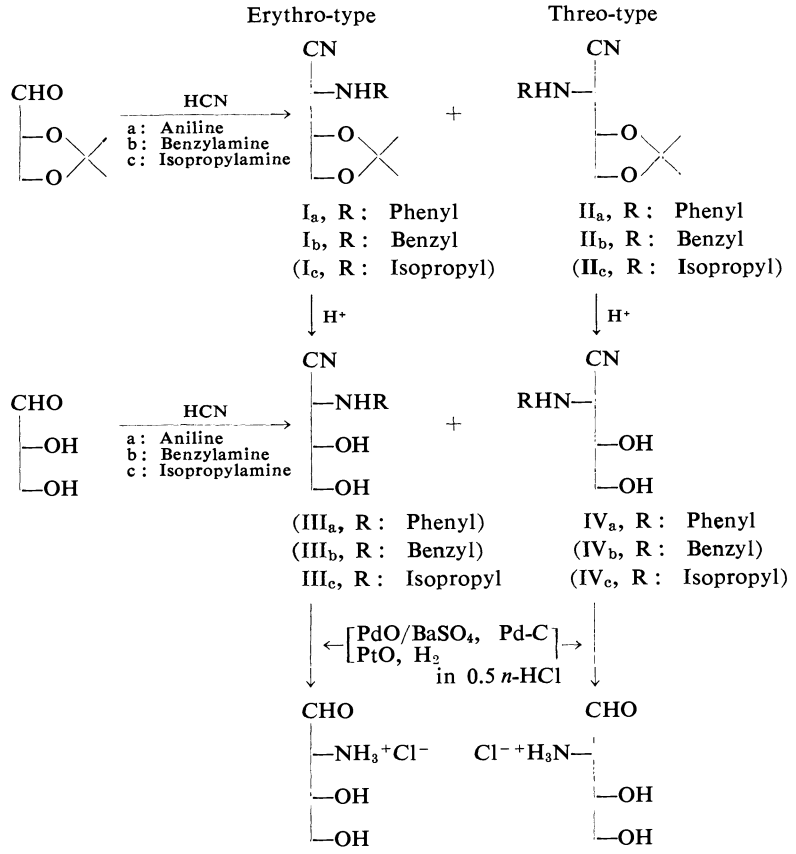



Fig. 1. Substances in parentheses could not be isolated as crystals.

*N*-phenyl-D-threosaminonitrile $IV_a$ and *N*-phenyl-D-erythrosaminonitrile $III_a$ which was derived by hydrolysis of $I_a$ were subjected to catalytic half reduction in hydrochloric acid solution to afford D-threosamine hydrochloride and D-erythrosamine hydrochloride which showed the same behavior as depicted by Kuhn et al.[3]

The authors gratefully thank Mr. Hiroichi Ono for his help throughout this work and Dr. Asaji Kondo for microanalyses.

*Laboratory of Organic Chemistry*
*Tokyo Institute of Technology*
*Meguro-ku, Tokyo*

## *The Preparation of Carrier-free $^{234}Th(UX^1)$ by Anion Exchange from Nitric Acid-Alcohol Mixed Solution of Uranyl Nitrate*

By Jun AKAISHI

(Received June 15, 1961)

The preparation of thorium-234 by solvent extraction[1-6] and ion exchange[7-10] from uranyl nitrate have been reported by many

1) O. Erbacher, W. Herr and M. Wiedmann, *Z. anorg. Chem.*, **252**, 282 (1944).
2) A. Norström and L. G. Sillén, *Svensk Kem. Tidskr.*, **60**, 227 (1948).
3) J. B. Th. Aten and F. Barendregt, *Physica*, **16**, 760 (1950).
4) G. A. Cowan, *US AEC Report*, LA-1721, 227 (1954).
5) L. Kosta, *J. Stefan Inst. Repts.* (*Ljubligna*), **3**, 157 (1956).
6) R. Muxart, *Bull. soc. chim. France*, No. 5, 803 (1960).
7) D. Dyrssen, *Svensk Kem. Tidskr.*, **62**, 153 (1950).
8) B. G. Harvey, Brit. Pat. 704602 (1954).
9) R. Lumbroso and J. Petit, *Compt. rend.*, **243**, 145 (1956).
10) S. S. Berman, L. E. Mackinney and M. E. Bednas, *Talanta*, **4**, 153 (1960).

workers. In nitric acid medium, thorium-234 was separated by anion exchanger Amberlite IRA-400[11]. Recently, Korkisch et al.[12] reported that the adsorption of thorium onto anion-exchange resin is very strong, but that of uranium is rather weak, in a nitric acid-alcohol mixed solution.

The author studied the procedure of the preparation of carrier-free thorium-234 using an anion exchanger Dowex 1-X8. The preparation procedure is as follows. One gram of commercial reagent grade uranyl nitrate hexahydrate crystal was dissolved without further purification in 5~6 ml. of 0.2 N nitric acid-ethyl alcohol 80%, mixed solution*, and the solution was passed through Dowex 1-X8 resin column (100~200 mesh, 1.0 g., 0.70 $cm^2$ ×2.8 cm., pretreated with a few milliliters of the nitric acid-alcohol mixed solution) at a flow rate 0.7 ml. per min., and then the column was washed with 30~40 ml. of the nitric acid-alcohol mixed solution. The elution of thorium from the resin column could be attained with a small amount of 0.2 N nitric acid or water. When the elution was carried out with 0.2 N nitric acid, thorium was almost completely eluted with 4~5 column volumes of the nitric acid solution at a flow rate 1.0 ml. per min.

The result shown in Fig. 1 was obtained using the procedure described above. The activity measurement of the solution was as follows; an aliquot of the solution was transferred to a glass counting dish, and evaporated to dryness. The $\alpha$ and $\beta$ activities were counted using a gas flow proportional counter and G-M counter respectively. In Fig. 2, decay curve of the eluate is shown.

The yield of thorium-234 from one gram of uranyl nitrate crystal was $4.6\times10^5$ d.p.m.($^{234}$Th $+^{234}$Pa), and the radiochemical impurities were not observed by $\beta$ and $\gamma$ energy measurements.

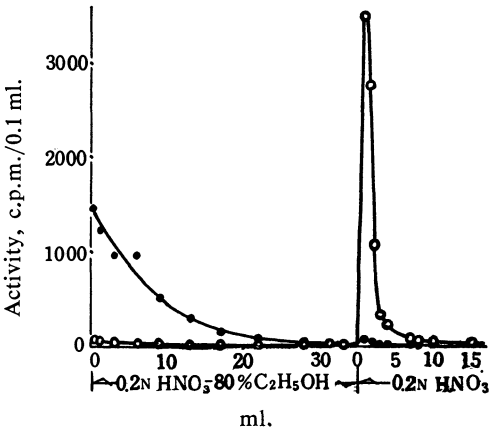



Fig. 1. Elution curve of thorium-234.
•—•: $\alpha$-activity, ○—○: $\beta$-activity

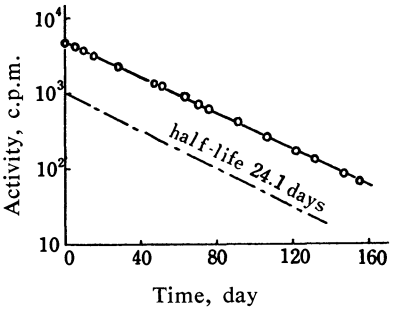



Fig. 2. Decay curve.

The author wishes to express his thanks to Mrs. Junko Iwamoto and Mr. Toshio Okamoto of the Division of Health Physics, JAERI for their kind assistance.

*Japan Atomic Energy Research Institute*
*Tokai-mura, Ibaraki-ken*

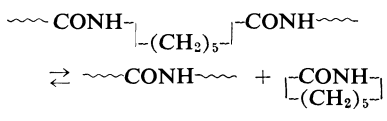
11) Y. M. Chen, *J. Chinese Chem. Soc. (Taiwan)*, [2], 4, 47 (1957).
12) F. Tera, J. Korkisch and F. Hecht, *J. Inorg. Nucl. Chem.*, 16, 345 (1961).
* For example, 2 ml. 1 N $HNO_3$+8 ml. 99.5 vol. % $C_2H_5OH$.

# *Studies on Polymerization and Depolymerization of ε-Caprolactam Polymer. IX*. Reformation Reaction of ε-Caprolactam from Poly-ε-capramide*

By Naoya OGATA

(Received January 24, 1961)

The mechanism of the polymerization reaction of ε-caprolactam in the presence of water has been studied in detail by many investigators[1-6]. It has been generally accepted that the initial reaction of the polymerization is caused by the hydrolysis of ε-caprolactam and that the chain growth occurs mainly through the addition of ε-caprolactam to $-NH_2$ end-groups, being catalyzed by -COOH end-groups. If this mechanism is correct, ε-caprolactam is reformed in the depolymerization reaction rolling out successively from $-NH_2$ end-groups of the polymer chain because the polymerization is an equilibration reaction. Therefore, no ε-caprolactam can be expected from poly-ε-capramide having modified end-groups. In the previous paper[6], however, it was presumed that the addition reaction of ε-caprolactam would take place even on amide groups near the center of the polymer chain. In this case the reverse process of this intramolecular amide-interchange reaction called "Einrollung Reaktion"[1] as shown below is responsible for the reformation of ε-caprolactam from poly-ε-capramide.



## Experimental

ε-Caprolactam with water content less than 0.01% was polymerized in the presence of 1/20, 1/50 or 1/100 mol./mol. of hexamethylenediamine or adipic acid at 257°C. Polymers were washed with boiling water, and then heated in a solid phase at 180°C for 10 hr. at 1 mmHg pressure. The analytical results of the polymers having almost exclusively $-NH_2$ or -COOH end-groups thus obtained are shown in Table I. The polymer having $-NH_2$ end-groups was heated in refluxing acetic anhydride for 4 hr. and $-NH_2$ end-groups were acetylated almost completely. The polymer having $-NH_2$ end-groups was also dissolved in phenol and $-NH_2$ end-groups in the polymer were neutralized by titrating with aqueous hydrochloric acid in the presence of thymol blue as an indicator. The polymer having -COOH end-groups was dissolved in hot benzyl alcohol and the solution was neutralized by titrating with alcoholic sodium hydroxide solution in the presence of phenolphthalein. The polymers having $-NH_3^+Cl^-$ or -COONa end-groups were precipitated by adding methanol to the neutralized solutions.

TABLE I. THE ANALYTICAL RESULTS OF THE POLYMERS

| Kind of end-group | Basic group mol./mol. | Acidic group mol./mol. | $[\eta]$ |
|---|---|---|---|
| $NH_2$—$NH_2$ | $9.8\times10^{-2}$ | $3.9\times10^{-4}$ | 0.21 |
| | $16.5\times10^{-2}$ | $7.2\times10^{-4}$ | 0.16 |
| HOOC—COOH | $11.8\times10^{-4}$ | $9.5\times10^{-2}$ | 0.20 |
| | $8.2\times10^{-4}$ | $7.8\times10^{-2}$ | 0.20 |
| NaOOC—COONa | 0 | 0 | 0.22 |
| | $2.7\times10^{-4}$ | 0 | 0.27 |
| | 0 | 0 | 0.41 |
| | 0 | 0 | 0.50 |
| $ClH\cdot H_2N$—$NH_2\cdot HCl$ | 0 | — | 0.25 |
| AcHN—NHAc | $8.8\times20^{-4}$ | $2.3\times10^{-4}$ | 0.23 |
| | $9.3\times10^{-4}$ | $2.7\times10^{-4}$ | 0.27 |
| | 0 | 0 | 0.43 |
| | $3.4\times10^{-4}$ | 0 | 0.52 |

Each of the polymers was washed with refluxing methanol and dried at 110°C in vacuo of 2 mmHg for 24 hr. in order to decrease the water content to less than 0.01%. The polymer samples, each 2 g. in weight, were sealed within glass tubes under a nitrogen atmosphere and heated for a certain period of time at 230 or 257°C in a vapor bath of thymol or Dowtherm A. The amount of ε-caprolactam reformed from the polymers was determined for the extract in chloroform. The number of end-groups in the polymers was determined and the intrinsic viscosity $[\eta]$ for the polymers was measured in 98% sulfuric acid. The polymerization degree $\bar{P}_n$ of the polymers was calculated by the following equation[7].

$$\bar{P}_n = 124[\eta] - 5$$

## Results

The rates of reformation of ε-caprolactam from the polymers are shown in Tables II—V.

* VIII, This Bulletin, 33, 1584 (1960).

1) F. Wiloth, *Kolloid-Z.*, **144**, 58 (1955); *Z. physik. Chem.*, **11**, 78 (1957).

2) P. H. Hermans, D. Heikens and P. F. van Velden, *J. Polymer Sci.*, **30**, 81 (1958): **44**, 437 (1960).

3) A. V. Tobolsky and A. Eisenberg, *J. Am. Chem. Soc.*, **81**, 2302 (1959).

4) H. Yumoto, This Bulletin, **28**, 94, 101 (1955).

5) H. Yumoto and N. Ogata, *Makromol. Chem.*, **25**, 71 (1957).

6) N. Ogata, ibid., **30**, 212 (1959).

7) A. Matthes, ibid., **5**, 165 (1950).

TABLE II. THE RATE OF REFORMATION OF ε-CAPROLACTAM FROM THE POLYMER OF $\overline{P}_n \fallingdotseq 20$

| Kind of end-group | Temp. °C | Time hr. | Lactam % | Basic group mol./mol. | Acidic group mol./mol. | [η] |
|---|---|---|---|---|---|---|
| $H_2N—NH_2$ | 230 | 0 | 0 | $9.8\times10^{-2}$ | $3.9\times10^{-4}$ | 0.21 |
| | | 1 | 0.51 | 8.9 〃 | 7.2 〃 | 0.32 |
| | | 2 | 1.33 | 8.9 〃 | 7.2 〃 | 0.33 |
| | | 5 | 3.34 | — | 8.6 〃 | — |
| | | 10 | 4.53 | 8.9 〃 | 10.0 〃 | 0.22 |
| | | 25 | 4.94 | 8.4 〃 | 10.4 〃 | — |
| | | 50 | 5.32 | 9.7 〃 | 8.5 〃 | — |
| | 257 | 0 | 0 | $16.5\times10^{-2}$ | $7.2\times10^{-4}$ | 0.16 |
| | | 1 | 4.60 | 11.9 〃 | 9.6 〃 | 0.14 |
| | | 2 | 6.74 | 12.0 〃 | 6.7 〃 | 0.16 |
| | | 5 | 8.45 | 12.0 〃 | 5.4 〃 | 0.16 |
| | | 10 | 8.97 | 12.1 〃 | 8.8 〃 | 0.17 |
| | | 25 | 9.85 | 11.4 〃 | 9.6 〃 | 0.16 |
| | | 50 | 10.23 | 11.5 〃 | 10.8 〃 | 0.17 |
| HOOC—COOH | 230 | 0 | 0 | $11.8\times10^{-4}$ | $9.5\times10^{-2}$ | 0.20 |
| | | 1 | 0.02 | 7.8 〃 | 9.5 〃 | 0.20 |
| | | 2 | 0.11 | 8.0 〃 | 9.2 〃 | 0.24 |
| | | 5 | 0.70 | 9.2 〃 | 9.0 〃 | 0.24 |
| | | 10 | 0.80 | 9.2 〃 | 9.0 〃 | 0.23 |
| | | 25 | 2.02 | 9.2 〃 | 9.5 〃 | 0.22 |
| | | 50 | 4.48 | 9.0 〃 | 9.5 〃 | 0.21 |
| | 257 | 0 | 0 | $8.2\times10^{-4}$ | $7.8\times10^{-2}$ | 0.20 |
| | | 1 | 1.40 | 6.3 〃 | 6.8 〃 | 0.20 |
| | | 2 | 2.22 | 6.3 〃 | 6.7 〃 | 0.21 |
| | | 5 | 4.69 | 6.9 〃 | 6.8 〃 | 0.20 |
| | | 10 | 6.72 | 6.5 〃 | 6.7 〃 | 0.23 |
| | | 25 | 7.84 | 6.7 〃 | 6.8 〃 | 0.20 |
| | | 50 | 7.75 | 6.3 〃 | 6.7 〃 | 0.20 |
| NaOOC—COONa | 230 | 0 | 0 | — | 0 | 0.22 |
| | | 25 | 0.22 | — | 0 | 0.22 |
| | | 50 | 0.63 | — | 0 | 0.21 |
| | 257 | 0 | 0 | — | 0 | 0.22 |
| | | 1 | 5.51 | — | 0 | 0.24 |
| | | 2 | 5.58 | — | 0 | 0.26 |
| | | 5 | 5.80 | — | 0 | 0.27 |
| | | 10 | 7.05 | — | 0 | 0.20 |
| | | 25 | 14.65 | — | 0 | 0.27 |
| | | 50 | 16.69 | — | 0 | 0.26 |
| $ClH\cdot H_2N—NH_2\cdot HCl$ | 230 | 0 | 0 | 0 | — | 0.24 |
| | | 1 | 1.74 | 0 | — | 0.24 |
| | | 2 | 2.06 | 0 | — | 0.23 |
| | | 5 | 3.40 | 0 | — | 0.24 |
| | | 10 | 4.74 | 0 | — | 0.22 |
| | | 25 | 9.35 | 0 | — | 0.21 |
| | | 50 | 11.21 | 0 | — | 0.22 |
| | 257 | 2 | 7.18 | 0 | — | 0.23 |
| | | 10 | 11.43 | 0 | — | 0.23 |
| | | 25 | 13.60 | 0 | — | 0.22 |
| | | 50 | 13.80 | 0 | — | 0.22 |
| AcHN—NHAc | 230 | 0 | 0 | $8.8\times10^{-4}$ | $2.3\times10^{-4}$ | 0.23 |
| | | 2 | 0.07 | 2.4 〃 | 2.9 〃 | — |
| | | 5 | 0.08 | 2.2 〃 | 2.9 〃 | 0.23 |
| | | 10 | 0.26 | 2.2 〃 | 2.4 〃 | 0.22 |
| | | 25 | 0.11 | 3.0 〃 | 2.5 〃 | 0.23 |
| | | 50 | 0.59 | 3.7 〃 | 2.9 〃 | 0.23 |
| | 257 | 0 | 0 | $8.6\times10^{-4}$ | $4.2\times10^{-4}$ | 0.23 |
| | | 1 | 0.31 | 6.9 〃 | 0.2 〃 | 0.24 |
| | | 5 | 0.87 | 9.2 〃 | 0.3 〃 | 0.25 |
| | | 10 | 1.57 | 15.0 〃 | 0.3 〃 | 0.25 |
| | | 25 | 2.50 | 15.0 〃 | 0.3 〃 | 0.25 |
| | | 50 | 4.98 | 17.7 〃 | 0.3 〃 | 0.24 |

Table III. The rate of reformation of ε-caprolactam from the polymer of $\bar{P}_n$=30

| Kind of end-group | Temp. °C | Time hr. | Lactam % | [η] |
|---|---|---|---|---|
| AcHN—NHAc | 230 | 0 | 0 | 0.27 |
| | | 50 | 0 | 0.28 |
| | | 100 | 0 | 0.28 |
| | | 150 | 0 | 0.28 |
| | 257 | 0 | 0 | 0.27 |
| | | 25 | 3.64 | 0.28 |
| | | 50 | 8.75 | 0.27 |
| | | 75 | 10.00 | 0.27 |
| | | 100 | 10.00 | 0.27 |
| | | 150 | 10.88 | 0.27 |
| NaOOC—COONa | 230 | 0 | 0 | 0.27 |
| | | 50 | 0 | 0.28 |
| | | 100 | 0 | 0.28 |
| | | 150 | 0 | 0.28 |
| | 257 | 0 | 0 | 0.27 |
| | | 25 | 5.79 | 0.28 |
| | | 50 | 7.61 | 0.28 |
| | | 75 | 8.60 | 0.28 |
| | | 100 | 8.29 | 0.28 |
| | | 150 | 9.25 | 0.28 |

Table IV. The rate of reformation of ε-caprolactam from the polymer of $\bar{P}_n$=40

| Kind of end-group | Temp. °C | Time hr. | Lactam % | [η] |
|---|---|---|---|---|
| AcHN—HNAc | 230 | 0 | 0 | 0.43 |
| | | 50 | 0 | 0.46 |
| | | 100 | 0 | 0.43 |
| | | 150 | 0.63 | 0.44 |
| | 257 | 0 | 0 | 0.43 |
| | | 25 | 2.96 | 0.43 |
| | | 50 | 3.90 | 0.41 |
| | | 75 | 7.07 | 0.42 |
| | | 100 | 7.72 | 0.42 |
| | | 150 | 8.17 | 0.42 |
| NaOOC—COONa | 230 | 0 | 0 | 0.41 |
| | | 50 | 0 | 0.47 |
| | | 100 | 0 | 0.45 |
| | | 150 | 0 | 0.43 |
| | 257 | 0 | 0 | 0.41 |
| | | 25 | 2.89 | 0.38 |
| | | 50 | 6.06 | 0.37 |
| | | 75 | 8.66 | 0.37 |
| | | 100 | 8.93 | 0.37 |
| | | 150 | 8.58 | 0.37 |

No change in the number of end-groups was observed during the heat treatment. As shown in Tables II—V, at 230°C, ε-caprolactam is reformed from the polymer of which the end-groups are exclusively -COOH or $-NH_2$ while no ε-caprolactam is reformed from the polymer having -NHAc or -COONa end-groups. However, at 257°C, ε-caprolactam is reformed even from the polymer having -NHAc or -COONa end-groups. The rate of the reformation of ε-caprolactam is not influenced by the polymerization degree of the modified polymers. The rate of the reformation of ε-caprolactam from the polymer having $-NH_3^+$ end-groups is very fast.

Table V. The rate of reformation of ε-caprolactam from the polymer of $\bar{P}_n$=50

| Kind of end-group | Temp. °C | Time hr. | Lactam % | [η] |
|---|---|---|---|---|
| AcHN—NHAc | 230 | 0 | 0 | 0.52 |
| | | 50 | 0 | 0.54 |
| | | 100 | 0 | 0.54 |
| | | 150 | 0.70 | 0.51 |
| | 257 | 0 | 0 | 0.52 |
| | | 25 | 4.41 | 0.53 |
| | | 50 | 3.98 | 0.50 |
| | | 75 | 6.51 | 0.51 |
| | | 100 | 8.52 | 0.51 |
| | | 150 | 8.90 | 0.51 |
| NaOOC—COONa | 230 | 0 | 0 | 0.50 |
| | | 50 | 0 | 0.57 |
| | | 100 | 0 | 0.53 |
| | | 150 | 0 | 0.52 |
| | 257 | 0 | 0 | 0.50 |
| | | 25 | 3.03 | 0.43 |
| | | 50 | 6.87 | 0.43 |
| | | 75 | 7.41 | 0.44 |
| | | 100 | 8.30 | 0.44 |
| | | 150 | 7.75 | 0.44 |

## Discussion

The re-equilibration of poly-ε-capramide has been studied[8-11] on the dry polymers having modified end-groups. It has been reported[8,9] that the rate of reformation of ε-caprolactam from the acetylated polymer is very much slower than that of normal polymer. From these results, it seems very probable that no re-equilibration would take place in a dry polymer having all its end-groups modified.

As shown in the experimental results, no ε-caprolactam is formed at 230°C from the polymer having COONa or -NHAc end-groups. However, above 230°C, it is presumed that the addition or reformation of ε-caprolactam must take place on the amide groups in the polymer chain through the intramolecular amide-interchange reaction. As the rate of the reformation of ε-caprolactam from the polymer having $-NH_3^+$ end-groups is very fast, it is ascertained[2,5] that the addition or the reformation of ε-caprolactam on the $-NH_2$ end-groups, catalyzed by the hydrogen ion, occurs fast.

Assuming that reformation reaction of ε-caprolactam from the polymer having modified end-groups may be caused by the intramolecular interchange reaction between two adjacent

8) S. Smith, *J. Polymer Sci.*, **30**, 459 (1958).
9) G. M. Van der Want, ibid., **37**, 547 (1959).
10) D. Heikens, P. H. Hermans and S. Smith, ibid., **38**, 265 (1959).
11) N. D. Katorzhnow and A. A. Strepikeev, *Zh. priklad Khim.*, **32**, 625 (1959).

amide groups in polymer chain, it can be expressed as follows:

$$M_n \underset{k_2}{\overset{k_1}{\rightleftarrows}} M_{n-1}+L \quad (1)$$

where $M_n$ and $M_{n-1}$ are polymer chains, L is ε-caprolactam, $k_1$, $k_2$ the rate constant of the reformation or addition reactions, respectively. The rate of the reformation reaction of ε-caprolactam can be expressed as follows, when the concentration of polymer chain is expressed in mole fraction of structural unit:

$$dx/dt=k_1(1-x)-k_2x \quad (2)$$

where $x$ is the mole fraction of ε-caprolactam reformed at $t$ hr. At equilibrium,

$$k_2=k_1(1-x_\infty)/x_\infty \quad (3)$$

where the equilibrium concentration of ε-caprolactam $x_\infty$ is about 0.07[4] and $(1-x_\infty)$ can be fixed as equal to 1. Then, from Eqs. 2 and 3,

$$dx/dt=k_1(1-x/x_\infty) \quad (4)$$

Integration of Eq. 4 gives Eq. 5.

$$2.303 \log x_\infty/(x_\infty-x)=k_1t/x_\infty \quad (5)$$

From Eq. 5, the rate constant of the reformation reaction of ε-caprolactam can be calculated for the polymer having modified end-groups, as shown in Table VI. The values of $k_1$ are roughly the same, being independent

TABLE VI. THE VALUES OF $k_1$ AT 257°C

| Kind of end-group | $\bar{P}_n$ | Time hr. | $k_1$ mol./mol.hr. |
|---|---|---|---|
| | | 1 | $0.33\times10^{-2}$ |
| | | 5 | 0.18 〃 |
| AcHN—NHAc | 26 | 10 | 0.18 〃 |
| | | 25 | 0.12 〃 |
| | | 50 | 0.18 〃 |
| | | 25 | 0.18 〃 |
| AcHN—NHAc | 29 | 50 | 0.42 〃 |
| | | 25 | 0.36 〃 |
| | | 50 | 0.32 〃 |
| NaOOC—COONa | 30 | 75 | 0.33 〃 |
| | | 100 | 0.21 〃 |
| | | 25 | 0.15 〃 |
| | | 50 | 0.11 〃 |
| AcHN—NHAc | 48 | 75 | 0.20 〃 |
| | | 100 | 0.20 〃 |
| | | 25 | 0.14 〃 |
| NaOOC—COONa | 46 | 50 | 0.20 〃 |
| | | 75 | 0.42 〃 |
| | | 25 | 0.24 〃 |
| | | 50 | 0.11 〃 |
| AcHN—NHAc | 59 | 75 | 0.16 〃 |
| | | 100 | 0.28 〃 |
| | | 25 | 0.15 〃 |
| NaOOC—COONa | 57 | 50 | 0.32 〃 |
| | | 70 | 0.30 〃 |
| Mean value | | | $0.23\times10^{-2}$ |

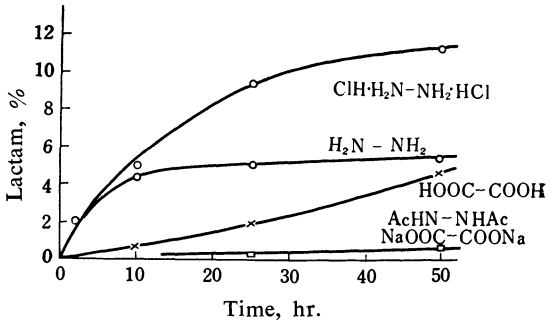



Fig. 1. The rate of reformation of ε-caprolactam from the polymer of $\bar{P}_n=20$ at 230°C.

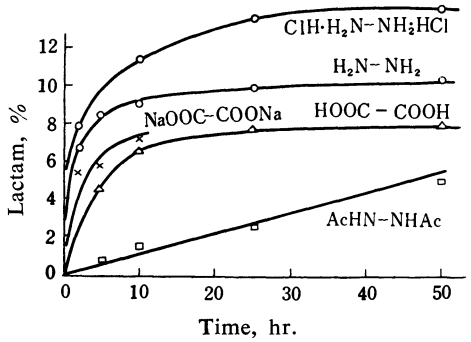



Fig. 2. The rate of reformation of ε-caprolactam from the polymer of $\bar{P}_n=20$ at 257°C.

of the polymerization degree of the polymer. The mean value of $k_1$ is $0.23\times10^{-2}$ mol./mol.hr. Yumoto[4] reported that the rate constant of the reformation of ε-caprolactam from the polymer $[\eta]_{cresol}=1.1$ was $2.26\times10^{-2}$ mol./mol.hr. at 257°C. In this case, as the number of amino- or carboxyl-groups in the polymer is $(0.5\sim0.7)\times10^{-2}$ mol./mol., it is presumed that the reformation of ε-caprolactam may be caused mainly by the reaction rolling out ε-caprolactam succesively from the ends of the polymer chain.

Compared with this value, the reformation velocity of ε-caprolactam from the polymer having modified end-groups is about 1/10 and it can be found that the end-groups of the polymer play a very important role for the addition or the reformation reactions of ε-caprolactam. However, the rate of the reformation of ε-caprolactam from the polymer having modified end-groups is independent of the polymerization degree of the polymer and it is presumed that ε-caprolactam is reformed also by the reaction between two adjacent amide groups in the polymer chain.

In the previous paper[6], it was reported from the results of the amide-interchange reaction of an *N*-alkyl acid amide and ε-caprolactam,

that the rate constant of the reformation reaction of ε-caprolactam at 252°C was $3.6\times10^{-2}$ mol./mol.hr. This value is considerably greater than that for the polymer having modified end-groups. This is probably due to the difference in activity of the components.

It is concluded for the polymerization and reformation reactions in the system of ε-caprolactam and poly-ε-capramide that the reaction occurs predominantly on the end-groups of the polymer and that the intramolecular amide-interchange reaction between two adjacent amide groups in the polymer chain occurs slowly.

## Summary

The reformation reaction of ε-caprolactam from poly-ε-capramide having modified end-groups has been studied. It was found that no ε-caprolactam was reformed at 230°C from the polymer of which all of the end-groups were -COONa or -NHAc groups, while ε-caprolactam was reformed slowly at 257°C. The rate of the reformation of ε-caprolactam from the polymer having -COONa or -NHAc end-groups is about 1/10 of that from the polymer having normal end-groups at 257°C and it is independent of the polymerization degree of the polymer.

The polymerization and the depolymerization reactions of ε-caprolactam polymer occur predominantly on the end-groups and the interchange reaction between two adjacent amide groups in the polymer chain occurs slowly.

The author wishes to express his sincere gratitude to Dr. H. Kobayashi for his permission to publish these results and also to Dr. T. Yoshino and Mr. T. Takayanagi for their helpful discussion. He is indebted to Mr. S. Yoshikawa for his assistance in the experiments.

*Research Department*
*Toyo Rayon Co., Ltd.*
*Minato-ku, Nagoya*

# *Studies on Organophosphorus Compounds. III. On Phosphite Copper Cyanide Complex Compounds*[*1]

By Yoshihiko NISHIZAWA

(Received January 27, 1961)

In a previous paper[1], it has been reported on a few new properties of phosphite[*2] cuprous halide complex compounds. During the course of an investigation of organophsphorus complex compounds, the present author has also found that phosphites react with copper cyanide to give new complex compounds[2] having strong fungicidal action[3].

There has been no report on copper cyanide complex compounds having the phosphorus atom, but recently Birum[4] prepared independently the same compounds as those of the present author and reported that they have insecticidal activity towards a few insects.

**Preparation of Phosphite Copper Cyanide Complex Compounds.**—Phosphite copper cyanides were prepared from phosphites and copper cyanides in a benzene solution. After copper cyanide was dissolved in benzene solution, and the benzene was evaporated under reduced pressure, the complex compounds were obtained as white crystals or colorless oil.

According to the mole ratio of phosphites to copper cyanide two complex compounds were obtained; namely, phosphite copper cyanide (I) and bis-phosphite copper cyanide (II), but tri-phosphite copper cyanide could not be prepared from three moles of phosphite and one mole of copper cyanide; instead, a product was one mole of bis-phosphite copper cyanide (II) and one mole of phosphite was unreacted.

$$(RO)_3P + CuCN \rightarrow (RO)_3PCuCN \quad (I)$$

$$2(RO)_3P + CuCN \rightarrow ((RO)_3P)_2CuCN \quad (II)$$

[*1] Presented at the Annual Meeting of Chemistry of Complex Compounds of Japan, Fukuoka, October, 1959.

[*2] The phosphorus compounds in this paper were named according to the Drake Committee's Report (*Chem. Eng. News*, **30**, 4515 (1952)).

1) Y. Nishizawa, This Bulletin, **34**, 1170 (1961).

2) Y. Nishizawa, and M. Nakagawa, Japanese Pat. Applied No. 12895 (1959).

3) J. Hattori and Y. Nishizawa, Japanese Pat. Applied No. 12896 (1959).

4) G. H. Birum, U. S. Pat., 2909544 (1959).

$$3(RO)_3P + CuCN \rightarrow ((RO)_3P)_2CuCN + (RO)_3P$$
(II)

Phosphite copper cyanides (I) gave bis-phosphite copper cyanides (II) by adding one mole ratio of phospite and II gave also I by adding one mole ratio of copper cyanide, and II were converted to phosphite copper cyanide (I) by heating under a reduced pressure.

$$(RO)_3PCuCN + (RO)_3P \rightarrow ((RO)_3P)_2CuCN$$
(I) (II)

$$((RO)_3P)_2CuCN + CuCN \rightarrow 2(RO)_3PCuCN$$
(II) (I)

$$((RO)_3P)_2CuCN \xrightarrow{heat} (RO)_3PCuCN + (RO)P\uparrow$$
(II) (I)

It is clear from the following experimental facts that these complex compounds have the phosphite group in their molecules. The compounds I and II reacted with benzoyl chloride in benzene solution to give *O,O*-dialkylbenzoyl phosphonates (A) and copper cyanide. The melting point of 2,4-dinitrophenylhydrozone of the phosphonate A coincided with that of 2,4-dinitrophenylhydrazone of the product prepared from trialkyl phosphite and benzoyl chloride by Kosolapoff's method[5]

$$((RO)_3P)_nCuCN + n\ C_6H_5COCl$$

$$\rightarrow n\ (RO)_2\overset{\overset{O}{\|}}{P}\cdot CO\cdot C_6H_5 + CuCN + n\ RCl$$
(A)

2,4-Dinitrophenylhydrazone

$$(RO)_3P + C_6H_5COCl \rightarrow (RO)_2P\text{-}COC_6H_5$$
(5)

The infrared absorption spectra*3 of these compounds, I and II, showed the absorption band of P–O-isopropyl group at 1010 $cm^{-1}$ (see Fig. 1). But the absorption bands of P–O stretching vibration[6] of phosphite at 857 and 769 $cm^{-1}$ shift to 879 and 779 $cm^{-1}$, respectively. From this shift, it is considered that P–O bonds are shortened by formation of the complex; namely, P–O bonds in these complex compounds become stronger than that of phosphite (see Fig. 1).

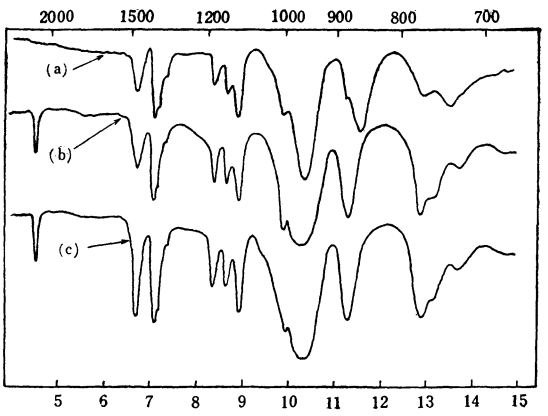



Fig. 1. (a) Infrared absorption spectrum of triisopropyl phosphite (in Nujol). (b) Infrared absorption spectrum of triisopropyl phosphite copper cyanide (Id) (in Nujol). (c) Infrared absorption spectrum of bis-(triisopropyl phosphite) copper cyanide (IId) (in Nujol).

In the ultraviolet absorption spectra*4 of these compounds, the absorption maximum did not appear.

**Molecular Weights of Bis-phosphite Copper Cyanide Complex Compounds.**—In many cases, it has been reported that organometallic cyanide complex compounds form the polymer[7,8], so the present author measured the molecular weights of the crystalline bis-phosphite copper

TABLE I. YIELDS, PHYSICAL CONSTANTS AND MICROANALYTICAL DATA OF PHOSPHITE AND BIS-PHOSPHITE COPPER CYANIDES, I AND II, $((RO)_3P)_nCuCN$

| No. | R | n | Yield % | M. p., °C or $n_D^{(t°C)}$ | Nitrogen, % | | Phosphorus, % | | Copper, % | |
|---|---|---|---|---|---|---|---|---|---|---|
| | | | | | Found | Calcd. | Found | Calcd. | Found | Calcd. |
| Ia | $CH_3$ | 1 | 98.6 | $1.5299^{(27)}$ | 6.41 | 6.56 | 13.5 | 13.4 | 29.3 | 29.7 |
| Ib | $C_2H_5$ | 1 | 97.9 | $1.5031^{(25)}$ | 5.63 | 5.47 | 12.2 | 12.1 | 25.1 | 24.9 |
| Ic | *n*-$C_3H_7$ | 1 | 98.4 | $1.5000^{(27)}$ | 4.76 | 4.71 | 10.2 | 10.4 | 21.4 | 21.3 |
| Id | iso-$C_3H_7$ | 1 | 98.6 | $1.4830^{(25)}$ | 4.75 | 4.71 | 10.6 | 10.4 | 21.0 | 21.3 |
| Ie | *n*-$C_4H_9$ | 1 | 99.1 | $1.4850^{(27)}$ | 4.01 | 4.12 | 9.3 | 9.1 | 18.3 | 18.7 |
| IIa | $CH_3$ | 2 | 99.3 | 60~61 | 4.15 | 4.15 | 18.3 | 18.4 | 18.6 | 18.8 |
| IIb | $C_2H_5$ | 2 | 99.6 | 121~122 | 3.61 | 3.32 | 14.9 | 14.7 | 15.0 | 15.1 |
| IIc | *n*-$C_3H_7$ | 2 | 98.9 | $1.4708^{(25)}$ | 2.61 | 2.77 | 12.3 | 12.3 | 12.8 | 12.6 |
| IId | iso-$C_3H_7$ | 2 | 98.7 | 85~86 | 2.69 | 2.77 | 12.4 | 12.3 | 12.9 | 12.6 |
| IIe | *n*-$C_4H_9$ | 2 | 98.4 | $1.4742^{(25)}$ | 2.99 | 2.75 | 12.0 | 12.1 | 12.3 | 12.5 |

*3 A Perkin Elmer 21 spectrophotometer was used.
*4 A Shimadzu QB-50 spectrophotometer was used.

5) G. M. Kosolapoff, *J. Am. Chem. Soc.*, **69**, 2112 (1947).
6) J. Bellamy, "The Infrared Spectra of Complex Molecules", John Wiley, New York (1958).
7) R. F. Phillips, *Chem. Abstr.*, **34**, 1532 (1940).
8) A. Burawoy, *J. Chem. Soc.*, **1935**, 1024.

TABLE II. THE MOLECULAR WEIGHTS OF BIS-PHOSPHITE COPPER CYANIDE (II) $[(RO)_3P]_2CuCN$

| No. | R | Cryoscopic solvent ($k$) | Ebullioscopic solvent ($k$) | Concn. (g./$G$ %) | $\Delta T$, °C | Molecular weight: Experimental | Molecular weight: Calcd. (Monomeric) | Degree of association |
|---|---|---|---|---|---|---|---|---|
| IIa | $CH_3$ | Benzene (5120) | | **0** | — | **1346** | 337.7 | 3.99 |
| | | | | 0.445 | 0.017 | 1340 | | |
| | | | | 1.651 | 0.041 | 1312 | | |
| | | | | 2.326 | 0.092 | 1294 | | |
| | | | Benzene (2570) | **0** | — | **630** | | 1.87 |
| | | | | 0.417 | 0.017 | 631 | | |
| | | | | 1.452 | 0.060 | 621 | | |
| | | | | 2.725 | 0.112 | 625 | | |
| | | Bromoform (14050) | | **0** | — | **556** | | 1.65 |
| | | | | 0.387 | 0.097 | 561 | | |
| | | | | 1.263 | 0.350 | 507 | | |
| | | | | 2.509 | 0.703 | 501 | | |
| | | Cyclohexane (20100) | | **0** | — | **651** | | 1.93 |
| | | | | 0.335 | 0.104 | 647 | | |
| | | | | 0.681 | 0.211 | 649 | | |
| | | | | 1.511 | 0.473 | 642 | | |
| | | | | 2.255 | 0.721 | 629 | | |
| | | | | 2.901 | 0.918 | 635 | | |
| | | | | 3.751 | 1.201 | 628 | | |
| | | | | 4.338 | 1.397 | 624 | | |
| | | | | 4.903 | 1.600 | 616 | | |
| IIb | $C_2H_5$ | Benzene | | **0** | — | **1676** | 421.5 | 3.98 |
| | | | | 0.384 | 0.012 | 1681 | | |
| | | | | 1.623 | 0.050 | 1661 | | |
| | | | | 2.553 | 0.078 | 1671 | | |
| | | | Benzene | **0** | — | **840** | | 1.99 |
| | | | | 1.035 | 0.032 | 831 | | |
| | | | | 2.315 | 0.073 | 815 | | |
| | | | | 2.659 | 0.084 | 814 | | |
| | | Bromoform | | **0** | — | **678** | | 1.61 |
| | | | | 0.381 | 0.079 | 678 | | |
| | | | | 1.025 | 0.219 | 658 | | |
| | | | | 2.472 | 0.527 | 659 | | |
| | | Cyclohexane | | **0** | — | **856** | | 2.03 |
| | | | | 0.438 | 0.104 | 846 | | |
| | | | | 1.250 | 0.302 | 832 | | |
| | | | | 2.081 | 0.516 | 811 | | |
| IId | iso-$C_3H_7$ | Benzene | | **0** | — | **999** | 505.5 | 1.98 |
| | | | | 0.369 | 0.019 | 994 | | |
| | | | | 1.156 | 0.059 | **1003** | | |
| | | | | 2.462 | 0.127 | 993 | | |
| | | | Benzene | **0** | — | **1020** | | 2.02 |
| | | | | 0.436 | 0.011 | 1019 | | |
| | | | | 1.396 | 0.037 | 970 | | |
| | | | | 2.599 | 0.069 | 968 | | |
| | | Bromoform | | **0** | — | **975** | | 1.93 |
| | | | | 0.375 | 0.054 | 976 | | |
| | | | | 1.443 | 0.213 | 952 | | |
| | | | | 2.769 | 0.412 | 944 | | |
| | | Cyclohexane | | **0** | — | **1040** | | 2.06 |
| | | | | 0.201 | 0.039 | 1036 | | |
| | | | | 1.518 | 0.296 | 1031 | | |
| | | | | 2.485 | 0.492 | 1015 | | |

cyanide as represented in these compounds. Molecular weights of these complex compounds were measured by the cryoscopic method[9] in benzene, bromoform, and cyclohexane and by the ebullioscopic method[10] in benzene. All of these solvents were prepared by purification of guaranteed reagents in the usual manner[11].

The results of these experiments are shown in Table II.

It is made clear from Table II that the complex compounds having methyl or ethyl groups as alkyl form tetramer in benzene solution at the freezing point and that they form dimer in other solvents, such as bromoform and cyclohexane, and moreover by the ebullioscopic method in benzene they also form dimer.

With isopropyl group as alkyl, the compound forms dimer in all cases.

It seems to be possible that the apparent values of molecular weights may be smaller, if the associated molecules dissociate in organic solvents. These possibilities are supported by the fact that the degree of association in non-polar solvents are greater than that in a polar solvent. So the present author measured the molecular weight of bis-(trimethyl phosphite) copper cyanide (IIa) by cryoscopy in cyclohexane in various concentrations ranging from 0.3 to 5 per cent.

If the associated molecules dissociate in organic solvents, the apparent values of molecular weight will become greater with the increase of concentration.

As shown in Table II, an increase of apparent values of molecular weight could not be found in the above range of concentration. So it seems to be right that the compound IIa forms dimer in cyclohexane, and does not form dimer from the dissociation of tetramer.

These problems of their structures or degree of association must be determined by X-ray analysis.

## Experimental

**Preparation of Phosphites.**—Trialkyl phosphites were prepared by Ford-Moore's method[12] and their yields, physical constants and microanalytical data are shown in Table III.

**Preparation of Phosphite or Bis-phosphite Copper Cyanides.**—The following examples illustrate the preparations of phosphite and bis-phosphite copper cyanides, I and II. Other examples are shown in Table I and their molecular weights are shown in Table II.

**Preparation of Triethyl Phosphite Copper Cyanide (Ib).**—To a solution of 33.2 g. (0.2 mol.) of triethyl phosphite in 50 ml. of benzene was gradually added 17.8 g. (0.2 mol.) of copper cyanide. The temperature rose gradually and copper cyanide dissolved in benzene. After stirring one hour, the reaction mixture was filterd and concentrated under reduced pressure. Colorless oil (49.6 g.) was obtained, $n_D^{25}$ 1.5031.

Found: N, 5.63; P, 12.2; Cu, 25.1. Calcd. for $C_6H_{15}O_3PCuCN$: N, 5.47; P, 12.1; Cu, 24.9%.

To a solution of 8.5 g. of Ib in 20 ml. of benzene, was added 5.6 g. of triethyl phosphite. The temperature did not rise. After concentrating the benzene solution, 13.9 g. of a white crystalline substance were obtained and the melting point of this substance was 121°C upon recrystallization from ligroin. This melting point coincided with that of authentic bis-(triethyl phosphite) copper cyanide (IIb) and a mixed melting point showed no depression.

**Preparation of Bis-(trimethyl phosphite) Copper Cyanide (IIa).** — This compound was prepared from 24.8 g. (0.2 mol.) of trimethyl phosphite and 8.9 g. (0.1 mol.) of copper cyanide in benzene solution as above mentioned. White crystals (33.5 g. 99.3%) were obtained and melted at 60~61°C.

Found: N, 4.15; P, 18.3; Cu, 18.6. Calcd. for $C_6H_{18}O_2P_2CuCN$; N, 4.15; P, 18.4; Cu, 18.8%.

To a solution of 11.2 g. of the compound IIa in 20 ml. of benzene was added 4.3 g. of trimethyl phosphite. After the benzene was evaporated, 15.1 g. of colorless oil were obtained and gave $n_D^{26}$ 1.5296. The refractive index, the infrared spectrum and the microanalytical data of this compound coincided with authentic trimethyl phosphite copper cyanide (Ia).

**Pyrolysis of Bis-(triethyl phosphite) Copper Cyanide (IIb).** — The compound IIb (21.1 g. 0.05 mol.) was set in a distillation flask (50 mol.) which was combined with the trap cooled at −50°C, and heated at 130°C under 0.1 mmHg pressure for 8 hr.

The colorless oil which was captured in the trap,

TABLE III. YIELDS, PHYSICAL CONSTANTS AND MICROANALYTICAL DATA OF PHOSPHITES $(RO)_3P$

| R | Yield % | B. p. °C | B. p. mmHg | $n_D^{(t°C)}$ | Phosphorus, % Found | Phosphorus, % Calcd. | Carbon, % Found | Carbon, % Calcd. | Hydrogen, % Found | Hydrogen, % Calcd. |
|---|---|---|---|---|---|---|---|---|---|---|
| $CH_2$ | 71 | 111~112 | 760 | 1.4096(21) | 24.9 | 25.0 | 29.17 | 29.03 | 7.31 | 7.26 |
| $C_2H_5$ | 82 | 55~ 57 | 19 | 1.4135(20) | 19.8 | 19.9 | 46.31 | 46.15 | 9.25 | 9.04 |
| $n$-$C_3H_7$ | 85 | 82~ 83 | 10 | 1.4263(20) | 15.1 | 14.9 | 52.06 | 51.92 | 10.09 | 10.10 |
| iso-$C_3H_7$ | 80 | 60~ 61 | 9 | 1.4079(29) | 15.0 | 14.9 | 51.88 | 51.92 | 10.41 | 10.10 |
| $n$-$C_4H_9$ | 87 | 119~120 | 10 | 1.4329(21) | 12.1 | 12.4 | 57.51 | 57.60 | 10.83 | 10.80 |

9) J. Sameshima, "Buturi-kagaku Jikken Hō", Shōkabō, Tokyo. p. 227.
10) J. Sameshima, ibid., p. 220.
11) T. Kuwata, "Yōzai, (Solvents)", Maruzen, Tokyo.
12) A. H. Ford-Moore, "Organic Syntheses", Vol. 31 (1951), p. 111.

was 7.1 g. and was distilled at 55~56°C/19 mmHg, $n_D^{20}$ 1.4133.

Found: P, 19.7; C, 46.05; H, 9.18. Calcd. for $C_6H_{15}O_3P$: P, 19.9; C, 46.15; H, 9.04%.

To a solution of 4.1 g. of this oil in 5 ml. of benzene was added 1.1 g. of copper cyanide. After filtering and concentrating, 5.0 g. of white crystals were obtained and melted at 121°C (recryst. from petroleum ether). This melting point coincided with that of authentic bis-(triethyl phosphite) copper cyanide (IIb) and the mixed melting point did not go down. So it was made clear that this oil was triethyl phosphite.

On the other hand, residual oil in a distillating flask gave 11.6 g. and had $n_D^{25}$ 1.4999, and the microanalytical data and the infrared absorption spectrum of this oil coincided with that of authentic triethyl phosphite copper cyanide.

Found: P, 12.5; N, 5.21; Cu, 24.6. Calcd. for $C_6H_{15}O_3PCuCN$: P, 12.1; N, 5.48; Cu, 24.9%.

To a solution of 5.1 g. of this oil in 10 ml. of benzene was added 3.3 g. of triethyl phosphite. After the benzene was evaporated off, 8.0 g. of white crystals were obtained and melted at 121°C. This melting point coincided with that of authentic bis-(triethyl phosphite) copper cyanide (IIb) and the mixed melting point did not go down. So, it was determined that the residual oil was triethyl phosphite copper cyanide (Ib).

**Reaction of Triethyl Phosphite Copper Cyanide (Ib) with Benzoyl Chloride.** — To a solution of 5.1 g. of triethyl phosphite copper cyanide (Ib) in 10 ml. of ether was added gradually 2.8 g. of benzoyl chloride. The temperature rose and copper cyanide was precipitated. The reaction mixture was filtered and concentrated. The residual oil was distilled under reduced pressure, b. p. 140°C/2.5 mmHg, $n_D^{23}$ 1.5068, yield 3.6 g.

Found: P, 12.6; C, 54.39; H, 6.18. Calcd. for $C_{11}H_{15}O_4P$: P, 12.8; C, 54.55; H, 6.20%.

2,4-Dinitrophenylhydrazone of this product was prepared in the usual manner and melted at 171~172°C (recryst. from ethanol). This melting point coincided with that of 2,4-dinitrophenylhydrazone of authentic *O,O*-diethylbenzoyl phosphonate[4] and mixed melting point did not go down.

## Summary

Trialky phosphite reacts with copper cyanide to give phosphite or bis-phosphite copper cyanides according to the mole ratio of phosphite to copper cyanide.

It is made clear from their molecular weights that these products form polymer in various organic solvents. Moreover, these products have strong fungicidal action but this will be reported in another paper.

The author wishes to express his thanks to Professor Shinichiro Fujise and Professor Taro Yamazaki of Tohoku University and to Professor Ryutaro Tutida of Osaka University for their helpful suggestions in the preparation of this manuscript. He also wishes to thank the Sumitomo Chem. Co., Ltd. for permission to publish this work. He is indebted to coworkers in the analytical section in this laboratory. He also wishes to express his thanks to Mr. M. Nakagawa for his assistance.

*Osaka Work Sumitomo Chem. Co., Ltd.*
*Konohana-ku, Osaka*

# *Infrared Spectra of Isotactic Poly-α-olefins**

By Hiroyuki TADOKORO, Tohru KITAZAWA**, Shun'ichi NOZAKURA and Shunsuke MURAHASHI

(Received January 18, 1961)

In the previous paper[1], we have reported that the infrared absorption bands at 1364, 1314, 1297 and 1185 $cm^{-1}$ of isotactic polystyrene (IPS) and its derivatives are considered to be closely associated with the helical structure of the isotactic polymers (mainly due to the $CH_2$, CH and C-C vibrations of the main chain having the alternate sequence of gauche and trans conformations) and that these bands may be used as the criterion for the isotactic structure. Furthermore, it has been confirmed from the infrared spectra of the mixture of IPS and isotactic poly-α, β, β-trideuterostyrene (IPTDS) that these bands are originated from the intramolecular interactions in the helical chain[2]. In this communication we wish to report the results obtained

* Presented at the 9th Annual Meeting of the Society of Polymer Science, Osaka, May, 1960.

** Present address: Research Laboratories, Kanegafuchi Spinning Co., Ltd., Tomobuchi-chô, Miyakojima-ku, Osaka.

1) H. Tadokoro, S. Nozakura, T. Kitazawa, Y. Yasuhara and S. Murahashi, This Bulletin, **32**, 313 (1959).

2) H. Tadokoro, T. Kitazawa, S. Nozakura and S. Murahashi, *Chem. High Polymers* (*Kôbunshi Kagaku*), **17**, 231 (1960).

from the infrared spectra measured on the following polymers in order to examine whether similar bands appear or not.

*Polypropylene.*—We have used the ethyl ether extract of Moplen MS as the atactic sample (APP), and its *n*-heptane residue as the isotactic sample (IPP).

*Isotactic and Atactic Poly-3-deuteropropene-1 (IPP-3D and APP-3D)* $-(-CH_2-\underset{\displaystyle CH_2D}{\underset{|}{CH}}-)_n-$.—Prepared according to the following scheme, and separated by the same procedure as in the case of polypropylene:

$$CH_2{=}CH{-}CH_2Cl \xrightarrow{Mg} CH_2{=}CH{-}CH_2MgCl \xrightarrow{D_2O}$$

$$CH_2{=}CH{-}CH_2D \xrightarrow{\text{Natta catalyst}} -(-CH_2-\underset{\displaystyle CH_2D}{\underset{|}{CH}}-)_n-$$

*Polybutene-1.*—Polymerized with Ziegler catalyst. We used the ethyl ether extract as the atactic sample (APB), and its residue as the isotactic sample (IPB).

*Isotactic Polyvinylcyclohexane (IPVCH) and Poly-α-deuterovinylcyclohexane (IPDVCH)* —$-(-CH_2-\underset{\displaystyle H}{\underset{|}{CD}}-)_n-$.—(kindly given by Professor C. G. Overberger of the Polytechnic Institute of Brooklyn).

Figure 1 shows the infrared dichroism (LiF optics) of IPP, IPP-3D and IPB as well as IPS for reference. The bands in the 3$\mu$ region appear at nearly the same frequencies as the characteristic values of the $CH_2$ and $CH_3$ stretching modes of *n*-paraffins (2960(∥) 2953 (⊥): $\nu_a$ ($CH_3$), 2920(⊥) : $\nu_a$ ($CH_2$) (*E*), 2905 (∥): $\nu_a$ ($CH_2$) (*A*), 2876(⊥) : $\nu_s$ ($CH_3$) (*E*), 2844(no): $\nu_s$ ($CH_2$) (*A* and *E*) for IPP). As we have already reported, no (or weak) dichroism of the 2849 $cm^{-1}$ $\nu_s$ ($CH_2$) band and the distinguished perpendicular dichroism of the 2924 $cm^{-1}$ $\nu_a$ ($CH_2$) band of IPS may be interpreted by the inclination of the $CH_2$ group. This dichroic feature may be expected to be found in the spectra of all kinds of helical isotactic polymers[3]. In fact, this feature has been

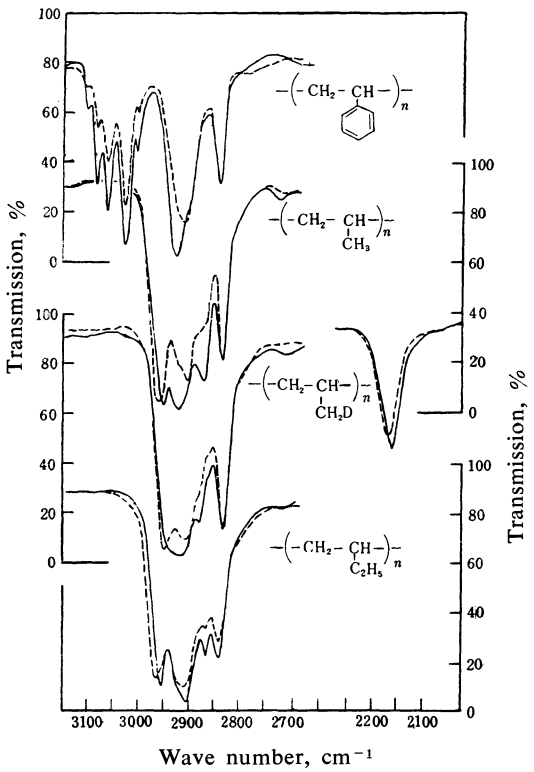



Fig. 1. Infrared dichroism of isotactic polystyrene, polypropylene, poly-3-deuteropropene-1 and polybutene-1 (LiF optics).

—— Electric vector perpendicular to elongation

---- Electric vector parallel to elongation

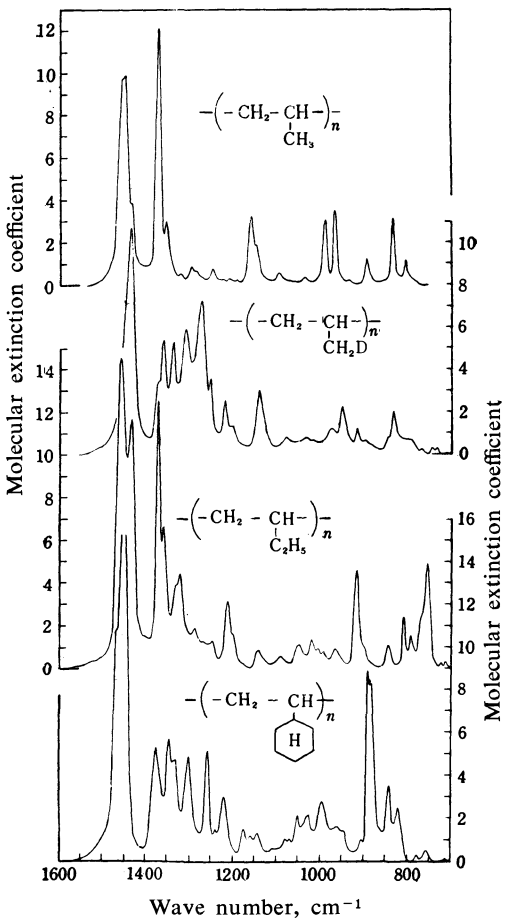



Fig. 2. Infrared spectra of isotactic poly-α-olefins.

3) S. Murahashi, S. Nozakura and H. Tadokoro, This Bulletin, 32, 534 (1959).

observed in the spectra of IPP and IPP-3D. Although IPP-3D has another $CH_2$ group in the side chain besides the $CH_2$ group in the main chain, it will be clear from a simple consideration that the dichroism of the $\nu_s$ ($CH_2$) band may be absent, if the $CH_2$ group assumes the three stable positions about the C-$CH_2$D axis with equal probability. This dichroic feature is obscured in the cases of IPB, IPVCH and IPDVCH, because of the complexity due to the existence of $CH_2$ groups in the side chain. In the spectra of IPS and IPP, there are appreciable shifts between perpendicular and parallel components of the $\nu_a$ ($CH_2$) band, and furthermore the perpendicular component occurs at higher frequencies and parallel ones at lower in both spectra. The splitting of the perpendicular and parallel components are also observed in the $\nu_a$ ($CH_3$) bands in the spectra of IPP and IPB, but in these cases the perpendicular ones occur at lower frequencies. The splitting of the $\nu_a$ ($CH_2$) bands may be explained from the factor group consideration reported already in the case of IPS[4]. The band splitting of the $\nu_a$ ($CH_3$) modes involves an interesting problem in relation to the perturbation of the environment to the local degeneracy of the $CH_3$ group.

Figure 2 is the infrared spectra (1600~700 $cm^{-1}$) of isotactic poly-α-olefins rewritten on the scale of molecular extinction coefficient. In Fig. 3, the spectra of the isotactic and atactic samples of poly-α-olefins at room temperature were compared with those of the molten states of the isotactic samples. Figure 4 shows the infrared dichroism (NaCl region) of isotactic poly-α-olefins. We have found that several bands at 1400~1100 $cm^{-1}$ region of the spectra of isotactic poly-α-olefins show behavior similar to that of the bands of IPS and its derivatives mentioned at the beginning of this article. The bands observed at 1364

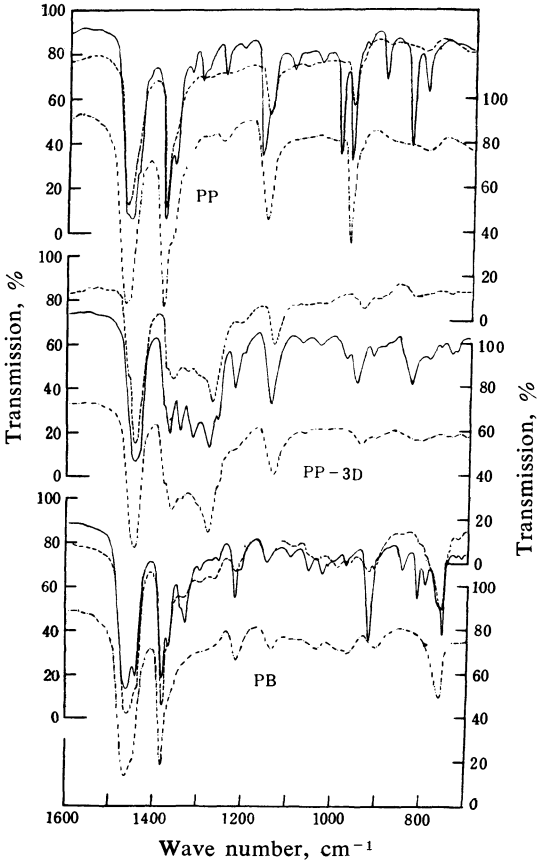



Fig. 3. Infrared spectra in various states of poly-α-olefins.
—— Isotactic samples
---- Atactic samples
-·-· Molten states of isotactic samples

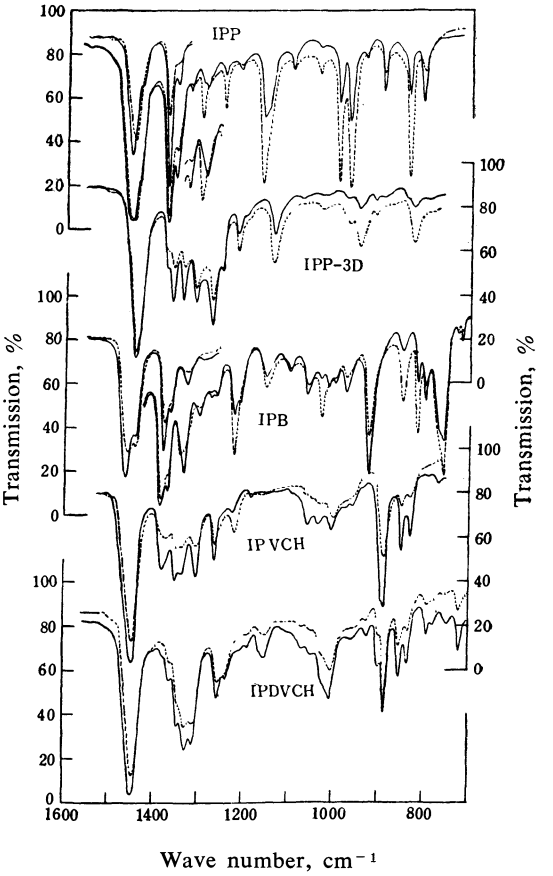



Fig. 4. Infrared dichroism of isotactic poly-α-olefins (NaCl optics).
—— Electric vector perpendicular to elongation
---- Electric vector parallel to elongation

4) H. Tadokoro, N. Nishiyama, S. Nozakura and S. Murahashi, ibid., 34, 381 (1961).

$cm^{-1}$ in the spectra of IPS and its derivatives[1,3,5] appear also in the spectra of IPP, IPP-3D, IPB and IPP-3, 3, $3D_3$[6] at the same frequency, and moreover exhibit the same characteristic behavior: (1) the perpendicular dichroism, (2) similar intensity (2~5 in molecular extinction coefficient), (3) absence in the cases of the atactic samples and (4) decrease of the intensity with heating and disappearance at molten state. This band is not observed in the spectra of IPTDS, isotactic poly-$\alpha D_1$-styrene[7], IPP-1, $1D_2$[6], IPP-2D[6]. The above mentioned inference for this band may be considered to be supported strongly by these experimental evidences. Especially, the constancy of the frequency (1365~1360 $cm^{-1}$) extending over the various samples of IPS, its derivatives and isotactic poly-$\alpha$-olefin swill suggest the approximate localization of the vibrations in the skeleton and the attached hydrogen atom, comparing them to the bands described subsequently. Some bands similar to the 1185 $cm^{-1}$ band of IPS (and 1183 $cm^{-1}$ of isotactic poly-*p*-deuterostyrene, 1184 $cm^{-1}$ of isotactic poly-*p*-methylstyrene, 1190 $cm^{-1}$ of isotactic poly-*m*-methylstyrene, 1184 $cm^{-1}$ of isotactic poly-*p*-trimethylsilylstyrene) are observed in the spectra of IPP (1167 $cm^{-1}$), IPP-3D (1216 $cm^{-1}$), IPB (1217 $cm^{-1}$) and IPVCH (1217 $cm^{-1}$) with the same parallel dichroism, the similar intensity (2.5~4.5 in molecular extinction coefficient) and the similar band shapes. In addition this band is absent in the spectra of atactic samples and IPTDS, IPDVCH, IPP-1, $1D_2$[6], IPP-2D[6] and IPP-3, 3, $3D_3$[6]. Consequently these bands are considered to be due to similar origin. In spite of the approximate constancy of the frequency in the case of IPS and its derivatives, the frequency differs considerably in the spectra of poly-$\alpha$-olefins. This fact suggests that in the mode assignable for this type of band the vibration in the main chain would couple with those of the side chain appreciably in the cases of poly-$\alpha$-olefins, while it would not do so with the phenyl side group.

5) M. Kobayashi, K. Nagai and E. Nagai, ibid., 33, 1421 (1960).
6) C. Y. Liang, M. R. Lytton and C. J. Boone, *J. Polymer Sci.*, 44, 549 (1960).
7) M. Kobayashi, This Bulletin, 33, 1416 (1960).

*Department of Polymer Science*
*Faculty of Science*
*Osaka University*
*Kita-ku, Osaka*

# *Molecular Rotations of Polyhydroxycyclohexanes in Relation to their Structures. II*[1]. *(−)-1, 2, 3, 5/4-Cyclohexanepentol*

By Shukichi YAMANA

(Received February 6, 1961)

$[M]_D^{20}$(W) of (−)-1, 2, 3, 5/4-cyclohexanepentol ((−)-epi-quercitol[2]) was calculated by using PM-method and Whiffen's method[3], respectively. The orientation of the unit groups, (OH). in the molecule is shown in Table I (Fig. 1).

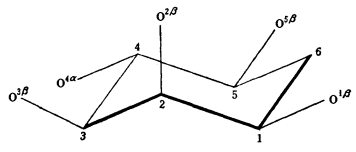



Fig. 1. Perspective drawing of the molecular model of (−)-1,2,3,5/4-cyclohexanepentol.

TABLE I

| Name | Orientation of unit group, (OH) | Calcd. $\sum[\mu]_{D\,obs}^{20}$ | Calcd. Whiffen |
|---|---|---|---|
| Cyclohexane | | | |
| (−)-1,2,3,5/ 4-pentol | [(1β), (2β), (3β), (4α), (5β)] | −6.8 (−10.9)[5] | 0 |

**PM-Method.**— $[M]_D^{20}$(W) of (−)-1, 2, 3, 5/4-cyclohexanepentol$\equiv\sum[\mu]_{D\,obs}^{20}$ of (−)-1, 2, 3, 5/4-cyclohexanepentol = (1β) Λ (2β) + (1β) Λ (3β) + (1β) Λ (4α) + (1β) Λ (5β) + (2β) Λ (3β) + (2β) Λ (4α) + (2β) Λ (5β) + (3β) Λ (4α) + (3β) Λ (5β) + (4α) Λ (5β) = $A+0+0+0-A-B+0-A+0+A$[4] = $-B=-6.8$ $(-10.9)$[5].

1) Part I: S. Yamana, This Bulletin, 33, 1741 (1960).
2) "Advances in Carbohydrate Chemistry", Vol. 14, Academic Press, New York (1959), p. 190.
3) D. H. Whiffen, *Chem. & Ind.*, 1956, 964.
4) Table II in the previous paper[1] is used, here.
5) The values, calculated by supposing that the optical center of (OH) is located at its O atom, are given in parentheses.

**Whiffen's Method.**

along $C^1-C^2$
C|C−C|O+O|O−O|H+H|H−H|C
along $C^2-C^3$
C|H−C|C+O|C−O|O+H|O−H|H
along $C^3-C^4$
C|C−C|H+O|H−O|O+H|O−H|C
along $C^4-C^5$
C|H−C|C+O|O−O|H+H|C−H|O
along $C^5-C^6$
C|C−C|H+O|H−O|H+H|H−H|C
along $C^6-C^1$
C|H−C|C+H|C−H|O+H|O−H|H
Total=0

As seen above, $[M]_D^{10}$(W) of (−)-1, 2, 3, 5/4-cyclohexanepentol is presumed to be −6.8 (−10.9)[5] (by PM-method) or 0 (by Whiffen's method). The corresponding observed value has not been found in any referential literatures, but $[M]_D$(W) was observed at 27°C as −8.9[6]. This is nearly equal to −6.8 (−10.9)[5], the value calculated by PM-method at 20°C. This fact indicates that in this case also, PM-method is more suitable for estimating $[M]_D^{20}$ (W) than Whiffen's method.

*Department of Chemistry*
*Kyoto Gakugei University*
*Fushimi-ku, Kyoto*

6) B. Magasanik, R. E. Franzl and E. Chargaff, *J. Am. Chem. Soc.*, **74**, 2618 (1952).

# *Studies on Surface Heterogeneity in Adsorption of Carbon Dioxide on Nickel by Use of the Isotopic Desorption Method*[1]

Kozo Hirota, Yasushi Kobayashi* and Jitsuo Kiji

(Received January 30, 1961)

A number of printed works on the active center of catalysts have appeared, since Taylor proposed the idea in 1925. However, though its existence on actual catalysts is recognized unequivocally by most researchers, some ambiguities remain yet as to its nature. In some cases the experimental grounds in favour of the active center may be explained by other causes, i. e., by the "induced heterogeneity" or by the mutual interaction between adsorbed molecules. Such situations regarding this important problem of catalysis may be brought about because researchers have taken it up by the kinetic or calorimetric methods, which are deficient in giving decisive conclusions.

Therefore, in order to attack the problem, now called heterogeneity of catalyst surface, it seems interesting to apply the isotopic desorption method of Roginsky[2], who applied it with success by the use of deuterium to determine the heterogeneity of nickel, when hydrogen was chemisorbed[3]. The process of the method consists in two procedures: firstly successive chemisorption of two gaseous portions of isotopically labelled and non-labelled species, to the catalyst to be investigated, and secondly, determination of the isotopic composition of the gases desorbed from the catalyst. Now, if the isotopic composition of the desorbed gases is the same as that of the mean of the chemisorbed gases, it is highly probable that the catalyst surface is homogeneous, while if it is not the same, the catalyst surface is likely to be heterogeneous. Since then, the method has been applied by others; e. g., chemisorption of carbon monoxide on a promoted iron catalyst by Kummer and Emmett[4], making radioactive carbon as the tracer, and chemisorption of hydrogen on nickel-silica by Schuit[5], who, however refused to accept the result of Roginsky.

Such being the situation it will be interesting to apply it to other systems under the condition of least ambiguity, so as to check the criticism against this method. In the present paper, the heterogeneity of nickel surface will be investigated by use of carbon dioxide,

* Present address: Radiation Center of Osaka Prefecture, Shike-cho, Sakai, Osaka.

1) Preliminary report: Preprint of the Catalyst Symposium of Japan, Osaka, April, 1959, p. 1.

2) S. R. Roginsky and O. Todes, *Acta Physicochim.* (*U. R. S. S.*), **21**, 519 (1946). This method is called the differential isotopic method in Russian literatures.

3) M. P. Keier and S. R. Roginsky, *Izvest, AN, URSS*, **1**, 27 (1950); Cf., "Advances in catalysts", **5**, 247 (1955).

4) J. K. Kummer and P. H. Emmett, *J. Am. Chem. Soc.*, 73, 2886 (1951).

5) G. C. Z. Schuit, *Chem. Abstr.*, **48**, 11, 869i (1954). Cf. P. M. Gundry and F. C. Thomkins, *Quart. Rev.*, **14**, 257 (1960).

making heavy carbon dioxide $CO^{18}O$ as the labelled species of adsorbent, and effecting desorption at the adsorbed temperatures. Selection of this adsorbate may be appropriate, because, besides its possible immobility on the surface, it will evolve little adsorption heat, as compared with hydrogen and carbon monoxide hitherto selected, so that the disturbing effect of evolved heat would be small on adsorption.

## Experimental

**Apparatus.**—The apparatus used in the measurement is shown in Fig. 1. During the experiment, caution was always taken that no mercury vapor might penetrate into catalyst A by constant use of trap T kept at ca. −78°C.

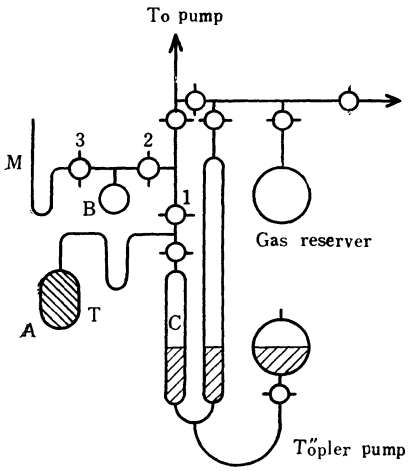



Fig. 1. Apparatus.

**Nickel Catalyst.**—Nickel carbonate, obtained by the reaction of aqueous nickel nitrate solution with an ammonium carbonate solution, was washed with water, dried and heated in the air for 10 hr. at 300°C. Nickel oxide thus prepared was turned into nickel powders by reducing it with hydrogen for 80 hr. at 350~380°C. Before each experimental run, the nickel powders were treated with hydrogen followed by evacuation at the same temperature at $10^{-6}$ mmHg. The specific area of the catalyst determined by the BET method (adsorbate, nitrogen) was 1.18 $m^2/g$.

**Gases.**—Heavy carbon dioxide $CO^{18}O$ was prepared in the present laboratory by the thermal diffusion method[6]. Its concentration was 29.9~15.2 atom %. Normal carbon dioxide was obtained by evaporation of commercial dry ice, and purified with aqueous sodium chromate, followed by dehydration with liquid nitrogen and phosphorus pentoxide. The hydrogen used for reduction was prepared by electrolysis of aqueous sodium hydroxide solution, and was purified finally by being effused through a palladium filter. The last treatment was indispensable for the reproducibility of the result.

**Adsorption Isotherm.**—For the sake of discussion, the adsorption isotherm for carbon dioxide on the nickel powders (28.1 g.) which were used in the experiment was determined at −78°C. This is shown in Fig. 2. It was found that 0.17$_8$ cc./g. was necessary in order to complete the monomolecular layer.

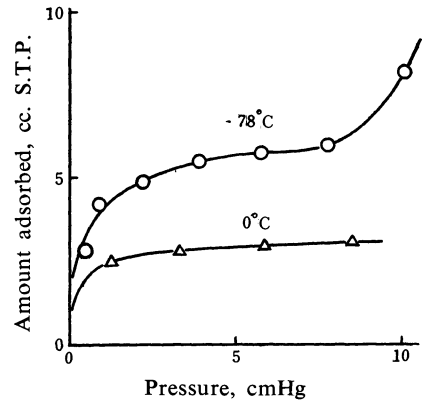



Fig. 2. Adsorption isotherms for carbon dioxide at 0 and −78°C (cat. 28.1 g.)

**Reduction of Nickel Surface.**—In order to determine the permissible degree of reduction the amount of adsorbed oxygen was measured with the isotopic dilution method by use of $CO^{18}O$, i. e., introducing the gas to the vessel which contained nickel and determining the degree of dilution in the gas collected from the vessel. When the $O^{18}$% of the original $CO_2$ was 15.2 atom % and when the reduction at 380°C was continued for 20 hr., the collection was made at two temperature intervals, the result being as follows :—between 0°C and room temperature, 0.3 cc. and 14.2%, and between room temperature and 300°C, ca. 1 cc. and 12.2%. Dilution of the original carbon dioxide occurred to such an extent that the residual oxygen was found not to be negligible by the above treatment of reduction, suggesting that the nickel surface did not reach a state sufficiently free from oxygen. However, it was found that eighty hours of reduction as actually adopted in the experimental runs was found to be satisfactory so that the heterogeneity could be discussed by this method. Such difficulty in cleaning the surface as was found above has been pointed out already, e. g., recently by Roberts and Sykes[7].

**Exchange Reaction.**—After the nickel catalyst charged in the reaction vessel A was reduced with hydrogen, it was evacuated and was kept at the adsorption temperature, which was adopted to be −78°C if otherwise not stated. Then a known amount $V_1$ of heavy carbon dioxide (or normal carbon dioxide) was introduced into the vessel A from the measuring pipette C. After the scheduled time which was set at 30 min. of contact, the gaseous sample was collected by opening the taps

6) K. Hirota, Y. Kobayashi et al., "Isotopes and Radiation" (Tokyo), 2, 235 (1959); Y. Kobayashi et al., "Mass-spectroscopy" (Japan), No. 13, 79 (1959).

7) M. W. Roberts and K. W. Sykes, *Trans. Faraday Soc.*, 54, 548 (1958).

1 and 2, and being condensed in the trap B cooled at −78°C. Amount $v$ of the condensed gas was determined by evaporating it in the known volume of space between the taps 3 and 2 with the manometer M. The residual carbon dioxide adsorbed tightly on the nickel could be calculated as the difference between $V_1$ and $v$. Then normal carbon dioxide (or heavy carbon dioxide), the amount of which was measured to be $V_2$, was again introduced to the catalyst already covered to some extent by heavy carbon dioxide. After the scheduled time of contact, the gaseous part of the carbon dioxide was again condensed in B, and was measured by the same procedure as described above. This procedure was done several times. The first desorption was made at the same temperature as the adsorption, and subsequent desorption was carried out by raising the temperatures gradually up to 300°C. The isotopic abundance and gaseous composition of each collected gas were determined by a mass-spectrometer.

## Results

For the sake of making the effect evident, the adsorption was carried out at temperatures as low as possible, i. e., mostly at −78°C and also at 19 and 0°C. However, the amount of the desorbed gas was determined at several temperatures up to 300°C. Experimental data are summarized in Table I in the order of the runs actually carried out. The first and second portions, denoted as I and II in Table I, of the gas introduced into the vessel are heavy and normal carbon dioxide if otherwise not stated. The numerals marked by→after $V_1$ denote the amount of the gas strongly adsorbed after desorption at the adsorption temperature.

The reproducibility of the experiment may be shown by the residual amount of the gas remaining after evacuation in Nos. 1 and 4, where the adsorbed and desorbed temperatures were the same (−78°C) while other experimental conditions were practically identical with each other. It is noteworthy that such strongly adsorbed gas amounted to ca. 1.85 cc. in both runs in spite of the difference of the first portion introduced. The tendency that

Table I. Experimental result

Catalyst: 28.1 g., BET area = 1.18 m²/g. = 5.0 m²/28.1 g.
Gaseous volume is expressed by STP, while concn. of $^{18}O$ by atom %.

| Run No. | Adsorption procedure | | | | Desorption procedure | | | | |
|---|---|---|---|---|---|---|---|---|---|
| | Temp. °C | Order of addition | Added amount cc. | $^{18}O$ Concn. % | Temp. °C | Evacuated time min. | Desorbed amount cc. $v$ | Residual amount cc. | $^{18}O$ Concn. % |
| 1 | | I | $V_1$=1.35 | 29.9 | −78 | 110 | (5.31) | 1.87 | 2.0 |
| | −78 | | →1.35 | | 0 | 100 | 0.21 | 1.66 | 11.4 |
| | | II | $V_2$=5.83 | 0.2 | 20~21 | 80 | 0.03 | 1.63 | 12.8 |
| | | | | | 150 | 60 | 0.06 | 1.57 | 12.5 |
| | | | | | 300 | 60 | 0.67 | 0.90 | 12.0 |
| 2* | | I | $V_1$=11.49 | 0.2 | −78 | 120 | (13.05) | 1.44 | 28.4 |
| | −78 | | →2.31 | | 0 | 120 | 0.25 | 1.19 | 10.8 |
| | | II | $V_2$=12.18 | 29.9 | 100 | 90 | 0.07 | 1.12 | 8.0 |
| | | | | | 300 | 80 | 0.94 | 0.18 | 7.2 |
| 3 | | I | $V_1$=2.36 | 28.4 | 0 | 120 | (4.35) | 2.26 | 3.5 |
| | 0 | | →2.18 | | 100 | 90 | 0.47 | 1.79 | 16.3 |
| | | II | $V_2$=4.43 | 0.2 | 300 | 100 | 1.02 | 0.77 | 17.4 |
| 4 | | I | $V_1$=5.62 | 29.9 | −78 | 120 | (5.01) | 1.83 | 2.8 |
| | −78 | | →1.88 | | 0 | 120 | 0.26 | 1.57 | 15.7 |
| | | II | $V_2$=4.96 | 0.2 | 100 | 90 | 0.09 | 1.48 | 17.9 |
| | | | | | 300 | 90 | 0.55 | 0.93 | 15.9 |
| 5** | | I | $V_1$= 2.32 | 15.2 | (a) Desorbed $CO_2$ was 0.1 cc. $CO_2/CO$=1/50, because CO desorbed at −78°C was 5.18 cc. | | | | |
| | −78 | | | | | | | | |
| | | II | $V_2$=12.24 (CO) | 0.2 | (b) $^{18}O$ concn. of CO became 1.0% | | | | |
| 6 | | I | $V_1$=5.69 | 29.1 | 19 | 120 | (4.81) | 2.40 | 3.3 |
| | 19 | | →2.36 | | 100 | 120 | 0.42 | 1.98 | 10.7 |
| | | II | $V_2$=4.85 | 0.2 | 300 | 120 | 1.02 | 0.96 | 19.0 |

* The first gas I was normal $CO_2$ and the second II $CO^{18}O$.
** The second gas was carbon monoxide instead of carbon dioxide.

Table II. Residual amount of $C^{18}O_2$ in Nos. 1 and 4

No. 1 ($C^{18}O_2$ adsorbed=0.40 cc.)

| Desorbed temp. °C | Heavy carbon dioxide | |
|---|---|---|
| | Desorbed cc. | Not desorbed cc. |
| −78 | 0.096 | 0.31 |
| 0 | 0.022 | 0.29 |
| 20~21 | 0.004 | 0.28 |
| 150 | 0.007 | 0.28 |
| 300 | 0.079 | 0.20 |

No. 4 ($C^{18}O_2$ adsorbed=0.56 cc.)

| Desorbed temp. °C | Heavy carbon dioxide | |
|---|---|---|
| | Desorbed cc. | Not desorbed cc. |
| −78 | $0.13_0$ | 0.43 |
| 0 | $0.04_0$ | 0.39 |
| 100 | $0.01_6$ | 0.37 |
| 300 | $0.08_6$ | 0.28 |

the first portion was adsorbed more tightly than the second could be observed in No. 2, where heavy carbon dioxide was made the second portion. From the comparison of Nos. 1 and 4 with No. 2, the residual gas at −78°C is evidently small in the case where heavy carbon dioxide was introduced as the second gas. This may be explained by the isotopic effect of adsorption. Though the discussion along this line is interesting, it will not be taken up in the present report, because there may be some accidental error*.

By comparing the result Nos. 3 and 6 where the adsorption and first desorption were carried out at 0°C and 19°C, respectively, with those of Nos. 1 and 4, it is clear that the strongly adsorbed carbon dioxide increases in amount as the temperature of adsorption becomes higher.

In order to obtain knowledge on the state of adsorption of carbon dioxide, a similar experiment was attempted making carbon monoxide the second gas in No. 5. Since carbon monoxide can be adsorbed on nickel very strongly as shown by the great heat of adsorption (35 kcal.)[8], carbon dioxide which has been adsorbed may be expelled from a nickel surface. Such an effect is moreover possible due to the heat evolution when carbon monoxide is chemisorbed. However, as described in Table I, the amount of the desorbed carbon dioxide was only ca. 0.1 cc., though carbon monoxide was desorbed more than carbon dioxide ($5.1_8$ cc.). This suggests a firm bonding of carbon dioxide with nickel. However the fact that $^{18}O$ concentration of carbon monoxide in the desorbed gas could not be neglected will become a matter of discussion; i. e. it was 1.0%. This indicates the occurrence of an exchange reaction such as

$$CO^{18}O + CO \rightarrow CO_2 + C^{18}O \qquad (I)$$

on nikel surface in parallel with desorption.

Such a firm bonding between the first chemisorbed* carbon dioxide and nickel can be concluded also from the isotopic balance of heavy oxygen in each run. According to No. 1, where 0.40 cc. of heavy carbon dioxide was chemisorbed as the first gas, only a part of it could be desorbed at each desorbing procedure, as shown in Table II, where the nautral abundance of $^{18}O$ was taken to be 0.2%. The same tendency can be seen also in No. 4, where 0.56 cc. of heavy carbon dioxide was first chemisorbed. It will be noteworthy that though the absolute amount of heavy carbon dioxide adsorbed at −78°C is different in both runs, their ratios to those at 300°C is the same i. e., 0.65. A similar result is found easily, in others runs, by the same method of calculation.

## Discussion

As pointed out above, a part of the nickel surface has a nature to chemisorb carbon dioxide so strongly that carbon monoxide added as the second gas can not expel the carbon dioxide practically from the surface. This nature of the nickel surface will be supported also from the fact that the molecules once chemisorbed at low temperature were not desorbed even by evacuation at 300°C. By use of the data of No. 1, the situation will be shown quantitatively. The residual amount 1.87 cc at the desorbed temperature corresponds to surface coverage ($\theta$) of 0.37, which decreases gradually down to $\theta$=0.18 (0.9 cc.) after the desorption process at 300°C, because the amount of carbon dioxide necessary to cover the catalyst surface monomolecularly is 5.0 cc.

Now the nature of such a special surface, which extends to about one third of BET area of the nickel, will be discussed from the standpoint of isotopic exchange of heavy oxygen with regard to possible occurrence of the induced heterogeneity. The data of No. 1 will be taken up again. If the bonding of carbon dioxide to nickel is extremely firm on

* The residual gas remaining at 300°C is only 0.18 cc. in No. 2. Such a small numeral will probably be brought out by an increased error due to the large amount of the second gas ($12.1_8$ cc.).

8) O. Beeck, "Advances in Catalysts", 2, 151 (1950).

* Chemisorption will hereafter be used often as a technical term not defined to be clearly different from adsorption.

some special sites on the surface, it may be possible that $^{18}O$ concentration in the first portion of desorbed gas is natural, i. e. 0.2%, because $V_1$ was 1.35 cc., which was less than the volume corresponding to the chemisorption on the special sites (1.87 cc.), leaving some vacant sites for the second gas. Actually, dilution of $^{18}O$ in the strongly adsorbed carbon dioxide occurred up to 2.0%, as shown in the last column of Table I. The degree of dilution will be given approximately as follows: 0.096/0.40=0.24. This suggests that there occurred some exchange of oxygen between strongly adsorbed carbon dioxide and that which was weakly adsorbed.

Now it is natural to assume that the difference of adsorptive power or the surface mentioned above might be due to the primary property of sites but not induced secondarily by the mutual interaction of absorbed molecules. This is because if the difference is brought about by the latter reason, the degree of the exchange reaction II between adsorbed carbon dioxide would occur much more markedly and increase according as the adsorption temperature rises, and evacuation at 300°C would take away most of the adsorbed carbon dioxide, due to a relatively weak interacting energy. Another fact will be shown against the induced heterogeneity by use of the data of No. 2, where heavy carbon dioxide added as the second gas ($3.6_5$ cc.) was taken out from the surface practically without exchange by the first desorption at the adsorption temperature, due to the weak bonding of the second gas with adsorptive sites.

Since the surface heterogeneity is confirmed, its nature will be discussed in more detail. According to the analysis of the data, it has been shown that even the special sites extending as much as one third of the total are not of a homogeneous nature in adsorptive power, three fourths of it making firmer bonding to carbon dioxide than the remaining one third. The existence of such heterogeneity is possible also from the data of No. 5, which can be explained by an exchange reaction I of weakly adsorbed carbon monoxide and strongly adsorbed carbon dioxide. Assuming that the amount of the strongly adsorbed carbon dioxide is 1.85 cc. and also that $^{18}O$ concentration of the strongly adsorbed carbon monoxide ($7.0_6$ cc.) is the same as that of the desorbed one, $^{18}O$ lost from carbon dioxide by the contact of carbon monoxide will be approximately equal to $(1.0\times12.24/1.85\times15.2)\times100\%=22\%$. It is noteworthy that this numeral nearly equals that (24%) obtained in the discussion of the above paragraph. Here it will be mentioned that no exchange of this type I could be observed on silver catalyst even at 220°C[9], suggesting that there was a difference in the chemisorped state between nickel and silver. The result may be caused by the chemisorptive power of nickel to carbon monoxide which is so strong that they can form stable carbonyl compounds, though the chemisorptive power of both metals to carbon dioxide is not very different, so that the exchange reaction

$$O_2^*+CO \rightarrow CO_2^*+O_2 \qquad \text{(III)}$$

proceeds at the same order of temperature 100~200°C[10].

In short, it can be concluded that there are two or three types of sites on nickel surface differing in chemisorptive power. It will be our next problem to investigate the real nature of these special sites, e. g., to see whether they exist as groups or as isolated ones. However, the problem of surface heterogeneity is very complicated, and the present data can not give an answer to all the questions to be discussed. Here it will be mentioned that, since the ratio of the active surface to the total is considerably large and reproducibility of the catalytic activity is very good, the heterogeneity here observed may be brought about by the different catalytic activity of each crystal plane and not by isolated sites on some planes. Further discussion concerning the nature of heterogeneity is to be continued in the investigation which will be reported soon.

## Summary

By applying the isotopic desorption method of Roginsky under the experimental condition of least ambiguity, heterogeneity of nickel surface has been studied on the chemisorption of carbon dioxide by making heavy oxygen as the tracer. It has been shown that about one third of the surface can chemisorb carbon dioxide very strongly at −78, 0 and 19°C, and a part of carbon dioxide chemisorbed is not desorbed even by the evacuation at 300°C. Considering the isotopic balance of heavy oxygen, it can be said that the above effect is brought about by the primary heterogeneity of surface sites but not by the "induced heterogeneity" of adsorbate. However, it has been found difficult to make the detailed nature of such heterogeneity by the present data alone.

9) Hirota and Kobayashi, Preprint of the Catalyst symposium of Japan, Kyoto, April, 1956.

10) K. Hirota and Y. Kobayashi, This Bulletin., 29, 996 (1956); Y. Kobayashi, M. Hatada and K. Hirota, unpublished.

A part of the expense for the present investigation has been defrayed from a grant given by the Ministry of Education to which the authors' thanks are due.

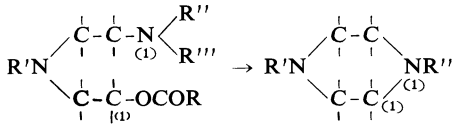
*Department of Chemistry*
*Faculty of Science*
*Osaka University*
*Nakanoshima, Osaka*

# *A New Method for the Preparation of Piperazines. III. Mechanism of Ring-closure Reactions with Elimination of Ester*

By Kazuo NAKAJIMA

(Received January 11, 1961)

The new synthesis of piperazines proposed by the author in the preceding papers[1], consists in heating a compound A to obtain a piperazine-derivative B under elimination of an ester C, as can be seen from the following over-all Scheme 1;



[A] [B]

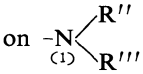
$$+ \mathrm{RCOOR'''} \qquad (1)$$

[C]

The compound A is an ester. It is generally accepted that the alkyl-ogygen bond in carboxylic acid ester of primary or secondary alcohols remains unattacked in hydrolysis or in other reactions in which these esters are concerned. However, esters of tertiary alcohols in some of their reactions may suffer the rupture of the alkyl-oxygen bond. For example, *tart*-butyl acetate, heated under reflux, is completely converted by dry hydrogen chloride into *tart*-butyl chloride and acetic acid, while *n*- and *sec*-butyl acetate undergo no reaction by the same treatment.

According to Eq. 1, however, the $C_{(1)}$-O bond should break up and the liberated acetoxyl group should combine with an alkyl group which comes out of $N_{(1)}$ to build up an ester molecule C, thus leaving a piperazine-ring system B.

The $-C-C_{(1)}-$ linkage in A may be regarded as an alkyl, so the piperazine-ring formation 1 may be considered to be a reaction which involves a replacement of R''' by $-C-C_{(1)}-$ grouping.

In other words, the ester part of A reacts as an alkylating reagent on  to drive out R'''.

In order to see the reactivities of alkyl acetates with tertiary amines, triethylamine and dimethylaniline were heated with *n*-butyl acetate under reflux for 20 hr.

However, no reaction could be observed and the starting materials were recovered unchanged. An attempt in an autoclave (at 280°C for 3 hr.) gave the same result.

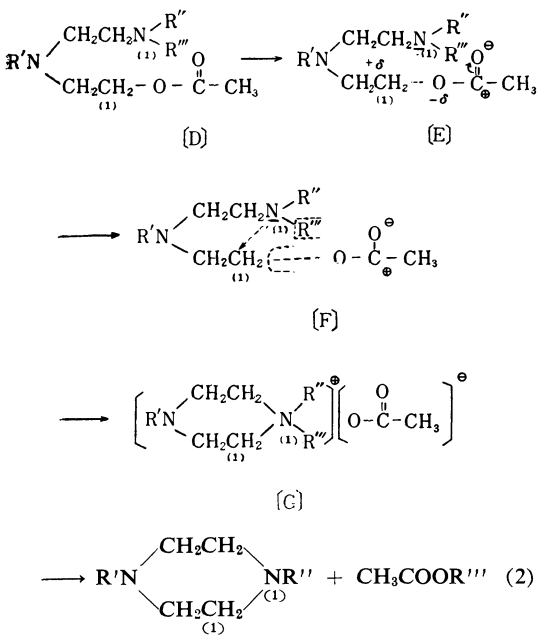
Even when *tert*-butyl acetate which has tendency to rupture at the alkyl-oxygen bond was used, reaction between the ester and triethylamine or dimethylaniline did not proceed.

In contrast to the very smooth progress of reaction 1 (R', R'', R''': $CH_3$), a ring-closure reaction for obtaining the same product by heating *N*, *N*, *N'*, *N'*-tetramethylethylenediamine and ethylenediacetate in an autoclave for 3 hr. at 280°C proved to be a failure.

In reaction 1 (R', R'', R'''; $CH_3$), the dialkylated amino group and the ester grouping are held in one molecule and are able to stay very close to each other on account of their special configuration. This proximity of the two groups is the most remarkable difference between the two cases of cyclization reaction and it seems to be plausible to attribute the cause of reaction 1 to the close situation of these groups.

The mechanism of the piperazine-ring formation might be written as follows;

1) K. Nakajima, This Bulletin, 34, 651, 655 (1961).

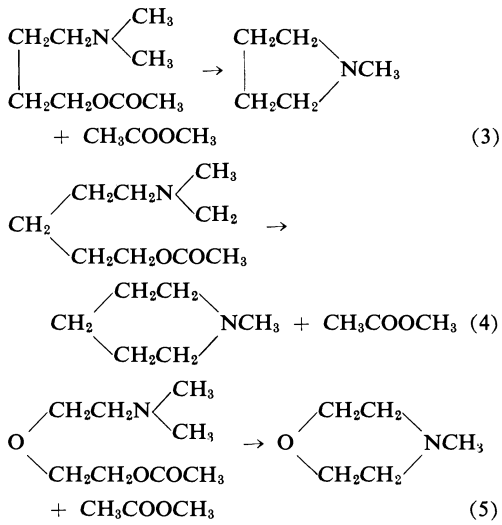


The first stage of the reaction mechanism is assumed to be the formation of a polarized state in the molecule D under the influence of heat as shown in E. In the second stage the union of $N_{(1)}$ and $C_{(1)}$ takes place and the carboxyl group is released as an anion. Then in the third stage the salt-like compound G thus formed is considered to be broken into a piperazine-derivative H and an ester $CH_3COOR'''$ at that elevated temperature. The decomposition of G may be regarded as a similar type of reaction to the thermal decomposition of the quarternary ammonium halides, which was reported by Hofmann[2].

This assumption for the similiarity can be explained by the fact that ease in liberation of the alkyl group R''' is identical to that of Hofmann's reaction, as briefly refered to in preceding report[1].

On inspecting the reaction mechanism shown in Scheme 2, an important question naturally arises as to what kind of compounds having a disubstituted amino and an ester-grouping in suitable positions in the molecule can undergo cyclization in the same way as these described above.

In order to give an answer to this question, several trials have been made with 4-dimethylamino-*n*-butyl acetate, 5-dimethylamino-*n*-pentyl acetate and β-acetoxy-β'-dimethylaminodiethyl ether. They have successfully proved that these compounds also undergo similar ring-closure reaction at about 200°C with elimination of an ester, giving *N*-methylpyrrolidine (3), *N*-methylpiperidine (4) and *N*-methylmorpholine (5), respectively.



These reactions make it easy to suppose that β-acetoxy-β'-dimethylaminodiethyl sulfide may have the possibility of being converted into *N*-methylthiomorpholine under similar conditions.

Synthesis of the sulfide, however, has not yet been attained.

## Experimental

***tert*-Butyl Chloride from *tert*-Butyl Acetate by Hydrogen Chloride.**—Dry hydrogen chloride was passed into *tert*-butyl acetate boiling in a flask fitted with a fractionating column, at such a rate that *tert*-butyl chloride formed distilled over at 50~60°C.

The reaction proceeded smoothly, leaving acetic acid in the reaction flask. *n*-Butyl and *sec*-butyl acetate remained intact by the same treatment.

***N*-Methylpyrrolidine from 4-Dimethylamino-*n*-butyl Acetate.**—*4-Dimethylamino-1-butanol.*—A mixture of 22 g. (0.2 mol.) of tetramethylene chlorohydrin and 50 g. of a 40% aqueous solution of dimethylamine was allowed to react in a bottle, plugged with a stopper holding a thermometer and an outlet tube connected to another bottle fed with water. By occasional shaking and timely cooling in water, the exothermic but moderate reaction was regulated so that no methylamine gas came to the bottle with water.

After adding 9 g. of powdered sodium hydroxide cautiously in small portions, the mixture was distilled. The crystals of sodium chloride which prevented the further distillation were removed by filtration and the filtrate was submitted to a careful fractionation. There was obtained about 15 g. of 4-dimethylamino-1-butanol as a colorless, viscous liquor boiling at 184°C.

Found: N, 11.82. Calcd. for $C_6H_{15}ON$: N, 11.95%.

*4-Dimethylamino-n-butyl Acetate.*—Twelve grams (0.12 mol.) of acetic anhydride was gradually

2) A. W. Hofmann, *Proc. Roy. Soc.*, **1860**, 10, 595.

added to 12 g. (0.12 mol.) of 4-dimethylamino-1-butanol with stirring and cooling in water. The reaction mixture was then dissolved in about 50 cc. of water and neutralized with sodium bicarbonate added in small portions until no more evolution of carbon dioxide was observed. The resultant solution was extracted with ether in a continuous extraction apparatus.

Distillation of the ether followed by a careful distillation in vacuo gave a 90~95% yield of the acetate.

Colorless liquid, b. p. 85°C/15 mmHg. Picrate, m. p. 126°C.

Found: N, 8.69. Calcd. for $C_8H_{17}O_2N$: N, 8.80%.

*N-Methylpyrrolidine.*—Sixteen grams (0.1 mol.) of 4-dimethylamino-*n*-butyl acetate was distilled slowly and carefully using a small Claisen flask, which is equipped with two thermometers, one being inserted in the liquid through the straight neck of the flask to read the internal temperature and the other fitted in the side neck to read the distillation temperature. When the internal temperature was raised to above 200°C, boiling commenced with the splitting into *N*-methylpyrrolidine and methyl acetate, both of which distilled over at 50~100°C as they were formed.

Redistillation of the distillate gave about 6 g. (about 75%) of pure *N*-methylpyrrolidine. *N*-Methylpyrrolidine is a well-known compound, a colorless liquid, b. p. 80~81°C. Picrate, m. p. 218°C.

**N-Ethylpyrrolidine from 4-Diethylamino-*n*-butyl Acetate.** — *4-Diethylamino-1-butanol.* — A mixture of 27 g. (0.25 mol.) of tetramethylene chlorohydrin and 36.5 g. (0.5 mol.) of diethylamine was boiled under reflux for 10 hr. The crystals of diethylamine hydrochloride, gradually formed during the heating, were filtered off and the filtrate was fractionally distilled. After a forerun of tetrahydrofuran (ca. 5 g.) formed in a side reaction 6, there was obtained about 15 g. of 4-diethylamino-1-butanol boiling at 208°C, as a colorless, viscous liquid.

$$HO(CH_2)_4Cl + HN(C_2H_5)_2 \rightarrow \begin{array}{l} CH_2\text{-}CH_2 \\ | \quad | \\ CH_2 \quad CH_2 \\ \diagdown \quad \diagup \\ \quad O \end{array} + (C_2H_5)_2NH\cdot HCl \qquad (6)$$

Found: N, 9.51. Calcd. for $C_8H_{19}ON$: N, 9.64%.

*4-Diethylamino-n-butyl Acetate.*—Obtained similarly as in the methyl derivative mentioned above. Colorless liquid, b. p. 98°C/12 mmHg.

Found: N, 7.31. Calcd. for $C_{10}H_{21}O_2N$: N, 7.48%.

*N-Ethylpyrrolidine.* — Obtained in the same way as in the methyl derivative above. Colorless liquid, b. p. 104~106°C. Picrate, m. p. 185°C.

**N-Methylpiperidine from 5-Dimethylamino-*n*-pentyl Acetate.**—On the whole, the actual procedure here is analogous to that of *N*-methylpyrrolidine.

*5-Dimethylamino-1-pentanol.*—A mixture of 24.5 g. (0.2 mol.) of pentamethylene chlorohydrin and 50 g. of a 40% aqueous solution of dimethylamine was allowed to react. After the reaction was completed the resultant homogenous solution was distilled until the internal temperature indicated 180°C. To the cooled mixture was added a concentrated solution of potassium hydroxide in methyl alcohol and the precipitate of potassium chloride was filtered off and the filtrate was distilled.

Colorless, viscous liquid, b. p. 205~206°C. Yield 21 g. (80%).

Found: N, 10.39. Calcd. for $C_7H_{17}ON$: N, 10.68%.

*5-Dimethylamino-n-pentyl Acetate.* — The procedure described in the case of the corresponding butyl derivative was also employed here.

Colorless oily liquid, sparingly soluble in water, b. p. 114°C/22 mmHg.

Found: N, 7.78. Calcd. for $C_9H_{19}O_2N$: N, 8.09%.

*N-Methylpiperidine.*—This compound was obtained by the slow distillation of 5-dimethylamino-*n*-pentyl acetate followed by the fractionation of the distillate, and was identified by comparison with the authentic sample.

Colorless liquid, b. p. 107°C.

**N-Ethylpiperidine from 5-Diethylamino-*n*-pentyl Acetate.** — *5-Diethylamino-1-pentanol.*—From 24.5 g. (0.2 mol.) of pentamethylene chlorohydrin and 30 g. (ca. 0.4 mol.) of diethylamine, about 25 g. (ca. 80%) of this compound was obtained as a colorless viscous liquid boiling at 127~130°C/22 mmHg.

Found: N, 8.75. Calcd. for $C_9H_{21}ON$: N, 8.80%.

*5-Diethylamino-n-pentyl Acetate.* — Colorless oil, sparingly soluble in water, b. p. 127°C/22 mmHg.

Found: N, 7.02. Calcd. for $C_{11}H_{23}O_2N$: N, 6.96%.

*N-Ethylpiperidine.* — The acetate above was split into *N*-ethylpiperidine and ethyl acetate at a temperature higher than 200°C. The reaction proceeded slowly but steadily. *N*-Ethylpiperidine is, of course, a well-known compound.

**N-Methylmorpholine from β-Acetoxy-β'-dimethylaminodiethyl Ether.**—*β-Hyroxy-β'-dimethylaminodiethyl Ether.*—The ether was prepared by the reaction of 2 mol. proportions of ethylene oxide on 1 mol. proportion of aqueous solution of dimethylamine.

In 110 g. (1 mol.) of a 40% aqueous solution of dimethylamine was absorbed ethylene oxide, generated by dropping a solution of 80 g. (2 mol.) of sodium hydroxide in 160 cc. of water onto a boiled mixture of 200 g. (2.5 mol.) of ethylene-chlorohydrin and 100 cc. of water under reflux. The reaction between ethylene oxide and dimethylamine is exothermic.

Suitable control of the dropping rate of the sodium hydroxide solution and occasional water-cooling were applied in order to bring the ethylene oxide entirely into action. The gain in weight of the reaction mixture was about 90 g. and indicated that in this way about 2 mol. of ethylene oxide could be generated and be made to enter into the reaction.

To the brown and viscous mixture was added portion-wise about 60 g. of anhydrous potassium

3) I. G. Farfen Ind., D. R. P. 432803; *Chem. Zentr.*, **1926**, II. 1693.

carbonate. Then there were formed two layers, of which the upper was separated and distilled fractionally. There was obtained about 15 g. of β-dimethylamino ethyl alcohol (b. p. 130~135°C) and about 50 g. of β-hydroxy-β'-dimethylamino-diethyl ether (b. p. 205°C).

Found: N, 10.68. Calcd. for $C_6H_{15}O_2N$: N, 10.52%.

*β-Acetoxy-β'-dimethylaminodiethyl Ether.* — Acetic anhydride (26 g. 0.25 mol.) was added dropwise to 35 g. (0.2 mol.) of β-hydroxy-β'-dimethylamino-diethyl ether with cooling in water.

After heating to boiling under reflux and subsequent cooling to room temperature, the mixture was dissolved in about 100 cc. of water, neutralized with about 30 g. of sodium bicarbonate added in small portions and extracted with ether in a continuous extractor. Distillation of the ether followed by fractionation of the residual liquid under reduced pressure gave almost a quantitative yield of β-acetoxy-β'-dimethylaminodiethyl ether as a colorless liquid boiling at 132°C/50 mmHg or 110°C/30 mmHg.

*N-Methylmorpholine.*—Distillation of β-hydroxy-β'-dimethylaminodiethyl ether, carried out slowly and carefully at atmospheric pressure, gave a mixture of methyl acetate and *N*-methylmorpholine in a good yield.

The *N*-methylmorpholine was identified by an authentic sample.

Colorless liquid, b. p. 215~216°C. Picrate m. p. 220°C. Chloroplatinate, m. p. 225~226°C.

**N-Ethylmorpholine from β-Acetoxy-β'-diethylaminodiethyl Ether.**—The procedure employed was substantially analogous to that of the methyl derivative.

*β-Hydroxy-β'-diethylaminodiethyl Ether**.—Obtained by the action of ethylene oxide on β-diethylaminoethyl alcohol in equimolecular proportions, or on an aqueous diethylamine solution in mole proportions of 2 to 1. Colorless, viscous oily liquid, b. p. 142°C/52 mmHg.

Found: N, 8.57. Calcd. for $C_8H_{19}O_2N$: N, 8.69%.

*β-Acetoxy-β'-diethylaminodiethyl Ether.*—Colorless oily liquid, b. p. 143~145°C/42 mmHg.

Found: N, 6.60. Calcd. for $C_{10}H_{21}O_3N$: N, 6.89%.

Chloroplatinate, yellow plates from concentrated solution, decomposed at 174°C.

Found (for chloroplatinate): Pt, 24.00. Calcd. for $(C_{10}H_{21}O_3N)_2 \cdot H_2PtCl_6$: Pt 23.90%.

*N-Ethylmorpholine.*—Obtained by a slow distillation of the above ether. The formation of *N*-ethylmorpholine proceeded very slowly but in an excellent yield. Colorless liquid, b. p. 139°C. Picrate, m. p. 190°C. Chloroplatinate, orange-yellow needles, m. p. 198°C. These data were identified with the authentic samples.

The auther wishes to express his heartfelt thanks to Professor Dr. Ryozo Goto, Kyoto University for his encouragement and numerous suggestions throughout this work.

*Kyoto Works, Teikoku Chemical Industry Co., Ltd.*
*Nakagyo-ku, Kyoto*

* Preparation by the action of mono-sodium compound of ethylene glycol on diethyl-(β-chloroethyl)-amine had been known; Bayer & Co., D. R. P. 398010; *Chem. Zentr.*, **1924**, II. 1399.

# *Reaction of Trypsin with S-Methylisothiourea and with S-Methylglucosylisothiourea*

By Kazuyuki MAEKAWA and Kyoko ISHIMOTO

(Received January 16, 1961)

*O*-Methylisourea has long been used to introduce amidyl residue into amino acids and peptides. The reaction of *O*-methylisourea with proteins takes place only in ε-amino group of lysine, and homoarginine is produced by the hydrolysis of the product[1]. Hughes et al. have shown that in treating serum albumin with *O*-methylisourea, the more the value of Sakaguchi's reaction increased, the less amino nitrogen became[2]. Roche and his associates treated bovine serum albumin, casein, and ovalbumin etc. with *O*-methylisourea in concentrated ammonium hydroxide, and after the hydrolysis of the reaction products, they identified homoarginine by means of paper chromatography[3]. Lately Chervenka et al. demonstrated that all of the 13 lysines changed into homoarginine and no more changes were caused in the reaction of chymotrypsin with

1) R. M. Herriott, "Advances in Protein Chem.", III, Acad. Press Inc., New York (1947), p. 215.

2) W. L. Hughes, H. A. Saroff and A. L. Carney, *J. Am. Chem. Soc.*, **71**, 2476 (1949).

3) J. Roche, M. Mourgue and R. Baret, *Bull. Soc. chim. biol.*, **36**, 85 (1954).

*O*-methylisourea[4]. On the other hand, Schütte employed *S*-methylisothiourea instead of *O*-methylisourea[5]. Later on, this reaction was applied to the δ-amino group of ornithine[6].

By the application of a similar reaction, that is, the condensation reaction which liberates mercaptan from substituted isothiourea, Micheel et al. have treated case in and gelatin etc. with *S*-methylglucosylisothiourea. They supposed that the ε-amino group of lysine undergoes the reaction, since the amount of combined sugar runs parallelly only to the lysine content of protein[7].

It has already been illustrated that concerning the reaction of *S*-methylglucosylisothiourea upon histidine, the carbon of position 4 or 2 in the imidazole ring is more reactive than the α-amino group of amino acids or the ε-amino group of lysine[8].

Authors have undertaken the study of the reaction of *S*-methylglucosylisothiourea and trypsin as an enzyme, as it has already been suggested that histidine is an essential site of the enzymatic activity[9].

In respect to trypsin, various active and inactive derivatives have already been reported[10-16], but no work on the reaction of *S*-methylisothiourea and *S*-methylglucosylisothiourea has been reported yet.

The results showed that trypsin molecule[17] was combined with 6~7 mol. of glucosylamidyl residue, and yet the enzymatic activity was retained, but the autodigestion was remarkably depressed. The amidinated trypsin was more stable than the glucosylamidyl derivative. These facts described in this report were not owing to the mercaptan produced by the reaction, but evidently owing to glucosylamidination or amidination. The mercaptan produced during the reaction had no part in the stabilization of trypsin, which fact is consistent with the result obtained by using 2, 3-dimercapto-1-propanol[18].

## Experimental

**Amidination and Glucosylamidination of Trypsin.** — One hundred milligrams of crystalline trypsin (Motida Pharm. Co.) was dissolved in 20 ml. of 1/15 M phosphate buffer, pH 8.0 (or Palitzsch's borate buffer) in the presence of 0.01 M calcium chloride[12,19]. The protein concentration of trypsin was determined spectrophotometrically, using values proposed by Green and Neurath[20]. Thus, enzyme solution was 0.695 mg./ml. Five milliliters of this enzyme solution was added to 3 ml. of aqueous solution of *S*-methylglucosylisothiourea hydroiodide (70 mg./ml.) and to the equal volume of *S*-methylisothiourea (50 mg./ml.) respectively. Then the reaction mixture was adjusted to pH 8 with a few ml. of 0.1 N sodium hydroxide, and covered with ether to dissolve mercaptan evolving. The solutions were allowed to stand at 10°C.

**Determination of Combined Glucosylamidyl Residue.**—To 1 ml. of the solution described above, which was taken out at certain time intervals, 5 ml. of 0.4 M solution of trichloroacetic acid (TCA) was added, and the mixture was warmed for a while at 50°C. The enzyme derivative precipitated was collected by centrifuge, then washed several times with TCA in order to remove the sugar compound which did not react. As for the precipitate, the

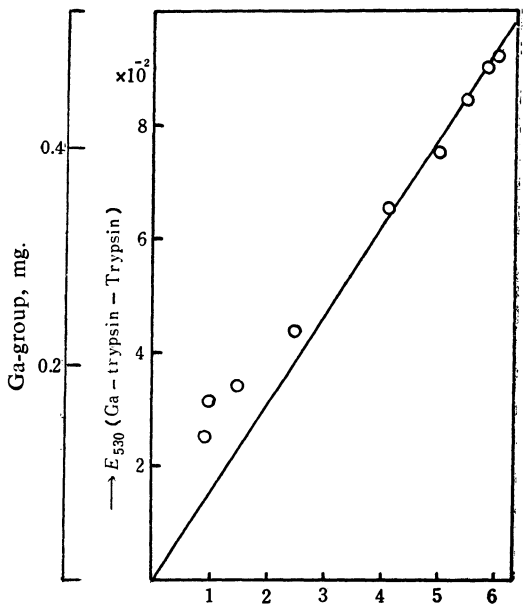



Fig. 1. Estimation of the Ga-group combined with enzyme.

4) C. H. Chervenka and P. E. Wilcox, *J. Biol. Chem.*, **222**, 621, 635 (1956).
5) E. Schütte, *Z. physiol. Chem.*, **279**, 52, 59 (1943).
6) J. N. Christensen, *J. Biol. Chem.*, **160**, 75 (1945).
7) F. Micheel and B. Herold, *Z. physiol. Chem.*, **293**, 187 (1953).
8) K. Maekawa and K. Ishimoto, *J. Chem. Soc. Japan, Pure Chem. Sec.* (*Nippon Kagaku Zasshi*), in press.
9) H. Gutfreund, *Trans. Faraday Soc.*, **51**, 441 (1955).
10) S. Korman and H. T. Clarke, *J. Biol. Chem.*, **221**, 139 (1956).
11) L. Terminiello, J. S. Ram, M. Bier and F. F. Nord, *Arch. Biochem. Biophys.*, **57**, 252 (1955).
12) T. Viswanatha and I. E. Liener, *J. Biol. Chem.*, **221**, 961 (1956).
13) J. S. Ram, L. Terminiello, M. Bier and F. F. Nord, *Arch. Biochem. Biophys.*, **52**, 464 (1954); F. F. Nord and M. Bier, *Biochim. Biophys. Acta*, **12**, 56 (1953).
14) I. Rychlik and F. Sorm, *Chem. Listy*, **47**, 618 (1953); c. f., *Chem. Abstr.*, **48**, 3405 (1954).
15) E. F. Jansen and A. K. Balls, *J. Biol. Chem.*, **194**, 721 (1952).
16) L. W. Cunningham, ibid., **211**, 13 (1954),
17) E. Sheppard and A. D. Mclaren, *J. Am. Chem. Soc.*, **75**, 2587 (1953).
18) M. Zacco and L. Fiore-Donato, *Fisiol. e med.*, **16**, 325 (1948); c. f., *Chem. Abstr.*, **44**, 3618 (1950).
19) M. Bier and F. F. Nord, *Arch. Biochem. Biophys.*, **33**, 320 (1951).
20) N. M. Green and H. Neurath, *J. Biol. Chem.*, **204**, 379 (1953).

combined glucosylamidyl residue was determined by the modified Brückner's method[21] as follows: Namely, 1 ml. of water and 1 ml. of 4% aqueous solution of orcinol were added to the resulting precipitate of enzyme-derivative. Then, 8 ml. of 31.2 N sulfuric acid, cooled with cold water, was added to it. After mixing them completely, it was heated in a boiling water bath exactly for 5 min., then cooled with tap water. The absorbance of the solution was measured at 530 mμ, using a whole blank solution which contains the same concentration of untreated enzyme and which has been treated similarly in the reference cell. The value of the combined glucosylamidyl residue was calculated by multiplying the molecular ratio for the value obtained from the estimation of glucosylamidyl glycine.

**Measurement of the Activity.**—One half milliliter of the reaction mixture was transferred into 10 ml. of 1/15 M phosphate buffer, pH 7.1 at certain time intervals. By using 1 ml. of this diluted solution, the enzymatic activity was measured according to the modified Anson's method by using casein as substrate[22].

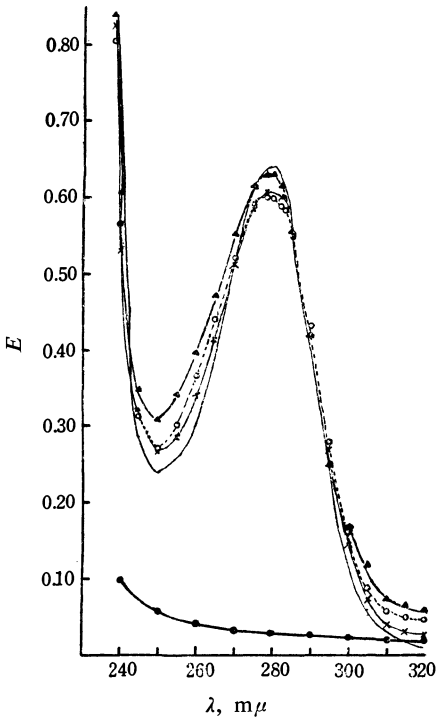



Fig. 2. UV-absorption spectrum of Ga-trypsin.
——— Trypsin
×—× Ga-trypsin
○···○ Ga-trypsin heated for 10 min. at 100°C
▲—▲ Ga-trypsin heated for 60 min. at 100°C
●—● Ga-glycine

**Determination of the Guanidino-group and Amino Nitrogen.**—The guanidino-group was determined by Sakaguchi's reaction. The sample was treated in the same manner as described in the determination of glucosylamidyl residue, because the Sakaguchi's reaction was inhibited by *S*-methylisothiourea and *S*-methylglucosylisothiourea. Namely, 0.5 ml. from the reaction mixture described above was pipetted out and the enzyme was precipitated by adding TCA solution and washed several times with TCA solution, then further washed with absolute alcohol. The precipitate was dissolved in 0.1 N sodium hydroxide and the guanidino-group was determined by Weber's method[24].

The amino group of the precipitate which was prepared by the same method as in the determination of glucosylamidyl residue was determined by ninhydrin reaction according to the method of Troll and Cannan[23].

**Absorption Spectrum and Optical Rotation.**—The sample for measurement of absorption spectrum was prepared by exhaustive dialysis against water of pH 3 (with hydrochloric acid). The optical rotation was determined by using the sample prepared as follows. A large amount of the reaction mixture was brought to pH 3.4 with hydrochloric acid, and precipitated at 70 per cent saturation of ammonium sulfate and washed several times with 70% ammonium sulfate. The precipitate was dissolved in water.

$$[\alpha]_D^{25}=\frac{+0.16\times 6000}{35\times 0.5\times 1.058}=+51.8^\circ$$

Table I. Reaction of *S*-methylglucosylisothiourea and trypsin

| Reaction time | Combined sugar component, mg. / mol. protein | Relative activity % | $NH_2$-group mol. / mol. protein |
|---|---|---|---|
| 24 hr. | 3.3 | 89 | 7.86 |
| 48 〃 | 4.6 | 78 | |
| 72 〃 | 5.7 | 71 | |
| 96 〃 | 6.0 | 65 | 6.76 |
| 6 days | 6.3 | 58 | |
| 14 〃 | 6.5 | 53 | 6.07 |
| 20 〃 | 6.5 | 53 | |

Table II. Reaction of *S*-methylisothiourea and trypsin

| Reaction time | Increase of amidine group % | Relative activity % | Relative activity (with 0.01 M $CaCl_2$) | $NH_2$-group mol. / mol. protein |
|---|---|---|---|---|
| 24 hr. | 115 | 95 | 78 | 7.86 |
| 48 〃 | | 94 | 68 | |
| 72 〃 | | 94 | 57 | |
| 96 〃 | 190 | 93 | 49 | 6.92 |
| 193 〃 | 220 | 93 | 43 | |
| 15 days | | 92 | 38 | |

21) J. Brückner, *Biochem. J.*, **60**. 201 (1955).
22) M. Laskowski, "Methods in Enzymology", Vol. II. Ed. by S. P. Colowick and O. Kaplan, Acad. Press Inc., New York (1955), p. 33.
23) W. Troll and R. K. Cannan, *J. Biol. Chem.*, **200**, 803 (1953).
24) C. J. Weber, ibid., **86**, 217 (1930).

Table III. Enzymatic hydrolysis of glucosylamidyl casein by glucosylamidyl trypsin or amidyl trypsin*

| Substrate | Enzyme | | |
|---|---|---|---|
| | Trypsin (with 0.01 M) $CaCl_2$, % | Glucosylamidyl trypsin | Amidyl trypsin |
| Casein | 82 | 93 | 100 |
| Glucosylamidyl casein | 70 | 79 | 93 |

* Enzyme preparation of trypsin and the two trypsin derivatives were taken from the incubating mixture in 24 hr. from starting.

## Results and Discussion

The results are shown in Tables I to III. Under the condition presented, trypsin (mol. wt. 23800)[15,16] was combined with 6~7 mol. of glucosylamidyl residue in 4 days. As the result, the color intensity of ninhydrin reaction decreased about 14 per cent. The Sakaguchi's reaction has no change by being combined with glucosylamidyl residue. By the reaction of trypsin and *S*-methylisothiourea, the guanidino group of enzyme derivative clearly increases.

By glucosylamidination or amidination of trypsin, the enzyme does not suffer from the loss of the enzymatic activity, but becomes rather stable against the autodigestion. It is well known that peptide linkage which involves $\alpha$-amino group of lysine becomes less easily digested by trypsin, by blocking the $\varepsilon$-amino group of the substrate with acetyl group and others[25,26]. From the result reported here, it is proved that glucosylamidyl casein and amidyl casein are resistive to the tryptic digestion, in accordance with a report of Weil et al.[26]

On the other hand, amidyl trypsin and glucosylamidyl trypsin have enzymatic activity, but it seems likely that homoarginine or glucosylhomoarginine linkage which exists in the modified enzyme molecule is not digested by trypsin and the modified trypsins.

It is probably deduced that $\varepsilon$-amino group of lysine and other groups which are to be glucosylamidinated or amidinated have nothing to do with the tryptic activity.

The authors wish to express their thanks to Mr. N. Aizawa of the Motida Pharm. Co. for a generous supply of trypsin.

*Laboratory of Biological Chemistry*
*Faculty of Agriculture*
*Ehime University*
*Matsuyama, Ehime*

25) J. E. Folk: *Arch. Biochem. Biophys.*, **64**, 6 (1956).
26) L. Weil and M. Telka, ibid., **71**, 473 (1957).

# *Electronic Structure and Biochemical Activities in Diethyl Phenyl Phosphates*

By Kenichi FUKUI, Keiji MOROKUMA, Chikayoshi NAGATA and Akira IMAMURA

(Received February 2, 1961)

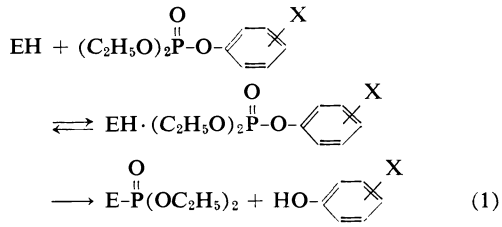
In the recent fifteen years thousands of organo phosphorus compounds have been found to be endowed with effective insecticidal properties and some of them—TEPP, parathion, paraoxon and so forth—are now in practical use[1]. It become apparent that the toxicity of these compounds to insect or to human being is mainly related to the reaction with the cholinesterase enzyme system in the body[2-5].

Diethyl substituted phenyl phosphates, which are treated in the present paper, have been tested in detail of their toxicities to insects, their effciencies of cholinesterase inhibition[3-5] and their hydrolysis constants[5-7], and each of the three has been found to be in line with the other[1,5,7]: phosphates are more toxic when their inhibiting activities are larger and when their hydrolysis constants are larger.

Diethyl phenyl phosphates are bound by a covalent bond to the esteratic site of cholinesterase in an irreversible phosphorylation, this inhibiting the hydrolysis of acetyl choline in a normal biochemical cycle. The enzyme-inhibiting mechanisms are proposed by Aldridge

1) R. L. Metcalf, "Organic Insecticides", Interscience Publishers, Inc., New York (1955), pp. 251-315.
2) J. E. Casida, *J. Agr. Food Chem.*, **4**, 772 (1956).
3) R. L. Metcalf and R. B. March, *J. Econ. Entomol.*, **42**, 721 (1949).
4) H. S. Hopf, *Ann. Appl. Biol.*, **41**, 248 (1954).
5) T. R. Fukuto and R. L. Metcalf, *J. Agr. Food Chem.*, **4**, 930 (1956).
6) W. N. Aldridge, *Chem. & Ind.* **1954**, 473.
7) W. N. Aldridge and A. N. Davidson, *Biochem. J.*, **51**, 62 (1952).

et al.[7-10] to be such as represented by the following scheme:



(1)

where EH is the enzyme, and the second step is assumed to be rate-determining. It was often said that the initial stage of the step is the attack of the electron-releasing, that is, the nucleophilic site or atom of cholinesterase on the P–O bond of phosphates, and this mechanism seems to be analogous to that of the alkali hydrolysis of the phosphates[1] and that the enzyme-inhibitory activity of the phosphate is, therefore, related to the lability of P–O bond[5,7]. And furthermore Aldridge estimated the strength of the bond by the ionization constant of the hydrolysis product[7]; the esters derived from strongly acidic phenols are highly toxic and vice versa. According to his opinion, paraoxon is toxic because *p*-nitrophenol is a strong acid.

In contrast with phosphates, it is interesting that highly purified parathion and its homologues—diethyl substituted phenyl thionophosphates— are little active as inhibitors of enzyme systems. They are oxidized in the tissue to the corresponding phosphates, which attack the cholinesterase, showing the poisoning action in vivo experiments[2,11,12].

The present authors have established the frontier electron theory, one of the quantum mechanical theories of chemical reactivity, of conjugated molecules, and found that the superdelocalizability, the index of reactivity in the theory, represents the experimental results better than those in other theories[13-15]. The theory has been successfully applied to biochemical problems as well, for instance, the carcinogenic activity of condensed aromatic hydrocarbons[16] and azo dyes[17], the plant growth activity of substituted benzoic acids[18], the nicotine-like activity of choline phenyl ethers[19] and the fungicidal activity of quinoline-*N*-oxides[20]. It is noteworthy, as theoretically indicated by the present authors, that these activities are directly related to the interaction of the conjugated molecule with a nucleophilic (electron releasing) atom or group of the tissue; and in this connection a discussion will be given in a later section.

Superdelocalizability on the *r*th atom of phenyl phosphates that is to be used in this paper is that for a nucleophilic reaction (the reagent attacking phosphates has been considered nucleophilic in nature[1,8]) and has the following form:

$$S_r^{(N)} = 2\sum_{j}^{\text{unocc}} \frac{(C_r^j)^2}{-\lambda_j} \qquad (2)$$

where $C_r^j$ is the coefficient of the *r*th atomic orbital in the *j*th molecular orbital, $\lambda_j$ is the coefficient of its energy $\varepsilon_j = \alpha + \lambda_j\beta$, $\alpha$ and $\beta$ are the standard coulomb and resonance integrals, and the summation covers unoccupied orbitals. The larger its magnitude is, the more reactive the molecule is. The phosphorus atom is considered to offer one orbital and one electron conjugable with other atoms, as has been discussed in our previous paper on ATP[21]. The coulomb integral of the atom X and the resonance integral between the atoms X and Y are written as $\alpha + a_X\beta$ and $l\beta$, respectively; and in Table I are listed the energy parameters used in the paper, which are not so different from those in previous papers[17,18,21],*.

## Results and Discussion

We calculated the superdelocalizability and the electron density on various positions of fifteen diethyl substituted phenyl phosphates, assuming that in the enzyme-inhibition the intermediate complex formation does not affect the electronic structure, and comparing with experimental results, found that the super-

8) D. Nachmansohn and I. B. Wilson, "Advances in Enzymol.", **12**, 259 (1951).
9) B. S. Hartley and B. A. Kiljby, *Biochem. J.*, **56**, 288 (1954).
10) W. N. Aldridge, ibid., **54**, 442 (1953).
11) R. L. Metcalf and R. B. March, *Ann. Entomol. Soc. Amer.*, **46**, 63 (1953).
12) R. L. Metcalf and R. B. March, *Science*, **117**, 527 (1953).
13) K. Fukui, T. Yonezawa and H. Shingu, *J. Chem. Phys.*, **20**, 722, (1952); K. Fukui, T. Yonezawa, C. Nagata and H. Shingu, ibid., **22**, 1433 (1954).
14) K. Fukui, T. Yonezawa and C. Nagata, This Bulletin, **27**, 423 (1954).
15) K. Fukui, T. Yonezawa and C. Nagata, *J. Chem. Phys.*, **26**, 831 (1957); ibid., **27**, 1247 (1957).
16) C. Nagata, K. Fukui, T. Yonezawa and Y. Tagashira, *Cancer Research*, **15**, 233 (1955).
17) C. Nagata, K. Fukui, T. Yonezawa, H. Kitano, Y. Inamoto, K. Kanai and Y. Tagashira, *Gann*, **46**, 346 (1955); K. Fukui, C, Nagata, T. Yonezawa, Y. Inamoto and A. Imamura, ibid., **51**, 67 (1960).
18) K. Fukui, C. Nagata and T. Yonezawa, *J. Am. Chem. Soc.*, **80**, 2267 (1958).
19) K. Fukui, C. Nagata and A. Imamura, *Science*, **132**, 87 (1960).
20) K. Fukui, A. Imamura and C. Nagata, This Bulletin, **33**, 122 (1959).
21) K. Fukui, K. Morokuma and C. Nagata, ibid., **33**, 1214 (1960).
* The energy parameter of the sulfur atom seems unsettled yet. Here we adopted $a_{=S} = 0.8$ so that the difference $\Delta a = a_{=O} - a_{=S}$ comes to 1.2 in accordance with Pullmans'[22].
22) B. Pullman and A. Pullman, *Rev. Mod. Phys.*, **32**, 428 (1960).

TABLE I. ENERGY PARAMETERS EMPLOYED IN THE CALCULATION*

| | | | |
|---|---|---|---|
| Phosphate part | $a_P=-1$ | | |
| | $a_{=O}=2$ | $l_{P=O}=1$ | |
| | $a_{=S}=0.8$ | $l_{P=S}=0.85$ | |
| | $a_{OC_2H_5}=2$ | $l_{P-OC_2H_5}=0.6$ | |
| | $a_{-O-}=2$ | $l_{P-O-}=0.6$ | |
| Substituent | | | |
| Nitro | $a_N=1$ | $l_{C'-N}=1$ | $a_{C'}=0.2$ |
| | $a_O=1.5$ | $l_{N-O}=1$ | |
| Formyl | $a_{=O}=2$ | $l_{C=O}=\sqrt{2}$ | $a_C=0.2$ |
| Cyano | $a_{=N}=1$ | $l_{C=N}=1$ | $a_C=0.1$ |
| Chloro | $a_{Cl}=2$ | $l_{C-Cl}=0.8$ | $a_{C'}=0.5$ |
| Methyl | $a_{CH_3}=3$ | $l_{C-CH_3}=0.7$ | |
| Methoxy | $a_{OCH_3}=2$ | $l_{C-OCH_3}=0.9$ | |
| Dimethylamino | $a_{CH_3}=3$ | $l_{CH_3-N}=0.7$ | |
| | $a_N=1$ | $l_{N-C'}=1$ | $a_{C'}=0.1$ |

* C' means the carbon atom adjacent to the substituent.

TABLE II. SUPERDELOCALIZABILITY AND TOTAL $\pi$ ELECTRON DENSITY ON PHOSPHORUS ATOM AND ALKALI HYDROLYSIS CONSTANT, CHOLINESTERASE INHIBITORY ACTIVITY AND INSECTICIDAL ACTIVITY OF DIETHYL SUBSTITUTED PHENYL PHOSPHATES

| Substituents | $S_P^{(N)}$ Superdelocalizability | $q_P$ Total $\pi$ electron density | Alkali hydrolysis constant ($min^{-1}$)*1 | Median inhibitory molar concentration (fly-brain ChE)*1 | Insecticidal activity*3 |
|---|---|---|---|---|---|
| 2,4-Dinitro | 1.132 | 0.278 | $5.7\times10^{-3}$ | $3.0\times10^{-9}$ | + |
| *o*-Nitro | 1.120 | 0.279 | $(3\times10^{-4})$*2 | $5.0\times10^{-8}$ | ++ |
| *p*-Nitro | 1.119 | 0.279 | $2.7\times10^{-4}$ | $2.6\times10^{-8}$ | ++ |
| *p*-Formyl | 1.106 | 0.279 | | $1.5\times10^{-7}$ | − |
| *p*-Cyano | 1.106 | 0.280 | | $1.3\times10^{-7}$ | ++ |
| 2,4,6-Trichloro | 1.100 | 0.280 | $7.9\times10^{-5}$ | $6.0\times10^{-9}$ | ++ |
| 2,4-Dichloro | 1.100 | 0.280 | $4.8\times10^{-5}$ | $5.0\times10^{-7}$ | + |
| *o*-Chloro | 1.099 | 0.280 | $5.1\times10^{-5}$ | $2.0\times10^{-5}$ | ± |
| *p*-Chloro | 1.099 | 0.280 | $3.2\times10^{-5}$ | $3.0\times10^{-5}$ | ± |
| Non | 1.097 | 0.281 | $9.2\times10^{-5}$ | $1.0\times10^{-8}$ | − |
| *m*-Nitro | 1.097 | 0.281 | $9.8\times10^{-5}$ | $5.0\times10^{-8}$ | ++ |
| *p*-Methyl | 1.097 | 0.281 | | $1.0\times10^{-3}$ | − |
| *m*-Methoxy | 1.096 | 0.281 | $8.9\times10^{-6}$ | $1.3\times10^{-4}$ | − |
| *p*-Methoxy | 1.096 | 0.281 | | $1.0\times10^{-3}$ | − |
| *p*-Dimethylamino | 1.094 | 0.282 | $1.9\times10^{-6}$ | $4.0\times10^{-7}$ | + |

*1 Taken from Ref. 5.
*2 Estimated from the data of Ref. 6.
*3 Deduced from the data of median lethal dosage to various insects of Refs. 3, 4 and 5. ++: very highly active, +: highly active, +: active, ±: less active, −: almost inactive.

delocalizability for a nucleophilic reaction on the phosphorus atom has close correlations with the case of alkali hydrolysis, and therefore, with the cholinesterase (ChE) inhibitory power and insecticidal activity, as is clearly seen in Table II. The total electron density on the phosphorus atom seems to show similar relations but even the largest difference is 0.004 at the utmost and would not be enough to elucidate large differences in the hydrolysis constants. Indexes of other positions or for other kinds of reaction (electrophilic and radical) had no such parallelism. These results suggest that in the alkali hydrolysis of phosphates the attack of hydroxyl anion to the phosphorus atom is rate-determining and the susceptibility of P–O bond to hydrolysis is nothing but the reactivity of the phosphorus atom, and would support the existing interpretation that both to the enzyme-inhibitory and to the insecticidal activities the hydrolytic attack of a nucleophilic site, probably of the esteratic site of cholinesterase, makes a controlling contribution.

Interactions of the substrates with the anionic site of cholinesterase, which become important in the hydrolysis of acetylcholine, are also probable for some phosphates; and they will

serve as a cause of discrepancy between activities of alkali hydrolysis and of esterase-inhibition, since in the former the reagent is a hydroxyl group only and has no subsidiary anionic site. In this series of compounds, however, these interactions do not seem to be significant, for we could find no such index on any atom in the substituted phenyl group, sterically suitable for the interactions, that would rationary explain the discrepancy.

In Table II, 2,4-dinitrophenyl phosphate is less toxic to insects than expected from the inhibitory power, this being explained as that it would be hydrolytically deactivated in its way to the effective site because of its too large reactivity[5]. This situation is well understood in terms of the superdelocalizability and its threshold for an effective insecticide seems to lie between 1.20 and 1.25. The lack of insecticidal toxicity of *p*-formylphenyl phosphate which could not be elucidated by experimental results[5] is difficult to explain even by this theoretical study, and some other factors would have to be considered.

Furthermore the striking difference of activities between phosphates and thionophosphates is to be discussed. We calculated as an example the superdelocalizability on the phosphorus atom of diethyl *p*-nirophenyl thionophosphate, which amounted to 1.056. Comparing this value with those of diethyl *p*-nitrophenyl phosphate (1.119) and other phosphates discussed above (1.132~1.094), one would clearly see the reason why the thionophosphate in itself is inactive in the inhibition of the enzyme system in vitro. As most thionophosphates substituted by other substituents are less reactive than the *p*-nitro compound, they are well understood to be inactive. The metabolic oxidation to phosphates thus has a meaning, we may say, in elevating the reactivity for a nucleophilic attack.

The nucleophilic nature of the cholinesterase inhibition and toxicity of phenyl phosphates, that is, the nature that the phosphate is attacked by an electron-releasing group, is very interesting in connection with our theoretical indication that the carcinogenic activity and at the same time the anti-tumor activity of conjugated compounds appear to be nucleophilic in their essential character as well as some other biochemical activities, for instance, the anti-fungal activity[20] or nicotine like activity[19]. The high nucleophilic reactivity of the phosphates in question suggests to us, that they would be endowed with the carcinogenic ability or with the carcinostatic ability, though the active site in the tissue will be different in each activity. In fact, paraoxon was found to have the carcinostatic activity[23]. On this point a more elaborate discussion will be given elsewhere[24].

*Faculty of Engineering*
*Kyoto University*
*Sakyo-ku, Kyoto*

23) B. Mendel, D. K. Myers, I. E. Uyldert, A. C. Ruys and W. M. De Bruy, *Brit. J. Pharmacol.*, **8**, 217 (1953).
24) K. Fukui, C. Nagata, A. Imamura and Y. Tagashira, *Gann*, **52**, 127 (1961).

# *Mass Spectra at Low Ionizing Voltage and Bond Dissociation Energies of Molecular Ions from Hydrocarbons*

By Itiro OMURA

(Received January 18, 1961)

Since Eyring and co-workers[1] first introduced the statistical theory to the interpretation of mass spectra of hydrocarbons, several authors[2-4] have reported similar results on simple organic molecules. King and Long[3] pointed out that the theory is inadequate at low ionizing voltages although it seems qualitatively satisfactory at high ionizing voltages such as 70 V. except for some of the rearrangement and hydrogen abstraction processes. Hence, it seems very important for the purpose of clarifying ion dissociation mechanisms to study mass spectra at low ionizing voltages.

In this paper, the experimental results on the mass spectra of some paraffins and olefins, especially on the characteristic features of ion yield in relation to the ionizing voltages, are

1) H. M. Rosenstock, M. B. Wallenstein, A. L. Wahrhaffig and H. Eyring, *Proc. Natl. Acad. Sci.*, **38**, 669 (1952).
2) L. Friedman, F. A. Long and M. Wolfsberg, *J. Chem. Phys.*, **27**, 613 (1957).
3) A. B. King and F. A. Long, ibid., **29**, 374 (1958).
4) A. Krope, E. M. Eyring, A. L. Wahrhaffig and H. Eyring, ibid., **32**, 149 (1960).

presented, and discussion is carried out on the bond dissociation of molecular ions.

## Experimental

The instrument used in this work is a Hitachi mass spectrometer: type RMS-3, of a single focusing, 60° sector type with a radius of 100 mm. Positive ions going into the ion collector are detected through a negative feedback amplifier with an electrometer tube, Raytheon 5886 tetrode. In order to measure appearance potentials, however, some slight modifications are made in the ion source and the electric circuit belonging to it. A shielding electrode is inserted between the filament and the ionization chamber of an ordinary ion source, the filament is heated by DC currents and the ionizing voltage can be changed by 0.1 V. step by means of a potentiometer.

In the experiment, the pressure in the sample reservoir and the operating conditions, except the ionizing voltage, of the ion source are kept nearly constant.

The extrapolation method[5] is applied to obtain the appearance potentials, and krypton (ionization potential spectroscopically obtained: 14.03 eV.[6]) is used as the calibrating gas.

TABLE I. APPEARANCE POTENTIALS AND ACTIVATION ENERGIES OF PARAFFINS, eV.

| | | | | |
|---|---|---|---|---|
| $C_2H_6^+$ 11.78 | 1.19 | $C_2H_5^+$ 12.97 | | $C_2H_3^+$ |
| | 0.38 | $C_2H_4^+$ 12.16 | | $C_2H_2^+$ |
| $C_3H_8^+$ 11.20 | 0.56 | $C_3H_7^+$ 11.76 | 3.0 | $C_3H_5^+$ 14.76 |
| | 1.0 | $C_3H_6^+$ 12.20 | | $C_3H_4^+$ |
| | 1.04 | $C_2H_5^+$ 12.24 | 3.22 | $C_2H_3^+$ 15.46 |
| | 0.64 | $C_2H_4^+$ 11.84 | | $C_2H_2^+$ |
| $n$-$C_4H_{10}^+$ 10.23 | 0.78 | $C_4H_9^+$ 11.11 | | |
| | 0.63 | $C_3H_7^+$ 10.86 | 2.54 | $C_3H_5^+$ 13·40 |
| | 0.54 | $C_3H_6^+$ 10.77 | | |
| | 2.32 | $C_2H_5^+$ 12.55 | | $C_2H_3^+$ |
| | 1.22 | $C_2H_4^+$ 11.45 | | |
| iso-$C_4H_{10}^+$ 10.23 | 1.37 | $C_4H_9^+$ 11.6 | | |
| | 0.93 | $C_3H_7^+$ 11.16 | 3.39 | $C_3H_5^+$ 14.55 |
| | 0.65 | $C_3H_6^+$ 10.88 | | |
| | 3.57 | $C_2H_5^+$ 13.80 | | $C_2H_3^+$ |
| | 3.84 | $C_2H_4^+$ 14.07 | | |

## Experimental Results

**Paraffins.**—The appearance potentials obtained for straight and branched paraffins are shown in Table I together with bond energies calculated from the appearance potentials. Numerals under the chemical formula of ions represent the appearance potentials in electron volts and those above the arrows the bond energies or the activation energies in unimolecular decomposition. These energy values are in good agreement with the values reported by Field and Franklin[7].

In Figs. 1, 2 and 3, relative yields of principal ions are shown in relation to the ionizing voltage. The abscissa, $V_e-I$, is the excess energy of the ionizing electron over the ionization potential of the parent molecules. Since M/e 29 peak in a mass spectram of isobutane results from the summation of a rearrangement peak ($C_2H_5^+$) and isotopic peaks, correction is necessary for the estimation of

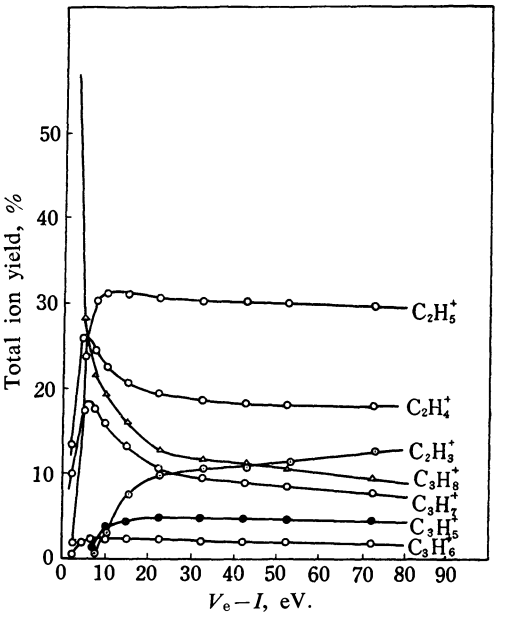



Fig. 1. Low voltage yield of ions from propane.
△ : Type I ○ : Type II
● : Type III ⊙ : Type IV

5) T. Mariner and W. Bleakney, *Phys. Rev.*, **72**, 807 (1947).
6) J. D. Morrison, *Revs. Pure Appl. Chem.*, **5**, 22 (1955).
7) F. H. Field and J. L. Franklin, "Electron Impact Phenomena and the Properties of Gaseous Ions", Academic Press Inc., New York (1957).

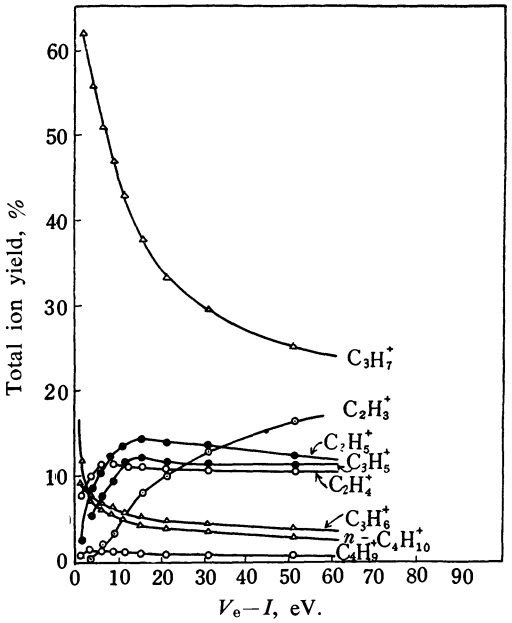



Fig. 2. Low voltage yield of ions from *n*-butane.
△ : Type I ○ : Type II
● : Type III ⊙ : Type IV

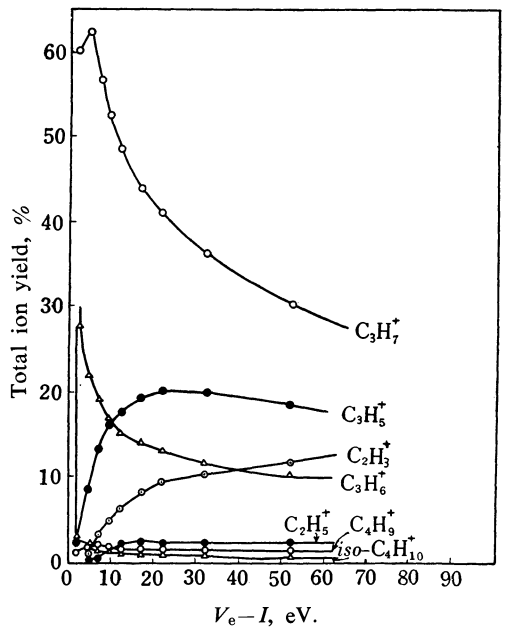



Fig. 3. Low voltage yield of ions from isobutane.
△ : Type I ○ : Type II
● : Type III ⊙ : Type IV

the $C_2H_5^+$ yield from the spectrum. The curve for $C_2H_5^+$ in Fig. 3 is a curve corrected by Washburn's method[8].

8) G. P. Barnard, "Modern Mass Spectrometry", the Institute of Physics, London (1953), p. 201.

These curves can be classified into four types, though it is difficult to classify some ions because they show medium aspects between two neighboring types. Type I curves are for those ions whose relative yield is very high at very low excess energies and decreases rapidly with the increase of ionizing voltage. Type II curves are for those ions whose relative yield rises rapidly to a maximum at an excess energy of 5~10 eV., and decreases to a nearly constant value. Type III curves are for those ions whose relative yield rises to a nearly constant value without passing a distinct maximum or after passing through a slight maximum at an excess energy higher than 10 eV. Type IV curves are for those ions whose relative yield increases slowly and does not level off until much higher ionizing voltages.

Parent ions and fragment ions of low activation energies belong to Type I. The activation energies of ions belonging to Type II are in a range between about 0.3. and 2 eV., and those to Type III in a range between about 2 and 3.5 eV., while those to Type IV are larger than 3 eV. The classification of principal ions from four paraffins are listed in Table II.

Table II. Classification of principal ions

| Type | Substance | | | |
|---|---|---|---|---|
| | Ethane | Propane | *n*-Butane | Isobutane |
| I | $C_2H_6^+$ | $C_3H_8^+$ | $n$-$C_4H_{10}^+$<br>$C_3H_7^+$<br>$C_3H_6^+$ | iso-$C_4H_{10}^+$<br>$C_3H_6^+$ |
| II | $C_2H_5^+$<br>$C_2H_4^+$ | $C_3H_7^+$<br>$C_3H_6^+$<br>$C_2H_4^+$ | $C_4H_9^+$<br>$C_2H_4^+$ | $C_4H_9^+$<br>$C_3H_7^+$ |
| III | $C_2H_3^+$<br>$C_2H_2^+$ | $C_3H_5^+$<br>$C_3H_4^+$<br>$C_2H_6^+$<br>$C_2H_5^+$ | $C_4H_8^+$<br>$C_3H_5^+$<br>$C_2H_5^+$ | $C_4H_8^+$<br>$C_4H_7^+$<br>$C_3H_5^+$<br>$C_2H_5^+$ |
| IV | $CH_3^+$ | $C_3H_3^+$<br>$C_3H_2^+$<br>$C_2H_3^+$<br>$C_2H_2^+$<br>$C_2H^+$<br>$CH_3^+$ | $C_4H_7^+$<br>$C_3H_3^+$<br>$C_2H_3^+$ | $C_3H_4^+$<br>$C_3H_3^+$<br>$C_2H_4^+$<br>$C_2H_3^+$ |

**Olefins.**—Similar results are obtained for straight olefins. The appearance potentials and the activation energies obtained are shown in Table III. These data are also in good agreement with the values of Field and Franklin[7]. Comparing Table III with Table I, the ionization potentials of olefins are considerably lower than those of paraffins with the same carbon numbers. This may be caused by the fact that $\pi$-electrons are concerned in the ionization of olefins. Activation energies, on the other hand, are higher for olefins than for paraffins.

TABLE III. APPEARANCE POTENTIALS AND ACTIVATION ENERGIES OF OLEFINS, eV.

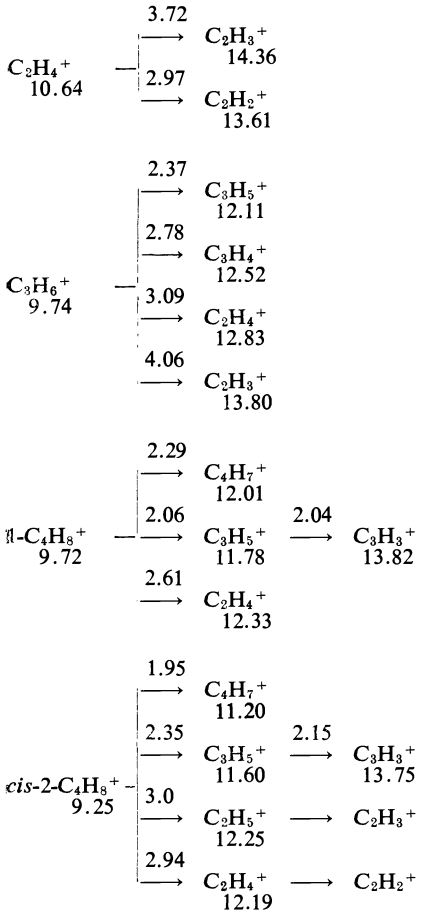



TABLE IV. CLASSIFICATION OF PRINCIPAL IONS

| Type | Substance | | | |
|---|---|---|---|---|
| | Ethylene | Propylene | 1-Butene | *cis*-2-Butene |
| I | $C_2H_4^+$ | $C_3H_6^+$ | *1*-$C_4H_8^+$ | *2*-$C_4H_8^+$ |
| II | | $C_3H_5^+$<br>$C_3H_4^+$ | $C_4H_7^+$<br>$C_3H_5^+$<br>$C_3H_4^+$ | $C_4H_7^+$<br>$C_3H_5^+$ |
| III | $C_2H_3^+$<br>$C_2H_2^+$ | $C_3H_3^+$<br>$C_3H_2^+$<br>$C_2H_5^+$<br>$C_2H_2^+$ | $C_4H_6^+$<br>$C_4H_5^+$<br>$C_4H_4^+$<br>$C_4H_3^+$<br>$C_3H_7^+$<br>$C_3H_6^+$<br>$C_3H_3^+$<br>$C_2H_5^+$<br>$C_2H_4^+$<br>$C_2H_2^+$ | $C_4H_6^+$<br>$C_4H_5^+$<br>$C_4H_4^+$<br>$C_4H_3^+$<br>$C_3H_6^+$<br>$C_3H_4^+$<br>$C_3H_3^+$<br>$C_3H_2^+$<br>$C_2H_5^+$<br>$C_2H_4^+$ |
| IV | $C_2H^+$<br>$C_2^+$ | $C_3H^+$<br>$C_3^+$<br>$C_2H_4^+$<br>$C_2H_3^+$<br>$C_2H^+$<br>$CH_3^+$<br>$CH_2^+$ | $C_4H_2^+$<br>$C_3H_2^+$<br>$C_3H^+$<br>$C_2H_3^+$ | $C_2H_3^+$<br>$C_2H_2^+$ |

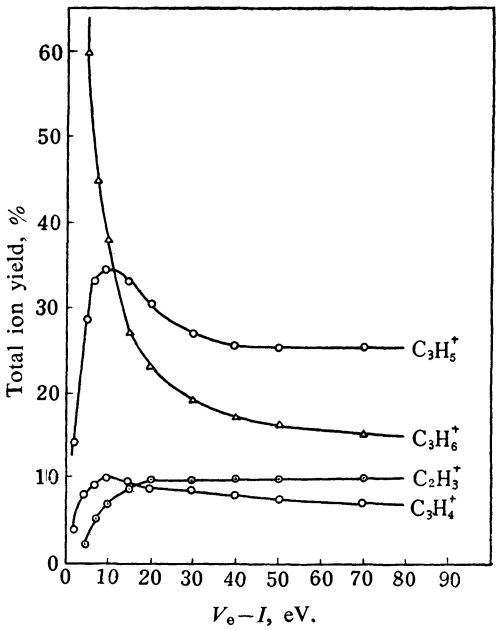



Fig. 4. Low voltage yield of ions from propylene.

△ : Type I ○ : Type II
● : Type III ⊙ : Type IV

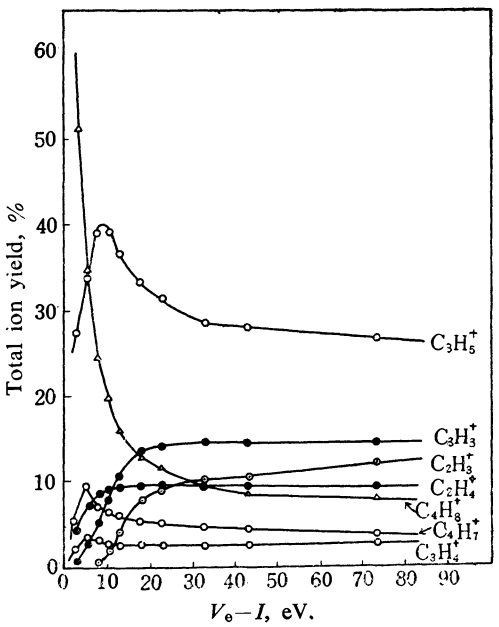



Fig. 5. Low voltage yield of ions from isobutene.

△ : Type I ○ : Type II
● : Type III ⊙ : Type IV

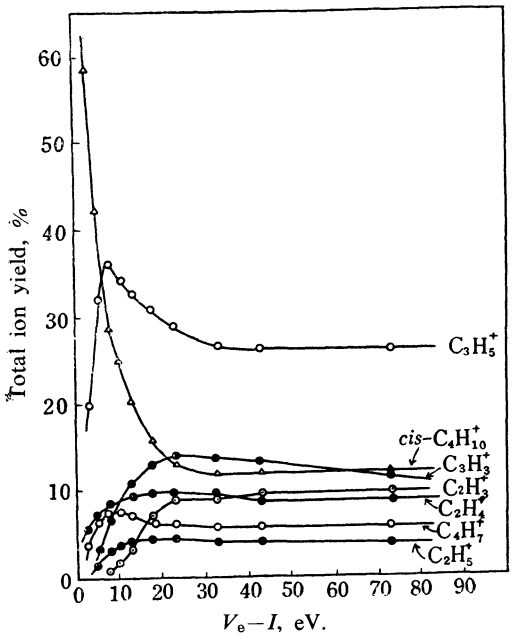



Fig. 6. Low voltage yield of ions from *cis*-2-butene.
△ : Type I ○ : Type II
● : Type III ⊙ : Type IV

Relative yields of principal ions are shown in Figs. 4, 5 and 6. The $C_2H_5^+$ yield in Fig. 6 is a corrected curve by Washburn's method[8]. As in the case of paraffins, the curves can be classified into four groups and the activation energies generally become larger from Type I to Type IV.

## Discussion

It has been believed that the statistical theory of unimolecular reaction[1] can be applied to the interpretation of decomposition of molecular ions by the impact of electrons with comparatively high energies. The theory is based on the presumption that molecular ions do not decompose instantaneously into ionized and neutral fragments, but the electron energies are uniformly distributed to whole bonds of molecular ions and then they are concentrated in a specific bond, causing the decompotision related with the electronic state of fragment ions.

According to the theory, a positive charge is distributed to a C-C or C-H bond and the bond rupture of a molecular ion is closely related with the distribution of the positive charge[7]. For instance, a parent ion of propane is presumed to be a hybrid of the following three structures[1] explained in terms of resonance:

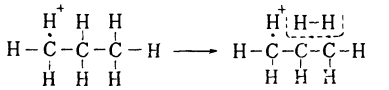
$$H_3{\equiv}C\dot{+}CH_2{-}C{\equiv}H_3 \qquad (1)$$

$$H_3{}^+{\doteq}C{-}CH_2{-}C{\equiv}H_3 \qquad (2)$$

$$H_3{}^+{\doteq}C{-}\underset{H}{\overset{H}{CH}}{=}CH_2 \qquad (3)$$

Fragment ions $C_2H_5^+$ and $C_3H_7^+$ can be expected from simple primary decompositions of the first and second structures, respectively. If a neutral molecule H-H is removed from the third structure, an ionic structure would be expected, $H_3{}^+{\doteq}C\text{-}CH{=}CH_2$, regarded as an olefinic molecular ion[9]. Thus the ionic structures concerned with the distribution of positive charge are very important for the primary rupture of C-C or C-H bond.

As mentioned above, a probable process for the $C_3H_6^+$ creation from $C_3H_8^+$ is a primary decomposition as follows:


(4)

or simply

$$C_3H_8{}^+ \longrightarrow C_3H_6{}^+ + H_2 \qquad (5)$$

As seen in Table I, the activation energy of $C_3H_6^+$ is a little less than twice the activation energy of $C_3H_7$. This seems to be an energy transfer effect showing that the energy in the rearrangement of hydrogen atoms is given away from a hydrogen molecule to a resonant ion. From the relation of decomposition energy, the $C_3H_6^+$ ions can not be expected through a secondary decomposition given by[9]

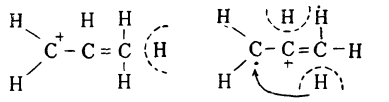
$$C_3H_8{}^+ \longrightarrow C_3H_7{}^+ + H \longrightarrow C_3H_6{}^+ + 2H \qquad (6)$$

The fragment ions $C_3H_5^+$, on the other hand, are expected through a secondary decomposition as follows:

$$\begin{aligned} C_3H_8{}^+ &\longrightarrow C_3H_7{}^+ + H \\ &\longrightarrow C_3H_5{}^+ + H_2 + H \end{aligned} \qquad (7)$$

In this case, energy transfer may also take place between a neutral hydrogen molecule and a resonant ion.

The $C_3H_5^+$ ions from paraffins are caused by a secondary decomposition, but those from olefins by a primary decomposition. For instance, the $C_3H_5^+$ ions from propylene are produced through both or either of the following process:


(8)

These two ionic structures are based on the assumption of electron migration[10], though

9) D. P. Stevenson and J. A. Hipple, Jr., *J. Am. Chem. Soc.*, 64, 1586 (1942).
10) G. R. Lester, "Advances in Mass Spectrometry", Symposium Publications Division, Pergamon Press (1959), p. 287.

unfortunately their relative importance has not been exactly proved by experiment. The positive charge is distributed more probaly on C-C bond than on C-H bond, but the principal ions intensities have shown that the "no-bond structures" give an effect of greater importance for the bond rupture. In case of butene, however, the rupture of C-C bond is more probable. The reason may be in the fact that the effects of double bond or no-bond structures are weaker in case of butene than in case of propylene.

It was reported that there might be a simple relation between the yield of fragment ions caused by the rupture of C-H bond of the parent ions and the number of bonds[11], but this theory has not been proved by experiment[1]. The results of the present experiment shown in Table V also contradict the theory. If the

TABLE V. RELATIVE AMOUNT OF PRINCIPAL IONS TO TOTAL IONS AND RATIO OF C-H BONDS TO TOTAL BONDS IN A HYDROCARBON

| Substance | $\frac{\text{C-H bonds}}{\text{Total bonds}}$ | $\frac{C_nH^+{}_{2n+1}}{\text{Total ions}}$ | $\frac{C_nH^+{}_{2n-1}}{\text{Total ions}}$ |
|---|---|---|---|
| $C_2H_6$ | 0.87 | 0.09 | |
| $C_3H_8$ | 0.80 | 0.08 | |
| $n$-$C_4H_{10}$ | 0.77 | 0.007 | |
| iso-$C_4H_{10}$ | 0.77 | 0.008 | |
| $C_2H_4$ | 0.8 | | 0.24 |
| $C_3H_6$ | 0.75 | | 0.24 |
| 1-$C_4H_8$ | 0.74 | | 0.05 |
| *cis*-2-$C_4H_8$ | 0.74 | | 0.05 |

distribution of positive charge on C-C and C-H bonds are calculated more precisely by the orbital theory, the process of decomposition of molecular ions might be explained more clearly.

Since the fragment ions $C_2H_4^+$ from isobutane are believed to be of olefinic structure and can not be expected to result from $C_2H_5^+$ ions, the process may be as follows:

$$\text{iso-}C_4H_{10}^+ \longrightarrow CH_3-\dot{C}H^+ + CH_3-CH_3$$
$$\longrightarrow CH_2\therefore CH_2^+ + C_2H_6 \qquad (9)$$

The energy necessary for reaction 9 is about 3.84 eV. The fragment ions $C_2H_5^+$ from isobutane also seem to be caused by primary decomposition; and a referred process may be as follows:

$$\text{iso-}C_4H_{10}^+ \longrightarrow CH_3-\dot{C}H^+ + CH_3-CH_3$$
$$\longrightarrow CH_3-CH_2^+ + C_2H_5 \qquad (10)$$

The energy necessary for the $C_2H_5^+$ creation is about 3.57 eV. and a little less than that for the $C_2H_4^+$. These processes 9 and 10 may be explained by the presumption of hydrogen transfer and rearrangement respectivly.

The $C_2H_4^+$ and $C_2H_5^+$ ions from *cis*-2-butene may be produced through the following processes, respectively:

$$\textit{cis}\text{-}2\text{-}C_4H_8^+ \longrightarrow CH_3-\dot{C}H^+ + CH-CH_3$$
$$\longrightarrow CH_2\therefore CH_2^+ + C_2H_4 \qquad (11)$$

and

$$\textit{cis}\text{-}2\text{-}C_4H_8^+ \longrightarrow CH_3-\dot{C}H^+ + CH-CH_3$$
$$\longrightarrow CH_3-CH_2^+ + C_2H_3 \qquad (12)$$

Hydrogen migration and rearrangement are related, as in cases of the reactions 9 and 10. Contrary to the case of isobutane, the activation energy for $C_2H_5^+$ ions is much greater than that for the $C_2H_4^+$ ions. This may be one of the double bond effects. Another double bond effect is shown in Table VI. The

TABLE VI. DOUBLE BOND EFFECT OF OLEFINS

| Substance | Ionization potential | Activation energy C-H | Activation energy C-C | Type of total ion yield C-H | Type of total ion yield C-C |
|---|---|---|---|---|---|
| $n$-$C_4H_{10}$ | 10.23 | 1.57 | 0.63 | 2 | 1 |
| 1-$C_4H_8$ | 9.72 | 2.29 | 2.06 | 2 | 2 |
| *cis*-2-$C_4H_8$ | 9.25 | 1.95 | 2.35 | 2 | 2 |

activation energy for a bond rupture is greater in cases of 1-butene and *cis*-2-butene than in the case of *n*-butane, especially for the rupture of C-C bond.

In order to examine chain branching effects, the results on propane, *n*-butane, and isobutane are compared in Table VII. The

TABLE VII. CHAIN BRANCHING EFFECT OF PARAFFINS IONS

| Substance | Ionization potential | Activation energy C-H | Activation energy C-C | Type of total ion yield C-H | Type of total ion yield C-C |
|---|---|---|---|---|---|
| $C_3H_8$ | 11.20 | 0.56 | 1.04 | 2 | 3 |
| $n$-$C_4H_{10}$ | 10.23 | 1.57 | 0.63 | 2 | 1 |
| iso-$C_4H_{10}$ | 10.23 | 1.37 | 0.93 | 2 | 2 |

activation energies for both C-C bond rupture and C-H bond rupture of iso-$C_4H_{10}^+$ are between those of $C_3H_8^+$ and $n$-$C_4H_{10}^+$, respectively.

## Summary

Relative yields of parent and principal fragment ions from four paraffins and olefins by electron impact are measured for the first time. The characteristic features of the ion yields can be classified into four types related with the ionizing voltages. The decomposition processes for some fragment ions can be explained under some assumptions, and those for forbidden ions $C_2H_5^+$ from isobutane and *cis*-2-butene under the assumption of hydrogen rerrangement.

11) F. L. Mohler, L. Williamson and H. M. Dean, *J. Research NBS*, 45, 235 (1950).

The author wishes to thank Dr. N. Morito and all the members of the mass spectrometry section of the Hitachi Central Research Laboratory for their helpful discussions throughout this work. Thanks are also due to Professor K. Higasi of Hokkaido University as well as Professor S. Nagakura of the University of Tokyo for the discussions in the broader aspects of the problems treated.

*Hitachi Central Research Laboratory*
*Kokubunji, Tokyo*

# *Rheological Properties of Hydrogels of Agar-agar*

By Kiyoshi ARAKAWA

(Received February 1, 1961)

Hydrogels of agar-agar are typical examples of polymeric thermo-reversible gels, and have long been the objects of the researches in colloid chemistry for these several decades[1]. Much remains unknown, however, concerning these gels even at present. In the study of thermo-reversible gels rheological methods are the most appropriate ones, and especially, the recent development of rheology has brought to light many new means for that purpose. The author has made a series of rheological studies on thermo-reversible gels[2,3], and a stress relaxation experiment has been made on the hydrogels of agar-agar, a part of the result of which was reported previously[2]. In this paper more comprehensive results and discussion are given.

## Experimental

**Sample.** — Sample I was given by Nihon Kaiso Kogyo Co., whose specification is shown in Table I together with that of sample II used in the previous experiment[2] for comparison. The intrinsic viscosity $[\eta]_{25}$ at 25°C of the aqueous solution of agar-agar was obtained by means of a capillary viscometer of the Ostwald type, and the molecular weight was calculated from the value of the intrinsic viscosity according to the following formula 1[4].

$$[\eta]_{25} = (3.7 \times 10^{-4}) M_v \qquad (1)$$

The obtained molecular weight is, however, an approximate one, because the reproducibility in the viscosity measurement at 25°C is not so good as that in the measurement at 60°C described below. The preparation of cylindrical gels for the stress relaxation experiment was made as follows. A powder sample was mixed with water in a vessel, and was dissolved by heating on an oil bath with a reflux condenser for two hours, and then was poured into cylindrical moulds. After the surfaces of the cylinders were covered with liquid paraffin in order to avoid the evaporation of water, the specimens were annealed in a thermostat. After 24 hr. specimen gels were taken out from the moulds and were aged at room temperature for more than two weeks. The dimension of the specimen was about 3 cm. in height and 2 cm. in diameter. The preparation of the solution for the measurement of viscosity was made according to the same procedure as that described above, and the measurement was made directly after the preparation.

**Apparatus.**—A chainomatic relaxometer was used to measure the relaxation of Young's modulus of the cylindrical gels, which was the same one as that used previously[2,3].

TABLE I. SAMPLES

| | Sample I | Sample II |
|---|---|---|
| Ashes, % | 2.9 | 1.5 |
| $[\eta]_{25}$, 100 cc./g. | 16.1 | 2.9 |
| Molecular weight | 40000 | 8000 |

## Results and Discussion

**Viscosity of Agar-agar Solution.** — The data of viscosity for the solution of sample I at 60°C are given in Fig. 1. As is seen in Fig. 1, the curve of $\eta_{sp}/C$ vs. $C$ relation rises with decrease of concentration after passing through a minimum point. This is the characteristic of the solution of polyelectrolyte in general and the same behavior of solutions of agar-agar was reported recently by Sakamoto and Kishimoto[5].

**Stress Strain Relation.** — The setress $\sigma$ of 2.6% gel of sample I at 25°C is plotted against the compressional strain $\gamma$ in Fig. 2. The stress $\sigma$ was measured accurately 2 min. after the instant of loading for all strains. It is

1) T. Nakagawa, *J. Chem. Soc. Japan, Pure Chem. Sec.* (*Nippon Kagaku Zasshi*) **72**, 390, 626 (1951), F. Hirata, ibid., **58**, 1156 (1937); **59**, 1, 7 (1938); N. Hirai, ibid., **72**, 837 (1951); **73**, 65, 68 (1952); K. Ninomiya, ibid., **76**, 72 (1955).

2) K. Arakawa and K. Atsumi, ibid., **80**, 133 (1959).

3) K. Arakawa, This Bulletin, **31**, 842 (1958); **32**, 1248 (1959); **33**, 1568 (1960).

4) N. Hirai and N. Nishimura, *J. Chem. Soc. Japan, Pure Chem. Sec.* (*Nippon Kagaku Zasshi*), **75**, 248 (1954).

5) M. Sakamoto and A. Kishimoto, *Bull. Japan. Soc. Sci. Fisheries*, **26**, 25 (1960).

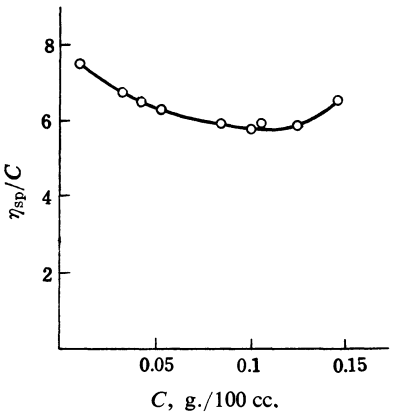



Fig. 1. Viscosity vs. $C$ relation.

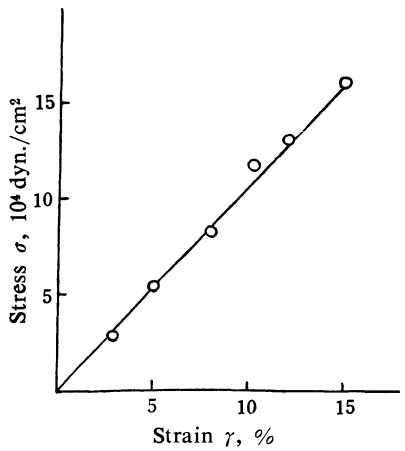



Fig. 2. Stress strain curve at 25°C.

clearly seen in Fig. 2 that the stress strain relation is linear within the amount of strain, 15%.

**Stress Relaxation.** — The relaxation Young's modulus $E_r(t)$ of 2.6% gel of sample I under constant strain at various temperatures is plotted against $\log t$ in Fig. 3, where $t$ is time and $E_r(t)$ is $\sigma/\gamma$. The amount of the imposed strain $\gamma$ is 5% for all temperatures, which is within the range of the linear relation between stress and strain.

The data of stress relaxation on the hydrogel of sample II of the same concentration, which were reported previously[2], are plotted again in Fig. 4 for comparison, but without the multiplication factor $298/T$ in this case. The relaxation curves in Fig. 3 show the inversion of the mutual position with lapse of time. It may be said that in the short time region and at the comparatively low temperature rubber elasticity appears predominantly, but with the lapse of time the junction cleavage occurs more frequently at the higher temperatures. However, in Fig. 4 no inversion is seen. This

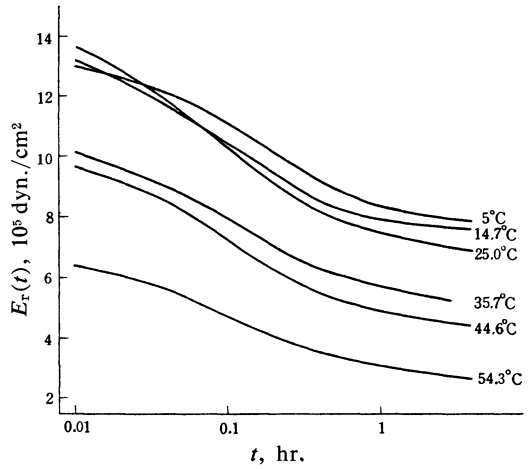



Fig. 3. Relaxation Young's modulus of 2.6% gel (sample I).

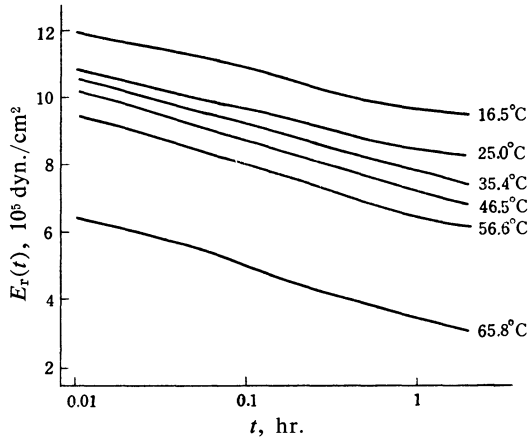



Fig. 4. Relaxation Young's modulus of 2.6% gel (sample II).

may be partly attributed to the difference in the molecular weight of agar-agar.

**Analysis of Relaxation Data by Mechanical Model.** — The mechanical behavior of these gels is represented by the 6-elements mechanical model shown in Fig. 5. According to this model, $E_r(t)$ under constant strain is expressed by Eq. 2,

$$E_r(t) = E_1 e^{-t/\tau_1} + E_2 e^{-t/\tau_2} + E_3 e^{-t/\tau_3} \qquad (2)$$

where $\tau_1 = \eta_1/E_1$, $\tau_2 = \eta_2/E_2$, and $\tau_3 = \eta_3/E_3$.

The results obtained from the curves in Fig. 3 and Fig. 4 by means of Eq. 2 are given in Table II. The calculation of the model constants was made by repeating the procedure described in the previous paper[2], when the following condition (3) was assumed.

$$\tau_1 \gg \tau_2 \gg \tau_3 \qquad (3)$$

As seen in Table II, this is satisfied.

The Maxwellian element of the relaxation time $\tau_1$ may be regarded as the representation

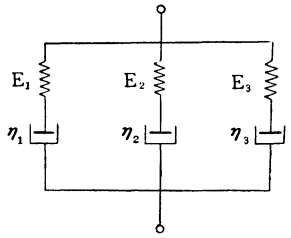



Fig. 5. Mechanical model.

TABLE II. CONSTANTS OF MECHANICAL MODEL OF 2.6% GEL

| Sample I °C | $E_1$ | $E_2$ | $E_3$ | $\tau_1$ | $\tau_2$ | $\tau_3$ |
|---|---|---|---|---|---|---|
| | $10^5$ dyn./cm$^2$ | | | hr. | min. | min. |
| 5 | 8.2 | 4.3 | 1.5 | 90 | 16 | 1 |
| 14.7 | 8.0 | 4.3 | 2.2 | 90 | 12 | 1 |
| 25.0 | 7.8 | 4.2 | 3.0 | 40 | 11 | 1 |
| 35.7 | 5.8 | 2.8 | 2.9 | 34 | 17 | 3.5 |
| 44.6 | 5.0 | 2.5 | 3.5 | 26 | 18 | 3.8 |
| 54.3 | 3.2 | 1.5 | 2.2 | 13 | 18 | 3.8 |
| Sample II | | | | | | |
| 16.5 | 10.0 | 1.5 | 1.5 | 42 | 12 | 1 |
| 25.0 | 8.8 | 1.6 | 1.6 | 42 | 13 | 0.8 |
| 35.4 | 8.4 | 1.2 | 1.9 | 18 | 17 | 1.4 |
| 46.5 | 7.9 | 1.8 | 1.3 | 15 | 10 | 1 |
| 56.6 | 7.0 | 1.8 | 1.2 | 17 | 12 | 0.8 |
| 65.8 | 3.9 | 1.4 | 1.7 | 9.8 | 17 | 1.4 |

of the main network structure. The linkage supporting this network may be of secondary nature, considering that the hydrogel of agar-agar makes sol-gel transition reversible, and the bond cleavage process in the gels under constant strain may occur at the junctions in the network, not along the network chains. From the $\tau_1$ vs. $1/T$ relation shown in Fig. 6, the average activation energy $\Delta\overline{H}$ is obtained for the dotted line, and is given in Table III, together with the values calculated from the previous data[2] for 4.0 and 1.0% gel of sample II.

$$\Delta H = R\frac{\partial \ln \tau_1}{\partial(1/T)} \qquad (4)$$

In the agar-agar gels the chain skeleton is composed of the chain of galactose. In natural cellulose the activation energy for the cleavage of hydrogen bonds along a-axis in crystalline region is 7~8 kcal./mol.[6] The value given in Table III is 4.5~6.6 kcal./mol., which is smaller than the above value in natural cellulose, and is camparable with the activation energy of the hydrogen bond between water molecules, 4.5 kcal./mol., and that for ethyl alcohol, 6.2 kcal./mol.[7] From the above consideration it may

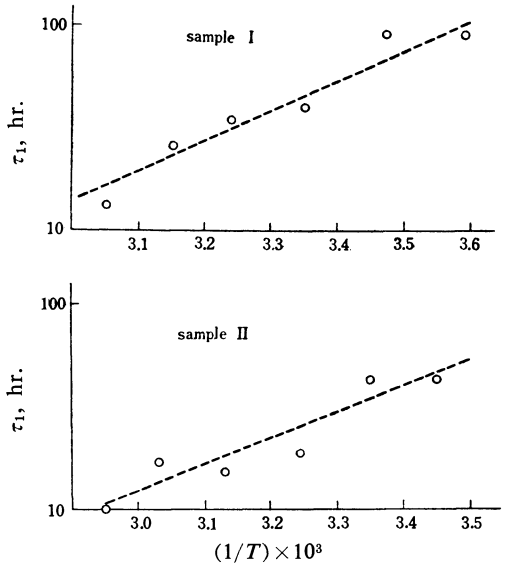



Fig. 6. $\tau_1$ vs. $1/T$ relation of 2.6% gel.

TABLE III. AVERAGE ACTIVATION ENERGY $\Delta\overline{H}$

| | Sample I | | Sample II | |
|---|---|---|---|---|
| Concn., % | 2.6 | 1.0 | 2.6 | 4.1 |
| $\Delta\overline{H}$, kal./mol. | 6.6 | 4.8 | 5.8 | 4.5 |

be said that in the hydrogel of agar-agar the secondary bond between each agar-agar molecule which constructs the gel structure is the hydrogen bond between galactose, and that the bond is a little weakened by the effect of solvent molecule, compared with the hydrogen bond in the micelle of natural cellulose.

## Summary

A rheological study was made for the hydrogels and the solution of agar-agar. The viscosity vs. concentration relation exhibits the character of polyelectrolyte. From the stress relaxation data obtained by a chainomatic balance relaxometer the following results were obtained.

1) The behavior of hydrogels of agar-agar is represented by the 6-elements mechanical model.

2) The activation energy of the secondary bond between agar-agar molecules which constructs the gel structure is 4.5~6.6 kcal./mol.

Then, there was some discussion on the structure of the hydrogels of agar-agar.

The author is indebted to Mr. Mineo Watase for his cooperation in carrying out this study.

*Department of Chemical Industry*
*Faculty of Engineering*
*Shizuoka University*
*Oiwake, Hamamatsu*

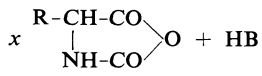
6) N. Saito, "High Polymer Physics", Shokabo, Tokyo (1958), p. 8.
7) L. Pauling, "The Nature of the Chemical Bond", Cornell Univ. Press, Ithaca (1940), Chap. 9.

# *Studies on Long Chain Alkyl Amides of Water-soluble Poly-α-amino Acids. I. Amphipathic Properties of Poly-DL-alanine Dodecylamide*

By Toshizo ISEMURA, Shoichi IKEDA, Fumikatsu TOKIWA* and Junzo NOGUCHI**

(Received February 3, 1961)

It has been established that poly-α-amino acid can be synthesized by the polymerization of *N*-carboxy-α-amino acid anhydride[1,2], and a basic substance such as sodium hydroxide, sodium methoxide or organic amines (e. g., *n*-hexylamine, triethylamine) initiates the polymerization effectively[1-3]. The polymerization reaction, initiated by a base (HB) capable of generating an active hydrogen, proceeds as a stepwise addition of amino acid residues in the following manner:



$$\rightarrow \text{H-(-NH-}\underset{\text{R}}{\text{CH}}\text{-CO-)}_x\text{-B} + x\ CO_2$$

The free amino group of poly-α-amino acid produced in each step of the reaction reacts with another molecule of *N*-carboxy anhydride. The stepwise polymerization then goes on until all the *N*-carboxy anhydride molecules are consumed, and the resulting poly-α-amino acid would have a number average degree of polymerization ($x$) equal to the initial anhydride-initiator molar ratio ([A]/[I]).

The poly-α-amino acid prepared in this way would have a basic residue (B) at the terminal carboxyl group linked by an amide bond, if an organic amine such as primary alkyl amine has been chosen as the initiator for polymerization. Thus an amphipathic poly-α-amino acid amide, which has both hydrophilic and hydrophobic groups in a molecule, may be readily synthesized by the above method, if the following conditions are satisfied. The poly-α-amino acid is soluble in water, the basic residue is composed of a hydrophobic group such as long paraffin chain, and the hydrophility of the poly-α-amino acid part is well balanced with the hydrophobicity of the basic residue, i. e., the initial [A]/[I] ratio is properly chosen.

Aside from the difference in chemical structure, the chain conformation and other related properties of poly-α-amino acid are greatly dependent on the constituent amino acid residue[4] as well as on the degree of polymerization, medium and temperature. The manifold possibility in the use of various water-soluble poly-α-amino acids would make the studies of amphipatic poly-α-amino acid alkylamide significant for elucidating the hydrophilic nature of different amino acid residues and the effect of the type of residue on the properties of amphipathic polymer and its hydrogen bonding nature. Furthermore, it is expected that the polymers would find practical uses as surface active agents.

It is noted that the reaction mechanism of polymerization of *N*-carboxy-α-amino acid anhydride is apparently analogous to that of ethylene oxide[5] and the structure of poly-α-amino acid amide resembles that of polyoxyethylene alkyl amine or ether.

The present paper deals with the synthesis and amphipathic nature of poly-DL-alanine alkyl amide, especially, of poly-DL-alanine dodecylamide, in relation to the degree of polymerization of polyamino acid part in a molecule.

## Synthesis

*N*-Carboxy-DL-alanine anhydride (DL-alanine NCA) was prepared from DL-alanine by the phosgene method[6]. The polymerizations were initiated with either dodecylamine, cetylamine or *N*-myristyl-β-alanine at [A]/[I] ratios which varied from 5 to 30. The polymers obtained were dodecylamide (I), cetylamide (II) or *N*-carboxyethyl-myristylamide (III) of poly-DL-alanine:

$$C_{12}H_{25}NH\text{-(-CO-}\underset{\text{CH}_3}{\text{CH}}\text{-NH-)}_x\text{-H} \qquad \text{(I)}$$

$$C_{16}H_{33}NH\text{-(-CO-}\underset{\text{CH}_3}{\text{CH}}\text{-NH-)}_x\text{-H} \qquad \text{(II)}$$

* Present Address: Research Laboratory, Kao Soap Co., Ltd., Wakayama.
** Present address: Faculty of Science, Kanazawa University, Kanazawa.

1) E. Katchalski and M. Sela, *Adv. Protein Chem.*, **13**, 243 (1958).
2) E. Katchalski, ibid., **6**, 123 (1951).
3) E. R. Blout and R. H. Karlson, *J. Am. Chem. Soc.*, **78**, 941 (1956).
4) e. g., E. R. Blout, C. de Lozé, S. M. Bloom and G. D. Fasman, ibid., **82**, 3787 (1960).
5) P. J. Flory, ibid., **62**, 1561 (1940).
6) A. C. Farthing, *J. Chem. Soc.*, **1950**, 3213; J. L. Bailey, ibid., **1950**, 3461.

$$C_{14}H_{29}N\text{-}(\text{-}CO\text{-}\underset{\displaystyle CH_2CH_2COOH}{\underset{|}{CH}}\text{-}NH\text{-})_x\text{-}H \qquad (III)$$

Among them, poly-DL-alanine dodecylamide (I, abbreviated to PADA) was investigated in some detail, and some of its characteristics are listed in Table I, with reference to the [A]/[I] ratio.

Table I. Characteristics of PADA and poly-DL-alanine

| Sample No. | [A]/[I] | $x$ | pH of suspension or solution[a] | Mole of HCl required for dissolution $10^{-3}$ mol./g. |
|---|---|---|---|---|
| PADA(A431) | 5 | 5.4 | 7.4 | 1.13 |
| 〃 (A432) | 10 | 10.2 | 6.7 | 0.50 |
| 〃 (A433) | 15 | 14.6 | 6.5 | 0.24 |
| 〃 (A434) | 20 | 18.5 | 6.1 | 0 |
| Poly-DL-alanine (J928) | 50 | 28.8 | 3.7 | 0 |

a) 0.75 g. sample in 100 ml. water

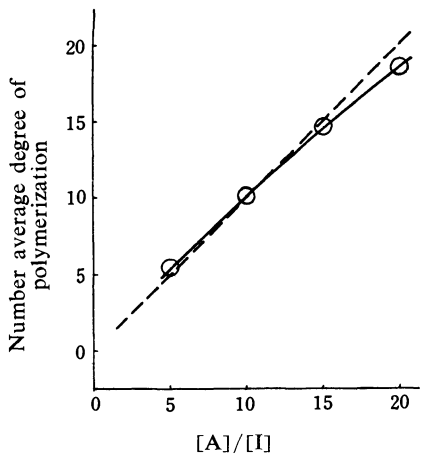
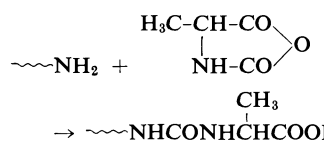



Fig. 1. PADA from polymerization in dioxane with dodecylamine initiator; number average degree of polymerization ($x$) as a function of anhydride-initiator ratio ([A]/[I]), (dashed line represents "theoretical" $x$-[A]/[I] relationship).

The number average degree of polymerization of PADA was determined by the titration of a terminal amino group with perchloric acid[7]. It should be equal to the [A]/[I] value, and Table I and Fig. 1 show that this relation is nearly fulfilled. Hereafter, the designation $x$ is used instead of [A]/[I] for specifying a PADA preparation, although the value of $x$ is not strictly equal to that of [A]/[I]. Values of $x$ were slightly lower than the [A]/[I] value at higher [A]/[I] ratios. The discrepancy may be ascribed either to the error in the titration which is enhanced at higher [A]/[I] ratios or to the presence of a few thermal carboxyl groups which has been formed in a termination reaction during the polymerization in the following manner[7]:



The results of the terminal amino analysis and infrared data as described below confirm the formation of PADA, i. e., poly-DL-alanine linked with dodecylamine in its terminal carboxyl group, in the case of the polymerization of *N*-carboxy-DL-alanine anhydride initiated with dodecylamine.

PADA is insoluble in ordinary organic solvents such as acetic acid, chloroform, and dimethylformamide, but is soluble in formic acid, dichloroacetic acid and *m*-cresol.

PADA of $x > 17$ is soluble in water, but PADA of $x < 17$ gives a turbid solution in water, the turbidity increasing with decreasing $x$. Polyoxyethylene dodecylamine becomes soluble in water for the degree of polymerization higher than 8[8]. However, PADA of any $x$ value is soluble in an aqueous acid solution, the free terminal amino group being ionized.

While the aqueous solutions of polyoxyethylene derivatives are known to exhibit the clouding phenomenon when heated[9], no such phenomenon is observed for PADA solution. This may be attributed to the formation of stronger hydrogen bonding between DL-alanyl residue and water molecule than that between oxyethylene residue and water molecule, the former being kept unbroken even at high temperatures.

## Experimental

***N*-Carboxy-DL-alanine Anhydride.** — DL-Alanine (20 g.) was suspended in dry dioxane (300 ml.), stirred and phosgene bubbled in for about 3 hr., maintaining the temperature at 35~40°C. After the completion of the reaction carbon dioxide was passed through the solution until free of phosgene. The solvent was removed at reduced pressure. Then anhydrous ether was added and evaporated under reduced pressure, and this procedure was repeated several times. Dry petroleum ether was poured into an oily residue, and DL-alanine NCA was recrystallized after keeping the oil for 24 hr. at −15°C. DL-Alanine NCA was recrystallized from ether-petroleum ether. M. p. 45°C, yield 80%.

7) A. Berger and M. Sela, *J. Am. Chem. Soc.*, **77**, 1893 (1955).

8) T. Otsuka, personal communication.

9) L. Raphael, *Ist. Int. Cong. on Surface Active Agent*, **1**, 52 (1954).

**Poly-DL-alanine Dodecylamide.**—After an appropriate amount of dodecylamine (for example, 1.6 g. at [A]/[I]=10) was dissolved in dry dioxane (200 ml.), DL-alanine NCA (10 g.) was added to it at room temperature. Polymerization was allowed to proceed for several hours. The suspension of PADA was poured into a large amount of ether, the precipitate was gathered by centrifugation and dried in vacuo.

**Other Derivatives of Poly-DL-alanine.**—Poly-DL-alanine cetylamide and poly-DL-alanine *N*-carboxyethyl-myristylamide were synthesized in the same manner as described above, using cetylamine and *N*-myristyl-β-alanine as initiator, respectively. Poly-DL-alanine was prepared by polymerizing with triethylamine-initiation at [A]/[I]=50, the average $x$ of which was found to be 28.8 by end-group analysis.

**Titration of Terminal Amino Groups.** — A N/20 perchloric acid solution was prepared by adding calculated amount of 70% perchloric acid to glacial acetic acid. After standing overnight, this solution was standardized by titration with pure sodium carbonate in glacial acetic acid, using crystal violet (0.2% glacial acetic acid solution) as indicator.

A sample of 50~80 mg. was weighed into a 50 ml. Erlenmeyer flask, dissolved in 2 ml. of dichloroacetic acid, and then 8 ml. of glacial acetic acid was added to the solution. The solution was titrated to green end-point of crystal violet indicator with the standard perchloric acid solution which was delivered from a 5 ml. micro-burette; the titer of solvent alone was subtracted from sample titer.

To check the procedure, a known amount of dodecylamine was titrated, and the agreement with calculated value was obtained at the green end-point. The point of color change was made somewhat obscure in the presence of dichloroacetic acid, but the accuracy of titration was within about 5%.

**Infrared Measurements.** — All infrared measurements were performed on a Shimadzu Type AR-275 double beam spectrometer using a sodium chloride prism. The samples for infrared measurements were prepared as dispersions either in potassium chloride disks or in Nujol.

**Titration with an Aqueous Hydrochloric Acid Solution.** — pH measurements were made with a Horiba Type M-3 pH-meter. A given amount of sample was dispersed or dissolved in distilled water, and titrated with a standard hydrochloric acid solution (0.06 N) to obtain a titration curve. Concentration of each sample was 0.75 g. polymer in 100 ml. solution.

**Measurements of Surface Tension.** — Surface tension was measured by drop weight method. The apparatus was placed in a thermostat of 25.0°C. The observed values were corrected by using the correction factor of Harkins and Jordan. The pH of sample solutions was adjusted to pH 5.0 by hydrochloric acid, unless otherwise stated, because all the samples were soluble at this pH.

**Measurements of Surface Pressure.** — Surface pressure was measured by a balance of hanging plate type at room temperature. Samples were spread from solutions in a mixed solvent, formic acid-isopropyl alcohol-water (1 : 2 : 7), on distilled water and on an aqueous solution of 0.01 M potassium carbonate or 0.2 M potassium chloride.

## Results and Discussion

**Infrared Absorption Spectra.** — The infrared spectra of PADA and poly-DL-alanine were recorded in the solid state from potassium bromide disks and Nujol suspensions. Some of the infrared data are summarized in Table II.

The absorption bands at 2970 and 2930 $cm^{-1}$ from a potassium bromide disk are assigned to the C-H stretching modes of $CH_3$ and $CH_2$ groups, respectively. The intensity of the former, relative to that of the latter, becomes stronger with increasing $x$, and is the strongest for poly-DL-alanine. This observation supports the formation of poly-DL-alanine linked with dodecylamine.

PADA and poly-DL-alanine show amide I absorption at 1661 and 1629 $cm^{-1}$ and amide III absorption at 1240 and 1220 $cm^{-1}$. The lower frequency in the amide III band was observed in Nujol suspension but not in potassium bromide disk. A band due to N-H stretching lies at 3310 and 3280 $cm^{-1}$. The lower frequency appeared in potassium bromide disk for PADA of $x=5$ but not in Nujol suspension. In amide I band the higher frequency

TABLE II. CHARACTERISTIC ABSORPTIONS OF PADA AND POLY-DL-ALANINE

| Characteristic band | | Frequency, $cm^{-1}$ PADA ($x=5$) | PADA ($x=10$) | PADA ($x=15$) | PADA ($x=20$) | Poly-DL-alanine |
|---|---|---|---|---|---|---|
| N-H(str.)[a] | | 3280 (s) | — | 3310 (s) | — | 3310 (s) |
| | | | — | | — | |
| Amide I | | 1661 (sh) | 1661 (sh) | 1661 (s) | 1661 (s) | 1661 (s) |
| | | 1629 (s) | 1629 (s) | 1629 (s) | 1629 (s) | 1629 (s) |
| Amide II | | 1530 (s) | 1530 (s) | 1530 (s) | 1530 (s) | 1530 (s) |
| Amide III[b] | | 1240 (w) | 1240 (w) | 1240 (m) | 1240 (m) | 1240 (m) |
| | | 1220 (m) | 1220 (m) | 1220 (m) | 1220 (w) | 1220 (sh) |
| C-H(str.)[a] | $CH_3$- | 2970 (w) | — | 2970 (w) | — | 2970 (m) |
| | $CH_2$- | 2930 (s) | — | 2930 (m) | — | 2930 (w) |

str.=stretching mode, s=strong, m=medium, w=weak, sh=shoulder
a) from KBr disk, b) from Nujol suspension

of the two amide bands is characteristic of the random conformation of polypeptide and the lower is of the β-conformation[10-13],*. The dependence of the relative intensity of two frequencies in the amide III and the N–H stretching bands upon the value of $x$ is also related to the presence of these two conformations. In all the three bands the intensity of the higher frequency of PADA relative to that of the lower increases with $x$, and poly-DL-alanine absorbs the higher frequency strongly. The results indicate that the random conformation is predominant for PADA with higher $x$ ($x \geq 20$) and poly-DL-alanine, the portion of the β-conformation increases with lowering $x$, and PADA with $x=5$ is mostly in the β-conformation**.

However, the above correlation of infrared frequency with the conformation of polypeptides could not be found in amide II band.

**Titration with an Aqueous Hydrochloric Acid Solution.** — When PADA or poly-DL-alanine is dispersed or dissolved in water, the solution shows an acidic pH. Poly-DL-alanine gives the most acidic pH, 3.7. Table I shows the pH's of the solution of 0.75 g. polymer in 100 ml. A value of pH, 2.8, of poly-DL-alanine ($x=30$) solution has been reported already[15]. This might be ascribed partly to the presence of the terminal carboxyl groups produced by the termination reaction during polymerization, as mentioned before[7].

The solution of PADA exhibits lower pH with increasing $x$, because an equal gram of polymer contains less terminal amino groups with increasing $x$. This effect is enhanced by the more complete solubility of PADA with higher $x$, since the amino groups of insoluble molecules would remain unionized.

When the solution of PADA is titrated with an aqueous hydrochloric acid solution, the pH is gradually lowered and then suddenly decreases. Fig. 2 shows the pH of solution plotted against mole of hydrochloric acid added when 0.75 g. PADA is dispersed or dissolved in 100 ml. solution. On this titration curve, a

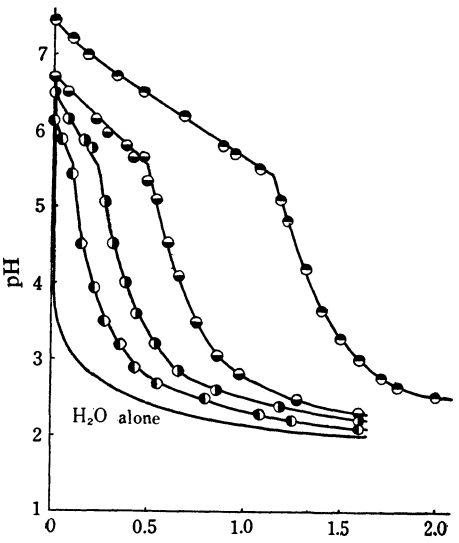



Fig. 2. Plots of pH of PADA solution against added amout of hydrochloric acid at 25°C. ◓, $x=5$; ◒, $x=10$; ◑, $x=15$; ◐, $x=20$

break point exists at about pH 5.5, irrespective of $x$. At this point the turbid dispersion of PADA with $x<17$ becomes almost transparent. If all the terminal amino groups could be titrated with hydrochloric acid, the break point should be the end point, and the mole of hydrochloric acid consumed should be equal to mole of terminal amino groups obtained from anhydrous perchloric acid titration. Nevertheless, the former was found to be considerably smaller than the latter. The discrepancy might arise from the fact that the PADA molecules in aqueous acid media aggregate into a "micelle". The micelle is composed of ionized molecules together with unionized molecules, the latter being not titratable with hydrogen ions. Evidence for the micelle formation is provided by surface tension data and preliminary experiments of ultracentrifugation and solubilization.

**Surface Tension.** — The surface tension of aqueous solutions of PADA together with poly-DL-alanine and dodecylamine hydrochloride was measured at pH 5.0. Dodecylamine hydrochloride was a sample recrystallized several times from acetone-benzene. The surface tension vs. concentration curves at pH 5.0 are shown in Fig. 3. The result obtained for dodecylamine hydrochloride was in good agreement with that already reported[16].

The surface tension of PADA solution is

10) A. Elliott, *Nature*, **170**, 1066 (1952).
11) C. H. Bamford, A. Elliott and W. E. Hanby, "Synthetic Polypeptides", Academic Press, New York (1956), p. 153.
12) A. Elliott, *Proc. Roy. Soc.*, **A221**, 104 (1953).
13) T. Miyazawa and E. R. Blout, *J. Am. Chem. Soc.*, **83**, 712 (1961).
* Following Elliott and others[10-12], the absorption at 1661 $cm^{-1}$ arises from the α-form.
** It is reported[14] that a low molecular weight poly-γ-benzyl-L-glutamate differs from a high molecular weight polymer in its conformation, while the latter is in the α-helical conformation.
14) E. R. Blout and A. Asadourian, *J. Am. Chem. Soc.*, **78**, 955 (1956).
15) K. Linderstøm-Lang, "Symposium on Protein Structure", Ed. by A. Neuberger, Methuen and Co. Ltd., London (1958), p. 23.
16) E. J. Hoffman, G. E. Boyd and A. W. Ralston, *J. Am. Chem. Soc.*, **64**, 408 (1942).

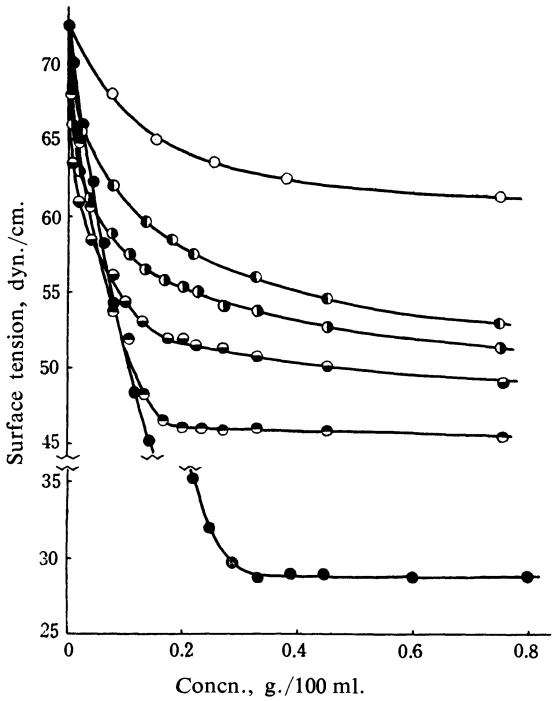



Fig. 3. Surface tension vs. concentration curves for aqueous solution of PADA, poly-DL-alanine and dodecylamine hydrochloride at pH 5.0 25°C. PADA: ◓, $x=5$; ◒, $x=10$; ◑, $x=15$; ◐, $x=20$; ○, poly-DL-alanine; ●, dodecylamine hydrochloride

characterized by a sharp initial decrease followed by a gradual flattening, as the concentration becomes higher. This behavior is commonly observed for surface active agents. The break point corresponds to the critical micelle concentration, although it becomes obscure for PADA of higher $x$. The critical micelle concentration of PADA lies in more dilute concentration than that of dodecylamine hydrochloride, and shifts towards lower concentration as $x$ increases.

In a PADA molecule, a sequence of DL-alanyl residues is between the dodecyl group and the ionized or unionized hydrophilic amino group at pH 5.0, where PADA is partially ionized. In this case the part of poly-DL-alanine reduces the repulsion between ionized hydrophilic groups due to the intermolecular hydrogen bonding. Thus the micelle formation takes place readily at lower concentration as $x$ increases. It is noticeable that the critical micelle concentration of PADA lies at about $10^{-3}$ mole per liter which is compared with

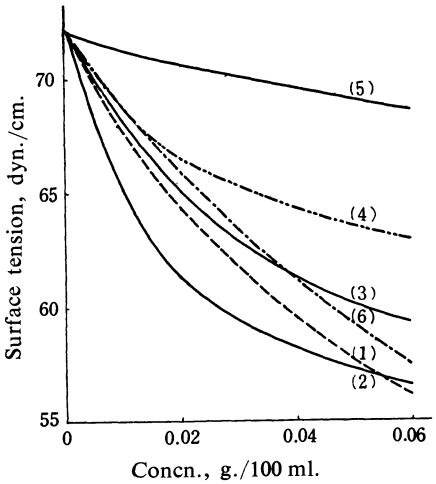



Fig. 4. Surface tension vs. concentration curves of PADA, poly-DL-alanine and dodecylamine hydrochloride at dilute concentrations. pH 5.0, 25°C. PADA: (1) $x=5$, (2) $x=10$, (3) $x=15$, (4) $x=20$, (5) poly-DL-alanine, (6) dodecylamine hydrochloride

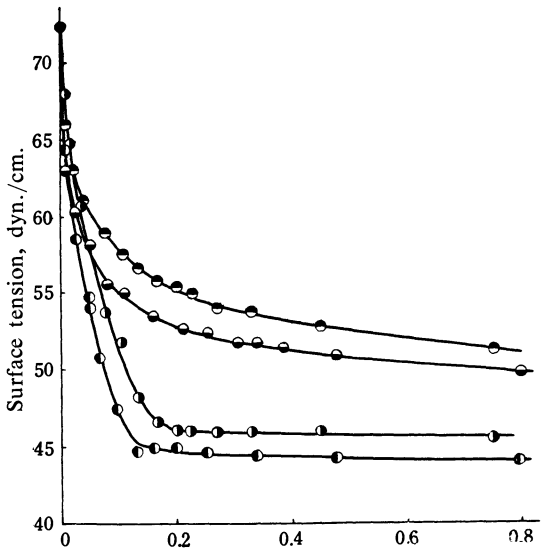



Fig. 5. Effect of acid on surface tension of PADA at 25°C. $x=5$: ◑, pH 5.0; ◐, pH 2.2, $x=15$: ◓, pH 5.0; ◒, pH 2.2

that of polyoxyethylene derivatives with long alkyl chain, $10^{-4}$ mol. per liter[17].

At low concentrations the slope of surface tension vs. concentration curve is the steepest for PADA of $x=10$ and is more gentle when $x$ is either smaller or larger than this value, as shown in Fig. 4. For $x<10$, the explanation is as described before. For $x>10$ the attraction

17) L. Hsioa, H. M. Dunning, P. B. Lorenz, *J. Phys. Chem.*, **60**, 657 (1956). E. Gonick and J. W. McBain, *J. Am. Chem. Soc.*, **69**, 334 (1947).

due to hydrogen bonding between DL-alanyl residues predominates over van der Waals cohesion between alkyl chains and the characteristics of poly-DL-alanine become obvious and reduce the effect of alkyl chain, thus surface tension being less lowered.

Fig. 5 show the effect of acid on surface tension of PADA. The more acidic the solution of PADA is, the lower the surface tension becomes and the break point shift to more dilute concentration. This fact indicates that the excess acid added beyond pH 5.5 remains free in solution and behaves like a simple neutral salt, suppressing the electrostatic repulsion between ionized amino groups.

**Surface Film of PADA.** — Fig. 6 illustrates surface pressure vs. area curves of PADA and poly-DL-alanine films on distilled water. They are of condensed type. The limiting area, $A_{\Pi\to 0}$ ($m^2$/mg.), of PADA increases with $x$, tending to that of poly-DL-alanine, as listed in Table III. The film of PADA occupies a larger area on the aqueous subphase containing salt than on distilled water, as shown in Fig. 7, but salt has no influence on poly-DL-alanine film.

The limiting area expressed in $m^2$/mg. is reduced to that in $Å^2$ per average DL-alanyl residue by

$$A_{\Pi\to 0}(Å^2/\text{residue}) = \frac{10^{23}}{N}\left(M_A + \frac{M_B}{x}\right) A_{\Pi\to 0}\ (m^2/\text{mg.}) \quad (1)$$

if the residue weight of dodecylamine is equally distributed over alanyl residues. Here $N$ is the Avogadro number, and $M_A$ and $M_B$ are residue weight of alanine (71) and dodecylamine (184), respectively. In Eq. 1 $x$ is assumed to be infinite for poly-DL-alanine film.

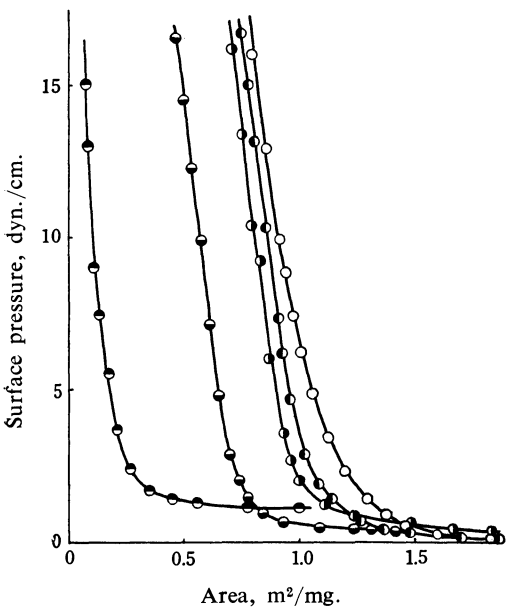



Fig. 6. Surface pressure vs. area curves of PADA and poly-DL-alanine on distilled water at 18°C. PADA: ◓, $x$=5; ◒, $x$=10; ◑, $x$=15; ◐, $x$=20; ○, poly-DL-alanine

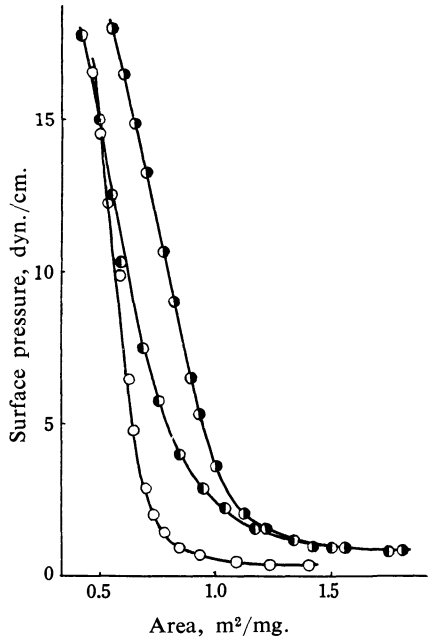



Fig. 7. Effect of salts on the surface pressure vs. area curves of PADA with $x$=10 at 18°C. ○, no salt; ◐, 0.01 M potassium carbonate; ◑, 0.2 M potassium chloride

TABLE III. LIMITING AREAS AND $f$ VALUES OF PADA AND POLY-DL-ALANINE

| $x$ | On distilled water $A_{\Pi\to 0}$ | | | On 0.01 M $K_2CO_3$ $A_{\Pi\to 0}$ | | | On 0.2 M KCl $A_{\Pi\to 0}$ | | |
|---|---|---|---|---|---|---|---|---|---|
| | $m^2$/mg. | $Å^2$/residue | $f$ | $m^2$/mg. | $Å^2$/residue | $f$ | $m^2$/mg. | $Å^2$/residue | $f$ |
| 5 | 0.26 | 4.7 | 0.05 | — | — | — | — | — | — |
| 10 | 0.74 | 11.0 | 0.64 | 0.89 | 13.3 | 0.81 | 1.07 | 15.9 | 0.99 |
| 15 | 0.98 | 13.5 | 0.87 | 1.09 | 15.0 | 0.98 | 1.11 | 15.3 | 1.00 |
| 20 | 1.06 | 14.1 | 0.94 | — | — | — | — | — | — |
| Poly-DL-alanine | 1.18 | 14.0 | — | — | — | — | 1.18 | 14.0 | — |

Since the limiting area of long chain alkylamine or alkylamide is about 20 Å$^2$ per molecule[18] and that of poly-DL-alanine is 14 Å$^2$ per residue, PADA should have a limiting area

$$A_{\Pi\to 0}(\text{Å}^2/\text{residue}) = \frac{20+14x}{x} \qquad (2)$$

if it spreads completely as a monomolecular film. While the observed value of the limiting area of PADA on aqueous salt solution such as 0.01 M potassium carbonate or 0.2 M potassium chloride is found to agree with the value calculated from Eq. 2, that obtained on distilled water is smaller than the calculated value. In the latter case, a part of hydrophilic poly-DL-alanine part might be submerged into water. If it is assumed that $xf$ DL-alanyl residues and a dodecylamino residue in a PADA molecule form a surface film and $x(1-f)$ DL-alanyl residues are submerged into water the limiting area of PADA may be expressed by

$$A_{\Pi\to 0}(\text{Å}^2/\text{residue}) = \frac{20+14xf}{x} \qquad (3)$$

Substituting the observed values of limiting area for $A_{\Pi\to 0}$(Å$^2$/residue) in Eq. 3, the values of $f$ are obtained as given in Table III.

It is interesting to note that, while PADA becomes more hydrophilic and more soluble in water as $x$ is larger, in surface film it spreads more; that is, more DL-alanyl residues in a molecule exist on an aqueous surface. This observation may be interpreted as follows: When PADA of lower $x$ is compressed, the van der Waals attraction between dodecyl groups is so strong that some of DL-alanyl residues are forced to be submerged into water. For PADA of higher $x$, however, a hydrogen-bonded conformation[19-21] of poly-DL-alanine part will remain unbroken on compression, since the hydrogen bonding is more predominant than van der Waals cohesion.

18) N. K. Adam, "Physics and Chemistry of Surfaces", Oxford University Press (1940), p. 50.
19) C. W. N. Cumper and A. E. Alexander, *Trans. Faraday Soc.*, **46**, 235 (1950).
20) J. T. Davies, ibid., **49**, 949 (1953).
21) T. Isemura and S. Ikeda, This Bulletin, **32**, 178 (1959).

**Summary**

Poly-DL-alanine alkyl amide has been synthesized by the polymerization of *N*-carboxy-DL-alanine anhydride initiated with alkyl amine at different anhydride-initiator ratios ([A]/[I]). The amphipathic properties of poly-DL-alanine dodecylamide (PADA) with [A]/[I] = 5 to 20 have been investigated in comparison with poly-DL-alanine.

The degree of polymerization of poly-DL-alanine part can be easily controlled by the initial [A]/[I] ratio. The number average degree of polymerization ($x$) is found to be approximately equal to [A]/[I].

The solubility of PADA in water is higher as $x$ increases, and PADA with $x>17$ is transparently soluble. PADA with any $x$ value is soluble in aqueous acid solutions, the pH of which is lower than 5.5. The titration curve with an aqueous acid solution shows a break at this pH.

The infrared spectra of PADA in the solid state indicate that PADA with higher $x$ is almost in the random conformation and the portion of the $\beta$-conformation increases as $x$ becomes lower.

Surface tension of PADA in aqueous acid solution exhibits typical characteristics of amphipathic substances. The degree of surface tension lowering at low concentration region is the largest for PADA of $x=10$.

The surface film of PADA is of condensed type and the limiting area is larger as $x$ increases. PADA with higher $x$ becomes more spread as surface film, more DL-alanyl residues being on the aqueous surface.

*Institute for Protein Research and Faculty of Science*
*Osaka University, Kita-ku, Osaka*

# *On the Temperature Dependence of Spectra of Solvated Anions*

By Akira MARUYAMA*, Mitsuo SHIMOJI and Kichizo NIWA

(Received February 20, 1961)

Recently it has been noticed that the ultraviolet spectra of solvated halide ions depend upon the temperature. The bands in the ultraviolet region are considered to be due to the charge transfer from the ion to the solvent. However, with respect to the details of the mechanism, different models have been proposed by several authors. In particular, these models seem to lead to different conclusions on the effect of temperature.

In this paper, it is shown that the differences existing among the previous theories are only apparent in character, and some experimental data on the temperature dependence of the ultraviolet spectra of solvated iodide ions are given.

## Experimental and Results

Measurements of absorption spectra were carried out with a Hitachi EPU-2 type spectrophotometer. The temperature was varied in the range 5~60°C and was kept constant within ±1°C, circulating the thermostatted water in the cell box by means of a small pump.

The absorption spectra for potassium iodide, ammonium iodide, codmium iodide, cobalt(II) iodide and bismuth(III) iodide in their aqueous solutions ($10^{-5}$ mol./l.) have a common maximum wavelength irrespective of the cations (for example 225 mμ at 12°C) in agreement with the data of many authors[1,2]. As is well known, this maximum can be ascribed to the existence of the iodide ion in such dilute solutions. In Table I the values of

TABLE I. WAVELENGTHS OF MAXIMUM ABSORPTION (mμ) OF IODIDES ($10^{-5}$ M IN WATER) AT SEVERAL TEMPERATURES

| Temp., °C | KI | $CdI_2$ | $BiI_3$ |
|---|---|---|---|
| 6.5 | 225.4 | 225.3 | 225.2 |
| 25.2 | 226.1 | 226.0 | 226.0 |
| 41.6 | 227.2 | 227.0 | 227.1 |
| 60.5 | 228.1 | 228.5 | 228.3 |

the maximum wavelength ($\lambda_{max}$) of potassium iodide, cadmium iodide and bismuth(III) iodide ($10^{-5}$ mol./l. aqueous solution) are shown with the error of ±0.2 mμ. In Fig. 1 the temperature dependence of the energy maximum ($h\nu_{max}$) calculated from $\lambda_{max}$ obtained is recorded. The slope in Fig. 1 gives $d(h\nu_{max})/dT = -32$ cal. deg$^{-1}$ mol$^{-1}$, where $h$ is Planck's constant. This is in agreement with the value of Smith and Symons[2]. Present results, that $d(h\nu_{max})/dT \approx -30$ cal. deg$^{-1}$ mol$^{-1}$ in these solutions, are in agreement with those obtained in many solvent systems[2-4]. Some theoretical considerations for this fact, i. e. the shift to longer wavelength with increasing temperature, will be given in the next section.

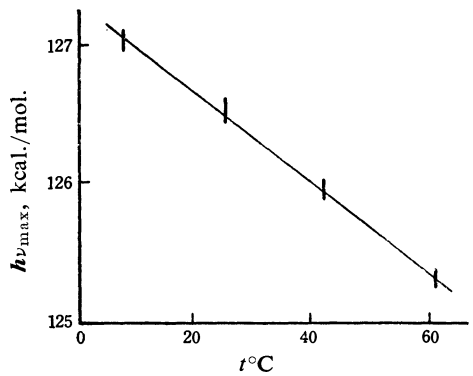



Fig. 1. $h\nu_{max}$ of $I^-$ in aqueous solution ($10^{-5}$ mol./l.).

## Discussion

Many anions dissolved in polar liquids such as water exhibit absorption spectra in the ultraviolet region. These spectra are considered to be due to an electron transfer from the solvated anion to a quantum state, which is yielded by the resultant atom, the adjacent water molecules, and the external polarized dielectrics. The electron transfer is so fast that the positions of all atomic nuclei in all solvent molecules may be regarded as fixed throughout the transition process in accordance with the Franck-Condon principle. In other words the process may be regarded as a sort of non-equilibrium state associated with electron transition. From this point of view Platzman and Franck[5] calculated the positions of the absorption bands of the aqueous halide

* Present adress: Totsuka works, Hitachi Ltd., Yokohama.

1) G. Scheibe, *Z. physik. Chem.*, **B5**, 355 (1929).

2) M. Smith and M. C. R. Symons, *Trans. Faraday Soc.*, **54**, 338 (1958).

3) E. Lederle, *Z. physik. Chem.*, **B10**, 121 (1930).

4) E. M. Kosower, R. L. Martin and V. W. Meloch, *J. Chem. Phys.*, **26**, 1353 (1957).

5) R. Platzman and J. Franck, *Z. Physik.*, **138**, 411 (1954).

ions. Their theoretical expression for the energy of the absorption $h\nu$ is as follows.

$$h\nu = E_x + L_{x^-} + \{\chi - L_x\} - B \quad (1)$$

Here $E_x$ is the electron affinity of the atom X, and $L_x$ and $L_{x^-}$ are the differences of energies associated with the solvation of the atom and of the ion, respectively. $\chi$ is the energy required to form the average solvation configuration of the solvent molecules (i. e. the correction term based on the Franck-Condon principle), and $B$ is the energy of the excited electron resulting from the Coulombic force of the polarized solvent (i. e. hydrogen-like states) and from the electronic polarization induced by the electron in the excited state.

$$B = \frac{2\pi^2 me^4}{h^2 2^2} Z^2_{\text{eff}} + \frac{1}{3}\frac{\pi^2 e^4 m}{h^2} Z_{\text{eff}}\left(1 - \frac{1}{D_{\text{op}}}\right) \quad (2)$$

and

$$Z_{\text{eff}} = \left(\frac{1}{D_{\text{op}}} - \frac{1}{D_s}\right) \quad (3)$$

where $D_{\text{op}}$ and $D_s$ are the optical and static dielectric constants, $m$ is the mass of an electron. The values of $h\nu$ calculated by using Eq. 1 were in good agreement with the experiment.

However, Smith and Symons[6,7], and Stein and Treinin[8] pointed out that the theory of Platzman and Franck fails to explain changes in the position of the absorption bands caused by changing temperature or solvent. Smith and Symons attempted to avoid the difficulties by adopting the "square well" model. According to this theory the electron after detachment from the ion still remains in the cavity previously occupied by the ion. Then the energy of the absorption $h\nu$ is given by

$$h\nu = E_x + \frac{h^2}{8mr_o^2} \quad (4)$$

where $r_o$ is an empirical parameter which was introduced by Smith and Symons. This parameter may roughly be regarded as the radius of the spherical cavity. However, it is unlikely that the order of magnitude of $r_o$ corresponds to any physically meaningful value, because it is greater (for example 4Å for $I^-$) than any value that may be reasonably expected. Stein and Treinin[8] modified the Platzman-Franck theory by introducting the concept of a variable radius parameter $r^*$ as suggested by Smith and Symons. Their equation is given as

$$h\nu = E_x + (S_{\text{ion}} + E_p) - L_x - B \quad (5)$$

where

$$S_{\text{ion}} + E_p = \frac{e^2}{r^*}\left(\frac{1}{2} + \frac{1}{2D_{\text{op}}} - \frac{1}{D_s}\right) \quad (6)$$

The difference between Platzman-Franck's Eq. (1) and Smith-Symon's (5) is that $(S_{\text{ion}} + E_p)$ in Eq. 5 takes the place of $(I_{x^-} + \chi)$ in Eq. 1. According to Stein and Treinin the valnes of the radius parameter $r^*$ obtained from the spectroscopic data on the basis of Eq. 5 were in good agreement with the apparent ionic radii estimated from partial ionic volumes. The temperature dependence of $h\nu$ was also explained in terms of the change of the radius of the cavity (or ionic radii), $dr^*/dT$. They emphasized that Franck and Platzman's procedure, taking into account $L_{x^-}$ and $\chi$, is inadequate for the treatment of the temperature dependence.

However, the concept of ionic radii in liquids corresponds to the rigid sphere model of liquids, and may be regarded as an appoximation for the behavior of liquids. The apparent ionic radii should be determined more rigorously from the relation between the total energy and ion-molecule distances. Thus Eq. 5 should in principle coincide with Eq. 1 apart from minor differences of mathematical expressions. Hence, the temperature dependence of $h\nu$ will be considered here without using the concept of the radius parameter $r_o$.

In Platzman-Franck's equation the effect of temperature may be prominent in the terms $L_{x^-}$, $\chi$ and $L_x$, since these factors strongly depend on the positions of nuclei. The terms caused by the electronic polarization or the electronic motion can be unimportant, since $dD_{\text{op}}/dT$ and $dD_s/dT$ are so small that the calculated value for $d(h\nu_{\max})/dT$ is at most about 1/10 of the observed values. Thus one can write

$$\frac{d(h\nu)}{dT} = \frac{d\{L_{x^-} - (I_x - \chi)\}}{dT} \quad (7)$$

It seems to be impossible to define $d(L_x - \chi)/dT$ in Eq. 7 by the usual thermodynamic method, though $d(L_{x^-})/dT$ simply denotes the change of the thermodynamic specific heats $\Delta C_{x^-}$ as the following:

$$\frac{d(L_{x^-})}{dT} = \Delta C_{x^-} = C^g_{x^-} - C^s_{x^-} \quad (8)$$

where $C^g_{x^-}$ and $C^s_{x^-}$ show the specific heats of the ion in vacuo and in the solvent, repectively. As was noted by Stein and Treinin, $\Delta C_{x^-}$ of the process $X^-$ (in solvent) $\rightarrow X^-$ (in

6) M. Smith and M. C. R. Symons, *Discuss. Faraday Soc.*, **24**, 206 (1957).
7) M. Smith and M. C. R. Symos, *Trans. Faraday Soc.*, **54**, 346 (1958).
8) G. Stein and A. Treinin, ibid., **55**, 1086 (1959).

vac.) can be positive. On the other hand, for the neutral atom X one can write

$$\frac{d(L_x-\chi)}{dT}=\Delta C_{x^*}=C^g{}_{x^*}-C^s{}_{x^*} \qquad (9)$$

corresponding to Eq. 8. However, $C^s{}_{x^*}$ does not denote the specific heat of the ion in the solvent to be defined in the equilibrium state, since $(L_x-\chi)$ does not correspond to the stable configuration for the atom. Substituting Eqs. 8 and 9 into Eq. 7, one obtains

$$\frac{d(h\nu)}{dT}=(C^g{}_{x^-}-C^g{}_{x^*})-(C^s{}_{x^-}-C^s{}_{x^*}) \qquad (10)$$

Approximately $C^g{}_{x^-}$ is equal to $C^g{}_x$, because both ion and atom are monatomic particles in the gaseous phase and the contribution of electronic states may be disregarded in the range of room temperature. Thus

$$\frac{d(h\nu)}{dT}\approx-(C^s{}_{x^-}-C^s{}_{x^*}) \qquad (11)$$

The configuration of the atomic nuclei, including the solvent molecules, will be similar in $C^s{}_{x^-}$ and $C^s{}_{x^*}$, though the ion-dipole interaction in $C^s{}_{x^-}$ may disappear in $C^s{}_{x^*}$ (i. e. only van der Waals interaction and the exchange repulsive energy). This means that the energy of interaction between the solute and the solvent will be much smaller in $C^s{}_{x^*}$ than in $C^s{}_{x^-}$. Then it is assumed that i) the ion-dipole interaction is so strong that the potential energy between the ion and the solvent molecule can be regarded as a classical vibration energy, and that ii) the interaction between the atom and the solvent molecule is negligibly weak compared with the ion-dipole interaction. Hence, it may be concluded that $(C^s{}_{x^-}-C^s{}_{x^*})$ is mainly due to the vibrational heat capacities (in the sense of classical mechanics) being proportional to the number of solvated molecules (or dipoles), $n$. Thus, from Eq. 11

$$\frac{d(h\nu)}{dT}\approx-kn \qquad (12)$$

where $k$ is the Boltzmann constant. As the order of magnitude of $n$ is usually 10 (for example, 6 to 8 for the first layer of hydration in aqeous solution[9]), $d(h\nu)/dT$ calculated may be about $-20$ cal. deg$^{-1}$ mol$^{-1}$ in agreement with the observed values. The present consideration (12) will, essentially, not be different from the Smith-Symons and Stein-Treinin theories, since the increase of the radius of cavity $r_0$ should correspond to the change in the free energy of the solvated ion caused by the temperature rise. Examples of this sort are found in the models of the free volume for liquids i. e. the harmonic oscillator model and smoothed potential model[10].

## Summary

The effect of temperature on the ultraviolet spectra of solvated anions is examined experimentally and theoretically. The shift of the spectrum to the longer wavelength with increasing temperature can be explained in terms of the oscillator model of the solvent molecules. This corresponds to the increase of the ionic radii (or the radius of the cavity) with the temperature rise.

*Department of Chemistry*
*Faculty of Science*
*Hokkaido University*
*Sapporo*

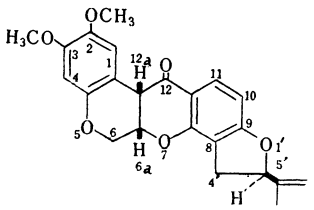
9) E. J. W. Verwey, *Rec. trav. chim.* **61**, 127 (1942).
10) R. H. Fowler and E. A. Guggenheim, "Statistical Thermodynamics", Cambridge, (1939).

# *The Absolute Configuration of Rotenone*[1]

By Masao NAKAZAKI and Hisao ARAKAWA

(Received February 9, 1961)

Rotenone, one of the most powerful vegetable insecticides, was first isolated by Nagai[2] from *Milletia taiwaniana* Nagai, a native of Formosa, and was found to be identical with tubotoxin[4] obtained from *Derris elliptica* which is now widely cultivated.



I

The accepted formula I[5] was advanced independently by Takei[6], Butenandt[7] and LaForge[8] at about the same time (1932).

To study the interesting relationship between the insecticidal action of rotenone and its stereochemistry, the establishment of the absolute configuration is essential. This contribution is concerned with the determination of the absolute configuration at C-5′ carbon atom of rotenone (I).

Tubaic acid (IIa) obtained by the alkaline degradation of rotenone was catalytically hydrogenated to give (−)-dihydrotubaic acid (IIb)[10], which was dissolved in acetic acid and exhaustively ozonolyzed[11] by passing ozone through it for 25 hr. After further oxidation with hydrogen peroxide, oxalic acid was removed as the calcium salt and the solution was passed through the column of Amberite IR-120 to be freed of the excess of calcium ions. The solvent was removed in vacuo and crude 3-hydroxy-4-methyl-pentanoic acid (III) (or IV in Fischer projection) was esterified with diazomethane to give the methyl ester IVb, b. p. 77~86°C/18 mmHg, $[\alpha]_D$+19.0°.

To correlate IVb with D-valine, the methyl ester IVb was converted into the hydrazide IVc, m. p. 152~153°C, $[\alpha]_D$+43°, which was treated with nitrous acid[12] to give (−)-5-isopropyloxazolidone (V), m. p. 113~114°C, $[\alpha]_D$ −44.5°, the structure of which was confirmed by the comparison of the infrared spectrum with the racemic V, m. p. 87~88°C, prepared from the racemic hydroxylic acid IVa[13,14].

(−) Methyl 2-hydroxy-3-methylbutanoate (VIIb), b. p. 62~63°C/15 mmHg, $[\alpha]_D$ −1.4°, which was prepared from D-valine (VI)[15] with retention of configuration[16], was treated with liquid ammonia in a steel bomb to give the (+)-amide VIIc, m. p. 99~101°C, $[\alpha]_D$ +65.10. Lithium aluminumhydride redcution of the amide VIIc afforded the aminoalcohol VIIIa

1) A preliminary note appeared in This Bulletin, **34**, 453 (1961).

2) K. Nagai, *J. Chem. Soc. Japan, Pure. Chem. Sec.* (*Nippon Kagaku Zasshi*), **23**, 744 (1902).

3) T. Kariyone, K. Atsumi and M. Shimada, *J. Pharm. Soc. Japan* (*Yakugaku Zasshi*), **43**, 736 (1923).

4) T. Ishikawa, *Tokyo Igaku Zasshi*, **31**, 187 (1917).

5) In the structure formula I is shown the numbering of carbon atoms employed by Büchi and Crombie (vide infra). The asymmetric carbon atom C-5′, about which this paper is concerned is C-2 according to the numbering used by Miyano and Matsui (vide infra) in their recent synthetic works.

6) S. Takei, S. Miyajima and M. Ono, *Ber.*, **61**, 1041 (1932).

7) A. Butenandt and W. McCartney, *Ann.*, **494**, 17 (1932).

8) F. B. LaForge and H. L. Haller, *J. Am. Chem. Soc.*, **54**, 810 (1932).

9) The configurations of carbon atoms at 6a and 12a seem not to be crucial to the insecticidal action; e. g. (−)-deguelin shows almost the same physiological action as that of (±)-deguelin (S. Takei and S. Miyajima, *Scientific Papers Inst. Phys. Chem. Research* (*Tokyo*), **12**, 946 (1933)). Cahn and coworkers (R. S. Cahn, R. F. Phillipers and J. J. Boam, *J. Chem. Soc.*, **1938**, 513). obtained (+)-isorotenone, the enantiomer of (−)-isorotenone which keeps the original configuration of rotenone at 6a and 12a carbon atoms, from "mutarotenone"; but there seems to have been no study on the comparison of the physiological properties between them. Although Miyano amd Matsui (M. Miyano, A. Kobayashi and M. Matsui, *Chem. Ber.* in press) reported the total synthesis of natural rotenone, the effect of the configuration C-5′ carbon atom has remained unknown, since the enantiomer of natural rotenone could not be prepared.

10) S. Takei and M. Koide, *Ber.*, **62**, 3030 (1929).

11) H. Arakawa and M. Nakazaki, *Chem. & Ind.*, **1959**, 671; **1960**, 173; *Ann.*, **636**, 111 (1960); H. Arakawa, This Bulletin, **33**, 200 (1960).

12) C. Schöpf, G. Dummer and W. Wüst, *Ann.*, **676**, 134 (1959); C. Shcöpf and W. Wüst, ibid., **676**, 150 (1959) employed 5-phenyloxazolidone as a relay intermediate when they ralated the absolute configuration of (−)-sedamine and (−)-allosedamine with (+)-mandelic acid.

13) Methyl ester of racemic IVa, b. p. 92~93°C/20mmHg, was prepared by sodium borohydride reduction of ethyl isobutyroylacetate (X). Racemic hydrazide IVc melted at 148~149°C.

14) G. Büchi, J. S. Kaltenbron, L. Crombie, P. J. Godin and D. A. Whiting (*Proc. Chem. Soc.*, **1960**, 274) obtained the racemic IVa by the Reformatsky reaction of isobutyraldehyde and benzyl bromoacetate followed by hydrogenolysis.

15) We are grateful to Dr. Setsuji Sakurai, Ajinomoto Co. for his generous gift of D-valine.

16) W. Klyne, "Pprogress in Stereochemistry", Vol. 1, Butterworth Pub., London (1950), p. 195; E. Fisher and H. Scheibler, *Ber.*, **41**, 2891 (1908); P. D. Bartlett, M. Kuna and P. A. Levene, *J. Biol. Chem.*, **118**, 303 (1937).

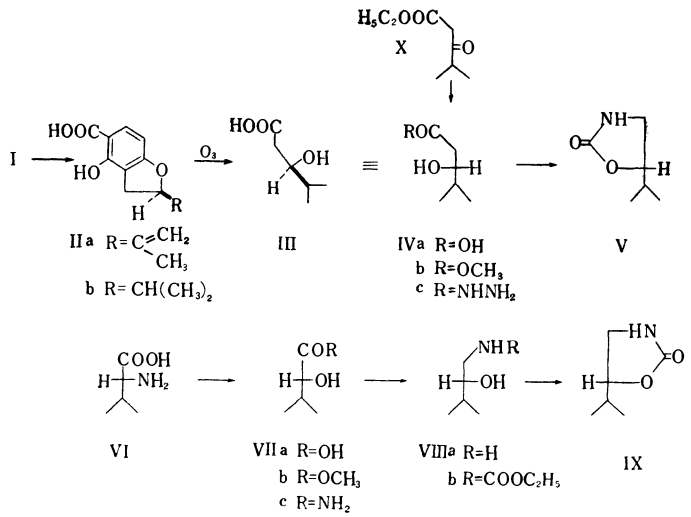



Fig. 1.

which was transformed, via the carbamate VIIIb, into (+)-5-isopropyloxazolidone (IX), m. p. 113~114°C, $[\alpha]_D$ +44.2°.

The fact that 5-isopropyloxazolidone (V and IX) were enatiomorphous was established by comparison of their intrared spectra, which can be superimposed in every detail, moreover, a mixed melting point determination of the 5-isopropyloxazolidone synthesized from the racemic hydroxylic acid IVa with the racemic compound prepared by mixing equal parts of (−)-5-isopropyloxazolidone from rotenone and (+)-5-isopropyloxazolidone from D-valine and recrystallization from benzene showed no depression. These facts clearly show, as can be seen from Fig. 1, that rotenone has (R)-configuration at the carbon atom C-5′ as illustrated in I.

During the course of this investigation, Büchi and Crombie[14] published a short communication in which they reported the same conclusion. They ozonolyzed (−)-dihydrotubaic acid (IIb) to obtain (+)-3-hydroxy-4-methylpentanoic acid (IVa). In order to secure enough starting material, they synthesized (±)-IVa and resolved via the quinine salt obtaining (−)-acid (enantiomer of III from rotenone) which they converted via three steps into (−)-2-methylpenta-3-ol with known configuration.

Thus we could confirm Büchi and Crombie's result[17], although our approach appears more direct and simple, giving well defined crystalline compounds in each step, which will be proved to be useful as key compounds in establishing absolute configuration of other compounds.

17) They also succeeded in establishing (S)-configuration at 6a carbon atom by the exhaustive ozonolysis of acetyldihydrorotenone to obtain D-glyceric acid in the form of its *p*-bromophenacyl ester. See Ref. 14.

## Experimental

**Dihydrotubaic Acid (IIb).**—IIb was prepared according to Takei and Koide's procedure, m. p. 166°C, $[\alpha]_D^{25}$ −103.7° (*c* 1.08, methanol).

Found: C, 64.88; H, 6.25. Calcd. for $C_{12}H_{14}O_4$: C, 64.85; H, 6.35%. (literature[10], m. p. 168°C, $[\alpha]_D$ −82.67°, chloroform).

**Exhaustive Ozonolysis of Dihydrotubaic Acid (IIb).**—To a solution of 4.4 g. of dihydrotubaic acid (IIb) in 70 cc. of 95% acetic acid, was passed ozone at room temperature for 25 hr. The color of the solution changed from colorless to brown after 5 min., and pale yellow after 30 min. and then colorless again. After 8 cc. of 30% hydrogen peroxide was added, the solution was kept at room temperature for 17 hr, then 50 cc. of water was added with a small amount of palladium-carbon to decompose the excess of hydrogen peroxide. In order to remove oxalic acid, 2 g. of calcium acetate was added and the resulting precipitate was filtered. After the solution was freed from excess calcium ion by passing through a column of Amberite IR-120, the solution was concentrated in vacuo to give a syrup which was dried in a vacuum desiccator overnight. The viscous hydroxylic acid III was dissolved in a small amount of methanol and esterified with excess diazomethane solution in ether. After being allowed to stand overnight and being dried over anhydrous sodium sulfate, the solution was concentrated, giving a pale yellow residue which was distilled in vacuo, b. p. 77~86°C/18 mmHg, 0.95 g. $[\alpha]_D^{20}$ +19.0° (*C* 5.77, ethanol).

**(+)-3-Hydroxy-4-methylpentanhydrazide (IVc).**—To a solution of 0.95 g. of the methyl ester IVb in 20 cc. of ethanol, 2 g. of 80% hydrazine hydrate solution was added and the mixture was heated on a water bath for 1 hr. After standing in a refrigerator overnight, the solid mass obtained was

recrystallized from ethanol giving crystals, m. p. 151~153°C, $[\alpha]_D^{19}$ +38~−40° (ethanol), 0.32 g. To prepare an analytical sample the product was recrystallized from ethanol, m. p. 152~153°C, $[\alpha]_D^{19}$ +43°) (*c* 1.01, ethanol).

Found: N, 19.14. Calcd. for $C_6H_{14}O_2N_2$: N, 19.17%.

**(−)-5-Isopropyloxazolidone (V).**—After 10 cc. of benzene was added to a solution of 0.3 g. of the hydrazide IVc in 10 cc. of 1N hydrochloric acid, a solution of 1.5 g. of sodium nitrite in 2 cc. of water was added during 10 min. at 5~6°C with stirring. After being kept at room temperature for 1 hr., the benzene layer was separated and washed with saturated aqueous sodium hydrogen carbonate and dried over calcium chloride for 30 min. When the benzene solution, being freed from the drying reagent, was heated on a water bath at 75°C, generation of nitrogen was observed, and the solution was refluxed for 30 min. Removal of the solvent gave crystals (0.22 g.) which were recrystallized from benzene to afford an analytical sample, m. p. 113~114°C, $[\alpha]_D^{18}$ −44.5° (*c* 1.01, ethanol), 70 mg. infrared spectrum (solvent: chloroform) was found completly superimposable on the one of (−)-isomer IX prepared from D-valine.

Found: C, 55.93; H, 8.55; N, 10.98. Calcd. for $C_6H_{11}O_2N$: C, 55.79; H, 8.58: N, 10.84%.

**(−)-Methyl 2-Hydroxy-3-methylbutanoate (VIIb).**—According to Fischer's procedure[16], 4.9 g. of D-valine ($[\alpha]_D^{16}$ −27.6° *c* 2.68, 6N hydrochloric acid) was converted into 2-hydroxy-3-methylbutanoic acid (VIIa). The hydroxylic acid was esterified with diazomethane in ether and the methyl ester VIIb was distilled to give an oil, boiling at 62~63°C/15 mmHg, $[\alpha]_D^{17}$ −1.4° (*c* 9.18, ethanol), 2.4 g.

**(+)-2-Hydroxy-3-methylbutanamide (VIIc).**—A mixture of 2.4 g. of methyl ester VIIb and 8 cc. of liquid ammonia was placed in a steel bomb and kept at 30°C overnight. After heating at 40~45°C for 2 hr., the excess of ammonia was evaporated, giving a residue, which was dissolved in ethanol. Removal of the solvent gave a viscous oil which was caused to solidify by trituration with benzene, m. p. 98~100°C, $[\alpha]_D^{15}$ +62° (*c* 1.0, methanol), 620 mg. The mother liquor was concentrated and the residue was again ammonolyzed with 80 cc. of liquid ammonia by heating at 140°C for 1 hr., and at 100°C for 15 hr. to give 600 mg. of the amide. The crude amides were recrystallized from ethanol-benzene to give crystals, m. p. 95~100°C, $[\alpha]_D^{15}$ +50° (*c* 1.02, methanol), 370 mg. For an analytical sample, the product was recrystallized from benzene, then from methanol, m. p. 99~101°C, $[\alpha]_D^{15}$ +65.1° (*c* 0.76, methanol).

Found: N, 11.82. Calcd. for $C_5H_{11}O_2N$: N, 11.96%.

**(+)-5-Isopropyloxazolidone (IX).**—In the thimble of a modified Soxhlet extractor inserted between the reflux condenser and the reaction flask which contained a slurry of 900 mg. of lithium aluminum-hydride in 100 cc. of tetrahydrofurane, was placed 940 mg. of the amide VIIc. After refluxing for 6 hr., a small amount of water, just enough to decompose the reaction complex, was added and the precipitated aluminum hydroxide was filtered. The aluminum hydroxide was continuously extracted with tetrahydrofurane for 2 hr., and the extract was combined with the filtrate. After 2 cc. of concentrated hydrochloric acid was added, the solvent was removed in vacuo, water was added to the residue and the solution was washed with ether three times. The acidic solution was made alkaline with 6 cc. of 50% potassium hydroxide and saturated with potassium carbonate, and then extracted with ether. After the ether extract was dried over anhydrous potassium carbonate, the solvent was removed to give the aminoalcohol VIIIa, which has an odor reminiscent of amine. The oil was dissolved in 15 cc. of benzene and was allowed to stand overnight. After the precipitated amide (140 mg.) was recovered, 0.7 cc. of pyridine was added with a solution of 0.65 g. of ethyl chloroformate in 4 cc. of benzene. After stirring for 1 hr., the reaction mixture was allowed to stand at room temperature for 1 hr. Ten cubic centimeters of water was added and the aqueous layer, after separating from the benzene layer, was extracted twice with benzene. The combined benzene extract was washed twice with 1 cc. of 1N hydrochloric acid and then with water. After the solvent was removed in vacuo, 10 cc. of benzene was added and evaporated to remove any trace of water by azeotropic distillation giving the carbamate VIIIb, 450 mg. To a sodium methoxide solution which was prepared from 50 mg. of sodium and 3 cc. of methanol, 10 cc. of toluene was added and the methanol was removed by heating with free flame. A solution of 450 mg. of the carbamate VIIIb in 17 cc. of toluene was added to the sodium methoxide suspension and heated at 100~105°C for 1 hr. with stirring. The reaction mixture was chilled in an ice bath and 10 cc. of water was added with stirring. The aqueous layer which separated from the toluene layer, was extracted twice with toluene. The combined toluene extract was concentrated to 5 cc. in vacuo to precipitate crystals which were recrystallized from benzene-benzine (b. p. 70~80°C), m. p. 111~112°C, 200 mg. Recrystallization from benzene raised the melting point to 113~114°C. $[\alpha]_D^{14}$ +44.2° (*c* 1.04, ethanol).

Found: C, 56.18; H, 8.68; N, 11.13. Calcd. for $C_6H_{11}O_2N$: C, 55.79; H, 8.58; N, 10.84%.

**(±)-Ethyl 3-Hydroxy-4-methylpentanoate.**—To a chilled solution of 8 g. of ethyl isobutyroylacetate in 40 cc. of methanol, 5 g. of sodium borohydride was added with stirring during 1 hr., and the reaction mixture was allowed to stand at room temperature for 1 hr. After the methanol was evaporated, water was added and the whole was extracted with choloroform. The chloroform extract was washed with diluted sulfuric acid and then with saturated sodium hydrogen carbonate solution. After drying over anhydrous sodium sulfate, the solvent was removed to give an oil, which distilled at 92~93°C/20 mmHg, 2.9 g.

**(±)-3-Hydroxy-4-methylpentanhydrazide.**—To a solution of 2.6 g. of the above-mentioned ester in 6 cc. of ethanol, was added 6 g. of 80% hydrazine hydrate and the reaction mixture was heated on a water bath for 1 hr. and allowed to stand in a refrigerator overnight. The precipitated crystals

were recrystallized from ethanol yielding crystals, m. p. 148～149°C, 1.72 g.

Found: N, 19.22. Calcd. for $C_6H_{14}O_2N_2$: N, 19.17%.

**(±)-5-Isopropyloxazolidone.**—Following the procedure described for the preparation of the (−)-isomer V, 1.7 g. of the racemic hydrazide was converted into (±)-5-isopropyloxazolidone, m. p. 87～88°C, 0.65 g.

Found: C, 55.88; H, 8.50; N, 11.12. Calcd. for $C_6H_{11}O_2N$: C, 55.79; H, 8.55; N, 10.84%.

The mixed melting point of the synthetic (±)-5-isopropyloxazolidone, m. p. 87～88°C, with the racemic compound, m. p. 87～88°C, which was prepared by mixing equal amounts of (−)-isomer V, m. p. 113～114°C from rotenone and (+)-isomer IX, m. p. 113～114°C from D-valine and recrystallization from benzene, was 87～88°C.

We are indebted to Mr. Mitsuru Notake for his effort in obtaining *Derris elliptica*, and to Nitto Kasei Co. for financial support.

*Department of Chemistry*
*Institute of Polytechnics*
*Osaka City University*
*Kita-ku, Osaka*

# *On Some Dark-colored Chlorocuprates(I, II) and Related Compounds. III. X-Ray Study and Reflectance Measurements*

By Masayasu MORI

(Received February 20, 1961)

In the majority of mixed valence compounds that exhibit abnormal light absorption, the metal atoms in different valence states are bound by atomic bridges or metal-metal bonds[1]. The abnormal light absorption in these compounds is explained as due to an electron transfer through these bonds or bridges[2]. In certain mixed valence halometallates as e. g. $Rb_2SbCl_6$, however, such bonds or bridges are hardly conceivable from crystallographic data, though they also are highly colored. The mechanism of interaction absorption in these compounds may not be essentially different, but is probably more complicated. Examples of such compounds are few: as far as the author is aware they are represented by one of the two general formulae, $M_2SbX_6$[3] and $[M^{III}A_6][PbCl_6]$[4,5]. The X-ray study which will be described below has proved that compounds, $[M^{III}A_6][CuCl_5]_x[CuCl_4]_{1-x}$,[6] constitute another such series. Diffuse reflectance of powdered chlorocuprates was also measured in order to examine the existence and the qualitative feature of the light absorption in these compounds, especially in connection with the problem of interaction color.

## Experimental

**Samples.**—The samples of chlorocuprates used for measurements of reflection were prepared according to the method described in the previous paper. The crystal used in the X-ray analysis was obtained by digesting the precipitate in the mother liquor at 30~40°C.

Hexamminechromium(III) chloride monohydrate which was used in the reflectance measurement and in the preparation of chlorocuprates was prepared by a procedure analogous to that for the preparation of $[Cr(NH_3)_6]_2(SO_4)_3 \cdot 2H_2SO_4 \cdot 3H_2O$, reported previously[7]. At the stage of precipitating the complex, 300 ml. of 12 N hydrochloric acid was used instead of 200 ml. of 12 N sufuric acid, and the yield of the chloride was 23~24 g. (48~50%). The undesirable effect of the impurities in zinc, pointed out in the previous paper could be minimized by amalgamation of metal surfaces by warming granular or mossy zinc in ca. 5% solution of mercury(II) chloride in 1 N hydrochloric acid.

Potassium copper(II) chlorides were prepared by Meyerhoffer's method[8]

**Reflectance Measurements.**—The diffuse reflectance, $R_d$, of chlorocuprates, i. e. the ratio of the

1) J. C. Bailar, Jr. et. al., "The Chemistry of the Coordination Compounds", Reinhold Publishing Corp., New York (1956), p. 19.
2) R. Tsuchida and S. Yamada, *Nature*, **174**, 1064 (1954).
3) K. A. Jensen, *Z. anorg. Chem.*, **232**, 193 (1937); ibid., **233**, 295 (1937); ibid., **252**, 317 (1944).
4) M. Mori, This Bulletin, **24**, 285 (1951).
5) M. Atoji and T. Watanabe, *J. Chem. Phys.*, **20**, 1045 (1952).
6) M. Mori, This Bulletin, **33**, 985 (1960); the chlorocuprates (I, II) in Ref. 6 is expressible in the above formula when the ratio, Cu(II)/Cu(total), is greater than 0.5. The water of crystallization is tentatively omitted in the expression since the percentage is very low (~1%) and hardly distinguishable from that of the adherent humidity.
7) M. Mori, *J. Chem. Soc. Japan, Pure Chem. Sec.* (*Nippon Kagaku Zasshi*), **74**, 253 (1953).
8) W. Meyerhoffer, *Z. physik. Chem.*, 3, 339 (1889)., ibid., **5**, 98 (1890).

quantity of light reflected by a powdered sample to the quantity of light reflected by magnesium oxide powder was measured with a Shimazu spectrophotometer, Type QR-50, with its integration sphere attachment, in the wave number range of $(1.4\sim3.0)\times10^4$ cm$^{-1}$.

**Crystal Analysis.**—Oscillation photographs of a small crystal of $[Cr(NH_3)_6][CuCl_5]_x[CuCl_4]_{1-x}$ were taken using Cu-$K\alpha$ radiation. The relative intensities of reflections were visually estimated and corrected for Lorenz and polarization factors by means of Cochran's chart[9]. The observed structure factors obtained in this way were compared with the calculated factors by the trial and error method. The lattice constant was determined with an X-ray diffractometer using Cu-$K\alpha_1$ radiation ($\lambda=1.5405$ Å).

## Results and Discussion

**The Crystal Structure of $[Cr(NH_3)_6][CuCl_5]_x[CuCl_4]_{1-x}$.**—From the oscillation data the crystal was found to have an $O_h$ symmetry, and only those reflections were observed which fulfilled the following conditions:

1) $h+k=2n$, $k+l=2n$, $l+h=2n$;

2) $h+k=4n$ for $(h\,k\,0)$ reflections;

3) $h\neq k$, $k\neq l$, $l\neq h$ for odd indices.

The space group is therefore determined to be $O_h^8$–Fd3c. The unit cube edge is $a=22.19+0.02$ Å, and the unit cell contains 32 of the above formula units. The observed density was 1.89 g./cc. and the calculated density is 1.84 g./cc. for $x=0.5$ and 1.92 g./cc. for $x=1$. There has been an ambiguity as to the $x$ value, i. e. the ratio, Cu(II)/Cu(total) for the sample used in X-ray work*.

General features of the intensity distribution were found to be similar to those observed for the chlorocuprate(II) of the same complex cation studied by Mori, Saito and Watanabe[10]. In the latter compound, 160 chlorine atoms in the unit cell are classified into two groups, those in 64 (e) equivalent positions and those in 96 (g) equivalent positions. In the case of chlorocuprate(I, II) the number of chlorine atoms should be smaller than 160 by $32(1-x)$. An attempt was made to obtain the value of $x$ by the method of least square, on the assumption that in chlorocuprate(I, II), either (e) or (g) equivalent positions are incompletely occupied. However, either assumption gave an $x$ value slightly greater than unity ($\sim1.03$). It is ridiculous to assume an $x$ value greater than unity, but it is probable that $x$ has been close to unity, for the sample crystal was prepared by a long digestion of the precipitate in the mother liquor, during which the quantity of univalent copper has probably decreased by air oxidation. The observed structure factors were, therefore, compared with those calculated on a tentative assumption of $x=1$ and the same atomic coordinates as those obtained for the chlorocuprate(II) (Table I). This comparison gave a fairly low $R$ (reliability factor) value, namely 0.152 for $(h\,k\,0)$ reflections (unobserved reflections included as $F_0=0$), and 0.212 for $(h\,k\,l)$ reflections up to $l=8$ (unobserved reflections excluded). Thus the present research could not find out the difference between the crystal structure of chlorocuprate (I, II) and that of chlorocuprate(II), although the sample crystal of chlorocuprate(I, II) appeared almost black in contrast to the yellow chlorocuprate(II) crystal. Because of the presence of heavy atoms, further refinement including the determination of the structure of chlorocuprate(I) ion probably necessitates more accurate intensity data for a sample with a higher Cu(I) content as well as a simultaneous study of chromium and cobalt compounds.

Table I. Atomic coordinates in chlorocuprate(I, II)

32 Cu: (b), 1/4, 1/4, 1/4, etc.
32 Cr: (c), 0, 0, 0, etc.
(64) Cl: (e), $u$, $u$, $u$ ($u=0.190$), etc.
(96) Cl: (g), 1/4, $v$, $-v$ ($v=0.075$), etc.
192 N: (h), $x$, $y$, $z$ ($x=0.070$, $y=0.050$, $z=-0.030$), etc.
$B$ (overall temperature factor): 2.5.

The information obtained is, therefore, that in hexamminechromium(III) chlorocuprate(I, II), too, the Cr and Cu atoms are arranged in the NaCl type and that the ionic species of Cu(II) is the trigonal-bipyramidal $[CuCl_5]^{3-}$ ion, the same ion as is found in the chlorocuprate(II). The chart prepared with a self-recording X-ray diffractometer for a powder sample of chlorocuprate(I, II) for which $x$ was nearly equal to 0.5 also showed relative intensities similar to those for the chlorocuprate(II). The essential feature of the crystal structure of chlorocuprate(I, II), therefore, seems to be unaltered even when $x$ approaches 0.5**. In particular, the Cu–Cu distance should remain about the same ($\sqrt{2}a/4=7.79$ Å), since any change in the Cu coordinate must result in a remarkable change in the structure factors. It

9) W. Cochran, *J. Sci. Instr.*, **25**, 253 (1948).

* Attention was not at first paid to this problem, for it was some time later that the author found the composition of the chlorocuprate(I, II) to be changeable.

10) M. Mori, Y. Saito and T. Watanabe, This Bulletin, **34**, 295 (1961).

** For $x$ below this value the ratio Cu/Cr is not 1:1 any more (Ref. 6).

is, therefore, difficult to assume anything like an atomic bridge between copper atoms in hexamminechromium(III) chlorocuprate(I, II) of a low Cu(I) content.

**Reflectance of Powdered Chlorocuprates.**—In presenting the data of reflectance measurements it seems convenient to use Kubelka and Munk's expression[11], $f(R_d)=(1-R_d)^2/2R_d$, for there is a certain parallelism between this quantity and the extinction coefficient of the crystal—they should be proportional to one another when the effect of the specular reflection at crystal surfaces is small compared with the diffuse reflection. Kortüm and Schöttler[12] stated that this condition is nearly fulfilled for potassium permanganate and its mixed crystals when the powder is very fine. Kondo and others[13] examined this problem in detail by comparing the reflection data with the absorption curve of a single crystal and found that even when the powder is sufficiently fine some effect of specular reflection makes the curve of $(1-R_d)^2/2R_d$ somewhat different from the true extinction curve of potassium permanganate, and that some caution must be exercised when reflectance is measured for substances of varying refractive indices.

In the present research, use was made of this powder method, because: (1) the process of measurement is very simple and the experiment is at any rate possible even when the compound does not crystallize in thin plates; (2) the light reflected from crystal surfaces of most chlorocuprates studied appeared white to the naked eye, so that at least in the visible region the effect of the specular reflection was thought to be smaller than in the case of potassium permanganate, in which case the light reflected from crystal surfaces seems green; and (3) the main purpose was to examine the existence and the qualitative feature of usually very broad interaction absorption in the visible region. In Figs. 1—4 is plotted the quantity, $\log[(1-R_d)^2/2R_d]$ for various chlorocuprates against wave number.

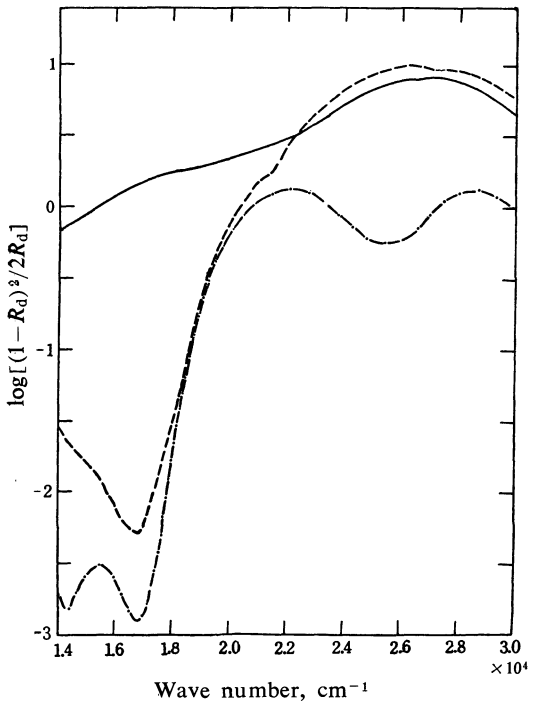



Fig. 1. Curves of $\log[(1-R_d)^2/2R_d]$ for hexamminechromium(III) chlorocuprates.

—— Curve $A_1$, $[Cr(NH_3)_6][CuCl_5]_x[CuCl_4]_{1-x}$ ($x\sim0.5$)
---- Curve $B_1$, $[Cr(NH_3)_6][CuCl_5]$
-·-· Curve $C_1$, $[Cr(NH_3)_6]Cl_3\cdot H_2O$

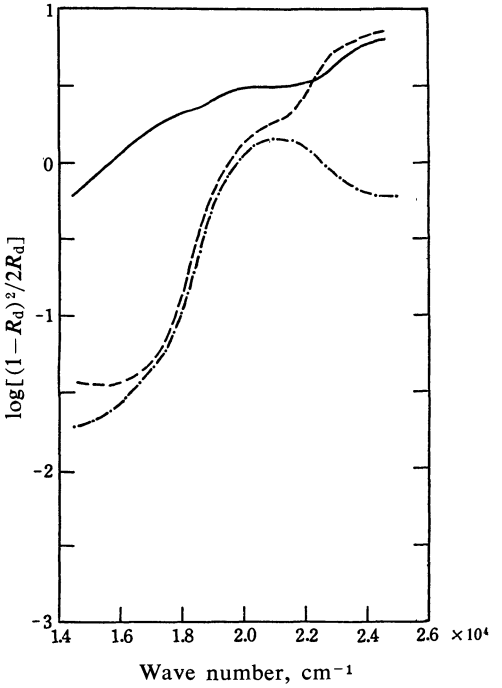



Fig. 2. Curves of $\log[1-R_d)^2/2R_d]$ for hexamminecobalt(III) chlorocuprates.

—— Curve $A_2$, $[Co(NH_3)_6][CuCl_5]_x[CuCl_4]_{1-x}$*
---- Curve $B_2$, $[Co(NH_3)_6][CuCl_5]$
-·-· Curve $C_2$, $[Co(NH_3)_6]Cl_3$

* The value of $x$ was determined by iodometry to be in the neighborhood of 0.7 although this analytical method is not adequate for the cobalt compound (Ref. 6).

11) P. Kubelka and F. Munk, *Z. techn. Physik.*, **12**, 593 (1931).
12) G. Kortüm and H. Schöttler, *Z. Elektrochem.*, **57**, 353 (1953).
13) Y. Kondo and T. Uemura, Pvesented at the Symposium on Coordination Chemistry of the Chemical Society of Japan, November, 1957; T. Uemura, Y. Kondo and S. Fujieda, ibid., September, 1960.

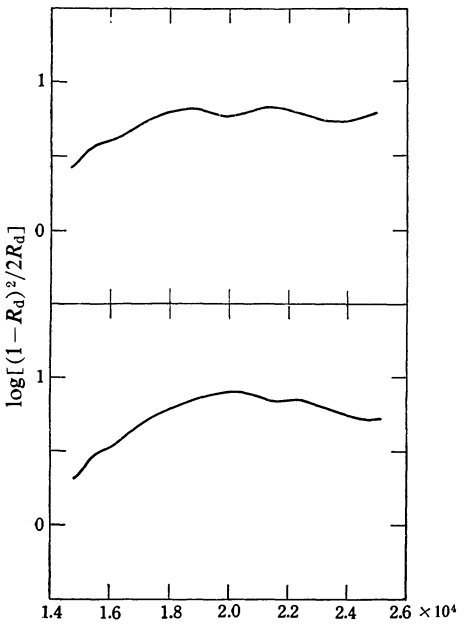



Fig. 3. Curves of $\log[(1-R_d)^2/2R_d]$ for chloroplumbates(II, IV).
Upper: Curve $A_3$, $[Co(NH_3)_6][PbCl_6]$
Lower: Curve $B_3$, $[Cr(NH_3)_6][PbCl_6]$

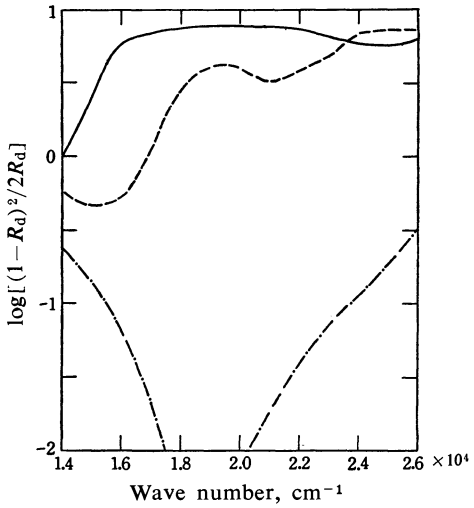



Fig. 4. Curves of $\log[(1-R_d)^2/2R_d]$ for some copper complexes.
—— Curve $A_4$, $[Cr(NH_3)_6][CuBr_5]$
-·-· Curve $B_4$, $[CuCl_2(H_2O)_2]\cdot 2KCl$
---- Curve $C_4$, $KCuCl_3$

*Hexamminechromium(III) Chlorocuprate(I, II), Hexamminechromium(III) Chlorocuprate(II) and Hexamminechromium(III) Chloride Monohydrate (Curves $A_1$, $B_1$ and $C_1$ Respectively in Fig. 1).*— Curve $A_1$ of the chlorocuprate(I, II) shows an existence of interaction absorption in the entire visible region, which is not observed in the case of the chlorocuprate(II) (curve $B_1$) or the chloride (curve $C_1$). At the same time both curves $A_1$ and $B_1$ show very great value of $\log[(1-R_d)^2/2R_d]$ (poor reflection) in the neighborhood of $2.7\times10^4$ cm$^{-1}$, suggesting the existence of strong absorption bands. It seems difficult to determine the exact positions of their peaks, owing to the insufficient accuracy of this method for low reflection values*, to the probable contribution of the specular reflection in this region and also to the effect of the complex cation; but there seems to be little doubt as to their high intensity. These absorption bands are probably charge transfer spectra[14,15] of $[CuCl_5]^{3-}$ ion; the chloride shows no such strong absorption in this region (curve $C_1$). That similar bands are observed for both chlorocuprate(II) and chlorocuprate(I, II) seems to be consistent with the result of X-ray analysis, which shows that in either compound the ionic species of Cu(II) included is the trigonal-bipyramidal $[CuCl_5]^{3-}$ ion.

The qualitative features of curves $A_1$ and

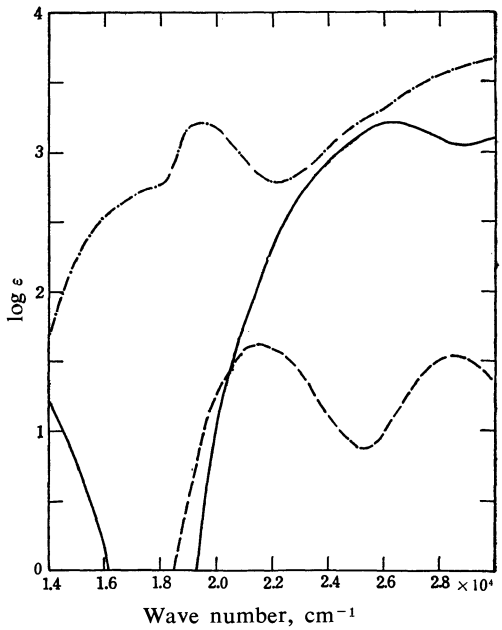



Fig. 5. Absorption spectra (in log ε*) of some aqueous solutions.
—— Curve $A_5$, 0.000124 M $CuSO_4$ in 10 N HCl
-·-· Curve $B_5$, 0.000087 M $CuSO_4$ in 8.7 N HBr
---- Curve $C_5$, 0.0216 M $[Cr(NH_3)]Cl_3$
* ε is expressed on the basis of g. ion Cu or Cr.

* Prof. Yukio Kondo of St. Paul's University kindly suggested that measurements with samples diluted with white substances are effective in these instances. The present author, therefore, wishes to apply this method to a more comprehensive study of halocuprates(II) as soon as possible.

14) E. Rabinowitch, *Rev. Modern Phys.*, 14, 112 (1942).
15) L. E. Orgel, *Quart. Rev.*, 8, 422 (1953).

$B_1$ are somewhat similar to those of the absorption curves of systems, copper(II)-copper (I) and copper(II) respectively, in concentrated calcium chloride solution, studied by Doehlemann and Fromherz[16], when the effect of the complex cation is taken into account (cf. also curves $A_5$ and $C_5$ in Fig. 5). The resemblance is probably not sufficient to prove that the ionic species is the same, but it may be worth noting that the compounds of this series are the only chlorocuprates in which an interaction color of copper(I) and copper(II) is observable, just as in the case of chloride solution.

Usefulness of reflectance measurements for samples with weak absorption bands may be exemplified by the comparison of the $\log f(R_d)$ curve of the powder sample (curve $C_1$, Fig. 1) with the $\log \varepsilon$ curve of an aqueous solution (curve $C_5$, Fig. 5) for the same stable complex compound, $[Cr(NH_3)_6]Cl_3 \cdot H_2O$. The peaks of the two absorption bands are found at almost the same positions although the heights of the peaks are found to be somewhat different. Moreover, a low peak is clearly perceptible at $1.55 \times 10^4$ cm$^{-1}$ in curve $C_1$, which probably corresponds to the transition of the $d_\varepsilon$ electron. It is not easy to find this peak even by absorption measurements when a sample solution is dilute.

*Hexamminecobalt(III) Chlorocuprate(I, II), Hexamminecobalt(III) Chlorocuprate(II) and Hexamminecobalt(III) Chloride (Curves $A_2$, $B_2$ and $C_2$, Respectively in Fig. 2).*—The general feature of the curves is quite similar to that of the corresponding chromium(III) compounds, except in the case of the difference of the position of the absorption peaks of hexammine complex cation.

*Hexamminecobalt(III) and Hexamminechromium(III) Chloroplumbates(II, IV) (Curves $A_3$ and $B_3$ Respectively in Fig. 3).*—Reflectance is very small in the entire visible region showing an existence of interaction absorption of Pb(II) and Pb(IV).

*Hexamminechromium(III) Pentabromocuprate (II) (Curve $A_4$ in Fig. 4).*—Reflectance is very small in the visible region, but it increases a little toward the lower wave number region. The relationship is somewhat similar to the absorption curve of $CuSO_4$ in 48% hydrobromic acid (curve $B_5$, Fig. 5)**. The flattening of the curve at the range of low reflectance is probably due to the effect of the specular reflection.

*Dipotassium Copper(II) Tetrachloride Dihydrate and Potassium Copper(II) Trichloride (Curves $B_4$ and $C_4$ Respectively in Fig. 4).*—Reflectance of these salts was measured for comparison with that of chlorocuprates described above. The former compound, which is known to have the structure, $[CuCl_2(H_2O)_2] \cdot 2KCl$[17,18], shows much weaker absorption in the neighborhood of $2.7 \times 10^4$ cm$^{-1}$ than do the chlorocuprates described above, and the charge transfer band seems to lie at the region of higher wave number. This has been ascertained by measurements up to wave number $3.0 \times 10^4$ cm$^{-1}$, though the curve is given only in the range, $(1.4 \sim 2.6) \times 10^4$ cm$^{-1}$.

In the case of $KCuCl_3$ the curve obtained is very different from those of other chloro complexes of copper studied in the present research or the absorption curve of copper(II) in a solution of high chloride concentration. This difference suggests that in $KCuCl_3$, copper(II) exists in a state quite different from those in the usual chlorocomplexes;—a polynuclear structure with chlorine bridges might, for example, be assumed as in the case of $CsCuCl_3$[19].

## Summary

The ionic species of Cu(II) in hexamminechromium(III) chlorocuprate(I, II) has been found to be a trigonal-bipyramidal $[CuCl_5]^{3-}$ ion. Reflectance measurements have shown the existence of diffuse interaction absorption in some chlorocuprates(I, II) and chloroplumbates (II, IV). A strong charge transfer band of $[CuCl_5]^{3-}$ was also found in the neighborhood of $2.7 \times 10^4$ cm$^{-1}$ for hexamminechromium(III) chlorocuprate(I, II) and hexamminechromium (III) chlorocuprate(II).

The present author is pleased to express his sincere thanks to Dr. Masayoshi Nakahara of St. Paul's University who kindly advised him to undertake reflectance measurements of chlorocuprates. He is grateful to Professor Yoshihiko Saito of the University of Tokyo for his kind guidance in X-ray study. The research would never have been possible without many valuable suggestions and constant encouragement accorded by Professor Shin'ichi Kawaguchi of our Institute. The author could utilize the spectrophotometer through the kindness of the Faculty of the Science of Living of our University.

*Institute of Polytechnics*
*Osaka City University*
*Kita-ku, Osaka*

16) E. Doehlemann and H. Fromherz, *Z. physik. Chem.*, **171A**, 353 (1934).

** The value of log $\varepsilon$ in the absorption curve of $CuSO_4$ in 48% hydrobromic acid given in the previous paper (Fig. 1 in Ref. 6) has been too small by unity. The correct values are given in Fig. 5 in the present paper.

17) S. B. Hendricks and R. G. Dickinson, *J. Am. Chem. Soc.*, **49**, 2149 (1927).

18) L. Chrobak, *Z. Krist.*, **88**, 35 (1934).

19) A. F. Wells, *J. Chem. Soc.*, **1947**, 1662.

# *Solvent Extraction of Inorganic Nitrates with Diphosphonate Ester. II. Thorium and Uranyl Nitrates*

By Hideo SAISHO

(Received March 10. 1961)

In the previous paper[1], was studied the solvent extraction behavior of zirconium, yttrium and several lanthanide elements (cerium, promethium, europium and lutetium) with tetra-*n*-butyl ethylene-diphosphonate* (TBEDP), $(BuO)_2P(O)(CH_2)_2(O)P(BuO)_2$. The distribution ratio of each element between nitric acid solution and TBEDP diluted with kerosene was determined in the range of nitric acid concentration from 0.01 to 13 M and TBEDP concentration from 0.1 to 0.2 M. The extractability of zirconium increased with increasing acidity. However, in the extraction of yttrium and lanthanide elements, the distribution ratios were very high in the low acidity region and decreased sharply with increasing acidity. This extracting reagent is very excellent for the extraction of trivalent elements such as lanthanide elements especially in the low acidity region.

The present paper describes in detail the solvent extraction behavior of thorium and uranium in the system of TBEDP-kerosene and nitric acid solution.

Infrared absorption studies have also been undertaken to obtain the information on the organic phase containing uranium.

## Experimental

**Sources of Materials.**—TBEDP received from the Tama Chem. Co., Tokyo, Japan was used without any further purification. TBEDP was diluted to the desired concentrations with kerosene, which had its flash point above 60°C and was not specially purified. Nitric acid solutions were prepared by diluting concentrated nitric acid, special grade. The acidity was checked volumetrically, whenever necessary.

Uranyl nitrate was of guaranteed reagent grade, and was used as $1.24\times10^{-3}$ M solution in the whole acidity region studied.

Thorium-234 ($UX_1$) separated from uranium was chosen to study the extractability of thorium by TBEDP. Thorium-234 tracer[2] was obtained as nitrate by means of the usual ethyl ether extaction method followed by cation exchange.

**Determination of Distribution Ratios.** — The details of the method used in the previous report[1] were also adopted in the present study. The distribution ratio was measured after shaking the two phases for thirty minutes in a thermostat kept at 25±0.5°C.

The uranium concentration in the aqueous phase was determined colorimetrically or by fluorimetry and that in the organic phase was measured in the same way after extraction into an aqueous solution of sodium carbonate. For colorimetry, the oridinary hydrogen peroxide method[3] was employed. The method adopted for fluorimetry was similar to that of Grimaldi et al.[4] The procedure was as follows: Aliquot portions containing uranium were transferred to a small platinum dish and carefully dried up under an infrared lamp. Fluoride flux was then added to the dish and the flux was melted for about five minutes in an electric furnace kept at 700°C. After cooling the melt, the fluorescence was measured, using excitation by radiation of 365 mμ wavelength. A blank and a standard were run at the same time. The fluoride flux used here consisted of 9% sodium fluoride, 45.5% sodium carbonate and 45.5% potassium carbonate, which were fused in platinum at about 500°C and then thoroughly ground and mixed. Both colorimetric and fluorimetric measurements were made with a Shimadzu recording photoelectric spectrophotometer, type RS.

Amounts of thorium-234 were determined radiochemically in the same way as those described in the previous paper[1]. Infrared spectra were measured with a Hitachi EPI-II double-beam infrared spectrophotometer equipped with a sodium chloride prism. All the measurements were made in the liquid state.

## Results and Discussion

**Effect of Nitric Acid Concentration.**—Figures 1 and 2 show the variation of distribution ratio, $K_d$, of uranium(VI) and thorium(IV) in the range of nitric acid concentration from 0.1 to 13 M, keeping the TBEDP concentration 0.1 M. Other authors'[5,6] results for both elements in the extraction with TBP from nitric acid are added for comparison.

1) H. Saisho, This Bulletin, **34**, 859 (1961).

* Tetra-*n*-butyl ethylene-diphosphonate is abbreviated as TBEDP.

2) D. Dyrssen, *Svensk. Kem. Tidskr.*, **62**, 153 (1950).

3) C. J. Rodden, editor-in-chief, "Analytical Chemistry of the Manhattan Project" (NNES VIII-1), McGraw-Hill Book Co., Inc., New York (1950), p. 83.

4) F. S. Grimaldi, I. May, M. H. Fletcher and J. Titcomb, "Collected Papers on Methods of Analysis for Uranium and Thorium", United States Government Printing Office, Washington (1954), p. 43.

5) K. Alcock, G. F. Best, E. Hesford and H. A. C. McKay, *J. Inorg. Nucl. Chem.*, **6**, 328 (1958).

6) E. Hesford, H. A. C. McKay and D. Scargill, ibid., **4**, 321 (1957).

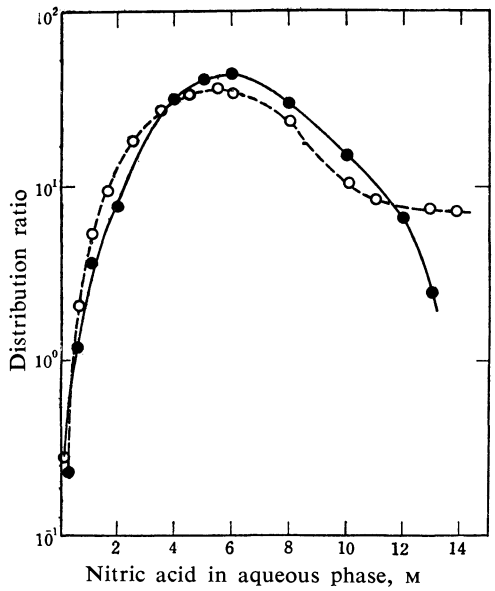



Fig. 1. Distribution ratio of uranium(VI).
—●—●—: 0.1 M TBEDP in kerosene
--○--○--: McKay et al.[5], 19% TBP in kerosene

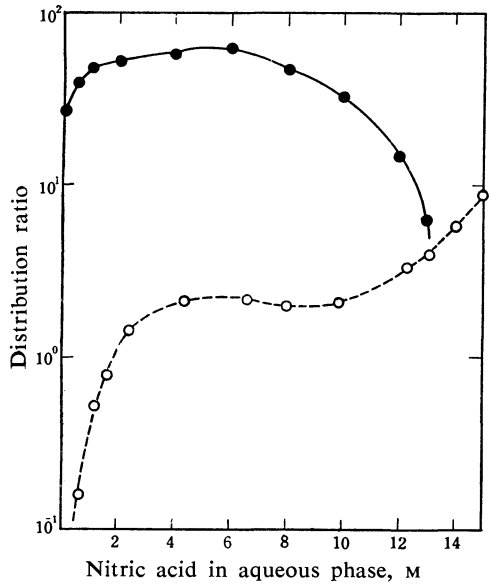



Fig. 2. Distribution ratio of thorium(IV).
—●—●—: 0.1 M TBEDP in kerosene
--○--○--: McKay et al.[6], 19% TBP in kerosene

As shown in Fig. 1, the acid dependence curves for TBEDP and TBP have a considerable resemblance; maximum extractions of uranium-(VI) from nitric acid solutions are observed at about 6 M nitric acid concentration in both cases.

As Fig. 2 shows, similarity in the shape of the acid dependence curves for TBEDP and TBP is also found in the acidity range up to about 6 M nitric acid; the $K_d$ values for thorium-(IV) increase with increasing acidity. In the higher acidity range, the $K_d$ values by TBEDP tend to decrease gradually, whereas those by TBP have an increasing tendency, especially in the acidity region over about 10 M nitric acid.

**Effect of TBEDP Concentration on Extraction of Uranium(VI).** — Figure 3 shows two series of results in the range of $1\times10^{-3}$ to $1\times10^{-1}$ M TBEDP concentration in the organic

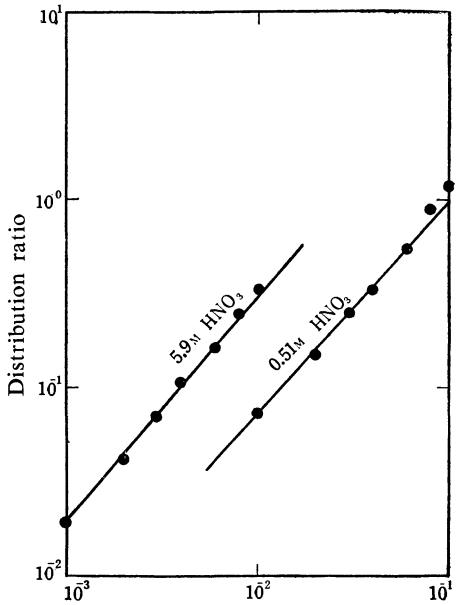



Fig. 3. Power dependence of distribution ratio on TBEDP concentration.

phase, keeping the acidity of the aqueous phase constant. In the plots of log $K_d$ vs. logarithmic TBEDP concentration, the slope of the lines through the points is 1.1 for both 0.51 and 5.9 M nitric acid up to about $6\times10^{-2}$ M TBEDP concentration. The first power dependence of the $K_d$ values on the TBEDP concentration indicates the 1 : 1 TBEDP to uranium ratio. The complex formed in the organic phase may be $UO_2\cdot(NO_3)_2\cdot$TBEDP, analogous to the corresponding uranium(VI) compound in TBP extraction[5,7]. It is in good agreement with the results obtained by Healy and Kennedy[8] for benzene solutions of diphosphoryl reagents containing the group =P(O)Y(O)P= (where Y

7) H. A. C. McKay, "Proceedings of International Conference on Peaceful Uses of Atomic Energy", Vol. VII, p/441, United Nations Publication, New York (1956).
8) T. V. Healy and J. Kennedy, *J. Inorg. Nucl. Chem.*, **10**, 128 (1959).

is oxygen, methylene or ethylene), saturated with uranyl nitrate.

**Infrared Studies on the Organic Phase.** — Infrared absorption studies may provide some information on the extracting behavior of uranyl nitrate by TBEDP. Infrared spectra were recorded for the following samples: (I) kerosene, (II) pure TBEDP, (III) 0.2 M kerosene solution of TBEDP, (IV) 0.2 M kerosene solution of TBEDP after being shaken with 6 M nitric acid, and (V) 0.2 M kerosene solution of TBEDP after being shaken with 0.5 M uranyl nitrate solution in 6 M nitric acid. The spectra in the region of 900 to 1700 $cm^{-1}$ are illustrated in Fig. 4.

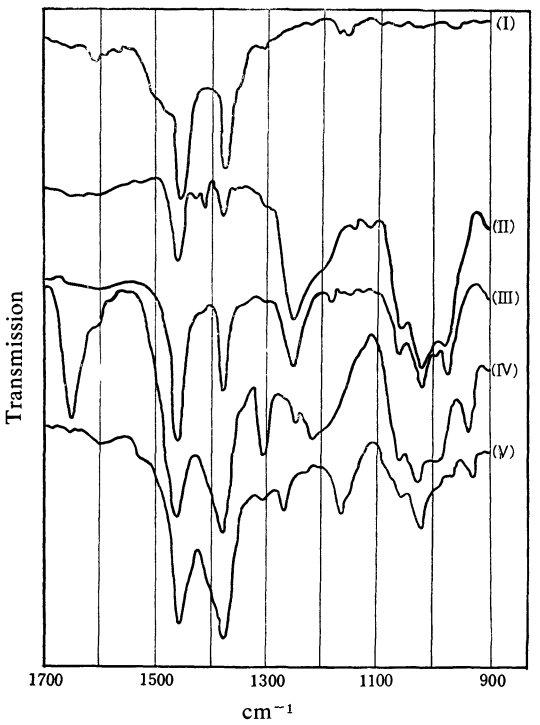



Fig. 4. Infrared absorption spectra of samples I—V.

(I) Kerosene
(II) Pure TBEDP
(III) 0.2 M Kerosene solution of TBEDP
(IV) 0.2 M Kerosene solution of TBEDP after being shaken with 6 M nitric acid
(V) 0.2 M Kerosene solution of TBEDP after being shaken with 0.5 M uranyl nitrate in 6 M nitric acid

The spectrum of the sample III can be explained as a mixture of the samples I and II. In the spectrum of III, the bands at 1462 and 1380 $cm^{-1}$ are assigned to the deformation vibrations of methyl groups in TBEDP and kerosene. The band at 1255 $cm^{-1}$ and the bands in the region of 1100 to 950 $cm^{-1}$ are due to TBEDP. The 1255 $cm^{-1}$ band is assignable to the P=O stretching frequency, while the other bands are associated with the stretching vibrations of the P-O-C linkage and the C-C bond.

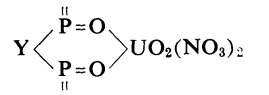
In the spectrum of IV, three new absorption bands were observed at 1649, 1305 and 944 $cm^{-1}$. According to Peppard et al.[9], four absorption bands are found in the infrared spectrum of 100% nitric acid at 1680, 1308, 924 and 769 $cm^{-1}$. The addition of water to 100% nitric acid causes the appearance of bands at 828 and 1380～1410 $cm^{-1}$ which have been attributed to the nitrate ion[10-13]. Thus, these three new bands are possibly due to nitric acid. The band due to the nitrate ion in the 1380～1410 $cm^{-1}$ region appears to overlap the 1380 $cm^{-1}$ band observed for TBEDP. These results indicate that nitric acid is extracted into the TBEDP organic phase.

The P=O stretching band, which appears at 1255 $cm^{-1}$ in pure TBEDP, shifts to about 1220 $cm^{-1}$. The corresponding band in the spectrum of V is observed at 1169 $cm^{-1}$. On the other hand, the bands near 1030 $cm^{-1}$ do not show any change in the spectra for III, IV and V. Therefore, the P=O bond takes part in the extractability of nitric acid and uranyl nitrate by TBEDP, but the P-O-C linkage does not appear to participate.

It is noticeable that the strong band of nitric acid observed at 1649 $cm^{-1}$ for IV disappears in the spectrum of V. The bands at 1305 and 944 $cm^{-1}$, which are also due to nitric acid, can not be found. Consequently, nitric acid seems to be nearly absent in V. These results suggest that uranium(VI) is extracted into the TBEDP organic phase more predominantly than nitric acid.

A band at 937 $cm^{-1}$ is observed in the spectrum of V instead of the absence of 944 $cm^{-1}$. This band may be assignable to the U=O stretching frequency[14-16].

Healy and Kennedy[8] have proposed the structure




9) D. F. Peppard and J. R. Ferraro, ibid., 15, 365 (1960).
10) G. Herzberg, "Infrared and Raman Spectra of Polyatomic Molecules", Van Nostrand, New York (1945), p. 322.
11) D. Redlich and L. E. Nielsen, *J. Am. Chem. Soc.*, 65, 654 (1943).
12) D. K. Ingold and D. J. Millen, *J. Chem. Soc.*, 1950, 2612.
13) R. A. Robinson and R. H. Stokes, "Electrolyte Solutions", Academic Press, New York (1959).
14) G. K. T. Conn and C. K. Wu, *Trans. Faraday Soc.*, 34, 1483 (1938).
15) L. H. Jones, *J. Chem. Phys.*, 23, 2105 (1955).
16) B. M. Gatehouse and A. E. Comyns, *J. Chem. Soc.*, 1958, 3965.

for the chelate complex formed between diphosphoryl reagents and uranyl nitrate This model is consistent with the present results.

The author wishes to express his sincere thanks to Dr. Hiroshi Ohinouye, Director of the Laboratory of the Mitsubishi Atomic Power Industries, Inc., and Mr. Kazumu Sugimoto, Chief of the Chemistry Section of the Laboratory for their support and permission to present this work.

Thanks are also due to Professor Nobufusa Saito and Assistant Professor Yuji Yokoyama of the University of Tokyo for their suggestions and guidance, to Mr. Mitsuo Tasumi for the infrared measurements, and to Mr. Ryoichi Uehara for his effort in the synthesis of tetra-*n*-butyl ethylene-diphosphonate.

*Engineering & Research Laboratory*
*Mitsubishi Atomic Power Industries, Inc.*
*Ohmiya, Saitama*

# *Über die Einwirkung von Brom auf 9-Acetylfluoren*

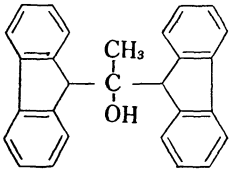
Von Mitsuo MASAKI und Masaki OHTA

(Eingegangen am 21 Februar, 1961)

Die Halogenierung von Fluorenen[1] oder Dibenzofulvenen[2] ist ausführlich berichtet worden. Über 9-Acylfluorene fehlen unseres Wissens aber bisjetzt entsprechende Untersuchungen.

Um das Ziel, 9-Glycylfluoren darzustellen, das durch Umsetzung von 9-Bromacetylfluoren mit Amin erhalten werden mag, haben wir zunächst Bromierung von 9-Acetylfluoren ins Auge gefasst. Es schien uns auch interessant zu sein, die Halogenierungsfähigkeit der 2-, 7- und 9-Stellungen des Fluorenrings, in dessen 9-Stellung Acetylgruppe vorliegt, und der Acetylgruppe aufzuschliessen.

Über die Synthese von 9-Acetylfluoren (I) sind von Miller u. a.[3] die Umsetzung von 9-Fluorenyl-lithium mit Acetylchlorid und von Wagner u. a.[4] die Claisen-artige Ester-Kondensation von Fluoren mit Essigsäureäthylester berichtet worden. Nach dieser Methode haben wir I erhalten können. Da auf jener Methode es aber einige Fragen[4,5] gibt, haben wir die Reaktion von 9-Fluorenyl-lithium mit Acetylchlorid versucht. Dabei erhält man nicht I, sondern eine Substanz vom Schmp. 182°C, deren Molekularformel $C_{28}H_{22}O$ darstellt. Durch Infrarot-Absorptionen bei 1060 und 3570 $cm^{-1}$ wie die typischen Banden beim tertiären Alkohol (Abb. 1) und durch Ultraviolet-Spektren wurde die Struktur der Substanz als $\alpha$-Di-9-fluorenyl-äthanol (II) festgestellt, das




(II)

offenbar durch weitere Einwirkung von 9-Fluorenyllithium auf primär gebildetes 9-Acetylfluoren entstanden war.

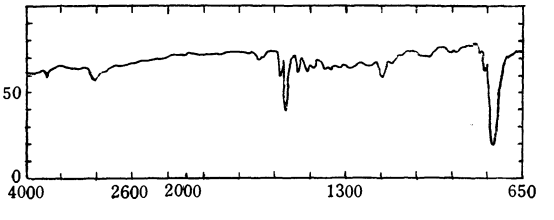



Abb. 1. Infrarot-Spectrum von II.

Nach Schlenk[6] entsteht bei der Einwirkung von Benzoylchlorid auf 9-Fluorenyl-lithium neben 9-Benzoylfluoren Di-9-fluorenyl-phenyl-carbinol. Bei Acetylchlorid erhält man jedoch nur II selbst dann, wenn 9-Fluorenyl-lithium

1) a) Ch. Courtot und C. Vignati, *Bull. soc. chim.*, **41**, 58 (1927). b) J. R. Sampey und E. E. Reid, *J. Am. Chem. Soc.*, **69**, 234 (1947). c) R. C. Fuson und H. D. Porter, *J. Am. Chem. Soc.*, **70**, 896 (1948).

2) a) W. Dilthey und P. Huchtemann, *J. prakt. Chem.*, (2) **154**, 238 (1940). b) E. Bergmann und A. v. Christiani, *Ber.*, **63**, 2559 (1930). c) E. Bergmann und A. v. Christiani, ebenda, **64**, 1491 (1931).

3) H. F. Miller und G. B. Bachman, *J. Am. Chem. Soc.*, **57**, 766 (1935).

4) I. Von und E. C. Wagner, *J. Org. Chem.*, **9**, 155 (1944).

5) E. J. Greenhow, E. N. White und D. McNeil, *J. Chem. Soc.*, **1953**, 3099.

6) W. Schlenk und E. Bergmann, *Ber.*, **62**, 745 (1929).

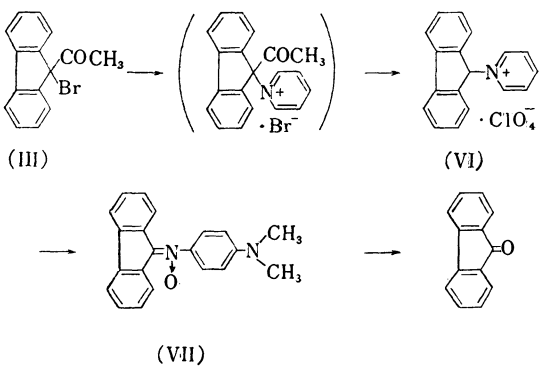
sich zur ätherischen Lösung von überschüssigem Acetylchlorid langsam hinzutropfen lässt. Daher kann man sich so vorstellen, dass die Reaktion von 9-Fluorenyl-lithium mit 9-Acetylfluoren in bestimmten Temperatursbereichen schneller als die mit Acetylchlorid sei.

Bei der Einwirkung von äquivalentem Brom auf I in Äther bei Raumtemperatur erhält man zwei Produkte, nähmlich Monobrom-körper (III) vom Schmp. 109～110°C (9.1 Tl.) und Dibrom-körper(IV) vom Schmp. 162～164°C (0.9 Tl.).

Beim Erhitzen mit Anilin liefert III Anilino-Körper(V), der in Säure unlöslich ist. Beim längeren Erwärmen von III in Pyridin erhält man eine schwarzbraune Substanz, die man sich als Pyridiniumsalz von III vorstellen kann. Aber die Elementaranalyse des Perchlorats zeigt, dass diese Molekularformel $C_{18}H_{14}O_4N$ darstellt, dass also unter Hydrolyse im Verlauf der Reaktion Acetylgruppe sich abspalten lässt und daher dass das Bromatom in III an einen Fluoren-Kern gebunden ist.

Die Konstitution des Perchlorates(VI) ergibt sich aus seiner Umsetzung über Nitron zum 9-Fluorenon.

Bei der Einwirkung von *p*-Nitroso-dimethyl-anilin auf VI in Pyridin erhält man entsprechendes Nitron (VII), das sich mit Säure zu 9-Fluorenon zersetzen lässt.



(III) (VI) (VII)

Aus den oben erwähnten Tatsachen und Ultraviolet-Absorptions-spektren kann geschlossen werden, wie in der Abbildung gezeigt, dass VI das Pyridiniumsalz des 9-Bromfluorens ist, und also dass die Verbindung vom Schmp. 109～110°C (III) 9-Brom-9-acetylfluoren darstellt.

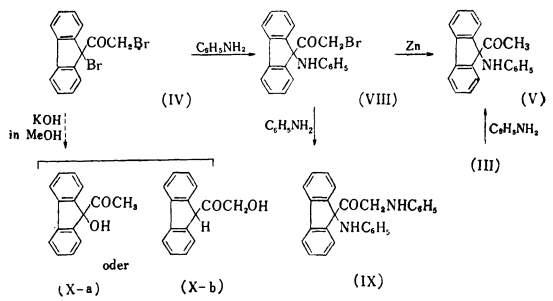
Erhitzt man Dibrom-körper vom Schmp. 162～164°C (IV), der auch bei der Einwirkung von 2 Mol Broms auf I quantitativ entsteht, mit überschüssigem Anilin in Benzol, so erhält man neben Anilinhydrobromid, ein Mono-anilino-monobrom-derivat (VIII), das sich bei der Reduzierung mit Zinkpulver Monoanilino-derivat überführen lässt, das nicht anders als die aus III gewonnene Verbindung (V) ist. Der Dibrom-körper enthält also eins der zwei Bromatome in 9-Stellung.

Beim längeren Erhitzen mit Anilin setzt sich VIII zu Dianilino-körper (IX) um. Aus dieser Tatsache und aus der Umsetzung von IX mit Kaliumhydroxyd in Alkohol ergibt sich die Stellung des zweiten Broms.

Bei der Einwirkung von methanolischem Kaliumhydroxyd auf IV bei Raumtemperatur erhält man das bromfreie Produkt, dessen Bruttoformel $C_{15}H_{12}O_2$ darstellt.

Nach einigen Vorschlägen[1a,7] kann man sich leicht vorstellen, dass das an 2- oder 7-Stellung von Fluoren-kern gebundene Brom nicht unter den oben erwähnten Bedingungen reagieren könne, und dass die Brome in IV nicht an 2- oder 7-Stellung gebunden sei: So sei die Verbindung (IV) 9-Brom-9-bromacetylfluoren, und diese Vermutung wurde durch Ultraviolet-Absorptionsspektren bestätigt.

Als Konstitution des oben erwähnten Produkt ($C_{15}H_{12}O_2$) kann man sich Formel X-a oder X-b vorstellen, die aber noch jetzt untersucht wird.



(IV) (VIII) (V) (III) (X-a) (X-b) (IX)

Die Bromierung von I mittels *N*-Bromsuccinimids ist uns nicht gelungen.

Es ist bemerkenswert, dass Acetylfluoren sich mit Brom zuerst in die 9-Stellung bromieren lässt und keine Bromierung mit NBS stattfindet, indessen Fluoren selbst sich bei der Einwirkung von Brom bei 0～5°C in 2- oder 2-, 7-Stellung[1a] bromieren lässt und bei der Bromierung mit NBS 9-Bromfluoren[1c] entsteht.

### Beschreibung der Versuche

***α*-Di-9-fluorenyl-äthanol (II).** — Eine ätherische Lösung von 9-Fluorenyl-lithium, aus 8 g Fluoren nach der Methode von Burtner und Cusic[8] dargestellt, wird unter mechanischem Rühren zu einer eisgekühlten Lösung von 5 g Acetylchlorid in 30 ccm abs. Äther langsam hinzugetropft, die Reaktionslösung lässt sich noch 2 Std bei Raumtemperatur rühren und darauf in ein Gemisch von Eis und Ammoniumacetat giessen. Die ätherische Schicht wird zusammen mit dem mit wässeriger

7) J. Schmidt und K. Bauer, ebenda, **38**, 3751 (1905).
8) R. R. Burtner und J. W. Cusic, *J. Am. Chem. Soc.*, **65**, 264 (1943).

Schicht noch 2 Mal geschüttelten Äther mit Natriumsulfat getrocknet. Der nach dem Abdamppen des Äther erhaltene Rückstand wird 2 Mal mit Petroläther und darauf mit wenigem Äthanol gewaschen, und aus Äthanol umkristallisiert. Hellrötliche Nadeln vom Schmp. 182°C. Ausb. 3.5 g.

Gef.: C 89.16; H 6.07. Ber. für $C_{28}H_{22}O$: C 89.84; H 5.88%.

**9-Brom-9-acetylfluoren (III).**—Man versetzt einer Lösung von 7.2 g des nach der Methode von Von und Wagner[4] erhaltenen 9-Acetylfluorens in 120 ccm Äther mit 5.5 g Brom bei Raumtemperatur und schüttelt das Gemisch um: Sofort verliert sich die Farbe des Broms. Nach 4~5 stündigem Stehen bei Raumtemperatur wird der abgeschiedene Niederschlag durch Dekantierung abgetrennt, der 1.3 g wiegt, nach dreimaligen Umkristallisierungen den Schmp. 160~161°C und bei Mischprobe mit IV keine Depression zeigt, und die ätherische Reaktionslösung ergibt beim Abdampfen des Äthers das kristallinische Produkt. Ausb. 8.3 g. Farblose Nadeln vom Schmp. 109~110°C (aus Äthanol, Essigsäure oder Ligroin).

Gef.: C 62.90; H 4.04. Ber. für $C_{15}H_{11}OBr$: C 62.72; H 3.83%.

**9-Brom-9-bromacetylfluoren (IV).**—Zu einer Lösung von 5.3 g 9-Acetylfluoren in 100 ccm abs. Äther setzt man unter Umschütteln langsam 8.2 g Brom zu. Nach eintägigem Stehen der Mischung wiegen die abgeschiedenen delben Nadeln 7 g und werden aus Äthanol umkristallisiert. Farblose Nadeln vom Schmp. 162~164°C.

Gef.: C 50.25; H 2.86. Ber. für $C_{15}H_{10}OBr_2$: C 49.18; H 2.73%.

**Einwirkung von Pyridin auf 9-Brom-9-acetylfluoren.** — In 10 ccm reinem trocknem Pyridin löst man 2.1 g III, wobei es sich leicht erwärmt, verschliesst den Kolben mit einem Calciumchlorid-Rohr, lässt es 3 Std bei Raumtemperatur stehen, darauf erwärmt man dieses ungefähr 3~4 Std auf dem Wasserbad und dann fügt man 200 ccm Benzol hinzu. Das ausgefallene, harzförmige Produkt wird nach der Entfernung von der benzolischen Lösung durch Dekantierung mit 80 ccm heissem Wasser extrahiert. Nach dem Erkalten versetzt man die wässerige Lösung mit Aktivkohle, filtriert sie ab und fügt eine Lösung von Perchlorsäure zum Filtrat hinzu. Im Eisschrank scheidet sich *N*-9-Fluorenyl-pyridiniumperchlorat (VI) vollständig ab. Es wird abfiltriert und aus Äthanol umkristallisiert. Blass-orange Nädelchen vom Schmp. 213~214°C. Ausb. 1.1 g.

Gef.: N 4.18. Ber. für $C_{18}H_{14}O_4NCl$: N 4.08%.

**9-Fluorenon-(*p*-dimethylaminophenyl)nitron (VII).** — In 6 ccm Pyridin löst man 0.7 g VI auf, versetzt es mit 0.27 g *p*-Nitrosodimethylanilin und fügt 1.8 ccm 2 N Natriumhydroxyd unter Umschütteln hinzu. Unter leichter Erwärmung scheidet sich ein Niederschlag ab. Nach 5~6 Std wird er abfiltriert und aus Äthanol umkristallisiert. Ausb. 0.5 g. Orange Prismen vom Schmp. 237~239°C.

Gef.: N 9.27. Ber. für $C_{21}H_{18}ON_2$: N 8.92%.

**Hydrolyse von VII.** — Im Scheidetrichter werden 0.5 g VII mit 20 ccm 3 N Salzsäure durchge schüttelt und 2~3 mal mit je 20 ccm Äther ausgeschüttelt. Den vereinigten Ätherextrakt wäscht man mit Wasser, trocknet mit Natriumsulfat und dampft ein. Es bleiben 0.22 g 9-Fluorenon, das als Hydrazon festgestellt wurde hinter. Schmp. 149~150°C (Lit.[9]: 149~150°C).

Gef. N 14.10%.

**9-Anilino-9-acetylfluoren (V).**—Zu einer Lösung von 0.4 g Anilin in 20 ccm Äthanol setzt man 1 g III zu, erwärmt dieses 4 Std bei 60~70°C auf dem Wasserbad, nach der Versetzung mit Aktivkohle erhitzt man dies im Rückfluss und darauf filtriert man das Gemisch ab, aus dem sich beim Erkalten Schuppen auskristallisieren. Ausb. 0.9 g. Aus Äthanol umkristallisiert, verwandeln sie sich in farblose Prismen vom Schmp. 142~144°C.

Gef.: N 4.55. Ber. für $C_{21}H_{17}ON$: N 4.68%.

**9-Anilino-9-bromacetylfluoren (VIII).**—Zu einer Lösung von 5 g Anilin in 40 ccm trocknem Benzol setzt man 5 g IV zu und erhitzt sie 2 Std auf dem Wasserbad. Nach der Entfernung des gebildeten Anilinhydrobromids nach dem Erkalten lässt sich die Lösung unter vermindertem Druck einengen und mit Äthanol versetzen, wobei langsam farblose

Fluoren

| | | | | | | |
|---|---|---|---|---|---|---|
| $\lambda_{max}$, Å | 2260* | 2545* | 2610 | 2720* | 2895 | 3010 |
| log ε | 3.91 | 4.23 | 4.28 | 4.13 | 3.81 | 3.98 |

α-Di-9-fluorenyl-äthanol

| | | | | | |
|---|---|---|---|---|---|
| $\lambda_{max}$, Å | 2600* | 2695 | 2810* | 2920 | 3040 |
| log ε | 4.43 | 4.50 | 4.33 | 3.96 | 3.97 |

*N*-(9-Fluorenyl)-pyridiniumperchlorat

| | | | | | |
|---|---|---|---|---|---|
| $\lambda_{max}$, Å | 2260 | 2330 | 2690 | 2815* | |
| log ε | 4.45 | 4.35 | 4.25 | 4.11 | |

9-Acetyl-9-fluorenol oder 9-(2'-Hydroxyacetyl)-fluoren

| | | | | | | |
|---|---|---|---|---|---|---|
| $\lambda_{max}$, Å | 2240 | 2555 | 2640 | 2740* | 2845 | 3190 |
| log ε | 4.38 | 4.50 | 4.70 | 4.10 | 4.08 | 4.12 |

9-Brom-9-acetylfluoren

| | | | | |
|---|---|---|---|---|
| $\lambda_{max}$, Å | 2475 | 2620* | | 2850* |
| log ε | 4.45 | 4.14 | | 3.89 |

9-Brom-9-bromacetylfluoren

| | | | | | |
|---|---|---|---|---|---|
| $\lambda_{max}$, Å | 2545 | 2640 | 2720* | 2850 | 3180 |
| log ε | 4.41 | 4.39 | 4.03 | 3.95 | 3.66 |

9-Anilino-9-acetylfluoren

| | | | | | | |
|---|---|---|---|---|---|---|
| $\lambda_{max}$, Å | 2250* | 2330 | 2465 | 2675 | 2770* | 3080* |
| log ε | 4.39 | 4.32 | 4.35 | 4.25 | 4.11 | 3.40 |

9-Anilino-9-bromacetylfluoren

| | | | | |
|---|---|---|---|---|
| $\lambda_{max}$, Å | 2240* | 2335 | 2465 | 2680* |
| log ε | 4.41 | 4.36 | 4.36 | 4.24 |

9-Fluorenon-hydrazon

| | | | | |
|---|---|---|---|---|
| $\lambda_{max}$, Å | 2370 | 2540 | 2940~3050 | 3320 |
| log ε | 4.75 | 4.37 | 3.96 | 4.07 |

9-Fluorenon-(*p*-dimethylaminophenyl)nitron

| | | |
|---|---|---|
| $\lambda_{max}$, Å | 2405 | 2625 |
| log ε | 4.68 | 4.69 |

* Schulter (in 99.5% Äthanol)
UV-Absorptions-spektren

9) H. Staudinger und O. Kupfer, *Ber.*, **44**, 2207 (1911).

Nadeln auskristallisieren. Ausb. 4.2 g. Aus Äthanol umkristallisiert, entstehen farblose Nadeln order Schuppen vom Schmp. 137~139°C.

Gef.: N 3.55 Ber. für $C_{21}H_{16}ONBr$: N 3.70%.

**9-Anilino-9-anilinoacetylfluoren (IX).** — Zu einer Lösung von 1 g Anilin in 12 ccm trocknem Benzol setzt man 1.7 g VIII zu und erhitzt dieses 20 Std im Rückfluss. Nach der Entfernung des gebildeten Anilinhydrobromids engt man die Lösung ein, versetzt sie mit ein wenig Äthanol und lässt sie bei Raumtemperatur stehen. Nach einer Woche erhält man 1 g gelbroten Niederschlag, der sich aus Benzol in farblose Nädelchen umkristallisiert. Schmp. 178~179°C.

Gef.: N 7.22. Ber. für $C_{27}H_{22}ON_2$: N 7.18%.

**Reduzierung von VIII mit Zinkpulver.**—In einen Gemisch von 90 ccm Äthanol, 20 ccm Benzol und 5 ccm Wasser löst man 2 g VIII auf, versetzt dieses mit 5 g Zinkpulver, erhitzt es 5 Std im Rückfluss unter mechanischem Rühren und dann filtriert man das Gemisch ab. Das Filtrat wird unter vermindertem Druck eingeengt, wobei ein kristallinisches Produkt zurückbleibt. Ausb. 1.3 g. Aus Äthanol umkristallisiert, erzeugen sich farblose Schuppen vom Schmp. 140~143.5°C und bei Mischprobe mit V zeigen sie keine Depression.

**Einwirkung von Kaliumhydroxyd auf IV in Methanol.**—Man löst 0.5 g Kaliumhydroxyd in 40 ccm abs. Methanol auf, versetzt es mit 1.7 g IV und schüttelt das Gemisch um, wobei die farblose Lösung intensiv gelb gefärbt wird und Nadeln ausscheidet. Nach 1~2 stündigem Umschütteln lässt man die Lösung 10 Std bei Raumtemperatur stehen, filtriert den gebildeten Niederschlag ab und wäscht ihn mit Wasser, der 0.6 g wiegt: Aus dem methanolischen Filtrat kann man noch ein 0.6 g Produkt erhalten. Aus Alkohol oder Petroläther umkristallisiert, erhält man gelbe Nadeln von Schmp. 110~112°C.

Gef.: C 80.87; H 5.25. Ber. für $C_{15}H_{12}O_2$ (X): C 80.36; H 5.36%.

Dr. Asaji Kondo danken wir bestens für seine Ausführung der Mikro-analyse.

*Organisch-Chemisches Laboratorium*
*Technische Hochschule zu Tokyo*
*Meguro-ku, Tokyo*

# *The Viscosity of Concentrated Aqueous Solutions of Strong Electrolytes*

By Takeshi SATOH and Koreaki HAYASHI

(Received October 29, 1960)

It has been pointed out that the viscosity $\eta$ of aqueous solutions of strong electrolytes can be expressed by the following empirical equation given by Jones and Dole[1],

$$\eta/\eta_0 = 1 + Ac^{1/2} + Bc \qquad (1)$$

where $\eta_0$ is the viscosity of pure water, $A$ and $B$ are parameters independent of concentration $c$ (mol./l. solution). Moreover, it is indicated that contrary to the positive value of $A$, the $B$-parameter can possess either sign corresponding to each pair of individual ionic species, and that the magnitude of $B$ is several times greater larger than that of $A$. It is noteworthy that the second term in Eq. 1 can be derived from the Debye-Hückel limiting law, and that the accord of theoretical derivation with the $A$-parameter obtained experimentally is very satisfactory. This excellent work focused in the ion-ion interaction was done by Falkenhagen and his coworkers[2]. On the other hand, the consideration of the parameter $B$ has probably been treated more qualitatively compared with $A$. It is generally accepted that $B$ may be determined additively from the specific value of the individual ion[3] and its temperature coefficient can be used as a measure indicating the effect of ion-solvent interaction in flow[3,4]. However, we should bear in mind the fact that the above-mentioned consideration should be limited to a narrow range of extremely dilute solutions. Frank and Thompson[5] have recently given fundamental reconsideration to some thermodynamic quantities and called our attention to the limit of the validity of the Debye-Hückel theory. According to their conclusion the Debye-Hückel formalism breaks down around the critical concentration $c_0$ owing to

1) E. g., H. S. Harned and B. B. Owen, "Physical Chemistry of Electrolytic Solutions", Reinhold Publ. Corp., New York (1950), p. 172.

2) H. Falkenhagen and E. L. Vernon, *Phys. Z.*, 33, 140 (1932); *Phil. Mag.*, (7) 14, 537 (1932).

3) E. C. Bingham, *J. Phys. Chem.*, 45, 885 (1941); M. Kaminsky, *Discuss. Faraday Soc.*, 24, 171 (1957).

4) R. J. Podolsky, *J. Am. Chem. Soc.*, 80, 4442 (1958).

5) H. S. Frank and P. T. Thompson, *J. Chem. Phys.*, 31, 1086 (1959); "The Structure of Electrolytic Solutions", John Wiley & Sons, Inc., New York (1959), p. 113.

TABLE I. RELATIVE VISCOSITIES OF 1-1 ELECTROLYTE SOLUTIONS

| Lithium chloride, 25°C | | Lithium bromide, 27°C | | Sodium chloride, 30°C by Suryanarayana and Venkatesan | | Sodium bromide, 25°C | |
|---|---|---|---|---|---|---|---|
| $c$, mol./l. | | $c$, mol./l. | | $c$, mol./l. | | $c$, mol./l. | |
| 0.7141 | 1.119 | 0.597 | 1.065 | 1.00 | 1.107 | 0.496 | 1.028 |
| 1.189 | 1.188 | 1.055 | 1.104 | 1.50 | 1.152 | 0.973 | 1.058 |
| 1.666 | 1.265 | 1.505 | 1.147 | 2.00 | 1.212 | 1.458 | 1.095 |
| 2.123 | 1.343 | 1.968 | 1.199 | 2.50 | 1.284 | 1.946 | 1.146 |
| 2.608 | 1.433 | 2.441 | 1.250 | 3.00 | 1.356 | 2.429 | 1.197 |
| 3.078 | 1.517 | 2.897 | 1.320 | 3.50 | 1.434 | 2.918 | 1.256 |
| 3.540 | 1.634 | 3.376 | 1.380 | 4.00 | 1.522 | 3.403 | 1.345 |
| 4.016 | 1.735 | 3.802 | 1.441 | 4.50 | 1.614 | 3.888 | 1.437 |
| 4.485 | 1.879 | 4.265 | 1.516 | 5.00 | 1.709 | 4.373 | 1.528 |
| 4.964 | 2.020 | 4.728 | 1.654 | | | 4.861 | 1.651 |

| Sodium iodide, 23°C | | Potassium fluoride, 26°C | | Potassium chloride, 25°C by Kume and Tanaka | |
|---|---|---|---|---|---|
| $c$, mol./l. | | $c$, mol./l. | | $c$, mol./l. | |
| 0.499 | 1.022 | 0.525 | 1.067 | 0.4985 | 0.998 |
| 0.998 | 1.042 | 1.034 | 1.135 | 0.7321 | 0.996 |
| 1.487 | 1.055 | 1.564 | 1.218 | 0.9692 | 0.995 |
| 1.982 | 1.094 | 2.081 | 1.291 | 1.0000 | 0.997 |
| 2.470 | 1.127 | 2.582 | 1.382 | 1.433 | 0.997 |
| 2.963 | 1.212 | 3.107 | 1.474 | 1.883 | 1.002 |
| 3.457 | 1.247 | 3.619 | 1.588 | 2.318 | 1.010 |
| 3.951 | 1.371 | 4.149 | 1.701 | 2.742 | 1.020 |
| 4.450 | 1.447 | 4.661 | 1.816 | 3.528 | 1.053 |
| 4.937 | 1.596 | 5.220 | 1.944 | 3.550 | 1.054 |
| | | 6.032 | 2.194 | 3.728 | 1.064 |
| | | 6.445 | 2.320 | 3.932 | 1.078 |
| | | | | 4.132 | 1.093 |
| | | | | 4.174 | 1.097 |

| Potassium bromide, 21°C | | Potassium iodide, 21°C | | Cesium chloride, 25°C | |
|---|---|---|---|---|---|
| $c$, mol./l. | | $c$, mol./l. | | $c$, mol./l | |
| 0.4315 | 0.983 | 0.610 | 0.964 | 0.5975 | 0.980 |
| 0.8439 | 0.967 | 1.208 | 0.931 | 1.509 | 0.964 |
| 1.271 | 0.953 | 1.817 | 0.904 | 2.267 | 0.956 |
| 1.692 | 0.942 | 2.426 | 0.919 | 3.088 | 0.977 |
| 2.104 | 0.943 | 3.015 | 0.925 | 4.058 | 1.010 |
| 2.524 | 0.937 | 3.626 | 0.943 | | |
| 2.942 | 0.947 | 4.831 | 1.022 | | |
| 3.379 | 0.954 | 6.039 | 1.152 | | |
| 3.802 | 0.966 | | | | |
| 4.206 | 0.986 | | | | |

the failure of the fine-grainedness* of the ion cloud. It is estimated that $c_0 \approx 10^{-3}$ mol./l. for 1-1 electrolytes at 25°C.

The aim of this paper is directed to the concentrated range reaching the saturation specified at a given temperature.

* It is noticeable that the various quantities defined in the ion cloud are to be essentially nonfluctuating. Let us consider one volume element in the cloud. Then, the frequency with which one ion happens to exist there should be sufficiently small. They introduce a new term of "fine-grainedness" to express the degree of averaging. Of course, in the limiting case of extremely dilute solution this requirement would be strictly justified.—The ion cloud would have the character of infinitely fine-grained matter.

## Experimental

The measurements of viscosity were made with conventional Ostwald viscometers in a water bath. According to the Hagen-Poiseuille law, the viscosity can be generally determined by

$$\eta = K\rho t \qquad (2)$$

where $\rho$ is the density of solution; $t$ is the efflux time and $K$ is a constant of the viscometer for a constant charge of liquid. Kinetic energy correction term $K'\rho/t$ ($K'$=constant) can be omitted in our present systems because the amount is negligible. The values of $K$ of two viscometers used were $3.214\times10^{-5}$ and $2.895\times10^{-5}$, respectively. These

values were determined by blank tests with pure water at different temperatures. The density $\rho$ of each solution was measured with a picnometer.

Lithium chloride, lithium bromide, sodium bromide, sodium iodide, potassium fluoride, potassium bromide, potassium iodide and cesium chloride were used as electrolytes. These samples were all special-grade commercial products. They were dried in a thermostat long enough before they were made into solutions.

## Results

Our experiments were carried out at room temperature by varying the concentration of solutions.

Suryanarayana and Venkatesan[6] have already reported the viscosities of sodium chloride solutions from 1 molal to saturation and from 30 to 55°C. Kume and Tanaka[7] have also presented a paper on some kinds of electrolytic solutions, in which the data of sodium chloride and potassium chloride are included. Consequently, for sodium chloride and potassium chloride we can utilize these data. In Table I our results are listed together with some of them. All the results are also shown in Fig. 1.

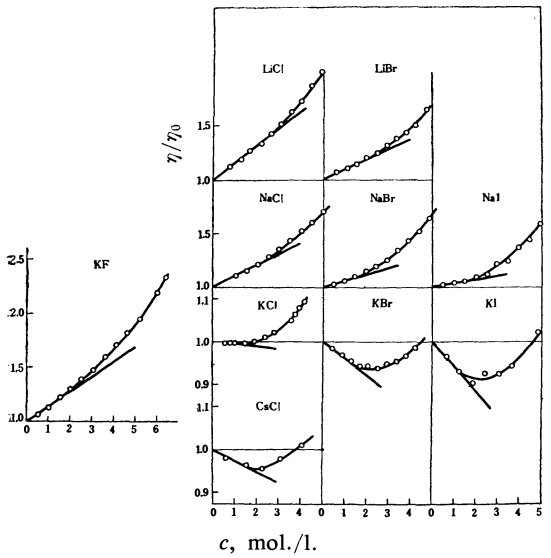



Fig. 1. Plots of relative viscosity against concentration.

## Discussion

One might easily admit that the relative viscosity vs. concentration curves could be generally classified into two groups. In the first type the relative viscosity varies almost linearly with the concentration in the dilute range (the slope is all positive) and then deviates clearly from the linearity after passing a critical point of concentration. The second type is one that indicates so-called negative viscosity — the behavior as a whole is not greatly different from the former, but it can be distinguished on one point, namely that its slope in the dilute range is negative. We would claim that the concentration corresponding to deflection point might be closely related with a critical concentration that is characterized in our model concerning the structure of electrolytic solutions. As general tendencies, with increasing temperature the absolute value of the tangent becomes greater and the deflection point moves to a higher concentration. But the displacement of the latter is so small that it can be neglected in the present problem. Derived from the data by Suryanarayana and Venkatesan[6] the temperature coefficient of the displacement under consideration is estimated as the order of 0.02 mol./l. deg$^{-1}$. These behaviors are shown in Fig. 2.

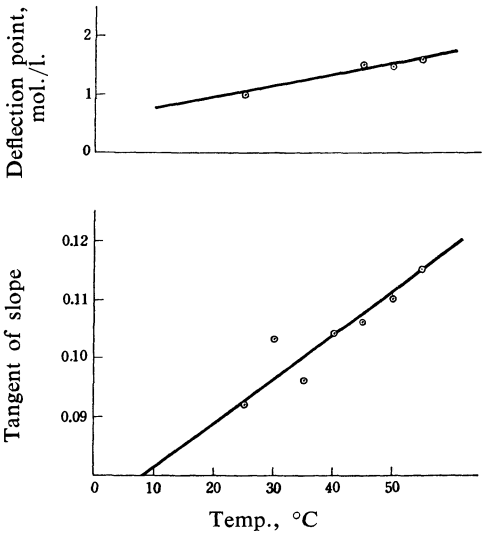



Fig. 2. Temperature coefficient of deflection point and tangent of slope against concentration (NaCl solution). After Suryanarayana and Venkatesan.

Let us continue the consideration in more detail. It is convenient to take series, e.g. anion series—in one series a cation is substituted corresponding to a fixed anion. In Fig. 3 the dependence of the ionic radius upon the tangent is plotted. One may notice the general feature that the tangent becomes smaller with increasing ionic radius (at a virtual value** its sign changes from positive

6) C. V. Suryanarayana and V. K. Venkatesan, *Trans. Faraday Soc.*, **54**, 1709 (1958).

7) T. Kume and M. Tanaka, *J. Chem. Soc. Japan, Pure Chem. Sec. (Nippon Kagaku Zasshi)*, **81**, 534 (1960).

** It is interesting to note that a critical value may probably satisfy a condition, in which a sum of both radii of the ions involved in one series is equal to 3.1~3.3Å. In the Cl series $K^+$ is incidentally fitted in this relationship.

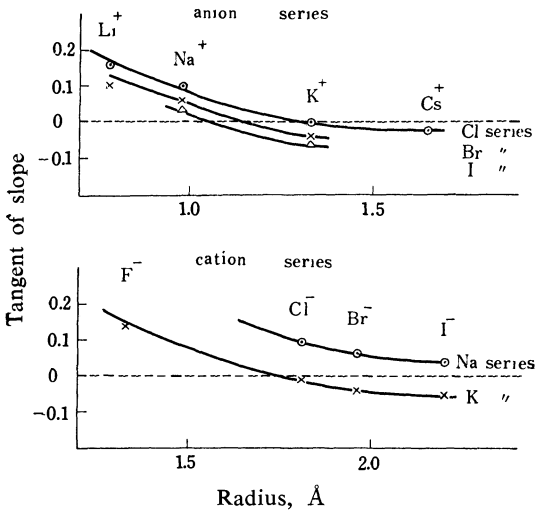



Fig. 3. Tangent of slope vs. ionic radius.

to negative) and the deflection point moves to a lower concentration***. Concerning the dilute range in which the viscosity varies linearly with the concentration, we would conform to Broersmas' treatment[8]. According to his assumption of local viscosity, the viscosity $\eta$ can be set,

$$\eta \approx \eta_{0-0} + 2\sum \frac{n_i v_i}{N v_0}(\eta_{i-j} - \eta_{0-0}) \qquad (3)$$

where $\eta_{i-j}(=\eta_{j-i})$ is a local viscosity in a region containing neighboring water molecules in the $i$th and $j$th hydration layers, consequently $\eta_{0-0}$ is a local viscosity in a region containing both free waters; $v_i$, $n_i$ and $v_0$, $n_0$ are the volume and the number per unit volume of water molecules existing in these respective states. $N$, the total number of water molecules per unit volume can be written:

$$N = n_0 + n(n_{1(+)} + n_{1(-)} + n_{2(+)} + n_{2(-)})$$

where $n_{1(+)}$, $n_{1(-)}$ and $n_{2(+)}$, $n_{2(-)}$ are the hydration numbers of primary and secondary layers surrounding a cation and an anion respectively. Equation 3 is considered to be based upon the following fundamental concepts. Local friction force is proportional to the total cross-sectional area of the molecules which are proportional to their volumes and the velosity gradient (a const) and the resultant of these effects contribute to the bulk viscosity. Factor 2 enters because the layers considered are identical so that element $i$ and $j$ can meet either way. The higher terms containing more than the square of concentration, $(n_i/N)^2$, are neglected. In other words the bulk viscosity is assumed to be givin by averaging the effect of local viscosity with the weights of relative volume and concentration of the water molecule in different state.

From the standpoint of our model Eq. 3 can be written,

$$\begin{aligned}\eta \approx \eta_{0-0} &+ 2\frac{n_{1(+)} n v_{1(+)}}{N v_0}(\eta_{1(+)-2(+)} - \eta_{0-0}) \\ &+ 2\frac{n_{2(+)} n v_{2(+)}}{N v_0}(\eta_{2(+)-0} - \eta_{0-0}) \\ &+ 2\frac{n_{1(-)} n v_{1(-)}}{N v_0}(\eta_{1(-)-2(-)} - \eta_{0-0}) \\ &+ 2\frac{n_{2(-)} n v_{2(-)}}{N v_0}(\eta_{2(-)-0} - \eta_{0-0}) \qquad (4)\end{aligned}$$

If we assume that $\eta_{1(+)-2(+)} \approx \eta_{1(-)-2(-)}$, $\eta_{2(+)-0} \approx \eta_{2(-)-0}$, the equation can be transformed to,

$$\begin{aligned}\frac{\eta}{\eta_0} \approx 1 + 2\frac{n}{N}\Bigg[&(n_{1(+)} + n_{1(-)})\frac{v_1}{v_0}\left(\frac{\eta_{1-2}}{\eta_{0-0}} - 1\right) \\ &+ (n_{2(+)} + n_{2(-)})\frac{v_2}{v_0}\left(\frac{\eta_{2-0}}{\eta_{0-0}} - 1\right)\Bigg] \qquad (5)\end{aligned}$$

Since $n = cN/1000$, where $N$ is the Avogadro number, we find that the relative viscosity varies linearly with the concentration. The factor of the linear term can clearly possess either sign. Since an inequality $\eta_{1-2} > \eta_{0-0}$ is admitted as being always valid, the correlation between $\eta_{2-0}$ and $\eta_{0-0}$ is likely to have a casting vote in the determination of the sign. When $\eta_{2-0} > \eta_{0-0}$, the sign shows positive. When $\eta_{2-0} < \eta_{0-0}$, the sign shows positive or negative corresponding to the inequality:

$$(\eta_{1-2} - \eta_{0-0})/(\eta_{0-0} - \eta_{2-0}) \gtrless (v_2/v_1)(n_{2(+)} + n_{2(-)})/(n_{1(+)} + n_{1(-)})$$

It turns out, therefore, that the condition of negative viscosity is given by

$$\eta_{2-0} < \eta_{0-0},\ (\eta_{1-2} - \eta_{0-0})/(\eta_{0-0} - \eta_{2-0}) < 5 \qquad (6)$$

in rough approximation[9].

It should be understood that the above-mentioned consideration does not contradict Eq. 1. As the concentration reaches nearly 0.1 mol./l., the linear term becomes predominant compared with the Debye-Hückel-Falkenhagen term. Of course, we could not express the relationship exactly only with a linear term. Kaminsky[10] has recently clarified the fact that we have to supply a quadratic term in order to obtain a more precise formula even in the range up to 0.5 mol./l. However, since the factor of linear term is larger than two other

*** This facts can be deduced from our data in spite of slight differences of temperature.

8) S. Broersma, *J. Chem. Phys.*, 24, 659 (1956).

9) T. Satoh and K. Hayashi, *J. Phys. Soc. Japan*, 15, 1658 (1960).

10) M. Kaminsky, *Z. Phys. Chem.*, 5, 154 (1955); 8, 173 (1956).

terms by one degree of order of magnitude, it is apparent that it plays a leading role in the concentrated range over 0.1 mol./l.

Suryanarayana and Venkatesan[6] have proposed that if one plotted a function $\ln(\eta/\eta_0)/C_*$ against reduced concentration $C_*$, where $C_*$ is the ratio of the mole fraction to that at saturation, one could probably represent the entire behavior except in dilute solutions. We suppose that the breakdown in their formalism may be essentially due to our critical phenomenon.

## Summary

The coefficients of the viscosity of concentrated aqueous solutions of 1-1 type electrolytes were measured at room temperature. Judging from the relationship between relative viscosity and concentration the electrolytes would be classified into two groups. One is normal and the other shows negative viscosity. It is the linear term that makes the most predominent contribution in the dilute range. We analyzed its factor by the use of Broersma's concept of local viscosity. From the expression obtained, a condition of negative viscosity was derived as 6 in approximation. According to our interpretation, negative viscosity does not result from individual characters of ions of each electrolyte in question, but from delicate correlations between the local viscosities of neighboring hydration layers.

The authors are very grateful to Professor Tatsuro Watari for his valuable and stimulating discussions. They also wish to thank Mr. Tatsundo Hakuya warmly for his assistances throughout the course of this work.

*Department of Physics*
*Defense Academy*
*Obaradai, Yokosuka*

# *Physicochemical Properties of Dilute Aqueous Solutions of Amylose. Optical Rotatory, Viscometric and Osmometric Studies*

By Takashi KUGE* and Sôzaburo ONO

(Received February 15, 1961)

Amylose is metastable in a neutral aqueous solution, and tends to retrograde. In the retrograded precipitates, amylose molecules take linear extended configurations and form well-ordered crystallites[1]. It has also been well known that amylose can be precipitated as complexes having a helical configuration from the aqueous solutions by the addition of various complexing agents[1]. Hence, it is natural to suppose that the configuration as well as the degree of aggregation of amylose molecules in solution can be changed, depending on the condition under which they are dissolved[2]. Accordingly, it may be inferred that a dilute aqueous solution of amylose has characteristic properties due to the high tendency to associate and the possibility of the transition among various probable configurations of amylose molecules. However, there have been very few experiments[3] concerning the physicochemical properties of the solution. Therefore, in the present experiments, in order to obtain further knowledge of the properties of dilute aqueous solutions of amylose, optical rotatory power, viscosity and osmotic pressure of the solution at various temperatures have been investigated.

## Experimental

**Materials.** — Amylose was obtained from potato strach by a selective precipitation method with *n*-butyl alcohol and isoamyl alcohol[4]. This amylose was recrystallized twice from boiling water in the presence of excess butanol and the resulting pure amylose was used in this investigation unless otherwise indicated. The $\beta$-limit dextrin used was prepared from glutinous rice starch by digestion with soyabean $\beta$-amylose which was given by Dr. Yamamoto of Osaka City University. The method of digestion was essentially similar to that described

* Present address: The Shimane Agricultural College, Nogi, Matsue City, Shimane Pref.

1) For a review, see H. Fuwa, "Starch Chemistry" (Denpun Kagaku), Ed. by Z. Nikuni, Asakura Syoten, Tokyo (1951), Chapter III.

2) C. T. Greenwood, *Adv. Carbohydrate Chem.*, **11**, 359 (1956).

3) a) E. F. Paschall and J. F. Foster, *J. Polymer Sci.*, **9**, 73, 85 (1952); b) *J. Am. Chem. Soc.*, **75**, 1177 (1953); c) J. F. Foster and E. F. Paschall, ibid., **75**, 1181 (1953); d) W. W. Everett and J. F. Foster, ibid., **81**, 3459, 3464 (1959).

4) E. J. Wilson, T J. Schoch and C. S. Hadson, ibid., **65**, 1380 (1943).

by Meyer and Bernfeld[5]. The β-limit dextrin obtained was found to be a 41% degraded product of the parent material by measuring the reducing power of the digested mixture.

**Optical Rotatory Power.** — A Rudolph photoelectric polarimeter model 200 was used for the measurements of the dispersion of rotatory power. A Hitachi polarimeter having a vernier scale of one handredth degree, was used for the measurements of the temperature dependence of rotatory power with a jacketed polarimeter tube which enables thermoregulated water to circulate. All measurements were made with two-decimeter tubes.

About 500 mg. of the amylose was dispersed in 70 ml. of 0.5 M aqueous potassium hydroxide and allowed to stand overnight to complete the dispersion and then filled up to 100 ml. with the same solvent. The solution thus obtained was diluted 2.5-fold either with distilled water, after neutralization (pH 5.4~6.0) with hydrochloric acid, or with the 0.5 M potassium hydroxide. The solutions were filtered and the filtrates were used for measurements. Likewise, the β-limit dextrin was also used.

For the measurements of the variations of rotatory power with temperature, the temperature of the circulating water was changed at an average rate of 3 degrees per 10 min. The temperature of the solution investigated was read from a thermometer immersed in the circulating water. The temperature seemed to be controlled to ±1.0°C. At a given constant temperature six readings were made and the average was taken.

**Viscosity.**—A usual Ostwald type viscometer was used throughout this investigation. For the solutions investigated the viscometer had flow times of 123~271 sec. at the experimental temperatures. Temperature control within ±0.01°C could be achieved by keeping a thermostated water-bath in an outer larger thermostat.

The procedure used for determining the viscosities was as follows: The amylose solution prepared as described in the above section was filtered through a glass filter. Ten milliliters of the filtrate was pipetted into the viscometer which was placed in the thermoregulated water-bath set at 25.0°C and allowed to stand for 20 min. The flow time was then determined three times and the average was taken. Thereafter the temperature of the water-bath was raised to another given temperature and after a further 20 min. the flow time was determined. This process was repeated at 5 degree intervals, until 50.0°C. The temperature was then decreased and the flow time was redetermined in the same way. This required approximately seven hours. Another aliquot of the solution was allowed to stand at 25.0°C during the period of the above experiment and thereafter its viscosity was also measured.

**Osmotic Pressure.** — Amylose obtained by a method similar to that described by Azumi and Nakajima[6] was recrystallized three times from water by the addition of *n*-butanol and the resulting pure potato amylose was used in this experiment.

The amylose was first dissolved in 0.5 M aqueous potassium hydroxide solution by stirring under nitrogen atmosphere for about two hours in a flask having a glass stopper which was then sealed and stored at 5.0°C for a night. This stored solution was then neutralized with hydrochloric acid and diluted with distilled water to yield 0.2 M solution with respect to potassium chloride containing 0.1~0.5% amylose which was used for the measurements. The concentration of amylose was calculated from the dry weight of the sample dissolved.

The osmometer employed was a modified Zimm-Myerson type osmometer[7,8]. The inner diameter of the measuring capillary was about 0.8 mm. The amount of the solution required to fill the osmometer was about 9 ml. Toluene was used as a pressure indicator, for the solutions examined tended to stick in the measuring capillary. Collodion membranes prepared in the manner described by Fuoss[9] could be useful in this study.

Setting the meniscus in an appropriate position, the measuring apparatus was allowed to stand at a given temperature controlled within ±0.05°C. The approach of the meniscus to equilibrium was followed by a cathetometer. The equilibrium value was attained within six hours in this case. The experimental error with regard to the equilibrium value was within ±0.1 cm.

## Results and Discussion

Specific rotations obtained at room temperature at different wavelengths using solutions of 0.2% concentration are given in Table I. The rotatory dispersions of the amylose and the β-limit dextrin were normal. That is, when the reciprocal of the specific rotation was plotted against the square of the wavelength, the points lay on a straight line (Fig.

TABLE I. SPECIFIC ROTATIONS OF AMYLOSE AND β-LIMIT DEXTRIN AT VARIOUS WAVELENGTHS

| Wavelength mμ | Specific rotation | | | |
|---|---|---|---|---|
| | Amylose | | β-Limit dextrin | |
| | 0.2 M KCl | 0.5 M KOH | 0.2 M KCl | 0.5 M KOH |
| 589.3 | — | 150.0 | 190.6 | 165.0 |
| 577.0 | 196.2 | 156.2 | 197.3 | 175.3 |
| 546.1 | 217.8 | 175.5 | 224.6 | 197.5 |
| 491.6 | 274.9 | 215.6 | 259.4 | 232.5 |
| 435.8 | 363.0 | 290.0 | 369.9 | 326.6 |
| 404.7 | 428.9 | 343.8 | 430.0 | 381.5 |
| 365.0 | 549.6 | 437.1 | 545.1 | 481.8 |
| 312.6 | 809.9 | 633.4 | — | — |

5) K. H. Meyer and P. Bernfeld, *Helv. Chim. Acta*, **23**, 875 (1940).
6) H. Azumi and T. Nakajima, *Sci. Rep. Tohoku Univ., Series I*, **36**, 278 (1952).
7) T. Kawai, "Zikken Kagaku Kōza", Vol. 8, Maruzen Co., Tokyo (1956), Chapter 3.
8) T. Matsuo, *High Polymers Chem. (Kōbunshi Kagaku)*, **15**, 640 (1958).
9) R. M. Fuoss and D. J. Mead, *J. Phys. Chem.*, **47**, 59 (1943).

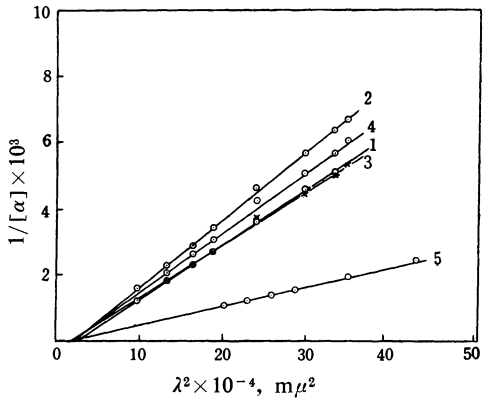



Fig. 1. The rotatory dispersions of amylose, $\beta$-limit dextrin and D-glucose. The date for D-glucose are taken from International Critical Table. Only for glucose, the ordinate scale should be read in one tenth of the presented. 1, amylose in 0.2 M KCl; 2, amylose in 0.5 M KOH; 3, $\beta$-limit dextrin in 0.2 M KCl; 4, $\beta$-limit dextrin in 0.2 M KOH; 5, D-glucose in $H_2O$.

1). Hence, the variation in the rotation measured can be expressed by a single term Drude equation

$$[\alpha]_\lambda = A/(\lambda^2-\lambda_c^2) \qquad (1)$$

where $[\alpha]_\lambda$ is the specific rotation at a given wavelength, $\lambda$, and $A$ and $\lambda_c$ are the rotation constant and the critical wavelength, respectively. $A$ and $\lambda_c$ can be obtained from the slope and the intercept of the straight line with the abscissa, respectively. Their values calculated by the least square method are given in Table II. Already determined correlations between rotatory properties and molecular structure make it apparent that optical rotatory dispersion is one of the best qualitative methods for detecting changes in configuration of very large optically active molecules[10]. Particularly, the helical configuration of protein and polypeptide could be well reflected in $\lambda_c$. Murakami[11] pointed out from a theoretical viewpoint that the helical structure in which many identical groups are asymmetrically arranged shifts apparently an original $\lambda_c$ corresponding to random structure towards longer wavelengths. Hence, it may be considered that amylose taking a helical configuration should possess a distinctively different $\lambda_c$ from that of amylose which has no helical configuration. All of the $\lambda_c$ found for the amylose and the $\beta$-limit dextrin in the two solvents are in close agreement with each other. It seems that the $\beta$-limit dextrin never takes a helical configuration because of its highly branched structure[1]. Moreover, D-glucose has also a nearly equal $\lambda_c$, as can be seen in Fig. 1 and Table II. Wolff et al.[12] also gave 147 m$\mu$ for $\lambda_c$ of corn amylose in 1 M potassium hydroxide, though they obtained 103 m$\mu$ for corn amylopectin. Hence, it can be stated that the wavelength near 140 m$\mu$ is an intrinsic $\lambda_c$ for D-glucopyranose residue, and the amylose in the two solvents at room temperature does not take a well-oriented helical configuration. Although there are some possibilities that right handed and left handed helices exist in the same amount, this seems to be rather rare.

TABLE II. CRITICAL WAVELENGTH AND ROTATION CONSTANT

| Substance | Solvent | $\lambda_c$, m$\mu$ | $A$ |
|---|---|---|---|
| Amylose | 0.2 M KCl | 151 | 60.2 |
| | 0.5 M KOH | 145 | 48.8 |
| $\beta$-Limit dextrin | 0.2 M KCl | 134 | 62.1 |
| | 0.5 M KOH | 141 | 54.4 |
| D-Glucose | $H_2O$ | 141[a] | |

a) The value was calculated from the data given in International Critical Table.

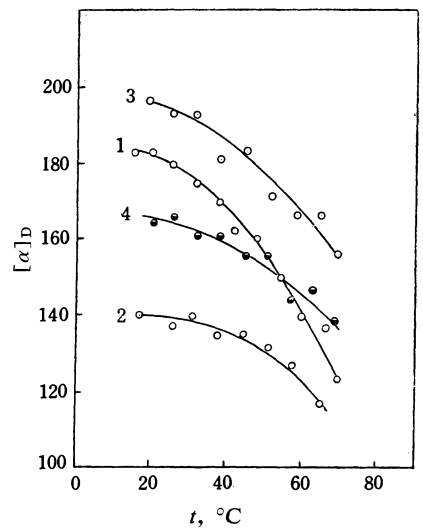



Fig. 2. The temperature dependences of specific rotations: 1, 0.2% amylose in 0.2 M KCl; 2, 0.2% amylose in 0.5 M KOH; 3, 0.2% $\beta$-limit dextrin in 0.2 M KCl; 4, 0.2% $\beta$-limit dextrin in 0.5 M KOH.

Figure 2 shows temperature dependence of the specific rotations of the amylose and $\beta$-limit dextrin in the two solvents at a wavelength 589 m$\mu$ (Na-D line). Although the rotation of the amylose in 0.2 M potassium

10) For a review, see C. Djerassi, "Optical Rotatory Dispersion, Applications to Organic Chemistry", McGraw Hill Book Co., Inc., New York (1960), Chapter 17.
11) H. Murakami, *J. Chem. Phys.*, **27**, 1231 (1957).
12) I. A. Wolff, P R. Watson and C. E. Rist, *J. Am. Chem. Soc.*, **74**, 3064 (1952).

chloride solution is considerably larger than that of the amylose in 0.5 M potassium hydroxide at 25°C, the former approaches the latter with increasing temperature, having a large temperature coefficient of negative sign. The rate of the change of the specific rotation is $-1.4°/°C$ in the region of the most rapid change, which is unusually large compared with those of carbohydrates of low molecular weight; for example, sucrose has the rate $\sim 0.01°/°C$[13].

Changing temperature can affect the optical rotation in four possible ways: 1) Configuration of the chain of amylose might change, namely, the helix-coil transition might occur. This was seen in cases of proteins and polypeptides[10]. 2) Ring conformation of glucopyranose residue might differ. Reeves[14] considered that the different specific rotations of corn amyloses in neutral aqueous solution and alkaline solution may be ascribed to different conformations of their glucopyranose rings, that is, B1 may be the conformation in neutral solution and 3B in alkaline solution (the symbols follow Reeves' convention). 3) The vicinal action of solvent might change[15]. This generally decreases with increasing temperature. 4) Hindrance to free rotation around bond axis might change. This would change axial symmetry.

Among these possibilities, the first is unlikely, since the $\beta$-limit dextrin also shows qualitatively the same behavior as to temperature dependence as the amylose does (Fig. 2). In addition, the specific rotation at the higher temperature is close to that of $\alpha$-D-glucose, which may suggest no contribution due to the helical structure to the rotation at the higher temperature. The second and the third possibilities are not clear at present. However, judging from the small temperature coefficients of the rotations of the carbohydrates having low molecular weights, the possibilities appear to be unimportant. Even if the transition between the two ring conformations mentioned above occurs, that would not explain the whole change of the rotation without other causes, since the rotation in neutral solution (corresponding to B1) becomes smaller than that in alkaline solution at room temperature (corresponding to 3B) with increasing temperature. The fourth seems to be most important in the present case. According to Kauzmann and Eyring[15], those influences which tend to restrict freedom of orientation about bonds connecting groups to the asymmetric carbon atom will tend to increase the order of magnitude of the optical activity, causing the first order contribution defined by them. At the lower temperature, the ability of free rotation around bonds such as C–O–C, C–OH and $C\text{-}CH_2\text{-}OH$ in amylose molecule seems to be strongly hindered owing to hydrogen bonds occurring between hydroxyl groups which come close to each other. This will lead to the higher rotation due to the first order contribution. With increase in temperature, the hydrogen bonds will be more or less ruptured and the free rotation will become easier. This process must also be taken into consideration in order to explain the anomalous behavior of viscosity of amylose, as can be seen later. Consequently, the lower rotation of amylose at the higher temperature may be ascribed to the vanishing of the first order contribution.

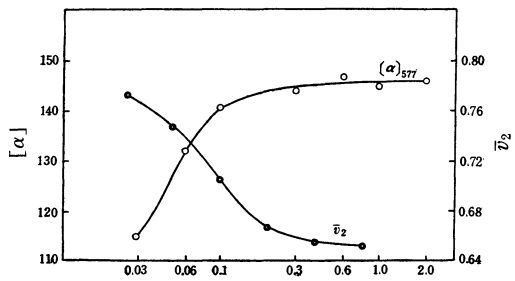



Fig. 3. The variations of specific rotation, $[\alpha]_{577}$, and partial specific volume, $\bar{v}_2$, of amylose in 0.5 M KOH with change in the concentration of amylose. $[\alpha]_{577}$ was measured by the Rudolph photoelectric polarimeter.

In Fig. 3 the variation of the specific rotation with that of partial specific volume which was found by Yoshikawa[16] by measuring density of amylose solution, is shown. Although the experimental error increases as the concentration becomes lower, it may be said that both the specific rotation and the partial specific volume sharply alter with decreasing concentration in the region of low concentration below 0.1%. These facts seem to be explained by the decrease of segment-segment interaction with decreasing concentration, and support the authors' opinion concerning the temperature dependence of the rotatory power.

From the point of view given above, it may be suggested that the large rotation of the $\beta$-limit dextrin compared with that of amylose would arise from the inability of free rotation around the bonds between carbon 5 and carbon 6 at branch points in the $\beta$-limit dextrin; besides, the highly branching structure would

13) T. R. P. Gibb, Jr., "Optical Methods of Chemical Analysis", McGraw Hill Book Co., Inc., New York (1942), Chapter 8.
14) R. E. Reeves, *J. Am. Chem. Soc.*, **76**, 4595 (1954).
15) W. Kauzmann and H. Eyring, *J. Chem. Phys.*, **9**, 41 (1941).
16) Y. Yoshikawa, Dissertation for Degree of Master, College of Agriculture, Univ. of Osaka Prefecture (1958).

increase segment-segment interaction occurring inside the molecule. On the contrary, in amylose which has no branch point, all of the bonds between carbon 5 and carbon 6 can rotate freely unless the hydrogen bond at carbon 6 is formed with another segment which comes into contact with it. The well known fact that amylopectin shows a greater rotation than that of amylose may be explained by the same consideration.

As for the viscosity, its change may be qualitatively parallel with that of the rotation. Figures 4 and 5 show the variations of the reduced viscosities of 0.2% amylose in 0.2 M potassium chloride and 0.5 M potassium hydroxide, respectively. Arrows marked on the curves in these figures indicate directions of the temperature change. Cross marks in the figures represent viscosities of the samples allowed to stand at 25.0°C for seven hours. It can be seen in these figures that the reduced viscosities in the two solvents decrease with increase in temperature, independent of the

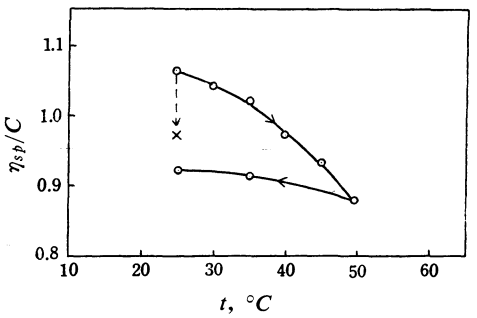



Fig. 4. The variation of reduced viscosity of 0.2% amylose in 0.2 M KCl with temperature.

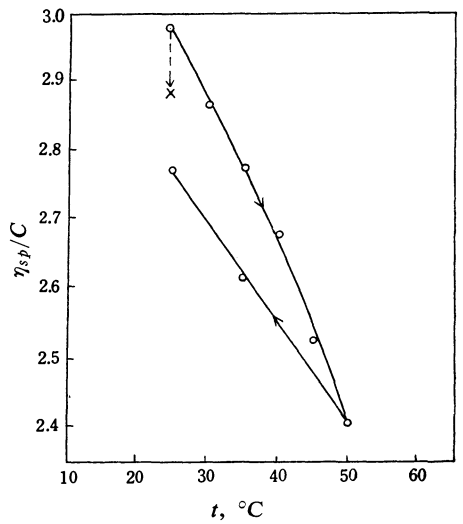



Fig. 5. The variation of reduced viscosity of 0.2% amylose in 0.5 M KOH with temperature.

nature of the solvents used. In a poor solvent, the intrinsic viscosity should increase with increasing temperature, according to the theory of viscosity. Flory[17] gave the following expression for intrinsic viscosity of polymer, assuming a random coil configuration.

$$[\eta] = \Phi(\bar{r}_0^2/M)^{3/2} M^{1/2} \alpha^3 \quad (2)$$

$$\alpha^5 - \alpha^3 = 2C_M \psi_1 (1-\theta/T) M^{1/2} \quad (3)$$

$$\theta = \kappa_1 T/\psi_1 \quad (4)$$

where meanings of the letters are the same as those given by Flory. Although a change in temperature may affect the intrinsic viscosity through alteration of both $(\bar{r}_0^2/M)^{3/2}$ and $\alpha^3$ occurring in Eq. 2, the change of the latter of these factors is likely to be dominant in a usual case. In a poor solvent, where both $\kappa_1$ and $\psi_1$ generally are positive, $\theta$ also will be positive, while negative $\kappa_1$ and positive $\psi_1$ in a good solvent will result in a negative $\theta$. Consequently, in general, the intrinsic viscosity of polymer in a poor solvent should increase with increasing temperature, since $\alpha$ should increase with increasing temperature according to Eq. 3. The increase of $\alpha$ should be most rapid in the immediate vicinity of $T=\theta$.

The viscosity of the amylose even in the aqueous potassium chloride solution, which is a poor solvent having a $\theta$-temperature of 25°C[3d], decreases with increase in temperature, though the reduced viscosity instead of the intrinsic viscosity is dealt with. The anomalous behavior of the viscosity should be accounted for by assuming that $(\bar{r}_0^2/M)$ of the amylose displays an unusually rapid alteration with temperature. $\bar{r}_0^2$ is modified by hindrance to free rotation around bond linking monomers, being greater with increase in the restriction. It is probable that the free rotation around glycosidic bond is strongly hindered by hydrogen bondings between segments through many hydroxyl groups of amylose. With increasing temperature, these hydrogen bonds will be ruptured and the restriction will decrease, which in turn will result in the decrease of $\bar{r}_0^2$. That is, the flexibility of the amylose chain seems to be considerably increased with increasing temperature through the decrease of the degree of the hydrogen bonding.

In the potassium hydroxide solution the possibility of the degradation of the amylose due to oxidation might be considered; however, in the potassium chloride solution the possibility can be ruled out[18]. Figure 4 shows that the solution recooled to 25.0°C does not completely recover its viscosity, and the viscosity

17) P. J. Flory, "Principles of Polymer Chemistry", Cornell Univ. Press, Ithaca, New York (1953), Chapter 14.
18) J. F. Foster and E. F. Paschall, *J. Am. Chem. Soc.*, 74, 2105 (1952).

of the solution after aging at 25°C is lower than that of the solution before aging. These facts may probably arise from the metastability of the amylose solutions having a tendency to retrograde. Possibly the change of the state of the amylose including hydrogen bonding cannot be completely reversible.

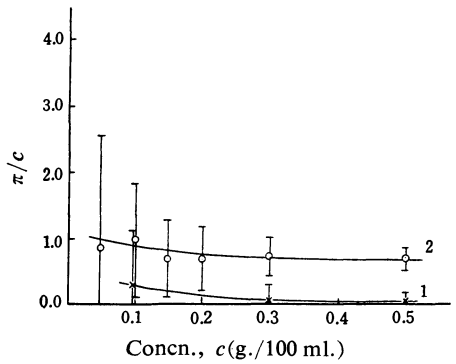



Fig. 6. $\pi/c$ ratio plotted against concentration of amylose in 0.2 M KCl: 1, at 25°C; 2, at 35°C. The vertical lines drawn represent the ranges of experimental error.

In Fig. 6, the ratio of the osmotic pressure to the concentration of the amylose, $\pi/c$, is plotted against the concentration, $c$. The vertical lines drawn in the figure represent the ranges of experimental error. The results of the osmotic measurements are not satisfactory because the experimental error is relatively great compared with the observed osmotic pressure. It may be, however, stated from Fig. 6 that osmotic pressure at 35°C is greater than that at 25°C, and the initial slopes of the curves of $\pi/c \sim c$ plot are negative. These facts seem to indicate that a significant amount of association of amylose occurs in the solutions examined. The amount may decrease with increase in temperature, and also decrease with decrease in concentration. It should be considered that the solutions used by Everett and Foster[3d] (solutions of amylose in aqueous potassium chloride, aqueous potassium hydroxide and dimethyl sulfoxide) to investigate molecular configuration of amylose in solution, are by no means molecularly dispersed solutions, judging from the above results. Therefore, their conclusion concerning the molecular configuration should not be accepted without modification.

Thus it may be said that all of the anomalous phenomena observed, indicate that hydrogen bonding plays a significant role in the properties of the dilute aqueous amylose solutions used in these experiments just as in those of more concentrated solutions or pastes[19]. In other words, any interpretation of the behavior of amylose aqueous solutions may be impossible without postulating hydrogen bondings, even in the case of such dilute solutions as 0.1% or so. At present, however, it is unfortunate that intermolecular and intramolecular hydrogen bondings can not be distinguished with respect to their effects acting on the described properties of the solution except in the case of osmotic pressure. The osmotic measurements may show the existence of the intermolecular hydrogen bondings. However, it seems natural to suppose that the intramolecular hydrogen bondings also exist and have great influence on the properties of the solution together with intermolecular hydrogen bondings.

As already stated above, the well-oriented helix of the amylose in the neutral aqueous solution can be excluded. However, the possibility of the existence of the deformed helix of amylose suggested by Holló and Szejtli[20] remains uncertain, and it seems worth while to reconsider this problem. According to them, the viscosity of acid solution of amylose is unchanged by the addition of iodine, as far as the added iodine is taken up to form the complex. Only when excess iodine is added, is the viscosity changed. If the configuration were substantially altered by the addition of iodine, it would affect the viscosity of the solution. Therefore keeping in mind the helical configuration in amylose-iodine complexes, the configuration of amylose in the solution should not be supposed to be substantially different from the helical configuration. The amylose in the neutral aqueous solutions may be permitted to take the deformed helical configuration, if it is assumed that the deformed helix has no contribution to the optical rotation. In the previous paper[21], the present authors suggested that the vanishing of the blue color of amylose-iodine complex at high temperature (70°C or so) appears to be ascribed to the random configuration of the amylose molecules. Considering these facts with the ease of the amylose-iodine reaction at room temperature, it seems probable that the amylose in neutral solution at room temperature may take the configuration of the deformed helix, which may easily be transformed into the well-oriented helix, rather than take a quite disordered random configuration. The deformed helical molecules appear to be more disordered with increasing temperature. Accordingly, the helical configuration of amylose in the solution at higher temperature may be

19) G. V. Caeser, "Chemistry and Industry of Starch", Ed. by R. W. Kerr, Academic Press, Inc., New York (1950), Chapter 9.

20) J. Holló and J. Szejtli, *Periodica Polytechnica*, **1**, 223 (1957); **2**, 25 (1958); *Die Stärke*, **10**, 49 (1958).

21) T. Kuge and S. Ono, This Bulletin, **33**, 1273 (1960).

more unreasonable than that at lower temperature.

Although Everett and Foster[3d] suggested a random coil configuration of amylose in aqueous neutral solutions from the studies of viscosity and light scattering, their results should be reconsidered, taking the above stated high degree of molecular association of amylose into account. If we assume the high degree of association of molecules having some flexibility, it may be reasonably supposed that the molecules must behave as a random coil in appearance, since a real polymer chain that is restricted in free rotation may be approximated by an equivalent freely jointed chain[22]. Associated amylose molecules, as a whole, may be statistically equivalent to a random coil polymer having great molecular weight.

As a consequence, the most probable configuration of amylose molecules dissolved in neutral aqueous solutions at room temperature, seems to be associated deformed helix which is tentatively drawn in Fig. 7.

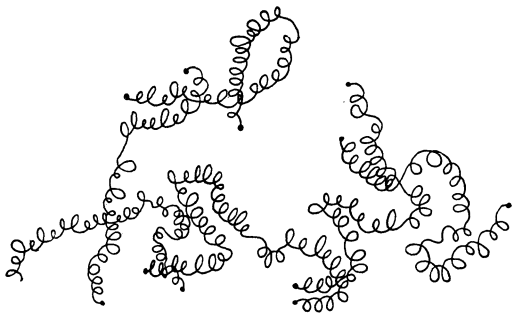
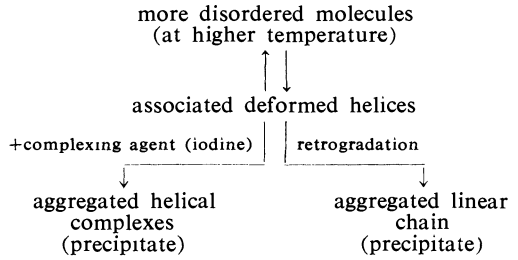


Fig. 7. Supposed configuration of amylose molecules dissolved in aqueous solutions. Dot drawn represents the end of molecule. The length of chain corresponding to each molecule is conveniently drawn to be shorter than that of real molecule.

It should be noted that amylose is metastable in neutral aqueous solutions. Hence, the supposed configuration drawn in Fig. 7, which seems to correspond to "native aggregate" proposed by Paschall and Foster[3a], is a metastable form and then may be stabilized by retrogradation (phase separation). Paschall and Foster also found that the native aggregate can not retrograde at room temperature without first undergoing at least partial disaggregation, and the disaggregation continues along with retrogradation. Therefore, the linear extended configuration of amylose seems to be formed only when retrogradation (crystallization) takes place. Consequently, the following scheme for molecular configuration change of amylose in aqueous solution may be proposed;




22) P. J. Flory, "Principles of Polymer Chemistry", Cornell Univ. Press, Ithaca, New York (1953), p. 411.

## Summary

Optical rotatory power, viscosity and osmotic pressure of dilute aqueous solutions of amylose have been studied. Optical rotatory dispersions of amylose and $\beta$-limit dextrin in 0.2 M potassium chloride and 0.5 M potassium hydroxide are normal and can be well expressed by a single term Drude equation. All of the $\lambda_c$ obtained from the analysis of the dispersion curves are close to 140 m$\mu$ which may be considered as a characteristic value of glucopyranose residue. This seems to indicate that there is no well-oriented helix of amylose in the solutions. With increasing temperature, the optical rotations of amylose and $\beta$-limit dextrin decrease. Amylose, especially in a neutral aqueous solution, has an unusually great temperature coefficient of specific rotation amounting to $-1.4°/°C$ as the largest value. Parallel with this change, the viscosities of the amylose solutions decrease with increasing temperature. These results seem to be well explained by assuming that the flexibility of amylose molecules is considerably influenced by temperature through the change of the degree of hydrogen bonding between segments of the molecules. Osmotic measurements have given evidence to prove the occurrance of the association of amylose molecules in the solution examined. The degree of the association has been found to decrease with increasing temperature. These facts indicate that hydrogen bonding plays a significant role in the properties of the dilute aqueous solution.

The molecular configuration of amylose in aqueous solutions has been discussed. It seems to be most probable that amylose molecules in the solutions take the configuration of deformed helix, and associate highly with each other. No linear extended configuration is possible. The figure of the supposed configuration is drawn.

The present authors are indebted to Professor S. Akabori and Professor R. Tsuchida of Osaka University for their permission to use of their Polarimeters, and also to Mr. A. Maeda, former member of Akabori Laboratory, for his kind

help in making the measurements. The authors thank Dr. T. Yamamoto of Osaka City University for the gift of $\beta$-amylase.

*Laboratory of Biophysical Chemistry*
*College of Agriculture University of*
*Osaka Prefecture Sakai, Osaka*

# *Thermodynamical Studies on Binary Systems Consisting of Polar and Non-polar Liquids. I. Construction of a Semi-automatic Microcalorimeter Suitable for the Rapid Measurement of Heats of Mixing of Binary Solutions*

By Kazuo AMAYA*

(Received March 1, 1961)

For the full understanding of thermodynamical properties of binary systems, it seems to be very important to know about the relation between the termodynamical properties of binary systems and the structure of the constituent molecules.

The accumlation of this knowledge may contribute not only to the development of the theory of solutions but also to the application of it to practical purposes. To see how the dipole moment of polar molecules affects the thermodynamical properties of binary systems containing them, the measurements of heats of mixing for binary solutions consisting of polar and non-polar liquids were attempted.

The main obstacles which prevent the systematic study of heats of mixing for a large number of binary systems of non-electrolytes have been the difficulty, and the laboriousness, of the precise measurement of the small amount of heat evolved or absorbed on mixing two kinds of liquids of non-electrolytes.

Therefore, in designing a calorimeter the following points are taken into account.

1) Ease of the measurement, particularly the shortening of the time required for one measurement by an economical use of waiting time. It is essentially necessary to perform a large number of measurements in a short time.

2) Saving of the amounts of the samples required for each measurement.

3) Elimination of the errors due to evaporation or condensation of the components on mixing.

4) Durability for continuous operation of the thermostat for a long period.

By bearing the above points in mind, a semi-automatic microcalorimeter with the following features is constructed.

1) Five removable mixing vessels are attached to the calorimeter. They can be fitted to or removed from the calorimeter from the outside of the calorimeter chamber without seriously affecting its thermal equilibrium. This device cuts down the time required for the calorimeter to reach thermal equilibrium, after which the next measurement can be carried out, and hence is capable of shortening the waiting time required for each measurement.

2) An automatic measurement of the integrated time from $10^{-4}$ to 100 sec. during which the electrical current is passed through the calorimeter heater is carried out with an electronic counter, a gate circuit and a standard crystal oscillator.

3) An automatic thermal compensation is possible when the system is endothermic.

4) The quantities of samples required for each measurement are less than 1 cc. for each component.

5) The vapor phase is completely eliminated. This eliminates the error due to evaporation or condensation of the components.

## Principle of the Construction of the Apparatus

The whole apparatus consists of a thermostat, a calorimeter, a thermister resistance thermometer, an automatic thermal compensation circuit composed the of constant current supply for the calorimeter heater and a relay circuit which exchange connection of a constant current supply from a dummy heater to the calorimeter heater, the automatic time measuring apparatus consisting of an electronic

* Present adress: Government Industrial Research Institute, Tokyo, Shibuya-ku, Tokyo.

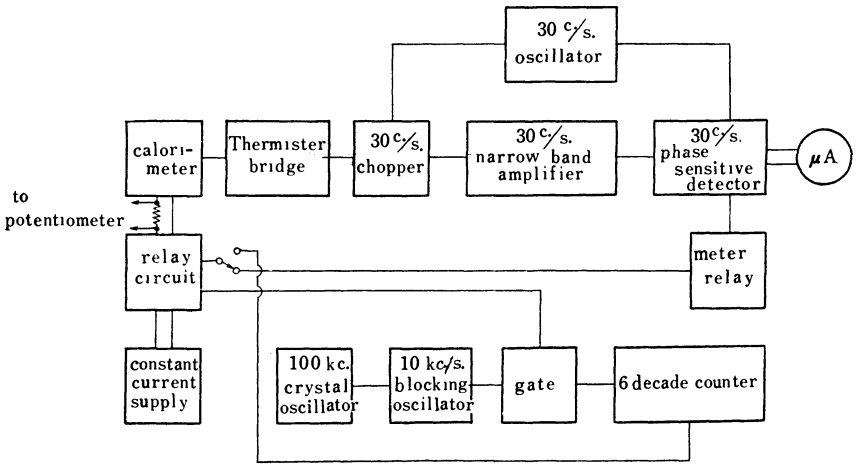



Fig. 1. Block diagram of the apparatus.

counter and the standard crystal oscillator and the gate, and a potentiometer for measuring the electric current of the calorimeter heater. The block diagram of the whole apparatus is shown in Fig. 1. The principle of the operation is as follows.

When the endothermic change occurs in the calorimeter, the signal from the thermometer is amplified by the vacuum tube amplifier and its output automatically operates the relay and changes the connection of the switch from the dummy heater to the calorimeter heater and supplies electrical energy to the calorimeter. At the same time, the gate circuit of the counter is opened and the signal of constant frequency of 10 kc. from a blocking oscillator synchronized by the 100 kc. crystal oscillator enters into the counter and begins to register the time. When sufficient energy has been supplied, the relay returns to its original position and ceases the supply of electrical energy to the calorimeter, and at that instance, the gate circuit is closed, and the integral value of the time during which the current is passed through the calorimeter heater is registered on the counter. For the part of the heat change which is not compensated perfectly, correction is made thereafter. For exothermic reaction, the change of temperature is plotted against time and the temperature change is referred to that caused by feeding a known amount of electrical energy.

### The Details of the Apparatus

**The Calorimeter.** — The calorimeter consists of the mixing vessel holder rotatable around the horizontal axis, the removable mixing vessels, and the mixing vessel container. All of these are contained in the calorimeter chamber which consists of a liquid-tight

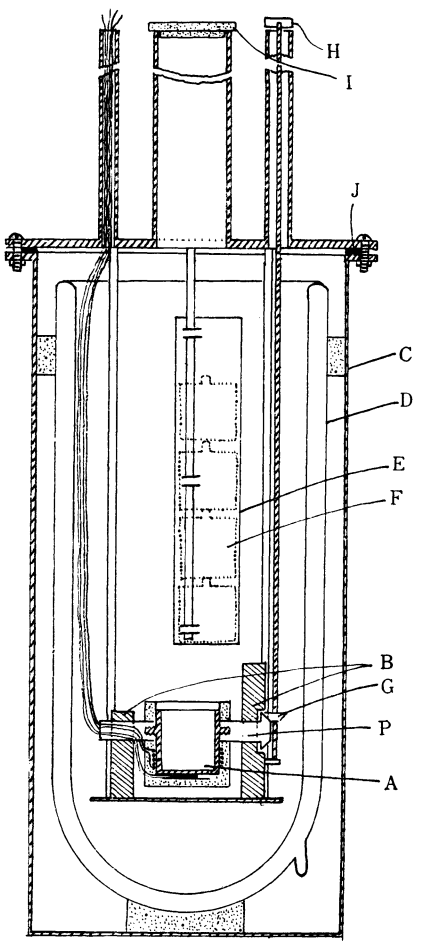



Fig. 2. Calorimeter.

A: Mixing vessel holder
B: Bearing
C: Brass chamber
D: Dewer vessel
E: Mixing vessel container
F: Mixing vessel
G: Bebel gear
H: Handle
I: Lid
J: Rubber packing

cylindrical brass chamber with a large Dewer vessel in it. By this calorimeter a large number of measurements can be made without much labor. The calorimeter from which the mixing vessel is taken away is shown in Fig. 2.

Inside the holder, the removable mixing vessel is just fitted. This can be placed or removed the by use of a long bakelite rod. The mixing procedure is to make the holder upside down by turning it around the pivot P through the manipulation of the handle from the outside of the calorimeter chamber.

**The Mixing Vessel Holder.** — The mixing vessel holder is shown in Fig. 3. A is the

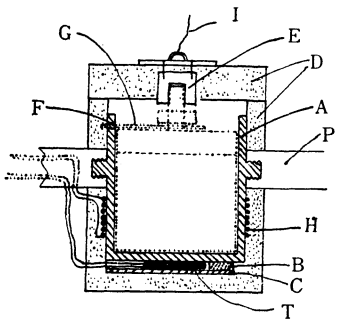



Fig. 3. Mixing vessel holder.

A: Brass vessel
B: Spacer
C: Copper plate
D: Foam styrene
E: Rubber cap
F: Small hole
G: Iron pin
H: Heater
I: String
P: Bakelite pivot
T: Thermister

mixing vessel holder made of a brass cylinder closed at one end and equipped with the pivot P. The cylinder is 3 cm. in inner diameter, 3.4 cm. in outer diameter, and 3.3 cm. in height. Around the outside wall of the cylinder, the calorimeter heater H of double silk covered manganin wire was wound non-inductively, and was fixed by Araldite resin. The resistance of the manganin wire is 45.850 Ω. The outside of the bottom wall of the mixing vessel holder is equipped with a thermister T of about 100 kΩ in resistance at 25°C. The thermister is enclosed in a thin polyvinyl chloride tube and sandwiched between the bottom of the holder and the cupper plate with a brass plate spacer of 2 mm. thickness with a slot, into which the thermister is just fitted, in order that the thermister may not be crushed. The pivot P, made of bakelite for thermal insulation, is fixed to the holder by a male screw extruding from the wall of the holder.

The pivot P is held by a bearing. The holder can be rotated around the pivot P through a bebel gear by rotating the pivot P with the handle outside the calorimeter chamber.

The leads of the thermister and the calorimeter heater are passed through the small holes bored along the axis of the pivot P and are drawn from the one end of the pivot P in order not to be entangled by the turning over of the holder.

The outside of the holder is all covered by foam styrene for thermal insulation.

**The Container for the Mixing Vessels.** — In a large space of the Dewer vessel, there is the mixing vessel container E which can contain four mixing vessels. The five mixing vessels filled with liquid samples to be mixed, are introduced into the calorimeter at one time. One of the five is held in the mixing vessel holder, and the other four are held in the mixing vessel container. When one measurement is finished, the mixing vessel in the holder is taken out of the calorimeter chamber and the one in the container is placed into the mixing vessel holder within the calorimeter chamber by the long bakelite rod without affecting the thermal equilibrium inside it.

**The Mixing Vessel.** — The mixing vessel is shown in Fig. 4. The mixing vessel consists

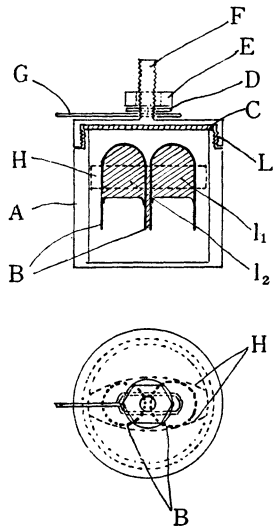



Fig. 4. Cross section and upper side view of the mixing vessel.

A: Iron vessel
B: Glass bells
C: Polyethylene sheet
D: Washer
E: Nut
F: Male screw
G: Iron pin
H: Spring steel plates
$l_1, l_2$: Liquid 1 and 2

of an iron vessel A and a lid L which are tightly fitted to each other by a screw, and two glass bells B fixed together by araldite resin. To make the vessel liquid-tight, a round sheet of polyethylene packing, 0.3 mm. in thickness, is placed between the vessel and the

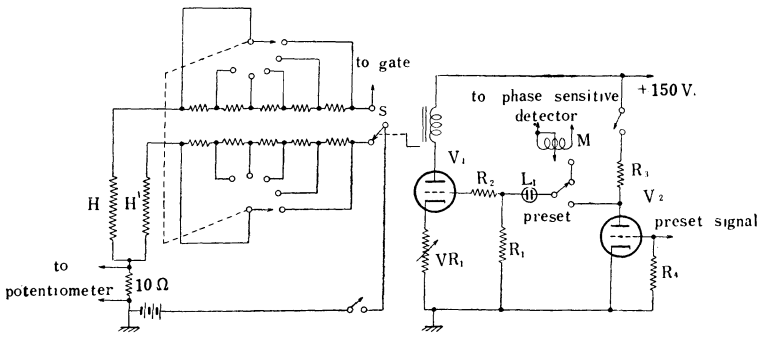



Fig. 5. Electrical circuit of automatic thermal compensation.

| | | | |
|---|---|---|---|
| $R_1$: 1 MΩ | $R_4$: 100 KΩ | S: Micro switch | L: Neon lamp |
| $R_2$: 1 MΩ | $VR_1$: 3 KΩ | H: Calorimeter heater | $V_1$: 1/2 6SN7 |
| $R_3$: 100 KΩ | M: Meter relay | H': Dummy heater | $V_2$: TY66G |

lid. The mixing vessel is a cylindrical iron vessel 2.6 cm. in inner diameter, 3.2 cm. in outer diameter and 3.1 cm. in height. The vessel is filled with mercury and then the two kinds of liquid to be mixed are introduced into two glass bells by two syringes, one for each liquid; therefore they are confined above the mercury separately.

To prevent the bells from being raised above the surface of the mercury by bouyancy when the liquids are introduced into them, two spring steel plates the length of each being a little longer than the inner diameter of the iron vessel, are stuck to the inner wall of the vessel by their restoring force across the diameter of the vessel and the bells are clamped by them.

The syringe used in introducing the liquid into the bell is the usual one modified by attaching a screw driver and by bending the end of the needle.

The upper side of the lid is equipped with a male screw and a nut.

The male screw is used when the mixing vessel is placed into, or is removed from the holder from the outside of the calorimeter chamber by the long bakelite rod, at the one end of which there is a female screw just fitted to the male screw. The nut clamps the iron pin which prevents the mixing vessel from falling down out of the holder when it is turned upside down.

Through the upper part of the wall of the holder a small hole is bored, into which the pin at the upper side of the mixing vessel is put (see Fig. 3).

Before placing the mixing vessel into the holder, the iron pin is loosely held between the nut and the upper side of the lid. When the vessel is put into the holder, the end of the pin is guided into the hole above mentioned by a small piece of permanent magnet, held at the other end of the long bakelite rod described above, and then the nut is screwed by a nut driver from the outside of the calorimeter chamber. After these procedures have been finished, the upper side of the mixing vessel is covered with a foam-stylene lid. The lid is fixed to the mixing vessel by fitting a rubber cap put at the center of the lid to the top of the male screw attached to the lid of the mixing vessel. The rubber cap prevents the foam styrene lid from falling off when the vessel holder is turned. Thus all sides of the calorimeter are covered by foam styrene, and good thermal insulation is assured. The inside of the calorimeter chamber can be illuminated by a miniature lamp in order that these procedures can be performed with ease.

**The Thermometer.**—The thermometer bridge, the converter and the thermister resistance thermometer are the same as those described in the previous paper[1]. The amplifier is also similar to that previously described except that the first stage vacuum tube 6SH7 is replaced by 12AT7 tube in which the two triode plate load resistors are wire wound resistors of 100 kΩ. By the use of the wire wound resister as the plate load, the excess noise is reduced and the signal to noise ratio is raised about three times higher than before.

**The Electrical Circuit for the Automatic Thermal Compensation.** — The electrical circuit for the automatic thermal compensation consists of the constant current supply, the dummy heater, the calorimeter heater, and the relay which converts the connection of the constant current supply from the dummy heater to the calorimeter heater by a lowering of the temperature of the calorimeter.

The electrical circuit is shown in Fig. 5.

The output of the phase sensitive detector

1) K. Amaya and R. Fujishiro, This Bulletin, 29, 270 (1956).

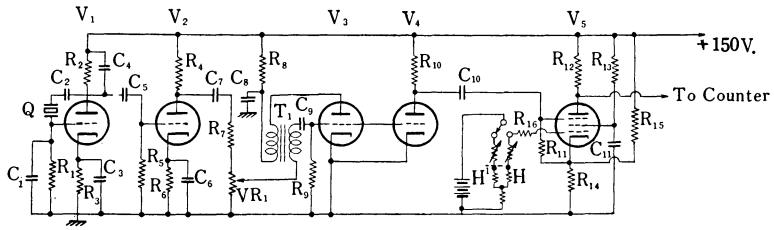



Fig. 6. The electrical circuit of the oscillator and the gate.

| | | | | |
|---|---|---|---|---|
| $R_1$: 100 kΩ | $R_9$: 150 kΩ | $C_1$: 250 pF | $C_9$: 250 pF | $VR_1$: 3 kΩ |
| $R_2$: 20 kΩ | $R_{10}$: 50 kΩ | $C_2$: 0.01 μF | $C_{10}$: 0.001 μF | H: Calorimeter heater |
| $R_3$: 1 kΩ | $R_{11}$: 100 kΩ | $C_4$: 0.1 μF | $C_{11}$: 0.1 μF | H': Dummy heater |
| $R_4$: 20 kΩ | $R_{12}$: 100 kΩ | $C_3$: 250 pF | $C_{12}$: 0.001 μF | $T_1$: Blocking trans |
| $R_5$: 500 kΩ | $R_{13}$: 150 kΩ | $C_5$: 250 pF | $V_1, V_2$: 1/2·5692 | |
| $R_6$: 1 kΩ | $R_{14}$: 1 kΩ | $C_6$: 0.1 μF | $V_3, V_4$: 1/2·6SN7 | |
| $R_7$: 30 kΩ | $R_{15}$: 20 kΩ | $C_7$: 250 pF | $V_5$: 6AS6 | |
| $R_8$: 50 kΩ | $R_{16}$: 100 kΩ | $C_8$: 1 μF | Q: 100 kc. crystal | |

of the thermometer amplifier is fed to a meter relay with sensitivity of 200 μA. When the needle of the meter relay touches the one contact point, the grid of the 1/2·6SN7 tube is connected to high potential through a neon discharge tube and the increased plate current operates the microswitch B and changes the path of electric current from the dummy heater to the calorimeter heater. This operation occurs when the temperature of the calorimeter changes by about $10^{-4}$°C.

A standard 10 Ω resistor is connected in a series with both the dummy and the calorimeter heater. The current which passes through the calorimeter heater is obtained by measuring the electric potential across the 10 Ω standard resistor with the potentiometer. The constant current supply is a heavy duty battery of 6 V. terminal voltage.

The terminal of the microswitch which is connected to the calorimeter heater has a lead to the grid of the gate tube, and when the switch operates, the potential of 6 V. is applied to the grid of the gate tube. $R$ and $R'$ are pairs of resistors having the same resistance and are connected in series with the calorimeter and the dummy heater respectively. By changing the position of the arm of the rotary switch, the total resistance of $R$ and $R'$ is changed, with the resistance kept equal to each other and thereby the current is adjusted from about 15 mA to 120 mA in five steps.

The dummy heater is the resistor having an almost equal value of resistance to the calorimeter heater. Before starting the experiment, the current is passed through the dummy heater and the battery is made to be at a steady state. By the operation of the switch, the total load is nearly the same and the steady state is not disturbed.

**The Time Measuring Apparatus.**—It consists of the standard 10 kc. oscillator with the gate circuit and the six decade electronic counter. The electrical circuits of the former is shown in Fig. 6.

The standard 10 kc. oscillator is a blocking oscillator synchronized by the standard 100 kc. crystal oscillator. The frequency of the 100 kc. crystal oscillator is not corrected by the standard frequency. The gate tube is a 6AS6 tube. The 10 kc. signals from the blocking oscillator are fed to the third grid of the 6AS6 tube. When no voltage is applied to the first grid of 6AS6, a 10 kc. signal sufficiently large to operate the counter is not produced across the plate load resistor of the 6AS6 tube. But, when the gate signal of 6 V. is applied to the first grid of 6AS6, the 10 kc. signal, sufficiently large to operate the counter, comes out. This operation follows in an instant when the electric current from the constant current supply is passed through the calorimeter heater, and so there occurs no delay. By this electronic device, the errors otherwise introduced, of individual persons caused by delay of pushing stop watches or a delay caused by the mechanical inertia of electromagnetic switches, are completely eliminated.

The six decade electronic counter is made of six discharge tube type decatrons of multi-output type manufactured by Japan Radio Communication Co. For the first stage a single pulse decatron is used which responds to signals of up to 20 kc./sec., and the other five are the double pulse decatrons which respond only to signals of up to 5 kc./sec.

By this counter the integral time from $10^{-4}$ to 100 sec. can be measured with an error of $\pm 10^{-4}$ sec. multiplied by the number of operations of the gate circuit.

The counter is also able to pass electrical current through the calorimeter heater for a

pre-determined time from 0 to 100 sec. in steps of $10^{-2}$ sec. But between the actual time and that pre-determined there is a difference of $3\times10^{-2}$ sec. due to the mechanical inertia of the mechanical switch system.

The device stated above is convenient for supplying a known amount of electrical energy to the calorimeter.

**The Thermostat.** — The thermostat and the regulator are practically the same as those described previously. The only improvement is the replacement of the leather belt-pulley type stirrer with the V-belt gear driven one by which the continuous operation for about three months was made possible.

The temperature of the thermostat was kept constant within $10^{-4}$°C at 25±0.1°C.

## Procedures

**Filling of the Bells with the Samples.** — The mixing vessel with two glass bells in it is immersed into a pool of mercury and is turned two or three times in order to exclude the air in the bells and fill them completely with mercury.

Making sure that no air remains in the bells, the two kinds of liquid to be mixed are introduced into each of the two bells by two syringes one for each component.

The quantity of the liquid introduced is determined by weighing the difference of the weight of the syringe by a chemical balance to 0.5 mg. before and after introducing the liquids into the bells.

After the liquids are introduced into the bells, mercury is poured into the vessel until the mercury overflows the edge of the mixing vessel.

Then the round sheet of polyethylene, the size of which is sufficient to cover the whole cross section of the mixing vessel, is placed over the surface of the mercury in the mixing vessel. Making sure that no air exists between mercury and the sheet of polyethylene, the lid of the mixing vessel is put on it and is tightly screwed.

Similar procedures are carried out for the other four mixing vessels containing the same kinds of liquid but of different ratios. The amount of the liquids taken is so chosen that the concentration of the resultant mixture is made about 10, 30, 50, 70 and 90% in voluo.

**The Measurement of the Temperature Change on Mixing.**—The five mixing vessels filled with the sample are introduced into the calorimeter chamber, which is immersed into the thermostat, and one of the five into the mixing vessel container. Then the end of a pin on the lid of the mixing vessel placed in the mixing vessel holder is guided to the hole of the mixing vessel holder and tightly clamped. Then the foam styrene lid is fixed over it. They are then left over night.

After thermal equilibrium is attained, the resistance of the thermister is read every minute and then the liquids are mixed. The mixing is performed by rotating the mixing vessel holder by 180°C, and then by rocking it within a small angle for several times with the handle, from the outside of the calorimeter chamber. Before mixing, the battery for the constant current supply to the calorimeter heater is connected to the dummy heater in order to keep it in a steady state.

When the heat of mixing is endothermic, the thermal compensation takes place automatically. In this case the current passes through the calorimeter heater intermittently from two to four times according to the rate of heat evolution and to the magnitude of electric current passed, until the heat absorbed is nearely compensated for. Then the operation of the automatic thermal compensation circuit is stopped and the resistance of the thermister is read every minute for 15 to 20 min. by manually adjusting the resistance box of the thermometer bridge so as to make the output of the phase sensitive detector null.

The current which has passed through the calorimeter heater is measured to a fraction of second desimals of mA within the interval during which the thermal compensation operates and the current is passed through the calorimeter heater.

The integrated time during which the current is passed through is automatically registered on the electronic counter. Then the known small amount of electrical energy is supplied to the calorimeter to evaluate the part of the heat not perfectly compensated. And again the values of resistance are read for 15 to 20 min. to construct a resistance-time curve.

When the heat of mixing is exothermic, automatic thermal compensation is impossible. In this case the resistance of the thermister is read for 15 to 20 min. after mixing and the resistance-time curve is constructed. Then again a known amount of electrical energy which is nearly equal to the heat evolved on mixing is supplied to the calorimeter and the resistance-time curve is constructed in a way similar to what was done before.

**Calculation of the Heats Evolved or Absorbed by the Use of Resistance-time Curves.**—Typical plots of resistance versus time for endothermic heat of mixing with automatic thermal compensation are shown in Fig. 7.

Within the intervals during which the automatic thermal compensation circuit is in

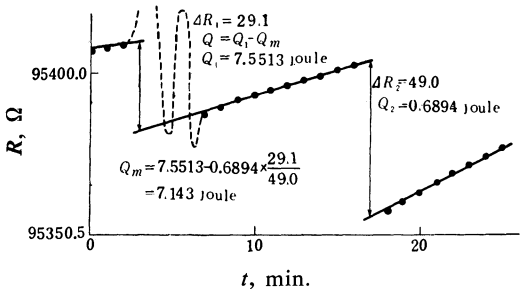



Fig. 7. Typical resistance vs. time curve for endothermic heat of mixing with automatic thermal compensation.

operation, the resistance of the thermister cannot be measured. The dotted line in the figure shows the plot that would be expected if it were actually made.

As the plots of resistance versus time after the thermal compensation ceases to operate are almost linear, it is extrapolated linearly to the time when the mixing was done.

This change of resistance, corresponding to the net change after mixing and the thermal compensation is denoted by $\Delta R_1$, and the total electrical energy supplied by thermal compensation by $Q_1$, and the change of resistance after supplying a known amount of electrical energy $Q_2$ is denoted by $\Delta R_2$, which is obtained by the similar procedure. The change of temperature is very small and the $\Delta R_1$ and $\Delta R_2$ is assumed to be proportional to the corresponding temperature change $\Delta T_1$ and $\Delta T_2$. Then the heat of mixing $Q_m$ is given by

$$Q_m = Q_1 - \Delta R_1/\Delta R_2 \cdot Q_2$$

Typical plots of resistance versus time for the exothermic change, are shown in Fig. 8. In this case the change of resistance on mixing

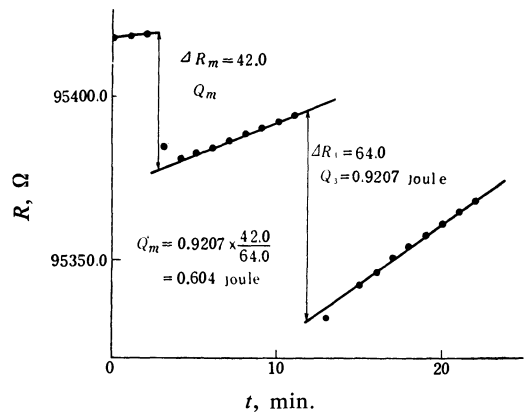



Fig. 8. Typical resistance vs. time curve for exothermic heat of mixing.

$\Delta R_m$ is obtained by linear extrapolation of the plots of resistance-versus time as described above. If the change of resistance due to the supply of a known amount of electrical energy $Q_3$ be $\Delta R_3$, the heat of mixing for this case is given by,

$$Q_m = \Delta R_m/\Delta R_3 \cdot Q_3$$

by assuming again that $\Delta R_m$ and $\Delta R_3$ are proportional to the corresponding change of temperature $\Delta T_m$ and $\Delta T_3$.

**The Sensitivity and the Errors.** — The heat sensitivity is about $10^{-2}$ joule/Ω and the change of resistance can be measured precisely to 0.1 Ω, and thus the change of heat of $10^{-3}$ joule can be detected.

The errors in the final result may arise from the following sources;

1) the error due to the measurement of time,

2) that due to the measurement of the current which passes through the calorimeter heater,

3) that due to the weighing and the filling of the samples,

4) that due to the omission of the correction of heat exchange between the calorimeter and the surroundings.

For 1 the frequency of the crystal oscillator is precise to $\pm 10^{-5}$, and the error in counting is $\pm N$ count, where $N$ is the number of operation of the gate circuit. $N$ is usually within five, and one count corresponds to $10^{-4}$ sec. and the integral time registered on the counter is from 10 to 100 sec., the relative error in the measurement of time is between $5\times10^{-5}$ and $5\times10^{-6}$.

Thus the total number of errors due to 1 is at most $\pm 5\times10^{-5}$.

For 2 the potential drop acrose the 10 Ω standard resistor is measured accurately to $\pm 0.5\times10^{-4}$ V. The current is of the order of a few to several tens of mA, then the potential drop across the standard 10 Ω resistor is of the order of several tenths of a volt. The relative error is at most $\pm 5\times10^{-4}$.

The resistance of the calorimeter heater is measured accurately to ±0.005 Ω in about 50 Ω. The relative error in the precision is $\pm 10^{-4}$.

For 3 the weighing of the samples is performed with the error of 0.5 mg. and the minimum weight of the samples taken is of the order of 100 mg. Then the relative errors would be at most $\pm 5\times10^{-3}$.

In the filling processes is sometimes occurs that a very small quantity of mercury enters into the needle of the syringe which can not be noticed until the next filling. When it is noticed, the drop of mercury is taken into a

weighing bottle and is weighed and the correction is made to the former weight of the liquids.

If it is left unnoticed or noticed in the fillings after the next or further filling, then the correction cannot be made and this amounts to a few milligrams. In this case, the errors from this source may amount to a few per cent at most.

For 4 no quantitative evaluation can be made because during the course of thermal compensation the temperature versus time relation can not be recorded by this apparatus.

In a course of inspection of the data, it was noticed that when the compensation currents had been large, the values of heats absorbed obtained by the above mentioned procedure were a little greater than that when the compensating current had been small.

The errror due to the heat exchange in the endothermic cases might be a few per cent. In the exthermic cases the error due to linear extrapolation might be a few per cent, and in endothermic cases this kind of error may be extremely small due to thermal compensation.

The final error arising from all these sources above mentioned, though the errors from 3 and 4 are the largest, may amount to a few per cent.

**Summary**

A semi-automatic microcalorimeter is constructed which is convenient for a large number of the measurements of heats of mixing of two kinds of liquid.

The calorimeter is equipped with a removable mixing vessel, its holder, and a container, by which the efficiency of the measurement is much increased. Automatic registering of the time intervals during which the electrical current is supplied to the calorimeter, as well as automatic thermal compensation for endothermic systems, are performed. It is another feature of the apparatus to require only less than 1 cc. of each component for each measurement. The elimination of the vapor phase of the liquids in the mixing vessel makes the results certain. The heat sensitivity is $10^{-3}$ joule.

The author wishes to express his thanks to Professor R. Fujishiro of Osaka City University and to Professor Y. Morino of the University of Tokyo for their constant encouragement throughout this work.

*Department of Chemistry*
*Faculty of Science*
*Kobe University*
*Higashinada-ku, Kobe*

# *Thermodynamical Studies on Binary Systems Consisting of Polar and Non-polar Liquids. II. The Measurement of the Heats of Mixing for Binary Systems of Polar and Non-polar Liquids*

By Kazuo AMAYA*

(Received March 1, 1961)

The heats of mixing for 22 binary systems of polar and non-polar liquids were measured. Each pair of polar and non-polar liquids had nearly equal molecular volume. This was done in order to see how the magnitude of the dipole moment of the constituent polar molecules relates to the thermodynamical properties of the binary systems.

## Samples

**Selection of the Pairs of Polar and Non-polar Liquids.**—In selecting pairs of polar and non-polar liquids which are suitable for use in investigating the effect of the dipole moments of the constituent molecules on the heats of mixing the following points were taken into account.

1) The molecular volumes of polar and non-polar components in each pair are nearly equal to each other. This eliminates the effect of the difference of molecular size and makes the effect of the dipoles as clear as possible.

2) The polar molecules have various degrees of magnitudes of dipole moment.

The pairs of polar and non-polar components for which the heats of mixing were measured are shown in Table I with their molar volumes and dipole moments.

It is considered that the observed heats of

* Present adress: Government Chemical Industrial Research Institute, Tokyo, Shibuya-ku, Tokyo.

TABLE I. PAIRS OF POLAR AND NON-POLAR LIQUIDS FOR WHICH THE HEAT OF MIXING WERE MEASURED, ILLUSTRATING SIMILARITY OF THEIR MOLAR VOLUMES

| Non-polar substances | Molar volume at 25°C, cc. | Polar substances | Molar volume at 25°C, cc. | Dipole moment in Debye unit |
|---|---|---|---|---|
| Cyclohexane | 108.09 | Chlorobenzene | 101.74 | 1.56 |
| | | Bromobenzene | 105.51 | 1.73 |
| | | Nitrobenzene | 103.16 | 4.21 |
| | | Benzonitrile | 103.50 | 4.39 |
| | | *n*-Butylchloride | 105.73 | 2.07 |
| | | *n*-Butylcyanide | 105.15 | 4.09 |
| | | Diethyl ketone | 106.40 | 2.71 |
| | | Methyl propyl ketone | 106.40 | 2.71 |
| | | Cyclohexanone | 104.67 | 2.75 |
| | | (Toluene | 106.85 | 0.37) |
| Toluene | 106.85 | Chlorobenzene | 101.74 | 1.56 |
| | | Bromobenzene | 105.51 | 1.73 |
| | | Nitrobenzene | 103.16 | 4.21 |
| | | Benzonitrile | 103.50 | 4.39 |
| | | *n*-Butylchloride | 105.73 | 2.07 |
| | | *n*-Butylcyanide | 105.15 | 4.09 |
| | | Cyclohexanone | 104.67 | 2.75 |
| Methylcyclohexane | 128.38 | Chlorocyclohexane | 119.37 | 2.07 |
| | | Bromocyclohexane | 124.43 | 2.15 |
| *trans*-Dichloroethylene | 77.28 | *cis*-Dichloroethylene | 76.12 | 1.89 |
| Benzene | 89.40 | Pyridine | 81.31 | 2.20 |
| 1,4-Dioxane | 85.80 | Pyridine | 81.31 | 2.20 |

mixing of polar and non-polar liquids contain both contributions from the non-electrostatic dispersion forces and those from the electrostatic dipolar and higher multipolar forces.

The former contribution may be small if the pair of polar and non-polar molecules have molecular structures similar to each other except in the case of the dipole moment. For such binary mixtures, the observed heats of mixing may be considered to be approximately equal to the contribution only from the dipoles of the polar molecules.

Thus at the beginning of the experiment, the measurements were made for the pairs of polar and non-polar molecules not only of similar molecular volume but also of similar molecular structure such as toluene—benzene derivatives (chlorobenzene, bromobenzene, nitrobenzene and benzonitrile), benzene—pyridine, *trans*-dichloroethylene—*cis*-dichloroethylene, methylcyclohexane—halocyclohexanes and cyclohexane—cyclohexanone systems. Although toluene is not strictly non-polar, its polar effect may be small enough to regard it as non-polar.

In the course of the experiment, anomalies were noticed in a group of the systems which contain aromatic compounds.

To make clear whether these anomalies come from the aromatic character of its polar component or of the non-polar component of the pairs of liquids, the experiment was extended to the pairs of aromatic non-polar—aliphatic polar as well as aliphatic non-polar—aromatic polar molecules.

TABLE II. BOILING POINT OF THE SAMPLES

| Substance | B. p. (obs.), °C | B. p. (lit. value), °C |
|---|---|---|
| Chlorobenzene | 131.5~131.6 | 131.687 |
| Bromobenzene | 155.7~155.8 | 155.908 |
| Nitrobenzene | 207.9~208.1 | 210.80 |
| Benzonitrile | 188.7~189.0 | 191.10 |
| *n*-Butylchloride | 78.2~ 78.3 | 78.44 |
| *n*-Butylcyanide | 140.0~140.8 | 142.25 |
| Diethylketone | 101.7~101.8 | 101.70 |
| Methyl propyl ketone | 101.8 | — |
| Cyclohexanone | 155.2~155.3 | 155.65 |
| Chlorocyclohexane | — | |
| Bromocyclohexane | — | |
| Pyridine | 115.0 | 115.58 |
| *cis*-Dichloroethylene | 60.3~ 60.4 | 60.36 |
| Cyclohexane | 80.4 | 80.4 |
| Toluene | 110.3~110.4 | 110.623 |
| Benzene | 80.1 | 80.103 |
| Methlycyclohexane | 100.8 | — |
| 1,4-Dioxane | 101.2 | 101.32 |
| *trans*-Dichloroethylene | 47.3 | 47.67 |

Cyclohexanone, diethyl ketone, and methyl propyl ketone were selected to show the effect of molecular shape and that of the position of the dipole in the molecule.

**Purification of the Samples.** — Most samples were purified from the commercially available purest products according to the methods described in the literature[1] and were finally distilled under normal pressure, with a concentric vaccum jacketed column of about 40 theoretital plates.

Bromocyclohexane and chlorocyclohexane were kindly donated by Dr. M. L. Huggins of the Eastman Kodak Co. Both compounds decompose at their boiling point under normal pressure, so they were used without further purification.

In Table II the boiling points of the samples are shown with the values given in the literature. The thermometer used for the distillation was not corrected by a standard thermometer. Also the boiling points were not corrected for the atmospheric pressure.

## Results and Discussion

The results of the heat of mixing for the 22 binary systems of polar and non-polor liquids are shown in Tables III and IV, in which the following notations are used.

$v_2$: Volume fraction of the polar liquids.

$x_2$: Mole fraction of the polar liquid.

$w_2$: Weight of the polar component taken for the measurement in grams.

$w_1$: Weight of the non-polar component taken for the measurement in grams.

$\Delta H_{\mathrm{m\ obs}}$: The observed heat of mixing in joule.

$\Delta H_{\mathrm{m}}$/cc.: The observed heat of mixing per unit volume of the mixture in joule.

$H^{\mathrm{E}}$: The heat of mixing per mole of the mixture in joule.

$\alpha$: The coefficient of the van Laar formula for heats of mixing of liquids. It is related to the heat of mixing by the relation

$$\Delta H_{\mathrm{m}} = \alpha \cdot V(1-v_2) \cdot v_2$$

where $V$ is the total volume of the mixture.

The volues of $\alpha$ are plotted against $v_2$ in Figs. 1 and 2, $\Delta H_{\mathrm{m}}$/mol. is plotted against $x_2$ in Figs. 3 and 4.

For the systems in which the non-polar component is non-aromatic, the coefficient $\alpha$ can be expressed approximately by the following quadratic expressions except for nitrobenzene-cyclohexane systems. For the systems in which the non-polar component is aromatic, $\alpha$ cannot be expressed by a simple formula.

TABLE III. HEATS OF MIXING OF POLAR AND NON-AROMATIC NON-POLAR LIQUIDS

| System | $w_1$ | $w_2$ | $v_2$ | $x_2$ | $\Delta H_{\mathrm{m\ obs}}$ | $\Delta H_{\mathrm{m}}$/cc. | $H^{\mathrm{E}}$ | $\alpha$ |
|---|---|---|---|---|---|---|---|---|
| | 0.126 | 1.154 | 0.866 | 0.873 | 3.221 | 2.660 | 274.1 | 22.86 |
| Chlorobenzene | 0.266 | 0.862 | 0.695 | 0.708 | 5.831 | 5.179 | 538.9 | 24.43 |
| + | 0.454 | 0.621 | 0.490 | 0.506 | 7.416 | 6.445 | 679.6 | 25.79 |
| Cyclohexane | 0.631 | 0.341 | 0.275 | 0.288 | 6.151 | 5.468 | 584.3 | 27.41 |
| | 0.898 | 0.150 | 0.105 | 0.111 | 3.508 | 2.705 | 292.3 | 28.76 |
| | 0.114 | 1.572 | 0.878 | 0.881 | 3.114 | 2.587 | 273.9 | 24.08 |
| Bromobenzene | 0.259 | 1.125 | 0.693 | 0.700 | 6.188 | 5.674 | 604.2 | 26.68 |
| + | 0.439 | 0.812 | 0.490 | 0.498 | 7.634 | 6.860 | 734.9 | 27.45 |
| Cyclohexane | 0.628 | 0.514 | 0.299 | 0.305 | 7.058 | 6.101 | 657.4 | 29.13 |
| | 0.756 | 0.135 | 0.085 | 0.087 | 2.688 | 2.518 | 273.1 | 32.38 |
| | 0.093 | 0.959 | 0.889 | 0.894 | 4.376 | 4.057 | 420.6 | 40.96 |
| Benzonitrile | 0.266 | 0.706 | 0.672 | 0.684 | 10.864 | 10.354 | 1085.6 | 47.00 |
| + | 0.446 | 0.544 | 0.485 | 0.499 | 14.330 | 12.800 | 1355.0 | 51.52 |
| Cyclohexane | 0.635 | 0.299 | 0.267 | 0.278 | 13.226 | 11.816 | 1266.2 | 60.37 |
| | 0.829 | 0.112 | 0.095 | 0.099 | 7.690 | 6.500 | 703.1 | 75.89 |
| | 0.116 | 1.221 | 0.872 | 0.879 | 7.143 | 6.112 | 625.6 | 54.64 |
| Nitrobenzene | 0.265 | 0.969 | 0.703 | 0.715 | 13.833 | 11.978 | 1266.7 | 58.71 |
| + | 0.416 | 0.625 | 0.493 | 0.510 | 15.497 | 14.632 | 1537.1 | 58.54 |
| Cyclohexane | 0.588 | 0.391 | 0.300 | 0.315 | 14.589 | 13.432 | 1430.0 | 63.92 |
| | 0.835 | 0.135 | 0.095 | 0.101 | 8.359 | 7.014 | 757.7 | 81.90 |

1) A. Weissberger and E. S. Porskauer, "Organic Solvent", Interscience Publishers Inc., New York (1955).

TABLE III. (Continued)

| System | $w_1$ | $w_2$ | $v_2$ | $x_2$ | $\Delta H_{m\ obs}$ | $\Delta H_m$/cc. | $H^E$ | $\alpha$ |
|---|---|---|---|---|---|---|---|---|
| | 0.114 | 0.879 | 0.871 | 0.875 | 2.240 | 1.956 | 206.2 | 17.45 |
| *n*-Butylchloride | 0.278 | 0.693 | 0.693 | 0.694 | 4.687 | 4.126 | 434.4 | 19.38 |
| + | 0.433 | 0.476 | 0.491 | 0.500 | 5.790 | 5.264 | 562.8 | 21.07 |
| Cyclohexane | 0.579 | 0.322 | 0.328 | 0.336 | 5.636 | 5.061 | 543.7 | 22.95 |
| | 0.828 | 0.100 | 0.096 | 0.099 | 2.658 | 2.246 | 243.4 | 25.90 |
| | 0.103 | 0.815 | 0.885 | 0.889 | 4.655 | 4.019 | 442.1 | 39.52 |
| *n*-Butylcyanide | 0.284 | 0.643 | 0.688 | 0.696 | 10.226 | 8.696 | 920.5 | 40.51 |
| + | 0.442 | 0.442 | 0.493 | 0.503 | 12.558 | 11.141 | 1188.2 | 44.57 |
| Cyclohexane | 0.642 | 0.246 | 0.272 | 0.279 | 11.841 | 10.396 | 1118.4 | 52.54 |
| | 0.844 | 0.107 | 0.110 | 0.114 | 7.028 | 5.747 | 621.1 | 58.64 |
| | 0.098 | 0.785 | 0.885 | 0.887 | 3.771 | 3.440 | 366.9 | 33.67 |
| Diethylketone | 0.145 | 0.261 | 0.632 | 0.638 | 4.135 | 8.110 | 869.9 | 34.90 |
| + | 0.265 | 0.263 | 0.487 | 0.492 | 6.498 | 9.738 | 1047.6 | 38.98 |
| Cyclohexane | 0.268 | 0.138 | 0.330 | 0.335 | 4.967 | 9.610 | 1037.6 | 43.47 |
| | 0.815 | 0.088 | 0.094 | 0.095 | 5.355 | 4.609 | 500.2 | 54.33 |
| | 0.097 | 0.820 | 0.890 | 0.892 | 4.047 | 3.556 | 379.2 | 36.29 |
| Methyl propyl ketone | 0.137 | 0.256 | 0.641 | 0.646 | 4.479 | 9.082 | 973.7 | 39.47 |
| + | 0.268 | 0.256 | 0.477 | 0.483 | 6.841 | 10.326 | 1111.2 | 41.39 |
| Cyclohexane | 0.256 | 0.142 | 0.346 | 0.351 | 5.050 | 9.951 | 1073.9 | 43.99 |
| | 0.826 | 0.098 | 0.102 | 0.104 | 6.113 | 5.144 | 558.1 | 56.84 |
| | 0.095 | 0.859 | 0.885 | 0.890 | 3.318 | 3.093 | 328.8 | 30.51 |
| Cyclohexanone | 0.271 | 0.725 | 0.687 | 0.696 | 7.800 | 6.965 | 735.3 | 32.41 |
| + | 0.421 | 0.503 | 0.495 | 0.506 | 9.479 | 8.794 | 935.9 | 35.18 |
| Cyclohexane | 0.629 | 0.302 | 0.283 | 0.292 | 9.233 | 8.147 | 875.9 | 40.16 |
| | 0.806 | 0.101 | 0.093 | 0.097 | 4.901 | 4.266 | 462.0 | 50.48 |
| | 0.103 | 1.019 | 0.884 | 0.891 | 1.264 | 1.089 | 131.1 | 10.62 |
| Chlorocyclohexane | 0.266 | 0.770 | 0.690 | 0.705 | 2.761 | 2.459 | 300.1 | 11.49 |
| + | 0.406 | 0.584 | 0.525 | 0.543 | 3.473 | 3.104 | 383.3 | 12.44 |
| Methylcyclohexane | 0.562 | 0.382 | 0.343 | 0.360 | 3.403 | 3.040 | 380.6 | 13.48 |
| | 0.730 | 0.144 | 0.132 | 0.140 | 1.922 | 1.749 | 222.2 | 15.26 |
| | 0.111 | 1.333 | 0.875 | 0.880 | 1.518 | 1.306 | 163.4 | 11.94 |
| Bromocyclohexane | 0.262 | 1.007 | 0.692 | 0.698 | 3.060 | 2.754 | 346.0 | 12.92 |
| + | 0.443 | 0.728 | 0.489 | 0.497 | 3.952 | 3.483 | 440.2 | 13.94 |
| Methylcyclohexane | 0.625 | 0.436 | 0.289 | 0.296 | 3.750 | 3.262 | 414.8 | 15.88 |
| | 0.822 | 0.166 | 0.105 | 0.108 | 1.880 | 1.565 | 200.2 | 16.60 |
| | 0.816 | 0.125 | 0.082 | 0.084 | 1.463 | 1.259 | 161.2 | 16.71 |
| | 0.141 | 1.178 | 0.891 | 0.893 | 0.580 | 0.559 | 42.63 | 5.75 |
| *cis*-Dichloroethylene | 0.413 | 0.897 | 0.679 | 0.684 | 1.458 | 1.411 | 108.2 | 6.47 |
| + | 0.694 | 0.667 | 0.484 | 0.490 | 2.001 | 1.850 | 142.5 | 7.41 |
| *trans*-Dichloroethylene | 0.929 | 0.391 | 0.291 | 0.296 | 1.883 | 1.787 | 128.8 | 8.65 |
| | 1.178 | 0.128 | 0.096 | 0.098 | 0.883 | 0.843 | 65.55 | 9.72 |
| | 0.130 | 0.992 | 0.889 | 0.895 | 0.217 | 0.190 | 15.48 | 1.93 |
| Pyridine | 0.182 | 0.321 | 0.650 | 0.663 | 0.250 | 0.495 | 40.79 | 2.17 |
| + | 0.343 | 0.329 | 0.502 | 0.517 | 0.418 | 0.625 | 51.96 | 2.50 |
| 1,4-Dioxane | 0.360 | 0.157 | 0.315 | 0.327 | 0.357 | 0.609 | 58.79 | 3.24 |
| | 1.061 | 0.116 | 0.103 | 0.109 | 0.422 | 0.367 | 31.26 | 3.93 |
| | 0.096 | 0.857 | 0.889 | 0.891 | 2.342 | 2.095 | 224.3 | 21.25 |
| Toluene | 0.265 | 0.665 | 0.693 | 0.696 | 5.206 | 4.675 | 502.2 | 21.96 |
| + | 0.420 | 0.456 | 0.494 | 0.498 | 6.075 | 5.670 | 611.2 | 22.68 |
| Cyclohexane | 0.589 | 0.267 | 0.289 | 0.293 | 5.464 | 5.103 | 552.1 | 24.83 |
| | 0.823 | 0.110 | 0.107 | 0.109 | 2.796 | 2.348 | 254.8 | 24.55 |

TABLE IV. HEATS OF MIXING POLAR AND AROMATIC NON-POLAR LIQUIDS

| System | $w_1$ | $w_2$ | $v_2$ | $x_2$ | $\Delta H_{m\ obs.}$ | $\Delta H_m$/cc. | $H^E$ | $\alpha$ |
|---|---|---|---|---|---|---|---|---|
| | 0.113 | 1.107 | 0.885 | 0.889 | −0.497 | −0.437 | −44.9 | −4.28 |
| Chlorobenzene | 0.300 | 0.799 | 0.674 | 0.686 | −0.971 | −0.904 | −93.8 | −4.12 |
| + | 0.475 | 0.584 | 0.491 | 0.502 | −1.346 | −1.245 | −130.2 | −4.98 |
| Toluene | 0.643 | 0.358 | 0.304 | 0.313 | −1.107 | −1.033 | −108.9 | −4.89 |
| | 0.828 | 0.104 | 0.090 | 0.093 | −0.438 | −0.415 | −44.2 | −5.09 |
| | 0.126 | 1.463 | 0.871 | 0.864 | −0.400 | −0.354 | −37.1 | −3.15 |
| Bromobenzene | 0.301 | 0.999 | 0.658 | 0.646 | −0.776 | −0.761 | −78.8 | −3.38 |
| + | 0.481 | 0.809 | 0.494 | 0.480 | −0.959 | −0.871 | −89.4 | −3.49 |
| Toluene | 0.684 | 0.474 | 0.287 | 0.276 | −0.770 | −0.693 | −70.3 | −3.39 |
| | 0.900 | 0.163 | 0.095 | 0.090 | −0.369 | −0.320 | −31.9 | −3.72 |
| | 0.102 | 1.050 | 0.899 | 0.902 | 0.088 | 0.076 | 7.8 | 0.83 |
| Benzonitrile | 0.305 | 0.758 | 0.682 | 0.689 | 0.080 | 0.072 | 7.5 | 0.33 |
| + | 0.481 | 0.534 | 0.489 | 0.498 | 0.006 | 0.005 | 0.5 | 0.02 |
| Toluene | 0.651 | 0.328 | 0.303 | 0.310 | $0.001_5$ | 0.001 | $0.1_5$ | $0.00_7$ |
| | 0.898 | 0.114 | 0.099 | 0.102 | 0.118 | 0.104 | 10.9 | 1.15 |
| | 0.113 | 1.129 | 0.878 | 0.882 | 1.169 | 1.089 | 112.4 | 10.16 |
| Nitrobenzene | 0.289 | 0.870 | 0.684 | 0.693 | 2.106 | 1.985 | 206.4 | 9.19 |
| + | 0.488 | 0.632 | 0.482 | 0.492 | 2.442 | 2.234 | 234.1 | 8.95 |
| Toluene | 0.687 | 0.455 | 0.323 | 0.331 | 1.929 | 1.640 | 173.1 | 7.50 |
| | 0.871 | 0.106 | 0.081 | 0.084 | 0.849 | 0.841 | 82.3 | 11.35 |
| | 0.097 | 0.817 | 0.892 | 0.893 | −0.604 | −0.581 | −61.2 | −6.02 |
| *n*-Butylchloride | 0.161 | 0.291 | 0.639 | 0.643 | −0.764 | −1.477 | −156.2 | −6.40 |
| + | 0.298 | 0.282 | 0.481 | 0.485 | −1.085 | −1.629 | −172.7 | −6.54 |
| Toluene | 0.297 | 0.145 | 0.322 | 0.327 | −0.780 | −1.532 | −162.8 | −7.02 |
| | 0.868 | 0.090 | 0.092 | 0.094 | −0.672 | −0.603 | −58.4 | −7.21 |
| | 0.113 | 0.707 | 0.871 | 0.873 | −0.614 | −0.599 | −63.1 | −5.35 |
| *n*-Butylcyanide | 0.155 | 0.263 | 0.648 | 0.653 | −0.682 | −1.336 | −140.8 | −5.86 |
| + | 0.303 | 0.263 | 0.485 | 0.490 | −1.113 | −1.631 | −172.5 | −6.53 |
| Toluene | 0.290 | 0.136 | 0.337 | 0.342 | −0.761 | −1.498 | −159.1 | −6.71 |
| | 0.848 | 0.075 | 0.087 | 0.089 | −0.378 | −0.351 | −37.4 | −4.39 |
| | 0.094 | 0.873 | 0.895 | 0.897 | −0.540 | −0.521 | −54.5 | −5.54 |
| Cyclohexanone | 0.290 | 0.673 | 0.680 | 0.685 | −1.277 | −1.215 | −127.6 | −5.58 |
| + | 0.480 | 0.499 | 0.488 | 0.494 | −1.603 | −1.475 | −155.7 | −5.90 |
| Toluene | 0.641 | 0.312 | 0.308 | 0.314 | −1.461 | −1.359 | −144.1 | −6.38 |
| | 0.815 | 0.086 | 0.088 | 0.090 | −0.373 | −0.359 | −38.3 | −4.47 |
| | 0.114 | 0.974 | 0.884 | 0.894 | −0.007 | −0.006 | −0.5 | −0.06 |
| Pyridine | 0.301 | 0.702 | 0.676 | 0.697 | −0.032 | −0.030 | −2.5 | −0.14 |
| + | 0.502 | 0.532 | 0.486 | 0.511 | 0.007 | 0.006 | 0.5 | 0.03 |
| Benzene | 0.715 | 0.309 | 0.279 | 0.299 | 0.040 | 0.035 | 3.1 | 0.18 |
| | 0.918 | 0.113 | 0.099 | 0.108 | 0.023 | 0.020 | 1.7 | 0.22 |

Chlorobenzene—Cyclohexane:

$$\alpha = 29.53 - 7.52_7 v_2 - 0.073_7 v_2^2$$

Bromobenzene—Cyclohexane:

$$\alpha = 32.72 - 10.02 v_2 + 0.405 v_2^2$$

Benzonitrile—Cyclohexane:

$$\alpha = 82.60 - 87.44 v_2 + 46.88 v_2^2$$

Nitrobenzene—Cyclohexane:

*n*-Butylchloride—Cyclohexane:

$$\alpha = 27.12 - 13.50_4 v_2 + 2.876 v_2^2$$

*n*-Butylcyanide—Cyclohexane:

$$\alpha = 64.48 - 54.01 v_2 + 28.75 v_2^2$$

Cyclohexanone—Cyclohexane:

$$\alpha = 54.91 - 57.44 v_2 + 34.31 v_2^2$$

Diethyl ketone—Cyclohexane:

$$\alpha = 59.73 - 60.62 v_2 + 35.05 v_2^2$$

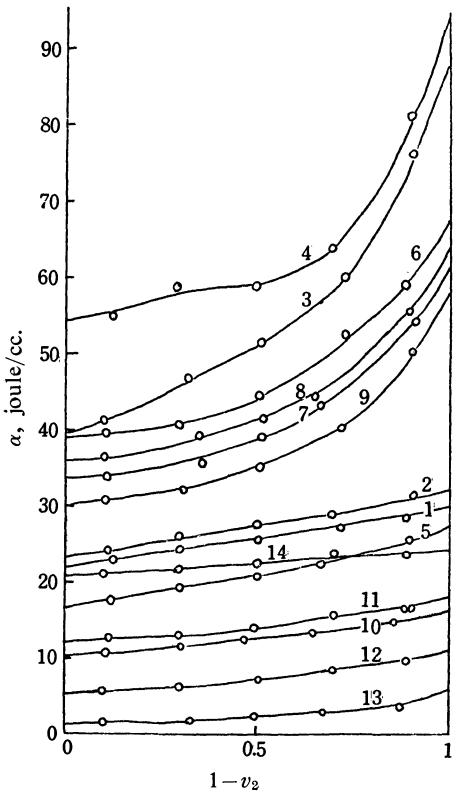



Fig. 1. The plots of van Laar coefficient $\alpha$ vs. volume fraction for the systems of group I.

1. Chlorobenzene—Cyclohexane
2. Bromobenzene—Cyclohexane
3. Benzonitrile—Cyclohexane
4. Nitrobenzene—Cyclohexane
5. *n*-Butylchloride—Cyclohexane
6. *n*-Butylcyanide—Cyclohexane
7. Diethyl ketone—Cyclohexane
8. Methyl propyl ketone—Cyclohexane
9. Cyclohexanone—Cyclohexane
10. Chlorocyclohexane—Methylcyclohexane
11. Bromocyclohexane—Methylcyclohexane
12. *cis*-Dichloroethylene—*trans*-Dichloroethylene
13. Pyridine—1,4-Dioxane
14. Toluene—Cyclohexane

Methyl propyl ketone—Cyclohexane:

$$\alpha = 62.22 - 61.38v_2 + 36.92v_2^2$$

Chlorocyclohexane—Methylcyclohexane:

$$\alpha = 16.01_5 - 7.36_2v_2 + 1.299v_2^2$$

Bromocyclohexane—Methylcyclohexane:

$$\alpha = 17.50 - 6.61v_2 + 0.396v_2^2$$

*cis*-Dichloroethylene—*trans*-Dichloroethylene:

$$\alpha = 10.438 - 7.172v_2 + 2.094v_2^2$$

Toluene—Cyclohexane:

$$\alpha = 24.78 - 3.971v_2$$

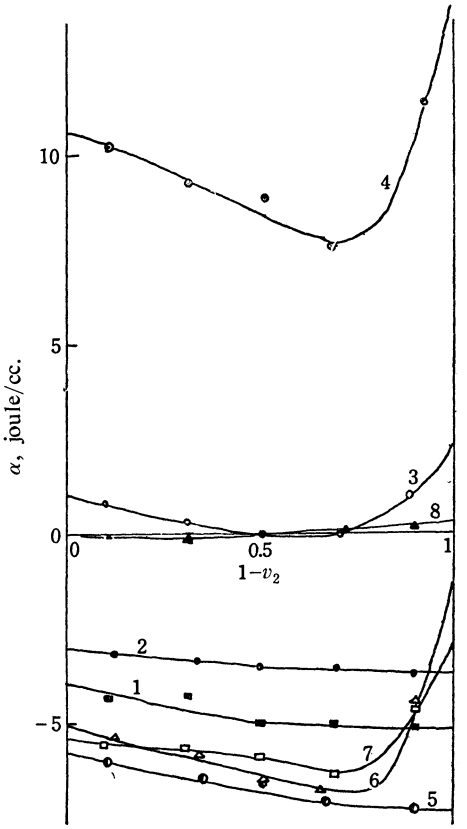



Fig. 2. The plots of van Laar coefficients $\alpha$ vs. volume fraction for the systems of group II.

1. Chlorobenzene—Toluene
2. Bromobenzene—Toluene
3. Benzonitrile—Toluene
4. Nitrobenzene—Toluene
5. *n*-Butylchloride—Toluene
6. *n*-Butylcyanide—Toluene
7. Cyclohexanone—Toluene
8. Pyridine—Benzene

Pyridine—1,4-Dioxane:

$$\alpha = 4.92_9 - 7.42_5v_2 + 4.69_2v_2^2$$

It is obvious from the above figures that for the systems where non-aromatic molecules such as cyclohexane and methyl cyclohexane are selected for the non-polar component (denoted as group I hereafter) the values of $\alpha$ are positive and increase smoothly as the volume fractions of polar component $v_2$ decrease. It is in sharp contrast to the cases of mixing of two non-polar liquids where the values of $\alpha$ are nearly constant over the whole range of concentrations[2].

The larger the dipole moment of the polar molecules the larger the variation of the values of $\alpha$ with concentration. This suggests that

2) J. H. Hildbrand, "The Solubility of Nonelectrolytes", Reinhold Publishing Corporetion, New York (1950).

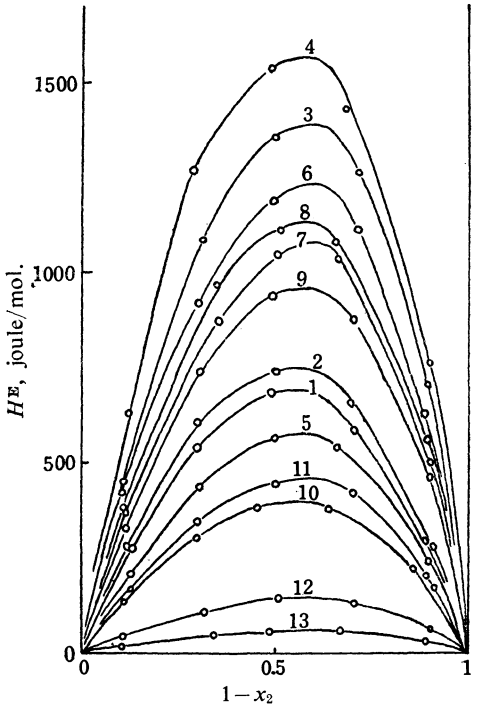



Fig. 3. The plots of $H^E$ vs. mole fraction for the systems of group I.

1. Chlorobenzene—Cyclohexane
2. Bromobenzene—Cyclohexane
3. Benzonitrile—Cyclohexane
4. Nitrobenzene—Cyclohexane
5. *n*-Butylchloride—Cyclohexane
6. *n*-Butylcyanide—Cyclohexane
7. Diethyl ketone—Cyclohexane
8. Methyl propyl ketone—Cyclohexane
9. Cyclohexanone—Cyclohexane
10. Chlorocyclohexane—Methylcyclohexane
11. Bromocyclohexane—Methylcyclohexane
12. *cis*-Dichloroethylene—*trans*-Dichloroethylene
13. Pyridine—1,4-Dioxane

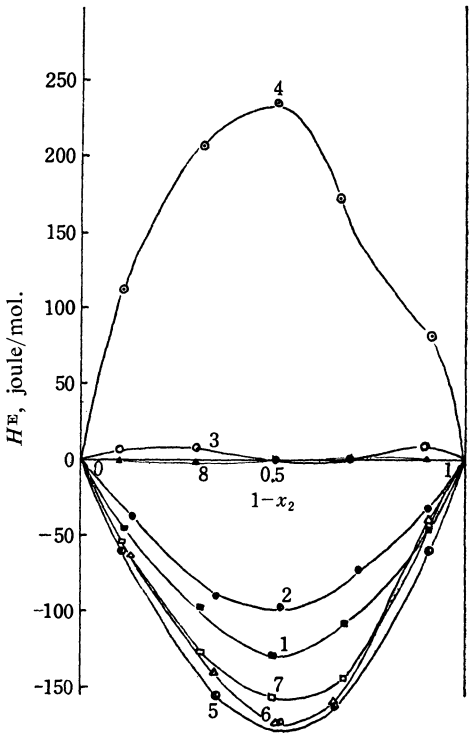



Fig. 4. The plots of $H^E$ vs. mole fraction for the systems of group II.

1. Chlorobenzene—Toluene
2. Bromobenzene—Toluene
3. Benzonitrile—Toluene
4. Nitrobenzene—Toluene
5. *n*-Butylchloride—Toluene
6. *n*-Butylcyanide—Toluene
7. Cyclohexanone—Toluene
8. Pyridine—Benzene

the change of the values of $\alpha$ with concentration originated from the effect of the dipoles of the polar constituents.

However, for the systems in which aromatic compounds such as toluene or benzene are the non-polar components (denoted as group II hereafter), most of the values of $\alpha$ decrease with the decrease of $v_2$ in most concentration ranges, and their variation seems to have no aparent relation with the dipole moment of the polar components.

Furthermore the values of $\alpha$ are much smaller than the corresponding systems of group I containing the same polar component and cyclohexane and are negative for most of these systems. This is a marked difference in comparison with group I.

It is difficult to interpret these differences by electrostatic energy only, for the dielectric constant of toluene does not differ so much from that of cyclohexane, and the electrostatic energy for both can also not be expected to differ greatly. It is concluded from the experimental results that the structural difference between aliphatic and aromatic non-polar liquids is responsible for these differences, for these anomalies are independent of whether the polar components are aromatic or not. This is in accordance with the fact that benzene shows an anomalous solvent effect in dielectric measurement.

As is seen from Fig. 2, for the systems of group II non-polar components, most of the values of $\alpha$ are negative, and if positive, these are small and do not change greatly with concentration as those systems in group I.

The effect of the dipole of the polar component, as is observed in the systems of group I, is also shown for such systems of group II as contain polar molecules of large dipole moment, in which the values of $\alpha$ begin to

increase with the decrease of $v_2$ at low concentrations of polar molecules. This may be interpreted as follows: in the systems of group II two effects must be taken into account; the one is that governed by the magnitude of the dipole moment of the polar component, and is similar to that observed in the systems of group I and the other is a kind of stabilizing effect, specific, or coherent to the aromatic character of non-polar liquids such as toluene or benzene.

For *cis*-dichloroethylene—*trans*-dichloroethylene and pyridine—dioxane systems the values of $\alpha$ are smaller than that of the other group of the systems of polar-non-aromatic non-polar pairs. This may be due to the quadrupole of their components.

## Summary

The heats of mixing were measured for 22 binary systems of polar and non-polar liquids where the pairs of liquids have similar molecular sizes.

For the systems in which the non-polar components are non-aromatic, the van Laar coefficients $\alpha$ are positive and increase smoothly as the concentration of polar liquids decrease. This variation of $\alpha$ with concentration is attributed to the effect of dipole of the polar component.

However, for the systems where the non-polar components are aromatic, the values of $\alpha$ are smaller than that of the corresponding non-aromatic system and are even negative for most of the cases and decrease with concentration of polar component in most concentration ranges.

The sharp difference between two groups of the binary systems, was attributed to the structural difference of aromatic and non-aromatic non-polar components.

The effect presumably due to the quadrupole of the non-polar components was noticed.

The author wishes to express his thanks to Professor R. Fujishiro of Osaka City University and to Professor Y. Morino of the University of Tokyo for their constant encouragement and discussions.

*Department of Chemistry*
*Faculty of Science*
*Kobe University*
*Higashinada-ku, Kobe*

# *Studies on Leucomycin. V. Isolation of Mycarose-4-isovalerate from Leucomycin $A_1$*

By Tetsuo WATANABE, Hisao NISHIDA and Kazuo SATAKE

(Received February 21, 1961)

Leucomycin $A_1$ is a main component of the basic antibiotic complex produced by *Streptomyces kitasatoensis Hata*[1,2]. As described in the previous papers, the main antibiotic isolated from the complex by counter current distribution with the use of a solvent system composed of benzene, chloroform, methanol and water[3], possessed one nitrogen and gave an amino sugar, mycaminose ($C_8H_{17}NO_4$) on drastic acid-hydrolysis[4]. In this paper, we wish to report the isolation of another sugar moiety from the mild acid-hydrolyzate and the identification of it as mycarose-4-isovalerate or its steric isomers.

By the action of methanolic hydrogen chloride, leucomycin $A_1$ ($C_{46}H_{81}NO_{17}$, m. p. 135~138°C, $pK'_a$ 7.1) was split into another basic compound I ($C_{34}H_{59}NO_{13}$, m. p. 154~155°C, $pK'_a$ 8.1) and a neutral oily substance II ($C_{13}H_{24}O_5$, b. p. 115~117°C/1.5 mmHg). The latter oil showed reducing properties only after the removal of the one acid-labile *O*-methyl group. These facts seemed to indicate that there had occurred a methanolysis of the neutral sugar moiety of leucomycin $A_1$. The methyl glycoside possessed an intense infrared absorption at 1745 $cm^{-1}$ and did not consume periodic acid under usual conditions*1. On alkaline hydrolysis at room temperature, however, II gave a mixture of two isomeric methyl

1) T. Hata, Y. Sano, M. Ohki, Y. Yokohama, A. Matsumae and S. Ito, *J. Antibiotics, Ser. A*, 6(2), 87 (1953).
2) T. Hata, F. Koga and H. Kanamori, ibid., 6(3), 109 (1953).
3) T. Watanabe, H. Nishida and K. Satake, This Bulletin, 33, 8, 1104 (1960).
4) T. Watanabe, ibid., 34, 15 (1961).

*1 The present author had no evidences to presume whether II was $\alpha$-, $\beta$- or a mixture of both glycoside isomers.

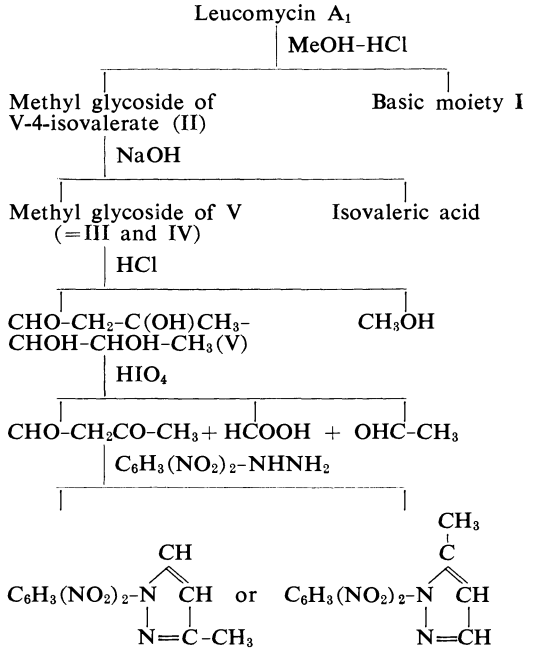
glycosides, III ($C_8H_{16}O_4$, m. p. 59~61°C) and IV ($C_8H_{16}O_4$, b. p. 115°C/1.5 mmHg), both of which consumed periodic acid; isovaleric acid was also obtained which was identified as the *S*-benzylthiouronium salt (m. p. 153°C). These results indicate that II is an isovarelyl ester of a neutral sugar glycoside.

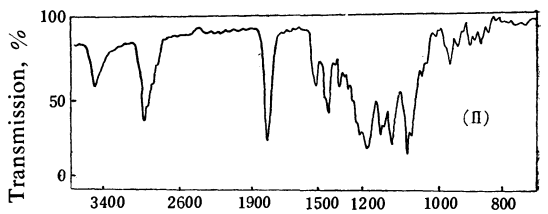
The *O*-methyl group of III was easily split with dilute mineral acid at room temperature, giving a reducing sugar V ($C_7H_{14}O_4 \cdot H_2O$, m. p. 89~90°C). The sugar V which possessed two *C*-methyl groups and three hydroxyl groups, gave a positive iodoform reaction, and rapidly consumed one mole of slightly alkaline iodine, indicating that V was a branched deoxyaldose. The sugar V dissolved in concentrated sulfuric acid with an intense red brown color, a behavior similar to that of intact leucomycin[3,4], and V as well as II showed a characteristic color with vanillineperchloric acid reagent on paper, which had been reported to be specific to 2-desoxyaldose[5].

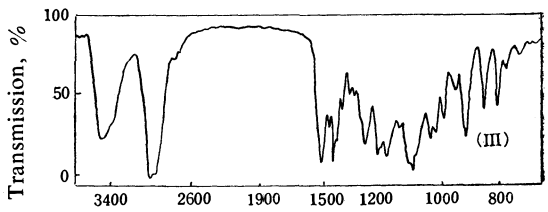
Upon periodate-oxidation, the sugar V consumed one mole of the oxidant rather rapidly and an additional one mole slowly, and produced one mole each of formic acid and acetaldehyde. The former was identified as the *p*-bromophenacyl ester (m. p. 100~101°C) and determined quantitatively by alkaline titration, while the latter was identified as the 2, 4-dinitrophenylhydrazone (m. p. 160~161°C) and assayed photocolorimetrically with the use of *p*-hydroxybiphenyl[6]. Beside the abovementioned two products, 1-(2, 4-dinitrophenyl)-3(or 5)-methylpyrazole ($C_{10}H_8N_4O_4$, m. p. 139~140°C) could be isolated from the reaction mixtures of periodate-oxidized products*2 of V with 2, 4-dinitrophenylhydrazine, indicating the formation of acetacetaldehyde from V[7,8].

These results seemed to indicate that the sugar V was a 2, 6-deoxy-3-methylaldose, thus mycarose which had already been isolated from magnamycin by Woodward et al.[9], or its steric isomer.

Isovaleric acid liberated from II by the action of alkali seemed to be originally attached to the C-4-position of V as the ester. This was because the derivative II, unlike the free V, had an intense infrared absorption at 1745 $cm^{-1}$ (see Fig. 1) presumably due to the presence of the ester linkage and because it did not



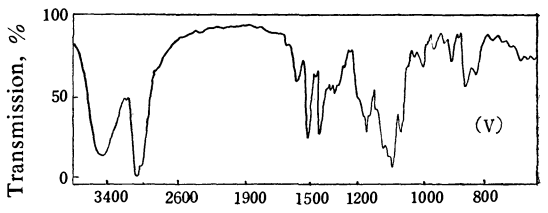




Fig. 1. Infrared absorption spectrum of II, III and V.

*2 An oxidized mixture resulted from one mole of periodate per mole of V, as the mixture contained acetaldehyde in a much lower ratio.

5) A. P. MacLennan and H. M. Randall, *Anal. Chem.*, 31, 2020 (1959).
6) B. A. Neidig and W. C. Hess, ibid., 24, 1627 (1952).
7) L. Claisen and N. Stylos, *Ber.*, 21, 1149 (1888).
8) L. Claisen and N. Stylos, ibid., 24, 1888 (1891).
9) P. P. Regna, F. A. Hochstein, R. L. Wagner, Jr. and R. B. Woodward, *J. Am. Chem. Soc.*, 75, 4625 (1953).

consume periodate under the usual conditions.

Intact leucomycin $A_1$ has one *O*-methyl group, that is acid-stable[10], while the methyl glycoside II derived from leucomycin $A_1$ with methanolic hydrogen chloride at room temperature is acid-labile. Accordingly the neutral sugar moiety (V-4-isovalerate) appears to be linked with another moiety I containing the basic mycaminose residue, as a glycoside, and to be methanolyzated by the above-mentioned treatment. In this respect, a marked difference should be emphasized among the $pK'_a$ of the basic moiety I ($pK'_a$ 8.1), intact leucomycin $A_1$ ($pK'_a$ 7.1) and diacetyl leucomycin $A_1$ ($pK'_a$ 5.1)*[3,11]. Sucha stepwise decrease in the $pK'_a$ values of the dimethylamino group[4] of mycaminose residue, might be interpreted by a successive blocking effect of two hydroxyl groups adjacent to the dimethylamino group. Thus V-4-isovalerate might be linked to the 4- or 2-position of mycaminose residue.

## Experimental

**Leucomycin $A_1$.**—The leucomycin complex used in this experiment was a commercial bulk, Lot No. 9LM-47, which was kindly given by the Research Institute, Toyo Jozo Co., Ltd. Leucomycin $A_1$ was isolated from the complex by a counter current distribution technique, as already reported by the present authors[3].

**Methanolysis of Leucomycin $A_1$.**—Leucomycin $A_1$ (20 g.) was dissolved in 100 ml. of methanol containing 1% hydrogen chloride and the solution mixture was allowed to stand for 18 hr. at 5°C. Thereafter, the reaction mixture was neutralized to pH 4 with diluted sodium hydroxide, concentrated under reduced pressure to remove methanol, diluted with water and extracted with ether (three times, 200 ml.-, 100 ml.- and 100 ml.-portions). The ether extract gave 4 g. of colorless oily liquid II, b. p. 115~117°C/1.5 mmHg, $[\alpha]_D^{25}$ −9.87 (*c* 3 in chloroform).

Found: C, 59.38; H, 9.59; $OCH_3$, 11.51. Calcd. for $C_{13}H_{24}O_5$: C, 59.98; H, 9.29; $OCH_3$, 11.90%. From the remaining aqueous layer, 8 g. of I was crystallized out on adjusting the pH to 8, m. p., 154~155°C (recrystallized from acetone-water)+.

Found: C, 59.14; H, 8.73; N, 1.97. Calcd. for $C_{34}H_{59}NO_{13}$: C, 59.22; H, 8.56; N, 2.03%.

**Alkaline Hydrolysis of II.**—Two grams of II was dissolved in 40 ml. of aqueous sodium hydroxide (1 N) and the solution was allowed to stand for 3 days at room temperature. The hydrolyzate was neutralized to pH 7 with hydrochloric acid, concentrated to dryness in vacuo and the residue was extracted continuously with chloroform. The chloroform extract gave 700 mg. of III (b. p., 76~78°C/1.5 mmHg, m. p., 59~61°C) and 500 mg. of IV (b. p., 115~116°C/1.5 mmHg, not solidified).

Found (for III): C, 54.76; H, 8.97; $OCH_3$, 17.03. Calcd. for $C_8H_{16}O_4$: C, 54.63; H, 9.15; $OCH_3$, 17.62%.

Found (for IV): C, 54.70; H, 9.02; $OCH_3$, 17.23%.

The chloroform-insoluble residues were dissolved into 0.1 N sulfuric acid and steam-distillated. The distillate gave a crystalline *S*-benzylthiouronium salt (m. p., 152~153°C, recrystallized from ethanol) which showed no depression on admixture with authentic *S*-benzylthiouronium isovalerate.

Found: C, 57.95; H, 7.39. Calcd: for $C_5H_9O_2 \cdot C_8H_{11}N_2S$: C, 58.24; H, 7.42%.

**Acid Hydrolysis of III.**—Seven hundred milligrams of III was dissolved in 40 ml. of 0.1 N sulfuric acid and allowed to stand for 45 min. The hydrolyzate was neutralized with aqueous barium hydroxide and the filtrate from barium sulfate was condensed in vacuo to 5 ml. and extracted with ether. The ether layer gave 580 mg. of crystalline solid V, m. p., 89~90°C (recrystallized from ethanol), $[\alpha]_D^{25}$ −25.08 (*c* 3 in water)

Found: C, 46.60; H, 9.40. Calcd. for $C_7H_{14}O_4 \cdot H_2O$: C, 46.41: H, 9.39%.

**Periodate Oxidation of V.**—*Quantitative Oxidation.*—The oxidation was achieved in 0.5% acetic acid at 20°C, with the uses of 0.52 mM of the sugar V and of 4.8 mM of sodium metaperiodate, and an aliquot of the reaction mixture was pipetted out after a given period, for the following analysis. The amounts of periodate consumed, was determined, after the addition of potassium iodide, by the titration with thiosulfate. The amounts of acetaldehyde formed was determined spectrophotometrically with *p*-hydroxbiphenyl[6]. The amounts of formic acid formed was determined by the alkali-titration on the oxidation mixture in aqueous solution instead of 0.5% acetic acid solution. Acetaldehyde and formic acid in the reaction mixture were identified as the 2, 4-dinitrophenylhydrazone (m. p., 160~161°C) and the *p*-bromophenacyl ester (m. p., 100~101°C), respectively. The melting points of these derivatives showed no depression on admixture with each authentic sample, respectively.

*Identification of 1-(2, 4-Dinitrophenyl)-3(or 5)-methylpyrazole with One Mole of Periodate.*—Five hundred milligrams of sugar V (2.78 mM) was dissolved in 50 ml. of water and 600 mg. (2.86 mM) of sodium periodate was added. The solution was allowed to stand for 20 min., then treated with 2, 4-dinitrophenylhydrazine. The bright red precipitate appeared in the solution, was purified on a column of silicagel (1.5×40 cm.) with a mixture of benzene, ethanol and petroleum ether as the developer. The second main band eluted from column gave 75 mg. of a crystal, m. p., 139~140°C (recrystallized from ethanol-ether). Admixture with authentic sample (1-(2, 4-dinitrophenyl)-3(or 5)-methylpyrazole synthesized from acetacetaldehyde and 2, 4-dinitrophenylhydrazine) caused no lowering of the melting point.

Found: C, 48.67; H, 3.60; N, 22.89. Calcd. for $C_{10}H_8N_4O_4$: C, 48.39; H, 3.25; N, 22.57%.

*3 Free mycaminose, itself, possessed a $pK'_a$ at 8.1[4].

10) T. Watanabe, unpublished.

11) T. Watanabe, unpublished.

+ It was chromatographically homogeneous[3].

13) G. L. Miller and A. L. Burton, *Anal. Chem.*, 31, 1790 (1959).

**Other Analyses.**—Aldose reaction with alkaline iodine[13], 2-desoxyaldose reaction with perchloric acid-vanilline reagent[5], iodoform-[14], anthrone-[15] and Fehling-[14] reactions were achieved under the conditions reported in the references cited, respectively. Infrared absorption spectra of II, III and V dispersed in potassium bromide disk or Nujol, were recorded with Koken infrared spectrophotometer, type D-101.

The authors wish to express their appreciation to Mr. T. Fujimoto, Mr. A. Take and Mr. S. Suda for their assistance in the elemental analysis and functional group analysis.

*Department of Chemistry*
*Faculty of Science*
*Tokyo Metropolitan University*
*Setagaya-ku, Tokyo*

14) Y. Mizuno, "Methods of Organic Analysis (Yuki Teisei Bunseki Ho)", Tokyo (1956), pp. 71, 80.
15) D. L. Morris, *Science*, **107**, 254 (1948).

# *Thermo-magnetic Study of Mercury and Dilute Amalgams of Sodium and Potassium*

By S. SRIRAMAN and V. SHANMUGASUNDARAM

(Received February 9, 1961)

The idea of the probable existence of definite compounds between mercury and an alkali element has been suggested by several investigators from their work on vapor pressure[1], surface tension[2] and electrical conductivity[3] measurements of these amalgams. But similar investigations by different authors[4-8] on these amalgams have failed to show any such compound formation. Rao and Aravamuthachari[9] have studied the magnetic susceptibility of dilute alkali amalgams at room temperature. At very low concentration of amalgams lithium showed an increase of diamagnetic susceptibility while the other alkali metals indicated a decrease. Klemn and Hauschulz[10] made magnetic measurements on alkali amalgams at 20 and $-180$°C. The maximum and minimum in $\chi$-concentration curves have been explained as due to the formation of compounds. The magnetic study of dilute alkali amalgams at higher temperatures may throw more light on the structure of the alkali amalgams. Hence the present investigation has been taken up.

## Experimental

Sodium, potassium and mercury used in this investigation were of the highest purity. The amalgams were prepared in vacuum with a specially prepared pyrex apparatus (Fig. 1) by distillation.

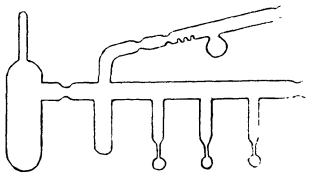


Fig. 1. The pyrex apparatus to prepare the amalgam.

The estimation of alkali content was carried out in accordance with improved procedure for the alkalimetric titration given by Lewis Adams and Lanman and described in detail by Rao and Aravamuthachari[9].

The specific susceptibilities of mercury, the two alkali metals and the amalgams were found by the Curie retorsion method using the vacuum arrangement described by Venkateswarlu and Sriraman[11]. For each specimen $\chi$ values were determined for four different field currents. Graphs were drawn between $\chi$ and $1/H$ for each specimen and in all cases the points were found to plot themselves in a horizontal straight line showing the complete

1) H. E. Bent and J. H. Hilderbrand, *J. Am. Chem. Soc.*, **49**, 3011 (1927).
2) S. S. Bhatnagar, Mata Prasad and D. M. Mukerji, *J. Ind. Chem. Soc.*, **1**, 81 (1924).
3) D. Boohariwala, G. R. Paranjapee and Mata Prasad, *Indian. J. Phys.*, **4**, 147 (1929).
4) R. W. Millar, *J. Am. Chem. Soc.*, **49**, 3003 (1927).
5) P. P. Pugachevich and O. A. Timsfeevicheva, *Doklady Akad. Nauk SSSR*, **94**, 285 (1954).
6) P. P. Pugachevich and O. A. Timsfeevicheva, ibid., **104**, 98 (1955).
7) T. B. Hine, *J. Am. Chem. Soc.*, **39**, 882 (1917).
8) W. J. Davis and E. J. Evans., *Phil. Mag.*, **10**, 569 (1930).
9) S. R. Rao and S. Aravamuthachari, *Proc. Ind. Acad. Sci.*, **9**, 181 (1939).
10) W. Klemn and B. Hauschulz, *Z. Elektrochem.*, **45**, 346 (1939).
11) K. Venkateswarlu and S. Sriraman, *Z. Naturforsch.*, **13a**, 451 (1958).

TABLE I. SUSCEPTIBILITY OF MERCURY, SODIUM AND POTASSIUM

| Substance | Number of bulbs studied | $\chi_s$ Observed | $\chi_s$ by others | | | |
|---|---|---|---|---|---|---|
| Mercury | 5 | −0.169 | −0.1675[12] | −0.166[9] | −0.1610[13] | −0.1667[10] |
| Sodium | 4 | +0.599 | +0.644[10] | +0.60[11] | +0.60[9] | +0.59[14] |
| Potassium | 4 | +0.462 | +0.532[10] | +0.460[11] | +0.52[9] | +0.51[14] |

absence of ferromagnetic impurities. For the calculation of $\chi$ the value for benzene ($0.702\times10^{-6}$) is taken as standard.

## Results

The results obtained for mercury and the two alkali metals are given in Table I. The values of susceptibility given in this report indicate those in $10^{-6}$ c. g. s. units.

Two mercury bulbs were studied at different temperatures between 30°C and 240°C. The results obtained are given in Table II. The fall in $\chi$-values of mercury is found to be slightly larger than reported by Bates and Baker[12].

TABLE II. $\chi_s$ (DIA) OF MERCURY AT DIFFERENT TEMPERATURES

| Temp. °C | $\chi_s$ | |
|---|---|---|
| | $Bulb_1$ | $Bulb_2$ |
| 30 | 0.169 | 0.169 |
| 60 | 0.169 | 0.169 |
| 90 | 0.167 | 0.167 |
| 120 | 0.166 | 0.166 |
| 150 | 0.166 | 0.165 |
| 180 | 0.165 | 0.164 |
| 210 | 0.164 | 0.164 |
| 240 | 0.163 | 0.163 |

In Table III are given the results obtained for sodium and potassium amalgams at room temperature. The last column gives the additive value calculated. Figures 2 and 3 represent the graphical representation of the results

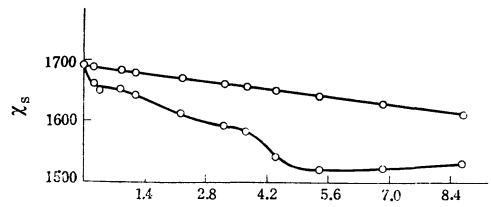



Fig. 2. The magnetic susceptibility of sodium amalgam as a function of atomic per cent of sodium metal in the amalgam.

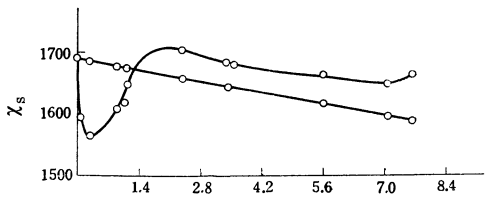



Fig. 3. The magnetic susceptibility of potassium amalgam as a function of atomic per cent of potassium metal in the amalgam.

TABLE III. $\chi_s$ (DIA) OF SODIUM AND POTASSIUM AMALGAMS

| Bulb No. | Sodium amalgam | | | | | Potassium amalgam | | | | |
|---|---|---|---|---|---|---|---|---|---|---|
| | Weight of amalgam g. | Concentration Weight % | Concentration At. % | $\chi_s$ Observed | $\chi_s$ Additive | Weight of amalgam g. | Concentration Weight % | Concentration At. % | $\chi_s$ Observed | $\chi_s$ Additive |
| 1 | 0.4910 | 0.008 | 0.070 | 0.166 | 0.169 | 0.4561 | 0.007 | 0.037 | 0.159 | 0.169 |
| 2 | 0.4132 | 0.024 | 0.209 | 0.166 | 0.169 | 0.4904 | 0.054 | 0.277 | 0.156 | 0.169 |
| 3 | 0.3940 | 0.043 | 0.374 | 0.165 | 0.169 | 0.5049 | 0.174 | 0.887 | 0.161 | 0.168 |
| 4 | 0.3876 | 0.097 | 0.839 | 0.165 | 0.168 | 0.3836 | 0.200 | 1.017 | 0.162 | 0.168 |
| 5 | 0.5298 | 0.137 | 1.179 | 0.164 | 0.168 | 0.3762 | 0.202 | 1.020 | 0.162 | 0.168 |
| 6 | 0.4765 | 0.263 | 2.248 | 0.161 | 0.167 | 0.5740 | 0.232 | 1.180 | 0.165 | 0.168 |
| 7 | 0.4098 | 0.379 | 3.211 | 0.159 | 0.166 | 0.4852 | 0.466 | 2.316 | 0.171 | 0.166 |
| 8 | 0.3841 | 0.440 | 3.713 | 0.158 | 0.166 | 0.6683 | 0.705 | 3.436 | 0.168 | 0.165 |
| 9 | 0.4670 | 0.530 | 4.443 | 0.154 | 0.165 | 0.6145 | 0.717 | 3.576 | 0.168 | 0.165 |
| 10 | 0.4757 | 0.638 | 5.316 | 0.152 | 0.164 | 0.3791 | 1.146 | 5.613 | 0.167 | 0.162 |
| 11 | 0.5012 | 0.840 | 6.880 | 0.152 | 0.163 | 0.5206 | 1.466 | 7.089 | 0.165 | 0.160 |
| 12 | 0.3461 | 1.080 | 8.696 | 0.153 | 0.161 | 0.5012 | 1.583 | 7.620 | 0.166 | 0.159 |

12) L. F. Bates and C. J. W. Baker, *Proc. Phys. Soc.*, **50**, 409 (1938).

13) A. Pacualtt, *Ann. Chim.* (*12*), **1**, 527-87 (1946).

14) W. Sucksmith, *Phil. Mag.*, **2**, 21 (1926).

TABLE IV. $\chi_s$ (DIA) OF SODIUM AND POTASSIUM AMALGAMS AT DIFFERENT TEMPERATURES

| Temperature °C | Sodium amalgam $\chi_s$ | | | | Potassium amalgam $\chi_s$ | | | | | | |
|---|---|---|---|---|---|---|---|---|---|---|---|
| Bulb No. | 1 | 5 | 7 | 10 | 1 | 2 | 5 | 6 | 7 | 8 | 10 |
| 30 | 0.166 | 0.164 | 0.159 | 0.152 | 0.159 | 0.156 | 0.163 | 0.165 | 0.171 | 0.168 | 0.167 |
| 60 | 0.166 | 0.164 | 0.159 | 0.152 | 0.159 | 0.156 | 0.162 | 0.164 | 0.170 | 0.169 | 0.166 |
| 90 | 0.166 | 0.165 | 0.158 | 0.153 | 0.159 | 0.156 | 0.162 | 0.165 | 0.170 | 0.169 | 0.166 |
| 120 | 0.165 | 0.165 | 0.159 | 0.152 | 0.160 | 0.157 | 0.162 | 0.163 | 0.170 | 0.169 | 0.165 |
| 150 | 0.166 | 0.164 | 0.159 | 0.151 | 0.159 | 0.156 | 0.161 | 0.165 | 0.171 | 0.168 | 0.166 |
| 180 | 0.166 | 0.164 | 0.160 | 0.152 | 0.159 | 0.156 | 0.162 | 0.166 | 0.170 | 0.168 | 0.165 |
| 210 | 0.166 | 0.164 | 0.159 | 0.152 | 0.159 | — | 0.163 | 0.165 | 0.171 | 0.168 | 0.166 |
| 240 | — | — | — | — | — | — | 0.162 | — | — | 0.169 | — |

obtained. Four of the above sodium amalgam bulbs and seven of the above potassium amalgam bulbs have been subjected to temperature study in the range 30°C to about 210°C. The results obtained (Table IV) show that, for each specimen, the $\chi_s$ values of the two amalgams remain practically constant at all temperatures.

## Discussion

When very small quantities of a metal goes into solution in mercury one of the three things may hapen; (1) a compound may be formed (2) the metallic atoms may exist in a state of solid solution in mercury and (3) the metal may get dispersed into atoms, each atom, being surrounded by a group of mercury atoms forming a complex molecule.

Bent and Hildebrand[1] suggest the presence of a compound $NaHg_{16}$ as it would explain both vapor pressure and electromotive force data. Inoue[15] and his co-workers claim to identify a compound $NaHg_{14}$ by electrolyzing a saturated sodium chloride solution with mercury cathode. These compounds correspond to about 5.5 and 6.5 atomic per cent of sodium. If such compounds are really formed a pronounced change in the susceptibility will normally be obtained at these concentration. Our results show only a very broad minimum at about 6 atomic per cent as illustrated in Fig. 2. In the case of potassium amalgam the variation of susceptibility at very low concentrations is so rapid (Fig. 3) that compound formation could not account for the change. A study of susceptibility of amalgams at these concentrations and at different temperatures may give us some indications regarding the formation or otherwise of a compound. Our results (Table IV) do not show any such indication. The $\chi_s$ values for amalgams of these concentrations are found to be practically constant at all temperatures. It may be observed that for potassium amalgams the minimum is fairly sharp at 0.3 atomic per cent of potassium. The magnetic investigations of alkali amalgams at 18°C by Klemn and Hauschulz[10] have not indicated the formation of compounds at such low concentrations.

According to Rao and Aravamuthachari[9] the alkali atoms do not even exist in a state of solid solution and they have advanced reasons from electrical conductivity data. Inoue and his co-workers[16] have discussed the structure of sodium amalgam with reference to the amalgamation potential, equilibrium potential, electrophoresis, surface tension and viscosity. The structure of the amalgam was considered as a colloidal state.

Rao and Aravamuthachari[9] suggest that when an exceedingly small quantity of an alkali metal is introduced into mercury it is likely that it is dispersed into atoms and each atom is surrounded by a group of mercury atoms forming a complex molecule. It seems quite probable that the initial fall in the diamagnetic susceptibility of mercury is due to this cause. As concentration increases the alkali atoms join in pairs and these pairs of alkali atoms are surrounded by a group of mercury atoms, the decrease of diamagnetism would rapidly disappear and diamagnetism increases. For these to occur, single atoms of the alkali elements should possess a high paramagnetic component and double atoms a strong diamagnetic component. Ample evidence for the former property is borne out by the experiments of Bates and Tai[17], who find that many metals which are diamagnetic in the solid state appear to possess a large paramagnetic component in the amalgam. Also a few metals like manganese which are paramagnetic in the solid state appear to possess nearly 20 times the paramagnetic susceptibility when dissolved in mercury. That two paramagnetic atoms joining together producing a

15) Y. Inoue and A. Osugi, *J. Electrochem. Soc. Japan*, **20**, 502-513 (1952).

16) Y. Inoue, A. Osugi and T. Amawa, ibid., **22**, 121-6 (1954).

17) L. F. Bates and L. C. Tai, *Proc. Phys. Soc.*, **48**, 795 (1936); ibid., **49**, 230 (1937).

diamagnetic molecule is illustrated by the example of hydrogen. Both the amalgams studied exhibit these effects though in the case of sodium amalgam the initial fall is not as rapid as in potassium amalgam.

The problem could be considered from the point of view of the influence of change in the specific volumes. Maey[18] has shown that the specific gravity of alkali amalgam diminishes rapidly even at low concentrations. The addition of only 0.6% by weight of sodium changes the specific gravity from 13.596 to 12.956. This change corresponds to what would have been obtained, if the mercury had been heated from 0 to 260°C. According to Stoner such an increase in volume would be accompanied by an increase of the paramagnetic susceptibility component of the free electrons. The fall observed in the susceptibility of the mercury at higher temperatures may be due to this cause.

As the amalgam is heated the volume increases. From the above argument this expansion should lead one to expect a further decrease in susceptibility. But the values for the two amalgams for the concentrations studied are not affected by rise of temperature. Is it possible that the lowering of susceptibility due to heating might be compensated by the rise in diamagnetic susceptibility due to the formation of more pairs of alkali atoms in the amalgam? This will mean that such pair formation is induced by temperature.

18) E. Maey, "A Comprehensive Treatise on Inorganic and Theoretical Chemistry", by Mellor, Vol. IV, Longmans Green & Co. (1923), p. 1016.

## Summary

The susceptibility of pure mercury was determined at different temperatures. Sodium and potassium amalgams were prepared in a pure state and the susceptibility of the amalgams of different concentrations at different temperatures was studied. The $\chi$-values of amalgams were found to be practically constant in the range of temperature employed.

The authors wish to express their grateful thanks to Dr. K. Venkateswarlu for his keen and continued interest throughout this investigation.

*Department of Physics*
*Annamalai University*
*Annamalainagar*
*South India*

# *Note on the Electron Spin Resonance of Cupric Oxide-Alumina Catalysts*

By Yoshio MATSUNAGA*

(Received February 20, 1961)

Cupric oxide-alumina is one of the supported catalyst systems examined by Selwood's susceptibility-composition isotherm method. The presence of a plateau of susceptibility of cupric ion at low concentrations is characteristic in this oxide system. The plateau found in the isotherm seemed to suggest that the cupric ions are effectively isolated from each other at low concentrations. However, the paramagnetism which is to be expected for isolated copper atoms in the reduced catalyst samples was not observed[1,2]. Here we wish to present the results of an electron spin resonance study of this oxide catalyst system.

Pure gamma-alumina was impregnated with cupric nitrate solution. The mixture was filtered after standing overnight, dried without washing, and heated in a stream of air at 400°C for six hours. The catalysts containing 0.44 to 16.6 per cent of copper were prepared. Using a Gouy balance as described previously, the magnetic susceptibility measurements were carried out at room temperature[3]. The alumina used in this study was found to have a value of $-0.36\times10^{-6}$ per gram. The gram susceptibility of the cupric ion was estimated on the assumption that the magnetic susceptibilities of cupric, aluminum, and oxide ions are additive and those of the latter two are independent of the composition of catalysts. Curve A in Fig. 1 shows the susceptibility of

* Present address: Cyanamid European Research Institute, Cologny, Geneva, Switzerland.

1) P. W. Selwood and N. S. Dallas, *J. Am. Chem. Soc.*, **70**, 2145 (1948).

2) P. E. Jacobson and P. W. Selwood, ibid., **76**, 2641 (1954).

3) Y. Matsunaga, This Bulletin, **30**, 868 (1957).

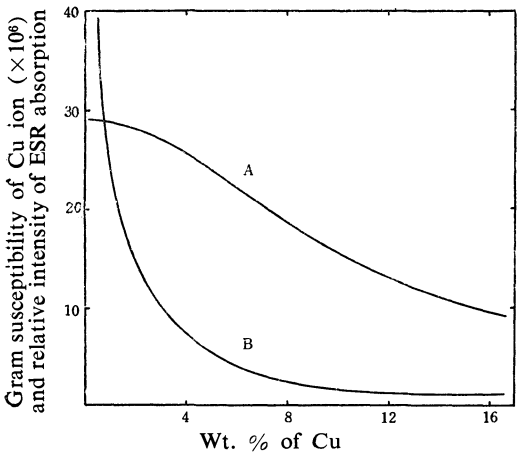



Fig. 1. Relation of susceptibility (curve A) and relative intensity of ESR absorption (curve B) of cupric ion supported on gamma-alumina to its concentration.

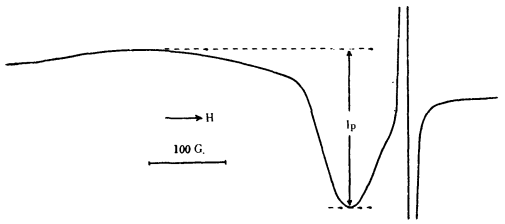



Fig. 2. Derivative of ESR of cupric oxide-alumina catalyst. The sharp peak on the right hand side is due to DPPH ($g=2.00$).

cupric ion plotted against the copper concentration. The value below three per cent of copper appears to be nearly constant. The general feature of curve A is quite similar to the curve reported by Jacobson and Selwood[2].

The electron spin resonance absorption was recorded on a spectrometer made by Japan Electron Optics Laboratory Ltd. at room temperature and at a frequency of 10 kMc./sec. No resonance absorption was found in massive cupric oxide with a field modulation of 15 gauss; on the other hand, the derivative of resonance absorption as shown in Fig. 2 was obtained from all of our catalysts. The spectrum seems to arise from the cupric ions with random orientation of tetragonal symmetry axes. The value of $g_\perp$ was estimated to be 2.05 using the method proposed by Kneubühl[4].

4) F. K. Kneubühl, *J. Chem. Phys.*, 33, 1074 (1960).

This absorption must be attributed to the cupric ions in the dispersed state and its intensity can be a measure of the amount of such cupric ions. The relative intensity was given by the ratio of the peak-to-peak intensity to the copper concentration, see $I_p$ of the derivative curve of resonance absorption in Fig. 2. Curve B in Fig. 1 gives the plot of relative intensity to the copper concentration. If our supported cupric oxide consists of a mixture of massive crystalline oxide and the cupric ions which contribute to the resonance absorption, curve B must show a plateau at low concentrations. The relative intensity of resonance absorption was found in a sharp increase in the range where the susceptibility value was nearly constant. Therefore, we may conclude that the above view is incorrect. The presence of another kind of dispersed state, in which the cupric ions do not give resonance absorption but do contribute to the increase of susceptibility value observed at low concentrations, must be taken into consideration. We may assume that the decrease of copper concentration is accompanied by a continuous diminution in the average number of neighboring cupric ions surrounding each cupric ion. At low concentrations each cupric ion may have only a few paramagnetic neighbors, possibly separated farther than in massive crystalline oxide. The interaction between such dispersed cupric ions may be too weak to affect the susceptibility value of these cupric ions, but may contribute to the broadening of resonance absorption to some extent. It seems likely that the observed asymmetric resonance absorption arises from the completely isolated cupric ions, probably dissolved in alumina in the course of the preparation of catalysts, and the cupric ions dispersed on the surface of a carrier and under the weak interaction with neighboring cupric ions give too broad resonance absorption to be detected.

The author wishes to express his hearty thanks to Professor Shizuo Fujiwara for his interest and encouragement.

*Department of Chemistry*
*Faculty of Science*
*The University of Tokyo*
*Hongo, Tokyo*

# *Note on the Oxidation of Perylene in Strong Acids*

By Yoshio MATSUNAGA*

(Received February 20, 1961)

The color reaction in concentrated sulfuric acid is one of the characteristic properties of polycyclic aromatic hydrocarbons and quinones, and has been used by organic chemists for their identification. Handa has measured the absorption spectra of a number of aromatic compounds dissolved in sulfuric acid of various concentrations, and attempted to estimate their basicities[1]. On the other hand, it has been pointed out by several authors that aromatic hydrocarbons in sulfuric acid show ESR absorption[2,3]. The paramagnetic species has been assigned by Weissman as a positive ion formed by oxidation. Hoijtink and Weijland have reported that the visible spectrum of a perylene solution in sulfuric acid resembles very closely that of a mononegative ion of this hydrocarbon[4].

In order to elucidate the nature of the species existing in sulfuric acid we attempted to study the oxidation of perylene by the optical and ESR methods. We examined the absorption spectrum of perylene dissolved in 70 per cent perchloric acid and observed two bands, at 503 and 530 m$\mu$, which are located at nearly the same position as the one in sulfuric acid (see Fig. 1a and c.). We attempted also the oxidation of perylene in perchloric acid using potassium ferricyanide and the isolation of the product. Weiss reported in 1941 that the salts of some other aromatic hydrocarbons were prepared by oxidation in strongly acidic media[5]. The black reaction mixture was washed with a slightly diluted perchloric acid, in which the oxidized perylene was found to be only very sparingly soluble, and examined by an ESR spectrometer at a frequency of 9 kMc./sec. and at room temperature. A sharp line with a width of about 2.4 gauss at a half power was found. The $g$-value corresponding to the center of the line was estimated, by comparison with DPPH, to be $2.0025\pm0.0003$. The solubility of the product in 70 per cent perchloric acid was found to be much higher than that of the original hydrocarbon, so the main product seems to be ionic, probably the hydrocarbon perchlorate as described by Weiss. Unfortunately the solubility is still not high enough to examine ESR absorption in the dissolved state.

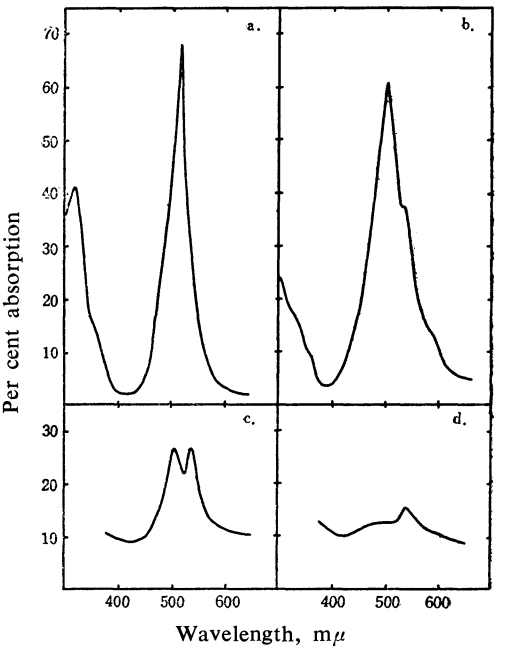



Fig. 1. Absorption spectrum of perylene in strong acids.
a, Dissolved in concentrated sulfuric acid
b, Oxidized perylene in 70 per cent perchloric acid
c, Dissolved in 70 per cent perchloric acid
d, After warming of c for a short time

The spectrum of the oxidized perylene has two bands which are located exactly at the same positions as those obtained by the direct dissolution of the hydrocarbon in perchloric acid. However, as shown in Fig. 1b, after oxidation the intensity of the band at lower wavelength became appreciably higher than the other. Although Dallinga and others have observed a similar spectrum of perylene by the dissolution in hydrogen fluoride and by the contact with oxygen, the band at higher wave-

* Present address: Cyanamid European Research Institute, Cologny, Geneva, Switzerland.

1) T. Handa, This Bulletin, **28**, 483 (1955).
2) Y. Yokozawa and I. Miyashita, *J. Chem. Phys.*, **25**, 796 (1956).
3) S. I. Weissman, E. de Boer and J. J. Conradi, ibid., **26**, 963 (1957).
4) G. J. Hoijtink and W. P. Weijland, *Rec. trav. chim.*, **76**, 836 (1957).
5) J. Weiss, Nature, **147**, 512 (1941).

length was found to be stronger in their case[6]. It seems to be evident that the band at lower wavelength is due to the paramagnetic ion formed by oxidation and the other is due to some other species derived from perylene. It is unlikely that the latter species is the protonated perylene, because no strong band was observed in this region of the spectrum of perylene in oxygen-excluded hydrogen fluoride[6]. The oxidation of perylene without the addition of an oxidizing reagent seems to be due to the presence of molecular oxygen dissolved in perchloric acid or combined with the hydrocarbon**. An attempt to accelerate the oxidation reaction of perylene in perchloric acid was made by warming. However, the band at 503 m$\mu$ decreased its intensity quickly (see Fig. 1d.). This observation shows that the band at the low wavelength side is due to a unstable species and seems to be not inconsistent with the above conclusion.

As it is convincing that only a part of perylene dissolved in concentrated sulfuric acid is paramagnetic[2,7], there must be again two or more species derived from perylene. Therefore, it seems likely that, as shown by the presence of a shoulder on the low wavelength side, the band due to the monopositive ion in sulfuric acid overlaps the band due to some other species.

The author attempted also the oxidation of tetracene in perchloric acid using ferricyanide and obtained a deep green solution and an unstable black precipitate. The absorption spectra of tetracene oxidized in perchloric acid and tetracene dissolved in sulfuric acid are rather complicated and the intensity ratios of bands depend on the time. Although the complete assignment has not yet been made, it appeared that there are three or more common species in these two solutions.

*Department of Chemistry*
*Faculty of Science*
*The University of Tokyo*
*Hongo, Tokyo*

6) G. Dallinga, E. L. Mackor and A. A. Verrijn Stuart, *Mol. Phys.*, **1**, 123 (1958).

** Although we have no direct evidence that perylene molecule combines with oxygen, mesonaphthodianthrene, which has a similar molecular structure to perylene, was found to give a paramagnetic molecular complex with oxygen, see Y. Matsunaga, *Can. J. Chem.*, **38**, 323 (1960).

7) Y. Matsunaga, This Bulletin, **31**, 776 (1958).

# *Reduction of Organic Compounds with Urushibara Catalysts under High Pressure. IX*[1]. *Reduction of Some Carbonyl Compounds with Urushibara Catalysts Prepared by Various Modified Methods*

By Shin-ichi TAIRA

(Received March 17, 1961)

In the preceding paper[1] of this series, catalytic reduction of acetophenone with various Urushibara nickel catalysts, especially with the catalyst prepared from preserved precipitated nickel and with the regenerated catalyst, was reported. The procedure for preparing the Urushibara catalysts has been successively modified and some varieties of the catalysts, namely, U-Ni-B[2-7], U-Ni-BA[5,6,8], U-Ni-$NH_3$[9], U-Ni-CB[7], U-Ni-A[3-7,10], U-Ni-AA[11], U-Ni-CA[7], U-Co-B[7,9,12,13], U-Co-CB[7], U-Co-A[7,13], U-Co-CA[7], U-Cu[7] and U-Cu-C[7], were developed. Each of them has intrinsic characteristics and can be used properly in accordance with the substance to be reduced. The preparation of the Urushibara catalysts is divided into two steps, that is, the preparation of precipitated metals and the digestion of them with acid or alkali. Therefore the

1) Part VIII: S. Taira, This Bulletin, **34**, 1072 (1961).
2) Y. Urushibara and S. Nishimura, ibid., **27**, 480 (1954).
3) Chem. Soc. Japan, ed., "Jikken Kagaku Kōza", Vol. 17, Part 2, Maruzen, Tokyo (1956), p. 311.
4) Y. Urushibara and K. Hata, *Kagaku Kōgyō*, **7**, 15 (1956).
5) K. Hata and S. Taira, *Kagaku Gijutsu*, **2**, 42 (1958).
6) K. Hata and S. Taira, *J. Soc. Org. Synth. Chem. Japan* (*Yūki Gōseikagaku Kyōkai-shi*), **16**, 596 (1958).
7) S. Taira, This Bulletin, **34**, 261 (1961).
8) K. Hata, S. Taira and I. Motoyama, ibid., **31**, 776 (1958).
9) S. Nishimura and A. Sugimori, *J. Chem. Soc. Japan, Pure Chem. Sec.* (*Nippon Kagaku Zasshi*), **81**, 314 (1960).
10) Y. Urushibara, S. Nishimura and H. Uehara. This Bulletin, **28**, 446 (1955).
11) K. Hata, K. Watanabe and H. Watanabe, ibid., **32**, 6 (1959).
12) S. Saito, *J. Pharm. Soc. Japan* (*Yakugaku Zasshi*), **76**, 351 (1956).
13) Chem. Soc. Japan, ed., "Jikken Kagaku Kōza", Vol. 17, Part 2, Maruzen, Tokyo (1956), p. 334.

nature of an Urushibara catalyst is decided by the method of preparation and digestion of precipitated metal.

In the present paper, reductions of deoxybenzoin, benzoin, benzil and furil with the Urushibara catalysts prepared by various methods are studied, and the further modifications of the preparation of the catalyst are presented.

## Experimental

**Apparatus.**—Reductions were carried out in an electro-magnetically stirring type autoclave having a capacity of 100 ml. (the Sakashita SE-10 type). For the reduction of furil, SE-20 (200 ml. capacity) was used.

**Materials.**—Deoxybenzoin was prepared from phenylacetyl chloride and benzene by the Friedel-Crafts reaction[14]. The crude material was purified by distillation under reduced pressure and then recrystallized from methanol, b. p. 159.5~160.5°C/6 mmHg, m. p. 55~56°C.

Benzoin was prepared from benzaldehyde[15]. The crude product was recrystallized three times from ethanol, m. p. 133~134°C.

Benzil was prepared by catalytic oxidation of the benzoin with ammonium nitrate[16]. The raw product was recrystallized from methanol, m. p. 96.5~97°C.

Furil was obtained by the same manner from furoin prepared from furfural[17], m. p. 165°C.

**General Procedure for Reduction.**—Catalyst was carefully transferred with ethanol into the autoclave. Then the air present in the autoclave was replaced by hydrogen gas four times. Most operations were carried out under the following conditions: (1) Catalyst was prepared so as to contain 0.5 g. of nickel metal. (2) Sample; 0.05 mol. (deoxybenzoin 9.8 g., benzoin 10.6 g., benzil 10.5 g., furil 9.5 g.). (3) Solvent; ethanol (99%) 50 ml. (4) pH; 9~11. When U-Ni-A, U-Ni-CA or U-Cu-C was used, 0.5 ml. of 5% sodium hydroxide solution was added. (5) Agitation; 40~45 strokes per minute. (6) Reaction temperature; 60~68°C. Agitation was started when the temperature in the autoclave reached 60°C. The heating of the autoclave was regulated so as to get to 60°C within 30~35 min., and then the temperature was kept between 60 and 68°C throughout the operation. (7) Initial pressure; 50~100 kg./cm². As it has been recognized[7] that initial pressure affected only slightly the velocity of reduction of the carbonyl group under 100 kg./cm², the effect of initial pressure was ignored. Depression of pressure was observed at intervals of 5 min. When U-Cu-C was used, reduction was carried out with the catalyst prepared so as to contain 1 g. of copper and at about 130°C.

**Reduction Products.**—*Phenylbenzylcarbinol.*—After the reduction of deoxybenzoin was finished, the catalyst was filtered off and washed with ethanol. The major part of ethanol was distilled off and the hot residue was poured into hot water with stirring and the mixture was cooled in an ice-bath. The precipitate was filtered off and dried. It was recrystallized from petroleum benzin into colorless needles, m. p. 66~67°C. Yield, 91~94% of the theoretical.

*Hydrobenzoin.* — After the reduction of benzoin was finished, the catalyst, mixed with some crystals separated out, was filtered off and washed with hot ethanol to dissolve the crystals. From the combined filtrate, the major part of ethanol was removed by distillation. The hot residue was poured into hot water with stirring. After cooling, the crude hydrobenzoin was filtered off and dried. It was recrystallized from aqueous ethanol into colorless scales, m. p. 139~140°C. Yield, 90~93% of the theoretical.

**Benzoin.**—After the partial reduction of benzil was finished, the contents were filtered off and washed throughly with hot ethanol. After removal of the major part of ethanol from the combined filtrate, benzoin crystallized in prisms, m. p. 132~134°C. Yield, 76~80% of the theoretical.

*Furoin.*—After the reduction of furil, the product was treated by the same procedure as is described above. Pale yellow prisms, m. p. 137~138°C. Yield, 79~81% of the theoretical.

**Preparation of Catalysts.**—The U-Ni-B[2-6], U-Ni-A[3-6,10], U-Ni-CB[7] and U-Ni-CA[7] were prepared by the methods described in the references cited. The others were prepared by the methods described below.

*Precipitated Nickel Prepared by a Simplified Method.*—To the well mixed zinc dust (10 g.) and water (4 ml.) placed in a 50 ml. beaker 4.04 g. of the crystals of commercially available nickel chloride ($NiCl_2 \cdot 6H_2O$) is added at once and the mixture is stirred with a glass rod. Soon reaction begins and a vigorous reaction takes place suddenly within a few minutes. The reaction mixture swells up into a slushy mass. It is washed with 200 ml. of cold water, and then the washing is filtered or removed by decantation. Thus about 13.5 g. of precipitated nickel, containing about 1 g. of nickel contaminated with a quantity of zinc, zinc oxide and basic zinc chloride, was obtained.

*U-Ni-B* was prepared from the above described precipitated nickel (containing 0.5 g. of nickel) by digesting with 80 g. of 10% sodium hydroxide solution at about 50°C for 15 min. The upper liquor was decanted and the residue was washed with two 50 ml. portions of water and then with the same amount of ethanol. The obtained catalyst was less bulky than the usual U-Ni-B and carried a black color (the usual U-Ni-B has rather grayish appearance). Every washing was removed by decantation.

*U-Ni-A* was prepared from the same precipitated nickel (containing 0.5 g. of nickel) by treatment with 75 ml. of 20% acetic acid at ordinary temperature until the generation of hydrogen gas subsided and a solid came up to the surface of the green solution. The solid was collected on a glass filter and washed with each 100 ml. portions of water and ethanol.

14) C. F. H. Allen and W. E. Barker, "Organic Syntheses", Coll, Vol. II (1948), p. 156.
15) R. Adams and C. S. Marvel, ibid., Coll. Vol. I, p. 94.
16) M. Weiss and M. Appel, *J. Am. Chem. Soc.*, **70**, 3666 (1948).
17) W. W. Hartman and J. B. Dickey, ibid., **55**, 1228 (1933).

*U-Ni-A Obtained by Treatment of the Precipitated Nickel with Hydrochloric Acid, Abbreviated as U-Ni-A(HCl).*—The precipitated nickel (containing 0.5 g. of nickel), prepared by normal or simplified method, was digested with 240 ml. of 0.75 N hydrochloric acid at ordinary temperature for about one minute until a solid came up to the surface of the green solution. The solid was collected on a glass filter and washed with 200 ml. of water and then with 100 ml. of ethanol.

*U-Cu-C.*—The precipitated copper was prepared by the same way as was reported in the previous paper[7]. It was treated with 200 ml. of 20% acetic acid on a boiling water bath at 80~90°C for about 20 min. At the end of the digestion a solid, adsorbing hydrogen gas, came up to the surface of the solution likely in case of preparing the U-Ni-A. The solid was collected on a glass filter and washed with 200 ml. of water and then with 150 ml. of ethanol. About 2.3~2.5 g. of bulky catalyst, containing copper (about 1 g.) and zinc, was obtained.

In all procedures, distilled water was used for washing except for the preparations of precipitated metals. The solid should be protected from contact with air as far as possible after the treatment of precipitated metals with acid or alkali.

## Results and Discussion

In the reduction of benzophenone[7] and acetophenone[1] to the corresponding alcohols with various Urushibara catalysts, the U-Ni-A was found to be the most useful catalyst. The same conclusion was confirmed also in the reduction of deoxybenzoin, benzoin and benzil. The U-Ni-CB was also found to be highly active (Tables I, II and III).

**Modification of the Preparation of the Catalyst.**—As was reported in the preceding paper[1], the preparation of the Urushibara nickel catalyst was fairly simplified. The

TABLE I. REDUCTION OF DEOXYBENZOIN

Deoxybenzoin 9.8 g. (0.05 mol.); solvent: ethanol (99%, about 50 ml.)

| Exp. No. | Catalyst[a] | Total weight of catalyst, g.[b] | Initial press. kg./cm² | Initial temp. °C | Reaction temp. °C | Time[c] min. |
|---|---|---|---|---|---|---|
| 11 | U-Ni-B | 3.2 | 56 | 22 | 60~62 | 30 |
| 12 | U-Ni-CB | 4.3 | 58 | 27 | 62~65 | 18 |
| 13 | U-Ni-A[d] | 0.7 | 56 | 18 | 60~61 | 17 |
| 14 | U-Ni-CA[d] | 0.4 | 60 | 20 | 60~63 | 22 |

a) Each catalyst was prepared so as to contain 0.5 g. of nickel.
b) The figures were obtained by weighing the dried catalyts after use for reduction.
c) The figures show the time required from the start of agitation (when the temperature reached to 60°C) till the cease of pressure depression, which had been observed every minute.
d) 0.5 ml. of 5% sodium hydroxide solution was added.

TABLE II. REDUCTION OF BENZOIN WITH VARIOUS URUSHIBARA NICKEL AND URUSHIBARA COPPER CATALYSTS

Benzoin 10.6 g. (0.05 mol.); solvent: enhanol (99%, about 50 ml.)

| Exp. No. | Catalyst[a] | Total weight of catalyst, g.[b] | Initial press. kg./cm² | Initial temp. °C | Reaction temp. °C | Time min. |
|---|---|---|---|---|---|---|
| 21 | U-Ni-B | 3.5 | 59 | 22 | 60~61 | 100 |
| 22 | U-Ni-B | 3.3 | 55 | 16 | 60~65 | 50 |
| 23 | U-Ni-B[c] | 2.8 | 64 | 30 | 60~66 | 60 |
| 24 | U-Ni-B[c] | 2.6 | 54 | 20 | 60~64 | 50 |
| 25 | U-Ni-CB | 5.5 | 60 | 30 | 60~61 | 50 |
| 26 | U-Ni-CB | 4.6 | 60 | 26 | 61~63 | 17 |
| 27 | U-Ni-A[d] | 0.7 | 55 | 21 | 65~67 | 10 |
| 28 | U-Ni-A[d] | 0.6 | 60 | 23 | 60~64 | 20 |
| 29 | U-Ni-A[c,d] | 0.4 | 67 | 26 | 62~64 | 35 |
| 210 | U-Ni-A[c,d] | 0.5 | 57 | 23 | 61~64 | 25 |
| 211 | U-Ni-A(HCl)[d] | 0.25 | 53 | 28 | 60~66 | 115 |
| 212 | U-Ni-A(HCl)[c,d] | 0.3 | 56 | 26 | 62~64 | 85 |
| 213 | U-Cu-C[d] | 2.3 | 38 | 23 | 130~132 | 30 |

a) Each U-Ni catalyst was prepared so as to contain 0.5 g. of nickel. The U-Cu catalyst was prepared so as to contain 1 g. of copper.
b) The figures were obtained by weighing the dried catalysts after use for reduction.
c) The catalyst was prepared from the newly developed precipitated nickel (cf. Experimental part).
d) 0.5 ml. of 5% sodium hydroxide solution was added.

TABLE III. REDUCTION OF BENZIL WITH VARIOUS URUSHIBARA NICKEL AND URUSHIBARA COPPER CATALYSTS

Benzil 10.5 g. (0.05 mol.); solvent: ethanol (99%, about 50 ml.)

| Exp. No. | Catalyst[a] | Total weight of catalyst, g.[b] | Initial press. kg./cm² | Initial temp. °C | Reaction temp. °C | Time[c] min. |
|---|---|---|---|---|---|---|
| 31 | U-Ni-B | 3.4 | 93 | 22 | 60~64 | 120(45,75) |
| 32 | U-Ni-B | 4.9 | 96 | 26 | 60~68 | 165(60,105) |
| 33 | U-Ni-B[d] | — | 80.5 | 30 | 60~66 | 75(20,55) |
| 34 | U-Ni-B[d] | 2.8 | 90 | 23 | 60~65 | 100(35,65) |
| 35 | U-Ni-CB | 5.6 | 97.5 | 25 | 63~66 | 35(10,25) |
| 36 | U-Ni-CB | 4.2 | 101 | 26 | 59~66 | 95(20,75) |
| 37 | U-Ni-A[e] | 0.65 | 95 | 20 | 60~66 | 25(10,15) |
| 38 | U-Ni-A[e] | 0.7 | 84 | 20 | 58~61 | 110(40,70) |
| 39 | U-Ni-A[d,e] | 0.35 | 42.5[f] | 23 | 60~68 | 55(20,35) |
| 310 | U-Ni-A[d.e] | 0.35 | 42[f] | 22 | 60~66 | 90(30,60) |
| 311 | U-Cu-C[e] | 2.3 | 80 | 24 | 128~138 | 55(20,35) |

a) Each U-Ni catalyst was prepared so as to contain 0.5 g. of nickel. The U-Cu catalyst was prepared so as to contain 1 g. of copper
b) The figures were obtained by weighing the dried catalysts after use for reduction.
c) The figures in the parentheses are the time required for reducing each carbonyl group, the first figures being for the first carbonyl group.
d) The catalyst was prepared from the newly developed precipitated nickel (c. f. Experimental part).
e) 0.5 ml. of 5% sodium hydroxide solution was added.
f) Supplementary hydrogen gas was charged three times when the pressure dropped to 30 kg./cm².

activity of U-Ni-A or U-Ni-B, prepared from the preserved precipitated nickel, being the same as that of the catalyst obtained from the freshly prepared precipitated nickel, time can be saved to prepare the catalyst if a large quantity of the precipitated nickel is previously reserved. On the other hand, the recovered Urushibara nickel catalysts can be repeatedly used by a simple process of regeneration, especially in form of the U-Ni-A.

As the process for the preparation of the Urushibara nickel catalyst is divided into the preparation of the precipitated nickel and the treatment of it with acid or alkali, the modification of preparing a catalyst can be devised in each of both procedures. Already many modifications have been accomplished, and varieties of the catalyst were reported. The precipitated nickel prepared at low temperature gives a highly active Urushibara nickel C. But the preparation of it requires so much time, that a favorable feature of the Urushibara catalysts to be prepared in a short time is lost. In case of preparing the precipitated nickel from hot aqueous nickel chloride solution and zinc dust on a boiling water bath, a vigorous exothermic reaction is observed. If the heat of the reaction is utilized, the time for preparing the precipitated nickel will be shortend and the procedure may be simplified. For the purpose of attaining this request, it may be suitable to use the concentrated solution of nickel chloride in place of the diluted solution used in the usual preparation. Thus, the first attempt was the addition of a very concentrated nickel chloride solution onto a dry zinc dust, but this method was unsuccessful as the reaction was so vigorous that an uniform agitation was impossible and an uniform deposition of nickel metal on the particles of zinc could not be expected. After several trials, it was found that the most profitable method consists in adding crystals of nickel chloride to the mixture of zinc dust and a little water, and a good precipitated nickel could be prepared in a few minutes.

In the preparation of the U-Ni-A by digesting the precipitated nickel with acid, acetic or propionic acid has been used and formic, butyric and hydrochloric acids had been regarded as unprofitable[3,4,10]. Supposing the action of the acid is to activate the precipitated nickel by generating hydrogen gas, removing the deactivating substances and eroding the surfaces of nickel particles[1], there is no reason that hydrochloric acid cannot be applicable except for some special poisonous action to a nickel catalyst. Therefore the nickel catalyst obtained from the precipitated nickel by treatment with hydrochloric acid is expected to have ability of hydrogenation though it may be lower than those of the other Urushibara nickel catalysts.

**Comparison of the Activities of Various Catalysts.**—The results of reduction of benzoin and benzil with the usual Urushibara nickel

TABLE IV. PARTIAL REDUCTION OF α-DIKETONES

| Exp. No. | α-Diketone | Solvent | Catalyst[a] | Initial press. kg./cm² | Reaction temp. °C | Time min. | Reduction product | Yield % |
|---|---|---|---|---|---|---|---|---|
| 41 | Benzil 10.5 g. (0.05 mol.) | Ethanol (50 ml.) | U-Ni-A | 80 | 20 | 100 | Benzoin | 76 |
| 42 | Benzil 10.5 g. (0.05 mol.) | Ethanol (50 ml.) | U-Ni-A[b] | 85 | 22 | 115 | Benzoin | 80 |
| 43 | Furil 9.5 g. (0.05 mol.) | Ethanol (100 ml.) | U-Ni-A | 56 | 60～63 | 90 | Furoin | 81 |
| 44 | Furil 9.5 g. (0.05 mol.) | Ethanol (100 ml.) | U-Ni-A[b] | 60 | 60～62 | 100 | Furoin | 79 |

a) Each catalyst was prepared so as to contain 0.5 g. of nickel, and in each operation 0.5 ml. of 5% sodium hydroxide solution was added.
b) The catalyst was prepared from the newly developed precipitated nickel (cf. Experimental part).

catalysts and with the newly developed ones are tabulated in Tables II and III. In consideration of the condition of preparing the newly developed precipitated nickel, it is expected that it possesses both natures of the precipitated nickels prepared in hot and in cold conditions. Accordingly the nature of the catalyst obtained from it may be situated between those of the usual Urushibara nickel and the Urushibara nickel C. When the Urushibara nickel catalysts of B type (prepared by digestion with alkali) are used for the reduction in an autoclave, the rates of reduction are influenced by the factors such as the fineness and dispersability of the catalyst, the bulk and the kind of carrier (e. g. zinc, zinc oxide) ete. On the other hand, as the Urushibara nickel catalysts of the A type (prepared by digestion with acid) contain only small quantities of zinc and zinc compounds, if any, and are less bulky than the B type, the inherent activities of the catalysts may dominate the velocities of reduction. In consideration of these facts, the time required for the completion of reduction with various Urushibara nickel catalysts is compared with each other. The activity of each catalyst is not always constant, but it can be approximately estimated by repeated experiments. Both for the reduction of benzoin and benzil, the usual U-Ni-A gives the best results. The U-Ni-A prepared from the newly developed precipitated nickel is somewhat inferior to the usual U-Ni-A, but has enough activity for practical use. The activity of the Urushibara nickel catalysts has been studied[3,18], in connection with the size of their crystallites, which was estimated by X-ray diffraction method. According to the authors, the more vigorous the reaction to prepare the precipitated nickel takes place, the smaller the crystallites of the obtained catalyst become, and the activity of the catalyst is lowered with the growth of the size of crystallites. The size of crystallites of the highly active Urushibara nickel catalysts was reported to be about 40 Å and the same as that of the Raney nickel catalyst. The values obtained by the present author were 39～45 Å for the usual U-Ni-A, and 33～41 Å for the modified U-Ni-A obtained from the newly developed precipitated nickel. On the whole the size of crystallites of the modified U-Ni-A was found to be smaller than that of the usual U-Ni-A. Therefore, the activities of the freshly prepared catalysts may not be discussed only from a standpoint of the size of crystallites, although the catalyst used in Exp. No. 39 gave a smaller value (33 Å) than that (37 Å) of the catalyst used in Exp. No. 310.

The U-Ni-A prepared by digesting the precipitated nickel with hydrochloric acid was proved to be still active though it was inferior to the other U-Ni-A. The cause may be partly due to the small contents of nickel metal and partly to the adsorption of some chlorine compound on the surface of the catalyst. As it has been previously reported[7], the Urushibara copper catalyst has an activity for reduction of a carbonyl group and the U-Cu-C is superior. But the treatment of the precipitated copper with acetic acid at room temperature requires much time. If the temperature of digesting the precipitated metal with acid affects the activity only slightly, it is advantageous to operate the digestion at high temperature. The results obtained with such catalyst are given as Exp. Nos. 213 and 311 in Tables II and III.

**Partial Reduction of α-Diketones.**—In every experiment on the reduction of benzil, a sudden fall of hydrogen uptake was observed after a certain quantity of hydrogen had been absorbed. It is conceivable that the reduction of one carbonyl group of the two has been finished at this point. Then, the partial reduction of α-diketones to α-ketols is expected to be possible under suitable condition. It was realized in the reduction of benzil and furil,

18) Y. Urushibara, M. Kobayashi, S. Nishimura and H. Uehara, *Shokubai*, 12, 107 (1956).

and the results of the partial reduction are shown in Table IV. In case of reducing a carbonyl group to the corresponding alcohol, it has been noticed that the velocity of hydrogen uptake increases at about 60°C and that the reduction is promoted by a trace of an alkali. The reduction in neutral solution being presumed to require a long time for the completion[7], the reduction of benzil to benzoin was carried out with the U-Ni-A added with a little quantity of alkali at room temperature. On the other hand, the partial reduction of furil was practised at about 60°C and in a large quantity of ethanol, as furil dissolves only slightly in ethanol at room temperature.

## Summary

The catalytic reduction of deoxybenzoin, benzoin, benzil and furil with various Urushibara catalysts under high pressure were studied. It was found that benzil and furil was converted into the corresponding $\alpha$-ketols by the partial reduction under proper condition.

Some modifications for the preparation of the Urushibara catalyst were attained. The newly developed precipitated nickel prepared by a very simple way proved to give a catalyst as active as the usual Urushibara nickel catalyst for practical use. Hydrochloric acid was found to be applicable for the digestion of the precipitated nickel in place of acetic acid.

The author expresses his sincere gratitude to Professor K. Hata for his helpful advice and encouragement throughout this work.

*Department of Chemistry*
*Faculty of Science*
*Tokyo Metropolitan University*
*Setagaya-ku, Tokyo*

# *Conformation and Reactivity of 4-Methylcyclohexylmethyl p-Tosylates*

By Nobuo Mori

(Received January 23, 1961)

The important relation between conformation and reactivity in a cyclohexane system which contains a departing group directly bound to the cyclohexane ring and in an acyclic system has been applied in many areas of organic chemistry[1].

The present work desires to confirm the effect of conformation on the reactivity in a cyclohexane system which contains a departing group bound through a methylene group to the ring, especially by means of substituted cyclohexylmethyl *p*-tosylates. For this purpose, novel *cis*- and *trans*-4-methylcyclohexylmethyl *p*-tosylates have been prepared from the corresponding carbinols which form the basis of the *p*-tosylates, and they were solvolyzed. The *cis*- and *trans*-4-methylcyclohexylcarbinols are prepared by hydrogenolysis of the corresponding 4-methylcyclohexanecarboxylic acid esters under severe conditions, at 250°C under 200 atm. in the presence of copper-barium-chromium oxide catalyst for 10 hr.[2] The author has used advantageously lithium aluminum hydride in dry ether for conversion of the esters into the carbinols.

1) For example, see M. S. Newman, "Steric Effects in Organic Chemistry", John Wiley & Sons, Inc., New York (1956).

2) R. G. Cooke and A. K. Macbeth, *J. Chem. Soc.*, **1939**, 1245.

## Experimental

**Samples.**—*Cyclohexylmethyl p-Tosylate.*—Benzaldehyde (20 g.) in ethanol (30 cc.) was hydrogenated under 80 initial atm. at a temperature gradually raised to 100°C in the presence of Raney nickel (10 g.) until no more hydrogen was absorbed. The filtered solution was distilled under reduced pressure to give the cyclohexylcarbinol, b. p. 74.5°C/20 mmHg. The carbinol was treated with an equimolecular amount of *p*-toluenesulfonyl chloride in pyridine at 0~5°C, to give the *p*-tosylate as needles, m. p. 30.5°C after recrystallization from aqueous methanol.

Found: C, 62.65; H, 7.51. Calcd. for $C_{14}H_{20}O_3S$: C, 62.55; H, 7.44%.

*cis*-4-*Methylcyclohexylmethyl p-Tosylate.*—A neutral solution of *p*-toluic acid (15 g.) in 10% sodium hydroxide solution in an autoclave was hydrogenated at 180~200°C under 90 initial atm. in the presence of Raney nickel (10 g.) for 2.5 hr. until no more hydrogen was absorbed. The filtered solution was worked up in the usual way, by making it acid with concentrated hydrochloric acid,

extracting the separated oily product with ether, evaporating the ether and distilling the residue under reduced pressure, to give the semi-solid mass (12 g.), b. p. 129~130°C/15 mmHg, which melted at 107~108°C (reported 111°C[3]) after one recrystallization from aqueous methanol. The acid (1.5 g.) so obtained was esterified by refluxing it in ethanol (30 cc.) containing concentrated sulfuric acid (1 g.) for 2 hr., to give the ethyl ester (1.6 g.), b. p. 92~93°C/28 mmHg. The ester in dry ether (5 cc.) was added stepwise into a suspension of lithium aluminum hydride (0.5 g.) in dry ether (50 cc.) at 0~5°C. After stirring for another half an hour, the reaction mixture was treated with a small volume of dilute sulfuric acid sufficiently to make the ether layer clear, and the layer was dried over potassium carbonate and evaporated to dryness. The oily product, which consisted mainly of *cis*-4-methylcyclohexylcarbinol, was treated with *p*-toluenesulfonyl chloride (1.5 g.) in pyridine (3 cc.) and after 3 hr. poured into a mixture of concentrated hydrochloric acid and ice to separate the oily mass which solidified after a few minutes. The solid was recrystallized from aqueous methanol to give the *cis*-tosylate (1.3 g.) as plates, m. p. 44.5~44.7°C.

Found: C, 64.00; H, 8.05. Calcd. for $C_{15}H_{22}O_3S$: C, 63.79; H, 7.85%.

*trans-4-Methylcyclohexylmethyl p-Tosylate.*—*p*-Toluic acid (8 g.) in glacial acetic acid (60 cc.) which had previously been treated with potassium permanganate, was hydrogenated at 70~80°C under atmospheric pressure in the presence of Adams platinic oxide catalyst (0.5 g.)[4] for about 2 hr. without any aeration of the catalyst until no more hydrogen was absorbed. The acetic acid was removed from the filtered solution under reduced pressure and the residue was distilled to give the hexahydro-acid (5 g.), b. p. 133~134°C/20.4 mmHg (reported 135°C/20 mmHg[3]). The acid (2 g.) was similarly converted into the *trans*-tosylate as needles, m. p. 30.5~31.0°C and yield 1 g. after recrystallizations with slight difficulty from methanol in a dry ice-acetone bath.

Table I. Summary of rate constants at 99.8°C

| 4-Substituent | Tosylate $\times 10^2$ mol./l. | Solvent | $k_1 \times 10^4$ $min^{-1}$ |
|---|---|---|---|
| H | 1.57 | HAcO | 2.27 |
| | 1.60 | EtOH | 8.42 |
| *cis*-$CH_3$ | 1.78 | HAcO | 4.34 |
| | 1.79 | EtOH | 7.68 |
| *trans*-$CH_3$ | 1.80 | HAcO | 1.79 |
| | 1.79 | EtOH | 11.0 |
| Ethyl tosylate* | 3.8~4.3 | HAcO | 5.08 |
| Isobutyl tosylate* | 2.5~2.8 | HAcO | 2.28 |

* Calculated from $8.47 \times 10^{-6}$ $sec^{-1}$ and $3.79 \times 10^{-6}$ $sec^{-1}$ respectively in Ref. 6.

3) G. H. Keats, ibid., 1937, 2003.

4) This catalyst was prepared according to the method described in "Organic Synthesis", Coll. Vol. 1 (1948), p. 463.

Found: C, 63.75; H, 7.84. Calcd. for $C_{15}H_{22}O_3S$: C, 63.79; H, 7.85%.

Solvolysis rates were measured at 99.8°C in ethanol (98.5% by weight) and in acetic acid containing a slight excess of acetic anhydride by the usual ampoule technique[5]. The reactions were followed by titrating at intervals for the sulfonic acid liberated during the solvolysis to ca. 50% completion because of slow velocity. The observed kinetics were nicely first order and the precision of the measurements was usually better than 5%. The calculated first order rate constants for the tosylates and also alkyl tosylates for a comparision are summarized in Table I.

## Discussion

Difference in reactivity between the two departing groups restricted respectively in axial and equatorial orientation depends on the difference in energy of the ground state, rather than the transition state; and when the departing group is axial, there is a compensating steric acceleration due to relief of crowding between this axial group and the axial hydrogen atoms in $\gamma$-position, and as a result of this the solvolysis should be quite facile for the axial group, for example as shown by the typical fact[7] that *cis*-4-*tert*-butylcyclohexyl *p*-tosylate is solvolyzed at a rate about 3 times as fast as the corresponding trans-isomer. As a matter of course, the difference disappears in the isomeric 1,2-dimethylcyclohexyl bromides[8] which are nearly equal in the energy of their ground states, and also in the isomeric 1,3-dimethylcyclohexyl chlorides[9].

Thus, in general, the high steric repulsion acting on the departing group as described above results in fast departure of the group, provided the transition state for solvolysis does not include at least any higher electronic effect, such as the inductive effect by substituents especially in $\beta$-position or internal participation of neighboring groups or hydrogens, as shown in the fact[10] that *tras*-2-acetoxylcyclohexyl *p*-tosylate is acetolyzed much faster than the corresponding cis-isomer. Such an electronic effect is probably not included in the transition states of the isomeric tosylates used in the present work.

**Preferred Conformation and Acetolysis.**—The possible chair conformations of the isomeric tosylates used in the present work are as follows:

5) N. Mori, *J. Chem. Soc. Japan, Pure Chem. Sec.* (*Nippon Kagaku Zasshi*), **80**, 1458 (1959); This Bulletin, **33**, 1144 (1960).

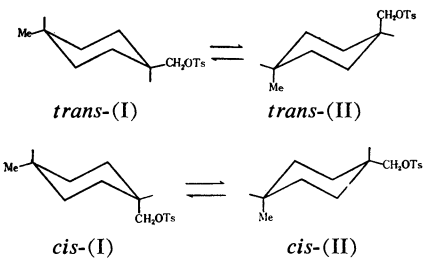
6) S. Winstein and H. Marshall, *J. Am. Chem. Soc.*, **44**, 1120 (1952).

7) S. Winstein and H. J. Holness, ibid., **77**, 5562 (1955).

8) T. D. Nevitt and G. S. Hamond, ibid., **76**, 4124 (1954).

9) H. C. Brown et al., ibid., **73**, 212 (1951).

10) S. Winstein et al., ibid., **70**, 821 (1948).

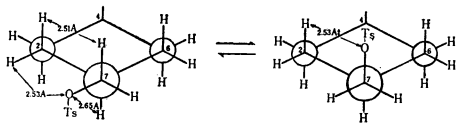



*trans*-(I) *trans*-(II)

*cis*-(I) *cis*-(II)

Fig. 1

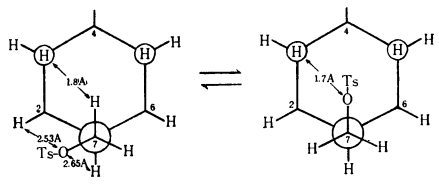
where Ts is the *p*-toluenesulfonyl group. The *trans*-(I) should be more stable than the *trans*-(II). On the other hand, the difference in stability between the *cis*-(I) and *cis*-(II) may be very small, and thus the cis-isomer is in the form of the *cis*-(I) in a considerable ground state concentration. Moreover, a favorable conformation of the *p*-toluenesulfoxymethyl group is very important, and for one in equatorial orientation it may be represented by the *e*-(III) and *e*-(IV) in Fig. 2, which are projected along the $C_7$ to $C_1$ axis and also accompanied by distances between non-bonded atoms in question,



*e*-(III) *e*-(IV)

Fig. 2

in which the conformation *e*-(III) will be more stable than *e*-(IV), because in the former only the bulky tosyl group eclipses the equatorial hydrogen on carbon atom 2 while in the latter the tosyl group eclipses the two axial hydrogens on carbon atoms 2 and 6. On the other hand, the toluenesulfoxymethyl group in axial orientation has two possible conformations which are represented respectively by the *a*-(III) and *a*-(IV) in Fig. 3, similarly projected



*a*-(III) *a*-(IV)

Fig. 3

The former, in which only the bulky tosyl group and equatorial hydrogen on carbon atom 2 are opposite one another, should be of lower energy than the latter, in which the distance between the tosyl group and the two axial hydrogens on carbon atoms 3 and 5 is very short. Thus, in such preferred conformations *e*-(III) and *a*-(III), the magnitude of repulsive action on the tosyl group in the axial toluenesulfoxymethyl group may be of the same order as that in the equatorial one; and therefore it will be expected that the isomeric 4-methylcyclohexylmethyl *p*-tosylates are solvolyzed at a nearly equal rate, if only the steric repulsion in the ground states is the governing factor. However, in the present work, the solvolysis in acetic acid as a poor nucleophilic solvent gave the result that the ratio of $k_{cis}/k_{trans}$ was 2.4. The fact may be explained on the possible assumption that, if the solvolysis is a simple carbonium ion process and the solvolysis of the cis-isomer proceeds, at least in part, via the conformation *a*-(III), the difference in energy between the ground state and the consequent possible carbonium ion, such as the *a*-(V) in Fig. 4, for the cis-isomer is very low as compared to that between the ground state *e*-(III) and the carbonium ion *e*-(V) for the trans-isomer. This assumption is probably right, since the high strain on the hydrogen atom in the methylene group in the ground state can substantially disappear in the consequent transition state, though the simple carbonium ion process is not always the governing consideration.

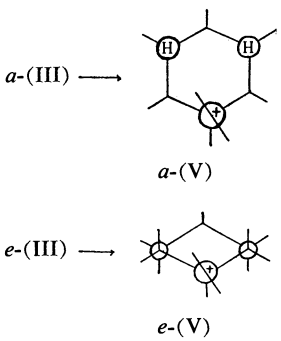



Fig. 4

**Solvent Effect and Ethanolysis.**—The rate of solvolysis of a given compound is generally altered by the solvating power or nucleophilic nature of a given solvent and the solvolysis includes usually solvation of the carbonium ion intermediate and nucleophilic assistance from the solvent molecules. Primary alkyl tosylates tend to be solvolyzed more rapidly in nucleophilic solvents such as ethanol than in acetic acid, and further the relative rates of $k_{EtOH}/k_{HAcO}$ for linear lower alkyl tosylates is higher than that for $\beta$-branched alkyl tosylates. For example, the ratio[6] at 75°C is 39 for ethyl tosylate, 6.2 for isobutyl tosylate and

0.28 for neopentyl tosylate. This would be partly due to the fact that variation from primary tosylate to $\beta$-branched alkyl tosylate would decrease the amount of nucleophilic assistance from the solvent. As the tosylates used in the present work are represented as the $\beta$-branched alkyl compounds in structure, it is expected that behavior of the tosylates in various solvents is approximately in agreement with that of isobutyl tosylate.

From Table II, it is seen that the rate of solvolysis of the trans-form increases according as the solvent changes from acetic acid to ethanol, in agreement with the behavior of primary alkyl tosylates, and the rate enhancing degree, that is, the ratio of $k_{EtOH}/k_{HAcO}$ is 6.1. This rate increasing trend is partly due to the fact that, in the conformation *e*-(III) of the trans-form, ethanol molecules approach more easily to the reaction center atom $C_7$, along the $C_1-C_6$ axis through the two hydrogens on carbon atom 6 in a back side attack manner.

On the other hand, the rate for the cis-form increases slightly under the same solvent sequence and the ratio is 1.7. This lower ratio would be mainly due to that in the conformation *a*-(III) of cis-form the axial hydrogen on carbon atom 5 hinders a similar entrance of solvent molecules along the $C_1-C_6$ axis.

TABLE II. RELATIVE RATES IN DIFFERENT SOLVENTS

| 4-Substituent | H | *cis*-$CH_3$ | *trans*-$CH_3$ |
|---|---|---|---|
| $k_{EtOH}/k_{HAcO}$ | 3.7 | 1.77 | 6.1 |

The author expresses his sincere thanks to Professor Yojiro Tsuzuki for his advice.

*Department of Chemistry*
*Tokyo College of Science*
*Shinjuku-ku, Tokyo*

# *Studies on the Silk-platinum Catalyst. II. General Properties*

By Akira AKAMATSU, Yoshiharu IZUMI and Shiro AKABORI

(Received February 27, 1961)

In the previous paper[1] of this series, the preparation of a silk-platinum catalyst, and its activity and stability were reported. This catalyst is extremely active for the hydrogenation of aromatic nitro compounds.

In the present work it was found that this catalyst was relatively less active for the hydrogenation of other compounds, and showed behaviors in the catalytic reactions, quite unlike the so far known reactions of other platinum catalysts. It is probable that the difference is mainly due to the nature of the carrier silk-fibroin in this catalyst. Various reactions of this catalyst with poisons of catalysts are also described in the present paper.

## Catalytic Efficiency with Various Compounds

In order to examine the catalytic efficiency of the silk-platinum catalyst[1], various compounds were tested for their power of reduction of 200 mg. of the catalyst per mole of hydrogen theoretically taken up, with 90 kg./cm$^2$ of hydrogen, in a 100 ml. autoclave. The results are summarized in Table I, in which are recorded the conditions used for the hydrogenation reaction, the ratios of hydrogen taken up to the theoretical amount, and reaction products and their yields.

**Hydrogenation of Ketones.**—This catalyst was found to be capable of catalyzing the hydrogenation of acetone and ethyl methyl ketone to the corresponding alcohols, but was quite inactive for the cardonyl groups of mesityloxide and acetophenone. In general, it is probable that simple aliphatic ketones can be reduced in the presence of this catalyst, while reduction of carbonyl groups, conjugated with the C=C double bonds and attached to aromatic rings, may be impossible.

**Hydrogenation of Aldehydes.**—A very interesting phenomenon was observed on the hydrogenation of both acetaldehyde and benzaldehyde in the presence of this catalyst. When hydrogen was introduced into the reaction vessel before the reactant had been heated to the reaction temperature, reduction of these aldehydes did not take place. But, when previously heated reactant was shaken with hydrogen (indicated by an asterisk* in the

1) A. Akamatsu, Y. Izumi and S. Akabori, This Bulletin, 34, 1067 (1961).

TABLE I. CATALYTIC REACTIONS WITH VARIOUS COMPOUNDS

| Substrate (g.) | Solvent (ml.) | Cat. mg. | Temp. °C | $H_2$-Uptake % | React. time min. | Product | Yield % |
|---|---|---|---|---|---|---|---|
| Acetone (29) | | 100 | 85 | 100 | 376 | Isopropyl alcohol | 79 |
| Ethyl methyl ketone (36) | | 100 | 85 | 100 | 207 | *sec*-Butyl alcohol | 89 |
| Acetophenone (24) | | 40 | 85 | 12 | 201 | — | — |
| Acetaldehyde (22) | | 100 | 50 | 0 | — | — | — |
| Acetaldehyde (22) | | 100 | 50* | 92 | 451 | Ethyl alcohol | 90** |
| Benzaldehyde (27) | | 100 | 50 | 0 | — | — | — |
| Benzaldehyde (27) | | 100 | 15 | 140 | 310 | Benzyl alcohol<br>Toluene | 87**<br>10** |
| Benzaldehyde (27) | | 100 | 60* | 130 | 66 | Benzyl alcohol<br>Toluene | 92**<br>6** |
| Allyl alcohol (29) | | 100 | 100 | 71 | 253 | *n*-Propyl alcohol | 70 |
| Maleic acid (12) | aq. NaOH (65) | 20 | 165 | 95 | 106 | Succinic acid | 81 |
| Mesityloxide (25) | | 100 | 13 | 88 | 1475 | Isobutyl methyl ketone | 60** |
| Acrolein (28) | | 100 | 100 | 20 | 917 | — | — |
| Crotonaldehyde (35) | | 100 | 70* | 0 | — | — | — |
| Nitromethane (6) | $(CH_3CO)_2O$ (50) | 60 | 45* | 100 | 196 | Methyl acetamide | 90 |
| Diethyl nitro malonate (21) | $(CH_3CO)_2O$ (50) | 60 | 78 | 100 | 68 | Diethyl acetaminomalonate | 64 |
| Acetophenoxime (14) | $CH_3OH$ (50) | 40 | 70 | 95 | 934 | $\alpha$-Phenethyl amine<br>$\alpha, \alpha'$-Diphenethyl amine | 72<br>20 |
| Ethyl cyanide (11) | $CH_3OH$ (50) | 80 | 60 | 0 | — | — | — |
| $\alpha$-Ketoglutaric acid (7) | $CH_3OH$ (35)<br>28%aq. $NH_3$ (15) | 10 | 100 | 0 | — | — | — |

* Hydrogen was introduced into the autoclave, after the reactant had been heated to this temprature.
** Estimated directly by gas-chromatography of the reaction mixture.

table), the reaction occurred. Moreover, benzaldehyde could be reduced even at room temperature. As a matter of further interest, it was found that the catalyst which was recovered after having failed to catalyze the reduction of benzaldehyde, showed a considerable increase in activity to hydrogenate nitrobenzene. Its reaction velocity ($v$)[1] was 100 at 21°C.

Unlike the case with ketones, this catalyst seems to be more active for the reduction of aromatic aldehydes than for that of aliphatic aldehydes, as shown by comparison of the reduction of acetaldyde and benzaldehyde shown in the table. With the aliphatic aldehyde groups conjugated with the C=C double bonds in acrolein and crotonaldehyde, hydrogen uptake hardly occurred.

**Hydrogenation of the C=C Double Bonds.**—Tests on the redudtion of allyl alcohol and maleic acid showed that this catalyst is rather active in hydrogenating the C=C double bonds. In the hydrogenation of allyl alcohol, the reaction velocity was influenced by the pressure of hydrogen. The reaction proceeded slowly at a low pressure of hydrogen. On the other hand, it was somewhat difficult to reduce the C=C double bonds conjugated with the carbonyl groups in mesityloxide, acrolein and crotonaldehyde. The double bonds in benzene rings were not reduced in the presence of the catalysts.

**Reduction of Aliphatic Nitro Compounds.**—This catalyst was found to be extremely active in hydrogenating nitro groups attached to aromatic rings, as described in the previous paper[1]. However, nitromethane and diethyl nitro malonate in acetic anhydride were both reduced much more slowly to give methyl acetamide and diethyl acetaminomalonate, respectively.

**Reduction of Acetophenoxime.**—Hydrogenation of acetophenoxime took place rather slowly with this catalyst, yielding $\alpha$-phenethyl amine and some $\alpha, \alpha'$-diphenethyl amine.

**Reduction of Ethyl Cyanide.**—Ethyl cyanide could not be reduced at all in the presence of this catalyst.

**Reductive Amination of $\alpha$-Ketoglutaric Acid.**—It was expected that this catalyst would convert $\alpha$-ketoglutaric acid to glutamic acid in the presence of ammonia and hydrogen, but the result was negative.

As seen in the results described above, the catalytic reactions effected by the silk-platinum catalyst are quite different from the known reductions effected by other platinum catalysts. It may be inferred that the difference is due to

the characteristic spacing of the active centers on the silk-platinum catalyst, which are the result of the structure of the carrier fibroin protein.

The difference between the catalytic efficiency of the silk-platinum and that of the platinic oxide catalyst in the hydrogenation of aromatic nitro compounds, was described in the previous paper[1] of this series.

### Poisoning of the Catalyst

The silk-platinum catalyst was found to be sensitive to poisonous substances or to chemical treatments. But the behavior towards catalytic poisons were somewhat different from that of the silk-palladium catalyst[2]. In examining these inhibitory effects, hydrogenation of nitrobenzene to aniline was adopted as the test system and the reaction velocity ($v$) was calculated as previously described[1].

**Inhibition by Carbon Monoxide.**—Activity of the silk-platinum catalyst in hydrogenating nitrobenzene in the presence of carbon monoxide was tested in comparison with that of the silk-palladium catalyst. For this purpose, carbon monoxide was mixed with hydrogen in various proportions, and introduced into the reaction system. The results obtained are shown in Table II.

Table II. Inhibition by carbon monoxide

| Catalyst | Addition of CO % | Temp. °C | React. vel. $v$ |
|---|---|---|---|
| Silk-Pt (40 mg.) | 0 | 19 | 41.7* |
| | 0.1 | 23 | 8.3* |
| | 0.1 | 50 | 35.7 |
| | 5.0 | 21 | 0 |
| | replaced with pure $H_2$ | 21 | 8.2 |
| | 5.0 | 110 | 5.0 |
| | 10.0 | 100 | 0 |
| | (recovered cat.) 0 | 16 | 15.0 |
| Silk-Pd (200 mg.) | 0 | 30 | 11.1 |
| | 0.1 | 30 | 0.12** |
| | replaced with pure $H_2$ | 30 | 0 |
| | 1.0 | 80 | 0.34 |

* See Fig. 1. ** Calculated value.

The silk-palladium catalyst was much more inhibited by carbon monoxide than the silk-platinum catalyst. The silk-platinum catalyst that had no catalytic action in the presence of carbon monoxide, recovered its activity to some extent in the absence of carbon monoxide. Furthermore, when little carbon monoxide was added (0.1%), the activity was restored even in the course of the reaction, as shown in Fig. 1. It is probable that carbon monoxide is adsorbed by the active metals, sometimes forming coordinate linkages, thus preventing the catalytic action. The activity may be restored when the adsorption is partially removed by hydrogenation of the carbon monoxide (as in the case shown in Fig. 1), or by washing the poisoned catalysts with methanol. It seems that palladium adsorbs carbon monoxide more easily than platinum, and thus the silk-palladium catalyst was more inhibited than the silk-platinum catalyst.

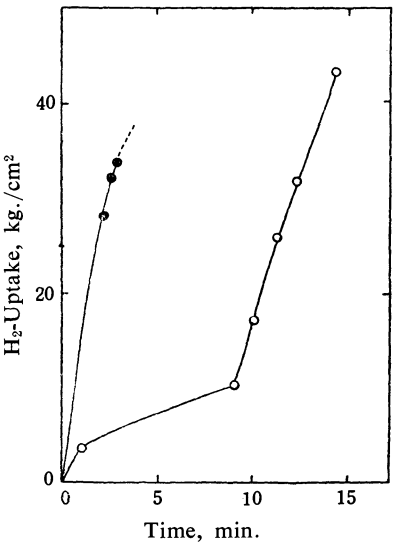



Fig. 1. Hydrogenation of nitrobenzene,
● in the absence of CO, at 19°C,
○ in the presence of 0.1% CO, at 23°C.

**Inhibition by Benzyl Mercaptan.**—As shown in Table III, treatment of the catalyst with benzyl mercaptan and its addition to the substrate resulted in a remarkable decrease in the catalytic activity in hydrogenating nitrobenzene. It is probable, that the mercaptan inhibits the catalyst by directly blocking active platinum, as in the case of the silk-palladium catalyst[2].

Table III. Inhibition by benzyl mercaptan

| Treatment | Addition | React. vel. $v$ at 32°C |
|---|---|---|
| — | — | 48.2 |
| $CH_3OH$ | — | 33.8 |
| $C_6H_5CH_2SH$*/$CH_3OH$ | — | 1.5 |
| — | $C_6H_5CH_2SH$ 2 mg.** | 1.1 |

* 1 mol. per mol. of platinum in the catalyst used.
** 0.25 mol. per mol. of platinum in the catalyst used.

**Inhibition by Metal Ions.**—In the case of the silk-palladium catalyst[2], the activity was greatly lowered in the presence of ferric and cupric ions supplied as nitrates. Cupric ion

2) Y. Izumi, ibid., 32, 936 (1959).

was somewhat more toxic than ferric ion. The silk-platinum catalyst was scarcely inhibited by ferric ion, as shown in Table IV. Cupric ion inhibited this catalyst considerably. The catalyst could not be reactivated by treatment with ethylenediamine tetra-acetic acid (EDTA). When the silk-palladium catalyst was similarly treated, however, it showed very powerful catalytic activity. These metal ions may form chelate linkages, though in a manner different from that of the silk-palladium catalyst, with the carrier protein to prevent the reactant from approaching the active platinum atoms.

TABLE IV. INHIBITION BY METAL IONS

| Metal ion | | React. vel. $v$ at 32°C |
|---|---|---|
| — | | 48.2 |
| $Fe(NO_3)_3 \cdot 12H_2O$ | 8 mg. ($10^{-4}$ mol.) | 36.8 |
| | 40 mg. | 26.5 |
| $Cu(NO_3)_2 \cdot 3H_2O$ | 5 mg. ($10^{-4}$ mol.) | 20.3 |
| | 10 mg. | 8.8 |
| | (treated with EDTA)* | 2.6 |
| | 25 mg. | 1.0 |

* The catalyst was recovered (80%) and treated with 0.5% ethylenediamine tetra-acetic acid.

**Effect of Acetylation.**—The activity of this catalyst remained unaffected by acetylation; the reaction velocity ($v$)[1] with an acetylated silk-platinum catalyst was 33.0 at 32°C. This is not the case with the silk-palladium catalyst[2].

## Experimental

**Preparation of the Catalyst.**—The catalysts used in this work were prepared by the method of Ref. 1 for the silk-platinum, and Ref. 3 for the silk-palladium catalyst.

**Isolation of the Products.**—*Reduction of Acetone.*—The reaction mixture was filtered and the filtrate was distilled; b. p. 80~82°C. The product was identified as isopropyl alcohol by means of gaschromatography.

*Reduction of Ethyl Methyl Ketone.*—The product was isolated as above (b. p. 97.5~98.5°C), and identified as *sec*-butyl alcohol by gaschromatography.

*Reduction of Acetaldehyde.*—The reaction mixture was filtered and the filtrate was treated by gaschromatography. The product was identified as ethyl alcohol, and the yield estimated.

*Reduction of Benzaldehyde.*—The products were identified as benzyl alcohol and toluene and their yields were estimated by gaschromatography.

*Reduction of Allyl Alcohol.*—The product distilling at 97~98°C was identified as *n*-propyl alcohol by means of gaschromatography.

*Reduction of Maleic Acid.*—An aqueous solution of maleic acid adjusted to pH 7.0 with sodium hydroxide was subjected to reduction. The reaction mixture was filtered and the filtrate evaporated to 20 ml. It was then acidified with 20 ml. of concentrated hydrochloric acid. After standing overnight, 9.5 g. of succinic acid (m. p. 184°C) was obtained. It was confirmed by ultraviolet spectroscopy that the product was devoid of unsaturated bonds.

*Reduction of Mesityloxide.*—The reaction mixture was filtered and the filtrate was subjected to gaschromatography. The product was identified as methyl isobutyl ketone, and the yield estimated. Unreacted mesityloxide was also detected.

*Reduction of Nitromethane.*—After filtration of the reaction mixture, the filtrate was fractionally distilled under reduced pressure. The product, boiling at 95~96°C/17 mmHg, was identified as methyl acetamide by gaschromatography and infrared spectroscopy.

*Reduction of Diethyl Nitro Malonate.*—The reaction mixture was filtered and the filtrate evaporated to 20 ml. Thirty milliliters of water were added. After standing overnight, 14 g. of diethyl acetamino malonate (m. p. 93~95°C) was obtained.

Found: N, 6.41. Calcd. for $C_9H_{15}O_5N$: N, 6.45%.

*Reduction of Acetophenoxime.*—The reaction mixture, from which the catalyst had been removed, was evaporated to 30 ml. To this was added 15 ml. of concentrated hydrocholoric acid and then 30 ml. of ether. After standing the solution in a refrigerator overnight, the crystals were filtered off, recrystallized from water, and identified as $\alpha$, $\alpha'$-diphenethyl amine hydrochloride (sublimed above 240°C).

Found: C, 73.52; H, 7.73; N, 5.22; Cl, 13.56. Calcd. for $C_{16}H_{20}NCl$: C, 73.55; H, 7.66; N, 5.32; Cl, 13.47%.

The filtrate was evaporated to dryness and the residue dissolved in 20 ml. of methanol, to which was added 30 ml. of ether. After standing overnight, $\alpha$-phenethyl amine hydrochloride was obtained. It was recrystallized from alcohol and ether; m. p. 158°C.

Found: C, 61.04; H, 7.80; N, 8.75, Cl, 22.45. Calcd. for $C_8H_{12}NCl$: C, 60.95; H, 7.68; N, 8.89; Cl, 22.49%.

**Poisoning of the Catalyst.**—The reaction velocity ($v$) of the hydrogenation of nitrobenzene to aniline was measured and calculated by the method of the previous paper[1].

*Inhibition by Carbon Monoxide.*—Carbon monoxide was mixed with hydrogen in varying proportions and introduced into the reaction system.

*Preparation of Inhibited Catalyst.*—Two hundred milligrams of the silk-platinum catalyst (containing 1/3000 mol. of platinum) was suspended in 100 ml. of methanol or in 100 ml. of 0.04% benzyl mercaptan methanol solution (containing 1/3000 mol. of mercaptan), stirred for 15 min. washed with methanol and ether, and then dried in vacuo. Forty milligrams of this catalyst was used for the test.

*Treatment of the Inhibited Catalyst by Ethylenediamine Tetra-acetic Acid (EDTA).*—The inhibited catalyst was boiled with a 0.5% aqueous solution of EDTA for 5 min., filtered, washed with water, methanol, and then ether, and finally dried in vacuo; 32 mg. (80%).

3) Y. Izumi, ibid., 32, 932 (1959).

*Acetylation of the Catalyst.*—One hundred milligrams of the catalyst was boiled with 50 ml. of acetic anhydride for 2 hr., filtered, washed with ether, and dried in vacuo. Forty milligrams of this catalyst was used for the test.

## Summary

1. The silk-platinum catalyst showed quite different behaviors with various compounds from that of other platinum catalysts. The difference is probably due to the characteristic spacing of the active centers on the silk-platinum catalyst, due to the structure of the carrier silk-fibroin protein.

2. The catalyst was found to catalize the hydrogenation of some aldehydes, unconjugated aliphatic ketones and C=C double bonds, aliphatic nitro groups and oxime, more weakly, than that of the aromatic nitro groups.

3. Carbon monoxide, benzyl mercaptan and cupric ion poisoned the catalyst, and the activity of the catalyst inhibited by cupric ion, was not recovered by treatment with ethylenediamine tetra-acetic acid.

4. Ferric ion scarcely inhibited the catalyst and acetylation of the catalyst scarcely decreased its activity, unlike that of the silk-palladium catalyst.

*Division of Organic Chemistry*
*Institute for Protein Research*
*Osaka University*
*Nishi-ku, Osaka*

# *Studies on the Composition and Properties of Less Familiar Metal Cyano Complexes. I. Composition of Nickel and Cobalt Octacyanomolybdates by Electrometric Methods*

By Wahid U. MALIK and S. Iftikhar ALI

(Received December 27, 1960)

The chemical literature abounds in references on the properties and composition of metal complexes of alkali ferro- and ferricyanides but very little attention appears to have been paid to the study of the metal complexes of alkali octacyanomolybdates. The only work worth mentioning is that of Wardlaw and co-workers[1] who carried out studies on the metal complexes of silver, thallium, copper, etc. by the method of chemical analysis. It is a well known fact that the physical methods have got certain advantages over the methods of chemical analysis in as far as that they not only provide precise information of the composition of the freshly precipitated complex but are able to eliminate the errors which might creep in during the washing and drying of precipitate possessing adsorptive and hydrolytic properties. Attention to this point was drawn by Bhattacharya[2] on the basis of the work carried out by him and his students on metal ferro- and ferricyanides. Since the metal complexes of alkali octacyanomolybdates appear to belong to the class of metal ferrocyano complexes, it was thought worthwhile to employ physical methods for the elucidation of their composition.

The present communication deals with our studies on the nickel and cobalt complexes of potassium octacyanomolybdate employing conductometric, potentiometric and amperometric methods. Moreover these complexes have not so far been studied and are likely to open a new field for the physico-chemical studies on metal cyano complexes.

## Experimental

The method recommended by Fieser[3] was followed for the preparation of potassium octacyanomolybdate. All chemicals, molybdenum(VI) oxide, potassium thiocyanate, pyridine and potassium cyanide, used were A. R. samples. The crystallized product (golden yellow in color) was dried over calcium chloride in a vaccum dessicator. It was dissolved in water twice distilled by a all-glass apparatus and its concentration was determined by titrating potentiometrically against the potassium permanganate solution of a known concentration. Potassium octacyanomolybdate(V) was prepared by the method

1) W. Wardlaw and co-workers, *J. Chem. Soc.*, **1927**, 2981.

2) A. K. Bhattacharya, "Proc. Symp. Coordination Compounds, Part I", National Academy of Science, India (1959), p. 139.

3) L. F. Fieser, *J. Am. Chem. Soc.*, **52**, 5204 (1930).

recommended by Kolthoff[4] and standardized potentiometrically against potassium ferrocyanide.

Nickel and cobalt chlorides of A. R. grade were used for preparing their solutions and their concentrations were estimated gravimetrically after precipitating as nickel dimethylglyoxime and cobalt ammonium phosphate respectively.

Conductometric titrations were done with the help of Cambridge conductivity bridge (No. L-350140) with a bridge type conductivity cell (No. L-355234 and cell constant 0.36). Potentiometric titrations were performed with Tinsley potentiometer (Type 338713) with a lamp and scale arrangement. The indicator electrode was the $K_4Mo(CN)_8 \rightleftarrows K_3Mo(CN)_8 + e$ couple obtained by dipping a bright platinum electrode in a solution of potassium octacyanomolybdate(IV) containing a little potassium octacyanomolybdate(V).

In order to carry out amperometric studies, the constant potential to be applied during the course of titrations was first of all determined, taking in the polarographic cell 1 cc. of 0.1 M salt solution in 0.1 M potassium chloride as supporting electrolyte, 0.0003% sodium methyl red for nickel(II) and 0.01% gelatin for cobalt(II) as maximum suppressor, the total volume made up to 20 cc. The current was measured with Fischer Elecdropode in conjunction with Multiflex galvanometer (type MGF 2, sensitivity 1 : 10), in the external circuit. Polarograms were drawn and from the plateau the potentials to be applied for the amperometric titrations were found out. The potential applied during the course

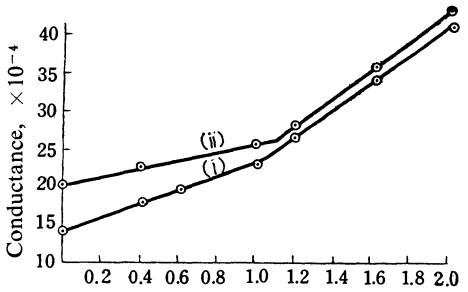



Fig. 1A. 40 cc., 0.0025 M (i) $NiCl_2$ and (ii) $CoCl_2$ vs. 0.05 M $K_4Mo(CN)_8$.

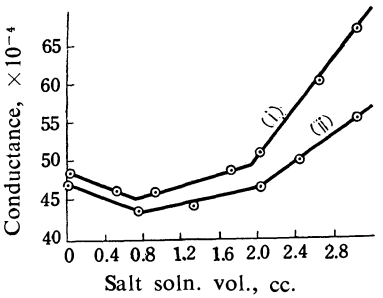



Fig. 1B. 40 cc. $K_4Mo(CN)_8$ 0.0025 M vs. 0.1 M (i) $NiCl_2$ and (ii) $CoCl_2$.

4) I. M. Kolthoff and W. J. Tomsicek, *J. Phys. Chem.*, **40**, 247 (1936).

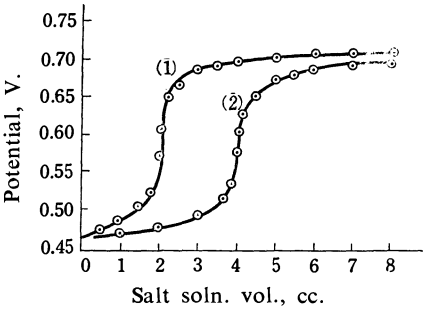



Fig. 2A. Curve (1), 10cc. 0.01M $K_4Mo(CN)_8$ vs. 0.1 M $NiCl_2$. Curve (2), 10 cc. 0.02 M $K_4Mo(CN)_8$ vs. 0.1 M $CoCl_2$.

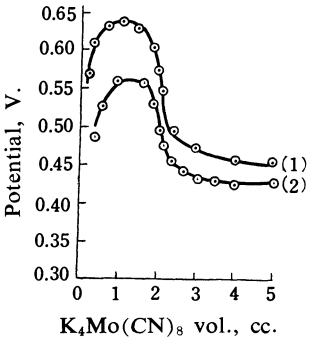



Fig. 2B. 10 cc. 0.02 M (1) $NiCl_2$ and (2) $CoCl_2$ vs. 0.05 M $K_4Mo(CN)_8$.

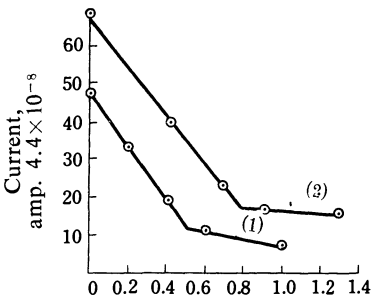



Fig. 3A. 20 cc. (1) 0.005 M $NiCl_2$ and (2) 0.0075 M $CoCl_2$ vs. 0.1 M $K_4Mo(CN)_8$.

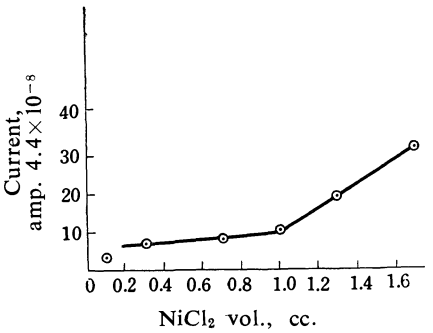



Fig. 3B. 20 cc., 0.0025 M $K_4Mo(CN)_8$ vs. 0.1 M $NiCl_2$.

of titrations for nickel(II) and cobalt(II), being −1.2 and −1.4 V. respectively. Electrodes used were the dropping mercury electrode and the S.C.E. Pure nitrogen was passed in order to maintain the inert atmosphere. All measurements were made at 30±0.1°C. Both direct (salt solution in the cell) and reverse ($K_4Mo(CN)_8$ in the cell) titrations were performed with different concentrations of the reactants.

The results are summarized below. A few typical curves are shown in Figs. 1A, 1B, 2A, 2B and 3A, 3B.

## Results

TABLE I. CONDUCTOMETRIC TITRATIONS

Direct: Salt soln. in the cell.

| Salt Soln. in the cell Vol., cc. | Concn., M | Vol. of 0.05 M $K_4Mo(CN)_8$ from the curves, cc. $NiCl_2$ | $CoCl_2$ | Ratio $Ni^{2+}$: $Mo(CN)_8^{4-}$ | $Co^{2+}$: $Mo(CN)_8^{4-}$ |
|---|---|---|---|---|---|
| 40 | 0.00075 | 0.4 | 0.38 | 2 : 1.25 | 2 : 1.1 |
| 40 | 0.00125 | 0.53 | 0.55 | 2 : 1.05 | 2 : 1.08 |
| 40 | 0·0020 | 0.90 | 1.0 | 2 : 1.09 | 2 : 1.1 |
| 40 | 0.0025 | 0.98 | 1.08 | 2 : 1.0 | 2 : 1.08 |

Reverse: Potassium molybdocyanide in the cell.

| $K_4Mo(CN)_8$ in the cell Vol., cc. | Concn., M | Vol. of 0.1 M salt soln. from the curves, cc. $NiCl_2$ | | $CoCl_2$ | | Ratio $Ni^{2+}$: $Mo(CN)_8^{4-}$ | $Co^{2+}$ : $Mo(CN)_8^{4-}$ |
|---|---|---|---|---|---|---|---|
| 40 | 0.0020 | 0.6 | 1.32 | 0.7 | 1.6 | 1 : 1.3 ; 2 : 1.04 | 1 : 1.3 ; 2 : 1 |
| 40 | 0.0025 | 0.76 | 1.85 | 0.88 | 2.0 | 1 : 1.2 ; 2 : 1.08 | 1 : 1.1 ; 2 : 1 |

TABLE II. POTENTIOMETRIC TITRATIONS

Direct: Potassium molybdocyanide in the cell.

| $K_4Mo(CN)_8$ Vol., cc. | Concn., M | Vol. of salt soln. from the curves, cc. $NiCl_2$ | $CoCl_2$ | Ratio $Ni^{2+}$: $Mo(CN)_8^{4-}$ | $Co^{2+}$: $Mo(CN)_8^{4-}$ |
|---|---|---|---|---|---|
| 10 | 0.02 | 3.8 | 4.1 | 2 : 1.05 | 2.05 : 1 |
| 10 | 0.0125 | 2.4 | 2.6 | 2 : 1.04 | 2.01 : 1 |
| 10 | 0.01 | 2.0 | 2.1 | 2 : 1.0 | 2.0 : 1 |

Reverse: Salt soln. in the cell.

| Salt soln. in the cell Vol., cc. | Concn., M | Vol. of 0.05 M $K_4Mo(CN)_8$ from the curves, cc. $NiCl_2$ | $CoCl_2$ | Ratio $Ni^{2+}$: $Mo(CN)_8^{4-}$ | $Co^{2+}$: $Mo(CN)_8^{4-}$ |
|---|---|---|---|---|---|
| 10 | 0.02 | 2.15 | 2.0 | 2 : 1.07 | 2 : 1.0 |
| 10 | 0.0125 | 1.3 | 1.7 | 2 : 1.04 | 2 : 0.87 |
| 10 | 0.01 | 1.0 | 1.0 | 2 : 1.0 | 2 : 1.0 |

TABLE III. AMPEROMETRIC TITRATIONS

Direct: Salt soln. in the cell.

| Salt solution Vol., cc. | Cocn., M | Vol. of 0.1 M $K_4Mo(CN)_8$ from the curves, cc, $NiCl_2$ | $CoCl_2$ | Ratio $Ni^{2+}$: $Mo(CN)_8^{4-}$ | $Co^{2+}$: $Mo(CN)_8^{4-}$ |
|---|---|---|---|---|---|
| 20 | 0.005 | 0.53 | 0.54 | 2 : 1.01 | 2 : 1.08 |
| 20 | 0.0075 | 0.77 | 0.77 | 2 : 1.02 | 2 : 1.02 |

Reverse: $K_4Mo(CN)_8$ in the cell.

| $K_4Mo(CN)_8$ Vol., cc. | Concn., M | Vol. of 0.1 M $NiCl_2$ from the curves, cc. | Ratio $Ni^{2+}$ : $Mo(CN)_8^{4-}$ |
|---|---|---|---|
| 20 | 0.0025 | 1.0 | 2 : 1 |
| 20 | 0.0030 | 1.2 | 2 : 1 |
| 20 | 0.00375 | 1.5 | 2 : 1 |

## Discussion

The reaction between nickel chloride/cobalt chloride and potassium molybdocyanide may be represented by the following stoichiometric equations:

$$MCl_2 + K_4Mo(CN)_8 = K_2MMo(CN)_8 + 2KCl \quad (1)$$

$$3MCl_2 + 2K_4Mo(CN)_8 = K_2M_3(Mo(CN)_8)_2 + 6KCl \quad (2)$$

$$2MCl_2 + K_4Mo(CN)_8 = M_2Mo(CN)_8 + 4KCl \quad (3)$$

$$MCl_2 + xK_4Mo(CN)_8 = K_2MMo(CN)_8 \cdot (x-1)K_4Mo(CN)_8 + 2KCl \quad (4)$$

(adsorption complex)

The results on conductometric, potentiometric and amperometric titrations summarized in the foregoing paragraph give a ratio of $2M^{2+}$ : $1Mo(CN)_8^{4-}$ pointing towards the formation of the complex $M_2Mo(CN)_8$ (M being Ni/Co) in accordance with Eq. 3 given above. Further, a ratio of 1 : 1 for the reactants is also found in the case of conductometric titration when the metal salt is added to the potassium molybdocyanide in the conductivity cell. For this ratio the complex formed would have the composition $K_2MMo(CN)_8$.

The combining ratios (both 2 : 1 and 1 : 1) show a slight discrepancy from the stoichiometric equations. For almost all the different concentrations of the reactants employed for these titrations, the amount of potassium molybdocyanide required is larger than the theoretical values. This behavior can well be explained by assuming that the freshly precipitated complexes have got the property of adsorbing $Mo(CN)_8^{4-}$ ion. An indirect proof of the adsorptive capacity of the complexes was forthcoming from our preliminary experiments. There it was found that the green precipitate of nickel molybdocyanide can be transformed into a stable sol when nickel chloride is added to a little excess of potassium molybdocyanide. However, mixing in the reverse order ($K_4Mo(CN)_8$ to $NiCl_2$) resulted in a thick precipitate rather than a sol. A similar behavior was found with cobalt molybdocyanide which could be obtained in the form of a stable orange colored sol by using excess of potassium molybdocyanide.

The potentiometric studies need a special mention here. We observed that potentiometric titrations for this precipitation reaction can be successfully performed by employing a $Mo(CN)_8^{4-} \rightleftarrows Mo(CN)_8^{3-} + e$ couple at bright platinum electrode. Typical curves (Fig. 2A) are obtained when the metal solution is added to the solution of potassium molybdocyanide containing a little potassium molybdicyanide. But in the case of reverse titrations (Fig. 2B) the curves are of a different nature, the e. m. f. increasing in the initial stages before showing a downward slope. This behavior points towards the fact that the molybdo-molybdicyanide couple attains equilibrium condition when an optimum amount of the reagent is present in the titrating cell. When sufficient amount of molybdocyanide has been added from the burette the curves have got the typical nature.

Amperometric titrations carried out with potassium molybdocyanide in the polarographic cell are different in shape than those which should be obtained on theoretical considerations, for such titrations (reducible ions added to non-reducible ions in the cell). The current increases appreciably on adding the titrant (Fig. 3B) and this is more so for $Co^{2+}$ solution (results not given). It was thought that the increase in current might be due to the formation of some intermediate soluble complex. The products of interactions at different stages in this region were taken separately and polarograms drawn. The $E_{1/2}$ in each case corresponded to the $E_{1/2}$ of $Ni^{2+}$ (−1.1 V.) and $Co^{2+}$ (−1.2 V.) thereby showing the non-existence of a soluble complex in between. Titrations with the metal solution in the cell (Fig. 3A) were of the same nature as required on theoretical grounds. It is quite likely that the colloidal nature of the solution in the former case influence the performance of the dropping mercury electrode and typical curves are not obtained there.

## Summary

The composition of the freshly precipitated nickel and cobalt cyano molybdates was determined using conductometric, potentiometric and amperometric methods. The nickel compound is green in color and its composition may be represented as $Ni_2Mo(CN)_8$. The orange precipitate of the cobalt cyano molybdate has also got the composition $Co_2Mo(CN)_8$. Reverse conductometric titration (salt solution added to molybdocyanide) give evidence of the complexes $K_2NiMo(CN)_8$ and $K_2CoMo(CN)_8$. These titrations provide information of the adsorption of $Mo(CN)_8^{4-}$ ions by the freshly precipitated complex. Both the compounds show tendency to pass into the colloidal state when the salt solution is added to excess of potassium octacyano molybdate.

Thanks are due to Professor M. O. Farooq for providing facilities and to the Ministry of

Scientific Research and Cultural Affairs, Government of India for the award of a fellowship to one of us (S. I. A.) to carry out this work.

*Chemical Laboratories*
*Muslim University*
*Aligarh, India*

# *Studies on the Composition and Properties of Less Familiar Metal Cyano Complexes. II. Composition of Copper Octacyano Molybdate and the Existence of the Redox System* $Cu^{+}+Mo(CN)_8^{3-} \rightleftharpoons Cu^{2+}+Mo(CN)_8^{4-}$

By Wahid U. MALIK and S. Iftikhar ALI

(Received December 27, 1960)

In continuation to our studies on the composition of the complex molybdocyanides of heavy metals by electrometric methods (Part I, this Bulletin*), investigations were extended to the copper complexes. The study of such complexes, besides providing information regarding the composition of cupric molybdocyanide, opens a new aspect for further investigation, viz., the existence of redox potential in the system $Cu^{+}+Mo(CN)_8^{3-} \rightleftarrows Cu^{2+}+Mo(CN)_8^{4-}$. Little work has been done in this direction even for the well-known metal ferrocyanogen complexes and very few references are available in the literature on this aspect of the problem.

For the first time Davidson[1] in 1937 drew attention towards the existence of $Fe^{3+}+Fe(CN)_6^{4-} \rightleftarrows Fe(CN)_6^{3-}+Fe^{2+}$ couple in the slow formation of ferric-ferrocyanide while carrying out experiments on the iron blues. Very recently systematic studies on these lines have been carried out by Malik[2] for systems like $Cu^{+}+Fe(CN)_6^{3-} \rightleftarrows Fe(CN)_6^{4-}+Cu^{2+}$; $Mn^{3+}+Fe(CN)_6^{4-} \rightleftarrows Fe(CN)_6^{3-}+Mn^{2+}$; $Cr^{2+}+Fe(CN)_6^{3-} \rightleftarrows Cr^{3+}+Fe(CN)_6^{4-}$ etc., applying amperometric methods.

The present communication deals with two aspects of the problem of copper complexes of alkali cyanomolybdates: i) the composition of the freshly precipitated cupric molybdocyanide by electrometric methods and ii) the study of the cuprous chloride potassium molybdicyanide reaction employing a cuprous-cupric couple at the bright platinum electrode.

## Experimental

Solutions of potassium molybdo- and molybdicyanide were prepared and standardized as given in Part I. Copper sulfate solution was prepared by dissolving a weighed amount of A. R. crystals of the salt in redistilled water and its concentration determined iodometrically[3]. Cuprous chloride[4] was prepared and a weighed amount of it dissolved in 1 M potassium chloride solution (acidified with a little hydrochloric acid). The solution was kept under a layer of paraffin to avoid oxidation. The concentration of the solution was determined by titrating against 0.1 M ammonium thiocyanate, using ferric alum[5] as the indicator.

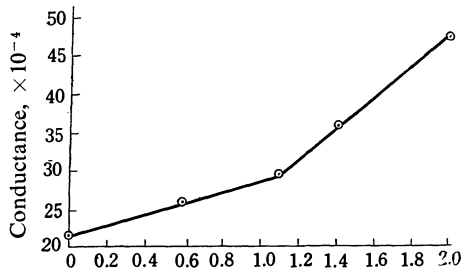



Fig. 1A. 40 cc. 0.0025 M $CuSO_4$ vs. $K_4Mo(CN)_8$ 0.05 M.

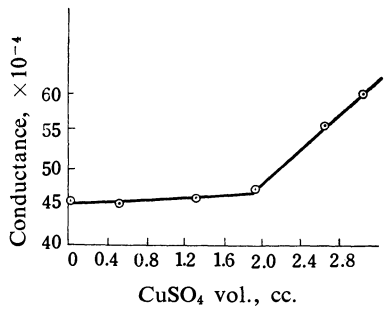



Fig. 1B. 40 cc. 0.0025 M $K_4Mo(CN)_8$ vs. 0.1 M $CuSO_4$.

* Part I, This Bulletin, 34 1306 (1961).

1) D. Davidson, *J. Chem. Educ.*, 14, 238 (1937).

2) W. U. Malik, *J. Ind. Chem. Soc.*, in press.

3) "Scott's Standard Method of Chemical Analysis", by Furman, Vol. I, Ed V, p. 368.

4) Fernelius, "Inorganic Syntheses", Vol. II, p. 1.

5) W. U. Malik and Co-workers, *Z. anorg. u. allgem. Chem.*, 299, 322 (1959).

Conductometric, potentiometric and amperometric titrations between copper sulfate and potassium molybdocyanide were carried out as described earlier. Potentiometric titrations between cuprous chloride and potassium molybdicyanide were carried out, using $Cu^{+} \rightleftarrows Cu^{2+}+e$ couple, obtained by dipping bright platinum electrode in a solution of cuprous chloride containing a little cupric chloride.

All the experiments were performed in the dark room and the vessels were also wrapped with black paper to avoid the decomposition of potassium molybdicyanide.

The results are summarized below. A few typical curves are shown in Figs. 1A, 1B, 2, 3A, 3B and 4A, 4B.

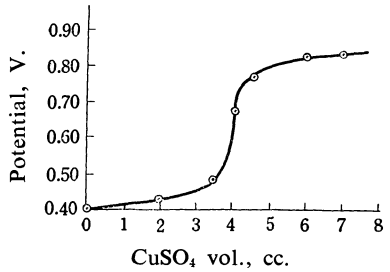



Fig. 2. 10 cc. 0.02 M $K_4Mo(CN)_8$ vs. 0.1 M $CuSO_4$.

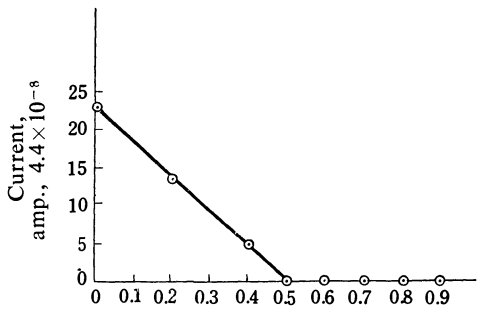



Fig. 3A. 20 cc. 0.005 M $CuSO_4$ vs. $K_4Mo(CN)_8$ 0.1 M.

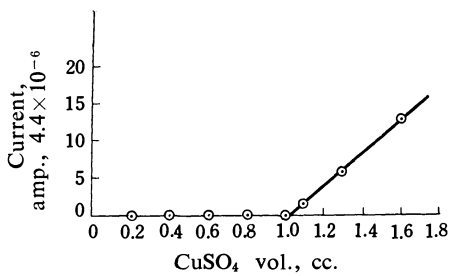



Fig. 3B. 20 cc. 0.0025 M $K_4Mo(CN)_8$ vs. 0.1 M $CuSO_4$.

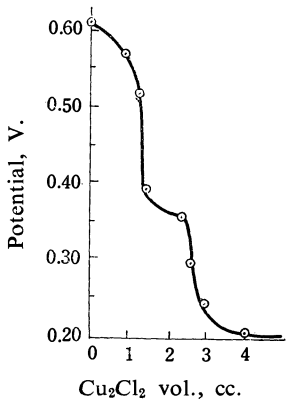



Fig. 4A. 5 cc. 0.0368 M $K_3Mo(CN)_8$ vs. 0.0794 M $Cu_2Cl_2$.

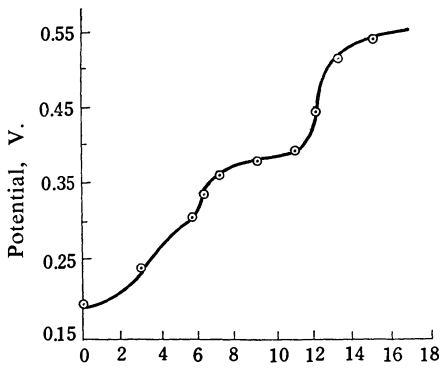



Fig. 4B. 5cc. 0.0619 M $Cu_2Cl_2$ vs. 0.046 M $K_3Mo(CN)_8$.

## Results

TABLE I. CONDUCTOMETRIC TITRATIONS

Direct: Copper sulfate solution in the cell.

| $CuSO_4$ in the cell Vol., cc. | Concn., M | Vol. of 0.05 M $K_4Mo(CN)_8$ from the curves, cc. | Ratio $Cu^{2+}$ : $Mo(CN)_8^{4-}$ |
|---|---|---|---|
| 40 | 0.00075 | 0.3 | 2 : 1.0 |
| 40 | 0.00125 | 0.54 | 2 : 1.05 |
| 40 | 0.0020 | 0.84 | 2 : 1.05 |
| 40 | 0.0025 | 1.10 | 2 : 1.09 |

Reverse: Potassium molybdocyanide in the cell.

| $K_4Mo(CN)_8$ Vol., cc. | Concn., M | Vol. of 0.1 M $CuSO_4$ from the curves, cc. | Ratio $Cu^{2+}$ : $Mo(CN)_8^{4-}$ |
|---|---|---|---|
| 40 | 0.00075 | 0.54 | 2 : 1.1 |
| 40 | 0.00125 | 0.86 | 2 : 1.16 |
| 40 | 0.0020 | 1.48 | 2 : 1.08 |
| 40 | 0.0025 | 1.80 | 2 : 1.1 |

TABLE II. POTENTIOMETRIC TITRATIONS

Direct: Potassium molybdocyanide in the cell.

| $K_4Mo(CN)_8$ Vol., cc. | $K_4Mo(CN)_8$ Concn., M | Vol. of 0.1 M $CuSO_4$ from the curves, cc. | Ratio $Cu_2^{+} : Mo(CN)_8^{4-}$ |
|---|---|---|---|
| 10 | 0.02 | 3.9 | 2 : 1.02 |
| 10 | 0.0125 | 2.45 | 2 : 1.02 |
| 10 | 0.01 | 1.90 | 2 : 1.05 |

TABLE III. AMPEROMETRIC TITRATIONS

Direct: Copper Sulfate Soln. in the cell.

Voltage applied, −0.4 V. Temp., 30±0.1°C

| copper sulphate Vol., cc. | copper sulphate Concn., M | Vol. of 0.1 M $K_4Mo(CN)_8$ from the curves, cc. | Ratio $Cu^{2+} : Mo(CN)_8^{4-}$ |
|---|---|---|---|
| 20 | 0.003 | 0.30 | 2 : 1 |
| 20 | 0.005 | 0.50 | 2 : 1 |
| 20 | 0.0075 | 0.72 | 2 : 1 |

Reverse: Potassium molybdocyanide in the cell.

| $K_4Mo(CN)_8$ Vol., cc. | $K_4Mo(CN)_8$ Concn., M | Vol. of 0.1 M $CuSO_4$ from the curves, cc. | Ratio $Cu^{2+} : Mo(CN)_8^{4-}$ |
|---|---|---|---|
| 20 | 0.0015 | 0.6 | 2 : 1 |
| 20 | 0.0025 | 1.0 | 2 : 1 |
| 20 | 0.00375 | 1.46 | 2 : 1.02 |

TABLE IV. POTENTIOMETRIC TITRATIONS BETWEEN CUPROUS CHLORIDE AND POTASSIUM MOLYBDICYANIDE

Direct: Potassium molybdicyanide in the cell.

| $K_3Mo(CN)_8$ Vol., cc. | $K_3Mo(CN)_8$ Concn., | Vol. of 0.0794 M $Cu_2Cl_2$ from the curves, cc. | | Ratio $Cu^{+} : Mo(CN)_8^{3-}$ | |
|---|---|---|---|---|---|
| 5 | 0.0276 | 1.0 | 2.0 | 1.12 : 2 | 1.12 : 1 |
| 5 | 0.0368 | 1.3 | 2.6 | 1.12 : 2 | 1.12 : 1 |
| 5 | 0.046 | 1.6 | 3.2 | 1.10 : 2 | 1.12 : 1 |

Reverse: Cuprous chloride in the cell.

| $Cu_2Cl_2$ Vol., cc. | $Cu_2Cl_2$ Concn., M | Vol. of 0.046 M $K_3Mo(CN)_8$ from the curves, cc. | | Ratio $Cu^{+} : Mo(CN)_8^{3-}$ | |
|---|---|---|---|---|---|
| 5 | 0.0397 | 3.8 | 7.7 | 1.13 : 1 | 1.13 : 2 |
| 5 | 0.0619 | 6.0 | 12.0 | 1.14 : 1 | 1.14 : 2 |
| 5 | 0.0794 | 7.2 | 14.4 | 1.19 : 1 | 1.19 : 2 |

## Discussion

Conductometric titrations between copper sulfate and potassium molybdocyanide (Figs. 1A and 1B) give the ratio $Cu^{2+}$ to $Mo(CN)_8^{4-}$ as 2 : 1. Potentiometric titrations carried out with copper sulfate solution in the cell did not give typical titration curves and there was a sharp rise in potential on the addition of even a small amount of molybdocyanide (containing a little molybdicyanide) from the burette. Titrations carried out in the reverse manner, viz., by adding copper sulfate solution to the molybdocyanide in the cell ($Mo(CN)_8^{4-} \rightleftarrows Mo(CN)_8^{3-} + e$ couple at the bright platinum electrode) gave very satisfactory results (Fig. 2) and here too a ratio of 2 : 1 was found to exist. However, both these methods gave a little more of potassium molybdocyanide than required by the stoichiometric equation: $2 \cdot CuSO_4 + K_4Mo(CN)_8 = Cu_2Mo(CN)_8 + 2K_2SO_4$ for the formation of the complex. Here this may also be attributed to the adsorption of $Mo(CN)_8^{4-}$ by the freshly precipitated complex although the adsorption effect is not so marked as in the case of cobalt and nickel complexes (Part I). The behavior of copper molybdocyanide is also slightly different from those of cobalt and nickel molybdocyanides in as much as that the precipitate of the latter pass into colloidal solution more readily than the former. Amperometric titrations (Figs. 3A and 3B) both

direct and reverse give the ratio 2 : 1, again pointing towards the formation of the complex $Cu_2Mo(CN)_8$.

Conductometric titrations as well as the amperometric titrations were unsuccessful in investigating the reaction between cuprous chloride and potassium molybdicyanide. In the latter suitable potential to be applied could not not be found while in the former sharp points of intersection at the equivalence point were not realized. However, potentiometric titrations at the $Cu^+ \rightleftarrows Cu^{2+}+e$ couple (Pt electrode dipped in a solution of cuprous chloride containing a little cupric chloride) gave typical titration curves with two sharp breaks (Figs. 4A and 4B). The values for the ratio $Cu^+$ : $Mo(CN)_8^{3-}$ being nearly 1 : 2 and 1 : 1 respectively.

Before assigning a particular formula to the complex formed by this reaction it is important to consider the oxidation reduction reaction : $Cu^+ + Mo(CN)_8^{3-} \rightleftarrows Cu^{2+} + Mo(CN)_8^{4-}$. Taking the redox potentials of $Mo(CN)_8^{4-} \rightleftarrows Mo(CN)_8^{3-}+e$ as $-0.82$ V. and that of $Cu^+ \rightleftarrows Cu^{2+}+e$ as $-0.17$ V., the equilibrium constant of the above mentioned redox reaction comes out to be $1.5\times10^{12}$. It means that during the interaction of cuprous chloride and potassium molybdicyanide, a large amount of cuprous is oxidized to the cupric state and the molybdicyanide is reduced to the molybdocyanide.

On the basis of the above explanation the reaction should take place in the following two steps.

$Cu_2Cl_2+2K_3Mo(CN)_8+2KCl=2CuCl_2+2K_4 \cdot Mo(CN)_8$ followed by, $2CuCl_2+2K_4Mo(CN)_8= 2K_2CuMo(CN)_8+2KCl$. The ratio 1 : 2 ($Cu^+$ : $Mo(CN)_8^{3-}$) found on the basis of potentiometric titration support the above mechanism since the overall reaction would be $Cu_2Cl_2+ 2K_3Mo(CN)_8=2K_2CuMo(CN)_8+2KCl$, giving the complex $K_2Cu^{II}Mo^{IV}(CN)_8$.

Whether an oxidation-reduction equilibrium ($K=1.5\times10^{12}$) can completely hold good in the case of precipitation reactions is rather difficult to say. It is quite probable that some of the cuprous chloride is precipitated by potassium molybdicyanide before mutual oxidation reduction takes place and some cuprous molybdicyanide is also formed. Under these conditions a ratio of 1 : 1 for the reactants should be realized. This is what we actually get from the second break of the direct and the first break of the reverse titrations. To sum up it may be said that the products of interaction between cuprous chloride and potassium octacyanomolybdate(V) are predominantly $K_2Cu^{II}Mo^{IV}(CN)_8$ although a little amount of $KCu_2^{I}Mo^{V}(CN)_8$ is also formed.

## Summary

The reaction between copper sulfate and potassium molybdocyanide was studied using conductometric, potentiometric and amperometric methods. The stoichiometric ratio of 2 : 1 for $Cu^{2+}$ to $Mo(CN)_8^{4-}$ correspond to the formation of $Cu_2Mo(CN)_8$. The interaction of cuprous chloride and potassium molybdicyanide resulted in the formation of $K_2Cu^{II}Mo^{IV}(CN)_8$. Evidence for the existence of a redox potential in the system $Cu^+ + Mo(CN)_8^{3-} \rightleftarrows Cu^{2+}+Mo(CN)_8^{4-}$ could be obtained for the latter reaction on the basis of potentiometric titrations.

Thanks are due to Professor M. O. Farooq for providing facilities and to the Ministry of Scientific Research and Cultural Affairs, Government of India for the award of a Fellowship to one of us (S. I. A.) to carry out this work.

*Chemical Laboratories*
*Muslim University*
*Aligarh, India*

# *On the Erlenmeyer Reaction. I. Mechanism of Threo-β-phenylserine Formation**

By Takeo KANEKO and Kaoru HARADA**

(Received December 9, 1960)

The Erlenmeyer reaction[1] of glycine with benzaldehyde in the presence of excess of alkali results in the formation of *N*-benzal-β-phenylserine alkali salt and *N*-benzal-α, β-diphenyl-β-hydroxyethylamine. Recently many stereochemical studies of β-phenylserine have been published in connection with chloramphenicol. Vogler[2] has determined chemically that the structure of Erlenmeyer's phenylserine was only of the threo-type. The diastereoisomeric erythro-β-phenylserine was first isolated in pure state by Shaw and Fox[3] in 1950. They prepared pure erythro-β-phenylserine using a new method for separation of the threo and erythro isomers, and they also found a paper chromatographic solvent (S-F solvent) to separate these two diasteromers.

An interesting point in the Erlenmeyer synthesis of β-phenylserine is that the threo isomer is the predominant product. The erythro isomer, which is expected to form in the aldol condensation of glycine and benzaldehyde, has not been isolated from the final crystalline product. Shaw and Fox found by use of their paper chromatographic solvent that the threo isomer increased and the erythro isomer decreased during the reaction.

Quantitative analyses of the threo- and the erythro-phenylserine and glycine in the reaction mixture at different intervals of the reaction time have now been carried out to determine the ratio of these three amino acids. Table I shows the ratio of these three amino acids produced in the Erlenmeyer reaction.

TABLE I. AMINO ACID RATIO IN THE ERLENMEYER REACTION

| hr. | Gly | Threo-phe. ser. | Erytho-phe. ser. |
|---|---|---|---|
| 1/4 | 48 | 28 | 24 |
| 1/2 | 39 | 39 | 22 |
| 1 1/2 | 23 | 52 | 25 |
| 4 1/2 | 18 | 62 | 20 |
| 24 | 11 | 73 | 16 |
| 50 | 9 | 77 | 14 |

From the results of the analyses, it may be inferred that the erythro isomer is converted into the threo isomer during the reaction.

In order to prove the hypothesis, either erythro or threo-phenylserine was mixed with ethanol, water, benzaldelyde and sodium hydroxide as in the Erlenmeyer reaction. It was found that if equimolar or less sodium hydroxide was used, threo- or erythro-phenylserine was not converted into its diastereomer. The resulting reaction mixture gave only the original threo or erythro isomer, which was identified by paper chromatography using the S-F solvent. However, by the use of an excess of alkali as in the Erlenmeyer reaction, both threo- and erythro-phenylserine were converted into a mixture of the isomers. When threo-, erythro- or a mixtuer of threo- and erythro-phenylserine were treated under Erlenmeyer's condition, one of the sodium salts of isomeric *N*-benzal-phenylserine crystallized out from the reaction mixture as the predominant product. After debenzalation of the crystalline

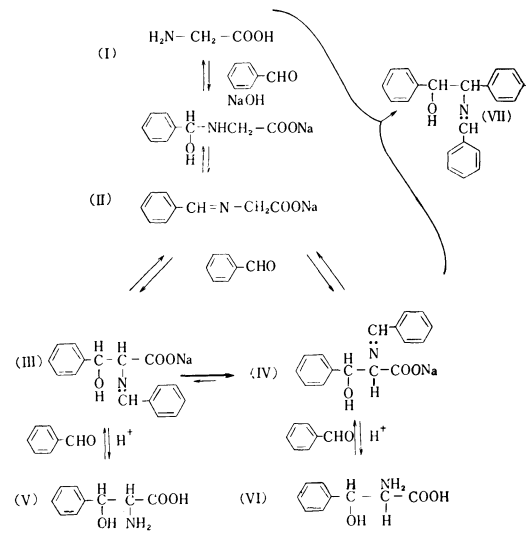



Fig. 1. Flow sheet of postulated mechanism of Erlenmeyer reaction.

* Presented in part at the 9th Annual Meeting of the Chemical Society of Japan, Kyoto, April, 1956.

** Present address: Florida State University, Oceanographic Institute, Tallahassee, Florida, U. S. A.

1) E. Erlenmeyer Jr., *Ber.*, **25**, 3445 (1892); E. Erlenmeyer, Jr. and E. Frustuck, *Ann.*, **284**, 36 (1894); E. Erlenmeyer, Jr., ibid., **307**, 70 (1899).

2) K. Vogler, *Helv. Chim. Acta*, **33**, 2111 (1950).

3) K. N. F. Shaw and S. W. Fox, *Abstr. of Papers, 18th Am. Chem. Soc. Meeting.*, p. 28N (1950); K. N. F. Shaw and S. W. Fox, *J. Am. Chem. Soc.*, **75**, 3417, 3421 (1953).

product, paper chromatography showed that the product consisted of only the threo isomer. Each of the mother liquors arising from the above mentioned three different reactions, however, contained glycine and the threo- and erythro-phenylserine. These results suggest a possible-mechanism for the formation of Erlenmeyer's threo-phenylserine. The postulated pathways of the reaction are shown in Fig. 1.

Glycine (I) reacted with benzaldehyde to yield benzal glycine (II). The resulting II reacted again with benzaldehyde forming erythro-*N*-benzal-phenylserine (III) and threo-*N*-benzalphenylserine (IV). In solution both III and IV exist as a mixture. However,

(A) if the solubility of IV is small and it crystallizes easily, and

(B) if there is an equilibrium between III and IV under the reaction conditions,

the erythro isomer III is converted in to threo isomer IV by crystallization. Erlenmeyer's threo-phenylserine formation may be considered as a typical asymmetric transformation reaction.

In the conversion of V→III→IV, about 65～75% of the threo isomer was isolated in crystal form IV. It is necessary to use more than twice the equivalent of alkali to crystallize IV in the conversion of erythro to threo isomer. The filtrate of the crystalline reaction product contains III, IV and glycine, the last being an alkali degradation product of phenylserine. The reaction yielded *N*-benzal-$\alpha$, $\beta$-diphenyl-$\beta$-hydroxyethylamine (VII) as a by-product. Paper chromatography showed that a longer reaction time resulted in an increased formation of VII.

In the conversion reaction, the $\alpha$- or $\beta$-carbon atom or both carbon atoms must be racemized or inverted. Optically active erythro-phenylserine was used to determine which carbon atom racemized or inverted during the reaction. When D-erythro-phenylserine was treated with benzaldehyde and alkali as in Erlenmeyer's reaction, condition, the mixture had a very high rotatory power which decreased rapidly as is shown in Fig. 2. After about 4.5 hr., the solution lost almost all optical activity and crystals were precipitated out. The expected optically active threo isomer was not obtained, but the crystal was identified as sodium salt of racemic *N*-benzal-threo-phenylserine (IV).

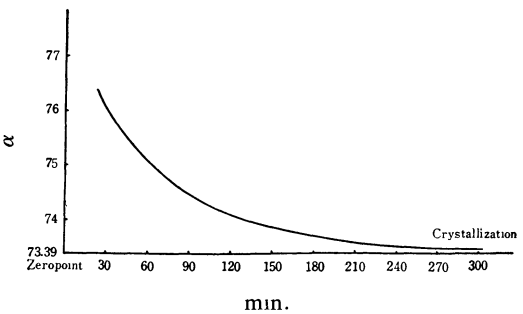



Fig. 2. Mutarotation of D-erythro-$\beta$-phenylserine.

This study showed that both the $\alpha$- and $\beta$-carbon atoms were racemized during the reaction. In the absence of benzaldehyde, D-erythro-phenylserine did not racemize so rapidly and it retained more than 75% of its optical activity after 4.5 hr. The racemization at the $\alpha$- and $\beta$-carbon atoms is not only due to the alkali but the *N*-benzal residue, which is important in the conversion process. Such knowledge suggests the equilibrium between III and IV as is shown in Fig. 3.

Optically active erythro-phenylserine has been isolated by Fone[4] using an enzymic method and he determined its configuration

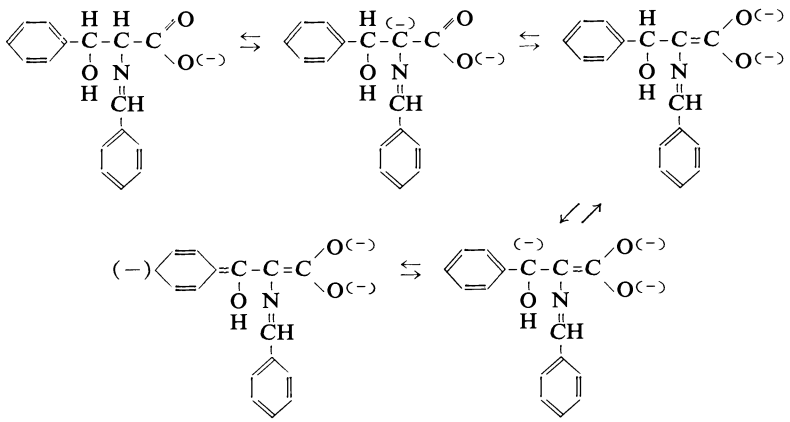


Fig. 3. Equilibrium between III and IV.

4) W. S. Fone, *J. Biol. Chem.*, **204**, 323 (1953).

biologically. In this study D- and L-erythro-phenylserine were prepared by resolution of *N*-benzoyl-DL-erythro-phenylserine using quinine. The D-isomer was isolated in an optically pure state but the L-isomer had only 75% of its optical activity. The configuration of these isomers was also determined chemically. The (−)-erythro-phenylserine was reduced with hydrogen iodide and red phosphorus giving D(+)-phenylalanine. The (−)-erythro isomer has a sweet taste, and (+)-erythro-phenylserine has a bitter taste. These results show that the (−)-erythro isomer has the $D_S$-configuration and (+)-erythro isomer has the $L_S$-configuration.

## Discussion

The fact that the mechanism of threo-phenylserine formation is based on the racemization of $\alpha$- and $\beta$-carbon atoms has been mentioned above. However, another explanation is possible: the $\alpha-\beta$ carbon linkage could be cleft during the reaction and the resulting benzaldehyde and *N*-benzal-glycine could react again to reform the threo isomer IV. Such a mechanism is conceivable since the linkage of the $\alpha-\beta$ carbon is not stable in the alkaline condition; phenylserine is completely decomposed to glycine and benzaldehyde after boiling for 1 hr. with 1 N sodium hydroxide. Elphimoff-Felkin[5] studied the transformation of ethyl threo-*p*-nitro-$\beta$-phenylserinate to the corresponding erythro isomer in alcoholic solution. The conversion reaction was explained by the cleavage of the $\alpha-\beta$ carbon bond of the threo isomer and consequent reforming of the erythro isomer from the resulting *p*-nitro-benzaldehyde and glycine ethylester. However, the explanation can not be applied successfully in the Erlenmeyer reaction. In the reaction of threo-*p*-nitro-phenylserine[6] with benzaldehyde and alkali, the sodium salt of *N*-benzal-threo-*p*-nitro-penylserine was crystallized out easily from the reaction mixture. The mother liquor contained threo- and erytho-*p*-nitro-phenylserine and only a trace amount of glycine. After two days' standing at room temperature, however, the mother liquor of the reaction mixture contained threo- and erythro-*p*-nitro-phenylserine, glycin and also a small amount of phenylserine, the last being a reaction product of benzaldehyde and glycine produced by the cleavage reaction. These results showed that the cleavage and resynthesis of phenylserine are not so important in the cases of short reaction time, although it may be important in the cases of prolonged reaction time. The fact that the phenylserine was not formed rapidly in the reaction of *p*-nitro-phenylserine and benzaldehyde, suggests that the mechanism shown in Figs. 1 and 3, which contains racemization of the $\alpha$- and $\beta$-carbon atoms and asymmetric transformation is a more reasonable pathway in the Erlenmeyer reaction.

The *N*-benzal residue in the reaction is important in the racemization and also in the formation and stabilization of many equilibrium systems. The $\beta$-carbon atom connected with the hydroxyl group is also interesting in regard to the formation of the conjugated double bond system from the $\beta$-phenyl residue to the *N*-benzal residue or to the carboxylate group. In the same reaction condition, L-tyrosine was not racemized at all with benzaldehyde and alkali.

The racemization mechanism of the Erlenmeyer reaction is complex. Two asymmetric carbons are racemized simultaneously. The observed data by rotatory power showed that the racemization proceeded as a pseudo 1st order reaction; the racemization constant, *K*, is 0.156 $min^{-1}$. The specific rotation of *N*-benzal D-erythro-phenylserine at zero time has a tremendously high value $[\alpha]_D^{27} = 13000°$ which is calculated from the racemization constant.

## Experimental

**Quantitative Analysis of the Amino Acid in the Erlenmeyer Reaction.**—A mixture of glycine (37.0 g.), water (400 ml.) and sodium hydroxide (70.0 g.) was shaken vigorously with a mixture of ethyl alcohol (100 ml.) and benzaldehyde (1.06 g.) under cooling. The mixture became clear and then a crystalline paste was formed gradually which solidified after several hours. About 0.5 g. of aliquot was taken from the reaction mixture after 15 min., 30 min., 1.5 hr., 4.5 hr., 24 hr. and 50 hr. These samples were acidified immediately with acetic acid, and a small amount of water was added. The resulting benzaldehyde was extracted with ether. The aqueous layer was adjusted to pH 10 with sodium carbonate solution, then extracted with ether to eliminate diphenylethanolamine. The aqueous solution was neutralized and evaporated in vacuo, and the residue was subjected to paper chromatography and also to dinitrophenylation of glycine and phenylserine. The ratio of glycine to phenylserine was determined by paper chromatography (solvent: *n*-BuOH : AcOH : $H_2O$/4 : 1 : 1). The corresponding spots were cut off and these were eluted with hot water. The ratio of glycine to phenylserine was determined colorimetrically, using the standard ninhydrin method[7]. The threo- and erythro-phenylserines were isolated by the Seki's method[8]. The DNP-amino acid mixture of each

5) I. Elphimoff-Felkin et al., *Compt. rend.*, **234**, 154, 1627 (1952).
6) G. Ehrhart, *Chem. Ber.*, **86**, 483 (1953).
7) S. Akabori and S. Mizushima, "Protein Chemistry (Tampakushitsu Kagaku)", Vol. 1, Kyoritsushuppan, (1954), p. 209.
8) T. Seki, *J. Biochem.* (*Tokyo*), **47**, 253 (1960).

sample was columnchromatographed, using Amberlite IR-112 resin ($Na^+$) and an elution solvent composed of pH 3.1 citric acid buffer (1/10 M) : ethyl methyl ketone : tetrahydrofurane/10 : 1 : 1.

Eluted solutions were collected with a fraction collector. The DNP-derivatives were separated into 3 fractions; the first band was composed of DNP-erythro-phenylserine and DNP-glycine, the second was dinitrophenol and the third was DNP-threo-phenylserine. The second band at 430 mμ disappeared on acidification to pH 1. The ratio of glycine and erythro-phenylserine to threo-phenylserine was determined colorimetrically at 430 mμ. The ratios of glycine, threo- and erythro-phenylserine were calculated from the data measured above. The results are shown in Table I.

**Reaction of Phenylserine with Benzaldehyde and Alkali.**—(A) *When a Small Proportion of Alkali was Used.*—In either case threo-phenylserine monohydrate (1.0 g.) or erythro-phenylserine (0.91 g.) was mixed with water (15 ml.), sodium hydroxide (0.2 g.), benzaldehyde (1.0 ml.) and ethanol (6 ml.). The mixture was shaken until it became clear and was allowed to stand overnight. The reaction mixture was diluted with hydrochloric acid; the resulting benzaldehyde was extracted with ether. The solution was neutralized and then examined by paper chromatography with the S-F solvent. Neither the threo nor the erythro isomer was converted.

(B) *When a Large Proportion of Alkali was Used.*—(1) Threo-phenylserine monohydrate (1.0 g.) was mixed with water (5 ml.), sodium hydroxide (0.6 g.), benzaldehyde (1 ml.) and ethanol (2 ml.). The clear solution began to deposit crystals after 1 hr. It was allowed to stand overnight at room temperature. After filtration and washing with ethanol, 1.30 g. of the crystalline *N*-benzal derivative IV was obtained. The IV was treated with 1 N hydrochloric acid and the resulting benzaldehyde was extracted with ether and the aqueous layer was evaporated to dryness. The phenylserine hydrochloride in the residue was extracted with absolute alcohol. After evaporation of the alcohol, the residual syrup was treated with silver carbonate and hydrogen sulfide to eliminate hydrochloric acid. The aqueous solution was evaporated. The resulting crude phenylserine was recrystallized from water, 0.75 g. of the threo-phenylserine monohydrate was obtained. The isolated phenylserine was shown to consist of pure threo isomer by paper chromatography with the S-F solvent (Found: N, 7.07%).

(2) A mixture of threo-phenylserine monohydrate (0.50 g.) and erythro-phenylserine (0.46 g.) was treated with sodium hydroxide (0.7 g.), water (5 ml.), benzaldehyde (1 ml.) and ethanol (2 ml.) as in the previous experiment. The clear solution began to deposit crystals after 2 hr. or earlier on seeding with IV. After standing overnight at room temperature, 0.95 g. of IV was isolated. The crystals were treated in the same way as above, 0.62 g. of pure threo-phenylserine monohydrate was isolated (Found: N, 7.18%).

(3) Erythro-phenylserine (0.91 g.) was treated with sodium hydroxide (1.0 g.), water (5 ml.), benzaldehyde (1 ml.) and ethanol (2 ml.). After 2 hr. crystallization began. The crystallization proceeded more rapidly after seeding of IV, 1.0 g. of crystals was isolated. It was treated as above, 0.65 g. of pure threo-phenylserine monohydrate was isolated. The threo isomer was converted into its copper complex.

Found: N, 6.48. Calcd. for $(C_9H_{10}O_3N)_2Cu$: N, 6.43%.

(4) D(−)-Erythro-phenylserine dioxane adduct (89.8 mg.) and benzaldehyde (80 mg.) were dissolved in 5 ml. of a mixture of water (10 ml.), ethanol (2 ml.) and sodium hydroxide (0.8 g.). The rotatory power of the solution was observed. In the first 30 min. of the reaction, the value of $[\alpha]_D$ was too great to observe. The mutarotation curve is shown in Fig 2. After 4.5 hr. the $[\alpha]_D$ reached almost zero and crystallization began in the solution. The crystals were filtered off. The analytical data of the crystals, paper chromatography and the rotatory power (in 2 N hydrochloric acid) of the isolated phenylserine showed that the crystal was the pure DL-threo-*N*-benzal-phenylserine sodium salt.

Found: N, 4.74. Calcd. for $C_{16}H_{14}O_3NNa$: N, 4.81%.

In the above reaction without benzaldehyde, D(−)-erythro-phenylserine maintained about 76% of its optical activity after 4.5 hr. of treatment.

**Reaction of Threo-*p*-nitro-phenylserine with Benzaldehyde and Alkali.** — The threo-*p*-nitro-phenylserine was prepared by the method of Ehrhart[6]. Threo-*p*-nitro-phenylserine (1.13 g.) was treated with sodium hydroxide (0.2 g.), water (15 ml.), benzaldehyde (1 ml.) and ethanol (4 ml.). The clear solution began to deposit crystals after 2 hr. The crystals were filtered off after 6 hr., and were converted into free *p*-nitro-phenylserine. The product was found to consist of the pure threo isomer by chromatography. The mother liquor of the reaction mixture contained both the threo- and the erythro-*p*-nitro-phenylserine and a trace amount of glycine. However, after 50 hr. of standing at room temperature, the mother liquor was found to contain phenylserine and an increased amount of glycine in addition to the threo- and erythro-*p*-nitro-phenylserine.

**Benzoyl Erythro- and Threo-phenylserine.**—Benzoyl-DL-erythro-phenylserine was prepared by the method of Shaw and Fox. Erythro-phenylserine was treated with benzoylchloride in the usual manner. M. p. 183~183.5°C (decomp.).

Found: C, 67.53; H, 5.48; N, 4.81%.

Benzoyl-DL-threo-phenylserine was prepared as above. M. p. 158°C (decomp.).

Found: C, 67.40; H, 5.43%.

**Resolution of Benzoyl-DL-erythro-phenylserine.**—*N*-Benzoyl-DL-erythro-phenylserine (28.5 g.) and quinine (27.2 g.) were dissolved in hot mixture of methanol (60 ml.) and acetone (40 ml.). When the solution had cooled down, crystallization of quinine salt began after seeding with an authentic specimen which was obtained during the crystallization experiment. After standing overnight in a refrigerator, the crystals were collected by filtration. The product after washing with cold acetone weighed 17.0 g. The quinine salt was recrystallized from 300 ml. of

99% ethanol, 14.0 g. of the quinine salt was obtained; m. p. 214~217°C (decomp.). The mother liquor from the recrystallization was combined with original mother liquor. From this, an additional 7.7 g. of quinine salt was isolated.

Found: C, 70.63; H, 6.31; N, 6.88. Calcd. for $C_{36}H_{39}O_6N_3$: C, 70.91; H, 6.45; N, 6.89%.

$[\alpha]_D^{22} = -105.0°$ (*c* 0.401, 99% ethanol).

Fifteen grams of the quinine salt was dissolved in ethanol, and to this solution, concentrated aqueous ammonia was added. The solution was then evaporated in vacuo to remove alcohol. The aqueous ammonia was added again and the evaporation was repeated until the ethanol was completely removed. The separated quinine base began to crystallize. The mixture was allowed to stand for a few hours for complete precipitation. The quinine was filtered off, then the filtrate was extracted three times with ether in order to remove residual quinine. The aqueous solution was concentrated in vacuo to 80 ml. and then acidified with 6 N hydrdrochloric acid to pH 2. The precipitated optically active benzoyl-erythro-phenylserine was filtered off. It was recrystallized from 35% ethanol, 5.7 g. of active benzoyl-erythro-phenylserine was obtained. M. p. 188~189°C (decomp.).

$[\alpha]_D^{23} = -29.3°$ (*c* 0.647, 99% ethanol).

Found: C, 67.27; H, 5.38; N, 4.90. Calcd. for $C_{16}H_{15}O_4N$: C, 67.36; H, 5.30; N, 4.91%.

**D-Erythro-phenylserine.**—(−)-*N*-Benzoyl-erythro-phenylserine (8.0 g.) was heated under reflux with 90 ml. of 15% hydrobromic acid for 3 hr. After hydrolysis, the solution was extracted three times with ether. After evaporation of the aqueous fraction under reduced pressure, water was added and the process repeated to remove the excess of hydrobromic acid. The residue was treated with silver carbonate and hydrogen sulfide. The dehydrobrominated solution was evaporated in vacuo, and the residue was dissolved in 15 ml. of hot water, then 15 ml. of dioxane was added to the solution. Two and a half grams of (−)-erythro-phenylserine dioxane adduct was crystallized out.

$[\alpha]_D^{26} = -53.7°$ (*c* 1.091, 2 dm, 2 N hydrochloric acid).

Found: C, 58.65; H, 6.70; N, 6.19. Calcd. for $(C_9H_{11}O_3N)_2C_4H_8O_2$: C, 58.65; H, 6.71; N, 6.22%.

Free (−)-erythro-phenylserine was prepared from the aqueous solution of the free amino acid by addition of much ethanol. The (−)-erythro-phenylserine has a sweet taste.

M. p. 193°C (decomp.). $[\alpha]_D^{25} = -68.0°$ (*c* 0.426, 2 N hydrochloric acid).

Found: C, 59.61; H, 6.12; N, 7.74. Calcd. for $C_9H_{11}O_3N$: C, 59.66; H, 6.12; N, 7.73%.

**Reduction of (−)-Erythro-phenylserine.**—A half gram of (−)-erythro-phenylserine dioxane adduct was heated at 150~160°C for 2 hr. with 15 ml. of hydrogen iodide and 0.6 g. of red phosphorus. The reaction mixture was filtered. It was then evaporated under reduced pressure, water was added and the process was repeated to remove the excess of hydrogen iodide. The residue was treated with silver carbonate and hydrogen sulfide, 160 mg. of D-phenylalanine was obtained.

$[\alpha]_D^{25} = +31.4°$ (*c* 0.780, 2 dm., water)

Found: C, 65.53; H, 6.65; N, 8.46. Calcd. for $C_9H_{11}O_2N$: C, 65.44; H, 6.71; N, 8.48%.

**L-Erythro-phenylserine.** — *N*-Benzoyl-L-erythro-phenylserine was isolated from the mother liquor of the quinine salt as shown above for the separation of D-erythro isomer, (+)-*N*-benzoyl-erythro-phenylserine, m. p. 182~183°C (decomp.).

$[\alpha]_D^{25} = +22.6°$ (*c* 0.973, 99% ethanol).

Found: C, 67.52; H, 5.44; N, 4.97. Calcd. for $C_{16}H_{15}O_4N$: C, 67.36; H, 5.30; N, 4.91%.

L-Erythro-phenylserine, m.p. 179~183°C (decomp.).

The L-erythro isomer has a bitter taste.

$[\alpha]_D^{25} = +51.2°$ (*c* 0.757, 2 N hydrochloric acid).

Found: N, 7.59. Calcd. for $C_9H_{11}O_3N$: N, 7.73%.

The authors wish to express their thanks to Professor Y. Yukawa of the Institute of Scientific and Industrial Research of this University for his helpful suggestions.

*Department of Chemistry*
*Faculty of Science*
*Osaka University*
*Nakanoshima, Osaka*

# *Forschung über den katalytischen Abbau des Kolophoniums*

Von Akira MITSUTOMI

(Eingegangen am 26. September, 1960)

Seit Berichterstattung durch Schulze[1] in 1877 über den thermischen Abbau des Kolophoniums sind mehr als 90 Jahre verflossen, aber wir haben vor uns nur ungefähr 10 Mitteilungen über das betreffende Thema. Vezes Dupont[2], Chevalier und andere[3] haben entweder durch direkte Kolophonium-Destillation oder seine Destillation mit organischen Säuren das Leichtöl für Brennstoff gewonnen. Es ist ruhig anzunehmen, dass es sich bei der Operation um einen thermischen Abbau des Kolophoniums bei 350～360°C handelt. Es ist beachtenswert, dass das brennstoffliche Leichtöl aus Kolophonium durch diese Forschung gewinnbar geworden ist. Tsukamoto[4] stellt auch bei Trockendestillation des Kolophoniums im gemeinsamen Einsatz von Aktivkohle und der japanischen Säureerde gasförmige und flüssige Produkte dar und ermittelt bei dem Letzteren Anthracen, Phenanthren, Reten u. s. w. Als Erster hat Newbery[5] den Abbau nach dem Gasphase-Verfahren vorgenommen. Als Katalysator wurde Aluminiumoxyd eingesetzt, wobei zweierlei flüssige Produkte, Sdp. 27～170°C oder 50～250°C, gewonnen wurden. Fast zu der gleichen Zeit hat Hoge[6] unterm Einsatz des Aluminiums als Katalysators bei 370～590°C den Abbau vorgenommen. Später in 1936 hat Lee[7] unterm Einsatz von Calciumoxyd, Ätzkali, der japanische Säurerde mit Calciumoxyd das Kolophonium abgebaut und Benzin, Kelosin u.s.w. dargestellt.

Es wurde durch solche Forschungsergebnisse klargemacht, dass durch Abbau des Kolophoniums Benzin-analoges Leichtöl zu gewinnen ist und die weitere Forschung hat ergeben, dass das Gasphase-Verfahren dabei das erfolgreichste Verfahren ist. Desalbres[8] berichtet, dass man unterm Einsatz der Fullererde den gesättigten Kohlenwasserstoff von Sdp. 60～130°C und flüssige Produkte von Sdp. 130～200°C gewinnen und diese Letzteren zum trocknenden Öl verwenden kann. Es ist aber Brodshi[9], der als Erster von den bisherigen Forschern den Reaktionszustand beim nach dem Gasphase-Verfahren erfolgenden Kolophonium-Abbau genau verfolgt hat. Er hat unterm Einsatz des Kupfers bei 500～700°C Kolophonium abgebaut und die Alkohole von Sdp. 30～200°C und flüssige Produkte von Sdp. 200°C und darüber erfasst. Er hat ferner jene Alkoholen auf analoge Weise abgebaut und ein Gemisch aus den aromatischen und ungesättigten Kohlenwasserstoffe von Sdp. 30～200°C dargestellt. Er hat bei den flüssigen hochsiedenden Produkten Naphthalin, Anthracen, Phenanthren, Reten nachgewiesen.

Wie oben beschrieben, sind durch Abbau des Kolophoniums die aus aromatischem Kohlenwasserstoff bestehenden flüssigen Produkte erhältlich. Annehmbar ist, dass diese für Brennstoff, Lösungsmittel, Schmierstoff, Emulgiermittel und andere Gebiete auch nützlich zu verwenden sind. Aber für einen kontinuierlich nach dem Gasphase-Verfahren erfolgenden Abbau des Kolophoniums vermisst man diesbezügliche Forschungsarbeiten. Fundamentale genaue Untersuchung ist erforderlich.

Es sollen nämlich in verschiedenen Punkten noch ergründet werden: Die Auswahl der haltbarsten Katalysatoren, die Festlegung der optimalen Temperatur, die nur den Abbau des Kolophoniums selbst einleitet, ohne aber dabei die Katalysatoren abbauen zu lassen, und die Ermittelung der ausbeutemässigen Veränderlichkeit der flüssigen Produkte bei kontinuierlichem Einsatz der Katalysatoren, sowie die Ermittelung der Zusammenhänge der katalysatorischen Einsatzmale mit der Anlagerungsmenge freien Kohlenstoffs an den Katalysatoren. Zur Gewinnung nützlicher flüssiger Produkte hat der Verfasser über den kontinuierlichen Abbau des Kolophoniums und des rohen Kieferharzes nach dem Gasphase-Verfahren Untersuchung gestellt.

## Experimentelle Vorrichtung und Operation

Die zu dieser Forschung herangezogene Vorrichtung wird in Abb. 1 gegeben. D stellt das verzinkte Eisenrohr von 90 ccm Länge und 2.8 ccm

1) G. Schulze, *Ber.*, **10**, 114 (1877).
2) Vezes Dupont, „Resines et Jerebenthine" (1924) S. 461.
3) J. M. A. Chevalier, P. Bourcet und H. Regnault, Franz. Pat. 552038 (1923).
4) T. Tsukamoto, *Pharm. Bull. (Japan)*, 170 (1928).
5) C. W. Newbery, *Amer.* P. 1902073 (1933).
6) D. W. Hoge, *Chem. Abstr.*, **27**, 3350 (1933).
7) M. Lee, *Ind. Research (China)*, **5**, 417 (1936), *Chem. Abstr.*, **31**, 842 (1937).
8) L. Desalbres, Franz. Pat. 871333, *Chem. Abstr.*, **43**, 4873 (1949).
9) J. Brodshin, *Bull. Inst. Pin.*, **1938**, 89, 118, 159, 203; *Chem. Abstr.*, 33, 4803 (1939).

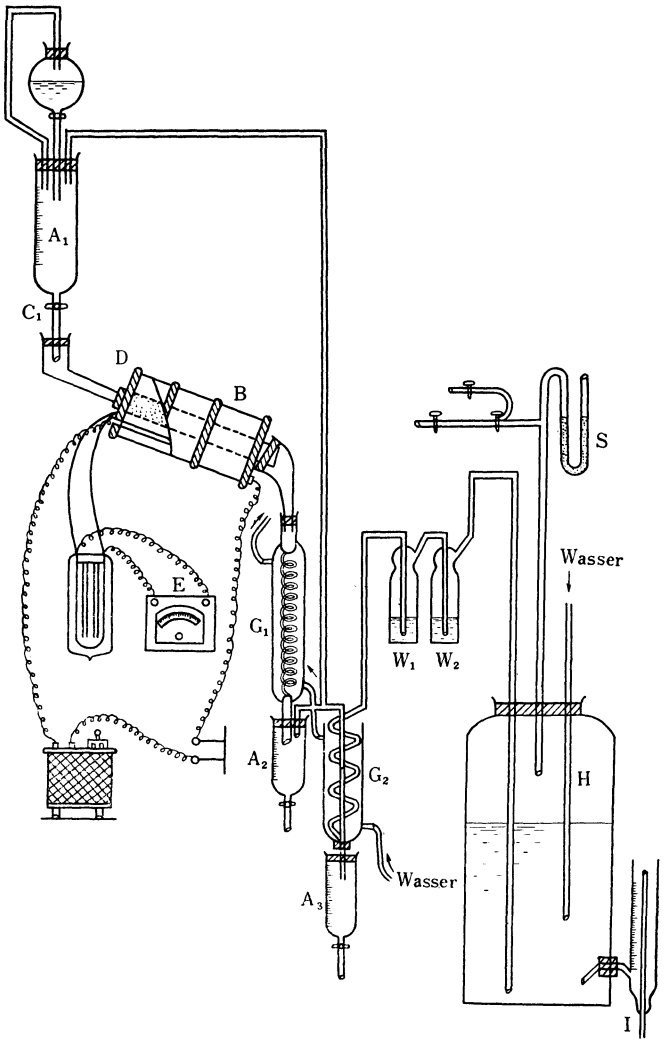



Abb. 1. Experimentelle Vorrichtung.

| | | | | | |
|---|---|---|---|---|---|
| $A_1, A_2, A_3$ : | Scheidetrichter mit Skalen | D : | Reaktionsrohr | I : | Vorlage |
| | | E : | Thermometer | S : | V-Rohr |
| B : | Elektroofen | $G_1, G_2$ : | Rückflusskühler | $W_1, W_2$ : | Waschflasche |
| $C_1$ : | Hahn | H : | Gassammler | | |

Durchmesser dar. Das mit gewisser Menge Katalysatoren eingefüllte Reaktionsrohr wird in den Elektroofen eingebracht und 3~5 Std erhitzt, damit die Katalysatoren aktiviert werden. Dann wird gewisse Menge wasserfreies Benzol (100 oder 200 ccm) in $A_1$ in 1 eingegossen und unter Regelung des Hahns $C_1$ und mit vorgeschriebener Raumgeschwindigkeit ununterbrochen abtröpfeln gelassen. Die flüssigen Reaktionsprodukte werden in $A_2$ und $A_3$ gesammelt, während die gasförmigen Produkte in den Gassammler H zugeführt werden. Währenddessen sollen die Oberflächen der Flüssigkeiten inner- und ausserhalb des U-Rohrs S stets unter einem vermindertem Druck gehalten bleiben. Unter dieser Regelung wird der ganze Versuch durchgeführt.

Nach dem fertigen Abtröpfeln der ganzen Probenmenge in das Reaktionsrohr wird die Erhitzung eine weitere Stunde fortgesetzt. Die flüssigen Produkte werden dann destilliert, nach verschiedenen Siedepunkten eingeteilt und analysiert.

**Zubereitung der Proben.**—Da das in der Wärme verflüssigte Kolophonium auch bei über 150°C behaltener Temperatur zufolge eventuell eintretenden Temperaturabsinken weitgehende Viskositätsveränderung erfährt, ist es äusserst schwierig, das Kolophonium mit einer konstanter Raumgeschwindigkeit in das Reaktionsrohr zu bringen.

Rohes Kieferharz ist auch mit der ähnlichen schwierigkeit verbunden. Diese Schwierigkeiten wurden von uns dadurch behoben, dass das Kolophonium und das rohe Kieferharz jeweils in gewisser Menge Benzol zuerst gelöst und als solche Lösungen in das Reaktionsrohr eingebracht werden.

Es wurde 500 g davon in absolutem Benzol gelöst und 1 Liter Lösung wurde erhalten. Eine Entnahme dieser Lösung wurde auf dem Wasserbad bei der möglichst niedrigen Temperatur abgedämpft und das gemessene Gewicht des Rückstandes wurde zum Gewicht des Kolophoniums gemacht.

**Zubereitung des Katalysators.**—Es wurden beim Versuche 12 Sorten Katalysatoren eingesetzt. Einzelkatalysatoren: Japanische Säureerde, Kieselgur, Bimsstein, Kaolin und Bentonit.

Mischkatalysatoren: Japanische Säureerde—Aluminiumoxyd (70 : 30), —Aktivkohle (50 : 50), —Zinkoxyd (70 : 30), —Titanoxyd (70 : 30), Eisenoxyd (70 : 30), —Kieselsäureanhydrid (70 : 30), Zinksulfat (70 : 30).

Die Mischkatalysatoren wurden folgenderweise zubereitet. Zinkoxydpulver wurde, z. B., mit Wasser von ca. 50°C gut gerührt und im Mörser unter Zusetzung mit der japanischen Säureerde möglichst homogen vermischt. Anschliessend werden davon Kugeln von 5~8 mm Durchmesser hergestellt, bei 60°C 2 Std angetrocknet, weiter bei 110~120°C 1 Std vollständig abgetrocknet. Dann werden sie nach Packung im Reaktionsrohr bei 500°C ca. 3 Std zur Aktivierung erhitzt.

**Berechung der Ausbeute.** — Das Kolophonium besteht hauptsächlich aus Harzsäure, Abietinsäure und Dextropimarsäure, während das rohe Kieferharz daneben noch Terpene gemischt enthält. Daher ist mit Recht zu erwarten, dass als seine Abbauprodukte gesättigte und ungesättigte aliphatische Säuren und aromatische Kohlenwasserstoffe u. s. w. gegeben sind. In folgerichtiger Überlegung, dass diese Substanzen nach weiterem Abbauen auch Benzole bilden würden, wurde noch vor Einschickung der Proben-Benzollösung in dem Reaktionsrohr eine gewisse Menge absolutes Benzol ins Rohr eingeschickt und unter gleichen Bedingungen wie bei der Probelösung erhitzt. Die als Destillate auslaufenden Benzolmengen wurden bestimmt und das an Katalysatoren absorbierten Benzol gemessen, um die Resultate dem Berechnen in dem richtigen Versuche zugrunde zu legen.

Es wird z. B. angenommen, dass als Katalysator japanische Säureerde benutzt und bei 450°C reagieren gelassen wird. Zuerst werden $A$ ccm absolute Benzol zugegeben und erhitzt, wobei $b$ ccm Produkte als Destillate erhalten werden. Und $d$ ccm Benzol werden davon festgestellt.

Andererseits werden $M$ ccm Kolophonium-Benzollösung gleicherweise reagieren gelassen, wobei $E$ ccm als Destillate von dem Vorlauf bis 85°C aufgefangen werden. Dann ist die Menge der flüssigen Reaktionsprodukte, die bis zur Temperatur von 85°C tatsächlich zu erhalten sind, mit folgender Gleichung auszudrücken:

$$E-M\times\frac{107}{200}\times\frac{d}{A}\text{ ccm}$$

Werden die Destillate von 85 bis 200°C zu $F$ ccm und solche über 200°C zu $G$ ccm gesetzt, so ist die Gesamtmenge der Destillate, $N$ ccm, folgenderweise ausdrückbar:

$$N=\left(E-M\times\frac{107}{200}\times\frac{d}{A}\right)+F+G$$

Für das rohe Kieferharz wurde es auch anhand obiger Methode berechnet. Es ist bekannt, dass Benzol bei ihrer Druckströmung durch erhitztes Eisenrohr zufolge der dann eintretenden Polymerisation Diphenyl und Triphenyl erzeugen. Da aber diese Bildung nur insgesamt weniger als 1% bezogen auf die eingesetzten Benzole geschieht war in dieser Versuchsreihe solcher Fehler unberücksichtigt.

Falls Zinkoxyd—japanische Säureerde und Zinkchlorid—japanische Säureerde als Katalysatoren benutzt wurden, wurden Abbauprodukte zweifelsohne festgestellt, die niedriger sieden als Benzol. Diese Tatsache wurde natürlich bei Durchführung der Versuche berücksichtigt.

TABELLE I. ERGEBNISSE DER KONTINUIERLICHEN VERSUCHE*

| Sorten der Katalysatoren | Kieselgur | | | Japanische Säureerde | | | Japanische Säureerde und Aluminiumoxyd (70 : 30) | | |
|---|---|---|---|---|---|---|---|---|---|
| Male der Kontinuierlichen Anwendung | 1 | 2 | 3 | 1 | 2 | 3 | 1 | 2 | 3 |
| Diverse Gase, l | 4.8 | 4.8 | 4.8 | 17.5 | 15.6 | 14.2 | 6.7 | 4.4 | 10.2 |
| Flüssige Produkte von niedrigen Siedepunkt, g | 34.8 | 23.5 | 28.7 | 28.4 | 32.2 | 26.1 | 33.9 | 33.0 | 24.4 |
| von hohen Siedepunkt, g | 18.9 | 43.9 | 47.7 | 40.2 | 37.8 | 42.2 | 20.9 | 23.8 | 39.7 |

* Abbaureaktion von je 100 g Kolophonium mit 94 g Katalysatoren bei 450°C.

TABELLE II. VERÄNDERUNGEN DES PROZENTUALEN AUSBEUTEVERHÄLTNISSES DER FLÜSSIGEN PRODUKTE IM ZUSAMMENHANG MIT DEN VERMEHRTEN WIEDERHOLUNGEN DER KONTINUIERLICHEN ANWENDUNGEN*

| Male der kontinuierlichen Anwendung | 1 | 2 | 3 | 4 | 5 | 6 | 7 | 8 |
|---|---|---|---|---|---|---|---|---|
| Flüssige Abbauprodukte von niedrigen Siedepunkt, % | 9.6 | 20.0 | 26.2 | 21.3 | 20.0 | 15.5 | 14.2 | 14.0 |

* Abbaureaktion von je 100 g Kolophonium mit 97 g Kieselgur bei 450°C.

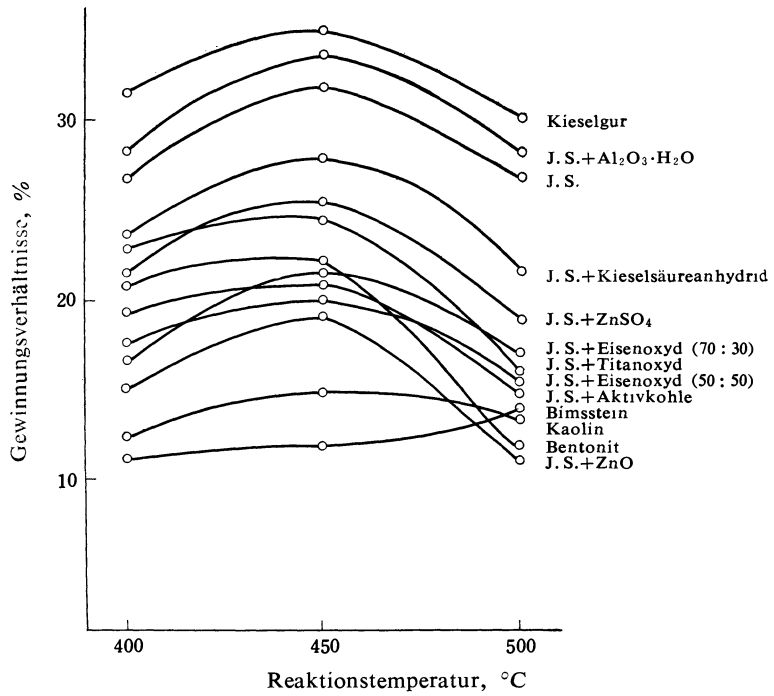



Abb. 2. Zusammenhang zwischen der Reaktionstemperatur und Gewinnungsverhältnisse der flüssigen Produkte von niedrigem Siedepunkte.

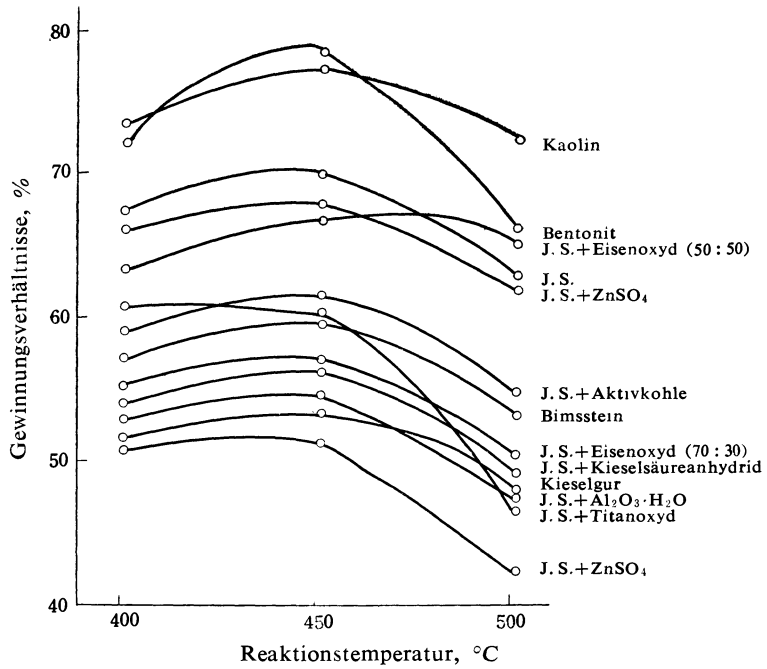



Abb. 3. Zusammenhang zwischen der Reaktionstemperatur und Gewinnungsverhältnisse der flüssigen Produkte.

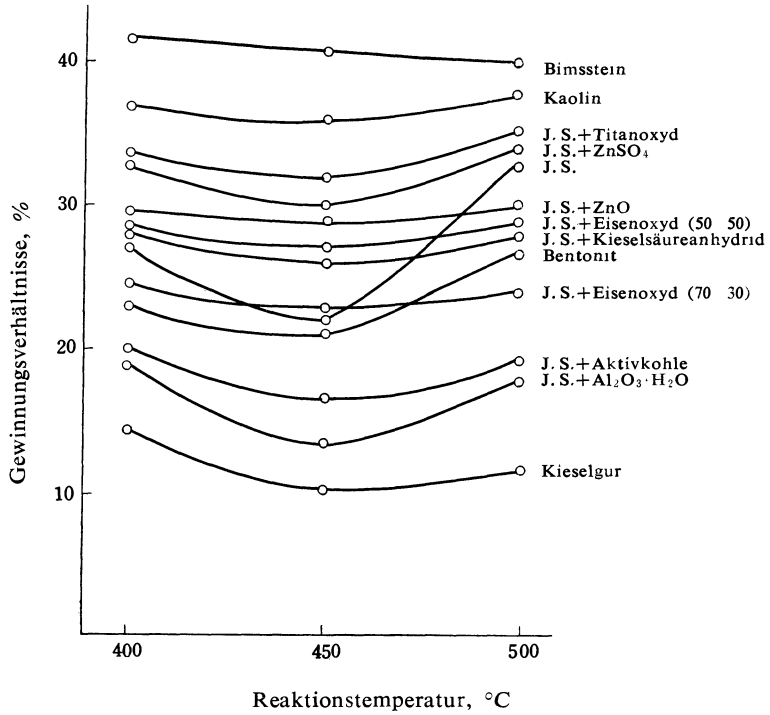



Abb. 4. Zusammenhang zwischen der Reaktionstemperatur und Gasentwicklungsmenge.

Flüssige Produkte in Abb. 1 — $A_2$ werden nach mehrmaligem Wäschen der Feindestillation unterzogen, und zwar dreiteilig abdestilliert, nämlich von dem Vorlauf bis zu 85°C, von 85 bis zu 200°C und von 200°C bis zu Trockenpunkt.

Der Destillationsverlust wurde nämlich nur bei dem niedersiedenden Fraktionen berücksichtigt. Der Verlust während des Wäschens und Abtrockenens ist aber über dis ganzen Fraktionen gleichmässig, so dass er zu $W$ ccm und der Destillationsverlust zu $L$ ccm gesetzt wird. Nach folgender Gleichung wird die Ausbeute berechnet:

Fraktion bis zu 200°C.....

$$\left(E-M\times\frac{107}{200}\times\frac{d}{A}\right)+F+L+W\times\frac{E+F}{E+F+G}$$

Fraktion über 200°C hinaus.....

$$G+W\times\frac{G}{E+F+G}$$

Gasförmige Produkte werden aus der Flasche H genommen, nach dem Hempel'schen Verfahren Kohlendioxyd etc. mengenmässig geprüft, dann mit 64% Schwefelsäure auf Isobutylen, mit 87% Schwefelsäure auf Butylen und Propylen, ferner mit 100% Schwefelsäure auf Äthylen analysiert.

## Versuchsergebnisse

Kolophonium besteht hauptsächlich aus Harzsäure, ferner Abietinsäure und Dextropimarsäure. Bei katalytischem Abbau trennt sich die Carboxyl-Gruppe los, um sich in Kohlendioxyd, Wasserstoff und Kohlenmonoxyd oder Wasser umzuwandeln. In Tabelle I sind mit der Beziehung als „diverse Gase" ihr Produktionsverhältnis angegeben. Bei diesen Gasen handelt es sich meistens um Kohlenmonoxyd und Wasserstoff mit geringem Anteil an Paraffin von niedriger Klasse. Bekanntlich ist aus Dextropimarsäure die Äthylen-Gruppe und aus Abietinsäure die Isopropyl-Gruppe leicht abspaltbar. Bei der katalytischen Abbau wie in vorliegendem Versuch müssen aber äusserst komplizierte Änderungen wie Polymerisation oder Verschiebung der Doppelbindung geschehen. Somit wird es nicht angebracht sein, direkt aus dem Bildungsverhältnis von Olefin auf des Abbauvermögen der Katalysatoren zu schliessen.

Kurz gefasst, ist es aus dem Versuchsergebnissen klar geworden, dass es zwischen der Ausbeute der flüssigen niedersiedenden Produkte und der Entwicklungsmenge der diversen Gase einen untrennbaren Zusammenhang besteht. Es wird demnach zu folgern, dass die geeignetesten Bedingungen für die Abbaureaktion mit vorzüglichen Katalysatoren eine erhöhte Bildung der niedersiedenden Fraktion und eine verminderte Gasentwicklung logischerweise ergeben.

Um zu finden, wie sich die Ausbeute an niedrigsiedenden flüssigen Produkten in Anhängigkeit von Reaktionstemperaturen verändert, wurden verschiedene Katalysatoren zum Abbau des Kolophoniums eingesetzt. Die Ergebnisse dieser Versuche wurden in Abb. 2

und 3 abgebildet, während die Gasentwicklungsmengen in Abb. 4 miteinander vergleichend gezeigt sind.

Die Ergebnisse der 8-malig kontinuierten Reaktion sind in Tabelle II aufgestellt. Es sei noch bemerkt, dass sich die an den Katalysatoren sich anlagernde freie Kohlenstoffmenge bei 3-maliger und 8-maliger kontinuierlicher Anwendung jeweils als 11 und 45 aufwies.

Die Ergebnisse bezüglich der Haltbarkeit, des Vermögens und der Regenerierbarkeit der Katalysatoren zeigen, dass als Katalysator für Abbau des Kolophoniums die Kieselgur der Beste ist. Dabei wird nämlich die höchste Produktionsmenge von flüssigen Fraktionen von niedrigem Siedepunkt schon bei verhältnismässig niedriger Temperatur erzielt. Andererseits liefern japanische Säureerde und das Gemisch derselben mit Aluminiumoxyd (70 : 30) gleiche gute Ergebnisse wie Kieselgur, sie besitzen aber den Nachteil einer kürzeren Haltbarkeit.

Von den Mischkatalysatoren zeigen das Gemisch der japanischen Säureerde mit Kieselsäureanhydrid (70 : 30) und dasselbe mit Zinksulfat (70 : 30) sowie dasselbe mit Titanoxyd (70 : 30) verhältnismässig gute Ergebnisse, sie liegen aber hinter der obengenannten Kieselgur zurück.

### Kohlenstoffanlagerung

Die Bestimmung der Anlagerung freien Kohlenstoffs an 100 g Katalysator bei Abbau von 100 g Kolophonium ergab die Ergebnisse in Tabelle III. In der Annahme, dass nach dem bei gleicher Temperatur erfolgten Abbau die Katalysatoren an ihrem eignen Gewicht keine Veränderung erfahren, wurde die Gewichtszunahme der Katalysatoren mit der angelagerten Kohlenstoffmenge gleichgestellt. Mit dieser Methode ist allerdings die aktuelle Anlagerungsmenge des Kohlenstoffs nicht zu ermitteln, aber sie ist insofern anwendar, als das „anscheinende Gewicht" nur zum Vergleich der Katalysatoren untereinander in Frage kommt. Diese zeigen, dass die Kieselgur oder das Gemisch von japanischer Säureerde mit Aktivkohle als Katalysator die geringste Anlagerung und Kaolin die nächst-geringste ergibt.

TABELLE III. ZUSAMMENHANG ZWISCHEN DEN KATALYSATORENSORTEN UND KOHLENSTOFF ANLAGERUNGSMENGE BEI DER ABBAUREAKTION VON KOLOPHONIUM

| Katalysatoren, 100 g | | A | B °C | C g |
|---|---|---|---|---|
| Japanische Säureerde | | — | 450 | 6.4 |
| 〃 | | — | 500 | 4.4 |
| Kieselgur | | — | 450 | 1.8 |
| Bentonit | | — | 450 | 4.2 |
| Kaolin | | — | 450 | 2.6 |
| Bimsstein | | — | 450 | 8.0 |
| Japanische Säureerde | Aluminiumoxyd | 70 : 30 | 450 | 6.3 |
| 〃 | Zinkoxyd | 70 : 30 | 500 | 9.2 |
| 〃 | Titaniumoxyd | 70 : 30 | 500 | 8.5 |
| 〃 | 〃 | 70 : 30 | 450 | 7.7 |
| 〃 | Eisenoxyd | 70 : 30 | 450 | 5.0 |
| 〃 | Kieselsäureanhydrid | 70 : 30 | 500 | 5.7 |
| 〃 | Aktivkohle | 50 : 50 | 450 | 1.7 |

A: Mischverhältnis
B: Reaktionstemperatur
C: Kohlenstoffanlagerung bezogen auf 100 g Einsatz des Ausgangsmaterials

### Haltbarkeit der katalysatorisch eingesetzten Kieselgur

Um die Kieselgur auf ihre katalysatorische Haltbarkeit zu prüfen, ein Zapfen für Umschaltung angebracht wurde, um bei fertigem Tröpfeln einer gewissen Menge des Kolophoniums jedesmals die flüssigen Produkte und Gas aufzufangen. Die flüssigen Produkte wurden destilliert und in 2 Fraktionen bis 200°C und über 200°C eingeteilt. Von den Gasen wurden die Anteile an Kohlendioxyd, Wasserstoff, Olefinen, Parafinen und so weiter prozentual analytisch bestimmt.

Als Katalysator wurden 108 g Kieselgur, eingesetzt und 100 g Kolophonium mit einer Raumgeschwindigkeit von 18 ccm/Std ins Reaktionsrohr bei 450°C geschickt.

Die an dem Katalysator angelagerte Menge freien Kohlenstoffs betrug nur 64 g erst nach dem beendeten Abbau von 1700 g Kolophonium. Daher ist anzunehmen, dass die Haltbarkeit dieses Katalysators verhältnismässig lang ist.

### Bestandteilmässige Untersuchung der flüssigen Produkte

Es wurden die flüssigen Produkten zuerst in die zwei Fraktionengruppen, nämlich in die bis zu 200°C und die däruber, eingeteilt. Die Erste wurde weiterer Feindestillation unterworfen. Hiervon wurden die Fraktion von Sdp. 85～90°C in Eisessig gelöst, brominiert, destilliert, um Brombenzol ergeben zu lassen, damit Benzol ermittelt wurde.

Auch zur Ermittelung des Toluols wurden die Fraktion von Sdp. 108～115°C weiterer Feindestillation unterzogen und in 2,4-Dinitrotoluol überführt. Dann wurde die Fraktion von Sdp. 128～145°C weiterer Feindestillation unterzogen, oxydiert, wonach Terephthalsäure zur Ermittelung des *p*-Xylol erfasst wurde. Von der Fraktion von Sdp. 149～159°C

wurde Cumol, von derselben von Sdp. 159～171°C Pseudocumol, und von derselben *p*-Cumol als sulfonsaures Barium gesondert und ermittelt. Trennung weiterer Bestandteile war äusserst erschwert, so dass eine Reindarstellung unmöglich war.

Als Bestandteile der flüssigen Produkte von höherem Siedepunkt als 200°C wurden Naphthalin, Anthracen, Phenanthren, Reten ermittelt. Naphthalin war von den Kondensaten bei Sdp. 215～235°C leicht als Pikrat ermittelt.

Die aus dem Kondensat von Sdp. 320～360°C ausgeschiednen Kristalle konnten nach Umkristallisierung aus Alkohol mit anschliessender Oxydation zu Anthrachinon als Anthrachinon nachgewiesen wurde. Ferner wurde Phenanthren nachgewiesen, indem die aus der Mutterlauge der Anthracen-Umkristallisierung erhaltenen Kristalle mit Chromsäureanhydrid zu Phenanthrachinon oxydiert wurden.

Die Trennung des Retens war äusserst schwierig. Die Kondensate über Sdp. 360°C wurden nämlich stark abgekühlt. Die dabei ausgeschiedenen Kristalle wurden getrennt. Durch ihre Umkristallisation wurde das dabei zuerst zur Abscheidung kommende Anthracen getrennt. Die Mutterlauge wurde mit Pikrinsäure-Benzollösung zugesetzt, wodurch Retenpikrat zur Ausfällung kam. Dies wurde durch Mischprobe nachgewiesen.

**Zusammenfassung**

Es wurden gefunden, dass als Katalysator zur Herstellung nützliche Kohlenwasserstoffe beim katalytischen Abbau des Kolophoniums nach dem Gasphaseverfahren bei gewöhnlichem Druck die Kieselgur auch für kontinuierliche Arbeit der Hervorragendste ist.

Die Reaktionstemperaturen um 450°C sind die Optimalen, wobei der prozentuale Gewinnungssatz für die flüssigen Produkte 53.7% beträgt. Diese flüssige Produkte werden in die Fraktion bis zu 200°C und dieselbe darüber eingeteilt. Aus der Vorderen wurden Benzol, Toluol, Xylol, Cymol, Pseudocymol, *p*-Cymol nachgewiesen, während aus der Letzteren Naphthalin, Anthracen, Phenanthren, Reten ermittelt wurden.

Bei den gasförmigen Produkten betrug der prozentuale Gewinnungssatz 8.6%. Sie bestanden hauptsächlich aus Kohlendioxyd, Olefine, Kohlenmonoxyd, Wasserstoff und Paraffinen.

Zum Schluss sei es noch bemerkt, dass die vorliegende Arbeit unter der Leitung von Herrn Professor Dr. Eiichi Funakubo an der Technischen Fakultät der Universität zu Osaka durchgeführt wurde.

*Chemisches Institut der*
*Technischen Fakultät der*
*Universität zu Osaka*
*Miyakojima-ku, Osaka*

# *Forschung über den katalytischen Abbau des rohen Kieferharzes*

Von Akira MITSUTOMI

(Eingegangen am 26. September, 1960)

Da das rohe Kieferharz als Gemisch aus Kolophonium und Terpenen gehalten werden kann, hat der Verfasser zum Versuch genau dieselbe Vorrichtung wie beim Kolophonium eingesetzt und fast gleicher Weise der katalytische Abbau des rohen Kieferharzes durchgeführt. Dabei wurde natürlich genau geprüft, ob die Kieselgur auch als Katalysator für kontinuierliche Abbau nach dem Gasphaseverfahren angepasst ist, wie es bei dem Kolophonium der Fall ist, und welche andere Katalysatoren dann die besten Ergebnissen darbringen.

### Zubereitung der Katalysatoren

Es wurden für vorliegende Versuchsreihe 17 folgende Katalysatoren eingesetzt.

Japanische Säureerde Nr. 1: Mit Wasser zugesetzt, verformt und aufgetrocknet.

Japanische Säureerde Nr. 2: In 10% Salzsäure eingetränkt, ca. 5 Std lang erhitzt, durch Dekantierung von Salzsäure getrennt mit Wasser gewaschen, bis das Spülabwasser neutral wird, und dann aufgetrocknet.

Japanische Säureerde Nr. 3: Mit 38% Salzsäure, wie oben beschrieben, behandelt.

Kupferoxyd: Marktbefindliches Kupferoxyd in Wasser aufgelöst, mit Ätznatronlauge behandelt: Nach Abspülen des gebildeten Hydroxyds erhitzt.

Zinkoxyd: Marktbefindliches Zinkoxyd behandelt, wie oben beschrieben.

Mischkatalysatoren:

Japanische Säureerde-Aluminiumoxyd (80 : 20), (70 : 30), (50 : 50), (30 : 70).

Japanische Säureerde-Zinkoxyd (90 : 10), (70 : 30).

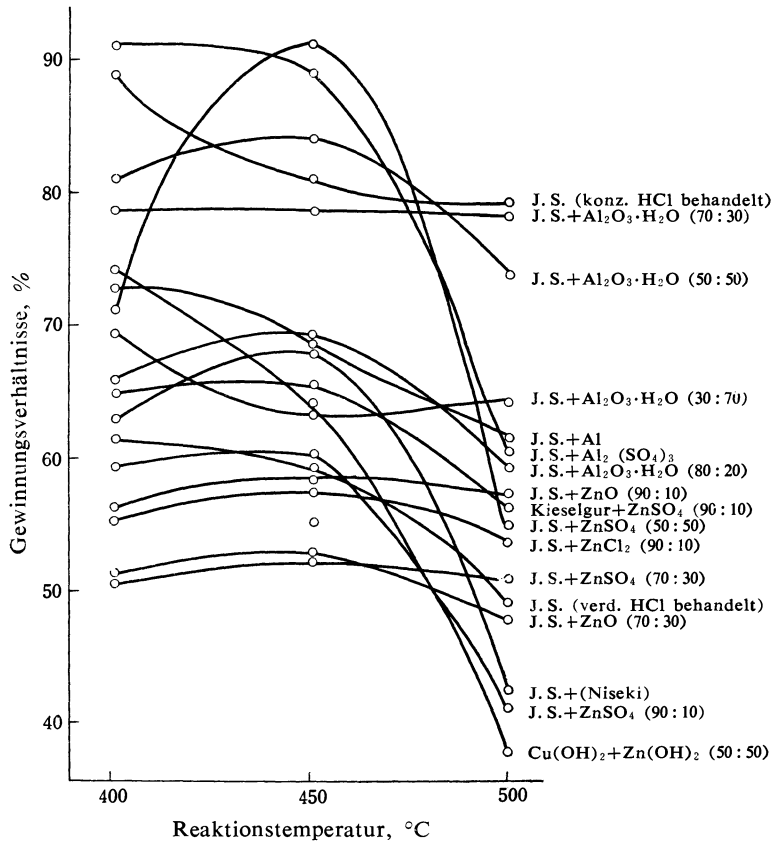



Abb. 1. Zusammenhang zwischen der Reaktionstemperatur und dem Gewinnungsverhältnisse der flüssigen Produkte.

J. S. : Japanische Säureerde

Japanische Säureerde-Zinkchlorid (90 : 10).
Japanische Säureeerde-Zinksulfat (90 : 10), (70 : 30), (50 : 50).
Japanische Säureerde-Aluminiumsulfat (70 : 30).
Japanische Säureerde-Magnesiumoxyd (70 : 30).
Kieselgur-Zinksulfat (90 : 10).
Kupferoxyd-Zinkoxyd (50 : 50).

Die oben genannten Katalysatoren wurden zu Kugeln mit gleich grossem Durchmesser vorformt wie es beim Abbau von Kolophonium der Fall war, und in gleichförmige Reaktionsanlage eingefüllt, vorgehitzt und aktiviert.

### Versuchsergebnisse und Beitrag darüber

Unter Verwendung gleichartiger Reaktionsvorrichtung wie bei vorher beschriebenem Kolophonium, wurde das rohe Kieferharz bei 400, 450 und 500°C Erhitzung gespaltet. Gleichzeitig mit Bestimmung des Gesamtvolumens der dabei produzierten Gase, des prozentualen Gehaltes an Kohlendioxyd, Olefinen, Wasserstoff, Paraffinen u. s. w. wurden flüssige Produkte auf ihr Bildungsverhältnis geprüft, indem sie in zwei Franktionen von denselben von 85 bis 200°C und über 200°C eingeteilt wurden.

Aus diesen Werten wurde das Abbauverhältnis von rohem Kieferharz errechnet. Daraufhin wurde das Abbauvermögen der Katalysatoren miteinander verglichen. Die Ergebnisse sind zum erleichterten Vergleich in Abb. 1 und 2 veranschaulicht. Basierend auf diesen Ergebnissen wurde folgende Batrachtung gestellt. Es war der Zweck der Versuche, rohen Kieferharz dem katalytischen Abbau zu unterziehen und das Gemisch von verschiedenen Kohlenwasserstoffen vom Siedepunkt unterhalb von 200°C mit guter Ausbeute darzustellen. Aus diesem Standpunkt ist zu finden, dass, zwar mit einigen Ausnahmen, der Abbau bei 450°C das beste Ergebnis lieferte. Alle als Katalysatoren eingesetzten Stoffe ergaben mit Ausnahme von dem Gemisch des Kupferoxyds mit Zinkoxyd gute Resultaten, und zwar wurde die Ausbeute von durchschnittlich 35 bzw. 50% erhalten. Vor allem erwies sich das Gemisch der japanischen Säureerde mit Aluminiumoxyd (50 : 50) als das Beste. Die dreimalig kontinuierlich erfolgte Spaltung von je 100 g rohem Kieferharz bei 450°C wies für flüssige

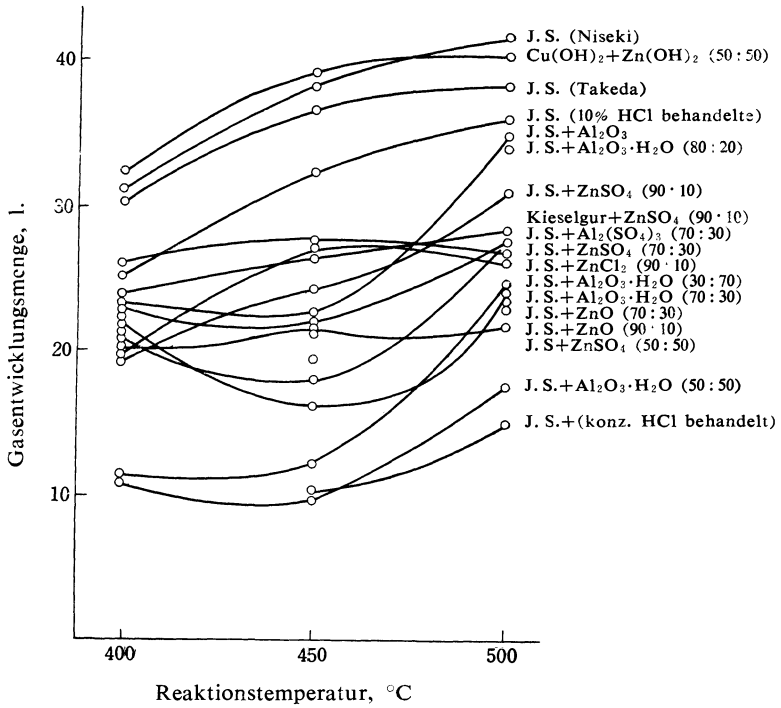



Abb. 2. Zusammenhang zwischen der Reaktionstemperatur und der Gasentwicklungsmenge.
J. S. : japanische Säureerde

Produkte von niedrigem Siedepunkt die Ausbeute von 44.5, 58.8 und 65.4% jeweils auf. Dabei wurde ferner bei Beendigung der dritten Reaction die Anlagerung freien Kohlenstoffs auf dem Katalysator nur als 10 g verwogen.

Als der nächstbeste erwies sich die mit konz. Salzsäure behandelte japanische Säureerde. Der bei 400°C und 450°C dreimal fortgesetztem Abbau von je 500 g Ausgangsmaterial zeigte für niedrigsiedende flüssige Produkte einen Mittelwerte von 50% Ausbeute auf.

Demgegenübre wurde bei dem Mischkatalysator von japanischer Säureerde und Zinksulfat (50 : 50), japanischer Säureerde und Zinkoxyd (90 : 10) eine Durchschnittsausbeute von 45% erzielt, aber eine erhöhte Anlagerung freien Kohlenstoffs auf den katalysatoren wurde mit weniger Haltbarkeit ermittelt.

**Anlagerung des Kohlenstoffs.** — Messung der Anlagerung freien Kohlenstoffs auf 100 g Katalysator beim Abbau von 100 g Roh-Kieferharz ergab die Ergebnisse von Tabelle I. Aus diesen Ergebnissen ist klar geworden, dass bei Katalysatoren aus Aluminiumoxyd, vor allem bei japanische Säureerde und Aluminiumoxyd Gemisch, die geringste Anlagerung freien Kohlenstoffs mit der längsten Haltbarkeit zu finden ist. Beim Gemisch der japanischen Säureerde mit Zinkchlorid wurde die höchste Anlagerung freien Kohlenstoffs mit dem Angriff des durch Abbau des Katalysators zu bildenden Chlors auf die Reaktionsanlage bestätigt, so dass dasselbe als katalysator unmöglich anzuwenden ist.

**Haltbarkeit des Mischkatalysator aus japanischer Säureerde und Aluminiumoxyd.** — Nach den obigen Untersuchungsergebnissen hat es sich herausgestellt, das der Mischkatalysator der japanischen Säureerde mit Aluminiumoxyd als Abbauskatalysator für rohes Kieferharz das geeigneteste ist.

Die Prüfung der Haltbarkeit erfolgte in gleicher Vorrichtung wie es bei Kolophonium der Fall war; 178 g Mischkatalysator aus japanischer Säureerde und Aluminiumoxyd (70 : 30), 223 ccm nach Volumen, wurden ins Reaktionsrohr eingeschickt. Dadurch wurden 2 kg rohes Kieferharz mit 18 ccm/Std Raumgeschwindigkeit bei 450°C gespaltet. Die Ergebnissen sind in Tabelle II verzeichnet. Nach diesen Versuchsergebnissen kann man wissen, dass sich die Ausbeute für niedrigsieden den flüssigen Produkte bei Auftragung von 500 g rohes Kieferharz als maximal erweist. Von

TABELLE I. ZUSAMMENHANG ZWISCHEN DEN KATALYSATOREN UND KOHLENSTOFFANLAGERUNGSMENGE

| Katalysatoren | | A | B | C | D |
|---|---|---|---|---|---|
| Japanische Säureerde | | — | 450 | 400 | 1.7 |
| J. Säureerde (mit 38% HCl behandelt) | | — | 500 | 400 | 0.9 |
| 〃 | 〃 | — | 500 | 500 | 1.0 |
| J. Säureerde | Aluminiumoxyd | 70 : 30 | 450 | 300 | 1.0 |
| 〃 | 〃 | 80 : 20 | 450 | 300 | 0.6 |
| 〃 | 〃 | 50 : 50 | 450 | 300 | 1.0 |
| 〃 | 〃 | 30 : 70 | 450 | 300 | 1.0 |
| 〃 | 〃 | 30 : 70 | 450 | 600 | 1.0 |
| 〃 | Zinkoxyd | 90 : 10 | 450 | 200 | 9.0 |
| 〃 | 〃 | 90 : 10 | 500 | 200 | 9.0 |
| 〃 | 〃 | 70 : 30 | 450 | 500 | 3.0 |
| 〃 | Zinkchlorid | 90 : 10 | 450 | 150 | 18.0 |
| 〃 | 〃 | 90 : 10 | 400 | 150 | 20.0 |
| 〃 | Aluminiumsulfat | 70 : 30 | 450 | 400 | 1.0 |
| 〃 | Zinksulfat | 70 : 30 | 500 | 400 | 3.3 |
| 〃 | 〃 | 50 : 50 | 450 | 300 | 6.0 |
| 〃 | Zinkoxyd | 50 : 50 | 400 | 400 | 2.9 |
| 〃 | 〃 | 50 : 50 | 500 | 400 | 2.6 |

A : Mischverhältnis
B : Reaktionstemperatur, °C
C : Einsatz des Ausgangsmaterials, g
D : Kohlenstoffanlagerung (g) bezogen auf 100 g Einsatz des Ausgangsmaterials.

TABELLE II. VERÄNDERUNGSZUSTAND DER GEWINNUNGSVERHÄLTNISSE DER ABBAUPRODUKTE AUS ROHEM KIEFERHARZ BEI KONTINUIERLICHEN EINSATZ MIT MISCHKATALYSATOR, JAPANISCHE SÄUREERDE-ALMINIUMOXYD (70 : 30) BEI 45°C

| | | flüssige Produkte | | gasförmige Produkte | | | |
|---|---|---|---|---|---|---|---|
| A g | B Std | Sdp. bis 200°C % | Sdp. bis 200°C % | C l | D % | E % | F % |
| 100 | 6 | 37.5 | 28.2 | 16.7 | 14.6 | 13.3 | 53.1 |
| 200 | 12 | 37.0 | 28.5 | 18.8 | 15.2 | 14.4 | 47.6 |
| 300 | 18 | 41.2 | 29.5 | 24.9 | 15.8 | 12.1 | 47.4 |
| 400 | 24 | 43.2 | 32.6 | 19.4 | 14.4 | 12.2 | 52.3 |
| 500 | 30 | 45.5 | 33.2 | 20.8 | 12.6 | 12.8 | 60.1 |
| 600 | 36 | 35.5 | 43.4 | 21.3 | 13.2 | 11.9 | 58.8 |
| 700 | 42 | 32.1 | 45.1 | 21.5 | 14.4 | 13.1 | 55.1 |
| 800 | 48 | 27.3 | 40.6 | 19.5 | 15.6 | 13.8 | 53.9 |
| 900 | 54 | 25.8 | 38.4 | 18.8 | 15.1 | 11.9 | 58.2 |
| 1000 | 60 | 25.9 | 39.2 | 18.3 | 14.1 | 14.6 | 54.4 |
| 1100 | 66 | 25.3 | 44.1 | 20.2 | 14.7 | 14.1 | 55.8 |
| 1200 | 72 | 23.8 | 40.8 | 18.2 | 12.8 | 11.7 | 53.9 |
| 1300 | 78 | 23.9 | 39.8 | 17.6 | 13.1 | 13.5 | 55.2 |
| 1400 | 84 | 22.5 | 42.5 | 17.2 | 12.6 | 15.3 | 59.4 |
| 1500 | 90 | 23.9 | 38.6 | 19.4 | 13.8 | 11.8 | 61.2 |
| 1600 | 96 | 22.4 | 34.5 | 16.2 | 10.1 | 13.2 | 60.8 |
| 1700 | 102 | 23.1 | 38.2 | 16.4 | 13.5 | 13.7 | 55.7 |
| 1800 | 108 | 20.1 | 34.6 | 17.3 | 13.7 | 13.9 | 53.5 |
| 1900 | 114 | 16.3 | 29.8 | 14.8 | 15.1 | 11.6 | 47.7 |
| 2000 | 120 | 17.4 | 30.6 | 17.2 | 12.6 | 13.3 | 49.2 |

A : Abtröpfelungsmenge des rohen Kieferharzes
B : Reaktionsdauer
C : Entwicklungsvolumen
D : $CO_2$
E : Olefine
F : Diverse Gase

dem erreichten fertigen Abbau des 900 g Roh-Kieferharzes an weist nunmehr der Abbau ein ungefähr konstantes Bild auf. Aber nachher verschlechtert sich der Abbau selbst. Es erweist sich endlich die Ausbeute von den flüssigen Produkten mit niedrigem Siedepunkt als 30%. Die während dieses ganzen kontinuierlichen Abbaus auf den Katalysatoren angelagertin Menge des freien Kohlenstoffs betrug nur 84 g.

**Bestandteile der flüssigen Produkte.** — Das rohe Kieferharz ist als Kolophonium mit Terpenen-Zusatz zu betrachten. Bei den durch den katalytischen Abbau hergestellten Produkten zeigt das Klophonium keinen grösseren Unterschied von dem rohen Kieferharz. Insbesondere bei Abbau bei einer hohen Temperatur über 400°C können die meisten Terpenen mit grosser Möglichkeit in gasige Substanzen ungewandelt werden. Dieser Umstand ist leicht einzusehen, wenn man die gebildete Gasmenge bei dem 450°C kontinuier-lichen Kolophonium-Abbau unter Verwendung der Kieselgur als Katalysator und dieselbe von der gleicherweise erfolgten Roh-Kieferharzspaltung bei 450°C vergleicht.

Die Untersuchnng der durch Abbau des rohen Kieferharzes dargestellten flüssigen Produkte stellte Benzol, Toluol, Xylol, Cumol, Pseudocumol, *p*-Cymol, Naphthalin, Anthracen, Phenanthren und Reten fest. Es waren also gleiche Ergebnisse wie bei dem bereits beschriebenen Kolophonium.

Als gasförmige Produkte wurde Wasserstoff, Kohlendioxyd, Kohlenoxyd, Olefinen festgestellt. Aber die chemische Zusammensetzung der Olefine wurde nicht geforscht.

## Zusammenfassung

Für kontinuierliche Gewinnung der flüssigen Produkte von niedrigem Siedepunkte durch den katalytischen Abbau des rohen Kieferharzes hat sich das Verfahren mit den Mischkatalysator aus der japanischen Säureerde und Aluminiumoxyd anzuwenden als das Erfolgreichste erwiesen.

Die Reaktionstemperatur wird am besten 450°C gewählt, wie es bei Kolophonium der Fall war. Es ist interessant, dass die Kieselgur, die sich bei Kolophonium bewährt hat, bei dem rohen Kieferharz nicht so sehr gute Ergebnisse dargebracht hat. Es wurde erkannt, dass es sich bei den Abbauprodukten bestandteilmässig fast um die gleichen Verbindungen wie bei dem Kolophonium.

Zum Schluss sei es noch bemerkt, dass die vorliegende Arbeit unter der Leitung von Herrn Professor Dr. Eiichi Funakubo an der Technischen Fakultät der Universität zu Osaka durchgeführt wurde.

*Chemisches Institut der*
*Technischen Fakultät der*
*Universität zu Osaka*
*Miyakojima-ku, Osaka*

# *An Analysis of Ishikawa's Equation of State as Applied to the Critical Region of Isopentane*

By Tetsuya ISHIKAWA and Minoru IKEDA

(Received September 29, 1960)

In the last report of this series of study[1], one of the present authors (Ishikawa) made a close investigation of his equation of state: for one mole of gas

$$p+\frac{a}{V^{2-\varepsilon}}=\frac{RT}{V-b}$$

where $a=3p_cV_c^2$, $b=V_c/3$ and $\varepsilon$ is an empirically determinable parameter which depends upon molecular association, its factor, $A$, being defined by him as the ratio of observed $P_cV_c/RT_c$ to its van der Waals' value 8/3, or $A=(1+3V_c^{\varepsilon})/4$ at the critical point. He remarked that $\varepsilon$ varies but little with the volume and that $\varepsilon$-$V$ curves of xenon and neopentane, $C(CH_3)_4$, in the critical region appear alike to

1) T. Ishikawa, This Bulletin, **26**, 78, 530 (1953); ibid., **27**, 226, 570 (1954); ibid., **28**, 89, 515 (1955); T. Ishikawa and M. Ikeda, ibid., **26**, 516 (1953).

consist of three parts, the first part being concave up to the critical point, or more precisely speaking, at first probably showing a minimum which is situated at the volume corresponding to the minimum of $p$-$V$ curve plotted by his equation, taking $\varepsilon$ to be that at the critical point, and finally a nearly straight line, the second part being undoubtedly a long straight line starting from the critical point; or, at the critical point the second and higher derivatives of $\varepsilon$ with respect to the volume appear to be zero, and the third part being convex upward to the maximum which may correspond to the volume at which the other form of van der Waals' equation ($b=V_c/3$) takes the critical pressure. This paper is intended to analyze the $\varepsilon$-$V$ curve by making use of Young's precise $PVT$-measurements on

TABLE I. CRITICAL ISOTHERM OF ISOPENTANE, 187.8°C

| $V$ cm$^3$ g$^{-1}$ | $p$ atm. | $\varepsilon_{obs}$ | $\varepsilon_{obs} V^{1/3}$ | $\varepsilon_1$ | $\varepsilon_1+\varepsilon_{obs}$ | $\varepsilon_g$ | $\varepsilon_1+\varepsilon_g$ | $\varepsilon_{calcd}$ | $n$ | $p_{calcd}$ atm. | Deviation % |
|---|---|---|---|---|---|---|---|---|---|---|---|
| 2.4 | 64.58 | 0.08025 | 0.44730 | 0.07993 | | | | 0.07993 | | 65.35 | +1.19 |
| 2.5 | 53.37 | 0.07890 | 0.44580 | 0.07885 | | | | 0.07885 | | 53.48 | +0.21 |
| 2.6 | 46.03 | 0.07769 | 0.44470 | 0.07782 | | | | 0.07782 | | 45.77 | −0.56 |
| 2.7 | 41.14 | 0.07665 | 0.44434 | 0.07685 | | | | 0.07685 | | 40.73 | −1.00 |
| 2.8 | 38.08 | 0.07567 | 0.44401 | 0.07592 | | | | 0.07592 | | 37.68 | −1.18 |
| 2.9 | 36.08 | 0.07483 | 0.44424 | 0.07504 | | | | 0.07504 | | 35.75 | −0.91 |
| 3.0 | 34.82 | 0.07460 | 0.44791 | 0.07420 | | | | 0.07420 | | 34.77 | −0.14 |
| 3.2 | 33.54 | 0.07323 | 0.4455 mean | 0.07262 | 0.14585 | 0.06779 | 0.14041 | 0.07323 | | 33.54 | ±0.00 |
| 3.4 | 33.07 | 0.07270 | | 0.07117 | 0.14387 | 0.06917 | 0.14034 | 0.07277 | | 33.11 | +0.12 |
| 3.6 | 32.96 | 0.07227 | | 0.06982 | 0.14209 | 0.07050 | 0.14032 | 0.07236 | | 32.88 | −0.24 |
| 3.8 | 32.93 | 0.07308 | | 0.06858 | 0.14166 | 0.07179 | 0.14037 | 0.07312 | | 32.89 | −0.12 |
| 4.0 | 32.92 | 0.07366 | | 0.06741 | 0.14107 | 0.07302 | 0.14043 | 0.07364 | | 32.94 | +0.06 |
| 4.3 | 32.91 | 0.07479 | | 0.06581 | 0.14060 | 0.07481 | 0.14062 | 0.07458 | | 33.09 | +0.55 |
| 4.6 | 32.89 | 0.07609 | | 0.06434 | 0.14043 | const. range | | 0.07607 | | 32.91 | +0.06 |
| 5.0 | 32.88 | 0.07782 | | 0.06258 | 0.14040 | | | 0.07783 | | 32.87 | −0.03 |
| 5.5 | 32.82 | 0.07978 | | 0.06062 | 0.14040 | | | 0.07979 | | 32.81 | −0.03 |
| 6.0 | 32.68 | 0.08146 | | 0.05889 | 0.14035 | 0.08359 | | 0.08144 | | 32.68 | ±0.00 |
| 6.5 | 32.45 | 0.08284 | | 0.05734 | 0.14018 | 0.08585 | | 0.08289 | 4 | 32.43 | −0.06 |
| 7.0 | 32.11 | 0.08404 | | 0.05594 | 0.13998 | 0.08800 | | 0.08402 | | 32.12 | +0.03 |
| 7.5 | 31.67 | 0.08513 | | 0.05467 | 0.13980 | 0.09005 | | 0.08510 | | 31.68 | +0.03 |
| 8.0 | 31.20 | 0.08597 | | 0.05351 | 0.13948 | 0.09200 | | 0.08599 | 3 | 31.19 | −0.03 |
| 8.5 | 30.70 | 0.08663 | | 0.05244 | 0.13907 | 0.09388 | | 0.08667 | | 30.69 | −0.03 |
| 9.0 | 30.17 | 0.08717 | | 0.05145 | 0.13862 | 0.09569 | | 0.08714 | | 30.17 | ±0.00 |
| 9.5 | 29.61 | 0.08765 | | 0.05053 | 0.13818 | 0.09743 | | 0.08755 | | 29.63 | +0.07 |
| 10.0 | 29.00 | 0.08822 | | 0.04967 | 0.13789 | 0.09911 | | 0.08816 | | 29.01 | +0.03 |
| 11.0 | 27.84 | 0.08894 | | 0.04819 | 0.13713 | 0.10231 | | 0.08906 | 2 | 27.82 | −0.07 |
| 12.0 | 26.71 | 0.08947 | | 0.04674 | 0.13621 | 0.10532 | | 0.08956 | | 26.70 | −0.04 |
| 13.0 | 25.66 | 0.08955 | | 0.04551 | 0.13506 | 0.10817 | | 0.08967 | | 25.64 | −0.08 |
| 14.0 | 24.63 | 0.08965 | | 0.04440 | 0.13405 | 0.11087 | | 0.08941 | | 24.66 | +0.12 |
| 15.0 | 23.66 | 0.08971 | | 0.04339 | 0.13310 | 0.11345 | | 0.08977 | | 23.65 | −0.04 |
| 16.0 | 22.71 | 0.09018 | | 0.04247 | 0.13265 | 0.11592 | | 0.09011 | | 22.71 | ±0.00 |
| 17.0 | 21.84 | 0.09029 | | 0.04161 | 0.13191 | 0.11828 | | 0.09030 | 4/3 | 21.84 | ±0.00 |
| 18.0 | 21.04 | 0.09019 | | 0.04083 | 0.13102 | 0.12056 | | 0.09036 | | 21.03 | −0.05 |
| 19.0 | 20.26 | 0.09046 | | 0.04010 | 0.13056 | 0.12275 | | 0.09030 | | 20.27 | +0.05 |
| | | | | | | | | | | mean | ±0.21 |
| 20.0 | 19.53 | 0.09067 | | | | 0.12487 | | 0.09027 | | 19.56 | +0.15 |
| 30.0 | 14.41 | 0.08848 | | | | 0.14294 | | 0.09103 | 1 | 14.33 | −0.56 |
| 40.0 | 11.28 | 0.09049 | | | | 0.15732 | | 0.08811 | | 11.32 | +0.35 |
| 50.0 | 9.30 | 0.08897 | | | | 0.16947 | | 0.08912 | | 9.30 | ±0.00 |
| 60.0 | 7.90 | 0.08878 | | | | 0.18009 | | 0.08935 | | 7.90 | ±0.00 |
| 80.0 | 6.07 | 0.08766 | | | | 0.19822 | | 0.08830 | 2/3 | 6.07 | ±0.00 |
| 90.0 | 5.44 | 0.08790 | | | | 0.20615 | | 0.08725 | | 5.44 | ±0.00 |
| 100.0 | 4.93 | 0.08720 | | | | 0.21352 | | 0.08597 | | 4.93 | ±0.00 |
| | | | | | | | | | | total mean | ±0.20 |

isopentane at the temperature range of 170～200°C, the critical temperature being 187.8°C[2].

### Analysis of $\varepsilon$-$V$ Curves

For the estimation of $\varepsilon$ at each isotherm of isopentane, we take the following values: $T_c$=187.8+273.16°K, $p_c$=25000 mmHg (32.89 atm.), $d_c$=0.2343 cm$^3$ g$^{-1}$, these values being quoted from the same observer's values on the border curve of this substance[3], $M$=72.151, $R$=82.06 cm$^3$ atm. deg$^{-1}$ mol$^{-1}$, log $a$=6.9711254, and $b$=102.68 cm$^3$ mol$^{-1}$.

In the liquid portion below the critical temperature, it is highly probable as estimated that $\varepsilon \times V^{1/3}$ is constant at each isotherm, the mean values being 0.4674 (2.4～2.5), 0.4564 (2.4～2.7), 0.4513(2.4～2.8) and 0.4472(2.4～3.0) at 170, 176, 180 and 185°C, respectively, the numbers in the parentheses showing volume ranges in cm$^3$ g$^{-1}$, and so we have conducted similar operation on the $\varepsilon$ values at and above the critical temperature, 187.8, 190, 195 and 200°C, their mean values being 0.4455(2.4～3.0), 0.44305(2.4～3.0), 0.4376(2.4～2.8) and 0.4320 (2.5～2.6), respectively. These constants are denoted by $c_1$'s.

All these values except that at 170°C, multiplied by each temperature in the absolute scale $T$, gave a constant value 204.89±0.34 (0.17% probable error), and therefore each value can be written as $204.89/T$. Let $\varepsilon$ in the liquid portion be denoted by $\varepsilon_l$, then $\varepsilon_l$ is the product of the above obtained value at each isotherm by $V^{-1/3}$ or is briefly expressed by $204.89/TV^{1/3}$. In the region of liquid and gaseous coexistence, however, $\varepsilon$ may become very complicated as supposed from the critical isotherm stated above, so we will make trial by taking the sum of $\varepsilon_l$ and $\varepsilon$ in this region to search for $\varepsilon$ in gaseous form in this region which is denoted $\varepsilon_g$. Unfortunately as Young's data are lacking in this region, we are obliged to study the functional form of $\varepsilon_g$ in the isotherms of from 187.8 to 200°C, above which the constant range of $\varepsilon \times V^{1/3}$ in the liquid portion apparently disappears.

As seen from Table I, the values of $(\varepsilon_l+\varepsilon_{obs})$ decrease at first, then approach nearly a constant, and again decrease.

For a supplementary test we will quote from the later $PVT$-measurements[4] on neopentane by Beattie, Douslin and Levine together with their earlier measurements[5] at 160.50～160.70°C, the critical temperature being 160.60°C already treated (see Table II). The constancy of $\varepsilon \times V^{1/3}$ in the liquid portion, $V$=142.9～222.2 cm$^3$·mol$^{-1}$, is not so good as those which appeared in Table I, yet we dare take their geometric mean values as 0.4246. The constant range in the region of coexistence distinctly occurs between 304.9 and 400 cm$^3$ mol$^{-1}$, their mean value being 0.13721, the range of which is a little beyond the upper limit of coexistence at 160.00°C as referred to Fig. 1 in the earlier paper of these observers.

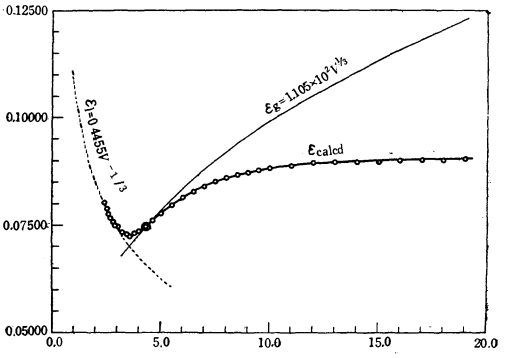



Fig. 1. $\varepsilon$-$v$ Diagram of isopentane at 187.8°C.

The existence of a constant range of $(\varepsilon_l+\varepsilon_{obs})$ as observed in this example has given us a clue for analyzing the first decreasing range up to a constant range: Putting the value $\varepsilon_{obs}-\{(\varepsilon_l+\varepsilon_{obs})-0.13721\}$, where $\varepsilon_l=0.4246V^{1/3}$, to be the form $c_2V^n$, $n$ and $c_2$ being constants, we have obtained $n=1/3$ and $c_2=1.106\times10^{-2}$. Similar calculations have given us the respective values for isopentane as follows: $n=1/3$ for all the cases and $c_2$'s are 1.105, 1.097, 1.081 and $1.064\times10^{-2}$ at 187.8, 190, 195 and 200°C, respectively, and $c_2=1.1145\times10^{-2}$ at 185°C has been graphically obtained from the preceding values which are quite linear against temperature. At the critical temperature where $V=V_c$, for neopentane $1.106\times10^{-2}\,V_c^{1/3}$ ($V_c$=303.0 cm$^3$ mol$^{-1}$)=0.07429, which is fairly coincident with the observed $\varepsilon$=0.07411, for isopentane $1.105\times10^{-2}\,V_c^{1/3}$ ($V_c$=4.268 cm$^3$ g$^{-1}\times$72.151=307.94)=0.07479, which is also coincident with the observed $\varepsilon$=0.07486. Thus it is highly probable that the common form of $c_2V^{1/3}$ obtained above is no other than the required $\varepsilon_g$ in each isotherm. This result shows us that in the critical isotherm $\varepsilon_l+\varepsilon_g$=a constant for the volume range up to the critical volume, or in other words, the molecular complexities of liquid and gaseous states are in equilibrium for this range.

In the isotherms above the critical temperature, the same phenomenon is also observed,

2) S. Young, *Proc. Roy. Dub. Soc.*, **12**, 374 (1910).
3) "International Critical Tables", Vol. III (1928), p. 244.
4) J. A. Beattie, D. R. Douslin and S. W. Levine, *J. Chem. Phys.*, **20**, 1619 (1952).
5) J. A. Beattie, D. R. Douslin and S. W. Levine, ibid., **19**, 948 (1951).

TABLE II. ISOTHERM OF NEOPENTANE, 160.50~160.70°C

| $V$ cm³ mol⁻¹ | $\varepsilon_{obs}$ | $\varepsilon_{obs} V^{1/3}$ | $\varepsilon_1$ | $\varepsilon_1+\varepsilon_{obs}$ | $c_2\times10^2$ | $\varepsilon_g$ | $\varepsilon_1+\varepsilon_g$ |
|---|---|---|---|---|---|---|---|
| 142.9 | 0.06630 | (0.3466) | | | | | |
| 166.7 | 0.07382 | 0.4063 | | | | | |
| 200.0 | 0.07356 | 0.4302 | | | | | |
| 222.2 | 0.07231 | 0.4380 | | | | | |
| | | 0.4246 geom. mean | | | | | |
| 250.0 | 0.07210 | | 0.06740 | 0.13950 | 1.108 | 0.06967 | 0.13707 |
| 259.7 | 0.07224 | | 0.06655 | 0.13879 | 1.108 | 0.07056 | 0.13711 |
| 266.7 | 0.07242 | | 0.06596 | 0.13838 | 1.107 | 0.07124 | 0.13720 |
| 270.3 | 0.07255 | | 0.06565 | 0.13820 | 1.107 | 0.07151 | 0.13716 |
| 277.8 | 0.07283 | | 0.06507 | 0.13790 | 1.106 | 0.07217 | 0.13724 |
| 285.7 | 0.07319 | | 0.06447 | 0.13768 | 1.104 | 0.07284 | 0.13731 |
| 292.4 | 0.07352 | | 0.06397 | 0.13749 | 1.103 | 0.07341 | 0.13738 |
| 298.5 | 0.07385 | | 0.06353 | 0.13738 | 1.102 | 0.07392 | 0.13745 |
| 304.9 | 0.07421 | | 0.06308 | 0.13729 | 1.106 mean | | |
| 312.5 | 0.07466 | | 0.06257 | 0.13723 | | | |
| 319.5 | 0.07508 | | 0.06211 | 0.13719 | | | |
| 328.8 | 0.07565 | | 0.06152 | 0.13717 | | | |
| 333.3 | 0.07592 | | 0.06124 | 0.13716 | mean | | |
| 340.1 | 0.07634 | | 0.06083 | 0.13717 | 0.13721 | | |
| 357.1 | 0.07733 | | 0.05985 | 0.13718 | | | |
| 363.6 | 0.07771 | | 0.05949 | 0.13720 | | | |
| 370.4 | 0.07812 | | 0.05912 | 0.13724 | | | |
| 377.4 | 0.07846 | | 0.05875 | 0.13721 | | | |
| 400.0 | 0.07961 | | 0.05763 | 0.13724 | | | |
| 500.0 | 0.08331 | | 0.05349 | 0.13680 | | | |
| 666.7 | 0.08585 | | 0.04860 | 0.13445 | | | |
| 1000.0 | 0.08701 | | 0.04246 | 0.12947 | | | |

but the constant range becomes short and shifts to greater volume than the critical volume.

In these ranges $\varepsilon_{calcd}$ can be estimated from a transformed relation: $\varepsilon_{calcd}=\varepsilon_{obs}-(\varepsilon_1+\varepsilon_g-\text{a constant})$, without doing the direct analysis of $\varepsilon_{obs}$. Next we consider $\varepsilon$-$V$ curve beyond the critical volume. Since in the critical isotherm of isopentane $\varepsilon_g=1.105\times10^{-2}V^{1/3}$ coincides numerically with the observed $\varepsilon$ in case $V=V_c$ and so $\varepsilon_1=0.4455\,V^{-1/3}$ vanishes as would be expected, we may put the change in molecular complexity in gaseous state to be the difference between the thus computed $\varepsilon_g$ and $\varepsilon_{obs}$ at the same volume, and assume that this difference is proportional to $V^n$, or $\varepsilon_{obs}=\varepsilon_g-c_3V^n$, $n$ and $c_3$ being constants. This calculation necessitates dividing the $\varepsilon$-$V$ curve into at least six parts: $n=4$ and $c_3=6.115\times10^{-14}$ (6.0~7.0), $n=3$ and $c_3=3.124\times10^{-11}$ (7.5~9.0), $n=2$ and $c_3=2.103\times10^{-8}$ (9.5~14), $n=4/3$ and $c_3=2.131\times10^{-6}$ (15~19), $n=1$ and $c_3=2.398\times10^{-5}$ (20~40), and $n=2/3$ and $c_3=3.416\times10^{-4}$ (50~100), the parentheses being volume range in $cm^3\,g^{-1}$. Similarly $n$'s and $c_3$'s of other isotherms have been obtained with expected results. For an example of the above results, we adopt from Table I (critical isotherm) with Fig. 1, in which $\varepsilon_{obs}$ is denoted by ○, $\varepsilon_{obs}$ at the critical point by ◎, $\varepsilon_{calcd}$ by a thick line, $\varepsilon_1=0.4455\cdot V^{-1/3}$ and $\varepsilon_g=1.105\times10^{-2}V^{1/3}$ by dotted and fine lines respectively.

## Discussion of the Results

Ishikawa's equation of state, though it is superior to most of the hitherto published equations of state, does not hold quantitatively in the critical region, so long as $\varepsilon$ is assumed to be a constant throughout the whole range of volume. However, if we consider it to consist of sets of volume functions having one ($c_1$ for the liquid portion) or two ($c_1$ and $c_2$, $c_2$ and $c_3$ for the coexistence and gaseous portions) constants analytically obtained from $\varepsilon_{obs}$, his equation holds for a certain range of volume during which the same molecular complexity continues.

In the liquid portion the increase in $V^{1/3}$ or in average molecular distance (if it is assumed that a molecule is spherical with a diameter $\sigma$, $V=\pi\sigma^3N/6$ where $N$=Avogadro's number, and average molecular distance is the distance

between the centers of the nearest molecules) causes the decrease in $\varepsilon$, this being consistent with the ordinary physico-chemical conception, whereas in the liquid and gaseous coexistence portion up to the critical volume the increase in average molecular distance causes the decrease in $\varepsilon$ of liquid form, $\varepsilon_l$, and at the same time the increase in $\varepsilon$ of gaseous form, $\varepsilon_g$, this being a case which is usually explained by the LeChatelier principle of mobile equilibrium. In the gaseous portion the decreasing rate from $\varepsilon_g$ is propotional to the $n$th power of average molecular distance thus: $n=12$ for 1.15~1.18 times, $n=9$ for 1.21~1.28 times, $n=6$ for 1.31~1.45 times, and $n=4$ for 1.50~1.67 times the average molecular distance at the critical point (9.95 Å according to the above assumption).

According to Warren's study[6] from Stewart's X-ray diffraction measurements on normal paraffins from pentane to pentadecane[7], the long-chain molecules are straight in liquids and neighboring molecules are roughly parallel, 5.65 Å apart from each other, as if it were the diffraction of diatomic molecules, and also according to Müller the diffraction ring in normal paraffins observed by Stewart is due to assemblages of molecules (cybotactic groups), the average distance of the nearest approach near their melting points being 4.5~5.0 Å[8]. As computed from the relation $A=(1+3V_c^e)/4$, the molecular association factors of neopentane, isopentane and *n*-pentane at their critical points are estimated to be 1.395, 1.402 and 1.471, respectively, the last being the value quoted from the critical constants measured by Beattie, Levine and Douslin[9]. These values are near to slightly polar substances such as methyl acetate (1.45), ethyl acetate (1.46) and propyl acetate (1.47) than to diatomic molecules such as nitrogen (1.29), oxygen (1.20), chlorine (1.35) and bromine (1.30). As a summery of the present analyses, we give in columns 10 and 11 in Table I the thus computed pressures, $p_{calcd}$, and their percentage deviations from the observed pressures, $p_{obs}$. On the whole, these deviations are so small that they are supposed to be experimental errors, since they are within less than 0.27% on the average up to 19~20 $cm^3g^{-1}$.

It is worth mentioning that Ishikawa's equation of state to which the thus suitable analyses are applied yields no such discrepancy from experiments in the critical region as all other equations of state generally do. Fig. 2 shows

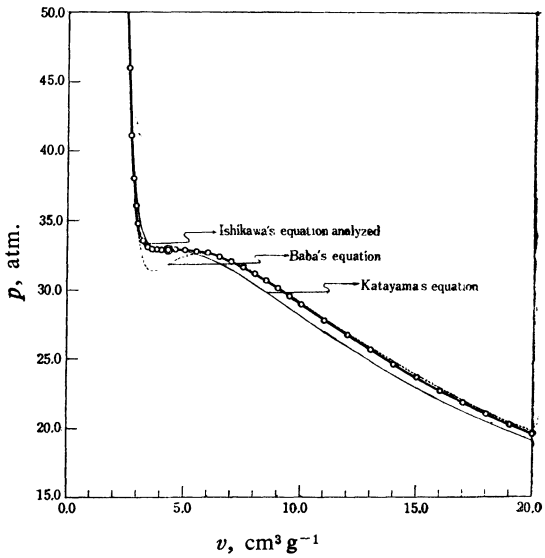



Fig. 2. Critical isotherm of isopentane.

the comparison of Ishikawa's equation adopted from Table I (thick line, 0.21% deviation up to 19 $cm^3g^{-1}$) with Katayama's equation[10] (fine line, 1.81% deviation up to 20 $cm^3g^{-1}$) and Baba's equation[11] (dotted line, 1.96% deviation up to 19 $cm^3g^{-1}$) which were applied by themselves to the same Young's data of isopentane.

## Conclusion

The above results lead to the following conclusions (1) that liquid associated molecules still exist at least 12°C above the critical temperature, and that they are assembled up to the critical volume, as judged from the coexistence condition for liquid and gaseous states: $\varepsilon_l+\varepsilon_g=$ a constant, where $\varepsilon_l=c_1V^{-1/3}$ and $\varepsilon_g=c_2V^{1/3}$, the former corresponding to the functional form of $\varepsilon$ for liquid assemblages and the latter to the base functional form of $\varepsilon$ for gaseous assemblages, (2) that gaseous associated molecules exist from the lower point on the border curve to the gaseous region, and are disassembled from the base functional form proportional to the average distance stepwise with volume increase by van der Waals' forces of the 12th, 9th, 6th, 4th, 3rd and 2nd powers of average distance for their respective volume ranges, and therefore (3) that the nature of the $p$-$V$ curve is, from the analytical standpoint of view, not continuous but discontinuous, and a clear difference in the functional forms between $\varepsilon_l$ and $\varepsilon_g$, and

6) B. E. Warren, *Phys. Rev.*, **44**, 969 (1933).
7) G. W. Stewart, *Proc. Natl. Acad. Sci.*, **13**, 787 (1927); *Phys. Rev.*, **31**, 174 (1928).
8) A. Müller, *Trans. Faraday Soc.*, **29**, 990 (1933).
9) J. A. Beattie, S. W. Levine and D. R. Douslin, *J. Am. Chem. Soc.*, **74**, 4778 (1952).
10) M. Katayama, *J. Chem. Soc. Japan (Nippon Kwagaku Kwaishi)*, **43**, 609 (1922).
11) T. Baba, *J. Technol. Res. Kantogakuin Univ.*, **5**, 1 (1960).

the disappearance of the former at the critical volume is a strong proof contrary to the hitherto accepted conception of continuity of liquid and gaseous states.

*Junior College of Commerce*
*Nagasaki University*
*Nagasaki*

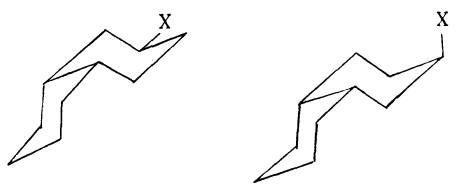
# *The Effect of Conformation on Reactivity. III*[1]. *Acetolysis of the cis-Decalyl p-Toluenesulfonates*

By Ichiro MORITANI*, Shinya NISHIDA and Masuo MURAKAMI

(Received January 14, 1961)

It has been shown that the strain arising from the compression between the tosyl group and the hydrogen atom in the 1, 3-diaxial positions to each other in the 1- and 2-*p*-toluenesulfonates of *trans*-decalol plays an important role in controlling the rate of acetolysis[1].

Theoretically no isomeric forms would be possible with the *trans*-decalin molecule due to its rigid comformation[1], but some rotational isomers are found to exist with the *cis*-decalin, the case being analogous to the cyclohexane system. Introduction of a substituent into the *cis-trans*-2-decalin molecule would give the following two conformations, the equatorial I and the axial II. Each of the three other *cis*-

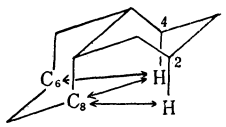



I II

*cis-trans*-2-Decalyl derivative

decalyl derivatives will give similar conformational isomers[2]. Therefore it would not be possible to utilize the interpretation given for the *trans*-decalyl system in predicting reactivities of the *cis*-decalyl derivatives.

The *cis*-decalin was found to be less stable than the *trans*-decalin[3]. This instability would be due to a non-bonded interaction between the atoms which constitute the *cis*-decalin ring. In other words, 1, 3-diaxial interactions are regarded as being responsible for the instabilities. This is apparent by the examination of the structure represented by III; there




III

*cis*-Decalin

is a steric compression between the $CH_2$ group at $C_6$ and the hydrogen atoms in the axial position at $C_2$ and $C_4$. The group involved in giving rise to strains in the system under consideration differs therefore, as seen above, from that found to be participating in the system previously studied, i. e., the $CH_2$ group rather than the tosyl group. It is of considerable interest to see how this type of 1, 3-diaxial interaction will affect *cis*-decalyl derivatives.

Hückel[4] has made studies on the methanolysis of *cis*-decalyl *p*-toluenesulfonates[4], but has not correlated the reactivities with conformations.

It seems desirable therefore to study the reaction on a quantitative basis to find the relationships between conformation and reactivity. In this regard, we have undertaken a study on rates of acetolysis of the four isomers of the *cis*-decalyl *p*-toluenesulfonates.

* Present address: Department of Applied Chemistry, Osaka University, Miyakojima-ku, Osaka.

1) Parts I and II of this series: I. Moritani, S. Nishida and M. Murakami, *J. Am. Chem. Soc.*, **81**, 3420 (1959); S. Nishida, ibid., **82**, 4290 (1960).

2) Dauben [Ref. W. G. Dauben, R. C. Tweit and C. Mannerskantz, ibid., **76**, 4424 (1954)] proposed the preferred conformation of various *cis*-decalyl amines.

3) W. G. Dauben and K. S. Pitzer, "Steric Effects in Organic Chemistry", Ed. by M. S. Nerman, John Wiley & Sons, Inc., New York (1956), p. 25.

4) W. Hückel, *Ber.*, **77**, 805 (1944); W. Hückel, R. Bross, O. Fechig, H. Feltkamp, S. Geiger, M. Hanack, M. Heinzel, A. Hubele, J. Kurg, M. Maier, D. Maucher, G. Näher, R. Neidlemd and R. B. Rasingkar, *Ann.*, **624**, 142 (1959).

TABLE I. SUMMARY OF THE RATE CONSTANTS OF THE ACETOLYSIS OF *cis*-DECALYL *p*-TOLUENESULFONATES

| Decalyl *p*-toluene sulfonate | Temp. °C | $10^5 \cdot k_1$ sec$^{-1}$ | $\Delta H^{\neq}$ kcal./mol. | $\Delta S^{\neq}$ e. u. |
|---|---|---|---|---|
| *cis-cis*-1 | 75.0 | 73.3 | | |
| | 64.77 | 25.3±0.01 | 23.6 | −5.3 |
| | 51.04 | 5.39±0.06 | | |
| | 41.32 | 1.70±0.03 | | |
| *cis-trans*-1 | 95.42 | 41.4±0.3 | 28.2 | −2.1 |
| | 85.08 | 13.3±0.1 | | |
| | 75.0 | 4.08 | | |
| | 70.45 | 2.33±0.02 | | |
| | 60.26 | 0.647±0.014 | | |
| *cis-cis*-2 | 90.21 | 42.5±0.4 | 27.3 | +0.6 |
| | 75.36 | 7.84±0.02 | | |
| | 75.0 | 7.15 | | |
| | 60.33 | 1.32±0.01 | | |
| *cis-trans*-2 | 90.29 | 45.4±0.2 | 27.4 | +1.3 |
| | 75.61 | 8.88+0.04 | | |
| | 75.0 | 8.53 | | |
| | 60.33 | 1.34±0.004 | | |

TABLE II. RELATIVE RATES OF ACETOLYSIS OF *cis*- AND *trans*-DECALYL *p*-TOLUENESULFONATES AT 75.0°C

| Decalyl *p*-toluene-sulfonate | Rel. rate 75.0°C | Decalyl *p*-toluene-sulfonate | Rel. rate 75.0°C | cis/trans |
|---|---|---|---|---|
| *cis-trans*-1 | 2.1 | *trans-trans*-1 | 0.53 | 3.9 |
| *cis-cis*-1 | 36.9 | *trans-cis*-1 | 27.6 | 1.3 |
| *cis-trans*-2 | 4.3 | *trans-trans*-2 | 3.1 | 1.4 |
| *cis-cis*-2 | 3.6 | *trans-cis*-2 | 1.0 | 3.6 |

TABLE III. PERCENTAGE OF OLEFIN FORMED ON THE ACETOLYSIS OF DECALYL *p*-TOLUENESULFONATES at 100°C

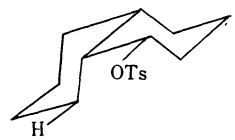
| Decalyl *p*-toluenesulfonate | Conformation | Percentage of Olefin, % |
|---|---|---|
| *trans-trans*-1 | 1 e | 66 |
| *trans-cis*-1 | 1 a | 90 |
| *trans-cis*-2 | 2 e | 68 |
| *trans-trans*-2 | 2 a | 80 |
| *cis-trans*-1 | | 81 |
| *cis-cis*-1 | | 100 |
| *cis-cis*-2 | | 79 |
| *cis-trans*-2 | | 74 |

The rates of acetolysis of *cis-cis*-1, *cis-trans*-1, *cis-cis*-2, *cis-trans*-2-decalyl *p*-toluenesulfonate were measured at several temperatures. The results are given in Table I. Straight-line relationships between the rate constants and reciprocal of the absolute temperatures were obtained.

The rates of acetolysis of the *cis*-decalyl derivatives were found to be always faster than those of the *trans*-decalyl derivatives. The rate acceleration in the *cis*-decalyl system appears to be due to 1, 3-diaxial interaction, consisting of a strain between ring A and B (Table II).

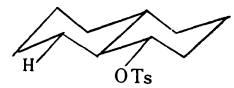
To provide further evidence, the products formed in the acetolysis of the *p*-toluenesulfonates were determined and the results are summarized in Table III. The acetolysis of *cis-cis*-1-decalyl *p*-toluenesulfonate yielded—octalin as the principal product. The olefin obtained gave only the white nitroso chloride, m. p. 138°C (decomp.), of $\Delta^{1,9}$-octalin[5] by treatment with amyl nitrite and concentrated hydrochloric acid. The olefin was also identified by the infrared and ultraviolet absorption spectra* (Figs. 1 and 2).

On the other hand, *cis-cis*-2-decalyl *p*-toluenesulfonate gave 80% of an olefin which was identified to be disubstituted by the ultraviolet absorption spectrum, Fig. 2 and 20% of acetate. The rate of acetolysis of *cis-cis*-1-decalyl *p*-toluenesulfonate is expected to be comparable to that of *trans-trans*-1-decalyl *p*-toluenesulfonate as illustrated in IV and V.




IV
*cis-cis*-1-Decalyl tosylate
70

:




V
*trans-trans*-1-Decalyl tosylate
1

However, the rate of the former was found to be 70 times faster than that of the latter. This marked difference in reactivity would then be ascribed to characteristics inherent to the ring systems or their conformation, since it has been known that *cis*-decalin is less stable than the *trans*-decalin by 2.2 kcal./mol.[3]. It would then be reasonable to suppose that the 1, 3-diaxial interaction present in the ground state of *cis*-decalin ring system is responsible for the exceedingly fast rate of the *cis*-decalyl derivatives. The mechanism involved contains obviously a weakening of the strain in the course of attaining the transition state by loosening the carbon-hydrogen bond at $C_9$ with simultaneous formation of a partial double bond between $C_1$ and $C_9$. This decrease in strain is due to a displacement of $C_9$ from the axial to the equatorial position with respect to the A ring as shown in

5) A. C. Cope and G. Holzman, *J. Am. Chem. Soc.*, **72**, 3062 (1952).

* An olefin obtained from an acetolysis of *trans-cis*-1-decalyl *p*-toluenesulfonate showed exactly the same infrared and ultraviolet absorption spectra as those of the olefin obtained in this study.

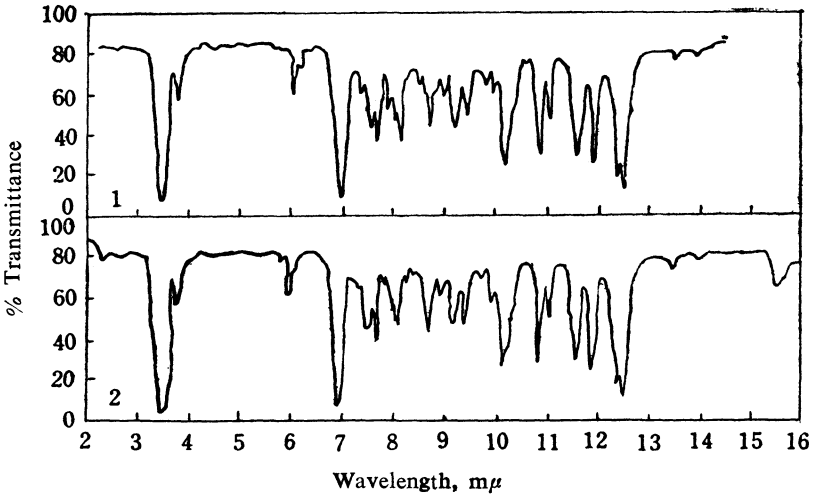



Fig. 1. ------ Infrared absorption spectra; curve 1, the olefin obtained on the acetolysis of *cis-cis*-1-decalyl *p*-toluenesulfonate; curve 2, $\Delta^{1,9}$-octalin[6].

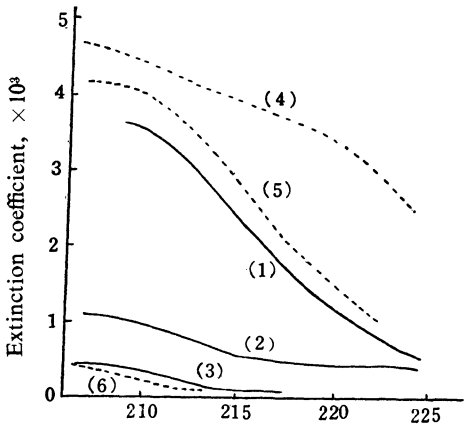
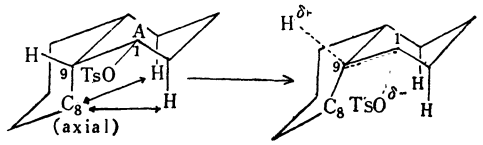



Fig. 2. Ultraviolet absorption spectra; curve 1, the olefin obtained on the acetolysis of *cis-cis*-1-decalyl *p*-toluenesulfonate; curve 2, the olefin obtained on the acetolysis of *cis-trans*-1-decalyl *p*-toluenesulfonate; curve 3, the olefin obtained on the acetolysis of *cis-cis*-2-decalyl *p*-toluenesulfonate; curve 4, tetrasubstituted olefin[7]; curve 5, trisubstituted olefin (exo-double bond)[7]; curve 6, disubstituted olefin[7].




VI
*cis-cis*-1-Decalyl tosylate
(more strained)

VII
(transition state)
(less strained)

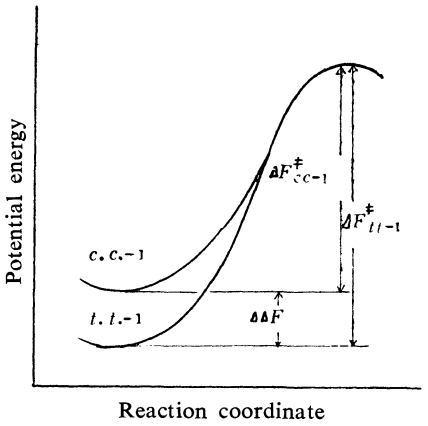



Fig. 3

VI and VII. Supposing the conformation of the transition state of *trans-trans*-1- to be similar to that of *cis-cis*-1-, the free energy of activation which controls reactivity can be represented as shown in Fig. 3, in which $\Delta F^{\ddagger}_{cc-1}$ indicates the free energy of activation for *cis-cis*-1- and $\Delta F^{\ddagger}_{tt-1}$ for *trans-trans*-1-decalyl *p*-toluenesulfonate. The energy difference between *cis*- and *trans*-decalin in the ground state would then be $\Delta\Delta F$. Thus *cis-cis*-1-decalyl *p*-toluenesulfonate should contain less free energy of activation than does the *trans-trans*-1-decalyl *p*-toluenesulfonate by $\Delta\Delta F$ indicating a higher reactivity of the former.

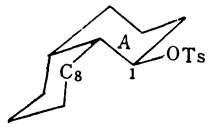
This rate-accelerating factor participates only in the elimination reaction. In other words, the rate-accelerating factor is operating only when $\Delta^{1,9}$-octalin is formed as a result of the cleavage of the *cis*-decalin ring. Our result that the acetolysis of *cis-cis*-1-1-decalyl *p*-toluenesulfonate yielded only $\Delta^{1,9}$-octalin is

6) A. C. Cope, R. J. Cotter and G. G. Roller, *J. Am. Chem. Soc.*, 77, 3594 (1955).
7) P. Bladon, H. B. Henbest and G. W. Wood, *J. Chem. Soc.*, 1952, 2737.

well in accord with the interpretation based on the above consideration.

*cis-trans*-1-Decalyl *p*-toluenesulfonate, an epimer of *cis-cis*-decalyl *p*-toluenesulfonate, was found to be less reactive than the *cis-cis*-1-decalyl derivative, the former being 17 times less reactive than the latter.

The preferred conformation of the *cis-trans*-1-decalyl derivative is represented by VIII and it will be seen that the $C_8$ is in the equatorial position with respect to ring A*). Accordingly,

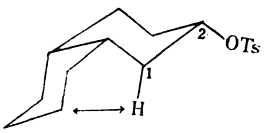



VIII
*cis-trans*-1-Decalyl tosylate

in the transition state a partial double bond should be formed between $C_1$ and $C_9$, in conformity with the explanation given for the *cis-cis*-1-decalyl derivative. But the decrease of the strain of the *cis*-decalin ring will be expected to be much smaller than that observed with the *cis-cis*-1-decalyl derivative. Thus, the contribution of strain in the acceleration of the reaction rate would be exceedingly small. This prediction was well supported by our experimental results, which showed that reactivity of *cis-trans*-1-decalyl *p*-toluenesulfonate was smaller than that of *cis-cis*-1-decalyl *p*-toluenesulfonate but greater than that of *trans-trans*-1-decalyl *p*-toluenesulfonate by a factor of 3.9, and that the olefin obtained in 80% yield consisted of a mixture of tri- and disubstituted octalin instead of trisubstituted $\Delta^{1,9}$-octalin as a major product (Fig. 2).

The distance between the carbon atom at the reaction center and the site of the ring fusion at $C_9$-$C_{10}$ in the *cis*-2-decalyl derivatives is not sufficiently small to affect their reaction rates, as observed with the 1-decalyl derivatives, but strains of the type we have proposed are considered to participate in giving higher reactivities compared with the *trans-cis*-2-decalyl derivative (2-equatorial).

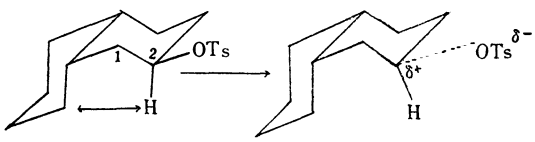
The preferred conformation of the *cis-cis*-2-decalyl *p*-toluenesulfonate shows that the hydrogen in the axial position at $C_1$ or $C_3$ is involved in giving rise to 1, 3-diaxial interaction. In the transition state, there will be a decrease in strain by partial breaking away of the hydrogen in the axial on either $C_1$ or $C_3$ after having formed a partial double bond between $C_1$ and $C_2$ or $C_3$. This requires less free energy of activation and consequently *cis-cis*-2-decalyl *p*-toluenesulfonate is expected to be more reactive than *trans-cis*-2-decalyl *p*-toluenesulfonate with which no such situation is possible. The prediction is well supported




IX
*cis-cis*-2-Decalyl tosylate
(more strained)

by the results that *trans-cis*-2-decalyl *p*-toluenesulfonate gives the olefin in only 68% while *cis-cis*-2-decalyl *p*-toluenesulfonate 80%.

Since the $C_2$ in the *cis-trans*-2-decalyl *p*-toluenesulfonate molecule, represented by X as the preferred conformation, takes a planar structure in the transition state in both the




X
*cis-trans*-2-Decalyl tosylate (more strained)

XI
(transition state)
(less strained)

substitution and elimination reactions, a decrease of 1, 3-diaxial interaction which has been present in the ground state would be expected, resulting in the increased reactivity. This is well demonstrated by the results of the kinetic studies; the *cis-trans*-2-decalyl derivative is 4.3 and 1.4 times more reactive than *trans-cis*-2-decalyl *p*-toluenesulfonate (2-equatorial) and *trans-trans*-decalyl *p*-toluenesulfonate (2-axial), respectively.

The present study with the *cis*-decalyl *p*-toluenesulfonates and the previous one with the *trans*-decalyl sulfonates point to the fact that 1, 3-diaxial arrangement, rather than the nature of the atoms or groups, is important in giving rise to strain. The data presented here and the foregoing discussion have provided further evidence to support the importance of 1, 3-diaxial interaction in controlling reactivities of the conformational isomers of the decalin derivatives.

## Experimental

**Materials.** — *cis-cis-1-Decalol.* — α-Naphthol was reduced with Raney nickel and the crystalline material formed in the reaction mixture after

* The other conformation (Ref. 2) of *cis-trans*-1-decalyl *p*-toluenesulfonate is expected to show a reactivity comparable to that of *cis-cis*-1-derivative. This is not the case however. Our results were not in agreement with this.

collection and recrystallization from petroleum ether, had m. p. 92~93°C[8].

*cis-trans-1-Decalol.*—The last fraction collected from the distillation of the reduction product of α-naphthol was distilled through a 45-cm. distilling column, under reduced pressure and the fraction boiling at 130~132°C/20 mmHg was collected. *cis-cis*-1-Decalol was removed by collecting crystalline material from a solution of the distillate in petroleum ether (50~60°C) and also crystals formed on concentrating the mother liquor. The oily filtrate weighing 6 g. was allowed to react with 5.8 g. of phthalic anhydride for 6 hr. at 135~140°C. The solid product obtained on cooling was recrystallized three times from benzene, twice from carbon tetrachloride and once from benzene, to give 7 g., m. p. 140~142°C[9].

The ester weighing 7 g. was hydrolyzed with 100 ml. of a 5% alcoholic solution of potassium hydroxide under reflux for one hour. After addition of water, it was extracted five times with 50 ml. portion of ether. The combined ether extracts were washed with water and dried over anhydrous magnesium sulfate. The ether was removed by distillation and the residue distilled to give 3 g. (83% yield), b. p. 116~117°C/20 mmHg.

*cis-cis-2-Decalol.*—A solution of 300 g. of β-naphthol in 300 ml. of ethanol was hydrogenated at 140~145°C under 200 atmospheric pressure, using 25 g. of Raney nickel as catalyst. The reaction mixture contained some crystalline material. The product was liquified by warming and the catalyst separated by filtration while warm. After cooling solution, the crystalline needles were collected and recrystallized once from alcohol and once from petroleum ether to give 80 g. of *cis-cis*-2-decalol, m. p. 104~105°C[10].

*cis-2-Decalone*[10].—To a solution of 30 g. (0.19 mol.) of *cis-cis*-2-decalol in 120 ml. of glacial acetic acid was added cautiously 15 g. (0.15 mol.) of chromium trioxide in a concentrated aqueous solution so that the temperature did not rise above 50°C. After allowing the reaction mixture to stand for two days at room temperature, it was heated on a water bath for two hours. It was cooled and a solution of 40 g. of potassium hydroxide in 200 ml. of water was added dropwise under ice cooling. The reaction mixture was extracted four times with ether and the ether solution washed with a saturated solution of sodium bicarbonate, followed by a saturated solution of sodium chloride. After drying the ether solution over anhydrous magnesium sulfate, the ether was removed and the residue distilled to give 24 g. (81% yield) of material, b. p. 124.5~125.5°C/20 mmHg, $n_D^{41}$ : 1.4945.

*cis-trans-2-Decalol*[11].—To a solution of 5.3 g. (0.035 mol.) of *cis*-2-decalone in 100 ml. ethanol was added 5 g. (0.22 mol.) of metallic sodium. When the reaction was complete, water was added and the oil which had separated was extracted five times with ether. The combined ether extracts were washed with water, dried over anhydrous magnesium sulfate, the ether removed, and the residue distilled to give 4 g. (75% yield) of material, b. p. 120~121°C/13 mmHg. After standing overnight the distillate, *cis-cis*-2-decalol in crystalline form (2.5 g.) was separated from the oil (1.5 g).

A reaction product formed by treating 4.3 g. of the oil with 4.3 g. of phthalic anhydride for six hours at 135~140°C was treated with petroleum ether to give a solid product. It was dissolved in a small amount of acetone to remove some insoluble material and the crystalline material obtained upon adding some petroleum ether was recrystallized from ethyl acetate to give 7.7 g. of the phthalate of *cis-trans*-2-decalol, m. p. 151~152°C[12].

The fraction boiling at 134~135°C/20 mmHg, 13.5 g., obtained from the reduction product of β-naphthol was treated with 13 g. of phthalic anhydride for six hours at 135~140°C. After treating the reaction product in the manner described above, 11 g. of the ester was obtained, m. p. 146~150°C.

Upon hydrolysis of the phthalic acid ester as described previously, 4.3 g. (75% yield) of the fraction boiling at 120~123°C/12 mmHg was obtained.

*cis-trans*-2-Decalyl *p*-nitrobenzoate[12] was prepared by the reaction of the fraction obtained above with *p*-nitrobenzoyl chloride in dry pyridine, m. p. 73~74.5°C.

Found : C, 67.35 ; H, 7.26 ; N, 4.49. Calcd. for $C_{17}H_{21}O_4N$ : C, 67.31 ; H, 6.98 ; N, 4.62%.

A solution of 7 g. (0.023 mol.) of the *p*-nitrobenzoate in 100 ml. anhydrous ether was added dropwise to a mixture of 3.5 g. (0.092 mol.) of lithium aluminum hydride in 50 ml. anhydrous ether and the reaction mixture refluxed for six hours. After allowing it to stand overnight, the excess hydride was decomposed by adding a small piece of ice and 100 ml. of 6 N hydrochloric acid. The ether layer was separated, washed with water, and dried over anhydrous magnesium sulfate. After removing the ether, the residue was distilled to give 3 g. (84% yield) of material, b. p. 121~123°C/12 mmHg.

*cis-Decalyl p-Toluenesulfonates*[4]. — The method employed was identical with that described for the preparation of the *trans*-decalyl *p*-toluenesulfonates. However, for the preparation of *cis-cis*-2-decalyl *p*-toluenesulfonate, it was found necessary to use 1.5 mol. equivalent of *p*-toluenesulfonyl chloride for one mole of the decalol in order to obtain a pure product. *cis-cis*-1-Decalyl *p*-toluenesulfonate was found to be very unstable and the analytical results obtained did not check closely with the calculated values, but the melting point of the decalol and the *p*-toluenesulfonate were in good agreement with those reported.

*cis-trans*-1-Decalyl *p*-toluenesulfonate was purified by recrystallizing from methanol to remove *cis-cis*-1-decalyl-*p*-toluenesulfonate, which was readily

8) W. Hückel and E. Brinkmann, *Ann.*, **441**, 21 (1925).
9) W. Hückel, R. Danneel, A. Gross and H. Naab, ibid., **502**, 99 (1933).
10) W. Hückel, *Nach. Ges. Wiss. Göttingen Math.-Phys. Klasse*, 1923, No. 1, 43-56; W. Hückel and R. Mentzel, *Ann.*, **441**, 8 (1925).
11) W. Hückel, R. Mentzel, E. Brinkmann and E. Kamenz, ibid., **451**, 109 (1926).
12) W. Hückel and K. Kumetat, *Ber.*, **67**, 1890 (1934).

decomposed by this treatment. Other *p*-toluenesulfonates were recrystallized from petroleum ether of appropriate boiling point.

The melting points and analytical results of the *cis*-decalyl *p*-toluenesulfonates prepared are given in Table IV.

TABLE IV. THE MELTING POINTS AND ANALYTICAL DATA OF THE *cis*-DECALYL *p*-TOLUENESULFONATES

| Decalyl *p*-toluenesulfonate | M. p.[3], °C | Found: % | % |
|---|---|---|---|
| *cis-trans*-1 | 88~89 | C: 66.13 | H: 7.98 |
| *cis-cis*-1 | 96 | C: 65.85 | H: 7.79 |
| *cis-trans*-2 | 88~89.5 | C: 65.94 | H: 7.83 |
| *cis-cis*-2 | 76~77 | C: 66.14 | H: 8.05 |
| | | Calcd. for $C_{17}H_{24}O_3S$ | |
| | | C: 66.20 | H: 7.84 |

TABLE V. REPRESENTATIVE KINETIC DATA FOR THE ACETOLYSIS OF 0.0179 mol./l. *cis-cis*-2-DECALYL *p*-TOLUENESULFONATE WITH 0.0185 mol./l. POTASSIUM ACETATE AT 90.21°C

| Time sec. | $HClO_4$ ml. | $10^4 \cdot k_1$ $sec^{-1}$ |
|---|---|---|
| 0 | 3.661 | — |
| 600 | 2.894 | 4.24 |
| 1500 | 2.073 | 4.17 |
| 2100 | 1.644 | 4.26 |
| 2400 | 1.476 | 4.26 |
| 2700 | 1.316 | 4.30 |
| 3120 | 1.175 | 4.18 |
| 3660 | 0.963 | 4.27 |
| 4200 | 0.828 | 4.22 |
| 5520 | 0.562 | 4.32 |
| — | — | — |
| ∞ | 0.248 | |
| | Mean | 4.25±0.04 |

**Rate Measurements.**—The rate determinations were made by the procedure previously described[1]. A typical kinetic run is shown in Table V.

**Determination of the Proportion of Unsaturated Products.** — Amounts of unsaturated substances formed in the reaction were determined by the bromide-bromate method[13].

**Acetolysis of *cis-cis*-1-Decalyl *p*-Toluenesulfonate.**—Twelve grams of *cis-cis*-1-decalyl *p*-toluenesulfonate were dissolved in 290 ml. of an acetic acid solution of 14 g. of potassium acetate. This solution was warmed for fifteen minutes at 100°C on a steam bath. After cooling 250 ml. of 25% aqueous solution of sodium hydroxide was added to the above solution. The solution was extracted with ether, dried over anhydrous magnesium sulfate, the ether was removed and distilled to give 4 g. (76% yield) of material, b.p. 84~86°C/23 mmHg. The acetate was not obtained.

One gram of this product was mixed with 3 ml. of acetic acid solution of two grams of isoamyl nitrite. Cooling the solution, 2 ml. of concentrated hydrochloric acid was added dropwise with swirling. The white precipitate was separated by filtration and washed with a few milliliters of acetone. The residual white nitrosochloride of $\Delta^{1,9}$-octalin (0.9 g.) had 128~130°C (decomp.)[14]. Two recrystallizations of this white nitrosochloride from acetone gave an analytically pure substance, 138°C (decomp.)[14]. The blue nitrosochloride of $\Delta^{1,9}$-octalin was not obtained from the acetone filtrate.

Found: C, 59.16; H, 7.88; N, 6.98. Calcd. for $C_{10}H_{16}NOCl$: C, 59.55; H, 8.00; N, 6.95%.

This work was supported partly by the grant in aid provided by the Ministry of Education and we express our gratitude.

*The Institute of Scientific ana Industrial Research*
*Osaka University*
*Sakai, Osaka*

13) J. D. Roberts and V. C. Chambers, *J. Am. Chem. Soc.*, 73, 5039 (1951); H. G. Lucas and D. Pressman, *Ind. Eng. Chem., Anal. Ed.*, 10, 140 (1938).
14) R. A. Bendeser, R. E. Robinson, D. M. Sauve and O. H. Thomas, *J. Am. Chem. Soc.*, 77, 3230 (1955).

# SHORT COMMUNICATIONS

## *The Polymerization of Vinyl Acetate Catalyzed by Iodine*

By Kozo HIROTA and Fukuo TAKEMURA

(Received July 12, 1961)

Recently it was reported by the present authors[1] that $\alpha$-methylstyrene ($\alpha$MS) could be polymerized with iodine, making an example of iodine-catalyzed high-polymerization in addition to vinylether[2]. Now, it has been confirmed that vinyl acetate (VAc) also belongs to another monomer of this kind. Since the polymerization of this monomer, however, is slightly different from those of $\alpha$MS and vinylether, and moreover, the peculiar behavior of iodine in polymerizing VAc was not mentioned at all by Bartlett et al.[3] who studied rather the role of iodine as inhibitor at its low concentration, essential points of this reaction will be reported.

Vinyl acetate was sealed in glass tubes together with iodine after degassed and dehydrated. The reaction was carried out at room temperature by shaking the tubes, because the reaction system remained heterogeneous in the case of a large amount of iodine. Besides the increase of viscosity the polymerization could be recognized by gradual precipitation of deep violet substance on the wall from the solution, but the precipitation did not occur so rapidly, e. g. it occurred after a day in the solution of 9 wt.% iodine. Such a tendency of separating colored "polymers" was not observed in the case of $\alpha$MS, where the polymers could be separated by the addition of methanol. Conversions of the monomer obtained at 160 hr. are plotted against the initial concentration of iodine in Fig. 1. Iodine begins to exhibit its polymerizing power at the concentration of 1 wt.% as suggested by the shape of the curve and this fact agrees with the finding of Bartlett and Kwait[3] as mentioned above.

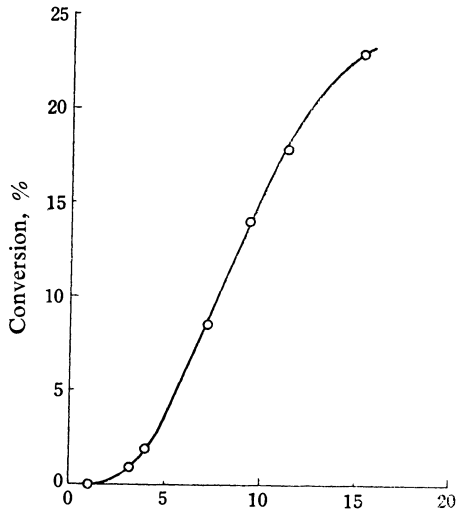



Fig. 1. Conversion of vinyl acetate to the insoluble polymer against the concentration of iodine.

The polymer is hard, brittle and amorphous, according to the X-ray pattern. It does not melt below 310°C. Iodine content is about 14~18%, though the concentration of iodine in the solution is varied from 4~15%. Infrared spectrum of the polymer shows that this polymer includes carbonyl and methyl groups. It is insoluble in ordinary organic solvents*, and hardly soluble even in aqueous potassium iodide solution at 80°C, suggesting that iodine is firmly occluded or bonded to the polymer. The molecular weight therefore can not be determined yet. This result presents a sharp contrast to the case of vinylether. According to preliminary measurement, this polymer seems to have specific resistance of about the order of $10^8$~$10^9$ ohm/cm.

We express our sincere thanks to Dr. Kenji Osaki of the Physical Department for the

1) K. Hirota, G. Meshitsuka, F. Takemura and T. Tanaka, This Bulletin, 33, 1316 (1960).
2) D. D. Eley and A. W. Richard, *Trans. Faraday Soc.*, 45, 425 (1949).
3) P. D. Bartlett and H. Kwait, *J. Am. Chem. Soc.*, 72, 1051 (1950).

* Besides the main polymer as described, a small amount of polymerized product which was soluble in petroleum benzine could be obtained.

X-ray measurement of the samples, and also to Mrs. Kiyoko Kishi for the help of the experiment.

*Department of Chemistry*
*Faculty of Science*
*Osaka University*
*Nakanoshima, Osaka*
(*K. H.*)

*Department of Chemistry*
*Faculty of Science*
*Nara Women's University*
*Nara*
(*F. T.*)

## *On the Formation of Benzoin by the Reaction of Carbon Monoxide with Organometallic Compounds**

By Membo RYANG and Shigeru TSUTSUMI

(Received July 20, 1961)

In the previous papers, the present authors reported that the reaction of carbon monoxide with organometallic compounds produced a coordinate complex as an intermediate, followed by the formation of the carbon monoxide adducts A.

$$RM+CO \longrightarrow (\text{Coordinate complex}) \longrightarrow R\text{-}\underset{\underset{O}{\|}}{C}\text{-}M$$

where M=MgX[1], Li[2], Na[3]. (A)

The adduct A is reactive and further reacts with excess of organometallic compounds, producing various reaction products, in which included acyloin, the dimerization product of the adducts A.

$$2\ R\underset{\underset{O}{\|}}{C}\text{-}M \longrightarrow 2\ R\text{-}\underset{\cdot\cdot}{C}\text{-}OM \longrightarrow$$

$$R\text{-}\underset{\underset{M}{|}}{\overset{\overset{O}{|}}{C}}\!=\!\underset{\underset{M}{|}}{\overset{\overset{O}{|}}{C}}\text{-}R \longrightarrow R\text{-}\underset{\underset{O}{\|}}{C}\text{-}\underset{\underset{OH}{|}}{CH}\text{-}R \qquad (1)$$

Fisher and Stoffers already reported the formation of acyloin by the reaction of carbon monoxide with Grignard reagents at high temperature and elevated pressure[4].

This report deals with an attempt to prepare acyloin under more mild conditions and it was found that, in the reaction of carbon monoxide with phenylmagnesium bromide in ethyl ether solution at −35°C, the addition of cobalt(II) chloride led to the formation of benzoin as a main product (Table run 3).

TABLE. THE REACTION OF CARBON MONOXIDE WITH PHENYLMAGNESIUM BROMIDE IN THE PRESENCE OF COBALT(II) CHLORIDE

| | Temp. °C | Time hr. | Theoretical yields of products, % | | | |
|---|---|---|---|---|---|---|
| | | | Diphenyl | Benzoin | Benzophenone | Triphenylcarbinol |
| 1. | −10 | 1 | 80 | trace | 5.5 | trace |
| 2. | −25 | 2 | 44.2 | 12.5 | 22 | 12 |
| 3. | −35 | 2 | 30 | 35 | trace | 5 |

On the other hand, the absence of cobalt(II) chloride under the same conditions gave a very poor yield.

From the above results, it is considered that although phenylcobalt chloride, which is formed by the reaction of phenylmagnesium bromide with cobalt(II) chloride (Eq. 2), is unstable, it reacts with carbon monoxide at low temperature, producing benzoin as a main product.

$$PhMgBr+CoCl_2 \longrightarrow PhCoCl+MgBrCl \qquad (2)$$

On the other hand, when reaction temperature is rather high (−10 or −20°C), phenyl radical is formed as a result of homolytic cleavage of the carbon-cobalt bond and dimerizes to diphenyl (run 1) or reacts with carbon monoxide in producing benzophenone (run 2).

$$PhCoCl \longrightarrow Ph\cdot + \cdot CoCl$$

$$2\ Ph\cdot \longrightarrow Ph\text{-}Ph$$

$$2\ Ph\cdot + CO \longrightarrow Ph\text{-}\underset{\underset{O}{\|}}{C}\text{-}Ph$$

Furthermore, in the reaction of carbon monoxide with phenyl potassium, which is prepared by the reaction of anisole with metallic potassium in pentane solution, benzoin (25%), benzhydrol (2.3%), benzoic acid (4%) and benzaldehyde (trace) are produced.

All these results mentioned above seem to support the opinion that, in the reaction of carbon monoxide with organometallic compounds, the carbon monoxide adduct A is formed and dimerizes to acyloin or further reacts with excess of organometallic compounds, producing various reaction products.

*Department of Chemical Technology*
*Faculty of Engineering*
*Osaka University*
*Miyakojima-ku, Osaka*

---

* Presented at the 14th Annual Meeting of the Chemical Society of Japan, Tokyo, April, 1961.

1) M. Ryang and S. Tsutsumi, *J. Chem. Soc. Japan, Pure Chem. Sec. (Nippon Kagaku Zasshi)*, **82**, 878 (1961).

2) M. Ryang and S. Tsutsumi, ibid., **82**, 880 (1961).

3) M. Ryang and S. Tsutsumi, ibid., in press; M. Ryang and S. Tsutsumi, *Tech. Rep. Osaka Univ.*, **11**, 181 (1961).

4) F. G. Fisher and O. Stoflers, *Ann.*, **500**, 253 (1930).

## *A Novel Resin Spot Test for Copper(II) Using a Chelating Resin**,[1]

By Masatoshi FUJIMOTO

(Received August 10, 1961)

"Resin spot test[2]" has proved its widespread utilities by many interesting works of the present author and other chemists[3]. This sensitive test is based mainly on the intense coloration of a few grains of light-colored ion exchangers by the up-take of trace amounts of colored substances from outer solution phase, and are easily attained much higher sensitivities as compared with those of ordinary spot test[4].

In this communication the author suggests a new possibility to lend high selectivities to the resin spot tests through applications of a sort of special resins having chelate-forming groups as functional groups. The resin used here is "Dowex A-1 Chelating Resin", a resin of styrene-divinylbenzene basis with imino-diacetate group, whicih adsorbs preferentially palladium(II) and copper(II) at about pH 5[5].

The commercial resin supplied as sodium form, 50—100 mesh, was packed in a column, converted into ammonium form via free-acid form, washed with de-ionized water, and dried at room temperature. A buffer solution of pH

TABLE I

| Ion | Coloration[a] | Limiting proportion[b], Cu(II) ($\mu$g): Foreign ion ($\mu$g) | | Ion | Coloration | Limiting proportion, Cu(II) ($\mu$g): Foreign ion ($\mu$g) | |
|---|---|---|---|---|---|---|---|
| Ti(V) | cl(W↓) | 1.4 : 42 | (1 : 63)[c] | Zn(II) | cl(cl) | 0.4 : 800 | (0.5 : 600) |
| V(IV) | lmYe(Ol) | 1 : 20− | (0.4 : 64) | Cd(II) | cl(cl) | 0.4 : 800+ | (0.4 : 800+) |
| Cr(III) | blPu(dlGry) | 1 : 2† | (1.8 : 2.2) | Hg(II) | cl(cl) | 1 : 390 | (1 : 390−) |
| Cr(VI) | yeGry(Ol) | 0.4 : 32† | (1.4 : 13) | Al(III) | cl(cl) | 0.5 : 1400+ | (1 : 1000−) |
| Mn(II) | cl(cl) | 1 : 900 | (0.5 : 1300) | Ga(III) | cl(cl) | 0.7 : 530 | (0.7 : 530) |
| Fe(III) | dlOr(cl) | 0.7 : 27− | (1 : 540) | In(III) | cl(cl) | 0.3 : 330 | (0.5 : 290) |
| Co(II) | puRe(cl) | 0.4 : 180† | (0.4 : 180†) | Tl(I) | cl(cl) | 0.3 : 680 | (0.3 : 680) |
| Ni(II) | plGrn(cl) | 1.4 : 8 | (0.2 : 21) | Ge(IV) | cl(cl) | 0.4 : 90+ | (0.4 : 90+) |
| **Cu(II)** | **ltgrnBl(ltgrnBl)** | **0.2** | **(0.2)** | Sn(II) | cl(cl) | 1 : 800+[d] | (——) |
| Zr(IV) | cl(W↓) | 0.4 : 580+ | (0.4 : 580+) | Pb(II) | cl(W↓) | 0.4 : 2000+ | (1 : 1250) |
| Mo(VI) | cl(cl) | 0.2 : 720+ | (0.2 : 720+) | Sb(III) | W↓(W↓) | 1.3 : 70+†† | (1.6 : 40) |
| Pd(II) | YeOc(YeOc) | 1.6 : 48† | (1.8 : 24−) | Bi(III) | W↓(W↓) | 1.3 : 760+†† | (1.6 : 460+) |
| Ag(I) | cl(ltYe) | 1 : 400+† | (0.7 : 520) | Te(IV) | cl(cl) | 1.4 : 27 | (1.2 : 32) |
| W(VI) | cl(cl) | 0.7 : 275+ | (0.7 : 275+) | Mg(II) | cl(cl) | 0.2 : 1800 | (0.4 : 1600) |
| Pt(IV) | ltYe↓(ltYe↓) | 0.7 : 200+ | (0.7 : 200+) | Ca(II) | cl(cl) | 0.25 : 1420+ | (0.4 : 1300+) |
| Au(III) | dlreOr↓(ltReYe↓) | 1.6 : 67 | (1.6 : 67) | Sr(II) | cl(cl) | 0.3 : 3000 | (0.4 : 2800) |
| Th(IV) | cl(cl↓) | 0.7 : 270 | (1.2 : 160+) | Ba(II) | cl(cl) | 0.4 : 1140+ | (1 : 720+) |
| U(VI) | lmYe(plYe) | 0.2 : 360 | (0.4 : 320) | | | | |

a Coloration of the resin beads after about an hour caused by the large amounts of foreign ion only. Color code: bl, bluish; Bl, blue; cl, colorless; dl, dull; grn, greenish; Grn, green; Gry, gray; lm, lemon; lt, light; Oc, ocre; Ol, olive; Or, orange; pl, pale; pu, purplish; Pu, purple; re, reddish; Re, red; W, white; ye, yellowish; Ye, yellow. ↓ shows the precipitation on the resin beads.

b + : The limiting proportion was improved with the lapse of time. − : The limiting proportion was rather lowered with time. † : The color at the very edge of the resin beads was observed. †† : A drop of supernatant solution after mixing each one drop of the buffer solution and the test solution was subjected to the test.

c In parentheses are shown the articles in the case, when after about 10 min. a drop of 1 F phosphoric acid is added.

d This value of limiting proportion was obtained only after being kept overnight in a moist chamber.

* Microanalysis with the Aid of Ion-exchange Resins. XVII.

1) Part XVI of the Series: M. Fujimoto, This Bulletin, 33, 864 (1960).

2) M. Fujimoto, ibid., 30, 283 (1957).

3) M. Fujimoto, *Chemist-Analyst*, 49, 4 (1960).

4) M. Fujimoto, This Bulletin, 29, 600 (1956).

5) W. I. Childs, "Properties of a Chelating Resin", Preprint of a paper from 135th Meeting, American Chemical Society, Boston, Mass., April, 1959; "Dowex A-1 Chelating Resin", Brochure of The Dow Chemical Company, Code No. 164—80 (1959), p. 2.

TABLE II

| Time after mixing | | 10 min. | 20 min. | 3 hr. | 2 d. |
|---|---|---|---|---|---|
| Limit of identification for copper(II) in $\mu$g. by | Resin spot test | 0.8 | 0.4 | 0.16 | 0.1 |
| | Resin centrifuge method | 0.2 | — | — | 0.2 |

4.7 was prepared from 1 F acetic acid and 1 F ammonium acetate.

In Table I are shown colorations of the resin beads with diverse metal ions under various conditions. In some cases the coloration in the resin beads for copper(II) was found to be rather improved in a slightly acid medium added with phosphoric acid. The following procedure was thus proposed for the specific detection of minute amount of copper(II) with the chelating resin without any specific reagents added.

In a depression of a white spot plate mix a few grains of Dowex A-1 Chelating Resin in the ammonium form with a drop (0.04 ml.) of the 1 F acetate buffer of pH 4.7. (Minute amount of tiny resin beads can easily be added in the depression only by touching a clean tip of a thin glass rod with the resin beads in a reservoir and by tapping gently the rim of the deppression with the tip portion of the rod). After a few minutes, add a drop of the test solution and allow to stand for about ten minutes. Then observe a more or less intense yellowish green to light greenish blue color developed in the *edge* of the resin beads under magnification. If the beads are covered with some other colors, add a drop of 1 F phosphoric acid and again observe the change in color at the edge of the resin beads. Since the chelate formation in the resin phase seems to be somewhat delayed, it would be desired to wait for an hour or more, preferably overnight, the spot plate being kept in a moist chamber free from any dust. It is also recommended to use the "resin centrifuge method[1]" to attain rapidly the highest sensitivity (see Table II). The time-dependency of the limit of identification for copper(II) in the present test is shown in Table II.

The influences of diverse metal ions on the present test are also summarized in Table I, in which are shown the limits of identification for copper(II) and limiting proportions in the presence of other metal ions. Further details for the proposed method will be reported elsewhere.

The author is indebted to Dr. A. J. Barnard, Jr., The J. T. Baker Chemical Company, and to Dr. J. R. Skidmore, Dow Chemical Company, for their kindness supplying him a sample of Dowex A-1 Chelating Resin and many valuable informations through the data sheet.

*Laboratory of Analytical Chemistry*
*Department of Chemistry*
*Faculty of Science*
*The University of Tokyo*
*Hongo, Tokyo*

## *Effects of High Energy Ionizing Radiation on Crystallinities of Cellulose II, III and IV*

By Hiroshi Sobue and Yoshitami Saito

(Received July 24, 1961)

Several reports of the effects of ionizing radiation on cellulose I[1] are known. In this communication, the effects of ionizing radiation on the crystalline regions of cellulose II, III and IV were reported.

We used viscose rayon as cellulose II. Cellulose III was prepared by treatments of the cellulose II in liquid ammonia at about $-78°C$ for four hours, and the ammonia was removed above $0°C$, and then the sample was dried at room temperature. Cellulose IV was made from cellulose II by treatments in glycerin at $260\sim265°C$ for one hour, then glycerin was washed off with ethanol and then the sample was dried in vacuo.

The samples were wrapped with aluminum foil and irradiated, cooling at about $-78°C$ with dry ice, by electron beam from a van de Graaff till total dosages were attained to $10^7$, $5\times10^7$, $10^8$ and $3\times10^8$ rad.

The crystallinities of the samples were determined by acid hydrolysis method and also by X-ray diffraction method, estimating the crystallinity by the ratio of crystalline diffraction areas to total diffraction areas (Hermans method[2]).

1) R. E. Glegg and Z. I. Kertesz, *J. Polymer Sci.*, **26**, 289 (1957); F. A. Blouin and J. C. Arthur, *Text. Res. J.*, **28**, 198 (1958); Y. Shinohara and H. Tanzawa, High Polymer Chemistry Meeting of Japan, November, 1958.

2) P. H. Hermans and A. Weiding, *J. Polymer Sci.*, **4**, 135 (1949).

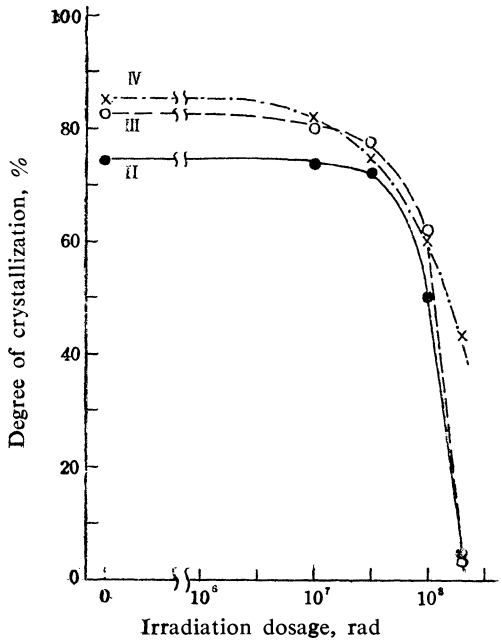



Fig. 1. The relationship between irradiation dosage and crystallinities by acid hydrolysis of celluloses.

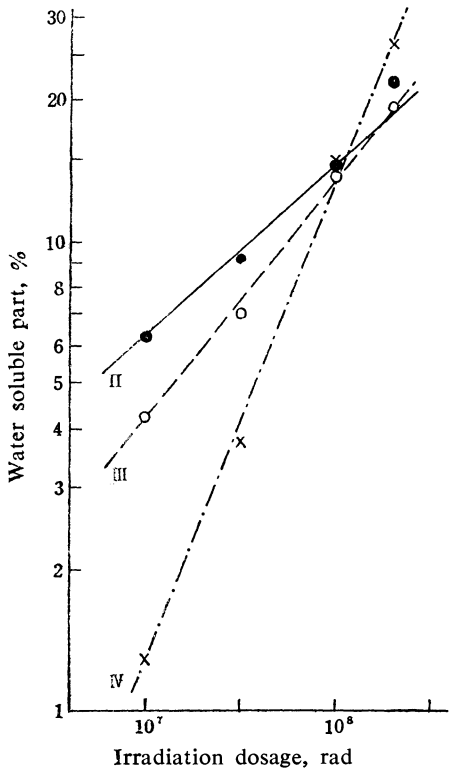



Fig. 2. The relationship between irradiation dosage and water soluble parts of celluloses.

The relationship between dosage and crystallinties by acid hydrolysis of celluloses is shown in Fig. 1. By the irradiation up to $5\times10^7$ rad, the decrease of crystalline regions is not observed for all celluloses. But by the irradiation of above $5\times10^7$ rad, in all types of celluloses remarkable lowering of crystallinities was observed.

The relationship between dosage and crystallinities by X-ray diffraction method is illustrated in Table I. There are not remarkable differences between X-ray diffractive crystallinities of unirradiated samples and those of samples irradiated with $10^7\sim3\times10^8$ rad.

Thus, the crystallinities of these celluloses are quite different depending on the measuring methods. The reason is explained as follows; large crystallites in the samples are degraded into small ones by the irradiation, but total crystalline areas determined by X-ray diffraction almost do not change. However, the velocity of acid hydrolysis becomes much greater as the crystallites are smaller.

TABLE I

| Radiation Dose (rad) | Crystallinities by X-ray diffraction method, % | | |
|---|---|---|---|
| | Cellulose II | Cellulose III | Cellulose IV |
| Unirradiated | 62.9 | 73.5 | 62.7 |
| $10^7$ | 62.0 | 78.1 | 63.2 |
| $5\times10^7$ | 62.2 | 65.0 | 64.2 |
| $10^8$ | 61.7 | 65·8 | 59.9 |
| $3\times10^8$ | 61.7 | 62.5 | 59.0 |

In Fig. 2, plots of water-soluble parts of celluloses versus dosage are shown. For each cellulose, the water soluble part increases rapidly by irradiation of above $10^8$ rad. Saeman et al.[3] reported that almost all parts of cotton linter become water soluble by $5\times10^8$ roentgen of Cathode ray in the Resonant-Transformer. From these results it is clear that cellulose is degraded to lower molecular weight substance by $3\sim5\times10^8$ rad.

*Department of Applied Chemistry*
*Faculty of Engineering*
*The University of Tokyo*
*Hongo, Tokyo*

3) J. F. Saeman, M. A. Millett and E. J. Lawton, *Ind. Eng. Chem.*, **44**, 2848 (1952).

## *Transformation of Swertiamarin to Gentiopicrin. The Structure of Gentiopicrin*

By Takashi KUBOTA and Yutaka TOMITA

(Received July 17, 1961)

In a preceding communication, it was reported that swertiamarin, the bitter component of *Swertia japonica* Makino, is represented by structure I[1], and that dehydration of the tertiary hydroxyl group of swertiamarin acetate (II) with potassium bisulfate and acetic anhydride affords monoanhydroswertiamarin acetate, $C_{24}H_{28}O_{13}$ (III), m. p. 143~144°C which shows bands in its ultraviolet absorption spectrum at 246 mμ log ε 3.44 and 269 μ log ε 3.37[1].

However, on further purification by chromatography and by recrystallization the melting point of II was raised to 151~152°C (IIIA), and the ultraviolet absorption spectrum showed a band at $\lambda_{max}$ 245 mμ log ε 3.65 and no band at 269 mμ. On the other hand, II treated with $BF_3$ in AcOH at low temperature for 3 hr. afforded a dehydrated product (IIIB) as colorless plates, m. p. 137~138°C. The ultraviolet absorption spectrum showed a band only at 270 mμ log ε 3.8 and none at 246 mμ. Therefore, the monoanhydroswertiamarin acetate (III) described in the previous paper[1] is a mixture of IIIA and IIIB and from the ultraviolet absorption spectra the following formulae are given for IIIA and IIIB respectively. (Fig. 1). The fact that a greater amount of IIIA is produced by the dehydration reaction with potassium bisulfate than the more stable triene type isomer IIIB, indicates the relationship between the hydroxyl group at $C_4$ and the hydrogen atom at $C_5$ to be in cis to each other. In the case of the dehydration reaction with $BF_3$, double bond migration of IIIA occurs by the action of $BF_3$ and consequently II gives the stable IIIB.

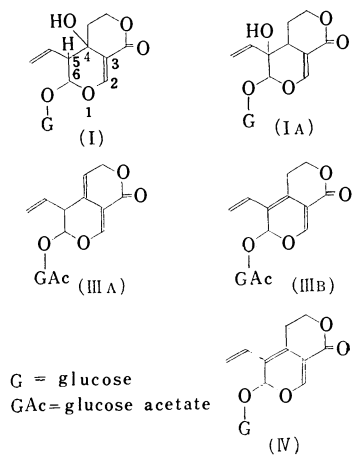



Fig. 1

The infrared absorption spectrum of IIIA shows a band at 12.2 μ which is due to the tri-substituted double bond. Therefore the tertiary hydroxyl group of I must exist at $C_4$ and not at $C_5$. From these results, an alternative structure of swertiamarin IA[1] can be excluded.

In order to establish the structure of gentiopicrin a detailed study on its degradation reactions was carried out by Asahina, Asano, Tanase and Ueno[2]. On the basis of their data the several possible structures were suggested by Sakurai[3], Korte[3] and Canonica and Pelizzoni[4], respectively. Although, Canonica and Pelizzoni[5] have recently proposed the formula IV as the most probable structure for gentiopicrin, the definite evidence for its carbon skeleton is lacking in their paper. If the structure IV is correct, IIIB, a monoanhydro derivative of II should be identical with gentiopicrin acetate.

Now it has been confirmed that IIIB and the acetate, m. p. 139°C, of gentiopicrin, extracted from the root of *Gentiana scabrae*, are identical in their infrared absorption spectra.

Concerning the structure of swertiamarin, the correctness of the carbon skeleton of I has been definitely demonstrated by synthesis of erythrocentaurin[6], the hydrolysis product of swertiamarin with emulsin, and by transformation of swertiamarin to gentianin[7] as reported in the previous papers. Although several structures were suggested for gentiopicrin, the structure IV proposed by Canonica and Pelizzoni has been established to be correct from the above-mentioned results.

*Faculty of Science*
*Osaka City University*
*Kita-ku, Osaka*

1) T. Kubota and Y. Tomita, *Tetrahedron Letters*, **5**, 176 (1961).

2) Y. Asahina, J. Asano, Y. Tanase and Y. Ueno, *Ber.*, **69**, 771 (1936); Y. Asahina and Y. Sakurai, ibid., **72**, 1534 (1939).

3) F. Korte, *Chem. Ber.*, **87**, 512, 780 (1954).

4) L. Canonica and F. Pelizzoni, *Gazz. chim. ital.*, **87**, 1251 (1957).

5) L. Canonica, F. Pelizzoni, P. Manitto and G. Jomi, *Tetrahedron Letters*, **24**, 7 (1960).

6) T. Kubota, Y. Tomita and K. Suzuki, ibid., **6**, 223 (1961).

7) T. Kubota and Y. Tomita, ibid., in press.

## *Reactions of Picryl Ether with Amino Compounds*

By Kazuo SATAKE, Masaru TANAKA, Yasuharu TSUZUKIDA and Shoji SHIMA

(Received June 26, 1961)

The cleavage of phenyl ether linkage, either in acidic or alkaline medium, has been achieved only under vigorous conditions. In this respect, ammonolysis of picryl ether was proved to be an exceptional case. Picryl ether (TNP-$OC_2H_5$* m. p. 77.5~78.5°C[1]; TNP-$OC_6H_5$ m. p. 151~152°C[2]) gave picramide (m. p. 187~188°C; $\lambda_{max}$ m$\mu$ ($\varepsilon \times 10^{-4}$): 325 (1.14), 415 (0.86)) and *N*-methylpicramide (m. p. 109~110°C; $\lambda_{max}$ m$\mu$ ($\varepsilon \times 10^{-4}$): 346 (1.60) with a marked shoulder at 418 m$\mu$) only by dissolving the ether into hydrated ethanol solution of ammonia (7.5 N) and methylamine (5 N), at room temperature, respectively. The results of spectrophotometric investigation[3], as illustrated in Fig. 1, indicated that the ammonolysis of picryl ether proceeded almost immediately with quantitative yield.

The most remarkable fact was different behaviors of the both picryl ethers with dimethylamine; thus the phenyl ether gave *N*, *N*-dimethylpicramide (m. p. 137~138°C[4]; $\lambda_{max}$ m$\mu$ ($\varepsilon \times 10^{-4}$): 380 (1.38)) immediately, while the ethyl ether did not even after 24 hr. under the conditions described in Fig. 1. With the use of excess amounts of dimethylamine (Tokyo Chemical Industry Co., Ltd.; Guaranteed Reagent), there was observed some formation of *N*-methylpicramide, presumably being originated from the contaminated methylamine.

Reaction of the same type occurred in much less alkaline medium (pH 8), and not only with amine but also with amino acid. Thus equimolar mixtures of glycine and picryl ethyl ether and of proline and picryl phenyl ether in borate buffer (pH 8.0) at room temperature gave TNP-glycine (m. p. 161°C; $\lambda_{max}$ m$\mu$ ($\varepsilon \times 10^{-4}$): 340 (1.25)[5]) and TNP-proline (m. p. 164~165°C; $\lambda_{max}$ m$\mu$ ($\varepsilon \times 10^{-4}$); 362 (1.29)[5]) with excellent yield, respectively. Some typical results on the reaction in analytical scale are summarized in Fig. 2, together with those of

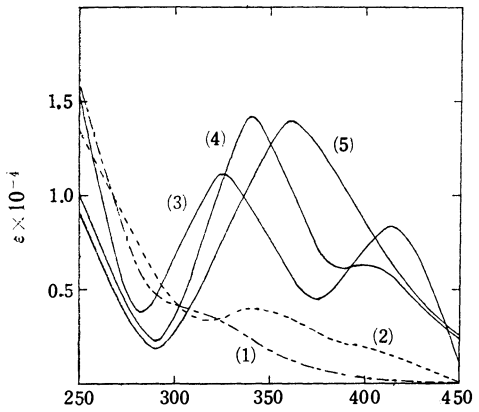



Fig. 1. Aminolysis of picryl phenyl ether (1) TNP-$OC_6H_5$ in N/10 HCl in 50% ethanol TNP-$OC_6H_5$ was previously dissolved into (2) N NaOH, (3) 7.5 N $NH_3$, (4) 5 N $CH_3NH_2$ and (5) 3.6 N $(CH_3)_2NH$, in 50% ethanol, and the mixture was acidified with HCl exactly after 1 min. Final concentrations were $1.0 \times 10^{-4}$ M in all cases. The spectra (3), (4) and (5) were just the same as those of picramide, *N*-methyl- and *N*, *N*-dimethylpicramide of $1.0 \times 10^{-4}$ M, respectively. The spectrum (2) indicated some formation of picric acid under the action of alkali.

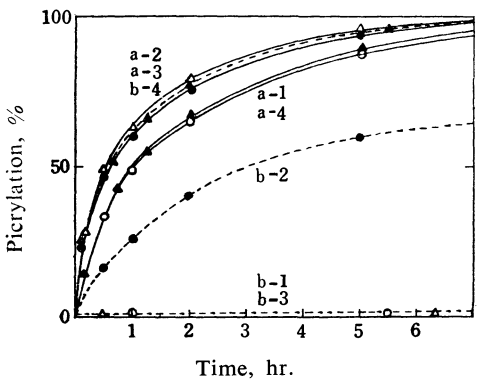



Fig. 2. Picrylation of glycine (——) and proline (----)
1) with TNP-$OC_2H_5$ (—○—)
2) with TNP-$OC_6H_5$ (—●—)
3) with TNP-$SO_3H$ (—△—)
4) with TNP-Cl (—▲—)

The initial concentrations of amino acid and picryl compounds were $1.0 \times 10^{-4}$ M in an equi-volume mixture of M/15 borate buffer (pH 8.0) and ethanol.

The picrylations of glycine (a) and proline (b) were estimated from the increment of optical density at 340 m$\mu$ and at 360 m$\mu$ respectively (see Fig. 1).

* TNP is an abbreviation for picryl (2, 4, 6-trinitrophenyl).

1) C. Willgerodt, *Ber.*, **12**, 1277 (1879).
2) C. Willgerodt, ibid., **12**, 1278 (1879).
3) The details of procedure were described in K. Satake, M. Tanaka and H. Shino, *J. Biochem.*, **50**, 6 (1961).
4) van Romburgh, *Rec. trav. chim.*, **2**, 105 (1883).

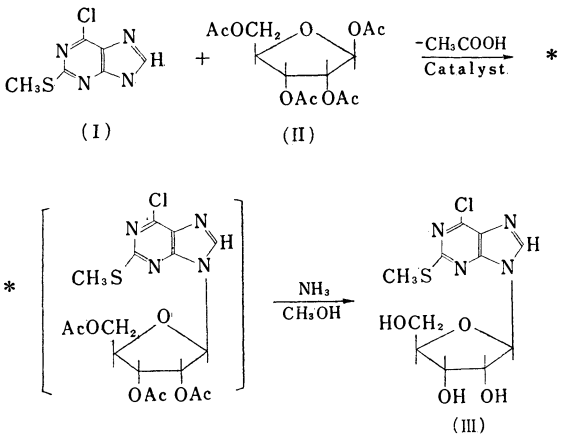
trinitrophenylations with TNP-Cl[5] and TNP-$SO_3H$[5,6] under the similar conditions.

It will be of interest that picryl ether is a powerful trinitrophenylating agent even under physiological condition. The ether as well as the chloride, a well-known trinitrophenylating reagent of protein, has been already reported to produce allergic dermatitis and to produce an antibody which reacts with TNP-protein on their repeated contact with skin[7]. The facts described in this paper will explain why picryl ether is a precursor of antigenic TNP-protein in vivo.

The details on trinitrophenylation of protein with picryl ether will be described elsewhere.

*Department of Chemistry*
*Faculty of Science*
*Tokyo Metropolitan University*
*Setagaya-ku, Tokyo*

5) T. Okuyama and K. Satake, *J. Biochem.*, **47**, 454 (1960).
6) K. Satake, T. Okuyama, M. Ohashi and T. Shinoda, ibid., **47**, 654 (1960).
7) I. A. Brownie and W. K. Cumming, *Biochem. J.*, **40**, 640 (1946); P. G. H. Gell, *Brit. J. Exptl. Path.*, **25**, 174 (1944).



## *New Catalysts for the Nucleoside Synthesis by Fusion Method*

By Yoshiharu Ishido and Tetsuo Sato

(Received June 27, 1961)

Recent studies[1] in this laboratory indicated that purine nucleosides could be synthesized merely by fusing a mixture of purine and 1-*O*-acyl sugar derivatives under reduced pressure in the presence of *p*-toluenesulfonic acid or zinc chloride. For example, the synthesis of 9-β-D-ribofuranosyl 2-methylthio-6-chloropurine (III) from 2-methylthio-6-chloropurine (I) and 1,2,3,5-tetra-*O*-acetyl-β-D-ribofuranose (II) may be formulated as follows:

For the synthesis of *O*-glycosides by the similar fusion method, various acidic catalysts have been used[2].

Recently, Helferich et al.[3] scrutinized the catalytic effect of several acids, including newly hydrochloric acid, sulfuric acid, oxalic acid and phosphoric acid, for the *O*-glycoside formation and found anhydrous methanesulfonic acid to be the most effective catalyst as far as being examined.

The present authors wish to report that anhydrous methanesulfonic acid was less effective than concentrated sulfuric acid and that concentrated phosphoric acid was almost ineffective for nucleoside (*N*-glycoside) synthesis.

7-β-D-Ribofuranosyl theophylline (VI):—To a fused mixture of an equivalent amount of theophylline (V) and II, concentrated sulfuric acid was added, and the mixture was subjected to react at 130～140°C for about ten minutes, in vacuo. The cooled reaction mixture was then dissolved into chloroform, and a small amount of unchanged V was filtered off. After neutralization of the filtrate with methanolic ammonia, the solvent was removed in vacuo to dryness, and then deacetylated with methanolic ammonia in the usual manner. The deacetylated syrup was crystallized by trituration with a small amount of ethanol and recrystallized from ethanol. IV was obtained as fine needles in 48% yield of theoreticals, m. p. 189～190°C, $[\alpha]_D^{15}+25°$ (*c* 0.50, water). This showed no depression on admixture with an authentic specimen[4]. When anhydrous methanesulfonic acid was used as a catalyst, the yield was 41% theoreticals (m. p. 182～186°C).

In the similar manner, III (in both cases of concentrated sulfuric acid and of anhydrous methanesulfonic acid, the yields were 39 and 15%

1) T. Sato, T. Simadate and Y. Ishido, *J. Chem. Soc. Japan. Pure Chem. Sec.* (*Nippon Kagaku Zasshi*), **81**, 1440 (1960); ibid., **81**, 1442 (1960); T. Simadate, Y. Ishido and T. Sato, ibid., in print, T. Simadate, ibid., in print.

2) B. Helferich and E. Schmitz-Hillebrecht, *Ber.*, **66**, 378 (1933); ibid., **67**, 1667 (1934); ibid., **68**, 790 (1935); K. Sisido, *J. Soc. Chem. Ind. Japan* (*Kōgyō Kwagaku Zasshi*), **39**, 456, 459 (1936); H. Bretschneider and K. Beran, *Monatsh.*, **80**, 262(1949); B. Helferich and D. V. Kasheliker, *Chem. Ber.*, **90**, 2094 (1957); B. Helferich and F. Eckenstein, ibid., **93**, 2467 (1960) etc.

3) B. Helferich and L. Forstoff, ibid., **94**, 158 (1961).

4) G. A. Howard, B. Lythgoe and A. R. Todd, *J. Chem. Soc.*, **1947**, 1052.

respectively), 9-β-D-ribofuranosyl 2-methythio-6-bromopurine (30.5% yield, in the former case) and 9-β(?)-D-ribofuranosyl 2-methylthio-6-iodopurine {44.8% yield, in the former, m. p. 188 ~189°C (decomp.), $[\alpha]_D^{24}$ −24.1° (*c* 0.38, 50% methanol), $\lambda_{max}$ = 237 mμ (ε = 17490), 262 mμ (ε = 14840) in water. Found: C, 31.39; H, 3.11; N, 13.35. Calcd. for $C_{11}H_{13}N_4O_4SI$: C, 31.37; H, 3.07; N, 13.21%} were obtained.

Detailed results will be published elsewhere.

The authors wish to express their deep gratitude to Mr. Kiyoshi Korida for his help in carrying out the experiment.

*Department of Organic Chemistry*
*Tokyo Institute of Technology*
*Meguro-ku, Tokyo*

# *Thermodynamical Studies on Binary Systems Consisting of Polar and Non-polar Liquids. III. Calculation of the Electrostatic Part of the Thermodynamic Excess Functions due only to the Dipole of the Polar Molecule for the Binary System Composed of Polar and Non-polar Liquids according to Onsager's Model*

By Kazuo AMAYA

(Received March 4, 1961)

In the previous paper it has been shown that in the systems containing non-aromatic non-polar components, the increase of van Laar coefficient with the decrease of the concentration of the polar component may be due to its dipole moment and that a kind of stabilizing effect exists in the systems containing aromatic non-polar components. In order to confirm the fact that such a variation of the van Laar coefficient with concentration in the former group of the systems is due to the dipoles of the polar components and to elucidate the cause of the stabilization effect in the latter group of the systems, theoretical formulas based on Onsager's model of polar liquids are derived to explain the electrostatic part of the excess thermodynamic quantities due only to the dipole of the polar component, by neglecting the effect of higher multipoles for a binary system of polar and non-polar liquids, and are applied to the actual systems for which the heats of mixing were measured.

## Derivation of Theoretical Expressions

In deriving the expressions of the electrostatic part of the thermodynamic excess functions due only to the dipole of the polar component for a binary system of polar and non-polar liquids, the following assumptions are made according to Onsager[1]:

1) The polar molecules is spherical.
2) The dipole is a point dipole and is located at the center of the molecule.
3) The medium surrounding the polar molecule is a continuous one having macroscopic isotropic dielectric constant.
4) The polarizability of the polar molecule is isotropic.

Then further the following assumption is imposed:

5) There is no volume change on mixing.

If a molecule of dipole moment $\mu$ and of polarizability $\alpha$ is placed at a cavity of radius $a$ in a medium of dielectric constant $\varepsilon$, the reaction field $R$ due to the dielectric is

$$R=\mu\cdot g \tag{1}$$

where $g$ is given by

$$g=\frac{2(\varepsilon-1)}{2\varepsilon+1-(2\alpha/a^3)(\varepsilon-1)}\cdot\frac{1}{a^3} \tag{2}$$

The electrostatic work $w$ required for the formation of a dipole $\mu$ in the medium is given by

$$w=-1/2\cdot g\cdot\mu^2 \tag{3}$$

Then according to Barker[2], the electrostatic part of the free energy of mixing $F^{\mathrm{Eel}}$, which is equal to $G^{\mathrm{Eel}}$ for a condensed system, for 1 mol. of a binary mixture in which the two components have the same molecular size and polarizability but different dipole moments $\mu_1$ and $\mu_2$, is given by

$$F^{\mathrm{Eel}}=G^{\mathrm{Eel}}=\frac{1}{2}N_{\mathrm{A}}(\mu^2{}_1-\mu^2{}_2)\times\left(x_1\int_{x_1}^{1}g\mathrm{d}x_1-x_2\int_{0}^{x_1}g\mathrm{d}x_1\right) \tag{4}$$

where $N_{\mathrm{A}}$ is the Avogadro Number, $x_1$ and $x_2$ denote the mole fraction of the components 1 and 2 respectively. For a binary solution in which one component is polar and the other is non-polar, the electrostatic part of the free energy of mixing is given by

$$G^{\mathrm{Eel}}=\frac{1}{2}N_{\mathrm{A}}\mu^2\left\{x_2\int_{x_2}^{1}g\mathrm{d}x_1-(1-x_2)\int_{0}^{x_2}g\mathrm{d}x_2\right\} \tag{5}$$

where $\mu$ denotes the dipole moment of the polar molecule, and $x_2$ the mole fraction of the polar component in the solution.

Then other thermodynamic functions may be derived from the well-known thermodynamic relations:

$$H^{\mathrm{Eel}}=G^{\mathrm{Eel}}-T\cdot\frac{\partial G^{\mathrm{Eel}}}{\partial T}$$

1) L. Onsager, *J. Am. Chem. Soc.*, **58**, 1486 (1936).

2) J. A. Barker, *Proc. Roy. Soc.*, **A219**, 367 (1953).

$$S^{\mathrm{Eel}}=-\frac{\partial G^{\mathrm{Eel}}}{\partial T}$$

and the following expressions are obtained.

$$H^{\mathrm{Eel}}=\frac{1}{2}N_{\mathrm{A}}\mu^2\left\{x_2\int_{x_2}^{1}h\mathrm{d}x_2-(1-x_2)\int_{0}^{x_2}h\mathrm{d}x_2\right\} \tag{6}$$

$$S^{\mathrm{Eel}}=\frac{1}{2}N_{\mathrm{A}}\mu^2\left\{x_2\int_{x_2}^{1}s\mathrm{d}x_2(1-x_2)\int_{0}^{x_2}s\mathrm{d}x_2\right\} \tag{7}$$

where

$$h=g-T\cdot\partial g/\partial T \tag{8}$$

and

$$s=-\partial g/\partial T \tag{9}$$

If the polarizability $\alpha$ of the polar molecule is expressed by

$$\frac{{n_2}^2-1}{{n_2}^2+2}=\frac{4}{3}\pi N\alpha \tag{10}$$

where $N$ is the number of polar molecules in a unit volume of the pure liquid and $n_2$ is the refractive index of the polar liquid, and the molar volume of the polar molecule, $V_{\mathrm{M}}$ is taken as $4/3\cdot\pi N_{\mathrm{A}}a^3$. Then $g$ is expressed as

$$g=\frac{8}{3}\pi\frac{1}{V_{\mathrm{M}}}\cdot N_{\mathrm{A}}\cdot\frac{\varepsilon(x_2)-1}{2\varepsilon(x_2)+{n_2}^2}\cdot\frac{{n_2}^2+2}{3} \tag{11}$$

For 1 mol. of solution the above quantities are given as follows.

$$G^{\mathrm{Eel}}=\frac{4}{3}\pi\frac{{N_{\mathrm{A}}}^2}{V_{\mathrm{M}}}\cdot\frac{{n_2}^2+2}{3}\mu^2\times\left\{x_2\int_{x_2}^{1}\frac{\varepsilon(x_2)-1}{2\varepsilon(x_2)+{n_2}^2}\mathrm{d}x_2-(1-x_2)\int_{0}^{x_2}\frac{\varepsilon(x_2)-1}{2\varepsilon(x_2)+{n_2}^2}\mathrm{d}x_2\right\} \tag{12}$$

$$H^{\mathrm{Eel}}=\frac{4}{3}\pi\frac{{N_{\mathrm{A}}}^2}{V_{\mathrm{M}}}\cdot\frac{{n_2}^2+2}{3}\mu^2\times\left\{x_2\int_{x_2}^{1}\frac{\varepsilon(x_2-1)}{2\varepsilon(x_2)+{n_2}^2}(1-A(x_2)\cdot T)\mathrm{d}x_2-(1-x_2)\int_{0}^{x_2}\frac{\varepsilon(x_2)-1}{2\varepsilon(x_2)+{n_2}^2}\times(1-A(x_2)\cdot T)\mathrm{d}x_2\right\} \tag{13}$$

$$S^{\mathrm{Eel}}=\frac{4}{3}\pi\frac{{N_{\mathrm{A}}}^2}{V_{\mathrm{M}}}\cdot\frac{{n_2}^2+2}{3}\mu^2\times\left\{x_2\int_{x_2}^{1}\frac{\varepsilon(x_2)-1}{2\varepsilon(x_2)+{n_2}^2}A(x_2)\mathrm{d}x_2-(1-x_2)\int_{0}^{x_2}\frac{\varepsilon(x_2)-1}{2\varepsilon(x_2)+{n_2}^2}A(x_2)\mathrm{d}x_2\right\} \tag{14}$$

where $A(x_2)$ is given by

$$A(x_2)=\frac{1}{V_{\mathrm{M}}}\frac{\mathrm{d}V_{\mathrm{M}}}{\mathrm{d}T}+\left(\frac{1}{\varepsilon(x_2)-1}-\frac{2}{2\varepsilon(x_2)+{n_2}^2}\right)\frac{\mathrm{d}\varepsilon(x_2)}{\mathrm{d}T}+\left(\frac{1}{{n_2}^2+2}-\frac{1}{2\varepsilon(x_2)+{n_2}^2}\right)2n_2\frac{\mathrm{d}n_2}{\mathrm{d}T} \tag{15}$$

which is easily derived by taking the logarithm of $g$ and differentiating it with temperature. In the above expressions the following notations are used:

$\varepsilon(x_2)$: the dielectric constant of the solution in which the mole fraction of the polar component is $x_2$,

$n_2$: the refractive index of the polar liquid,

$N_{\mathrm{A}}$: Avogadro's number,

$V_{\mathrm{M}}$: the molar volume of the polar liquid, and

$T$: absolute temperature.

## The Application of the Theory to the Actual Systems

**The Necessary Data for the Calculation.**—In applying the theory to the actual systems, it is necessary to have the numerical values of the following quantities:

1) the thermal expansion coefficient of the polar liquid,

2) the dielectric constant of the pure polar liquid, $\varepsilon_2$,

3) the temperature dependence of $\varepsilon_2$, $\mathrm{d}\varepsilon_2/\mathrm{d}T$,

4) the refractive index of the pure polar liquid, $n_2$,

5) the temperature dependence of $n_2$, $\mathrm{d}n_2/\mathrm{d}T$,

6) the density of the pure polar liquid, $d$,

7) the dipole moments of the polar component in vacuum, $\mu$,

8) the dielectric constant of the solution, $\varepsilon_{12}$, and

9) the temperature dependence of $\varepsilon_{12}$, $\mathrm{d}\varepsilon_{12}/\mathrm{d}T$.

It is preferable to use the values of these constants which are determined experimentally, but unfortunately they are not available for all the systems considered in this experiment. In fact, for 1, 2, 4, 6 and 7 the values are available for all the components, but for 3 and 5 the values are only partly available and for 8 and 9 none of the values are available for all the systems. For those which are not available in the literature, they are derived from the relevant values on reasonable assumptions or the experimental rules as described in the following.

**The Derivation of the Values of the Quantities which are not Available in the Literature.**—(1) The temperature dependence of the dielectric constant of the polar liquid. According to Onsager, the dielectric constant of a

TABLE I. PHYSICAL CONSTANTS OF THE COMPONENTS USED FOR THE CALCULATION

| Substance | Therm.exp. coeff., $\times 10^3$ per °C | Dielectric const., $\varepsilon$ | Refractive index for Na D line $n_D$ | Temp. dependence of $\varepsilon \times 10^2$ per °C | Temp. dependence of $n_D \times 10^4$ per °C | Molecular volume cc. | Dipole moment Debye unit |
|---|---|---|---|---|---|---|---|
| Chlorobenzene | 0.981 | 5.612 | 1.52211 | −1.6 | −5.4 | 101.74 | 1.70 |
| Bromobenzene | 0.887 | 5.40 | 1.55762 | −1.76* | −4.9 | 105.51 | 1.74 |
| Benzonitrile | 0.88 | 25.2 | 1.5265 | −8.7 | −3.4 | 103.50 | 4.39 |
| Nitrobenzene | 0.824 | 34.89 | 1.55057 | −18.6 | −4.0 | 103.16 | 4.21 |
| Diethyl ketone | 1.203 | 17.00 | 1.39003 | −8.43* | −4.7 | 106.40 | 2.71 |
| Methyl propyl ketone | 1.203 | 17.00 | 1.39003 | −8.43* | −4.7 | 106.40 | 2.71 |
| *n*-Butylchloride | 1.25 | 7.39 | 1.39954 | −3.24* | −5.0 | 105.73 | 2.07 |
| *n*-Butylcyanide | 1.15 | 20.3 | 1.38170 | −8.87* | −4.3 | 105.15 | 4.09 |
| Cyclohexanone | 0.947 | 18.3 | 1.44941 | −8.58* | −4.9 | 104.67 | 2.75 |
| Chlorocyclohexane | 0.949 | 7.906** | 1.46555 | −3.28* | −5.1 | 119.37 | 2.07 |
| Bromocyclohexane | 0.891 | 7.945** | 1.5020 | −3.23* | −5.2 | 124.43 | 2.15 |
| Pyridine | 1.029 | 12.3 | 1.5067 | −5.59 | −5.0 | 81.31 | 2.22 |
| *cis*-Dichloroethylene | 1.288 | 9.0 | 1.44903 | −4.45* | −6.5 | 76.17 | 1.80 |
| *trans*-Dichloroethylene | 1.67 | 2.14 | 1.4405 | −0.263* | −10.1 | 77.28 | 0 |
| Methylcyclohexane | 1.13 | 2.020 | 1.42058 | −0.16 | −5.1 | 128.38 | 0 |
| Cyclohexane | 1.197 | 2.0199 | 1.42353 | −0.16 | −5.4 | 108.09 | 0 |
| Toluene | 1.109 | 2.3661 | 1.49413 | −0.24 | −5.6 | 106.85 | 0(0.37) |
| Benzene | 1.197 | 2.284 | 1.49790 | −0.20 | −6.4 | 89.40 | 0 |
| 1,4-Dioxane | 1.34 | 2.209 | 1.42025 | −0.226* | −4.3 | 85.80 | 0 |

* Calculated according to the formula 16.
** Kindly measured by Mrs. K. Sasaki of this Institute.

TABLE II. THE CALCULATED VALUES OF THE ELECTROSTATIC PART OF THERMODYNAMIC EXCESS FUNCTIONS FOR BINARY SYSTEMS CONTAINING POLAR AND NON-AROMATIC NON-POLAR COMPONENTS

| System | $x_2$ | $G^{Eel}_{calcd}$ | $H^{Eel}_{calcd}$ | $TS^{Eel}_{calcd}$ |
|---|---|---|---|---|
| Chlorobenzene —Cyclohexane | 1.000 | 0 | 0 | 0 |
| | 0.916 | 36.8 | 58.4 | 21.6 |
| | 0.829 | 70.2 | 112.6 | 42.4 |
| | 0.743 | 97.3 | 158.4 | 61.6 |
| | 0.653 | 119.0 | 196.7 | 77.7 |
| | 0.559 | 133.6 | 224.7 | 91.1 |
| | 0.462 | 139.2 | 239.2 | 100.0 |
| | 0.360 | 133.5 | 234.9 | 101.4 |
| | 0.251 | 113.2 | 203.0 | 89.9 |
| | 0.132 | 72.1 | 131.8 | 59.7 |
| | 0 | 0 | 0 | 0 |
| Bromobenzene —Cyclohexane | 1.000 | 0 | 0 | 0 |
| | 0.914 | 38.7 | 62.5 | 23.8 |
| | 0.827 | 72.7 | 118.9 | 46.2 |
| | 0.738 | 101.7 | 168.2 | 66.5 |
| | 0.647 | 123.9 | 208.5 | 84.6 |
| | 0.553 | 138.5 | 237.3 | 98.8 |
| | 0.456 | 144.0 | 251.3 | 107.3 |
| | 0.354 | 137.9 | 245.2 | 107.3 |
| | 0.246 | 111.5 | 211.8 | 100.3 |
| | 0.130 | 70.3 | 137.5 | 67.2 |
| | 0 | 0 | 0 | 0 |

| System | $x_2$ | $G^{Eel}_{calcd}$ | $H^{Eel}_{calcd}$ | $TS^{Eel}_{calcd}$ |
|---|---|---|---|---|
| Benzonitrile —Cyclohexane | 1.000 | 0 | 0 | 0 |
| | 0.908 | 234.3 | 216.6 | −17.7 |
| | 0.816 | 452.4 | 426.4 | −26.0 |
| | 0.722 | 652.8 | 626.2 | −26.6 |
| | 0.628 | 829.2 | 812.2 | −17.0 |
| | 0.532 | 974.0 | 978.6 | 4.6 |
| | 0.435 | 1073.4 | 1113.9 | 40.5 |
| | 0.337 | 1107.3 | 1199.0 | 91.7 |
| | 0.231 | 1032.7 | 1189.0 | 156.9 |
| | 0.129 | 823.5 | 1015.8 | 192.3 |
| | 0.070 | 541.3 | 713.5 | 172.2 |
| | 0 | 0 | 0 | 0 |
| Nitrobenzene —Cyclohexane | 1.000 | 0 | 0 | 0 |
| | 0.908 | 199.9 | 130.3 | −69.6 |
| | 0.814 | 389.8 | 262.0 | −127.8 |
| | 0.720 | 566.0 | 394.4 | −171.6 |
| | 0.625 | 725.0 | 527.6 | −197.4 |
| | 0.529 | 859.2 | 658.9 | −200.3 |
| | 0.431 | 959.4 | 788.7 | −170.7 |
| | 0.333 | 1007.6 | 902.4 | −105.2 |
| | 0.232 | 970.2 | 977.3 | 7.1 |
| | 0.127 | 777.1 | 913.5 | 136.4 |
| | 0.069 | 519.6 | 719.6 | 200.0 |
| | 0 | 0 | 0 | 0 |

TABLE II. (Continued)

| System | $x_2$ | $G^{Eel}_{calcd}$ | $H^{Eel}_{calcd}$ | $TS^{Eel}_{calcd}$ |
|---|---|---|---|---|
| | 1.000 | 0 | 0 | 0 |
| | 0.910 | 59.9 | 89.2 | 29.3 |
| | 0.819 | 113.2 | 178.6 | 65.4 |
| | 0.727 | 158.6 | 259.8 | 101.2 |
| *n*-Butylchloride | 0.633 | 194.7 | 326.6 | 131.9 |
| —Cyclohexane | 0.538 | 219.9 | 378.9 | 159.0 |
| | 0.440 | 230.8 | 411.3 | 180.5 |
| | 0.340 | 223.4 | 414.3 | 190.9 |
| | 0.236 | 191.5 | 371.9 | 180.4 |
| | 0.124 | 124.0 | 254.3 | 130.3 |
| | 0 | 0 | 0 | 0 |
| | 1.000 | 0 | 0 | 0 |
| | 0.906 | 85.9 | 87.2 | 1.3 |
| | 0.811 | 165.3 | 171.9 | 6.6 |
| | 0.716 | 236.3 | 252.6 | 16.3 |
| Diethyl ketone | 0.620 | 296.9 | 327.6 | 30.7 |
| (Methyl | 0.524 | 344.1 | 384.2 | 40.1 |
| propyl ketone) | 0.427 | 373.4 | 448.1 | 74.7 |
| —Cyclohexane | 0.328 | 377.7 | 489.9 | 112.2 |
| | 0.227 | 343.9 | 470.9 | 127.0 |
| | 0.121 | 244.6 | 369.7 | 125.1 |
| | 0.064 | 152.1 | 246.9 | 94.8 |
| | 0 | 0 | 0 | 0 |
| | 1.000 | 0 | 0 | 0 |
| | 0.902 | 104.0 | 99.2 | −4.8 |
| | 0.809 | 194.7 | 190.0 | −4.7 |
| | 0.715 | 276.4 | 277.1 | 0.7 |
| | 0.620 | 346.6 | 358.8 | 12.2 |
| Cyclohexanone | 0.525 | 401.9 | 432.1 | 30.2 |
| —Cyclohexane | 0.428 | 436.8 | 491.7 | 54.9 |
| | 0.329 | 442.7 | 527.8 | 85.1 |
| | 0.227 | 403.7 | 518.4 | 114.7 |
| | 0.119 | 283.5 | 403.2 | 119.7 |
| | 0.060 | 169.1 | 258.8 | 89.7 |
| | 0 | 0 | 0 | 0 |
| | 1.000 | 0 | 0 | 0 |
| | 0.906 | 185.4 | 170.2 | −15.2 |
| | 0.812 | 358.1 | 336.9 | −21.2 |
| | 0.717 | 514.2 | 497.3 | −16.9 |
| | 0.621 | 649.8 | 648.9 | −0.9 |
| *n*-Butylcyanide | 0.524 | 757.5 | 786.0 | 28.5 |
| —Cyclohexane | 0.427 | 828.3 | 901.6 | 73.3 |
| | 0.328 | 845.8 | 977.5 | 131.7 |
| | 0.227 | 780.3 | 976.1 | 195.8 |
| | 0.121 | 565.4 | 789.0 | 223.6 |
| | 0.062 | 347.0 | 529.0 | 182.0 |
| | 0 | 0 | 0 | 0 |

| System | $x_2$ | $G^{Eel}_{calcd}$ | $H^{Eel}_{calcd}$ | $TS^{Eel}_{calcd}$ |
|---|---|---|---|---|
| | 1.000 | 0 | 0 | 0 |
| | 0.915 | 49.5 | 69.9 | 20.4 |
| | 0.828 | 94.2 | 135.7 | 41.5 |
| | 0.740 | 133.2 | 196.4 | 63.2 |
| Chlorocyclohexane | 0.649 | 165.1 | 249.8 | 84.7 |
| —Methylcyclohexane | 0.555 | 188.0 | 292.9 | 104.9 |
| | 0.459 | 199.3 | 320.9 | 121.6 |
| | 0.358 | 195.3 | 326.6 | 131.3 |
| | 0.251 | 169.9 | 297.4 | 127.5 |
| | 0.134 | 112.2 | 208.1 | 95.9 |
| | 0 | 0 | 0 | 0 |
| | 1.000 | 0 | 0 | 0 |
| | 0.912 | 53.9 | 75.5 | 21.6 |
| | 0.824 | 102.3 | 146.0 | 43.7 |
| | 0.734 | 144.0 | 210.1 | 66.1 |
| Bromocyclohexane | 0.642 | 177.7 | 266.0 | 88.3 |
| —Methylcyclohexane | 0.548 | 201.5 | 310.6 | 109.1 |
| | 0.452 | 212.8 | 338.9 | 126.1 |
| | 0.352 | 207.8 | 343.5 | 135.7 |
| | 0.246 | 180.2 | 301.5 | 131.3 |
| | 0.131 | 118.8 | 216.8 | 98.0 |
| | 0 | 0 | 0 | 0 |
| | 1.000 | 0 | 0 | 0 |
| | 0.908 | 64.1 | 103.5 | 39.4 |
| | 0.815 | 121.3 | 199.6 | 78.3 |
| *cis*-Dichloro- | 0.727 | 166.9 | 280.6 | 113.7 |
| ethylene | 0.626 | 208.7 | 360.7 | 152.0 |
| —*trans*-Dichloro- | 0.529 | 240.5 | 419.4 | 178.9 |
| ethylene | 0.430 | 256.8 | 454.9 | 198.1 |
| | 0.328 | 247.5 | 456.6 | 209.1 |
| | 0.222 | 209.3 | 405.2 | 195.9 |
| | 0.107 | 126.5 | 260.2 | 133.7 |
| | 0 | 0 | 0 | 0 |
| | 1.000 | 0 | 0 | 0 |
| | 0.913 | 91.5 | 107.0 | 15.5 |
| | 0.824 | 175.3 | 209.7 | 34.4 |
| | 0.734 | 249.9 | 306.3 | 56.4 |
| Pyridine | 0.643 | 312.6 | 394.2 | 81.6 |
| —1,4-Dioxane | 0.550 | 360.9 | 470.2 | 109.3 |
| | 0.454 | 388.9 | 527.0 | 138.1 |
| | 0.356 | 389.9 | 554.2 | 164.3 |
| | 0.253 | 351.6 | 530.2 | 178.6 |
| | 0.141 | 251.0 | 408.6 | 157.6 |
| | 0 | 0 | 0 | 0 |

TABLE III. THE CALCULATED VALUES OF THE ELECTROSTATIC PART OF THERMODYNAMIC EXCESS FUNCTIONS FOR BINARY SYSTEMS CONTAINING POLAR AND AROMATIC NON-POLAR COMPONENTS

| System | $x_2$ | $G^{Eel}_{calcd}$ | $H^{Eel}_{calcd}$ | $TS^{Eel}_{calcd}$ |
|---|---|---|---|---|
| Chlorobenzene —Toluene | 1.000 | 0 | 0 | 0 |
| | 0.905 | 34.5 | 55·3 | 20.8 |
| | 0.806 | 64.6 | 105.1 | 40.5 |
| | 0.707 | 87.8 | 145.3 | 57.5 |
| | 0.613 | 103.4 | 173.5 | 70.1 |
| | 0.498 | 112.4 | 192.1 | 79.7 |
| | 0.386 | 110.2 | 192.0 | 81.8 |
| | 0.269 | 94.5 | 168.9 | 74.4 |
| | 0.143 | 61.2 | 111.9 | 50.7 |
| | 0.005 | 2.8 | 5.2 | 2.4 |
| | 0 | 0 | 0 | 0 |
| Bromobenzene —Toluene | 1.000 | 0 | 0 | 0 |
| | 0.902 | 36.4 | 64.2 | 27.8 |
| | 0.802 | 67.3 | 120.3 | 53.0 |
| | 0.700 | 92.2 | 166.5 | 74.3 |
| | 0.595 | 109.2 | 200.5 | 91.3 |
| | 0.488 | 117.3 | 218.9 | 101.6 |
| | 0.376 | 114.5 | 216.5 | 102.0 |
| | 0.248 | 98.0 | 185.9 | 87.9 |
| | 0.133 | 57.3 | 115.8 | 58.5 |
| | 0 | 0 | 0 | 0 |
| Benzonitrile —Toluene | 1.000 | 0 | 0 | 0 |
| | 0.906 | 224.9 | 204.8 | −20.1 |
| | 0.810 | 434.4 | 401.4 | −33.0 |
| | 0.714 | 624.8 | 587.8 | −37.0 |
| | 0.618 | 789.7 | 759.2 | −30.5 |
| | 0.519 | 922.1 | 910.0 | −12.1 |
| | 0.421 | 1007.4 | 1026.9 | 19.5 |
| | 0.321 | 1025.7 | 1091.1 | 65.4 |
| | 0.214 | 932.6 | 1053.3 | 120.7 |
| | 0.109 | 648.6 | 794.4 | 145.8 |
| | 0.049 | 349.9 | 457.6 | 107.7 |
| | 0 | 0 | 0 | 0 |
| Nitrobenzene —Toluene | 1.000 | 0 | 0 | 0 |
| | 0.905 | 189.3 | 121.0 | −68.3 |
| | 0.810 | 367.9 | 242.9 | −125.0 |
| | 0.714 | 532.1 | 364.2 | −167.9 |
| | 0.617 | 677.7 | 483.8 | −193.9 |
| | 0.519 | 798.5 | 599.7 | −198.8 |
| | 0.420 | 884.2 | 707.3 | −176.9 |
| | 0.320 | 916.8 | 795.4 | −121.4 |
| | 0.218 | 861.7 | 835.2 | −26.5 |
| | 0.112 | 631.2 | 719.7 | 88.5 |
| | 0.054 | 377.9 | 491.0 | 113.1 |
| | 0 | 0 | 0 | 0 |

| System | $x_2$ | $G^{Eel}_{calcd}$ | $H^{Eel}_{calcd}$ | $TS^{Eel}_{calcd}$ |
|---|---|---|---|---|
| *n*-Butylchloride —Toluene | 1.000 | 0 | 0 | 0 |
| | 0.901 | 56.1 | 86.4 | 30.3 |
| | 0.802 | 104.6 | 168.3 | 63.7 |
| | 0.701 | 144.5 | 240.2 | 95.7 |
| | 0.600 | 174.0 | 298.9 | 124.9 |
| | 0.496 | 191.4 | 339.5 | 148.1 |
| | 0.390 | 193.1 | 355.2 | 161.2 |
| | 0.281 | 174.6 | 334.7 | 160.1 |
| | 0.168 | 128.9 | 259.7 | 130.8 |
| | 0.046 | 43.8 | 92.8 | 49.0 |
| | 0 | 0 | 0 | 0 |
| Cyclohexanone —Toluene | 1.000 | 0 | 0 | 0 |
| | 0.908 | 89.0 | 84.8 | −4.2 |
| | 0.802 | 181.9 | 178.1 | −3.8 |
| | 0.705 | 257.1 | 258.8 | 1.7 |
| | 0.607 | 320.1 | 333.2 | 13.1 |
| | 0.508 | 367.5 | 397.9 | 30.4 |
| | 0.409 | 393.8 | 447.3 | 53.5 |
| | 0.307 | 390.0 | 470.5 | 80.5 |
| | 0.203 | 339.8 | 443.3 | 103.5 |
| | 0.092 | 205.9 | 298.0 | 92.1 |
| | 0.031 | 81.7 | 126.9 | 45.2 |
| | 0 | 0 | 0 | 0 |
| *n*-Butylcyanide —Toluene | 1.000 | 0 | 0 | 0 |
| | 0.903 | 181.0 | 167.6 | −13.4 |
| | 0.805 | 348.0 | 330.3 | −17.7 |
| | 0.707 | 497.9 | 486.4 | −11.5 |
| | 0.609 | 625.9 | 632.1 | 6.2 |
| | 0.510 | 725.5 | 762.2 | 36.7 |
| | 0.410 | 786.6 | 866.9 | 80.3 |
| | 0.309 | 792.9 | 928.0 | 135.1 |
| | 0.205 | 714.1 | 903.4 | 189.1 |
| | 0.098 | 482.8 | 674.5 | 191.7 |
| | 0.040 | 206.1 | 318.9 | 112.8 |
| | 0 | 0 | 0 | 0 |
| Pyridine —Benzene | 1.000 | 0 | 0 | 0 |
| | 0.914 | 88.7 | 107.0 | 18.3 |
| | 0.827 | 170.2 | 210.0 | 39.8 |
| | 0.738 | 243.3 | 308.4 | 65.1 |
| | 0.647 | 304.9 | 398.3 | 93.4 |
| | 0.553 | 352.3 | 475.5 | 123.2 |
| | 0.456 | 379.6 | 533.4 | 153.8 |
| | 0.356 | 379.5 | 559.6 | 180.1 |
| | 0.249 | 339.0 | 530.9 | 191.9 |
| | 0.134 | 233.5 | 394.9 | 161.4 |
| | 0 | 0 | 0 | 0 |

polar liquid $\varepsilon_2$ is related to temperature as

$$\varepsilon_2-n_2^2=\frac{3\varepsilon_2}{2\varepsilon_2+n_2^2}\cdot\frac{(n_2^2+2)^2}{3}\cdot\frac{4\pi N}{3kT}\mu^2 \quad (16)$$

By assuming that the dipole moment $\mu$ of the polar molecule is independent of temperature, we obtain the following expression, by taking the logarithm of both sides of the formula 16 and differentiating it with the temperature:

$$\left(\frac{1}{\varepsilon_2-n_2^2}+\frac{2}{2\varepsilon_2+n_2^2}-\frac{1}{\varepsilon_2}\right)\frac{d\varepsilon_2}{dT}+\left(\frac{1}{2\varepsilon_2+n_2^2}-\frac{1}{\varepsilon_2-n_2^2}-\frac{2}{n_2^2+2}\right)2n_2\frac{dn_2}{dT}=\frac{1}{N}\cdot\frac{dN}{dT}-\frac{1}{T} \quad (17)$$

where $1/N\cdot dN/dT$ is the thermal expansion coefficient of the polar liquid reversed in sign. All the values in the above expression are available except $d\varepsilon_2/dT$. Then the values of $d\varepsilon_2/dT$ can be derived by the relevant values such as $\varepsilon_2$, $n_2$, $dn_2/dT$, $T$ and the thermal expansion coefficient.

(2) The temperature dependence of the refractive index of the liquid. The refractive index $n$ of a liquid can approximately be expressed as $(n^2-1)/(n^2+2)\cdot 1/\rho=\text{const.}$ where $\rho$ is the density of the liquid. Differentiating it with temperature, we obtain

$$\frac{dn}{dT}=\frac{(n^2-1)(n^2+2)}{6n}\cdot\frac{1}{\rho}\cdot\frac{d\rho}{dT} \quad (18)$$

$1/\rho\cdot d\rho/dT$ is the thermal expansion coefficient of the liquid reversed in sign. Then we can derive the values of $dn/dT$ from the refractive index and the thermal expansion coefficient of the liquid.

(3) The dielectric constant of the solution, $\varepsilon_{12}$. According to Onsager, the dielectric constant of a binary solution of polar and non-polar liquid is expressed as

$$\frac{3(1-v_2)(\varepsilon_{12}-n_1^2)\varepsilon_{12}}{2\varepsilon_{12}+n_1^2}+\frac{3v_2(\varepsilon_{12}-n_2^2)}{2\varepsilon_{12}+n_2^2}=\frac{4\pi Nv_2\mu^2}{3kT}\left\{\frac{\varepsilon_{12}(n_2^2+2)}{2\varepsilon_{12}+n_2^2}\right\}^2 \quad (19)$$

where $v_2$ is the volume fraction of the polar components.

By replacing $\mu^2$ in the above expression with

$$\frac{9(\varepsilon_2-n_2^2)(2\varepsilon_2+n_2^2)kT}{\varepsilon_2(n_2^2+2)^2\cdot 4\pi N}=\mu^2 \quad (20)$$

which is obtained from Onsager's expression of the dielectric constant for a pure polar liquid, we obtain[3]

3) T. Hanai, N. Koizumi and R. Gotō, *J. Chem. Soc. Japan, Pure Chem. Sec.* (*Nippon Kagaku Zasshi*), **80**, 17 (1959).

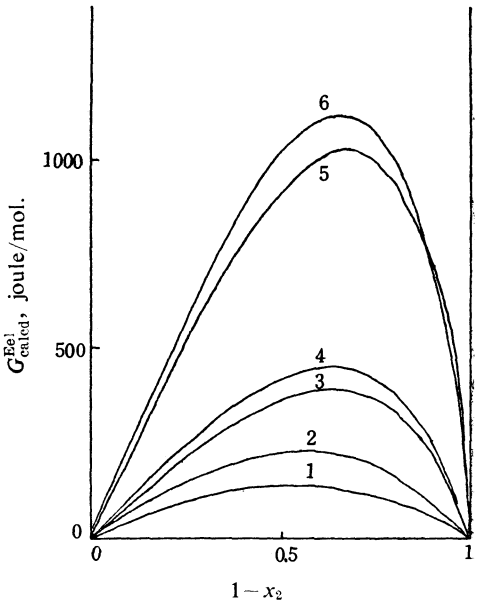



Fig. 1. $G^{Eel}_{caled}$ vs. mol. fraction.
1. Chlorobenzene—Cyclohexane
2. *n*-Butylchloride—Cyclohexane
3. Diethyl ketone—Cyclohexane
4. Cyclohexanone—Cyclohexane
5. Nitrobenzene—Cyclohexane
6. Benzonitrile—Cyclohexane

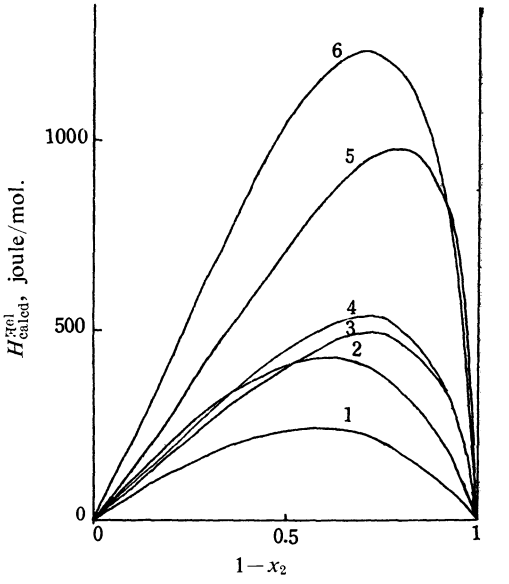



Fig. 2. $H^{Eel}_{caled}$ vs. mol. fraction.
1. Chlorobenzene—Cyclohexane
2. *n*-Butylchloride—Cyclohexane
3. Diethyl ketone—Cyclohexane
4. Cyclohexanone—Cyclohexane
5. Nitrobenzene—Cyclohexane
6. Benzonitrile—Cyclohexane

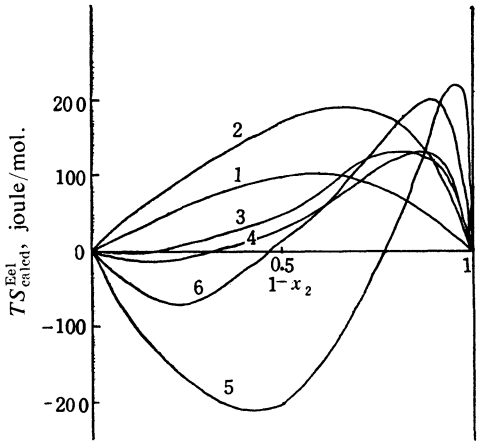



Fig. 3. $TS^{Eel}_{calcd}$ vs. mol. fraction.

1. Chlorobenzene—Cyclohexane
2. *n*-Butylchloride—Cyclohexane
3. Diethyl ketone—Cyclohexane
4. Cyclohexanone—Cyclohexane
5. Nitrobenzene—Cyclohexane
6. Benzonitrile—Cyclohexane

$$\frac{\varepsilon_{12}-\varepsilon_1}{2\varepsilon_{12}-n_1^2}\cdot(1-v_2)+\frac{(\varepsilon_{12}-\varepsilon_2)(2\varepsilon_{12}\varepsilon_2+n_2^4)}{\varepsilon_2(2\varepsilon_{12}+n_2^2)^2}v_2=0 \tag{21}$$

where $\varepsilon_1$ and $n_1$ are the dielectric constant and refractive index of the non-polar liquid respectively, other notation being the same as those already described. All the values in the above expression 21 are known except $\varepsilon_{12}$ and $v_1$. The dielectric constant of the solution $\varepsilon_{12}$ can be calculated from the expression 21 for any given values of concentration $v_2$.

(4) The temperature dependence of $\varepsilon_{12}$, $d\varepsilon_{12}/dT$. It is approximated by a weighted mean such as

$$\frac{d\varepsilon_{12}}{dT}=\frac{\varepsilon_2-\varepsilon_{12}}{\varepsilon_2-\varepsilon_1}\cdot\frac{d\varepsilon_1}{dT}+\frac{\varepsilon_{12}-\varepsilon_1}{\varepsilon_2-\varepsilon_1}\cdot\frac{d\varepsilon_2}{dT} \tag{22}$$

$d\varepsilon_1/dT$ is the temperature dependence of the dielectric constant of the non-polar liquid. If $d\varepsilon_1/dT$ is not available, it is derived by using the following expression

$$\frac{\varepsilon_1-1}{\varepsilon_1+2}\cdot\frac{1}{\rho}=\text{constant} \tag{23}$$

TABLE IV. THE ELECTROSTATIC PART OF VAN LAAR COEFFICIENTS, $\alpha^{el}_{calcd}$ CALCULATED ACCORDING TO ONSAGER'S MODEL FOR BINARY SYSTEMS CONSISTING OF POLAR AND NON-AROMATIC NON-POLAR MOLECULES

| System | $v_2$ | $\alpha^{el}_{calcd}$ joule/cc. | System | $v_2$ | $\alpha^{el}_{calcd}$ joule/cc. |
|---|---|---|---|---|---|
| | 1.000 | 7.18 | | 1.000 | 23.21 |
| | 0.9115 | 7.07 | | 0.9045 | 24.13 |
| | 0.8203 | 7.43 | | 0.8089 | 26.44 |
| | 0.7312 | 7.80 | | 0.7132 | 29.22 |
| Chlorobenzene | 0.6387 | 8.20 | | 0.6173 | 32.68 |
| —Cyclohexane | 0.5441 | 8.67 | Benzonitrile | 0.5208 | 37.12 |
| | 0.4468 | 9.20 | —Cyclohexane | 0.4244 | 42.98 |
| | 0.3460 | 9.81 | | 0.3269 | 51.15 |
| | 0.2395 | 10.47 | | 0.2236 | 64.03 |
| | 0.1256 | 11.19 | | 0.1239 | 87.05 |
| | 0 | 12.03 | | 0.0672 | 105.58 |
| | | | | 0 | 131.96 |
| | 1.000 | 7.28 | | 1.000 | 13.67 |
| | 0.9123 | 7.39 | | 0.9036 | 14.45 |
| | 0.8235 | 7.72 | | 0.8071 | 16.17 |
| | 0.7332 | 8.10 | | 0.7106 | 18.31 |
| Bromobenzene | 0.6412 | 8.52 | | 0.6139 | 21.09 |
| —Cyclohexane | 0.5470 | 8.98 | Nitrobenzene | 0.5171 | 24.78 |
| | 0.4498 | 9.50 | —Cyclohexane | 0.4199 | 30.17 |
| | 0.3485 | 10.09 | | 0.3223 | 37.98 |
| | 0.2417 | 10.75 | | 0.2235 | 50.93 |
| | 0.1267 | 11.52 | | 0.1214 | 75.65 |
| | 0 | 12.35 | | 0.0664 | 101.21 |
| | | | | 0 | 141.11 |

TABLE IV. (Continued)

| System | $v_2$ | $\alpha^{el}_{calcd}$ joule/cc. | System | $v_2$ | $\alpha^{el}_{calcd}$ joule/cc. |
|---|---|---|---|---|---|
| | 1.000 | 9.34 | | 1.000 | 7.10 |
| | 0.9080 | 10.08 | | 0.9091 | 7.04 |
| | 0.8154 | 11.18 | | 0.8176 | 7.53 |
| | 0.7227 | 12.17 | | 0.7253 | 8.10 |
| *n*-Butylchloride | 0.6278 | 13.11 | Chlorocyclohexane | 0.6320 | 8.77 |
| —Cyclohexane | 0.5323 | 14.25 | —Methylcyclohexane | 0.5373 | 9.55 |
| | 0.4350 | 15.63 | | 0.4407 | 10.48 |
| | 0.3352 | 17.33 | | 0.3411 | 11.61 |
| | 0.2315 | 19.44 | | 0.2371 | 13.04 |
| | 0.1214 | 22.12 | | 0.1256 | 14.90 |
| | 0 | 25.22 | | 0 | 17.15 |
| | 1.000 | 17.50 | | 1.000 | 7.14 |
| | 0.9038 | 18.57 | | 0.9098 | 7.37 |
| | 0.8074 | 20.50 | | 0.8190 | 7.87 |
| | 0.7109 | 22.83 | | 0.7273 | 8.44 |
| | 0.6143 | 25.79 | Bromocyclohexane | 0.6345 | 9.12 |
| *n*-Butylcyanide | 0.5173 | 29.54 | —Methylcyclohexane | 0.5403 | 9.91 |
| —Cyclohexane | 0.4199 | 34.65 | | 0.4439 | 10.84 |
| | 0.3216 | 41.83 | | 0.3444 | 11.98 |
| | 0.2218 | 52.64 | | 0.2401 | 13.41 |
| | 0.1181 | 70.32 | | 0.1277 | 15.23 |
| | 0.0625 | 87.26 | | 0 | 17.37 |
| | 0 | 109.10 | | | |
| | 1.000 | 8.83 | | 1.000 | 15.23 |
| | 0.9045 | 9.48 | | 0.9062 | 15.97 |
| | 0.8088 | 10.42 | | 0.8120 | 17.12 |
| | 0.7129 | 11.55 | | 0.7236 | 18.34 |
| Diethyl ketone | 0.6167 | 12.95 | *cis*-Dichloroethylene | 0.6213 | 20.00 |
| (Methyl propyl ketone) | 0.5202 | 14.36 | —*trans*-Dichloroethylene | 0.5244 | 21.91 |
| —Cyclohexane | 0.4230 | 17.10 | | 0.4257 | 24.19 |
| | 0.3248 | 20.77 | | 0.3244 | 27.04 |
| | 0.2245 | 25.54 | | 0.2188 | 30.71 |
| | 0.1196 | 32.54 | | 0.1056 | 35.62 |
| | 0.0632 | 38.65 | | 0 | 40.74 |
| | 0 | 46.69 | | | |
| | 1.000 | 9.81 | | 1.000 | 15.44 |
| | 0.8991 | 10.41 | | 0.9083 | 15.73 |
| | 0.8039 | 11.45 | | 0.8163 | 17.04 |
| | 0.7084 | 12.70 | | 0.7237 | 18.57 |
| | 0.6127 | 14.27 | Pyridine | 0.6306 | 20.41 |
| Cyclohexanone | 0.5165 | 16.28 | —1,4-Dioxane | 0.5365 | 22.69 |
| —Cyclohexane | 0.4197 | 18.16 | | 0.4411 | 25.52 |
| | 0.3217 | 22.62 | | 0.3436 | 29.18 |
| | 0.2216 | 28.01 | | 0.2425 | 34.09 |
| | 0.1157 | 36.60 | | 0.1346 | 41.19 |
| | 0.0583 | 43.69 | | 0 | 51.24 |
| | 0 | 52.08 | | | |

TABLE V. THE ELECTROSTATIC PART OF VAN LAAR COEFFICIENTS, $\alpha^{el}_{calcd}$ CALCULATED ACCORDING TO ONSAGER'S MODEL FOR BINARY SYSTEMS CONSISTING OF POLAR AND AROMATIC NON-POLAR MOLECULES

| System | $v_2$ | $\alpha^{el}_{calcd}$ joule/cc. | System | $v_2$ | $\alpha^{el}_{calcd}$ joule/cc. |
|---|---|---|---|---|---|
| | 1.000 | 6.06 | | 1.000 | 8.31 |
| | 0.9005 | 6.04 | | 0.9004 | 9.10 |
| | 0.7978 | 6.34 | | 0.8002 | 9.94 |
| | 0.6972 | 6.67 | | 0.6992 | 10.77 |
| Chlorobenzene | 0.6011 | 6.98 | *n*-Butylchloride | 0.5970 | 11.70 |
| —Toluene | 0.4855 | 7.37 | —Toluene | 0.4934 | 12.78 |
| | 0.3747 | 7.81 | | 0.3878 | 14.06 |
| | 0.2595 | 8.33 | | 0.2792 | 15.62 |
| | 0.1371 | 8.92 | | 0.1661 | 17.58 |
| | 0.0051 | 9.59 | | 0.0456 | 20.21 |
| | 0 | 9.67 | | 0 | 21.03 |
| | 1.000 | 6.61 | | 1.000 | 16.65 |
| | 0.9007 | 6.79 | | 0.9014 | 17.91 |
| | 0.7998 | 7.29 | | 0.8028 | 19.78 |
| | 0.6972 | 7.45 | | 0.7039 | 22.09 |
| Bromobenzene | 0.5923 | 7.83 | | 0.6049 | 24.99 |
| —Toluene | 0.4844 | 8.25 | *n*-Butylcyanide | 0.5055 | 28.77 |
| | 0.3727 | 8.71 | —Toluene | 0.4057 | 33.87 |
| | 0.2557 | 9.17 | | 0.3050 | 41.16 |
| | 0.1315 | 9.51 | | 0.2026 | 52.51 |
| | 0 | 9.64 | | 0.0961 | 72.80 |
| | | | | 0.0388 | 79.91 |
| | | | | 0 | 91.86 |
| | 1.000 | 21.37 | | 1.000 | 8.93 |
| | 0.9027 | 22.46 | | 0.8963 | 8.61 |
| | 0.8053 | 24.58 | | 0.7985 | 10.53 |
| | 0.7077 | 27.20 | | 0.7004 | 11.71 |
| | 0.6099 | 30.45 | | 0.6021 | 13.18 |
| Benzonitrile | 0.5114 | 34.65 | Cyclohexanone | 0.5032 | 15.36 |
| —Toluene | 0.4131 | 40.18 | —Toluene | 0.4036 | 17.54 |
| | 0.3136 | 47.92 | | 0.3028 | 20.99 |
| | 0.2082 | 60.20 | | 0.1994 | 26.10 |
| | 0.1056 | 79.09 | | 0.0901 | 34.09 |
| | 0.0470 | 95.65 | | 0.0303 | 40.48 |
| | 0 | 112.10 | | 0 | 44.22 |
| | 1.000 | 12.41 | | 1.000 | 15.74 |
| | 0.9023 | 13.26 | | 0.9068 | 15.44 |
| | 0.8045 | 14.87 | | 0.8133 | 16.72 |
| | 0.7066 | 16.86 | | 0.7194 | 18.32 |
| | 0.6086 | 19.42 | Pyridine | 0.6249 | 20.19 |
| Nitrobenzene | 0.5104 | 22.87 | —Benzene | 0.5294 | 22.47 |
| —Toluene | 0.4119 | 27.75 | | 0.4328 | 25.35 |
| | 0.3128 | 35.02 | | 0.3341 | 29.07 |
| | 0.2124 | 47.09 | | 0.2321 | 34.08 |
| | 0.1085 | 69.87 | | 0.1235 | 41.32 |
| | 0.0521 | 93.30 | | 0 | 50.97 |
| | 0 | 122.20 | | | |

By differentiation with temperature, we obtain

$$\frac{d\varepsilon_1}{dT}=\frac{1}{\rho}\frac{d\rho}{dT}\frac{(\varepsilon_1-1)(\varepsilon_1+2)}{3} \quad (24)$$

which can be calculated from the values of $\varepsilon_1$ and the thermal expansion coefficient of the non-polar liquid.

The values used for the calculations are shown in Table I.

## The Results and Discussions

The calculation is carried out for the systems for which the heats of mixing were measured. For the systems where toluene is the non-polar component, it is assumed that the dipole-moment of toluene is zero. No serious difference occurs even if the finite value of its dipole moment is taken into account (the difference being only 4% at most). The results obtained are shown in Tables II and III and some of them are shown in Figs. 1—3.

As is seen from the above tables, the electrostatic part of the excess free energy and the excess enthalpy of mixing for the above systems derived on the Onsager model, are all positive over all the concentrations and the quantities for 1 mol. of mixture deviate from the parabola expressed by $Kx_2(1-x_2)$, where $K$ is a constant and $x_2$ is the mole fraction of the polar components. The larger the dipole moments of the polar components are, the larger are the deviations and the larger the shift of $x_{max}$, $x_{max}$ designating the concentration where these quantities are maximum.

The electrostatic part of the excess entropy of mixing for 1 mol. of the mixture shows a specific behavior. For the systems containing polar components of small dipole moments, they are positive over the whole concentration, but for those of large dipole moments, the values are negative over the range of larger values of $x_2$, and rapidly increase and take very large positive values as $x_2$ decreases.

It is naturally expected that these values do not differ so much if the non-polar component, cyclohexane, is replaced by toluene, because of the similar dielectric constant, since according to the assumption of the theory the values are the function of dielectric constant only.

The calculated values of the electrostatic part of van Laar coefficients $\alpha^{el}_{calcd}$ were also calculated by the relation: $\alpha^{el}_{calcd}=H^{Eel}_{calcd}/v_2(1-v_2)\cdot V$, where $V$ is the molar volume of the mixture. They are shown in Tables IV and V.

It is seen from the results that the values of $\alpha^{el}_{calcd}$ are positive and increase with the decrease of concentration $x_2$ of polar component, and the larger the dipole moments, the larger the values of $\alpha^{el}_{calcd}$ as well as their variations with concentration.

## Summary

The electrostatic part of the excess functions for 21 binary systems consisting of polar and non-polar liquids were calculated according to Onsager's model. The electrostatic part of the excess free energy and excess enthalpy are positive over all the concentrations for all of these systems and these quantities are unsymmetric with regard to the mole fractions $x$ against the value at the point $x=0.5$.

The concentrations $x_{max}$ where these quantities have maximum values, shift to a lower concentration of polar component. The larger the dipole moment of the polar components, the larger the maximum values and the shifts are. The electrostatic part of excess entropies have positive values over the whole concentration for systems consisting of a polar component of small dipole moment, but for those consisting of one with a larger dipole moment, these quantities take negative values for a high concentration of polar component, but take positive values for a low concentration range. The electrostatic part of van Laar coefficients is also calculated and these values increase with the decrease of concentration of polar component.

The author wishes to express his thanks to Professor R. Fujishiro of Osaka City University and to Professor Yonezo Morino of the University of Tokyo for their constant encouragement and discussions.

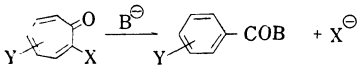
*Government Chemical Industrial Research Institute*
*Shibuya-ku, Tokyo*

# *Studies on the Mechanism of Rearrangement Reaction of 2-Phenyl-4-bromotropone to 2-Phenylbenzoic Acid*[1]

By Yoshio KITAHARA, Ichiro MURATA and Tadashi MUROI*

(Received January 26, 1961)

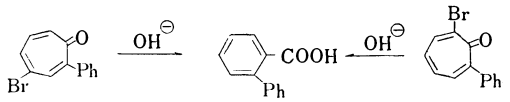
It had been found in the early period of studies on troponoid chemistry that the tropone derivatives having the halogen or methoxyl group in the 2-position undergo rearrangement to benzoic acid derivatives when treated with bases[2]. This rearrangement reaction has often been utilized for deriving unknown troponoid to known benzene derivatives to determine the position of various substituents in the seven-membered ring by the organic chemical method[2].



X=halogen, methoxyl

Two kinds of mechanism may be considered for this rearrangement reaction. One, route-A, involves the attack of the base on the carbonyl carbon (C-1), followed by ring contraction concerted with liberation of the substituent in C-2 as an anion[3]. The other, route-B, is the attack of the base on C-2 and subsequent rearrangement[4]. If the rearrangement proceeds through route-A, the carbon atom in the carboxyl group of the benzoic acid produced corresponds to the carbonyl carbon of tropone, and if the reaction goes through route-B, it will be the carbon atom at C-2 of the tropone. An investigation of the rearrangement with carbonyl-labeled 2, 7-dibromo- and 2, 4, 7-tribromotropone proved that the modified mechanism of route-A is the correct one[5].

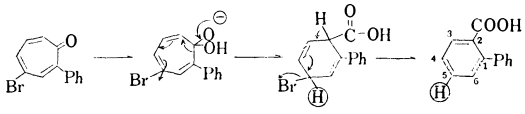
One of the authors (T. M.) found that the product obtained by treatment of 2-phenyl-4-bromotropone (I) with alkali was unexpectedly 2-phenylbenzoic acid (III), the same as the rearrangement product of 2-phenyl-7-bromotropone (II)[6].



I III II

Differing from II, I does not possess any group easily liberated as an anion at the carbon adjacent to the carbonyl group and the rearrangement product, III, no longer possesses bromine atom. Consequently, the mechanism proposed by Doering and Denney[5] cannot be applied to this rearrangement reaction.

The following mechanism was considered for this abnormal rearrangement reaction and tracer technique using heavy water was utilized to prove this assumption.



If the rearrangement proceeds through this route, the reaction carried out in a system containing deuterium as an origin of hydrogen should give a product with the carbon-bound deuterium only in the 5-position of the biphenyl formed.

A solution of I dissolved in a solution of deuterium oxide[7], sodium hydroxide-*d*, and methanol-*d*[8] was refluxed for 30 min. and 2-phenylbenzoic acid was isolated from the acid portion. To remove deuterium from the carboxyl group, the acid was converted into its methyl ester with diazomethane and the ester was hydrolyzed to deuterated 2-phenylbenzoic acid (III) of m. p. 108~110°C[9]. The

---

i) Paper read at the Tohoku Local Meeting of the Chemical Society of Japan, Akita, October, 1959.

* Present address: Hitachi Research Laboratory, Hitachi Ltd., Sukekawa-machi, Hitachi, Ibaraki.

2) T. Nozoe, *Sci. Repts. Tohoku Univ.*, *I*, **34**, 199 (1950); T. Nozoe, *Nature*, **167**, 1055 (1951); J. W. Cook and J. D. London, *Quart. Revs.* (*London*), **5**, 99 (1951); P. L. Pauson, *Chem. Revs.*, **55**, 9 (1950).

3) W. von E. Doering and L. H. Knox, *J. Am. Chem. Soc.*, **73**, 828 (1951); T. Nozoe, Y. Kitahara and S. Masamune, *Proc. Japan Acad.*, **27**, 649 (1951); Y. Kitahara, *Sci. Repts. Tohoku Univ.*, *I*, **39**, 250 (1956).

4) W. von E. Doering and L. H. Knox, *J. Am. Chem. Soc.*, **74**, 5683 (1952).

5) W. von E. Doering and D. B. Denney, ibid., **77**, 4619 (1955).

6) T. Muroi, *J. Chem. Soc. Japan, Pure Chem. Sec.* (*Nippon Kagaku Zasshi*), **80**, 303 (1959).

7) Norsk Hydro-electrisk; purity, 99.78%. $d_4^{20}$ 1.10514.

8) D. H. Hill, B. Stewart, S. W. Kantor, W. A. Judge and C. R. Hauser, *J. Am. Chem. Soc.*, **76**, 5129 (1954).

9) Under this rearrangement condition, 2-phenylbenzoic acid was proved to be free from secondary deuteration on aromatic nucleus, since the infrared absorption spectrum of the product obtained by treatment of 2-phenylbenzoic acid under the same conditions as for rearrangement of I was identical with that of the original substance. D. J. G. Ives (*J. Chem. Soc.*, **1938**, 81) also reported that deuteration did not take place on the benzene ring when benzoic acid was treated in a deuterium oxide-sodium hydroxide-*d* system.

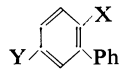
TABLE I. COMPARISON OF INFRARED ABSORPTION BANDS OF DEUTERATED COMPOUNDS AND CORRESPONDING NON-DEUTERATED COMPOUNDS*

| III' | III | IV' | IV | V' | V |
|---|---|---|---|---|---|
| 3070 | 3065 | 3370 | 3370 | 3275 | 3270 |
| 3030 | | 3175 | 3175 | 3230 | 3215 |
| 2890 | 2920 | 3055 | | 3020 | 3010 |
| 2655 | 2670 | | | | |
| 2520 | 2525 | | | | |
| | 2280 | | | | |
| 1949 | 1955 | | | | |
| 1692 | 1695 | 1692 | 1692 | 1658 | 1658 |
| 1601 | 1597 | 1640 | 1640 | | 1598 |
| | 1502 | 1619 | 1618 | 1587 | 1583 |
| 1483 | 1481 | 1602 | 1594 | 1533 | 1530 |
| 1456 | 1450 | 1582 | 1578 | 1497 | |
| 1445 | | | 1498 | 1477 | 1473 |
| 1408 | 1412 | 1482 | 1477 | 1453 | 1444 |
| | 1400 | 1455 | | 1437 | |
| 1290 | 1282 | 1442 | 1447 | | 1403 |
| 1260 | 1252 | | 1418 | 1372 | 1370 |
| 1180 | 1182 | 1400 | | 1303 | 1303 |
| 1164 | | | 1383 | | 1287 |
| 1139 | 1143 | 1150 | 1150 | 1254 | 1248 |
| | 1110 | 1112 | 1111 | 1157 | 1154 |
| 1094 | | 1075 | 1074 | | 1125 |
| 1073 | 1073 | 1010 | 1005 | 1112 | |
| 1047 | 1049 | 957 | | 1073 | 1073 |
| 1007 | 1003 | | 905 | 1047 | 1051 |
| 929 | | | 860 | 1010 | 1004 |
| 910 | 908 | 841 | | 975 | 975 |
| | 884 | 800 | 800 | 941 | |
| | 856 | 778 | 774 | 922 | 916 |
| 694 | 694 | 743 | 751 | | 904 |
| 673 | 673 | | 725 | | 832 |
| 654 | 651 | 696 | 696 | 776 | 772 |
| | | | 670 | 756 | |
| | | | | 742 | 740 |
| | | | | 705 | 701 |
| | | | | 662 | 655 |

* IR spectra are measured using a Perkin-Elmer Model 21 double beam spectrophotometer in KBr pellet.

infrared absorption spectrum of III (Table I.) was different from that of III'[10], and this fact indicated that it contained the deuterium atom.

In order to determine the position of the deuterium atom in III, the following reaction was carried out. III was allowed to react with thionyl chloride at room temperature and the resulting acid chloride, treated with ammonia water, gave the amide (IV), m. p. 172.5~173°C. The Hofmann reaction of IV by the method of




III: X=COOH, Y=D
IV: X=$CONH_2$, Y=D
V: X=$NHCOCH_3$, Y=D
VI: X=$NHCOCH_3$, Y=Br
III': X=COOH, Y=H
IV': X=$CONH_2$, Y=H
V': X=$NHCOCH_3$, Y=H

Graebe[11] yielded the corresponding amine and the product was acetylated to give deuterated 2-acetamidobiphenyl (V), m. p. 113~114°C. The infrared absorption spectra of IV and V so obtained (Table I) and determination of deuterium by mass analysis (cf. Experimental) indicated that the deuterium atom has remained during the series of these reaction steps.

Bromination of V and V' with 1 mol. of bromine in glacial acetic acid gives the known 2-acetamido-5-bromobiphenyl (VI)[12] of m. p. 127.5~128.5°C in a quantitative yield from both. The infrared absorption spectra of VI derived from both V and V' were entirely identical, indicating that the deuterium atom in V had been substituted with a bromine atom in this bromination procedure. VI is a known substance and the position of its bromine atom has already been determined. These facts have proved that the deuterium atom in II, IV and V is in 5-position in the biphenyl ring and, consequently, the reaction mechanism assumed for this abnormal rearrangement might be proved to be correct.

## Experimental[13]

**Rearrangement Reaction of 2-Phenyl-4-bromotropone (I) in Heavy Water System.**—To a solution of sodium (1.38 g.) dissolved in methanol-*d* (35 ml.), deuterium oxide (25 ml.) and I (4.9 g.) were added and the mixture, provided with a calcium chloride tube, was refluxed for 30 min. on a water bath. Methanol was evaporated in a reduced pressure, the residue was diluted with 10 ml. of water, and extracted with chloroform to remove the neutral portion. The aqueous layer was acidified with hydrochloric acid to Congo red, the precipitated acid portion was extracted with chloroform, and the extract was washed with water. After drying over magnesium sulfate, chloroform was evaporated from the extract and the residue was sublimed in reduced pressure, from which 2.3 g. of crude crystals, m. p. 99~104°C, was obtained.

Without further purification, this product was dissolved in ether and ether solution of diazomethane was added to effect esterification. The residue obtained on evaporation of ether was dissolved in ethanol (30 ml.), 2 N sodium hydroxide (10 ml.) was added, and the mixture was refluxed

10) The same reaction was carried out in parallel, using 2-phenylbenzoic acid synthesized from fluorene[11]. The compounds not containing deuterium are represented by the same compound number as the corresponding deuterated compounds but with a prime.

11) C. Graebe and A. S. Rateanu, *Ann.*, **279**, 257 (1894).

12) H. A. Scarborough and W. A. Waters, *J. Chem. Soc.*, **1927**, 89.

13) All melting points are uncorrected.

for 2.5 hr. to effect hydrolysis. Ethanol was evaporated, the residue was acidified with diluted hydrochloric acid extracted with chloroform. The crystals obtained from this extract were sublimed in reduced pressure and afforded 2.15 g. (61.6%) of crystals melting at 95~103°C. Recrystallization from cyclohexane gave III m. p. 108~110°C.

Found: D, 8.93. Calcd. for $C_{13}H_9DO_2$: D, 10.00 atom%.

**2-Carbamoylbiphenyl-5-*d* (IV).**—The addition of thionyl chloride (2 ml.) to III (1.9 g.) resulted in vigorous reaction with evolution of hydrogen chloride. The mixture was allowed to stand at room temperature for 1.5 hr., excess thionyl chloride was distilled off in reduced pressure, and the oily residue was added to 28% ammonia water under ice-cooling, by which white precipitates formed at once. The precipitates were collected and the crude amide (1.8 g) of m. p. 145~158°C so obtained was recrystallized from hydrous ethanol to IV, m. p. 172.5~173°C.

Found: D, 8.37. Calcd. for $C_{13}H_{10}DNO$: D, 9.08 atom%.

**2-Acetamidobiphenyl-5-*d* (V).**—IV (1.75 g.) was triturated with water (10 ml.) in a mortar and transferred to a beaker. A solution of sodium hypobromide, prepared from bromine (1.75 g.), sodium hydroxide (3.5 g.), and water (22 ml.) at 0°C, was added into the beaker with ice-cooling and the mixture was stirred for 1 hr. A trace of insoluble matter was removed by filtration, the filtate was heated at 50~55°C for 1 hr., and submitted to steam distillation. The distillate was extracted with chloroform, the extract was washed with water, dried, and chloroform was evaporated. The residue (1 g.) was dissolved in dehydrated pyridine (3 ml.) and acetyl chloride (0.7 g.) was added dropwise under ice-cooling. The mixture was allowed to stand for 30 min. and poured into 2 N hydrochloric acid containing cracked ice. The crystals that separated out were collected by filtration (1.1 g.), m. p. 104~108°C. Recrystallization from hydrous ethanol gave V, m. p. 113~114°C.

Found: D, 6.60. Calcd. for $C_{14}H_{12}DNO$: D, 7.70 atom%.

**2-Acetamido-5-bromobiphenyl (VI).**—A solution of bromine (390 mg.) in glacial acetic acid (2 ml.) was added to a solution of V (500 mg.) dissolved in glacial acetic acid (3 ml.), with stirring, and the mixture was allowed to stand overnight. The mixture was then poured into ice-water, and crude crystals (750 mg.) of m. p. 115~118°C were sublimed in reduced pressure. Recrystallization of the sublimate from hydrous ethanol gave V as colorless needles m. p. 127.5~128.5°C.

Found: C, 57.64; H, 4.40; N, 4.37. Calcd. for $C_{14}H_{12}ONBr$: C, 57.93; H, 4.17; N, 4.83%.

The determination of deuterium by mass analysis was carried out by Dr. Sumio Horibe, Faculty of Science, Tokyo Metropolitan University, and the infrared spectral measurement was made by Mr. Hideji Aono of this Institute, to both of whom the authors express their sincere gratitude.

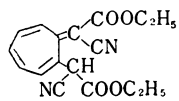
*The Chemical Research Institute*
*of Non-Aqueous Solutions*
*Tohoku University*
*Katahira-cho, Sendai*

# *Condensation Reaction of Troponoids and Ethyl α-Cyano-β-aminoglutaconate. I*

By Shingo MATSUMURA

(Received February 2, 1961)

Nozoe and others have studied the reaction mechanism whereby azulene derivatives are formed by condensation of troponoids and cyanoacetic ester, and have considered the formation of an intermediate A during the course of this reaction[1]. There is also a possibility, in addition to the above mechanism,



(A)

of formation of a dimer of cyanoacetic ester followed by its condensation with troponoids in the formation of 2-aminoazulene derivatives.

This paper describes some results obtained on examination of this point.

Reaction of 2-chlorotropone (I) and a dimer[2] of ethyl cyanoacetate, i. e. ethyl α-cyano-β-aminoglutaconate (II) in absolute ethanol, in the presence of sodium ethoxide, affords red needles (III), m. p. 165°C, orange scales (IV), m. p. above 260°C, and colorless scales (V), m. p. 197°C. The use of a tertiary amine as the condensation agent results in the formation of III and IV but not of V.

1) T. Nozoe, S. Seto, S. Matsumura and T. Asano, *Proc. Japan Acad.*, 32, 339 (1956).

2) S. Matsumura, This Bulletin, in press.

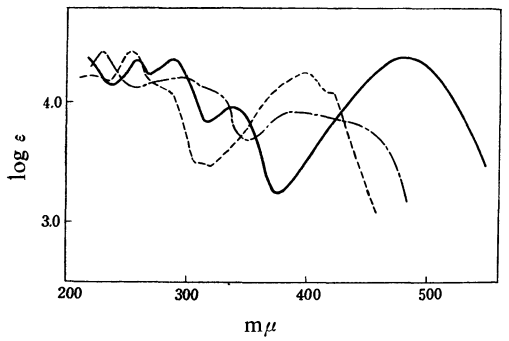
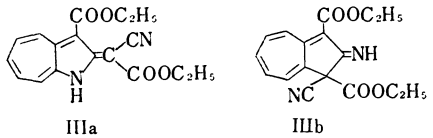



Fig. 1. UV absorption spectra of III, IV and V in methanol.
—— III, ----- IV, -·-·- V

Examinations were made on the structure of these products. The ultraviolet absorption spectra[3] of III, IV and V are given in Fig. 1.

These absorption spectra indicate that these products are not 2-aminoazulene derivatives. The analytical values of III correspond to molecular formula of $C_{17}H_{16}O_4N_2$ and structures like IIIa and IIIb may be assumed from this molecular formula.




The infrared absorption spectrum[4] of III, as indicated in Fig. 2a, exhibits absorption bands at 3220 $cm^{-1}$ for the imino or hydroxyl group, at 2200 $cm^{-1}$ for the cyano group conjugated with unsaturated bond, at 1688 $cm^{-1}$ for ester carbonyl conjugated with unsaturated bond, and at 1650 $cm^{-1}$ for stretching vibration of ester carbonyl conjugated with unsaturated bond or that due to NH deformation vibration.

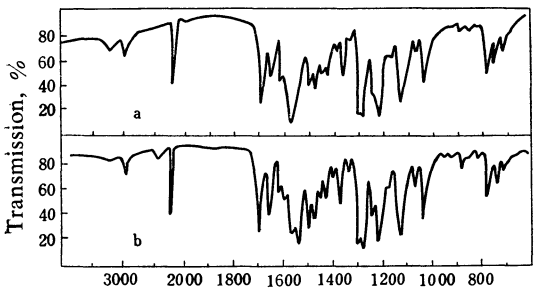



Fig. 2. IR absorption spectra of III (a) and $III_D$ (b) in KBr.

The structure of III which satisfies these infrared spectral results is the formula IIIa.

III undergoes reaction with sodium alkoxide to form a red substance (VI) which is decomposed by water or dilute acid to revert to III. This shows that VI is a sodium salt of III.

III does not form a picrate on addition of an ethanolic solution of picric acid but a prolonged heating of such a solution produces a picrate of m. p. 156°C (decomp.), sparingly soluble in ethanol. III easily reacts with dilute hydrochloric acid to form a labile product of red needles (VII), m. p. 155°C.

Other structurally unknown substances of various colors are obtained but they are all unstable and cannot be isolated in pure form. VII forms a picrate of m. p. 156°C.

The passage of dry hydrogen chloride gas through dehydrated benzene solution of III gives yellow needles (VIII) assumed to be the hydrochloride of III. VIII is extremely labile and decomposes when left in the air. The neutralization of VIII with sodium hydrogen carbonate solution liberates VII, whose ultraviolet absorption spectrum, as indicated in Fig. 3, is similar to that of 1-azaazulene derivatives.

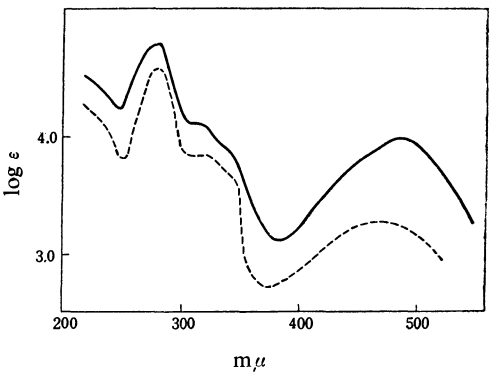



Fig. 3. UV absorption spectra of VII (——) and 3-ethoxycarbonyl-2-(diethoxycarbonylmethyl)-1-azaazulene (----) in methanol.

III is insoluble in water but dissolves in an aqueous solution of potassium hydroxide, from which it is extracted with an organic solvent. These foregoing facts show that III is an amphoteric substance and its behavior resembles that of pyrrole or indole to acids and alkalis.

These experimental results support the structure of IIIa for III.

Recently, Seto and others[5] prepared 2-chloro-3-ethoxycarbonyl-1-azaazulene (X) from 3-ethoxycarbonyl-1-azaazulan-2-one (IX) and

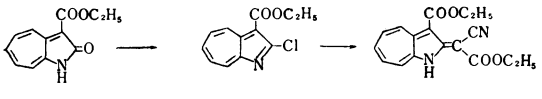
3) Measured by a Beckman Model DU spectrophotometer.

4) IR spectra are measured using a Perkin-Elmer Model 21 double beam spectrophotometer by Mr. S. Aono of this Institute, to whom the author is deeply indebted.

5) S. Seto et al., to be published.

obtained corresponding condensates by condensation of X with diethyl malonate and ethyl cyanoacetate.

Comparative examination of III with the condensate, m. p. 165°C, of X with ethyl cyanoacetate showed that they are the same substances. Consequently, III was proved to have IIIa structure, i. e. 2-(cyano-ethoxycarbonylmethylene)-3-ethoxycarbonyl-1-azaazulane.



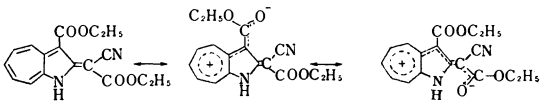
IX X III

Further examination was made on the absorption band at 1650 $cm^{-1}$ in the infrared spectrum of III to see whether it is due to the ester carbonyl conjugated with unsaturated bond, stretching vibration of C=C, or to deformation vibration of N–H group. In order to confirm this point, a deuterated compound ($III_D$) of III was prepared.

$III_D$ was easily obtained on decomposition of VI with deuterium oxide. Admixture of $III_D$ with III showed no depression in the melting point and the ultraviolet absoption spectrum of $III_D$ in anhydrous cyclohexane agreed with that of III. The infrared spectrum of $III_D$, indicated in Fig. 2b, shows that the absorption bands at 3220, 1225 and 710 $cm^{-1}$ in III have disappeared and new bands have appeared at 2420, 1533 and 1186 $cm^{-1}$ in the spectrum of $III_D$, with decreased intensity of the absorption band at 1563 $cm^{-1}$.

The wave number ratio of 3220 $cm^{-1}$ in III and 2420 $cm^{-1}$ in $III_D$ is 1.330, which approximately agrees with the usual value of $\nu$(N–H)/$\nu$(N–D)[6]. Since the absorption band at 710 $cm^{-1}$ in III is active to deuteration, this absorption can be assigned to the out-of-plane deformation vibration of the N–H group. The absorption band at 1650 $cm^{-1}$ in III is still present in $III_D$ so that it is not due to any deformation vibration of the N–H group but should be the stretching vibration of ester carbonyl or the exo-methylene group. If it were due to the carbonyl, the absorption has a very much lower frequency for that of unsaturated ester carbonyl. This fact indicates that there is a large contribution of ionic structures such as those shown in Scheme 1 in III.

In oder to determine the assignment of absorption bands at 1688 and 1650 $cm^{-1}$, 2-(dicyanomethylene)-3-ethoxycarbonyl-1-azaazulane (XI) and 2-(cyano-ethoxycarbonylmethylene)-3-cyano-1-azaazulane (XII) were prepared and their infrared spectra were measured. Condensation of X and sodiomalononitrile in dry dioxane afforded lustrous red crystals XI, m. p. above 260°C.



Scheme 1.

Condensation of 2-chloro-3-cyano-1-azaazulene (XIII) and ethyl sodiocyanoacetate in dehydrated dioxane produced dark red crystals (XII), m. p. 230°C. The ultraviolet absorption spectra of XI and XII are indicated in Fig. 4 and the infrared spectra of XI and XII are shown respectively in Fig. 5a and b. These infrared spectra exhibit an absorption band due to ester carbonyl at 1690 $cm^{-1}$ in XI and at 1645 $cm^{-1}$ in XII.

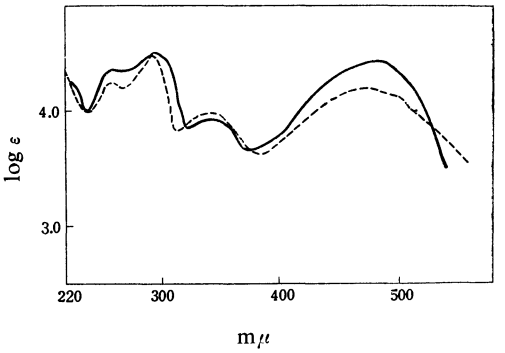



Fig. 4. UV absorption spectra of XI and XII in methanol.
—— XI, ----- XII

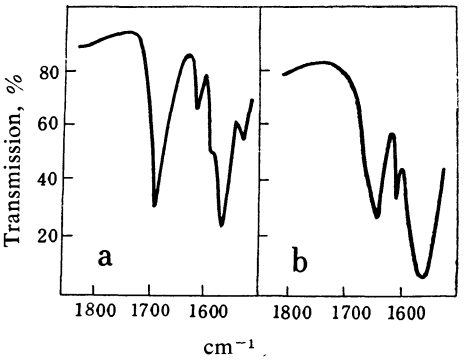



Fig. 5. IR absorption spectra of XI (a) and XII (b) in KBr disk.

These facts prove that the absorption band at 1688 $cm^{-1}$ in III is due to the carbonyl group in the ester at 3-position and that at 1650 $cm^{-1}$ is the absorption of the ester carbonyl group bonded to the methylene group

6) L. J. Bellamy, "The Infrared Spectra of Complex Molecules", Methuen (1958), p. 257.

and that it is not due to the stretching vibration of exo-methylene.

Analytical values of IV correspond to the molecular formula of $C_{15}H_{12}O_4N_2$ and its ultraviolet spectrum is similar to the absorption curve of 1-oxaazulan-2-one or 1-azaazulan-2-one derivatives. The infrared spectrum of IV, as indicated in Fig. 6a, exhibits the absorptions at 3380 and 3278 $cm^{-1}$ for primary amino group, at 2205 $cm^{-1}$ for cyano group conjugated with unsaturated bond, at 1740 $cm^{-1}$ for carbonyl in unsaturated $\gamma$-lactone, and at 1675 $cm^{-1}$ for ester carbonyl conjugated with unsaturated bond. From these results, IV is assumed to be a 1- oxaazulan-2-one derivative.

Seto obtained 1-oxaazulan-2-one (XIV), by decomposition of 3-ethoxycarbonyl-1-oxaazulan-2-one or 3-acetyl-1-oxaazulan-2-one with concentrated sulfuric acid.[7]

The same decomposition of IV with concentrated sulfuric acid afforded XIV, m. p. 69°C, and this has proved that IV is $\alpha$-amino-$\alpha$-(1-oxaazulan-2-on-3-yl)-$\beta$-cyano-$\beta$-ethoxycarbonyl-ethylene.

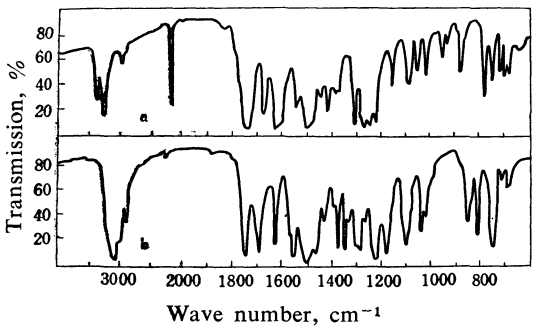
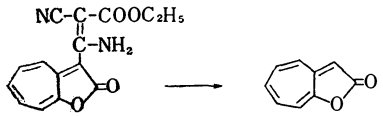



Fig. 6. IR absorption spectra of IV(a) and V(b) in KBr disk.




IV XIV

Analytical values of V correspond to the molecular formula of $C_{17}H_{18}O_5N_2$ and the infrared spectrum of V, indicated in Fig. 6b, exhibits a strong and broad absorption band at around 3100 $cm^{-1}$, absorption of cyano group at 2260 $cm^{-1}$, that of ester carbonyl at 1740 $cm^{-1}$, and that due to ester carbonyl conjugated with unsaturated bond at 1688 $cm^{-1}$.

Sometimes V is not obtained by condensation of I and II and the yield of V is generally poor. Further examination of this product was not made.

7) S. Seto, *Sci. Repts. Tohoku Univ.* (*I*), 37, 367 (1953).

Reaction of 2-methoxytropone (XV) and II in the presence of an alkoxide results in almost complete recovery of XV and III, IV and V are not obtained.

From the foregoing results, it was shown that 2-aminoazulene derivative was not formed in the condensation of troponoids with II.

## Experimental

**Reaction of 2-Chlorotropone (I) and Ethyl $\alpha$-Cyano-$\beta$-aminoglutaconate (II).**—a) To a solution of sodium ethoxide, prepared from 250 mg. of metallic sodium and 10 ml. of absolute ethanol, 2.45 g. of II was added and a solution of 1.5 g. of I dissolved in 30 ml. of absolute ethanol was added to it with stirring under ice-cooling. The solution colored red immediately. The mixture was allowed to stand at room temperature for 3 hr. and the red crystals that separated out were collected by filtration. The collected crystals were dissolved in benzene to separate them from colorless inorganic salt and evaporation of benzene left red crystals of m. p. 155~159°C. Repeated recrystallization from ethanol afforded 800 mg. of red needles (III), m. p. 163~165°C.

The reaction mixture left after the removal of the above crystals was evaporated to dryness under reduced pressure and the residue separated into crystalline and oily substances. This residual mixture was dissolved in benzene to be separated into benzene-soluble and insoluble portions.

The benzene-soluble portion afforded 350 mg. of III.

Found: C, 65.52; H, 5.38; N, 8.56. Calcd. for $C_{17}H_{16}O_4N_2$: C, 65.37; H. 5.16; N, 8.97%.

UV $\lambda_{max}^{MeOH}$ m$\mu$ (log $\varepsilon$): 260 (4.32), 289.5 (4.37), 340 (3.98), 490 (4.37).

Addition of water to the benzene-insoluble portion precipitated 200 mg. of orange crystals insoluble in water. This substance is extremely sparingly soluble in various organic solvents. Its recrystallization from a large quantity of chloroform afforded orange-yellow scales (IV), m. p. above 260°C.

Found: C, 63.58; H, 4.01; N, 9.85. Calcd. for $C_{15}H_{12}O_4N_2$: C, 63.38; H, 4.26; N, 9.86%.

UV $\lambda_{max}^{MeOH}$ m$\mu$ (log $\varepsilon$): 254 (4.43), 282 (4.14), 399 (4.27).

The water-soluble portion of this mixture produced, upon neutralization with dilute nitric acid, 750 mg. of brown precipitate and five recrystallizations from ethanol afforded 150 mg. of colorless scales V, m. p. 195~197°C.

Found: C, 61.85; H, 5.71; N, 8.83. Calcd. for $C_{17}H_{18}O_5N_2$: C, 61.81; H, 5.49; N, 8.48%.

UV $\lambda_{max}^{MeOH}$ m$\mu$ (log $\varepsilon$): 230 (4.43), 300 (4.21), 388 (3.92).

b) To a solution of 1 g. of I and 1.7 g. of II dissolved in 30 ml. of absolute ethanol, 1.4 g. of tributylamine was added under ice-cooling and the solution changed from orange to red. After allowing the mixture to stand for 5 hr. at room

8) All melting points are uncorrected. The microanalyses were carried out by Mr. S. Ohyama and Miss. Y. Endo of this Institute, to whom the author is deeply indebted.

temperature, the red leaflet crystals that separated out were collected by filtration and treated with chloroform to be separated into chloroform-soluble and insoluble portions.

Red needle crystals separated from the chloroform-soluble portion and recrystallization from ethyl acetate gave 550 mg. of III. The solid sparingly soluble in chloroform was recrystallized from a large quantity of chloroform to 420 mg. of orange-yellow crystals IV.

The reaction mixture after separation of the above products was evaporated, the residue was dissolved in chloroform, and the solvent was evaporated to dryness from the chloroform extract. The red crystalline residue thereby obtained was recrystallized from ethanol to 140 mg. of III.

**Sodium Compound (VI) of III.**—A solution of sodium ethoxide, prepared from 10 mg. of metallic sodium and 1 ml. of absolute ethanol, was added to the solution of 100 mg. of III dissolved in 1 ml. of dehydrated benzene by which 100 mg. of amorphous orange-red solid (VI), m. p. above 260°C, formed immediately. The solid was collected, washed with benzene, and dried.

VI was dissolved in water and extracted with benzene. The benzene extract was dried over anhydrous sodium sulfate and evaporation of benzene left 70 mg. of III. The residual aqueous solution was adjusted to pH 7 and extracted with benzene. The benzene extract was dried over anhydrous sodium sulfate and evaporated, leaving 20 mg. of III.

Found: N, 8.46. Calcd. for $C_{17}H_{15}O_4N_2Na$: N, 8.35%.

**Reaction of III and Picric Acid.**—a) A mixture of 50 mg. of III and saturated solution of picric acid in ethanol was warmed on a water bath to effect solution and the solution was allowed to stand at room temperature. The red needle crystals that separated out were recrystallized from ethyl acetate and 40 mg. of III was recovered.

b) A mixture of 50 mg. of III and 100 mg. of picric acid was placed in a test tube and the tube was heated in a water bath at 90°C to effect solution. Addition of ethanol to this solution separated 120 mg. of orange-yellow crystals, m. p. 156~158°C (decomp.), sparingly soluble in ethanol.

Found: N, 12.81. Calcd. for $C_{23}H_{19}O_{11}N_5$: N, 12.79%.

**Action of Aqueous Alkali Solution on III.**—A solution of 20 mg. of III dissolved in 1 ml. of 10% potassium hydroxide aqueous solution was heated on a water bath for 1 hr., cooled, and adjusted to pH 7. The red crystals thereby produced were recrystallized from ethanol and ca. 15 mg. of III was recovered.

**Action of Acetic Anhydride on III.**—A solution of 50 mg. of III dissolved in 1 ml. of acetic anhydride to which was added 1 drop of pyridine was heated at 120°C for 3 hr. Acetic anhydride was evaporated and the residue was recrystallized from ethanol, by which 30 mg. of III was recovered.

**Action of Diazomethane of III.**—The excess of ether solution of diazomethane was added to the solution of 20 mg. of III dissolved in 30 ml. of ether and the mixture was allowed to stand at room temperature for 4 hr. Evaporation of ether left crystals which were recrystallized from ethyl acetate and III was recovered.

**Action of Acid on III.**—a) Dropwise addition of 0.2 ml. of 2 N hydrochloric acid to a solution of 50 mg. of III dissolved in 1 ml. of ethanol by application of heat resulted in yellowing of the solution. Ethanol was evaporated from this mixture, the residue was neutralized with sodium hydrogencarbonate solution, and the dark red precipitate that formed was extracted with benzene. The benzene extract was dried over anhydrous sodium sulfate and passed through a column of alumina, by which the product separated into red, blue and green bands.

Elution of the red band with benzene afforded ca. 5 mg. of red leaflets VII, m. p. 153~155°C.

Elution of the green band with ethyl acetate failed to give any crystalline product.

VII formed a picrate of m. p. 156~158°C on addition of saturated ethanol solution of picric acid.

Found: N, 13.02. Calcd. for $C_{23}H_{19}O_{11}N_5$: N, 12.79%.

b) Dry hydrogen chloride gas was passed through a solution of 50 mg. of III dissolved in dehydrated benzene and the yellow needle crystals (VIII) that separated out were collected by filtration. This product underwent a change by atmospheric moisture. The product was dissolved in water, neutralized with sodium hydrogencarbonate, and the precipitate was extracted with benzene from which 10 mg. of a substance agreeing with VII, m. p. 153~155°C, was obtained.

**Deuterated Compound ($III_D$).**—A solution of 100 mg. of VI dissolved in 1 ml. of deuterium oxide to which was added 1 drop of acetic anhydride was allowed to stand at room temperature for 1 hr. The red needle crystals that separated out were recrystallized from dehydrated benzene-cyclohexane mixture and 60 mg. of $III_D$, m. p. 163~164°C, undepressed on admixture with III, was obtained.

**Synthesis of 2-(Dicyanomethylene)-3-ethoxycarbonyl-1-azaazulane (XI).**—To a sodium ethoxide solution prepared from 50 mg. of metallic sodium and 2 ml. of absolute ethanol, 250 mg. of malononitrile was added to form its sodio compound and ethanol was evaporated completely. The residue was suspended in 2 ml. of dehydrated dioxane, 250 mg. of 2-chloro-3-ethoxycarbonyl-1-azaazulene (X) was added to it, and the mixture was heated at 90°C for 1 hr. The reaction mixture colored dark red and orange precipitate separated gradually. Dioxane was evaporated from this mixture, the residue was dissolved in water, and the solution was acidified with acetic acid by which a lustrous crystalline precipitate was produced. Recrystallization from acetone gave 120 mg. of lustrous red crystals XI, m. p. above 260°C.

Found: C, 67.74; H, 4.08; N, 15.98. Calcd. for $C_{15}H_{11}O_2N_3$: C, 67.91; H, 4.18; N, 15.84%.

UV $\lambda_{max}^{MeOH}$ mμ (log ε): 259 (4.23), 295 (4.47), 340 (3.92), 483 (4.43).

**Synthesis of 2-(Cyano-ethoxycarbonylmethylene)-3-cyano-1-azaazulane (XII).**—To a suspension of 50 mg. of sodium in 2 ml. of dehydrated dioxane,

400 mg. of ethyl cyanoacetate was added and the mixture was warmed to form the sodio compound. A mixture of this sodio compound and 200 mg. of 2-chloro-3-cyano-1-azaazulene (XIII) was heated at 90°C for 1 hr., by which the solution became dark red and a reddish orange precipitate began to separate out. Dioxane was evaporated, the residue was dissolved in water, and the aqueous solution was acidified with acetic acid. The dark red precipitate thereby formed was recrystallized from acetone and 280 mg. of dark red needles XII, m. p. 230°C (decomp.), was obtained.

Found: C, 67.83; H, 4.26; N, 15.67. Calcd. for $C_{15}H_{11}O_2N_3$: C, 67.91; H, 4.18; N, 15.84%.

UV $\lambda_{max}^{MeOH}$ $m\mu$ (log $\varepsilon$): 256 (4.21), 293 (4.46), 340 (3.80), 490 (4.18).

**Formation of 1-Oxaazulan-2-one (XIV).** — A solution of 100 mg. of IV dissolved in 0.2 ml. of concentrated sulfuric acid was heated on a water bath for 1 hr. and the brownish orange solution that formed was diluted with water. This was extracted with benzene, the extract was washed thoroughly with water, and dried over anhydrous sodium sulfate. Evaporation of benzene left an oily substance with aroma.

This residue was digested with hot cyclohexane, the orange crystals thereby obtained were sublimed in reduced pressure, and the sublimate was recrystallized from cyclohexane, affording XIV, m. p. 69~71°C.

The author takes this opportunity to express his sincere gratitude to Professor Tetsuo Nozoe and Professor Shuichi Seto for their kind guidance throughout the course of this work, and to Mr. Fumio Sato for his cooperation in carrying out the experiments.

*The Chemical Research Institute of Non-Aqueous Solutions*
*Tohoku University*
*Katahira-cho, Sendai*

# *Studies on Micro-paraffin. III. Properties and Spectra of Each Fraction of Micro-paraffin Separated by Urea Method and Chromatography*

By Kazuo NEGORO

(Received December 20, 1960)

Since Bengen's discovery in 1940[1,2], it has been observed with interest that crystalline molecular compounds, that is to say, urea adductible components, were formed by urea and organic compounds of straight-chain structure and numerous studies on this reaction have been reported. The application of this reaction has been remarkably developed as one of the excellent separation methods of organic compounds[3]. Phillips[4] explained that 20~90% of urea adductible compenents were contained in microcrystalline waxes.

Molecular compounds, formed by urea and ordinary paraffin waxes, were previously reported[5,6], and the studies on micro-paraffins will be explained in this report. The micro-paraffin was separated into two groups of compounds; one was of the straight-chain structure forming adducts with urea and the other was of the non-straight-chain structure forming no adducts. Then, each group was separated into three fractions soluble in pentane, benzene, and alcohol, successively, by chromatography with silica gel. The crystal properties of each soluble fraction were studied and its ultraviolet and infrared absorption spectra were measured.

As a result of these experiments, it was confirmed that it was reasonable to consider that the cause of the micro-crystallization of the so-called micro-paraffin should be not essential, but derived by secondary factor. It was also confirmed that about 60% of the micro-paraffins obtained from the tank residue of Arabian crude oil (Aramo oil in Saudi-Arabia)[7] consisted of urea adductible paraffins which had higher melting points and lower refractive indices than those of non-adductible ones. However, it was found when the ultraviolet spectra of each soluble fraction was separated by chromatography that small quantities of various aromatics were mixed with the fractions and an absorption band due to the double band was observed on the infrared

1) F. Bengen, German Pat. O. Z 12438 (1940).
2) F. Bengen, *Angew. Chem.*, **63**, 207 (1951).
3) "The Chemistry of Petroleum Hydrocarbons" (Sekiyu Tankasuiso Kagaku) I, Kyoritsu Shuppan Co., Tokyo (1956), p. 26.
4) J. Phillips, *Petroleum Refiner*, **38**, No. 9, 193 (1959).
5) E. Kuraku, S. Yagi and K. Negoro, *Science (Kagaku)*, **22**, 216 (1952).
6) E. Kuraku, S. Yagi and K. Negoro, ibid., **22**, 363 (1952).
7) K. Negoro, *J. Chem. Soc. Japan, Ind. Chem. Sec. (Kogyo Kagaku Zasshi)*, **64**, 295 (1961),

spectrum of the benzene soluble fraction. After recrystallization of each fraction with ethyl alcohol, it was observed by the microscope that the adductible paraffin formed plate crystals, and the fractions soluble in pentane and benzene separated from micro-paraffin by chromatography also formed plate crystals. These phenomena were proved by the infrared spectra indicating that each fraction showed the characteristic crystal band[8] in the wavelength of 13.7~13.9 $\mu$ (wave number of 730~710 $cm^{-1}$).

On the contrary, the non-adductible paraffin showed a micro-crystalline state; the only exception was the pentane soluble fraction separated from non-adductible micro-paraffins by chromatography, which formed plate crystals.

## Experimental

**Formation of Urea Adducts.**—Micro-paraffin was dissolved in benzene and treated with solid urea. The activators for the reaction were water and methyl alcohol. The formed molecular compounds of urea and straight chain paraffins (urea adducts) were separated from the non-adductible paraffin with urea by a suction filter with a vacuum pump.

The adducts were dried to constant weight watching the temperature to avoid decomposition, and finally, were decomposed with hot water. The adductible paraffins were separated from urea by dissolving them in hot water.

They were separated by filtration as they solidified with the drop of temperature. They were completely dried in a desiccator and weighed. The so-called urea reject or adductible paraffin, was weighed after benzene, methyl alcohol and water were expelled by solvent recovery apparatus. The conditions of the experiments are shown in Table I.

TABLE I. UREA ADDUCTS REACTION

| | |
|---|---|
| Micro-paraffin | 112.5 g. |
| Benzene | 1700 cc. |
| Urea | 450.0 g. |
| Methyl alcohol for activator | 45 cc. |
| Water | 4.5 cc. |
| Reaction temp. | 33°C |
| Reaction time | 50 min. |
| Drying temp. of adducts | 35~45°C |
| Drying time of adducts | 60 hr. |
| Hot water | 6000 cc. |
| Temp. of hot water | 70~80°C |

The materials used in the experiment were as follows:

Methyl alcohol: b. p. 65°C, refined from commercial first grade product by distillation.

Benzene: b. p. 80°C, refined from commercial product by ordinary method[9].

Urea: m. p. 132.6°C, refined by recrystallization method.

**Chromatography.** — Each of the adductible and non-adductible paraffins was dissolved in a large quantity of pentane.

Twenty grams of the adductible paraffin was weighed out and dissolved in 16 l. of pentane; and 20 g. of the non-adductible paraffin was weighed out as above and dissolved in 12 l. of pentane.

Each of the two was charged into the column for chromatography, and treated with pentane, benzene, and ethyl alcohol to be separated into their soluble fractions.

The column used was a glass tube of 160 cm. in length and 6 cm. in diameter, and packed with 3 kg. of 80 mesh silica gel that had been dried for 8 hr. at 120°C.

**Measurement of Physical Properties.** — *Mean Molecular Weight.*—Measured by the depression of freezing point[10] in refined benzene.

*Melting Point.*—Measured by the method of dropping point[11].

*Refractive Index.*—Measured by an Abbe refractometer at 70°C (higher than melting point of paraffins).

**Observation of Crystals**[12].—The adductible and non-adductible paraffins and their pentane, benzene and ethyl alcohol soluble fractions separated by chromatography were recrystallized with solvent (ethyl alcohol; b. p. 78°C). The crystals were observed with ordinary or phase-contrast microscopes. One gram of each paraffin sample was dissolved in 300 cc. of ethyl alcohol and the solution was warmed to 70°C in a thermostat. Then, it was gradually cooled to room temperature and recrystallized.

**Measurement of Ultraviolet Absorption Spectrum.** — A photo-electric spectrophotometer of Type EPU-2 manufactured by Hitachi Mfg., Co. was used for the measurement of ultraviolet absorption spectrum. About 0.5 g. of the sample was taken and weighed accurately, and then dissolved in 5 g. of refined *n*-hexadecane to make up the solution of concentration of 10 wt. %. The solution was diluted to a tenth its former strength by the weighing method, successively, to make concentrations of 1, 0.1 and 0.01%. The ultravioled spectra of these solutions were measured at room temperature. *n*-Hexadecane, refined from commercial special grade product by the same process as the previous report[13], was confirmed to be fit for a diluent by measuring the degree of transparency in the range of wavelength of 220~420 m$\mu$.

8) K. Negoro, *J. Chem. Soc. Japan, Pure Chem. Sec.* (*Nippon Kagaku Zasshi*), **82**, 229 (1951)..

9) "Text-book of Chemical Experiment" (Jikken Kagaku Koza) 2 (Fundamental Technique II), Maruzen, Tokyo (1956), p. 73.

10) J. Sameshima, "Experimental Methods of Physical Chemistry" (Butsuri Kagaku Jikkenho), Shokabo, Tokyo (1941), p. 227.

11) Nippon Oil Co., "Test-methods of Petroleum" (Sekiyu Shikenho), Sekiyu-keizai-kenkyukai, Tokyo (1954), p. 218.

12) S. Yagi and K. Negoro, *Chem. Ind. Japan* (*Kagaku Kogyo*), **8**, 1112 (1957).

13) K. Negoro, *Report of Central Research Laboratory, Nippon Mining Co.* (*Nikko Chuo Shikenjo Shoho*), **11**, No. 3, 1139 (1960).

**Measurement of Infrared Absorption Spectrum.** — A infrared spectrophotometer of Perkin Elmer Model-21 was used for the measurement of infrared spectrum. The sample of the adductible or non-adductible paraffins and each fraction separated by chromatography were applied on the spectrophotometer and measured.

## Results and Discussions

**Results of Urea Adducts Formation.** — The micro-paraffins which were obtained from the tank residues of Arabian crude oil were treated with urea, and the results are shown in Table II.

TABLE II. UREA TREATMENT OF MICRO-PARAFFIN

| Material | Weight, g. | Yield, % |
|---|---|---|
| Micro-paraffin | 112.5 | 100.0 |
| Urea adductible paraffin | 69.5 | 61.8 |
| Urea non-adductible paraffin | 33.1 | 28.9 |
| Loss | 9.9 | 9.3 |

According to Philips[4], it was reported that micro-crystalline waxes contained 20~90% of urea adductible components. Turner et al.[14] reported that ordinary crystalline waxes contained 80~90% of *n*-paraffin by the results of the examination by mass-spectra on 16 sorts of paraffins. As results of the above reports, it is considered that the so-called micro-paraffins have higher molecular weight than that of the ordinary crystalline waxes and that the former contain side chain substances in a larger amount than the latter. It seems to be reasonable to consider that isoparaffins which have some side chains and the paraffins which have one or two aromatic or naphthene rings form adducts with urea as reported by Zimmerschied[15].

It will not be stated that all the components of such urea adductible paraffins consist of *n*-paraffin alone (small quantities of side-chain paraffins may be contained). The above consideration will also be confirmed by the results of chromatography, ultraviolet spectroscopy, and infrared spectroscopy as mentioned below.

**Results of Chromatography and Properties of Each Fraction.** — The adductible and non-adductible paraffins were separated by chromatography with silica gel.

The yields of each fraction are shown in Table III.

Great differences of the yields of each fraction were not seen between the two paraffins. However, there were great differences between the results of the physical properties of each fraction as shown in Table IV.

The non-adductible paraffins have higher mean molecular weights, lower melting points, and very much higher refractive indices than the adductible paraffins. Then, it was shown that in micro-paraffins, straight-chain hydrocarbons were separated effectively from substances having side-chains and aromatics.

TABLE III. RESULTS OF CHROMATOGRAPHY

| | Micro-paraffin | Urea adductible paraffin | Urea non-adductible paraffin |
|---|---|---|---|
| Pentane soluble fraction | 75.4 (76.8)* | 79.0 (86.8) | 76.5 (84.5) |
| Benzene soluble fraction | 17.0 (17.3) | 9.5 (10.4) | 9.5 (10.5) |
| Ethyl alcohol soluble fraction | 5.8 (5.9) | 2.5 (2.8) | 4.5 (5.0) |
| Loss | 1.8 (—) | 9.0 (—) | 9.5 (—) |
| Total | 100.0 (100.0) | 100.0 (100.0) | 100.0 (100.0) |

* The values in ( ) show the yield (%) of each fraction, from which loss is subtracted.

TABLE IV. PHYSICAL PROPERTIES OF EACH FRACTION

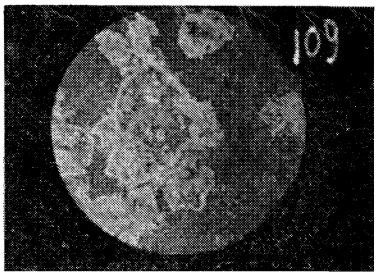
| | Mean molecular weight | | M. p., °C | | Refractive index, $n_D^{70}$ | |
|---|---|---|---|---|---|---|
| | A Urea adductible paraffin | B Urea non-adductible paraffin | A | B | A | B |
| Base micro-paraffin | 613 | 620 | 67.0 | 54.4 | 1.4400 | 1.4460 |
| Pentane soluble fraction | 607 | 636 | 65.0 | 54.0 | 1.4390 | 1.4410 |
| Benzene soluble fraction | 591 | 602 | 20 | 20 | 1.5050 | 1.5200 |
| Alcohol soluble fraction | 636 | 627 | 67.0* | 46.5* | —** | —** |

* Though each fraction was dropped at 57.0 or 46.5°C in measuring, some parts of the residues were solid. It was difficult to determine the melting point.

** Measurements were impossible.

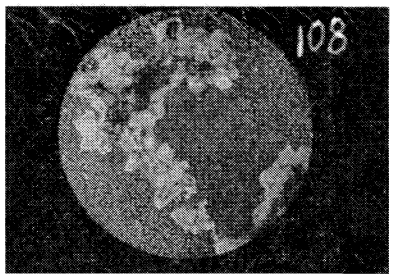
14) W. R. Turner et al., *Ind. Eng. Chem.*, **47**, 1219 (1955).

15) W. J. Zimmerschied et al., ibid., **42**, 1300 (1950).



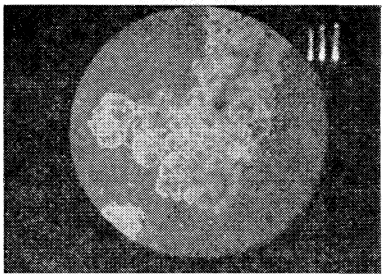

×100

Fig. 1. Urea adductible paraffin (A).



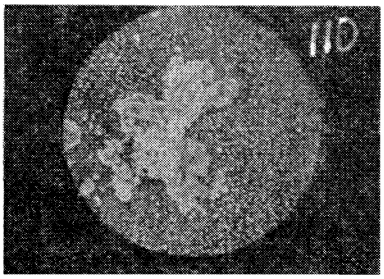

×100

Fig. 2. Urea non-adductible paraffin (B).



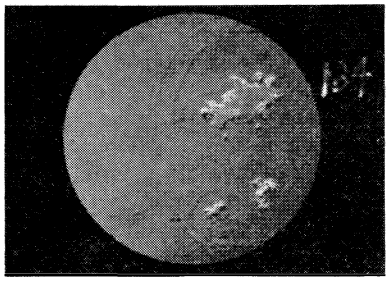

×100

Fig. 3. Pentane franction of A.



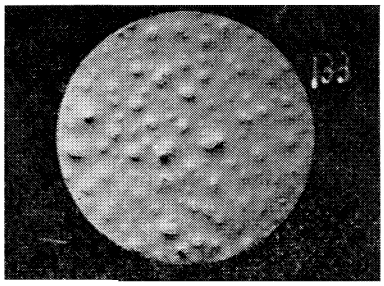

×100

Fig. 4. Pentane fraction of B.



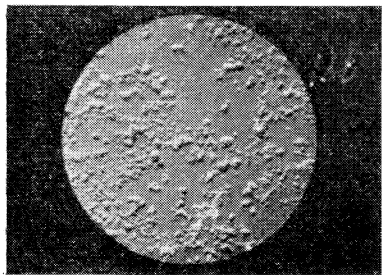
×100

Fig. 5. Benzene fraction of A.



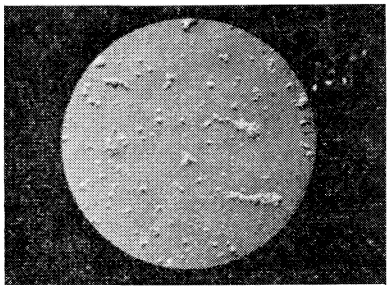
×100

Fig. 6. Benzene fraction of B.



×100

Fig. 7. Alcohol fraction of A.



×100

Fig. 8. Alcohol fraction of B.

In particular, by the fact that the non-adductible paraffins have very high refractive indices, it should be suggested that they consist of complicated compounds[16].

It has already been known that hydrocarbons with side-chains and aromatic or naphtheric substances have lower melting points and higher refractive indices[17,18].

16) P. T. Edwards, *Petroleum Refiner*, **36**, 180 (1957).
17) A. N. Sachanen, "The Chemical Constituents of Petroleum", Reinhold Publ. Corp., New York (1945), pp. 289—296.
18) K. Negoro, *Chemistry (Kagaku)*, **15**, No. 5, 16 (1960).

**Results of the Observation of Crystals.**—Each fraction obtained by chromatography from the non-adductible paraffins was recrystallized with ethyl alcohol and observed through a microscope.

The results of the observation are shown in Figs. 1—8. Figure 1 shows the adductible paraffin which forms plate crystals smaller than those of the ordinary crystalline paraffin wax.

On the other hand, the non-adductible paraffin is in a very micro-crystalline state as shown in Fig. 2.

The growth of plate crystals of the pentane soluble fraction of urea adductible paraffin (Fig. 3) has progressed further than those of base paraffin, and the pentane soluble fraction of urea non-adductible paraffin (Fig. 4) also develops to plate crystals. The benzene soluble fraction of urea adductible paraffin from plate crystals as shown in Fig. 5, but that of urea non-adductible paraffin is microcrystalline as shown in Fig. 6. The ethyl alcohol soluble fractions of the two (adductible and non-adductible) were very fine and amorphous as shown in Figs. 7 and 8. These were very different from the other fractions.

The results of such observations through the microscope conformed to the results of measurement of infrared spectra of each paraffin, and these facts are interesting for the investigation on microcrystallization of micro-paraffin.

**Results of Measurement of Ultraviolet Spectrum.** — Each fraction of urea adductible or non-adductible paraffins was diluted with *n*-hexadecane, and its degree of transparency

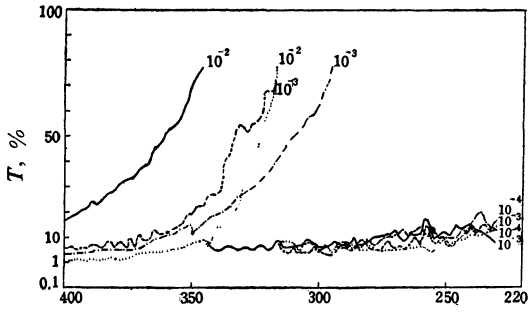



Fig. 9. Urea adductible paraffins.
——— Urea adductible paraffin (A)
– – – – Pentane fraction of A
—·—· Benzene fraction of A
····· Alcohol fraction of A

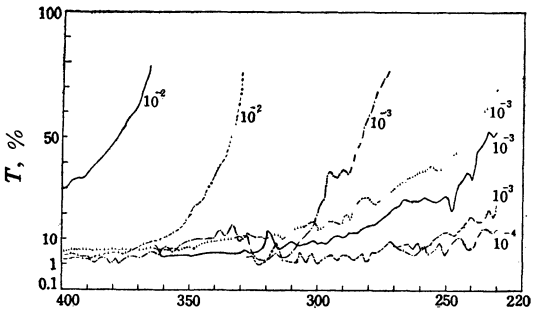



Fig. 10. Urea non-adductible paraffins.
——— Urea non-adductible paraffin (B)
– – – – Pentane fraction of B
—·—· Benzene fraction of B
····· Alcohol fraction of B

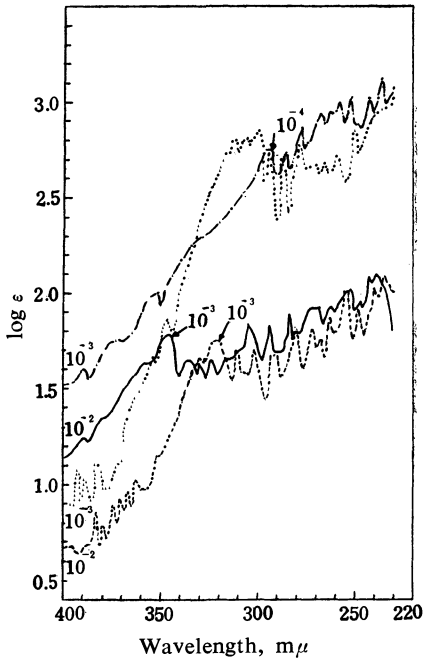



Fig. 11. Ultraviolet spectra of urea adductible paraffins.
——— Urea adductible paraffin (A)
– – – – Pentane fraction of A
—·—· Benzene fraction of A
····· Alcohol fraction of A

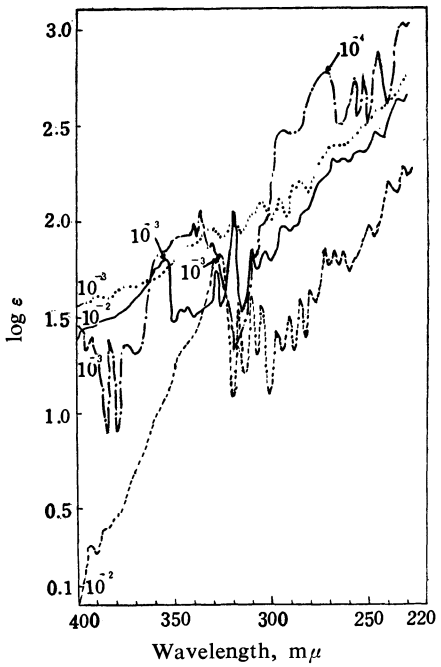



Fig. 12, Ultraviolet spectra of urea non-adductible paraffins.
——— Urea non-adductible paraffin (B)
– – – – Pentane fraction of B
—·—· Benzene fraction of B
····· Alcohol fraction of B

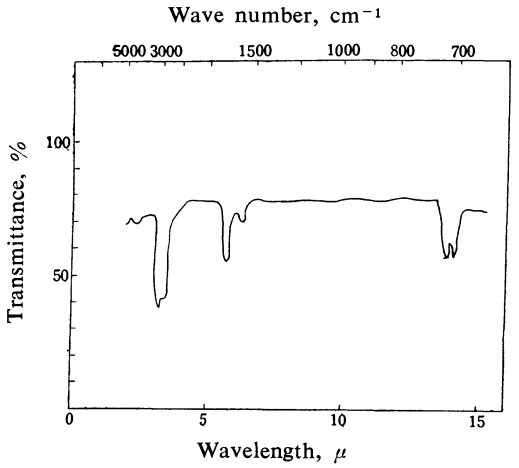



Fig. 13. Infrared spectrum of the urea adductible paraffins.

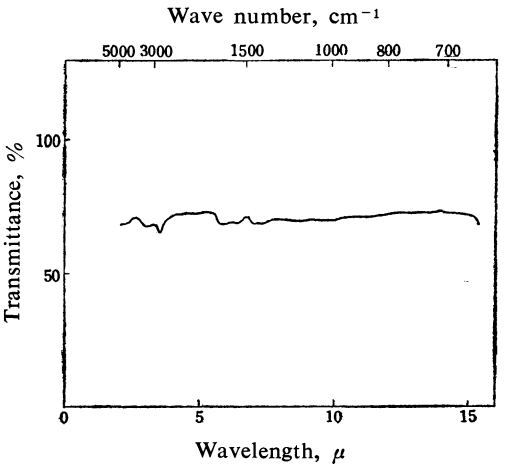



Fig. 16. Infrared spectrum of the alcohol fraction of urea adductible paraffins.

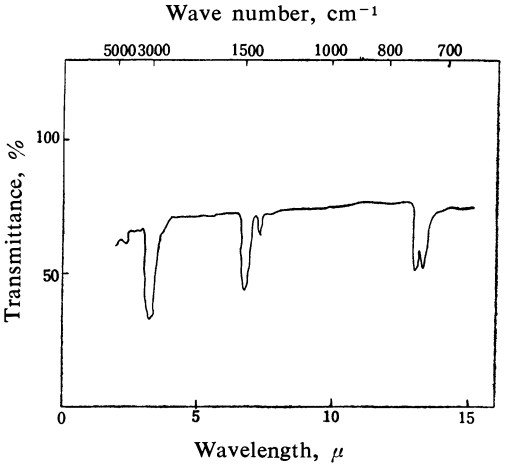



Fig. 14. Infrared spectrum of the pentane fraction of urea adductible paraffins.

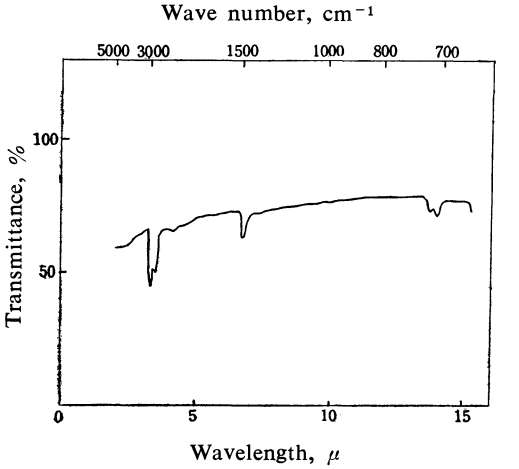



Fig. 17. Infrared spectrum of the urea non-adductible paraffins.

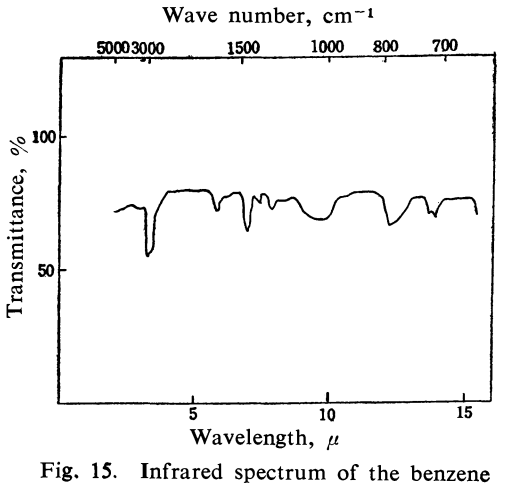



Fig. 15. Infrared spectrum of the benzene fraction of urea non-adductible paraffins.

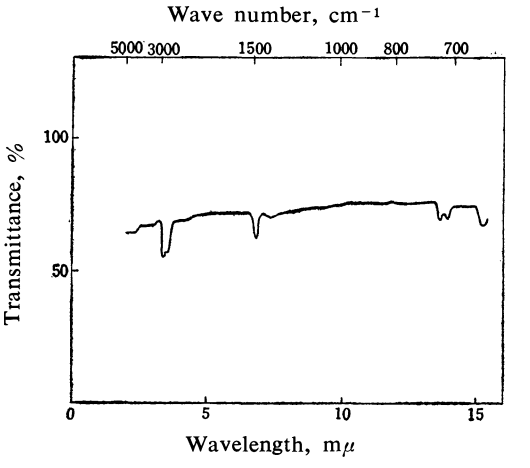



Fig. 18. Infrared spectrum of the pentane fraction of urea non-adductible paraffins.

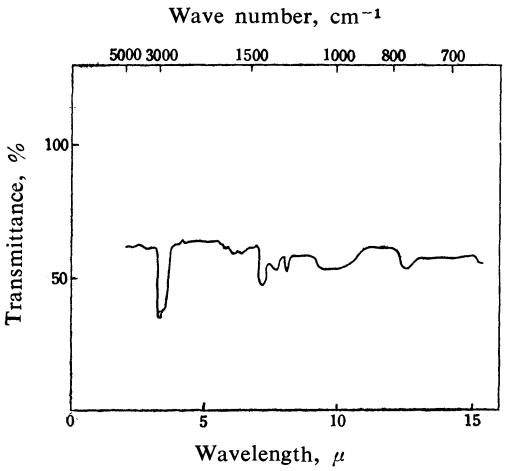



Fig. 19. Infrared spectrum of the benzene fraction of urea non-adductible paraffins.

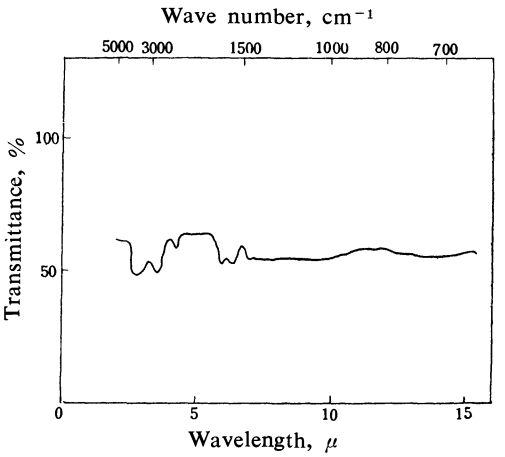



Fig. 20. Infrared spectrum of the alcohol fraction of urea non-adductible paraffins.

Tabble V. Infared spectrum of the urea adductible paraffin

| Wavelength, μ | Wave number, cm⁻¹ | Assignment of vibrations |
|---|---|---|
| 3.35 | 2990 | C-H (aliphatic) stretching vibration |
| 3.43 | 2850 | C-H (aliphatic) stretching vibration |
| 6.85 | 1458 | Deg-C-H bending vibration |
| 7.29 | 1369 | Syn-C-H bending vibration |
| 13.83 | 723 | Crystal band |
| 14.04 | 712 | Crystal band |

Table VI. Infared spectrum of the pentane fraction of the urea adductible paraffin

| Wavelength, μ | Wave number, cm⁻¹ | Assignment of vibrations |
|---|---|---|
| 3.37 | 2950 | C-H (aliphatic) stretching vibration |
| 3.44 | 2820 | C-H (aliphatic) stretching vibration |
| 6.84 | 1460 | Deg-C-H bending vibration |
| 7.27 | 1372 | Syn-C-H bending vibration |
| 13.82 | 723 | Crystal band |
| 14.02 | 713 | Crystal band |

Table VII. Infrared spectrum of the benzene fraction of the urea adductible paraffin

| Wavelength, μ | Wave number, cm⁻¹ | Assignment of vibrations |
|---|---|---|
| 2.90 | 3450 | O-H stretching vibration |
| 3.37 | 2950 | C-H (aliphatic) stretching vibration |
| 3.40 | 2850 | C-H (aliphatic) stretching vibration |
| 5.85 | 1708 | C=O stretching vibration |
| 6.25 | 1597 | Conjugated double bond stretching vibration ? |
| 6.84 | 1460 | Deg-C-H bending vibration |
| 7.27 | 1373 | Syn-C-H bending vibration |
| 7.96 | 1254 | Aromatic derivative vibration ? |
| 12.62 | 792 | |
| 13.83 | 724 | Crystal band |
| 14.02 | 713 | Crystal band |

Table VIII. Infrared spectrum of thf alcohol fraction of the urea adductible paraffin

| Wavelength, μ | Wave number, cm⁻¹ | Assignment of vibrations |
|---|---|---|
| 2.95 | 3390 | O-H stretching vibration |
| 3.40 | 2880 | C-H (aliphatic) stretching vibration |
| 5.83 | 1710 | C=O stretching vibration |

Table IX. Infrared spectrum of the urea non-adductible paraffin

| Wavelength, $\mu$ | Wave number, $cm^{-1}$ | Assignment of vibrations |
|---|---|---|
| 3.36 | 2950 | C-H (aliphatic) stretching vibration |
| 3.44 | 2820 | C-H (aliphatic) stretching vibration |
| 4.00 | 2380 | |
| 6.83 | 1461 | Deg-C-H bending vibration |
| 13.84 | 723 | Crystal band |
| 14.03 | 713 | Crystal band |

Table X. Infrared spectrum of the pentane fraction of the urea non-adductible paraffin

| Wavelength, $\mu$ | Wave number, $cm^{-1}$ | Assignment of vibrations |
|---|---|---|
| 3.36 | 2950 | C-H (aliphatic) stretching vibration |
| 3.44 | 2820 | C-H (aliphatic) stretching vibration |
| 6.85 | 1580 | Deg-C-H bending vibration |
| 7.31 | 1365 | Syn-C-H bending vibration |
| 13.85 | 722 | Crystal band |
| 14.04 | 712 | Crystal band |

Table XI. Infrared spectrum of the benzene fraction of the urea non-adductible paraffin

| Wavelength, $\mu$ | Wave number, $cm^{-1}$ | Assignment of vibrations |
|---|---|---|
| 2.55 | 3930 | |
| 3.37 | 2950 | C-H (aliphatic) stretching vibration |
| 3.44 | 2820 | C-H (aliphatic) stretching vibration |
| 5.88 | 1700 | C=O stretching vibration |
| 5.99 | 1695 | |
| 6.27 | 1590 | Conjugated double bond stretching vibration ? |
| 6.87 | 1455 | Deg-C-H bending vibration |
| 7.29 | 1360 | Syn-C-H bending vibration |
| 7.97 | 1254 | Aromatic derivatives vibration ? |
| 12.55 | 797 | |
| 14.07 | 712 | $-(CH_2)-$ rocking vibration |

Table XII. Infrared spectrum of the alcohol fraction of the urea non-adductible paraffin

| Wavelength, $\mu$ | Wave number, $cm^{-1}$ | Assignment of vibrations |
|---|---|---|
| 2.50 | 4000 | |
| 2.58 | 3880 | |
| 2.86 | 3500 | O-H stretching vibration |
| 3.37 | 2950 | C-H (aliphatic) stretching vibration |
| 3.44 | 2820 | C-H (aliphatic) stretching vibration |
| 4.20 | 2760 | |
| 5.82 | 1715 | C=O stretching vibration |
| 5.87 | 1700 | |
| 6.05 | 1650 | |
| 6.21 | 1610 | Conjugated double bond stretching vibration ? |
| 6.49 | 1540 | |
| 6.85 | 1458 | |
| 7.32 | 1358 | |

($T\%$) was measured; the results are shown in Figs. 9 and 10.

The ultraviolet spectra of the two paraffins are shown in Figs. 11 and 12, in which ordinate means $\log \varepsilon$ and abscissa wavelength ($m\mu$) calculated from the above results.

As [the results of such ultraviolet spectra, it is considered that both of the urea adductible and non-adductible paraffins contain various aromatics though their quantities are small.

**Results of Measurement on Infrared Spectrum.** —The results of the infrared spectra measured on each fraction of urea adductible and non-adductible paraffins are shown in Figs. 13—20. Though it is difficult to analyze any spectra on each fraction, the assignment of the main

vibrations has been considered as shown in Tables V—XII in reference to the results of Randall and others[19].

It was reported in our previous paper[7,8] that the results of the observation by microscope was noteworthy, showing that any substances in plate crystals had a crystal band in the range of wave number of 710~730 $cm^{-1}$ (or wavelength of 13.7~13.9 $\mu$).

## Conclusion

Comparing the urea adductible with non-adductible paraffin, there have been considerable differences in each fraction. In particular, it is very interesting that the alcohol fraction has the spectrum assigned to O-H streching vibration, which has been suggested to be the cause of micro-crystallization. It is considered that the substances which are the cause of micro-crystallization shall be contained in the alcohol fraction of urea non-adductible paraffins.

The author expresses his sincere appreciation to Professor Ryozo Goto and Professor Saburo Yagi, Kyoto University, for their cordial guidance in these studies, and is also grateful to the personnel in Osaka Ind. Tech. Lab., who co-operated with the author on the experiments of infrared spectrum.

*Central Research Laboratory*
*Nippon Mining Co.*
*Kitaadachi-gun, Saitama*

19) H. N. Randall et al., "Infra-red Determination of Organic Structure", O. van Nostrand Co., New York (1949).

# *Studies on Micro-paraffin. IV. On the Transformation of Paraffin Crystal by Addition of Pure Substances*

By Kazuo NEGORO

(Received January 23, 1961)

Numerous phenomena, concerning the micro-crystallization of microparaffin derived by secondary cause, were previously reported[1]. Many investigations were made for the crystal growth of paraffin wax in the field of lubricating oils, because it was supposed to have great effects on the pour points of oils[2]. The pour points of lubricating oils are not the melting points of oils, but it seems to be reasonable to consider that the pouring phenomenon happens when the whole fluidity of lubricating oils is lost by the crystallization of wax components contained in the oils. Therefore, additional agents are used for pour point depressants to keep the fluidity of lubricating oils in low temperature inhibiting the crystal growth of paraffin waxes. They are supposed to inhibit the crystal growth of paraffin waxes, because they are adsorbed by paraffin waxes rather than oils.

The addition of any inorganic and organic substances to ordinary crystalline paraffin waxes were examined and their structure which should inhibit the crystal growth of paraffin waxes. In particular, as seen in the report[3], the cause of micro-crystallization of microparaffins was considered to be affected by substance with hydroxyl groups derived by the results of studies on ultraviolet and infrared spectra, etc. of the components separated from the microparaffin by a propane deasphalting method, urea adducts method, and chromatography: hence, the behavior of various organic compounds having OH groups should be noticed. Then, many pour point depressants for lubricating oils, additional agents to paraffin waxes[4], and direct dyes[5] were examined at the same time. Furthermore, pure organic substances considered to be effective for the crystal growth of paraffin waxes were studied at the base of pure *n*-dotriacontane (forming plate crystals), and their effects on crystal growth of *n*-hydrocarbon (simple substance, but not mixture) were investigated.

As the above results, such as Santopour or pour point depressants for lubricating oils, picric acid, *p*-hydroxydiphenyl, and some direct

1) K. Negoro, *J. Chem. Soc. Japan, Ind. Chem. Sec.* (*Kogyo Kagaku Zasshi*), **64**, 295 (1961).
2) K. Horiguchi, "Junkatsuyu Kagaku" (The Chemistry of Lubricating Oils), Sankyo, Tokyo (1958), p. 295.
3) K. Negoro, *J. Chem. Soc. Japan, Pure Chem. Sec.* (*Nippn Kagaku Zasshi*), **82**, 229 (1961).
4) K. Negoro, *Oil Chemistry* (*Yukagaku*), **7**, 23 (1958).
5) S. Inokawa, *J. Chem. Soc. Japan, Pure Chem. Sec.* (*Nippon Kagaku Zasshi*), **76**, 726 (1955).

dyes were found to be the substances affected on the transformation of crystal growth of paraffins.

These behaviors shall be cleared by future studies, they are now being investigated by X-ray diffraction, and infrared spectra of microparaffins. However, it is very interesting that the existence of the above organic substances with hydroxyl groups and similar molecular structure, affects the transformation of the crystal of paraffin waxes. It was found, also, that there was a difference between the paraffin waxes (mixture of various hydrocarbons) and *n*-dotriacontane for such effects of addition. Therefore, the composition of paraffin was considered to be effective for the micro-crystallization of microparaffins.

## Experimental

**Materials.**—*Crystalline Paraffin.*—The sample of wax was made in the Funakawa Refinery, Nippon Mining Co., m. p. 53.5°C, and refractive index $1.4308^{70.0}$.

*n-Dotriacontane.*—The product of Fischer Scientific Co., and purchased from Pacific Gulf Oil Co.,[6] m. p. 69.2°C, sp. gr. $0.7831^{70.0}$, and refractive index $1.4308^{70.1}$.

*n*-Dotriacontane was of a high purity, but a content of some impurities was recognized by the result of the ultraviolet spectrum (wavelength 220~400 mμ) measurement with purified *n*-hexadecane as diluent. Accordingly, purification was conducted with 10% of activated clay at 75°C (yield of 78%). Such purified *n*-dotriacontane was confirmed to contain no impurities by a measurement of the ultraviolet spectrum as above, m. p. 69.5°C and refractive index $1.4315^{73.0}$.

The above values were confirmed to be almost equal to those in the literature[7].

*Chemicals.*—Many inorganic and organic chemicals, added to the crystalline paraffin or *n*-dotriacontane, were of special or 1st grade made by Kanto Kagaku Co.

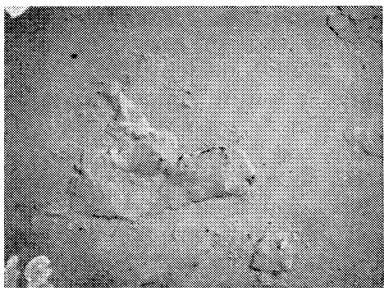
*Solvents.*—Ethyl alcohol was purified by a general method[8], and its boiling point was 78.0°C.

**Crystallization.**—Crystalline paraffin or *n*-dotriacontane was weighed accurately on a chemical balance; and 10, 1 and 0.1 wt.% of each inorganic or organic chemicals (as additive) were also weighed accurately. Both the paraffin and the additive were placed in an Erlenmeyer's flask and melted at 80°C in a thermostat. Even when there were some chemicals not melted at 80°C, the next operation was started; 1 g. of purified ethyl alcohol was added to 300 cc. of each sample with a pipette, and was warmed at 75±1°C in the thermostat to make the sample soluble in ethyl alcohol with intermittent stirring. Then, it was gradually cooled to room temperature for the growth of the crystal of the paraffin.

**Observation of Crystals by Microscope**[9].—The crystal of each sample was placed on a slide glass with a syringe, and was observed with an ordinary or phase-contrast microscope; and then, photographs of the state of each crystal were taken.

## Results and Discussion

**Effects of Various Substances on Crystallization of Crystalline Paraffin.**—*Effects of Inorganic Substances.*—The effects of the existence of various inorganic substances on the crystallization of crystalline paraffin were investigated. The crystalline paraffin at the base forms thin and large plate crystals as shown in Fig. 1, which mainly consists of *n*-paraffin (containing 88~90% of the straight chain adductible paraffin), and it is supposed that the average number of carbon chains of hydrocarbons contained to be 27*[1].



×225

Fig. 1. Crystals of crystalline paraffin.

In the case of each 10% of various metals, oxides, acids, alkalis, salts, etc., such as sulfur, zinc powder, manganese dioxide, silica, zinc oxide, aluminum chloride, sodium bicarbonate, potassium chlorate, alum, silver nitrate, ammonium vanadate, sulfuric acid, hydrochloric acid, sodium hydroxide, etc., existed with crystalline paraffin, no transformation were observed in the crystallization of the crystalline paraffins.

*Effects of Organic Substances.*—Next, the effects of 0.1~10% of various pure organic substances on crystalline paraffin were also examined. Experiments were conducted on various organic compounds; and at the same time, as explained above by the investigation of the crystal properties[1,3], ultraviolet spectra and infrared spectra on each fraction of microparaffin separated by the application of propane deasphalting method, urea adducts method, chromatography etc., the compound with hydoroxyl or carbonyl groups was considered

6) Personal communication from H. I. Goodman (Pacific Gulf Oil Co.).

7) F. Francis, O. M. Watkins and R. W. Wallington, *J. Chem. Soc.*, **121**, 1529 (1922).

8) "Text-book on Chemical Experiments" (Jikken Kagaku Koza), 2 (Fundamental Technique II), Maruzen, Tokyo (1956), p. 78.

9) S. Yagi and K. Negoro. *Chem. Ind., Japan (Kagaku Kogyo)*, **8**, No. 12, 32 (1957).

*1 It is presumed by X-ray diffraction method (X-ray diffraction of various paraffins will be mentioned in the later report of this series to be continued).

TABLE I. EFFECTS OF ORGANIC SUBSTANCES ON THE CRYSTALLIZATION OF PARAFFIN

| Sample | Molecular formula | M. p.*1 | Solubility in alcohol*2 | Effects on crystallization of paraffin |
|---|---|---|---|---|
| *p*-Hydroxydiphenyl | $C_6H_5C_6H_4OH$ | 161.5 | Sol. | Transformation (micro-crystallization) |
| Picric acid | $HOC_6H_2(NO_2)_3$ | 118 | Sol. | Transformation (micro-crystallization) |
| Glucose | $C_6H_{12}O_6$ | 134 | Sol. | Transformation |
| Quinizarine | $C_6H_4\langle^{CO}_{CO}\rangle C_6H_2(OH)_2$ | 177.5 | Sol. | Transformation (micro-crystallization) |
| Calcium stearate | $(C_{17}H_{35}COO)_2Ca$ | 110~115 | Insol. | Transformation |
| Barium stearate | $(C_{17}H_{35}COO)_2Ba$ | 195~200 | Insol. | Transformation |
| Aluminum stearate | $(C_{17}H_{35}COO)_3Al$ | 118~120 | Insol. | Transformation |
| Zinc naphthate | $(C_6H_{11}COO)_2Zn$ | | Sol. | Transformation |
| Lead naphthate | $(C_6H_{11}COO)_2Pb$ | | Sol. | Transformation |

*1 Melting point measured by the capillary tube method.
*2 Sol, soluble Insol, insoluble

to give effects on the micro-crystallization of microparaffin. Under the above circumstances, in particular, the various types of organic compounds with functional groups such as hydroxyl or carbonyl group were examined in a wide scope. In the case of each 10% of various aromatics, alcohols, aldehydes, ketones, acids, esters, salts, phenols, amines, nitrogen compounds, sulfur compounds, etc., such as naphthalene, *tert*-butyl alcohol, cetyl alcohol, cholesterol, phenol, $\alpha$- and $\beta$-naphthol, resorcinol, glycerine, pyrogallol, *p*-hydroxydiphenyl, picric acid, *m*- and *p*-nitrophenol, *o*-, *m*- and *p*-dinitrobenzene, aniline, lauril amine, triethanolamine, phenylhydrazine, azobenzene, methyl orange, hydroxyazobenzene, dinitrophenyl hydrazine, benzaldehyde, glucose, methylisobutyl ketone, acetophenone, $\alpha$- and $\beta$-naphthoquinone, quinizarine, benzoic acid, acetic acid, naphthenic acid, oleic acid, stearic acid, oxalic acid, adipic acid, 2.3- and 2.5-dihydroxybenzoic acid, salicylic acid, calcium acetate, calcium, barium and aluminum stearate, lead oleate, zinc and lead naphthate, amyl acetate benzyl acetate, ethyl chloride, trichloroethylene, methylchlorostearate, *n*-heptyl mercaptane, dibenzyl disulfide, etc. exist with crystalline paraffin, were observed in the crystallization of the crystalline paraffin, were observed in the crystallization of the crystalline paraffins. Each of the various organic compounds which transformed the crystalline properties of paraffin when being added to it, are shown in Table I.

The substances having hydroxyl groups combined with an alkyl group or a benzene ring, were hardly affected on crystallization of paraffins. Glycerine, ethylene glycol, pyrogallol, etc.[2] which were said to drop the pour points of lubricating oils when being added, were not much affected on the crystal growth of paraffins. However, in the case of *p*-hydroxydiphenyl and picric acid, the crystal growth of crystalline paraffins was evidently inhibited as shown in Figs. 2 and 3, respectively, and it is very interesting that they show a microcrystalline state.

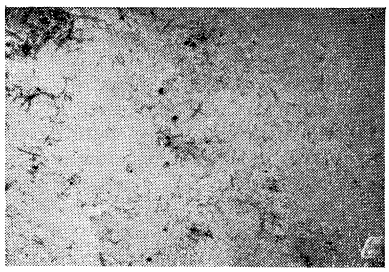

×225

Fig. 2. Transformation of crystals of crystalline paraffin caused by the addition of *p*-hydroxydiphenyl.

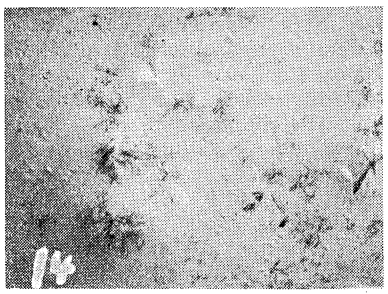

×225

Fig. 3. Transformation of crystals of crystalline paraffin caused by the addition of picric acid.

In the next stage, nitrogen compounds such as compounds having nitro, amino or azo groups, etc. were examined. But almost no effects were observed on such compounds as shown above. As the results of investigations on the compounds having aldehyde or ketone groups, quinizarine (having two hydroxyl groups in addition to ketone groups and

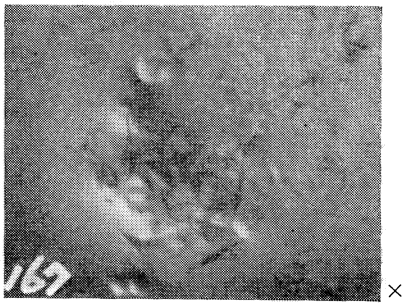

×225

Fig. 4. Transformation of crystals of crystalline paraffin caused by the addition of quinizarine.

benzene nucleus) formed the microcrystallization of crystalline wax as shown in Fig. 4. Almost no effects were given by various types of organic acids having hydroxyl groups. However, in the presence of metallic salts of stearic or naphthenic acid, microcrystalline crystals were found accompanied by plate crystals of crystalline paraffin. The metallic soaps of fatty acids are used for the pour point depressant of lubricating oils[10], and they are said to have larger effects when their molecular weights are larger. For instance, the effects of the existence of metallic salts of stearic and naphthenic acids on the crystals of a crystalline paraffin are shown in Figs. 5 and 6, respectively.

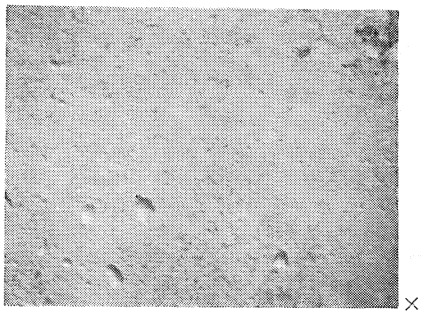

×225

Fig. 5. Transformation of crystals of crystalline paraffin caused by the addition of calcium stearate.

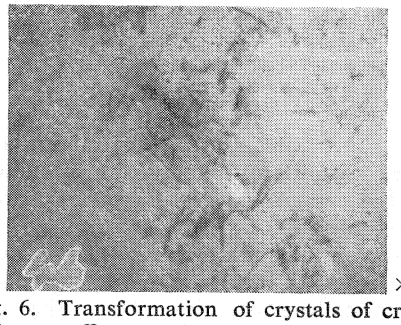

×225

Fig. 6. Transformation of crystals of crystalline paraffin caused by the addition of zinc naphthate.

Though effects of the addition of a few compounds of sulfur were investigated, so far, substances inhibiting the crystal growth of crystalline paraffins have not been found.

The substances giving effects on the transformation of crystallization are shown in Table I.

*Effects of Addition Agents.*—The results of the investigations on addition agents of paraffin waxes had been already reported[11]. The effects of the existence of such agents on the crystals of paraffin waxes were examined. Also the pour point depressants, recently being in practical use in the field of lubricating oils, are considered to have effects on keeping the fluidity of lubricating oil in lower temperature[2] by inhibiting the growth of paraffin crystals mixed in oils. Then, the effects of depressants on sale upon the crystallization of crystalline paraffins when mixed in the paraffins were also examined as above, and the results are shown in Table II.

It was found that the substance, having the most remarkable effect on the change of the crystals of paraffin wax, was Santopour. In

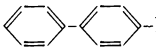
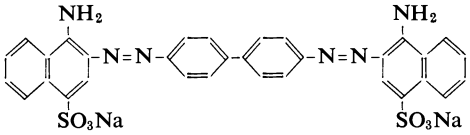
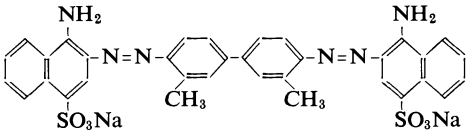
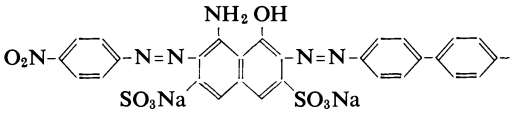
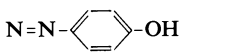
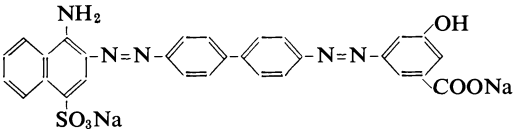
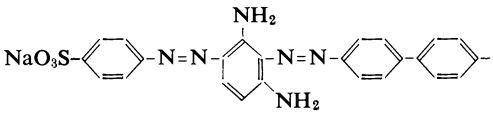
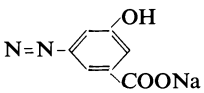
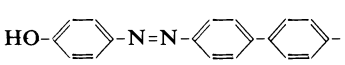
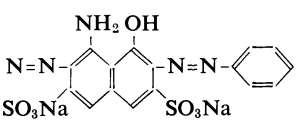
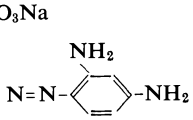
Table II. Effects of addition agents on the crystallization of paraffin

| Sample | Effects on crystallization of paraffins | Summary |
|---|---|---|
| Polyethylene | no | Improver of m. p. which micronizes the structure of paraffin |
| Acra wax c | no | Synthetic paraffin. Improver of m. p. |
| Carbo wax | no | Poly (ethylene glycol) (mol. wt. 4000) |
| Vistac | no | Polybutene (mol. wt. 1100 and 3400) |
| Ar wax | no | Paraffin added by polyethylene |
| Stroba wax | no | Paraffin mixed with a small quantity of resin |
| Adva wax | Somewhat transformation | Microparaffin added by polyethylene |
| Chloro-naphthalene | Transformation | Chlorinated naphthalene |
| Santopoid 23RI | no | Addition agents of lubricating oils |
| Ionol | no | Addition agents of lubricating oils |
| Santopour | Transformation (micro-crystallization) | Addition agents of lubricating oils |
| Santolube 70 | no | Addition agents of lubricating oils |

10) Y. Tanaka, R. Kobayashi and T. Tsukuda, *J. Soc. Chem. Ind. Japan* (*Kōgyō Kwagaku Zassi*) **38**, 10, 28, 1033 (1935).

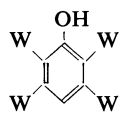
11) K. Negoro, *Oil Chemistry* (*Yukagaku*), **7**, 97 (1958).

Table III. Effect of direct dyes

| Sample | Structural formula | Effects on crystallization of paraffin |
|---|---|---|
| *p*-Aminodiphenyl |  | no |
| Congo red |  | no |
| Benzopurprine |  | no |
| Nippon green B conc. |   | Transformation (micro-crystallization) |
| Nippon orange R |  | Transformation |
| Nippon brown 3G |   | Transformation |
| Nippon dark green B conc. |   | Transformation |
| Nippon deep black ex. conc. |   | Transformation |

this case, the phenomenon of micro-crystallization as picric acid, *p*-hydroxydiphenyl, etc. was confirmed by microscopy as shown in Fig. 7.

Santopour is the product made from phenol and paraffin wax[12], and it is said to form the following structure. It is attractive that the structure is similar to that of picric acid which caused the crystals of the crystalline paraffins to micro-crystallize.



(W; paraffinic chain)

Chloronaphthalene*, which was made by blowing chlorine into naphthalene, was added to the crystalline paraffin. Then, the crystal growth of paraffin was inhibited, and almost no crystal of paraffin appeared by cooling under the same condition; it was attractive

12) N. Iimure, "Guide-book of Petroleum Products", Sangyo Tosho, Tokyo (1956), p. 162.

* The trial product by K. Hashizume (Fukushima Paraffin Paper Co.), was used and its composition is obscure.

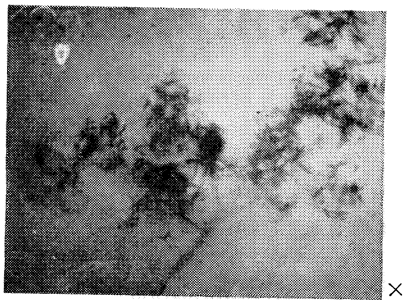

×225

Fig. 7. Transformation of crystals of crystalline paraffin caused by the addition of Santopour.

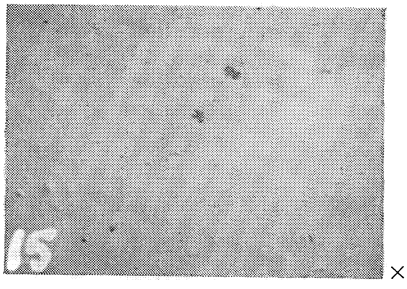

×225

Fig. 8. Transformation of crystals of crystalline paraffin caused by the addition of chloronaphthalene.

that only a small amount of amorphous crystals was observed as shown in Fig. 8.

*Effects of Direct Dyes.*—It has been reported[5] that the direct dyes having functional groups such as hydroxyl group, amino group, etc. made the gelatin of methyl cellulose by bridge-making through each molecule. Then, the effects of such dyes on crystal growth of the paraffin were examined. The results of experiments on 9 sorts of dyes are shown in Table III.

It is very interesting that in the case of direct dyes also, only the compounds having hydroxyl groups gave effects on crystal growth of the crystalline paraffin.

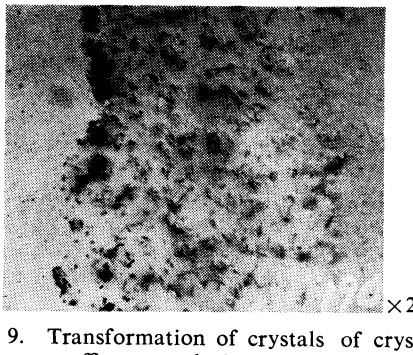

×225

Fig. 9. Transformation of crystals of crystalline paraffin caused by the addition of Nippon green B conc.

*Effects of Asphalt Components.*—Similarly, the asphalt component separated from heavy oil containing microparaffin[1] by propane deasphalting method was added to the crystalline paraffin. Then, the crystals of the paraffin were microcrystallized as shown in Fig. 10, and it was interesting that the micro-crystalline state was very closely similar to that caused by the addition of Santopour, picric acid, *p*-hydroxydiphenyl, etc.

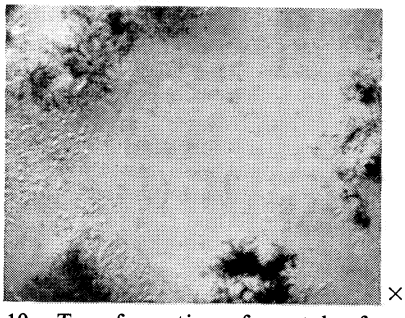

×225

Fig. 10. Transformation of crystals of crystalline paraffin caused by the addition of asphalt component.

**Effects of Various Substances on Crystallization of *n*-Dotriacontane.**—Each of the various organic compounds which transformed the crystalline properties of paraffin when being added to it, were added to a purified *n*-dotriacontane (formed thin plate crystals as shown in Fig. 11) as the above examination. Then, its effects on the crystallization of *n*-dotriacontane were investigated. These results are shown in Table IV.

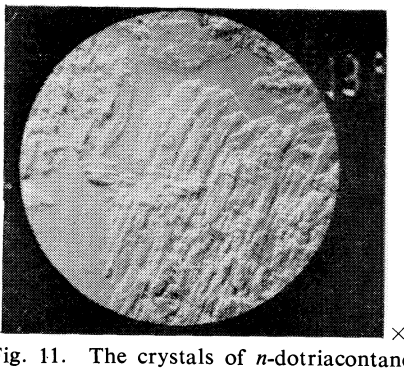
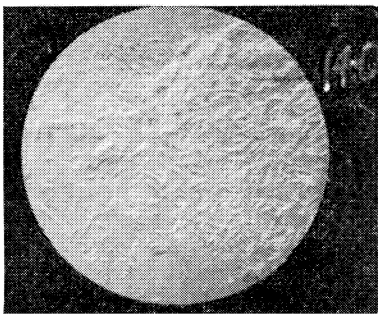

×225

Fig. 11. The crystals of *n*-dotriacontane.

The phenomena of micro-crystallization which gave effects on the crystal when *p*-hydroxydiphenyl or picric acid was added to *n*-dotriacontane are in Figs. 12 and 13, respectively. Figure 14 shows the photograph of crystal transformations of *n*-dotriacontane when Santopour, addition agent of lubricating oils, was added to it, and it is easy to find out crystals of needles.

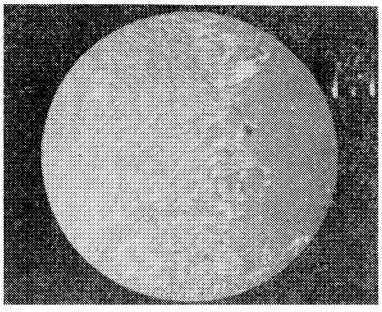
Table IV. Effects of various organic substances on the crystallization of *n*-dotriacontane

| Sample | Effects on crystallization of *n*-dotriacontane | Sample | Effects on crystallization of *n*-dotriacontane |
|---|---|---|---|
| *p*-Hydroxydiphenyl | Transformation (micro-crystallization) | Adva wax | Almost no transformation |
| Picric acid | Transformation (micro-crystallization) | Santopour | Transformation (micro-crystallization) |
| Glucose | Almost no transformation | Nippon green B conc. | Transformation |
| Quinizarine | Almost no transformation | Nippon orange R | Almost no transformation |
| Calcium stearate | Almost no transformation | Nippon brown 3G | Almost no transformation |
| Barium stearate | Almost no transformation | Nippon dark green B conc. | Almost no transformation |
| Aluminum stearate | Almost no transformation | Nippon deep black ex. conc. | Almost no transformation |
| Zinc naphthate | Almost no transformation | Chloronaphthalene | Almost no transformation |
| Lead naphthate | Almost no transformation | Asphalt component | Transformation |



×150

Fig. 12. Transformation of crystals of *n*-dotriacontane caused by the addition of *p*-hydroxydiphenyl (micro-crystallized).

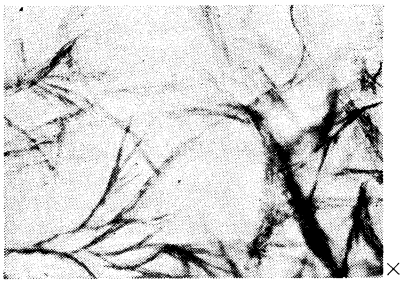


×150

Fig. 13. Transformation of crystals of *n*-dotriacontane caused by the addition of picric acid (micro-crystallized).

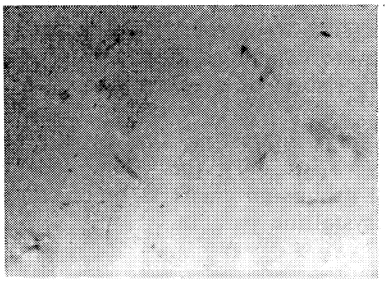
Though the dyes in general gave no remarkable effects, only in the case of "Nippon green B conc." formed micro-crystallization in some parts as shown in Fig. 15.

The examples of almost no effects were the results of photomicrographs of the addition of chloronaphthalene or barium stearate to *n*-dotriacontane, which are shown in Figs. 16 and 17, respectively.



×225

Fig. 14. Transformation of crystals of *n*-dotriacontane caused by the addition of Santopour (micro-crystallized).

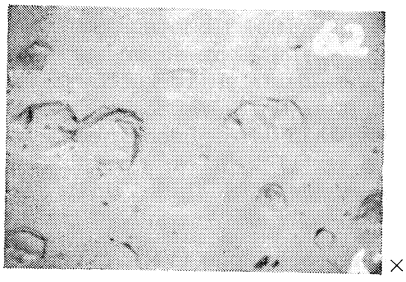


×225

Fig. 15. Transformation of crystals of *n*-dotriacontane caused by the addition of "Nippon green B conc." (hardly micro-crystallized).

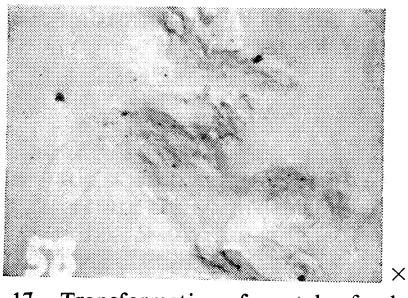
In the case of the asphalt component obtained by propane deasphalting method, its effect was not so remarkable though a little transformation of the crystals of *n*-dotriacontane was seen (Fig. 18).

As mentioned above, two cases were considered; one was of crystalline paraffin, a mixture of various hydrocarbons, in which the



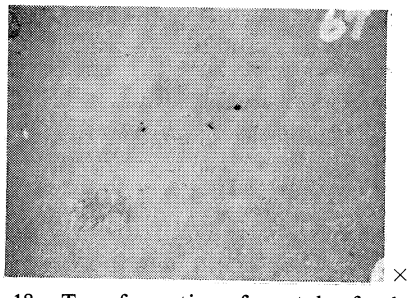
×225

Fig. 16. Transformation of crystals of *n*-dotriacontane caused by the addition of chloronaphthalene (almost no change).



×225

Fig. 17. Transformation of crystals of *n*-dotriacontane caused by the addition of barium stearate (almost no change).



×225

Fig. 18. Transformation of crystals of *n*-dotriacontane caused by the addition of asphalt component (hardly micro-crystallizad).

content of straight paraffins was nearly 90% and containing paraffin side chains, naphthene rings, and aromatic rings; and other was of *n*-dotriacontane, *n*-paraffin series hydrocarbon of carbon number 32. Then, the effects of addition of various organic compounds were different between both, and the composition of the paraffin gave effects on the facility of micro-crystallization of the paraffin. It had already been found[3] that the content of the adductible compounds of the straight chain in the microparaffin was nearly 60%. Accordingly, the easiness of micro-crystallization of microparaffin should be considered to be caused by the existence of more side chains of paraffin in microparaffin than in the crystalline paraffin wax. By observation with the microscope, the phenomenon of micro-crystallization is seemd to be that very fine crystals of plate are rolled up to make minute crystals of needle.

It was found that Santopour, picric acid, *p*-hydroxydiphenyl, and a few direct dyes formed a considerable micro-crystallization of pure hydrocarbons of a straight chain too. It is interesting that all these compounds contain hydroxyl groups and being in somewhat similar structures. Essential investigation will be made by X-ray diffraction, infrared spectrum, observation by electron microscope etc. with regard to the reason why these substances form micro-crystallization of the crystals of paraffin. It should be caused by the fact that the properties of paraffin molecules arranging regularly and growing up to the fundamental crystal of plate are inhibited or obstructed. However, it will be cleared in detail by future studies.

The author expresses his sincere appreciation to Professor Ryozo Goto and Professor Saburo Yagi, Kyoto University, for their cordial guidance and discussion throughout this research.

*Central Research Laboratory*
*Nippon Mining Co.*
*Kitaadachi-gun, Saitama*

# *On 2-Aminotropothione Derivatives*

By Tetsuo Nozoe and Kazuo Matsui

(Received March 22, 1961)

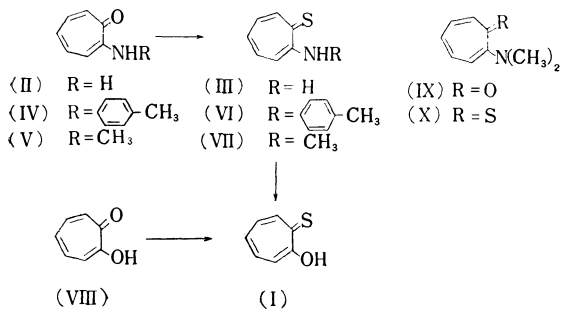
2-Mercaptotropone (I) with two possible tautomeric structures, A and B, was synthesized in 1953 in our laboratory[1,2]. Although the structure of 2-mercaptotropone (B) was assigned at that time from its chemical behaviors, further examinations on its physicochemical properties as well as those of its homologs suggested that I should take the structure A of 2-hydroxytropothione rather than B, in a static state[3].



(A) (B)

As another type of tropothione derivatives, 2-aminotropothiones (1-amino-7-thioxo-1, 3, 5-cycloheptatrienes) were recently synthesized by Brasen et al.[4] from 2-aminotroponeimines (1-amino-7-imino-1, 3, 5-cycloheptatrienes) by the action of hydrogen sulfide. This report deals with another synthesis of 2-aminotropothiones, probably identical with Brasen's compounds and reactions thereof.

Heating 2-aminotropone (II) with excess of phosphorus pentasulfide in pyridine for 2 hr. on a water bath yields 2-aminotropothione (III) as orange red prisms, m. p. 135~136°C, in 60% yield. III is neutral substance and stable in air, and gives benzoate, m. p. 136~137°C. Hydrolysis of III with excess of potassium hydroxide in ethanol affords I.



(II) R=H (III) R=H (IX) R=O
(IV) R=C6H4-CH3 (VI) R=C6H4-CH3 (X) R=S
(V) R=CH3 (VII) R=CH3

(VIII) (I)

Similarly, 2-*p*-toluidinotropothione (VI), orange red plates of m. p. 98~99°C, and 2-methylaminotropothione (VII), orange needles of m. p. 67~68°C, are obtained respectively from 2-*p*-toluidinotropone (IV) and 2-methylaminotropone (V). Both VI and VII are stable substances and benzene layer colors dark red with cupric acetate by the formation of chelate compound.

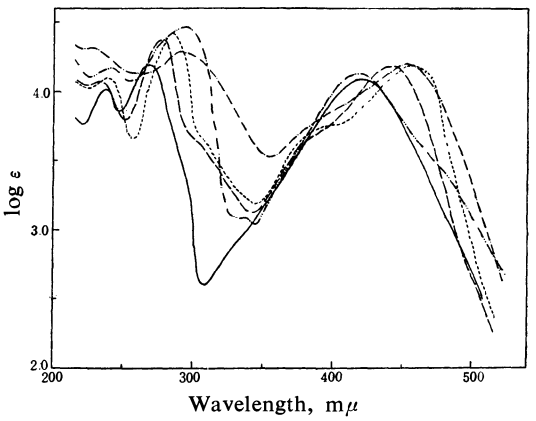



Fig. 1. Ultraviolet absorption spectra of I (——), III (——), VI (-·-·), VII (----) and benzoate of III (-···-) in methanol.

Reaction of tropolone (VIII) with phosphorus pentasulfide gives I even in a lower yield. But 2-dimethylaminotropone (IX) failed to give any objective 2-dimethylaminotropothione (X) except resinous materials by the same method.

These facts imply that hydrogen bond formation between C=S and NH or OH group considerably affects the stability of tropothione derivatives.

As electrophilic substitution, bromination of III in acetic acid was carried out, but only a yellow complex was obtained and heating of it with water ended in decomposition with the recovery of the original substance (III).

There can be two tautomeric structures, C and D, for each III, VI and VII. But their ultraviolet spectra fairly resemble that of 2-hydroxytropothione (I) (structure A) (Fig. 1). This fact suggests, that all these should exist as 2-aminotropothiones (structure C).



(C) (D)

1) T. Nozoe, M. Sato and K. Matsui, *Proc. Japan Acad.*, **29**, 22 (1953).
2) Idem., *Sci. Repts. Tohoku Univ., Ser. I*, **37**, 211 (1953).
3) T. Nozoe and K. Matsui, This Bulletin, **34**, 616 (1961).
4) W. R. Brasen, H. E. Holquist and R. E. Benson, *J. Am. Chem. Soc.*, **82**, 995 (1960).

Infrared spectrum of III is shown in Fig. 2. Absorption assignable to SH group usually seen at 2600~2550 $cm^{-1}$ is absent, and according to Mecke's law,[5] strong absorption at 1045 $cm^{-1}$ must correspond to $\nu_{C=S}$. Thus, the infrared spectrum also supports the structure C for III. This result is in agreement with that obtained by Brasen from nuclear magnetic resonance studies[4].

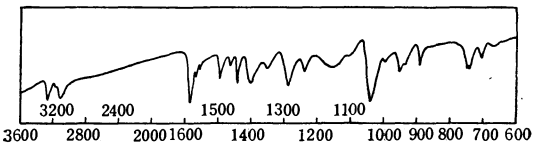



Fig. 2. Infrared absorption spectum of III (KBr disk).

It is known that although I takes structure A in the static state, it behaves like 2-mercaptotropone (structure B) during various reactions, affording only *S*-substituted derivatives[1,2]. However, the possibility of the structure of 2-mercaptotroponeimine (D) for III is excluded even during chemical reactions from its inertness toward diazomethane and the formation of *N*-benzoate as described below.

Two possible structures are assumed for benzoate of III, i. e. *N*- and *S*-benzoate. Its ultraviolet spectrum, however, considerably resembles that of III itself (Fig. 1), and $\nu_{C=S}$ appears at 1065 $cm^{-1}$ in its infrared spectrum. It has therefore been clarified, that this must be *N*-benzoate.

These experiments thus show an essential difference in the chemical properties between I and III.

## Experimental[6]

**2-Aminotropothione (III).**—A mixture of 0.5 g. of 2-aminotropone (II), 1.5 g. of phosphorus pentasulfide and 5 ml. of pyridine was stirred on a water bath for 2 hr. After removal of pyridine under a reduced pressure, water was added to the residue and separated crystals were collected by filtration and dried. This was extracted with methanol for 1 hr. and left cooling. Precipitated crystals were filtered off and methanol was evaporated. The residue was extracted with hot benzene and the crystals obtained was recrystallized from benzene to give 0.3 g. of III as orange red prisms, m. p. 136~137°C.

Found: C, 61.42; H, 4.83; N, 10.00. Calcd. for $C_7H_7NS$: C, 61.27, H, 5.15, N, 10.21%.

Benzoate: Prepared from III and benzoyl chloride in pyridine, and recrystallized from ethanol to red leaflets, m. p. 136~137°C.

Found: C, 69.66; H, 4.45; N, 5.40. Calcd. for $C_{14}H_{11}ONS$: C, 69.68; H, 4.59; N, 5.81%.

**Hydrolysis of III; Formation of 2-Mercaptotropone (I).**—A mixture of 30 mg. of III, 1 ml. of 20% potassium hydroxide and 4 ml. of ethanol was refluxed for 6 hr., ethanol was evaporated under a reduced pressure, water was added to the residue and the solution was treated with activated carbon. The filtrate thereby obtained was acidified with 6 N sulfuric acid and the crystals that separated out were collected by filtration. Sublimation of this product under 3 mmHg pressure afforded I as orange red crystals m. p. 54~55°C. Yield, 15 mg. This was identified by mixed fusion with authentic sample.

**2-*p*-Toluidinotropothione (VI).**—A mixture of 0.3 g. of 2-*p*-toluidinotropone (IV), 1 g. of phosphorus pentasulfide and 5 ml. of pyridine was stirred on a water bath for 2 hr. Pyridine was removed under a reduced pressure, water was added to the residue and extracted with chloroform. Extract was washed with 2 N hydrochloric acid and the solvent was evaporated in vacuo. The residue was extracted with hot ethanol, and the substance so obtained was recrystallized first from cyclohexane then from ethanol to give VI as orange red plates, m. p. 98~99°C. Yield, 50 mg.

Found: C, 74.31; H, 5.49; N, 5.85. Calcd. for $C_{14}H_{13}NS$: C, 73.99; H, 5.76; N, 6.17%.

**2-Methylaminotropothione (VII).**—A mixture of 0.3 g. of 2-methylaminotropone (V), 1.5 g. of phosphorus pentasulfide and 5 ml. of pyridine was stirred on a water bath for 1.5 hr. Pyridine was removed under a reduced pressure, water was added to the residue and extracted with chloroform. After evaporation of chloroform, the residue was triturated with 5 ml. of methanol and insoluble materials were filtered off. Methanol was evaporated in vacuo and the residue was extracted with hot cyclohexane. Extracted material was recrystallized two times from cyclohexane to give 50 mg. of VII as orange needles, m. p. 67~68°C.

Found: C, 63.92; H, 5.68; N, 9.27. Calcd. for $C_8H_9NS$: C, 63.53; H, 6.00; N, 9.27%.

**Reaction of Tropolone (VIII) and Phosphorus Pentasulfide; Formation of I.**—A mixture of 0.2 g. of VIII, 0.5 g. of phosphorus pentasulfide and 5 ml. of pyridine was stirred on a water bath for 30 min. Pyridine was evaporated under a reduced pressure, 10 ml. of 2 N potassium hydroxide was added to the residue, and the solution was treated with activated carbon. The filtrate thereby obtained was acidified with 6 N sulfuric acid and the crystals that separated were collected by filtration. Sublimation of this product under 3 mmHg pressure and recrystallization of the sublimate from petroleum ether afforded I as orange red prisms, m. p. 53~55°C. Yield, 20 mg. This was identified by admixture.

**Reaction of Dimethylaminotropone (IX) and Phosphorus Pentasulfide.**—To a solution of 1 g. of IX dissolved in 5 ml. of pyridine, 1.5 g. of phosphorus pentasulfide was added under stirring. The solution colored red immediately and darkened after a short time. After stirring for 1.5 hr. at room temperature, pyridine was evaporated under a reduced pressure, water was added to the residue and separated dark

5) R. Mecke. R. Mecke and A. Lüttringhaus, *Chem. Ber.*, **90**, 975 (1957).

6) All m. p. are uncorrected. The microanalyses were carried out by Miss A. Iwanaga and Miss M. Suzuki to whom the authors express their deep gratitude.

crystals were collected by filtration. This was extracted with methanol for 1 hr., but only small amounts of resinous materials were obtained.

**Bromination of III.**—A solution of 40 mg. of bromine in 0.5 ml. of acetic acid was added to 30 mg. of III dissolved in 3 ml. of acetic acid under stirring. Yellow crystals that separated were collected by filtration. This substance, m. p. over 280°C, is insoluble in benzene or ethanol. By heating it with water, followed by extraction with chloroform and sublimation of the extract under 3 mmHg pressure, 15 mg. of III, m. p. 130~135°C, was recovered, identified by mixed fusion.

*Department of Chemistry*
*Faculty of Science*
*Tohoku University*
*Katahira-cho, Sendai*

# *Synthesis of Some 8, 8-Disubstituted Heptafulvene Derivatives*[1]

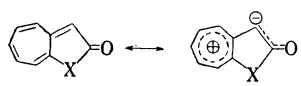
By Tetsuo NOZOE, Toshio MUKAI, Kazutoshi OSAKA*
and Nobuyuki SHISHIDO**

(Received March 23, 1961)

Heptafulvene (methylenecycloheptatriene) (A) can be regarded as a methylene analog of tropone and is also one of the typical non-alternant hydrocarbones with a cyclic conjugated double bond system. Its structure suggests more or less the contribution of a 6-$\pi$



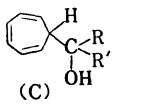
(A)



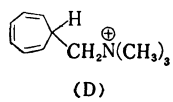
(B)

electron system as tropylium ion. Consequently, it seems of interest to examine the aromaticity and reactivity of this type of compounds comparing with those of azulenes and azulane-2-one type of compounds (B: X=O or NH)[2]. Theoretical interests on the unique ring system attracted also much attention of physical chemists as well as organic chemists and calculation by molecular orbital method has been carried out by Berthier and Pullman[3], Bergman et al.[4] and Julg and Pullman[5,6].

Attempts have already been made for synthesis of heptafulvene derivatives. In 1953, Grundmann, Ottman and Gollner[7], and van Aardt[8] in 1954, attempted the elimination of water from tropyl carbinols (C) but a facile formation of a polymer or styrenes as a rearrangement product was observed and the desired compound could not be obtained. In 1954, Doering and Wiley[9] succeeded in obtaining heptafulvene by the Hofmann elimination of



(C)



(D)

the quaternary ammonium salt (D), obtained from norcaradienecarboxamide, under special conditions. Recently details of this work have been published[10]. According to Doering and Wiley, heptafulvene is a very unstable compound and easily undergoes polymerization but its structure has been proved from the formation of methylcycloheptane by hydrogenation and of dimethyl azulene 1, 2-dicarboxylate by addition with dimethyl acetylene dicarboxylate followed by oxidation. Matteson, Drysdale and Sharkey[11] also obtained heptafulvene, though in a minute amount, by pyrolytic decomposition of methylenecycloheptadienes.

The reason for the larger lability of heptafulvene compared with tropone is considered to be due to the difference in the electron-withdrawing power of the carbonyl and methylene

1) A part of this work was presented at the Local Meeting of Tohoku District of the Chemical Society of Japan, Yamagata, June, 1959.

* Present address: Research Institute of Asahi Chemical Industries, Ltd., Itabashi-ku, Tokyo.

** Present address: Mitsubishi Chemical Industries, Ltd., Yawata, Fukuoka Japan.

2) T. Nozoe, S. Seto, S. Matsumura and T. Terasawa, *Chem. & Ind.*, **1954**, 1356.

3) G. Berthier and B. Pullman, *Trans. Faraday Soc.*, **45**, 484 (1949).

4) E. D. Bergman, E. Fischer, D. Ginsburg, Y. Hirshberg, D. Lavie, M. Mayot, A. Pullman and B. Pullman, *Bull. soc. chim. France*, **V18**, 684 (1951).

5) A. Julg, *J. Chem. Phys.*, **52**, 50 (1955).

6) A. Julg and B. Pullman, ibid., **52**, 481 (1955).

7) C. Grundmann, G. Ottman and G. Gollner, *Ann.*, **582**, 178 (1953).

8) Van Aardt, *J. Chem. Soc.*, **1954**, 2965.

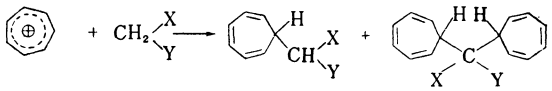
9) Abstract of papers presented at The 126th Meeting of the American Chemical Society, New York, N. Y., September, 1954, p. 10.

10) W. von E. Doering and D. W. Wiley, *Tetrahedron*, **11**, 183 (1960).

11) D. S. Matteson, J. J. Drysdale and W. H. Sharkey, *J. Am. Chem. Soc.*, **82**, 2853 (1960).

group, that is, the difference in the contribution of the tropylium-type structure. If this is the case, it may be anticipated that a more stable heptafulvene derivative would be obtained by the introduction of an electron-withdrawing group, such as cyano or ethoxycarbonyl, into the 8-position of heptafulvene. The present series of work was undertaken on such assumption.

Condensation of tropylium ion and active methylene compound has been reported by Vol'pin, Ahrem and Kursanov[12], and by Conrow[13]. Similar to their method, reaction of tropylium ion and malononitrile gave tropylmalononitrile (I) and ditropylmalononitrile (II). Further reaction of I with tropylium ion also afforded II. Such a fact and the ultraviolet and infrared spectra in Table I supported the structures of I and II to be correct.



X=Y=CN or $CO_2Et$ (I) X=Y=CN (II) X=Y=CN

(III) X=CN, Y=$CO_2Et$ (IV) X=CN, Y=$CO_2Et$

(V) X=Y=$CO_2Et$

Table I. Ultraviolet and infrared spectrum

| Compd. | UV in MeOH mμ (log ε) | IR, $cm^{-1}$ |
|---|---|---|
| I | 260(3.71) | 2900, 2260(CN), 1406, 1340, 1330, 1289, 1184, 1064, 930, 900, 813, 764, 695 (a) |
| II | 255(3.81) | 3010, 2870, 2260(CN), 1615, 1530, 1445, 1440, 1275, 1210, 1196, 772, 735, 695 (a) |
| III | 256(3.46) | 2980, 2260(CN), 1740(CO), 1468, 1448, 1404, 1370, 1332, 1285, 1250, 1207, 1095, 1028, 850, 735, 700 (b) |
| IV | 256(3.76) | 2990, 2250(CN), 1732(CO), 1610, 1445, 1396, 1270, 1257, 1211, 1197, 1107, 1015, 1005, 747, 740, 702, 687 (a) |
| V | 257.5 (3.49)(c) | 2967, 1730(CO), 1443, 1440, 1365, 1305, 1265, 1230, 1170, 1112, 1095, 1030, 860, 744, 703 (b) |
| VI | 225(4.01) 255(4.08) 384(4.36) | 2205(CN), 1633*, 1585, 1520*, 1490*, 1406, 1269*, 885*, 830*, 763* (a) |
| VIII | 254(3.96) 386(4,22) | 2200(CN), 1693(CO), 1630*, 1530*, 1500*, 1483, 1420, 1412, 1390, 1255*, 1215, 1135, 1105, 1033, 830*, 820*, 780* (a) |
| X | 246 355 (d) | 1718(CO), 1685(CO), 1635*, 1545*, 1515*, 1430, 1369, 1260*, 1205, 1070, 1031, 877, 806*, 782*, 740, 704 (b) (d) |

(a) KBr disk
(b) Liquid state
(c) Conrow's datum. See Ref. 12.
(d) X is comtaminated with V.

Condensation of tropylium ion and ethyl cyanoacetate proceeded in the same way by which ethyl tropylcyanoacetate[12] (III) and ethyl ditropylcyanoacetate (IV) were obtained. IV was also obtained by the reaction of III with tropylium ion. The structures of III and IV were supported by their ultraviolet and infrared spectroscopic data given in the Table.

It is already known that diethyl tropylmalonate (V) is obtained by the reaction of tropylium ion and diethylmalonate[12,13], but the reaction of V with tropylium ion failed to afford diethyl ditropylmalonate. This is probably rather attributed to the smaller electron-withdrawing power of the ethoxycarbonyl group than that of the cyano group or to the steric hindrance of the bulky ethoxycarbonyl group.

As was expected, application of a dehydrogenation agent to the tropilidene derivatives, I, III and V, successfully afforded the desired 8,8-disubstituted heptafulvenes. Application of one mole of bromine to I in chloroform, and subsequent heating of the bromide thereby obtained, resulted in the formation of reddish crystals (VI), $C_{10}H_6N_2$, m.p. 200°C, in 50% yield, with liberation of hydrogen bromide. Oxidation of I with *N*-bromosuccinimide in *tert*-butanol containing pyridine and water also gave VI, in 70% yield, accompanying a small amount of rearrangement product, benzalmalononitrile (VII)[14]. VI could be obtained by refluxing I with chloranil in xylene. The infrared absorption of the cyano group in VI shifted to a smaller wave number by 55 $cm^{-1}$ than in I (cf. Table) and shows there is a fair degree of conjugation of the cyano group with the unsaturated system. The ultraviolet spectrum of VI is similar to that of 1-oxa-azulan-2-one derivatives (Fig. 1). These facts

12) M. E. Vol'pin, I. S. Ahrem, D. N. Kursanov, *Isvest. Akad. Nauk U. S. S. R., Otdel Khim. Nauk*, **1957**, 1501; *Zhur. Obschchei Khim.*, **30**, 1187 (1960).

13) K. Conrow, *J. Am. Chem. Soc.*, **81**, 5461 (1959).

14) B. B. Corson and R. W. Stroughton, ibid., **50**, 2830 (1928).

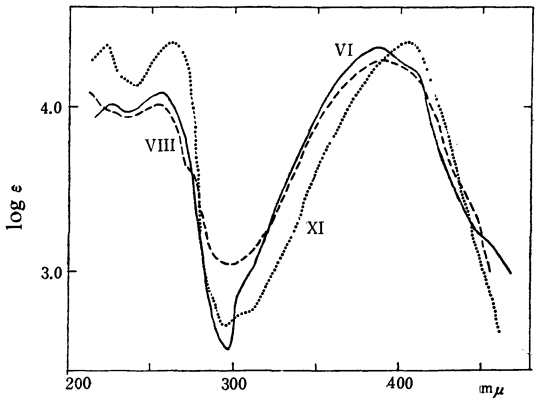
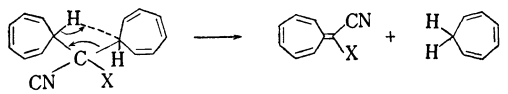



Fig. 1. Ultraviolet absorption spectra of VI (——), VIII (----) and XI (·····) in methanol.

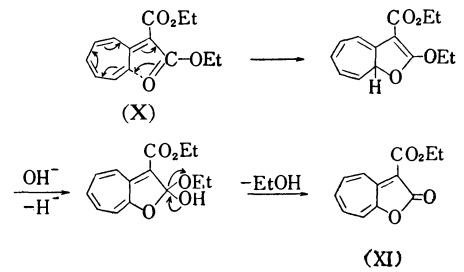
support that VI possesses the structure of 8, 8-dicyanoheptafulvene (heptafulvene-8, 8-dicarbonitrile). Heating of ditropylmalononitrile (II) at 140~150°C for 30 min. resulted in formation of VI and tropilidene in an almost quantitative yield. This reaction is considered to proceed through the intermediate depicted below (four-centered type reaction)[15].



(II) X=CN (VI) X=CN
(IV) X=$CO_2Et$ (VIII) X=$CO_2Et$

8-Cyano-8-ethoxycarbonylheptafulvene (VIII) as red crystals, m. p. 63.5°C was successfully synthesized in about a 40% yield by dehydrogenation of ethyl tropylcyanoacetate (III) with chloranil in boiling xylene. Pyrolysis of ethyl ditropylcyanoacetate (IV) gave also VIII in about a 25% yield. The reason why IV gave a poorer yield of VIII than in the case of pyrolysis of II can be attributed to the smaller electron-withdrawing power of ethoxycarbonyl than in the cyano group to split the bond between the tropyl group and the carbon atom to which it is attached. It was found that the reaction of III with *N*-bromosuccinimide under the condition described previously for I gave ethyl α-cyanocinnamate[16] (IX) rather than the expected VIII in a good yield. The absorption maxima of the infrared spectrum of VIII are given in the Table I. The shift of absorption bands of the carbonyl and cyano groups to a smaller wave number than those of III indicates the conjugation of these functional groups with the unsaturated system. On comparison of the infrared spectra of the two kinds of heptafulvenes, VI and VIII, it is learned that there are some absorption maxima characteristic to them. (indicated by an asterisk in the Table).

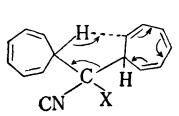
8, 8-Diethoxycarbonylheptafulvene (X) was obtained as a red oil by dehydrogenation of diethyl tropylmalonate (V) with chloranil. X was somewhat more labile than VI or VIII and tended to undergo polymerization on being left in the air. The structure of X is evident from the similarity of its ultraviolet spectrum with those of VI and VIII, and from the presence of absorption bands in its infrared spectrum characteristic to heptafulvenes (see Table 1). The absorption of carbonyl in X shifted to a small wave number from that of V. Bromination-dehydrobromination of diethyltropylmalonate (V) gave 3-ethoxycarbonyl-1-oxaazulan-2-one (XI)[17] whose formation may have passed through X as an intermediate, but this point requires further examination.



(X) (XI)

In parallel with this work, Doi synthesized 3, 4-dihydroxy-8, 8-dicyanoheptafulvene by the reaction of 3-iodotropolone and malononitrile in the presence of sodium amide in liquid ammonia[18]. A few months later, Kitahara and Doi et al. successfully synthesized VI by condensation of tropone and malononitrile[19], and recently they obtained VI, VIII and X from tropylium ion and bromo compounds of malononitrile, ethyl cyanoacetate and diethyl malonate[20]. Their examination of the properties of heptafulvenes revealed some interesting facts as mentioned in Refs. 21 and 24.

15) A similar reaction mechanism involving an intermediate of a five membered ring can be possible. The examples of this type of reaction mechanism can be found in the explanation of the Cope Rearrangement. A. C. Cope, K. E. Hoyle and D. Heyl, *J. Am. Chem. Soc.*, 63, 1843 (1941); E. G. Foster, A. C. Cope and F. Daniels, ibid., 69, 1893 (1947).



16) J. T. Carrik, *J. Prakt. Chem.*, 45, 500 (1892).

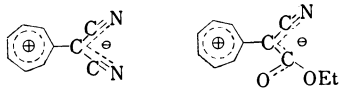
17) S. Seto, *Science Repts. Tohoku Univ., Ser. I*, 37, 367 (1954).

18) Paper presented at the Local Meeting of Tohoku District of the Chemical Society of Japan, Yamagata, June, 1959.

19) Paper presenteted at the General Meeting of Tohoku District of the Chemical Society of Japan, Akita, October, 1959.

20) Paper presented at the General Meeting of Hokkaido District of the Chemical Society of Japan, Sapporo, July, 1960.

8,8-Dicyanoheptafulvene (VI) is sparingly soluble in organic solvent and has a fairly high melting point, but 8-cyano-8-ethoxycarbonyl- (VIII) and 8,8-diethoxycarbonylheptafulvene (X) are more soluble than VI. VI and VIII do not form perchlorate, picrate, styphnate, or trinitrobenzene complex. VI and VIII are fairly stable to acids and do not change on being refluxed for 2 hr. with 6 N hydrochloric acid, while VI changes into a yellow solid on being heated with 75% sulfuric acid. On the other hand, VI and VIII are labile towards alkali[21]. Such behavior of 8,8-substituted heptafulvenes is different from that of heptafulvene (A)[10]. This is reminiscent of the fact that cyano and ethoxycarbonyl groups situated at 1- or 3-position of azulene are also difficult to hydrolyse with acids[22]. VI is stable to bromination and neither substitution nor addition reaction occurs on application of excess bromine in chloroform. These facts can be explained by the great contribution of the 6-$\pi$ electron structures E and F due to electron-attracting groups at 8-position. In fact, as has been published[23], measurement of the dipole moment has shown that the value are 7.49 D (dioxane, 25°C) for VI and 4.40 D (benzene, 25°C) for VIII.



(E) (F)

In order to examine the aromaticity and double bond character of heptafulvenes, Diels-Alder reaction and hydrogenation were carried out. 8,8-Diethoxycarbonylheptafulvene (X) tends to undergo polymerization, while 8,8-dicyanoheptafulvene (VI) does not form an adduct even on being refluxed with maleic anhydride in xylene. 8-Cyano-8-ethoxycarbonylheptafulvene (VIII) shows an intermediate reactivity and partially undergoes addition reaction with maleic anhydride to form the adduct (XII), which has an absorption at 247 m$\mu$. VI resists catalytic hydrogenation over palladium carbon but easily absorbs three moles of hydrogen by the use of platinum oxide as catalyst and forms a pale yellow oil[24], which still retains the absorption at 239 m$\mu$ in its ultraviolet spectrum. On the other hand, X easily absorbs 4 mol. of hydrogen and forms an octahydro compound XIII, which was converted to cycloheptylmalonic acid[25] on hydrolysis.

These experimental results have shown that the stability of 8,8-disubstituted heptafulvenes depends on the nature of the substituent present and the high stability of the compound with a strongly negative group like the cyano group which agrees with the presumption.

## Experimental[26,27]

**The Condensation Reaction of Tropylium Bromide and Malononitrile.**—To a solution of 2.41 g. (0.037 mol.) of malononitrile in 30 ml. of pyridine was gradually added 6 g. (0.035 mol.) of crude tropylium bromide[28] with stirring for 30 min. After stirring for 2 hr. at room temperature, the mixture was poured into 110 ml. of 6 N hydrochloric acid and extracted with benzene. The benzene extract was washed with water, diluted sodium hydrogen carbonate and water, dried over sodium sulfate and evaporated. The brown oily residue crystallized partly on standing. Addition of ethanol and cooling afforded 1.6 g. of crystals, m.p. 58~60°C, as first crop, 1.4 g. of crystals, m.p. 89~99°C, as second crop, and 2 g. of crystals, m.p. 38~48°C containing oil as third crop. Recrystallization of the first crop from benzene gave 1.24 g. (yield 22.7 %) of tropylmalononitrile (I) as colorless crystals, m.p. 61~62°C, which showed m.p. 62.8~63.5°C on recrystallization from benzene once more.

Found: C, 77.38; H, 5.26; N, 17.73. Calcd. for $C_{10}H_8N_2$: C, 76.90; H, 5.16; N, 17.94%.

The solution of the third crop in petroleum ether-benzene (1 : 2) was chromatographed through a column containing 40 g. of alumina. An elution with the same solvent gave 0.64 g. of crystals, m. p. 94~105°C. This substance and the second crop were combined and recrystallized from ethanol to give ditropylmalononitrile (II) as colorless prisms, m. p. 107~108°C.

Found: C, 82.78; H, 5.57; N, 11.15. Calcd. for $C_{17}H_{14}N_2$: C, 82.90; H, 5.73; N, 11.37%.

**The Condensation Reaction of Tropylium Bromide and Tropylmalononitrile (I).**—To a solution of 0.31 g. (2 mmol.) of I in 6.3 ml. of pyridine 0.35 g. (2 mmol.) of crude tropyl bromide was added and the solution resulted was heated on a water bath for 1.5 hr. After addition of 21.7 ml. of 6 N hydrochloric acid under ice-cooling, the mixture was extracted with benzene. The benzene extract was washed with diluted sodium hydrogen carbonate and water, dried over sodium sulfate and distilled to give 0.39 g. (yield 80%) of crystals, m.p. 102~104°C. Recrystallization from ethanol gave colorless crystals, m.p. 104~105.5°C, which showed no depression on admixture with II.

21) Y. Kitahara et al. reported that VI and VIII rearranged to the corresponding styrene derivatives on treating with dilute alkali.

22) Unpublished work by T. Asano and M. Tada in this Laboratory.

23) M. Yamakawa, H. Watanabe, T. Mukai, T. Nozoe and M. Kubo, *J. Am. Chem. Soc.*, **82**, 5665 (1960).

24) Y. Kitahara et al. found that VI absorbed 4 mol. of hydrogen to give an octahydro compound which on hydrolysis gave cycloheptylmalonic acid.

25) I. Vogel, *J. Chem. Soc.*, **1928**, 2025.

26) All melting points and boiling points were uocorrected.

27) The microanalyses were performed by Mr. S. Azumi and Miss A. Iwanaga to whom the authors expressed their gratitude.

28) Tropylium bromide was synthesized from tropilidene by the method of Doering and Knox. *J. Am. Chem. Soc.*, **79**, 352 (1957).

**The Condensation Reaction of Tropylium Bromide and Ethyl Cyanoacetate.**—To a solution of 16.4 g. (0.145 mol.) of ethyl cyanoacetate in 150 ml. of pyridine, 20.4 g. (0.12 mol.) of crude tropyllium bromide was gradually added with stirring under ice-cooling. The reaction mixture was allowed to stand overnight at room temperature to which 260 ml. of concentrated hydrochloric acid was added dropwise under ice-cooling. The acidic solution was extracted with ether and the ether extract was filtered off, washed with diluted sodium hydrogen carbonate and water, and dried over sodium sulfate. Evaporation of ether gave 22.30 g. of a brown oil which crystallized partially on standing. Filtration afforded 6.3 g. of crystals, m.p. 115~117°C, which were recrystallized from ethanol to give 5.3 g. (yield 15%) of ethyl ditropylcyanoacetate (IV) as colorless prisms, m.p. 124~125°C.

Found: C, 78.12; H, 6.35; N, 4.84. Calcd. for $C_{19}H_{19}O_2N$, C, 77.79; H, 6.53; N, 4.77%.

Distillation of the filtrate in reduced pressure gave 10.97 g. (yield 45.0%) of ethyl tropylcyanoacetate (III) as orange viscous oil, b.p. 130~135°C /4 mmHg. After one more distillation, the oil of b.p. 125~130°C/2 mmHg was submitted for microanalysis and spectrum determination.

Found: C, 70.22; H, 6.45; N, 7.06. Calcd. for $C_{12}H_{13}O_2N$. C, 70.91; H, 6.45; N, 6.89%.

**The Condensation Reaction of Tropylium Bromide and Ethyl Tropylcyanoacetate (III).**—A solution of 0.43 g. (2.5 mmol.) of crude tropyl bromide and 0.5 g. (2.5 mmol.) of III in 10 ml. of pyridine was warmed at 40~50°C in a water bath for 30 min. Under ice-cooling, the reaction mixture was neutralized by adding 36 ml. of 6 N hydrochloric acid and extracted with benzene. The benzene extract was washed with water, dried over sodium sulfate and evaporated. Recrystallization of residual crystals from ethanol gave 0.57 g. (yield 78%) of colorless crystals, m. p. 122~123°C, which were proved to be identical with IV by mixed melting point determination.

**Bromination and Dehydrobromination of Tropylmalononitrile (I).**—A solution of 0.32 g. (2 mmol.) of bromine in 0.3 ml. of chloroform was added dropwise to a solution of 0.31 g. (2 mmol.) of I in 3 ml. of chloroform at room temperature. During stirring for 40 min., the color of bromine disappeared and evaporating chloroform in reduced pressure at room temperature gave a pale orange oil. Heating the oil in a boiling water bath for 10 min., it changed to orange red crystals with the evolution of hydrogen bromide gas. Addition of ethanol and filtration affored 150 mg. (yield 50%) of reddish crystals, m.p. 180~185°C, which on recrystallization from ethanol gave 8, 8-dicyanoheptafulvene (VI) as red needles, m.p. 198~199°C.

Found: C, 78.09; H, 4.20; N, 17.77. Calcd. for $C_{10}H_6N_2$: C, 77.90; H, 3.92; N, 18.17%.

**Dehydrogenation of Tropylmalononitrile (I) with *N*-Bromosuccinimide.**—Five hundred milligrams (3.2 m mol.) of I and 550 mg. (3.0 m mol.) of *N*-bromosuccinimide were added to a solution of 11 ml. of *tert*-butanol, 2 ml. of pyridine and 1 ml. of water and the mixture was allowed to stand at room temperature for 90 hr. During this period, reddish needles separated. The filtration gave 250 mg. of red needles, m.p. 194~199°C. After adding 60 ml. of water, the filtrate was extracted with ether. The ether extract was washed with water, dried over magnesium sulfate and evaporated to 160 mg. red needles, m. p. 195~198°C and the filtrate was dissolved in benzene and chromatographed using 3 g. of alumina. After evaporation, the first elutes with benzene gave 65 mg. of colorless needles, m. p. 81~82°C, (VII) which showed no depression on admixture with benzalmalononitrile, m. p. 83°C[14]. The second elutes with benzene gave 60 mg. of red needles, m. p. 194~198°C. Three hundred and fifty milligrams (yield 70%) of total red needles were combined and recrystallized from ethanol to give red needles, m. p. 198~199°C, which is identical with VI.

**Dehydrogenation of Tropylmalononitrile (I) with Chloranil.**—Three hundred milligrams (1.9 mmol.) of I and 510 mg. (2.1 mmol.) of chloranil were added to 5 ml. of xylene and the mixture was refluxed for 2 hr. The dark brown precipitate separated on cooling was filtered and dissolved in benzene. The benzene solution was washed with 1 N sodium hydroxide solution and water and dried over sodium sulfate. Epaporation of benzene gave 60 mg. of orange red crystals, m. p. 179~188°C. Recrystallization from ethanol gave 50 mg. (yield 17%) of red needles, m. p. 189~199°C, which showed no depression on admixture with the authentic sample VI.

**Thermal Decomposition of Ditropylmalononitrile (II).**—One gram (6.4 mmol.) of II was placed in the sublimation apparatus with a cold-finger condenser and heated at 140~150°C in an oil bath for 30 min. Sublimation in 2 mmHg at the same temperature gave 540 mg. (yield 86%) of red needles, m.p. 188~193°C. Recrystallization from ethanol afforded red crystals, m.p. 199~200°C, which showed to be identical with VI on admixture with the authentic sample. During thermal decomposition and sublimation, about 200 mg. of a yellowish oil was caught in a trap cooled with dry ice-acetone. One hundred and twenty five milligrams of this oil and 147 mg. (1.5 mmol.) of maleic anhydride were added to 1.5 ml. of xylene and the mixture was refluxed for 4.5 hr. An addition of 5 ml. of petroleum ether to the solution gave 110 mg. (yield 41%) of pale yellow crystals, m. p. 98~99°C, on cooling. Recrystallization from carbon tetrachloride afforded crystals, m. p. 99~100°C, which showed no depression on admixture with adduct, m. p. 99~100°C. of tropilidene and maleic anhydride[29].

**Dehydrogenation of Ethyl Tropylcyanoacetate (III) with Chloranil.**—To 100 ml. of xylene, 19.6 g. (0.08 mol.) of chloranil and 10 g. (0.051 mol.) of III were added and the mixture was refluxed for 1.5 hr., while a lot of dark brown crystals separated. The crystals (A) obtained by filtration were digested several times with methanol (B) and then benzene (C). Thus 7.1 g. of chloranil was recovered as an insoluble part. The residue obtained from ethanol washings (B) by evaporation was digested with benzene (D) to give 2.1 g. of dihydrochloranil. The washings C and D were

29) K. Alder and G. Jacobs, *Ber.*, **86**, 1528 (1953).

combined and chromatographed through a column containing 60 g. of alumina. Elution of a dark red band with benzene and evaporation of benzene gave 2.84 g. of dark red oil (E) which crystalized partially. The xylene filtrate from A was evaporated in reduced pressure and the residue obtained was washed with methanol (F) to give 2.1 g. of chloranil. Methanol washings were evaporated and the residue was dissolved in benzene and chromatographed using 60 g. of alumina. Evaporation of red benzene eluates affored 1.66 g. of red crystals (G), m.p. 46~54°C. Four and a half grams (yield 45%) of the combined red crystals, E and G were dissolved in benzene and chromatographed again using alumina to give 8-cyano, 8-ethoxycarbonylheptafulvene (VIII) as red crystals, m. p. 61~63°C. Recrystallization from petroleum ether gave red prisms, m. p. 63.5°C.

Found: C, 72.06; H, 5.50; N, 6.78. Calcd. for $C_{12}H_{11}O_2N$: C, 71.62; H, 5.51; N, 6.9%.

**Thermal Decomposition of Ethyl Ditropylcyanoacetate (IV).**—One gram (3.4 mmol.) of IV in a small Claisen flask was heated at 170~195°C in an oil bath and distilled in 2 mmHg at the same temperature to give a red viscous oil. Addition of a little amount of ethanol afforded yellow crystals, m.p. 118~120°C, which proved to be starting IV, by mixed m.p. determination. The red filtrate, after evaporating ethanol, was dissolved in benzene and chromatographed using alumina. An elution of a red absorption band with benzene and evaporation of benzene gave 150 mg. (yield 22%) of a red oil which crystallized on standing and showed m.p. 55~60°C. Repeated recrystallization from petroleum ether gave red prisms, m.p. 63°C, which showed no depression on admixture with VIII.

**The Reaction of Ethyl Tropylcyanoacetate (III) and *N*-Bromosuccinimide.** — Four hundred milligrams (2 mmol.) of III and 420 mg. (2.4 mmol.) of *N*-bromosuccinimide were dissolved in a mixture of 10 ml. of *tert*-butanol, 2 ml. of pyridine and 1 ml. of water. The reaction mixture was allowed to stand at room temperature for about 1 week, then poured to 30 ml. of water and extracted with ether. The ether extracts were washed with diluted hydrochloric acid and water, dried over magnesium sulfate and evaporated to 340 mg. of brown oil. On adding a small amount of ethanol. it crystallized to give 300 mg. of crystals, m.p. 45~47°C. Recrystallization from petroleum ether afforded colorless plates (IX), m. p. 49~50°C, which showed no depression on admixture with authentic ethyl α-cyanocinnamate, m. p. 50°C[16].

**Dehydrogenation of Diethyl Tropylmalonate (V) with Chloranil.**—To boiling xylene were added 7.5 g. (0.03 mol.) of V and 8.8 g. (0.036 mol.) of chloranil and the reaction mixture was refluxed for 1.5 hr. After cooling, dark red crystals separated, and this was filtered to give 2.8 g. of dihydrochloranil as crystals, m.p. 228°C. Distillation of xylene from the filtrate under reduced pressure afforded precipitates from which 2.0 g. of chloranil, m.p. 285°C, were obtained by washing with methanol (A). The washings A were evaporated and the residue was dissolved in benzene and chromatographed through a column containing 50 g. of alumina. An elution of a red band with benzene and evaporation of solvent gave 4.1 g. of red oil (B). It seemed to contain a little amount of starting material, because of the presence of infrared absorption at 705 and 740 $cm^{-1}$ due to tropilidene nucleus. The distillation of the oil (B) in reduced pressure gave the following fractions. 1) 0.32 g. of oil, b.p. 122~130°C/3 mmHg. 2) 1.00 g. of red oil, b.p. 130~140°C/3 mmHg. 3) 0.63 g. of red oil, b.p. 140~150°C/3 mmHg and a considerable amount of residue.

Found: C, 67.77; H, 6.54 (for fr. 3); C, 67.42; H, 6.91 (for fr. 2). Calcd. for $C_{14}H_{16}O_4$: C, 67.73; H, 6.50%.

Fraction 2 (0.68 g.) was allowed to stand at room temperature for about 2 weeks, thereby red gelatinous material was obtained. On being dissolved in hot ethanol and cooled, it gave 0.35 g. of pale yellow amorphous product which softens at about 120°C. This is sparingly soluble in ether and ethanol, but soluble in acetone, benzene and ethyl acetate. It has a weak absorption maximum at 255 mμ.

Found: C, 67.46; H, 6.24. Calcd. for $C_{14}H_{16}O_4$: C, 67.73; H, 6.50%. mol. wt.: 1000 (by Rast method using camphor).

**Bromination and Dehydrobromination of Diethyl Tropylmalonate (V).**—To a solution of 0.96 g. (4 mmol.) of V in 5 ml. of chloroform was added a solution of 0.64 g. of bromine (4 mmol.) in 2 ml. of chloroform. After stirring for 30 min., the solvent was evaporated from the mixture to give 1.5 g. of a pale yellow oil. Heating the oil in a boiling water bath for 60 min. resulted in evolution of hydrogen bromide gas to give 1.1 g. of a brownish oil. It was dissolved in benzene and the benzene layer was washed with diluted sodium hydrogen carbonate and water, dried over sodium sulfate and chromatographed through a column containing 20 g. of alumina. The evaporation of benzene elutes gave 350 mg. of red oil which has an ultraviolet absorption maxima at 274 and 355 mμ. An elution with ethyl acetate afforded 300 mg. of brown oil which crystallized. Recrystallization from ethanol gave 50 mg. of yellow crystals (XI), m.p. 130°C, which proved to be identical with 3-ethoxycarbonyl 1-oxaazulan-2-one, m.p. 130°C, by mixed melting point determination[17].

**Behavior of 8,8-Disubstituted Heptafulvene, VI and VIII against Acid and Alkali.** — a) 6 N Hydrochloric acid and ethanol: 60 mg. of VI was dissolved in a mixture of 3 ml. of concentrated hydrochloric acid and 3 ml. of ethanol and the solution was refluxed for 2 hr. On cooling, red needles were crystallized and 40 mg. of starting material, m.p. 198°C, was collected by filtration.

One hundred miligrams of VIII was treated in the same way as above and the reaction mixture was poured into 50 ml. of water and extracted with benzene. The benzene extracts were washed with water, dried over sodium sulfate and evaporated to 85 mg. of red oil which crystallized and showed m.p. 59~61°C. Recrystallization from petroleum ether gave red prisms, m.p. 62~63°C, which was proved to be identical with starting VIII.

b) 75% sulfuric acid: 100 mg. of VI was added to 2.5 ml. of 75% sulfuric acid and the mixture was heated in a boilding water bath. After 6 hr.,

all crystals were dissolved and no carbon dioxide evolved. Dilution with 5 ml. of water and addition of sodium hydrogen carbonate to pH 2.5 separated an yellow amorphous material which is sparingly soluble in water or ether, but soluble in sodium hydrogen carbonate.

c) 2 N potassium hydroxide and ethanol solution: 50 mg. of VI was dissolved in 1 ml. of 6 N potassium hydroxide and 2 ml. of ethanol and the resulted mixture was refluxed for 1 hr. 20 mg. of solid resinous material separated. Extraction of the filtrate with benzene gave no starting VI.

**Bromination of 8, 8-Dicyanoheptafulvene (VI).**—To a solution of 80 mg. (0.55 mmol.) of VI in 3 ml. of chloroform was added a solution of 160 mg. of bromine (1 mmol.) in 0.6 ml. of chloroform and the reaction mixture was stirred at room temperature for 4 hr. Bromine still remained. Evaporation of chloroform at room temperature gave 70 mg. of red needles, m.p. 192~194°C, which were recrystallized from ethanol to give a starting material (VI) as crystals, m.p. 199~200°C.

**Reaction of 8-Cyano, 8-Ethoxycarbonylheptafulvene (VIII) and Maleic Anhydride.**—A solution of 300 mg. (1.5 mmol.) of VIII and 176 mg. (1.8 mmol.) of maleic anhydride in 6 ml. of xylene was refluxed for 34 hr. After xylene was distilled under reduced pressure and a small amount of methanol was added, a red viscous oil crystallized. Sixty milligrams (yield 13.4%) of light yellow crystals, m. p. 170~174°C, were obtained by filtration and recrystallized from methanol to give an adduct (XII) as crystals, m.p. 177°C.

Found: C, 63.67; H, 4.08; N, 4.62. Calcd. for $C_{16}H_{13}O_5N$: C, 64.21; H, 4.38; N, 4.68%. $\lambda_{max}^{MeOH}$ 297 mμ (log ε 4.23).

Evaporation of methanol from the filtrate gave 250 mg. of a red oil which was dissolved in benzene and chromatographed through column containing 6 g. of alumina. An elution with benzene afforded 100 mg. (yield 33%) of VIII as red crystals, m.p. 50~55°C.

**Reaction of 8, 8-Dicyanoheptafulvene (VI) and Maleic Anhydride.**—Two hundred and fifty milligrams (1.7 mmol.) of VI and 190 mg. (1.9 mmol.) of maleic anhydride was added to 6 ml. of xylene and the resulted mixture was refluxed for 13 hr. On cooling, red needles crystallized. Evaporation of xylene and addition of ethanol to residue gave 200 mg. of starting VI as red needles, m. p. 195°C.

**Catalytic Reduction of 8, 8-Dicyanoheptafulvene (VI).**—a) One hundred milligrams (0.65 mmol.) of VI was dissolved in 40 ml. of ethanol and hydrogenated in the presence of 30 mg. of Pd-carbon (5%) at ordinary temperature and pressure. Only 20 ml. (0.9 mmol.) of hydrogen was absorbed for 6 hr. Treated in the usual way, 90 mg. of red needles, m.p. 184~188°C were obtained which was identical with VI.

b) With Pt-oxide. A solution of 120 mg. (0.82 mmol.) of VI in 55 ml. of ethanol was hydrogenated in the presence of 15 mg. of Pt-oxide at ordinary temperature and pressure. After 42 ml. (2.3 mmol.) of hydrogen had been absorbed, the color of the solution changed and at 57 ml. (3.1 mmol.) of hydrogen the velocity became slow and at 61 ml. (3.3 mmol.) hydrogenation was stopped. Catalysts were filtered and the filtrate was evaporated to give 120 mg. of yellow oil which showed infrared absorption at 3345, 3445 $cm^{-1}$ due to $NH_2$ group. It was dissolved in benzene and passed through a column containing 9 g. of alumina. Evaporation of the benzene eluate gave 30 mg. of a colorless oil which has no infrared absorption maximum due to $NH_2$ or NH group, but showed an absorption maximum at 239 mμ in methanol. Evaporation of the ether eluates gave 45 mg. of a brown oil which has infrared absorption at 3345 and 3445 $cm^{-1}$.

**Catalytic Reduction of 8, 8-Diethoxycarbonylheptafulvene (X).**—A solution of 500 mg. (2 mmol.) of X in 40 ml. of ethanol was hydrogenated in the presence of 10 mg. of Pt-oxide as catalyst at ordinary temperature and pressure. After 107 ml. (4.9 mmol.) of hydrogen had been absorbed, the red color of the solution disappeared and the absorption of hydrogen almost ceased at 175 ml. (7.8 mmol.). The filtrate obtained by removal of the catalyst was evaporated to 400 mg. of an yellow oil (XIII). It has no absorption maximum in the ultraviolet spectrum.

Two hundred and fifty milligrams of XIII was added to a mixture of 2.5 ml. of 6 N potassium hydroxide and 2.5 ml. of ethanol and the solution was refluxed for 2 hr. After evaporating ethanol and diluting with water, the reaction mixture was acidified with diluted hydrochloric acid and extracted with ether. The ether extracts were washed with water, dried over sodium sulfate and evaporated to 200 mg. of colorless crystals, m. p. 145~149°C (decomp.). Repeated recrystallization from a mixture of carbon tetrachloride and acetone gave colorless crystals, m. p. 160~161°C (decomp.).

Found: 60.49; H, 7.72. Calcd. for $C_{10}H_{16}O_4$: C, 59.98; H, 8.05%.

Reported melting point for cycloheptylmalonic acid is 164.5°C[25].

The authors express their gratitude to Shell Petroleum Company for the kind donation of tropilidene used as the starting material, and to Sankyo Co., Ltd. for donation of a research fund which covered a part of the expenses for this work. The authors also thank Mr. H. Tsuruta for repeating some experiments.

*Department of Chemistry*
*Faculty of Science*
*Tohoku University*
*Katahira-cho, Sendai*

# *Intramolecular Interaction between Hydroxyl Group and π-Electrons. XIII*[1]. *$\nu_{O-H}$ Absorption of 2,6-Diphenylphenol and the Related Compounds*

By Michinori Ōki, Haruo Hosoya and Hiizu Iwamura

(Received March 27, 1961)

It has been clarified, by a series of reports[2] from this laboratory, that, if a hydroxyl group and the π-electrons are located at suitable positions, the intramolecular interaction takes place to the extent which is determined by the structure of the molecule, the strength of the proton-donor, and the strength of the proton-acceptor. Thus, in a usual case, two O-H stretching ($\nu_{O-H}$) absorption bands corresponding to the free and the interacting hydroxyl groups appear in the 3μ region. The above consideration leads to the deduction that, if the steric factors force the hydroxyl group to approach the π-electrons, there would be no free hydroxyl group. Tribenzylcarbinol[3] will be one of the examples in this category.

Pauling suggested[4] that the hydrogen atom of the phenolic hydroxyl group is located in the plane of the aromatic nucleus because of the resonance stabilization. Later, the suggestion was found to be true when 2,6-dichlorophenol was found[5] to possess only an O-H··· Cl bonded hydroxyl group from the O-H stretching absorption in the infrared region and the microwave data also[6] led to the same conclusion as Pauling's suggestion. Therefore, if a phenol carries two groups at both ortho-positions of the hydroxyl group, which contain π-electrons, the compound can be another example which has no free hydroxyl group. In this paper, 2,6-diphenylphenol and the related compounds are taken as examples and absence or presence of the free hydroxyl group will be discussed in terms of the steric factor.

## Experimental

**Measurement and Calculation.** — The measurement of the absorption in the 3μ region was carried out with a Perkin Elmer 112G grating spectrometer and quartz cells of 2 and 5 cm. lengths as required. Carbon tetrachloride was used as a solvent. The concentration was $1\sim2\times10^{-3}$ mol./l. and the spectral slit width 1 $cm^{-1}$ in this region. The calculation of the band intensities was performed as reported previously[7], the integrated intensities being the authors' choice. However, on some occasions, the assumption that the appearance of the two peaks or the asymmetric curve indicates the overlap of the two symmetric curves, each of which is expressed by the Lorentz function, is proved to be false, suggesting the presence of the third band. In such cases, the molecular extinction coefficients were taken instead of the integrated intensities for the convenience of the calculation.

**Materials.**—The compounds used for this work are known unless otherwise mentioned and their physical constants agreed with those reported in the literature.

*4-Nitro-2,6-diphenylphenol.* — This compound was prepared by condensation of nitromalonaldehyde and dibenzyl ketone according to the method described by Hill[8]. The melting point of the compound was 115°C after four recrystallizations from ethanol. However, the melting point was suddenly raised up to 135°C when a large crystal was scratched, and the compound melting at 115°C has never been obtained thereafter. This phenomenon must be a type of polymorphism but the physical measurement was not carried out with the unstable form because of the lack of the sample. The melting point of the stable form was 135~136°C (lit.[8], 135~136°C).

*3,5-Dimethyl-2,6-dipropenylphenol.* — A mixture of 20 g. (0.123 mol.) of 2-allyl-3,5-dimethylphenol, 15.7 g. (0.13 mol.) of allyl bromide, 18.0 g. (0.13 mol.) of potassium carbonate and 50 ml. of acetone was refluxed for ten hours. The filtrate from the reaction mixture was fractionated and gave 22 g. (87%) of allyl 2-allyl-3,5-dimethylphenyl ether, b. p., 148~150°C/15 mmHg. The ether was refluxed with an equal amount of *N,N*-diethylaniline for three hours and, after cooling, the mixture was diluted with petroleum ether. The solution was shaken with dilute hydrochloric acid to remove *N,N*-diethylaniline and then extracted with Claisen's alkali. When the alkaline solution was diluted with water, an oil separated, which was distilled to give 83% 2,6-diallyl-3,5-dimethylphenol, b. p., 105~106°C/2 mmHg, $n_D^{19}$ 1.5410.

Found: C, 82.94; H, 9.05. Calcd. for $C_{14}H_{18}O$: C, 83.12; H, 8.97%.

The phenol (10 g.) was dissolved in 30 ml. of

1) Part XII: M. Ōki and H. Iwamura, *Tetrahedron*, in press.
2) See Part XII of this series and the preceding papers cited therein.
3) M. Ōki and H. Iwamura, This Bulletin, 33, 1632 (1960).
4) L. Pauling, *J. Am. Chem. Soc.*, 58, 94 (1936).
5) O. R. Wulf, U. Liddel and S. B. Hendricks, ibid., 58, 2287 (1936).
6) Presented by T. Kojima before the 13th Annual Meeting of the Physical Society of Japan at Kyoto, October 1958. Also private communication from Prof. K. Shimoda, The University of Tokyo.
7) M. Ōki and H. Iwamura, This Bulletin, 32, 567 (1959).
8) H. B. Hill, *Am. Chem. J.*, 24, 1 (1900).

methanol containing 10 g. of potassium hydroxide and the solvent was evaporated until the temperature of the solution rose to 130°C. The mixture was refluxed for twenty hours at that temperature, cooled, diluted with water and extracted with ether. The ethereal extract was dried over potassium carbonate and fractionated to give 7.3 g. of 3,5-dimethyl-2,6-dipropenylphenol, b. p., 155°C/18 mmHg. The compound solidified and was recrystallized from petroleum ether. The melting point was 59~60°C.

Found: C, 83.04; H, 9.12. Calcd. for $C_{14}H_{18}O$: C, 83.12; H, 8.97%.

## Results and Discussion

The $\nu_{O-H}$ absorptions of substituted 2,6-diphenylphenols and of 2-chloro-6-phenylphenol are summarized in Table I. As expected, these phenols did not possess absorption at the position (ca. 3600 $cm^{-1}$) where ordinary phenols do, but at the position which is too low a wave number to be assigned to the free hydroxyl group. Absorptions of 4-substituted 2,6-diphenylphenols are symmetric and appear at lower wave numbers as the substituent at 4 position is more electronegative, the phenomenon being common for the ordinary phenols[9] and 4-substituted 2,6-di-*tert*-butylphenols[10].

TABLE I. $\nu_{O-H}$ ABSORPTIONS OF PHENOLS [2,4,6-XY($C_6H_5$)$C_6H_2$OH]

| Substituent X | Substituent Y | $\nu_{max}$ $cm^{-1}$ | $\varepsilon_{max}$ | $A\times10^{-4}$ $mol^{-1}$ l. $cm^{-2}$ |
|---|---|---|---|---|
| $C_6H_5$ | $NO_2$ | 3531.2 | 366 | 2.54 |
| $C_6H_5$ | H | 3553.3 | 305 | 1.93 |
| $C_6H_5$ | $NH_2$ | 3567.9 | 305 | 1.85 |
| Cl | H | 3550.2<br>3535.6 | 41<br>184 | 0.30<br>1.22 |

Since the hydroxyl group of the 4-substituted 2,6-diphenylphenols is considered to be all interacting with the $\pi$-electrons of the adjacent phenyl groups, it may be interesting to compare the absorptions of these compounds with those of the corresponding phenols in benzene. Thus the $\nu_{O-H}$ absorption of *p*-nitrophenol was measured in benzene solution, the absorption maximum being at 3527.4 $cm^{-1}$. The difference (3.8 $cm^{-1}$) from 4-nitro-2,6-diphenylphenol is rather small and supports the above mentioned idea. However, it must be considered that this difference is the combination of the solvent effect and the electronic effect of the substituent. 4-Nitro-2,6-diphenylphenol in benzene showed the $\nu_{O-H}$ absorption at 3523.3 $cm^{-1}$. Therefore, the difference between 3527.4 $cm^{-1}$ and 3523.3 $cm^{-1}$ may be attributed to the effect of two phenyl groups at *o*-positions. Phenol in benzene is known to show its $\nu_{O-H}$ maximum at 3562 $cm^{-1}$ [11]. The deviation from 3553.3 $cm^{-1}$ may be interpreted similarly.

2-Chloro-6-phenylphenol has its $\nu_{O-H}$ absorption maximum at 3535.6 $cm^{-1}$ but the curve shows a shoulder at the higher wave number side. Therefore, the curve was divided into two, assuming that it was an overlap of two symmetric curves which could be expressed by the Lorentz function (Fig. 1). The authors

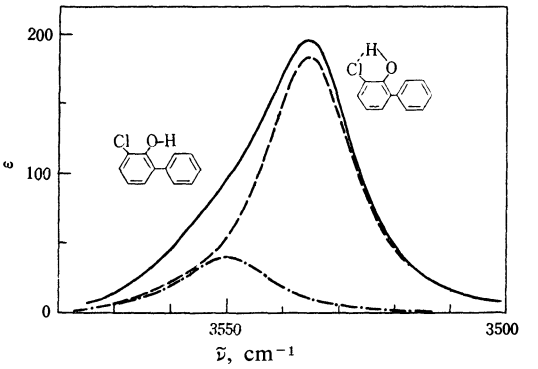



Fig. 1. $\nu_{O-H}$ absorption of 3-chloro-2-hydroxybiphenyl.
——— the observed curve
– – – O-H···Cl
—·—· O-H···$\pi$

have data, concerning the interacting form of 2-hydroxybiphenyl and the hydrogen-bonded form of *o*-chlorophenol, which reveal the fact that the former is located at 3565.0 $cm^{-1}$ and the latter at 3547.0 $cm^{-1}$. Then it will be most probable to assign the band maximum at 3535.6 $cm^{-1}$ to the hydrogen-bonded form of the hydroxyl group with ortho chlorine atom and that at 3550.2 $cm^{-1}$ to the interacting form with $\pi$-electrons. The lowering of the wave number must be derived from the effect of the electron-drawing substituents. As to the integrated intensities of each component, the O-H···Cl bonded form is apparently large, but it may not necessarily mean that the molecule having the hydrogen bond between the hydroxyl group and the chlorine atom is greatly in the majority, since it is a well-known fact that the absorption intensity per molecule becomes stronger on O-H···Cl hydrogen bond formation.

As the source of the $\pi$-electrons, the propenyl group might be considered equally effective with the aromatic nucleus. Thus, various phenols containing propenyl groups are prepared and their $\nu_{O-H}$ absorptions examined. The results are summarized in Table II. As is clear from Table II, replacement of a phenyl

9) P. J. Stone and H. W. Thompson, *Spectrochim. Acta*, **10**, 17 (1957).
10) K. U. Ingold, *Can. J. Chem.*, **38**, 1092 (1960).
11) M. L. Josien, P. Dizabo and P. Saumagne, *Bull. soc. chim. France*, **1957**, 423.

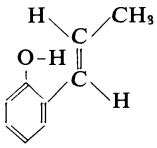
Table II. $\nu_{O-H}$ absorption of phenols containing propenyl group

[2,6-X($CH_3CH{=}CH$)$C_6H_3OH$]

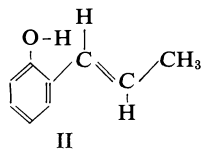
| X | O-H | $\nu_{max}$ $cm^{-1}$ | $\varepsilon^a{}_{max}$ | $\Delta\nu_{max}$ $cm^{-1}$ |
|---|---|---|---|---|
| H | f* | 3611.1 | 159.0 | 58.8 |
| | i* | 3552.2 | 34.0 | |
| $CH_3CH{=}CH$- | f | 3603.5 | 78.0 | 57.5 |
| | i | 3546.0 | 72.0 | |
| $C_6H_5$ | f | 3607.4 | 21.3 | 44.2 |
| | i | 3563.2 | 241.6 | |

* f and i denote the free and the interacting forms, respectively.

group by a propenyl group gives rise to the appearance of an absorption due to the free form of the hydroxyl group and this phenomenon is enhanced when two propenyl groups are introduced in place of the phenyl groups of 2,6-diphenylphenol. One of the possibilities which reasonably explains the phenomenon is the concept of the rotational isomerism. *o*-Propenylphenol is taken as an example for the explanation, because of its simplicity. In this case, the consideration of the cis form[4] will suffice to cover the possibilities, since 2,6-dipropenylphenol contains only this form whichever direction the O-H points.



I



II

The authors are assured that *o*-propenylphenol assumes the trans form with respect of the ethylenic linkage[12]. Then there will be two rotational isomers about the $C_{Ph}-C_\alpha$ axis, being represented by I and II. Structure II will possess a free hydroxyl group, if a pair of π-electrons are necessary for the interaction and/or if the hydrogen atom of the hydroxyl group must approach from the upper side to the π-electron cloud in order to establish the interaction. Thus, structure I may be the only form which possesses the interaction in *o*-propenylphenol. The availability of the π-electrons of 2,6-diphenylphenol, on the other hand, will not be altered no matter what rotational position is taken, because the structure corresponding to I is always involved in this compound. If the above assumption is correct, a compound which is forced to take structure I will have no free hydroxyl group. The enforcement may be given by the steric hindrance. 3,5-Dimethyl-2-propenylphenol and 3,5-dimethyl-2,6-dipropenylphenol were chosen as examples. The results are shown in Table III.

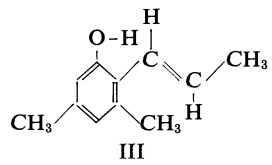
12) It is supported by the fact that *o*-propenylphenol possesses an absorption at 968.6 $cm^{-1}$ due to C-H out-of-plane deformation.

Table III. $\nu_{O-H}$ absorptions of 6-substituted 3,5-dimethyl-2-propenylphenols

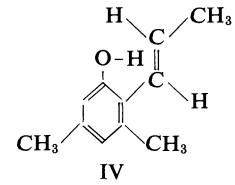
[6,3,5,2-X$(CH_3)_2$($CH_3CH{=}CH$)$C_6H$-OH]

| X | O-H | $\nu_{max}$ $cm^{-1}$ | $\varepsilon^a{}_{max}$ | $\Delta\nu_{max}$ $cm^{-1}$ |
|---|---|---|---|---|
| H | f | 3607.7 | 19.4 | 68.5 |
| | i | 3539.2 | 101.9 | |
| $CH_3CH{=}CH$- | f | — | — | — |
| | i | 3526.5 | 120.2 | |

The steric effect of the methyl group may be too great to assume structure III and the structure IV becomes favorable. Therefore, the structure of 3,5-dimethyl-2-propenylphenol may be represented by IV. The structure IV is, at the same time, favorable for the internal interaction and these considerations predict that 3,5-dimethyl-2-propenylphenol contains more interacting molecules than 2-propenylphenol in spite of the fact that the methyl group is the electron-donating group which weakens the proton donating power of the phenols. Comparison of the data in Tables II and III indicates that this is really the case. Since 2,6-dipropenyl-3,5-dimethylphenol has two propenyl groups which are sterically enforced to take the structure as IV, it is naturally expected that this compound will possess single $\nu_{O-H}$ absorption at a rather low frequency. Actually a perfectly symmetrical band is found at 3526.5 $cm^{-1}$. Hence, it is proved that the propenyl group can also be the source of the π-electrons which give th $\nu_{O-H}$ absorption at extraordinarily low frequency.



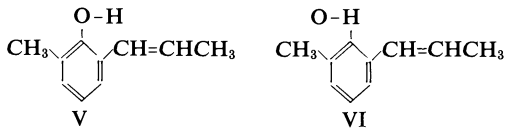
III



IV

As to the steric effect on the interaction, it may also be interesting to examine the $\nu_{O-H}$ absorption of 2-methyl-6-propenylphenol. Since the hydroxylic hydrogen atom is located on the plane of the benzene nucleus, it is reasonably expected that, in *o*-cresol, the molecule will be more stable when the hydroxylic hydrogen is located on the opposite side of the methyl group. Therefore, in 2-methyl-6-propenylphenol, the contribution of structure V may be more than that of structure VI. This consideration suggests that there will be more molecules, which have the intramolecular interaction between the hydroxyl group and π-electrons, in 2-methyl-6-propenylphenol than in 2-propenylphenol. The former compound has one absorption maximum at 3617.0 $cm^{-1}$

($\varepsilon^a_{max}=83.8$) and another at 3548.3 $cm^{-1}$ ($\varepsilon^a_{max}=39.3$). Comparison of the results with these compounds indicates that the above consideration is correct, since both $\Delta\nu_{max}$ and $\varepsilon_i/\varepsilon_f$ are greater in 2-methyl-6-propenylphenol.




V VI

The $\nu_{O-H}$ absorptions of the precursors of the propenyl compounds, the phenols carrying allyl groups, are also examined in connection with the freedom of rotation and the basicity of the ethylenic linkage. The results are shown in Table IV. The diagrams of the $\nu_{O-H}$ absorptions of 2-allyl-3, 5-dimethylphenol and 2, 6-diallyl-3, 5-dimethylphenol are also given in Fig. 2, because of the difficulty of understanding the matter from the mere numericals. The $\varepsilon_i/\varepsilon_f$ of the phenols carrying allyl groups are always greater than those of the propenylphenol derivatives unless they carry methyl groups at 3 and 5 positions. This will mean that the effect of the basicity of the ethylenic

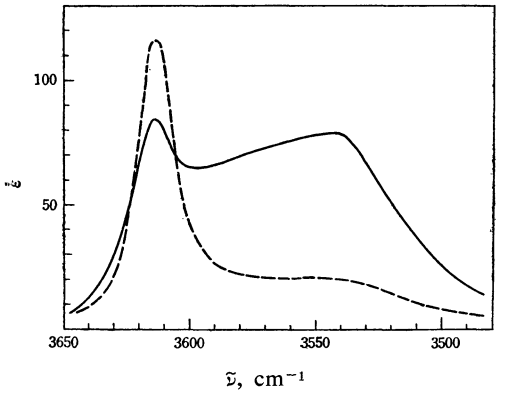


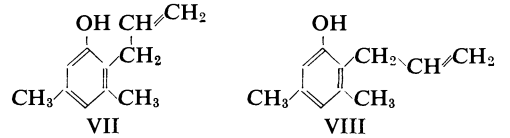

Fig. 2. The apparent $\nu_{O-H}$ absorption of 2, 6-diallyl-3, 5-dimethylphenol (——) and 2-allyl-3, 5-dimethylphenol (– – –).

TABLE IV. $\nu_{O-H}$ ABSORPTIONS OF PHENOLS CARRYING ALLYL GROUPS

| Phenol | O-H | $\nu_{max}$ $cm^{-1}$ | $\varepsilon^a_{max}$ | $\Delta\nu_{max}$ $cm^{-1}$ |
|---|---|---|---|---|
| 3-Allyl-2-hydroxy-biphenyl | f | 3609.2 | 13.9 | 46.0 |
| | i | 3563.2 | 259.5 | |
| 2, 6-Diallylphenol | f | 3616.0 | 45.5 | 71.7 |
| | i | 3544.3 | 88.3 | |
| 2-Allyl-3, 5-dimethyl-phenol | f | 3614.0 | 116.0 | 66.8 |
| | i | 3547.2 | 20.6 | |
| 2, 6-Diallyl-3, 5-dimethylphenol | f | 3614.0 | 84.5 | 72 |
| | i | 3542* | 79 | |
| 2-Allyl-6-methyl-phenol | f | 3619.0 | 77.8 | 71.0 |
| | i | 3548.0 | 52.3 | |

* Four place number is given because of the uncertainty due to the broadness of the band (see Fig. 2).

bond plays the major role and the rotation about $C_{Ph}-C_\alpha$ axis the minor role, for the interaction. This is because the basicity of the ethylenic linkage in the propenylphenols is rather low due to the conjugation with the benzene nucleus. In contrast with the above situation, when methyl groups are present at 3 and 5 positions, the allylphenols show smaller $\varepsilon_i/\varepsilon_f$ value than those of the corresponding propenylphenols. This is without doubt caused by the freedom of rotation. That is, it is possible for "cis" 2-allyl-3, 5-dimethylphenol to take the conformations illustrated, for example, by VII and VIII, which are unfavorable for the intramolecular interaction. The possibilities of taking these unfavorable structures are owing to the rotation about $C_{Ph}-C_\alpha$ and $C_\alpha-C_\beta$ axes, while, in 3, 5-dimethyl-2-propenylphenol, the rotation about the $C_{Ph}-C_\alpha$ is at least partially restricted due to the resonance stabilization and the steric interference of the methyl group, possibly causing all the cis forms to be the interacting. Baker and Shulgin[13] have mentioned that the steric effect of the methyl group in 2-allyl-3, 5-dimethylphenol is favorable for the interaction, when compared with 2-allylphenol, probably because the contribution of structures such as VIII is less. Nevertheless, the conclusion is not contradictory, since it may be possible for




VII VIII

structure VIII to be present to a small extent and it is out of the question at the present time which structure is the main contribution for the free cis form.

When an asymmetrical band is assumed to be an overlap of the symmetrical bands, the compounds which contain one or two propenyl groups at ortho positions of the hydroxyl group usually possess three $\nu_{O-H}$ bands unless the absorption corresponding to the interacting form is very strong. In the case of 2-phenyl-6-propenylphenol, the three bands may be reasonably assigned to the free, the interacting with the phenyl group, and the interacting with the propenyl group. However, the situation must be further studied with other compounds before obtaining a general conclusion.

The authors are indebted to Professors Yoshiyuki Urushibara and Saburo Nagakura for their valuable advice and encouragement throughout this work. A part of the cost

13) A. W. Baker and A. T. Shulgin, *J. Am. Chem. Soc.*, **80**, 5358 (1958).

was defrayed from the Grant in Aid for Fundamental Scientific Research of the Ministry of Education, for which the authors' thanks are due.

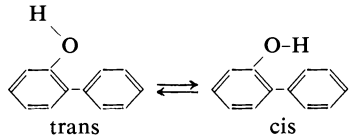
*Department of Chemistry*
*Faculty of Science*
*The University of Tokyo*
*Hongo, Tokyo*

# *Intramolecular Interaction between Hydroxyl Group and π-Electrons. XIV*[1]. *Electronic Effect of the Substituents on the Interaction in 2-Hydroxybiphenyls*

By Michinori Ōki and Hiizu Iwamura

(Received March 27, 1961)

Since the observation by Wulf and his co-workers[2], it has been occasionally reported that 2-hydroxybiphenyl shows doublet O–H stretching band in the infrared absorption spectrum. The phenomenon was explained on the assumption that 2-hydroxybiphenyl would be composed of cis and trans isomers. Such an explanation had been adopted by Pauling[3] for the like phenomenon observed in the infrared spectrum of *o*-chlorophenol. As the cis isomer seems to be less stable because of




the steric interference, there must exist a cause which makes the appearance of this form possible. Wulf and his co-workers attributed stabilizing force to the approach of the hydroxyl group to the first carbon atom of the benzene ring which is ortho to the hydroxyl group and to the consequent attraction between them, but failed to show the true nature. Later, Mecke[4] explained the phenomenon from the polarizable nature of the π-electrons in the benzene nucleus and assumed that a so-called π-complex was formed intramolecularly, without giving further details. Recently Musso and von Grunelius[5] reported some $\nu_{O-H}$ absorptions of 2,2′-dihydroxybiphenyl and their derivatives and discussed the competitive intramolecular hydrogen bond formation between O–H···O and O–H···π systems, with special reference to the geometrical consideration. The examples are, however, too complicated to help us to understand the nature of the latter interaction separately.

The present authors have preliminarily reported[6] that the energies of the intramolecular interaction between the hydroxyl group and the π-electrons in 2-hydroxy-4- and -4′-nitrobiphenyls are 2.5 and 0.9 kcal./mol., respectively. The present study was initiated on the expectation that the electronic effect of the substituents on the interaction will provide additional informatin in regard to the true nature of the interaction.

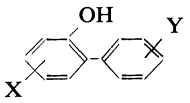
## Experimental

Measurement and treatment of the infrared spectra were carried out as described previously[7]. The known samples were prepared according to the literature, and the new as described below. Their physical constants and analytical data are listed in Table I.

**Materials.** — *2-Hydroxyl-4-methoxybiphenyl.* — 2-Amino-4-methoxybiphenyl[13] (0.02 mol., 4.0 g.) was dissolved in aqueous sulfuric acid (4.5 ml. of concentrated sulfuric acid and 6 ml. of water) and diazotized with 1.5 g. of sodium nitrite in 3 ml. of water. The excess of nitrite was decomposed by a lump of urea and the solution was poured into 20 ml. of boilng 30% aqueous sulfuric acid. The separated dark oil was taken up in ether and the ether layer was extracted thrice with 20% aqueous sodium hydroxide solution. The alkaline extract was acidified and extracted with ether. The ether extract was treated with active charcoal, filtered and evaporated. The tarry residue was extracted with hot petroleum ether and the extract deposited prisms after cooling. The pure sample was obtained by recrystallization from petroleum ether.

1) Part XIII: M. Ōki, H. Hosoya and H. Iwamura, This Bulletin, **34**, 1391 (1961).
2) O. R. Wulf, U. Liddel and S. B. Hendricks, *J. Am. Chem. Soc.*, **58**, 2290 (1936).
3) L. Pauling, ibid., **58**, 94 (1936).
4) W. Lüttke and R. Mecke, *Z. Elektrochem.*, **53**, 241 (1949).
5) H. Musso and S. von Grunelius, *Ber.*, **92**, 3101 (1959).
6) M. Ōki, H. Iwamura and Y. Urushibara, This Bulletin, **31**, 770 (1958).
7) M. Ōki and H. Iwamura, ibid., **32**, 567 (1959).

TABLE I. PHYSICAL CONSTANTS AND ANALYTICAL DATA OF THE SUBSTITUTED 2-HYDROXYBIPHENYLS



| Substituent X | Substituent Y | M. p. or b. p. observed (lit.) | Analytical Data: Found C | Found H | Found N | Calcd. C | Calcd. H | Calcd. N |
|---|---|---|---|---|---|---|---|---|
| H | H | 59°C (59°C[8]) | | | | | | |
| 4-MeO | H | 66~67°C | 78.08 | 6.25 | | 77.98 | 6.04 | |
| 4-Cl | H | 38.5~39°C | 70.46 | 4.43 | (Cl=17.39) | 70.42 | 4.43 | (Cl=17.33) |
| 4-$NO_2$ | H | 103~105°C (102°C[9]) | | | | | | |
| 5-Et | H | 122°C/2 mmHg (171~172°C/18 mmHg[10]) | 84.92 | 7.09 | | 84.81 | 7.12 | |
| 5-$PhN_2$ | H | 95~96°C (94~95°C[11]) | | | | | | |
| 5-$CO_2Me$ | H | 128~129.5°C | 73.81 | 5.52 | | 73.67 | 5.30 | |
| 5-$NO_2$ | H | 128°C (128°C[11]) | | | | | | |
| H | 3'-MeO | 90~91°C | 78.13 | 6.09 | | 77.98 | 6.04 | |
| H | 3'-$CO_2Me$ | 88~89°C | 73.77 | 5.48 | | 73.67 | 5.30 | |
| H | 3'-$NO_2$ | 99.5~100°C | 66.78 | 4.22 | 6.44 | 66.97 | 4.22 | 6.51 |
| H | 4'-MeO | 65~65.5°C | 78.13 | 6.15 | | 77.98 | 6.04 | |
| H | 4'-Cl | 51~52°C (53°C[12]) | | | | | | |
| H | 4'-Br | 60°C (60~61°C[12]) | | | | | | |
| H | 4'-I | 74°C | 48.79 | 3.15 | | 48.67 | 3.06 | |
| H | 4'-$CO_2Me$ | 133~133.5°C | 73.85 | 5.43 | | 73.67 | 5.30 | |
| H | 4'-$NO_2$ | 123~124°C (122°C[12]) | | | | | | |

*4-Chloro-2-hydroxybiphenyl.*—A half moles (86.3 g.) of 4-chloro-2-nitroaniline[14] was diazotized in 150 ml. of concentrated hydrochloric acid with 35 g. of sodium nitrite in 50 ml. of water, and decomposed in the presence of 2 l. of thiophene free benzene by adding an excess of sodium acetate. Stirring was continued over-night. The benzene layer was washed with aqueous sodium hydroxide and the solvent evaporated. 4-Chloro-2-nitrobiphenyl distilled at 160~166°C/2 mmHg, and solidified in the receiver. It was recrystallized from petroleum ether-benzene to give prisms melting at 53°C (lit.[15], 52~53°C). The nitro-compound (23 g., 0.1 mol.) was catalytically hydrogenated over platinized Raney nickel[16] in ethanol, 6.5 l. of hydrogen being absorbed in 2 hr. 2-Amino-4-chlorobiphenyl was, without further purification, diazotized in aqueous sulfuric acid with sodium nitrite and decomposed by pouring into 30% aqueous sulfuric acid. 4-Chloro-2-hydroxybiphenyl was recrystallized from carbon tetrachloride to form prisms.

*5-Ethyl-2-hydroxybiphenyl.*—To a solution of 5 g. of 5-acetyl-2-hydroxybiphenyl[10] in 100 ml. of acetic acid was added a few drops of 3 N hydrochloric acid and 100 mg. of platinum oxide. On shaking under hydrogen atmosphere, 1.1 l. of hydrogen was absorbed under the atmospheric pressure and at the room temperature. The solvent was evaporated under reduced pressure and the residue was distilled at 122°C/2 mmHg, giving the desired phenol, $n_D^{15}$ 1.5893.

*2-Hydroxy-5-methoxycarbonylbiphenyl.*—5-Acetyl-2-hydroxybiphenyl[10] in pyridine was oxidized with iodine to the corresponding β-ketoalkylpyridinium iodide, which was cleft by aqueous alcoholic sodium hydroxide to 2-hydroxybiphenyl-5-carboxylic acid, as is specified by King[17]. The carboxylic acid was recrystallized from benzene to give plates melting at 148°C (lit.[18], 148~149°C). A suspension of 8 g. of the hydroxycarboxylic acid in 100 ml. of methanol was saturated with hydrogen chloride, refluxed on a water bath for two hours and then poured into 500 ml. of ice-water. The crystals were collected and recrystallized from benzene to give plates.

*2-Hydroxy-3'-methoxybiphenyl.*—To a mixture of 30 g. of *m*-bromoanisole and 50 g. of *o*-nitrochlorobenzene was added in five portions 50 g. of copper bronze at 200°C. The temperature was kept at 200~240°C for five hours longer. After cooling, the solid mass was extracted with acetone and the extract was fractionally distilled under diminished pressure, the fraction boiling at 150~175°C/1~2 mmHg being collected. On fractional recrystalliza-

8) W. Hückel, O. Neunhoeffer, A. Gercke and E. Frank, *Ann.*, **477**, 123 (1930).
9) C. Finzi and A. Mangini, *Gazz. chim. ital.*, **62**, 664 (1932),
10) K. von Auwers and G. Wittig, *J. prakt. Chem.*, **108**, 99 (1924).
11) W. Borsche and B. G. B. Scholten, *Ber.*, **50**, 600 (1917).
12) J. C. Colbert and R. M. Lacy, *J. Am. Chem. Soc.*, **68**, 271 (1946).
13) F. C. Coppa and L. P. Walls, *J. Chem. Soc.*, **1950**, 314.
14) M. A. F. Holleman, *Rec. trav. chim. Pay-Bas*, **34**, 207 (1915).
15) K. Hoegerle and P. L'Écuyer, *Can. J. Chem.*, **37**, 2074 (1959).
16) S. Nishimura, This Bulletin, **32**, 61 (1959).
17) L. C. King, *J. Am. Chem. Soc.*, **66**, 894 (1944).
18) K. H. Stotta and A. E. Nold, *Ber.*, **68**, 2230 (1935).

tion of the distillate from methanol, 10 g. of 3'-methoxy-2-nitrobiphenyl, melting at 83~84°C was obtained. Found: N, 6.28. Calcd. for $C_{13}H_{11}O_3N$: N, 6.11%. Catalytic reduction of the nitrocompound gave 2-amino-3'-methoxybiphenyl which was characterized as the acetyl derivative (m. p., 114°C) and analyzed. Found: C, 74.88; H, 6.48; N, 5.81. Calcd. for $C_{15}H_{15}O_2N$: C, 74.66; H, 6.27; N, 5.81%. Diazotization of the amine and the subsequent hydrolysis gave 2-hydroxy-3'-methoxybiphenyl.

*2-Hydroxy-3'-methoxycarbonylbiphenyl.*—2-Amino-3'-methoxycarbonylbiphenyl[19] was diazotized in aqueous sulfuric acid and decomposed at 80°C. The oily layer was extracted with ether and washed with aqueous sodium carbonate solution. The solvent was evaporated and the residue was recrystallized from carbon tetrachloride, to give prisms.

*2-Hydroxy-3'-nitrobiphenyl.*—To a solution of 3 g. of 2-methoxy-3'-nitrobiphenyl (m. p., 68.5~69°C)[20] in 50 ml. of acetic acid was added 20 ml. of 48% aqueous hydrobromic acid. The mixture was warmed on a water bath for five hours, when the oily layer disappeared. The solution was concentrated under reduced pressure and the residue was diluted with 50 ml. of water. Brown oil was extracted with benzene and the benzene layer was extracted with 20% aqueous sodium hydroxide. The aqueous layer was acidified and the product recrystallized from methanol to form needles.

*2-Hydroxy-4'-methoxybiphenyl.*—4'-Methoxy-2-nitrobiphenyl[21] (2.3 g., 0.01 mol.) was reduced with 13 g. of stannous chloride dihydrate and 15 ml. of concentrated hydrochloric acid in 20 ml. of alcohol by refluxing for two hours. The amine[22] in 30 ml. of water and 2 ml. of sulfuric acid was diazotized with 0.7 g. of sodium nitrite in 2 ml. of water and hydrolyzed as usual to the desired phenol. The phenol was recrystallized from a mixture of carbon tetrachloride and petroleum ether (1 : 1).

*2-Hydroxy-4'-iodobiphenyl.*—4'-Amino-2-hydroxybiphenyl[23] (3.7 g., 0.02 mol.) was diazotized in aqueous sulfuric acid (2.4 g. of concentrated sulfuric acid and 20 ml. of ice-water) with 1.5 g. of sodium nitrite in 3 ml. of water. The diazonium solution was added dropwise to the boiling aqueous potassium iodide solution (4 g. of potassium iodide in 5 ml. of water) and the separated brown oil was extracted with ether. On evaporation the ether extract gave heavy oil which was heated with hot petroleum ether and decanted. Repetition of the process gave thick prisms.

*2-Hydroxy-4'-methoxycarbonylbiphenyl.*—To a mixture of 50 g. (0.32 mol.) of *o*-nitrochlorobenzene and 26 g. (0.1 mol.) of methyl *p*-iodobenzoate, heated at 230~240°C, was added 80 g. of copper bronze for three hours. After cooling, the mass was extracted with acetone using a Soxlet extractor. The acetone extract deposited a large amount of 2,2'-dinitrobiphenyl, which was filtered off. The mother liquor was evaporated and the residue was refluxed with 500 ml. of ethanol and 160 ml. of 10% aqueous sodium hydroxide for three hours. The mixture was diluted with water to make up 1 l. and boiled for several minutes with active charcoal and then filtered. The filtrate was acidifed and the precipitate was collected. Recrystallization from acetic acid gave 6 g. of 2-nitrobiphenyl-4'-carboxylic acid, melting at 247°C (lit.[24], 250°C). It was catalytically hydrogenated over platinum oxide, as described in the literature[24]. The aminocarboxylic acid was diazotized and hydrolyzed as usual. The crude hydroxycarboxylic acid was used, without further purification, for the preparation of the corresponding ester. Esterification was carried out by saturating the methanolic suspension with hydrogen chloride nd refluxing the mixture for two hours. Recrystallization from carbon tetrachloride gave prisms.

## Results and Discussion

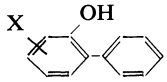
It must be confirmed in the first place that two bands which appear in the 3 μ region in the infrared are not derived from the intermoleculer hydrogen bonding but from the intramolecular origin. With 2-hydroxybiphenyl, the infrared spectra were measured over the concentration range from 0.5 to 0.001 mol./l. in carbon tetrachloride. At concentration of over 0.1 mol./l., a third band appears at 3460 $cm^{-1}$, which is assigned to the $\nu_{O-H}$ of the associated hydroxyl group, but, below 0.01 mol./l., this band disappears and the ratio of intensities of the remaining ones scarcely depend upon concentraion. All the following data were obtained in these conditions, usually 0.001 mol./l. solution being employed.

The absorption at the higher wave number of 2-hydroxybiphenyl is located at 3607 $cm^{-1}$ and, referring to the free $\nu_{O-H}$ of phenol, 3610 $cm^{-1}$ [25], is assigned to the trans form of the molecule having the free hydroxyl group (f). The other absorption at the lower wave number is tentatively assigned to the cis form having the intramolecular interaction with π-electrons of another benzene ring and having a less force constant of the O-H stretch (i). The intensities and the maxima of these two bands vary considerably with different substituents on each benzene ring. The apparent effect of the substituents on the infrared absorption spectra is shown in Figs. 1 and 2, and the numerical data are in Tables II and III. If the varied band properties can be explained reasonably in terms of the intramolecular interaction with π-electrons, the above assignment will be justified.

Substitution has been confined to the positions at 4, 5, 3' or 4' of the hydroxyl group

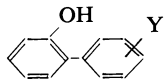
19) R. Adams and T. L. Cairns, *J. Am. Chem. Soc.*, **61**, 2179 (1939).
20) W. J. Dunstan and G. K. Hughes, *J. Proc. Roy. Soc. N. S. Wales*, **80**, 77 (1947); *Chem. Abstr.*, **42**, 4161a (1948).
21) B. Jones and F. Chapman, *J. Chem. Soc.*, **1952**, 1832.
22) I. G. M. Campbell and D. J. Morrill, ibid., **1955**, 1666.
23) W. G. Christiansen and S. E. Harris, *J. Am. Pharm. Assoc.*, **22**, 723 (1933); *Chem. Abstr.*, **29**, 4382 (1935).
24) I. G. M. Campbell, *J. Chem. Soc.*, **1950**, 3113.
25) P. J. Stone and H. W. Thompson, *Spectrochim. Acta*, **10**, 17 (1957).

Table II. $\nu_{O-H}$ absorptions of 2-hydroxybiphenyls substituted in A-ring



| X | OH | $\nu_{max}$ cm$^{-1}$ | $\Delta\nu^a_{1/2}$ cm$^{-1}$ | $A\times10^{-4}$ mol$^{-1}$ l. cm$^{-2}$ | $\Delta\nu_{max}$ cm$^{-1}$ | $A_i/A_f$ |
|---|---|---|---|---|---|---|
| H | f | 3607.0 | 18.2 | 0.20 | 42.0 | 6.4 |
| | i | 3565.0 | 15.0 | 1.28 | | |
| 4-MeO | f | 3606.0 | 22.8 | 0.20 | 43.2 | 7.2 |
| | i | 3562.8 | 15.8 | 1.44 | | |
| 4-Cl | f | 3601.5 | 20.8 | 0.20 | 43.3 | 7.3 |
| | i | 3558.2 | 15.6 | 1.45 | | |
| 4-$NO_2$ | f | 3597.8 | 19.6 | 0.23 | 44.0 | 7.4 |
| | i | 3553.8 | 19.4 | 1.70 | | |
| 5-Et | f | 3610.2 | 20.3 | 0.23 | 41.5 | 5.6 |
| | i | 3568.7 | 16.0 | 1.27 | | |
| 5-$PhN_2$ | f | 3599.0 | 24.0 | 0.21 | 45.8 | 8.3 |
| | i | 3553.2 | 16.8 | 1.74 | | |
| 5-$CO_2$Me | f | 3596.7 | 18.6 | 0.18 | 46.1 | 8.8 |
| | i | 3550.6 | 15.8 | 1.59 | | |
| 5-$NO_2$ | f | 3590.0 | 24.6 | 0.22 | 47.4 | 8.6 |
| | i | 3542.6 | 16.6 | 1.90 | | |

Table III. $\nu_{O-H}$ absorptions of 2-hydroxybiphenyls subsituted in B-ring



| Y | O-H | $\nu_{max}$ cm$^{-1}$ | $\Delta\nu^a_{1/2}$ cm$^{-1}$ | $A\times10^{-4}$ mol$^{-1}$ l. cm$^{-2}$ | $\Delta\nu_{max}$ cm$^{-1}$ | $A_i/A_f$ |
|---|---|---|---|---|---|---|
| H | f | 3607.0 | 18.2 | 0.20 | 42.0 | 6.4 |
| | i | 3565.0 | 15.0 | 1.28 | | |
| 3'-MeO | f | 3607.1 | 17.4 | 0.15 | 47.9 | 9.3 |
| | i | 3559.2 | 17.0 | 1.40 | | |
| 3'-$CO_2$Me | f | 3605.0 | 18.8 | 0.44 | 30.7 | 2.4 |
| | i | 3574.3 | 17.0 | 1.06 | | |
| 3'-$NO_2$ | f | 3602.6 | 19.0 | 0.99 | 20.4 | 0.66 |
| | i | 3582.2 | 16.6 | 0.65 | | |
| 4'-MeO | f | 2607.1 | 18.0 | 0.15 | 47.6 | 9.7 |
| | i | 3559.5 | 17.6 | 1.45 | | |
| 4'-Cl | f | 3605.0 | 17.8 | 0.37 | 35.0 | 3.1 |
| | i | 3570.0 | 15.6 | 1.14 | | |
| 4'-Br | f | 3606.0 | 14.8 | 0.36 | 34.9 | 3.3 |
| | i | 3576.1 | 16.0 | 1.19 | | |
| 4'-I | f | 3605.3 | 13.4 | 0.32 | 35.1 | 4.1 |
| | i | 3570.2 | 16.0 | 1.32 | | |
| 4'-$CO_2$Me | f | 3304.4 | 17.2 | 0.34 | 33.0 | 3.6 |
| | i | 3571.4 | 16.2 | 1.21 | | |
| 4'-$NO_2$ | f | 3602.1 | 17.2 | 0.79 | 22.5 | 0.97 |
| | i | 3579.6 | 17.6 | 0.77 | | |

Added in proof: After this paper had been received, W. Beckering (*J. Phys. Chem.*, **65**, 206 (1961)) reported O-H$\cdots\pi$ interaction in some of the examples included in the present study.

at 2-position in biphenyl skeleton in order to avoid either another intramolecular hydrogen bond[1] and/or steric influence[26], which make the consideration more complex. For the sake of convenience, the substituted 2-hydroxybiphenyls are calssified into two groups; one is those with the substituent on the benzene ring (A) which bears the hydroxyl group and the other those on the other ring (B).

The varied $\Delta\nu_{max}$ and $A_i/A_f$ in Tables II and III may be considered to correspond to the strength of the interaction, since the former is known to be approximately proportional to the enthalpy (Eq. 1)[27] and the latter to the equilibrium constant (Eq. 2)[28] of the interaction. Therefore, neither value should be independent of the other and the relation between $\Delta\nu_{max}$ and $\log(A_i/A_f)$ must be linear (Eq. 3) if $\Delta S$ of the interaction, and the constants $a$ and $b$ are independent of the

26) Unpublished work. See also Ref. 5.

27) R. M. Badger and S. H. Bauer, *J. Chem. Phys.*, **5**, 839 (1937).

28) M. Ōki and H. Iwamura, This Bulletin, **33**, 1600 (1960).

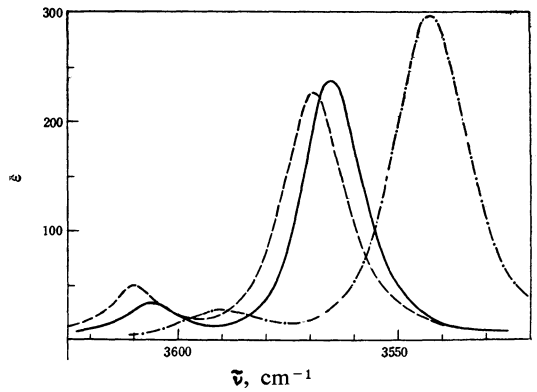



Fig. 1. The apparent $\nu_{O-H}$ absorptions of 2-hydroxybiphenyls (A).

——— 2-hydroxybiphenyl
——— 5-ethyl-2-hydroxybiphenyl
—·—· 2-hydroxy-5-nitrobiphenyl

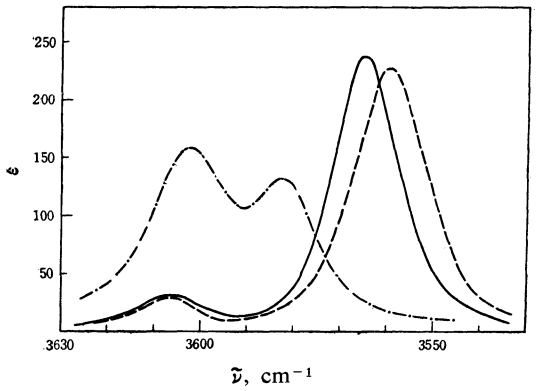



Fig. 2. The apparent $\nu_{O-H}$ absorptions of 2-hydroxybiphenyls (B).

——— 2-hydroxybiphenyl
——— 2-hydroxy-3'-methoxybiphenyl
—·—· 2-hydroxy-3'-nitrobiphenyl

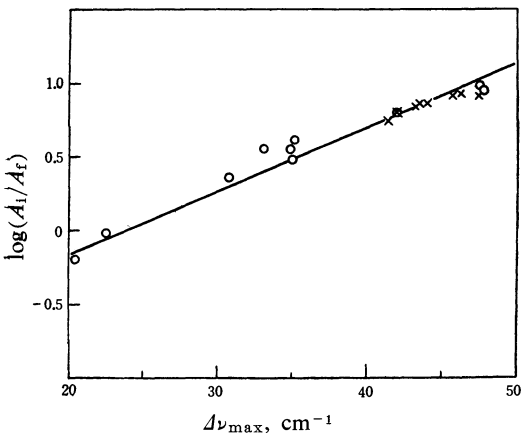



Fig. 3. Relation between $\log(A_1/A_f)$ and $\Delta\nu_{max}$, the cross and circle representing 2-hydroxybiphenyls substituted in the A and B ring, respectively.

substituents. The case is realized from Fig. 3. Strictly speaking, however, the line has a little convex curvature upwards, which may be attributed to the second order term neglected in

$$-\Delta H = a\Delta\nu_{max} \quad (1)$$

$$K = bA_1/A_f \quad (2)$$

$$RT\cdot\ln(A_1/A_f) = a\Delta\nu_{max} + (T\Delta S - RT\cdot\ln b) \quad (3)$$

the approximation, assuming the constancy of $a$, $b$ and $\Delta S$. From the gradient of the line, a constant $a$ in the equation can be estimated to be 0.057 kcal.cm$^{-1}$ at the measured temperature. It may be expressed otherwise by saying that the wave number shift of 18 cm$^{-1}$ corresponds to the energy of the interaction of one kcal./mol. Compared with the ordinary hydrogen bonding, in which displacement of $\nu_{O-H}$ by 40 cm$^{-1}$ corresponds to one kcal./mol. of the enthalpy change[27], these interactions seem to have the characteristic that a smaller $\Delta\nu_{max}$ corresponds to an appreciable enthalpy change. This is, however, overestimated, since the term $T\Delta S$ in Eq. 3 is some what dependent on $\Delta\nu_{max}$ and the greater $\Delta\nu_{max}$ makes the absolute value of $\Delta S$, which is inherently negative, greater. It will tend to make its value less.

It is further shown in Fig. 3, that the points representing 2-hydroxybiphenyls substituted on the B-ring spread wider by about five times than those having the substituent on the A-ring; that is, the effect of the substituents on the phenomenon is more fully developed in the B-ring. As the first approximation, the strength of the intramolecular interaction between the hydroxyl group and π-elctrons is expected to be influenced by the substituent on the B-ring by directly affecting the π-electron density and the proton accepting character of the B-ring, while the substituent on the A-ring will not touch the π-electron density of the B-ring but affect the proton donating character of the hydroxyl group. The above observation means that the former effect is predominant.

As to the latter effect, it is well known that acid dissociation constant ($pK_a$) of phenols[29] and spectroscopically free $\nu_{O-H}$ of phenols in carbon tetrachloride solution[30], are in linear relationship with Hammett's sigma constants of the substituents. The free $\nu_{O-H}$ of 2-hydroxybiphenyls substituted in the A-ring have been examined in this connection and the results are presented in a Hammett sigma-rho plot in Fig. 4. A line with rho value of −13.8 is

29) H. C. Brown, D. H. McDaniel and O. Häfliger, "Determination of Organic Structures by Physical Methods", Ed. by E. A. Braude and F. C. Nachod, Academic Press Inc., New York (1955), p. 589.
30) L. L. Ingraham, J, Corse, G. F. Bailey and F. Stitt, *J. Am. Chem. Soc.*, **74**, 2297 (1952).

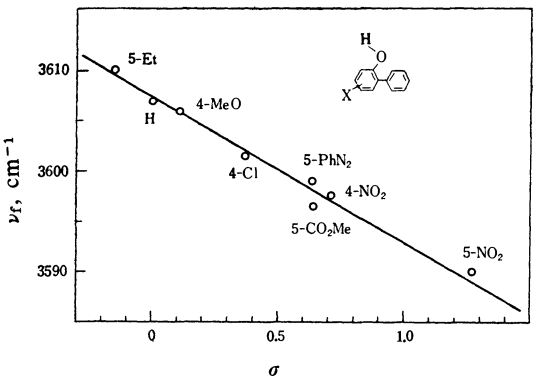



Fig. 4. $\nu_{O-H}$ frequencies of the free hydroxyl group in 2-hydroxybiphenyls substituted in the A ring versus the Hammett sigma constants.

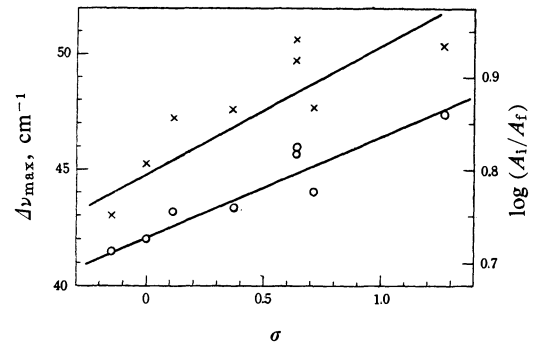



Fig. 5. Dependence of the two band properties, $\Delta\nu_{max}$ (the circles to the left ordinate) and $\log(A_i/A_f)$ (the crosses to the right ordinate) on the substituents in A-ring.

obtained, comparable to $\rho=-12.6$ in the substituted phenols[30]. This suggests that the substituents in the A-ring are really pertaining to the proton donating character of the hydroxyl group just as in phenols and thus must be affecting the strength of the intramolecular interaction. In Fig. 5, it is illustrated to what extent the strength of the interaction, i.e., $\Delta\nu_{max}$ and $\log(A_i/A_f)$ depends on the sigma constants of the substituents. It can be concluded from Figs. 4 and 5, that the intramolecular interaction between the hydroxyl group and $\pi$-electrons strengthens as the electron drawing power of the substituents or the acidity of the hydroxyl group enhances, and weakens with the electron-donating substituents.

As the substituents on the ring B govern the density and polarizability of $\pi$-electrons acting as the hydrogen accepter, it is natural that the variation in the B-ring substituent causes a salient change in the degree of the interaction in such a direction that the electron donating substituents (e.g., methoxyl) enhance the interaction, while the electron-attracting substituents (e.g., nitro) disfavor the interaction. Two kinds of band properties, $\Delta\nu_{max}$ and $\log(A_i/A_f)$ have again been tested for Hammett's sigma-rho relation, in the expectation that $\pi$-electron density and/or polarizability at the site of the interaction will be expressed in terms of sigma values, just as in the case of the electrophilic nuclear substitution reaction[31]. Although Wulf et al.[2] suggested that the hydroxyl group would approach the first carbon atom (1′-carbon), there is no a priori reason which of the 3′- or 4′- substituents may be regarded as *m*- or of *p*-position in respect of the site of the interaction. In the previous papers[32,33] the authors have succeeded in assigning the position of the hydroxylic proton in the interaction in benzyl and phenethyl alcohols by plotting $\log(A_i/A_f)$ against Hammett's sigma values considering the various possibilities, and by choosing the assignment of better linearity. The trial has again been applied to the present system but failed to obtain the precise linearity in either case. In Fig. 6 is shown the relation between $\log(A_i/A_f)$s' relative to that for 2-hydroxybiphenyl and the Hammett sigma constants, *m*- and *p*-values of which are allotted to 4′- and 3′-substituents, respectively. These are

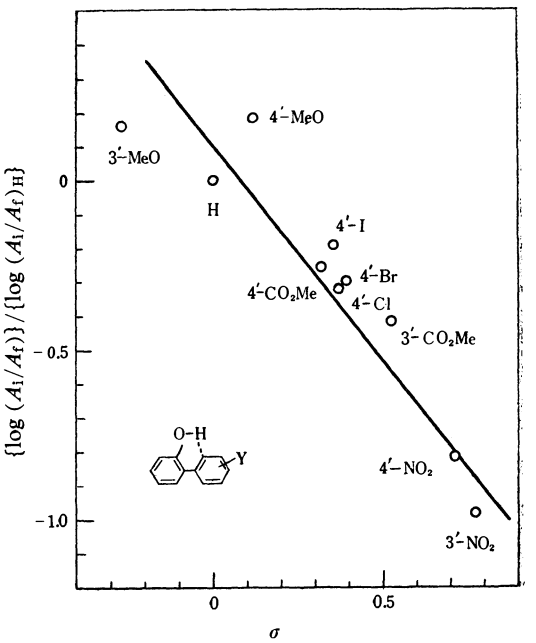



Fig. 6. Relation between $\{\log(A_i/A_f)\}/\{\log(A_i/A_f)_H\}$ and the Hammett sigma constants in 2-hydroxybiphenyl substituted in B-ring.

31) C. W. McGary, Jr., Y. Okamoto and H. C. Brown, ibid., 77, 3037 (1955).
32) M. Ōki and H. Iwamura, This Bulletin, 32, 955 (1959).
33) M. Ōki and H. Iwamura, ibid., 32, 1135 (1959).

in better linearity than the reverse assignment in so far as 3′-electrophilic substituents (e. g., nitro) disfavor the interaction more than the 4′-ones. Here it may be said that the hydroxylic proton is more concerned with π-electrons at 2′-carbon than at the 1′. Methoxyl group at 3′- and 4′-positions, however, favors the interaction equally, in spite of the fact that their sigma constants are of opposite sign and differ by 0.38. If the interaction is solely concerned with π-electrons at 2′-carbon, the methoxyl group at 4-position would not have favored the interaction. Putting the emphasis upon the last observation and regarding the difference in the electrophilic substituents minor, it may tentatively be concluded that the hydroxylic proton is concerned with π-electron density between 1′ and 2′ carbon atoms, like the structure of the complex formed between silver ion and benzene[34].

It has been assumed that the electronic effect of the substituents might be confined to the ring to which it is attached. Biphenyls are, however, characteristic of its conjugation between two phenyl rings, and a considerable conjugation has been demonstrated by the kinetic study[35] and the ultraviolet spectroscopy[36], even when it is substituted at one ortho-position by a rather small group[37]. Although there is no datum available for the 2-hydroxybiphenyl system, if the conjugation exists between two rings in this system, the free $\nu_{O-H}$ must also be dependent on the substituents on the B-ring. In Fig. 7 the wave number where the free $\nu_{O-H}$ appears is plotted to Hammett's sigma constants, *m*- and *p*-sigma values being alloted to the substituents at 3′- and 4′-positions, respectively. A line having an inclination of −3.9 is obtained and, compared with that of Fig. 4, −13.8, it can be

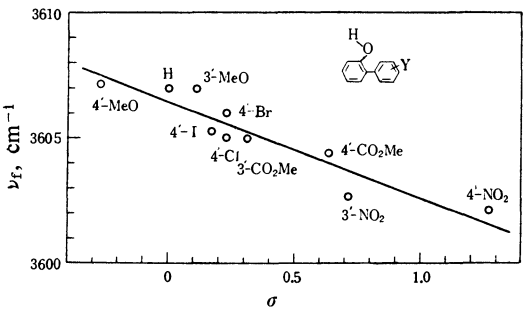



Fig. 7. $\nu_{O-H}$ frequencies of the free hydroxyl group in 2-hydroxybiphenyls substituted in the B-ring, versus the Hammett sigma constants.

34) R. E. Rundle and J. H. Goring, *J. Am. Chem. Soc.*, **72**, 5337 (1950).
35) E. Berliner and L. H. Liu, ibid., **75**, 2417 (1953).
36) V. P. Kreiter, W. A. Bonner and R. H. Eastmann, ibid., **76**, 5770 (1954).
37) G. H. Beaven, D. M. Hall, M. S. Lesslie and E. E. Turner, *J. Chem. Soc.*, **1952**, 854.

stated that in 2-hydroxybiphenyls 28% of the electronic effect of the substituents can be transmitted across the pivot bond through mesomerism and/or induction. The degree of conjugation is rather great in spite of the ortho substitution when compared with biphenyls free from the substituent[35,36], because Berliner obtained, for example, $\rho=0.37$ from the dissociation constants of the substituted biphenyl-4-carboxylic acids, deducing 37% propagation of the substituent effect[38]. This may be reasonable, however, because the data obtained for 2-hydroxybiphenyls are for free $\nu_{O-H}$ of trans configration, which, unlike cis form, has only a little excessive steric hindrance compared with a hydrogen atom.

With these new informations of conjugative effect, the effect of the substituents at the A and the B-rings on the electron donating power of the B-ring and on the proton donating character of the hydroxyl group, respectively, must be reevaluated. Since the effect of the substituents is more strongly exerted by affecting the proton accepting power than the proton donating one, as shown in Fig. 3, the effect of the B-ring substituents on the apparent interaction by affecting the proton donating character of the hydroxyl group of the A-ring may be neglected. On the other hand, the effect of the A-ring substituents on the proton accepting character of the B-ring must be taken into account, since it amounts to 28% of that caused by the B-ring substituents and has as much influence on the interaction as the effect on the proton donatining power of the hydroxyl group. The electron attracting substituents (e. g., nitro), for example, influence the interaction as a result of two opposing effects. That is, they favor the interaction by strengthening the proton donating character of the hydroxyl group and disfavor it by lessening the proton accepting charactor of the B-ring. Although it is as yet impossible to separate the two competing effects quantitatively, it is clear that the pure effect of A-ring substituents on the proton donating character of the hydroxyl group is more pronounced than is estimated from Fig. 3.

The authors are indebted to Professor Yoshiyuki Urushibara for his encouragement and discussuion throughout this work. The authors' thanks are also due to the Ministry of Education for the Grant in Aid for Fundamental Scientific Research.

*Department of Chemistry*
*Faculty of Science*
*The University of Tokyo*
*Hongo, Tokyo*

38) E. Berliner and E. A. Blommers, *J. Am. Chem. Soc.*, **73**, 2479 (1951).

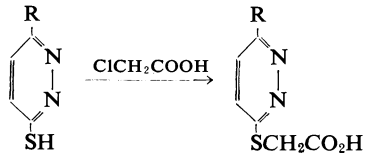
# *Studies on Meso-ionic Compounds. XIV*[1]. *Synthesis of Meso-ionic Compounds from Pyridazine Derivatives Having a Carboxymethylmercapto Group*

By Masaki OHTA and Kimio KISHIMOTO

(Received April 3, 1961)

In the previous paper of this series, the reaction of several kinds of azoles (5-phenyl-1, 3, 4-triazole, 5-phenyl-1, 3, 4-oxadiazole, 1, 5-diphenyl-1, 3, 4-triazole, benzothiazole, benzoxazole, cyclohexeno- and cyclopentenothiazoles) having a carboxymethylmercapto group with acetic anhydride was reported[2]. Although no formation of pigments had been reported by Duffin et al.[3], it was demonstrated that not only the corresponding meso-ionic compounds but also pigments are formed in the reaction.

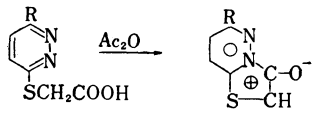
In this paper, the present authors further extended this reaction to pyridazine derivatives and studied whether the meso-ionic compounds are obtained or not from the pyridazine derivatives possessing a carboxymethylmercapto group by the loss of one mole of water. The structure of the resulting meso-ionic compounds from pyridazine derivatives was confirmed by infrared absorption, hydrolysis, and the reaction of the compounds with phenylhydrazine or mercuric chloride.




I (a—f) II (a—f)

a: R=$CH_3$ d: R=Cl
b: R=$SCH_3$ e: R=Ph
c: R=$SCH_2Ph$ f: R=SH

Pyridazine derivatives possessing a carboxymethylmercapto group[4] were prepared from the corresponding mercapto pyridazine derivatives by the reaction with monochloroacetic acid. By the action of acetic anhydride or acetic anhydride-pyridine on 3-methyl-6-(carboxymethylmercapto)-pyridazine (IIa), violet pigment, which was not prosecuted for detailed investigation because of its difficult purification, was formed, and no corresponding meso-ionic compound was formed. But the present authors have found that IIa reacts readily with acetic anhydride-pyridine-triethyl amine to give a red meso-ionic compound IIIa by the loss of one mole of water, and in the same manner as in the case of IIa the other meso-ionic compounds IIIa—IIIe are obtained from those corresponding parent acids IIa—IIe, respectively. Unlike those reported previously[2], however, the present compounds are not formed in the absence of triethylamine as a more basic tertiary base, and by moisture in the air or in the solvent of recrystallization the new red compounds IIIa—IIIe immediately are turned into pale yellow compounds of which analytical values show their structures to be meso-ionic compounds IIIa—IIIe having a water of crystallization and which reversibly return to the red compounds of IIIa—IIIe on drying. These

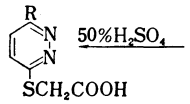



II (a—e) III (a—e)

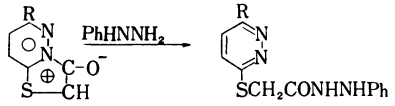
meso-ionic compounds are heat-unstable solids which are readily soluble in polar and non-polar solvents. For example, meso-ionic compounds give yellow aqueous solutions with the exception of IIIe and red solution in absolute ethanol or dry benzene. The influence of the substituent in 3-position of pyridazine on the ring closure of II by acetic anhydride was scarecely observed. Only 3-mercapto-6-(carboxymethylmercapto)-pyridazine (IIf) gave no mese-ionic compound. On storage, IIIa deteriorated and became black after about two weeks at room temperature. Though the other compounds IIIb—IIIe are stable, IIIa—IIIe turn black in pyridine or 10% aqueous sodium hydroxide. The infrared spectra of IIIa—IIIe respectively, in comparison with those of the parent acids, have a new strong absorption at 1630～1650 $cm^{-1}$ with the disappearance of a band near 1700 $cm^{-1}$ due to carbonyl vibration of the carboxy group. This similar remarkable change of the spectra of meso-ionic compounds from these pyridazine derivatives has been observed also in infrared spectra of meso-ionic

1) Part XIII, This Bulletin, **34**, 668 (1961).
2) M. Hashimoto and M. Ohta, ibid., **33**, 1394 (1960).
3) G. F. Duffin and J. D. Kendall, *J. Chem. Soc.*, **1951**, 734; ibid., **1956**, 361.
4) M. Kumagai, *J. Chem. Soc. Japan, Pure Chem. Sec.* (*Nippon Kagaku Zasshi*), **81**, 1604, 1886 (1960).

compounds derived from 2-(carboxymethylmercapto)-pyridine, whose structure had been confirmed synthetically[3], and from azoles having a carboxymethylmercapto group[2]. By 50% aqueous sulfuric acid IIIa—IIIe were easily hydrolyzed to the corresponding parent acids IIa—IIe respectively. The meso-ionic compounds IIIa, IIIb and IIIe reacted with




II (a—e)




III IV(a, b and e)

mercuric chloride in methanol respectively to give pale yellow precipitates, whose analytical values suggest the structures to be IIIa+2$HgCl_2$, IIIb+HgCl and IIIe+HgCl respectively[5,6], but in the case of the parent acids IIa—IIe no such precipitates were formed. When meso-ionic compounds IIIa, IIIb and IIIe were heated with phenyl hydrazine in ethanol, the corresponding phenylhydrazides (IVa, IVb and IVe) were obtained. The fact that the corresponding phenylhydrazones were not formed, suggests that the C-O bond of the meso-ionic compounds has no ketonic character.

## Experimental

**3-Benzylmercapto-6-mercaptopyridazine.**—A solution of benzylchloride (0.8 g.) in methanol (2 ml.) was poured into a solution of 3,6-dimercaptopyridazine[4] (0.8 g.) and sodium hydroxide (0.2 g.) in methanol (14 ml.). The solution was heated at 70°C on a water bath for 5 min., and 10% aqueous sodium hydroxide was added. The insoluble substance was filtered off. The filtrate was neutralized with aqueous hydrochloric acid to precipitate 3-benzylmercapto-6-mercaptopyridazine. Recrystallization from glacial acetic acid gave pale yellow needles (0.9 g.), m. p. 178~179°C. Yield 68.7%.

Found: N, 11.90. Calcd. for $C_{11}H_{10}N_2S_2$: N, 11.96%.

The alkali insoluble substance described above was recrystallized from ethanol to give white needles of 3,6-bis(benzylmercapto)-pyridazine, m. p. 121~122°C.

Found: N, 8.74. Calcd. for $C_{18}H_{16}N_2S_2$: N, 8.64%.

**3-Methyl-6-(carboxymethylmercapto)-pyridazine (Ia).**—A solution of chloroacetic acid (3.75 g.) and sodium hydroxide (1.6 g.) in water (16 ml.) was

Table I. 3-Substituted pyridazine derivatives having a carboxymethylmercapto group in the 6-position

| | R | Appearance | M. p., °C | Yield, % | Formula | Anal. N% Found | (Calcd.) |
|---|---|---|---|---|---|---|---|
| IIb | $SCH_3$ | White plates | 183~184 | 78.3 | $C_7H_8O_2N_2S_2$ | 13.04 | (12.96) |
| IIc | $SCH_2Ph$ | White plates | 108~109 | 72.5 | $C_{13}H_{13}O_2N_2S_2$ | 9.67 | (9.59) |
| IId | Cl | 7) | | | | | |
| IIe | Ph | White plates | 149~150 | theor. | $C_{12}H_{10}O_2S$ | 11.60 | (11.38) |
| IIf | SH | Yellow prisms | 180 (decomp.) | 71.4 | $C_6H_6O_2N_2S_2$ | 13.56 | (13.86) |

Table II. Meso-ionic compounds from acids IIb—IIe

| | M. p., °C | Yield, % | Formula | Anal. C% Found (Calcd.) | H% Found (Calcd.) | N% Found (Calcd.) |
|---|---|---|---|---|---|---|
| IIIb | > 300 | theor. | $C_7H_6ON_2S_2$ | 42.20 (42.43) | 3.14 (3.05) | 14.20 (14.14) |
| IIIc | 167~168 | 81.8 | $C_{13}H_{10}ON_2S_2$ | 57.07 (56.93) | 3.89 (3.68) | 10.19 (10.22) |
| IIId | > 250 | 80.0 | $C_6H_3ON_2SCl$ | 38.30 (38.57) | 1.96 (1.61) | 14.87 (11.38) |
| IIIe | 110 (decomp.) | (60.0) | $C_{12}H_{10}O_2N_2S$ (having $H_2O$) | 60.43 (58.53) | 4.38 (4.09) | 11.38 (11.38) |
| | 122 (decomp.) | 60.0 | $C_{12}H_8ON_2S$ | 62.78 (63.16) | 3.55 (3.53) | 12.13 (12.28) |

5) G. F. Duffin and J. D. Kendall, *J. Chem. Soc.*, **1956**, 3189.
6) H. Kato et al., *J. Chem. Soc. Japan, Pure Chem. Sec.* (*Nippan Kagaku Zasshi*), **78**, 707 (1957).
7) J. Kinugawa et al., *J. Pharm. Soc. Japan* (*Yakugaku Zasshi*), **80**, 1559 (1960).

added to a solution of 3-methyl-6-mercapto-pyridazine (5.0 g.)[4] and sodium hydroxide (1.6 g.) in water (16 ml.). The solution was warmed on a water bath at 60~65°C for an hour. After cooling, the reaction mixture was neutralized with 10% aqueous hydrochloric acid and the resulting precipitate was filtered off. Recrystallization from ethanol gave white plates (4.3 g.) m. p. 138~139°C. Yield 58.9%.

Found: C, 45.50; H, 4.52; N, 14.90. Calcd. for $C_7H_8O_2N_2S$: C, 45.65; H, 4.34; N, 15.22%.

**IIb, IIc, IId, IIe and IIf[4].** — These acids were prepared by the same procedure as used for Ia. The following Table I set forth these results.

**Meso-ionic Compound IIIa from IIa.**—The acid IIa (4.0 g.) was dissolved at room temperature in a mixture of acetic anhydride, pyridine and triethylamine (volume ratio of 1 : 1 : 1) (5 ml.). The solution immediately turned red and after a few minutes orange crystals were separated, which were filtered off, and completely washed with ether. Recrystallization from ethanol-ligroin gave pale yellow needles, m. p. 106°C (decomp.), which have a water of crystallization.

Found: C, 45.60; H, 4.45; N, 15.14. Calcd. for $C_7H_6ON_2S \cdot H_2O$: C, 45.65; H, 4.38; N, 15.21%.

When this compound was heated at about 65°C under reduced pressure, the water of crystallization was removed, affording red crystals of IIa, m. p. 135°C (decomp.). Yield 2.0 g. (50.0%).

Found: C, 50.30; H, 3.72; N, 16.54. Calcd. for $C_7H_6ON_2S$: C, 50.60; H, 3.64; N, 16.87%.

**Meso-ionic Compound IIIb, IIIc, IIId and IIIe Derived from Acids IIb, IIc, IId and IIe Respectively.**—In exactly the same manner as in the case of IIa, these meso-ionic compounds were obtained from the corresponding parent acids IIb, IIc, IId and IIe respectively, and are listed in Table II.

**Action of Aqueous Sulfuric Acid on IIIa.**—A suspension of IIIa (0.3 g.) in 50% aqueous sulfuric acid (1 ml.) was refluxed gently for 5 min. The solution slowly turned red to yellow. After cooling, the solution was neutralized with 10% aqueous sodium hydroxide and was concentrated under diminished pressure. Absolute ethanol (50 ml.) was added to the concentrated solution and the resulting precipitate was filtered off. Crude crystals obtained by concentration of the filtrate were recrystallized twice from ethanol, to afford white plates (0.15 g.), m. p. 139°C, which were undepressed by admixture with an authentic sample of IIa.

**Action of Aqueous Sulfuric Acid on IIIb and IIIe.**—The reaction product, from IIIb or IIIe by a method similar to that for IIa, was undepressed by the admixture with authentic sample of IIb or IIe. Yield of IIb, 81.7% and that of IIe 40%.

**Action of Aqueous Sulfuric Acid on IIIc.** — A suspension of IIIc (0.1 g.) with 50% aqueous sulfuric acid (2 ml.) was gently boiled for 10 min., and after cooling, the solution was neutralized with 10% aqueous sodium hydroxide and was extracted with ether. The extract was dried over anhydrous sodium sulfate and was evaporated to dryness. The residue was recrystallized from glacial acetic acid affording 0.07 g. of white plates m. p. 108~109°C, which showed no depression on admixture with an authentic specimen of IIc.

**Action of Aqueous Sulfuric Acid on IIId.** — In the same manner as in the case of IIIc, the parent acid IIc was obtained.

**Reaction of IIIa, IIIb and IIIe Respectively, with Mercuric Chloride[5,6].** — The solution of IIIa (0.7 g.) and sodium acetate (0.7 g.) in 50% aqueous methanol (20 ml.) was added to a solution of mercuric chloride (1.1 g.) in 50% aqueous methanol (5 ml.). The solution immediately turned yellow to separate a yellow precipitate (1.3 g.). Recrystallization from ethanol gave pale yellow crystals, m. p. > 230°C.

Found: N, 4.22. Calcd. for $C_7H_6ON_2SHg_2Cl_4$: N, 3.94%.

Yellow precipitate from IIIb or IIIe was prepared by the same method as used for IIIa and yellow precipitate from IIIb has m. p. > 300°C.

Found: N, 6.71. Calcd. for $C_7H_5ON_2S_2HgCl$: N, 6.47%. M. p. 250°C (decomp.) from IIIe, Found: N, 5.73, 5.71. Calcd. for $C_{12}H_7ON_2SHgCl$: N, 6.05%.

**Action of Phenylhydrazine on IIIa.**—A solution of phenylhydrazine (0.1 g.) in absolute ethanol (1 ml.) was added to a solution of IIIa (0.1 g.) in absolute ethanol (2 ml.) and the solution was refluxed on a water bath for 15 min. and decolorized with charcoal. The residual oil obtained by evaporation of alcohol solidified giving crude crystals (0.1 g.), m. p. 125~126°C, on cooling in an ice bath for 1 hr. Twice recrystallization from ethanol-ligroin yielded a pure sample of the corresponding phenylhydrazide (IVa) as orange needles, m. p. 138~139°C.

Found: C, 56.43; H, 5.21; N, 20.32, 20.24. Calcd. for $C_{13}H_{14}ON_4S$: C, 56.92; H, 5.15; N, 20.43%.

**Action of Phenylhydrazine on IIIb and IIIe.**—In exactly the same manner as described above, phenylhydrazides (IVb and IV) were prepared, IVe was plates (33.9%), m. p. 181~181.5°C.

Found: C, 64.14; H, 4.93; N, 16.42. Calcd. for $C_{18}H_{16}ON_4S$: C, 64.27; H, 4.80; N, 16.66%. IV, m. p. 152~153°C. Found: N, 18.75. Calcd. for $C_{13}H_{14}ON_4S_2$: N, 18.29%.

The authors are indebted to Dr. Asaji Kondo for microanalyses.

*Laboratory of Organic Chemistry*
*Tokyo Institute of Technology*
*Meguro-ku, Tokyo*

# *The Crystal Structure of Orthorhombic Aniline Hydrobromide, $C_6H_5NH_3Br$*

By Isamu NITTA*, Tokunosuké WATANABÉ and Inao TAGUCHI†

(Received March 13, 1961)

It has been reported in the previous paper[1], that aniline hydrobromide, $C_6H_5NH_3Br$, shows a phase transition of $\lambda$-type in the neighborhood of room temperature. It is monoclinic below 27.5°C, and is orthorhombic above this temperature. In the present paper, the crystal structure of the high temperature modification will be given.

## Experimental

Crystals of aniline hydrobromide were obtained by slow evaporation from methanol solutions. They were made into small cylindrical rods parallel to the b- and c-axis, less then 0.1 mm. in diameter, by partial dissolution with filter paper moistened with methanol. The hot air stream method[2] was applied to take oscillation and Weissenberg photographs. The temperature of the crystals was maintained at $70\pm1$°C during exposure.

The unit cell containing four formula units was found to have the following dimensions:

$$a=16.77\pm0.06\,\text{Å}$$

$$b=6.05\pm0.03\,\text{Å}$$

and

$$c=6.86\pm0.03\,\text{Å}$$

The space group was uniquely determined, from missing reflections, to be $D_{2h}^{10}$-Pnaa.

In order to collect intensity data, unfiltered Cu-$K$ radiations were used for taking Weissenberg photographs. This allowed us to make use of $K\beta$ in addition to $K\alpha$[3]. The multiple-film technique was applied, and the relative intensities of reflections were visually estimated by comparison with standard intensity scales for each series due to $K\alpha$ and $K\beta$. Corrections for Lorentz and polarization factors were made in the usual way. Corrections for absorption were made using Bradley's method for cylindrical specimens[4]. The linear absorption coefficients for Cu-$K\beta$ were calculated using Walter's rule[5] from the values for Cu-$K\alpha$. The extinction effect was more or less minimized by putting larger weights on the relative intensity values obtained from smaller specimens.

## Structure Determination

Since there are four formula units in the unit cell, four bromine atoms must lie on one of the four-fold equivalent positions, a, b, c and d, given by $D_{2h}^{10}$-Pnaa[6]. Two of these, a and b, have the eigen symmetry $C_i$-$\bar{1}$, and the other two, c and d, have $C_2$-2. Inspection of the observed intensities of reflections ($h\,0\,0$) ruled out the possibility of placing these four bromine atoms either on a or b, hence they must lie either on c or d. There are four aniline molecules in the unit cell and their longest molecular axis on which lie the atoms, N, $C_1$ and $C_4$ must occupy either c or d. Now neither the bromine atoms nor aniline molecules can occupy simultaneously the same equivalent positions, neither c nor d, since the axial length $a$ is too short to be accommodated with these. This case is definitely eliminated also by a qualitative disagreement between observed and calculated structure factors ($0\,k\,l$) even for lower order reflections. Therefore, if the bromine atoms are placed on c, the atoms N, $C_1$ and $C_4$ must be placed on d, or vice versa. The choice of these two alternatives is immaterial, since it depends only on the choice of origin. Thus, the atomic coordinates for each atom are those given in Table I.

TABLE I. ATOMIC COORDINATES ASSIGNED TO EACH ATOM

| | |
|---|---|
| 4Br | $x\,\frac{1}{4}\,\frac{1}{4}$, $\bar{x}\,\frac{3}{4}\,\frac{3}{4}$, $\frac{1}{2}+x\,\frac{1}{4}\,\frac{1}{4}$, $\frac{1}{2}-x\,\frac{3}{4}\,\frac{3}{4}$; |
| 4N, 4$C_1$ and 4$C_4$: | $x\,\frac{3}{4}\,\frac{1}{4}$, $\bar{x}\,\frac{1}{4}\,\frac{3}{4}$, $\frac{1}{2}+x\,\frac{3}{4}\,\frac{1}{4}$, $\frac{1}{2}-x\,\frac{1}{4}\,\frac{3}{4}$; |
| 8$C_2$ and 8$C_3$: | $x\,y\,z$, $x\,\frac{1}{2}-y\,\frac{1}{2}-z$, $\frac{1}{2}-x\,\frac{1}{2}+y\,\bar{z}$, $\frac{1}{2}-x\,\bar{y}\,\frac{1}{2}+z$, $\bar{x}\,\bar{y}\,\bar{z}$, $\bar{x}\,\frac{1}{2}+y\,\frac{1}{2}+z$, $\frac{1}{2}+x\,\frac{1}{2}-y\,z$, $\frac{1}{2}+x\,y\,\frac{1}{2}-z$ |

The number of positional parameters to be determined is ten in all. However, if we assume the usual bond distances and bond angles for the aniline molecule, they can be reduced to only three. They are $x_{Br}$, $x_N$ and $\alpha$, the last one representing the angle between the benzene ring and the plane (010). An approximate value 0.025 for $x_{Br}$ was easily obtained from the Patterson synthese, $P(xz)$ and $P(xy)$. Using this value, trial and error methods gave

* Present address: Department of Chemistry, Kwansei Gakuin University, Uegahara, Nishinomiya.
† Deceased, 26 May, 1959.

1) I. Taguchi, This Bulleten, **34**, 392 (1961).
2) I. Taguchi, *Annual Report Inst. Fibre Research, Osaka Univ.*, **8**, 45 (1945).
3) T. Watanabé and I. Taguchi, *Acta Cryst.*, **14**, 67 (1961).
4) A. J. Bradley, *Proc. Roy. Soc.*, **A47**, 879 (1935).
5) "Internationale Tabellen zur Bestimmung von Kristallstrukturen", II., Gebrüder Bornträger, Berlin (1935), p. 576.
6) "International Tables for X-Ray Crystallography", I, The Kynoch Press, Birmingham (1952), p. 144.

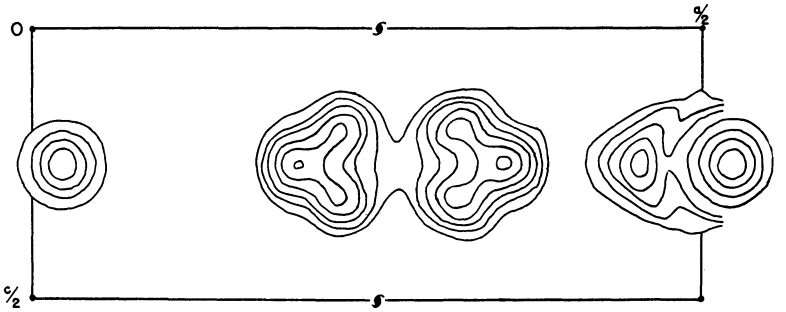



Fig. 1. Electron density projection along the b-axis. Contours for the carbon and nitrogen atoms are drawn at intervals of 1 $Å^{-2}$, starting at the 3 e$Å^{-2}$ level. Contours for the bromine atom are drawn at intervals of 10 e$Å^{-2}$, starting at the 10 e$Å^{-2}$ level.

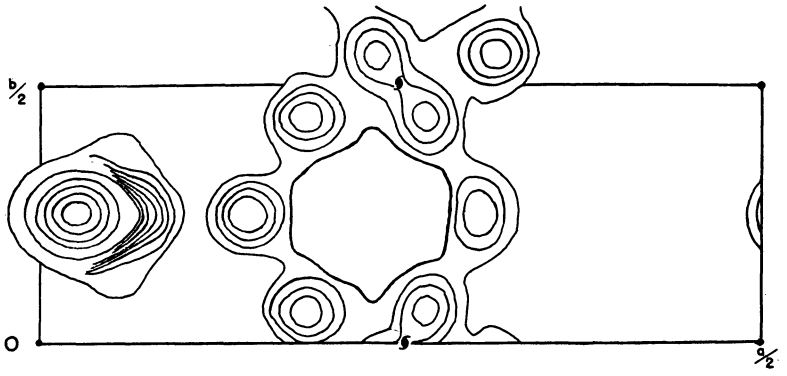



Fig. 2. Electron density projection along the c-axis. Contours intervals are the same as in Fig. 1.

approximate values, $x_N=0.43$ and $\alpha=25°$, from $(0kl)$ reflections.

The electron density projections along the b- and c-axis were then calculated, based on this trial structure, a few terms of doubtful sign being ommitted. They showed all the atoms except nitrogen. Afer three cycles of refinement, there were no terms whose signs were to be changed. The final electron density projections, $\rho(xz)$ and $\rho(xy)$, are shown in Figs. 1 and 2. From the $\rho(xz)$ projection, a more accurate value for $x_{Br}$ was obtained assuming the Gaussian curvature near the peak. Those of the carbon atoms were also obtained graphically from these two projections. As the nitrogen atom in these projections is partially masked by the bromine atom, the location of the nitrogen atom was evaluated by subtracting the observed electron density distribution of the bromine atom from $\rho(xz)_{z=(1/4)}$, assuming that the former has the same distribution along $+X$ and $-X$ from $x_{Br}$. Using the atomic coordinates thus obtained, the discrepancy factors were found to be 11.5% for $(h0l)$ and 11.2% for $(hk0)$ reflections, the overall temperature factor being assumed to be isotropic, with a value 4.0 $Å^2$.

### Refinement of the Structure

Two difference syntheses, $D(xz)$ and $D(xy)$, prepared at this stage indicated an appreciable anisotropy of thermal vibration of the bromine atom, in addition to a slight shift of the atomic coordinates for each atom. The bromine parameter was refined, using mainly $(h0l)$ reflections, and those of the other atoms were made, using both $(h0l)$ and $(hk0)$ reflections. Since the direction of the maximum vibration of the bromine atom is along the c-axis, its atomic scattering factor can be given by[7]

$$f_{Br}=f_{Br}\text{ (free atom) }\exp(-\gamma)$$
$$\gamma=(A+B\sin^2\varphi)\sin^2\theta/\lambda^2$$

where $\varphi$ is the angle between $\boldsymbol{a}$ and $\boldsymbol{h}$, and $A$ and $B$ are unknown quantities to be determined. In order to allow for the anisotropic vibration of the bromine atom, the variation of the temperature parameter with $\varphi$ was first determined

7) E. W. Hughes, *J. Am. Chem. Soc.*, 63, 1717 (1941).

in the following way. The contributions of the carbon and nitrogen atoms were subtracted from the observed structure factors to give a set of $F'_O$ values. These $F'_O$ values were divided into groups with $\varphi=0\sim15°$, $15\sim30°$,……, $75\sim90°$, and for each group $\gamma$ was obtained from a plot, log $F_{Br}/F'_O$ against $(\sin\theta/\lambda)$, where $F_{Br}$ stands for the calculated bromine contribution without temperature factor. Further refinement followed, assuming that the temperature factors for the carbon and nitrogen atoms were the same and isotropic.

At this stage, the secondary extinction effect was corrected using the equation[8], $I_o=I_c \exp(-gI_c)$.

Finally the contributions of the hydrogen atoms were allowed for. It was assumed that the hydrogen atoms attached to the carbon atoms were located in the outward directions bisecting the angle between consecutive C–C bonds, at a distance 1.05 Å, and that the hydrogen atoms attached to the nitrogen atom were distributed tetrahedrally with respect to the C–N bond, at a distance 1.01 Å. It was further assumed that these hydrogen atoms were rotating freely around the C–N bond as in the case of methylammonium chloride[9]. Now the contribution from the rotating hydrogen atoms to the structure factor can be written by

$$\pm 12 f_H \exp -(\sin\theta/\lambda)^2 B_H \times J_o(K \sin\theta/\lambda) \begin{matrix}\cos 2\pi h x_H \\ \sin 2\pi h x_H\end{matrix}$$

where $J_o$ is the zeroth order Bessel function and the argument $K$ is $4\pi r_o \sin\theta_o$. In this expression, $r_o$ and $\theta_o$ are the radius of the orbit and the angle between $\boldsymbol{a}$ and $\boldsymbol{h}$ respectively, and $x_H$ is the common $x$ parameter for hydrogen atoms. The temperature factor for hydrogen, $B_H$, was assumed to be isotropic with a value 6.5 Å$^2$. The agreement between observed and calculated strucrure factors was found definitely improved especially for lower order reflections. The discrepancy factors were decreased to 7.9% and 6.5% for $(h0l)$ and $(hk0)$ reflections, including all the non-observed terms up to $\sin\theta/\lambda = 0.67$. The final positional parameters and temperature factors for each atom are listed in Table II. The interatomic distances and bond angles calculated from these positional parameters are given in Tables III and IV. In Tables V and VI, the observed and calculated structure factors for $(h0l)$ and $(hk0)$ reflections are given.

## Discussion

The crystal structure of aniline hydrobromide can be said to belong to a distorted CsCl-type, consisting of bromine and anilinium ions. The $C_2$–$C_3$ distance in the benzene ring is slightly shorter than the other C–C distances. The $C_1$–N distance is 1.47 Å, suggesting a single bond nature.

The structue can also be described as built up with alternating layers, parallel to the (100) plane, one layer containing anilinium ions and the other bromine ions. The structure may further be taken as a superstructure along the a-axis, since every other layer contains anilinium ions in different orientations, as can be seen in Fig. 4. The inclination of the benzene ring to the plane (010) is ±22.5°, so that the angle between the neighboring benzene rings is 45°. The bromine ions lie nearly on the same plane, the deviation from the plane being 0.386 Å.

The shortest intermolecular atomic distances are found between carbon atoms. These distances (see Table IV) are somewhat shorter than the usually accepted van der Waals' contact, 3.70 Å.

Between the consecutive layers, the strongest interactions will be those between the bromine ion and the nitrogen atom of the anilinium ion. Each bromine ion is surrounded by four nitrogen atoms, and each nitrogen atom by four bromine ions, which from a rhomb parallel to

Table II. Positional parameters and temperature factors

| | Positional parameter | | | Temperature factor, Å$^2$ | | |
|---|---|---|---|---|---|---|
| | $x$ | $y$ | $z$ | $Bx$ | $By$ | $Bz$ |
| Br | 0.0230 | 0.25 | 0.25 | 4.3 | 3.7 | 5.3 |
| N | 0.4441 | 0.75 | 0.25 | | | |
| $C_1$ | 0.3564 | 0.75 | 0.25 | | | |
| $C_2$ | 0.3152 | 0.5650 | 0.1833 | | 6.0 | |
| $C_3$ | 0.2323 | 0.5650 | 0.1833 | | | |
| $C_4$ | 0.1914 | 0.75 | 0.25 | | | |

Table III. Bond distances and bond angles

| Bond distance, Å | | Bond angle | |
|---|---|---|---|
| $C_1$–$C_2$ | 1.42 | $\angle N$–$C_1$–$C_2$ | 121°34′ |
| $C_2$–$C_3$ | 1.39 | $\angle C_2$–$C_1$–$C_2'$ | 116°52′ |
| $C_3$–$C_4$ | 1.42 | $\angle C_1$–$C_2$–$C_3$ | 121°34′ |
| N–$C_1$ | 1.47 | | |

Table IV. Intermolecular atomic distances, Å

| | |
|---|---|
| $C_4$(I)……$C_5$(II) | 3.76 |
| $C_2$(I)……$C_5$(II) | 3.61 |
| $C_3$(I)……$C_5$(II) | 3.57 |
| $C_4$(I)……$C_6$(II) | 3.54 |
| Br(A)……N(II) | 3.30 |
| Br(A)……N(III) | |
| Br(C)……N(II) | 3.48 |
| Br(E)……N(II) | |

8) J. Houstry and J. Clastre, *Acta Cryst.*, **10**, 696 (1957).
9) E. W. Hughes and W. N. Lipscomb, *J. Am. Chem. Soc.*, **63**, 1737 (1941).

the (100) plane. Of the interatomic distances between the nitrogen and bromine atoms, two are shorter, 3.3 Å, and the other two are longer, 3.48 Å. The angles subtended at the nitrogen atom by the four bromine atoms are 99° and 114°. The direction of the maximum thermal vibration of the bromine atom within the layer is nearly parallel to the longer distance of Br

TABLE V. OBSERVED AND CALCULATED STRUCTURE FACTORS FOR ($h0l$) REFLECTIONS

| $h$ 0 $l$ | $F_O$ | $F_C$ | $h$ 0 $l$ | $F_O$ | $F_C$ |
|---|---|---|---|---|---|
| 0 0 0 | | 344.0 | 0 0 4 | 66.0 | 71.2 |
| 2 0 0 | 58.8* | 61.2 | 2 0 4 | 50.8 | 56.4 |
| 4 0 0 | 115.6* | 114.4 | 4 0 4 | 36.0 | 40.0 |
| 6 0 0 | 75.2* | 73.2 | 6 0 4 | 30.4 | 31.6 |
| 8 0 0 | 8.8 | 12.0 | 8 0 4 | 12.4 | 11.6 |
| 10 0 0 | — | 0.8 | 10 0 4 | — | 0.8 |
| 12 0 0 | 10.4 | − 9.6 | 12 0 4 | 10.4 | − 6.4 |
| 14 0 0 | 17.2 | −17.6 | 14 0 4 | 8.0 | − 7.2 |
| 16 0 0 | 11.6 | −12.0 | 16 0 4 | 10.0 | − 8.8 |
| 18 0 0 | 17.2 | −16.8 | 18 0 4 | 11.6 | − 9.6 |
| 20 0 0 | 11.6 | −12.4 | | | |
| | | | 2 0 5 | 11.6 | − 9.6 |
| 2 0 1 | 11.6 | 3.6 | 4 0 5 | 13.5 | −15.6 |
| 4 0 1 | 42.0 | −41.6 | 6 0 5 | 28.4 | −25.6 |
| 6 0 1 | 70.8* | −70.8 | 8 0 5 | 24.8 | −25.2 |
| 8 0 1 | 33.2 | −41.6 | 10 0 5 | 19.6 | −19.2 |
| 10 0 1 | 67.2* | −70.4 | 12 0 5 | 27.2 | −26.0 |
| 12 0 1 | 39.2 | −42.4 | 14 0 5 | 11.6 | −11.6 |
| 14 0 1 | 32.8 | −37.6 | 16 0 5 | 8.8 | − 8.4 |
| 16 0 1 | 16.8 | −17.2 | | | |
| 18 0 1 | 10.4 | −10.4 | 0 0 6 | 24.0 | −25.6 |
| 20 0 1 | — | 2.4 | 2 0 6 | 26.4 | −30.8 |
| | | | 4 0 6 | 15.6 | −16.4 |
| 0 0 2 | 189.6* | −190.4 | 6 0 6 | 15.6 | −15.2 |
| 2 0 2 | 58.8* | −72.8 | 8 0 6 | 7.2 | − 6.4 |
| 4 0 2 | 78.8* | −82.0 | 10 0 6 | — | − 0.4 |
| 6 0 2 | 57.2* | −55.6 | 12 0 6 | 7.2 | 3.6 |
| 8 0 2 | 12.4 | −14.0 | 14 0 6 | — | 2.8 |
| 10 0 2 | — | − 1.2 | 16 0 6 | 4.4 | 5.2 |
| 12 0 2 | 10.8 | 8.8 | | | |
| 14 0 2 | 13.6 | 14.0 | 2 0 7 | 5.6 | 4.8 |
| 16 0 2 | 12.0 | 11.2 | 4 0 7 | 5.6 | 4.8 |
| 18 0 2 | 16.0 | 14.4 | 6 0 7 | 14.0 | 11.6 |
| 20 0 2 | 10.0 | 10.8 | 8 0 7 | 13.2 | 11.6 |
| | | | 10 0 7 | 7.2 | 7.6 |
| 2 0 3 | 10.8 | 11.6 | 12 0 7 | 15.6 | 12.0 |
| 4 0 3 | 25.6 | 28.8 | | | |
| 6 0 3 | 46.4 | 48.0 | 0 0 8 | 9.2 | 8.8 |
| 8 0 3 | 35.2 | 39.6 | 2 0 8 | 12.0 | 12.0 |
| 10 0 3 | 42.4 | 44.0 | 4 0 8 | 5.6 | 6.0 |
| 12 0 3 | 35.2 | 36.8 | 6 0 8 | 6.8 | 5.6 |
| 14 0 3 | 23.6 | 24.8 | 8 0 8 | 3.6 | 2.4 |
| 16 0 3 | 12.8 | 13.6 | | | |
| 18 0 3 | 8.4 | 8.0 | | | |
| 20 0 3 | — | 2.0 | | | |

* Corrected for extinction

TABLE VI. OBSERVED AND CALCULATED STRUCTURE FACTORS FOR ($hk0$) REFLECTIONS

| $h$ $k$ 0 | $F_O$ | $F_C$ | $h$ $k$ 0 | $F_O$ | $F_C$ |
|---|---|---|---|---|---|
| 2 1 0 | 62.8* | −60.0 | 0 4 0 | 68.8 | 68.8 |
| 4 1 0 | 80.4* | −81.6 | 2 4 0 | 54.8 | 53.6 |
| 6 1 0 | 68.4* | −73.3 | 4 4 0 | 38.0 | 39.2 |
| 8 1 0 | 82.4* | −84.0 | 6 4 0 | 32.4 | 30.4 |
| 10 1 0 | 47.6 | −53.2 | 8 4 0 | 14.0 | 12.0 |
| 12 1 0 | 35.2 | −39.6 | 10 4 0 | 5.6 | 1.6 |
| 14 0 1 | 26.8 | −26.8 | 12 4 0 | 6.4 | − 6.0 |
| 16 1 0 | 18.4 | −19.6 | 14 4 0 | 8.4 | − 7.6 |
| 18 1 0 | 8.4 | − 8.0 | 16 4 0 | 8.0 | − 9.2 |
| 20 1 0 | 4.0 | − 3.6 | 18 4 0 | 8.8 | −12.4 |
| 22 1 0 | — | 0.0 | | | |
| | | | 2 5 0 | 21.6 | −16.4 |
| 0 2 0 | 104.4* | −110.0 | 4 5 0 | 21.6 | −21.2 |
| 2 2 0 | 116.8* | −123.2 | 6 5 0 | 26.0 | −25.2 |
| 4 2 0 | 57.2* | −60.4 | 8 5 0 | 32.0 | −31.2 |
| 6 2 0 | 54.0 | −53.2 | 10 5 0 | 20.4 | −20.0 |
| 8 2 0 | 18.8 | −20.8 | 12 5 0 | 19.2 | −19.6 |
| 10 2 0 | — | − 0.4 | 14 5 0 | 10.4 | −11.2 |
| 12 2 0 | 15.2 | 11.6 | 16 5 0 | 7.6 | −10.4 |
| 14 2 0 | 6.4 | 9.2 | | | |
| 16 2 0 | 15.2 | 14.8 | 0 6 0 | 40.0 | 36.8 |
| 18 2 0 | 14.8 | 14.8 | 2 6 0 | 22.8 | −21.6 |
| 20 2 0 | 6.4 | 8.8 | 4 6 0 | 22.0 | −22.4 |
| 22 2 0 | 6.8 | 8.0 | 6 6 0 | 16.4 | −15.6 |
| | | | 8 6 0 | 5.6 | − 6.0 |
| 2 3 0 | 28.8 | 25.2 | 10 6 0 | — | − 1.2 |
| 4 3 0 | 58.4 | 56.4 | 12 6 0 | — | 2.8 |
| 6 3 0 | 41.2 | 42.8 | 14 6 0 | 6.4 | 5.2 |
| 8 3 0 | 45.6 | 46.8 | | | |
| 10 3 0 | 15.2 | 11.6 | 2 7 0 | 7.6 | 5.2 |
| 12 3 0 | 13.6 | 16.8 | 4 7 0 | 11.2 | 10.8 |
| 14 3 0 | 28.8 | 27.6 | 6 7 0 | 11.2 | 10.8 |
| 16 3 0 | 12.4 | 11.6 | 8 7 0 | 11.6 | 12.4 |
| 18 3 0 | 6.0 | 6.4 | 10 7 0 | 10.0 | 11.6 |
| 20 3 0 | — | 2.8 | | | |
| | | | 0 8 0 | 8.0 | 10.4 |
| | | | 2 8 0 | 11.2 | 11.6 |
| | | | 4 8 0 | 6.4 | 8.0 |

* Corrected for extinction

TABLE VII. MELTING POINTS AND TEMPERATUER FACTORS OF SEVERAL AMINE HYDROHALIDES

| Substance | M. p. °C | Mean temp. factor, Å² |
|---|---|---|
| Aniline hydrochloride[a)] | 198 | 4.0 |
| Aniline hydrobromide[b)] | 283 | 5.8 |
| Aniline hydroiodide[c)] | 365 | 6.0 |
| Cyclohexylamine hydrochloride[d)] | 206 | 5.0 |

a) C. J. Brown, *Acta Cryst.*, **2**, 228 (1949).
b) Present investigation
c) I. Nitta, I. Taguchi and H. Hiyama, to be published.
d) A. Shimada, Y. Okaya and M. Nakamura, *Acta Cryst.*, **8**, 819 (1955).

···Br. The cleavage plane, (001), is also perpendicular to this longer distance.

Since the anilinium ion in this structure should have the two-fold rotational symmetry demanded by the space group, the three hydrogen atoms bound to the nitrogen atom must occupy statistical positions by some means.

Two plausible models of arrangement of these three hydrogen atoms are shown in Fig. 5. Case A, in Fig. 5, includes two strong and one weak hydrogen bonds. On the other hand, in case B there are one strong and two weak hydrogen bonds. These are the two extremes. A model of free rotation around the C–N axis is another extreme. This model of free rotation was incorporated into the structure factor calculations as described in the section of refinement.

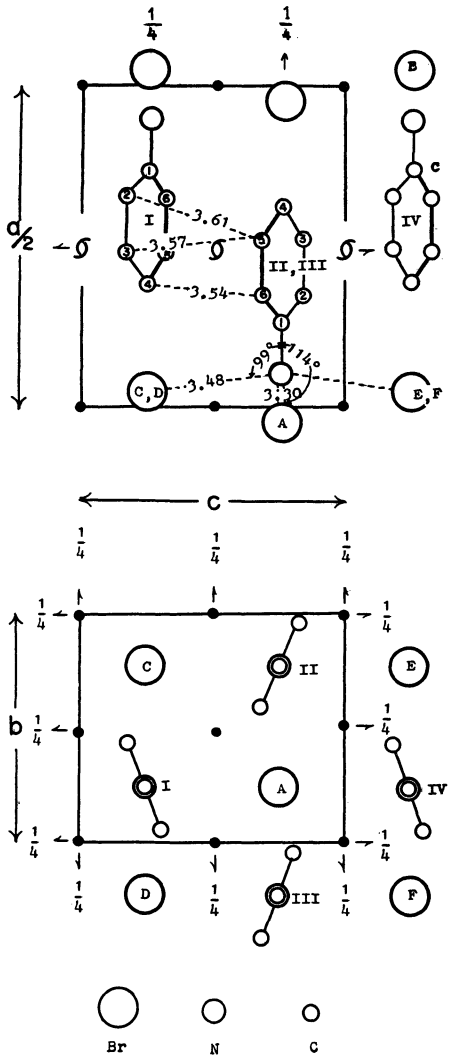



Fig. 3. The structure of the orthorhombic aniline hydrobromide projected on to the (010) and (100) planes.

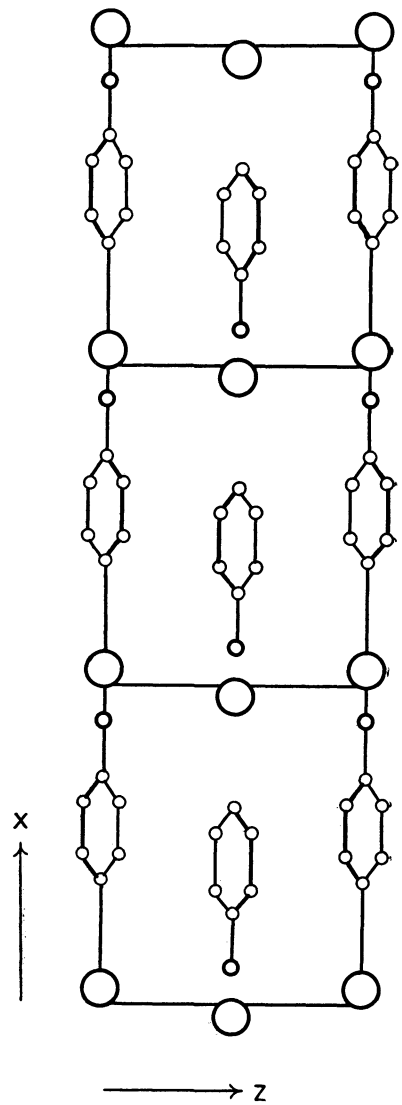



Fig. 4. A schematic representation of the superstructure along the b-axis.

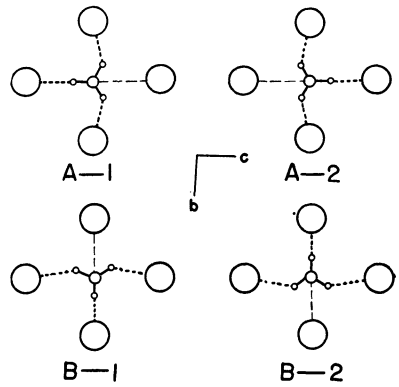



Fig. 5. Statistical arrangements of the three hydrogen atoms bound to the nitrogen atom.

Now, the actual structuer may be represented by an average of all the possible states arising from these extremes stated above, with an appropriate weight on each. Such a statistical arrangement of the hydrogen atoms will vanish when the phase transition takes place.

The mean temperature factor is 5.8 Å$^2$. This value is considerably large for a crystal whose melting poing is as high as 283°C. The temperature factors and melting points of several related compounds are listed in Table VI. That these amine hydrohalides have large thermal vibration and relatively high melting points will probably be due to the partially ionic and partially molecular character of these compounds. The large thermal motion will arise from their molecular character, whereas the ionic character will be responsible for their high melting points. It is interesting to note that these amine hydrohalides have these common characteristics notwithstanding their different crystal structures.

Let us now compare the crystal structure of aniline hydrobromide with those of alkylamine hydrohalides. Both methyl- and propyl-ammonium chlorides crystallize in the tetragonal system, and the alkylammonium ions are characterized by the four-fold axial symmetry. In methylammonium chloride, the three hydrogen atoms attached to nitrogen occupy statistical positions, or they are in rotation. In propylammonium chloride, not only these hydrogen atoms but also the nitrogen and carbon atoms, too, are rotating. The difference between the four-fold axial symmetry of the alkylammonium ions and the two-fold axial symmetry of the anilinium ions may be due to the difference in their molecular shape. All these crystals are apolar, so that their structures can be described as an alternating disposition or antiparallel arrangement of dipoles along their principal axes. The nitrogen atoms in these alkylammonium chlorides have four halogen atoms as their immediate neighbors, so also the nitrogen atoms in aniline hydrobromide, though these four distances in the latter are not exactly the same.

There are some indications of a possible hindered oscillation of the anilinium ion around its longest axis. The final difference projection, $D(xz)$, shows that the temperature factors of $C_2$ and $C_3$ are larger than those of $C_1$ and $C_4$. Some reflections such as (112) whose structure factors have contributions from $C_2$ and $C_3$ alone are associated with diffuse spots, presumably due to the thermal motion stated above.

*Faculty of Science*
*Osaka University*
*Nakanoshima, Osaka*

# *Some Electrophilic Substitution Reactions of 4-Aminotropolone**

By Kozo Doi

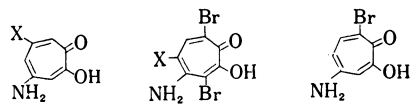
(Received March 29, 1961)

In the course of investigations of 4-aminotropolone (I) and its derivatives, the author has established general methods of their syntheses, which include amination of 3-iodotropolones with potassium amide in liquid ammonia[1], applications of the Schmidt reaction to acetyl-, formyl- and isopropenyltropolones[2] and of the Curtius reaction to 4-carboxytropolones[1], and amination of 4-bromotropolone with aqueous ammonia[3].

On the other hand, there have been little informations on reactivities of 4-aminotropolones except on a diazotization of 4-amino-6-methyltropolone (II)[4], whereas the reactions of the isomeric 3- and 5-amino derivatives have been much investigated[5]. Recently the author has reported in brief the synthetic applications of I, involving preparations of some pyridotropolones[6] and of 4-aminotropone[7]. In this communication the author wishes to take up some electrophilic substitution reactions of the aminotropolone (I).

* This work was presented at the 12th Annual Meeting of the Chemical Society of Japan, Kyoto, April, 1959.

1) K. Doi, This Bulletin, **34**, 497 (1961).
2) K. Doi, ibid., **34**, 501 (1961).
3) K. Doi, ibid., **34**, 504 (1961).
4) W. D. Crow, R. D. Haworth and P. R. Jefferies, *J. Chem. Soc.*, **1952**, 3705.
5) Cf. P. L. Pauson, *Chem. Revs.*, **55**, 9 (1955).
6) K. Doi, *Bull. Chem. Res. Inst. Non-Aqueous Solutions, Tohoku Univ.*, **9**, 19 (1959).
7) K. Doi, This Bulletin, **33**, 887 (1960).



I: X=H III: X=Br IV
II: X=Me V: X=H

On bromination the aminotropolone (I) has been found to give nuclear substitution products in the same manner as many other tropolones. For example, in the presence of sodium acetate as a hydrogen bromide acceptor, I consumes three molar equivalents of bromine to afford in a good yield the tribromotropolone (III). On the other hand, in the absence of any hydrogen bromide acceptor, I reacts with one molar equivalent of bromine to give not only a monobromo derivative, IV, which was identified with that obtained from an application of the Schmidt reaction to the known 6-acetyl-3-bromotropolone[2], but also a dibromo compound, V, whose respective yield is better in the latter than the former. Such a preferential formation of dibromo compound by one molar equivalent of bromine has also been observed in the case of tropolone itself[5].

In Fig. 1 are indicated the ultraviolet absorption spectra of the above two substitution products, III and V, comparing with that of the monobromo compound IV. Tsuboi[8] observed that an introduction of one bromine atom into the 3 (or 7)- and 5-position of tropolone caused a red shift of the maximum in the longest wavelength by 10 and 15 mμ, respectively. Now, the above three bromotropolones (III, IV and V) have the maximum in the longest wavelength at 410, 380 and 390 mμ, respectively. The difference of the maxima of V and IV is 10 mμ, and that of III and V is 20 mμ, the fact of which suggests that the dibromotropolone (V) may be a 3, 7-dibromo derivative rather than a 3, 5-dibromo one.

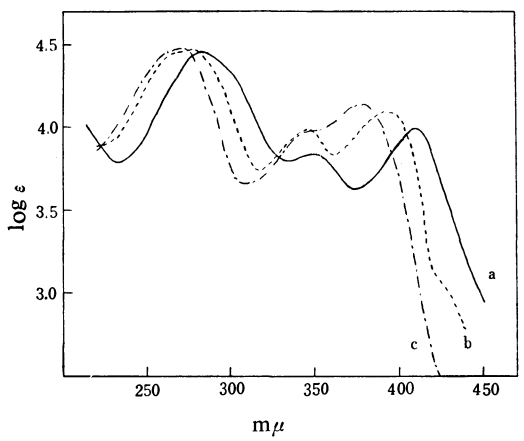



Fig. 1. The ultraviolet absorption spectra.
(a): 4-Amino-3, 5, 7-tribromotropolone (III)
(b): 4-Amino-3, 7-dibromotropolone (V)
(c): 6-Amino-3-bromotropolone (IV)

8) M. Tsuboi, This Bulletin, 25, 369 (1952).

The position of the two bromine atoms of the dibromo compound V is also understood from a comparison of the characteristic bands due to the CH out-of-plane vibration (864cm$^{-1}$) with those of some other 3, 4, 7-trisubstituted tropolones, which possess bands in the 820~875 cm$^{-1}$ region[9], in the infrared absorption spectra. Table I indicates frequencies of the CH out-of-plane vibration of V, comparing with those of some other 3, 4, 7-trisubstituted tropolones.

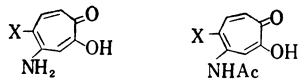
Table I. Frequencies of the CH out-of-plane vibration of some 3,4,7-trisubstituted tropolones

| Compound | $\nu_{CH}$ cm$^{-1}$ | Ref. |
|---|---|---|
| 4-Amino-3, 7-dibromotropolone (V) | 864 | |
| 4-Isopropyl-3, 7-dibromotropolone | 835 | 10 |
| 7-Bromo-3-iodo-4-methyltropolone | 847 | 11 |
| 7-Bromotropolone-3, 4-dicarboxylic anhydride | 872 | 12 |
| 7-Hydroxytropolone-3, 4-dicarboxylic anhydride | 882 | 12 |

4-Aminotropolone (I), differing from its isomeric 3- and 5-amino derivatives, has been found to be fairly stable in pace of the action of nitric acid. Thus an attempt to obtain a nitro compound from I in an usual reaction condition for nitration of tropolones causes to yield not any substitution product but merely a nitrate, possessing a composition of $C_7H_7O_2N \cdot HNO_3 \cdot H_2O$. With fuming nitric acid, however, I reacts vigorously to form in a poor yield 4-amino-5-nitrotropolone (VI), whose structure was confirmed by the fact that the ultraviolet absorption is practically identical with that of the product obtained by an application of the Schmidt reaction to 4-acetyl-5-nitrotropolone[2].

In order to obtain further informations with respect to orientation of electrophilic substitution, nitration has also been carried out on 4-acetylaminotropolone (VII), which is readily prepared from the reaction of I and acetyl chloride in pyridine. Nitration of VII with fuming nitric acid in an acetic acid solution gives also a 5-nitro derivative, VIII, whose structure is confirmed by the formation of VI on its alkaline hydrolysis.

9) Y. Ikegami, *J. Japanese Chem.* (*Kagaku-no-Ryoiki*), Extra No. 38, 33 (1959).
10) T. Nozoe, E. Sebe, S. Mayama and S. Iwamoto, *Sci. Repts. Tohoku Univ. Ser. I*, 36, 184 (1952).
11) T. Nozoe, K. Doi, K. Kitahara and K. Omura, to be published.
12) T. Nozoe, K. Doi and T. Hashimoto, This Bulletin, 33, 1071 (1960).



VI: X=$NO_2$ VII: X=H
IX: X=$NH_2$ VIII: X=$NO_2$
X: X=*p*-Tolylazo

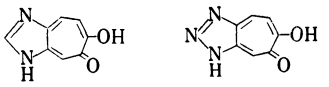
The absorption maximum at 400 mμ (log ε 3.90) of VIII indicates more decreased values both in wavelength and absorption intensity than that at 435 mμ (log ε 4.41) of 5-nitrotropolone itself[13]. This is not consistent with the bathochromic effect of the acetylamino group, having been attributed recently to the steric inhibition of resonance between the nitro group and the tropolone nucleus by the adjacent acetylamino group[14].

From a catalytic hydrogenation of the 5-nitro derivative VIII over palladized charcoal, 4,5-diaminotropolone (IX) is readily obtained. In the previous paper[2], the author found that an application of the Schmidt reaction to 4-acetyltropolone resulted in the formation of 4-aminotropolone sulfate instead of the expected acetylamino derivative VII, attributing this mechanism to the hydrolyzable nature of VII in the condition employed. Actually it has now been found that the acetylamino compound VII affords easily 4-aminotropolone sulfate on being merely dissolved in concentrated sulfuric acid even at room temperature. This fact justifies the previous mechanism in the Schmidt reaction of the acetyltropolones.

Bromination and nitration of 5-aminotropolones have already been reported, but in no cases has isolation of the substitution products been described[15]. With 3-aminotropolone, some electrophilic substitutions involving bromination, nitration, and azo coupling have been attempted with no isolation of any reaction products[16]. On the contrary, 4-aminotropolone (I) gives easily nuclear substitution products in some electrophilic reactions. This fact is probably considered to be connected with that the amino and hydroxyl groups in the aminotropolone (I) are situated at the positions where they cooperate with each other to increase the reactivity of the tropolone ring, whereas the two groups in the 3- and 5-isomers are not in such positions.

The aminotropolone (I), similarly to the other tropolones, undergoes azo coupling to give a nuclear substitution product of red dyestuff, not a diazoamino derivative. Thus on being treated with diazotized *p*-toluidine in an alkaline solution, I affords in a good yield 4-amino-5-*p*-tolylazotropolone (X), whose hydrogenolysis leads to the diaminotropolone (IX).

In a similar manner to *o*-phenylenediamine, the diamino compound IX gives an imidazole, XI, on being heated with formic acid, and a



XI XII

triazole, XII, on being diazotized. Informations on tautomerism between these reaction products and their possible isomers of the aza-azulene type have not been obtained in detail, but it is probably concluded that they may not be their possible dihydroxy-azaazulene derivatives, since their respective ultraviolet absorption is resembling that of imidazolo[d]tropone[17] and of triazolo[d]tropone[18] (Fig. 2).

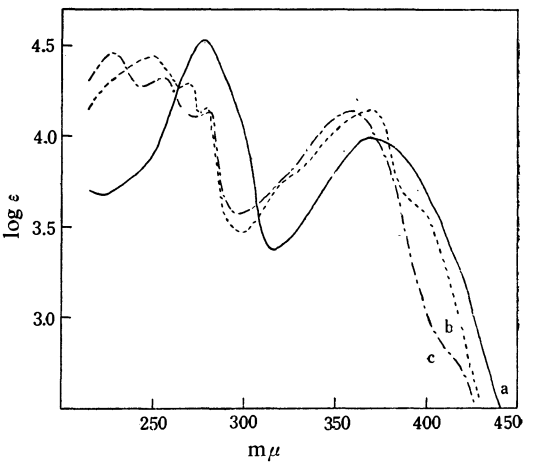



Fig. 2. The ultraviolet absorption spectra.
(a): 4,5-Diaminotropolone (IX)
(b): Imidazolo[d]tropolone (XI)
(c): Triazolo[d]tropolone (XII)

## Experimental

All of the ultraviolet absorption spectra were measured in methanol solution with a Beckman model DU quartz spectrophtometer. The infrared spectra were measured on potassium bromide disks with a Perkin-Elmer model 21 infrared spectrometer, using a rock salt prism.

**Tribromination of 4-Aminotropolone (I).**—To a stirred mixture of I (70 mg.), sodium acetate trihydrate (200 mg.) and methanol (2 ml.) was added dropwise a cold solution of bromine (240 mg.) in methanol (2 ml.). The reaction mixture was

13) T. Nozoe, Y. Kitahara, K. Doi and T. Arai, *Bull. Chem. Res. Inst. Non-Aqueous Solutions, Tohoku Univ.*, 7, 13 (1957).
14) Y. Kitahara, K. Doi and T. Hashimoto, ibid., 9, 91 (1960).
15) T. Nozoe, S. Ebine, S. Ito and A. Konishi, *Proc. Japan Acad.*, 27, 10 (1951); T. Nozoe, S. Seto, S. Ito and M. Sato, ibid., 27, 426 (1951).
16) K. Doi, unpublished work.
17) T. Nozoe, M. Sato, S. Ito, K. Matsui and T. Matsuda, *Proc. Japan Acad.*, 29, 565 (1953).
18) T. Nozoe, S. Ito and K. Matsui, ibid., 30, 313 (1954).

diluted with water, and the precipitated solid, after collection by filtration, sublimation in vacuo, and subsequent recrystallization from acetic acid, gave 4-amino-3, 5, 7-tribromotropolone (III, 160 mg.) as yellow needles, m. p. 203°C.

Found: N, 3.80. Calcd. for $C_7H_4O_2NBr_3$: N, 3.75%.

$\lambda_{max}$ mμ (log ε): 282 (4.47), 350 (3.84), 410 (4.00).

**Monobromination of I.**—To a stirred cold solution of I (0.41 g.) in methanol (10 ml.) was added dropwise a solution of bromine (0.48 g.) in methanol (2 ml.). After 30 min., the solution was evaporated in vacuo, the residue was diluted with water (5 ml.), and the deposited solid, after collection by filtration, was crystallized fractionally from methanol to give less soluble 4-amino-3,7-dibromotropolone (V, 016 g.) as yellow prisms, m. p. 224~225°C.

Found: N, 5.01. Calcd. for $C_7H_5O_2NBr_2$: N, 4.75%.

$\lambda_{max}$ mμ (log ε): 276 (4.46), 345 (3.99), 390 (4.10). From the more soluble portion, 6-amino-3-bromotropolone (IV) as yellow needles, m. p. and mixed[2] m. p. 214°C, was obtained. Further bromination of the preceding products, IV and V, afforded respectively the tribromotropolone (III).

**Nitration of 4-Aminotropolone (I).**—a) To a stirred solution of I (0.41 g.) and acetic acid (3 ml.) was added dropwise at room temperature a solution of fuming nitric acid (0.2 g., *d* 1.84) and acetic acid (1 ml.). After evaporation of the solvent, the residual solid was recrystallized from a mixed solvent of acetic acid and methanol to give 4-aminotropolone nitrate (0.26 g.) in the form of colorless needles, m. p. 163~164°C (decomp.).

Found: C, 41.96; H, 4.06; N, 13.80. Calcd. for $C_7H_7O_2N \cdot HNO_3 \cdot H_2O$: C, 42.00; H, 4.03; N, 14.00%. This substance is soluble in water and its aqueous solution decomposes sodium hydrogen carbonate.

b) Addition of fuming nitric acid (0.2 g.) to the aminotropolone (I, 0.41 g.) resulted in a vigorous reaction to form a deep red solution, which was immediately chilled in ice and allowed to stand for 30 min. Then this solution was diluted with water (2 ml.), the residual solid was collected by filtration, and crystallized from acetic acid to yield 4-amino-5-nitrotropolone (VI) as yellow needles, m. p. above 300°C, which was identified with an authentic specimen[2] through ultraviolet absorption.

**4-Acetylaminotropolone (VII).**—After acetyl chloride (3.1 g.) was added dropwise during 10 min. to a stirred cold solution of I (2.8 g.) in pyridine (10 ml.), the reaction mixture was allowed to stand for 4 hr. The mixture was diluted with water, allowed to stand overnight, and then acidified to Congo red with dilute hydrochloric acid. The solid which separated on chilling this mixture was collected and recrystallized from methanol to afford 4-acetylaminotropolone (VII, 2.2 g.) as colorless needles, m. p. 166~167°C.

Found: C, 55.43; H, 5.33; N, 7.14. Calcd. for $C_9H_9O_3N \cdot H_2O$: C, 54.82; H, 5.62; N, 7.10%.

$\lambda_{max}$ mμ (log ε): 267 (4.54), 365 (3.84).

**4-Acetylamino-5-nitrotropolone (VIII).**—To a stirred mixture of VII (1.3 g.) and acetic acid (4 ml.) was added dropwise at room temperature a solution of fuming nitric acid (0.5 g.) and acetic acid (1 ml.), the deep red solution so formed was allowed to be stirred for further 1 hr., diluted with water (40 ml.), and extracted with four 25-ml. portions of ether. The ether extract, after evaporation of the solvent followed by recrystallization from a mixed solvent of acetic acid and methanol, gave VIII (0.46 g.) as yellow needles, m. p. 230°C (decomp.).

Found: C, 48.53; H, 3.88; N, 12.31. Calcd. for $C_9H_8O_5N_2$: C, 48.53; H, 3.60; N, 12.50%.

$\lambda_{max}$ mμ (log ε): 274 (4.53), 400 (3.90).

**Hydrolysis of VIII.**—A mixture of VIII (0.2 g.), potassium hydroxide (0.2 g.), and water (8 ml.) was heated at 60°C on a water bath for 30 min., and then the resulting red solution was acidified with dilute hydrochloric acid to separate the aminotropolone (VI, 0.15 g.), whose structure was confirmed by the comparison of the ultraviolet absorption with that of an authentic sample[2].

**4, 5-Diaminotropolone (IX).**—A mixture of the nitroamine (VI, 0.18 g.), 5% palladium-on-carbon (50 mg.) and methanol (100 ml.) was shaken in an hydrogen atmosphere until the uptake of hydrogen had ceased. Then the catalyst was removed by filtration, the filtrate evaporated in vacuo, and the residue crystallized twice from ethyl acetate to give 4,5-diaminotroplone (IX, 60 mg.) as yellow prisms, m. p. 215°C (decomp.).

Found: C, 54.98; H, 5.21; N, 18.57. Calcd. for $C_7H_8O_2N_2$: C, 55.25; H, 5.30; N, 18.41%.

$\lambda_{max}$ mμ (log ε): 278 (4.54), 371 (3.99).

**4-Amino-5-*p*-tolylazotropolone (X).**—A diazonium chloride solution prepared from *p*-toluidine (2 g.) was added dropwise during 10 min. to a stirred cold solution of I (2.8 g.), potassium hydroxide (6 g.) and water (100 ml.). After 30 min., the reaction mixture was acidified with acetic acid, the solid which separated was collected, and recrystallized from ethyl acetate to afford X (4.5 g.) of red needles, m. p. 230°C (decomp.).

Found: N, 16.22. Calcd. for $C_{14}H_{13}O_2N_3$: N, 16.46%.

$\lambda_{max}$ mμ (log ε): 260 (4.37), 300 (4.38), 375 (4.11), 470 (4.41).

Hydrogenation of X in methanol over 5% palladized carbon afforded easily a diamino derivative IX.

**Imidazolo[d]tropolone (XI).**—A mixture of IX (0.15 g.) and 80% formic acid (10 ml.) was heated under reflux for 2 hr., the solvent was evaporated to dryness, and the residue, after sublimation in vacuo, was recrystallized from acetic acid to give XI (60 mg.) of colorless prisms, m. p. above 275°C

Found: C, 59.08; H, 3.55; N, 17.60. Calcd. for $C_8H_6O_2N_2$: C, 59.26; H, 3.73; N, 17.28%.

$\lambda_{max}$ mμ (log ε): 250 (4.44), 268 (4.28), 280 (4.14), 372 (4.14).

**Triazolo[d]tropolone (XII).**—A solution of sodium nitrite (60 mg.) in water (1 ml.) was added dropwise during 5 min. to a stirred cold solution of IX (0.15 g.), acetic acid (0.2 ml.), concentrated hydrochloric acid (0.4 ml.) and water (6 ml.). After 2 hr., the mixture was diluted with water (40 ml.), neutralized with sodium hydrogen carbonate, and extracted continuously with ether for 5 hr. The ether extract, after evaporation of the solvent, sublimation of the residue in vacuo followed by

crystallization from acetic acid, gave XII (50 mg.) of colorless prisms, m. p. 265°C (decomp.).

Found: C, 51.20; H, 2.98; N, 25.78. Calcd. for $C_7H_5O_2N_3$: C, 51.54; H, 3.09; N, 25.76%.

$\lambda_{max}$ m$\mu$ (log $\varepsilon$): 228 (4.48), 256 (4.34), 282 (4.14), 360 (4.17).

The author wishes to express his sincere gratitude to Professor Yoshio Kitahara for his kind guidance throughout the course of the present experiment, to Mr. Hideji Aono for the infrared spectral measurements, and to Messrs. Shin-ichi Ohyama, Kuni Kato and Ayako Iwanaga for microanalyses.

*The Chemical Research Institute*
*of Non-Aqueous Solutions*
*Tohoku University*
*Katahira-cho, Sendai*

# *Molecular Rotations of Terpenes in Relation to their Structures. I. The Internal Conformation of Isopropyl Group in Menthol-like Substance*[1]

By Shukichi YAMANA

(Received December 27, 1960)

In liquid or dissolved state, $C^9H_3$ and $C^{10}H_3$ in the isopropyl group of menthol-like substance are considered to be free to rotate about the axis of $C^4$-$C^8$ bond and the position which has minimal potential and makes these methyl groups rest, may be decided by steric repulsions and intramolecular van der Waals' forces etc. between the atoms in the molecule (Fig. 1).

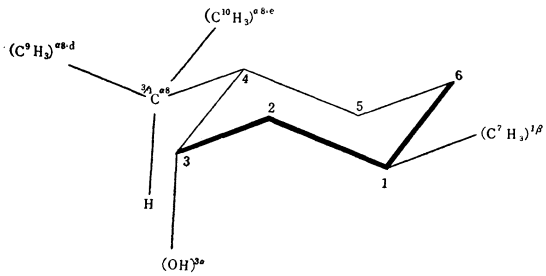



Fig. 1[2]. Perspective drawing of the molecular model of (+)neomenthol.

On the other hand, by uing the PM-method, the author recently tried to explain the molecular rotations of polyhydroxycyclohexanes[3,4]. From the standpoint of the fact that a menthol-like substance is a kind of polyhydroxy (or monohydroxy)-cyclohexane, the type of the internal conformation of its isopropyl group at an equilibrium state, above mentioned, is discussed in this article.

1) Presented at the Symposium on the Structural Chemistry of the Chemical Society of Japan, Sapporo, August, 1960.

2) $C^{\alpha 8}$-Atom is $C^8$-atom which is situated in $\alpha$-orientation (i. e. under the cyclohexane-ring in Fig. 1). $(CH_3)^{\alpha 8}$ means the $CH_3$ group which combines with $C^{\alpha 8}$-atom. Concerning the symbols, d- and e-, refer to "Method Proposed" in this article.

3) S. Yamana, This Bulletin, 33, 1741 (1960).

## Molecular Model and Data Used

According to Jefferies' investigation of menthol-like substances by infrared spectrum[5], it was concluded that in their molecules, isopropyl group usually takes equatorial orientation and that two methyl groups repulse each other. Referring to Jefferies' work, only the compounds which have a six-membered ring of C 1 conformation are treated in this article.

The unit groups in their molecules and their corresponding molecular rotations are given in Table I.

The molecular model and the optical properties of the hydroxyl group (except the value of $\zeta$-coefficient), used in the preceding article[3] were adopted here without any correction. Values of mean polarizability $\alpha$ and of anisotropy ratio $\beta$ of methyl group are $2.27\times10^{-24}$ (cc.) and 0.35 respectively[17]. The optical

4) In the previous paper[3], by using $[M]_D^{20}$(W) of (−) 1, 3/2, 4 cyclohexanetetrol, the value of $(\zeta_{OH})^2$ was calculated as 3.6402 $\{3/(n^2+2)\}$. But strictly speaking, it was apparent there that if 3.6402 $\{3/(n^2+2)\}$ is used, $\sum[\mu]_{Dobs}^{20}$ of (−)1/2 cyclohexanediol becomes somewhat smaller than its corresponding $[M]_D^{20}$(W) and $\sum[\mu]_{Dobs}^{20}$ of (+) 3, 5, 6/1, 2, 4 cyclohexanehexitol becomes somewhat larger than its corresponding $[M]_D^{20}$(W). That fact can be explained superficially by the assumption of the changeability of $(\zeta_{OH})^2$ according to the number of hydroxyl groups in a molecule. When $[M]_D^{20}$(W) of (−) 1/2 cyclohexanediol is used, the value of $\zeta_{OH}^2$ is calculated as follows;

$$\sum[\mu]_{Dobs}^{20} \text{ of } (-)\ 1/2 \text{ cyclohexanediol} = (OH)\cdot {}^{1\beta}\chi(OH)^{2\alpha} + (OH)^{1\beta}\chi\text{ch.R} + (OH)^{2\alpha}\chi\text{ch.R}$$

$$= -11.73\{(n^2+2)/3\}\zeta_{OH}^2 + 0 + 0 \equiv -48.2$$

$$\therefore\ \zeta_{OH}^2 = 4.1091\{3/(n^2+2)\} \qquad (4)^*$$

(Ref. Tables I and II of the previous paper[3]).

5) A. R. H. Cole and P. R. Jefferies, *J. Chem. Soc.*, 1956, 4391.

TABLE I.

| Name | Unit groups | $[M]_D^{20}$ [6] |
|---|---|---|
| (−)1/2 Cyclohexanediol | [$(OH)^{1\beta}$, $(OH)^{2\alpha}$, ch. R[7]] | $-48.2_w$[8] |
| (−)*trans*-2-Methylcyclohexanol | [$(OH)^{1\beta}$, $(CH_3)^{2\alpha}$, ch. R ] | $-42.4$[9] |
| (+)Neomenthol | [$(CH_3)^{1\beta}$, $(OH)^{3\alpha}$, $(iso\text{-}C_3H_7)^{4\alpha}$, ch. R ] | $30.6$[10] |
| (−)*cis*-2-Hydroxyneomenthol | [$(CH_3)^{1\beta}$, $(OH)^{2\alpha}$, $(OH)^{3\alpha}$, $(iso\text{-}C_3H_7)^{4\alpha}$, ch. R ] | $-50.6_{ch}$[11] |
| (+)*trans*-2-Hydroxyneomenthol | [$(CH_3)^{1\beta}$, $(OH)^{2\beta}$, $(OH)^{3\alpha}$, $(iso\text{-}C_3H_7)^{4\alpha}$, ch. R ] | $70.3_{ch}$[11] |
| (−)*trans*-2-Hydroxymenthol | [$(CH_3)^{1\beta}$, $(OH)^{2\alpha}$, $(OH)^{3\beta}$, $(iso\text{-}C_3H_7)^{4\alpha}$, ch. R ] | $-16.0_{ch}$[11] |
| (−)*cis*-2-Hydroxymenthol | [$(CH_3)^{1\beta}$, $(OH)^{2\beta}$, $(OH)^{3\beta}$, $(iso\text{-}C_3H_7)^{4\alpha}$, ch. R ] | $-56.7_{ch}$[11] |
| (−)Isomenthol | [$(CH_3)^{1\alpha}$, $(OH)^{3\beta}$, $(iso\text{-}C_3H_7)^{4\alpha}$, ch. R ] | $-39.4_{ch}$[12] |
| (−)Menthol | [$(CH_3)^{1\beta}$, $(OH)^{3\beta}$, $(iso\text{-}C_3H_7)^{4\alpha}$, ch. R ] | $-77.5_{et}$[13] |
| (−)Carvomenthol | [$(CH_3)^{1\beta}$, $(OH)^{2\alpha}$, $(iso\text{-}C_3H_7)^{4\alpha}$, ch. R ] | $-41.2$[14] |
| (+)*cis*-1,2-Menthanediol | [$(CH_3)^{1\beta}$, $(OH)^{1\alpha}$, $(OH)^{2\alpha}$, $(iso\text{-}C_3H_7)^{4\alpha}$, ch. R ] | $24.1_{ac}$[15] |
| (+)Neocarvomenthol | [$(CH_3)^{1\beta}$, $(OH)^{2\beta}$, $(iso\text{-}C_3H_7)^{4\alpha}$, ch. R ] | $65.2$[14] |
| (+)*trans*-1-Hydroxyneocarvomenthol | [$(CH_3)^{1\beta}$, $(OH)^{1\alpha}$, $(OH)^{2\beta}$, $(iso\text{-}C_3H_7)^{4\alpha}$, ch. R ] | $79.2_{ac}$[16] |

w: water solution, ch: chloroform solution, et: ethyl alcohol solution, ac; acetone solution.

center of a unit group is located at the center of the mass of its corresponding bond. In order to simplify the calculations, the refractive indices of the homogeneous substances and of the solutions under discussion are all assumed to be about 1.46[18].

## Method Proposed

Strictly speaking, as isopropyl group has no optical axis of cylindrical symmetry, the calculations of $[\mu]^{20}_{D\,calcd}$ which are concerned with isopropyl group are impossible. In order to avoid this difficulty, the following two simplifications are introduced.

Simp. I

$$(iso\text{-}C_3H_7)^{4\alpha} = (C^8H)^{4\alpha} + (C^9H_3)^{\alpha 8} + (C^{10}H_3)^{\alpha 8} \simeq^{2)} (C^8H_3)^{4\alpha} + (C^9H_3)^{\alpha 8} + (C^{10}H_3)^{\alpha 8}$$

Simp. II

$$(iso\text{-}C_3H_7)^{4\alpha}\chi A = \{(C^8H)^{4\alpha} + (C^9H_3)^{\alpha 8} + (C^{10}H_3)^{\alpha 8}\}\chi A \simeq (C^8H)^{4\alpha}\chi A + (C^9H_3)^{\alpha 8}\chi A + (C^{10}H_3)^{\alpha 8}\chi A$$

From Simps. I and II,

$$(iso\text{-}C_3H_7)^{4\alpha}\chi A \simeq (C^8H_3)^{4\alpha}\chi A + (C^9H_3)^{\alpha 8}\chi A + (C^{10}H_3)^{\alpha 8}\chi A \quad (1)$$

Next, the positions of minimal potential for $(C^9H_3)^{\alpha 8}$ or $(C^{10}H_3)^{\alpha 8}$ will be mentioned. Referring to the steric repulsion between one of these methyl groups and the C-atom in the cyclohexane-ring ($C^3$- and $C^5$-atoms), it can be easily understood that there should be three positions of minimal potential for methyl groups. The author names these three positions d-, e- and f-positions, respectively (Fig. 2).

But, d-position is trans to $C^4$–$C^5$ bond and e-position is trans to $C^4$–$C^3$ bond and f-position is gauche to both $C^4$–$C^5$ and $C^4$–$C^3$ bonds. As

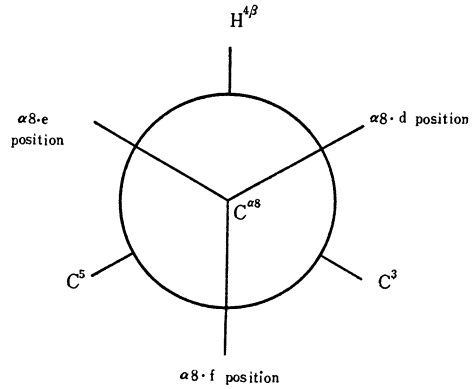



Fig. 2. Positions of minimal potential of $CH_3$ in $iso\text{-}C_3H_7$, viewed along $C^{\alpha 8}$–$C^4$ axis.

6) $[M]^{20}_D$ of pure materials in liquid state or of chloroform solutions are adopted, preferentially. Some values were presumed from $[M]_D$ which had been observed in the neighborhood of 20°C. (Ref. 3).

7) ch. R is an abbreviated symbol of a cyclohexane-ring.

8) Th. Posternak, D. Reymond and H. Friedli, *Helv. Chim. Acta*, **38**, 205 (1955).

9) G. A. C. Gough, H. Hunter and J. Kenyon, *J. Chem. Soc.*, **1926**, 2052.

10) O. Zeitshel and H. Schmidt, *Ber.*, **59**, 2298 (1926).

11) P. R. Jefferies and B. Milligan, *J. Chem. Soc.*, **1956**, 2363.

12) W. Hückel and H. Miggemeyer, *Ber.*, **72**, 1354 (1939).

13) J. Read and W. J. Grubb, *J. Chem. Soc.*, **1934**, 313.

14) R. G. Johnston and J. Read, ibid., **1935**, 1138.

15) H. Schmidt, *Suomen Kemistilehti B.*, **31**, 61 (1958); *Chem. Abstr.*, **52**, 20226 (1958).

16) P. Ham, G. Dupont, J. Wiemann and R. Dulou, *Compt. rend.*, **249**, 700 (1959).

17) S. Yamana, This Bulletin, **31**, 564 (1958).

18) The refractive index, $n$, is as follows; homogeneous state (1.46), chloroform solution (1.45), acetone solution (1.36), ethyl alcohol solution (1.36). If $n$ changes from 1.46 to 1.36, $\{(n^2+2)/3\}$ changes by $\partial/\partial n\{(n^2+2)/3\}\delta n \simeq 0.0973$. The magnitude of this value of $\{(n^2+2)/3\}$-change is about 7% of the value of $\{(n^2+2)/3\} \simeq 1.3772$.

movable groups in isopropyl group are $(C^9H_3)^{\alpha 8}$, $(C^{10}H_3)^{\alpha 8}$ and one H atom, it is obvious that any two of these three positions (d-, e- and f-positions) must be occupied by two methyl groups and the remaining one position should be occupied by one H atom. Then, the following three types of the internal conformation of $(iso\text{-}C_3H_7)^{4\alpha}$ are possible (Table II).

TABLE II. THE TYPE OF THE INTERNAL CONFORMATION OF $(iso\text{-}C_3H_7)^{4\alpha}$

| Name of type | $\alpha 8$·d-Position | $\alpha 8$·e-Position | $\alpha 8$·f-Position |
|---|---|---|---|
| Symmetrical | $CH_3$ | $CH_3$ | H |
| Unsymmetrical I | H | $CH_3$ | $CH_3$ |
| Unsymmetrical II | $CH_3$ | H | $CH_3$ |

**Substances which Have $(OH)^{3\alpha}$.**—It is apparent in Table III that the distance between O-atom in $(OH)^{3\alpha}$ and f-position is 2.52 Å and is shorter than the sum of van der Waals' radius of methyl group and that of $(OH)^{3\alpha}$.

TABLE III. THE DISTANCES BETWEEN O-ATOM IN $(OH)^3$ AND THREE POSITIONS OF MINIMAL POTENTIAL OF METHYL GROUP IN $(iso\text{-}C_3H_7)^{4\alpha}$

| | $\alpha 8$·d-Position | $\alpha 8$·e-Position | $\alpha 8$·f-Position |
|---|---|---|---|
| $(OH)^{3\alpha}$ | 3.49 Å | 4.30 Å | 2.52 Å |
| $(OH)^{3\beta}$ | 2.52 Å | 4.30 Å | 3.49 Å |

Then, owing to the steric repulsion, $(OH)^{3\alpha}$ may refute the idea that any movable methyl group in isopropyl group stays at f-position. In this case, the symmetrical type is only one possible type of the internal conformation of isopropyl group. For these reasons, it is concluded that in $(iso\text{-}C_3H_7)^{4\alpha}$ of (+)neomenthol in the liquid or dissolved state, two $(CH_3)^{\alpha 8}$'s are forced to stay at d- and e-positions (Fig. 1).

$$\therefore\ (iso\text{-}C_3H_7)^{4\alpha} = (C^8H)^{4\alpha} + (C^9H_3)^{\alpha 8\cdot d}\ ^{20)} + (C^{10}H_3)^{\alpha 8\cdot e} \simeq (C^8H_3)^{4\alpha} + (C^9H_3)^{\alpha 8\cdot d} + (C^{10}H_3)^{\alpha 8\cdot e}\ ^{21)} \quad (2)$$

Referring to Table I and Eq. 2, $\sum [\mu]^{20}_{D\ obs}$ of (+)neomenthol can be calculated by the following equation.

$$\begin{aligned}\sum [\mu]^{20}_{D\ obs} \text{ of (+)neomenthol} &= (CH_3)^{1\beta}\text{⅄}(OH)^{3\alpha} + (CH_3)^{1\beta}\text{⅄}(CH_3)^{4\alpha} + (CH_3)^{1\beta}\text{⅄}(CH_3)^{\alpha 8\cdot d} + (CH_3)^{1\beta}\text{⅄}(CH_3)^{\alpha 8\cdot e} \\ &+ (CH_3)^{1\beta}\text{⅄ch. R} + (OH)^{3\alpha}\text{⅄}(CH_3)^{4\alpha} \\ &+ (OH)^{3\alpha}\text{⅄}(CH_3)^{\alpha 8\cdot d} + (OH)^{3\alpha}\text{⅄}(CH_3)^{\alpha 8\cdot e} \\ &+ (OH)^{3\alpha}\text{⅄ch. R} + (CH_3)^{4\alpha}\text{⅄}(CH_3)^{\alpha 8\cdot d} \\ &+ (CH_3)^{4\alpha}\text{⅄}(CH_3)^{\alpha 8\cdot e} + (CH_3)^{4\alpha}\text{⅄ch. R} \\ &+ (CH_3)^{\alpha 8\cdot d}\text{⅄}(CH_3)^{\alpha 8\cdot e} + (CH_3)^{\alpha 8\cdot d}\text{⅄ch. R} \\ &+ (CH_3)^{\alpha 8\cdot e}\text{⅄ch. R} \quad (3)\end{aligned}$$

On the other hand, $[\mu]^{20}_{D\ calcd}\{3/(n^2+2)\}$, caused by the dynamical coupling effect between any two members of unit groups in menthol-like substance, can be calculated by using the theoretical formulae[19]. The results of calculation are shown in Table IV.

By using Table IV, Eq. 3 is rewritten as follows;

$$\begin{aligned}\sum [\mu]^{20}_{D\ obs} \text{ of (+)neomenthol} &= (-4.04\zeta'_{CH_3}\zeta'_{OH}{}^{22)} + 0 - 4.41\zeta'^2_{CH_3} + 4.41\zeta'^2_{CH_3} + 0 + 25.30\zeta'_{CH_3}\zeta'_{OH} + 3.09\zeta'_{CH_3}\zeta'_{OH} - 4.04\zeta'_{CH_3}\zeta'_{OH} + 0 + 0 + 0 + 0 + 0)\{(n^2+2)/3\} + D - D \\ &= 20.31\zeta'_{CH_3}\zeta'_{OH}\{(n^2+2)/3\}\end{aligned}$$

The corresponding observed value is 30.6[23].

$$\therefore\ 20.31\zeta'_{CH_3}\zeta'_{OH}\{(n^2+2)/3\} \equiv 30.6$$

or

$$\zeta'_{CH_3}\zeta'_{OH} = 1.5066\{3/(n^2+2)\} \quad (4)$$

On the other hand, the value of $\zeta_{CH_3}\zeta_{OH}$ in the case of hydroxycyclohexane can be calculated by using (−)*trans*-2-methylcyclohexanol as below;

$$\begin{aligned}\sum [\mu]^{20}_{D\ obs} \text{ of (−)}trans\text{-2-methylcyclohexanol} &= (OH)^{1\beta}\text{⅄}(CH_3)^{2\alpha} + (OH)^{1\beta}\text{⅄ch. R} + (CH_3)^{2\alpha}\text{⅄ch. R}^{23)} \\ &= -25.30\{(n^2+2)/3\}\zeta_{CH_3}\zeta_{OH} + 0 + 0^{24)} \\ &\equiv -42.4\end{aligned}$$

$$\therefore\ \zeta_{CH_3}\zeta_{OH} = 1.6759\{3/(n^2+2)\} \quad (5)$$

The value of $\zeta'_{CH_3}\zeta'_{OH}$ of menthol-like substance, shown in Eq. 4 is almost equal to that of $\zeta_{CH}\zeta_{OH}$ of methylcyclohexanol given in Eq. 5. This fact indicates that the value of $\zeta'_{CH_3}\zeta'_{OH}$ in Eq. 4 is trustworthy. Moreover, by using Eq. 4, $\sum [\mu]^{20}_{D\ obs}$ of (+)*trans*-2-hydroxyneomenthol which has $(OH)^{3\alpha}$ in its molecule is calculated to be 69.5. This calculated value is almost equal to the corresponding observed value, 70.3. This fact may mean that the value of $\zeta'_{CH_3}\zeta'_{OH}$ in Eq. 4 is a suitable one for the calculation of $\sum [\mu]^{20}_{D\ obs}$ of menthol-like substances.

Next, by using a method similar to that described above, an equation can be obtained as follows;

19) S. Yamana, This Bulletin, 30, 203 (1957).

20) $(CH_3)^{\alpha 8\cdot d}$ means $(CH_3)^{\alpha 8}$ which stays at d-position, and so on (Ref. 2).

21) Simp. I is used here.

22) $\zeta'$ is $\zeta$-coefficient of a unit group in the case of menthol-like substance.

23) Ref. Table I.

24) Table IV is used, here.

TABLE IV. $[\mu]^{20}_{D\,calcd}\{3/(n^2+2)\}$, CAUSED BY THE DYNAMICAL COUPLING EFFECT BETWEEN ANY TWO MEMBERS OF UNIT GROUPS IN MENTHOL-LIKE SUBSTANCE OF C 1 CONFORMATION

| | $(CH_3)^{\alpha 8\cdot f}$ | $(CH_3)^{\alpha 8\cdot e}$ | $(CH_3)^{\alpha 8\cdot d}$ | $(CH_3)^{4\alpha}$ | $(OH)^{3\beta}$ | $(OH)^{3\alpha}$ | $(OH)^{2\beta}$ | $(OH)^{2\alpha}$ |
|---|---|---|---|---|---|---|---|---|
| ch. R | 0 | $-D$ | $D$ | 0 | 0 | 0 | 0 | 0 |
| $(OH)^{1\alpha}$ | 0 | −0.74 | 0.74 | 0 | 1.88 | 0 | 0 | 11.73 |
| $(CH_3)^{1\alpha}$ | 0 | −1.75 | 1.75 | 0 | 4.20 | 0 | 0 | 25.30 |
| $(CH_3)^{1\beta}$ | 0 | 4.41 | −4.41 | 0 | 0 | −4.04 | 25.30 | −25.30 |
| $(OH)^{2\alpha}$ | −4.74 | 0 | 4.74 | 0 | 11.73 | −11.73 | | |
| $(OH)^{2\beta}$ | 0 | 4.64 | −0.11 | −4.04 | −11.73 | 0 | | |
| $(OH)^{3\alpha}$ | 0 | −4.04 | 3.09 | 25.30 | | | | |
| $(OH)^{3\beta}$ | −3.07 | 4.04 | 0 | −25.30 | | | | |
| $(CH_3)^{4\alpha}$ | 0 | 0 | 0 | | | | | |
| $(CH_3)^{\alpha 8\cdot d}$ | 0 | 0 | 0 | | | | | |
| $(CH_3)^{\alpha 8\cdot e}$ | 0 | 0 | 0 | | | | | |
| $(CH_3)^{\alpha 8\cdot f}$ | 0 | 0 | 0 | | | | | |

Note: $D$ cannot be calculated, theoretically.

TABLE V. $\sum[\mu]^{20}_{D\,obs}$ OF MENTHOL-LIKE SUBSTANCE

| Name | Type S | Type I | Type II |
|---|---|---|---|
| (−)*trans*-2-Hydroxymenthol | −12.8 | $-29.4-D$ | $-33.0+D$ |
| (−)*cis*-2-Hydroxymenthol | −43.4 | $-45.5-D$ | $-63.4+D$ |
| (−)Isomenthol | −25.7 | $-31.3-D$ | $-35.5+D$ |
| (−)Menthol | −32.0 | $-34.3-D$ | $-45.1+D$ |
| (−)Carvomenthol | −31.0 | $-42.9-D$ | $-40.5+D$ |
| (+)*cis*-1,2-Menthanediol | 19.2 | $6.2-D$ | $10.8+D$ |
| (+)Neocarvomenthol | 38.9 | $41.4-D$ | $29.5+D$ |
| (+)*trans*-1-Hydroxyneocarvomenthol | 38.9 | $40.3-D$ | $30.6+D$ |

S: Symmetrical type, I: Unsymmetrical I type, II: Unsymmetrical II type.

$$\sum[\mu]^{20}_{D\,obs} \text{ of } (-)cis\text{-2-hydroxyneomenthol} \equiv(-11.73\zeta'^{2}_{OH}-0.25\zeta'_{CH_3}\zeta'_{OH}) \times\{(n^2+2)/3\}\equiv-50.6 \quad (6)$$

Combining Eq. 4 with Eq. 6,

$$\zeta'^{2}_{OH}=4.2796\{3/(n^2+2)\} \quad (7)$$

or

$$\zeta'_{OH}=2.0687\{3/(n^2+2)\}^{1/2} \quad (7')$$

The value of $\zeta'^{2}_{OH}$ in Eq. 7 is nearly equal to that of $\zeta^{2}_{OH}$, $4.1091\{3/(n^2+2)\}$ which was obtained for the case of (−)1/2 cyclohexanediol[25]. This fact can easily be understood by considering that both (−)*cis*-2-hydroxyneomenthol and (−) 1/2 cyclohexanediol have only two hydroxyl groups which are adjacent to each other in their molecules. Thus, the value of $\zeta'^{2}_{OH}$ Eq. 7 seems to be reliable. From Eqs. 4 and 7′,

$$\zeta'_{CH_3}=0.7283\{3/(n^2+2)\}^{1/2}$$

and

$$\zeta'^{2}_{CH_3}=0.5304\{3/(n^2+2)\} \quad (8)$$

**Substances which Have $(OH)^{3\beta}$.** — Referring to Table III, the nearest position from O-atom in $(OH)^{3\beta}$ is $\alpha$8·d-position. Then, owing to the steric repulsion, $(OH)^{3\beta}$ may refute the idea that any movable $(CH_3)^{\alpha 8}$ in $(iso\text{-}C_3H_7)^{4\alpha}$ stays at $\alpha$8·d-position. In this case, the internal conformation of $(iso\text{-}C_3H_7)^{4\alpha}$ may be forced to take the unsymmetrical I type. But if an atom or group which combines whith $C^2$-atom attracts $(OH)^{3\beta}$ off $\alpha$8·d-position, the influence of $(OH)^{3\beta}$ on the type of the internal conformation of $(iso\text{-}C_3H_7)^{4\alpha}$ may be greatly weakened. Now, by using Eqs. 4 and 7, $\sum[\mu]^{20}_{D\,obs}$ of the menthol-like substances which have $(OH)^{3\beta}$ are calculated in each type of the internal conformation of $(iso\text{-}C_3H_7)^{4\alpha}$. The results of calculation are shown in the upper part of Table V.

For lack of experimental data in relation to the cyclohexane-ring, $D$ cannot be calculated theoretically. Then, the author resorted to a quasi-empirical evaluation of it. (−)Menthol has $(OH)^{3\beta}$ but it has no atom or group which combines with the $C^2$-atom and attracts $(OH)^{3\beta}$. And moreover, as the orientation of its $(CH_3)^{1\beta}$ is equatorial, the influence of $(CH_3)^{1\beta}$ on the type of the internal conformation of its $(iso\text{-}C_3H_7)^{4\alpha}$ will be very small. Then, the internal conformation of its $(iso\text{-}C_3H_7)^{4\alpha}$ is expected

25) Ref. Eq. 4* in the foot-note 4.

TABLE VI. COMPARISON OF $[M]_D^{20}$ WITH $\sum[\mu]_{D\,obs}^{20}$

| Name | at $C^3$ | $[M]_D^{20}$ [23] | $\sum[\mu]_{D\,obs}^{20}$ S | I | II | % |
|---|---|---|---|---|---|---|
| (+)Neomenthol | $(OH)^{3\alpha}$ | 30.6 | 30.6 | | | 100% S |
| (−)*cis*-2-Hydroxyneomenthol | $(OH)^{3\alpha}$ | −50.6 | −50.6 | | | 100% S |
| (+)*trans*-2-Hydroxyneomenthol | $(OH)^{3\alpha}$ | 70.3 | 69.5 | | | 100% S |
| (−)*trans*-2-Hydroxymenthol | $(OH)^{3\beta}$ | −16.0 | −12.8 | −72.6 | 10.2 | 95% S + 5% I |
| (−)*cis*-2-Hydroxymenthol | $(OH)^{3\beta}$ | −56.7 | −43.4 | −88.7 | −20.2 | 71% S +29% I |
| (−)Isomenthol | $(OH)^{3\beta}$ | −39.4 | −25.7 | −74.5 | 7.7 | 72% S +28% I |
| (−)Menthol | $(OH)^{3\beta}$ | −77.5 | −32.0 | −77.5 | −1.9 | 100% I |
| (−)Carvomenthol | none | −41.2 | −31.0 | −86.1 | 2.7 | 82% S +18% I |
| (+)*cis*-1,2-Menthanediol | none | 24.1 | 19.2 | −37.0 | 54.0 | 86% S +14% II |
| (+)Neocarvomenthol | none | 65.2 | 38.9 | −1.8 | 72.7 | 22% S +78% II |
| (+)*trans*-1-Hydroxyneocarvomenthol | none | 79.2 | 38.9 | −2.9 | 73.8 | 100% II |

S: Symmetrical type, I: Unsymmetrical I type, II: Unsymmetrical II type.

to be of the unsymmetrical I type. Accordingly, by referring to Table V, $\sum[\mu]_{D\,obs}^{20}$ of (−) menthol should be $(-34.3-D)$. The corresponding observed value is −77.5[23].

$$\therefore \quad -34.3-D\equiv -77.5$$

or

$$D=43.2 \qquad (9)$$

By using Eq. 9, Table V can be rewritten into Table VI.

The seventh column of Table VI indicates the percentage of two types in order to explain the corresponding observed value. But, as the observed value, $[M]_D^{20}$, has some probable errors and the calculated value, $\sum[\mu]_{D\,obs}^{20}$, was obtained by using some assumptions, the absolute values of the percentage in the seventh column should not be considered to be conclusive. Thus, it becomes apparent that even in this series, the symmetrical type can be prevalent when there are some groups which attract $(OH)^{3\beta}$ or to not allow any $(CH_3)^{\alpha 8}$ to say at the $\alpha 8$·f-position. But the ratio of these two types is affected greatly by the orientations of the other atoms or groups in the molecules.

**Substances which Have no (OH)$^3$.**—By using a method similar to those mentioned above, $\sum[\mu]_{D\,obs}^{20}$ of the substances which have not $(OH)^3$ are calculated and the results are shown in the lower parts of Tables V and VI. In this case also, the symmetrical type is prevalent. But it is strange that in (+)neocarvomenthol and (+)*trans*-1-hydroxyneocarvomenthol, the unsymmetrical II type is prevalent among the three types. This may mean that there is a kind of intramolecular (or intermolecular) van der Waals' attractive force between $(CH_3)^{\alpha 8}$ and the hydroxyl group which combines with the $C^2$- or $C^1$-atom, but this point is left for future study.

## Summary

From the standpoint of the fact that a menthol-like substance is a kind of hydroxycyclohexane, the molecular rotations of menthol-like substances are calculated by using the PM-method. A comparison of the calculated values with the corresponding observed values seems to make it possibe to presume the type of the internal conformation of $(iso\text{-}C_3H_7)^{4\alpha}$.

*Department of Chemistry*
*Kyoto Gakugei University*
*Fushimi-ku, Kyoto*

# *Structure of Enteromycin. I*. Derivatives and Products in Various Reactions of Enteromycin*

By Kōmei MIZUNO

(Received April 4, 1961)

*Streptomyces albireticuli* isolated by Nakazawa[1] in 1951 produces several biologically active antibiotics including eurocidine[2], enteromycin[3], carbomycin[4] (magnamycin)[5,6] and tertiomycin[7], which are different from each other in properties and they all show low toxicity. Nakazawa et al. isolated eurocidin[2] from a methanolic extract of the mycelium of the microorganism and carbomycin[4] from an ethyl acetate extract of the filtered broth which had been made alkaline beforehand, and Miyake et al. obtained tertiomycin[8] from the mother liquor of carbomycin. Nakazawa et al. also isolated enteromycin, an antibiotic active against Gram-negative bacteria, from the ethyl acetate extract of the above filtered broth which had been made acid, and assigned to it an empirical formula of $C_6H_8O_5N_2$, but its structure has so far remained unclarified. The present author, however, from the results of experiments to be published in four reports hence, has made clear that the antibiotic is *N*-(*O*-methyl-*aci*-nitroacetyl)-3-aminoacrylic acid. It is a peptide-type[9] compound and seems to be the first so far isolated from natural products as a substance having a *O*-methyl-*aci*-nitro group.

Enteromycin (I) is sparingly soluble in water and other solvents, but can be recrystallized from plenty of hot methanol and gives two kinds of interchangeable crystals Ia and Ib according to the extent of cooling. The p*K*a of this compound is 4.3, and from its molecular weight calculated from the amount of the alkali consumed and from its analytical values the molecular formula of $C_6H_8O_5N_2$ was assigned to it. Enteromycin has a methoxy group, and is optically non-active and negative to the phenolic OH reaction (referred to as Barton[10] reaction hereafter) by the ferric chloride-potassium ferricyanide reagent, but reduces the Fehling's reagent. A methanolic solution of this compound exhibits three absorption maxima at $\lambda$ 230 m$\mu$ ($\varepsilon$ 9000), 275 m$\mu$ ($\varepsilon$ 13000) and 298 m$\mu$ ($\varepsilon$ 16000) (Fig. 1), and the infrared spectra of Ia and Ib show absorptions at the following wavelengths ($\nu_{max}^{Nujol}$ $cm^{-1}$): 3300~3330 (NH), 2560~2670 (COOH), 1680~1690 (CO), 1620~1640 (conj. C=N), 1600 (conj. C=C), 1560 (-CO-NH-), 992 (Ia), 988 (Ib) (trans C=C). When methylated with diazomethane Ia and Ib gave the same product II [m. p. 141°C (decomp.), $C_7H_{10}O_5H_2$] and the infrared spectrum (Fig. 4) of the product clearly exhibited the absorption (1720 $cm^{-1}$) of COOR. II, having two methoxy groups, is obviously the methyl ester of I and so I seems sure to have a methoxy group detectable by the Zeisel method and a free carboxyl group, and therefore the formula A was assigned to it.

$$C_6H_8O_5N_2 \quad (C_4H_4O_2N_2)\rightarrow\begin{matrix}-COOH\\-OCH_3\end{matrix}$$

A

Since further reaction of II with diazomethane yielded a product (III) [m. p. 121°C (decomp.), $C_8H_{12}O_5N_4$] suspected to be a molecular compound from its molecular formula, the skeleton of I was assumed to have one or more double bonds.

I is unstable to heat, acid and alkali, and when heated with water it gave off formaldehyde (IV), acetaldehyde (V), carbon dioxide (VI), and others. In addition to V and VI, I also produced ammonia (VII), glyoxylic acid (VIII), oxalic acid (IX), etc. by heating with diluted hydrochloric acid, and acetaldehyde when reacted with hydroiodic acid, but no formaldehyde was yielded in these acid decompositions. Heating of I with sodium hydrogen carbonate solution afforded oxamic acid (XI). When subjected as such to thermal decomposition, I changed, under evolution of formaldehyde, into a substance which was positive to

* This constitutes Part XXXV of a series entitled "Studies on Antibiotics" by S. Tatsuoka, and was reported at the Forum on Natural Organic Compounds held on October 16, 1960.

1) K. Nakazawa, *J. Agr. Chem. Soc. Japan*, (*Nippon Nôgei-kagaku Kaishi*), **29**, 647 (1955).
2) K. Nakazawa, ibid., **29**, 650 (1955).
3) K. Nakazawa, ibid., **29**, 659 (1955).
4) K. Nakazawa et al., ibid., **29**, 661 (1955).
5) F. W. Taaner et al., *Antibiotics & Chemotherapy*, **2**, 441 (1952).
6) R. B. Woodward, *Angew. Chem.*, **69**, 50 (1957).
7) R. Utahara et al., *J. Antibiotics*, A, **7**, 120 (1954).
8) A. Miyake et al., ibid., **12**, 59 (1959).
9) A. J. Birch and H. Smith, Ciba Foundation Symposium. Amino Acids and Peptides with Antimetabolic Activity, Spottitwoode, Ballantyne & Co., Ltd., London and Colchester (1958), p. 247.
10) G. M. Barton et al., *Nature*, **170**, 249 (1952).

the Barton reaction and easily soluble in water and methanol. The substance was recrystallized from water in plates (XII) [m. p. 175°C (decomp.), $C_5H_6O_4N_2$] and needle-like crystals XIII [m. p. 169°C (decomp.), $C_{11}H_{14}O_9N_4$], and XII further afforded two kinds of interchangeable products XIIa and XIIb when recrystallized from water. XII (p*K*a 4.3 and 8.3) is an acid substance consuming two moles of alkali, and it is positive to the Barton reaction and reduces the Fehling's reagent but has no methoxyl group detectable by the Zeisel method. A methanolic solution of this substance exhibited two absorption maxima at $\lambda$ 225 m$\mu$ ($\varepsilon$ 16500) and 280 m$\mu$ ($\varepsilon$ 18000), and from infrared spectra of XIIa and XIIb (Figs. 6, 7) the presence of OH (3450 $cm^{-1}$), NH (3330), COOH (2560~2670), CO (1680), conj. C=N (1630), conj. C=C (1610) and trans C=C (975, 990) was presumed.

XIII has a methoxy group and from its ultraviolet spectrum (Fig. 8) and antibiotic activity,

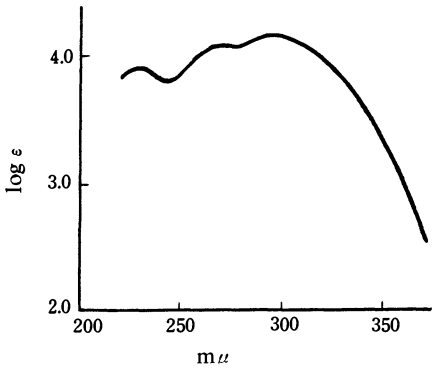



Fig. 1. Ultraviolet absorption spectrum of enteromycin (Ia, Ib) in methanol.

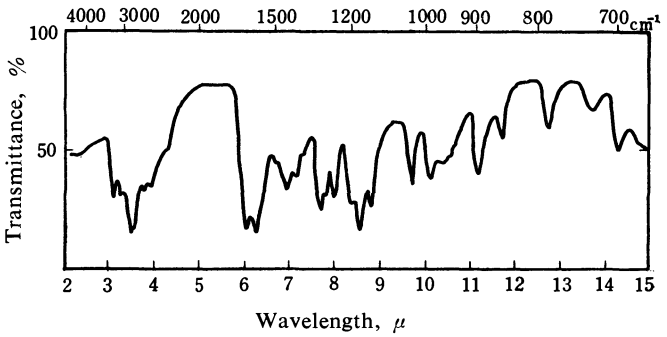



Fig. 2. Infrared absorption spectrum of enteromycin (Ia).

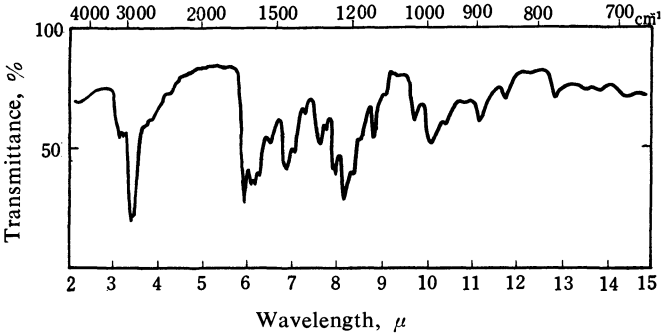



Fig. 3. Infrared absorption spectrum of enteromycin (Ib).

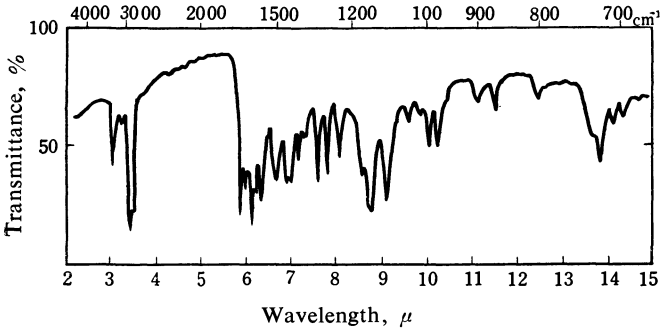



Fig. 4. Infrared absorption spectrum of enteromycin methylester (II).

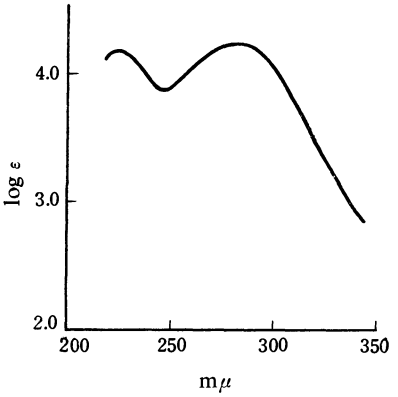



Fig. 5. Ultraviolet absorption spectrum of demethoxyenteromycin (XII) in methanol.

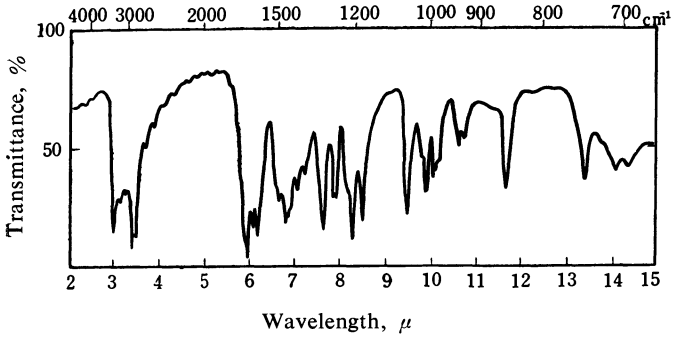



Fig. 6. Infrared absorption spectrum of demethoxy-enteromycin (XIIa).

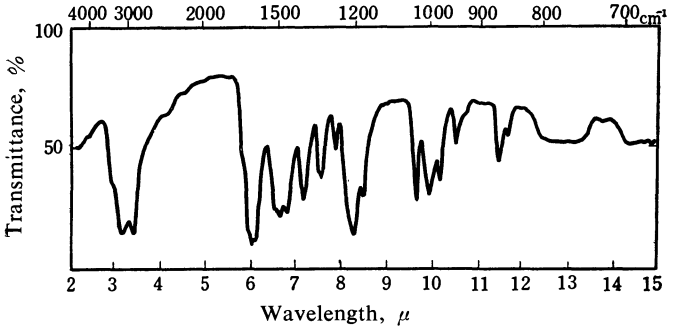



Fig. 7. Infrared absorption spectrum of demethoxy-enteromycin (XIIb).

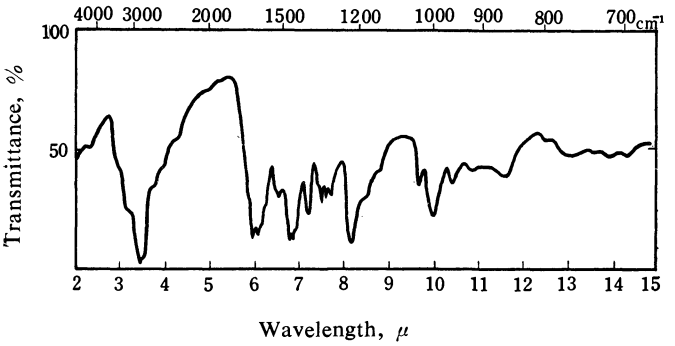



Fig. 9. Infrared absorption spectrum of XIII.

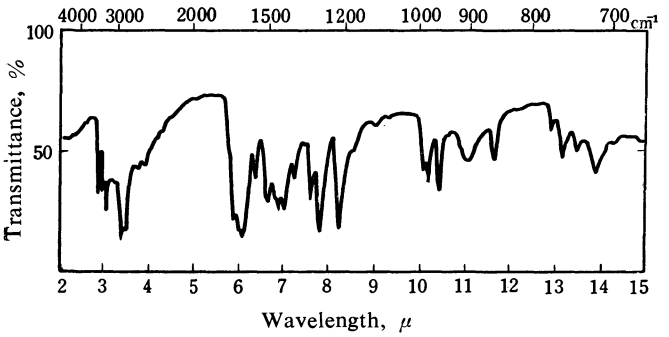



Fig. 10. Infrared absorption spectrum of enteromycin amide (XIV).

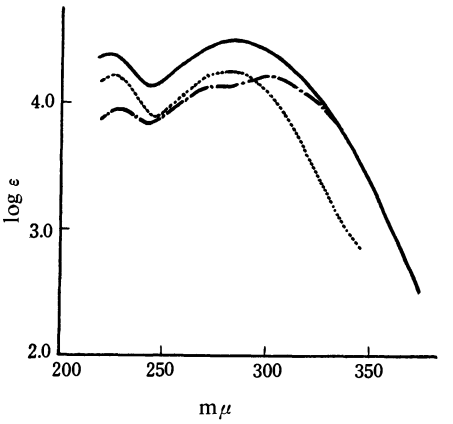



Fig. 8. Ultraviolet absorption spectra of I (—·—·—), XII (----), and molecular complex XIII (——) in methanol.

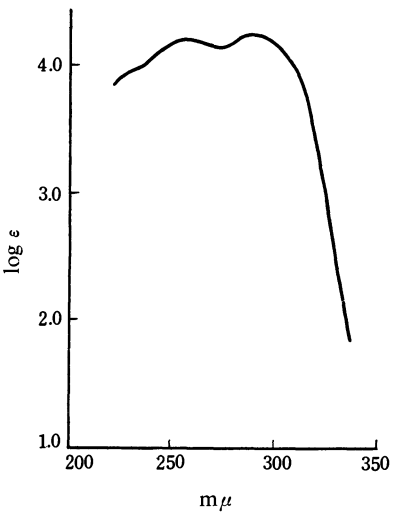



Fig. 11. Ultraviolet absorption spectrum of XIV in methanol.

it is assumed to be a molecular compound consisting of I and XII, and this assumption was confirmed by the infrared spectrum (Fig. 9) of the product prepared from equimolecular amounts of the two components. Demethoxylation** of I by heating afforded XII or XIII as mentioned above depending on the temperature and time of heating, and from the kind and amount of the product the progress of the demethoxylation could be checked. The thermal decomposition proceed to a considerable extent when I was left standing at 30°C for some ten days. However, since neither formaldehyde nor a substance positive to the Barton reaction was produced when I was allowed to stand in a methanolic solution of trimethylamine at 0°C for a long time, I seems to have no such a group as $-CH_2OH$ which produces formaldehyde by general dehydroxymethylation. Considered together with the results of decompositions of I with acid and water, the methoxy group detectable by the Zeisel method appears to be split off as formaldehyde, and therefore I is assumed to have a specific functional group including a methoxy group. So XII may be called demethoxyenteromycin. Amidation of I produced light yellow crystals, m. p. 163°C (decomp.) (neither urotropine nor IV was found in the mother liquor), which were converted into stable prisms (XIV) [m. p. 208°C (decomp.), $C_5H_7O_4N_3$], when treated with diluted acetic acid. As this product was positive to the Barton reaction and its infrared spectrum (Fig. 10) exhibited various absorptions characteristic of amides, it may be called enteromycin amide. The ultraviolet spectrum (Fig. 11) of the product showed two maxima at $\lambda$ 255 m$\mu$ ($\varepsilon$ 15000) and 290 m$\mu$ ($\varepsilon$ 18000), but as the spectrum did not resemble that of I, the product is likely to have a structure considerably different from that of I.

As mentioned before, I seems to have one or more double bonds, so it was subjected to catalytic reduction to make its skeleton clear, whereupon XII was produced first but the final product was XV [m. p. 225°C (decomp.), $C_5H_{10}O_3N_2$]. This product has no methoxy group and is positive to the ninhydrin reaction, and it may be called dehydroxytetrahydrodemethoxyenteromycin from its molecular formula.

From the above results the methoxyl group of I appears to be split off by catalytic reduction, and though I seems apparently to be amidated, it has no $COOCH_3$ group, so the amidation must be due to a specific functional group mentioned before. The carbon dioxide produced in the acid decomposition of I seems to have derived from the COOH group, and since acetaldehyde was produced in the same decomposition, the molecule of I ought to have $-CH=CH-$ or $-CH_2-CH=$ combination. Further the fact that ammonia, oxalic acid, and glyoxylic acid were produced in the decomposition and that oxamic acid was obtained in the alkali decomposition seems to suggest that I has $-NH-CO-\overset{|}{C}H-$ or $=N-CO-\overset{|}{C}H-$ combination.

Chart 1.

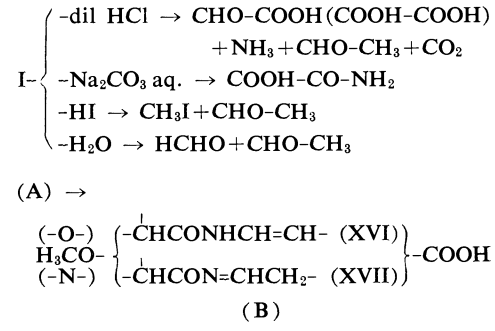
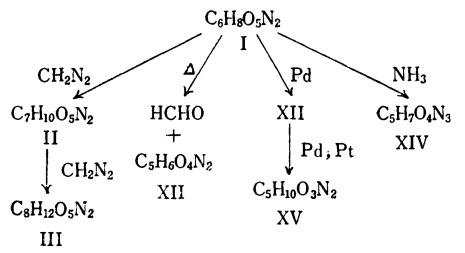



Chart 2.




## Experimental

**Enteromycin (I).** — A hot solution of 1 g. of enteromycin in 500 cc. of methanol was filtered with 100 g. of decolorizing charcoal and the filtrate was left standing, separating 500 mg. of long needle-like crystals Ib. Concentration of the mother liquor gave an additional crop of 300 mg. A solution of 200 mg. of Ib in 150 cc. of hot methanol was concentrated to about 50 cc. under reduced pressure and cooled to yield fine prisms Ia. Working up of the mother liquor afforded another crop, making the total yield 180 mg. Ia and Ib were clearly distinguishable in infrared spectrum. They dissolved in aqueous sodium hydrogen carbonate solution with evolution of carbon dioxide and colored yellow at 142°C, brown at 158°C and melted at 172°C with decomposition.

Found: C, 38.21; H, 4.41; N, 15.14; O-$CH_3$, 16.14. Calcd. for $C_6H_8O_5N_2$: C, 38.30; H, 4.29; N, 14.89; O-$CH_3$, 16.54% (one O-$CH_3$).

The p$K$a of this compound is 4.3 and its molecular weight is 180±10 when calculated from the amount of the alkali consumed.

** Whether this phenomenon is to be called demethoxylation or deformaldehyde reaction was unknown at first, but preference was given to the former as experiments proceeded.

**Enteromycin Methylester (II).**—To a suspension of 600 mg. of pure I in 60 cc. of ethanol was added an ether solution of diazomethane produced from 5 g. of nitrosomethylurea in several portions at 10~15°C. When evolution of nitrogen subsided, the almost colorless reaction mixture was concentrated under reduced pressure, giving 630 mg. of white crystals, which melted at 141°C (decomp.) after recrystallization from ethanol. This product gives off no carbon dioxide in sodium hydrogen carbonate solution and is negative to the ferric chloride-potassium ferricyanide reaction.

Found: C, 41.86; H, 4.75; N, 13.48; O-$CH_3$, 30.01. Calcd. for $C_7H_{10}O_5N_2$: C, 41.58; H, 4.99; N, 13.86; O-$CH_3$, 30.70% (two O-$CH_3$).

**Diazomethane Addition Product of Enteromycin Methylester (III).**—To a solution of 200 mg. of II in 20 cc. of ethanol was added a solution of diazomethane in 50 cc. of ether which was produced from 2 g. of nitrosomethylurea, and the reaction mixture was left standing at room temperature for 10 hr. and then concentrated at low temperature under diminished pressure to precipitate crystals. The crystals, after washing with ethanol, were dissolved in hot methanol, the solution was filtered, and the crystals obtained from the filtrate were recrystallized from ethanol, giving 100 mg. of needles, m. p. 121°C (decomp.). This compound is positive to the ferric chloride-potassium ferricyanide reaction and gives orange-red color with the Dragendorff[11] reagent.

Found: C, 39.40; H, 5.02; N, 22.50; O-$CH_3$, 25.02. Calcd. for $C_8H_{12}O_5N_4$: C, 39.24; H, 4.95; N, 22.94; O-$CH_3$, 25.42% (two O-$CH_3$).

**Decomposition of Enteromycin with Hot Water.**—A suspension of 100 mg. of I in 6 cc. of water was heated at 100°C for 1 hr. in vessel A under introduction of nitrogen. The aldehydes and carbon dioxide evolved were collected in receivers B and C containing pure water and baryta water, respectively. After the reaction, about 25 mg. of barium carbonate was obtained. A solution of 20 mg. of 2,4-dinitrophenylhydrazine in 5 cc. of concentrated hydrochloric acid was added to the receiver B, the mixture was allowed to stand for 3 hr. and the resulting hydrazones were extracted with ethyl acetate. The extract was washed with water, dried over anhydrous sodium sulfate and concentrated at low temperature under reduced pressure, separating 25 mg. of yellowish orange 2,4-dinitrophenylhydrazones (referred to as 2,4-DNPH hereafter). Paper chromatography of a solution of the products in chloroform-acetone (1 : 1) by the method of Gasparic[12] gave the two yellow spots at $R_f$ 0.25 and 0.38, which were identified as of 2,4-DNPH of formaldehyde (IV) and that of acetaldehyde (V).

**Decomposition of Enteromycin with Hydrochloric Acid.**—A suspension of 200 mg. of I in 2 cc. of 1 N hydrochloric acid was treated as above at 95°C for 1 hr. In addition to 140 mg. of barium carbonate, the following substances were obtained.

*Acetaldehyde (V).*—The aldehyde produced was converted to 2,4-DNPH with a solution of 2,4-dinitrophenylhydrazine in hydrochloric acid and the resulting crude product, m. p. 141°C (ca. 40 mg.) was purified by recrystallization from ethanol, when m. p. rose to 160°C. The $R_f$ value in paper chromatography and infrared spectrum of the product where in complete accord with those of 2,4-DNPH of synthetic acetaldehyde, and a mixed melting point determination of both substances showed no depression.

Found: C, 43.37; H, 3.73; N, 24.83. Calcd. for $C_8H_8O_4N_4$: C, 42.86; H, 3.60; N, 24.99%.

*Oxalic Acid (IX).*—The reaction mixture was extracted with 20 cc. of ether and the extract was concentrated to give 20 mg. of white crystals, m. p. 96°C, which was subjected to paper chromatography by the method of Stark[13] et al. (solvent: 75% phenol containing 1% of formic acid), affording a spot at $R_f$ 0.20, suspected to be of oxalic acid. The sodium salt of the product was converted to *S*-benzylthiuronium salt and purified by recrystallization from ethanol, m. p. 193°C.

Found: N, 13.17. Calcd. for $C_{18}H_{22}O_4N_4S_2$: N, 13.27%.

*Glyoxylic Acid (VIII).*—A solution of 2,4-dinitrophenylhydrazine in hydrochloric acid was added to the reaction mixture which had been extracted with ether, and after 3 hr. the resulting hydrazone was extracted with ethyl acetate. Concentration of the extract yielded a small amount of yellow crystals, which when paper-chromatographed in parallel with 2,4-DNPH of synthetic glyoxylic acid, gave a spot of 2,4-DNPH of glyoxylic acid at $R_f$ 0.40.

*Ammonia (VII).*—The reaction mixture from which 2,4-DNPH of glyoxylic acid had been separated was made alkaline and steam-distilled. The evolving basic gas was collected in diluted hydrochloric acid and the solution was evaporated to dryness to yield some plates. The product was identified as ammonium chloride because it gave, on paper chromatography (solvent: the upper layer of a mixture of *n*-butanol, acetic acid and water (4 : 1 : 5)), a spot at $R_f$ 0.14 which was positive to the ninhydrin reaction and took on a grayish brown color with the ammonical silver nitrate solution.

**2, 4-DNPH of Glyoxylic Acid.**—One and three tenths grams of ethyl diethoxyacetate, $(EtO)_2CH$-COOEt, synthesized by Moffett's method[14] was hydrolyzed by heating in 5 cc. of 5 N sodium hydroxide at 65°C for one hour and the reaction mixture, after neutralizing with hydrochloric acid, was shaken with ether to remove the unreacted material. One gram of 2,4-dinitrophenylhydrazine was dissolved in the aqueous layer, 25 cc. of concentrated hydrochloric acid was added, the mixture was stirred for 30 min. at 80°C, yielding 1.5 g. of yellow crystals. The crystals were dissolved in a solution of 1.5 g. of sodium bicarbonate in 30 cc. of water, the solution was acidified with hydrochloric acid and extracted with ethyl acetate, and the extract, after being washed with water and dried, was evaporated under reduced pressure, leaving 1.1 g. of a residue, which crystallized from hot methanol into yellow needlelike crystals, m. p. 193°C (decomp.).

11) A. Zaffaroni et al., *J. Biol. Chem.*, **177**, 109 (1949).

12) J. Gasparic and M. Vecera, *J. Chromatog.* **1**, xviii (1958).

13) J. B. Stark et al., *Anal. Chem.*, **23**, 413 (1951).

14) R. B. Moffett, *Org. Syntheses*, **35**, 59 (1955).

Found: C, 37.89; H, 2.66; N, 21.79. Calcd. for $C_8H_6O_6N_4$: C, 37.80; H, 2.38; N, 22.05%.

**Paper Chromatography of 2,4-DNPH of Glyoxylic Acid.** — Each of 2,4-DNPH of various aldehydes, dissolved in a 1 : 1 mixture of chloroform and acetone, was developed by the ascending method on a piece of Tōyō filter paper No. 7 (4×45 cm.) acetylated by Micheel's method[15], using a solvent of cyclohexane-benzene-chloroform-ethyl acetate-acetone (5 : 5 : 10 : 1 : 5). $R_f$ values of various 2,4-DNPH at the time when the solvent front migrated about 20 cm. from the starting point were as shown below.

| Substance | $R_f$ value |
|---|---|
| 2,4-Dinitrophenylhydrazine | 1.00 |
| 2,4-DNPH of acetone | 0.90~0.95 |
| 〃 of formaldehyde | 0.84 |
| 〃 of acetaldehyde | 0.73 |
| 〃 of glyoxylic acid | 0.40 |

Under ultraviolet rays all the spots were observed as light absorbing spots and all of them exhibited a peculiar brownish purple color when immersed in 90% ethanol containing 2% of sodium hydroxide.

**Decomposition of Enteromycin with Hydroiodic Acid.** — Fifty milligrams of I was heated with 4 cc. of the hydroiodic acid mixture (hydroiodic acid-phenol-propionic anhydride) at 60~80°C for 40 min. and at 80~120°C for 2 hr. under introduction of nitrogen, and the aldehyde in the distillate was converted to 2,4-DNPH. On paper chromatography as before, the 2,4-DNPH gave a single yellow spot at $R_f$ 0.35, which was identified as 2,4-DNPH of acetaldehyde.

**Decomposition of Enteromycin with Alkali Carbonate.** — *Oxamic Acid (XI).* — A mixture of 500 mg. of I and 5 cc. of 10% sodium carbonate solution was heated on the water bath and after being concentrated to 1.2 cc. cooled to yield ca. 100 mg. of crystals. The crystals were dissolved in 3 cc. of water, the solution was passed through a column of Amberlite IR-120 (H-form), and the effluent, after concentration under reduced pressure, was mixed with a little ethanol to separate 50 mg. of yellowish white crystals. The crystals were dissolved again in water and reprecipitated with ethanol, giving 30 mg. of white crystals, m. p. 203°C (decomp.). The product, melting at 210°C after drying at 120°C for 2 hr. in vacuo, was identified as oxamic acid having one mole of water of crystallization.

**Thermal Decomposition of Enteromycin (1).** — Three hundred milligrams of I was heated at 110~120°C for 40~50 min. in a 5 cc. flask connected through a Liebig condenser with a vessel containing 5 cc. of cold pure water, under gentle introduction of nitrogen which was washed with an alkaline pyrogallol solution and dried with calcium chloride. And the following substances were obtained.

*Demethoxyenteromycin (XII).* — The yellow contents of the flask were dissolved in 3 cc. of methanol and the solution, after being filtered to remove the unreacted material (70 mg.), was evaporated at low temperature under diminished pressure. The white residue was dissolved in 2 cc. of hot water and cooled to separate about 40 mg. of needles XIII. The mother liquor from the needles was concentrated, yielding 140 mg. of prisms XIIa, which, after several recrystallizations from water, gave about 40 mg. of plates XIIb. Both kinds of the crystals colored brown at 157°C and melted at 175°C with decomposition. They were positive to the ferric chloride-potassium ferricyanide reaction and could be distinguished from each other by their infrared spectra.

Found (XIIa): C, 37.82; H, 3.91; N, 17.85. Found (XIIb): C, 37.78; H, 3.97; N, 17.97; O-$CH_3$, undetected. Calcd. for $C_5H_6O_4N_2$: C, 37.98; H, 3.83; N, 17.72%.

*Formaldehyde (IV).* — The aldehyde collected in the water-containing vessel was converted to 2,4-DNPH (ca. 30 mg.), which afforded a single yellow spot at $R_f$ 0.25 on paper chromatography[12]. The product melted at 168°C after recrystallization from methanol and it was identified as 2,4-DNPH of formaldehyde from its infrared spectrum and by mixed melting point determination.

Found: C, 40.38; H, 3.08; N, 27.00. Calcd. for $C_7H_6O_4N_4$: C, 40.00; H, 2.88; N, 26.66%.

**Thermal Decomposition of Enteromycin (2).** — *Enteromycin Demethoxyenteromycin Molecular Compound.* — When I was left standing at room temperature for more than several months, it gave off the smell of formaldehyde and colored yellow. The product was treated as in the case of XII to give needle-like crystals (XIII), m. p. 169°C (decomp.), which were positive to the ferric chloride-potassium ferricyanide reaction and had about one half antibiotic activity of that of I.

Found: C, 38.52; H, 3.88; N, 16.68. Calcd. for $C_{11}H_{14}O_9N_4(C_6H_8O_5N_2 \cdot C_5H_6O_4N_2)$: C, 38.10; H, 4.05; N, 16.20%.

Fifty milligrams of I and 50 mg. of XII were dissolved in 5 cc. of hot water and the solution was cooled to yield needle-like crystals having the same infrared spectrum as XIII.

*Non-dehydroxymethylation.* — A solution of 50 mg. of I in 5 cc. of 1% methanolic trimethylamine solution was left standing at 5°C for one week and concentrated at low temperature under reduced pressure. The residue (ca. 50 mg.) was dissolved in 3 cc. of water and the solution was acidified with several drops of acetic acid, giving about 45 mg. of crystals showing the same infrared spectrum as I.

**Enteromycin Amide (XIV).** — A solution of 500 mg. of I in 100 cc. of methanol saturated with ammonia was allowed to stand overnight at room temperature, and the solvent was distilled off, leaving 450 mg. of crude crystals. The crystals were dissolved in 7 cc. of water and the solution was filtered and made acid with acetic acid to separate 380 mg. of crystals, m. p. 196~203°C (decomp.). The product, after recrystallization from methanol, melted at 208°C (decomp.) and was positive to the ferric chloride-potassium ferricyanide reaction.

Found: C, 34.59; H, 4.02; N, 24.50; O-$CH_3$,

15) F. Micheel and H. Schweppe, *Microchim. Acta*, **1954**, 60.

undetected. Calcd. for $C_5H_7O_4N_3$: C, 34.68; H, 4.08; N, 24.24%.

A solution of 30 mg. of 2,4-dinitrophenylhydrazine in 10 cc. of concentrated hydrochloric acid was added to the above acid mother liquor and the mixture, after being heated at 100°C for 10 min. and left standing for one hour, was extracted with ethyl acetate. The 2,4-DNPH obtained from the extract showd the spot of 2,4-DNPH of acetaldehyde at $R_f$ 0.35 on paper chromatography[12].

**Catalytic Reduction of Enteromycin.**—*Demethoxyenteromycin (XII).* — A solution of 300 mg. of I in 300 cc. of hot pure methanol was rapidly cooled and catalytically reduced on palladium-carbon, when one mole of hydrogen was absorbed in about 30 min. The catalyst was filtered off and the filtrate was concentrated at low temperature under reduced pressure, separating crystals. The mother liquor from the crystals was further concentrated and a solution of the residue (ca. 200 mg.) in 5 cc. of hot water was allowed to stand to deposite needle-like crystals. The crystals were filtered and the filtrate was concentrated to about 3 cc., yielding ca. 150 mg. of plates, m. p. 175°C (decomp.). The infrared spectrum of the product was in complete agreement with that of XIIa.

Found: C, 38.10; H, 4.00; N, 17.62. Clacd. for $C_5H_6O_4N_2$: C, 37.98; H, 3.83; N, 17.72%.

*Dehydroxytetrahydrodemethoxyenteromycin (XV).*— A solution of 300 mg. of I in 300 cc. of hot pure methanol was cooled and reduced in the presence of 100 mg. of Adams platinum oxide when 4 mol. of hydrogen was absorbed about 2 hr. The catalyst was filtered and washed well with water, and the combined filtrate and washing were concentrated at low temperature under reduced pressure. The resulting white crystals (200 mg.), after recrystallization from aqueous methanol, melted at 225°C and were positive to the ninhydrin reaction.

Found: C, 40.97; H, 7.11; N, 18.92; $-NH_2$, 11.55. Calcd. for $C_5H_{10}O_3N_2$: C, 41.09; H, 6.90; N, 19.17; $-NH_2$, 10.45% (one-$NH_2$).

On paper chromatography by the method of Consden[16] et al. (80 g. phenol, 19.3 cc. water and 0.7 cc. concentrated aqueous ammonia) the product afforded a spot at $R_f$ 0.68, which with the ninhydrin reagent gave a color changing from yellow to blue.

16) R. Consden et al., *Biochem. J.*, **38**, 224 (1944).


## Summary

In order to know its functional groups and the combining state of the groups, enteromycin was subjected to such reactions as methylation, amidation, degradation, and catalytic reduction, and the properties of the products were investigated.


*Research Laboratories*
*Takeda Chemical Ind., Ltd.*
*Higashiyodogawa-ku, Osaka*

# *Structure of Enteromycin. II*. Derivatives and Products in Various Reactions of Dimethoxyenteromycin*

By Kōmei MIZUNO

(Received April 4, 1961)

Dehydroxytetrahydrodemethoxyenteromycin (XV)[1] obtained by the catalytic reduction of enteromycin (I) or demethoxyenteromycin (XII) seems to have the same skeleton as that of the latter two. And from the course of changes of I, XII appears to be in the closest relation with I. In the present work, the structure of XV was established, and the functional group of XII and its derivatives were investigated in detail.

The infrared spectrum (Fig. 1) of XV exhibited the absorptions of NH, COOH and $COO^- \cdot NH_3^+$ (2100, 1620, 1370 $cm^{-1}$), but its ultraviolet spectrum showed no specific absorption at the long wave region beyond $\lambda$ 220 m$\mu$. Also, an amino group was detected in this compound by azotometry. Since the compound was considered to be a saturated peptide in view of the above facts, it was hydrolyzed with hydrochloric acid and the product was subjected to paper chromatography, detecting glycine (XXIII) and $\beta$-alanine (XXV). The DNP derivatives[2] of both amino acids were also confirmed by paper chromatography. Hydrolysis of the DNP derivative of XV produced no DNP-amino acid, but since $\beta$-alanine was obtained as a free amino acid, XV was.

* This constitutes part XXXVI of a series entitled "Studies on Antibiotics" by S. Tatsuoka, and was reported at the Forum on Natural Organic Compounds held on October 16, 1960.

1) K. Mizuno, This Bulletin, **34**, 1419 (1961).

2) W. W. Bromer, *J. Am. Chem. Soc.*, **79**, 2794 (1957).

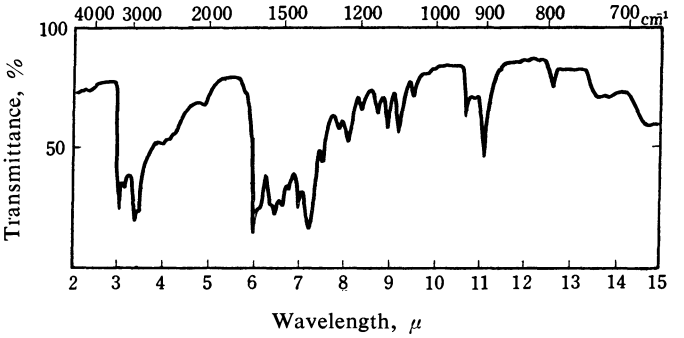
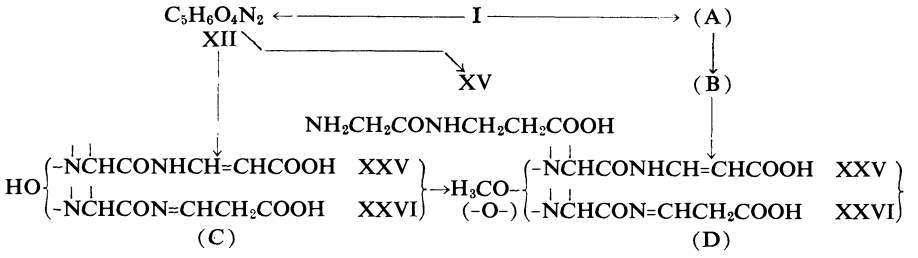



Fig. 1. Infrared absorption spectrum of dehydroxytetrahydrodemethoxyenteromycin (glycyl-β-alanine) (XV).




assumed to be glycyl-β-alanine. So *N*-formylglycine was condensed with β-alanine ethyl ester in the presence of dicyclohexylcarbodiimide and the resulting *N*-formylglycyl-β-alanine ethyl ester was hydrolyzed with sodium hydroxide to give *N*-formyl-β-alanine. The product was deformylated by the method of Miyamoto[3] et al., and the infrared spectrum, melting point (decomp.), and $R_f$ value in paper chromatography of the resultant product were found to be in full accord with those of XV. From these results the formula C was presumed for XII and the formula D for I.

The two acidic groups[1] in XII were confirmed by acetylation and methylation of XII. The product was obtained as prisms (XVIII) [m. p. 181°C (decomp.), $C_7H_8O_5N_2$] negative to the Barton reaction, and since its infrared spectrum (Fig. 2) showed a clear absorption of >NO-COR[4] (1775 $cm^{-1}$), it was called *O*-acetyldemethoxyenteromycin.

Reaction of XII with diazomethane products, one of which (XIX) [m. p. 159°C, $C_7H_{10}O_4N_2$] was obtained as prisms and had a methoxy group and the other (XX) [m. p. 137°C, $C_7H_{10}O_4N_2$] was yielded as needles and had two methoxy groups. As the infrared spectra (Figs. 3 and 4) of both products showed the absorption of COOR (1710 $cm^{-1}$), they were called *N*-methyldemethoxyenteromycin methyl ester and *O*-methyldemethoxyenteromycin methyl ester, respectively.

From the formation of these compounds, it is obvious that XII representable by the formula C has a phenolic hydroxyl group in addition to a free carboxyl group. Decomposition of XII with hydrochloric acid produced acetaldehyde (V), carbon dioxide (VI), ammonia (VII), and glyoxylic acid (VIII), but not formaldehyde, and boiling of XII with water also afforded no formaldehyde, and therefore the structure of XII would be almost the same as that of I, except the special functional[1] group including a methoxy group. Amidation of XII gave a compound (XXI) m. p. 168°C (decomp.), $C_5H_9O_4N_3$] as needles, which positive to the ninhydrin reaction and reverted to the original compound by treatment with heat, water, or diluted acetic acid. And as the infrared spectrum (Fig. 5) of this product exhibited the absorption characteristic of amides, it was called demethoxyenteromycin amide. Also similarity of the ultraviolet spectrum of the product to that of XII suggested that it has a structure considerably different from that of entromycin amide (XIV).

Finally the course of the change of XII to XV by catalytic reduction was investigated in detail. Namely, catalytic reduction of XII on palladium-carbon first yielded prisms (XXII) [m. p. 203°C (decomp.), $C_5H_8O_3N_2$] which were sparingly soluble in cold water and gave a

3) M. Miyamoto et al., *J. Pharm. Soc. Japan* (*Yakugaku Zasshi*), in press.
4) H. Bredereck et al., *Chem. Ber.*, **89**, 1533 (1956).

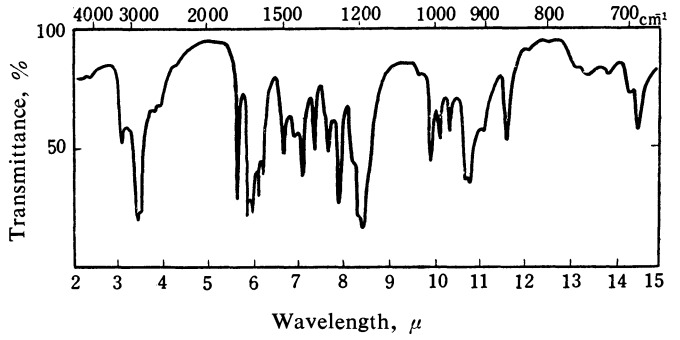



Fig. 2. Infrared absorption spectrum of *O*-acetyldemethoxyenteromycin (XVIII).

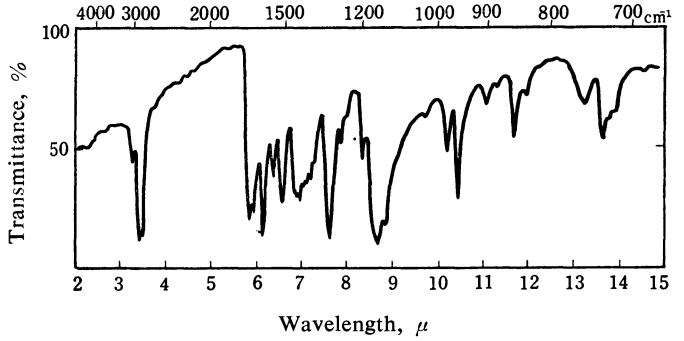



Fig. 3. Infrared absorption spectrum of *N*-methyldemethoxyenteromycin methyl ester (XIX).

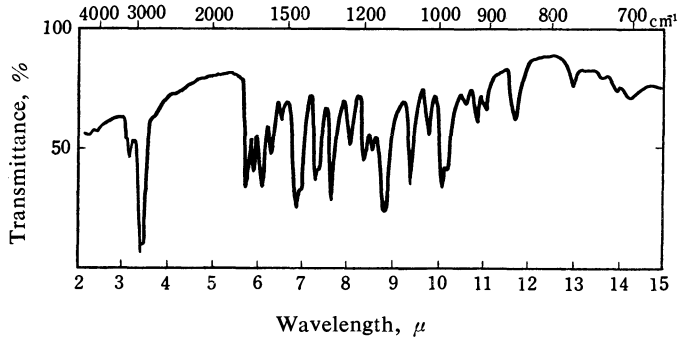



Fig. 4. Infrared absorption spectrum of *O*-methyldemethoxyenteromycin methyl ester (XX).

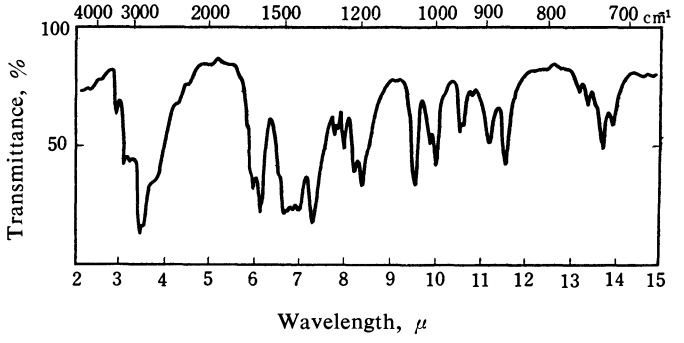



Fig. 5. Infrared absorption spectrum of demethoxyenteromycin amide (XXI).

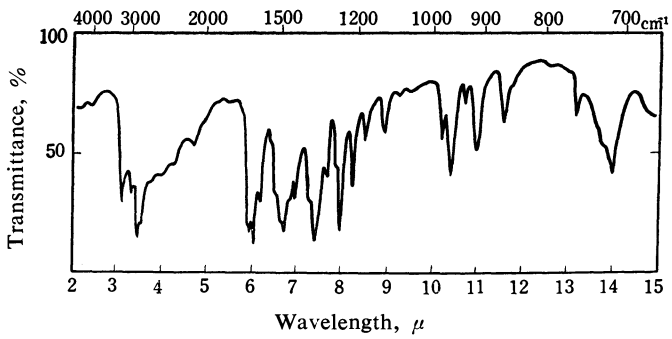



Fig. 6. Infrared absorption spectrum of dehydroxydihydrodemethoxyenteromycin (XXII).

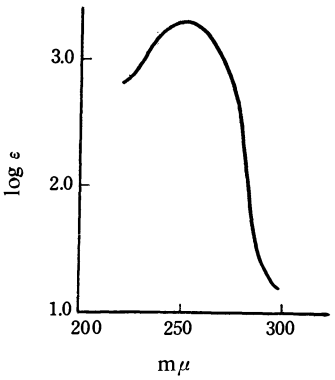
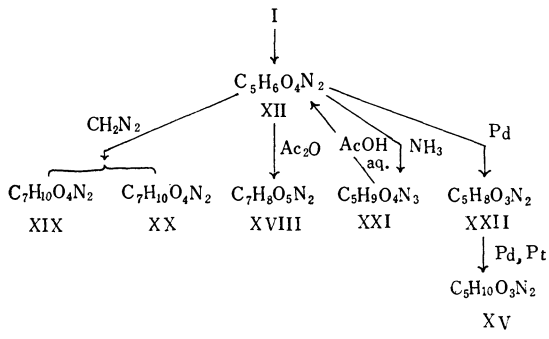



Fig. 7. Ultraviolet absorption spectrum of XXII in water.

yellow ninhydrin reaction, and further reduction resulted in the formation of glycyl-β-alanine (XV). From its molecular formula, XXII was called dehydroxydihydrodemethoxyenteromycin, and since its infrared spectrum (Fig. 6) exhibited the absorptions of NH, COOH and $COO^- \cdot NH_3^+$, it was considered to be a peptide. The ultraviolet spectrum (Fig. 7) of the compound showed a single absorption maximum ($\varepsilon_{max}$ 2000) at $\lambda_{max}$ 250 mμ.




## Experimental

**Hydrolysis of Dehydroxytetrahydrodemethoxyenteromycin (XV).**—A solution of 10 mg. of XV in 1 cc. of 6 N hydrochloric acid was heated at 110°C for 5 hr. in a sealed tube, the air in which was replaced with nitrogen. The reaction mixture was evaporated to dryness, the residue was dissolved in 1 cc. of water, and part of the solution was subjected to paper chromatography according to the method described in Report I, giving two spots at $R_f$ 0.42 and 0.65. The former spot colored brownish pink with ninhydrin and the latter, blue, and they were identified as glycine and β-alanine, respectively. Five tenths cc. of the above aqueous solution was adjusted to pH 8 with 30 mg. of sodium hydrogen carbonate, the mixture was allowed to react with a solution of 8 mg. of 1-fluoro-2,4-dinitrobenzene in 0.5 cc. of ethanol, and the product was extracted by the method of Bromer[2]. The product was developed in the dark on filter paper, Whatman No. 1, with the upper layer of *n*-butanol-0.1% aqueous ammonia (1 : 1), giving two yellow spots at $R_f$ 0.28~0.33 and 0.37~0.40. They were identified as DNP-glycine and DNP-β-alanine. Each of the two spots was extracted with 4 cc. of hot water, and the absorption of the extracts was measured, finding that the two products were contained in the material in equimolecular amounts.

**Hydrolysis of DNP-Dehydroxytetrahydrodemethoxyenteromycin.**—To a solution of 10 mg. XV in 2 cc. of water was added a solution of 7 mg. of 1-fluoro-2,4-dinitrobenzene in 2 cc. of ethanol, followed by 20 mg. each of sodium hydrogen carbonate and sodium carbonate, and the mixture was treated as in the preceding experiment. The reaction mixture was extracted first with ether at acid pH to remove 2,4-dinitrophenol and then with isobutanol to obtain the DNP-derivative of the peptide compound. Part of the product was subjected to two dimensional paper chromatography; namely it was, developed first with the same solvent system as in the preceding experiment to detect a yellow spot at $R_f$ 0.26, which migrated to $R_f$ 0.26 in the second development with a solution of sodium dihydrogen phosphate (1 M) and disodium hydrogen phosphate (0.5 M) in 1 l. of water. The above DNP-derivative was hydrolyzed by heating with 0.5 cc. of 10 N hydrochloric acid at 100°C for 3 hr. and the ether soluble portion of the product was chromatographed as above, detecting the spot of 2,4-dinitrophenol at $R_f$ 0.44~0.49 (in the first development) and 0.26 (in the second development) and the spot of 2,4-dinitroanilin at 0.85~0.95 (in the first development) and 0.00 (in the second development), but no spot of DNP-glycine was observed. The acid solution from which the ether solube portion had been separated was evaporated to dryness and the residue was chromatographed as in the preceding experiment, whereupon a spot coloring blue with ninhydrin was detected at $R_f$ 0.65, which was identified as β-alanine.

**Synthesis of Glycyl-β-alanine.**—To a solution of 2.1 g. of *N*-formylglycine in 20 cc. of ethanol was added 2.4 g. of β-alanine ethyl ester, followed by

4.2 g. of dicyclohexylcarbodiimide, and the mixture was allowed to stand overnight with cooling. The separated urea derivative was filtered off, the filtrate was evaporated under reduced pressure, and the residue was dissolved in 20 cc. of ethyl acetate. The solution was filtered and the needle-like crystals, m. p. 72°C (ca. 2.5 g.) obtained from the filtrate was purified by recrystallization from ethyl acetate. The product melted at 75°C.

Found: C, 47.81; H, 7.09; N, 14.13. Calcd. for $C_8H_{14}O_4N_2$ (*N*-formylglycyl-β-alanine ethyl ester): C, 47.52; H, 6.97; N, 13.85%.

One gram of the product dissolved in 20 cc. of dioxane was hydrolyzed by standing with 6~7 cc. of 1 N sodium hydroxide at room temperature, the reaction mixture was passed through a column of Amberlite IR-120 (H-form) to remove sodium ion, and the effluent was concentrated under diminished pressure to give white crystals, which were recrystallized from ethanol in prisms, m. p. 121°C (600 mg.).

Found: C, 41.68; H, 5.81; N, 15.84. Calcd. for $C_6H_6O_4N_2$ (*N*-formylglycyl-β-alanine): C, 41.38; H, 5.79; N, 16.09%.

To a solution of 450 mg. of the product in 2 cc. of methanol was added 0.25 cc. of hydrazine hydrate (80%), and the mixture was heated for 5 hr. on the water bath. The resulting crystals were washed with methanol and recrystallized from aqueous methanol, yielding 250 mg. of prisms, m. p. 225°C (decomp.). The infrared spectrum, $R_f$ value in paper chromatography and coloration in the ninhydrin reaction of the product were in complete agreement with those of XV described in Report I.

Found: C, 40.75; H, 7.10; N, 18.84. Calcd. $C_5H_{10}O_3N_2$ (glycyl-β-alanine): C, 41.09; H, 6.90; N, 19.17%.

**O-Acetyldemethoxyenteromycin (XVIII).**—To a solution of 300 mg. of demethoxyenteromycin (XII) in 15 cc. of hot water was added dropwise 2 cc. of acetic anhydride at 55~60°C over a period of about 15 min. with vigorous stirring. The mixture once became clear, but white crystals m. p. 180°C (decomp.) (ca. 320 mg.), gradually separated there from, which were recrystallized from methanol in prisms, m. p. 181°C (250 mg.). The product is negative to the ferric chloride-potassium ferricyanide reaction and resists ester exchange with methanol and decomposes when dried at a temperature over 70°C in vacuo.

Found: C, 42.33; H, 4.33; N, 13.97; -$COCH_3$, 20.50. Calcd. for $C_7H_8O_5N_2$: C, 42.00; H, 4.03; N, 14.00; -$COCH_3$, 21.50%.

**N-Methyldemethoxyenteromycin Methyl Ester (XIX).**—To a solution of 600 mg. of XII in 30 cc. of ethanol was added a solution of diazomethane (produced from 7 g. of nitrosomethylurea) in 80 cc. of ether and the mixture was left standing at room temperature for 10 hr. The solvent was distilled off and the resulting white crystals, m. p. 120°C (150 mg.) were recrystallized from 1.5 cc. of methanol in needles (XIX), m. p. 159°C (ca. 60 mg.). This product is negative to the ferric chloride-potassium ferricyanide reaction.

Found: C, 45.16; H, 5.21; N, 15.22; O-$CH_3$, 16.38. Calcd. for $C_7H_{10}O_4N_2$: C, 45.16; H, 5.41; N, 15.05; O-$CH_3$, 16.67%.

**O-Methyldemethoxyenteromycin Methyl Ester (XX).**—The mother liquor from XIX was concentrated to 0.7 cc. and left standing, separating 70 mg. of needles, which after crystallization from methanol melted at 137°C. Like XIX, the product is negative to the phenolic OH reaction, and its molecular weight is 180±20 when measured by the Rast method, using camphor as solvent.

Found: C, 45.15; H, 5.45; N, 15.04; O-$CH_3$, 32.45. Calcd. for $C_7H_{10}O_4N_2$: C, 45.16; H, 5.41; N, 15.05; O-$CH_3$, 33.30%.

**Decomposition of Demethoxyenteromycin with Hydrochloric Acid.**—According to the method described in Report I, a mixture of 100 mg. of XII and 3 cc. of 1 N hydrochloric acid was heated in the atmosphere of nitrogen at 100°C for about one hour in flask A, which was connected with vessel B containing pure water and vessel C containing baryta water. The reaction mixture changed from brown to redish brown and plenty of barium carbonate deposited. After the reaction, the aldehyde in the vessel B was converted to the 2,4-DNPH derivative with a solution of 2,4-dinitrophenylhydrazine in hydrochloric acid, and the product was chromatographed as before, detecting a single spot of the 2,4-DNPH of acetaldehyde at $R_f$ 0.38.

A solution of 2,4-dinitrophenylhydrazine in hydrochloric acid was added to one half of the contents of the flask A, the resulting 2,4-DNPH derivative was extracted with ethyl acetate, and the extract was shaken with sodium hydrogen carbonate solution. The aqueous layer was made acid and extracted again with ethyl acetate, and the extract, after washing with water and drying, was concentrated under reduced pressure to give yellow crystals, which on paper chromatography exhibited the spot of the 2,4-DNPH derivative of glyoxylic acid at $R_f$ 0.42. The remaining half of the contents of the flask A was made alkaline and steam-distilled, and the distillate neutralized with hydrochloric acid was evaporated to dryness, affording white crystals, which, when paper chromatographed as described in Report I, gave the spot of ammonium chloride at $R_f$ 0.14.

**Demethoxyenteromycin Amide (XXI).**—An amount of 500 mg. of XII was dissolved in 100 cc. of methanol saturated with ammonia and the solution, after standing overnight, was concentrated in the atmosphere of nitrogen at low temperature under reduced pressure, giving about 200 mg. of a residue which became light yellow prisms melting at 168°C (decomp.) after washing with a mixture of acetone and ethanol. The same treatment of the mother liquor yielded 250 mg. of unchanged XII. The product, m. p. 168°, colors blue with ninhydrin and is positive to the ferric chloride-potassium ferricyanide reaction. It produces XII quantitatively when treated with diluted acetic acid or hot water.

Found: C, 34.54; H, 5.49; N, 23.93. Calcd. for $C_5H_9O_4N_3$: C, 34.28; H, 5.18; N, 23.99%.

**Dehydroxydihydrodemethoxyenteromycin (XXII).**—A 200 mg. portion of XII dissolved in 20 cc. of pure methanol was reduced on 150 mg. of palladium

carbon (1 : 10) until about 2 mol. of hydrogen was absorbed. The catalyst was filtered and washed with hot water, the combined washing and filtrate were concentrated under reduced pressure, and methanol was added to the concentrate, giving about 150 mg. of crystals. The product was treated with a little cold water and the insoluble portion was recrystallized from water, yielding 70 mg. of prisms, m. p. 203°C (decomp.), which colored yellow with ninhydrin and gave a spot at $R_f$ 0.63 on paper chromatography[2].

Found: C, 41.46; H, 5.79; N, 19.48; $-NH_2$, 11.06. Calcd. for $C_5H_8O_3N_2$: C, 41.66; H, 5.59; N, 19.44; $-NH_2$, 9.86%.

Catalytic reduction of a solution of 30 mg. of XXII in 10 cc. of a mixture of glacial acetic acid and methanol on about 30 mg. of Adams platinum oxide (or palladium-carbon) afforded about 20 mg. of glycyl-β-alanine.

**Summary**

The structure of dehydroxytetrahydrodemethoxyenteromycin was established to be glycyl-β-alanine. Demethoxyenteromycin yielded *O*-acetyldemethoxyenteromycin by acetylation, *N*-methyl- and *O*-methyldemethoxyenteromycins by methylation, and demethoxyenteromycin amide by amidation. Catalytic reduction of demethoxyenteromycin gave first dehydroxydihydrodemethoxyenteromycin and then glycyl-β-alanine. Acid decomposition products of demethoxyenteromycin were the same those of enteromycin, except methyliodide.

*Research Laboratories*
*Takeda Chemical Ind., Ltd.*
*Higashiyodogawa-ku, Osaka*

# *Infrared Absorption Spectra of Water of Crystallization in Cobaltous Chloride Hexa- and Dihydrate Crystals*

By Itaru GAMO

(Received February 13, 1961)

The infrared absorption spectra of cobaltous chloride hexahydrate and dihydrate have been separately subject to two investigations[1,2]. However, there has been no comparative study of the two crystals in relation to their structural difference.

In the present paper, observed spectra were examined in relation to the difference of the binding states of the water molecules in them. The two crystals have an advantage over the hydrated salts of oxy-acids such as hydrated sulfates, because all the observed bands can be attributed to the vibrations of water molecules without ambiguity except for those due to the skeletal vibrations of the metal atom and ligands. Furthermore their structures are well determined by X-ray diffraction[3] and by electron diffraction[4] respectively.

## Experimental

**Preparation.** — Commercial cobaltous chloride hexahydrate of guaranteed grade was recrystallized from water. Cobaltous chloride dihydrate was obtained by keeping the purified hexahydrate over calcium chloride at ordinary temperature for 24 hr.[5]

**Measurement.**—Spectra were recorded by means of a Kôken DS 301 infrared spectrophotometer using a sodium chloride or potassium bromide prism. The potassium bromide disk technique was employed.

## Results

The spectra are given in Fig. 1. In the 3 $\mu$ region one peak is observed for the hexahydrate at 3430 $cm^{-1}$, and one shoulder and two peaks for the dihydrate at 3564, 3444 and 3226 $cm^{-1}$. These are comparable to the peaks of various inorganic hydrated salts[6] in this region, and can be assigned to the O–H stretching vibrations of water molecules affected by coördination on a cobalt atom and by the hydrogen bonding with a chlorine atom or an oxygen atom of an outer water molecule. Overlapping of several stretching bands is probably responsible for the broadness of the band for the hexahydrate. In the 6 $\mu$ region, two bands of medium intensity are observed at 1625 and 1599 $cm^{-1}$ for the hexahydrate. The latter is fairly sharp. Both can be assigned to the bending mode of water molecules, the former being presumably due to a ligand water

1) J. Lecomte, *J. chim. phys.*, **50**, C 53 (1953).
2) O. Glemser and E. Hartert, *Naturwiss.*, **42**, 534 (1955).
3) J. Mizuno, K. Ukei and T. Sugawara, *J. Phys. Soc. Japan*, **14**, 383 (1959).
4) B. K. Vainstein, *Doklady Akad. Nauk. S. S. S. R.*, **68**, 301 (1949).
5) L. Gmelin, "Handbuch der anorganischen Chemie", Verlag Chemie, Berlin (1932), No. 58, p. 276.
6) I. Gamo, This Bulletin, **34**, 760 (1961).

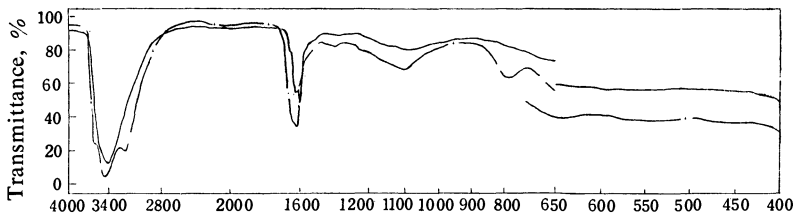



Fig. 1. Observed bands of $CoCl_2 \cdot 6H_2O$ and $CoCl_2 \cdot 2H_2O$.
..... $CoCl_2 \cdot 6H_2O$ —·—· $CoCl_2 \cdot 2H_2O$

molecule and the latter to a water molecule free from coördination. For the dihydrate, one band of medium intensity is observed at 1610 $cm^{-1}$. It can be assigned to the bending mode of a ligand water molecule. In the 9 $\mu$ region, the spectrum of the hexahydrate shows a very broad weak band at 1090 $cm^{-1}$, and that of the dihydrate shows a similar one at 1100 $cm^{-1}$. The origins of these bands cannot be decided at present. Probably they are the combinations or overtones of some restricted rotation modes of water molecules. The band observed at 790 $cm^{-1}$ for the dihydrate can be attributed to the wagging vibration of a ligand water molecule affected by hydrogen bonding, because of its position, intensity and shape. The bands so far reported were observed in the sodium chloride region.

In the potassium bromide region, no band was observed for the hexahydrate. For the dihydrate only one very broad band was observed at 642 $cm^{-1}$. It is tentatively attributed to the rocking mode of the water molecule which is responsible for the wagging band at 790 $cm^{-1}$, because the twisting band of a water molecule is usually too weak to be observed. It cannot be assigned to any skeletal vibration of the metal atom and ligands since the skeletal vibration bands should appear in a lower frequency region.

Tables I and II summarize these results.

Table I. Observed frequencies of $CoCl_2 \cdot 6H_2O$

| Wave number, $cm^{-1}$ | Assignment |
|---|---|
| 3430 s | O-H stretch. |
| 1625 m | H-O-H bend. |
| 1599 m, sh | H-O-H bend. |
| 1090 w, v.b | |

Table II. Observed frequencies of $CoCl_2 \cdot 2H_2O$

| Wave number, $cm^{-1}$ | Assignment |
|---|---|
| 3564 s, shoulder | |
| 3444 s | O-H stretch. |
| 3226 s | O-H stretch. |
| 1610 m | H-O-H bend. |
| 1100 w, v.b | |
| 790 w, b | $H_2O$ wag. |
| 642 m, v.b | $H_2O$ rock. |

Abbreviations: s, strong; m, medium; w, weak; v, very; b, broad; sh, sharp.

## Discussion

According to X-ray analysis[3], four water molecules and two chlorine atoms in cobaltous chloride hexahydrate are coördinated on the cobalt atom, making an octahedron with the cobalt atom at the center. Two other water molecules are far distant from the cobalt atom, and each of their oxygen atoms forms a hydrogen bond with one of the two O–H bonds of a ligand water molecule. The other O–H bond of this water molecule forms another hydrogen bond with a chlorine atom of a neighboring octahedron (for details, see Fig. 2).

An electron diffraction study[4] shows that two water molecules and two chlorine atoms in

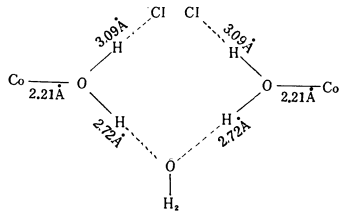



Fig. 2. Arrangement of atoms in $CoCl_2 \cdot 6H_2O$.

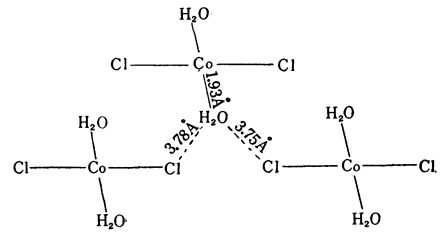



Fig. 3. Arrangement of atoms in $CoCl_2 \cdot 2H_2O$*.

* The three parallelograms are respectively in different planes. The values 3.75 and 3.78 Å were calculated from the data in Ref. 4.

cobaltous chloride dihydrate are coördinated on the cobalt atom, making a parallelogram with the cobalt atom at the center (Fig. 3).

As in the previous studies[6,7], it shall be assumed that the water frequencies are influenced by coördination and hydrogen bonding.

As is seen from Fig. 2, at least four O–H stretching frequencies are expected theoretically for the hexahydrate: one for the O–H bond of the ligand water molecule which forms the hydrogen bond O–H···Cl, one for the bond O–H···O, and two (symmetric and antisymmetic) for the almost free water molecule. The peak observed at 3430 $cm^{-1}$ probably corresponds to either one of the first two, because the frequency shift from the value of the vapor state is of the same order as in many cases[6] where the water molecule is affected by coördination and hydrogen bonding. The last two frequencies should appear in a higher region since they correspond to an almost free water molecule. Probably they are weak and hidden in the above-mentioned band.

In the dihydrate, the nearest distance between a ligand water molecule and a chlorine atom of a neighboring parallelogram is 3.75 Å, and the next to the nearest distance is 3.78 Å. The two observed bands, at 3444 and 3226 $cm^{-1}$ can be explained in relation to the crystal structure by the following assumption: one of the O–H bonds of the ligand water molecule forms a hydrogen bond with one of these two chlorine atoms, and the other is free from hydrogen bonding. We can correlate the 3226 $cm^{-1}$ band with the fomer O–H bond and the 3444 $cm^{-1}$ band with the latter since hydrogen bonding lowers the stretching frequency and the coördination effects are equal in the two cases. It is unlikely that one of the O–H bonds forms a hydrogen bond of distance 3.75 Å and the other forms a hydrogen bond of distance 3.78 Å respectively with each of the two chlorine atoms, because the frequency difference of 218 $cm^{-1}$ is far too great to be explained by the difference of the hydrogen bond distances 0.03 Å since the stretching frequency is relativery insensitive to the hydrogen bonding effect. The shoulder at 3564 $cm^{-1}$ cannot be interpreted for the present.

For the bending vibration in the hexahydrate two frequencies are observed. They can be explained readily from the crystal structure. The higher frequency (1625 $cm^{-1}$) can be attributed to the mode of the coördinated and hydrogen bonded water molecule, and the lower frequency (1599 $cm^{-1}$), the value of which is almost equal to that of the vapor state frequency (1595 $cm^{-1}$), can be assigned to the almost free water molecule since in general the two effects are likely to increase the bending frequency[8]. For the dihydrate there is observed only one bending frequency (1610 $cm^{-1}$), corresponding to the fact that there is only one kind of water molecule in the unit cell of the crystal. It is 15 $cm^{-1}$ lower than that for the ligand water molecule in the hexahydrate. This indicates that the additive effect of coördination and hydrogen bonding is greater in the hexahydrate than in the dihydrate although the coördination distance between the cobalt atom and the water molecule is somewhat shorter, and so the coördination effect is greater in the dihydrate.

The position and the shape of the wagging band at 790 $cm^{-1}$ for the dihydrate are reasonable as compared with those in the usual cases. For the hexahydrate no band was observed in this region. (These results suggest that the band at 781 $cm^{-1}$ reported for the hexahydrate in a previous paper[6] may be in fact due to the dihydrate which may have happened to be produced by partial dehydration of part of the hexahydrate during the vacuum process in the preparation of the KBr disk.)

The position and the shape of the rocking band at 642 $cm^{-1}$ for the dihydrate seem also to be reasonable. The frequencies of the wagging and the rocking band are somewhat lower than the corresponding frequencies for aluminum sulfate octodecahydrate[8] respectively.

## Summary

The observed spectra of the water of crystallization were interpreted by the effects of coördination and hydrogen bonding. The total difference in the spectra of the two crystals was explained in relation to the difference in their atomic arrangements.

The author wishes to express his thanks to Professor Takehiko Shimanouchi of the University of Tokyo for his helpful guidance.

*Institute for Science and Engineering Research*
*Waseda University*
*Shinjuku-ku, Tokyo*

7) I. Gamo, ibid., 34, 764 (1961).

8) I. Gamo, ibid., to be published.

# *Infrared Absorption Spectra of Water of Crystallization in Ferrous Chloride Tetrahydrate Crystal*

By Itaru GAMO

(Received February 13, 1961)

The crystal structure of ferrous chloride tetrahydrate has been determined in detail by X-ray diffraction[1]. Therefore it is possible to correlate the infrared absorption spectra of the water of crystallization with the structure.

In the present study, the characteristic bands of the water of crystallization in the crystal were determined for this purpose. Like cobaltous chloride hexahydrate and dihydrate[2], the crystal has an advantage in that observed bands can be attributed to the vibrations of water molecules almost uniquely. The spectra have an interesting feature in the bending region that has not been observed in other cases in this series of studies[2-6].

## Experimental

**Preparation.**—Commercial ferrous chloride tetrahydrate of guaranteed grade was recrystallized from water.

**Measurement.** — Spectra were recorded by a Kôken DS 301 infrared spectrophotometer equipped with a sodium chloride prism. The potassium bromide disk technique was employed.

## Results

The spectra are given in Fig. 1. In the 3 $\mu$ region, one peak is observed at 3442 $cm^{-1}$ and one shoulder at 3238 $cm^{-1}$. These are comparable to the peaks of various inorganic hydrated salts in this region, and can be assigned to the O–H stretching vibrations of water molecules affected by the interaction with an iron atom and by the hydrogen bonding with a chlorine atom. The overlapping of several stretching bands is probably responsible for the somewhat broad feature of the band. In the 5 $\mu$ region, a broad and very weak band is observed at 2301 $cm^{-1}$. It can be assigned to the combination of the bending and the wagging mode of a water molecule. It is somewhat overlapped by the carbon dioxide band at 2352 $cm^{-1}$. A similar band observed at 1740 $cm^{-1}$ is probably due to an overtone of some restricted rotation mode or a combination of such modes. In the 6 $\mu$ region, two remarkably sharp peaks of medium intensity are observed at 1626 and 1603 $cm^{-1}$, the former being a little weaker than the latter. They are assigned to the bending vibrations of water molecules affected by the same effects as in the cases of streching modes. They are the sharpest bending bands that have been observed in this series of studies. Hitherto only one bending band was observed or in the case of two peaks at least one was not sharp[2,4]. This is not because the present instrument is better in resolving power than that used in most of the previous measurements. An infrared study of the crystal by the latter instrument gave two equally sharp bands in the same region. The shoulder at 1492 $cm^{-1}$ is too low to be assigned to the bending mode and therefore should be attributed to the first overtone of the wagging mode (see below). Probably the weak band at 1229 $cm^{-1}$ has its origin in a combination or an overtone. The 755 $cm^{-1}$ band can be

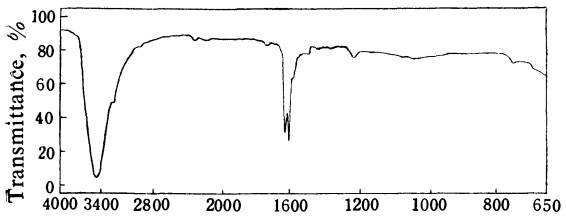



Fig. 1. Observed bands of $FeCl_2 \cdot 4H_2O$.

TABLE I. OBSERVED FREQUENCIES OF $FeCl_2 \cdot 4H_2O$

| Wave number, $cm^{-1}$ | Assignment |
|---|---|
| 3442 v. s | $\nu(H_2O)$ stretch. |
| 3238 m, shoulder | $\nu(H_2O)$ stretch. |
| 2301 v. w, b | $\nu_2+\nu_R$ ($H_2O$) bend.+wag. |
| 1740 v. w, b | |
| 1626 m, v. sh | $\nu_2(H_2O)$ bend. |
| 1603 m, v. sh | $\nu_2(H_2O)$ bend. |
| 1492 w, shoulder | $2\nu_R(H_2O)$ |
| 1229 w, b | |
| 755 w, b | $\nu_R(H_2O)$ wag. |

Abbreviations: s, strong; m, medium; w, weak; v, very; b, broad; sh, sharp.

1) B. R. Penford and J. A. Grigor, *Acta Cryst.*, **12**, 850 (1959).
2) I. Gamo, This Bulletin, **34**, 1430 (1961).
3) I. Gamo, ibid., **34**, 760 (1961).
4) I. Gamo, ibid., **34**, 764 (1961).
5) I. Gamo, ibid., to be published.
6) I. Gamo, ibid., to be published.

assigned to the wagging mode of a water molecule because of its position and shape.

Table I summarizes these results.

## Discussion

According to X-ray analysis[1], the crystal is monoclinic and belongs to space group $P2_1/c$ with $a=5.91$, $b=7.17$, $c=8.44$ Å and $\beta=112°10'$. The structure consists of discrete groups, two per unit cell. Each group contains one iron atom, four water molecules, and two chlorine atoms. It is a distorted octahedron. There are two iron-oxygen distances: 2.09 and 2.59 Å. Hereafter the corresponding oxygen atoms will be called oxygen I and II, and the corresponding water molecules will be called type I and type II, respectively. The distance 2.59 Å is considerably greater than the sum of the ionic radii of iron and oxygen (2.16 Å). Therefore oxygen II is very weakly held in the group. The analysis suggests that oxygen I forms a pair of hydrogen bonds with two chlorine atoms in the manner shown in Fig. 2, and in oxygen II two hydrogen atoms are used to form three hydrogen bonds (Fig. 3). Therefore they are likely to be more or less bifurcated.

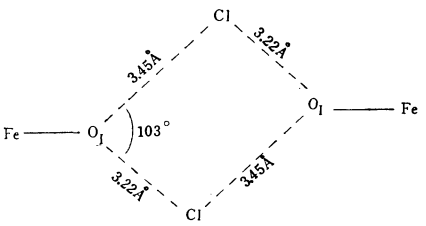



Fig. 2. Suggested hydrogen bonds for $O_I$. The error in each bond length is ±0.04 Å.

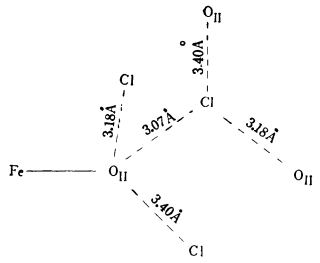



Fig. 3. Suggested hydrogen bonds for $O_{II}$. The error in each bond length is ±0.025 Å.

As in the previous studies[2-5], it will be assumed that the water frequencies are influenced by coördination and hydrogen bonding.

Figure 2 may suggest, at first sight, couplings between vibrations of two water molecules of type I due to hydrogen bonding. But it is unlikely because of the considerable difference between the distances of the two hydrogen bonds connected by the same chlorine atom. The situation is similar in the case of type II (Fig. 3). Therefore the observed two stretching frequencies are not due to splitting by hydrogen bonding. Further, there is a considerable difference between two O-H distances in each molecule because the corresponding hydrogen bonds are different in length. This suggests that the observed bands are not due to the symmetric and the antisymmetric vibration respectively.

The stretching frequency of water is in general likely to decrease by the effect of coördination, as suggested by comparison of the frequency of the ammonium ion with that of the ammonia molecule[7]. Hydrogen bonding of course lowers the frequency; therefore the two effects will be additive.

From this standpoint, it will first be assumed that the observed two bands at 3442 and 3238 $cm^{-1}$ are both due to water of type II. Since the metal-to-oxygen bond is almost purely electrostatic in this case, we have only to take into account the hydrogen bonding effect. Then, from Glemser's relationship[8] between the stretching frequency and the hydrogen bond length, the corresponding O-H···Cl distances are estimated to be 3.32 and 3.11 Å, respectively. Both values seem to be compatible with the above-mentioned suggestion concerning hydrogen bonding for oxygen II, indicating the validity of the assumption. Bands due to water of type I should appear in a lower region because the coördination effect is fairly large (distance 2.09 Å). Probably they escape detection due to their weak intensity.

The two effects influence the bending frequency also. Hydrogen bonding increases the frequency as seen in the case of ice. The observed two frequencies 1626 and 1603 $cm^{-1}$ are lower than the value 1644 $cm^{-1}$ in ice, which is free from coördination. This suggests that coördination lowers the bending frequency. The situation may be similar to that in the case of the degenerate deformation frequency of the ammonia molecule in a metal ammine complex[9], which is somewhat lower than the corresponding value of the vapor state. Probably in the case of water in general the effect of coördination should cancel partly the effect of hydrogen bonding. This seems to be responsible for the relatively small change in the bending frequency by the two effects, as compared with that in the stretching frequency.

From the above-mentioned standpoint, the stronger coördination results in the lower

7) I. Gamo, *J. Chem. Soc. Japan, Pure Chem. Sec.* (*Nippon Kagaku Zasshi*), 73, 594 (1952).
8) O. Glemser and E. Hartert, *Naturwiss.*, 42, 534 (1955).
9) G. F. Svatos, D. M. Sweeny, S. Mizushima, C. Curran and J. V. Quagliano, *J. Am. Chem. Soc.*, 79, 3313 (1957).

bending frequency. Thus the observed bands at 1626 and 1603 $cm^{-1}$ can be reasonably attributed to water molecules of type II and of type I, respectively, since the coördination is considerably weaker in the former and the hydrogen bonding effects are approximately equal in the two cases. For the present, their remarkable sharpness cannot be correlated with the crystal structure.

Experimental results[3,5] show that either of the two effects increases the wagging frequency. The band at 755 $cm^{-1}$ is reasonably attributed to the wagging mode of water of type I, the metal-oxygen distance being 2.09 Å. The wagging band due to type II should appear in a lower region, because in this case the coördination effect is very small (distance 2.59 Å) and the hydrogen bond strength is of the same order as in ice, which is free from coördination and has a wagging band near 600 $cm^{-1}$.

**Summary**

The observed spectra of the water of crystallization were correlated with the crystal structure determined by X-rays. They were interpreted as affected by coördination and hydrogen bonding. The coördination was concluded to lower the bending frequency of water in general. Two remarkably sharp bending bands were found.

The author wishes to express his thanks to Professor Takehiko Shimanouchi of the University of Tokyo for his helpful guidance.

*Institute for Science and Engineering Research*
*Waseda University*
*Shinjuku-ku, Tokyo*

# *Absorptiometric Determination of Micro-amounts of Iron in Nuclear Grade Graphite and Urania-Graphite Fuel; Nitroso R Salt Method after Coprecipitation of Iron with Manganese Dioxide**

By Masatoshi MIYAMOTO

(Received January 24, 1961)

It has been necessary, in the author's laboratory, to determine micro-amounts of iron in nuclear grade graphite and urania-graphite fuel for a nuclear reactor. Spectrographic methods have been used to estimate the iron impurity in graphite. Recently[1], the impurity in graphite of high purity was determined after concentration by a chemical method. Little literature on absorptiometric determination of the impurity in nuclear grade graphite and urania-graphite fuel is seen at present. The author has applied a method with nitroso R salt, sodium 1-nitroso-2-naphthol-3, 6-disulfonate[2,3], to these samples because the reagent has the highest sensitivity to iron at present giving very stable green color[4]. In this paper, the effect of diverse ions, preliminary separation and contamination with foreign iron are discussed.

## Experimental

**Apparatus and Materials.** — A Hitachi spectrophotometer, model EPU-2, was used for all measurements of absorbancy, matched 1 cm. cells being used. A Beckman pH-meter, model H-2, was used for acidity measurements. An electric furnace used for the ashing of samples was equipped with a protector assembled with fused silica plates to keep the sample out of possible contamination with dust from the wall of the furnace.

All the chemicals were of JIS special grade including starting materials in the following preparation of chemicals unless otherwise stated. Nitroso R salt was recrystallized from 50% aqueous ethanol. Hydrochloric acid and aqueous ammonia were purified by distillation. Cobalt sulfate was prepared by the pyrolysis of chloropentaminecobalt(III) chloride followed by furming with sulfuric acid and recrystallization. The cobalt complex was prepared according to the description by M. Biltz and W. Biltz[5]. Manganese chloride was prepared from iron-free potassium permanganate by reduction with

* Presented at the Tohoku Local Meeting of the Chemical Society of Japan, Sendai, September, 1960.

1) A. A. Demidov and L. B. Gorbunova, *Zavodskaya Lab.*, **25**, 956 (1959); *Chem. Abstr.*, **54**, 10634 (1960).

2) C. P. Sideris, *Ind. Eng. Chem., Anal. Ed.*, **14**, 756 (1942).

3) Y. Oka and M. Miyamoto, *Japan Analyst*, (*Bunseki Kagaku*), **1**, 23 (1952); *Bull. Res. Inst. Min. Dress. Met., Tohoku Univ.*, **9**, 25 (1953).

4) Y. Oka and M. Miyamoto, *J. Chem. Soc. Japan, Pure Chem. Sec.* (*Nippon Kagaku Zasshi*), **75**, 864 (1954); *Sci. Rep. RITU.*, **A7**, 84 (1955); *J. Chem. Soc. Japan, Pure Chem. Sec.* (*Nippon Kagaku Zasshi*), **76**, 672 (1955); *Sci. Rep. RITU.*, **A7**, 482 (1955).

5) M. Biltz and W. Biltz, "Ubungsbeispiele aus der unorganischen Experimentalchemie", (1920), p. 166.

ethanol and dissolution of resulting manganese dioxide followed by recrystallization. For the removal of iron impurity, the permanganate was dissolved in water containing a small amount of aluminum sulfate followed by the precipitation of aluminum hydroxide with aqueous ammonia.

*Standard Iron Solution.* — A solution containing 2 mg. of iron per milliliter was made by dissolving ammonium ferric sulfate in 0.1 N hydrochloric acid. The iron concentration was checked titrimetrically with a standard permanganate solution after the reduction of iron by stannous chloride. The iron solution was appropriately diluted in time for use.

*Nitroso R Salt Solution.* — 0.500 g. of the reagent was dissolved in 100 ml. of water.

*Buffer Solution.* — A 4.00 M solution of recrystallized sodium acetate.

*Hydroxylamine Sulfate Solution.* — 5.00 g. of the salt was dissolved in 100 ml. of water.

*Manganese Solution.*—A 0.2 M solution of manganese chloride.

*Ammonium Carbonate Solution.*—A 0.1 M solution was made by dissolving the salt in 0.3 N aqueous ammonia followed by standing over night and filteration.

*Acidified Hydroxylamine Solution.*—Three parts of the hydroxylamine sulfate solution were mixed with 1 part of 6 N hydrochloric acid.

**Method.** — The absorptiometric determination of iron was made as follows unless otherwise stated: a test solution was taken in a 25 ml. volumetric flask and neutralized with dilute aqueous ammonia either against a drop of a methyl orange indicator solution or till just before the precipitation of iron. Two milliliters of 0.1 N hydrochloric acid and 1.0 ml. of the hydroxylamine sulfate solution were added and the liquid was swirled well followed by dilution to about 20 ml. Two milliliters each of the reagent solution and the buffer solution were added in the order with stirring. The liquid was diluted to the mark. The flask was immersed in boiling water for about 10 min. followed by cooling to room temperature with running water. The intensity of the resulting color was measured at 715 and 650 mμ., the wavelength widths being 1.0 mμ.

The coprecipitation of iron with manganese dioxide was made as follows unless otherwise stated: to a test solution, 10 ml. of the manganese solution was added and the solution was diluted to about 100 ml. Ten milliliters of the ammonium carbonate solution was added. Five milliliters of about 3% hydrogen peroxide was added with stirring and the solution was heated on a boiling water bath for 30 to 40 min. The resulting precipitate was centrifuged at 3,000 r. p. m. for 10 min. followed by washing with about 15 ml. of water. It was dissolved in 5 ml. of the acidified hydroxylamine solution. The resulting solution was transferred into a quartz dish and evaporated on a water bath till dryness. The residue was taken with 2.0 ml. of hot 0.1 N hydrochloric acid and transferred into a 25 ml. volumetric flask for the determination of iron.

## Results and Discussion

In the following discussions, a deviation within 2% was allowed.

**Adjustment of Acidity and Effect of Diverse Ions.**—An optimum pH-range for the full color development was reported by the present author[3] to be 5.3 to 6.5. The acidity of a test solution, which contains 0.5 to 4.0 ml. of 0.1 N hydrochloric acid can be satisfactorily adjusted within the optimum range by the addition of 2.0 ml. of the buffer solution.

Griffing and Mellon[6] reported the effect of many diverse ions. The present results obtained with several ions are shown in Table I. According to the previous workers, vanadium-(V) interferes strongly because of its color formation. The present result, however does not indicate any interference with the color intensity of iron complex by the presence of at least 10 p. p. m. of the ion. Manganese(II) gives an absorption band around 440 mμ. The strong effect of an increased amount of the reagent or the metal ion on the intensity of the band suggests that the manganese(II) complex formed is unstable. The instability of the complex permits the presence of a large amount of the metal ion without interference in the color development of iron. An intense red color of cobalt(III) complex, which has disappeared by the heating for completion of the color reaction of iron, gradually appears again when the solution is left to stand. Fortunately, the red complex does not give absorption at 715 mμ. Because of the high stability of the red complex, however, the use of increased amounts of the reagent is required for the full color development of iron. Uranium(VI) does not give any absorption in long wavelength region. The presence of a very large amount of the ion is thus permitted. This is parallel with Nageswara Rao and

TABLE I. EFFECT OF DIVERSE IONS ON THE DETERMINATION

Each test solution contains 2.00 p. p. m. of iron at the final concentration.

| Diverse ions* added, p. p. m. | | Errors, % 715 mμ | Errors, % 600 mμ | Amounts of the reagent soln. used, ml./25 ml. |
|---|---|---|---|---|
| Sodium | 4,600 | −0 | 1 | 2.00 |
| Vanadium(V) | 10 | 1 | 0 | 2.00 |
| Manganese(II) | 835 | 2 | 12 | 2.00 |
| Cobalt(II) | 10 | 2 | 45 | 4.00 |
| Nickel | 10 | 2 | 9 | 2.00 |
| Uranium(VI) | 4,760 | 1 | 5 | 2.00 |

* Added as sodium chloride, ammonium metavanadate, manganese chloride, nickel nitrate and uranyl nitrate, respectively.

6) M. Griffing and M. G. Mellon, *Anal. Chem.*, **19**, 1014 (1947).

Raghava Rao's results[7] on the reaction of uranyl ion with the reagent.

**Removal of Diverse Ions by Coprecipitation of Iron with Manganese Dioxide.** — Dean and Lady[8] selectively decomposed colored complexes of diverse ions with hydrazine under a carefully controlled condition without affecting the color intensity of the iron complex. Very recently, Ishii[9] extracted iron with tributyl phosphate for absorptiometric determination of iron impurity in uranium metal with 1, 10-phenanthroline. The present author coprecipitated iron with manganese from an ammoniacal carbonate solution leaving the diverse ions as well as uranium in the solution. The manganese was precipitated as dioxide by the oxidation of manganese(II) ion. The method is simple and appropriate for the extraction of iron out of sample solutions which contain "concentrated" uranium. Coprecipitation of iron with aluminum hydroxide was found unsuitable for the present purpose because of the resistance of the precipitate to dissolution in a dilute acid and of possible precipitation of aluminum hydroxide at the stage of the color development of the iron.

*Coprecipitation of Iron.*—Figure 1 shows the completeness of the coprecipitation of iron with 1.2 mg. of manganese. Increases in the blank absorption at 715 and 600 m$\mu$. may be attributed to iron impurity in the reagents used. Figure 2 shows the amounts of manganese required for complete precipitation of iron. It also indicates that 2 ml. of bromine water may be used as an oxidizing agent instead of hydrogen peroxide when the solution is boiled for 10 to 15 min. Hydrogen peroxide, however, is superior to bromine water because the former gives a well coagulated precipitate by warming on a water bath. Three milliliters of 3% hydrogen peroxide is sufficient for complete precipitation of manganese(II) ion. Precipitation of manganese by the reduction of permanganate[10] with formate, sulfite or ethanol[11] was found unsuitable for the present purpose because of difficulty in the collection of a very fine precipitate formed.

Filteration of the precipitate by a filter paper is unsuitable because of possible contamination with foreign iron from the filter. The amounts of iron impurity found in the Toyo, No. 5B (7 cm.) were 0.6 to 2.6 $\mu$g. per each filter. The precipitate is dissolved in the acidified hydroxylamine solution with ease. The minimum amount of the solvent required to dissolve the precipitate is 1.25 ml. A hot hydrogen peroxide solution containing hydrochloric or sulfuric acid, as the solvent, is inferior to the former.

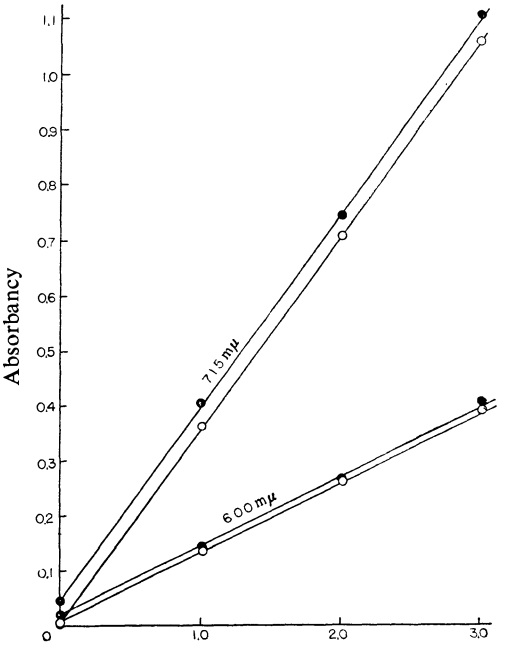



Fig. 1. Amounts of iron and color intensity. The final volume was 25 ml. ○, coprecipitation was not made; ●, coprecipitation with 1.2 mg. of manganese was made.

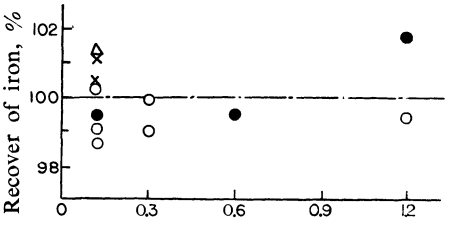



Fig. 2. Amounts manganese and recovery of iron by the coprecipitation.

Amounts of iron taken are: ●, 50 $\mu$g. (oxidation with bromine water); △, 25 $\mu$g.; ○, 50 $\mu$g. and ×, 75 $\mu$g.

*Separation of Iron from Diverse Ions.* — Results shown in Table II indicate that the separation by this method is effective to eliminate the diverse ions. One fourth milligram of platinum associated with uranium is satisfactorily removed from iron (cf. No. 5 in Table

7) M. Nageswara Rao and Bh. S. V. Raghava Rao, Z. *Anal. Chem.*, **142**, 161 (1954).
8) J. A. Dean and J. H. Lady, *Anal. Chem.*, **23**, 1096 (1951).
9) D. Ishii, *Japan Analyst* (*Bunseki Kagaku*), **9**, 693 (1960).
10) H. N. Stokes and J. R. Cain, *J. Am. Chem. Soc.*, **29**, 409 (1907).
11) E. B. Sandell, "Colorimetric Determination of Traces of Metals", Interscience Publishers, New York (1950), p. 374.

TABLE II. ERRORS OF THE DETERMINATION AFTER THE PRELIMINARY SEPARATION

Each test solution contains 50.00 $\mu$g. of iron

| No. | Divers ions added, mg. | Errors, % | | Amounts of the reagent soln. used, ml./25 ml. |
|---|---|---|---|---|
| | | 715 m$\mu$ | 600 m$\mu$ | |
| 1 | Cu(II), 0.25 | −1 | −1 | 2.00 |
| | | 0 | 1 | 2.00 |
| | | −1 | −1 | 2.00 |
| 2 | Cr(VI), 0.25 | −0 | −2 | 2.00 |
| | | −0 | −1 | 2.00 |
| | | 2 | 1 | 2.00 |
| 3 | Co(II), 5.0 | −13 | −5 | 4.00 |
| 4 | Pt(VI), 2.0 | 12 | 19 | 2.00 |
| | | 12 | 18 | 2.00 |
| 5 | Pt(VI), 0.25; U(VI), 100 | −0 | −1 | 2.00 |
| | | −1 | −1 | 2.00 |
| | | −1 | −0 | 2.00 |
| 6 | Cu(II), V(V), P (phosphate), Cr(VI), Co(II) and Ni; 0.25 of each. U(VI), 100 | 0 | 4 | 2.00 |
| | | 0 | 21 | 2.00 |
| | | 0 | 17 | 2.00 |
| | | −0 | 30 | 4.00 |
| | | −0 | 32 | 4.00 |
| 7 | Cu(II), V(V), P(phosphate), Cr(VI), Co(II), Ni and Pt(IV); 0.25 of each. U(VI), 100 | 2 | 19 | 2.00 |
| | | 3 | 31 | 2.00 |
| | | 3 | 30 | 2.00 |

II) while the presence of the same amount of platinum associated with many diverse ions altogether tends to give a slight positive error (cf. No. 7). The removal of cobalt is not effective (cf. No. 3). Sixty five to seventy-one percent of the original cobalt was found in manganese dioxide precipitated from a solution containing 0.25 mg. of cobalt and 50 $\mu$g. of iron.

**Determination of Iron Impurity in Nuclear Grade Graphite and Urania-Graphite Fuel.** — Copper and Chromium, which may strongly interfere with the absorptiometry, are scarcely found in appreciable amounts in nuclear grade graphite. This enables us to apply the method to samples of the graphite without any preliminary separation. The method can be applied to samples of ordinary grade graphite in the same way because iron forms the greater part of the impurities in general. In this case, absorption at 600 m$\mu$. may be used to check the degree of interference by diverse impurities comparing the intensity of the absorption with that obtained at 715 m$\mu$. Preliminary separation is required in the case of urania-graphite fuel because of comparatively large amounts of impurities in the urania component.

*Sampling.*—Contamination with foreign iron should be avoided during the sampling of analytical specimens. The use of a drill tipped with a tungsten-cobalt alloy, G2[12], is suitable for the sampling from graphite blocks by drilling. In the author's experience, the weight loss of the drill was 1.2 mg. when 2 kg. of graphite was pulverized by the drilling while the loss of an alloyed steel drill was about 6 mg. (3 p. p. m. as to the graphite) under the same conditions. The average hardness of the graphite blocks used was 27.3 by Shore unit. Crashing with a press and pulverizing in an agate mortor may also be done.

*Contamination with Foreign Iron from Platinum Crucibles.* — It was said that[11] platinum wares contain iron impurity which may be dissolved out with hot acids, giving erroneous results in determinations of micro-amounts of iron. The present author evaporated 4 ml. each of 18 N sulfuric acid in platinum crucibles on a hot plate till dryness. The crucibles were cleaned by pyrosulfate fusion and immersion in 1 to 1 hydrochloric acid successively before use. Each residue was taken with 1 ml. of hot water followed by the determination of iron. Results are shown in Fig. 3. The amounts of iron extracted from the platinum crucibles do not depend on the fuming time. This was confirmed by a statistical treatment of the data. The average amount of the iron extracted is 1 $\mu$g. which is the same amount as that found in the sulfuric acid used. From the results, platinum crucibles cleaned carefully may be used for ashing of samples and fuming with sulfuric or perchloric acid. Porcelain crucibles, "SCP" Brand, may also be used. The above fuming test applied to the crucibles gave substantially

12) JIS, H 5501 (1953).

TABLE III. IRON IMPURITY IN GRAPHITE AND URANIA-GRAPHITE FUEL

| | Iron found, p. p. m. | | | | | |
|---|---|---|---|---|---|---|
| | Without the preliminary septn. | | | With the preliminary septn. | | |
| | 715 mμ | 600 mμ | Difference | 715 mμ | 600 mμ | Difference |
| Natural graphite | 151×10 | 158×10 | 7×10 | — | — | — |
| Nuclear grade graphite, A | 40.4 | 40.5 | 0.1 | — | — | — |
| B | 24.4 | 26.2 | 1.8 | — | — | — |
| C | 5.4 | 7.0 | 1.6 | 5.3 | 5.4 | 0.1 |
| Urania-graphite fuel, A | 47.0 | 60.2 | 13.2 | 59.4 | 59.1 | 0.3 |
| B | 32.0 | 41.9 | 9.9 | 52.1 | 51.6 | 0.5 |

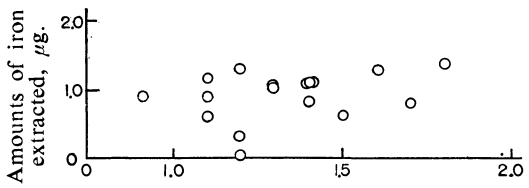



Fig. 3. Fuming time and amounts of iron extracted from platinum crucibles
Capacity of platinum curcibles, 30 ml.; 18 N sulfuric acid, 4.00 ml.; heated on a hot plate.

the same results as those obtained in the case of the platinum crucibles.

*Recommended Procedure.* — Five grams of a graphite sample is ashed in a platinum crucible at about 800°C. Washed oxygen gas may be introduced into the furnace, if necessary. The ash is treated with 2 ml. of 6 N hydrochloric acid on a water bath and evaporated to dryness. The ash dissolves during the evaporation. Colored insoluble matter, if any, should be completely dissolved with the aid of 1 ml. of hydrofluoric acid followed by fuming with 1 ml. of perchloric or sulfuric acid till dryness. The resulting residue is taken with 10 ml. of 0.1 N hydrochloric acid. The solution is diluted to 50.00 ml. Ten milliliter portions of the test solution are taken in a 25 ml. volumetric flask. One milliliter of the hydroxylamine sulfate solution is added and the determination is made as described in the section "Experimental", the color intensity being measured at 715 mμ. For the preparation of the working curve a set of standard iron solutions containing 0, 1, 2 and 3 p. p. m. at the final concentrations is used.

The amount of a sample to be taken may be reduced to less than 1 g. depending on the content of iron impurity in the sample when the whole of the test solution is used for the color development. The author, however, recommends the use of 5 g. of a sample, which contains a very small amount of iron impurity, to reduce errors due to contamination and segregation of the iron impurity. The lower limit of the determination may be expected to be 2 p. p. m.

In the case of samples of urania-graphite fuel, the coprecipitation of iron should be made as described in the section "Experimental." In this case, the fuming with perchloric acid is made prior to the coprecipitation to convert chromium impurity into chromate ion. Blank tests are required when either or both the fuming and the coprecipitation are carried out.

Iron impurities in several samples determined by the method are shown in Table III. Results obtained at 600 mμ. are also shown for comparison. In the case of samples of the urania-graphite fuel, low results were obtained when the removal of diverse ions was ommitted. They are thought to be due to the consumption of the reagent by large amounts of diverse ions present.

## Summary

An absorptiometric determination of micro-amounts of iron with nitroso R salt was satisfactorily applied to the routine analysis of nuclear grade graphite. An ashed sample is brought into a solution and the color of iron is developed by the reagent with the aid of hydroxylamine sulfate. Adjustment of pH to the optimum range is easily made by the addition of a definite amount of an acetate buffer. The intensity of the color is measured at 715 mμ. The range of the determination covers 2 to 75 p. p. m. when 1 g. of a sample is taken, the final volume being 25 ml. In the case of a sample of urania-graphite fuel, the ash is fumed with perchloric acid and a preliminary separation is made by coprecipitation with manganese dioxide which is produced by the oxidation of manganese(II) ion with hydrogen peroxide in a hot ammoniacal carbonate solution. The recovery of

iron is quantitative and the removal of diverse ions is satisfactory. All of the uranium is also removed here. Contamination with foreign iron from a drill used for sampling and from the platinum or percelain crucibles used is negligible. The effect of diverse ions on the absorptiometry was also examined.

The author is indebted to Mr. H. Nihei and Miss Fukamachi for their experimental work. Acknowledgment is made to Drs. K. Ono and Y. Oka, Professors of Tohoku University, for their encouragement and also to Tokai Electrode Mfg. Co. Ltd. for their permission to publish the results.

*Technical Research Laboratory*
*Tokai Electrode Mfg. Co. Ltd.*
*Fujisawa-shi, Kanagawa-ken*

# *Photochemical Processes due to n-π* and π-π* Transitions of 2-Picoline N-Oxide in the Vapor Phase*

By Norisuke HATA*1

(Received February 8, 1961)

As reported in the previous paper[1], the main photolytic product of pyridine *N*-oxide due to irradiation by 3261 or 2537 Å was pyridine in both cases. We observed a remarkable difference in the relation between the quantum yield of pyridine produced and the temperature.

In the case of 2-picoline *N*-oxide, however, it may be expected that the introduction of a methyl group in the 2-position of the pyridine ring might cause photochemical behavior different from that of pyridine *N*-oxide. In order to investigate the effect of 2-methyl substitution on the photolysis of pyridine *N*-oxide, the present author carried out the gaseous photolysis of 2-picoline *N*-oxide by irradiating with the 3261 Å (Cd $^3P_1$) or 2537 Å (Hg $^3P_1$) resonance line, which corresponds to absorption due to an $n$-$\pi^*$ or a $\pi$-$\pi^*$ transition of this substance, respectively. It was found from this experiment that 2-picoline *N*-oxide undergoes a photochemical rearrangement to isomerize to 2-pyridinemethanol at 3261 Å and a fission of N→O bond to produce 2-picoline at 2537 Å.

## Experimental

The 2-picoline *N*-oxide used in this experiment was prepared by the method described by Ochiai and purified by vacuum distillation several times[2]. B. p., 105~106°C/4 mmHg.

A pyrex cadmium resonance lamp was used as a light source for the photolysis in the $n$-$\pi^*$ absorption region, while a quartz mercury resonance lamp was used in the $\pi$-$\pi^*$ absorption region, and these lamps were those used for the photolysis of pyridine *N*-oxide.

The gaseous photolysis of 2-picoline *N*-oxide was carried out by a procedure similar to that of pyridine *N*-oxide described in the previous paper[1]. Photolytic products were also divided into fractions A, B, C and D just as those of pyridine *N*-oxide, where

Fraction A: Gaseous product not condensed at −196°C (liquid nitrogen).

Fraction B: Gaseous product condensed at −196°C and not condensed at −95°C (liquid nitrogen in methanol).

Fraction C: Liquid product condensed at −95°C and not condensed at −75°C (dry ice in methanol).

Fraction D: Dark brown polymer.

The pressures of fractions A and B were each measured with a Toepler-gauge, and analyzed by using a mass-spectrometer and a low-pressure gas-chromatograph (column: benzyl ether). The analysis of fraction C was done with a Shimadzu quartz spectrophotometer QB-50 and also a Shimadzu gas-chromatograph GC-1A (column: cetyl alcohol). The analysis of fraction D was not carried out.

## Results and Discussion

The ultraviolet absorption spectra of several methylpyridine *N*-oxides have been measured in polar solvents by Ikekawa et al.[3], where they discussed a relation between the maximum of $\pi$-$\pi^*$ absorption and the position of the methyl group in the pyridine ring. The author has also observed a weak shoulder absorption

*1 Present address: Tokyo Electrical Engineering College, Kanda, Chiyoda-ku, Tokyo.

1) N. Hata *J. Chem. Phys.*, in press.

2) E. Ochiai, *J. Org. Chem.*, **18**, 534 (1953),

3) N. Ikekawa and Y. Sato, *Pharm. Bull.*, **2**, 400 (1954).

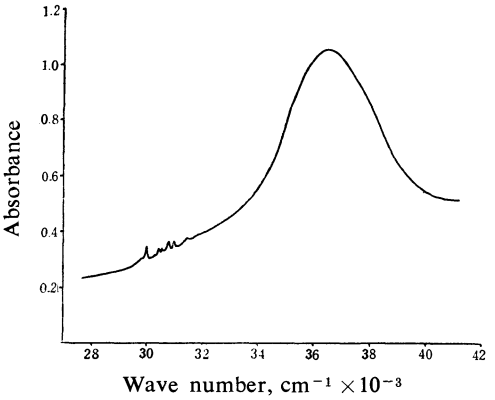



Fig. 1a. Vapor spectrum of 2-picoline *N*-oxide at room temperature. (Absorption region due to $n$-$\pi^*$ and $\pi$-$\pi^*$ transition.)

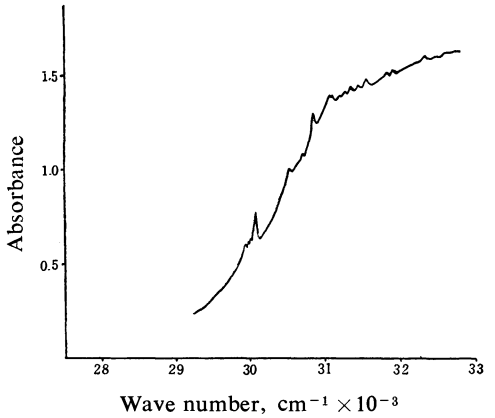



Fig. 1b. Vapor spectrum of 2-picoline *N*-oxide at 80°C. (Absorption region due to $n$-$\pi^*$ transition.)

with three isomeric picoline *N*-oxides in a non-polar solvent and in the vapor[4]. The absorption was regarded as due to an $n$-$\pi^*$ transition. Figure 1 shows the vapor spectrum of 2-picoline *N*-oxide which was measured with a Cary recording spectrophotometer 14 M*[2].

As described in the experimental part, the photolytic products at 3261 or 2537 Å irradiation were divided into fractions A, B, C and D. Fraction A was mainly hydrogen but included a small amount of oxygen, and fraction B was identified as carbon dioxide. Fraction C obtained as a liquid product was 2-pyridinemethanol at 3261 Å irradiation, whereas it was 2-picoline in the case of 2537 Å irradiation. The experimental results were expressed as quantum yields of fractions A, B and C at different temperatures as shown in Figs. 2 and 3.

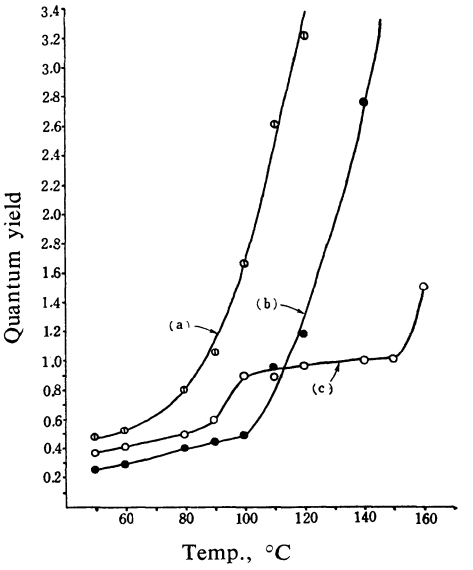



Fig. 2. Quantum yields of products versus temperature in the case of 2537 Å irradiation.
(a) —◑—: Fraction A
(b) —●—: Fraction B
(c) —○—: Fraction C

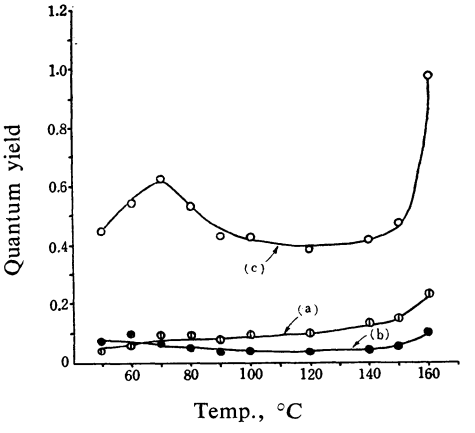
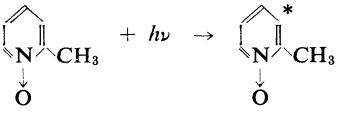


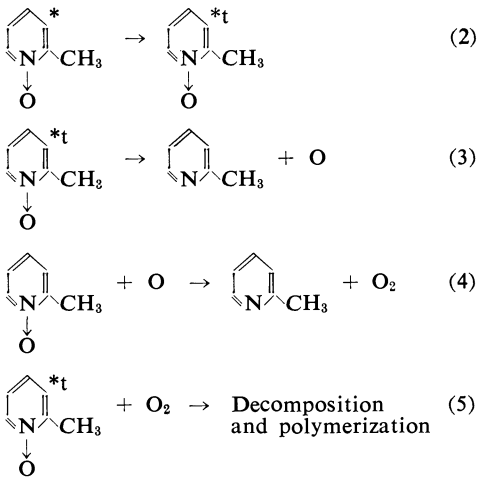

Fig. 3. Quantum yields of products versus temperature in the case of 3261 Å irradiation.
(a) —◑—: Fraction A
(b) —●—: Fraction B
(c) —○—: Fraction C

The processes succeeding to a $\pi$-$\pi^*$ transition of 2-picoline *N*-oxide may be expressed as follows, assuming that the excited molecule passes through a triplet state as in the case of pyridine *N*-oxide[1]. That is,




(1)

4) N. Hata, This Bulletin, to be published.
*2 The spectral measurement was performed by Dr. A. Kuboyama, to whom the author's thanks are due.



(2)

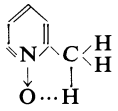
(3)

(4)

(5)

(* and *t denote the excited singlet and triplet states, respectively.)

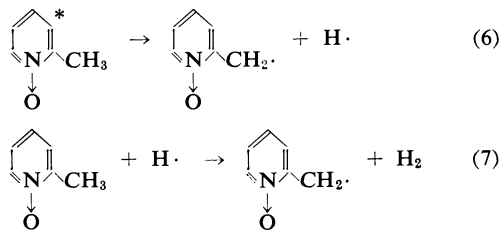
Fig. 2 indicates how the quantum yield of each photolytic product at 2537Å irradiation changes with temperature. Although the quantum yield of fraction C (2-picoline) is 0.4~0.5 at low temperatures, it increases steeply at about 90°C to a saturated value (0.9~1.0) at temperatures above 100°C. (Such a temperature dependence of the quantum yield has not been observed in the case of pyridine *N*-oxide at 2537Å irradiation, in which case the quantum yield of pyridine produced did not change substantially with temperature.) This observation suggests that an activation energy would be required for the production of 2-picoline. This may be interpreted qualitatively as follows. Excited 2-picoline *N*-oxide, due to a $\pi$-$\pi^*$ transition, presumably passes into a triplet state crossing with the excited singlet state to dissociate to 2-picoline and atomic oxygen in a predissociative manner as in the case of pyridine *N*-oxide (cf. Fig. 3 in Ref. 1). Since, for the pyridine *N*-oxide[1] or 3-picoline *N*-oxide[5] which does not possess a methyl group in the 2-position of the pyridine ring, the quantum yield of fraction C is independent on the temperature, the temperature dependence observed in the case of 2-picoline *N*-oxide must be associated with the interaction between the methyl group and the N→O group. The N→O bond energy of 2-picoline *N*-oxide is approximately the same as in pyridine *N*-oxide, i. e. ca. 110 kcal. $mol^{-1}$, although it may be smaller than 110 kcal. $mol^{-1}$ owing to the decrease of N→O double bond character caused by the hyperconjugative effect of 2-methyl group. Therefore, the process 3, by which the excited triplet 2-picoline *N*-oxide dissociates to 2-picoline and atomic oxygen, possibly does not need an activation energy. Thus, process 4 which is the alternative reaction producing 2-picoline is probably influenced by the interaction between the 2-methyl group and the N→O group. Investigation of the ultraviolet absorption spectrum of 2-picoline *N*-oxide[3,4], suggests the formation of a weak hydrogen bond between the methyl group and N→O group as shown in A. Such a weak



(A)

hydrogen bond formation may bring about a retarding effect for process 4 at low temperatures. Since the hydrogen bond is broken by the thermal perturbation caused by the increasing temperature, however, the abstraction reaction 4 would be facilitated by increasing temperature. Therefore, it is expected that the quantum yield of 2-picoline may rapidly increase to become about twice the value at low temperature. Figure 2 indicates distinctly the existence of such a tendency. The activation energy necessary for the production of 2-picoline estimated from the temperature-dependence of the quantum yield is about 1.1 kcal. $mol^{-1}$.

2-Picoline *N*-oxide gives rise also to substantial amounts of hydrogen upon irradiation with 2537Å, where the quantum yield increases remarkably with rising temperature as shown in Fig. 2. This is probably due to a participation of the following processes in addition to the process 5.



(6)

(7)

Although $D(CH_2\text{-}H)$ in 2-picoline *N*-oxide is not known, it is reasonable to assume processes 6 and 7, since the gaseous photolysis of toluene produces hydrogen[6].

In addition to processes 6 and 7, the production of fractions A, B and D probably resulted from the process 5 between excited 2-picoline *N*-oxide and oxygen produced by process 4 as in the case of pyridine *N*-oxide. To confirm the correctness of this reaction the gaseous photolysis was attempted for the mixture of 2-picoline *N*-oxide and oxygen, expecting that the 2-picoline would decrease and other products

5) N. Hata, This Bulletin, **34**, 1444 (1961).

6) R. R. Hentz and M. Burton, *J. Am. Chem. Soc.*, **73**, 536 (1953); G. Porter, *Chem. Soc. (London), Spec. Publ.* p. 139, No. 9 (1957).

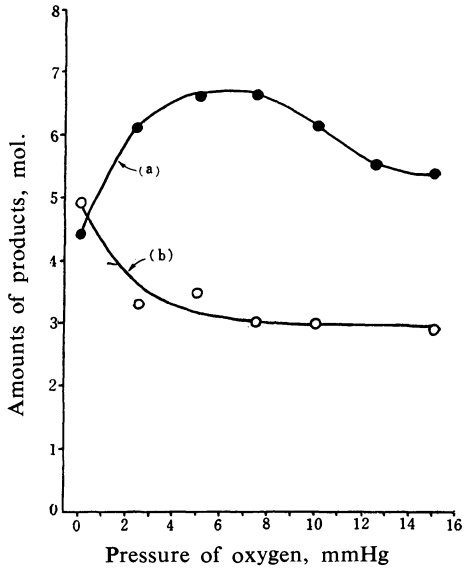



Fig. 4. Amounts of products versus oxygen pressure in the photolysis for the mixture of 2-picoline *N*-oxide and oxygen at 2537 Å (irradiation time: 10 min., temperature: 90°C).
(a) —●—: Fraction B
(b) —○—: Fraction C

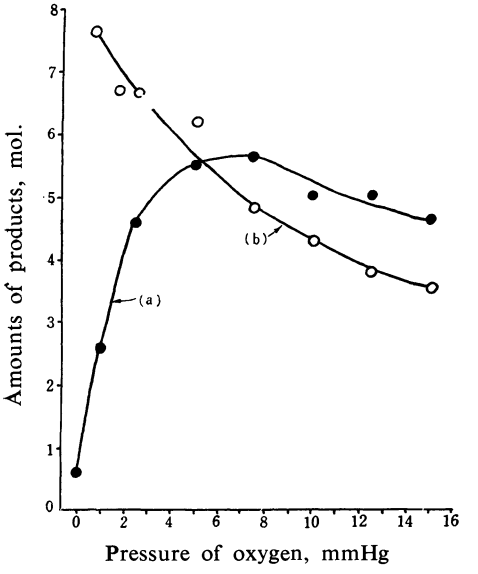
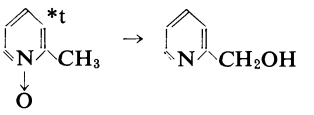



Fig. 5. Amounts of products versus oxygen pressure in the photolysis for the mixture of 2-picoline *N*-oxide and oxygen at 3261 Å (irradiation time: 2 hr., temperature: 70°C).
(a) —●—: Fraction B
(b) —○—: Fraction C

would increase with increasing oxygen pressure. The experimental results are expressed as amounts of fractions B (carbon dioxide) and C (2-picoline) in the decomposed products under the different pressures of oxygen. The results support clearly the occurence of process 5 described above.

In the case of 3261 Å irradiation ($n$-$\pi^*$ transition), 2-picoline *N*-oxide isomerizes to 2-pyridinemethanol by a rearrangement of the oxygen atom of N→O group to the methyl group as shown in process 8 and the production of fractions A, B and D were very small.




(8)

As seen from Fig. 3, the quantum yield of fraction C shows a maximum value at about 70°C and approximate temperature-independence at temperatures greater than 100°C. The fact that the quantum yield is affected by changes in temperature seems to indicate that process 8 requires some activation energy. Its activation energy estimated from the quantum yield and the temperatures*3 is about 3.4 kcal. $mol^{-1}$. This production of 2-picoline from its *N*-oxide at 3261 Å irradiation requires, presumably, an activation energy of about 11～12 kcal. $mol^{-1}$, considering the fact that the activation energy for the production of pyridine[1] or 3-picoline[5] from its *N*-oxide is about 11～12 kcal. $mol^{-1}$. Since the activation energy necessary for the photoisomerization of 2-picoline *N*-oxide to 2-pyridinemethanol is estimated to be about 3.4 kcal. $mol^{-1}$, however, the excited triplet molecule resulting from 3261 Å irradiation may largely undergo process 8 involving a smaller potential barrier than that for the N→O bond split.

If the photochemical behavior due to $n$-$\pi^*$ transition is only the rearrangement process described above, its products should be 2-pyridinemethanol alone. However, the fact that small amounts of decomposed and polymerized products are detected in the products as seen in Fig. 3 seems to indicate that processes 3—7 occur simultaneously with process 8. The experimental results of the photolysis for the mixture of constant amounts of 2-picoline *N*-oxide and different pressures of oxygen suggest that the above assumption is reasonable. That is, as seen from Figs. 4 and 5 the fact that fraction B increases rapidly and fraction C decreases with increasing pressures of oxygen

*3 The quantum yield of 2-pyridinemethanol (fraction C) decreases at temperatures above 80°C, which may probably be ascribed to the increase of quenching of the excited molecule with increasing pressures of 2-picoline *N*-oxide. Therefore, the calculation of the activation energy necessary for the production of 2-pyridinemethanol was performed by using some of the quantum yields at temperatures below 80°C.

may be regarded as evidence for the reaction between excited 2-picoline *N*-oxide and oxygen.

**Summary**

The gaseous photolysis of 2-picoline *N*-oxide was carried out by irradiation with the 3261 Å (Cd $^3P_1$) or 2537 Å (Hg $^3P_1$) resonance lines corresponding to an $n$-$\pi^*$ or a $\pi$-$\pi^*$ absorption of this substance, respectively.

In the case of 3261 Å irradiation, the major product was 2-pyridinemethanol, whose quantum yield showed a marked temperature-dependence. The activation energy necessary for the production of 2-pyridinemethanol was estimated to be about 3.4 kcal. mol$^{-1}$.

On the other hand, the photolytic products at 2537 Å irradiation were 2-picoline and other decomposition products and polymers. The quantum yield of 2-picoline showed a marked temperature-dependence, which may be attributed to the interaction between the 2-methyl group and the N→O group. The activation energy necessary for the production of 2-picoline was estimated to be about 1.1 kcal. mol$^{-1}$.

In conclusion, the author wishes to express his hearty thanks to Professor Ikuzo Tanaka for his kind guidance and encouragement. Thanks are also due to Mr. Y. Mori and Dr. K. Naiki for their helpful discussions during the course of this work.

*Laboratory of Physical Chemistry*
*Tokyo Institute of Technology*
*Meguro-ku, Tokyo*

# *Photochemical Processes due to n-π* and π-π* Transitions of 3-Picoline N-Oxide in the Vapor Phase*

By Norisuke HATA*1

(Received February 15, 1961)

The photochemical reactions caused by an $n$-$\pi^*$ or a $\pi$-$\pi^*$ transition of pyridine *N*-oxide and 2-picoline *N*-oxide were previously studied in the vapor phase[1,2], by irradiating with the 3261 Å (Cd $^3P_1$) or 2537 Å (Hg $^3P_1$) resonance line, respectively. As reported in the previous paper[2], the introduction of the 2-methyl group in pyridine *N*-oxide strongly influences the photochemical behavior of pyridine *N*-oxide both in $n$-$\pi^*$ and $\pi$-$\pi^*$ transitions. However, it is considered that the photochemical reactions of 3-picoline *N*-oxide are similar to those of pyridine *N*-oxide, because the hyperconjugative effect and also the interaction with the N→O group could be neglected with the 3-methyl group. Therefore, the present author has attempted the gaseous photolysis of 3-picoline *N*-oxide by irradiation with 3261 Å (Cd $^3P_1$) and 2537 Å (Hg $^3P_1$) resonance lines, each of which corresponds respectively to the absorption region due to an $n$-$\pi^*$ or a $\pi$-$\pi^*$ transition of 3-picoline *N*-oxide.

## Experimental

The synthesis of the 3-picoline *N*-oxide used in this experiments was done by a method similar to that of pyridine *N*-oxide*2. The product was purified by vacuum distillation several times[3]. B. p., 123°C/5 mmHg.

The light sources employed for the photolysis in the $n$-$\pi$ or $\pi$-$\pi^*$ absorption region were a pyrex cadmium resonance lamp or a quartz mercury resonance lamp, respectively, which were used in the case of pyridine *N*-oxide[1] and 2-picoline *N*-oxide[2].

Since the experimental methods are similar to those of pyridine *N*-oxide and 2-picoline *N*-oxide as reported in a previous paper[1], the description of the experimental techniques are omitted in this paper. The photolytic products were divided into fractions A, B, C and D just as in the photolysis of pyridine *N*-oxide or 2-picoline *N*-oxide, where

Fraction A: Gaseous products not condensed at −196°C (liquid nitrogen).

Fraction B: Gaseous products condensed at −196°C and not condensed at −95°C (liquid nitrogen in methanol)

Fraction C: Liquid products condensed at −95°C and not condensed at −75°C (dry ice in methanol).

Fraction D: Dark brown polymers.

The pressures of fractions A and B were each measured with a Toepler-gauge, and analyzed by using a mass-spectrometer and a low pressure gas-chromatograph (column: benzyl ether). The analysis of fraction C was done with a Shimadzu

*1 Present address: Tokyo Electrical Engineering College, Kanda, Chiyoda-ku, Tokyo.

1) N. Hata and I. Tanaka, *J. Chem. Phys.*, in press.

2) N. Hata, This Bulletin, **34**, 1440 (1961).

3) E. Ochiai, *J. Org. Chem.*, **18**, 534 (1953).

*2 The 3-picoline used in the synthesis of 3-picoline *N*-oxide was supplied by Dr. T. Kubota, to whom the author's thanks are due.

quartz spectrophotometer QB-50 and also a Shimadzu gas-chromatograph (column: cetyl alcohol). The analysis of fraction D was not carried out.

## Results and Discussion

3-Picoline *N*-oxide has two absorption systems in the region of the near ultraviolet both in the solution of a non-polar solvent and in the vapor[4]. Figure 1 shows the absorption curves of 3-picoline *N*-oxide in the vapor phase, which was measured with a Cary recording spectrophotometer 14 M*[3]. As seen from Fig. 1, there are two absorption regions between 28000 and 40000 $cm^{-1}$, one of which is the weak absorption at about 30000 $cm^{-1}$ and the other a stronger absorption at about 35500 $cm^{-1}$. As will be described in a later paper[4], the weak absorption at the longest wavelength which consists of sharp vibrational structures having an O–O band at 29368 $cm^{-1}$ corresponds to the $n$-$\pi^*$ absorption due to an excitation of non-bonding electrons localized on the oxygen atom to the antibonding $\pi$-orbital. On the other hand, the strong absorption having its absorption maximum at about 35703 $cm^{-1}$ is considered to be due to a $\pi$-$\pi^*$ transition.

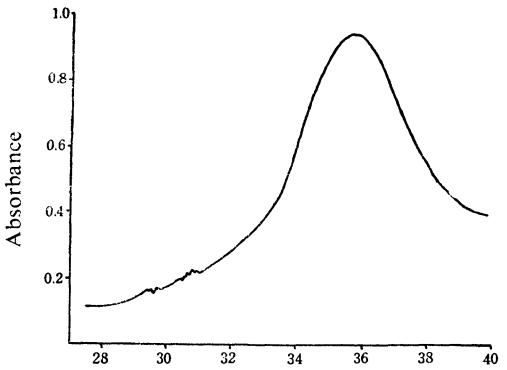



Fig. 1a. Vapor spectrum of 3-picoline *N*-oxide at 70°C. (Absorption region due to $n$-$\pi^*$ and $\pi$-$\pi^*$ transitions.)

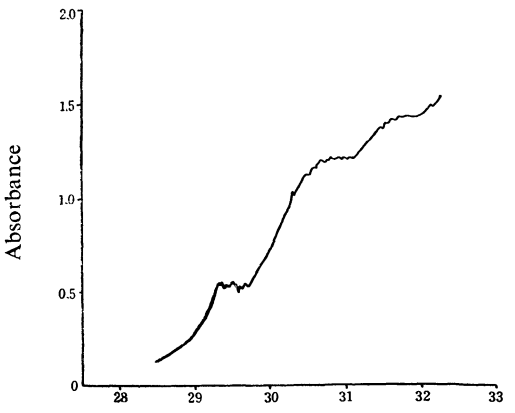



Fig. 1b. Vapor spectrum of 3-picoline *N*-oxide at 100°C. (Absorption region due to $n$-$\pi^*$ transition.)

As described in the experimental part, the photolytic products due to irradiation with 3261 or 2537 Å were divided into fractions A, B, C and D. Fraction A was largely hydrogen, although small amounts of oxygen were detected in this fraction. Fraction B was identified as carbon dioxide. Fraction C, obtained as a liquid product, was 3-picoline. The experimental results were expressed as the quantum yield of fractions A, B and C at different temperatures as shown in Figs. 2 and 3. The quantum yields of the products at temperatures greater than 160°C were not shown in these figures, because the thermal decomposition of 3-picoline *N*-oxide occurs simultaneously with the photochemical decomposition at these higher temperatures.

The experimental results of the photolysis for 3-picoline *N*-oxide are summarized as follows.

*a) A Relation between the Quantum Yield of Fraction C (3-Picoline) and the Temperature.* —In the case of 3261 Å irradiation ($n$-$\pi^*$ transition), the quantum yield increases markedly at about 80~100°C, although it has a comparatively low value at temperatures below 80°C. A further increase of the temperature causes a decrease in the quantum yield to some extent. On the other hand, the quantum yield at 2537 Å irradiation ($\pi$-$\pi^*$ transition) is independent of the temperature, and has a value of about 0.55.

*b) A Relation between the Quantum Yield of Fraction A (Mainly Hydrogen) or Fraction B (Carbon Dioxide) and the Temperature.* — The quantum yields of fractions A and B increase continuously with rising temperature with both 3261 and 2537 Å irradiation.

*c)* In either case (i.e., 3261 and 2537 Å) comparatively greater amounts of fraction D (dark brown polymer) are obtained.

*d)* When the photolysis of a mixture of 3-picoline *N*-oxide and oxygen was carried out at different pressures of oxygen, the amount of fraction B markedly increased with increasing oxygen pressure, but that of fraction C decreased.

From the experimental results described above, it is concluded that the photochemical reaction of 3-picoline *N*-oxide is quite similar to that of pyridine *N*-oxide, but not to that

4) N. Hata, This Bulletin, to be published.

*3 The spectral measurement was performed by Dr. A. Kuboyama, to whom the author's thanks are due.

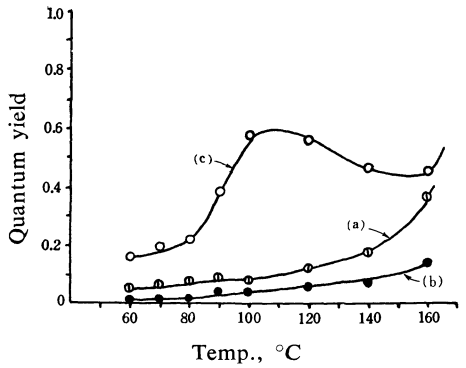



Fig. 2. Quantum yields of products versus temperature in the case of 3261 Å irradiation.
(a) —◑—: Fraction A
(b) —●—: Fraction B
(c) —○—: Fraction C

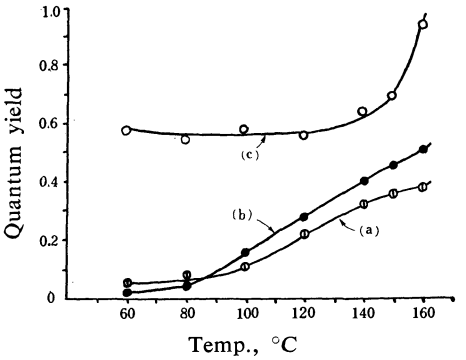
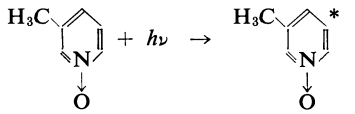
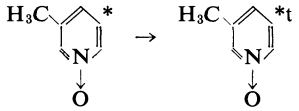
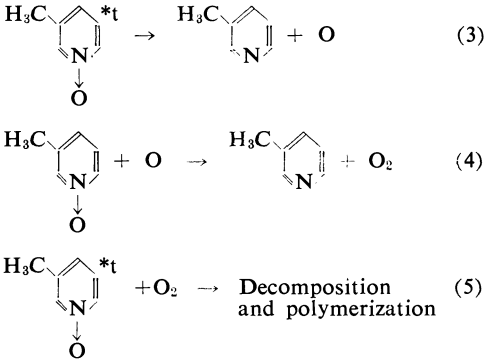



Fig. 3. Quantum yields of products versus temperature in the case of 2537 Å irradiation.
(a) —◑—: Fraction A
(b) —●—: Fraction B
(c) —○—: Fraction C

of 2-picoline *N*-oxide. This fact suggests that the hyperconjugative effect of methyl group or the interaction between N→O group and methyl group may be neglected in the photolysis of 3-picoline *N*-oxide. Therefore, it may be considered that the mechanism of the photochemical reaction of 3-picoline *N*-oxide would be similar to that of pyridine *N*-oxide. Thus, we assumed the following mechanism as the processes succeeding to an $n$-$\pi^*$ and a $\pi$-$\pi^*$ transitions of 3-picoline *N*-oxide.


(1)


(2)


(3)

(4)

(5) Decomposition and polymerization

(* and *t denote the excited singlet and triplet states, respectively.)

First the 3-picoline *N*-oxide molecule is excited to the corresponding excited singlet state due to an $n$-$\pi^*$ or a $\pi$-$\pi^*$ transition caused by an absorption of 3261 or 2537 Å radiation. (Cf. the schematic potential curves for pyridine *N*-oxide as depicted in Fig. 4 of Ref. 1 for the succeeding description). Such an excited molecule probably decomposes to 3-picoline and atomic oxygen in a predissociative manner, in which a triplet state crossing with the first excited state exists presumably as a short lived intermediate. As seen from Figs. 2 and 3, the quantum yield of 3-picoline at 3261 Å irradiation shows a remarkable temperature dependence as pointed out in the experimental results a, while at 2537 Å irradiation it is independent of the temperature. This fact means that activation energy would be required for the production of 3-picoline at 3261 Å, but not at 2537 Å. The activation energy necessary for the production of 3-picoline in the case of 3261 Å irradiation is about 11.5 kcal. $mol^{-1}$, which was estimated from the relation between the quantum yield of produced 3-picoline and the temperature, and this value coincides nearly with that of pyridine *N*-oxide. Of the processes 3 and 4, which are possibly the essential reactions producing 3-picoline, the process 3 might be the only reaction requiring an activation energy. If an appreciable activation energy is required for process 4, the quantum yield of 3-picoline must also depend on the temperature even at 2537 Å irradiation. (However, the experimental results do not show any temperature-dependence of the quantum yield of 3-picoline at 2537 Å irradiation). As reported in a previous paper for the case of 2-picoline *N*-oxide[2], the temperature-dependence of the quantum yield of 2-picoline observed at 2537 Å irradiation was attributed to the interaction between the 2-methyl group and the N→O group as one of the main factors. Therefore, in the case of 3-picoline *N*-oxide the experimental result obtained at 2537 Å irradiation

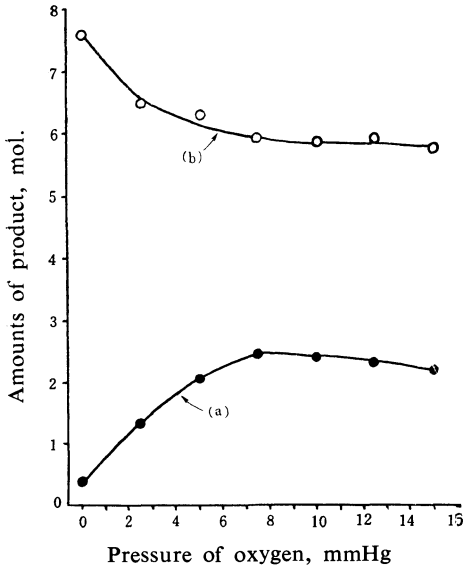



Fig. 4. Amounts of products versus oxygen pressure in the photolysis of mixtures of 3-picoline *N*-oxide and oxygen at 3261 Å (irradiation time: 2 hr., temperature: 100°C).
(a) —●—: Fraction B
(b) —○—: Fraction C

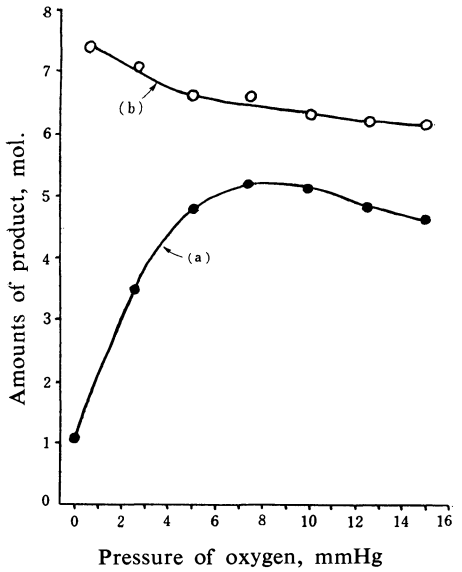



Fig. 5. Amounts of products versus temperature in the photolysis of mixtures of 3-picoline *N*-oxide and oxygen at 2537 Å (irradiation time: 10 min., temperature: 80°C).
(a) —●—: Fraction B
(b) —○—: Fraction C

(which is similar to that of pyridine *N*-oxide) supports the idea of the importance of the interaction between 2-methyl group and N→O group in the photolysis of 2-picoline *N*-oxide.

The results of the photolysis of mixtures of constant amounts of 3-picoline *N*-oxide and different pressures of oxygen are shown in Figs. 4 and 5 for the cases of 3261 and 2537 Å irradiations, respectively. These results indicate that the amounts of 3-picoline decrease and that of fraction B (carbon dioxide) increases with increasing oxygen pressure. This is regarded as evidence for the occurrence of the reaction 5 between the excited molecule and oxygen. In Figs. 4 and 5, the tendency for the amounts of products observed at oxygen pressures greater than about 7.5 mmHg to approach a saturated value may be ascribed to collisional deactivation of the excited molecule by oxygen with increasing pressures of oxygen.

## Summary

Gaseous photolysis of 3-picoline *N*-oxide was attempted by irradiation with the 3261 Å (Cd $^3P_1$) or 2537 Å (Hg $^3P_1$) resonance line corresponding to an $n$-$\pi^*$ or a $\pi$-$\pi^*$ absorption region, respectively, of this substance. In either case, the photolytic products were mainly 3-picoline, and we observed a remarkable temperature-dependence for the quantum yield of 3-picoline in the case of 3261 Å irradiation but not in the case of 2537 Å irradiation. This observation suggests that an activation energy would be required for the production of 3-picoline at 3261 Å only. The activation energy estimated from the relation between the quantum yield of produced 3-picoline and the temperature at 3261 Å irradiation was about 11.5 kcal. mol$^{-1}$, which is almost about the same value as that of pyridine *N*-oxide. The reactions succeeding to an $n$-$\pi^*$ or a $\pi$-$\pi^*$ transition of 3-picoline *N*-oxide were considered to be similar to the case of pyridine *N*-oxide.

In conclusion, the author wishes to express his hearty thanks to Professor Ikuzo Tanaka for his kind guidance and encouragement. Thanks are also due to Mr. Y. Mori and to Dr. K. Naiki for their helpful discussion during the course of this work.

*Laboratory of Physical Chemistry*
*Tokyo Institute of Technology*
*Meguro-ku, Tokyo*

# *Infrared Spectra of Acyclic Imides. IV. Effects of Alkali Halides on the Infrared Spectra of Diacetamide*

By Toyozo UNO, Katsunosuke MACHIDA and Ikuko HAMANAKA

(Received February 6, 1961)

Anomalies in the infrared spectra of some polar molecules in the alkali halide disk technique have often been reported[1]. In case of benzoic acid[2], potassium iodide disks have been recommended to obtain the same infrared spectra as those of pastes. On the other hand, molecules containing the -CONHCO- group such as succinimide[3], cyanuric acid[4] and barbituric acid[5], have been reported to undergo spectral changes depending on the method of preparation of samples. In the present paper, we will report that diacetamide ($CH_3$-CONHCO-$CH_3$), which has been revealed to exhibit dimorphism[6], also shows an analogous anomaly. An inversion of configuration of the -CONHCO- group is suggested to take place in the course of this spectral change. The ionic radii of the anions and the cations of alkali halides involved as well as the amount of water contained in the sample have been proved to influence the spectral change. The effect of compression in the disk technique has also been examined.

## Results and Discussion

**Alkali Halide Anomaly and Dimorphism of Diacetamide.** — The crystal of diacetamide in form A undergoes marked changes in infrared spectra on the addition of various alkali halides. This phenomenon was observed at first for potassium iodide, in the course of measurements in the disk technique. As reported in the preceding paper[6], diacetamide in form A shows two C=O stretching bands at 1734 and 1700 $cm^{-1}$, the stronger one being the band at 1700 $cm^{-1}$. This was always the case for Nujol or hexachlorobutadiene pastes. For potassium bromide disks however, both of these bands sometimes underwent changes in relative intensities so that the band at 1734 $cm^{-1}$ became the stronger one. In an attempt to prevent this spectral change, the use of potassium iodide as the matrix[2] was made to result in a marked spectral change of different type over the whole region measured.

On the other hand, another crystal form (form B) was found for diacetamide[6] and a close similarity in infrared spectra was observed between pastes of the form B and potassium iodide disks of form A. Furthermore, form A and form B were proved to involve the trans-cis and the trans-trans -CONHCO- group respectively, giving rise to infrared spectra markedly different from each other. Thus, the above fact concerning potassium iodide suggests that the configuration of the -CONHCO- group is changed from the trans-cis to the trans-trans configuration in the course of preparation of potassium iodide disks from form A. To confirm this, further investigations with the use of various alkali halides have been made and the following results have been obtained.

**Effects of Various Alkali Halides.** — *1) Potassium Iodide, Sodium Iodide and Sodium Bromide.*—The presence of these alkali halides gives rise to analogous changes in infrared spectra of the form A of diacetamide not only in the disk technique but also in the paste method. Here, the paste method means the technique in which the mixture of diacetamide in form A and one of potassium iodide, sodium iodide and sodium bromide (the molar ratio being approximately one to one) is mulled with Nujol or hexachlorobutadiene. It is seen from this fact that the primary factor for the spectral change is not in the disk technique itself but in the alkali halide used. By the application of the paste method, the effect of water adsorbed on alkali halides or other impurities can be made negligible since in this case the amounts of diacetamide and alkali halide are comparable to each other. Furthermore, the paste method is preferable to examine the corresponding spectral changes for diacetamide-*d* since the infrared spectra of highly pure diacetamide-*d* can be obtained only with a rapid technique such as the paste method. Considering these advantages of the paste method, we have carried out the measurements in the present study mainly on the

1) For example, see O. Amakasu and A. Ito. *J. Chem. Soc. Japan, Pure Chem. Sec.* (*Nippon Kagaku Zasshi*), **81**, 683 (1960). A number of literatures were cited in it.
2) V. C. Farmer, *Spectrochim. Acta*, **8**, 374 (1957).
3) A. W. Baker, *J. Phys. Chem.*, **61**, 453 (1957).
4) W. M. Padgett, II., J. M. Talbert and W. F. Hamner, *J. Chem. Phys.*, **26**, 959 (1957).
5) B. Cleverley and P. P. Williams, *Chem. & Ind.*, **1959**, 49.
6) T. Uno and K. Machida, This Bulletin, **34**, 545 (1961).

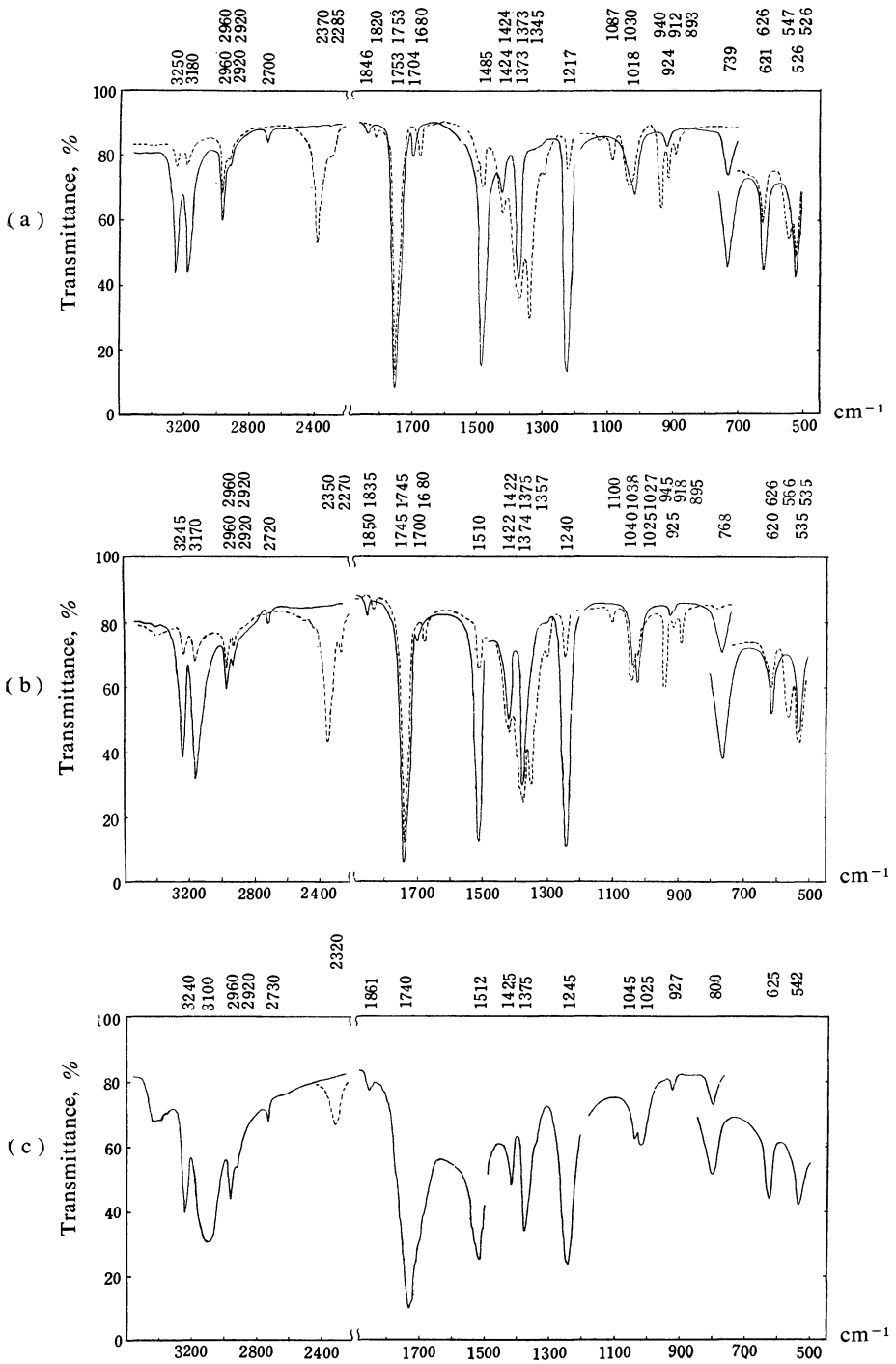



Fig. 1. Infrared spectra of diacetamide in the two-component systems containing alkali halides.

(a) Diacetamide-KI (3600～2200 $cm^{-1}$ and 1550～1200 $cm^{-1}$, hexachlorobutadiene paste; 1900～1550 $cm^{-1}$ and 1200～500 $cm^{-1}$, Nujol paste).

(b) Diacetamide-NaBr (3600～2200 $cm^{-1}$ and 1490～1200 $cm^{-1}$, hexachlorobutadiene paste; 1900～1490 $cm^{-1}$ and 1200～500 $cm^{-1}$, Nujol paste).

(c) Diacetamide-LiCl (3600～2200 $cm^{-1}$ and 1490～1200 $cm^{-1}$, hexachlorobutadiene paste; 1900～1490 $cm^{-1}$ and 1200～500 $cm^{-1}$, Nujol paste).

solid lines: undeuterated species.

broken lines: *N*-deuterated species.

pastes of the two-component systems of diacetamide and various alkali halides[7].

The infrared spectra of the two-component systems containing potassium iodide and sodium bromide are shown in Figs. 1, (a) and (b) respectively. It is obviously seen that these spectra resemble that of diacetamide in the form B[6]. These two-component systems show the sharp symmetric imide I band near 1750 $cm^{-1}$ as well as the weak but well resolved antisymmetric imide I band near 1700 $cm^{-1}$. The latter band has been supposed to be overlapped by the broad symmetric imide I band in the spectrum of the undeuterated species in form B[8]. Furthermore, the low-frequency shift of the antisymmetric imide I band on deuteration is obviously observed for these two-component systems. There is only a little difference in the corresponding characteristic frequencies between the system containing sodium iodide and that containing potassium iodide. The system containing sodium bromide shows however, the infrared spectrum in which some characteristic frequencies related mainly to the N-H bond are appreciably different from those observed for the systems containing iodides. The similarity in the infrared spectra between form B and the two-component system containing one of these alkali halides is also observed in the case of diacetamide-*d*.

*2) Potassium Bromide, Potassium Chloride and Sodium Chloride.*—The infrared spectrum of the two-component system consist of form A and one of these alkali halides is identical with that of form A. In other words, these alkali halides bring about no spectral change. The comparison of alkali halides described in 1 and 2 suggests that both the cation and the anion of alkali halides participate in the spectral change under consideration.

*3) Lithium Iodide, Lithium Bromide and Lithium Chloride.*—These lithium salts bring about the spectral change. Infrared spectra analogous to Figs. 1, (a) and (b) are obtained for the systems containing lithium iodide and lithium bromide respectively. The infrared spectrum of the system containing lithium chloride is shown in Fig. 1, (c), which is appreciably different from either (a) or (b) in the regions 3600 to 2000 $cm^{-1}$ and 1000 to 700 $cm^{-1}$. Since lithium halides adsorb an appreciable amount of water during the preparation of pastes, the examination of the spectral change for diacetamide-*d* on addition of lithium halides seriously suffers from the interference of the undeuterated species. Consequently, the characteristic bands of diacetamide-*d* in the two-component systems containing lithium halides could hardly be identified except for the N-D stretching band.

On the basis of the above fact, those infrared spectra obtained by the addition of these alkali halides may be conveniently classified into three types $B_1$, $B_2$ and $B_3$ according to the anion involved. Thus, we have three iodides, two bromides and one chloride giving rise to the spectral types $B_1$, $B_2$ and $B_3$ in that order. Differences among the types $B_1$, $B_2$ and $B_3$, as represented by Figs. 1, (a), (b) and (c) respectively, are mainly in the N-H (and N-D) stretching and the imide V (and V′) frequencies[6,8,9]. Table I shows these frequencies for each spectral type. The other characteristic frequencies[8] of diacetamide in the two-component systems are shown in Table II. Discussions on these frequencies will be given later.

TABLE I. THE CHARACTERISTIC FREQUENCIES (IN $cm^{-1}$) OF DIACETAMIDE DEPENDING ON THE ANION

| Anion | $I^-$ | $Br^-$ | $Cl^-$ | Form B[6] |
|---|---|---|---|---|
| Spectral types*1 | $B_1$ | $B_2$ | $B_3$ | |
| N-H Stretch.*2 | 3250m*3 | 3245m | 3240m | 3280 s |
| | 3180m | 3170 s | 3100 s | 3205 s |
| Imide V | 739m | 768m | 800m | 739m |
| N-D Stretch. | 2370m | 2350m | 2320m | 2405 s |
| Imide V′ | 547m | 566m | — | 547m |

*1 : See also Table III.
*2 : The origin of the splitting of this band was discussed in Ref. 9.
*3 : s, strong; m, medium.

TABLE II. THE CHARACTERISTIC FREQUENCIES (IN $cm^{-1}$) OF DIACETAMIDE DEPENDING ON BOTH THE ANION THE CATION

| | | $Li^+$ | $Na^+$ | $K^+$ |
|---|---|---|---|---|
| $Cl^-$ | Sym. imide I | 1740 s | | |
| | Imide II | 1512 s | | |
| | Imide III | 1245 s | | |
| | Imide II′ | ? | | |
| | Imide III′ | ? | | |
| $Br^-$ | Sym. imide I | 1740 s | 1745 s | |
| | Imide II | 1510 s | 1510 s | |
| | Imide III | 1245 s | 1240 s | |
| | Imide II′ | ? | 1357m | |
| | Imide III′ | ? | 945m | |
| $I^-$ | Sym. imide I | 1742 s | 1748 s | 1753 s |
| | Imide II | 1500 s | 1490 s | 1485 s |
| | Imide III | 1237 s | 1220 s | 1217 s |
| | Imide II′ | ? | 1349m | 1345m |
| | Imide III′ | ? | 941m | 940m |

**Effect of Water.** — Since lithium halides are extremely hygroscopic and it is difficult to

7) For the method of preparation of samples, see Experimental Part 2.
8) T. Uno and K. Machida, This Bulletin, 34, 551 (1961).
9) T. Uno and K. Machida, ibid., 34, 821 (1961).

avoid the adsorption of water during the preparation of pastes, the effect of a small amount of water on this spectral change must be taken into account if lithium halides are involved. Instead of removing water from the systems containing lithium halides, the other alkali halides were re-examined in the presence of a small amount of water[10]. The result was such that sodium chloride and potassium bromide partly give rise to the spectral change in the presence of water while potassium chloride does not.

These results are summarized in Table III, from which it is seen that the presence of water favors this spectral change. This may

Table III. The spectral types* of diacetamide-alkali halide systems

| | | $Li^+$ | $Na^+$ | $K^+$ |
|---|---|---|---|---|
| $Cl^-$ | Without water | — | A | A |
| | With water | $B_3$ | $B_3$ (partly) | A |
| $Br^-$ | Without water | — | $B_2$ | A |
| | With water | $B_2$ | $B_2$ | $B_2$ (partly) |
| $I^-$ | Without water | — | $B_1$ | $B_1$ |
| | With water | $B_1$ | $B_1$ | $B_1$ |

* A is the identical spectrum with that of form A. B's are the spectra analogous to that of form B. Suffices differentiate the features of the N-H stretching and the imide V band (see text and Table I).

be understood in connection with the fact that the recrystallizing solvent for form B is water[6]. It is also seen however, that the ionic radii of the anion and the cation are concerned with this spectral change in both samples with and without water. In the alkali halide disk technique, the contamination of water is hardly avoidable since an excess of alkali halides which are usually hygroscopic must be used in comparison with the sample. As seen from Table III, the spectral change of diacetamide in the two-component system containing potassium bromide takes place only in the presence of water. Situations may be analogous for potassium bromide disks. The water adsorbed on the matrix partly gives rise to the spectral change related to the changes in intensities of the C=O stretching bands at 1734 and 1700 $cm^{-1}$ previously mentioned.

**Effect of Compression in the Disk Technique.**— When the disk technique is applied to form B of diacetamide with potassium bromide or potassium chloride as the matrix, it is observed that the absorption bands due to form A appear partly[11]. This fact may be interpreted in terms of the degradation of crystal lattices under pressure as has been reported for substances with melting points below 90°C[3]. Since diacetamide (m. p. 81°C) is crystallized in form A from the molten liquid[6], it is not surprising that the degradation of form B is followed by the formation of form A. Thus, in the potassium bromide disk technique, the presence of water favors the change from form A to form B[12] while the compression favors the reverse change. The infrared spectra of diacetamide in potassium bromide disks may vary with changes in these two factors.

**Interaction between Diacetamide and Various Alkali Halides.** — Differences in the characteristic frequencies among the two-component systems under consideration may be interpreted in terms of interaction between the -CONHCO- group and the ions of alkali halides. As seen from Table I, the N-H (and N-D) stretching and the imide V (and V′) frequencies depend only on the anion. This fact suggests the occurrence of an ion-dipole interaction between the imide hydrogen atom and the anion. Such an interaction, if any, is expected to become weaker as the ionic radius of the anion increases. The tendency of frequency shifts shown in Table I is in accord with this expectation. As the anion is changed from $Cl^-$ through $Br^-$ up to $I^-$, the N-H (and N-D) stretching frequency increases while the imide V (and V′) frequency decreases. On the other hand, as seen from Table II, the frequencies of the bands due mainly to the vibrations of the C=O or C-N bonds depend on both the cation and the anion, suggesting that there occurs another ion-dipole interaction between the C=O oxygen atoms and the cation of alkali halides. If otherwise, the frequencies shown in Table II should depend also only on the anion. Thus, the frequency differences shown in Tables I and II suggest that the ion-dipole interaction between the anion and the N-H bond and that between the cation and the C=O bonds occur simultaneously. Table II shows that the imide I frequency increases with the ionic radii of both the anion and the cation, while the imide II, III and II′ frequencies show the reverse shifts. The frequency shifts of the characteristic bands of monosubstituted amides depending on the polarity of the molecule have been well investigated[13]. Since similar shifts on the change of polarity are expected for the corresponding characteristic frequencies of acyclic imides, the above fact may be taken as indicating that the polar

10) Estimation of the amount of water added was described in Experimental Part 3.

11) For the conditions of preparations of disks, see Experimental Part 4.

12) Strictly speaking, a certain form in which the -CONHCO- group takes a configuration similar to that in form B.

13) T. Miyazawa, *J. Chem. Soc. Japan, Pure Chem. Sec.* (*Nippon Kagaku Zasshi*), 77, 321, 619 (1956).

character of the molecule of diacetamide becomes more predominant as the ionic radii of the anion and the cation of alkali halide decrease. Furthermore, the symmetric imide I frequencies shown in Table II are higher than that of form B of diacetamide (1734 $cm^{-1}$). This fact means that the bond order of the C=O bond involved in the ion-dipole interaction with the cations is greater than that of the C=O bond involved in hydrogen bond in form B. The ion-dipole interaction between the cations and the C=O bonds seems to be so weak that this does not affect the nature of the N-H bond appreciably, resulting in the independence of the frequencies shown in Table I on the cation.

All the molecules of diacetamide in the two-component system under consideration can be involved in the ion-dipole interactions supposed from the spectral change only if the crystal lattice of form A degrades completely. This was confirmed by the powder X-ray diffraction measurement. Figure 2, (a) shows the diffraction pattern of the intimate mixture of diacetamide and potassium iodide (the molar ratio being approximately one to one)[14]. The diffraction pattern of diacetamide in form A is shown in Fig. 2, (b). It is seen that no diffraction line in (a) appears in (b). Thus, the crystal lattice of form A of diacetamide does not remain in the two-component system with potassium iodide. Furthermore, the appearance of new diffraction lines in (b) obviously indicates the formation of different lattices. These results give support to the explanation of the spectral change in terms of the ion-dipole interactions suggested above.

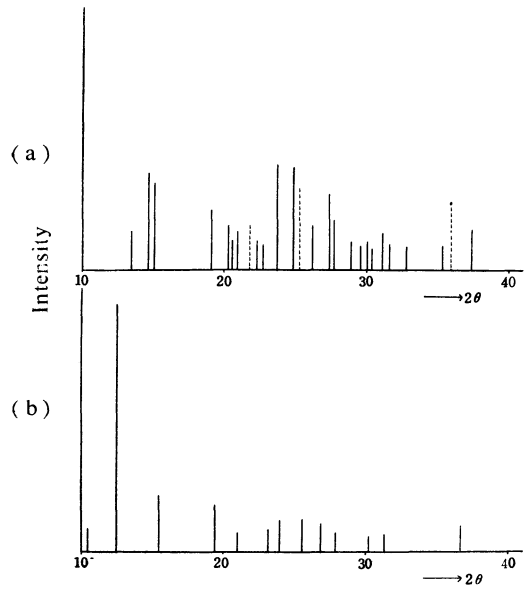



Fig. 2. Powder X-ray diffraction patterns.
(a) Diacetamide-KI system (Broken lines indicate the lines due to KI).
(b) Diacetamide in form A.

Table III shows that larger anions and smaller cations are favorable to give rise to the spectral change. Discussions will now be conducted regarding this fact on the basis of the ion-dipole interactions. The spectral change under consideration seems to be the evidence for the change in the configuration of the -CONHCO- group. Owing to the repulsive force between two oxygen atoms of the -CONHCO- group in the trans-trans configuration, the molecule in this configuration is expected to be less stable than that in the trans-cis configuration. In fact, as reported in the preceding paper[6], this is true for diacetamide. However, if a large anion such as $I^-$ approaches the hydrogen atom of a molecule in the trans-cis configuration, a strong repulsive force will be exerted between this anion and the oxygen atom at the cis position with respect to the hydrogen atom This repulsive force may be expected to increase with the ionic radius of the anion. On the other hand, if a cation approaches the oxygen atoms of a molecule in the trans-trans configuration, the repulsive force between these two oxygen atoms will be partly compensated for by the attractive forces between this cation and the oxygen atoms. The smaller the cation is, the more closely it can approach these oxygen atoms, so that the repulsive force between these two oxygen atoms decreases with the ionic radius of the cation. Thus, the simultaneous effects of the cation and the anion will give rise to the inversion from the trans-cis configuration to the trans-trans one and, as the experiment shows, the larger the anion and the smaller the cation of alkali halide are, the more easily the inversion takes place.

The actual situation in the crystalline state may be somewhat different from the monomolecular model for the ion-dipole interaction supposed above. However, it is noticed here that such a simplified model is sufficient for the qualitative elucidation of the marked spectral change. From the above discussions, it is expected that the energy difference between the trans-cis and the trans-trans configuration is rather small for diacetamide. Besides the electrostatic and the steric contribution to the energy, the energy of the formation of hydrogen bond must be taken into account to estimate the energy difference between these two configurations. However, as the problem is related to the solid state, it is difficult to determine which of these two configurations has the greater advantage for the formation of

14) See Experimental Part 5.

hydrogen bond, whose natures may be very different from each other for these two configurations.

## Conclusion

It has been found that the alkali halide disk technique gives rise to marked changes in infrared spectra of diacetamide under some conditions. This phenomenon has been proved to be related to the contamination of water, to the compression in this technique and to the ionic radii of the anion and the cation of alkali halide used. Similar spectral changes of diacetamide on the addition of various alkali halides have been interpreted in terms of the inversion of the -CONHCO- group from the trans-cis to the trans-trans configuration. In a qualitative consideration on the basis of both the electrostatic interactions and the steric effect, it has been pointed out that the possibility of the inversion is closely related to the ionic radii of both the cation and the anion.

## Experimental

1) **Materials.** — Commercially available G. P. grade sodium chloride and potassium chloride were purified according to Hales' method[15]. Commercially available E. P. grade lithium iodide and lithium bromide, G. P. grade potassium iodine, potassium bromide, sodium iodide, sodium bromide and lithium chloride were used without further purification. These alkali halides were ground to 200 mesh, dried over phosphorus pentoxide at 150~200°C, in 5~10 mmHg for 10~15 hr., and stocked over phosphorus pentoxide in a vacuum desiccator. The preparation of form A and form B of diacetamide and diacetamide-*d* has been described[6].

2) **Preparation of Pastes.** — Each of the alkali halides (2~3 mg.) described in 1 was added on a drop of Nujol or hexachlorobutadiene in an agate mill and ground by hand carefully. Then form A of diacetamide or diacetamide-*d* (2~3 mg.) was added and ground by hand rapidly for ca 30 sec. The pastes thus obtained were immediately subjected to measurement. The preceding paper will be referred to for the details of the measurement[6].

3) **Effect of Water.** — Water was added with a thin glass rod on the sample containing each of potassium iodide, potassium bromide, potassium chloride, sodium iodide, sodium bromide and sodium chloride, and pastes were prepared as described in 2. The amounts of both water and diacetamide were adjusted so that the relative intensities of the O-H and the N-H stretching bands were similar to those of the corresponding bands observed for the samples containing lithium halides. In most cases the transmittance for the band maxima near 3400 and 3200 $cm^{-1}$ were 60~70% and 30~50% respectively.

4) **Preparation of Disks.** — Potassium chloride or potassium bromide (ca. 500 mg.) and diacetamide in form B (1~2 mg.) were ground by hand in an agate mill for 3~5 min., and pressed under 120 kg./$cm^2$ in 2~3 mmHg for ca. 5 min. to prepare a disk.

5) **X-Ray Diffraction Measurement.** — Form A of diacetamide (ca. 500 mg.) and potassium iodide (ca. 830 mg.) were ground by hand carefully for 20~30 min., allowed to stand in a vacuum desiccator containing phosphorus pentoxide for a day, and subjected to the diffraction measurement (Fig. 2, (a)). Form A of diacetamide was treated similarly except for the addition of potassium iodide (Fig. 2, (b)). A Rigaku Denki X-ray diffractometer with GM counter was used and the Cu-$K_\alpha$ line was adopted.

The authors express their thanks to Dr. Tatsuo Miyazawa of Osaka University for his kind advice. Thanks are also due to Dr. Kiyoshi Nakamura of Research Laboratory, Dainihon & Co. Ltd. for his kind advice and for X-ray diffraction measurements.

*Faculty of Pharmacy*
*Kyoto Uuiversity*
*Sakyo-ku, Kyoto*

15) J. L. Hales and W Kynaston, *Analyst*, **79**, 702 (1954).

# *Some Observations on the Process of Dehydration and Rehydration of Gypsum by Means of Proton Magnetic Resonance*

By Tatsuo SAITO

(Received February 15, 1961)

In the previous paper[1], the proton resonance spectra of thermally dehydrated products of alumina trihydrate in vacuo and their rehydrated specimens were measured and the relations between the phase transformation and the movements of bound water were investigated.

In the present paper, the process of thermal dehydration of natural gypsum in vacuo and their rehydration by saturated water vapor were investigated by the variation of line shapes of proton resonance spectra.

On the study of the process of dehydration and rehydration of gypsum extensive literatures have appeared. Several authors[2-8] deduced that the hemihydrate obtained from the partial dehydration of gypsum has a zeolitic type of structure such that water molecules can enter and leave it without destroying the lattice. Other authors[9] deduced that the calcium sulfate hemihydrate has a definite chemical composition and that the process of dehydration is not zeolitic in character. On the other hand, Mitsuki[10] and Razouk[8] explained that the dehydration of gypsum in vacuo leads directly to the formation of a soluble anhydrite.

The present author found by the observations of the proton resonance spectra that the soluble anhydrite produced by the thermal dehydration of gypsum occludes some quantity of movable water in the space of its crystal lattice and that the hemihydrate obtained by the rehydration of dehydrated gypsum has a definite crystal water and some quantity of movable water.

## Experimental

**Experimental Apparatus.**—The NMR measurements were performed at room temperature using the modulation technique described by Bloembergen, Purcell and Pound[11]. The detecting apparatus[12] has the ordinary constitution, which is composed of an r−f oscillator, an r−f amplifier, a detector, an audio frequency amplifier, a lock-in amplifier and a recorder. The pole face diameter of the permanent magnet is 140 mm. and the air gap length is 40 mm. The magnet has the field intensity of 4140 gauss, with a uniformity of $2\times10^{-5}$ over the whole sample volume. Continuous variation of the static magnetic field linear with time was achieved by an automatic current scanning apparatus[13].

**Specimens.**—The starting material used in this experiment was fibrous gypsum (Produces in Iwasawa, Iwate Prefecture) containing the stoichiometric amount of water according to the formula, $CaSO_4 \cdot 2H_2O$. The X-ray diffraction diagram of this material is shown in Fig. 1.

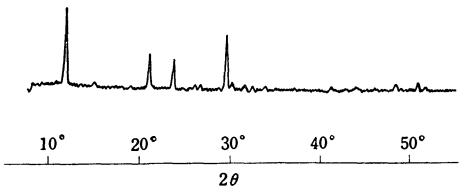
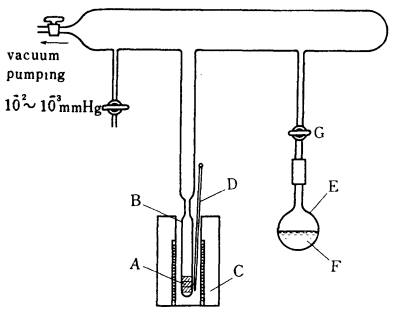



Fig. 1. X-ray diagram of the starting material, gypsum.




A: sample cake (dia. 8 mm.) B: resonance sample tube C: electric furnace D: thermometer E: flask (100 cc.) F: distilled water in evacuated flask G: cock.

Fig. 2. Apparatus used for the preparation of the specimens.

1) T. Saito, This Bulletin, **34**, 757 (1961).
2) G. Linck and H. Jung, *Z. anorg. allgem. Chem.*, **137**, 407 (1924).
3) C. S. Gibson and S. Holt, *J. Chem. Soc.*, **1933**, 638.
4) W. A. Caspari, *Proc. Roy. Soc.*, A, **155**, 41 (1936).
5) C. W. Bunn, *J. Sci. Instru.*, **18**, 70 (1941).
6) S. J. Gregg and E. G. J. Willing, *J. Chem. Soc.*, **1951**, 2916.
7) R. Kiriyama and H. Ibamoto, This Bulletin, **26**, 109 (1953).
8) R. I. Razouk, A. S. Salem and R. S. Mikhail, *J. Phys. Chem.*, **64**, 1350 (1960).
9) H. B. Weiser, W. O. Milligan and W. C. Ekholm, *J. Am. Chem. Soc.*, **58**, 1261 (1936); H. B. Weiser and W. O. Milligan, ibid., **59**, 1456 (1937).
10) C. Mitsuki, *J. Ceram. Assoc. Japan*, **60**, 92 (1952).
11) N. Bloembergen, E. M. Purcell and R. V. Pound, *Phys. Rev.*, **73**, 679 (1948).
12) S. Yano, *J. Phys. Soc. Japan*, **14**, 952 (1959).
13) T. Sidei, S. Yano and S. Sasaki, *J. Appl. Phys. Japan*, **27**, 513 (1958).

Each dehydration-specimen or rehydration-specimen was prepared in the vacuum system illustrated in Fig. 2. To prepare each specimen by thermal dehydration in vacuo, about 2 g. of powdered gypsum was pressed in the form of small cakes A and put into the resonance sample tube B which was connected to the high vacuum system. This sample tube B was heated from outside by an electric furnace C for 3 hr. in a high vacuum and was then sealed off. The dehydration temperatures were 70, 80, 90, 95, 100, 105, 110, 115, 125, 150 and 200°C. For the preparation of rehydration-specimens, each sample after the treatment of the thermal dehydration in vacuo was immediately exposed for 15 hr. to saturated water vapor which was introduced through the cock G from the flask E at room temperature. Then, each sample tube containing this rehydrated specimen was pumped out to a high vacuum for 12 hrs. at room temperature and was then sealed off. In this experiment, the temperature of the dehydration in vacuo was 80, 95, 110, 125, 135, 150, 165, 180, 220, 250 and 300°C.

X-Ray powder diffraction was made with a "Geigerflex" recording X-ray spectrometer using filtered $CuK_\alpha$ radiation.

## Results and Discussion

**Thermal Dehydration in vacuo.**—The experimental derivative curves of the proton resonance obtained from the dehydrated products are shown in Figs. 3 and 4. The photographs of a and b in Fig. 4 show the recorded spectra of the typical derivative curves.

As is seen in Fig. 3, the derivative curve of the starting material shows a typical line shape of two spin system[14] with broad width of about 14 gauss. While in the line shape of the specimen dehydrated at 70°C a single peak appeared overlapping the line of the starting material at its center, for the specimen dehydrated at 90°C only the center peak was observed. This characteristic single sharp peak was also observed for the specimen dehydrated at 150°C, while for the specimen dehydrated at 200°C no proton resonance signal was observed. It is known that this single sharp peak of proton resonance originates from the water molecules which are in the thermal motion.

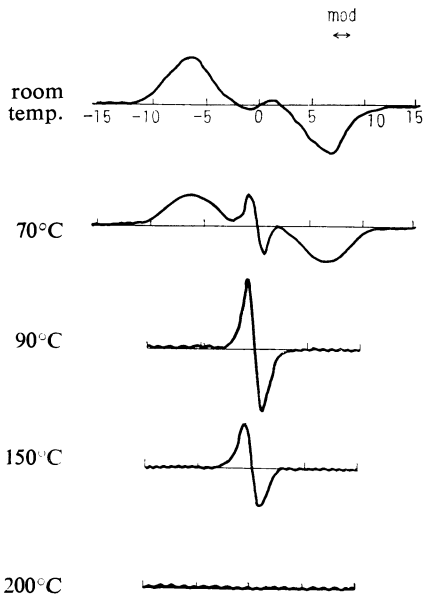
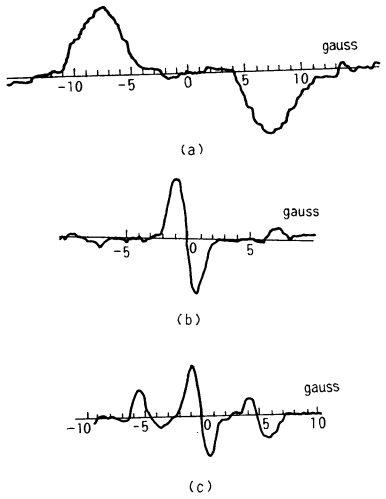
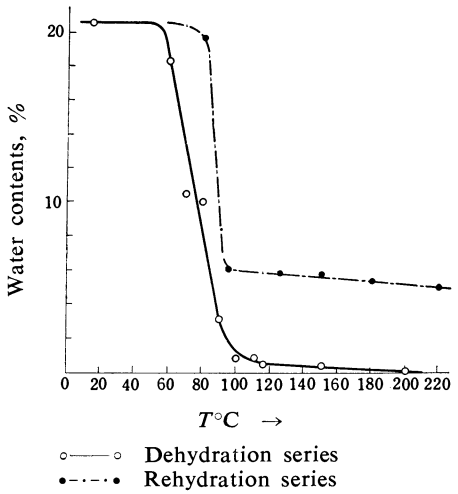



Fig. 3. Experimental derivative curves of proton resonance in the dehydration-specimens.




(a) starting material, gypsum.
(b) dehydrated gypsum at 95°C.
(c) rehydrated product of (b)

Fig. 4. Recorded derivatives of proton resonance in the dehydration or rehydration-specimens.




o——o Dehydration series
•-·-·• Rehydration series

Fig. 5. Variation of water contents in the dehydration or rehydration-specimens the dehydration temperature.

14) G. E. Pake, *J. Chem. Phys.*, **16**, 327 (1948).

To compare the above results with the change of chemical composition, the water content of each dehydration-specimen was measured and the values of percentage of weight loss at 800°C were plotted in Fig. 5 as the function of the dehydration temperature.

As is seen in Fig. 5, the water content decreases suddenly at about 70°C from the value corresponding to dihydrate to the value of 1~2% corresponding to soluble anhydrite, while the remaining water can not be completely removed even at 150°C and in this process of dehydration the steps corresponding to the formation of hemihydrate were not observed. This is in agreement with the results obtained by other authors[8,10].

In the X-ray diffraction studies, the crystallographical phase transformation was observed for the dehydration at about 70°C as shown in Fig. 6.

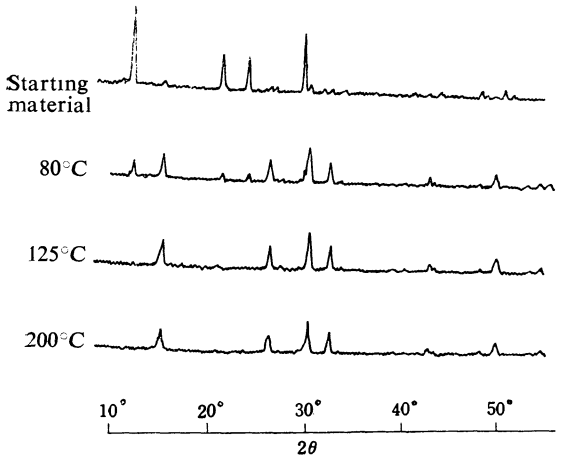



Fig. 6. X-ray diffraction diagrams of the dehydration-specimens.

From these experimental results, it is assumed that the decomposition of this gypsum occurs at 60~70°C, that some quantity of water released during the dehydration remains in the space of the crystal lattice which is introduced by the dehydration and that this movable water is gradually removed with rises of temperature, having no influence upon the crystal lattice.

On the other hand, the crystal structure of gypsum[15] may be described as a complex layer structure in which the layers are bound together by bonds from water molecules, each of which is joined to a $Ca^{2+}$, 0 atom of a $SO_4^{2-}$ ion of one layer and an 0 atom of $SO_4^{2-}$ ion of an adjacent layer.

It might be concluded from the experiments described above that these O-H-O bonds are so weak that the crystal structure of gypsum can be broken down even at low temperature and that the evolution of the binding water may occur at the same time, while some quantity of this water may remain in the space of the lattice which is introduced by the decomposition at low temperature.

**Rehydration of the Dehydration-Specimens in vacuo.**—The NMR measurements were carried out on the specimens prepared by the rehydration of gypsum thermally dehydrated in vacuo. The typical experimental derivative curves obtained from these measurements are shown in Fig. 7.

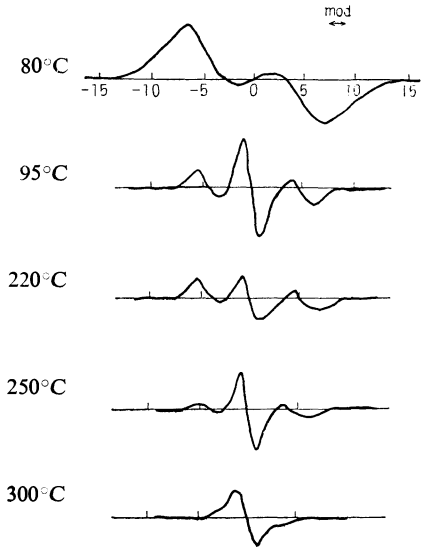



Fig. 7. Experimental derivative curves of proton resonance in the rehydration-specimens.

As is seen in Fig. 7, the rehydrated specimens of gypsum dehydrated at the temperature from 95 to 250°C show the same line shapes. The photograph of c in Fig. 4 shows the recorded spectrum of this typical derivative curve, while the rehydrated specimen of gypsum dehydrated at 80°C shows the same line shape as that of the starting material. From the measurements of the water content of these rehydrated specimens, it was found that the line shapes observed for the rehydrated specimens of gypsum dehydrated from 95 to 250°C correspond to the phase of hemihydrate, $CaSO_4 \cdot 1/2\,H_2O$. The values of the water content of these specimens were also plotted in Fig. 5 as the function of the dehydration temperature.

While these rehydration-specimens corresponding to hemihydrate were crystallographically quite similar to the dehydrated gypsum corresponding to soluble anhydrite from the result of the X-ray study, the line

15) A. F. Wells, "Structural Inorganic Chemistry", Oxford University Press, London (1950), p. 440.

shapes observed for these rehydration-specimens are different from that for the dehydrated gypsum and are presumably understood as the signal of three spin type with an intensive center peak. The line width of this line shape (the separation between peaks in side band) was about 11～12 gauss.

The product obtained from this hemihydrate by the thermal treatment at 100°C for 3 hr. in vacuo showed only the single center peak corresponding to the movable water. This movable water may also be explained as the zeolitic water existing in the space of the crystal lattice which was introduced by the dehydration of hemihydrate.

On the other hand, the rate of rehydration of gypsum dehydrated at 125°C by saturated water vapor was examined by NMR measurements and it was found that all the specimens obtained from the rehydration for one to 48 hr. showed the same line shapes as that corresponding to hemihydrate. This result means that hemihydrate is considerably stable against saturated water vapor and that the rate of hydration of soluble anhydrite is very high. This result is in agreement with the result obtained by other authors[8].

However, gypsum dehydrated at 80°C is easily rehydrated by saturated water vapor directly to dihydrate. This fact means that the product dehydrated at 80°C has the pseudolattice of gypsum and transforms easily to the phase of dihydrate by the addition of water molecules.

## Summary

1) On the thermal dehydration in vacuo, the characteristic single sharp peak of proton resonance was observed for the specimens dehydrated at the temperature from 70 to 150°C.

It is assumed that this single sharp peak is attributed to the zeolitic water probably existing in the space of the crystal lattice of soluble anhydrite and that this zeolitic water can be interpreted as being a part of the water molecules which originate from dihydrate during the thermal decomposition.

2) Calcium sulfate hemihydrate was formed by the rehydration of gypsum dehydrated in vacuo. This hemihydrate showed the proton resonance spectrum corresponding to the signal of three spin type with an intensive center peak. This intensive center peak can be interpreted as an indication of the movable water existing in the space of the crystal lattice of hemihydrate.

3) This hemihydrate was considerably stable under the atmosphere of saturated water vapor. This was ascertained by the NMR measurements.

The author wishes to express his sincere thanks to Dr. Y. Kotera of this Institute for his kind advice.

The author also wishes to express his hearty thanks to Professor Tokutaro Hagiwara of Hiroshima University for his kind direction and also to Professor Tunahiko Sidei and Dr. Syukuro Yano of Kyoto University for their continual guidance and encouragement throughout this study.

*Government Chemical Industrial Research Institute, Tokyo*
*Shibuya-ku, Tokyo*

# *Studies on the Surface Structure of Porous Materials*

By Akie TSURUIZUMI

(Received December 29, 1960)

It has been generally accepted that the adsorption of gases on adsorbents such as active carbon and silica gel is both physical and chemical in nature, the latter being caused by the formation of complex surface compounds with residual active groups as well as by an ion exchange effect on the surface. The chemisorption plays a role in the earlier stage of the adsorption process, while the general behavior of the adsorption is characterized by the physical behavior.

Pore structure of the surface, which is important for both the theoretical and practical studies, could be visualized by combining

various methods such as porosimetries and adsorption measurements. A preferential physical adsorption of adsorbates with various molecular sizes could be used most effectively for classification of the pore-sizes.

In the present paper, the pore structures of various adsorbents such as active carbon and silica gel were studied. The results of adsorption measurements with water vapor and various organic vapors, the BET method using nitrogen, and mercury and water prosimetry were analyzed, and the size, shape and chemical nature of the pores were discussed in detail.

An emphasis was placed on the deviations from the prevailing theories, which are based on a simple pore model such as the cylindrical one. The analysis of the deviations enabled us to depict the shape of the pore, being of narrow-neck or ink-bottle shape. In addition, a new term, 'sieving coefficient' was proposed, which would be quite profitable for classification of the adsorbents.

## Theoretical

The pores are classified into the following three groups: micro-pores, ca. 10 Å in radii; transitional pores, 100~500 Å; micro-pores, 10000 Å. The transitional and micro-pore distributions are determined empirically by a mercury porosimetry[1]. The micro-pore distribution is calculated by Thomson's formula,

$$r=-\frac{2v\sigma\cos\theta}{RT\ln P/P_0} \qquad (1)$$

where $v$ is the molecular volume, $\theta$ the contact angle, $\sigma$ the surface tension, $r$ the pore radius, $P$ the vapor pressure of the meniscus, and $P_0$ that of the bulk phase.

A total volume of pores with a radius in a range between $r$ and $r+dr$ is represented by

$$dv=D(r)dr \qquad (2)$$

where $v$ is the total volume of the pores, and $D(r)$ the distribution function of the pore radii. The function $D(r)$ is obtained by graphical differentiation of a curve drawn by plotting the total amount of adsorption against the radii of the pores. A plot of $dv/d\log r$ vs. $\log r$ was similar to the Gaussian probability curve.

Thomson's equation is implicitly based on the following assumptions: i) Adsorption of water is caused by the capillary condensation. ii) The pore is cylindrical in shape with a uniform diameter. iii) The water adsorbed in the pore has the same density as that in bulk phase.

Cohan[2], McBain[3] and Higuchi[4] have pointed out that the size distribution function of pores having diameters less than 10 Å can not be calculated by Thomson's equation. If the radii of pores are less than 10 Å, the condensation of water vapor inside the pore is impossible, because the diameter of the void space in the pore is reduced to 2~3 molecular sizes by preliminary formation of a monolyer on the inside wall in the earlier stage of the adsorption process.

In the range of higher radius, a minor correction for pore radius less than six per cent is necessary[5]. This is due to the reduction of the pore space by the formation of the adsorption film on the wall. This correction was, however, not applied in the present study. Actually, pore-size distribution curves obtained by using Thomson's equation are in good agreement with those obtained from the adsorption of nitrogen as has been shown by Joyer[6], with those obtained by the adsorption of benzene vapor and by the mercury porosimetry reported by the present author[7].

The radius of a cylindrical pore is given by the equation[8]

$$pr=2\pi\sigma\cos\theta \qquad (3)$$

where $p$ is the applied pressure to press the mercury into the pore, $\sigma$ the surface tension of mercury, $r$ the redius of the pore and $\theta$ the contact angle.

Expressing $p$ in kg./cm$^2$, $r$ in cm., and putting $\delta=480$ dyn./cm. and $\theta=140°$C[9,10], Eq. 3 is reduced to

$$pr=7.5\times10^{-4} \qquad (4)$$

If the pores are ink-bottle or bottle-neck shaped, the appearent radii obtained by the porosimetry are those of narrow-neck shape, being less than the true ones.

## Experimental

**Materials.**—*Sugar Charcoals* ($S_3$, $S_4$, $SZ_3$, $SZ_4$).—$S_3$, $S_4$[11]: An aqueous solution of commercial white sugar decolored with an active carbon was passed through a column of ion exchange resins (Amberlite

1) H. L. Ritter and L. C. Drack, *Ind. Eng. Chem., Anal. Ed.*, **17**, 782 (1945).

2) L. H. Cohan, *J. Am. Chem. Soc.*, **60**, 433 (1938).

3) J. W. McBain, ibid.. **57**, 691 (1935).

4) I. Higuchi, *Sci. Pap. Inst. Phys. Chem. Res.*, **20**, 130 (1941).

5) M. M. Dubinin, *Quart. Rev.*, **9**, 109 (1955).

6) L. G. Joyer, E. P. Barset and R. Skold, *J. Am. Chem. Soc.*, **73**, 3155 (1951).

7) A. Tsuruizumi, *J. Chem. Soc. Japan, Pure Chem. Sec. (Nippon Kagaku Zasshi)*, **81**, 870 (1960).

8) E. W. Washburn, *Proc. Natl. Acad. Sci.*, **7**, 115 (1921).

9) H. L. Ritter and L. C. Drake, *Ind. Eng. Chem., Anal. Ed.*, **17**, 782, 787 (1945).

10) A. J. Juhola and E. O. Wiig, *J. Am. Chem. Soc.*, **71**, 2069, 2078 (1949).

11) A. Tsuruizumi, *J. Chem. Soc. Japan, Pure Chem. Sec. (Nipoon Kagaku Zasshi)*, **79**, 266 (1957).

TABLE I. CLASSIFICATION OF PORE VOLUME

| Sample | A $v_1$ Micro-P. vol. to 50 Å ($r$) cc./g. | B[a] $v_2$ Trans.-P. vol. 75~1000 Å cc./g. | C[b] $v_3$ Macro-P. vol. 1000~43000 Å cc./g. | D Pressed total mercury vol. B+C cc./g. | E $V_t$ Total pore vol. A+D=A+B+C cc./g. |
|---|---|---|---|---|---|
| $S_3$ | 0.1205 | 0.0152 | 0.0590 | 0.0742 | 0.1947 |
| $S_4$ | 0.1554 | 0.0162 | 0.0410 | 0.0572 | 0.2126 |
| $SZ_3$ | 0.7950 | 0.0350 | 0.0680 | 0.1030 | 0.8980 |
| $SZ_4$ | 0.8850 | 0.0370 | 0.2200 | 0.2570 | 1.1420 |
| M. S.[c] | 0.2140 | 0.0680 | 0.1330 | 0.2010 | 0.4150 |
| Silica[d] | 0.3750 | 0.0800 | 0.0410 | 0.1210 | 0.4960 |

a) B, b) C calculated from mercury porosimetry.
c) Molecular sieve 5 A.
d) Silica gel No. 28.

IRA 400 and IRC 120) repeatedly until its electrical conductivity was reduced to as low as 4~6 $\mu\mho$/cm. The crystals of the sugar purified by recrystallization from ethanol were dried at 40°C under 5~10 mmHg. The ashes in 10 g. of the purified sugar were undetectable with a chemical balance. The sugar placed on a quartz boat in a quartz combustion tube in an electric furnace was carbonized in a stream of nitrogen gas with a flow rate of 20~30 ml./min. The traces of oxygen in this were removed beforehand by passing through a layer of heated reduced copper. The temperature of the furnace was raised at a rate of 5°C/min., and then kept at a required temperature for 30 min. The rate of temperature rise was a factor to determine the pore structure. Carbonization temperatures and yields were as follows: $S_3$, 800°C and 23.44%; $S_4$, 1000°C and 21.30%. Granules of 70~100 meshes were collected with sieves. Spectroscopic analysis: Al (−), Si (+),·····.

$SZ_3$, $SZ_4$: A mixture of 10 g. of the purified sugar and 20 g. of zinc chloride (G. P. grade) with a few drops of hydrochloric acid was heated to 200°C on a evaporating dish. The charcoals obtained by the same carbonization process as that mentioned above from the residues were boiled with hydrochloric acid (1 : 1) to remove zinc chloride, washed with distilled water till pH values of the filtrates became 5~6, and dried for 4~6 hr. at 150~170°C. Granules of 70~100 meshes were collected. Ashes in 1 g. of the sample were undetectable with a chemical balance. No traces of zinc were detected by the dichizon method[12]. Spectroscopic analysis: Al (−), Mg(±), Si(+).

*Molecular Sieve 5A**. — Composition: $Me^{12}/n\{(AlO_2)_{12}-(SiO_2)_{12}\}27-30H_2O$, (Me: Ca, Na). Highly polar. Pore diameter noted by the manufacturer was 5 Å.

*Silica Gel No. 28.* — A gel precipitated from 3 N sodium silicate and 4 N sulfuric acid at a controlled pH of 5.5 was washed with water, electrodialized for 100 hr., dried at 20~30°C, and finally at 120~150°C. 70~100 meshes.

*3SZ$_4$, 6SZ$_4$.*—A sample of $SZ_4$ impregnated with 2 per cent nitrobenzene solution of polyvinyl chloride (Geon 103EP) was carbonized by the same method as that mentioned above at 1000°C. The process was repeated three times for $3SZ_4$ and six times for $6SZ_4$. The pore volumes and internal total wall areas were shown in Tables I and II.

TABLE II. TOTAL PORE VOLUME BY WATER OR MERCURY DISPLACEMENT METHODS

| Sample | F Water displ. vol. cc./g. | G Mercury displ. vol. cc./g. | H Total pore vol. G−F cc./g. |
|---|---|---|---|
| $SZ_3$ | 0.540 | 1.541 | 1.001 |
| $SZ_4$ | 0.528 | 1.580 | 1.051 |

TABLE III. EQUIVALENT INTERNAL WALL AREA OF EACH OF DISPERSE PORTIONS

| Sample | Surface area by $S=2V_t/\bar{r}$: $S_1$ Surface area of micro-P. $m^2/g.$ | $S_2$ Surface area of trans.-P. $m^2/g.$ | $S_3$ Surface area of macro-P. $m^2/g.$ | Surface area BET $m^2/g.$ |
|---|---|---|---|---|
| $S_3$ | 241 [8.0][e] (10)[f] | 2.4 (125.9) | 0.11 (10.000) | 400 |
| $S_4$ | 380 [7.5] (8.2) | 2.5 (125.9) | 0.08 (10.000) | 450 |
| $SZ_3$ | 800 [15] (18.0) | 2.0 | 0.14 | 1400 |
| $SZ_4$ | 1180 [10] (15.0) | 6.0 | 0.44 | 1600 |
| M. S.[c] | 660 [2.0] (6.5) | 13.0 | 2.0 | 460 |
| Silica[d] | 681 [7.5] (11.0) | 16.0 | 0.08 | 720 |

e) [Å] maximum distribution radius.
f) (Å) mean radius.

*Formic Acid.* — A guaranteed grade reagent was dehydrated with a boric acid of high melting point by being allowed to stand for a few days, and distilled under reduced pressure. The process was repeated. $N_D^{20}$: 1.3716.

*n-Propionic Acid and n-Butyric Acid.*—Guaranteed grade reagents supplied by Tokyo Oka Co., were

12) E. B. Sandell, "Colorimetric Determination of Metals", Interscience Publishers, Inc., New York (1950).
* The product of Linde Air Product Co., U. S. A.

used without further purification. $N_D^{20}$: 1.3873 and 1.3990.

*n-Valeric Acid.*—A guaranteed grade reagent supplied by Tokyo Oka Co., was used without further purification.

*Benzene.* — A guaranteed grade reagent supplied from Wako Junyaku Co., was dehydrated with metallic sodium and distilled under reduced pressure.

**Measurements of Adsorption.** — The adsorption of water vapor was measured at 30°C with a quartz spring balance of sensitivity of 2.4630 mg./mm. using a cathetometer graduated to 1/20 mm. The samples were out-gased at various temperatures for 6 hr. under $10^{-5}$ mmHg. The temperatures are: for sugar carbons, 300~350; for molecular sieve 5A, 250~300; for silica gel No. 28, 150~200°C. The poresize distribution was calculated from the desorption isotherm, the contact angle being assumed to be $\cos\theta=0.49$[10]. Adsorptions of monocarboxylic acids and benzene were measured with a quartz spring balance at 38±0.1°C. The adsorbents were out-gased by heating at 300~350°C and $10^{-5}$ mmHg.

**Measurement of Pore Volume.** — The total pore volume was measured by a water and mercury displacement method using a modified Juhola and Wiig's apparatus[10] shown in Fig. 1. The liquid water was introduced into a flask from an upper reservoir after the samples in the flask adsorbed such an amount of water vapor from a side tube that the adsorption equilibrium was reached. The total pore volume was calculated from the difference of volum of water and mercury displaced.

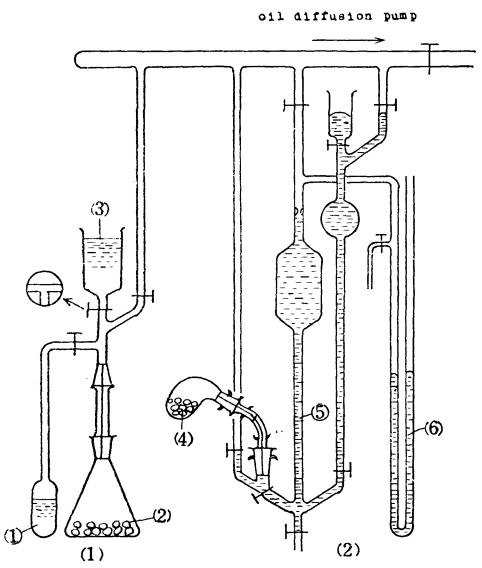



Fig. 1. Displacement volume measurement apparatus.
(1) Apparent density measurement by liquid displacement
(2) Apparent density measurement by mercury displacement
①③ Water ②④ Adsorbent
⑤ Mercury burette
⑥ Mercury manometer

**Measurement of BET Area.** — The BET surface area was obtained with a usual adsorption apparatus using nitrogen gas as an adsorbate.

**Mercury Porosimetry.**—A usual mercury porosimeter was used. In order to obtain high accuracy, the diameter of both platinum wire and dilatometer were made as small as possible. The applied pressure was measured with a gauge, and the maximum pressure reached was 1500 kg./cm². The temperature was kept at 0°C.

## Experimental Results and Discussion

**Pore Distribution.**—*$S_3$ and $S_4$.*— Plots of $dv/d\log r$ vs. $\log r$ (Å) for the samples $S_3$ and $S_4$ are shown in Fig. 2, where a tri-disperse distribution is observed. The peaks are designated as micro-, transitional and macro-pore from left to right in the figure. The shape of the transitional distribution curve is changed by modification of the carbonization or activation condition as is shown later. The distribution curves for a range 3~4 in $\log r$ are not shown as they are less than $10^{-4}$, being scaled out.

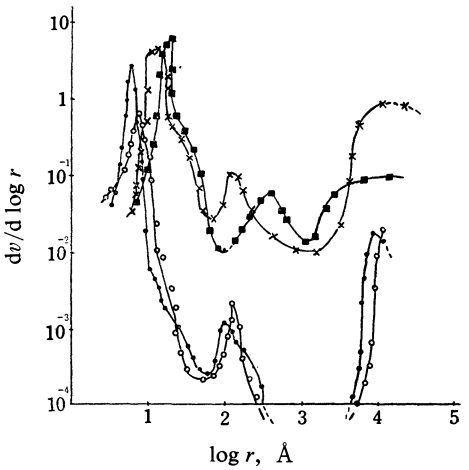



Fig. 2. Pore-size distribution in sugar carbons.
—●— $S_4$ —■— $SZ_3$
—○— $S_3$ —×— $SZ_4$

*$SZ_3$ and $SZ_4$.* — The pore-size distribution curves are also tri-disperse as a shown in Fig. 2. As is seen in Table IV, the total pore volume estimated from the results of mercury and water displacement method is in good agreement with that calculated as the total sum of the respective volumes of micro-, transitional, and macro-pores. The greater part of the surface areas of the sugar carbons ($S_3$, $S_4$, $SZ_3$ and $SZ_4$) being composed of the areas of the internal wall of the micro-pores, the number of transitional and macro-pores are too low to give any influence on the adsorption characteristics.

TABLE IV. CLASSIFICATION OF PORE VOLUME

| Sample | A $v_1$ Micro-P. vol. to 50 Å ($r$) cc./g. | B[b] $v_2$ Trans.-P. vol. 75~1000 Å cc./g. | C[b] $v_3$ Macro-P. vol. 1000~43000 Å cc./g. | D Total mercury vol. pressed in B+C cc./g. | E $V_t$ Total P. vol. A+D =A+B+C cc./g. | F[a] Water displ. vol. cc./g. | G[a] Mercury displ. vol. cc./g. | H Total pore vol. G−F cc./g. |
|---|---|---|---|---|---|---|---|---|
| $SZ_4$ | 0.885 | 0.037 | 0.220 | 0.257 | 1.142 | 0.528 | 1.580 | 1.051 |
| $3SZ_4$ | 0.730 | 0.023 | 0.079 | 0.102 | 0.832 | 0.539 | 1.337 | 0.798 |
| $6SZ_4$ | 0.620 | 0.018 | 0.065 | 0.083 | 0.703 | 0.535 | 1.207 | 0.672 |
| $S_4$ | 0.155 | 0.016 | 0.041 | 0.057 | 0.212 | — | — | — |
| Silica gel No. 28 | 0.375 | 0.080 | 0.041 | 0.121 | 0.496 | — | — | — |

a) Pore volume by water and mercury displacement methods.
b) Calculated from mercury porosimetry.

*Molecular Sieve 5A.* — The micro-pore distribution curves of molecular sieve 5A were obtained by assuming $\cos\theta=1$ in Thomson's equation because of its high polarity. A di-disperse distribution curve with sharp peaks is seen in Fig. 3.

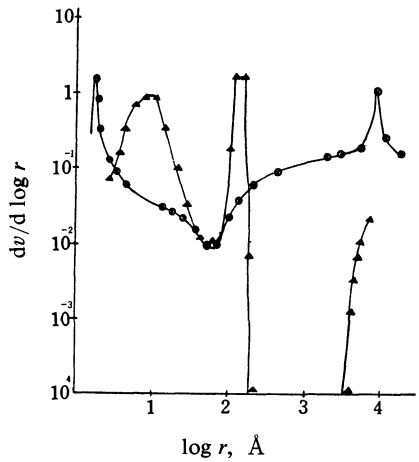



Fig. 3. Pore-size distribution in a silica gel and the molecular sievs 5A.
—▲— $SiO_2$ gel —⊗— M. S. (5A)

*Silica Gel No. 28.* — As is seen in Fig. 3, a tri-distribution curve is observed. The curve is, however, broken at a range $\log r=2\sim3$. The macro-pores are presumed to be produced by the secondary treatment, and the distribution curve is originally di-disperse. The total volumes of pores calculated from the respective peaks in the figures are shown in Table IV.

If it is assumed that the pore is a cylinder with a circular section, the total volume of the pores, $V_t$, and the inner surface area, $S$, in each peak can be calculated by the formula

$$V_t=\pi(\bar{r})^2L \qquad (5)$$

where $\bar{r}$ is an average radius of pores and $L$ the length of the cylinder. The inner surface area is related to the pore radius by the equation

$$S=2\pi\bar{r}L \qquad (6)$$

In Tables III and V, the inner wall areas calculated by the equation

$$S=2V_t/\bar{r} \qquad (7)$$

and the BET area are compared, where the coincidence is noted only in the case of the silica gel. The discrepancy seen in the tables may be ascribed to both the complexity of the pore structure and a per-sorption[13]. Another minor factor to be taken into account is the difference of densities of nitrogen in the submicro-pore and in bulk phase. The BET area is usually greater than the true area.

TABLE V. INTERNAL WALL AREA OF DISPERSE

| Sample | Surface area by $S=2V_t/\bar{r}$: Surface area of micro-P. m²/g. | Surface area of trans.-P. m²/g. | Surface area of macro-P. m²/g. | Surface area by BET m²/g. |
|---|---|---|---|---|
| $SZ_4$ | 1180 [10][a] (15.0)[b] | 6.0 | 0.44 | 1600 |
| $3SZ_4$ | 1000 [9.5] (14.5) | 3.2 | 0.16 | 1460 |
| $6SZ_4$ | 858 [9.0] (14.1) | 2.8 | 0.13 | 1300 |
| $S_4$ | 380 [7.5] (8.2) | 2.5 | 0.08 | 450 |
| Silica gel No. 28 | 681 [7.5] (11.0) | 16.0 | 0.08 | 720 |

a) [Å] maximum distribution radius.
b) (Å) mean radius.

The total wall area of the silica gel No. 28, $S$ (total sum of the areas of the micro-pores, transitional pores and macro-pores) is approximately 700 m./g. (Table V), and is in

13) A. Tsuruizumi, *J. Chem. Soc. Japan, Pure Chem. Sec.* (*Nippon Kagaku Zasshi*), **79**, 142 (1957),

agreement with the nitrogen BET area of 720 m./g. The areas obtained by the various fatty acids are ranged between 680 and 750 $m^2/g$. as will be shown later. These facts prove that there are only a few pores of a narrow-neck or ink-bottle type, which complicate the nature of the adsorption. The radius of the maximum distribution in the molecular sieve 5A is ca. 2Å.

### Adsorption of Organic Vapors

The adsorption isotherms of both monocarboxylic acids and benzene vapor were S-shape for all the adsorbents studied, and fit the BET equation well. The adsorption isotherms of benzene vapor on the samples $3SZ_4$ and $6SZ_4$ are shown in Fig. 4. The samples

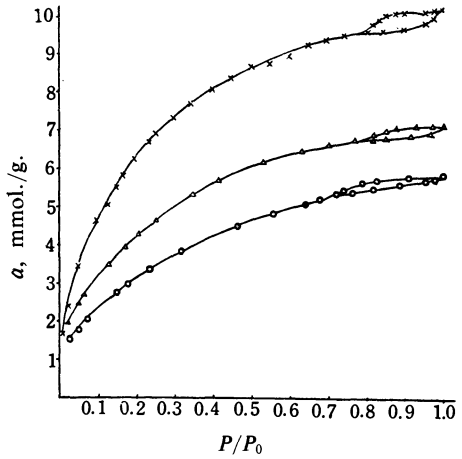



Fig. 4. Adsorption isotherm of benzene.
—×— $SZ_4$ —△— $3SZ_4$ —○— $6SZ_4$

$3SZ_4$ and $6SZ_4$ were prepared by carbonizing the sample $SZ_4$ impregnated with the nitrobenzene solution of polyvinyl chloride. The pores of the $SZ_4$ carbon were filled up to some extent, and the transitional pores were affected most sensitively. The transitional pore distribution curves for $SZ_4$, $3SZ_4$ and $6SZ_4$ obtained from the desorption isotherms of benzene vapor by using Thomson's equation are shown in Fig. 5, and the full distribution curves drawn by annexing the distribution curves estimated from the data of mercury porosimetry are shown in Fig. 6. The tri-disperse distribution is seen in the figure, and in each peak shift regularly according to the decrease in the pore volumes. The displacement of the transitional peaks are most conspicuous.

The distribution curve of the transitional pores estimated from the benzene adsorption shown in Fig. 4 was slightly higher than those obtained by the mercury porosimetry (Fig. 5).

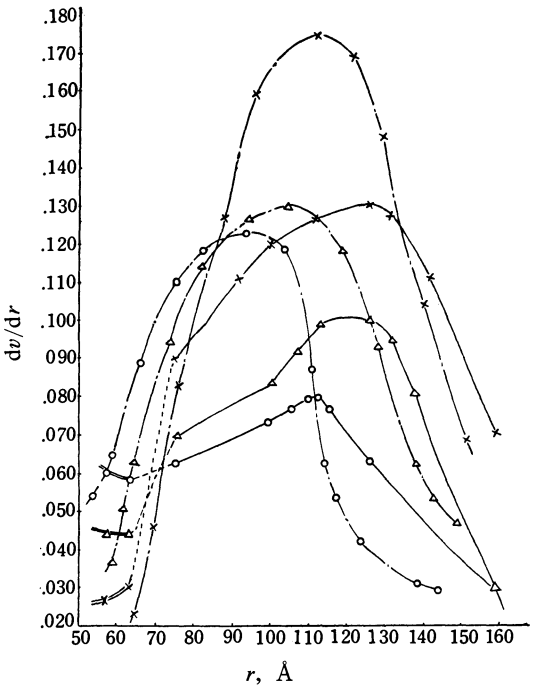



Fig. 5. Distribution of transitional-pores.
—·—· Calculated from benzene adsorption
——— Calculated from mercury porosimetry
═══ Calculated from water vapor adsorption (in the range of micro-pore distribution).
—×— $SZ_4$ —△— $3SZ_4$ —○— $6SZ_4$

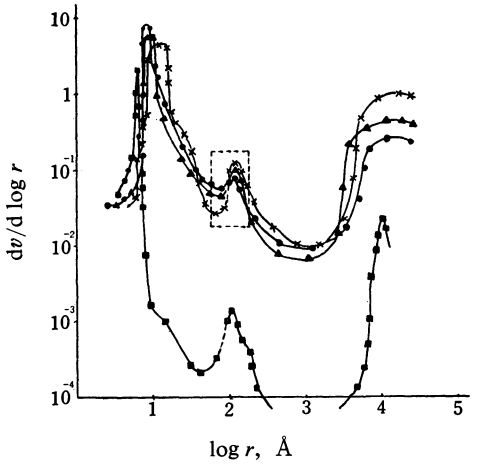



Fig. 6. Carbons pore-size distribution in sugar.
—×— $SZ_4$ —●— $6SZ_4$
—▲— $3SZ_4$ —■— $S_4$

The disagreement of the two curves may be ascribed to the errors arising from the application of Thomson's equation which is based on a number of assumptions inadequate in the

present case. Since in the mercury porosimetry no ambiguous assumptions are adduced other than the independency of the contact angle with respect to the applied pressure, the result of the porosimetry is most reliable.

A range of the distribution curve (shown by dotted lines in Figs. 5 and 6) between the micro-pore and transitional pore can not be determined precisely by the mercury porosimetry. Since the curves shown by broken lines with dots in Fig. 5 obtained by the adsorption method using benzene vapor were continuous in full range, it is quite resonable to bridge the gap between the solid line of the mercury porosimetry and the double line of the water adsorption with the dotted line as is shown in Fig. 5.

In the previous papers[11,13,14], the present author has suggested that the pore distribution of the active carbon is tri-disperse. The existence of the micro-pores of about molecular diameter size, the transitional pores (ca. 100 Å), and the macro-pores (ca. 100 $\mu$) as cracks or cavities is hereby confirmed.

Effective areas of the adsorbents, calculated from the amounts of adsorbates in a monolayer coverage (Figs. 7, 8 and 9) by using the B-point method[15] are shown in Table VI. The

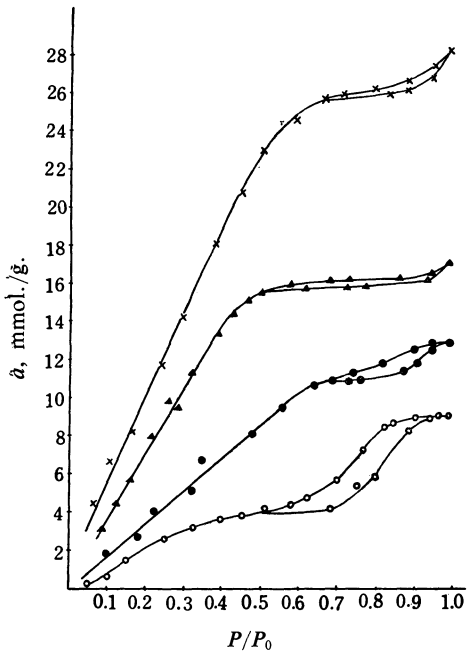



Fig. 7. Adsorption isotherms of *n*-carboxylic acid vapors ($SZ_4$, 38±0.1°C).
—○— *n*-Butyric acid —▲— Acetic acid
—○— *n*-Propionic acid —×— Formic acid

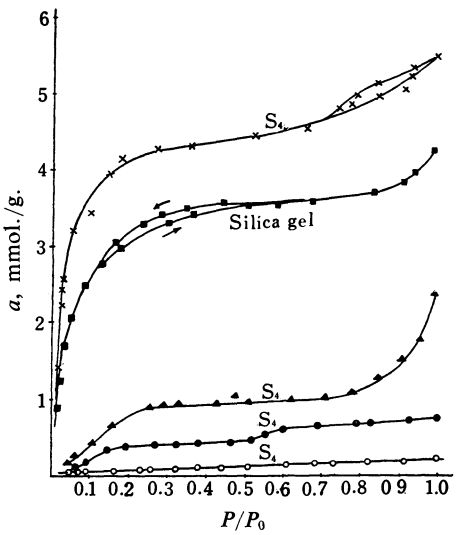



Fig. 8. Adsorption isotherms fo *n*-carboxylic acid vapors (38±0.1°C).
—○— *n*-Butyric acid —×— Formic acid
—●— *n*-Propionic acid —■— Benzene
—▲— Acetic acid

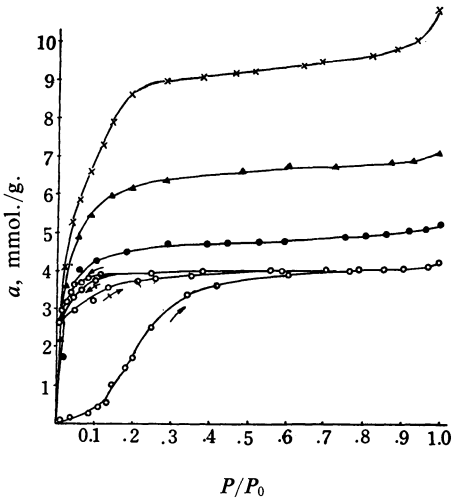



Fig. 9. Adsorption isotherms of *n*-carboxylic acid vapors (silica gel, 38±0.1°C).
⟶ —|→ Adsorption ⟵⟶ First process
⟵ ←|— Desorption —|→ ←|— Second process
—○— *n*-Butyric acid —▲— Acetic acid
—●— *n*-Propionic acid —×— Formic acid

sectional areas of the adsorbate molecules used for the calculation of the surface area are listed in Table VI. These were determined by the adsorption on $SZ_4$, $S_4$ and silica gel No. 28. The surface areas of sugar carbons obtained with formic and acetic acid are higher than the BET areas, while the higher acids gave lower

14) A. Tsuruizumi, ibid., **79**, 273 (1957).
15) A. Blackburn and J. J. Kipling, *J. Chem. Soc.*, **1955**, 1493.

TABLE VI. SURFACE AREA OBTAINED FROM ADSORPTION ISOTHERM

| Adsorbates | Adsorptive sectional area, Å² | Surface area, m²/g. $S_4$ [450][a] | $SZ_4$ [1600] | Silica gel No. 28 [720] |
|---|---|---|---|---|
| Formic acid | 13.38 | 342.0 | 2365.0 | 717.0 |
| Acetic acid | 19.58 | 106.0 | 1828.0 | 755.0 |
| *n*-Propionic acid | 25.01 | 55.0 | 1600.0 | 716.0 |
| Benzene | 29.13 | 26.5 | 1100.0 | 723.0 |
| *n*-Heptane | (29.20)[b] | 19.0 | 850.0 | 680.0 |
| *n*-Butyric acid | 31.35 | 0.9 | 717.0 | 730.0 |

a) [ ] Surface area from BET method.
b) If adsorptive section is circle from Fig. 10, its radius get 3.05Å as adsorptive sectional area is calculated 29.20Å².

values. This discrepancy can be explained as follows. The molecules of formic and acetic acid are small enough to diffuse into fine pores, and before the formation of a uniform monolayer, a capillary condensation takes place. This increases the apparent surface area. The critical temperatures of the formic and acetic acid are lower than those of the higher acids, but this is not the predominant factor for the earlier occurrence of the capillary condensation. The same situation was found in the adsorption of nitrogen gas as has been reported previously by the present author[13]. These effects of molecular size of the adsorbates on the adsorption characteristics suggest the existence of a number of pores of irregular shapes such as narrow-neck or ink-bottle on the sugar carbon surface.

BET type adsorption isotherms were observed for all the acids on $S_4$ as is shown in Fig. 8. A surface area of $S_4$ calculated by the B-point method is, however, remarkably smaller than the nitrogen BET area as is seen in Table VI, and this disagreement increased with the c-number of the acid molecule. This sieving effect of the carbon $S_4$ is presumed to be due to the special pore-distribution, a greater part of the surface being composed of the micropores of average radius less than 8.2Å. An adsorption isotherm of benzene (non-polar adsorbate) on silica gel No. 28 (polar adsorbent) obtained under the same conditions shows no hysteresis as is shown in Fig. 8, and a surface area calculated by the B-point method was identical with the nitrogen BET area as is shown in Table VI.

As is seen in the Fig. 8, the desorption curve of benzene vapor from the silica gel returns back to the original point, These facts indicate that no chemisorption takes place on the silica gel. BET type adsorption isotherms were observed for various carboxylic acids on silica gel No. 28 as is shown in Fig. 9. Values of the effective surface area of silica gel obtained by the B-point method for the series of carboxylic acids are equal to the nitrogen BET area as is seen in Table VI. These results lead us to conclude that there exist no pores of narrow-neck or ink-bottle shape on the surface of the silica gel, and the pore size is large enough to accommodate such large adsorbate molecules as the carboxylic acids.

In Fig. 9, the anomalous behavior of the adsorption of the carboxylic acids (*n*-butyric acid) on the silica gel is shown. According to a number of reports[16-23], the heat treatment in vacuo reduces the number of OH groups and changes the nature of S–O bonds. The OH groups on the silica gel were not exterminated by the usual calcination, and a greater part of the group are thought to remain in the samples of the present study. The unclosed hysteresis loop of the *n*-butyric acid is presumed to be due to the chemisorption with these residual OH groups. When the adsorption-desorption process is repeated once again from a point $P/P_0=0$, the loop returns back to the original point as is seen in Fig. 9. Clearly the second adsorption process was physical in nature, and no anomality appears in further repetitions of the process.

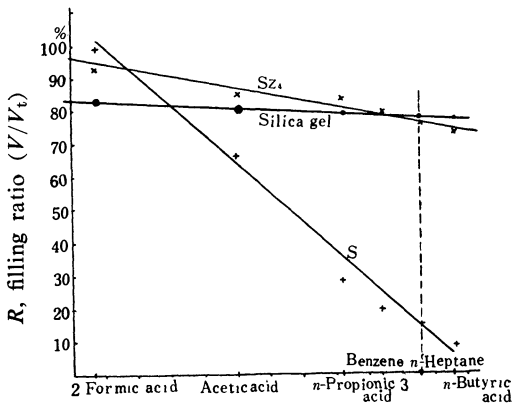



Fig. 10. Sieving coefficient.

16) J. J. Kipling and D. B. Peakall, ibid., **1957**, 834.
17) J. H. de Boer, M. E. A. Hermans and J. M. Vleeskens, *Konnikl. Ned. Akad. Wetenschap. Proc., Ser.* **B60**, 45 (1957).
18) J. H. D. de Boer and J. W. Vleeskens. ibid., **B60**, 234 (1957).
19) L. D. Belyakova and A. V. Kiselev, *Doklady Akad. Nauk S. S. S. R.*, **119**, 298 (1958).
20) A. V. Kiselev, V. V. Khopina and Yu. A. Elekov, *Izvest. Akad. Nauk S. S. S. R., Chem. Sci. Sec.*, 664 (1958).
21) K. G. Krasil'nikov, V. F. Kiselev and E. T. Sysoec., *Doklady Akad. Nauk S. S. S. R.*, **116**, 990 (1957).
22) S. P. Zhdanow and A. V. Kiselev., *Zhur. Fiz. Khim.*, **31**, 2213 (1957).
23) D. D. Belvakova, O. M. Dzhigit and A. V. Kiselev, ibid., **31**, 1577 (1958).

In Fig. 10, the filling ratio, $R=V/V_t$, is plotted against the radii of the adsorption sectional area of the adsorbate molecules, $r$, where $V_t$ is the total volume of adsorbent (Tables IV and VII) and $V$, the total volume of the adsorbate adsorbed on the adsorbent (Table VII).

TABLE VII. ADSORBED VOLUME, A, OF ADSORBATES AT $P/P_0=1.0$

| Adsorbate | Adsorbed volum, $V$ | | |
|---|---|---|---|
| | $S_4$ | $SZ_4$ | Silica gel |
| Formic acid | 0.21 | 1.06 | 0.41 |
| Acetic acid | 0.14 | 0.97 | 0.40 |
| *n*-Propionic acid | 0.06 | 0.95 | 0.39 |
| Benzene | 0.04 | 0.90 | 0.387 |
| *n*-Heptane | 0.03 | 0.86 | 0.38 |
| *n*-Butyric acid | 0.018 | 0.83 | 0.38 |
| Total pore vol., $V_t$ | 0.2126 | 1.142 | 0.4960 |

The adsorbed volume was calculated on the assumption that the density of the adsorbed liquid is the same as that in bulk. As for the *n*-heptane, the length and width of the molecule is reported to be 11.6 and 4.9Å, respectively, but the radius of the cross section, $r$, is unknown. If the values of the filling ratio of *n*-heptane are marked on the lines in Fig. 10, the three points lie on a line which meets with the abscissa at right angles. The radius can be estimated from the cut on the abscissa as 3.05Å which is proper in order of magnitude compared with the width.

The filling ratios change linearly with the radii of the adsorptive sectional area for respective adsorbents. The new term "sieving coefficient" is defined as the slope of these lines, which signifies an ability of the physical selective adsorption or the sieving effect. The sieving coefficient increases with the sharpness of the peak in the pore-size distribution curve. The coefficients for the adsorbents studied are as follows:

$S_4$ $0.947_3$, $SZ_4$ $0.155_5$, Silica gel No. 28 0.057.

The sieving coefficient would be quite a useful term to specify the adsorptive behavior of the adsorbents.

## Summary

1. The adsorption characteristics of the sugar carbon prepared by carbonization or activation and silica gel were studied in detail by the adsorption of water, benzene and fatty acid vapors, and mercury porosimetry.

The pore distribution of the active carbon was tri-disperse. The effects of the partial filling of the pores were examined. The missing link in the distribution curve between the micro-pore and transitional pore in the previous reports was replenished.

2. The narrow-neck or ink-bottle structure of the pores of sugar carbon complicated the adsorption characteristics. The pores of the silica gel were cylindrical with a uniform section.

3. In order to specify the physical selective adsorption, the new term "sieving coefficient" was defined from the relation between the pore radii and cross sections of the adsorbates.

The author expresses his gratitude to Professor I. Sano of Nagoya University for his encouragement.

*Department of Chemistry*
*Nagoya Municipal Industrial*
*Research Institute*
*Atsuta-ku, Nagoya*

# *Non-empirical Study of the π-Electronic Structure of Vinyl Chloride Molecule by Valence Bond Method*

By Shozaburo TAKEKIYO

(Received October 21, 1960)

In the year 1956, a semi-empirical consideration of conjugation in vinyl chloride molecule with molecular orbital method was performed by Goldstein[1] and recently the self-consistent field calculations of the π-electronic energy levels and the wave functions for the ground state have been carried out non-empirically by Simonetta and others[2].

On the other hand, it seems that no considerations by valence bond method have ever been made, except a semi-empirical calculation of the double bond character due to the resonance of the C–Cl bond in the molecule[3].

In this paper, the HLSP method[4] is applied to the non-empirical calculation of the π-electronic energy levels and other electronic properties of the molecule and the results are compared with those obtained by the method of LCAO self-consistent field.

## Energy Levels and Wave Functions

The skeleton of the molecule is shown in Fig. 1.

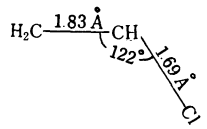



Fig. 1. Skeleton of vinyl chloride molecule.

For the carbon atoms and the chlorine atom, Slater $2p_\pi$- and $3p_\pi$-orbitals with $Z_C=3.18$, $Z_{Cl}=6.099$ have been assumed.

The approximate Hamiltonian operator $H$ employed here is

$$H=\sum_i [T(i)+U_{\text{core}}(i)]+(1/2)\sum_{\substack{i,\ j\\ i\neq j}}(e^2/r_{ij})$$

where $T(i)$ is the kinetic energy operator for electron $i$ and $U_{\text{core}}(i)$ is the potential energy operator for this electron in the field of the core.

Numerical values of integrals over atomic orbitals have been taken from Simonetta and others[2].

All the π-type resonance structures, whose corresponding bond eigenfunctions are linearly independent, and the energy values for these structures are shown in Fig. 2.

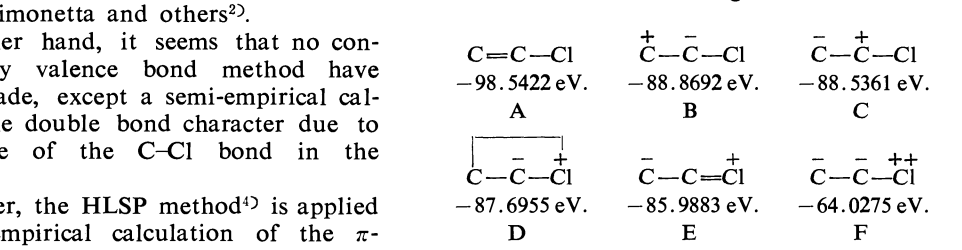



Fig. 2. Canonical structures and the energy values for the structures.

In the calculations all kinds of overlap and exchange integrals have been considered.

Wave functions for the molecule and the corresponding energy values are shown in Table I, where $\Phi_i$ is the wave function, corresponding to the energy $E_i$, and $\Psi_K$ is the normalized bond eigenfunction for structure K.

TABLE I. WAVE FUNCTIONS FOR THE MOLECULE AND THE ENERGY VALUES

$$\Phi_1=0.73595\Psi_A+0.21845\Psi_B+0.22127\Psi_C+0.16156\Psi_D+0.11523\Psi_E+0.00667\Psi_F \qquad E_1=-100.91\text{ eV.}$$

$$\Phi_2=0.09265\Psi_A-0.01220\Psi_B-0.29470\Psi_C-0.31017\Psi_D+1.09225\Psi_E-0.30640\Psi_F \qquad E_2=-89.50\text{ eV.}$$

$$\Phi_3=0.09583\Psi_A-0.57177\Psi_B+0.71265\Psi_C-0.49640\Psi_D-0.04121\Psi_E+0.00000\Psi_F \qquad E_3=-85.50\text{ eV.}$$

$$\Phi_4=0.04141\Psi_A-0.05625\Psi_B-0.01469\Psi_C+0.02055\Psi_D-0.03334\Psi_E-0.00362\Psi_F \qquad E_4=-82.37\text{ eV.}$$

$$\Phi_5=0.61285\Psi_A-0.31888\Psi_B-0.78240\Psi_C-0.52176\Psi_D+0.70541\Psi_E+0.11148\Psi_F \qquad E_5=-76.41\text{ eV.}$$

$$\Phi_6=0.03309\Psi_A-0.00686\Psi_B-0.09569\Psi_C-0.07927\Psi_D+0.38669\Psi_E-1.02578\Psi_F \qquad E_6=-61.47\text{ eV.}$$

1) J. H. Goldstein, *J. Chem. Phys.*, **24**, 507 (1956).
2) M. Simonetta, G. Favini and S. Carra, *Mol. Phys.*, **1**, 181 (1958).
3) J. A. A. Ketelaar, *Rec. trav. chim.*, **58**, 266 (1939).
4) W. Heitler and F. London, *Z. Phys.*, **44**, 455 (1927); J. C. Slater, *Phys. Rev.*, **37**, 481 (1931); L. Pauling, *J. Am. Chem. Soc.*, **53**, 1367 (1931).

### Probabilities of Resonance Structures, Charge Densities, and Bond Orders

Probability $P_K$ for structure K has been calculated by the most popular expression

$$P_K = C_K \sum_L C_L \int \Psi_K \Psi_L d\tau$$

where $C_K$ is the coefficient of bond eigenfunction $\Psi_K$ in the wave function for the ground state of the molecule and $d\tau$ is the product of the volume elements for the four π-electrons. The results are as follows:

$$P_A = 0.6846 \qquad P_B = 0.1110 \qquad P_C = 0.1198$$
$$P_D = 0.0543 \qquad P_E = 0.0300 \qquad P_F = 0.0003$$

Then π-electron density $D_i$ for atom $i$ and bond order $B_{ij}$ between atoms $i$ and $j$ have been evaluated by the following equations:

$$D_i = \sum_K P_K m_i^K$$

$$B_{ij} = \sum_K P_K (n_{ij}^K + 1)$$

where $m_i^K$ is the number of π-electrons on atom $i$ in structure K and $n_{ij}^K$ is the number of the covalent π-bonds between atoms $i$ and $j$ in structure K. These results are shown in Fig. 3.

$$\underset{1.0391}{H_2C} \overset{1.6846}{\text{——}} \underset{1.0458}{CH} \overset{1.0300}{\text{——}} \underset{1.9151}{Cl}$$

Fig. 3. π-Electron densities and bond orders.

### Discussion

The transition energy between the ground state and the first excited state is 11.41 eV. (Table I) The value, calculated by the method of LCAO self-consistent field, is

$$E_{V23} - E_N = 11.1842 \text{ eV}.^{2)}$$

The numerical difference between the two methods seems to be due to the neglect of the self-consistent procedure for the calculation of the excited state in the latter.

The formula of Pauling and others[5] has been used to evaluate the C–C and the neighboring C–Cl bond lengths from the semi-empirical values of bond radii[6]; and the results are as follows:

$$R_{C-C} = 1.358 \text{ Å} \qquad R_{C-Cl} = 1.744 \text{ Å}$$

The values, obtained by Simonetta and others, are $R_{C-C} = 1.448$ Å and $R_{C-Cl} = 1.73$ Å[2], and the experimental values are 1.38 and 1.69 Å respectively[7].

The positive charge on the chlorine atom is evaluated as $2 - 1.9151 = 0.0849$ and the interpreted value from observation is 0.06[8].

The ionic character of the molecule, calculated from the values of the probabilities, is 31.54%.

### Summary

π-electronic energy levels, probabilities of the resonance structures, π-electron densities, and the bond orders of the vinyl chloride molecule have been calculated non-empirically by the standard valence bond method, based on a complete set of the π-type resonance structures. Slater $2p_\pi$- and $3p_\pi$-orbitals have been assumed for the carbon and chlorine atoms and all the multiple exchange integrals have been considered. The calculated transition energy between the ground state and the first excited state is 11.41 eV., the ionic character is 31.54%, and the positive charge on the chlorine atom is 0.0849 (experimental value is 0.06.).

The author wishes to express his sincere thanks to Professor Kyosuke Omori, Kyushu University, for many helpful criticisms and suggestions. Thanks are also due to Professor Saburo Nagakura, the University of Tokyo, for his advice and valuable assistance.

*Faculty of Liberal Arts*
*Nagasaki University*
*Ohashi, Nagasaki*

5) L. Pauling, L. O. Brockway and J. Y. Beach, *J. Am. Chem. Soc.*, **57**, 2705 (1935); L. Pauling and L. O. Brockway, ibid., **59**, 1223 (1937).

6) L. Pauling, "The Nature of the Chemical Bond", Cornell University Press (1939), p. 154.

7) P. W. Allen and L. E. Sutton, *Acta Cryst.*, **3**, 46 (1950).

8) J. H. Goldstein and J. K. Bragg, *Phys. Rev.*, **78**, 347 (1950).

# *Preparation of Perfluorocarboxylic Acids from Esters by Electrochemical Fluorination**

By Shunji NAGASE and Rimpei KOJIMA

(Received December 26, 1960)

Perfluorocarboxylic acids have been prepared from carboxylic acids, acid halides, acid anhydrides and acid amides, ketones, ethers etc. by electrochemical fluorination[1-4].

In a previous paper[5], it was shown that perfluorocarboxylic acids were prepared in a significant yield from alcohols which were known to give only fluorocarbons by electrochemical fluorination[1,6]. A possible mechanism of the fluorination of alcohols to perfluorocarboxylic acid fluorides was assumed to involve the first attack by fluorine on $\alpha$-carbon atom of the alcohols, and dehydrofluorination followed by exhaustive fluorination of acid fluorides formed as intermediates to perfluoro-acid fluorides.

The present paper deals with the work extended further to the fluorination of esters to obtain perfluorocarboxylic acids.

So far, there has been no detailed report on the electrochemical fluorination of simple esters. Simons[2] carried out the fluorination of butyl acetate and made decafluorobutane.

In the present series of work, ethyl, propyl and butyl acetates, ethyl, propyl and butyl propionates, and ethyl, propyl and butyl butyrates were fluorinated and trifluoroacetic, perfluoropropionic, and perfluorobutyric acids were obtained in good yields.

Again, the mechanism of dehydrofluorination at $\alpha$-carbon atom of alcohols which takes place after hydrofluorolysis of esters into carboxylic acid fluorides and alcohols, could be applied to the formation of perfluorocarboxylic acid fluorides from esters.

The perfluorocarboxylic acid fluorides formed were converted into perfluorocarboxylic acids by treatment with water. No detectable amount of partially fluorinated esters and alcohols were found in the residue in the electrolytic cell but the presence of acid fluorides and unreacted esters, etc. was confirmed.

## Experimental

**Materials.**—*Esters.*—Special or first grade commercial reagents were used after distillation through a fractionation column. Some of the esters were prepared in the usual manner in this laboratory.

*Hydrogen Fluoride.*—Hydrogen fluoride purity of 99.4% was supplied from a commercial cylinder.

**Apparatus.**—The apparatus used for this work essentially consisted of an electrolytic cell, a sodium fluoride tube, and an absorber, as described previously[5].

The electrolytic cell of 1 l. in capacity was a 10-cm. cylindrical nickel vessel provided with a copper condenser at the top to cool down vaporizing hydrogen fluoride and a drain at the bottom, and having 8 and 9 pieces of nickel plates (0.5 mm. in thickness) as anodes and cathodes, fastened together, suspended alternately from the top, and insulated from each other by Teflon pieces. The distance between the plates was 1.7 mm. and the effective surface area of the anodes and cathodes was 9.2 $dm^2$. A copper tubing was provided inside the cell to keep the optimum temperature by circulation of ice water during the reaction.

The sodium fluoride tube was an iron pipe containing sodium fluoride pellets to remove hydrogen fluoride.

The absorber used was a pair of polyethylene bottles containing 200 and 50 ml. of water.

**Procedure.**—One liter of hydrogen fluoride was introduced into the cell through the polyethylene container, and electrolysis was carried out without a sample to remove a trace of water in the hydrogen fluoride at an average of 5.2 V. for about 13 amp. hr. in nitrogen atmosphere. About 35 g. of the sample was then dissolved in this solution and electrolysis was carried out with the anodic current density of 2.5 to 3.5 amp./$dm^2$ at an average of 4.8 V., at 4~6°C for designated amp. hr. At the end, the voltage rose up to 5.2~5.3 V.

It was found that the amount of the electricity used up to this point corresponded to about 1.3 times that assumed to be required to form fluorine with discharging fluoride ion which would substitute with hydrogen in the sample and combine with it to form hydrogen fluoride.

The gaseous product generated from the cell, containing fluorocarbons, oxygen difluoride, perfluoro-acid fluorides, hydrogen, etc. was passed through

---

* Presented in part at the Tokai Local Meeting of the Chemical Society of Japan, Nagoya, November, 1960.

1) J. H. Simons et al., *J. Electrochemical Soc.*, **95**, 47 (1949).

2) J. H. Simons, U. S. Pat., 2519983 (1950).

3) A. R. Diesslin, E. A. Kauck and J. H. Simons, U. S. Pat., 2567011 (1951); U. S. Pat, 2593737 (1952).

4) E. A. Kauck and A. R. Diesslin, *Ind. Eng. Chem.*, **43**, 2332 (1951).

5) S. Nagase and R. Kojima, *J. Chem. Soc. Japan, Ind. Chem. Sec.* (*Kogyo Kagaku Zasshi*), in press.

6) J. Burdon and J. C. Tatlow, "Advances in Fluorine Chemistry", Vol. 1, Ed. by M. Stacey, J. C. Tatlow and A. G. Sharpe, Butterworths Scientific Publications Ltd., London (1959), p. 157.

the condenser and the sodium fluoride tube, and bubbled through water in the absorber where the perfluoro-acid fluorides reacted, and converted into perfluorocarboxylic acids. In this system, the gases which are inert to water should escape as gases.

When the reaction was over, the hydrogen fluoride in the cell was distilled into the polyethylene container which was used repeatedly by adding it into the new hydrogen fluoride for the next run, but for different kinds of esters, hydrogen fluoride freshly supplied from the cylinder was used. About 50 ml. of a residue consisting mainly of hydrogen fluoride remained at the bottom of the cell and its other components were investigated further by the method described earlier[5].

The aqueous solution of the perfluorocarboxylic acids in the absorber was neutralized with sodium carbonate, filtered and the filtrate was dried. The sodium perfluorocarboxylates formed were then extracted with absolute ethanol.

Quantitative analysis of the products was made by the base line method with potassium bromide pellet infrared absorption spectrum using 11.88 $\mu$ (for sodium trifluoroacetate), 9.68 $\mu$ (for sodium perfluoropropionate), and 10.65 $\mu$ (for sodium perfluorobutyrate) as key bands. The standard sodium carboxylates were prepared from trifluoroacetic acid secured from the Eastman Kodak Co., and perfluoropropionic and perfluorobutyric acids secured from the Minnesota Mining and Manufacturing Co. by treatment with sodium carbonate.

When several runs were repeated, the electrodes were stained with a grey substance, which was removed by electropolishing in 0.5% of potassium carbonate solution.

## Results and Discussion

The effect of anodic current density on the yield was mainly examined in a similar manner as in the fluorination of alcohols. Trifluoroacetic acid was obtained from ethyl acetate and the results are shown in Table I. The yields shown were calculated on the basis that 1 mol. of ethyl acetate would give 2 mol. of sodium trifluoroacetate. The fluorination of ethanol also yielded trifluoroacetic acid, but the yield was usually less than that in the case of ester.

The calculation of current efficiencies shown was based on the amount of the electricity assumed to be required to form fluorine with a discharging fluoride ion which would substitute hydrogen in the ester and combine with it to form hydrogen fluoride. This means that the electricity to make 8 mol. of fluorine would be required for the fluorination of 1 mol. of ethyl acetate to form 2 mol. of sodium trifluoroacetate.

The results obtained from the fluorination of propyl acetate, from which trifluoroacetic and perfluoropropionic acids were obtained, are shown in Table II. The yields shown were also calculated on the basis that 1 mol. of propyl acetate would give 1 mol. of sodium trifluoroacetate and 1 mol. of sodium perfluoropropionate, which means that the acyl and the alkyl groups in the ester would give perfluorocarboxylic acids whose number of carbon atoms corresponds to those of the acyl and the alkyl group in the ester.

Table I. Fluorination of ethyl acetate

Electricity passed: 211 amp. hr.
Sample taken: 34.5 g.

| $D_A$[a] amp./dm$^2$ | Product obtained g. | Yield % | Current efficiency % |
|---|---|---|---|
| 2.5 | 45.6 | 43.4 | 34.0 |
| 2.7 | 47.2 | 44.9 | 35.2 |
| 3.0 | 52.0 | 49.5 | 38.8 |
| 3.3 | 54.2 | 51.6 | 40.5 |
| 3.5 | 54.9 | 52.3 | 41.0 |

a) $D_A$: Anodic current density.

The current efficiency was also calculated by the same method as for ethyl acetate, i. e. the electricity assumed to make 10 mol. of fluorine would be required for the fluorination of 1 mol. of propyl acetate to form 1 mol. of sodium trifluoroacetate and 1 mol. of sodium perfluoropropionate.

The results obtained from the fluorination of butyl acetate, ethyl, propyl and butyl propionates, and ethyl, propyl and butyl butyrates are shown in the Tables. All of the yields and current efficiencies shown were calculated in the same way as was mentioned above.

It was found that the yield of the perfluorocarboxylic acid obtained from the fluorination of propyl propionate or butyl butyrate was much higher than that from propyl or butyl alcohol, but the degree of cleavage which would result in the formation of perfluorocarboxylic acids consisting of a smaller number of carbon atom than that of corresponding alcohol, or acyl or alkyl group in the ester was essentially the same in alcohols and esters.

It is of interest to know which side of the ester, acyl or alkyl group, would give perfluorocarboxylic acid more easily. Comparison between the results obtained from butyl acetate and ethyl butyrate or butyl propionate and propyl butyrate indicated that perfluorobutyric acid was obtained in better yield from ethyl and propyl butyrates than from butyl acetate and butyl propionate. This showed that perfluorocarboxylic acids are formed more easily from acyl than alkyl group in the ester.

When the number of carbon atoms increased in the ester, the degree of cleavage increased, as is usually observed in electrochemical fluorination. For example, propyl acetate gave sodium trifluoroacetate and sodium perfluoropropionate in molar ratio of about 1 to 0.9, but butyl acetate gave sodium trifluoroacetate

TABLE II. FLUORINATION OF PROPYL ACETATE
Electricity passed: 228 amp. hr.

| Sample taken | $D_A$ | Product obtained | Yield | Current efficiency | Composition[a] | |
|---|---|---|---|---|---|---|
| g. | amp./dm² | g. | % | % | $CF_3COONa$ | $C_2F_5COONa$ |
| 34.5 | 2.5 | 35.7 | 32.7 | 26.1 | 46 | 54 |
| 34.5 | 2.7 | 42.0 | 38.5 | 30.7 | 45 | 55 |
| 34.5 | 3.0 | 34.3 | 31.5 | 25.1 | 45 | 55 |
| 34.6 | 3.3 | 36.7 | 33.6 | 26.8 | 44 | 56 |
| 34.5 | 3.5 | 46.3 | 42.5 | 33.8 | 46 | 54 |

a) The composition of the products analyzed by infrared spectrophotometer is given in weight per cent.

TABLE III. FLUORINATION OF BUTYL ACETATE
Electricity passed: 240 amp. hr.

| Sample taken | $D_A$ | Product obtained | Yield | Current efficiency | Composition, wt. % | | |
|---|---|---|---|---|---|---|---|
| g. | amp./dm² | g. | % | % | $CF_3COONa$ | $C_2F_5COONa$ | $C_3F_7COONa$ |
| 34.6 | 2.5 | 32.7 | 29.5 | 23.5 | 60 | 2.4 | 38 |
| 34.5 | 2.7 | 27.1 | 24.5 | 19.4 | 63 | 1.9 | 33 |
| 34.5 | 3.0 | 32.7 | 29.6 | 23.5 | 56 | 4.7 | 40 |
| 34.5 | 3.3 | 30.8 | 27.9 | 22.2 | 64 | 1.9 | 34 |
| 34.6 | 3.5 | 39.7 | 35.8 | 28.6 | 54 | 2.7 | 43 |

TABLE IV. FLUORINATION OF ETHYL PROPIONATE
Electricity passed: 228 amp. hr.
Sample taken: 34.5 g.

| $D_A$ | Product obtained | Yield | Current efficiency | Composition, wt. % | |
|---|---|---|---|---|---|
| amp./dm² | g. | % | % | $CF_3COONa$ | $C_2F_5COONa$ |
| 2.5 | 17.2 | 15.8 | 12.6 | 46 | 54 |
| 2.7 | 38.9 | 35.7 | 28.4 | 45 | 55 |
| 3.0 | 43.4 | 39.8 | 31.7 | 44 | 56 |
| 3.3 | 35.1 | 32.2 | 25.7 | 46 | 54 |
| 3.5 | 53.5 | 49.1 | 39.1 | 47 | 53 |

TABLE V. FLUORINATION OF PROPYL PROPIONATE
Electricity passed: 240 amp. hr.
Sample taken: 34.5 g.

| $D_A$ | Product obtained | Yield | Current efficiency | Composition, wt. % | |
|---|---|---|---|---|---|
| amp./dm² | g. | % | % | $CF_3COONa$ | $C_2F_5COONa$ |
| 2.5 | 29.6 | 26.7 | 21.3 | 7.3 | 93 |
| 2.7 | 33.2 | 29.9 | 23.9 | 5.1 | 95 |
| 3.0 | 36.2 | 32.6 | 26.1 | 6.8 | 93 |
| 3.3 | 38.5 | 34.7 | 27.7 | 5.3 | 95 |
| 3.5 | 38.6 | 34.8 | 27.7 | 7.1 | 93 |

TABLE VI. FLUORINATION OF BUTYL PROPIONATE
Electricity passed: 250 amp. hr.
Sample taken: 34.5 g.

| $D_A$ | Product obtained | Yield | Current efficiency | Composition, wt. % | | |
|---|---|---|---|---|---|---|
| amp./dm² | g. | % | % | $CF_3COONa$ | $C_2F_5COONa$ | $C_3F_7COONa$ |
| 2.5 | 30.3 | 27.1 | 21.5 | 6.5 | 65 | 28 |
| 2.7 | 30.7 | 27.5 | 21.7 | 6.9 | 67 | 26 |
| 3.0 | 33.6 | 30.0 | 23.8 | 7.7 | 62 | 31 |
| 3.3 | 29.7 | 26.6 | 21.1 | 7.8 | 64 | 29 |
| 3.5 | 43.1 | 38.6 | 30.6 | 6.3 | 64 | 30 |

Table VII. Fluorination of ethyl butyrate

Electricity passed: 240 amp. hr.
Sample taken: 34.5 g.

| $D_A$ | Product obtained | Yield | Current efficiency | Composition, wt, % | | |
|---|---|---|---|---|---|---|
| amp./dm² | g. | % | % | $CF_3COONa$ | $C_2F_5COONa$ | $C_3F_7COONa$ |
| 2.5 | 31.8 | 28.9 | 23.1 | 50 | 3.9 | 46 |
| 2.7 | 27.3 | 24.8 | 18.8 | 49 | 4.9 | 46 |
| 3.0 | 35.6 | 32.3 | 25.9 | 56 | 2.3 | 42 |
| 3.3 | 35.8 | 32.5 | 26.0 | 55 | 2.8 | 43 |
| 3.5 | 32.4 | 29.4 | 23.5 | 49 | 4.1 | 47 |

Table VIII. Fluorination of propyl butyrate

Electricity passed: 250 amp. hr.
Sample taken: 34.5 g.

| $D_A$ | Product obtained | Yield | Current efficiency | Composition, wt. % | | |
|---|---|---|---|---|---|---|
| amp./dm² | g. | % | % | $CF_3COONa$ | $C_2F_5COONa$ | $C_3F_7COONa$ |
| 2.5 | 24.2 | 21.7 | 17.2 | 6.3 | 60 | 34 |
| 2.7 | 31.3 | 28.0 | 22.2 | 6.2 | 59 | 35 |
| 3.0 | 31.5 | 28.2 | 22.3 | 6.4 | 55 | 38 |
| 3.3 | 28.0 | 25.1 | 19.9 | 6.2 | 56 | 38 |
| 3.5 | 30.1 | 26.9 | 21.3 | 6.3 | 58 | 36 |

Table IX. Fluorination of butyl butyrate

Electricity passed: 258 amp. hr.
Sample taken: 34.5 g.

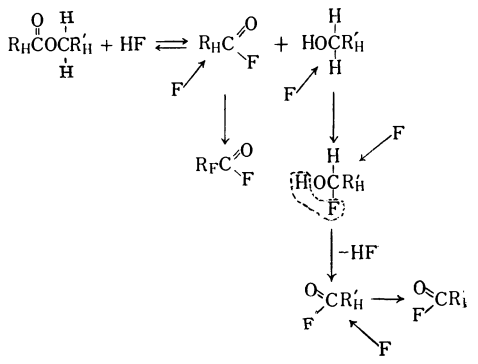
| $D_A$ | Product obtained | Yield | Current efficiency | Composition, wt. % | | |
|---|---|---|---|---|---|---|
| amp./dm² | g. | % | % | $CF_3COONa$ | $C_2F_5COONa$ | $C_3F_7COONa$ |
| 2.5 | 19.0 | 16.8 | 13.4 | 9.1 | 13 | 78 |
| 2.7 | 22.2 | 19.7 | 15.6 | 8.8 | 8.8 | 82 |
| 3.0 | 26.0 | 23.0 | 18.3 | 9.4 | 7.1 | 83 |
| 3.3 | 31.1 | 27.5 | 21.9 | 8.8 | 6.6 | 85 |
| 3.5 | 36.8 | 32.5 | 25.9 | 7.1 | 5.4 | 87 |

and sodium perfluorobutyrate in molar ratio of about 1 to 0.4, which indicates that butyl radical is degradated considerably as compared with propyl radical.

In the fluorination of alcohols, the maximum yield of perfluorocarboxylic acids was obtained with anodic current density of 3.3 amp./dm², and the yield decreased sharply with higher or lower current densities, irrespective of the kind of alcohols used, but there seemed to be no such simple relationship between the anodic current density and yield for the esters within the range of the current density applied. However, the yield generally increased with increasing current density.

The presence of a small amount of unreacted ester remaining in the residue in the cell along with the acetyl fluoride and partially fluorinated carboxylic acid fluorides was confirmed. The grey precipitate consisting mainly of nickel and copper fluorides was also found in the residue.

The mechanism of the fluorination of esters to form perfluorocarboxylic acid fluorides, although this reaction obviously could and probably did follow different routes simultaneously, might involve, in the first place, hydrofluorolysis of the esters in hydrogen fluoride to form acid fluorides and alcohols as shown below. Alcohols formed in this way would be converted into acid fluorides through the mechanism of dehydrofluorination at the $\alpha$-carbon atom.



In these formulae, $R_H$ and $R_H'$ are hydrocarbon radicals, and $R_F$ and $R_F'$ are perfluorocarbon radicals. Acid fluorides $R_H$–COF and $R_H'$–COF thus formed would be fluorinated further to perfluorocarboxylic acid fluorides.

## Conclusion

1) Perfluorocarboxylic acids were obtained from esters in a good yield by electrochemical fluorination and the relationship between anodic current density and yield was examined. Generally, the yield increased with increasing anodic current density.

2) The result of electrochemical fluorination of esters was compared with that of alcohols. A better yield was obtained from the esters.

3) The presence of a larger number of carbon atoms in the acyl or alkyl group in the ester caused more degradation than those of smaller numbers.

4) The mechanism of the formation of perfluorocarboxylic acid fluorides from esters was discussed.

The authors wish to express their sincere thanks to Osaka Metal Industries Co. for supplying hydrogen fluoride.

*Government Industrial Research Institute, Nagoya*
*Kita-ku, Nagoya*

# *Molecular Structure Investigation of Chlorotrifluoroethylene by Electron Diffraction*

By Takeshi KAWAI, Hiroshi SEKINE and Masato IGARASHI

(Received January 30, 1961)

The molecular structures of chlorine and fluorine derivatives of ethylene such as tetrachloroethylene[1-3] and tetrafluoroethylene[4,5] have been studied by electron diffraction using a sector-microphotometer or visual methods (Table I).

In order to see the carbon-halogen bond distances and the valence angles of ethylene derivative including two kinds of halogens, we investigated chlorotrifluoroethylene (Kel F monomer) by electron diffraction using the visual method and compared it with those of the related compounds.

## Experimental

The sample was prepared by Osaka Kinzoku Industrial Co.

The apparatus of electron diffraction was the same as that in the previous report[6]. In order to reduce the vapor pressure of the sample the liquid-sample reservoir was cooled by a mixture of dry ice and alcohol during the diffraction experiment. The diffraction photographs were measured by the visual method (Fig. 1).

## Analysis and Results

The radial distribution and theoretical intensity curves have been calculated by the usual method. The thermal factors were omitted for convenience in all the theoretical intensity curves except curves D′ and D″ in which the mean amplitudes listed in Table III were used. Some of the intensity curves are shown in Fig. 1 and the molecular parameters of the corresponding models are listed in Table II.

As can be seen from the first peak of the radial distribution curve (Fig. 2), it is difficult to distinguish the C=C and the three C-F bond distances separately. The mean value of them is 1.31 Å. The second peak shows that the C-Cl bond distance is 1.71 Å.

When the angles FCF and FCCl of the models are varied, the C=C and all the C-F bond distances being fixed at 1.31 Å and the C-Cl band distance at 1.71 Å, the features of the maxima or the shelves at about $q=28\sim41$ of the theoretical intensity curves change appreciably and the curves C and D, in which the two angles are equal to 115 and 114°, respectively, fit better with the observed curve

1) L. O. Brockway, J. Y. Beach and L. Pauling, *J. Am. Chem. Soc.*, **57**, 2693 (1935).
2) W. N. Lipscomb, Ph. D. Thesis, California Institute of Technology, 1946.
3) I. L. Karle and J. Karle, *J. Chem. Phys.*, **20**, 63 (1952).
4) I. L. Karle and J. Karle, ibid., **18**, 963 (1950).
5) T. T. Broun and R. L. Livingston, *J. Am. Chem. Soc.*, **74**, 6084 (1952).
6) T. Yuzawa and M. Yamaha, This Bulletin, **26**, 414 (1953).

TABLE I. MOLECULAR STRUCTURES OF TETRACHLOROETHYLENE AND TETRAFLUOROETHYLENE

Tetrachloroethylene

| Reference | C-Cl, Å | C=C, Å | ∠ClCCl | ∠CCCl | Method |
|---|---|---|---|---|---|
| 1 | 1.73±0.02 | 1.38 | | 123.7±1° | visual |
| 2 | 1.71±0.02 | 1.34±0.05 | 115.5±2° | 122.1±1° | visual |
| 3 | 1.72±0.01 | 1.30±0.03 | 113.5±1.5° | | sector |

Tetrafluoroethylene

| Reference | C-F, Å | C=C, Å | ∠FCF | Method |
|---|---|---|---|---|
| 4 | 1.313±0.010 | 1.313±0.035 | 114±2° | sector |
| 5 | 1.30 ±0.02 | 1.33 ±0.06 | 114±2° | visual |

TABLE II. PARAMETERS OF MOLECULAR MODELS FOR THE THEORETICAL INTENSITY CURVES AND $q_{calcd}/q_{obs}$ VALUES

| Model | C=C Å | C-F Å | C-Cl Å | ∠FCF | ∠FCCl | ∠CCCl | $q_{calcd}/q_{obs}$ | Average deviation |
|---|---|---|---|---|---|---|---|---|
| A | 1.31 | 1.31 | 1.71 | 120° | 120° | 120° | | |
| B | 1.31 | 1.31 | 1.71 | 117° | 117° | 121.5° | | |
| C | 1.31 | 1.31 | 1.71 | 115° | 115° | 122.5° | 1.000 | 0.017 |
| D | 1.31 | 1.31 | 1.71 | 114° | 114° | 123° | 1.004 | 0.015 |
| E | 1.31 | 1.31 | 1.71 | 112° | 112° | 124° | | |
| F | 1.31 | 1.31 | 1.71 | 114° | 117° | 121.5° | | |
| G | 1.31 | 1.31 | 1.71 | 114° | 120° | 117° | | |
| H | 1.31 | 1.31 | 1.71 | 114° | 114° | 120° | | |
| I | 1.31 | 1.31 | 1.71 | 114° | 114° | 126° | 0.993 | 0.012 |
| J | 1.31 | 1.31 | 1.71 | 114° | 114° | 128° | | |
| K | 1.31 | 1.27 | 1.73 | 114° | 114° | 123° | | |
| L | 1.31 | 1.29 | 1.71 | 114° | 114° | 123° | 1.003 | 0.016 |
| M | 1.31 | 1.33 | 1.71 | 114° | 114° | 123° | 0.993 | 0.014 |
| N | 1.31 | 1.35 | 1.73 | 114° | 114° | 123° | | |
| O | 1.31 | {1.31(2) {1.29(1) | 1.73 | 114° | 114° | 123° | 0.995 | 0.016 |
| P | 1.31 | 1.31 | 1.67 | 114° | 114° | 123° | | |
| Q | 1.31 | 1.31 | 1.69 | 114° | 114° | 123° | 1.003 | 0.017 |
| R | 1.31 | 1.31 | 1.73 | 114° | 114° | 123° | 0.996 | 0.015 |
| S | 1.31 | 1.31 | 1.75 | 114° | 114° | 123° | 0.995 | 0.017 |
| T | 1.29 | 1.31 | 1.73 | 114° | 114° | 123° | | |
| U | 1.35 | 1.31 | 1.73 | 114° | 114° | 123° | | |
| V | 1.37 | 1.30 | 1.70 | 116° | 116° | 122° | 0.990 | 0.018 |
| W | 1.39 | 1.29 | 1.69 | 117° | 117° | 121.5° | 0.987 | 0.022 |
| X | 1.25 | 1.32 | 1.73 | 112° | 112° | 124° | 1.003 | 0.014 |
| Y | 1.23 | 1.33 | 1.73 | 111° | 111° | 124.5° | | |
| D' | 1.31 | 1.31 | 1.71 | 114° | 114° | 123° | 0.998 | 0.015 |
| D'' | 1.31 | 1.31 | 1.71 | 114° | 114° | 123° | 0.994 | 0.017 |

than any other curves of different bond angles.

By comparing the features and $q_{calcd}/q_{obs}$ values of the intensity curves of the models which have bond angles different from those of models C and D, the acceptable regions of the two bond angles FCF and FCCl were determined as 114±2° and the bond angle CCCl as 123±2°.

And then by comparing the intensity curves of the models in which C-Cl bond distance was varied from 1.67Å to 1.75Å, the C-Cl bond distance was determined as 1.72±0.02Å.

If either one of the C=C or the C-F bond distance is longer and the other is shorter than 1.31Å, a considerably good intensity curve is obtained by altering both the bond angles and C-Cl distance in the acceptable regions which have been described previously. But as the contribution of the C-F atomic pairs to the total intensity curve is much greater than that of C=C atomic pair, the acceptable region of C=C distance is much larger than these of C-F distances. They were 1.31±0.06Å for C=C and 1.31±0.02Å for C-F, respectively.

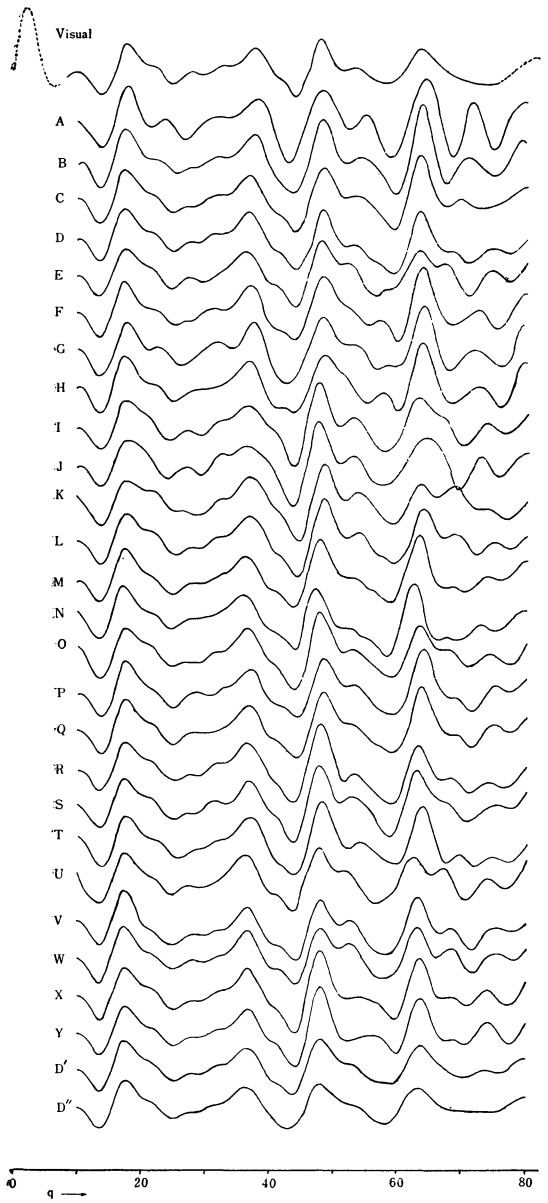
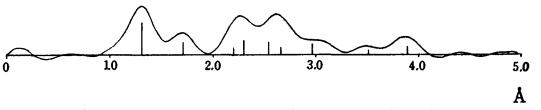



Fig. 1. Intensity curves.

Finally the theoretical intensity curves of model D including thermal factors listed in Table III are compared. They are not greatly different from that of the rigid model, but curve D' seems a little better than curve D''.




Vartical lines show the interatomic distances of model D.

Fig. 2. Radial distribution curve.

TABLE III. MEAN AMPLITUDES USED FOR THE CALCULATIONS OF INTENSITY CURVES D' AND D''

| Atomic pair | Mean amplitude, Å | |
|---|---|---|
| | Model D' | Model D'' |
| C=C | 0.04 | 0.04 |
| C-F | 0.04 | 0.05 |
| C-Cl | 0.05 | 0.05 |
| C···F | 0.06 | 0.06 |
| C···Cl | 0.06 | 0.06 |
| F···F | 0.06 | 0.09 |
| cis F···F | 0.09 | 0.09 |
| trans F···F | 0.06 | 0.11 |
| Cl···F | 0.06 | 0.09 |
| cis Cl···F | 0.09 | 0.09 |
| trans Cl···F | 0.06 | 0.11 |

When the above results are compared with those in Table I, all the parameters of the molecule are practically identical with those of Refs. 3 and 4, although the present results by visual method have broader limits of uncertainty than those of the sector-microphotometer method.

The authors wish to express their sincere gratitude to Professor Akira Kotera for his kind guidance throughout this study. They also owe much to Dr. Nobuo Yamada, The Electrical Communication Laboratory, Nippon Telegraph and Telephone Public Corporation, to whom their thanks are due.

*Department of Chemistry*
*Faculty of Science*
*Tokyo University of Education*
*Koishikawa, Tokyo*

# *Energy Distribution of Secondary Electrons from Copper-Beryllium Alloy by Positive Ions of Inert Gases. I. Electro-polished Surface*

By Toshio SUGIURA

(Received January 17, 1961)

A series of studies of electron ejection from copper-beryllium (4%) alloy by positive ions have been extended in this work. In a previous paper[1], the yields of the secondary electron emission from the variously treated copper-beryllium targets by inert gas ions and some hydrocarbons and their fragment ions were measured, and the surface composition of these alloy targets were also determined by electron diffraction analysis in order to discuss the correlation between the yields of the secondary electron emission and the surface composition of the ion targets.

The secondary electron emission by inert gas ions had been studied by Hagstrum[2-6] on the atomically clean surfaces of some transition metals. The energy distribution of the secondary electrons ejected by the Auger process obeying the assumed mechanism had been theoretically calculated by Hagstrum[7], and a good agreement had been obtained between the theory and his experimental results.

Generally, the ejection of secondary electrons from a metal surface by impact of a positive ion proceeds at the expense of the potential or kinetic energy of the incident ion. Potential ejection may take place only if the ionization potential of the incident ion exceeds twice the work function of the target metal. Kinetic ejection, on the other hand, is expected to increase with increasing ion energy, and is the dominant process for all ions with kinetic energy above a few thousand electron volts, and it also proceeds for positive ions whose ionization potential is less than twice that of the work function of the metal.

Recently, Waters[8] had intended to confirm this kinetic ejection, and had measured the kinetic energy distribution of the ejected electrons from the atomically clean surface of tungsten impacted by alkali ions.

Unfortunately, the theory of the kinetic ejection by the positive ion having low kinetic energy had not yet been clarified, but the mechanism of secondary electron emission by the impact of high speed ions had been made the analysis by Sternglass[9]. He had studied the process of secondary electron emission regarded as the component of two essentially important parts, namely the formation of secondaries inside the metal and their subsequent escape from the surface. Also he had postulated that the energy loss of the primary particle as a result of the excitation and ionization of the target materials results in the formation of internal secondary electrons, and that the secondaries formed might lose their energy by various collison processes so that only a fraction of them may be able to reach the surface of the metal with sufficient energy to escape from the surface. The assumption of Sternglass seems to be suggestive for the secondary electron emission from the practical (not atomically clean) surfaces by impact of the ions.

The main points of interest of the present work are the direct measurements of the kinetic energy distribution of the secondary electrons ejected from the practical surface usable as the first dynode of the secondary electron multiplier tube, and the confirmation of the correlation between the yield of the secondary electron emission and the energy distribution of the secondary electron emission and the energy distribution of the secondary electrons. The results reported in this paper are concerned with the energy distribution of the secondary electrons ejected from the electro-polished copper-beryllium surface by impact of the singly- and doubly-charged argon and neon ions and singly-charged herium ions, together with the influence of the kinetic energy of these incident ions.

## Experimental

In the experimentals of the electron ejection, the beam of ions which is homogeneous in constitution and kinetic energy was allowed to impinge upon a target surface. In order to measure the yield of secondary electrons ($\gamma_1$, number of electrons per incident ion) and the distribution in kinetic energy

1) T. Hayakawa and T. Sugiura, This Bulletin, **34**, 58 (1961).
2) H. D. Hagstrum, *Rev. Sci. Instr.*, **24**, 1122 (1953).
3) H. D. Hagstrum, *Phys. Rev.*, **89**, 244 (1953).
4) H. D. Hagstrum, ibid., **91**, 543 (1953).
5) H. D. Hagstrum, ibid., **96**, 325 (1954).
6) H. D. Hagstrum, ibid., **104**, 317, 672, 1516 (1956).
7) H. D. Hagstrum, ibid., **96**, 336 (1954).
8) P. M. Waters, ibid., **109**, 1053 (1958); **111**, 1466 (1958).
9) E. J. Sternglass, ibid., **108**, 1 (1957).

of ejected electrons, both as functions of the ion and target and of the ion kinetic energy, the apparatus must incorporate an ion source, a mass analyzer, an arrangement of target and surrounding electron collector, and the means to vary the velocity of the ion beam while keeping it focused on the target.

**Mass Spectrometer.** — The present experiments were performed by a mass spectrometer constructed in our laboratory, and their details were already reported in the previous paper[1]. In this studies, in order to eliminate the influence of the fringing field of the analyzing magnet on the slow electrons, the magnetic shield composed of six sheets of soft iron plates of 1.0 mm. in thickness was attached to the middle part between the ion collector region and the analyzing magnet. By this shielding, the influence of the fringing field on the energy distribution of secondary electrons was considered negligible, as described below.

**Ion Target and Electron Collector.** — Since the measurements of the energy distribution of the ejected electrons were made by the retarding potential method, the target was made relatively small and placed at the center of the spherical electron collector.

The ion target and the electron collector designed for the study of energy distribution of secondary electrons are schematically shown in Figs. 1a and b. In Figs. 1a and b, T indicates the ion target box

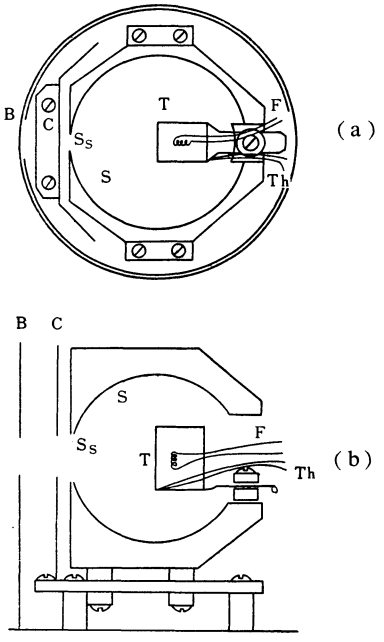



Fig. 1. Schematic top view (a) and side view (b) of the electron collector and ion target for the study of secondary electron emission by ion impact. T denotes the ion target, S the spherical electron collector, B, C and Ss the buffer, the collector and ion entrance slit, F the tungsten filament prepared for the heating of the ion target, Th the nickel-palladium thermocuple.

shaped from the copper-beryllium (4%) plate, and the front area of this box is $6\times12$ mm$^2$ and the target was mounted at the center of the spherical electron collector S by the steatite insulator. S was constructed by two pieces of the brass blocks fastened to each other and the inside of these brass blocks were spherically excavated, the diameter of this sphere is 27 mm., and the area of the ion entrance slit Ss is $10\times3$ mm$^2$. In order to minimize the tertiary electron emission by secondary electrons and the variation of the contact potential with contamination by adsorped gases, the inside surface of the electron collector was covered with evaporated gold films. C is the collector slit of $8\times2$ mm$^2$ in area and shaped from a molybudenum plate of 0.2 mm. in thickness, and B is the buffer slit of $10\times5$ mm$^2$ in area formed by a copper plate of 0.4 mm. in thickness. The tungsten filament F was prepared inside the ion target box for heating the ion target by electron bombardment, and the temperature of the ion target was measured by a nickel-palladium thermocouple Th.

By these assemblies, all ions strike only the front surface of the ion target inside the spherical electron collector, since the focusing of the mass analyzer is determined by ion beam width less than 0.3 mm. at the collector slit during the course of studies.

**Measurements of Energy Distributions of Secondary Electrons.**—Electron energy distributions were measured in this work by means of the retarding potential method. Currents $I_s$ at the electron collector were measured as a function of the voltage $V_{sT}$ supplied between the ion target and the electron collector. The net ion currents $I_i$ were measured by the ion target to which $-18$ V. was supplied against the electron collector through a battery in order to eliminate secondary electrons, and the ratio of the currents $I_s/I_i$ was obtained as a function of the retarding potential $V_{sT}$.

Typical retarding potential data for the singly-charged argon ions are shown in Fig. 2. The kinetic energy distributions of the ejected electrons $(N_0(E_k)=d(I_s/I_i)/dV_r)$ have been obtained from the retarding potential data in the following way where $V_r$ denotes the retarding potential corrected to the contact potential difference between copper-beryllium and gold against $V_{sT}$. The differences in $I_s/I_i$ for each 0.25 V. retarding potential difference was plotted vs. $V_r$. Typical energy distribution curves obtained from the data shown in Fig. 2 are shown in Fig. 3 in which the unit of $N_0(E_k)$ is electrons per ion per electron volt. A UX-54 tube was used as the primary tube of the d. c. amplifier, and the output current was recorded by two galvanometers of different sensitivities. Since a high resistance of $1\times10^{10}$ ohm was used and the measured current was less than $1\times10^{-11}$ amp. in all measurements, the inaccuracy of the retarding potential caused by the incident electrons or the primary ions is less than 0.1 V. and this causes no effective error in this study.

**Measurement of Contact Potential Difference.**— The apparatus used for the measurements of the contact potential difference is shown in Fig. 4a. The vacuum line of apparatus was all constructed

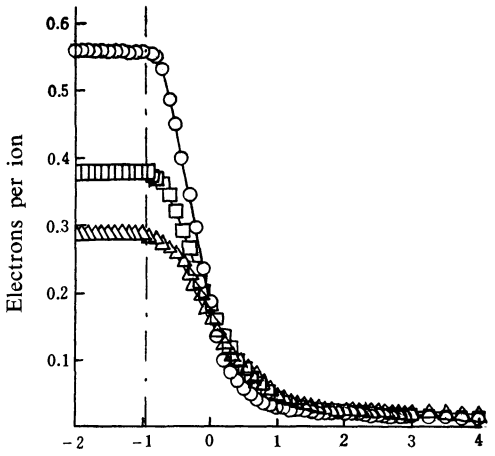



Fig. 2. Polt of ejected electron current $I_S$ in electrons per ion as a function of the retarding potential $V_{ST}$ for argon ions impinged on the electro-polished Cu-Be surface. Circule, square and triangle points denote impinged ion energy of 1240, 840 and 540 V., respectively.
The vertical line show on the electron energy scale indicates the contact potential difference between Au and electro-polished Cu-Be.

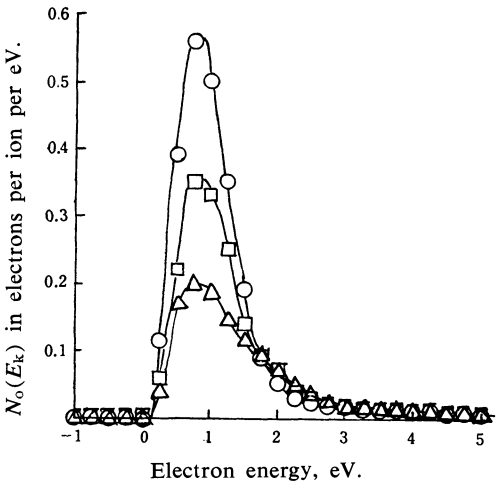



Fig. 3. Plot of the numbers of electrons per incident ion per eV. as a function of retarding potential $V_r$ corrected for the contact potential difference. The curves plotted by circular, square and triangular points were obtained by differentiating the curves shown in Fig. 2.

by molybdenum glass and R in Fig. 4a is the measurement tube, and these were evacuated by the Hickman type oil diffusion pump through a liquid nitrogen trap, and the vacuum during the measurements was $1\times10^{-6}$ mmHg. In Fig. 4b the electrode system is shown, the cylindrical electrode P was formed from a nickel plate of 0.2 mm. in thickness and the inside of this cylinder was covered

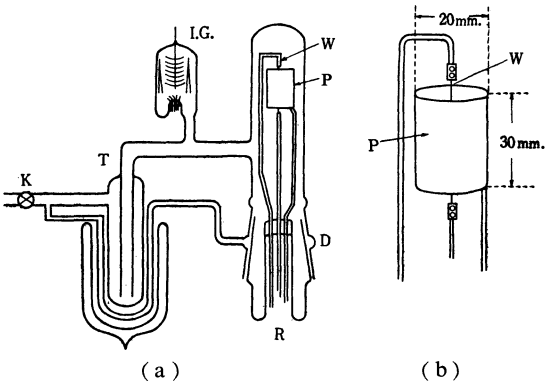



Fig. 4. Schematic diagram of the apparatus for the measurements of the contact potential difference (a). (b) show the electrode assembly. R denotes the measurement tube, P the retardation plate and the thermal electron collector, W the tungsten filament which supplying thermal electrons, I. G. the Bayard-Alpert ionization gauge, and T the liquid nitrogen trap.

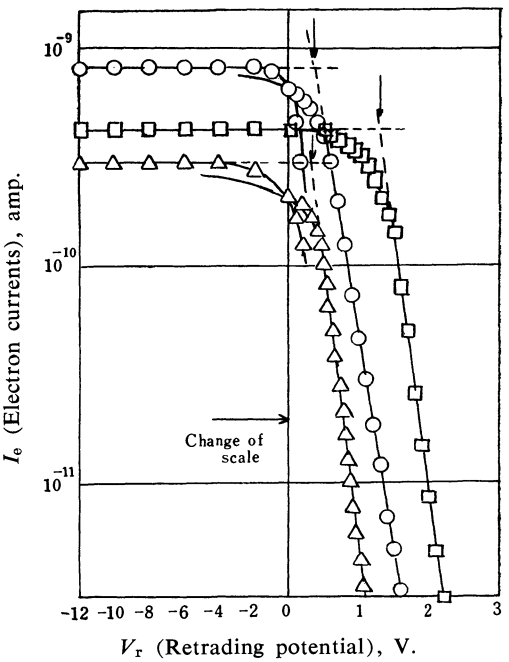



Fig. 5. Retarding potential data on thermoionic electron for the heated tungsten used to determine the contact potential difference between gold and electro-polished Cu-Be. The circle points show the Au—W system, the square points show the Cu-Be—W system, and the triangular points show the data of Hagstrum for Au—W system, in which the electron current scale is arbitrary for the Hagstrum's plot. The vertical arrow on each curve indicates the value for the zero field in each system.

with the evaporated gold film for the measurements of the contact potential difference between gold and tungsten, while for measurements of the contact potential difference between copper-beryllium and tungsten P was formed from a copper-beryllium plate of 0.15 mm. in thickness and was treated in the same manner as the ion target was. The tungsten filament F of 0.07 mm. in diameter was strung at the central axis of the electrode P. The electrode P and the tungsten filament F were mounted on a molybdenum rod in the measurement tube R. The geometry of the cylindrical electrode P was 20 mm. in inner diameter and 30 mm. in length. The stabilized 0.85 V. and 0.8 amp. were supplied to the filament in order to minimize the positive ion emission from the filament, the ionization of the residual gases and the photon radiation. Under these conditions, the thermal electron current of about $10^{-9}$ amp. was measured by a $\mu\mu$ ammeter. The retarding potential for the thermal electrons was applied on the center of the filament potential to the electrode P by dividing the battery potential. Typical results of the retarding potential curves for the thermal electrons emitted from the tungsten filament onto the gold plate or the copper-beryllium plate are shown in Fig. 5.

**Materials.**—The copper-beryllium ion target was shaped in a box-form after tempering and mechanical polishing with fine emery papers, and successively electro-polished in the solution which had been reported in the previous paper[1]. Spectroscopically pure argon and neon were used in the present experiments as well as in the previous sutdies, and also spectroscopically pure helium of the Teikoku Oxygen Co. was used without any further purifications. The mass spectrometric analyses of these gaseous samples revealed that the total impurities were less than 0.005% in volume.

## Results

**Contact Potential between Gold and Electro-polished Copper-Beryllium.** — Typical retarding potential data obtained from the manner described above are shown in Fig. 5. In Fig. 5, the circle points indicate the retarding potential curve between the tungsten filament and the gold surface, while the square points show the retarding potential curve between tungsten filament and the electro-polished copper-beryllium surface. The triangle points in Fig. 5 indicate the results of the tungsten~gold system measured by Hagstrum[2] in which the electron current scale was shown in an arbitarary unit. As seen in Fig. 5, the retarding potential portion had been observed to be linear from 0.5 to 1.6 V. for the tungsten ~gold system, and to be linear from 1.4 to 2.2 V. for the tungsten~copper-beryllium system, while in Hagstrum's data the linear portion is from 0.5 to 1.1 V. The point of zero field has been determined by the intersection of the extrapolated straight lines through the saturated current and retarding portions as shown by arrows in each curve in Fig. 5.

These treatments of semilog plot are strictly correct only for plane parallel geometry[10], although the present author measured by geometry of cylindrical symmetry and Hagstrum[2] had measured by spherical geometry. But the present results of the tungsten—gold system are in close agreement with Hagstrum's result, and the discrepancies between these observed values and the true values are expected to be smaller than 0.1 V. The observed value of the contact potential difference between gold and electro-polished copper-beryllium alloy is 0.95 eV., while the surface potential of the electro-polished copper-beryllium is 0.95 eV. more positive than that of gold.

**Kinetic Energy Distribution of Secondary Electrons.** — The distribution curves of the kinetic energy of the secondary electron by singly- and doubly-charged argon and neon ions and by singly-charged herium ions are shown in Figs. 3, 6, 7, 8 and 9, respectively. In these figures the results obtained for the incident ion energies of 1240, 840 and 540 V. are respectively indicated by circles, squares and triangles, and the correction of the contact potential difference between the ion target and

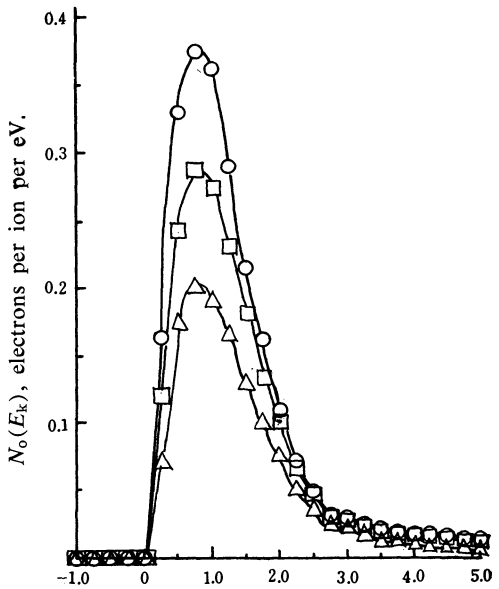



Fig. 6. Energy distributions of electron ejected from electro-polished Cu-Be by doubly-charged argon ions. Circular, square and triangular points denote the kinetic energy of incident ions of 1240, 840 and 540 V. respectively.

10) K. T. Compton and I. Langmuir, *Rev. Modern Phys.*, 3, 225 (1931).

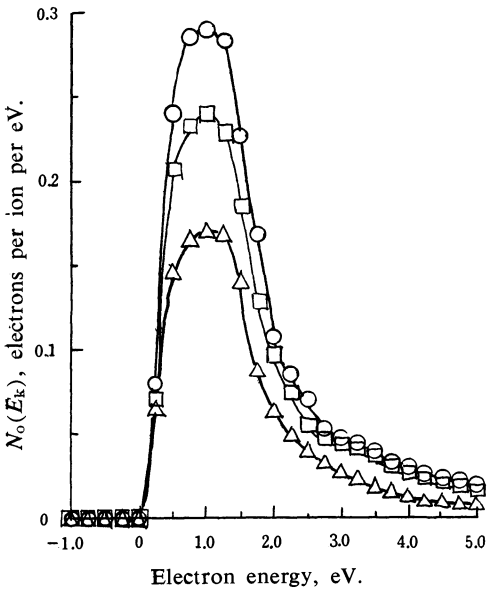



Fig. 7. Energy distributions of electron ejected from electro-polished Cu-Be by singly-charged neon ions. Circular, square and triangular points denote the kinetic energy of incident ions of 1240, 840 and 540 V. respectively.

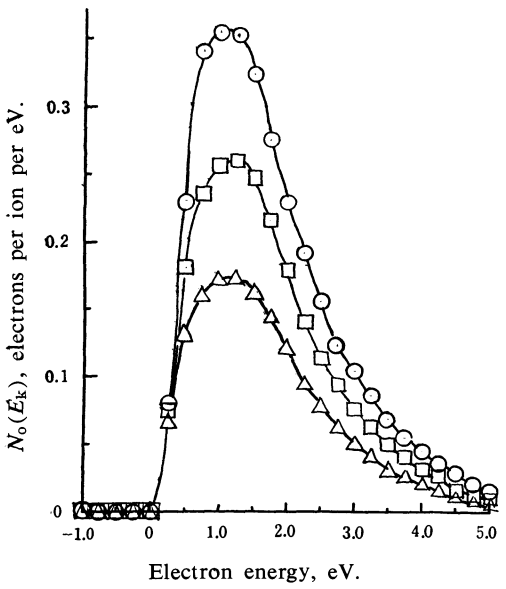



Fig. 8. Energy distributions of electron ejected from electro-polished Cu-Be by doubly-charged neon ions. Circular, square and triangular points denote the kinetic energy of incident ions of 1240, 840 and 540 V. respectively.

the electron collector was made for the retarding potential $V_r$.

These curves show that the fringing field of the analyzing magnet is negligible around the electron collector. If the fringing field is effective around the electron collector, then the electrons having low kinetic energy could not reach the electron collector and the distribution curves of the electron kinetic energy would have drifted to the low energy side. This effect has been studied by Hagstrum[3]. In the present studies, the magnetic field for the mass analyzer was varied for the focusing of ions having the various masses and kinetic energies, but every distribution curve obtained in this work practically showed that $N_0(E_k) = 0$ at the zero field in the retarding potential scale and no low energy tail has been observed.

The kinetic energy distribution shown by the half widths of each distribution curve and

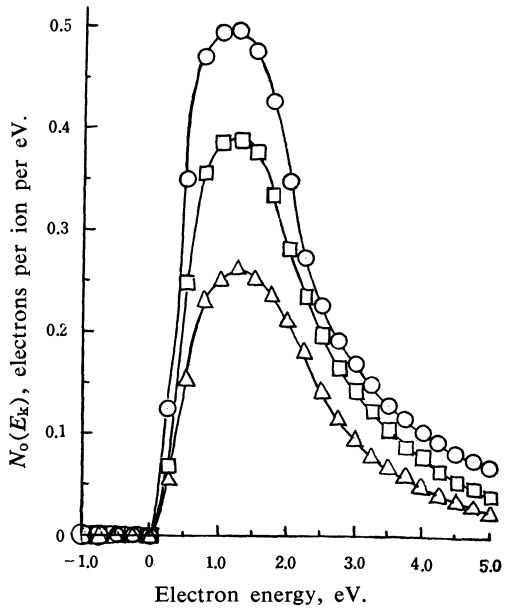



Fig. 9. Energy distributions of electron ejected from electro-polished Cu-Be by singly-charged herium ions. Circular, square and triangular points denote the kinetic energy of incident ions of 1240, 840 and 540 V. respectively.

TABLE I. VARIATION OF THE HALF WIDTHS OF THE ENERGY DISTRIBUTION CURVES AND YIELDS OF SECONDARY ELECTRONS FORM ELECTRO-POLISHED Cu-Be SURFACE WITH ION ENERGIES OF PRIMARY INERT GAS IONS

| | Half widths of the energy distribution curves of secondary electrons in eV. | | | Yield of the secondary electrons $\gamma_1$ in electrons per ion. | | |
|---|---|---|---|---|---|---|
| Ion energy | 1240 | 840 | 540 | 1240 | 840 | 540 |
| Ion | | | | | | |
| $A^+$ | 1.00 | 1.05 | 1.20 | 0.56 | 0.38 | 0.27 |
| $A^{2+}$ | 1.30 | 1.35 | 1.40 | 0.58 | 0.43 | 0.36 |
| $Ne^+$ | 1.40 | 1.45 | 1.50 | 0.57 | 0.43 | 0.31 |
| $Ne^{2+}$ | 1.90 | 1.95 | 2.05 | 0.82 | 0.56 | 0.39 |
| $He^+$ | 2.00 | 2.05 | 2.15 | 1.35 | 0.94 | 0.68 |

the yield $\gamma_i$ of the secondary electrons are summarized in Table I.

## Discussion

**General Features of Energy Distribution Curves.**—As seen in Figs. 3, 6, 7, 8 and 9, all distribution curves have their maximum at about 1 eV. But the sharpness of each distribution curve is more similar to that of the lithium ions and the tungsten surface by Waters[8] than that of the argon ions and the tungsten surface by Hagstrum[6], both shown in Fig. 10. Although the surface in this work

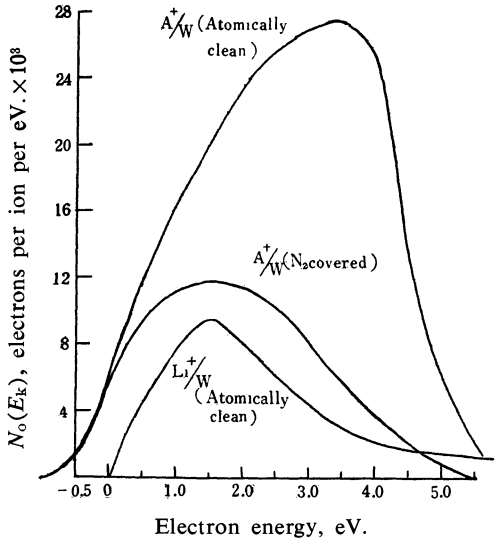



Fig. 10. Energy distributions of secondary electrons ejected by 10 eV. $A^+$ ions from atomically clean tungsten (W) and tungsten covered with the monolayer of nitrogen ($N_2$/W) given by Hagstrum[8], and the distribution curve of electron ejected by 1000 eV. $Li^+$ ions from atomically clean tungsten surface ($Li^+$) given by Waters[8].

was not atomically clean, the energy distribution curves observed in this work are not similar to that for the nitrogen covered surface of tungsten observed by Hagstrum shown in Fig. 10. The electron yields obtained in these studies are much greater than the results of Hagstrum and Waters. Since the present results were obtained from the alloy surface covered by residual gases and Hagstrum and Waters worked on the atomically clean surfaces of pure metals, the direct comparison of these data has no significant meaning, but the general features of the present distribution curves show much similarity of the kinetic ejection.

**Effect of Ion Kinetic Energy.** — As seen in Table I, the yield of the secondary electrons is clearly increased by increasing the kinetic energies of the incident ions, while the half width of the energy distribution curve of the secondary electrons is slightly decreased by increasing the ion kinetic energies. The difference between two distribution curves of different ion kinetic energies indicates the difference in the distribution of the different numbers of the secondary electrons emitted by different ion kinetic energies. In these different energy distributions, it is clearly shown that the increase in the electron yield as increasing the ion kinetic energies is mainly contributed to low energy electrons. This effect may be qualitatively explainable from the following idea similar to that of Sternglass[9]. Since the incident ions penetrate deeper as the ion kinetic energy increases, the number of secondary electrons formed in the alloy may be proportionally increased with the increase in the penetration depth. The formed secondary electrons may lose their energies in various types of collision processes, so that only a small fraction of them can reach the surface with sufficient energy to escape from the surface. But an increased number of electrons with the increase in the ion kinetic energy are formed in the deeper layer in the alloy, thus the detected secondary electrons might lose their initial energies during the passage through the layers in the alloy. The dependency of the distribution curves on the ion kinetic energy in these studies has previously been explained.

**Influence of Ion Species.**—As seen in Table I and Figs. 3, 7 and 9, the yield of the secondary electrons at any definite ion energy for the singly-charged inert gas ions is clearly increased in sequence from the argon, neon to helium ions, and this sequence has a correlation to their ionization potentials. Then, higher yield of the secondary electrons may be obtained by impact of the ion having the higher ionization potential.

As seen in Figs. 3, 7 and 9 and Table I, the energy distribution curves are broader for light ions than for heavier ions. These phenomena can not be explained by any similar explanation of the influence of the effect of the ion kinetic energy, since the ions of different masses are formed in the mass spectrometer with constant kinetic energy when the ions were accelerated by the acceleration voltage. If the penetration depth of the ions is assumed[9] to be simply dependent upon the ion kinetic energy, the penetration depth of the lighter ions is the same as that of the heavier ions. But the present results on the energy distribution clearly show the existence of the higher energy electrons in the case of lighter ions. They also indicate that the higher

energy electrons emitted by the ions have a higher ionization potential.

These phenomena indicate that the mechanism of the secondary electron ejection from the electro-polished copper-beryllium surface is not simple. The ionization potentials of argon, neon and helium are 15.76, 21.59 and 24.58 eV., respectively, and though the work function of the electro-polished copper-beryllium is not certain it may be presumed to be less than 6 eV. Then, it is considered from the present experimental conditions that the ionization potentials of the ions of the present consideration are larger then twice the work function of the alloy surface. Consequently, it remains open to discussion as to the mechanism of the potential ejection[7], but the general features of the distribution curves of the electron energies show considerable similarity to the kinetic ejection. For the reason mentioned above, it is difficult to deduce any simple conclusion on the mechanism of the electron emission by inert gas ions from the present work.

**Effect of Ionic Charges.**—From a comparison of Figs. 3 and 6 for argon ions and Figs. 7 and 8 for neon ions, the energy distribution curves by the doubly-charged ions are broader than those by the singly-charged ions, and the yield of the secondary electrons by the doubly-charged ions are greater than that by the singly-charged ions at any definite ion kinetic energy. Thus the energy distribution indicates that the doubly-charged ions ejected the higher energy electrons than the singly-charged ions do. This tendency is similar to the influence of the ion species on the yield and energy distribution of secondary electrons. The secondary ionization potential of the argon and neon ions are 43.52 and 62.57 eV., respectively, then the mechanism of the secondary electron emission from copper-beryllium may occur according to the complex mechanisms in which the secondary electron is ejected by contribution of both of the kinetic and the potential energies of the incident ions.

## Summary

The distribution curves of the kinetic energies of the secondary electrons from the electro-polished copper-beryllium surface by inert gas ions were measured by the retarding potential method together with the yield of the secondary electron emission. The contact potential difference between the ion target (electro-polished copper-beryllium) and the electron collector (gold) was also measured by the retarding potential method for the thermal electrons from tungsten, and the correction of this contact potential difference was made for the kinetic energies of secondary electrons. The main results obtained are as follows.

(1) The contact potential difference between gold and electro-polished copper-beryllium (4%) is 0.95 eV. (gold, negative).

(2) The general features of the distribution curves of secondary electrons are similar to the distribution curves of the kinetic ejection measured by Waters.

(3) The present results of the energy distribution curves of secondary electrons by the inert gas ions indicate that the yield of secondary electrons is increased by increasing the kinetic energy of the primary ions, and that this increment in the yield is mainly contributed from the secondary electrons which have lower kinetic energies than that of the secondary electrons emitted by the incident ions of low kinetic energies. These phenomena are able to be postulated qualitatively by the idea of sternglass.

(4) The total number of emitted electrons is increased with the increase in the value of the ionization potential of incident ions, and the kinetic energies of emitted electrons become greater by increasing the potential energy of incident ions. These phenomena are difficult to explain by the mechanism of the kinetic ejection, therefore the electron emission from the electro-polished copper-beryllium surface by inert gas ions may occur according to the complicated mechanism in which the potential energies of incident ions contribute to the electron emission together with their kinetic energies.

(5) In contrast with the singly-charged ions, the doubly-charged ions give rise to the broadening of the energy distribution curves. This also suggests the occurrence of the complicated ejection mechanisms.

The author wishes to acknowledge his indebtedness to Professor Shoji Shida of the Tokyo Institute of Technology, Professor Teruo Hayakawa and Professor Osamu Toyama of University of Osaka Prefecture, under whose direction and guidance this work was carried out.

The expense has been defrayed in part from a grant given by the Ministry of Education, to which the author's thanks are due.

*Department of Applied Chemistry*
*Faculty of Engineering*
*University of Osaka Prefecture*
*Sakai, Osaka*

# *On the Structures of p-tert-Butyl Phenol Resin and α-Naphthol Resin. II. Infrared Absorption Spectra of p-tert-Butyl Phenol and α-Naphthol*

By Reisuke SODA

(Received February 28, 1961)

It was previously reported[1] that a polymer, synthesized from *p-tert*-butyl phenol and formaldehyde, was a suitable material for coating the fiber of a dust respirator to obtain a high efficiency of filtration. This polymer showed anomalous phenomena in its benzene solution.

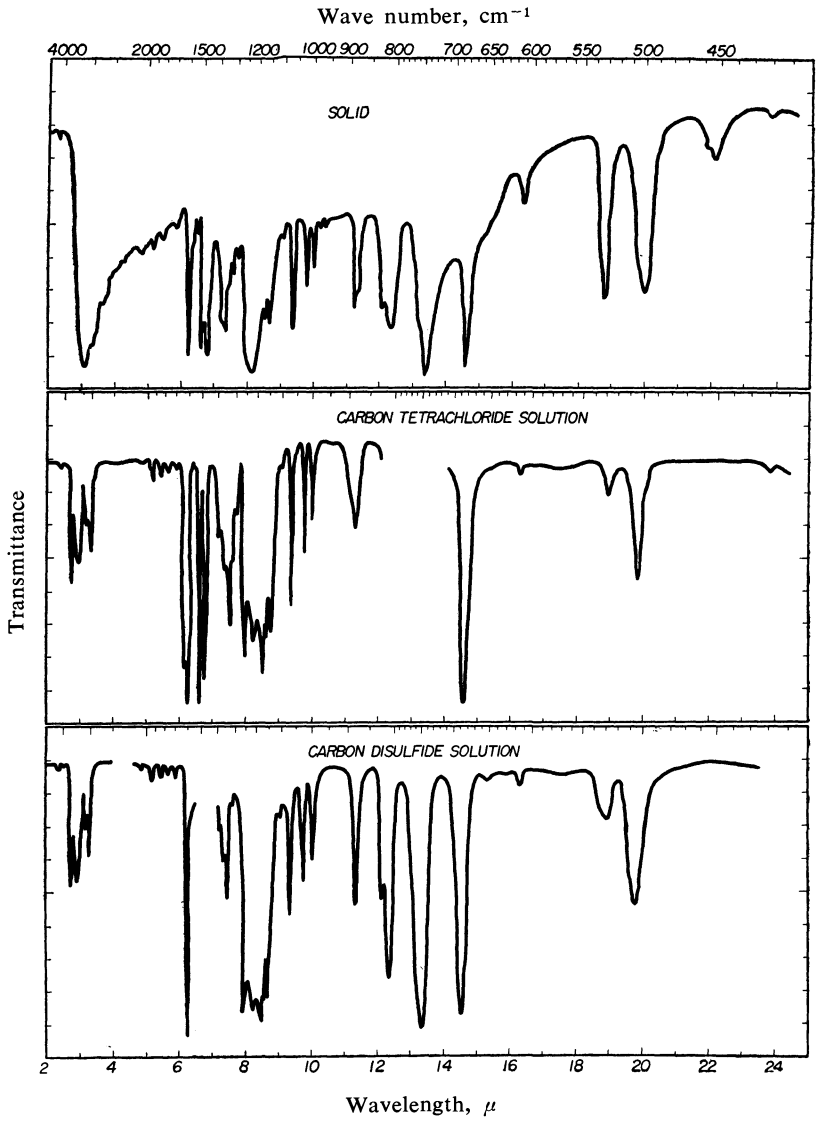



Fig. 1. Spectra of phenol in solid and solutions. Spectrum is cut off in the region of interference due to solvents. Concentration of solution is about 0.1 M in carbon tetrachloride and 0.5 M in carbon disulfide.

1) R. Soda, *Bull. Natl. Inst. Ind. Health*, No. 3, 40 (1960).

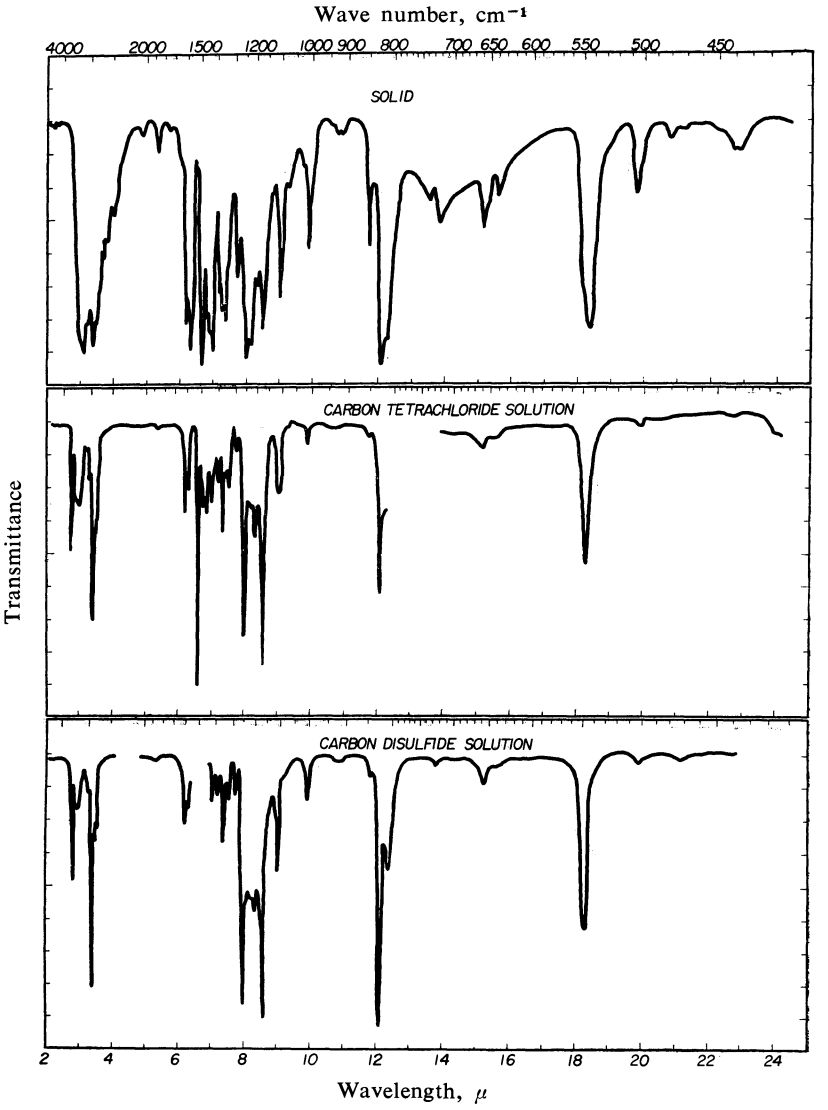



Fig. 2. Spectra of *p-tert*-butyl phenol in solid and solutions. Spectrum is cut off in the region of interference due to solvents. Concentration of solution is about 0.3 M in carbon tetrachloride and 0.4 M in carbon disulfide.

The polymer had a relatively small molecular weight and both sides of the polymer chain were *p-tert*-butyl phenol. Also the OH bonds of the polymer were bound by a very strong intramolecular hydrogen bonding and this intramolecular hydrogen bonding was made partly loose only when the polymer was dissolved in benzene. Bands of the spectrum obtained in the region of sodium chloride prism were assigned, but some ambiguity remained in these assignments.

In the present work, to eliminate the above stated doubtfulness of the assignment, the infrared absorption spectra of *p-tert*-butylphenol and the other O–H compounds were precisely measured and the observed region was extended to about 33 μ in the region of cesium bromide optics, particularly the in-plane and the out-of-plane O–H deformation vibration were investigated in more detail.

## Experimental

*p-tert*-Butyl phenol was purified by recrystallizing it from its saturated benzene solution and by vacuum distillation. α-Naphthol was recrystallized from ethyl alcohol. Phenol was purified by distillation. The solvents used were carbon tetrachloride and carbon disulfide, each being distilled once. The potassium bromide powder used for the measurement of the solid spectrum, was heated, ground to particle size of 200 to 300 mesh and dried by heating at 200°C. For the measurement of the spectrum of a solid some samples were resolidified

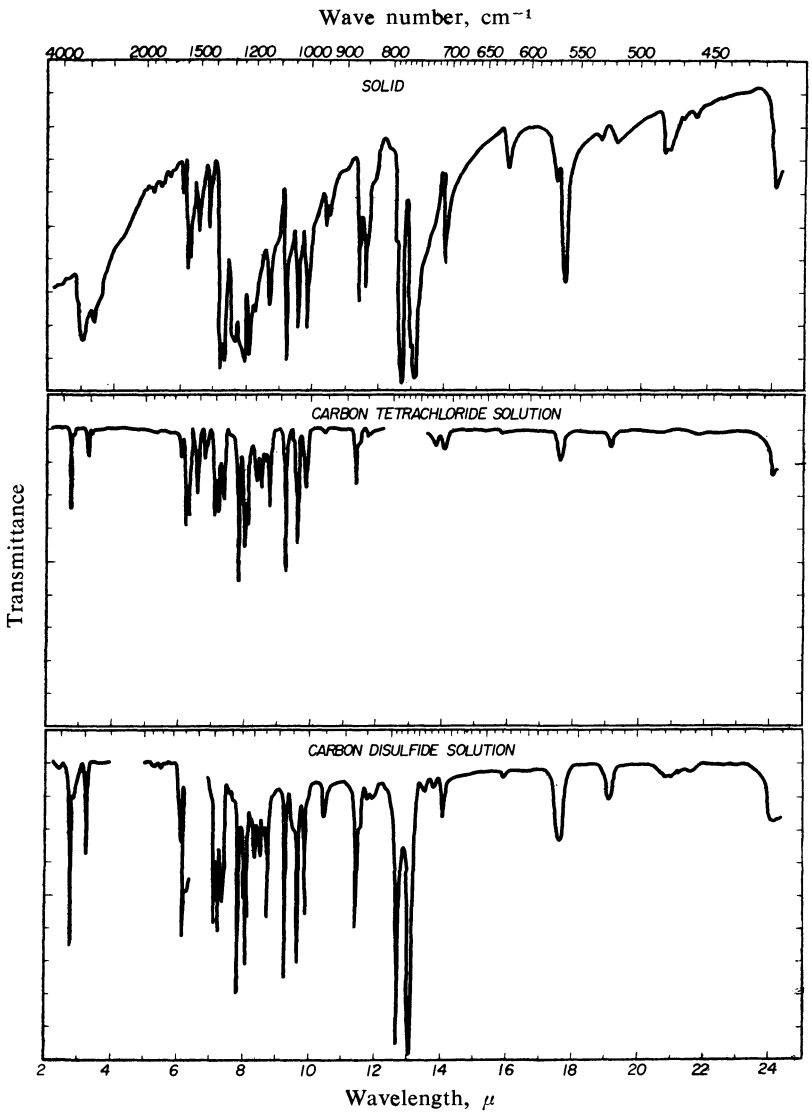



Fig. 3. Spectra of α-naphthol in solid and solutions. Spectrum is cut off in the region of interference due to solvents. Concentration of solution is about 0.05 M in carbon tetrachloride and 0.1 M in carbon disulfide.

between two rock salt plates or potassium bromide plates which were polished at both surfaces to make flat. The sample powder was sandwiched between two heated window plates and cooled moderately to make a solid film. The other spectra were obtained with potassium bromide disks.

The cell used for the solution had the thickness of 1 mm. and its window was of potassium bromide or rock salt. The infrared spectrum was observed by a Perkin-Elmer Model 137 Infracord spectrophotometer, Perkin-Elmer Model 21 spectrophotometer and Perkin-Elmer Model 221 spectrophotometer.

## Results and Discussion

The spectrum of solid of fused film between window plates was approximately the same as that of a potassium bromide pellet. It may be considered that the orientation effect does not exist in this case. Therefore the spectrum of solid obtained could be analyzed without caution of experimental condition. The spectra of phenol in the solid state, in solutions of carbon tetrachloride and of carbon disulfide are shown in Fig. 1. Those of *p-tert*-butyl phenol and of α-naphthol are illustrated in Figs. 2 and 3, respectively. The spectra of solids of these three compounds differ from those of solutions in several regions. The spectra of these compounds in solution change their features with the concentration of solution in some regions. Those changes of spectra are illustrated in Figs. 5 to 16. The spectra

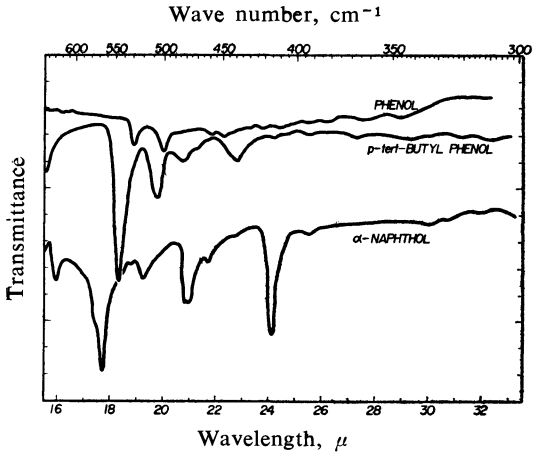



Fig. 4. Spectra of *p-tert*-butyl phenol and α-naphthol in CsBr region (KBr disk).

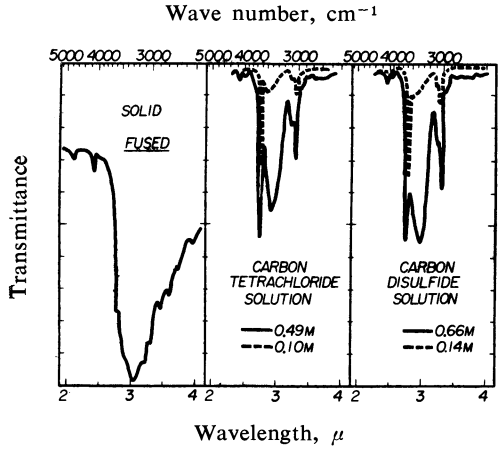



Fig. 5. Spectra of phenol in 3 μ region.

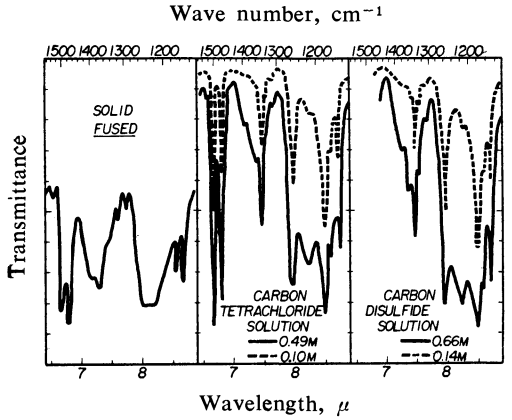



Fig. 6. Spectra of phenol in the region of 1500~1150 $cm^{-1}$. Spectrum is cut off in the region of interference due to solvents.

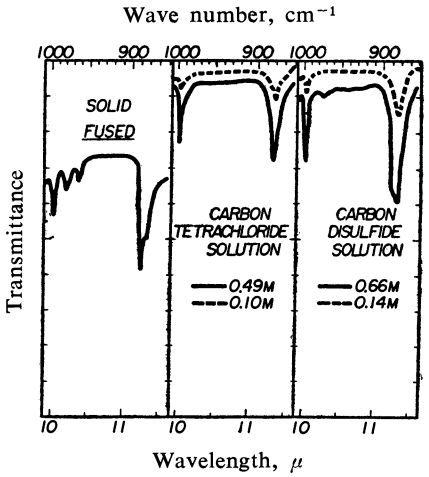



Fig. 7. Spectra of phenol in the region near 1000 $cm^{-1}$.

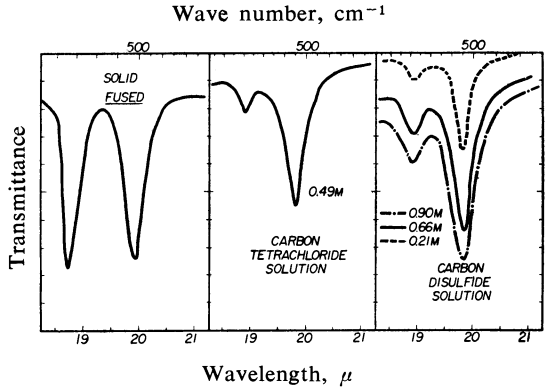



Fig. 8. Spectra of phenol in the region close to 500 $cm^{-1}$.

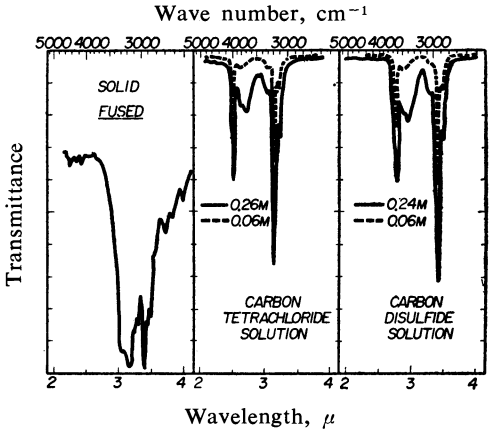



Fig. 9. Spectra of *p-tert*-butyl phenol in 3 μ region.

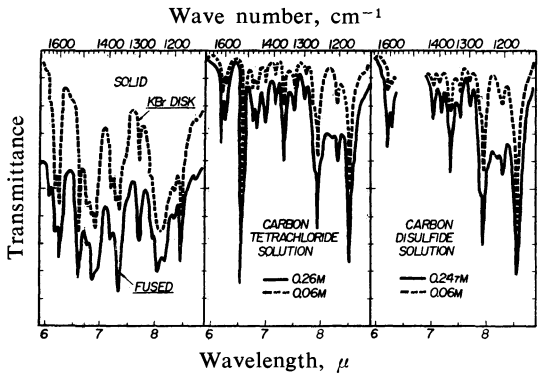



Fig. 10. Spectra of *p-tert*-butyl phenol in the region of 1600~1150 $cm^{-1}$. Spectrum is cut off in the region of interference due to solvents.

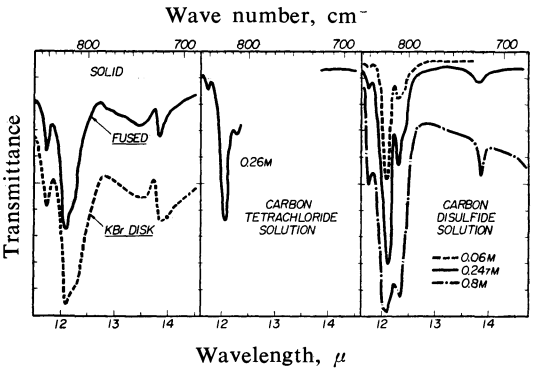



Fig. 11. Spectra of *p-tert*-butyl phenol in the region near 800 $cm^{-1}$. Spectrum is cut off in the region of interference due to solvents.

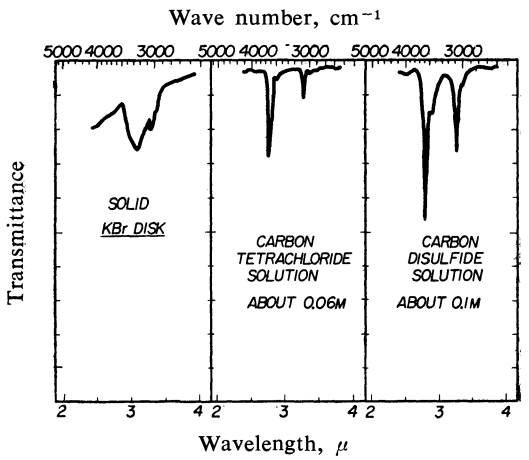



Fig. 13. Spectra of α-naphthol in 3 μ region.

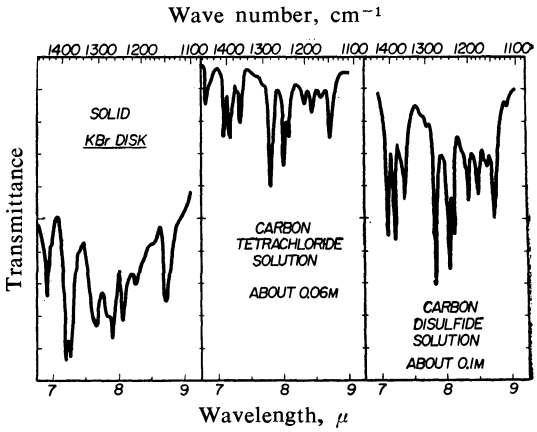



Fig. 14. Spectra of α-naphthol in 8 μ region. Spectrum is cut off in the region of interference due to solvents.

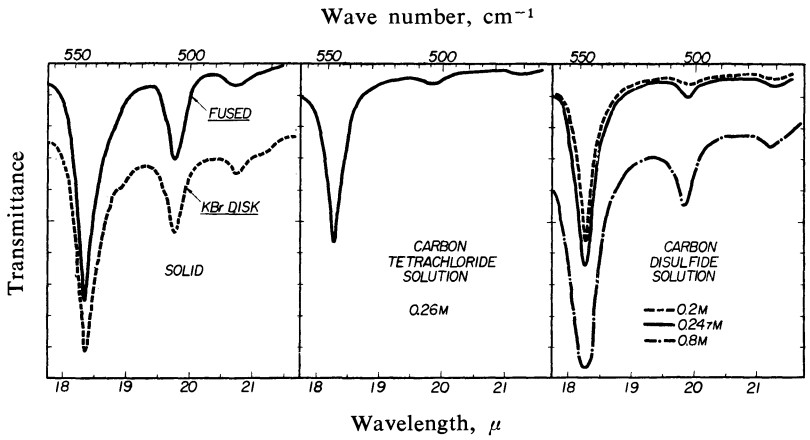



Fig. 12. Spectra of *p-tert*-butyl phenol in the region of 550~460 $cm^{-1}$.

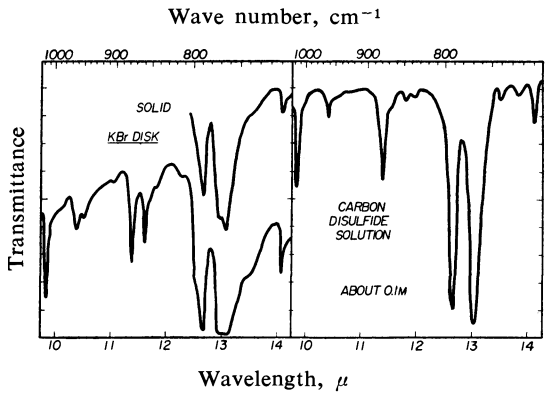



Fig. 15. Spectra of α-naphthol in the region of 1000~700 cm$^{-1}$.

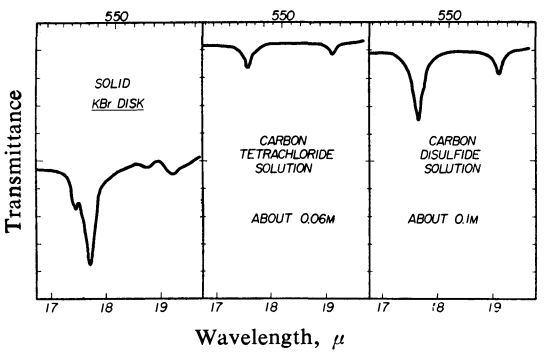



Fig. 16. Spectra of α-naphthol in the region near 550 cm$^{-1}$.

of these compounds in the region of cesium bromide optics are shown in Fig. 4. No strong band which is observable at ordinary concentration is found in the region of 25 to 34 μ. Considerable changes of spectra of these compounds are observed in three regions at 3, 7 to 8 and near 18 μ when the phase and the concentration alter. The other remarkable changes are found in the regions of 6, 11 and 14 μ, but these changes are much less than those in the former regions. The changes in the regions at 6, 11 and 14 μ are observed when the solids are brought into solution but are not observed when the concentrations of solutions alter. Changes of spectral region at 18 μ of *p-tert*-butyl phenol and α-naphthol are not clear compared with that of phenol.

**Phenol.** — The spectrum of phenol has been investigated by several authors. Kuratani[2] assigned OH deformation vibrations to it and concluded that this vibration coupled with C-O stretching vibration. He reported that these vibrations gave rise to the bands at 1280 and 1195 cm$^{-1}$ respectively. Mecke and Rossmy[3] reported that these bands which occurred at 1339 and 1174 cm$^{-1}$ shifted by complete deuteration to 1294 and 915 cm$^{-1}$, respectively, and that the band at 1174 cm$^{-1}$ had a larger part of O-H deformation vibration character than the band at 1339 cm$^{-1}$.

In the present experiment, as shown in Figs. 1 and 6, the appreciable change is found in region at 1200 cm$^{-1}$ with the change of phase and concentration of solution. The change at 1300 cm$^{-1}$ region is so complex that it is not easy to make a unique assignment. The band at 1220 cm$^{-1}$ of solid spectrum shifts to 1210 cm$^{-1}$ in solution spectrum and the intensity of this band decreases when the concentration of solution is lower. In the solution, a new band appears near 1180 cm$^{-1}$ and its relative intensity to that of 1210 cm$^{-1}$ band increases at the lower concentration. The 1390 cm$^{-1}$ band of solid decreases its intensity and a strong band appears near 1340 cm$^{-1}$ in the solution. The relative intensity of the latter band to the former increases in a lower concentration of solution. Then it may be concluded that the bands 1390 and 1220 cm$^{-1}$ in solid state and the bands 1380 and 1210 cm$^{-1}$ in solution are assigned to coupled modes of C-O stretching vibration and hydrogen-bonded O-H deformation vibration. The bands at 1340 and 1180 cm$^{-1}$ may be assigned to the coupled modes of C-O stretching vibration and free O-H deformation vibration. These conclusions do not contradict the results of other papers[2-5]. These conclusions agree with what is observed in 3 μ region. In this region the stretching vibration of the O-H bond gives rise to a broad at its center at 3300 cm$^{-1}$ in solid but in solution sharp band at 3600 to 3620 cm$^{-1}$ and broad band at 3370 cm$^{-1}$ or higher. The phenol molecule will associate to a large aggregate through the hydrogen bonding in the solid state. In the solution these molecules are dispersed into monomer with free O-H bond and partly associate to build up a small polymer through O-H···O linkage. Therefore the O-H vibration of solid shows the strong hydrogen bonding character due to a larger associated molecule and that of solution shows the characters of free hydroxyl bond and partly of the weakly hydrogen-bonded bond. Other changes are observed

2) K. Kuratani, *J. Chem. Soc. Japan, Pure Chem. Sec.* (*Nippon Kagaku Zasshi*), 73, 758 (1952).

3) R. Mecke, and C. Rossmy, *Z. Elektrochem.*, 59, 866 (1955).

4) L. J. Bellamy, "The Infrared Spectra of Complex Molecules", Metheu & Co., Ltd., London, J. Wiley & Sons Inc., New York (1954), pp. 64~69 and 96.

5) "Chemical Application of Spectrocopy", Ed. by W. West, Interscience Pub., Ltd., London (1956), pp. 388~434,

TABLE I. BAND POSITIONS AND ASSIGNMENT OF SPECTRUM OF PHENOL

| Band, $cm^{-1}$ | | Assignment |
|---|---|---|
| Solid | Solution | |
| | 3610 | $\nu$(O-H), free |
| | 3480 | $\nu$(O-H), bonded |
| 3360 | 3380 | $\nu$(O-H), bonded |
| 3090 | 3070 | $\nu$(C-H), aromatic |
| 3010 | 3030 | $\nu$(C-H), aromatic |
| 1605 | 1605 | Ring vibration |
| 1597 | 1597 | Ring vibration |
| 1502 | 1501 | Ring vibration |
| 1473 | 1470 | Ring vibration |
| 1389 | 1387 to 1380 | $\delta$(O-H), bonded and $\nu$(C-O)? |
| 1370 | 1355 | $\delta$(O-H), bonded and $\nu$(C-O)? |
| | 1341 | $\delta$(O-H), free and $\nu$(C-O) |
| 1337 | 1330 | Skeletal vibration |
| 1318 | 1310 | Skeletal vibration |
| 1245 | 1256 | Skeletal vibration |
| 1222 | 1211 | $\delta$(O-H), bonded and $\nu$(C-O) |
| | 1177 | $\delta$(O-H), free and $\nu$(C-O) |
| 1168 | 1166 | $\delta$(C-H) or skeletal vibration |
| 1153 | 1150 | $\delta$(C-H) or skeletal vibration |
| 1071 | 1067 | $\delta$(C-H) or skeletal vibration |
| 1024 | 1023 | $\delta$(C-H) or skeletal vibration |
| 998 | 998 | Skeletal vibration |
| 883 | 882 | Skeletal vibration |
| 822 | 824 | |
| 810 | 809 | |
| 752 | 750 | $\delta$(C-H), out-of-plane |
| 689 | 687 | $\delta$(C-H), out-of-plane |
| 663 | 656 | |
| 615 | 616 | Skeletal vibration |
| 533 | 527 | $\delta$(O-H), out-of-plane? |
| 503 | 505 | $\delta$(O-H), out-of-plane? |

near 890 and 980 $cm^{-1}$. But these changes do not clearly show its origin and are smaller than those in the above-mentioned regions. Furthermore the changes in this region are not observed with variation of concentration of solution. These changes may be explained as influence of crystal field[6]. Each band is tentatively assigned as shown in Table I. Out-of-plane O-H deformation vibration is considered to give rise to the band in lower frequency region. As shown in Fig. 4, the main intense bands arise at 530 and 500 $cm^{-1}$. These bands change their relative intensities when this substance is dissolved from a solid. The frequency shifts are slight as shown in Fig. 8. In carbon disulfide solution and in a solid form this relative absorbance ratio ($E_{530}/E_{500}$) varies as follows:

| State | Relative intensity Ratio |
|---|---|
| Solid | 1.10 |
| $CS_2$ soln. | |
| 0.9 M | 0.22 |
| 0.66 M | 0.21 |
| 0.21 M | 0.19 |
| $CCl_4$ soln. | |
| 0.49 M | 0.19 |

Then the band at 530 $cm^{-1}$ is tentatively assigned to OH out-of-plane deformation vibration of a solid and the 500 $cm^{-1}$ band to that of free O-H bond and some other vibrations. No benzene gives rise to absorption bands in these regions but with toluene a weak band arises at 521 $cm^{-1}$. Chlorobenzene, bromobenzene and iodobenzene give rise to a strong band near 450 to 460 $cm^{-1}$ and ethylbenzene at 486 $cm^{-1}$. Therefore the bands at 530 and 500 $cm^{-1}$ may be connected with the O-H out-of-plane deformation vibration and the other skeletal vibration[5].

***p-tert*-Butyl Phenol.** — The spectra of this compound as illustrated in Figs. 2, 4, 9, 10, 11 and 12, are similar to those of phenol, particulary the bands which concern the O-H vibrations. Phenol is a monosubstituted benzene derivative and *p-tert*-butyl phenol is a 1,4 disubstituted derivative. These spectra differ from each other at the bands due to some benzene ring vibrations and ring C-H vibrations. As the latter substance has further a tertiary butyl group, there appear also the bands due to the methyl group and the C·$(CH_3)_3$ group vibrations.

The change of phase and concentration causes changes of its association degree and state of molecule. This resembles that of phenol and hence O-H stretching vibration and O-H in-plane deformation vibration change their frequencies and intensities. These facts are illustrated in Figs. 9, 10 and 12. In Fig. 11, the bands at 820 and 760 $cm^{-1}$ change slightly their features with phase. The reason is still unexplained exactly but may be attributed to the crystal field effect[6]. The assignments of bands are summarized in Table II.

The spectrum of phenol in the region at 18 to 22 $\mu$ is different from that of *p-tert*-butyl phenol. It is generally accepted that in this region the band is highly sensitive to the substituent[5]. 1, 4-Dimethyl benzene gives rise to a weak band at 645 $cm^{-1}$ and a very strong band at 480 $cm^{-1}$. This strong band shifts to 432 $cm^{-1}$ in 1, 3-dimethyl benzene and to 436 $cm^{-1}$ in 1, 2-dimethyl benzene. Therefore it may be reasonable to conclude[5] that disubstituted

6) R. J. Grisemthwaite, and R. F. Hunter, *J. Appl. Chem.*, 6, 324 (1956).

Table II. Band positions and assignment of spectrum of *p-tert*-butyl phenol

| Band, $cm^{-1}$ | | Assignment |
|---|---|---|
| Solid | Solution | |
| | 3610 | ν(O-H), free |
| | 3480 | ν(O-H), bonded |
| 3230 | 3380 | ν(O-H), bonded |
| 3060 | | ν(C-H), aromatic |
| 3020 | 3030 | ν(C-H), aromatic |
| 2950 | 2960 | ν(C-H), $-CH_3$ |
| 2900 | 2910 | ν(C-H), $-CH_3$ |
| 2860 | 2880 | ν(C-H), $-CH_3$ |
| 1613 | 1612 | Ring vibration |
| 1597 | 1595 | Ring vibration |
| 1520 | 1521 | Ring vibration |
| 1477 | 1477 | δ(C-H), $-CH_3$ |
| 1460 | 1463 | δ(C-H), $-CH_3$ |
| 1442 | 1425 | δ(O-H), bonded and ν(C-O) |
| 1391 | 1391 | δ(C-H), $-CH_3$ |
| 1361 | 1363 | δ(C-H), $-CH_3$ |
| | 1328 | δ(O-H), free and ν(C-O) |
| 1298 | 1294 | Skeletal vibration |
| 1263 | 1256 | C-$CH_3$ rocking |
| 1230 | 1217 | δ(O-H), bonded and ν(C-O) |
| 1200 | 1203 | δ(C-H), aromatic and C-$CH_3$ rocking |
| | 1173 | δ(O-H), free and ν(C-O) |
| 1112 | 1110 | δ(C-H), aromatic |
| 1084 | 1083 | δ(C-H), aromatic |
| 931 | 931 | ν(C-C), C-$CH_3$ |
| 851 | 849 | ν(C-C), C-$CH_3$ |
| 827 | 828 | δ(C-H), out-of-plane |
| 818 | 812 | δ(C-H), aromatic or ν(C-C), C-$CH_3$ |
| 723 | 724 | |
| 660 | 659 | Skeletal vibration or substituent characteristic |
| 641 | 641 | Substituent characteristic or skeletal vibration |
| 545 | 546 | δ(O-H), out-of-plane ? |
| 507 | 503 | δ(O-H), out-of-plane and others |
| 472 | 473 | |
| | 469 | δ(O-H), out-of-plane : free O-H |
| 442 | 442 | |
| 416 | | C-C bending, C-$CH_3$ |

benzene gives rise to the band at 500 to 400 $cm^{-1}$. Solid of *p-tert*-butyl phenol absorbs at 545 $cm^{-1}$ (strong), 506 $cm^{-1}$ (medium), 482 $cm^{-1}$ (weak) and 472 $cm^{-1}$ (very weak). The band at 545 $cm^{-1}$ remains unchanged when the compound is dissolved. The band at 482 $cm^{-1}$ disappears and a new band appears at 470 $cm^{-1}$. No regularity is found among the relative intensities of bands at 545, 506, 482 and 470 $cm^{-1}$. The effect of the condition of measurement on these values is so remarkable that a quantitative argument has little meaning. Qualitatively, the bands at 506 and 480 $cm^{-1}$ of solid and those at 503 and 472 $cm^{-1}$ of solution are perhaps concerned with O-H out-of-plane deformation vibration, considering that of phenol. The other vibration may couple with this vibration. Further discussion can not be carried out now.

Other assignments are nearly the same as in the previous report[1] in the region of sodium chloride optics. These assignments are obtained with consideration of those of phenol, 1,4-disubstituted benzene and *tert*-butyl compounds.

**α-Naphthol.**—α-Naphthol is an aromatic O-H compound which has one group of three adjacent free hydrogen atoms and one group of four adjacent free hydrogen atoms. α-Naphthylamine in solid gives rise to a broad band near 3200 $cm^{-1}$ but in solution gives rise to a sharp band at 3620 $cm^{-1}$ and a weak band at 3500 $cm^{-1}$. This aspect of OH stretching vibration band is the same as those of phenol and *p-tert*-butyl phenol stated already. Regions 1400 to 1350 $cm^{-1}$, 1330 to 1250 $cm^{-1}$ and 1210 to 1160 $cm^{-1}$ vary with the change of phase. From those results it may be considered that the band due to OH deformation vibration appears near 1170 and 1330 to 1340 $cm^{-1}$ for free α-naphthol molecule. There is also some possibility of considering the coupling of OH deformation vibration with the other mode of vibration rather than with the C-O stretching vibration. Then the above-mentioned regions which show the different features with the change of phase and concentration of solution, may be concerned with the OH deformation vibration. Tentatively for free α-naphthol, the bands near 1180 and 1359 $cm^{-1}$ are assigned to those vibrations.

Out-of-plane deformation vibration of aromatic C-H bonds may give rise[4,5,7] to the bands at 760 to 740 $cm^{-1}$ and 780 to 760 $cm^{-1}$ (more generally 800 to 760 $cm^{-1}$) or 770 to 735 $cm^{-1}$ and 810 to 750 $cm^{-1}$ for α-naphthol. The other characteristic bands to the substitution may be considered to appear near 725 to 680 $cm^{-1}$, or more precisely at 740 to 710 $cm^{-1}$, (720 to 710 $cm^{-1}$), 710 to 690 and 650 $cm^{-1}$. Then the bands at 789 and 765 $cm^{-1}$ may be assigned to that mode of vibration and other characteristic bands may be attributed to those at 730, 710 and 629 $cm^{-1}$. According to the literature[5,7] the three bands at 730, 710 and 629 $cm^{-1}$ can be assigned to the in-plane deformation vibration of aromatic C-H bond.

The change of spectra in the region below 1000 $cm^{-1}$ with phase change is yet to be explained clearly. The doublet of 959 $cm^{-1}$,

7) H. Luther and H. Gunzler, *Z. Naturforsch* **10b**, 445 (1955).

the band at 867 $cm^{-1}$ and bands at 769 and 765 $cm^{-1}$ in solid are different from these in solution. The doublet bands disappear and the single band appears at 959 and 767 $cm^{-1}$, and the band 867 $cm^{-1}$ disappears completely when the solid sample is dissolved. It is not suitable to consider that these bands are attributable to the vibration mode concerned with O-H vibration because O-H vibration does not give rise to bands in these regions in general. These changes may be caused from crystal field effect[6].

TABLE III. BAND POSITIONS AND ASSIGNMENT OF SPECTRUM OF α-NAPHTHOL

| Band, $cm^{-1}$ Solid | Band, $cm^{-1}$ Solution | Assignment |
|---|---|---|
| | 3620 | ν(O-H), free |
| | 3500 | ν(O-H), bonded |
| 3240 | | ν(O-H), bonded |
| 3110 | | ν(O-H), bonded |
| 3050 | 3060 | ν(C-H), aromatic |
| 1634 | 1634 | Ring vibration |
| 1600 | 1600 | Ring vibration |
| 1582 | 1582 | Ring vibration |
| 1560 | 1546 | Ring vibration |
| 1515 | 1517 | Ring vibration |
| 1453 | 1453 | Ring vibration |
| 1439 | 1404 | |
| 1387 or 1377 | 1388 | δ(O-H), bonded and ν(C-O) |
| | 1358 | δ(O-H), free and ν(C-O) |
| 1315 | 1312 | δ(O-H), bonded and ν(C-O)? |
| 1300 | 1297 | δ(O-H), bonded and ν(C-O)? |
| 1264 | 1276 | Skeletal vibration |
| 1253 | 1245 | Skeletal vibration |
| 1239 | 1235 | Skeletal vibration |
| | 1199 | δ(O-H), free and ν(C-O)? |
| | 1181 | δ(O-H), free and ν(C-O)? |
| 1172 | 1175 | Skeletal vibration |
| 1148 | 1145 | δ(C-H) |
| 1083 | 1082 | δ(C-H) or skeletal vibration |
| 1044 | 1040 | Skeletal vibration |
| 1015 | 1015 | δ(C-H) |
| 959 | 958 | Skeletal vibration |
| 875 | 877 | Skeletal vibration |
| 856 | 850 | δ(C-H), out-of-plane ? |
| 843 | 837 | δ(C-H), out-of-plane |
| 789 | 790 | δ(C-H), out-of-plane |
| 768 | 768 | δ(C-H), out-of-plane |
| 740 | 742 | Skeletal vibration or δ(C-H), out-of-plane |
| 731 | 725 | δ(C-H), out-of-plane |
| 712 | 710 | δ(C-H), out-of-plane |
| 628 | 629 | Skeletal vibration |
| 573 or 564 | 568 | δ(O-H), out-of-plane ? |
| 521 | 524 | δ(O-H), out-of-plane ? |
| 482 | 480 | Substituent characteristic skeletal vibration |
| 478 | 476 | Substituent characteristic skeletal vibration |
| 461 | 461 | Substituent characteristic skeletal vibration |
| 416 | 416 | Substituent characteristic skeletal vibration |

The tentative assignments are summarized in Table III. In the present experiment the concentration of solution is not altered. Therefore the assignment of the band concerned with OH vibration can not be carried out decidedly. Out-of-plane OH deformation vibration is expected to give rise to the bands in the region near 500 $cm^{-1}$ with consideration of these bands of phenol and *p-tert*-butyl phenol: But α-naphthol shows such a complex aspect in this region that a simple assignment can not be carried out at present. Perhaps bands at 530, 520 and 460 $cm^{-1}$ may be concerned with this vibration mode.

It may be accepted as true that the above three compounds give rise to the bands near 3600 $cm^{-1}$ due to OH stretching vibration, those near 1170 $cm^{-1}$ and near 1330 $cm^{-1}$ due to free OH in plane deformation vibration and those near 500 $cm^{-1}$ concerned in OH out-of-plane deformation vibration. These bands are attributed to free OH bond, but in a case of solid state or associated state, the bands at 3300 $cm^{-1}$, those at 1200 to 1230 $cm^{-1}$ and 1380 to 1430 $cm^{-1}$, and those near 500 $cm^{-1}$ may be assigned to the above mentioned vibration modes respectively. The bands in the region of 500 $cm^{-1}$ can not be decidedly assigned now but may be determined by deuteration of OH bond, considering the argument given above.

In the next paper the assignment will be made of the absorption bands of *p-tert*-butyl phenol resin and α-naphthol resin according to the result of this work.

## Summary

In connection with the work on a resin for dust respirator, the spectra of phenol, *p-tert*-butyl phenol and α-naphthol were observed in solid and in solution. Infrared absorption spectra can be explained by considering that these compounds associate by hydrogen bonding in solid form and that they hold the equilibrium between monomer and associated molecule in solution. Reasonable assignments were made to some of the bands observed. The deformation vibration of O-H (free) and stretching vibration of C-O seem to couple with each other and give rise to bands near 1340 and 1180 $cm^{-1}$ in any of these three compounds. Bands due to the out-of-plane O-H deformation vibration could not be determined but it was found that the bands in the

550～500 $cm^{-1}$ region were concerned with this vibrational mode.

The author wishes to express his hearty thanks to Assistant Professor T. Miyazawa and his collaborators at the Institute for Protein Research, Osaka University, for their kindness in permitting the use of a Perkin-Elmer Model 221 spectrophotometer. He wishes to express his thanks to Mr. M. Kawano at the Railway Technical Research Institute for the measurement of the spectrum in cesium bromide region. He also expresses his thanks to Dr. S. Koshi of this Institute for his kind supply of samples.

*National Institute of Industrial Health*
*Kawasaki-shi, Kanagawa-ken*

# *Infrared Absorption Spectra of Quartz and Some other Silica Modification*

By Reisuke SODA

(Received February 28, 1961)

Recently it was reported that the surface of a quartz particle was forced to change its structure by grinding[3-5]. Infrared absorption spectra of the quartz perticle showed that the band near 950 $cm^{-1}$ appeared as the result of grinding and disappeared when the particle was leached[1,2]. The origin of the band near 3400 $cm^{-1}$ was assumed to be the stretching vibration of O–H bond and its intensity changed depending upon the treatment of the particle. The parallel relation was observed between the intensity of 3400 $cm^{-1}$ band and that of 950 $cm^{-1}$. The intensities of the two bands increased with the degree of grinding. Another silica modification such as carplex gave rise to the 950 $cm^{-1}$ band and the intensities of both the 950 $cm^{-1}$ band and the 3400 $cm^{-1}$ band of this compound were stronger than those bands of other silica modifications. Previously the author assigned it tentatively to the deformation vibration of O–H link of silanol group at the surface layer of the particle[1]. In the present paper more evidence will be given to confirm the assignment of this band.

## Experimental

A quartz sample was prepared by grinding and in some cases by leaching the ground particle. The ground particle was fractionated by the particle size suspending it in water and separating it with centrifugal force. This procedure was reported in the other paper[1]. Ten per cent aqueous solution of sodium hydroxide was used to leach the particle. A quartz sample used was that was produced at Ishikawayama. The carplex was supplied by the Shionogi Co., Ltd. It was fine powder of particle size less than 0.5 $\mu$. The sample powder was mixed with potassium bromide in an agate mortar. The potassium bromide used was c. p. grade and pulverized in agate mortar into particle size of 200 to 300 mesh by sieving with a stainless steel sieve and dried by heating above 200°C for about one day. The mixed powder was dried by heating at about 150°C for 3 hr. and poured into the die to be pressed under 10 tons per square centimeter after evacuation for about 10 min. A shaped disk was inserted into the cell for the potassium bromide disk method.

Infrared absorption spectra were measured with Perkin-Elmer model 137 infracord spectrophotometer and Perkin-Elmer model 221 spectrophotometer.

Notations showing kinds of sample particles are as follows[1]:

Q-I-2M is the sample Ishikawayama quartz ground for 2 min., Q-I-6H that ground for 6 hr., Q-I-24H for 24 hr., O-I-100H for 100 hr. and Q-I-2M-L is the sample Ishikawayama quartz ground for 2 min. and leached with aqueous sodium hydroxide.

## Results

The spectrum of Q-I-2M gives rise to the bands at 1180, 1150 and 1070 $cm^{-1}$. These are very strong, but those at 800, 780 and 695 $cm^{-1}$ are sharp and have medium intensities. Sometimes a band near 3400 $cm^{-1}$ is observed with only a very weak intensity. The spectrum of Q-I-6H gives rise to the very weak band at 950 $cm^{-1}$ and to a weak but clear band at 3300 to 3400 cm other than those of Q-I-2M. In

1) H. Sakabe et al., *Bull. Natl. Inst. Ind. Health*, No. 4 (1961), in press.
2) R. Soda, ibid., (1961), in press.
3) J. Brown, W. J. Jaap and P. D. Ritchie, *J. Appl. Chem.*, **9**, 153 (1959).
4) K. Wheatley, ibid., **9**, 159 (1959).
5) J. A. Van Lier, P. J. De Bruyn and J. Th. G. Overbeek, *J. Phys. Chem.*, **64**, 1675 (1960).

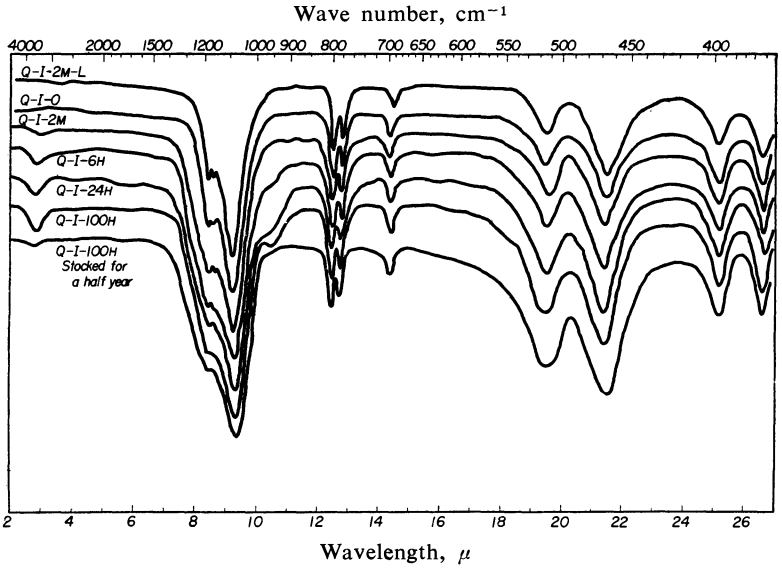



**Fig. 1.** Spectra of quartz particles prepared by various procedures. The range of particle size is 0.5~2 $\mu$ and mean size is about 1 $\mu$. Samples are Ishikawayama quartz ground by hand (Q-I-0), ground mechanically for 2 min. (Q-I-2M), for 6 hr. (Q-I-6H), for 24 hr. (Q-I-24H) and for 100 hr. (Q-I-100H). Q-I-2M-L designates Ishikawayama quartz ground for 2 min. and leached by NaOH aq.

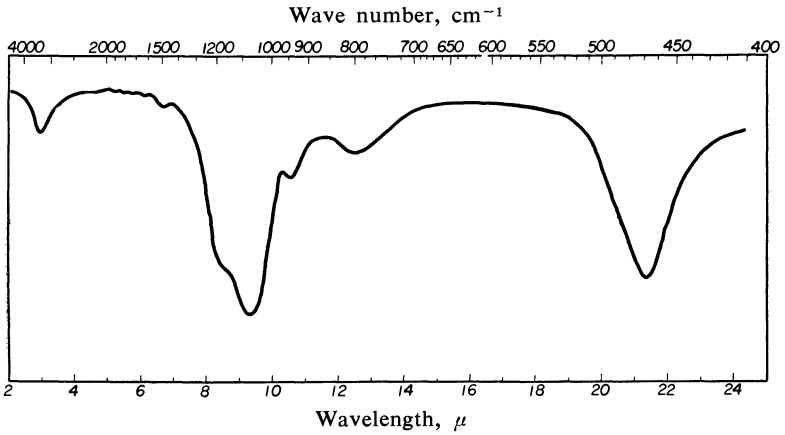



Fig. 2. Spectrum of amorphous silica "Carplex".

spectra of Q-I-24H and Q-I-100H the bands at 3300 to 3400 $cm^{-1}$ and at 950 $cm^{-1}$ are more intense than those of Q-I-6H. The intensities of those bands increase with grinding times. In the spectrum of Q-I-100H which has been kept in a desiccator for a half year, the intensities of the bands at 3400 and 950 $cm^{-1}$ decrease and sometimes the band at 950 $cm^{-1}$ is scarcely observed. The spectrum of carplex gives rise to the strongest bands at 1160 and 1090 $cm^{-1}$ and to a very weak broad band near 800 $cm^{-1}$. Besides those bands, it gives rise to a band of medium intensity at 3300 $cm^{-1}$ and to a well defined band near 950 $cm^{-1}$ as shown in Fig. 2.

The spectrum of Q-I-2M-L gives rise to no bands at 3400 and 950 $cm^{-1}$. The three bands near 1100 $cm^{-1}$ changed their aspects with their grinding times and with leaching. These band groups are sharply separated with leached quartz and lose their defined aspects with the grinding process. The band at 1070 $cm^{-1}$ is broader and first the band at 1150 $cm^{-1}$ becomes like the shoulder of 1070 $cm^{-1}$ band and finally is masked by the latter band with the increment of grinding time. The band at 1180 $cm^{-1}$ is like the shoulder of 1070 $cm^{-1}$ band also when the grinding time is longer than about 20 hr. These changes are illustrated in Fig. 1. In the region of the cesium bromide

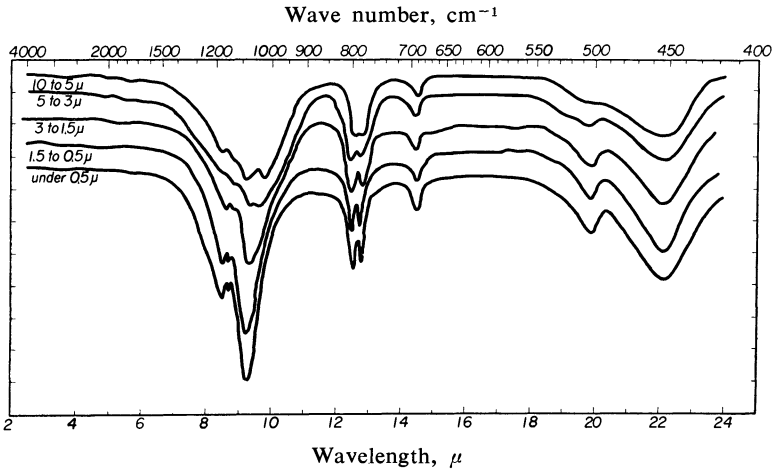



Fig. 3. Spectra of quartz in several range of particle size. Sample is Ishikawayama quartz ground for 2 min. and leached by NaOH aq.

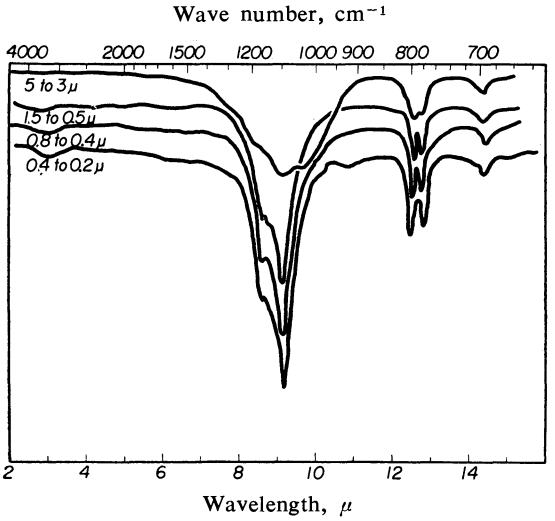



Fig. 4. Spectra of quartz in several range of particle size. Sample is Ishikawayama quartz ground for 100 hr.

optics, the spectrum of quartz powder is not influenced by the grinding times.

The spectrum of quartz powder changes its aspect with particle size in several regions. These changes are shown in Figs. 3 and 4. Figure 3 illustrates the spectra of Q-I-2M-L samples which have the particle size of the order of ten to zero microns. Figure 4 illustrates the spectra of Q-I-100H samples stocked for a half year, the particle sizes of which are from the order of 10 to that of 0.2 $\mu$. The particle size has a remarkable influence on the spectrum in the region of 8 to 9 $\mu$, and less remarkably on those in the regions of 12 and 20 $\mu$. Particularly this effect is markedly seen when the particle size is larger than 3 $\mu$. These results are summarized in Table I.

## Discussion

In general, silica modifications give rise to strong bands in the region of 1200 to 1050 $cm^{-1}$. These bands may be assigned to stretching vibration of Si-O[6,7]. The bands at 800, 780 and 694 $cm^{-1}$ of quartz are also attributed to the silica structure and are very sensitive to skeletal structure of silica. In the longer wavelength region of cesium bromide optics, the bands at 519, 470, 398 and 376 $cm^{-1}$ are attributed to the vibrations concerned with skeletal structure. Beyond those bands, the bands at 3400 and 950 $cm^{-1}$ which appear in the spectrum of carplex, Q-I-6H, Q-I-24H and Q-I-100H are not attributable to the above-mentioned structure sensitive vibrations but may be assigned mainly to hydroxyl group vibration of the silanol group[8-10]. Particle size has a very appreciable influence on the spectrum in the region of 8.5 to 9 $\mu$ and less but an effect which cannot be neglected on that in the region of 12 and 20~24 $\mu$ particularly when the particle size is larger than 3 $\mu$. These phenomena have been observed by several investigators and explained in a few ways[11]. At present the author has little interest in these explanations of the phenomena,

6) E. R. Lippincott, A. Van Valkenburg, C. E. Weir and E. N. Bunting, *J. Res. Nat. Bur. Stds.*, **61**, 61 (1958).
7) J. M. Hunt, M. P. Wisherd and L. C. Bonham, *Anal. Chem.*, **22**, 1478 (1950).
8) R. McDonald, *J. Phys. Chem.*, **62**, 1168 (1958).
9) H. A. Benesi and A. J. Jones, ibid., **63**, 179 (1959).
10) H. Scholze, *Naturwiss.*, **47**, 226 (1960).
11) W. M. Tuddenham and R. J. P. Lyon, *Anal. Chem.*, **32**, 1630 (1960).

TABLE I. INFRARED ABSORPTION BANDS AND THEIR CHARACTERISTICS OF SILICA

| Band positions $cm^{-1}$ | Remarks |
|---|---|
| 3400 to 3300 | Band intensity: strong to weak; carplex, Q-I-100H, Q-I-24H, Q-I-6H, Q-I-2M and Q-I-2M-L. Generally assigned to O-H stretching. |
| 1180, 1150 and 1070 | Very strong band region of quartz. The sharp feature with Q-I-2M and Q-I-2M-L is lost and the broadth of 1070 $cm^{-1}$ band develops with grinding; 1150 $cm^{-1}$ band appears as shoulder of 1070 $cm^{-1}$ band with Q-I-6H and Q-I-24H, the former being covered by the latter with Q-I-100H. 1180 $cm^{-1}$ band also appears as the shoulder of 1070 $cm^{-1}$ band. Particle size influences features of these bands, and a new band occurs at 1040 $cm^{-1}$ and this shifts towards lower wave number side as the particle size is larger than 3 $\mu$. In that case, this band group is diffuse and seems to be less intense. |
| 1160 and 1090 | Very strong band with carplex. |
| Close to 950 | Intensity: medium to weak; carplex, Q-I-100H, Q-I-24H, and probably Q-I-6H. This band cannot be found out with Q-I-2M and Q-I-2M-L. |
| 800 | Broad weak band with carplex. |
| 800, 780 and 694 | Characteristic bands of quartz with medium intensity. No appreciable change in the feature is observed by grinding. Particle sizes larger than 3 $\mu$ have an influence on the aspects of bands at 800 and 780 $cm^{-1}$ but no influence on 694 $cm^{-1}$ band. |
| 520, 470, 400 and 380 | Characteristic bands of quartz. No appreciable change occurs with grinding. Particle size influences their aspects as it is larger than 3 $\mu$. |

but would like to remark on the fact that as the particle size of ground quartz is smaller the band at 950 $cm^{-1}$ is more intense and the band group in the region of 8 to 9 $\mu$ is more diffuse. This will be concerned in the considerably irregular structure different from the original quartz structure. These aspects are illustrated in Figs. 3 and 4.

From spectral change with grinding and leaching as illustrated in Fig. 1, it may be recognized that the bands at 3400 and 950 $cm^{-1}$ also change their aspects in parallel. These two characteristic bands increase their intensities with the grinding times, decrease during the stock of sample in desiccator under the reduced pressure and disappear when the particle is leached. The relative intensity of these two bands scarcely differs with the samples treated in various ways.

It is generally accepted[3-5] that quartz particle ground mechanically has a disturbed and easily soluble layer around the surface, the structure of which is different from quartz itself but not completely amorphous like silica gel. In this case it was observed by means of the BET method with argon or krypton that the surface area of particles increases with the grinding. The interior parent structure does not change its original structure during the grinding but the surface layer is gradually disturbed and the amount of disturbed layer or the thickness of this layer increases with grinding times. The leached sample decreases its surface area and it is considered that the spectrum of this sample is essentially the same as those of the original sample. The change of spectrum in the region of 8 to 9 $\mu$ is responsible for this disturbed structure on the particle surface. The more disturbed the layer is, the more diffuse bands appear in this spectral region. This will be caused by the superposition of the spectrum of the disturbed layer on the original spectrum[1]. According to the above consideration, it is concluded that the intensities of the bands at 3400 and 950 $cm^{-1}$ increase with the increment of the amount of the disturbed layer surrounding the surface of the particle. The more the surface area increases, the more the number of SiOH bonds appears. Therefore the SiOH bonds exist mainly on the particle surface, particularly in the disturbed structure. The band at 3400 $cm^{-1}$ which is assigned to the stretching vibration of OH bond will increase its intensities not only with the SiOH group but also with the absorbed water molecule. But the absorbed water molecule gives rise to the bands near 1600 $cm^{-1}$ and does not at 900 to 1000 $cm^{-1}$ generally[10]. From this consideration, the band at 950 $cm^{-1}$ may be assigned to O-H deformation vibration of silanol group.

In the lower frequency region on new band was observed by the grinding. Therefore it is inadequate to consider that the band at 950 $cm^{-1}$ be assigned to the overtone or combination tone. This argument supports indirectly above assignment of the band at 950 $cm^{-1}$ to O-H deformation vibration. From the result of spectra obtained in this work, the band at 950 $cm^{-1}$ may be reasonably assigned to the

O-H deformation vibration of silanol group on the surface of ground quartz particle.

**Summary**

Some silica modification such as carplex and ground quartz particle, gives rise to the bands near 950 $cm^{-1}$. This band has no relation with the skeletal structure of Si-O bond and can not be explained as overtone or combination tone. It is reasonable to assign this band to O-H deformation vibration of silanol group. The effect of particle size and grinding time on the spectrum of quartz was examined and it was concluded that the ground quartz particle was covered by some irregular structure on its surface, which was different from quartz structure. In this surface structure, the silanol group seems to be constructed.

The author wishes to express his thanks to Mr. A. Masuda at the University of Tokyo for the use of an infracord spectrophotometer. He wishes to express his thanks to Mr. M. Kawano at the Railway Technical Research Institute for their measurement of the spectrum in cesium bromide region. He also desires to express his hearty gratitude to Assistant Professor T. Miyazawa at the Institute for Protein Research, Osaka University for the use of a Perkin-Elmer model 221 spectrophotometer and also for valuable advice. Finally he wishes to thanks Mr. A. Hamada of this Institute for his kind supply of the dust sample to him.

*National Institute of Industrial Health*
*Kawasaki-shi, Kanagawa-ken*

# *Silanes. Vibrational Assignments and Frequency Correlations*

By George J. JANZ and Yukio MIKAWA*

(Received February 17, 1961)

Silanes have received widespread attention during the last decade and are of continuing current interest[1-4]. As part of a program in this laboratory on the vibrational spectra, molecular structure, and thermodynamic properties of this class of compounds, a review of the widely scattered results was undertaken to assess the status of our information. It became apparent in the course of this review that a need existed for a critical evaluation of the vibrational assignments, and for the interpretation of the normal frequencies on a series of simplified vibrational modes. This communication reports the results thus obtained, together with a useful table of generalized characteristic frequencies and bond distances based on this work.

## Status

Information for about one hundred silanes, widely scattered in the published literature, was reviewed relative to the subjects: frequency assignment (FA), infrared spectra (IR), Raman spectra (R) molecular structure (M), thermodynamic properties (T), normal coordinate vibrational analyses (NC) and force constants (FC). For reference and guidance, the status of knowledge is presented in summary form in Table I.

## Vibrational Spectra

Relative to the vibrations associated with the silicon atom and the surrounding four atoms attached with tetrahedral angles, all of the silanes considered can be classified into three groups based on the symmetry of molecule; $SiX_4$, $SiXY_3$ and $SiX_2Y_2$. The designation of normal vibrations, symmetry class and selection rules for each type of molecules are shown in Table II, where the symbols $\nu$, $\delta$ and $\tau$ denote stretching, deformation and twisting vibrations, respectively, and the suffixes a, e, f and b denote the class of symmetry group to which the vibration belongs. The simplified vibrational modes for each type of molecule are illustrated in Figs. 1—3. It is recognized that the exact feature of the normal mode differs from molecule to molecule depending on the masses of atoms and the force constants of the bonds, and can be calculated by the normal

* Present address: Research Laboratory, Mitsubishi Chemical Industries, Ltd. Kawasaki-shi.

1) H. Kriegsmann, *Z. anorg. Chem.*, **299**, 138 (1959).
2) A. L. Smith and N. C. Angelotti, *Spectrochim. Acta*, **1959**, 412.
3) R. N. Kniseley, V. A. Fassel and E. E. Conrad, ibid., **1959**, 651.
4) H. W. Thompson, ibid., **16**, 238 (1960).

TABLE I. STATUS OF KNOWLEDGE FOR SILANES

| Silane | FA | IR | R | M | T | NC | FC | Ref. |
|---|---|---|---|---|---|---|---|---|
| $SiH_4$ | × | × | × | × | × | × | × | 7—17 |
| $H_2SiD_2$ | × | × | | | × | | | 17, 18 |
| $HSiD_3$ | × | × | | × | × | | | 17—20 |
| $SiD_4$ | × | × | | | × | | | 17—19 |
| $H_3Si(CH_3)$ | × | × | | × | | × | × | 3, 21—23 |
| $H_2Si(CH_3)_2$ | × | × | × | | | × | × | 21—25 |
| $HSi(CH_3)_3$ | × | × | × | × | | × | × | 21—23 |
| $Si(CH_3)_4$ | × | × | × | × | × | × | × | 16, 17, 26—40 |
| $H_3SiCH=CH_2$ | × | × | | | | | | 21 |
| $H_3SiC_2H_5$ | | × | | | | | | 21 |
| $H_2Si(C_2H_5)_2$ | | × | | | | | | 21, 41 |
| $HSi(C_2H_5)_3$ | | × | | | | | | 21 |
| $Si(C_2H_5)_4$ | × | × | × | | | | | 21, 42, 43 |
| $H_nSi(C_3H_7)_{4-n}$* | | × | | | | | | 41, 44, 45 |
| $Si(CH_2CH=CH_2)_4$ | | × | | | | | | 46 |
| $H_3Si(C_4H_9)$ | | × | | | | | | 21, 45 |
| $H_2Si(C_4H_9)_2$ | | × | | | | | | 41 |
| $H_2Si(C_5H_{11})_2$ | | × | | | | | | 45 |
| $H_3Si(C_6H_5)$ | | × | | | | | | 3, 73 |
| $H_2Si(C_6H_5)_2$ | × | × | × | | | | | 41, 73 |
| $HSi(C_6H_5)_3$ | | × | | | | | | 44, 73 |
| $Si(C_6H_5)_4$ | | | | × | | | | 47 |
| $D_3Si(C_6H_5)$ | | × | | | | | | 3 |
| $DSi(C_6H_5)_3$ | | × | | | | | | 44 |
| $H_3SiC_6H_{11}$ | | × | | | | | | 45 |
| $H_2Si(C_6H_{11})_2$ | | × | | | | | | 41 |
| $H_3SiC_{10}H_9$ | | × | | | | | | 45 |
| $(CH_3)_nSi(C_2H_5)_{4-n}$* | | | × | | | | | 35 |
| $(CH_3)_2Si(C_3H_7)_2$ | | × | | | | | | 21 |
| $(CH_3)_3Si(C_6H_5)$ | | × | × | | | | | 48 |
| $Si(OCH_3)_4$ | × | × | × | | | | × | 49—53 |
| $Si(OC_2H_5)_4$ | × | × | × | | | | | 49, 51, 54 |
| $Si(OC_3H_7)_4$ | | × | × | | | | | 49 |
| $R_3Si(OR')$** | × | × | × | | | | | 55 |
| $R_2Si(OR')_2$** | × | × | × | | | | | 55, 56, 115 |
| $RSi(OR')_3$** | × | × | × | | | × | | 55, 56, 109 |
| $SiF_4$ | × | × | × | × | × | × | × | 16, 17, 57—62 |
| $H_3SiF$ | × | × | | × | × | | × | 17, 63—65 |
| $H_2SiF_2$ | × | × | | | × | | | 17, 66, 67 |
| $HSiF_3$ | × | × | | × | × | | | 17, 65—68 |
| $D_3SiF$ | × | × | | × | × | | | 17, 64, 65, 67, 69 |
| $D_2SiF_2$ | × | × | | | × | | | 17, 66 |
| $DSiF_3$ | × | × | | | × | | | 17, 66, 67 |
| $(CH_3)_3SiF$ | × | × | × | × | | | | 70, 71 |
| $(CH_3)_2SiF_2$ | × | × | × | | | | | 25 |
| $(CH_3)SiF_3$ | × | × | × | × | × | | × | 17, 65, 72 |
| $CH_3SiH_2F$ | × | × | | | | | | 24 |
| $(C_6H_5)_nSiF_{4-n}$* | × | × | × | | | | | 73 |
| $SiCl_4$ | × | × | × | × | × | × | × | 5, 6, 14, 16, 17, 26—28, 52, 61, 62, 74, 79 |
| $H_3SiCl$ | × | × | | × | × | | | 14, 17, 75—78, 111 |
| $H_2SiCl_2$ | × | × | × | × | × | | | 3, 17, 24, 42, 80, 81, 85 |
| $HSiCl_3$ | × | × | × | × | × | × | × | 17, 19, 82—87 |
| $D_3SiCl$ | × | × | | × | | | | 67, 69 |

TABLE I. (Countinued)

| Silane | FA | IR | R | M | T | NC | FC | Ref. |
|---|---|---|---|---|---|---|---|---|
| $(CH_3)_3SiCl$ | × | × | × | × | × | × | × | 5, 17, 26—28, 43, 71, 83, 91, 93—95 |
| $(CH_2)_2SiCl_2$ | × | × | × | × | × | × | × | 5, 17, 25—28, 43, 89, 92 |
| $(CH_3)SiCl_3$ | × | × | × | × | × | × | × | 5, 17, 26—28, 43, 83, 88—91 |
| $CH_2=CHSiCl_3$ | × | × | | | | | | 97 |
| $(C_2H_5)_3SiCl$ | × | | × | | | | | 42, 43 |
| $(C_2H_5)_2SiCl_2$ | × | | × | | | | | 42, 43 |
| $(C_2H_5)SiCl_3$ | × | × | × | | | | | 42, 43, 51 |
| $(CH_2=CH-CH_2)_nSiCl_{n-4}$* | | × | | | | | | 46 |
| $(C_3H_7)SiCl_3$ | | × | | | | | | 51 |
| $(C_4H_9)SiCl_3$ | | × | | | | | | 51 |
| $(C_{10}H_7)SiCl_3$ | | × | | | | | | 96 |
| $(C_6H_5)_nSiCl_{4-n}$* | × | × | × | | | | | 73 |
| $CH_3SiCl_2H$ | × | | × | | | | | 43 |
| $C_2H_5SiCl_2H$ | × | | × | | | | | 43 |
| $(CH_3O)_nSiCl_{4-n}$* | × | × | × | | | | | 50, 52, 55, 113 |
| $(C_2H_5O)_nSiCl_{4-n}$* | × | | × | | | | | 54, 114 |
| $SiBr_4$ | × | | × | × | × | × | × | 5, 12, 16, 17, 29, 74, 98 |
| $H_3SiBr$ | × | | × | × | × | × | × | 12, 13, 17, 63, 100, 101 |
| $H_2SiBr_2$ | × | × | × | | × | × | × | 13, 17, 80, 100, 102 |
| $HSiBr_3$ | × | | × | × | × | × | × | 12, 13, 17, 98, 102, 103 |
| $(CH_3)_3SiBr$ | × | | × | × | | | | 29, 95, 104 |
| $(CH_3)_2SiBr_2$ | × | × | × | × | | | | 25, 29, 104 |
| $(CH_3)SiBr_3$ | × | | × | × | | | | 29, 104 |
| $SiI_4$ | × | | × | × | × | × | × | 6, 17, 74, 105 |
| $H_3SiI$ | × | × | | × | | | × | 106—108 |
| $H_2SiI_2$ | | × | | | | | | 24, 106 |
| $D_3SiI$ | × | × | | | | | × | 108 |
| $(CH_3)_3SiI$ | × | | × | × | | | | 95, 110 |
| $F_3SiCl$ | | | | × | | | | 26, 65 |
| $F_3SiBr$ | | | | × | | | | 65 |
| $F_2SiBr_2$ | | | | × | | | | 65, 98 |
| $Cl_nSiBr_{n-4}$* | × | × | × | × | × | × | × | 6, 17, 74, 99, 111 |
| $Cl_3SiI$ | × | | × | | × | × | × | 6, 17, 74 |
| $Cl_2SiI_2$ | × | | × | | | × | × | 6, 74 |
| $ClSiI_3$ | × | | × | | × | × | × | 6, 17, 74 |
| $(CH_3)_3SiOH$ | × | × | × | | | | | 71, 112 |
| $(C_6H_5)_nSi(OH)_{4-n}$* | × | × | × | | | | | 73 |
| $(CH_3)_3SiSH$ | × | × | × | | | | | 71 |

* $n=1, 2, 3$ ** R, R′=$CH_3$ or $C_2H_5$


5) T. Shimanouchi, I. Tsuchiya and Y. Mikawa, *J. Chem. Phys.*, **18**, 1306 (1950).
6) M. Dewaulle, *J. Phys. Chem.*, **56**, 355 (1952); *J. Am. Chem. Soc.*, **74**, 5768 (1952).
7) K. Venkateswarlu and S. Sundaran, *J. Chem. Phys.*, **23**, 2365 (1955).
8) C. H. Tindal, J. W. Straley and H. H. Nielson, *Phys. Rev.*, **62**, 151 (1942).
9) W. D. Steward and H. H. Nielson, ibid., **47**, 828 (1935).
10) C. H. Tindal, J. W. Straley and H. H. Nielson, ibid., **58**, 1002 (1940).
11) F. B. Stett and D. M. Yost, *J. Chem. Phys.*, **4**, 82 (1936).
12) H. Murata and K. Kawai, ibid., **23**, 2451 (1955).
13) T. Shimanouchi, ibid., **17**, 245 (1949).
14) C. Cerny and E. Erdos, *Collection Czechoslov. Chem. Commun.*, **19**, 646 (1954).
15) A. P. Atlshuler, *J. Chem. Phys.*, **23**, 761 (1955).
16) T. Shimanouchi, ibid., **17**, 848 (1949).
17) Y. Mikawa, *J. Chem. Soc. Japan, Pure Chem. Sec.* (*Nippon Kagaku Zasshi*), **81**, 1521 (1960). "Selected Values of Properties of Chemical Compounds", Ed. by F. D. Rossini, MCA Research Project, Carnegie Institute of Technology, Pittsburgh, Pa., to be published.
18) J. H. Meal and M. Kent Wilson, *J. Chem. Phys.*, **24**, 385 (1956).

19) S. R. Pola and M. K. Wilson, Harvard University, Project No. R-351-30-13 (1954).
20) D. R. J. Boyd, *J. Chem. Phys.*, **23**, 922 (1955).
21) S. Kaye and S. Tannenbaum, *J. Org. Chem.*, **18**, 1750 (1953).
22) A. C. Bond and L. O. Brockway, *J. Am. Chem. Soc.*, **76**, 3312 (1954).
23) I. F. Kovalev, *Optics and Spectroscopy*, **8**, 166 (1960).
24) E. A. V. Ebsworth, M. Onyszchuk and N. Sheppard, *J. Chem. Soc.*, **1958**, 1453.
25) H. Kriegsmann, *Z. Elektrochem.*, **62**, 1033 (1958).
26) R. L. Livingston and L. O. Brockway, *J. Am. Chem. Soc.*, **66**, 94 (1944).
27) A. L. Smith, *J. Chem. Phys.*, **21**, 1997 (1953).
28) J. Goubeau, H. Siebert and M. Winterwerb, *Z. anorg. u. allgem. Chem.*, **259**, 240 (1949).
29) H. Murata and S. Hayashi, *J. Chem. Phys.*, **19**, 1217 (1951).
30) D. H. Rank, B. D. Saksean and E. R. Shull, *Discussions Faraday Soc.*, **9**, 187 (1950).
31) C. W. Young, J. S. Kohler and D. S. Mckinney, *J. Am. Chem. Soc.*, **66**, 1410 (1947).
32) F. Wall and C. R. Eddy, *J. Chem. Phys.*, **6**, 107 (1938).
33) D. H. Rank and E. R. Bordner, ibid., **3**, 248 (1935).
34) S. Silver, ibid., **8**, 919 (1940).
35) V. A. Kolesova, E. V. Kukharskaya and D. N. Andrew, *Izvest. Akad. Nauk. S. S. S. R., Otdel. Khim. Nauk*, 294 (1953).
36) I. Simon and H. O. McMahon, *J. Chem. Phys.*, **20**, 905 (1952).
37) J. G. Aston and R. M. Kennedy, *J. Am. Chem. Soc.*, **62**, 2567 (1940).
38) I. F. Kovalev, *Optics and Spectroscopy*, **5**, 387 (1957).
39) K. Shimizu and H. Murata, *J. Mol. Spectroscopy*, **5**, 44 (1960).
40) H. Siebert, *Z. anorg. u. allgem. Chem.*, **268**, 177 (1952).
41) R. West and E. G. Rochow, *J. Org. Chem.*, **18**, 303 (1953).
42) H. Murata, *J. Chem. Phys.*, **18**, 1308 (1950).
43) H. Murata, *J. Chem. Soc. Japan, Pure Chem. Sec. (Nippon Kagaku Zasshi)*, **73**, 465 (1952).
44) L. Kaplan, *J. Am. Chem. Soc.*, **76**, 5880 (1954).
45) H. E. Opitz, J. S. Peake and W. H. Nebergall, ibid., **78**, 292 (1956).
46) R. E. Scott and K. C. Firsch, ibid., **73**, 2599 (1951).
47) M. Yokoi, *J. Chem. Soc. Japan, Pure Chem. Sec. (Nippon Kagaku Zasshi)*, **73**, 822 (1952).
48) C. C. Cerato, J. L. Lauer and H. C. Beachell, *J. Chem. Phys.*, **22**, 1 (1954).
49) H. Kriegsmann and K. Licht, *Z. Elektrochem.*, **62**, 1163 (1958).
50) H. Murata, *J. Chem. Phys.*, **20**, 347 (1952).
51) A. L. Smith, *Spectrochim. Acta*, **16**, 87 (1960).
52) J. Goubeau and H. Behr, *Z. anorg. u. allgem. Chem.*, **272**, 2 (1953).
53) K. Iguchi, *J. Chem. Phys.*, **22**, 1937 (1954).
54) H. Murata, ibid., **20**, 1184 (1952).
55) R. Forneris and E. Funck, *Z. Elektrochem.*, **62**, 1130 (1958).
56) R. E. Richards and H. W. Thompson, *J. Chem. Soc.* **1949**, 124.
57) D. M. Yost, E. M. Lassettre and S. T. Gross, *J. Chem. Phys.*, **4**, 325 (1936).
58) H. Urey and C. Bradley, *Phys. Rev.*, **28**, 1970 (1932).
59) F. L. Voelz, A. G. Meister and F. F. Cleveland, *J. Chem. Phys.*, **19**, 1084 (1951); **20**, 1498 (1952).
60) E. A. Jones, Kirby-Smith, Woltz and Nielsen, ibid., **19**, 242 (1951).
61) L. Pauling and L. O. Brockway, *J. Am. Chem. Soc.*, **57**, 2684 (1935).
62) H. Siebert, *Z. anorg. u. allgem. Chem.*, **274**, 34 (1953).
63) C. Newman, J. K. O'Loane, S. R. Polo and M. K. Wilson, *J. Chem. Phys.*, **25**, 855 (1956).
64) F. A. Andersen and B. Bak, *Acta Chem. Scand.*, **8**, 738 (1954).
65) J. Sheridan and W. Gordy, *Phys. Rev.*, **77**, 719 (1950).
66) M. K. Wilson, ASTIA-AD-120452 (Harvard 1957).
67) C. Newman, S. R. Polo and M. K. Wilson, *Spectrochim. Acta*, **15**, 793 (1959).
68) G. A. Heath, L. F. Thomas and J. Sheridan, *Trans. Faraday Soc.*, **50**, 779 (1954).
69) B. Bak, J. Bruhn and J. Rastrup-Andersen, *J. Chem. Phys.*, **21**, 753 (1953).
70) R. G. Gunton, J. F. Ollom and H. N. Rexroad, ibid., **22**, 1942 (1954).
71) H. Kriegsmann, *Z. anorg. u. allgem. Chem.*, **294**, 113 (1958).
72) R. L. Collins and J. R. Nielsen, *J. Chem. Phys.*, **23**, 351 (1954).
73) H. Kriegsmann and K. H. Schowtka, *Z. Phys. Chem. (Leipzig)*, **209**, 261 (1958).
74) Y. Kakiuchi, This Bulletin, **26**, 260 (1953).
75) A. Monfils, *J. Chem. Phys.*, **19**, 138 (1951).
76) A. Monfils, *Compt. rend.*, **236**, 795 (1953).
77) H. Sharabaugh, *Phys. Rev.*, **74**, 1870 (1948).
78) B. P. Dailey, J. M. Mays and C. H. Townes, ibid., **76**, 136 (1949).
79) L. O. Brockway and J. Y. Beach, *J. Am. Chem. Soc.*, **60**, 1836 (1938).
80) J. Hawkins, S. Polo and M. K. Wilson, *J. Chem. Phys.*, **21**, 1122 (1953).
81) J. A. Hawkins and M. K. Wilson, ibid., **21**, 360 (1953).
82) T. G. Gibian and D. S. McKinney, *J. Am. Chem. Soc.*, **73**, 1431 (1951).
83) R. C. Mockler, J. H. Bailey and W. Gordy, *J. Chem. Phys.*, **21**, 1710 (1953).
84) M. H. Pirene, *Compt. rend.*, **206**, 516 (1938).
85) L. O. Brockway and I. E. Coop, *Trans. Faraday Soc.*, **34**, 1429 (1938).
86) K. Yamasaki, A. Kotera, M. Iwasaki and N. Tatematsu, *J. Chem. Soc. Japan, Pure Chem. Sec. (Nippon Kagaku Zasshi)*, **69**, 104 (1953).
87) T. G. Gibian and D. S. Mckinney, *J. Am. Chem. Soc.*, **73**, 1431 (1951).
88) L. Burnelle and J. Duchesne, *J. Chem. Phys.*, **20**, 1324 (1952).
89) M. C. Tobin, *J. Am. Chem. Soc.*, **75**, 1788 (1953).
90) K. Shimizu and H. Murata, This Bulletin, **32**, 46 (1959).
91) K. Shimizu and H. Murata, *J. Mol. Spectroscopy*, **4**, 201 (1960).
92) K. Shimizu and H. Murata, ibid., **4**, 214 (1960).
93) J. Duchesne, *J. Chem. Phys.*, **16**, 1006 (1948).
94) R. L. Livingston and L. O. Brockway, *J. Am. Chem. Soc.*, **68**, 719 (1946).
95) J. Goubeau and H. Sommer, *Z. anorg. u. allgem. Chem.*, **289**, 1 (1957).
96) J. W. Gilkey and L. J. Tyler, *J. Am. Chem. Soc.*, **73**, 4982 (1951).
97) E. R. Shull, R. A. Thursoch and C. M. Birdsall, *J. Chem. Phys.*, **24**, 147 (1956).
98) R. Spitzer, W. J. Howell, Jr., and V. Schomaker, *J. Am. Chem. Soc.*, **64**, 62 (1942).
99) B. Schneider and J. Pliva, *Collection Czechoslov. Chem. Commun. Suppl.*, **19**, 653 (1954).
100) D. W. Mayo, H. E. Opitz and J. S. Peake, *J. Chem. Phys.*, **23**, 1344 (1955).
101) A. H. Sharbaugh, J. K. Bragg, T. C. Madison and V. G. Thomas, *Phys. Rev.*, **76**, 1419 (1949).
102) F. Francois and M. Buisset, *Compt. rend.*, **230**, 1946 (1950).
103) J. Wouters, M. Hemptinne and P. Capron, *Am. Soc. Sci., Burxelles, Ser. I*, **57**, 25 (1937).
104) K. Yamasaki, A. Kotera, M. Yokoi and M. Iwasaki, *J. Chem. Phys.*, **17**, 1355 (1949).
105) P. W. Allen and L. E. Sutton, *Acta Cryst.*, **3**, 46 (1950).
106) H. J. Emeléus, A. G. Macdiarmid and A. G. Maddock, *J. Inorg. Nuclear Chem.*, **1**, 194 (1955).
107) R. N. Dixon and N. Sheppard, *Trans. Faraday Soc.*, **53**, 282 (1957).
108) H. R. Linton and E. R. Nixon, *Spectrochim. Acta*, **12**, 41 (1958).
109) T. Tanaka, This Bulletin, **33**, 446 (1960).
110) H. N. Rexroad, D. W. Howgate, R. C. Gunton and J. Ollom, *J. Chem. Phys.*, **24**, 625 (1956).
111) B. P. Dailey, J. M. Mays and C. H. Towns, *Phys. Rev.*, **76**, 136 (1949).
112) W. S. Tatlock and E. G. Rochow, *J. Org. Chem.*, **17**, 1560 (1952).
113) H. Murata, K. Kawai and M. Yokoo, *J. Chem. Soc. Japan, Pure Chem. Sec. (Nippon Kagaku Zasshi)*, **77**, 893 (1956).
114) H. Murata and K. Kawai, ibid., **77**, 1542 (1956).
115) M. Hayashi, ibid., **79**, 436 (1958).

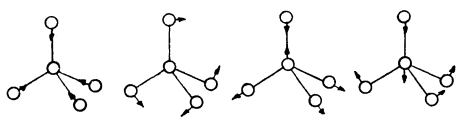
TABLE II. DESIGNATION OF NORMAL VIBRATIONS, SYMMETRY CLASS AND SELECTION RULES

| Type of molecule | Symmetry class | Designation | Activity | | Interpretation |
|---|---|---|---|---|---|
| | | | Raman | Infrared | |
| $SiX_4$ | $A_1$ | $\nu_a(SiX_4)$ | p*1 | i*3 | Symmetrical stretching |
| | E | $\delta_e(SiX_4)$ | d*2 | i | The 1st kind of deformation |
| | $F_2$ | $\nu_f(SiX_4)$ | d | a*4 | Asymmetrical stretching |
| | $F_2$ | $\delta_f(SiX_4)$ | d | a | The 2nd kind of deformation |
| $SiXY_3$ | A | $\nu_a(SiX)$ | p | a | Stretching vibration |
| | A | $\nu_a(SiY_3)$ | p | a | Symmetrical stretching |
| | A | $\delta_a(SiY_3)$ | p | a | The 2nd kind of deformation |
| | E | $\nu_e(SiY_3)$ | d | a | Asymmetrical stretching |
| | E | $\delta_e(SiY_3)$ | d | a | The 1st kind of deformation |
| | E | $\delta_e(SiXY_3)$ | d | a | Bending of SiX or wagging of $SiY_3$ |
| $SiX_2Y_2$ | $A_1$ | $\nu_a(SiX_2)$ | p | a | Symmetrical stretching |
| | $A_1$ | $\nu_a(SiY_2)$ | p | a | Symmetrical stretching |
| | $A_1$ | $\delta_a(SiX_2)$ | p | a | The 1st kind of deformation |
| | $A_1$ | $\delta_a(SiY_2)$ | p | a | The 1st kind of deformation |
| | $A_2$ | $\tau(SiX_2Y_2)$ | d | i | Twisting |
| | $B_1$ | $\nu_b(SiX_2)$ | d | a | Asymmetrical stretching |
| | $B_1$ | $\delta_b(SiX_2Y_2)$ | d | a | Rocking of $SiX_2$ or wagging of $SiY_2$ |
| | $B_2$ | $\nu_b(SiY_2)$ | d | a | Asymmetrical stretching |
| | $B_2$ | $\delta_b(SiY_2X_2)$ | d | a | Rocking of $SiY_2$ or wagging of $SiX_2$ |

*1 polarized *2 depolarized *3 inactive *4 active

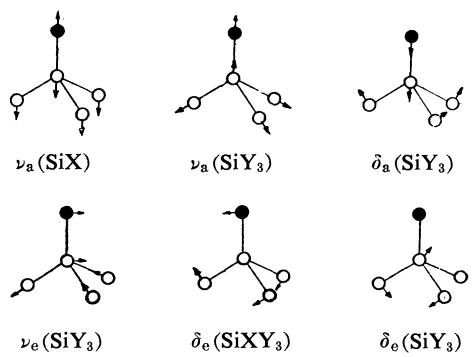
coordinate treatment for the individual molecule.

$\nu_a(SiX_4)$ in $SiX_4$, $\nu_a(SiX_3)$ in $SiX_3Y$, $\nu_a(SiX_2)$ in $SiX_2Y_2$ and $\nu_a(SiX)$ in $SiXY_3$ are interpreted as symmetrical stretching vibrations of Si–X in which X atoms vibrate in phase back and forth in the direction of the bonds. $\nu_f(SiX_4)$ in $SiX_4$, $\nu_e(SiX_3)$ in $SiX_3Y$ and $\nu_b(SiX_2)$ in $SiX_2Y_2$ are interpreted as asymmetrical stretching vibrations of Si–X in which X atoms vibrate out of phase in the direction of the bonds. The deformation vibrations $\delta_e(SiX_4)$ in $SiX_4$, $\delta_e(SiX_3)$ in $SiX_3Y$ and $\delta_a(SiX_2)$ in $SiX_2Y_2$ make one group called the first kind of deformation vibrations. This kind produces the change in the angle between the two adjacent bonds. The second kind of deformation vibrations which inculdes $\delta_f(SiX_4)$ in $SiX_4$ and $\delta_a(SiX_3)$ in $SiX_3Y$ is a symmetrical deformation vibration with respect to the threefold axes. As for $\delta_e(SiXY_3)$, two alternative ways for interpretation are possible. If X is a lighter atom than Y, $\delta_e(SiXY_3)$ should be interpreted as a bending of X, whereas, in the opposite case it should be interpreted as a wagging of $Y_3$. $\delta_b(SiX_2Y_2)$ may be interpreted either as a wagging vibration in which



$\nu_a(SiX_4)$ $\delta_e(SiX_4)$ $\nu_f(SiX_4)$ $\delta_f(SiX_4)$

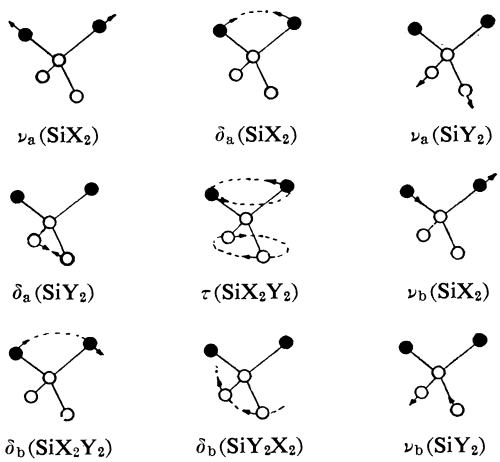
Fig. 1. Normal vibrations of $SiX_4$.



$\nu_a(SiX)$ $\nu_a(SiY_3)$ $\delta_a(SiY_3)$

$\nu_e(SiY_3)$ $\delta_e(SiXY_3)$ $\delta_e(SiY_3)$

Fig. 2. Normal vibrations of $SiXY_3$.



$\nu_a(SiX_2)$ $\delta_a(SiX_2)$ $\nu_a(SiY_2)$

$\delta_a(SiY_2)$ $\tau(SiX_2Y_2)$ $\nu_b(SiX_2)$

$\delta_b(SiX_2Y_2)$ $\delta_b(SiY_2X_2)$ $\nu_b(SiY_2)$

Fig. 3. Normal vibrations of $SiX_2Y_2$.

two X atoms swing as a unit in $SiX_2$ plane or as a rocking vibration in which two Y atoms swing back and forth parallel to the same plane. The situation is the same for $\delta_b(SiY_2X_2)$ if X is replaced by Y and vice versa. $\tau(SiX_2Y_2)$ is interpreted as a twisting vibration of $SiX_2$ in respect to $SiY_2$. This vibration depends upon the nature of the X atom as well as of the Y atom.

All of the published data are tabulated in Tables III—V in accordance with the above designations. Some values are from Raman spectra of the liquid state and some from infrared spectra of the liquid or gaseous states. In most instances, the differences in the frequencies reported with the different methods or by various investigators were not sufficiently

TABLE III. NORMAL FREQUENCIES OF $SiX_4$ TYPE MOLECULES

| $SiX_4$ | $\nu_a(SiX_4)$ | $\delta_e(SiX_4)$ | $\nu_f(SiX_4)$ | $\delta_f(SiX_4)$ |
|---|---|---|---|---|
| $SiH_4$ | 2187 | 974.6 | 2190.6 | 914.2 |
| $SiD_4$ | (1582)[c] | (689)[c] | 1597 | 681 |
| $SiF_4$ | 800 | 268 | 1031 | 391 |
| $SiCl_4$ | 424 | 150 | 610 | 221 |
| $SiBr_4$ | 249 | 90 | 487 | 137 |
| $SiI_4$ | 168 | 63 | 405 | 94 |
| $Si(CH_3)_4$ | 598 | 202 | 696 | 239 |
| $Si(C_2H_5)_4$ | 553 | 160 | 736 | 303 |
| $Si(OCH_3)_4$ | 640 | 251 | 844 | 308 |
| $Si(OC_2H_5)_4$ | 654 | 240 | 792 | 305 |

c: Calculated value

TABLE IV. NORMAL FREQUENCIES OF $SiXY_3$ TYPE MOLECULES

| $SiXY_3$ | $\nu_a(SiX)$ | $\nu_a(SiY_3)$ | $\delta_a(SiY_3)$ | $\nu_e(SiY_3)$ | $\delta_e(SiY_3)$ | $\delta_e(SiXY_3)$ |
|---|---|---|---|---|---|---|
| $SiHD_3$ | 2182 | 1573 | 683 | 1598 | 683 | 851 |
| $SiHF_3$ | 2314.5 | 858.6 | 425.2 | 998.6 | 305.5 | 844.5 |
| $SiHCl_3$ | 2274 | 497 | 250 | 600 | 179 | 810 |
| $SiHBr_3$ | 2234 | 360 | 168 | 470 | 113 | 767 |
| $SiDF_3$ | 1688 | 854 | 421.9 | 994.4 | 302.2 | 628.5 |
| $SiFH_3$ | 872.0 | 2206 | 989.7 | 2196 | 943.4 | 728.1 |
| $SiFD_3$ | 888 | 1577 | 704 | 1615 | (764)[c] | 549 |
| $SiClH_3$ | 551 | 2201 | 949 | 2195 | 954.4 | 664.0 |
| $SiClD_3$ | 538 | 1581 | 702 | 1616 | (734)[c] | 488 |
| $SiClBr_3$ | 583 | 291 | 173 | 489 | 102 | 159 |
| $SiClI_3$ | 557 | 220 | 114 | 411 | 73 | 134 |
| $SiH(CH_3)_3$ | 2118 | 625 | 219 | 718 | 251 | 908 |
| $SiF(CH_3)_3$ | 898 | 620 | 206 | 695 | 259 | 290 |
| $SiCl(CH_3)_3$ | 487 | 640 | 242 | 700 | 188 | 330 |
| $SiCl(C_2H_5)_3$ | 464 | 592 | 221 | 739 | 160 | 295 |
| $SiCl(OCH_3)_3$ | 510 | 717 | 264 | 845 | — | 357? |
| $SiCl(OC_2H_5)_3$ | 520 | 695 | 290 | 799 | — | — |
| $SiBrH_3$ | 430 | 2200 | 930 | 2196 | 950.4 | 632.6 |
| $SiIH_3$ | 362 | 2192 | 903 | 2206 | 941 | 592 |
| $SiID_3$ | 352 | 1575 | 664 | 1607 | — | 435 |
| $SiBrCl_3$ | 368 | 545 | 191 | 610 | 205 | 135 |
| $SiICl_3$ | 333 | 519 | 169 | 600 | 197 | 123 |
| $SiBr(CH_3)_3$ | 373 | 632 | 238 | 704 | 177 | 214 |
| $SiI(CH_3)_3$ | 331 | 627 | 231 | 704 | 164 | 198 |
| $Si(CH_3)H_3$ | 700 | 2167 | 940 | 2167 | 980 | 540 |
| $Si(CH_3)F_3$ | 700 | 900 | 390 | 982 | 332 | 229 |
| $Si(CH_3)Cl_3$ | 764 | 458 | 229 | 577 | 163 | 229 |
| $Si(CH_3)Br_3$ | 746 | 314 | 153 | 453 | 98 | 186 |
| $Si(C_2H_5)Cl_3$ | 715 | 447 | 187 | 580 | 152 | 224 |
| $Si(OCH_3)Cl_3$ | 808 | 450 | 226 | 602 | 170 | 295 |
| $Si(OC_2H_5)Cl_3$ | 775 | 475 | 215 | 603 | 171 | 249 |

C: calculated value

great to be of concern relative to the problem of the characteristic frequencies for the molecules. The assignments in the literature were, in large part, without ambiguity for most of the silanes in Tables III—V. Some new assignment are proposed in the light of the correlation rule developed in this work. For $Si(CH_3)_3Cl$, 188 $cm^{-1}$ should be assigned to $\delta_e(SiC_3)$ because the first kind of deformation vibration of Si–C usually appears near 200 $cm^{-1}$; and $\delta_e(SiC_3)$ should lie at a lower frequency than $\delta_a(SiC_3)$ as in the case of ethyl chlorosilanes. For $Si(CH_3)_2Cl_2$, 241 $cm^{-1}$ should be assigned to $\delta_b(SiC_2Cl_2)$, which belongs to $B_1$

TABLE V. NORMAL FREQUENCIES OF $SiX_2Y_2$ TYPE MOLECULES

| $SiX_2Y_2$ | $\nu_a(SiX_2)$ | $\nu_a(SiY_2)$ | $\delta_a(SiX_2)$ | $\delta_a(SiY_2)$ | $\nu_b(SiX_2)$ | $\nu_b(SiY_2)$ | $\delta_b(SiX_2Y_2)$ | $\delta_b(SiY_2X_2)$ | $\tau(SiX_2Y_2)$ |
|---|---|---|---|---|---|---|---|---|---|
| $SiH_2D_2$ | 2189 | 1587 | 944 | 682.5 | 2183 | 1601 | 743 | 862 | (844)[c] |
| $SiH_2F_2$ | 2245 | 870 | 984.8 | 321.7 | 2250 | (978)[c] | 728.2 | (905)[c] | (785)[c] |
| $SiH_2Cl_2$ | 2200 | 531 | 953 | 188 | 2200 | 592 | 610 | 877 | 710 |
| $SiH_2Br_2$ | 2206 | 393 | 925 | 122 | 2232 | 456 | 556 | 828 | 688 |
| $SiH_2(CH_3)_2$ | 2143 | 954 | 658 | 228 | 2165 | 732 | 875 | 472 | 703 |
| $SiD_2F_2$ | 1614 | 878.5 | 708 | 319 | 1619 | 950 | 579.2 | 680.2 | (563)[c] |
| $SiCl_2Br_2$ | 563 | 326 | 191 | 111 | 605 | 508 | 144 | 182 | 122 |
| $SiCl_2I_2$ | 538 | 276 | 160 | 83 | 589 | 418 | — | 149 | 111 |
| $Si(CH_3)_2F_2$ | 670 | 828 | 213 | 330 | 786 | 952 | 271 | 496 | 213 |
| $Si(CH_3)_2Cl_2$ | 688 | 473 | 232 | 168 | 805 | 553 | 241 | 298 | 177 |
| $Si(C_2H_5)_2Cl_2$ | 695 | 458 | 190 | 157 | 746 | 650 ? | 241 | 299 | — |
| $Si(OCH_3)_2Cl_2$ | 772 | 481 | 250 | 183 | 851 | 590 | 315 | 364 | — |
| $Si(OC_2H_5)_2Cl_2$ | 744 | 490 | 240 | — | 813 | 598 | 295 | — | — |
| $Si(CH_3)_2Br_2$ | 682 | 355 | 208 | 118 | 797 | 426 | 208 | 208 | 166 |

c: Calculated value

TABLE VI. CHARACTERISTIC FREQUENCIES FOR SILANES

| | | Number of data |
|---|---|---|
| **Si-H** | | |
| Stretching | | |
| a) symm. | 2118~2315 $cm^{-1}$ | 16 |
| b) asymm. | 2142~2250 $cm^{-1}$ | 11 |
| Deformation | | |
| a) 1st kind | 925~ 985 $cm^{-1}$ | 11 |
| b) 2nd kind | 903~ 990 $cm^{-1}$ | 6 |
| **Si-D** | | |
| Stretching | | |
| a) symm. | 1573~1688 $cm^{-1}$ | 8 |
| b) asymm. | 1597~1649 $cm^{-1}$ | 7 |
| Deformation | | |
| a) 1st kind | 683~ 708 $cm^{-1}$ | 6 |
| b) 2nd kind | 664~ 704 $cm^{-1}$ | 5 |
| **Si-C** | | |
| Stretching | | |
| a) symm. | 553~ 764 $cm^{-1}$ | 18 |
| b) asymm. | 695~ 805 $cm^{-1}$ | 13 |
| Deformation | | |
| a) 1st kind | 160~ 232 $cm^{-1}$ | 12 |
| b) 2nd kind | 221~ 303 $cm^{-1}$ | 8 |
| **Si-O** | | |
| Stretching | | |
| a) symm. | 640~ 808 $cm^{-1}$ | 8 |
| b) asymm. | 782~ 851 $cm^{-1}$ | 6 |
| Deformation | | |
| a) 1st kind | 240~ 251 $cm^{-1}$ | 4 |
| b) 2nd kind | 264~ 308 $cm^{-1}$ | 4 |
| **Si-F** | | |
| Stretching | | |
| a) symm. | 800~ 900 $cm^{-1}$ | 10 |
| b) asymm. | 950~1031 $cm^{-1}$ | 7 |
| Deformation | | |
| a) 1st kind | 268~ 332 $cm^{-1}$ | 7 |
| b) 2nd kind | 390~ 425 $cm^{-1}$ | 4 |
| **Si-Cl** | | |
| Stretching | | |
| a) symm. | 424~ 583 $cm^{-1}$ | 23 |
| b) asymm. | 577~ 610 $cm^{-1}$ | 15 |
| Deformation | | |
| a) 1st kind | 150~ 205 $cm^{-1}$ | 15 |
| b) 2nd kind | 169~ 250 $cm^{-1}$ | 8 |
| **Si-Br** | | |
| Stretching | | |
| a) symm. | 249~ 373 $cm^{-1}$ | 10 |
| b) asymm. | 426~ 507 $cm^{-1}$ | 7 |
| Deformation | | |
| a) 1st kind | 90~ 118 $cm^{-1}$ | 7 |
| b) 2nd kind | 137~ 173 $cm^{-1}$ | 4 |
| **Si-I** | | |
| Stretching | | |
| a) symm. | 168~ 362 $cm^{-1}$ | 7 |
| b) asymm. | 405~ 418 $cm^{-1}$ | 3 |
| Deformation | | |
| a) 1st kind | 63~ 83 $cm^{-1}$ | 3 |
| b) 2nd kind | 94~ 114 $cm^{-1}$ | 2 |

TABLE VII. BOND LENGTHS

(a) $SiX_4$

| | $SiH_4$ | $SiD_4$ | $SiF_4$ | $SiCl_4$ | $SiBr_4$ | $SiI_4$ | $Si(CH_3)_4$ |
|---|---|---|---|---|---|---|---|
| Si-X(Å) | 1.48 | 1.48 | 1.54 | 2.02 | 2.15 | 2.46 | 1.90 |

(b) $SiX_3Y$

| | $SiH_3F$ | $SiF_3H$ | $SiD_3F$ | $SiF_3D$ | $SiH_3Br$ | $SiBr_3H$ | $SiHCl_3$ | $SiCl_3H$ |
|---|---|---|---|---|---|---|---|---|
| Si-X | 1.48 | 1.56 | 1.48 | 1.56 | 1.48 | 2.16 | 1.48 | 2.02 |
| Si-Y | 1.59 | 1.48 | 1.59 | 1.48 | 2.21 | 1.48 | 2.05 | 1.48 |
| | $SiCl_3Br$ | $SiBr_3Cl$ | $SiD_3H$ | $SiF_3(CH_3)$ | $SiCl_3I$ | $SiI_3Cl$ | $Si(CH_3)_3Cl$ | $SiCl_3(CH_3)$ |
| Si-X | 2.02 | 2.15 | 1.48 | 1.55 | 2.02 | 2.46 | 1.87 | 2.02 |
| Si-Y | 2.15 | 2.02 | 1.48 | 1.88 | 2.46 | 2.02 | 2.03 | 1.88 |

(c) $SiX_2Y_2$

| | $SiH_2F_2$ | $SiD_2F_2$ | $SiH_2Br_2$ | $SiH_2Cl_2$ | $SiCl_2Br_2$ | $SiH_2D_2$ | $Si(CH_3)_2Cl_2$ |
|---|---|---|---|---|---|---|---|
| Si-X | 1.48 | 1.48 | 1.48 | 1.48 | 2.02 | 1.48 | 1.87 |
| Si-Y | 1.59 | 1.59 | 2.21 | 2.05 | 2.15 | 1.48 | 2.03 |

and 298 $cm^{-1}$ to $\delta_b(SiCl_2C_2)$, which belongs to $B_2$. This assignment is justified from the result of the normal coordinate treatment in which 245 $cm^{-1}$ and 304 $cm^{-1}$ were calculated[5] for $\delta_b(SiC_2Cl_2)$ and $\delta_b(SiCl_2C_2)$, respectively. For the antisymmetrical stretching vibration of Si-I in $SiCl_2I_2$ two Raman lines 418 $cm^{-1}$ and 346 $cm^{-1}$ are reported by Dewaulle[6]. 418 $cm^{-1}$ should be assigned to $\nu_b(SiI_2)$ but 436 $cm^{-1}$ is preferably assigned as a combination, $276+160=436$ $cm^{-1}$.

## Discussion of Characteristic Frequency Assignments

The survey of the normal frequencies listed in Tables III—V shows that symmetrical stretching vibrations, or $\nu_a(SiX_4)$ in $SiX_4$, $\nu_a(SiX_3)$ in $SiX_3Y$, $\nu_a(SiX_2)$ in $SiX_2Y_2$ and $\nu_a(SiX)$ in $SiXY_3$ appear in a narrow frequency range characteristic for the Si-X. In Table VI the characteristic frequencies ranges and the number of the data from which the ranges have been decided are tabulated. The generalized values of the bond lengths, similarly from this review, are listed in Table VII. More detailed inspection shows the correlation: $\nu_a(SiX_4) < \nu_a(SiX_3) < \nu_a(SiX_2) < \nu_a(SiX)$, where X represents C, O, F, Cl, Br and I. Since the Raman line due to this vibration is generally a sharp, strong, and polarized line, this frequecy may be used as a key frequency for the S-X symmetrical stretching mode.

The asymmetrical stretching vibrations: $\nu_f(SiX_4)$ in $SiX_4$, $\nu_e(SiX_3)$ in $SiX_3Y$, and $\nu_b(SiX_2)$ in $SiX_2Y_2$, also occur in a narrow range, characteristic for Si-X. These occur, without exception, in a higher frequency range than the corresponding symmetrical stretching vibrations. Since the infrared band due to this vibration is very strong, this may be used as a key band for Si-X if it lies in a region available for infrared measurements.

If the term "deformation vibration" defines the type of nomal vibration in which some of the atoms vibrate in the direction perpendicular to bands then all the other types of vibrations are included in this category. Among these, the first and the second kind of deformation vibrations may be expected as characteristic frequencies, since these fall in a rather narrow range as defined by the bonds concerned. These are included in Table VI. For Si-H or Si-D, the ranges for the first kind and the second kind of deformation vibrations overlap each other. For the rest, in most of the cases, the second kind of deformation occurs at a higher frequency range than the first kind.

The other types of vibrations such as $\delta_e(SiXY_3)$, $\delta_b(SiX_2Y_2)$ and $\tau(SiX_2Y_2)$ are generally found as broad frequency ranges so that it is difficult to assign a characteristic frequency. However, if one or more hydrogens are present, the modes: $\delta_e(SiHX_3)$, $\delta_e(SiH_3X)$, $\delta_b(SiH_2X_2)$, $\delta_b(SiX_2H_2)$ and $\tau(SiH_2X_2)$ could be characteristic, each for their own structure since the mass of the hydrogen is so very small, relative to the rest of the system.

Generally, as the mass of the atom attached to the silicon atom increases, there is a corresponding decrease in frequency for both the stretching and deformation vibrations. The effect of electronegativity on the frequency of a particular vibration is, however, striking. Thus, for example, the symmetric stretching vibrations of Si-F occcur in a higher frequency range than those of Si-C even though the atomic weight of fluorine is greater than that of carbon.

**Si-H.**—The symmetrical stretching vibration

of Si–H appears in the range 2118～2315 $cm^{-1}$. If the molecule has more than two Si–H bonds, the asymmetrical stretching vibration is also observed in the range 2142～2250 $cm^{-1}$ in addition to the symmetrical vibration. The asymmetrical mode falls, as expected, in a higher range than the symmetrical mode. The general correlation: $\nu_a(SiH_3X) < \nu_a(SiH_2X_2) < \nu_a(SiHX_3)$ is true for all of the halogenated silanes. It is striking that in the series of methyl silanes the Si–H symmetric stretching frequencies decrease appreciably as the number of methyl groups increases.

Relative to the deformation vibration, both the first and the second kinds of deformations appear in an almost identical frequency range, 903～990 $cm^{-1}$. The separation is rather small and, in most of the cases, the higher frequency is assigned to the first kind of deformation.

Since the mass of the hydrogen atom is very small compared with the others, vibrations such as $\delta_e(SiX_3H)$, $\delta_e(SiH_3X)$, $\delta_b(SiH_2X_2)$, $\delta_b(SiX_2H_2)$ and $\tau(SiH_2X_2)$ may be considered as the hydrogen bending or deformation vibrations. Although examples for these modes are very limited at present, it is apparent that these are to be found in the following ranges:

| | | |
|---|---|---|
| $\delta_e(SiX_3H)$ | 767～908 $cm^{-1}$ | (5 examples) |
| $\delta_e(SiH_3X)$ | 540～728 $cm^{-1}$ | (5 examples) |
| $\delta_b(SiH_2X_2)$ | 469～919 $cm^{-1}$ | (5 examples) |
| $\delta_b(SiX_2H_2)$ | 828～919 $cm^{-1}$ | (5 examples) |
| $\tau(SiH_2X_2)$ | 688～844 $cm^{-1}$ | (5 examples) |

**Si–D.**—Eight deuterated silanes were used in assigning the frequency range of the Si–D vibration. Although deuterium has twice the atomic weight of hydrogen, the Si–D vibration can still be regarded as that of a very light atom vibrating against an atom of infinite mass. Thus many features of this class resemble the case of Si–H.

The symmetrical stretching vibrations occur in the range of 1573～1688 $cm^{-1}$ while the asymmetrical stretching vibrations occur in the region 1597～1649 $cm^{-1}$. The higher frequencies are always assigned to the non-symmetrical vibrations. It is striking that the stretching vibration of Si–D in $SiDF_3$ has very high frequency (1688 $cm^{-1}$) compared with the stretching vibration of Si–D in the other compounds. This is the same as in the case of $SiHF_3$, where $\nu_a(SiH)$ was assigned to 2314.5 $cm^{-1}$, which seems an extraordinarily high value for the stretching vibration of Si–H.

The Si–D deformation vibrations, both the first kind and the second kind, occur in the frequency range 664～708 $cm^{-1}$, and higher frequencies are assigned to the second kind of deformation.

**Si–C.**—The Si–C symmetrical stretching vibrations occur in the frequency range of 553～764 $cm^{-1}$ while the asymmetrical stretching vibrations occur in the range of 695～805 $cm^{-1}$. The tendency of the frequency shift depending on the number of the carbon atoms attached to the silicon atom is apparent, i. e., $\nu_a(SiC_4) < \nu_a(SiC_3) < \nu_a(SiC_2) < \nu_a(SiC)$. For the asymmetrical stretching vibrations, the relation, $\nu_f(SiC_4) < \nu_e(SiC_3) < \nu_e(SiC_2)$ is also true, if a particular series, such as $Si(CH_3)_4-Si(CH_3)_3Cl-Si(CH_3)_2Cl_2$, is considered. The deformation vibrations occur in the frequency range 160～259 $cm^{-1}$ for the first kind, and 206～303 $cm^{-1}$ for the second kind. The latter appaears, without exception, in a higher frequency range than the former.

**Si–O–C.**—The Si–O symmetrical stretching vibrations in the linkage of Si–O–C occur in the frequency range of 640～808 $cm^{-1}$, while the asymmetrical stretching vibrations occur in the range of 792～851 $cm^{-1}$. The frequencies of the symmetrical stretching vibrations decrease as the number of methoxy or ethoxy groups attached to the silicon atom increases, i. e.: $\nu_a(SiO_4) < \nu_a(SiO_3) < \nu_a(SiO_2) < \nu_a(SiO)$. The asymmetric vibration frequencies are concentrated in a rather narrow range, and the correlation $\nu_f(SiO_4) < \nu_e(SiO_3) < \nu_e(SiO_2)$ is true for any series, such as: $Si(OCH_3)_4-Si(OCH_3)_3Cl-Si(OCH_3)_2Cl_2$.

Owing to the very limited data, the frequency range for the deformation vibrations can not be decided with any certainty. From the available information, it appears that the first and second kinds of deformation vibrations occur in the range 240～308 $cm^{-1}$.

**Si–Halogen.** — The Si–halogen stretching modes occur in the range of 168～1031 $cm^{-1}$. The broad frequency range is due to the large variations in atomic weights for the halogen atoms, i. e.: F=19.00 to I=126.9. As the atomic weight of the atom attached to the silicon atom increases, a corresponding decrease in the frequency of the symmetrical and asymmetrical Si–X stretching vibrations is observed. For example, in the $SiX_4$ series, the Si–X stretching frequency decreases in the order: 800～424–249～168 $cm^{-1}$, for $SiF_4$, $SiCl_4$, $SiBr_4$ and $SiI_4$ respectively. In any series of the type $SiX_4$–$SiX_3Y$–$SiX_2Y_2$–$SiXY_3$, where X is a halogen atom and Y is different or a non-halogen atom, the frequencies of the symmetrical stretching vibration, i. e., $\nu_a(SiX_4)$, $\nu_a(SiX_3)$, $\nu_a(SiX_2)$, $\nu_a(SiX)$, increase as the number of the halogen atoms attached to the silicon atom decreases. By contrast, the frequencies of the asymmetrical stretching vibrations: $\nu_f(SiX_4)$, $\nu_e(SiX_3)$ and $\nu_b(SiX_2)$ do not show this trend. It is apparent that these are limited to narrower ranges than

the symmetrical vibrations. Thus, for Si–Cl, the range of the symmetrical frequencies is 424～583 $cm^{-1}$ whereas the range of the asymmetrical is 577～610 $cm^{-1}$. It is also seen that the asymmetrical modes always occur in a higher frequency range than the corresponding symmetrical stretching modes. The first kind of deformation vibrations occurs in a definite region for each kind of halogen, e. g.: $\delta_e(SiCl_4)$ in $SiCl_4$, $\delta_e(SiCl_3)$ in $SiCl_3Y$ and $\delta_a(SiCl_2)$ in $SiCl_2Y_2$. All are in the range, 150～205 $cm^{-1}$. The second kind of deformation vibrations usually occurs in a higher frequency range than the first kind. The other deformation vibrations occur in a range so wide that to list it would be of little significance.

## Summary

The status of knowledge relative to the vibrational assignments, molecular structure, and spectral data for a series of about one hundred silanes has been surveyed and is reported in brief tabular form. A scheme of simplified vibrational modes is discussed, and used to develop the assignment of fundamentals for some fifty five silanes. Some new assignments are proposed in the light of a correlation rule which has been developed. Tables of characteristic frequencies, and the best values for bond distances, based on this work, are presented.

The authors wish to thank Fred Behnke for assitance with the compilation of the literature and the summary in Table I. This work was made possible, in part, by a grant from the National Science Foundation, Washington, D. C.

*Department of Chemistry*
*Rensselaer Polytechnic Institute*
*Troy, New York, U. S. A.*

# *Syntheses and Infrared Absorption Spectra of Deuterated Polyvinyl Alcohols* $-(-CD_2-CD-)_n-$ [*1]
$OH(D)$

By Hiroyuki TADOKORO, Hiroshi NAGAI[*2], Syûzô SEKI and Isamu NITTA[*3]

(Received February 20, 1961)

We have previously reported[1] that the 1141 $cm^{-1}$ band in the infrared absorption spectra of polyvinyl alcohol (PVA) increases the intensity sensitively with crystallization (heat-treatments), and the optical density of this band is approximately in linear relationship with the degree of crystallinity determined by the methods of density and of the sorption of water vapor. We have further concluded that the 1141 $cm^{-1}$ band is a so-called "crystallization-sensitive" band. We have also made the deuteration of the OH group of PVA in order to clarify the assignment of this band[2-4], and further we have undertaken the deuteration of the main-chain of this polymer for the same purpose. In addition we have measured the infrared pleochroism of the doubly oriented PVA samples, and have shown that the experimental facts obtained so far can be explained fairly well, when we tentatively assign this band to the skeletal vibration of the planar zig-zag chain in the crystalline region[3,5,6].

On the other hand, Krimm, Liang and Sutherland[7] have reported that this band

*1 Read at the Annual Meeting of the Society of Polymer Science, Osaka, May, 1960.

*2 Present address: Electrical Communication Laboratory, Nippon Telegraph & Telephone Public Corporation, Musashino, Tokyo.

*3 Present address: Kwansei Gakuin University, Uegahara, Nishinomiya-shi.

1) H. Tadokoro, S. Seki and I. Nitta, This Bulletin, **28**, 559 (1955).

2) H. Tadokoro, S. Seki and I. Nitta, *J. Chem. Phys.*, **23**, 1351 (1955).

3) H. Tadokoro, S. Seki and I. Nitta, *J. Polymer Sci.*, **22**, 563 (1956).

4) H. Tadokoro, This Bulletin, **32**, 1252 (1959).

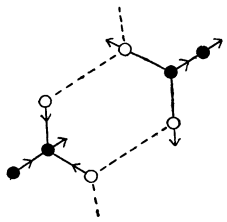
5) H. Tadokoro, S. Seki, I. Nitta and R. Yamadera, *J. Polymer Sci.*, **28**, 244 (1958).

6) H. Tadokoro, This Bulletin, **32**, 1334 (1959).

7) S. Krimm, C. Y. Liang and G. B. B. M. Sutherland, *J. Polymer Sci.*, **22**, 227 (1956).

should not be assigned to the crystalline band, but to the C–O–C stretching mode of the ether linkage produced between the molecular chains by heat-treatment. On the contrary, we have reconfirmed the linear relationship between the band intensity and the density for a number of samples subjected to heat-treatments under various conditions, by using the density-gradient tube method[6,8,9]. And furthermore we have accumulated experimental evidences for assigning this band to the crystalline band, such as comparison with the X-ray diffraction data on the formalized samples, swollen samples, etc.[6,8]

Quite recently Krimm[10] has considered the band to be a crystalline band and suggested that this band may be associated with the $\nu$(CO) mode of a portion of a chain in which an intramolecular hydrogen bond is formed between two neighboring OH groups that are on the same side of the plane of the carbon chain. On the other hand Liang and Pearson[11] have made the factor group analysis of PVA crystal based upon the symmetry of the average crystal structure deduced from X-ray analysis[12]. Then they have assigned the 1141 $cm^{-1}$ band to the symmetric skeletal stretching modes as follows:



In order to make such detailed assignments, further accumulation of the experimental data as well as the calculation of the normal modes of vibrations*4 would be necessary.

In this paper we wish to report the syntheses

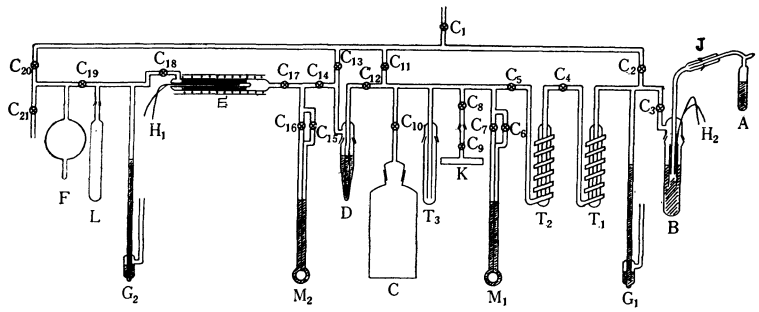



Fig. 1. The apparatus for the synthesis of $\alpha, \beta, \beta$-trideuterovinyl acetate.

A: $D_2O$. B: $CaC_2$ (vessel made of Telex). C: Gas vessel for $C_2D_2$ (20 l.). D: $CH_3COOD$. E: Reaction tube (made of Telex). F: Gas vessel for adjusting the pressure. G: Safety valve. $H_1$: Thermocouple (copper-Constantan). $H_2$: Thermocouple (Chromel-Almel). J: Joint K: Gas cell for infrared measurements. M: Mercury manometer. $T_1$ and $T_2$: Trap. $T_3$: Trap made of Telex. L: Trap for product. $C_1$–$C_{21}$: Cock.

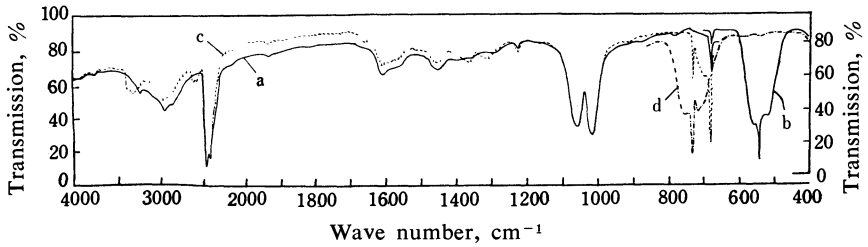



Fig. 2. Infrared spectra of acetylene-$d_2$ and acetylene.
a: $C_2D_2$ (degree of deuteration 97% at 200 mmHg)
b: $C_2D_2$ (degree of deuteration 97% at 70 mmHg)
c: $C_2D_2$ (degree of deuteration 94% at 200 mmHg)
d: $C_2H_2$ (at 70 mmHg)

8) H. Tadokoro, K. Kôzai, S. Seki and I. Nitta, ibid., 26, 379 (1957).
9) H. Tadokoro, K. Kôzai, S. Seki and I. Nitta, *Chem. High Polymers* (*Kôbunshi Kagaku*), 16, 418 (1959).
10) S. Krimm, *Fortschr. Hochpolym.-Forsch.*, 2, 51 (1960).
11) C. Y. Liang and F. G. Pearson, *J. Polymer Sci.*, 35, 303 (1959).
12) C. W. Bunn, *Nature*, 161, 929 (1948).
*4 The calculation of the normal modes of vibration of PVA is going on at Professor T. Shimanouchi's Laboratory of the University of Tokyo (T. Shimanouchi and M. Tasumi, Annual Meeting of the Society of Polymer Science, May, 1960).

and the infrared spectra of the deuterated PVA's $-(-CD_2-\underset{\underset{OH(D)}{|}}{CD}-)_n-$, and also the spectra of the intermediate products.

### Preparation of the Samples

As has already been reported, the OH group of PVA can be easily deuterated by the isotope exchange reaction with deuterium oxide, but the CH group can not be deuterated by such a simple method. Hence we have synthesized deuterated PVA's according to the following scheme:

$$CaC_2 \xrightarrow{D_2O} C_2D_2$$

$$(CH_3COO)_2O \xrightarrow{D_2O} CH_3COOD$$

$$C_2D_2 + CH_3COOD \xrightarrow{(CH_3COO)_2Zn} CD_2{=}CD{-}OCOCH_3$$

$$\xrightarrow{\text{polymerization}} -(-CD_2-\underset{\underset{OCOCH_3}{|}}{CD}-)_n-$$

$$\xrightarrow{\text{saponification}} -(-CD_2-\underset{\underset{OH}{|}}{CD}-)_n-$$

$$\xrightarrow{D_2O} -(-CD_2-\underset{\underset{OD}{|}}{CD}-)_n-$$

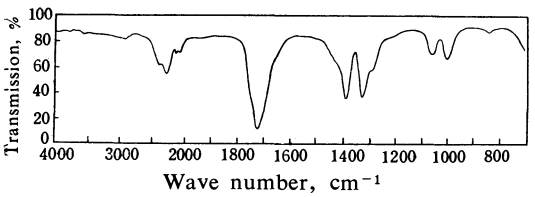



Fig. 3. Infrared spectrum of acetic acid-*d* (degree of deuteration 92%, at liquid state).

Fig. 1 shows the outline of the apparatus used for the synthesis of $\alpha, \beta, \beta$-trideuterovinyl acetate. The system can be highly evacuated by using a mercury diffusion pump and a rotary pump. The vessel B made of Telex*5 holds calcium carbide which was dried at about 580°C for about four hours under high vacuum ($10^{-4}$ mmHg or below). The container of deuterium oxide A may be rotated at the joint J, and acetylene-$d_2$ is generated by dropping deuterium oxide into B. The generated acetylene-$d_2$ is transferred to the trap $T_1$ cooled with liquid nitrogen, and then warmed up to the dry-ice temperature by exchanging the refrigerant. The same procedure was repeated at the trap $T_2$ and then acetylene-$d_2$ is transferred to the trap $T_3$ cooled with liquid nitrogen. In this way impurities and excess deuterium oxide were eliminated from acetylene-$d_2$. Then acetylene-$d_2$ is held in the gas vessel C (about 20 l.). The purity of the acetylene-$d_2$ gas was checked by measuring the infrared spectra. K is the gas cell for this purpose equipped with the windows of AgCl plates.

Acetic acid-*d* was prepared by heating the equal mole mixture of acetic anhydride and deuterium oxide at 110°C for about four hours in a sealed tube. The acetic anhydride used had been purified by distillation, standing for several days with sodium metal and subsequent distillation (b. p.:

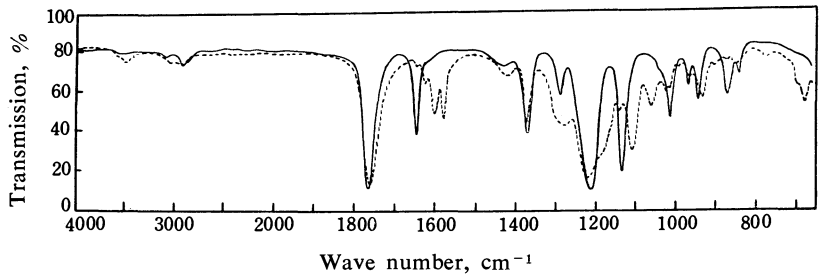



Fig. 4. Infrared spectra of $\alpha, \beta, \beta$-trideuterovinyl acetate (----) and vinyl acetate (——) at liquid state.

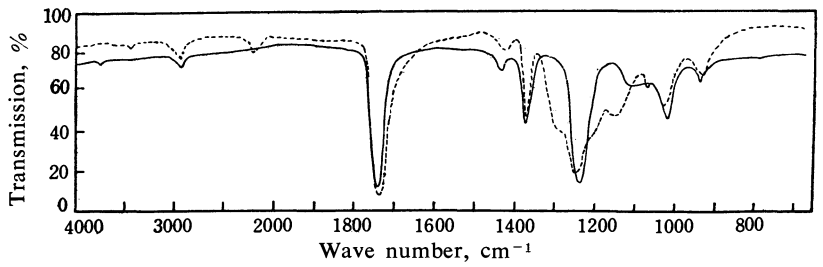



Fig. 5. Infrared spectra of poly-$\alpha, \beta, \beta$-trideuterovinyl acetate (----) and polyvinyl acetate (——).

*5 Boro-silicate glass manufactured by Tôshiba Electric Co., Ltd.

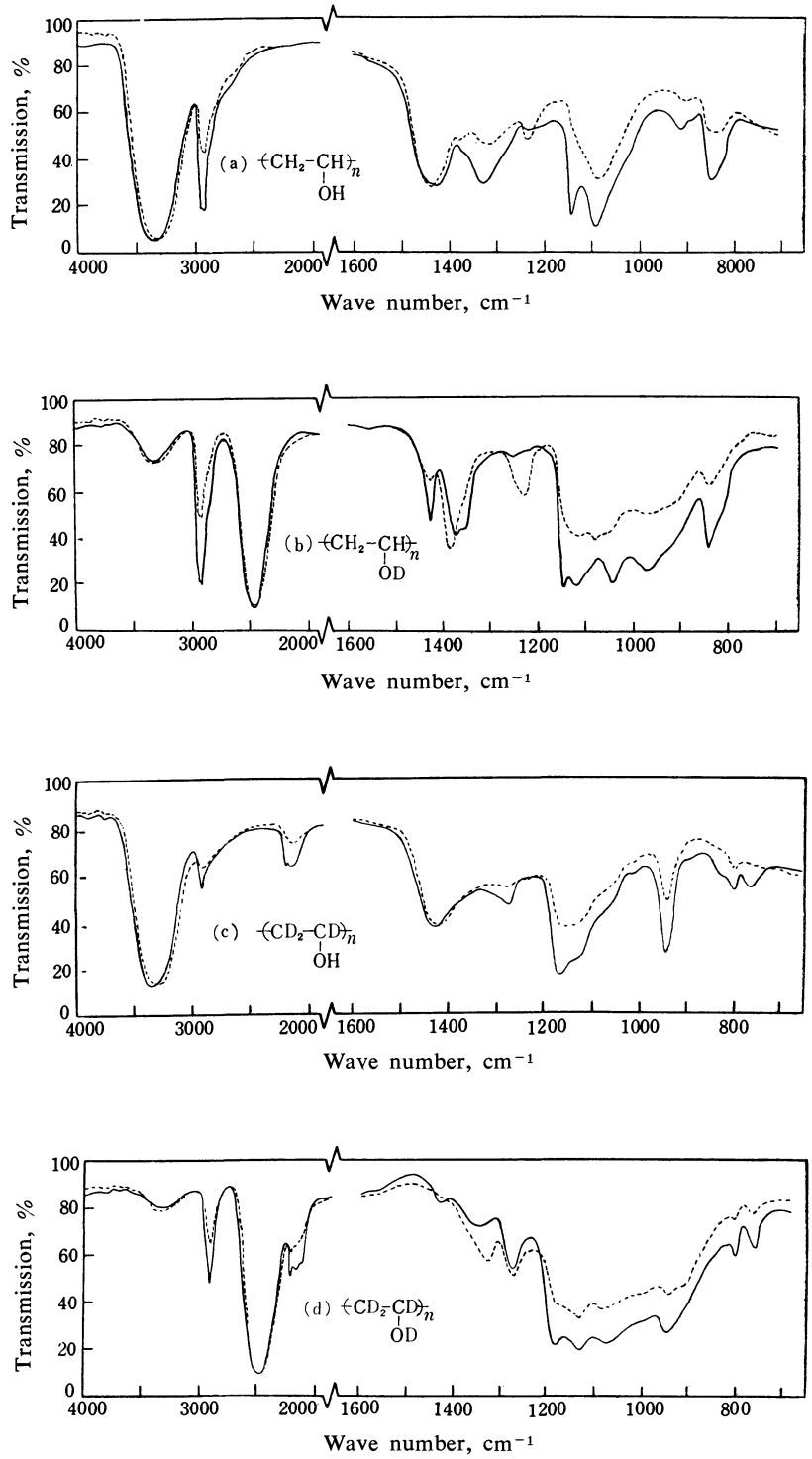



Fig. 6. Infrared dichroism of (a) PVA, (b) PVA-*d*, (c) PV-$d_3$A and (d) PV-$d_3$A-*d*.
—— Electric vector perpendicular to elongation.
---- Electric vector parallel to elongation.

TABLE I. INFRARED SPECTRA AND TENTATIVE

| PVA | | | PVA-*d* | | | PV-$d_3$A | | |
|---|---|---|---|---|---|---|---|---|
| Frequency $cm^{-1}$ | Plechroism | Intensity | Frequency $cm^{-1}$ | Dichroism | Intensity | Frequency $cm^{-1}$ | Dichroism | Intensity |
| 3340[a] | — | vs | | | | 3340[a] | — | vs |
| 2937 | ⊥ (⊥)[g] | s | 2937 | ⊥ | s | | | |
| | | | | | | (2905)[b] | ⊥ | m |
| 2908 | ⊥ (∥) | s | 2908 | ⊥ | s | | | |
| 2840 | ⊥ | sh | 2840 | ⊥ | sh | | | |
| | | | 2470[a] | — | vs | | | |
| | | | | | | 2200 | ⊥ | m |
| | | | | | | 2145 | ⊥ | m |
| | | | | | | 2105 | ⊥ | sh |
| 1440[c] | ∥ | s | | | | | | |
| | | | 1428 | ⊥ | m | 1425[c] | ⊥ | m |
| 1420[c] | ⊥ | m | | | | 1420[c] | ∥ | m |
| | | | 1383 | ∥ | s | | | |
| 1376 | ⊥ | w | 1376 | ⊥ ? | m | | | |
| | | | 1360 | ⊥ | sh | | | |
| 1326[d] / 1315 | ⊥ | m | | | | | | |
| | | | 1256 | ⊥ ? | sh | 1265 | ⊥ | m |
| 1232 | ∥ | w | 1230 | ∥ | m | | | |
| 1141 | ⊥ (∥) | s | 1148 | ⊥ | s | 1165 | ⊥ | s |
| | | | | | | 1125 | ⊥ | sh |
| | | | 1122 | ⊥ | s | | | |
| 1093 | ⊥ (⊥) | s | | | | | | |
| 1083 | ∥ | m | 1083 | ∥ | m | | | |
| | | | | | | 1055 | ⊥ | sh |
| | | | 1094 | ⊥ | s | | | |
| | | | 977 | ⊥ | m | | | |
| | | | | | | 940 | ⊥ | s |
| | | | 930 | ⊥ | sh | | | |
| 913 | ⊥ (∥) | m | | | | | | |
| 890 | ⊥ (∥) | vw | | | | | | |
| 849 | ⊥ (∥) | m | 842 | ⊥ | m | | | |
| 835 | ⊥ (⊥) | sh | 825 | ⊥ | sh | | | |
| | | | | | | 823 | ⊥ | sh |
| | | | | | | 797 | ⊥ | w |
| | | | | | | 760 | ⊥ | w |
| 640[e] | ∥ | sh | | | | | | |
| 610 | ⊥ | m | | | | | | |
| 480 | ⊥ | m | | | | | | |
| 410 | ? | w | | | | | | |
| 360 | ⊥ | w | | | | | | |

a) The $\nu$(OH) band at about 3340 $cm^{-1}$ shows no appreciable dichroism at the absorption peak, but shows a perpendicular and parallel nature at the higher frequency and lower frequency sides, respectively. The $\nu$(OD) band at about 2470 $cm^{-1}$ also shows the same behavior.

b) The wave numbers in parentheses are for the bands associated with the residual hydrogen atoms because of the incompleteness of deuteration.

c) The band at about 1430 $cm^{-1}$ splits into 1440 and 1420 $cm^{-1}$ in the polarized spectra because of the difference of their dichroism.

ASSIGNMENTS OF PVA, PVA-*d*, PV-$d_3$A AND PV-$d_3$A-*d*

| Frequency $cm^{-1}$ | PV-$d_3$A-*d* Dichroism | PV-$d_3$A-*d* Intensity | Tentative assignments[f] |
|---|---|---|---|
| | | | $\nu$(OH) |
| | | | $\nu_a(CH_2)$ |
| (2905)[b] | ⊥ | m | $\nu$(residual CH) |
| | | | $\nu_s(CH_2)$ |
| 2470[a] | — | vs | $\nu$(OD) |
| 2200 | ⊥ | m | $\nu_a(CD_2)$ |
| 2145 | ⊥ | m | $\nu_s(CD_2)$ |
| 2105 | ⊥ | sh | |
| (1428)[b] | ⊥ | vw | Superposition of $\delta(CH_2)$ and a coupling band (coupling of $\delta$(OH) and 1383 $cm^{-1}$ band of PVA-*d*). 1428 $cm^{-1}$ band of PVA-*d* is $\delta(CH_2)$ |
| | | | $w$(CH) or $w(CH_2)$ |
| | | | $\delta$(CH) ? |
| 1330 | ∥ | m | |
| | | | Coupling of $\delta$(OH) and 1383 $cm^{-1}$ band of PVA-*d* |
| 1272 | ⊥ ? | m | |
| | | | $w(CH_2)$ or $w$(CH) |
| 1185 | ⊥ | s | Crystalline band (see text) |
| 1135 | ∥ | m | |
| 1130 | ⊥ | s | |
| | | | Mainly due to $\nu$(CO) |
| 1085 | ∥ | m | |
| 1080 | ⊥ | s | |
| | | | Mainly due to $\nu$(CO) |
| | | | $\delta$(OD) |
| 940 | ⊥ | s | |
| | | | Skeletal or CH ? |
| 905 | — | sh | |
| | | | Skeletal or $CH_2$ |
| | | | $r(CH_2)$ |
| 797 | ⊥ | w | |
| 757 | ⊥ | w | |

d) The band at about 1325 $cm^{-1}$ has its absorption peaks at 1326 and 1315 $cm^{-1}$ in the cases of perpendicular and parallel radiation, respectively.

e) The data in the region lower than 640 $cm^{-1}$ is reproduced from the paper by Krimm et al.[7]

f) $\nu$: stretching, $\nu_a$: antisymmetric stretching, $\nu_s$: symmetric stretching, $\delta$: bending, $w$: wagging, $r$: rocking.

g) The notation ⊥ and ∥ in parentheses refer to the polarization with respect to the plane of the zig-zag carbon chain[5,14].

139~140°C). Acetic acid-*d* was put in the vessel D. Acetylene-$d_2$ gas, after bubbling through vessel D, was introduced into the reaction-vessel E. Then the gas mixture was caught in the vessel L cooled with liquid nitrogen. The catalyst used was zinc acetate carried on active charcoal kindly supplied by Dr. T. Omae of the Nippon Gôsei Kagaku Co., Ltd. The reaction temperature was about 200°C. The obtained vinyl-$d_3$-acetate was purified by using a concentric distillation column (Taika Kôgyô Co., Ltd., Osaka). The polymerization of vinyl-$d_3$-acetate was carried out in a sealed glass tube with $\alpha,\alpha'$-azobisisobutyronitrile catalyst at 60°C for about 24 hr.

**Infrared Spectra of the Intermediate Products.** —Fig. 2 is the infrared spectra of acetylene-$d_2$. The degree of deuteration was estimated by using the $\nu_5$ band (CH symmetric deformation, $C_2H_2$: 729.2 $cm^{-1}$, $C_2HD$: 676 $cm^{-1}$, $C_2D_2$: 538.7 $cm^{-1}$) assuming that the absorption coefficients of the above bands are equal in the spectra of $C_2H_2$, $C_2HD$ and $C_2D_2$. A spectrum of the sample of lower degree of deuteration (about 94%) was reproduced for reference. The intensity of the 676 $cm^{-1}$ band, which is absent in the spectrum of $C_2H_2$ (curve d), is very strong in the spectrum of the 94% $C_2D_2$ (curve c), but weak in the case of the 97% $C_2D_2$ (curve b). Accordingly the $\nu_5$ mode of $C_2HD$ is considered to be assigned to the 676 $cm^{-1}$ band, although this mode has been so far assigned to the 687 $cm^{-1}$ band by Stitt[13].

Fig. 3 is a spectrum of acetic acid-*d*, the degree of deuteration of which was estimated to be about 92% by using the intensity ratio of the bands of OH and OD stretching.

Fig. 4 shows the spectra of vinyl-$d_3$-acetate (broken line) and of vinyl acetate (solid line). Fig. 5 shows the spectra of polyvinyl-$d_3$-acetate (broken line) and of polyvinyl acetate (solid line). It should be noticed that the spectra of the monomer and polymer in the 1300~1100 $cm^{-1}$ region show a change similar to that of deuteration. The 1235 $cm^{-1}$ band of polyvinyl acetate and the 1212 $cm^{-1}$ band of vinyl acetate, which are considered to be assigned to the stretching mode of ester linkage, shift to the higher frequency 1245 and 1220 $cm^{-1}$, respectively. This behavior is interesting in relation to the shift of the 1141 $cm^{-1}$ band of PVA to higher frequency with deuteration as will be discussed later.

**Spectra of PVA and Deuterated PVA's.** —In Fig. 6 the polarized infrared spectra of PVA, PVA-*d*, poly-$\alpha,\beta,\beta$-trideuterovinyl alcohol (PV-$d_3$A) and poly-$\alpha,\beta,\beta$-trideuterovinyl alcohol-*d* (PV-$d_3$A-*d*) are shown. The solid and broken curves represent the spectra obtained with radiation polarized, respectively, perpendicular and parallel to the direction of elongation. The spectral data and the tentative assignments for PVA and deuterated PVA's are given in Table I. In the column of pleochroism of PVA the notations $\perp$ and $\parallel$ in parenthesis refer to the polarization with respect to the plane of the zig-zag carbon chain[5,14].

The OH stretching band at 3340 $cm^{-1}$ shifts to 2470 $cm^{-1}$ with the deuteration of the OH group, but the $CH_2$ stretching bands at about 2930 $cm^{-1}$ are not affected by this type of deuteration. By the deuteration of the CH group these bands shift to about 2200 $cm^{-1}$. Both these bands due to the OH and CH groups shift to lower frequencies, when all the hydrogen atoms are deuterated. The residual 2930 $cm^{-1}$ band is due to the incomplete deuteration of the CH group.

The 1141 $cm^{-1}$ band of PVA and the 1165 $cm^{-1}$ band of PV-$d_3$A are inferred to be due to the similar origins of absorption mechanism from the following similarities:

1) The distinguished dichroism,
2) The similar intensity,
3) The increase of the intensity with heat-treatment (Fig. 7), and

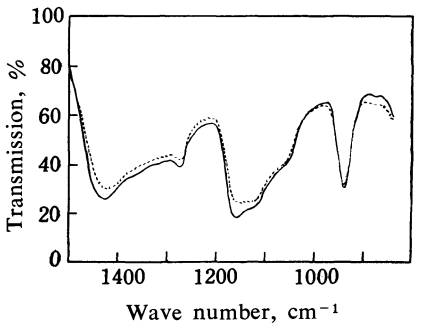



Fig. 7. Spectral change of PV-$d_3$A by heat-treatment.
---- No-treatment
—— Treated at 160°C for 20 min.

4) The small shift to higher frequencies with deuteration of the OH group. The 1141 $cm^{-1}$ band of PVA shifts to 1148 $cm^{-1}$ and the 1165 $cm^{-1}$ band of PV-$d_3$A to 1185 $cm^{-1}$ with deuteration of the OH group.

Thus the 1165 $cm^{-1}$ band of $-(-CD_2-\underset{\underset{OH}{|}}{CD}-)_n-$ is considered to be the crystalline band corresponding to the 1141 $cm^{-1}$ band of PVA.

The experimental facts we have found so far abou' the 1141 $cm^{-1}$ band are summarized as follows:

13) F. Stitt, *J. Chem. Phys.*, **8**, 56 (1940).

14) E. J. Ambrose, A. Elliott and R. B. Temple, *Proc. Roy. Soc.*, **A199**, 183 (1949).

1) The intensity increases with crystallization by heat-treatment, and shows a parallel relationship with the crystallinity determined by the density and the sorption of water vapor[1,8,9].

2) The band behaves in a parallel way with the X-ray diffraction rings due to the crystalline region, when the sample is formalized or swollen in water[6,8].

3) The band exhibits strong perpendicular dichroism in the case of an elongated sample, and distinguished pleochorism in the doubly oriented sample of PVA. The transition moment of this band is parallel to the zig-zag plane, while that of the 1093 $cm^{-1}$ band is perpendicular to the zig-zag plane[3-6]. Furthermore, we have obtained another new experimental fact as follows.

4) The shift of this band with deuteration of the CH or OH group is small. This new experimental fact also supports our tentative assignment of 1141 $cm^{-1}$ band mainly due to the stretching vibration of the extended zig-zag chain in the crystalline region. Here, of course, a considerable coupling of the vibration of the oxygen atom with the skeletal vibrations should be expected.

Next, we proceed to the interpretation of the other bands. Although we can not make any conclusive assignments of these bands merely from the present data, we may discuss here the tentative assignments of the several main bands. We have reported already that the 1430 $cm^{-1}$ band of PVA should be a superposition of $\delta(CH_2)$ and some other band related to the OH group (probably $\delta(OH)$), since the intensity of this band decreases sensitively on deuteration and there remains a sharp band which is certainly attributed to the $\delta(CH_2)$ mode. The 1383 $cm^{-1}$ band was tentatively considered to be $w(CH_2)$ or $w(CH)$, and the 1376 $cm^{-1}$ to be $\delta(CH)$. This inference was confirmed, since these bands disappear in the spectra of PV-$d_3$A-$d$.

The bands near 850 $cm^{-1}$ of PVA were considered to be skeletal or of $CH_2$ vibrations, because there was quite a little effect of deuteration. Especially the 835 $cm^{-1}$ band having the pleochroism perpendicular to the plane of zig-zag chain was assigned to $r(CH_2)$. All these bands disappear by the deuteration of the main chain. The bands near 760 $cm^{-1}$ of PV-$d_3$A and PV-$d_3$A-$d$ are supposed to be due to $r(CD_2)$ mode. But further inference about the origin of the bands may be difficult, because of the complexity which is possibly due to the strong coupling among the group vibrations.

At present we are aiming to accumulate results of further experiments such as the infrared measurements of the highly doubly oriented samples of $-(-CD_2-\underset{\underset{OH(D)}{|}}{CD}-)_n-$, the preparation of the more highly deuterated samples, and of the selectively deuterated samples, $-(-CD_2-\underset{\underset{OH(D)}{|}}{CH}-)_n-$, $-(-CH_2-\underset{\underset{OH(D)}{|}}{CD}-)_n-$, etc.

The authors wish to express their sincere thanks to Professor S. Murahashi of this Faculty, Professor T. Shimanouchi of the University of Tokyo and Dr. T. Omae of Nippon Gôsei Kagaku Co., Ltd. for helpful advice and criticism. The authors are also indebted to Mr. A. Nozaki for his cooperation in the construction of the apparatus.

*Department of Polymer Science* (*H. T.*)
*Department of Chemistry*
(*H. N., S. S. & I. N.*)
*Faculty of Science*
*Osaka University*
*Nakanoshima, Osaka*

# *The Study of Adsorption of Detergents at a Solution-Air Interface by Radiotracer Method. IV. The Valency and Concentration Effects of Added Electrolytes on the Adsorption of Alkyl Sulfate Ion*

By Ryohei MATUURA, Hideo KIMIZUKA and Akira MATSUBARA

(Received February 18, 1961)

The preceding study on the effect of excess electrolytes on the adsorption of dodecyl sulfate ion using the radiotracer method has confirmed directly the fact that the presence of excess electrolytes increases both the equilibrium amount and the rate of adsorption of the dodecyl sulfate ion[1], the result which was deduced by a number of authors from surface tension measurements of the solution[2]. However, in the presence of a large excess of electrolytes the rate of adsorption was too rapid to be measured accurately and also the adsorption isotherm was nearly independent of the type of added electrolytes.

We may expect to obtain further data concerning the effects of added electrolytes on the rate and the amount of adsorption of the detergent if we explore the region of the more dilute concentrations of the added electrolytes and/or the detergent. The present paper describes the results of such experiments and the discussions about them.

## Experimental and Results

The method of preparation and purification of the samples and the procedure used for the experiments have already been described[1,3]. The specific activities of the radioactive sodium dodecyl sulfate (SDS), sodium tetradecyl sulfate (STS) and sodium hexadecyl sulfate (SHS) used were ca. 10 mc. per millimole. The temperatures of the experiments were 29.5 $\pm$1.5°C.

In the study on the valency effect, the concentrations of electrolytes were all $10^{-4}$ mol./l., and those of SDS ranged from $5\times10^{-6}$ to $5\times10^{-5}$ mol./l. In the study on the effect of the excess salt the concentrations of detergents were $4\times10^{-6}$ mol./l. for SDS and $2\times10^{-6}$ mol./l. for STS and SHS and those of salt were changed from $10^{-3}$ mol./l. to 1 mol./l.

The rate of adsorption and the adsorption isotherm of dodecyl sulfate ion ($DS^-$) in the presence of electrolytes are shown in Figs. 1 and 2, respectively. In Fig. 1, $K$ represents the constant in the rate equation

$$\Gamma_t = K\sqrt{t} \qquad (1)$$

where $\Gamma_t$ denotes the amount of adsorption at time $t$[4].

As is seen from these figures, both the rate and the equilibrium amount of the adsorption of $DS^-$ increase with the increase in cationic valency of the electrolyte, while they are almost independent of the anionic valency. Table I shows the values of rate constant $K_0$ of the equation

$$K = K_0 C \qquad (2)$$

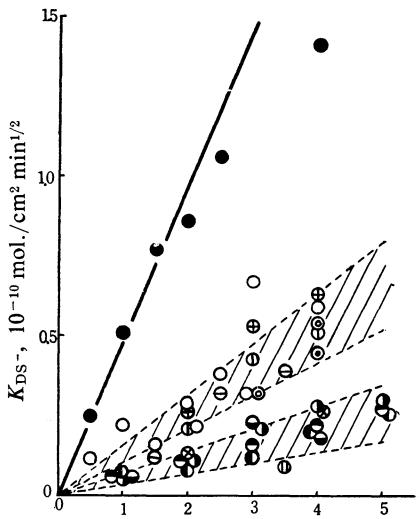



Fig. 1. Effect of added electrolytes on the rate of adsorption of $DS^-$, 29.5$\pm$1°C. Concentrations of electrolytes are all $10^{-4}$ mol./l.

I ◑ NaCl, ◐ $Na_2SO_4$, ⓓ $Na_2CO_3$, ◓ $K_3Fe(CN)_6$, ◒ KCl.
II ○ $MgCl_2$, ⓘ $CoCl_2$, ⊖ $HgCl_2$, ⊕ $MnCl_2$, ⊗ $Zn(CH_3COO)_2$, ◎ $CaCl_2$, ⊙ $Ca(OH)_2$.
III ● $AlCl_3$.

1) R. Matuura, H. Kimizuka and K. Yatsunami, This Bulletin, 32, 646 (1959).
2) N. K. Adam and H. L. Shute, *Trans. Faraday Soc.*, 34, 758 (1938); G. C. Nutting, F. A. Long and W. D. Harkins, *J. Am. Chem. Soc.*, 62, 1496 (1940), etc.
3) R. Matuura, H. Kimizuka, S. Miyamoto and R. Shimozawa, This Bulletin, 31, 532 (1958).
4) R. Matuura, H. Kimizuka, S. Miyamoto, R. Shimozawa and K. Yatsunami, ibid., 32, 404 (1959).

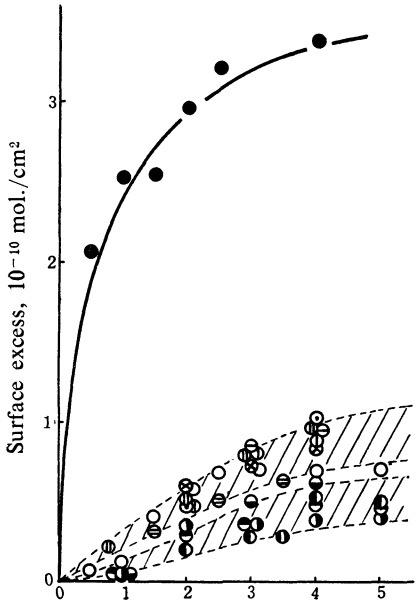



Fig. 2. Effect of added electrolytes on the equilibrium adsorption of $DS^-$, 29.5±1°C. Concentrations of electrolytes are all $10^{-4}$ mol./l.

I ◑ NaCl, ◐ $Na_2SO_4$, ◑ $Na_2CO_3$, ◓ $K_3Fe(CN)_6$ ◒ KCl.
II ○ $MgCl_2$, ⓘ $CoCl_2$, ⊜ $HgCl_2$, ⓘ $MnCl_2$, ⊙ $Zn(CH_3COO)_2$, ⊖ $CaCl_2$, ⊗ $Ca(OH)_2$.
III ● $AlCl_3$.

TABLE I. RATE CONSTANT $K_0$ OF THE ADSORPTION OF $DS^-$ IN THE PRESENCE OR ABSENCE OF ELECTROLYTE. THE CONCENTRATIONS OF SDS, $5\times10^{-6}\sim5\times10^{-5}$ mol./l.; THE CONCENTRATION OF ELECTROLYTE, $10^{-4}$ mol./l. $K_0$ IN $10^{-3}$ cm./min$^{1/2}$. 29.5±1.5°C

| | No added salt | Added electrolyte | | |
|---|---|---|---|---|
| | | Valency of cation | | |
| | | 1 | 2 | 3 |
| $K_0$ | 0.35±0.1 | 0.52±0.2 | 1.35±0.3 | 4.30±0.5 |

where $C$ is the concentration of SDS[4].

The value of $K_0$ in the absence of added electrolyte calculated according to the simple diffusion theory[5] is $22.8\times10^{-3}$ cm./min$^{1/2}$. It is seen from Table I that the rate constants increase in the presence of electrolyte, showing a greater increase the higher the cationic valency, but the values are less than the rate constant of the simple diffusion theory.

The effects of electrolyte concentrations on the rate constants and the equilibrium adsorptions of $DS^-$, tetradecyl sulfate ion ($TS^-$) and

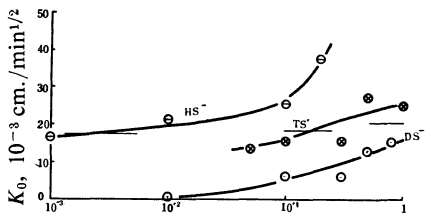



Fig. 3. Effect of salt concentration on the rate constant of adsorption of the alkyl sulfate ion. 29.5±1.5°C. Concentrations of detergents are $4\times10^{-6}$ mol./l. for SDS and $2\times10^{-6}$ mol./l. for STS and SHS. Horizontal lines indicate the values expected from the simple diffusion theory.

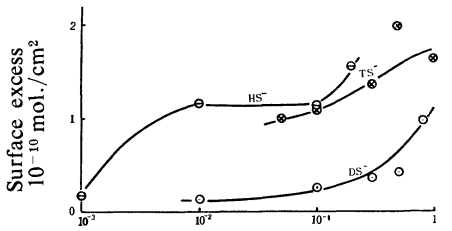



Fig. 4. Effect of salt concentration on the adsorption of the alkyl sulfate ion. 29.5±1.5°C. Concentrations of detergents are $4\times10^{-6}$ mol./l. for SDS and $2\times10^{-6}$ mol./l. for STS and SHS.

hexadecyl sulfate ion ($HS^-$) are shown in Figs. 3 and 4, respectively. These figures indicate that the presence of excess sodium chloride remarkably increases the equilibrium adsorption as well as the rate constants of the alkyl sulfate ions. It must be noted here that the rate constant does exceed the value of the simple diffusion theory when the concentration of the salt becomes great as indicated in the cases of $TS^-$ and $HS^-$. Unfortunately the diffusion coefficients of $TS^-$ and $HS^-$ in the presence of excess salt have not been known, and so we calculated the rate of adsorption by the simple diffusion theory using the diffusion coefficient in the absence of added electrolyte. But the condition described above will be held even when the diffusion coefficient in the presence of added salt is used, because it may generally be considered as less than that in the absence of salt*.

5) A. F. H. Ward and L. Tordai, *J. Chem. Phys.*, **14**, 453 (1946).

* We have measured the self-diffusion coefficient of $DS^-$ at the concentration of $4\times10^{-4}$ mol./l. in the presence (0.1 N) and absence of sodium chloride and found the values, at 25°C, to be $5.6\times10^{-6}$ and $6.5\times10^{-6}$ cm$^2$/sec., respectively. We are going to measure the corresponding values of $TS^-$ and $HS^-$, the result of which will be published in a separate paper after the work has been completed.

## Discussion

The simple diffusion theory proposed by Ward and Tordai[5] assumed that the adsorption takes place as a result of the formation of the subsurface of zero concentration, which is taken to be the region of the thickness of a few molecular diameters being situated in the immediate vicinity of the surface. The formation of a subsurface of zero concentration is explained by the fact that the surface active solute finds a position of lower potential energy in the surface than in the bulk. According to this theory, at the initial stage of the formation of the adsorbed layer, the solute molecules will diffuse from the bulk to the subsurface more slowly than they do from the subsurface to the surface, on the assumption that the equilibrium is established instantaneously between the latter two regions.

It has, however, been shown that the simple diffusion theory fails to explain quantitatively our experimental results of the adsorption of alkyl sulfate ions without added inorganic electrolytes[4], and the present result also shows that the simple diffusion theory does not hold for the adsorption of $DS^-$ in the presence of a small concentration of inorganic electrolytes, as is shown in Table I. Also the results of the experiments on the adsorption of non-electrolytes from the solution so far reported by several authors can not be explained by the simple diffusion theory[6]. All these results showed that the rate of adsorption is smaller than the value expected from the simple diffusion theory.

As the factors responsible for the delay in the rate of adsorption Blair[6] proposed an energy barrier for the adsorption of non-electrolytes and Doss[7] an electrical potential barrier for the surface active electrolytes. Some other factors, e. g., the reorientation[8] and the surface pellicle formation[9], have also been considered. Of course, these various factors taken together are responsible for the retardation of the adsorption rate of alkyl sulfate ions at the solution-air interface. It is difficult to cover the whole experimental result by any single theory. For example, let us consider Doss' theory of electrical potential barrier. According to this theory, the electrical double layer at the surface resists the adsorption of surface active ion owing to the electrical repulsion. The rate differs from the value of the diffusion theory, which may be regarded as being essentially identical with the simple diffusion theory, by a factor

$$\exp\left(-\frac{x\varepsilon\psi_0}{kT}\right) \tag{3}$$

where $x$ denotes the fraction of surface covered by the adsorbed molecules, $\varepsilon$, the elementary charge, $k$, the Boltzmann constant and $T$, the absolute temperature. $\psi_0$ is given by

$$\psi_0 = -\frac{4\pi\rho}{D}\sqrt{\frac{1000\,DkT}{4\pi N\varepsilon^2\sum_i c_i z_i^2}} \tag{4}$$

where $\rho$ is the surface charge density at monolayer adsorption, $D$, the dielectric constant of medium, $N$, the Avogadro number and $c_i$, the concentration of $i$-th ion having valency $z_i$. Eqs. 3 and 4 predict that the rate of adsorption at the given amount of adsorption depends upon the ionic strength of the solution. From Fig. 1 and Table I it may be seen that the rate of adsorption does not depend on the anionic valencies in spite of their different ionic strengths of added electrolytes, but depends essentially on the cationic valencies. These facts can not be explained by Doss' theory mentioned above. Cassie and Palmer[10] deduced from their consideration on the structure of the adsorbed film, assuming Gouy-Chapman's diffuse double layer, that the film of long chain anions will be remarkably influenced by the presence of a high valent cation, while it will be independent of the nature of the anion in solution. Our result agrees with this view and also with observation on the surface[2] or interfacial tension[11]. Of course, the electrical double layer formed at the surface will be supposed to resist the adsorption of surface active ion, but the quantitative explanation for it should be given in a somewhat different way.

As the concentration of the added electrolyte becomes larger, the rate of adsorption of alkyl sulfates becomes faster until it reaches the value predicted by the simple diffusion theory in the case of $DS^-$, while in the cases of $TS^-$ and $HS^-$ the rate constants exceed the simple diffusion values, as shown in Fig. 3. It is not easy to explain by the prevailing theories the reason why the rates of adsorption of $TS^-$ and $HS^-$ exceed the values of simple diffusion theory in the presence of a large excess of electrolyte.

Addison[12] proposed that the difference between the dynamic and the static surface tension is a measure of the driving force for the adsorption, which is introduced in his theory

6) C. M. Blair, Jr., ibid., **16**, 113 (1948).
7) K. S. G. Doss, *Kolloid-Z.*, **86**, 205 (1939).
8) A. E. Alexander, *Trans. Faraday Soc.*, **37**, 15 (1941).
9) J. W. McBain and L. H. Perry, *Ind. Eng. Chem.*, **31**, 35 (1939); M. E. L. McBain and L. H. Perry, *J. Am. Chem. Soc.*, **62**, 989 (1940).
10) A. B. D. Cassie and R. C. Palmer, *Trans. Faraday Soc.*, **37**, 156 (1941).
11) C. Robinson, *Nature*, **139**, 626 (1937).
12) C. C. Addison, *J. Chem. Soc.*, **1944**, 477.

explicitly as the surface activity. At equilibrium there is a concentration gradient near the surface. Since the ordinary diffusion takes place from higher to lower concentrations, the equilibrium state may be supposed to be the state at which the osmotic force due to the concentration gradient is equilibrated with an adsorptive force such as the driving force suggested by Addison.

In general, both the driving force and the activation energy may be considered to be the factors responsible for the rate of adsorption. It may be pointed out here that the difference between the amount of solute in a dynamic surface and that in an equilibrium surface is a measure of the driving force and so the equilibrium adsorption becomes a measure of the driving force at the instant of the formation of the fresh surface. Thus the higher surface active molecule may drift to the surface faster than the lower surface active one providing the activation energy remains in the constant. The change in the rate of adsorption caused by the foreign substance should, therefore, be attributed not only to the change in activation energy, but also to the change in surface activity.

By comparing Figs. 1 and 2 it is seen that the presence of polyvalent cation increases both the rate and the amount of equilibrium adsorption of $DS^-$ at a given concentration of SDS. This means that the higher rate of adsorption should be related to the larger amount of adsorption in addition to the lowering of activation energy. This is also true for the case of Figs. 3 and 4. The fact that the rate constants of $TS^-$ and $HS^-$ exceed the predicted value of the diffusion theory indicates clearly that the surface activity should be taken into account in the theory of the rate of adsorption of detergent at the solution surface.

## Summary

The adsorption of dodecyl sulfate ion in the presence of various inorganic electrolytes whose concentrations are all $10^{-4}$ mol./l. and the adsorption of alkyl sulfate ions in the presence of the excess salt were measured by using S-35 labeled alkyl sulfates.

In the presence of various electrolytes, both the rate of adsorption and the equilibrium adsorption of dodecyl sulfate ion increase with the cationic valency of added electrolyte, while they are almost independent of the anionic valency.

In the presence of the excess salt, both the rate and the equilibrium adsorption of the alkyl sulfate ions increase with the salt concentration. With increasing concentration of salt the rate of adsorption of the dodecyl sulfate ion approaches the rate of the simple diffusion theory, while that of tetradecyl- and hexadecyl sulfate ion exceeds the value predicted by the simple diffusion theory.

It was pointed out that the higher rate of adsorption is attributed to the higher surface activity of solute.

The idea of surface activity was explicitly introduced in the explanation for the adsorption process and the discussions for the theories proposed earlier were given.

*Department of Chemistry*
*Faculty of Science*
*Kyushu University*
*Hakozaki, Fukuoka*

# *Determination of Ortho-, Pyro- and Tripolyphosphate by the Use of a Small Column of Ion-exchange Resin*

By Shigeru OHASHI* and Shichiro TAKADA

(Received February 27, 1961)

The determination of ortho-, pyro- and tripolyphosphate in their mixture is usually carried out by paper chromatography[1] or ion-exchange chromatography[2]. In paper chromatographic determination satisfactory separation of the chain phosphates can be obtained only in acid chromatographic solvent mixtures. Therefore, care must be taken about partial hydrolysis of the condensed phosphates during a chromatographic separation. When paper chromatographic separation is performed at room temperature (15~30°C), a correction due to the hydrolysis of the condensed phosphates should be applied, depending on the temperature. When the separation is performed at a lower temperature then 5°C, the correction due to the hydrolysis is negligible, but a long time is consumed for the separation. On the other hand in the ion-exchange chromatographic determination the phosphates adsorbed by a column are successively eluted with a buffered solution of potassium chloride of pH 4~9. Therefore in the process of the elution the condensed phosphates are not hydrolyzed practically, but by the use of a column of the usual scale a long time is consumed for the separation.

The purpose of this paper is to present a rapid method for the determination of mixed ortho-, pyro- and tripolyphosphate by the use of a small column of ion-exchange resin. The continuous-gradient elution method by Jameson[2h] was applied and a paper micro-fraction collector was used.

## Experimental

The assembly of apparatus used in this investigation is shown in Fig. 1.

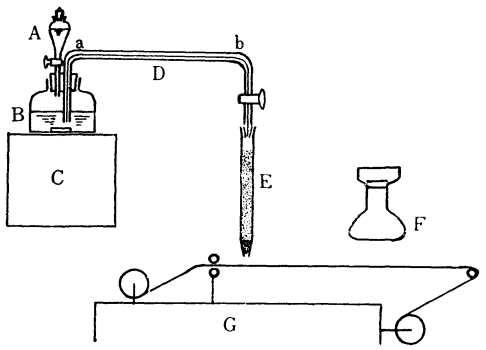



Fig. 1. Apparatus.
A : Stock bottle, B : Mixing bottle,
C : Magnetic stirrer, D : Capillary,
E : Column, F : Infrared lamp,
G : Paper micro-fraction collector.

**Ion-exchange Column.**—A coarser part of Dowex 1-X 4 (200~400 mesh) of chloride form was filled in a capillary, 2.6 mm. in diameter and 60 mm. in height.

**Phosphate Samples.**—Disodium hydrogen orthophosphate dodecahydrate, tetrasodium pyrophosphate decahydrate and pentasodium tripolyphosphate hexahydrate were used.

**Elution.** — Solutions of potassium chloride of various concentrations were buffered with sodium formate and formic acid. The concentrations of sodium formate and formic acid were kept constant (HCOONa 5.1 g./l. and 80% HCOOH 2.5 ml./l.) and the pH of the solution was regulated with aqueous ammonia. The solution of potassium chloride in a stock bottle was continuously added to a mixing bottle which contained 10 ml. of water initially. Then the solution in the mixing bottle was introduced to the ion-exchange column. The flow rate was regulated to be about 30 sec./drop.

**Fraction Collector.** — By the use of a paper micro-fraction collector[3] manufactured by Mitamura the eluted solution was collected drop by drop on a piece of filter paper and was dried immediately with an infrared lamp.

* Present address: Department of Chemistry, Faculty of Science, Kyushu University, Fukuoka.

1) a) J. P. Crowther, *Anal. Chem.*, **26**, 1383 (1954), b) H. Grunze and E. Thilo, *Sitz. ber. deut. Akad. Wiss. Berlin, Kl. Math. allgem. Naturw.*, **1953**, No. 5, 26 pp., c) E. Karl-Kroupa, *Anal. Chem.*, **28**, 1091 (1956), d) H. Hettler, *J. Chromatog.*, **1**, 389 (1958), e) D. N. Bernhart and W. B. Chess, *Anal. Chem.*, **31**, 1026 (1959), and f) M. J. Smith, ibid., **31**, 1023 (1959).

2) a) S. Lindenbaum, T. V. Peters, Jr., and Wm. Rieman III, *Anal. Chim. Acta*, **11**, 530 (1954), b) C. E. Higgins and W. H. Baldwin, *Anal. Chem.*, **27**, 1780 (1955), c) J. A. Grande and J. Beukenkamp, ibid., **28**, 1497 (1956), d) J. P. Ebel and N. Busch, *Compt. rend.*, **242**, 647 (1956), e) M. Matsuhashi, *J. Biochem.*, **44**, 65 (1957), f) W. B. Chess and D. N. Bernhart, *Anal. Chem.*, **31**, 1116 (1959), g) R. H. Kolloff, *ASTM Bull.*, No. **237**, 74 (1959), and h) R. F. Jameson, *J. Chem. Soc.*, **1959**, 752.

3) N. Tamiya, T. Soda and Y. Yoshino, This Bulletin, **27**, 393 (1954).

**Qualitative Observation on the Separation of Phosphates.** — After the separation the filter paper containing phosphates was sprayed with a solution which was made by mixing 5 ml. of 60% perchloric acid, 1 ml. of concentrated hydrochloric acid, and 1 g. of ammonium heptamolybdate tetrahydrate and diluting this to 100 ml. with water. The sprayed paper was dried under the infrared lamp, then placed under an ultraviolet lamp and irradiated until blue spots appeared.

**Quantitative Analysis of Phosphate Mixtures.**— The paper area containing each phosphate species was cut into small pieces and was burned to ashes in a crucible. The ash was digested with nitric acid and the acid solution was evaporated to dryness. The residue was dissolved in a diluted solution of sulfuric acid and the phosphate was determined colorimetrically according to the method of Karl-Kroupa[1c].

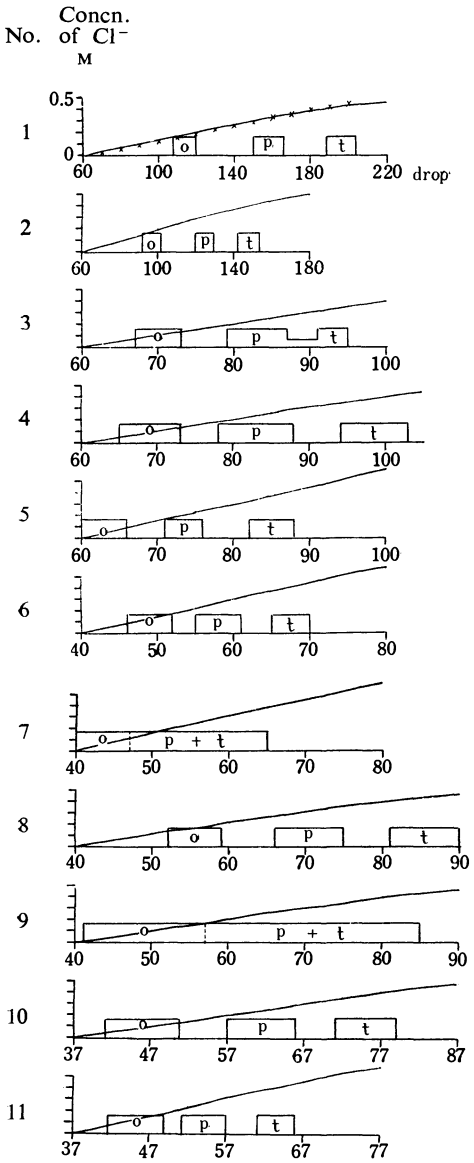



Fig. 2. Separation of phosphate mixtures.
o : Orthophosphate, p : Pyrophosphate,
t : Tripolyphosphate.

## Results and Discussion

Experimental results for the dependence of separation of phosphate mixtures on the elution conditions are summarized in Fig. 2 and Table I. The rectangles in Fig. 2 indicate only the positions of phosphate species in the elutions but not their concentrations. The variation of the concentration of chloride ion in the eluant is expressed by the equation,

$$x = a(1 - e^{-ft/v}) \qquad (1)$$

where $x$ (mol./l.) is the concentration of chloride ion in the mixing bottle, $a$ (mol./l.) is the concentration of chloride ion in the stock bottle, $f$ (ml./min.) is the flow rate, $v$(ml.) is the volume of solution in the mixing bottle and $t$ (min.) is the time from the start of mixing. The curves in Fig. 2 indicate the concentration of chloride ion in the eluant calculated from Eq. 1. The cross marks in Fig. 2-1 indicate the concentration of chloride ion determined experimentally.

Table I. Conditions of experiments shown in Fig. 2

| No. | Amount of phosphate μg. | | Concn. of KCl in the stock bottle M | pH of KCl soln. |
|---|---|---|---|---|
| 1 | Each | 20 | 0.75 | 5.5 |
| 2 | 〃 | 20 | 1 | 5.5 |
| 3 | 〃 | 20 | 2 | 5.5 |
| 4 | 〃 | 20 | 2 | 4.5 |
| 5 | 〃 | 20 | 3 | 4.5 |
| 6 | 〃 | 20 | 3 | 4.5 |
| 7 | 〃 | 100 | 3 | 4.5 |
| 8 | 〃 | 100 | 2 | 4.5 |
| 9 | 〃 | 300 | 2 | 4.5 |
| 10 | 〃 | 100 | 2 | 4.5 |
| 11 | Ortho<br>Pyro<br>Tripoly | 100<br>10<br>10 | 3 | 4.5 |

The capillary between a and b in Fig. 1 was shortened step by step to promote the efficiency of the elution. In the experiments of Fig. 2-1～5, 6～9 and 10～11, the capillaries of the length 41.5, 24.0 and 20.7 cm. were used, respectively.

Jameson[2h] used 0.75 M solution of potassium chloride of pH 5.5 as a stock solution to determine the compositions of strong phosphoric acids. Using a potassium chloride solution of the same concentration and pH as those used by Jameson, the authors tested the separation of the phosphate mixture. The separation of 20 μg. as phosphorus of each phosphate species is complete, but too much eluant is consumed

(Fig. 2-1). The same amounts of the phosphate mixture can be separated by the use of 1 M potassium chloride of pH 5.5 (Fig. 2-2), but in the case of 2 M potassium chloride of pH 5.5 the separation of pyro- and tripolyphosphate is incomplete (Fig. 2-3). The use of 2 or 3 M potassium chloride of pH 4.5 can separate 20 $\mu$g. as phosphorus of each phosphate species (Fig. 2-4 and 5, and 6). The separation of 100 $\mu$g. as phosphorus of each phosphate species can not be achieved by the use of 3 M potassium chloride of pH 4.5 (Fig. 2-7). On the other hand 2 M potassium chloride of pH 4.5 should be used for that purpose (Fig. 2-8 and 10). However, 2 M potassium chloride of pH 4.5 can not separate 300 $\mu$g. as phosphorus of each phosphate species (Fig. 2-9).

As shown in Fig. 2-10, 100 $\mu$g. as phosphorus of each phosphate species can be separated by letting only 79 drops of the eluant flow. Similarly 100 $\mu$g. of orthophosphate, 10 $\mu$g. of pyrophosphate and 10 $\mu$g. of tripolyphosphate, as phosphorus in all cases, can be separated satisfactorily by letting only 66 drops of the eluant flow (Fig. 2-11).

TABLE II. RESULTS OF ANALYSES OF PHOSPHATE MIXTURES

| Sample | Phosphate species | % P | | |
|---|---|---|---|---|
| | | Calcd. | Found, this method | Found, paper chromatography[1c] |
| Pure phosphate mixture | Ortho- | 50.1 | 50.4 | 50.8 |
| | Pyro- | 49.9 | 49.6 | 49.2 |
| Pure phosphate mixture | Ortho- | 66.8 | 67.5 | — |
| | Pyro- | 33.2 | 32.5 | — |
| Commercial sodium tripolyphosphate | Ortho- | — | 0.0 | 0.0 |
| | Pyro- | — | 7.6 | 7.2 |
| | Tripoly- | — | 92.4 | 92.8 |

The results of the quantitative analyses obtained by the precent procedure are shown in Table II. The first and the second sample are synthetic mixtures of pure alkali orthophosphate and pyrophosphate and the third sample is a commercial sodium tripolyphosphate. For comparison, the paper chromatographic analyses were carried out for the first and the third sample by the method of Karl-Kroupa[1c]. The data obtained by the present method were well coincident with the calculated values and the data obtained by paper chromatography.

**Summary**

The authors presented the new rapid method for the determination of ortho-, pyro- and tripolyphosphate in the mixture by the use of a small column, 2.6 mm. in diameter and 60 mm. in height, of ion-exchange resin, Dowex 1−X4 (200∼400 mesh). The continuous-gradient elution method was applied and the paper micro-fraction collector was used. For example, by the use of 2 M potassium chloride of pH 4.5 as the stock solution, 100 $\mu$g. as phosphorus of each phosphate species can be separated by letting only 79 drops of the eluant flow. The quantitative data obtained by the present method were well coincident with the calculated values or the data obtained by the paper chromatography.

*Department of Chemistry*
*Faculty of Science*
*Kanazawa University*
*Kanazawa*

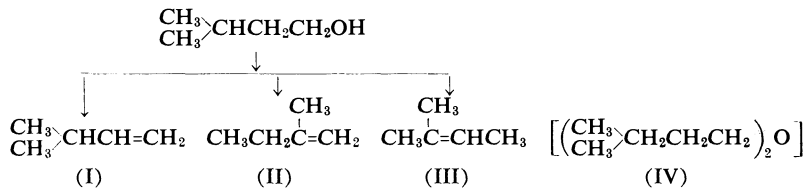
# *Forschung über die katalytische Entwässerung des Isoamylalkohols. I.*

Von Akira MITSUTOMI

(Eingegangen am 26. September, 1960)

Die Gewinnung der Olefine durch Entwässerung des Isoamylalkohols geschieht entweder nach dem sogenannten „Flüssigkeits oder Gasphase-verfahren". Bei dem erst genannten Flüssigkeitsverfahren liefert Isoamylalkohol in der unter Zusatz von konzentrierter Schwefelsäure unterhalb von 100°C erfolgenden Entwässerung Amylen in 15～18%iger Ausbeute sowie Isoamyläther in ca. 27%iger Ausbeute, wie die Arbeiten von Norris und Reuter[1], und von Cramer und Cambell[2] klar zeigen. Die hier entstehenden Amylene sind zwar nach ihrem Siedepunkt, 32～42°C, als ein Gemisch aus Methyläthyläthylen und Trimethyläthylen

1) J. P. Norris und R. Reuter, *J. Am. Chem. Soc.*, **49**, 2624 (1927).
2) P. I. Cramer und J. M. Campbell, *Ind. Eng. Chem.*, **29**, 234 (1937).



anzunehmen, sie sind aber auf das Mischverhältnis, die chemischen Zusammensetzung noch nicht geprüft.

Abgesehen von der Diskontinuierlichkeit von diesem Verfahren, kann es wenn auch nur für Olefine-Herstellung als geeignet nicht angesprochen werden. Aus dem Standpunkt, für die industrielle Produktion das kontinuierlich arbeitende Gasphase-Verfahren technisch fertigzubringen, hat der Verfasser diese Forschung durchgeführt.

Ipatiew[3] berichtet für das Gasphase-Verfahren, dass man durch Zuführung des Isoamylalkohols durch das bei 540°C vorher erhitzte mit Aluminiumoxyd gefüllte Eisenrohr ein Gemisch des Isopropyläthylens (I) mit kleiner Menge Methyläthyläthylen (II) und Trimethyläthylen (III) erhält, ohne dabei aber Isoamyläther (IV) festzustellen.

Ipatiew[4] hat ferner bei der Prüfung der Isomerisation von Isopropyläthylen erkannt, dass bei Abwesenheit von Katalysatoren diese Isomerisation auch bei Erhitzung bis zu 400, 500 und 540°C immer ausbleibt, während bei Anwesenheit von Aluminiumoxyd als Katalysator bereits im Bereich von 450～535°C das Isopropyläthylen ca. 50～60% zu Trimethyläthylen isomerisiert wird. In der Genenwart von Kieselgur wird es ca. 20%.

Auch Adams, Kamm und Marvel[5] haben berichtet, dass durch Entwässerung des Isoamylalkohols bei 500～540°C unter Anwendung des Aluminiumoxyds und Bimssteins als Katalysator Isopropyläthylen mit 70～80%iger Ausbeute dargestellt werden konnte, ohne aber Trimetyläthylen bilden zu lassen.

Nach Norris und Reuter[6] bildet sich nur Isopropyläthylen, wenn Isoamylalkohol durch Aluminiumoxyd als Katalysator bei 375～400°C entwässert wird, und das wird erst nach Erhitzung bei 375～450°C in der Gegenwart von Aluminiumsulfat als Katalysator nur um 45% zu Trimethyläthylen isomerisiert, während beim Vorhandensein der Phosphorsäure als Katalysator die genannte Isomerisation des Isopropyläthylens bei 450°C absolut ausbleibt und erst bei 500°C nur um 15～29% eintritt.

Es ist zwar von Kashima[7] angegeben, dass aus *n*-Amylalkohol bei Anwendung der japanischen Säureerde als Katalysator *n*-Amylen und *n*-Amyläther dargestellt wurden. Aber von der Stellung der Doppelbindung von diesem *n*-Amylen ist keineswegs erwähnt. Fujita[8] hat unter Erhitzung des mit Aktivkohle gefüllten Kupferrohrs bei 320～340°C ein Gemisch aus Isoamylalkohol und Wasser hindurchgezogen, und ausser Isobutylen und Isopropyläthylen noch die Bildung von Isoamyläther, Isobutan, Isovaleraldehyd und Isovalersäure ermittelt.

Es muss von den oben genannten Arbeiten überhaupt gesagt werden, dass sie mit Ausnahme von Fujita die Trennung der Reaktionsprodukte und deren Ermittelung sehr ungründlich behandelten und weiterer eingehender Prüfung bedürfen.

Die Olefine, der Gegenstand der Arbeiten, die durch Entwässerung der niedrigen Alkohole gebildet werden, haben einander sehr naheliegende Siedepunkte, so dass die Trennung der einzelnen Olefinen mit grösseren Schwierigkeiten verbunden sind. Üblicherweise wird das Gemisch unter Benutzung des unterschiedlichen Löslichkeitsgrades gegenüber 60%iger Schwefelsäure getrennt. Mit solch einer Methode können die einzelnen Olefine in ihrem primären Zustande keineswegs alle voneinander getrennt werden. Solche in verhältnismässig geringer Menge vorhandenen Olefine können als reiner Verlust weder erfasst noch rein dargestellt werden.

Ferner kann als für diese Arbeiten überhaupt gemeinsamer Nachteil angeschprochen werden, dass ausgerechnet die Frage immer noch offengelassen ist, nämlich welche Typen Katalysatoren geeignet sind, um gewisse Typen Olefinen durch Entwässerung von Alkohol zu gewinnen.

Dieser Umstand kommt selbstverständlich daher, dass, wie bereits beschrieben, die Bestimmung der chemischen Zusammensetzung und des Mischverhlätnisses von den Reaktionsprodukten äusserst unbeachtet behandelt ist. Der Verfasser hat die unentbehrlichen Bedingungen bestimmt, Trimethyläthylen durch das Gasphase-Verfahren kontinuierlich herzustellen, und den Reaktionsmechanismus geklärt.

3) W. I. Ipatiew, *Ber.*, **36**, 2000 (1903).
4) W. I. Jpatiew, ebenda, **36**, 2003 (1903).
5) R. Adams, O. Kamm und C. S. Marvel, *J. Am. Chem. Soc.*, **40**, 1950 (1918).
6) J. F. Norris and R. Reuter, ebenda., **49**, 2627 (1927).
7) K. Kashima, Dieses Bulletin, **4**, 177 (1929).
8) Y. Fujita, ebenda, **9**, 11 (1934).

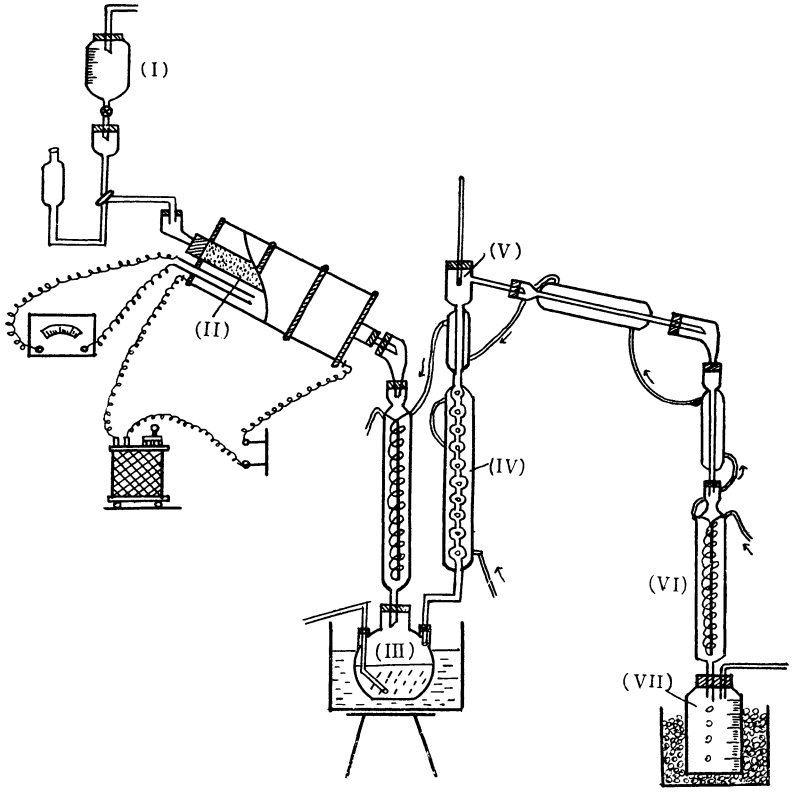



Abb. 1. Experimentelle Vorrichtung.

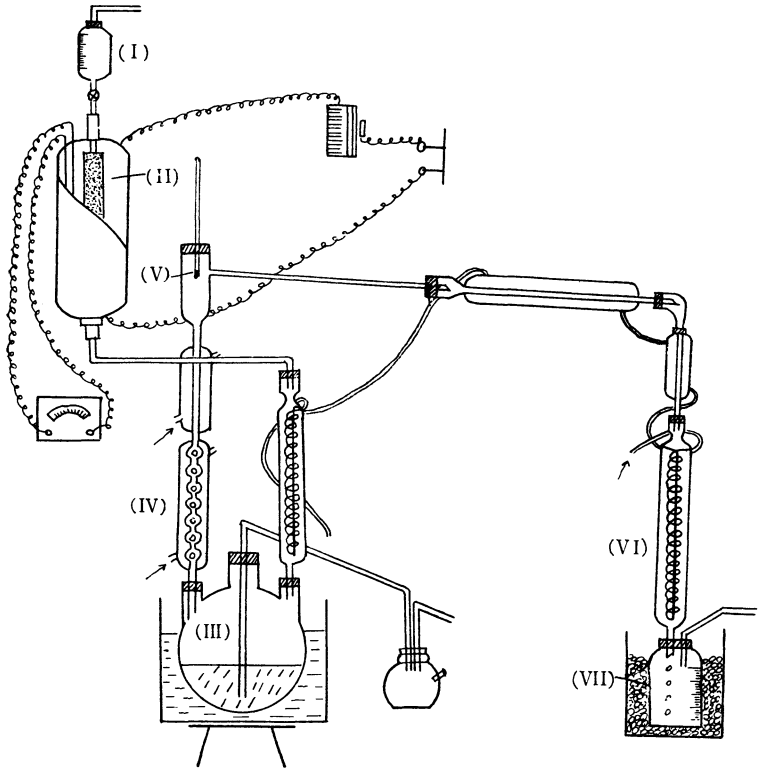



Abb. 2. Experimentelle Vorrichtung.

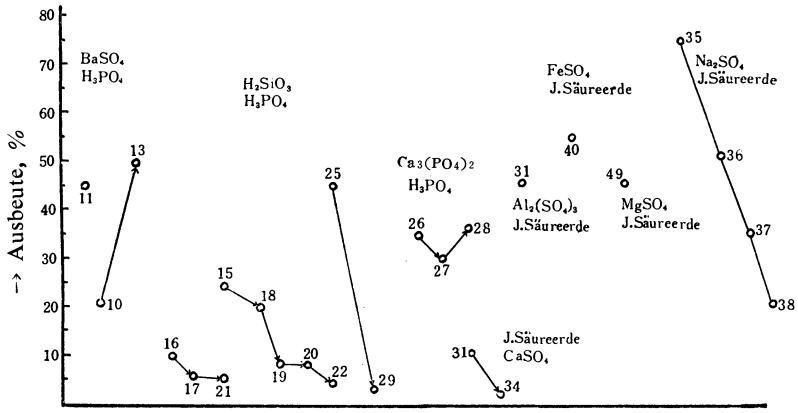



Abb. 3. Verglich der Ausbeute von der vierten Fraktion bei verschiedenen katalystoren.

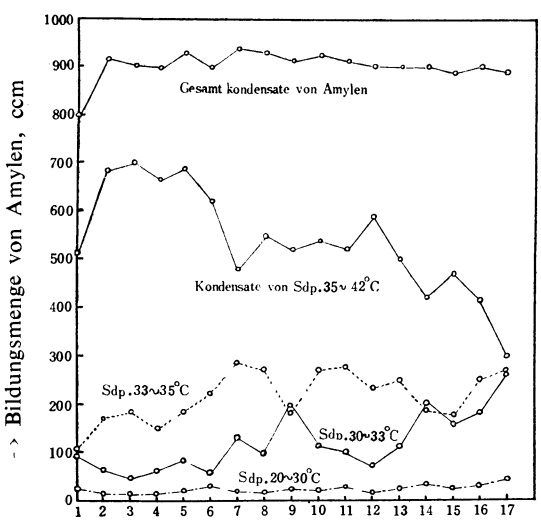



Abb. 4

Aggregateinheit Nr. 1
Versuchsreihenummer 59～75
Dauer der kontinuierlichen Anwendung 186 Std.

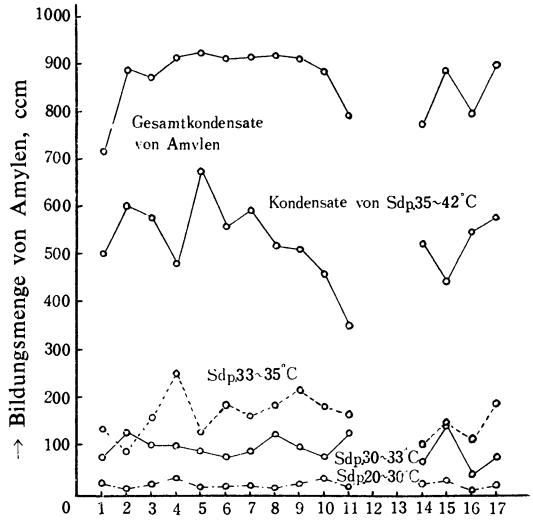



Abb. 5

| Aggregateinheit | Nr. 3 | Nr. 2 |
|---|---|---|
| Versuchsreihenummer | 80～90 | 76～79 |

Zu diesem Zweck wurden die Hochfeindestillation, Fluoreszenz Indikator Adsorptionsanalyse, Infrarot Spektrographie sowie Gas-Chromatographie herangezogen.

### Beschreibung der Versuche

Die beiden Vorrichtungen, einmal die horizontale Type, andersmal die vertikale Type, wurden für Entwässerung von Isoamylalkohol nach dem Gasphase-Verfahren verwendet, mit aber annähernd gleichen Ergebnissen. Das Ausgangsmaterial, Isoamylalkohol, tritt tröpfenweise in gewissen Zeitabständen von dem kalibierten Behälter ins Reaktionsrohr aus. In dem Reaktionsrohr sind die in Korngrösse vereinheitlichten Katalysatoren eingepackt und von Aussern her elektrisch geheizt. Die durch Reaktion zu bildenden Olefine und weitere gasförmige Substanzen wandern über den Kühler in den Behälter ein. Dieser Behälter liegt in dem Wasserbad und bleibt unterhalb von 100°C.

Das unverwandelte Isoamylalkohol verbleiben in dem Behälter, während die Olefine mit niedrigem Siedepunkte allein durch den Kühler hinaufsteigen, in den Kühler, wo sie stark abgekühlt werden, und die Vorlage aufgesammelt werden.

Die Kondensate werden nach Feindestillation in 4 Fraktionen eingeteilt: 20～30°C, 30～33°C, 33～35°C, 35～42°C.

Die vierte Fraktion bestehen hauptsächlich aus Trimethyläthylen. Anhand deren prozentualen Ausbeute wurde das katalysatorische Vermögen beurteilt.

Als Katalysatoren wurden 15 folgende Substanzen in verschiedenen Kombinationen eingesetzt: $Al_2O_3$,

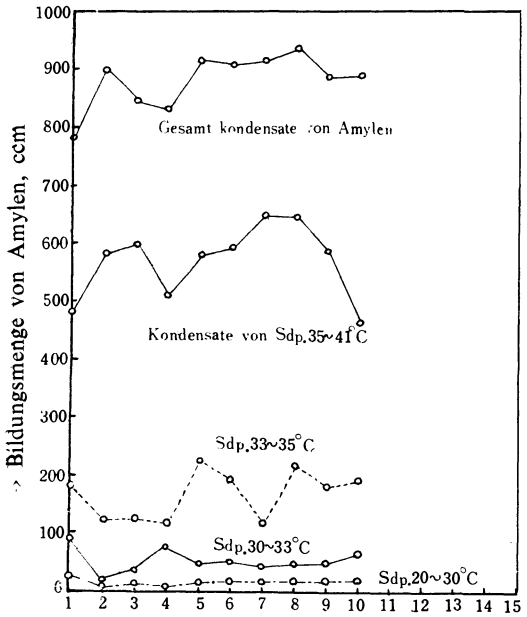



Abb. 6

| | |
|---|---|
| Aggregateinheit | Nr. 4 |
| Versuchsreihenummer | 91～100 |

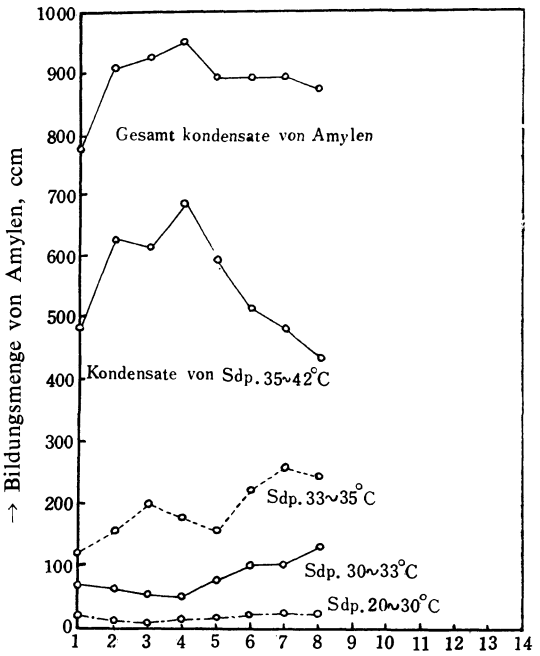



Abb. 7

| | |
|---|---|
| Aggregateinheit | Nr. 5 |
| Versuchsreihenummer | 101～108 |

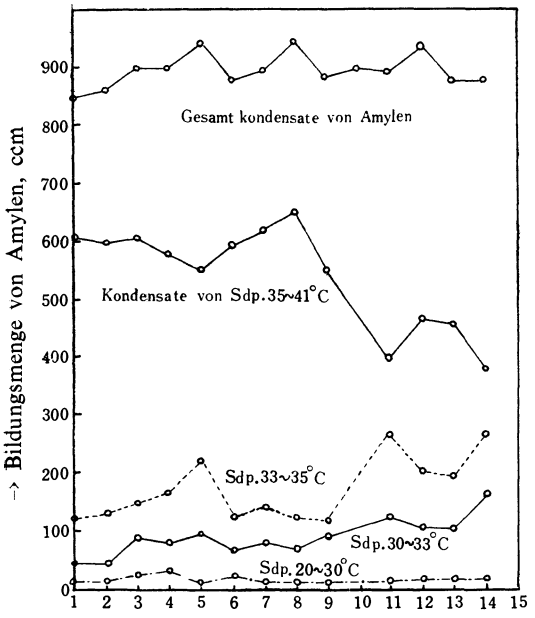



Abb. 8

| | |
|---|---|
| Aggregateinheit | Nr. 6 |
| Versuchsreihenummer | 109～122 |

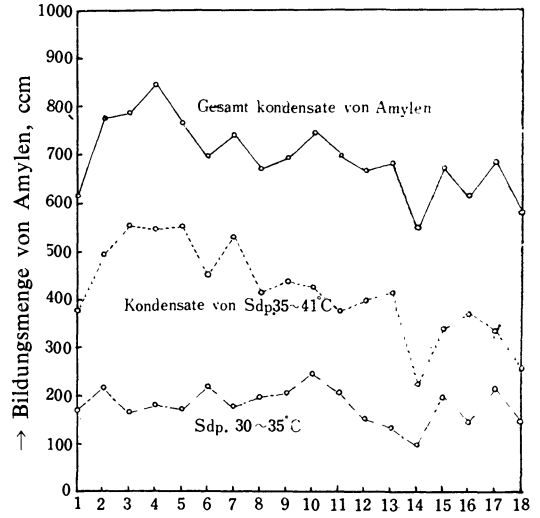



Abb. 9

| | |
|---|---|
| Aggregateinheit | Nr. 7 |
| Versuchsreihenummer | 123～140 |
| Dauer der kontinuierlichen Anwendung | 220 Std. |

$BaSO_4$, $H_3PO_4$, $H_2SiO_3$, $ZnSO_4$, $FeSO_4$, $MgSO_4$, $ZnCl_2$, $Ca_3(PO_4)_2$, $Al_2(SO_4)_3$, $CaSO_4$, $Na_2SO_4$, $KHSO_4$, Stärke, japanische Säureerde.

Der Kakalysator wurde in geeignetem Verhältnis gemischt, mit etwas Wasser zugesetzt, angeteigt, in geeignete Korngrösse verformt, zuerst bei 60°C für 2 Std, dann bei 120°C für 1 Std erhitzt und aufgetrocknet.

## Ergebnisse

Die Versuchsergebnisse liessen folgenden Schluss ziehen: Bei dem Aluminiumoxyd als Katalysator zeigte sich die Gesammtmenge von den dritten und vierten Fraktionen nur als 5.5%, ausserdem dieselbe von den Ersten und Zweiten auch als 27%. Unter allen Umständen war Aluminiumoxyd als Katalysator für vorliegenden Versuch unbrauchbar.

Die Resultaten beim Einsatz anderer Katalysatoren sind in Tabelle I aufgezeichnet.

Die Tabelle I umfasst die beiden extremen Ausbeute, nämlich des Maximum und Minimum an der Ausbeute von der vierten Fraktion, die beim gleichen, mehr als zweimal kontinuierlich eingesetzten Mischkatalysator erhalten wurde. Die in der Tabelle I angegebenen Versuchsnummer sind identisch mit denselben in der Tabelle II. In der Tabelle II weisen sie die Beschreibung der verwendeten Reaktionsröhre auf.

Kurz gefasst, ist der Aluminiumoxyd-Katalysator für Fabrikation des Trimethyläthylens ungeeignet. Wenn daher solche Katalysatoren, die über 50%ige Ausbeute des Trimethyläthylens erzielen lassen, aus Tabelle I gesucht werden, können Mischkatalysatoren aus Kieselsäure und Phosphorsäure, aus Natriumsulfat, Eisensulfat oder Magnesiumsulfat mit jeweiligem Zusatz von japanischer Säureerde gefunden werden. Besonders beim Natriumsulfat ist durch Reaktion bei 400°C die Ausbeute von 72% an Trimethyläthylen erzielbar. Die genannte Ausbeute gilt aber nur für das erste Mal. Bei kontinuierlichen Reaktionen vermindert sich diese in einer fortwährenden Abschwächung wie 72.0→53.0→36.5→20.0%.

Auch der Mischkatalysator aus Kieselsäure und Phosphorsäure wies anfangs 55%ige Ausbeute auf, sank aber nach viermaliger kontinuierlicher Anwendung auf 5.5%ige Ausbeute ab. Bei anderen Katalysatoren blieb es fast gleich. Nach 70 bzw. 120 Std kontinuierlicher Anwendung ist das Entwässerungs- und Isomerisations-vermögen fast restlos verlorengegangen, somit sind alle für vorliegenden Versuch vollkommen ungeeignet.

Daher hat der Verfasser zwei Reaktionsröhre in Serie gestellt. In dem ersten Reaktionsrohr soll hauptsächlich die Entwässerung erfolgen, während in dem zweiten die Isomerisation gefördert wird, um die Ausbeute von Trimethyläthylen steigen zu lassen. Mit dieser Absicht wurden die Versuche unter Einsatz verschiedener Katalysatoren angestellt. Die Reaktionstemperatur betrug im ersten Reaktionsrohr 350～450°C und im zweiten 275～320°C. Auch in diesem Fall vermindert sich die Ausbeute an Trimethyläthylen mit Vermehrung der kontinuierlichen Reaktionsmale, um endlich bei dem fünften Mal bis auf 20.0% abzusinken, wie die Tabelle III klar anzeigt.

Die Versuchsergebnisse, die in Tabelle III

Tabelle I. Beziehung zwischen Katalysatorensorten und Ausbeute an Trimethyläthylen

| Mischkatalysatoren | | Ausbeute an vierten Fraktion | | | |
|---|---|---|---|---|---|
| | | min. Werte | | max. Werte | |
| Basis-Substanz | Zusatz | Versuchs Nr. | % | Versuchs Nr. | % |
| $BaSO_4$ | $H_3PO_4$ | 12 | 6.0 | 13 | 45.0 |
| $H_2SiO_3$ | $H_3PO_4$ | 21 | 5.5 | 24 | 55.5 |
| $Ca_3(PO_4)_2$ | $H_3PO_4$ | 27 | 30.0 | 28 | 37.5 |
| $CaSO_4$ | J. S.[a)] | 34 | 9.5 | 31 | 42.0 |
| $Al_2(SO_4)_3$ | J. S. | — | — | 30 | 44.5 |
| $Na_2SO_4$ | J. S. | 38 | 20.0 | 35 | 72.0 |
| $KHSO_4$ | J. S. | — | — | 39 | 30.0 |
| $FeSO_4$ | J. S. | — | — | 40 | 56.0 |
| $MgSO_4$ | J. S. | — | — | 41 | 50.0 |

a) J. S.: Japanische Säureerde.

Tabelle II. Beziehung zwischen Grösse der Reaktionsröhre und Versuchsreihe Nummern

| Grösse des Reaktionsröhre | | Material | Versuchsreihe Nummer |
|---|---|---|---|
| Durchmesser<br>Länge | 5 cm<br>54 cm | Eisen | 13, 24, 30, 34, 35, 38, 39 |
| Durchmesser<br>Länge | 3.4 cm<br>62.5 cm | Silica | 12, 21, 27, 28, 31, 40, 41 |

TABELLE III. AUSBEUTE AN DER VIERTEN FRAKTION BEI ANORDNUNG DER ZWEIEN REAKTIONSRÖHRE IN SERIE

| Inhalt des Mischkatalysators | | Ausbeute an der vierten Fraktion | | | |
|---|---|---|---|---|---|
| das erste Reaktionsrohr | das zweite Reaktionsrohr | min. Werte Versuchs Nr. | % | max. Werte Versuchs Nr. | % |
| $Ca_3(PO_4)_2+H_3PO_4$ | $Al_2(SO_4)_3$ | 47 | 20.0 | 44 | 67.5 |
| $Na_2SO_4$ | $Al_2(SO_4)_3$ | 58 | 20.0 | 51 | 72.0 |
| $FeSO_4$ | $Al_2(SO_4)_3$ | — | — | 56 | 56.0 |
| $MgSO_4$ | $Al_2(SO_4)_3$ | — | — | 57 | 50.0 |

TABELLE IV. BEZIEHUNG ZWISCHEN MALENANZAHL DER KONTINUIERLICHEN ANWENDUNG UND DER AUSBEUTE DER FLÜSSIGEN PRODUKTE UND DES TRIMETHYLÄTHYLENS

| | | | | | | | | | | |
|---|---|---|---|---|---|---|---|---|---|---|
| Reaktionstemp. °C | 450 | 420～450 | 450 | 450 | 450 | 450 | 450 | 450 | 450 | 445 |
| Abtröpfelungsmenge von Alkohol, ccm/Std | 100 | 100 | 90 | 80 | 80 | 100 | 100 | 100 | 100 | 200 |
| Male der kontinuierlichen Anwendung | 1 | 2 | 3 | 4 | 5 | 6 | 7 | 8 | 9 | 10 |
| Gesamtausbeute der Amylen, vol. % | 80.0 | 92.0 | 92.0 | 91.0 | 93.0 | 91.0 | 94.0 | 94.0 | 93.0 | 94.0 |
| Ausbeute des Trimethyläthylens, vol. % | 52.5 | 66.0 | 69.0 | 65.8 | 67.5 | 63.5 | 48.0 | 55.0 | 52.0 | 53.9 |
| Unverwandelte Alkohol, vol. % | 6 | 3.5 | 2.5 | 1.5 | 2.0 | 2.0 | 1.0 | 2.0 | 2.5 | 2.0 |

TABELLE V. BEZIEHUNG ZWISCHEN DEN EINSATZBEDINGUNGEN UND DEN GRÖSSENORDUNGEN DER REAKTIONSRÖHRE

| Nummer des Reaktionsrohrs | Durchmesser cm | Länge cm | Material | Versuchsreihennummer | kontinuirliche Anwendung Male | kontinuirliche Anwendung Dauer, Std | Durchschnittsausbeute von Gesamtamylen vol. % | Durchschnittsausbeute von Fraktion von Sdp. 35～41°C vol. % |
|---|---|---|---|---|---|---|---|---|
| 1 | 3.4 | 62.5 | Eisen | 1 | 17 | 170 | 90.8 | 54.9 |
| 2 | 3.4 | 62.5 | 〃 | 2 | 4 | 40 | 82.1 | 53.1 |
| 3 | 3.4 | 62.5 | 〃 | 3 | 11 | 110 | 86.8 | 51.2 |
| 4 | 5.0 | 54.0 | 〃 | 4 | 10 | 100 | 88.9 | 56.3 |
| 5 | 3.4 | 62.5 | 〃 | 5 | 10 | 100 | 88.3 | 56.5 |

verzeichnet sind, zeigten, dass die Haltbarkeit des Vermögens arm und somit für kontinuierliche Reaktion ungeeignet ist.

Der Mischkatalysator aus Zinksulfat und japanischer Säureerde zeigte im Unterschied von den anderen in der Ausbeute von Trimethyläthylen bei der ersten Anwendung 52.5%, und die der Zweiten noch eine Höhe von 66%, also deutete auf Möglichkeit einer kontinuierlichen Anwendung an. Daher wurden 64 Male Versuche angestellt, womit endlich festgestellt wurde, dass diesser Katalysator für Entwässerung und Isomerisation des Isoamylalkohols zur hochprozentigen Gewinnung des Trimethyläthylens fabrikatorisch sehr geeignet ist. Der Auszug aus den zahlreichen Versuchsergebnissen wird zum Beispiel in Tabelle IV gegeben.

Wenn also mit dem in Tabelle V bezeichneten Reaktionsrohr Nr. 1 Isoamylalkohol 1000 ccm bei 420～450°C reagiert wird, beträgt die Ausbeute des Trimethyläthylens auch nach 10-maliger kontinuierlicher Anwendung ein- und desselben Katalysators stets über 50%, mit nur geringfügiger Nebenbildung von Isopropyläthylen und Methyläthyläthylen.

Dies liefert den Beweis dafür, dass der Zinksulfat-Katalysator zu dem Zweck des Verfassers befriedigenderweise vorzüglich ist. Dieser Umstand ist auch bei 52 Male, unter Einsatz der Reaktionsröhrenummer 2, 3, 4 und 5 klar feststellbar.

Um diejenigen Ergebnisse handelt es sich bei den Versuchen Nr. 1—5. Tabelle V zeigt eine zum Vergleich derer zusammengefasste Aufstellung.

Es sei noch hinzugefügt, dass die Ausbeute an Trimethyläthylen in solcher Versuche fast die Gleichen wie in Tabelle IV sind und somit hier fortgelassen wurden.

## Zusammenfassung

Die Methode, die hauptsächlich aus Trimethyläthylen bestehenden Olefine aus Isoamylalkohol nach dem Gasphase-Verfahren zu gewinnen, wurde ausgearbeitet. Nach der Feststellung, dass der von Ipatiew vorgeschlagene Katalysator, Aluminiumoxyd, zu diesem

Zweck ungeeignet ist, wurden verschiedene Katalysatoren, auf ihr Vermögen, Trimethyläthylen zu liefern, untersucht, mit dem Ergebnis, dass ein Gemisch des Zinksulfat es mit der japanischen Säureerde das beste Vermögen besitzt. Ihre Eignung wurde nach weiterer Forschung unter Modifizierung der Bedingungen ermittelt.

Zum Schluss sei noch davon erwähnt, dass die vorliegende Arbeit der Leitung von Herrn Professor Dr. Eiichi Funakubo an der Technischen Fakultät der Universität zu Osaka verdankt ist.

*Chemisches Institut der Technischen Fakultät der Universität zu Osaka*
*Miyakojima-ku, Osaka*

# *Forschung über die katalytische Entwässerung des Isoamylalkohols. II. Prüfung der Bedingungen für kontinuierliche Dehydratisierung bei Zinksulfat-Katalysator*

Von Akira MITSUTOMI

(Eingegangen am 26. September, 1960)

Der Verfasser hat bereits in der I. Mitteilung[1] betont, dass für kontinuierliche Fabrikation der hauptsächlich aus Trimethyläthylen bestehenden Olefinen, ausgehend von Isoamylalkohol, der Zinksulfat-Katalysator das beste Vermögen besitzt.

Um die Entwässerung und Isomerisation beim Einsatz dieses Katalysators genauer zu forschen und unter Anwendung der labormässig grösstmöglichen Apparatur die geeigneten Bedingungen für Olefin-Produktion zu ermitteln, wurden folgende Reihen Versuche gestellt.

## Beschreibung der Versuche

**Zubereitung der Katalysatoren.** — Es wurden kristallines Zinksulfat und japanische Säureerde gut vermischt, mit Zusatze von etwas Wasser genügend angeteigt, in passende Korngrösse verarbeitet, zuerst bei 60°C 2 Std, dann bei 120°C 1 Std erhitzt und abgetrocknet. Die Erhitzungsgewichtsabnahme u. s. w. stehen in Tabelle I.

Es wurden von den Katalysatoren 3 Sorten, nämlich Nr. 1, 2 und 3, wie in Tabelle II angegeben, präpariert und auf katalysatorisches Vermögen, Haltbarkeit u. s. w. geprüft.

Für Reaktionsröhre wurden die Eiserne verwendet. Die einzelnen Grössen, die Versuchsnummern, wobei die Betreffenden eingesetzt wurden, und weitere Angaben sind in Tabelle III verzeichnet.

**Versuchsmethode.** — Mittelgrosse und grosse Reaktionsröhre, deren Grössenordnung bereits in Tabelle III angegeben ist, wurden in gleicher Weise aufgestellt wie in der I. Mitteilung. Drein wurden unter Variierung der Temperaturen 1000 ccm Isoamylalkohol eingeschickt, wasserabgespaltet, isomerisiert und die Produkte, eingeteilt in 3 folgenden Fraktionen, und die Ausbeute wurde geprüft: bis 30°C, 30~35°C, 35~41°C.

Indem andererseits mit 1000 ccm Isoamylalkohol als einmaliger Einschickung ein und derselbe Katalysator kontinuierlich angewandt wurde, wurde derselbe unter Beobachtung der Änderungen von Ausbeute auf seine Haltbarkeit geprüft.

Ferner wurden unter folgendem Grundsatz Versuche angestellt: (I) Bei Versuchsreihennummer 1 bis 6 wurde unterm Einsatz der mittelgrossen Reaktionsröhre bei Einhaltung der Temperatur zu ca. 398~540°C der Katalysator Nr. 1 auf das Vermögen geprüft. (II) Bei Versuchsreihennummer 7 bis 9 wurde unterm Einsatz der Reaktionsröhr mit etwas grösserem Durchmesser bei ca. 380~451°C Reaktionstemperatur der Katalysator Nr. 1 geprüft. (III) Bei Versuchsreihennummer 10 bis 12 wurde der Katalysator Nr. 1 bei Absenkung der Reaktionstemperatur auf 320~410°C auf das Vermögen geprüft. (IV) Bei Versuchsreihennummer 16~18 wurde der Katalysator Nr. 2 und bei denen 13~15 derselbe Nr. 3 auf das Vermögen geprüft. (V) Unter dem Einsatz des labormässig zulässigen möglichstgrossen Reaktionsrohrs wurde der Katalysator Nr. 1 auf das Vermögen geprüft. Unter variierten Temperaturen wurden 96 Male Versuche angestellt. (VI) Mit gleichgrossem Reaktionsrohr wie oben wurde der Katalysator Nr. 2 geprüft. Es waren die Versuchsreihe Nr. 16~18.

## Versuchsergebnisse

Unter Einhaltung der gleichen Bedingungen mit Ausnahme der Reaktionstemperatur wurden unabhängig voneinander 290 Male Experimente durchgeführt, indem ein neuer Katalysator

1) A. Mitsutomi, This Bulletin, 34, 1518 (1961).

TABELLE I. GEWICHTSABNAHME DER KATALYSATOREN NACH ERHITZUNG

| | Gewicht g | Kornzahl | Gewicht g | Kornzahl | Gewicht g | Kornzahl |
|---|---|---|---|---|---|---|
| Vor Trocknen | 10 | 37 | 50 | 186 | 100 | 302 |
| Nach Trocknen | 6 | 37 | 29.6 | 186 | 58 | 302 |
| Erhitzungsgewichtsabnahme | 4 | 37 | 20.4 | 186 | 42 | 302 |
| Durchschnittsgewicht eines Korns | 0.4 | | 0.592 | | 0.58 | |
| Durchschnittsdurchmesser eines Korns, mm | 6.4 | | 6.4 | | 6.4 | |

TABELLE II. ZUSAMMENSETZUNG DER KATALYSATOREN UND VERSUCHAREIHENNUNMERN

| Sorten | Katalysator Zusammensetzung | | | Reaktionsrohr | |
|---|---|---|---|---|---|
| | Zinksulfat | Japanische Säureerde | Zusatz | Mittelgrosses Versuchsnummer | Grosses Versuchsnummer |
| Nr. 1 | 30 | 70 | $H_2O$ | 1～ 9 | 10～12 |
| Nr. 2 | 50 | 50 | $H_2O$ | | 16～18 |
| Nr. 3 | 30 | 70 | $NH_4OH$ | 13～15 | |

TABELLE III. REAKTIONSROHRGRÖSSE UND VERSUCHSREIHENUMMERN

| Reaktionsrohr | | Einfüllungs-volumen $cm^3$ | Katalysatoren | | Versuchs-nummer | Reaktions-temperatur °C |
|---|---|---|---|---|---|---|
| Durchmesser cm | Länge cm | | Sorten | Einpackungs-menge kg | | |
| 5.2 | 56 | 1560 | Nr. 1 | 1.156 | 1～ 6 | 398～540 |
| 2.9 | 65 | 1560 | Nr. 1 | 1.156 | 7～ 9 | 380～451 |
| 2.9 | 56 | 1560 | Nr. 3 | 1.170 | 13～15 | 380～450 |
| 5.1 | 122 | 2512 | Nr. 1 | 1.86 | 10～12 | 320～410 |
| 5.1 | 122 | 2512 | Nr. 2 | 1.93 | 16～18 | 300～370 |

TABELLE IV. FABRIKATIONSERGEBNIS VON AMYLEN NACH DEM GASPHASE-VERFAHREN

| Versuchs-reihen-nummer | Reaktions-temperatur, °C | Ausbeute, vol. % | | | | unver-wandelter Alkohol, Vol. % |
|---|---|---|---|---|---|---|
| | | Gesamte Amylene | Fraktion von | | | |
| | | | bis 30° | 30～35° | 35～41° | |
| 1 | 455～511 | 68.0 | 0 | 22.0 | 66.1 | 1.8 |
| 2 | 450～540 | 67.0 | 0 | 26.4 | 62.8 | 3.5 |
| 3 | 450～499 | 76.0 | 0 | 22.1 | 70.2 | 2.2 |
| 4 | 410～450 | 62.0 | 0 | 27.2 | 57.0 | 3.0 |
| 5 | 400～450 | 78.0 | 0 | 28.3 | 63.5 | 4.0 |
| 6 | 398～451 | 84.0 | 0 | 27.3 | 63.8 | 2.5 |
| 7 | 400～445 | 74.0 | 0 | 19.8 | 69.6 | 2.1 |
| 8 | 380～449 | 78.0 | 0 | 29.0 | 57.0 | 3.5 |
| 9 | 380～450 | 71.0 | 0 | 28.2 | 57.9 | 4.2 |
| 13 | 390～430 | 82.0 | 3.8 | 30.3 | 57.8 | 16.7 |
| 14 | 380～430 | 84.0 | 2.1 | 30.5 | 59.5 | 8.8 |
| 15 | 380～450 | 84.0 | 2.4 | 31.3 | 59.2 | 7.5 |
| 10 | 350～410 | 70.0 | 6.3 | 23.5 | 69.0 | 9.0 |
| 11 | 320～400 | 78.0 | 0.8 | 21.6 | 73.0 | 17.5 |
| 16 | 300～345 | 78.0 | 1.9 | 13.1 | 73.0 | 12.5 |
| 17 | 300～350 | 70.0 | 1.1 | 15.2 | 72.0 | 12.0 |
| 18 | 300～370 | 80.0 | 1.5 | 16.0 | 72.5 | 19.0 |
| 12 | 320～390 | 81.0 | 1.1 | 22.3 | 74.0 | 6.4 |

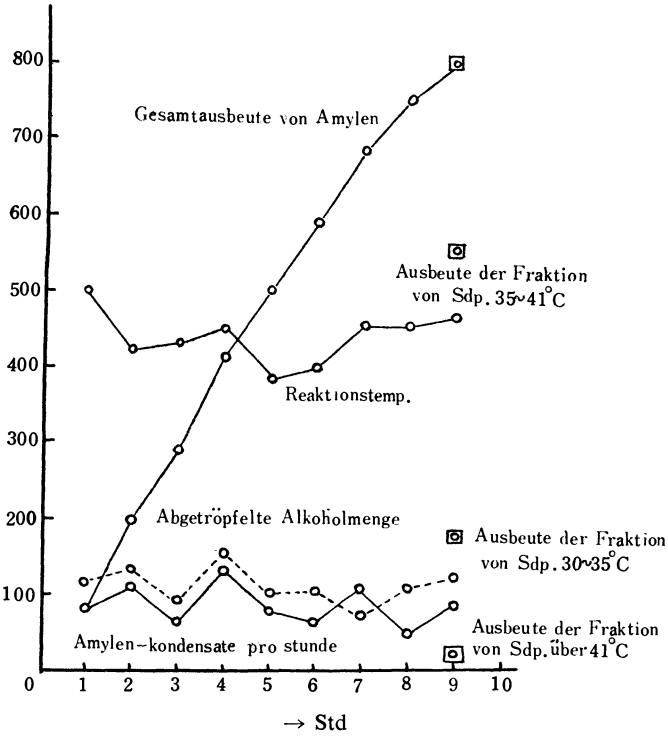



Abb. 1
Versuchsreihennummer 125 Reaktionstemp. 390~455°C

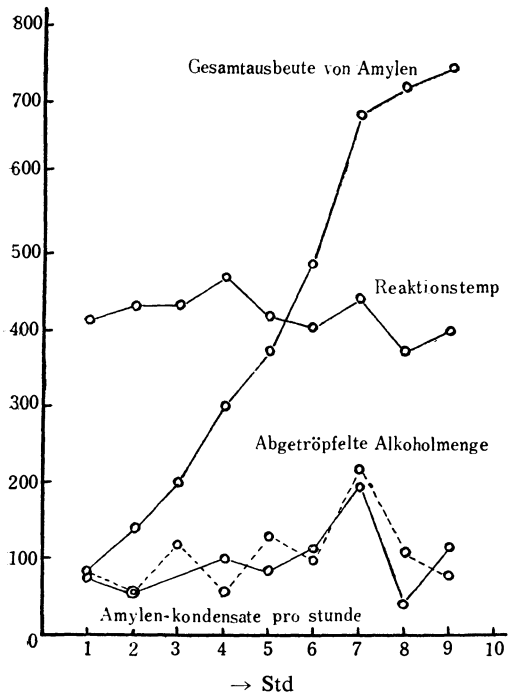



Abb. 2
Versuchsreihennummer 127
Reaktionstemp. 360~450°C

jeweils eingesetzt wurde. Von den Versuchsergebnissen wurden die als typisch Erscheinenden ausgesucht und zum Vergleich auf eine Tabelle IV gebracht.

Wird die Überlegenheit durch die Fraktion von Sdp. 35~41°C, Ausbeute an Amylen und des Wiedergebungsvermögen entschieden, so lässt sich finden, dass die Reaktionstemperatur von gegen 350±30°C herum für den Zweck vorliegender Versuche die optimal Bedingung darstellt, wie die Ergebnisse bei der aus Exp. Nr. 10, 11, 12, 16, 17 und 18 bestehenden Gruppe zeigen.

Bei einer höheren Temperatur erhält man nur in seltenen Fällen gute Ausbeute, wie es bei Exp. Nr. 3 der Fall ist, aber es lässt sich nicht gut wiedergeben. Im Gegensatz hierzu ist das Wiedergebungsvermögen von den Resultaten bei Exp. Nr. 8, 9, 13, 14 und 15 ausgezeichnet gut, aber ausgerechnet die Ausbeute an Trimethyläthylen ist als verhältnismässig schlecht zu bezeichnen. Im Gegenteil davon verbessert sich die Ausbeute der Fraktion von Sdp. 30~35°C. Die dabei herschende Reaktionstemperatur von ca. 400±30°C ist als geeignet für unsere Forschung nicht anzusprechen.

Ferner, die mit dem Fortschreiten der Reaktion ununterbrochen eintretenden Destillatsmengen von Amylen und die drei,

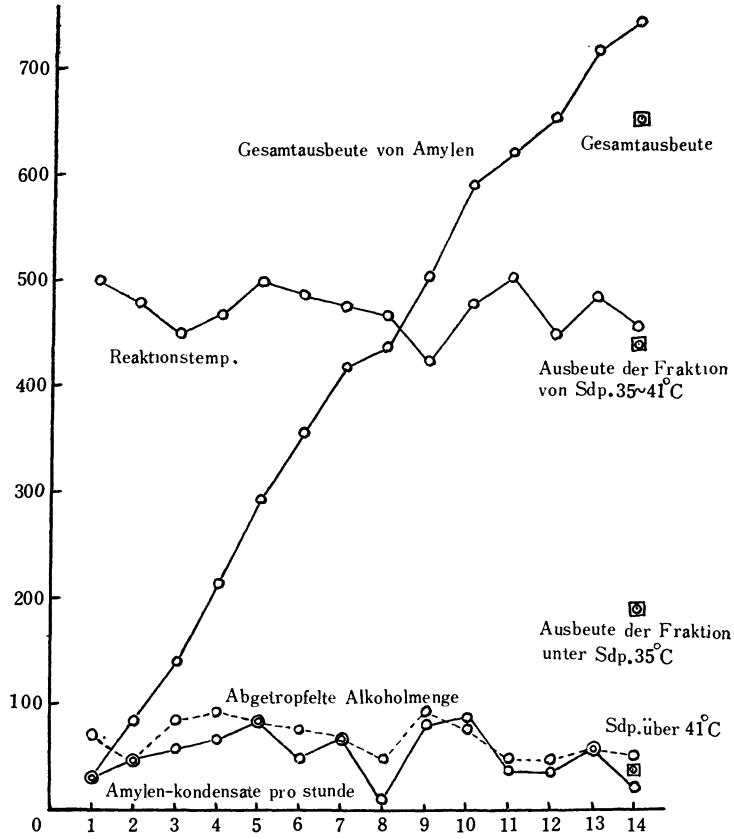



Abb. 3

Versuchsreihennummer 129 Reaktionstemp. 450～499°C

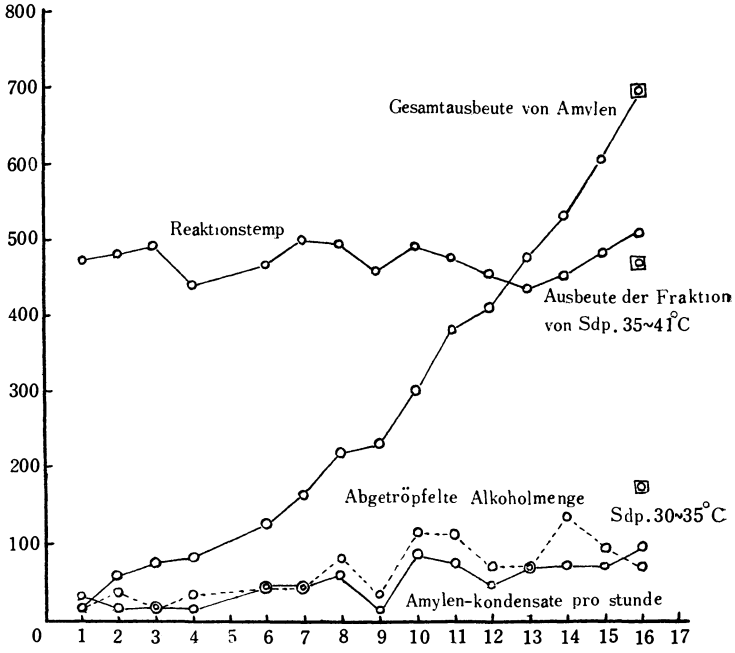



Abb. 4

Versuchsreihennummer 130 Reaktionstemp. 450～510°C

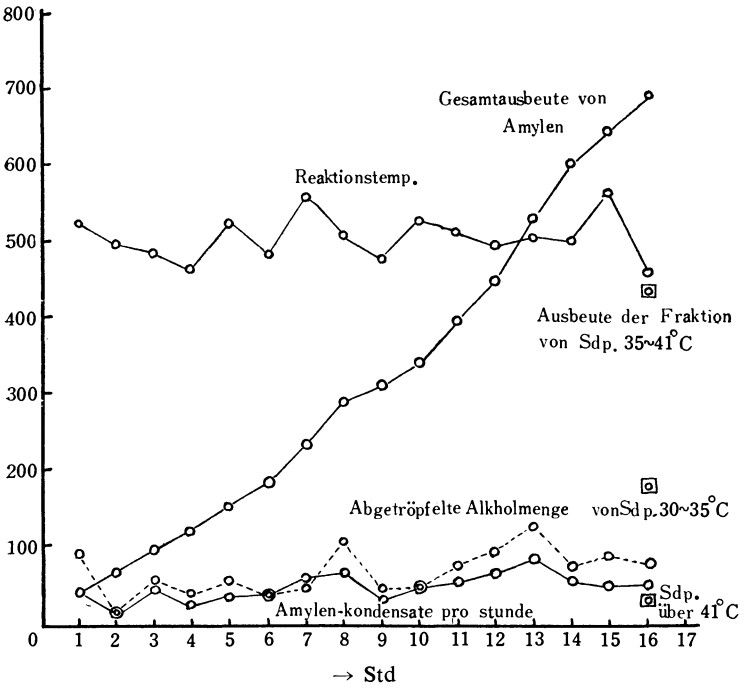



Abb. 5

Versuchsreihennummer 134 Reaktionstemp. 450～540°C

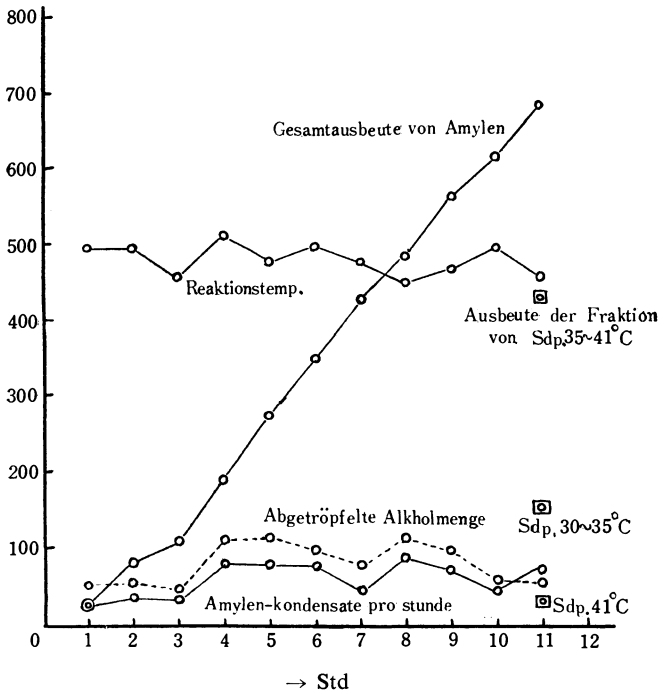



Abb. 6

Versuchsreihennummer 135 Reaktionstemperatur 455～511°C

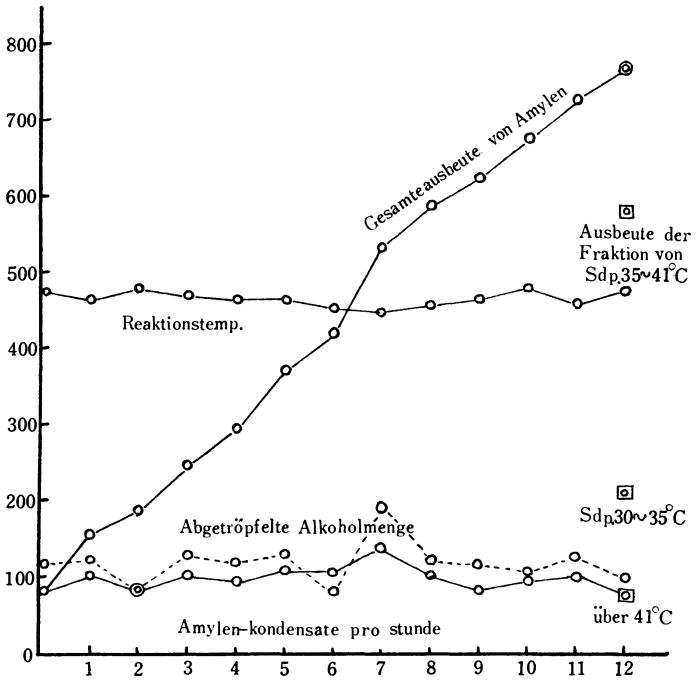



Abb. 7
Versuchsreihennummer 142 Reaktionstemperatur 405~437°C

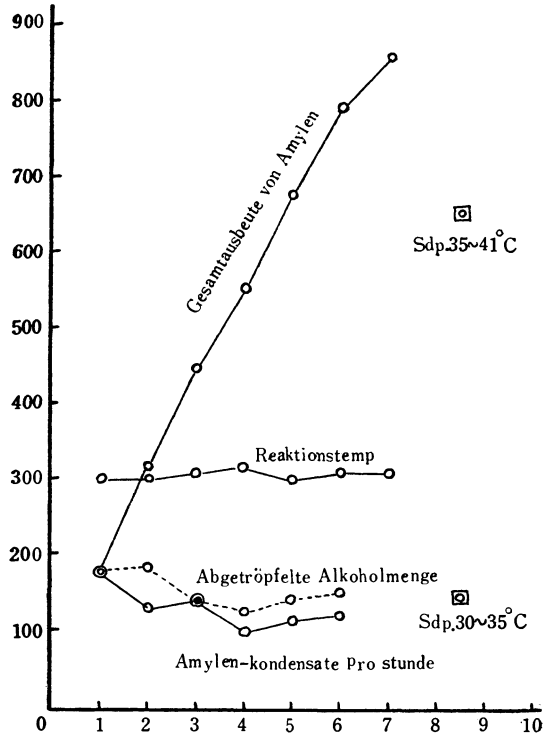



Abb. 8
Versuchsreihennummer 159
Reaktionstemperatur 300~315°C

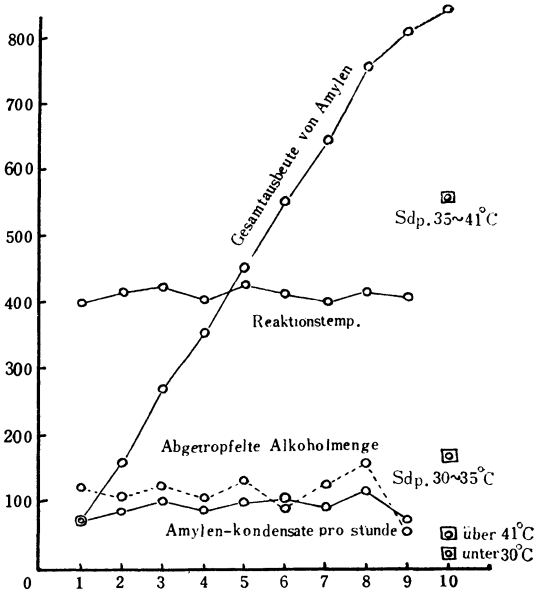



Abb. 9
Versuchsreihennummer 172
Reaktionstemperatur 405~420°C

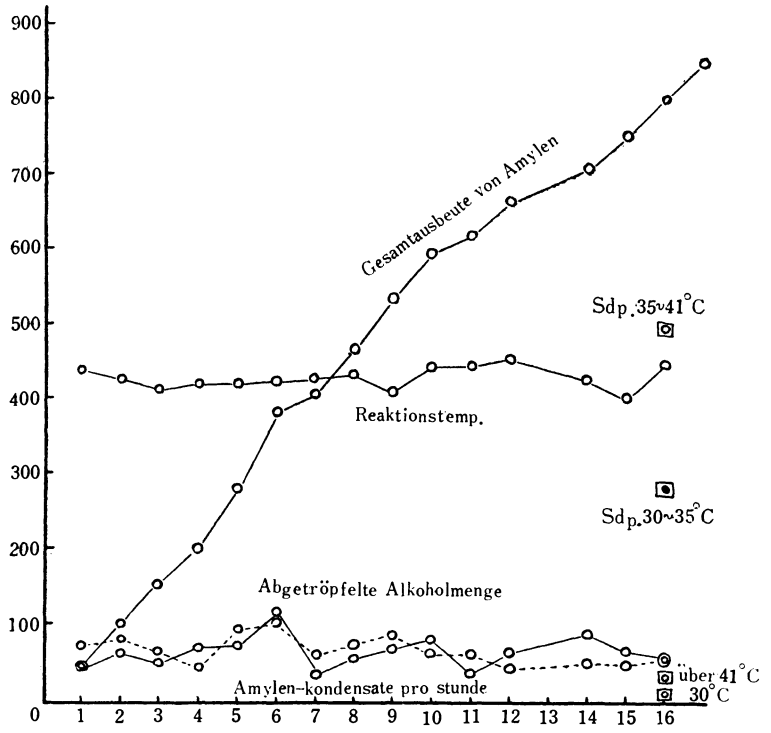



Abb. 10
Versuchsreihennummer 179 Reaktionstemperatur 400~450°C

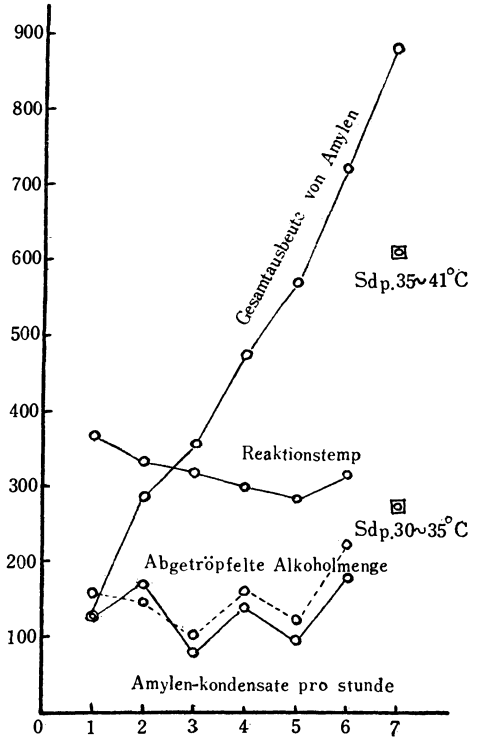



Abb. 11
Versuchsreihennummer 185
Reaktionstemperatur 280~365°C

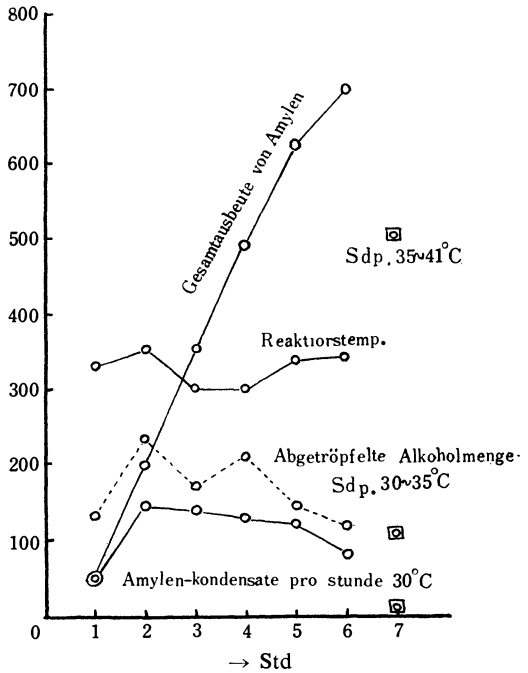



Abb. 12
Versuchsreihennummer 199
Reaktionstemperatur 300~350°C

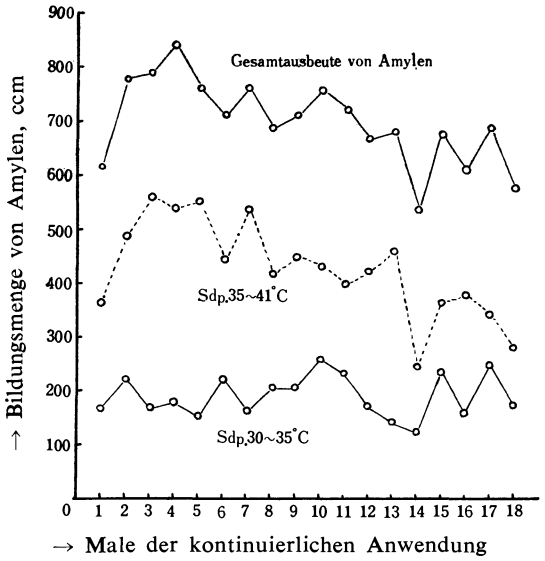



Abb. 13

| | |
|---|---|
| Versuchsreihennummer | 123~140 |
| Dauer der kontinuierlichen Anwendung | 220 |
| Male der kontinuierlichen Anwendung | 18 |
| Katalysator | Nr. 1 |

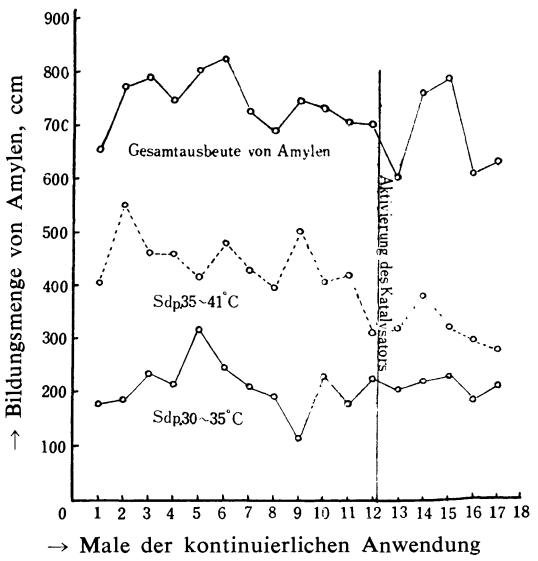



Abb. 14

| | |
|---|---|
| Versuchsreihennummer | 141~157 |
| Dauer der kontinuierlichen Anwendung | 234 |
| Male der kontinuierlichen Anwendung | 17 |
| Katalysator | Nr. 1 |

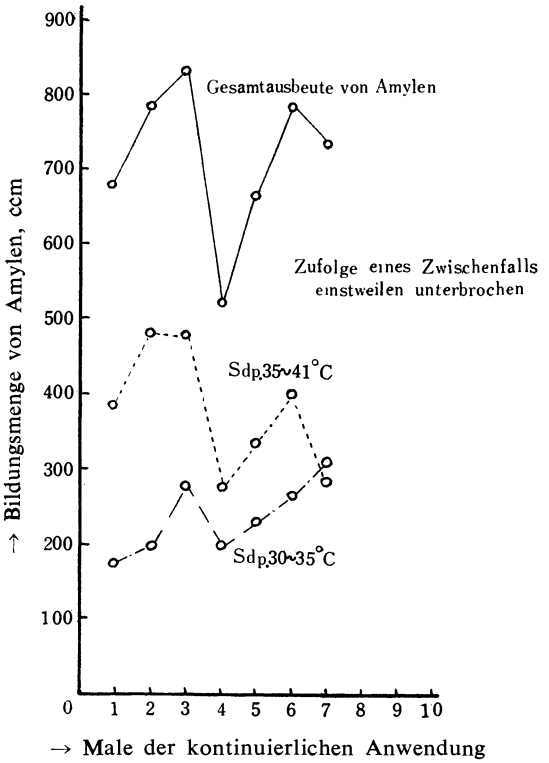



Abb. 15

| | |
|---|---|
| Versuchsreihennummer | 164~170 |
| Dauer der kontinuierlichen Anwendung | 86 |
| Male der kontinuierlichen Anwendung | 7 |
| Katalysator | Nr. 2 |

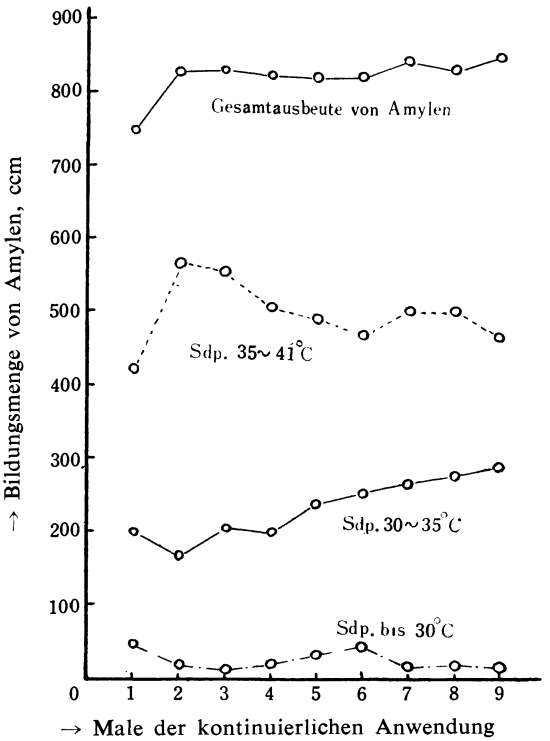



Abb. 16

| | |
|---|---|
| Versuchsreihennummer | 171~179 |
| Dauer der kontinuierlichen Anwendung | 99 |
| Katalysator | Nr. 3 |
| Temperatur | 28~35°C |

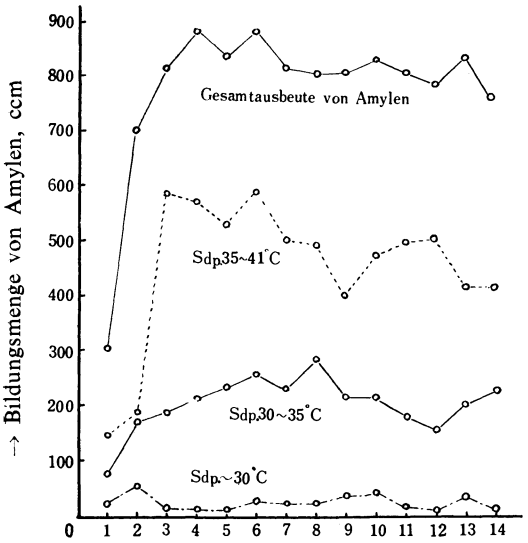



Abb. 17

| | |
|---|---|
| Versuchsreihennummer | 180～193 |
| Dauer der kontinuierlichen Anwendung | 87 |
| Male der kontinuierlichen Anwendung | 14 |
| Katalysator | Nr. 1 |
| Temperatur | 15～23°C |
| Grosses Reaktionsrohr | (122×5.1) |

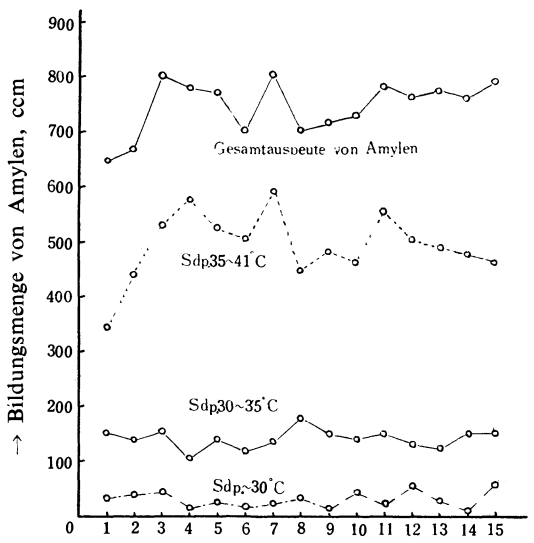



Abb. 18

| | |
|---|---|
| Versuchsreihennummer | 194～208 |
| Dauer der kontinuierlichen Anwendung | 100 |
| Male der kontinuierlichen Anwendung | 15 |
| Katalysator | Nr. 2 |
| Temperatur | 11～19°C |
| Grosses Reaktionsrohr | |

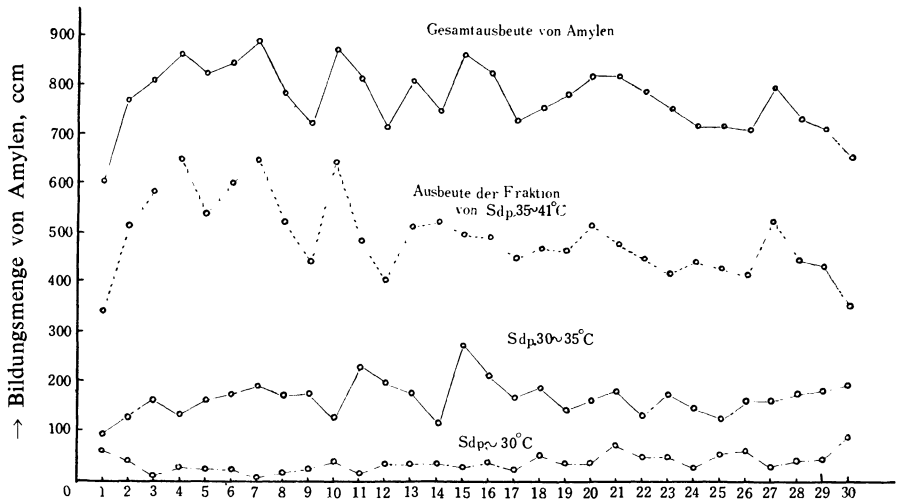



Abb. 19

| | |
|---|---|
| Versuchsreihennummer | 209～238 |
| Dauer der kontinuierlichen Anwendung | 174 |
| Male der kontinuierlichen Anwendung | 30 |
| Katalysator | Nr. 1 |
| Temperatur | 6～13.5°C |
| Grosses Reaktionsrohr | |

unabhängig davon bei der fraktionierten Destillation erhaltenen Sorten von Olefinen wurden auf ein Diagramm gebracht und die mit dem Ablauf der Zeit herlaufende Bildung von Olefinen wurde beobachtet. Dann wurden zwei im Labor anwendbare grösstmögliche Reaktionsröhre wurden für längere Zeit kontinuierlich erfolgende Versuche eingesetzt. Hierbei wurden die Katalysatoren Nr. 1, 2 und 3 (Tabelle V) in Unabhängigkeit voneinander eingesetzt und die Reaktionstemperaturen wurden nur auf drei Bedingungsarten, nämlich 450±30°C, 380 ±30°C und 400±30°C, beschränkt. Und jeweils für 220, 100 und 99 Stunden wurde die Reaktion fortgesetzt. Eine Einsicht in diese Versuchsergebnisse lässt wissen, dass die Bildung von Olefinen beim Einsatz von Katalysator Nr. 3 höchst glatt erfolgt und das Dehydratisierungsvermögen des Katalysators fast nicht nachlässt. Von den gebildeten Amylenen verhält sich die vorwiegend aus Trimethyläthylen bestehende Fraktion bei Sdp. 35～40°C regelmässig und sie ist mengenmässig mehr als die zwei anderen Fraktionen.

TABLE V. DIE ZUSAMMENSETZUNG DER ZINKSULFAT-KATALYSATOREN

| Sorten der Katalysatoren | Zinksulfat, % | Japanische Säureerde, % | Zusatz |
|---|---|---|---|
| Nr. 1 | 30 | 70 | Wasser |
| Nr. 2 | 50 | 50 | Wasser |
| Nr. 3 | 30 | 70 | Ammoniak |

Es lässt sich ausserdem vermuten, dass irgendeines Verhältnis unter diesen Dreien besteht.

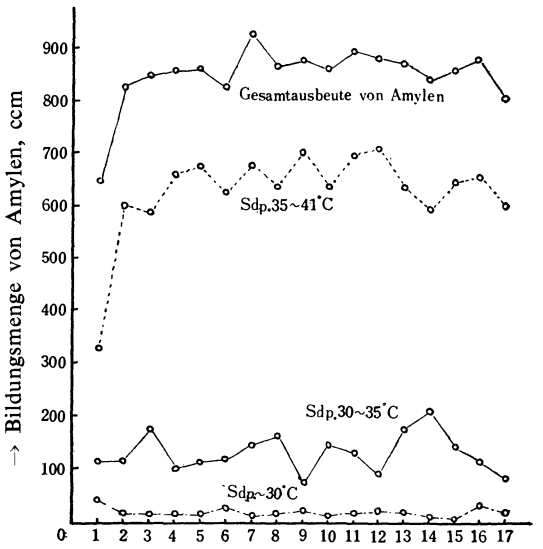



Abb. 20

| | |
|---|---|
| Versuchsreihennummer | 239～255 |
| Dauer der kontinuierlichen Anwendung | 104 |
| Male der kontinuierlichen Anwendung | 17 |
| Katalysator | Nr. 1 |
| Grosses Reaktionsrohr | |
| Temperatur | 5～14°C |

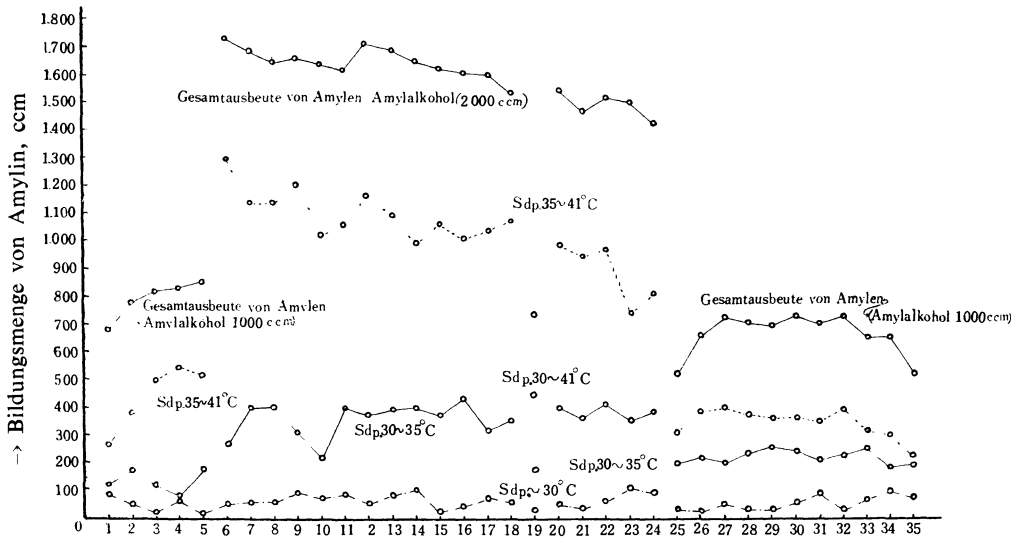



Abb. 21

| | | | |
|---|---|---|---|
| Versuchsreihenummer | 256～290 | Katalysator | Nr. 1 |
| Dauer der kontinuierlichen Anwendung | 246 | Temperatur | 6.5～11.5°C |
| Male der kontinuierlichen Anwendung | 35 | Grosses Reaktionsrohr | (122×5.1) |

Aus der obigen Forschungsarbeit wurden folgende Folgerungen gezogen:

(I) Das Gemisch des Zinksulfates mit der japanischen Säureerde erweist sich für Gewinnung des Trimethyläthylens aus Isoamylalkohol als das beste.

(II) Die Katalysatoren mit drei folgenden Zusammensetzungen wurden in bezug auf Leistungen verglichen. Es wurde gefunden, dass der Katalysator Nr. 3 die besten Ergebnissen aufweist, und dass derselbe Nr. 1 als der nächstbeste in Frage kommt. Der Katalysator Nr. 2 ist als der schlechteste ausgefallen.

Das heisst, bei Zinksulfat ist es unnötig, viel zu verwenden. Mit 30% davon ist es ausreichend. Bei Zusatz geringer verd. Ammoniak werden die besten Ergebnisse erzielt.

(III) Die optimale Reaktionstemperatur liegt bei ca. 400°C. Bei unzweckmässig höherer Temperatur tritt Abbau des Katalysators und weitere unzweckdienliche chemische Änderung mit schlechten Ergebnissen ein.

(IV) Als Katalysator ist solcher in Kugeln mit ca. 8～10 mm Durchmesser angebracht.

(V) Nach Einpackung des Katalysators in Reaktionsrohr ist es nötig, zuerst denselben zur Aktivierung bei ca. 500°C zu erhitzen.

(VI) Die Reaktion soll unter gewöhnlichem Druck erfolgen. Eine Druckerhöhung ist unnötig.

(VII) Als das Reaktionsrohr kann ruhig gewöhnliches Eisen benutzt werden.

(VIII) Der Zinksulfat-Katalysator lässt auch nach einer ununterbrochenen Verwendung keinerlei beachtenswerte Veränderung an der Leistung feststellen. Er hat solche von anderen Katalysatoren nicht erreichbar Haltbarkeit. Es ist somit klar geworden, dass Amylen in der kontinuierlichen Arbeitsweise herstellbar ist.

(IX) Selbst in einem äusserst unglücklichen Fall wird bei dieser Arbeitsweise Isoamylalkohol nur noch um ca. 15% unverändert und immer noch zurückgewonnen. Dies kann nach Trennung von Wasser wiederum ins Reaktionsrohr eingeschickt werden.

## Zusammenfassung

Um die höchst geeigneten Bedingungen zu bestimmen, worunter aus Isoamylalkohol die hauptsächlich aus Trimethyläthylen bestehenden Olefine gewonnen werden, wurden labormässig zulässige grösste Vorrichtung herangezogen und das Zinksulfat Gemisch als Katalysatoren auf ihre Leistungen untersucht. Bei dem Mischverhältnis von 30 : 70 erwies sich das Gemisch des Zinksulfates mit der japanischen Säureerde als das Beste. Auch nach 246 stündigem ununterbrochenem Einsatz wurde noch keinerlei grössere Änderung an seiner katalysatorischen Leistung ermittelt.

Hinsichtlich des vorteilhaften Umstandes, dass die Reaktion unterm Einsatz gewöhnlichen Eisenmaterials bei normalem Druck und dem Temperaturbereich von 350±30°C erfolgt, wurde der Zinksulfat-Katalysator als höchst geeignet für Entwässerung und Isomerisation des Isoamylalkohols beurteilt.

Zum Schluss sei noch davon erwähnt, dass die vorliegende Arbeit der Leistung von Herrn Professor Dr. Eiichi Funakubo an der Technischen Fakultät der Universität zu Osaka verdankt ist.

*Chem. Institut der Techn. Fakultät der Universität zu Osaka Miyakojima-ku Osaka*

# SHORT COMMUNICATIONS

## *On the Influence of Sodium Oxide upon the Crystal Structure of Tricalcium Silicate*

By Goro YAMAGUCHI and Hiroshi UCHIKAWA

(Received August 10, 1961)

The crystal structure of pure $3CaO \cdot SiO_2$ and the solid solution of the system $3CaO \cdot SiO_2$-$Al_2O_3$-MgO, so-called alite, had been determined[1,2]. No results, however, had been reported on the influence of $Na_2O$ upon $3CaO \cdot SiO_2$ and there existed a need for detailed investigation on this system.

In the present paper, the authors describe the results of the investigation on the formation and decomposition of the solid solution of the system $3CaO \cdot SiO_2$-$Na_2O$ and its crystal structure.

Pure $3CaO \cdot SiO_2$ was synthesized by following procedures, that is, the mixtures of alkali free guaranteed reagent of $CaCO_3$ and $SiO_2$ were heated in platinum crucible at 1500°C, then cooled rapidly, pulverized, reheated several times until no free CaO was found. Then various amount of guaranteed reagent of $Na_2CO_3$ were added to $3CaO \cdot SiO_2$ and mixed sufficiently, heated at 1450°C for 30 min. and then cooled rapidly to room temperature.

This procedure was necessary to obtain the well-crystallized $3CaO \cdot SiO_2$-$Na_2O$ solid solution. Chemical compositions, refractive indices and specific gravity of the solid solution of this system are shown in Table I.

X-Ray diffraction pattens of the characteristic peaks at 51～52°C in $2\theta$ corresponding to (220) of Jeffery's trigonal cell[1,2] of the $3CaO \cdot SiO_2$-$Na_2O$ solid solution measured by slow scanning and high resolution are shown in Fig. 1.

These characteristic peaks were triplet until $Na_2O$ content increased to 0.33% and then changed to doublet. Further increase of a $Na_2O$ content made no remarkable change of the X-ray diffraction patterns of the $3CaO \cdot SiO_2$-$Na_2O$ solid solution until 0.71%. More further addition of $Na_2CO_3$ decomposed it into $\beta$-$2CaO \cdot SiO_2$, $Na_2O \cdot CaO \cdot SiO_2$ and free CaO.

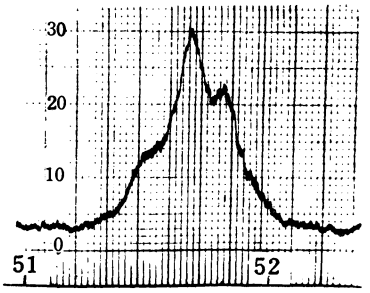



Fig. 1. X-Ray diffraction pattern of the characteristic peak of $3CaO \cdot SiO_2$-$Na_2O$ solid solution (specimen No. 6).

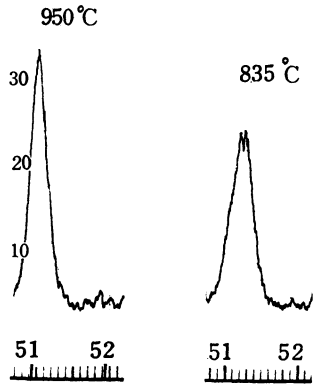



Fig. 2. High temperature X-ray diffraction patterns of the solid solution of the system $3CaO \cdot SiO_2$-$Na_2O$ (specimen No. 6).

The triplet ⇄ doublet change seemed corresponding to triclinic ⇄ monoclinic transition.

In differential thermal analysis, the low $Na_2O$ samples showed two endothermic and exothermic peaks at 900～1000°C corresponding to the reversible transitions of triclinic ⇄ monoclinic ⇄ trigonal, but the high $Na_2O$ (0.3～0.7% of $Na_2O$) samples showed one endothermic and exothermic peak of the monoclinic ⇄ trigonal transition.

In high temperature X-ray diffraction, doublet peaks of the high $Na_2O$ sample changed to singlet at about 900°C as shown in Fig. 2.

From the results of X-ray diffraction and differential thermal analysis, the high $Na_2O$ solid solution was considered to be monoclinic structure. Assuming that this solid solution have Yamaguchi and Miyabe's monoclinic cell[2] corresponding to pseudo-orthorhombic cell

1) J. W. Jeffery, *Acta Cryst.*, 5, 26 (1952).
2) G. Yamaguchi and H. Miyabe, *J. Am. Ceram. Soc.*, 43, 219 (1960).

TABLE I. CHEMICAL COMPOSITION, REFRACTIVE INDICES AND SPECIFIC GRAVITY OF SYNTHESIZED PURE $3CaO \cdot SiO_2$ AND THE SOLID SOLUTION OF THE SYSTEM $3CaO \cdot SiO_2$-$Na_2O$

| | Notation of specimen | $SiO_2$ | CaO | $Na_2O$ | Total | F. CaO | Sp. gr. | Refractive Indices | |
|---|---|---|---|---|---|---|---|---|---|
| | | | | | | | | $\alpha$ | $\gamma$ |
| Pure $3CaO \cdot SiO_2$ | | 26.14 | 73.85 | — | 99.99 | 0.00 | 3.149 | 1.718±0.002 | 1.723±0.002 |
| $3CaO \cdot SiO_2$-$Na_2O$ solid solution | No. 1 | 26.13 | 73.81 | 0.05 | 99.99 | 0.12 | — | — | — |
| | No. 2 | 26.10 | 73.74 | 0.14 | 99.98 | 0.34 | — | — | — |
| | No. 3 | 26.08 | 73.67 | 0.25 | 100.00 | 0.73 | — | — | — |
| | No. 4 | 26.05 | 73.61 | 0.33 | 99.99 | 0.85 | — | 1.717±0.002 | 1.721±0.002 |
| | No. 5 | 26.02 | 73.50 | 0.48 | 100.00 | 1.36 | — | 1.716±0.002 | 1.720±0.002 |
| | No. 6 | 25.97 | 73.34 | 0.71 | 100.02 | 2.92 | — | 1.715±0.002 | 1.718±0.002 |

derived from Jeffery's trigonal cell[1], lattice constants were determined by precise X-ray diffraction as follows:

$a=12.262$ a. u., $b=7.053$ a. u., $c=25.086$ a. u., $\beta=90°07'$.

Calculated value of interplaner spacing from these lattice constants coinside with those obtained by the precise measurement of the diffraction peaks.

By heating for three hours at 1450°C, the monoclinic high $Na_2O$ solid solution released $Na_2O$ and changed into the triclinic low $Na_2O$ solid solution.

The gradual decomposition of $3CaO \cdot SiO_2$ into $2CaO \cdot SiO_2$ and free CaO occurred at about 1250°C was fairly accelerated in the solid solution, compared with that of pure $3CaO \cdot SiO_2$.

The rate of hydration of the solid solution was larger than that of pure $3CaO \cdot SiO_2$.

This solid solution seems significant because alite in commercial portland cement clinker contains a few amount of $Na_2O$ and effect of $Na_2O$ can not be little.

*Department of Applied Chemistry*
*Faculty of Engineering*
*The University of Tokyo*
*Hongo, Tokyo* (*G. Y.*)

*Central Research Laboratory of*
*Onoda Cement Company*
*Toyosu, Tokyo* (*H. U.*)

# *Zur einfachen Bestimmung im Wasser Milliardestelmenge vorhandenen Kupfers(II) durch Anreicherung mit Mikroschicht der Chelatbildungsharze**

Von Masatoshi FUJIMOTO

(Eingegangen am 2. August, 1961)

In einer vorhergehenden Mitteilung[1] wurde eine spezifische „Harztüpfelmethode[2,3]“ zum Nachweise geringer Menge Kupfers(II) mit den Kugeln eines Chelatbildungsharzes, „Dowex A-1 Chelating Resin[4],*1“, vorgeschlagen, dessen Haftgruppe, Iminodiacetat-gruppe, durch starke Chelatbildung mit Kupfer(II) am Rande der Kugeln ohne Zusatz spezifischer Reagens eine charakteristische Himmelblaufarbe liefert. Bei der vorliegenden Arbeit wurde es neu gezeigt, daß beim Durchlaufen einer Wasserprobe, die nur Spurenmenge Kupfers(II) enthalten ist, eine dünne Mikroschicht des genannten Chelatbildungsharzes eine deutliche und der Kupfer-(II)-menge entsprechende Hellgrün- bzw. Blaufarbe annimmt, welche eine eindeutige und leistungsfähige, halbquantitative Analyse der Milliardestelmenge Kupfers(II) an der Wasserprobe ermöglicht.

---

* Mikroanalyse mit Hilfe von Ionenaustauscherharzen. XVIII. (Eine vorläufige Mitteilung für eine Reihe der Untersuchungen über Ultramikroanreicherungsverfahren mit Ionenaustauscherschicht).

1) XVII. Mitteilung der Reihe: M. Fujimoto, Dieses Bulletin, **34**, 1342 (1961).

2) M. Fujimoto, ebenda, **30**, 283 (1957).

3) Zusammensetzung der Daten für Harztüpfelmethode bei M. Fujimoto, *Chemist-Analyst*, **49**, 4 (1960).

4) Vgl. „Dowex A-1 Chelating Resin“, The Dow Chemical Co., Code No. 164-180 (1959); T. Richard und Wm. Rieman III, *Anal. Chim. Acta*, **24**, 202 (1961).

*1 Die Probe des Dowex A-1 Chelatbildungsharzes wurde von Herren Dr. A. J. Barnard, Jr., sowie Dr. J. R. Skidmore gegeben, wofür der Verfasser zum herzlichsten Dank verpflichtet ist.

TABELLE I. RESULTATE DER GEGENWÄRTIGEN ULTRAMIKROSCHÄTZUNG VON KUPFER(II)-GEHALT BEI DEN VERSCHIEDENEN WASSERPROBEN

| Probewasser | | Durchlaufgeschwindigkeit ($\mu$l/Sek) | (cm/Sek) | $V_B$[c] (ml) | scheinbare Farbintensität[d] (nach 500 ml Durchlauf) | Farbton der Harzschicht | ausgeschätzter Kupfer(II)-gehalt |
|---|---|---|---|---|---|---|---|
| Probe-A | | 70 | 0.56 | $\gg$100 | − | blaßgelb | $<4\times10^{-9}$ |
| Probe-B | | 100 | 0.80 | $\simeq$200 | ++ | hell grünlich blau | $\simeq4\times10^{-8}$ |
| Probe-C | | 140 | 1.1 | $\gg$1000 | − | blaßgelb | $<4\times10^{-9}$ |
| Probe-D | | 90 | 0.72 | $\gg$1000 | − | blaßgelb | $<4\times10^{-9}$ |
| 1 | | 70 | 0.56 | $\gg$1000 | − | blaßgelb | |
| 2 | | 70 | 0.56 | >1000 | − | blaßgelb | |
| 4 | $\mu$g Cu(II)[a] | 70 | 0.56 | $\simeq$1000 | ± | blaßgelb ? | |
| 10 | pro 1 | 66 | 0.52 | $\simeq$450 | (+) | hell grünlich gelb | |
| 20 | Liter | 50 | 0.40 | $\simeq$300 | + | hell bläulich grün | |
| 40 | Probe- | 95 | 0.76 | $\simeq$200 | ++ | hell grünlich blau | |
| 100 | wassers | 100 | 0.80 | $\simeq$75 | ++ | grünlich blau | |
| 200 | | 60 | 0.48 | $\simeq$40 | +++ | intensiv grünlich blau (himmelblau) | |
| 10[b] | | 3.2 | 0.14 | $\simeq$80 | + (nach 80 ml Durchlauf) | hell grünlich gelb | |

Probe-A: durch UNIBED-Austauschersäule entionisiertes Wasser; B: mit einem Messingapparat destilliertes Wasser; C: mit Schliffglasapparat umdestilliertes Wasser; D: Trinkwasser aus Wasserleitung. a Umkristallisiertes Kupfersulfat wurde mit dem entionisierten Wasser versetzt. b Es wurde hier eine Kapillarharzschicht wie Abb. 1-c angewandt, wobei starker Einfluß der Durchlaufgeschwindigkeit auf die Färbung der Harzschicht beobachtet wurde. c Ein Volumen des Wassers, nach dessen Durchlauf erste Grünfarbe an den Harzkugeln in der Schicht sicher erkennbar wird. d −: nicht erkennbar, ±: unsicher, (+): schwach, +: sicher, ++, +++: intensiv.

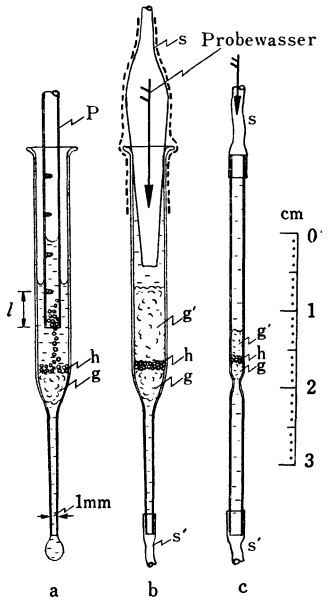



Abb. 1 Mikroharzschicht zur Anreicherung kleinster Menge der Ionen.

Man dreht ein Glasröhrchen 4 mm im Durchmesser und 3 bis 5 cm lang wie Abb. 1 aus[5], und verstöpft dieses etwa 5 mm lang mit einer Watte der feinsten Glaswolle g. Dann läßt man darauf gerade 10 $\mu$l der genannten Harzkugeln (50-100 mesh und in der Ammoniumform) mit entionisiertem Wasser zusammen mittels einer vorher je 10 $\mu$l eingeteilten Kapillarpipette P*[2] absinken.

Man packt locker andere Glaswolle g' um etwa 5-10 mm lang gerade auf diese Harzschicht h wie Abb. 1-b ein. Man steckt einen gereinigten, feinen Polyäthylenschlauch*[3] s ins Probewasser ein und läßt dieses mit Hilfe eines Aspirators durch die obenerwähnte Harzschicht h und den Schlauch s' mit mäßiger Geschwindigkeit durchfließen*[4]. Je 10 bzw. 100 ml Durchlaufen des Probewassers beobachtet man die Färbung an der Harzschicht h unter Vergrößerung mit einer Lupe. Tabelle I zeigt die einigen Beispiele über verschiedene Wasserproben ausgeführter Bestimmungen.

5) Vgl. M. Fujimoto, Dieses Bulletin, **29**, 595 (1956).

*2 Aus der einem Tropfen (etwa 0.04 ml) entionisierten Wassers entsprechenden Länge der Kapillarpipette kann man die gerade 10 $\mu$l-Gehalt entsprechende Länge ($l$) leicht bestimmen.

*3 Einen feinen Polyäthylenschlauch von beliebigem Durchmesser kann man aus einem Schlauche 1 cm im Durchmesser leicht ausdrehen, indem man diesen über einer kleinen Flamme eines Brenners bis zur anscheinenden Durchsichtigkeit gelind erhitzen läßt, und diesen etwas weichenden Schlauch langsam und stark bis zum gewünschten Durchmesser auszieht und im kalten Wasser rasch erstarren läßt.

*4 Anwendung des Wasserdrucks an Stelle des Absaugens zum Durchlaufen des Probewassers ermöglicht noch einfache Anreicherung, worüber der Verfasser zur Zeit noch eingehenden Versuch durchführt.

Die oben mit einem Chelatbildungsharze ausgeführte Ultramikroanreicherungsmethode für außerordentlich verdünnten Bestandteil sei dadurch bis zur noch niedrigen Konzentration wie Billionstel oder weniger ($<10^{-12}$) erfolgreich zu erweitern, daß man, unter genau regulierter Durchlaufgeschwindigkeit der Flüssigkeit, verschiedenartige Adsorptionsmittel, z. B., Kationen- oder Anionenaustauscher sowie anorganische Austauscher, mit empfindlichsten und spezifischen Reagenzien zusammen verwendet. Der Verfasser führt darüber eine Reihe der Untersuchungen aus, die später genau berichtet werden.

*Laboratorium für analytische Chemie*
*Chemisches Institut der wissenschaftlichen Fakultät*
*Universität Tokyo*
*Tokyo, Hongo*

## *Experimental Evidence for the Theoretical Condensation Isotherm on Spheres Arranged in the Closest Packing*

By Izumi HIGUCHI, Yataro USHIKI and Reiko SUZUKI

(Received August 3, 1961)

One of the contentions of the capillary condensation theory is that the shape of isotherms in the range of high relative pressure is determined by the pore distribution of the sorbent. Hitherto, however, we have not known any process to control precisely the pore distribution of sorbent in its preparation. Therefore the contention seems to have no experimental evidence.

In the former report[1,2] one of us calculated three types of theoretical capillary condensation isotherms which were given by spheres of the sorbent when they were arranged linearly, or two dimensionally, or in the closest packing. A number of experimental isotherms given by corpuscular sorbents, consisting of non-porous particles, exhibited unquestionably the capillary condensation in the range of relative pressure, which was anticipated from the theory and the size of particles, arranged in the two dimensional closest packing. If we can get a corpuscular sorbent of which packing type is previously known, the theoretical condensation isotherms will be confirmed experimentally. Experimental isotherms of benzene and methanol at 0°C on the porous Vycor glass are shown in Figs. 1 and 2. The shape of sorption and desorption isotherms are very similar to what we can theoretically obtain for the corpusclar sorbent if the elementary spheres are arranged in the closest packing. Porous Vycor glass, considering from its preparation process and

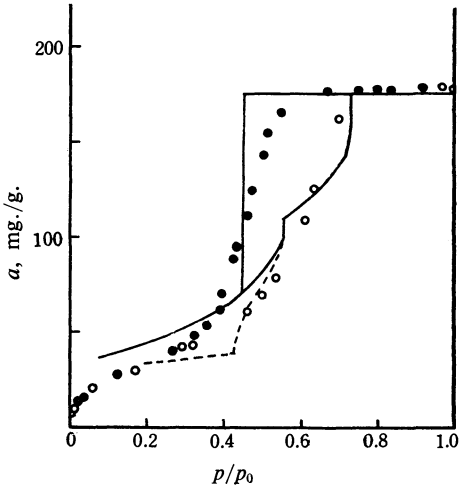



Fig. 1. Sorption isotherm of benzene at 0°C on porous Vycor glass. Circles, sorption data; solid circles, desorption data; the solid line, the theoretical condensation isotherm; the dotted line, the theoretical one, taking into account the vapor pressure correction.

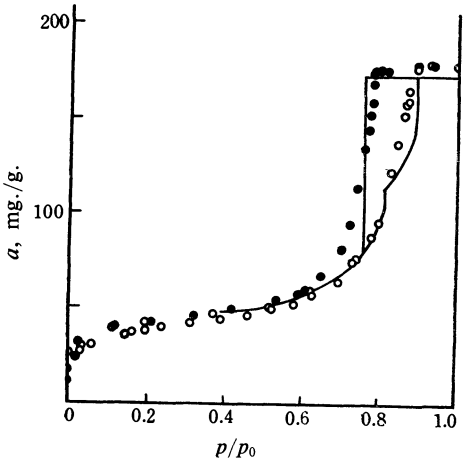



Fig. 2. Sorption isotherm of methanol on porous Vycor glass at 0°C. Circles, sorption data; solid circles, desorption data; the solid line, the theoretical condensation isotherm.

1) I. Higuchi and H. Utsugi, *J. Chem. Phys.*, **20**, 1180 (1952).
2) I. Higuchi and H. Utsugi, *Sci. Repts. Tohoku Univ. Ser. I*, **36**, 27 (1952); *J. Chem. Soc. Japan, Pure Chem. Sec. (Nippon Kagaku Zasshi)*, **73**, 395, 397 (1952).

its hardness, seems to be the most suitable sorbent which is idealized to be consisting of spherical silica particles arranged in the closest packing. The average diameter of elementary particles assumed to be spherical can be calculated from BET area, which is obtained experimentally with benzene isotherm. Then, theoretical condesation isotherms for benzene or methanol can be calculated from the $V(y)$-$y$ relation given in the previous report[2], wherein $V(y)$ denotes the condensed liquid volume per the unit volume of sorbent and $y$ is the radius of curvature of the condensed liquid surface divided by the radius of spherical particles.

The theoretical ones, exhibited by solid lines in the figures, are in good agreement with the experimental values. This is a more satisfactory agreement than expected, because the packing model used in the calculation is quite an idealized one.

From the success mentioned above, we can draw a number of important conclusions for the sorption phenomena : (1) The structure of porous Vycor glass is idealized to be consisting of almost spherical particles arranged in the closest packing. (2) Both sorption and desorption isotherms in the range of high relative pressure are due to the capillary condensation of the sorbate. (3) Kramer-McBain mechanism for the hysteresis[3] in isotherms is confirmed experimentally to be very reasonable.

Both works of Barrer et al[4]. and Kiselev et al.[5] seem to be excellent extensions from the similar standpoint for the capillary condensation theory and hysteresis mechanism. Barrer et al. calculated various theoretical condensation isotherms for a number of single pores different in their shapes and gave a reasonable formula to compute the isotherm for the contact zone between spheres. According to our precise numerical estimations, it is not adequate to calculate the condensed liquid volume between contact spheres by their scheme because the difference in volume between their model and ours is so minor as to be practically negligible. On the other hand, calculations of vapor pressure of the sorbate by our approximation using the usual Thomson equation is rather serious for the linear packing of spheres. Fortunately, however, it is not so serious, as mentioned previously[2] for the closest packing wherein true two dimensional concave meniscus is prevalent between spheres. The correction for this effect is shown by the dotted line in Fig. 1, indicating that our approximation adapted previously may not essentially influence the theory.

The authors gratefully express their appreciation to Dr. Goodman in Corning Glass Corp. and Dr. A. T. Ree for the donation of porous Vycor glass.

*College of Arts and Sciences*
*Tohoku University*
*Sendai*

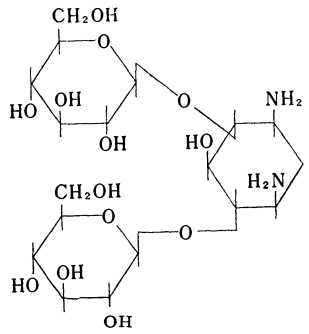
3) J. W. McBain, *J. Am. Chem. Soc.*, 57, 691 (1935).
4) R. M. Barrer, N. McKenzie and J. S. S. Reay, *J. Coltoid Sci.*, 11, 479 (1957).
5) A. P. Karnaukhov, and A. V. Kiselev, *Zhur. Fiz. Khim.*, 31, 3635 (1957); *Chem. Abstr.*, 52, 5928 (1958).

## *Synthesis of 4,6-Di-(D-glucopyranosyl)-deoxystreptamine*

By Sumio UMEZAWA and Yukio ITO

(Received August 9, 1961)

Recently, it has been shown that a essential group for antibiotic character of neomycin[1], kanamycin[2] and paromomycin[3] belongs to the glucosides of deoxystreptamine, however, synthesis of the allied glucosides has not been reported as yet*. In continuation of our work[2d] on kanamycin, we have synthesized 4, 6-di-(β-D-glucopyranosyl)deoxystreptamine (IV).




1) F. A. Kuehl, M. N. Bishop and K. Folkers, *J. Am. Chem. Soc.*, **73**, 881 (1951); K. L. Rinehart and P. W. K. Woo, ibid., **83**, 643 (1961).

2) a) H. Umezawa, K. Maeda, M. Murase and H. Mawatari, *J. Antibiotics (Japan), Ser. A*, **11**, 163 (1958). b) M. J. Cron, O. B. Fardig, D. L. Johnson, D. F. Whitehead, I. R. Hooper and R. U. Lemieux, *J. Am. Chem. Soc.*, **80**, 4115 (1958). c) H. Ogawa, T. Ito, S. Kondo and S. Inoue, *J. Antibiotics (Japan), Ser. A*, **11**, 169 (1958); *Bull. Agr. Chem. Soc. Japan*, **23**, 289 (1959). d) S. Umezawa, Y. Ito and S. Fukatsu, *J. Antibiotics (Japan), Ser., A*, **11**, 162 1958); This Bulletin, **32**, 81 (1959).

3) T. S. Haskell, J. C. French and Q. R. Bartz, *J. Am. Chem. Soc.*, **81**, 3483 (1959).

* It should be noted that a related compound, *O*-(β-D-2-amino-2-deoxyglucopyranosyl) derivative of *d, l-trans*-2-aminocyclohexanol was synthesized: T. Suami and S. Umezawa, This Bulletin, to be published.

Addition of excess carbobenzoxychloride in toluene to an aqueous solution of deoxystreptamine made alkaline with sodium hydroxide gave, in 48% yield, *N*, *N'*-dicarbobenzoxydeoxystreptamine (I), m. p. 233~235°C. Found: C, 62.06; H, 6.23; N, 6.55. Calcd. for $C_{22}H_{26}O_7N_2$: C, 61.38; H, 6.09; N, 6.51%.

*N*, *N'*-Dicarbobenzoxydeoxystreptamine (I) failed to react with acetobromoglucose in benzene, chloroform, dioxane or dimethylformamide, however, it has been found that the condensation proceeded in nitromethane. To a suspension of I (1.63 mmol.) in nitromethane was added acetobromoglucose (5.35 mmol.) and powdery mercuric cyanide (5.5 mmol) and the suspension was stirred for twenty-four hours at 27°C. Extraction with chloroform followed by evaporation of the solvent gave a crude product, which was recrystallized from absolute ethanol to afford, in 76% yield, *N*, *N'*-dicarbobenzoxy-4, 6-di-(tetraacetyl-D-glucosyl) deoxystreptamine (II), m. p. 253~254°C, $[\alpha]_D^{17.5}$ −9.6° (*c* 1.965, chloroform). Found: C, 54.83; H, 5.53; N, 2.85. Calcd. for $C_{50}H_{62}O_{25}N_2$: C, 55.05; H, 5.73; N, 2.57%.

Infrared spectrum: $\nu_{max}^{Nujol}$ 3480, 3340 (OH, NH); 1760 (acetyl C=O); 1700 (C=O in $OCOCH_2C_6H_5$); 1520 (CONH); 1220; 1160, 1075 (glucoside); 1035 (alicyclic secondary alcohol); 903 (β-glucoside); 733, 695 (monosubstituted benzene).

Hydrolysis of II (1.0 g.) with methanolic ammonia at room temperature followed by evaporation in vacuo and washing with ethyl acetate gave a crude product, which was recrystallized from water-dioxane-ethanol (5: 1: 10) to afford colorless needles (0.38 g.) of *N*, *N'*-dicarbobenzoxy-4,6-di-(D-glucosyl) deoxystreptamine (III), m.p. 288~290°C (decomp.), $[\alpha]_D^{17.5}$ −5.67° (*c* 1.43, pyridine). Found: C, 54.16; H, 6.06; N, 3.81. Calcd. for $C_{34}H_{46}N_2O_{17}$: C, 54.11; H, 6.14; N, 3.71%. Infrared spectrum: $\nu_{max}^{Nujol}$ 3350, 1700, 1545, 1295, 1230, 1165, 1075, 1035, 890, 735, 695 $cm^{-1}$.

Hydrogenolysis of III (0.5 g.) with palladium catalyst in water-dioxane (1:1) followed by evaporation in vacuo and washings with dioxane, ether and ethanol gave a crude product, which was recrystallized from water-ethanol to afford colorless crystals of 4,6-di-(β-D-glucosyl) deoxystreptamine (IV), $[\alpha]_D^{20}$ −4.69° (*c* 1.01, water). The product darkened and decomposed at about 190~230°C. Found: C, 43.91; H, 7.26; N, 5.37. Calcd. for $C_{18}H_{34}O_{13}N_2$: C, 44.43; H, 7.06; N, 5.76%. Infrared spectrum: $\nu_{max}^{Nujor}$ 3340, 1600 ($NH_2$), 1165, 1075, 1035, 890 $cm^{-1}$.

The positions of attachment of two D-glucoses to deoxystreptamine was substantiated by periodate oxidation of 4, 6-di-(tetraacetyl-D-glucosyl) deoxystreptamine diacetate (V), which was obtained by hydrogenolysis of II with palladium catalyst in dioxane-acetic acid -water. The compound decomposed at about 270°C (darkening at about 180°C). Found: C, 48.62; H, 6.46; N, 3.14. Calcd. for $C_{34}H_{50}N_2O_{21}\cdot 2CH_3CO_2H$: C, 48.40; H, 6.21; N, 2.97%.

Upon oxidation with sodium periodate in aqueous 50% dioxane for twenty-nine hours, V did not consume the oxidant, while, in parallel experiments, methyl α-D-glucoside and β-pentaacetyl-D-glucose consumed 1.97 and 0.1 mol. of the oxidant respectively. The glucosidic linkages in III or IV are therefore on C-4 and C-6 of deoxystreptamine.

Infrared spectra of the products (III, IV) showed absorption at 890 $cm^{-1}$ which is characteristic of β-glucosidic linkage, Moreover, a rough calculation** of the anomeric contribution (A) of the glucosidic linkages in IV gave a negative value (−13141), the presence of two β-linkages being suggested.

The structure of IV has a close resemblance to that of kanamycin, however, there is a characteristic difference regarding the configuration of anomeric carbon atoms. IV showed no antibiotic activity. The syntheses of allied compounds containing α-linkages of amino sugars are in progress.

The authors are indebted to Mr. S. Nakada for the microanalyses.

*Department of Applied Chemistry*
*Faculty of Engineering*
*Keio University, Tokyo*

** By substitution of 2B (24000) of D-glucose into the equation $[M]_D = 2A+2B$: $-2281 = 2A+24000$.

## *Effect of Impurities on the $^{81}Br$ Quadrupole Resonance in p-Dibromobenzene*

By Juro MARUHA, Jun KOIZUMI, Masahiko SUHARA and Tokuzo TONOMURA

(Received September 6, 1961)

Some investigations have been done concerning the effect of impurities on the nuclear quadrupole resonance absorption of $^{35}Cl$ in molecular crystals[1,2]. In particular Monfils

1) See for instance: J. Duchesne, "Advances in Chemical Physics", Vol. II, Ed. by I. Prigogine, Interscience Publishers, Inc., New York (1959), p. 190.
2) S. Kojima, S. Ogawa, M. Minematsu and M. Tanaka, *J. Phys. Soc. Japan*, **13**, 446 (1958).

and Grosjean derived an equation for the line height ($I$) of the absorption curve as follows[3]:

$$I = I_0 \exp(-NC) \qquad (1)$$

where $C$ is the concentration of impurity, and $N$, a "characteristic number", represents the number of resonant nuclei per impurity molecule whose resonance have been perturbed so they can no longer contribute to the central portion of the line. The main effect of impurity was considered the lattice defect due to the volume difference between the resonant atom and the substituted one[1,2]. For bromine compound, however, only one investigation has been reported. Dreyfus and Dautreppe studied the intensity of the resonance line of $^{79}Br$ in $p$-dibromobenzene[4]. The present paper contains the study of the effect of impurities on the resonance line of $^{81}Br$ in $p$-dibromobenzene.

The spectrometer used was similar one reported by Kojima[5]. The intensity of resonance line war observed with a video amplifier and an oscilloscope. The frequency of the resonace was about 224 Mc/sec. Samples are carefully purified and mixed, then sealed into glass tubes. The mixed sample in each tube was melted and crystallized slowly by standing overnight. The tube containing the mixed crystal was placed in a r-f coil of the spectrometer. All the measurements were carried out at 4±1°C, hence $p$-dibromobenzene exists in the $\alpha$-phase.

The results are shown in Fig. 1, graphically. In each case plots of log ($I/I_0$) vs. $C$ is not a single straight line but is nearly hyperbolic. If a linear relation is assumed in the small impurity region, the characteristic number is calculated according to Eq. 1, from the slope. These values are listed in Table I. The values

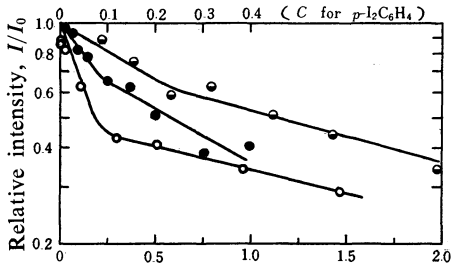



Fig. 1. Variation of relative intensities with concentration of impurities.
◒ $p$-$BrC_6H_4Cl$ ● $p$-$I_2C_6H_4$ ○ $p$-$Cl_2C_6H_4$

obtained for $p$-dichlorobenzene and $p$-diiodobenzene are not consistent with the Dreyfus and Dautreppe's values. In their experiment log ($I/I_0$) decreases linearly with $C$ over wide concentration range for the above two cases, whereas it is hyperbolic for the case of $p$-bromochlorobenzene, and they considered the latter is an exceptional case. On the contrary Kojima et al. showed in their experiment concerning the $^{35}Cl$ resonance[2] that the results are always hyperbolic, as we obtained. Thus the results of Dreyfus and Dautreppe are considered to be dubious.

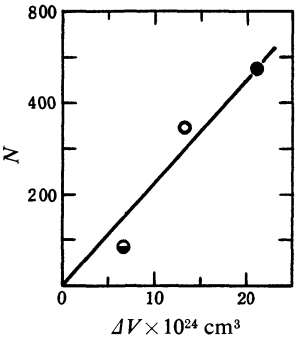



Fig. 2. Relation between characteristic number and volume difference.
● $p$-$I_2C_6H_4$ ○ $p$-$Cl_2C_6H_4$ ◒ $p$-$BrC_6H_4Cl$

TABLE I. CHARACTERISTIC NUMBER AND VOLUME DIFFERENCE

| Impurity molecule | $N$ | $\Delta V$ ($10^{-24}$ cm$^3$) | $N'$[a] |
|---|---|---|---|
| $p$-$BrC_6H_4Cl$ | 82 | − 6.63 | — |
| $p$-$Cl_2C_6H_4$ | 348 | −13.26 | 32 |
| $p$-$I_2C_6H_4$ | 475 | +21.14 | 80 |

a) Dreyfus and Dautreppe's value.

The relation between the characteristic number ($N$) and the volume difference ($\Delta V$) is shown in Fig. 2, and can be expressed by

$$N = k\Delta V \qquad (2)$$

where $k$ is $22.5 \times 10^{24}$ cm$^{-3}$. Compared with the corresponding results for chlorine compounds[6], it may also be true for the bromine compound that the main effect of impurity is attributed to the volume difference between the Br atom and the substituted one.

*Department of Chemistry*
*Faculty of Science*
*Kanazawa University*
*Sengoku-cho, Kanazawa*

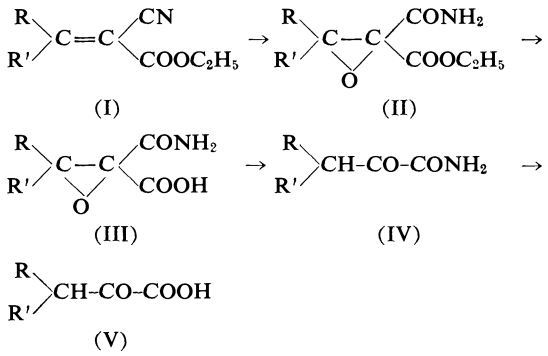
3) A. Monfils and D. Grosjean, *Physica*, **22**, 541 (1956).
4) B. Dreyfus and D. Dautreppe, *Compt. rend.*, **243**, 1517 (1956).
5) S. Kojima, K. Tsukada, K. Shimauchi and A. Hinaga, *J. Phys. Soc. Japan*, **9**, 795 (1954).
6) R. E. Michel and R. D. Spence, *J. Chem. Phys.*, **26**, 954 (1957).

## *Syntheses of α-Keto Amides and Acids from Ethyl Alkylidenecyanoacetate*

By Minoru IGARASHI and Hiroshi MIDORIKAWA

(Received September 9, 1961)

The present paper deals with a novel preparation of α-keto amides and acids from ethyl alkylidenecyanoacetate as starting material. The synthetic steps are shown in the following scheme.




Payne and Williams[1] have shown that α, β-unsaturated acids such as crotonic and maleic

TABLE I. PREPARATION OF EPOXYAMIDE II FROM ETHYL ALKYLIDENECYANOACETATE (I)

$RR'C(O)C(CONH_2)COOEt$

| R | R' | M. p., °C | Yield, % | Formula | Calcd. C | Calcd. H | Calcd. N | Found C | Found H | Found N% |
|---|---|---|---|---|---|---|---|---|---|---|
| Methyl | Methyl | 101 | 61 | $C_8H_{13}O_4N$ | 51.33 | 7.00 | 7.48 | 50.89 | 6.53 | 7.45 |
| Methyl | Ethyl | 77 | 80 | $C_9H_{15}O_4N$ | 53.72 | 7.51 | 6.96 | 53.28 | 7.45 | 7.01 |
| Methyl | Isobutyl | 69 | 71 | $C_{11}H_{19}O_4N$ | 57.62 | 8.35 | 6.11 | 57.37 | 8.01 | 6.15 |
| Methyl | Hexyl | 88 | 64 | $C_{13}H_{23}O_4N$ | 60.98 | 9.01 | 5.44 | 60.62 | 8.78 | 5.42 |
| Propyl | Propyl | 99 | 50 | $C_{12}H_{21}O_4N$ | 59.24 | 8.70 | 5.76 | 58.85 | 8.40 | 5.84 |
| Methyl | Phenyl | 91 | 70 | $C_{13}H_{15}O_4N$ | 62.64 | 6.07 | 5.62 | 62.40 | 6.01 | 5.59 |
| Cyclohexyl | | 111 | 65 | $C_{11}H_{17}O_4N$ | 58.13 | 7.54 | 6.16 | 58.23 | 7.45 | 6.07 |
| Cyclopentyl | | 123 | 75 | $C_{10}H_{15}O_4N$ | 56.32 | 7.09 | 6.57 | 55.99 | 6.83 | 6.53 |

TABLE II. PREPARATION OF α-KETOAMIDE IV FROM III

$RR'CHCOCONH_2$

| R | R' | M. p., °C | Yield, % | Formula | Calcd. C | Calcd. H | Calcd. N | Found C | Found H | Found N% |
|---|---|---|---|---|---|---|---|---|---|---|
| Methyl | Methyl | 112 | 50 | $C_5H_9O_2N$ | 52.16 | 7.88 | 12.17 | 51.89 | 7.77 | 11.99 |
| Methyl | Ethyl | 71 | 52 | $C_6H_{11}O_2N$ | 55.79 | 8.58 | 10.85 | 55.81 | 8.59 | 10.85 |
| Propyl | Propyl | 63 | 80 | $C_9H_{17}O_2N$ | 63.13 | 10.00 | 8.18 | 62.84 | 9.49 | 8.20 |
| Methyl | Phenyl | 116 | 64 | $C_{10}H_{11}O_2N$ | 67.78 | 6.26 | 7.91 | 67.53 | 6.11 | 7.84 |
| Cyclohexyl | | 120 | 48 | $C_8H_{13}O_2N$ | 61.91 | 8.44 | 9.03 | 62.07 | 8.18 | 9.02 |
| Cyclopentyl | | 144 | 40 | $C_7H_{11}O_2N$ | 59.55 | 7.85 | 9.92 | 59.37 | 7.62 | 9.91 |

TABLE III. PREPARATION OF α-KETO ACID V FROM III

$RR'CHCOCOOH$

| R | R' | M. p., °C (B. p., °C/mmHg) | Yield, % | Oxime M. p., °C | Oxime Formula | Oxime Calcd. N | Oxime Found N% |
|---|---|---|---|---|---|---|---|
| Methyl | Ethyl | 40 (82~84/18) | 75 | 164 | $C_6H_{11}O_3N$ | 9.65 | 9.51 |
| Methyl | Isobutyl | 89 (140~143/7) | 80 | 132 (decomp.) | $C_8H_{15}O_3N$ | 8.09 | 8.03 |
| Methyl | Hexyl | (126~129/8) | 92 | 90 (decomp.) | $C_{10}H_{19}O_3N$ | 6.96 | 6.81 |
| Propyl | Propyl | (145~148/7) | 80 | 144 (decomp.) | $C_9H_{17}O_3N$ | 7.48 | 7.33 |
| Methyl | Phenyl | 53 | 90 | 120 (decomp.) | $C_{10}H_{11}O_3N$ | 7.25 | 7.02 |
| Cyclohexyl | | 50 | 98 | 170 | $C_8H_{13}O_3N$ | 8.18 | 8.18 |
| Cyclopentyl | | 54 | 60 | 131 (decomp.) | $C_7H_{11}O_3N$ | 8.91 | 8.92 |

1) G. B. Payne and P. H. Williams, *J. Org. Chem.*, **24**, 54 (1959).

acids are efficiently epoxidized with hydrogen peroxide using sodium tungstate as catalyst, and Payne[2] has also established that ethyl isopropylidenecyanoacetate is converted to the corresponding epoxyamide by the use of hydrogen peroxide and sodium hydroxide.

In the present work, ethyl alkylidenecyanoacetate was epoxidized at 70~80°C in ethanol containing 30% hydrogen peroxide and sodium tungstate dihydrate. The resulting epoxyamide II reacted with alcoholic alkali at room temperature to give the compound III. Decarboxylation and rearrangment of III to α-ketoamide IV was readily accomplished by heating with a small amount of water. Further, the treatment of III and IV with dilute hydrochloric acid affored α-keto acid V in a good yield. The compounds IV and V formed the corresponding oximes. The compounds which were prepared by this process are listed in Tables I–III.

The method appears to be generally applicable in the synthesis of α-keto amide and acid.

Details of this study will be published elsewhere.

The authors wish to express their sincere thanks to Dr. Taro Hayashi and Dr. Tatsuo Takeshima for their kind advice.

*The Institute of Physical and Chemical Research*
*Komagome, Bunkyo-ku, Tokyo*

2) G. B. Payne, ibid., 26, 654 (1961).

## *Rhodium-Platinum Oxide as a Catalyst for the Hydrogenation of Organic Compounds. II*[1]. *Catalyst Preparation and Effects of Platinum in Rhodium-Platinum Oxide*

By Shigeo NISHIMURA

(Received September 20, 1961)

It was reported previously[1-3] that rhodium-platinum(3 : 1) oxide prepared exactly in the same way as Adams platinum oxide is easily reduced with hydrogen to the metals at the ordinary temperature and pressure and that the resulting rhodium-platinum black is an excellent catalyst retaining the nature of a pure rhodium catalyst and is substantially superior to Adams platinum and palladium catalysts both in activity and in selectivity in the hydrogenation of various organic compounds.

It has been found that the activity of rhodium-platinum(3 : 1) oxide and also that of rhodium oxide are considerably enhanced by fusing the corresponding chlorides with sodium nitrate for a shorter time at a lower temperature than as directed in the preparation of platinum oxide[4]. The rhodium-platinum(3 : 1) catalyst prepared in this way is not only more active, but also more easily dissolved in aqua regia than reported previously. This fact prompted the author to prepare a catalyst which retains the nature of a rhodium catalyst and can be completely recovered with aqua regia. Rhodium-platinum oxide of various compositions has been prepared by the improved procedure and the activity and selectivity have been studied in the hydrogenation of toluene and acetophenone in acetic acid. The results are summarized in Table I. The catalysts containing 70 to 90% of rhodium are the most active and selective. On the other hand, those containing about 30% or more of platinum dissolve on gently heating in aqua regia without leaving any insoluble residue. Thus the requirements mentioned above are satisfied to a large extent by the catalyst consisting of 70% of rhodium and 30% of platinum, which dissolves in aqua regia practically with no residue, and yet is nearly as active and as selective as rhodium-platinum(3 : 1) oxide.

Though rhodium oxide is not easily reduced with hydrogen as noted previously[2], that prepared by the improved procedure can be reduced to the metal in 3~4 hr. at 30°C or in about 1 hr. at 45~50°C in acetic acid under the atmospheric pressure of hydrogen. The resulting rhodium black, however, is unexpectedly less active than rhodium-platinum (3 : 1) oxide as shown in the hydrogenation of toluene. The proportion of hydrogenolysis in the hydrogenation of acetophenone is somewhat greater with rhodium oxide than with rhodium-platinum(3 : 1) oxide (see Table I). Thus, the platinum in rhodium-platinum oxide promotes the reduction of the oxide to the metals, makes the resulting catalyst more active and selective than the pure rhodium catalyst, and makes it possible to recover the metals with aqua regia.

1) Part I: S. Nishimura, This Bulletin, **34**, 32 (1961).
2) S. Nishimura, ibid., 33, 566 (1960).
3) S. Nishimura, T. Onoda and A. Nakamura, ibid., 33, 1356 (1960).
4) R. Adams, V. Voorhees and R. L. Shriner, "Organic Syntheses", Col. Vol. 1, 2nd Ed., John Wiley & Sons, Inc., New York (1941), p. 463.

TABLE I. CATALYTIC HYDROGENATION OF TOLUENE AND OF ACETOPHENONE WITH RHODIUM-PLATINUM OXIDE OF VARIOUS COMPOSITIONS[a]

| Catalyst | | Time for the reduction of oxide to metal | Hydrogenation of toluene (0.921 g.) | | Hydrogenation of acetophenone (0.601 g.) | |
|---|---|---|---|---|---|---|
| | | | Initial rate[b] | Time | $H_2$ uptake | Time |
| Rh(%) | Pt(%) | min. | ml./min. | min. | mol./mol. | min. |
| 100 | 0 | 210 | 88 | 23 | 4.08 | 30 |
| 90 | 10 | 50 | 110 | 15 | 4.03 | 20 |
| 80 | 20 | 30 | 106 | 16 | 4.02 | 22 |
| 75 | 25 | 24 | 108 | 15 | 4.02 | 20 |
| 70 | 30 | 20 | 103 | 16 | 4.02 | 20 |
| 60 | 40 | 16 | 91 | 16 | 4.05 | 24 |
| 50 | 50 | 11 | 87 | 17 | 4.08 | 36 |
| 25 | 75 | 5 | 49 | 25 | 4.15 | 50 |
| 0 | 100 | 2 | 19 | 83 | 4.65 | 75 |

a) Each hydrogenation was carried out with 50 mg. of oxide in 20 ml. of acetic acid at 30°C under the atmospheric pressure of hydrogen. The substance to be hydrogenated was added after the oxides was reduced to the metal.

b) Initial rate refers to 50 mg. of catalyst metal.

**Procedure for the Preparation of Rhodium-Platinum (7 : 3) Oxide.** — A mixture of the chlorides corresponding to 0.30 g. of rhodium and 0.13 g. of platinum in the weights of the metals is fused with 20 g. of sodium nitrate in the same way as in the preparation of platinum oxide[5]. After a violent evolution of the oxides of nitrogen has almost subsided, the temperature is raised and kept at 460~480°C for about 10 min. After cooling, the solidified mass is rinsed in distilled water. The solid is collected, washed with 100 ml. of 0.5% aqueous sodium nitrate, and then dried over calcium chloride. The yield is 0.665 g., which is quantitative on the basis of the metal content (65%) of the oxide.

The author wishes to express his sincere gratitude to Professor Yoshiyuki Urushibara for his continued encouragement.

*Department of Chemistry*
*Faculty of Science*
*The University of Tokyo*
*Hongo, Tokyo*

5) Cf. Ref. 4, p. 463.

# *Naphthalene as an Isolatable Reaction Intermediate in the Catalytic Vapor-phase Oxidation of Methylnaphthalenes to Phthalic Anhydride*

By Charles J. NORTON

(Received August 22, 1961)

Naphthalene has not been reported previously as a reaction intermediate in the heterogeneous vapor-phase oxidation of either monomethylnaphthalenes or dimethylnaphthalenes with air over vanadia catalyst at reactions which yield phthalic anhydride[1-3]. Recently, Morita tried unsuccessfully to detect naphthalene as an intermediate in the oxidation of 2-methylnaphthalene and naphthalene-1- and 2-carboxylic acid. For this reason, he concluded that naphthalene is not a reaction intermediate in the oxidation of methylnaphthalenes to phthalic anhydride[4].

The purpose of this communication is to report the discovery and isolation of naphthalene as an isolatable reaction intermediate under reaction conditions which are well known to effect its further oxidation to phthalic anhydride[1-6].

1) J. K. Dixon and J. E. Longfield, "Catalysis", Ed. by P. H. Emmett, Vol. VII., Reinhold (1960), Chap. 3, pp. 196-222.
2) R. N. Shreve and R. W. Welborn, *Ind. Eng. Chem.*, 35, 279 (1943).
3) C. R. Kinney and I. Pincus, ibid., 43, 2880 (1951).
4) S. Morita, This Bulletin, 33, 511 (1960).
5) N. L. Franklin, P. H. Pinchbeck and F. Popper, *Trans. Inst. Chem. Eng.*, 43, 280 (1956).
6) A. F. D'Alessandra and A. Farkas, *J. Colloid Sci.*, 11, 653 (1956).

TABLE I. FLUID-BED OXIDATIONS IN AIR OVER VANADIA CATALYST[1]

| Feed | Reaction condition: Temp. °C | Contact time sec. | Air-to-feed ratio l.(air)/g.(feed) | Mol. % coversion to various product: PA[2] | MA[3] | NQ[4] | HC[5] | N[6] | $CO_2$[7] |
|---|---|---|---|---|---|---|---|---|---|
| A. Oxidations at conditions for good phthalic anhydride pronduction | | | | | | | | | |
| Naphthalene | 375 | 0.69 | 29 | 50.5 | 2.2 | 1.4 | 25.8[8] | — | 20.1 |
| 22% 1-Methylnaphthalene, 78% 2-Methylnaphthalene | 375 | 0.66 | 91 | 30.9 | 2.6 | 3.1 | 3.8 | (0.5)[10] | 59.6 |
| 22% 1-Methylnaphthalene, 78% 2-Methylnaphthalene | 375 | 0.45 | 82 | 37.4 | 2.3 | 1.8 | 19.5 | (2.3)[10] | 39.1 |
| 2-Methylnaphthalene | 375 | 0.49 | 99 | 37.8 | 5.9 | 3.6 | 13.4 | (1.7)[10] | 39.3 |
| 1,2-Dimethylnaphthalene | 375 | 0.48 | 148 | 19.7 | 22.7 | 4.2 | 13.2 | (1.0)[10] | 40.2 |
| 1,7-Dimethylnaphthalene | 375 | 0.48 | 165 | 15.5 | 3.0 | 1.1 | 4.9 | (0.0)[10] | 75.5 |
| 2,3-Dimethylnaphthalene | 375 | 0.41 | 133 | 49.0 | 2.5 | 2.9 | | 8.8[11] | 36.8 |
| B. Oxidations at milder conditions than required for good phthalic anhydride production | | | | | | | | | |
| 1-Methylnaphthalene | 324 | 0.26 | 7.34 | low[9] | — | — | — | 4.02[12] | — |
| 1-Methylnaphthalene | 324 | 0.15 | 6.78 | low[9] | — | — | — | 4.34[12] | — |
| 1-Methylnaphthalene | 347 | 0.10 | 4.71 | low[9] | — | — | — | 2.18[12] | — |

1) Davison powdered vanadia oxidation catalyst, 100~200 mesh, activated in air at 430°C for 2 hr.
2) PA=Phthalic anhydride
3) MA=Maleic anhydride
4) NQ=Naphthoquinone
5) HC=Total recovered hydrocarbons
6) N=Naphthalene
7) $CO_2$ determined by difference
8) Largely naphthalene
9) Phthalic anhydride produced in low yield, but not determined.
10) Determined by elution chromatography; too little to confirm by auxiliary analyses.
11) Determined by elution chromatography and confirmed by melting point and infrared and ultraviolet spectrometry.
12) Determined by gas-liquid chromatographic analyses.

The experiments related below were carried out in a laboratory fluid-bed catalytic flow reactor equipped with air and liquid feed devices, and a temperature controller. The condensable reaction products were caught in a series of traps and analyzed by a combination of gravimetric, spectrometric, and chromatographic procedures. Experimental conditions a reults are summarized in Table I.

Naphthalene was first isolated in an 8.8 mol. per cent conversion in the reaction product mixture obtained from 2, 3-dimethylnaphthalene under conditions which gave a 49.0 weight per cent conversion to phthalic anhydride. This naphthalene was separated from the product mixture by means of elution chromatography with petroleum ether over alumina. The identity and purity of the reaction product were established by m. p., 80.1~80.7°C, and gas-liquid chromatographic, infrared and ultraviolet spectrometric comparisons with an authentic sample of naphthalene.

Only small amounts of naphthalene were detected by elution chromatograms in the product mixtures obtained from the oxidation of 1-methylnaphthalene under the reaction conditions for good phthalic anhydride yields. However, improved conversions of 2.18 to 4.34 mol. per cent naphthalene were obtained under milder reaction conditions, which gave low yields of phthalic anhydride (see Part B, Table I). These reaction product mixtures were distilled to obtain a 15.2 g. naphthalene cut, b. p. 214~223°C/629 mmHg, which on recrystallization from ethanol gave an infrared spectrum entirely superimposable with one of an authentic naphthalene sample.

These experimental results conclusively demonstrate that naphthalene is an isolatable reaction intermediate in the heterogeneous vapor-phase oxidation of 2, 3-dimethylnaphthalene to phthalic anhydride. Although the naphthalene conversions were too small to be confirmed under conditions favoring good phthalic anhydride production from either 1- or 2-dimethylnaphthalene, larger naphthalene conversions were demonstrated and confirmed in the oxidation of 1-methylnaphthalene at milder reaction conditions, which are less favorable for good phthalic anhydride production. Consequently, any reaction mechanism or kinetic analysis for the heterogeneous vapor-phase

oxidation of methylnaphthalenes over vanadia must consider naphthalene as an isolatable reaction intermediate which is produced in sufficient quantities to be desorbed from the catalyst and detected.

The author wishes to acknowledge the assistance of T. E. Moss in the experimental work.

*The Denver Research Center*
*The Ohio Oil Company*
*Littleton, Colorado*

## *Sudachitin, a New Flavone Pigment of Sudachi*

By Tokunaru HORIE, Mitsuo MASUMURA and F. Shigeo OKUMURA

(Received August 14, 1961)

A new flavone pigment was isolated in a 0.005% yield from the ether extract of the green fruit of *Citrus sudachi Hort ex Shirai*, one of the species of the family Rutaceae, which is produced only in Tokushima prefecture, Shikoku. The name, sudachitin is suggested for this new flavone. A better yield was obtained from the alcohol extract (0.014%) accompanying a second new flavone of m. p. 271~273°C from the mother liquor of sudachitin purifications in 0.004% yield.

Sudachitin crystallized as yellow needles from a mixture of ethyl acetate and methanol (1 : 1), 239.5~240.5°C, and its analytical values agreed with the formula $C_{18}H_{16}O_8$. When treated with metallic magnesium and hydrochloric acid, it gave typical reddish-orange color reaction for flavone pigments. It gave a greenish brown color with ferric chloride, indicating the presence of free hydroxyl groups.

The conversion of sudachitin (I) into a triacetate (II), $C_{24}H_{22}O_{11}$, m. p. 167.5~168.5°C, with acetic anhydride, and into a trimethyl ether (III), $C_{21}H_{22}O_8$, m. p. 135.5~136.5°C, with dimethyl sulfate, or into a triethyl ether (IV) $C_{24}H_{28}O_8$, m. p. 143~144°C, with diethyl sulfate, revealed the presence of three hydroxyl groups. These three derivatives gave the positive flavone color test with metallic magnesium and hydrochloric acid, but did not show a ferric chloride test. Diazomethane converted sudachitin into a dimethyl ether (V), $C_{20}H_{20}O_8$, m. p. 143~144°C, suggesting the existence of a free hydroxyl group at the 5-position of the flavone ring, at this stage, the similarity of the above two derivatives of sudachition to the nobiletin previously isolated by Robinson and coworkers[1], the structure of which has been confirmed as 3′, 4′, 5, 6, 7, 8-hexamethoxy flavone[2,3] (III), was noticed. The ultraviolet spectra of sudachitin trimethyl ether (III) and nobiletin*, and of sudachitin dimethyl ether (V) and 5-hydroxy-3′, 4′, 6, 7, 8-pentamethoxy flavone* were shown to be identical. The mixed melting point of the above two pairs also did not show any depression. From the above evidence, it is clear that the position of six substituents in sudachitin should be at 3′, 4′, 5, 6, 7 and 8

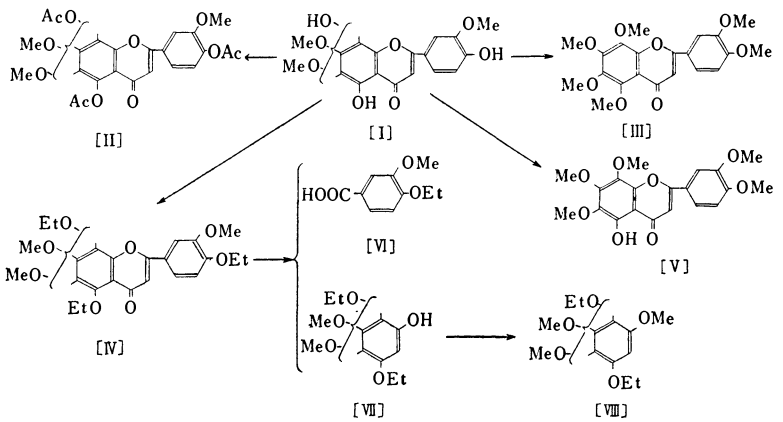



Fig. 1

1) Kwong-Fong Tseng, *J. Chem. Soc.*, **1938**, 1003; R. Robinson, Kwong-Fong Tseng, ibid., **1938**, 1004.
2) Z. Horii, *J. Pharm. Chem. Japan* (*Yukagaku Zasshi*), **60**, 614 (1940).
3) A. Tsukamoto and T. Ohtaki, ibid., **67**, 9 (1947).
* Samples of nobiletin and 5-hydroxy-3′, 4′, 6, 7, 8-pentamethoxy flavone were kindly provided by Dr. Z. Horii, University of Osaka.

positions, and one of the three free hydroxyl groups should be at the 5-position in the flavone ring.

In order to obtain furthur evidence regarding the position of the remaining two free hydroxyl groups, sudachitin triethyl ether (IV) was refluxed for 6 hr. in 10% potassium hydroxide solution. Acidificatin of the mother liquor from the ether extract of the hydrolysis mixture, gave a white precipitate in an 84% yield, which recrystallized from benzene, gave colorless needles, m. p. 193~194°C[4], (Found: C, 60.95; H, 6.23. Calcd. for $C_{10}H_{12}O_4$: C, 61.22; H, 6.16%). The mixed melting point with 4-ethoxy-3-methoxybenzoic acid[4] (VI) synthesized from vanillin was not depressed. From this fact, the position of the second free hydroxyl group was proved to be the 4'-position in the flavone ring. From the ether extract of the above mentioned hydrolysis mixture which had been saturated with carbon dioxide before ether extraction, there was obtained an oily product VII which gave a positive phenol test with ferric chloride. This was converted with dimethyl sulfate into a methyl ether, a diethoxy-trimethoxy benzene (VIII), whose analytical values agreed with the formula $C_{13}H_{20}O_5$ (Found: C, 61.04; H, 7.95. Calcd. for $C_{13}H_{20}O_5$: C, 60.92; H, 7.87%).

In the light of these findings, it was concluded that sudachitin most probably is the trihydroxy-trimethoxy flavone shown as structure I in Fig. 1.

An attempt to establish the relative positions of the hydroxyl- and methoxyl-groups on the benzene ring of VIII by direct comparison with three isomeric diethoxy-trimethoxybenzenes failed, because the amount of diethoxy-trimethoxybenzene from sudachitin was too small to purify.

The synthesis of three isomeric triethoxy-trimethoxy flavone which is only remaining way to confirm the final structure of sudachitin, is now in progress.

*Department of Applied Chemistry*
*Faculty of Engineering*
*University of Tokushima*
*Tokushima*

4) F. Tiemann, *Ber.*, **8**, 1130 (1875).

# *Stress Relaxation of Gels of Polyvinyl Alcohol-Glycerin-Water System*

By Kiyoshi ARAKAWA

(Received March 2, 1961)

In the previous paper[1] the results of the stress relaxation study on the gels of the polyvinyl alcohol-glycerin-water system were reported. This was taken as an example of non-electrolytic thermo-reversible gel systems of polymeric nature, and some discussions were held concerning the concentration dependence of relaxation spectrum.

The average molecular weight of the sample of polyvinyl alcohol used in the previous study was $1.1\times10^4$, which was comparatively low as a polymer. Another study on the mechanical behavior of polyvinyl alcohol-glycerin-water gels has been attempted for a polyvinyl alcohol sample of higher molecular weight in order to investigate the effect of the molecular weight difference on its mechanical behavior and to obtain further knowledge concerning the concentration dependence of relaxation spectrum.

## Experimental

**Sample.** — A commercial sample of polyvinyl alcohol was used. The amount of residual acetyl group of this powder sample was 1.0% by mole, which was determined by the titration method. The intrinsic viscosity $[\eta]_{25}$ obtained by means of a capillary viscometer of Ostwald type was 1.27 (100 cc./g.), and the viscosity average molecular weight which was calculated from the value of viscosity by Diew's formula[2] was $8.5\times10^4$.

The preparation of specimen gels was made according to the same procedure as that described in the previous paper[1] and also the mixing ratio of glycerin and water was made to be precisely the same as before. Gels of three different concentrations of polyvinyl alcohol were prepared, namely: 6.05, 7.95 and 9.07% by weight.

**Apparatus and Procedure for Measurements.** — The same relaxometer as has been used in the preceding studies[3] on the rheological properties of thermo-reversible gels was used in this experiment. The measurement of relaxation Young's modulus under a given constant strain was carried out for two hours after sudden imposition of the strain. The imposed strain was 5% for 7.95% and 9.07% gels, and 20% for 6.05% gels, respectively. The temperature was varied with about 10°C interval.

1) K. Arakawa, This Bulletin, **31**, 842 (1958).
2) H. Diew, *J. Polymer Sci.*, **12**, 147 (1954).
3) K. Arakawa, This Bulletin, **32**, 1248 (1959); ibid., **33**, 1568 (1960); K. Arakawa and K. Atsumi, *J. Chem. Soc. Japan, Pure Chem. Sec.* (*Nippon Kagaku Zasshi*) **80**, 133 (1959).

## Results and Discussion

**Relaxation Data.** — The relaxation Young's modulus under constant compressional strain at various temperatures is plotted in the form of $(298/T)E_r$ versus log $t$, where $(298/T)$ is a reduction factor to 25°C concerning rubber-like elasticity. The results are shown in Figs. 1(a), 1(b) and 1(c) for each concentration.

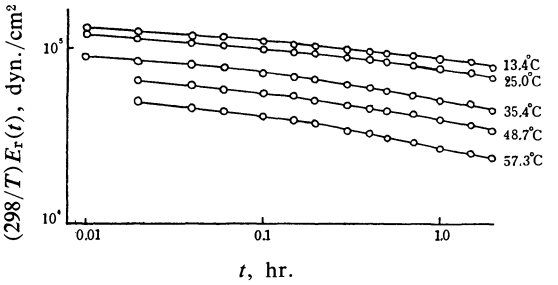



Fig. 1 (a). Reduced relaxation Young's modulus $(298/T)E_r(t)$ of 6.05% gel.

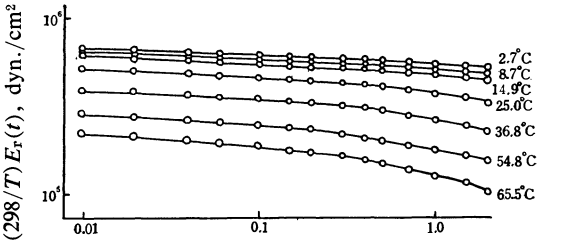



Fig. 1 (b). Reduced relaxation Young's modulus $(298/T)E_r(t)$ of 7.95% gel.

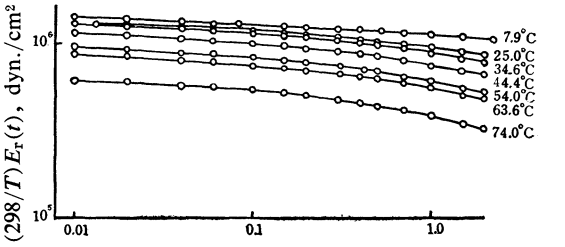



Fig. 1 (c). Reduced relaxation Young's modulus of 9.07% gel.

According to the time-temperature superposition principle[4], a master relaxation curve at 25°C for each concentration is obtained by shifting the relaxation curves at different temperatures horizontally along the $\log t$ axis. The master relaxation curves, thus obtained, are shown in Fig. 2. The coincidence of each relaxation curve by superposition is good as seen in Fig. 2.

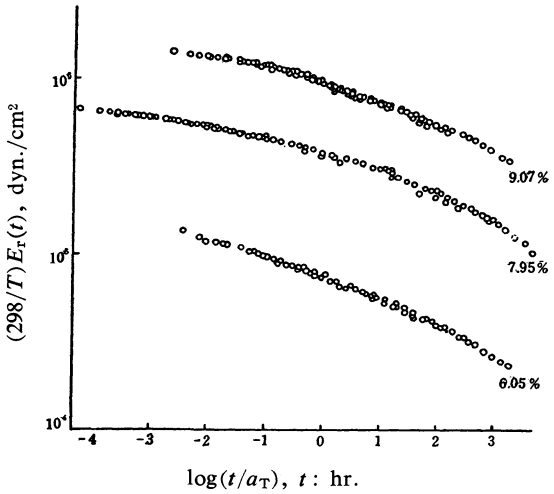



Fig. 2. Master relaxation curves at 25°C.

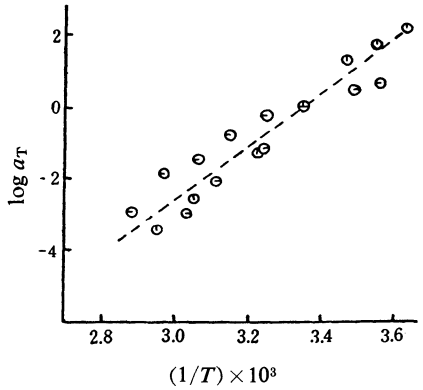



Fig. 3. $\log a_T$ versus $1/T$ relation.
⊖ 6.05%, ⏀ 7.95%, ⊖ 9.07%

The shift factors $\log a_T$ are plotted against $1/T$ in Fig. 3. This plotting shows a nearly linear relation, as in the case of the previous study[1], where the molecular weight of the polyvinyl alcohol was $1.1\times10^4$. Thus, the apparent activation energy $H_a$ calculated from the gradient of the $\log a_T$ versus $1/T$ curve is kept constant within the temperature and concentration ranges in the present study. When the apparent activation energy is constant, shift factors $a_T$ are expressed as follows,

$$a_T = A\exp(H_a/RT) \quad (1)$$

The values of $\log A$ and $H_a$ are given in Table I, together with those of molecular weight $1.1\times10^4$ in the previous paper[1].

TABLE I. VALUES OF $\log A$ AND $H_a$

| Mol. wt. of polyvinyl alcohol | $8.5\times10^4$ | $1.1\times10^4$ |
|---|---|---|
| $\log A$ | −25.7 | −43.8 |
| $H_a$ (kcal./mol.) | 35 | 60 |

The constancy of $H_a$ as well as the good coincidence of each relaxation curve by superposition is said to support the adequacy of the application of the superposition method, which exhibits the equality of the temperature dependence of all relaxation mechanisms within these ranges of temperature and concentration[5].

In order to compare the temperature dependence of shift factors in this case with the equation of the WLF form[6], the values of $\log a_T$ referred to $T_S$ are plotted against $T-T_S$ in Fig. 4, where $T_S$ is a reference temperature. The values of $\log a_T$ agree with the curve of

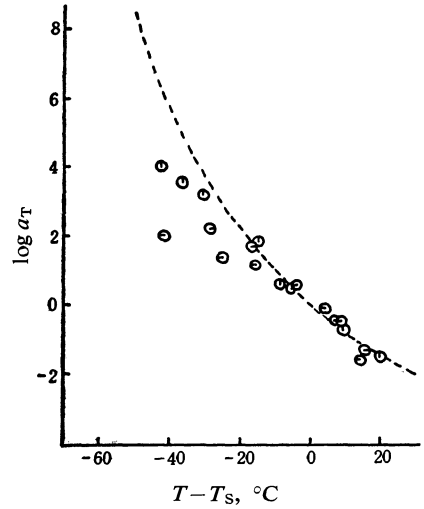



Fig. 4. $\log a_T$ versus $T-T_S$ relation.
⊖ 6.05%, ⏀ 7.95%, ⊖ 9.07%
---- Equation of WLF form, $C_1$: 8.86, $C_2$: 101.6
Values of $T_S$ 315°K for 6.05%
319°K for 7.95%
323°K for 9.07%

WLF equation within the range of $(T-T_S)=-20\sim20$°C, but outside of this range they deviate from the curve.

**Concentration Dependence of Distribution Functions of Relaxation Times.**—From the

4) A. V. Tobolsky, "Properties and Structure of Polymers", John Wiley and Sons, Inc., Publishers, New York (1960), Chapter 4, Sec. 2 and 3.

5) C. A. Dahlquist and M. R. Hatfield, *J. Colloid Sci.*, 7, 253 (1952).

6) M. L. Williams, R. F. Landel and J. D. Ferry, *J. Am. Chem. Soc.*, 77, 3701 (1955).

master curves shown in Fig. 2 distribution functions of relaxation times, $H(\log\tau)$, which are defined by Eq. 2 are obtained by Alfrey's first order approximation, Eq. 3.

$$E_r(t)=\int_0^\infty H(\log\tau)e^{-(t/\tau)}\mathrm{d}\log\tau \qquad (2)$$

$$H(\log\tau)=-2.303\left[E_r\frac{\mathrm{d}\log E_r}{\mathrm{d}\log t}\right]_{t=\tau} \qquad (3)$$

The distribution functions, thus obtained, are shown in Fig. 5. As is seen clearly, they are of typical box type character. When seen in details, there appears a fairly broad flat region in the curve for the gel of 7.95% and a peak in the curve for the gel of 9.07%. The curve for the gel of 6.05% is regarded as the one in the rubbery flow region which follows after the flat region. The distribution functions of the gels described in the previous paper[1] are shown together for comparison by dotted lines.

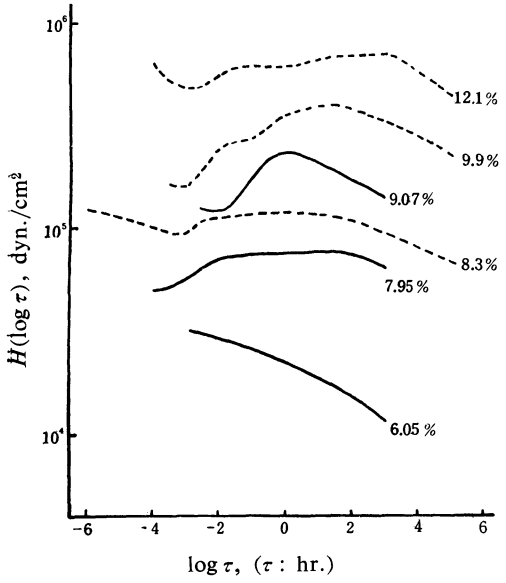



Fig. 5. Distribution functions of relaxation times.
—— Molecular weight, $8.5\times10^4$
---- Molecular weight, $1.1\times10^4$

When we see in detail the change in the shape of the curves with increase of concentration, it may certainly be said that the simple reduction rule concerning concentration which was proposed by Ferry et al.[7] and also the modified reduction rule by DeWitt et al.[8] on polymer solutions do not hold in this case, and that the circumstances are more complicated. However, when we seen all curves including dotted lines, it is found that the curves change their shapes continuously with the increase of concentration and that there is no marked difference among them in the tendency of the change in shape in spite of the fairly great difference in molecular weight.

The curve for the gel of 6.05% decreases monotonously. This corresponds to the rubbery flow region, and there appears a broad flat region in the curve of the gel of 7.95%, and the broad flat region is levelled up for the gel of 8.3%. Then there appears a peak in the flat region for the gel of 9.9%, and the peak shifts with the increase of concentration, accompanying the ascent of the curve.

Then it may be said that the difference in molecular weight has no marked effect on the distribution functions of relaxation times and that there are two or more mechanisms which behave differently with the increase of concentration.

In order to investigate the concentration dependence of distribution functions, the average values of $H(\log\tau)$ in the whole box type region, $\bar{H}$, which is regarded as the height of the idealized box type spectrum, are calculated and plotted in the form of $\log\bar{H}$ versus $\log C$, where $C$ is concentration in weight %, in Fig. 6, including those for the case of molecular weight $1.1\times10^4$. Then we see in Fig. 6 that a linear relation holds between $\log\bar{H}$ and $\log C$ as follows,

$$\log\bar{H}=\alpha+\beta\log C \qquad \alpha=0.45,\ \beta=5 \qquad (4)$$

As is shown in the equation above described, the value of $\bar{H}$ is proportional to the fifth

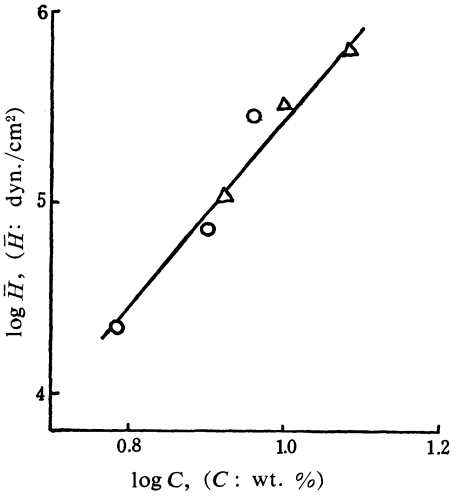



Fig. 6. Concentration dependence of average value of distribution functions of relaxation times in box type region.
○ Molecular weight, $8.5\times10^4$
△ Molecular weight, $1.1\times10^4$

7) J. D. Ferry, ibid., **72**, 3746 (1950).
8) T. W. DeWitt, H. Markovitz, F. J. Padden and L. J. Zapas, *J. Colloid Sci.*, **10**, 174 (1955).

power of concentration. Then it is said that in the case of thermo-reversible gels there exists much more sensitive dependence of distribution functions on concentration, compared with the case of concentrated polymer solutions[7,8].

## Summary and Conclusion

A stress relaxation study was made for the gels of the polyvinyl alcohol-glycerin-water system using a chainomatic balance relaxometer, where the molecular weight of polyvinyl alcohol was $8.5\times10^4$. Relaxation Young's moduli under constant strain were measured up to two hours after sudden imposition of the strain for the gels of three different concentrations of polyvinyl alcohol: 6.05, 7.95 and 9.07% by weight. The relaxation curves at various temperatures were successfully superposed to a master relaxation curve for each concentration, and relaxation spectra were obtained from the master curves by Alfrey's approximation. The main results obtained are as follows.

1) The relaxation spectrum of the gel of the polyvinyl alcohol-glycerin-water system has a typical box type character.

2) The difference in molecular weight of polyvinyl alcohol has no marked effect on the relaxation spectrum of the gel.

3) The concentration dependence of the relaxation spectrum are fairly complicated in its details.

4) The average value of the distribution function of relaxation times in the box type region is proportional to the fifth power of concentration, rather than to the first or the second power.

*Department of Chemical Industry*
*Faculty of Engineering*
*Shizuoka University*
*Oiwake, Hamamatsu*

# *The Infrared Absorption Spectrum of 1, 2, 4, 5-Tetrachlorobenzene in Vapor State*

By Shinnosuke SAËKI*

(Received March 4, 1961)

The molecular spectra of 1, 2, 4, 5-tetrachlorobenzene have been studied by some investigators[1]. All of these studies were, however, mainly concerned with a number of benzene derivatives to find the relation between the position of substituents in the benzene ring and C–H out-of-plane characteristic frequencies. Also 1, 2, 4, 5-tetrachlorobenzene was treated only as a member of the substituted benzenes. The assignment of the observed bands of this substance has been little discussed with the exception of its out-of-plane C–H vibration. Besides, all the spectra were taken in solid or liquid state or in solution, and the spectra taken in these states are not suitable to be used for the assignment of the bands. We measured the spectra of ordinary and deuterated 1, 2, 4, 5-tetrachlorobenzene in vapor state with the aid of a high temperature cell to make some tentative assignments of the observed infrared absorption bands.

## Experimental and Results

The measurements were carried out on ordinary and deuterated 1, 2, 4, 5-tetrachlorobenzenes, from 5000 to 2000 $cm^{-1}$ with a lithium fluoride prism, from 2000 to 700 $cm^{-1}$ with a sodium chloride prism and from 700 to 400 $cm^{-1}$ with potassium bromide prism using the Perkin-Elmer 112 infrared spectrometers. As the boiling points of these substances are considerably high, in order to observe the spectra in vapor state we used the high temperature cell which was described in a previous paper[2]. The partial pressure of each substance was not measured. The substance was simply put in the cell which has been previously heated but not evacuated, and regulated the quantity of the substance in the cell so that it might give a good spectrum.

The ordinary 1, 2, 4, 5-tetrachlorobenzene used in this experiments was extra pure grade on the market, and the deuterated one was kindly provided by Dr. Leitch in Canada.

* Present address: Government Chemical Industrial Research Institute, Shibuya-ku, Tokyo.

1) For example, E. K. Plyler, H. C. Allen, Jr. and E. D. Tidwell, *J. Research Nat. Bur. Standards*, **58**, 255 (1957).

2) S. Saëki, This Bulletin, 33, 1021 (1960).

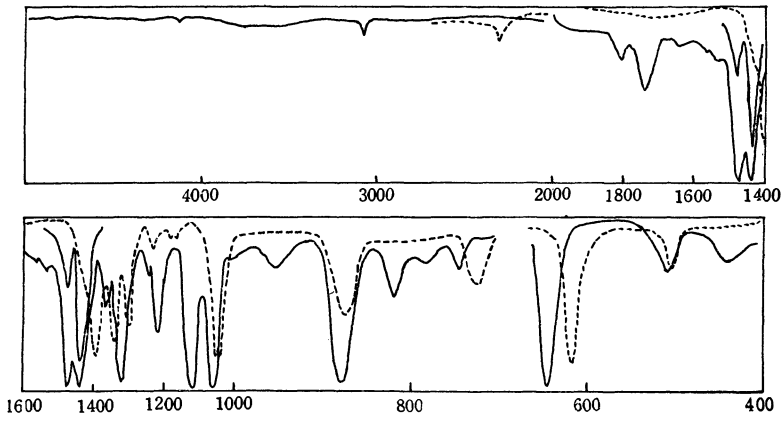



Fig. 1. Infrared absorption spectra of ordinary and deuterated 1,2,4,5-tetrachlorobenzenes.
$C_6H_2Cl_4$ —— $C_6D_2Cl_4$ ----

TABLE I. INFRARED ABSORPTION BANDS OF 1,2,4,5-TETRACHLOROBENZENES

| $C_6H_2Cl_4$ | $C_6D_2Cl_4$ | $C_6H_2Cl_4$ | $C_6D_2Cl_4$ |
|---|---|---|---|
| 3094 m | 2300 m | | 1175 w |
| 2775 w | | 1116 s | 1054 s, 1047 s |
| 2680 w | | 1060 s | |
| 2630 w | | 947 w | |
| 1802 w | | 880 s | 874 s |
| 1740 w | | 820 m | 725 m |
| 1474 m | 1425 w | 782 w | |
| 1436 s | 1392 s | 745 w | |
| 1367 m | 1345 s | 645 s | 617 s |
| 1319 s | 1297 s | 509 m | 504 m |
| 1241 w | 1235 m | 440 w | |
| 1218 m | 1187 w | | |

The observed spectra of each substance are shown in Fig. 1, and the observed frequencies are shown in Table I.

## Assignment

The symmetry of this substance belongs to the point group $V_h$ as *p*-dichlorobenzene does. So it has thirteen infrared active normal vibrations of which five belong to the species $B_{1u}$ (in-plane), five to the species $B_{2u}$ (in-plane) and three to the species $B_{3u}$ (out-of-plane)*. These expected vibrational modes are listed in Table II.

Among these vibrations, the C–Cl bending vibration of each species is expected to be unobservable under the experimental conditions because of its low frequency, and some of the ring deformation frequencies might also exist beyond the experimental region. Therefore we should expect to observe from seven to ten fundamental frequencies under the experimental conditions. In the spectra nine or ten strong bands were observed for $C_6H_2Cl_4$ and eight strong bands for $C_6D_2Cl_4$. In addition to these strong bands a medium or weak band in shorter wavelength region was observed; that is, a band at 3094 $cm^{-1}$ of $C_6H_2Cl_4$ and at 2300 $cm^{-1}$ of $C_6D_2Cl_4$ which are evidently the fundamental bands of C–H and C–D stretching vibrations respectively.

Between 1500 and 1200 $cm^{-1}$ three fundamental bands, might be expected that is, the ring stretching vibrations of the species $B_{1u}$ and $B_{2u}$ and the ring in-plane deformation vibration of the species $B_{2u}$. It should be mentioned here that the third vibration, which is called a ring deformation vibration, might probably have a considerably high frequency, because the mode of this ring deformation is necessarily accompanied by a ring stretching mode. Taking into account the relative intensities of these bands and the product rule, we consider that the

TABLE II. INFRARED ACTIVE NORMAL VIBRATIONS OF 1,2,4,5-TETRACHLOROBENZENES

| Species | Mode |
|---|---|
| $B_{1u}$ (in-plane) | C–H or C–D stretching |
| | Ring stretching |
| | Ring deformation |
| | C–Cl stretching |
| | C–Cl bending |
| $B_{2u}$ (in-plane) | C–H or C–D bending |
| | Ring stretching |
| | Ring deformation |
| | C–Cl stretching |
| | C–Cl bending |
| $B_{3u}$ (out-of-plane) | C–H or C–D bending |
| | Ring deformation |
| | C–Cl bending |

* In this case, x axis was taken along the symmetry axis perpendicular to the molecular plane, and z axis along the symmetry axis combining two hydrogen atoms.

three bands at 1474, 1436 and 1319 $cm^{-1}$ of $C_6H_2Cl_4$ correspond to the three bands at 1345, 1392 and 1297 $cm^{-1}$ of $C_6D_2Cl_4$ respectively, and assigned the first pair of bands to the ring stretching vibration of species $B_{2u}$, the second to the ring stretching vibration of species $B_{1u}$ and the third to the ring in-plane deformation vibration of species $B_{2u}$.

It appeared somewhat curious that in the region between 1200 and 1000 $cm^{-1}$ we found two bands of $C_6H_2Cl_4$ at 1116 and 1060 $cm^{-1}$, but only one band of $C_6D_2Cl_4$ at 1051 $cm^{-1}$ corresponding to them. The intensities of both of the two bands of $C_6H_2Cl_4$ were too remarkable to be considered as overtone or combination bands. On closer examination of the shape of the band at 1051 $cm^{-1}$ of $C_6D_2Cl_4$, we found the two absorption maxima at 1054 and 1047 $cm^{-1}$ which were not known to be the branches of a single band or to be the peaks of two independent bands. Badger and Zumwalt[3] gave the band envelopes of several types of unsymmetrical rotator molecules. The $\rho$*1 and S values of the molecule of $C_6D_2Cl_4$ are 1.8 and $-0.7$ respectively for which the band envelope is not given in their paper. But the estimation from the different band envelopes described in their paper told us that the splitting of the two maxima would not be greater than 3 $cm^{-1}$.

Dennison[4] also showed that the diagrams of the fine structure of the band, but it was difficult to estimate the splitting of the two absorption maxima from these diagrams. If one approximates the molecule of 1, 2, 4, 5-tetrachlorobenzene by a symmetric rotator*2, the approximate value of the splitting can be found to be about 5 $cm^{-1}$ *3. Actually this splitting distance was found to be about 7 $cm^{-1}$, a little larger than the above-mentioned estimated and calculated values. But such an amount of discrepancy between the observed and calculated (or estimated) values is not enough to favor the supposition that these two absorption maxima would be caused by the two independent bands. However, we shall take this supposing at present, for it appears to explain more easily the correspondence between the absorption bands of each substance. Thus we assigned the band at 1116 and 1060 $cm^{-1}$ of $C_6H_2Cl_4$ to the C–H in-plane bending vibration of species $B_{2u}$ and to the ring deformation vibration of species $B_{1u}$ respectively, and for their corresponding bands of $C_6D_2Cl_4$ we considered that the band at 1047 $cm^{-1}$ of $C_6D_2Cl_4$ corresponds to the former band and the band at 1054 $cm^{-1}$ of $C_6D_2Cl_4$ to the latter.

In the region below 1000 $cm^{-1}$ were found four remarkable bands of each substance, that is, 880, 820, 645 and 509 $cm^{-1}$ for $C_6H_2Cl_4$, and 874, 725, 617 and 504 $cm^{-1}$ for $C_6D_2Cl_4$. Kakiuchi[5] assigned the band at 867 $cm^{-1}$ of $C_6H_2Cl_4$ to the out-of-plane C–H bending vibration. It is evident that this is the band which was observed at 880 $cm^{-1}$ in our experiments*4. But we found in the spectrum of $C_6D_2Cl_4$ a remarkable band at 874 $cm^{-1}$ which evidently corresponds to the band at 880 $cm^{-1}$. It means that the frequency shift caused by the replacement of hydrogen atoms by deuterium atoms is only 6 $cm^{-1}$. This frequency shift is too small for a vibration mainly concerned with the C–H bond. Thus we assigned the band at 820 $cm^{-1}$ to the out-of-plane C–H vibration, for its corresponding band of $C_6D_2Cl_4$ was found at 725 $cm^{-1}$, showing a great frequency shift. But the intensities of these bands appear to be too weak for the out-of-plane C–H and C–D vibrations, and we have not found a plausible explanation for this fact. As for the above-mentioned band at 880 $cm^{-1}$ (874 $cm^{-1}$ for $C_6D_2H_4$) we assigned it to the C–Cl stretching vibration of species $B_{1u}$. And to the other C–Cl stretching vibration which belongs to species $B_{2u}$, we assigned the band at 645 $cm^{-1}$ (617 $cm^{-1}$ for $C_6D_2Cl_4$). The last pair of bands which were found at 509 $cm^{-1}$ (for $C_6H_2Cl_4$) and at 504 $cm^{-1}$ (for $C_6D_2Cl_4$) were assigned to the out-of-plane deformation vibration of the ring. The assignment given above is shown in Table III.

It should be mentioned here that the assignment shown in Table III based on the assumption that the band at 1051 $cm^{-1}$ of $C_6D_2Cl_4$ is composed of two closely positioned independent bands. If not, the assignment should be quite changed as follows.

We regarded the absorption maxima at 1054 and 1047 $cm^{-1}$ observed in the spectrum of $C_6D_2Cl_4$ as the branches of one band which corresponds to the band at 1116 or at 1060 $cm^{-1}$ of $C_6H_2Cl_4$. Then one of these two bands has no corresponding band of $C_6D_2Cl_4$ except the band at 874 $cm^{-1}$. If we consider the band

3) R. M. Badger and L. R. Zumwalt, *J. Chem. Phys.*, **6**, 711 (1938).

*1 Badger and Zumwalt defined $\rho=(a-c)/b$, where $a$, $b$ and $c$ are the reciprocals of three principal moments of inertia, $I_A$, $I_B$ and $I_C$ respectively.

4) D. M. Dennison, *Rev. Mod. Phys.*, 33, 280 (1931).

*2 For this molecule three principal moments of inertia were calculated as $I_A=688\times10^{-40}$, $I_B=1752\times10^{-40}$ and $I_C=2440\times10^{-40}$. Thus the approximation by the symmetric rotator is not very bold.

*3 In this calculation we assumed that $I_B=2000\times10^{-40}$. This is the approximate mean value of the real $I_B$ and $I_C$ values.

5) Y. Kakiuchi, *J. Chem. Soc. Japan, Pure Chem. Sec.* (*Nippon Kagaku Zasshi*), **80**, 356 (1959).

*4 He used the frequencies observed by Plyler and his collaborators[2]. Those frequencies were observed in the liquid state, so it is quite natural that there are small discrepancies between their frequencies and our frequencies observed in the vapor state.

TABLE III. ASSIGNMENT I

| Species | $C_6H_2Cl_4$ | $C_6D_2Cl_4$ | Mode |
|---|---|---|---|
| $B_{1u}$ | 3094 | 2300 | C-H or C-D stretching |
| | 1436 | 1392 | Ring stretching |
| | 1060 | 1054 | Ring deformation |
| | 880 | 874 | C-Cl stretching |
| | — | — | C-Cl bending |
| $B_{2u}$ | 1474 | 1345 | Ring stretching |
| | 1319 | 1297 | Ring deformation |
| | 1116 | 1047 | C-H or C-D bending |
| | 645 | 617 | C-Cl stretching |
| | — | — | C-Cl bending |
| $B_{3u}$ | 820 | 725 | C-H or C-D bending |
| | 509 | 504 | Ring deformation |
| | — | — | C-Cl bending |

at 874 $cm^{-1}$ of $C_6D_2Cl_4$ as corresponding to the band at 1116 or at 1060 $cm^{-1}$, this great frequency shift suggests that the pair is to be assigned to the C-H (C-D) in-plane bending vibration of species $B_{2u}$. Then there are two possible assignments of the other pair (the band at 1060 or at 1116 $cm^{-1}$ of $C_6H_2Cl_4$ and the band at 1051 $cm^{-1}$ of $C_6D_2Cl_4$), that is, an assignment to the ring deformation vibration and an assignment to the C-Cl stretching vibration of species $B_{1u}$. In the case of this molecule the frequency of the ring deformation vibration of species $B_{1u}$ might be rather low, for it could occur without coupling with a stretching mode of the ring. The frequency of a C-Cl stretching vibration which is generally expected at about 700 $cm^{-1}$ might easily couple with the vibrations of other modes in this case, and its frequency might change over a wide region. From these considerations we concluded that the pair of bands in question is to be assigned to the C-Cl stretching vibration of species $B_{1u}$. Concerning the question as to which of the above-mentioned two bands at 1116 $cm^{-1}$ and at 1060 $cm^{-1}$ of $C_6H_2Cl_4$ is to be assigned to C-H in-plane bending vibration of species $B_{2u}$, we decided to assign the former band to this normal vibration from the consideration of the product rule.

As for the other fundamental bands, we assigned the pair of bands at 509 $cm^{-1}$ ($C_6H_2Cl_4$) and 504 $cm^{-1}$ ($C_6D_2Cl_4$) to the ring in-plane deformation vibration of species $B_{1u}$ and the pair of bands at 645 $cm^{-1}$ ($C_6H_2Cl_4$) and 617 $cm^{-1}$ ($C_6D_2Cl_4$) to the C-Cl stretching vibration of species $B_{2u}$. In addition to the above-mentioned change in the assignment, the correspondence of three pairs of ring stretching vibrations (in the region 1300~1500 $cm^{-1}$) is also changes from the consideration of the product rule as is shown in Table IV.

This is the second assignment which seems to us to be as plausible as the former one. This assignment is shown in Table IV.

TABLE IV. ASSIGNMENT II

| Species | $C_6H_2Cl_4$ | $C_6D_2Cl_4$ | Mode |
|---|---|---|---|
| $B_{1u}$ | 3094 | 2300 | C-H or C-D stretching |
| | 1474 | 1392 | Ring stretching |
| | 1060 | 1047 | Ring deformation |
| | 509 | 504 | C-Cl stretching |
| | — | — | C-Cl bending |
| $B_{2u}$ | 1436 | 1345 | Ring stretching |
| | 1319 | 1297 | Ring deformation |
| | 1116 | 874 | C-H or C-D bending |
| | 645 | 617 | C-Cl stretching |
| | — | — | C-Cl bending |
| $B_{3u}$ | 880 | 725 | C-H or C-D bending |
| | — | — | Ring deformation |
| | — | — | C-Cl bending |

## Discussion

According to the product rule the theoretical value of the ratio of products of the frequencies is 1.407 for all three species ($B_{1u}$, $B_{2u}$ and $B_{3u}$) in the case of this molecule. As we could not observe all of the fundamental frequencies under our experimental conditions, it was not possible to apply the product rule to the results obtained perfectly, but it was possible to ascertain whether the ratio of products calculated from the observed frequencies alone exceeds the theoretical value or not. We carried out this calculation for every species of both of the above-mentioned assignments. The results are shown in Table V.

TABLE V. CALCULATED RATIOS OF THE PRODUCTS OF OBSERVED FREQUENCIES

| | Species | Calculated ratio | Number of observed frequency |
|---|---|---|---|
| Assignment I | $B_{1u}$ | 1.405 | 4 of 5 |
| | $B_{2u}$ | 1.242 | 4 of 5 |
| | $B_{3u}$ | 1.142 | 2 of 3 |
| Assignment II | $B_{1u}$ | 1.456 | 4 of 5 |
| | $B_{2u}$ | 1.449 | 4 of 5 |
| | $B_{3u}$ | 1.214 | 1 of 3 |

None of the calculated ratios of assignment I exceeded the theoretical value 1.407, while two of the three calculated ratios of assignment II exceed the theoretical values. From the theoretical point of view assignment I shows no contradiction. But on closer examination one will find some points of discussion. In the first place the value of the ratio for species $B_{1u}$ of assignment I is almost equal

to the theoretical value, so the ratio of the unobserved fifth frequencies must be nearly 1. As the fifth frequency is that of the C–Cl bending vibration (or skeletal vibration), this requirement will probably be fulfilled. In the second place those ratios for the species $B_{2u}$ and $B_{3u}$ of the assignment I are so small that the ratios of the last unobserved frequency of these species must be considerably great, that is, 1.144 and 1.232 for the species $B_{2u}$ and $B_{3u}$ respectively. Considering the fact that both of these values are ratios of the frequencies of C–Cl bending vibrations, they are evidently too great to attribute to the single ratios of frequencies. This appears to be an absolute defect of assignment I as well as of the above-mentioned ambiguity in the explanation of the band at 1051 $cm^{-1}$ of $C_6D_2Cl_4$.

As for assignment II, as we mentioned previously, there are two ratios exceeding the theoretical values. However, a discrepancy of a few per cent must be expected between the observed and theoretical ratios, as there are various factors which cause the deviation, such as small mechanical errors of the spectrometer, the unharmonicity of the vibrations, Fermi resonance, etc. Therefore, provided that the ratios of C–Cl bending frequencies are nearly 1, the discrepancies found for species $B_{1u}$ and $B_{2u}$ might not absolutely deny assignment II.

In the case of species $B_{3u}$, since only one of the three frequencies was observed, the application of the product rule was quite impossible. But the ratio of 1.214 obtained for the first pair of frequencies of this species seems to be perfectly plausible for the C–H (or C–D) out-of-plane bending vibration, and this assignment appears to be strongly preferable to that for species $B_{3u}$ of assignment I.

After all, although we could not find an adequate difference between two assignments shown in Table V to draw out any unambiguous conclusion, assignment II seems to us a little more plausible than the other. In order to remove this ambiguity it may be necessary to carry out the measurement of the spectra of these substances in the far infrared region or to observe the precise shape of each fundamental band or to find out the exact force constants which will allow us to calculate the normal frequencies of these molecules with sufficient accuracy.

## Summary

The infrared absorption spectra of ordinary and deuterated 1, 2, 4, 5-tetrachlorobenzenes were measured in the vapor state using the high temperature cell. For the results obtained by the measurements we proposed two possible assignments of the fundamental infrared bands, and made the discussion comparing these two tentative assignments. However, at present we have no experimental base upon which we can decide the superiority of one to the other. In order to solve this difficulty we are going to make an investigation of the spectra of these molecules in the far infrared region as well as the calculation of the exact force constants of the chlorobenzenes.

This work was done at the laboratory of Professor J. Lecomte of the Laboratoire des Recherches Physiques, Faculté des Sciences de Paris. The author acknowledges greatefully Professor Lecomte's encouragement and advice. He also wishes to thank Dr. Leitch of the National Research Council at Ottawa for kindly sending deuterated 1, 2, 4, 5-tetrachlorobenzene prepared by him.

*Laboratoire des Recherches Physiques*
*Faculté des Sciences de Paris*

# π Electronic Structure of Cinnamaldehyde

By Kōzō Inuzuka

(Received March 6, 1961)

In two previous papers[1,2] we studied the electronic structure of the acrolein molecule. This molecule has an intense absorption band of $(\pi, \pi^*)$ type in the region near 2000 Å, which was assigned to an intramolecular charge transfer band by Nagakura[3]. Cinnamaldehyde is regarded as a derivative of acrolein, in which a hydrogen atom is substituted by a phenyl group. From this point of view the comparison of the spectra of acrolein and cinnamaldehyde may be interesting.

The absorption spectrum of cinnamaldehyde was measured in *n*-hexane solution in the 2000~3000 Å region. Molecular orbital calculation was made for the π electronic structure of the cinnamaldehyde molecule with a view to understanding its absorption band, as there has scarcely been any theoretical work done on the electronic structure of this molecule.

## Ultraviolet Absorption Spectra

The ultraviolet absorption spectra of cinnamaldehyde and acrolein are shown in Fig. 1.

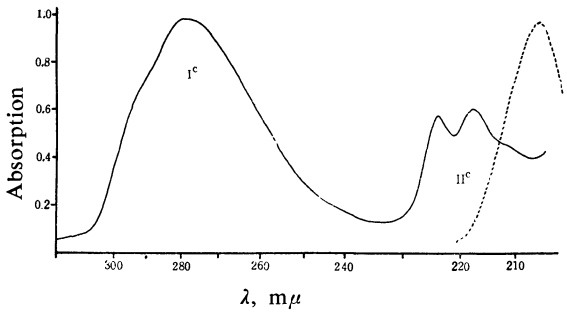



Fig. 1. Ultraviolet absorption spectra of cinnamaldehyde and acrolein.

Solid line: cinnamaldehyde in *n*-hexane
Broken line: acrolein in *n*-hexane

The spectra of these molecules were measured with a Hitachi self-recording quartz spectrophotometer of type E. P. S. The solvent was *n*-hexane carefully purified by the method of Weissberger and Proskauer[4]. It appears that the cinnamaldehyde band is displaced to the red with respect to the acrolein band, owing to the extension of conjugation within the molecule. In order to ascertain that the transition in cinnamaldehyde corresponding to the absorption in the 2000 Å region is of the $\pi-\pi^*$ type, the effect on the spectrum of changing the solvent from *n*-hexane to ethanol was also studied.

## Calculation of Energy Levels

Although the methods of Pariser and Parr[5] and others simplify the calculation of molecular energy levels in very ingenious ways, it is still not easy to apply the theory to a molecule such as cinnamaldehyde. In the present calculation the MO's of cinnamaldehyde were obtained by the simple LCAO-MO method and we took account of the interaction of electrons by including configuration interaction to some extent[6]. As the molecular dimension of cinnamaldehyde is not known, we relied on the structure inferred from the result of the electric dipole moment value by Bently et al.[7] The molecular structure is shown in Fig. 2,

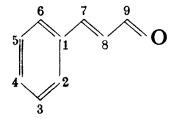



Fig. 2. Cinnamaldehyde.

but in our calculation a somewhat more simplified model was used. Actually cinnamaldehyde has not $C_{2v}$ symmetry, but the orbitals obtained in our approximation are what would be found if $C_1$-$C_7$=$C_8$-$C_9$=O was linear. Thus the cinnamaldehyde MO's may be said to resemble those with $C_{2v}$ symmetry. The MO's of cinnamaldehyde were obtained by the simple LCAO-MO method with neglect of overlap integrals. The Coulomb integral $\alpha_o$ and the resonance integral $\beta_{co}$ are expressed as

$$\alpha_o = \alpha + \delta_o\beta$$

$$\beta_{co} = \rho_{co}\beta$$

1) K. Inuzuka, This Bulletin, 34, 6 (1961).
2) K. Inuzuka, ibid., 34, 729 (1961).
3) S. Nagakura, *Mol. Phys.*, 3, 105 (1960).
4) A. Weissberger and E. S. Proskauer, "Organic Solvents", Interscience Publishers, Inc., New York, N. Y. (1955).
5) R. Pariser and R. G. Parr, *J. Chem. Phys.*, 21, 466, 767 (1953).
6) H. Baba and S. Suzuki, ibid., 32, 1706 (1960).
7) J. B. Bentley, K. B. Everard, R. J. B. Marsden and L. E. Sutton, *J. Chem. Soc.*, 1947, 2957.

Table I. Orbital energies and orbitals for cinnamaldehyde

| $i$ | Symmetry | Orbital energy $(e_i-\alpha)/\beta$ | Orbital $\phi_i$ |
|---|---|---|---|
| 1 | $b_1$ | 2.481 | $0.0956\chi_1+0.0508(\chi_2+\chi_6)+0.0303(\chi_3+\chi_5)+0.0245\chi_4+0.1544\chi_7+0.2644\chi_8+0.5374\chi_9+0.7751\chi_o$ |
| 2 | $b_1$ | 2.100 | $0.4826\chi_1+0.3928(\chi_2+\chi_6)+0.3423(\chi_3+\chi_5)+0.3260\chi_4+0.2593\chi_7+0.1065\chi_8-0.0775\chi_9-0.1825\chi_o$ |
| 3 | $b_1$ | 1.429 | $0.3051\chi_1-0.0094(\chi_2+\chi_6)-0.3185(\chi_3+\chi_5)-0.4458\chi_4+0.5174\chi_7+0.4171\chi_8+0.0126\chi_9-0.2515\chi_o$ |
| 4 | $a_2$ | 1.000 | $1/2(\chi_2+\chi_3-\chi_5-\chi_6)$ |
| 5 | $b_1$ | 0.815 | $0.4091\chi_1+0.2871(\chi_2+\chi_6)-0.1752(\chi_3+\chi_5)-0.4298\chi_4-0.2739\chi_7-0.5158\chi_8-0.1237\chi_9+0.2555\chi_o$ |
| 6 | $b_1$ | −0.429 | $0.1751\chi_1-0.2630(\chi_2+\chi_6)-0.0622(\chi_3+\chi_5)+0.2897\chi_4+0.5130\chi_7-0.3310\chi_8-0.4883\chi_9+0.3580\chi_o$ |
| 7 | $a_2$ | −1.000 | $1/2(-\chi_2+\chi_3-\chi_5+\chi_6)$ |
| 8 | $b_1$ | −1.117 | $0.4721\chi_1-0.1815(\chi_2+\chi_6)-0.2694(\chi_3+\chi_5)+0.4824\chi_4-0.1870\chi_7-0.1824\chi_8+0.4632\chi_9-0.2248\chi_o$ |
| 9 | $b_1$ | −1.650 | $0.0747\chi_1+0.1169(\chi_2+\chi_6)-0.2675(\chi_3+\chi_5)+0.3243\chi_4-0.4061\chi_7+0.5347\chi_8-0.4723\chi_9+0.2121\chi_o$ |
| 10 | $b_1$ | −2.129 | $0.4909\chi_1-0.3811(\chi_2+\chi_6)+0.3204(\chi_3+\chi_5)-0.3010\chi_4-0.3218\chi_7+0.2245\chi_8-0.1275\chi_9+0.0497\chi_o$ |

Table II. Energies and wave functions for lower excited states of cinnamaldehyde

| Symmetry | Excitation energy, eV. calcd. | Excitation energy, eV. obs. | Wave function | Oscillator strength |
|---|---|---|---|---|
| $B_2^-$ | 4.10 | | $0.946V_{46}-0.326V_{57}$ | 0.000 |
| $A_1$ | 4.11 | 4.41 | $V_{56}$ | 0.806 |
| $B_2^+$ | 5.50 | 5.53 | $0.326V_{46}+0.946V_{57}$ | 0.337 |

where $\alpha=\alpha_c$ and $\beta=\beta_{cc}$. We adopted the values of the parameters $\delta_o=1.5$ and $\rho_{co}=2^{1/2}$ as given by Baba et al.[6] Other Coulomb integrals were assumed to be equal to $\alpha$. The resonance integrals except those of the benzene ring and carbonyl group, were calculated by the approximation generally adopted

$$\beta_{rs}=(S_{rs}/S)\beta$$

were $S_{rs}$ is the overlap integral between neighboring atom r and s, and $S$ the overlap integral for benzene. In Table I the MO energies and orbitals of cinnamaldehyde are given. For the resonance integral values which are necessary for determining the energies of configurations the values given by Goodman and others[8,9]

$$\beta(B_2)=2.98\text{ eV.}$$

$$\beta(A_1)=3.30\text{ eV.}$$

were used. The configuration interaction was considered between those configurations with lower energy and belonging to the same symmetry. The matrix element of the total Hamiltonian $\mathbf{H}$ between the configurations $V_{ik}$ and $V_{jl}$ is given by

$$\int V_{ik}^*\mathbf{H}V_{jl}\,d\upsilon=2[ki|jl]-[kl|ji] \qquad (i\neq j,\ k\neq l)$$

where

$$[ij|kl]=\int\phi_i^*(1)\phi_k^*(2)(e^2/r_{12})\phi_j(1)\phi_l(2)d\upsilon$$

MO's $\phi_i$ are obtained by the simple LCAO procedure neglecting differential overlap. The integral $[ij|kl]$ can be expressed in terms of atomic orbitals as

$$[pp|qq]=\int\chi_p^*(1)\chi_q^*(2)(e^2/r_{12})\chi_p(1)\chi_q(2)d\upsilon$$

For the integrals of this type we employed Pariser and Parr's results[5]. To avoid difficult calculation only the interaction between $V_{46}$ and $V_{57}$ belonging to the same symmetry is considered. In this way the value of the matrix element

$$\int V_{46}^*\mathbf{H}V_{57}\,d\upsilon=0.449\text{ eV.}$$

is obtained. If we assume that there is approximately no interaction between $V_{56}$ and other configurations, the energy of the state represented by $V_{56}$ is calculated directly. The energies of the states resulting from the interaction of $V_{46}$ and $V_{57}$ were obtained including the

8) L. Goodman and H. Shull, *J. Chem. Phys.*, **27**, 1388 (1957).
9) E. G. McRae and L. Goodman, *J. Mol. Spectroscopy*, **2**, 464 (1958).

configuration interaction energy between them as given above. The oscillator strength, $f$, is calculated by the method described by Mulliken and Rieke[10],

$$f=1.085\times10^{11}\times\omega\sum_{r}Q_r^2 \quad (r=x, y, z)$$

where $\omega$ is the frequency of the transition in $cm^{-1}$ and $Q_r$ is the transition moment defined by

$$Q_r=\int\Psi_i^* r \Psi_j \, dv$$

$\Psi_i$ is a state wave function. The results are shown in Table II.

## Discussion

The electronic spectrum of cinnamaldehyde in *n*-hexane solution has three absorption peaks at about 280, 224 and 218 mμ (Fig. 1). Among these three peaks the one at 280 mμ is the strongest, having two weak shoulders near 293 and 300 mμ. In Fig. 3 the orbital energy level

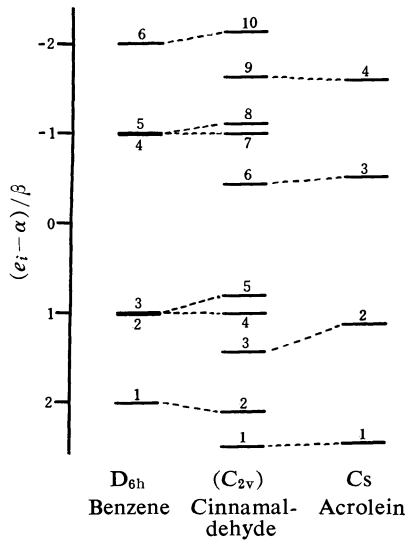



Fig. 3. Orbital energy level diagram.

diagram of cinnamaldehyde is given with those of benzene and acrolein. From this figure the occupied levels 4, 5 and the vacant levels 7, 8 of cinnamaldehyde may be assigned to the degenerate levels 2, 3 and 4, 5 of benzene. The levels 3 and 6 of cinnamaldehyde may be assigned to the levels 2 and 3 of acrolein in ground and upper states, respectively. We assigned the band at 280 mμ (4.41 eV.) to the calculated value 4.11 eV. ($A_1$), because the value of calculated oscillator strength of $A_1$ state is much greater than that of $B_2^-$ state. Therefore, the band at 280 mμ corresponds to the transition from $\phi_5$ to $\phi_6$. In our experiment no band corresponding to the calculated value 4.10 eV. ($B_2^-$) was found. The reason why we could not find the band ($B_2^-$) may be explained by the interpretation that the band ($A_1$) of cinnamaldehyde is displaced to the longer wavelength side by the greater extension of conjugation and covers the band ($B_2^-$). This interpretation conforms with the result of our calculation and with the work of Thomas et al.[11]

It should be mentioned here about the electron distribution associated with $\phi_3$, $\phi_5$ and $\phi_6$ of cinnamaldehyde. Table III shows the

Table III. Distribution of an electron in MO's $\phi_3$, $\phi_5$ and $\phi_6$

| | $\phi_3$ | $\phi_5$ | $\phi_6$ |
|---|---|---|---|
| $C_1^2$ | 0.0931 | 0.1674 | 0.0307 |
| $C_2^2$ | 0.0001 | 0.0824 | 0.0692 |
| $C_3^2$ | 0.1015 | 0.0307 | 0.0039 |
| $C_4^2$ | 0.1987 | 0.1848 | 0.0839 |
| $C_7^2$ | 0.2677 | 0.0750 | 0.2631 |
| $C_8^2$ | 0.1739 | 0.2660 | 0.1096 |
| $C_9^2$ | 0.0002 | 0.0153 | 0.2385 |
| $C_0^2$ | 0.0632 | 0.0651 | 0.1281 |

distribution of an electron occupying the MO's $\phi_3$, $\phi_5$ and $\phi_6$ in terms of squares of coefficients of atomic orbitals. It seems that the excitation of an electron from $\phi_5$ to $\phi_6$ transfers the electronic charge from the benzene ring to the acrolein group. This suggests that the transition from $\phi_5$ to $\phi_6$ corresponds to an intramolecular charge transfer band. In the region of the band II$^e$ there are two peaks at 224 and 218 mμ. Of these the 218 mμ peak is higher than the 224 mμ peak. There may arise a question as to whether or not the two main peaks constituting the band II$^e$ reveal the vibrational structure of an electronic transition, or represent two different transitions. The frequency separation between them is 1230 in *n*-hexane and 1030 $cm^{-1}$ in ethanol solutions, respectively, at room temperature. The change of 200 $cm^{-1}$ is too great. It may be reasonable to interpret the two peaks as two different transitions. The band at 224 mμ (5.53 eV.) may be assigned to the calculated excitation energy 5.56 eV. ($B_2^+$), and may correspond to the $A_{1g}$-$B_{2u}$ transition in benzene.

On the other hand, from the energy level diagram Fig. 3, we tentatively assign the band at 218 mμ (5.69 eV.) to a transition $V_{36}$ which has the lowest energy among the transitions $V_{36}$, $V_{58}$, $V_{47}$ and $V_{48}$. The transition energies for them are directly obtained from the

10) R. S. Mulliken and C. A. Rieke, *Rep. Progr. Phys.*, **8**, 231 (1941).

11) J. F. Thomas and G. Branch, *J. Am. Chem. Soc.*, **75**, 4793 (1953).

orbital energies in Table I, this is, $1.858\beta$, $1.932\beta$, $2.000\beta$, $2.117\beta$. Since cinnamaldehyde has in reality no $C_{2v}$ symmetry and the energies of these configurations are close to each other, the configuration interaction between them must be taken into consideration in order to ascertain the above assignment for $V_{36}$. For simplicity only the interaction is here considered between configurations of apparently the same symmetry type. Accordingly, the interaction between $V_{36}$, $V_{58}$ and $V_{47}$ is taken into consideration. The state energies for them were calculated including configration interaction. The results of the calculation are shown in Table IV. The calculated value for $V_{36}$ is

TABLE IV. EXCITATION ENERGIES FOR LOWER EXCITED STATES OF CINNAMALDEHYDE

| | $(m_i-m_j)\beta$ eV. | Including C. I. | Obs. |
|---|---|---|---|
| $V_{36}$ | 6.13 | 5.53 | 5.69 |
| $V_{58}$ | 6.38 | 6.22 | |
| $V_{47}$ | 6.60 | 7.37 | |

in good agreement with the observed value within present approximation. The calculated value 5.53 eV. for $V_{36}$ conforms rather with the band at 224 m$\mu$ (5.53 eV.), but we may tentatively assign the transition from $\phi_3$ to $\phi_6$ to the band at 218m$\mu$ within the present approximation. Since the orbitals $\phi_3$ and $\phi_6$ of cinnamaldehyde correspond to the orbitals $\phi_2$ and $\phi_3$ of acrolein in Fig. 3, it may be said that the 218 m$\mu$ band corresponds to the transition in the substituent group.

## Summary

State energies of the cinnamaldehyde molecule are calculated by the simple LCAO-MO method, including configuration interaction and assuming the $C_{2v}$ symmetry. The results of the calculation conform well with the observed absorption bands lying in the 2000~3000Å region. In cinnamaldehyde the 280 m$\mu$ band is assigned to the intramolecular charge transfer band. The $B_2^-$ band which we could not find in spectrum of cinnamaldehyde may be covered under the charge transfer band which is greatly shifted toward the red as the result of extension of conjugation. In the region of the band II$^c$ two peaks at 224 and 218 m$\mu$ represent two different transitions, respectively. The former is assigned to the $B_2^+$ type transition and the latter to the transition in the acrolein group.

The author expresses his sincere thanks to Professor Sunao Imanishi and Dr. Yoshiya Kanda for their encouragement throughout this work. He thanks also Dr. Rhōichi Shimada and Mr. Akira Sadō for their kind advice.

*Department of Chemistry*
*Faculty of Science*
*Kyushu University*
*Hakozaki, Fukuoka*

# *The Diamagnetic Susceptibility of Benzoate, Salicylate, Propionate, Butyrate and Succinate Ions*

By S. SRIRAMAN and S. THIRUVENGADATHAN

(Received February 9, 1961)

Magnetic susceptibilities of simple ions were evaluated by a number of workers. The importance of such a study was clearly brought out by the work of Hoare and Brindley[1], Varadachari[2] and Subramaniam[3]. In the present investigation a few alkali and alkaline earth compounds containing benzoate, salicylate, propionate, butyrate and succinate radicals have been studied in the solid state and the susceptibilities of the anions calculated assuming the previously accepted values for the cations.

## Experimental

The substances used were mostly either Merck's G. R. or B. D. H., A. R. and a few whose purity was not definite were recrystallized befor use. The salts were all found to be free from ferromagnetic impurities. Great care was taken to prevent the solids from absorbing atmospheric moisture and where this tendency existed the salts were analyzed for the moisture content by gravimetric methods and kept in vacuum desiccator before use.

Measurements of the susceptibilities of the acids

1) F. E. Hoare and G. W. Brindley, *Proc. Roy. Soc.*, **147A**, 88 (1934).
2) P. S. Varadachari, *Proc. Ind. Acad. Sci.*, **2A**, 16 (1935).
3) K. C. Subramaniam, ibid., **4A**, 404 (1936).

and their salts were made with a Curie balance. The retorsion method[4] was employed. A correction for the displaced air was applied for every bulb. For every salt and acid more than half a dozen bulbs containing different masses of the salts were examined at three field currents, viz. 4, 5 and 6 amp. Benzene (B. D. H., A. R. grade) was used as the standard and its specific susceptibility was taken as 0.702*. The susceptibilities of the salts were calculated from the usual formula.

$$\frac{\theta_S}{\theta_B} = \frac{m_S\chi_S - K_a v_S}{m_B\chi_B - K_a v_B}$$

Here $\theta_S$, $\theta_B$ and $m_S$, $m_B$ represent the deflections for and the masses of, the substance and benzene respectively; $v_S$ and $v_B$ represent the volume of the air displaced by the substance and benzene respectively. $K_a$ refers to the paramagnetic susceptibility of air at the room temperature. Its value at N. T. P. is $0.029\times10^{-6}$ (I. C. T. 6, 354, 1929) and its value at the room temperature (30°C) was found from the relation $K_a/T^2$ is constant where $K_a$ is the susceptibility of air at absolute temperature $T$°K.

## Results

The susceptibilities obtained for the acids and their salts are recorded in Table I. For the evaluation of ionic susceptibilities of the anions under investigation, Flordal and Frivold's[5] values derived from salts in dissolved

Table I. Susceptibility values for the acids and their salts

| No. | Substance | Mol. wt. | $\chi_S$ | $\chi_M$ | $\chi_{Ma}$* | $\chi_{Ma}$ (others) |
|---|---|---|---|---|---|---|
| 1 | Benzoic acid, $C_6H_5COOH$ | 122.20 | 0.5832 | 71.27 | 71.27 | 67.78[6] 70.29[7] 70.28[8] 70.62[9] |
| 2 | $NaC_7H_5O_2$ | 144.11 | 0.5350 | 77.10 | 77.10 | 77.60[10] |
| 3 | $KC_7H_5O_2$ | 160.25 | 0.5332 | 85.45 | 85.45 | 82.62[10] |
| 4 | $Ca(C_7H_5O_2)_2\cdot3H_2O$ | 336.15 | 0.5575 | 187.40 | 148.52 | 151.00[10] |
| 5 | $Sr(C_7H_5O_2)_2$ | 311.63 | 0.4912 | 153.07 | 153.07 | 166.70[10] |
| 6 | $Ba(C_7H_5O_2)_2\cdot2H_2O$ | 415.16 | 0.4589 | 190.52 | 164.60 | 177.30[10] |
| 7 | Salicylic acid, $HOC_6H_4COOH$ | 137.12 | 0.5367 | 73.59 | 73.59 | 72.23[9] |
| 8 | $NaC_7H_5O_3$ | 160.11 | 0.5138 | 82.26 | 82.26 | 85.70[10] |
| 9 | $KC_7H_5O_3$ | 176.21 | 0.5146 | 90.68 | 90.68 | 93.70[10] |
| 10 | $Ca(C_7H_5O_3)_2$ | 314.33 | 0.5050 | 158.74 | 158.74 | 162.00[10] |
| 11 | $Sr(C_7H_5O_3)_2$ | 361.88 | 0.4700 | 170.08 | 170.08 | 176.10[10] |
| 12 | $Ba(C_7H_5O_3)_2$ | 411.60 | 0.4305 | 177.19 | 177.19 | 188.00[10] |
| 13 | Propionic acid, $CH_3CH_2COOH$ | 74.04 | 0.5898 | 43.67 | 43.67 | 43.60[11] |
| 14 | $NaC_3H_5O_2$ | 96.07 | 0.5308 | 50.99 | 50.99 | 48.90[10] |
| 15 | $KC_3H_5O_2$ | 112.18 | 0.5347 | 59.98 | 59.98 | 57.20[10] |
| 16 | $Ca(C_3H_5O_2)_2$ | 186.24 | 0.5475 | 101.97 | 101.97 | 100.40[10] |
| 17 | $Sr(C_3H_5O_2)_2$ | 234.00 | 0.4423 | 103.50 | 103.50 | 107.90[10] |
| 18 | $Ba(C_3H_5O_2)_2$ | 283.52 | 0.4118 | 116.75 | 116.75 | 123.50[10] |
| 19 | Butyric acid, $CH_3CH_2CH_2COOH$ | 88.10 | 0.6146 | 54.15 | 54.15 | 55.70[12] |
| 20 | $NaC_4H_7O_2$ | 110.09 | 0.5391 | 59.35 | 59.35 | 61.60[10] |
| 21 | $KC_4H_7O_2$ | 126.10 | 0.5220 | 65.82 | 65.82 | 70.00[10] |
| 22 | $Ca(C_4H_7O_2)_2$ | 214.29 | 0.4988 | 106.89 | 106.89 | 119.50[10] |
| 23 | $Sr(C_4H_7O_2)_2$ | 261.81 | 0.4400 | 115.20 | 115.20 | 129.60[10] |
| 24 | $Ba(C_4H_7O_2)_2$ | 311.59 | 0.4018 | 125.20 | 125.20 | 145.60[10] |
| 25 | Succinic acid, $COOH(CH_2)_2COOH$ | 118.09 | 0.4804 | 56.73 | 56.73 | 57.10[13] |
| 26 | $Na_2C_4H_4O_4$ | 162.16 | 0.4159 | 67.44 | 67.44 | 76.82[10] |
| 27 | $K_2C_4H_4O_4$ | 194.31 | 0.4480 | 87.05 | 87.05 | 89.22[10] |
| 28 | $CaC_4H_4O_4$ | 156.20 | 0.4245 | 66.31 | 66.31 | 54.84[10] |
| 29 | $SrC_4H_4O_4$ | 203.75 | 0.3584 | 73.02 | 73.02 | 71.50[10] |
| 30 | $BaC_4H_4O_4$ | 253.43 | 0.3345 | 84.77 | 84.77 | 97.60[10] |

* $\chi_{Ma}$=Anhydrous molar susceptibility.

* All susceptibility values given in this paper indicate the diamagnetic susceptibilities in $10^{-6}$ c. g. s. unit.

4) S. R. Rao, ibid., **1**, 123 (1934).

5) V. M. Flordal and D. E. Frivold, *Ann. Physik*, **23**, 425 (1935).

6) F. M. Gray and W. M. Birse, *J. Chem. Soc.*, **105**, 2715 (1914).

7) K. Kido, *Sci. Rep. Tohoku, Imp. Univ.*, **24**, 701 (1936).

8) C. M. French, *Trans. Faraday. Soc.*, **50**, 1321 (1954).

9) K. Venkateswarlu and S. Sriraman., ibid., **53**, 438 (1957).

10) Mata Prasad et al., (a) *Proc. Ind. Acad. Sci.*, **16A**, 307 (1942); (b) ibid., **20A**, 224 (1944); (c) *J. Chem. Phys.*, **17**, 819 (1949); (d) ibid., **18**, 936 (1950); (e) ibid., **18**, 941 (1950); (f) ibid., **20**, 129 (1952).

11) P. Pascal, (a) *Compt. rend.*, **149**, 342 (1909); (b) ibid., **158**, 158 (1914); (c) ibid., **159**, 429 (1914); (d) ibid., **173**, 144 (1921).

12) K. Kido, *Sci. Rep. Tohoku. Imp. Univ.*, **21**, 869 (1932); ibid., **22**, 835 (1933).

13) B. K. Singh, *Proc. Ind. Acad. Sci.*, **22A**, 163 (1945).

TABLE II. SUSCEPTIBILITIES OF THE CATIONS

| Ion | $Na^+$ | $K^+$ | $Ca^{2+}$ | $Sr^{2+}$ | $Ba^{2+}$ |
|---|---|---|---|---|---|
| $\chi_{ion}$ | 6.90 | 15.00 | 8.80 | 18.30 | 29.30 |

state for $Na^+$, $K^+$, $Ca^{2+}$, $Sr^{2+}$ and $Ba^{2+}$ are used and these are given in Table II for ready reference.

The susceptibilities of the anions are evaluated using Pascal's law. Also the acid values were taken to represent the value of the corresponding ion on the assumption that $H^+$ does not contribute anything[14]. The mean values obtained for the anions under study are given in Table III.

TABLE III. IONIC SUSCEPTIBILITIES

| Ion | Mean value from salts | $\chi_{ion}$ from acid | Mean |
|---|---|---|---|
| Benzoate $C_7H_5O_2^-$ | 69.11 | 71.27 | 70.19 |
| Salicylate $C_7H_5O_3^-$ | 75.17 | 73.59 | 74.38 |
| Propionate $C_3H_5O_2^-$ | 44.39 | 43.67 | 44.03 |
| Butyrate $C_4H_7O_2^-$ | 49.74 | 54.15 | 51.95 |
| Succinate $C_4H_4O_4^{2-}$ | 55.68 | 56.73 | 56.21 |

## Discussion

The general method adopted for the evaluation of the ionic susceptibilities is on the basis that the molar susceptibility of a heteropolar salt is the sum of the constituent ions. The data available on the subject show that in the case of several ions, the values given by different authors differ sometimes by large amounts. Bhatnagar and co-workers[15] and Mata Prasad and co-workers[10] have followed a statistical method in which they subtracted all the known values of the susceptibilities of anions from the molar susceptibilities of a number of salts of a cation and took the arithmetical mean of the values thus obtained as the correct value for the cation. Kido[12], Joos[16] and Ikenmeyer[17] have observed that a linear relation exists between the susceptibilities of ions of chemically related elements belonging to the same group of the periodic table and their atomic numbers. This method of evaluation of the ionic susceptibilities has been questioned by Trew[18] and Selwood[19] on the ground that it is open to theoretical objection. Mata Prasad and co-workers[10] have followed Kido's[12] suggestion. Their results show that the susceptibility values of the anions deduced from the salts of Li, Na, K etc., are distinctly different from those deduced from the salts of Ca, Sr and Ba. This difference is large in some cases and small in others. If the linear relation is assumed then the assignment of ionic value could be done by measuring the molar susceptibilities of only two salts containing the cations of the same column of the periodic table.

When two ions combine there is every likelihood of a deformation taking place in both the ions. It is quite possible that the degree of deformations in ions may be different for the different groups of cations. To what extent this will affect the susceptibility of the anions is a question which is worth considering. On the basis of Pascal's additive law[11] the $\chi$ of anions can be calculated assuming the values of alkali and alkaline earth metallic ions. In Table IV this calculation has been made with the values obtained by Mata Prasad and co-workers[10], Rao and Sriraman[20] and Venkateswarlu and Sriraman[9] for formate, acetate and oxalate ions.

The anion values given in Table IV show definitely that they do not change abruptly as we pass from one group of metallic ions to another. All the values are of the same order subject to the error in the measurements of the susceptibility of the salts.

It is interesting to compare these values for a few typical ions with the values (Table V) obtained by Prasad and others by graphical method on the basis of linearity. For four ions the values from alkali salts are larger than from alkaline earth salts, for the last two ions the change is the other way about and for the oxalate ion no change is observed. If the values of the various ions are calculated from their own measurements on the basis of additivity, such marked variations are not found. Considering the graphical method adopted, Trew[18] has definitely pointed out that the graphs do not show linearity and the points do not lie on a single straight line. Our results in the present investigation also confirm this point. The linearity may be approximately true in a very few cases as Kido[12] found but it is certainly not applicable in all cases. The large amount of literatures available on the subject and the convincing facts brought out by Trew[18] show that the additivity method

14) K. Reichender, *Ann. Physik*, **1**, 169 (1929).
15) S. S. Bhatnagar et al., *Phil. Mag.*, **18**, 449 (1934).
16) V. G. Joos, *Z. Physik*, **19**, 347 (1923).
17) K. Ikenmeyer, *Ann. Physik*, **1**, 169 (1929).
18) V. C. G. Trew, *Trans. Faraday, Soc.*, **37**, 476 (1941).
19) P. W. Selwood, "Magnetochemistry", Interscience Publishers Inc., New York (1952).
20) S. R. Rao and S. Sriraman, *Phil. Mag.*, **24**, 1025 (1937).

TABLE IV

| Substance | Prasad and co-workers | | Rao and Sriraman | |
|---|---|---|---|---|
| | $\chi_{Ma}$ | $\chi_{Anion}$ | $\chi_{Ma}$ | $\chi_{Anion}$ |
| Sodium formate, NaHCOO | 24.50 | 17.60 | 24.80 | 17.90 |
| Calcium formate, $Ca(HCOO)_2$ | 45.30 | 18.30 | 39.50 | 15.35 |
| Barium formate, $Ba(HCOO)_2$ | 73.70 | 22.20 | 66.60 | 18.65 |
| Sodium acetate, $NaCH_3COO$ | 39.22 | 32.22 | 37.60 | 30.70 |
| Barium acetate, $Ba(CH_3COO)_2$ | 99.49 | 35.10 | 88.04 | 29.37 |
| | | | Venkateswarlu and Sriraman | |
| Sodium oxalate, $Na_2C_2O_4$ | 51.20 | 37.40 | 47.74 | 33.94 |
| Potassium oxalate, $K_2C_2O_4$ | 65.64 | 35.64 | 64.89 | 34.89 |
| Calcium oxalate, $CaC_2O_4$ | 44.30 | 35.50 | 42.08 | 33.28 |
| Strontium oxalate, $SrC_2O_4$ | 54.64 | 36.34 | 51.20 | 32.90 |
| Barium oxalate, $BaC_2O_4$ | 64.80 | 35.50 | 63.10 | 33.80 |

TABLE V

| Anion | $\chi_{anion}$, graphical | | $\chi_{anion}$ additive |
|---|---|---|---|
| | Li, K, Na | Ca, Sr, Ba | |
| Formate | 20.50 | 15.00 | 17.30[20] |
| Acetate | 34.00 | 25.00 | 29.80[20] |
| Oxalate | 34.40 | 34.00 | 33.86[9] |
| Succinate | 58.80 | 36.00 | 55.67[21] |
| Salicylate | 81.00 | 74.50 | 74.62[21] |
| Malonate | 45.00 | 53.00 | — |
| Stearate | 206.00 | 212.00 | — |

21) S. Sriraman and S. Thiruvengadathan, This paper.

of evaluating the ionic value is more reliable subject to the accuracy of the measurements and the small error involved in the assumption of the cation values.

The authors wish to express their grateful thanks to Dr. K. Venkateswarlu for his keen and continued interest throughout this investigation.

*Department of Physics*
*Annamalai University*
*Annamalainagar, South India*

# *Refractometric Study of Some Cyano and Oxalato Complex Anions*

By Yoshio MATSUNAGA*

(Received February 20, 1961)

The molar refraction of simple salts, particularly in the dissolved state, has been studied extensively by Fajans and others; however, little attention has been paid to that of complex salts. It seemed of great interest to examine the following two effects based on this physical quantity;

(1) polarization effect; the decrease of mobility of electrons in ligands due to the field of a central metal ion, and

(2) delocalization effect; the increase of mobility of electrons by the formation of $\pi$-bonds.

The former effect is expected to contribute to the decrease of molar refraction and the latter to the increase. With this hope we studied the molar refraction of some cyano and oxalato complex salts. Because of the high polarizability and the great ability for $\pi$-bond formation of ligand, cyano complex anions of the inner orbital type were chosen to demonstrate the above-mentioned two effects. On the other hand, oxalato complex anions are of the outer orbital type and the interaction between the constituents may not be very strong.

## Experimental

**Materials.**—They were prepared by the methods described in the references cited. $K_3Cu(CN)_4$, prepared from cupric sulfate and potassium cyanide, and dried at 150°C[1]. $K_2Zn(CN)_4$, prepared from zinc sulfate and potassium cyanide, and dried at

* Present address: Cyanamid European Research Institute, Cologny, Geneva, Switzerland.

1) W. Biltz, *Z. anorg. u. allgem. Chem.*, **170**, 161 (1928).

105°C[2]. $K_2Cd(CN)_4$, prepared from cadmium sulfate and potassium cyanide, and dried at 105°C[1]. $K_2Hg(CN)_4$, prepared from mercuric cyanide and potassium cyanide, and dried at 80°C[1]. $K_3Cr(CN)_6$, prepared from potassium dichromate and potassium cyanide, and dried at 100°C[3]. $K_3Mn(CN)_6$, prepared from potassium cyanide and manganese(III) phosphate[3]. $K_3Fe(CN)_6$ and $K_4Fe(CN)_6$, Dog brand guaranteed reagents supplied by Koso Chemical Co., Ltd. Tokyo. $K_3Co(CN)_6$, prepared from cobalt chloride and potassium cyanide[3]. $K_2Ni(CN)_4$, prepared from nickel sulfate and potassium cyanide, and dried at 105°C[3]. $K_3Al(C_2O_4)_3 \cdot 3H_2O$, prepared from aluminum sulfate, potassium oxalate and oxalic acid[4]. $K_3Fe(C_2O_4)_3 \cdot 3H_2O$, prepared from ferric sulfate, barium oxalate, and potassium oxalate[4]. $K_2C_2O_4 \cdot H_2O$, prepared from oxalic acid and potassium carbonate.

**Measurements.**—The refractive index $n$ of aqueous solutions was measured with a Pulfrich refractometer using the NaD line. The density $d$ of the same solution was determined with Ostwald's pycnometers of about 10 cc. Most salts involved in this study are easily soluble in water, so that a concentration higher than three per cent by weight was applied. The specific refraction $r$ of the respective solution was calculated from these data using the Lorentz-Lorenz formula,

$$r=(n^2-1)/(n^2+2)\times 1/d$$

The molar refraction $R$ of the dissolved salt was derived from this specific refraction by the application of the additivity rule,

$$R=MW[r(\text{soln.})-(100-w)\times r(\text{water})]/w$$

where $w$ is the concentration of salt and $MW$ is the molecular weight. The value $R$ was found to be independent of concentration in the measured range.

TABLE I. MOLAR REFRACTION OF COMPLEX SALTS

| | Molar refraction, cc. | | |
|---|---|---|---|
| | Solution | | Crystal[c] |
| Salt | Obs. | Lit. | |
| $K_3Cu(CN)_4$ | 46.8 | — | 44.9[d] |
| $K_2Zn(CN)_4$ | 37.8 | — | 37.5 |
| $K_2Cd(CN)_4$ | 39.9 | — | 40.5 |
| $K_2Hg(CN)_4$ | 43.1 | — | 43.2 |
| $K_3Cr(CN)_6$ | 55.5 | — | 56.2 |
| $K_3Mn(CN)_6$ | 61.0 | — | — |
| $K_3Fe(CN)_6$ | 61.2 | 61.44[a], 60.91[b] | 58.4 |
| $K_4Fe(CN)_6$ | 67.4 | 67.8[a], 69.06[b] | — |
| $K_3Co(CN)_6$ | 59.2 | — | — |
| $K_2Ni(CN)_4$ | 42.1 | — | — |
| $K_2Al(C_2O_4)_3$ | 59.5 | — | — |
| $K_2Fe(C_2O_4)_3$ | 66.4 | — | — |
| $K_2C_2O_4$ | 22.5 | — | — |

a See Ref. 5.
b See Ref. 6.
c The values of density were taken from Ref. 1, and those of refractive index from Ref. 7 except that for $K_3Cu(CN)_4$.
d Refractive indices were taken from Ref. 8.

## Results and Discussion

In Table I are presented our observed values of molar refraction of the complex salts in the dissolved state together with a few recorded values and also some estimated values for the crystalline salts. The molar refraction of aqueous complex anion was estimated, assuming that the contributions of cation and anion are additive. The value for aqueous $K^+$ ion was taken as 2.255 cc.[9] The molar refraction of aqueous ions is generally smaller than that of gaseous ions. For example the values: 0.20, 0.50 and 0.28 cc. were given by Fajans and Joos for gaseous $Li^+$, $Na^+$ and $Mg^{2+}$ ions, respectively[10]. On the other hand, they gave −0.42, +0.200 and −1.57 cc. for the above-mentioned ions in the dissolved state. The difference between the values in the two states can be ascribed to the polarization, or the decrease of mobility of electrons in water molecules by the electrostatic force due to the cation concerned. Great polarizing power is expected from small ions of high valency. The negative values assigned to aqueous $Li^+$ and $Mg^{2+}$ ions arise from the large polarization effect on the water molecules in the hydration sphere. However, the magnitude of this effect in hydrated ions seems to be too small and inaccurate to be discussed quantitatively. The size of complex anions is much larger than that of simple ions, therefore we may consider that the molar refraction of aqueous complex anion is approximately equal to that of gaseous complex anion.

We assume that the molar refraction of complex anions is given by the sum of the following three terms:

(1) The sum of the molar refractions of the constituents in the gaseous state. The term $A$ in Table II gives the molar refraction of the imaginary complex anion in which there is neither metal-ligand nor ligand-ligand interaction.

2) G. Bauer, "Handbuch der Präparativen Anorgachen Chemie", F. Enke, Stuttgart (1954), pp. 807, 819.
3) W. C. Fernelius, "Inorganic Syntheses", vol. 2, McGraw-Hill Book Co., New York (1946), pp. 203, 213, 225, 227.
4) H. S. Booth, ibid., Vol. 1., Mc Graw-Hill Book Co., New York (1939), p. 35.
5) A. Heydweiller, *Physik. Z.*, **26**, 526 (1925).
6) M. T. Rogers and J. G. Malik, *J. Am. Chem. Soc.*, **77**, 6515 (1955).
7) A. N. Winchell and R. C. Emmons, "The Microscopic Characters of Artificial Inorganic Solid Substances or Artificial Minerals", John Wiley & Sons, Inc., New York (1931), pp. 173, 177, 178.
8) E. G. Cox, W. Wardlaw and K. C. Webster, *J. Chem. Soc.*, **1936**, 775.
9) K. Fajans and R. Lühdemann, *Z. physik. Chem.*, **B29**, 150 (1935).
10) K. Fajans and G. Joos, *Z. Physik*, **23**, 1 (1924).

(2) The contribution of polarization of ligands: the term $P$ in Table II. The ligand-ligand interaction may be ignored because of the rather large size of cyanide and oxalate ions. Therefore, the magnitude of this term may be assumed to be proportional to the polarizing power of central metal ion; namely to the valency of metal ion and to the reciprocal of the square of metal-ligand distance.

(3) The contribution of delocalization of electrons by the formation of $\pi$-bonds: the term $D$ in Table II. The magnitude of this term may depend on the configuration of complex ion and the number of available electrons.

Table II. Molar refraction of complex anions

| Anion | $R$ for anion cc. | $A$, cc. (additive) | $P$, cc. (polarization) | $D$, cc. (delocalization) |
|---|---|---|---|---|
| $Cu(CN)_4^{3-}$ | 40.1 | 34.7 | − 6.4 | 11.8 |
| $Zn(CN)_4^{2-}$ | 33.3 | 34.3 | −12.8 | 11.8 |
| $Cd(CN)_4^{2-}$ | 35.4 | 36.3 | −12.8 | 11.9 |
| $Hg(CN)_4^{2-}$ | 38.6 | 36.7 | −12.8 | 14.7 |
| $Cr(CN)_6^{3-}$ | 48.8 | 50.9 | −16.5 | 15.4 |
| $Mn(CN)_6^{3-}$ | 54.3 | 50.9 | −16.5 | 20.9 |
| $Fe(CN)_6^{3-}$ | 54.4 | 50.9 | −16.5 | 21.0 |
| $Fe(CN)_6^{4-}$ | 58.2 | 51.1 | −11.0 | 19.1 |
| $Co(CN)_6^{3-}$ | 52.5 | 50.9 | −16.5 | 19.1 |
| $Ni(CN)_4^{2-}$ | 37.6 | 34.3 | − 8.7 | (12) |
| $Al(C_2O_4)_3^{3-}$ | 52.8 | 54.1 | − 1.3 | 0 |
| $Fe(C_2O_4)_3^{3-}$ | 59.7 | 54.5 | − 1.3 | 6.5 |

The molar refraction of gaseous cyanide ion was estimated to be 8.40 cc. based on the value observed for potassium cyanide in the dissolved state[11] and that of gaseous oxalate ion 18.0 cc. similarly. Pauling has given the following values for gaseous cations; $Cu^+$ 1.08, $Zn^{2+}$ 0.72, $Cd^{2+}$ 2.74, $Hg^{2+}$ 3.14 and $Al^{3+}$ 0.136 cc.[12] We assumed 0.7 cc. for $Ni^{2+}$ and $Fe^{2+}$ ions and 0.5 cc. for trivalent ions of the first transition metals. The terms $A$ given in Table II were calculated using these values. It must be noted that the values of tetrahedral complex anions are in good agreement with the observed molar refractions except in the case of $Cu(CN)_4^{3-}$ ion, However, as is shown in the following paragraph, this agreement arises from the compensation between the terms $P$ and $D$.

For the estimation of the term $P$ we must know the distance between ligand and central metal ion. Only the following values are available; Zn–CN (center) 2.61, Cd–CN 2.67 and Hg–CN 2.65 Å[13]. We may assume that the required distances are the same in the series of tetrahedral cyano complex anions including $Cu(CN)_4^{3-}$. The maximum error arising from this assumption may not be more than 10 per cent of the term $P$ or about 1 cc., as seen in Table II. The positive charge on central metal ion is mostly neutralized as a result of polarization of ligands. The magnitude of the term $D$ for the isoelectronic $Cu(CN)_4^{3-}$ and $Zn(CN)_4^{2-}$ ions may be assumed to be roughly the same. Therefore, the chief difference between the two is that of the valency of the central metal ions, and the term $P$ for $Cu(CN)_4^{3-}$ ion may be about one half of that for $Zn(CN)_4^{2-}$ ion. Consequently the difference between $(A-R)$ for $Zn(CN)_4^{2-}$ ion and that for $Cu(CN)_4^{3-}$ ion gives the magnitude of the term $P$ for the latter. The term $P$ estimated for $Zn(CN)_4^{2-}$ ion was assumed to be applicable to the other two tetrahedral complex anions. The $Cu(CN)_4^{3-}$ ion has been known to dissociate appreciably in dilute solution[14]. However, we ignored this fact in our treatment of molar refraction because rather concentrated solutions were used for our measurements.

For octahedral cyano complex anions the isoelectronic ions $Fe(CN)_6^{4-}$ and $Co(CN)_6^{3-}$ were used for the basis of discussion. We assumed again that the distance between metal ion and ligand is nearly constant in these five complex anions, therefore the term $P$ for $Fe(CN)_6^{4-}$ ion may be about two thirds of that for $Co(CN)_6^{3-}$ ion and the term $D$ for this pair may be roughly the same. The term $P$ estimated for $Co(CN)_6^{3-}$ ion was applied to the other trivalent cyano complex anions.

The contribution of polarization effect on a cyanide ion was found to be about 1.6 cc. per unit charge on central metal ion for tetrahedral anions and about 0.9 cc. per unit charge for octahedral ones. The similar polarization found in the reaction,

$$H^+ + CN^- \rightarrow \text{gaseous HCN } (6.47\,\text{cc.})^{15}$$

1.93 cc. may be compared with the above two estimations. As the mutual repulsion of cyanide ions in a complex anion must be weaker in a tetrahedral configuration than in an octahedral one, the cyanide ions in the former are closer to the central metal ion than those in the latter. Therefore, the observed order of polarization of a cyanide ion; HCN > tetrahedral complex anion > octahedral complex anion seems to be reasonable. The contribution of electron-delocalization to molar refraction was estimated to be around 3 cc. per cyanide ion for both tetrahedral and octahedral complex

11) M. Le Blanc and P. Rohland, *Z. physik. Chem.*, **19**, 261 (1896).
12) L. Pauling, *Proc. Roy. Soc.*, **A114**, 181 (1927).
13) R. G. Dickinson, *J. Am. Chem. Soc.*, **44**, 774 (1922).
14) J. H. Baxendale and D. T. Westcott, *J. Chem. Soc.*, **1959**, 2347.
15) K. Fajans, *Z. physik. Chem.*, **B24**, 103 (1934).

anions. The term $P$ for the square planar $Ni(CN)_4^{2-}$ ion was obtained using a value of $4\times3$ cc. for its term $D$, and the polarization of a cyanide in per unit charge in this anion seems to be nearly the same as that for octahedral complex anions.

In the case of oxalato complex anions, the observed molar refraction of $Al(C_2O_4)_3^{3-}$ ion, in which the aluminum ion has no $d$-electron for $\pi$-bonding, is only slightly smaller than its term $A$ or we may say in agreement with its term $A$ within the limit of estimations. This agreement suggests that the polarization of the oxalate ions by the field of the aluminum ion is very small. The term $D$ for $Fe(C_2O_4)_3^{3-}$ ion was found to be about 6.5 cc. This value is much less than that for cyano complex anions of the inner orbital type.

TABLE III. COMPARISON BETWEEN MOLAR REFRACTION AND MOLAR VOLUME OF CYANO COMPLEX ANIONS

| Anion | Molar refraction cc. | Molar volume[a] cc. |
|---|---|---|
| $Cu(CN)_4^{3-}$ | 40.1 | 93 |
| $Zn(CN)_4^{2-}$ | 33.3 | 118 |
| $Cd(CN)_4^{2-}$ | 35.4 | 128 |
| $Hg(CN)_4^{2-}$ | 38.6 | 126 |
| $Cr(CN)_6^{3-}$ | 48.8 | 135 |
| $Mn(CN)_6^{3-}$ | 54.3 | — |
| $Fe(CN)_6^{3-}$ | 54.4 | 129 |
| $Fe(CN)_6^{4-}$ | 58.2 | 126 |
| $Co(CN)_6^{3-}$ | 52.5 | 129 |
| $Ni(CN)_4^{2-}$ | 37.6 | 98 |

a These values were taken from Ref. 1.

Recently Hieber and his collaborators have discussed the molar volumes of some complex cyano anions[16,17]. They have observed the following series of molar volumes for the isoelectronic anions with the configuration of rare gas type,

$$Zn(CN)_4^{2-} > Cu(CN)_4^{3-} > Ni(CN)_4^{4-}$$

and $$Co(CN)_6^{3-} > Fe(CN)_6^{4-} > Mn(CN)_6^{5-}$$

and concluded that the decrease of molar volume can be correlated with the increasing double bond character of metal-carbon bonds. The importance of polar structures as the determining factor was also pointed out for the molar volume of anions of non-rare gas type. Although molar refraction is a measure of size of complex anion, these two physical quantities have no simple correlation as seen in Table III. For the pairs of isoelectronic complex anions; $Cu(CN)_4^{3-}$ and $Zn(CN)_4^{2-}$, and $Fe(CN)_6^{4-}$ and $Co(CN)_6^{3-}$, the molar refractions were found in the reverse order to the molar volumes.

16) W. Hieber, R. Nast and J. G. Floss, *Z. anorg. u. allgem. Chem.*, **283**, 188 (1956).
17) W. Hieber and O. Vohler, ibid., **294**, 219 (1958).

**Summary**

The molar refractions of ten cyano and two oxalato complex salts were measured in the dissolved state using the NaD line. The molar refractions of complex anions were assumed to be given by the sum of (1) the molar refractions of the ligands and the central metal ion in the gaseous state, (2) the polarization of the ligands due to the field of the central metal ion, and (3) the delocalization of electrons by the metal-ligand $\pi$-bonding. The estimation of each term was attempted on the assumption that the chief difference between isoelectronic anions, for example $Cu(CN)_4^{3-}$ and $Zn(CN)_4^{2-}$, is that of the valency of the central metal ions and the contribution of delocalization is roughly the same in such a pair. The polarization of a cyanide ion was found to be about 1.6 cc. per unit charge of metal ion for tetrahedral anions and about 0.9 cc. for octahedral ones. The contribution of $\pi$-bonding was estimated to be around 3 cc. per metal-ligand bond for both of the above-mentioned cyano complex anions. The small polarization and delocalization effects were observed in the case of oxalato complex anions.

The author wishes to express his hearty thanks to Professors Eiichi Minami and Shizuo Fujiwara for their interest and encouragement.

*Department of Chemistry*
*Faculty of Science*
*The University of Tokyo*
*Hongo, Tokyo*

# *The Preparation of cis- and trans-4-tert-Butylcyclohexyl-1-carbinols*

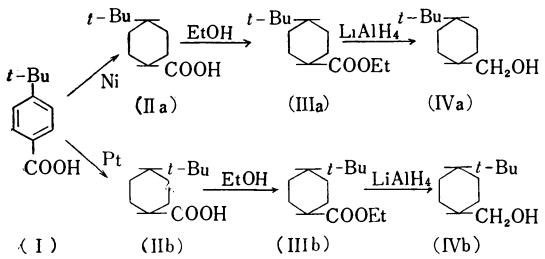
By Nobuo MORI

(Received March 18, 1961)

In the course of the investigation[1] concerning the conformation of a toluenesulfoxymethyl group directly bound to a cyclohexane ring, it was found to be desirable to study *cis*- and *trans*-4-*tert*-butylcyclohexyl-1-carbinyl *p*-toluenesulfonates.

The present work relates to a process for the preparation of the hitherto unknown *cis*- and *trans*-4-*tert*-butylcyclohexyl-1-carbinols and their *p*-toluenesulfonates.

The *cis*- and *trans*-carbinols have now been prepared from 4-*tert*-butylbenzoic acid by hydrogenating them over platinum oxide in acetic acid and over Raney nickel in neutral aqueous medium, respectively. The resulting *cis*- and *trans*-4-*tert*-butylhexahydrobenzoic acids were converted into their ethyl esters which were treated with lithium aluminum hydride to give the *cis*- and *trans*-carbinols respectively, and they were converted into the *p*-toluenesulfonates. The process carried out is shown in the following scheme.




*tert*-Butylbenzoic acid (I) used as starting material was obtained by reacting dry benzene with *tert*-butyl alcohol over aluminum chloride[2], brominating the resulting *tert*-butylbenzene with bromine over iron powder[3] and treating a Grignard reagent of the 4-*tert*-butylbromobenzene with carbon dioxide according to the method[4] for the conversion of *tert*-butyl chloride into *tert*-butylacetic acid.

The hydrogenation of substituted benzene compounds in neutral medium with Raney nickel generally gives thermodynamically stable hydrogenated benzene compounds as main products and on the contrary in acetic acid with platinum oxide less stable stereoisomers. For example, the hydrogenation[1,5] of 4-methyl- or isopropylbenzoic acid over Raney nickel gives mainly the corresponding *trans*-hexahydrobenzoic acid melting at a higher temperature and over platinum oxide the corresponding cis-isomer melting at a lower temperature. The hydrogenation of the 4-isopropylbenzoic acid by either of the above methods does not proceed so readily as with the 4-methylbenzoic acid. The 4-methylbenzoic acid is completely hydrogenated with Raney nickel under an initial pressure of 90 atm. at 180~200°C in 2 hr. to give the hexahydrobenzoic acid, while the hydrogenation of the isopropylbenzoic acid[5] is effected under 150~200 atm. 200°C for 4~5 hr. On the other hand, the hydrogenation[1,5] of the methyl- and isopropylbenzoic acids with platinum oxide is completed under atmospheric pressure in 2~4.5 and 6 hr., respectively.

In the present work, the butylbenzoic acid (I) was hydrogenated in a neutral aqueous solution with Raney nickel under an initial pressure of 90 atm. 250~260°C in 5 hr., although the uptake of hydrogen was not complete and this reaction was probably accompanied by hydrogenolysis, and the *trans*-hexahydrobenzoic acid melting at 175~176°C after recrystallization was obtained in a 40% yield. On the other hand, the butylbenzoic acid (I) was not hydrogenated in acetic acid with platinum oxide within 4 hr. at 60~70°C under atmospheric pressure, but the uptake of hydrogen was very readily and completely effected under an initial pressure of 60 atm. at about 100°C in 1 hr. and the *cis*-hexahyrobenzoic acid (IIb) was obtained as scales, m. p. 115~117°C after recrystallization, in a good yield. The difficulty in hydrogenation of these 4-alkylbenzoic acids increases as the alkyl group goes from methyl to *tert*-butyl. These acids were converted into their anilides by the method without the danger of isomerization.

The above acids were converted into their ethyl esters by refluxing in ethyl alcohol with a small amount of sulfuric acid in a short

1) N. Mori, This Bulletin, **34**, 1299 (1961).
2) C. S. Marvel et al., *J. Am. Chem. Soc.*, **66**, 914 (1944).
3) R. C. Huston, W. B. Fox and M. N. Binder, *J. Org. Chem.*, **3**, 251 (1938).
4) H. Gilman and R. H. Kirby, "Organic Syntheses", Coll. Vol. I, Second edition (1941), p. 361.
5) R. G. Cooke and A. K. Macbeth, *J. Chem. Soc.*, **1939**, 1245.

period. The refractive index and the density of the cis-ester (IIIb) are higher than those of the trans-ester (IIIa). In Table I, the physical constants of the *cis*- and *trans*-4-*tert*-butylhexahydrobenzoic acids and their derivatives obtained in the present work are shown with those of 4-methyl and isopropylhexahydrobenzoic acids and their derivatives for comparison.

Table I. Physical constants of isomeric 4-alkyl-hexahydrobenzoic acids and their derivatives

| 4-Alkyl | Free acid M. p., °C | Anilide M. p., °C | Ethyl ester $n_D^{20}$ | Ethyl ester $d_4^{20}$ |
|---|---|---|---|---|
| *trans-tert*-Bu | 175~176 | 139.5 | 1.4515 | 0.9282 |
| *cis-tert*-Bu | 115~117 | 191 | 1.4593 | 0.9400 |
| *trans*-isoPr[5] | 94 | — | — | — |
| *cis*-isoPr[5] | liq. | — | 1.4491 | — |
| *trans*-Me[6] | 111 | — | 1.4392 | 0.9361 |
| *cis*-Me[6] | 13 | — | 1.4425 | 0.9448 |

These trans- and cis-esters IIIa and IIIb were converted into the corresponding carbinols IVa and IVb by treatment with lithium aluminum hydride, according to the method[1] for the conversion of the isomeric 4-methylhexahydrobenzoic acid ethyl esters into their carbinols. It is well known that hydrogenolysis of esters with lithium aluminum hydride proceeds with complete retention of configuration while that with sodium in alcohol and over copper chromite catalyst proceeds with some isomerization. The purified *cis*-carbinol is in needles melting at 56~57°C and the trans-isomer is in needles of m. p. 25~27°C. The refractive index and the density of the *cis*-carbinol which was in a super-cooled liquid form before purification are higher than those of the super-cooled *trans*-carbinol, as shown in Table II, which also includes those of 4-methyl- and isopropyl-cyclohexyl-1-carbinols for comparison, and this fact is in accordance with the Auwers-Skita rule[7].

Table II. Physical constants of isomeric 4-alkylcyclohexyl-1-carbinols and their tosylates

| 4-Alkyl | Carbinol $n_D^{20}$ | Carbinol $d_4^{20}$ | Tosylate M. p., °C |
|---|---|---|---|
| *trans-tert*-Bu | 1.4683 | 0.9092 | 83 ~84 |
| *cis-tert*-Bu | 1.4781 | 0.9243 | 95 ~95.5 |
| *trans*-isoPr[5] | 1.4661* | 0.9007* | — |
| *cis*-isoPr[5] | 1.4682* | 0.9051* | — |
| *trans*-Me[5] | 1.4578* | 0.8962* | 44.5~44.7[1] |
| *cis*-Me[5] | 1.4617* | 0.9074* | 30.5~31.0[1] |

* Values at 30°C.

6) G. H. Keats, ibid., **1937**, 2003.
7) K. von Auwers, *Ann.*, **420**, 84 (1920); A. Skita, *Ber.*, **53**, 1792 (1920); A. Skita and W. Faust, ibid., **64**, 2878 (1931).

## Experimental

**4-*tert*-Butylbenzoic Acid (I).**—A Grignard reagent solution was prepared in the usual way by adding dropwise 4-*tert*-butyl-bromobenzene (70 g.) in dry ether (200 cc.) to magnesium strips (8 g.) covered with ether (50 cc.) while warming on steam bath and stirring. The solution was cooled to −15~−10°C in an ice-salt bath and then treated with a stream of dry carbon dioxide until the temperature rose no more. The reaction mixture was decomposed with dilute sulfuric acid and the ethereal layer was washed with aqueous sodium hydroxide solution. The aqueous layer separated was acidified with concentrated hydrochloric acid to give an acid product which melted at 163~164.4°C (lit.[2] 164°C) after one recrystallization from aqueous methanol.

***trans-tert*-Butylhexahydrobenzoic Acid (IIa).**—A solution (pH=8.0) of the butylbenzoic acid (12 g.) in 7% sodium hydroxide solution was hydrogenated in the presence of Raney nickel (6 g.) under an initial pressure of 90 atm. at 250~260°C. The reaction was stopped after 5 hr. although the uptake of hydrogen was not complete. After removal of the catalyst, the solution was acidified with concentrated hydrochloric acid and the precipitated material (10 g.) was repeatedly recrystallized from aqueous methanol to give the pure *trans*-hexahydrobenzoic acid (3 g.) as plates, m. p. 175~176°C (lit.[8] 174°C).

Found: C, 71.8; H, 10.9. Calcd. for $C_{11}H_{20}O_2$: C, 71.7; H, 10.9%.

A part of the acid was converted into an anilide by refluxing for 10 min. with one equivalent each of thionyl chloride and pyridine in dry benzene and then for 2 min. with two equivalents of aniline. Recrystallization of the anilide from aqueous ethanol readily gave fine plates, m. p. 139.5°C.

Found: N, 5.6. Calcd. for $C_{17}H_{25}ON$: N, 5.4%.

***cis-tert*-Butylhexahydrobenzoic Acid (IIb).**—A solution of the butylbenzoic acid (10 g.) in purified glacial acetic acid (60 cc.) was hydrogenated with platinum oxide (0.5 g.) under an initial pressure of 60 atm. at 90~100°C until no more hydrogen was absorbed. After removal of the catalyst and the solvent, the crystalline residue was taken up in a small volume (about 20 cc.) of petroleum ether and the undissolved parts were filtered off. The filtrate was concentrated and cooled. The separated plates were filtered off and recrystallized repeatedly from aqueous methanol to give the pure *cis*-hexahydrobenzoic acid (6 g.) as scales, m. p. 115~117°C (lit.[8] 116°C).

Found: C, 71.7; H, 10.6. Calcd. for $C_{11}H_{20}O_2$: C, 71.7; H, 10.9%.

The anilide of the cis-acid was obtained by the method used for the trans-acid as long needles from aqueous methanol and ligroin, m. p. 191°C which was depressed to 124~127°C on admixture with the trans-anilide.

Found: N, 5.6. Calcd. for $C_{17}H_{25}ON$: N, 5.4%.

8) Eliel and Acharya reported that the acids were first obtained by Stolow, but the details of preparation are not described. See E. L. Eliel and R. V. Acharya, *J. Org. Chem.*, **24**, 151 (1959).

**Ethyl *trans*-*tert*-Butylhexahydrobenzoate (IIIa).**—The trans- acid (3 g.) was refluxed in ethanol (30 cc.) with concentrated sulfuric acid (0.5 cc.) for 2 hr. After concentration of the reaction mixture, the residue was taken up in ether, washed with water, 10% sodium carbonate solution and then water, dried with sodium sulfate and concentrated. The residue was distilled under reduced pressure to give the ethyl ester (3 g.) which boiled at 125~137°C (mainly 135~136°C)/25 mmHg and had $n_D^{20}$ 1.4522. Redistillation gave the pure ester which had b. p. 146~148°C/29 mmHg, $n_D^{20}$ 1.4515 $d_4^{20}$ 0.9282 and $MR_D$ 61.70 (Calcd. 61.69).

**Ethyl *cis*-*tert*-Butylhexahydrobenzoate (IIIb).**—The cis- acid (3.5 g.) gave similarly the cis-ethyl ester (3.5 g.) which, after redistillation, had b. p. 134~137°C/28 mmHg, $n_D^{20}$ 1.4593, $d_4^{20}$ 0.9400 and $MR_D$ 61.74 (Calcd. 61.69).

***trans*-*tert*-Butylcyclohexylcarbinol (IVa).**—The trans-ester (2.5 g.) in dry ether (30 cc.) was added dropwise to a suspension of lithium aluminum hydride (1.0 g.) in dry ether (60 cc.) at 0~5°C and the reaction mixture was stirred for another hour. This mixture was then treated with a small amount of cold dilute sulfuric acid until the ether layer was clear and then filtered. The filtrate and washings of the filter cake were combined, dried with potassium carbonate and concentrated. The residue was distilled to give the carbinol (1.8 g.) as a viscous oil which had b. p. 140~140.5°C/28.5 mmHg, $n_D^{20}$ 1.4683, $d_4^{20}$ 0.9092, $MR_D$ 52.13 (Calcd. 52.32), which solidified in a refrigerator and melted at 25~27°C.

Found: C, 77.5; H, 12.9. Calcd. for $C_{11}H_{22}O$: C, 77.6; H, 13.0%.

The carbinol (1.1 g.) was treated with *p*-toluenesulfonyl chloride (1.5 g.) in dry pyridine (5 cc.) by the usual way[1] at 0~5°C and allowed to stand overnight in a refrigerator with occasional shaking. The mixture was poured into a mixture of ice and concentrated hydrochloric acid. The separated crystalline solid was filtered off and recrystallized twice from aqueous ethanol to give the *trans*-*p*-toluenesulfonate (1.4 g.) as needles, m. p. 83~84°C.

Found: C, 66.8; H, 8.6. Calcd. for $C_{18}H_{28}O_3S$: C, 66.6; H, 8.66%.

***cis*-*tert*-Butylcyclohexylcarbinol (IVb).**—A similar treatment of the cis-ester (3.0 g.) with lithium aluminum hydride (1.2 g.) gave the *cis*-carbinol (1.4 g.) as a viscous oil, b. p. 133~136°C/27 mmHg, $n_D^{20}$ 1.4781, $d_4^{20}$ 0.9243 and $MR_D$ 52.16 (Calcd. 52.32), which soon partially solidified on being allowed to stand in a refrigerator. The semi-solid mass was pressed on a porous tile and recrystallized from aqueous ethanol to give the pure *cis*-carbinol as long needles, m. p. 56~57°C.

Found: C, 78.2; H, 12.8. Calcd. for $C_{11}H_{22}O$: C, 77.6; H, 13.0%.

The pure carbinol was treated by the method used for the *trans*-carbinol with *p*-toluenesulfonyl chloride to give the *cis*-*p*-toluenesulfonate. Recrystallization from methanol gave needles, m. p. 95~95.5°C.

Found: C, 66.7; H, 8.8. Calcd. for $C_{18}H_{28}O_3S$: C, 66.6; H, 8.66%.

*Tokyo College of Science*
*Shinjuku-ku, Tokyo*

# *Semiconductivity and Absorption Spectrum of Perylene Single Crystal*

By Mizuka SANO and Hideo AKAMATU

(Received March 6, 1961)

Concerning the electronic conduction in organic solids, most of which are aromatic compounds, the investigation on single crystals is of special interest. For instance, it is desirable to determine the anisotropy of the electrical conductivity. If it is presumed that the conduction takes place in association with the overlapping of $\pi$-electron orbitals, the resistivity should be the lowest in such a direction where the overlapping is the largest. Mette and Pick[1] have observed such an anisotropy in the anthracene single crystal. We have found a similar anisotropy of thin evaporated films of perylene, coronene and violanthrene in which minute crystals are in alignment along the textured structure[2]. In this note, the investigation on the perylene single crystal is presented. It contributes to the above argument and suggests the correlation between the conduction level and the electronic absorption band in the molecular crystal.

Perylene, which was synthetized from naphthalene following Scholl[3], was recrystallized from the benzene solution and the gracial acetic acid solution successively, then sublimed in vacuo. However, these procedures could not

1) H. Mette and H. Pick, *Z. Phys.*, **134**, 566 (1953).

2) H. Inokuchi, H. Kuroda and H. Akamatu, This Bulletin, **34**, 749 (1961).

3) R. Scholl, *Ber.*, **43**, 2202 (1910).

eliminate a trace of reddish substance, terrylene ($C_{30}H_{16}$). Finally, the chromatographic technique with alumina was applied to its benzene solution in the dark. Subsequent sublimation yielded a faint yellow product.

Thin perfect single crystals were obtained when the sublimation procedure was carefully controlled and made to be slow. In a favorable condition, flake-like crystals were produced on the glass wall, which possessed the area of about $4\times6\,mm^2$ with the thickness of $60\sim280\,\mu$. It was proved by means of the X-ray diffraction that the surface plane of the flake-like crystal is the (001) plane.

The electrical resistivity was measured by applying the voltage perpendicularly to the (001) plane, or in parallel to the plane. Aquadag was employed as the electrodes. The voltage source was a battery of dry elements with a voltage up to 450 V. The measurement was carried out, with the aid of direct current amplifier, in vacuo ($10^{-3}$ mmHg) over a temperature range from 40 to 110°C.

No departure from Ohm's law was observed in the voltage region employed (up to $1.6\times10^3$ V./cm.). The resistivity decreased with increasing temperature and a good linear realationship was obtained between the logarithm of the resistivity ($\rho$) and the reciprocal of the temperature, (Fig. 1), which indicates the applicability of the following formula.

$$\rho=\rho_0\exp(\varepsilon/2kT)$$

where $\varepsilon$ is the energy gap.

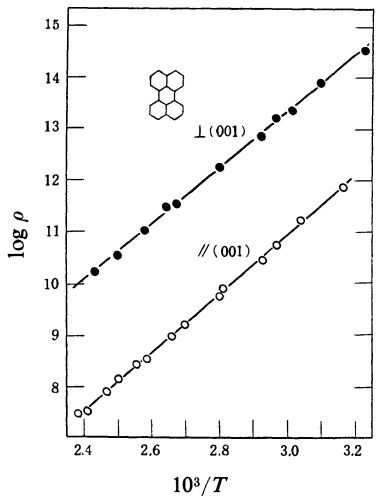



Fig. 1. The relation between resistivity and temperature for perylene single crystal.

It was found that the resistivity is isotropic in the (001) plane. But in the direction perpendicular to this plane, the resistivity is higher by a factor of $10^2$ than that in the (001) plane, (Table I).

TABLE I. THE VALUES OF $\varepsilon$ AND $\rho_{15°C}$ AND THE ABSORPTION SPECTRUM OF PERYLENE CRYSTAL

| | $\varepsilon$ eV. | $\rho_{15°C}$ Ω·cm. |
|---|---|---|
| ⊥ (001) | 2.1 | $6.5\times10^{15}$ |
| ∥ (001) | 2.2 | $4.1\times10^{13}$ |
| Film* | | |
| from the sandwich-type cell | 2.0 | $10^{18}\sim10^{19}$ |
| from the surface-type cell | 2.2 | $10^{13}$ |
| Absorption spectrum | | |
| the peak of the *p*-band | 2.67 | |
| the onset of the *p*-band | 2.26 | |

* after Inokuchi, Kuroda and Akamatu[2]

The absorption spectra of the perylene crystal and its solution in ethyl alcohol were recorded by the spectrophotometer (Cary model 11). The spectrum of the single crystal resembles closely that of the solution, excepting some broadening and a small shift toward the long wavelength side. In consequence, according to Clar's classification[4], the absorption bands of the crystal can be assigned to the *p*-, $\alpha$- and $\beta$-band respectively, referring to the absorption bands of the solution.

In the neighborhood of the absorption edge, it is rather difficult to decide precisely the threshold value. However, the onset of the *p*-band is found in the vicinity of 466 m$\mu$ for the solution and 550 m$\mu$ for the crystal. The value of light quantum for the latter is in agreement with the observed value of $\varepsilon$, (Table I).

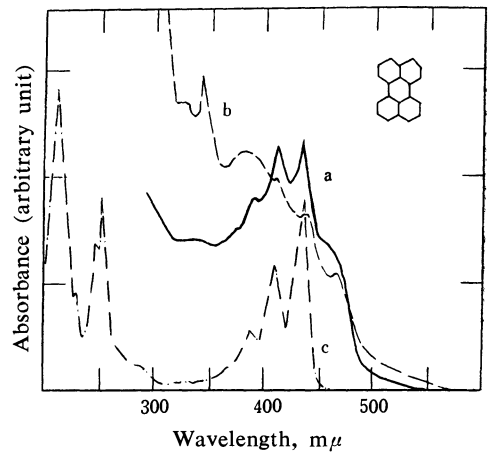



Fig. 2. Absorption spectra of perylene. (a) Single crystal, (b) Evaporated film, (c) Solution in ethyl alcohol

The anisotropy was found in regard to the conductivity, but not to the value of the energy gap. The same result has been obtained for

4) E. Clar, "Aromatische Kohlenwasserstoffe", Springer Verlag, Berlin (1952).

the evaporated film of perylene[2]. It can be concluded that the anisotropy arises due to the difference in the mobility of free carriers which is dependent on the direction of drift, but not due to the difference in the number of carriers which are in thermal equilibrium.

The direction of $\pi$-bond orbitals in each molecule extends perpendicularly from the molecular plane, and molecules are arranged in the crystal in such a way that the molecular planes are parallel with each other with a distance of 3.47 Å and nearly perpendicular to the (001) plane[5]. Therefore, the direction of the lowest resistivity is coincident with the direction of the extending of $\pi$-bond orbitals of molecules in the crystal. The maximum overlapping of the orbitals is expected to be between neighboring molecules in this direction.

If a conduction level could be assumed in the molecular crystal, the observed value of the energy gap implies that it lies in the neighborhood of the onset of the *p*-absorption band. No theory has yet explained the reason why the lowest excited state contributes to the conduction, but it is likely that the excitation of $\pi$-electrons to the lowest excited singlet state is the first process of electronic conduction in the perylene crystal.

*Department of Chemistry*
*Faculty of Science*
*The University of Tokyo*
*Hongo, Tokyo*

5) D. M. Donaldson, J. M. Robertson and J. G. White, *Proc. Roy. Soc.*, A220, 311 (1953).

# *Syntheses of γ-Ionone Analogues. I–II.*

By Atsuaki ARAI and Iwao ICHIKIZAKI

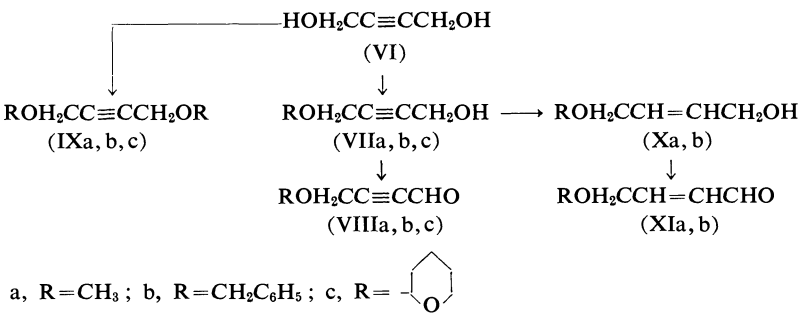
(Received March 18, 1961)

## I. Several Asymmetric Bifunctional Dienophiles and their Diels-Alder Adducts with 2, 3-Dimethyl-1, 3-butadiene

Tetrolaldehydes or crotonaldehydes containing an adequate functional substituent in the γ-position seem to be suitable as the dienophiles for the preparation of the Diels-Alder adducts which can be used as the key intermediates for a certain synthetical project concerning γ-ionone analogues. In spite of their apparently simple structure, such compounds and their Diels-Alder adducts have hitherto scarcely been reported.

One of the present authors and his co-workers[1] synthesized the diethylacetals of γ-hydroxytetrolaldehyde (I), γ-dialkylaminotetrolaldehyde (II) and of γ-dialkylaminocrotonaldehyde (III), and then explained that all these acetals could neither give the free parent aldehydes nor behave as a dienophile, while they reported that γ-methoxycrotonaldehyde (XIa) was proved to be a dienophile. In this paper the authors wish to describe the preparation of several dienophiles in such series and the Diels-Alder reactions of them with a typical symmetric diene, 2, 3-dimethyl-1, 3-butadiene.

Five dienophiles — γ-methoxy-, γ-benzyloxy- and γ-tetrahydropyran-2-yloxytetrolaldehyde (VIIIa, VIIIb and VIIIc), γ-methoxy- and γ-benzyloxycrotonaldehyde (XIa and XIb)—were prepared successfully by the manganese dioxide oxidation of the corresponding carbinols (VIIa, VIIb, VIIc, Xa and Xb) as shown by the following scheme:




where: a, $R=CH_3$; b, $R=CH_2C_6H_5$; c, R= 

1) I. Ichikizaki, Ching-Chung Yao, Y. Fujita and Y. Hasebe, This Bulletin, **28**, 80 (1955).

4-Methoxy-2-butyn-1-ol (VIIa) was prepared in 43% yield through a partial methylation of 2-butyn-1,4-diol (VI) with dimethyl sulfate in an aqueous alkali. A modified procedure was applied for the preparation of 4-benzyloxy-2-butyn-1-ol (VIIb) by adding benzyl chloride at 110~115°C into a xylene suspension of monosodium butyndiolate prepared beforehand from a large excess of VI with sodamide in liquid ammonia. In both cases appreciable amounts of 1,4-dialkoxy-2-butynes (IXa and IXb) were isolated.

Catalytic hydrogenation of the acetylenic carbinols, VIIa and VIIb, in the presence of a palladium-calcium carbonate catalyst in ethyl acetate gave the corresponding ethylenic carbinols, Xa and Xb, in good yields.

An attempted preparation of 4-tetrahydropyran-2′-yloxy-2-butyn-1-ol (VIIc) directly from VI and dihydropyran was proved to be unsatisfactory, since it was extremely difficult to separate the pure product from the reaction mixture containing 1,4-bistetrahydropyran-2′-yloxy-2-butyne (IXc), unchanged VI besides VIIc. IXc was, therefore, prepared at first by heating VI with two moles of dihydropyran in the presence of a catalytic amount of concentrated hydrochloric acid or *p*-toluenesulfonic

TABLE I. 4-ALKOXY-2-BUTYN-1-ALS AND 4-ALKOXY-2-BUTEN-1-ALS
$ROCH_2C{\equiv}CCHO$ (VIII), $ROCH_2CH{=}CHCHO$ (XI)

| Compound Number | R | B. p. °C/mmHg | $n_D^T$ | Yield, % based on the parent carbinol | Molecular formula | Analysis, % Found C | Found H | Calcd. C | Calcd. H |
|---|---|---|---|---|---|---|---|---|---|
| VIIIa | $-CH_3$ | 68~69/25 | $1.4504^{20}$ | 41 | $C_5H_6O_2$ | 59.99 | 6.58 | 61.21 | 6.16 |
| VIIIb | $-CH_2C_6H_5$ | 116~117/1.0<br>111~112/0.7 | $1.5383^{21}$ | 55 | $C_{11}H_{10}O_2$ | 75.58 | 5.93 | 75.84 | 5.79 |
| VIIIc[a] |  | 83~84/0.8 | $1.4902^{16}$ | 68 | $C_9H_{12}O_3$ | 64.55 | 7.54 | 64.27 | 7.19 |
| XIa | $-CH_3$ | 73~74/27 | | 45 | $C_5H_8O_2$ | 59.76 | 8.15 | 59.98 | 8.05 |
| XIb | $-CH_2C_6H_5$ | 111~113/1.0 | $1.5310^{18.5}$ | 52 | $C_{11}H_{12}O_2$ | 74.92 | 6.88 | 74.97 | 6.86 |

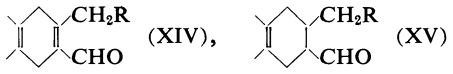
a) $\nu_{max}$(liquid film) 2245, 2200 (C≡C); 1670 (C=O, conj.); 1185, 1125, 1083, 1060, 1031, 967, 944, 904, 874 $cm^{-1}$ (C-O-C); no absorption band of hydroxyl group is observed.
$\lambda_{max}^{n\text{-hexane}}$ 221 mμ (ε 26400)

TABLE II. SOLID DERIVATIVES OF 4-ALKOXY-2-BUTYN-1-ALS AND 4-ALKOXY-2-BUTEN-1-ALS
$ROCH_2C{\equiv}CCHO$ (VIII), $ROCH_2CH{=}CHCHO$ (XI)

| Parent aldehyde Number | R | Semicarbazone Appearance | M. p. °C | $\lambda_{max}^{EtOH}$ mμ (ε) | Molecular formula | Analysis, % Found N | Calcd. N | 2,4-Dinitrophenylhydrazone Appearance | M. p. °C | Molecular formula | Analysis, % Found N | Calcd. N |
|---|---|---|---|---|---|---|---|---|---|---|---|---|
| VIIIa | $-CH_3$ | | | | | | | Orange-yellow needles | 111~112.2 | $C_{11}H_{10}O_5N_4$ | 19.90 | 20.14 |
| VIIIb | $-CH_2Ph$ | Slightly yellow needles | 138.5~139[a] | 236 (33700)<br>281 (41500) | $C_{18}H_{17}O_2N_3$ | 13.47 | 13.67 | Yellow needles | 121~122 | $C_{17}H_{14}O_5N_4$ | 15.89 | 15.81 |
| VIIIc |  | | | | | | | Yellow needles | 120~120.5[b] | $C_{10}H_8O_5N_4$ | 21.13 | 21.21 |
| XIa | $-CH_3$ | | | | | | | Red-orange needles | 140~141 | $C_{11}H_{12}O_5N_4$ | 19.83 | 19.99 |
| XIb | $-CH_2Ph$ | Needles | 148~149 | 264 (34500) | $C_{12}H_{15}O_2N_3$ | 18.27 | 18.02 | Orange silk-like needles | 166.5 | $C_{17}H_{16}O_5N_4$ | 15.68 | 15.72 |

a) Phenylsemicarbazone
b) This 2,4-dinitrophenylhydrazone was identical with that of 4-hydroxy-2-butyn-1-al (I).

TABLE III. DIELS-ALDER ADDUCTS OF γ-SUBSTITUTED TETROL- AND CROTONALDEHYDES WITH 2,3-DIMETHYL-1,3-BUTADIENE




| Dienophiles Number | Condition of D-A reaction Temp. °C | Time hr. | Adduct Number | R | Yield % | B. p. °C/mmHg | $n_D^T$ | Molecular formula | Analysis, % Found C | Found H | Calcd. C | Calcd. H |
|---|---|---|---|---|---|---|---|---|---|---|---|---|
| VIIIa | 140~150 | 13 | XIVa | $-OCH_3$ | 84.3 | 113~117 /3 | $1.5161^{18}$ | $C_{11}H_{16}O_2$ | 71.68 | 8.93 | 73.30 | 8.95 |
| VIIIb | 145~153 | 14 | XIVb | $-OCH_2Ph$ | 81.6 | 141~145 /0.03 | $1.5554^{20}$ | $C_{17}H_{20}O_2$ | 79.37 | 7.83 | 79.65 | 7.86 |
| VIIIc | 120~130 | 21 | XIVc[a] |  | 72 | 146~147 /0.75 | $1.5221^{20}$ | $C_{15}H_{22}O_3$ | 71.60 | 8.80 | 71.97 | 8.86 |
| XIa | 125~135 | 13 | XVa | $-OCH_3$ | 73 | 82~84[b] /2.5 | | $C_{11}H_{18}O_2$ | 72.58 | 9.81 | 72.49 | 9.96 |
| XIb | 125~135 | 13 | XVb | $-OCH_2Ph$ | 71.5 | 130~135 /0.01 | | $C_{17}H_{22}O_2$ | 79.12 | 8.49 | 79.03 | 8.58 |
| Croton-aldehyde | 140~150 | 9 | XVI | $-H$ | 72.4 | 98/18[c] | $1.4731^{20}$ | $C_{10}H_{16}O$ | 78.70 | 10.68 | 78.89 | 10.59 |

a) $\lambda_{max}^{EtOH}$ 235 mμ (ε 7600); $\nu_{max}$ (liquid film) 1675 (C=O); 1198, 1181, 1118, 1078, 1057, 1028, 973, 907, 873 $cm^{-1}$ (C-O-C-O)

b) Ref. 1, b. $p._{2.5}$ 82~84°C.

c) O. Diels and K. Alder, *Ann.*, **470**, 62 (1929), reported b. $p._{12}$ 89°C.

acid in tetrahydrofuran, then it was similarly treated with one equivalent of VI to afford pure VIIc in a good yield. The tetrahydropyranyl ether thus prepared was fairly soluble in water and afforded the 2,4-dinitrophenylhydrazone of 5-hydroxypentanal (XII) in quantitative yield by the Brady reagent.

So far as the authors were aware, none of the acetylenic primary carbinols had ever been reported to be oxidized into the aldehydes by the technique after Attenburrow[2], however, all of the 4-alkoxy-2-butyn-1-ols (VIIa, VIIb and VIIc) and the 4-alkoxy-2-buten-1-ols (Xa and Xb) were successfully oxidized by the usual method with active manganese dioxide to yield the corresponding aldehydes (VIIIa, VIIIb, VIIIc, XIa and XIb), which were all proved to be the dienophiles of moderate activity as descrided later. Their properties and analytical data are shown in Table I and their solid derivatives are summarized in Table II.

It is worth noticing in this connection that the same oxidation technique seems not to be applicable to γ, γ-dialkoxyacetylenic carbinol, because 4,4-diethoxy-2-butyn-1-ol (XIII)[1,3] was recovered unchanged on treatment with active manganese dioxide under more vigorous conditions than that generally adopted[2,4,5].

Treatment of 4-tetrahydropyran-2′-yloxy-2-butyn-1-al (VIIIc) with the Brady reagent afforded in an excellent yield 2,4-dinitrophenylhydrazones of 5-hydroxypentanal (XII) and that of 4-hydroxy-2-butyn-1-al (I), while the latter was also obtained in a good yield by similar treatment of 4,4-diethoxy-2-butyn-1-ol (XIII). This means that VIIIc is readily hydrolyzed and quantitatively affords the above two aldehydes, namely XII and I.

The condensation between each of the aldehydes (VIIIa, VIIIb, VIIIc, XIa and XIb) and 2,3-dimethyl-1,3-butadiene under the conditions as listed in Table III essentially afforded only a sole adduct. Some chemical evidences, which will be described in the following paper, of the adducts and the ultraviolet absorption data of their semicarbazones listed in Table IV demonstrate that they all have normal structures as expected.

On the Diels-Alder reaction involving α,β-acetylenic carbonyl compound, only a few examples which have resulted in the formation of an inhomogeneous product owing to the migration of the double bonds or the partial aromaticization have been reported[6,7]. It

2) J. Attenburrow, A. F. B. Cameron, I. H. Chapman R. M. Evans, B. A. Hem, A. B. A. Jansen and T. Walker, *J. Chem. Soc.*, **1952**, 1094.

3) R. G. Jones and M. G. Main, *J. Am. Chem. Soc.*, **75**, 4048 (1953).

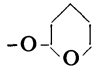
4) M. Harfenist and A. Bavley, *J. Org. Chem.*, **19**, 1608 (1954).

5) B. C. L. Weedon et al., *J. Chem. Soc.*, **1953**, 1578, 3286.

6) J. C. Lunt and F. Sondheimer, ibid., **1950**, 3361.

7) E. A. Braude, E. R. H. Jones, F. Sondheimer and J. B. Toogood, ibid., **1949**, 607.

TABLE IV. SOLID DERIVATIVES OF THE DIELS-ALDER ADDUCTS

| Adduct | | 2,4-Dinitrophenylhydrazone | | | | Semicarbazone | | | | |
|---|---|---|---|---|---|---|---|---|---|---|
| Number | R | Appearance | M. p. °C | Molecular formula | Analysis, % Found / Calcd. N | Appearance | M. p. °C | $\lambda_{max}^{EtOH}$ mμ (ε) | Molecular formula | Analysis, % Found / Calcd. N |
| XIVa | $-OCH_3$ | Red-orange needles | 203～204 | $C_{17}H_{20}O_5N_4$ | 15.93 / 15.55 | Needles | 218.5～219.5 (decomp.) | 272.5 (23400) | $C_{12}H_{19}O_2N_3$ | 17.89 / 17.71 |
| | | | | | | Prisms | 175～177 | 273 (28100) | $C_{18}H_{23}O_2N_3$ | 13.55 / 13.41 |
| XIVb | $O-CH_2Ph$ | Red-orange needles | 203 | $C_{23}H_{24}O_5N_4$ | 12.86 / 12.84 | Needles | 179～180[b] | 237 (11700) 284 (32900) | $C_{24}H_{27}O_2N_3$ | 11.07 / 10.79 |
| XIVc |  | Dark-red needles | 209～210[a] | $C_{21}H_{26}O_6N_4$ | 13.60 / 13.02 | Needles | 187～188 | 272 (28300) | $C_{16}H_{25}O_3N_3$ | 13.50 / 13.67 |
| XVa | $-OCH_3$ | Yellow needles | 159～160 | $C_{17}H_{22}O_5N_4$ | 15.54 / 15.46 | Needles | 152～153[c] | 232.5 (12400) 269 (33700) | $C_{12}H_{21}ON_3S$ | 16.40 / 16.46 |
| XVb | $O-CH_2Ph$ | Yellow needles | 134.5～135 | $C_{23}H_{26}O_5N_4$ | 12.41 / 12.78 | Plates | 143[b] | 248 (27100) | $C_{24}H_{29}O_2N_3$ | 10.64 / 10.73 |
| XVI | $-H$ | Bright yellow needles | 193～194 | $C_{16}H_{20}O_4N_4$ | 16.64 / 16.86 | | | | | |

a) Found: C, 58.38; H, 6.02. Calcd. C, 58.59; H, 6.09%; $\lambda_{max}^{CHCl_3}$ 234 mμ (ε 25300), 259 (15100), 378 (31400)
b) Phenylsemicarbazone
c) Thiosemicarbazone, Ref. 1, m.p. 152°C

should be noted, therefore, that when the condensation between VIIIc and 2, 3-dimethyl-1, 3-butadiene was carried out at 140°C the expected adduct (XIVc) was obtained in only 24% yield and the principal product was colorless crystals, m.p. 60°C, formulated as $C_{10}H_{12}O$, which could also be obtained in 34% yield by heating XIVc with *p*-toluenesulfonic acid in tetrahydrofuran. This crystalline product has a strong menthol-like odor and becomes gradually a dark-brown resinous matter on exposure to air and light. By considering the fact that its properties and the infrared spectrum closely resemble those of phthalane[8] the authors estimated its structure as 5, 6-dimethyl-1, 3-dihydroisobenzofuran (XVII). The nuclear magnetic resonance spectrum[9] of this compound, obtained at 56.4 mc., was in complete accord with the structure XVII. The spectrum of XVII displayed three singlet peaks at −2.53, 1.55 and 2.84 p.p.m. whose area varied in a ratio of approximately 1 : 2 : 3, respectively. The resonance of −2.53 p.p.m. can be assigned to the aromatic hydrogens, while that of 2.84 p.p.m. is definitely associated with the hydrogens of methyl groups. The methylene groups linked with oxygen atom satisfactorily were accounted for by the peak of 1.55 p.p.m.

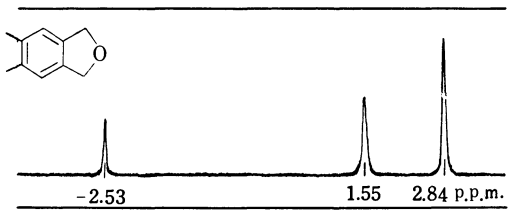


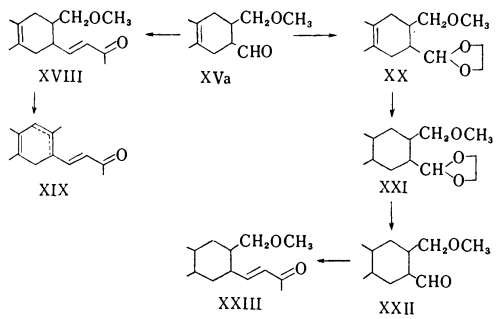

Fig. 1. NMR spectrum of 5,6-dimethyl-1,3-dihydroisobenzofuran.

## II. Synthesis of 2-Methylene-4, 5-dimethylcyclohexylmethanol and Related Compounds

In this paper the authors wish to describe the preliminary work which has been carried out in the course of study for the preparation of an analogue of γ-cyclogeraniol and related compounds by employing the Diels-Alder adducts reported in the preceding paper.

An attempt was made at first to synthesize 4-(2′-methylene-4, 5-dimethyl-4′-cyclohexenyl)-but-3-en-2-one by employing 3, 4-dimethyl-6-methoxymethyl-3-cyclohexenylmethanal (XVa) as the starting substance. Condensation of XVa with acetone in the presence of barium hydroxide afforded in 69% yield 4-(3′,4′-dimethyl-6′-methoxymethyl-3′-cyclohexenyl)-but-3-en-2-one (XVIII) which on heating with hydrogen bromide at 130°C gave a crude oil, from which a considerable amount of only one orange 2, 4 dinitrophenylhydrazone was obtained. Since the infrared spectrum of the hydrazone did not exhibit a characteristic absorption band of exocyclic methylene group, its parent aldehyde was considered to be a triply unsaturated ketone as represented by XIX which resulted from XVIII after elimination of methyl alcohol. Consequently the use of such a methoxymethyl compound as XVIII for the preparation of γ-ionone analogue was regarded as being practically unsuitable.

In order to hydrogenate a double bond in the ring of XVa a carbonyl group was once protected as the acetal. By the method of Salmi[10] XVa was converted into the corresponding ethylendioxy compound XX in 79% yield, which was hydrogenated over a palladium-charcoal catalyst in ethanol to give the saturated acetal XXI. The XXI was readily hydrolyzed, when heated under reflux in tetrahydrofuran with 2 N aqueous sulfuric acid, to yield the free aldehyde XXII which was condensed with acetone in the usual method giving 4-(4′, 5′-dimethyl-2′-methoxymethylcyclohexyl)-but-3-en-2-one (XXIII).




Since the conversion of a side methoxymethyl group into an exocyclic methylene had failed, a formyl group that is another functional group of such an adduct as XVa was investigated for the same purpose by employing 3, 4, 6-trimethyl-3-cyclohexenylmethanal (XVI) as a simple model.

In an autoclave XVI was hydrogenated in the presence of Raney nickel catalyst and anhydrous dimethylamine to afford in 80% yield *N*, *N*-dimethyl-2, 4, 5-trimethylcyclohexylmethylamine (XXV), together with an appreciable amount of 2, 4, 5-trimethylcyclohexylmethanol (XXIV). Though it is well known[11]

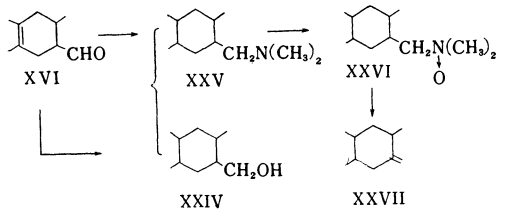
8) J. Entel, C. H. Ruof and H. C. Howard, *J. Am. Chem. Soc.*, **74**, 441 (1952).

9) The NMR spectra were determined on a Varian Associates V-4300C high resolution NMR spectrometer with ca. 10% solution in $CCl_4$ with water as an external reference standard.

10) E. I. Salmi, *Ber.*, **71**, 1803 (1938).

11) W. S. Emerson, "Organic Reactions", Vol. IV, (1948), pp. 174—255.

that primary and secondary amines are generally converted into tertiary amines by reductive condensation with various carbonyl compounds, no case with alicyclic aldehyde has been reported until the above preparation was completed[12].

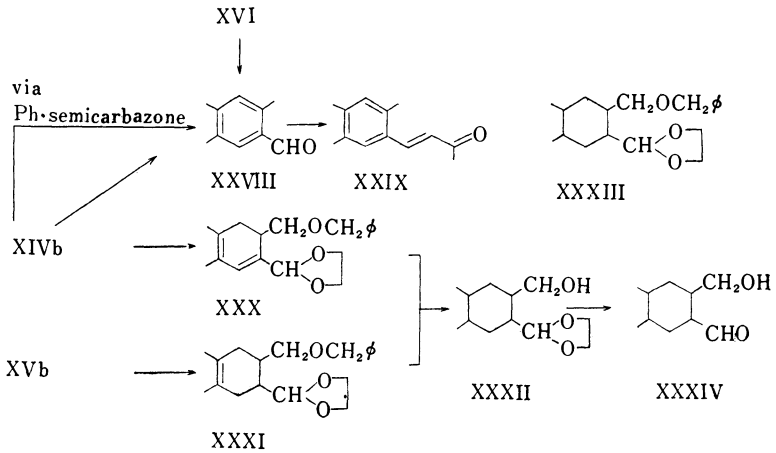



Oxidation of the tertiary amine XXV with 30% aqueous hydrogen peroxide gave in 82% yield an amine oxide XXVI as a colorless syrup which was characterized as crystalline picrate. The amine oxide XXVI was pyrolyzed in the manner described by Cope and his co-workers[13]. The decomposition proceeded smoothly at 120 ~130°/2.5 mmHg under nitrogen, and gave in yield of 61% based on XXV, a colorless mobile liquid, $C_{10}H_{18}$, which showed b.p. 59~59.2°/16.2 mmHg, $n_D^{20}$ 1.4601 and was proved to be homogeneous by vapor phase chromatography. From the infrared absorption bands at 3077, 1648 and 885 $cm^{-1}$ indicative of exocyclic methylene group, 1-methylene-2, 4, 5-trimethylcyclohexane (XXVII) was assigned for the hydrocarbon. The above result demonstrates that the thermal decomposition of XXVI gave exclusively the expected unsaturated hydrocarbon and also provided a further example in support of the specific formation of methylene cycloalkanes previously reported by Cope and his co-investigator[14,15].

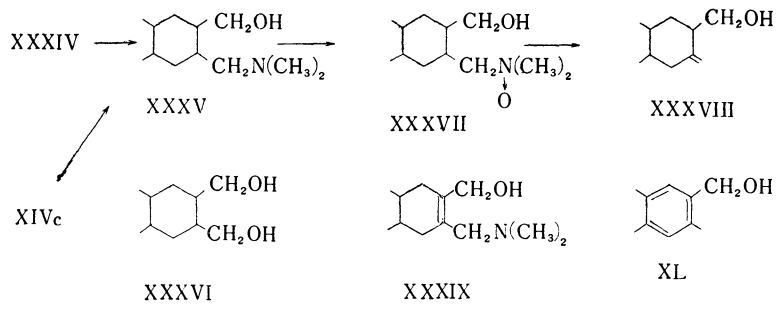
Since three of the new Diels-Alder adducts —XIVb, XIVc and XVb—have all a functional group readily convertible to a hydroxyl group, an attempt was made to prepare from them 2-methylene-4, 5-dimethylcyclohexylmethanol (XXXVIII) which can be regarded as an analogue of γ-cyclogeraniol.

In order to isolate XIVb of high purity the phenylsemicarbazone obtainable in yield of 96% from the original adduct was hydrolyzed on steam distillation in the presence of concentrated sulfuric acid and *o*-phthalic acid, whereas 2, 4, 5-trimethylbenzaldehyde (XXVIII), m. p. 43°C (lit.[16] m. p. 42°C), was obtained in 60% yield with benzyl alcohol. The compound XXVIII was also formed in 20% yield by heating XIVb under reflux in xylene with a catalytic amount of *p*-toluenesulfonic acid, and it was characterized as the semicarbazone and 2, 4-dinitrophenylhydrazone, both of which were identical with those of an authentic sample prepared by the sulfur dehydrogenation of 3, 4, 6-trimethyl-3-cyclohexenylmethanal (XVI). On condensation with acetone, the aldehyde XXVIII afforded 4-(2′, 4′, 5′-trimethylphenyl)-but-3-en-2-one (XXIX) which showed m. p. 49.5°C (semicarbazone, m. p. 223~224°C; 2, 4-dinitrophenylhydrazone, m. p. 247~249°C).

An attempted acid-catalyzed reaction of XIVb with ethylene glycol following the method of Salmi[10] gave in only 33.5% yield an acetal which was probably XXX[17], while a considerable amount of XXVIII was yielded from




12) The 12th Annual Meeting of the Chemical Society of Japan, Kyoto, April, 1959.
13) A. C. Cope, R. A. Pike and C. F. Spencer, *J. Am. Chem. Soc.*, **75**, 3212 (1953).
14) A. C. Cope, C. L. Bumgardner and E. E. Schweizer, ibid., **79**, 4729 (1957).
15) A. C. Cope, E. Ciganek, C. F. Howell and E. E. Schweizer, ibid., **82**, 4663 (1960).
16) L. Gattermann, *Ann.*, **347**, 347 (1906).
17) Such migration of double bonds in the presence of acid will be discussed in the following paper, Part III.




the elimination of benzyl alcohol. However, 6-benzyloxymethyl-3,4-dimethyl-3-cyclohexenylmethanal (XVb) could be converted into the corresponding acetal XXXI in a good yield without the elimination of benzyl alcohol.

XXX as well as XXXI usually afforded XXXII on hydrogenation over a palladium-charcoal catalyst; however, they occasionally afforded an appreciable amount of 2-benzyloxymethyl-4, 5-dimethylcyclohexylmethanal ethylene acetal (XXXIII), when hydrogenated with a catalyst prepared from less active charcoal. This result suggests that the hydrogenation of double bonds proceeded more rapidly than the hydrogenolysis of the benzyloxy group. On hydrolysis with diluted aqueous sulfuric acid in tetrahydrofuran the acetal XXXII was readily converted into the hydroxy aldehyde XXXIV.

On catalytic hydrogenation with dimethylamine over Raney nickel catalyst, XXXIV afforded in 60% yield *N*, *N*-dimethyl-4, 5-dimethyl-2-hydroxymethylcyclohexylmethylamine (XXXV) and simultaneously a considerable amount of 1, 2-bishydroxymethyl-4, 5-dimethylcyclohexane (XXXVI), m. p. 113~115°C. XXXV was successively oxidized with 30% hydrogen peroxide in the usual method to the *N*-oxide XXXVII, which was decomposed at 120~130°C to exclusively yield 2-methylene-4, 5-dimethylcyclohexylmethanol (XXXVIII), b. p. 94~97°C/17.5 mmHg, $n_D^{27}$ 1.4729, as shown by its infrared absorption bands at 3058, 1642 and 884 $cm^{-1}$.

In another attempt to prepare the hydroxy amine XXXV directly from XIVc by similar reductive alkylation of dimethylamine with the aldehyde XXXIV as described above, XXXV was obtained in yield of 43.5% and it was usually contaminated with a base which was assumed from the methiodide to be the unsaturated aminoalcohol XXXIX. In this reduction a neutral compound, $C_{10}H_{14}O$, which shows m.p. 84.5°C; $\lambda_{max}^{EtOH}$ 217 mμ (ε 175), 267 (338) and 274 (322), was also isolated in 32% yield. The infrared spectrum exhibited the presence of hydroxyl group (~3360, 1038) as well as of 1, 2, 4, 5-tetra-substituted aromatic group (879 $cm^{-1}$), and clearly suggested that this compound was to be 2, 4, 5-trimethylbenzyl alcohol (XL) which had been reported elsewhere to show m. p. 168°C[18]. The NMR spectrum provided an independent confirmation of its structure. The spectrum[9] consisted of five peaks at −2.23, −2.10, 0.30, 2.25 and 2.50 p. p. m. the chemical shifts of which permit the unequivocal assignment. The two non-equivalent hydrogens on the ring are accounted for by the peaks of −2.23 and −2.10 p. p. m. The three methyl groups were found at 2.50 p. p. m. as a singlet peak, while the methylene group with hydroxyl group was found at a lower magnetic field (0.30 p. p. m.). The resonance at 2.25 p. p. m. can be assigned to the proton of hydroxyl group.

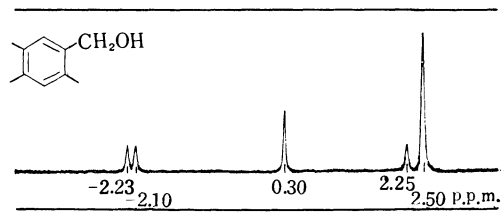



Fig. 2. NMR spectrum of 2,4,5-trimethylbenzyl alcohol.

## Experimental[19]

**4-Methoxy-2-butyn-1-ol (VIIa) and 4-Methoxy-2-buten-1-ol (Xa).**—These compounds were prepared by the method of Ichikizaki et al[1]. 4-Methoxy-2-butyn-1-ol (VIIa), b. p. 105.5~106°C/20.5 mmHg, $n_D^{20}$ 1.4595, was obtained in 43% yield. In addition to VIIa, 1, 4-dimethoxy-2-butyne (IXa), b.p. 63~65°C/20 mmHg, was obtained in 9% yield as a by-product. 4-Methoxy-2-buten-1-ol (Xa), b.p. 88~89°C/20 mmHg, $n_D^{12}$ 1.4490, was obtained by hydrogenation of VIIa with a palladium-calcium carbonate catalyst (5% Pd) in 89% yield.

18) W. J. Hickinbottom, "Chemistry of Carbon Compounds", Vol. III-A, Ed. by E. H. Rodd, Elsevier Pub. Co. (1954), p 499.

19) All melting points were determined on the Kofler block and are uncorrected. The ultraviolet spectra were determined with a Hitachi EPU-2A spectrophotometer and the infrared spectra were obtained with a Perkin-Elmer model 112, a Kōken model DS-301, and a Nippon Bunkō model IR-S recording spectrophotometers with sodium chloride optics.

**4-Benzyloxy-2-butyn-1-ol (VIIb).** — 2-Butyne-1, 4-diol (VI) (200 g.) was added portionwise to a solution of sodamide (prepared from 35 g. of sodium) in liquid ammonia (1 l.) under vigorous stirring at −45∼−50°C over a period of 10 min. After being stirred for additional 2 hr. under cooling, the reaction mixture was diluted with xylene (800 ml.) and then set aside overnight to evaporate ammonia. The residual suspension was heated gradually to 100°C under stirring to remove the remaining ammonia as completely as possible. To it benzyl chloride (200 g.) was added dropwise over a period of 30 min. under vigorous stirring at 110∼115°C and the mixture was stirred for an additional hour. After being cooled, the reaction mixture was poured into cold water (500 ml.) and the xylene layer separated was washed with 10% sulfuric acid and water and dried over sodium sulfate. Distillation gave two fractions, 198 g. (69.2%), b. p. 142∼147°C/4 mmHg and 9 g., b. p. 170∼175°C/2 mmHg. Upon redistillation the lower boiling fraction afforded pure 4-benzyloxy-2-butyn-1-ol (VIIb), b. p. 143∼146°C/2.5 mmHg, $n_D^{25}$ 1.5379.

Found: C, 73.76; H, 7.07. Calcd. for $C_{11}H_{12}O_2$: C, 74.97; H, 6.86%.

Upon redistillation the higher boiling fraction afforded pure 1, 4-dibenzyloxy-2-butyne (IXb), b. p. 169∼170°/1.5 mmHg, $n_D^{19.5}$ 1.5590.

Found: C, 81.20; H, 6.71. Calcd. for $C_{18}H_{18}O_2$: C, 81.17; H, 6.81%.

**4-Benzyloxy-2-buten-1-ol (Xb).**—A solution of 4-benzyloxy-2-butyn-1-ol (VIIb) (100 g.) in ethyl acetate (140 ml.) was hydrogenated with a palladium-barium carbonate catalyst (2.5% Pd, 1.5 g.) at 22°C until 14515 ml. of hydrogen (1.05 equiv.) had been absorbed. After removal of the catalyst and solvent the residue was distilled to afford 4-benzyloxy-2-buten-1-ol (Xb) (83 g., 82%), b. p. 125∼127.5°C/2 mmHg, $n_D^{25}$ 1.5267.

Found: C, 74.08; H, 7.88. Calcd. for $C_{11}H_{14}O_2$: C, 74.13; H, 7.92%.

**1, 4-Bistetrahydropyran-2′-yloxy-2-butyne (IXc).**—A solution of dihydropyran (18.5 g., 0.22 mol.) in tetrahydrofuran (20 ml.) was added dropwise to a solution of VI (8.6 g., 0.1 mol.) in tetrahydrofuran (20 ml.) containing 2 drops of concentrated hydrochloric acid with stirring at 60°C over a period of 30 min. and the resulting mixture was gently refluxed for additional 3 hr. After being cooled, the reaction mixture was made alkaline with a cold 5% aqueous sodium carbonate solution and extracted with three 80 ml. portions of ether. The combined extracts were washed 4 times with a saturated aqueous sodium chloride solution, dried over potassium carbonate and evaporated. Distillation of the residue under nitrogen gave the bis-ether IXc (17 g., 67%), b.p. 144∼146°C/1.0 mmHg, $n_D^{16}$ 1.4913; $\nu_{max}^{film}$ 2226 (C≡C), 1186, 1120, 1081, 1056, 1022, 973, 946, 905 and 872 cm$^{-1}$ (C-O-C-O).

Found: C, 65.66; H, 8.70. Calcd. for $C_{14}H_{22}O_4$: C, 66.11; H, 8.72%.

**4-Tetrahydropyran-2′-yloxy-2-butyn-1-ol (VIIc).**—A solution of the bis-ether IXc (25.4 g., 0.1 mol.) in tetrahydrofuran (10 ml.) was added dropwise to a solution of VI (8.6 g., 0.1 mol.) in tetrahydrofuran (30 ml.) containing 3 drops of concentrated hydrochloric acid under gentle reflux and then boiled for 3 hr. The resultant reaction mixture was worked up as described in the preceding section to leave a pale yellow oil which was distilled through a 8 cm. Vigreux column to yield VIIc (23.0 g., 68%), b. p. 122∼124°C/0.8 mmHg, $n_D^{19}$ 1.4913; $\nu_{max}^{film}$ 3470∼3450 (OH) and 2220 cm$^{-1}$ (C≡C). The characteristic absorption bands in its finger-print region were almost superimposable on those of the bis-ether IXc.

Found: C, 63.27; H, 8.46. Calcd. for $C_{11}H_{14}O_3$: C, 63.51; H, 8.29%

Upon treatment with the Brady reagent, this compound yielded 2, 4-dinitrophenylhydrazone of 5-hydroxypentanal which was crystallized from aqueous methanol and showed m. p. 115°C, undepressed on admixture with the authentic sample.

**4, 4-Diethoxy-2-butyn-1-ol (XIII).**—This compound was obtained in 57.7% by the method of Ichikizaki et al.[1], and had b.p. 118∼119°C/3 mmHg and $n_D^{26}$ 1.4335 (lit.[1] b. p. 88°C/0.5 mmHg, $n_D^{25}$ 1.4493).

The 2, 4-dinitrophenylhydrazone crystallized from 50% methanol in yellow needles, m. p. 120∼120.5°C (lit.[1] m. p. 119°C).

Found: N, 21.13. Calcd. for $C_{10}H_8O_5N_4$: N, 21.21%.

**General Procedure for Oxidation of Carbinols (VII and X) with Manganese Dioxide.**—A solution of the carbinol (5 g.) obtained above in benzene (5 ml.) was added dropwise to a suspension of manganese dioxide (50 g.) prepared by the method of Attenburrow et al.[2] in the same solvent (350 ml.) over a period of 5∼15 min. under vigorous stirring at room temperature and the resultant mixture was stirred for additional 3∼5 hr. During this period the initial temperature increased 10∼12°C. The reaction mixture was filtered and the precipitate was washed with petroleum ether. The washing was combined with the filtrate and evaporated in a nitrogen atmosphere under reduced pressure. Fractionation of the residue afforded the desired aldehydes whose properties and elemental analyses are listed in Table I. The solid derivatives prepared from these aldehydes are summarized in Table II.

**Attempted Oxidation of 4, 4-Diethoxy-2-butyn-1-ol (XIII) with Manganese Dioxide.** — XIII was treated with manganese dioxide according to the general procedure described above. Distillation afforded a trace of fore-run and unchanged starting material (76%). Although XIII was treated with a large excess of the oxidizing agent in boiling benzene for 10 hr., the unchanged starting material was recovered (78%), and the desired aldehyde could not be obtained.

**Reaction of 4-Tetrahydropyran-2′-yloxy-2-butyn-1-al (VIIIc) with the Brady Reagent.**—VIIIc was treated with the Brady reagent in the usual manner giving a mixture of two 2,4-dinitrophenylhydrazones. Recrystallization from aqueous methanol yielded 2, 4-dinitrophenylhydrazone of 4-hydroxy-2-butyn-1-al in yellow needles, m. p. 120∼120.5°C, undepressed on admixture with a sample prepared from XIII.

On addition of water the mother liquor afforded

2, 4-dinitrophenylhydrazone of 5-hydroxypentanal in orange-yellow leaflets, m. p. 115°C, undepressed on admixture with the authentic sample prepared as described below.

**5-Hydroxypentanal (XII).**—This compound was prepared in 65% yield by the method of Schniepp et al.[20] and showed b. p. 61~61.5°C/5 mmHg and $n_D^{17}$ 1.4510 (lit. b. p. 54~55°C/3 mmHg, $n_D^{25}$ 1.4514[20]; b. p. 80°C/12 mmHg, $n_D^{20}$ 1.4510[21]).

The 2, 4-dinitrophenylhydrazone crystallized from 50% methanol in orange-yellow leaflets, m. p. 115~116°C (lit. m. p. 109°C[22]; m. p. 107~109°C[23]).

Found: N, 20.19. Calcd. for $C_{11}H_{14}O_5N_4$: N, 19.85%.

**General Procedure for Diels-Alder Addition of 2, 3-Dimethyl-1, 3-butadiene to γ-Alkoxytetrolaldehydes VIII and γ-Alkoxycrotonaldehydes XI.**—A solution of freshly distilled aldehyde (1 equiv.), 2, 3-dimethyl-1, 3-butadiene (1.05 equiv.) and a trace of quinol in an appropriate solvent was taken in a 50~100 ml. glass bomb and was heated under nitrogen in an oil bath under the conditions described in Table III. After removal of the solvent the residue was distilled under reduced pressure to afford a crude product which was purified by redistillation through a short Vigreux column to give a pure adduct.

Some physical properties and sold derivatives of the adducts thus obtained are summarized in Tables III and IV.

**Phenylsemicarbazone of 2-Benzyloxymethyl-4, 5-dimethylcyclohexa-1, 4-dienylmethanal (XIVb).**—A solution of the aldehyde XIVb (4.0 g.) in ethanol (20 ml.) and phenylsemicarbazide (3.8 g.) in the same solvent (12 ml.) were refluxed for 5 min. The cooled reaction mixture was diluted with water and allowed to stand overnight at room temperature. A white precipitate which had been separated was collected and crystallized from ethanol-ethyl acetate to afford phenylsemicarbazone of XIVb (5.8 g., 96%) in needles, m. p. 179~180°C.

The elemental analysis and the ultraviolet absorption data are listed in Table IV.

**5, 6-Dimethyl-1, 3-dihydroisobenzofuran (XVII).**—*a) From 4-Tetrahydropyran-2'-yloxy-2-butyn-1-al (VIIIc) and 2, 3-Dimethyl-1, 3-butadiene.*—A solution of the aldehyde VIIIc (3.06 g.) in benzene (10 ml.) was treated with 2, 3-dimethyl-1, 3-butadiene (1.8 g.) in the presence of a trace of quinol at 140°C for 10 hr. by the general procedure described above. Distillation afforded two fractions: b. p. 90~110°/1.5 mmHg (1.5 g., 55.5%) and b. p. 133~135°C/0.55 mmHg (1.1 g., 24.1%).

The lower boiling fraction of colorless oil solidified immediately after distillation and crystallized from aqueous methanol in colorless fine plates which melted at 60°C and had a characteristic menthol-like odor. The infrared spectrum (KBr disk) showed absorption bands at 1606 (w), 1543 (m), 1495 (m), 1440 (s), 1418 (m), 1389 (s), 1320 (m), 1214 (m), 1127 (m), 1086 (m), 1028 (s), 890 (s) and 768 $cm^{-1}$ (s), and also indicated the absence of the carbonyl group.

Found: C, 80.82; H, 8.40. Calcd. for $C_{10}H_{12}O$: C, 81.04; H, 8.16%.

Upon treatment with the Brady reagent this compound yielded red 2, 4-dinitrophenylhydrazone which crystallized from ethanol-ethyl acetate in red needles, m. p. 208~209°C.

Found: C, 55.11; H, 5.62; N, 15.74. Calcd. for $C_{16}H_{16}O_5N_4$: C, 55.48; H, 5.24; N, 16.18%.

An attempt to prepare the semicarbazone of this product in the usual manner was unsuccessful.

These evidences, therefore, strongly suggest that the lower boiling product is probably 5, 6-dimethyl-1, 3-dihydroisobenzofuran (XVII).

The higher boiling fraction of a pale yellow viscous oil was an expected adduct which was proved to be identical with XIVc (Tables III and IV) by mixed melting point determination of their 2, 4-dinitrophenylhydrazones and by infrared comparison.

*b)—From 4, 5-Dimethyl-2-tetrahydropyran-2'-yloxymethylcyclohexa-1, 4-dienylmethanal (XIVc).*—A solution of the aldehyde XIVc (0.5 g.) in tetrahydrofuran (20 ml.) was heated with *p*-toluenesulfonic acid (0.1 g.) under reflux for 3 hr. After removal of the solvent the residue was taken in ether and the ethereal solution was washed with a 2% aqueous sodium carbonate solution and water, dried and evaporated. Distillation of the residue afforded an oil which boiled at 130°C (bath temperature)/15 mmHg and solidified rapidly. Recrystallization from petroleum ether yielded colorless plates which melted at 60°C and proved to be identical with XVII obtained from a) by mixed melting point determination and infrared comparison.

The compound XVII was unstable and on exposure to air or light furnished a dark-brown resinous material.

**3, 4-Dimethyl-6-methoxymethyl-3-cyclohexenylmethanal Ethylene Acetal (XX).**—A mixture of the aldehyde XVa (6.6 g.), ethylene glycol (4.0 g.), *p*-toluenesulfonic acid (20 mg.) and benzene (30 ml.) was taken in a flask provided with an azeotropic water separator and heated under reflux in an oil bath (120~130°C) until no more aqueous phase has been separated from an azeotropic distillate (for ca. 4 hr.). The solvent was removed under reduced pressure and the residual brown oil was thoroughly extracted with ether. The combined ethereal extracts were washed with a 10% aqueous sodium carbonate solution and with water, dried over sodium sulfate and evaporated under reduced pressure. Distillation of the residue afforded the acetal XX (6.5 g., 79.3%) as a colorless liquid, b. p. 105~106°C/2.0 mmHg, $n_D^{25}$ 1.4868.

Found: C, 68.90; H, 9.97. Calcd. for $C_{13}H_{22}O_3$: C, 68.99; H, 9.80%.

This compound afforded 2, 4-dinitrophenylhydrazone, m. p. 160°C, undepessed on admixture with that of XVa.

**4, 5-Dimethyl-2-methoxymethylcyclohexylmethanal Ethylene Acetal (XXI).**—The acetal XX (6.5 g.) in absolute ethanol (40 ml.) was hydrogenated in the presence of 5% palladium-on-charcoal (0.2 g.) at 100°C and a pressure of 120 kg./$cm^2$ for 2 hr.

20) L. E. Schniepp and H. H. Geller, *J. Am. Chem. Soc.*, **68**, 1646 (1946).
21) C. D. Hurd and W. H. Saunders Jr., ibid., **74**, 5326 (1952).
22) G. F. Woods and H. Sanders, ibid., **68**, 2111 (1946).
23) G. F. Woods and D. N. Kramer, ibid., **69**, 2246 (1947).

The catalyst was removed by filtration and the filtrate was evaporated under reduced pressure. Distillation of the residue yielded the saturated acetal XXI (5.0 g., 77%), b.p. 103~105°C/2.5 mmHg, $n_D^{29}$ 1.4659.

Found: C, 68.44; H, 10.48. Calcd. for $C_{13}H_{24}O_3$: C, 68.38; H, 10.59%.

The 2, 4-dinitrophenylhydrazone crystallized from ethanol in yellow plates, m. p. 129~130°C.

Found: N, 15.40. Calcd. for $C_{17}H_{24}O_5N_4$: N, 15.38%.

**4, 5-Dimethyl-2-methoxymethylcyclohexylmethanal (XXII).**—A mixture of the acetal XXI (1.8 g.), tetrahydrofuran (30 ml.) and 2 N sulfuric acid (30 ml.) was heated under reflux for 24 hr. The cooled reaction mixture was made slightly alkaline with a 10% sodium carbonate solution, concentrated under reduced pressure and then extracted with ether. The ethereal extract was washed with water, dried and evaporated. Distillation of the residue afforded the aldehyde XXII (1.0 g., 69%), b.p. 93~95°C/1.0 mmHg, $n_D^{17}$ 1.4710; $\nu_{max}^{liquid}$ 1730 $cm^{-1}$ (C=O), $\nu_{max}^{CCl_4}$ 1725.2 $cm^{-1}$ (C=O); $\lambda_{max}$ 226 mμ (ε 499), 294 (59) in 75% aqueous dioxane.

Found: C, 71.58; H, 10.67. Calcd. for $C_{11}H_{20}O_2$: C, 71.69; H, 10.94%.

The 2, 4-dinitrophenylhydrazone showed m. p. 130°C, undepressed on admixture with that of XXI.

**4-(3', 4'-Dimethyl-6'-methoxymethyl-3'-cyclohexenyl)-but-3-en-2-one (XVIII).**—The aldehyde XVa (3.6 g.) was added dropwise to a boiling solution of barium hydroxide (0.7 g.) in 90% aqueous acetone (20 ml.) and the resultant mixture was refluxed for 7.5 hr. The cooled reaction mixture was neutralized with 1 N hydrochloric acid, concentrated under reduced pressure and then extracted with ether. The dried ethereal solution was fractionated to yield the unsaturated ketone XVIII (3.0 g., 68.5%), b. p. 122~123°C/3 mmHg, $n_D^{22.5}$ 1.5000; $\nu_{max}^{liquid}$ 1680 (C=O), 1624 (C=C), 1115 (C-O-C) and 983 $cm^{-1}$ (trans-CH=CH-).

Found: C, 75.42; H, 10.10. Calcd. for $C_{14}H_{22}O_2$: C, 75.63; H, 9.97%.

The 2, 4-dinitrophenylhydrazone crystallized from ethanol in red prisms, m. p. 155~156°C.

Found: N, 14.05. Calcd. for $C_{20}H_{26}O_5N_4$: N, 13.92%.

**4-(4', 5'-Dimethyl-2'-methoxymethylcyclohexyl)-but-3-en-2-one (XXIII).**—The aldehyde XXII (1.7 g.) was added dropwise to a boiling solution of barium hydroxide (0.3 g.) in 90% aqueous acetone (10 ml.) and the resultant mixture was refluxed for 10 hr., and was then treated in the same manner as that described above to yield the ketone XXIII (1.2 g., 58%), b. p. 120~122°C/2 mmHg, $n_D^{32}$ 1.4781.

Found: C, 74.34; H, 10.65. Calcd. for $C_{14}H_{24}O_2$: C, 74.95; H, 10.78%.

The 2, 4-dinitrophenylhydrazone crystallized from ethanol in red-orange plates, m. p. 127~129°C.

Found: N, 14.06. Calcd. for $C_{20}H_{28}O_5N_4$: N, 13.85%.

**Reaction of 4-(3', 4'-Dimethyl-6'-methoxymethyl-3'-cyclohexenyl)-but-3-en-2-one (XVIII) with Hydrobromic Acid.**—A mixture of the unsaturated ketone XVIII (0.3 g.) and a constant boiling hydrobromic acid (b. p. 123°C, 12 ml.) was heated in a 50 ml. glass bomb at 130°C for 4 hr. The black tarry oil formed was poured into an ice-cooled 10% aqueous sodium carbonate solution and extracted with ether. The ethereal extract was washed, dried and evaporated. Distillation of the residue afforded a colorless oil (0.11 g.), b. p. 90~100°C/0.8 mmHg, $n_D^{24.5}$ 1.5241. This oily product gave a positive Beilstein test and a 2, 4-dinitrophenylhydrazone which contained no bromine atom and crystallized from ethanol in orange needles, m. p. 174~175°C.

Found: C, 61.15; H, 6.13. Calcd. for $C_{19}H_{22}O_4N_4$: C, 61.61; H, 5.99%.

Although the position of the double bonds on the ring could not be confirmed, the derivative obtained above was seen clearly to be 2, 4-dinitrophenylhydrazone of 4-(2', 4', 5'-trimethylcyclohexadienyl)-but-3-en-2-one, since elemental analysis was very satisfactory and the infrared spectrum exhibited no absorption band attributable to the exocyclic methylene group.

**2, 4, 5-Trimethylcyclohexylmethanol (XXIV).**—3, 4, 6-Trimethyl-3-cyclohexenylmethanal (XVI) (3.04 g.) in ethanol (30 ml.) was hydrogenated over a Raney nickel catalyst (1.5 g.) in a 100 ml. stainless-steel autoclave at 192°C and a pressure of 192 kg./cm² for 1 hr. The catalyst was removed by filtration and the filtrate was evaporated. Distillation of the residue afforded XXIV (2.9 g., 93%) as a colorless oil, b. p. 110°C/16 mmHg, $n_D^{17}$ 1.4700.

Found: C, 76.62; H, 13.02. Calcd. for $C_{10}H_{20}O$: C, 76.86; H, 12.90%.

***N*, *N*-Dimethyl-2, 4, 5-trimethylcyclohexylmethylamine (XXV).**—A mixture of XVI (7.4 g.), anhydrous dimethylamine (2.9 g.), a Raney nickel catalyst (1.2 g.) and ethanol (50 ml.) was shaken with hydrogen at 180~220°C and a pressure of 121 kg./cm² for 4 hr., after which time a pressure of 58 kg./cm² of hydrogen was absorbed. The catalyst was removed by filtration and the filtrate was evaporated under reduced pressure. Distillation of the residue afforded a crude product (7.9 g.) b. p. 100~105°C/16 mmHg, $n_D^{21}$ 1.4622~1.4658. This oil was taken up in ether and extracted with diluted hydrochloric acid. The aqueous extracts were combined, neutralized with aqueous sodium hydroxide and then extracted with ether. The dried ethereal solution was distilled under reduced pressure to yield a pure amine XXV (6.6 g., 80%), b. p. 98~99°C/15 mmHg, $n_D^{17.5}$ 1.4607.

Found: C, 78.77; H, 13.52. Calcd. for $C_{12}H_{25}N$: C, 78.61; H, 13.75%.

The methiodide crystallized from ethanol in leaflets, m. p. 262°C (decomp.).

Found: C, 48.19; H, 8.83; N, 4.18; I, 38.5. Calcd. for $C_{13}H_{28}NI$: C, 48.0; H, 8.6; N, 4.3; I, 39.0%.

The picrate was obtained as a yellow oil which could not be induced to crystallize.

The ethereal solution which had been shaken with acid was dried and then distilled under reduced pressure to yield a neutral compound (0.8 g., 10.8%), b. p. 114~116°C/17 mmHg, $n_D^{20.5}$ 1.4668. This compound was proved to be identical with

XXIV obtained above by comparison of their infrared spectra.

***N*, *N*-Dimethyl-2, 4, 5-trimethylcyclohexylmethylamine Oxide (XXVI).**—To a solution of the amine XXV (6.11 g., 1/30 mol.) in methanol (5 ml.) was added dropwise 30% aqueous hydrogen peroxide (13 g., 1/10 mol.) under vigorous stirring at 0°C and the resultant mixture was allowed to warm to room temperature. The mixture was stirred for 11.5 hr. and set aside overnight, after which time all of the reaction mixture was homogeneous. The excess of hydrogen peroxide was then decomposed with platinum foil (0.3 g.) under stirring for 35 hr. at room temperature. After removal of the platinum foil the solution was evaporated under reduced pressure (15~17 mmHg) at below 35°C to leave a syrupy residue which was taken up in absolute ethanol (10 ml.). The solution was evaporated through a 25 cm. Vigreux column under reduced pressure. This work-up was repeated 4 times to remove the last traces of water and afforded the amine oxide XXVI as a very viscous colorless liquid. The product thus obtained was used in the next preparation without further purification, since its practical purity was indicated by the determination of an amine oxide prepared in another run described below.

When an excess of picric acid in aqueous ethanol was mixed with an aqueous ethanolic solution of a crude amine oxide prepared from the amine XXV (0.46 g.) in the manner described above, there was obtained a picrate which crystallized from absolute ethanol in yellow plates, m. p. 165~166.5°C. The yield was 0.82 g. (82%).

Found: C, 50.36; H, 6.80; N, 12.69. Calcd. for $C_{18}H_{28}O_8N_4$: C, 50.46; H, 6.59; N, 13.08%.

**1-Methylene-2, 4, 5-trimethylcyclohexane(XXVII).**—The amine oxide XXVI obtained above was taken in a 100 ml. flask fitted with a 15 cm. Vigreux column and heated to 110°C, at this temperature decomposition of the amine oxide occurred. After 30 min. the distillation became slower and the bath was heated to 180°C. The pyrolysis products, which distilled mainly at 120~130°C (bath temperature), were swept with nitrogen through a trap cooled with a freezing mixture and then through a liquid nitrogen cooled trap. The products were combined and taken up in ether. The ethereal solution was washed twice with 10% hydrochloric acid and 3 times with water, dried over magnesium sulfate and then in the presence of a small amount of quinol concentrated under a 25 cm. Vigreux column at atmospheric pressure. The residue was distilled under nitrogen to yield the hydrocarbon XXVII (2.8 g., 61.0% based on XXV), b. p. 59~59.2°C/16.2 mmHg, $n_D^{20}$ 1.4601. This hydrocarbon decolorized rapidly a dilute solution of bromine in carbon tetrachloride and readily consumed potassium permanganate in acetone solution. $\nu_{max}^{liquid}$ 3077, 1648, 885 (>C=$CH_2$); 1464, 1384 (-$CH_2$- and $CH_3$) and 1770 $cm^{-1}$ (over-tone of δ CH).

Found: C, 87.12; H, 12.63. Calcd. for $C_{10}H_{18}$: C, 86.88; H, 13.12%.

The aqueous washings were combined and concentrated under reduced pressure to leave a crystalline residue, which was taken up in absolute ethanol. The solution was evaporated to dryness yielding a crude *N*, *N*-dimethylhydroxylamine hydrochloride (2.0 g., 61.5%), m. p. 103~105°C. A sample recrystallized from absolute ethanol in needles, m. p. 105~106.5°C (lit. m. p. 104.5~106.5°C[13] and m. p. 106.5~109°C[24]).

**2-Benzyloxymethyl-4, 5-dimethylcyclohexa-4, 6-(or -1, 4-) dienylmethanal Ethylene Acetal (XXX).**—A mixture of the aldehyde XIVb (47.2 g.), *p*-toluenesulfonic acid (0.05 g.), ethylene glycol (26.2 g.) and benzene (250 ml.) was taken in a flask provided with an azeotropic water separator and heated under reflux at 120°C for 4 hr. The water was drawn off from time to time. After the excess of benzene was removed under reduced pressure the residue was extracted with ether. The ethereal solution was washed with a 10% aqueous sodium carbonate solution and with water, dried over sodium sulfate and then evaporated. Distillation of the residue afforded a lower boiling fraction (5.8 g.), b. p. 52~80°C/0.001 mmHg, and an acetal XXX (18.5 g., 33.5%) as a pale yellow viscous oil, b. p. 144~148°C/0.001 mmHg, $n_D^{26}$ 1.5429.

Found: C, 75.73; H, 8.21. Calcd. for $C_{19}H_{24}O_3$: C, 75.97; H, 8.05%.

The lower boiling fraction on treatment with the Brady reagent yielded a 2, 4-dinitrophenylhydrazone. Recrystallization from ethanol-ethyl acetate gave a pure sample, m. p. 226°C, undepressed on admixture with the 2, 4-dinitrophenylhydrazone of 2, 4, 5-trimethylbenzaldehyde.

**6-Benzyloxymethyl-3, 4-dimethyl-3-cyclohexenylmethanal Ethylene Acetal (XXXI).**—A mixture of the aldehyde XVb (8.3 g.), ethylene glycol (9.0 g.), *p*-toluenesulfonic acid (0.05 g.) and benzene (40 ml.) was refluxed at 130~135°C for 4 hr. The reaction mixture was worked up in the manner described above to yield the acetal XXXI (7.2 g., 74.2%), b. p. 150~155°C/0.017 mmHg.

Found: C, 73.98; H, 8.55. Calcd. for $C_{19}H_{26}O_3$: C, 75.46; 8.67%.

**4, 5-Dimethyl-2-hydroxymethylcyclohexylmethanal Ethylene Acetal (XXXII).**—*a) From XXX.*—The acetal XXX (16.5 g.) in ethanol (40 ml.) was hydrogenated over a 5% palladium-on-charcoal catalyst (1.0 g.) in a stainless-steel autoclave at 120°C and a pressure of 120 kg./$cm^2$ for 8 hr. The catalyst was filtered off and the filtrate was evaporated. Distillation of the residue afforded a saturated acetal XXXII (3.9 g., 33%) as a viscous oil, b. p. 112~120°C/1.3 mmHg, $n_D^{25.5}$ 1.4786.

Found: C, 66.90; H, 10.62. Calcd. for $C_{12}H_{22}O_3$: C, 67.25; H, 10.35%.

The 2, 4-dinitrophenylhydrazone crystallized from methanol-light petroleum in orange-yellow leaflets, m. p. 194~196°C.

Found: N, 16.19. Calcd. for $C_{16}H_{22}O_5N_4$: N, 15.99%.

Further distillation afforded a higher boiling viscous oil (6.7 g.), which boiled at 120~125°C/0.001 mmHg and was thought probably to be 2-benzyloxymethyl-4, 5-dimethylcyclohexylmethanal ethylene acetal (XXXIII), since it afforded readily

24) A. C. Cope, N. A. LeBel, H. H. Lee and W. R. Moore, ibid., 79, 4720 (1957).

XXXII on hydrogenolysis under the same conditions as those described above.

*b) From XXXI.*—The acetal XXXI (11.4 g.) in ethanol (50 ml.) was hydrogenated over 5% palladium-on-charcoal (1.0 g.) for 5 hr. in the manner described above to yield XXXII (6.2 g., 77.5%), b. p. 131~134°C/3.0 mmHg.

The 2, 4-dinitrophenylhydrazone prepared from this liquid showed m. p. 195~196°C, undepressed on admixture with a sample obtained in a).

The 3, 5-dinitrobenzoate crystallized from benzene-petroleum ether in plates, m. p. 110~111°C.

Found: C, 55.47; H, 5.96; N, 7.01. Calcd. for $C_{19}H_{24}O_8N_2$: C, 55.87; H, 5.92; N, 6.86%.

**4,5-Dimethyl-2-hydroxymethylcyclohexylmethanal (XXXIV).**—A mixture of the acetal XXXII (3.1 g.), tetrahydrofuran (16 ml.) and 2 N sulfuric acid (16 ml.) was refluxed for 2.5 hr. The cooled reaction mixture was neutralized with a 30% aqueous sodium carbonate solution and extracted with ether. The ethereal solution was washed with a saturated sodium chloride solution, dried over sodium sulfate and then evaporated. Distillation of the residue under nitrogen afforded the hydroxyaldehyde XXXIV (1.9 g., 77.3%), which boiled at 99~105°C/2.0 mmHg and solidified rapidly. Recrystallization from methanol-light petroleum yielded colorless plates, m. p. 84°C; $\nu_{max}^{KBr}$ 3333, 1724, 1456, 1124, 1087, 1047, 971, 899 and 877 $cm^{-1}$; $\lambda_{max}$ 225 m$\mu$ ($\varepsilon$ 37.3), 294 (29.1) in 75% aqueous dioxane.

Found: C, 70.81; H, 10.62. Calcd. for $C_{10}H_{18}O_2$: C, 70.54; H, 10.66%.

The 2, 4-dinitrophenylhydrazone crystallized from methanol in orange-yellow leaflets, m. p. 194~195°C, undepressed on admixture with that of XXXII.

***N*, *N*-Dimethyl-4,5-dimethyl-2-hydroxymethylcyclohexylmethylamine (XXXV).**—*a) From XXXIV.*—A mixture of the aldehyde XXXIV (1.2 g.), anhydrous dimethylamine (0.8 g.), Raney nickel catalyst (1.2 g.) and absolute ethanol (30 ml.) was shaken with hydrogen in a 100 ml. autoclave at 180~190°C and a pressure of 118 kg./cm² for 1.6 hr. The catalyst was filtered off and the solution was evaporated to leave an oil, which was taken up in ether and extracted twice with 2 N hydrochloric acid. The aqueous extracts were combined, made alkaline with a 10% sodium hydroxide solution and then extracted with ether. The dried ethereal solution on distillation afforded the aminoalcohol XXXV (0.8 g., 57%), b. p. 100~105°C/2.0 mmHg, $n_D^{29.5}$ 1.4666.

Found: C, 71.73; H, 12.40. Calcd. for $C_{12}H_{25}ON$: C, 72.30; H, 12.64%.

The methiodide crystallized from ethanol-ethyl acetate in prisms, m. p. 221°C.

Found: C, 45.40; H, 8.33. Calcd. for $C_{13}H_{28}ONI$: C, 45.87; H, 8.28%.

The ethereal solution which had been shaken with hydrochloric acid was distilled to yield an oil (0.15 g., 12%), which boiled at 115~121°C/2.0 mmHg and solidified on being set aside for a short time. Recrystallization from light petroleum afforded colorless plates, m. p. 113~115°C.

Found: C, 69.01; H, 11.23. Calcd. for $C_{10}H_{20}O_2$: C, 69.72; H, 11.70%.

This compound is thought probably to be 1, 2-bishydroxymethyl-4, 5-dimethylcyclohexane (XXXVI), since the elemental analysis is very satisfactory and the infrared spectrum exhibits strong absorption bands of the hydroxyl group at 3310 and 1045 $cm^{-1}$ but no band attributable to an aldehyde group.

*b) From XIVc.*—A mixture of the aldehyde XIVc (2.9 g.), anhydrous dimethylamine (2.0 g.), Raney nickel (2.0 g.) and ethanol (40 ml.) was shaken with hydrogen at 200~220°C and a pressure of 197 kg./cm² for 3 hr. When the resultant reaction mixture was worked up as in the case of XXXIV, there were obtained a crude amino compound (1.2 g., 43.5%) and a neutral one (0.8 g., 31.6%).

The amino compound boiled at 80°C/0.55 mmHg, $n_D^{15}$ 1.4755, and the infrared spectrum exhibited strong absorption bands of hydroxyl group at 3370 and 1066 $cm^{-1}$ and characteristic bands attributable to the *tert*-amino group at 2838, 2800 and 2742 $cm^{-1}$.

Found: C, 72.53; H, 12.80; N, 7.10. Calcd. for $C_{12}H_{25}ON$: C, 72.30; H, 12.64; N, 7.03%.

The methiodide crystallized from methanol-ethyl acetate in leaflets, m. p. 221°C, undepressed on admixture with that of XXXV obtained in a).

From the crude methiodide, there was obtained a small amount of crystals which were slightly soluble in methanol-ethyl acetate. Recrystallization afforded a pure sample, m. p. 271~272°C.

Found: C, 46.30; H, 7.93. Calcd. for $C_{13}H_{26}ONI$: C, 46.00; H, 7.73%.

The elemental analysis indicates that the methiodide is probably that of *N*, *N*-dimethyl-4, 5-dimethyl-2-hydroxymethyl-1-cyclohexenylmethylamine (XXXIX).

The neutral product of colorless liquid obtained above boiled at 95~105°C/0.6 mmHg and solidified rapidly. Recrystallization from petroleum ether yielded 2,4, 5-trimethylbenzyl alcohol (XL) in needles, m. p. 84.5°C.

The infrared spectrum (KBr disk) exhibited strong absorption bands of hydroxyl group at 3360 and 1038 $cm^{-1}$ and other principal bands at 1621 (w), 1513 (m), 1450 (s), 1078 (s), 1009 (s), 996 (s), 899 (m), 888 (m), and 877 $cm^{-1}$ (s). $\lambda_{max}^{EtOH}$ 217 m$\mu$ ($\varepsilon$ 175), 265 (338) and 274 (322).

Found: C, 80.02; H, 9.51. Calcd. for $C_{10}H_{14}O$: C, 79.95; H, 9.39%.

***N*, *N*-Dimethyl-4, 5-dimethyl-2-hydroxymethylcyclohexylmethylamine Oxide (XXXVII).**—To a solution of the amine XXXV (0.6 g.) in methanol (3.6 ml.) was added 30% aqueous hydrogen peroxide (1.5 g.) and the resultant mixture was stirred at 30°C for 50 hr., after which time the reaction mixture gave no color with phenolphthalein. The excess of hydrogen peroxide was then decomposed with a small amount of platinum foil and the solution was worked up as in the case of XXVI to yield the amine oxide XXXVII (0.55 g., 84.6%) as a colorless glass, which was characterized as the picrate which could not be induced to crystallize. The product thus obtained was used in the next pyrolysis without further purification.

**4, 5-Dimethyl-2-methylenecyclohexylmethanol (XXXVIII).**—The amine oxide XXXVII (0.4 g.) obtained above was pyrolysed as in the case of XXVII to yield a neutral XXXVIII (0.12 g., 42%),

b. p. 94~97°C/17.5 mmHg, $n_D^{27}$ 1.4729. The infrared spectrum (liquid film) exhibited absorption bands of hydroxyl group at 3385 and 1053 $cm^{-1}$, the bands attributable to exocyclic double bond at 3058, 1642 and 884 $cm^{-1}$ and other principal bands at 1765, 1459 and 1384 $cm^{-1}$.

Found: C, 77.79; H, 11.85. Calcd. for $C_{10}H_{18}O$: C, 77.86; H, 11.76%.

**2, 4, 5-Trimethylbenzaldehyde (XXVIII).**—*a) By Sulfur Dehydrogenation of 3, 4, 6-Trimethyl-3-cyclohexenylmethanal (XVI).*—The aldehyde XVI (2.3 g.) was heated under reflux with sulfur (1.2 g.) at 220~230°C in an oil bath until the evolution of hydrogen sulfide ceased (for ca. 40 min.). The resultant yellowish dark-brown mixture was distilled to yield a yellow oil (0.45 g.), b. p. 128~130°C/18 mmHg, $n_D^{20}$ 1.5591 (lit.[25] b. p. 55~60°C/5~10 mmHg).

The 2, 4-dinitrophenylhydrazone crystallized from ethanol-ethyl acetate in red needles, m. p. 223~224.5°C.

Found: C, 58.40; H, 5.07. Calcd. for $C_{16}H_{16}O_4N_4$: C, 58.53; 4.91%.

The semicarbazone crystallized from ethanol-ethyl acetate in needles, m. p. 239°C; $\lambda_{max}^{EtOH}$ 226 mμ (ε 16500), 285 (23400),

Found: C, 64.36; H, 7.35. Calcd. for $C_{11}H_{15}ON_3$: C, 64.36; H, 7.37%.

*b) By the Action of p-Toluenesulfonic Acid on 2-Benzyloxymethyl-4, 5-dimethylcyclohexa-1, 4-dienylmethanal (XIVb).*—A mixture of the unsaturated aldehyde XIVb (1.0 g.), *p*-toluenesulfonic acid (0.3 g.) and xylene (10 ml.) was heated under reflux for 4 hr. The cooled reaction mixture was neutralized with a 10% aqueous sodium carbonate solution and extracted with ether. The ethereal solution was washed with water, dried over sodium sulfate and then evaporated. Distillation of the residue afforded a colorless oil (0.2 g., 35%), b. p. 80~90°C/0.6~0.8 mmHg.

The 2, 4-dinitrophenylhydrazone crystallized from ethanol-ethyl acetate in bright red prisms, m. p. 225~226.5°C, undepressed on admixture with that of XXVIII obtained in a).

*c) By Hydrolysis of Phenylsemicarbazone of 2-Benzyloxymethyl-4, 5-dimethylcyclohexa-1, 4-dienyl methanal (XIVb).*—Steam distillation of the phenylsemicarbazone (4.5 g.) of XIVb from a mixture of *o*-phthalic acid (4.5 g.), ethylene glycol (40 ml.), concentrated sulfuric acid (14.0 g.) and water (40 ml.) afforded benzyl alcohol (0.3 g.) and the aldehyde XXVIII (1.3 g., 60%) as a colorless liquid after the usual workup. The regenerated aldehyde was distilled to yield a pure compound, which boiled at 87°C/1.0 mmHg and was crystallized upon treatment with petroleum ether. Recrystallization from methanol-petroleum ether afforded colorless plates, m. p. 43°C (lit.[16] m. p. 42°C); $\lambda_{max}^{EtOH}$ 215 mμ (ε 22400), 261 (14700), 298 (2400). The infrared spectrum (KBr disk) exhibited a strong absorption band of carbonyl group at 1686 $cm^{-1}$, and other principal bands at 3000 (m, sh), 2934 (m), 2856 (m), 2742(m), 1608 (s), 1551 (s), 1501 (m), 1454 (s), 1386 (m), 1255 (m), 1187 (s), 1082 (m), 887 (m) and 775 $cm^{-1}$ (s).

Found: C, 80.95; H, 8.21. Calcd. for $C_{10}H_{12}O$: C, 81.04; H, 8.16%.

The 2, 4-dinitrophenylhydrazone crystallized from ethyl acetate in bright red needles, m. p. 226~227°C.

The semicarbazone crystallized from chloroform-ethyl acetate in fine needles, m. p. 239~240°C.

The melting points of mixtures of the above derivatives with samples obtained in a) showed no depression.

**4-(2', 4', 5'-Trimethylphenyl)-but-3-en-2-one (XXIX).**—A solution of the aldehyde XXVIII (0.4 g.) obtained in c) in acetone (5 ml.) was added dropwise to a boiling mixture of barium hydroxide (0.2 g.), acetone (8 ml.) and water (2 ml.) and the resulting mixture was heated under reflux for 18.5 hr. The cooled reaction mixture was acidified with 1 N hydrochloric acid, concentrated under reduced pressure and then extracted with ether. The ethereal extracts were combined, washed and dried. Distillation of the residue afforded a colorless oil (0.2 g., 40%), which boiled at 120~140°C (bath temperature)/3.0 mmHg and solidified on standing. Recrystallization from petroleum ether yielded XXIX in colorless prisms, m. p. 49.5~50°C (lit.[26] m. p. 51°C); $\lambda_{max}^{EtOH}$ 216.5 mμ (ε 12600), 233 (10700), 305 (21900); $\nu_{max}^{KBr}$ 1683 (conjugated C=O), 1660 (conjugated C=C), 978 (trans -CH=CH-) and 869 $cm^{-1}$.

The 2, 4-dinitrophenylhydrazone crystallized from methanol-chloroform in dark-red needles, m. p. 247~249°C.

Found: N, 15.29. Calcd. for $C_{19}H_{20}O_4N_4$: N, 15.21%.

The semicarbazone crystallized from ethanol-ethyl acetate in leaflets, m. p. 223~224°C; $\lambda_{max}^{EtOH}$ 237 mμ (ε 18600), 307 (42600).

Found: N, 17.20. Calcd. for $C_{14}H_{19}ON_3$: N, 17.13%.

We wish to thank Dr. Asaji Kondo of the Tokyo Institute of Technology for the microanalyses; Drs. Tadashi Sato of Waseda University and Kenji Kuratani of the Aeronautical Research Institute, the University of Tokyo, for the infrared spectra; and Dr. Ichiro Yamaguchi of the Japan Atomic Energy Research Institute for the nuclear magnetic resonance spectra.

*Laboratory of Organic Chemistry*
*Kobayasi Institute of*
*Physical Research*
*Kokubunji, Tokyo*

25) C. D. Shacklett and H. A. Smith, ibid., 75, 2654 (1953).
26) W. John et al., *Z. Physiolo. Chem.*, 268, 104 (1941).

# *Thermodynamical Studies on Binary Systems Consisting of Polar and Non-polar Liquids. IV. Estimation of the Electrostatic Part of the Excess Enthalpy from the Observed Values aud Comparison with the Calculated Values*

By Kazuo AMAYA

(Received March 13, 1961)

In a previous paper[1], the author calculated the electrostatic part of the excess enthalpy of binary systems composed of polar and non-polar liquids according to Onsager's model. In this paper the observed values of these quantities have been derived under reasonable assumptions and are compared with the calculated values.

## The Principle of the Estimation of the Electrostatic Part of the Excess Enthalpy from the Experimental Results

In order to derive the electrostatic part of the excess enthalpy due only to the permanent dipole of the polar molecule from the experimental result of the heat of mixing, the non-electrostatic part of the excess enthalpy must be estimated under reasonable assumptions and subtracted from the experimental value, since the observed excess enthalpy contains not only the electrostatic but also the non-electrostatic part.

As a first approximation, it may be assumed that the intermolecular interaction enery of polar molecules is the sum of the non-electrostatic part of the energy due to dispersion forces and the electrostatic one due to dipoles if higher multipoles are neglected.

From this assumption the cohesive energy for 1 mol. of pure polar liquid, $\Delta U_2$, may be given by

$$\Delta U_2 = \Delta U_2^{el} + \Delta U_2^{n-el} \tag{1}$$

where $\Delta U_2^{el}$ and $\Delta U_2^{n-el}$ are the electrostatic and the non-electrostatic part of cohesive energy respectively.

Since the electrostatic intermolecular energy is absent in non-polar liquids, the cohesive energy for non-polar liquid $\Delta U_1$ is given by the non-electrostatic intermolecular energy due to dispersion forces of non-polar molecules:

$$\Delta U_1 = \Delta U_1^{n-el} \tag{2}$$

Further, if the non-electrostatic part of the energy due to dispersion forces is assumed to be the sum of the energy due to dispersion forces of the nearest neighbor pairs, then for 1 mol. of polar liquid $\Delta U_2^{n-el}$ is given by

$$\Delta U_2^{n-el} = 1/2 \cdot N_A z \omega_{22} \tag{3}$$

and similarly for 1 mol. of non-polar liquid,

$$\Delta U_1^{n-el} = 1/2 \cdot N_A z \omega_{11} \tag{4}$$

where $N_A$ is Avogadro's number, $z$ is the number of the nearest neighbors and $\omega_{22}$ and $\omega_{11}$ are the non-electrostatic part of interaction energy due to dispersion forces of the nearest neighbor pairs of polar and non-polar molecules respectively.

When 1 mol. of the solution is formed from $x_2$ mole of polar liquid and $(1-x_2)$ mol. of non-polar liquid, both liquids being composed of molecules of similar size, the total energy of the system $\Delta U_{12}$ is given by

$$\Delta U_{12} = \frac{1}{2} x_2^2 N_A z \omega_{22} + x_2(1-x_2) N_A z \omega_{12} + \frac{1}{2}(1-x_2)^2 N_A z \omega_{11} + \Delta U_{12}^{el} \tag{5}$$

where $\omega_{12}$ is the non-electrostatic part of the nearest neighbor pair interaction energy of the pair consisting of polar and non-polar molecules and $\Delta U_{12}^{el}$ is the electrostatic part of the energy due to dipoles for 1 mol. of the solution. Thus the excess energy $U^E$ is given by

$$U^E = x_2(1-x_2) N_A z \omega + \Delta U_{12}^{el} - x_2 \Delta U_2^{el} \tag{6}$$

where $\omega$ is the part of interchange energy due to dispersion forces given by

$$2\omega = 2\omega_{12} - \omega_{22} - \omega_{11} \tag{7}$$

In a similar way the electrostatic part of the excess energy due to dipole-dipole interaction as well as the non-electrostatic contribution due to dispersion forces may be expressed as a function of volume fraction $v_2$ of the polar liquid:

$$U^E = V \alpha^{n-el} v_2(1-v_2) + \Delta U_{12}^{el}(v_2) - v_2 \cdot \Delta U_2^{el} \tag{8}$$

where $V$ is the volume of 1 mol. of the solution.

1) K. Amaya, This Bulletin, 34, 1349 (1961).

TABLE I. VALUES OF $\alpha^{el}_{obs}(0)$, $\alpha^{el}_{obs}(1)$, $\Delta\alpha^{el}_{obs}$ AND $\alpha^{el}_{obs}(0)/\alpha^{el}_{obs}(1)$ FOR THE SYSTEMS IN WHICH NON-POLAR COMPONENTS ARE NON-AROMATIC

| System | $\alpha^{el}_{obs}(0)$ joul./cc. | $\alpha^{el}_{obs}(1)$ joul./cc. | $\Delta\alpha^{el}_{obs}$ joul./cc. | $\alpha^{el}_{obs}(0)/\alpha^{el}_{obs}(1)$ |
|---|---|---|---|---|
| Chlorobenzene—Cyclohexane | 12.5 | 4.9 | 7.6 | 2.54 |
| Bromobenzene—Cyclohexane | 15.7 | 6.1 | 9.6 | 2.58 |
| Benzonitrile—Cyclohexane | 65.6 | 25.0 | 40.6 | 2.62 |
| Nitrobenzene—Cyclohexane | 75 | 37 | 38 | 2.03 |
| Cyclohexanone—Cyclohexane | 54.9 | 31.8 | 23.1 | 1.73 |
| Diethylketone—Cyclohexane | 54.4 | 28.9 | 25.5 | 1.89 |
| Methylpropylketone—Cyclohexane | 56.9 | 32.5 | 24.4 | 1.75 |
| *n*-Butylchloride—Cyclohexane | 21.8 | 11.2 | 10.6 | 1.95 |
| *n*-Butylcyanide—Cyclohexane | 59.2 | 33.9 | 25.3 | 1.75 |
| Chlorocyclohexane—Methylcyclohexane | 16.0 | 9.95 | 6.0$_5$ | 1.61 |
| Bromocyclohexane—Methylcyclohexane | 17.5 | 11.3 | 6.2 | 1.55 |
| *cis*-Dichloroethylene—*trans*-Dichloroethylen | 10.4 | 5.4 | 5.0 | 1.95 |
| Pyridine—1,4-Dioxane | 4.7 | <1.9 | >2.8 | 2.24 |

It may be assumed that $\alpha^{n-el}$, the contribution of dispersion forces to the van Laar coefficient is constant over the whole concentration range, because the coefficients $\alpha$ for binary systems of non-polar liquids are nearly constant. In addition it is also assumed that there is no volume change on mixing. Then $U^E$ is equal to $H^E$:

$$U^E = H^E = V\alpha^{n-el}v_2(1-v_2) + H^{E-el} \quad (9)$$

$$U^{E-el} = H^{E-el} = U^{E-el} - \Delta U_{12}{}^{el}(v_2) - v_2 \cdot \Delta U_2{}^{el} \quad (10)$$

Further, if the electrostatic part is expressed in the form

$$H^{E-el} = V\alpha^{el}v_2(1-v_2) \quad (11)$$

then

$$H^E = V(\alpha^{n-el} + \alpha^{el})v_2(1-v_2) \quad (12)$$

where $\alpha^{el}$ is the electrostatic contribution to $\alpha$.

## The Estimation of $\alpha^{n-el}$, Non-electrostatic Part of $\alpha$

The values of $\alpha^{el}$ can be obtained if the values of $\alpha^{n-el}$ are estimated under reasonable assumptions. And for estimating the non-electrostatic part of the heat of mixing, the following procedures are employed:

**(1) The Systems of Cyclohexane—Aliphatic Polar Molecule.** — For cyclohexane—*n*-hexane system the heat of mixing per mole of cyclohexane at the extreme dilution is about 573 joul./mol.[2] corresponding to the value of 5.3 joul./cc. for $\alpha$. Since for non-polar liquid systems the values of $\alpha$ do not vary with concentration, it may be reasonable to use the above value over all the concentration range. Even for the binary systems of cyclohexane and polar aliphatic hydrocarbon derivatives, it may be permissible, as an approximation, to take the value of 5.3 joul./cc. non-electrostatic part of $\alpha$, neglecting the difference for between $CH_3$, $CH_2$ and the polar groups.

**(2) The Systems of Cyclohexane—Benzene Derivative.**—In (1) the observed values of the electrostatic part of $\alpha$ at the two extreme concentrations of $v_2=1$ and 0, $\alpha^{el}_{obs}(1)$ and $\alpha^{el}_{obs}(0)$, are obtained by subtracting the value of 5.3 joul./cc. from the observed values at the corresponding concentrations. If the ratios, $\alpha^{el}_{obs}(0)/\alpha^{el}_{obs}(1)$, are calculated, they are found to lie between 2.0 and 1.5 as shown in Table I. Accordingly, if may be permissible to approximate the corresponding ratio in the cyclohexane—toluene system to be 2. Then, by empolying the observed value of $\alpha_{obs}(0) = 24.78$ joul./cc., $\alpha_{obs}(1) = 20.81$ joul./cc. for this system, the non-electrostatic part of $\alpha$ of 17.0 joul./cc. is obtained. As an approximation, neglecting the difference between $CH_3$ group of toluene and polar groups in other benzene derivatives, it may be plausible to assume the value of 17.0 joul./cc. as the non-electrostatic part of $\alpha$ for cyclohexane—benzene derivative systems.

The ratios of $\alpha^{el}_{obs}(0)/\alpha^{el}_{obs}(1)$ for the systems in which the non-polar components are non aromatic are shown in Table I.

It is seen from the table that the values of the ratio $\alpha^{el}_{obs}(0)/\alpha^{el}_{obs}(1)$ for the aromatic polar molecules are nearly equal to about 2, but slightly larger than those for non-aromatic molecules.

**(3) The Systems of Cyclohexane—Cyclohexanone, Methylcyclohexane — Harocyclohexane and *cis*- and *trans*-Dichloroethylene Systems.**—It is assumed that the non-electrostatic part of $\alpha$ is equal to zero because of the similarity of the two components.

2) Landolt-Bernstein, Physikalische-Chemiche Tabellen, III. Erg., p. 2826.

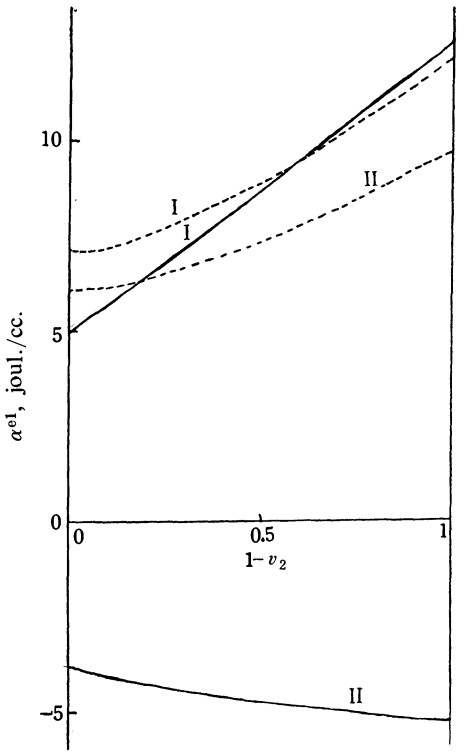



Fig. 1.1. Chlorobenzene—cyclohexane (I) and chlorobenzene—toluene (II) systems.

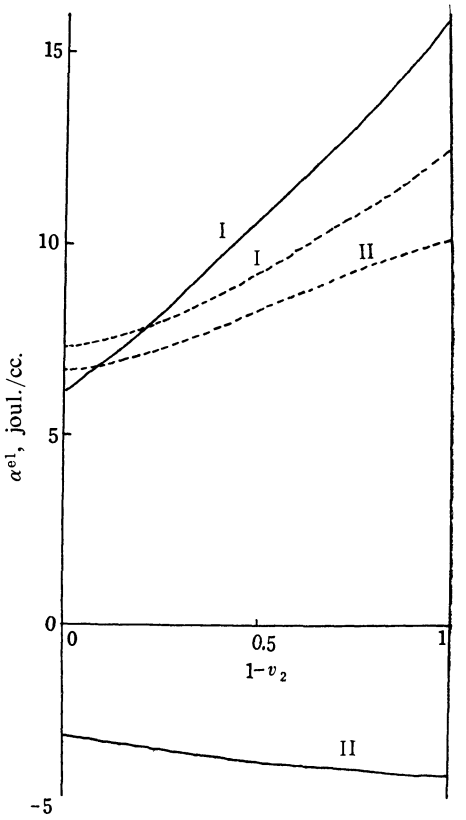



Fig. 1.2. Bromobenzene—cyclohexane (I) and bromobenzene—toluene (II) systems.

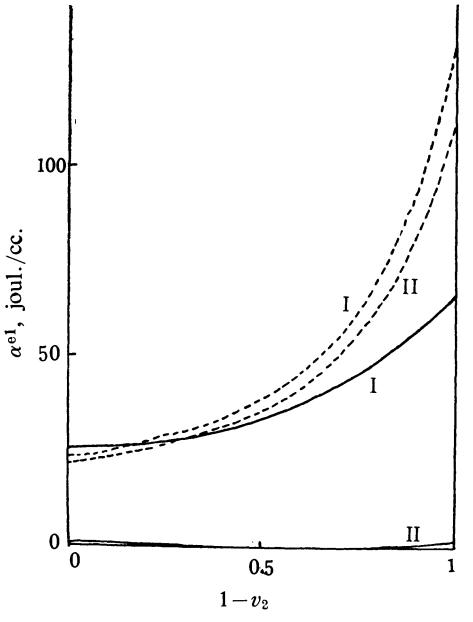



Fig. 1.3. Benzonitrile — cyclohexane (I) and benzonitrile—toluene (II) systems.

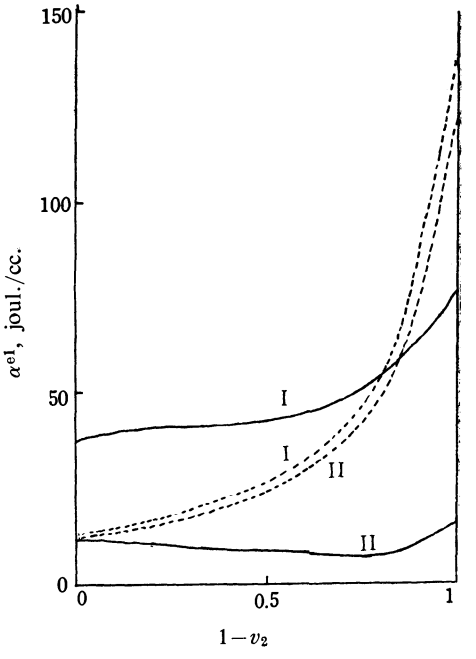



Fig. 1.4. Nitrobenzene — cyclohexane (I) and nitrobenzene—toluene (II) systems.

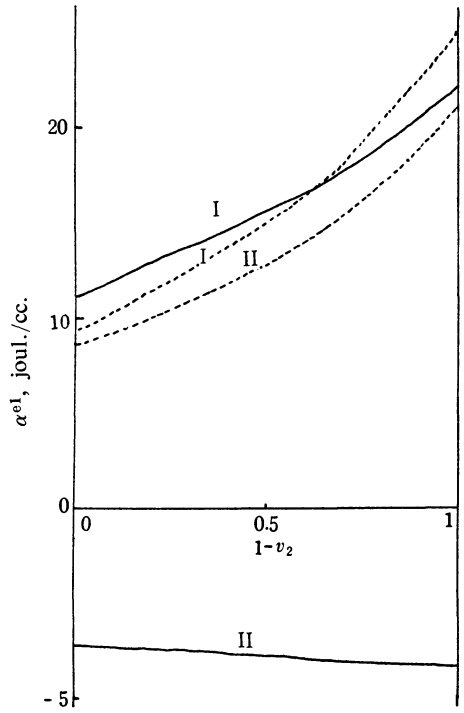



Fig. 1.5. Butylchloride — cyclohexane (I) and butylchloride—toluene (II) systems.

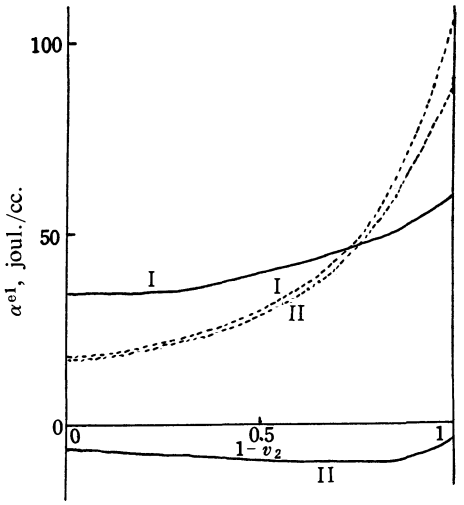



Fig. 1.6. Butylcyanide — cyclohexane (I) and butylcyanide—toluene (II) systems.

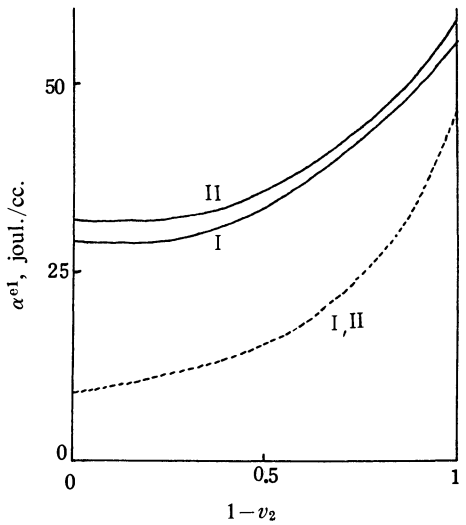



Fig. 1.7. Diethylketone — cyclohexane (I) and methylpropylketone — cyclohexane (II) systems.

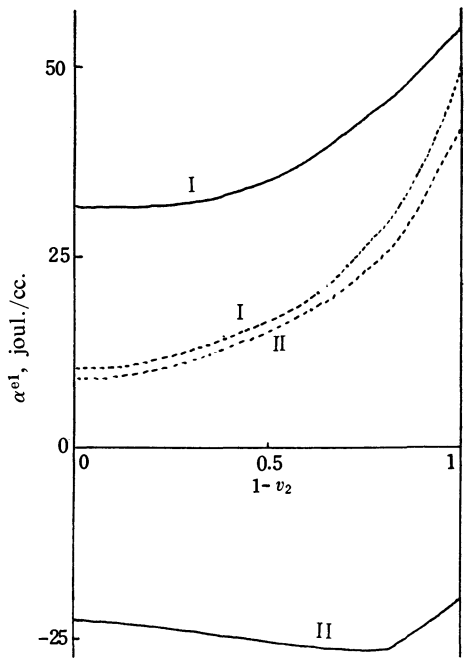



Fig. 1.8. Cyclohexanone—cyclohexane (I) and cyclohexanone—toluene (II) systems.

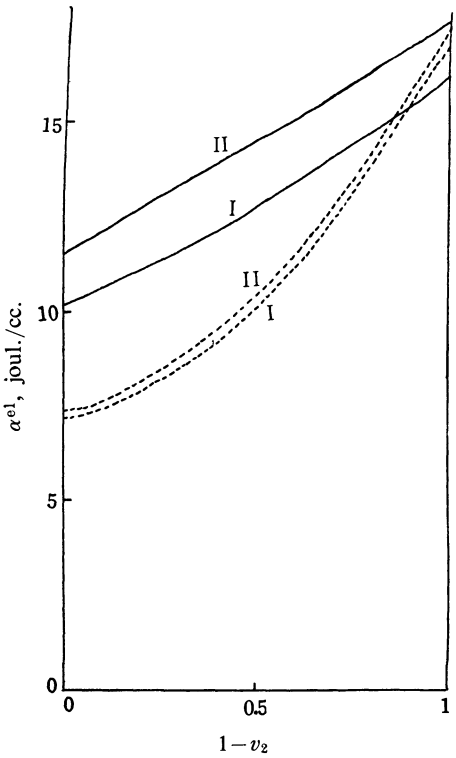



Fig. 1.9. Chlorocyclohexane—methylcyclohexane (I) and bromocyclohexane—methylcyclohexane (II) systems.

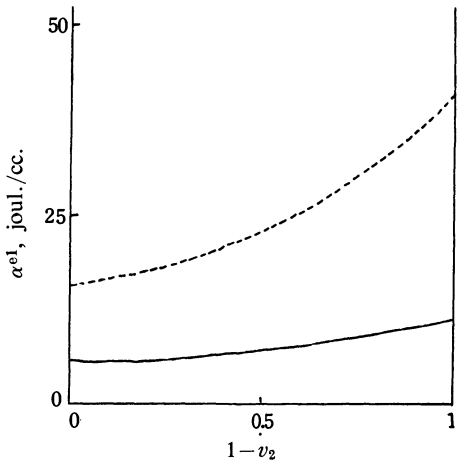



Fig. 1.10. *cis*-Dichloroethylene—*trans*-dichloroethylene system.

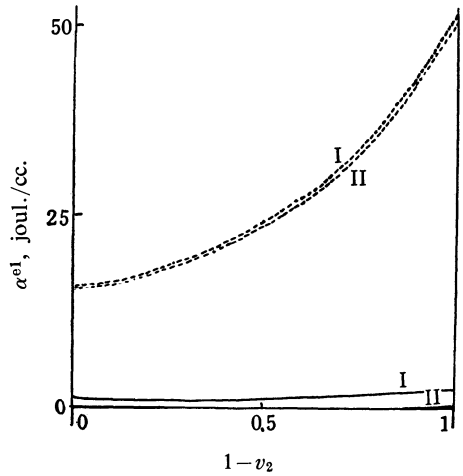



Fig. 1.11. Pyridine—1,4-dioxane (I) and pyridine—benzene (II) systems.

Fig. 1.1—1.11. The observed and the calculated values of electrostatic part of van Laar coefficient $\alpha^{el}$ plotted against volume fraction.
—— Observed ----- Calculated

For the systems in which non-polar components are aromatic such as toluene or benzene, $\alpha^{n-el}$, the non-electrostatic part of $\alpha$, is estimated as follows.

**(4) The Systems of Toluene—Aromatic Polar Molecule.**—For the systems of toluene—benzene derivatives and of benzene—pyridine, the $\alpha^{n-el}$ are assumed to be zero for their structural similarity.

**(5) The Systems of Toluene—Aliphatic Polar Molecule.** — For butylchloride — toluene, and butylcyanide—toluene systems, the values of $\alpha^{n-el}$ are estimated from the data of heat of mixing for the toluene—*n*-heptane system[3], by neglecting the differences between the polar group and $CH_3$ or $CH_2$ groups as before. For the present cases the value of $\alpha$ for *n*-heptane (1.5 joul./cc.) are assumed to be $\alpha^{n-el}$.

For the cyclohexanone-toluene system $\alpha^{n-el}$ is assumed to be 17.0 joul./cc. as before.

3) Landolt-Bernstein, Physikalische-Chemische Tabellen, H. W. II, p. 1567.

## Results and Discussion

The values of the electrostatic part of the van Laar coefficient $\alpha^{el}_{obs}$ were plotted against volume fraction with solid lines in Figs. 1.1—1.11.

Before comparing them with the calculated values, it will be examined whether there exist any regularity between these values and dielectric constants of the polar component or not.

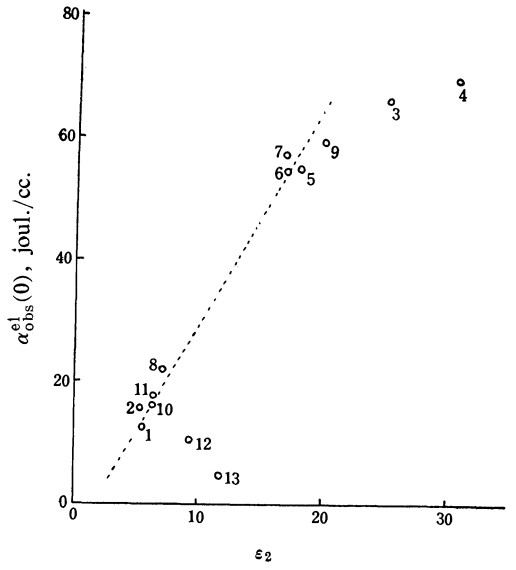



Fig. 2.

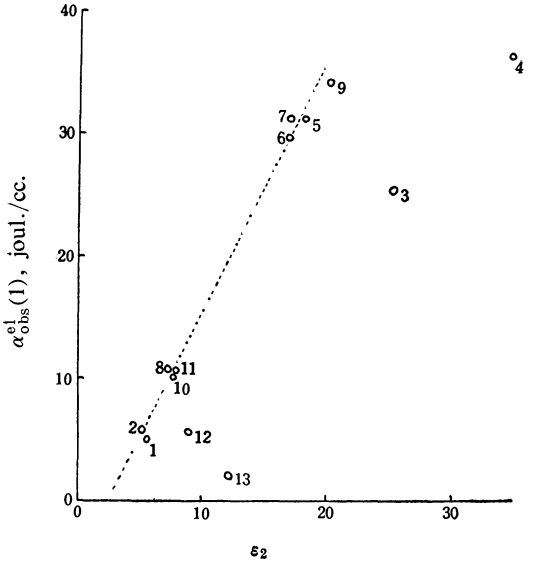



Fig. 3.

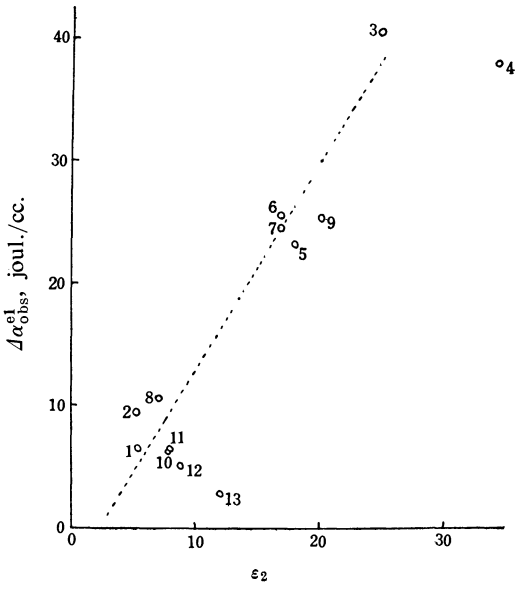



Fig. 4.

Figs. 2, 3 and 4. The plots of observed values of electrostatic part of van Laar coefficients at concentration $v_2=0$ and $v_2=1$ and their difference, $\alpha^{el}_{obs}(0)$, $\alpha^{el}_{obs}(1)$ and $\Delta\alpha^{el}_{obs}$ respectively vs. dielectric constant of polar components $\varepsilon_2$ for systems with non-aromatic non-polar components.

1. Chlorobenzene—Cyclohexane
2. Bromobenzene—Cyclohexane
3. Benzonitrile—Cyclohexane
4. Nitrobenzene—Cyclohexane
5. Cyclohexanone—Cyclohexane
6. Diethylketone—Cyclohexane
7. Methylpropylketone—Cyclohexane
8. *n*-Butylchloride—Cyclohexane
9. *n*-Butylcyanide—Cyclohexane
10. Chlorocyclohexane—Methylcyclohexane
11. Bromocyclohexane—Methylcyclohexane
12. *cis*-Dichloroethylene—*trans*-Dichloroethylene
13. Pyridine—1,4-Dioxane

For systems in which non-polar components are non-aromatic such as cyclohexane and methyl cyclohexane etc.,. the values of $\alpha^{el}_{obs}$ at $v_2=1$ and $v_2=0$, $\alpha^{el}_{obs}(1)$ and $\alpha^{el}_{obe}(0)$ respectively, are shown in Table I.

The difference of $\alpha^{el}_{obs}(0)$ and $\alpha^{el}_{obs}(1)$, $\Delta\alpha^{el}_{obs}$, for the above systems are also shown in Table I.

The values of $\alpha^{el}_{obs}(0)$, $\alpha^{el}_{obs}(1)$ and $\Delta\alpha^{bl}_{obs}$ are plotted against the dielectric constants $\varepsilon_2$ of the polar components, in Figs. 2—4.

As is seen from the above figures, it is likely that $\alpha^{el}_{obs}(1)$, $\alpha^{el}_{obs}(0)$ and $\Delta\alpha^{el}_{obs}$ have a kind of correlation to the dielectric constants of the polar components, that is, each plot gives approximately a straight line which intersects the abscissa at about $\varepsilon_2=2$. It should be noted, however, that a slight deviation is observed for butylcyanide and nitrobenzene which have much larger dipole moments than the others. The fact that the straight line intersects the absissa at about $\varepsilon_2=2$, which is neary equal to the dielectric constant of the non-polar components shows that on mixing these non-polar liquids with liquids having a dielectric constant of about 2, which might be non-polar, the electrostatic part of the heat of mixing vanishes.

This indicates that the estimation of $\alpha^{n-el}$ mensioned above was not so inappropriate.

For *cis*-dichloroethylene—*trans*-dichloroethylene and pyridine—dioxane systems the plots

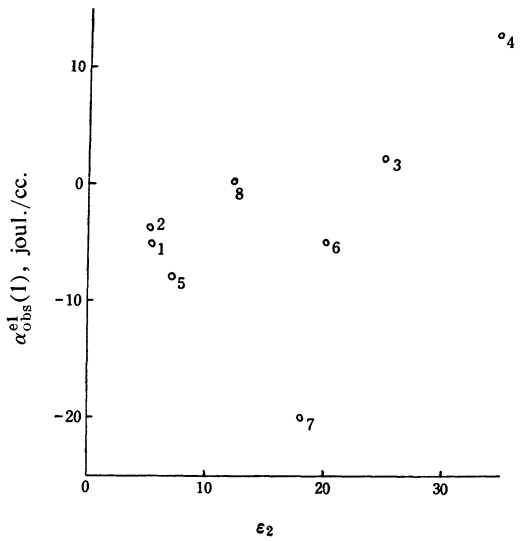



Fig. 5.

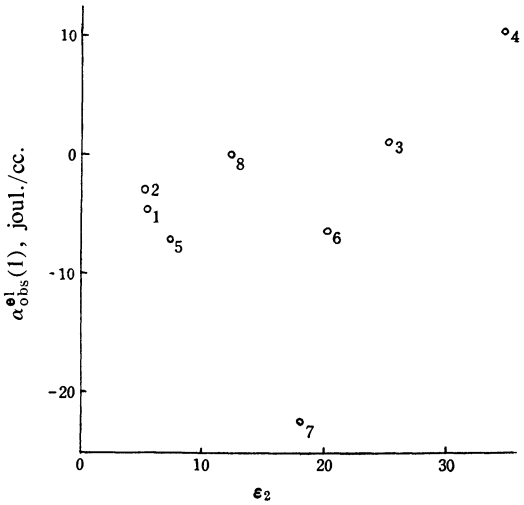



Fig. 6.

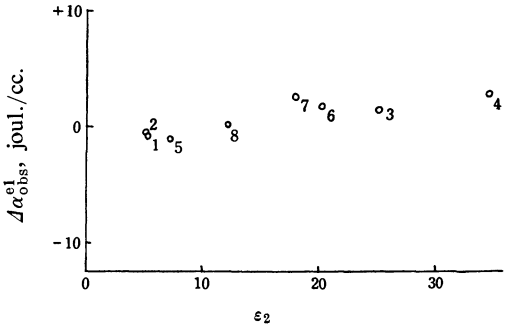



Fig. 7.

Figs. 5, 6, 7. The plots of observed values of electrostatic part of van Laar cofficients at concentrations $v_2=0$ and $v_2=1$ and their difference, $\alpha^{el}_{obs}(0)$, $\alpha^{el}_{obs}(1)$ and $\Delta\alpha^{el}_{obs}$ respectively vs. dielectric constant of polar components $\varepsilon_2$ for systems with aromatic non-polar components.

1. Chlorobenzene—Toluene
2. Bromobenzene—Toluene
3. Benzonitrile—Toluene
4. Nitrobenzene—Toluene
5. *n*-Butylchloride—Toluene
6. *n*-Butylcyanide—Toluene
7. Cyclohexanone—Toluene
8. Pyridine—Benzene

of $\alpha^{el}_{obs}(1)$, $\alpha^{el}_{obs}(0)$ and $\Delta\alpha^{el}_{obs}$ versus $\varepsilon_2$ deviate largely from the other systems. This might be due to the quadrupole moment of the non-polar component molecules. These non-polar molecules behave apparently as non-polar so far as the dielectric constant is concerned, but energetically not. The contribution from the local dipoles of these molecules which is not considered here, should be introduced, in systems containing molecules with quadrupole moment. The assumption of a single point dipole is drastic for the *cis*-dichloroethylene molecule, which has two large bond dipoles at a finite distance, and this may also be one of the reasons of the deviations for the system of *cis*- and *trans*-dichloroethylenes. For the pyridine—dioxane system the deviation is much greater than the above system, and this may be attributed to the large quadrupole moments of dioxane or the special interaction between pyridine and dioxane.

For the nitrobenzene—cyclohexane system, the plot of $\alpha^{el}_{obs}$ versus $v_2$ has a peculiar shape compared with the remaining systems of this group. This may be attributed to the antiparallel orientation of nitrobenzene molecules in pure liquid and its concentrated solution, which is evidenced by the increase of the dielectric constant on application of a strong electric field[4]. This antiparallel orientation exists only at a concentration higher than about 80 mol. %, and at a lower concentration antiparallel orientation vanishes. As the antiparallel orientation of dipoles in pure liquid and concentrated solution is stable, the vanishing of the antiparallel orientation requires some energy and this contributes to make the values of $\alpha^{el}$ increase. This effect is important in a concentration higher than 80 mol. %, and in the actual system the values of $\alpha$ are rather shifted in the positive direction in this concentration range compared with the other systems.

For systems in which non-polar components are aromatic such as toluene and benzene, the values of $\alpha^{el}_{obs}(1)$ and $\alpha^{el}_{obs}(0)$ and their differences $\Delta\alpha^{el}_{obs}$ are obtained by graphical extrapolation, and are shown in Table II.

4) A. Piekara, Achelekowski, *J. Chem. Phys.*, **25**, 794 (1956).

TABLE II. VALUES OF $\alpha^{el}_{obs}(0)$, $\alpha^{el}_{obs}(1)$ AND $\Delta\alpha^{el}_{obs}$ IN joul./cc. FOR THE SYSTEMS IN WHICH NON-POLAR COMPONENTS ARE AROMATIC

| System | $\alpha^{el}_{obs}(0)$ | $\alpha^{el}_{obs}(1)$ | $\Delta\alpha^{el}_{obs}$ |
|---|---|---|---|
| Chlorobenzene—Toluene | −5.1 | −4.3 | −0.8 |
| Bromobenzene—Toluene | −3.7 | −3.1 | −0.6 |
| Benzonitrile—Toluene | 2.5 | 1.1 | 1.4 |
| Nitrobenzene—Toluene | 13.2 | 10.5 | 2.7 |
| *n*-Butylchloride—Toluene | −8.1 | −7.2 | −0.9 |
| *n*-Butylcyanide—Toluene | −4.7 | −6.5 | 1.8 |
| Cyclohexanone—Toluene | −20.0 | −22.5 | 2.5 |
| Pyridine—Benzene | 0.3 | 0 | 0.3 |

The values of $\alpha^{el}_{obs}(1)$, $\alpha^{el}_{obs}(0)$ and $\Delta\alpha^{el}_{obs} = \alpha^{el}_{obs}(0) - \alpha^{el}_{obs}(1)$ are plotted against the dielectric constant of the polar components and are shown in Figs. 5—7.

It is seen from the figures that no regulality is observed for $\alpha^{el}_{obs}(1)$ and $\alpha^{el}_{obs}(0)$ but for $\Delta\alpha^{el}_{obs}$ and they are nearly independent of the dielectric constants of the polar component. These are not on a line intersecting the abscissa at about $\varepsilon_2=2$.

Now the observed value will be compared with the calculated value. In Figs. 1.1—1.11, the values of $\alpha^{el}_{calcd}$ together with $\alpha^{el}_{obs}$ are plotted against the volume fractions of the polar component for the 21 binary systems of polar and non-polar liquids.

It is seen from the figures that for the systems in which non-polar components are non-aromatic both $\alpha^{el}_{obs}$ and $\alpha^{el}_{calcd}$ are positive and increase as the volume fraction of the polar component $v_2$ decreases. This confirms the fact that the variations of $\alpha$ with concentration are essentially due to the dipole of the polar component. However, quantitative agreements are poor for some of systems. For those in which non-polar components are aromatic, then differ in the manner of the change of $\alpha$ with concentration and sometimes even in their signs giving no qualitative agreement. This also confirms the fact that for the latter group of the systems, some kind of effect coherent to the aromaticity of the non-polar component which is not taken into consideration in the assumption of the derivation of the theory, occurs in the actual cases, and this may be the reason for the qualitative disagreement.

Further, quantitative comparison of $\alpha^{el}_{obs}$ and $\alpha^{el}_{obs}$ for the systems in which non-polar components are non-aromatic are made for the former group of the systems whose $\alpha^{el}$ may be considered to be explained principally by dipolar forces. The ratios of the calculated value to the experimental one, $\alpha^{el}_{calcd}/\alpha^{el}_{obs}$ are calculated for those systems at five values of concentration $v_2=1.00$, 0.75, 0.50, 0.25 and 0. The values of these ratios are plotted against the volume fraction in Fig. 8.

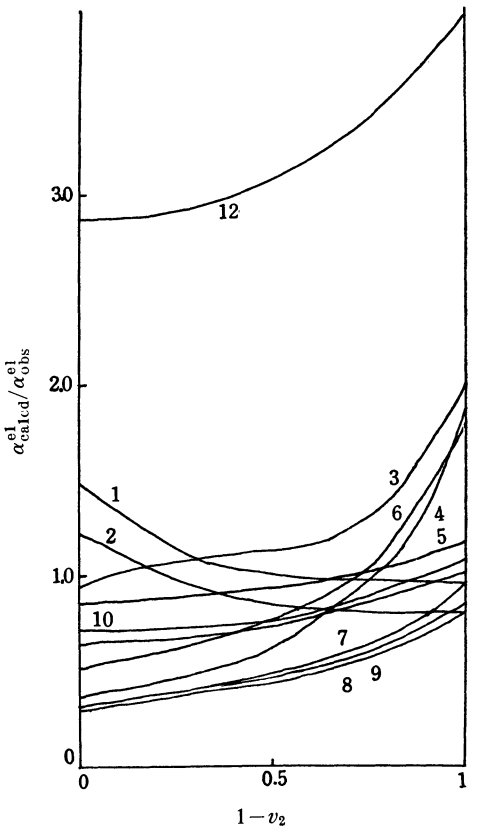



Fig. 8. Ratio $\alpha^{el}_{calcd}/\alpha^{el}_{obs}$ vs. volume fraction.

1. Chlorobenzene—Cyclohexane
2. Bromobenzene—Cyclohexane
3. Benzonitrile—Cyclohexane
4. Nitrobenzene—Cyclohexane
5. *n*-Butylchloride—Cyclohexane
6. *n*-Butylcyanide—Cyclohexane
7. Cyclohexanone—Cyclohexane
8. Diethylketone—Cyclohexane
9. Methylpropylketone—Cyclohexane
10. Chlorocyclohexane—Methylcyclohexane
11. Bromocyclohexane—Methylcyclohexane
12. *cis*-Dichloroethylene—*trans*-Dichloroethylene

It is seen from the result that most of the values of $\alpha^{el}_{calcd}/\alpha^{el}_{obs}$ are less than 2, whereas for the two systems, namely, of *cis*- and *trans*-dichloroethylene and of pyridine—dioxane, they differ considerably from the rest. Especially for the latter, it is too large to show in the figure. This indicates that the contribution due to the effect which cannot be explained merely with dipolar forces, presumably due to the quadrupole of the constituent molecules, is contained in the above two systems.

It indicates that in calculating electrostatic energy, contributions from multipoles higher than dipole such as quadrupole etc. must be taken into account for such systems.

It also indicates that for the rest of the group of the systems except the system containing the component molecules with larger dipole moments, such as nitrobenzene, benzonitrile and butylcyanide, the heats of mixing at infinite dilution of polar liquid in non-polar liquid are rather in good agreement with the theory despite of its rough assumptions. Rather good agreement obtained in a very dilute region for the systems with polar molecules of moderate magnitude of dipole moment, may be evidence that in these dilute regions, the assumptions made in the theory are not far from the actual circumstances.

Disagreement in the concentrated region may principally be due to the roughness of the theory such as the neglect of the short range interaction.

For systems containing polar molecules of large dipole moment the calculated values differ greatly from the experimental values.

This suggests that the larger the dipole moments is, the less satisfied is the condition of the assumption made in the theory in the actual circumstances.

**Summary**

The electrostatic part of the van Laar coefficients were derived from the observed value of heats of mixing and some regularity was found between these values and the dielectric constant of polar components if non-polar components are non-aromatic (group I). However, no regularity exists between them if non-polar components are aromatic (group II). These values were also compared with the calculated values. For group I, qualitative agreements were obtained and this confirms the fact that the variation of $\alpha$ with concentration is due to dipolar interaction of the polar components. The agreement is poor for systems containing a polar component with large dipole moments or for one containing a non-polar component with quadrupole moment. For group II, no qualitative agreement was obtained.

The author wishes to express his thanks to Professor Ryoichi Fujishiro of Osaka City University and to Professor Yonezo Morino of the University of Tokyo for their constant encouragement and discussions.

*Government Chemical Industrial Research Institute*
*Shibuya-ku, Tokyo*

# *Thermodynamical Studies on Binary Systems Consisting of Polar and Non-polar Liquids. V. The Anomalies in the Binary Systems of Polar Liquid with Aromatic Non-polar Liquid*

By Kazuo AMAYA

(Received March 30, 1961)

In a previous paper it has been shown that an anomalous stabilization effect exists in those systems consisting of polar and aromatic non-polar components. To elucidate the cause of these phenomena, plausible explanations are proposed from the molecular view point.

## Experimental Evaluation of the Anomalous Stabilization Effect

As is stated above, the binary systems containing the aromatic non-polar molecule and polar molecule show anomalous behavior in the heats of mixing.

First the decrease of the van Laar coefficient $\alpha$ due to the anomalous effect which was observed in aromatic non-polar solvents but not in non-aromatic solvents, will be estimated on reasonable assumptions.

Consider an imaginary non-polar liquid which is normal in nature such as cyclohexane, and its dielectric constant is the same as that of toluene. It may be reasonable to assume that the electrostatic part of the imaginary heat of mixing of the above imaginary non-polar liquid with polar liquids, if observed, would deviate from the theoretical values calculated for systems containing toluene in a previous paper, to the same extent as that of the deviation of the experimental value from the calculated one in the corresponding systems consisting of the same polar liquid and cyclohexane, because the dielectric constant of

toluene and cyclohexane differs only slightly. Then the van Laar coefficient due to the electrostatic part of imaginary heat of mixing may be estimated according to the following expression by the use of $\alpha^{el}_{c.obs}$ and $\alpha^{el}_{c.calcd}$ for the cyclohexane-polar liquid system and the $\alpha^{el}_{t.calcd}$ for the toluene-polar liquid system.

$$\alpha^{el}_{i.obs}=\alpha^{el}_{c.obs}\cdot\alpha^{el}_{t.calcd}/\alpha^{el}_{c.calcd} \quad (1)$$

where $\alpha^{el}_{i.obs}$ is the van Laar coefficient for an imaginary binary system mentioned above. The results obtained are shown in Table I.

TABLE I. VAN LAAR COEFFICIENT DUE TO STABILIZATION ENERGY $\alpha_{stab}$ AND THE VALUES OF STABILIZATION ENERGY $\Delta E_{stab}$ IN THE SYSTEMS COMPOSED OF POLAR LIQUID AND TOLUENE

| System | $v_2$ | $\alpha^{el}_1$ joul./cc. | $\alpha_{stab}=\alpha^{el}_{obs}-\alpha^{el}_1$ joul./cc. | $\Delta E_{stab}$ joul./mol. |
|---|---|---|---|---|
| | 1.0 | 4.16 | − 8.5 | 0 |
| Chlorobenzene | 0.75 | 5.76 | −10.1 | 196 |
| —Toluene | 0.50 | 7.18 | −12.1 | 319 |
| | 0.25 | 8.57 | −13.6 | 269 |
| | 0 | 10.07 | −15.2 | 0 |
| | 1.0 | 5.54 | − 8.6 | 0 |
| Bromobenzene | 0.75 | 7.73 | −11.0 | 218 |
| —Toluene | 0.50 | 9.59 | −13.1 | 348 |
| | 0.25 | 11.37 | −15.0 | 299 |
| | 0 | 12.28 | −16.0 | 0 |
| | 1.0 | 23.07 | −22.0 | 0 |
| Benzonitrile | 0.75 | 24.44 | −23.9 | 467 |
| —Toluene | 0.50 | 30.88 | −30.9 | 812 |
| | 0.25 | 42.52 | −42.3 | 840 |
| | 0 | 55.87 | −53.4 | 0 |
| | 1.0 | 33.60 | −23.1 | 0 |
| Nitrobenzene | 0.75 | 37.00 | −27.4 | 533 |
| —Toluene | 0.50 | 37.63 | −29.1 | 762 |
| | 0.25 | 44.13 | −36.2 | 718 |
| | 0 | 64.95 | −51.8 | 0 |
| | 1.0 | 9.95 | −17.3 | 0 |
| *n*-Butylchloride | 0.75 | 11.60 | −19.4 | 384 |
| —Toluene | 0.50 | 13.64 | −21.3 | 565 |
| | 0.25 | 15.75 | −24.5 | 488 |
| | 0 | 18.20 | −26.9 | 0 |
| | 1.0 | 32.29 | −38.8 | 0 |
| *n*-Butylcyanide | 0.75 | 33.45 | −40.6 | 808 |
| —Toluene | 0.50 | 37.54 | −45.5 | 1210 |
| | 0.25 | 45.25 | −53.4 | 1067 |
| | 0 | 50.26 | −55.0 | 0 |
| | 1.0 | 28.92 | −51.4 | 0 |
| Cyclohexanone | 0.75 | 28.48 | −51.0 | 1003 |
| —Toluene | 0.50 | 32.34 | −55.2 | 1456 |
| | 0.25 | 41.15 | −64.6 | 1286 |
| | 0 | 46.61 | −66.6 | 0 |

These values would be the corresponding electrostatic part of the van Laar coefficient for heats of mixing of toluene and the polar liquids if toluene were normal in nature as cyclohexane is, and do not show any anomalous behavior. The difference between such apparent values and the observed values may be considered to be the contribution from the anomalous effect. The part of the contribution of the anomalous effect to the van Laar coefficient $\alpha_{stab}$ thus obtained are also shown in the same table together with the stabilization energy per mole of the solution. It is seen that $\alpha_{stab}$ is dependent on the concentration.

## The Origin of the Anomalous Stabilization Effect

**The Anisotropy of the Aromatic Non-polar Molecules.**—If an anisotropic non-polar molecule is placed in an electric field, it tends to orient its most polarizable axis to be parallel to the direction of the electric field. In a region near the polar molecule, a strong electric field is produced arouud it and hence aromatic molecules in this region would tend to orient their most polarizable axis along the direction of the electric field. Then the effective dielectric constant of this region increases somewhat more than the original macroscopic value, the extent of which depends on the anisotropy of the non-polar molecule and the magnitude of the dipole moment of the polar molecule.

The increase of the dielectric constant of the non-polar liquid makes the calculated values of the van Laar coefficient decrease as is seen from the above results that the calculated values of the electrostatic part of the van Laar coefficient $\alpha^{el}_{calcd}$ for tolune-polar liquid system is an amount of 80~90% of those for the corresponding system of cyclohexane-polar liquid. Anisotropy constants for benzene and toluene are reproduced for reference from the literature:

$$\text{for benzene}\begin{cases}\alpha_1=123.1\\ \alpha_2=123.1\\ \alpha_3=\ 63.5\end{cases}\quad\bar{\alpha}=103.2,\quad\frac{\alpha_1}{\bar{\alpha}}=1.193$$

$$\text{for toluene}\begin{cases}\alpha_1=156.4\\ \alpha_2=136.6\\ \alpha_3=\ 74.8\end{cases}\quad\bar{\alpha}=122.6,\quad\frac{\alpha_1}{\bar{\alpha}}=1.276$$

If we suppose that the non-polar molecules given above orient their most polarizable axis completely along the direction of the electric field produced by the polar molecule, the effective dielectric constant may be increased from 2.366 of toluene to about 3.

The values calculated with the values of 3

for the dielectric constant of non-polar liquid indicate the maximum contribution of this effect. In actual cases, however, the orientation of the non-polar molecule along the direction of the electric field is disturbed by thermal agitation and the effective dielectric constant may be less than 3.

The orientational effect in the solution consisting of anisotropic non-polar molecules accompanying the increase of effective dielectric constant in the region of small $x_2$ would make the values of $\alpha^{el}_{calcd}$ smaller than before.

But with this consideration alone it is impossible to make the values of $\alpha^{el}$ negative and also to explain the concentration dependence of $\alpha_{stab}$.

**The Addition Stabilizing Effect due to Orientation of Anisotropic Non-polar Molecules in an Electric Field.**—The molecules of toluene and benzene are somewhat anisotropic, and when they are placed in a strong electric field, they tend to orient their most polarizable axis in the direction of the applied electric field. In the gaseous state this effect results in the increase of polarizability, and hence somewhat stabilizes the molecules. But this effect makes little contribution as was explained above.

In the liquid state, however, molecules interact with each other, and if we are admitted to assume the orientation of these molecules increases the intermolecular interaction energy, these stabilizing effects may be explained consistently.

Anisotropic non-polar molecules near a polar molecule are in a more ordered state than those far from the polar molecule because of the strong dipolar field of the latter. It may be reasonable to assume that in a region near the dipolar molecule, anisotropic non-polar molecules stick together more or less as they do in their solid state and the degree or the extent of the orientation depends on the magnitude of the dipolar field.

Let us consider an anisotropic non-polar molecule whose polarizabilities along three principal axes x, y and z are $\alpha_x$, $\alpha_y$ and $\alpha_z$ respectively.

When this molecule is placed in an electric field $F$, then the electrostatic energy of the molecule, $E$ is expressed as

$$E=-\frac{1}{2}(\alpha_x\cos^2\theta_{\mu x}+\alpha_y\cos^2\theta_{\mu y}+\alpha_z\cos^2\theta_{\mu z})F^2 \tag{2}$$

where $\theta_{\mu x}$, $\theta_{\mu y}$ and $\theta_{\mu z}$ denote the angles between the direction of the electric field and each principal x, y and z axis respectively.

For simplicity, assuming that

$$\alpha_x=\alpha_y \tag{3}$$

the electrostatic energy $E$ is given by

$$E=-\frac{1}{2}(\alpha_z\cos^2\theta_{\mu z}+\alpha_x\sin^2\theta_{\mu z})F^2$$
$$=-\frac{1}{2}\{(\alpha_z-\alpha_x)\cos^2\theta_{\mu z}+\alpha_x\}F^2 \tag{4}$$

then

$$\overline{\cos^2\theta_{\mu z}}=\frac{2\int_{\pi/2}^{0}\int_0^{2\pi}\cos^2\theta_{\mu z}\cdot\exp\left[\frac{1}{2}\{(\alpha_z-\alpha_x)\cos^2\theta_{\mu z}+\alpha_x\}\times(F^2/kT)\right]\cdot\sin\theta_{\mu z}d\theta_{\mu z}d\varphi}{\int_{\pi/2}^{0}\int_0^{2\pi}\exp\left[\frac{1}{2}\{(\alpha_z-\alpha_x)\cos^2\theta_{\mu z}+\alpha_x\}\times(F^2/kT)\right]\cdot\sin\theta_{\mu z}d\theta_{\mu z}d\varphi}$$
$$=\frac{\int_{\pi/2}^{0}\cos^2\theta_{\mu z}\exp\left[\frac{1}{2}(\alpha_z-\alpha_x)(F^2\cos^2\theta_{\mu z}/kT)\right]\times\sin\theta_{\mu z}d\theta_{\mu z}}{\int_{\pi/2}^{0}\exp\left[\frac{1}{2}(\alpha_z-\alpha_x)F^2\cos^2\theta_{\mu z}/kT\right]\cdot\sin\theta_{\mu z}d\theta_{\mu z}} \tag{5}$$

Putting $\cos^2\theta_{\mu z}=x$, and $1/2\cdot(\alpha_z-\alpha_x)F^2/kT=a$, then the above expression becomes

$$\overline{x^2}=\frac{\int_0^1 x^2e^{ax^2}dx}{\int_0^1 e^{ax^2}dx}=\frac{\left[\frac{x}{2a}e^{ax^2}\right]_0^1}{\int_0^1 e^{ax^2}dx}-\frac{1}{2a} \tag{6}$$

As the integration in the denominater, $\int e^{ax^2}dx$ can not be expressed in a simple formula, the integrand is expanded in a power series, and is integrated, and then the following expression is obtained

$$\int e^{ax^2}dx=\int\left(1+ax^2+\frac{a^2x^4}{2!}+\frac{a^3x^6}{3!}+\cdots\right)dx$$
$$=x+\frac{a}{3}x^3+\frac{a^2x^5}{5\cdot2!}+\frac{a^3x^7}{7\cdot3!}+\cdots \tag{7}$$

For extreme cases of $a\ll1$ and $a\gg1$, the following approximate formula are obtained.

For $a\ll1$

$$\int_0^1 e^{ax^2}dx=1+\frac{a}{3}+\frac{a^2}{10}+\cdots \tag{8}$$

$$\left[\frac{x}{2a}e^{ax^2}\right]_0^1=\frac{1}{2a}+\frac{1}{2}+\frac{a}{4}+\cdots \tag{9}$$

then

$$\frac{\left[\frac{x}{2a}e^{ax^2}\right]_0^1}{\int_0^1 e^{ax^2}dx}=\left(\frac{1}{2a}+\frac{1}{2}+\frac{a}{4}+\cdots\right)\times\left(1+\frac{a}{3}+\frac{a^2}{10}+\cdots\right)^{-1}$$
$$=\frac{1}{2a}+\frac{1}{3}+\frac{7}{90}a+\cdots \tag{10}$$

Then

$$\overline{\cos^2\theta_{\mu z}}=\frac{1}{3}+\frac{7}{90}a+\cdots \tag{11}$$

For $a \gg 1$, $\overline{\cos^2\theta_{\mu z}}$ tend to unity.

For the molecule with $\alpha_z > \alpha_x = \alpha_y$, $\overline{\cos^2\theta_{\mu z}}$ tends to 1/3 as $a$ approaches to zero, and to 1 as it approaches to infinite. For the molecule $\alpha_z < \alpha_y = \alpha_y$, $\overline{\cos^2\theta_{\mu z}}$ tends to 1/3 as $a$ approaches to zero and to 0 as it approaches to infinite.

As the value of $\overline{\cos^2\theta_{\mu z}}$ varies with the order of the molecular arrangement, it may be reasonable to define an order parameter as

$$s = (\overline{\cos^2\theta_{\mu z}} - 1/3)/(1-1/3) \quad \text{for } \alpha_z > \alpha_x \quad (12)$$

and

$$s = (1/3 - \overline{\cos^2\theta_{\mu z}})/1/3 \quad \text{for } \alpha_z < \alpha_x \quad (13)$$

$s$ is proportional to $a$ for small values of $a$ and tends to approach to 1 for large values of $a$ like the Langevin function. It may reasonably be assumed that the stabilization energy due to orientation of the anisotropic non-polar molecules is proportional to $s$ and as a result it may be saturated in a strong electric field corresponding to a great value of $a$.

Now, the order of magnitude of $a$ for actual cases will be considered. For the values of $(\alpha_z - \alpha_x)$ the value $\approx 60 \times 10^{-25}$ cc. per molecule of toluene is taken, and for $F$, if the values of an electric field at a distance of 3Å from a point dipole of 1D is taken, the value of $F$ is $3.7 \times 10^4$ e. s. u., there $a$ for $T = 300°K$ becomes 0.05 for 1D, and 0.82 for 4D. For chlorobenzene $a$ is about 0.15 and for nitrobenzene this value is about 0.8.

Now, let us consider the order of magnitude of this effect. Since this effect is cooperative with respect to an aromatic non-polar molecule, it is natural that the contribution from this effect vanishes in a limit at zero concentration of aromatic non-polar component. Then it may be resonable to attribute the concentration dependent part of $\alpha_{stab}$ to this effect.

At infinite dilution of polar liquids, this stabilization energy per mole of polar liquid is from about 700 to 3200 joul.

On the other hand, heats of fusion, which may be considered to be a measure of orientational energy for benzene and toluene are about 9840 joul. and 6620 joul. per mole, respectively. As one polar molecule is surrounded by several of the nearest neighboring non-polar molecules at infinite dilution, a slight extent of ordered state in the group of molecules is possible to introduce considerable stabilization energy to their systems. Therefore, the magnitude of the above values of stabilizing energy seems to be not unreasonable as the contribution from this effect.

The stabilization energy of toluene at an infinite dilution of the polar molecule caused by 1 mol. of polar molecule is plotted against $\mu^2$ in Fig. 1.

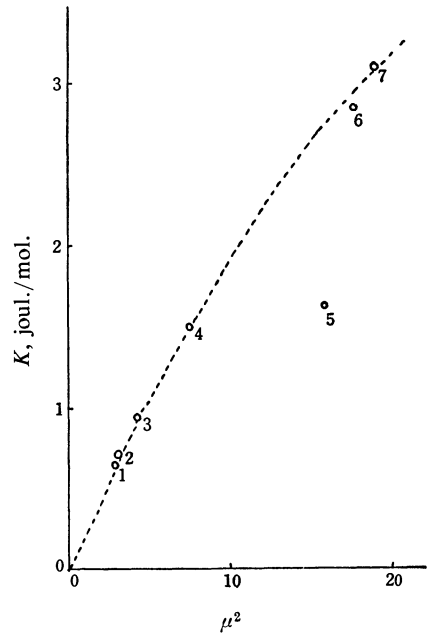



Fig. 1. Concentration dependent part of stabilization energy per mole of polar components at infinite dilution in toluene plotted against square of dipole moment of the polar molecules.

1. Chlorobenzene
2. Bromobenzene
3. *n*-Butylchloride
4. Cyclohexanone
5. *n*-Butylcyanide
6. Nitrobenzene
7. Benzonitrile

It is seen from the figure that the saturation effect is only slightly observed as the theory predicts. This fact makes the above explanation plausible. As for a concentration independent part of $\alpha_{stab}$, further investigations will be necessary.

## Summary

The anomalous stabilization energy for the systems containing polar and aromatic non-polar liquids was evaluated on reasonable assumptions. The van Laar coefficient due to this stabilizing effect was found to be dependent on the concentration. The stabilization effect corresponding to the concentration dependent part of the van Laar coefficient was explained by the cooperative orientation of aromatic non-polar molecules around the polar molecules.

The author wishes to express his thanks to Professor Ryoichi Fujishiro of Osaka City University and to Professor Yonezo Morino of the University of Tokyo for their constant encouragement and discussions.

*Government Chemical Industrial Research Institute*
*Shibuya-ku, Tokyo*

# *Mass-spectrometric Study on Ionization and Dissociation of Diethyl Ether by Electron Impact*

By Ichiro KANOMATA

(Received March 28, 1961)

Since 1930 many studies on ionization and dissociation of organic molecules by electron impact have been made by means of a mass-spectrometer. The reason for using a mass-spectrometer for these kinds of studies is to obtain the information on the decomposition processes through determination of M/e values and of the appearance potentials of ions formed by electron impact.

The study on the processes of ionized decomposition by electron impact is not only fundamental for the radiation chemistry of organic compounds but also helpful for the researches on molecular structures and chemical reactions.

The author previously reported the mass-spectrometric study on ionization and dissociation of the ethyl alcohol molecule by electron impact[1,2]. The present report relates to the decomposition of the diethyl ether molecule which has one oxygen atom, and the ionization of the molecule is thought to "cause the removal" of one of the lone pair 2 p electrons of this oxygen atom as well as in the case of ethyl alcohol in the previous study.

## Experimental

The mass spectrometer[3] used for this study was a 90° sector type ($R=12$ cm.), and the appearance potentials (AP) of ions were determined by the extrapolated difference method[4]. The ionization potential of the molecule was calibrated with the ionization potential of argon (15.76 eV.) and the appearance potentials of fragment ions were determined by referring to the ionization potential of the molecule. The sample was chemically pure and was not particularly refined.

## Results

The appearance ratios of ions produced from the molecule by 75 eV. electron impact are shown in Table I. From the table it is obviously recognized that the M/e=31 ion ($CH_2OH^+$ or $CH_3O^+$) is the most abundant, and the M/e=29, 59, 45 and 74 ions are also abundant. The appearance potentials of these five species of ions obtained are tabulated in Table II.

TABLE I. APPEARANCE RATIOS

| M/e | Ion | Appearance ratio |
|---|---|---|
| 75 | Isotope peak | 0.3 |
| 74 | $(C_2H_5)_2O^+$ | 25.7 |
| 60 | $(CH_3)(C_2H_5)O^+$, isotope peak | 2.1 |
| 59 | $(CH_2)(C_2H_5)O^+$ | 46.0 |
| 46 | $C_2H_5OH^+$, isotope | 0.4 |
| 45 | $(C_2H_5)O^+$ | 31.3 |
| 44 | $C_2H_4O^+$ | $3.1_5$ |
| 43 | $C_2H_3O^+$ | $12.7_5$ |
| 42 | $C_2H_2O^+$ | 3.0 |
| 41 | $C_2HO^+$ | 6.0 |
| 31 | $CH_2OH^+$ or $CH_3O^+$ | 100.0 |
| 30 | $CH_2O^+$ | $3.1_5$ |
| 29 | $CHO^+$ or $C_2H_5^+$ | 63.5 |
| 28 | $CO^+$ or $C_2H_4^+$ | 10.2 |
| 27 | $C_2H_3^+$ | 37.1 |
| 26 | $C_2H_2^+$ | 8.0 |
| 15 | $CH_3^+$ | 14.3 |
| 14 | $CH_2^+$ | 2.7 |

TABLE II. APPEARANCE POTENTIALS (eV.)

| M/e | Ion | Appearance potential |
|---|---|---|
| 74 | $(CH_3CH_2)O^+(CH_2CH_3)$ | $9.55\pm0.02$ |
| 59 | $CH_2O^+CH_2CH_3$ | $10.80\pm0.08$ |
| 45 | $CH_3CH_2O^+$ | $13.23\pm0.04$ |
| 31 | $CH_2O^+H$ or $CH_3O^+$ | $12.3_5\pm0.1$ |
| 29 | $C_2H_5^+$ or $CHO^+$ | $14.0\pm0.2$ |

## Discussion

When a molecule $R_1R_2$ is composed of $R_1$ and $R_2$ atoms (or radicals), the appearance potential of $R_1^+$ ions is given by

$$A(R_1^+) = I(R_1R_2) + D(R_1^+ - R_2) \quad (1)$$

$$= I(R_1) + D(R_1 - R_2) \quad (2)$$

Here, $I(R)$ is the ionization potential of atom (radical) R, and $D(R_1-R_2)$ is the bond dissociation energy between $R_1$ and $R_2$. Of course, radicals or atoms produced may generally have some excitational or kinetic energy. In case the molecule consists of many atoms as organic compounds, however, the potential

1) T. Kambara and I. Kanomata, *Buturi* 4, 71 (1949).
2) T. Kambara and I. Kanomata, *Hitachi Hyoron Rombunshu*, No. 7, 15 (1949).
3) I. Kanomata, Y. Kaneko and T. Oguri, *Mass Spectroscopy*, No. 3, 12 (1954).
4) J. W. Warren, *Nature*, 165, 811 (1950).

surfaces that give the binding energies between atoms approach each other, and therefore the excess energy may be small as reported by some authors[5,6]. From this point of view the neglect of this excess energy will not be serious in the course of this discussion.

The processes of production of ions are as follows:

$$M/e=74 \quad (C_2H_5)_2O^+, \quad AP \ 9.55 \text{ eV}.$$

This ion is the parent ion and the appearance potential is the ionization potential of diethyl ether molecule. This value was obtained by Morrison[7] as 9.72 eV. by critical slope method and by Price[8] spectroscopically as 10.2 eV. These results are largely different from each other beyond their errors of measurement, though the reason can not be explained.

It must be considered what kind of electron in the molecule is concerned with its ionization. Mulliken[9] reported that the lone pair electrons of the oxygen atom in the molecules, such as water and alcohol, have the lowest ionization potential by charge transfer effect. Hence the ionization occurs at first by the removal of one of these electrons. The fact that the ionization potentials decrease in the order of H-O-H (12.76 eV.), $CH_3$-O-H (10.95 eV.), $CH_3$-O-$CH_3$ (10.5 eV.) and $C_2H_5$-O-$C_2H_5$ (9.55 eV.) can be explained by this charge transfer effect. This postulate was also used when the present author and Kambara studied the ionization and dissociation of ethyl alcohol[1,2], propyl alcohol[10,11], acetone and acetic acid[12] molecules by electron impact, and will be required to discuss the dissociation process for the production of M/e=59 ion from diethyl ether. From these facts, the ionization potential 9.55 eV. is thought to be that of the oxygen atom in the molecule.

$$M/e=59 \quad (CH_2\text{-}O\text{-}C_2H_5)^+, \quad AP \ 10.80 \text{ eV}.$$

Equation 1, in this case, leads to $A(R_{59}^+)=I(R_{74})+D(R_{59}^+-R_{15})$. Inserting the observed values, $D(R_{59}^+-R_{15})=10.80-9.55=1.25$ eV. is obtained. This dissociation energy of the ionic state should correspond to the dissociation energy of the C-C bond of the neutral molecule. The reason why the dissociation energy for such an ionized molecule is apparently low may be elucidated as follows.

If one of the lone pair electrons of the oxygen atom in the molecule is removed by ionization in accordance with Mulliken's postulate, the other electron left in the atom may have new binding activity, that is, the trivalency of the $O^+$ ion. Therefore, when the structure of M/e=59 ion is assumed as $\begin{matrix}H\\H\end{matrix}\!\!>\!C\!=\!O^+\text{-}C_2H_5$, this ion should be more stabilized, by the energy of formation of trivalent structure, than the structure of $\cdot\begin{matrix}H\\C\\H\end{matrix}\!\!\text{-}O^+\text{-}C_2H_5$ which is yielded by only removing a $CH_3$ radical from the parent ion.

In order to estimate this stabilization energy of formation of trivalent bond, it is assumed that the dissociation energy of the C-C bond of the diethyl ether molecule is equal to that of ethane.

$$D(R_{59}-R_{15})=D(CH_3-CH_3)=80\pm6 \text{ kcal.}^{13}$$
$$=83.3\pm1 \text{ kcal.}^{14}$$
$$=3.6 \text{ eV}.$$

Then the stabilization energy becomes $3.6-1.25=2.35$ eV. $=54$ kcal./mol. Consequently, under the assumption of the additivity of bond energy, the total binding energy of trivalent bond of $O^+$ in this case is obtained as (3.26 eV. $\times2+2.35$ eV. $=8.87$ eV. $=)204$ kcal./mol., where 3.26 eV. is the value of $D$(C-O).

It may be recognized that in this ion resonance occurs as in carbon monoxide molecule, causing the stabilization near 58 kcal. of resonance energy of carbon monoxide[15].

$$M/e=45 \quad (C_2H_5\text{-}O)^+, \quad AP \ 13.23 \text{ eV}.$$

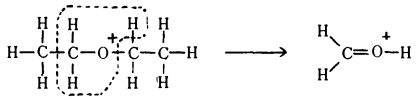
This ion is thought to be produced by the removal of a $C_2H_5$ radical from the parent ion. Therefore the relation $A(C_2H_5-O\cdot^+)=I(C_2H_5-O\cdot)+D(R_{45}-R_{29})$ exists. According to Syrkin and Dyatkina's data[16] on heat of dissociation, $D$(C-O) for diethyl ether is 75 kcal./mol. (3.26 eV.), hence from the above equation $I(C_2H_5-O^+\cdot)=10.0$ eV. is obtained. This value is somewhat greater than the ionization potential of the parent molecule (9.55 eV.). This seems to be due to the charge transfer effect which is adopted to explain the low value of the ionization potential of the parent molecule. As regards this ion, of course, the stabilization due to trivalency of $O^+$ can not take place.

5) F. H. Field and J. L. Franklin, "Electron Impact Phenomena", Academic Press Inc. Publishers, New York (1957).
6) C. E. Berry, *Phys. Rev.*, **78**, 597 (1950).
7) J. D. Morrison and A. J. C. Nicholson, *J. Chem. Phys.*, **20**, 1021 (1951).
8) T. M. Sugden, A. D. Walsh and W. C. Price, *Nature*, **148**, 373 (1941).
9) R. S. Mulliken, *J. Chem. Phys.*, 3, 506 (1935).
10) T. Kambara, *J. Phys. Soc. Japan*, 5, 31 (1950).
11) T. Kambara, ibid., 5, 36 (1950).
12) T. Kambara, ibid., 5, 84 (1950).
13) M. Szwarc, *Chem. Revs.*, **47**, 75 (1950).
14) J. S. Roberts and H. A. Skinner, *Trans. Faraday Soc.*, **45**, 339 (1949).
15) L. Pauling, "The Nature of the Chemical Bond", Cornell University Press, Ithaca (1939).
16) Y. U. Syrkin and M. E. Dyatkina, "Structure of Molecules and Chemical Bond", Interscience Publishers, Inc., New York (1950).

M/e=31 $(CH_3\text{-}O\text{-}H)^+$, AP 12.3$_5$ eV.

The structure of this ion may be thought to be either $CH_3O^+$ or $CH_2OH^+$. Though this ion is the most abundant among those produced by 75 eV. electron impact, it can not be produced through a simple process, as the rupture of only one bond in the cases of M/e =59 and 45. Thus, in this dissociation process, rearrangement of atoms in the molecule is necessary.

The following dissociation process is energetically reasonable.



That is, it is thought that with the ionization of the oxygen atom, the rupture of bonds and the formation of O-H bond take place simultaneously. Assuming the bond energy additivity, the energy necessary for this process will be calculated as follow:

| | |
|---|---|
| ionization of oxygen atom | 9.55 eV. |
| rupture of C-C bond | 3.6 eV. |
| rupture of C-O bond | 3.26 eV. |
| rupture of C-H bond[17] | 2.9 eV. |
| formation of O-H bond | −4.8 eV. |
| formation of $>C=O^+\text{-}$ structure | −2.35 eV. |

The sum of these energies is 12.16 eV. in total and agrees well with the appearance potential obtained.

On the contrary, if this ion is assumed to have the structure of $CH_3O^+$, the energy necessary for the reaction becomes more than 16 eV. Therefore the structure of M/e =31 ion is concluded to be $H_2C=O^+\text{-}H$.

M/e=29 $C_2H_5^+$ or $CHO^+$, AP 14.0 eV.

If the M/e=29 ion is $C_2H_5^+$, Eq. 2 leads

$$A(C_2H_5^+) = I(C_2H_5) + D(C_2H_5\text{-}OC_2H_5)$$

Then $I(C_2H_5) = 14.0 - 3.26 = 10.74$ eV.

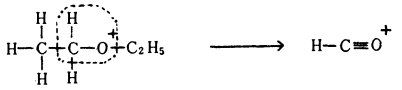
The ionization potential of $C_2H_5$ radical can be estimated from various data. For example, Bleakney gave a rather high value of 9.8 eV. from the decomposition of ethyl alcohol, and the mean value of the data given from various ionized decompositions of organic compounds is 8.75 eV.[5] Moreover, the energy for direct ionization of $C_2H_5$ radical has the rather low value of 8.60 eV.[18] Therefore, this ion should not be $C_2H_5^+$ ion, but $CHO^+$.

If it is assumed that radicals of H, $CH_3$ and $C_2H_5$ are produced in the course of the formation of $CHO^+$, the heat of reaction can be calculated from the thermochemical data as follows.

$$A(CHO^+) = \Delta H_f(CH_3) + \Delta H_f(C_2H_5) + \Delta H_f(H) + \Delta H_f(CHO^+) - \Delta H_f(C_2H_5OC_2H_5) = 14.3 \text{ eV.}$$

The calculated value agrees well with the experimental result.

From the standpoint of bond energy additivity, and the assumed reaction of



as in the case of M/e=31 ion, the energy necessary for the reaction will be calculated as follows.

| | |
|---|---|
| ionization of the molecule | 9.55 eV. |
| rupture of C-C bond | 3.6 eV. |
| rupture of C-O bond | 3.26 eV. |
| rupture of C-H bond | 2.9 eV. |
| $H\text{-}C\text{-}O^+\text{-} \rightarrow H\text{-}C\equiv O^+$ | $-2.35\times2$ eV. |

The sum of these energies is 14.6 eV. The difference between this value and the measured appearance potential is somewhat great, but this is unavoidable under such a loose assumption and rough calculation.

The total bond energy of $O^+$ ion in the case of $CHO^+$ is also calculated as in the case of M/e=59 ion. That is to say, provided that the energy of the C-O bond 3.26 eV. is conserved in one of the triple bond of $CHO^+$ ion, the total energy of $O^+$ is calculated as

$$3.26 + 2.35\times2 = 7.96 \text{ eV.} = 182 \text{ kcal./mol.}$$

This value is rather small compared with that of M/e=59 ion.

The reason why the stabilization is smaller in this case than in the case of M/e=59 ion is thought to be due to the existence of fewer resonance structures.

## Summary

A mass spectrometric study on ionization and dissociation of diethyl ether has been carried out.

The M/e=31 ion is the most abundant among the ions produced by 75 eV. electron impact and the M/e=29, 59, 45 and 74 ions are abundant in this order next to M/e=31 ion.

The appearance potential measurement of these ions leads to the following conclusion. The ions are formed by the removal of one of the lone pair electrons of the oxygen atom in the molecule.

17) C. E. Cumming and M. E. Bleakney, *Phys. Rev.*, **58** 787 (1940).
18) J. A. Hipple and D. P. Stevenson, ibid., **63**, 121 (1943).

By considering the trivalent structure of $O^+$ and by applying the bond energy additivity, which is adequate for hydrocarbons, to such an ionized dissociation process the producing processes of such ions can be satisfactorily revealed.

The stabilization energy for the formation of $\rangle C=O^+-$ structure is obtained as 54 kcal./mol. by such a calculation.

The author would like to express his deep appreciation to Professor K. Kido and Professor T. Titani for their kind guidance and to Mr. Y. Kaneko and Mr. T. Oguri for their earnest coorporation.

*Department of Physics*
*Tokyo Metropolitan University*
*Setagaya-ku, Tokyo*

# *Proton Magnetic Resonance Spectra of Methylthiophenesulfonylchlorides*

By Kensuke TAKAHASHI, Yasuo MATSUKI, Yoshiteru MIYAKE and Genjiro HAZATO

(Received March 31, 1961)

In the previous communication[1], the relative magnitude of the coupling constants for the ring protons in thiophene derivatives was assumed to be $J_{23}>J_{34}>J_{25}>J_{24}$, in which the values for $J_{25}$ and $J_{24}$ could not be determined experimentally. This assumption is in accordance with the recent experimental works by Gronowitz and Hoffman[2]. In this note, the experimental results of the proton magnetic resonance spectra for the six isomers of methylthiophenesulfonylchloride are presented. Those results complement the previous communication on the substituted thiophenes. The observed values of $J_{25}$ and $J_{24}$ and some experimental coupling constants for the methyl group and the ring proton are also presented. Some qualitative results of the solvent effect on the chemical shifts of these isomers are also presented.

## Experimental

The apparatus and procedure were similar to those previously described[1], and cyclohexane was used as an internal reference. The compounds used in the present observations were synthesized by Matsuki and his collaborators. Details of the preparation of these new compounds will be given later in Journal of the Chemical Society of Japan, Ind. Chem. Sec. The boiling points and the measured conditions of the samples are given in Table I; with respect to these six isomers, 2-methyl-5-thiophenesulfonylchloride is the only one which is reported in the literature[3], as far as we know.

TABLE I

| Substituent | B. p. °C/mmHg | Measured condition wt. % Sample | $CCl_4$ | $C_6H_{12}$ |
|---|---|---|---|---|
| 2-$CH_3$, 3-$SO_2Cl$ | 91~93/3 | 77.9 | | 22.1 |
| 2-$CH_3$, 4-$SO_2Cl$ | 92~94/3 | 56.9 | 30.7 | 12.4 |
| 2-$CH_3$, 5-$SO_2Cl$ | 96~98/3 | 81.9 | | 18.1 |
| 3-$CH_3$, 2-$SO_2Cl$ | 98~100/2.5 | 83.2 | | 16.8 |
| 3-$CH_3$, 4-$SO_2Cl$ | 96.2~97/3 | 82.7 | | 17.3 |
| 3-$CH_3$, 5-$SO_2Cl$ | 100~101/3 | 78.9 | | 21.1 |

## Results and Discussion

The chemical shifts for the ring protons and for the methyl protons are given in Table II, in c. p. s. at 40 Mc./sec. The values given here are reproducible within the deviation of about 1 c.p.s. Each of the two substituents, methyl and chlorosulfonyl groups, as previously

TABLE II. THE PROTON MAGNETIC RESONANCE DATA IN METHYLTHIOPHENESULFONYLCHLORIDES, REFERRED TO CYCLOHEXANE IN C. P. S. AT 40 Mc./sec.

| Substituent | Assignment 2-H | 3-H | 4-H | 5-H | $CH_3$ |
|---|---|---|---|---|---|
| 2-$CH_3$, 3-$SO_2Cl$ | — | — | 234 | 226 | 52 |
| 2-$CH_3$, 4-$SO_2Cl$ | — | 226 | — | 257 | 44 |
| 2-$CH_3$, 5-$SO_2Cl$ | — | 216 | 247 | — | 46 |
| 3-$CH_3$, 2-$SO_2Cl$ | — | — | 223 | 250 | 47 |
| 3-$CH_3$, 4-$SO_2Cl$ | 228 | — | — | 270 | 44 |
| 3-$CH_3$, 5-$SO_2Cl$ | 239 | — | 247 | — | 36 |

1) K. Takahashi, Y. Matsuki, T. Mashiko and G. Hazato, This Bulletin, 32, 156 (1959).

2) S. Gronowitz and R. A. Hoffman, (a) *Arkiv för Kemi*, 13, 279 (1958); (b) ibid., 15, 45 (1959); (c) ibid., 16, 501 (1960); (d) ibid., 16, 515 (1960); (e) idid., 16, 539 (1960); (f) ibid., 16, 563 (1960); (g) *Acta Chem. Scand.*, 13, 1687 (1959).

3) W. E. Truce and M. F. Amos, *J. Am. Chem. Soc.*, 73, 3013 (1951).

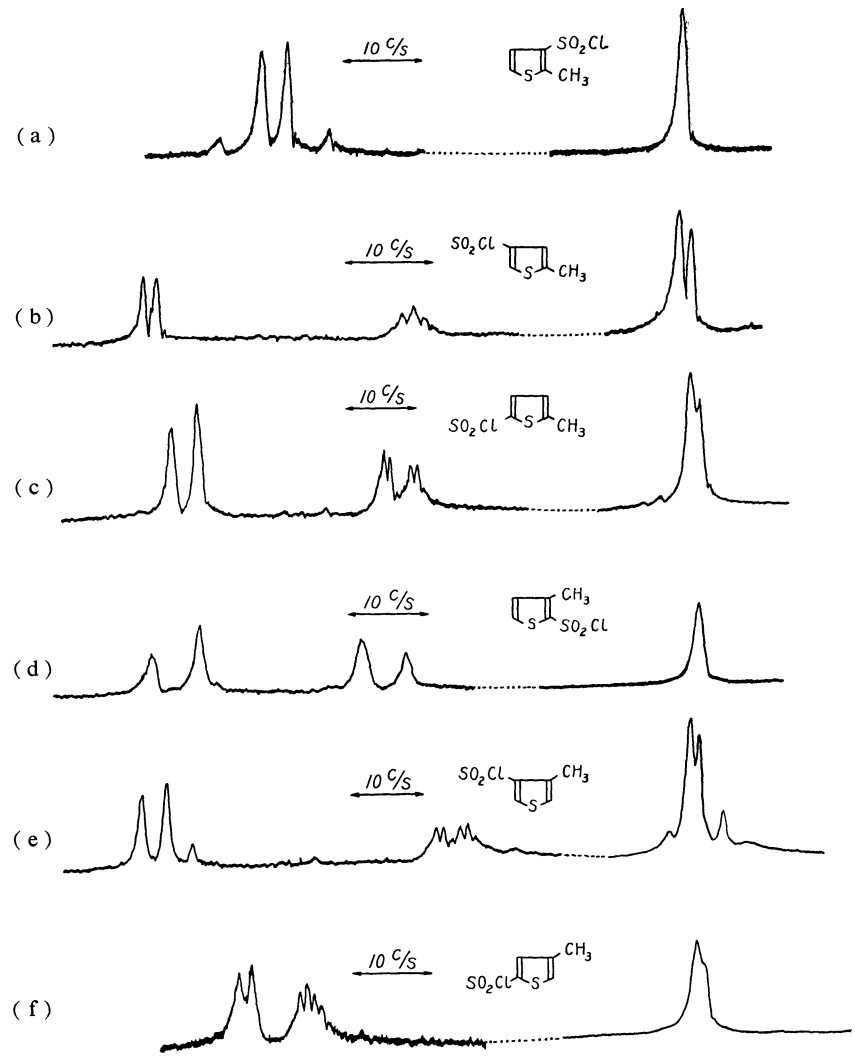



Fig. 1. The proton magnetic resonance spectra at 40 Mc./sec., showing
(a) 2-methyl-3-thiophenesulfonylchloride
(b) 2-methyl-4-thiophenesulfonylchloride
(c) 2-methyl-5-thiophenesulfonylchloride
(d) 3-methyl-2-thiophenesulfonylchloride
(e) 3-methyl-4-thiophenesulfonylchloride
(f) 3-methyl-5-thiophenesulfonylchloride.
Applied magnetic field increases from left to right in all figures. Some extra peaks probably due to the presence of the small isomeric impurities are observed in c, e and f.

reported[1], gives the reverse effect on the chemical shift, so that all spectra here observed can be assigned easily from the standpoint of the chemical shift. In a case where the signal is split by the indirect spin-spin interaction, the shift given in Table II is that for the center of the resonance pattern, so that the difference of the values given for two ring protons in a compound (for example, in 2-methyl-3-thiophenesulfonylchloride, 234 minus 226 equals to 8 c.p.s.) does not equal the true chemical shift for those ring protons, but equals $(J^2+\delta^2)^{1/2}$. The analysis of the two-proton system was reported very early by Hahn and Maxwell[4], and later by Bannerjee, Das and Saha[5]. In this system, the spectrum consists of two

4) E. L. Hahn and D. E. Maxwell, *Phys. Rev.*, **88**, 1070 (1952).
5) M. K. Bannerjee, T. P. Das and A. K. Saha, *Proc. Roy. Soc.*, **A226**, 490 (1954).

doublets; the separation in each doublet just gives the coupling constant between two protons. The disubstituted thiophenes are also the typical model of the two-proton system in which the analysis of the spectrum can be done very easily. But sometimes, as in the case of some methylthiophenesulfonylchlorides, the spectra are somewhat complicated owing to the small interaction between the ring protons and the substituents. The magnitude of the coupling constant for the ring proton and its neighboring methyl protons, as previously reported[1], has the order of about 1.0 c.p.s.; however, the chemical shift between them is more than 170 c.p.s. at 40 Mc./sec. The chemical shifts are here so large compared with the coupling constants ($J/\delta$ <0.006) that the spectra can be analyzed by the simple method of the two-proton system. The results of the simple treatment are given in Table III.

Table III. The coupling constants ($J$) and the chemical shifts ($\delta$) of two ring protons in methylthiophenesulfonylchlorides in c. p. s. at 40 Mc./sec. Measured conditions are summarized in Table I

| Substituent | $J$ | $\delta$ |
|---|---|---|
| 2-$CH_3$, 3-$SO_2Cl$ | 5.3±0.1 | 6.6±0.1 |
| 2-$CH_3$, 4-$SO_2Cl$ | 1.5±0.1 | 29.5±0.6 |
| 2-$CH_3$, 5-$SO_2Cl$ | 4.1±0.1 | 30.6±0.1 |
| 3-$CH_3$, 2-$SO_2Cl$ | 5.2±0.1 | 26.2±0.1 |
| 3-$CH_3$, 4-$SO_2Cl$ | 3.5±0.1 | 40.2±0.3 |
| 3-$CH_3$, 5-$SO_2Cl$ | 1.8±0.1 | 7.5±0.1 |

The proton magnetic resonance spectra of the six isomers studied are reproduced in Fig. 1, in which the ring proton spectra are shown at the left-hand side and the methyl proton spectra at the right-hand side. With respect to the ring proton spectra, a and d in Fig. 1 show the typical type of two-proton system; on the other hand, the other figures in Fig. 1 show some small splittings caused by methyl protons. For 2-methyl-3-thiophenesulfonylchloride, each of the two ring proton spectra is a little asymmetric as shown in a of Fig. 1. The doublet at the low field side is somewhat broader than the doublet at the high field side. Similar broadening is observed also in the doublet at the high field side, the 4-proton spectrum in 3-methy-2-thiophenesulfonylchloride, as shown in d of Fig. 1. For 2-methyl-4-, 2-methyl-5-, 3-methyl-4- and 3-methyl-5-thiophenesulfonylchloride, as shown in b, c, e and f in Fig. 1*, the ring proton spectra consist of two doublets. The one at the low field side has a simple structure and the other doublet at the high field side shows the fine structure caused by the interaction with methyl protons. The methyl proton spectra at the higher field side show also a doublet. In these four isomers, the 2-methyl group couples to 3-proton with a coupling constant of 1.1 c. p. s. However, the 3-methyl group couples to 2-proton with the same value but does not couple to 4-proton with the same order of coupling constant. This trend was also obseved in the spectrum of 3-methyl-2-thiophenesulfonylchloride, as shown in d of Fig. 1., in which no resolved fine structure was observed. The interaction between 4-proton and the adjacent methyl group is small. But the spectra of 4-proton are somewhat broader than those of 5-proton in 2-methyl-3- and 3-methyl-2-thiophenesulfonylchloride, as shown in a and d of Fig. 1. Consequently, it can be assumed that 2-methyl or 3-methyl group couples to 4-proton with a small coupling constant but couples to 5-proton with no appreciable constant. Similar results on the long range coupling in thiophene derivatives also have been obtained by others[2f,2g,6].

The coupling constants between two ring protons in the six isomers studied are 5.3 and 5.2 c.p.s. for $J_{23}$, 4.1 c.p.s. for $J_{34}$, 3.5 c.p.s. for $J_{25}$, and, 1.5 and 1.8 c.p.s. for $J_{24}$, as shown in Table III. The previous assumption[1] that the coupling constants between the ring protons for thiophene derivatives are $J_{23} > J_{34} > J_{25} > J_{24}$, is also consistent with the present observed values. It is very interesting to note that the observed coupling constant between the two protons by way of the sulfur atom ($J_{25}$) are relatively large, as compared with the meta-coupling constants for the benzene derivatives[7]; this trend is also obtained in thiophene which was analyzed recently by several authors[2b,8,9].

Chemical shifts depend upon the nature and the concentration of the solvents, so that the observation of the solvent effects on the chemical shift in the present compounds has also been made. The measured conditions and the results are summarized in Table IV. Three typical solvents were used, cyclohexane and carbon tetrachloride as nonpolar solvents, and acetone as a polar solvent. The experiment was carried out with the definite dilute solution of the compounds in each solvent, because of the limited amount of the synthesized material

* In c, e and f in Fig. 1, some extra peaks probably due to the presence of small isomeric impurities are observed.

6) P. L. Corio and I. Weinberg, *J. Chem. Phys.*, **31**, 569 (1959).
7) H. S. Gutowsky, C. H. Holm, A. Saika and G. A. Williams, *J. Am. Chem. Soc.*, **79**, 4596 (1957).
8) T. Isobe, *Bull.Chem. Res. Inst. Non-Aqueous Solutions, Tohoku Univ.*, **9**, 115 (1960).
9) R. J. Abraham and H. J. Bernstein, *Can. J. Chem.*, **37**, 2095 (1959).

TABLE IV. DISPLACEMENTS OF THE PROTON RESONANCES WHEN THE SAMPLES ARE DILUTED WITH CYCLOHEXANE, CARBON TETRACHLORIDE AND ACETONE, IN C. P. S. AT 40 Mc./sec., REFERRED TO THE VALUES GIVEN IN TABLE II, MINUS SIGN SHOWING THE DISPLACEMENT TO THE HIGHER FIELD

| Substituent | Measured Solution, wt. % | | | | Displacement, c. p. s. | | | | |
|---|---|---|---|---|---|---|---|---|---|
| | Sample | $C_6H_{12}$ | $CCl_4$ | $(CH_3)_2CO$ | 2-H | 3-H | 4-H | 5-H | $CH_3$ |
| 2-$CH_2$, 3-$SO_2Cl$ | 10.6 | 89.4 | | | — | — | −1.5 | −6.5 | −0.5 |
| 2-$CH_3$, 4-$SO_2Cl$ | 10.6 | 83.7 | 5.7 | | — | −2.0 | — | −5.5 | −2.5 |
| 2-$CH_3$, 5-$SO_2Cl$ | 8.0 | 92.0 | | | — | −8.0 | −6.0 | — | −3.5 |
| 3-$CH_3$, 2-$SO_2Cl$ | 11.5 | 88.5 | | | — | — | −7.5 | −10.0 | −2.0 |
| 3-$CH_3$, 4-$SO_2Cl$ | 12.4 | 87.6 | | | −8.5 | — | — | −7.5 | −1.5 |
| 3-$CH_3$, 5-$SO_2Cl$ | 11.3 | 88.7 | | | −9.0 | — | −5.0 | — | −2.5 |
| 2-$CH_3$, 3-$SO_2Cl$ | 6.7 | 1.9 | 91.4 | | — | — | +1.0 | −1.5 | +2.5 |
| 2-$CH_3$, 4-$SO_2Cl$ | 5.0 | 1.1 | 93.9 | | — | 0.0 | — | −1.5 | +1.0 |
| 2-$CH_3$, 5-$SO_2Cl$ | 4.4 | 1.0 | 94.6 | | — | −3.0 | −1.5 | — | +0.5 |
| 3-$CH_3$, 2-$SO_2Cl$ | 6.4 | 1.3 | 92.3 | | — | — | −4.0 | −5.0 | 0.0 |
| 3-$CH_3$, 4-$SO_2Cl$ | 7.2 | 3.7 | 89.2 | | −5.0 | — | — | −3.5 | 0.0 |
| 3-$CH_3$, 5-$SO_2Cl$ | 8.2 | 2.2 | 89.6 | | −3.5 | — | −1.5 | — | +1.0 |
| 2-$CH_3$, 3-$SO_2Cl$ | 14.6 | 15.4 | | 70.0 | — | — | +4.5 | +13.5 | +3.0 |
| 2-$CH_3$, 4-$SO_2Cl$ | 9.1 | 13.6 | 5.0 | 72.3 | — | +7.5 | — | +16.0 | +2.5 |
| 2-$CH_3$, 5-$SO_2Cl$ | 12.8 | 14.5 | | 72.7 | — | +8.0 | +8.0 | — | +4.0 |
| 3-$CH_3$, 2-$SO_2Cl$ | 13.2 | 14.3 | | 72.5 | — | — | +7.5 | +14.5 | +1.5 |
| 3-$CH_3$, 4-$SO_2Cl$ | 15.3 | 14.4 | | 70.3 | +13.0 | — | — | +12.0 | +0.5 |
| 3-$CH_3$, 5-$SO_2Cl$ | 14.0 | 15.1 | | 70.9 | +16.0 | — | +8.0 | — | +2.0 |

at hand, and a small amount of cyclohexane was used also as an internal reference. One of our aims in this experiment was to find a key for the assignment of the chemical structure by the NMR spectrum. As shown in Table IV, it is clear that, in the six compounds studied, all $\alpha$-protons are sensitive to the polarity of the solvents as compared with $\beta$-protons, notably in the case of the solution in acetone. It should be kept in mind that the self-polarizabilities given by de Heer[10] for $\alpha$- and $\beta$-carbon atoms in thiophene are qualitatively in agreement with the present results of the solvent effect.

*The Chemical Institute of*
*Non-Aqueous Solution*
*Tohoku University*
*Katahira-cho, Sendai*

10) J. de Heer, *J. Am. Chem. Soc.*, 76, 4802 (1954).

# *Proton Magnetic Resonanace Spectra of p-Cresol*

By Ichiro YAMAGUCHI

(Received March 28, 1961)

Schaefer and Schneider[1] investigated the ring proton resonance spectra of the *p*-substituted toluene derivatives and obtained many fruitful results concerning the interaction between ring protons and solvent molecules. The present author previously reported an NMR study of several hydrogen-bonded systems[2-5]. In these reports, explanations of the NMR behavior of the ring protons were made when the protons are affected by a change in the hydrogen-bonding situation in the molecule. In the present work, the NMR spectra of *p*-cresol, which gives rather a simple spectrum for the ring protons, were measured in various solutions and the NMR behaviors of methyl, hydroxyl and ring protons were interpreted in terms of hydrogen bond formation.

1) T, Schaefer and W. G. Schneider, *J. Chem. Phys.*, 32, 1218 (1960).

2) I. Yamaguchi, This Bulletin, 34, 353 (1961).
3) I. Yamaguchi, ibid., 34, 744 (1961).
4) I. Yamaguchi, ibid., 34, 451 (1961).
5) I. Yamaguchi, to be published.

## Experimental

The NMR measurements were made with a Varian NMR spectrometer at a resonance frequency of 56.4 Mc./sec. and at a temperature of 20°C. Chemical shifts of methyl, hydroxyl and ring protons from an external reference of water proton were determined by the side band technique and the susceptibility corrections were applied. *p*-Cresol was a guaranteed grade reagent and was purified by distillation. The solvents used were benzene, chloroform, carbon tetrachloride, dioxane, acetone and pyridine. These were purified with a Podobielniak distillator. Solutions with concentrations between 0.02 and 1 mol. fractions were prepared for each solvent.

## Results and Discussion

Figure 1 shows the concentration dependence of the chemical shifts of the methyl, hydroxyl and ring protons in carbon tetrachloride solutions. The hydroxyl proton resonance curves show characteristic behavior of each solution as shown in Fig. 2. On the other hand, the methyl and ring proton resonance curves show slight dependence on the solvent. Generally, the resonance fields of the methyl and ring protons decrease on dilution. The greater part of the causes of this inclination can be ascribed to the diamagnetic anisotropy effect of aromatic rings in the solution[6]. The resonance in the ring protons shows an interesting concentration dependence: Pure cresol liquid gives a single line spectrum while it gives a spectrum with

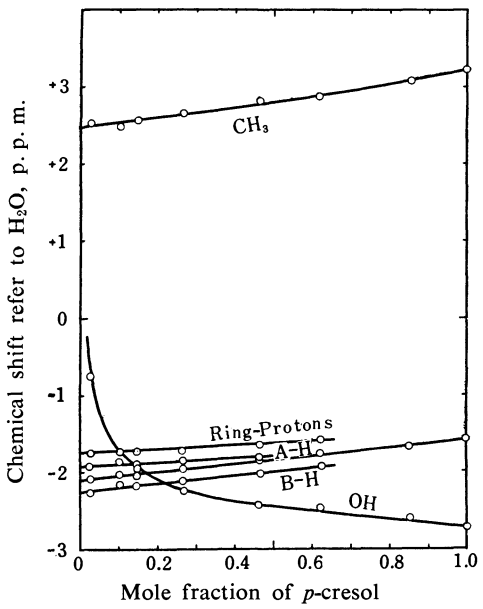



Fig. 1. Concentration dependence of chemical shift for *p*-cresol in $CCl_4$ solution.

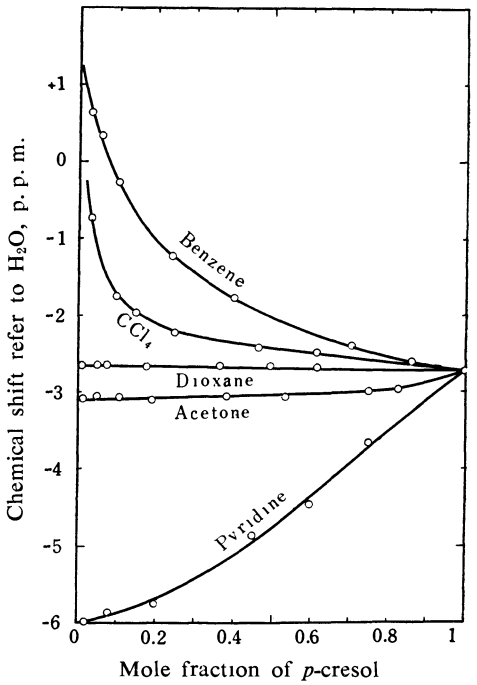



Fig. 2. Concentration dependence of OH proton chemical shift for *p*-cresol in various solutions.

a structure in dilute solution, arising from the proton pairs being chemically different from each other.

**Methyl Proton.** — The chemical shift of the methyl protons for benzene and pyridine solutions is apparently independent of the concentration because the net content of aromatic rings in the solutions is almost invariable. Those for the other solutions show the concentration dependence which is characteristic of the anisotropic effect of benzene rings of the solute in these solvents. The dilution shifts are almost the same as those for ring protons in benzene[6]* for the same solutions. The slope of the curve for the acetone solution is smaller than the others and this finding is parallel to the case of the ring protons in benzene. There seemed to be no notable effect of the hydrogen bonding on the methyl proton resonance.

**Hydroxyl Proton.** — Pure *p*-cresol gives a hydroxyl proton resonance line at slightly lower field than that in pure phenol[7]. This may be caused by the strengthening of the hydrogen bond by the hyperconjugation effect of the *p*-methyl group, although the hydrogen bond energies for the two compounds are comparable

6) A. A. Bothner-By and R. E. Glick, *J. Chem. Phys.*, **26**, 1651 (1957).

* The curves appeared in Ref. 6 were corrected for the susceptibility of the solutions.

7) R. L. Batdorf, Ph. D. Thesis, Univ. of Minnesota, 1955.

to each other[8]. The solvent and concentration dependences of the hydroxyl proton resonance are shown in Fig. 2. The curves for benzene, chloroform and carbon tetrachloride solutions show the dissociation process of the hydrogen bond between the solute molecules on dilution. The curves for dioxane, acetone and pyridine solutions suggest new hydrogen bond forms between the solute and the solvents on dilution.

The curves for the carbon tetrachloride solution are as similar as those for phenol in carbon tetrachloride solution[9], exhibiting a representative NMR behavior of the dissociation process of a hydrogen bond system. The curve for the concentration above the concentration of about 0.3 mol. fraction is considered to correspond to the dissociation process of polymer species. In the range below about 0.05 mol. fraction the dissociation of dimer molecules is considered to be dominant. The resonance field for the benzene solution increases simply on dilution. This behavior of the curve is caused by several factors; the dissociation of the associated molecules, the ring current effect of benzene and the hydrogen bond formation with the $\pi$-electron system of the solvent molecule. The last may cause the rapid increase of the resonance field on dilution.

In dioxane and acetone solutions, the solute is considered to form a new hydrogen bond with the solvent molecules on dilution while the associated *p*-cresol molecules dissociate. The new hydrogen bonds are probably weaker ones than the intermolecular hydrogen bond of *p*-cresol. This is because the resonances at the infinite dilution are due to a more shielded proton than that in the intermolecular hydrogen bond of *p*-cresol. Pyridine, a strong proton acceptor, appeared to form a strong hydrogen bond with *p*-cresol as suggested by the curve. Pyridine seems to destroy the hydrogen-bonded association or chelation[2] of a compound by its strong proton accepting power.

**Ring Proton.**—The ring proton resonance in solutions appears at a slightly higher field than those for benzene in respectively the same solvents. This is due to the electron-releasing substituents of methyl and hydroxyl groups in *p*-cresol. *p*-Cresol liquid gives a single resonance line for the ring protons while diluted *p*-cresol with any solvent gives a spectrum with a characteristic structure of the $A_2B_2$ system[10] as shown in Fig. 1. The slope of the concentration-dependence curves for ring protons is due mainly to the anisotropic effect of the aromatic rings in the solutions. The slope of the curves for B-protons (ortho to methyl group) in chloroform, carbon tetrachloride, dioxane and acetone solutions are slightly gentler than those for benzene in respectively the same solutions[6]. This easier characteristic of the slope may be ascribed to the bulkier molecular size of *p*-cresol compared to that of benzene[11]. Therefore the B-protons can plausibly be assumed to be scarcely affected by the varying situations of the hydrogen bonding but to some effect proper to the proton in an aromatic ring. The slope for A-protons (ortho to hydroxyl group) is much easier than that for the B-protons.

If the effect of the ring current is removed for simplicity's sake from considerations of NMR behavior of the ring protons, the B-proton resonance is nearly independent of the concentration of the solutions, while the A-proton resonance is displaced to a higher field on dilution. The cause of this inclination for the A-protons may be ascribed to some changes in the following effects affected by the hydrogen bond formation; (i) the inductive and mesomeric effects of the hydroxyl group, (ii) the electrostatic field which originated from the hydroxyl bond moment, (iii) effect of magnetic anisotropy of the solvent molecule in the proximity of A-proton, (iv) preferential hydrogen bond formation between A-proton and solvent molecule, and (v) dispersion effect of solvent molecule on the A-proton. The effects (i) and (ii) have their origin in the molecule itself while (iii), (iv) and (v) come from the interaction with the solvent. Since the behavior for the A-proton is common to all solutions, the effects (iii) and (iv) are ruled out. It is difficult to consider a preferential dispersion effect on the A-proton, and the effect (v) is also ruled out. On hydrogen bond formation, the length and the polarization of the O–H bond may increase[12] and hence the electrostatic field at the A-protons originating from the bond moment may be altered. This electric field might cause the displacement of the A-proton resonance. However, the direction of the displacement is to a higher field with increasing bond moment. Therefore, the contribution of the effect (ii) should be small. For this reason, the effect (i) is considered to be dominant to cause the displacement of the resonance in A-proton. With the effect (i), this inclination for the A-protons

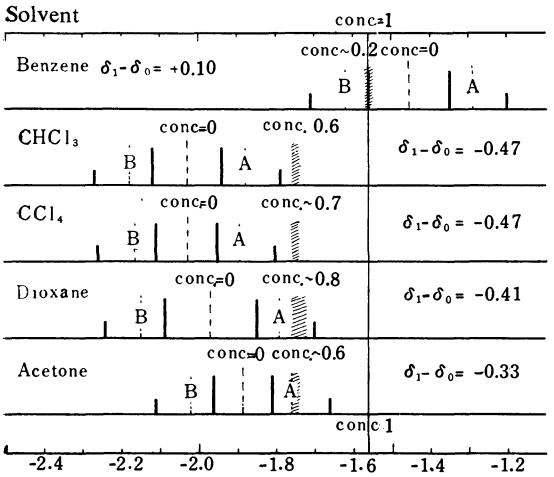
8) G. C. Pimentel and A. L. McClellan, "The Hydrogen Bond", Freeman, San Francisco (1960), Appendix B.
9) C. M. Huggins, G. C. Pimentet and J. N. Shoolery, *J, Phys. Chem.*, **60**, 1311 (1956).
10) H. J. Bernstein, J. A. Pople and W. G. Schneider, *Can. J. Chem.*, 35, 65 (1957); R. E. Richards and T. P. Schaefer, *J. Mol. Spectroscopy*, 2, 1280 (1958).
11) J. A. Pople, W. G. Schneider and H. J. Bernstein, "High Resolution Nuclear Magnetic Resonance, "McGraw-Hill, New York (1959), p. 426.
12) See for example: A. Burawoy, "Hydrogen Bondnig", Ed. by D. Hadzi, Pergamon Press, New York (1959), p. 259.

TABLE I. CHEMICAL SHIFTS, DILUTION SHIFT, COUPLING CONSTANT AND COALESCENT CONCENTRATION OF RING PROTON SPECTRUM IN *p*-CRESOL

| Solvent | $\delta_{ring}$ (p. p. m.) conc.=1 | $\delta_{ring}$ (p. p. m.) conc.=0 | Dilution shift (p. p. m.) $\delta_1-\delta_0$ | $\delta_{AB}$ (c./sec.) | $J_{AB}$ (c./sec.) | Coalese. conc. (mol. fraction) |
|---|---|---|---|---|---|---|
| Benzene | −1.56 | −1.46 | +0.10 | 18.6 | 8.5 | ~0.2 |
| $CHCl_3$ | 〃 | −2.03 | −0.47 | 16.6 | 〃 | ~0.6 |
| $CCl_4$ | 〃 | −2.03 | −0.47 | 15.3 | 〃 | ~0.7 |
| Dioxane | 〃 | −1.97 | −0.41 | 20.3 | 〃 | ~0.8 |
| Acetone | 〃 | −1.89 | −0.33 | 14.7 | 〃 | ~0.6 |

may be interpreted as follows: On formation of a strong intermolecular hydrogen bond between *p*-cresol molecules, the electron density on the oxygen atom should increase. This dense distribution of the negative charge is supplied from the ring, especially from the ortho-positions by inductive and mesomeric mechanisms. Thus the chemical shift of the A-proton is displaced to a lower field in the concentrated range. This qualitative explanation is plausible for the systems of hydroxyl hydrogen bond so far investigated by the present author[2,3].

Table I gives the chemical shift of the ring proton systems ($\delta_{ring}$) at the concentrations of zero and 1 mol. fractions, the dilution shift ($\delta_1-\delta_0$), the relative chemical shift and the spin coupling constant between A and B protons at infinite dilution, and the concentration where the lines of the spectrum coalesce. Figure 3 shows the position of the spectra of the ring protons schematically for the solutions investigated. The spectrum for benzene solution is displaced to a considerably high field compared to those for the other solutions. This is due to the anisotropic effect of benzene. The B-proton resonance at the infinite dilution for chloroform, carbon tetrachloride and dioxane solutions occur at about the same field in relation to one another, whereas the A-proton resonance for them occurs at fields different from one another. This fact also supports the inactiveness of the B-protons against the change in the environments. The B-proton resonance for acetone solution is the only exception: The resonance occurs at a slightly higher field than for the other solutions mentioned above. The same is observed for the ring protons of benzene in acetone solution[6]. Therefore, the preferential hydrogen bond interaction of an acetone molecule with the B-proton as suggested by Schneider and Schaefer[1] is denied in this case. This discrepancy may partly be attributed to the large dielectric constant of acetone[1].




Chemical shift refer to $H_2O$

Fig. 3. Ring proton spectra for *p*-cresol in various solutions.

In Fig. 3, the field where the resonance lines coalesce to a single line is indicated by a shaded range. It is surprising that the fields are almost the same for all solutions (about −1.74 p.p.m.) except benzene solution although the concentrations are different from one another. The coincidence of the field may have some meaning concerning the structure of the solutions or may rather be an accident. However, in this work, this phenomenon could not be well interpreted with the anisotropic effect of the aromatic rings in the solutions at the coalescent concentration. The single coalesced line in the concentrated range may suggest that only the same species of associated polymers as in pure *p*-cresol exists in this range. In benzene solution, the coalescence occurs at an exceptionally low concentration. This may be ascribed to the poor ability of the benzene molecule to disrupt the hydrogen bonds due to the geometrical similarity of the flat molecular shape of benzene and *p*-cresol.

It may be noted that the resonance fields of the methyl protons at the coalescent concentration for the four solutions are approximately +2.95 p. p. m., and this value is also nearly independent of the solvent. Accompanying the ring proton resonance data, this fact may also supply some information about the structure of the solutions.

**Summary**

The proton magnetic resonance spectra of *p*-cresol in several solutions were measured. The concentration dependence of the resonance in methyl protons suggests no remarkable effect of the hydrogen bonding on methyl protons. The resonance in the hydroxyl proton shows characteristic concentration dependences which are ascribed to the dissociation of the associated molecule in benzene, chloroform and carbon tetrachloride solutions and to the formation of new hydrogen bonds with solvent in acetone, dioxane and pyridine solutions. The ring proton resonance spectrum is a single line in concentrated range whereas it is an $A_2B_2$ type spectrum in dilute range. The splitting of the spectrum in dilute solutions is ascribed to the change in the screening of the proton ortho to the hydroxyl group affected by the change in the intermolecular hydrogen-bonding situation. The shielding of the proton ortho to the methyl group appeared to be unaffected by the same change.

*Japan Atomic Energy Research Institute*
*Division of Radiation Applications*
*Tokai, Ibaraki-ken*

# *Nuclear Magnetic Resonance in Amino-group of Aniline Derivatives*

By Ichiro YAMAGUCHI

(Received March 28, 1961)

The association of aniline molecules by their weak hydrogen bonds was suggested by several authors[1,2]. However, the association is still not well ascertained. Nuclear magnetic resonance measurements of aniline derivatives have not yet been made and are expected to give valuable information about the intermolecular hydrogen bond of these compounds and, in connection with the work on dimethyl phenols[3], about the effects of the ortho-methyl group on the proton resonance chemical shift of the amino-group. Thus this paper presents the study of the hydrogen bond of the amino-group by NMR measurements.

## Experimental

All the NMR measurements were carried out with a Varian NMR spectrometer at a radio frequency of 56.4 Mc./sec. and at a temperature of 20°C. The compounds investigated were aniline, *o*-, *m*- and *p*-toluidines and 2, 3-, 2, 4-, 2, 5-, 2, 6- and 3, 4-dimethylanilines. These were all guaranteed grade reagents and purified by distillation immediately before making solutions. The solvents used were carbon tetrachloride and acetone. These were purified with a Podobielniak fractional distillator. Solutions with concentrations of between 0.01 and 1 mol. fractions were made for all liquid aniline derivatives. 3, 4-Dimethyl aniline is solid and the concentrations of the solutions measured were up to saturated solution. The chemical shifts from water as an external reference were determined by the side band technique. Corrections for bulk diamagnetic susceptibility of the solutions were made. The values of the volume susceptibility were obtained by applying Pascal's rule and appropriate extrapolations. Their values were 0.676 for aniline, 0.70 for all toluidine isomers and 0.68 for all dimethyl aniline isomers.

## Results and Discussion

The concentration dependence of the amino proton resonance for carbon tetrachloride solutions are shown in Fig. 1a and those for acetone solutions in Fig. 1b. Pure aniline derivatives investigated give amino proton resonance at $+1.7 \sim +1.9$ p. p. m. The resonance fields are remarkably higher than those of hydroxyl proton resonance in phenols. Figure 2 shows an example of the concentration dependence of the chemical shifts for dimethyl aniline isomers. The resonance of the amino protons in carbon tetrachloride solutions was a sharp single absorption while that in acetone solutions was generally broad, especially in dilute solutions.

In Fig. 1, curves for the amino protons in various aniline derivatives investigated are observed to fall in a rather narrow field range and apparently there is no notable feature connecting the relative position of the methyl group to the amino group. This fact is remarkably in contrast with the hydroxyl proton resonance of dimethyl phenol isomers[3]. In

1) E. Fischer, *Z, Naturforsch.*, **9a**, 90 (1954); A. E. Lutskii, *Zhur. Obshchei. Khim.*, **26**, 2299 (1956).
2) J. C. Dearden and W. F. Forbes, *Can. J. Chem.*, **38**, 896 (1960).
3) I. Yamaguchi, This Bulletin, **34**, 774 (1961).

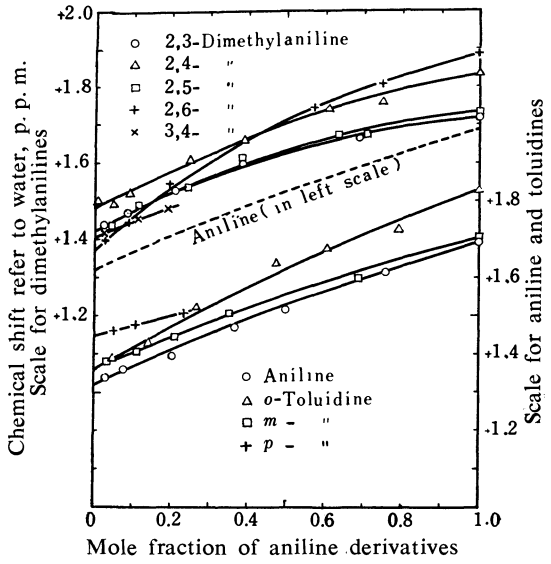



Fig. 1a. Concentration dependence of amino proton chemical shift for aniline derivatives in carbon tetrachloride solution.

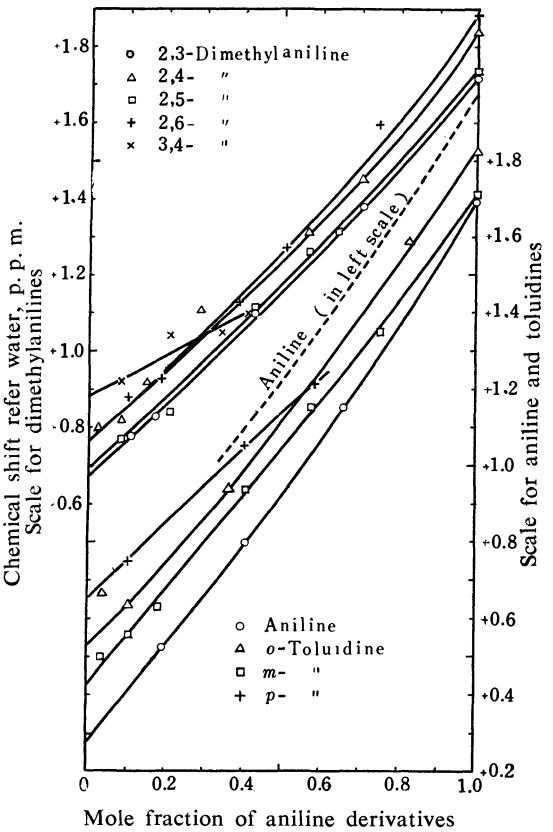



Fig. 1b. Concentration dependence of amino proton chemical shift for aniline derivatives in acetone solution.

this narrow range, the curves for dimethyl aniline isomers appear at the highest field side, those for toluidine isomers at the middle and that for aniline at the lowest side. This order seems to correspond exactly to the order of the base strength of these compounds. The cause of this arrangement of the shifts would mainly be the inductive effect of the methyl groups. In each group of the isomers, the curves for compounds with ortho- or para-methyl group appear at a higher field than those with the meta-methyl group. This result suggests that the mesomeric effect of the methyl group also has an important role to the chemical shift of the amino protons.

Dodd and Stephenson[4] showed a correlation between the basicity of amines and the NH frequency shift in the infrared absorption spectrum caused by hydrogen bond formation between amines and acetone or pyridine. Thus it seems to be natural to expect some correlations between basicity and hydrogen bond shift of proton resonance spectrum of an aniline. Several authors[5,6] pointed out that the basicity of aniline derivatives is strongly dependent on the position and the inductive and mesomeric effects of a substituent in the ring. For example, among *m*- and *p*-toluidines and aniline the base strength of *p*-toluidine is the strongest and that of aniline is the weakest, and this fact was ascribed to the inductive and mesomeric effects of the methyl group. However, the effect of an ortho-substituent on the basicity is not simple because of the additional specific ortho effect[5].

The base strengths of aniline derivatives were reported by several authors[5,7]. Although the $pK_a$ value of a compound reported in one paper is slightly different from that in another, due partly to the solvent and concentration used, the order of the magnitude of the $pK_a$ values is almost the same. The following is the increasing sequence of the $pK_a$ values of aniline derivatives: 3, 4-diMe-, *p*-Me-, 2, 4-diMe-, 3, 5-diMe-, *m*-Me-, 2, 3-diMe-anilines, aniline, 2, 5-diMe-, *o*-Me- and 2, 6-diMe-anilines. The order of the values of the chemical shift in carbon tetrachloride solutions seems to correlate approximately with that of the base strengths of the compounds although some lack of accordance between the two orders is observed. Qualitatively, the factor which

4) R. E. Dodd and G. W. Stephenson, "Hydrogen Bonding", Ed. by Hadzi, Pergamon Press, New York (1959), p. 177.
5) R. N. Beale, *J. Chem. Soc.*, **1954**, 4494.
6) M. Gillois and P. Rumph, *Bull. soc. chim. France*, **1954**, 112.
7) N. F. Hall and M. R. Sprinkle, *J. Am. Chem. Soc.*, **54**, 3469 (1932); G. Thomson, *J. Chem. Soc.*, **1946**, 1113; van Helden et al., *Rec. trav. chim.*, **73**, 39 (1954); B. M. Wepster, ibid., **76**, 357 (1957).

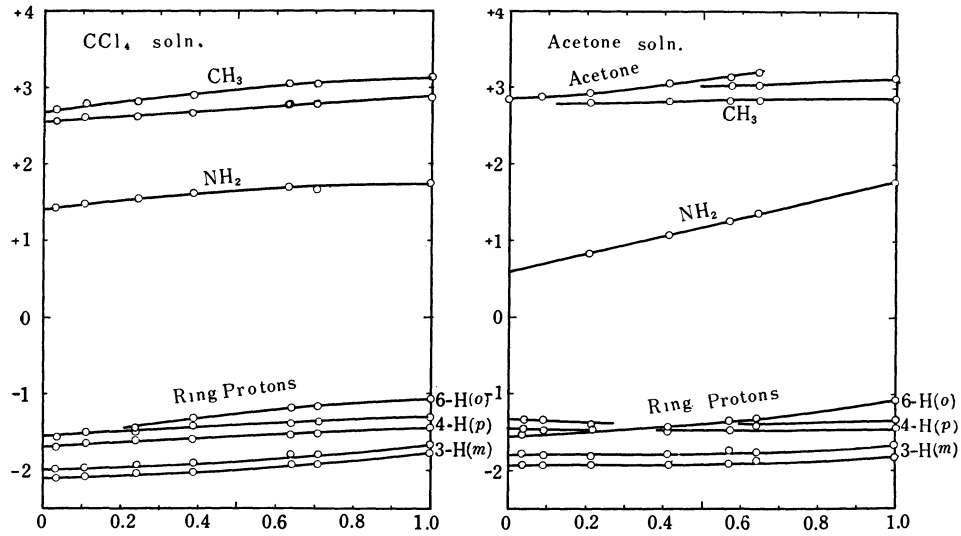



Fig. 2. Concentration dependence of chemical shift for 2,5-dimethyl aniline in carbon tetrachloride and acetone solutions.

determines the base strength of an amine is the charge density on the nitrogen atom[8] and not that on the proton in the amino group. The effective charge density on the nitrogen atom, which has lone pair electrons as well as valence electrons, may be affected in a complicated way rather by changes in the structural and chemical circumstances of the amino-group than by the electronic effect of substituents. Therefore the slight lack of accordance between the order of the proton resonance chemical shifts and that of the base strengths may be observed.

For carbon tetrachloride solutions, the slope of the concentration dependence curve for the amino protons is considerably small and is nearly the same as, but slightly smaller than, that for methyl protons in toluidine and dimethylaniline isomers. The positive slope of the curves is caused by the magnetic anisotropy effect of the aromatic rings in the solutions[9]. If the slope of the curves for methyl protons is assumed to arise merely from the anisotropic effect and if the amino protons are assumed to be affected by the same anisotropic field as that for methyl protons, the curves for the amine protons which are subtracted by the anisotropic effect can be obtained. These curves have a negative slope which might be an indication of a dissociation process of hydrogen bonds on dilution. The association of aniline molecules by intermolecular hydrogen bonds is not well ascertained, although it is, with less confidence, pointed out by several authors with physicochemical measurements[1] and infrared studies[2]. If a hydrogen bond with the same order of strength as an OH hydrogen bond exists between solute molecules, the slope would be more concentration dependent. The slopes which were observed are much smaller than those of dissociation processes of the OH hydrogen-bonded systems. This difference in the NMR behavior between the system might be partly due to the difference between the effective charge in the electronic shielding of the OH group and that of the amino group on formation of hydrogen bonds. It is unfortunate that the data available for estimation of bond energies of the N-H···N hydrogen-bonded systems as well as NMR data for amino protons are very scarce, and at the present stage, no decisive conclusion on the extent of the hydrogen bonding for aniline derivatives can be drawn from the NMR shift data. However, from the knowledge of the NMR measurements so far made with the OH hydrogen-bonded systems, it may be said that the hydrogen-bonded association of aniline derivatives occurs and the strength of it is fairly weak.

For acetone solutions, the effect of the hydrogen bond formation between the solute and the solvent is remarkable and the dilution shifts are large compared with those for carbon tetrachloride solutions. The order of the magnitude of the chemical shifts of the amino protons in acetone solutions is almost the same as that for carbon tetrachloride solutions.

A measure for the ability of the hydrogen

8) See for example: G. W. Wheland, "Resonance in Organic Chemistry", John & Wiley, New York (1955).
9) A. A. Bothner-By and R. E. Glick, *J. Chem. Phys.*, **26**, 1651 (1957).

TABLE I. CHEMICAL SHIFTS, DILUTION SHIFTS AND $\Delta$ VALUE OF $NH_2$ PROTON IN ANILINE DERIVATIVES (IN p. p. m.)

| Compound | Pure *p*-cresol | $CCl_4$ soln. | | Acetone soln. | | $\Delta$ |
|---|---|---|---|---|---|---|
| | | Concn.=0 | $\delta_1-\delta_0$ | Concn.=0 | $\delta_1-\delta_0$ | |
| Aniline | +1.69 | +1.33 | 0.36 | +0.28 | 1.41 | 1.05 |
| *o*-Toluidine | +1.82 | +1.37 | 0.45 | +0.53 | 1.29 | 0.84 |
| *m*-Toluidine | +1.71 | +1.37 | 0.34 | +0.44 | 1.27 | 0.93 |
| *p*-Toluidine | — | +1.44 | — | +0.66 | — | 0.78 |
| 2,3-Dimethyl aniline | +1.72 | +1.42 | 0.30 | +0.67 | 1.05 | 0.75 |
| 2,4-Dimethyl aniline | +1.84 | +1.48 | 0.36 | +0.78 | 1.06 | 0.70 |
| 2,5-Dimethyl aniline | +1.73 | +1.43 | 0.30 | +0.68 | 1.05 | 0.75 |
| 2,6-Dimethyl aniline | +1.88 | +1.38 | 0.50 | +0.76 | 1.08 | 0.62 |
| 3,4-Dimethyl aniline | — | +1.5 | — | +0.9 | — | 0.6 |

bond formation of a compound, $\Delta$ value*, proposed by the present author[10] is listed in Table I for the aniline derivatives investigated. The values of the chemical shift and the dilution shifts for the amino protons in carbon tetrachloride and acetone solutions are also listed in Table I. The magnitudes of the $\Delta$ value are about 1 and this value suggests the weakness in the ability of hydrogen bond formation of the compounds. This value nearly corresponds to the ability of 2,6-di-*tert*-butyl-*p*-cresol[10]. The $\Delta$ values for aniline and *m*-toluidine are large while that of 2,6-dimethyl aniline is remarkably small. With the data of the dilution shift for carbon tetrachloride solutions, the extent of the hydrogen bond formation of the aniline derivatives is clearly dependent on the existence of the ortho-methyl group.

Among the curves of the amino proton resonance for carbon tetrachloride solutions the behavior of the curves for 2,*x*-dimethyl anilines ($x=3, 4$ and 5) are peculiar as indicated by their small dilution shifts compared with that of 2,6-dimethyl aniline. The value is even smaller than that of *o*-toluidine. Considering the behavior of the curves by subtracting the anisotropic effect of the rings in the solution medium, this peculiarity apparently means that 2,*x*-dimethylanilines ($x=3, 4$ and 5) associate to a higher extent than *o*-toluidine does. However, this intrerpetation can not be accepted from the standpoint of the $\Delta$ values of these compounds. This discrepancy may possibly be caused by an additional effect of the *x*-(meta- or para-) methyl group on the amino proton resonance and this effect counterbalances the effect of the ortho-methyl group.

The ring proton spectra for dimethyl aniline isomers show slight concentration dependence. The displacement of the ortho-proton resonance line to a lower field on dilution is observed. The displacement is more remarkable for acetone solutions than for carbon tetrachloride solutions. This inclination is opposed to the behavior of the ortho-proton curves for phenol derivatives[3,11]. On association of aniline derivatives, the charge migration from the ring to the amino group would not be so much as for phenol derivatives because, possibly, the hydrogen bonding is very weak. However, the proton in the amino group is attracted by the proton-accepting group and this results the change in the electrostatic field at the ortho-proton[12]. In this way, the association would cause the displacement of the resonance field of the ortho-proton to a higher field. In acetone solutions, a weak hydrogen bond between the acetone and the ortho-proton would form and the displacement of the ortho-proton resonance to a lower field on dilution is observed as in the case of dimethyl phenols in acetone solution[3].

## Summary

Concentration dependenec of the chemical shift of amino protons in aniline derivatives in carban tetrachloride and acetone solutions were measured. The chemical shift of the amino proton in aniline derivatives is revealed to be clearly dependent on the existence of the ortho-methyl group. In carbon tetrachloride solutions, the concentration dependence of the resonance lines is slight, suggesting that the association of the solute molecules by hydrogen bonding is very weak. In acetone solutions, the dependence suggests hydrogen bond formation between solute and acetone. The base strength of aniline derivatives appeared to have no direct correlation with the

10) I. Yamaguchi, This Bulletin, 34, 451 (1961).

* $\Delta$ is defined as the difference between the chemical shift of a hydnogen-bonded proton at infinite dilution for carbon tetrachloride solution and that for an acetone solution.

11) I. Yamaguchi, This Bulletin, 34, 353 (1961).

magnitude of the chemical shift of amino proton in these compounds. The ring proton spectra of dimethyl aniline are slightly concentration dependent. The resonance in the ortho-protons appears to be displaced to a lower field on dilution and this tendency was ascribed to the change in the electrostatic field at the proton arising from the N–H bond moment change by hydrogen bond formation.

*Japan Atomic Energy Research Institute*
*Division of Radiation Applications*
*Tokai, Ibaraki-ken*

# *Synthesis and Reactions of Cyano- and Carboxytropones*

By Katsuo KIKUCHI

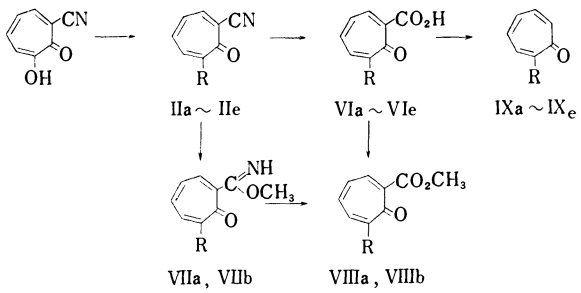
(Received March 20, 1961)

It has been reported that several kinds of cyanotropolones[1-4] can be obtained by the reaction of bromotropolones with cuprous cyanide or with potassium cyanide. In the case of cyanotropone, however, only the synthesis of 2-cyanotropone from 2-bromotropone and cuprous cyanide has been reported.[5]

In the present paper it is shown that several kinds of Grignard reagents react with 3-cyanotropolone (I)[1-4] to give corresponding 2-aryl- or 2-alkyl-7-cyanotropones. In this respect it is interesting to note that the cyano group of I is rather inactive to the Grignard reagents used and that the expected 3-aroyl- or 3-acyltropolones are not obtained.

The reaction of phenylmagnesium bromide and I afforded 7-cyano-2-phenyltropone (IIa) as yellow plates. Proof of the structure of IIa was obtained both by decarboxylation and by decarboxylative bromination of 2-phenyltropone-7-carboxylic acid (VIa) from IIa to yield 2-phenyltropone[6-9] and 7-bromo-2-phenyltropone[8,10], respectively.

Similarly, the reaction of I with $\alpha$- and $\beta$-naphthylmagnesium bromide each afforded 7-cyano-2-$\alpha$-naphthyltropone (IIb) as yellow needles and 7-cyano-2-$\beta$-naphthyltropone (IIc) as yellow plates. A similar reaction of I with methylmagnesium iodide afforded 7-cyano-2-methyltropone (IId) as colorless needles in rather poor yield. The treatment of I with benzylmagnesium chloride, however, resulted in the formation of 2-benzyl-7-cyanotropone (IIe) as yellow needles of m. p. 102°C and yellow prisms (III) of m. p. 145°C, with the latter predominating. The ultraviolet absorption spectra of IIa—IIe are shown in Fig. 1.




R a, $C_6H_5$; b, $\alpha$-$C_{10}H_7$; c, $\beta$-$C_{10}H_7$; d, $CH_3$; e, $C_6H_5CH_2$

III was easily reacted both with concentrated hydrochloric acid and with ethanolic hydrogen chloride to give colorless needles (IV) and colorless prisms (V), respectively. Detailed studies on the structures of III, IV and V are now under way.

The cyanotropones (IIa-IIe) obtained above were easily hydrolyzed with sulfuric acid to give corresponding tropone carboxylic acids. Thus, 2-phenyltropone-7-carboxylic acid (VIa), 2-$\alpha$-naphthyltropone-7-carboxylic acid (VIb), 2-$\beta$-naphthyltropone-7-carboxylic acid (VIc), 2-methyltropone-7-carboxylic acid (VId) and

1) B. J. Abadir, J. W. Cook, J. D. Loudon and D. K. V. Steel, *J. Chem. Soc.*, **1952**, 2350.
2) T. Nozoe, Y. Kitahara and S. Masamune, *Proc. Japan Acad.*, **29**, 17 (1953).
3) T. Nozoe and Y. Kitahara, ibid., **30**, 204 (1954).
4) Y. Kitahara, *Sci. Repts. Tohoku Univ., Ser. I*, **40**, 74 (1956).
5) T. Nozoe, S. Seto and S. Matsumura, *Proc. Japan Acad.*, **28**, 483 (1952).
6) T. Nozoe, T. Mukai and J. Minegishi, ibid., **27**, 419 (1951).
7) W. E. Doering and C. F. Hiskey, *J. Am. Chem. Soc.*, **74**, 5688 (1952).
8) W. E. Doering and J. R. Mayer, ibid., **75**, 2387 (1953).
9) T. Nozoe, T. Mukai, J. Minegishi and T. Fujisawa, *Sci. Repts. Tohoku Univ., Ser. I*, **37** 388 (1953).
10) T. Mukai, ibid., **38**, 280 (1954).

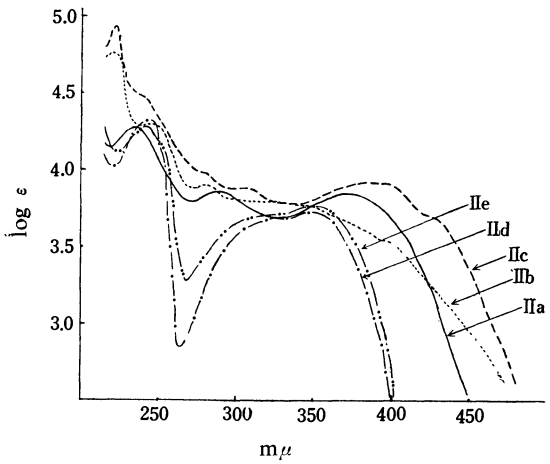



Fig. 1. Ultraviolet absorption spectra of IIa—IIe in methanol.

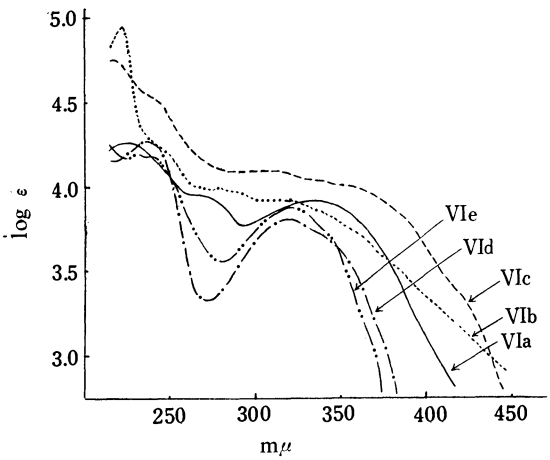



Fig. 2. Ultraviolet absorption spectra of VIa—VIc in methanol.

2-benzyltropone-7-carboxylic acid (VIe) were obtained. The ultraviolet absorption spectra of VIa–VIe are shown in Fig. 2.

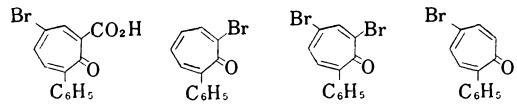
When treated with methanolic hydrogen chloride, 7-cyano-2-phenyltropone (IIa) afforded methyl 2-phenyltropone-7-carboximidate (VIIa) as pale yellow needles, the structure of which was ascertained by the hydrolysis of VIIa with dilute hydrochloric acid to give methyl 2-phenyltropone-7-carboxylate (VIIIa). Similar treatment of 7-cyano-2-$\alpha$-naphthyltropone (IIb) afforded methyl 2-$\alpha$-naphthyltropone-7-carboximidate (VIIb) as an oil, the hydrolysis of which afforded methyl 2-$\alpha$-naphthyltropone-7-carboxylate (VIIIb).

Attempted synthesis of formyltropones by Stephen's method did not succeed.

When heated to reflux in acetic anhydride, VIa, VIb and VIc were easily decarboxylated to give 2-phenyltropone (IXa), 2-$\alpha$-naphthyltropone (IXb)[11] and 2-$\beta$-naphthyltropone (IXc)[11] respectively.

The treatment of VIa with 2 mol. equivalents of bromine in acetic acid afforded an acid (X) accompanied with 7-bromo-2-phenyltropone (XI) or with 5, 7-dibromo-2-phenyltropone (XII)[12]. The structures of the latter two compounds were identified by respective admixture with authentic samples.

When heated to its decomposition points, X was submitted to decarboxylation to give yellow needles (XIII). Both X and XIII were converted by bromine in acetic acid to 5, 7-dibromo-2-phenyltropone (XII). This fact indicates that X and XIII are 5-bromo-2-phenyltropone-7-carboxylic acid and 5-bromo-2-phenyltropone, respectively.




X XI XII XIII

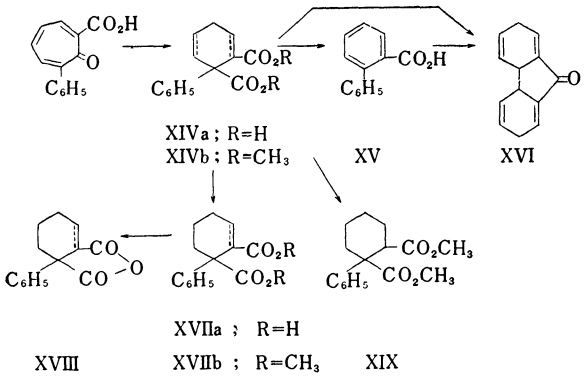
The action of bromine on IIb and IIc gave no satisfactory results.

The action of alkali on 2-phenyltropone-7-carboxylic acid (VIa) was next examined. It was already reported that the action of sodium hydroxide solution on tropone-4-carboxylic acid[12] gave terephthalic acid. The behavior of VIa to alkali, however, was somewhat different. VIa, when heated with dilute sodium hydroxide solution, was easily submitted to rearrangement to form a dibasic acid XIVa of m. p. 217~218°C (decomp.), in good yield. Analysis of XIVa and its dimethyl ester XIVb are in agreement with the formulae $C_{14}H_{12}O_4$ and $C_{16}H_{16}O_4$ respectively. XIVa reduces Fehling's solution and ammoniacal silver nitrate solution. Mild oxidation of XIVa with alkaline-ammoniacal silver nitrate solution gave colorless crystals (XV) which were identified as *o*-biphenylcarboxylic acid. The treatment of XV with concentrated sulfuric acid yielded fluorenone (XVI), which was also obtained directly from XIVa by the action of the same acid under evolution of gas.

XIVa absorbed one mole of hydrogen on palladium-charcoal and on Adam's catalyst to give colorless needles (XVIIa), m. p. 223~225°C (decomp.); dimethyl ester (XVIIb) of XVIIa, m. p. 81~82°C. Analysis of XVIIa and XVIIb are in agreement with the formulae $C_{14}H_{14}O_4$ and $C_{16}H_{18}O_4$, respectively. XVVIIa, when

11) K. Kikuchi, *J. Chem. Soc. Japan, Pure Chem. Sec.* (*Nippon Kagaku Zasshi*), **77** 1439 (1956).
12) J. R. Bartels-Keith, A. W. Johnson and A. Langemann, *J. Chem. Soc.*, **1952**, 4461.

heated above its melting point, gave an anhydride (XVIII) of m. p. 125~127°C, which gave the original acid by sodium carbonate solution. The uptake of two moles of hydrogen by XIVa was difficult, but on one occasion, it was reduced on palladium-charcoal to give a small yield of colorless crystals, m. p. 160~170°C which without further purification, was converted to its dimethyl ester (XIX), m. p. 77~78°C. The analysis of XIX is in agreement with the formula $C_{16}H_{20}O_4$.



XIVa ; R=H
XIVb ; R=$CH_3$ XV XVI

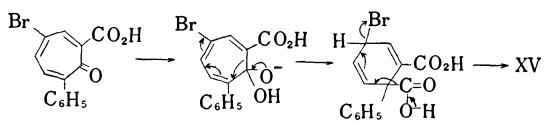
XVIIa ; R=H
XVIII XVIIb ; R=$CH_3$ XIX

From these facts, it seems almost certain that XIVa is 1-phenylcyclohexadiene-1, 2-dicarboxylic acid but the exact location of double bonds in the cyclohexadiene ring is not clarified yet.

Similar treatment of 2-α-naphthyltropone-7-carboxylic acid (VIb) with dilute sodium hydroxide gave a dicarboxylic acid (XX)($C_{18}H_{14}O_4$) of m. p. 237~238°C (decomp.), which was converted to benzanthrone (XXI) with concentrated sulfuric acid. XX is considered to be 1-α-naphthylcyclohexadiene-1, 2-dicarboxylic acid formed in a manner similar to that in the case of XIVa.

The reaction of 5-bromo-2-phenyltropone-7-carboxylic acid (X) with dilute alkali, however, gave *o*-biphenylcarboxylic acid (XV). The mechanism of its formation is tentatively assumed as follows.

Recently it was reported[13] that the reaction of 4-bromo-2-phenyltropone and 4-mercapto-2-phenyltropone with alkali gave the same *o*-biphenylcarboxylic acid (XV). It seems interesting that the rearrangement of troponoid compounds is accompanied with the formation of hydroaromatic compounds or with the elimination of substituents other than in 2-(i. e. 7-) position.



13) T. Muroi, *J. Chem. Soc. Japan, Pure Chem. Sec.* (*Nippon Kagaku Zasshi*), **80**, 303 (1959).

## Experimental

**7-Cyano-2-phenyltropone (IIa).**—To a solution of phenylmagnesium bromide, prepared from 9.6 g. of bromobenzene, 1.7 g. of magnesium and 30 cc. of absolute ether, and subsequently diluted with 40 cc. of anhydrous tetrahydrofuran, was added 3.0 g. of powdered 3-cyanotropolone (I) during 10 min. with stirring. The resulting clear solution was stirred for 2.5 hr. at 45~55°C, decomposed with dilute sulfuric acid and extracted with chloroform. The chloroform solution was washed with water, dried and the solvent was removed by distillation. The yellow crystals thereby obtained were recrystallized from a mixture of benzene and petroleum ether to give yellow plates (IIa), m. p. 134~135°C. Yield, 2.22 g.

Found: C, 80.69; H, 3.89; N, 7.04. Calcd. for $C_{14}H_9ON$: C, 81.14; H, 4.38; N, 6.76%.

**7-Cyano-2-α-naphthyltropone (IIb).**—To a solution of α-naphthylmagnesium bromide, prepared from 2.8 g. of α-bromonaphthalene, 0.34 g. of magnesium and 5 cc. of absolute ether, was added a solution of 0.5 g. of I dissolved in dehydrated dioxane and was stirred for 7 hr. at 75~80°C. After being left overnight, the reaction mixture was decomposed with dilute sulfuric acid and extracted with chloroform. The chloroform extract was washed with water, dried and the solvent was removed. The residual oil provided 0.34 g. of IIb, m. p. 160~162°C. Recrystallization from benzene gave yellow needles, m. p. 163~164°C.

Found: C, 84.52; H, 4.18; N, 5.78. Calcd. for $C_{18}H_{11}ON$: C, 84.03; H, 4.31; N, 5.44%.

**7-Cyano-2-β-naphthyltropone (IIc).**—To a solution of β-naphthylmagnesium bromide, prepared from 2.8 g. of β-bromonaphthalene, 0.34 g. of magnesium, a small amount of iodine and 5 cc. of absolute ether, was added a solution of 0.5 g. of I dissolved in dehydrated dioxane, and the reaction mixture was treated as in the case of IIb. The residual oil provided 0.42 g. of IIc, m. p. 177~180°C. Recrystallization from dioxane gave yellow plates, m. p. 180~181°C.

Found: C, 84.51; H, 4.01; N, 5.56. Calcd. for $C_{18}H_{11}ON$: C, 84.03; H, 4.31; N, 5.44%.

**7-Cyano-2-methyltropone (IId).**—To a solution of methylmagnesium iodide, prepared from 2.56 g. of methyl iodide, 0.5 g. of magnesium and absolute ether and subsequently diluted with dehydrated tetrahydrofuran, was added 0.8 g. of powdered I with stirring. After being stirred for another 4 hr. at 45~50°C, the mixture was treated as in the case of IIa to give 0.12 g. of IId. Recrystallization from ethanol gave colorless needles, m. p. 119~120°C.

Found: C, 74.41; H, 4.66; N, 9.72. Calcd. for $C_9H_7ON$: C, 74.47; H, 4.86; N, 9.65%.

**Reaction of 3-Cyanotropolone (I) and Benzylmagnesium Chloride.**—To a solution of Grignard reagent prepared from 3.78 g. of benzyl chloride, 0.75 g. of magnesium and 15 cc. of absolute ether

and diluted with 15 cc. of dehydrated tetrahydrofuran, was added 1.5 g. of I with stirring. The mixture was stirred for another 2 hr. at 45~50°C, decomposed with dilute sulfuric acid and extracted with chloroform. The chloroform extract was washed with water, the solvent was removed under reduced pressure, and 530 mg. of yellow crystals (III) thereby obtained, were collected by filtration. Chromatographic separation of the filtrate over silica gel gave 40 mg. of III and 120 mg. of 2-benzyl-7-cyanotropone (IIe).

IIe was recrystallized from ethanol to give pale yellow prisms, m. p. 101~102°C.

Found: C, 81.16; H, 4.72; N, 6.51. Calcd. for $C_{15}H_{11}ON$: C, 81.43; H, 5.01; N, 6.33%.

III was recrystallized from ethanol to give yellow prisms, m. p. 144~145°C.

Found: C, 79.81; H, 6.22; N, 4.51. Calcd. for $C_{22}H_{19}O_2N$: C, 80.22; H, 5.81; N, 4.25%.

**Reaction of Compound (III) and Concentrated Hydrochloric Acid.**—The addition of 0.5 cc. of concentrated hydrochloric acid to 100 mg. of III at room temperature gave viscous syrup which soon solidified to colorless crystals. They were collected by filtration and recrystallized from a large amount of *n*-butanol to give colorless microneedles (IV), m. p. 225°C (decomp.).

Found: C, 76.04; H, 6.62; N, 4.24. Calcd. for $C_{22}H_{21}O_3N$: C, 76.06; H, 6.09; N, 4.03%.

**Reaction of Compound (III) and Ethanolic Hydrogen Chloride.**—The addition of 0.5 cc. of ethanol, saturated with hydrogen chloride, to 100 mg. of III at room temperature yielded a clear solution. After being left for 10 min., the solvent was removed and the crystals that were obtained were recrystallized from ethanol to give colorless prisms (V), m. p. 173~174°C.

Found: C, 76.25; H, 6.98; Calcd. for $C_{24}H_{25}O_3 \cdot N$: C, 76.77; H, 6.71%.

**2-Phenyltropone-7-carboxylic Acid (VIa).**—A mixture of 1.7 g. of IIa and 17 cc. of 75% sulfuric acid was heated at 140~150°C for one hour and the mixture was poured onto ice. The crystals that separated out were recrystallized from ethanol to give yellow plates, m. p. 107~108°C. Yield, 1.6 g.

Found: C, 74.18; H, 4.47. Calcd. for $C_{14}H_{10}O_3$: C, 74.33; H, 4.46%.

*Methyl Ester (VIIIa).*—Obtained by the reaction of VIa and ethereal diazomethane. Recrystallization from methanol gave yellow needles, m. p. 99~100°C.

Found: C, 74.88; H, 4.87. Calcd. for $C_{15}H_{12}O_3$: C, 74.99, H, 5.03%.

*p-Toluidide.*—Obtained by the usual method. Recrystallization from ethanol gave orange-yellow crystals, m. p. 121~122°C.

Found: N, 4.56. Calcd. for $C_{21}H_{17}O_2N$: N, 4.44%.

**2-α-Naphthyltropone-7-carboxylic Acid (VIb).**—Obtained by heating a mixture of 100 mg. of IIb, 1 cc. of 50% sulfuric acid and 1 cc. of glacial acetic acid at 150~160°C for one hour. Recrystallization from ethanol gave orange yellow prisms, m. p. 139~140°C. Yield, 80 mg.

Found: C, 78.01; H, 4.51. Calcd. for $C_{18}H_{12}O_3$: C, 78.25; H, 4.38%.

*Methyl Ester (VIIIb).*—Yellow prisms of m. p. 105~106°C.

Found: C, 78.17; H, 4.72. Calcd. for $C_{19}H_{14}O_3$: C, 78.60; H, 4.85%.

**2-β-Naphthyltropone-7-carboxylic Acid (VIc).**—Obtained as in the case of VIb. Recrystallization from *n*-butanol gave reddish orange microcrystals, m. p. 189~190°C.

Found: C, 78.17; H, 4.38. Calcd. for $C_{18}H_{12}O_3$: C, 78.25; H, 4.38%.

*Methyl Ester.*—Yellow plates, m. p. 81~82°C.

Found: C, 78.53; H, 5.07. Calcd. for $C_{19}H_{14}O_3$: C, 78.60; H, 4.85%.

**2-Methyltropone-7-carboxylic Acid (VId).**—Obtained as in the case of VIa. Recrystallization from ethanol gave colorless plates, m. p. 146~147°C.

Found: C, 65.75; H, 4.72. Calcd. for $C_9H_8O_3$: C, 65.85; H, 4.91%.

**2-Benzyltropone-7-carboxylic Acid (VIe).**—Obtained as in the case of VIa. Pale yellow needles of m. p. 128~129°C.

Found: C, 74.76; H, 4.75. Calcd. for $C_{15}H_{12}O_3$: C, 74.99; H, 5.03%.

**Methyl 2-Phenyltropone-7-carboximidate (VIIa).**—A mixture of 100 mg. of IIa and 2 cc. of absolute methanol was saturated with dry hydrogen chloride under ice-chilling, and the resulting clear red solution was left overnight at 0°C. Benzene and water were added successively to the solution, and the aqueous layer was neutralized cautiously with cold dilute aqueous solution of sodium carbonate. The crystals that separated out were collected by filtration, yield 70 mg. Recrystallization from ether gave pale yellow needles (VIIa) m. p. 85~86°C.

Found: N, 6.04. Calcd. for $C_{15}H_{13}O_2N$: N, 5.85%.

*Picrate.*—Reddish orange prisms, m. p. 141~142°C.

Found: N, 12.03. Calcd. for $C_{21}H_{16}O_9N_4$: N, 11.96%.

**Acid Hydrolysis of VIIa.**—A solution of 30 mg. of VIIa in 2 N hydrochloric acid was warmed on a water bath for 10 min. and cooled. The crystals that separated out were collected by filtration and recrystallized from methanol to give yellow crystals, m. p. 98~100°C. These crystals showed no depression of melting point on admixture with VIIIa.

**Methyl 2-α-Naphthyltropone-7-carboximidate (VIIb).**—Similar treatment of IIb as in the case of IIa provided VIIb as an oil which could not be solidified. This oil was subjected to acid hydrolysis with 2 N hydrochloric acid by which yellow crystals, m. p. 105~106°C were obtained. These crystals showed no depression of melting point on admixture with VIIIb.

**Decarboxylation of 2-Phenyltropone-7-carboxylic Acid (VIa).**—A solution of 50 mg. of VIa in 0.5 cc. of acetic anhydride was heated to reflux for 1.5 hr., shaken with water to decompose the acetic anhydride and extracted with benzene. The benzene extract was washed with 2 N sodium carbonate and water, dried and the solvent was evaporated. The pale yellow crystals (IXa) m. p. 82~83°C thereby obtained showed no depression of melting point on admixture with 2-phenyltropone.

**Decarboxylation of 2-α-Naphthyltropone-7-carboxylic Acid (VIb).**—Treatment of VIb similar to that in the case of VIa yielded pale yellow crystals m. p. 110°C which showed no depression of melting point on admixture with an authentic sample of 2-α-naphthyltropone (IXb).

**Decarboxylation of 2-β-Naphtyltropone-7-carboxylic Acid (VIc).**—Treatment of VIc similar to that in the case of VIa yielded pale yellow crystals of m. p. 132~134°C, undepressed on admixture with an authentic sample of 2-β-naphthyltropone (IXc).

**Bromination of VIa.**—a) To a solution of 50 mg. of VIa in 0.5 cc. of acetic acid was added 70 mg. of bromine. After standing for 5 hr. the whole was heated for 10 min. on a water bath, diluted with water and extracted with benzene. The benzene extract was washed with dilute sodium carbonate solution and the aqueous layer was acidified with dilute hydrochloric acid by which 30 mg. of 5-bromo-2-phenyltropone-7-carboxylic acid (X) was obtained as yellow needles. Recrystallization from ethanol raised the melting point to 174~175°C (decomp.).

Found: C, 55.10; H, 3.11. Calcd. for $C_{14}H_9O_3Br$: C, 55.11; H, 2.96%.

The benzene layer was washed with water, dried and the solvent was evaporated. Residual oil provided some crystals on standing which were recrystallized from cyclohexane to give pale yellow plates (XI), m. p. 78~80°C. These crystals showed no depression of melting point on admixture with 7-bromo-2-phenyltropone.

b) Similar treatment of 50 mg. of VIa with 70 mg. of bromine, except when heating was prolonged to one hour, afforded 20 mg. of X and several milligrams of pale yellow needles (XII) m. p. 131~132°C, which showed no depression of melting point on admixture with 5, 7-dibromo-2-phenyltropone.

**Decarboxylation of X.**—Acid (X), when heated to its melting point and subsequently sublimed under reduced pressure, was easily decarboxylated to give 5-bromo-2-phenyltropone (XIII). Recrystallization from ethanol gave pale yellow needles, m. p. 130~131°C.

Found: C, 59.34; H, 3.17. Calcd. for $C_{13}H_9OBr$: C, 59.79; H, 3.47%.

**Bromination of X.**—To a solution of 40 mg. of X in acetic acid was added 40 mg. of bromine and the mixture, after standing for one hour, was heated on a water bath for one hour, diluted with water and extracted with benzene. The benzene extract was washed successively with water, 2 N sodium carbonate and water, and the solvent was removed. The crystals thereby obtained were recrystallized from ethanol to give yellow needles (XII), m. p. 130~131°C, with undepressed melting point on admixture with 5, 7-dibromo-2-phenyltropone (XII).

**Bromination of XIII.**—To a solution of 30 mg. of XIII dissolved in 0.5 cc. of acetic acid was added 50 mg. of bromine and the mixture was allowed to stand for two days. The mixture was then diluted with water, extracted with benzene and the benzene solution was washed successively with water, 2 N sodium carbonate and water. The residual oil, obtained upon removal of the solvent, was heated on a water bath for 30 min. and cooled. The crystals thereby obtained were repeatedly recrystallized from ethanol to give yellow crystals (XII) m. p. 127~130°C, with undepressed melting point on admixture with 5, 7-dibromo-2-phenyltropone.

**Reaction of VIa and Alkali.**—A solution of 100 mg. of VIa dissolved in 1 cc. of 1 N sodium hydroxide was heated on a water bath for an hour, treated with active charcoal and then acidified with 2 N hydrochloric acid by which 80 mg. of 1-phenylcyclohexadiene-1, 2-dicarboxylic acid (XIVa) was obtained. Recrystallization from dilute ethanol gave colorless prisms, m. p. 216~217°C (decomp.).

Found: C, 68.60; H, 4.96. Calcd. for $C_{14}H_{12}O_4$: C, 68.84; H, 4.95%. Neutral equivalent as a dibasic acid, 122; Found. 126.

These crystals gradually reduced Fehling's solution and the ammonical silver nitrate solution.

*Dimethyl Ester (XIVb).*—Obtained by the reaction of XIVa and ethereal diazomethane. Recrystallization from methanol gave colorless prisms, m. p. 95~96°C.

Found: C, 70.41; H, 5.64. Calcd. for $C_{16}H_{16}O_4$; C, 70.57; H, 5.92%.

**Oxidation of XIVa.**—A solution of 50 mg. of XIVa dissolved in 1.5 cc. of alkaline-ammoniacal silver nitrate solution (prepared by dissolving 0.3 g. of silver nitrate in 3 cc. each of concentrated aqueous ammonia and 10% sodium hydroxide solution) was heated on a water bath for 30 min. After removal of the precipitate that formed, the filtrate was acidified and the crystals that separated out were collected by filtration. Recrystallization from dilute ethanol gave colorless prisms (XV), m. p. 108~109°C. Treatment of XV with concentrated sulfuric acid at room temperature yielded crystals (XVI), m. p. 80~82°C. XV and XVI were identified as *o*-biphenylcarboxylic acid and fluorenone, respectively, by the mixture melting point determination.

**Action of Concentrated Sulfuric Acid on XIVa.**—Addition of 0.3 cc. of concentrated sulfuric acid to 30 mg. of XIVa at room temperature resulted in deep reddish purple solution under evolution of gas. After being warmed slightly on a water bath, the reaction mixture was poured onto crushed ice. The crystals that separated out were collected by filtration and recrystallized from dilute ethanol to give yellow prisms (XVI), m. p. 80~82°C, with undepressed melting point on admixture with fluorenone.

**Catalytic Reduction of XIVa.**—a) A solution of 250 mg. of XIVa dissolved in 10 cc. of methanol was catalytically reduced at ordinary temperature and pressure, with the addition of 30 mg. of Adam's catalyst. Absorption of hydrogen was 35 cc. After removal of the catalyst by filtration, methanol was removed, and the crystalline residue was recrystallized from methanol to give colorless needles (XVIIa) of m. p. 223~224°C (decomp.). Yield, 100 mg.

Found: C, 67.77; H, 5.53. Calcd. for $C_{14}H_{14}O_4$; C, 68.28; H, 5.73%.

*Dimethyl Ester (XVIIb).*—Colorless needles, m. p. 81~82°C.

Found: C, 69.68; H, 6.25. Calcd. for $C_{16}H_{18}O_4$: C, 70.05; H, 6.61%.

*Anhydride (XVIII).*—Acid (XVIIa) was heated above its melting point for one minute and cooled. The crystalline mass was recrystallized from methanol to give colorless needles of m. p. 125~127°C.

Found: C, 72.71; H, 5.17. Calcd. for $C_{14}H_{12}O_3$: C, 73.67; H, 5.30%.

b) A solution of 150 mg. of XIVa dissolved in 5 cc. of methanol was catalytically reduced at ordinary temperature and pressure, with the addition of 100 mg. of palladium-charcoal (5%). The absorption of hydrogen was about 30 cc. After removal of the catalyst by filtration, methanol was removed, and the crystalline residue was washed with a small amount of ether. These crystals of m. p. 160~170°C were, without further purification, converted to their dimethyl ester (XIX) by the action of ethereal diazomethane. Recrystallization from methanol gave colorless prisms, m. p. 77~78°C. These crystals showed depression of the melting point on admixture with XVIIb.

Found: C, 69.88; H, 7.13. Calcd. for $C_{16}H_{20}O_4$: C, 69.54; H, 7.30%.

**Reaction of 2-α-Naphthyltropone-7-carboxylic Acid (VIb) and Alkali.**—Similar treatment of VIb as in the case of VIa gave 1-α-naphthylcyclohexadiene-1, 2-dicarboxylic acid (XX) as colorless prisms, m. p. 237~238°C (decomp.).

Found: C, 73.68; H, 5.00. Calcd. for $C_{18}H_{14}O_4$: C, 73.46; H, 4.80%.

**Action of Sulfuric Acid on XX.**—Similar treatment of XX with concentrated sulfuric acid as in the case of XIVa gave yellow needles (XXI), m. p. 169~170°C, with undepressed melting point on admixture with benzanthrone.

**Reaction of 5-Bromo-2-phenyltropone-7-carboxylic Acid (X) and Alkali.**—A solution of 20 mg. of X dissolved in 0.4 cc. of 1 N sodium hydroxide was heated for one hour on a water bath and acidified with dilute hydrochloric acid. The crystals thereby obtained were collected by filtration and recrystallized from ethanol to give colorless crystals (XV), m. p. 105~108°C, with undepressed melting point on admixture with *o*-biphenylcarboxylic acid. By treatment with concentrated sulfuric acid, XV was converted to fluorenone (XVI) and identified by mixture melting point determination.

The author wishes to express his sincere thanks to Professor Tetsuo Nozoe of Tohoku University for his guidance and encouragement throughout this work, as well as to Professor Shuichi Seto, Professor Yoshio Kitahara and Assistant Professor Toshio Mukai of Tohoku University for their kind advice and suggestions. He is also grateful to Mrs. Kuniko Kodaira for the measurements of ultraviolet absorption spectra and to Mr. Shinichi Ohyama and Miss Ayako Iwanaga for the elemental analyses.

*Department of Chemistry*
*Faculty of Liberal Arts and Science*
*Yamagata University*
*Yamagata*

# *Infrared and Raman Spectra of Dialkoxymethanes in Various Phases and the Assignment of Spectra of Methoxyethoxymethane*

By Kenkichi NUKADA

(Received March 23, 1961)

The study of internal rotation around the C–C bond has been carried out in great detail by several authors[1], but detailed discussion of that arround the C–O bond has not been carried out so far.

In this paper, the rotational isomerism of compounds containing two C–O bonds such as dialkoxymethanes ($R_1OCH_2OR_2$) is discussed from the spectroscopical point of view. Infrared spectra of vapor, liquid and solid phases and Raman spectra of liquid phase were obtained, and the possible interpretation of these results was given by referring to other available data such as dipole moment.

With the conclusion thus obtained, the assignments of vibrational frequencies of dimethoxymethane and diethoxymethane are reported in the other papers[2,3], and that of methoxyethoxymethane is presented in this paper.

## Experimental

The samples used were dimethoxymethane (DMM, $CH_3OCH_2OCH_3$), methoxyethoxymethane

1) S. Mizushima, "Structure of Molecules and Internal Rotation", Academic Press, New York (1954).

2) K. Nukada, *Spectrochim. Acta*, to be published.

3) K. Nukada, This Bulletin, to be published.

(MEM, $CH_3OCH_2OC_2H_5$), diethoxymethane (DEM, $C_2H_5OCH_2OC_2H_5$) and diisopropoxymethane (DPM, $(CH_3)_2CHOCH_2OCH(CH_3)_2$). All the compounds were synthesized in our laboratory and their purity was checked by gas chromatography[4,5].

Infrared spectra of vapor and liquid phases were obtained by means of Perkin Elmer 21 spectrophotometer and those of solid phase were obtained by means of Perkin Elmer 12C spectrophotometer, both equipped with a sodium chloride prism. Infrared spectra at an elevated temperature were obtained with a gas celll designed and constructed by Mr. H. Tomita of our laboratory[6]. Because dialkoxymethanes are rapidly decomposed at high temperature by oxygen in air, care should be taken to remove oxygen as completely as possible from a gas cell in a high temperature experiment. Solid infrared spectra were obtained with a low temperature cell designed by us[7].

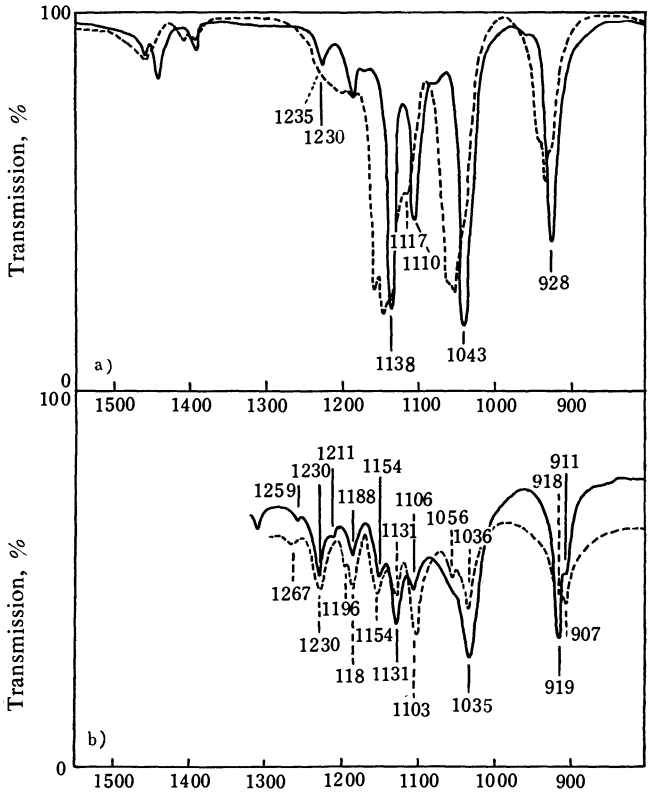
Raman spectra were taken by means of Cary 81 spectrophotometer. The degree of depolarization was measured by wrapping two types of polaroids around a Raman tube.

## Results and Discussion

**Infrared Spectra of Dimethoxymethane in Various Phases.** — The spectra of vapor and liquid phases are shown in Fig. 1a.

The intensity of vapor bands at 1235 and 1110 $cm^{-1}$ shows an appreciable decrease as compared with that of liquid bands. Of these, the liquid band at 1110 $cm^{-1}$ is known as a branch of "methylal's doublet", and it is a remarkable fact that in vapor phase a branch of the doublet turns to be a shoulder. As will be described in the following section and in the other paper[8], in other dialkoxymethanes and in ethylidene dialkyl ethers ($R_1OCH(CH_3)OR$) the smae behavior of spectra were also observed.

The low temperature infrared spectra are shown in Fig. 1b. It was found that two types of spectra are obtained at low temperature below melting point. It is dependent upon




Wave number, $cm^{-1}$

Fig. 1. Infrared spectra of dimethoxymethane ($CH_3OCH_2OCH_3$).

a) Solid line, $CCl_4$ solution, cell thickness: 0.15 mm., 1.5%. Dashed line, vapor
b) Solid line, Type A spectrum of solid phase. Dashed line, Type B spectrum of solid phase

4) K. Nukada, *Reports Govn. Chem. Ind. Research Inst. Tokyo*, **55**, 92 (1960).
5) K. Nukada, ibid., to be published.
6) H. Tomita, unpublished.
7) K. Nukada, *J. Chem. Soc. Japan, Pure Chem. Sec.* (*Nippon Kagaku Zasshi*), **80**, 218 (1959).
8) K. Nukada, This Bulletin, to be published.

the critical condition of freezing the material. An example of freezing procedure is as follows: After cooling gradually, spectrum A (solid line in Fig. 1b) was obtained at −150°C, then after once melting and cooling again, spectrum B (dashed line in Fig. 1b) was obtained at −134°C. The last procedure was repeated and spectrum B was obtained again. After once melting and cooling again, spectrum A was obtained at −135°C. Lastly, on raising the temperature, spectrum B was obtained at −110°C. It is not clear at present that the difference of these spectra is due either to the difference of crystallized states between two types of solid phase, or is due to the fact that one of them is in a super-cooled state. Spectrum A is more similar to that of the solution except for the band at 1230 $cm^{-1}$, the relative intensity of which is greater than that of liquid phase spectrum, and for new bands at 1259, 1211, 1051 and 911 $cm^{-1}$, appearing as shoulders. Spectrum B is, on the other hand, quite different from that of the solution, that is, the intensity ratio of the band at 1131 $cm^{-1}$ to one at 1103 $cm^{-1}$ changes appreciably.

From these results the following assumption seems to be possible. In DMM, two rotational isomers exist, namely $\alpha$ and $\beta$ forms. The bands at 1138, 1043 and 928 $cm^{-1}$ are due to vibrations belonging to the $\alpha$ form, and the bands at 1230 and 1110 $cm^{-1}$ are due to vibrations belonging to the $\beta$ form. If this assumption is true, both forms are mixed moderately in liquid phase and the $\alpha$ form exists predominatingly in vapor phase. In solid phase, both forms are still mixed but the abundance ratio of the two forms changes as compared with that in the case of the liquid phase, that is, the $\beta$ form is more predominant. The possible forms may be gauche-gauche form (or less polar form), two methyl groups of which rotate about 120° from the central OCO plane in an anticlockwise sence, and trans-trans form (or more polar form), the COCOC skeleton of which is planar.

If this assumption is ture,

1) The dipole moment of vapor and liquid phase should be considerably different at room temperature,

2) Some solvent effect is expected since the dipole moments of two isomers are considerably different, and

3) The appearance of the vapor spectrum should change to some extent with increasing temperature.

In the following description, the above-mentioned assumption is examined by checking these three items in detail.

1) In his prewar paper, Kubo illustrated the diagram showing the correlation between dipole moment and azimuthal angles of rotation of methyl groups in DMM[9]. From this diagram together with the observed value of dipole moment, Kubo has concluded that in the vapor phase DMM has one stable configuration, in which two methyl groups rotate to the opposite sides of central OCO plane (gauche-gauche form). Recently, Uchida et al. measured the dipole moment of DMM in liquid phase at 25°C (0.67D) and found that it is in good agreement with the value of vapor extrapolated to 25°C (0.69D)[10]. Uchida et al. has concluded that DMM is a mixture of rotational isomers, most of which is helical or almost helical in structure (gauche-gauche form). These results lead to a definite conclusion that at least at room temperature, the abundance ratio of isomers are, if they exist, almost equal in vapor and liquid phases.

Therefore, the cause of appreciable change between infrared spectra of vapor and condensed phases is not due to the change of abundance ratio of isomers between two phases, but due to some other kind of effect such as the change of intermolecular interaction between two phases.

2) In Fig. 2, the infrared spectrum of acetonitrile solution of DMM is shown. As acetonitrile is a very polar solvent (dielectric constant of which is 38), there must be some systematic change of spectra between acetonitrile solution and non-polar solvent solution, if the rotational isomerism actually exists in solution. From Fig. 2, the ratio of absorbance of the band at 1140 $cm^{-1}$ to that of the band at 1111 $cm^{-1}$ ($K_{1140}/K_{1111}$) is calculated to be 0.374.

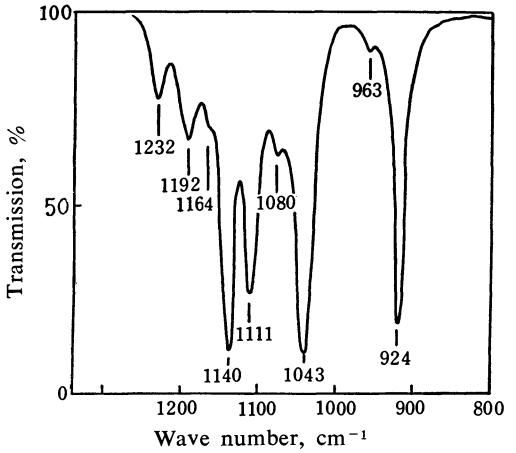



Fig. 2. Infrared spectrum of dimethoxymethane ($CH_3OCH_2OCH_3$). Acetonitrile solution, cell thickness: 0.015 mm., 20%.

9) M. Kubo, *Sci. Papers Inst. Phys. Chem. Research*, **29**, 179 (1936).

10) J. Uchida, Y. Kurita and M. Kubo, *J. Polymer Sci.*, **19**, 365 (1956).

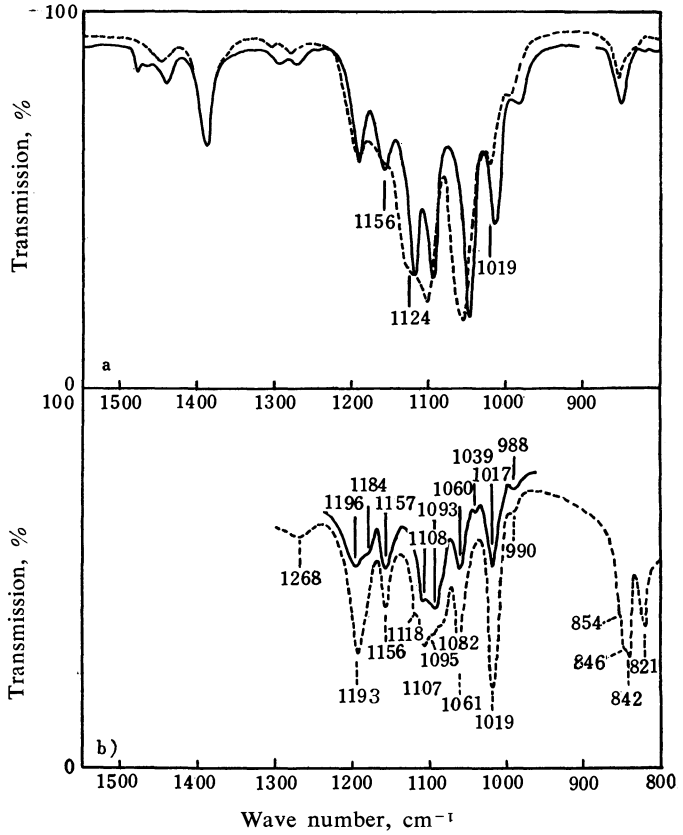



Fig. 3. Infrared spectra of diethoxymethane ($C_2H_5OCH_2OC_2H_5$).

a) Solid line, $CCl_4$ and $CS_2$ solutions, cell thickness: 0.15 mm., 2%. Dashed line, vapor.
b) Solid phase spectra, solid line, cell thickness: 0.015 mm. Dashed line, cell thickness: 0.05 mm.

The ratio is also calculated to be 0.331 in the case of carbon tetrachloride solution. Though it is impossible to obtain such a ratio in the case of vapor (Fig. 1a), it is clear that is has a very high value. Hence if these two bands belong to another type of rotational isomers, a more polar form must be predominant in the vapor phase, but this is inconsistent with the measurement of dipole moment[9]. From these considerations, it is reasonable to assume that these two bands belong to the same type of isomers.

3) Vapor spectra of DMM were taken at the temperature range between 24 and 100°C. No change in the appearance of the spectra was observed. The dipole moment of the vapor varies with the temperature as mentioned by Uchida et al., and they have explained this as the change of abundance ratio between isomers with temperature variation[10]. The present observation seems to be inconsistent with the conclusion of them. The most reasonable interpretation to make a compromise between the results of infrared spectra and those of dipole moment is as follows. This molecule has one form (gauche-gauche form) below 100°C, both in the vapor and liquid phases. The variation of dipole moment with temperature is due to the increase of amplitude of torsional oscillation, while the change of appearance of spectra among three phases is due to the change of intermolecular interaction.

As will be described in detail in the other papers[2,3], the change of band intensity among different phases is sometimes a useful measure in assigning spectra. One example is as follows. If an infrared band is strong in the liquid phase but weak in the vapor phase and the corresponding Raman band is strong and polarized, this band is safely assigned to a totally symmetrical vibration. The change of band intensity between vapor and liquid phases is also observed in the case of DMM-$d_2$ ($CH_3 \cdot OCD_2OCH_3$), DMM-$d_6$ ($CD_3OCH_2OCD_3$), DMM-$d_8$ ($CD_3OCD_2OCD_3$), DEM and DEM-$d_2$ ($C_2H_5OCD_2OC_2H_5$). The author has found that in all cases the above-mentioned rule can be used in the assignment of spectra.

**Infrared and Raman Spectra of Diethoxymethane in Various Phases.** — Since DEM has four internal rotational axes, a possible number of rotational isomers may be larger than that of DMM. But from the spectroscopical point of view, isomers concerning C–ethoxy axes are important and those concerning C–C axes are less important.

In Fig. 3a, infrared spectra of vapor and liquid phases of DEM are shown. As in the case of DMM, the appearance of spectra is rather different between two phases, that is, the intensity of vapor bands at 1156, 1124 and 1019 $cm^{-1}$ shows an appreciable decrease as compared with those of liquid phase spectra.

Solid infrared spectra of DEM are shown in Fig. 3b. Just as in the case of DMM, two types of spectra, namely A and B, are observed according to the slight change of the critical condition of freezing the material. In the type A spectrum, the intensity of the bands at 1193, 1019, 842 and 821 $cm^{-1}$ shows an appreciable increase and that of the band at 1095 $cm^{-1}$ shows a decrease as compared with those of carbon tetrachloride solution. The appearance of the type B spectrum is similar to that of the carbon tetrachloride solution, except for the doublet at 1100 $cm^{-1}$.

In Fig. 4, the infrared spectrum of acetonitrile solution is shown. There exists no difference between the spectra of carbon tetrachloride and of acetonitrile solutions.

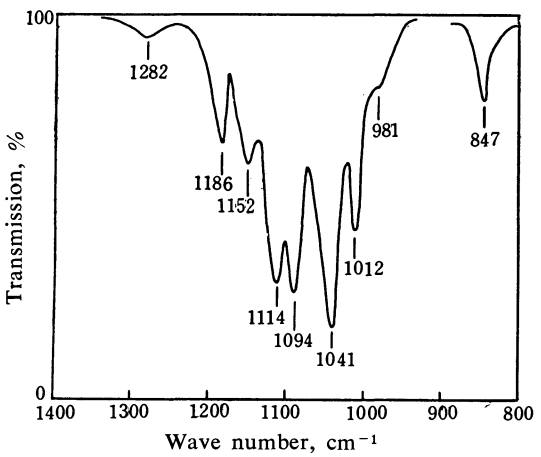



Fig. 4. Infrared spectrum of diethoxymethane ($C_2H_5OCH_2OC_2H_5$). Acetonitrile solution.

In Fig. 5, Raman spectra of carbon tetrachloride and acetonitrile solutions of DEM are shown. The intensity of the band at 1047 $cm^{-1}$ increases and that at 1187 $cm^{-1}$ decreases in acetonitrile solution. There is, however, no other experimental evidence that the former band belongs to the more polar form and the

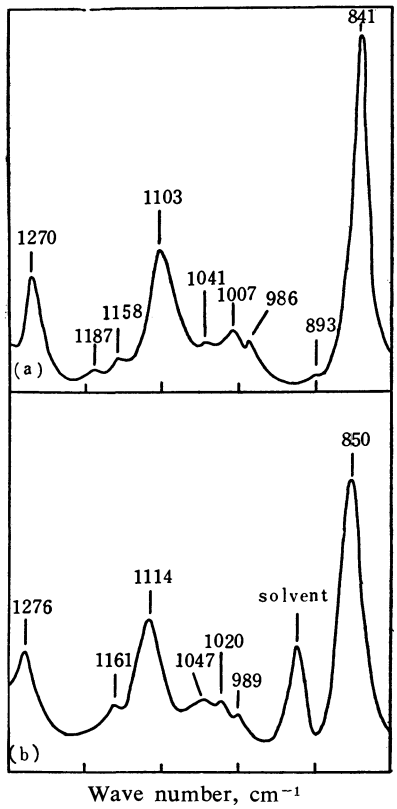



Fig. 5. Raman spectra of diethoxymethane ($C_2H_5OCH_2OC_2H_5$).

a) Pure liquid.
b) Acetonitrile solution (60%).

latter to the less polar form, hence the intensity change is probably due to simple solvent effect, that is, is due to the difference of intermolecular interaction between two kinds of solutions.

Vapor spectra of DEM were taken at the temperature range between 24 and 100°C. As no change was observed in the appearance of spectra within the temperature range, DEM has almost one and the same form in vapor phase below 100°C.

According to the measurement of Kubo, dipole moment of DEM is, in vapor phase, 1.22D at 56°C and slightly increases with rising temperature (1.26D at 203°C). Kubo has concluded that this molecule has one stationary form in vapor and that the difference of dipole moment between DMM and DEM (0.5D) is due to the difference of azimuthal angles of alkyl groups from the central OCO plane[11]. Since there is no dipole measurement on liquid phase the molecular structure of DEM of liquid phase is not clear, but from the analogy

11) M. Kubo, *Sci. Papers Inst. Phys. Chem. Research*, **30**, 169 (1936).

with DMM one could assume that the molecular form is the same both in vapor and liquid phases (nearly gauche-gauche form, but that the azimuthal angles of ethyl groups from central OCO plane are smaller than those of methyl groups in DMM), and that the change of appearance of spectra among different phases is dependent on the difference of intermolecular interaction. The detail of assignment will be reported elsewhere[3].

**Infrared Spectra of Methoxyethoxymethane in Various Phases.**—In Figs. 6 and 7, infrared spectra of vapor, liquid and solid phases of MEM are shown.

The vapor bands at 1131 and 926 $cm^{-1}$ become weaker as compared with the liquid bands, and the doublet at 1112 $cm^{-1}$ (and 1096 $cm^{-1}$) in the liquid phase is distorted in the vapor phase,that is, it becomes singlet in the vapor phase. The solid bands at 1218 $cm^{-1}$ and 1013 $cm^{-1}$ become much stronger and one at 1135 $cm^{-1}$ becomes weaker as compared with the liquid bands.

It is quite hard, as in the case of DMM and DEM, to interpret such a complicated change of spectra among various phases as the change of abundance ratio of the rotational isomers. It is better to assume that from the analogy of

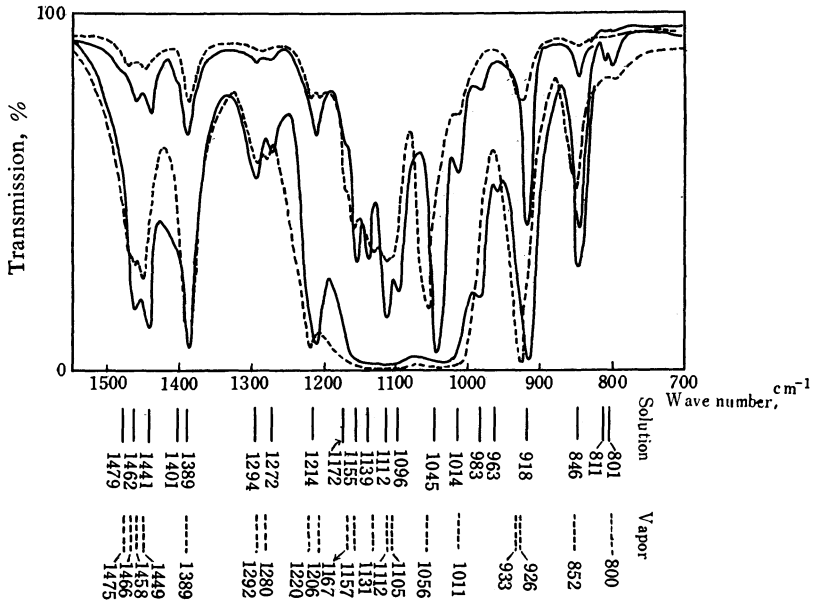



Fig. 6. Infrared spectra of methoxyethoxymethane ($CH_3OCH_2OC_2H_5$).
Solid line, $CCl_4$ and $CS_2$ solutions, cell thickness: 0.15 mm., 20% and 2%. Dashed line, vapor.

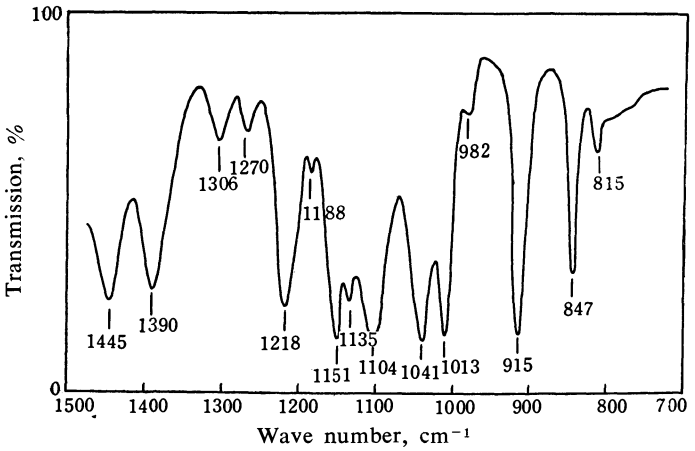



Fig. 7. Infrared spectrum of methoxyethoxymethane ($CH_3OCH_2OC_2H_5$).
Solid, cell thickness: 0.015 mm.

DMM, MEM has also one form in the liquid and vapor phases at least near room temperature. If the dipole moment of the vapor and liquid phases are observed, one can establish the validity of the above-mentioned assumtion.

**Assignment of Infrared and Raman Spectra of Methoxyethoxymethane.** — In this section the assignment of the infrared and Raman spectra (Fig. 8) of MEM is given by assuming that this molecule has only one form in its vapor and liquid phases.

The assignment of bands at 3000 $cm^{-1}$ has

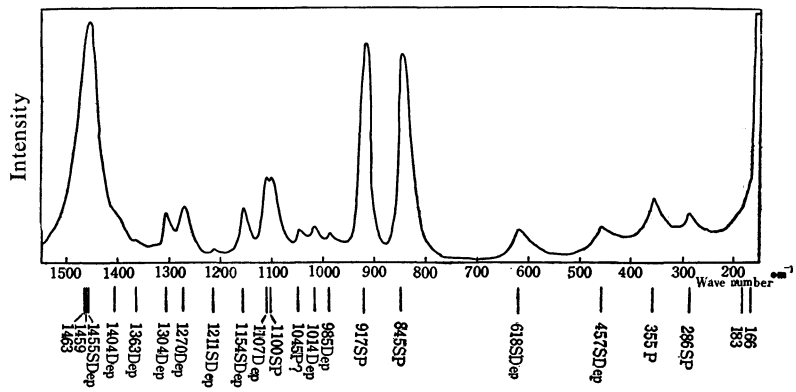



Fig. 8. Raman spectrum of methoxy ethoxy methane ($CH_3OCH_2OC_2H_5$).

TABLE I. VIBRATIONAL FREQUENCIES OF METHOXYETHOXYMETHANE

| Infrared | | Raman | Assignment |
|---|---|---|---|
| Vapor | Liq. | | |
| 1475 (vw) | 1479 (w) | | $CH_2$ scissoring (MeO and EtO) |
| 1466 } (m) 1458 } | 1462 (m) | 1463 (m, sh) | sym. $CH_3$ deformation (MeO) |
| | | 1459 (m, sh) | |
| 1449 (m) | 1441 (m) | 1455 ( s ) S. Dep. | asym. $CH_3$ deformation (MeO and and EtO) |
| | 1401 (w) | | |
| 1389 (m) | 1389 (m) | 1404 (w) Dep. | sym. $CH_3$ deformation (EtO) |
| | | 1363 (w) Dep. | $CH_2$ wagging ($OCH_2O$) ? |
| 1292 (vw) | 1294 (w) | 1304 (m) S. Dep. } | $CH_2$ rocking (EtO) |
| 1280 (w) | 1272 (w) | 1270 (m) S. Dep. } | $CH_2$ twisting ($OCH_2O$ and EtO) |
| 1220 } (w) 1206 } | 1214 (m) | 1211 (w) S. Dep. | $CH_3$ rocking (MeO) |
| 1167 (w) | 1172 (w) | | |
| 1157 (m) | 1155 ( s ) | 1154 (m) S. Dep. | |
| 1131 (sb) | 1139 ( s ) | | asym. COCOC stretching |
| 1112 } ( s ) 1105 } | 1112 ( s ) | 1107 ( s ) Dep. ? | CC stretching |
| 1011 (w) | 1014 (m) | 1014 (w) Dep. | $CH_2$ rocking (EtO) |
| | 983 (w) | 985 (w) Dep. | $CH_3$ rocking (EtO) |
| | 963 (vw) | | |
| | 1096 ( s ) | 1100 ( s ) S. P. | sym. COCOC stretching |
| 1056 ( s ) | 1045 ( s ) | 1045 (w) P. ? | asym. COCOC stretching |
| 933 } (m) 926 } | 918 ( s ) | 917 ( s ) S. P. | $CH_3$ rocking (MeO) |
| 852 (w) | 846 (m) | 845 ( s ) S. P. | sym. COCOC stretching |
| | 811 (w) | | |
| 800 (vw) | 801 (w) | | |
| | | 618 (m) S. Dep. | asym. COCOC deformation |
| | | 457 (m) S. Dep. | sym. COCOC deformation |
| | | 355 (m) P. | sym. COCOC deformation |
| | | 286 (m) S. P. | CCO deformation |
| | | 183 (sh) } 166 (sh) } | torsional vibration ? |

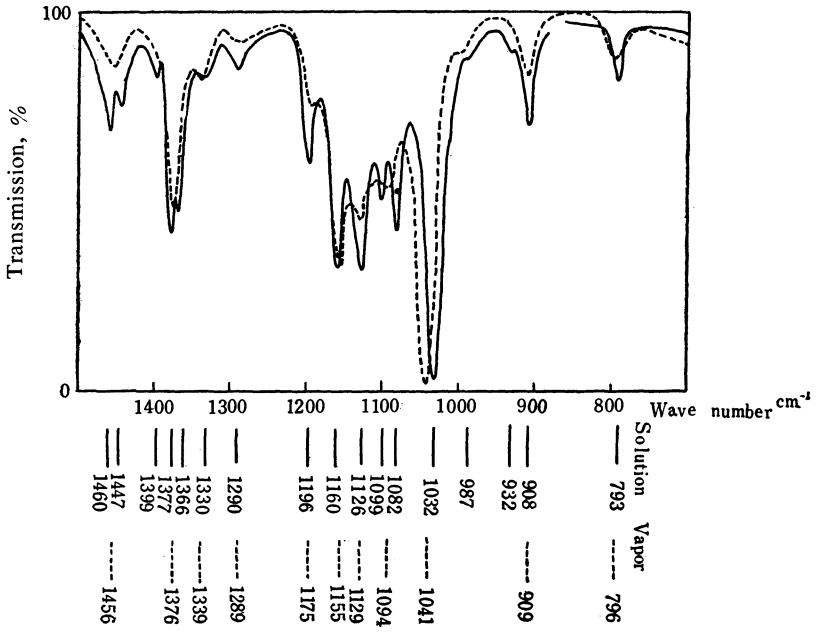



Fig. 9. Infrared spectra of diisopropoxymethane ($(CH_3)_2CHOCH_2OCH(CH_3)_2$).
Solid line, $CCl_4$ and $CS_2$ solutions, cell thickness: 0.15 mm., 2%. Dashed line, vapor.

already been given by the same author[12].

The appearance of infrared spectra between 1500 and 1250 $cm^{-1}$ is quite similar to that of DEM and DEM-$d_2$, except for the lack of a very weak band a 1360 $cm^{-1}$. It means that the absorbance of bands in the ethoxyl group is greater than that of the methoxyl group. The appearance of Raman bands is, on the other hand, slightly different from that of DEM and DEM-$d_2$, that is, the intensity of the band at 1404 $cm^{-1}$ decreases and that at 1304 $cm^{-1}$ increases.

As the interaction between methoxyl and ethoxyl groups may be weak, the spectra of MEM within this region may be reasonably explained by assuming the simple superimposition of spectra, of methoxyl and ethoxyl compounds as shown in Table I.

A medium infrared band at 1214 $cm^{-1}$ (having a corresponding weak Raman band) is assigned to the methyl rocking of methoxyl group. This is consistent with the fact that at this frequency many compounds containing methoxyl group have a medium infrared band and that the homologues of these compounds having no methoxyl group have no infrared band[2,3,13,14].

Spectra between 1150 and 800 $cm^{-1}$ are very complicated not only in this molecule but in many other molecules containing oxygen atoms such as ethers, other dialkoxymethanes, ethyldene alkyl ethers, 2,2-dialkoxypropane and orthoaliphatic acid esters. The skeletal COCOC stretching should clearly exist within this region. As shown in the discussion of DMM and its deuterated compounds[2], DEM and DEM-$d_2$[3] and dimethyl ether and dimethyl ether-$d_6$[15,16], skeletal stretchings are mixed with CH deformation vibrations to some extent, and from inspection without exact calculation it is quite hard to give a rigorous assignment. Nevertheless, some bands could be assigned reasonably from the strong similarity of spectra among homologues.

The strong liquid infrared band at 1096 $cm^{-1}$ (having no vapor infrared band and a strong and strongly polarized Raman band) is assigned to the symmetrical COCOC stretching. In DMM and DEM, liquid infrared bands around 1100 $cm^{-1}$ have a corresponding very weak vapor infrared band and a medium or strong and strongly polarized Raman band. They have been assigned to the symmetrical COCOC stretching in good agreement with the present assignment.

The strongest infrared band at 1045 $cm^{-1}$ (having a corresponding weak Raman band) is assigned to the asymmetrical COCOC stretching by the analogy with DMM.

Two very strong and strongly polarized

12) K. Nukada, *J. Chem. Soc. Japan, Pure Chem. Sec.* (*Nippon Kagaku Zasshi*), **80**, 976 (1959).
13) K. Nukada, ibid., **80**, 1112 (1959).
14) K. Nukada, ibid., **81**, 1028 (1960).
15) Y. Kanazawa and K. Nukada, This Bulletin, to be published.
16) Y. Kanazawa and S. Saeki, ibid., to be published.

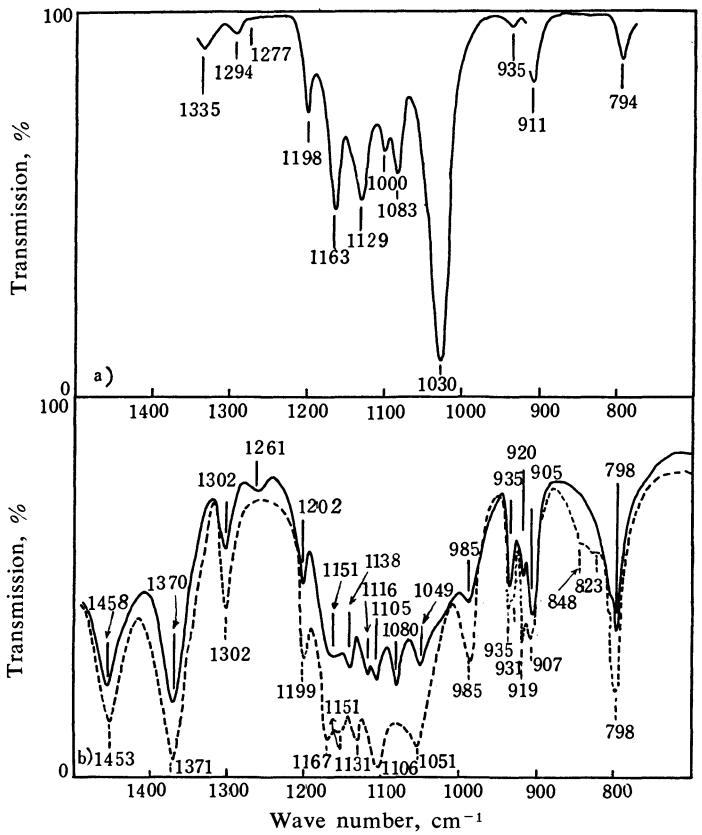



Fig. 10. Infrared spectra of diisopropoxymethane $(CH_3)_2CHOCH_2OCH(CH_3)_2$.

a) Acetonitrile solution, cell thickness: 0.015 mm., 20%

b) Solid, solid line, cell thickness: 0.015 mm. Dashed line, cell thickness: 0.05 mm.

Raman bands at 917 and 845 $cm^{-1}$ (having corresponding strong and weak infrared bands, respectively) are assigned to the methyl rocking of the methoxy group and the symmetrical COCOC stretching, respectively. The basis of the assignment will be described in other papers[2,3].

The assignment of the remaining bands between 1150 and 800 $cm^{-1}$ is very difficult only from the comparison of the spectra of homologues. They may be mixtures of asymmetrical COCOC stretchings, CC stretching, methylene rocking of ethoxyl group, and methyl rocking of methoxyl and ethoxyl groups.

The bands below 700 $cm^{-1}$ are due to the skeletal deformation and torsional vibrations.

In DMM, DMM-$d_2$, DMM-$d_6$, DMM-$d_8$[2], DEM and DEM-$d_2$[3], three medium Raman bands appear at 640~560 $cm^{-1}$ (depolarized), 450~370 $cm^{-1}$ (depolarized) and at 325~295 $cm^{-1}$ (polarized). The present data of MEM are completely consistent with these results. Therefore, they could be assigned to the asymmetrical, symmetrical (central angle OCO and two terminal angles COC vibrate in the opposite phases) and symmetrical (all angles vibrate in the same phase) COCOC skeletal deformations, respectively, from the analogy with the case above mentioned. In DEM and DEM-$d_2$, an additional strongly polarized Raman band appears at 240 $cm^{-1}$. In MEM, the band at 286 $cm^{-1}$ is strongly polarized and the origin of this band is probably like that of the band at 240 $cm^{-1}$ in DEM and DEM-$d_2$, hence this band is assigned to OCC deformation as in the case of DEM and DEM-$d_2$.

Torsional vibrations are expected to exist below 250 $cm^{-1}$, and Raman bands at 183 and 166 $cm^{-1}$ may be assigned to these vibrations, although the assignment is somewhat doubtful as these bands are very weak and appear as a shoulder of very strong exciting line.

**Infrared Spectra of Diisopropoxymethane in Various Phases.**—Infrared spectra of DPM in vapor and liquid phases are shown in Fig. 9. As in the case of other dialkoxymethanes, the intensity of some bands (1175, 1129 and 1094 $cm^{-1}$) become smaller in the vapor phase.

No appreciable difference is found between the spectra of carbon tetrachloride and acetonitrile solutions (Fig. 10a).

Solid infrared bands have at least two different shapes, which are dependent on the critical condition of freezing the material, as shown in Fig. 10b.

The vapor spectra were taken at the temperature range between 24 and 106°C, but no change was observed.

The results are thus very similar to those in the case of DMM, DEM and MEM. Therefore, the same assumption as the above-mentioned one may also be held in this case. Because DPM has great bulk at the terminals (isopropyl groups) and the steric repulsion between isopropyl groups and the central methylene group is expected to be very large, this molecule may take a nearly planar zig-zag form.

## Summary

The rotational isomerism of dialkoxymethanes ($CH_3OCH_2OCH_3$, $CH_3OCH_2OC_2H_5$, $C_2H_5OCH_2OC_2H_5$ and $(CH_3)_2CHOCH_2OCH\cdot(CH_3)_2$) is discussed from the spectroscopical point of view. The experimental results are as follows.

1) The appearance of infrared spectra is appreciably different among the vapor, liquid and solid phases. Of these, the solid spectrum gives the most complicated figure.

2) No solvent effect is obtained in acetonitrile solution.

3) No change is observed in the vapor infrared spectrum between room temperature and 100°C.

It is concluded from these results and data of dipole moment that dimethoxymethane exists as one configuration in the liquid and vapor phases, the terminal methyl groups of which are rotating about 120° anticlockwise sense from the central OCO plane.

The configuration of other dialkoxymethanes are assumed to be of one form by the analogy of experimental results.

Finally, the assignment of vibrational spectra of methoxyethoxymethane is presented.

The author wishes to express his sincere thanks to Dr. Y. Mashiko for his valuable discussion.

*Government Chemical Industrial Research Institute of Tokyo*
*Shibuya-ku, Tokyo*

# *Infrared and Raman Spectra of Diethoxymethane and Diethoxymethane-$d_2$*

By Kenkichi NUKADA

(Received March 30, 1961)

In previous papers, the author has reported the characteristic vibrations of infrared spectra of dialkoxymethanes[1] and ethylidene dialkyl ethers[2], and more recently the assignment of vibrational spectra of dimethoxymethane ($CH_3OCH_2OCH_3$) and its deuterated compounds[3].

In this paper, infrared and Raman spectra of diethoxymethane (DEM, $C_2H_5OCH_2OC_2H_5$) and diethoxy methane-$d_2$ (DEM-$d_2$, $C_2H_5OCD_2 \cdot OC_2H_5$) are presented and the assignment of spectra are given by referring to the above-mentioned results[1-3].

DEM has four internal rotational axes and there is a possibility of more than two rotational isomers existing in it. The author has examined the rotational isomerism of dialkoxymethanes and concluded that dimethoxymethane, the simplest homologue of DEM, takes one form in vapor and liquid phases near room temperature. He did not obtain such a definite conclusion in the case of DEM, but from the similarity of the change of infrared spectra among various phases between dimethoxymethane and DEM, he suggested that DEM also takes one and the same form in vapor and liquid phases (two ethoxyl groups rotate about 120° in an anticlockwise sense from the central OCO plane) near room temperature[4]. In this paper, the assignment is given with the assumption mentioned above.

1) K. Nukada, *J. Chem. Soc. Japan, Pure Chem. Sec.* (*Nippon Kagaku Zasshi*), **80**, 1112 (1959).
2) K. Nukada, ibid., **80**, 976 (1959).
3) K. Nukada, *Spectrochim. Acta*, to be published.
4) K. Nukada, This Bulletin, to be published.

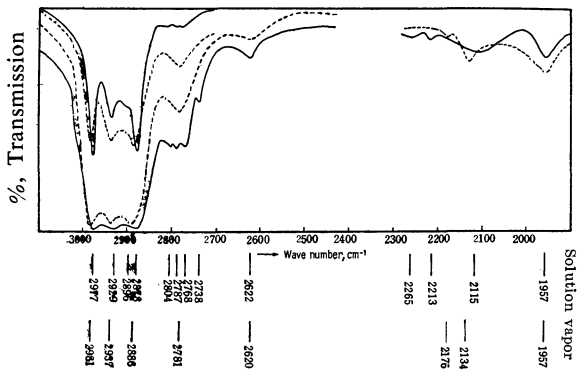



Fig. 1a. Infrared spectra of DEM (C-H and C-D stretching region).

Solid line, $CCl_4$ solution (25 and 5 vol. %, 0.15 mm.) Dashed line, vapor

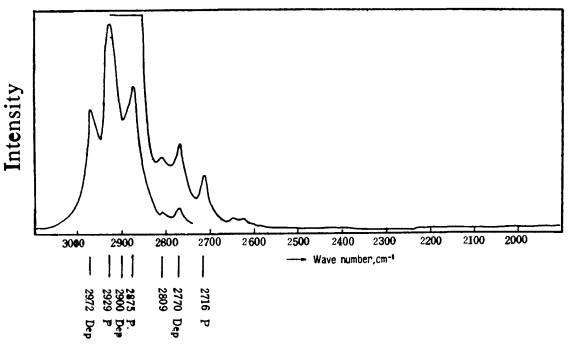



Fig. 1b. Raman spectra of DEM (C-H and C-D stretching region).

Pure liquid

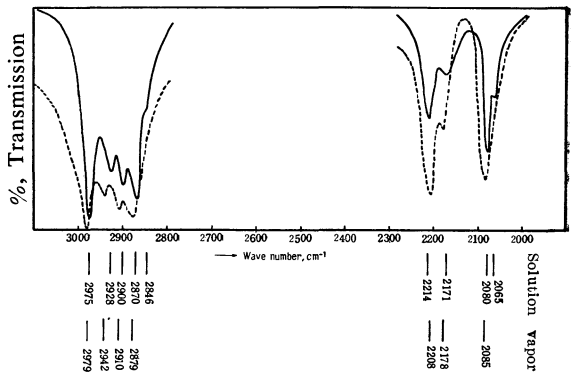



Fig. 1c. Infrared spectra of DEM-$d_2$ (C-H and C-D stretching region).

Solid line, $CCl_4$ solution, (10 vol.%, 0.15 mm.) Dashed line, vapor

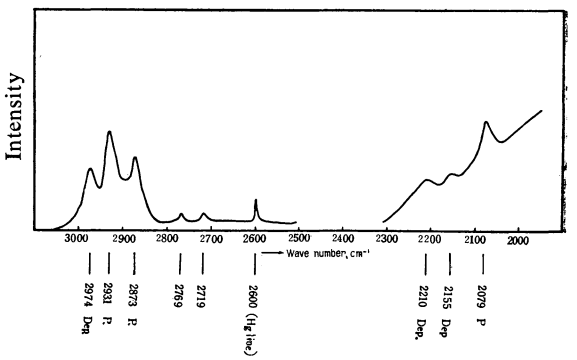



Fig. 1d. Raman spectra of DEM-$d_2$ (C-H and C-D stretching region).

Pure liquid

## Experimental

DEM and DEM-$d_2$ were prepared from ethanol and formaldehyde, and from ethanol and formaldehyde-$d_2$, respectivity. The detailed description of the prepatation will be reported elsewhere[5].

Infrared spectra were obtained by means of a Perkin Elmer 12C spectrophotometer equipped with a lithium fluoride prism and a 21 spectrophotometer equipped with a sodium chloride or a cesium bromide prism.

Raman spectra were obtained by means of a Cary 81 spectrophotometer. In the case of DEM-$d_2$, a capillary tube, the capacity of which is 0.2 cc. was used. The degree of depolarization was measured by wrapping two kinds of polaroids around a Raman tube.

The spectra thus obtained are illustrated in Figs. 1—3.

## Results and Discussion

**C-H and C-D Stretching Vibrations.** — The features of the Raman spectra of DEM and DEM-$d_2$ are quite similar in the 3000 $cm^{-1}$ region. They have two strongly polarized bands at 2929～2931 $cm^{-1}$ and at 2873～2875 $cm^{-1}$, and one depolarized band at 2972～2974 $cm^{-1}$. The features of the infrared spectra are, on the other hand, slightly different from each other. Thus, the intensity ratios of the bands at 2928～2929 $cm^{-1}$ to those at 2896～2900 $cm^{-1}$ are different in these two compounds.

The strongest infrared bands at 2977～2975 $cm^{-1}$ in DEM and DEM-$d_2$ (the corresponding Raman bands being strongly depolarized) are assigned to the asymmetrical methyl stretching of the ethoxyl group[2].

The strong infrared bands at 2870～2878 $cm^{-1}$, having corresponding strongly polarized Raman bands, in DEM and DEM-$d_2$ are assigned to the symmetrical methyl stretching[1].

In dimethoxymethane-$d_6$ ($CD_3OCH_2OCD_3$), bands at 2932 and 2887 $cm^{-1}$ are assigned respectively to the asymmetrical and the symmetrical methylene stretchings of $OCH_2O$ group[3]. The corresponding $CD_2$ stretchings

5) K. Nukada, *Reports Gov. Chem. Ind. Research Inst. Tokyo*, to be published.

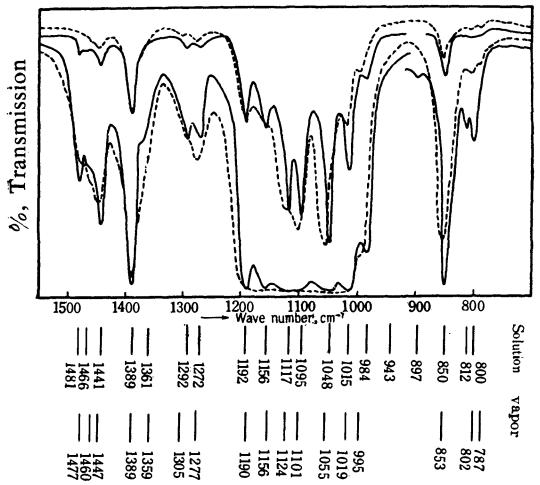



Fig. 2a. Infrared spectra of DEM (finger print region).

Solid line, $CCl_4$ and $CS_2$ solution (0.15 mm., 20 and 3 vol.%), dashed line, vapor

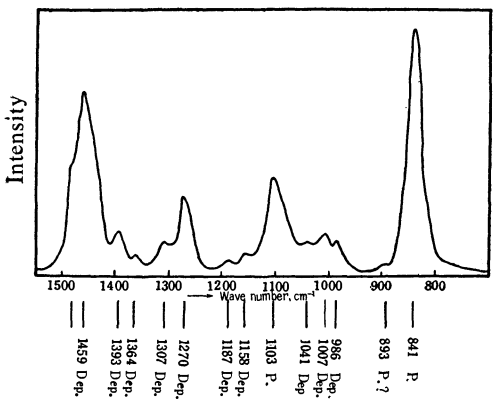



Fig. 2b. Raman spectrum of DEM (finger print region).

Pure liquid

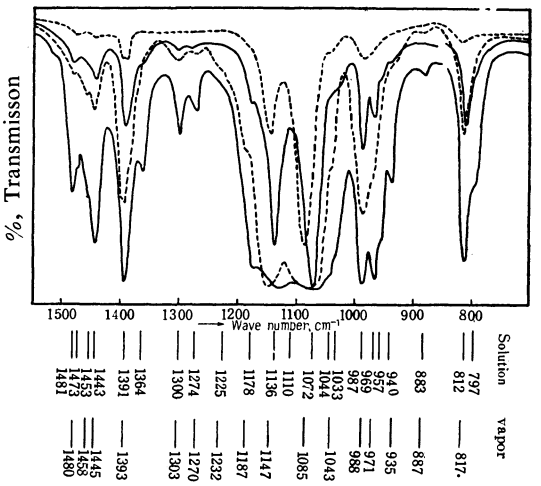



Fig. 2c. Infrared spectra of DEM-$d_2$ (finger print region).

Solid line, $CCl_4$ and $CS_2$ solution, (0.15 mm., 20 and 3 vol.%), dashed line, vapor

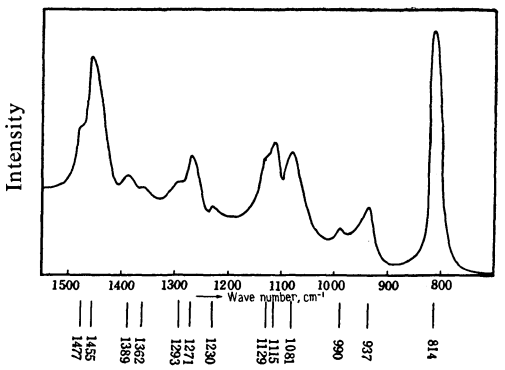



Fig. 2d. Raman Spectrum of DEM-$d_2$ (finger print region).

Pure liquid

are found in dimethoxymethane-$d_2$ ($CH_3OCD_2 \cdot OCH_3$) to be at 2188 (strongly depolarized in Raman) and at 2080 $cm^{-1}$ (strongly polarized in Raman), respectively. In DEM-$d_2$, two strong infrared bands appear at 2214 (the corresponding Raman band being strongly depolarized) and at 2080 $cm^{-1}$ (the corresponding Raman band being strongly polarized); hence they are assigned to the asymmetrical and the symmetrical $CD_2$ stretchings of the $OCD_2O$ group, respectivery, on the analogy of the above mentioned results. The asymmetrical and symmetrical methylene stretchings of the $OCH_2O$ group in DEM are then expected to appear near 2930 and 2890 $cm^{-1}$, respectively. The relative intensity of the infrared band at 2928~2929 $cm^{-1}$ becomes lower in DEM-$d_2$ as compared with the one in DEM, while that at 2870~2878 $cm^{-1}$ does not chow an appreciable change between DEM and DEM-$d_2$. Then it is certain that the asymmetrical methylene stretching of the $OCH_2O$ group exists at 2930 $cm^{-1}$ in DEM, and that it is probably overlapped by the other type of vibration. The overlapping band is presumably the asymmetrical methylene stretching of ethoxy group[2]. The bands at 2870~2878 $cm^{-1}$ in DEM and DEM-$d_2$ are assigned to the symmetrical methylene stretching of the ethoxyl group, overlapped by the symmetrical methylene stretching of the $OCH_2O$ group, as described above, and also by the symmetrical methyl stretching of the ethoxyl group. Since the intensity of these bands does not alter appreciably between DEM DEM-$d_2$, the absorbance of the symmetrical methylene stretching

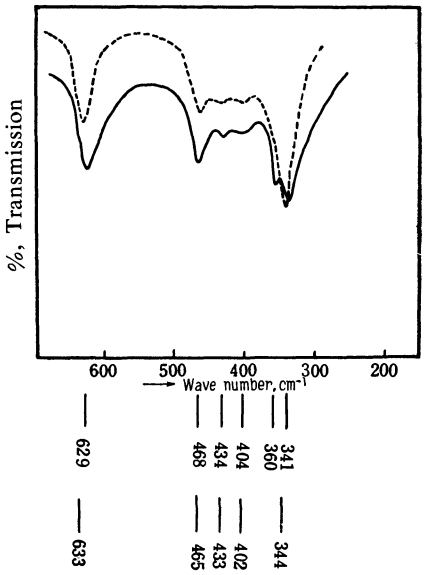



Fig. 3a. Infrared spectra of DEM (skeletal deformation region).

Solid line, pure liquid (0.2 mm.), dashed line vapor

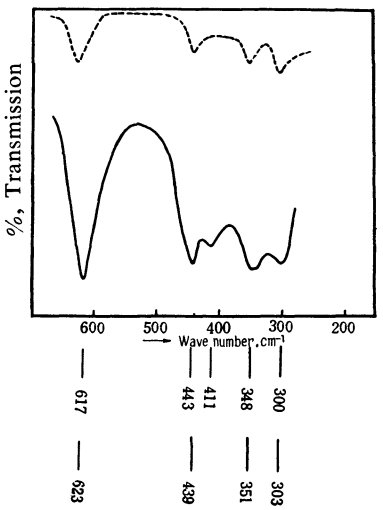



Fig. 3c. Infrared spectra of DEM-$d_2$ (skeletal deformation region).

Pure liquid (0.2 mm.)

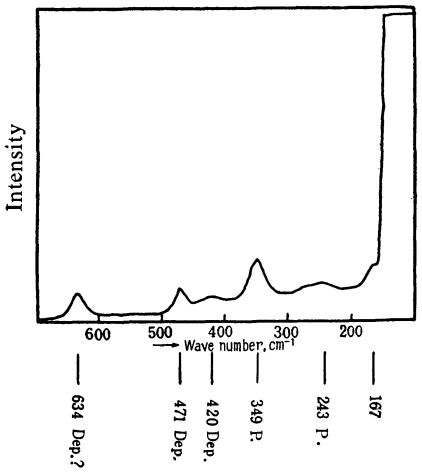



Fig. 3b. Raman spectrum of DEM (skeletal deformation region).

Pure liquid

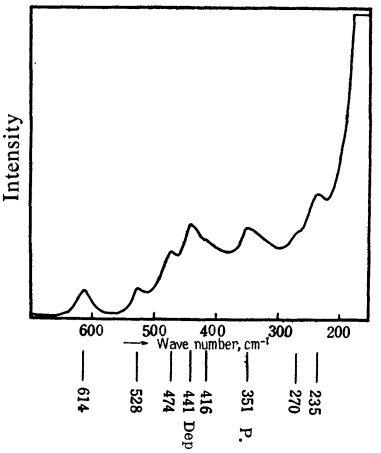



Fig. 3d. Raman spectrum of DEM-$d_2$ (skeletal deformation region).

Pure liquid

of the $OCH_2O$ group is concluded to be small.

The possibility of the Fermi resonance occurring between two types of methylene groups may be small, because the interaction between them is believed to be negligible.

The remaining weak bands may be overtone and/or combination.

**Skeletal Stretching and C–H and C–D Deformation Vibrations.** — The appearance of the spectra of DEM and DEM-$d_2$ is quite similar in the range between 1480 and 1270 $cm^{-1}$ both in infrared and Raman. Therefore, the absorbance of the ethoxyl group is more predominant than that of the $OCH_2O$ group in this frequency region.

Medium infrared and Raman bands appear at 1477~1481 $cm^{-1}$ both in DEM and DEM-$d_2$. In ethylidene diethyl ether ($C_2H_5OCH(CH_3)\cdot OC_2H_5$), ethylidene methyl ethyl ether ($CH_3OCH(CH_3)OC_2H_5$), 2, 2-diethoxypropane ($C_2H_5OC(CH_3)_2OC_2H_5$)[6], triethyl orthoformate ($HC(OC_2H_5)_3$) and in triethyl orthopropionate

6) K. Nukada, ibid., to be published.

TABLE I. VIBRATIONAL FREQUENCIES OF DIETHOXYMETHANE AND DIETHOXYMETHANE-$d_2$*

| DEM | | | DEM-$d_2$ | | | Assignment |
|---|---|---|---|---|---|---|
| IR | | Raman | IR | | Raman | |
| Vapor | Liq. | | Vapor | Liq. | | |
| 2981(s) | 2977(s) | 2972(s) Dep. | 2979(s) | 2975(s) | 2974(s) Dep. | asym. $CH_3$ stretching |
| 2937(m) | 2929(m) | 2929(s) S. P. | 2942(m) | 2928(m) | 2931(s) S. P. | asym. $CH_2$ stretching ($OCH_2O$, EtO) |
| | 2896(w) | | 2910(m) | 2900(m) | | combination or overtone |
| 2886(m) | 2878(s) | 2875(s) S. P. | 2879(s) | 2870(s) | 2873(s) S. P. | sym. $CH_3$ stretching / sym. $CH_2$ stretching ($OCH_2O$, EtO) |
| | | | 2208(s) | 2214(s) | 2210(w) Dep. | asym. $CD_2$ stretching |
| | | | 2178(m) | 2171(m) | 2155(w) Dep. | $CD_2$, combination or overtone |
| | | | 2085(s) | 2080(s) | 2079(m) S. P. | sym. $CD_2$ stretching |
| | | | 2063(sh) | 2065(sh) | | $CD_2$, combination or overtone |
| 1477(vw) | 1481(m) | 1481(m, sh) | 1480(vw) | 1481(m) 1473(vw) | 1477(m, sh) | $CH_2$ scissoring ($OCH_2O$, EtO) |
| 1460(vw) | 1466(vw) | 1459(s) S. Dep. | 1458(vw) | 1453(vw) | 1455(s) S. Dep. | asym. $CH_3$ deformation |
| 1447(w) | 1441(vw) | | 1445(w) | 1443(m) | | EtO, combination or overtone (COCOC) |
| 1389(m) | 1389(m) | 1393(m) Dep. | 1393(m) | 1391(m) | 1389(m) | sym. $CH_3$ deformation / $CH_2$ wagging ($OCH_2O$) |
| 1359(vw) | 1361(vw) | 1364(w) Dep. | | 1364(vw) | 1362(w) | $CH_2$ wagging (EtO) |
| 1305(w) | 1292(w) | 1307(w) Dep. | 1303(vw) | 1300(w) | 1293(w) | $CH_2$ rocking (EtO) |
| 1277(w) | 1272(w) | 1270(s) Dep. | 1270(vw) | 1274(w) | 1272(s) Dep. | $CH_2$ twisting (EtO) |
| | | | 1232(vw) | 1255(w) | 1230(w) P. ? | $CD_2$ scissoring or twisting+COCOC stretching |
| 1190(m) | 1192(m) | 1187(w) Dep. | | | | $CH_2$ twisting or wagging ($OCH_2O$) |
| 1156(w) | 1156(m) | 1158(w) Dep. | | | | $CH_2$ rocking ($OCH_2O$) |
| 1124(m) | 1117(s) | | 1147(s) | 1136(s) | 1129(w) | asym. COCOC streching |
| | | | | 1110(vvw) | 1115(s) P. | $CD_2$ scissoring or twisting |
| 1101(s) | 1095(s) | 1103(s) P. | 1085(s) | 1072(s) | 1081(s) | sym. COCOC stretching |
| 1055(s) | 1048(s) | 1041(w) Dep. | 988(m) | 987(s) | 990(m) | asym. COCOC stretching |
| 1019(m) | 1015(s) | 1007(m) Dep. | 935(vw) | 940(w) | 937(m) Dep. | sym. CC stretching |
| 995(w) | 984(w) | 986(w) Dep. | 971(w) | 969(m) | | asym. CC stretching |
| 853(m) | 850(m) | 841(s) S. P. | 817(w) | 812(s) | 814(s) S. P. | sym. COCOC stretching |
| | 943(vw) | | | | | |
| | 897(vw) | 893(w) P. ? | 887(vw) | 883(vw) | | |
| 802(vw) | 812(vw) | | | | | |
| 787(vw) | 800(vw) | | | 797(vw) | | |
| 633(s) | 629(s) | 634(m) Dep. ? | 623(s) | 617(s) | 614(m) | asym. COCOC deformation |
| | | | | | 528(w) | |
| | | | | | 474(w) | |
| 465(m) | 468(s) | 471(m) Dep. | 439(s) | 443(s) | 441(m) Dep. | sym. COCOC deformation |
| 433(w) | 434(m) | 420(w) Dep. | | 411(m) | 416(w) | |
| 402(w) | 404(m) | | | | | |
| | 360(w) | | | | | |
| 344(s) | 341(s) | 349(m) S. P. | 351(s) | 348(s) | 351(m) P. | sym. COCOC deformation |
| | | | 303(m) | 300(m) | | |
| | | | | | 270(vw) | |
| | | 243(w) S. P. | | | 235(w) | sym. OCC deformation |
| | | 167(w) | | | | |

* P. and Dep. mean "polarized" and "depolarized", and S. means "strongly".

$(C_2H_5C(OC_2H_5)_3)$[7], a weak or medium infrared band is observed in this region. But in diisopropoxymethane $((CH_3)_2CHOCH_2OCH\cdot(CH_3)_2)$[8], ethylidene dimethyl ether $(CH_3\cdot OCH(CH_3)OCH_3)$, trimethyl orthoformate $(HC(OCH_3)_3)$, trimethyl orthoacetate $(CH_3C\cdot(OCH_3)_3)$ and in trimethyl ortho-*n*-valerate $(CH_3(CH_2)_3C(OCH_3)_3)$[7], no band exists in this region. Hence the bands at 1477~1481 $cm^{-1}$ are assigned to the methylene vibration of the ethoxyl group, certainly the scissoring vibration. The methylene scissoring of the $OCH_2O$ group can also exist at this frequency[3], but the absorbance of the latter may probably smaller than that of the former and it is hard to observe it.

All compounds containing oxygen atoms which the author has studied[1-4,6-8] have weak infrared and strong and depolarized Raman bands around 1460 $cm^{-1}$ except for dimethoxymethane and dimethoxymethane-$d_8$ $(CD_3\cdot OCD_2OCD_3)$. The last two compounds contain no methyl group, thus the bands in this region should be due to the methyl group. Therefore the bands at 1455~1466 $cm^{-1}$ (very weak in infrared and strong and depolarized in Raman) in DEM and DEM-$d_2$ are assigned to the asymmetrical methyl deformation of the ethoxyl group.

The origin of infrared bands at 1440~1443 $cm^{-1}$ both in DEM and DEM-$d_2$ is not clear, but they must be due to the vibration of the ethoxyl group, or the combination or overtone of skeletal vibrations.

The medium infrared and polarized Raman bands at 1389~1393 $cm^{-1}$ both in DEM and DEM-$d_2$ are assigned to the symmetrical methyl deformation of the ethoxyl group. From the result on dimethoxymethane and its deuterated compounds[3] the methylene wagging of the $OCH_2O$ group could exist in this region. So in DEM, these two bands may probably overlap.

The very weak infrared and weak Raman bands at 1359~1362 $cm^{-1}$ in DEM and DEM-$d_2$ are assigned to the methylene wagging of the ethoxyl group.

The features of doublet at 1292~1307 $cm^{-1}$ and 1270~1274 $cm^{-1}$ do not alter strongly between DEM and DEM-$d_2$, thus these bands are also due to the ethoxyl group. Of these, the former bands are assigned to the methylene rocking and the latter to the methylene twisting, because the Raman intensity of the latter is greater than that of the former and it is expected that the twisting vibration, the species of which is A, should give a stronger band.

In conclusion, it becomes clear that bands due to the ethoxy group are at 1477~1481, 1455~1466, 1441~1443, 1389~1393, 1361~1364, 1292~1307 and at 1270~1274 $cm^{-1}$ (all the values are those of liquid phase). The skeletal vibrations may not appear in such a high frequency region.

The weak Raman band at 1230 $cm^{-1}$ (having a corresponding very weak infrared band) in DEM-$d_2$ may be due to $CD_2$ vibration coupled with the COCOC skeletal vibration. Since the Raman band is polarized, it is assigned to the $CD_2$ scissoring or twisting, being coupled with an A type skeletal stretching, to some extent.

The medium bands at 1187~1192 $cm^{-1}$ both in infrared and Raman in DEM disappear in DEM-$d_2$ (in which a very weak infrared band appears at 1178 $cm^{-1}$, though the origin of this band may be different as the intensity is too low). Hence these bands are due to the methylene vibration of the $OCH_2O$ group, probably the twisting or wagging.

The bands at 1156~1158 $cm^{-1}$ in DEM both in infrared and Raman disappear in DEM-$d_2$. In dimethoxymethane and dimethoxymethane-$d_6$, weak infrared bands at this freqencey are assigned to the methylene rocking of the $OCH_2O$ group[3]. According to these results, these bands are assigned to the methylene rocking of the $OCH_2O$ group.

From the study on dimethoxymethane and its deuterated compounds, the skeletal COCOC stretching should exist between 1150~800 $cm^{-1}$ [3]. In DEM and DEM-$d_2$, the additional skeletal stretchings due to CC bonds could exist in this region. But the absorbance of the latter ones may be smaller than that of the former, hence the features of the spectra of DEM and DEM-$d_2$ are actually similar to those fo dimethoxymethane at this frequency region.

The infrared bands at 1117 and at 1136 $cm^{-1}$ in DEM and DEM-$d_2$ are the next strongest bands in the liquid phase, and the corresponding Raman bands are very weak. In dimethoxymethane and its deuterated compounds, the strong infrared bands around 1140 $cm^{-1}$, the corresponding Raman bands of which are extremely weak, are assigned to the asymmetrical skeletal stretching[3]. These bands are then assigned to one of the asymmetrical COCOC stretchings.

The Raman band at 1115 $cm^{-1}$ in DEM-$d_2$ is due to the $OCD_2O$ methylene vibration. As it is strongly polarized, it may be assigned to the scissoring or twisting being coupled with the symmetrical skeletal stretching to some extent.

The strong infrared band at 1095 $cm^{-1}$ in

7) K. Nukada, *J. Chem. Soc. Japan, Pure Chem. Sec.* (*Nippon Kagaku Zasshi*), **81**, 1028 (1960).
8) K. Nukada, This Bulletin, to be published.

DEM corresponds to the band at 1072 $cm^{-1}$ in DEM-$d_2$. As the corresponding Raman bands are strong and strongly polarized (in DEM), these bands are assigned to one of the symmetrical COCOC stretchings.

The strong infrared band appears at 1048 $cm^{-1}$ in DEM, but no corresponding band exists in DEM-$d_2$ near that frequency. In DEM-$d_2$, the remaining band, the intensity of which is rather high, is the band at 987 $cm^{-1}$. Furthermore the intensity of the corresponding Raman bands is not so high in both cases, thus it is reasonable to correlate the two bands as the same type of skeletal vibration. The remaining modes are one symmetrical and one asymmetrical vibration, but as described in detail later the symmetrical one should appear at 800~850 $cm^{-1}$ both in DEM and DEM-$d_2$. Accordingly these bands are assigned to the asymmetrical COCOC stretching.

The bands at 1015 and 984 $cm^{-1}$ in DEM and those at 940 and 969 $cm^{-1}$ in DEM-$d_2$, may be due to CC stretchings. The former ones are assigned to the symmetrical mode and the latter to the asymmetrical one, respectively, since the intensity of the corresponding Raman bands of the former is higher than that of the latter.

The strongest and strongly polarized Raman bands exist at 841 and 814 $cm^{-1}$ in DEM and DEM-$d_2$, respectively. In dimethoxymethane, its deuterated compounds[3], methoxyethoxymethane and in diisopropoxymethane[9], there appear the strongest and strongly polarized Raman bands, being assigned to the symmetrical skeletal stretching, between 900 and 800 $cm^{-1}$. Thus these bands are also definitely assigned to the symmetrical COCOC stretching. Just as in the case of dimethoxymethane and its deuterated compounds[3], the corresponding infrared bands are not so strong, and in the vapor phase its intensity becomes lower than that of the liquid phase. As already mentioned in the study of dimethoxymethane, the mode of this vibration is such that two terminal ethoxyl groups vibrate symmetrically and the central OCO group does not move much.

**Skeletal Deformation Vibrations.** — It is expected that five skeletal angle deformations appear over 200 $cm^{-1}$ and six torsional vibrations below 250 $cm^{-1}$. At the present, no infrared band below 280 $cm^{-1}$ is obtained because of the experimental limitation and Raman band below 200 $cm^{-1}$ is hardly observable since the strong exiting line disturbs the observation of weak Raman band. All the skeletal deformations could then be observed either in infrared or in Raman, while the torsional vibrations are hardly observable.

There are three pairs of strong Raman bands in DEM and DEM-$d_2$, namely at 634 and 614, 471 and 441, and 349 and 351 $cm^{-1}$. In dimethoxymethane, its deuterated compounds[3] and in methoxyethoxymethane[4], there appear such pairs of Raman bands. The appearance of infrared spectra is also quite similar between DEM and DEM-$d_2$, that is, three pairs of strong infrared bands appear at the same frequency regions. Hence they are certainly due to the skeletal deformations

Of these, the bands at 349~351 $cm^{-1}$ are strongly polarized in Raman, so they are assigned to the symmetrical COCOC deformation. As in the case of dimethoxymethane and its deuterated compounds, these are the vibrations all skeletal angles of which move in the same phase.

The degree of depolarization of the remaining two bands is not clear, but on the analogy of dimethoxymethane the bands at 614~634 $cm^{-1}$ in DEM and DEM-$d_2$ are assigned to the asymmetrical deformation and the last bands at 441~470 $cm^{-1}$ to the other symmetrical one, two COC angles and the OCO angle of which vibrate in the opposite phases.

As the Raman bands at 235~243 $cm^{-1}$ in DEM and DEM-$d_2$ are strongly polarized, they are assigned to the symmetrical OCC deformation. The assignment of the asymmetrical one is not clear.

The remaining weak bands may be overtone and/or combination of torsional vibrations.

## Summary

Infrared spectra between 3000 and 280 $cm^{-1}$ (vapor and liquid phases) and Raman spectra (liquid phase) of diethoxymethane ($C_2H_5 \cdot OCH_2OC_2H_5$) and of diethoxymethane-$d_2$ ($C_2H_5OCD_2OC_2H_5$) were observed and the assignment of the spectra is presented with the assumption that these molecules take one form both in the vapor and liquid phases. In the assignment, that of the homologues such as dimethoxymethane, its deuterated compounds, methoxyethoxymethane and diisopropoxymethane, are taken into consideration.

The author wishes to express his sincere thanks to Dr. Y. Mashiko for his valuable discussions.

*Government Chemical Industrial Research Institute of Tokyo*
*Shibuya-ku, Tokyo*

9) K. Nukada, ibid., to be published.

# *Structure of Enteromycin. III.* Structure of Demethoxyenteromycin*

By Kōmei MIZUNO

(Received April 4, 1961)

The present work was initiated with a view to knowing the structure of dehydroxydihydrodemethoxyenteromycin (XXII)[1] and establishing the structure of demethoxyenteromycin (XII) by making clear the partial structures of *O*-acetyldemethoxyenteromycin (XVIII), *N*-methyldemethoxyenteromycin methyl ester (XIX), and *O*-methyldemethoxyenteromycin methyl ester (XX).

XXII has a molecular formula having one mole less hydrogen than dehydroxytetrahydrodemethoxyenteromycin (XV), namely glycyl-$\beta$-alanine, and its hydrolysis with hydrochloric acid gives glycine, acetaldehyde and others. The infrared spectum (Report II, Fig. 6) of this compound shows the absorption of C=C and the ultraviolet spectrum (Report II, Fig. 7) inhibits an adsorption similar to that of $\alpha, \beta$-unsaturated carboxylic acids. Further the infrared spectra (Report II, Figs. 2 and 4) of XVIII and XX reveals the clear absorption of NH. From these facts it is reasonable to assign the structure of *N*-glycyl-3-aminoacrylic acid to XXII. Accordingly, of the presumptive formulas, D

$$NH_2CH_2CONHCH=CHCOOH \qquad (XXII)$$

and C, for enteromycin and demethoxyenteromycin described in Report II, the $\alpha, \beta$-unsaturated ones would be preferential.

Catalytic reduction of XVIII on Adams platinum oxide yielded acetic acid (XXVII) and glycyl-$\beta$-alanine, and this fact ascertained the presence of $\rangle$NOAc in XVIII. On the other hand, the position of the $\rangle$NOH group in XII was clarified to be at the terminal N in the formula C. Catalytic reduction of XIX and hydrolysis of the resulting viscous substance (ester) (XX) yielded sarcosine (XXIX) and $\beta$-alanine. The same treatment of XX gave glycine and $\beta$-alanine. From these results, it is proper to think that the remaining hand of the hydroxyimino group (HO-N$\langle$C) in XII is not used for a N-N combination (the infrared spectra of XVIII and XX reveal the absorption of NH) or for a N-C combination (in a N-C combination is present, it must be split off by catalytic reduction before the formation of XXII which is a readily saturable unsaturated compound). In other words, the terminal N of XII ought to participate in aldoxime. Since thus XII is a strongly phenolic aldoxime compound, it gives two methyl derivatives ($CH_3$-$\overset{\overset{O}{\uparrow}}{N}$=CH- and $H_3CO$·N=CH-) as Fuson[2] pointed out, and XIX is understood as the *N*-methyl derivative taking

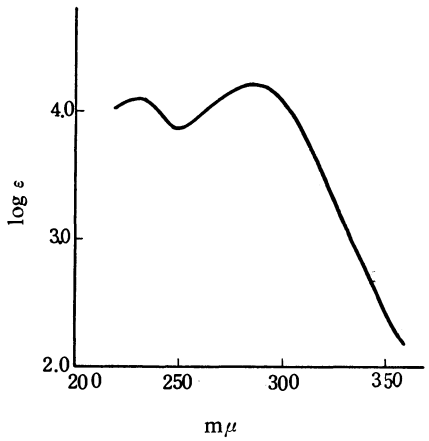



Fig. 1. Ultraviolet absorption spectrum of *O*-methyldemethoxyenteromycin methyl ester (XX) in methanol.

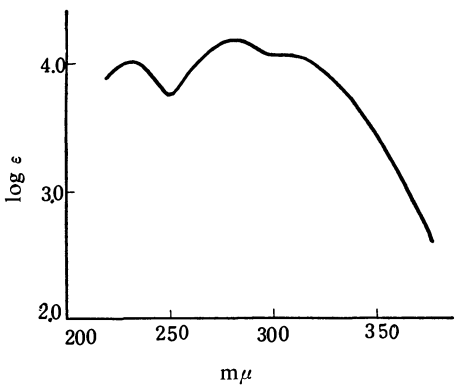



Fig. 2. Ultraviolet absorption spectrum of *N*-methyldemethoxyenteromycin methyl ester (XIX) in methanol.

* This constitutes Part XXXVII of a series entitled "Studies on Antibiotics" by S. Tatsuoka, and was reported at the forum on Natural Organic Compounds, October 1960.

1) K. Mizuno, This Bulletin, 34, 1425 (1961).

2) R. C. Fuson, "Advanced Organic Chemistry" (1950), p. 515.

oxide-form, and XX as the *O*-methyl derivative taking ether-form. The ultraviolet spectrum (Fig. 1) of XX, like that of XVIII, showed such strong absorptions at $\lambda$ 225 m$\mu$ and 280 m$\mu$ as those of diketone[3] compounds, whereas the ultraviolet spectrum (Fig. 2) of XIX exhibited such a strong absorption at $\lambda$ 295 m$\mu$ as the conjugate nitrone-form[4] may show. These facts seem to be in good accord with the above-mentioned structures.

Namely, the structure of XII must be *N*-(hydroxyiminoacetyl)-3-aminoacrylic acid,

$$HON=CHCONHCH=CHCOOH \quad (XII)$$

and consequently the structure of methyl *N*-(*N*-oxy-methyliminoacetyl)-3-aminoacrylate

$$H_3\overset{\overset{O}{\uparrow}}{C}N=CHCONHCH=CHCOOCH_3 \quad (XIX)$$

is presumed for XIX, and the structure of methyl *N*-(*O*-methylhydroxyiminoacetyl)-3-aminoacrylate

$$H_3CON=CHCONHCH=CHCOOCH_3 \quad (XX)$$

for XX.

## Experimental

**Acid Decomposition of Dehydroxydihydrodemethoxyenteromycin.**—A solution of 30 mg. of dehydroxydihydrodemethoxyenteromycin (XXII) in 3 cc. of 6 N hydrochloric acid was heated at 100°C for 6 hr. in a sealed tube, the air of which was replaced with nitrogen. One half of the reaction mixture was allowed to react with 2, 4-dinitrophenylhydrazine dissolved in hydrochloric acid, and the product was subjected to paper chromatography to detect the spot of the 2, 4-DNPH of acetaldehyde at $R_f$ 0.35. The remaining half was evaporated to dryness and the residue was chromatographed, finding a single spot of glycine at $R_f$ 0.40.

**Catalytic Reduction of *O*-Acetyldemethoxyenteromycin.** — A solution of 30 mg. of *O*-acetyldemethoxyenteromycin in 50 cc. of pure methanol was reduced in the presence of 20 mg. of Adams platinum oxide. The reaction mixture was diluted with 20 cc. of pure water and filtered, and 10 cc. of the filtrate was passed through a column of Amberlite IR-120 (H-form). The effluent, after addition of aqueous ammonia, was concentrated under diminished pressure and the residue was chromatographed by the method of Kennedy et al[5]. (solvent system: 95% ethanol containing ammonia. Detective reagent: a solution of B.P.B. in 70% ethanol, made acid with citric acid) to detect a blue spot, which was identified as ammonium acetate, and hence the presence of acetic acid in the reaction mixture was confirmed. It is evident that the spot is not formic acid because it does not reduce the ammoniacal silver nitrate solution of Brown et al.[6] The remaining filtrate (60 cc.) was concentrated under reduced pressure, giving 10 mg. of crystals, m.p. 225°C (decomp.), the infrared spectrum and $R_f$ value in paper chromatography of which were in complete accord with those of glycyl-$\beta$-alanine.

**Catalytic Reduction of *N*-Methyldemethoxyenteromycin Methyl Ester and Hydrolysis of the Product.**— A solution of 30 mg. of *N*-methyldemethoxyenteromycin methyl ester in 10 cc. of pure methanol was reduced on 20 mg. of Adams platinum oxide. The reaction mixture was filtered and concentrated under reduced pressure, leaving a small amount of a very viscous substance (XXVIII). The infrared spectrum of the substance showed the absorption of COOR, but its ultraviolet spectrum revealed no specific absorption in the long wave region beyond $\lambda$ 220 m$\mu$. Part of the substance was hydrolyzed with 6 N hydrochloric acid and the resulting free amino acid was investigated by the ninhydrin reaction and paper chromatography, whereupon a blue spot was detected at $R_f$ 0.65 and a pink spot at $R_f$ 0.73. The former spot was identified as $\beta$-alanine and the latter as sarcosine. The substance, after dinitrophenylation, gave three yellow spots; i.e. a spot at $R_f$ 0.37 in the first development, at $R_f$ 0.30 in the second development, a spot at $R_f$ 0.52 in the first development, at $R_f$ 0.28 in the second development, and a spot at $R_f$ 0.40 in the first development, at $R_f$ 0.43 in the second development, and they were identified as DNP-alanine, 2, 4-dinitrophenol, and DNP-sarcosine, respectively. The spots of DNP-$\beta$-alanine and DNP-sarcosine were extracted with hot water, and from the absorptions of the extracts the two compounds were found to be contained in equimolecular amounts.

The rest of the substance (XXVIII) was dinitrophenylated and the ether soluble portion of the product was hydrolyzed with hydrochloric acid and chromatographed, when no spot of DNP-sarcosine was detected, and the presence of only free $\beta$-alanine was confirmed.

**Catalytic Reduction of *O*-Methyldemethoxyenteromycin Methyl Ester and Hydrolysis of the Product.**— A solution of 30 mg. of *O*-methyldemethoxyenteromycin methyl ester in 10 cc. of pure methanol was reduced on 20 mg. of Adams platinum oxide. The reaction mixture was filtered and concentrated under reduced pressure to give a viscous substance. The product was hydrolyzed with hydrochloric acid and chromatographed as before, detecting glycine and $\beta$-alanine.

## Summary

The structure of dehydroxydihydrodemethoxyenteromycin was assumed to be *N*-glycyl-3-aminoacrylic acid. From the fact that catalytic reduction of *O*-acetyldemethoxyenteromycin afforded acetic acid and glycyl-$\beta$-alanine, and that *N*-methyl- and *O*-methyldemethoxyenteromycin methyl ester have the partial structures of *N*-(*N*-oxy-methyliminoacetyl)- and *N*-(*O*-

3) L. Dorfmann, *Chem. Revs.*, 1953, 80.
4) W. D. Emmons, *J. Am. Chem. Soc.*, **79**, 5739 (1957); **78**, 6208 (1956).
5) E. P. Kennedy and H. A. Barker, *Anal. Chem.*, **23**, 1033 (1951).
6) F. Brawn and C. P. Hall, *Nature*, **166**, 66 (1950).

methylhydroxyiminoacetyl)-, respectively, it was made clear that demethoxyenteromycin is an aldoxime having the structure of *N*-(hydroxyiminoacetyl)-3-aminoacrylic acid.

*Research Laboratories*
*Takeda Chemical Industries, Ltd.*
*Higashiyodogawa-ku, Osaka*

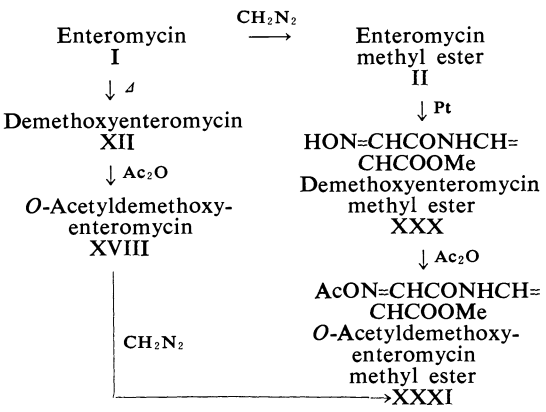
# *Structure of Enteromycin. IV**

By Kōmei MIZUNO

(Received April 4, 1961)

As reported in the previous papers[1-3], enteromycin (I) differs from demethoxyenteromycin (XII) in molecular formula only by $CH_2O$, but they are greatly different in property. From the fact that enteromycin is demethoxylated by heating under evolution of formaldehyde, and from the results of the decomposition of I and XII, enteromycin seems to have a specific functional group containing a methoxyl group. Therefore, the clarification of the functional group was considered to be the most important problem for establishing the structure of I. So the course of the conversion of I to XII by catalytic reduction was restudied first of all. On the other hand, attempts were made to know the position of the functional group by clarifying the structure of the amido compounds, XIV[1] and XXI[2], of I and XII.

Enteromycin methyl ester[1] (II) is soluble in many solvents and its catalytic reduction gives prisms (XXX) [m. p. 196°C (decomp.), $C_6H_8O_4N_2$], which are positive to the reaction of Barton et al.[1] The product has a methoxyl group, and though its infrared spectrum (Fig. 1) shows no absorption of $COOCH_3$ (1710 $cm^{-1}$), its ultraviolet spectrum exhibits two absorption maxima at $\lambda$ 225 m$\mu$ ($\varepsilon$ 11000) and 280 m$\mu$ ($\varepsilon$ 16000). However, as the product was positive to the Barton reaction, it was assumed to be demethoxyenteromycin methyl ester and the assumption was confirmed by the following experiments. Acetylation of XXX with acetic anhydride in warm water afforded prisms (XXXI) [m. p. 127°C, $C_8H_{10}O_5N_2$] negative to the Barton reaction. As the infrared spectrum (Fig. 2) of this product showed a clear absorption of $\equiv NOCOCH_3$ (1775 $cm^{-1}$), it was assumed to be *O*-acetyldemethoxyenteromycin methyl ester, and the assumption was confirmed by the formation of the same compound by methylation of *O*-acetyldemethoxyenteromycin (XVIII) with diazomethane. From the above fact, it was found that II is demethoxylated only by catalytic reduction without heating, and that such a phenomenon seems to be due to the specific position of the methoxyl group in the functional group in I and II.




Catalytic reduction of enteromycin amide (XIV) on palladium-carbon yielded prisms (XXXII) [m. p. 179°C (decomp.), $C_5H_9O_4N_3$] and the product was called dihydroenteromycin amide. It was positive to the Barton reaction but negative to the ninhydrin reaction and the reaction of the hydrazino group[4], and though its ultraviolet spectrum (Fig. 3) showed an absorption maximum at $\lambda$ 250 m$\mu$ ($\varepsilon$ 5100), its infrared spectrum (Fig. 4) exhibited no absorption of C=C. Hydrolysis of the product with hydrochloric acid afforded $\beta$-alanine but neither glyoxylic acid nor acetaldehyde, and alkaline

* This constitutes Part XXXVIII of a series entitled "Studies on Antibiotics" by S. Tatsuoka, and was reported at the forum on Natural Organic Compounds, October 1960.

1) K. Mizuno, This Bulletin, **34**, 1419 (1961).
2) K. Mizuno, ibid., **34**, 1425 (1961).
3) K. Mizuno, ibid., **34**, 1631 (1961).
4) F. H. Pollard and A. J. Banister, *Anal. Chim. Acta*, **14**, 70 (1956).

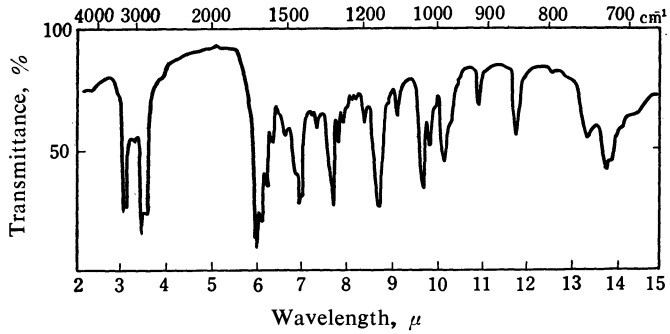



Fig. 1. Infrared absorption spectrum of demethoxyenteromycin methyl ester (XXX).

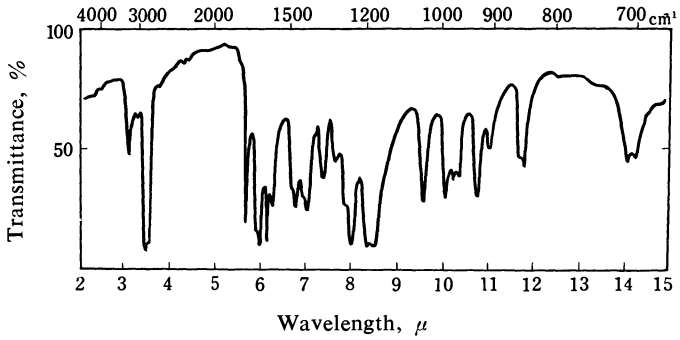



Fig. 2. Infrared absorption spectrum of *O*-acetyl demethoxyenteromycin methyl ester (XXXI).

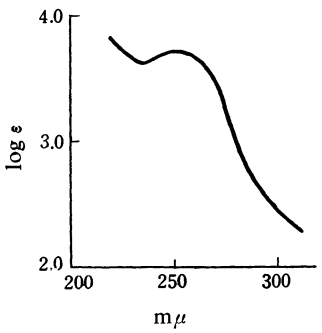



Fig. 3, Ultraviolet absorption spectrum of dihydroenteromycin amide (XXXII) in methanol.

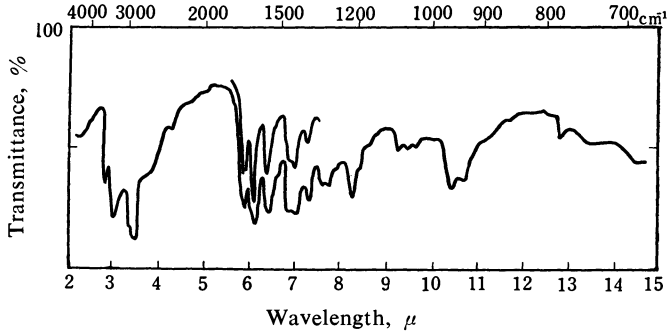



Fig. 4. Infrared absorption spectrum of XXXII.

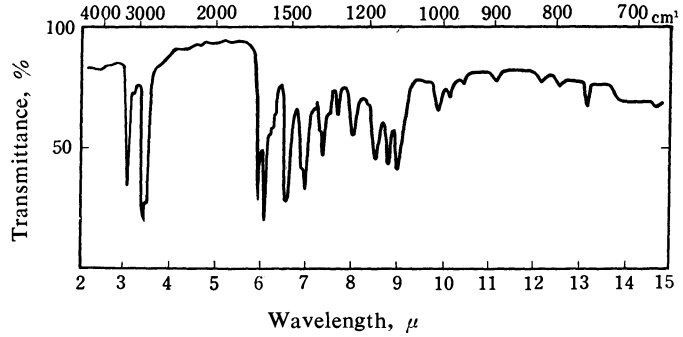
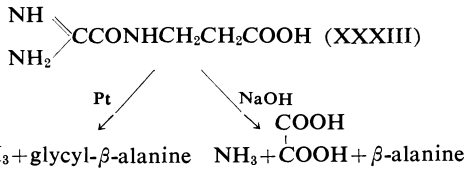


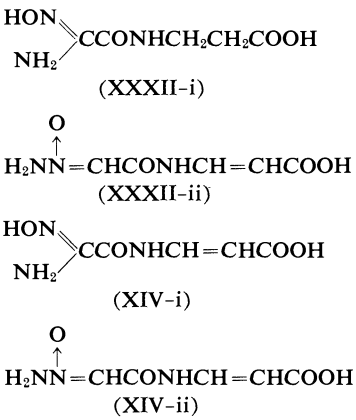

Fig. 5. Infrared absorption spectrum of a pyrazoline derivative (III) of enteromycin methyl ester.

hydrolysis of the product furnished β-alanine and oxalic acid under evolution of a basic gas.

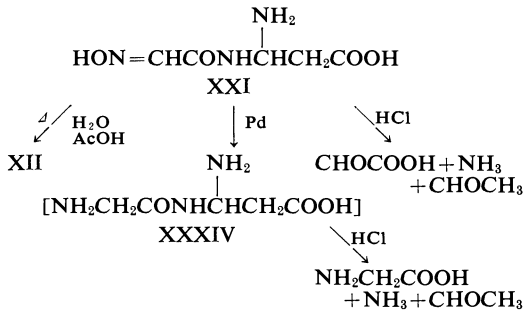
Catalytic reduction of XXXII for a long time in the presence of palladium-carbon gave a light pink product readily soluble in water (XXXIII) [m. p. 213°C (decomp.), $C_5H_9O_3N_3$], which was negative to the Barton reaction but positive to the ninhydrin reaction. The product was hydrolyzed with alkali, and in the reaction mixture were detected β-alanine, ammonia and oxalic acid, by paper chromatography. Further reduction of the above product on Adams platinum oxide produced ammonia and glycyl-β-alanine. From these results, amidinocarbonyl-β-alanine was assigned as the structure of XXXIII.




Accordingly, XXXII was considered to have the structure of *N*-(hydroxyamidinocarbonyl)-β-alanine (XXXII-i) and XIV the structure of *N*-(hydroxyamidinocarbonyl)-3-aminoacrylic acid (XIV-i) among the four formulas shown below:

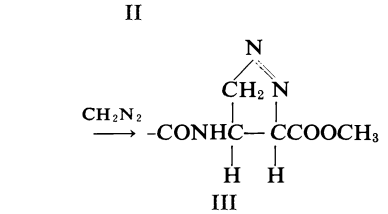



An aqueous solution of the product (XXXIV) obtained by catalytic reduction of demethoxy-enteromycin amide (XXI) on palladium-carbon showed no specific absorption in the long wave region beyond λ 220 mμ, and hydrolysis of the product with hydrochloric acid produced acetaldehyde, ammonia and glycine. On the other hand, XXI furnished acetaldehyde and glyoxylic acid when hydrolyzed with hydrochloric acid, and its infrared spectrum (Report II, Fig. 5) exhibited no absorption of C=C. From this fact, XXI was presumed to be 3-amino *N*-(hydroxyiminoacetyl)-β-alanine.



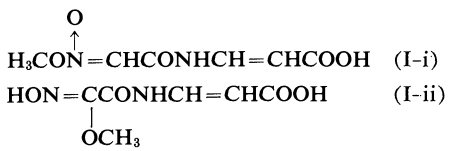

The amidation product of XII has not the same structure as that (XIV-i) of enteromycin amide. Judging from the structure of XIV-i, it is evident that the $-OCH_3$ group of the functional group characteristic of I is situated on the HO-N=CH-CO- side of XII and its position seems to be the nitrogen of the oxime or the α-carbon atom.

To make clear that enteromycin also has a 3-amino acrylic acid portion, the structure of the diazomethane addition product[1] (III) of enteromycin methyl ester was investigated. Catalytic reduction of III on Adams platinum oxide and hydrolysis of the product with hydrochloric acid yielded glycine but not β-alanine. The infrared spectrum (Fig. 5) of III exhibited no absorption of C=C. From these results the addition product was considered to be a pyrazoline[5] derivative formed by addition of diazomethane to the α, β-double bond. This suggested that II also has such a double bond.




Namely, enteromycin also contains a 3-amino-acrylic acid portion.

From these results and considerations, the following two formulas were presumed as the structure of enteromycin.




Of the two formulas, (I-i) was preferred from the following experimental data.

i) Glyoxylic acid was produced by acid hydrolysis.

5) K. V. Auwers and O. Ungemach, *Ber.*, **66**, 1205 (1933)

ii) Methylation with diazomethane gave not *N*- or *O*-methyl compound but a pyrazoline derivative.

iii) The products obtained in various stages of catalytic reduction had no methoxy group[6].

iv) Ultraviolet Spectrum showed at $\lambda$ 298 m$\mu$ a strong absorption suspected to be due to conjugated nitrone.

v) To be negative to the reaction of Barton et al. for the phenolic hydroxyl group.

vi) Infrared spectra of I and II exhibited no absorption of -OH.

vii) Only one acidic group was observed.

Arndt et al.[7] once synthesized *O*-methyl-*aci*-nitroacetate and found that this compound was converted by heating into the corresponding oxime under evolution of formaldehyde. Gilman[8] explained the mechanism as this; a proton of the methoxyl is attracted by the coordinating oxygen and as a result the methoxyl converts into formaldehyde, while the corresponding oxime is formed. The formula I-i, having such a functional group, well explains the mechanism of the demethoxylation of enteromycin by heating. Since formation of formaldehyde from a methoxyl group may not be possible in any other group than the functional group, the formula I-i seems to be conclusively right from this point alone.

The problem still to be solved is whether or not amidation of a compound having such a specific structure as I-i furnishes a substance similar to XIV-i.

To clarify this point, ethyl *O*-methyl-*aci*-nitroacetate $C_5H_9O_4N$; $H_3CO\overset{O}{\uparrow}N=CHCOOC_2H_5$ synthesized by the method of Arndt et al. was amidated under the same conditions as in I and detailed investigation was made on the product (XXXV) [m. p. 171°C (decomp.), $C_2H_5O_2N_3$]. The product was positive to the Barton reaction and its ultraviolet spectrum (Fig. 6) showed an absorption at $\lambda$ 250 m$\mu$ ($\varepsilon$ 5100), which was in accord with that of dihydroenteromycin amide (XXXII). Alkaline hydrolysis of XXXV evolved a basic gas and produced oxalic acid, and acetylation of it with acetic anhydride in warm water gave an *O*-acetyl compound [m. p. 168°C (decomp.), $C_4H_7O_3N_3$], which was negative to the Barton reaction and the infrared spectrum of which showed the absorption of AcON= (1755 cm$^{-1}$).

Next, XXXV was reduced for a long time in the presence of palladium-carbon, and the light pink product (XXXVI) yielded ammonia and oxalic acid when hydrolyzed with alkali, and oxamide (XXXVII) when treated with hot water. Since, however, XXXVI was not isolated, the following experiments were carried out. XXXV was reduced on Adams platinum oxide and the product was hydrolyzed with hydrochloric acid, giving glycine. Catalytic reduction of the *O*-acetyl derivative of XXXV with palladium-carbon in acetic anhydride yielded a light pink product assumed to be *N*, *N'*-diacetyldiaminoacetamide [m. p. 257°C (decomp.), $C_6H_{11}O_3N_3$], and the structure was confirmed from the formation of glyoxylic acid by the hydrolysis of the product with hydrochloric acid.

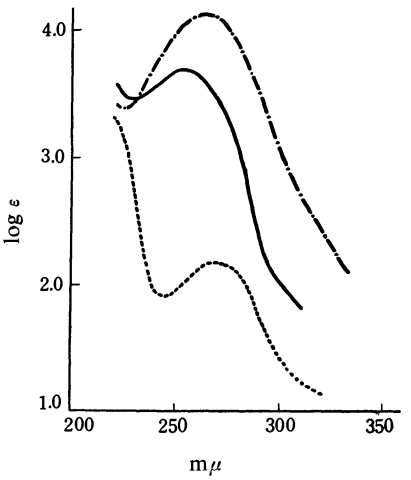



Fig. 6. Ultraviolet absorption spectra of ethyl *O*-methyl *aci*-nitroacetate (-·-·-), oxamide monoxime (XXXV) (——), and ethyl nitroacetate (----) in methanol.

From these results, XXXV is represented by the formula below and may be called oxamide monoxime. Thus XXXV was found to have a structure similar to XIV-i.

Thus, conversion of I-i to XIV-i was considered possible, and hence the plane structure of enteromycin was established as *N*-(*O*-methyl-*aci*-nitroacetyl)-3-aminoacrylic acid (I-i).

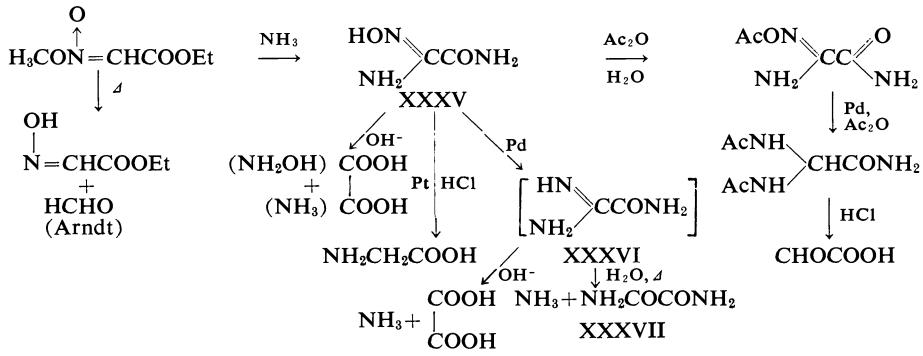
The steric configuration of I was investigated next. The infrared spectra of III, XXI, XXXII and XXXIII, which are considered to be saturated in the 3-aminoacrylic acid portion, scarcely showed the absorption of trans[9] C=C (960~990 cm$^{-1}$), whereas I, II, XII, XIV, XVIII, XIX, XX, XXII, XXX and XXXI, which are considered to be unsaturated in the portion, exhibited the absorption without exception, and therefore the configuration of the portion is assumed to be trans.

6) K. Johnson and E. F. Degering, *J. Am. Chem. Soc.*, **61**, 3194 (1939).

7) F. Arndt and J. D. Rose, *J. Chem. Soc.*, **1935**, 7.

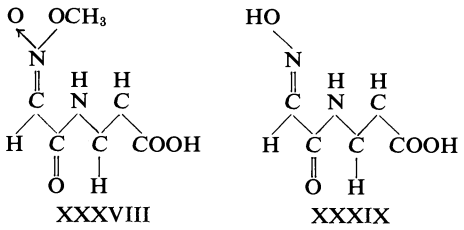
8) H. Gilman, "Organic Chemistry Advanced Treatise 1", 1st. ed. (1938), p. 627.

9) L. J. Bellamy, "The Infrared Spectra of Complex Molecules", Methuen & Co., Ltd., London, John Wiley & Sons, Inc., New York (1954), p. 40.



XII is an aldoxim and takes two crystal forms, but its *O*-acetyl derivative (XVIII) takes only one crystal form. Treatment of XVIII with alkali carbonate afforded XIIa but not the corresponding nitrile.

According to the rule proposed by Hantzsch et al.[10] and corrected by Brady et al.[11,12] and Meisenheimer et al.[13,14], and if all the compounds of the present work follow the rule, the configuration of the hydroxyiminoacetyl group of XII is assumed to be *syn*, and the hydrogen attached to the $\alpha$-carbon atom is on the same side of the double bond as the coordinating oxygen in the *aci*-nitroacetyl group of I-i, and therefore** XXXVIII and XXXIX may be assigned to enteromycin and demethoxyenteromycin, respectively.



## Experimental

**Demethoxyenteromycin Methyl Ester (XXX).**—A solution of 200 mg. of enteromycin methyl ester (II) in 40 cc. of pure methanol was reduced on 80 mg. of Adams platinum oxide until 0.8~0.9 mol. of hydrogen was absorbed. The catalyst was filtered off and the filtrate was evaporated at low temperature under reduced pressure, leaving about 150 mg. of crystals, m. p. 178°C (decomp.), which were recrystallized from methanol to give ca. 70 mg. of needles, m. p. 196°C (decomp.). The product is positive to the ferric chloride·potassium ferricyanide reaction.

Found: C, 42.00; H, 4.87; N, 15.86; O-$CH_3$, 18.29. Calcd. for $C_6H_8O_4N_2$: C, 41.86; H, 4.68; N, 16.28; O-$CH_3$, 18.03%.

***O*-Acetyldemethoxyenteromycin Methyl Ester (XXXI).**—a) To a solution of 50 mg. of XXX in 3 cc. of hot water was added several drops of acetic anhydride and the mixture, after standing for 10 min., was adjusted to pH 6.0 with sodium hydrogen carbonate and extracted with ethyl acetate. The extract was washed with water and evaporated at low temperature under reduced pressure, and the residual prisms, m. p. 116°C (ca. 20 mg.) were recrystallized from acetone. The product melted at 127°C.

b) A suspension of 300 mg. of *O*-acetyldemethoxyenteromycin (XVIII) in 7 cc. of ethyl acetate was allowed to react with a solution of diazomethan (produced from 1 g. of nitrosomethylurea) in 20 cc. of ether for 30 min. and the colorless reaction mixture was evaporated at low temperature under reduced pressure to leave a syrupy substance. The syrupy substance was left standing with a little ether and the resulting crystals (ca. 250 mg.) were recrystallized from acetone in prisms, m. p. 127°C. The product and that in a) gave the same infrared spectrum and their mixed melting point showed no depression.

Found: C, 45.16; H, 4.86; N, 12.76; O-$CH_3$, 13.96. Calcd. for $C_8H_{10}O_5N_2$: C, 44.86; H, 4.71; N, 13.08; O-$CH_3$, 14.36%.

**Dihydroenteromycin Amide (XXXII).**—A solution of 500 mg. of enteromycin amide (XIV) in 400 cc. of hot pure methanol was cooled and reduced on 150 mg. of palladium-carbon (1 : 10) until about one mole of hydrogen was absorbed (ca. 90 min.). The reaction mixture was evaporated at low temperature under reduced pressure, the syrupy residue was dissolved in 10 cc. of methanol, and ether was added to the filtered solution to deposit light pink crystals. The crystals were filtered off, the filtrate was concentrated, and ether was added to the syrupy residue, separating about 380 mg. of crystals, m. p. 176°C (decomp.), which were recrystallized

10) A. Hantzsch and A. Werner, *Ber.*, **23**, 11 (1890); **24**, 13 (1891).

11) D. L. Brady and G. Bischop, *J. Chem. Soc.*, **127**, 1357 (1925).

12) G. W. Wheland, "Advanced Organic Chemistry", (1949), p. 338.

13) J. Meisenheimer et al., *Ann.*, **495**, 249 (1932).

14) H. Gilman, "Organic Chemistry Advanced Treatise 1", 2nd ed., (1948) p. 467.

** Recently, Nishikawa et al.[15] conducted infrared spectroscopic analysis on the compounds of the present work and on their deuterium-substituted derivatives and reported that the intramolecular hydrogen bond observed between NH and coordinating oxygen in enteromycin methyl ester (II) could be explained only by its *anti*-configuration. If their assumption is right, the configuration of enteromycin is in reverse with that of XXXVIII and does not apply to the rule of Hautzsch et al.

15) M. Nishikawa et al., *J. Pharm. Soc. Japan* (*Yakugaku Zasshi*), in press.

from methanol in white plates, m.p. 179°C (decomp.) (250 mg.). The product is positive to the ferric chloride-potassium ferricyanide reaction, gives yellowish brown color with ninhydrin, and furnishes a spot at $R_f$ 0.55 on Consden's paper chromatography described in Report I.

Found: C, 34.56; H, 5.49; N, 24.18. Calcd. for $C_5H_9O_4N_3$: C, 34.28; H, 5.18; N, 23.99%.

**Decomposition of Dihydroenteromycin with Hydrochloric Acid.** — A solution of 10 mg. of XXXII in 1 cc. of 6 N hydrochloric acid was heated under reflux at 100°C for one hour. In one half of the reaction mixture 5 mg. of 2,4-dinitrophenylhydrazine was dissolved and the solution was investigated by paper chromatography to detect no 2,4-DNPH of acetaldehyde or of glyoxylic acid. The remaining half of the reaction mixture was evaporated to dryness and the residue was chromatographed, giving the spot of β-alanine at $R_f$ 0.65.

**Decomposition of Dihydroenteromycin with Alkali.**—A solution of 10 mg. of XXXII in 1 cc. of 1 N sodium hydroxide was refluxed for one hour, when a basic gas evolved copiously. The reaction mixture was passed through a column of Amberlite IR-120 (H-form) and the effluent was subjected to paper chromatography, detecting the spot of oxalic acid at $R_f$ 0.20. The substance adsorbed on Amberlite IR-120 was eluted with 1 N ammonium hydroxide and the solution was chromatographed as above to give a spot of β-alanine.

**Dehyroxydihydroenteromycin Amide (XXXIII).** —A solution of 700 mg. of XXXII in 40 cc. of acetic acid was catalytically reduced for about 40 hr. in the presence of 200 mg. of palladium-carbon and the reaction mixture was concentrated at low temperature under reduced pressure in the atmosphere of nitrogen, leaving crystals, which, after washing first with ether and then with methanol, afforded about 350 mg. of light pink crystals, m.p. 205°C (decomp.). The product is positive to the ninhydrin reaction (light blue color) and gives a spot at $R_f$ 0.77 on paper chromatography (Consden's method).

Found: C, 38.02; H, 6.00; N, 26.86. Calcd. for $C_5H_9O_3N_3$: C, 37.73; H, 5.70; N, 26.41%.

Addition of 1 cc. of 1 N sodium hydroxide to 20 mg. of the product evolved a gas, which was basic to pH test paper and reddened the Nessler's reagent, suggesting that it is ammonia. The mixture was boiled for one hour under reflux and subjected to paper chromatography, detecting oxalic acid and β-alanine.

**Desaminodehydroxytetrahydroenteromycin [Glycyl-β-alanine] (XV).** — A solution of 30 mg. of XXXIII in 5 cc. of 70% methanol was reduced on 20 mg. of Adams platinum oxide and the reaction mixture, after being filtered, was concentrated, leaving about 13 mg. of glycyl-β-alanine.

**Catalytic Reduction of Demethoxyenteromycin Amide and Hydrolysis of the Product.**—A solution of 30 mg. of demethoxyenteromycin amide (XXI) in 10 cc. of pure methanol was reduced on 15 mg. of palladium-carbon. The reaction mixture was neutral and evolved no ammonia, and it exhibited no specific absorption in the long wave region beyond 220 mμ. The reaction mixture was diluted with 3 cc. of water, the catalyst was filtered off, and the filtrate was concentrated at low temperature under reduced pressure, leaving a white residue, which was hydrolyzed by heating with 4 cc. of 3 N hydrochloric acid at 100°C for 2 hr. A 2 cc. portion of the reaction mixture was allowed to react with 2,4-dinitrophenylhydrazine and the resulting 2,4-DNPH was chromatographed to find the spot of the 2,4-DNPH of acetaldehyde at $R_f$ 0.36. The rest of the reaction mixture was evaporated to dryness under diminished pressure and the residue was also chromatographed, detecting a large amount of glycine and traces of β-alanine.

**Ethyl *O*-Methyl-*aci*-nitroacetate.**—An amount of 2.7 g. of ethyl nitroacetate ($K_p$ 79~81°C) prepared from ethyl acetoacetate by the method of Arndt et al.[8] was dissolved in 10 cc. of ether, and the solution was left standing with 40 cc. of an ether solution of diazomethane produced from 5 g. of nitrosomethylurea. The reaction mixture was evaporated at low temperature under reduced pressure, leaving an oily substance showing an absorption maximum (ε 13500) at λ 262 mμ.

Found: C, 41.05; H, 6.45; N, 9.02. Calcd. for $C_5H_9O_4N$ (ethyl *O*-methyl-*aci*-nitroacetate): C, 40.81; H, 6.17; N, 9.52%.

**Oxamide Monoxime (XXXV).**—To a solution of 1.5 g. of ethyl *O*-methyl-*aci*-nitroacetate in 10 cc. of methanol was added 50 cc. of methanol saturated with ammonia, and the yellowish orange-colored mixture, after standing at room temperature overnight, was concentrated at low temperature under reduced pressure, giving 1 g. of light yellow crystals, m.p. 165°C (decomp.). The crystals were dissolved in hot methanol, decolorized with carbon, and the solution was cooled to furnish about 600 mg. of colorless prisms, m.p. 171°C (decomp.), positive to the ferric chloride-potassium ferricyanide reaction but negative to the ninhydrin reaction.

Found: C, 23.58; H, 4.83; N, 40.27. Calcd. for $C_2H_5O_2N_3$: C, 23.30; H, 4.89; N, 40.77%.

An amount of 20 mg. of the product was boiled with 2 cc. of 1 N sodium hydroxide for one hour, when a basic gas evolved copiously. The reaction mixture was passed through a column of Amberlite IR-120 (H-form) and the effluent was chromatographed, giving the spot of oxamide at $R_f$ 0.20.

***O*-Acetyloxamide Monoxime.**—To a solution of 2.5 g. of oxamide monoxime (XXXV) in 7 cc. of hot water was added dropwise 2 cc. of acetic anhydride at 60°C with vigorous stirring. After about 20 min. the reaction mixture was concentrated at low temperature under reduced pressure and the separated crystals were recrystallized from acetone in prisms, m.p. 168°C (decomp.).

The product was negative to the ferric chloride-potassium ferricyanide reaction and showed the infrared spectrum characteristic of =NOCOR (1755 $cm^{-1}$).

Found: C, 33.32; H, 4.83; N, 29.04. Calcd. for $C_4H_7O_3N_3$ (*O*-acetyloxamide monoxime; $CH_3COON{=}C(NH_2)CONH_2$: C, 33.10; H, 4.86; N, 28.96%.

***N*, *N'*-Diacetyldiaminoacetamide.**—A solution of 1 g. of *O*-acetyloxamide monoxime $AcON{=}C(NH_2)\cdot CONH_2$ in a mixture of 20 cc. of glacial acetic acid and 7 cc. of acetic anhydride was reduced on 500 mg.

of palladium-carbon (1 : 10) for about 6 hr. The reaction mixture, after addition of water, was concentrated under reduced pressure, and the part sparingly soluble in hot acetone of the product was recrystallized from water to give about 800 mg. of light pink crystals, m. p. 257°C (decomp.).

Found : C, 41.51 ; H, 6.49 ; N, 24.41. Calcd. for $C_6H_{11}O_3N_3$ *N*,*N'*-diacetyldiaminoacetamide, $(CH_3CO\cdot NH)_2CHCONH_2$ : C, 41.61 ; H, 6.60 ; N, 24.27%.

A solution of 50 mg. of the product in about 1 cc. of water was heated with a solution of 2,4-dinitrophenylhydrazine in hydrochloric acid for about 2 hr. to hydrolyze and at the same time to produce the 2,4-DNPH derivative. The reaction mixture was extracted with ethyl acetate and the extract was shaken with a sodium hydrogen carbonate solution. The alkaline solution was made acidic and extracted again with ethyl acetate, and the extract, after washing with water and drying, was evaporated at low temperature under reduced pressure, giving yellowish white needles, m. p. 192°C. The infrared spectrum of the product was in accord with that of the 2,4-DNPH of glyoxylic acid and the product showed the same color reaction (orange-brown with alkali) and the same $R_f$ value (0.40) in paper chromatography as the 2,4-DNPH of glyoxylic acid.

**Oxamide (XXXVII).**—Catalytic reduction of a solution of 700 mg. of XXXV in a mixture of 10 cc. of methanol and 10 cc. of glacial acetic acid absorbed one mole of hydrogen in about 30 min. The reaction mixture had not the absorption maximum at $\lambda$ 250 m$\mu$ and gave a light blue color with ninhydrin. The reaction mixture was concentrated at low temperature under reduced pressure and the syrupy residue was crystallized by addition of ether. The product was washed with ether, treated with cold water and warm water successively, and recrystallized from hot water to give about 200 mg. of crystals, m. p. above 300°C, negative to the ninhydrin reaction.

Found : C, 27.27 ; H, 4.76 ; N, 31.84. Calcd. for $C_2H_4O_2N_2$ (oxamide) : C, 27.27 ; H, 4.58 ; N, 31.81%.

The ninhydrin positive substance (XXXVI) detected immediately after the reduction could not be isolated.

**Catalytic Reduction of Oxamide Monoxime.**—A solution of 10 mg. of XXXV in 10 cc. of glacial acetic acid was reduced to 20 mg. of Adams platinum oxide for about 2 hr. The reaction mixture was concentrated under reduced pressure and hydrolyzed by heating with 3 cc. of 6 N hydrochloric acid at 100°C for about one hour. Paper chromatography of the white residue of the hydrolysis mixture gave a spot of glycine.

**Decomposition of *O*-Acetyldemethoxyenteromycin with Sodium Carbonate.**—A mixture of 100 mg. of *O*-acetyldemethoxyenteromycin (XVIII) and 4 cc. of 5% sodium carbonate solution was allowed to stand at room temperature for 70 min. The reaction mixture was neutralized with acetic acid and extracted with ethyl acetate. The plates, m. p. 175°C (decomp.) (70 mg.) obtained from the extract were positive to the ferric chloride-potassium ferricyanide reaction and exhibited the same infrared spectrum as demethoxyenteromycin (XII).

Found : C, 38.12 ; H, 3.77 ; N, 17.52. Calcd. for $C_5H_6O_4N_2$ : C, 37.98 ; H, 3.83 ; N, 17.02%.

## Summary

Catalytic reduction of enteromycin methyl ester afforded demethoxyenteromycin methyl ester. Since demethoxyenteromycin amide was presumed to be 3-amino-*N*-(hydroxyiminoacetyl)-$\beta$-alanine, while enteromycin amide was considered to be *N*-(hydroxyamidinocarbonyl)-3-aminoacrylic acid, the two presumptive formulas, I–i and I–ii, were proposed for enteromycin. As the amido compound prepared by amidation of synthetic ethyl *O*-methyl-*aci*-nitroacetate was assumed to have the structure of hydroxyamido carbonyl amide (oxamide monoxime) and as enteromycin was demethoxylated by heating under evolution of formaldehyde, the formula I–i was found to be preferential, considering together other properties of the compound, and therefore the plane structure of enteromycin was established to be *N*-(*O*-methyl-*aci*-nitroacetyl)-3-aminoacrylic acid. The steric configuration of the 3-amino acrylic acid seems to be trans and that of the *O*-methyl *aci*-nitroacetyl group (the configuration of the hydrogen attached to the $\alpha$-carbon atom and of the coordinating oxygen) to be syn.

The author is grateful to Dr. S. Kuwada, Director of the Laboratories for his kindness to give the chance to conduct the present work and for his encouragement throughout the work. Thanks are to Drs. K. Tanaka, A. Miyake, M. Miyamoto, Y. Ueno, J. Ueyanagi and T. Kanzawa for their kind advice. The author is also indebted to Messrs. Y. Kawamatsu, T. Yoshikawa for their kind assistance, to Dr. K. Nakazawa, Messrs. M. Shibata, M. Inowe and their coworkers who gave the starting material, to Messrs. M. Nishikawa, H. Nakamachi for their infrared spectroscopic analyses, to Dr. Y. Asahi for his measurement of dissociation constants, to Messrs. M. Kan, H. Kashiwagi and Mrs. Y. Tsukamoto, Misses F. Suzuki, M. Ueda, and H. Nabekura for their elementary analyses and Mr. T. Nakata for his azotometric determination.

*Research Laboratories*
*Takeda Chemical Industries, Ltd.*
*Higashiyodogawa-ku, Osaka*

# *Oxidation of Ferrous Ions in Aqueous Solutions by Cobalt-60 Gamma Rays. II*[1]. *Effect of Anions at High Dose*

By Hiroshi HOTTA and Shin-ichi OHNO

(Received April 18, 1961)

It is well-known that the Fricke dosimeter ($G(Fe^{3+})=15.6$) is the best secondary standard dosimeter, but it has the upper limit of applicable doses due to the solubility of oxygen in the solution. The air-free system may also be applicable up to higher doses as a good dosimeter ($G(Fe^{3+})=8.2$) for the same kind of radiations with the Fricke dosimeter, if the procedure of degassing oxygen is not minded. For this purpose, the property at high dose was examined.

The reaction scheme for the air-free system is usually assumed as follows:

$$Fe^{2+}+OH=Fe^{3+}+OH^- \quad (1)$$

$$Fe^{2+}+H_2O_2=Fe^{3+}+OH^-+OH \quad (2)$$

$$Fe^{2+}+H+H^+=Fe^{3+}+H_2 \quad (3)$$

As the dose increases, $G(Fe^{3+})$ decreases gradually above a certain dose due to re-reduction of ferric ion produced, by the reaction

$$Fe^{3+}+H=Fe^{2+}+H^+ \quad (4)$$

competing with reaction 3. However, this reaction may not be so simple, for ferric ion is usually associated with anions in the solution, as discussed later.

On the other hand, sodium chloride is usually added by 0.001 M as a stabilizer for the Fricke dosimeter to suppress the effect of organic impurities, for chloride ion scavenges OH radical, which reacts with the impurities, like

$$Cl^-+OH+H^+=Cl+H_2O \quad (5)$$

and this reaction does not affect the $G(Fe^{3+})$ due to the following reaction[2]

$$Fe^{2+}+Cl=Fe^{3+}+Cl^- \quad (6)$$

The effect of anions, especially halide ions, on the radiolysis of ferrous solutions at high dose was investigated in the present study to obtain the detailed information of reaction 4.

## Experimental

The preparation of solutions and the irradiation method by 10 kc. cobalt-60 gamma rays were the usual ones as was mentioned in Part I[1]. The composition of the solutions used is listed in Table I. All the solutions containing halide salts were dissolved in the "standard solution", which contained 0.04 M ferrous ammonium sulfate in 0.8 N sulfuric acid.

The concentration of ferric ion was usually measured by a Shimadzu spectrophotometer. The molar extinction coefficient of ferric ion at 304 m$\mu$, which was 2150 $cm^{-1}$ at 24°C, was constant between 0.2 N and 1.2 N sulfuric acid, but increased by 0.8% for

TABLE I. COMPOSITION OF SOLUTIONS USED IN M AND THEIR $k_4/k_3$ IN Eq. iii

| Run | $FeSO_4(NH_4)_2SO_4$ | $H_2SO_4$ | $Na_2SO_4$ | NaCl | KBr | KF | $O_2$ | $k_4/k_3$ |
|---|---|---|---|---|---|---|---|---|
| a | 0.5 | 0.4 | — | — | — | — | Free | 9.77 |
| b | 0.5 | 1.4 | — | — | — | — | Free | 0.85 |
| c | 0.5 | 2.4 | — | — | — | — | Free | 0.80 |
| d | 0.5 | 4.0 | — | — | — | — | Free | 0.63 |
| e | 0.5 | 0.4 | 1.0 | — | — | — | Free | 2.7 |
| f | 0.04 | 0.4 | — | 0.001 | — | — | Free | 0.77 |
| g | 0.04 | 0.4 | — | 0.01 | — | — | Free | 2.1 |
| h | 0.04 | 0.4 | — | 0.1 | — | — | Free | 14 |
| i | 0.04 | 0.4 | — | 0.5 | — | — | Free | 54 |
| j | 0.04 | 0.4 | — | 0.001 | — | — | Satur. | — |
| k | 0.04 | 0.4 | — | 0.01 | — | — | Satur. | — |
| l | 0.04 | 0.4 | — | 0.1 | — | — | Satur. | — |
| m | 0.04 | 0.4 | — | — | 0.1 | — | Free | 2.1 |
| n | 0.04 | 0.4 | — | — | — | 0.1 | Free | 0.14 |
| p | 0.04 | 0.4 | — | — | — | — | Free | 0.67 |

1) Part I: H. Hotta, A. Terakawa and S. Ohno, This Bulletin, 33, 442 (1960).

2) H. A. Dewhurst, *Trans. Faraday Soc.*, **48**, 965 (1952).

the rise of one degree centigrade between 13 and and 38°C. However, this was measured by the titration method of potassium permanganate for solutions containing fluoride ion or a large amount of ferric ion.

## Results

**Dependence of the Concentration of Ferrous and Sulfate Ions.**—The oxidation of ferrous ion in the nitrogen-saturated solution of 0.5 M ferrous ammonium sulfate in 0.8 N sulfuric acid is shown as "a" in Fig. 1. The $G(Fe^{3+})$ was initially 8.2, and gradually decreased above $7\times10^6$r (0.05 M in ferric ion). The result for the 0.1 M ferrous solution, measured up to 0.09 M in ferrous ion, was almost the same as solution a. The $G(Fe^{3+})$ for the 0.04 M ferrous solution began to come down at $4\times10^6$ r (0.03 M in ferric ion). The decrease of $G(Fe^{3+})$ at high dose is due to reaction 4 as mentioned in the "Introduction". On the other hand, the reaction

$$OH+H_2=H+H_2O \qquad (7)$$

may promote reaction 4 at high dose, at which hydrogen molecules are accumulated in the closed medium. The conversion ratio of ferric ion to initial ferrous ion at the bending point of the $(Fe^{3+})$-dose curve is different between the above solutions.

The effect of sulfate concentration on $G(Fe^{3+})$ at high dose in nitrogen-saturated 0.5 M ferrous ammonium sulfate solutions is shown in Fig. 1, that is, solutions b, c and d were dissolved in 2.8, 4.8 and 8 N sulfuric acid, respectively, and solution f contained 1 M sodium sulfate in 0.8 N sulfuric acid. The decrease of $G(Fe^{3+})$ is considerably suppressed by 2.8 N sulfuric acid, but this effect does not increase much by the more concentrated sulfuric acid. Sulfuric acid is more effective than sodium sulfate as compared between solutions b and e which contained the same amount of sulfate group (1.4 M).

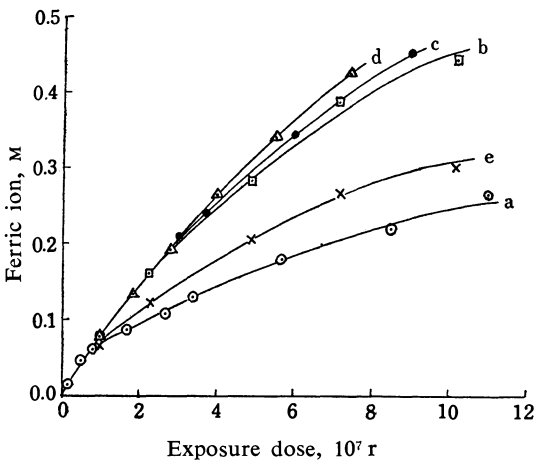



Fig. 1. Oxidation of ferrous ion in the nitrogen-saturated solutions a (⊙), b (▣), c (●), d (△) and e (×).

**Effect of Halide Ions.** — The oxidation of ferrous ion in the nitrogen-saturated standard solutions containing f 0.001 M, g 0.01 M, h 0.1 M and i 0.5 M sodium chloride, respectively, is shown in Fig. 2. As the concentration of of sodium chloride increases, the observed points depart at the lower dose from the straight line of solution f, and the $G(Fe^{3+})$ decreases with the increase of the dose.

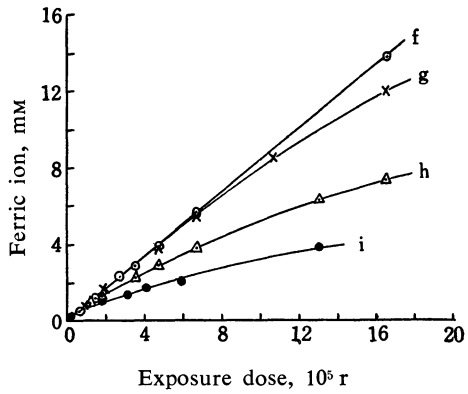



Fig. 2. Oxidation of ferrous ion in the nitrogen-saturated solutions f (⊙), g (×), h (△) and i (●).

On the other hand, the oxidation of ferrous ion in the oxygen-saturated standard solutions containing j 0.001 M, k 0.01 M, and l 0.1 M sodium chloride, respectively, is shown in Fig. 3. The thermal air oxidation of ferrous ion catalyzed by chloride ion, corrected in Fig. 3, were $(2.5\pm0.5)\times10^{-4}$ M in these solutions. The effect of chloride ion as seen in Fig. 2 does not appear even in solution l till oxygen is consumed.

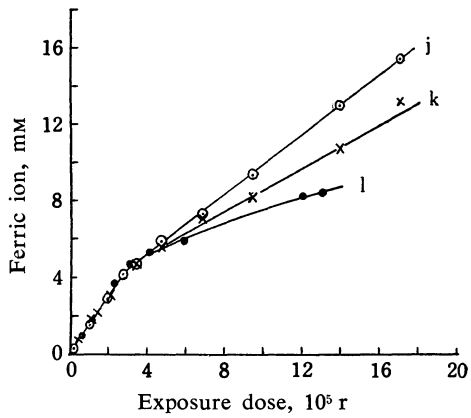



Fig. 3. Oxidation of ferrous ion in the oxygen-saturated solutions j (⊙), k (×) and l (●).

TABLE II. CONCENTRATION OF COMPLEXES IN M

| Run | X | $Fe^{III}$ | $Fe^{3+}$ | $FeSO_4^+$ | $Fe(SO_4)_2^-$ | $FeX^{2+}$ | $FeX_2^+$ | $FeX_3$ | $X^-$ |
|---|---|---|---|---|---|---|---|---|---|
| h | Cl | 0.01 | $9.1\times10^{-5}$ | $2.6\times10^{-3}$ | $7.3\times10^{-3}$ | $3.8\times10^{-5}$ | $4.9\times10^{-6}$ | $2.0\times10^{-9}$ | 0.1 |
| i | Cl | 0.01 | $9.0\times10^{-5}$ | $2.55\times10^{-3}$ | $7.2\times10^{-3}$ | $1.9\times10^{-4}$ | $1.2\times10^{-4}$ | $2.5\times10^{-6}$ | 0.5 |
| m | Br | 0.01 | $9.2\times10^{-5}$ | $2.6\times10^{-3}$ | $7.4\times10^{-3}$ | $4.6\times10^{-6}$ | ? | ? | 0.1 |
| n | F* | 0.01 | $5.3\times10^{-5}$ | $1.5\times10^{-3}$ | $4.2\times10^{-3}$ | $1.3\times10^{-3}$ | $2.6\times10^{-3}$ | $1.6\times10^{-4}$ | $1.55\times10^{-4}$ |
| p | None | 0.01 | $9.2\times10^{-5}$ | $2.6\times10^{-3}$ | $7.4\times10^{-3}$ | — | — | — | — |

Note: * On assumption that $\frac{(H^+)(F^-)}{(HF)}=1.17\times10^{-3}$ ($\mu=0.5$)[4].

TABLE III. ASSOCIATION CONSTANT OF FERRIC COMPLEXES AT 25°C

| Ligand | $K_1$ | $K_2$ | $K_3$ | Ionic strength | Reference |
|---|---|---|---|---|---|
| $SO_4$ | 95 | 9.4 | — | 1.0 | 5 |
| F | $1.62\times10^5$ | $8.9\times10^3$ | 500 | 0.5 | 4 |
| Cl | $4.2\pm0.2$ | $1.3\pm0.4$ | $0.04\pm0.02$ | 1.0 | 6 |
| Br | 0.5 | — | — | 1.0 | 6 |

Note: $K_n=\frac{(FeX_n^{n-3})}{(FeX_{n-1}^{n-4})(X^-)}$

Furthermore, the effect of 0.1 M various halide ions, namely, h sodium chloride, m potassium bromide n potasium fluoride, and p nothing, in the nitrogen-saturated standard solution, was studied as shown in Fig. 4. The effectiveness on the $G(Fe^{3+})$ is in the order of

$$Cl^- > Br^- > SO_4^{2-} > F^- \qquad \text{(i)}$$

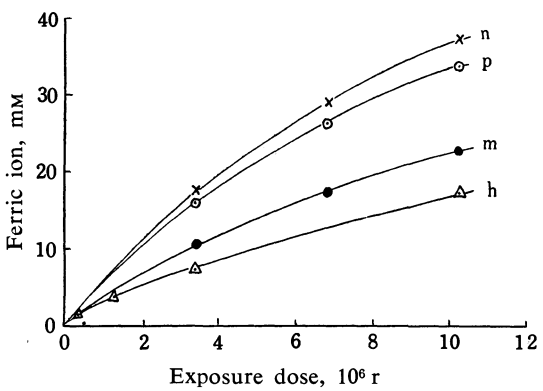



Fig. 4. Oxidation of ferrous ion in the oxygen-saturated solutions h (△), m (●), n (×) and p (⊙).

## Discussion

If chloride ion is only a scavenger for OH radicals as mentioned in the "Introduction", the $G(Fe^{3+})$ should not be affected by the excess of chloride ion. However, the $G(Fe^{3+})$ in the air-free systems decreases at high dose with increase of chloride ion in Figs. 2 and 3. On the other hand, as mentioned already, ferric ions are more or less associated with anions; for example, as $FeCl^{2+}$, $FeCl_2^+$, $FeCl_3$ etc., and even if bare, hydrated with water molecules. Therefore, it is supposed that the reduction rate is different between those ferric complexes.

When the present hypothesis is correct, the observed series i for the effectiveness of various anions on the reduction of ferric ion might be understood by the properties and concentration of the complexes in the solutions. The concentrations of respective complexes in the irradiated standard solutions containing 0.1 M halide salt and 0.01 M ferric species are estimated in Table II without correction of activity on the asumption that ferrous and ammonium ions do not associate with any ion. The concentration of $SO_4^{2-}$ is assumed to be 0.30 M in those solutions from Kerker's result[3]. Furthermore, the association constants of respective complexes in Table III[4-6] are used directly in the evaluation, for the association constant is usually not so changed between 0.5 and 1.0 of ionic strength expected from the above estimation for sulfuric acid.

Ferrous ion is considered to be also associated with hydrogen ion in the acidic solution through the oxygen atom of a water molecule like

$$Fe^{2+}\cdots O\begin{matrix}H\\ \cdots H^+\cdots H\end{matrix} \qquad \text{(ii)}$$

3) M. Kerker, *J. Am. Chem. Soc.*, **79**, 3664 (1957).
4) J. Hudis and A. C. Wahl, ibid., 75. 4153 (1953).
5) R. A. Whiteker and N. Davidson, ibid., **75**, 3081 (1953).
6) E. Rabinowitch and W. A. Stockmayer, ibid., **64**, 335 (1942).

and the approach of a hydrogen atom to the hydrogen ion is assumed to be the rate-determining step of reaction 3. Therefore, if the effect of reaction 7 is ignored, the reaction scheme in the "Introduction" leads to the equation for the rate of oxidation in the mixture of ferric and ferrous ions[7].

$$\frac{d(F^{III})}{d(Dose)} = 2G(H_2) + \frac{2G(H)}{1+\frac{k_4(Fe^{III})}{k_3(Fe^{II})}} \quad \text{(iii)}$$

where $k_3$ and $k_4$ are the rate constants of reactions 3 and 4, respectively, and $(Fe^{III})$ and $(Fe^{II})$ are the concentration of ferric and ferrous species obtained by chemical analysis, respectively. Then, the appearent ratios, $k_4/k_3$, without considering complex formation, are obtained as listed in Table I as the measure of relative reduction rates. The larger value is more reliable.

Exactly speaking, since $(Fe^{III})$ and $(Fe^{II})$ do not always mean their free ion concentration $(Fe^{3+})$ and $(Fe^{2+})$, due to complex formation or imperfect dissociation, the apparent ratio should be rewritten as

$$\frac{k_4(Fe^{III})}{k_3(Fe^{II})} = \frac{1}{k_3(Fe^{2+})}\sum(c_i)k_4' \quad \text{(iv)}$$

where $c_1$ and $k_4'$ are the concentration and rate constant of reduction reaction in reference to the $i$'th ferric complex, respectively, as

$$FeX^{2+} + H = Fe^{2+} + X^- + H^+ \quad (8)$$

instead of reaction 4. If the difference between $(Fe^{II})$ and $(Fe^{2+})$ is ignored, the relative rate constant to reaction 3, the $k_4'/k_3$, for respective ferric complexes are obtained in Table IV

Table IV. Relative reduction rate and standard oxidation-reduction potential of ligand

| Ligand | $k_4'/k_3$ in Eq. iv | Standard oxidation-reduction potential V. |
|---|---|---|
| Br | 3000 | 1.065 |
| Cl | 3400±300 | 1.385 |
| $H_2O$ | 20~70 | 1.77 |
| $SO_4$ | <2 | 1.98 |
| F | ≈0 | 2.85 |

from the estimation in Table II. The contribution except for $Fe^{3+}$, $FeSO_4^+$, $FeX^{2+}$ is also ignored in the evaluation, for the concentration or reaction rate of ignored complexes is small in comparison with those species. The value for $FeCl^{2+}$ is obtained from $k_4/k_3$ of solutions g, h and i. The value of hydrated ferric ion corresponds to free ferric ion in Table II. The assumption for the concentration of $SO_4^{2-}$ is effective for the values in Table IV, but not effective for the ratio between them. It is concluded from Table IV that the reduction rate of ferric chloride and bromide complexes by hydrogen atom is more than fifty times as great as hydrated ferric ions. Also that ferric sulfate complexes are much less reductive than hydrated ferric ion, and ferric fluoride complexes are scarcely reductive at all. It is also understood by the lower reductivity of ferric sulfate complexes why the dose-yield curve is straight ($G(Fe^{3+})=8.2$) up to high dose in spite of the production of ferric ion.

The quantitative analysis is impossible for the result of the concentrated solutions as shown in Fig. 1 for the lack of fundamental constants. However, since the $k_4/k_3$ of sulfuric acid solution is approximately proportional to the ratio of concentration, $(Fe^{3+})/(Fe^{III})$ from Eq. iv, this ratio can give some information for those systems. That is, the ratio, $(Fe^{3+})/(Fe^{III})$, is a function of the concentration of sulfate ion, which suppresses the concentration of free ferric ion by the formation of ferric sulfate complexes as less-reductive species, including the dependence of association constant on ionic strength[5,8]. It is concluded from the ratios in Table I that the concentration of free ferric ion in the solutions decreases and that of free sulfate ion increases with increase of sulfuric acid up to 1 M, but neither concentration changes so much in the more concentrated sulfuric acid solution. The fact is confirmed by the study of the dissociation of sulfuric acid[3,9]. Sodium sulfate is not so effective as sulfuric acid for the suppresion of the reduction reaction in comparison between solutions b and e containing the same amount of sulfate group, for the dissociation of sulfuric acid is suppressed by sodium sulfate. The difference of $k_4/k_3$ between solutions a and p containing the same amount of sulfuric acid may be due to the effect of direct reaction with thermerized electron as suggested by Weiss[10] or other reactions in a hot track in the concentrated solution.

On the other hand, in Fig. 3, the $G(Fe^{3+})$ in the presence of oxygen is not affected by chloride ion even in solution till oxygen is consumed. It is because all hydrogen atoms from the radiolysis of water associate rapidly with oxygen as $HO_2$ which is an oxydizing reagent. According to Rothschild and Allen, the association rate is more than one hundred times as fast as the rate of reaction 3[7].

7) W. G. Rothschild and A. O. Allen, *Radiation Research*, **8**, 101 (1958).

8) B. N. Mattoo, *Z. phys. Chem.*, **19**, 156 (1959).

9) T. F. Young and L. A. Blatz, *Chem. Revs.*, **44**, 93 (1949).

10) J. Weiss, *Nature*, **186**, 751 (1960).

Silverman and Dodson reported that the rate of electron exchange reaction between ferric chloride complex and ferrous ion is about ten times as fast as that between free ferric and ferrous ions[11]. For such a case, the ligand atom gives a chance for multi-charged ions to anchor easily at the same site, and also serves as the bridge of electron transfer. Brown[12] suggested that the effectiveness may be a function of the electronegativity and polarizability[13]. Since the reactivity of the hydrogen atom for the present reaction is not due to electrostatic force but due to unpaired electron, some difference is expected between the two cases. In fact, the electron exchange reaction between $Tl^+$ and $Tl^{3+}$ is promoted in sulfuric acid[14], but ferric sulfate complex is less reductive for hydrogen atom than hydrated ferric ion as shown in Table IV. Anyhow, it is necessary for the reaction

$$Fe^{3+}-X^- + H \longrightarrow Fe^{2+} + XH \qquad (9)$$

even if XH is dissociated afterwards, that the ligand X loss one electron. The standard oxidation-reduction potential of the ligand to do so, $\Delta E$, which may be a function of electronegativity and polarizability, corresponds to the reductivity of complexes in Table IV. The discrepancy for the order of bromide complex may be due to the uncertainty of its association constant. When the reduction rate of complexes might be expressed as

$$k = A \exp\left(-\frac{\Delta E}{RT}\right) \qquad (v)$$

the $k_4'/k_3$ of fluoride complex is expected to be the order of 0.01.

## Summary

The $G(Fe^{3+})$ of air-free acidic ferrous sulfate solutions decreases gradually with the increase of dose due to the re-reduction of ferric ion produced. The decrement depends on the property of anion as well as sulfuric acid in the solution in the order of

$$Cl^- > Br^- > SO_4^{2-} > F^-$$

The relative reduction rate of ferric complexes is obtained in Table IV as a result of the estimation of respective complexes in the solution; that is, ferric chloride and bromide complexes promote the reduction of ferric ion, and ferric sulfate and fluoride complexes suppress it.

*Japan Atomic Energy Research Institute*
*Tokai, Ibaraki-ken*

11) J. Silverman and R. W. Dodson, *J. Phys. Chem.*, **56**, 846 (1952).
12) Discussion in Ref. 11.
13) J. R. Tessman, A. H. Kahn and Wm. Shockley, *Phys. Rev.*, **92**, 890 (1953).
14) C. H. Brubaker, Jr., K. O. Groves, J. P. Mickel and C. P. Knop, *J. Am. Chem. Soc.*, **79**, 4641 (1957).
15) L. Pauling, "General Chemistry", Chap. 32, W. H. Freeman & Co., (1953).

# *Synthesis of Several Tertiary Alcohols from Propanol-2 and Ethylene by Gamma-ray Irradiation**

By Kozo HIROTA and Motoyoshi HATADA

(Received April 22, 1961)

In previous reports[1,2], it was found that several higher ketones can be synthesized by a chain telomerization from acetaldehyde and terminal olefins by $\gamma$-ray irradiation with high $G$ values. Similar telomerization may also occur with a high yield in the system of propanol-2 and ethylene, considering Urry's research[3] on the peroxide- and light-induced additions of several alcohols to olefins. The chain-carrying radical of this system, however, is $(CH_3)_2\dot{C}OH$ instead of $CH_3\dot{C}O$ in the systems of acetaldehyde and olefins, as will be shown as follows:

Initiating step:

$$(CH_3)_2CHOH \rightsquigarrow (CH_3)_2\dot{C}OH + H$$

Propagating step:

* Chain Telomerization Induced by Gamma-rays. II.

1) K. Hirota and M. Hatada, This Bulletin, 33, 1682 (1960).

2) K. Hirota, S. Iizuka and M. Hatada, Abstract Papers of the 13th Annual Meeting of the Chemical Society of Japan (1960).

3) W. H. Urry et al., *J. Am. Chem. Soc.*, 76, 450 (1954).

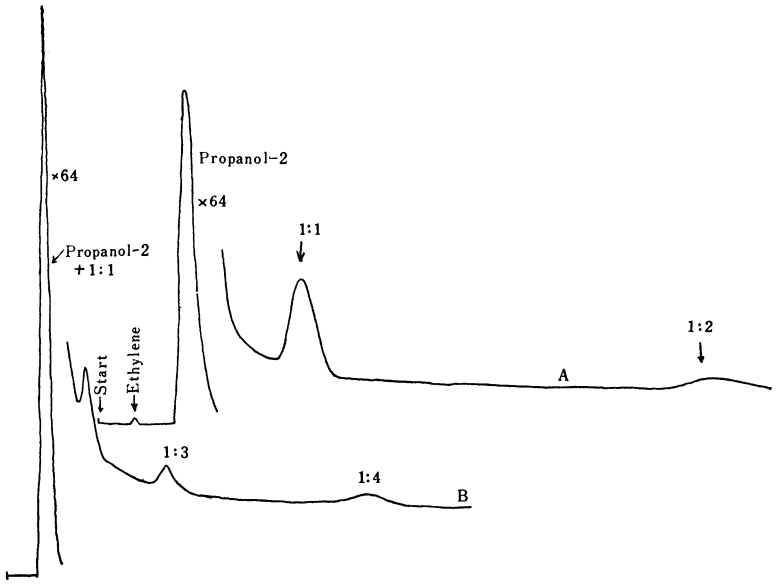



Fig. 1. Gaschromatograms of the samples after irradiation.
Curve A was obtained by using D. O. P. 3 m. column at 107°C.
Curve B was obtained by using H. V. O. 6 m. column at 180°C.

$$(CH_3)_2\dot{C}OH + C_2H_4 \xrightarrow{k_{p0}} (CH_3)_2C(OH)CH_2\dot{C}H_2$$

$$(CH_3)_2C(OH)CH_2\dot{C}H_2 \xrightarrow{+C_2H_4, k_{p1}}$$

$$+(CH_3)_2CHOH \swarrow^{k_{d1}} \quad (CH_3)_2C(OH)(CH_2)_3\dot{C}H_2$$

$$(CH_3)_2(C_2H_5)COH + (CH_3)_2\dot{C}OH$$

By a similar scheme $(CH_3)_2C(OH)(CH_2)_3\text{-}\dot{C}H_2$ will produce $(CH_3)_2\text{-}(OH)(CH_2)_3$ and $(CH_3)_2\cdot C(OH)(CH_2)_3CH_2CH_2\dot{C}H_2$ with velocity constants $k_{d2}$ and $k_{p2}$, respectively, etc.

It is the object of the present paper to report that the expected telomerization proceeds even at room temperature.

## Experimental

Commercial pure propanol-2 was used after distillation, while commercial ethylene (research grade) was used without further purification. No impurity was found in the gases by either gaschromatographical or mass-spectral analyses.

Every sample for irradiation was degassed and distillated into glass tubes (1.2 cm. in diameter; ca. 20 cm. in length), equipped with a breakable joints. After the tubes were sealed, they were irradiated by $\gamma$-rays from the Co-60 source (700 c) installed in this laboratory. Dosimetry was based on a ferrous oxidation yield of 15.5. After the irradiation, the samples were taken out through the breakable joint and were put through gaschromatographic analysis (Apparatus; Shimadzu GC1A type).

The initial ratios of propanol to ethylene in the sample were about ten if otherwise not described. These ratios will be denoted as $R$ hereafter, which, however, is not necessarily equal to that in solution, because ethylene is hardly soluble.

## Results

In the sample irradiated, *tert*-amyl alcohol (1 : 1 telomer) and *tert*-heptyl alcohol (1 : 2 telomer) were identified by the use of a 3.0 m. column of dioctyl phthalate, while *tert*-nonyl alcohol (1 : 3 telomer) and *tert*-undecyl alcohol (1 : 4 telomer) were also detected by the use of a 6.0 m. column of high vacuum-oil (Fig. 1). However, the existence of higher telomers will be estimated, especially when $R$ is large, as is done in the discussions.

In Fig. 2, the amount of the 1 : 1 telomer produced is plotted against the irradiated time. After an induction period is observed in the initial part of the curve, a linear increase is found in the amount. It is interesting to note that a similar induction period was also observed[4] in the gamma-ray-induced telomerization of acetaldehyde and ethylene. Such an effect may be due to the presence of some undetectable impurities, e. g. oxygen or other radical-scavengers. The $G$ value calculated from the linear part of the curve is ca. 1.2×

4) Cf. K. Hirota, H. Ochi and M. Hatada, *Isotopes and Radiation* (*Tokyo*), 3, No. 6 (1960). (Short communication).

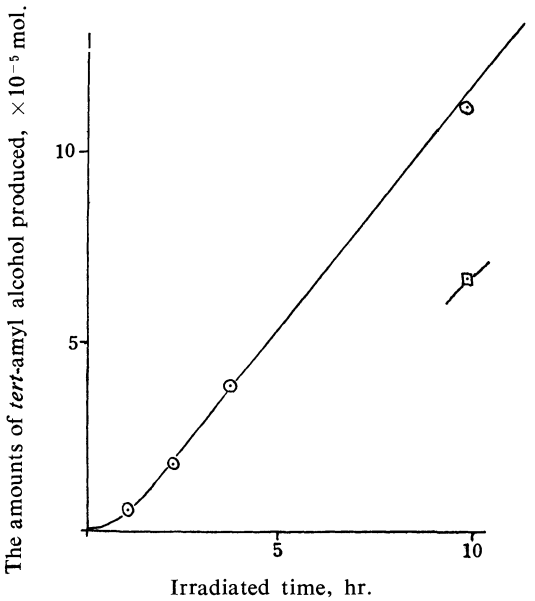



Fig. 2. The amounts of *tert*-amyl alcohol vs. irradiation time.
Dose rate, $5.7\times10^{4}$ r/hr.
$(CH_3)_2CHOH/C_2H_4(=R)$ in mole, 1 : 10
Irradiation temperature, 6°C

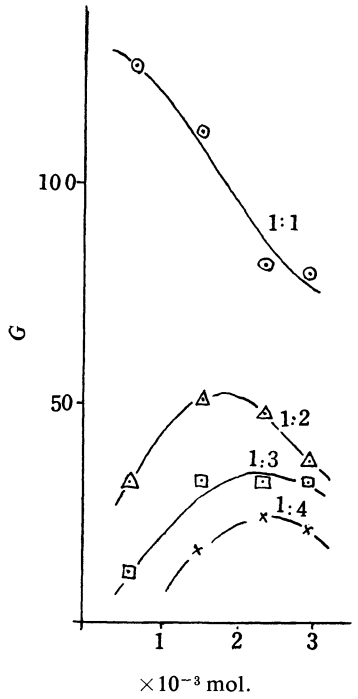



Fig. 3. *tert*-Alcohols produced vs. the amount of ethylene in the system.
Dose rate, $5.7\times10^{4}$ r/hr.
Energy absorbed, $8.5\times10^{19}$ eV.
Irradiation temp., 9°C

$10^2$, suggesting that this reaction proceeds by a chain mechanism. Figure 3 shows the relation between $R$ and $G$ values of the product at 9°C, where other variables are kept constant. By use of the data of Fig. 3 molar fraction $F_i$ of the $1:i$ telomers to the total telomers is plotted in Fig. 4, making $R$ as the ordinate. The full curves in the figure will be explained in the discussion.

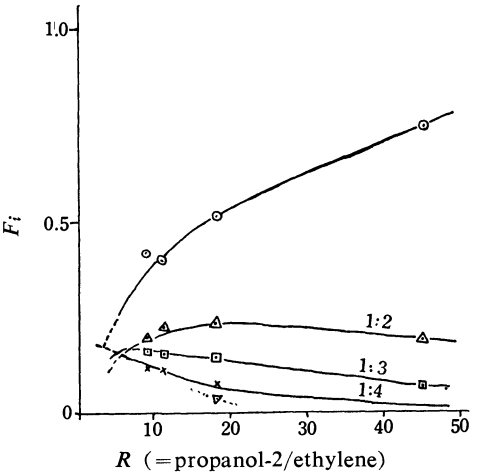



Fig. 4. Distribution of the telomers corresponding to the data of Fig. 3.
—— Calculated by

$$F_i=\frac{C_nR}{\prod_{i=1}^{n}(C_iR+1)}$$

▽ Assumed value for 1 : 5 telomer

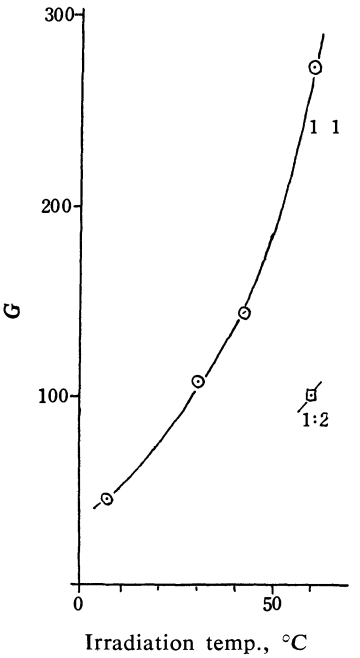



Fig. 5. *tert*-Amyl alcohols vs. irradiation temp.

Temperature dependency of $G$ values on the amount of the products is shown in Fig. 5. It is clear that the higher is the reaction temperature, the more *tert*-amyl alcohol is produced and $G$ value reaches about 300 at 60°C. Plots of logarithms of the $G$ values vs. $1/T$°K give a straight line as shown in Fig. 6, by which an activation energy of 6.3 kcal./mol. can be determined. This value, however, is not necessarily that of the reaction, but is of complex nature, because the solubility of ethylene into alcohol changes when the reaction temperature is changed as is seen in our experiment.

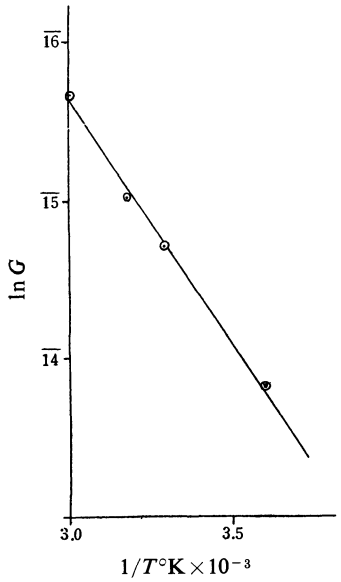



Fig. 6. $\ln G$(*tert*-amyl alcohol) vs. $1/T$°K. $E_A=6.3$ kcal./mol.

## Discussion

If the telomerization proceeds by the reaction scheme shown in the introduction, the distribution of the telomers produced will be given as molar fractions $F_i$ by the theoretical relation[5]:

$$F_i=\frac{C_iR}{\prod_{i=1}^{n}(C_iR+1)}$$

where $C_n$'s$=k_{dn}/k_{pn}$ are transfer constants. Assuming that the molar ratio of alcohol to ethylene in the solution is the same as that ($R$) of the starting material and that higher telomers are produced though small in amount, chain transfer constants $C_i$'s were calculated from the observed $F_i$'s in the sample of $R=18$, and were found to be 0.062, 0.056, 0.073 and 0.12 for $i=1$, 2, 3 and 4, respectively, if $G$ value of 1 : 5 telomer is assumed to be 8. The mean value of $C_1$, $C_2$ and $C_3$, i. e. 0.062, resembles Urry's average transfer constant, 0.057[3], obtained at 115~130°C, using di-*tert*-butyl peroxide as initiator. This means that the chain-propagating step of the radiation-induced reaction is similar to that of the reactions induced by chemical initiators, although the reaction temperatures, pressure and $R$ values are different in the two reactions.

However, exactly speaking, plots of $F_i$ determined from the observed data vs. $R$ do not lie on the full curves calculated from the above $C_i$'s so completely as shown in Fig. 4. Similar comparison of the theory and experiment was better in the systems of acetaldehyde and propylene[1] or isobutylene[2]. The discrepancy in this system may be brought about by the assumptions adopted in the calculation i. e., $G$ value of 1 : 5 telomer and neglect of the change of solubility of ethylene to propanol-2 with pressure. Though a better coincidence may be obtained by the introduction of solubility data, this correction could not be carried on, because of the absence of such data. On the other hand, production of higher alcohols, corresponding to $1:i$ telomer ($i\geq 5$), ought to be considered, as assumed to some extent in the calculation, because if they are completely neglected, the coincidence became more than that shown in Fig. 4.

The overall activation energy obtained above (6.3 kcal./mol.) nearly equals that of the abstraction reaction of hydrogen atom from $\alpha$-carbon of propanol-2, i. e., 7.3 kcal./mol.[6] Considering the ambiguity included in the former value, such a degree of coincidence indicates that the step which produces the chain-carrying radical may be regarded as being the rate-determining one in the above mechanism.

In the irradiated samples containing a small amount of iodine ($10^{-3}$ mol. in propanol-2), not even a trace of telomers was found, probably due to the radical-scavenging action of iodine. This finding may serve as an evidence of the radical mechanism as assumed by us. However, since formation of $CH_nI^+$ and $CH_4OI^+$ was recently observed mass spectrometrically by the ion-molecule reactions[7];

$$CH_n^+ + I_2 \rightarrow CH_nI^+ + I$$
$$\text{or}\quad CH_n^+ + I_2 \rightarrow CH_{n-1}I^+ + HI$$
$$CH_3OH^+ + I_2 \rightarrow CH_4OI^+ + I$$

an ion-scavenging action of iodine can be taken into account. It is possible therefore that some ion or ions also play some role in the

5) Cf. C. Walling, "Free Radicals in Solution", John Wiley & Sons, New York (1957), p. 245.

6) A. F. Trotman-Dickenson and E. W. R. Steacie, *J. Chem. Phys.*, **19**, 329 (1951); *Quart. Rev.*, **7**, 198 (1953).

7) A. Henglein, *Z. Elektrochem.*, **64**, 1015 (1960).

present reaction, but probably in some intermediate step which preceeds the production of $(CH_3)_2\dot{C}OH$. Then the initiating step above the mechanism will be composed of several elementary ones.

Though the $G$ value of this telomerization is of the same order of magnitude as the system of acetaldehyde and propylene or isobutylene, it is smaller by one or two orders of magnitude at the same temperature than that of the system where acetaldehyde was used instead of propanol-2[4]. This may be attributed to the difference in nature between the chain-carrying radicals, i. e., acetyl radical and isopropyl radical in both systems.

## Summary

Tertiary amyl and higher tertiary alcohols have been synthetized at 6~60°C by irradiating gamma-rays on mixture of propanol-2 and ethylene enclosed in glass vessels. It has been found that as the irradiation temperature the $G$ value of these telomers increases markedly, e. g. up to ca. 300 at 60°C. It has been concluded from the distribution of the telomers produced that this reaction proceeds by a chain mechanism, making isopropyl radical $(CH_3)_2\dot{C}OH$ as the chain-carrying radical. It has been estimated that the characteristic of gamma-rays will be found in the step prior to the production of the isopropyl radical. If the rays can play some role in this reaction.

The authors wish to express their sincere thanks to Mr. Hiroshi Ochi for his help in performing the present research.

*Osaka Laboratories*
*Japanese Association for Radiation Research on Polymers*
*Neyagawa, Osaka* (*M. H. & K. H.*)
*Department of Chemistry*
*Faculty of Science*
*Osaka University*
*Nakanoshima, Osaka* (*K. H.*)

# *Syntheses and Ultraviolet Spectra of Aromatic Azo Compounds. I. Bromo-methylazobenzenes*

By Yujiro NOMURA

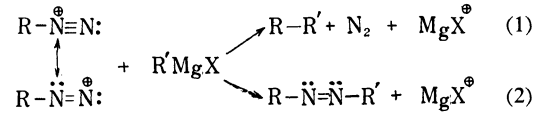
(Received April 22, 1961)

The reaction of Grignard reagents with aromatic diazonium salts was first investigated by Hodgson and Marsden[1], who found that the addition of the zinc chloride double salts of several diazonium chlorides to arylmagnesium bromides in refluxing dry ether gave azo compounds in low yields.

Oda and Nakano[2], on the other hand, reported that the zinc chloride double salt of benzenediazonium chloride reacted with alkyl- or arylmagnesium bromides in ether at 0°C to give 6~34% of the theoretical amount of alkyl- or arylbenzenes.

Curtin and Ursprung[3] reinvestigated these reactions following the procedure of Oda et al. and observed that azo compounds were formed in 2~35% yields and no significant amounts of biaryls, reported by Oda et al. to be products of these reactions, could be obtained. They postulated that small amounts of metal impurities might be contained in magnesium employed by Oda et al. which catalyzed the reaction in an abnormal way.

The formation of biarly or azo compound in the reaction of Grignard reagent with diazonium ion may be represented by the following equations:




(1)

(2)

If the reaction proceeded according to 1, the same mole of nitrogen as biaryl R-R′ should be evolved. But no significant amounts of nitrogen have been observed to evolve in these reactions in accordance with the observations of Curtin et al. Since azobenzenes initially formed by the reaction 2 might react further

1) H. H. Hodgson and E. Marsden, *J. Chem. Soc.*, **1945**, 274.
2) R. Oda and K. Nakano, *Repts. Inst. Chem. Res., Kyoto Univ.*, **19**, 91 (1949); R. Oda, *Mem. Fac. Eng. Kyoto Univ.*, **14**, 195 (1952).
3) D. Y. Curtin and J. A. Ursprung, *J. Org. Chem.*, **21**, 1221 (1956).

TABLE I. BROMO-METHYLAZOBENZENES

| No. | Compound | M.p., °C | Color | Found N, % (Calcd. for $C_{13}H_{11}BrN_2$: N, 10.18%) | Yield* |
|---|---|---|---|---|---|
| I | 2-Bromo-2'-methyl | 88~89[a] | Red | 10.10 | 64 |
| II | 2-Bromo-3'-methyl | 44.5~45.5[b] | Orange red | 9.99 | 40 |
| III | 2-Bromo-4'-methyl | 60.5~61.5[c] | Red orange | 10.03 | 60 |
| IV | 3-Bromo-2'-methyl | 49[c] | Red orange | 10.24 | 61 |
| V | 3-Bromo-3'-methyl | 79~79.5[c] | Orange | 10.23 | 52 |
| VI | 3-Bromo-4'-methyl | 119.5[d] | Orange yellow | 10.08 | 65 |
| VII | 4-Bromo-2'-methyl | 53.5~54[c] | Red orange | 10.14 | 42 |
| VIII | 4-Bromo-3'-methyl | 81.5[c] | Orange | 10.19 | 68 |
| IX | 4-Bromo-4'-methyl | 153[a] | Brown orange | 10.03 | 68 |
| X | 4-Bromo-2-methyl | 73~73.5[b] | Red orange | 9.97 | 73 |
| XI | 4-Bromo-3-methyl | 68.5[b] | Yellow orange | 10.35 | 74 |
| XII | 2-Bromo-4-methyl | 43.5~44[c] | Red orange | 10.20 | 65.6 |

a) Recrystallized from ethanol.
b) Distilled in vacuo and then recrystallized from methanol.
c) Distilled in vacuo and then recrystallized from dilute ethanol.
d) Recrystallized from ethanol containing a small amount of benzene.
* Based on bromocompound used.

with excess Grignard reagent to yield hydrazobenzenes[4] and their derivatives[5], it was suspected that the attack of Grignard reagents on azobenzenes might be responsible for the rather poor yields of azo compounds.

The present study was carried out for the purpose of applying the reactions of Grignard reagents with diazonium salts to the preparations of various azo compounds and always the excess of diazonium salts over Grignard reagents were used expecting better yields of azo compounds.

**General Procedure.**—The ethereal solution of tolylmagnesium bromide prepared from 1 mol. of bromotoluene and the excess of magnesium was added slowly with vigorous stirring to the suspension of 1.3~1.5 mol. of the zinc chloride double salt of bromobenzenediazonium chloride at a rate necessary to maintain refluxing. The resulting dark red mixture was stirred for an additional 60 min. at room temperature and then poured onto ice-cold dilute hydrochloric acid. The ether layer was separated and washed with water and dried. Evaporation of the ether gave a solid or oil, which crystallized upon standing. The crude bromo-methylazobenzenes thus obtained were recrystallized from alcohol or distilled in vacuo, followed by recrystallization from alcohol.

In the syntheses of 4-bromo-2-methylazobenzene (X), 4-bromo-3-methylazobenzene (XI) and 2-bromo-4-methylazobenzene (XII), phenyl magnesium bromide and the excess of the zinc chloride double salts of bromotoluene-diazonium chlorides were used.

The bromo-methylazobenzenes prepared by this method were shown in Table I. They are all new compounds except 4-bromo-4'-methylazobenzene (IX)[6] and 4-bromo-3-methylazobenzene (XI)[7], which showed no depression of their melting points on admixture with a respective authentic specimen prepared according to the literature.

Electronic absorption spectra were measured in an alcoholic solution. The maxima of the absorption spectra of bromo-methylazobenzenes were listed in Table II. It can be seen that the *K*-bands of bromo-methylazobenzenes shift

TABLE II. WAVELENGTHS AND INTENSITIES OF ELECTRONIC ABSORPTION MAXIMA (IN ETHANOL)

| | *K*-band | | *R*-band | |
|---|---|---|---|---|
| | $\lambda$, m$\mu$ | $\varepsilon_{max}$ | $\lambda$, m$\mu$ | $\varepsilon_{max}$ |
| I | 329 | 14400 | 465 | 420 |
| II | 324 | 15700 | 455 | 430 |
| III | 333 | 19550 | 456 | 460 |
| IV | 327 | 18700 | 454 | 510 |
| V | 321 | 19900 | 446 | 670 |
| VI | 329 | 22300 | 442 | 570 |
| VII | 332 | 22800 | 456 | 590 |
| VIII | 328 | 24600 | 446 | 460 |
| IX | 333 | 26100 | 441 | 570 |
| X | 333 | 26600 | 457 | 610 |
| XI | 327 | 25600 | 445 | 530 |
| XII | 331 | 18900 | 456 | 450 |

4) H. Franzen and W. Deibel, *Ber.*, **38**, 2716 (1905).
5) E. Bamberger and M. Tichvinsky, ibid., **35**, 4179 (1902).
6) 4-Bromo-4'-methylazobenzene was synthesized by D. Bigiavi et al., *Gazz. chim. ital.*, **57**, 557 (1927), by the condensation of *p*-nitroso-toluene and *p*-bromoaniline.
7) 4-Bromo-3-methylazobenzene was prepared by the bromination of 3-methylazobenzene or by the condensation of 5-amino-2-bromotoluene and nitrosobenzene. J. Burns et al., *J. Chem. Soc.*, **1928**, 2932.

towards a longer wavelength than unsubstituted azobenzene ($\lambda_{max}$ 318 m$\mu$, $\varepsilon_{max}=20900$ in alcohol) especially when methyl or bromine is in ortho or para positions. On the other hand, the molecular extinction coefficients ($\varepsilon_{max}$) became larger when methyl or/and bromine was situated in ortho, meta and para positions, in this order.

## Experimental

Ultraviolet absorption spectra were measured by a Hitachi EPU 2 type spectrophotometer using a 1 cm. quartz cell.

**Preparation of the Zinc Chloride Double Salt of Diazonium Chloride.**—The mixture of 1 mol. of amine and 3~4 mol. of hydrochloric acid (1 : 1) was diazotized at 0°C with sodium nitrite dissolved in a small amount of water. To the resulting solution of diazonium chloride was added a cold saturated solution of zinc chloride (200 cc.) with stirring, when the zinc chloride double salt of diazonium chloride was separated out. After being allowed to stand in ice water for some time with occasional stirring, the double salt was filtered by suction and washed several times with a little ice-cold alcohol and then with ether. The double salt was spread in air and then dried in vacuum desiccator. The yield was excellent in most cases.

A few examples of the preparation of the zinc chloride double salt of diazonium chloride was shown below.

Thirty two grams of 2-amino-5-bromotoluene were added to 100 cc. of dilute hydrochloric acid (1 : 1), and the resulting suspension of the amine hydrochloride was diazotized at 0°C. A saturated solution of zinc chloride (about 40 cc.) was added to the diazotized solution with stirring. The yield of the double salt was 40 g. or 98% of the theoretical. In the same manner, from 17.2 g. of *p*-bromoaniline was obtained 28.0 g. (95% yield) of the double salt, and from 17.2 g. of *m*-bromoaniline was obtained 28.3 g. of the double salt.

**Preparations of Bromo-methylazobenzenes.**—Twelve bromo-methylazobenzenes were prepared following the general procedure described above. An example is given below in the preparation of 2-bromo-2'-methylazobenzene (I).

Seventeen grams of the zinc chloride double salt of *o*-bromobenzenediazonium chloride and 150 cc. of dry ether were put in a 300 cc. flask equipped with an efficient stirrer, a reflux condenser and a dropping funnel. A Grignard solution prepared from 7 g. of *o*-bromotoluene and 1.3 g. of magnesium in ether and diluted to about 40 cc. with dry ether was introduced from the dropping funnel to the suspension of the diazonium salt with vigorous stirring over a period of 15 min. without external cooling. Exothermic reaction occurred and gentle reflux continued for some time after all the Grignard solution was added. The mixture was diluted to double its volume with ether and shaken with cold dilute hydrochloric acid and then with water, dried over calcium chloride and evaporated to give the red crystals, which were recrystallized from ethanol with a small amount of decolorizing charcoal. The yield of 2-bromo-2'-methylazobenzene was 7 g. or 64% of the theoretical amount based on *o*-bromotoluene.

## Summary

1) Twelve bromo-methylazobenzenes have been synthesized by the reactions of Grignard reagents with zinc chloride double salts of diazonium compounds. Ten of them are new compounds.

2) The ultraviolet absorption spectra of bromo-methylazobenzenes have been measured and some regularities of the absorption maxima have been observed in them.

The author is indebted to Dr. Nozomu Ebara for the determination of the ultraviolet absorption spectra.

*Department of Chemistry*
*College of General Education*
*The University of Tokyo*
*Meguro-ku, Tokyo*

# *Photoreduction of Methylene Blue by the Visible Light in the Aqueous Solution Containing Certain Kinds of Inorganic Salts. III. Kinetic Treatment of the Reaction*

By Yoshiharu Usui and Masao Koizumi

(Received April 13, 1961)

It has been established in the previous papers[1] that upon irradiation of the aqueous solution of methylene blue containing various kinds of salts by visible light, the formation of leuco dye takes place accompanied by demethylation and the irreversible decomposition of dye; and in particular its rate is quite high in the presence of phosphate, sodium hydroxide and borate. Leuco formation and demethylation proceed as simultaneous reactions and in most cases the rate of the former is higher than that of the latter, which can be suppressed almost completely under suitable conditions.

Now it is very remarkable that the leuco-formation can occur without any reducing agents in the ordinary sense, and how this occurs still awaits further studies and is a very important problem to be solved. In the previous paper two possibilities were suggested for the primary process, i. e., the reaction of the excited dye and that of the ground state on one hand and the reaction between the excited dye and hydroxide ion on the other. Of course the problem must be attacked from various standpoints, and the present paper is chiefly concerned with the investigation from the reaction kinetics.

## Kinetic Treatment

The present reaction as a whole is too complicated to be treated exactly, but it is desirable to get an approximate rate formula which can reproduce the experimental results, as a means for studying further the reaction scheme. Now the most reliable data supplied by the experiments are the decline of the main absorption band of the dye. But as already stated, the formation of leuco dye is accompanied with demethylation which causes the shift of the maximum toward the shorter wavelength. Therefore, by applying the minimum ratio method of Blaisdell[2] to the absorption spectra of the irradiated solution, the one due to the remaining methylene blue was evaluated and its analysis was undertaken. The decrease in dye concentration obtained from the above treatment is, of course the sum due to leuco-formation, demethylation and irreversible decomposition, but in view of the fact that these reactions take place with about the same ratio for a particular system during the most part of one run, the rate derived therefrom may well correspond to that of leuco-formation. It is necessary however, to pay due attention to this point when the rates for different systems are compared; for example, in case of phosphate the rate of demethylation is of about the same order of that of leuco-formation, while in case of sodium hydroxide the former is quite a good deal smaller than the latter.

In Fig. 1 plots of $\varepsilon_{max}$ against time are given for the typical results so far obtained, in which $\varepsilon_{max}$ pertains to the maximum of the absorption spectra of methylene blue after

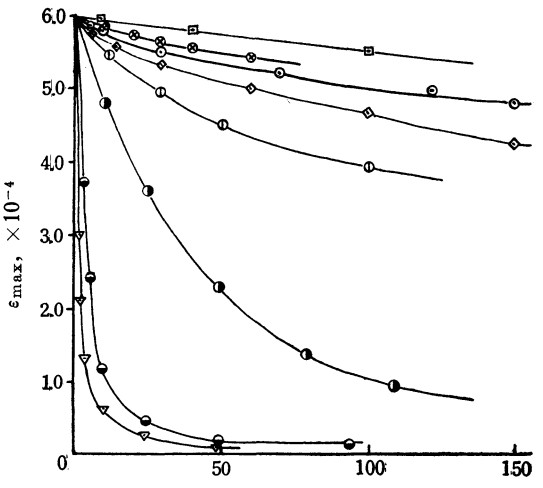



Fig. 1. Photobleaching of methylene blue in deaerated solutions containing various inorganic compounds.

◙ $HCl(1\times10^{-3}$ M), ◑ $NaOH(1\times10^{-3}$ M),
ⓘ $Na_2SO_4$, ⊗ NaCl, ⊙ NaI,
◈ Without any salt, ◑ Borate buffer,
▽ Phosphate buffer

1) Y. Usui, H. Obata and M. Koizumi, This Bulletin, 34, 1049 (1961); H. Obata, ibid., 34, 1057 (1961).
2) B. E. Blaisdell, *J. Soc. Dyers. & Colorists*, 65, 619 (1949).

Blaisdell's treatment*. It is seen that broadly speaking, they are classified into three groups on the grounds of the magnitude of bleaching. The first group with a very small rate contains sodium sulfate, sodium iodide, sodium chloride and the pure aqueous solution. The second group with a medium rate contains only borate buffer, and the third one with the largest rate are phosphate buffer and sodium hydroxide solution. As stated below the first and the second groups have the rate formula which is approximately of the first order in respect to dye while for the third group the second order rate formula fits the experimental data quite satisfactorily. Hence the first and second group may be lumped together. In the following the rate for borate buffer and that for phosphate buffer will be separately discussed, each as a representative of the two groups.

**Borate Buffer Solution.**—Approximately, the rate is represented as of the first order with respect to dye, but as the reaction proceeds it becomes progressively smaller than that calculated from the simple first order rate formula. The cause for this retardation may supposedly be due to the interference of a certain reaction product; for example, such a product as hydrogen peroxide and this was really confirmed by the following experiment. Thus into the solution of methylene blue of which 80~90% had previously been photobleached, a suitable quantity of dye was newly dissolved in vacuo to make the concentration about equal to that of the previous one. Using such a solution the photoreaction was once more repeated and its rate was compared with that of the previous experiment.

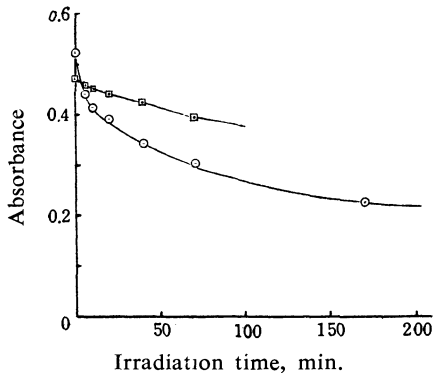



Fig. 2. Retardation by reaction product(s) in borate buffer at 30°C.
(◉: 1st run, ▣: 2nd run)

* Since the optical density of the solution during the course of the reaction is relatively small, the inner filter effect of the demethylated dye need not be taken into account.

As shown in Fig. 2, the rate in the second run is much smaller than that in the first one. On the basis of this result we now propose the following scheme as a tentative one.

$$\begin{array}{ccccccccc} \mathrm{MB} & \xrightarrow{h\nu} & \mathrm{MB^*} & \rightarrow & \mathrm{MB^t} & \cdots\cdots & \xrightarrow{a} \mathrm{X} & \xrightarrow{k_1} & \mathrm{P} \\ & & \downarrow & & \downarrow & & \downarrow k_d \quad \searrow^{k_2} & & +\mathrm{P} \\ & & \mathrm{MB} & & \mathrm{MB} & & \mathrm{MB} & & \mathrm{MB} \end{array} \qquad \text{(A)}$$

In this scheme it is assumed that the dye molecule goes via the triplet state to a certain intermediate X, and $a$ is a fraction of excited dye which attains to X. X then is assumed to react in three different ways, i.e., the product-forming reaction of the (apparent) first order (rate constant; $k_1$) the usual deactivation process (rate constant; $k_d$) and a process of particular deactivation caused by the attack of some reaction product (rate; $k_2[\mathrm{P}][\mathrm{X}]$). In fact it is entirely unknown how the reaction product may interfere with the reaction, but here the above scheme may conventionally be adopted rather as a trial one, partially because of the simplicity of the formula obtained therefrom.

If the reaction proceeds in a steady state according to the above scheme, the rate formula may be expressed as follows;

$$-\frac{\mathrm{d}[\mathrm{MB}]}{\mathrm{d}t}=k_1[\mathrm{X}]=\frac{ak_1C}{k_1+k_d+k_2(C_0-C)} \qquad (1)$$

in which $C_0$ is the initial concentration of dye. In the absence of the retarding effect of the product, this equation is reduced to the following,

$$-\frac{\mathrm{d}[\mathrm{MB}]}{\mathrm{d}t}=\frac{ak_1C}{k_1+k_d}$$

Here it is to be added that the absorption of light is assumed to be approximately proportional to the dye concentration $C$.

Below it will be shown that the above trial formula is satisfactory to some extent.

Integration of 1 leads to

$$\frac{\ln C_0-\ln C}{C_0-C}=\frac{k_2}{k_1+k_d+k_2C_0}+\frac{ak_1}{k_1+k_d+k_2C_0}\cdot\frac{t}{C_0-C} \qquad (2)$$

This equation requires a linear relation between $(\ln C_0-\ln C)/(C_0-C)$ and $t/(C_0-C)$, which in fact is well satisfied by most of the experimental results within the experimental error. This is shown in Fig. 3.

It is also evident from the figure that Eq. 2 does not hold in the case of phosphate buffer. The values for intercept, $S=k_2/(k_1+k_d+k_2C_0)$, inclination, $\alpha=ak_1/(k_1+k_d+k_2C_0)$ and the ratio of the latter to the former, $ak_1/k_2(=\alpha/S)$,

TABLE I. RESULTS OF KINETIC TREATMENT

| Condition of soln, M | pH | Concn. of dye*, M | $S\times10^{-5}$ | $\alpha\times10^{4}$ | $\alpha/S$, mol. $l^{-1}\cdot sec^{-1}$ |
|---|---|---|---|---|---|
| a) $Na_2SO_4$ ; $1.0\times10^{-2}$ | 6.10 | $1.2\times10^{-5}$ | 0.968 | 1.63 | $1.7\times10^{-9}$ |
| b) NaI ; $1.0\times10^{-2}$ | 6.10 | $1.2\times10^{-5}$ | 0.640 | 0.32 | $5.0\times10^{-10}$ |
| c) NaCl ; $1.0\times10^{-2}$ | 6.18 | $2.0\times10^{-5}$ | 0.676 | 0.69 | $1.0\times10^{-9}$ |
| d) Plain aq. soln. | 6.22 | $1.6\times10^{-5}$ | 0.566 | 0.71 | $1.3\times10^{-9}$ |
| e) Na-Borate ; $7.8\times10^{-3}$<br>HCl ; $1.6\times10^{-2}$ | 7.50 | $4.0\times10^{-6}$ | 6.96 | 17.7 | $2.5\times10^{-9}$ |
| f) Na-Borate ; $7.8\times10^{-3}$<br>HCl ; $1.6\times10^{-2}$ | 7.50 | $8.0\times10^{-6}$ | 2.46 | 4.84 | $2.0\times10^{-9}$ |
| g) Na-Borate ; $7.8\times10^{-3}$<br>HCl ; $1.6\times10^{-2}$ | 7.50 | $1.2\times10^{-5}$ | 1.34 | 3.10 | $2.3\times10^{-9}$ |
| h) Na-Borate ; $7.8\times10^{-3}$<br>HCl ; $1.6\times10^{-2}$ | 7.55 | $1.6\times10^{-5}$ | 1.16 | 3.68 | $3.2\times10^{-9}$ |
| i) Na-Borate ; $7.8\times10^{-3}$<br>HCl ; 0 | 9.15 | $1.2\times10^{-5}$ | 0.103 | 54.3 | $5.3\times10^{-7}$ |
| j) Na-Borate ; $7.8\times10^{-3}$<br>HCl ; $1.2\times10^{-2}$ | 8.30 | $1.2\times10^{-5}$ | 0.103 | 10.8 | $1.1\times10^{-8}$ |
| k) Na-Barate ; $7.8\times10^{-3}$<br>HCl ; $1.4\times10^{-2}$ | 7.85 | $1.2\times10^{-5}$ | 0.108 | 4.97 | $4.6\times10^{-9}$ |
| l) Na-Borate ; $7.8\times10^{-3}$<br>HCl ; $1.7\times10^{-2}$<br>NaCl ; $1.0\times10^{-1}$ | 7.61 | $1.2\times10^{-5}$ | 1.01 | 9.30 | $9.3\times10^{-9}$ |

* Analytical concentration of the initial solution.

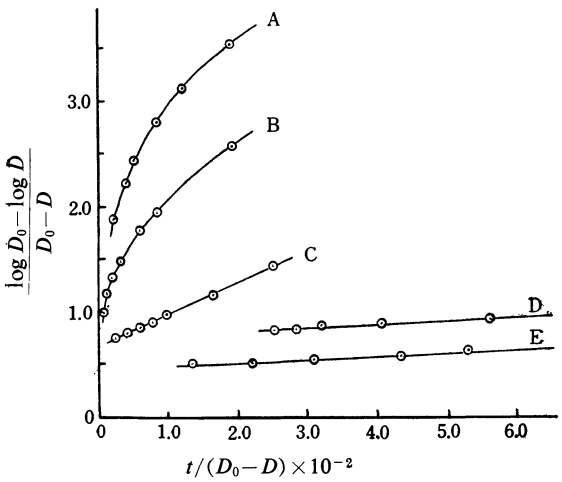



Fig. 3. Application of Eq. 2 for various salt solutions.
A. Phosphate buffer
B. NaOH aq. soln.
C. Borate buffer
D. $Na_2SO_4$ aq. soln.
E. aq. soln.

are summarised in Table I except for phosphate and sodium hydroxide for which Eq. 2 does not hold.

For the further support of Eq. 2, the effect of the initial concentration on the rate was examined in case of borate buffer. From Eq. 2 the reciprocal of the intercept ($=1/S$) should satisfy the following equation,

$$\frac{1}{S}=\frac{k_1+k_d}{k_2}+C_0 \qquad (3)$$

hence the plot of $1/S$ against $C_0$ should be a straight line of slope 1. The slope experimentally obtained is about 0.91 as shown in Fig. 4.

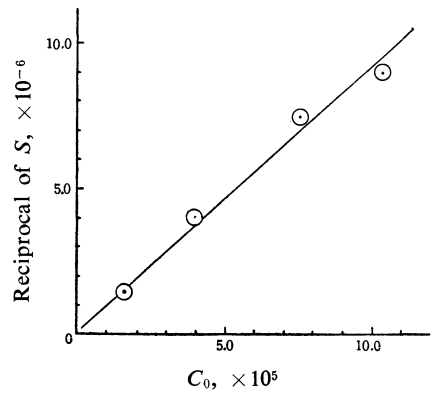



Fig. 4. Plot of $1/S$ against initial concn. $C_0$.

Further, the reciprocal of inclination of Eq. 2 being represented as follows,

$$\frac{1}{\alpha}=\frac{k_1+k_d}{ak_1}+\frac{k_2}{ak_1}C_0 \qquad (4)$$

the plot of $1/\alpha$ against $C_0$ should be linear with the inclination of $k_2/ak_1$. This was in fact satisfied by the experimental data, the value obtained being $4.4\times10^{8}$ ($mol^{-1}$ l. sec.)

which agrees approximately with the mean value of (e)—(h) in Table I ($S/\alpha=4.0\times10^8$).

Thus the reliability of Eq. 2 was substantiated to some extent, and so the effect of pH on the rate, which was examined in the region of pH, 7.40~9.15 keeping the concentration of borate ion constant, was analyzed by Eq. 2. The values of $\log \alpha/S(\alpha/S=ak_1/k_2)$ for the various pH values are shown in Table II.

Table II

| pH | log[OH⁻] | log $\alpha/S$ |
|---|---|---|
| 9.15 | −4.85 | −7.28(−7.69) |
| 8.30 | −5.70 | −7.97 |
| 7.85 | −6.15 | −8.32 |
| 7.55 | −6.45 | −8.63 |
| 7.40 | −6.60 | −8.48 |

It is apparent that the value of $\alpha/S$ increases approximately proportionally to the concentration of [OH⁻].

**Phosphate Buffer Solution.** — It is assumed that the essential difference against the case of borate lies only in the bimolecular reaction of X and MB, which leads to the production of leuco dye, all the other steps being quite similar as in the previous one. Thus

$$\mathrm{MB} \xrightarrow{h\nu} \mathrm{MB^*} \rightarrow \mathrm{MB^t} \cdots\cdots \xrightarrow{a} \mathrm{X} \xrightarrow[k_1']{\mathrm{MB}} \mathrm{P}$$

$$\mathrm{MB^*} \rightarrow \mathrm{MB}, \quad \mathrm{MB^t} \rightarrow \mathrm{MB}, \quad \mathrm{X} \xrightarrow{k_d'} \mathrm{MB}, \quad \mathrm{X} \xrightarrow{k_2'} \mathrm{P}$$

whence the rate is expressed as follows,

$$-\frac{\mathrm{d[MB]}}{\mathrm{d}t}=\frac{2ak_1'C^2}{k_1'C+k_d'+k_2'(C_0-C)}=\frac{2ak_1'C^2}{k_d'+(k_1'-k_2')C+k_2'C_0} \quad (5)$$

In view of the fact that the experimental data can quite satisfactorily be reproduced by the second order rate formula, it may be permissible to put $k_1'=k_2'$. Then,

$$-\frac{\mathrm{d[MB]}}{\mathrm{d}t}=\frac{2ak_1'C^2}{k_d'+k_2'C_0}=2kC^2 \quad (6)$$

where

$$k=\frac{ak_1'}{k_d'+k_2'C_0}$$

Some examples for the relation $1/C\sim t$ are shown in Fig. 5. Most of the experimental results satisfy the linear relation. (Table III).

When the initial concentration is varied, the following relation should hold between the reciprocal of $k$ and $C_0$

$$\frac{1}{k}=\frac{k_d'}{ak_1'}+\frac{k_2'}{ak_1'}C_0 \quad (7)$$

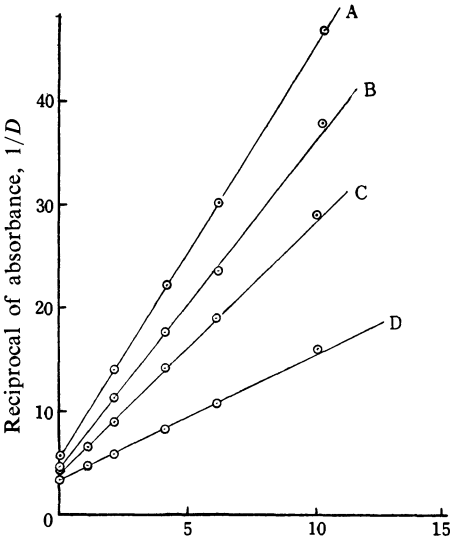



Fig. 5. Plot of the reciprocal of absorbance (D) against the irradiation time at constant pH.
Initial concn. of dye; A····· $4\times10^{-6}$ M
B····· $8\times10^{-6}$ M
C·····$1.2\times10^{-5}$ M
D·····$1.6\times10^{-5}$ M

Table III. Kinetic data and condition of the solution
(Concn. of total phosphate=$6.7\times10^{-2}$ M)

| Concn. of dye, M | pH | $k$, mol$^{-1}$ l. sec$^{-1}$ |
|---|---|---|
| $4\times10^{-6}$ | 7.56 | $2.00\times10^3$ |
| $8\times10^{-6}$ | 7.58 | $1.09\times10^3$ |
| $1.2\times10^{-5}$ | 7.54 | $1.03\times10^3$ |
| $1.6\times10^{-5}$ | 7.58 | $0.67\times10^3$ |
| $1.2\times10^{-5}$ | 6.94 | $0.94\times10^3$ |
| $1.2\times10^{-5}$ | 7.71 | $1.16\times10^3$ |
| $1.2\times10^{-5}$ | 8.07 | $1.30\times10^3$ |
| $1.2\times10^{-5}$ | 8.81 | $1.48\times10^3$ |

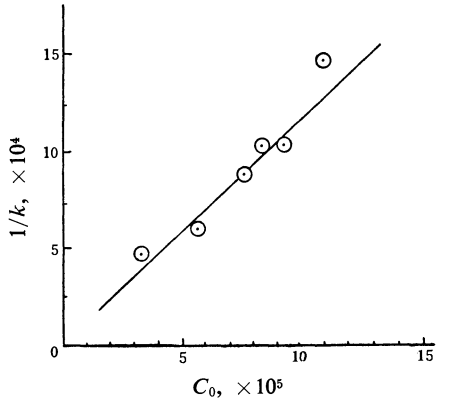



Fig. 6. Plot of $1/k$ against initial concn. $C_0$ for Eq. 7.

It was confirmed that the experimental results approximately satisfy the above relation. This is shown in Fig. 6.

The effect of pH on the rate was examined and the results are shown in Table IV.

TABLE IV

| pH | log[OH⁻] | log $k$ |
|---|---|---|
| 8.81 | −5.19 | 3.17 |
| 8.07 | −5.93 | 3.11 |
| 7.71 | −6.29 | 3.06 |
| 7.52 | −6.48 | 3.02 |
| 6.94 | −7.06 | 2.97 |

In contradistinction to the case of borate buffer, the rate is scarcely affected by the variation of pH.

### The Effect of Some Added Substances

**The Behavior when Ferric Chloride and *o*-Phenanthroline are Added.** — In the previous paper it was reported that when these substances are added to the borate buffer solution of methylene blue and irradiated, the complex between $Fe^{2+}$ and *o*-phenanthroline is formed, the quantity of which attains to more than ten times that of the dye. Thus, it was concluded from the above result, that no impurity contained in dye participates essentially in the reaction. In addition to this conclution, the investigation of this system is important with regard to the quantitative relation between the leuco-formation and the irreversible photodecomposition. So further description will be given below.

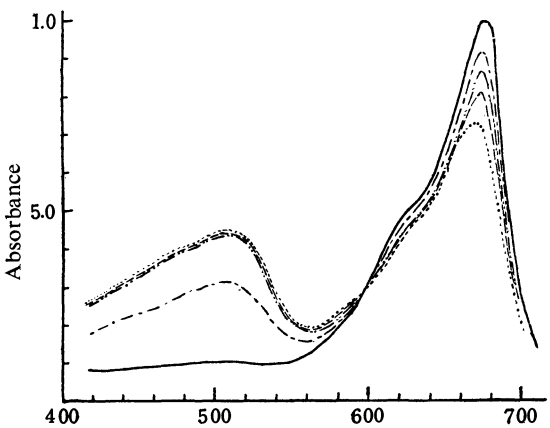



Fig. 7. The spectral change of the mixture of methylene blue-borate buffer, *o*-phenanthroline and ferric chloride solution when irradiated.
—— initial
– – – 2 min.-irradiation
—·— 5 min.-irradiation
—·· 20 min.-irradiation
····· 50 min.-irradiation

A typical result is shown in Fig. 7, in which the absorption band of 510 mμ is due to trisphenanthroline iron(II) complex. In this experiment the concentration of the complex produced by 2 min. irradiation is about fourteen times that of the decrease in dye concentration. This decrease is due to the irreversible bleaching, the solution not being decolorized by aeration. Thus it may be judged that if the formation of leuco dye takes place only by the accompanying irreversible decomposition of dye, then one molecule of dye decomposed ought to be able to produce more than ten molecules of leuco dye. This makes the above view highly improbable.

It is to be added that when the irradiation is continued after all the $Fe^{3+}$ has been consumed to produce trisphenanthroline iron(II) complex, the bleached dye partially recovers its color upon the introduction of air. Therefore it is certain that as long as $Fe^{3+}$ exists the produced leuco dye reduces $Fe^{3+}$, but after the disappearance of $Fe^{3+}$ the existence of the reduced dye persists.

It is regrettable that no such experiment can be performed for the phosphate solution on account of the small solubility of $Fe^{3+}$ salt.

**The Effect of the Addition of Pyruvate.** — It was reported in the previous paper that a small quantity of hydrogen peroxide was detected in case of borate buffer but not in phosphate buffer. Now it is well known that in general hydrogen peroxide is rapidly decomposed by the addition of pyruvate, and it is interesting to investigate the effect of the addition of pyruvate upon the rate and to compare the two cases when the phosphate or borate buffer is used. The concentrations of pyruvate ($C_{py}$) added to the borate buffer are $1.2\times10^{-4}$, $2.2\times10^{-4}$, and $2.4\times10^{-4}$ M. The results are shown in Fig. 8.

It is apparent from the figure that the slope becomes steeper with the increase of the concentration of pyruvate. Further, when $\alpha/S$-values for the two cases, one with pyruvate and the other without it but otherwise in the similar conditions are compared, the value for the former is definitely larger; thus from Fig. 8 for $C_{py}=2.2\times10^{-4}$ M, $\alpha/S=7.57\times10^{-9}$ and for $C_{py}=0$, $\alpha/S=2.97\times10^{-9}$(mol. $l^{-1}$ $sec^{-1}$). The above results are well comprehended if the $k_2$-value in the second term on the right side of Eq. 2 gets smaller with the addition of pyruvate. Although the possibility for other steps to be affected might not be neglected, it seems most plausible that the

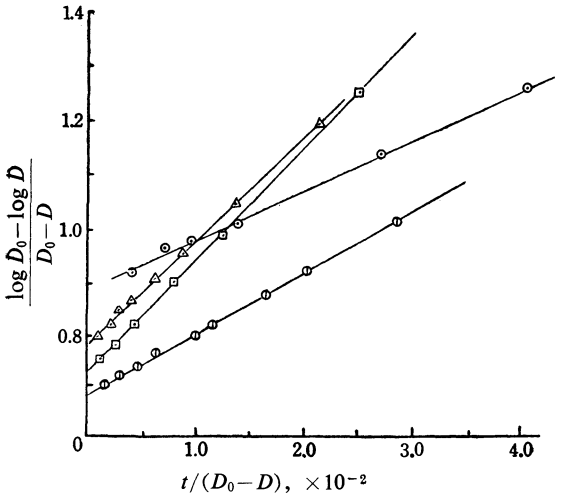



Fig. 8. The effect of the addition of pyruvate on Eq. 2 ($D$……optical density).

⊙ [Pyr]=0
① [Pyr]=$1.2\times10^{-4}$ M
△ [Pyr]=$2.2\times10^{-4}$ M
◙ [Pyr]=$2.4\times10^{-4}$ M

addition of pyruvate chiefly affects the $k_2$-value in view of the result obtained for phosphate buffer (described below).

When ten times as much pyruvate as the concentration of methylene blue was added to phosphate buffer, the rate was also represented as of the second order with respect to dye and the $k$ value of Eq. 6 was evaluated to be $5.3\times10^2$ ($mol^{-1}$ l. $sec^{-1}$). This is slightly smaller than $6.2\times10^2$, which is the $k$-value in the absence of pyruvate but otherwise having similar conditions. It is evident that the addition of pyruvate to the phosphate buffer scarcely affects the rate.

Thus the effect of pyruvate-addition is quite different in the case of phosphate and borate, and this is just what is expected from the results already obtained.

**The Effect of the Addition of Quinone.** — It was reported in the previous paper that in the case of phosphate buffer, neither hydrogen peroxide nor oxygen was detected. But it is premature to deny the formation of oxygen only on the basis of this analysis, because the produced oxygen may be consumed in the irreversible photodecomposition of dye. In order to detect the oxygen formed, it seems rather essential to make the experiment under conditions such that the oxygen which might be produced, be accumulated so rapidly that it is scarcely consumed in the photooxidation of dye.

With this view in mind and from the analogy of the Hill reaction in photosynthesis, the addition of quinone was tested. Thus if the quinone does not attack the excited dye but only oxidizes the leuco dye produced as in the case of the Hill reaction, the oxygen is expected to be accumulated.

Preliminary tests demonstrated, however, that the addition of quinone, the quantity being up to several times (in mole) that of the dye induces a quite complicated spectral change of methylene blue when the evacuated solution is irradiated. In addition, spectra of methylene blue in the above solution were found to change even in the dark though the rate was much slower.

Thus there is no doubt that the direct photoreaction does take place between dye and quinone. This reaction seems to be interesting from a different point of view, but it is clear that quinone is too reactive to be used for the above object. Hence further studies have been abandoned. Other kinds of quinones or other types of oxidants more mild in character should be searched.

## Quantum Yield

In both buffer solutions, the quantum yield ($\gamma$) for the initial stage was evaluated by using the inclination of the curve of optical density against time, and the number of photons ($I_{abs}$) absorbed by the solution, both in the initial stage. The latter quantity was measured with the combination of the thermopile (Moll and Burger standard thermopile) and White single potentiometer (Leeds and Northrup).

The following table shows the results obtained for borate and phosphate buffer solutions.

Table V. Quantum yield

| Condition | | $I_{abs}$ (photons. $sec^{-1}$ $cc^{-1}$) | $\Delta D/\Delta t$ ($D$, $min^{-1}$) | $\gamma$ |
|---|---|---|---|---|
| a) | Phosphate buffer | $7.2\times10^{15}$ | 0.089 | $9.2\times10^{-4}$ |
| | | $6.9\times10^{16}$ | 0.029 | $7.1\times10^{-4}$ |
| b) | Borate buffer | $3.5\times10^{15}$ | 0.006 | $3.0\times10^{-4}$ |
| | | $8.7\times10^{15}$ | 0.010 | $2.2\times10^{-4}$ |

## Discussion

It was found in the previous paper that the general feature of the reaction is somewhat different in borate and phosphate buffer. Now in the present paper additional differences were found from the kinetic standpoint. Thus the rate in borate buffer is approximately of the first order in dye while that of the phosphate buffer, is of the second order, and moreover the pH effect is quite different in two cases. Therefore, two cases will be separately discussed, anticipating the essential difference in mechanism.

In case of borate the rate being of the first order in dye, the interaction of two dye molecules of which one acts as an electron-donor and the other as an acceptor can safely be neglected. The result of the experiment pertaining to the formation of trisphenanthroline iron(II) chloride also denies such an interaction. Thus one cannot but consider that in this case the oxidation of water is taking place under some cooperative action of the salt. In fact, as reported in the previous paper, a small quantity of hydrogen peroxide was detected.

As regards the photofission of water by visible light, Yamafuji reported a long time ago[3] that hydrogen peroxide was produced when the solution of eosine or chlorophyll was irradiated by the solar light. Their experiments, however, were criticized by Rabinowitch[4] and at present their results seem to be judged to be doubtful.

Indeed the decomposition of water by the visible light by virtue of the following scheme

$$H_2O \rightarrow H+OH$$

or

$$HO^- \rightarrow e+OH \qquad (6)$$

must be almost impossible from the energetic reason, except for the case in which the absorption of more than two photons takes part in one act. However, if the reaction in the following molecular mechanism occurs,

$$D^+ + 2OH^- \rightarrow DH + HO^-_2 \qquad (7)$$

the free enthalpy change is not so great. It is ca. $\Delta G^\circ_{298}=49.65$ kcal./mol. so that with an efficient use of the energy of photon absorbed, ca. 43.0 kcal., only 6.6 kcal. needs to be provided for the reaction 7 to occur. If borate ion can afford a certain amount of free enthalpy in some way, then the quantum yield experimentally obtained would be attained by the process 7.

In connection with this it is tempting to recall that borate is an electron deficient substance and to suppose that some of the borate ions may be in a certain energy-rich state combining with hydroxide ion. Alternatively there might be a possibility that a certain species of dye such as $(D\cdots OH)H^+$ which Lewis[5] proposed, takes part in the reaction to make it energetically feasible. The result that the rate is approximately of the first order in $[OH^-]$ in spite of the second order for the stoichiometric equation, might be related with this.

Next the case of phosphate will be discussed. In this case neither hydrogen peroxide nor oxygen was detected and the reaction proceeds in the second order with regards to dye. These facts seem at first strongly to suggest that the initial process is the interaction of the excited dye with the ground-state-dye molecule, the electron transfer taking place between them according to

$$D^* + D \rightarrow D^- + D^+ \qquad (8)$$

and resulting in the leuco-formation from one dye molecule and the irreversible decomposition of another. But judging from the result that 70~80% of the bleached dye is recolorized by the introduction of air, it seems necessary that one molecule of dye decomposed ought to be able to reduce about three dye molecules and that the reducing power of the substances produced by dye-decomposition should be much larger; otherwise the quantity of reduced dye would be much less. Hence the above scheme would not be accepted unless it is confirmed experimentally that the above requirements are really satisfied. At the present stage it seems rather improbable that the leuco-formation only occurs through 8 though it may contribute to some extent.

On the other hand, the reaction

$$2D^+ + 2OH^- \rightarrow 2DH + O_2 \qquad (9)$$

seems not entirely impossible from the energetic view point. Thus its $\Delta G^\circ_{298}$ is 55.93 kcal. and taking the energy of photon, 43.0 kcal. into account, the free enthalpy is evaluated to be about 6.4 kcal. for one dye molecule. Should the phosphate ion be able to provied energy in some way, reaction 9 would be realized just as reaction 7.

The role of phosphate ion must be clarified irrespective of wether the reaction goes via 8 or 9.

The photoreduction which has been confirmed in this series of investigation would be expected to occur in other thiazine dyes and this has really been ascertained in the case of thionine. Since the demethylation need not be taken into account for thionine, the quantitative study would be more feasible particularly as regards the interrelation between leuco-formation and irreversible decomposition. These are now in course of study.

## Summary

Kinetic treatment was undertaken for the photobleaching of the aqueous solution of methylene blue containing various inorganic salts.

If a certain kind of inhibiting action due to

3) K. Yamafuji et al., *Biochem. Z.*, **301**, 404 (1939).
4) E. I. Rabinowitch, "Photosynthesis and Related Processes", Vol. I, Interscience Publishers, Inc., New York (1956), p. 78.
5) G. N. Lewis et al., *J. Am. Chem. Soc.*, **65**, 1150 (1943).

some reaction product(s) is taken into consideration, the rate for borate buffer is satisfactorily reproduced as the first order of excited dye, while for phosphate buffer it is second order with regard to dye. It was further found from this analysis that the rate of the essential step (or steps) of the reaction for the case of borate is approximately proportional to the concentration of $OH^-$, while for the case of phosphate it is almost independent of pH.

The quantity of irreversible decomposition of dye in case of borate buffer was estimated to be very small against that of the reversible bleaching, the former being a few tenths of the latter from the experimental results obtained when ferric chloride and *o*-phenanthroline were added to the borate buffer solution.

Judging from the results hitherto obtained, it is most plausible that the photoreduction of methylene blue in case of borate takes place through the decomposition of water. But in case of phosphate, there still remains some possibility that the reaction commences by the interaction of excited dye and ground state dye, electron transfer taking place between them.

The quantum yield of the bleaching reaction was measured and found to be $(2\sim3)\times10^{-4}$ for borate buffer and $(7\sim9)\times10^{-4}$ for phosphate buffer.

Thanks are due to Dr. Shunji Kato and Mr. Hiroshi Obata for helpful discussions.

*Department of Chemistry*
*Faculty of Science*
*Tohoku University*
*Katahira-cho, Sendai*

# *Raman Spectra of p-Dichlorobenzene and p-Dichlorobenzene-$d_4$*

By Shinnosuke SAËKI

(Received April 3, 1961)

The molecular spectra of *p*-dichlorobenzene have been studied by many investigators, and the author has reported on the infrared absorption spectra of ordinary and deuterated *p*-dichlorobenzene previously[1]. In this paper, the Raman spectra of the same substances will be reported upon, for it is essential for the assignment of the molecular vibration to study the Raman spectra as well as the infrared spectra.

As the molecule of *p*-dichlorobenzene has the center of symmetry, the thirty normal vibrations are divided into two groups according to the rule of mutual exclusion. Consequently, fifteen vibrations are active in Raman effect and eleven vibrations are active in infrared absorption spectrum. Though this fact does much to simplify the molecular spectra of this substance, the Raman spectrum of this substance is still rather complicated with the appearence of the overtone lines, combination lines and lines due to the Fermi resonance in addition to the above-mentioned eleven fundamental lines.

Concerning the Raman spectrum of *p*-dichlorobenzene, a number of papers have been published since many years ago[2-4]. In these papers, the assignment of the lines was carried out inductively, comparing the spectrum with those of other benzene derivatives of the same type and observing a frequency change between them for each corresponding band or line. Since the number and the variety of the treated substance were extensive, and since the conclusions were made after prudent examinations, one can put much confidence in most of the results obtained by this method. However, since in a different molecule the strength to the interatomic bonds (force constants) changes as well as the masses of atoms, a slight ambiguity appears to be left in the assignment which resulted from such inductive studies. Actually the proposed assignments of some Raman lines of *p*-dichlorobenzene seemed to be somewhat indefinite and arbitrary.

In the study reported here, as the Raman spectra were observed for completely deuterated *p*-dichlorobenzene as well as for the ordinary one, the product rule could be applied in order

1) S. Saëki, This Bulletin, 33, 1021 (1960).

2) A. Stojiljković and D. H. Whiffen, *Spectrochim. Acta*, **12**, 47 (1958).

3) D. H. Whiffen, ibid., **7**, 253 (1955).

4) C. Garrigon-Lagrange, J-M. Lebas and M-L. Josien, ibid., **12**, 305 (1958).

to verify the assignment proposed. In addition to the frequencies, the qualitative depolarization ratio of each line was also observed by the two exposure method using the polaroid cylinders in order to obtain more definite assignments than previous ones.

## Experimental

Ordinary *p*-dichlorobenzene of extra pure grade on the market was recrystallized three times from the ethanol solution, and then sublimed before being used for the measurement of the Raman spectra. The melting point of the obtained substance was 53°C.

The deuterated one was prepared and purified as follows. Ordinary *p*-dichlorobenzene was stirred at 105°C for six hours in heavy sulfuric acid. The reaction mixture was poured on ice and the precipitate filtered off and washed with water and dried. The exchange with heavy sulfuric acid was repeated until the strongest band of $C_6HD_3Cl_2$ could hardly be observed in the infrared absorption spectrum of the substance. It was necessary to repeat the exchange reaction two or three times in order to attain such purity. Then the obtained substance was further purified in the same way as that for ordinary *p*-dichlorobenzene, but because of the smallness of the quantity, the purification could not be carried out so thouroughly as in the case of ordinary *p*-dichlorobenzene. The deuterated substance was probably a little less pure than the ordinary one.

The Cary model 81 automatic recording Raman spectrophotometer was used for the measurements, of which the source was the mercury arc lamp of Toronto type, and the dispersion of the grating was 4 Å/mm. at 5000 Å.

The spectra were measured in the solution of 1 g. *p*-dichlorobenzene in 5 ml. carbon tetrachloride. The qualitative depolarization ratios were measured by placing the polaroid cylinder around the Raman tube and by polarizing the exciting light to the directions parallel or perpendicular to the axis of the tube.

## Results

The observed Raman spectra are shown in Figs. 1—4. As are shown in Figs. 3 and 4, the base lines of the spectra of deuterated *p*-dichlorobenzene rose gradually towards the higher frequency ends of the spectra, showing remarkable backgrounds. It might probably be caused by the slight resinous impurity, which could not be removed completely by the purification because of the small quantity of deuterated substance available, as we mentioned previously.

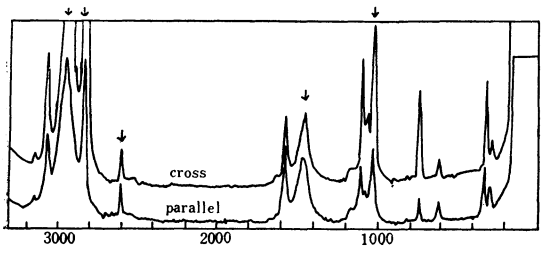



Fig. 1. Raman spectra of *p*-dichlorobenzene (1 g. in 5 ml. methanol).

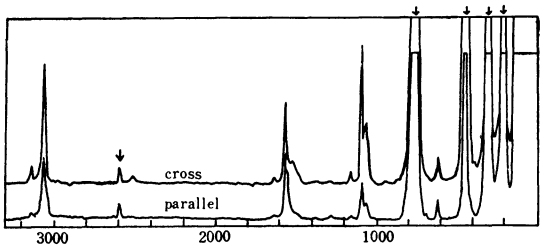



Fig. 2. Raman spectra of *p*-dichlorobenzene (1 g. in 5 ml. carbon tetrachloride).

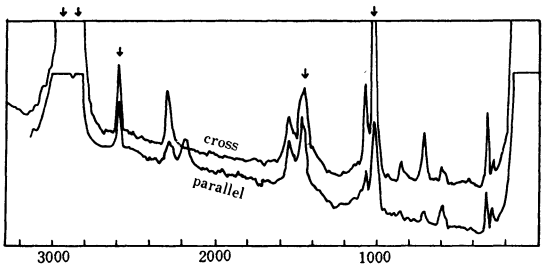



Fig. 3. Raman spectra of *p*-dichlorobenzene-$d_4$ (1 g. in 5 ml. methanol).

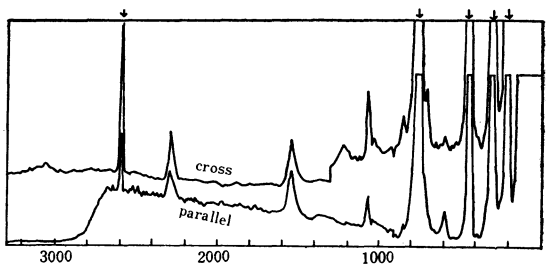



Fig. 4. Raman spectra of *p*-dichlorobenzene-$d_4$ (1 g. in 5 ml. carbon tetrachloride).

The observed frequencies and intensities of Raman lines are listed in Tables I and II. The intensities are described by the heights of lines measured on the chart. The notation "masked" means that the line could not be observed, due to the masking effect of a strong Raman line of the solvent in the spectra of that solution while it was observed in the other solution. Though the Raman spectra of the substances were observed in the solution in methanol or in carbon tetrachloride, there is no possibility that a Raman line is masked in both methanol and carbon tetrachloride solutions, for there is no frequency region

TABLE I. RAMAN SPECTRA OF *p*-DICHLOROBENZENE

| Methanol soln. | | | Carbon tetrachloride soln. | | | Depolarization ratio |
|---|---|---|---|---|---|---|
| $\tilde{\nu}$ | Intensity | | $\tilde{\nu}$ | Intensity | | |
| | Cross | Parallel | | Cross | Parallel | |
| 295 | 14 | 17 | | Masked | | dep. |
| 329 | 54 | 27 | | Masked | | p. |
| 349 | sh. | 1 | | Masked | | ? |
| | Unobserved | | 400 | 4 | 2 | ? |
| 623 | 13 | 14 | 625 | 16 | 16 | dep. |
| 744 | 56 | 16 | | Masked | | p. |
| 1067 | 19 | | 1067 | 16 | 5 | p. |
| 1077 | sh. | 10 | 1080 | 25 | 5 | p. |
| 1103 | 80 | 35 | 1103 | 83 | 25 | p. |
| 1177 | 6 | 3 | 1163 | 8 | 3 | p. |
| | Unobserved | | 1285 | 2 | 3 | dep. |
| | Unobserved | | 1378 | 2 | 0 | ? |
| | Masked | | 1531 | 12b | sh. | p. |
| 1571 | 38 | 39 | 1572 | 48 | 51 | dep. |
| | Unobserved | | 1630 | 4 | 3 | dep. |
| 2520 | 4 | 0 | 2523 | 5 | 1 | p. |
| 3071 | 66 | 33 | 3071 | 75 | 39 | p. |
| 3147 | 8 | 5 | 3147 | 11 | 4 | ? |

TABLE II. RAMAN SPECTRA OF *p*-DICHLOROBENZENE-$d_4$

| Methanol soln. | | | Carbon tetrachloride soln. | | | Depolarization ratio |
|---|---|---|---|---|---|---|
| $\tilde{\nu}$ | Intensity | | $\tilde{\nu}$ | Intensity | | |
| | Cross | Parallel | | Cross | Parallel | |
| 288 | 11 | 12 | | Masked | | dep. |
| 324 | 42 | 27 | | Masked | | p. |
| 607 | 12 | 14 | 606 | 11 | 17 | dep. |
| 708 | 30 | 9 | 710 | sh. | sh. | p. |
| 863 | 14 | 6 | 861 | 13 | 5 | p. |
| 937 | ? | | | | | |
| 1078 | 54 | 28 | 1078 | 39 | 18 | p. |
| ca. 1520 | 2 | 3 | ca. 1520 | sh. | 0 | p. |
| 1553 | 24 | 22 | 1553 | 28 | 30 | dep. |
| 2285 | | | 2285 | 8? | 12? | dep. |
| 2301 | 36 | 15 | 2301 | 31 | 19 | p. |

where both methanol and carbon tetrachloride have a strong Raman line. The only exception is the region between a line at 1460 $cm^{-1}$ of methanol and a line at 1530 $cm^{-1}$ of carbon tetrachloride. But fortunately, as neither of these lines was very strong, there was little possibility that a line would escape observation even in this region, so long as its intensity is not extremely weak.

The notation "unobserved" in the tables means that the line was not observed in one of the solutions while it was observed in the other solution. As all of these lines had very small intensities, it was not unreasonable that they were unobservable in one of the solutions. However, they could still not be adopted uncritically as the Raman lines of solute.

The notation "sh." means a line observed as a shoulder of a strong Raman line of the solute itself or the solvent, and "p." and "dep." represent a line which apparently changed and apparently did not change its intensity when excited by incident light polarized parallel and perpendicular to the axis of the Raman tube, respectively.

## Discussion

The molecule of *p*-dichlorobenzene belongs to a point group $V_h$, and its fifteen Raman active normal vibrations are factored into six of the species $A_g$ (in-plane), five of the species $B_{3g}$ (in-plane), one of the species $B_{1g}$ (out-of-plane) and three of the species $B_{2g}$ (out-of-plane). Therefore six polarized (and probably strong) lines and nine depolarized lines were expected to be observed in the Raman spectrum. The modes of these normal vibrations are shown in Table III.

TABLE III. THE MODES OF THE NORMAL VIBRATIONS OF *p*-DICHLOROBENZENE

| Species | No.* | Mode |
|---|---|---|
| $A_g$ | $\nu_1$ | C-H or C-D stretching |
| | $\nu_2$ | Ring stretching |
| | $\nu_3$ | C-H or C-D in-plane bending |
| | $\nu_4$ | Ring stretching |
| | $\nu_5$ | C-Cl stretching |
| | $\nu_6$ | Ring in-plane deformation |
| $B_{1g}$ | $\nu_9$ | C-H or C-D out-of-plane bending |
| $B_{2g}$ | $\nu_{15}$ | C-H or C-D out-of-plane bending |
| | $\nu_{16}$ | Ring out-of-plane deformation |
| | $\nu_{17}$ | C-Cl out-of-plane bending |
| $B_{3g}$ | $\nu_{23}$ | C-H or C-D stretching |
| | $\nu_{24}$ | Ring stretching |
| | $\nu_{25}$ | C-H or C-D in-plane bending |
| | $\nu_{26}$ | Ring in-plane deformation |
| | $\nu_{27}$ | C-Cl in-plane bending |

* The normal vibrations were numbered after Herzberg.

***p*-Dichlorobenzene.** — Seventeen Raman lines are observed in the spectrum of this substance. Therefore the number of observed lines exceedes the number of Raman active normal vibrations. However, since there were several lines which were apparently considered to be overtones or combinations, this fact does not mean that all of the Raman active normal vibrations have been observed.

As we mentioned previously, six polarized lines were expected to be observed, but actually nine polarized lines were found in the observed spectrum, as is shown in Table I. Considering its frequency value, one of these polarized lines observed at 2522 $cm^{-1}$ *1 must be explained as an overtone or a combination. The number of remaining observed lines was still more than the number of expected lines. Considering the vibrational modes shown in Table III, these six lines belonging to the species $A_g$, one was expected to appear near 3000 $cm^{-1}$, one at about 1500 $cm^{-1}$, and two between 1300 and 1000 $cm^{-1}$. Though the vibrational mode of $\nu_4$ was described as the ring stretching, it proved to be the "breathing" vibration of the benzene ring on closer examination. Therefore its frequency might be relatively low and expected to appear in this region, and two below 1000 $cm^{-1}$. Accordingly it was clear that the line at 3071 $cm^{-1}$ had to be assigned to C–H stretching vibration, the line at 1531 $cm^{-1}$ to the ring stretching vibration, the line at 774 $cm^{-1}$ to the C–Cl stretching vibration, and the line at 331 $cm^{-1}$ to the ring in-plane deformation vibration.

Concerning the assignment of the lines observed in the region 1000~1300 $cm^{-1}$, there were some points of discussion. While only two of the totally symmetric normal vibrations were expected to appear in this region, four polarized Raman lines were actually observed at 1067, 1080, 1103 and 1163 $cm^{-1}$ *2. As the line at 1103 $cm^{-1}$ had much greater intensity than the other three, this line may the most plausibly be assigned to the breathing vibration of the ring. From the facts that the line at 1067 $cm^{-1}$ was very close to the line at 1080 $cm^{-1}$, and that these two lines were hardly resolved in the spectrum of the methanol solution, these two lines might be considered to be brought out by a Fermi resonance between a fundamental and an overtone or a combination vibration (for example 545($b_{1u}$)[1] $\times 2 = 1090$ ($A_g$), 744 ($a_g$) + 331 ($a_g$) = 1075 ($A_g$)). Then the frequency of the in-plane bending vibration of C–H bonds was estimated to be about 1075 $cm^{-1}$, the mean value of these two frequencies. Provided that the two normal vibrations were assigned in such a way, the line at 1163 $cm^{-1}$ had to be considered as an overtone or a combination, or a fundamental which belongs to a species other than $A_g$. However it was also possible to take the line at 1163 $cm^{-1}$ for the in-plane bending vibration of C–H bonds, and to take the lines at 1067 and 1080 $cm^{-1}$ for the above-mentioned combination and overtone respectively. This alternative assignment seems to be somewhat unreasonable taking into account their relative intensities, nevertheless this could not be considered to be absolutely impossible. The superiority of one to the other will be revealed later by the application of the product rule.

The next step is to assign the other lines to the normal vibrations which belong to species other than $A_g$. These normal vibrations consist of four out-of-plane vibrations which belong to the species $B_{1g}$ or $B_{2g}$, and five in-plane vibrations which belong to the species $B_{3g}$. As is shown in Table II, two of the four out-of-plane vibrations are those of C–H bonds, and their frequencies must be higher than 819 $cm^{-1}$, which is the frequency of the infrared active out-of-plane vibration of C–H bonds (species $B_{3u}$[1]) in which the four C–H bonds vibrate from the plane of the molecule up and down in the same phase. Though the frequencies of these vibrations were estimated to be between 819 and 1100 $cm^{-1}$, no depolarized line was observed in this region. Since naturally too much confidence should not be put in the observed degrees of depolarization, it would not be impossible to assign the lines at 1067 and 1080 $cm^{-1}$ to these out-of-plane vibrations. However, since these lines had been well explained as a combination and as an overtone, as was mentioned above, and since the observed degrees of depolarization were not consistent with the above assignments, it appears better to consider that the normal vibrations in question were not observed and to assign the above lines to a combination and an overtone than to make a strained assignment. Further discussion concerning these lines will be seen later.

The other two out-of-plane vibrations are those of the ring and of the C–Cl bonds. Since the frequency of the former was expected to be about 400 $cm^{-1}$, the line observed at 400 $cm^{-1}$ in the solution of carbon tetrachloride was assigned to it. But it should be mentioned here that there remained a little ambiguity in this assignment, since the intensity of the line was so weak that it was not observed in the solution of methanol. As the out-of-plane bending vibrations of C–Cl bonds were expected to be observed in lower frequency region —probably in the vicinity of 300 $cm^{-1}$, the line at 294 $cm^{-1}$ was assigned to this vibration.

*1 As a slight discrepancy was generally seen between the frequency observed in methanol solution and that oserved in carbon tetrachloride solution, the mean value of these two was used in this paper as a rule. However, in the case that an apparent difference existed between the accuracies of two observed frequencies, the more accurate one was used.

*2 Since the second and the fourth lines were observed much more clearly in carbon tetrachloride than in methanol as is seen in Figs. 1 and 2, the frequencies observed in carbon tetrachloride solution were adopted as is mentioned in the last foot-note.

The last five normal vibrations to be assigned are those which belong to the species $B_{3g}$. The frequency of the stretching vibration of C–H bonds was naturally a little higher than 3000 $cm^{-1}$, and in the observed spectra a weak line was found at 3147 $cm^{-1}$ in addition to the strong line at 3071 $cm^{-1}$ which was already assigned to the vibration of the species $A_g$. The observation of the qualitative depolarization ratio showed that this weak line was considerably polarized. In addition to this fact, the frequency 3147 $cm^{-1}$ appeared to be too high even for an aromatic C–H stretching vibration. Therefore this line had to be assigned not to the C–H stretching vibration, but to the overtone of the ring stretching vibration of 1572 $cm^{-1}$ which will be discussed below. The C–H stretching vibration of the species $B_{3g}$ should be considered to overlap with that of the species $A_g$ at 3071 $cm^{-1}$.

Three of the remaining normal vibrations are the stretching vibration of the ring, the in-plane deformation vibration of the ring and the in-plane bending vibration of C–H bonds. There might be no objection to assigning three depolarized lines observed at 1572, 1285 and 623 $cm^{-1}$ to them respectively. As for the last remaining normal vibration, that is, the C–Cl in-plane bending vibration, there was no observed line except a very weak line at 349 $cm^{-1}$ to be assigned to it. Though the intensity of this line was very low, this line had been observed also by Whiffen et al.[2] And since there were no lines observed in the spectra to be assigned to the C–Cl bending vibrations except the two lines observed at 349 and at 294 $cm^{-1}$, it appeared to be quite plausible to assign the former line to the in-plane, and the latter line to the out-of-plane bending vibration of C–Cl bonds respectively.

A brief discussion should be given here concerning the lines which had not yet been treated above that is, the weak lines at 2520, 1630 and 1378 $cm^{-1}$, of which the degrees of depolarization could not be measured with adequate certainty. The line at 2520 $cm^{-1}$, though observed to be polarized, could not be explained as a line belonging to the species $A_g$. This line might probably be a combination line of the species $B_{3g}$, that is, 1405 ($b_{2u}$) + 1091($b_{1u}$). The line at 1630 $cm^{-1}$ was measured as a depolarized line, and explained as being 1091($b_{1u}$) + 545($_{3u}$). The line at 1378 $cm^{-1}$ was easily explained as 819($b_{3u}$) + 544($b_{3u}$).

**Deuterated *p*-Dichlorobenzene.** — The Raman lines observed for deuterated *p*-dichlorobenzene was not so many as for an ordinary one. The observed eleven lines were shown in Table II. According to the measurement of the qualitative polarization ratios, six of these lines were polarized. But the result obtained for the line at about 1520 $cm^{-1}$ was a little ambiguous, because its intensity was so weak that the observation of the depolarization ratio was very difficult even qualitatively. However, these six polarized lines were unambiguously assigned to the six normal vibrations of the species $A_g$, as is shown in Table IV. The comparison of this assignment with that for ordinary *p*-dichlorobenzene will be given later.

The remaining five observed lines are to be assigned to the remaining nine normal vibrations, of which four out-of-plane vibrations belong to the species $B_{1g}$ or $B_{2g}$, and five in-plane vibrations belong to the species $B_{3g}$. It might be apparent that two of the out-of-plane vibrations concerning C–D bonds have frequencies higher than 695 $cm^{-1}$, the frequency of the C–D out-of-plane vibration of the species $B_{3u}$ observed in the infrared absorption spectrum[1]. However no corresponding line was observed in such a region of frequency, so it had to be concluded that these vibrations had too low intensities to be observed. The other two out-of-plane vibrations were expected to appear from 350 to 400 $cm^{-1}$ and at about 250 $cm^{-1}$ respectively, considering their vibrational modes (Table III). But there was no line to correspond to the former vibration. The line corresponding to the latter vibration was observed at 288 $cm^{-1}$ with remarkable intensity, but it was difficult to determine whether this line was to be assigned to the out-of-plane or in-plane vibration of C–Cl bonds.

Concerning the in-plane normal vibrations belonging to the species $B_{3g}$, there might be no difficulty in assigning the line at 2285 $cm^{-1}$ to the C–D stretching vibration and the line at 1553 $cm^{-1}$ to the ring stretching vibration. As for the in-plane bending vibration of C–D bonds, since the corresponding vibration of ordinary *p*-dichlorobenzene was observed at 1285 $cm^{-1}$ with relatively low intensity, the frequency was expected to be a little lower than 1000 $cm^{-1}$ in the case of a deuterated one. No distinct line was observed in this frequency region at first sight, but the closer examination of the spectra revealed a very weak line at 937 $cm^{-1}$, the intensity of which was so weak that the line could hardly be distinguished from the noises. It might be a little questionable to consider it as a real Raman line. but if we remember that the line at 1285 $cm^{-1}$ of ordinary *p*-dichlorobenzene was also very weak and that the corresponding line of deuterated *p*-dichlorobenzene has to appear in the region of 900~1000 $cm^{-1}$, this line could be assigned to the C–D in-plane bending vibration.

The line at 607 $cm^{-1}$ was easily assigned to

the ring in-plane deformation vibration.

To the C–Cl in-plane bending vibration, it is possible to assign the line at 288 $cm^{-1}$, but, as is mentioned above, it might also be possible to assign it to the in-plane bending vibration of C–Cl bonds. As in the case of ordinary *p*-dichlorobenzene, the decision of the assignment for these vibrations appear to be impossible at this point.

**The Product Rule.**—According to the Teller-Radlich product rule, the theoretical ratios of the products of the frequencies for each substance are 1.998 for the species $A_g$, 1.249 for the species $B_{1g}$, 1.408 for the species $B_{2g}$ and 1.969 for the species $B_{3g}$, where the calculations were carried out using the following values for molecular constants:

| | |
|---|---|
| $m_H = 1.0081$ | (in physical atomic weight) |
| $m_D = 2.0147$ | (in physical atomic weight) |
| $m_C = 12.0038$ | (in physical atomic weight) |
| $m_{Cl} = 34.9801$ | (in physical atomic weight) |
| $r_{C-H} = 1.08$ | (Å) |
| $r_{C-Cl} = 1.68$ | (Å) |
| $r_{C-C} = 1.39$ | (Å) |

and 120° for all of the bond angles.

The assignments for the six normal vibrations of the species $A_g$ were unambiguously determined in the case of ordinary *p*-dichlorobenzene, but in the case of a deuterated substance there remained a question which of the two lines at 1163 $cm^{-1}$ and 1075 $cm^{-1}$ was to be assigned to the in-plane vibration of C–H bonds. If the ratio of the products of the frequencies was calculated assuming the latter assignment, the result was 1.825, a little less than the theoretical value 1.998. On the contrary, if the former assignment was assumed, the ratio became 1.991, in good accordance with the theoretical value. This result led us to the conclution that it was the line at 1163 $cm^{-1}$ to be assigned to the C–H bending vibration of the species $A_g$.

Here, in connection with this assignment a comment should be mentioned about the exchange of the vibrational modes. As was stated above, according to this assignment, $\nu_3$'s were 1163 and 1078 $cm^{-1}$ for ordinary and deuterated *p*-dichlorobenzene respectively, and $\nu_4$'s were 1103 and 863 $cm^{-1}$ for ordinary and deuterated ones respectively. The fact that the line at 1103 $cm^{-1}$ was much more intense than the line at 1163 $cm^{-1}$ in the spectra of ordinary *p*-dichlorobenzene suggests to us that the mode of the former is the breathing of the benzene ring and that of the latter is the C–H in-plane bending vibration. However, in the case of a deuterated substance, it was clear from the consideration of the frequency that

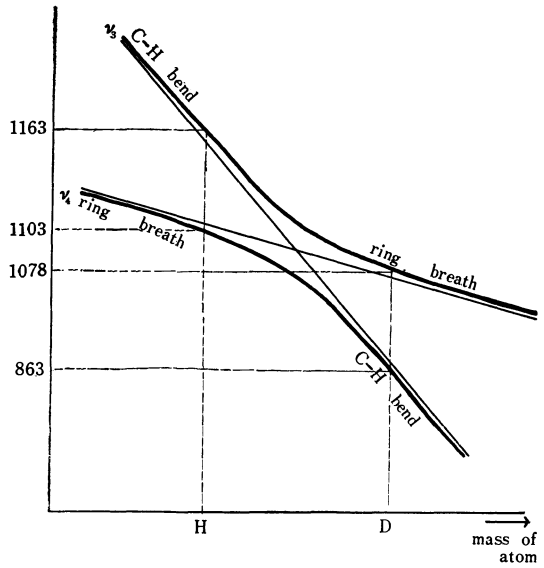



Fig. 5. The variation of vibrational mode with atomic mass.

the line at 1078 $cm^{-1}$ was the breathing of the benzene ring and that the line at 863 $cm^{-1}$ was the C–D in-plane bending vibration. Thus the exchange of the vibrational modes shown in Fig. 5 took place in the case of these molecules. This consideration suggested that the breathing vibration of the benzene ring strongly couples with the C–H or C–D in-plane bending vibration in these molecules, and that the modes of these vibrations are by no means simple, but rather complicated combinations of some simple modes.

It was impossible to apply the product rule to the species $B_{1g}$ and $B_{2g}$ because of the insufficient number of the observed lines. As was already stated above, only one normal vibration—the C–H or C–D out-of-plane vibration—belongs to the species $B_{1g}$. Therefore, provided that the line at 1067 or 1080 $cm^{-1}$ of ordinary *p*-dichlorobenzene corresponds to this vibration, the frequency of the corresponding vibration of deuterated substance could be estimated at about 850 $cm^{-1}$ by utilizing the product rule. As is shown in Table II, a remarkable line was indeed observed at 863 $cm^{-1}$ in the spectra of deuterated substance, but it was already assigned to a vibration of the species $A_g$, because the measurement of the depolarization ratio showed it to be polarized. In addition to such a lack of a corresponding line, both lines at 1067 and 1080 $cm^{-1}$ of the ordinary substance were themselves polarized, and so it seemed to be unreasonable to assign either of them to the vibration of the species $B_{1g}$.

As the C–Cl in-plane bending vibration of

TABLE IV. ASSIGNMENTS OF RAMAN LINES OF ORDINARY AND DEUTERATED *p*-DICHLOROBENZENES

| Species | No. | $\tilde{\nu}$ $C_6H_4Cl_2$ | $\tilde{\nu}$ $C_6D_4Cl_2$ | Mode |
|---|---|---|---|---|
| $A_g$ | $\nu_1$ | 3071 | 2301 | C-H or C-D stretching |
| | $\nu_2$ | 1531 | ca. 1520 | Ring stretching |
| | $\nu_3$ | 1163 | 1078 | C-H in-plane bending / Ring breathing |
| | $\nu_4$ | 1103 | 863 | Ring breathing / C-D in-plane bending |
| | $\nu_5$ | 744 | 708 | C-Cl stretching |
| | $\nu_6$ | 329 | 324 | Ring in-plane deformation |
| $B_{1g}$ | $\nu_9$ | — | — | C-H or C-D out-of-plane bending |
| $B_{2g}$ | $\nu_{15}$ | — | — | C-H or C-D out-of-plane bending |
| | $\nu_{16}$ | 400? | — | Ring out-of-plane deformation |
| | $\nu_{17}$ | 295 | 288 | C-Cl out-of-plane bending |
| $B_{3g}$ | $\nu_{23}$ | 3071 | 2285 | C-H or C-D stretching |
| | $\nu_{24}$ | 1572 | 1553 | Ring stretching |
| | $\nu_{25}$ | 1285 | 937? | C-H or C-D in-plane bending |
| | $\nu_{26}$ | 623 | 607 | Ring in-plane deformation |
| | $\nu_{27}$ | 349 | — | C-Cl in-plane bending |

deuterated *p*-dichlorobenzene, which corresponds to the line at 349 $cm^{-1}$ of the ordinary substance, was not observed, the exact application of the product rule was impossible for the species $B_{3g}$ also. However, the ratio of products of the frequencies calculated from four pairs of observed frequencies alone was 1.963, which was very near to the theoretical value 1.969 irrespective of the omission of the fifth pair. Generally speaking, a vibration directly concerned with C–H bonds naturally shows the sensitive frequency shift with the substitution of the hydrogen atoms by deuterium atoms. The other vibrations—especially when their frequencies are very different from the frequency of C–H vibration—show little frequency shift. Therefore the C–Cl bending vibration of deuterated *p*-dichlorobenzene was expected to have a frequency nearly equal to that of the corresponding vibration of ordinary *p*-dichlorobenzene, 349 $cm^{-1}$. This means that the ratio of the frequencies for the fifth vibration of the species $B_{3g}$ is probably little larger than 1, and therefore, if the above-mentioned calculation had been carried out taking account of this pair of frequencies, the result would be still in good accordance with the theoretical value. This consideration means that the application of the product rule could prove the correctness of the assignment for the species $B_{3g}$ too.

The assignment which was determined above is shown in Table IV.

## Summary

The Raman spectra of ordinary and deuterated *p*-dichlorobenzene were measured in solutions. The qualitative depolarization ratios of observed Raman lines were also measured by the two exposure method using the polaroid cylinders. On the basis of these results, the assignments of normal vibrations for these substances were determined. The assignments for the in-plane normal vibrations (species $A_g$ and $B_{3g}$) were verified applying the product rule.

The author gratefully acknowledges the encouragement and advice given him by Dr. Y. Mashiko.

*Government Chemical Industrial Research Institute of Tokyo*
*Shibuya-ku, Tokyo*

# *Decomposition of Mono- and Diethanolamine Carbamate in Glycerol Solution*

By Mamoru MATSUDA

(Received May 4, 1961)

Monoethanolamine (MEA) and diethanolamine (DEA) provide excellent methods to remove acidic gases from natural and refinery gases. At normal temperatures these amines have strong affinity for the gases, while at higher temperatures these amines are recovered by expulsion of the acidic gases.

Many papers have been published on the absorption reaction of carbon dioxide with MEA or DEA[1-5], and a few on the reverse reaction[6,7]. However, no kinetic study of the decomposition of the MEA and DEA carbamate or carbonate has hitherto been carried out.

The present paper reports the activation energies for decomposition and absorption obtained from the rate of decomposition, and the heats of formation, together with equilibrium constants, over the temperature range of 110 to 140°C.

## Experimental

**Chemicals.** — MEA, DEA and glycerol were of reagent grade and fractionally distilled in vacuo. Solvents such as xylene, *n*-butyl acetate, *n*-butyl alcohol, acetic acid, and toluene were also of reagent grade. Carbon dioxide from a steel cylinder was purified by passing through concentrated sulfuric acid and anhydrous calcium chloride.

**Preparation of Samples.** — MEA (1 part) was dissolved in glycerol (2 parts). The reaction between the solution, $n_D^{20}$ 1.4680, $d_{20}^{20}$ 1.187, and carbon dioxide took place by bubbling the latter through the former gently for 3 hr. The sample thus obtained had carbon dioxide 0.06385 g./g. sample (0.334 mol. $CO_2$/mol. MEA), $n_D^{20}$ 1.4803, $d_{20}^{20}$ 1.250. The DEA glycerol solution (1 : 2 by vol.), $n_D^{20}$ 1.4729, $d_{20}^{20}$ 1.211, was treated with the same procedure as above; 0.02485 g. $CO_2$/g. sample (0.220 mol. $CO_2$/mol. DEA), $n_D^{20}$ 1.4779, $d_{20}^{20}$ 1.228.

**Apparatus and Technique.** — The apparatus for the decomposition of the sample was shown in Fig. 1. The reaction tube R was a 50 ml. test tube, 2.5 cm. in diameter, charged with glass rods, 0.4 cm. $\phi \times 1.0$ cm. The manometer M was provided with an entraining liquid, a saturated aqueous solution of sodium chloride acidified with sulfuric acid containing a few drops of methyl orange. The cooling zone N was an effective, comparatively large, about 100 ml., heat exchanger, and the temperature of it was maintained constant by circulating water at 20°C. The graduated glass tube G, 3 mm. in diameter, lying horizontally, was calibrated exactly by measuring the length of mercury of known weight.

The experiment was carried out as follows: the apparatus consisting of R, M, N and G, was filled with pure carbon dioxide. About 9 g. of mercury was employed to stop the open end of the graduated glass G. The reaction temperature was maintained within ±0.2°C by the vapor of the boiling solvent which was heated by an oil-bath thermostat O regulated to ±1°C. When the system reached an equilibrium, as shown by a steady state of the colored solution inside the U-tube M and the mercury plug P, all the variables—barometric pressure, temperatures of cooling water $T_5$, of the room $T_3$, of the reaction tube $T_2$, and of the solvent vapor $T_1$—were recorded. Then the plug was set to zero

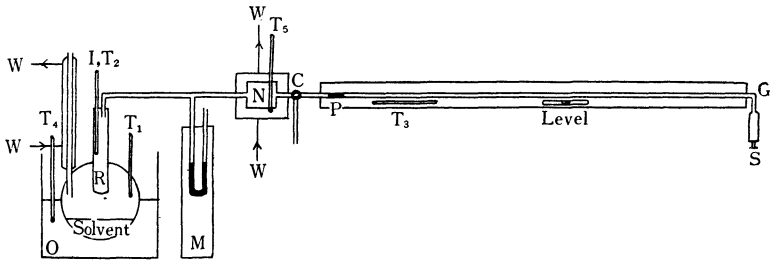



Fig. 1

1) J. W. Mason and B. F. Dodge, *Trans. Am. Inst. Chem. Engrs.*, 32, 27 (1936).
2) D. S. Cryder and J. O. Maloney, ibid., 37, 827 (1941).
3) A. L. Shneerson and A. G. Leibush, *J. Appl. Chem.*, (*U. S. S. R.*), 19, 867 (1946); *Chem. Abstr.*, 41, 4340 (1947).
4) D. W. Van Krevelen and P. J. Hoftijzer, *Chem. Eng. Prog.*, 44, 529 (1948).
5) F. Goodridge, *Trans. Faraday Soc.*, 49, 1324 (1953); 51, 1703 (1955).
6) R. M. Reed and W. R. Wood, *Trans. Am. Inst. Chem. Engrs.*, 37, 363 (1941).
7) H. C. Paulsen et al., U. S. Pat. 2701750 (1955).

by means of a two way cock C and a syringe S. A weighed sample was poured from 2 ml. syringe into the reaction tube through an open glass tube I. The glass tube was closed with a rubber plug. It took less than 3 seconds. The temperature in the tube did not substantially decrease. The sample began to evolve carbon dioxide pushing the mercury plug. The syringe S was operated manually to maintain the inside and outside pressures equal at all times by reading the manometer M. The position of the mercury plug, time, and other variables were recorded at short intervals. The experiment was repeated two or three times at the same temperature.

Gravimetric analyses of carbon dioxide of the fresh and the heated samples which still retained carbon dioxide were carried out. The apparatus and technique were the same as those of Knorr's method[8].

## Results and Discussion

Figures 2 and 3 are graphs of the increase in volume of the gases formed as a function of time due to the decomposition of the samples over the temperature range of about 110 to 140°C. It can not be assumed that the increase in volume was due only to the evolution of carbon dioxide. Vapor of the amines and the solvent, the change of atmospheric pressure and room temperature may affect the measurements. The temperature and the pressure were substantially constant during the experiments. As to the vapor of the amines and the solvent, a blank test showed that the vapor increased the volume by about 0.3 ml./g. sample at 136°C for the initial period of the reaction, in about half a minute. After that period the reaction system reached an equilibrium.

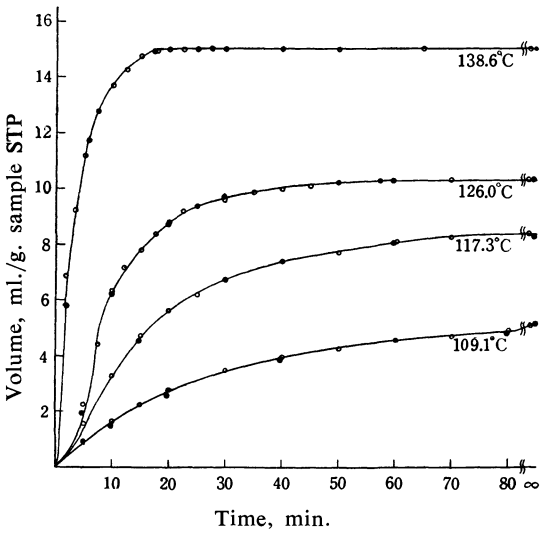



Fig. 2. Rate of decomposition of MEA carbamate in glycerol solution at constant pressure.
● Theoretical
○ Experimental

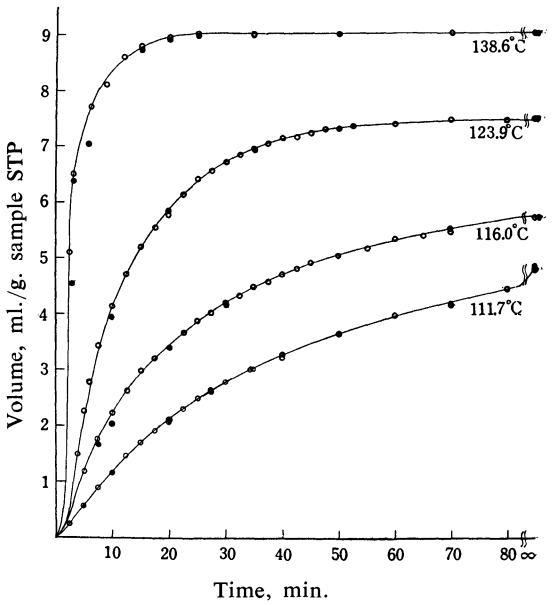



Fig. 3. Rate of decomposition of DEA carbamate in glycerol solution at constant pressure.
● Theoretical
○ Experimental

The results of gravimetric and volumetric analyses at equilibrium were listed in Table I.

TABLE I. THE AMOUNT OF CARBON DIOXIDE, EVOLVED AND RESIDUAL (ml. $CO_2$/g. sample STP)

| Temp., °C | Vol. of evolved gas, $u_e$ (volumetric) | Vol. of residual $CO_2$ (gravimetric) |
|---|---|---|
| MEA 138.6 | 15.0±0.5 | 17.3 ±0.2 |
| 126.0 | 10.3±0.4 | 22.0 ±0.1 |
| 117.3 | 8.4±0.2 | 23.8 ±0.1 |
| 109.1 | 5.1±0.2 | 27.2 ±0.1 |
| At room temp. | — | 32.27±0.05 |
| DEA 138.6 | 9.1±0.3 | 3.5 ±0.1 |
| 123.9 | 7.5±0.2 | 5.1 ±0.1 |
| 116.0 | 5.8±0.1 | 6.8 ±0.1 |
| 111.7 | 4.9±0.2 | 7.7 ±0.1 |
| At room temp. | — | 12.58±0.05 |

Concerning the reaction mechanism of the amines and carbon dioxide, Van Krevelen and Hoftijzer suggested that in aqueous solution the complete reaction took place in two steps, the first being a dissociation of the amine and the second the combination of the fragments, and the reaction was a third order[4]. As to

8) W. W. Scott, "Scott's Standard Method of Chemical Analysis", D. Van Nostrand Co., Inc., New York (1939), p. 235.

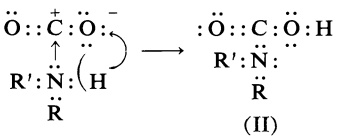
the reaction order a similar conclusion was reached by Cryder and Maloney[2], and Smola[9]. The work of Mason and Dodge[1], and of Shneerson and Leibush[3], showed that the concentration of carbon dioxide in aqueous solution of the amine at equilibrium varied about 0.5 to 0.9 mol. per amine as the temperature decreased from about 75 to 0°C, and the absorption would take place as follows:

$$2RR'NH + H_2O + CO_2 \rightleftarrows (RR'NH_2)_2CO_3$$

$$(RR'NH_2)_2CO_3 + CO_2 + H_2O \rightleftarrows 2RR'NH_2HCO_3$$

$$R = HOCH_2CH_2;\ R' = R \text{ or } H$$

Goodridge interpreted the reaction in terms of zero order as tentative, and presented the following mechanism in the absence of water[5]:



(II)

The amine carbamates in glycerol solution were decomposed, according to the following reactions:

$$RR'NCOONH_2RR' \underset{k_2}{\overset{k_1}{\rightleftarrows}} 2RR'NH + CO_2 \quad (1)$$

MEA $R = HOCH_2CH_2,\ R' = H$

DEA $R = R' = HOCH_2CH_2$

The partial pressure of carbon dioxide was constant at 1 atmospheric pressure. The reaction was reversible as the formula 1, and the following differential equation will be valid:

$$du/dt = k_1(a_0 - u) - k_2(a_0' + 2u)^2 p_{CO_2} \quad (2)$$

$$= k_1(a_0 - u) - k_2'(a_0' + 2u)^2 \quad (3)$$

where

$a_0$ = initial concentration of MEA or DEA carbamate, mol./g. sample,

$a_0'$ = initial concentration of MEA or DEA, mol./g. sample,

$k_1$ = rate constant of decomposition of the carbamate,

$k_2$ = rate constant of absorption of the MEA or DEA,

$u$ = moles of the decomposed carbamate at the time $t$, and

$p_{CO_2}$ = partial pressure of carbon dioxide.

When $u=0$ at $t=0$ and $u=u_e$ at $t=\infty$, the solution of the Eq. 3 is:

$$(Ka_0 - a_0'^2)/u = (\sqrt{K^2 + 8K(2a_0 + a_0')}/2) \cdot \coth(k_2' t \sqrt{K^2 + 8K(2a_0 + a_0')}/2) + (K + 4a_0')/2 \quad (4)$$

where $K = k_1/k_2' = (a_0' + 2u_e)^2/(a_0 - u_e)$ (5)

$$k_2' = k_2 p_{CO_2} \quad (6)$$

A relation between rate constants, $k_1$ and $k_2'$, and equilibrium constant $K$, should be expressed as $k_1/k_2' = K^{1/\nu(r)}$, where $\nu(r)$ = the number of occurrence of a rate determining step necessary to complete an overall reaction formula[10]. At present, however, $\nu(r) = 1$, as will be explained.

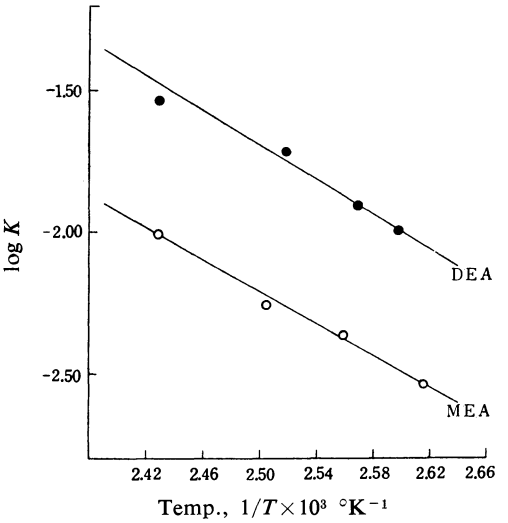



Fig. 4. Temperature dependence of equilibrium constant $K$; $\log K$ vs. $1/T$ ($\times 10^{-3}$).

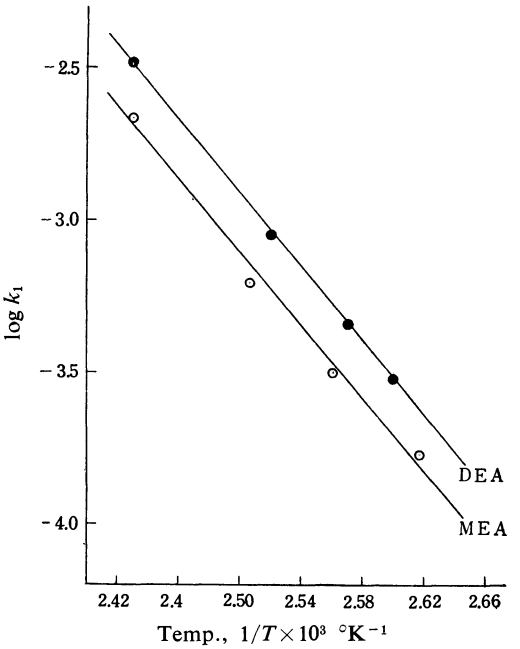



Fig. 5. Temperature dependence of rate constant $k_1$; $\log k_1$ vs. $1/T$ ($\times 10^{-3}$).

9) A. Smola, *Mitt, chem. Forsch.*, **2**. 38 (1948); **2**, 43 (1948).

10) J. Horiuti, *Chem. & Chem. Ind.* (*Kagaku to Kogyo*) **9**, 355 (1956).

On the basis of the amount of carbon dioxide at equilibrium, equilibrium constants were calculated. The temperature dependence of the equilibrium constants was shown in Fig. 4. From the slopes of the lines the heats of the reaction were calculated by the van't Hoff's equation, and were found to be 12.9 and 13.4 kcal./mol. $CO_2$ for MEA system and DEA system, respectively. Since $a_0$, $a_0'$, $K$, $t$ and $u$ were known by the experiment, the rate constants, $k_1$ and $k_2'$, at each temperature, were calculated. After the initial period the values of the rate constants became equal within the limits of experimental error. The calculated values of $u$ obtained from Eq. 4, using these rate constants and the others, were plotted against the time. The agreement with the experimental values supports the validity of Eqs. 1 to 6. The values of $\log k_1$ and $\log k_2'$ were plotted against the reciprocals of corresponding absolute temperatures, as shown in Figs. 5 and 6, and the Arrhenius' energies of activation of the decomposition and the absorption were calculated over the temperature range of 110 to 140°C, and were found to be 27.5 and 14.4 kcal./mol. for the MEA system, 27.8 and 13.6 kcal./mol. for DEA system, respectively.

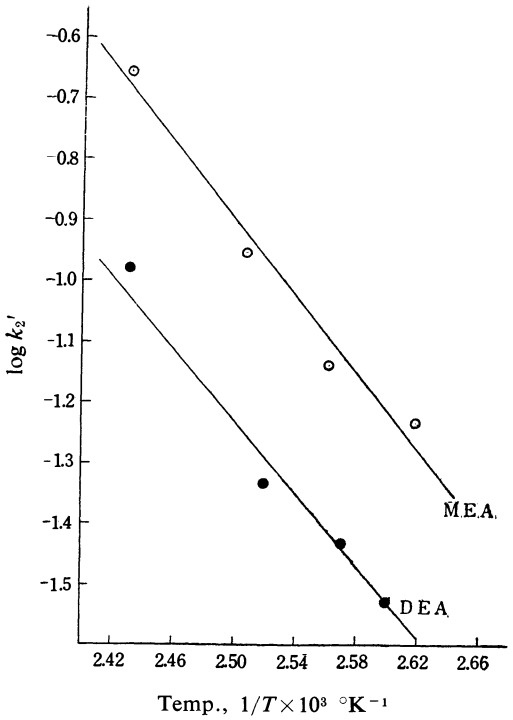



Fig. 6. Temperature dependence of rate constant $k_2'$; $\log k_2'$ vs. $1/T$ ($\times10^{-3}$).

As to the samples, the reaction products should have the formula $RR'NCOONH_2RR'$ (I), since the solution had still excess amine which would eventually change the products of the type RR'NCOOH (II), if present, to the type (I).

The author wishes to express his sincere thanks to Mr. Shûzô Kishida for his encouragement. This paper is published by the permission of the Technical Research and Development Institute, Defense Agency.

*2nd R & D Center*
*Technical Research*
*and Development Institute*
*Defense Agency Japan*
*Setagaya-ku, Tokyo*

# *Photoconductivity of Polycyclic Aromatic Compounds*

By Mizuka SANO

(Received May 10, 1961)

Since Akamatu and Inokuchi reported the photoconductivity of violanthrone[1], a number of investigations have been made on the photoconductive phenomena in aromatic compounds[2-7]. These investigations, however, have been concentrated mainly on compounds consisting of a small number of rings, such as anthracene and pyrene, which possess resistivities as high as $10^{20}$ ohm. cm. at room temperature[3]; hence, they may be classified as insulation photoconductors rather than semiconductors. Recently Kallmann and Pope[8] showed

1) H. Akamatu and H. Inokuchi, *J. Chem. Phys.*, **20**, 1481 (1952).
2) H. Inokuchi, This Bulletin, **27**, 22 (1954).
3) H. Inokuchi, ibid., **29**, 131 (1956).
4) D. M. J. Compton, T. C. Waddington and W. G. Schneider, *J. Chem. Phys.*, **27**, 160 (1957).
5) L. E. Lyons and G. C. Morris, *J. Chem. Soc.*, **1957**, 3648.
6) B. Rosenberg, *J. Chem. Phys.*, **29**, 1108 (1958).
7) D. C. Northrop and O. Simpson, *Proc. Roy. Soc.*, A **244**, 377 (1958).
8) H. Kallmann and M. Pope, *J. Chem. Phys.*, **32**, 300 (1960).

that the injected holes from an electrode contributed to the major conduction in anthracene, and Moore and Silver[9] concluded that anthracene is an extrinsic photoconductor rather than the intrinsic one.

On the other hand, relatively little work has been done on the photoconductive behaviors in multi-ring compounds, though it is known that the semiconductive properties are enhanced with the increase of the number of rings.

## Experimental

**Materials.**—Most of the materials were synthetized by Drs. Handa and Aoki in our laboratory. All of them were carefully purified by recrystallization from solutions. To the final process of the purification the vacuum sublimation method was applied repeatedly.

**Procedures.** — Two types of photocells, i. e., the surface-type cell and the sandwich-type cell, were employed for the investigation of photoconduction. The surface-type cell consisted of a uniform film of aromatic compound with a thickness of about one micron and an area of $15\times15$ mm$^2$. The film was deposited on a pyrex glass plate (the dimension of which was 20 mm.$\times$25 mm.) by slow sublimation in vacuo. Colloidal graphite, "Aquadag", was applied on the film to serve as the electrodes, which were 1 cm. in length and about 3 mm. in width, with a gap of 1 mm. between them. The sandwich-type cell was formed by sublimation of the compound onto a pyrex plate on which a transparent aluminum conducting film had been previously deposited. The second aluminum film, lying entirely on the organic film, completed a photocell with an area of $10\times5$ mm$^2$ and a thickness of a few microns.

The sublimation of organic compounds was carried out in vacuo ($10^{-3}$ mmHg) without decomposition over temperatures ranging from 80 to 380°C. The growth of a film was followed by observing the color of reflected light, and in this way the thickness could be estimated accurately enough to prepare an appropriate film for photoconduction.

Most of the aromatics employed absorb the light intensely in the spectrum region extending from near ultraviolet to near infrared, so that a tungsten lamp is one of the most convenient light sources. The Mazda 750-watt projector lamp was used, being associated with second-order interference filters to isolate narrow particular wavelength regions. The maximum transmissive wavelengths of the regions, which were 9~16 m$\mu$ in half band width, ranged from 392 to 1324 m$\mu$, with an interval of 50~100 m$\mu$.

Absolute measurements of intensity of incident light on an organic photocell were made with the Nihonbunko vacuum thermopile which was placed at the position of the photocell. The sensitivity of the thermopile was 5.6 microvolts per one microwatt with the time constant of 33 milliseconds and the resistance of 4.2 ohm. A germanium phototransistor and a PbS photocell were used as auxiliary instruments for the measurement of light intensity, because these detectors endure a higher intensity of light better than the thermopile. The maximum intensity, $6\times10^{18}$ photons/sec·cm$^2$, was obtained for the light which was isolated by the 1324 m$\mu$ filter.

Measurements of electric current were made with association of the Takeda Model V-IM dc amplifier. The ampplifier has the input resistance ranging from $4.5\times10^5$ to $4.4\times10^{11}$ ohm. The voltage source applying to an organic photocell was a battery of dry elements with voltage of up to 700 V.

The apparatus, as illustrated in Fig. 1, consisted of five parts; the outer glass cylinder, the liquid nitrogen container with the photocell holder, the radiation shield, the optical windows and four conducting leads. The photocell was mounted on the holder by being pressed with a polystyrene plate and nuts.

Measurements of temperature were made with the germanium resistor which had been calibrated with a pentane direct-readings thermometer. The resistance of the resistor changed from 27 to 10 ohm. following the temperature change from +15 to −196°C. The complete evacuation and the heat radiation shield prevented condensation of moisture on the surface of optical window. The apparatus was placed in a metal box, which served for shutting out the photocell from light and also for preventing electrical disturbance.

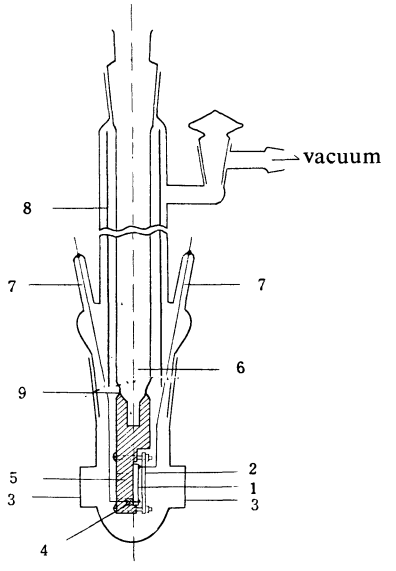



Fig. 1. The apparatus for conductivity measurement.

1 Photocell
2 Polystyrene plate
3 Optical windows
4 Germanium-registor thermometer
5 Specimen holder
6 Liquid nitrogen container
7 Conducting leads
8 Radiation shield
9 Copper-soft glass joint

9) W. Moore and M. Silver, ibid., 33, 1671 (1960).

## Results

**Change in Photocurrent with Electric Potential.** —The electric current was measured as a function of applied potential under the illumination of monochromatic light. Most of the observations were made with surface-type photocells in vacuo, to avoid the effects of space charge which were occasionally observed with sandwich-type photocells.

The current responded to potential variation instantaneously and then remained constant with time. The potential dependence of photocurrent was reproducible, as in the case of dark current similarly. When the logarithm of the current $i$ was plotted against the logarithm of the applied potential $V$, a linear relationship was obtained. This is illustrated in Fig. 2 for pyranthrene. From this, the potential-current relation could be expressed by the following formula,

$$i \propto V^{\alpha}$$

The values of $\alpha$ for pyranthrene, violanthrene and perylene are shown in Table I. In this table, it is seen that $\alpha$ is approximately unity, under different conditions of illumination with regard to wavelength and intensity of light. Hence, it can be concluded that the photocurrent obeys Ohm's law over the range of potential applied up to $7\times10^3$ V./cm.

**Change in Photocurrent with Light Intensity.** — The photocurrent in surface-type photocells was observed as a function of light intensity. The relation between photocurrent and light intensity yielded two regions generally, as illustrated in Figs. 3 and 4. In each region, the relationship between the photocurrent $i_p$ and the light intensity $L$ could be expressed by the formula,

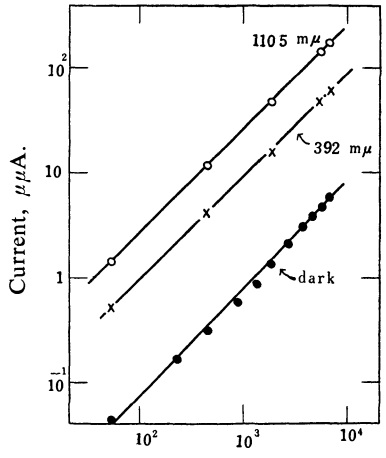



Fig. 2. The relation between current and applied potential for pyranthrene.

TABLE I. THE $\alpha$-VALUE FOR SURFACE-TYPE PHOTOCELLS

| | Illumination: Wavelength mμ | Illumination: Intensity photons/sec. cm² | α-Value |
|---|---|---|---|
| Pyranthrene (film) | Dark | — | 1.05 |
| | 392 | $10^{15}$ | 1.01 |
| | 529 | $10^{13}$ | 1.14 |
| | 1055 | $10^{15}$ | 1.10 |
| | 1105 | $10^{17}$ | 1.00 |
| Violanthrene (film) | Dark | — | 1.11 |
| | 557 | $10^{13}$ | 1.15 |
| Perylene (film) | 470 | $10^{13}$ | 1.20 |
| Perylene (single crystal) | 392 | $10^{16}$ | 1.17 |
| | 403 | $10^{16}$ | 1.15 |
| | 502 | $10^{16}$ | 1.17 |
| | 502 | $10^{17}$ | 1.19 |

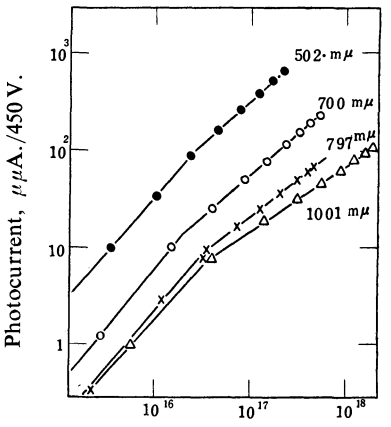



Fig. 3. The relation between photocurrent and light intensity for pyranthrene (surface-type photocell).

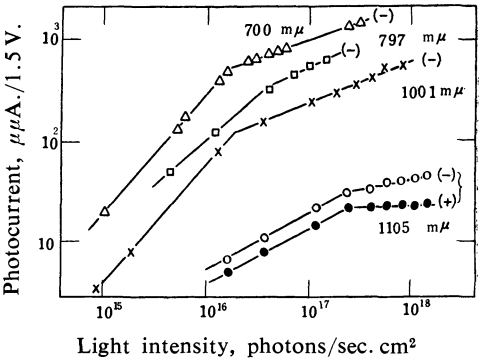



Fig. 4. The relation between photocurrent and light intensity for pyranthrene (sandwich-type photocell).

Illuminated electrode was biased positively, (+) and negatively (−).

$$i_p \propto L^n$$

In the region of low light intensity, usually not much exceeding $10^{16}$ photons/sec. cm$^2$, the photocurrent changed approximately in linearity with the light intensity, i. e., the exponent $n$ was nearly unity. This relation was seemingly independent of the wavelength of incident light, the atmosphere, the applied potential and the temperature.

While in the region of high light intensity, $n$ possessed a smaller value than unity, and was dependent on the wavelength of illumination. Nevertheless, no appreciable difference of $n$-value was noted according to the variation of temperature, potential, or atmosphere. The $n$-values are summarized in Table II.

No indication of saturation was observed with surface-type photocells even in the region of the highest light intensity, around $10^{18}$ photons/sec. cm$^2$. However, sandwich-type photocells showed the saturation of photocurrent at the light intensity of $2\times10^{17}$ photons/sec. cm$^2$, as illustrated in Fig. 4.

TABLE II. THE $n$-VALUE FOR PYRANTHRENE AND PERYLENE SURFACE-TYPE PHOTOCELLS IN THE REGION OF HIGH LIGHT INTENSITY

| Wavelength of illumination mμ | Pyranthrene film | | | Perylene single crystal | |
|---|---|---|---|---|---|
| | In vacuo* | | In dry air | In vacuo* | In dry air |
| | 290°K | 185°K | 290°K | 290°K | 290°K |
| 403 | 0.86 | | | 0.98 | 0.87 |
| 450 | 0.84 | | | 0.95 | 0.87 |
| 502 | 0.95 | | 1.06 | 1.12 | 1.15 |
| 552 | 1.00 | 1.03 | | 1.10 | 1.02 |
| 599 | 0.89 | | | 0.86 | 0.82 |
| 655 | 0.82 | | | 0.79 | 0.68 |
| 700 | 0.85 | 0.81 | 0.87 | | |
| 747 | 0.77 | | | | |
| 797 | 0.77 | | 0.74 | | |
| 853 | 0.61 | | | | |
| 901 | 0.62 | | | | |
| 945 | 0.73 | | | | |
| 1001 | 0.67 | | 0.63 | 0.78 | |
| 1105 | 0.76 | 0.78 | | 0.79 | |
| 1195 | 0.78 | | | 0.78 | |
| 1324 | 0.92 | 0.91 | 0.88 | | |

* $10^{-3}$ mmHg after being flushed with argon gas.

**Change in Photocurrent with Temperature.**—The temperature dependence for photocurrent was measured over the range from 173 to 290°K. The surface-type photocell was employed with association of the apparatus which is shown in Fig. 1. The photocurrent increased with an increase in the temperature. Plots of the logarithm of photocurrent $i_p$ against the reciprocal of temperature gave a straight line

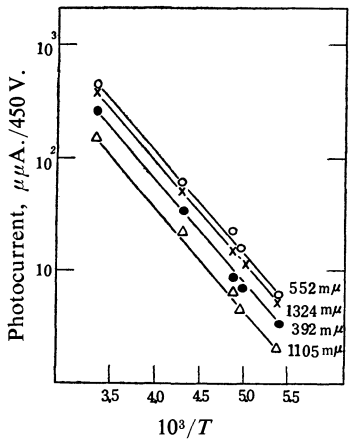



Fig. 5. The photocurrent vs. temperature for pyranthrene (surface-type photocell).

(Fig. 5), and the relation follows the equation,

$$i_p = i_0 \exp(-E/kT)$$

where $E$ is the activation energy of photocurrent.

It is of interest that the activation energy, e. g., 0.18 eV. for pyranthrene, was found to be independent of the intensity and the wavelength of incident light over the range from 392 to 1324 mμ employed.

**Generation of Charge Carriers.**—An attempt was made to measure the photocurrent which was produced by the illumination onto a limited area of the aromatic film between the electrodes of surface-type photocell. Aquadag electrodes were painted on the pyranthrene film with a gap of 7 mm. between them. When the whole area between the electrodes was illuminated, the maximum photocurrent, of the value of $12\times10^{-12}$ A./450 V., was observed. When the illumination was made onto the half part of the area between the electrodes by masking the other half, the magnitude of photocurrent was smaller than that expected if the photons in the same number had been uniformly distributed over the whole area. When the illumination was focused onto one of the electrodes alone, the increase of current was hardly observed. In addition, when the light fell onto a small limited area of the film, the magnitude of photocurrent assigned per unit area was nearly equal to that of the photocurrent produced by the illumination on the half area. Consequently it might be concluded that the charge carriers are not produced in a particular portion such as the Aquadag electrode or the contact area, but in the area between both elctrodes. Nevertheless, there is no explanation for the fact that the maximum photocurrent was produced by the illumination on the whole area. Probably the difference is

related to the decay pocess of charge carriers.

The photocurrent produced by an asymmetric illumination with respect to the polarity of ppalied potential was also measured. Onto a pyranthrene surface-type cell an image of slit of monochromatic light was collimated so that the illuminated strip lay parallel to the electrodes. Keeping the applied potential ($2.25\times\times10^2$ V./cm.) and light intensity ($2.8\times10^{17}$ photons/sec. cm$^2$ for 552 m$\mu$ illumination) constant, the photocurrent was measured as the image was moved from one electrode to the other. The photocurrent was always greater when the illuminated portion was located close to the negatively biased electrode. In this case, the photoelectromotive force due to the asymmetric illumination was undetectable, even under the illumination of the highest light intensity.

Also, a sandwich-type photocell possesses the asymmetry in itself, because the light intensity of illumination is diminished successively along the electric potential. The photocurrent of a pyranthrene film (about 10 $\mu$ in thickness), which was sandwiched between two evaporated aluminum films, was 1.5 times greater when the illuminated side was negatively biased than when it was positively biased at the applied potential of $1.5\times10^3$ V./cm.

The thermoelectromotive force, which was observed with compressed powder of isoviolanthrone, was of the order of $10^{-4}$ V./deg., indicating conduction predominantly by electrons.

## Discussion

The semiconductive behaviors of polycyclic aromatic compounds have been fairly extensively studied, but the theoretical interpretation of their electronic conduction has not been completed, because the intermolecular interactions in the solid state are scarcely known. However, a significant part of the behavior of organic semiconductors can be discussed, for convenience, in terms of the band model. It may be postulated that the empty band and the full band are formed from the energy levels of the excited states and the ground state of $\pi$-electrons of the molecule respectively. In this case, the band widths might be narrow; especially the width of the full band is so narrow because of poor overlapping of the wave functions for the ground state, that the full band may be regarded as a series of discrete levels. Consequently it is quite probable that the holes are almost confined to the particular molecules in which they are generated, and most of the electric current is conducted by electrons through the crystal. The model was supported by the signs of the thermoelectromotive force and the polarity for the maximum photocurrent which was produced by an asymmetric illumination. In addition, as the ohmic nature of photocurrent as well as the experiment on the limited-area illumination indicated, the generation of charge carriers took place in the bulk of aromatic film, neither from the electrode nor the electrode-film contact. Hence, the multi-ring compounds are seemingly intrinsic photoconductors. The light intensity dependence for photocurrent has been usually accounted for by the concept of the trapping process of charge carriers. For instance, Rose[10] explained the variation of the exponent $n$ from 1 to 0.5 by the population of the effective trapping centers which varies depending on the intensity of illumination. Our result showed that $n$ possesses unity at a low light intensity and possesses a smaller value than unity at a high light intensity. This result is coincident qualitatively with that shown by Rose. The temperature dependence for photocurrent can not be easily interpreted because more than one parameter can change with temperature. However, the activation energy of photocurrent was independent on the wavelength of light. This result seems to indicate that the activation energy is not associated with the formation of charge carriers, such as the dissociation of electron-hole pairs, but with the transport process of carriers. If the trapping centers are assumed to be of the same depth below the empty band, and the temperature dependence could be ascribed to the variation of the mobility of carriers, the activation energy indicates the depth of trapping center. However, the nature of the centers has not been established. As suggested by Nelson[11] for the case of cationic dyestuff, every molecule might be regarded as a trapping center in the polycyclic aromatic compounds.

## Summary

The voltage, light intensity, and temperature dependences for photocurrent in multi-ring compounds were studied as well as the photocurrent produced by the limited-area illumination. The photocurrent was found to be ohmic over the range of voltage employed. The photocurrent increased linearly with the intensity of light in the region of low light intensity, while it increased as the fractional power of the light intensity in the region of high intensity. The photocurrent increased with an increase of the temperature, and the activation energy of the photocurrent was found to be independent of the wavelength and the intensity of illumination.

10) A. Rose, *RCA Review*, **12**, 362 (1951).
11) R. C. Nelson, *J. Chem. Phys.*, **30**, 406 (1959).

The signs of the thermoelectric power as well as the polarity for the maximum photocurrent, and the experiment on the limited-area illumination indicated that the conduction in polycyclic aromatic compounds was due predominantly to electrons which were generated in the bulk of aromatic film.

The author expresses his hearty thanks to Professor Hideo Akamatu for his kind direction and advice, and also to Dr. Hiroo Inokuchi for his continuous advice in this work. The cost of this research has been defrayed from the Scientific Research Encouragement Grant from the Ministry of Education to which the author's thanks are due.

*Department of Chemistry*
*Faculty of Science*
*The University of Tokyo*
*Hongo, Tokyo*

# *Stereoregular Polymers. IX. Polymerization of Optically Active α-Olefins**

By Shun'ichi NOZAKURA, Shigeru TAKEUCHI, Heimei YUKI and Shunsuke MURAHASHI

(Received April 18, 1961)

In their previous work[1], the authors polymerized styrene with anionic catalysts containing the optically active alkyl group such as optically active amylsodium or triamylaluminum combined with titanium trichloride. The purpose was to obtain optically active polystyrene, in which one helical configuration (either right- or left-handed screw helix) presumably induced by the active group might be predominantly present. However, the attempt was not successful.

X-Ray analyses of various isotactic polymers have shown that the crystalline structure of the polymer, and accordingly the crystallinity and the melting temperature are largely dependent on the side group of the chain[2]. In other words, the type of helix, i.e. the number of monomeric units or of turns in the identity period, may be decided definitely by the shape and size of the substituent group of the chain.

The present work was carried out as one of the programs of attempting to regulate the direction of helical configuration of polymer chain in its screw sense. Two optically active α-olefins, *l*-4-methyl-1-hexene and *d*-3-methyl-1-pentene, were polymerized by the Ziegler catalyst and the nature of the polymer was examined in anticipation that the asymmetric substituent might induce the helical configuration, which exists with only one (right- or left-handed) screw sense, in the polymer chain.

## Experimental

**Preparation of Monomers.**—*l-2-Methyl-1-butanol.*—Commercial fusel oil was fractionally distilled by Stedman type column (about seventy theoretical plates) repeatedly. *l*-2-Methyl-1-butanol thus obtained showed b. p. 128°C and $\alpha_D^{28}$ −9.36° (*l*=20 cm.) (optical purity 98.7%)[3].

*d-1-Chloro-2-methylbutane.*—The alcohol was converted to the chloride by thionyl chloride. Yield 78.7%, b. p. 99°C, $[\alpha]_D^{30}$ +1.63° (optical purity 97%)[4].

*Optically Active 1-Bromo-2-ethoxy-4-methylhexane.*—2-Methylbutylmagnesium chloride derived from optically active *d*-1-chloro-2-mehthylbutane was made to react with α, β-dibromo ethyl ether[5] to give 1-bromo-2-ethoxy-4-methylhexane[6]. Yield 60.3%, b. p. 91~93°C/15 mmHg.

*l-4-Methyl-1-hexene*[7].—The ethoxyheptyl bromide gave *l*-4-methylhexene in 61% yield by refluxing an alcoholic solution with zine powder for 10 hr.

* This paper is based upon a portion of a thesis submitted by S. Takeuchi in partial fulfillment of the requirements for the Degree of Master of Science in Osaka University, March, 1960.

1) S. Murahashi, S. Nozakura and S. Takeuchi, This Bulletin, 33, 658 (1960).

2) G. Natta, *Angew. Chem.*, **68**, 393 (1956).

3) R. M. Ideda, R. E. Kepner and A. D. Webb, *Anal. Chem.*, **28**, 1335 (1956).

4) A. Mackenzie and G. W. Clough, *J. Chem. Soc.*, **103**, 698 (1913).

5) L. S. Swallen and C. E. Boord, *J. Am. Chem. Soc.*, **52**, 651 (1930); H. B. Dykstra, J. F. Lewis and C. E. Boord, ibid., **52**, 3396 (1930).

6) D. C. Rowland, K. W. Greenlee, J. M. Derfer and C. E. Boord, *J. Org. Chem.*, **17**, 807 (1952).

7) F. J. Soday and C. E. Boord, *J. Am. Chem. Soc.*, **55**, 3293 (1933).

TABLE I

| | Polymerization[a] | | | | Polymer | | | |
|---|---|---|---|---|---|---|---|---|
| | Monomer g. | $AlEt_3$ g. | $TiCl_4$ g. | Yield % | M. p. °C | $[\alpha]_D$(in toluene) | $[\eta]^b$ | $d_4^{13}$ |
| *l*-4-Methyl-1-hexene | 3.6 | 0.56 | 0.38 | 19 | 180～182 | +251°(27.5°) | 0.86 | 0.862[c] |
| 〃 | 5.7 | 0.75 | 0.50 | 7 | 171～174 | +249 (21) | 0.79 | 0.86 |
| 5-Methyl-1-hexene | 3.1 | 0.38 | 0.25 | 25 | 112～114 | + 54 (22) | — | —[d] |
| 〃 | 2.1 | 0.38 | 0.25 | 58 | 102～104 | + 52 (22) | — | — |
| 〃 | 1.6 | 0.38 | 0.25 | 46 | 96 | + 54 (22) | — | — |
| *d*-3-Methyl-1-pentene | 4.4 | 0.75 | 0.50 | 20 | 260～264 | +255 (24)[g] | — | 0.831[e] |
| *dl*-3-Methyl-1-pentene | 1.3 | 0.38 | 0.25 | 8 | 200～205 | — — | — | 0.832[f] |

a, Solvent: 20 ml. *n*-heptane. b, Toluene solution at 29.9°. c, Found: C, 84.94; H, 14.29. d, Found: C, 85.26; H, 14.10; Ash, 0.26. e, Found: C, 84.60; H, 14.09; Ash, 0.89. f, Unfractionated. Found: C, 85.38; H, 14.12; Ash, trace. All the samples contained traces of ash. Calcd. for $[C_nH_{2n}]_p$: C, 85.63; H, 14.37%. g, in petrolatum liquid.

B. p. 87～88°C, $[\alpha]_D^{31}$ −2.50° (optical purity 94%)[8] $n_D^{31}$ 1.3970, $d_4^{31}$ 0.692.

*5-Methyl-1-hexene.*— It was synthesized similarly from commercial isoamyl alcohol via isoamyl chloride in 16% yield based on the chloride. B. p. 83～85°C. The isoamyl chloride showed an optical activity ($[\alpha]_D^{22}$ +0.33°), which corresponded to that calculated for a mixture of 81% pure isoamyl chloride and 19% *d*-1-chloro-2-methylbutane[9].

*d-3-Methyl-1-pentanol.*—Optically active 3-methyl-1-pentanol was synthesized from formaldehyde and 2-methylbutylmagnesium chloride derived from *d*-1-chloro-2-methylbutane (b. p. 99～100°C, $[\alpha]_D^{10}$ +1.71°, optical purity ca. 100%), which was obtained from optically pure *l*-2-methyl-1-butanol, b. p. 127.5～128.5°C, $[\alpha]_D^{11}$ −9.55° (*l*=20 cm.). Gaseous formaldehyde was bubbled through the ethereal solution of the Grignard reagent with dry nitrogen. The subsequent decomposition and steam-distillation of the product gave *d*-3-methyl-1-pentanol in 38.3% yield, b. p. 147～149°, $[\alpha]_D^{10}$ +8.41° (literature[8]: $[\alpha]_D^{19.5}$ +8.53°).

*d-3-Methylpentyl Acetate.*— The acetate was obtained from the alcohol by using *p*-toluenesulfonic acid as a condensing catalyst, yield 69%, b.p. 156～158°C, $[\alpha]_D^{8}$ +8.53° (literature[8]: $[\alpha]_D^{19}$ +8.30°).

*d-3-Methyl-1-pentene.* — The methylpentyl acetate was dropped with a stream of nitrogen through a quartz tube packed with glass pieces at 500°C. The pyrolysis gave *d*-3-methyl-1-pentene in 36% yield. b. p. 54～55°C, $[\alpha]_D^{12}$ +32.95° (literature[8]: $[\alpha]_D^{17}$ +32.86°).

*dl-3-Methyl-1-pentanol.*—Ethylene oxide was bubbled through an ethereal solution of *sec*-butylmagnesium chloride using nitrogen as a carrier gas. The product was decomposed by saturated aqueous ammonium chloride and steam-distilled to give *dl*-3-methyl-1-pentanol. Yield 52%, b. p. 148～150°C.

*dl-3-Methyl-1-pentene.* — The racemic 3-methyl-1-pentene was obtained from the racemic methylpentanol via its acetate similarly as described on the optically active methylpentene. Yield 35% based on the alcohol, b. p. 54～56°C.

**Polymerization.** — The heptene monomers, *l*-4-methyl-1-hexene and 5-methyl-1-hexene, were polymerized in a five-necked flask described previously[10]. The vessel was flushed with dry nitrogen, and charged with *n*-heptane, titanium tetrachloride and aluminum triethyl (*n*-heptane solution), and the monomer was injected by a hypodermic syringe through a rubber cap fitted on the vessel. The mixture was heated for 10 hr. at 70°C. All procedures were done in a stream of dry nitrogen. The reaction mixture was then poured into a large volume of methanol containing a small amount of hydrochloric acid to decompose the catalyst. After being allowed to stand overnight the precipitated polymer was collected by centrifugation, washed with methanol, and dried.

The hexene monomers, *d*- and *dl*-3-methyl-1-pentene, were polymerized by analogous procedures but using a sealed tube as the reaction vessel and at 50°C for longer periods, 40 hr. for racemic and 144 hr. for *d*-monomer.

The results of polymerization were summarized in Table I.

The polyheptenes were soluble in chloroform, carbon tetrachloride, toluene, benzene, decalin, carbon disulfide, and hot *n*-heptane, and insoluble in ether, alcohol and acetone.

Poly-*d*-3-methyl-1-pentene was almost insoluble in usual organic solvents. This was slightly soluble above its melting point in petrolatum liquid, dibutyl phthalate and dioctyl phthalate. The solution in petrolatum liquid was maintained clear and stable even after it had cooled to room temperature, but the polymer precipitated from the phthalate solutions below about 290°C and no appreciable amount of polymer appeared from the liquid phases by adding methanol.

On the other hand, the polymeric product of *dl*-3-methyl-1-pentene was found to be largely contaminated with polyethylene produced from the Ziegler catalyst itself and was fractionated successively by boiling toluene and by boiling decalin. The toluene-soluble fraction (68%) containing a considerable amount of polyethylene melted between 130 and 190°C. The decalin-soluble fraction (17%) and the remaining insoluble fraction (15%) melted at 225～226°C and 245～247°C, respectively. The solubility of decalin-insoluble fraction seemed

8) P. Pino and L. Lardicci, *Chem. & Ind.*, **1959**, 483.
9) F. C. Witmore and J. H. Olewine, *J. Am. Chem. Soc.*, **60**, 2570 (1938).
10) S. Murahashi, S. Nozakura, M. Sumi and K. Hatada, This Bulletin, **32**, 1094 (1959).

to be slightly greater than that of poly-*d*-3-methyl-1-pentene but was about the same.

**Optical Rotation.**— For the determinations of optical rotatory dispersion and optical purity a Rudolph high-precision photoelectric spectropolarimeter model 200S-80 was used.

The observed optical rotation of a solution of poly-*d*-3-methyl-1-pentene in petrolatum liquid was $\alpha_D^{24}$ +4.68° ($l$=20 cm.) at $c$=0.0745. The petrolatum liquid, however, had an optical rotation $\alpha_D^{24}$ +2.15° ($l$=10 cm.), and the specific rotation of the polymer, $[\alpha]_D^{24}$ +255°, was calculated from the difference of rotations of the solution and the solvent.

**Density.**—Determination of polymer density was carried out by a density gradient tube using methanol and water as media.

**Melting Point.**—The polymer sample was placed on a metal block under the microscope. The metal block was heated by a hot plate and the melting point of the sample was measured.

## Results

The dependence of the optical rotation on the concentration of poly-*l*-4-methyl-1-hexene was examined in four solvents, toluene, decalin, carbon tetrachloride and carbon disulfide. The results are shown in Fig. 1. The linear ralationships between the rotation and the polymer concentration were obtained in each solvent. These led to the values of specific rotation $[\alpha]_D^{27.5}$ +251° (toluene), $[\alpha]_D^{24}$ +268° (decalin), $[\alpha]_D^{25}$ +236° (carbon tetrachloride) and $[\alpha]_D^{13}$ +290° (carbon disufide).

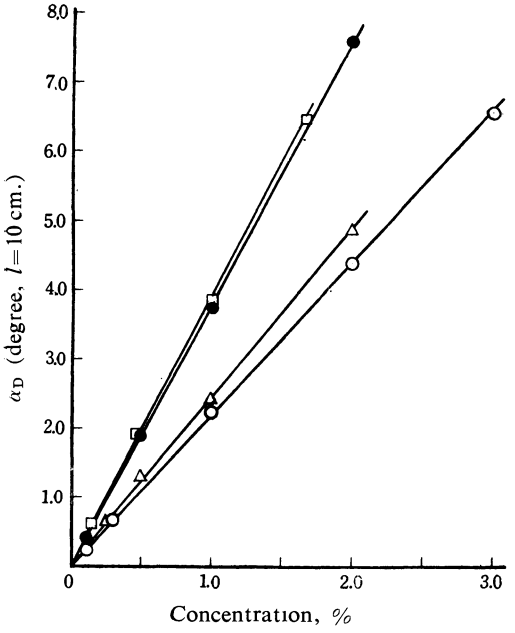



Fig. 1. Optical rotation vs. concentration of poly-*l*-4-methyl-1-hexene in various solvents: ○ in toluene at 27.5°C; △ in decalin at 24°C; □ in carbon tetrachloride at 25°C; ● in carbon disulfide at 13°C.

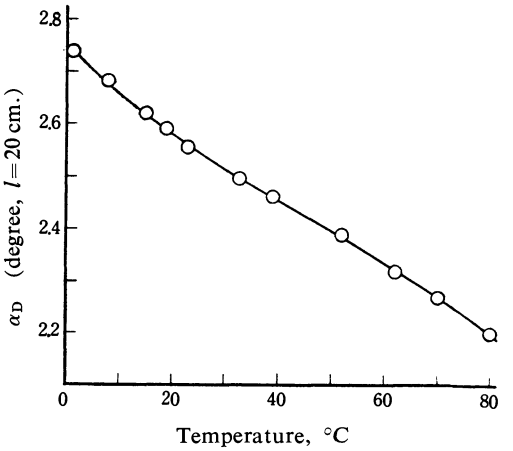



Fig. 2. Temperature dependence of optical rotation of 0.5% poly-*l*-4-methyl-1-hexene solution in decalin.

The plots of the optical rotation of 0.5% poly-*l*-4-methyl-1-hexene solution in decalin vs. temperature are shown in Fig. 2. The rotation decreased almost linearly with the elevation of temperature from 2 to 80°C.

To the toluene solution of the polymer (concentration 1.05%) *n*-heptane, a poor solvent for the polymer, was added successively and the change of optical rotation of the solution was followed. Similarly *n*-butanol, a precipitant against the polymer, was added in another series of this experiment. The results showed that the rotation was rather strictly linear to the concentration of the polymer alone (Fig. 3). In these experiments the ageing of the

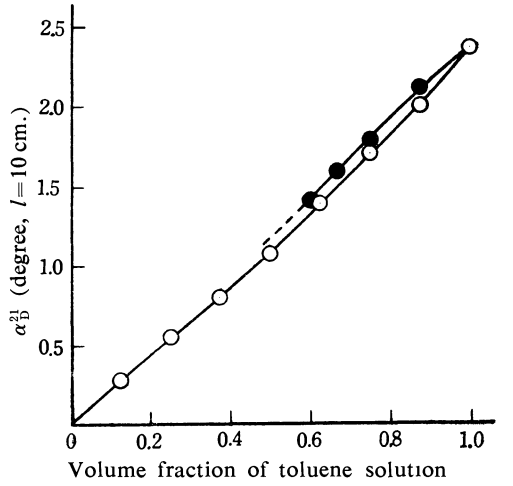



Fig. 3. Changes in optical rotation with the addition of *n*-heptane (○) and *n*-butanol (●) to 1.05% solution of poly-*l*-4-methyl-1-hexene in toluene. Dotted line, precipitation occurred.

solution caused no change in the optical rotation after adding the poor or the bad solvent.

The optical rotatory dispersion was measured with the polymer in two solvents, decalin ($c=0.4\%$, $l=10$ cm.) and toluene-*n*-heptane mixture (1 : 1 vol./vol., $c=0.6\%$, $l=10$ cm.). The results are shown in Figs. 4 and 5. The plots $\alpha_\lambda\lambda^2$ vs. $\alpha_\lambda$, where $\alpha_\lambda$ is the optical rotation at a wavelength $\lambda$, were linear as shown in Fig. 5, and no abnormal dispersion was observed.

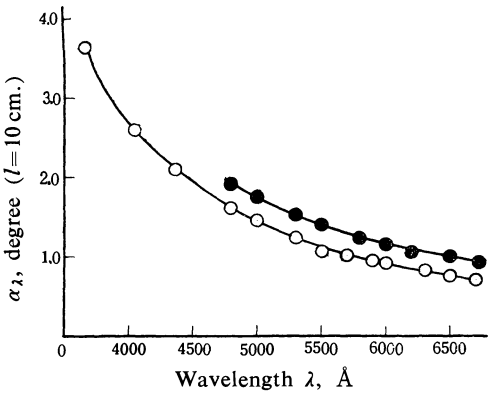



Fig. 4. Optical rotatory dispersion of poly-*l*-4-methyl-1-hexene: ○ in decalin ($c=0.4$) at 21°C; ● in toluene-*n*-heptane mixture (1 : 1 vol./vol., $c=0.6$) at 19°C.

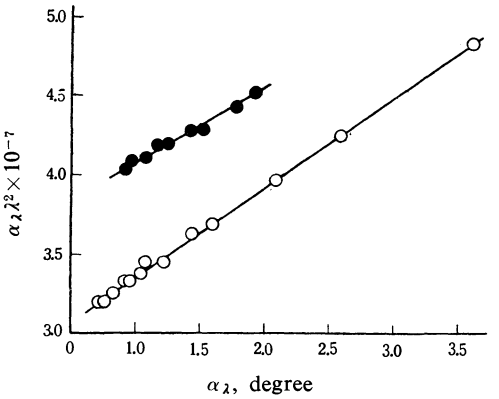



Fig. 5. $\alpha_\lambda\lambda^2$ vs. $\alpha_\lambda$ in the optical rotatory dispersion of poly-*l*-4-methyl-1-hexene: ○ in decalin; ● in toluene-*n*-heptane mixture.

All the polymers obtained here gave sharp crystalline X-ray patterns except the toluene-soluble fraction of poly-*dl*-3-methyl-1-pentene. The patterns given by poly-*d*-3-methyl-1-pentene and the decalin-insoluble fraction of poly-*dl*-3-methyl-1-pentene were completely different. The spacings obtained from the powder X-ray diagrams are summarized in Table II.

TABLE II. SPACINGS FOR POLY-*d*-3-METHYL-1-PENTENE AND POLY-*dl*-3-METHYL-1-PENTENE

| Poly-*d*-3-methyl-1-pentene | Poly-*dl*-3-methyl-1-pentene[a] |
|---|---|
| 9.60 Å (vs) | 9.26 (s) |
| 6.92 (vw) | 8.65 (s) |
| 6.18 (m) | 5.38 (s) |
| 5.55 (vw) | 4.74 (mw) |
| 5.09 (vw) | 4.20 (m) |
| 4.66 (s) | 3.91 (m) |
| 4.23 (vw) | |
| 4.05 (w) | |
| 3.26 (w) | |
| 3.07 (vw) | |
| 2.75 (vw broad) | |
| 2.53 (vw) | |
| 2.39 (vw) | |

a Decalin-insoluble fraction.

## Discussion

Both of the optically active polymers, poly-*l*-4-methyl-1-hexene and poly-*d*-3-methyl-1-pentene, showed enormously large optical rotations compared with those of the monomers. The large optical rotations seemed to be contributed not only by the neighboring groups around the asymmetric carbon atom of the side group but also by the molecular asymmetry of the helical configuration of the main chain, more practically by a predominant concentration of either right- or left-handed helix in the solution.

It is doubtful that the isotactic polymer such as poly-$\alpha$-olefin still maintains its helical structure in the solution. However, Takeda and his collaborators[11] recently stated from their infrared absorption study that in carbon disulfide isotactic polystyrene retained its helical structure[12] even in the solution state. This encouraged us to investigate the optical rotation of poly-*l*-4-methyl-1-hexene in solution by varying the conditions in order to learn its exact nature.

The concentration of the helix might vary with the concentration of the polymer, if it remained in the solution in any extent. The temperature might also affect the concentration of the helix. The concentration of the helix would be considered to be related to the interaction between the molecules of polymer and solvent. A good solvent may release the helical configuration of the polymer to transform it into a randomly coiled structure and, on the other hand, poor solvent might probably coil up the chain to a helix as shown by

11) M. Takeda, K. Iimura, A. Yamada and Y. Imamura, ibid., 32, 1150 (1959).
12) H. Tadokoro et al., ibid., 32, 313, 534 (1959); *J. Polymer Sci.*, 36, 553 (1959).

Doty and his coworkers[13] for poly(γ-benzyl L-glutamate).

However, the concentration, the temperature and the addition of bad solvent gave no distinct change in the specific rotation of the polymer in solution, compared with the large change observed in the helix-coil transformation of poly (γ-benzyl L-glutamate). In addition, the plots of optical rotatory dispersion fitted the equation $\alpha_\lambda\lambda^2=\lambda_c^2\alpha_\lambda+A'$[13] derived from the simple one-term Drude equation $[\alpha_\lambda]=A/(\lambda^2-\lambda_c^2)$, where $\lambda_c$, $A$ and $A'$ are the constants, respectively, and no complex dispersion was found. These facts strongly suggest that the optical rotation of this polymer is attributed to only one species, the asymmetric carbon atom of the substituent group, at least in solution.

The polymer formed from the 5-methyl-1-hexene monomer had a specific rotation $[\alpha]_D^{22}$ $+54^\circ$ in toluene. Obviously this was caused by *l*-4-methyl-1-hexene units in the polymer which had been contained in the monomer used. Reding[14] has reported that the polymer produced from a mixture of 4-methyl-1-pentene and 3-methyl-1-butene was a copolymer but not a mixture of the homopolymers of each monomer. Therefore, it may be preferable to consider the polymer obtained here as being also the copolymer of 5-methyl-1-hexene and *l*-4-methyl-1-hexene. It must be noted that the specific rotation of this polymer was about 20% of that of poly-*l*-4-methyl-1-hexene and the percentage was coincident with the content of *d*-1-chloro-2-methylbutane in amyl chloride mixture used as the starting material of the monomer, although many steps had been taken in the way from the chloride to the polymer.

The optical rotatory behavior of poly-*l*-4-methyl-1-hexene gave no positive evidence either for the existence of helical configuration in solution or, if any, for a predominant existence of right- or left-handed helices. This might be caused by the absence of strong intramolecular attraction such as hydrogen bond to coil up the chain to a helix in solution. Even if the helix was maintained in solution, the one carbon atom inserted between the main chain and the asymmetric carbon atom would weaken the steric influence of the neighboring groups around the asymmetric carbon atom. This might result in no regulation of the direction of helical configuration in a single screw sense.

The density of poly-*l*-4-methyl-1-hexene was coincident with the value reported for poly-*dl*-4-methyl-1-hexene by Natta[2]. The melting point was also approximately the same as those observed by Natta (188°C)[2] and Campbell (157~160°C)[15] with the polymer formed from the racemic monomer. These facts seem to suggest that there is almost no difference in the crystalline structure of either the optically active or the racemic polymer even in the solid state.

On the contrary, the melting point of poly-*d*-3-methyl-1-pentene is distinctly higher than that of the decalin-insoluble fraction of poly-*dl*-3-methyl-1-pentene, which seemed to have almost the same crystallinity and stereoregularity as those of the former polymer from its solubility behavior. Furthermore, the X-ray diffraction patterns of these two polymers are so different that the polymers appeared to be constituted with completely different monomeric units from each other.

The low conversion and also the very low stereospecificity in the polymerization of *dl*-3-methyl-1-pentene suggest the difficulty of isotactic propagation of this monomer. This may be caused by the copolymerization of the *d*- and *l*-monomers, in which the asymmetric tertiary carbon atoms are adjacent to the vinyl groups.

In the polymerization of racemic monomer three types are probable in the formation of its polymer: a mixture of homopolymers of *d*- and *l*-monomer each, a random copolymer and a block-copolymer of these. Furthermore, each type of these is able to form isotactic, atactic and stereo-block polymers in regard to the main chain of the polymer.

For the polymer of *dl*-3-methyl-1-pentene the authors obtained three fractions according to the solubility difference. The problem as to which of the above mentioned types correspond to the respective fractions is very interesting, although this is not certain at the present stage of this work.

In poly-3-methyl-1-pentene the asymmetric carbon atom of side chain is adjacent and so close to the main chain of the polymer that it may affect the configuration of the chain, contrary to the case of poly-4-methyl-1-hexene. Therefore, the predominant or exclusive formation of either the right- or left-handed helix may be expected in much more probability for poly-*d*-3-methyl-1-pentene than for poly-*l*-4-methyl-1-hexene. Unfortunately, the detailed investigation on the optical rotation of poly-*d*-3-methyl-1-pentene could not be done due to the extremely low solubility of the polymer, although the polymer showed a

13) P. Doty and J. T. Yang, *J. Am. Chem. Soc.*, **78**, 498 (1956); **79**, 761 (1957).
14) F. P. Reding, *J. Polymer Sci.*, **37**, 555 (1959).
15) T. W. Campbell and A. C. Haven, Jr., *J. Appl. Polymer Sci.*, **1**, 73 (1959).

very large specific rotation, $[\alpha]_D^{24}$ +255°, in petrolatum liquid.

After the completion of this work, papers by Pino and Lorenzi[16], and Bailey and Yates[17] appeared, which described the same subject independently. Bailey and Yates reported that the specific rotation of poly-*d*-3-methyl-1-pentene $[\alpha]_D^{25}$ was −257° in 1,1-ditolylethane. The present sample of the same polymer showed distinctly dextro rotation also in 1,1-ditolylethane, but the exact value could not be obtained, because the concentration of the solution was too small to be measured, due to the extremely low solubility of the polymer in 1,1-ditolylethane at room temperature. Pino and Lorenzi reported that the various soluble fractions of poly-*d*-3-methyl-1-pentene, which seemed to be atactic or stereoblock, had dextro rotations.

Pino and Lorenzi concluded in their paper that in dilute solution and in the molten state the isotactic and stereo-block polymers of optically active α-olefins may be at least in part spiralized and that helices of a single screw sense may largely prevail, because of the remarkable dependence of the optical rotation on stereoregularity and temperature. However, the temperature coefficient of optical rotation must also be dependent on the magnitude of specific rotation itself and in this respect the temperature coefficients of the optical rotation of optically active poly-α-olefins may be considered to be not so large. Other considerations seem to be necessary to explain the large optical rotations of these isotactic polymers formed from optically active α-olefins.

The authors wish to thank Dr. Yōzō Chatani for his help in the X-ray investigation.

*Department of Polymer Science*
*Faculty of Science*
*Osaka University*
*Nakanoshima, Osaka*

16) P. Pino and G. P. Lorenzi, *J. Am. Chem. Soc.*, **82**, 4745 (1960).
17) W. J. Bailey and E. T. Yates, *J. Org. Chem.*, **25**, 1800 (1960).

# *Studies on Phenolic Resins. IV. Physical and Chemical Properties of Coating Films of Japanese Lac (Urushi) (Rigidity Modulus-Temperature Relations Measured by Torsional Pendulum Method)*

By Tsutomu KUWATA, Jū KUMANOTANI and Seiji KAZAMA

(Received April 17, 1961)

Japanese lac (*urushi*) has been used as a natural coating material for more than two thousand years in Japan and China. It has been recognized that the coating film prepared from Japanese lac has many excellent properties and utility. The decorative coating film for artificial and wooden articles has a beautiful color tone and as the protective coating film, it is known by experience to have outstanding physical and chemical properties, compared with the films of the usual paints or varnishes. Traditional wooden crafts coated with *urushi* are very famous and used with appreciation all over the world, but our country imports a large quantity of raw Japanese lac from other Asian countries, because it produces only five per cent of the demand. Therefore, it has been hoped to make up industrial processes to synthesize some substance that can be used in place of natural Japanese lac, or some kind of compounding component or filler for it. There were two ways of attempting this aim.

One attempt was to synthesize the compouds chemically identical with the natural substance. The substance which is usually called Japanese lac is a sap of Rhus vernicifera D. C., produced in Japan and China. Chemical identification of urushiol, the principal component and polymerization unit of Japanese lac, was carried out by Majima[1] and Dawson[2] and the latter established that urushiol was composed of four

1) R. Majima, "Untersuchungen über den Japanlack", (1924).
2) S. V. Sunthankar and C. R. Dawson, *J. Am. Chem. Soc.*, **76**, 5070 (1954).

derivatives of catechol, substituted at 3-position with paraffinic, olefinic, diolefinic, and triolefinic straight chains of 15 carbons, and the average number of double bonds in the mixture were about two for one molecule. Some of these compounds were synthesized by Dawson[3] and Yukawa[4] but their processes cannot be applied to industrial production. Many chemically analogous compounds were synthesized in the past but they could not be used practically.

Another attempt was made in the industrial field for the purpose of obtaining substitutes or fillers for Japanese lac, and several kinds of coating materials, which formed a film apparrently similar to that of Japanese lac, were prepared and commercialized as "synthetic Japanese lac". But the interesting and important feature of Japanese lac, which must be taken into account, is that it contains an oxidation-reduction enzyme, laccase, and air-drying of Japanese lac proceeds through a characteristic oxidation-polymerization of urushiol with oxygen in the air, catalyzed with laccase[5]; also that the characteristic reaction is thought to be one of the factors that give good properties to the film. Though the molecular structure and reaction mechanism of laccase are not yet known, it was proved to act only on *ortho-* or *para*-polyhydroxy or polyamino aromatic compounds[5]. Therefore commercialized so-called "synthetic Japanese lacs", which are oil varnishes, are not affected by laccase, and they degrade the mechanical properties of the film when used as fillers for Japanese lac.

In another paper the authors studied the preparative method of compounds capable of polymerizing at room temperature together with urushiol, affected with laccase equally to it, when added to natural Japanese lac as fillers[6].

Evaluation of those compounds should be carried out in respect of the physical and mechanical properties of the coating films formed from the mixtures of them and Japanese lac, as compared with the properties of Japanese lac film.

Although it is well known by experience that the coating films of Japanese lac have ideal physical and mechanical properties, scientific studies have been limited to the subjects of resistance to chemical reagents and electrical insulation, and no data were available about the mechanical properties.

In this paper the authors first studied, by means of the torsional pendulum method, the mechanical properties of coating films, prepared through various processes from Japanese lac. This method had been developed to study the visco-elastic behavior of polymers, and in spite of its being a simple operation, it presented useful data such as rigidity modulus and decrement of oscillation at any temperature, and glass transition temperature of the film.

As the results of the observation of the mechanical properties of the coating films which were the oxidation polymerization products of urushiol under the action of laccase or heat, it was revealed that the Japanese lac films had excellent, characteristic properties, never found in other kinds of coating films.

Then the authors determined the mechanical data of three coating film samples each prepared from the mixtures of 10 parts of Japanese lac and 6 parts of the synthetic compound. These three compounds were chosen from a series of catechol derivatives, which had been synthesized by the authors for the purpose of obtaining a good filler for Japanese lac. It was evidently approved by the properties of the film samples that those compounds were excellent fillers for Japanese lac and able to be used in place of urushiol.

## Experimental by Torsional Pendulum Method

The torsional pendulum method developed by Inoue[7] to investigate the mechanical characteristics of polymer films is simple in operation, and gives reliable data. Torsional pendulum apparatus has as the main part an inertia bar attached at its center to the lower end of a pending sample film strip, and a mirror is set below the center. The period and the amplitudes of damping oscillation of the bar are measured by the lamp-and-scale system. Rigidity modulus ($G$) and logarithmic decrement ($\lambda$) are calculated from these data.

**Procedure.**—Torsional pendulum apparatus with sample film was set in a low temperature thermostat, slowly heated up to 40°C and kept at this temperature for 40 min. This duration was necessary for the internal structure of the sample to reach equilibrium at this temperature. Then the temperature was cotinuously dropped at the rate of 1°C/2 min. down to −60°C, while measuring the amplitudes and the period of 3~6 oscillation cycles every 5 or 10°C. The temperature was slowly raised to room temperature, and the apparatus with sample was kept there overnight. Next day it was set in an electric heating thermostat, and the temperature was continuously raised at the rate of 1°C/2 min. to about 150°C and the measurement was carried out every 5 or 10°C.

The rigidity modulus ($G$) of the sample film was calculated from the period, and the logarithmic

3) B. Love and C. R. Dawson, ibid., **78**, 4083 (1956).
4) T. Yukawa, Presented at the 13th Annual Meeting of Chem. Soc. Japan, Tokyo, April, 1960.
5) G. Bertrand, *Compt. rend.*, **124**, 1032, 1355 (1897).
6) T. Kuwata, J. Kumanotani and S. Kazama, *J. Chem. Soc. Japan, Ind. Chem. Sec.* (*Kogyo Kagaku Zasshi*), **64**, 1629 (1961).
7) Y. Inoue, ibid., **55**, 262 (1952).

decrement ($\lambda$) was calculated from the amplitude change.

$G$ and $\lambda$ were plotted against temperature, and the temperature where $\lambda$ was maximum was glass transition temperature ($T_g$) of the sample film.

TABLE I. LIST OF SAMPLES

| No. | Sample film |
|---|---|
| 1 | Air-dried film of kiurushi |
| 2 | Baked film of kiurushi |
| 3 | Air-dried film of sugurome urushi |
| 4 | Baked film of sugurome urushi |
| 5 | Air-dried film of sugurome urushi |
| 6 | Tested strip of sample No. 5, heated at 100°C for 2 hr. after measurement up to 110°C |
| 7 | Sample No. 5, kept in air for 25 days |
| 8 | Sample No. 1, kept in air for 30 months |
| 9 | Tested strip of sample No. 8, kept in air overnight after measurement up to 150°C |
| 10 | Sample No. 2, kept in air for 30 months |
| 11 | Sample No. 3, kept in air for 30 months |
| 12 | Tested strip of sample No. 11, kept in air overnight after measurement up to 150°C |
| 13 | Sample No. 5, kept in air for 30 months |
| 14 | Air-dried film of Thailand-sugurome urushi, kept in air for 30 months |
| 15 | Air-dried film of sugurome processed mixture of kiurushi and distilled urushiol (1 : 1 part) kept in air for 7 months |
| 16 | Air-dried film of sugurome-processed mixture of kiurushi (10 parts) and linseed oil (3 parts) |
| 17 | Air-dried film of sugurome-processed mixture of kiurushi (10 parts) and linseed oil (6 parts) |
| 18 | Sample No. 16, kept in air for 30 months |
| 19 | Air-dried film of sugurome-processed mixtre of kiurushi (10 parts), linseed oil (2 parts) and ester gum (1 part) |
| 20 | Baked film of sugurome-processed mixture of kiurushi (10 parts), linseed oil (2 parts) and ester gum (1 part) |
| 21 | Sample No. 20, kept in air for 30 months |
| 22 | Air-dried film of sugurome-processed mixture of kiurushi (10 parts) and catechol derivative A (6 parts) |
| 23 | Air-dried film of sugurome-processed mixture of kiurushi (10 parts) and catechol derivative B (6 parts) |
| 24 | Air-dried film of sugurome-processed mixture of kiurushi (10 parts) and catechol derivative C (6 parts) |
| 25 | Air-dried film of oil varnish of reactive *o*-cresol resin |
| 26 | Air-dried film of oil varnish of nonreactive *o*-cresol resin |

The inertia bar used in the experiment was made of aluminum, the length being 20.64 cm., weight 34.01 g. moment of inertia 1210 g. cm$^2$. The periods measured were 3~15 sec. It had been reported that in order to obtain reliable data the periods should lie in the range from 2 to 17 sec.[8]

**Sample Films.**—The sample films are listed in Table I. The meanings of several terms which are unique to Japanese lac are as follows.

*Kiurushi* (raw Japanese lac); this is the sap of the plant.

*Sugurome process*; this is a unique process in the preparation of usual commercial coating material of Japanese lac in Japan. Raw Japanese lac, alone or with other substances, is stirred in a wooden vessel for a time, then heated at about 38°C for about 7 hr. under stirring. During the process dehydration and partial oxidation of the lac take place.

*Sugurome urushi*; *sugurome-processed* Japanese lac. The raw Japanese lac of Samples Nos. 1—4, 8—12, 15—24, was taken from a lot produced in Moppo, China. The Samples Nos. 5, 6, 7, 13, were taken from another lot. Sample No. 14 was the film formed from Thailand lac, the main component of which is not urushiol but thithiol.

*Sugurome-proscess* in the preparation of Sample No. 5, was a little different from that of Sample No. 3, but details were not ascertained.

The torsional pendulum method required the sample film strip, of which the breadth $b$ was about 1 cm. and the thickness $h$ was more than 0.02 cm. because $b/h$ ratio should be 10~50 in order to obtain reliable data. But the thickness of the uniform film formed by one coating was 0.002~0.004 cm. The authors prepared the sample coating films by coating the sample lacs on tin plates (25 cm. × 15 cm.), repeating the coating and drying to touch-free state five to ten times until the films formed became thick enough.

Air-drying was carried out in a wet atmosphere in order to activate laccase. In case of baking, every coat was heated by an infrared lamp (40~60°C) to give a touch-free surface, and finally the film was heated at 100°C for 1 hr. in an electric drier.

The sample film thus formed on the tin plate was cut into strips, about 1 cm. broad, and these strips were torn off after amalgamation of the tin surface. The dimensions of the test strips we used were 13~15 cm. in length and 30~60 in $b/h$.

Samples Nos. 22—24 were the air-dried films of *sugurome-processed* mixtures of *kiurushi* (10 parts) and catechol derivatives (6 parts). Catechol derivative A was the ester of homoprotocatechuic acid and linseed oil alcohol; B, mixed glyceride of protocatechuic acid and linseed oil fatty acid (1 : 2); C, allyl ester of addition product of catechol and linseed oil fatty acid.

Samples Nos. 25 and 26 were the films of varnishes of phenolic resins, observed in comparison with Japanese lac.

All sample films except those of which the duration of exposure to air are noted in Table I were examined within 10 days after preparation.

8) J. Furuichi, *J. Appl. Phys., Japan*, **27**, 720 (1958).

TABLE II. PHYSICAL PROPERTIES OF JAPANESE LAC COATING FILMS

| Sample No. | $T_g$°C | $G_g$, dyn./cm² | $G_r$, dyn./cm² | $G_h$, dyn./cm² | $\lambda_{max}$ |
|---|---|---|---|---|---|
| 1 | 70 | $1.1\times10^9$ | $5.2\times10^9$ | $4.8\times10^8$ | 0.33 |
| 2 | 85 | $2.2\times10^9$ | $7.1\times10^9$ | $1.4\times10^9$ | 0.19 |
| 3 | 30 | $7.3\times10^8$ | $1.2\times10^9$ | $2.4\times10^8$ | 0.31 |
| 4 | 45 | $1.3\times10^9$ | $2.7\times10^9$ | $3.9\times10^8$ | 0.22 |
| 5 | 45 | $2.4\times10^9$ | $5.0\times10^9$ | $5.6\times10^8$ | 0.21 |
| 6 | 58 | $4.1\times10^9$ | $7.9\times10^9$ | $1.3\times10^9$ | 0.21 |
| 7 | 63 | $1.9\times10^9$ | $5.8\times10^9$ | $6.6\times10^8$ | 0.23 |
| 8 | 100 | $2.1\times10^9$ | $7.7\times10^9$ | $1.1\times10^9$ | 0.27 |
| 9 | 115 | $2.5\times10^9$ | $7.7\times10^9$ | $1.3\times10^9$ | 0.18 |
| 10 | 130 | $2.5\times10^9$ | $9.7\times10^9$ | $1.8\times10^9$ | 0.18 |
| 11 | 83 | $7.9\times10^8$ | $5.4\times10^9$ | $2.5\times10^8$ | 0.49 |
| 12 | 93 | $1.2\times10^9$ | $7.2\times10^9$ | $3.5\times10^8$ | 0.30 |
| 13 | 95 | $2.2\times10^9$ | $6.8\times10^9$ | $7.4\times10^8$ | 0.23 |
| 14 | 77 | $8.4\times10^8$ | $3.5\times10^9$ | $1.8\times10^8$ | 0.29 |
| 15 | 90 | $2.0\times10^9$ | $6.0\times10^9$ | $7.9\times10^8$ | 0.21 |
| 16 | 10 | $2.0\times10^9$ | $1.4\times10^9$ | $3.9\times10^8$ | 0.20 |
| 17 | −45 | $3.9\times10^9$ | $4.5\times10^8$ | $2.2\times10^8$ | 0.17 |
| 18 | 81 | $1.3\times10^9$ | $6.2\times10^9$ | $3.6\times10^8$ | 0.28 |
| 19 | 20 | $1.3\times10^9$ | $1.3\times10^9$ | $1.4\times10^8$ | 0.33 |
| 20 | 35 | $2.4\times10^9$ | $3.6\times10^9$ | $7.3\times10^8$ | 0.22 |
| 21 | 86 | $2.4\times10^9$ | $8.3\times10^9$ | $8.0\times10^8$ | 0.27 |
| 22 | 10 | $1.8\times10^9$ | $1.2\times10^9$ | $2.6\times10^8$ | 0.22 |
| 23 | 0 | $1.4\times10^9$ | $6.4\times10^8$ | $2.5\times10^8$ | 0.21 |
| 24 | 0 | $1.7\times10^9$ | $8.2\times10^8$ | $3.2\times10^8$ | 0.20 |
| 25 | 17 | $1.6\times10^9$ | $9.8\times10^8$ | $1.8\times10^8$ | 0.44 |
| 26 | 8 | $2.2\times10^9$ | $5.2\times10^8$ | — | 0.30 |

## Results and Discussion

The results of the experiments are shown in Table II and Figs. 1—5. The following abbreviations are used: $T$, temperature in °C; $G$, rigidity modulus in dyn./cm²; $\lambda$, logarithmic decrement; $T_g$, glass transition temperasure; $G_g$, rigidity modulus at glass transition temperature; $G_r$, rigidity modulus at 20°C; $G_h$, high temperature rigidity modulus or the minimum rigidity modulus above $T_g$; $\lambda_{max}$, the maximum logarithmic decrement shown at $T_g$. ($T_g$ was defined as the temperature at which $\lambda$ reached the maximum)

**Characteristic *G-T* Relations of Coating Films of Japanese Lac.**—All kinds of coating films formed from synthetic resins show glass transition phenomena. Not to mention the films of thermoplastic resins[9], those of cross-linked polymers, such as epoxy[10], alkyd[11] and phenolic resin varnish[12] change markedly in physical and mechanical properties as the temperature changes through $T_g$, over a relatively narrow temperature range. Below $T_g$ they are in the glassy state, being rigid and a little brittle, and values of $G$ are about $10^{10}$ dyn./cm². Above $T_g$ they are in the rubbery state, being soft and flexible, and values of $G$ range between $10^7$ and $10^8$ dyn./cm², so they lack in mechanical strength. The abrupt change in properties depending upon temperature is undesirable for practical use and, therefore, each kind of coating film can be used in a limited range of temperature.

But it is revealed by the authors' experiment that the coating films of Japanese lac were quite different from and superior to those from usual synthetic resins in their properties.

As shown in Fig. 1, in temperature range around $T_g$, temperature dependence of $G$ of air-dried and baked films of *kiurushi* and *sugurome-urushi* was less than that of Samples Nos. 25 and 26, which were air-dried films of oil varnishes of *o*-cresol resins presented as examples of phenolic resin. $G$ of Japanese lac films changed so mildly with temperature from lower to higher temperature ranges, as $T_g$ could not be determined distinctly from *G-T* curve. $T_g$ was determined from the $\lambda$-$T$ relation and the $\lambda$-$T$ curve, too, was smooth compared with that of the synthetic resin film.

At room temperature, three coating films, except the baked film of *kiurushi*, had ample flexibility in spite of their great rigidity modulus, compared with synthetic resin films.

9) Y. Inoue, *J. Chem. Soc. Japan, Ind. Chem. Sec.* (*Kogyo Kagaku Zasshi*), **63**, 1427 (1960).
10) K. Ueki, ibid., **64**, 1425 (1961).
11) L. W. Chen, unpublished.
12) J. Kumanotani, unpublished.

Among them the air-dried film of *sugurome-urushi* was the most rigid but as flexible as samples Nos. 25 and 26, which were in the rubbery state and had smaller values of $G_r$. Values of $G_h$ of Japanese lac films were, generally, larger than those of synthetic resin films, in which case it was reported that films with $G_h$ greater than $10^8$ dyn./cm$^2$ were insufficient in flexibility[13]. These data of mechanical properties of Japanese lac films showed that the films had an excellent tolerance to temperature change and good adaptability as protective coating films over a wide temperature range.

By $G$-$T$ and $\lambda$-$T$ relations, $G_h$ and $T_g$, we are able to know the deformation behavior of a polymer substance when loaded by mechanical force, and assume the internal polymeric structure of the polymers. $T_g$ increases with the increase of intermolecular forces caused by the polar group, and of the density of the cross-link of polymer molecules. This is because $T_g$ shows the temperature at which thermal energy becomes sufficient to allow segments of polymers to move beyond energy barriers of environments. $G_h$ increases with increase of density of cross-link, the deformation of polymer substance being restricted only by cross-links of molecules at the temperatures enough above $T_g$.

Japanese lac films are cross linked polymers formed by oxidation-polymerization of urushiol, activated with laccase or heat. The cross-linking points are catechol nucleus and double bonds of side chains of urushiol molecules. Therefore the films are considered to have some complicated three dimensional structure. In case of air-drying, the action of laccase contributes to the formation of this characteristic structure. The films are in transitional state, some parts being in the glassy state and the others in the rubbery state over a wide range of temperature and they do not show sharp glass transition. Also the rubber parts increase with the rise of temperature, $G$ and $\lambda$ changing smoothly.

The ideal combination of rigidity and flexibility of the films is also considered to be owing to the characteristic polymer structure of polymerized urushiol with rigid benzene ring and flexible long side chain.

The large values of $G_h$ of Japanese lac films suggested high density of cross-link, but it must be noted that the density of cross-link at high temperature was higher than that at room temperature, because thermal cross-linking reaction took place during the measurement up to the temperature at which $G_h$ was given. This fact was pointed out from comparison of $T_g$ and $G_h$ between Samples No. 8 and No. 9, and between No. 11 and No. 12. And it may be mentioned that the increase of $G$ with temperature above the temperature at which $G_h$ was given was due to both entropy elasticity effect and the increasing density of cross-link.

The above mentioned two characteristics in physical properties of Japanese lac films (1. They do not show sharp glass transition phenomenon. 2. They have ideally combined flexibility and rigidity.) are unique to them.

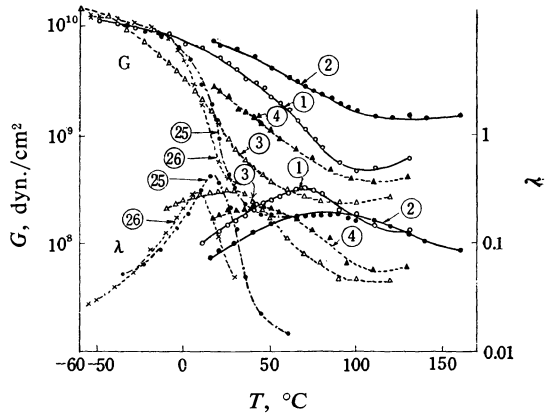



Fig. 1. Rigidity modulus-temperature relations.

① Air-dried film of kiurushi
② Baked film of kiurushi
③ Air-dried film of sugurome urushi
④ Baked film of sugurome urushi
㉕ Air-dried film of oil varnish of reactive *o*-cresol resin
㉖ Air-dried film of oil varnish of nonreactive *o*-cresol resin

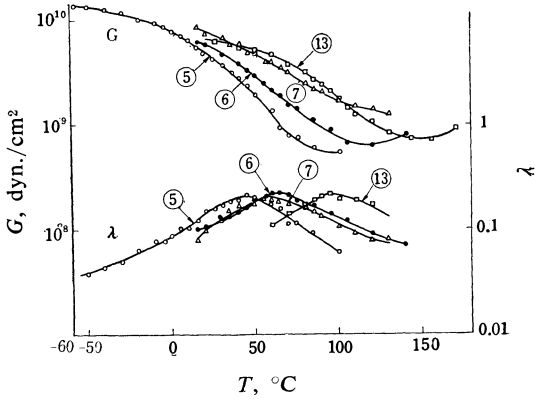



Fig. 2. Rigidity modulus-temperature relations.

⑤ Air-dried film of sugurome urushi
⑥ Tested strip of ⑤, heated at 100°C for 2 hr. after measurement
⑦ Sample ⑤, kept in air for 25 days
⑬ Sample ⑤, kept in air for 30 months

13) Y. Inoue, "Kōgyōkagaku Zensho", Vol. 30, Nikkan Kogyo Shimbunsha, Tokyo (1960), p. 120.

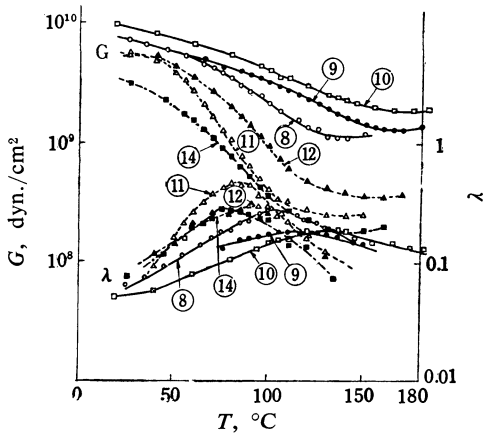



Fig. 3 Rigidity modulus-temperature relations.

⑧ Sample ①, kept in air for 30 months
⑨ Tested strip of ⑧, kept in air overnight after measurement
⑩ Sample ②, kept in air for 30 months
⑪ Sample ③, kept in air for 30 months
⑫ Tested strip of ⑪, kept in air overnight after measurement
⑭ Air-dried film of thailand-sugurome urushi, kept in air for 30 months

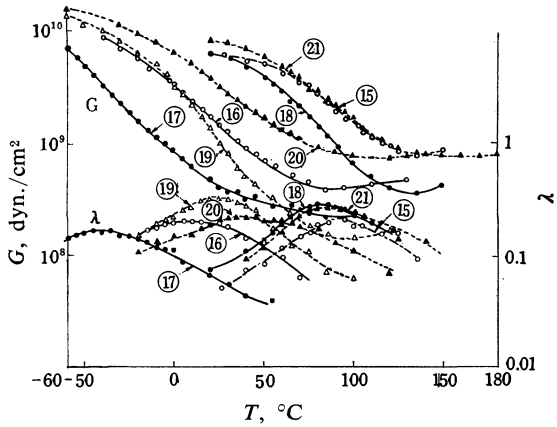



Fig. 4 Rigidity modulus-temperature relations.

⑮ Air-dried film of sugurome processed mixture of kiurushi and distilled urushiol (1 : 1 part), kept in air for 7 months
⑯ Air-dried film of sugurome processed mixture of kiurushi (10 parts) and linseed oil (3 parts)
⑰ Air-dried film of sugurome processed mixture of kiurushi (10 parts) and linseed oil (6 parts)
⑱ Sample ⑯, kept in air for 30 months
⑲ Air-dried film of sugurome processed mixture of kiurushi (10 parts), linseed oil (2 parts) and ester gum (1 part)
⑳ Baked film of sugurome processed mixture of kiurushi (10 parts), linseed oil (2 parts) and ester gum (1 part)
㉑ Sample ⑳, kept in air for 30 months

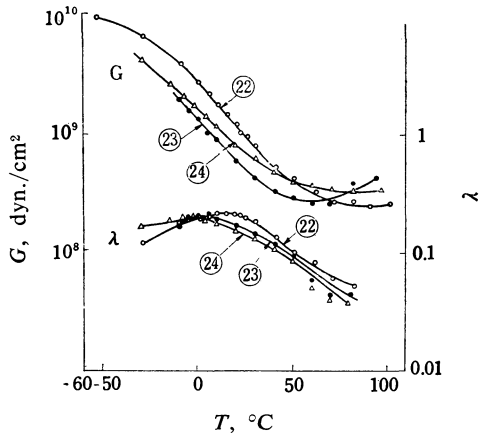



Fig. 5 Rigidity modulus-temperature relations.

㉒ Air-dried film of sugurome processed mixture of kiurushi (10 parts) and catechol derivative A (6 parts)
㉓ Air-dried film of sugurome processed mixture of kiurushi (10 parts) and catechol derivative B (6 parts)
㉔ Air-dried film of sugurome processed mixture of kiurushi (10 parts) and catechol derivative C (6 parts)

The films from synthetic Japanese lac may be necessary to be characterized by these points in order to exceed films from other synthetic resins. These characteristics were retained in Samples Nos. 5—21, which are used in practice as Japanese lac films.

**Effect of *Sugurome-process* on Physical and Chemical Properties of Coating Films.**— Coating films from *sugurome-urushi* (Samples Nos. 3, 4, 5, 11, 13) were more fiexible and had lower values of $T_g$, $G_r$ and $G_h$ than films from *kiurushi* (Samples Nos. 1, 2, 8 and 10). The differences in those physical properties were remarkable between them either in case of air-dried films (between No. 1 and No. 3) or baked (between No. 2 and No. 4), or after they were kept in air for 30 months (between No. 8 and No. 11). $T_g$ of baked film from *kiurushi* was valued at 85°C and it lacked in flexibility at room temperature. The cause of the difference is not clear but it may be due to the characteristic unit of polymerization induced by laccase-oxygen(air)-polymerization. Further investigation is needed about the chemical change during the *sugurome-process*. But this traditinal process proved to be very advantageous in preparing qualified coating material of Japanese lac to form air-dried film with a large value of $G_r$ and ample flexibility (Sample No. 3).

Sample No. 5 was also air-dried film of *sugurome-urushi*, but it differed from Sample

No. 3 in physical properties, because the lot of *kiurushi* and conditions of *sugurome-process* and drying process were respective for each. The properties of Sample No. 5 lay between those of Sample No. 1 (from *kiurushi*) and No. 3, and this relationship was retained after time elapsed (Samples Nos. 8, 11 and 13). The quality of Japanese lac may be modified to various extents by changing the condition of the *sugurome-process*.

**Effect of Fillers.**—Linseed oil is used today commonly as a filler for Japanese lac. A mixture of *kiurushi* and linseed oil is *sugurome-processed* and commercialized. Sample No. 16 which was air-dried film of *sugurome-processed* mixture of *kiurushi* (10 parts) and linseed oil (3 parts), had a lower value of $T_g$, about the same value of $G_r$ and a higher value of $G_h$ than Sample No. 3 (from *sugurome-urushi*). No considerable difference was found between *G-T* curves of the two (Figs. 1 and 4), and they were almost identical in mechanical properties. The decrease of $T_g$ was due to the decrease of intermolecular force caused by the addition of the drying oil, and the increase of $G_h$ was due to the increase of cross-link density induced by the reaction of the double bonds.

But in the case of Sample No. 17 (*kiurushi* 10 parts, linseed oil 6 parts), $T_g$ was much depressed to $-45°C$ and values of $G_r$ and $G_h$ also depressed. At high temperatures the oil oozed out of the film. The small values of $\lambda_{max}$ of these samples were due to their plasticity. Those facts indicate that if a large amount of linseed oil is added to Japanese lac, its plasticizing effect deteriorates the physical properties of the film.

*Sugurome-processed* mixture of *kiurushi*, linseed oil and ester gum is called "*shuai-urushi*" and is of general use. Owing to the polar group and polycondensed ring of ester gum, the $T_g$ of air-dried film of *shuai-urushi* (sample No. 19) was rather high but the small value of $G_h$ indicated the small density of cross-link. In baked film (Sample No. 20) values of $G_r$ and $G_h$ were greater than those of baked film from *sugurome-urushi*.

Sample No. 15 was air-dried film from *sugurome processed* mixture of 10 parts of *kiurushi* and 10 parts of urushiol isolated by molecular distillation of alcohol extract from kiurushi, and kept in air for 7 months. The content of laccase of the mixture equalled a half of that of No. 3 (*sugurome-urushi*). The film had a strong esthetic appeal and excellent flexibility, and what is more, values of $T_g$, $G_r$ and $G_h$ were higher than those of Sample No. 11 (Sample No. 3, kept in air for 30 months). Contrary to the case of linseed oil, laccase acted on urushiol very effectively, and it is concluded that if any compound similar to urushiol is obtained, a great amount can be added to Japanese lac.

The principal component of Thailand lac is not urushiol but thithiol, a mixture of 4-heptadecenylcatechols with 1.5~2 double bonds in average. It contains laccase but the content is less than in Japanese lac, and 4-substituted catechol seems to be inferior to 3-substituted catechol in chemical reactivity. Therefore its film formation takes a long time and it is used as a filler for Japanese lac. Sample No. 14 was air-dried film of *sugurome-processed* Thailand lac, kept in air for 30 months. The film was bad in its physical properties and color. Compared with No. 11 (*sugurome-urushi* of Japanese lac), values of $T_g$, $G_r$ and $G_h$ were lower, showing low density of cross-link.

**Effect of Heat and Exposure to Air.**—There are two ways of drying, namely, air-drying and baking. In most cases *sugurome-urushi* is air-dried on articles. Samples Nos. 2, 4 and 20 were baked films of *kiurushi*, *sugurome-urushi* and *shuai-urushi* respectively. Compared with Samples Nos. 1, 3 and 19 (air-dried films), baked films had higher values of $T_g$, $G_r$ and $G_h$, lower value of $\lambda_{max}$ and were less flexible and less glossy than the corresponding air-dried films. These differences in properties between them were also found in the case of No. 8 and No. 10 (after 30 months). The reaction mechanism in film formation is considered to be respective for each drying process.

Samples Nos. 1, 2, 3, 5, 16 and 20 were kept in air for 30 months to investigate changes in physical and chemical properties with time. They were Samples Nos. 8, 10, 11, 13, 18 and 21 respectively. As shown in Table II, changes of values of $T_g$ and $G_r$ for each were as follows:

| Sample | $T_g$, °C | $G_r \times 10^{-9}$, dyn./cm$^2$ |
|---|---|---|
| Air-dried film of kiurushi | 70→100 | 5.2→7.7 |
| Baked film of kiurushi | 85→130 | 7.1→9.7 |
| Air-dried film of sugurome-urushi (No. 3) | 30→ 83 | 1.2→5.4 |
| Air-dried film of sugurome-urushi (No. 5) | 45→ 95 | 5.0→6.8 |
| Air-dried film of sugurome-processed mixture of kiurushi (10 parts) and linseed oil (3 parts) | 10→ 81 | 1.4→6.2 |
| Air-dried film of shuai-urushi | 35→ 86 | 3.6→8.3 |

But concerning the values of $G_h$ of these samples, they were almost unchanged except in the case of air-dried film of *kiurushi* whose $G_h$ changed from $4.8\times10^8$ to $1.1\times10^9$ dyn./cm$^2$.

These facts indicated that the films were oxidized in air, polar groups being formed in polymer molecules. On account of the increase of intermolecular forces caused by the polar groups, the films became rigid at room temperature and values of $T_g$ rose. However, cross-liking did not take place during the exposure except in air-dried film of *kiurushi*. This phenomenon may be associated with the effect of heating or sugurome-process when the film was formed.

Even in the films kept in air for 30 months, thermal cross-linking occurred during the measurement up to 150°C, and as shown in Fig, 3, values of $T_g$, $G_r$ and $G_h$ increaed. (No. 8→ No.9, No. 11→No. 12)

**Evaluation of Synthetic Catechol Derivatives as Fillers.**—As reported in another paper[6], the authors synthesized a series of catechol derivatives for the purpose of obtaining good fillers for Japanese lac. From them the next three compounds were chosen;

A. Ester of homoprotocatechuic acid and linseed oil alcohol
B. Glyceride prepared from 1 mol. of protocatechuic acid, 2 mol. of linseed oil fatty acid and 1 mol. of glycerine.
C. Allyl ester of addition product of catechol and linseed oil fatty acid.

Mixtures of 10 parts of *kiurushi* and 6 parts of catechol derivatives were *sugurome-processed*, and air-dried films shown in Table I were formed, namely, Samples Nos. 22, 23 and 24 respectively. Velocity of the drying was not slow.

Physical data of these samples mesured by the torsional pendulum method are given in Table II and Fig. 5.

Values of $T_g$ of these samples ranged from 0∼10°C, closing that of Sample No. 16 (*kiurushi* 10 parts and linseed oil 3 parts) and far above that of No. 17 (*kiurushi* 10 parts and linseed oil 6 parts, $T_g$; −45°C). Therefore it was evidently approved that these catechol derivatives were much more advantageous than linseed oil as fillers for Japanese lac. Especially the $G-T$ curve of Sample No. 22 was almost identical with that of Sample No. 3 (*sugurome-urushi*). It is considered that catechol derivative A polymerizes together with urushiol under the action of laccase, to form a film almost identical with the film of pure Japanese lac in physical properties.

## Summary

As to Japanese lac some reports are found in literature concerning chemical identification of the lac component, or electrical insulation and resistance of the film to chemical reagents, but no physical and chemical properties related to internal polymer structure of the film had ever been investigated. In this paper the authors studied the physical and chemical properties of the film of Japanese lac by means of the torsional pendulum method.

As the results of the experiment, the following characteristics of the films prepared by various processes from Japanese lac were revealed:

1. The films do not show sharp glass transition phenomenon and are durable as a protective coating over a wide range of temperature.
2. The films from *sugurome-processed* Japanese lac have ample flexibility and considerable rigidity, ideally combined.
3. During exposure to air, the films are oxidized with formation of polar group in polymer molecules. But cross-linking does not take place except in air-dried film of raw Japanese lac.

The above mentioned physical and chemical properties of the film account for the characteristic, complicated three dimensional polymer structure caused by action of laccase and chemical structure of urushiol, and such excellent properties can not be found in any other films from synthetic resins. The results obtained are of practical use and they should be taken into consideration in the study of preparation of fillers or substitutes for Japanese lac.

Catechol derivatives synthesized by the authors were confirmed to be fairly good fillers.

The authors wish to thank Professor Y. Inoue of the Tokyo Institute of Technology for his valuable advice. They are also indebted to the Saitō Shōten, Ltd. for the preparation of the sample films.

*Department of Applied Chemistry*
*Faculty of Engineering*
*The University of Tokyo*
*Hongo, Tokyo*

# *Non-Empirical Calculation of the π-Electronic Structure of Cyclobutadiene Molecule by Valence Bond Method*

By Shozaburo TAKEKIYO

(Received October 21, 1960)

Non-empirical calculation of the energy levels of the cyclobutadiene molecule was first made by Craig[1] from the point of view of molecular orbital method and later a calculation by valence bond method was performed, by McWeeny[2-4] using orthogonalized atomic orbitals[5].

In the calculation by Craig a complete basis of antisymmetric molecular orbital configurations was taken into considerations and, on the other hand, in the working of McWeeny a complete set of canonical structures was included. Energy levels in both of the methods, therefore, should arrive at a complete agreement theoretically*. But it was pointed out by Shida and Kuri[6] that the numerical value 11.1289 eV. of molecular integral $\gamma_{22}$ in the paper of Craig should be corrected to 10.5586 eV. The difference between these two values may have some effects on the energy levels.

In this paper, therefore, the calculation of the π-electronic energy levels and the wave functions of the molecule is made by valence bond method, including the complete set of canonical structures and considering all kinds of overlap, single exchange, and multiple exchange integrals. The results are compared with those due to ASMO CI calculation.

Calculations are also made in the way of the orthogonalization of atomic orbitals, and Slater functions, and thus the magnitude of the ionic character of the molecule is found. The results are discussed in comparison with those due to the non-orthogonal orbitals.

## Calculation

Cyclobutadiene was assumed to be a square molecule in which the bond distance between two neighboring carbon atoms is 1.40 Å. Slater $2p_\pi$-orbitals were used for the atomic orbitals of the four carbon atoms, with the screening constant $Z_C = 3.18$. π-Electron repulsive integrals were taken from Craig[1] and penetration and core integrals were calculated directly by the present author according to the method of Parr and Mulliken[7]. The canonical structures and the corresponding energies are shown in Fig. 1.

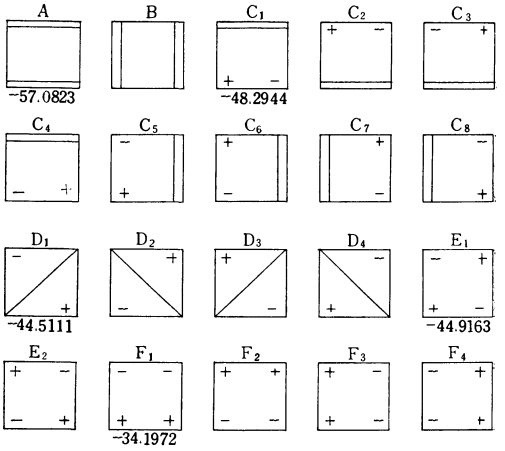



Fig. 1. Canonical structures and the energy values for the structures. (Energies are in electron volts and are relative to $4W_{2p}$, where $W_{2p}$ is the energy of a $2p_\pi$-electron of a carbon atom in its valence state.)

Bases $\Psi_i$'s for irreducible representations of the group, to which the molecule belongs, are given in Table I, where $N_i$ is the normalization constant and $\Psi_K$ is the normalized bond eigenfunction for structure K.

In our approximation the Hamiltonian operator $H$ is expressed in the form

$$H = \sum_i H_{\text{core}}(i) + (1/2)\sum_{\substack{i,\ j \\ i \neq j}} (e^2/r_{ij})$$

where

$$H_{\text{core}}(i) = T(i) + U_{\text{core}}(i)$$

$T(i)$ is the kinetic energy operator for electron $i$ and $U_{\text{core}}(i)$ is the potential energy operator for this electron in the field of the core.

Calculated wave functions $\Phi_i$'s for the molecule and the corresponding energy values $E_i$'s

1) D. P. Craig, *Proc. Roy. Soc.*, **A202**, 498 (1950).
2) R. McWeeny, ibid., **A223**, 63 (1954).
3) R. McWeeny, ibid., **A223**, 306 (1954).
4) R. McWeeny, ibid., **A227**, 288 (1955).
5) P.-O. Löwdin, *J. Chem. Phys.*, **18**, 365 (1951); P.-O. Löwdin, ibid., **21**, 496 (1953).
* Agreement of the results in both of the methods has been reported by McWeeny[4].
6) S. Shida and Z. Kuri, *J. Chem. Soc. Japan, Pure Chem. Soc. (Nippon Kagaku Zasshi)*, **76**, 322 (1955).
7) R. G. Parr and R. S. Mulliken, *J. Chem. Phys.*, **18**, 1338 (1950).

TABLE I. RELATIONS BETWEEN BOND EIGENFUNCTIONS AND BASES

$$
{}^1A_{1g}\begin{cases}
\Psi_1=(1/N_1)(\Psi_A+\Psi_B)\\
\Psi_2=(1/N_2)(\Psi_{C1}+\Psi_{C2}+\Psi_{C3}+\Psi_{C4}+\Psi_{C5}+\Psi_{C6}+\Psi_{C7}+\Psi_{C8})\\
\Psi_3=(1/N_3)(\Psi_{D1}+\Psi_{D2}+\Psi_{D3}+\Psi_{D4})\\
\Psi_4=(1/N_4)(\Psi_{E1}+\Psi_{E2})\\
\Psi_5=(1/N_5)(\Psi_{F1}+\Psi_{F2}+\Psi_{F3}+\Psi_{F4})
\end{cases}
$$

$$
{}^1B_{1g}\begin{cases}
\Psi_6=(1/N_6)(\Psi_{C1}-\Psi_{C2}+\Psi_{C3}-\Psi_{C4}+\Psi_{C5}-\Psi_{C6}+\Psi_{C7}-\Psi_{C8})\\
\Psi_7=(1/N_7)(\Psi_{D1}-\Psi_{D2}+\Psi_{D3}-\Psi_{D4})\\
\Psi_8=(1/N_8)(\Psi_{E1}-\Psi_{E2})
\end{cases}
$$

$$
{}^1B_{2g}\begin{cases}
\Psi_9=(1/N_9)(\Psi_A-\Psi_B)\\
\Psi_{10}=(1/N_{10})(\Psi_{C1}+\Psi_{C2}+\Psi_{C3}+\Psi_{C4}-\Psi_{C5}-\Psi_{C6}-\Psi_{C7}-\Psi_{C8})\\
\Psi_{11}=(1/N_{11})(\Psi_{F1}+\Psi_{F2}-\Psi_{F3}-\Psi_{F4})
\end{cases}
$$

TABLE II. WAVE FUNCTIONS FOR THE MOLECULE AND THE CORRESPONDING ENERGY VALUES

Based on non-orthogonal atomic orbitals

$$\Phi_1({}^1B_{2g})=0.80023\Psi_9+0.26085\Psi_{10}-0.01111\Psi_{11} \qquad E_1=4W_{2p}-58.3517\ \text{eV}.$$
$$\Phi_2({}^1A_{1g})=0.75393\Psi_1+0.32697\Psi_2-0.11784\Psi_3+0.09264\Psi_4-0.00386\Psi_5 \qquad E_2=4W_{2p}-56.3627\ \text{eV}.$$
$$\Phi_3({}^1B_{1g})=0.68396\Psi_6+0.24527\Psi_7+0.21925\Psi_8 \qquad E_3=4W_{2p}-52.6519\ \text{eV}.$$

Based on orthogonalized atomic orbitals

$$\bar{\Phi}_1({}^1B_{2g})=0.82284\bar{\Psi}_9+0.55729\bar{\Psi}_{10}-0.11117\bar{\Psi}_{11} \qquad \bar{E}_1=4\bar{\alpha}+41.8774\ \text{eV}.$$
$$\bar{\Phi}_2({}^1A_{1g})=0.78562\bar{\Psi}_1+0.55233\bar{\Psi}_2-0.01629\bar{\Psi}_3+0.25304\bar{\Psi}_4+0.11591\bar{\Psi}_5 \qquad \bar{E}_2=4\bar{\alpha}+44.0248\ \text{eV}.$$
$$\bar{\Phi}_3({}^1B_{1g})=0.75721\bar{\Psi}_6+0.49877\bar{\Psi}_7+0.42174\bar{\Psi}_8 \qquad \bar{E}_3=4\bar{\alpha}+46.9387\ \text{eV}.$$

are given in Table II. In the table, $\bar{\Phi}_i$'s are the wave functions for the molecule, obtained in the way of the orthogonalization of the atomic orbitals, $\bar{E}_i$'s are the corresponding energy values, and $\bar{\alpha}$ is as follows:

$$\bar{\alpha}=\int\bar{k}(i)H_{\text{core}}(i)\bar{k}(i)\mathrm{d}v_i$$

where $\bar{k}(i)$ is the orthogonalized expression of atomic orbital $k(i)$ of electron $i$ on atom $k$ and $\mathrm{d}v_i$ is the volume element of this electron.

## Ionic Character

Now, ionic characters, evaluated on the basis of non-orthogonal atomic orbitals are generally different from the values, obtained in their orthogonalized representation[5],*1.

Probabilities $P_K$'s of structure K's in both of the ground ${}^1B_{2g}$ state and the first excited ${}^1A_{1g}$ state were calculated from the following expression and the results are shown in Table III.

$$P_K=C_K\sum_L C_L\int\Psi_K\Psi_L\,\mathrm{d}\tau$$

where $C_K$ is the coefficient of normalized bond eigenfunction $\Psi_K$ in $\Phi_1({}^1B_{2g})$ or $\Phi_2({}^1A_{1g})$ and $\mathrm{d}\tau$ is the product of the volume element for all the $\pi$-electrons.

*1 It does not appear that considerations of such discrepancies for $\pi$-electronic systems have been made.

TABLE III. PROBABILITIES OF STRUCTURES

Based on non-orthogonal atomic orbitals

| $A=B$ | $C_i$ | $D_i$ | $E_i$ | $F_i$ |
|---|---|---|---|---|
| Ground ${}^1B_{2g}$-state | | | | |
| 0.3924 | 0.0265 | 0.0008 | 0 | 0 |
| First excite ${}^1A_{1g}$-state | | | | |
| 0.3503 | 0.0300 | 0.0054 | 0.0194 | −0.0002 |

Based on orthogonalized atomic orbital

| $A=B$ | $C_i$ | $D_i$ | $E_i$ | $F_i$ |
|---|---|---|---|---|
| Ground ${}^1B_{2g}$-states | | | | |
| 0.3385 | 0.0388 | 0.00309 | 0 | 0 |
| First excited ${}^1A_{1g}$-state | | | | |
| 0.3086 | 0.0381 | 0.0001 | 0.0320 | 0.0034 |

From these results, ionic characters are

$$
{}^1B_{2g}\text{ state}\begin{cases}
21.517\% & \text{based on } k(i)\\
32.293\% & \text{based on } \bar{k}(i)
\end{cases}
$$

$$
{}^1A_{1g}\text{ state}\begin{cases}
29.946\% & \text{based on } k(i)\\
38.280\% & \text{based on } \bar{k}(i)
\end{cases}
$$

In the ${}^1B_{2g}$ and ${}^1A_{1g}$ states the ionic characters based on $\bar{k}(i)$ are larger than on $k(i)$ by 10.776% and 8.334%, respectively.

Bond orders $B_{ij}$'s between neighboring two carbon atoms $i$ and $j$ were evaluated by formula

$$B_{ij}=\sum_K P_K(n_{ij}^K+1)$$

where $n_{ij}^K$ is the number of the $\pi$-electronic

covalent bonds between carbon atoms $i$ and $j$ in structure K. The results are

$^1B_{2g}$ state { 1.445 based on $k(i)$ ; 1.416 based on $\bar{k}(i)$

$^1A_{1g}$ state { 1.410 based on $k(i)$ ; 1.385 based on $\bar{k}(i)$

Double bond characters based on $k(i)$ are larger by 2.92% and 2.52% than these based on $\bar{k}(i)$ the $^1B_{2g}$ and $^1A_{1g}$ states, respectively.

## Discussion

Energy levels of the molecule, calculated by various methods, are shown diagrammatically in Fig. 2.

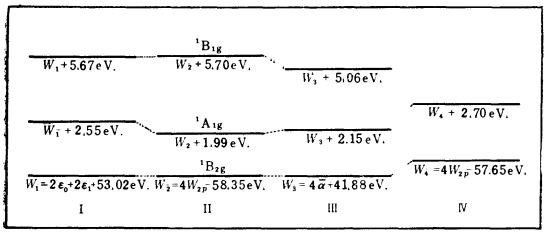



Fig. 2. Comparison of energy levels.

I. ASMOCI method[1]. II. VB method (based on non-orthogonal atomic orbitals). III. VB method (based on orthogonalized atomic orbitals). IV. Heitler-London method.

The $^1A_{1g}$ level evaluated by the present author (II) is lower by 0.56 eV. relatively than that of Craig. But influences of the difference in the values of the molecular integral on the other levels hardly appear at all*2.

One of the causes for the discrepancies of the ionic characters in the two ways is that, in the cases of the use of the orthogonalized atomic orbitals, exchange integrals which appear in the interactions of covalent structures give generally repulsive forces.

Actually, in the case of an exchange integral $\bar{J}$,

$$\bar{J}=\int\cdots\cdots\bar{a}(1)\bar{b}(2)\bar{c}(3)\bar{d}(4)\cdots\cdots H \cdots\cdots\bar{a}(1)\bar{c}(2)\bar{b}(3)\bar{d}(4)\cdots\cdots d\tau$$

is expanded as follows and $\bar{J}$ is, therefore, equal to $(\bar{b}\bar{c}|\bar{b}\bar{c})$.

$$\bar{J}=\sum_{\substack{k\\ k\neq b,\,c}}\bar{\alpha}_k\bar{S}_{bc}^2+2\bar{\beta}_{bc}\bar{S}_{bc}+(1/2)\sum_{\substack{k,\,l\\ k\neq b,\,c\\ l\neq b,\,c,\,k}}(\bar{k}\bar{k}|\bar{l}\bar{l})\bar{S}_{bc}^2+2\sum_{\substack{k\\ k\neq b,\,c}}(\bar{k}\bar{k}|\bar{b}\bar{c})\bar{S}_{bc}+(\bar{b}\bar{c}|\bar{b}\bar{c})$$

where

$$\bar{\alpha}_k=\int\bar{k}(i)H_{\mathrm{core}}(i)\bar{k}(i)\,dv_i\text{*3}$$

$$\bar{\beta}_{kl}=\int\bar{k}(i)H_{\mathrm{core}}(i)\bar{l}(i)\,dv_i$$

$$\bar{S}_{kl}=\int\bar{k}(i)\bar{l}(i)\,dv_i$$

$$(\bar{k}\bar{l}|\bar{p}\bar{q})=e^2\int(1/r_{ij})\bar{k}(i)\bar{l}(i)\bar{p}(j)\bar{q}(j)\,dv_i\,dv_j$$

From similar analyses multiple exchange integrals lead to zeros. In the use of the orthogonalized atomic orbitals, therefore, the weight of the covalent structures appears generally smaller than in the use of the non-orthogonal orbitals.

Accordingly, when $\pi$-electron densities or bond orders etc. are considered as the measure of chemical reactivities, it will be necessary for attention to be given to the discrepancies of these values in the two ways.

## Summary

$\pi$-Electronic energy levels, probalities of the resonance structures, and bond orders of cyclobutdiene molecule have been calculated by the valence bond method on the bases of two ways, one is based on non-orthogonal atomic orbitals and the other on their orthogonalization. Calculated ionic characters are 21.517% (ground $^1B_{2g}$ state), 29.946% (first excited $^1A_{1g}$ state) in the former and 32.293%, 38.280% in the latter. Bond orders between neighboring carbon atoms are 1.445, 1.410 and 1.416, 1.385 respectively.

The author wishes to express his hearty thanks to Professor Kyosuke Omori, Kyushu University, for his kind guidance and encouragement throughout this study.

Thanks are also due to Professor Saburo Nagakura, the University of Tokyo, for his valuable advice.

*Faculty of Liberal Arts*
*Nagasaki University*
*Ohashi, Nagasaki*

*2 Relative differences of levels between II and III in Fig. 2 seem to be due to the approximate orthogonalization of atomic orbitals[4,5].

*3 Since atoms except carbon are generally included in $\pi$-electronic system, $\bar{\alpha}_k$ is here to be distinguished from $\bar{\alpha}$ in the previous paragraph.

# *Statistical Thermodynamics of Solutions of Optically Active Substances. I. Excess Free Energy of Binary Solution of d- and l-Isomers*

By Kazuo AMAYA

(Received March 1, 1961)

In recent years considerable progress has been made in the field of the theory of solutions and the fundamental features of various types of binary solutions such as polymer solutions, and associated solutions, etc. were explained theoretically. However, there seem to be no papers which treat the problem of of the solutions containing optical isomers. In this paper the idea of interaction of surface points in groups will be introduced to elucidate the fundamental features of the solution consisting of optical isomers.

## The Model of the Solutions of Optical Isomers

In the statistical mechanical lattice theory of solutions of anisotropic molecules, the model usually adopted is that the surface of the molecule is devided into a definite number of contact points and each contact point is grouped into an energetically equivalent element and the number of contact points belonging to each group has a definite value. The configurational energy of the system is a sum of interaction energies of the pairs of each contact point. In such a model, however, the mutual configuration of different kinds of elements in one and the same molecule is not taken into account.

According to the above model, the molecules of *d*- and *l*-optical isomers have the same number of contact points of the same kind of elements, so that these two kinds of molecules cannot be distinguished. In order to distinguish one isomer from the other, mutual configuration of contact points of different kinds in one and the same molecule must be introduced into the above model, and at least three contact points of different kinds of elements must interact in groups at a time.

To meet the above requirement the following model is proposed.

(1) The molecule is a regular polyhedron composed of $z$ planes of which one consists of $a$-element and the remaining $z-1$ ones are consist of $b$-elements, and further, the $a$-element is composed of three sub-elements 1, 2, 3, the arrangement of these three elements, viewed toward the plane from the outside of the molecule along the direction normal to it, is in the order, 1, 2, 3 clockwise for *d*-isomers and 1, 3, 2 for *l*-isomers, the mirror image of *d*-isomers.

(2) Each molecule occupies one site of the quasi-crystalline lattice of $z$ nearest neighbors, and the molecular axis which passes the center of the molecule and the $a$-plane composed of $a$-element can take $z$ directions. When the direction is specified, it can take 3 further different arrangements by the rotation around the axis and thus the molecule at one site can have $3z$ orientational freedom in all*.

(3) The molecules contact with plane to plane and the total configurational energy of the system is the sum of the interaction energy of pairs of planes, the kind of pair of planes is $a-a$, $a-b$ and $b-b$ and the $a-a$ pair contains 6 kinds of sub pairs, 11, 22, 33, 12, 13 and 23 and ab pair 3 kinds of sub pairs, $b1$, $b2$ and $b3$. If $a$-elements of *l*-isomers and *d*-isomers are denoted by $a_l$ and $a_d$ respectively, the $a_l-a_l$ pair can take 3 configurations $\begin{pmatrix}1&2&3\\1&3&2\end{pmatrix}$, $\begin{pmatrix}1&2&3\\2&1&3\end{pmatrix}$ and $\begin{pmatrix}1&2&3\\3&2&1\end{pmatrix}$ with interaction energy $\omega_{11}+2\omega_{23}$, $2\omega_{12}+\omega_{33}$ and $2\omega_{13}+\omega_{22}$ respectively, where $\omega_{ij}$ denotes the interaction energy of a pair of $i$ and $j$ element.

For $a_d-a_d$ pair the same value of interaction energy is obtained for each configuration. For $a_l-a_d$ pair, three configurations are represeted $\begin{pmatrix}1&2&3\\1&2&3\end{pmatrix}$, $\begin{pmatrix}1&2&3\\3&1&2\end{pmatrix}$ and $\begin{pmatrix}1&2&3\\2&3&1\end{pmatrix}$ with interaction energy $\omega_{11}+\omega_{22}+\omega_{33}$, $\omega_{12}+\omega_{13}+\omega_{23}$ and $\omega_{12}+\omega_{13}+\omega_{23}$ respectively, can take place.

$\begin{pmatrix}1&2&3\\1&2&3\end{pmatrix}$ means the configuration in which sub elements 1, 2 and 3 of $a_d$ plane of *d*-isomers interact with sub element of 1, 2 and 3 of $a_l$ plane of *l*-isomers forming sub pairs 11, 22 and 33. Generally, distinguishable pairs are obtained by cycling the lower row of numbers without permutation.

## The Configurational Partition Function and the Excess Free Energy

Using the above model, the configurational partition functions and the excess free energy

* Strictly speaking the regular polyhedron must have a symmetry of $C_{3n}$ around all of $z$ axes passing through the center of the molecule and that of each of $z$ planes.

of the binary system of *d*- and *l*-optical isomers were derived based on the method of expansion of Kirkwood[1].

Generally configurational partition function $\Omega$ is, by definition, expressed as

$$\Omega=\sum e^{-E/kT} \tag{1}$$

where $E$ denotes the potential energy of a system for a particular configuration and summation is carried out over all configurations.

For the system of pure *l*-isomers, its configurational partition function $\Omega_l$ is represented

$$\begin{aligned}\Omega_l&=\sum e^{-E_l/kT}=e^{-\bar{E}_l/kT}(\sum e^{-(E_l-\bar{E}_l)/kT})\\&=e^{-\bar{E}_l/kT}(\sum e^{-W_l/kT})\end{aligned} \tag{2}$$

where $E_l$ denotes the potential energy of the system of pure *l*-isomers and $\bar{E}_l$ denotes the unweighted average of $E_l$ over all configurations and $W_l$ denotes $E_l-\bar{E}_l$. If $g_l$ denotes the number of distinguishable configurations of the system consisting of $N_l$ molecules of *l*-isomer, then the configurational partition function of the system is expressed, following Kirkwood[1], as

$$\ln\Omega_l-\ln g_l-\frac{N_l\chi_l}{\boldsymbol{kT}}=\sum\ln\frac{1}{g_l}\sum e^{-W_l(N_l)/kT} \tag{3}$$

where $N_l\chi_l=\bar{E}_l$ and $g_l$ according to the above model, is equal to $(3z)^{N_l}$.

By the use of an auxiliary quantity $h_l$ defined by

$$h_l=1-\frac{1}{g_l}\sum e^{-W_l(N_l)/kT} \tag{4}$$

Eq. 3 can be rewritten as

$$\begin{aligned}&\ln\Omega_l-N_l\ln 3z-\frac{N_l\chi_l}{\boldsymbol{kT}}\ln(1-h_l)\\&=-h_l-\frac{1}{2}h_l^2-\frac{1}{3}h_l^3-\frac{1}{4}h_l^4-\cdots\cdots\end{aligned} \tag{5}$$

If the $h_l$ in Eq. 4 is expanded in powers of $W_l(N_l)/\boldsymbol{kT}$, the following formula is obtained.

$$\begin{aligned}h_l=&\frac{\langle W_l(N_l)\rangle_{Av.}}{\boldsymbol{kT}}-\frac{\langle W_l^2(N_l)\rangle_{Av.}}{2!\ (\boldsymbol{kT})}\\&+\frac{\langle W_l^3(N_l)\rangle_{Av.}}{3!\ (\boldsymbol{kT})^3}-\cdots\cdots\end{aligned} \tag{6}$$

where $\langle W_l(N_l)\rangle_{Av.}$ denotes the unweighted average of $W_l(N_l)$ over all configurations, and similarly $\langle W_l^t(N_l)\rangle_{Av.}$ denotes the unweighted average of the $t$ th power of $W_l(N_l)$ over all configurations. Substituting 6 into 5 the following expression is obtained.

$$\begin{aligned}&\ln\Omega_l-N_l\ln 3z-\frac{N_l\chi_l}{\boldsymbol{kT}}=-\frac{\langle W_l(N_l)\rangle_{Av.}}{\boldsymbol{kT}}\\&-\{\langle W_l(N_l)\rangle^2_{Av.}-\langle W_l^2(N_l)\rangle_{Av.}\}/2!\ (\boldsymbol{kT})^2\\&-\{\langle W_l^3(N_l)\rangle_{Av.}\\&-3\langle W_l(N_l)\rangle_{Av.}\langle W_l(N_l)\rangle_{Av.}\}/3!\ (\boldsymbol{kT})^3\\&-\{2\langle W_l(N_l)\rangle^3_{Av.}\}/3!\ (\boldsymbol{kT})^3-\cdots\cdots\end{aligned} \tag{7}$$

As $\bar{E}_l$ is the unweighted average of $E_l$, it follows that

$$\langle W_l(N_l)\rangle_{Av.}=\overline{(E_l-\bar{E}_l)}=\bar{E}_l-\bar{E}_l=0 \tag{8}$$

Then Eq. 7 is rewritten as

$$\begin{aligned}&\ln\Omega_l-N_l\ln 3z-\frac{N_l\chi_l}{\boldsymbol{kT}}=\frac{\langle W_l^2(N_l)\rangle_{Av.}}{2!\ (\boldsymbol{kT})^2}\\&-\frac{\langle W_l^3(N_l)\rangle_{Av.}}{3!\ (\boldsymbol{kT})^3}-\cdots\cdots\end{aligned} \tag{9}$$

Similarly, for the system of $N_d$ *d*-isomers, the following expression is obtained.

$$\begin{aligned}&\ln\Omega_d-N_d\ln 3z-\frac{N_d\chi_d}{\boldsymbol{kT}}=\frac{\langle W_d^2(N_d)\rangle_{Av.}}{2!\ (\boldsymbol{kT})^2}\\&-\frac{\langle W_d^3(N_d)\rangle_{Av.}}{3!\ (\boldsymbol{kT})^3}-\cdots\cdots\end{aligned} \tag{10}$$

In the following, it will be shown that $\chi_l$ is equal to $\chi_d$. As $\chi_l$ is the unweighted average of $E_l$ over all configurations, $\chi_l$ is proportional to

$$\bar{\omega}_{a_l-a_l}+2(z-1)\bar{\omega}_{a_l-b}+(z-1)^2\bar{\omega}_{b-b} \tag{11}$$

and similarly $\chi_d$ is proportional to

$$\bar{\omega}_{a_d-a_l}+2(z-1)\bar{\omega}_{a_d-b}+(z-1)^2\bar{\omega}_{b-b} \tag{12}$$

where $-$ denotes the unweighted average and $\omega_{a_l-a_l}$, $\omega_{a_l-a_d}$, $\omega_{a_l-b}$, $\omega_{a_d-b}$ and $\omega_{b-b}$ denote the interaction energy of $a_l-a_l$, $a_d-a_d$, $a_l-b$, $a_d-b$ and $b-b$ plane pairs respectively.

Further, according to the assumption made above, the following relation is obtained.

$$\begin{aligned}\bar{\omega}_{a_l-a_l}&=\frac{1}{3}\{\omega_{11}+\omega_{22}+\omega_{33}+2(\omega_{12}+\omega_{23}+\omega_{31})\}\\&=\bar{\omega}_{a_d-a_d}\end{aligned} \tag{13}$$

Thus each of three different configurations of $a_l-a_l$ $a_d-a_d$ pair of plane have the same interaction energy. Further

$$\bar{\omega}_{a_l-b}=\omega_{1b}+\omega_{2b}+\omega_{3b}=\bar{\omega}_{a_d-b} \tag{14}$$

From 11, 12, 13 and 14, we obtain

$$\chi_l=\chi_d=\chi_0 \tag{15}$$

As is stated above, the interaction energy of the pairs of planes in *l*-isomers $\omega_{a_l-a_l}$, $\omega_{a_l-b}$ and $\omega_{b-b}$ and in *d*-isomers $\omega_{a_d-a_d}$, $\omega_{a_d-b}$ and $\omega_{b-b}$ have the same value, and the total energy $E$ is the sum of such interaction energies of pairs of planes. Further for one specified configuration in the system consisting of $N_0$ molecules of *l*-isomers, with a specified number of pairs of $a_l-a_l$, $a_l-b$ and $b-b$ plane contacts,

1) J. G. Kirkwood, *J. Chem. Phys.*, **6**, 70 (1938).

there exists the corrsponding configuration in the system contisting of $N_0$ molecules of *d*-isomers, for, one to one correspondence exists between both isomers.

Then the total configurational energy for one specified configuration for *l*-isomers is equal to that of the corresponding configuration in $\alpha$-isomers, that is

$$E_l = E_d \tag{16}$$

and hence

$$W_l(N_0) = W_d(N_0) = W_0(N_0) \tag{17}$$

For $d-l$ mixtures consisting of $N_l$ *l*-isomers and $N_d$ *d*-isomers, the configurational partition function $\Omega_{dl}$ is expressed as

$$\begin{aligned}
&\ln \Omega_{dl} - N\ln 3z - \ln \frac{N!}{(Nx)!\,\{N(1-x)\}!} \\
&- N\cdot\chi_{ld}(x)/\boldsymbol{kT} = -\langle W_{dl}(N,x)\rangle_{Av.}/\boldsymbol{kT} \\
&- \{\langle W_{dl}(N,x)\rangle^2_{Av.} \\
&- \langle W^2_{dl}(N,x)\rangle_{Av.}\}/2!\,(\boldsymbol{kT})^2 \\
&- \{\langle W^3_{dl}(N,x)\rangle_{Av.} - 3\langle W^2_{dl}(N,x)\rangle_{Av.} \\
&\cdot\langle W_{dl}(N,x)\rangle_{Av.}\}/3!\,(\boldsymbol{kT})^3 \\
&- 2\langle W_{dl}(N,x)\rangle^3_{Av.}/3!\,(\boldsymbol{kT})^3
\end{aligned} \tag{18}$$

where $N=N_l+N_d$ and $N\cdot\chi_{dl}(x)$ is the unweighted mean of interaction energy of the system and $x=N_l/N$. Since $\chi_{dl}(x)$ is proportional to

$$\begin{aligned}
&x^2\{\bar{\omega}_{a_l-a_l} + 2(z-1)\bar{\omega}_{a_l-b} + (z-1)^2\omega_{b-b}\} \\
&+ 2(1-x)x\{\omega_{a_l-a_d} + (z-1)(\omega_{a_l-b}+\omega_{a_d-b}) \\
&+ (z-1)^2\omega_{b-b}\} + (1-x)^2 \\
&\{\omega_{a_d-a_d} - 2(z-1)\bar{\omega}_{a_d-b} + (z-1)^2\omega_{b-b}\}
\end{aligned} \tag{19}$$

$\bar{\omega}_{a_l-a_d}$ is the mean of three interaction energies

$$\omega_{11}+\omega_{22}+\omega_{33},\ \omega_{12}+\omega_{23}+\omega_{31},\ \omega_{12}+\omega_{23}+\omega_{31}$$

Each term differs from that of $\omega_{a_l-a_l}$ or $\omega_{a_d-a_d}$ but the unweighted mean over these three configurations, becomes the same value as follows:

$$\begin{aligned}
\bar{\omega}_{a_d-a_l} &= \frac{1}{3}(\omega_{11}+\omega_{22}+\omega_{33}+\omega_{12}+\omega_{23}+\omega_{31} \\
&\quad +\omega_{12}+\omega_{23}+\omega_{31}) \\
&= \frac{1}{3}\{\omega_{11}+\omega_{22}+\omega_{33}+2(\omega_{12}+\omega_{23}+\omega_{31})\} \\
&= \omega_{a_l-a_l} = \omega_{a_d-a_d}
\end{aligned} \tag{20}$$

Hence, from 19, 20, 11 and 12, we have

$$\chi_{dl}(x) = \chi_l = \chi_d = \chi_0 \tag{21}$$

$$\langle W_{dl}(N,x)\rangle_{Av.} = \overline{(E_{dl}-\bar{E}_{dl})} = \bar{E}_{dl} - \bar{E}_{dl} = 0 \tag{22}$$

For the system consisting of $N$ *d*-isomers or $N$ *l*-isomers, free energy is expressed as

$$\begin{aligned}
F_d = F_l &= -\boldsymbol{kT}\ln\Omega_0 = N\boldsymbol{kT}\ln 3z + N\chi_0 \\
&+ \frac{\langle W^2_0(N)\rangle_{Av.}}{2!\,(\boldsymbol{kT})} - \frac{\langle W^3_0(N)\rangle_{Av.}}{3!\,(\boldsymbol{kT})^2} + \cdots\cdots
\end{aligned} \tag{23}$$

For $d-l$ mixtures consisting of $N_l(=Nx)$ molecules of *l*-isomer and $N_d$ $(=N(1-x))$ molecules of *d*-isomer, we obtain

$$\begin{aligned}
F_{dl} &= -\boldsymbol{kT}\ln\Omega_{dl} = N\boldsymbol{kT}\ln 3z + N\chi_0 \\
&+ N\boldsymbol{kT}\{x\ln x + (1-x)\ln(1-x)\} \\
&+ \frac{\langle W^2_{dl}(N,x)\rangle_{Av.}}{2(\boldsymbol{kT})} - \frac{\langle W^3_{dl}(N,x)\rangle_{Av.}}{3!\,(\boldsymbol{kT})^2} \\
&+ \cdots\cdots
\end{aligned} \tag{24}$$

As each configuration has a different energy, that is $W_{dl}=(N,x)\neq W_0(N)$, then the free energy of mixing $\Delta F_m$ is represented as

$$\begin{aligned}
\Delta F_m &= N\boldsymbol{kT}\{x\ln x + (1-x)\ln(1-x)\} \\
&+ \frac{1}{2(\boldsymbol{kT})}\{\langle W^2_{dl}(N,x)\rangle_{Av.} - \langle W^2_0(N_l)\rangle_{Av.} \\
&- \langle W^2_0(N_d)\rangle_{Av.}\} - \frac{1}{3!\,(\boldsymbol{kT})^2} \\
&\times\{\langle W^3_{dl}(N,x)\rangle_{Av.} - \langle W^3_0(N_l)\rangle_{Av.} \\
&- \langle W^3_0(N_d)\rangle_{Av.}\} + \cdots\cdots
\end{aligned} \tag{25}$$

Then the problem is reduced to a calculation of second and heigher powers of $W_{dl}(N,x)$, $W_0(N_l)$ and $W_0(N_d)$. Now $\langle W^2_0(N_l)\rangle$, $\langle W^2_0(N_d)\rangle$ and $W^2_{dl}(N)$ will be considered.

According to the model mentioned above, potential energy $E$ of the system consisting of $N$ molecules of *l*- or *d*-isomers with the particular configuration having $N_{bb}$ *bb* pairs, $N_{ab}$ *ab* pairs, $N_{aa_1}$ $aa_1$ pairs, $N_{aa_2}$ $aa_2$ pairs and $N_{aa_3}$ $aa_3$ pairs, where $aa_1$, $aa_2$ and $aa_3$ denote three kinds of *aa* contact, is expressed as

$$\begin{aligned}
E &= N_{bb}\omega_{bb} + N_{ab}\omega_{ab} + N_{aa_1}\omega^0_{aa_1} + N_{aa_2}\omega^0_{aa_2} \\
&+ N_{aa_3}\omega^0_{aa_3}
\end{aligned} \tag{26}$$

where $\omega^0_{aa_1}$, $\omega^0_{aa_2}$ and $\omega^0_{aa_3}$ denote those interaction energies corresponding to $aa_1$, $aa_2$ and $aa_3$ pairs respectively and these values are $\omega_{11}+2\omega_{23}$, $\omega_{22}+2\omega_{13}$ and $\omega_{33}+2\omega_{12}$ respectively. Then the average value $E$ becomes

$$\begin{aligned}
E &= \bar{N}_{bb}\omega_{bb} + \bar{N}_{ab}\omega_{ab} + \bar{N}_{aa_1}\omega_{aa_1} \\
&+ \bar{N}_{aa_2}\omega_{aa_2} + \bar{N}_{aa_3}\omega_{aa_3} \\
&= \frac{1}{2}zN\left\{\frac{(z-1)^2}{z^2}\omega_{bb} + \frac{2(z-1)}{z^2}\omega_{ab}\right. \\
&\left. + \frac{1}{z^2}\cdot\frac{1}{3}(\omega_{aa_1}+\omega_{aa_2}+\omega_{aa_3})\right\}
\end{aligned} \tag{27}$$

As $W_0(N)$ means the difference between the

potential energy of the system of particular configuration and that averaged over all configurations, $W_0(N)$ for the particular configuration mentioned above becomes

$$W_0(N)=E-\bar{E}=\left\{N_{bb}-\frac{1}{2}N\frac{(z-1)^2}{z}\right\}\omega_{bb}+\left\{N_{ab}-\frac{N(z-1)}{z}\right\}\omega_{ab}+N_{aa_1}\omega^0_{aa_1}+N_{aa_2}\omega^0_{aa_2}+N_{aa_3}\omega^0_{aa_3}-\frac{1}{6}\frac{N}{z}(\omega^0_{aa_1}+\omega^0_{aa_2}+\omega^0_{aa_3}) \quad (28)$$

In calculating $\langle W_0^2(N)\rangle_{Av.}$, we must strictly take the average over all possible configurations. However, since of all configurations the configurations with $N_{bb}=\bar{N}_{bb}$, $N_{ab}=\bar{N}_{ab}$ and $\sum_{i=1}^{3}N_{aa_i}=\bar{N}_{aa}$ occupy the predominant part, and the average over these configurations, may differ very little from that over all configurations, we approximately take the former average in place of the latter. Then

$$W_0(N)=\sum_{i=1}^{3}{}'N_{aa_i}\omega^0_{aa_i}-\frac{1}{6}\frac{N}{z}(\sum_{i=1}^{3}\omega^0_{aa_i}) \quad (29)$$

where $\sum'$ donates the summation under the restriction that $\sum_{i=1}^{3}N_{aa_i}=1/2\cdot N/z$ and $\langle W_0^2(N)\rangle_{Av.}$ becomes

$$\langle W_0^2(N)\rangle=\overline{(\sum_{i=1}^{3}{}'N_{aa_i}\omega^0_{aa_i})^2}-2\sum_{i=1}^{3}{}'N_{aa_i}\omega^0_{aa_i}\times\frac{1}{6}\frac{N}{Z}(\sum_{i=1}^{3}\omega^0_{aa_i})+\left(\frac{1}{6}\frac{N}{z}\sum_{i=1}^{3}\omega^0_{aa_i}\right)^2=(\sum_{i=1}^{3}{}'N_{aa_i}\omega^0_{aa_i})^2-\left(\frac{1}{6}\frac{N}{z}\sum_{i=1}^{3}\omega^0_{aa_i}\right)^2 \quad (30)$$

As all configurations of *aa* pair can take place with equal probability the first term of 30 becomes

$$(\sum_{i=1}^{3}{}'N_{aa_i}\omega^0_{aa_i})^2=\left(\frac{1}{2}\frac{N}{z}\right)^2\int_0^1\int_0^y[\{\omega^0_{aa_1}x+\omega^0_{aa_2}(y-x)\}+\omega^0_{aa_3}(1-y)]^2dxdy=\left(\frac{1}{2}\frac{N}{z}\right)^2\frac{1}{6}(\omega^{0^2}_{aa_1}+\omega^{0^2}_{aa_2}+\omega^{0^2}_{aa_3}+\omega^0_{aa_1}\omega^0_{aa_2}+\omega^0_{aa_2}\omega^0_{aa_3}+\omega^0_{aa}\omega^0_{aa_1}) \quad (31)$$

Substituting 31 into 30 the following formula is obtained:

$$\langle W_0^2(N)\rangle_{Av}=\left(\frac{1}{2}\frac{N}{z}\right)^2\cdot\frac{1}{36}\{(\omega^0_{aa_1}-\omega^0_{aa_2})^2+(\omega^0_{aa_2}-\omega^0_{aa_3})^2+(\omega^0_{aa_3}-\omega^0_{aa_1})^2\} \quad (32)$$

For the system consisting of $N_l$ molecules of *l*-isomers and $N_d$ molecules of *d*-isomer, $\langle W_{dl}^2(Nx)\rangle$, where $N=N_l+N_d$ and $x=N_l/(N_l+N_d)$, can be obtained in a similar way. In this case the average may be taken over the configurations in which $N^{ll}_{aa}=\overline{N^{ll}_{aa}}=Nx^2/2z$, $N^{dl}_{aa}=\overline{N^{dl}_{aa}}=Nx(1-x)/z$ and $N^{dd}_{aa}=\overline{N^{ll}_{aa}}=N(1-x)^2/2z$ where $N^{ll}_{aa}$, $N^{dl}_{aa}$ and $N^{dd}_{aa}$ are the number of pairs of $a_l-a_l$, $a_l-a_d$ and $a_d-a_d$ respectively. The $a_l-a_d$ pair can have three different configuration with corresponding interaction energies $\omega^{ld}_{aa_1}$, $\omega^{ld}_{aa_2}$ and $\omega^{ld}_{aa_3}$. As mentioned above $\omega^{ld}_{aa_1}=\omega_{11}+\omega_{22}+\omega_{33}$, $\omega^{ld}_{aa_2}=\omega^{ld}_{aa_3}=\omega_{12}+\omega_{13}+\omega_{23}$, then

$$\sum_{i=1}^{3}\omega^{ld}_{aa_i}=\omega_{11}+\omega_{22}+\omega_{33}+2(\omega_{12}+\omega_{13}+\omega_{23})=\sum_{i=1}^{3}\omega^{ll}_{aa_i}=\sum_{i=1}^{3}\omega^{dd}_{aa_i}=\sum_{i=1}^{3}\omega^0_{aa_i} \quad (33)$$

From 33 the following expressions are obtained.

$$W_{dl}(N,x)=\sum_{i=1}^{3}{}'(N^{ll}_{aa_i}\omega^{ll}_{aa_i}+N^{dd}_{aa_i}\omega^{ld}_{aa_i}+N^{dd}_{aa_i}\omega^{dd}_{aa_i})-\frac{1}{6}\frac{N}{z}(\sum_{i=1}^{3}\omega^0_{aa_i})=\sum_{i=1}^{3}{}'\left\{N^{ll}_{aa_i}\omega^{ll}_{aa_i}-\frac{Nx^2}{2z}\left(\frac{1}{3}\sum_{i=1}^{3}\omega^{ll}_{aa_i}\right)\right\}+\sum_{i=1}^{3}{}'\left\{N^{ld}_{aa_i}\omega^{ld}_{aa_i}-\frac{Nx(x-1)}{z}\left(\frac{1}{3}\sum_{i=1}^{3}\omega^{dl}_{aa_i}\right)\right\}+\sum_{i=1}^{3}{}'\left\{N^{dd}_{aa_i}\omega^{dd}_{aa_i}-\frac{N(1-x)^2}{2z}\left(\frac{1}{3}\sum_{i=1}^{3}\omega^{dd}_{aa_i}\right)\right\} \quad (34)$$

where $\sum'$ denotes the summation under the restrictions that $\sum_{i=1}^{3}N^{ll}_{aa_i}=Nx^2/2Z$, $\sum_{i=1}^{3}N^{dl}_{aa_i}=Nx(1-x)/z$ and $\sum_{i=1}^{3}N^{dd}_{aa_i}=(1-x)^2/2z$. Since the mean values in $\{\ \}$ of 34 become zero, then

$$\begin{aligned}\langle W_{dl}^2(N,x)\rangle_{Av}=&\left(\frac{1}{2}\frac{N}{z}x^2\right)^2\cdot\frac{1}{36}\{(\omega^{ll}_{aa_1}-\omega^{ll}_{aa_2})^2+(\omega^{ll}_{aa_2}-\omega^{ll}_{aa_3})^2+(\omega^{ll}_{aa_3}-\omega^{ll}_{aa_1})^2\}\\&+\left\{\frac{Nx(1-x)}{z}\right\}^2\cdot\frac{1}{36}\{(\omega^{dl}_{aa_1}-\omega^{dl}_{aa_2})^2+(\omega^{dl}_{aa_2}-\omega^{dl}_{aa_3})^2+(\omega^{dl}_{aa_3}-\omega^{dl}_{aa_1})^2\}\\&+\left\{\frac{1}{2}\frac{N}{z}(1-x)^2\right\}^2\cdot\frac{1}{36}\{(\omega^{dd}_{aa_1}-\omega^{dd}_{aa_2})^2+(\omega^{dd}_{aa_2}-\omega^{dd}_{aa_3})^2+(\omega^{dd}_{aa_3}-\omega^{dd}_{aa_1})^2\}\\=&\left(\frac{1}{2}\frac{N}{z}\right)^2\{x^4+(1-x)^4\}\cdot\frac{1}{36}\times\{(\omega^0_{aa_1}-\omega^0_{aa_2})^2+(\omega^0_{aa_2}-\omega^0_{aa_3})^2+(\omega^0_{aa_3}-\omega^0_{aa_1})^2\}+\left(\frac{N}{z}\right)x^2(1-x)^2\times\frac{1}{36}\{(\omega^{dl}_{aa_1}-\omega^{dl}_{aa_2})^2+(\omega^{dl}_{aa_2}-\omega^{dl}_{aa_3})^2+(\omega^{dl}_{aa_3}-\omega^{dl}_{aa_1})^2\}\end{aligned} \quad (35)$$

If the terms higher than second power of $W$ in 25 are neglected, free energy of mixing $\Delta_m F$ or excess free energy $F^E$ may be expressed as

$$\begin{aligned}\Delta_m F - NkT\{x\ln x+(1-x)\ln(1-x)\} &= F^E \\ &= -\frac{1}{2kT}\left[\left(\frac{1}{2}-\frac{N}{z}\right)^2\{x^4+(1-x)^4 \right. \\ &\quad -x^2-(1-x)^2\}\times\frac{1}{36}\{(\omega^0_{a_1a_1}-\omega^0_{a_2a_2})^2 \\ &\quad +(\omega^0_{a_2a_2}-\omega^0_{a_3a_3})^2+(\omega^0_{a_3a_3}-\omega^0_{a_1a_1})\} \\ &\quad \left.+\left(\frac{N}{z}\right)^2 x^2(1-x)^2\times\frac{1}{36}\{(\omega^{dl}_{a_1a_1}-\omega^{dl}_{a_2a_2})^2\right. \\ &\quad \left.+(\omega^{dl}_{a_2a_2}-\omega^{dl}_{a_3a_3})^2+(\omega^{dl}_{a_3a_3}-\omega^{dl}_{a_1a_1})^2\}\right] \qquad (36)\end{aligned}$$

## Discussions

As is seen from the above result the principal term of excess free energy $F^E$ is inversely proportional to absolute temperature. This is due to the fact that the optical *d*- and *l*-isomers are energetically identical in random mixture (see Eqs. 21 and 22), so that the first order terms are dropped in the expansion. It is in remarkable contrast to that of the usual binary solutions where the principal terms of $F^E$ are independent of temperature.

Dependency of the term on mole fraction $x$ of one component is complicated and is higher than quadratic in $x$. This is another feature of the system of optically active substances.

The term is usually very small and is quite negligible.

However, if the difference $|\omega^0_{a_ia_i}-\omega^0_{a_ja_j}|$ or $|\omega^{dl}_{a_ia_i}-\omega^{dl}_{a_ja_j}|$ happens to be great, the contribution from these terms may become appreciable. For instance consider an optical active molecule whose sub elements 1, 2 and 3 are $-NH_2$, $-C{=}O$ and $-OH$ group respectively. Then hydrogen bonding is formed between the pairs 1−2, 1−3, 2−3 and 3−3 but is not formed between pairs 1−1 and 2−2.

If we assume that interaction energies of these pairs which form hydrogen bonding are all equal and 5 kcal./mol. and those of the pairs which do not form hydrogen bonding are neglected, then $F^E$ becomes according to 36.

$$F^E \approx \frac{1.45}{(2z)^2}\ \text{kcal./mol.}$$

$$\text{at } T=300^\circ\text{K and } x=0.5$$

If we assume that $Z=4$, $F^E$ becomes $F^E\approx 22$ cal./mol. Although the value 22 cal./mol. obtained above is quite approximate because of the neglect of higher orders than the second, the order of magnitude of the value may not differ from that obtained by rigorous calculation.

## Summary

A statistical mechanical theory of solutions consisting of *d*- and *l*-optical isomers is developed based on a new model of optically active molecules, and the excess free energy of the system is also derived and the order of magnitude of this quantity is examined.

The auther wishes to express his hearty thanks to Peofessor Yonezo Morino of the University of Tokyo for his helpful discussions.

*Government Chemical Industrial Research Institute*
*Shibuya-ku, Tokyo*

# *Forschung über die katalytische Entwässerung des Isoamylalkohols. III. Prüfung über die Bestandteile der durch Zinksulfat-Katalysator-Entwässerung entstehenden Produkten*

Von Akira MITSUTOMI

(Eingegangen am 8. April, 1961)

Die im vorangehenden Bericht[1] beschriebenen Versuche zeigten klar, dass der Zinksulfat-Katalysator der Beste ist, wenn aus Isoamylalkohol die hauptsächlich aus Trimethyläthylen bestehenden Olefinen hergestellt werden sollen. Dass diese unter Anwendung des genannten Katalysators aus Isoamylalkohol hergestellten Olefine ein Gemisch aus Trimethyläthylen, Isopropyläthylen und Methyläthyläthylen darstellen, ist allerdings nach ihrem Siedepunkt und weiteren physikalischen Konstanten anzunehmen, ist aber keineswegs nach exakter Prüfung der Bestandteile bestätigt.

Der Verfasser schreibt im folgenden die

1) A. Mitsutomi, Dieses Bulletin, 34, 1525 (1961).

Ergebnisse der Forschung zur Bestimmung der Bestandteile nieder.

### Beschreibung der Versuche

Als Katalysatoren wurde nach den Versuchsergebnissen bis zu der II. Mitteilungen das Gemisch aus 330 g Zinksulfat ($ZnSO_4 \cdot 7H_2O$) und 770 g japanischer Säureerde mit Zusatz 100 ccm 28% Ammoniak eingesetzt, danach noch in Kugelformen verarbeitet, zuerst bei 60°C 2 Std, dann bei 120°C 5 Std erhitzt und aufgetrocknet, anschliessend ins Reaktionsrohr eingefüllt und bei 500°C 8 Std aktiviert.

TABELLE I. ERGEBNISSE DER FEINDESTILLATION VON DEN REAKTIONSPRODUKTEN

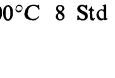
| Nummerierung der Fraktion | Destillationstemp. (Korr.) °C | Prozentuales Destillationsverhaltnis, % | $n_D^{20}$ |
|---|---|---|---|
| 1 | 21.7~30.8 | 14.4 | 1.3708 |
| 2 | 30.8~33.8 | 5.0 | 1.3852 |
| 3 | 33.8~35.8 | 6.6 | 1.3880 |
| 4 | 35.8 | 13.0 | 1.3880 |
| 5 | 35.8~42.8 | 5.0 | 1.3970 |
| | Rückstand | 32.0 | 1.4028 |

Probe $n_D^{20}=1.4059$

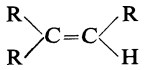
Ganz gleichartige, aber verkleinerte Versuchsanlage, wie sie im vorangehenden mitteilung beschrieben ist, wurde herangezogen und die Reaktionstemperatur auf 350~400°C eingestellt.

Zuerst wurden flüssige Reaktionspodukte der Feindestillation unterworfen, wodurch fünf Fraktionen erhalten wurden. Sie sind in Tabelle I aufgestellt.

**Prüfung der ersten Fraktion.**—Das Infrarotspektrum der ersten Fraktion ist in Abb. 1 gezeigt.

Es sind die für Isopropyl-Gruppe charakteristischen Gerüstschwingungen 6.9 $\mu$ und 7.27 $\mu$, die intensiv erscheinen. Ferner sind 10.1 $\mu$, 11.03 $\mu$, 11.32 $\mu$ usw. für  spezifisch bemerkbar.

Diese Umstände unterstreichen das Vorhandensein des Isopropyläthylens.

Ferner ist die Absorption 12.53 $\mu$ für  festzustellen, ausserdem sind 9.33 $\mu$, 8.25 $\mu$ für Trimethyläthylen schwach dargestellt.

Diese Umstände lassen beurteilen, dass diese Fraktion neben viel Mengen Isopropyläthylen das Mitvorhandensein geringer Menge Trimethyläthylen zulässt.

**Prüfung von Fraktion Nr. 2.**—Das Infrarotspektrum von Fraktion Nr. 2 ist in Abb. 2 gezeigt.

Die Besichtigung dieses Infrarotspektrums lässt

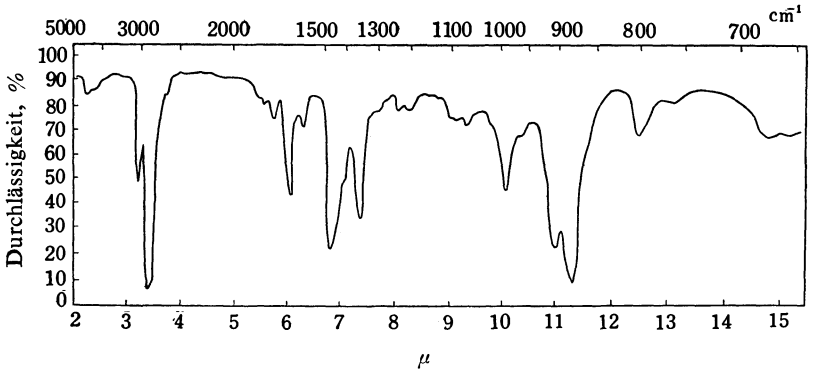



Abb. 1. Infrarotspektrum von Fraktion Nr. 1.

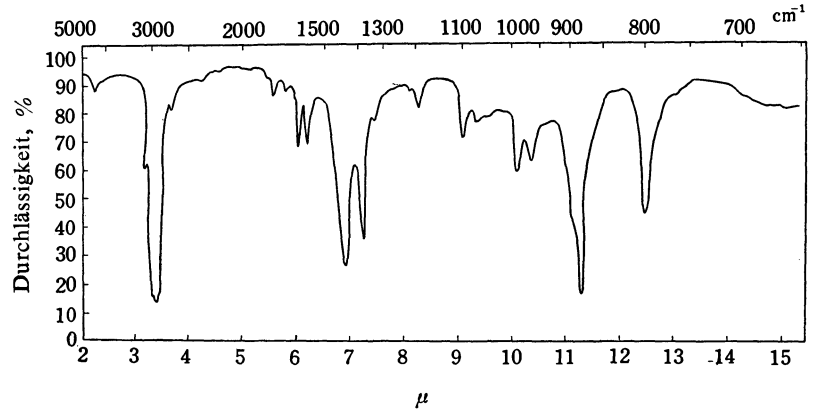



Abb. 2. Infrarotspecktrum von Fraktion Nr. 2.

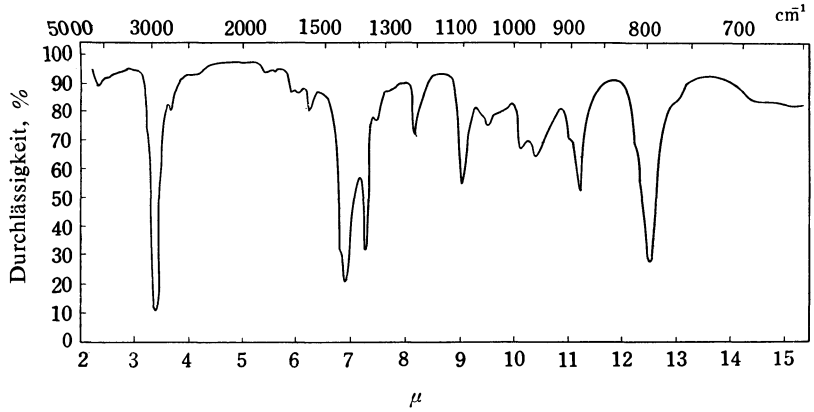



Abb. 3. Infrarotspektrum von Fraktion Nr. 3.

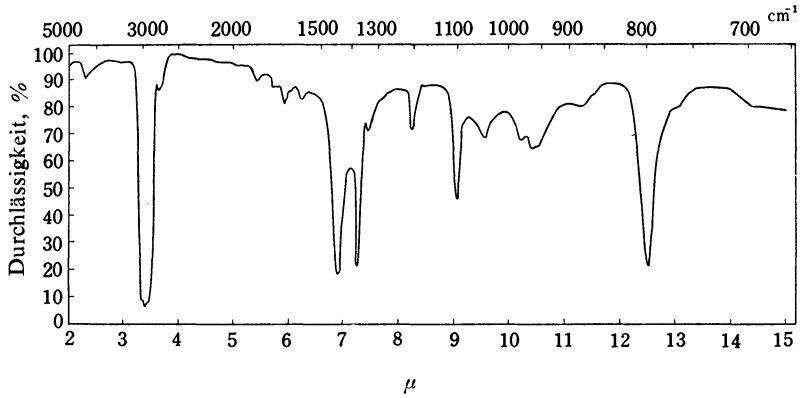
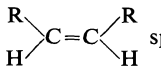
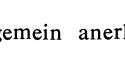
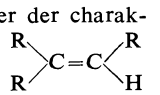



Abb. 4. Infrarotspectrum von Fraktion Nr. 4.

wissen, dass ausser der für  spezifischen 12.50 $\mu$ Wellenlänge die bei den obengenannten und unterstrichenen Wellenlängen mit den charakteristischen Gerüstschwingungen bei Trimethyläthylen gut übereinstimmen.

Ferner zu beachten ist die Absorption von 11.28 $\mu$, die als charakteristische Gerüstschwingung für Bindung von  allgemein anerkannt ist. Der Umstand, dass dies stark hervortritt, lässt wissen, dass die Fraktion Nr. 2 das Gemisch aus Trimethyläthylen und Methyläthyläthylen fast in gleichen Anteilen darstellt.

**Prüfung von Fraktion Nr. 3.**—Das Infrarotspektrum diesser Fraktion (Abb. 3) zeigt gute Übereinstimmung der Absorptionsstellungen mit denen in Abb. 2, nur dass die 12.50 $\mu$ stärker ist als bei Abb. 2, während die 11.28 $\mu$ schwächer ist, woraus mit Recht zu schliessen ist, dass diese Fraktion das Gemisch aus vielen Mengen Trimethyläthylen und geringer Menge Methyläthyläthylen darstellt.

**Prüfung von Fraktion Nr. 4.**—Der Brechungsindizes $n_D^{20}=1.3880$ dieser Fraktion ist fast mit den Literaturangaben von Trimethyläthylen $n_D^{20}=1.3874$, identisch, was annehmen lässt, dass es sich hierbei doch um reines Trimethyläthylen handelt. Bei ihrem Ultrarotspektrum (abb. 4) sind ausser der charakteristischen Gerüstgchwingungen für  die Gesamtkurvenverzeichnungen fast mit denen für Trimethläthylene übereinstimmend. Kein Vorhandensein anderer Verbindungen ist anzunehmen.

**Bestandteilmässige Untersuchung des Destillationsrückstandes.** — Wenn Reaktionstemperaturen der Entwässerung von Isoamylalkohol variieren und dabei die flüssigen Produkte (Rückstand von der Tabelle I) hinsichtlich ihres Brechungsindies miteinander verglichen werden, so lassen sich annähernd ein konstanten Wert finden (Tabelle II), dieser zeigt dass die Produkte bestandteilmässig keinerlei grössere unterschiede aufweisen.

Tabelle II. Zusammenhang der Reaktionstemperaturen mit den Brechungsindizien der Reactionsprodukte

| Reaktionstemperatur, °C | 375~425 | 350~400 | 325~375 |
|---|---|---|---|
| $n_D^{20}$ | 1.4050 | 1.4059 | 1.4048 |

Da ihre bestandteilmässige Untersuchung tatsächlich keine grösseren Unterschiede voneinander ergab,

TABELLE III. DESTILLATIONSERGEBNISSE VON DESTILLATIONSRÜCKSTANDGEMISCH

| Fraktion-nummern | Destillations-temperatur °C/mmHg | Destillate-menge ccm | $n_D^{20}$ | Anmerkung |
|---|---|---|---|---|
| 1 | 92～94/760 | 5 | 1.3961 | farblos, klar, stechendes Geruch |
| 2 | 94～96/760 | 7.5 | 1.3961 | ditto |
| 3 | 96～102/760 | 3.5 | 1.3993 | ditto |
| 4 | 50～72/46 | 3 | 1.4292 | hellgelb, aromatisches Geruch |
| 5 | 72～80/46 | 3.5 | 1.4326 | ditto |
| 6 | 931～15/7 | 1.5 | 1.4648 | gelbbraun, aromatisches Geruch |
| | Rückstand | 6 | | pechartig, dickklebrig |

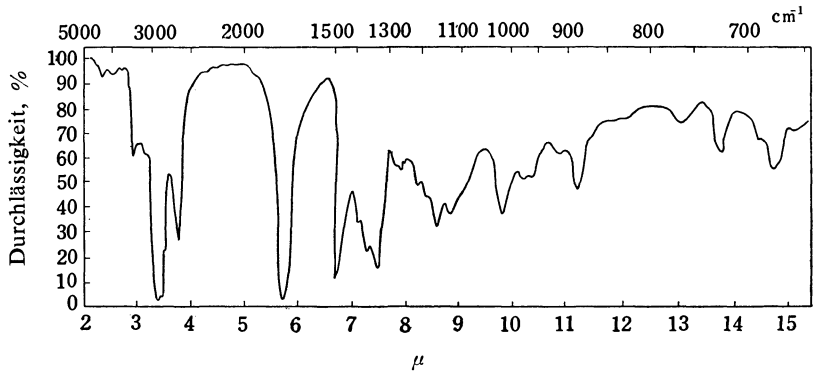



Abb. 5. Infrarotspektrum von Fraktion Nr. 2 (Tabelle III).

wurden diese drei Reaktionsprodukte voneinander abgesondert destilliert und die jeweiligen Destillate wurden zusammengebracht und dieses Rückstandsgemisch wieder der destillation unterzogen. Die Ergebnisse sind in Tabelle III aufgestellt.

Die Fluoreszenz-Indikator-Adsorptionsanalyse an der Fraction Nr. 2 hiervon ergab, dass das Gemisch aus Olefin 3.7%, aromatischartige Verbindungen 2.9% und gleich wie Alkohol polarisierte Substanzen 93.4% besteht.

Aus dem Infrarotspektrum der Fraktion Nr. 2 (Abb. 5) ist zu sehen, dass die für Aldehyde bzw. Keton-Radikal charakteristische Gerüstschwingungen



3.7 $\mu$ und 5.8 $\mu$ sowie die für  Radikal spezifischen 7.25 $\mu$ und 7.3 $\mu$ alle ausdrucksvoll in Erscheinung treten, das weist klar auf, dass Isovaleraldehyde in vielen Mengen enthalten sind. Die Absorption 2.9 $\mu$ zeigt das Vorhandensein des OH Radikals auf, während die 3.4 $\mu$ und 3.5 $\mu$ für Alkyl-Radikal klarsichtlich auftreten. Die Zusammenfassung dieser Tatsachen lässt beurteilen, dass diese Fraktion das Gemisch aus Isovaleraldehyde in vielen Mengen und unverwandte Isoamylalkohol in geringer Menge darstellt.

Ferner wurde nach chemischer Untersuchung erkannt, dass die Fraktionen von Nr. 1 bis 3, welche vollkommen gleiches stechendes Geruch besitzen, bestandteilmässig vollständig gleich sind wie die Fraktion Nr. 2. Wie aus Tabelle III ersichtlich, sind die Brechungsindizien miteinander fast identisch. Erst bei der Fraktion Nr. 4 steigt der Indizies etwas an und zwar immer höher mit den erhöhten Siedepunkten. Das Geruch geht von dem Stechenden nebenbei zum Aromatischen über. Hieraus ist das Vorhandensein der Polymere anzunehmen. Hinsichtlich der Tatsache, dass bei qualitativer Analyse des Schwefels mittels Nitroprussidnatrium und der Doktor-Lösung die Fraktionen Nr. 5, 6 und der Rückstand positiv sind, wurden die ebengenannten Nr. 5 und 6 gründlich gewaschen. Nämlich, bei der Fraktion Nr. 5 wurden 110 ccm Doktor-Lösung auf 3.1 ccm Proben in mehr als 10 Portionen eingeteilt angewandt und gewaschen. Die öligen Schichten blieben aber trotz des Waschens immer noch gelblich oder hellbraunlich, wurden nicht farblos.

Nun wurde 15 ccm der Fraktion Nr. 5 mit 500 ccm Doktor-Lösung in 20 Portionen gewaschen, aber die Farbtönung blieb immer noch unverändert. Der Brechungsindizies war $n_D^{20}=1.4550$ und die qualitative Analyse des Schwefels zeigte sich als positiv.

TABELLE IV. DESTILLATIONSERGEBNISSE DES GEWASCHENEN ÖLS (FRAKTION NR. 5 DER TABELLE III)

| Fraktionen | Destillations-temperatur °C/10 mmHg | $n_D^{20}$ | Schwefel-versuche | Anmerkung |
|---|---|---|---|---|
| 1 | 46～ 67 | 1.4420 | ± | Gelb |
| 2 | 67～ 85 | 1.4392 | + | 〃 |
| 3 | 112～135 | 1.4443 | + | 〃 |
| | Rückstand | | + | Schwarzbraunlich, dickklebrig |

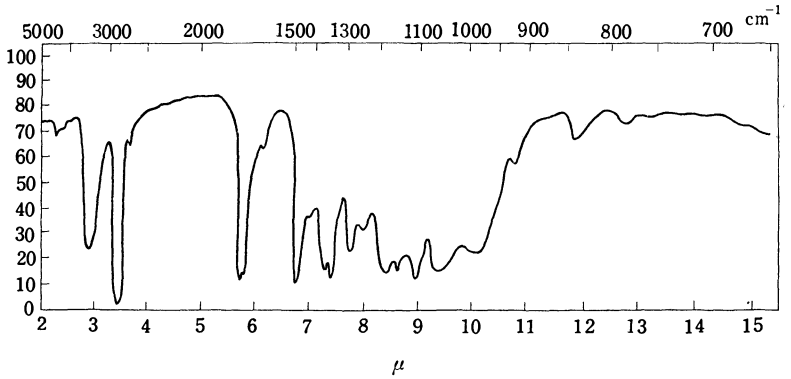



Abb. 6. Infrarotspektrum von Fraktion Nr. 3. (Tabelle IV)

Das gewaschene Öl wurde unterm verminderten Druck destlliert. Die Ergebnisse sind in Tabelle IV verzeichnet.

Bei infrarotspectraler Untersuchung (Abb. 6) der Fraktion Nr. 3 der Tabelle IV erwiesen sich die für Aldehyd oder Keton spezifischen Absorption 3.42 $\mu$ und 5.8 $\mu$ intensiv, während im Übrigen die weiteren Absorptionen mit denen als Isovaleraldehyde im grossen und ganzen übereinstimmten. Die Feststellbarkeit der Absorptionswellenlänge 2.9 $\mu$ für OH Radikal und der Absorption für Isopropyl-Radical ist klarer Nachweis für Isoamylalkohol. Es ist daher anzunehmen, dass es sich bei diesen öligen Substanzen um ein Gemisch aus Isovaleraldehyd und Isoamylalkohol handelt.

Die obigen Ergebnisse lassen für den Destillationsrückstand auf das Folgende schliessen.

Die Fluoreszenz-Indikator-Adsoptionsanalyse an dem ungewaschen Rückstand ergab, dass die jeglichen Fraktionen fast gleiche Zusammensetzung haben,

Tabelle V. Aufstellung der Ergebnisse bei Fluoreszenz-Indikator-Adsorptionsanalyse von dem ungewaschnen Rückstand der Tabelle IV

| Franktionsnummern | Olefine % | Schwefelverbindungen % | Gemisch von Isovaleraldehyde und Isoamylalkohol, % |
|---|---|---|---|
| 1 | 7.8 | 2.8 | 89.4 |
| 2 | 3.7 | 2.9 | 93.4 |
| 3 | 3.9 | 4.7 | 91.4 |
| 4 | 5.7 | 0.3 | 94.0 |

wie die Tabelle V zeigt. Die Untersuchungsergebnisse bei der Fraktion Nr. 2 können ruhig für die übrigen Fraktionen als gültig betrachtet werden. Damit könnte eine jeweilige untersuchung erübrigt sein.

Ferner bei dem gewaschenen Rückstand ist zu finden, dass ausser Isovaleraldehyd und Isoamylalkohol etwa mit Waschen leicht unentfernbare, nämlich fest gebundene Schwefelverbindungen wenn auch in geringer Menge vorhanden sind. Diese Schwefelverbindungen stammen zwar aus thermischer Zerlegung des Katalysators, aber ihr Urwesen konnte zufolge mengenmässiger Geringfügigkeit nicht festgestellt werden.

Ferner ist annehmbar, dass noch weitere hochsiedende Polymere mitvorhanden sind.

Zusammenfassung der obigen Ausführungen lautet wie folgt: Wenn Isoamylalkohol in Gegenwart des Zinksulfates als Katalysator das Wasser entzogen wird, entsteht ausser in einem Gemisch befindlichen vieren Mengen Trimethyläthylen mit geringer Menge Methyläthyläthylen sowie Isopropyläthylen, Isovaleraldehyd strukturmässig unbekannte Polymere und Schwefelverbindungen.

Zum Schluss sei noch davon erwähnt, dass die vorliegende Arbeit der Leistung von Herrn Professor Dr. Eiichi Funakubo an der Technischen Fakultät der Universität zu Osaka verdankt ist.

*Chemisches Institut der Technischen Fakultät der Universität zu Osaka*
*Miyakojima-ku Osaka*

# *Forschung über die katalytische Entwässerung des Isoamylalkohols. IV. Quantitative Untersuchung der durch unterm Einsatz des Zinksulfat-Katalysators erfolgende Dehydratisierung gebildeten Produkte auf ihre Bestandteile*

Von Akira MITSUTOMI und Eiichi FUNAKUBO

(Eingegangen am 8. April, 1961)

Um die Zusammensetzung der aus Isoamylalkohol dargestellten Olefine zu bestimmen, wurden unterm Einsatz des Zinksulfat-Katalysators, gleich wie in der letzten Mitteilung[1], durch Fluoreszenz-Indikator Adsorotionsanalyse und Silicagel Adsorption die betreffenden gesättigten Kohlenwasserstoffe und Olefine getrennt.

Daraufhin wurde durch Infrarot-Absorptionsspektrum und Gaschromatographie an den Feindestillaten das Wesentliche ermittelt, dann quantitativ der Verbreitungszustand von den Olefinen untersucht, schliesslich die Zusammensetzung derselben klargemacht und gleichzeitig über den Bildungsmechanismus thermodynamische Betrachtung durchgeführt. Die vorliegende Mitteilung beschreibt den Verlauf der Versuchsdurchführung.

## Beschreibung der Versuche

*Operation.*—Die Vorrichtung ist in Abb. 1 gezeigt. Es wird Isoamylalkohol in 100 ccm Glaszylinder (4) mit Skalen eingefüllt. Daraus wird je eine gewisse Menge hiervon in Verdampfer (III) abgegeben und drin mit Mantelerhitzer verdampft. Der Alkoholdampf wird beim Aufsteigen in Wärmeaustauscher (II) durch aus Reaktionsrohr (I) austretendes Gas stets bei 155～165°C erhitzt und in Reaktionsrohr (I) geführt.

Die Temperatur in Reaktionsrohr konnte während der ca. 6 Tage gedauerten kontinuierlichen Reaktion stets bei 350±3°C gehalten bleiben.

Die in Wärmeaustauscher kondensierten hochsiedenden flüssigen Substanzen laufen in Vorlage (IV) zusammen, während die übrigen gasförmigen Substanzen von Wärmeaustauscher her in Vorlage (V). Vorlage (V) wird auf Wasserbad auf 80°C erwärmt, so dass unveränderter Isoamylalkohol und durch Reaktion gebildetes Wasser kondensiert werden, während Olefine und weitere niedrigsiedende flüssige Substanzen, indem sie durch über Erhitzer (6) einlaufendes heisses Wasser in Kühler (VI), von aussen her gewärmt werden, aufsteigen und anschliessend in Kühler stark abgekühlt und in Sammler (VIII) angesammelt werden.

Gase werden über Messer mengenmässig erfasst und in Sammler aufgefangen. Als die Gesamtmenge der Probe eingetan und die Reaktion zum Abschluss gebracht wurde, wurde Stickstoffgas aus Zylinder ins Reaktionssystem eingedrückt, wodurch Reaktionsprodukte alle in Vorlage gebracht wurden, indem jeglicher Verlust weitgehendst verhindert wurde.

Als Katalysator wurde das Gemisch aus 3 Teilen Zinksulfat $ZnSO_4 \cdot 7H_2O$ und 7 Teilen japanischer Säureerde herangezogen, welches mit zugesetztem 28%igen Ammoniakwasser angeteigt, zu Klumpen gemacht, bei 60°C 2 Std und dann bei 120°C 5 Std aufgetrocknet, anschliessend in Reaktionsrohr eingepackt und durch 1 stündige Erhitzung bei 500°C aktiviert wurde.

Als Probe wurde handelsübliche Ware Isoamylalkohol abdestilliert, deren Fraktion bei Sdp 127～130°C angesammelt wurde.

Bei vorliegendem Versuche wurde darauf Wert gelegt, die Reaktionstemperatur bei 350±5°C zu behalten. In der Wirklichkeit gelang es uns daher, während der für Reagieren der ganzen Probenmenge von 4800 ccm benötigten Dauer von 115 Std und 50 Min die Temperatur bei 350±3°C zu sichern.

Durchmesser eines Teilchens vom Katalysator……durchschnittlich 6 mm
Gesamtpackungsmenge des Katalysators……1.505 kg, 1.723.9 ccm
Durchlaufgeschwindigkeit der Proben……41.44 ccm/Std
Raumgeschwindigkeit……1.44 ccm/Min

## Versuchsergebnisse

Nach der von uns vorgeschlagenen Methode* wurde die Typenanalyse an rohen Olefinen vorgenommen, deren Ergebnissen in Tabelle I, II, aufgestellt. Daraufhin wurde durch das Silicagel-Adsorptionsverfahren gesättigter Kohlenwasserstoff getrennt und die Gewinnung der reinen Olefinen vorgenommen. Zu diesem Zweck wurden 200 gm Silicagel** in das Adsorptions-Trennungsrohr eingepackt, darauf 80 ccm rohe Olefine zugegeben. Der Ansatz wurde unter

1) A. Mitsutomi, Dieses Bulletin, 34, 1681 (1961).

* Hierbei handelt es sich um ein für Leichtöl-Produkte von Steinkohlenteer anwendbares, durch Modifizierung der FIA-Methode von neuem ausgearbeitetes Verfahren, welches noch später bekanntgegeben wird.

** Tokai Gel F. I. Das Von der Fa. Tokai Kagaku Kogyo K. K. hergestellte, mit dem Olefin-Polymerisation verhindernden Vermögen versehne, für die Chromatographie einsetzbare Silica-gel.

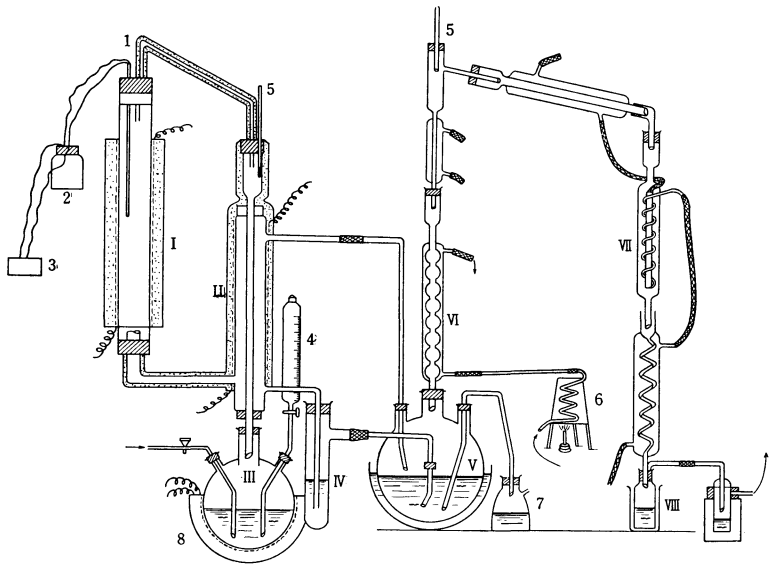



Abb. 1

I……Reaktionsrohr, Aussendurchmesser 70 mm
Innendurchmesser 60 mm
Länge 800 mm
Elektrisch zu erhitzender Reaktionsrohrteil: Länge 610 mm, Aussendurchmesser 120 mm
II……Wärmeaustauscher, Innendurchmesser 12 mm, Ausserdurchmesser 43 mm, Länge 430 mm
III……Verdampfer, Kapazität 300 ccm
IV……Vorlage, Durchmesser, 30 mm, Länge 210 mm
V……Trennungsvorlage für unveränderten Alkohol und für Wasser, Kapazität 300 ccm
VI, VII…Kühler
VIII……Vorlage für rohe Olefine.
(1)……Thermoelement
(2)……
(3)……Pyrometer
(4)……Messzylinder von 100 ccm Kapazität mit Skalen.
(5)……Thermometer
(6)……Heizkörper für zirkulierendes Wasser
(7)……Vorrichtung für Entnahme des unveränderten Alkohols und Wassers.
(8)……Falltür.

Tabelle I. Aufstellung der Reaktionsprodukte beim Ansatz von 4800 ccm Alkohol

| | Ausbeute ccm | Prozentuale Ausbeute, % | | $n_{20}^{D}$ |
|---|---|---|---|---|
| | | bezogen auf Probenmenge | bezogen auf aktuell reagierte Probenmenge | |
| Rohe Olefine | 2988 | 62.25 | 75.55 | 1.3849 |
| Wasser | 575 | 11.98 | 14.53 | |
| hochsiedende Produkte | 30 | 0.63 | 0.76 | |
| Wasermenge, kondensierts in Wärmeaustauscher | 10 | 0.21 | 0.25 | |
| gebildete Gasmenge | 319.6 l. | | 14.3 Mol. | |
| unveränderter Alkohol | 845 | 17.6 | | |

Tabelle II. Analytische Ergebnisse roher Olefine

| Versuchsnummer | 1 | 2 | Mittelwert |
|---|---|---|---|
| gesättigter Kohlenwasserstoff, % | 2.33 | 2.38 | 2.35 |
| Olefine, % | 97.67 | 97.62 | 97.65 |

TABELLE III. ERGEBNISSE DER ADSORPTIONSBEHANDLUNG FÜR ROHE OLEFINE

| Male der Versuche | 1 | 2 | 3 | 4 | 5 | 6 | 7 | 8 | 9 | 10 | 11 | 12 | 13 |
|---|---|---|---|---|---|---|---|---|---|---|---|---|---|
| SO-(I), ccm | 11.5 | 10 | 10 | 11 | 9.5 | 10 | 10.5 | 10.4 | 10.5 | 11 | 10 | 10 | 11 |
| rein Olefin-(I), ccm | 63.5 | 64.5 | 65.5 | 64 | 65.5 | 63 | 66.5 | 66.8 | 63.5 | 61.5 | 64 | 64.5 | 63.3 |
| OA-(I), ccm | 5.5 | 5 | 7.5 | 6.5 | 5.5 | 6 | 5.3 | 5 | 7 | 6 | 6 | 5.5 | 5.2 |

SO: Gemisch des gesättigten Kohlenwasserstoffs mit Olefin.
OA: Gemisch des Olefins mit Äthanol.

TABELLE IV. ERGEBNISSE DER ADSORPTIONS-REINIGUNG DES GEMISCHES AUS GESÄTTIGTEN KOHLENWASSERSTOFFEN UND OLEFINE SO-(I)

| Male der Versuche | | 1 | 2 | 3 | 4 | 5 |
|---|---|---|---|---|---|---|
| getrennte stoffe | SO-(II), ccm | 19.5 | 20 | 20 | 20 | 20 |
| | rein Olefine (II), ccm | 37.5 | 36 | 36.5 | 36.5 | 36 |
| | OA-(II), ccm | 3.5 | 4 | 3.5 | 3.5 | 4 |

TABELLE V. GASCHROMATOGRAPHIE DER OLEFINEN

| Probenzeichen | Bestandteile, % | | | | |
|---|---|---|---|---|---|
| | A | B | C | E | F |
| O-(I) | 3.3 | 8.1 | 14.7 | 74.2 | Spur |
| O-(II) | 0.8 | 11.2 | 18.4 | 69.6 | |
| O-(III) | 0.7 | 14.9 | 23.0 | 61.1 | |
| O-(IV) | 0.8 | 22.9 | 22.9 | 53.3 | |

TABELLE VI. ERSTE PRÜFUNGSERGEBNISSE VON OLEFINE O-I

| | Destillate | | | Prozentuales Verhältnis der Bestandteile | | | | |
|---|---|---|---|---|---|---|---|---|
| Nummer | Temperatur, °C | Menge, ccm | $n_D^{20}$ | A, % | B, % | C, % | E, % | F, % |
| 1 | 18 ~19.5 | 6 | 1.3672 (t=15) | 0.5 | 98.4 | 1.1 | — | — |
| 2 | 19.5~20 | 11.5 | | — | 92.7 | 7.3 | — | — |
| 3 | 20 ~28 | 24 | 1.3722 | 1.5 | 44.6 | 53.9 | — | — |
| 4 | 28 ~29 | 11.5 | | 2.3 | 11.5 | 86.2 | — | — |
| 5 | 29 ~30 | 21 | 1.3779 | 0.9 | 1.9 | 96.2 | — | 0.9 |
| 6 | 30 ~31 | 57 | | 0.5 | 0.5 | 84 | 13.5 | 1.5 |
| 7 | 31 ~35 | 60 | | — | — | 35.3 | 63.9 | 0.8 |
| 8 | 35 ~36.2 | 21.5 | | — | — | 16.3 | 82.9 | 0.8 |
| 9 | 36.2 | 20 | 1.3865 | — | — | 9.4 | 90.3 | 0.3 |
| 10 | 36.2~36.8 | 73.5 | 1.3870 | — | — | 3.2 | 96.8 | — |
| 11 | 36.8 | 36 | 1.3872 | — | — | 2.4 | 97.6 | — |
| 12a | 36.8 | 38 | 1.3873 | — | — | 1.6 | 98.4 | — |
| 12b | 36.8~36.9 | 31.5 | 1.3873 | — | — | 0.8 | 99.2 | — |
| 13 | 36.9 | 101 | 1.3875 | — | — | — | 100 | — |
| 14 | 36.9~37 | 40.5 | 〃 | — | — | — | 100 | — |
| 15 | 37 | 50 | 〃 | — | — | — | 100 | — |
| 16 | 37 ~37.1 | 10 | 〃 | — | — | — | 100 | — |
| | Rückstand | 14 | | | | | | |
| | Summe | 627, 78.4% | | | | | | |

Anwendung des Äthanols der Austauschentwicklung unterzogen. Tabelle III zeigt die Reinigungsergebnisse.

Dann wurde 60 ccm von dem auf diese Weise erhaltenen SO-(I) weiter abpipettiert und in das mit 200 g Silica-gel eingepackte Rohr eingegossen. Mit Äthanol wurde die Austauschentwicklung ausgeführt. Die erhaltenen Ergebnisse sind in Tabelle IV aufgestellt. Dieses Reinigungs verfahren wurde weiter wiederholt und die Ergebnisse sind in Abb. aufgestellt. Da die Olefine hinsichtlich ihrer Brechungsindizien zusammensetzungsmässige Ähnlichkeit zu zeigen schienen, wurde sie gaschromatographisch auf ihre Zusammensetzung untersucht (Tabelle V).

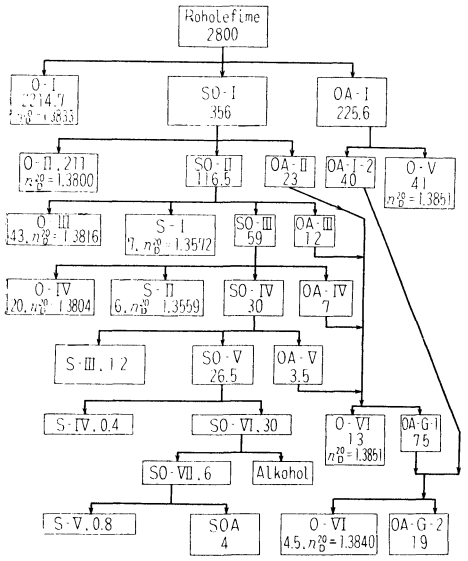


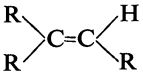

Abb. 2.*

* Nummer in ccm, S: gesättigte Kohlenwasserstoffe, O: Olefine.
Gesamtsumme S: 15.4 ccm, O: 2547.2 ccm.

Wie aus Tabelle V ersichtlich, hat die Probe O-(I) im Vergleich mit drei weiteren Proben anderes Mischverhältnis der Bestandteile aufgezeigt. Dementsprechend wurde darauf eingestellt, dass Olefin O-(I) alleine, O-(II), O-(III) und O-(IV) gemeinsam, auch O-(V), O-(VI), und O-(VIII) gemeinsam, gruppenweise gesondert destilliert werden. Um aber noch festzustellen, wurden die durch vorherige Destillation erhaltenen Fraktionen gaschromatographisch analysiert und der Verbreitungszustand der Bestandteile untersucht. Die Ergebnisse sind in Tabelle VI verzeichnet. Es wurde dabei erkannt, dass die drei Bestandteile B, C und E vorwiegend vorhanden sind, wobei die Beziehung der Siedepunkte auf Gehaltsmenge klar vortritt.

Von diesen Fraktionen sind diejenigen mit Sdp 36.9~37.1°C 100%ig reine E-Bestandteile, deren Brechnungsindies mit den Literaturangabe, von Trimethyläthylen $n_D^{20}=1.3874$, 1.3876 identisch ist.

Wegen weiterer Feststellung dieser Annahme wurde das Infrarot-Absorptionsspectrum gemessen. Dabei liess es sich finden, dass, wie Abb. 3 zeigt, das ganze Bild mit Standardsbild des 2-Methyl-2-buten übereinstimmt und die spezifische Absorptionswellenlänge 12.53 $\mu$ für




Type intensiv auftritt. Dadurch

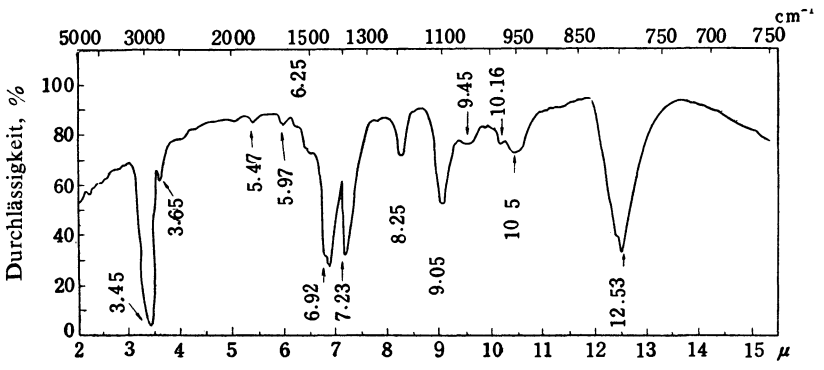



Abb. 2. Infrarot-Absorptionsspektrum von Fraktion Nr. 14.

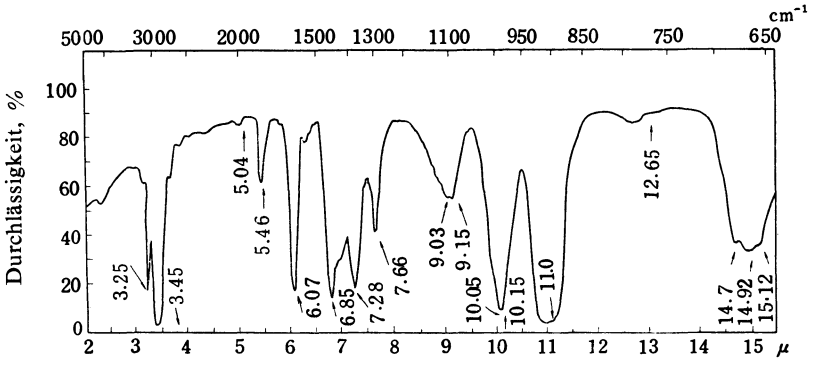



Abb. 3. Infrarot-Absorptionsspektrum von B-Bestandteil.

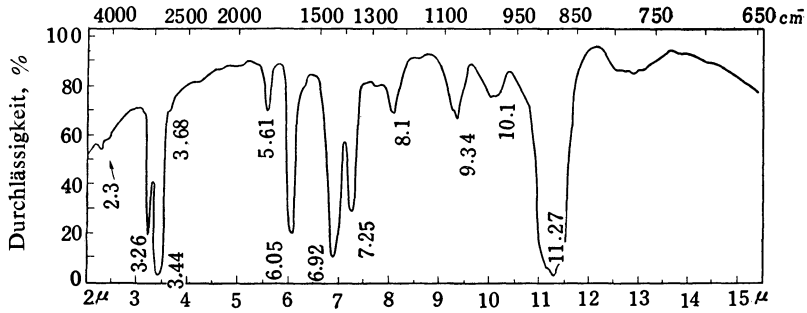



Abb. 4. Infrarot-Absorptionsspektrum von C-Bestandteil.

ist entschieden worden, dass der Bestandteil E Trimethyläthylen darstellt.

Die erste Fraktion, Sdp 18~19.5°C, zeigte das Brechungsindies, welches mit der Literaturangabe von 3-methyl-1-buten $n_D^{15}=1.3677$ übereinstimmt. Ausserdem zeigten die Messungen des Infrarot-Absorptionsspektrums (Abb. 4) einwandfreie Übereinstimmung mit dem Standardsbild für 3-Methyl-1-buten. Als spezifische Absorptionswellenlänge von $\begin{matrix}R\\H\end{matrix}\!\!>\!C$ $=CH_2$ sind die Werte von $10.05\pm0.02\,\mu$, und $10.98\pm0.02\,\mu$ nach K. E. Kitson und $10.98\pm0.02\,\mu$ nach J. A. Anderson order $10.95\pm0.02\,\mu$ nach E. L. Sailer angegeben und diese alle sind auch in unserem Bild als intensive Absorptionen aufgetreten. Demnach haben wir entschieden, dass der Bestandteil B 3-Methyl-1-buten ist. Im Infrarot-Absorptionsspektrum (Abb. 4) der Fraktion Nr. 5 tritt die spezifische Absorption, $11.27\,\mu$, fur $\begin{matrix}R\\R\end{matrix}\!\!>\!C=CH_2$ intensiv auf. Ausserdem stimmt das genze Spektraldiagramm mit dem Standardsdiagramm von Methyläthyläthylen einwandfrei überein. Aus dieser Tatsache und dem Messwerte von Brechungsindies ist entscheiden, dass der C-Bestandteil Methyläthyläthylen darstellt.

Die in Tabelle VI aufgezeichneten gaschromatohraphischen Analysenergebnisse zugrunde nehmend, wurde mengenmässige Verteilung der einzelnen Bestandteile in den einzelnen Fraktionen rechnerisch festgestellt. Kurz gefasst, gaschromatographische und infrarotabsorptionsspektrale Analyse an den durch Feindestillation fraktionierten Destillaten hat ergeben, dass die durch Silicagel-Adsorption gereinigten Olefine folgende Zusammensetzung besitzen: Trimethyläthylen 74.77, Methyläthyläthylen 19.96, Isopropyläthylen 4.78, und Olefine von unbekennter Konstitution 0.49%.

Dann wurden die Olefine O-(II), O-(III) und O-(IV), deren Brechungsindizien einander nähern, zusammengebracht und der Feindestillation unterzogen. Gaschromatographische Analyse an den Fraktionen ergaben die Resultaten in Tabelle VII.

Die Zusammensetzung von rein Olefin in dem Gemisch aus O-(II), O-(III) und O-(IV), war wie folgt: Trimethyläthylen 65.98, Methyläthyläthylen 21.95, Isopropyläthylen 11.63, und Unbekannte Olefin 0.44%.

Die Zusammensetzung von reinem Olefin in dem, Gemisch aus O-(V), O-(VI)und O-(VII), war von Tabelle VIII errechnet wie folgt: Trimethyläthylen 66.35, Methyläthyläthylen 30.17, Isopropyläthylen 0.43, und unbekannte Olefin 3.05%.

TABELLE VII. ERGEBNISSE DER FEINDESTILLATION AN REINEN OLEFINEN

| Fraktion | | | | Ergebnisse der gaschromatographische Analyse | | | |
|---|---|---|---|---|---|---|---|
| Nummer | Temperatur, °C | Menge, ccm | $n_D^{20}$ | A, % | B, % | C, % | E, % |
| 1 | 19.9~20 | 6 | 1.3644 | — | 100 | — | — |
| 2 | 20 | 6 | 1.3645 | — | 100 | — | — |
| 3 | 20.1~29.5 | 14 | 1.3680 | 4.5 | 53.6 | 42 | — |
| 4 | 29.5~30 | 9 | 1.3759 | 1.2 | 1.8 | 97.1 | — |
| 5 | 30 ~30.1 | 9 | 1.3778 | 0.2 | spur | 99.8 | — |
| 6 | 30.1~35.2 | 17 | 1.3808 | — | — | 50 | 50 |
| 7 | 35.2~36.6 | 20 | 1.3848 | — | — | 11.1 | 88.9 |
| 8 | 36.6~36.9 | 22 | 1.3857 | — | — | 7.6 | 92.4 |
| 9 | 36.9~37 | 35 | 1.3803 | — | — | 3.3 | 96.7 |
| 10 | 37 | 37 | 1.3872 | — | — | — | 100 |
| | Rückstand | 14 | 1.3921 | | | | |

Tabelle VIII. Ergebnisse der Feindestillation an reinen Olefine-Gemisch von O-(V), O-(VI) und O-(VII)

| Fraktion | | | | Ergebnisse von Gaschromatographie, % | | | | |
|---|---|---|---|---|---|---|---|---|
| Nummer | Temperatur, °C | Menge, ccm | $n_D^{20}$ | A | B | C | E | F |
| 1 | 26.9～30.2 | 4 | 1.3807 | spur | 1.9 | 94.9 | — | 3.2 |
| 2 | 30.2～35.5 | 4 | 1.3872 | — | spur | 33.3 | 59.1 | 7.4 |
| 3 | 35.5～36.3 | 3 | 1.3882 | — | — | spur | 97.1 | 2.9 |
| 4 | 36.3～36.6 | 4 | 1.3886 | — | — | — | 100 | — |
| 5 | 36.6 | 2 | 1.3889 | — | — | — | 100 | — |
| | Rückstand, ccm | 8 | 1.3919 | | | | | |

Tabelle IX. Ergebnisse der Destillation vom durch Reaktion gebildeten Wasser

| Fraktionen | | | Spezifikation | | |
|---|---|---|---|---|---|
| Einteilung | Temperatur °C | Menge ccm | obere Schicht (organische Phase) ccm | unter Schicht (Wasser-Phase) ccm | Anmerkung |
| 1 | 67～68 | 3.9 | 3.7 | 0.2 | Destillation unter normalem Druck. |
| 2 | 80～94 | 64.1 | 6.1 | 58 | unter gering vermindertem Druck destilliert. |
| 3 | 94～95 | 370 | 370 | — | gleichmässige Flüssigkeit. |
| 4 | 95～96 | 98 | 98 | — | |
| 5 | 97～99 | 11 | 11 | — | |
| 6 | Rückstand | 1 | 1 | — | |
| | Summe | 548 | 489.8 | 58.2 | |

**Untersuchung auf das durch Reaktion gebildete Wasser.**—Von dem durch Reaktion gebildeten Wasser wurden 550 ccm genommen und destilliert. Verlauf der Destillation und Eigenschaften der Fraktionen sind in Tabelle IX aufgestellt.

Die Fraktionen von Nr. 3 bis 5 waren homogene Flüssigkeiten, enthielten kein Wasser, verhielten den Schiff'schen Reagenz äusserst indifferent.

Bei den Fraktionen Nr. 1 und 2, die der Schiff'schen Reagenz intensiv positiv waren, wurde ihre organische Phase mit *p*-Nitrophenylhydrazin einwirken gelassen.

Von 0.2 ccm der Fraktion Nr. 1 wurden 275 mg *p*-Nitrophenylhydrazon Schmp 101.5～104°C, und von 0.5 ccm der Fraktion Nr. 2 619 mg derselben, aber Schmp 103～108°C, erhalten. Nach Umkristallisation wandelte sich das Vordere in Schmp 105.5～110°C, und das Letztere in Schmp 105～108°C um. Die Beiden wurden durch die Mischschmelzpunktsbestimmung als Isovaleraldehyd mit Sicherheit festgestellt.

**Thermodynamische Betrachtung über Isomerisationsgleichgewicht und Zusammenfassung.** — Mit der Absicht, aus Isoamylalkohol die vorwiegend aus Trimethyläthylen bestehenden Olefinen kontinuierlich zu fabrizieren, wurde das Gas-Phase Verfahren erforscht.

Zuerst wurden Katalysatoren aus 15 Sorten Substanzen ausgearbeitet, indem diese entweder als Einzelkörper oder als Kombination eingesetzt wurden. In 122 Versuchen wurde auf das katalysatorische Vermögen gründlich untersucht. Dabei haben wir den geeignetesten Katalysator in der Zinksulfat-japanischer Säureerde-Kombination gefunden. Dieser besteht aus 3 Teilen Zinksulfats und 7 Teilen japanischer Säureerde. Dieser Ansatz wird unter Zusatz von Ammoniak angeteigt, zu Kugeln verarbeitet, und aktiviert. Das auf diese Weise behandelte Material entwickelt ausgezeichnetes katalysatorisches Vermögen und zeigt auch nach 246 Std langem kontinuierlichem Einsatz und Behandlung des 52 betragenden Alkohol-Durchsatzes fast kein Nachlassen an der Wirkung.

Unter Anwendung der Reaktionsröhre von mittelgrossem und grossem Format wurden 290 Male Versuche angestellt, um die optimalne Reaktionsbedingungen zu finden. Die durch

Tabelle X. Vergleich der mehreren Versuchsergebnisse von hohen Ausbeuten

| Reaktionstemperatur °C | Ausbeute in % der einzelnen Fraktionen | | | |
|---|---|---|---|---|
| | ～30°C | 30～35°C | 35～41°C | Summe |
| 330～360 | 4.6 | 17.7 | 67 | 89.3 |
| 330～350 | 4.0 | 16.2 | 67 | 87.2 |
| 285～345 | 0.7 | 22.6 | 67.8 | 91.1 |
| 350～370 | 2.1 | 18.9 | 70 | 91.0 |
| 360～390 | 3.7 | 18.3 | 72.5 | 94.5 |
| 300～315 | 0 | 17.3 | 75.2 | 92.5 |

Reaktion erhaltenen rohen Olefine wurden einfach hinsichtlich der Siedepunkte in drei Gruppen eingeteilt, deren Ausbeute festgestellt wurde. Mehrere Sorten mit hohen Ausbeuten wurden beispielsweise in Tabelle X aufgestellt.

Daraus ist die Beurteilung entstanden, dass bei Fabrikation des Trimethyläthylens aus Isoamylalkohol die Ausführung der Reaktion bei 350°C und dergleichen die opimalen Ergebnisse ergibt. Darauf wurde die Reaktion von 4800 ccm Isoamylalkohol bei 350±3°C vorgenommen. Die dabei erhaltenen Reaktionsprodukte wurden durch solche verschiedene Methoden wie Fluoreszenz-Indikator Adsorptionsanalyse, Feindestillation, Infrarot-Absorptionsspektrum, Gaschromatographie usw., auf ihre Bestandteile geprüft, und zwar mit folgenden Ergebnissen: Trimethyläthylen, 74.77～75.14, Methyläthyläthylen, 19.96～20.06, und Isopropyläthylen, 4.78～4.80%.

Für diese dreien Olefine sind schon von Kistiaskowsky[2] zuverlässige thermodynamische Ergebnisse vorgebracht worden. Wir haben anhand dieser Ergebnisse nach folgender Formel theoretische Werte des Isomerisationsgleichgewichtes für die vorliegende Reaktion zu bildende Olefine gesucht.

$$\Delta F = -RT \ln K$$

worin $\Delta F$: Innere Energie, $R$: Gaskonstante, $K$: Gleichgewichtskonstante, $T$: Absolute Temperatur.

Für $\Delta F$ haben wir die folgende von Kistiaskowsky gefundene Hydrierungswärme herangezogen.

| | $-\Delta F$ (Cal./Mol.) | $K$ bei 350°C |
|---|---|---|
| Trimethyläthylen-Methyläthyläthylen | 1571 | 3.56 |
| Trimethyläthylen-Isopropyläthylen | 3416 | 15.8 |
| Methyläthyläthylen-Isopropyläthylen | 1845 | 4.44 |

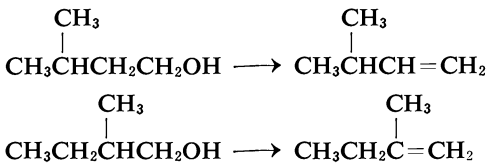
Aus diesen Ergebnissen wird das theoretische prozentuale Verhältnis der Bildung für die Dreien wie folgt abgeleitet:

| | Theoretische Werte (bei 350°C), % | Experimentelle Werte (bei 350°C), % |
|---|---|---|
| Trimethyläthylen | 74.45 | 75.14 |
| Methyläthyläthylen | 20.91 | 20.06 |
| Isopropyläthylen | 4.64 | 4.80 |

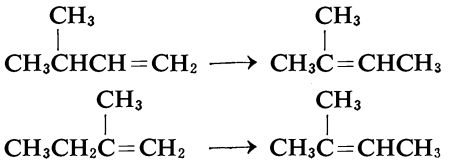
Es ist sehr interessant, dass die genannten theoretischen Werte mit den von uns experimentell erhaltenen Ergebnissen ganz einwandfrei übereinstimmen. Diese Tatsache dürfte eine interessante Hinweisung auf den Mechanismus dieser Reaktion und die Eigenschaften des Katalysators, geben.

Das Bildungsverhältnis von den durch diese Arbeit erhaltenen Olefinen ist nämlich mit dem thermodynamisch zu findenden Verhältnis identisch. Mit anderen Worten, das stimmt mit dem thermodynamisch zu findenden stabilen Gleichgewichtszustand der Isomerisation überein. Die herrschende Annahme ist es, dass der Hauptbestandteil des zu entwässernden Isoamylalkohols Isobutylcarbinol sei, während die Gehalte an *gem*-Methyläthyläthylalkohol geringfügig seien.

Wenn die Entwässerung ohne Isomerisationsreaktion erfolgt, würde aus Isobutylcarbinol Isopropyläthylen und aus *gem*-Methyläthyläthylalkohol Methyläthyläthylen gebildet.



Da nun Isopropyläthylen und Methyläthyläthylen ebenfalls die Isomerisation in Trimethyläthylen mit sich bringen, entstehen die folgenden Formeln.



Nun wird die Orientierung dieser Isomerisation im allgemeinen thermodynamisch bedingt. Mit anderen Worten, dies besagt, dass das Unstabile ins Stabile isomerisiert wird. Die Reihenfolge der Stabilität ist nach Kistiakowsky wie folgendes: Trimethyläthylen > Methyläthyläthylen > Isopropyläthylen. Wenn diese Stabilität elektronentheoretisch betrachtet wird, so ist sie abhängig von dem Hyperkonjugationseffekt, wie Ingold[3] bereits erwähnt. Somit ist die Annahme der Isomerisation von Isopropyläthylen in Trimethyläthylen und von Isopropyläthylen in Methyläthyläthylen begründet.

Wenn jetzt ein anderer Gesichtspunkt genommen wird, nämlich über das Isomerisationsvermögen des Katalysators Betrachtung geübt wird, so ist es zu sagen, dass derjenige Katalysator, der Theorie übereinstimmende Isomerisationsverhältnis aufzeigt, der Ausgezeichnete ist. Die Tatsache, dass das Isomerisationsverhältnis mit dem theoretischen

2) G. B. Kistiaskowsky et al., *J. Am. Chem. Soc.* **57**, 65, 876 (1935); **58**, 137, 146 (1936); **59**, 831 (1937).

3) M. L. Dhar, E. D. Hughes, C. K. Ingold, A. M. M. Mandour, G. A. Mow and L. I. Woolf, *J. Chem. Soc.*, **1948**, 2093.

Zahlenwert identisch ist, wie es bei der vorliegenden Arbeit der Fall ist, liefert den Beweis dafür, dass das dabei eigesetze Zinksulfat ausgezeichnetes katalysatorisches Vermögen bei Entwässerungsisomerisation ausübt.

Aus den obigen Betrachtungen ist es anzunehmen, dass bei der vorliegenden Entwässerungsisomerisation das thermodynamische Isomerisationsgleichgewicht erreicht worden ist, indem unabhängig von Verunreinigungen des zu entwässernden Alkohols die gebildeten Olefine isomerisiert werden (obgleich es unklar ist, ob die Isomerisierung gleichzeitig mit der Entwässerung oder erst nach der erfolgten Bildung der Olefine geschieht).

*Chemisches Institut der Technischen Fakultät der Universität zu Osaka*
*Miyakojima-ku, Osaka*

# *Hot-atom Chemistry of Hexamminechromium(III) Nitrate in the Solid State*

By Nagao IKEDA, Kenji YOSHIHARA, Hiroshi EBIHARA and Kiyomi SUZUKI

(Received November 21, 1960)

The hot-atom effect in trisethylenediaminechromium(III) nitrate[1,2] and hexamminecobalt-(III) nitrate[3] has been studied, but the same effect in hexamminechromium(III) nitrate has not yet been reported. Recently, the present authors succeeded in enriching $^{60}Co$ and $^{60m}Co$ recoil atoms produced in neutron-irradiated hexamminecobalt(III) nitrate with a high efficiency[4]. The method used by the authors was based on the heterogeneous extraction; the neutron-irradiated fine powders were shaken with a liquid which did not dissolve the target but dissolved the recoil species. As this method is very simple and rapid, it has sometimes been used for the enrichment of radioisotopes produced by (n, p)- and (n, $\alpha$)-reactions[5,6]. In the case of (n, $\gamma$)-reaction[7], however, it does not usually give a high yield because of the short recoil range. Therefore the results in the previous paper were rather striking. In this paper, we investigated a similar heterogeneous extraction method on hexamminechromium(III) nitrate and discussed the mechanism of the extraction process. This complex is insoluble in concentrated nitric acid, but chromic ion and chromate or dichromate ion are soluble in it. Therefore, recoil atoms of $^{51}Cr$ should be extracted and enriched in the aqueous phase by shaking the target powder with concentrated nitric acid.

On the chemical form of the recoil chromium, some results heve already been reported; e.g., in the case of chromium azo-dye Palatine Fast Blue GGN[8], 83% of the radioactive chromium is present as chromium(III) and 11% of it as chromium(VI)*. In the present paper, chemical forms of recoil chromium atoms were also investigated.

## Experimental

**Target Material.** — Hexamminechromium(III) nitrate was prepared by Mori's method[9].

**Irradiation.**—The cyclotron at the Institute of Physical and Chemical Research, Tokyo, and the nuclear reactor JRR-1 at the Japan Atomic Energy Research Institute were used for irradiation. The hot-atom effect of $^{55}Cr$ (half-life: 3.5 min.) was investigated by using the cyclotron, and that of $^{51}Cr$ (half-life: 27.8 day) by using the nuclear reactor. In the cyclotron, neutrons were generated by bombardment of beryllium with accelerated deuterons, and slowed down by a paraffin block. The neutron flux at the position of irradiation was about $10^6 \sim 10^7$ n/cm$^2$ sec.* The reactor, JRR-1 was operated at 50 kW/hr., and the neution flux

1) A. Turco and M. Scatena, *Ric. Sci.*, **25**, 2651 (1955).
2) A. Turco, *J. Inorg. Nucl. Chem.*, **13**, 200 (1960).
3) G. Kayas, *Bull. soc. chim. France*, **17**, 1145 (1950).
4) N. Ikeda, K. Yoshihara and N. Mishio, *Radioisotopes*, **8**, 242 (1959).
5) E. Bleurer and W. Zünti, *Helv. Phys. Acta*, **20**, 195 (1947).
6) P. Jordan, *Helv. Chim. Acta*, **34**, 699, 715 (1951).
7) P. Süe and T. Yuasa, *J. chim. phys.*, **41**, 160 (1944).
8) N. Shibata and K. Yoshihara, This Bulletin, **32**, 422 (1959); K. Yoshihara, M. Arai and T. Ishimori, *Proceedings of the 3rd Isotope Conference of Japan*, S18 (1959).
* In this paper, Cr(III) represents chromic ion, and Cr(VI) represent chromate or dichromate ion.
9) M. Mori, *J. Chem. Soc. Japan, Pure Chem. Sec.* (*Nippon Kagaku Zasshi*), **74**, 253 (1953).
* Contribution of fast neutrons to the radioactivation did not exceed about 5%.

was of the order of $10^{11}$ n/cm² sec. at the irradiation**. Temperature at the position did not exceed about 50°C.

**Measurement of Radioactivity.**—As $^{55}$Cr emitted only $\beta$-particles (2.85 MeV.), the radioactivity was measured by a GM-counter made by the Institute of Physical and Chemical Research, (end window type, mica window thickness: 1.4 mg./cm²). Radioactivity of $^{51}$Cr was measured by a single channel $\gamma$-ray spectrometer made by the Atomic Instrument Co., Model 810A, (well type, NaI crystal, $1^3/_4'' \phi \times 2''$). $\gamma$-Ray of 0.32 MeV. of $^{51}$Cr was measured at the photo-peak by this counter.

**Measurement of Solubility of Hexamminechromium(III) Nitrate in Nitric Acid.**—The solubility of hexamminechromium(III) nitrate in nitric acid was determined in advance. Each 0.2 g. of the sample was shaken with 25 ml. of nitric acid of various concentrations for two or four minutes at 20°C. Results are listed in Table I. The solubility was about 1 mg./25 ml. for the acidity of 8~12 N at 20°C, but it was slightly greater for 6 N. Therefore the acidity of 8~12 N is preferable for this extraction process.

TABLE I. SOLUBILITY OF HEXAMMINECHROMIUM-(III) NITRATE IN NITRIC ACID (20°C)

| Concentration of $HNO_3$, N | Shaking time min. | Solubility, mg. $[Cr(NH_3)_6](NO_3)_3$/ 25 ml. |
|---|---|---|
| 6 | 2 | 3.1 |
| 6 | 4 | 3.4 |
| 8 | 2 | 1.2 |
| 8 | 4 | 1.1 |
| 10 | 2 | 1.0 |
| 10 | 4 | 0.91 |
| 12 | 2 | 0.89 |
| 12 | 4 | 0.89 |

**Determination of Chromium.**—Amounts of extracted chromium in the liquid phase were determined colorimetrically. After the liquid phase was centrifuged, the complex salt in it was destroyed by boiling with concentrated nitric acid repeatedly, and tervalent chromium was oxidized to the sexivalent state with silver peroxide and the amounts of sexivalent chromium were determined by the diphenylcarbazide method[10]. The enrichment factors, $E$ were calculated by the following formula:

$$E = \frac{a}{a_t} = \frac{M}{m} Y$$

where $a$ and $a_t$ denote specific activities in the liquid phase and in the irradiated complex salt before the process, respectively. $M$ and $m$ denote the amounts of chromium in the original salt and in the liquid phase, respectively. $Y$ is the yield of $^{51}$Cr in the liquid phase.

**Extraction of Enriched $^{55}$Cr.**—About 1 g. of hexamminechromium(III) nitrate was bombarded with neutrons produced by the cyclotron for about an hour or two. After irradiation, the target was divided into two portions. One was subjected to the measurement of radioactivity by a GM-counter tracing its decay (Sample I), and the other to the extraction of $^{55}$Cr with 20~50 ml. of 8 N nitric acid in an Erlenmeyer flask by being shaken vigorously for 2 min. After the extraction and centrifugal separation, the solid was washed with ethanol and dried in air. Its radioactivity was measured by a GM-counter tracing its decay (Sample II). Samples I and II were weighed, and the retention was calculated from the ratio of the specific activities of the two samples at the same time. The extraction yield was given by subtracting the retention value from 100%. The results are listed in Table II. The extraction yield higher than 60% was obtained and the enrichment factor of 200~400 was obtained. The enrichment of $^{55}$Cr has been attained by these simple and rapid procedures.

**Preparation of Enriched $^{51}$Cr.**—Enrichment of $^{51}$Cr was studied in the same way as in the case of $^{55}$Cr. About 1 g. of the sample was irradiated in the pneumatic tube in the nuclear reactor for 2 hr. After irradiation, the sample was shaken with 50 ml. of 8 N nitric acid in an Erlenmeyer flask for 2 min. After being centrifuged from the solid, an aliquot of the liquid phase was subjected to the measurement of radioactivity by a $\gamma$-ray spectrometer. The solid was dissolved in water, and the radioactivity of an aliquot of the solution was measured by a $\gamma$-ray spectrometer. The yield of $^{51}$Cr was calculated from these values. The results are shown in Table III. A yield of 57~73% was obtained. The enrichment factor was 24~41 which was much lower than the values of $^{55}$Cr.

**Extraction Curves on Repeated Extraction.**—In order to investigate the extraction mechanism, extraction curves on repeated extractions were observed. An outline of the procedures for the repeated extractions is illustrated in Fig. 1. About 0.2 g. of the sample was irradiated in the pneumatic tube in JRR-1, and treated according to the

TABLE II. PREPARATION OF ENRICHED CHROMIUM-55

| Amount of target, g. | Irradiation time, hr. | Integrated deuteron current, $\mu$A·hr. | Volume of 8 N $HNO_3$ ml. | Radiochemical yield % | Enrichment factor |
|---|---|---|---|---|---|
| 1.292 | 2 | 20 | 50 | 86 | 230 |
| 0.972 | 2 | 20 | 25 | 66 | 240 |
| 1.270 | 1 | 14 | 20 | 61 | 400 |

** Contribution of fact neutrons to the radioactivation did not exceed about 5%.

10) M. Tanaka, This Bulletin, 23, 165 (1950); E. B. Sandell, "Colorimetric Determination of Traces of Metals", 2nd Ed., Interscience Pub. (1950), p. 260.

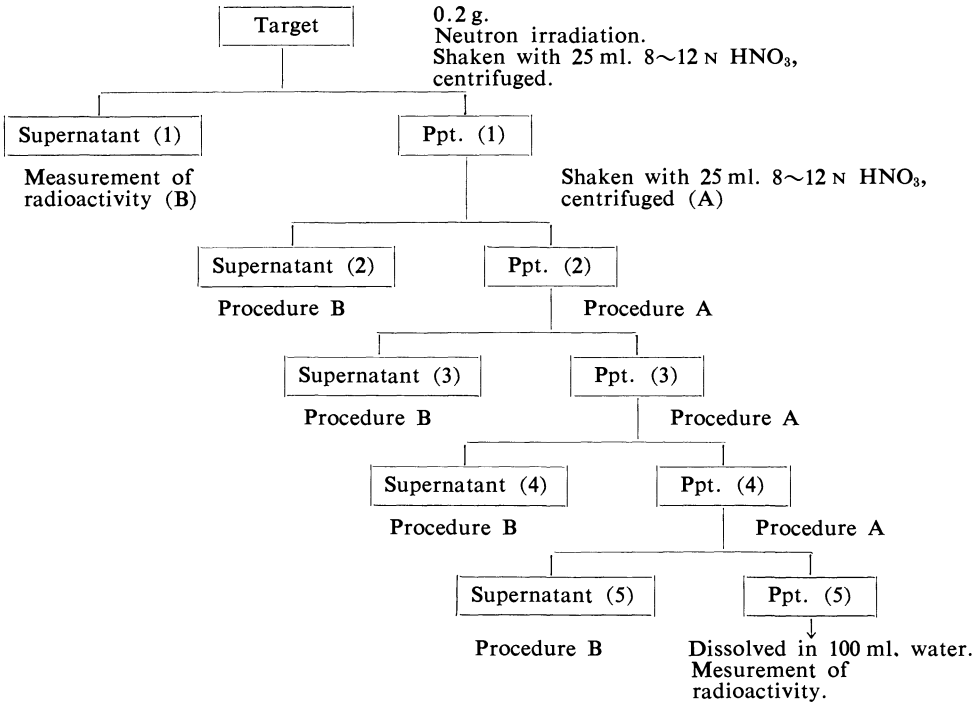



Fig. 1. Procedures in repetition of the extraction.

TABLE III. PREPARATION OF ENRICHED CHROMIUM-51

| Amount of target, g | Vol. of 8N $HNO_3$ ml. | Radiochemical yield % | Enrichment factor |
|---|---|---|---|
| 1.0 | 50 | 57 | 24 |
| 1.0 | 50 | 73 | 41 |

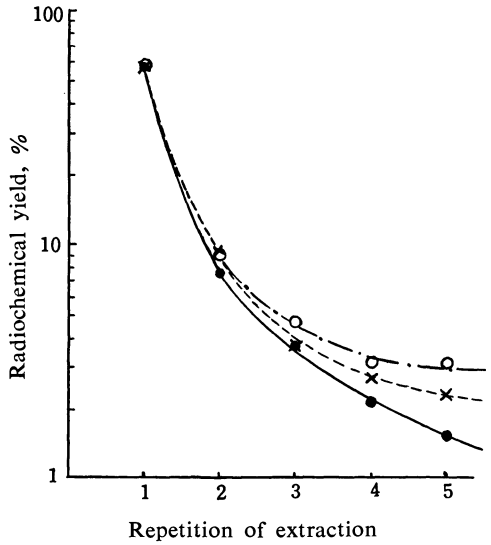



Fig. 2. Relationship between the radiochemical yield and the repetition of extraction (nitric acid only).
—●— 8 N $HNO_3$ -·-○·- 12 N $HNO_3$
···×··· 10 N $HNO_3$

procedures shown in Fig. 2, where the values of extraction yield at 20°C are plotted against the repetition number of extraction. The extraction yield was very large at the first extraction, and decreased first rapidly and then slowly. As is shown in Fig. 2, tails of the extraction curves are higher with the increasing concentration of nitric acid. The total extraction yield of five fold extraction is shown in Table IV. These values increase

TABLE IV. TOTAL RADIOCHEMICAL YIELD OF CHROMIUM-51 ON REPEATED HETEROGENEOUS EXTRACTIONS

| Series | 8 N $HNO_3$ % | 10 N $HNO_3$ % | 12 N $HNO_3$ % |
|---|---|---|---|
| No. 1 | 71.4 | 73.8 | 75.0 |
| No. 2 | 70.5 | 71.0 | 74.5 |
| No. 3 | 63.6 | 72.5 | 78.1 |

with the increasing concentration of nitric acid. In all experiments mentioned above, nitric acid was used for extraction. Howevere, as the target material is slightly soluble in nitric acid, it is necessary to investigate whether this small solubility plays an important role on the extraction process or not. Nitric acid solution saturated with hexamminechromium(III) nitrate was used as an extracting agent in order to suppress the dissolution of the target. The results are shown in Fig. 3. As a whole, no large difference is found between the results in Figs. 2 and 3, but the tails of the extraction curves seem to be slightly affected by using nitric acid saturated with the complex salt. All the extraction curves in Fig. 3 are similar in shape.

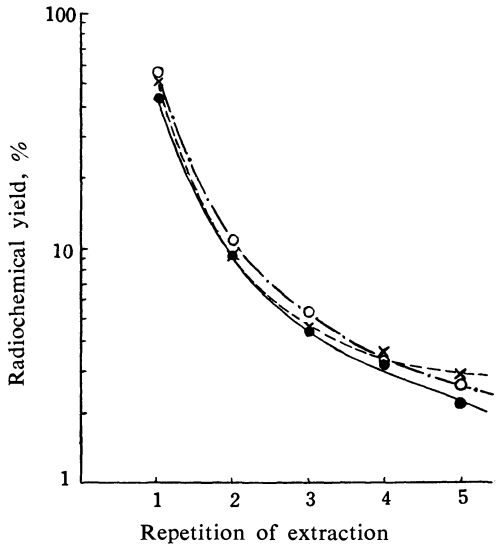



Fig. 3. Relationship between the radiochemical yield and the repetition of extraction (nitric acid saturated with hexamminechromium(III) nitrate).
—●— 8 N $HNO_3$ -·-○·- 12 N $HNO_3$
···×··· 10 N $HNO_3$

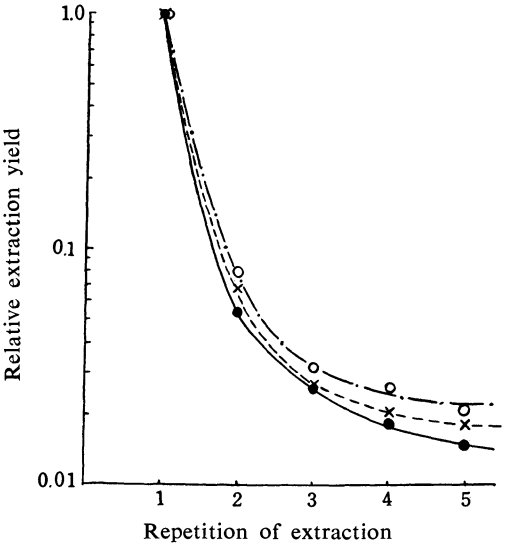



Fig. 4. Effects of shaking time on the extraction. 8 N $HNO_3$ was used for the extraction; shaking time: —●— 1 min. -·-○·- 10 min. ···×··· 6 min.

The effect of shaking time on the extraction yield was investigated, using 8 N nitric acid without addition of the complex salt as the extracting agent. The sample was shaken for 6 or 10 min. The results are shown in Fig. 4. The tails of the extraction curves become higher with the increase of shaking time.

**Determination of Enrichment Factors.** — To calculate the enrichment factor of $^{51}Cr$ in each extract, chromium was determined colorimetrically as described before. The results are listed in Table V. The chromium found in the aqueous phase is derived from the dissolved complex salt or of radiation- and thermal-decomposition of the complex salt in the reactor. In Table V, "amount of chromium" (in 25 ml. extract) represents the amount of chromium calculated in the form of the complex salt. Comparing the amounts of chromium in Table V with those of dissolved chromium in Table I, it is shown that the solubility of the irradiated complex salt was much greater than that of the salt before irradiation. Even if radiation- and thermal-decomposition of the compolex in the reactor was considered, this could not account for the increase of the amount of chromium in the aqueous phase. At the first extraction, the enrichment factor was the largest, and it fell down with the repetition of extraction. The effect of concentration of nitric acid is distinctly seen on the fourth and the fifth extraction in the table.

TABLE V. ENRICHMENT FACTORS OF CHROMIUM-51 ON EACH EXTRACTION

| Extraction number | | Amount of chromium, mg. $[Cr(NH_3)_6]\cdot(NO_3)_3$ | Enrichment factor |
|---|---|---|---|
| 8 N $HNO_3$ | 1 | 5.4 | 20 |
| | 2 | 2.8 | 5.4 |
| | 3 | 2.7 | 2.8 |
| | 4 | 3.0 | 1.5 |
| | 5 | 3.7 | 0.9 |
| 8 N $HNO_3$ | 1 | 5.6 | 20 |
| | 2 | 2.9 | 6.5 |
| | 3 | 2.5 | 3.2 |
| | 4 | 2.4 | 2.4 |
| | 5 | 2.1 | 2.3 |
| 8 N $HNO_3$ | 1 | 5.8 | 20 |
| | 2 | 3.0 | 5.5 |
| | 3 | 1.8 | 5.5 |
| | 4 | 1.9 | 3.7 |
| | 5 | 2.0 | 3.4 |

As dissolution of a small amount of the target is inevitable, the enrichment factor drops more or less in the heterogeneous extraction. Therefore, the enrichment factor of chromic ion which is the predominant species produced by the hot-atom effect was determined by the following procedures. The irradiated target was dissolved in water and an iron(III) carrier as well as chromate ion as a hold-back carrier was added to the solution. Ammonia was added to the mixture to precipitate ferric hydroxide with which chromic ion coprecipitates. After being washed with a very dilute aqueous ammonia, the precipitate was dissolved in hydrochloric acid and again ferric hydroxide was precipitated with ammonia. After being washed the precipitate was dissolved in 9 N hydrochloric acid, and the solution was extracted twice tri-*n*-butyl phosphate to remove the iron. The aqueous phase was washed twice with benzene to remove tri-*n*-butyl phosphate. The chromium content in the aqueous phase was determined colorimetrically. The enrichment factor of $^{51}Cr$(III) thus obtained was 150~230. As an enrichment factor of 20 was

obtained at the first extraction in Table V, dissolution of target material plays an important role in diminishing the enrichment factor of $^{51}Cr$ in the heterogeneous extraction.

**Determination of Chemical Forms of Recoil Products.**— In the hot-atom effect of chromium complex salts, formation of chromate ion besides chromic ion was observed[8]. Harbottle[11] suggested that ammonium ion might act as a reducing agent on the recoil event in chromate. As hexamminechromium(III) nitrate has six ammonia molecules in it, it was considered interesting to note whether sexivalent chromium was formed in the target or not.

This was investigated in the following way. At first, the percentage of chromium(III) was determined. After adding 10 mg. of iron(III) carrier as well as 20 mg. of chromate as a hold back carrier to the aqueous solution of the irradiated target, ammonia was added to this mixture to precipitate ferric hydroxide. By this procedure, $[Cr(NH_3)_6](NO_3)_3$ and chromium(VI) were not precipitated while chromium(III) was coprecipitated with ferric hydroxide almost completely. The precipitate was separated and the radioactivity was measured by a $\gamma$-ray spectrometer.

Next, formation of chromium(VI) was tested by the following two methods; one is based on the precipitation of lead chromate in the presence of chromic ion as a hold-back carrier, and the other on the extraction of chromate with tri-*n*-butyl phosphate[8]. The latter method was preferable because of its exactness, and was adopted to determine the percentage of chromate. The aqueous solution of the irradiated target was made to 1 N by hydrochloric acid, and it was extracted with tri-*n*-butyl phosphate. Chromate was extracted into the tri-*n*-butyl phosphate phase, while the complex salt and chromic ion were left in the aqueous phase. The radioactivity of the organic layer was measured by a $\gamma$-ray spectrometer. Thus the distribution of the chemical forms of the recoil products were determined; chromium(III) fraction 98~99%, chromium(VI) fraction $<0.2\%$ and the retention 1~2%.

**Measurement of the Surface Area of the Target***.— The surface area of the target was measured by the nitrogen adsorption method before and after irradiation. Before irradiation, the mean grain size of 140~300 m$\mu$ was obtained, and this value was not substantially changed by irradiation.

## Discussion

On heterogeneous extraction of recoil atoms in hexammimechromium(III) nitrate, extraction curves were affectd neither by concentration of nitric acid, nor by the extraction time. Therefore the extraction mechanism in this method is considered to be mainly due to the surface process, because if the leaching process from the interior part of the target were a principal feature, great changes would be brought about in the extraction curve by changing the concentration of nitric acid or the extraction time. However, the tail of the extraction curve becomes higher at the higher concentration of nitric acid or at the longer extraction time. These results may be interprete by assuming that the leaching process more or less contributes to the whole process.

If the surface process were a predominant one, the following problems would arise. (1) How does the slight dissolution of hexamminechromium(III) nitrate into nitric acid affect the whole process? The previous experiment will furnish an answer to this problem. The extraction curve is not markedly changed even though the extraction is done with the use of nitric acid saturated with the complex salt. Perhaps this shows that slight dissolution of the target in the aqueous phase does not markedly affect the whole process of the extraction. (2) In order to obtain a large extraction yield such as several times ten per cent by the surface process, the grain size of the target must be vevy small and must be of the comparable order to the recoil range[12]. However, the mean grain size of the target used in these experiments was 140~300 m$\mu$ (This value was not substantially changed by irradiation.). This value is much greater than the value of 10 m$\mu$ or less which is considered to be a recoil range of the (n, $\gamma$)-reaction. How is this fact interpreted?

It is difficult to solve this problem clearly, but we may assume as follows: Hexamminechromium(III) nitrate is relatively unstable to heat and is apt to be decomposed beyond 100°C. In the case of the $^{50}Cr$ (n, $\gamma$) $^{51}Cr$ reaction, the recoil energy of the order of 300 eV. is dissipated in the neighborhood of the recoil atom, and therefore high temperature appears locally around it. For example, Harbottle[13] suggested that several thousands of atoms around the recoil atom attain to several hundred degrees in a molecular crystal. The thermal decomposition by heat liberated locally is considered to be very probable in this case. Chromium nitrate and ammonia molecules would be irregularly present in this "thermal spike". This part would be easily dissolved into the aqueous phase on contact with nitric acid. This part may be considered to be the path to nitric acid. A recoil atom present in this "thermal spike" would be expected to be carried into the nitric acid solution on extraction, and a crack which reaches the

11) G. Harbottle, *J. Chem. Phys.*, **22**, 1083 (1954).

* This measurement was carried out by Dr. Izumi Higuchi of the Tohoku University.

12) J. Pauley and P. Süe, *J. phys. radium*, **18**, 22 (1957).

13) G. Harbottle and N. Sutin, *J. Phys. Chem.*, **62**, 1344 (1958).

surface after irradiation or on the extraction may be possible. Since ammonia is produced by decomposition of the complex salt, local high pressure may appear in the neighborhood of the "thermal spike". Calculating from the data of the recoil energy of the (n, $\gamma$)-reaction and the dissociation energy of the complex salt, ammonia molecules of the order of $10^4$ must be present around the "thermal spike". This high pressure may be apt to make a crack at the time of the extraction.

Owing to a thermal spike and/or a crack, the recoil atom would be extractable beyond the recoil range. A similar explanation is possible in the case of the hot-atom effect in hexamminecobalt(III) nitrate.

The heterogeneous extraction is applicale to the rapid separation of recoil atoms. Especially, it is very effective to separate the radioisotope such as $^{55}Cr$ which has a very short half-life. However, a very high enrichment factor is not expected by this method.

The authors wish to express their hearty thanks to Dr. Kenjiro Kimura, the Director of the Japan Atomic Energy Research Institute for his kind guidance and encouragement throughout this work, to Dr. Izumi Higuchi, Professor of Tohoku University for the measurement of the surface area of the target, to the members of the cyclotron group at the Institute of Physical and Chemical Research, Tokyo, for the bombardment of the samples, and also to Mr. Michimasa Arai for his helpful assistance. A part of the expense for this work was defrayed by a grant from the Ministry of Education, to which the authors' thanks are due.

*Tokyo University of Education*
*Otsuka, Tokyo (N. I. & K. S.)*

*Japan Atomic Energy Research Institute*
*Tokai-mura, Ibaragi-ken (K. Y. & H. E.)*

# *Spectroscopic Studies on Molecular Configurations of Some Aliphatic Dinitriles. I. Infrared Spectra of Succinonitrile and Bis(succinonitrilo)copper(I) Nitrate*

By Ikuo MATSUBARA

(Received April 24, 1961)

Although the infrared spectra of many substances with polymethylene chains of the type $X-(CH_2)_n-X$ have been studied in relation to their molecular configurations[1], no detailed spectroscopic studies seem to have been made on the series of aliphatic dinitriles except for the case of succinonitrile[2,3]. An interpretation of the spectra of such compounds is always a difficult problem because of the complexity caused by the existence of a number of rotational isomers. By the use of low-temperature techniques, however, the spectra of single rotational isomers in the crystalline solid state may be obtained. It is true that the spectra in the solid state may be explained in part by comparing them with those of like molecules, but it would be of great value if the direct determination of their molecular configurations in the crystalline solid state could be made by other physical methods such as by X-ray crystal structure analysis. Incidentally aliphatic dinitriles form stable copper(I) complexes of the type $[Cu\{NC-(CH_2)_n-CN\}_2]NO_3$ $(n=2, 3\cdots)$[4]. The crystal structures of the first few members of this homologous series were studied recently by X-ray method and the configuration of the ligand dinitrile molecule in the crystals of each complex was determined[5-7]. The infrared spectra of these complexes, which may be analyzed on the basis of these results, would supply much useful data for the complete understanding of the spectra of dinitrile molecules. Naturally a rigorous analysis of the spectrum of a complex compound would be a complicated problem. Therefore, it should

1) N. Sheppard, "Advances in Spectroscopy", Ed. by H. W. Thompson, Vol. 1, Interscience Publishers Inc., New York (1959), p. 288; see the references cited there.
2) W. E. Fitzgerald and G. J. Janz, *J. Molec. Spectroscopy*, **1**, 49 (1957).
3) I. Nakagawa and K. Tokumaru, Private communication.
4) H. H. Morgan, *J. Chem. Soc.*, **123**, 2901 (1923); H. Rath, H. Rehm, H. Rummler and E. Specht, *Melliand Textilber.*, **38**, 431, 538 (1957).
5) Y. Kinoshita, I. Matsubara and Y. Saito, This Bulletin, **32**, 741 (1959).
6) Y. Kinoshita, I. Matsubara and Y. Saito, ibid., **32**, 1216 (1959).
7) Y, Kinoshita, I. Matsubara, T. Higuchi and Y. Saito, ibid., **32**, 1221 (1959).

first be assumed that the interaction forces between the ligand molecules are so small that the main features of the spectrum may be explained from the consideration of an isolated ligand molecule[8].

This paper will report on the study of the infrared spectrum of bis(succinonitrilo)copper-(I) nitrate, $[Cu(NC-CH_2-CH_2-CN)_2]NO_3$, in connection with the configuration of the ligand succinonitrile. The result of X-ray analysis[5] shows that in the crystals of this complex the ligand succinonitrile molecule is coordinated tetrahedrally with its nitrogen atoms of both ends to two different copper atoms and takes the gauche configuration. Therefore, the infrared data of this complex may be of interest in relation to the results of the spectroscopic studies on succinonitrile by Fitzgerald and Janz[2], and Nakagawa and Tokumaru[3], who concluded that this molecule exists as a mixture of two rotational isomers, trans and gauche, the latter being the more stable configuration at low temperatures. The spectral changes due to decomposition of the complex as a result of interaction with alkali halides have been of help in assigning the vibrational frequencies of succinonitrile. The assignments of the skeletal deformation vibrations were successfully carried out on the basis of the result of a normal coordinate treatment.

## Experimental

The method of preparation and the properties of bis(succinonitrilo)copper(I) nitrate are as described in the previous paper[5].

The infrared spectra of the complex and of succinonitrile in the 4000~400 $cm^{-1}$ region were obtained using a Perkin-Elmer Model 21 and a Perkin-Elmer Model 13 spectrophotometer (with sodium chloride and potassium bromide optics, respectively). Spectra in the cesium bromide region were also obtained using a Perkin-Elmer Model 21 spectrophotometer*. The spectrum of succinonitrile was recorded at room temperature and at −50°C. A low-temperature transmission cell of the type described by Nukada[9] was used to obtain the spectra at low temperatures. The results shown in Figs. 1a and 1b are essentially the same as those obtained by Fitzgerald and Janz[2]. The spectrum of the complex was obtained using both Nujol mull and potassium bromide disk techniques. Nujol mulls of the complex gave different spectra depending on the type of alkali halide cell windows used as supporting plates. The spectrum obtained by using KRS-5 plates and that obtained by using sodium chloride plates were at first identical with each other, but the latter soon began to change gradually with time. This suggests that some interaction exists between the complex and sodium chloride plates. When potassium bromide plates were used the reaction occurred so rapidly that the spectrum changed while it was being recorded. These changes are clearly seen in Fig. 2. The spectrum in Fig. 2a is that obtained by using KRS-5 plates. The spectra in Figs. 2b and 2c are those obtained respectively by the use of sodium chloride and potassium bromide plates. (These were recorded after the specimens had been placed in the laboratory for one day.) These two spectra are in some respects different from each other, showing that the reaction products are not the same in the two cases. The spectrum obtained from a potassium bromide disk of the complex is shown in Fig. 3, which agrees quite well with that obtained from a Nujol mull by the use of potassium bromide plates (Fig. 2c). This means that the same type of reaction occurred between the complex and potassium bromide in the two cases. The absorption frequencies of succinonitrile and bis(succinonitrilo)copper(I) nitrate are listed in Table I together with the assignment.

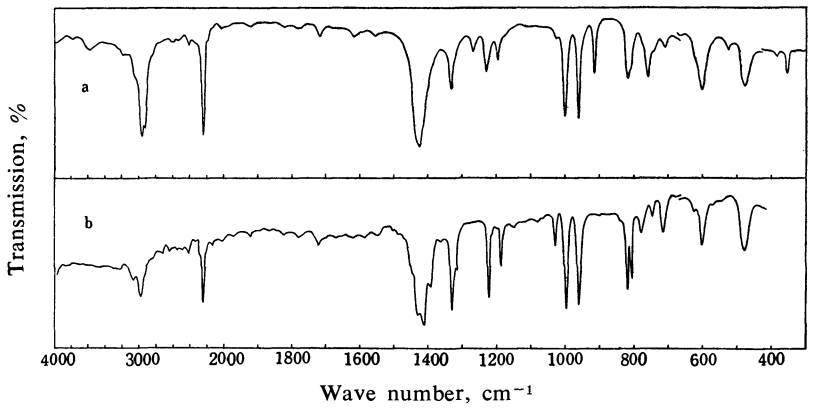



Fig. 1. Infrared spectra of succinonitrile. (a) at room temperature; (b) at −50°C.

8) See for example: F. A. Cotton, "Modern Coordination Chemistry", Ed. by J. Lewis and R. G. Wilkins, Interscience Publishers Inc., New York (1960), Chapter 5.

* By the courtesy of Government Chemical Industrial Research Institute of Tokyo.

9) K. Nukada, *J. Chem. Soc. Japan, Pure Chem. Sec.* (*Nippon Kagaku Zasshi*), **80**, 218 (1959).

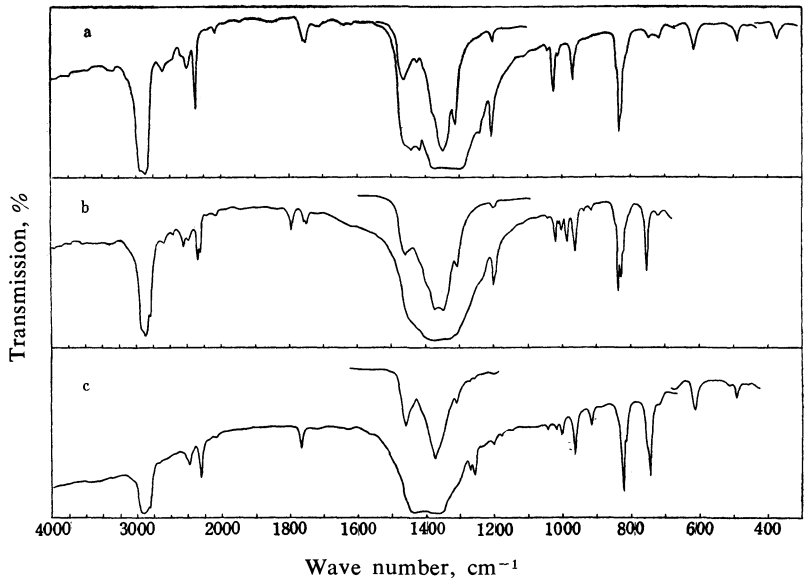



Fig. 2. Infrared spectra obtained from Nujol mulls of bis(succinonitrilo)copper(I) nitrate by using (a) KRS-5, (b) sodium chloride and (c) potassium bromide supporting plates.

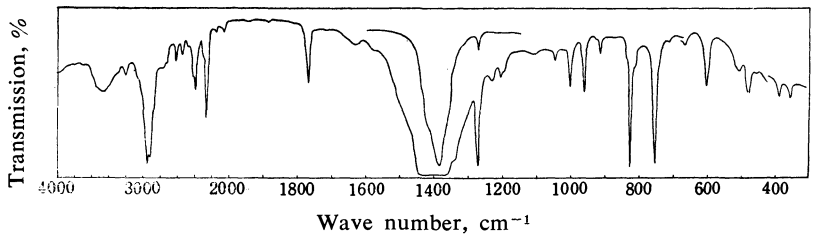



Fig. 3. Infrared spectrum obtained from a potassium bromide disk of bis(succinonitrilo)-copper(I) nitrate.

In Table II are included the absorption frequencies due to the nitrate ion in the complex.

## Results and Discussion

The spectral simplification that occurred when succinonitrile was cooled down to $-50°C$ is clearly seen in Fig. 1. In the $1400\sim400\ cm^{-1}$ region there are four absorption bands that disappear at low temperatures. Fitzgerald et al.[2] and Nakagawa et al.[3] assigned these bands, which are at frequencies of 1271, 917, 761 and $527\ cm^{-1}$, to the vibrations of the trans form (symmetry $C_{2h}$) and assigned all the remaining bands to the vibrations of the gauche form (symmetry $C_2$). As long as the ligand succinonitrile takes the gauche form in the crystals of bis(succinonitrilo)copper(I) nitrate[5], the spectrum of this complex should be closely correlated with that of succinonitrile at low the temperatures. In complete agreement with expectation, the Nujol mull spectrum of the complex (Fig. 2a) corresponds well with the low-temperature spectrum of succinonitrile (Fig. 1b) except for the regions where absorptions due to nitrate vibrations or skeletal vibrations of the complex take place. The fact that no absorptions occur at the four frequencies which were ascribed by the previous authors[2,3] to the vibrations of the trans form gives additional support to their conclusion. On the other hand, the spectra in Figs. 2b, 2c and 3 have absorptions corresponding to the trans vibrations and show spectral features similar to that of succinonitrile at room temperature (Fig. 1a). This means that splitting of copper-nitrogen coordinate bonds occurred and succinonitrile was isolated as a result of the interaction between the complex and alkali halides. The intense bands observed at 1348 and $830\ cm^{-1}$ in Fig. 2a must be ascribed to infrared active fundamentals of the nitrate ion in the complex. The weak doublet with peaks at 1757 and $1751\ cm^{-1}$ must be a certain combination band of the nitrate ion, because some

TABLE I. INFRARED ABSORPTION BANDS OF SUCCINONITRILE AND BIS(SUCCINONITRILO)-COPPER(I) NITRATE

| Succinonitrile | | Bis(succinonitrilo)copper(I) nitrate | | Assignment | |
|---|---|---|---|---|---|
| Solid (Room temp.) | Solid (−50°C) | Nujol mull[a] | KBr disk | Gauche($C_2$) | Trans($C_{2h}$) |
| | | 3300 vw | 3322 vw sh | | |
| | 3226 vw | | | | |
| 3205 w | | | 3205 w | | |
| 3058 mw sh | 3067 mw | | | | |
| 2985 vs | 2994 m | | 2950 s | C–H stretch. | C–H stretch. |
| 2950 s sh | 2959 w sh | | 2924 s | C–H stretch. | C–H stretch. |
| 2849 vw sh | 2849 vw | | | | |
| | | | 2786 w | | |
| | 2732 w | 2725 vw sh | 2740 vw sh | | |
| | | 2681 mw | | | |
| 2646 vw sh | 2639 w | | | | |
| 2597 vw | 2611 vw | | 2611 w | | |
| 2558 vw | 2545 vw | 2564 w sh | 2551 w | | |
| | 2494 vw | | | | |
| | | | 2475 vw | | |
| | 2445 vw | 2451 w sh | | | |
| 2427 w | 2421 w | | 2415 mw sh | | |
| | | 2398 mw | 2398 m | | |
| | 2283 w sh | 2283 ms | 2283 w sh | C≡N stretch. (bound) | |
| 2257 vs | 2257 s | | 2257 ms | C≡N stretch. (free) | C≡N stretch. |
| 2203 vw sh | 2203 vw | | | | |
| 2151 vw | 2141 w | | 2155 vw | | |
| 2045 vw | 2041 vw | 2066 w | 2066 vw | | |
| | | 1942 vw | 1942 vw | | |
| 1923 vw | 1923 w | | | | |
| | | | 1883 vw | | |
| 1825 vw | 1825 w | | | | |
| 1786 vw | 1786 w | | | | |
| 1721 w | 1721 mw | 1709 vw | | | |
| 1621 w | | 1639 vw | | | |
| | | 1613 vw | | | |
| | 1590 w | | 1570 vw sh | | |
| 1558 w | 1550 w | 1538 vw sh | | | |
| | 1445 mw sh | | | | |
| 1425 vs | 1431 vs sh | | | B $CH_2$ bend. | $B_u$ $CH_2$ bend. |
| 1416 s sh | 1414 vs | 1418 ms | 1410 m sh | A $CH_2$ bend. | |
| | 1395 m sh | | | | |
| | 1361 w | | | | |
| 1337 ms | 1332 s | 1310 vs | 1339 s sh | B $CH_2$ wag. | |
| 1323 w sh | 1319 m sh | | 1307 m sh | | |
| 1271 mw | | | 1272 s | | $B_u$ $CH_2$ wag. |
| 1231 ms | 1225 s | 1242 m sh | 1232 w | A $CH_2$ wag. | |
| 1198 m | 1189 m | 1202 ms | 1206 w | A $CH_2$ twist. | ($A_u$ $CH_2$ twist.) |
| | | | 1199 w sh | | |
| 1179 vw sh | | | | | |
| | 1152 w | | | | |
| | | 1105 vw | 1111 vw | | |
| | 1081 w | 1074 vw | | | |
| 1027 w | 1032 m | 1021 m | 1021 vw | A C–C stretch. | |
| 1001 s | 999 vs | 1010 w | 1003 m | B C–CN stretch. | |

TABLE I. (Continued)

| Succinonitrile | | Bis(succinonitrilo)copper(I) nitrate | | Assignment | |
|---|---|---|---|---|---|
| Solid (Room temp.) | Solid (−50°C) | Nujol mull[a] | KBr disk | Gauche($C_2$) | Trans($C_{2h}$) |
| 962 s | 963 vs | 966 m | 963 m | A $CH_2$ rock. | |
| | 954 mw sh | | | | |
| | | | 929 vw | | |
| 917 ms | | | 917 w | | $B_u$ C-CN stretch. |
| 839 vw sh | 842 w sh | 837 mw sh | 838 w sh | | |
| 818 ms | 820 s | 826 ms sh | | B $CH_2$ rock. | |
| 813 ms sh | 810 ms | 813 mw sh | 812 w sh | A C-CN stretch. | |
| 776 vw sh | 780 m | | | 603+170[b] | |
| 761 ms | | | 754 s | | $A_u$ $CH_2$ rock. |
| 746 mw sh | 750 mw | 746 w | | 385+356 | |
| 714 mw | 718 m | 719 w | 714 vw | 480+235[c]; 2×356 | |
| 668 vw | | | 667 vw | | 528+145[d] |
| 623 w sh | 628 w | | | | |
| 603 ms | 603 ms | 615 m | 602 m | B C-C-C bend. | |
| 578 vw sh | 576 vw | | | | |
| | | | 524 vw sh | | |
| 527 w | | | 509 w | | $B_u$ C-C-C bend. |
| 480 ms | 483 ms | 490 mw | 480 mw | A C-C-C bend. | |
| | | 458 vw | | | |
| 385 w | | | 389 w | A C-C≡N bend. | $A_u$ C-C≡N bend. |
| | | (369 mw) | | | |
| 356 m | | 360 w sh | 356 w | B C-C≡N bend. | |

a) KRS-5 supporting plates were used to obtain the spectrum.
b) Raman frequency for the A C-C≡N bending mode of the gauche form.
c) Raman frequency for the B C-C≡N bending mode of the gauche form.
d) Calculated frequency for the $B_u$ C-C≡N bending mode of the trans form.

TABLE II. INFRARED ABSORPTION BANDS DUE TO NITRATE IONS IN BIS(SUCCINONITRILO)-COPPER(I) NITRATE

| Nujol mull | | | KBr disk | $NaNO_3$[b] | $KNO_3$[b] |
|---|---|---|---|---|---|
| KRS-5[a] | NaCl[a] | KBr[a] | | | |
| | 1795 mw | | | 1790 vw | |
| | | 1770 m | 1770 m | | 1767 vw |
| 1757/51 mw | 1757/51 mw | | | | |
| | | 1377 vs | 1381 vs | | 1380 vs |
| | 1375/51 vs | | | 1358 vs | |
| 1348 vs | | | | | |
| 1043 w | 1043 vw | 1047 w | 1048 w | — | — |
| | 836 ms | | | 836 m | |
| 830 s | 830 ms | | | | |
| | | 824 s | 826 s | | 824 m |

a) Denotes the type of alkali halide cell windows used to support the mull.
b) See Ref. 10 in text.

inorganic nitrates show weak absorptions in this region[10]. As a result of reaction with sodium chloride these nitrate bands have decreased in their intensities and new absorptions appeared at 1795, 1375/51 and 836 $cm^{-1}$ as shown in Fig. 2b. The reaction with potassium bromide caused the appearance of new bands at 1770, 1377 (or 1381) and 824 (or 826) $cm^{-1}$ as shown in Figs. 2c and 3. These new bands observed in the two cases correspond quite well with those of sodium nitrate and potassium nitrate, respectively (see Table II). Considering these results the reaction of the complex with alkali halides should be ascribed largely

10) F. A. Miller and C. H. Wilkins, *Anal. Chem.*, **24**, 1253 (1952).

to an ion interchange between the two phases. A weak band observed at 1043 $cm^{-1}$ in the spectrum of the complex may correspond to an infrared inactive frequency of the nitrate ion which may have become active due to the effect of the crystalline field of the complex.

The remaining bands of the complex are assigned to the vibrations of the gauche form of succinonitrile with reference to the results of the previous authors[2,3]. Thus the bands observed at 1310 and 1242 $cm^{-1}$ should be assigned to the B and A $CH_2$ wagging modes, respectively. The bands at 1202 $cm^{-1}$ should correspond to the A $CH_2$ twisting mode. On the other hand, the B $CH_2$ twisting mode remains unidentified. According to the result of the normal coordinate treatment by Nakagawa et al.[3] the B $CH_2$ twisting mode should have a frequency lower than that of the A counterpart, but no appropriate band is found either in the spectrum of the complex or in that of succinonitrile. The weak band at 1027 $cm^{-1}$ and the strong band at 1001 $cm^{-1}$ in the spectrum of succinonitrile are assigned to the A C–C stretching and the B C–CN stretching modes, respectively. This is in agreement with the expectation that a symmetrical skeletal stretching mode is generally weaker than an asymmetrical one in the infrared spectrum. The Raman counterparts of these bands are found at frequencies of 1027 and 1006 $cm^{-1}$ (see Table VIII in Appendix). The fact that the former is much stronger than the latter supports the above assignment because a totally symmetric vibration is expected to be strong in the Raman spectrum. At low temperatures the 1027 $cm^{-1}$ band increases in intensity relative to the 1001 $cm^{-1}$ one (Fig. 1b), showing that the A C–C stretching mode is susceptible to the effect of crystalline field. In the spectrum of the complex a relatively strong band is observed at 1021 $cm^{-1}$. This band may be assigned to the A C–C stretching mode. To the B C–CN stretching mode may correspond the weak band at 1010 $cm^{-1}$. The fact that the intensity relation of these two bands is reverse to what is observed in the case of succinonitrile seems not to be in harmony with this assignment, but we may tentatively ascribe it to the effect of the crystalline field of the complex. The strong band at 966 $cm^{-1}$, which corresponds to the 962 $cm^{-1}$ band in succinonitrile, is assigned to the A $CH_2$ rocking mode. The 818 $cm^{-1}$ band of succinonitrile with a shoulder at 813 $cm^{-1}$ splits into two components at low temperatures as shown in Fig. 1. One of the components at 820 $cm^{-1}$ is ascribed to the B $CH_2$ rocking mode and the other at 810 $cm^{-1}$ to the A C–CN stretching mode. In the spectrum of the complex no well-defined band maxima corresponding to these vibrations are observed, due to overlapping by the strong nitrate band at 830 $cm^{-1}$. However, the shoulder bands at 826 and 813 $cm^{-1}$ are assigned with confidence to the B $CH_2$ rocking and the A C–CN stretching modes, respectively. The $CH_2$ rocking frequencies of 1, 2-disubstituted ethanes are known to change conspicuously depending on the azimuthal angle of internal rotation, and therefore can be used to determine the molecular configurations of rotational isomers[11]. The azimuthal angle of internal rotation of succinonitrile in the crystals of the complex has been determined by X-ray analysis to be 53° taking the cis position as the origin[5]. The gauche angle of free succinonitrile must be close to this value, for the two $CH_2$ rocking frequencies of this molecule agree quite well with the corresponding values of the complex. This conclusion is also in good agreement with what is expected from the calculated frequencies of these vibrations[3].

Assignment of the skeletal deformation vibrations are made with reference to the result of a normal coordinate treatment (see Appendix). The 615 and 490 $cm^{-1}$ bands of the complex correspond each to the 603 and 480 $cm^{-1}$ bands of succinonitrile which are assigned to the B and A C–C–C bending modes, respectively. The weak band at 527 $cm^{-1}$ of succinonitrile which disappears at low temperatures and has no counterpart in the spectrum of the complex (Fig. 2a) corresponds to the $B_u$ C–C–C bending mode of the trans form. The bands at 385 and 356 $cm^{-1}$ of succinonitrile are assigned to the A and B C–C≡N (out-of-plane) bending modes of the gauche form, respectively. The 385 $cm^{-1}$ band may also have some contribution from the $A_u$ C–C≡N out-of-plane bending mode of the trans form. As shown in Fig. 2a the spectrum of the complex has an absorption band at 369 $cm^{-1}$ which probably corresponds to the Cu–N stretching mode, and the shoulder band at 360 $cm^{-1}$ may be correlated with the B C–C≡N bending mode. The absorption corresponding to the A C–C≡N bending mode is not observed, probably due to the overlapping by the 369 $cm^{-1}$ band. The $B_u$ C–C≡N in-plane bending mode of the trans form has a calculated frequency of 145 $cm^{-1}$, while the A and B C–C≡N (in-plane) bending modes of the gauche form have calculated frequencies of 178 and 247 $cm^{-1}$, respectively (see Table VIII in Appendix). The values for the gauche form are in good agreement with the observed Raman frequencies, while the infrared data in the region below 300 $cm^{-1}$ are

11) I. Nakagawa, *J. Chem. Soc. Japan, Pure Chem. Sec.* (*Nippon Kagaku Zasshi*), **76**, 813 (1955).

not available for this investigation. The fact that the C–C–C bending modes of nitriles such as acrylonitrile[12], malononitrile[13] and propionitrile[14] always appear in a region as high as 600~450 $cm^{-1}$ and that the C–C≡N (in-plane) bending modes lie in a region as low as 250~150 $cm^{-1}$ suggests that there must be considerable mixing of the two bending coordinates in these skeletal deformation vibrations and no single coordinate may be associated with the individual frequencies. Calculation of the potential energy distributions for the skeletal deformation vibrations has shown that the energies associated with the C–C–C bending and the C–C≡N (in-plane) bending motions are of the same order in these two types of vibration (see Appendix). In the spectrum of succinonitrile there are three absorptions in the 800~700 $cm^{-1}$ region other than that corresponding to the $CH_2$ rocking mode of the trans form. These bands with peaks at 780, 750 and 718 $cm^{-1}$ are observed to increase remarkably in their intensities at low temperatures (Fig. 1b). As Fujiyama and Shimanouchi[15] suggested, these may be attributed to overtones or combinations of some skeletal deformation vibrations of the gauche form. The proposed assignments for these vibrations are included in Table I.

The sharp band observed at 2283 $cm^{-1}$ in the Nujol mull spectrum (Fig. 2a) may correspond to the C≡N stretching vibration of the complex. The C≡N vibrational shift of 26 $cm^{-1}$ towards higher frequencies as compared with the free succinonitrile may be understood by considering the structure of the complex. X-Ray analysis of this complex[5] has revealed that the carbon-nitrogen bond distance is 1.14 Å and that the Cu–N–C–$CH_2$ group is close to linear, from which it is expected that the carbon-nitrogen bond is essentially of a triple-bond character, the contributions of polar resonance structures such as $-C^+=N^-$ being decreased, and the C≡N stretching frequency is thereby increased. Califano et al.[16] have shown that in the cases of nitriloxides, R–C≡N→O, the C≡N stretching frequencies are about 70 $cm^{-1}$ higher than those of the corresponding nitriles and have explained this as due to the coupling with the N→O stretching vibration. In the case of this complex the effect of the interaction between the C≡N stretching and the Cu–N stretching vibrations, though small, may also contribute to the increase in the C≡N stretching frequency.

12) F. Halverson, R. F. Stamm and J. J. Whalen, *J. Chem. Phys.*, **16**, 808 (1948).
13) F. Halverson and R. J. Francel, ibid., **17**, 694 (1949).
14) N. E. Duncan and G. J. Janz, ibid., **23**, 434 (1955).
15) T. Fujiyama and T. Shimanouchi, Paper presented at the 14th Annual Meeting of the Chemical Society of Japan, Tokyo, April, 1961.
16) S. Califano, R. Moccia, R. Scarpati and G. Speroni, *J. Chem. Phys.*, **26**, 1777 (1957).

## Summary

The infrared spectrum of bis(succinonitrilo)-copper(I) nitrate, $[Cu(NC-CH_2-CH_2-CN)_2]NO_3$, has been studied in relation to the molecular configuration of the ligand succinonitrile, which is known from X-ray analysis to be the gauche form. The spectral features of this complex are quite similar to those of free succinonitrile at −50°C in agreement with the conclusion of the previous workers that the gauche isomer of succinonitrile is stable at low temperatures. Thus all the main absorption bands of the complex were satisfactorily explained as due to the vibrations of the gauche isomer. Decomposition of the complex occurs as a result of interaction with alkali halides such as sodium chloride and potassium bromide, which causes the appearance of absorption bands corresponding to the vibrations of the trans isomer. Considering the frequency shifts of the nitrate vibrations the reaction of the complex with alkali halides should be ascribed largely to an ion interchange between the two phases. The increase of 26 $cm^{-1}$ in the C≡N stretching frequency by complex formation may be understood from the linear structure of the Cu–N–C–$CH_2$ group which suggests that the carbon-nitrogen bond is essentially of a triple-bond character, the contributions of polar resonance structures such as $-C^+=N^-$ being decreased. Assignment of the skeletal deformation frequencies has been made with the help of a normal coordinate treatment which also made possible discussions concerning the nature of these vibrations.

The author wishes to express his sincere thanks to Professor S. Imanishi of Kyushu University for his kind encouragement in the course of this study. He also wishes to thank Dr. H. Murata of Hiroshima University and Dr. I. Nakagawa of the University of Tokyo for many valuable discussions. He is also grateful to Mr. D. Miura of Toyo Rayon Co., Ltd. for carrying out the mechanical calculations and to Messrs. T. Ito, H. Kataoka and K. Shirasaki of Toyo Rayon Co., Ltd. for their assistance in experiments.

## Appendix: Calculation of Skeletal Vibrations

The skeletal vibrations of succinonitrile were calculated as a six-body problem. The in-plane skeletal vibrations of propionitrile (symmetry $C_s$) were also calculated as a four-body problem in order to obtain more information on the nature of the skeletal deformation vibrations of aliphatic nitriles. A potential function of the Urey-Bradley

TABLE III. FORCE CONSTANTS OF PROPIONITRILE AND SUCCINONITRILE (in millidyne/Å)

| | |
|---|---|
| $K(CH_3\text{-}CH_2)=4.00$[a] | $H(CH_2\text{-}C\equiv N)=0.14_1$[b] |
| $K(CH_2\text{-}CH_2)=3.70$[a] | $F(CH_3\text{-}CH_2\text{-}C)=0.45$[a] |
| $K(CH_2\text{-}C)=3.50$[a] | $F(CH_2\text{-}CH_2\text{-}C)=0.45$[a] |
| $K(C\equiv N)=18.10$[b] | $F(CH_2\text{-}C\equiv N)=0.50$[b] |
| $H(CH_3\text{-}CH_2\text{-}C)=0.25$[a] | $k(C\text{-}C\equiv N)=0.12$ Å$^2$ [c] |
| $H(CH_2\text{-}CH_2\text{-}C)=0.25$[a] | |

a) Transferred from various hydrocarbons and their derivatives and adjusted to obtain better agreement with the observed values. See for example S. Mizushima, T. Shimanouchi, I. Nakagawa and A. Miyake, *J. Chem. Phys.*, **21**, 215 (1953); M. Hayashi, *J. Chem. Soc. Japan, Pure Chem. Sec. (Nippon Kagaku Zasshi)*, **78**, 222 (1957).

b) Transferred from acetonitrile with some modifications. See I. Nakagawa, "Infrared Absorption Spectrum" (in Japanese), Vol. 7, Nankodo Co., Ltd., Tokyo (1959) p. 1.

c) Interaction term between the C-C≡N in-plane and out-of-plane bending coordinates introduced to obtain better agreement with the observed values.

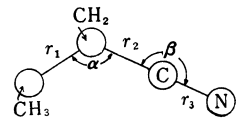



Fig. 4. Internal coordinates of propionitrile.

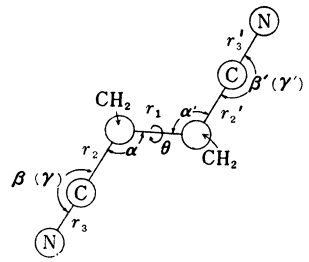



Fig. 5. Internal coordinates of succinonitrile. $\beta$ (or $\beta'$) and $\gamma$ (or $\gamma'$) denote bending of C≡N bond in and out of the plane of the adjacent C-C-C linkage, respectively. $\theta=180°$ for trans and $\theta=60°$ for gauche.

TABLE IV. SYMMETRY COORDINATES OF PROPIONITRILE

| | |
|---|---|
| $S_1=(\Delta r_1+\Delta r_2)/\sqrt{2}$ | ($CH_3\text{-}CH_2\text{-}C$ sym. stretching) |
| $S_2=(\Delta r_1-\Delta r_2)/\sqrt{2}$ | ($CH_3\text{-}CH_2\text{-}C$ antisym. stretching) |
| $S_3=\Delta r_3$ | ($C\equiv N$ stretching) |
| $S_4=\Delta\alpha$ | ($CH_3\text{-}CH_2\text{-}C$ bending) |
| $S_5=\Delta\beta$ | ($CH_2\text{-}C\equiv N$ bending) |

type[17] was used, and the values of force constants were transferred from other related molecules as shown in Table III. The symmetry coordinates of propionitrile and succinonitrile listed in Tables IV and V were constructed from the internal coordinates shown in Figs. 4 and 5, respectively. In the trans form of succinonitrile (symmetry $C_{2h}$) there is no coupling between the C-C≡N in-plane bending and out-of-plane bending motions, because they belong to different classes (see Table V). In the gauche form (symmetry $C_2$), however, these two motions belong to the same classes and accordingly a coupling occurs between them. In the Urey-Bradley type of potential function no cross term corresponding to the interaction between the two C-C≡N bending coordinates is considered, while such an interaction term, $k(C\text{-}C\equiv N)$, was introduced in this calculation to obtain better agreement with the observed frequencies. The value of $k(C\text{-}C\equiv N)$ used in this case is also included in Table III. For the calculation of the kinetic energy matrices the assumed bond lengths of $r(CH_3\text{-}CH_2)=1.54$ Å, $r(CH_2\text{-}CH_2)=1.54$ Å, $r(CH_2\text{-}C)=1.50$ Å and $r(C\equiv N)=1.15$ Å and the bond angle of 109°28′ were used. The result obtained for the in-plane vibrations (A′) of propionitrile agrees well with the observed values[14] as shown in Table VI. In Table VII are listed the diagonal terms of the potential energy distribution[18], which show that the energies associated with the coordinates $S_4$(C-C-C bending) and $S_5$(C-C≡N bending) are of the same order in the two skeletal deformation vibrations. The signs of

TABLE V. SYMMETRY COORDINATES OF SUCCINONITRILE

| $C_2$ | $C_{2h}$ | | |
|---|---|---|---|
| A | $A_g$ | $S_1=\Delta r_1$ | ($CH_2\text{-}CH_2$ stretching) |
| | | $S_2=(\Delta r_2+\Delta r_2')/\sqrt{2}$ | ($CH_2\text{-}C$ sym. stretching) |
| | | $S_3=(\Delta r_3+\Delta r_3')/\sqrt{2}$ | ($C\equiv N$ sym. stretching) |
| | | $S_4=(\Delta\alpha+\Delta\alpha')/\sqrt{2}$ | ($CH_2\text{-}CH_2\text{-}C$ sym. bending) |
| | | $S_5=(\Delta\beta+\Delta\beta')/\sqrt{2}$ | ($CH_2\text{-}C\equiv N$ sym. in-plane bending) |
| | $A_u$ | $S_6=(\Delta\gamma+\Delta\gamma')/\sqrt{2}$ | ($CH_2\text{-}C\equiv N$ sym. out-of-plane bending) |
| B | $B_u$ | $S_7=(\Delta r_2-\Delta r_2')/\sqrt{2}$ | ($CH_2\text{-}C$ antisym. stretching) |
| | | $S_8=(\Delta r_3-\Delta r_3')/\sqrt{2}$ | ($C\equiv N$ antisym. stretching) |
| | | $S_9=(\Delta\alpha-\Delta\alpha')/\sqrt{2}$ | ($CH_2\text{-}CH_2\text{-}C$ antisym. bending) |
| | | $S_{10}=(\Delta\beta-\Delta\beta')/\sqrt{2}$ | ($CH_2\text{-}C\equiv N$ antisym. in-plane bending) |
| | $B_g$ | $S_{11}=(\Delta\gamma-\Delta\gamma')/\sqrt{2}$ | ($CH_2\text{-}C\equiv N$ antisym. out-of-plane bending) |

17) T. Shimanouchi, ibid., **17**, 245, 734, 848 (1949).

18) Y. Morino and K. Kuchitsu, ibid., **20**, 1809 (1952).

TABLE VI. CALCULATED AND OBSERVED FREQUENCIES OF PROPIONITRILE (in $cm^{-1}$)

| Calcd. | Obs.[a] | | Assignment |
|---|---|---|---|
| | Infrared | Raman | |
| 2259 | 2252 | 2251 | C≡N stretching |
| 1016 | 1075 | 1078 | C-C-C antisym. stretching |
| 840 | 836 | 838 | C-C-C sym. stretching |
| 514 | 545 | 548 | C-C-C bending |
| 241 | — | 226 | C-C≡N bending |

a) See Ref. 14 in text.

TABLE VII. POTENTIAL ENERGY DISTRIBUTIONS OF PROPIONITRILE[a]

| $\nu_{calcd}$ | 2259 | 1016 | 840 | 514 | 241 |
|---|---|---|---|---|---|
| $S_1$ | − 4 | +17 | +79 | + 4 | 0 |
| $S_2$ | + 4 | +82 | −14 | 0 | 0 |
| $S_3$ | +95 | − 1 | + 4 | + 1 | 0 |
| $S_4$ | 0 | − 1 | −12 | +49 | +42 |
| $S_5$ | 0 | − 1 | − 1 | +41 | −57 |

a) The signs of the corresponding L matrix elements are also included.

TABLE VIII. CALCULATED AND OBSERVED FREQUENCIES OF SUCCINONITRILE (in $cm^{-1}$)

| Gauche($C_2$) | | | | Trans ($C_{2h}$) | | | | |
|---|---|---|---|---|---|---|---|---|
| Class | Calcd. | Obs. | | Class | Calcd. | Obs. | | Assignment |
| | | Infrared | Raman[a] | | | Infrared | Raman[a] | |
| A | 2259 | 2257 | 2260 | $A_g$ | 2258 | | 2260 | C≡N sym. stretching |
| | 1036 | 1027 | 1027 | | 1036 | | 1027 | C-C stretching |
| | 812 | 813 | 812 | | 883 | | 812 | C-CN sym. stretching |
| | 472 | 480 | 483 | | 460 | | 514 | C-C-C bending |
| | 178 | — | 170 | | 242 | | 235 | C-C≡N bending |
| | 390 | 385 | 386 | $A_u$ | 398 | 385 | | C-C≡N bending |
| B | 2259 | 2257 | 2260 | $B_u$ | 2260 | 2257 | | C≡N antisym. stretching |
| | 882 | 1001 | 1006 | | 874 | 917 | | C-CN antisym. stretching |
| | 601 | 603 | 604 | | 500 | 527 | | C-C-C bending |
| | 247 | — | 235 | | 145 | — | | C-C≡N bending |
| | 369 | 356 | 359 | $B_g$ | 398 | | 386 | C-C≡N bending |

a) Recorded from an aqueous solution with a Cary Model 81 spectrophotometer.

TABLE IX. POTENTIAL ENERGY DISTRIBUTIONS OF THE TRANS FORM OF SUCCINONITRILE[a]

| | $A_g$ | | | | | $A_u$ |
|---|---|---|---|---|---|---|
| $\nu_{calcd}$ | 2258 | 1036 | 883 | 460 | 242 | 398 |
| $S_1$ | 0 | +84 | +16 | + 5 | 0 | — |
| $S_2$ | + 8 | −24 | +55 | +12 | + 5 | — |
| $S_3$ | −95 | − 1 | + 3 | + 1 | + 1 | — |
| $S_4$ | 0 | 0 | −39 | +27 | +39 | — |
| $S_5$ | 0 | − 1 | − 3 | +44 | −52 | — |
| $S_6$ | — | — | — | — | — | +100 |

| | $B_u$ | | | | $B_g$ |
|---|---|---|---|---|---|
| $\nu_{calcd}$ | 2260 | 874 | 500 | 145 | 398 |
| $S_7$ | − 8 | +91 | − 1 | − 2 | — |
| $S_8$ | +95 | + 6 | 0 | 0 | — |
| $S_9$ | 0 | 0 | +41 | +61 | — |
| $S_{10}$ | 0 | 0 | +60 | −40 | — |
| $S_{11}$ | — | — | — | — | +100 |

a) See the footnote of Table VII.

TABLE X. POTENTIAL ENERGY DISTRIBUTIONS OF THE GAUCHE FORM OF SUCCINONITRILE[a]

| | A | | | | | |
|---|---|---|---|---|---|---|
| $\nu_{calcd}$ | 2259 | 1036 | 812 | 472 | 178 | 390 |
| $S_1$ | 0 | +87 | +14 | + 3 | 0 | 0 |
| $S_2$ | + 8 | −20 | +74 | 0 | 0 | 0 |
| $S_3$ | −95 | − 1 | + 4 | 0 | 0 | 0 |
| $S_4$ | 0 | − 3 | − 8 | +16 | +47 | −32 |
| $S_5$ | 0 | − 2 | − 2 | +42 | −58 | −13 |
| $S_6$ | 0 | 0 | 0 | +16 | +23 | +76 |

| | B | | | | |
|---|---|---|---|---|---|
| $\nu_{calcd}$ | 2259 | 882 | 601 | 247 | 369 |
| $S_7$ | + 8 | +88 | + 4 | + 1 | + 1 |
| $S_8$ | −95 | + 5 | + 1 | 0 | 0 |
| $S_9$ | 0 | −14 | +48 | +25 | +15 |
| $S_{10}$ | 0 | 0 | +28 | −84 | + 3 |
| $S_{11}$ | 0 | 0 | + 6 | +17 | −93 |

a) See the footnote of Table VII.

the L matrix elements have revealed that the vibrations assigned to the C-C-C bending and the C-C≡N bending modes correspond respectively to the in-phase and the out-of-phase coupling of the above two coordinates. The calculated and the observed frequencies of succinonitrile are compared in Table VIII, and the diagonal terms of the potential energy distribution for the trans and the gauche forms are listed in Tables IX and X, respectively. In the case of the trans form, where no coupling between the in-plane ($A_g$ and $B_u$) and out-of-plane ($A_u$ and $B_g$) vibrations occurs, situation is the same as in propionitrile and energetically the contributions of both the coordinates $S_4$(C-C-C bending)

and $S_5$(C-C≡N bending) or those of $S_9$(C-C-C bending) and $S_{10}$(C-C≡N bending) are important in producing two each of the skeletal deformation vibrations belonging to class $A_g$ or $B_u$. It is shown from the signs of the L matrices that the vibrations assigned to the C-C-C bending modes (600~450 $cm^{-1}$) correspond to the in-phase coupling and those assigned to the C-C≡N bending modes (250~150 $cm^{-1}$) to the out-of-phase coupling of the two types of bending coordinate. The potential energy distributions show that the $A_g$ vibration which corresponds to the symmetric C-CN stretching mode has a large contribution from the C-C-C bending motion. This is in agreement with the result obtained in the case of 1,2-dichloroethane[19]. In the case of the gauche form coupling occurs between $S_4$, $S_5$ and $S_6$ or $S_9$, $S_{10}$ and $S_{11}$ to produce three each of the skeletal deformation frequencies belonging to class A or B. However, it may be noted that the contribution of $S_6$ or $S_{11}$ (C-C≡N out-of-plane bending) is predominant in the vibrations assigned to the C-C≡N bending modes (400~350 $cm^{-1}$). As in the case of the trans form the energetical contributions of both $S_4$ and $S_5$ or of both $S_9$ and $S_{10}$ are important in two each of the remaining skeletal deformation vibrations belonging to class A or B. The signs of the L matrix elements show that the vibrations assigned to the C-C-C bending modes (600~450 $cm^{-1}$) correspond to the in-phase coupling and those assigned to the C-C≡N bending modes (250~150 $cm^{-1}$) to the out-of-phase coupling of the two types of bending coordinate.

*Central Research Laboratories*
*Toyo Rayon Co., Ltd.*
*Otsu, Shiga-ken*

19) I. Nakagawa and S. Mizushima, ibid., **21**, 2195 (1953).

# *Spectroscopic Studies on Molecular Configurations of Some Aliphatic Dinitriles. II. Infrared Spectra of Glutaronitrile and Bis(glutaronitrilo)copper(I) Nitrate*

By Ikuo MATSUBARA

(Received April 24, 1961)

In the preceding paper[1] the author has reported on the analysis of the infrared spectrum of bis(succinonitrilo)copper(I) nitrate, which proved to be quite useful for the understanding of the spectrum of succinonitrile. As a continuation of the spectroscopic studies on the series of aliphatic dinitriles, the infrared spectrum of bis(glutaronitrilo)copper(I) nitrate, $[Cu\{NC-(CH_2)_3-CN\}_2]NO_3$, has been investigated in connection with the molecular configuration of glutaronitrile. This molecule has four possible spectroscopically distinguishable rotational isomers, *TT*, *TG*, *GG* and *GG'*[2], and the complexity of its spectrum in the liquid state, which may be ascribed to the coexistence of these rotational isomers, makes its analysis almost impossible. Recently the author has studied the infrared spectrum of glutaronitrile by the use of low-temperature techniques and found that this molecule forms two different crystalline solid phases, depending on the mode of crystallization[3]. Determination of the molecular configuration of glutaronitrile in each crystalline solid phase has been made possible by comparing the two solid-state spectra with that of bis(glutaronitrilo)copper(I) nitrate, the X-ray analysis of which has revealed that in the crystals of this complex the ligand glutaronitrile molecule takes the *GG* configuration[4]. The detailed analysis of the infrared spectrum of this complex which will be presented in this paper has been undertaken to interpret the whole spectrum of glutaronitrile both in the liquid and in the crystalline solid states. Calculation of the skeletal vibrations for each isomeric form of glutaronitrile also proved useful in determining the configuration of this molecule.

## Experimental

Bis(glutaronitrilo)copper(I) nitrate was prepared in the same way as that described in the previous paper[4].

The infrared spectra in the 4000~400 $cm^{-1}$ region of glutaronitrile and the complex were recorded using a Perkin-Elmer Model 21 and a Perkin-Elmer Model 13 spectrophotometer (with sodium chloride

1) I. Matsubara, This Bulletin, 34, 1710 (1961).
2) For the nomenclature of the rotational isomers see S. Mizushima, "Structure of Molecules and Internal Rotation", Academic Press Inc., New York (1954), Part I, Chapter V.
3) I. Matsubara, *J. Chem. Phys.*, 35, 373 (1961).
4) Y. Kinoshita, I. Matsubara and Y. Saito, This Bulletin, 32, 1216 (1959).

and potassium bromide optics, respectively). The spectrum of glutaronitrile in the liquid state is shown in Fig. 1a. As has already been reported[3], glutaronitrile can form two different crystalline solid phases. By rapid cooling of the liquid down to −60°C a metastable crystalline form is obtained. This has the spectrum shown in Fig. 1b. When the solid is warmed up to −40°C an irreversible transition occurs giving a more stable crystalline form which has the spectrum shown in Fig. 1c. The spectrum of bis(glutaronitrilo)copper(I) nitrate was obtained using both Nujol mull and potassium bromide disk methods. The spectrum obtained from a Nujol mull of the complex by using KRS-5 supporting plates is shown in Fig. 2a. The spectrum in Fig. 2b is that obtained from a Nujol mull of the complex by using potassium bromide plates. (This spectrum was recorded after the specimen had been placed in the laboratory for one day.) These two spectra are very different from each other, showing that a reaction occurred between the complex and potassium bromide as in the case of bis(succinonitrilo)copper(I) nitrate[1]. The use of sodium chloride plates resulted in a spectrum identical with that in Fig. 2a and no time dependent change of the spectrum was observed. Potassium bromide disks of the complex gave different spectra depending on the pressure applied to prepare the disk. In Figs. 3a and 3b are shown the spectra obtained from the disks which were prepare by applying pressures of 8 tons and 10 tons, respectively. The potassium bromide disk having the spectrum shown in Fig. 3a, when repressed under a pressure of 10 tons, undergoes an irreversible change and

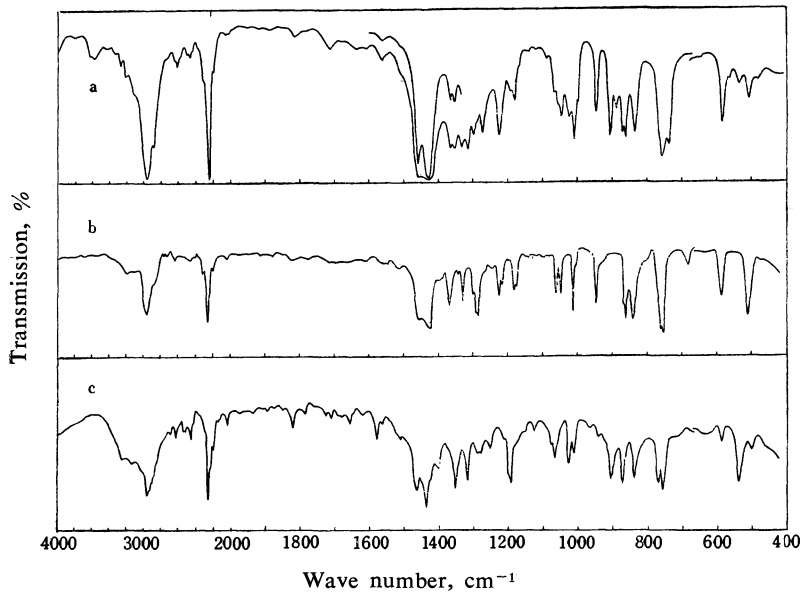



Fig. 1. Infrared spectra of glutaronitrile in various states. (a) liquid; (b) solid (metastable form); (c) solid (stable form).

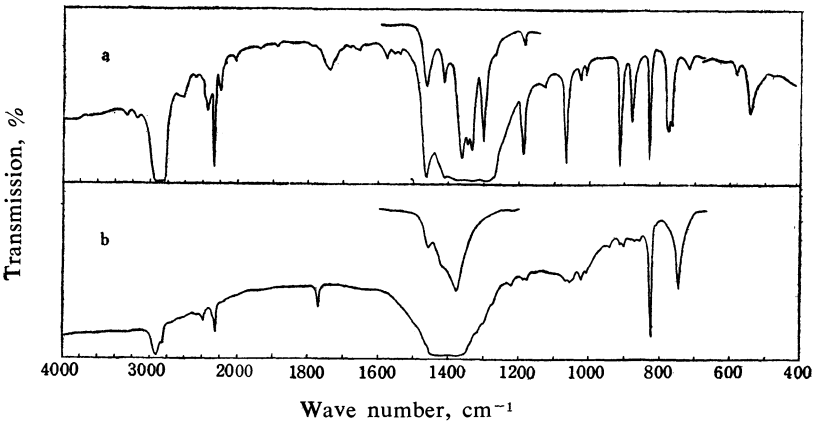



Fig. 2. Infrared spectra obtained from Nujol mulls of bis(glutaronitrilo)-copper(I) nitrate by using (a) KRS-5 and (b) KBr supporting plates.

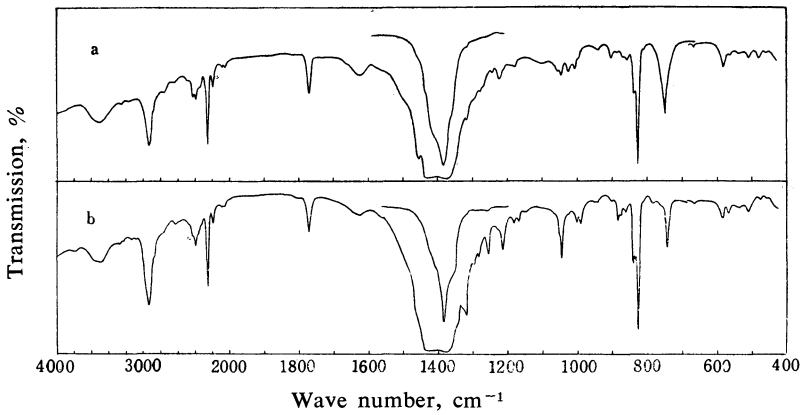



Fig. 3. Infrared spectra obtained from KBr disks of bis(glutaronitrilo)-copper(I) nitrate prepared by applying pressures of (a) 8 tons and (b) 10 tons.

comes to exhibit a spectrum identical with that shown in Fig. 3b. The absorption frequencies of glutaronitrile and bis(glutaronitrilo)copper(I) nitrate are listed in Table I together with the assignment.

## Results and Discussion

The symmetry types and the selection rules for the fundamental vibrations of glutaronitrile in the 1400~400 $cm^{-1}$ region[5,6] are given in Table II. All the fifteen fundamental vibrations in this region are expected to be infrared active for the *TG*, *GG* and *GG'* isomers, while for the *TT* isomer two $CH_2$ twisting and one $CH_2$ rocking modes belonging to class $A_2$ are infrared inactive. As long as the ligand glutaronitrile takes the *GG* configuration in the crystals of bis(glutaronitrilo)copper(I) nitrate[4], its spectrum should be explained as due to the vibrations of the *GG* form of glutaronitrile. The spectrum obtained from a Nujol mull of this complex by using KRS-5 supporting plates (Fig. 2a) seems to be in good agreement with the selection rules for the *GG* isomer of glutaronitrile. On the other hand, the Nujol mull spectrum obtained by the use of potassium bromide plates (Fig. 2b) and the potassium bromide disk spectrum (Fig. 3a) are very different from the spectrum in Fig. 2a and are quite similar to that of the liquid glutaronitrile (Fig. 1a). This means that free glutaronitrile has been produced as a result of interaction between the complex and potassium bromide. This interaction caused the shifts of the nitrate bands of the complex observed at 1748, 1361 and 830 $cm^{-1}$ in Fig. 2a to 1770, 1385 and 826 $cm^{-1}$, respectively, as shown in Figs. 2b and 3. The latter frequencies agree quite well with those of potassium nitrate[7], showing that the mechanism of reaction of the complex and potassium bromide should be ascribed largely to an ion interchange between the two phases as in the case of bis-(succinonitrilo)copper(I) nitrate[1].

As reported in the previous paper[3] the spectrum of glutaronitrile in the stable crystalline form (Fig. 1c) is closely correlated with that of bis(glutaronitrilo)copper(I) nitrate shown in Fig. 2a. The one to one correspondences between the individual bands of the two spectra are almost complete except for the regions where absorptions due to nitrate vibrations or skeletal vibrations of the complex take place. From this result it has been concluded that glutaronitrile takes the *GG* configuration in the stable crystalline solid state[3]. The vibrational assignment of these two spectra, though tentative in nature, are made with reference to the work of Brown and Sheppard[8] on trimethylene halides which were also found to take the *GG* configuration in the crystalline solid state. Thus, the bands observed at 1350, 1316 and 1250 $cm^{-1}$ in the spectrum of the stable solid form (Fig. 1c) may be assigned to the $CH_2$ wagging modes and those at 1287/79, 1190 and 1125 $cm^{-1}$ to the $CH_2$ twisting modes. The behaviors of the $CH_2$ wagging modes are somewhat anomalous in the case of the complex (Fig. 2a). There are quite intense bands at 1334 and 1300 $cm^{-1}$ but no band is observable around 1250 $cm^{-1}$. Although this may be ascribed to the effect of the crystalline force field of the complex, no further discussions will be made at this stage. The bands observed at 1271, 1188 and 1130 $cm^{-1}$ in the spectrum

5) J. K. Brown, N. Sheppard and D. M. Simpson, *Phil. Trans. Roy. Soc. London*, A247, 35 (1954).
6) E. Funck, *Z. Elektrochem.*, 62, 901 (1958).
7) F. A. Miller and C. H. Wilkins, *Anal. Chem.*, 24, 1253 (1952).
8) J. K. Brown and N. Sheppard, *Proc. Roy. Soc.*, A231, 555 (1955).

TABLE I. INFRARED ABSORPTION BANDS OF GLUTARONITRILE AND BIS(GLUTARONITRILO)COPPER(I) NITRATE

| Glutaronitrile | | | Bis(glutaronitrilo) copper(I) nitrate | | Assignment | |
|---|---|---|---|---|---|---|
| Liquid | Solid | | Nujol mull[a] | KBr disk[b] | | |
| | Metastable form | Stable form | | | | |
| | | 3247 vw | 3279 vw | 3257 vw | | |
| 3205 vw | 3195 vw | | | | | |
| | | | 3165 vw | | | |
| 3115 vw sh | | 3125 vw | | 3125 vw | | |
| 2959 s | 2950 ms | 2950 s | | 2933 ms | *TT*, *TG*, *GG* | C-H stretch. |
| | | 2924 s sh | | 2915 m sh | | |
| 2890 m | 2874 w | 2890 w sh | | 2874 w sh | *TT*, *TG*, *GG* | C-H stretch. |
| | | 2688 vw | 2695 vw | | | |
| 2646 vw sh | | | | | | |
| 2618 vw | 2625 w | 2625 w | 2632 w | 2618 vw | | |
| | | 2532 vw | | | | |
| 2506 vw | | 2500 vw | 2488 vw | | | |
| 2463 vw | 2451 w | | | | | |
| 2445 vw sh | | 2445 w | 2421 vw sh | 2427 w sh | | |
| | | | | 2398 mw | | |
| | | | 2353 mw | 2364 w sh | | |
| 2299 vw sh | 2304 w | 2288 vw sh | | | | |
| | | | 2278 s | | *GG* | C≡N stretch. (bound) |
| 2249 vs | 2245 ms | 2247 s | | 2252 ms | *TT*, *TG*, *GG* | C≡N stretch. (free) |
| 2198 vw | 2198 w | 2198 w | 2208 w | 2198 mw | | |
| | | | | 2096 vw | | |
| 2049 vw | | | | | | |
| 2016 vw | 2016 vw | 2020 w | 2037 w | | | |
| | | 1931 vw | 1942 vw | | | |
| 1890 vw | | 1890 vw | 1890 vw | | | |
| 1812 w | 1818 vw | 1818 w | | | | |
| 1786 vw | 1773 vw | 1783 vw | 1776 vw | | | |
| | | 1721 vw | 1724 vw sh | | | |
| 1712 w | | 1706 vw | 1706 w sh | | | |
| | | 1675 vw | 1672 vw | | | |
| 1634 vw | | 1653 w | 1658 vw | | | |
| 1608 vw | 1605 vw | 1613 vw | | | | |
| | 1570 vw | 1575 w | 1580 w | | | |
| 1563 w | 1553 vw | 1560 vw | 1558 vw | 1563 vw | | |
| 1548 vw sh | 1543 vw | 1536 vw sh | 1543 vw | | | |
| 1511 vw sh | 1508 w | 1508 vw | 1506 vw sh | | | |
| 1458 s | 1451 ms | 1460 ms | | | *TT*, *TG*, *GG* | $CH_2$ bend. |
| 1429 vs | 1420 s | 1433 s | 1414 s | | *TT*, *TG*, *GG* | $CH_2$ bend. |
| | 1395 vw | 1399 w | | | | |
| 1366 m | 1364 m | | | | *TG* | $CH_2$ wag. |
| 1355 m | | 1350 ms | 1334 vs | | *GG* | $CH_2$ wag. |
| | 1339 w | | | | | |
| 1333 m | 1328 m | | | 1328 w sh | *TG* | $CH_2$ wag. |
| 1314 m | | 1316 ms | 1300 vs | 1319 mw | *TT*, *GG* | $CH_2$ wag. |
| 1299 m | 1300 w | | | 1297 vw | *TG* | $CH_2$ twist. |
| 1289 vw sh | | 1287 w | 1271 ms sh | 1280 w | *GG* | $CH_2$ twist. |
| | 1289 ms sh | 1279 w | | | | |
| 1272 m | 1282 ms | | | 1272 vw sh | *TG* | $CH_2$ wag. |
| | | 1250 w | | 1256 mw | *TT*, *GG* | $CH_2$ wag. |
| | 1241 vw | | | | | |

TABLE I. (Continued)

| Glutaronitrile | | | Bis(glutaronitrilo) copper(I) nitrate | | Assignment | |
|---|---|---|---|---|---|---|
| Liquid | Solid | | Nujol mull[a] | KBr disk[b] | | |
| | Metastable form | Stable form | | | | |
| 1224 ms | 1224 m | | | 1224 vw sh | *TG* | $CH_2$ twist. |
| | 1214 mw | | | 1214 mw | *TT* | $CH_2$ twist. |
| | | 1208 vw | | | | |
| 1193 vw | | 1190 ms | 1188 s | | *GG* | $CH_2$ twist. |
| 1181 m | 1181 m | | | 1179 w | *TG* | $CH_2$ twist. |
| 1170 vw sh | 1174 m | | | 1168 w | *TT* | $CH_2$ twist. |
| 1145 vw | 1148 vw | | | 1149 vw | | |
| | 1140 vw | | | | | |
| 1120 vw | | 1125 w | 1130 w | | *GG* | $CH_2$ twist. |
| 1087 vw | | 1075 w | | | | |
| 1066 w sh | 1060 m | 1065 m | 1066 s | 1064 vw sh | *TG*, *GG* | C–C stretch. |
| 1056 w sh | | | | 1050 w sh | *TT* | C–C stretch. |
| 1047 m | 1045 m | | | 1044 m | *TT*, *TG* | C–C stretch. |
| 1022 m | | 1026 m | 1027 mw | 1026 vw sh | *GG* | C–C stretch. |
| 1008 ms | 1009 ms | 1010 m | 1009 w | | *TG*, *GG* | C–C stretch. |
| | 1003 w sh | | | | | |
| 998 w | | | | 1000 w | *TT* | C–C stretch. |
| 991 vw sh | | | | 990 w | | |
| | | 964 w | 971 vw | 953 vw | | |
| 945 m | 943 ms | 943 w | | 943 vw | *TG* | $CH_2$ rock. |
| 904 ms | | 903 ms | 913 s | 902 vw | *GG* | $CH_2$ rock. |
| | | 899 ms sh | | | | |
| 888 w | | | | 885 mw | *TT* | C–C stretch. |
| 870 ms | | 873 ms | 880 ms | 877 w | *GG* | C–C stretch. |
| | | 871 ms | | | | |
| | 864 m sh | 864 w sh | | | | |
| 860 ms | 859 ms | | | 861 w | *TG* | C–C stretch. |
| 835 ms | 839 ms | 837 ms | 830 s | 839 m | *TG*, *GG* | $CH_2$ rock. |
| | 835 ms sh | | | 833 m | | |
| | 800 vw | | 808 vw | 812 vw sh | | |
| 757 s | 757 s | 768 ms | 778 ms | 784 w | *TG*, *GG* | $CH_2$ rock. |
| | 751 s | 754 ms | 767 ms | 758 vw sh | | |
| 737 ms | | | | 742 m | *TT* | $CH_2$ rock. |
| | 681 mw | | | | | |
| | | | | 666 vw | | |
| 648 vw | | | | | | |
| 583 ms | 586 ms | 588 w | 586 w | 584 mw | *TG*, *GG* | C–C–C bend. |
| 565 w | | | | 564 w | *TT* | C–C–C bend. |
| 535 w | | 537 ms | 544 ms | 532 vw | *GG* | C–C–C bend. |
| 507 m | 511 ms | 503 vw | | 508 w | *TG* | C–C–C bend. |
| 481 vw | | | 475 vw | 473 vw | *TT* | C–C–C bend. |
| | | | | 458 vw | | |

a) KRS-5 supporting plates were used to obtain the spectrum.
b) The disk was prepared by applying a pressure of 10 tons.

of the complex are assigned to the $CH_2$ twisting modes. Absorptions corresponding to the C–C stretching modes are found at 1065, 1026, 1010 and 873 $cm^{-1}$ in the spectrum of the stable solid form and at 1066, 1027, 1009 and 880 $cm^{-1}$ in the spectrum of the complex. To the $CH_2$ rocking modes may correspond the bands observed at 903, 837 and 768/54 $cm^{-1}$ in the spectrum of the stable solid form and those observed at 913, 830 and 778/67 $cm^{-1}$ in the spectrum of the complex.

The configuration of glutaronitrile in the metastable crystalline solid state must be the *TG* form as the *TT* form can be excluded from

TABLE II. THE SYMMETRY TYPES AND SELECTION RULES FOR THE FUNDAMENTAL VIBRATIONS OF GLUTARONITRILE IN THE 1400～400 $cm^{-1}$ REGION

| Types of symmetry coordinates | | *TT*($C_{2v}$) | | | | *GG*($C_2$) | | *TG*($C_1$) | *GG'*($C_s$) | |
|---|---|---|---|---|---|---|---|---|---|---|
| | | $A_1$ | $A_2$ | $B_1$ | $B_2$ | A | B | | A' | A'' |
| $CH_2$ wagging | | 1 | 0 | 2 | 0 | 1 | 2 | 3 | 1 | 2 |
| $CH_2$ twisting | | 0 | 2 | 0 | 1 | 2 | 1 | 3 | 1 | 2 |
| C-C stretching | | 2 | 0 | 2 | 0 | 2 | 2 | 4 | 2 | 2 |
| $CH_2$ roking | | 0 | 1 | 0 | 2 | 1 | 2 | 3 | 2 | 1 |
| C-C-C bending | | 1 | 0 | 1 | 0 | 1 | 1 | 2 | 1 | 1 |
| Selection rules | IR | + | − | + | + | + | + | + | + | + |
| | Raman | + | + | + | + | + | + | + | + | + |

consideration of the selection rules and the existence of the *GG'* form is considered improbable from steric reasons[3]. The vibrational assignment of the spectrum shown in Fig. 1b was made on this basis. Thus, the bands observed at 1364, 1328 and 1289/82 $cm^{-1}$ may be assigned to the $CH_2$ wagging modes, and those at 1300, 1224/14 and 1181/74 $cm^{-1}$ to the $CH_2$ twisting modes of the *TG* form. The bands at 1060, 1045, 1009 and 859 $cm^{-1}$ correspond to the C-C stretching modes and those at 943, 839/35 and 757/51 $cm^{-1}$ must be ascribed to the $CH_2$ rocking modes.

The majority of the bands in the liquid-state spectrum of glutaronitrile (Fig. 1a) can be satisfactorily explained as due to the vibrations of the *TG* and the *GG* isomers, and a few remaining bands must be ascribed to the vibrations of the *TT* form, because one of them at 737 $cm^{-1}$ certainly corresponds to the $CH_2$ rocking vibration of the methylene chain of the planar all-trans configuration[5,9]. These conclusions are further confirmed by the calculation of the skeletal deformation vibrations for each isomeric form of glutaronitrile (see Appendix). The results of the calculation show that each isomer should have two C-C-C bending frequencies in the 650～450 $cm^{-1}$ region. From the potential energy distributions it is shown that the energetical contributions of both the C-C-C bending and the C-C≡N (in-plane) bending motions are important in these skeletal deformation vibrations as in the case of succinonitrile[1]. The frequencies of 586 and 511 $cm^{-1}$ observed in the spectrum of the metastable solid form (Fig. 1b) agree quite well with the values of 567 and 507 $cm^{-1}$ calculated for the *TG* form. The frequencies of 588 and 537 $cm^{-1}$ observed in the spectrum of the stable solid form (Fig. 1c) and those of 586 and 544 $cm^{-1}$ in the spectrum of the complex (Fig. 2a) are in excellent agreement with the values of 590 and 535 $cm^{-1}$ calculated for the *GG* form. In the spectrum of the liquid glutaronitrile there are weak bands at 565 and 481 $cm^{-1}$ which disappear at low temperatures. These frequencies correspond well with the values of 546 and 441 $cm^{-1}$ calculated for the *TT* form. The values of 616 and 510 $cm^{-1}$ calculated for the *GG'* form seem not to be appropriate to explain the observed frequencies in all cases. The potassium bromide disk spectrum of the complex shown in Fig. 3b is different from the spectrum in Fig. 3a in that the absorptions corresponding to the vibrations of the *TT* form as described above are anomalously intense. It seems that the applied pressure of 10 tons must have favored the selective formation of the *TT* isomer in the reaction of the complex with potassium bromide. The spectrum in Fig. 3b shows a few other anomalously intense bands besides those mentioned above. These bands must also correspond to the vibrations of the *TT* form which could not be identified in the spectrum of the liquid glutaronitrile because of the overlapping of absorptions due to the *TG* or the *GG* form.

Spectral features of the complex in the C≡N stretching frequency region are similar to those of bis(succinonitrilo)copper(I) nitrate[1]. The sharp band observed at 2278 $cm^{-1}$ in the Nujol mull spectrum (Fig. 2a) should correspond to the C≡N stretching mode of the complex. The C≡N vibrational shift of 29 $cm^{-1}$ towards higher frequencies as compared with the free glutaronitrile may be explained from a consideration of the structure of the complex. From X-ray analysis of this complex[4] it has been found that the carbon-nitrogen bond distance is 1.14 Å and that the Cu-N-C-$CH_2$ group is close to linear. This suggests that the carbon-nitrogen bond is essentially of a triple-bond character, the contributions of polar resonance structures such as $-C^+=N^-$ being decreased, and the C≡N stretching frequency is thereby increased. The effect of coupling between the C≡N stretching and the Cu-N stretching vibrations, though small, may also contribute to the increase in the C≡N stretching frequency. As shown in Figs. 2b and 3, reaction with potassium bromide results in the appearance of the band at 2252 $cm^{-1}$ which corresponds to the C≡N stretching frequency of the free glutaronitrile. The band observed at 2353 $cm^{-1}$ in

9) H. Tschamler, *J. Chem. Phys.*, 22, 1845 (1954).

the Nujol mull spectrum is considered to be characteristic of the tetrahedral configuration of the complex as in the case of bis(succinonitrilo)copper(I) nitrate[1]. The origin of the band observed at 2208 $cm^{-1}$ is hard to explain, because its intensity tends to vary from specimen to specimen and no other homologues of this series of complex show any absorption at the corresponding frequency. For the present, it may be ascribed to a certain combination vibration or to a vibration of some impurities in the complex.

## Summary

The infrared spectra of glutaronitrile and bis(glutaronitrilo)copper(I) nitrate, $[Cu\{NC-(CH_2)_3-CN\}_2]NO_3$, have been studied. The spectrum of the complex has been analyzed on the basis of the result of X-ray analysis which disclosed that the ligand glutaronitrile takes the *GG* configuration in the crystals of this compound. This complex reacts with alkali halides such as potassium bromide, resulting in the isolation of free glutaronitrile. Considering

Table III. Force constants of glutaronitrile (in millidyne/Å)[a]

| | |
|---|---|
| $K(CH_2-CH_2)=3.70$ | $H(CH_2-C\equiv N)=0.14_1$ |
| $K(CH_2-C)=3.50$ | $F(CH_2-CH_2-CH_2)=0.45$ |
| $K(C\equiv N)=18.10$ | $F(CH_2-CH_2-C)=0.45$ |
| $H(CH_2-CH_2-CH_2)=0.25$ | $F(CH_2-C\equiv N)=0.50$ |
| $H(CH_2-CH_2-C)=0.25$ | $k(C-C\equiv N)=0.12$ Å$^2$ |

a) Transferred from succinonitrile. See Appendix in Ref. 1.

Table IV. Symmetry coordinates of glutaronitrile

| $C_{2v}$ | $C_2$ | $C_s$ | | |
|---|---|---|---|---|
| $A_1$ | A | A' | $S_1=(\Delta r_1+\Delta r_1')/\sqrt{2}$ | ($CH_2$-$CH_2$ sym. stretching) |
| | | | $S_2=(\Delta r_2+\Delta r_2')/\sqrt{2}$ | ($CH_2$-C sym. stretching) |
| | | | $S_3=(\Delta r_3+\Delta r_3')/\sqrt{2}$ | (C≡N sym. stretching) |
| | | | $S_4=\Delta\alpha_0$ | ($CH_2$-$CH_2$-$CH_2$ bending) |
| | | | $S_5=(\Delta\alpha+\Delta\alpha')/\sqrt{2}$ | ($CH_2$-$CH_2$-C sym. bending) |
| | | | $S_6=(\Delta\beta+\Delta\beta')/\sqrt{2}$ | ($CH_2$-C≡N sym. in-plane bending) |
| $A_2$ | | | $S_7=(\Delta\gamma+\Delta\gamma')/\sqrt{2}$ | ($CH_2$-C≡N sym. out-of-plane bending) |
| $B_1$ | B | A'' | $S_8=(\Delta r_1-\Delta r_1')/\sqrt{2}$ | ($CH_2$-$CH_2$ antisym. stretching) |
| | | | $S_9=(\Delta r_2-\Delta r_2')/\sqrt{2}$ | ($CH_2$-C antisym. stretching) |
| | | | $S_{10}=(\Delta r_3-\Delta r_3')/\sqrt{2}$ | (C≡N antisym. stretching) |
| | | | $S_{11}=(\Delta\alpha-\Delta\alpha')/\sqrt{2}$ | ($CH_2$-$CH_2$-C antisym. bending) |
| | | | $S_{12}=(\Delta\beta-\Delta\beta')/\sqrt{2}$ | ($CH_2$-C≡N antisym. in-plane bending) |
| $B_2$ | | | $S_{13}=(\Delta\gamma-\Delta\gamma')/\sqrt{2}$ | ($CH_2$-C≡N antisym. out-of-plane bending) |

Table V. Calculated and observed frequencies of glutaronitrile (in $cm^{-1}$)

| *TT*($C_{2v}$) | | | *GG*($C_2$) | | | | *TG*($C_1$) | | *GG'*($C_s$) | |
|---|---|---|---|---|---|---|---|---|---|---|
| Calcd. | | Obs. Liquid[a] | Calcd. | Obs. Solid[b] | | Obs. Complex[c] | Calcd | Obs. Solid[d] | Calcd. | Assignment |
| $A_1$ 2259 | | | A 2259 | | | | 2259 | | A' 2259 | C≡N sym. stretching |
| 993 | | | 980 | | | | 984 | | 980 | C-C sym. stretching |
| 909 | | | 825 | | | | 829 | | 826 | C-CN sym. stretching |
| 441 | | 481 | 590 | 588 | | 586 | 507 | 511 | 616 | C-C-C bending |
| 315 | | | 358 | | | | 336 | | 364 | C-C-C bending |
| 107 | | | 157 | | | | 205 | | 226 | C-C≡N bending |
| $A_2$ 398 | | | 384 | | | | 368 | | 399 | C-C≡N bending |
| $B_1$ 2259 | | | B 2259 | | | | 2259 | | A'' 2259 | C≡N antisym. stretching |
| 1069 | | | 1062 | | | | 1067 | | 1062 | C-C antisym. stretching |
| 843 | | | 853 | | | | 883 | | 851 | C-CN antisym. stretching |
| 546 | | 565 | 535 | 537 | | 544 | 567 | 586 | 510 | C-C-C bending |
| 230 | | | 241 | | | | 174 | | 169 | C-C≡N bending |
| $B_2$ 398 | | | 387 | | | | 388 | | 365 | C-C≡N bending |

a) Obtained by subtracting the bands which correspond to the vibrations of the *GG* and the *TG* isomers.
b) Stable crystalline solid state.
c) Obtained from a Nujol mull by using KRS-5 supporting plates.
d) Metastable crystalline solid state.

TABLE VI. POTENTIAL ENERGY DISTRIBUTIONS OF THE *TT* FORM OF GLUTARONITRILE[a]

| | $A_1$ | | | | | | $A_2$ |
|---|---|---|---|---|---|---|---|
| $\nu_{calcd}$ | 2259 | 993 | 909 | 441 | 315 | 107 | 398 |
| $S_1$ | 0 | +82 | +11 | + 9 | + 3 | + 1 | — |
| $S_2$ | − 8 | −20 | +60 | + 1 | +13 | 0 | — |
| $S_3$ | +95 | − 1 | + 3 | 0 | + 1 | 0 | — |
| $S_4$ | 0 | − 1 | −20 | − 1 | +60 | −22 | — |
| $S_5$ | 0 | − 7 | −18 | +20 | + 6 | +53 | — |
| $S_6$ | 0 | − 1 | − 1 | +65 | − 7 | −26 | — |
| $S_7$ | — | — | — | — | — | — | +100 |

| | $B_1$ | | | | | $B_2$ |
|---|---|---|---|---|---|---|
| $\nu_{calcd}$ | 2259 | 1069 | 843 | 546 | 230 | 398 |
| $S_8$ | 0 | +93 | + 7 | 0 | − 2 | — |
| $S_9$ | + 8 | − 9 | +85 | + 1 | 0 | — |
| $S_{10}$ | −95 | 0 | + 5 | 0 | 0 | — |
| $S_{11}$ | 0 | 0 | − 5 | +58 | +41 | — |
| $S_{12}$ | 0 | 0 | 0 | +40 | −59 | — |
| $S_{13}$ | — | — | — | — | — | +100 |

a) The signs of the corresponding L matrix elements are also included.

TABLE VII. POTENTIAL ENERGY DISTRIBUTIONS OF THE *GG* FORM OF GLUTARONITRILE[a]

| | A | | | | | | |
|---|---|---|---|---|---|---|---|
| $\nu_{calcd}$ | 2259 | 980 | 825 | 590 | 358 | 157 | 384 |
| $S_1$ | 0 | +77 | +27 | + 1 | − 1 | 0 | 0 |
| $S_2$ | + 8 | −29 | +61 | + 5 | 0 | 0 | 0 |
| $S_3$ | −95 | − 1 | + 3 | 0 | 0 | 0 | 0 |
| $S_4$ | 0 | − 7 | 0 | −28 | −44 | +14 | +10 |
| $S_5$ | 0 | 0 | −11 | +31 | − 7 | +45 | −11 |
| $S_6$ | 0 | − 1 | − 2 | +20 | −46 | −47 | 0 |
| $S_7$ | 0 | 0 | 0 | + 5 | +20 | +15 | +74 |

| | B | | | | | |
|---|---|---|---|---|---|---|
| $\nu_{calcd}$ | 2259 | 1062 | 853 | 535 | 241 | 387 |
| $S_8$ | 0 | +96 | + 4 | + 3 | 0 | 0 |
| $S_9$ | + 8 | − 7 | +85 | + 2 | 0 | 0 |
| $S_{10}$ | −95 | 0 | + 5 | 0 | 0 | 0 |
| $S_{11}$ | 0 | − 3 | −12 | +39 | +27 | −23 |
| $S_{12}$ | 0 | − 1 | − 1 | +33 | −79 | − 2 |
| $S_{13}$ | 0 | 0 | 0 | + 7 | +26 | +83 |

a) See the footnote of Table VI.

TABLE VIII. POTENTIAL ENERGY DISTRIBUTIONS OF THE *TG* FORM OF GLUTARONITRILE[a]

| $\nu_{calcd}$ | 2259 | 984 | 839 | 507 | 336 | 205 | 368 | 2259 | 1067 | 883 | 567 | 174 | 388 |
|---|---|---|---|---|---|---|---|---|---|---|---|---|---|
| $S_1$ | 0 | +83 | +13 | + 5 | + 1 | 0 | + 1 | 0 | + 1 | − 1 | − 1 | 0 | + 1 |
| $S_2$ | − 7 | −21 | +57 | + 1 | + 2 | + 1 | + 1 | + 1 | 0 | −13 | 0 | 0 | 0 |
| $S_3$ | +80 | − 1 | + 3 | 0 | 0 | 0 | 0 | −15 | 0 | − 1 | 0 | 0 | 0 |
| $S_4$ | 0 | − 4 | − 1 | − 3 | +55 | + 4 | + 1 | 0 | 0 | +11 | − 8 | −14 | + 2 |
| $S_5$ | 0 | − 2 | −14 | +17 | 0 | +34 | +20 | 0 | − 2 | + 1 | + 6 | + 8 | − 1 |
| $S_6$ | 0 | − 1 | − 1 | +26 | + 3 | −54 | +14 | 0 | 0 | 0 | + 7 | − 8 | 0 |
| $S_7$ | 0 | 0 | 0 | +10 | + 1 | +16 | −73 | 0 | 0 | 0 | + 2 | + 1 | +13 |
| $S_8$ | 0 | + 1 | 0 | 0 | 0 | 0 | 0 | 0 | −93 | − 6 | − 1 | − 1 | 0 |
| $S_9$ | + 1 | 0 | −17 | 0 | + 3 | 0 | 0 | + 7 | + 9 | −59 | − 5 | 0 | + 1 |
| $S_{10}$ | −15 | 0 | − 1 | 0 | 0 | 0 | 0 | −80 | 0 | − 3 | − 1 | 0 | 0 |
| $S_{11}$ | 0 | − 2 | 0 | + 5 | − 1 | − 5 | + 1 | 0 | 0 | +11 | −32 | +32 | +15 |
| $S_{12}$ | 0 | 0 | 0 | +12 | −31 | + 6 | + 1 | 0 | + 1 | + 1 | −19 | −45 | 0 |
| $S_{13}$ | 0 | 0 | 0 | + 3 | +16 | − 2 | −10 | 0 | 0 | 0 | − 4 | +13 | −68 |

a) See the footnote of Table VI.

the frequency shifts of the nitrate vibrations the reaction of the complex with potassium bromide should be ascribed largely to an ion interchange between the two phases. The increase of 29 $cm^{-1}$ in the C≡N stretching frequency by complex formation may be understood from the linear structure of the Cu–N–C–$CH_2$ group which suggests that the carbon-nitrogen bond is essentially of a triple-bond character, the contributions of polar resonance structures such as $-C^+=N^-$ being decreased. Glutaronitrile can form two different crystalline solid phases, depending on the mode of crystallization. From comparison of the two solid-state spectra with that of the complex and from consideration of the vibrational selection rules it has been concluded that glutaronitrile takes the *GG* configuration in one crystalline solid state and the *TG* in the other, and that it exists as a mixture of three isomers, *GG*, *TG* and *TT* in the liquid state. Calculation of the skeletal deformation frequencies for each isomeric form has given the results which support this conclusion. Vibrational assignment of glutaronitrile in various states has been made satisfactorily on the basis of the above results.

The author wishes to express his hearty thanks to Professor S. Imanishi of Kyushu University for his kind encouragement in the course of this study. He is also indebted to Dr. H. Murata of Hiroshima University for many helpful discussions and to Mr. D. Miura

of Toyo Rayon Co., Ltd. for carrying out the mechanical calculations. The assistance of Messrs. T. Ito, H. Kataoka and K. Shirasaki of Toyo Rayon Co., Ltd. in experiments is also acknowledged.

## Appendix: Calculation of Skeletal Vibrations

The skeletal vibrations of glutaronitrile were calculated as a seven-body problem. Calculations were carried out on all the four isomeric forms, $TT(C_{2v})$, $GG(C_2)$, $GG'(C_s)$ and $TG(C_1)$. A potential function of the Urey-Bradley type[10] was used, and the values of force constants were transferred from succinonitrile[1] as shown in Table III. The symmetry coordinates of glutaronitrile listed in Table IV were constructed from the internal coordinates shown in Fig. 4. Except for the case

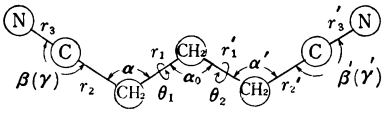



Fig. 4. Internal coordinates of glutaronitrile. $\beta$ (or $\beta'$) and $\gamma$ (or $\gamma'$) denote bending of C≡N bond in and out of the plane of the adjacent C-C-C linkage, respectively. $\theta_1=\theta_2=180°$ for $TT$, $\theta_1=\theta_2=60°$ for $GG$, $\theta_1=-\theta_2=60°$ for $GG'$, and $\theta_1=180°$ and $\theta_2=60°$ for $TG$.

of the $TT$ form, coupling between the C-C≡N in-plane and out-of-plane bending motions occurs. As in the case of succinonitrile[1] a cross term $k$(C-C≡N) corresponding to the interaction of the two C-C≡N bending coordinates was introduced into the potential function (Table III). For the calculation of the kinetic energy matrices the assumed bond lengths of $r(CH_2\text{-}CH_2)=1.54$ Å, $r(CH_2\text{-}C)=1.50$ Å and $r(C\equiv N)=1.15$ Å and the bond angle of 109°28′ were used.

The calculated frequencies are listed in Table V, in which the observed frequencies for the skeletal deformation vibrations are also included, although the observed data are not available for the region below 400 $cm^{-1}$. For each isomeric form there exist two vibrations corresponding to the C-C-C bending modes in the 650~450 $cm^{-1}$ region. The potential energy distributions listed together with the signs of the corresponding L matrix elements in Tables VI—IX show that these vibrations correspond to the in-phase coupling of the C-C-C bending and the C-C≡N (in-plane) bending motions. The agreement between the observed and the calculated frequencies of these vibrations are satisfactory, showing that the skeletal deformation frequencies of glutaronitrile are quite useful in determining the configurations of rotational isomers of this molecule.

Table IX. Potential energy distributions of the $GG'$ form of glutaronitrile[a]

| | A′ | | | | | | |
|---|---|---|---|---|---|---|---|
| $\nu_{calcd}$ | 2259 | 980 | 826 | 616 | 364 | 226 | 399 |
| $S_1$ | 0 | +77 | +27 | + 1 | + 1 | 0 | 0 |
| $S_2$ | + 8 | −29 | +59 | + 6 | 0 | 0 | 0 |
| $S_3$ | −95 | − 1 | + 3 | + 1 | 0 | 0 | 0 |
| $S_4$ | 0 | − 8 | 0 | −22 | +62 | +13 | 0 |
| $S_5$ | 0 | 0 | −13 | +41 | + 4 | +27 | −19 |
| $S_6$ | 0 | − 1 | − 2 | +16 | +34 | −63 | 0 |
| $S_7$ | 0 | 0 | 0 | + 3 | − 2 | +30 | +81 |
| | A″ | | | | | | |
| $\nu_{calcd}$ | 2259 | 1062 | 851 | 510 | 169 | 365 | |
| $S_8$ | 0 | +96 | + 4 | + 2 | 0 | 0 | |
| $S_9$ | − 8 | − 8 | +85 | + 1 | 0 | 0 | |
| $S_{10}$ | +95 | 0 | + 5 | 0 | 0 | 0 | |
| $S_{11}$ | 0 | − 3 | −10 | +23 | +49 | −18 | |
| $S_{12}$ | 0 | − 1 | − 1 | +41 | −56 | −18 | |
| $S_{13}$ | 0 | 0 | 0 | +13 | +11 | +91 | |

a) See the footnote of Table VI.

*Central Research Laboratories*
*Toyo Rayon Co., Ltd.*
*Otsu, Siga-ken*

10) T. Shimanouchi, ibid., **17**, 245, 734, 848 (1949).

# *Synthesis and Physical Properties of Normal Higher Primary Alcohols. IV. Thermal and X-Ray Studies on the Polymorphism of the Alcohols of Even Carbon Numbers from Dodecanol to Tetratriacontanol**

By Akira WATANABE

(Received April 20, 1961)

Since X-ray study on a series of normal paraffins was reported by Müller[1], several investigations have been made on the transition phenomenon of many long-chain compounds including acids[2-5], esters[3,6], bromides[7], and alcohols[8]. In these compounds, phase change is known to occur just below their freezing points accompanying the changes in a number of physical properties such as crystal structure, thermal property, and dipole moment in polar compounds. Recently nuclear magnetic resonance studies were also reported[9]. The $\alpha$ phase, which appears at the high temperature side, has been found to possess molecular freedom, the molecule being assumed to rotate about the long axis because of the characteristics of symmetrical crystal structure and high dielectric constant in this phase.

Although Hoffman et al.[10] recently summarized the results of the several investigations mainly on paraffins and bromides, some problems seemed to remain to be solved. The results on the higher alcohols appearing in the literature seemed to be somewhat ambiguous and the data for the alcohols with odd carbon atoms and with more than eighteen carbon atoms are too scanty to permit generalization of the series. On the other hand, the transition phenomenon has been known to be affected by the presence of extremely small amounts of impurities as well as variations in the technique of measurements and in thermal histories of the materials. Therefore it was felt to be important to examine the phenomenon with a series of pure compounds under conditions as comparable as possible. In view of these facts, the author has undertaken a study of synthesis and physical properties of normal higher alcohols with more than ten carbon atoms in order to establish the existence of transition in each member and its dependency on chain length. The reports on the synthesis have been published[11] and in this paper investigation of thermal analyses and X-ray studies on the alcohols of even carbon atoms from dodecanol to tetratricontanol are reported.

**Nomenclature of the Phases.**—*$\alpha$-Form.*—This form obtained on crystallization from the melt is somewhat transparent and on further cooling changes to the more opaque $\beta$ or $\gamma$ form at the transition point. X-Ray analysis indicates that the hydrocarbon chain is vertical to the plane of the end groups and the dielectric constant is higher than those of the $\beta$ or $\gamma$ or liquid phase. It has also been known that this form is unstable and gradually transforms into a more stable $\gamma$ form on standing.

*$\beta$-Form.*—This form, in which the hydrocarbon chain is vertical to the plane of the end groups, appears below the transition point mainly in odd members and in shorter members of the even alcohols. In the latter case, gradual transformation from $\beta$ to $\gamma$ form is known to exist in some of the members.

*$\gamma$-Form.*—This form, in which the hydrocarbon chain inclines to the plane, appears below the transition point only in even compounds and is stable at low temperature.

The correspondence of the present nomenclature to those adopted by other workers is as follows.

* This study has been carried out at the Department of Physics, Faculty of Science, Kyoto University, as a part of the cooperative research on "Synthesis and Physical Properties of Long Chain Compounds".

1) A. Müller, *Proc. Roy. Soc.*, **A138**, 514 (1932).
2) W. E. Garner and A. M. King, *J. Chem. Soc.*, **1929**, 1849.
3) J. D. Meyer and R. E. Reid, *J. Am. Chem. Soc.*, **55**, 1574 (1933).
4) F. Francis et al., *Proc. Roy. Soc.*, **A128**, 214 (1930); ibid., **A158**, 691 (1937).
5) E. Stenhagen and E. Sydow, *Arkiv. Kemi.*, **6**, 309 (1953).
6) W. O. Baker and C. P. Smyth, *J. Am. Chem. Soc.*, **60**, 1229 (1938).
7) R. W. Crowe and C. P. Smyth, ibid., **72**, 1098 (1950).
8) a) J. W. C. Phyllips and S. Munford., ibid., **55**, 1747 (1933). b) K. Higasi and M. Kubo, *Pap. Inst. Phys. Chem. Res.*, **36**, 286 (1939). c) J. D. Hoffman and C. P. Smyth, *J. Am. Chem. Soc.*, **71**, 431 (1949). d) Y. Kakiuchi and T. Sakurai, *J. Phys. Soc. Japan*, **4**, 365 (1949). e) Y. Kakiuchi, T. Sakurai and T. Suzuki, ibid., **5**, 369 (1950). f) D. G. Kolp and E. S. Lutton, *J. Am. Chem. Soc.*, **73**, 5593 (1951). g) K. Asai, *J. Phys. Soc. Japan*, **14**, 1084 (1959).
9) a) E. R. Andrew, *J. Chem. Phys.*, **18**, 607 (1950). b) S. Kojima and O. Ogawa, *J. Phys. Soc. Japan*, **8**, 283 (1953).
10) J. D. Hoffman and B. F. Decker, *J. Phys. Chem.*, **57**, 520 (1953).
11) A. Watanabe, This Bulletin, **32**, 1295 (1959); A. Watanabe, ibid., **33**, 531 (1960); A. Watanabe, ibid., **34**, 398 (1961).

| Present paper | Kolp, Lutton | Smyth et al. |
|---|---|---|
| $\alpha$ | Alpha | $\alpha$ |
| $\beta$ | Sub-alpha | $\beta_1$ |
| $\gamma$ | Beta | $\beta_2$ |

## Experimental

**Purity of the Materials.**—The alcohols used in this study were all prepared by the lithium aluminum hydride reduction of the corresponding fatty acids or their ethyl esters, the acids above octadecanoic being synthesized from the commercially available lower acids which were initially purified by fractional distillation followed by recrystallization. Since it is difficult to purify the compounds in high purity or to obtain a reliable method to establish their purity when the carbon chain is considerably long, the present efforts were made especially toward the purification of the alcohols above tetracosanol.

As is generally known, elemental analysis data which were presented in previous papers[11], are poor criterions for judging the purity of the compounds with more than about eighteen carbon atoms. It was found, however, in the present study that the transition point rather than the melting point proved to be reliable because repetition of the purification process resulted in the raising or disappearance of the transition points though the melting point did not vary noticeably. Table I gives the melting, freezing and transition points of pure and mixed alcohols.

X-Ray examinations also revealed the interesting facts that the presence of as much as 0.5% of hexadecanol in octadecanol resulted in the apparance of $\beta$ spacing while only $\gamma$ spacing was found in octadecanol assumed to be pure. Similar states were found in higher members. Fig. 1 shows this phenomenon clearly.

The purification of the final products were carried out extensively by means of high-vacuum distillation followed by recrystallization until the melting points, transition points and X-ray spacings became constant.

The facts that the melting points and transition points of the alcohols obtained fell on smooth curves (Fig. 8) and the X-ray spacings of the alcohols above hexadecanol gave only $\gamma$ form, indicate the high purity of the materials.

**Time-heating Curves.** — The melting points and transition points were determined by thermal analysis. A small drop of the molten substance was put on a junction of thermocouple which is made of copper and constantan of about 0.01 mm. in diameter and it was inserted into a doubly air-jacketed tube placed in a water bath.

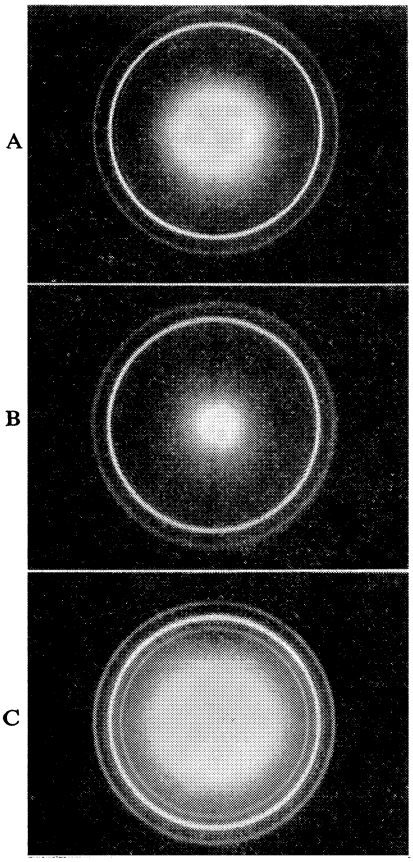



Fig. 1. X-Ray diffraction patterns of pure and mixed alcohols.
A Pure $C_{18}H_{37}OH$
B $C_{18}H_{37}OH$ containing 0.5%$C_{16}H_{33}OH$
C $C_{22}H_{45}OH$ containing 1% $C_{24}H_{49}OH$

Since a higher heating rate was found to be advantageous for good determination of the temperature, the measurements were carried out at the rate of about 2.0°C per minute, readings being taken every 10 sec. Each compound was run at least five times and the reproduciblity of the data was good. Probable errors of the temperatures determined on heating were estimated as being 0.1 to 0.3°C depending on the sharpness of the inflexion points and on the errors on calibration of

Table I. Weight percentage of lower compounds

| | | 0 | 0.5 | 1 | 3 | 97 | 99 | 99.5 | 100 |
|---|---|---|---|---|---|---|---|---|---|
| $C_{16}$—$C_{18}$ | M.p. | 57.3—58.1 | 57.1—58.0 | 56.7—57.6 | 55.7—56.6 | 48.1—49.7 | 48.2—49.3 | 48.1—49.1 | 48.3—49.3 |
| | F.p. | 57.0—56.9 | 56.8—56.6 | 56.5—56.4 | 56.7—56.5 | 48.0—47.8 | 48.3—48.1 | 48.4—48.2 | 48.4—48.2 |
| | T.p. | 51.3—51.1 | 49.0—48.9 | 48.6—48.5 | 47.0—46.7 | 37.8—37.6 | 39.2—39.0 | 40.9—40.8 | 41.8—41.7 |
| $C_{22}$—$C_{24}$ | M.p. | 74.0—75.0 | 73.8—75.0 | 73.8—75.0 | 73.7—74.6 | 69.2—69.8 | 69.5—70.0 | 69.5—70.1 | 69.5—70.2 |
| | F.p. | 74.3—74.1 | 74.0—73.8 | 73.8—73.6 | 73.6—73.3 | 69.0—68.8 | 69.2—69.0 | 69.8—69.6 | 69.6—69.4 |
| | T.p. | 69.5—69.2 | 67.9—67.7 | 66.9—66.6 | 66.1—65.9 | 58.6—58.4 | 60.5—60.2 | 61.0—60.7 | 61.7—61.4 |

The temperature was measured by capillary method and uncorrected.
The heating or cooling speed was 1°C per minute.

the thermocouple, but those of cooling were about 1°C because the high temperature forms tended to supercool before the transitions, as may be seen in Fig. 4.

**X-Ray Pattern Measurements.**—It is known that the crystal spacings of the alcohols so far investigated here consist of $\beta$ and or $\gamma$ modifications in their low temperature forms and $\alpha$ modification in their high temperature form. The three modifications indicate different long spacing depending on different angles of inclination of hydrocarbon chains with respect to the planes of end groups. The most inclined $\gamma$ form shows the shortest spacing. The short spacing also indicates a greater value in $\alpha$ and $\beta$ forms because the molecules are more loosely packed in these forms than in the $\gamma$ form. The data of all the compounds were reported in a previous paper[12] and are represented graphically here (Fig. 2). In the present investigation emphasis was laid on changes of spacings under various conditions especially on the correlations with thermal analyses using the same materials. The X-ray photographs were all taken using Cu-K radiation at 40 KV. and 20 ma. Camera distances and exposure times were varied depending on the chain lengths of the compounds.

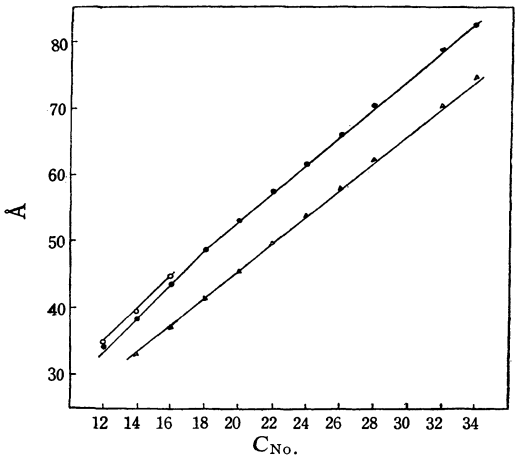



Fig. 2. Long spacings of *n*-higher alcohols.

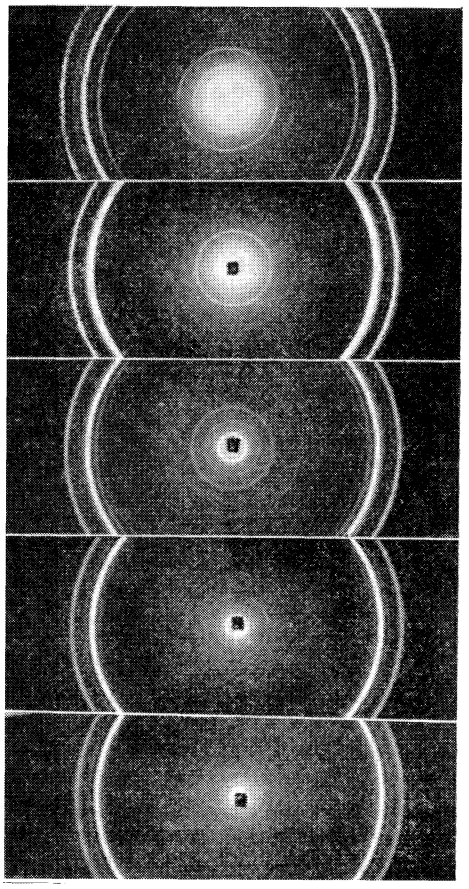


Fig. 3. Representative X-ray diffraction patterns of alcohols. The patterns in discending order are from $C_{12}$, $C_{16}$, $C_{18}$, $C_{24}$, $C_{28}$ alcohols.

Patterns such as Fig. 3 were taken by the method of sampling as follows. The melted samples were mounted on aluminum rings with about 1.2 mm. diameter and 0.8 mm. width and then solidified in the air. The beam was irradiated perpendicularly to the plane of the sample.

An effective method for the detection of $\alpha$ or $\beta$ form in $\gamma$ form was found to be the measurement of the short spacing rather than that of the long spacing. To prepare specimens for these measurements the melted materials were drawn into thin-walled capillary tubes of about 0.2 mm. diameter. The rapidly cooled specimens were obtained by plunging the capillary tube containing the melt into an ice bath. On taking a photograph the capillary tubes were rotated during exposure. An electrically heated brass furnace in which the capillary tube was inserted was used, if necessary. Accuracy of the temperatures measured by means of a copper-constantan thermocouple was within 0.5°C.

## Results and Discussion

The transition temperatures on cooling which were obtained by visual observation have been presented in earlier paper[11], but in this method it was experienced to be difficult to

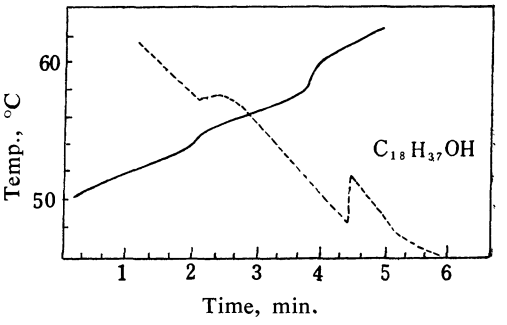



Fig. 4. Time-temperature curves for octadecanol.

12) a) K. Tanaka, T. Seto and T. Hayashida, *Bull. Inst. Chem. Res. Kyoto. Univ.*, 35, 123 (1957). b) K. Tanaka, T. Seto and A. Watanabe and T. Hayashida, ibid., 37, 281 (1959).

identify the transition point on heating. By the present study more reliable and detailed results could be obtained.

**Rotational Transition.**—Typical thermograms obtained for octadecanol are given in Fig. 4. Phase transitions, which occur at 54.5°C on heating and at 52.5°C on cooling, are shown by the break in the curves, latent heat absorption or evolution being indicated. Evidently the transition is of the first order and reversible. The previous X-ray diffraction patterns[12] and dipole moment measurements[13] indicated that the transition is rotational. For the alcohols from tetradecanol to hexacosanol similar thermograms were obtained as those presented above in contrast with the results of Phillips and other workers[8a,f] who reported the transitions only on cooling in most of these alcohols. However, the present results were very reproducible even when the thermal histories of the samples had been varied and, furthermore, the data were consistent with those obtained by the previous X-ray patterns[12],*.

Although the present thermal studies for tetradecanol and hexadecanol could not reveal three formes, the previous X-ray studies[12] indicated that these compounds are trimorphic in the solid state and the low temperature forms which consisted of $\beta$ and $\gamma$ forms, transform them into high temperature form ($\alpha$) at the different temperatures, the lower temperatures being the $\beta$ to $\alpha$ transition point; the alcohols above hexadecanol showed the simple $\gamma$ to $\alpha$ transitions.

The break in the heating curve of hexacosanol was barely detectable and the interval

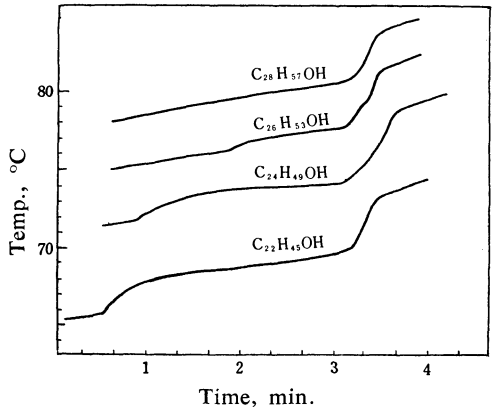



Fig. 5. Time-temperature curves for $C_{22}$, $C_{24}$, $C_{26}$, $C_{28}$ alcohols.

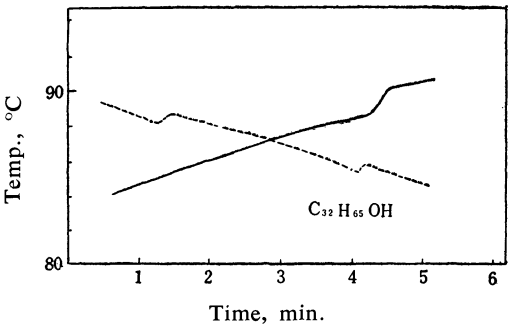



Fig. 6. Time-temperature curves for dotricontanol.

between the melting and transition points is narrow (1.2°C) (Fig. 5). The behaviors of the alcohols above hexacosanol differ markedly from those of the lower members of the series. The curves for octacosanol and dotriacontanol showed that the transitions on heation are missing while those on cooling are still present, However, both transitions were found to disappear at tetratriacontanol. These results are consistent with those by the present X-ray data, according to which in two shorter members ($C_{28}$, $C_{32}$) the $\gamma$ form persisted up to the melting points and in the last member ($C_{34}$) only the $\gamma$ form appeared at the temperature just below its freezing point.

Concerning the existence of transition in dodecanol some disagreements can be found in the literature[8ac,9ab,12a,14-16]. In the present study, non-existence of the transition was verified by the method such as thermal analysis using rapidly or slowly cooling technique, or X-ray pattern measurements made just below the freezing point with an exposure time of 15 min., and dielectric constant measurements

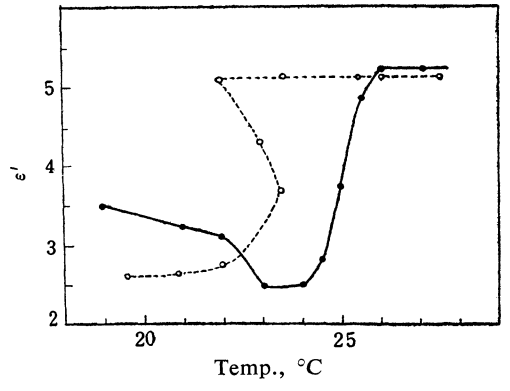



Fig. 7. Temperature dependence of the dielectric constant of dodecanol at 0.5 KC.
● Heating ○ Cooling

13) K. Asai, E. Yoda and S. Yamanaka, *J. Phys. Soc. Japan*, **10**, 634 (1955).

* Some disagreements will be found between the previous and present results. The former must be revised in view of the use of purer materials and more accurate techniques in measurements in the present study.

14) J. D. Bernal, *Nature*, **129**, 870 (1932).
15) E. Ott, *Z. physik. Chem.*, **193**, 218 (1944).
16) E. Frosch, *Ann. Physik*, **42**, 254 (1942).

at 0.5 (Fig. 7) and 5 KC. in which the results agreed with those of Smyth.

In Table II the data obtained by thermal analyses are given together with those obtained from the literature. The corresponding diagram is shown in Fig. 8.

TABLE II

| Alcohol | Carbon No. | M. p. °C | Transition points, °C Heating | Cooling |
|---|---|---|---|---|
| Dodcyl | 12 | 24.0 | — | —(21.6)Ph. |
| Tetradecyl | 14 | 38.0 | 36.2 | 33.5(35.0)Ph. (34.4)S. |
| Hexadecyl | 16 | 49.5 | 45.7 | 43.0(45.0)Ph. (43.2)S. (43.8)K. |
| Octadecyl | 18 | 58.5 | 54.5 | 52.5(53.6)Ph. (53.4)S. (54.7)K. |
| Eicosyl | 20 | 65.0 | 63.5 | 58.2 |
| Docosyl | 22 | 70.5 | 67.6 | 63.5(64.5)S. |
| Tetracosyl | 24 | 75.5 | 72.8 | 71.5 |
| Hexacosyl | 26 | 79.3 | 78.1 | 73.5 |
| Octacosyl | 28 | 82.5 | — | 77.5 |
| Dotriacontyl | 32 | 88.5 | — | 86.2 |
| Tetratriacontyl | 34 | 91.0 | — | — |

Ph.; Phillips and Munford (Thermal analyses).
S.; Smyth et al. (Dielectric measurements).
K.; Kolp and Lutton (Thermal analyses).

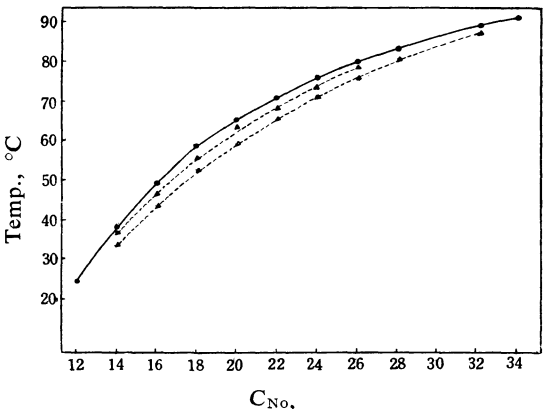



Fig. 8. Melting and transition points of *n*-higher alcohols.
● Melting point
▲ Transition point (heating)
△ Transition point (cooling)

It appears to be interesting that variations in properties of the $\alpha$ forms were observed as the chain length of the compounds increased. In the previous and present studies the following observations have been obtained.

I) Opacities of $\alpha$ forms increase in visual inspections.

II) Inflexions at the transition points become smaller (Fig. 5).

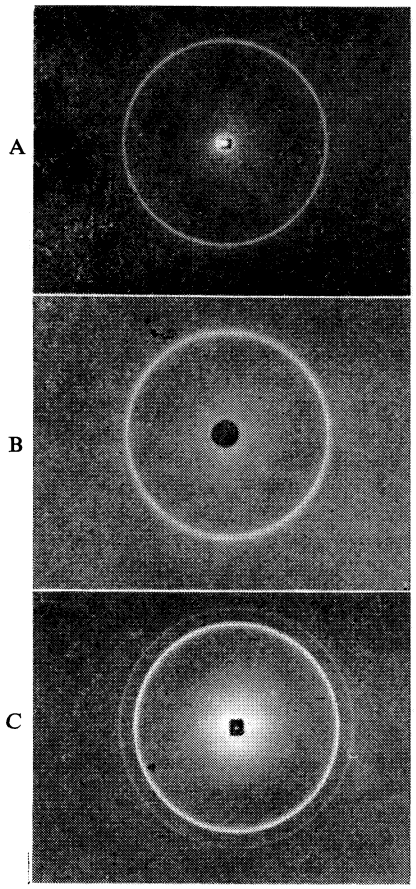



Fig. 9. X-Ray diffraction patterns of the $\alpha$ forms. The photographs were taken after the samples had been standing at the temperatures just below their freezing points for 2 hr.
A $C_{16}H_{33}OH$ C $C_{14}H_{29}OH$
B $C_{26}H_{53}OH$

III) Side spacings of $\alpha$ forms split into two lines (Fig. 9).

IV) In $\alpha$ forms inclination of the hydrocarbon chain to the plane of the ends increases (Fig. 2).

These facts would suggest that deviations in configurations or molecular motions from the typical rotational state may increase as the chain lengthens. Although it is necessary for complete interpretations of the data to await to obtain further data, a possible surmise is that molecular vibration around the axis, rather than rotation, may be caused in such longer compounds.

**$\beta$ to $\gamma$ Transformation***.—It was reported by Smyth et al.[8c] to explain their result by dielectric constant measurements that in octadecanol and other alcohols rotational transition

* According to Hoffman, the term transformation will be used here to denote phase changes such as $\beta$ to $\gamma$ or $\alpha$ to $\gamma$ which occur spontaneously on storage.

appeared when the sample was heated immediately after it was cooled from the melt while the transition failed to appear on heating the stored sample. Their argument suggests that the $\beta$ form obtained on cooling may transform into the $\alpha$ form but the transformation of this $\beta$ form into the $\gamma$ form which has occurred during the storage, may make it difficult for the transition to take place. The latter X-ray investigation made by Kolp and Lutton[8f] seemed to substantiate this fact although there appeared to remain some doubts in their thermal analysis. As described above, however, the present thermal studies showed that heating transitions invariably appeared in the materials which had been prepared under various conditions such as rapid cooling, slow cooling, or prolonged storage and X-ray data also revealed the existence of $\gamma$ to $\alpha$ transitions.

Apart from the facts described above, examination with $\beta$ to $\gamma$ transformation seemed to be so interesting that more detailed X-ray studies were undertaken. The results of the experiments with tetradecanol and hexadecanol indicated that this transformation took place as evidenced by the increasing intensity of the $\gamma$ spacings. They appeared to be very gradual, occurring over a wide temperature range. For example, after being kept at 42°C for 24 hr. a sample of hexadecanol showed nearly equal amounts of $\beta$ and $\gamma$ forms in their low temperature form which had consisted of about $2/3\beta$ and $1/3\gamma$ forms before the heating. Both compounds indicated no transformation on storage at about 25°C for 24 hr. It was also found that the low temperature forms of these alcohols contained more $\gamma$ forms when they were cooled slowly from the melt as compared with when they were cooled rapidly. This may be partly due to the $\beta$ to $\gamma$ transformations which occurred during the cooling and partly due to the $\alpha$ to $\gamma$ transformations which will be discussed in the next section.

Because of the absence of the $\beta$ form in alcohols above hexadecanol, this transformation can not be considered in these compounds. It may be concluded that the $\beta$ to $\gamma$ transformation exists only in tetradecanol and hexadecanol but it is so slow as to provide no appreciable effects on rotational transitions in qualitative measurements.

**$\alpha$ to $\gamma$ Transformation.**—This transformation, as well as $\beta$ to $\gamma$ transformation, was reported by Smyth, Kolp and other workers[8cf]. Recently Asai[13] demonstrated the stability of the $\alpha$ form in octadecanol in his dielectric constant measurements. In the present X-ray investigations the behaviors of $\alpha$ forms in the series were examined by careful control of the temperatures of the samples. It was found that the high temperature form of tetradecanol consists of $\alpha$ and $\gamma$ forms, the former being the less stable. The data were obtained by holding the compound at the temperature just below its freezing point for about 2 hr., indicating that about 2/3 of the initially existing $\alpha$ form was transformed into the $\gamma$ form (Fig. 9). In hexadecanol evidence of a smilar behavior was found at the temperature 1°C above its transition point, but at the temperature 1°C below its freezing point the observed spacing indicated only the $\alpha$ form. This $\alpha$ form proved to be stable so that no transformation could be observed within a few hours (Fig. 9). The $\alpha$ forms appearing in the alcohols above hexadecanol showed a considerable stability over the entire region of the temperatures. The relationship described above is illustrated diagrammatically in Fig. 10. It

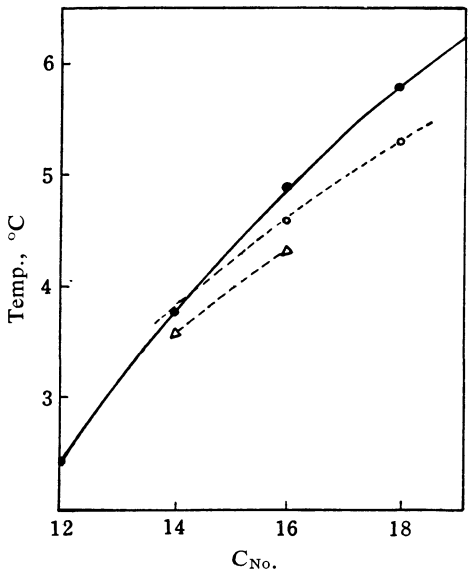



Fig. 10.

● Melting point
○ $\gamma$ to $\alpha$ transition point
△ $\beta$ to $\alpha$ transition point

will be apparent that $\gamma$ to $\alpha$ transition points are higher than $\beta$ to $\alpha$ transition points and that the $\alpha$ form is unstable only when it coexists with the $\gamma$ form but once $\gamma$ to $\alpha$ transformations have taken place the resulting $\alpha$ form is stable.

It is expected that the $\alpha$ form obtained only on cooling may be somewhat unstable. However, the X-ray examinations show that the $\alpha$ form in dotriacontanol is stable at least within about 2 hr.

## Summary

1. Determination of the melting points and transition points of the even carbon numbered alcohols from $C_{12}$ to $C_{34}$ was made by thermal analysis. The transition points of the alcohols above $C_{18}$, except $C_{22}$, have never been reported.

2. The reversible transition sets in at $C_{14}$ and terminates at $C_{26}$. The transition of $C_{28}$ and $C_{32}$ is irreversible, appearing only on cooling and both transitions disappear at $C_{34}$. Probably the pure sample of dodecanol may indicate no transition in any methods of measurements.

3. Properties of the $\alpha$ forms gradually change with increasing chain lengths.

4. The $\beta$ to $\gamma$ and $\alpha$ to $\gamma$ transformations were examined by X-ray pattern measurements and the results were discussed.

5. Transition points and X-ray spacings may be reliable criteria of purity of higher alcohols, and probably of some other long chain compounds.


The author wishes to express his sincere thanks to Professor Ryozo Goto and Professor Kenzo Tanaka of Kyoto University for their continual guidance and encouragement. He is also grateful to Dr. Tsuneo Seto of Kyoto University for his kind direction and criticism in the X-ray diffraction measurements. Thanks are also tendered to Dr. Kenjiro Asai of Kyoto University for his kind direction in the dielectric constant measurements.

*Department of Applied Chemistry*
*Himeji Technical College*
*Idei, Himeji*

# SHORT COMMUNICATIONS

## *A New Rapid Method of Determining Molecular Weight of Water Soluble Linear Polymers by the Measurement of Rate of Settling of Clay Suspensions*

By Yūkichi TOYOSHIMA

(Received April 25, 1961)

During the past decade it has been reported that certain water-soluble linear polymers can give rise to the aggregation of clay particles in a state of aqueous suspension[1,2]. In this communication this fact was investigated in a more quantitative manner by observing the relation between the rate of (hindered[3]) settling $v$ of clay suspensions under addition of a linear polymer and the molecular weight of the polymer.

Itaya clay (product of Yamagata Prefecture) levigated and after removing pebbles and large aggregates, was dried and used as suspensoid. Polymers used in this study were purified as described in a previous article[4].

The suspension was introduced in a sedimentation tube of 67.3 cm. long, which was agitated by rotating the tube for 15 min. at a speed of 5 revolutions per minute. After stopping agitation, settling rate of the suspension was measured at $30.0\pm0.1$°C. Intrinsic viscosity of the polymer freshly dissolved in aqueous 1 M sodium nitrate solution was also measured at $30.00\pm0.01$°C in a capillary viscometer of the Ubbelohde type, and the molecular weight of the polymer was determined from it.

In Figs. 1 and 2 $v\sim[\eta]^{30°C}_{1\,M\,NaNO_3}$ relation was shown for thy system in which 0.02% (to the amount of clay) of polymer was added to the 5% clay suspension. A linear relationship between $v$ and $[\eta]^{30°C}_{1\,M\,NaNO_3}$ was confirmed. A similar linearity was also found for a different content of polymers (below 0.02%) and a different concentrations of clay suspensions (above 5%) so long as the other experimental conditions were kept constant. We may discuss in details the mechanism of aggregation

1) A. S. Michaels, *Ind. Eng. Chem.*, **46**, 1485 (1954).
2) M. Noda, *Kōgyō Yōsui*, **30**, 33 (1961).
3) C. Orr, Jr. and J. M. DallaValle, "Fine Particle Measurement", The Macmillan Co., New York (1959), p. 48.
4) Y. Toyoshima, *J. Chem. Soc. Japan, Pure Chem. Sec.* (*Nippon Kagaku Zasshi*), **82**, 1295 (1961).

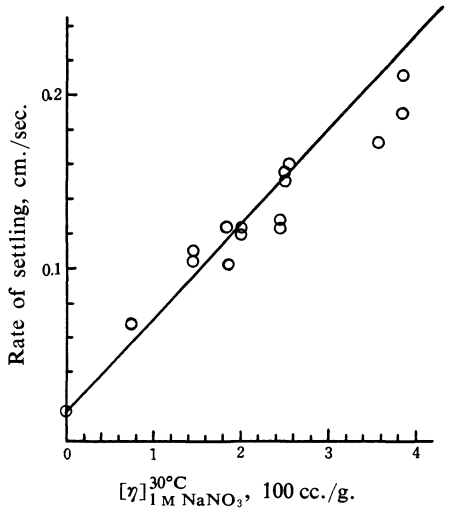



Fig. 1. The relationship between $[\eta]^{30°C}_{1\,M\,NaNO_3}$ and $v$ for polyacrylamides.

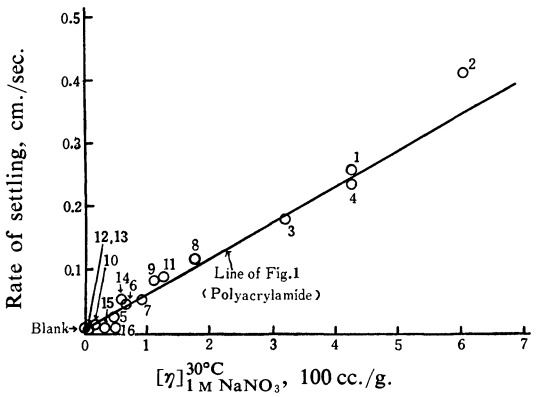



Fig. 2. The relationship between $[\eta]^{30°C}_{1\,M\,NaNO_3}$ and $v$ for various water soluble linear polymers.

1, 2, 3, 4 } Partially hydrolyzed polyacrylamide
5, 6, 7 } Polyvinyl alcohol
8, 9 } Sodium carboxymethylcellulose
10, 11 } Polyvinylpyrrolidone
12, 13 } Dialdehyde starch
14 Agar
15 Gelatin
16 Polyethylene oxide

of clay particles referring to this linearity in a separate reports*. Here we should like rather to draw attention to the fact that using this relation between $v$ and $[\eta]^{30°C}_{1\,M\,NaNO_3}$ together with the known relation between $[\eta]^{30°C}_{1\,M\,NaNO_3}$ and molecular weight $M$ of the polymer, we can correlate $v$ with $M$, and that using such a relationship we can determine the molecular weight from the measurement of sedimentation velocity, which is easier to practise than a similar and well known method of molecular weight determination by the measurement of intrinsic viscosity.

In the case of polyacrylamide, $v \sim [\eta]$ relation is expressed as

$$v = K[\eta]^{30°C}_{1\,M\,NaNO_3} + a \quad (1)$$

while that of $[\eta]$ and $M$ is

$$[\eta]^{30°C}_{1\,M\,NaNO_3} = 3.73 \times 10^{-4} M^{0.66} \quad (2)$$

therefore we obtain from 1 and 2,

$$\log(v-a) = 0.66 \log M + \log(3.73K \times 10^{-4}) \quad (3)$$

where $K$ is a constant, and $a$ the rate of settling without the addition of polymer. Measurement of $[\eta]^{30°C}_{1\,M\,NaNO_3}$, $v$ and $a$ shows that such a linear relationship really holds as shown in Fig. 3. Hence it enables a rapid

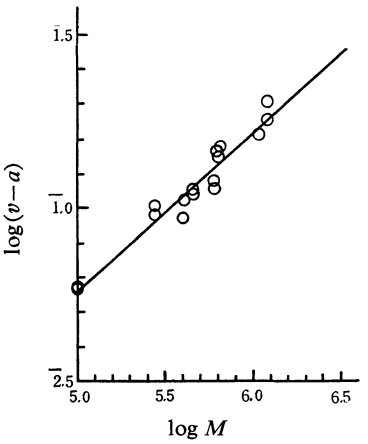



Fig. 3. The relationship between log $M$ and $\log(v-a)$ for polyacrylamides.

determination of the molecular weight of unknown polyacrylamide from the simple determination of rate of settling under the definite condition of sedimentation test using the clay suspension of the same origin. As for the other various water-soluble linear polymers, for instance, partially hydrolyzed polyacrylamide, polyvinyl alcohol, sodium carboxymethylcellulose, polyvinylpyrrolidone, dialdehyde starch, agar, gelatin, and polyethylene oxide, the same linear relationship as in Fig. 1 was also obtained as shown in Fig. 2. Hence their molecular weights can be rapidly determined from the rate of settling of

5) New Product Bulletin, No. 34, American Cyanamid Co., New York (1955), p. 2.

* The details will be published in a near future.

clay suspensions as in the case of polyacrylamide if the relationships between $[\eta]^{30°C}_{1\ M\ NaNO_3}$ and molecular weights for these polymers are determined previously by the method, for instance, of light scattering or osmotic pressure. As a routine procedure for product control, this new method is perhaps one of the rapid and simple methods for determining molecular weights of water-soluble linear polymers.

The author wishes to express his sincere thanks to Dr. Tsunetaka Sasaki of Tokyo Metropolitan University and Dr. Ryōhei Matsuura of Kyushu University for their advice and criticism, to Dr. Akira Nakatsuchi and Dr. Jirō Kato of our Institute for constant guidance, Mr. Takesada Akiba of our Institute for his permission to publish this work, and to Mr. Mitsuo Ōno for his technical assistance.

*Nitto Institute of Chemical Research*
*Kamikizaki, Urawa*

## *Cation-exchange Properties of Phosphoantimonic(V) Acid*

By Takuji Ito and Mitsuo Abe

(Received June 9, 1961)

Limitation of the use of organic ion-exchange resins, in recent years, brought much attention to the development of synthetic inorganic ion exchangers[1,2].

This paper describes some of the ion-exchange properties of phosphoantimonic(V) acid recently discovered. The experimental results indicate that the material is one of the very promising ion exchangers.

Experiment was made with an attempt to obtain the precipitate which was composed of antimony pentoxide and phosphoric acid. When antimony pentachloride was poured in the aqueous solution of phosphoric acid, the rate of formation of the precipitate obtained by the hydrolysis of the said chloride became extremely slow as the concentration of phosphoric acid increased. In case that the concentration of phosphoric acid was suitable relative to that of antimony pentachloride, gelatinous precipitate which was very difficult to filter was gradually formed in warming the solution. After filtering under suction and drying at 80°C, glassy materal was obtained. The material was physically and chemically stable against water, salt solutions and solutions of strong mineral acids, and showed strong cation-exchange properties even in dilute acid solutions.

When the material was added to 0.1 M ammonium nitrate solution its pH fell rapidly at first and then reached to a stational value (approximately 1.8), due to the liberation of $H^+$ produced by exchange with the cation in the solution. The adsorption of $NH_4^+$ on the material was 1.4 meq./g.

The analytical results of the glassy material indicate that the mole ratio of antimony pentoxide to phosphorus pentoxide contained was about 2 : 1.

This new material was provisionally given a name of "Phosphoantimonic Acid". This glassy acid was able to exchange reveresibly its $H^+$ with $NH_4^+$, alkali, alkaline earth and other metal ions (e. g. Ag, Cu etc.).

As one example of ion-exchange reversibility, 0.1 M ammonium nitrate solution was passed down a column (0.8 $cm^2 \times 7$ cm.) filled with this glassy ion exchanger of H-form. $H^+$ was liberated as a result of quantitative adsorption of $NH_4^+$. The adsorbed $NH_4^+$ was quantitatively eluted by treatment with 3 N nitric acid.

Extremely interesting is the strong adsorption of $K^+$ on the material in acid solutions. When the 0.01 M potassium chloride solution

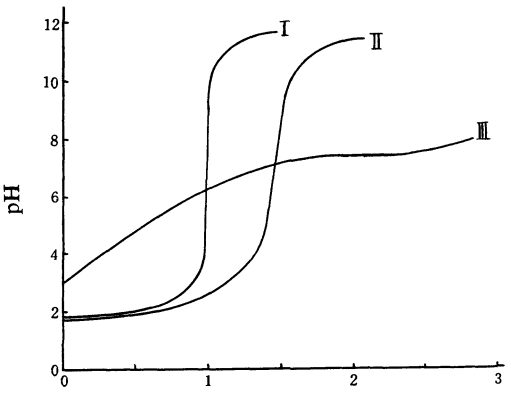



Fig. 1. pH-titration curve for phosphoantimonic acid.
I : 0.01 N $H_2SO_4$ 100 ml.
II : Phosphoantimonic acid
III : Zirconium phosphate (quoted from Ref. 2)

1) K. A. Kraus, H. O. Philips, T. A. Carlson and J. S. Johnson, Paper 1832 presented at the 2nd International Conference of the Peaceful Uses of Atomic Energy, Geneva, 1958.
2) C. B. Amphlett, L. A. McDonald and M. J. Redman, *J. Inorg. & Nuclear Chem.*, 6, 220 (1958).

was added to a column in H-form, $K^+$ was adsorbed very easily and completely just as $NH_4^+$ done. The adsorbed $K^+$ could not eluted even by treatment with 3 N hydrochloric acid or 3 N nitric acid and it was, however, easily eluted with 1 M ammonium nitrate solution. It seemed to us that the abnormal absorbability on this material in strong acid solution might be perhaps attributed to the unordinary structure of phosphoantimonic acid.

The pH-titration curve of the glassy material showed that it was a strong monobasic acid (Fig. 1). It seems extremely possible that phosphoantimonic acid shows strong acid cation-exchange property, because antimonic acid (formally, hexahydroxyl antimonic acid $H[Sb(OH)_6]$) itself is monobasic and has the same strength of acidity as that of acetic acid (viz. dissociation constant; $H[Sb(OH)_6] = 4 \times 10^{-5}$, $CH_3COOH = 1.66 \times 10^{-5}$).

*Research Laboratory of*
*Resources Utilization*
*Tokyo Institute of Technology*
*Meguro-ku, Tokyo*

## *Chemical Constitution of Enmein a Bitter Principle from Isodon trichocarpus Kudo*

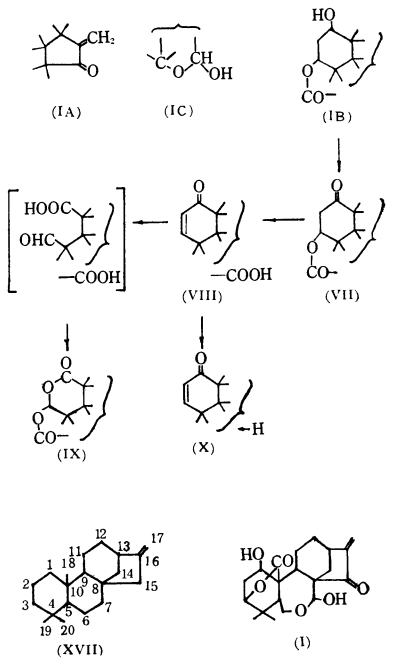
By Takashi KUBOTA, Teruo MATSUURA
Tsutomu TSUTSUI and Keizo NAYA

(Received September 11, 1961)

The partial structure IA was suggested by Takahashi, Fujita and Koyama[1] for enmein[2] (isodonin[3]), $C_{20}H_{26}O_6$, m. p. 274~275°C, $[\alpha]_D$ −156° (acetone). We now wish to propose the structure I for enmein from the following evidences.

Reduction reactions, carried out by us and by other investigators[1,2], of enmein are summarized as follows. Catalytic hydrogenation of enmein ($\lambda_{max}^{EtOH}$ 232.5 m$\mu$ ($\varepsilon$ 7400)) affords a mixture of dihydroenmein-a (IIa), $C_{20}H_{28}O_6$, m.p. 256~257°C (decomp.) ($\lambda_{max}^{EtOH}$ 297 m$\mu$ ($\varepsilon$ 36); $\nu_{max}$ 2.90, 5.72, 5.87 $\mu$), and dihydroenmein-b (IIb), $C_{20}H_{28}O_6$, m. p. 215~216°C (decomp.) ($\nu_{max}$ 2.82, 5.72, 5.82 $\mu$). On mild treatment with sodium borohydride IIb is epimerized to IIa. Dihydroenmein-a is also obtained by the sodium borohydride reduction of enmein in methanol at room temperature. Both dihydroenmeins give the same diacetate (III), $C_{24}H_{32}O_8$, m. p. 231~232°C (decomp.), which is obtained also by the reduction of diacetylenmein (IV), $C_{24}H_{30}O_8$, m. p. 221~223°C (decomp.). Both enmein and dihydroenmein are reduced with sodium borohydride in ethanol at 60°C to yield tetrahydroenmein (V), $C_{20}H_{30}O_6$, m. p. 260°C (decomp.) ($\nu_{max}$ 2.91, 5.86 $\mu$), (triacetate (VI), $C_{26}H_{36}O_9$, m. p. 193°C ($\nu_{max}$ 5.78 $\mu$, no hydroxyl)). Since dihydroenmein-a (IIa) ($\nu_{max}$ 5.87 $\mu$; exalted $\delta$-lactone) is recovered unchanged after consuming one mole of alkali on hydrolysis, it is suggested that enmein has a $\delta$-lactone group.

The partial structure IB is deduced from following results. Chromium trioxide-oxidation of dihydroenmein-a (IIa) affords bisdehydrodihydroenmein (VII), $C_{20}H_{24}O_6$, m. p. 251~253°C (decomp.), (monosemicarbazone, $C_{21}H_{27}O_6N_3$, m. p. 225~226°C). Bisdehydrodihydroenmein consumes one mole of dilute alkali (1/60 N) on hydrolysis to yield an acid (VIII),




$C_{20}H_{24}O_6 \cdot 1/3H_2O$, m. p. 233°C (decomp.) ($\nu_{max}$ 5.64, 5.75, 5.86, 6.01 $\mu$), (monomethylester, $C_{21}H_{26}O_6$, m.p. 245~246°C, monosemicarbazone, $C_{21}H_{27}O_6N_3$, m. p. 265~267°C (decomp.). Inspection of the ultraviolet spectra of VIII ($\lambda_{max}^{EtOH}$ 225 m$\mu$ ($\varepsilon$ 9600)) and its monosemicarbazone ($\lambda_{max}^{EtOH}$ 278 m$\mu$ ($\varepsilon$ 14300)) shows that the acid VIII possesses an $\alpha,\beta$-unsaturated

1) M. Takahashi, T. Fujita and Y. Koyama, *J. Pharm. Soc. Japan* (*Yakugaku Zasshi*), **78**, 699(1958); **80**, 594, 696(1960).
2) T. Ikeda and S. Kanatomo, ibid., **78**, 1123 (1958).
3) K. Naya, *J. Chem. Soc. Japan, Pure Chem. Soc.* (*Nippon Kagaku Zasshi*), **79**, 885 (1958). In comparison of infrared spectra, isodonin was identical with enmein which was kindly supplied by Dr. S. Kanatomo, Kanazawa University.

ketone group, –CO–CH=CH–. Ozonolysis of VIII affords a crystalline neutral substance (IX), $C_{19}H_{22}O_7$, m. p. 249~251°C (decomp.), which consumes two moles of dilute alkali (1/50 N) on hydrolysis, gives positive color reactions for an aldehyde and shows no more absorption of the enone group in its ultraviolet spectrum. On pyrolysis VIII is decarboxylated to yield a neutral substance (X), $C_{19}H_{24}O_4$, m. p. 169~172°C ($\lambda_{max}^{EtOH}$ 225 mμ (ε 8500)).

Bisdehydrodihydroenmein (VIII) consumes two moles of alkali (1/5 N) to yield an amorphous acid, while the neutral substance X is recovered unchanged after consuming one mole of alkali on hydrolysis. Therefore it is suggested that a lactone group is newly formed in oxidation of IIa to VII. On the other hand, treatment of dihydroenmein-a (IIa) with ethanolic sulfuric acid affords an *O*-ethyl derivative (XI), $C_{22}H_{32}O_6$, m. p. 193~195°C, (monoacetate, $C_{24}H_{34}O_7 \cdot 1/2C_6H_6$, m. p. 103~105°C, (no hydroxyl in its infrared spectrum)). Treatment of IIa with methanolic hydrogen chloride affords *O*-methyldihydroenmein(XII), $C_{21}H_{30}O_6$, m. p. 192~193°C, which reverts to dihydroenmein-a (IIa) on acid-catalyzed hydrolysis. The presence of a methoxyl group in XII was confirmed by the Zeisel analysis and the NMR spectrum (τ 6.68; three protons) of dehydro-*O*-methyldihydroenmein (XIII), $C_{21}H_{28}O_6$, m. p. 218~220°C, which is obtained from XII by chromium trioxide-oxidation. On hydrolysis XIII consumes one mole of alkali to yield a crystalline acid (XIV), $C_{21}H_{28}O_6 \cdot H_2O$, m. p. 190~192°C (decomp.) ($\lambda_{max}^{EtOH}$ 230 mμ (ε 9700); $\nu_{max}$ 5.75, 5.85, 5.97, 6.17 μ), (monomethyl ester $C_{22}H_{30}O_6$, m. p. 189~192°C ($\lambda_{max}^{EtOH}$ 228 mμ (ε 10400)), monosemicarbazone $C_{22}H_{31}O_6N_3 \cdot H_2O$, m. p. 205°C (decomp.) ($\lambda_{max}^{EtOH}$ 277.5 mμ (ε 14900)). Conversion of XII to XIV (via XIII) is easily recognized as the transformation, IB→VII→VIII, of the part IB in XII. From these results, it is concluded that the remaining oxygen atoms in the enmein molecule exist as a cyclic hemi-acetal group IC.

Recently two important degradation products were isolated by Kanatomo[4], namely 1-ethyl-4-(3, 3-dimethylcyclohexyl)benzene (XV) on dry distillation of enmein with baryta and retene (XVI) on selenium dehydrogenation of the lithium aluminum hydride-reduction product of dihydroenmein. Kanatomo suggested that enmein has the carbon skeleton of phyllocladene (XVII) and the ketonic and lactonic carbonyl groups exist at the $C_{15}$- and $C_{18}$-positions of XVII, respectively.

However, from the molecular formula and the partial structure, IA, IB and IC, of enmein, it is apparent that enmein must have a tricarbocyclic ring. Our proposed structure I for enmein is supported by the following evidences. The NMR spectra of diacetyldihydroenmein (III) and dehydro-*O*-methyldihydroenmein (XIII) show that the number of protons attached to the carbon atom, to which one or two oxygen atoms are bonded, is five (at the $C_1$-, $C_3$-, $C_6$- and $C_7$-positions) in III and four (at the $C_3$-, $C_6$- and $C_7$-positions) in XIII. Furthermore a sharp singlet (τ 3.80; one proton equivalent) attributed to the $C_7$-proton of the hemiacetal acetate[5] in III shows that the carbon atom adjacent to the hemiacetal group in enmein must have no hydrogen atom. From the biogenetic point of view, it is suggested that the hemiacetal group in the ring B may be formed from a 7-keto-diterpene by the Bayer-Villiger type oxidation followed by the reduction of a lactone formed.

*Faculty of Science*
*Osaka City University*
*Kita-ku, Osaka*

4) S. Kanatomo, *J. Pharm. Soc. Japan.* (*Yakugaku Zasshi*), 81, 1049 (1961).

5) J. A. Pople, W. G. Schneider and H. J. Bernstein, "High Resolution Nuclear Magnetic Resonance", McGraw-Hill Book Comp., Inc., New York (1959), p. 395.

## *Tritium and Carbon-14 in the Tree Rings*

By Kunihiko KIGOSHI and Yoshio TOMIKURA

(Received September 25, 1961)

The data on the atmospheric carbon-14 and tritium in recent years can be expected to furnish new information on the circulation problems of geophysics.

There are several data on the concentration of carbon-14 in the atmospheric carbon dioxide and of tritium in the rain water[1-3]. This note presents the results of measurements of the concentration of carbon-14 and tritium in the tree rings of recent years. The purpose of the measurements was to obtain the annual mean concentration of the atmospheric carbon-14 and of the tritium in the rain water.

1) T. A. Rafter and G. J. Fergusson, U. N. Conference on the Peaceful Uses of Atomic Energy, **18**, 526 (1958).
2) F.Begeman and W. F. Libby, AFOSR Report Number: Tn-56-561, ASTIA Document Number AD 110381 (1956).
3) H. v. Buttlar and W. F. Libby, *J. Inorg. & Nuclear Chem.*, **1**, 75 (1955).

TABLE I. TRITIUM AND CARBON-14 CONCENTRATION IN TREE RINGS

| Interval of growth of tree ring | Trritium concentration, $T/H \times 10^{18}$ | | Carbon-14 concentration** | |
|---|---|---|---|---|
| | Pine ; grown in Hiroshima* | Paulownia ; grown in Tokyo | Pine ; grown in Hiroshima* | Paulownia ; grown in Tokyo |
| Aug. 1953~Sept. 1954 | 92.2±6.2 | | 0.975±0.009 | |
| Aug. 1954~Sept. 1955 | 54.5±4.2 | 96.3±8.1 | 0.967±0.009 | 1.032±0.012 |
| Aug. 1955~Sept. 1956 | 80.7±8.9 | | 1.006±0.008 | |
| Aug. 1956~Sept. 1957 | 67.3±2.6 | 65.6±2.2 | 1.060±0.009 | 1.024±0.012 |
| Aug. 1957~Sept. 1958 | 138.7±3.9 | | 1.101±0.008 | 1.153±0.012 |
| Aug. 1958~Sept. 1959 | 304.4±3.0 | 261 ±3 | 1.192±0.012 | 1.196±0.013 |
| Aug. 1959~Sept. 1960 | 138.7±2.8* | 111 ±2.8 | 1.221±0.013- | 1.187±0.013 |

* This tree was cut down in April 1960, therefore the last tree ring corresponds to the period between Aug. 1959 and April 1960.

** The data are normalized to the concentration of Carbon-14 of the hypothetical modern wood which would not have been affected by industrial effect and nuclear tests.

The tree ring samples were previously dried in a vacuum desiccator at 110°C for several hours. The hydrogen in the tree ring was collected as water by combustion of the gas evolved by strong heating of the dried sample. The water obtained (100~150 ml.) was purified and electrolyzed in order of enrich the tritium. After the reduction of the volume of the water to about one hundredth, the deuterium content of the concentrate was measured by buoyancy method. The tritium disintegration rate was measured by an external quenched Geiger-Counter filled with hydrogen and propane. The preparation of hydrogen from the water and the operation of the counter were done in the similar manner to those developed by Östlund[4].

In Table I the measured tritium concentrations of the tree rings are shown together with the carbon-14 concentrations in the same tree rings. The carbon-14 concentrations were measured in the same manner as described in the previous paper[5]. The concentration of carbon-14 and tritium in the tree ring may be regarded as an annual mean value of the carbon-14 concentration in the atmosphere and that of the tritium concentration in the rain water respectively. The data on the carbon-14 presented here and in previous paper show a tendency of decrease after 1960 and seem to have a maximum value at the beginning of 1960.

The annual mean concentration of tritium in the rain water descreases after 1959 with the half life of about one year. Since the tritium in the troposphere has short mean life[2], the amount of tritium in the troposphere may be proportional to the amount of supply of tritium to the troposphere from the stratosphere. The observed decrease of tritium after 1959 and the annual variation of carbon-14 after 1959 suggest a stratospheric residence time of 1~2 years for these nuclides.

*Department of Physics and Chemistry, Gakushuin University*
*Toshima-ku, Tokyo*

4) H. G. Östlund, IAEA Tritium Symposium, Vienna, 1961, Paper TTS/17.

5) K. Kigoshi and T. Tomikura, This Bulletin, 33, 1576 (1960).

## *Variation of the Atmospheric Carbon-14 in Recent Years at Tokyo*

By Kunihiko KIGOSHI and Kunihiko ENDO

(Received September 25, 1961)

This note presents the results of measurements made in recent years of the atmospheric carbon-14. The data are expected to furnish informations about the circulation problems of geophysics as well as to contribute to the evaluation on the hazard from the man-made radionuclides. The atmospheric carbon dioxide was collected in Tokyo by means of the absorption in the sodium hydroxide solution. The radioactivities were measured by an acetylene filled proportional counter as described in the previous paper[1].

The results obtained are shown in Table I. The unit of the values of the carbon-14 concentration listed in the table is a concentration of atmospheric carbon-14 at eighteenth century

1) K. Kigoshi and Y. Tomikura, This Bulletin, 33, 1576 (1960).

TABLE I. ATMOSPHERIC CARBON-14 CONCENTRATION

| Collection date | Measured concentration of carbon-14* |
|---|---|
| 1959 | |
| 20 Oct. | 1.240±0.016 |
| 20 Nov. | 1.250±0.013 |
| 4—5 Dec. | 1.172±0.014 |
| 1960 | |
| 20 Jan. | 1.149±0.017 |
| 1—5 Feb. | 1.113±0.013 |
| 22—24 Feb. | 1.240±0.027 |
| 2 April<br>9 May | 1.121±0.011 |
| 25—26 May | 1.105±0.010 |
| 24—25 June | 1.105±0.010 |
| 27—29 July | 1.140±0.005 |
| 5—7 Sept. | 1.105±0.014 |
| 25—27 Sept. | 1.172±0.009 |
| 24—26 Oct. | 1.121±0.009 |
| 24—26 Nov. | 1.021±0.009 |
| 22—24 Dec. | 1.219±0.018 |
| 1961 | |
| 25—27 Jan. | 1.010±0.014 |
| 21—23 Feb. | 1.072±0.011 |
| 21—22 April | 1.265±0.016 |
| 24—26 May | 1.112±0.009 |

* The unit is a concentration of the atmospheric carbon-14 at eighteenth century.

calculated from the measured concentration of carbon-14 in the tree rings growing at that time.

Rafter and Fergusson[2] reported the carbon-14 concentrations in the atmosphere in New Zealand which showed regular increase of atmospheric carbon-14 concentration between December 1955 and December 1957 by nuclear tests. Compared to these data, Table I shows large fluctuation which might be due to the nature of the air mass at the collection date in Tokyo. The air mass into which carbon-14 from the stratosphere has been supplied at the latest time must have a high concentration of carbon-14. The exchange of carbon dioxide between the air and the surface ocean water may play an important role to surppress the atmospheric carbon-14 concentration. It has been observed by several authors[2-4] that the carbon-14 concentration in the surface ocean water showed large fluctuation due to the mixing of the surface water with the deep sea water. If this fluctuation has strong influence on the atmospheric carbon-14 concentration, the consideration on this line has to be taken for the evaluation of the Suess Effect and of the annual variation of the cosmic ray intensity measured by using the tree ring samples.

*Department of Physics and Chemistry, Gakushuin University*
*Toshima-ku, Tokyo*

2) T. A. Rafter and C. J. Fergusson, U. N. Con. on the Peacefull Uses of Atomic Energy, **18**, 526 (1958).
3) S. Fonselius and C. Östlund, *Tellus*, **11**, 77 (1959).
4) W. S. Broecker, R. Gerard, M. Ewing and B. C. Heezen, *J. Geophys. Res.*, **65**, 2903 (1960).

## *Dipole Moment and Infrared Spectrum of 2, 3, 5, 6-Tetraisopropylnitrobenzene*

By Ruka NAKASHIMA, Setsuo WATARAI and Toshio KINUGASA

(Received September 30, 1961)

Dipole moment and infrared spectrum of 2, 3, 5, 6-tetraisopropylnitrobenzene were examined. The process of the dipole moment measurement is the same as that described in the articles[1].

The dipole moment of this compound is 3.57D (in benzene solution, at 25±0.01°C), and is actually less than that of nitrobenzene (3.97D)[2], but not so different from that of nitrodurene (3.60D)[3].

The small value of the dipole moment observed is attributed, as generally accepted, to the decrease of the resonance moment of the nitro-group due to steric hindrance.

The infrared spectra were measured with a Perkin-Elmer Model 21 spectrophotometer (with rock salt prism) in chloroform solution in the region from 1670 to 1250 $cm^{-1}$.

Fig. 1 shows the infrared spectra of nitrodurene and 2, 3, 5, 6-tetraisopropylnitrobenzene, and the data are shown in Table I.

TABLE I

| Compound | N-O stretch. vib. Asym. $cm^{-1}$ | N-O stretch. vib. Sym. $cm^{-1}$ | Diff. from $C_6H_5$-$NO_2$ $\Delta As$ $cm^{-1}$ | Diff. from $C_6H_5$-$NO_2$ $\Delta S$ $cm^{-1}$ |
|---|---|---|---|---|
| $C_6H_5$-$NO_2$ | 1527 | 1348 | — | — |
| Nitrodurene | 1526 | 1378 | −1 | 30 |
| Nitro-tetra-iso Pr-$C_6H_5$ | 1524 | 1389 | −3 | 41 |

1) S. Mizushima and K. Higashi, *J. Chem. Soc. Japan (Nippon Kwagaku Kwaishi)*, **54**, 226 (1933).

2) Our observed data.

3) L. E. Sutton et al., *Rec. trav. chim.*, **78**, 790 (1959); In their paper, the dipole moment of nitrodurene was reported as 3.62 D, but they neglected $P_A$. So we recalculated their value in consideration of $P_A$ (≒5% of $P_E$) to fit to our data.

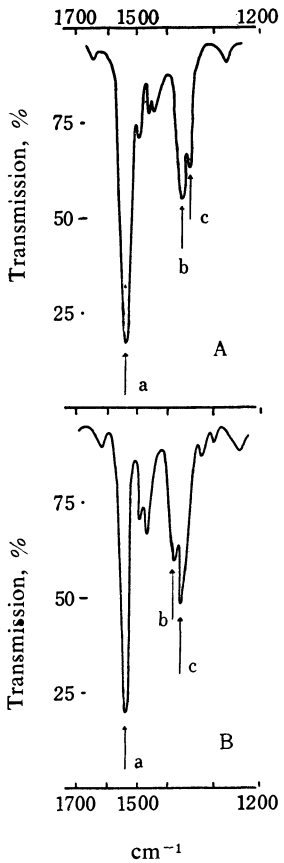



Fig. 1. Infrared spectra of nitrobenzenes (A: Nitrodurene, B: 2,3,5,6-tetra-isopropylnitrobenzene) in chloroform solution.

a: $\nu_{N-O}$ asym., b: $\nu_{N-O}$ sym., c: $\delta_{CH}$ in $-CH_3$

According to our previous observations on the general behavior of N–O sym. and asym. stretching vibrations of alkyl- and halogenonitrobenzenes[4], the N–O sym. was sensitive to the co-planarity of the nitro-group with the benzene plane, on the other hand, N–O asym. was affected by the polarity of substituents.

The infrared spectrum data obtained in the present investigation clearly reveal the general features mentioned above.

In comparing the value of $\Delta S$, which seemed to represent the magnitude of steric hindrance, it may be suggested that a larger steric hindrance was in 2, 3, 5, 6-tetraisopropylnitrobenzene than in nitrodurene.

There was a little discrepancy between the results obtained from the study with infrared spectrum and those from dipole moment.

A similar disagreement is found also in the series of the measurements of alkyl- and halogenonitrobenzenes, which will be discussed in elsewhere.

*Department of Chemistry*
*Faculty of Science*
*Kobe University*
*Higashinada-ku, Kobe*

4) R. Nakashima et al., The 7th. IR and Raman Symposium at Osaka, Proceeding papers, p. 151 (1960).

# *On the pH Dependence of Transport Behavior of Weak Acids and Weak Bases across Ion-exchange Membranes*

By Manabu Senō and Takeo Yamabe

(Received October 10, 1961)

We have pointed out that the transport behavior of weak acids and bases across ion-exchange membranes depends remarkably on the solution pH[1]. It is noticed that there is a range of pH at which the maximum transport takes place. This behavior is due to the suppression of dissociation of acids in the lower pH range, and to the contribution of the competitive transport of hydroxide ions in the higher pH range, in the case of weak acids for example. In this communication, this problem is treated in general and some useful conclusions are derived.

Let us consider the three-component system consisting of strongly dissociated ions $A^-$, e.g., chloride ions, weak acid ions $B^-$, and hydrogen or hydroxide ions. It is assumed that the concentration of each component of the sample solution remains unchanged in course of the electrodialysis experiment and all the electrolytes which are adsorbed in the membrane are in the dissociated state. Then, the permselectivity coefficient $T^{B}_{A+OH}$ is defined and written in terms of constant or known quantities as follows:

$$T^{B}_{A+OH}=\left(\frac{\bar{t}_B}{\bar{t}_A+\bar{t}_{OH}}\right)\Big/\left(\frac{C_{B_0}}{C_A+C_{OH}}\right)$$
$$=T'^{B}_{A}\cdot\frac{KC_{OH}}{1+KC_{OH}}\cdot\frac{1+(C_{OH}/C_A)}{1+T^{OH}_{A}(C_{OH}/C_A)} \quad (1)$$

1) T. Yamabe, M. Senō and N. Takai, This Bulletin, 32, 1383 (1959); *J. Chem. Soc. Japan, Ind. Chem. Sec.* (*Kogyo Kagaku Zasshi*), 64, 556 (1961); I. Kamii, T. Tanaka and T. Yamabe, *J. Pharm. Soc.* (*Yakugaku Zasshi*), 81, 931 (1961).

where $t$ transport number, $C$ concentration, $K=K_B/K_W$, $K_B$ and $K_W$ dissociation constants of weak acid BH and water, and

$$T'^{B}_{A}=\left(\frac{\bar{t}_B}{\bar{t}_A}\right)\Big/\left(\frac{C_B}{C_A}\right),\quad T^{OH}_{A}=\left(\frac{\bar{t}_{OH}}{\bar{t}_A}\right)\Big/\left(\frac{C_{OH}}{C_A}\right)$$

are permselectivity coefficients* which are constant independently of experimental conditions, and the absence and presence of bar above symbols refer to the solution and the membrane phase respectively. Subscript $B_0$ means total acid molecules in dissociated and undissociated states, and B weak acid ions.

The ratio of transport numbers which expresses the relative amount of weak acid transferred across an anion-exchange membrane is

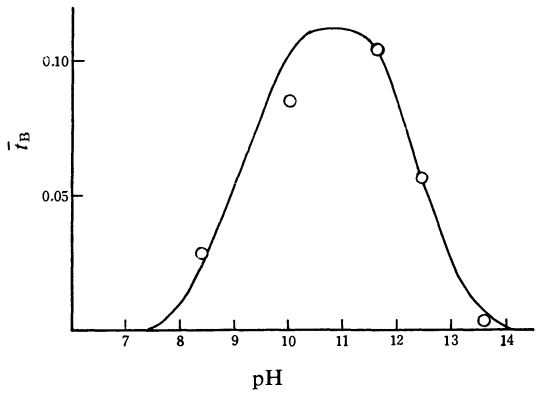



Fig. 1. Transport of boric acid across an anion-exchange membrane.
○ Experimental, —— Theoretical
Experimental conditions ; A five-compartment cell, 0.33 mA./cm², 1 hr.; Membranes, heterogeneous ones made from Amberlite IR-120 or IRA-400 ; Stock solution, 0.05 M $H_3BO_3$, 0.05 M NaCl, NaOH (for adjustment of pH).

$$\frac{\bar{t}_B}{\bar{t}_A+\bar{t}_B+\bar{t}_{OH}}=\frac{T^{B}_{A+OH}C_{B_0}}{C_A+T^{B}_{A+OH}C_{B_0}+C_{OH}} \qquad (2)$$

The experimental verification of these expressions was obtained in the case of boric acid across an anion-exchange membrane as shown in Fig. 1. The experimental procedure was the same as that in the preceding papers[1]. The transport number $t_B$ is the amount (equivalent**) of boric acid transferred across the anion-exchange membrane by passage of the electricity of 1 faraday. The theoretical curve was drawn according to Eqs. 1 and 2, in which quantities were estimated as follows; $T^{OH}_{Cl}$ is 2, $T'^{B}_{Cl}$ is 0.2*, $\bar{t}_{Cl}+\bar{t}_B+\bar{t}_{OH}$, the transport number of anions across the anion-exchange membrane***, is 0.7 and $K_B$ is $7.3\times10^{-10}$**.

This treatment leads us to the following general conclusion. The minimum pH at which the appreciable transport of a weak acid occurs depends primarily on its dissociation constant and nearly equals to $pK_B-1$, and the maximum transport takes place in the pH range between $pK_B+1$ and 12~13. The smaller is $T^{OH}_{A}$ and the larger are $C_A$ and $C_B$, the higher is the maximum pH. The same treatment can be applied to weak bases. The details will be presented in near future.

The authors express their thanks to Mr. Katuya Yanase for his experimental cooperation.

*The Institute of Industrial Science*
*The University of Tokyo*
*Yayoi-cho, Chiba*

* These are practically dependent on the current densities. $T'^{B}_{A}$ is known from the electrodialysis experiment in the pH range higher than $pK_B+1$, where $T^{B}_{A}=(\bar{t}_B/\bar{t}_A)/(C_{B_0}/C_A)=T'^{B}_{A}$.

** Only the dissociation of boric acid in the first step was considered. Further dissociations are so weak (dissociation constants $1.8\times10^{-13}$ and $1.6\times10^{-14}$) that these contributions are neglected in the pH range smaller than 13 and in the larger pH range the contribution of hydroxide ions becomes overwhelming.

*** Strictly, it contains the contribution of the transport number of anions across the adjacent cation-exchange membrane.

# *A New Method for the Determination of Boron by Spectrophotometry with Pyrocatechol Violet*

By Kazuo HIIRO

(Received December 7, 1960)

For the photometric determination of boron, most of the reagents such as oxyanthraquinones are used in concentrated sulfuric acid media, in another case using curcumin, the sample solution should be evaporated with the reagent solution under carefully controlled conditions for color development. Since these procedures are very tedious and time consuming, it would seem very useful if the color development could be substantiated simply and rapidly in aqueous media.

In previous publications it has been reported that some of the colorimetric reagents such as polyvinylalcohol[1,2], chromotropic acid[3], victoria violet[4,5] and H-resorcinol[6] can be used in aqueous media, and that some reagents are applied to indirect methods. However, many of them are not always applicable to routine work, as they are less accessible reagents, and in the case of chromotropic acid the measurements must be carried out in the ultraviolet region.

Pyrocatechol violet, a kind of sulfophthalein dye, is generally used as a metallochromic indicator for chelatometry and as photometric reagent for many metal ions such as zirconium[7,8], thorium[9], copper[10], bismuth[11], aluminum[12] and yttrium[13]. Patrovský[14] studied the detection of boron, niobium, germanium and tantalum using this reagent.

In this paper the application of the reagent to the determination of boron has been described, and the proposed method is very convenient and useful, because the procedure is carried out in an aqueous medium and the absorbance can be measured in the visible region. In this study, the absorption curves of dilute pyrocatechol violet solutions with various pH values were taken, and the existence of an isosbestic point at 494 m$\mu$ was confirmed, various facts including the effect of pH and of the reagent concentration, stability of the color and effect of temperature and of the sort of buffer solutions were examined. The interference of diverse metal ions is masked by adding ethylenediaminetetra-acetate solution as a sequestering agent. Beer's law is obeyed in the range 0.2 to 2.0 p. p. m. of boron at 494 m$\mu$.

## Experimental

**Apparatus.** — Spectrophotometric measurements were made with a Shimadzu quartz spectrophotometer, Model QB-50, with 1 cm. glass transmission cells. A Horiba glass electrode pH meter, Model H-3 was used for all pH measurements.

**Materials.**—*Standard Boron Solutions.* — Dissolve 0.5716 g. of reagent grade boric acid in 1000 ml. of water. One milliliter of the solution corresponds to 100 $\mu$g. of boron. Dilute an aliquot of the solution with water, and prepare 10.0 p. p. m. and 5.0 p. p. m. of standard boron solutions.

*Pyrocatechol Violet Solution.* — Prepare a $2\times10^{-3}$ M aqueous solution (Dotite PV).

*Buffer Solutions.*—Prepare an ammonium chloride-ammonium hydroxide buffer solution by mixing 8 parts of 0.5 M ammonium chloride solution and 1 part of 0.5 M aqueous ammonia solution, and adjust the pH to 8.55~8.60. Veronal buffer solution is prepared as follows. To 100 ml. of mixed solution of M/7 sodium diethylbarbiturate and M/7 sodium acetate add 40 ml. of 0.85% sodium chloride solution and 25 ml. of 0.1 N hydrochloric acid, and adjust to pH 8.55~8.60.

*Ethylenediaminetetraacetate Solution.* — Dissolve disodium ethylenediaminetetraacetate (dihydrate) in water to make the concentration of $5\times10^{-2}$ M.

Other various salt solutions are prepared from analytical grade reagents.

**Measurement of Absorption Spectra of Pyrocatecholviolet.** — Twenty milliliters of $10^{-4}$ M pyrocatechol violet solutions were mixed with 5 ml. of veronal buffer solutions of various pH values and diluted to 50 ml. with water. The absorption spectra of these solutions were measured with water as reference.

**Procedure.**—Pipet the boron solution containing

1) R. F. Muraca and E. S. Jacobs, *Chemist-Analyst*, **44**, 14 (1955).
2) A. J. Monte-Bovi, J. J. Sciarra and C. Martorana, *Drug Standards*, **27**, 15 (1959); *Anal. Abstr.*, **6**, 4307 (1959).
3) D. F. Kuemmel and M. G. Mellon, *Anal. Chem.*, **29**, 378 (1957).
4) C. A. Reynolds, *U. S. Atomic Energy Comm.*, Rep. AECU-3845, 12 (1958); *Anal. Abstr.*, **6**, 2499 (1959).
5) C. A. Reynolds, *Anal. Chem.*, **31**, 1102 (1959).
6) V. A. Griso and E. N. Poluektova, *Zhur. anal. Khim.*, **13**, 434 (1958).
7) J. P. Young, J. R. French and J. C. White, *Anal. Chem.*, **30**, 422 (1958).
8). Yu. A. Cherniknov, W. F. Lukyanov and E. M. Knyazeva, *Zhur. anal. Khim.*, **14**, 207 (1959).
9) M. Svach, *Z. anal. Chem.*, **149**, 414 (1956).
10) M. Svach, ibid., **149**, 417 (1956).
11) M. Svach, ibid., **149**, 325 (1956).
12) Communication, *Anal. Chem.*, **32**, 725 (1960).
13) J. P. Young, J. C. White and R. G. Ball, ibid., **32**, 928 (1960).
14) V. Patrovský, *Chem. listy*, **51**, 968 (1957); *Anal. Abstr.*, **4**. 3593 (1957).

25 μg. or 50 μg. of boron into a 25 ml. measuring flask, add 5 ml. of $2\times10^{-3}$ M pyrocatechol violet solution and 5 ml. of buffer solution at pH 8.55~8.60, and dilute to the mark with water. Measure the absorption at 494 mμ; use a mixed solution containing 5 ml. of pyrocatechol violet and buffer in 25 ml. as reference.

In order to study the effect of diverse salts, color developments were made using 25 μg. of boron with various amounts of 4% salt solutions, and measurements were made for the solution with 50 μg. of several cations.

The effect of the temperature upon the absorbance was investigated as follows. Solutions containing 2.0 p. p. m. of boron were warmed in a water bath at a proper temperature for 15 min., and the absorbance of the solutions was measured against a reference treated similarly. For the solutions containing 1.0 p. p. m. of boron, absorbance and temperature of the warm solutions were measured at proper intervals.

## Results

**Absorption Spectra of Pyrocatechol Violet Solution.**—Fig. 1 shows the absorption curves of $4\times10^{-5}$ M pyrocatechol violet solutions at various pH values. It is found that, as the pH of the solution decreases, a maximum (450 mμ) appears, while when the pH increases absorbance at the absorption maximum (600 mμ) increases, and there is an isosbestic point at 494 mμ. Since the absorbance at the isosbestic point is not affected by the pH value of solutions, and the absorbance of reagent blank is always constant at the wavelength, the use of this isosbestic point is very advantageous for the determination of boron.

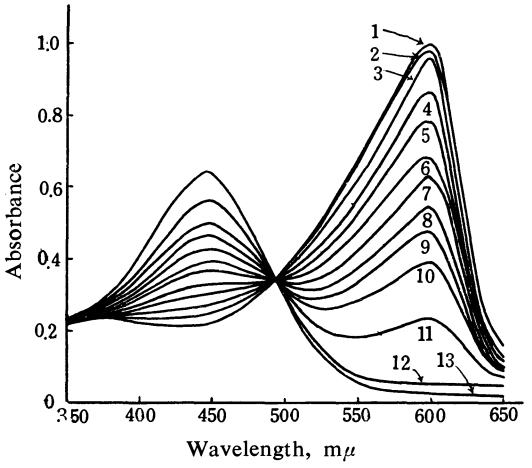



Fig. 1. Absorption spectra of pyrocatechol violet solution at various pH's.

| | | | | | |
|---|---|---|---|---|---|
| 1 | pH 9.32 | 6 | pH 8.21 | 11 | pH 7.21 |
| 2 | 8.98 | 7 | 8.10 | 12 | 5.80 |
| 3 | 8.72 | 8 | 7.95 | 13 | 4.55 |
| 4 | 8.53 | 9 | 7.79 | | |
| 5 | 8.41 | 10 | 7.63 | | |

**Effect of pH.** — As shown in Fig. 2, it is found that the maximum absorptions were obtained at pH range of 8.3~8.6.

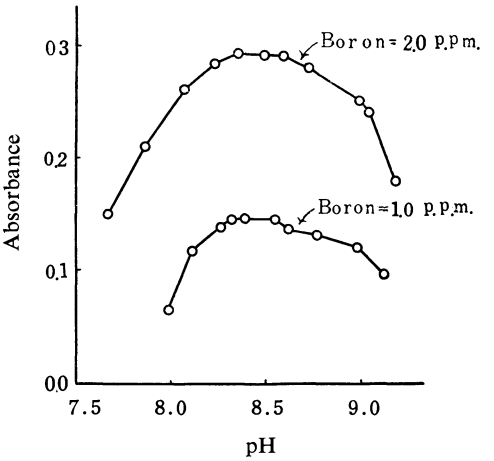



Fig. 2. Effect of pH value.
$2\times10^{-3}$ M Pyrocatechol violet soln.; 5.0 ml.,
Veronal buffer soln.; 5.0 ml.,
Measured at 494 mμ

**Absorption Spectra of Colored Boron-Pyrocatechol Violet Solution.**—Fig. 3 shows the absorption curves of the boron-pyrocatechol-violet solutions, obtained by the standard procedure. The maximum absorption is shown at 484 mμ.

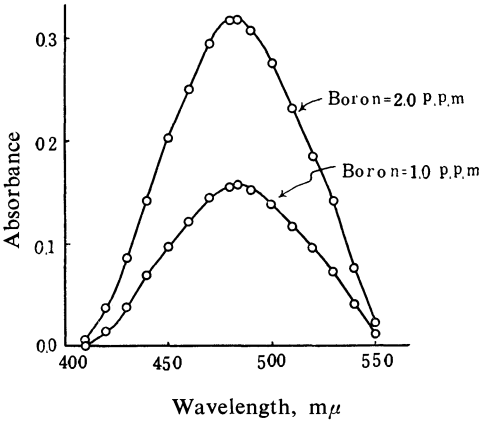
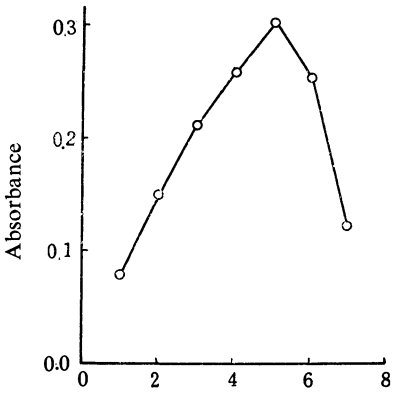



Fig. 3. Absorption spectra of colored boron-pyrocatechol violet solutions.
$2\times10^{-3}$ M Pyrocatechol violet soln.; 5.0 ml.
$NH_4Cl$-$NH_4OH$ buffer soln.; 5.0 ml.

**Reagent Concentration.**—In order to test the effect of concentration of pyrocatechol violet, a series of the absorbances was measured under various concentrations of the reagent, using the reagent blanks of the same concentration

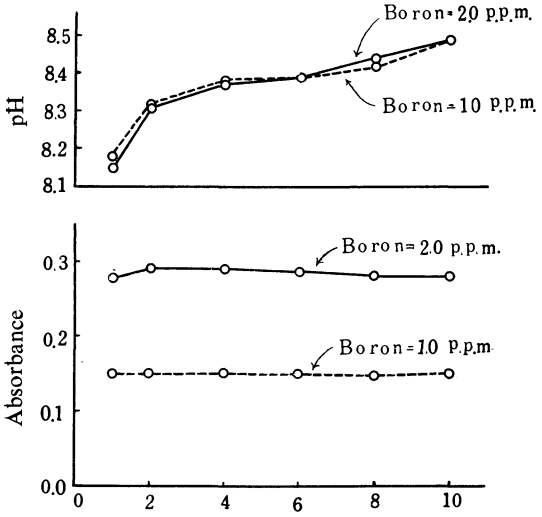
as references. As shown in Fig. 4, 5 ml. of $2\times10^{-3}$ M pyrocatechol violet solution in 25 ml. is the optimum amount.




$2\times10^{-3}$ M P. V. soln. added, ml.

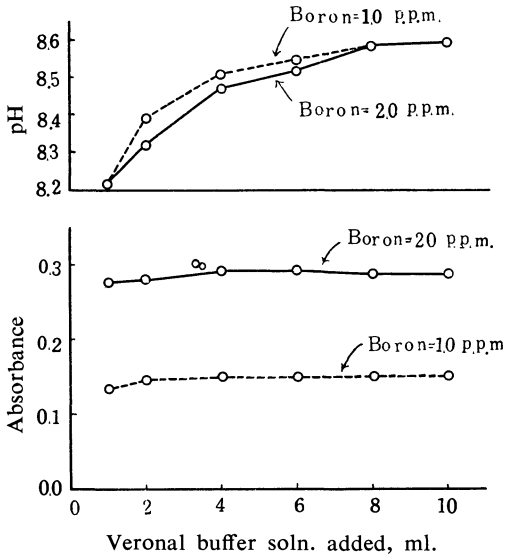
Fig. 4. Effect of pyrocatechol violet concentration.
Boron concentration; 2.0 p. p. m.
$NH_4Cl$-$NH_4OH$ buffer soln.; 5.0 ml.
Measured at 494 mμ.

**Effect of Buffer Solutions.** — The effect of buffer solution was tested with varying amounts of 0.5 M ammonium chloride-ammonia buffer solution or veronal buffer solution. At least 2 ml. of both buffer solutions are essential, as shown in Figs. 5 and 6, and 5 ml. is preferable, for the purpose of avoiding the pH change due to the addition of various salts in the following experiments.




$NH_4Cl$-$NH_4OH$ buffer soln. added, ml.

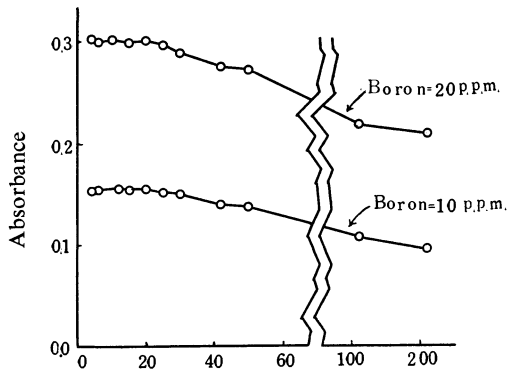
Fig. 5. Effect of buffer solution (I). In the case of ammonium chloride-ammonium hydroxide buffer solution.
$2\times10^{-3}$ M Pyrocatechol violet soln.; 5.0 ml.
Measured at 494 mμ




Veronal buffer soln. added, ml.

Fig. 6. Effect of buffer solution (II). In the case of veronal buffer solution.
$2\times10^{-3}$ M Pyrocatechol violet soln.; 5.0 ml.
Measured at 494 mμ

**Color Stability.**—Fig. 7 shows that the absorbance of colored solutions is constant for 20 min. Consequently the measurements should be done within 20 min. after color development.




Time of standing, min.

Fig. 7. Color stability of boron-pyrocatechol violet solutions.
$2\times10^{-3}$ M Pyrocatechol violet soln.; 5.0 ml.
Veronal buffer soln.; 5.0 ml.
Measured at 494 mμ
Temperature; 26~27°C

**Temperature.**—It is observed that the absorbance is affected by temperature, that is, the intensity of absorbance increases as temperature is lowered, and there is an apparent linear relationship between absorbance and temperature as shown in Fig. 8. The temperature coefficients are $0.927\times10^{-2}$/°C for 2.0 p. p. m. and $0.330\times10^{-2}$/°C for 1.0 p. p. m. of boron.

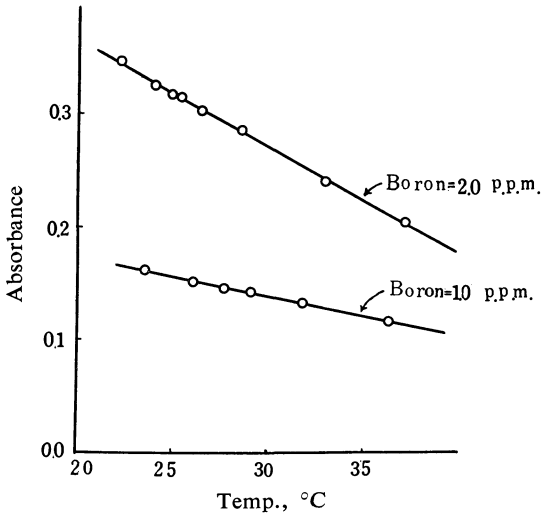



Fig. 8. Effect of temperature.

$2\times10^{-3}$ M Pyrocatechol violet soln.; 5.0 ml.
Veronal or $NH_4Cl$-$NH_4OH$ buffer soln.; 5.0 ml.
Measured at 494 mμ

**Stability of Pyrocatechol Violet Solution.**—The solution of pyrocatechol violet is stable for more than one month, as shown in Fig. 9.

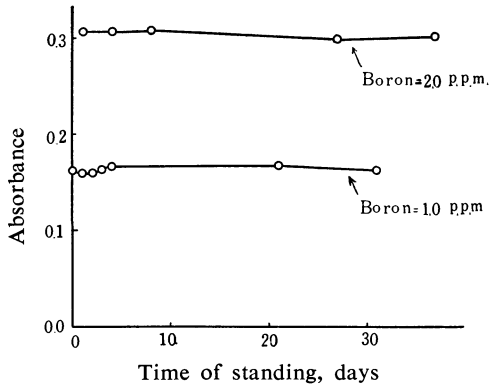



Fig. 9. Stability of pyrocatechol violet solution.

$2\times10^{-3}$ M Pyrocatechol violet soln.; 5.0 ml.
Veronal or $NH_4Cl$-$NH_4OH$ buffer soln.; 5.0 ml.
Measured at 494 mμ

**Diverse Salts.**—The results are presented in Table I. It was found that the presence of such salts as potassium fluoride, sodium chloride, potassium iodide, sodium sulfate, disodium hydrogenphosphate and potassium sodium tartrate do not interfere even at a concentration of 200 mg. per 25 ml. But sodium sulfite

Table I. Effect of diverse salts

| Salt | Added, mg. | | | | |
|---|---|---|---|---|---|
| | 0 | 40 | 80 | 120 | 200 |
| KF | 0.159 | 0.150 | 0.156 | 0.158 | 0.158 |
| NaCl | 0.164 | 0.163 | 0.155 | 0.151 | 0.145 |
| KI | 0.159 | 0.158 | 0.151 | 0.152 | 0.150 |
| $Na_2SO_4$ | 0.153 | 0.155 | 0.158 | 0.156 | 0.153 |
| $Na_2HPO_4\cdot12H_2O$ | 0.156 | 0.154 | 0.155 | 0.157 | 0.152 |
| $Na_2SO_3$ | 0.154 | 0.106 | 0.099 | 0.088 | 0.074 |
| $KNO_3$ | 0.153 | 0.171 | 0.183 | 0.181 | 0.181 |
| $KNaC_4H_4O_6\cdot4H_2O$ | 0.155 | 0.150 | 0.157 | 0.152 | 0.152 |
| $56Na_2O\cdot44SiO_2$ | 0.156 | 0.156 | 0.156 | 0.159 | 0.158 |
| $NaHCO_3$ | 0.153 | 0.154 | 0.154 | 0.155 | 0.156 |

Table II. Effect of diverse metal ions

| Ion | EDTA none | Added, mg. | $5\times10^{-2}$ M EDTA 0.5 ml. added | | |
|---|---|---|---|---|---|
| | 0 | 50 | 100 | 200 | 500 |
| Magnesium | 0.164 | 0.125 | 0.163 | 0.165 | 0.166 |
| Zinc | 0.158 | 0.091 | 0.161 | 0.155 | 0.157 |
| Copper(II) | 0.159 | 0.095 | 0.154 | 0.152 | 0.162 |
| Aluminum | 0.156 | −0.308 | −0.009 | −0.377 | −0.705 |
| Lead | 0.152 | 0.162 | 0.154 | 0.150 | 0.153 |
| Manganase(II) | | 0.030 | 0.160 | 0.157 | 0.158 |
| Nickel | | 0.070 | 0.159 | 0.153 | 0.150 |
| Cobalt(II) | | −0.015 | 0.155 | 0.152 | 0.153 |
| Cadmium | | 0.125 | 0.151 | 0.158 | 0.155 |

and potassium nitrate interfere when 40 mg. per 25 ml. are present.

**Diverse Metal Ions.**—As shown in Table II, the following ions interfere seriously: Magnesium, zinc, copper(II), manganase(II), nickel, cobalt(II), cadmium and aluminum. Since these cations form stable chelates with ethylenediaminetetraacetate, when disodium salt of ethylenediaminetetraacetate is present in concentration of $10^{-3}$ M, they are masked effectively and do not interfer even at the concentration of 20 p. p. m. However, the interference of aluminum can not be eliminated.

**Calibration Curve.**—Measurements were made for the solutions containing various amounts of boron. Beer's law is obeyed up to 2.0 p. p. m. of boron as shown in Fig. 10. The sensitivity of this method was 0.006085/$\mu$g. and the mean error was 1.59%. Standard deviation was 0.002528 in absorbance for ten reproducible measurements for each 1.0 p. p. m. of boron.

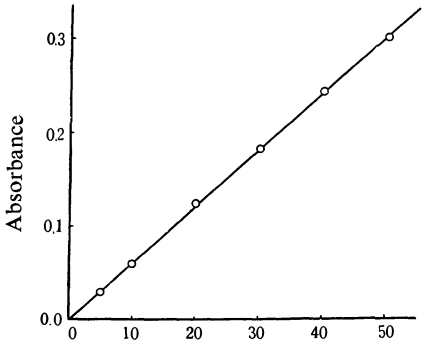



Fig. 10. Calibration curve.

$2\times10^{-3}$ M Pyrocatechol violet soln.; 5.0 ml.
$NH_4Cl$-$NH_4OH$ buffer soln.; 5.0 ml.
Measured at 494 m$\mu$
Temperature; 26~27°C.

## Discussion

The proposed new photometric method for the determination of boron by using pyrocatechol violet as a color reagent is simple in procedure as compared with the other methods.

From Fig. 1, considerations can be made as follows. Because pyrocatechol violet is a tetrabasic acid and consequently can release four protons, it may be formulated as $H_4F$, the absorption band with peak at 450 m$\mu$ can be considered as belonging exclusively to $H_3F^-$, and the peak at 600 m$\mu$ must be due to $H_2F^{2-}$ form.

As shown in Fig. 3, for the spectrophotometric measurements it is desired to choose the maximum wavelength at 482 m$\mu$, but because the absorbance of pyrocatechol violet solution is not affected by pH value at the isosbestic point 494 m$\mu$ it is preferable that the isosbestic point be chosen for the determination of boron, although photometric sensitivity is lowered slightly.

The proposed method has the feature of no preliminary separation of diverse ions, because many of them may be masked by ethylenediaminetetraacetate. This method can thus effectively be used for the determination of boron in such samples as metals, metallic oxides and alloys.

In this procedure, however, color intensity is considerably affected by temperature, so the absorption measurements must be done under constant temperature. Fortunately the effect of temperature difference will be corrected, provided that the calibration curves are made simultaneously.

Investigations for the effects of other diverse salts and metal ions and also the determination of boron for many metallic samples are now proceeding in this laboratory.

The author is indebted to Dr. Yuroku Yamamoto, Kyoto University, for his guidance and to Dr. Isao Muraki, Chief of the 5th Department of our Institute, for his useful suggestions.

*Osaka Industrial Research Institute*
*Oyodo-ku, Osaka*

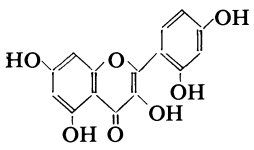
# *A New Method for the Spectrophotometric Determination of Boron with Quercetin*

By Kazuo HIIRO

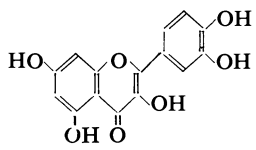
(Received January 12, 1961)

In previous publications it was reported that morin, a kind of oxyflavone, was used as a reagent for the fluorimeric and spectrophotometric determination of boron[1,2]. By an analogous consideration on the basis of the chemical constitution of the reagent, it may be said that there is a possibility of using quercetin instead of morin for the photometric determination of boron.

The formula for both compounds are:



Morin



Quercetin

In the field of photometry, quercetin was already used as a coloring reagent for germanium[3,4], zirconium[5] and molybdenum[6] etc. in previous publications. Wilson formerly reported the reactivity of boron with several kinds of flavone compounds including only a brief description on quercetin[7].

On the result of preliminary experiments the present author was confident that quercetin could be applicable to the determination of boron. In this paper, therefore, the application of the reagent to a new photometric method for boron has been described. The effects of reagent concentration, oxalic acid, and hydrogen ion concentration are examined. In addition, various conditions including temperature, duration of heating, and vessel material for evaporation of sample solution, and stability of the color, solvent of dried residue and diverse salts and the stability of the reagent solution have been investigated. It was found that the colored complex of boron-quercetin has a mole ratio of 1 : 1 under the proposed condition, and that Beer's law was obeyed over the range 0.00 to 0.50 p. p. m. of boron at 445 mμ.

The new photometric method for determination of boron was applied to graphite samples, and satisfactory results were obtained.

## Experimental

**Apparatus.** — Spectrophotometric measurements were made with a Shimadzu quartz spectrophotometer, Model QB-50, using 1 cm. glass transmission cells. For the operation of color development a water bath of 50×35×35 cm. and an air bath of ordinary type were used.

**Materials.** — Dissolve 0.5716 g. of reagent grade boric acid in 1 l. of water to make a solution corresponding to 100.0 μg. of boron per 1.0 ml. Dilute an aliquot of the solution with water, and prepare standard solutions containing 5.0 p.p.m. and 2.0 p.p.m. of boron. Prepare a 0.2% ethanolic quercetin solution. Dissolve oxalic acid of analytical reagent grade in 95% ethanol to make a 20% solution. Prepare 1 N hydrochloric acid solution. All other salt solutions are prepared from reagents of analytical grade.

**Standard Procedure.**—Pipet an aliquot of the boron solution containing about 5.0 μg. of boron into a 100 ml. quartz beaker, add a suitable amount of water up to 2.0 ml. and add successively 1.0 ml. of 1 N hydrochloric acid, 3.0 ml. of 20% oxalic acid solution and 1.0 ml. of quercetin solution. Mix thoroughly and evaporate the contents to dryness on a water bath at 55±3°C. Subsequent to complete dryness, place the beaker in an air bath at 60~90°C, and keep it there for about 1 hr. to make sure of complete color development. After cooling to room temperature, dissolve the residue in 10 ml. of acetone and measure the absorbance at 445 mμ with acetone as reference.

To ascertain the stability of the color, read absorbance of the solution at proper intervals of time after color development. In order to study the effect of diverse salts, color developments were made using 2.0 μg. of boron in the presence of various amounts of 0.5 or 2.0% salt solutions.

Measurements of absorption spectra were made in respect to the solution obtained by the abovementioned procedure at every 5 mμ intervals of wavelength.

**Determination of Boron in Graphite Samples.**— Determination of boron in graphite samples was

1) A. Murata and F. Yamauchi, *J. Chem. Soc. Japan, Pure Chem. Sec.* (*Nippon Kagaku Zasshi*), **79**, 231 (1958).
2) A. Murata and F. Yamauchi, ibid., **79**, 1454 (1958).
3) Y. Oka and S. Matsuo, ibid., **74**, 931 (1953).
4) Y. Oka and S. Matsuo, ibid., **76**, 610 (1955).
5) F. S. Grimaldi and C. E. White, *Anal. Chem.*, **25**, 1886 (1953).
6) G. Goldstein, D. L. Manning and O. Menis, ibid., **30**, 539 (1958).
7) C. W. Wilson, *J. Am. Chem. Soc.*, **61**, 2303 (1939).

made as follows[8]. Weigh powdered sample into a platinum boat, add 2.0 ml. of 3% calcium hydroxide aqueous suspension and mix well. Evaporate the graphite to dryness on a small heater, introduce the boat into a combustion tube in an electric furnace heated at 900°C and ash the sample in a current of oxygen. After cooling, remove carefully the ash into a distillation apparatus and distil off boron as methyl borate into a 100 ml. quartz beaker containing 1.4 ml. of 0.2 N sodium hydroxide solution and 9.0 ml. of water. Evaporate the contents in a quartz beaker to dryness on a water bath warmed at 40~50°C, and add 1.4 ml. of 0.2 N sulfuric acid to the dried residue and then treat as mentioned above.

## Results

**Absorption Spectra of the Complex.**—The absorption curves of colored solutions obtained by standard procedure are shown in Fig. 1. There is a maximum at 445 mμ, which suits for the spectrophotometric measurements.

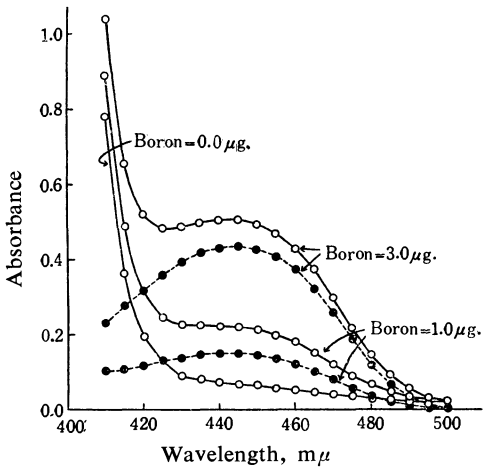



Fig. 1. Absorption spectra of colored complex of boron-quercetin.
Boron; 3.0 μg., 1.0 μg. and 0.0 μg.
Quercetin; 0.2% soln., 1.0 ml. (A-lot)
Oxalic acid; 20% soln., 3.0 ml.
HCl; 1 N soln., 1.0 ml. Water; 3.0 ml.
—○— Obtained against acetone as reference
—●— Obtained against blank as reference

**Reagent Concentration.**—Absorbances of a series of solutions contained 1.0 and 3.0 μg. of boron were measured in the presence of various amounts of the reagent. As shown in Fig. 2, 1.0 ml. of 0.2% quercetin solution is the optimum amount.

**Oxalic Acid Concentration.**—A test was made using 1.0 and 3.0 μg. of boron in the presence of varying amounts of 20% oxalic acid solution. The results indicate that 3.0 ml. of oxalic acid is recommended as shown in Fig. 3.

8) I. Muraki and K. Hiiro, *J. Chem. Soc. Japan, Pure Chem. Sec. (Nippon Kagaku Zusshi)*, **78**, 850 (1957).

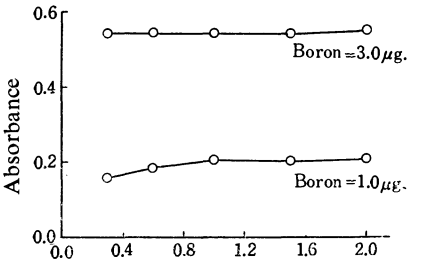



Fig. 2. Effect of quercetin added.
Boron; 3.0 μg. and 1.0 μg.
HCl; 1 N soln., 1.0 ml.
Oxalic acid; 20% soln., 3.0 ml.
Water; 3.0 ml. Quercetin; A-lot

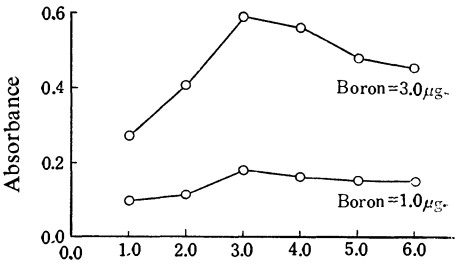



Fig. 3. Effect of oxalic acid added
Boron; 3.0 μg. and 1.0 μg.
Quercetin; 0.2% soln., 1.0 ml. (A-lot)
HCl; 1 N soln., 1.0 ml. Water; 3.0 ml.

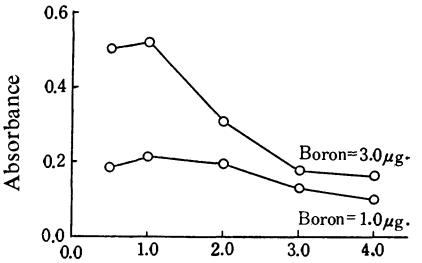



Fig. 4. Effect of hydrochloric acid added.
Boron; 3.0 μg. and 1.0 μg.
Quercetin; 0.2% soln., 1.0 ml. (A-lot)
Oxalic acid; 20% soln., 3.0 ml.
Water; 3.0 ml.

**Hydrochloric Acid Concentration.**—As shown in Fig. 4, it appears that the maximum absorption is obtained when 1.0 ml. of 1 N hydrochloric acid is used.

**Effect of Water.**—The absorbances were affected by the amount of water. As shown in Fig. 5, 3.0~4.0 ml. of water is always needed for complete color development in this procedure.

**Effect of Drying Conditions on Color Formation.**—As shown in Table I, the absorbance of the resulting solution containing 2.0 μg. of boron is affected by drying conditions for color development. Most satisfactory results were obtained when evaporation was made first on a water bath at 55±3°C for 4 hr. and then in an air bath at 60 to 90°C for 1 hr.

The effect of the kind of vessel on evaporation was tested. It was desired to use a quartz beaker or a platinum basin as shown in Table II. In the cases of a glass or polyethylene beaker some interferences were observed.

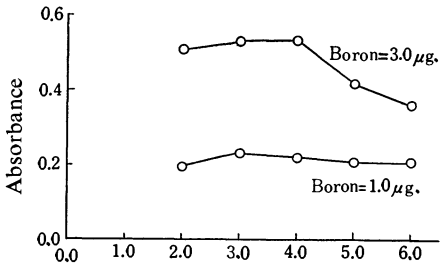



Fig. 5. Effect of water present.
Boron; 3.0 μg. and 1.0 μg.
Quercetin; 0.2% soln., 1.0 ml. (A-lot)
Oxalic acid; 20% soln., 3.0 ml.
HCl; 1 N soln., 1.0 ml.

Table I. Effect of drying conditions on color formation

Boron; 2.0 μg. Quercetin; 0.2% soln., 1.0 ml. (B-lot) Oxalic acid; 20% soln., 3.0 ml. HCl; 1 N soln., 1.0 ml. Water; 3.0 ml.

| Drying conditions | | | | Absorbance |
|---|---|---|---|---|
| On water bath (55±3°C) hr. | In air bath °C, hr. | In desiccator, hr. | In air bath °C, hr. | |
| 5.0 | | | | 0.435 |
| 6.0 | | | | 0.451 |
| 4.0 | 60, 1.0 | | | 0.466 |
| 4.0 | 60, 2.0 | | | 0.453 |
| 4.0 | 75, 0.5 | | | 0.388 |
| 4.0 | 75, 1.0 | | | 0.455 |
| 4.0 | 75, 2.0 | | | 0.466 |
| 4.0 | 90, 0.5 | | | 0.462 |
| 4.0 | 90, 1.0 | | | 0.455 |
| 4.0 | 90, 2.0 | | | 0.450 |
| 4.0 | 75, 1.0 | 40 | 75, 0.5 | 0.461 |
| 4.0 | 75, 1.0 | 40 | 75, 1.0 | 0.465 |

Table II. Effect of kinds of vessel

Boron; 2.0 μg. Quercetin; 0.2% soln., 1.0 ml. (B-lot) Oxalic acid; 20% soln., 3.0 ml. HCl; 1 N soln., 1.0 ml. Water; 3.0 ml.

| Kinds of vessel | Absorbance | Boron found μg. |
|---|---|---|
| 100 ml. Quartz beaker | 0.465 | $1.9_8$ |
| 50 ml. Quartz beaker | 0.470 | $2.0_0$ |
| 100 ml. Glass beaker | 0.503 | $2.1_6$ |
| 50 ml. Glass beaker | 0.484 | $2.0_7$ |
| Platinum basin, deep type | 0.468 | $1.9_9$ |
| Platinum basin, shallow type | 0.470 | $2.0_0$ |
| 100 ml. Polyethylene beaker | 0.558 | $2.4_3$ |

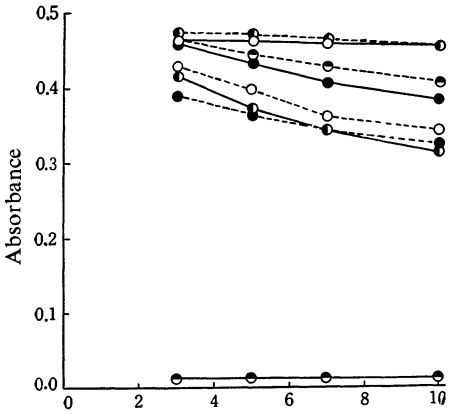



Fig. 6. Effect of kind of solvent.
Boron; 2.0 μg.
Quercetin; 0.2% soln., 1.0 ml. (B-lot)
Oxalic acid; 20% soln., 3.0 ml.
HCl; 1 N soln., 1.0 ml.
Water; 3.0 ml.
—○— Pure acetone
--○-- Acetone: Water=1:1
--●-- Ethyl alcohol
--◐-- Methyl isobutyl ketone
—◒— Toluene
—●— Acetone: Water=4:1
—◐— Methyl alcohol
--◒-- Butyl alchol
—◑— Carbon tetrachloride

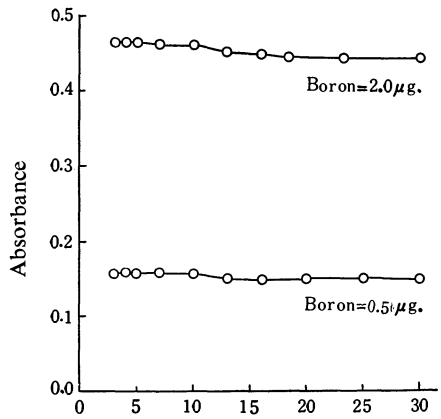



Fig. 7. Stability of the color.
Boron; 2.0 μg. and 0.5 μg.
Quercetin; 0.2% soln., 1.0 ml. (B-lot)
Oxalic acid; 20% soln., 3.0 ml.
HCl; 1 N soln., 1.0 ml.
Water; 3.0 ml.

**Effect of the Kind of Solvent on Colored Complex.**—Various kinds of solvent for extraction of boron-quercetin colored complex are tested with 2.0 μg. of boron. Fig. 6 shows that the best results are obtained in the case of pure acetone as a solvent.

**Color Stability.**—The absorbance of colored solutions is almost constant within 10 min., and then decreases slightly as shown in Fig. 7. It is thus desired to measure the absorbances within 10 min. after colored complex is dissolved with acetone.

**Stability of Quercetin Solution during Storage.**—It is found that the absorbance is increased as the duration of storage increases after preparation of the quercetin solution, and becomes constant after about 10 days as shown in Fig. 8. Hence, it is advisable to use the reagent solution after standing for about 10 days. It may be used at least 20 days after preparation.

**Effect of Diverse Salts.**—The effect of diverse ions on the spectrophotometry was examined. These salts cause interference seriously as shown in Fig. 9.

**Mole Ratio of Boron to Quercetin in Colored Complex.**—As shown in Fig. 10, maximum

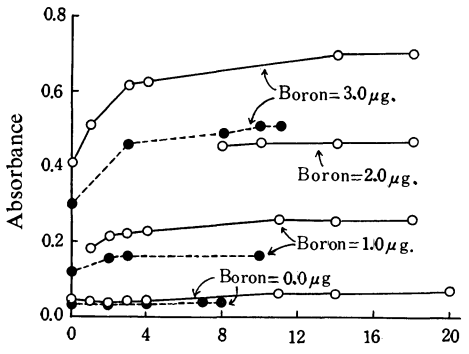



Fig. 8. Effect of duration of storage of quercetin solution.
Boron; 3.0 μg., 2.0 μg., 1.0 μg., and 0.0 μg.
Quercetin; 0.2% soln., 1.0 ml. (A- and B-lot)
Oxalic acid; 20% soln., 3.0 ml.
HCl; 1 N soln., 1.0 ml. Water; 3.0 ml.
—○— In the case of quercetin of B-lot
---●-- In the case of quercetin of A-lot

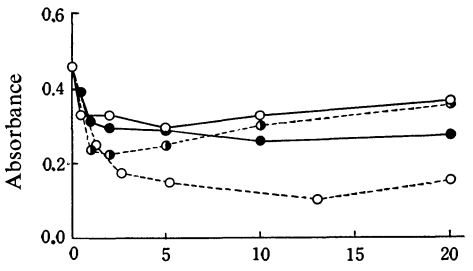



Fig. 9. Effect of diverse salts.
Boron; 2.0 μg.
Quercetin; 0.2% soln., 1.0 ml. (B-lot)
Oxalic acid; 20% soln., 3.0 ml.
HCl; 1 N soln., 1.0 ml. Water; 3.0 ml.
—○— NaCl —●— $Na_2SO_4$
---◑-- $CH_3COONa \cdot 3H_2O$
---○-- $Na_2HPO_4 \cdot 12H_2O$

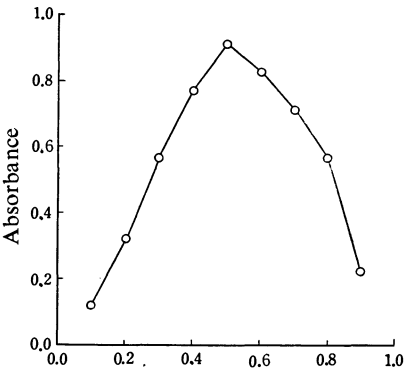



Fig. 10. Determination of ratio of boron to quercetin
Boron; $10^{-3}$ M soln., $(1.0-x)$ ml.
Quercetin; $10^{-3}$ M soln., $x$ ml. (B-lot)
Oxalic acid; 20% soln., 3.0 ml.
HCl; 1 N soln., 1.0 ml. Water; 3.0 ml.

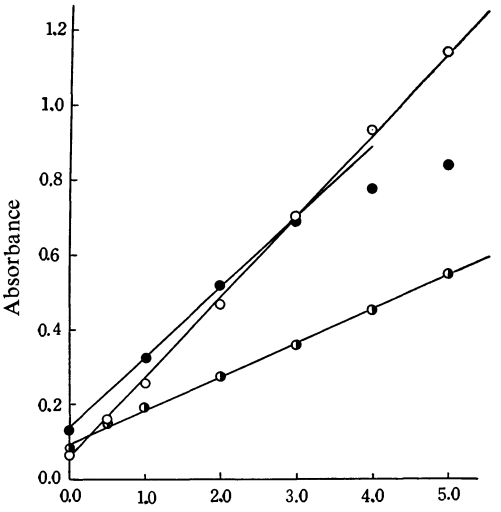



Fig. 11. Calibration curves.
Quercetin; 0.2% soln., 1.0 ml. (B-lot)
Oxalic acid; 20% soln., 3.0 ml.
HCl; 1 N soln., 1.0 ml. Water; 3.0 ml.
—○— Obtained by standard procedure
—◑— Obtained in the presence of 20 mg. of sodium sulfate
—●— Obtained after separation of boron by distillation

absorbance of the complex is obtained when the mole ratio of boron to quercetin has a value of 1 to 1[9].

**Calibration Curves.**—Measurements of absorbance were made with a number of the colored solutions containing varying amounts of boron. The results show that Beer's law is obeyed over the range 0.00 to 0.50 p. p. m. of boron as shown in Fig. 11. The sensitivity of this method, mean error and molar extinction coefficient were 0.204 $\mu$g., 4.90% and 22100 respectively. Even in the presence of 20 mg. of sodium sulfate, Beer's law is also obeyed over the range 0.00 to 0.50 p. p. m. of boron, but the sensitivity is decreased to 0.101 $\mu$g. in this case. After distillation of varying amounts of boron and evaporation of the distillate containing alkali and water to dryness, absorbances of the solutions of the dried residues were measured. As shown in Fig. 11, Beer's law is obeyed over the range 0.00 to 0.30 p. p. m. of boron.

**Determination of Boron in Graphite Samples.**—The results obtained by the above-mentioned experiments are presented in Table III.

TABLE III. RESULTS OF DETERMINATION OF BORON IN GRAPHITE SAMPLES

| Sample | Taken g. | Absorbance | Boron found $\mu$g. | Boron determined p.p.m. | Results obtained by curcumin method p.p.m. |
|---|---|---|---|---|---|
| Graphite-A | 0.5 | 0.660 | 2.8 | 5.6 | 5.53 |
| Graphite-B | 3.0 | 0.380 | 1.3 | 0.43 | 0.47 |
| Graphite-C | 2.0 | 0.450 | 1.7 | 0.85 | 0.90 |

9) W. C. Vosburgh and G. R. Cooper, *J. Am. Chem. Soc.*, 63, 437 (1941).

## Discussion

A sensitive new photometric method for the determination of boron by using quercetin as color reagent is proposed. The constitution of the boron-quercetin colored complex is considered to have the mole ratio of 1 : 1. In this procedure, if a different lot of quercetin, even though from the same maker, is used for color development, the absorbance is also varied, hence the determination of boron must be made using the calibration curve obtained by the same lot of quercetin as is used in the working operation. In this procedure, the color intensity of the solution is considerably affected by diverse salts, but the calibration curves are quite linear in the presence of a definite amount of salts. For the determination of boron in many kinds of practical samples, the proper separation of boron is desired. From the results of determination of boron in graphite samples, it was found that there is satisfactory agreement of the results obtained by the proposed method with those by the curcumin method in the limit of experimental error. This method may thus also be utilized for the determination of boron in other samples after preliminary separation of boron by distillation.

The author is indebted to Dr. Yuroku Yamamoto, Kyoto University, for his guidance and to Dr. Isao Muraki, Chief of the 5th Department of our Institute, for his useful suggestion.

*Osaka Industrial Research Institute*
*Agency of Industrial Science & Technology*
*Ministry of International Trade & Industry*
*Oyodo-ku, Osaka*

# *Normal Vibrations of Dimethyldimethoxysilane*

By Toshio TANAKA

(Received November 5, 1960)

The dipole moment of dimethyldimethoxysilane was previously reported to be 1.33 D at 25°C and 1.35 D at 50°C[1]. If ∠Si-O-C in this molecule was about 130° and the rotation about two Si-O bonds was free, the observed moment agreed with that calculated from bond moments. However, the ∠Si-O-C assumed there seems to be somewhat too large compared with that in tetramethoxysilane[2]. It was suggested, therefore, that the Si-O bond would perhaps rotate under some hindrance[1]. Thereafter, the Raman and the infrared spectra of dimethyldimethoxysilane were measured, and the probable form of this molecule was discussed. As the result,

1) A. kotera, K. Matsumura, H. Nomura, Y. Nakano and U. Maeda, presented at the Symposium on Organosilicon Compounds, Osaka, October, 1956, and private communication.

2) M. Yokoi, This Bulletin, **30**, 106 (1957).

it was concluded that this molecule would be *GG* form in the solid state* and have no rotational isomers[3].

This paper reports the calculation of the fundamental frequencies of this molecule and their normal mode of skeletal vibrations, under the assumption that this molecule belongs to the point group $C_{2v}$. In the calculation, a methyl group was regarded as a point mass. The normal coordinate treatment was carried out by the Wilson *FG* matrix method[4] with a Urey-Bradley potential function. No calculation of the normal vibration for $Y_2M(XZ)_2$ type molecules has been reported as far as the author knows.

## Normal Coordinate Treatment

The normal coordinate treatment has been carried out for parameters which are shown in Fig. 1. The symmetry of the molecule was assumed as $C_{2v}$. The interplanar angle for a Si-O-C plane and a C-Si-O plane including the same Si-O bond were also assumed to have an interplanar angle of $+60°$ or $-60°$.

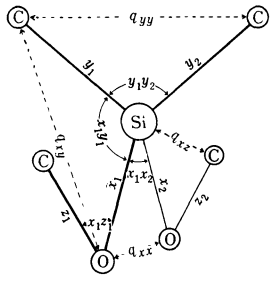



Fig. 1. Internal coordinates of the skeletal of dimethyldimethoxysilane.

According to the group theory, this molecule has fifteen skeletal vibrations, six of $a_1$, two of $a_2$, four of $b_1$ and three of $b_2$ species. Each one of the skeletal vibrations of $a_2$ and $b_2$ species is the torsional oscillation of a (Si-)$OCH_3$ group*. All vibrations of the $a_1$, $b_1$ and $b_2$ species are active both in infrared and Raman spectra, and those of the $a_2$ species are Raman active but infrared inactive.

From the internal coordinates indicated in Fig. 1, the following orthonormal symmetry coordinates have been found:

for the $a_1$ vibrations,

$$R_1=\Delta(z_1+z_2)/\sqrt{2}$$
$$R_2=\Delta(x_1+x_2)/\sqrt{2}$$
$$R_3=\Delta(y_1+y_2)/\sqrt{2}$$
$$R_4=\Delta(x_1z_1+x_2z_2)/\sqrt{2}$$
$$R_5=\Delta(x_1x_2-y_1y_2)/\sqrt{2}$$
$$R_6=\Delta(2x_1x_2+2y_1y_2-x_1y_1-x_1y_2-x_2y_1-x_2y_2)/\sqrt{12}$$

for the $a_2$ vibration,

$$R_7=\Delta(x_1y_1-x_1y_2-x_2y_1+x_2y_2)/2$$

for the $b_1$ vibrations,

$$R_9=\Delta(z_1-z_2)/\sqrt{2}$$
$$R_{10}=\Delta(x_1-x_2)/\sqrt{2}$$
$$R_{11}=\Delta(x_1z_1-x_2z_2)/\sqrt{2}$$
$$R_{12}=\Delta(x_1y_1+x_1y_2-x_2y_1-x_2y_2)/2$$

and for the $b_2$ vibrations,

$$R_{13}=\Delta(y_1-y_2)/\sqrt{2}$$
$$R_{14}=\Delta(x_1y_1-x_1y_2+x_2y_1-x_2y_2)/2$$

The numbering of these symmetry coordinates corresponds to the numbering of the fundamentals in Table I.

From the coefficients of the symmetry coordinates and the potential constants in a Urey-Bradley force field[5], the *F* matrix elements are obtained as follows:

for the $a_1$ vibrations,

$$F_{11}=K_z+s_{zx}{}^2F_{xz}+t_{zx}{}^2F_{xz}'$$
$$F_{12}=s_{xz}s_{zx}F_{xz}-t_{xz}t_{zx}F_{xz}'$$
$$F_{14}=(s_{zx}t_{xz}F_{xz}+s_{xz}t_{zx}F_{xz}')x$$
$$F_{22}=K_x+2s_{xx}{}^2F_{xx}+2s_{xy}{}^2F_{xy}+s_{xz}{}^2F_{xz}+2t_{xy}{}^2F_{xy}'+t_{xz}{}^2F_{xz}'$$
$$F_{23}=2(s_{xy}s_{yx}F_{xy}-t_{xy}t_{yx}F_{xy}')$$
$$F_{24}=(s_{xz}t_{zx}F_{xz}+s_{zx}t_{xz}F_{xz}')z$$
$$F_{25}=s_{xx}t_{xx}(F_{xx}+F_{xx}')x$$
$$F_{26}=\sqrt{2/3}\{s_{xx}t_{xx}(F_{xx}+F_{xx}')x-(s_{xy}t_{yx}F_{xy}+s_{yx}t_{xy}F_{xy}')y\}$$
$$F_{33}=K_y+2s_{yy}{}^2F_{yy}+2s_{yx}{}^2F_{xy}+2t_{yx}{}^2F_{xy}'$$
$$F_{35}=-s_{yy}t_{yy}(F_{yy}+F_{yy}')y$$
$$F_{36}=\sqrt{2/3}\{s_{yy}t_{yy}(F_{yy}+F_{yy}')y-(s_{yx}t_{xy}F_{xy}+s_{xy}t_{yx}F_{xy}')x\}$$
$$F_{44}=(H_{xz}+t_{xz}t_{zx}F_{xz}-s_{xz}s_{zx}F_{xz}')xz$$
$$F_{55}=\{(H_{xx}+t_{xx}{}^2F_{xx}-s_{xx}{}^2F_{xx}')x^2+(H_{yy}+t_{yy}{}^2F_{yy}-s_{yy}{}^2F_{yy}')y^2\}/2+3\kappa/\sqrt{8}$$
$$F_{56}=\{(H_{xx}+t_{xx}{}^2F_{xx}-s_{xx}{}^2F_{xx}')x^2-(H_{yy}+t_{yy}{}^2F_{yy}-s_{yy}{}^2F_{yy}')y^2\}/\sqrt{6}$$

* In the liquid state, the two Si—O bonds would rotate slowly centering in the *GG* form[3].

3) M. Hayashi, *J. Chem. Soc. Japan, Pure Chem. Sec. (Nippon Kagaku Zasshi)*, **79**, 436 (1958).

4) E. B. Wilson, Jr., *J. Chem. Phys.*, **7**, 1047 (1939).

* Represents the methoxyl group attached to silicon atom.

5) T. Shimanouchi, *J. Chem. Phys.*, **17**, 245, 734, 848 (1949).

$$F_{66}=\{(H_{xx}+t_{xx}^2F_{xx}-s_{xx}^2F_{xx}')x^2 + (H_{xy}+t_{xy}t_{yx}F_{xy}-s_{xy}s_{yx}F_{xy}')xy + (H_{yy}+t_{yy}^2F_{yy}-s_{yy}^2F_{yy}')y^2\}/3 + \kappa/\sqrt{8}$$

$$F_{13}=F_{15}=F_{16}=F_{34}=F_{45}=F_{46}=0$$

for the $a_2$ vibration,

$$F_{77}=(H_{xy}+t_{xy}t_{yx}F_{xy}-s_{xy}s_{yx}F_{ny}')xy - \kappa/\sqrt{8}$$

for the $b_1$ vibrations,

$$F_{99}=K_z+s_{zx}^2F_{xz}+t_{zx}^2F_{xz}'$$

$$F_{910}=s_{xz}s_{zx}F_{xz}-t_{xz}t_{zx}F_{xz}'$$

$$F_{911}=(s_{zx}t_{xz}F_{xz}+s_{xz}t_{zx}F_{xz}')x$$

$$F_{1010}=K_x+2s_{xy}^2F_{xy}+s_{xz}^2F_{xz}+2t_{xx}^2F_{xx}' + 2t_{xy}^2F_{xy}'+t_{xz}^2F_{xz}'$$

$$F_{1011}=(s_{xz}t_{zx}F_{xz}+s_{zx}t_{xz}E_{xz}')z$$

$$F_{1012}=\sqrt{2}\,(s_{xy}t_{yx}F_{xy}+s_{yx}t_{xy}F_{xy}')y$$

$$F_{1111}=(H_{xz}+t_{xz}t_{zx}F_{xz}-s_{xz}s_{zx}F_{xz}')xz$$

$$F_{1212}=(H_{xy}+t_{xy}t_{yx}F_{xy}-s_{xy}s_{yx}F_{xy}')xy + 3\kappa/\sqrt{8}$$

$$F_{912}=F_{1112}=0$$

and for the $b_2$ vibrations,

$$F_{1313}=K_y+2s_{yx}^2F_{xy}+2t_{yx}^2F_{xy}'+2t_{yy}^2F_{yy}'$$

$$F_{1314}=\sqrt{2}\,(s_{yx}t_{xy}F_{xy}+s_{xy}t_{yx}F_{xy}')x$$

$$F_{1414}=(H_{xy}+t_{xy}t_{yx}F_{xy}-s_{xy}s_{yx}F_{xy}')xy + 3\kappa/\sqrt{8}$$

where the following abbreviations have been adopted:

$s_{xx}=4x/3q_{xx}$ $\quad t_{xx}=\sqrt{8}\,x/3q_{xx}$

$s_{yy}=4y/3q_{yy}$ $\quad t_{yy}=\sqrt{8}\,y/3q_{yy}$

$s_{xy}=(3x+y)/3q_{xy}$ $\quad t_{xy}=\sqrt{8}\,y/3q_{xy}$

$s_{yx}=(3y+x)/3q_{xy}$ $\quad t_{yx}=\sqrt{8}\,x/3q_{xy}$

$s_{xz}=(x-z\cos\theta)/q_{xz}$ $\quad t_{xz}=z\sin\theta/q_{xz}$

$s_{zx}=(z-x\cos\theta)/q_{xz}$ $\quad t_{zx}=x\sin\theta/q_{xz}$

and the symbols used for the equilibrium values of the interatomic distances and of the interbond angles are $x$=Si—O, $y$=Si—C, $z$=O—C, $q_{xx}$=O···O, $q_{yy}$=C···(Si)···C, $q_{xy}$=O···C, $q_{xz}$=Si···C and $\theta=\angle$SiOC.

The $G$ matrix elements are obtained by the use of the table of Decius[6] and the method of Crawford[7]. Using the notations $\rho_x$, $\rho_y$ and $\rho_z$ for the reciprocals of Si—O, Si—C and O—C bond lengths, and $\mu_{Si}$, $\mu_O$ and $\mu_C$ for the reciprocals of the masses of silicon and oxygen atoms and methyl group, respectively, the following $G$ matrix elements have been obtained:

for the $a_1$ vibrations,

$$G_{11}=\mu_O+\mu_C$$

$$G_{12}=\mu_O\cos\theta$$

$$G_{14}=-\rho_x\mu_O\sin\theta$$

$$G_{15}=-\rho_x\mu_O\sin\theta$$

$$G_{16}=-\sqrt{3}\,\rho_x\mu_O\sin\theta/\sqrt{2}$$

$$G_{22}=2\mu_{Si}/3+\mu_O$$

$$G_{23}=-2\mu_{Si}/3$$

$$G_{24}=-\sqrt{8}\,\rho_x\mu_{Si}/3$$

$$G_{25}=-\sqrt{8}\,(\rho_x+\rho_y)\mu_{Si}/3$$

$$G_{26}=-2(\rho_x-\rho_y)\mu_{Si}/\sqrt{3}$$

$$G_{33}=2\mu_{Si}/3+\mu_C$$

$$G_{34}=\sqrt{8}\,\rho_x\mu_{Si}/3$$

$$G_{35}=\sqrt{8}\,(\rho_x+\rho_y)\mu_{Si}/3$$

$$G_{36}=2(\rho_x-\rho_y)\mu_{Si}/\sqrt{3}$$

$$G_{44}=4\rho_x^2\mu_{Si}/3+\rho_z^2\mu_C+(\rho_x^2+\rho_z^2 - 2\rho_x\rho_z\cos\theta)\mu_O$$

$$G_{45}=4\rho_x(\rho_x+\rho_y)\mu_{Si}/3+\rho_x(\rho_x-\rho_z\cos\theta)\mu_O$$

$$G_{46}=\sqrt{8}\,\rho_x(\rho_x-\rho_y)\mu_{Si}/\sqrt{3} + \sqrt{3}\,\rho_x(\rho_x-\rho_z\cos\theta)\mu_O/\sqrt{2}$$

$$G_{55}=4(\rho_x+\rho_y)^2\mu_{Si}/3+\rho_x^2\mu_O+\rho_y^2\mu_C$$

$$G_{56}=\sqrt{8}\,(\rho_x^2-\rho_y^2)\mu_{Si}/\sqrt{3} + \sqrt{3}\,(\rho_x^2\mu_O-\rho_y^2\mu_C)/\sqrt{2}$$

$$G_{66}=2(\rho_x-\rho_y)^2\mu_{Si}+3(\rho_x^2\mu_O+\rho_y^2\mu_C)/2$$

$$G_{13}=0$$

for the $a_2$ vibration,

$$G_{77}=3(\rho_x^2\mu_O+\rho_y^2\mu_C)/2$$

for the $b_1$ vibrations,

$$G_{99}=\mu_O+\mu_C$$

$$G_{910}=\mu_O\cos\theta$$

$$G_{911}=-\rho_x\mu_O\sin\theta$$

$$G_{912}=\rho_x\mu_O\sin\theta/\sqrt{2}$$

$$G_{1010}=4\mu_{Si}/3+\mu_O$$

$$G_{1011}=\sqrt{8}\,\rho_x\mu_{Si}/3-\rho_z\mu_O\sin\theta$$

$$G_{1012}=-2(\rho_x+3\rho_y)\mu_{Si}/3$$

$$G_{1111}=\rho_z^2(\mu_O+\mu_C)+\rho_x^2(2\mu_{Si}/3+\mu_O) - 2\rho_x\rho_y\mu_O\cos\theta$$

$$G_{1112}=-\sqrt{2}\,\rho_x(\rho_x+3\rho_y)\mu_{Si}/3 - \rho_x(\rho_x-\rho_z\cos\theta)\mu_O/\sqrt{2}$$

$$G_{1212}=(\rho_x^2\mu_O+3\rho_y^2\mu_O)/2+(\rho_x+3\rho_y)^2\mu_{Si}/3$$

for the $b_2$ vibrations,

$$G_{1313}=4\mu_{Si}/3+\mu_C$$

6) J. C. Decius, ibid., **16**, 1025 (1948).
7) B. Crawford, ibid., **21**, 1108 (1953).

$G_{1314} = -2(\rho_x + \rho_y/3)\mu_{Si}$

$G_{1414} = (3\rho_x{}^2\mu_O + \rho_y{}^2\mu_C)/2 + (3\rho_x + \rho_y)^2\mu_{Si}/3$

The molecular and potential constants used in the calculation are listed in Table I. These values are the same as those in the preceding paper[8] except $H_{yy}$, $F_{yy}$ and $\kappa$. The potential constants of $H(CH_3\text{-}Si\text{-}CH_3)$ and $F(CH_3\cdots CH_3)$ in tetramethylsilane[9] have been adopted for the $H_{yy}$ and $F_{yy}$ in the molecule under consideration. The $\kappa$ in this molecule has been assumed to be the mean between that in tetramethylsilane[9] and that in tetramethoxysilane[10]. The values of $F'$ have been assumed to be equal to $-F/10$ in the usual way.

Table I. Molecular and potential constants of dimethyldimethoxysilane

| Bond distance and angle | Potential constant | |
|---|---|---|
| | Type | md./Å |
| $x$=Si—O | $K_x$(Si—O) | 3.25 |
| =1.64 Å[a] | $K_y$(Si—$CH_3$) | 3.03 |
| $y$=Si—C | $K_z$(O—$CH_3$) | 4.88 |
| =1.888 Å[b] | $H_{xx}$(O—Si—O) | 0.13 |
| $z$=O—C | $H_{xy}$(O—Si—$CH_3$) | 0.12 |
| =1.42 Å[a] | $H_{yy}$($CH_3$—Si—$CH_3$) | 0.11 |
| ∠OSiC | $H_{xz}$(Si—O—$CH_3$) | 0.22 |
| =∠OSiC | $F_{xx}$(O···O) | 0.13 |
| =∠CSiC | $F_{xy}$(O···$CH_3$) | 0.08 |
| =109°28 | $F_{yy}$($CH_3$···$CH_3$) | 0.034 |
| =∠SiOC | $F_{xz}$(Si···$CH_3$) | 0.21 |
| =113° [a] | $\kappa$ | 0.185 Å$^2$ |

a) Values in $Si(OCH_3)_4$; M. Yokoi, This Bulletin, **30**, 100 (1957).
b) Value in $Si(CH_3)_4$; W. F. Sheehan, Jr. and V. Schomaker, *J. Am. Chem. Soc.*, **74**, 3956 (1952).

### Assignments of the Observed Frequencies

From the $F$ and $G$ matrix elements given above, the fundamental frequencies have been calculated by the use of the molecular and the potential constants listed in Table I, and the results are shown in Table II, together with the observed wave numbers[3] of the Raman and the infrared bands in the region of the skeletal vibrations. The skeletal vibrations have been assigned by the calculation of the potential energy distribution in the symmetry coordinates.

In the present calculation, the wave number of the Si-O symmetrical stretching vibration($a_1$) is higher than that of the Si-O nonsymmetrical stretching vibration($b_1$). Nevertheless, the observed frequencies near 690 and 735 $cm^{-1}$ have been assigned as $\nu_2(a_1)$ and $\nu_{10}(b_1)$, respectively (Table II), considering the intensities of Raman and infrared bands.

As is shown in Table II, the calculated values of $\nu_2$ and $\nu_{10}$ are considerably higher than the observed ones, respectively. In order to get a better agreement between the calculated wave number and the observed, it is necessary

Table II. Raman and infrared data, calculated wave numbers and the assignment for dimethyldimethoxysilane

| $\nu$. Obs. | | $\nu$. Calcd. | Assignment | Mode of vibration |
|---|---|---|---|---|
| Raman[a] | Infrared[a] | | | |
| 98 (1b) | | 136 | $\nu_6$ ($a_1$) | $Si(CH_3)_2$+$SiO_2$ sym. def. |
| | | 190 | $\nu_{12}$ ($b_1$) | $SiO_2$ rocking |
| 218 (4) | | 208 | $\nu_7$ ($a_2$) | $Si(CH_3)_2$ twisting |
| | | 238 | $\nu_5$ ($a_1$) | $Si(CH_3)_2$+$SiO_2$ nonsym. def. |
| 260 (2) | | 288 | $\nu_4$ ($a_1$) | SiOC sym. def. |
| 355 (0) | | 302 | $\nu_{14}$ ($b_2$) | $Si(CH_3)_2$ rocking |
| 380 (4bb) | | 400 | $\nu_{11}$ ($b_1$) | SiOC nonsym. def. |
| 618 (106) | 613 (w) | 618 | $\nu_3$ ($a_1$) | Si—C sym. str. |
| | 673 (w) | | | |
| 691 (3) | 690 (w) | 813 | $\nu_2$ ($a_1$) | Si—O sym. str. |
| 736 (2) | 730 (s) | 779 | $\nu_{10}$ ($b_1$) | Si—O nonsym. str. |
| 804 (5) | 797 (s) | 791 | $\nu_{13}$ ($b_2$) | Si—C nonsym. str. |
| 845 (1) | 849 (vs) | | } | (Si—)$CH_3$ rocking |
| 865 (2) | | | } | |
| 995 (1) | 998 (vw) | | | |
| 1080 (2) | 1073 (vs) | 1069 | $\nu_9$ ($b_1$) | C—O nonsym. str. |
| | 1088 (sh) | 1071 | $\nu_1$ ($a_1$) | C—O sym. str. |

a) Values in the liquid state

8) T. Tanaka, This Bulletin, **33**, 446 (1960).
9) T. Shimanouchi, *J. Chem, Soc. Japan, Pure Chem. Sec.* (*Nippon Kagaku Zasshi*), **74**, 266 (1953).
10) H. Murata, ibid., **77**, 893 (1956).

TABLE III. THE $L$ MATRICES OF THE SKELETAL NORMAL VIBRATIONS OF DIMETHYLDIMETHOXYSILANE

$a_1$ vibrations

| | $Q_1$ | $Q_2$ | $Q_3$ | $Q_4$ | $Q_5$ | $Q_6$ |
|---|---|---|---|---|---|---|
| $R_1$ (C—O sym. str.) | 0.36 | −0.03 | 0.02 | −0.02 | 0.00 | 0.01 |
| $R_2$ (Si—O sym. str.) | −0.10 | −0.23 | 0.14 | −0.04 | 0.00 | 0.00 |
| $R_3$ (Si—C sym. str.) | 0.01 | 0.22 | 0.20 | 0.01 | 0.01 | 0.00 |
| $R_4$ (SiOC sym. def.) | −0.07 | 0.23 | −0.15 | −0.18 | 0.10 | 0.06 |
| $R_5$ ($Si(CH_3)_2$+$SiO_2$ nonsym. def.) | −0.08 | 0.21 | −0.02 | −0.16 | −0.16 | −0.04 |
| $R_6$ ($Si(CH_3)_2$+$SiO_2$ sym. def.) | −0.12 | 0.05 | −0.04 | −0.06 | 0.15 | −0.14 |

$b_1$ vibrations

| | $Q_9$ | $Q_{10}$ | $Q_{11}$ | $Q_{12}$ |
|---|---|---|---|---|
| $R_9$ (C—O nonsym. str.) | 0.35 | −0.07 | 0.01 | 0.00 |
| $R_{10}$ (Si—O nonsym. str.) | −0.13 | −0.30 | −0.01 | −0.01 |
| $R_{11}$ (SiOC nonsym. def.) | −0.08 | 0.09 | 0.30 | −0.10 |
| $R_{12}$ ($SiO_2$ rocking) | 0.10 | 0.14 | −0.21 | −0.14 |

$b_2$ vibrations

| | $Q_{13}$ | $Q_{14}$ |
|---|---|---|
| $R_{13}$ (Si—C nonsym. str.) | −0.33 | −0.03 |
| $R_{14}$ ($Si(CH_3)_2$ rocking) | 0.18 | −0.28 |

TABLE IV. POTENTIAL ENERGY DISTRIBUTION $F_{ii}L_{ia}^2/\lambda_a$ FOR THE NORMAL VIBRATION OF SKELETAL IN DIMETHYLDIMETHOXYSILANE

$a_1$ vibrations

| | $\nu_1$ | $\nu_2$ | $\nu_3$ | $\nu_4$ | $\nu_5$ | $\nu_6$ |
|---|---|---|---|---|---|---|
| $R_1$ (C—O sym. str.) | 0.94 | 0.01 | 0.01 | 0.05 | 0.00 | 0.01 |
| $R_2$ (Si—O sym. str.) | 0.05 | 0.50 | 0.33 | 0.11 | 0.00 | 0.00 |
| $R_3$ (Si—C sym. str.) | 0.00 | 0.39 | 0.59 | 0.01 | 0.01 | 0.00 |
| $R_4$ (SiOC sym. def.) | 0.01 | 0.09 | 0.07 | 0.42 | 0.20 | 0.22 |
| $R_5$ ($Si(CH_3)_2$+$SiO_2$ nonsym. def.) | 0.01 | 0.07 | 0.00 | 0.32 | 0.53 | 0.08 |
| $R_6$ ($Si(CH_3)_2$+$SiO_2$ sym. def.) | 0.01 | 0.00 | 0.00 | 0.03 | 0.26 | 0.69 |

$b_1$ vibrations

| | $\nu_9$ | $\nu_{10}$ | $\nu_{11}$ | $\nu_{12}$ |
|---|---|---|---|---|
| $R_9$ (C—O nonsym. str.) | 0.91 | 0.08 | 0.01 | 0.00 |
| $R_{10}$ (Si—O nonsym. str.) | 0.09 | 0.89 | 0.01 | 0.02 |
| $R_{11}$ (SiOC nonsym. def.) | 0.00 | 0.01 | 0.66 | 0.33 |
| $R_{12}$ ($SiO_2$ rocking) | 0.01 | 0.03 | 0.32 | 0.64 |

$b_2$ vibrations

| | $\nu_{13}$ | $\nu_{14}$ |
|---|---|---|
| $R_{13}$ (Si—C nonsym. str.) | 0.96 | 0.04 |
| $R_{14}$ ($Si(CH_3)_2$ rocking) | 0.06 | 0.95 |

to adopt a lower value of $K_x$(Si—O), than the 3.25 md./Å of methyltrimethoxysilane[8]. Accordingly, it seems that the value of $K_x$(Si—O) in dimethyldimethoxysilane is rather lower than that in methyltrimethoxysilane. This may correspond to the tendency for the bond energy of Si-O bond which decreases as the number of oxygen atoms attached to silicon decreases; $-E_{Si-O}$ in $SiO_4$ unit $>-E_{Si-O}$ in $CSiO_3$ unit $>-E_{Si-O}$ in $C_2SiO_2$ unit, as reported by the present author[11].

The $L$ matrices and the distribution of potential energy in symmetry coordinates have been calculated for the skeletal normal modes; the results are shown in Tables III and IV, respectively. As shown in Table IV, some of the symmetry coordinates of totally symmetric species are related to several normal modes to a considerable extent; the $R_2$ and $R_3$ coordinates to both modes of $\nu_2$ and $\nu_3$, and the $R_4$ and $R_5$ coordinates to a mode of $\nu_4$.

The author wishes to express his sincere thanks to Professor Takeo Watase of this University, Professor Hiroshi Azumi of Tohoku University and Dr. Hiroshi Murata of Hiroshima University for much valuable discussion.

*Department of Applied Chemistry*
*Faculty of Engineering*
*Osaka University*
*Miyakojima-ku, Osaka*

11) T. Tanaka, *J. Inorg. Nucl. Chem.*, 13, 225 (1961).

# *Thermodynamic Studies on Cobalt Complexes. VIII. Some Information about Diaquotetramminecobalt(III) Complexes and Thermal Dissociation of the Corresponding Chloride**

By Motoshichi MORI, Ryokichi TSUCHIYA, Shuji TAKEMURA and Eisei MATSUDA

(Received December 19, 1960)

Although there have been a few reports[1,2] on the visible and ultraviolet absorption spectra of diaquotetramminecobalt(III) complexes, none can be found on the infrared absorption spectra of cobalt(III) diaquo-complexes except in the cases of $[Co(NH_3)_2(OH_2)_2Cl_2]Cl$ and $[Co\,en(OH_2)_2Cl_2]Cl$[3] containing chloride ions as the ligand. The investigation of diaquotetramminecobalt(III) complexes by X-ray diffraction method has never been reported. In the present study the infrared absorption and the X-ray diffraction of diaquotetramminecobalt(III) and aquopentamminecobalt(III) complexes were measured. From these some information about their crystal structures was brought out. Since little has been reported concerning the thermochemical properties of cobalt(III) diaquo-complexes, some of them will be described, with special reference to the thermal dissociation of the diaquotetramminecobalt(III) chloride.

## Experimental

Diaquotetramminecobalt(III) chloride, sulfate and perchlorate were prepared[4] by the aquation of carbonatotetramminecobalt(III) nitrate with hydrochloric, sulfuric and perchloric acids respectively. Their visible and ultraviolet absorption spectra were measured with a Hitachi EPU-2 type spectrophotometer. The infrared absorption of diaquotetramminecobalt(III) and aquopentamminecobalt(III) perchlorates were measured by the Nujol mull method with an Ōyō Kōgaku Kenkyūsho DS-201 infrared spectrophotometer, and the X-ray diffraction, with a Rigaku Denki X-ray diffractometer. The results obtained were compared with those of hexamminecobalt(III) perchlorate.

The thermal analysis was carried out for diaquotetramminecobalt(III) chloride, sulfate and perchlorate with a Shimadzu thermobalance. The thermal dissociation pressure of diaquotetramminecobalt(III) chloride was measured in vacuo with a mercury manometer.

## Results and Discussion

**Thermal Analyses of Diaquotetramminecobalt(III) Chloride, Sulfate and Perchlorate.**— In order to verify the fact that the complexes obtained were actually the desired ones, chemical analyses, determinations of coagulation values and thermal analyses were made with them. The weight losses of the complexes upon heating are plotted against the temperature in Fig. 1. It is presumed that the chloride and sulfate decompose according to the following schemes:

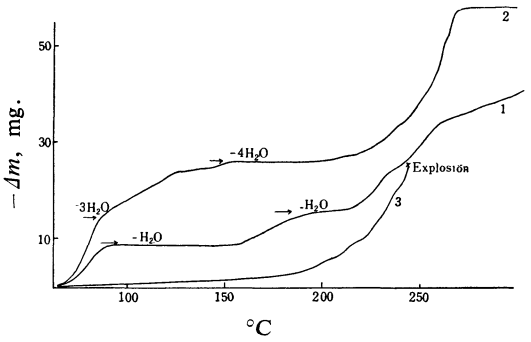



Fig. 1. The relationships between the weight loss and the temperature upon heating diaquotetramminecobalt(III) chloride (1), sulfate hydrate (2) and perchlorate (3). Both the weights of the chloride and of the perchlorate used are 0.2 g. respectively and that of the sulfate hydrate is 0.1 g. The expressions of $-nH_2O$ show the steps of dehydration of $n$ g molecule of water from oneg ram molecule of those complexes.

$$[Co(NH_3)_4(OH_2)_2]Cl_3 \xrightarrow[70\sim90°C]{-H_2O} [Co(NH_3)_4\cdot (OH_2)Cl]Cl_2 \xrightarrow[150\sim170°C]{-H_2O} cis\text{-}[Co(NH_3)_4Cl_2]Cl \xrightarrow[200\sim234°C]{} CoCl_2$$

* Read at the Symposium on Coordination Compounds of the Chemical Society of Japan, Sendai, September, 1960.

1) Y. Shimura and R. Tsuchida, This Bulletin, **29**, 312 (1956).

2) A. Kiss and D. Czeglédy, *Z. anorg. u. allgem. Chem.*, **235**, 407 (1938).

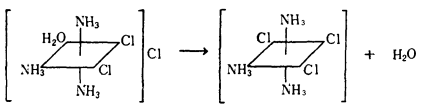
3) E. Kyuno, *J. Chem. Soc. Japan, Pure Chem. Sec.* (*Nippon Kagaku Zasshi*), **80**, 724 (1959).

4) S. M. Jörgensen, *Z. anorg. Chem.*, **2**, 296 (1892).

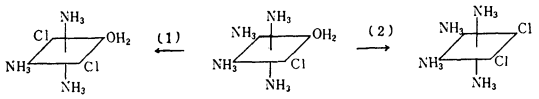
$$[Co(NH_3)_4(OH_2)_2]_2(SO_4)_3\cdot 3H_2O \xrightarrow[80°C]{-3H_2O} [Co(NH_3)_4(OH_2)_2]_2(SO_4)_3 \xrightarrow[90\sim150°C]{-4H_2O} [Co(NH_3)_4SO_4]_2SO_4 \xrightarrow[240\sim260°C]{} 2CoSO_4 + (NH_4)_2SO_4$$

The perchlorate begins to decompose gently at about 190°C and explodes at 243°C. The decomposition of the perchlorate does not take place in a stepwise manner as does the chloride and sulfate.

*trans*-Aquodichlorotriamminecobalt(III) chloride, $[Co(NH_3)_3(OH_2)Cl^{(1)}_{2(6)}]Cl$, does not decompose at 100°C, whereas even at this temperature the corresponding *cis*-chloride changes to trichlorotriamminecobalt(III) complex releasing water as shown below:



There has been a report[5] that this phenomenon might be explained by the so-called trans-effect[6]. If the trans-effect is to be applied to the decomposition of aquochlorotetramminecobalt(III) chloride, the product must be *trans*-aquodichlorotriamminecobalt(III) chloride, $[Co(NH_3)_3(OH_2)Cl^{(1)}_{2(6)}]Cl$. But the product actually obtained in our experiment is *cis*-dichlorotetramminecobalt(III) chloride, $[Co(NH_3)_4Cl^{(1)}_{2(2)}]Cl$; i. e. process 1 did not occur, but process 2 did take place:



This shows that the trans-effect can not be applied to this process. A better explanation may be that *cis*-dichlorotetramminecobalt(III) chloride is more stable than the corresponding trans-chloride in the same way as that *cis*-dinitrotetramminecobalt(III) chloride is thermodynamically more stable than the corresponding *trans*-chloride[7].

**Visible and Ultraviolet Absorption Spectra of Diaquotetramminecobalt(III) Complexes.**—The visible and ultraviolet absorption spectra of diaquotetramminecobalt(III) complex which have already been reported by Tsuchida and his co-worker[1] and Kiss and his co-worker[2] are not in agreement with each other. That is, the maxima of both the first and second absorption bands of the complex reported by the former workers* are remarkably lower than those by the latter. The absorption of the complex measured by us are given in Fig. 2. The maxima of the first and second absorption bands of the complex are found at $\nu_1=59.0\times10^{13}$ sec$^{-1}$ ($\log\varepsilon_1=1.73$) and $\nu_2=84.5\times10^{13}$ sec$^{-1}$ ($\log\varepsilon_2=1.66$) respectively, where $\nu$ is the frequency and $\varepsilon$ is the molar extinction coefficient.

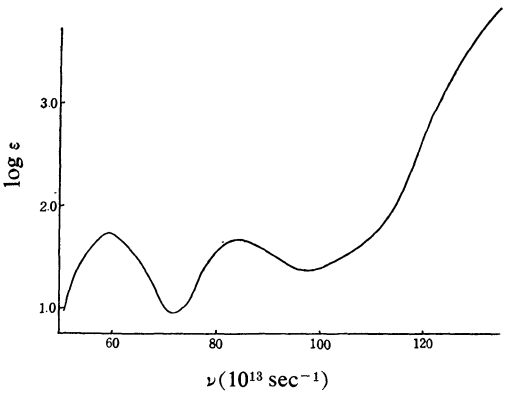



Fig. 2. The absorption spectrum of diaquotetramminecobalt(III) perchlorate.

**Dissociation Pressure of Diaquotetramminecobalt(III) Chloride.**—It was found above that diaquotetramminecobalt(III) chloride decomposed at 70~90°C as follows:

$$[Co(NH_3)_4(OH_2)_2]Cl_3(s) = [Co(NH_3)_4(OH_2)Cl]Cl_2(s) + H_2O(g)$$

The vapor pressure or dissociation pressure of diaquotetramminecobalt(III) chloride was measured at 7~36.5°C with the apparatus already described[8]. The results are listed in Table I.

The logarithm of the dissociation pressure, $p_{mm}$, is plotted against the reciprocal of the absolute temperature in Fig. 3. A straight

TABLE I. DISSOCIATION PRESSURE OF DIAQUOTETRAMMINECOBALT(III) CHLORIDE

| Temp. C° | $1/T\times10^3$ | Dissociation pressure $p_{mm}$ | $\log p_{mm}$ |
|---|---|---|---|
| 7 | 3.559 | 4.15 | 0.6181 |
| 19 | 3.425 | 5.40 | 0.7324 |
| 21 | 3.401 | 5.89 | 0.7701 |
| 31 | 3.290 | 6.99 | 0.8445 |
| 36.5 | 3.231 | 7.98 | 0.9020 |

5) M. Mori, M. Shibata, K. Hirota, K. Masuno and Y. Suzuki, *J. Chem. Soc. Japan, Pure Chem. Sec.*, (*Nippon Kagaku Zasshi*), **79**, 1251 (1958).
6) J. V. Quagliano and L. Schubert, *Chem. Revs.*, **50** 201 (1952).
7) M. Mori, R. Tsuchiya and H. Fukuda, This Bulletin, **33**, 1503 (1960).

* By private communication received from R. Tsuchida in Oct., 1959, $\nu_1=59.2$ ($\log\varepsilon_1=1.72$) and $\nu_2=84.6\sim84.7$ ($\log\varepsilon_2=1.64$).
8) M. Mori and R. Tsuchiya, This Bulletin, **32**, 467 (1959).

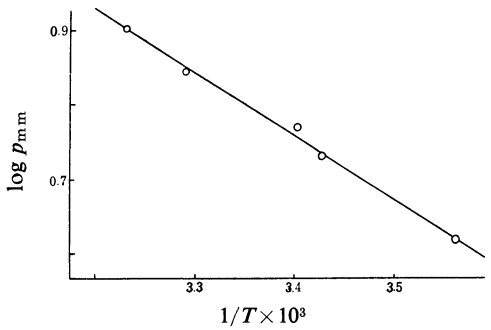



Fig. 3. The relationship between the dissociation pressure of diaquotetramminecobalt(III) chloride and the temperature.

line is obtained. The equation of the straight line is calculated by the method of least squares as,

$$\log p_{mm}=3.669-856.1/T$$

The free energy change for the dissociation is obtained as,

$$\Delta G^\circ=3916-3.604\,T,\quad \Delta G^\circ_{298}=2842\text{ cal.} \qquad (1)$$

From the free energy change for the dissociation of hexamminecobalt(III)[8] and aquopentamminecobalt(III) chlorides[9], the free energy change for the reaction in which one gram equivalent of $NH_3$ is replaced by one gram equivalent of $H_2O$ in the coordination sphere is calculated as below:

$$[Co(NH_3)_6]Cl_3(s)+H_2O(g)=[Co(NH_3)_5\cdot OH_2]Cl_3(s)+NH_3(g)$$
$$\Delta G^\circ=-296+8.32\,T \qquad (2)$$

The entropy change is $\Delta S^\circ=-8.32$ e. u. If it is assumed that the entropy change of the reaction,

$$[Co(NH_3)_5OH_2]Cl_3(s)+H_2O(g)=[Co(NH_3)_4(OH_2)_2]Cl_3(s)+NH_3(g) \qquad (3)$$

in which one gram equivalent of $NH_3$ in the reactant is replaced by one gram equivalent of $H_2O$, is equal to the entropy change of the reaction 2, i. e. $-8.32$ e. u., then the free energy change for reaction 3 is obtained by using the value of the above entropy change and the heats of formation of the substances[10,11] concerning the reaction as:

$$\Delta G^\circ=-1140+8.32\,T \qquad (4)$$

Since the free energies of formation of aquopentamminecobalt(III) chloride, water vapor and ammonia are known, from these values and Eq. 4 the free energy of formation of diaquotetramminecobalt(III) chloride in the solid state is calculated as,

$$\Delta G^\circ_f=-360600+363.2\,T$$
$$\Delta G^\circ_{f298}=-252300\text{ cal.} \qquad (5)$$

The free energy of formation of aquochlorotetramminecobalt(III) chloride, which is the decomposition product of diaquotetramminecobalt(III) chloride, is obtained from Eqs. 1 and 5 as follows:

$$\Delta G^\circ_f=-298900+349.0\,T$$
$$\Delta G^\circ_{f298}=-194900\text{ cal.}$$

From the above results the free energies of the reaction in which an ammonia molecule is successively replaced by a water molecule in the coordination sphere of hexamminecobalt(III) chloride are calculated and from these relationships it is concluded that the thermodynamic stabilities of these complexes are in the order:

$$[Co(NH_3)_6]Cl_3>[Co(NH_3)_5OH_2]Cl_3>[Co(NH_3)_4(OH_2)_2]Cl_3>[Co(NH_3)_4(OH_2)\cdot Cl]Cl_2>[Co(NH_3)_5Cl]Cl_2$$

**Infrared Absorption Spectra of Cobalt(III) Aquoammine-complexes.**—The infrared absorption spectra for diaquotetramminecobalt(III) and aquopentamminecobalt(III) perchlorates are listed in Table II together with those for hexamminecobalt(III) perchlorate already reported[12].

From the table it is seen that the wave numbers of the stretching vibration of N-H, $\nu_{N-H}$ for aquo-complexes are lower than those for hexammine-complex, whereas the wave numbers of the degenerate bending vibration, deg. $\delta_{NH_3}$, and the symmetric bending vibration, sym. $\delta_{NH_3}$, of $NH_3$ for the former are higher than those for the latter. The wave numbers of the rocking vibration of $NH_3$, $\rho_{NH_3}$, are remarkably higher for the former. This means that the coordinate bond character of Co—N in the coordination sphere of cobalt(III) ammine-complexes increases when one or two water moleclues coordinate in place of ammonia molecules.

**X-Ray Diffraction Data for Cobalt(III) Aquoammine-complexes.**—Some reports have been published on the X-ray diffraction for

9) M. Mori, R. Tsuchiya and Y. Okano, ibid., **32**, 1029 (1959).
10) K. B. Yatsimirskii and L. L. Pankowa, *Zhur. Obshchei Khim.*, **19**, 617 (1949); K. B. Yatsimirskii, "Thermochemie von Komplexverbindungen", Akademie-Verlag, Berlin (1956), p. 178.
11) F. D. Rossini et al., "Selected Values of Chemical Thermodynamic Properties", United States Government Printing Office, Washington (1952), p. 9.
12) J. Fujita, K. Nakamoto and M. Kobayashi, *J. Am. Chem. Soc.*, **79**, 3295 (1956).

TABLE II. WAVE NUMBER OF VIBRATION FOR O-H AND N-H BONDS IN THE INFRARED ABSORPTION SPECTRA OF HEXAMMINECOBALT(III), AQUOPENTAMMINECOBALT(III) AND DIAQUOTETRAMMINECOBALT(III) PERCHLORATES

| Complex | $\nu_{O-H}$ | $\nu_{N-H}$ | | deg. $\delta_{NH_2}$ | sym. $\delta_{NH_3}$ | $\rho_{NH_3}$ |
|---|---|---|---|---|---|---|
| $[Co(NH_3)_6](ClO_4)_3$ | | 3320 | 3240 | 1630 | 1352 | 803 |
| $[Co(NH_3)_5OH_2](ClO_4)_3$ | 3400 | 3257 | 3205 | 1634 | 1355 | 826 |
| $[Co(NH_3)_4(OH_2)_2](ClO_4)_3$ | 3390 | 3246 | 3195 | 1637 | 1346 | 839 |

TABLE III. X-RAY DIFFRACTION DATA FOR AQUOPENTAMMINECOBALT(III) AND DIAQUOTETRAMMINECOBALT(III) PERCHLORATES

| $[Co(NH_3)_5OH_2](ClO_4)_3$ | | | | $[Co(NH_3)_4(OH_2)_2](ClO_4)_3$ | | | |
|---|---|---|---|---|---|---|---|
| $d$(Å) | $I/I_0$ | $hkl$ | $a$(Å) | $d$(Å) | $I/I_0$ | $hkl$ | $a$(Å) |
| 4.019 | 100 | 220 | 11.37 | 4.001 | 100 | 220 | 11.32 |
| 3.276 | 5 | 222 | 11.35 | | | | |
| 2.842 | 18 | 400 | 11.37 | 2.829 | 20 | 400 | 11.32 |
| 2.319 | 4.3 | 422 | 11.36 | 2.307 | 5.5 | 422 | 11.30 |
| 2.184 | 13 | 333 | 11.35 | 2.174 | 11 | 333 | 11.30 |
| 2.009 | 5 | 440 | 11.36 | 2.000 | 5.5 | 440 | 11.31 |
| 1.796 | 6.5 | 620 | 11.36 | 1.789 | 7 | 620 | 11.31 |
| 1.518 | 6 | 642 | 11.36 | 1.511 | 5.5 | 642 | 11.32 |
| 1.340 | 3 | 822 | 11.37 | | | | |
| | | | $a_{mean}=11.36$ Å | | | | $a_{mean}=11.31$ Å |
| | | | $D=2.087$ | | | | $D=2.119$ |

hexamminecobalt(III) chloride[13] and perchlorate[14], but none for cobalt(III) aquoammine-complexes except $[Co(NH_3)_5(OH_2)]I_3$[15] and $[Co(NH_3)_4(OH_2)_2][TlCl_6]$[16]. The results of the X-ray diffraction measurement for aquopentamminecobalt(III) and diaquotetramminecobalt(III) perchlorates are shown in Table III. In this table $d$ is interplanar spacing, $I/I_0$, relative intensity, and $hkl$, indices of lattice planes.

The crystals of these complexes belong to the cubic system like $(NH_4)_3[FeF_6]$[17] and the number of chemical units in a unit cell is $Z=4$. By comparing the length of the edge of a unit cell, $a$, and the density, $D$, for the above two cobalt(III) aquoammine perchlorates with those for hexamminecobalt(III) perchlorate, $a=11.41$ Å and $D=2.048$[14], as already reported, it is found that the dimension of the unit cell becomes smaller when one gram equivalent of $NH_3$ is replaced by one gram equivalent of $H_2O$ in the coordination sphere of hexamminecobalt-(III) or aquopentamminecobalt(III) perchlorate. Such a tendency can be seen also in the cases of $[Co(NH_3)_6][TlCl_6]$ ($a=11.42$ Å)[18] and $[Co(NH_3)_4(OH_2)_2][TlCl_6]$ ($a=11.30$ Å)[16]. It makes us suppose that the change of the bond distance of Co–N is closely related to the increase of the coordination bond character which can be detected from the infrared absorption spectra.

13) F. M. Jäger, *Z. Kryst.*, **39**, 543 (1904).
14) R. W. G. Wyckoff, S. B. Hendricks and T. P. McCatcheon, *J. Am. Chem. Soc.*, **13**, 389 (1927).
15) G. Natta, *Gazz. chim. ital.*, **58**, 624 (1928).
16) M. Linhard, W. Manthey and K. Plieth, *Z. Elektrochem.*, **57**, 862 (1953).
17) V. Cagliotti and G. Giacomello, *Naturwissenschaften*, **26**, 317 (1938).
18) T. Watanabe, M. Atoji and C. Okazaki, *Acta Cryst.*, **3**, 405 (1950).


## Summary

The visible and ultraviolet absorption spectra of diaquotetramminecobalt(III) perchlorate were measured and its decomposition process was discussed on the basis of the thermal analytical data.

The decomposition pressure of diaquotetramminecobalt(III) chloride was measured and the free energy of formation of aquochlorotetramminecobalt(III) chloride which was the product of the decomposition was calculated.

The infrared absorption and X-ray diffraction were measured for diaquotetramminecobalt(III) and aquopentamminecobalt(III) perchlorates and the relationships between the dimension of the unit cell and the coordinate bond strength, Co–N, were discussed.



*Department of Chemistry*
*Faculty of Science*
*Kanazawa University*
*Kanazawa*

# *Thermodynamic Studies on Cobalt Complexes. IX. Chemical Equilibrium between Diaquotetramminecobalt(III) Complex and Oxalate Ion**

By Motoshichi MORI, Ryokichi TSUCHIYA and Eisei MATSUDA

(Received December 19, 1961)

The method of Schramm[1] has been well known for a long time as a general method of preparing oxalatotetramminecobalt(III) complexes. It depends on the reaction of oxalic acid upon diaquotetramminecobalt(III), hydroxoaquotetramminecobalt(III), chloroaquotetramminecobalt(III) or carbonatotetramminecobalt(III) complexes. However, the thermodynamic properties of the oxalatotetramminecobalt(III) complex thus formed have never been reported. In order to get information about these properties the chemical equilibrium between diaquotetramminecobalt(III) ion and oxalate ion was studied spectrophotometrically.

## Experimental

Diaquotetramminecobalt(III) complex was prepared as the perchlorate by the reaction of carbonatotetramminecobalt(III) nitrate with perchloric acid. The identity of the sample was confirmed by chemical and thermal analyses, the measurements of the coagulation values and those of absorption spectra[2]. Oxalic acid and potassium and ammonium oxalates were purified by recrystallization.

At first oxalic acid was added to a solution of diaquotetramminecobalt(III) perchlorate as the source of oxalate ion. But the reaction hardly proceeded at all even when the solution was heated. On the other hand, when potassium oxalate was used, the diaquo-complex was decomposed owing to the strong alkalinity of the solution. When ammonium oxalate was used in place of oxalic acid or potassium oxalate, the reaction with diaquotetramminecobalt(III) perchlorate did occur. But, in this case, oxalatotetramminecobalt(III) complex was not produced but cobalt(III) oxalatoammine complex which contained the oxalate ion as an unidentate ligand was obtained. This fact will be described later in detail.

At last, the mixed solution, or the buffer solution, of oxalic acid and potassium oxalate was used. Although the reaction between the buffer solution and diaquotetramminecobalt(III) perchlorate did not proceed at room temperature, it did when heated to 65°C, producing oxalatotetramminecobalt(III) ion.

From the above preliminary experiments the following method of the determination of the chemical equilibrium between the diaquo-complex and oxalate ion was selected. The mixture of 50 ml. of a solution of diaquotetramminecobalt(III) perchlorate and 50 ml. of a buffer solution consisting of oxalic acid and potassium oxalate was kept in the flask at 65°C for ten minutes and then it was immersed in the thermostat at 25°C. When the equilibrium was attained after about six hours, the absorbancy of the solution was measured with a Hitachi EPU-2 type spectrophotometer. The maximum of the first absorption band of diaquotetramminecobalt(III) ion is at $\nu=59.0\times10^{13}\,\mathrm{sec}^{-1}$ ($\log\varepsilon=1.73$)[2] and that of oxalatotetramminecobalt(III) ion, at $\nu=58.7\times10^{13}\,\mathrm{sec}^{-1}$ ($\log\varepsilon=1.91$)[3], where $\nu$ is the frequency and $\varepsilon$, the molar extinction coefficient. The measurement of absorbancy of the solution at equilibrium was made at 510 m$\mu$.

Since cobalt(III) oxalato-complexes are readily decomposed by sunlight, a brown flask was employed in order to protect the solution from the photodecomposition. The range of the initial concentration of the diaquotetramminecobalt(III) complex was 1/500~1/800 F and that of the oxalate ion was 1/80~1/5000 F. In order to diminish the ionic strength, the concentration of the diaquo complex must be lowered. But if it is lowered below 1/800 F the error of measurement of the absorbancy will grow larger. Therefore the concentration of the diaquo-complex could not be lowered below 1/800 F. The measurement of pH of the solution was made with a Horiba HRL Model M pH meter.

## Theoretical

The reaction between diaquotetramminecobalt(III) and oxalate ions is expressed by:

$$[Co(NH_3)_4(OH_2)_2]^{3+}(aq.)+C_2O_4^{2-}(aq.) = [Co(NH_3)_4C_2O_4]^{+}(aq.)+2H_2O(l) \quad (1)$$

If the initial concentration of the diaquo-complex ion is expressed by $C$, its concentration at equilibrium, by $C_1$ and the concentration of oxalatotetramminecobalt(III) ion at equilibrium, by $C_2$, then

$$C=C_1+C_2 \quad (2)$$

If the molar extinction coefficients of the diaquo-complex and oxalate ions at 510 m$\mu$ are expressed by $\varepsilon_1$[2] and $\varepsilon_2$[3] respectively, and the value corresponding to the molar extinction coefficient calculated from the absorbancy

* Read at the Symposium on Coordination Compounds of the Chemical Society of Japan, Sendai, September, 1960.

1) W. Schramm, *Z. anorg. u. allgem. Chem.*, **180**, 167, 177 (1929).

2) M. Mori, R. Tsuchiya, S. Takemura and E. Matsuda, This Bulletin, **34**, 1757 (1961).

3) Y. Shimura and R. Tsuchida, ibid., **29**, 312 (1956).

measured at the chemical equilibrium of reaction 1 is expressed by $\varepsilon$, there exists the relationship:

$$C\varepsilon = C_1\varepsilon_1 + C_2\varepsilon_2 \tag{3}$$

From Eqs. 2 and 3, the concentration of each complex ion is obtained by

$$C_1 = C\frac{\varepsilon_2 - \varepsilon}{\varepsilon_2 - \varepsilon_1} \quad \text{and} \quad C_2 = C\frac{\varepsilon - \varepsilon_1}{\varepsilon_2 - \varepsilon_1} \tag{4}$$

In the mixed solution of the diaquo-complex with oxalic acid and potassium oxalate, it is considered that the following three equilibria exist together with the equibrium 1;

$$H_2C_2O_4 \rightleftarrows H^+ + HC_2O_4^- \tag{5}$$

$$HC_2O_4^- \rightleftarrows H^+ + C_2O_4^{2-} \tag{6}$$

$$K_2C_2O_4 \rightleftarrows 2K^+ + C_2O_4^{2-} \tag{7}$$

The first and second dissociation constants of oxalic acid, $K_1$ and $K_2$, are given as follows respectively[4]:

$$K_1 = \frac{C_{H^+} \cdot C_{HC_2O_4^-}}{C_{H_2C_2O_4}} = 5.9\times10^{-2} \quad \text{and}$$

$$K_2 = \frac{C_{H^-} \cdot C_{C_2O_4^{2-}}}{C_{HC_2O_4^-}} = 6.4\times10^{-5}$$

where $C_{H_2C_2O_4}$, $C_{HC_2O_4^-}$, $C_{C_2O_4^{2-}}$ and $C_{H^+}$ are the concentrations of oxalic acid, hydrogenoxalate ion, oxalate ion and hydrogen ion at equilibrium respectively.

The concentrations of the species in the aqueous solution at equilibrium were calculated in the following two cases separately. The first is the case when the concentration of potassium oxalate is relatively small and the oxalate ion in the solution at equilibrium consists of those formed from potassium oxalate by the ionization process 7 and from oxalic acid by process 6. The second is the case when the concentration of potassium oxalate is relatively large and not only the oxalate ion at equilibrium is all formed from potassium oxalate alone but also a part of the hydrogenoxalate ion in process 5 is given by potassium oxalate.

The calculation in the first case is carried out in the following way. The oxalate ion is assumed to consist of those formed by the ionization of potassium oxalate 7 and the second ionization process of oxalic acid 6. So, if the initial concentration of potassium oxalate and the concentration of oxalate ion formed by process 6 are expressed by $C^\circ_{K_2C_2O_4}$ and $C_x$ respectively, the concentration of the oxalate ion at equilibrium is obtained by $C^\circ_{K_2C_2O_4} + C_x - C_2$, since the concentration of the oxalate ion consumed by the reaction with diaquo-complex is $C_2$. When the initial concentration of oxalic acid and the concentration of hydrogenoxalate ion are expressed by $C^\circ_{H_2C_2O_4}$ and $C_y$ respectively, the concentration of the oxalic acid remaining unionized at equilibrium is obtained by $C^\circ_{H_2C_2O_4} - (C_y + C_x)$ and therefore the first and second dissociation constants of oxalic acid are given by the following equations respectively.

$$\left.\begin{aligned} K_1 &= \frac{C_{H^+} \cdot C_y}{C^\circ_{H_2C_2O_4} - (C_y + C_x)} \\ K_2 &= \frac{C_{H^+}(C^\circ_{K_2C_2O_4} + C_x - C_2}{C_y} \end{aligned}\right\} \tag{8}$$

In these equations, $C^\circ_{H_2C_2O_4}$ and $C^\circ_{K_2C_2O_4}$ are known and $C_2$ is calculated by Eq. 4. The two variables, $C_x$ and $C_y$, can be obtained by solving the above Eq. 8 with respect to $C_x$ and $C_y$ as follows:

$$\left.\begin{aligned} C_x &= \frac{\left(K_1K_2C^\circ_{H_2C_2O_4} + (C_2 - C^\circ_{K_2C_2O_4})\right) \times (C^2_{H^+} + K_1C_{H^+})}{C^2_{H^+} + K_1C_{H^+} + K_1K_2} \\ C_y &= \frac{K_1C_{H^+}(C^\circ_{H_2C_2O_4} + C^\circ_{K_2C_2O_4} - C_2)}{C^2_{H^+} + K_1C_{H^+} + K_1K_2} \end{aligned}\right\} \tag{9}$$

The method of determining $C_{H^+}$ will be described later.

The apparent equilibrium constant, $K_C$, for reaction 1 is given as below,

$$K_C = \frac{C_2 \cdot C^2_{H_2O}}{C_1 \cdot C_{C_2O_4^{2-}}} = \frac{C_2 \cdot C^2_{H2O}}{C_1(C^\circ_{K_2C_2O_4} + C_x - C_2)} \tag{10}$$

where $C_{H_2O} = 1000/18 = 55.5$. This constant varies with the ionic strength of the solution. The ionic strength must be known to find the thermodynamic equilibrium constant. The concentrations and the ionic strengths of each ion at equilibrium are given as follows:

| | Concentration | Ionic strength |
|---|---|---|
| $[Co(NH_3)_4(OH_2)_2]^{3+}$ | $C_1$ | $(9/2)C_1$ |
| $[Co(NH_3)_4C_2O_4]^+$ | $C_2$ | $(1/2)C_2$ |
| $3ClO_4^-$ | $3(C_1+C_2)$ | $(3/2)(C_1+C_2)$ |
| $H^+$ | $C_{H^+}$ | $(1/2)C_{H^+}$ |
| $K^+$ | $2C^\circ_{K_2C_2O_4}$ | $C^\circ_{K_2C_2O_4}$ |
| $C_2O_4^{2-}$ | $C^\circ_{K_2C_2O_4} + C_x - C_2$ | $2(C^\circ_{K_2C_2O_4} + C_x - C_2)$ |
| $HC_2O_4^-$ | $C_y$ | $(1/2)C_y$ |

The total ionic strength, $\mu$, in the solution is calculated by

$$\mu = 6C_1 + 3C^\circ_{K_2C_2O_4} + 1/2C_{H^+} + 2C_x + 1/2C_y \tag{11}$$

The calculation in the second case is performed in the following manner. In this case the concentration of the oxalate ion ionized by reaction 7 is high enough to combine with

4) R. Gane and Ch. K. Ingold, *J. Chem. Soc.*, **1931**, 2153.

diaquo-complex to form oxalatoammine-complex and to compose a part of hydrogenoxalate ion. When the concentrations of hydrogenoxalate ion produced from potassium oxalate and oxalic acid are expressed by $C_y$ and $C_z$ respectively, the concentrations of hydrogenoxalate ion, unionized oxalic acid and oxalate ion at equilibrium are obtained as $C_y+C_z$, $C^\circ_{H_2C_2O_4}-C_z$ and $C^\circ_{K_2C_2O_4}-C_2-C_y$ respectively and therefore the first and second dissociation constants are given as follows:

$$K_1=\frac{C_{H^+}(C_y+C_z)}{C^\circ_{H_2C_2O_4}-C_z}$$
$$K_2=\frac{C_{H^+}(C^0_{K_2C_2O_4}-C_2-C_y)}{C_y+C_z} \qquad (12)$$

The two variables, $C_y$ and $C_z$, can be obtained by solving the above two Eq. 12 as below:

$$\left.\begin{aligned} C_y&=\frac{\left(\begin{array}{c}((C^2_{H^+}+K_1C_{H^+})(C^\circ_{K_2C_2O_4}-C_2))\\ -K_1K_2C^\circ_{H_2C_2O_4}\end{array}\right)}{C^2_{H^+}+K_1C_{H^+}+K_1K_2}\\ C_z&=\frac{\left(\begin{array}{c}-C^2_{H^+}(C^\circ_{K_2C_2O_4}-C_2)+K_1C_{H^+}\\ C^\circ_{H_2C_2O_4}+K_1K_2C^\circ_{H_2C_2O_4}\end{array}\right)}{C^2_{H^+}+K_1C_{H^+}+K_1K_2}\end{aligned}\right\} \qquad (13)$$

Therefore the concentration of hydrogenoxalate ion at equilibrium, $C_{HC_2O_4^-}$, is given by

$$C_{HC_2O_4^-}=C_y+C_z=\frac{\left(\begin{array}{c}K_1C_{H^+}(C^\circ_{H_2C_2O_4}+C^\circ_{K_2C_2O_4})\\ -C_2)\end{array}\right)}{C^2_{H^+}+K_1C_{H^+}+K_1K_2} \qquad (14)$$

The apparent equilibrium constant, $K_C$, is given as below:

$$K_C=\frac{C_2\cdot C^2_{H_2O}}{C_1\cdot C_{C_2O_4^{2-}}}=\frac{C_2\cdot C^2_{H_2O}}{C_1(C^\circ_{K_2C_2O_4}-C_2-C_y)} \qquad (15)$$

The total concentrations and the ionic strengths of each ion in this aqueous solution at equilibrium are given as follows:

| | Concentration | Ionic strength |
|---|---|---|
| $[Co(NH_3)_4\cdot(OH_2)_2]^{3+}$ | $C_1$ | $(9/2)C_1$ |
| $[Co(NH_3)_4\cdot C_2O_4]^+$ | $C_2$ | $(1/2)C_2$ |
| $3ClO_4^-$ | $3(C_1+C_2)$ | $(3/2)(C_1+C_2)$ |
| $H^+$ | $C_{H^+}$ | $(1/2)C_{H^+}$ |
| $K^+$ | $2C^\circ_{K_2C_2O_4}$ | $C^\circ_{K_2C_2O_4}$ |
| $C_2O_4^{2-}$ | $C^\circ_{K_2C_2O_4}-C_2-C_y$ | $2(C^\circ_{K_2C_2O_4}-C_2-C_y)$ |
| $HC_2O_4^-$ | $C_y+C_z$ | $(1/2)(C_y+C_z)$ |

The total ionic strength, $\mu$, in the solution is calculated by

$$\mu=6C_1+3C^\circ_{K_2C_2O_4}+1/2\,C_{H^+}-2C_y+1/2(C_y+C_z) \qquad (16)$$

## Results and Discussion

At first by measuring the absorbancy of the solution at equilibrium, the concentrations of diaquoammine complex and oxalatoammine-complex, $C_1$ and $C_2$, were calculated by Eq. 4. By using these values, the initial concentrations of oxalic acid and potassium oxalate, $C^\circ_{H_2C_2O_4}$ and $C^\circ_{K_2C_2O_4}$, the values of the first and second dissociation constants of oxalic acid, $K_1$ and $K_2$, and, by using the activity of hydrogen ion, $a_{H^+}$, in place of the concentration, $C_{H^+}$, the approximate concentrations of oxalic acid and hydrogenoxalate ion, $C_x$ or $C_y$, were estimated by Eq. 9 or 13. The approximate ionic strengths of the solution at equilibrium were also calculated by Eq. 11 or 16.

In order to know the true concentrations of oxalate and hydrogenoxalate ions, the above calculation must be carried out by using the concentration of hydrogen ion. In spite of it the value obtained by pH measurement is not the concentration of hydrogen ion but the activity. Therefore by finding the activity coefficient of hydrogen ion in each solution having the above approximate ionic strengths from Kielland's table[5], the concentration of hydrogen ion was obtained and the concentrations of oxalate ion and hydrogenoxalate ion and the ionic strengths were again calculated by Eqs. 9 and 11 or 13, 14 and 16 respectively.

Then the apparent equilibrium constant, $K_C$, was calculated by Eq. 10 or 15. These values calculated are all summarized in Table I.

The logarithm of the apparent equilibrium constant, $K_C$, is plotted against the square root of the ionic strength, $\mu$, in Fig. 1. If it is assumed that this plotting gives a quadratic curve, the equation of the curve is calculated by the method of least squares as,

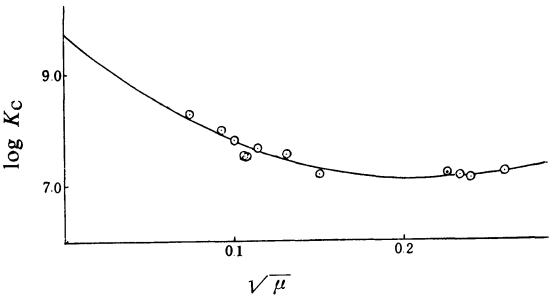



Fig. 1. The relationship between the apparent equilibrium constant of the reaction, $[Co\cdot(NH_3)_4(OH_2)_2]^{3+}+C_2O_4^{2-}=[Co(NH_3)_4C_2O_4]^+ +2H_2O$, and the ionic strength in the solution.

5) J. Kielland, *J. Am. Chem. Soc.*, **59**, 1675 (1937).

TABLE I. EQUILIBRIUM OF $[Co(NH_3)_4(OH_2)_2]^{3+}+C_2O_4^{2-}=[Co(NH_3)_4C_2O_4]^{+}+2H_2O$, AT 25°C
Measurement of extinction coefficient was made at $\lambda=510$ m$\mu$.

| Initial concn. of $[Co(NH_3)_4\cdot(OH_2)_2](ClO_4)_3$ $C\times10^3$ F | Initial concn. of $H_2C_2O_4$ $C^\circ_{H_2C_2O_4}\times10^3$ F | Initial concn. of $K_2C_2O_4$ $C^\circ_{K_2C_2O_4}\times10$ F | $\varepsilon$ | $C_1\times10^3$ | $C_2\times10^3$ |
|---|---|---|---|---|---|
| 1.250 | 1.250 | 1.250 | 76.3 | 0.225 | 1.025 |
| 1.250 | 0.500 | 0.500 | 67.0 | 0.648 | 0.603 |
| 2.00 | 2.00 | 2.00 | 75.9 | 0.393 | 1.607 |
| 1.250 | 2.50 | 2.50 | 78.8 | 0.112 | 1.138 |
| 2.00 | 1.00 | 1.00 | 68.2 | 0.946 | 1.114 |
| 2.00 | 0.667 | 0.667 | 63.7 | 1.275 | 0.725 |
| 2.00 | 0.500 | 0.500 | 62.0 | 1.395 | 0.605 |
| 2.00 | 3.125 | 3.125 | 71.5 | 0.550 | 1.450 |
| 2.00 | 6.250 | 6.250 | 75.5 | 0.422 | 1.578 |
| 2.00 | 12.50 | 12.50 | 72.0 | 0.675 | 1.325 |
| 10.00 | 10.00 | 10.00 | 70.0 | 3.17 | 6.83 |
| 10.00 | 10.00 | 10.00 | 68.0 | 3.74 | 6.26 |
| 2.00 | 25.00 | 25.00 | 75.0 | 0.354 | 1.646 |
| 10.00 | 20.00 | 20.00 | 73.9 | 2.08 | 7.92 |

| pH | $C_{H^+}\times10^3$ | $C_{C_2O_4^{2-}}\times10^4$ | $K_C\times10^{-7}$ | log $K_C$ | $\mu$ | $\sqrt{\mu}$ |
|---|---|---|---|---|---|---|
| 3.00 | 1.076 | 0.814 | 17.24 | 8.237 | 0.005352 | 0.0732 |
| 3.42 | 0.412 | 0.511 | 5.608 | 7.748 | 0.006065 | 0.0779 |
| 3.00 | 1.089 | 0.131 | 9.614 | 7.983 | 0.008379 | 0.0915 |
| 2.91 | 1.33 | 0.174 | 17.99 | 8.255 | 0.008602 | 0.0928 |
| 3.12 | 0.829 | 0.627 | 5.785 | 7.762 | 0.009850 | 0.0993 |
| 3.24 | 0.629 | 0.557 | 3.144 | 7.497 | 0.01047 | 0.1023 |
| 3.36 | 0.478 | 0.463 | 2.885 | 7.460 | 0.01059 | 0.1029 |
| 2.80 | 1.75 | 1.642 | 4.945 | 7.694 | 0.01278 | 0.1131 |
| 2.70 | 2.23 | 2.95 | 3.904 | 7.592 | 0.01665 | 0.1290 |
| 2.65 | 2.62 | 5.45 | 1.109 | 7.045 | 0.02162 | 0.1470 |
| 2.67 | 2.50 | 3.20 | 2.074 | 7.317 | 0.05073 | 0.225 |
| 2.67 | 2.50 | 3.30 | 1.562 | 7.194 | 0.05330 | 0.231 |
| 2.63 | 2.74 | 10.55 | 1.357 | 7.133 | 0.05650 | 0.238 |
| 2.60 | 2.97 | 6.50 | 1.804 | 7.256 | 0.06606 | 0.257 |

$$\log K_C=65.24\,\mu-25.98\sqrt{\mu}+9.687$$

The value of log $K_C$ at $\sqrt{\mu}=0$ is obtained by the extrapolation of this curve as,

$$\log K=9.7$$

This is the thermodynamic equilibrium constant of the reaction between diaquotetramminecobalt(III) and oxalate ions. The free energy change of the reaction is obtained as,

$$\Delta G^\circ_{298}=-13.2\text{ kcal.} \qquad (17)$$

Since the free energies of formation of diaquotetramminecobalt(III) ion, oxalate ion and water in unit activity are known as $-152.8$ kcal.[6], $-161.8$ kcal.[7] and $-56.69$ kcal.[8] respectively, the free energy of formation of oxalatotetramminecobalt(III) ion in unit activity is calculated as

$$\Delta G^\circ_{f298}=-213.9\text{ kcal.}$$

The heat of reaction between diaquotetramminecobalt(III) and oxalate ions is calculated as,

$$\Delta H=6.8\text{ kcal.} \qquad (18)$$

by using the heats of reaction of each compound concerned, i. e., $-235.7$ kcal.[9] for diaquotetramminecobalt(III) ion, $-197.0$ kcal.[7] for oxalate ion, $-68.32$ kcal.[8] for water and $-289.3$ kcal. for oxalatotetramminecobalt(III) ion. The last value is estimated from $\Delta H=-146.0$ kcal.[10] for hexamminecobalt(III) ion

6) A. B. Lamb and A. T. Larson, ibid., 42, 2038 (1920).
7) F. D. Rossini et al., "Selected Values of Chemical Thermodynamic Properties", United States Government Printing Office, Washington (1952), p. 120.
8) F. D. Rossini et al., l. c., p. 9.
9) K. B. Yatsimirskii, "Thermochemie von Komplexverbindungen", Akademie-Verlag, Berlin (1956), p. 178.
10) K. B. Yatsimirskii, l. c., p. 161.

and $\Delta H = -575.8$ kcal.[11] for trisoxalatocobaltate(III) ion. By using 17 and 18 the entropy change for the reaction between diaquotetramminecobalt(III) and oxalate ions is obtained as

$$\Delta S = 67.1 \text{ e. u.}$$

This large value suggests the great stability of oxalatotetramminecobalt(III) ion due to the chelate formation by oxalate ion.

The absorbancy of the solution produced by the reaction of diaquotetramminecobalt(III) perchlorate with ammonium oxalate was measured, and the spectra of the solution are shown in Fig. 2. The absorption spectra of oxalatopentamminecobalt(III) ion and oxalatotetramminecobalt(III) ion are also shown in the same figure. It is found that the absorption spectra of the compound produced at room temperatures by the reaction of the diaquo-complex with ammonium oxalate resembles that of oxalatopentamminecobalt(III) ion, whereas, when the reaction is promoted upon heating to 60°C, a shoulder of the absorption curve appears in the range of wavelengths corresponding to the second absorption band of oxalatotetramminecobalt(III) ion. It is presumed that a part of oxalate ion coordinated as a unidentate ligand at room temperatures undergoes transition to a bidentate ligand.

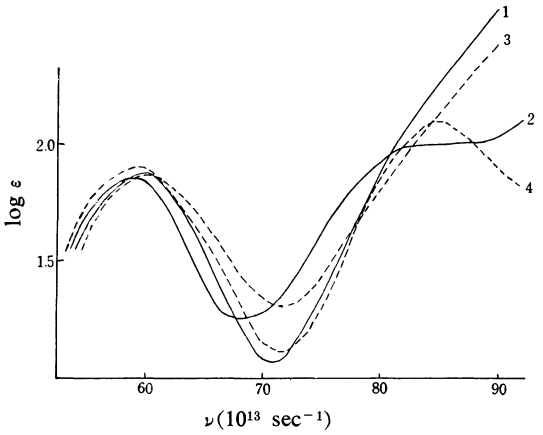



Fig. 2. The absorption spectra of the solution containing diaquotetramminecobalt(III) perchlorate and ammonium oxalate.
1. The solution at room temperature.
2. The solution after being heated at 60°C.
3. Oxalatopentamminecobalt(III) perchlorate.
4. Oxalatotetramminecobalt(III) perchlorate.

11) K. B. Yatsimirskiĭ and L. L. Pankowa, *Zhur. Obshcheĭ Khim.*, **19**, 623 (1949); K. B. Yatsimirskiĭ, "Thermochemie von Komplexverbindungen", Akademie-Verlag, Berlin (1956), p. 180; *Chem. Abstr.*, **43**, 7805 *d* (1949).

## Summary

The equilibrium of the reaction, $[Co(NH_3)_4(OH_2)_2]^{3+} + C_2O_4^{2-} = [Co(NH_3)_4C_2O_4]^+ + 2H_2O$ (1), was measured spectrophotometrically and the free energy of formation of oxalatotetramminecobalt(III) ion was calculated. The large increase of the entropy for the above reaction was interpreted by the chelate effect of oxalate ion.

When the mixture of oxalic acid and potassium oxalate reacts with diaquotetramminecobalt(III) complex, oxalate ion is coordinated as a bidentate ligand, whereas it is coordinated as an unidentate ligand when ammonium oxalate reacts with the same diaquo-complex.

*Department of Chemistry*
*Faculty of Science*
*Kanazawa University*
*Kanazawa*

# *Chemical Studies on Radioactive Indicators. XXIV. Separation of Rhenium from Technetium by the Distillation Method*

By Mutsuo KOYAMA

(Received December 22, 1960)

It has been considered that technetium has much resemblance in chemical properties to rhenium and the latter element has often been used as a carrier in the analysis of the former. An appropriate method is needed for the separation and the determination of technetium which is supposed to be present in natural ores or meteorites and also for the preparation of carrier-free rhenium or technetium produced by the bombardment of nuclear particles. Although several methods for separation, i. e., precipitation method[1], ion exchange method[2] and paper chromatography[3] have been proposed, it can not be said that any one of them is satisfactory in the analysis of the samples containing technetium and rhenium over a wide range of quantity.

The distillation of rhenium as $Re_2O_7$[4,5] has been a powerful method in the isolation from various elements other than technetium but the attempt to separate rhenium from technetium has not appeared yet.

In the previous paper[6], the author pointed out that the distillation of technetium from sulfuric acid is promoted by the addition of an oxidizing agent, such as nitric acid or potassium bichromate, and delayed by the addition of a reducing agent, such as hydroxylamine.

The resistance for the distillation of technetium in the presence of a reducing agent would be due to the formation of a lower oxidation state than +7. A similar experiment was performed on rhenium and it was found that reducing agent showed no effect on the distillation.

In this experiment, several kinds of gas were passed through the distilling flask as carrier and it was found that steam was the most effective on the separation of rhenium from technetium. The experiments were carried out with the solutions of carrier-free $^{95m}Tc$, $^{97m}Tc$, $^{183}Re$ and $^{184}Re$ in the presence or the absence of rhenium carrier.

The results were quite satisfactory as shown in Tables I and II.

## Experimental

**Reagents and Apparatus.**—*Isotopes.*—$^{95m}Tc$(60d) and $^{97m}Tc$(90d) were isolated as pertechnetate, from the proton-bombarded molybdenum target[6]. $^{183}Re$(71d) and $^{184}Re$(50d) were isolated as perrhenate from the proton-bombarded tungsten target[7].

*Stable Rhenium.*—Metallic powder of rhenium was obtained from Yokozawa Chemicals Co. and was converted to perrhenate by fusing it with sodium hydroxide and sodium peroxide in a nickel crucible.

*Distilling Apparatus.*—A pyrex glass distilling apparatus shown in Fig. 1 was prepared. Junctions were connected without grease.

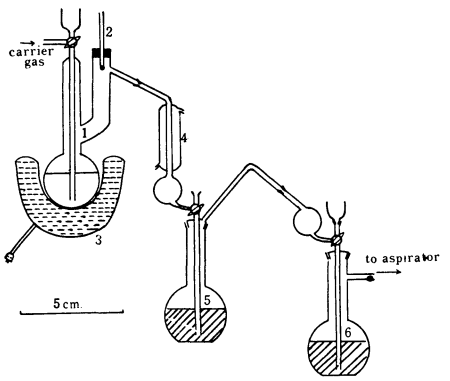



Fig. 1. Distilling apparatus.
1. Distilling flask 2. Thermometer
3. Mantle heater 4. Cooler
5. Receiver-1 (10 ml. of water)
6. Receiver-2 (20 ml of 4 N NaOH)

*Counters.*—A single channel $\gamma$-ray spectrometer (crystal: NaI(Tl), 1×1 inch) made by Kobe Kogyo Co., Ltd. and a G. M. counter (Tube: G. M. 132A, mica window 1.95 mg./cm$^2$) made by Metro Denki Co., Ltd. were used.

**Procedure.**—Six milliliters of the sample solution was taken in the distilling flask and heated with a mantle heater whose temperature was controlled with a transformer.

Carrier gas was conducted at the rate of 60

1) C. Perrier and E. Segrè, *J. Chem. Phys.*, **5**, 712 (1937).
2) E. Jacobi, *Helv. Chim. Acta*, **61**, 2118 (1948).
3) M. Lederer, *Anal. Chim. Acta*, **12**, 146 (1955).
4) W. Geilmann and E. Weibke, *Z. anorg. u. allgem. Chem.*, **199**, 120 (1931).
5) W. Geilmann and H. Bode. *Z. anal. Chem.*, **130**, 323 (1950).
6) M. Ishibashi, T. Fujinaga and M. Koyama, *J. Chem. Soc. Japan, Pure Chem. Sec.* (*Nippon Kagaku Zasshi*), **81**, 1260 (1960).
7) M. Ishibashi, T. Fujinaga and M. Koyama, ibid., **82**, 185 (1961).

bubbles per minute. Receivers were cooled with ice water, whenever necessary. Any adhering activity inside the cooler was washed out into the receiver with a small amount of water before the measurements of the activities of the distillate. All the solutions were brought to a known volume in a volumetric flask and an aliquot was taken in a 5 ml. glass counting dish and was mounted for the $\gamma$-ray measurement.

## Results and Discussion

**Effect of the Concentration of Sulfuric Acid.** —Carrier-free rhenium was used in the experiments for testing the effect of the concentration of sulfuric acid on the distillation of rhenium. Rhenium was not distilled out from the pure water solution. On heating the sulfuric acid solution, the temperature remained at about 98~100°C during the distillation of water. After the water was distilled over, the temperature decreased once and again rose gradually to about 250°C, while sulfuric acid began to be distilled. The distilling temperature (250°C) was changeable depending on the heating and bubbling conditions.

In Fig. 2, the amounts of distilled rhenium are plotted against the amounts of distilled sulfuric acid. When 60% of the total amount of sulfuric acid was distilled, nearly 100% of rhenium was distilled out, irrespective of the initial concentration of sulfuric acid. The rate of distillation of rhenium was the greatest with 6 N sulfuric acid and the smallest with 30 N sulfuric acid. However, no quantitative distillation could be expected by the use of dilute sulfuric acid, because the volume of distilling solution became too small to dissolve the residual materials in the course of distillation.

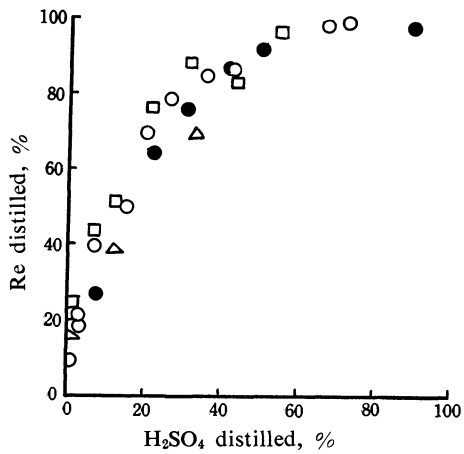



Fig. 2. Relationship between amount of Re distilled and that of $H_2SO_4$.
△ 6 N $H_2SO_4$ ○ 18 N $H_2SO_4$
□ 24 N $H_2SO_4$ ● 30 N $H_2SO_4$

Therefore, 18 N sulfuric acid was used in the following experiments.

**Effects of Reducing Agent and Carrier Gas on the Distillation of Rhenium and Technetium.** —In order to examine the effects of the atmosphere in the distilling flask on the distillation rate of rhenium and technetium, three kinds of gas, i.e., air, hydrogen and carbon dioxide, were bubbled respectively through the flask during the distillation.

Stannous chloride and hydroxylamine were used as the reducing agent, but the former

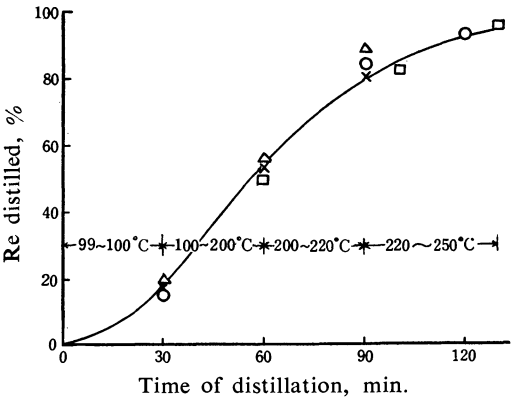



Fig. 3. Distillation rate of Re from 18 N $H_2SO_4$ in the presence or the absence of reducing agents.

| | Reducing agent | Carrier gas |
|---|---|---|
| ○ | None | Air |
| □ | 〃 | $CO_2$ |
| × | 10% $SnCl_2$ 1 ml. | 〃 |
| △ | 10% $NH_2OH \cdot HCl$ 1 ml. | 〃 |

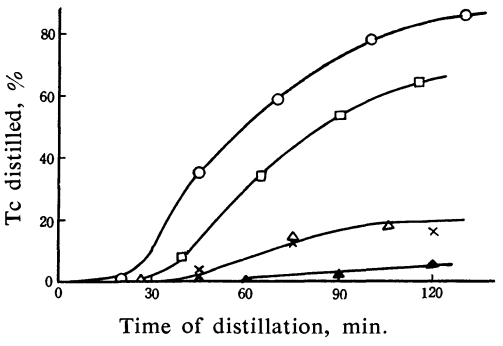



Fig. 4. Distillation rates of Tc from 18 N $H_2SO_4$ in the presence or the absence of reducing agents.

| | Reducing agent | Carrier gas |
|---|---|---|
| ○ | None | Air |
| □ | 10% $NH_2OH \cdot HCl$ 0.5 ml. | 〃 |
| △ | 〃 | $CO_2$ |
| × | 〃 | $H_2$ |
| ▲ | 10% $NH_2OH \cdot HCl$ 2 ml. | $CO_2$ |

TABLE I. DISTILLATION RATES OF RHENIUM

| Solution | Redistilled (%) at various times | | | | | | |
|---|---|---|---|---|---|---|---|
| | 20 min. | | 40 min. | | 60 min. | | Spot tests of residual solution |
| | c.p.m. | % | c.p.m. | % | c.p.m. | % | |
| Carrier-free | 3570 | 61.6 | 5540 | 95.6 | 5780 | 99.8 | — |
| Re alone | 3790 | 65.4 | 5250 | 90.5 | 5740 | 98.9 | |
| Carrier-free Re+10% $NH_2OH \cdot HCl$ 2 ml. | 3210 | 55.4 | 5170 | 89.2 | 5790 | 99.9 | — |
| Re 1 mg.+ | 2450 | 42.2 | 5200 | 89.6 | 5780 | 99.7 | None |
| 10% $NH_2OH \cdot HCl$ 2 ml. | 3090 | 53.2 | 5480 | 94.5 | 5790 | 99.8 | None |
| Re 10 mg.+ | 890 | 15.4 | 5450 | 94.5 | 5740 | 99.0 | 1γ>Re |
| 10% $NH_2OH \cdot HCl$ 2 ml. | 2200 | 38.2 | 5220 | 90.7 | 5790 | 99.9 | 1γ>Re |

* Carrier gas: steam, Total volume of solution to be distilled: 6 ml. of 18 N $H_2SO_4$, Radioactive Re added: 5800 c.p.m.

TABLE II. DISTILLATION RATES OF TECHNETIUM

| Solution | Tc distilled (%) at various times | | | | | | | | | |
|---|---|---|---|---|---|---|---|---|---|---|
| | 20 min. | | 40 min. | | 60 min. | | 80 min. | | 100 min. | |
| | c.p.m. | % | c.p.m. | % | c.p.m. | % | c.p.m. | % | c.p.m. | % |
| Tc alone | 4470 | 12.4 | 704 | 18.6 | 765 | 20.2 | 795 | 21.0 | — | — |
| | 628 | 16.6 | 784 | 20.7 | 832 | 22.0 | 835 | 22.0 | | |
| Tc+10% $NH_2OH \cdot HCl$ 2 ml. | 0 | 0 | 0 | 0 | 0 | 0 | 20 | 0.5 | — | — |
| | 0 | 0 | 0 | 0 | 0 | 0 | 10 | 0.3 | | |
| Tc+Re 10mg+ 10% $NH_2OH \cdot HCl$ 2 ml. | 0 | 0 | 0 | 0 | 0 | 0 | 0 | 0 | — | — |
| | 0 | 0 | 0 | 0 | 0 | 0 | 0 | 0 | | |
| Tc+$HNO_3$ 1 ml. | 1470 | 38.8 | 2000 | 52.8 | 2020 | 53.0 | 3090 | 81.7 | 3500 | 92.4 |
| | 1360 | 35.0 | 2360 | 62.3 | 2380 | 63.0 | 3190 | 84.5 | 3350 | 88.6 |

* At the same condition as in the case of rhenium. Tc added: 3800 c.p.m.

was partially distilled out. In Fig. 3, it can be seen that the distillation rate of rhenium from sulfuric acid is independent of the presence of hydroxylamine and bubbling gas. The fact that the addition of hydroxylamine had no effect on the distillation rate of rhenium shows that hydroxylamine can not reduce perrhenate[8].

In the case of technetium, the decrease in the distillation rate was distinctly observed by the addition of hydroxylamine, even when air was used as carrier gas.

In the same experiment, the bubbling of hydrogen or carbon dioxide caused a marked decrease in the distillation rate, especially in the period of the distillation of water, little technetium being found in the receiver.

The difference of the distillation rates between the use of air and that of carbon dioxide or hydrogen seems to be due to the difference of oxidizing ability against hydroxylamine. After the water was consumed in the flask, technetium gradually came to appear in the distillate. The increase in the amounts of hydroxylamine caused the decrease of the distillation rate of technetium.

**Separation of Rhenium from Technetium.**— In the foregoing method, as an appreciable amount of hydroxylamine is decomposed by heating with sulfuric acid solution, much hydroxylamine has to be added for the quantitative separation of rhenium from technetium.

To achieve smooth distillation, it is desirable to keep the amount of hydroxylamine as small as possible. Utilizing the fact that much rhenium but no technetium could be found in the distillate, the steam distillation method in the presence of hydroxylamine was examined.

Table I shows the distillation rates of rhenium obtained by steam distillation in the presence or the absence of hydroxylamine. It was found that by passing steam only at 100°C, little rhenium was distilled out, however, with gentle heating of the flask above 105°C, rhenium came to be distilled out with the steam.

8) S. Tribalat, *Ann. chim.*, 4, 289 (1949).

After distillation for 60 min., more than 99% of the rhenium was recovered. In the case when the distillation was carried out with stable rhenium, a spot test for the rhenium[9] remaining in the flask proved to be less than 1$\gamma$ of rhenium as shown in Table I.

The presence of hydroxylamine also had no effect on the distillation rate of rhenium in this method. In Table II, the distillation rates of technetium in the same condition as in the case of rhenium are shown. Distillation rates of technetium from 18 N sulfuric acid were smaller than that of rhenium even in the absence of hydroxylamine. In the presence of hydroxylamine no technetium appeared in the receivers, while most of the rhenium had been distilled off.

On the other hand, it was also observed that the presence of nitric acid promoted the distillation of technetium in the steam distillation. Therefore the separation of rhenium from technetium followed by the separation of technetium from other non-volatile materials by the distillation method could be attained by the proper use of hydroxylamine and nitric acid.

9) E. B. Sandell, "Colorimetric Determination of Traces of Metals", Interscience Publishers, New York (1959), p.754.

## Summary

The separation of rhenium from technetium was investigated. Pertechnetate is reduced to non-volatile species by the use of hydroxylamine, but perrhenate is not reduced by such an agent. Rhenium is distilled out with steam from sulfuric acid medium and technetium remains in the solution containing hydroxylamine. Rhenium from carrier-free amounts up to 10 mg. can be separated quantitatively from technetium by this method.

The author desires to express his hearty thanks to Professor Masayoshi Ishibashi and Professor Taitiro Fujinaga for their helpful advice and encouragement throughout this work. The author is also grateful to Dr. Kazuo Saito of the Institute for Nuclear Study, the University of Tokyo, for making preparation of radio-isotopes convenient.

*Chemistry Institute*
*Faculty of Science*
*Kyoto University*
*Sakyo-ku, Kyoto*

# *Chemical Use of the Absorption of Soft $\gamma$-Rays, $\beta$-Ray-excited X-Rays and K-Capture X-Rays*. I. Improvement in Fundamental Technique and Introduction of a Differential Absorption Method*

By Tadashi NOZAKI

(Received December 20, 1960)

Soft $\gamma$-rays, $\beta$-ray-excited X-rays and K-capture X-rays are absorbed mainly by the photoelectric effect in most cases, the absorption coefficient depending much on the atomic number of the absorber material. The mass absorption coefficient ($\sigma$) for the photoelectric absorption of a photon whose energy is over the absorption edge of the absorber material is expressed by[1]

$$\sigma = C(Z^5/A)E^{-\lambda} \qquad (8/3 < \lambda < 7/2) \quad (1)$$

where $Z$ and $A$ are respectively the atomic number and the atomic weight of the absorber material and $C$ is a constant.

This phenomenon is to be applied to a vast field of chemistry as well as radiography. Recently, several kinds of works by the use of the absorption of such photons have been published[2-4], including the determination of sulfur in petroleum, of chlorine and bromine in solid organic substances, and of uranium and heavy metal salts. The thickness and density of several kinds of material were also measured by similar techniques. The fundamental technique which has been adopted in these works, however, is useful only for either of the following two cases; (1) when a monoenergetic photon-beam source of a suitable

* A part of this paper was reported at the 2nd Isotope Conference of Japan, February, 1958.

1) e. g., E. Segrè, "Experimental Nuclear Physics", Vol. 1, John Wiley & Sons, Inc., New York (1953), p. 310.

2) W. W. Meinke, *Anal. Chem.*, **28**, 737 (1956).

3) W. W. Meinke, ibid., **30**, 688 (1958).

4) W. W. Meinke, ibid., **32**, No. 5-106R (1960).

energy is used (i. e. when the exponential absorption law holds), and (2) when a relationship between the absorbance and the quantity (or concentration) of the element (or substance) to be determined can easily be obtained empirically under a given condition.

To extend the applicability of the absorption phenomenon, according to the present author's opinion, it is essential to improve the fundamental technique so that an exponential absorption curve and an accurate absorption coefficient could be obtained for a photon-beam even when it is not exactly mono-energetic.

Thus, the following studies have been undertaken: (1) examination of a source giving photons of required energy, (2) examination of a detector which enables an efficient measurement of the radiation and gives an absorption curve as near as possible to the exponential with a given absorber, (3) introduction of the differential absorption method which is useful for obtaining a better absorption curve and a more accurate absorption coefficient in the presence of photons of different energies, (4) examination of apparent change in the absorption coefficient with geometrical arrangement, and (5) establishment of an empirical relationship between the absorption coefficient and the photon energy.

**Photon-beam Source.** — Absorptiometry in quantitative analysis is usually based on Lambert-Beer's law, regardless of the photon-beam energy (wavelength). For a mono-energetic photon-beam an exponential absorption curve can be obtained easily. Radio-isotopes emitting such photons are desirable as the source, and have been used in several works[2-4]. Various nuclides including the following are useful for this purpose: $^{51}Cr$, $^{133}Ba$, $^{203}Hg$, $^{139}Ce$, $^{141}Ce$, $^{185}W$, $^{153}Gd$, $^{97m}Tc$, $^{170}Tm$, $^{109}Gd$, $^{204}Tl$, $^{241}Am$, $^{145}Sm$, $^{73}As$, $^{210}Pb$ (RaD), $^{125}I$, $^{93}Mo$, $^{68}Ge$, $^{59}Ni$, $^{55}Fe$ and $^{49}V$. (The photon energy decreases in the order given.) In using a radio-isotope emitting also $\beta$-rays for the source, the Bremsstrahlung should be made as weak as possible with a suitable enveloping substance (e. g. polystyrene).

Since a relatively small number of nuclides among those written above are usually accessible, another kind of source, generating $\beta$-ray-excited X-rays, is required for increasing the energy variety. With $\beta$-ray-excited X-rays as the source, such improvements in the fundamental technique as shown later are necessary, as they are not exactly mono-energetic. The yield and the purity (absence of photons of unsuitable energies) depend on the target (converter) and the arrangement of the generator. For the present purpose the purity of the X-rays and the ease in the change of the target material are more important than the yield. A reflection-type generator with a $K_\beta$-filter holder, (Fig. 1) serves conveniently.

Figure 2 shows the spectra observed by a scintillation counter (sodium iodide $1'' \times 1''$ crystal with aluminum cover), and Fig. 3 those by the scintillation and a proportional counter.

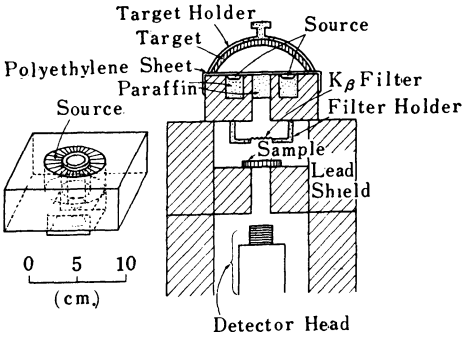



Fig. 1. Generator of $\beta$-ray-excited X-rays.

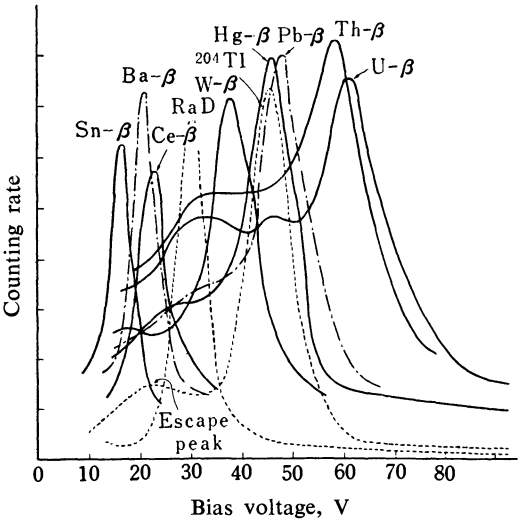



Fig. 2. Spectra of photon-beam sources.

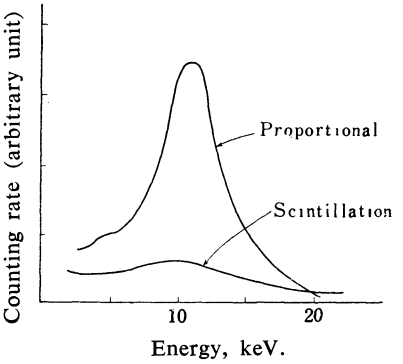



Fig. 3. Spectra of Br-$\beta$.

(For convenience, β-ray-excited X-ray of element M is written as M-β in this paper.)

**Detector.** — The counting efficiency and the shape of the absorption curve depend much on the detection method. When $^{55}Fe$ is used as a source, a simple G-M counter works satisfactorily. But this counter is a poor detector for a photon-beam having a higher energy than 10 keV. and the pulse height cannot be discriminated. Thus, an ordinary G-M counter can be used only for a few sources: e. g. $^{55}Fe$, $^{59}Ni$.

Measurement of photon-beams by counting only a narrow region of photo-peak (photo-peak counting) by a low-noise scintillation counter with a single channel analyzer offers a better result in general; the efficiency is high for photons of 20 to 300 keV. and the absorption curve is more similar to a typical exponential curve. For a photon having an energy under 20 keV., however, the following three problems are encountered: (1) the absorption by the cover of the scintillator, (2) the multiplier noise, and (3) the broadening of photo-peak (e. g. those in Fig. 2). The first can be made small by the use of a beryllium-covered crystal, which, however, is not always readily available. On the other hand, a proportional counter tube filled with xenon, krypton or a mixture of these serves, as a still better detector for such a measurement. Fig. 3 shows the spectra of Br-β measured by a xenon-filled proportional counter and by the scintillation counter. No marked photo-peak is observed by the latter. Though the photo-peak obtained by the proportional counter is not so sharp as inferred from literature[5], probably owing to the end effect, the counter is proved to be a very useful detector for such a photon-beam. A krypton-filled tube works as either a proportional or a G-M counter according to the applied voltage, though the dead time of the G-M tube is as long as 1 millisecond. By the use of an external quenching circuit, however, such a tube could be used also as a G-M tube and provides a cheaper technique for measuring photons below 50 keV.

In Fig. 4 the absorption curves of photon-beam from $^{204}Tl$ and of Hg-β are shown. Both emit the characteristic X-rays of mercury. The curve measured by a usual G-M counter is far from the exponential curve; the absorption coefficients are much larger at the initial stage, and an absorption tail is observed. The former phenomenon can be attributed to the L-series X-rays which are more sensitive to counter than the *K* X-rays. The same is seen

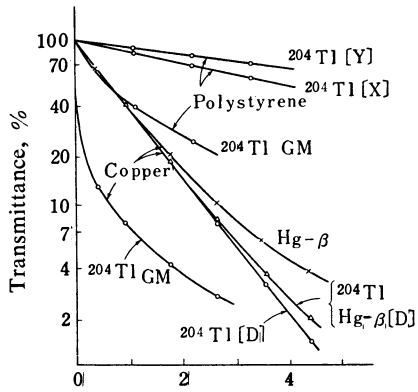



Fig. 4. Absorption curves.
GM; Measured by a G-M counter
[D]; The differential absorption curve
[X]; Absorber at the position in Fig. 1
[Y]; Absorber on the scintillator

with $^{203}Hg$, which emits a γ-ray and characteristic X-rays of thallium owing to internal conversion. The tailing should be due to the Bremsstrahlung. The curves obtained by the photo-peak counting with a scintillation counter are greatly superior. For $^{203}Hg$, the curve maintains the exponential form even when the counting rate decreases to 1/1000 of the initial. For other sources, especially for β-ray-excited X-rays, however, the absorption tailing exists to a considerable degree.

The energy resolution of the counter should be taken into account, since $K_\alpha$ X-rays of the β-ray-excited X-ray are always accompanied with $K_\beta$ rays and Bremsstrahlung of similar energies. On measuring a mono-energetic photon-beam by a scintillation or a proportional counter, the photo-peak is expressed by the Gaussian distribution curve,

$$R = k \exp[-h^2(E_m - E)^2] \quad (2)$$

where $R$ is the counting rate, $E$ is the energy, $E_m$ is the observed energy giving maximum $R$ on the spectrum, and $k$ and $h$ are constants. And,

$$(\Delta E)_{1/2} = C\sqrt{E_m} \quad (3)$$

where $(\Delta E)_{1/2}$ is the full width of photo-peak at 1/2 counting rate and $C$ is a constant. By the use of a good source, i. e. RaD, the value $C$ in Eq. 3 can be determined, and from this value and Eq. 2 the fraction of $K_\beta$ involved in the measurement range is calculated under a given experimental condition. For a common experimental condition described in the experimental part, the effect of $K_\beta$ is usually of less significance in case of a source giving a higher

5) W. Parrish et al., *Rev. Sci. Instr.*, **27**, 795 (1956).

energy than Hg-$\beta$, but must be considered for a source giving a lower energy than Ce-$\beta$. In the latter case a $K_\beta$ filter is useful to some extent; the shape in a higher energy region than the top of the photo-peak is improved and the photo-peak itself becomes sharper.

**Differential Absorption Method.** — As mentioned above, the absorption curve obtained by the above technique is in general not entirely satisfying for an accurate work. Inevitably there is absorption tailing to a certain degree, which is a nuisance when trying to obtain an accurate absorption coefficient, especially when the absorbance is large.

Two useful methods for the removal of the effect of absorption tailing (differential method and auxiliary absorption method) are presented, which have been devised anew in consideration of the causes of the tailing.

There must be three causes:

(1) Photons of a higher energy suffer the Compton scattering in the detector and escape with an energy loss in the vicinity of the measurement range.

(2) The same scattering also occurs in the absorber and surrounding materials, and a part of the scattered photons can have a similar energy as that of the main photo-peak and enter the detector.

(3) The escape-peak of a photon whose energy is higher by the energy of the $K_\alpha$ of the detector material appears in the measurement range.

For effects 1 and 2, the following relationship is known[6].

$$E_e = h\nu_0 \frac{2h\nu_0/mc^2}{1h+2\nu_0/mc^2} \tag{4}$$

where $E_e$ is the maximum energy that an electron can obtain after a collision. When $E_e$ is smaller than $mc^2/5$, $h\nu_0/E_e$ is greater than 7/2. This relathionship shows that photons giving the effect 1 must have had much higher energies than the observed range, when the photons were subjected to only one scattering. The chance of multiple scattering giving rise to effect 1 must be very small.

The effect 2 must result either from a small-angle scattering or from a multiple scattering. When the measurement is made in an arrangement shown in Fig. 1, the probability of the latter is negligible. A photon scattered with a small change of direction (e. g. a few degree), $\theta$, loses so small an amount of energy that it is hardly ever distinguished from the unscattered photon. The following familiar equation elucidates such a relationship[7]

$$h\nu = \frac{h\nu_0}{1+(h\nu_0/mc^2)(1-\cos\theta)} \tag{5}$$

where $h\nu$ and $h\nu_0$ are respectively the energy of the photon after and before the scattering. Thus, the tailing due to effect 2 is not serious.

Complete elimination of the effect 3 is practically impossible. But when the geometrical arrangement is so adjusted as to make the photon-beam enter the center of the detector, the escape-peak is less distinct.

Thus, the main cause of the tailing should be the single Compton scattering (in the detector) of photons having much higher energies.

*Differential Method.* — Several sheets of absorber made of the same material and having the same thickness are prepared. The counting rate is measured, the number of the sheets being changed one by one. When the decrease in the counting rate caused by placing one additional sheet is plotted against the number of the sheets used, the curve is more similar to an ideally exponential than the ordinary curve.

That curve, which is tentatively called "differential absorption curve" can be formulated as follows: the ordinary absorption curve is generally expressed by

$$R = A\exp(-\Phi T) + B(T) \tag{6}$$

where $\Phi$ and $T$ are respectively the absorption coefficient and the absorber thickness and $A$ is a constant, and $B(T)$ is written as

$$B(T) = \sum_n B_n \exp[-\Phi_n T] \tag{7}$$

For simplicity, the following case is considered.

$$B(T) = B\exp[-\Phi' T] + C \tag{8}$$

That is to say, the source gives only two kinds of photon, and there is a constant back ground. Then, the difference between the counting rates measured through $n$ and $n+1$ sheets of the absorber of thickness $\Delta T$ is expressed by

$$\begin{aligned} R_n - R_{n+1} &= A\exp(-\Phi n\Delta T)[1-\exp(-\Phi\Delta T)] \\ &\quad + B\exp(-\Phi' n\Delta T)[1-\exp(-\Phi'\Delta T)] \\ &= [1-\exp(-\Phi\Delta T)]\left[A\exp(-\Phi T)\right. \\ &\quad \left. + \frac{1-\exp(-\Phi'\Delta T)}{1-\exp(-\Phi\Delta T)} B\exp(-\Phi' T)\right] \end{aligned} \tag{9}$$

where $T = n\Delta T$. Comparison of Eq. 9 with Eq. 6 shows that the effect of a photon of a higher energy is reduced with the aid of the differential curve by a factor of $[1-\exp(-\Phi'\Delta T)]/[1-\exp(-\Phi\Delta T)]$. With an infinite number of

6) e. g. Ref. 1, p. 319.
7) e. g. ibid., p. 318.

infinitely thin absorbers this factor becomes $\Phi'/\Phi$, the ratio of the absorption coefficient for the photon of the higher energy to that for the lower energy. This ratio must be much less than unity. Because, as mentioned above, the energies of the two photons should differ largely from each other, and the absorption, at least for the photon of the lower energy, is mostly due to photoelectric effect. This is why the differential absorption curve is superior to the ordinary absorption curve. Such a consideration also holds in an actual case, where the source gives more photons of varying energies than shown in Eq. 8. When the counts taken are large enough in each measurement with varying numbers of the absorber sheet, the secondary differential absorption curve offers a still better result.

The differential absorption curves of $^{204}$Tl and Hg-$\beta$ with copper are shown in Fig. 4. For other kinds of source and absorber material a similar improvement is observed.

*Auxiliary Absorber Method.*—For the measurement of the differential absorption curve, several sheets of the same absorber material having the same thickness are required. Practically, this requirement is hardly fulfilled. The "auxiliary absorber method" finds more general use. A thin foil of a certain material (auxiliary absorber) having as large an absorption coefficient as possible specifically for the photon in question is placed in the path of the photon-beam. Further, the decrease in the counting rate caused by this absorber is measured both in the presence and the absence of the sample. When the decrease in counting rate in the presence of the sample is divided by that in its absence, the quotient gives a fairly accurate transmittance (denoted by fraction and not by percentage) of the photon through the sample. This is true even when the absorbance of the sample is considerably great. This can be explained by the following equations. (Subscript A indicates figures for auxiliary absorber.)

$$R(T)=A\exp(-\Phi T)+B(T)$$
$$R(0)=A+B(0)$$
$$R(T_A)=A\exp(-\Phi_A T_A)+B(T_A)$$
$$R(T+T_A)=A\exp(-\Phi T-\Phi_A T_A)+B(T+T_A)$$

Hence, the quotient $D$ becomes

$$D=\frac{R(T)-R(T+T_A)}{R(0)-R(T_A)}=\frac{\left(\begin{array}{c}A\exp(-\Phi T)\,[1-\exp(-\Phi_A T_A)]\\+B(T)-B(T+T_A)\end{array}\right)}{A[1-\exp(-\Phi_A T_A)]+B(0)-B(T_A)} \quad (10)$$

When

$$\left.\begin{array}{l}B(0)=B(T_A)\text{ and }B(T)=B(T+T_A)\\D=\exp(-\Phi T)\end{array}\right\} \quad (11)$$

The larger the $\Phi_A$ is and the smaller the $T_A$ is, the better are satisfied the assumptions in Eq. 11. It is clear from a similar argument given in the "differential absorption method" that the auxiliary absorber method offers an improved absorption curve. This curve is also always superior to the differential absorption curve. The differential method can be regarded as a special case of the auxiliary absorber method, each of the absorbers in the former being itself the auxiliary absorber in the latter.

Absorption curves of a solution of barium chloride (0.114 g./ml.) in dilute hydrochloric acid are shown in Fig. 5 with the absorption curve of hydrochloric acid containing the same quantity of chlorine. The auxiliary absorber is a thin tin foil, through which about 53% of photons transmit.

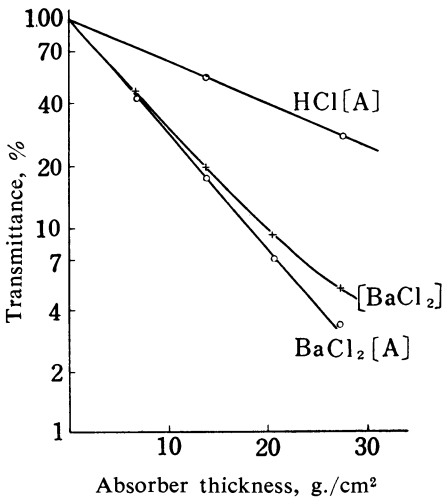



Fig. 5. Absorption curves. $BaCl_2$ [A] and HCl [A] are the auxiliary absorption curves. [$BaCl_2$] is the ordinary absorption curve.

**Effect of Geometrical Arrangement.**—A change of apparent absorption coefficient is clearly observed for an absorber having a small absorption coefficient according to the geometrical arrangement. For such an example, absorption curves of polystyrene for the photon from $^{204}$Tl are shown in Fig. 4. The curve denoted by [X] means that the absorber is placed as shown in Fig. 1, and the one denoted by [Y] means that it is placed on the scintillator. When a detector, an absorber and a source are placed close to one another, the apparent absorption coeffieient is small, and

increases toward a definite value with the increase in the distances between the source and the absorber and between the absorber and the detector.

This effect is attributable to the small-angle Compton scattering with a negligible energy loss. With such an absorber, the photolectric effect and the coherent scatterings contribute only slightly, and the absorption is caused almost entirely by the Compton scattering. However, the addition of the correction value, which can be obtained from the theoretical result[8], offers a definite value independent of the geometrical arrangement, unless the source, absorber and detector are close to one another. Such a corrected value is thought to be the true absorption coefficient. For the geometrical arrangement shown in Fig. 1, the correction value to be added is 0.007 $cm^2/g.$ for atoms in the absorber having an equal number of protons and neutrons. This value is about 1/20 of the total Compton-scattering cross section of the atom for a photon of 100 keV. Thus, this correction value can be used for all kinds of absorber material and for all kinds of photon-beam with quite a little final fractional error, so far as the absorption is mainly due to the photoelectric effect.

**Relationship between the Absorption Coefficient and the Photon Energy.** — Fairly good absorption curves and accurate absorption coefficients are obtained with the aid of techniques described above. The total cross section of the Compton scattering by an electron is almost independent of the binding state. The relationship between the total cross section of the Compton scattering and the photon energy is found in various literatures.

Amidst the coherent scatterings of photons[9] with which we are concerned here, only the Rayleigh scattering has a significant contributions, though its cross section is much smaller than that of the photoelectric absorption. The dependence of Rayleigh-scattering cross section on the photon energy is not greatly different from that of the photoelectric effect.

Thus, $\phi$, the absorption coefficient excluding the contribution of the Compton scattering is proportional to $E^{-\lambda}$, or,

$$\phi = kE^{-\lambda} \qquad (13)$$

where $8/3 < \lambda < 7/2$, and $k$ is a constant.

The experimental results shown in Fig. 6 agree with Eq. 13. They agree also with other absorber materials such as tungsten, neodymium, barium, iodine and aluminum. These experimental results indicate that Eq. 13 is valid not only above but also under the K-absorption edge, with a change of the magnitude of $k$ at the edge. This relationship plays an important role in further extension of the present study. However, it is doubtful, whether an extrapolation of a curve in Fig. 6 to a region of much lower energy (e. g. $^{55}Fe$ as the source) provides a correct value.

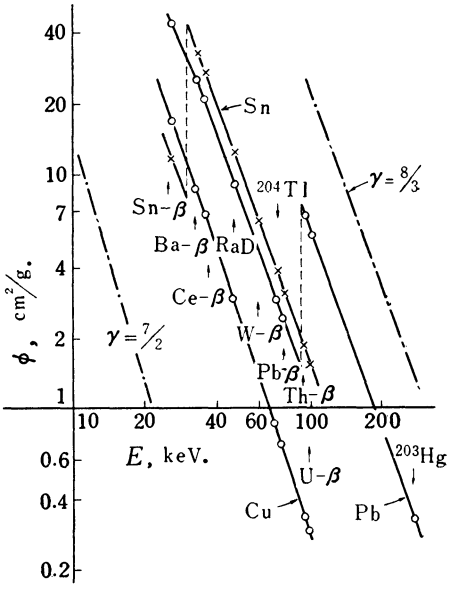



Fig. 6. Relationship between Absorption coefficient and photon energy.

There are numerical tables and charts calculated theoretically for the absorption coefficient against the photon energy. The value, however, is not entirely trustworthy for a photon having an energy not much larger than the binding energy of an electron in the absorber material, because of the invalidity of the Born approximation[10]. For the region under the K-absorption edge, the experimental values are usually considerably larger than the theoretical.

## Experimental

**Photon-beam Source.** — A solution containing radioisotopes of high specific activity emitting useful photons together with $\beta$-rays, was dried up in a hole dug in a small piece of polystyrene block, and the hole was filled with solid paraffin. When such a radioisotope was dried up in an iron dish or kept without $\beta$-ray absorber, the absorption curve, deviated further from the exponential curve. To improve the absorption curve, a solution containing $^{204}Tl$ was dried up on a crossing of polystyrene fibers at the center of a cubic polystyrene box of 5 cm. dimension, and the air in the box was replaced by hydrogen. However, only a little improvement was observed.

8) e. g. K. Siegbahn, "Beta- and Gamma-ray Spectroscopy", North Holland Pub. Co., Amsterdam (1954), p. 33.
9) e. g. ibid., p. 528.
10) e. g. ibid., p. 857.

About 50 mc. of $^{90}Sr$ of a high specific activity was dried up on a ring-formed filter paper for use as a $\beta$-ray source of the $\beta$-ray-excited-X-ray generator. It was essential to shield the detector from scattered photons by thick lead blocks. Targets of the generator were prepared as follows. Metal plates of a suitable thickness were formed as shown in Fig. 1, for use as the target. For other materials, compounds with lighter elements, such as uranium oxide, thorium oxide, mercury(I) chloride, tungsten oxide, cerium(IV) oxide, barium carbonate and ammonium bromide were placed on polystyrene target holders to a layer of due thickness with the aid of a benzene solution of polystyrene. The polyethylene sheet covering the lead block of the generator suffered radiation damage and had to be renewed with great care within a year.

**Detector.**—A scintillator (NaI, $1''\times1''$, Harshow) was mounted with the aid of a silicone oil on a photomultiplier tube (du Mont 6292), which was selected out of several tubes by examining their stability and thermal noise (a thinner crystal would be preferable for some cases). Heater voltage for the linear amplifier and preamplifier must be stabilized. The unit having the longest resolving time in the counter assembly was the pulse-height analyzer (5 $\mu$sec.), others having much smaller resolution time. Throughout the work, the gain of the linear amplifier and the preamplifier and the applied voltage to the photomultiplier tube were kept constant, unless a $\gamma$-ray having a higher energy than 200 keV. was measured. The scale in the abscissa of Fig. 2 was the bias voltage (base line) of the single channel analyzer under that condition. The window width for the photo-peak counting was 5.4 V. for a source of a higher energy than RaD and 3.6 V. for that of a lower energy than Ce-$\beta$ respectively under the same condition. The counting rate without absorber was about $10^4$ to $2\times10^4$ c. p. m. in other cases than $^{203}Hg$, in which the rate was about $10^5$ c. p. m.

Under the condition of the photo-peak counting, the fraction of $K_\beta$ rays appearing in the measurement range was as follows (denoted by percentage); U-$\beta$ 9, Th-$\beta$ 9, Pb-$\beta$ 15, Hg-$\beta$ 17, W-$\beta$ 22, Ce-$\beta$ 33, Ba-$\beta$ 35 and Sn-$\beta$ 44. For $K\beta$-filter, barium carbonate powder and iodoform were used for Ce-$\beta$ and Ba-$\beta$ respectively, both being painted on a thin filter paper in viscous benzene solution of polystyrene.

Proportional counter tubes (1.6 cm. diameter, 10 cm. effective length) of end-window type (1.9 mg./cm$^2$ mica) filled with methane (4 cm.Hg) and xenon, krypton or a mixture of these (ca. 40 cm.Hg) were set up and their characteristics measured. The output pulse of the tube was preamplified and introduced into the same electronic devices as those used with the scintillation head. The tube was also connected to a simple G-M counter circuit.

**Absorbers and Measurement of Absorption Coefficient.**—Metal-plate absorbers of aluminum, copper, tin, molybdenum and lead were obtained commercially or by rolling the pure metal to a desired thickness. A known quantity of pure iodine was dissolved in ethanol and made up to a definite volume. Pure barium and neodymium carbonates were dissolved in hydrochloric acid of a suitable concentration, and the content of the element was determined gravimetrically. Absorption curves of both the solution and the solvent were determined, and the absorption coefficient of the element was calculated, volume change due to the dissolution being taken into account.

## Summary

Studies for the improvement of fundamental techniques for the chemical use of the absorption of soft $\gamma$-rays, $\beta$-ray-excited X-rays and K-capture X-rays were undertaken. The exponential absorption curve, which is essential for the measurement of the accurate absorption coefficient and for many quantitative works, was obtained by the use of a proper detection method and the differential absorption technique, even in the presence of some photons having various energies. The relationship between the absorption coefficient thus obtained and the photon energy proved to agree with the theoretical result.

*The Electrical Communication Laboratory*
*Musashino, Tokyo*

# *Visible Absorption Spectra of 1, 3, 5-Trinitrobenzene and its Derivatives in Aqueous Alkaline Acetone*

By Takehiro ABE

(Received January 16, 1961)

In a previous short communication[1] it was reported that when an acetone solution of 1, 3, 5-trinitrobenzene was treated with aqueous sodium hydroxide intense 460 and weak 510~590 mμ bands appeared and when ammonia water was applied an intense 505 mμ band came out. In the present work, the same spectroscopic investigation has been made on similar reactions of aqueous sodium hydroxide and of aqueous ammonia with 1, 3, 5-trinitrobenzene derivatives of 1, 3, 5-trinitrobenzene, 2, 4, 6-trinitrotoluene, tetryl (2, 4, 6-trinitrophenylmethylnitramine) and picryl chloride, in acetone.

## Expermental

Commercial extra pure grade trinitro compounds and commercial grade acetone were purified by the same methods as in the previous paper[2]. Sodium hydroxide and ammonia water (ca. 28%) of commercial grade were used without further purification.

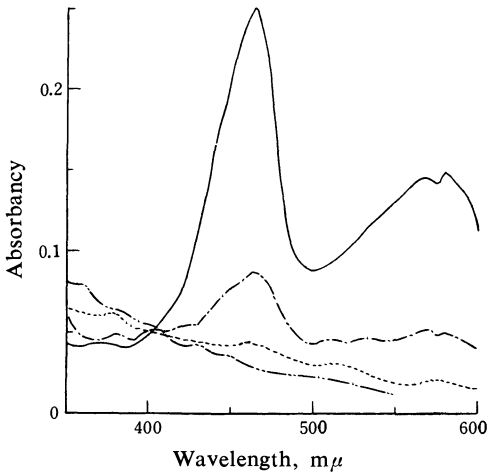



Fig. 1. Absorption spectra of 1,3,5-trinitrobenzene ($1.06\times10^{-5}$ M) in acetone (containing 4% water by volume) in the presence of sodium hydroxide ($4.16\times10^{-2}$ N) at room temperature.

1 ——— Immediately after the preparation
2 —·—· After 1 hr.
3 ------ After 2 hr.
4 —··— After 5 hr.

Each colored solution was made pipetting 1 cc. of an aqueous alkaline solution into 1 cc. of acetone solution of each trinitro compound and diluting the resulting solutions with acetone to 25 cc. Spectra of all the colored solutions were measured, using a Hitachi EPU-2 spectrophotometer at room temperature. The length of the absorption cells was 1 cm.

## Results and Discussion

**Absorption Spectra of the Trinitro Compounds in Aqueous Acetone Containing Sodium Hydroxide (Figs. 1-4).**—When dilute aqueous solutions of sodium hydroxide are added, all the

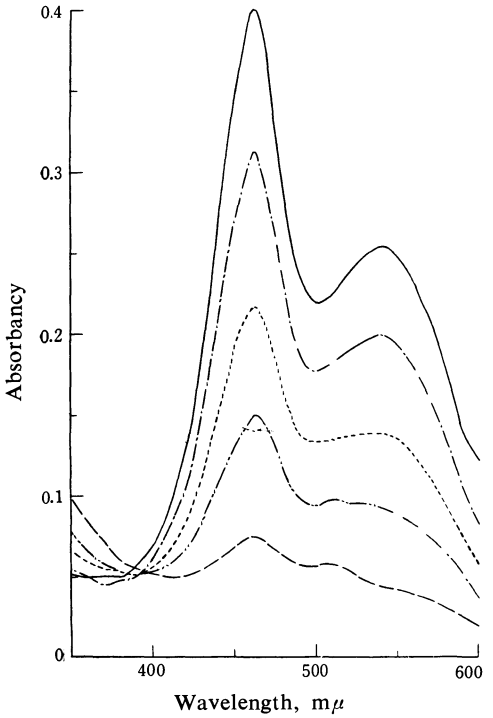



Fig. 2. Absorption spectra of 2,4,6-trinitrotoluene ($1.68\times10^{-5}$ M) in acetone (containing 4% water by volume) in the presence of sodium hydroxide ($4.16\times10^{-2}$ N) at room temperature.

1 ——— Immediately after the preparation
2 —·—· After 1 hr.
3 ------ After 2 hr.
4 —··— After 3 hr.
5 ——— After 5 hr.

1) T. Abe, This Bulletin, 32, 778 (1959).
2) T. Abe, ibid., 32, 339 (1959).

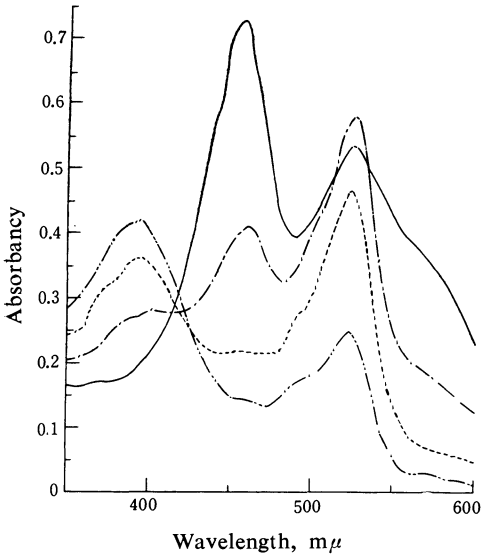



Fig. 3. Absorption spectra of tetryl ($3.95\times10^{-5}$ M) in acetone (containing 4% water by volume) in the presence of sodium hydroxide ($4.16\times10^{-2}$ N) at room temperature.

1 ——— Immediately after the preparation
2 —·—· After 1 hr.
3 ------ After 2 hr.
4 —··— After 4 hr.

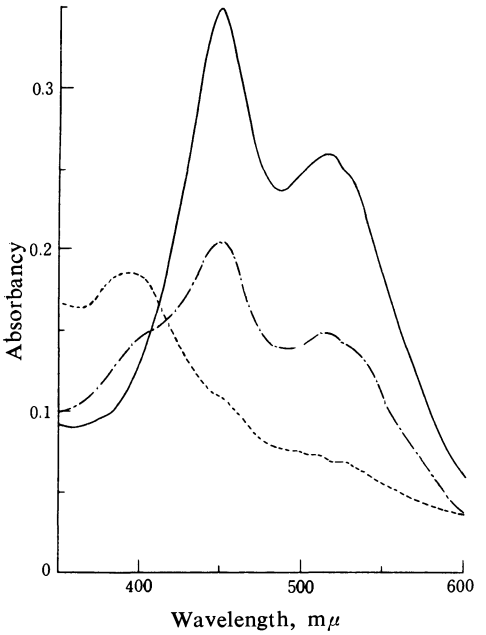



Fig. 4. Absorption spectra of picryl chloride ($1.73\times10^{-5}$ M) in acetone (containing 4% water by volume) in the presence of sodium hydroxide ($4.16\times10^{-2}$ N) at room temperature.

1 ——— Immediately after the preparation
2 —·—· After 1 hr.
3 ------ After 3 hr.

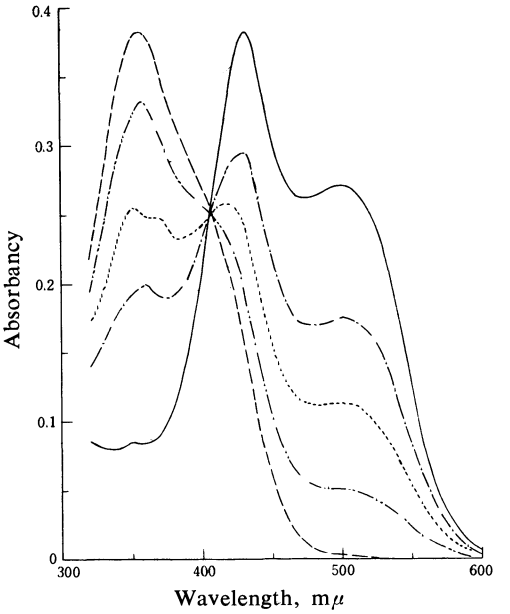
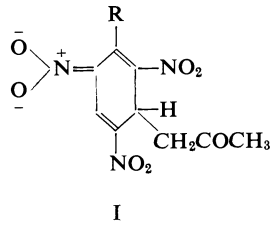


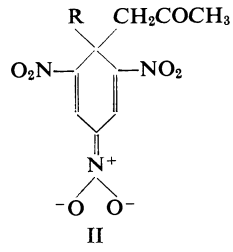

Fig. 5. Absorption spectra of tetryl in water containing sodium hydroxide at room temperature.

1 ——— Immediately after the preparation
2 —·—· After 1 hr.
3 ------ After 2 hr.
4 —··— After 4 hr.
5 ——— After a day

acetone solutions of these trinitro compounds initially show similar absorption curves 1. The analogy among the absorption curves 1 in Figs. 1–4 is not in perfect accord with Kimura's results[3]. He reported that a spectral pattern of a colored solution produced by treating trinitrobenzene with sodium hydroxide in a mixture of acetone and methanol (50% by volume) was different from patterns similarly made from trinitrotoluene and picryl chloride, and that the former was due to structure I while the latter ones were due to both structures I (mainly) and II.




I

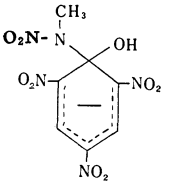



II

A change in an absorption curve of the aqueous alkali-treated colored solution of tetryl with time is indicated in Fig. 5. The colored solution made by adding a drop of aqueous

3) M. Kimura, *Pharm. Bull. (Japan)*, 3, 75 (1955).

sodium hydroxide solution (1 N) to a dilute aqueous solution of tetryl is decolorized at the highest measurable rate at room temperature among those of the four trinitro compounds. The decolorized solution shows an absorption curve 5 similar to that of picrate anion. It is well known that tetryl reacts with aqueous alkali to form picrate. Accordingly, as mentioned in the previous paper[2], a curve in Fig. 5 is expected to be due to Meisenheimer's intermediate III in the process of substitution reaction of tetryl to picric acid.



III

Recently such Meisenheimer's intermediates have been presented for many colored products of polynitrobenzene derivatives with alkalies*. From the close similarity of the absorption curves 1 in Figs. 1–4 with that 1 in Fig. 5 it seems likely that the curves 1 in Figs. 1–4 do not correspond to products such as I or II but do to such Meisenheimer's type complexes, III, formed between the trinitro compounds and sodium hydroxide.

When the colored solutions for Figs. 1–4 are allowed to stand for several hours, they become turbid. Their spectra can not, therefore, be measured thereafter. Figs. 3 and 4 suggest that both the colored species from tetryl and picryl chloride are gradually converted into a substance giving an absorption band at about 390 mμ. Picric acid in acetone also gives an absorption band at the same region in the presence of sodium hydroxide[4]. Accordingly, the colored species from tetryl and picryl chloride in acetone as well as in water are probably converted mainly into picric acid. On the other hand, the colored solutions of trinitrobenzene and trinitrotoluene do not have distinct bands at about 390 mμ even after decoloration, as indicated in Figs. 1 and 2. Therefore, those from trinitrobenzene and trinitrotoluene would undergo further complicated reactions like the reaction of trinitrobenzene with sodium carbonate in methanol, finally giving 3, 5-dinitroanisole through the formation of the Meisenheimer's intermediate[5].

**Absorption Spectra of the Trinitro Compounds in Acetone Containing Ammonia Water (Figs. 6-9).**—Figs. 6–9 show that colored solutions initially produced by additions of ammonia water to the acetone solutions of the trinitro compounds give absorption curves 1 similar to these for the colored solutions obtained by

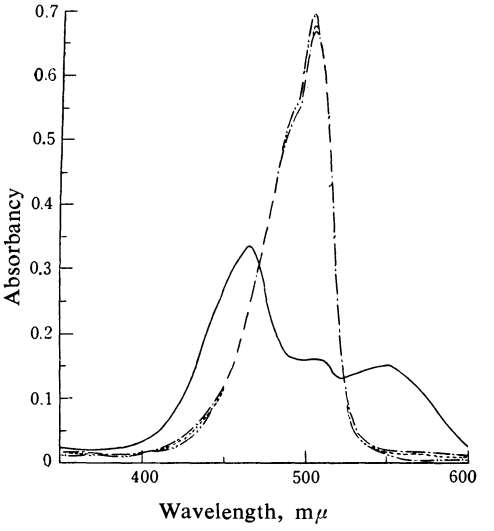



Fig. 6. Absorption spectra of 1,3,5-trinitrobenzene ($1.23\times10^{-5}$ M) in acetone (containing 4% water by volume) in the presence of ammonia (1.2%) at room temperature.

1 ——— Immediately after the preparation
2 —·—· After 1 hr.
3 ------ After 3 hr.
4 —··— After a day

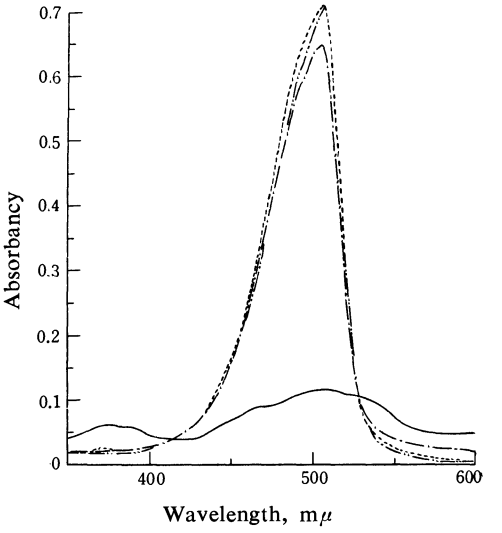



Fig. 7. Absorption spectra of 2,4,6-trinitrotoluene ($1.68\times10^{-5}$ M) in acetone (containing 4% water by volume) in the presence of ammonia (1.2%) at room temperature.

1 ——— Immediately after the preparation
2 —·—· After 1 hr.
3 ------ After 3 hr.
4 —··— After a day

* For example, see Ref. 4.

4) T. Abe, This Bulletin, 34, 21 (1961).
5) P. T. Izzo, *J. Org. Chem.*, 24, 2026 (1959).

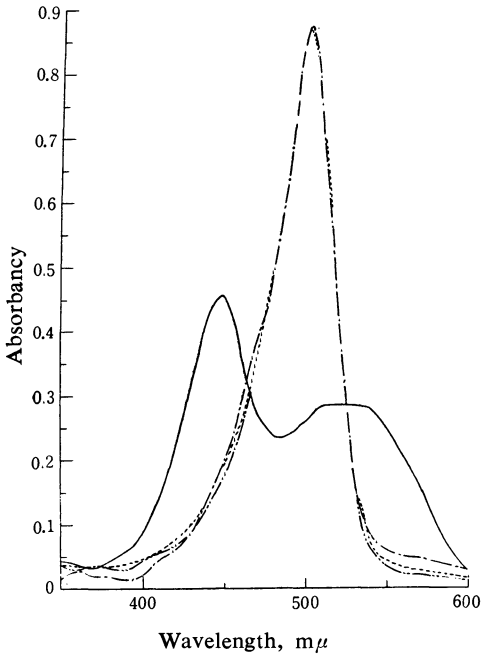



Fig. 8. Absorption spectra of tetryl ($2.00\times10^{-5}$ M) in acetone (containing 4% water by volume) in the presence of ammonia (1.2%) at room temperature.
1 ——— Immediately after the preparation
2 —·—· After 1 hr.
3 ------ After 3 hr.
4 —··— After a day

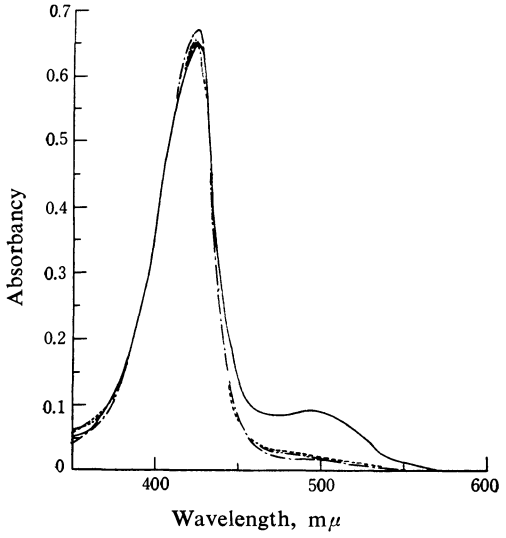



Fig. 9. Absorption spectra of picryl chloride ($1.65\times10^{-5}$ M) in acetone (containing 4% water by volume) in the presence of ammonia (1.2%) at room temperature.
1 ——— Immediately after the preparation
2 —·—· After 1 hr.
3 ------ After 3 hr.
4 —··— After a day

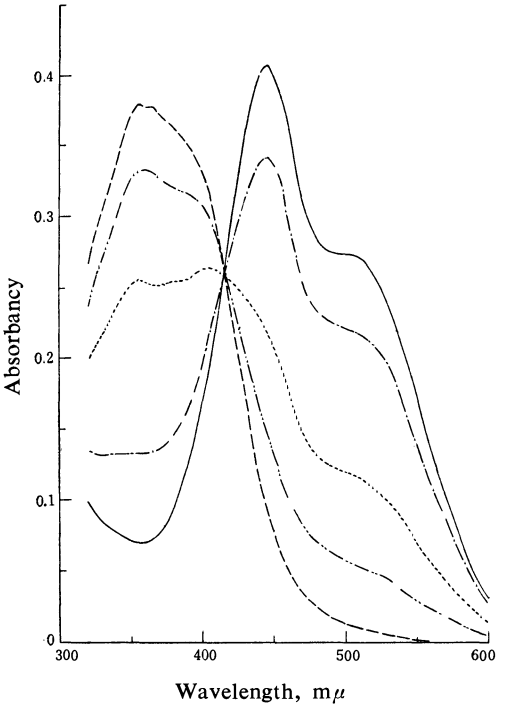



Fig. 10. Absorption spectra of tetryl in water containing ammonia at room temperature.
1 ——— Immediately after the preparation
2 —·—· After 1 hr.
3 ------ After 4 hr.
4 —··— After 8 hr.
5 ——— After a day

the addition of sodium hydroxide, except in the case of the solution from trinitrotoluene, and that the initially produced colored solutions change to the other solutions having different stable intense bands. The absorption curve 1 in Fig. 7 is the only one which does not correspond to the curve 1 in Fig. 2, but does to the curve[6,7] for a colored solution formed from trinitrotoluene in ethanol by the action of sodium ethoxide. Caldin et al.[6,7] have suggested a proton-transfer reaction. Miller and Wynne-Jones[8] also observed that a mixture of trinitrobenzene with diethylamine in acetone or in ethanol produced at first an intensely colored solution having absorption maxima at 470, 515 and 570 mμ and that the solution changed after a considerable period to that having an absorption band only at 515 mμ.

One can see from Fig. 10 that both ammonia water and sodium hydroxide react identically

6) E. F. Caldin and G. Long, *Proc. Roy. Soc.*, **A228**, 263 (1955).
7) J. B. Ainscough and E. F. Caldin, *J. Chem. Soc.*, **1956**, 2528.
8) R. E. Miller and W. F. K. Wynne-Jones, ibid., **1959**, 2375.

with tetryl in water. From the similarity of the absorption curves 1 in Figs. 1–5 and 10, the absorption curves 1 in Figs. 6, 8 and 9 are perhaps due to the colored intermediates such as III, except for the case of trinitrotoluene. These initially formed colored intermediates may further react to produce a stable colored species giving the final absorption curves 4 in Figs. 6–9. The stable colored species were provisionally considered to be Meisenheimer's intermediates in the previous paper[9]. However, it has not yet been proved that the stable colored species are converted further into picric acid. Therefore, at present one can not conclude that they are the Meisenheimer's intermediates. Kimura[10] reported that a darkish purple substance obtained by adding sodium bicarbonate to the acetone solution of trinitrobenzene was a product similar to II.

## Summary

The visible absorption spectra of the colored solutions produced by adding aqueous sodium hydroxide solution or ammonia water to the acetone solutions of 1, 3, 5-trinitrobenzene and its derivatives (2, 4, 6-trinitrotoluene, tetryl and picryl chloride) were measured at room temperature in order to investigate the difference of the chemical actions between stong-alkaline sodium hydroxide and weak-alkaline ammonia water.

These trinitro compounds in acetone containing sodium hydroxide show spectra similar to that of the aqueous sodium hydroxide solution of tetryl. The spectrum of this aqueous colored solution is considered to be due to an intermediate of the Meisenheimer type in the process of the substitution reaction of tetryl to picric acid. Consequently, all the spectra of the colored solutions from the trinitro componds are also probably due to the intermediates of the Meisenheimer type.

Each colored solution of the trinitro compounds in acetone containing ammonia water initially shows the same spectrum as that with sodium hydroxide, except for the case of trinitrotoluene, and changes to the other colored solution having an intense and stable band entirely different from the initial spectrum. The initially formed colored solutions of these trinitro compounds, except the solution from trinitrotoluene, may also be due to the Meisenheimer intermediates.

The author is particularly indebted to Professor Yōkan Nomura for helpful discussions.

*Department of Chemistry*
*Defense Academy*
*Yokosuka*

9) T. Abe, This Bulletin, 32, 997 (1959).
10) M. Kimura, *J. Pharm. Soc Japan* (*Yakugaku Zasshi*), 73, 1219 (1953).

# *Sur la Dissolution des Minerais Sulfurés en Divers Milieux. V. Dissolution de la Sphalérite*

Par Masami ICHIKUNI et Hiroshi KAMIYA

(Reçu le 20 Janvier 1961)

Lorsqu'on aborde le problème de la désagrégation des minerais sulfurés par voie chimique, on s'intéresse notamment aux réactions qui ont part à ce phénomène. Bien que de nombreux articles soint déjà parus à ce propos, ces études sont faites, dans la plupart des cas, avec l'utilisation des minerais et non des minéraux. L'interprétation des résultats était très difficile, car les analyses chimiques n'ont donné que l'aspect global du phénomène composé de nombreuses réactions qui s'avançaient chacune à vitesse différente. Il faut qu'on sache quelles réactions peuvent avoir lieu et ont lieu au cours de la désagrégation.

Pour l'analyse des résultats, la sphalérite semble se munir d'un caractère favorable grâce à la simplicité de sa composition chimique. Kuz'minykh et Yakhontova[1] ont déjà étudié l'extraction du zinc à partir de ce minéral en utilisant le sulfate de fer (III) comme réactif. Il s'agit de la dissolution du minéral en milieu extrêmement oxydant ; ce milieu ne représenterait pas celui de la nature. Ohashi[2] a examiné la dissolution des minéraux sulfurés dans les

1) I. N. Kuz'minykh et E. L. Yakhontova, *Zhur. Prinklad. Khim.* (*J. Applied Chem.*), **23**, 1121 (1950).
2) S. Ohashi, *J. Chem. Soc. Japan, Pure Chem. Sec.* (*Nippon Kagaku Zasshi*), **74**, 845 (1953).

eaux saturées d'air, mais il est regrettable que cet auteur n'ait pas montré les réactions de dissolution. Récemment, du point de vue électrochimique, Sato[3] a donné le mécanisme de la décomposition des minéraux sulfurés dans une solution choisie.

Les présents auteurs voudraient montrer les réactions de la décomposition de la sphalérite en diverses solutions et préciser les conditions qui favorisent la désagrégation, tout en tenant compte des composants mineurs en solution. Il est probable que ces derniers se chargent du rôle de catalyseur dans la nature. L'accélération des réactions est souvent due uniquement à l'action du catalyseur. On tâtonne encore quelles substances peuvent être un catalyseur dans la désagrégation des minerais sulfurés.

### Méthode d'Expérience

On suspend 500 mg. de sphalérite pulvérisée dans 200 ml. de liqueur à l'aide d'un agitateur magnétique, et effectue le prélèvement de 5 ml. de liqueur à des intervalles appropriés au cours de 2 hr. de traitement. Le ballon à fond plat à 300 ml. contenant la liqueur est plongé dans un bain-marie dont la température est maintenue constamment à 50°C. Le ballon est bien bouché avec un bouchon de caoutchouc, persé de 2 tuyaux de verre : le plus long, dont le bout de dessous se munit d'un hémisphère de verre fritté qui touche presque le fond du ballon, sert à produire de nombreuses petites bulles d'air dans la liqueur, lorsqu'on relie à une trompe le tuyau le plus court qui ne s'enfonce pas dans la liqueur. Le débit de l'air est réglé à 0,4 l./min.

La sphalérite produite à la mine de Hosokura, département de Miyagi, est pulvérisée et passée au tamis 60. Le Tableau I montre le résultat d'analyse de l'échantillon. Une certaine teneur en plomb s'explique par la présence de la galène qui est une des impuretés minéralogiques les plus communes. On a préparé ici deux échantillons en pulvérisant de nouveau de la sphalérite tamisée dans un mortier d'agate. Un échantillon qui a été utilisé pour l'examen de l'influence du pH sur la dissolution de ce minéral était moins fin que l'autre avec lequel on a effectué les autres expériences.

Tableau I. Résultat d'analyse chimique de la sphalérite

| Composant | Teneur, % |
|---|---|
| Zn | 61,78 |
| Fe | 1,29 |
| Cd | 0,38 |
| Mn | 0,06 |
| Cu | 0,01 |
| Pb | 2,62 |
| S | 31,53 |
| $SiO_2$ | 0,21 |
| Total | 97,88 |

3) M. Sato, *Econ. Geol.*, 55. 1202 (1960).

La liqueur prélevée est immédiatement filtrée et amenée à 25 ml. Sur cette solution diluée on effectue le dosage du zinc, et s'il y a lieu, du fer et du cuivre. Le dosage du zinc et du cuivre est fait par voie colorimétrique au moyen de la dithizone, et celui du fer, au moyen de l'*o*-phénanthroline. Le dosage de l'hydrogène sulfuré a été effectué par l'iodométrie après une filtration soigneuse de liqueur. L'ion sulfate est examiné avec une solution de chlorure de baryum.

### Résultats

**Effets du pH.**—Quand on a introduit de l'air, la vitesse de dissolution du zinc dépendait dans une grande mesure de l'acidité du milieu. La sphalérite s'est dissoute rapidement au début du traitement, et dont la vitesse de dissolution a ralenti graduellement et elle est devenue constante dans une demi-heure (voir la Fig. 2). Cette vitesse constante servait à établir une échelle de comparaison entre toutes les conditions des expériences.

Le résultat des expériences est indiqué sur la Fig. 1. Comme elle l'indique, la vitesse de dissolution décroit avec la diminution de l'acidité du milieu. L'ion sulfate n'a été décelé en aucun cas. On remarque donc une réaction qui suit :

$$(1) \qquad ZnS + 2H^+ \rightarrow Zn^{2+} + H_2S$$

A part de cette réaction, on en a une autre qui conduit à la formation du soufre libre :

$$(2) \quad ZnS + 2H^+ + O \rightarrow Zn^{2+} + S + H_2O$$

Comme la formation du soufre libre était négligeable, on admet que la première réaction est prédominante sous les conditions des expériences. On n'arrive pourtant pas à décider si la formation du soufre libre est attribuable à l'oxydation de l'hydrogène sulfuré, formé par la première réaction, ou à l'oxydation directe du minéral.

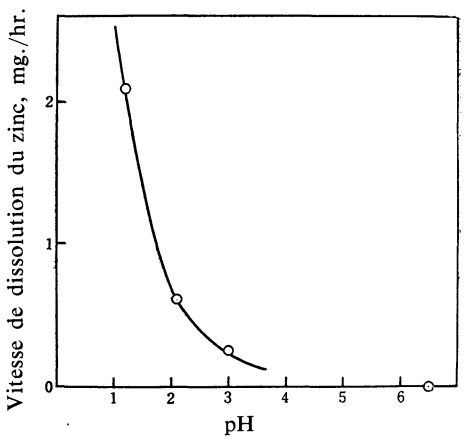



Fig. 1. Vitesse de dissolution de la sphalérite en fonction du pH (expériences effectuées avec barbotage d'air de 400 ml./min.).

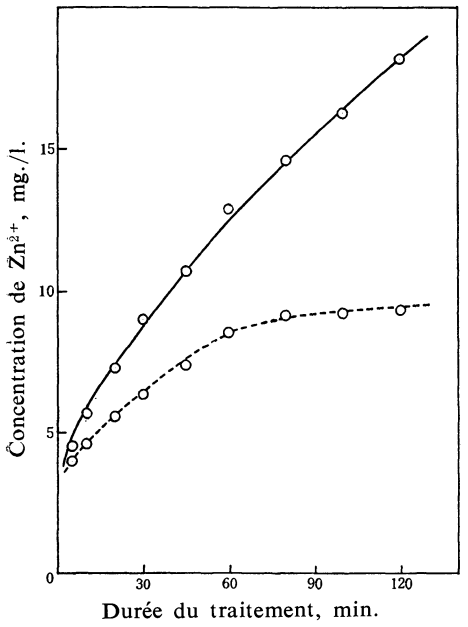



Fig. 2. Variation de concentration de $Zn^{2+}$ en fonction de la durée du traitement.
Trait plein : expérience effectuée avec l'introduction de l'air
Trait discontinu : expérience effectuée sans introduction de l'air

Il faut qu'on tienne compte de la granulométrie de l'échantillon utilisé dans cette expérience, lorsqu'on compare ce résultat avec celui des expériences exposées ci-après qui ont été effectuées avec l'échantillon plus fin.

**Effets du Barbotage de l'Air.**—Il faut qu'on sache d'abord si l'oxygène barboté agit en oxydant du minéral et de l'hydrogène sulfuré, ou simplement en entraîneur de celui-ci. A cet effet, deux expériences ont été entreprises: l'une, avec l'introduction de l'air, dont le débit était de 0,4 l./min., et l'autre, sans introduction de l'air. Dans la dernière expérience, l'air ne se comportait pas en entraîneur, et cela ne signifie pas l'expulsion entière de l'oxygène. Les deux ont été effectuées en milieu d'acide chlorhydrique 0,01 N et à la température de 50°C. Dans la Fig. 2, on dessine la concentration de zinc en fonction de la durée du traitement. Comme on voit dedans, deux courbes, correspondant chacune aux deux expériences décrites ci-dessus, s'approchent l'une de l'autre au début de la dissolution, cependant, elles s'éloignent rapidement avec le temps. La différence des deux expériences peut s'expliquer par l'accumulation de l'hydrogène sulfuré. Cette supposition sera très compréhensible, si l'on admet que le barbotage de l'air, entraînant avec celui-ci l'hydrogène sulfuré formé, favorise une dissolution remarquable du minéral. En fait, sans introduction de l'air, la teneur en hydrogène sulfuré a atteint une valeur de 2,1 mg./l. au bout de 2 hr. de traitement.

Examinons ensuite la possibilité de l'oxydation de l'hydrogène sulfuré par l'oxygène dissous. Si la réaction d'oxydation de ce composé s'avançait avec une vitesse considérable, l'empêchement de la dissolution n'aurait pas lieu, tout au moins, pendant un certain temps, car la liqueur contenait 5,0 mg./l. d'oxygène dissous avant l'addition du minéral. Au bout de 2 hr. de traitement, on a trouvé une concentration de zinc de 9,3 mg./l., correspondant à la formation de l'hydrogène sulfuré de 4,8 mg./l. Ce chiffre ne suffit pas à consumer entièrement l'oxygène dissous, même si l'hydrogène sulfuré soit complètement oxydé en soufre libre par l'oxygène contenu dans la liqueur. D'ailleurs la surface de la liqueur étant toujours en contact avec l'atmosphère, il n'y a aucune raison de croire que l'accumulation de l'hydrogène sulfuré a été causée par manque d'oxygène libre.

Par suite de ces considérations, on conclut que l'oxydation de l'hydrogène sulfuré par l'oxygène libre s'avance très lentement, et que l'hydrogène sulfuré ralentit la décomposition de la sphalérite, même en présence de l'oxygène atmosphérique. Il va sans dire qu'à l'état d'équilibre, la présence de l'hydrogène sulfuré n'est pas compatible avec celle de l'oxygène libre. Le système réalisé par les expériences était hors de l'équilibre, comme l'indique la co-présence de l'hydrogène sulfuré et de l'oxygène. La théorie de l'équilibre chimique ne sera pas très utile à expliquer le mécanisme des réactions qui ont lieu au cours du traitement.

Calculons ici le produit de concentration de zinc par celle d'ion sulfure avec les chiffres qu'on a obtenus sur l'expérience effectuée sans introduction de l'air, au bout de 2 hr. de traitement :

$$[Zn^{2+}] = 9{,}3 \text{ mg./l.} = 1{,}4 \times 10^{-4} \text{ mol./l.}$$

$$[H_2S] = 2{,}1 \text{ mg./l.} = 0{,}62 \times 10^{-4} \text{ mol./l.}$$

Comme $[H^+]^2[S^{2-}]/[H_2S] = 10^{-21}$, où $[H^+] = 10^{-2}$, on a :

$$[S^{2-}] = 0{,}62 \times 10^{-21} \text{ mol./l.}$$

donc,

$$[Zn^{2+}] \cdot [S^{2-}] = 0{,}87 \times 10^{-25}$$

Cette valeur est beaucoup moins grande que le produit de solubilité de la sphalérite : $10^{-23{,}3}$. On notera ici que la vitesse de dissolution du minéral est déjà très ralentie sous cette condition.

**Effets des Ions $Fe^{2+}$.**—Cet essai s'est fait à 50°C, en milieu d'acide chlorhydrique 0,01 N, avec l'introduction de l'air dont le débit était de 0,4 l./min. On a préparé une solution

étalon de $Fe^{2+}$ en dissolvant du chlorure de fer(II) hydraté dans l'acide chlorhydrique 0,01 N. Elle contenait 1,000 mg./l. de $Fe^{2+}$.

Les ions $Fe^{3+}$ exercent une action particulière sur la dissolution du minerai sulfuré, dans ce cas ils se réduisent en ions $Fe^{2+}$. Une solution qui est en contact avec un gisement de minerais sulfurés trouve son fer presque entièrement à l'état divalent. Les ions $Fe^{3+}$ se forment dans la nature par l'oxydation des ions $Fe^{2+}$ au moyen de l'oxygène atmosphérique. On a effectué ces expériences en prenant le mécanisme de la formation des ions $Fe^{3+}$ dans la nature en considération. Par l'introduction de l'air dans une solution contenant des ions $Fe^{2+}$, on a essayé de reproduire en quelque sorte la formation des ions $Fe^{3+}$. On avait déjà noté que l'action des ions $Fe^{2+}$ et de l'oxygène atmosphérique favorisait une forte dissolution de la chalcopyrite, et on l'avait attribué à la formation des ions $Fe^{3+}$ [4].

On montre sur la Fig. 3 un exemple tiré des expériences: la présence des ions $Fe^{2+}$ ralentit considérablement la dissolution du zinc. Même une teneur en ions $Fe^{2+}$ à 100 mg./l. produit le même effet, comme on voit sur la Fig. 4. Lorsqu'on dit vitesse de dissolution, il s'agit toujours de celle qui est mesurée à l'état stationnaire de dissolution. Ce résultat ne s'accorde pas avec celui de la chalcopyrite.

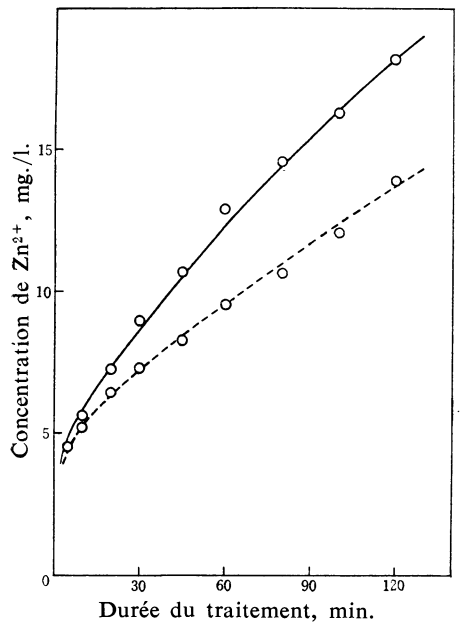



Fig. 3. Variation de concentration de $Zn^{2+}$ en fonction de la durée du traitement.
Trait plein: en l'absence des ions $Fe^{2+}$
Trait discontinu: en présence de 1.000 mg./l. de $Fe^{2+}$

4) M. Ichikuni, Ce Bulletin, 33, 1159 (1960).

**Effets des Ions $Fe^{3+}$.**—Cet essai a été effectué à 50°C, en milieu d'acide chlorhydrique 0,01 N, avec l'introduction de l'air, dont le débit restait toujours le même que les essais précédents. La solution étalon de $Fe^{3+}$ a été préparée à partir du chlorure de fer(III) hydraté. On en a dissous dans l'acide chlorhydrique, de manière à ce que la solution contienne 100 mg./l. de $Fe^{3+}$.

La réaction entre la sphalérite et des ions $Fe^{3+}$ est exprimée par l'équation suivante[1]:

$$(3)\quad ZnS + 2Fe^{3+} \rightarrow Zn^{2+} + S + 2Fe^{2+}$$

où la dissolution de 1 mol. de zinc correspond à la réduction de 2 mol. de $Fe^{3+}$ en $Fe^{2+}$. L'examen du résultat d'expériences, montré

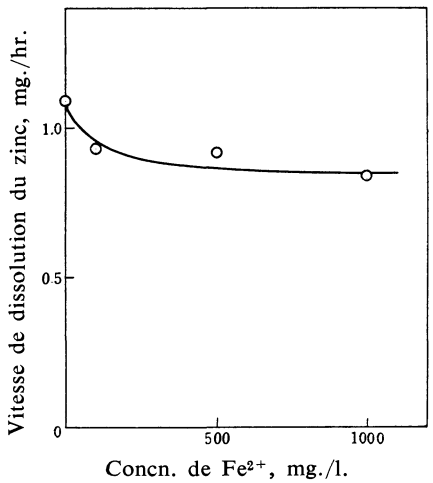



Fig. 4. Vitesse de dissolution de la sphalérite en fonction de la concentration en ions $Fe^{2+}$ de la liqueur.

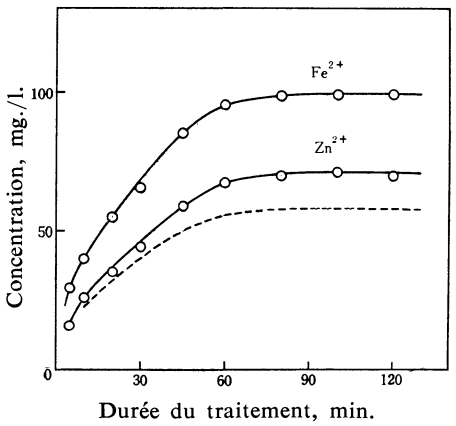



Fig. 5. Dissolution de la sphalérite par l'action des ions $Fe^{3+}$.
Trait plein: concentration de zinc dissous et defer réduit
Trait discontinu: concentration théorique de zinc, calculée à partir de la concentration trouvée de $Fe^{2+}$

sur la Fig. 5, révèle que la quantité dissoute de zinc est toujours supérieure à la quantité théorique de zinc, calculée d'après la réaction 3 à partir de la quantité trouvée de $Fe^{2+}$. Il est certain qu'une partie de zinc a été dissoute d'après la réaction 1, où l'hydrogène sulfuré a été partiellement entraîné par le courant d'air, sans être oxydé en soufre libre par l'action des ions $Fe^{3+}$.

**Effets des Ions $Cu^{2+}$.**—Il est bien connu que les ions de métaux lourds, notamment $Cu^{2+}$, jouent un rôle de catalyseur dans de diverses réactions. Comme les ions $Cu^{2+}$ se trouvent très fréquemment dans les eaux de mine, il est probable qu'ils contribuent d'une certaine manière à l'accélération ou à la retardation des réactions de désagrégation.

Bien que l'action des ions $Cu^{2+}$ ait été remarquée par certains chercheurs[5], la connaissance en est encore peu suffisante. Le comportement des ions $Cu^{2+}$ trouvé dans cette expérience permettra de révéler la fonction qu'ils exercent dans la désagrégation. Cet essai a été effectué sous les mêmes conditions que les précédents, sauf la présence des ions $Cu^{2+}$ qui ont été ajoutés saus forme du sulfate.

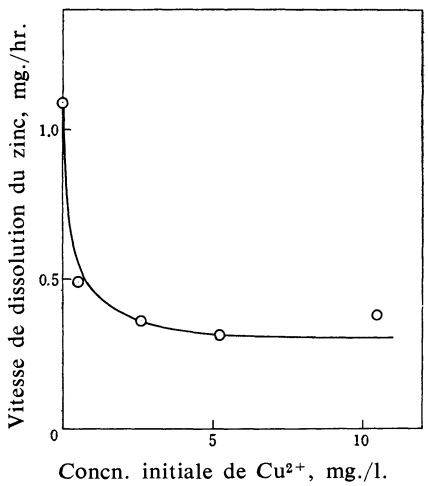



Fig. 6. Influence des ions $Cu^{2+}$ sur la dissolution de la sphalérite.

La vitesse de dissolution du zinc a été mesurée dans des solutions de diverses teneurs en $Cu^{2+}$. La Fig. 6 représente le résultat de l'essai. Les ions $Cu^{2+}$ ralentissent la dissolution. Une variation faible de concentration en $Cu^{2+}$ révélé qu'une petite portion de $Cu^{2+}$ avait disparu au cours de l'expérience. La diminution en a atteint 0,5 mg./l. près au bout de 2 hr. de traitement. Le cuivre aurait précipité sous forme du sulfure, dont la formation est attribuable au dégagement de l'hydrogène sulfuré, libéré par la décomposition du minéral. Toutefois la quantité fixée de cuivre était très faible par rapport à celle d'hydrogène sulfuré formé. On peut en déduire que la condition oxydante défavorise la fixation du cuivre, même en présence des ions sulfure. Comme le cuivre ajouté restait presque entièrement à l'état dissous, on admet qu'une réaction d'échange du zinc avec le cuivre n'avait pas lieu. Si la réaction d'échange intervenait, il y aurait une tendance d'augmenter la vitesse de dissolution à mesure que la concentration en $Cu^{2+}$ augmente.

Or, généralement dit, des solutions formées dans la zone d'oxydation du gisement des minerais sulfurés contiennent encore d'autres ions que les ions $Cu^{2+}$. La caractéristique des solution est donc la co-présence de divers ions, tels que des ions $Fe^{2+}$, $Fe^{3+}$, $Cu^{2+}$, $Mn^{2+}$ et ainsi de suite. L'action des ions $Cu^{2+}$ devrait être examinée en présence d'autres ions, notamment des ions de fer.

**Effets des Ions $Fe^{3+}$ et $Cu^{3+}$.**—Il est bien connu que les ions $Fe^{3+}$ sont efficaces à la décomposition des minerais sulfurés, mais il n'y a presque aucune étude sur la contribution des ions $Cu^{2+}$ à ce phénomène. Seulement Garrels et Thompson[6] ont mentionné que l'attaque des ions $Fe^{3+}$ contre la pyrite n'était pas accélérée par la présence des ions $Cu^{2+}$. On a entrepris ici un essai de dissolution de la sphalérite au moyen des ions $Fe^{3+}$ en présence des ions $Cu^{2+}$, et en a comparé le résultat avec celui de l'essai précédent qu'on avait effectué

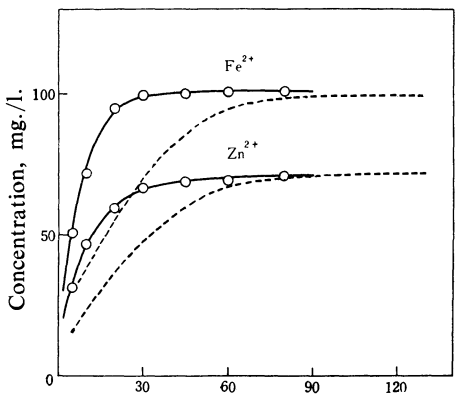



Fig. 7. Effets des ions $Cu^{2+}$ sur la dissolution de la sphalérite par l'action des ions $Fe^{3+}$.
Trait plein : expérience effectuée en présence de 5,25 mg./l. de $Cu^{2+}$
Trait discontinu : expérience effectuée en l'absence des ions $Cu^{2+}$

5) S. Koch et Gy. Grasselly, *Acta Univ. Szegediensis, Acta Mineral. Petrog.*, 6, 23 (1952).

6) R. M. Garrels et M. E. Thompson, *Am. J. Sci.*, **258** A, 57 (1960).

dans une liqueur contenant 100 mg./l. de $Fe^{3+}$, mais qui était exempte de cuivre.

La Fig. 7 donne les résultats de cet essai et du précédent. On voit que la présence des ions $Cu^{2+}$ favorise une décomposition rapide de la sphalérite. On ajoute encore que la diminution de concentration en $Cu^{2+}$ n'avait pas lieu au cours du traitement, tant que les ions $Fe^{3+}$ restaient en solution.

**Effets des Ions $Fe^{2+}$ et $Cu^{2+}$.**—Les résultats des essais précédents nous ont conduit à l'entreprise d'un autre essai mis sous les conditions qui ne sont das trop éloignées de celles de la nature. En considérant les eaux de mine, où les ions $Fe^{2+}$ sont prédominants dans la plupart des cas, on a imaginé que l'essai de la dissolution en présence des ions $Fe^{2+}$ et $Cu^{2+}$ réaliserait les réactions réelles dans la nature.

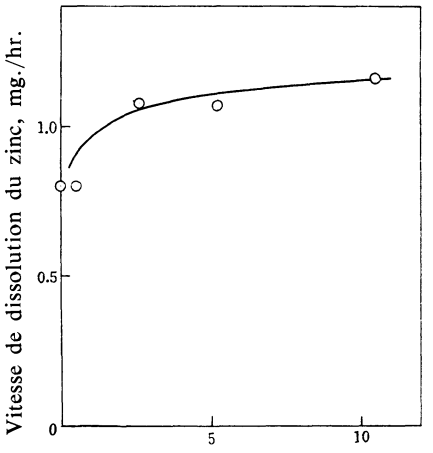



Fig. 8. Vitesse de dissolution de la sphalérite en présence de 700 mg./l. de $Fe^{2+}$ et de quantité variable de $Cu^{2+}$.

La Fig. 8 montre le résultat. Dans cette série d'expériences, la concentration de $Fe^{2+}$ était fixée à 700 mg./l. et celle de $Cu^{2+}$ variait de 0,53 à 10,5 mg./l. La concentration de $Cu^{2+}$ a diminué très lentement au cours du traitement. La diminution s'en est élevée à 0,5 mg./l. près au bout de 2 hr. de traitement. Toutefois on a remarqué une dissolution accélérée de la sphalérite, tant que l'ion cuivre restait en solution. On discutera plus loin le mécanisme possible de ce phénomène.

## Discussion

C'est le pH du milieu qui exerce une grande influence sur la décomposition du minéral, sans qu'on tienne compte des effets électrochimiques provenant du contact avec d'autres minéraux. Si le minéral existait indépendamment d'autres minéraux, il resterait assez stable en milieu neutre même en présence de l'oxygène atmosphérique.

La présence de l'oxygène libre et des ions $Fe^{2+}$ n'est pas capable d'accélérer sa décomposition, c'est que l'oxydation des ions $Fe^{2+}$ en ions $Fe^{3+}$ s'avance très lentement avec l'oxygène libre. Si les ions $Fe^{3+}$ étaient formés rapidement à partir des ions $Fe^{2+}$ par l'action de l'oxygène, l'introduction de l'air rendrait la décomposition du minéral d'autant plus facile que la teneur en ions $Fe^{2+}$ de la liqueur est plus grande.

Les ions $Cu^{2+}$, agissant souvent en catalyseur, ne sont pas tous seuls capables d'augmenter la vitesse de décomposition du minéral, par conséquent on ne peut pas attendre une réaction d'échange du zinc avec le cuivre. Il est intéressant que les ions $Fe^{2+}$ ainsi que les ions $Cu^{2+}$, loin d'accélérer la désagrégation de la sphalérite, la retardent considérablement. Ce phénomène offre des problèmes importants à la géochimie des gisements métallifères.

L'action des ions $Fe^{3+}$ avait été bien étudiée, mais on a trouvé ici, pour la première fois, qu'une petite quantité de cuivre accélérait la réaction entre le minéral et les ions $Fe^{3+}$. Toutefois les produits de réaction étaient toujours les ions $Zn^{2+}$ et le soufre libre en milieu acide, indépendamment de la présence du cuivre. On considère pour le moment le cuivre comme catalyseur.

On a eu ainsi l'idée d'examiner la dissolution du minéral en présence des ions $Fe^{2+}$ et $Cu^{2+}$ avec l'introduction de l'air. Si ces ions se comportaient indépendamment les uns des autres, ils en retarderaient la dissolution. Mais, au contraire, leur co-présence y était efficace. Ce fait insiste qu'il y a une interaction entre les ions $Fe^{2+}$, $Cu^{2+}$ et l'oxygène. Il est probable que les ions $Cu^{2+}$ facilite l'oxydation des ions $Fe^{2+}$ en ions $Fe^{3+}$ par l'oxygène atmosphérique. Ils accélèrent également l'attaque des ions $Fe^{3+}$ contre le minéral.

On conclut donc que la présence des ions $Cu^{2+}$ est indispensable à une décomposition rapide de la sphalérite, et que les ions $Cu^{2+}$ jouent ici un rôle de catalyseur. Toutefois des composés insolubles de cuivre n'en sont pas capables. On ajoute encore que, malgré l'action catalytique du cuivre, une formation abondante d'ions $Fe^{3+}$ n'aura pas lieu, le rapport $Fe^{3+}/Fe^{2+}$ étant réglé par le potentiel d'oxydo-réduction du milieu, par conséquent on ne peut pas attendre une dissolution rapide du minéral, tant que les réactions se passent en solution.

## Résumé

Les facteurs intervenant à la décomposition chimique de la sphalérite ont été examinés. Un petit pH ainsi que l'oxydant, notamment le

fer trivalent accélèrent la décomposition. La présence de l'hydrogène sulfuré la retarde considérablement. A pH 2, celle des ions $Fe^{2+}$ ou des ions $Cu^{2+}$ empêche une dissolution rapide du minéral, même avec l'introduction de l'air. La décomposition du minéral par les ions $Fe^{3+}$ est accélérée par les ions $Cu^{2+}$. La co-présence des ions $Fe^{2+}$ et $Cu^{2+}$ favorise, avec le barbotage de l'air, une dissolution remarquable du minéral, ce qui est attribuable à l'action catalytique des ions $Cu^{2+}$ qui facilitent probablement l'oxydation des ions $Fe^{2+}$ en ions $Fe^{3+}$, et l'attaque de ceux-ci contre le minéral.

Les auteurs se permettent d'exprimer leur remerciements sincères à Monsieur le professeur K. Noguchi et à Monsieur le professeur T. Hanya qui ont bien voulu donner des conseils utiles et participer à la discussion sur l'interprétation des résultats.

*Faculté des Sciences*
*Université Métropolitaine de Tokyo*
*Sétagaya-ku, Tokyo*

# *Physicochemical Studies on Cobalt Salts of Higher Fatty Acids. I. Preparation of Cobalt Soap by Metathesis*

By Hirotaro KAMBE*

(Received February 24, 1961)

Heavy metal salts of higher fatty acids, usually called heavy metal soaps, can be made by a substitution reaction between fatty acid and the salt of weak inorganic acid such as acetate. In place of inorganic salts, oxide or hydroxide may be used. These reactions can be accelerated by fusing the reactants. This is the principle of the fusion method, which is commonly used as a means of preparation of heavy metal soaps.

Cobalt soap may be prepared by the fusion method. The melting of fatty acid with cobalt(II) acetate or cobalt(II) hydroxide is followed by the reactions:

$$Co(CH_3COO)_2+2RCOOH = Co(RCOO)_2+2CH_3COOH$$

or $$Co(OH)_2+2RCOOH=Co(RCOO)_2+2H_2O$$

The cobalt soap made by the fusion method is not crystalline powder, but a glassy mass. Molten cobalt soap is easily oxidized and often becomes dark on prolonged heating in air. For these reasons we have concluded that the fusion method is not suited for preparing pure cobalt soap.

With water soluble salts of weak acid, fatty acid may react in solution. Kaufman and Lüssling[1] reported that when they shook a solution of fatty acid in petroleum ether with an aqueous solution of cobalt(II) acetate, the upper petroleum ether layer became blue as the formed cobalt soap dissolved into petroleum ether. They obtained cobalt oleate by this method. But our preliminary experiment has shown that it is difficult to prepare cobalt stearate with this technique, for the stearate is less soluble in petroleum ether than the oleate. When we use ethyl alcohol instead of petroleum ether as the solvent, the reaction advances very smoothly in a homogeneous solution and crystalline cobalt stearate powder can be prepared. This may be another means of preparing cobalt soap, as is shown later.

Water soluble inorganic salts, either of weak acid or of strong acid, react instantaneously with alkaline soap. This type of reaction is called double decomposition or metathesis. Metathesis is most important in preparing metal soaps, and it is the basis of the so-called precipitation method. The soaps made by metathesis are generally crystalline powder.

In the case of cobalt soap, cobalt(II) chloride, nitrate, sulfate, and acetate may be used as inorganic salts in metathesis. Reactions between these and sodium or potassium soap would proceed readily in solution to form cobalt soaps. For example,

$$CoCl_2+2RCOONa=Co(RCOO)_2+2NaCl$$

Kahlenberg[2] has shown very long ago that metathetic formation of heavy metal soaps

* Present address: Aeronautical Research Institute, the University of Tokyo, Meguro-ku, Tokyo.

1) H. P. Kaufmann and Th. Lüssling, *Fette und Seifen*, 55, 90 (1953).

2) L. Kahlenberg, *J. Phys. Chem.*, 6, 6 (1902).

could be carried out also in organic solvents. Koenig[3] prepared many metal soaps, including cobalt soap, by metathesis in warm water. The soap thus formed was dried in an air oven at 115~120°C for 10~12 hr., and the glassy solid obtained was then pulverized. Koenig observed a color change from pink to blue when cobalt soap was heated.

In Koenig's method an aqueous solution of sodium soap is used, and at the lower concentrations, alkaline soap may be hydrolyzed to free acid, which will contaminate the soap being formed. Whitmore and Lauro[4] proposed a method for preventing the hydrolysis of alkaline soap by the addition of ethanol to the solution.

Although Whitmore and Lauro did not prepare cobalt soap in this way, we have examined this method in detail and found that besides common pink hydrous cobalt soap, blue anhydrous and red hydrous soaps may be formed according to conditions. In this part of the study, metathetic preparation of cobalt soap was investigated, and particularly the effects of several factors on the color of the soap being formed were discussed.

## Experimental

**Materials.**—*Fatty Acids.*—Stearic, palmitic, myristic, and lauric acid were fractionally distilled products, made by Nihon Yushi Co., and were recrystallized from absolute ethanol.

*Solvents.*—Ethanol and methanol were dehydrated and distilled over anhydrous calcium oxide. Acetone was dehydrated by potassium carbonate anhydrate.

*Cobalt(II) Salts.*—Cobalt chloride, $CoCl_2 \cdot 6H_2O$, nitrate, $Co(NO_3)_2 \cdot 6H_2O$, sulfate, $CoSO_4 \cdot 7H_2O$, and acetate, $Co(CH_3COO)_2 \cdot 4H_2O$ were chemically pure reagents and were recrystallized from water. These salts, except sulfate, are very deliquescent, and they were used with some water.

**Metathesis.**—The following standard procedure was adopted to control experimental factors.

(i) Fatty acid, mostly stearic acid, was dissolved in absolute ethanol by warming in a constant temperature water-bath at 60°C, and neutralized exactly by an alkaline solution, with phenolphthalein as indicator. The alkaline solution used was usually 0.15 N potassium hydroxide solution in water or in ethanol. If necessary, some amount of either solvent was added to the alkaline soap solution to control the ratio of the volume of solvent (ethanol in this case) to that of water in the system; this is called the solvent ratio hereafter. When this ratio is comparatively low, the alkaline soap solution becomes turbid by hydrolysis of the soap. In such cases the reaction products tend to contain free fatty acid, which may be extracted, however, by acetone, as is shown below.

(ii) An excess of cobalt salt, mostly cobalt chloride, was dissolved in the same water-bath in water, or, if necessary, in pure or aqueous ethanol. The solution of cobalt chloride in water is considerably acidic, and also the solution after metathesis becomes slightly acidic. It is natural for the soap made in this way to contain some free fatty acid. When cobalt acetate is used instead of chloride, the solution is not so acidic that free acid is not included in the soap, as was pointed out by Whitmore and Lauro[4].

(iii) After both solutions were warmed to 60°C, a cobalt salt solution was stirred into the alkaline soap solution little by little. As cobalt soap is almost insoluble in the solution, it precipitated immediately. The reaction must be carried out always below 60°C, because above this temperature the reaction products become somewhat bluish.

The color of soap in the solution was observed directly after the reaction and also after having been left in the solution for some time with or without stirring. The alkaline soap solution, which had at first shown a pink color due to phenolphthalein, became blue after the addition of a little of the cobalt salt solution because cobalt ion shows a blue color in ethanol. When the whole salt solution was added, the color of the solution faded generally, and pink soap precipitated.

(iv) The precipitates were filtered off by suction, washed by absolute ethanol to remove free fatty acid, and dried overnight in a vacuum desiccator over calcium chloride anhydrate at room temperature. The color of the soap was preserved during drying in this way. The dried soaps were pulverized by an agate mortar. Free fatty acid was extracted with acetone over anhydrous potassium carbonate in a Soxhlet extractor.

## Results and Discussion

As a preliminary experiment, the colors of cobalt soaps formed at various solvent ratios, based on volume, were observed in the solution without stirring.

In pure ethanol, the yield of cobalt soap was very little. As metathesis is an ionic reaction, it is natural that the reaction is suppressed in a solvent, in which degrees of ionization of reactants are low. A solution of cobalt chloride in pure ethanol is blue, and metathesis in this solvent proceeded in a blue solution. But the reaction product was not pure blue; it seemed dark blue at first, and became pale violet after being left in the solution.

In pure water, the product was pink, but when dried, it gained a tinge of blue. If the solvent ratio was lower than 1 : 1, the color of the formed soap was pink as in pure water. When the ratio exceeded 1 : 1, although the formed soap was also pink at the beginning, often small blue particles grew overnight within pink precipitates. Sometimes the whole soap turned blue in a short time, less than an

3) A. E. Koenig, *J. Am. Chem. Soc.*, 36, 951 (1914).
4) W. F. Whitmore and M. Lauro, *Ind. Eng. Chem.*, 22, 646 (1930).

hour. These color changes were most rapid at a solvent ratio somewhat higher than 1 : 1.

**Effect of Stirring.**—As stated above, sometimes blue soap grew in addition to pink soap in the solution when it was left without stirring. First, we examined the effect of stirring on this color change.

In a standard procedure with the solvent ratio 5 : 1, pink soap turned blue without stirring, even if very slowly, but the color changed in 1 hr. with stirring. If some blue soap powder, prepared previously, was added to the solution, the color change was completed in 15 min.

When the solution was kept at 60°C after reaction, the color did not change even after 1 hr., but if it was taken out from the water-bath and cooled by stirring, the color began to change immediately and turned perfectly blue in 25 min.

From these facts, it is concluded that the blue soap has grown from pink soap. The addition of some blue soap advances the color change remarkably, for added soap powder forms nuclei for color change. At 60°C spontaneous occurrences of nuclei are suppressed, and the color change is not observed. Below 60°C nuclei of blue soap would appear, but they grow so slowly without stirring, that the color change proceeds locally and heterogeneously, and as a result small blue particles appear within pink precipitates. Therefore, to change color completely, cooling the solution by stirring is absolutely necessary.

The bubbling of air into the solution did not alter the speed of color change. Closing the vessel and stirring by a magnetic stirrer also did not influence the effect. It is evident that oxidation is not a cause of color change.

**Effect of Solvent Ratio.**—Next we examined again the effect of the solvent ratio on the color change, but with stirring.

Stearic acid (2 g.) was dissolved in ethanol and/or water (250 ml.) and neutralized by 0.15 N potassium hydroxide in ethanol or water (about 50 ml.). The solution was mixed at 60°C with cobalt chloride in ethanol and/or water (50 ml.), with various solvent ratios, and cooled by stirring. The time needed to turn blue was observed. The results are shown in Table I.

In series I, with larger solvent ratios, the colors of the products seemed violet or pale blue from an early stage. They did not readily turn blue and contained some white powder of potassium soap. Below the ratio 6 : 1, pink soap was formed at the beginning and changed blue soon, as stated before.

In series II, which contained more water than series I, the speed of the color change became larger with the lower solvent ratio. Sometimes blue soap turned violet soon and became red overnight. The red cobalt stearates formed in these systems are completely different in appearance from pink soaps formed directly after the reaction. When dried, they can be pulverized very easily, in contrast to plastic pink soaps.

TABLE I. EFFECT OF THE SOLVENT RATIO ON THE COLOR OF COBALT SOAPS

| System | No. | Solvent ratio based on volume | Color of product |
|---|---|---|---|
| Series I | 1 | (pure ethanol) | Bluish precipit. in blue soln., mixed with white K soap. |
| | 2 | 30 : 1 | Pale violet, turned blue in 2.5 hr., mixed with K soap. |
| | 3 | 15 : 1 | Violet, turned blue in 60 min., mixed with K soap. |
| | 4 | 9 : 1 | Reddish, turned blue in 60 min. |
| | 5 | 6 : 1 | Pink, turned blue in 60 min. |
| Series II | 6 | 5 : 1 | Pink, turned blue in 30 min. |
| | 7 | 4 : 1 | Pink, turned blue in 15 min., violet in 60 min., red overnight. |
| | 8 | 3.3 : 1 | Pink, turned blue in 15 min., violet in 40 min., red overnight. |
| | 9 | 2.8 : 1 | Pink, turned blue in 30 min. |
| | 10 | 2.3 : 1 | Pink, turned blue in 25 min. |
| Series III | 11 | 2 : 1 | Pink, turned blue in 10 min., red overnight. |
| | 12 | 1.5 : 1 | Pink, turned blue in 5 min., red overnight. |
| | 13 | 1.3 : 1 | Pink, turned blue in 10 min., red overnight. |
| Series IV | 14 | 1 : 1 | Pink, turned red overnight. |
| | 15 | 1 : 1.5 | Pink, turned red overnight. |
| | 16 | 1 : 2 | Pink, turned red overnight. |
| | 17 | 1 : 3 | Red, without change. |
| | 18 | 1 : 5 | Red, without change. |

In series III, with the greater water content, the speed of the color change became very rapid, and at the solvent ratio of about 1.5 : 1, it was at a maximum. The products turned completely red overnight.

The last series, where the solvent ratio is lower than 1 : 1, was very different from the preceding series. In this series soaps did not change blue, however long stirred, but became red gradually. The systems which contained the most little amount of ethanol were red rather than pink from the outset. It was hard to dry them in vacuum, for they contained a large amount of water.

Together with the other results obtained, the following facts were confirmed:

(i) The color of the product is determined by the solvent ratio after mixing. The addition of either solvent to the solution after reaction did not affect the color.

(ii) If the resultant solvent ratio is the same, the compositions of the reactant solutions are indifferent to the color of the product.

(iii) The extent of excess of cobalt chloride over stearic acid and the order of mixing solutions did not significantly affect the color of the soap formed.

(iv) The speed of the color change from blue to red depends on the solvent ratio and the time of stirring. Blue soap always turned red if it was left in solution for long a time.

**Effect of Degree of Neutralization.**—In these experiments, the solution of stearic acid was exactly neutralized by an alkaline solution. Next we examined the effect of the degree of neutralization on the color change of cobalt soap.

At the solvent ratio 1 : 2, when exactly neutralized, the cobalt soap did not change blue, though it later became red. If the amount of added alkaline solution was varied between 60 and 140% of the equivalent, different effects were observed. When the system was insufficiently neutralized, the products became red sooner and contained much free fatty acid. When the added alkali was more deficient, the color change became slower. However, when an excess of alkali was added to the system, the product became violet. When there is a large excess of alkali, the reaction would not readily proceed because, as will be discussed in the next part, the cobalt soap may be decomposed to free acid by the presence of much alkali.

At the solvent ratio 2 : 1, when exactly neutralized, the formed pink soap soon became blue with stirring and later turned red in the solution. But when alkali was added in excess, a color change from pink to blue was not observed and the soap turned red at last. On the contrary, when alkali was insufficient, the speed of becoming blue was more rapid. When the degree of neutralization was lower, the color change became quicker, although the yield was smaller.

As well as adding insufficient alkali to the fatty acid solution, the addition of hydrochloric acid to the cobalt chloride solution had the same effect on color change. But after the forming of the pink soap, the addition of hydrochloric acid was not effective.

From these results it is concluded that the solution must be acidic at mixing for realizing the color change.

**Effect of Using Other Solvents than Ethanol.**—Throughout the preceding experiments, the solvent was a mixture of ethanol and water. Next we used acetone and methanol in place of ethanol. Any solvent which dissolves fatty acid may be used, but when the solvent does not mix with water, as the petroleum ether used by Kaufmann and Lüssling[1], the procedure becomes somewhat difficult. With methanol or acetone, metathesis could be carried out as with ethanol. In particular, when the solvent ratio was lower than 1 : 1, only pink soaps were formed. With these solvents, even if the solvent ratio was higher than 1 : 1, the blue soap could not be obtained. But when acetone was used, the formed soap became red quickly.

**Effect of Using Other Cobalt Salts than Chloride.**—Instead of cobalt chloride we tried to use other cobalt salts. Cobalt nitrate and sulfate may be used in the same way as chloride. But cobalt acetate showed somewhat different effects.

Cobalt acetate may react directly with stearic acid in aqueous ethanol. In this substitution reaction, when the solvent ratio is 2 : 1, the color changed blue and subsequently turned red. But at the ratio 1 : 2, the color did not change at all.

The color change was suppressed markedly by the addition of alkali. If the fatty acid was exactly neutralized, that is, in metathesis, the formed pink soap did not change blue in any solvent ratio.

At the solvent ratio 2 : 1, pink soap made by metathesis turned blue in 60 min. with cobalt chloride, in 30 min. with cobalt nitrate, in 20 min. with cobalt sulfate, and never with cobalt acetate.

In a substitution reaction with cobalt acetate, the addition of alkali suppressed markedly the color change to blue. The substitution reaction could be carried out between cobalt acetate and stearic acid with acetone in place of ethanol.

However, when acetone was used, with the solvent ratio 2 : 1, pink soap turned blue, even if very slowly, but perfectly blue soap was not obtained.

**Effect of Using Other Fatty Acids than Stearic Acid.**—Other cobalt soaps may be prepared by metathesis in the same way as stearate. In place of stearic acid, palmitic, myristic, and lauric acid were used.

These reactions proceeded just the same way as with stearate. The color changes were also observed, but the speed of color change from pink to blue becomes slower, as the chain length of fatty acid decreases. The laurate could not turn blue under the same conditions.

The time for turning blue with the solvent ratio is tabulated in Table II. These reactions were obtained by stirring the solutions at 45°C for 1 hr. and later leaving them in the solution without stirring. The solutions were slightly acidic.

Table II. Time for turning blue of pink cobalt soaps

| Solvent ratio | 4 : 1 | 1.5 : 1 | 1 : 1.5 | 1 : 4 |
|---|---|---|---|---|
| Cobalt stearate | 15 min. | 10 min. | — | — |
| Cobalt palmitate | 2 days | 1~2 hr. | — | — |
| Cobalt myristate | 4~5 days | 1 day | — | — |
| Cobalt laurate | — | — | — | — |

— Did not become blue.

## Summary

As a method of preparation of cobalt soap, metathesis between alkaline soap and cobalt salt was investigated.

Cobalt stearate, palmitate and myristate were obtained in pink, blue and red forms according to conditions. Cobalt laurate in blue form was not observed.

Metathetic products were always pink at the beginning. If the system has a solvent ratio (solvent to water) higher than 1 : 1, and the solution after mixing is acidic, the color of soap will turn blue with stirring. It will change red later when left in the solution. The blue form could not be obtained with acetone or methanol as a solvent.

The speed of the color change became considerably slower with fatty acid of a shorter chain length.

In substitution reaction between stearic acid and cobalt acetate with a solvent ratio higher than 1 : 1, the same color changes were observed. But in this system the addition of some alkali suppressed markedly the color change, and at an exactly neutralized metathetic reaction the soap did not turn blue. Even in this case, when acetone was used instead of ethanol, the color change was observed, but the speed was very slow.

The author expresses his gratitude to Professor Bunnosuke Yamaguchi for his advice throughout this work and to Messrs. Itaru Mita, Hirokazu Watanabe and Hiroshi Kayano for their assistance in experiments.

*Institute for Science and Technology*
*The University of Tokyo*
*Meguro-ku, Tokyo*

# *Physicochemical Studies on Cobalt Salts of Higher Fatty Acids. II. Compositions of Cobalt Soaps*

By Hirotaro KAMBE*

(Received February 27, 1961)

Cobalt soap is generally a neutral salt between a bivalent cobalt cation and two univalent fatty acid anions. For example, the composition of cobalt stearate is ideally expressed by $Co(C_{17}H_{35}COO)_2$.

Oudemans[1] and Caspari[2] have pointed out that cobalt laurate is monohydrate. Kaufmann and Lüssling[3] found that while, under some conditions, cobalt oleate was obtained as an acidic salt, $Co(C_{17}H_{35}COO)_2 \cdot (C_{17}H_{35}COO)_2$, cobalt stearate was a neutral salt.

In the previous part of these studies[4], it was found that cobalt soaps obtained by metathesis in aqueous ethanol showed three different colors, that is, pink, blue and red.

* Present address: Aeronautical Research Institute, the University of Tokyo, Meguro-ku, Tokyo.

1) A. C. Oudemans, *J. prakt. Chem.*, [1], **89**, 206 (1863).
2) C. E. Caspari, *Am. Chem. J.*, **27**, 310 (1902).
3) H. P. Kaufmann and Th. Lüssling, *Fette und Seifen*, **55**, 90 (1953).
4) H. Kambe, This Bulletin, **34**, 1786 (1961).

In the present part they will be analyzed. As a result, it will be ascertained that different colors are principally due to the difference of hydration of the cobalt soap.

## Experimental

**Materials.**—Cobalt soaps are cobalt stearates, described in the previous paper[4]. Several specimens of each typical color were chosen from among many samples.

**Analyses.**—*Free Fatty Acid.*—Free fatty acid was extracted from soaps by the use of acetone for 1 hr. with a Soxhlet extractor. The color of the soaps was not altered by extraction. Acetone was dehydrated by anhydrous potassium carbonate. A glass cylinder was inserted around a cylindrical filter paper in order to improve the circulation of the solvent[5]. The amount of free acid was determined by evaporating the solution. The residue was dissolved in ethanol, and the solution was titrated by a standard alkaline solution.

*Combined Fatty Acid.*—Cobalt soaps were decomposed by boiling with 0.1 N sulfuric acid. Isolated fatty acid and unreacted soap melted and floated in a mass on the surface of the solution. The decomposition was continued until the molten mass became wholly colorless.

Cobalt soap can be decomposed also by a 0.1 N alkaline solution. This method was not adequate here, however, because the solution foamed so much, that it was feared that unreacted soap might overflow the vessel.

The solution was cooled, and the seperated fatty acid was filtered off. The filtrate obtained in this process was used for determining the content of the cobalt. Fatty acid was dried on filter paper, dissolved in hot ethanol, and titrated by a standard alkaline solution.

*Cobalt.*—The amount of cobalt was determined by several methods. (i) Soaps were burnt to ashes, which were weighed as $Co_3O_4$. (ii) Cobalt was precipitated from the solution as a complex salt by $\alpha$-nitroso-$\beta$-naphthol. (iii) Cobalt was deposited on a platinum electrode electrolytically. (iv) The cobalt solution was titrated by an EDTA solution.

*Burning Method.*—Cobalt soap was heated in a porcelain crucible by a Bunsen burner. Stearic acid was carbonized at first, and then the whole mass was ignited and completely oxidized by strong heating. The residue was weighed as $Co_3O_4$.

*$\alpha$-Nitroso-$\beta$-naphthol Method.*—By adding an excess of hydrogen peroxide to the acidic solution of cobalt, cobalt ions were oxidized from bivalent to tervalent. The black cobaltic hydroxide precipitated from the solution by the addition of a sodium hydroxide solution. The precipitate was dissolved again by glacial acetic acid, and the dark brown solution obtained was diluted with some warm water and mixed with the solution of $\alpha$-nitroso-$\beta$-naphthol in acetic acid. The reddish brown precipitate was filtered off, dried at 130°C, and weighed as $(C_{10}H_6ONO)_3Co$.

*Electrodeposition Method.*—Cobalt stearate (0.1 g.) was decomposed by 0.1 N sulfuric acid (20 ml.), and the separated fatty acid was filtered off. The filtrate was concentrated to 10 ml., ammonium sulfate (0.5 g.) was added, and the solution was made alkaline with 0.1 N ammonia solution (40 ml.), and sodium bisulfate (0.02 g.) was added. With platinum plates as electrodes, the golden solution was electrolyzed with a current 0.2 amp. and 3.5 V. at 60°C for 8 hr. The cobalt metal deposited on the cathode was weighed after drying in an air-oven at 110°C.

*EDTA Titration.*—Cobalt soap (30 mg.) was decomposed by 0.3 N hydrochloric acid (20 ml.). The fatty acid was solidified to a mass. The solution was diluted to 70 ml. by water, murexide (ammonium purpurate) was added as an indicator[6], and the solution was neutralized by 1 N ammonia solution in some excess. The yellow solution was titrated by 0.01 M EDTA (disodium ethylenediamine tetraacetate), until the color of the solution became pink. The concentration of EDTA solution was calibrated by a standard cuprous nitrate solution.

*Water of Hydration.*—Cobalt soaps had been dried in a vacuum at room temperature. Pink species gained a tinge of blue, but other soaps did not change their colors substantially in this process. Their colors did not change during storage in an ambient atmosphere.

Inorganic cobalt salts contain some water of hydration, some of which could not be removed in the vacuum. It is possible for cobalt soaps to have such a tightly combined water of hydration. The water content was determined (i) by a Karl-Fischer reagent and (ii) by weighing after heating in a vacuum.

*Karl-Fischer Titration.*—From among the several methods of this technique, the inverse dead-stop method with "magic eye" titrometer was carried out[7]. The titration vessel was equipped with a draining cock, as proposed by Campbell[8].

The standard methanol used was an extra pure reagent, made by Takeda Chemicals Co., the water content of which was about 0.5% by volume. The Karl-Fischer reagent was prepared as usual[9] and calibrated by sodium acetate trihydrate.

The cobalt soaps did not dissolve, but were well dispersed in mixtures of methanol and pyridine, which were basic solvents of the reagent. However, because the soap was powder, it was difficult to place it in titration vessel. This was the main origin of errors.

*Dehydration in Vacuum at Heating.*—The decrease of weights was measured by a quartz spring balance in an evacuated glass tube at $10^{-3}$ mmHg. An electric furnace was used to heat the soap up to 150°C. The sensitivity of the quartz balance was 7.54 cm./g., and its accuracy was 0.2 mg. in weight. A sample of 0.1 g. was usually taken for measurements.

5) K. J. Mysels, H. H. Pomeroy and G. H. Smith, *Anal. Chem.*, **20**, 878 (1948).

6) H. Flaschka, *Mikrochemie*, **39**, 38 (1952).

7) R. Kieselbach, *Anal. Chem.*, **21**, 1578 (1949).

8) D. E. Campbell, ibid,. **25**, 203 (1953).

9) J. Mitchell, Jr., and D. M. Smith, "Aquametry", Interscience Publishers, Inc., New York (1948).

## Results and Discussion

**Free Fatty Acid.**—The amounts of free fatty acid in several samples of each species of cobalt stearate were measured. The average values are shown in Table I. The amount of free acid was relatively little. It was most in pink, but very little in red, soap. The following analyses were carried out with samples, the free acid of which had been completely extracted.

Table I. Free fatty acid contents in cobalt stearates

| | |
|---|---|
| Pink | 4.14 % |
| Blue | 2.36 % |
| Red | 0.70 % |

**Compositions.**—Several analyses of each species of cobalt stearate were executed by various methods. These results are tabulated together in Table II. Although the values were scattered in some ranges, the average values of each method and their mean are shown.

Theoretical compositions calculated from several possible formulas of cobalt stearate are shown in Table III. In comparing Table II with Table III, it is certain that three forms of cobalt stearate are neither basic nor acidic salt.

The blue form corresponds to anhydrous neutral soap, for it shows no water content. The red form must be dihydrate, judging from the content of hydration water. The observed

Table II. Observed compositions of cobalt stearates

| | Cobalt, % | | | | Stearic acid, % | Hydration water, % | | Total, % |
|---|---|---|---|---|---|---|---|---|
| | By burning to ashes | With α-nitroso-β-naphthol | By electro-deposition | By EDTA titration | By neutral-ization | By Karl-Fischer reagent | By heating in vacuum | |
| | 8.12 | 9.1 | 9.29 | | 82.6 | | 3.56 | |
| | 8.95 | 9.4 | 9.65 | | 87.0 | | 4.55 | |
| | 9.01 | 9.4 | 9.12 | | 81.8 | | 3.97 | |
| | | 10.8 | 9.52 | | 85.5 | | 6.34 | |
| Pink | | 12.1 | 9.25 | | 87.3 | | 3.91 | |
| | | 9.0 | | | | | 3.71 | |
| | | | | | | | 4.35 | |
| | | | | | | | 6.26 | |
| | | | | | | | 3.65 | |
| | av. 8.65 | av. 10.0 | av. 9.38 | | av. 84.8 | | av. 4.36 | |
| | | mean 9.34 | | | mean 84.8 | | mean 4.36 | mean 98.50 |
| | 8.94 | | 9.35 | 9.32 | 88.0 | −0.8 | 0.0 | |
| | 10.43 | | 10.15 | 9.63 | 90.9 | −0.5 | | |
| | 9.91 | | 10.15 | 9.59 | 92.5 | 1.4 | | |
| Blue | | | 10.33 | 9.34 | 91.5 | 0.26 | | |
| | | | 10.78 | 9.51 | 88.1 | | | |
| | | | 9.78 | 9.58 | 89.1 | | | |
| | | | 10.12 | 9.48 | 92.4 | | | |
| | | | 10.54 | | | | | |
| | av. 9.76 | | av. 10.14 | av. 9.49 | av. 90.4 | av. 0.1 | | |
| | | mean 9.80 | | | mean 90.4 | mean 0.0 | | mean 100.20 |
| | 7.88 | | 9.04 | 9.04 | 84.5 | 3.46 | 5.43 | |
| | 9.65 | | 9.11 | 9.21 | 86.0 | 4.40 | 5.67 | |
| | 8.24 | | 9.36 | 9.11 | 86.9 | 1.28 | 5.41 | |
| | 8.57 | | 9.18 | 9.01 | 78.6 | 5.48 | 5.72 | |
| Red | | | 9.26 | 9.01 | 87.6 | | | |
| | | | 9.71 | 9.02 | 87.6 | | | |
| | | | | 9.04 | | | | |
| | | | | 9.06 | | | | |
| | av. 8.65 | | av. 9.34 | av. 9.06 | av. 85.1 | av. 3.66 | av. 5.56 | |
| | | mean 9.02 | | | mean 85.1 | mean 4.61 | | mean 98.73 |

TABLE III. CALCULATED COMPOSITIONS OF COBALT STEARATES

| | Cobalt, % | Stearic acid, % | Water, % |
|---|---|---|---|
| Neutral salts, $(C_{17}H_{35}COO)_2Co$ | 9.42 | 90.58 | — |
| Monohydrate, $(C_{17}H_{35}COO)_2Co \cdot H_2O$ | 9.15 | 88.05 | 2.80 |
| Dihydrate, $(C_{17}H_{35}COO)_2Co \cdot 2H_2O$ | 8.90 | 85.64 | 5.46 |
| Basic salt, $(C_{17}H_{35}COO)Co(OH)$ | 16.40 | 83.60 | — |
| Acidic salt, $(C_{17}H_{35}COO)_2Co(C_{17}H_{35}COOH)$ | 6.47 | 93.53 | — |

contents of cobalt of these soaps were somewhat larger than the calculated values, for some of the combined fatty acid might be hydrolyzed and removed during the extraction by acetone.

The pink form shows a composition nearer to red dihydrate than to blue anhydrate. Experimental values are particularly scattered in this species. As the pink soap is an incipient product in metathesis, it may be natural that its composition is somewhat indefinite.

**Mechanism of Color Change.**—From these results, it has been ascertained that the difference of color is due to the degree of hydration of these soaps. In the previous paper[4], it was found that under some conditions the pink soap thus formed soon turned blue and then red later in solution. This corresponds with the change of the amount of water of hydration, which first decreases and then increases again. This process seems very strange, but the following interpretation may be proposed.

The alkaline soap in aqueous ethanol takes the form of micelles, in which lyophilic ionic groups of soap molecules exist in the outer layer against solvent molecules. Ionic groups dissociate in different degrees, according to the solvent ratio in solution. When the cobalt ions are added, dissociated soap ions in the outer lyophilic layer react with cobalt ions immediately. Therefore, in the incipiently formed pink soap there remains the original micelle structure of alkaline soap, as will be discussed in the later part of these studies.

With the existence of sufficient alkali, cobalt soap turns gradually to red dihydrate, which is the most stable form in these solvents. When the alkali is insufficient, the dissociation of alkaline soap is greatly suppressed, and therefore the ionic reactions proceed limitedly. In these circumstances the yield of cobalt soap is little, and much free acid exists in the formed soap.

When the solvent ratio is higher than 1 : 1, the solvent becomes somewhat oleophilic and the formed pink soap turns blue, perhaps by an inversion of the micelle structure. In this case some of the lyophobic hydrocarbon chains appear outside. As the soap becomes less lyophilic in this system, blue crystals tend to rise to the surface of the solution.

In the following time, water molecules gradually penetrate into the interior of the micelles of blue soap and adhere to the hydrophilic cobalt ions as waters of hydration. As the penetration of water is difficult through such a thick layer of hydrocarbon chains, the change of color from blue to red generally occurs slowly.

## Summary

Pink, blue and red cobalt stearates were analyzed and their compositions were determined. From these results, it has been confirmed that blue soap is anhydrate and red soap is dihydrate. The pink soap has a rather indefinite composition nearer to red soap. A mechanism of the color changes was proposed based on the inversion of the micelle structure under some circumstances.

The author expresses his gratitude to Professor Bunnosuke Yamaguchi for his kind advice throughout this work. He is also indebted to Mr. Itaru Mita for his executions of EDTA titrations, and to Messrs. Hirokazu Watanabe, Satoshi Ayano and Takeo Ozawa for their assistance on experiments.

*Institute for Science and Technology*
*The University of Tokyo*
*Meguro-ku, Tokyo*

# *Physicochemical Studies on Cobalt Salts of Higher Fatty Acids. III. Spectrophotometric Specifications of Colors of Cobalt Soaps*

By Hirotaro KAMBE

(Received February 28, 1961)

Cobalt soaps of higher saturated fatty acids have been described generally as pink crystals. Recently Herron and Pink[1] described rose-pink cobalt laurate dihydrate and purple anhydrate, which was obtained by the dehydration of pink soap in boiling organic solvents.

In a previous paper of this series[2], three species of cobalt soap of different colors were obtained by metathesis in aqueous ethanol under some conditions. From results of analyses, it was ascertained that blue soap is anhydrate, red soap is dihydrate, and pink soap has a degree of hydration near to that of dihydrate[3].

In the present paper, the colors of these soaps will be specified by spectrophotometry. Reflection spectra and a chromaticity diagram of these colors will be shown. Relations of these colors with each other will also be discussed.

## Experimental

**Materials.**—The same samples of cobalt stearates were used as for the previous papers[2,3].

**Reflection Spectra.**—Reflection spectra of soaps were measured with a Shimadzu QR-50 quartz spectrophotometer, to which an integrating sphere was attached. Reflection coefficients expressed in percentages were plotted against wavelengths between 350 and 700 m$\mu$ to get reflection curves.

**Graphical Representation of Chromaticity.**—Reflection curves were analyzed by a method proposed by the International Commission on Illumination (I. C. I.)[4]. Tristimulus values, $X$, $Y$ and $Z$, were determined from reflection curves by graphical integrations with the thirty-selected-ordinate method[4].

$$X=0.03268\sum R_x(\lambda_n) \qquad Y=0.03333\sum R_y(\lambda_n)$$
$$Z=0.03938\sum R_z(\lambda_n) \qquad (1)$$

where $R(\lambda_n)$'s are reflection coefficients of the sample at selected wavelengths (Table I).

Trichromatic coefficients, $x$, $y$ and $z$ were calculated by the formulas

$$x=\frac{X}{X+Y+Z} \qquad y=\frac{Y}{X+Y+Z}$$

Table I. Thirty selected ordinates for illuminant C

| Ordinate number | ($X$) Wavelength m$\mu$ | ($Y$) Wavelength m$\mu$ | ($Z$) Wavelength m$\mu$ |
|---|---|---|---|
| 1 | 424.4 | 465.9 | 414.1 |
| 2 | 435.5 | 489.4 | 422.2 |
| 3 | 443.9 | 500.4 | 426.3 |
| 4 | 452.1 | 508.7 | 429.4 |
| 5 | 461.2 | 515.1 | 432.0 |
| 6 | 474.0 | 520.6 | 434.3 |
| 7 | 531.0 | 525.4 | 436.5 |
| 8 | 544.3 | 529.8 | 438.6 |
| 9 | 552.4 | 533.9 | 440.6 |
| 10 | 558.7 | 537.7 | 442.5 |
| 11 | 564.1 | 541.4 | 444.4 |
| 12 | 568.9 | 544.9 | 446.3 |
| 13 | 573.2 | 548.4 | 448.2 |
| 14 | 577.3 | 551.8 | 450.1 |
| 15 | 581.3 | 555.1 | 452.1 |
| 16 | 585.0 | 558.5 | 454.0 |
| 17 | 588.7 | 561.9 | 455.9 |
| 18 | 592.4 | 565.3 | 457.9 |
| 19 | 596.0 | 568.9 | 459.9 |
| 20 | 599.6 | 572.5 | 462.0 |
| 21 | 603.3 | 576.4 | 464.1 |
| 22 | 607.0 | 580.5 | 466.3 |
| 23 | 610.9 | 584.8 | 468.7 |
| 24 | 615.0 | 589.6 | 471.4 |
| 25 | 619.4 | 594.8 | 474.3 |
| 26 | 624.2 | 600.8 | 477.7 |
| 27 | 629.8 | 607.7 | 481.8 |
| 28 | 636.6 | 616.1 | 487.2 |
| 29 | 645.9 | 627.3 | 495.2 |
| 30 | 663.0 | 647.4 | 511.2 |

$$z=\frac{Z}{X+Y+Z} \qquad (2)$$

They were plotted on an I. C. I. chromaticity diagram. Dominant wavelength $\lambda_d$, purity $p_e$, and brightness $Y$ were determined for each sample.

## Results and Discussion

The reflection spectra of several samples of each typical color are shown in Figs. 1—3. Their tristimulus values and trichromatic coefficients have been calculated in Table II and plotted on an I. C. I. chromaticity diagram in Fig. 4. Their dominant wavelengths, purities,

* Present address. Aeronautical Research Institute, The University of Tokyo, Meguro-ku, Tokyo.

1) R. C. Herron and R. C. Pink, *J. Chem. Soc.*, **1956**, 3948.
2) H. Kambe, This Bulletin, **34**, 1786 (1961).
3) H. Kambe, ibid., **34**, 1790 (1961).
4) A. C. Hardy, "Handbook of Colorimetry", Cambridge, Mass. (1936).

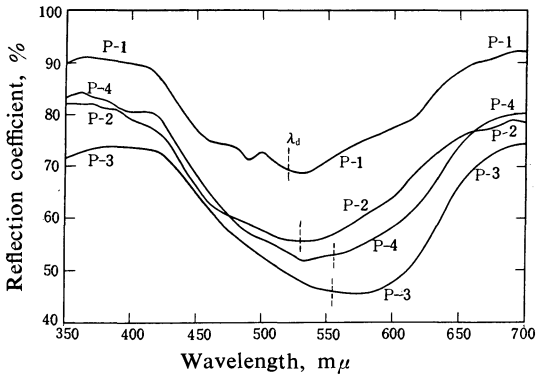



Fig. 1. Reflection curves of pink cobalt stearates.

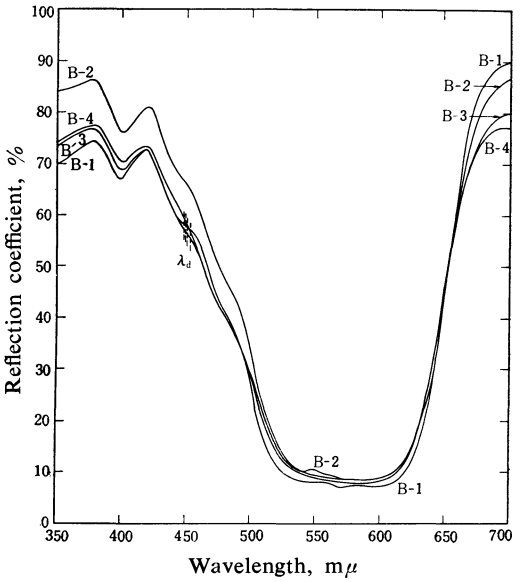



Fig. 2. Reflection curves of blue anhydrous cobalt stearates.

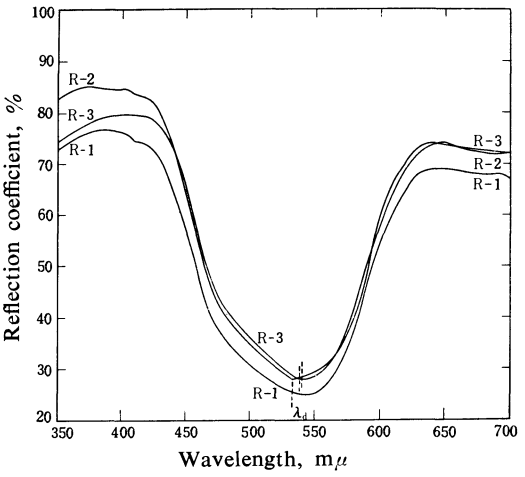



Fig. 3. Reflection curves of red cobalt stearate dihydrates.

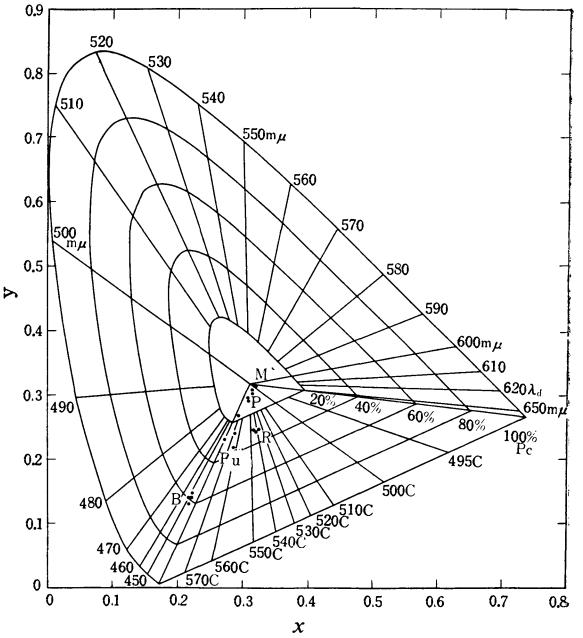



Fig. 4. I. C. I. chromaticity diagram.

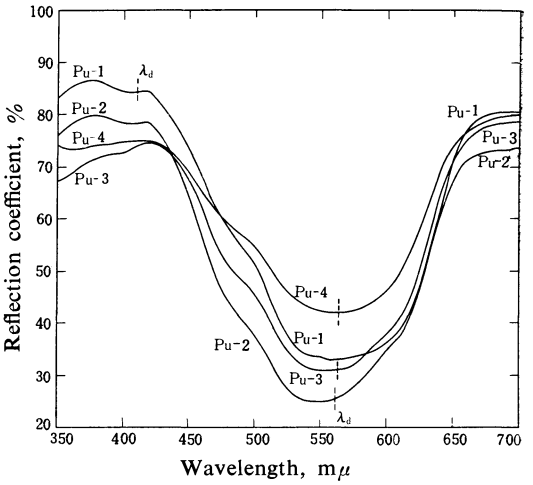



Fig. 5. Reflection curve of purple cobalt stearates.

and brightnesses are also tabulated in Table II.

The dominant wavelengths $\lambda_d$ of each spectrum are shown with dotted lines. In color language, blue and red soaps must be called violet and magenta respectively.

Pink soaps (Fig. 1) show a broad absorption band with a maximum at 530~540 mμ. The dominant wavelength of pink soaps varies within a wide range, from pure pink at 520c mμ to bluish pink at 565c mμ, but it does not essentially differ from that of red soaps. Pink soaps have smaller purities and larger brightnesses than red soaps.

TABLE II. CHROMATICITY COEFFICIENTS OF COLORS OF SEVERAL TYPICAL COBALT STEARATES

| System | Tristimulus values | | | Trichromatic coefficients | | | Dominant wavelength | Purity | Brightness |
|---|---|---|---|---|---|---|---|---|---|
| | $X$ | $Y$ | $Z$ | $x$ | $y$ | $z$ | $\lambda_d$, m$\mu$ | $p_c$, % | $Y$, % |
| (Pink soaps) | | | | | | | | | |
| P-1 | 76.24 | 73.81 | 91.78 | 0.315 | 0.305 | 0.380 | 520c* | 5.5 | 73.81 |
| P-2 | 63.38 | 59.74 | 77.52 | 0.316 | 0.298 | 0.386 | 530c | 8.5 | 59.74 |
| P-3 | 67.13 | 63.79 | 86.23 | 0.309 | 0.294 | 0.397 | 554c | 9.0 | 63.79 |
| P-4 | 59.65 | 55.86 | 77.89 | 0.308 | 0.289 | 0.403 | 555c | 10.5 | 55.86 |
| (Blue soaps) | | | | | | | | | |
| B-1 | 21.26 | 12.67 | 64.43 | 0.216 | 0.129 | 0.655 | 448 | 62.5 | 12.67 |
| B-2 | 24.45 | 15.45 | 73.07 | 0.216 | 0.137 | 0.647 | 452 | 60.5 | 15.45 |
| B-3 | 21.76 | 13.74 | 63.20 | 0.220 | 0.139 | 0.641 | 449 | 57.0 | 13.74 |
| B-4 | 22.63 | 14.78 | 64.49 | 0.222 | 0.145 | 0.633 | 450 | 56.5 | 14.78 |
| (Red soaps) | | | | | | | | | |
| R-1 | 48.84 | 36.22 | 62.96 | 0.330 | 0.245 | 0.425 | 533c | 32.5 | 36.22 |
| R-2 | 53.78 | 40.25 | 71.30 | 0.325 | 0.243 | 0.431 | 538c | 32.5 | 40.25 |
| R-3 | 53.34 | 40.25 | 71.21 | 0.324 | 0.244 | 0.432 | 540c | 31.5 | 40.25 |

* 520c m$\mu$ means complementary to color of 520 m$\mu$.

TABLE III. CHROMATICITY COEFFICIENTS OF SOME PURPLE COBALT STEARATES AND PINK COBALT STEARATES OBTAINED IN AQUEOUS METHANOL

| System | Tristimulus values | | | Trichromatic coefficients | | | Dominant wavelength | Purity | Brightness |
|---|---|---|---|---|---|---|---|---|---|
| | $X$ | $Y$ | $Z$ | $x$ | $y$ | $z$ | $\lambda_d$, m$\mu$ | $p_c$, % | $Y$, % |
| (Purple soaps obtained from blue soaps) | | | | | | | | | |
| Pu-1 | 46.22 | 39.17 | 84.23 | 0.272 | 0.231 | 0.497 | 410 | 27.5 | 39.17 |
| Pu-2 | 39.06 | 29.53 | 67.90 | 0.286 | 0.216 | 0.497 | 561c | 36.0 | 29.53 |
| (Purple soaps obtained from red and pink soaps) | | | | | | | | | |
| Pu-3 | 45.26 | 37.66 | 74.94 | 0.287 | 0.239 | 0.475 | 562c | 27.0 | 37.66 |
| Pu-4 | 52.34 | 47.41 | 78.73 | 0.293 | 0.266 | 0.441 | 564c | 17.0 | 47.41 |
| (Pink soaps obtained in aqueous methanol) | | | | | | | | | |
| M-1 | 83.21 | 81.61 | 95.46 | 0.320 | 0.314 | 0.367 | 493c | 3.0 | 81.61 |
| M-2 | 85.91 | 84.42 | 98.34 | 0.320 | 0.314 | 0.366 | 493c | 3.0 | 84.42 |

Blue anhydrates (Fig. 2) show a large absorption band with a broad maximum at 580~590 m$\mu$, and a shallow but sharp absorption band at 400 m$\mu$. The blue color of this species originates from a large reflection at shorter wavelengths.

Red dihydrates (Fig. 3) show a deep but relatively sharp absorption band at 540~550 m$\mu$. Sometimes the spectra of blue soaps have a small shoulder at a corresponding position, arising from the red soap also present.

When blue soap was taken out of the solution at a half-turned-red state, purple soap was obtained. Pink and red soaps also became purple when they were immersed in pure ethanol for a long time. These samples are shown in Figs. 4 and 5, and their trichromatic coefficients are tabulated in Table III.

Purple soaps have dominant wavelengths between those of pink and blue soaps. Purple soaps obtained from blue soap have relatively larger purities. In these samples the dominant wavelength seems to change abruptly from 564c m$\mu$ to 410 m$\mu$, but it is clear from the chromaticity diagram (Fig. 4) that these dominant wavelengths are continuous. The main origin of purple color changes in this range, however, from an absorption band at 560 m$\mu$ to a reflection band at 400 m$\mu$.

In this way, it is established that among cobalt soaps of different colors, red and pink soaps are the same in nature, although their colors differ in purity and brightness, and that blue soap continues to pink or red soap through purple soaps.

Cobalt stearate may be formed by metathesis in aqueous methanol instead of ethanol[2], but the color of the soaps thus formed is pale pink. Their reflection curves are very flat, with a maximum at about 500 m$\mu$, as shown in Fig. 6 and in Table III. It is characteristic for them that their purities are small and

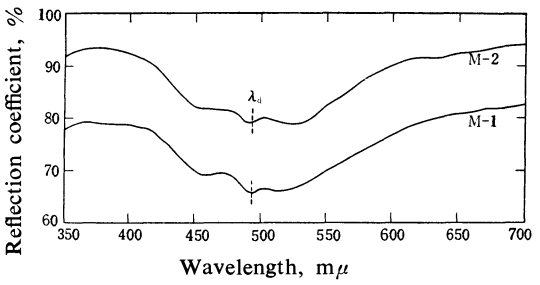



Fig. 6. Reflection curves of cobalt stearates obtained in aqueous methanol.

their brightnesses are large, and their maximum absorption occurs at a shorter wavelength.

## Summary

The colors of three species of cobalt stearates were specified by I. C. I. chromaticity coefficients. Reflection spectra have been compared with each other, and it has been found that these colors are continuous in nature.

Pink soaps have dominant wavelengths in a wide range from 520c~555c mμ and show small purities and large brightnesses. Red soaps have essentially the same dominant wavelengths as that of pink soaps at 530c~540c mμ, but they show comparatively large purities and small brightnesses, because they are darker than pink soaps. They must be called magenta in color language.

Blue soaps must be called violet rigorously, for they show dominant wavelengths at about 450 mμ. They have larger purities and smaller brightnesses. Between blue and pink, many tones of color from violet to purple exist continuously. It is certain that these colors are related to each other.

The pale pink cobalt stearates obtained in aqueous methanol were specified in the same way.

The author expresses his gratitude to Professor Bunnosuke Yamaguchi, for his advice throughout this work. He is also indebted to Messrs. Hiroshi Kayano and Teijiro Mizuno for their assistance in spectrophotometry.

*Institute for Science and Technology*
*The University of Tokyo*
*Meguro-ku, Tokyo*

# *Physicochemical Studies on Cobalt Salts of Higher Fatty Acids. IV. Ionic Nature of Cobalt Soaps, Revealed in Infrared Absorption Spectra and Magnetic Susceptibilities*

By Hirotaro KAMBE* and Itaru MITA*

(Received March 11, 1961)

In the previous papers of these studies[1-3], three forms of cobalt soap with different colors —in other words, with different degrees of hydration—were found. As they are salts of fatty acid, they must be composed of cobalt and fatty acid ions.

In the present paper, their infrared absorption spectra and magnetic susceptibilities are measured. It is concluded that as the infrared absorption bands of carboxylate ion are found, these soaps are essentially ionic in nature. Magnetic moments of cobalt ion in these soaps, calculated from magnetic susceptibilities, support this conclusion.

Infrared spectra of cobalt salts of normal fatty acids, from formic to stearic acid, were observed by Duval, Lecomte, and Douvillé[4]. They confirmed that the carboxylic groups in these salts are essentially ionic in nature.

Herron and Pink[5] measured the magnetic susceptibilities of cobalt stearate and laurate, and of cobalt laurate dihydrate. The magnetic moments of cobalt ions in these soaps were given as $\mu_{eff}=5.00$, 5.06 and 5.07 BM respectively. Moreau and Vatteroni[6] measured the magnetic susceptibilities of the cobalt salts of fatty acids with carbon numbers between 1

* Present address: Aeronautical Research Institute, The University of Tokyo, Meguro-ku, Tokyo.

1) H. Kambe, This Bulletin, **34**, 1786 (1961).
2) H. Kambe, ibid., **34**, 1790 (1961).
3) H. Kambe, ibid., **34**, 1794 (1961).
4) C. Duval, J. Lecompte and F. Douvillé, *Ann. phys.*, [11], **17**, 5 (1942).
5) R. C. Herron and R. C. Pink, *J. Chem. Soc.*, **1956**, 3948.
6) C. Moreau and M. Vatteroni, *Compt. rend.*, **237**, 1090 (1953).

and 18. They have found that the susceptibilities of cobalt salts of higher fatty acids are somewhat larger than that of inorganic cobalt sulfate.

The experimental results obtained in the present paper will be discussed in comparison with these investigations.

## Experimental

**Materials.**—Cobalt stearate, palmitate, and myristate, of each typical color, obtained in the previous paper[1] were used as samples. Stearic acid, sodium stearate, and cobalt hydroxide, which had been purified as usual, were used references to the infrared investigations.

**Infrared Absorption Spectra.**—Infrared absorption spectra were measured chiefly with a Perkin Elmer Model 112 single beam spectrophotometer, using a sodium chloride or calcium fluoride prism. Some samples were measured also with a Perkin Elmer Model 12B double beam spectrophotometer at the Laboratories of Mitsubishi Kasei Co*2.

As cobalt soaps are generally insoluble in common solvents, powdered samples were used in the form of potassium bromide disks, or mulls in Nujol or in hexachlorobutadiene (HCB).

The potassium bromide disk method was used mainly in the range of wave number below 1700 $cm^{-1}$. The sample soaps and potassium bromide were carefully dried and pulverized to pass through a sieve of 200~250 meshes per inch. A small percentage was mixed with potassium bromide powder and pressed at 10,000 $kg./cm^2$ to form a disk.

Above 2700 $cm^{-1}$, the Nujol mull or HCB mull method was used exclusively. Mulls were placed between rock salt plates. Nujol shows strong absorptions of C-H bond, which overlap C-H absorptions of the soap. Although HCB is so volatile that it is difficult to make mulls with it, it was chiefly used in the range of 2700~4000 $cm^{-1}$, for it shows no absorption above 1700 $cm^{-1}$.

**Magnetic Constants.**—The magnetic susceptibility $\chi_H$ of cobalt soap, mixed with zinc oxide, was measured by Gouy's method*3. $\chi_H$ was corrected for ferromagnetic imprities by plotting susceptibilities against reciprocal field strength. Extrapolation to infinite field strength gives $\chi_\infty$, which is substantially free from ferromagnetic effects.

As the specific susceptibility of zinc oxide, $\chi_{ZnO}$, had been given as $-0.26\times10^{-6}$ c. g. s., the specific susceptibility of soap, $\chi$, was determined by the following formula:

$$\chi_\infty=\frac{w}{100}\chi+\frac{100-w}{100}\chi_{ZnO} \qquad (1)$$

in which $w$ is the concentration of soap in per cent by weight. Molar susceptibility is calculated by a formula:

$$\chi_M=M\cdot\chi \qquad (2)$$

in which $M$ is the molecular weight of soap.

The diamagnetic component of susceptibility, $\sum\chi_{dia}$, was corrected by a formula

$$\chi_M=\chi_{para}+\sum\chi_{dia} \qquad (3)$$

The diamagnetic susceptibilities of the constituents of which are shown in Table I.

The magnetic moments in Bohr magneton (BM) were calculated by a formula:

$$\mu_{eff}=2.839\sqrt{\chi_{para}\cdot T} \quad (BM) \qquad (4)$$

TABLE I. SPECIFIC DIAMAGNETIC SUSCEPTIBILITIES, $-\chi_{dia}\cdot10^6$ (c.g.s./g.)

| | |
|---|---|
| Stearate ion | 209* |
| Hydration water | 13[7] |
| Cobalt(II) ion | 12[8] |

* This value was found in magnesium, zinc and cadmium stearates[7].

## Results and Discussion

**Infrared Absorption Spectra.**—The wave numbers of the absorption maxima in the infrared spectra of cobalt soaps are assigned and tabulated in Tables II and III.

*Absorptions by Hydrocarbon Chain.* — Among species of the same color, the chain length of fatty acid did not significantly influence the spectrum. Band progression at 1200~1300 $cm^{-1}$, due to hydrocarbon chain, depends to some extent upon the length of the chain, but the absorption bands of cobalt soaps are weaker than that of stearic acid.

The absorption bands of C-H stretching vibrations, i. e. the out-of-phase vibration of $CH_2$ at 2865, the in-phase one at 2935, and the asymmetrical vibration of $CH_3$ at 2970 $cm^{-1}$, and the bands of symmetrical bending of $CH_2$ at 1465 $cm^{-1}$ were always observed in all soaps, without distinction of color. The symmetrical bending vibration band of $CH_3$ at 1375 $cm^{-1}$ was found in red soaps, but in other soaps it was not readily indentified.

*Absorptions by Carboxylate Ion.* — Absorption spectra in the range of 1250~1800 $cm^{-1}$ are shown in Figs. 1—3.

It is well known that in free fatty acid carboxyl groups of two molecules are donded by hydrogen bonds to take a dimeric form. The absorption of a carboxyl group in this state reveals its C=O stretching vibration band near 1700 $cm^{-1}$ (cf. Table III). In cobalt soaps, two absorption bands of carboxyl group were found at 1400 and 1550 $cm^{-1}$, instead of one band at 1700 $cm^{-1}$. They correspond to the symmetric and antisymmetric stretching vibrations of carboxylate ion, $-\left[C\begin{matrix}O\\O\end{matrix}\right]^-$, as

*2 With the latter instrument, measurements were executed by Mr. S. Morita.

*3 Magnetic measurements were carried out by Dr. Y. Matsunaga at Department of Chemistry, Faculty of Science, The University of Tokyo.

7) M. Prasad, C. R. Kanekar, S. P. Walvekar and D. D. Khanolkar, *J. Chem. Phys.*, **18**, 936 (1950).

8) P. W. Selwood, *Chem. Revs.*, **38**, 41 (1946).

TABLE II. INFRARED ABSORPTION SPECTRA OF COBALT SOAPS MEASURED WITH A P. E. 112 SPECTROPHOTOMETER ($cm^{-1}$)*

| System | Progression bands | | | | | Sym. bend. $CH_3$ | Sym. str. $COO^-$ | Asym. bend. $CH_3$ | Sym. bend. $CH_2$ | Asym. str. $COO^-$ | Out-of-phase str. $CH_2$ | In-phase str. $CH_2$ | Asym. str. $CH_3$ | Str. OH | |
|---|---|---|---|---|---|---|---|---|---|---|---|---|---|---|---|
| (Pink soaps) | | | | | | | | | | | | | | | |
| Cobalt stearate | w 1270 | w 1284 | w 1303 | w 1320 | w 1336 | | s 1410 | s 1441 | s 1467 | s 1559 | s 2870 | s 2940 | m 2970 | s 3300 | |
| Cobalt palmitate | w 1260 | w 1288 | w 1297 | w 1318 | w 1334 | | s 1410 | s 1441 | s 1467 | s 1559 | s 2870 | s 2940 | m 2970 | s 3290 | |
| Cobalt myristate | | w 1290 | | w 1316 | w 1334 | | s 1410 | s 1441 | s 1467 | s 1559 | s 2870 | s 2940 | m 2970 | s 3300 | |
| (Blue soaps) | | | | | | | | | | | | | | | |
| Cobalt stearate | | w 1287 | 1307 | w 1322 | w 1340 | m 1396 | | | m 1461 | s 1525 | s 2860 | s 2935 | m 2970 | | |
| Cobalt palmitate | | | w 1297 | w 1322 | w 1340 | m 1396 | | | m 1461 | s 1523 | s 2860 | s 2935 | m 2970 | | |
| Cobalt myristate | | | w 1296 | w 1322 | w 1341 | m 1396 | | | m 1461 | s 1523 | s 2860 | s 2935 | m 2970 | | |
| (Red soaps) | | | | | | | | | | | | | | | |
| Cobalt stearate | | w 1285 | w 1305 | w 1322 | w 1336 | w 1374 | s 1412 | | s 1470 | s 1535 | s 2865 | s 2935 | m 2970 | s 3260 | s 3400 |
| Cobalt palmitate | | w 1278 | w 1296 | w 1322 | w 1340 | w 1376 | m 1412 | | s 1469 | s 1534 | s 2865 | s 2935 | m 2970 | s 3260 | s 3400 |
| Cobalt myristate | | | w 1292 | w 1318 | w 1340 | m 1374 | s 1412 | | s 1468 | s 1532 | s 2865 | s 2935 | m 2970 | s 3260 | s 3400 |

TABLE III. INFRARED ABSORPTION SPECTRA OF COBALT SOAPS MEASURED WITH A P. E. 21B, BY KBr DISK METHOD ($cm^{-1}$)*

| System | Rocking $CH_2$ | Out-of-plane deform. OH | Str. C–C | Progression bands | Sym. str. $COO^-$ | Asym. bend. $CH_3$ | Sym. bend. $CH_2$ | Asym. str. $COO^-$ | Str. C=O | Str. OH | Out-of-phase str. $CH_2$ | In-phase str. $CH_2$ | Asym. str. $CH_3$ |
|---|---|---|---|---|---|---|---|---|---|---|---|---|---|
| Blue cobalt stearate | w 720 | | w 1110 | v. w several | m 1400 | | m 1468 | m 1532 | | | s 2850 | s 2920 | sh 2970 |
| Red cobalt stearate | w 720 | | w 1110 | v. w several | m 1415 | | m 1470 | s 1532 | | | s 2850 | s 2920 | sh 2970 |
| Sodium stearate | w 720 | | v. w 1110 | v. w several | m 1424 | m 1445 | m 1475 | s 1560 | | | s 2850 | s 2920 | sh 2960 |
| Stearic acid | m 720 m 730 | m 940 | w 1110 | w 1190～1300 | m 1412 m 1432 | | m 1468 | | s 1700 | d. m 2650 | s 2850 | s 2920 | sh 2960 |

* s: strong; m: medium; w: weak; v. w: very weak; sh: shoulder; d: diffuse

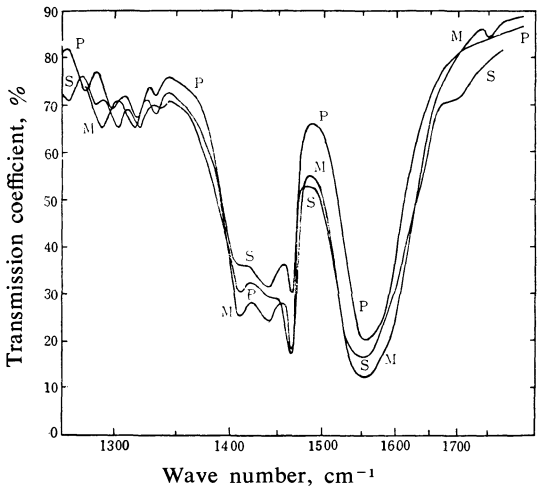



Fig. 1. Infrared absorption spectra of pink cobalt soaps.
S: Cobalt stearate P: Cobalt palmitate
M: Cobalt myristate

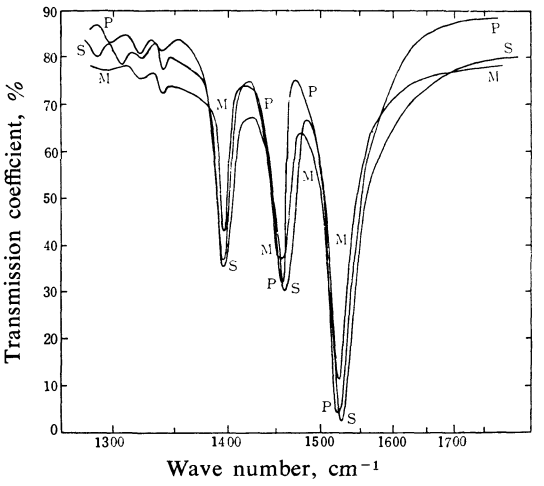



Fig. 2. Infrared absorption spectra of blue cobalt soaps.
S: Cobalt stearate P: Cobalt palmitate
M: Cobalt myristate

pointed out by Duval, Lecompte and Douvillé[4]. Their conclusion was based on the deformation vibration modes of carboxylate ions, appearing at lower frequency range than ours. Their results were stated to be uncertain at a higher frequency range owing to the insufficient resolving power of their instrument.

From this result it has been concluded definitely that all cobalt soaps obtained in our experiments are ionic in nature. As a reference, spectra of free stearic acid and sodium stearate are shown in Table III. Stearic acid distinctly shows a stretching vibration of C=O at 1700

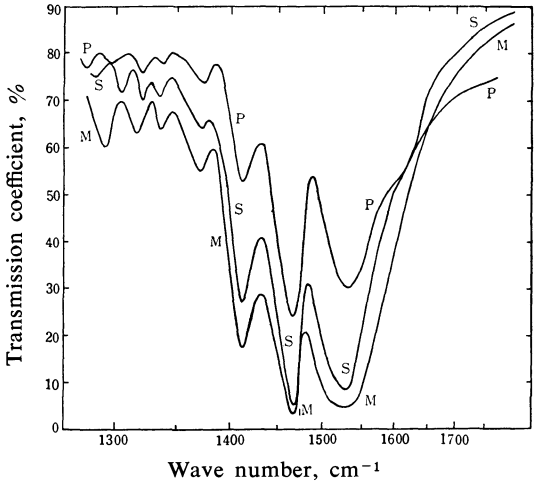



Fig. 3. Infrared absorption spectra of red cobalt soaps.
S: Cobalt stearate P: Cobalt palmitate
M: Cobalt myristate

$cm^{-1}$, while no band was found at 1550 $cm^{-1}$ corresponding to the antisymmetric vibration of carboxylate ion. In place of the symmetric stretching band of carboxylate ion at 1400 $cm^{-1}$, there appeared the C–O stretching band and O–H in-plane deformation band of $-C\begin{matrix}O\\OH\end{matrix}$. Naturally, the OH stretching band at 2650 $cm^{-1}$ and the OH out-of-plane deformation band at 940 $cm^{-1}$ appeared in the spectrum of stearic acid.

Sodium stearate shows carboxylate bands at 1424 and 1560 $cm^{-1}$ and an absorption by the asymmetrical bending of $CH_3$ at 1445 $cm^{-1}$, which appears in pink soaps, exclusively. This may indicate the similarity between sodium soap and pink cobalt stearate.

*Absorptions by Hydroxyl Bond.* — In spectra of cobalt soaps with different colors of the same fatty acid, several differences were found.

In red and pink soaps, absorptions by stretching vibration of OH bonds appeared in the 3200~3400 $cm^{-1}$ region, but in blue soaps they were completely lacking. This is in accordance with the results of analyses of water content[2]. In pink soaps, a broad peak reveals itself at 3300 $cm^{-1}$, but in red soap, two peaks appear at 3260 and 3400 $cm^{-1}$.

The hydroxyl bond of cobalt hydroxide shows a very sharp band of free OH vibration at 3640 $cm^{-1}$, which does not exist in the spectrum of every soap. Liquid water shows a peak of hydrogen-bonded OH at 3410 $cm^{-1}$. In comparison with these data, water molecules in cobalt soaps were attached to cobalt ion with stronger bonds than hydrogen-bonds in

TABLE IV. MAGNETIC CONSTANTS OF COBALT SOAPS ($T$=297°K)

| | $\chi_H \cdot 10^6$ | | $\chi_\infty \cdot 10^6$ | w | $\chi \cdot 10^6$ | $\chi_M \cdot 10^6$ | $\sum\chi_{dia}10^6$ | $\chi_{para} \cdot 10^6$ | $\mu$ |
|---|---|---|---|---|---|---|---|---|---|
| | $H$=22500 | 16400 | (calcd.) | wt. % | | | | | BM |
| | $1/H \cdot 10^4$=0.444 | 00610 | 0 | | | | | | |
| Red cobalt stearate dihydrate | | | | | | ($M$=661.89) | | | |
| | 3.16 | 3.37 | $2.59_8$ | | | | | | |
| | 3.07 | 3.27 | $2.53_5$ | | | | | | |
| | | | Av. 2.57 | 19.8 | $14.0_3$ | 9286.3 | −456 | 8830.3 | $4.59_7$ |
| Blue cobalt stearate anhydrate | | | | | | ($M$=625.86) | | | |
| | 2.48 | 3.57 | $2.23_9$ | | | | | | |
| | 2.51 | 2.61 | $2.24_2$ | 18.8 | $13.0_3$ | 8155.0 | −430 | 7725.0 | $4.30_0$ |
| | | | Av. 2.24 | | | | | | |

TABLE V. ELECTRONIC CONFIGURATIONS OF COBALT(II) COMPLEXES[9,10]

| Type | Coordination number | Geometry of complex | Electronic configurations (3d 4s 4p 4d 5s) | Hybrid orbitals | Observed magnetic moment $\mu_{eff}$, BM |
|---|---|---|---|---|---|
| Free $Co^{2+}$ ion | | | ↑↓ ↑↓ ↑ ↑ ↑ \| □ \| □ □ □ \| □ □ □ □ □ \| □ | | |
| Spin-free or ionic covalent | 6 | octahedral | ↑↓ ↑↓ ↑ ↑ ↑ \| ×× \| ×× ×× ×× \| ×× ×× ×× \| □ | $(4s)(4p)^3(4d)^2$ | 4.9～5.6 |
| | 4 | tetrahedral | ↑↓ ↑↓ ↑ ↑ ↑ \| ×× \| ×× ×× ×× \| □ □ □ □ □ \| □ | $(4s)(4p)^3$ | 4.3～4.8 |
| | 4 | square, planar | ↑↓ ↑↓ ↑ ↑ ↑ \| ×× \| ×× ×× □ \| ×× □ □ □ □ \| □ | $(4s)(4p)^2(4d)$ | 4.8～5.4 |
| Spin-paired covalent | 4 | square, planar | ↑↓ ↑↓ ↑↓ ↑ ↑ \| ×× \| ×× ×× □ \| □ □ □ □ □ \| □ | $(3d)(4s)(4p)^2$ | 2.1～2.9 |
| | 6 | presumably tetragonal (a) | ↑↓ ↑↓ ↑↓ ↑ ↑ \| ×× \| ×× ×× ×× \| ×× □ □ □ □ \| □ | $(3d)(4s)(4p)^3(4d)$ | 1.7～2.0 |
| | | (b)* | ↑↓ ↑↓ ↑↓ ×× ×× \| ×× \| ×× ×× ×× \| □ □ □ □ □ \| ↓ | $(3d)^2(4s)(4p)^3$ | |

×× : Bonding orbitals.

* Figgis and Nyholm[9] proposed originally this configuration, but considered later that this improbable.

free water. Therefore, it was concluded that water in cobalt soaps exists as hydration water.

**Magnetic Susceptibilities.** — Observed values of magnetic susceptibilities and magnetic moments, calculated as stated above, of red and blue cobalt stearates are shown in Table IV.

Figgis and Nyholm[9] have shown that, according to magnetic moment, cobalt(II) compounds may be classified into two types, that is, the spin-free or ionic covalent type and the spin-paired covalent type, as shown in Table V. The number of unpaired electrons, $n$, in these configurations is three and one. Therefore, the spin only value of magnetic moment, $\mu_{eff}=\sqrt{n(n+2)}$, is 3.88 and 1.73 BM, respectively. The observed values of many complexes of each type were 4.2～5.6 BM in the spin-free type, and 1.7～2.9 BM in the spin-paired type, as shown in Table V.

On the basis of these facts it has been concluded that the cobalt soaps used in the present paper were spin-free or ionic covalent complexes. This conclusion is completely consistent with the results of infrared absorption measurements.

Observed values of magnetic moments of cobalt(II) complexes are generally larger than spin only values, for the contribution of the orbital motion of electrons was not completely quenched in them owing to the presence of ligand fields and spin-orbit couping. Among ionic covalent complexes, the orbital contribution is smaller in tetrahedral $sp^3$ orbitals than in octahedral $sp^3d^2$ orbitals. This is based on the difference of multiplicities of ground states in these configurations[10].

Although our values are somewhat smaller than that of Figgis and Nyholm, blue and red cobalt soaps must correspond to the $(4s)(4p)^3$ tetrahedral four-covalent complex and the $(4s)(4p)^3(4d)^2$ octahedral six-covalent complex respectively. Holm and Cotton[10] have proposed the $(4s)(4p)^2(4d)$ square planar, ionic covalent type for some cobalt(II) complexes, but this configuration may be excluded from our cases by considerations of color.

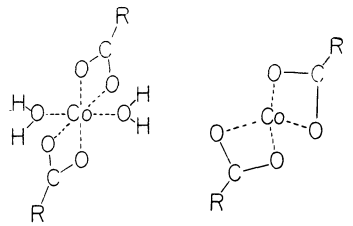
9) B. N. Figgis and R. S. Nyholm, *J. Chem. Soc.*, **1954**, 12; **1959**, 331, 338.

10) R. H. Holm and F. A. Cotton, *J. Chem. Phys.*, **31**, 788 (1959); **32**, 1168 (1960); *J. Am. Chem. Soc.*, **82**, 2979, 2983 (1960).

The magnetic moments of rose-pink cobalt laurate dihydrate and purple anhydrate of cobalt stearate and laurate obtained by Herron and Pink[5] were larger than our values, as has been shown before. In contrast with our results, they found no difference in magnetic moments between anhydrate and dihydrate of cobalt laurate. As their purple anhydrate was prepared by boiling rose-pink dihydrate with solvent, it might be a glassy form recovered from a molten state. In our experiments, which will be discussed in a later part of these studies, a once-melted soap showed a somewhat larger magnetic moment than a true blue form. The orbital contribution is so much affected by a crystal field[10] that the melted form must have a different contribution of orbital motion to the magnetic moment.

Moreau and Vatteroni[6] compared the magnetic susceptibilities of cobalt soaps with that of cobalt sulfate and found that the values of cobalt soaps were somewhat larger than inorganic salt. They concluded that these soaps were regarded as structure complexes. This is also consistent with our results.

**Structure Formulas of Cobalt Soaps.**—From these results, it may be concluded that red dihydrate and blue anhydrate of cobalt stearate have a geometry of octahedral and tetrahedral coordination complex respectively. The structure formulas of these soaps may be described as shown in Fig. 4, following Herron and Pink[5]. Such a formula was proposed for cupric salts of lower fatty acids by French and Lowry[11] and opposed by Sidgwick[12]. Sidgwick's main reason for rejecting this formula was that the strain in the chelate ring of four members makes them exceedingly unstable. The alternative formula, in which the carboxyl group occupies two coordination positions attaching themselves to two different cobalt ions, so as to form a ring of more than four members, must be proposed. This was done in cupric soaps[5], but not yet for cobalt soaps.



(a) (b)

Fig. 4. Proposed structure formulas of cobalt soaps.
(a) Red dihydrate (b) Blue anhydrate

## Summary

The infrared absorption spectra and the magnetic susceptibilities of red dihydrate and blue anhydrate of cobalt stearate were measured. The infrared spectra showed the existence of carboxylate ion in these soaps, and magnetic measurements confirmed that they are ionic in nature.

The magnetic moments of red and blue cobalt stearates showed that they are spin-free or ionic covalent complexes. The geometry of red soap is six-covalent octahedral, and that of blue is four-covalent tetrahedral. Structure formulas were proposed for them in correspondence with these geometries, but they may be improbable because of the existence of unstable rings of four members. Alternative formulas, in which a carboxyl group joins two cobalt ions, might be considered but have not yet been given.

The authors express their gratitude to Professor Bunnosuke Yamaguchi for his advice throughout this work, and to Dr. Yoshio Matsunaga and Mr. Shiro Morita for their accomplishments in magnetic and some infrared absorption measurements.

*Institute for Science and Technology*
*The University of Tokyo*
*Meguro-ku, Tokyo*

11) H. S. French and T. M. Lowry, *Proc. Roy. Soc.*, **106A**, 489 (1924).
12) N. V. Sidgwick, "The Electronic Theory of Valency", Oxford Univ. Press, Oxford (1927), p. 252.

# *Statistical Thermodynamics of Solutions of Optically Active Substances. II. Solubility of d- and l-Isomers in Optically Active Solvents*

By Kazuo AMAYA

(Received March 1, 1961)

It is expected theoretically that when *d*- and *l*-optical isomers are independently dissolved in an optically active liquid, the solubilities of *d*- and *l*-isomers may be different. To elucidate the special feature of this problem, the theoretical expression for the solubilities of *d*- and *l*-optical isomers is based on the model described in a previous paper[1]. Further a possibility of optical resolution is discussed.

## Theory

Let us consider two kinds of systems, the one of which contains optically active liquid substance A and *l*-isomer of optically active molecule B (which is denoted by $B_l$) and the other contains A and *d*-isomer of optically active molecule B (which is denoted by $B_d$). For simplicity it is assumed that the two components are completely immiscible in the solid state and completely miscible in the liquid state.

The chemical potential of $B_l$ molecule in crystal $\mu^{K}_{B_l}$ is a function of absolute temperature, $T$, alone while the chemical potential of the same molecule in solution $\mu^{S}_{B_l}$ is a function of, $T$, mole fraction of $B_l$, $x_{B_l}$, and interaction parameter between A and $B_l$ molecules, $\omega_{AB_l}$. For a saturated solution of $B_l$ in A the chemical potential of $B_l$ is equal to that in the crystal, then it follows that

$$\mu^{K}_{B_l}(T) = \mu^{S}_{B_l}(T, x_{B_l}, \omega_{AB_l}) \quad (1)$$

In a similar way for a saturated solution of $B_d$ in the following expression is obtained

$$\mu^{K}_{B_d}(T) = \mu^{S}_{B_d}(T, x_{B_d}, \omega_{AB_d}) \quad (2)$$

where $\mu^{K}_{B_d}$ and $\mu^{S}_{B_d}$ are the chemical potentials of $B_d$ molecule in the crystal and in the saturated solution respectively, and $x_{B_d}$ is the mole fraction of $B_d$ in the solution and $\omega_{AB_d}$ is an interaction parameter between A and $B_d$ molecules.

As $B_l$ and $B_d$ molecules are mirror images for each other, the chemical potential of $B_l$ molecule is equal to that of $B_d$ molecule in the crystal at the same temperature. Then it follows from 1 and 2 that

$$\mu^{K}_{B_l}(T) = \mu^{K}_{B_d}(T) = \mu^{S}_{B_l}(T, x_{B_l}, \omega_{AB_l}) = \mu^{S}_{B_d}(T, x_{B_d}, \omega_{AB_d}) \quad (3)$$

Since $\omega_{AB_l}$ and $\omega_{AB_d}$ have different values, $x_{B_l}$ and $x_{B_d}$ in each saturated solution have different values. It means that the solubility of $B_d$ and $B_l$ optical isomers differ from each other. In the following, explicit expressions for $\mu^{S}_{B_l}$ and $\mu^{S}_{B_d}$ will be derived. In deriving the theoretical expressions, the following assumptions are made:

(1) Molecule A, $B_l$ and $B_d$ are equal in size and each occupies a site of quasi-crystalline lattice and has $3z$ orientational freedoms.

(2) Molecule A is covered by $z$ planes, one of which is composed of *a* element, and the others $(z-1)$ are composed of *b* elements. The *a* element is composed of three subelements 1, 2 and 3 and their arrangement is in the order 1, 2, 3 clockwise viewed from outside of the molecule.

(3) Molecule B (both $B_l$ and $B_d$) is also covered by $z$ planes, one of which is composed of $a'$ element and the others $(z-1)$ are composed of $b'$ elements. $a'$ element is composed of three subelements $1'$, $2'$ and $3'$ and their arrangement is in the order $1'$, $2'$, $3'$ clockwise for $B_l$ molecule and $1'$, $3'$, $2'$ clockwise for $B_d$ molecule viewed from outside of the molecule.

(4) The configurational energy of the system is the sum of interaction energies of plane-plane pairs.

If the interaction energy of plane $i$ and plane $j$ is denoted by $\omega_{ij}$, all possible kinds of $\omega_{ij}$ and their interaction energies become as follows.

A−A $\quad \omega_{bb}, \omega_{ab}, \omega_{aa_1} = \omega_{11} + 2\omega_{23}$
$\omega_{aa_2} = \omega_{22} + 2\omega_{13}$
$\omega_{aa_3} = \omega_{33} + 2\omega_{12}$

B−$B_l$, B−$B_d$ $\quad \omega_{b'b'}, \omega_{a'b'}, \omega_{a'a'_1} = \omega_{1'1'} + 2\omega_{2'3'}$
$\omega_{a'a'_2} = \omega_{2'2'} + 2\omega_{1'3'}$
$\omega_{a'a'_3} = \omega_{3'3'} + 2\omega_{1'2'}$

A−$B_l$ $\quad \omega_{bb'}, \omega_{ab'}, \omega_{a'b}, \omega^{l}_{aa_1} = \omega_{11'} + \omega_{23'} + \omega_{32'}$
$\omega^{l}_{aa'_2} = \omega_{22'} + \omega_{13'} + \omega_{31'}$
$\omega^{l}_{aa'_3} = \omega_{33} + \omega_{12'} + \omega_{21'}$

1) K. Amaya, This Bulletin, **34**, 1689 (1961).

$$\mathrm{A}-\mathrm{B}_d \qquad \omega_{bb'},\ \omega_{ab'},\ \omega_{a'b},\ \omega^d_{aa'_1}=\omega_{11'}+\omega_{22'}+\omega_{33'}$$
$$\omega^d_{aa'_2}=\omega_{13'}+\omega_{21'}+\omega_{32'}$$
$$\omega^d_{aa'_3}=\omega_{12'}+\omega_{23'}+\omega_{31'}$$

The total configurational energy of the system is expressed as a sum of these energies. For a system composed of $N_A$ molecules of A and $N_{B_l}$ molecules of $B_l$, the configurational partition function $\Omega_{AB_l}$ is given by

$$\ln \Omega_{AB_l}-\ln\frac{(N_A+N_{B_l})!}{N_A!\,N_{B_l}!}-\ln(3z)^{N_A+N_{B_l}}-\frac{N_A\chi_A+N_{B_l}\chi_{B_l}}{kT}$$
$$=\frac{\langle W_{AB_l}(N_A,N_{B_l})\rangle}{kT}-\frac{\langle W_{AB_l}(N_A,N_{B_l})\rangle^2-\langle W^2{}_{AB_l}(N_A,N_{B_l})\rangle}{2!\,(kT)^2}-\cdots\cdots \tag{4}$$

where

$$\chi_A=\frac{z}{2}\cdot\frac{1}{z^2}\left\{(z-1)^2\omega_{bb}+2(z-1)\omega_{ab}+\frac{1}{3}(\omega_{aa_1}+\omega_{aa_2}+\omega_{aa_3})\right\} \tag{5}$$

$$\chi_B=\frac{z}{2}\cdot\frac{1}{z^2}\left\{(z-1)^2\omega_{b'b'}+2(z-1)\omega_{a'b'}+\frac{1}{3}(\omega_{a'a'_1}+\omega_{a'a'_2}+\omega_{a'a'_3})\right\} \tag{6}$$

and $W_{AB_l}(N_A, N_{B_l})$ is the excess potential energy of the system and $\langle W_{AB_l}(N_A, N_{B_l})\rangle$ and $\langle W_{AB_l}{}^2(N_A, N_{B_l})\rangle$ denote the unweighted mean over all configurations of this quantity and of the square of it respectively. Then $\langle W_{AB_l}(N_A, N_{B_l})\rangle$ is given by

$$\langle W_{AB_l}(N_A,N_{B_l})\rangle=(N_A+N_{B_l})\{(1-x_{B_l})^2\chi_A+2x_{B_l}(1-x_{B_l})\chi_{AB_l}+x^2{}_{B_l}\chi_{B_l}\}-N_A\chi_A-N_{B_l}\chi_{B_l}$$
$$=(N_A+N_{B_l})x_{B_l}(1-x_{B_l})(2\chi_{AB_l}-\chi_A-\chi_{B_l})^* \tag{7}$$

where

$$x_{B_l}=N_{B_l}/(N_A+N_{B_l})$$
$$\chi_{AB_l}=\frac{1}{z}\left\{(z-1)^2\omega_{bb'}+(z-1)(\omega_{ab'}+\omega_{a'b})+\frac{1}{3}(\omega^l_{aa'_1}+\omega^l_{aa'_2}+\omega^l_{aa'_3})\right\}$$

In evaluating $\langle W^2{}_{AB_l}(N_A, N_{B_l})\rangle$, the average value over most probable configurations is taken as an approximation, since it is very difficult to evaluate the exact value of this quantity averaged over all possible configurations. For most probable configurations, the number of plane-plane pairs for each kind of pair becomes as shown in Table I.

The average value over the above configurations becomes as follows with a procedure similar to that described in the previous paper[1].

$$\langle W_{AB_l}(N_A,N_{B_l})\rangle^2-\langle W^2{}_{AB_l}(N_A,N_{B_l})\rangle=-\frac{(N_A+N_{B_l})^2}{4z^2}\Big[(1-x_{B_l})^4\cdot\frac{1}{36}\{(\omega_{aa_1}-\omega_{aa_2})^2+(\omega_{aa_2}-\omega_{aa_3})^2+(\omega_{aa_3}-\omega_{aa1})^2\}$$
$$+4x^2{}_{B_l}(1-x_{B_l})^2\cdot\frac{1}{36}\{(\omega^l_{aa'_1}-\omega^l_{aa'_2})^2+(\omega^l_{aa'_2}-\omega^l_{aa'_3})^2+(\omega^l_{aa'_3}-\omega^l_{aa'_1})^2\}$$
$$+x^4{}_{B_l}\cdot\frac{1}{36}\{(\omega_{a'a'_1}-\omega_{a'a'_2})^2+(\omega_{a'a'_2}-\omega_{a'a'_3})^2+(\omega_{a'a'_3}-\omega_{a'a'_1})^2\}\Big] \tag{8}$$

By substituting 8 into 4, the following expression for configurational partition function $\Omega_{AB_l}$ is obtained.

TABLE I

| The kind of pairs | | Number of pairs | |
|---|---|---|---|
| A−A | $b-b$ | $(z-1)^2/z^2\cdot N_{AA}$ | |
| | $a-b$ | $2(z-1)/z^2\cdot N_{AA}$ | $N_{AA}=\frac{1}{2}(N_A+N_{B_l})z(1-x_{B_l})^2$ |
| | $a-a$ | $1/z^2\cdot N_{AA}$ | |
| $B_l-B_l$ | $a'-b'$ | $(-1)^2/z^2\cdot N_{B_lB_l}$ | |
| | $a'-b'$ | $2(z-1)/z^2\cdot N_{B_lB_l}$ | $N_{B_lB_l}=\frac{1}{2}(N_A+N_{B_l})zx^2{}_{B_l}$ |
| | $a'-a'$ | $1/z^2\cdot N_{B_lB_l}$ | |
| $A-B_l$ | $b-b'$ | $(z-1)^2/z^2\cdot N_{AB_l}$ | |
| | $a-b'$ | $(z-1)/z^2\cdot N_{AB_l}$ | $N_{AB_l}=(N_A+N_{B_l})z\cdot x_{B_l}(1-x_{B_l})$ |
| | $a'-b$ | $(z-1)/z^2\cdot N_{AB_l}$ | |
| | $a-a'$ | $1/z^2\cdot N_{AB_l}$ | |

* Mean cohesive energy of a B molecule in an imagi- nary liquid state.

$$\ln \Omega_{AB_l}=\ln \frac{(N_A+N_{B_l})!}{N_A!\,N_{B_l}!}+\ln(3z)^{N_A+N_{B_l}}+\frac{N_A\chi_A+N_{B_l}\chi_{B_l}}{kT}\cdot\frac{(N_A+N_B)}{kT}(2\chi_{AB_l}-\chi_A-\chi_{B_l})x_{B_l}(1-x_{B_l})+\frac{1}{2(kT)^2}\frac{(N_A+N_{B_l})^2}{4z^2}\Big[(1-x_{B_l})^4\cdot\frac{1}{36}\{(\omega_{aa_1}-\omega_{aa_3})^2+(\omega_{aa_2}-\omega_{aa_3})^2+(\omega_{aa_3}-\omega_{aa_1})^2\}+4x^2{}_{B_l}(1-x_{B_l})^2\cdot\frac{1}{36}\{(\omega^l_{a'a'_1}-\omega^l_{a'a'_2})^2+(\omega^l_{a'a'_2}-\omega^l_{a'a'_3})^2+(\omega^l_{a'a'_3}-\omega^l_{a'a'_1})^2\}+x^4{}_{B_l}\cdot\frac{1}{36}\{(\omega_{a'a'_1}-\omega_{a'a'_2})^2+(\omega_{a'a'_2}-\omega_{a'a'_3})^2+(\omega_{a'a'_3}-\omega_{a'a'_1})^2\}\Big] \tag{9}$$

Then the chemical potential of $B_l$ molecules $\mu^S{}_{B_l}$ can be obtained by partial differentiating $-kT\ln\Omega_{AB_l}$ with respect to $N_{B_l}$

$$\mu^S{}_{B_l}=-\frac{\partial kT\ln\Omega_{AB_l}}{\partial N_{B_l}}=kT\ln x_{B_l}-\chi_{B_l}+(1-x_{B_l})^2(2\chi_{AB_l}-\chi_A-\chi_{B_l})-\frac{1}{36}\frac{N}{z^2}\frac{1}{kT}\Big[-(1-x_{B_l})^4\{(\omega_{aa_1}-\omega_{aa_2})^2+(\omega_{aa_2}-\omega_{aa_3})^2+(\omega_{aa_3}-\omega_{aa_1})^2\}+x_{B_l}(1-x_{B_l})^3\{(\omega^l_{a'a'_1}-\omega^l_{a'a'_2})^2+(\omega^l_{a'a'_2}-\omega^l_{a'a'_3})^2+(\omega^l_{a'a'_3}-\omega^l_{a'a'_1})^2\}+x^3{}_{B_l}(2-x_{B_l})\{(\omega_{a'a'_1}-\omega_{a'a'_2})^2+(\omega_{a'a'_2}-\omega_{a'a'_3})^2+(\omega_{a'a'_3}-\omega_{a'a'_1})^2\}\Big] \tag{10}$$

where $N=N_A+N_{B_l}$.

For the system consisting of $N_A$ molecules of A and $N_{B_d}$ molecules of $B_d$, the chemical potential $\mu_{B_d}$ for the $B_d$ molecule can be derived in quite the same way. Then $\mu^S{}_{B_d}$ becomes

$$\mu^S{}_{B_d}=kT\ln x_{dB}-\chi_{B_d}+(1-x_{B_d})^2(2\chi_{AB_d}-\chi_A-\chi_{B_d})-\frac{1}{36}\frac{N}{z^2}\frac{1}{kT}\Big[-(1-x_{B_d})^4\{(\omega_{aa_1}-\omega_{aa_2})^2+(\omega_{aa_2}-\omega_{aa_3})^2+(\omega_{aa_3}-\omega_{aa_1})^2\}+x_{B_d}(1-x_{B_d})(3\{(\omega^d_{a'a'_1}-\omega^d_{a'a'_2})^2+(\omega^d_{a'a'_2}-\omega^d_{a'a'_3})^2+(\omega^d_{a'a'_3}-\omega^d_{a'a'_1})^2\}+x^3{}_{B_d}(2-x_{B_d})\{(\omega_{a'a'_1}-\omega_{a'a'_2})^2+(\omega_{a'a'_2}-\omega_{a'a'_3})^2+(\omega_{a'a'_3}-\omega_{a'a'_1})^2\}\Big] \tag{11}$$

where

$$\chi_{AB_d}=\frac{1}{z}\Big\{(z-1)^2\omega_{bb'}+(z-1)(\omega_{ab'}+\omega_{a'b})+\frac{1}{3}(\omega^d_{aa'_1}+\omega^d_{aa'_2}+\omega_2{}^d_{aa'_3})\Big\} \tag{12}$$

Now compare 10 with 11. Since $B_l$ is a mirror image of $B_d$ and $B_l$ molecules are energetically equivalent, it follows that

$$\chi_{B_l}=\chi_{B_d} \tag{13}$$

and from the relation

$$\omega^l_{aa'_1}+\omega^l_{aa'_2}+\omega^l_{aa'_3}=\omega_{11'}+\omega_{23'}+\omega_{32'}+\omega_{22'}+\omega_{13'}+\omega_{31'}+\omega_{33'}+\omega_{12'}+\omega_{21'}=\omega_{11'}+\omega_{22'}+\omega_{33'}+\omega_{13'}+\omega_{21'}\,\omega_{32'}+\omega_{12'}+\omega_{23'}+\omega_{31'}=\omega^d_{aa'_1}+\omega^d_{aa'_2}+\omega^d_{aa'_3}$$

it follows that

$$\chi_{AB_l}=\chi_{AB_d} \tag{14}$$

Then the only difference between 10 and 11 is the second term in the bracket [ ] which contain the coefficient $x_B(1-x_B)^3$ *.

By using new notations that $\chi_B=\chi_{B_l}=\chi_{B_d}$ and $\chi_{AB}=\chi_{AB_l}=\chi_{AB_d}$, and expressing mole fractions of $B_l$ and $B_d$ molecules in their saturated solutions by $x_l$, and $x_d$ respectively, $x_l$ and $x_d$ are correlated by the following equations

$$\mu^S{}_{B_l}(x_l)=kT\ln x_l-\chi_B+(1-x_l)^2(2\chi_{AB}-\chi_A-\chi_B)-\frac{1}{36}\frac{N}{z^2}\frac{1}{kT}\{-(1-x_l)^4C_{AA}+x_l(1-x_l)^3C_{AB_l}+x_l^3(2-x_l)C_{BB}\} \tag{15}$$

$$=\mu^S{}_{B_d}(x_d)=kT\ln x_d-\chi_B+(1-x_d)^2(2\chi_{AB}-\chi_A-\chi_B)-\frac{1}{36}\frac{N}{z^2}\frac{1}{kT}\{-(1-x_d)^4C_{AA}+x_d(1-x_d)^3C_{AB_d}+x_d^3(2-x_d)C_{BB}\} \tag{16}$$

where

$$C_{AA}=(\omega_{aa_1}-\omega_{aa_2})^2+(\omega_{aa_2}-\omega_{aa_3})^2+(\omega_{aa_3}-\omega_{aa_1})^2$$

$$C_{BB}=(\omega_{a'a'_1}-\omega_{a'a'_2})^2+(\omega_{a'a'_2}-\omega_{a'a'_3})^2+(\omega_{a'a'_3}-\omega_{a'a'_1})^2$$

$$C_{AB_l}=(\omega^l_{aa'_1}-\omega^l_{aa'_2})^2+(\alpha^l_{aa'_2}-\omega^l_{aa'_3})^2+(\omega^l_{aa'_3}-\omega^l_{aa'_1})^2$$

$$C_{AB_d}=(\omega^d_{aa'_1}-\omega^d_{aa'_2})^2+(\omega^d_{aa'_2}-\omega^d_{aa'_3})^2+(\omega^d_{aa'_3}-\omega^d_{aa'_1})^2$$

* $x_B$ denotes $x_{B_l}$ or $x_{B_d}$.

## Discussions

The chemical potentials of $B_l$ and $B_d$ molecules in the solution $\mu^{S}{}_{B_l}(x)$ and $\mu^{S}{}_{B_d}(x)$ respectively, can be expressed as a function of their mole fraction $x$ by the same formula except for the term containing $C_{AB_l}$ and $C_{AB_d}$. If the common part is expressed by $F(x)$, the following formula is obtained.

$$\mu^{S}{}_{B_l}(x) = F(x) + \frac{1}{36}\frac{N}{z^2}\frac{1}{kT}C_{AB_l}x(1-x)^3 + \cdots\cdots$$

$$\mu^{S}{}_{B_d}(x) = F(x) + \frac{1}{36}\frac{N}{z^2}\frac{1}{kT}C_{AB_d}x(1-x)^3 + \cdots\cdots$$

This formula is represented schematically in Fig. 1. It is clear from the above expression that the higher the temperature the greater the difference between the two curves is. The straight line parallel to the $x$ axis representing $\mu=\mu^{K}$ crosses the curves representing $\mu^{S}{}_{B_l}(x)$ and $\mu^{S}{}_{B_d}(x)$ at points $P_l$ and $P_d$. Projections of $P_l$ and $P_d$ on $\chi$ axis represent $x_l$ and $x_d$ respectively. As these two curves generally do not coincide with each other, $x_l$ and $x_d$ have different values. This shows that the solubilities of *d*- and *l*-optical isomers in optical active solvent differ from each other and the magnitude of the difference is determined by the difference between $C_{AB_l}$ and $C_{AB_d}$. It is clear from the above argument that in principle the optical resolution is possible using the difference of solubility of *d*- and *l*-optical isomers in optical active solvents and by choosing a proper kind of molecule of A, which makes the difference of $C_{AB_l}$ and $C_{AB_d}$ large, the difference between $x_l$ and $x_d$ can be made large enough to obtain an efficient optical resolution.

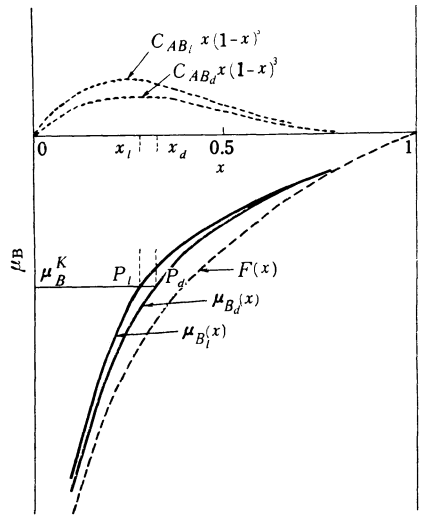



Fig. 1. Schematic diagram of $\mu_{B_l}$ and $\mu_{B_d}$ as a function of $x$.

The above argument is confined only to the mixture in which $B_l$ and $B_d$ molecules form no racemic compound. For the case where a racemic compound is formed more elaborate consideration must be made.

## Summary

The statistical mechanical expression relating the solubilities of *d*- and *l*-optical isomers in optically active solvent is derived.

It is shown that there exists a difference between these two solubilities.

The possibility of optical resolution is also discussed.

The auther wishes to express his hearty thanks to Professor Yonezo Morino of The University of Tokyo for his helpful discussions.

*Government Chemical*
*Industrial Research Institute*
*Shibuya-ku, Tokyo*

# *Liquid-Vapor Equilibrium of Isotope Mixture under Centrifugal Force*

By Kazuo AMAYA

(Received March 30, 1961)

In order to estimate the efficiency of concentrating one of the isotopic compounds by distillation of the mixture under centrifugal force, a theoretical expression for liquid-vapor equilibrium of the isotopic mixture under centrifugal force was derived and a concentration factor under practical condition was estimated for actual cases.

## Derivation of the Expression for the Distribution of Isotope Mixture in Liquid-Vapor Phase System under Centrifugal Force

Consider an isotopic mixture composed of $N_1$ molecules of isotope 1 of mass $m_1$ and $N_2$ molecules of isotope 2 of mass $m_2$.

If the mole fraction of isotope 1 in the mixture is denoted by $x$, then

$$N_1 = Nx \tag{1}$$

$$N_2 = N(1-x) \tag{2}$$

where $N = N_1 + N_2$.

Suppose that the mixture is confined in a closed box with cross section area $S$ and height $H$ and is placed in a field of homogeneous centrifugal force $g$*, the direction of which is perpendicular to the cross section.

If the densities of molecules of isotope 1 and 2 in the vapor phase at a distance $h^v$ from the liquid surface are denoted by $n^v_{1g}(h^v)$ and $n^v_{2g}(h^v)$ respectively and those in the liquid phase by $n^l_{1g}(h^l)$ and $n^l_{2g}(h^l)$ respectively, and suppose that the vapor density is sufficiently low and the liquid is not compressible, then following relations hold.

$$n^v_{1g}(h^v) = n^v_{1g}(0) \cdot \exp(-m_1 g h^v / kT) \tag{3}$$

$$n^v_{2g}(h^v) = n^v_{2g}(0) \cdot \exp(-m_2 g h^v / kT) \tag{4}$$

$$n^l_{1g}(h^l) + n^l_{2g}(h^l) = n^l_{1g}(0) + n^l_{2g}(0) = N_0 = \text{const.} \tag{5}$$

$$n^l_{1g}(h^l) = N_0 \cdot n^l_{1g}(0) \cdot \exp(m_1 g h^l / kT) / \{n^l_{1g}(0) \cdot \exp(m_1 g h^l / kT) + n^l_{2g}(0) \cdot \exp(m_2 g h^l / kT)\} \tag{6}$$

$$n^l_{2g}(h^l) = N_0 \cdot n^l_{2g}(0) \cdot \exp(m_2 g h^l / kT) / \{(n^l_{1g}(0) \cdot \exp(m_1 g h^l / kT) + n^l_{2g}(0) \cdot \exp(m_2 g h^l / kT)\} \tag{7}$$

where $k$ is the Boltzmann constant and $T$ is the absolute temperature of the box.

If the vaporization energy of isotope 1 is assumed to be equal to that of isotope 2, then it follows that,

$$n^l_{1g}(0) = K_T n^v_{1g}(0) \tag{8}$$

$$n^l_{2g}(0) = K_T n^v_{2g}(0) \tag{9}$$

where $K_T$ is a constant at a given temperature, $T$. From the principle of conservation of mass in a closed system, the following relations are obtained.

$$S\int_0^{H^v_g} n^v_{1g}(h^v)\mathrm{d}h_v + S\int_0^{H^l_g} n^l_{1g}(h^l)\mathrm{d}h_l = Nx \tag{10}$$

$$S\int_0^{H^v_g} n^v_{2g}(h^v)\mathrm{d}h_v + S\int_0^{H^l_g} n^l_{2g}(h^l)\mathrm{d}h_l = N(1-x) \tag{11}$$

where $SH^v_g$ and $SH^l_g$ are the volume of the space in the box occupied by the vapor and the liquid respectively at equilibrium under centrifugal force $g$ and namely $H = H^v_g + H^l_g$.

If, at equilibrium, mole fraction of isotope at the interface of liquid and vapor is denoted by $x_g$ it follows from 5 that

$$n^l_{1g}(0) = N_0 x_g \tag{12}$$

$$n^l_{2g}(0) = N_0(1-x_g) \tag{13}$$

then Eqs. 6 and 7 are rewritten as

$$\begin{aligned} n^l_{1g}(h^l) &= N_0 x_g \cdot \exp(m_1 g h^l / kT) / \{x_g \cdot \exp(m_1 g h^l / kT) + (1-x_g) \cdot \exp(m_2 g h^l / kT)\} \\ &= N_0 \Big/ \left[1 + \frac{1-x_g}{x_g} \cdot \exp\{(m_2 - m_1) g h^l / kT\}\right] \end{aligned} \tag{14}$$

$$\begin{aligned} n^l_{2g}(h^l) &= N_0(1-x_g) \cdot \exp(m_2 g h^l / kT) / \{x_g \cdot \exp(m_1 g h^l / kT) + (1-x_g) \cdot \exp(m_2 g h^l / kT)\} \\ &= N_0 \Big/ \left[1 + \frac{x_g}{1-x_g} \cdot \exp\{(m_1 - m_2) g h^l / kT\}\right] \end{aligned} \tag{15}$$

and from 3, 4, 8 and 9

* For the sake of simplicity, the values of $g$ are assumed to be constant along the direction of height.

$$n^{v}_{1g}(h^{v}) = N_0/K_T \cdot x_g \cdot \exp(-m_1 g h^{v}/\boldsymbol{kT}) \quad (16)$$

$$n^{v}_{2g}(h^{v}) = N_0/K_T \cdot x_g \cdot \exp(-m_2 g h^{v}/\boldsymbol{kT}) \quad (17)$$

Substituting 14 and 16 into 10, and 15 and 17 into 11, and integrating them, we obtain

$$Nx = N_0 S\Big[ x_g/K_T \cdot \boldsymbol{kT}/m_1 g\{1-\exp(-m_1 g H^{v}_g/\boldsymbol{kT})\} + H^{l}_g - \boldsymbol{kT}/(m_2-m_1)g \times \ln\Big\{\frac{1+(1-x_g)/x_g \cdot \exp((m_2-m_1)gH^{l}_g/\boldsymbol{kT})}{1+(1-x_g)/x_g}\Big\}\Big] \quad (18)$$

$$N(1-x) = N_0 S\Big[ (1-x_g)/K_T \cdot \boldsymbol{kT}/m_2 g\{1-\exp(-m_2 g H^{v}_g/\boldsymbol{kT})\} + H^{l}_g - \boldsymbol{kT}/(m_1-m_2)g \times \ln\Big\{\frac{1+x_g/(1-x_g)\cdot\exp((m_1-m_2(gH^{l}_g/\boldsymbol{kT})}{1+x_g/(1-x_g)}\Big\}\Big] \quad (19)$$

## Calculation of Concentration Factor for Actual Cases

Now, the change of composition of isotope in the mixture by distillation under centrifugal force will be considered. When $g=0$, Eqs. 18 and 19 become

$$Nx = N_0 S x_0 (1/K_T \cdot H^{v}_0 + H^{l}_0) \quad (20)$$

$$N(1-x) = N_0 S(1-x_0)(1/K_T \cdot H^{v}_0 + H^{l}_0) \quad (21)$$

where $H^{v}_0$, $H^{l}_0$ and $x_0$* are the values of $H^{v}_g$, $H^{l}_g$ and $x_g$ when $g=0$ respectively. By Eqs. 18 and 19 to 20 and 21 respectively and from the relation

$$H^{l}_0 + H^{v}_0 = H^{l}_g + H^{v}_g \quad (22)$$

the values of $x_g/x_0$ may be obtained in principle. However, the exact solution of these equations is very complicated.

In order to obtain a workable formula, we may expand the logarithm of the last terms in 18 and 19 in powers of $(m_2-m_1)gH^{l}_g/\boldsymbol{kT}$, and the following relations are obtained

$$x_g/K_T \cdot [\boldsymbol{kT}/m_1 g \cdot \{1-\exp(-m_1 g H^{v}_g/\boldsymbol{kT})\} + H^{l}_g] + 1/2 \cdot \{(1-x_g)-(1-x_g)^2\}(m_1-m_2)gH^{l}_g/\boldsymbol{kT} + \cdots\cdots = x_0(H^{v}_0/K_T + H^{l}_0) \quad (23)$$

$$(1-x_g)/K_T \cdot [\boldsymbol{kT}/m_2 g \cdot \{1-\exp(-m_2 g H^{v}_g/\boldsymbol{kT})\} + H^{l}_g] + 1/2 \cdot (x_g - x_g^2)(m_2-m_1)gH^{l}_g/\boldsymbol{kT} + \cdots\cdots = (1-x_0)(H^{v}_0/K_T + H^{l}_0) \quad (24)$$

If we assume that

$$|m_1-m_2| = 3,$$

$$H^{l}_g \approx 0.1 \text{ cm.}$$

$$g = 10^7 \text{ dyn.}$$

$$T \approx 300^\circ\text{K}$$

then the order of magnitude of the second term of the left side of 23 or 24 is about $1/2 \cdot |m_1-m_2| \times 10^{-5} = 1.5 \times 10^{-5}$ and can be neglected as being sufficiently small. Using the following notation

$$x_g = x_0(1+\delta) \quad (25)$$

$$H^{l}_g = H^{l}_0 + \Delta h, \quad H^{v}_g = H^{v}_0 - \Delta h \quad (26)$$

and adding 23 and 24, we obtain

$$x_0(1+\delta)\boldsymbol{kT}/m_1 g \cdot [1-\exp\{-m_1 g(H^{v}_0 - \Delta h)/\boldsymbol{kT}\}] + \{1-x_0(1+\delta)\}\boldsymbol{kT}/m_2 g \times [1-\exp\{-m_2 g(H^{v}_0 - \Delta h)/\boldsymbol{kT}\}] - H^{v}_0 = -K_T \Delta h \quad (27)$$

To obtain the approximate value of $\Delta h$, the mixture may be assumed to be of single component of mass $\bar{m} = m_1 x_0 + m_2(1-x_0)$, then

$$\boldsymbol{kT}/\bar{m}g\{1-\exp(-\bar{m}gH^{v}_0/\boldsymbol{kT}) \cdot (1+\bar{m}g\Delta h/\boldsymbol{kT})\} - H^{v}_0 = -K_T \Delta h \quad (28)$$

The value of $\Delta h$ thus obtained is then substituted into 23 and 24, and we can obtain $\delta$ from the relation

$$\frac{\boldsymbol{kT}/m_1 g \cdot \{1-(1+m_1 g\Delta h/\boldsymbol{kT})\exp(-m_1 g H^{v}_0)\} + K_T(H^{l}_0 + \Delta h)}{\boldsymbol{kT}/m_2 g \cdot \{1-(1+m_2 g\Delta h/\boldsymbol{kT})\}\exp(-m_2 g H^{v}_0) + K_T(H^{l}_0 + \Delta h)} = \frac{1-x_0(1+\delta)}{(1-x_0)(1+\delta)} \quad (29)$$

Now consider the value of $\delta$ for an actual case. For example, consider $UF_6$ and assume that

$$m_1 = 350, \quad m_2 = 353$$

$$K_T \fallingdotseq 300,^* \quad g = 10^7 \text{ dyn.}$$

$$T = 333^\circ\text{K}, \quad H^{v}_0 + H^{l}_0 = 20 \text{ cm.}, \quad H^{l}_0 = 0.1 \text{ cm.}$$

TABLE I. VALUES OF $\delta$, $x'_g$ AND THE CONCENTRATION FACTOR $(x'_g - x_0)/x_0$ AS FUNCTIONS OF ORIGINAL CONCENTRATION $x_0$ OF $^{235}UF_6$ IN $^{238}UF_6 - ^{235}UF_6$ MIXTURE WITH $g = 10^7$ dyn., $H = 20$ cm. AND $H^{l}_0 = 0.1$ cm.

| $x_0$ | $\delta \times 10^{-3}$ | $x'_g$ | $(x'_g - x_0)/x_0$ % |
|---|---|---|---|
| 0.01 | −0.95 | 0.010205 | 2.05 |
| 0.1 | −0.87 | 0.10186 | 1.86 |
| 0.2 | −0.77 | 0.20330 | 1.65 |
| 0.3 | −0.67 | 0.30432 | 1.44 |
| 0.4 | −0.58 | 0.40493 | 1.23 |
| 0.5 | −0.48 | 0.50513 | 1.03 |
| 0.6 | −0.39 | 0.60491 | 0.82 |
| 0.7 | −0.29 | 0.70429 | 0.61 |
| 0.8 | −0.19 | 0.80326 | 0.41 |
| 0.9 | −0.10 | 0.90183 | 0.20 |
| 1.0 | 0 | 1.0 | 0 |

* By dividing 20 by 21, it follows that $x_0 = x$

* The vapor is assumed to be an ideal gas, and the molar volume of vapor of 22.4 l. is divided by molar volume of $UF_6$ in liquid state 75.4 cc., to obtain 22.4/0.0754 = 297.

and $\delta$ are calculated for $x_0=0.01$, 0.05, 0.1 and 0.9 and are shown in Table I. Using these values of $\delta$ we can calculate the composition of the isotope mixture at the top of the box. The composition $x_g'$ thus obtained is also shown in Table I. The concentration factors $x_g'/x_0$ are about 1.02 and the concentration of the isotope may become quite efficient by the proper design of an apparatus for successive distillation.

## Summary

Expressions for the distribution of the isotope mixture in liquid-vapor phase system under centrifugal force were derived. By the use of these expressions, the efficiency of the isotope concentration was estimated for actual cases under accessible conditions. It was found that an efficient concentration of the isotope from their mixture was possible by the proper design of an apparatus for successive distillation.

*Government Chemical Industrial Research Institute, Tokyo*
*Shibuya-ku, Tokyo*

# *Adsorbabilities of Diacidotetrammine Type Cobalt(III) Complex Ions on a Cation Exchanger*[1]

By Motoshichi MORI, Muraji SHIBATA and Kuniko HORI

(Received March 3, 1961)

Since King and Walter[2] reported the separation of the cis and trans isomers of dinitrotetramminecobalt(III) ions by ion-exchange chromatography, the same kind of study has been extensively developed in our laboratory on other isomers of the diacidoteterammine type complex, and as a result it has been found that the trans isomers were, as a general rule, eluted faster than the corresponding cis isomers[3,4]. In the present work, some supplementary experiments for confirming the above rule are attempted by using the complexes which are relatively unstable in aqueous solutions. Furthermore, the adsorbabilities of all the complexes, including the previous ones, on a cation exchanger are compared.

## Experimental

**Complexes.** — All the complexes were prepared according to the literatures[5], and their identity and purity were examined with the absorption spectra in an alcoholic aqueous solution. The complexes used were as follows: the trans-cis and cis-trans isomers of $[Co\,en(NH_3)_2Cl_2]Cl$ and the trans and cis isomers of $[Co\,en_2Cl_2]$, $[Co\,en_2Br_2]Br$ and $[Co\,en_2(NO_2)Cl]Cl$.

**Elution Methods.**—A column (1×10 cm.) which contained 5 g. of Ammberlite IR-120 (50~100 mesh) in sodium form was used, and the sample solution was prepared in concentrations ranging from 0.01 to 0.06 M depending on the solubility of the complexes. Fifteen milliliters of each sample solution was applied to the column, and then the column was eluted with 0.15 M sodium chloride ethanol-water (1 : 1) solution. The velocity of elution was 0.5 ml./min. Examination of the eluted species was made by measuring the optical density of the eluted fraction at particular wavelengths. The ethanol-water solution was used as the eluant to minimize the aquation rections of the complexes.

The measurement of the optical density was carried out with a Hitachi model EPU-2 spectrophotometer.

## Results and Discussion

The elution curve of a mixture of the isomeric $[Co\,en(NH_3)_2Cl_2]^+$ is shown in Fig. 1, in which the measurement of the optical density was performed at an absorption maximum and a minimum of the trans-cis ion (460 and 560 mμ). As is seen in the figure, an elution maximum for the trans-cis ion appears in the fraction 10 and one for the cis-trans ion in the fractions 20 and 21. When only the trans-cis complex was applied to the

1) Separation of metal complex isomers by the ion-exchanger, Part III Partly presented at the 10th Annual Meeting of the Chemical Society of Japan, Tokyo, April, 1957.

2) E. L. King and R. R. Walter, *J. Am. Chem. Soc.*, **74**, 4471 (1952).

3) M. Mori, M. Shibata and J. Azami, *J. Chem. Soc. Japan, Pure Chem. Sec. (Nipoon Kagaku Zasshi)*, **76**, 1003 (1955).

4) M. Mori, M. Shibata and M. Nanasawa, This Bulletin, **29**, 947 (1956).

5) J. C. Bailar and D. F. Peppard, *J. Am. Chem. Soc.*, **62**, 105 (1940); A. Werner, *Ber.*, **34**, 1733 (1901); *Ann.* **386**, 48, 107, 111, 248 (1912).

column, the elution curve had its maximum in the fraction 9 and dropped to zero at the fraction 20. On the other hand, the cis-trans ion began to appear in the fraction 9 and showed the maximum elution at the fraction 21. It is, therefore, clear that each portion of the fractions 9—20 in Fig. 1 is, more or less, contaminated with both species.

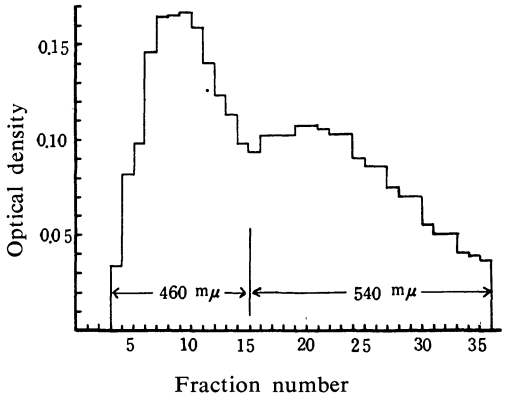



Fig. 1. Elution curve of $[Co\,en(NH_3)_2Cl_2]Cl$ isomers.

The elution curves of *trans*- and *cis*-$[Co\,en_2NO_2Cl]^+$ are shown in Figs. 2 and 3. The maximum concentration of the trans compound is observed in the fraction 8, and that for the cis in the fractions 21 and 22. The elution of a mixture of these isomers was examined, but the elution curve is omitted because the absorption spectra of both isomers are quite similar, and hence no perceptible peak was obtained.

Figure 4 is the elution curve for *trans*-$[Co\,en_2Br_2]^+$ and shows the elution peak in the fraction 7. The experiment of the elution for the cis ion was unsuccessful because of the extremely low solubility of the complex.

The elution curve for the isomeric $[Co\,en_2\cdot Cl_2]^+$ in a mixed solution is shown in Fig. 5, where the elution maxima are in the fractions

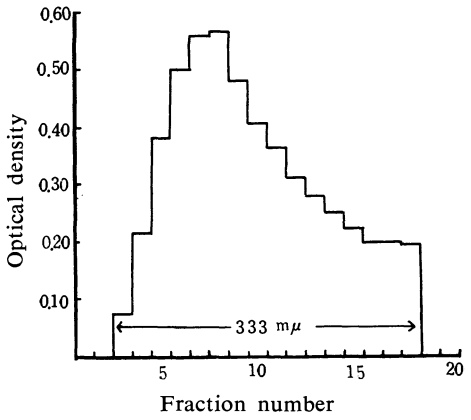



Fig. 2. Elution curve of *trans*-$[Co\,en_2NO_2Cl]Cl$.

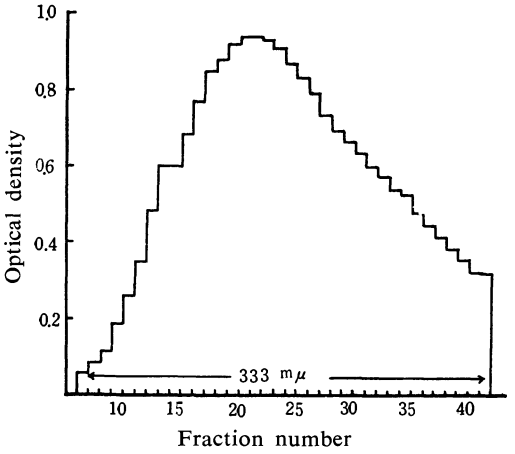



Fig. 3. Elution curve of *cis*-$[Co\,en_2NO_2Cl]Cl$.

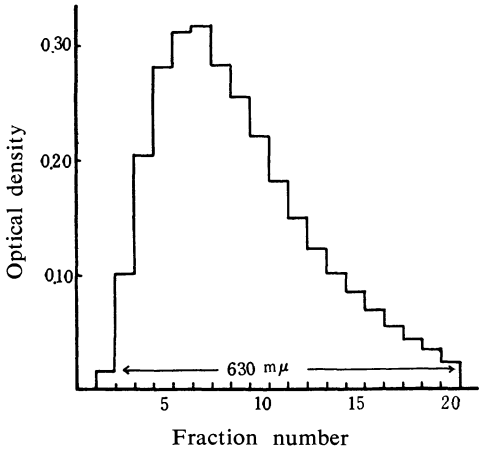



Fig. 4. Elution curve of *trans*-$[Co\,en_2Br_2]Br$.

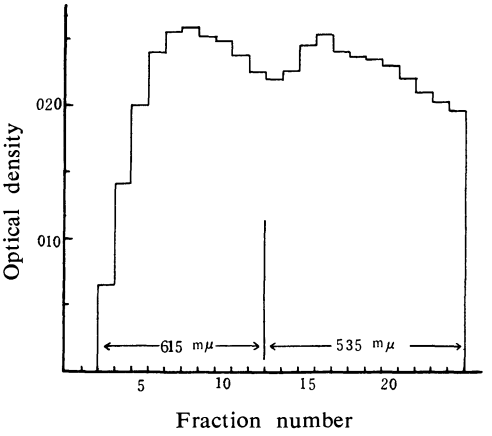



Fig. 5. Elution curve of $[Co\,en_2Cl_2]Cl$ isomers.

8 and 16. In the case of the individual solution, the trans ion was eluted with the maximum in the fraction 7 and finished its elution at the fraction 15, while the cis ion began to elute in fraction 5 and showed the maximum in the fraction 16.

From these results, it is again found that the trans ion is eluted faster than the cis ion. Furthermore, it is possible to predict the relative adsorbabilities as follows:

For the trans ions,

$$[Co\ en_2Br_2]^+ < [Co\ en_2Cl_2]^+ \simeq [Co\ en_2NO_2Cl]^+ < [Co\ en(NH_3)_2Cl_2]^+$$

For the cis ions,

$$[Co\ en_2Cl_2]^+ < [Co\ en(NH_3)_2Cl_2]^+ \simeq [Co\ en_2NO_2Cl]^+$$

Now, we are in a position to discuss the relative adsorbabilities of all the complex ions studied in the present and previous papers[3,4].

Table I. Comparison of elution maxima

| Complex ion | Eluant | Fraction no. of elution max. trans | cis |
|---|---|---|---|
| $[Co\ en(NH_3)_2Cl_2]^+$ | 0.15 M NaCl alcoholic aqueous soln. | 10 | 21—22 |
| $[Co\ en_2Cl_2]^+$ | | 8 | 16 |
| $[Co\ en_2NO_2Cl]^+$ | | 8* | 21—22* |
| $[Co\ en_2Br_2]^+$ | | 7* | — |
| $[Co\ en_2Cl_2]^+$ | 0.5 M NaCl aqueous soln. | 7 | 12 |
| $[Co\ en_2(NO_2)_2]^+$ | | 6 | 17 |
| $[Co\ en_2(NCS)_2]^+$ | | 5 | 14 |
| $[Co(NH_3)_4(NO_2)_2]^+$ | 0.5 M NaCl aqueous soln. | 13 | 35 |
| $[Co\ en_2(NO_2)_2]^+$ | | 11 | 31 |

* Fraction number in individual solution.

Unfortunately, it was impossible to perform all of the elutions under identical conditions. It is, therefore, difficult to derive a definite adsorbability order directly, but it is possible to predict such an order from a comparison of the elution maxima (Table I).

For the trans ions.

$$[Co\ en_2(NCS)_2]^+ < [Co\ en_2(NO_2)_2]^+ \simeq [Co\ en_2Br_2]^+ < [Co\ en_2Cl_2]^+ \simeq [Co\ en_2NO_2Cl]^+ < [Co(NH_3)_4(NO_2)_2]^+ < [Co\ en(NH_3)_2Cl_2]^+$$

For the cis ions.

$$[Co\ en_2Cl_2]^+ < [Co\ en_2(NCS)_2]^+ < [Co\ en(NH_3)_2Cl_2]^+ \simeq [Co\ en_2NO_2Cl]^+ < [Co\ en_2(NO_2)_2]^+ < [Co(NH_3)_4(NO_2)_2]^+$$

For the trans ions of the diacido-bisethylenediamine complexes, the adsorbabilities increase in the order of the dithiocyanato-, the dinitro-, the dibromo- and the dichloro-complexes; this trend may be attributed to the differences of the ionic radii of the complex ions since the distance between the cobalt and the ligand ion increases in the order $Cl^-$, $Br^-$, $NO_2^-$ and $NCS^-$. On the other hand, such a trend was not observed for the cis ions. It must, however, be said that the ammine-complexes always have a stronger affinity for a cation exchanger than the corresponding ethylenediamine-complexes; this also be due to the differences of size between ammonia and ethylenediamine molecules.

In the present work, we wanted to study many complexes of the diacido-type, but we were limited by the solubility of the complexes. However, through all the experiments it is to be noted that this kind of technique is useful for distinguishing isomeric forms of complexes, apart from the practical separation of the isomers.

## Summary

Additional elution experiments for confirming the fact that the trans ions of the diacido-tetrammine-type complexes are always eluted faster than the corresponding cis ions have been performed by using several diacido-type complexes which are relatively unstable. By comparing the elution maxima for the whole complex ions which have been used to date, the relative adsorbabilities of the isomeric ions on a cation exchanger have been predicted as follows:

For the trans ions,

$$[Co\ en_2(NCS)_2]^+ < [Co\ en_2(NO_2)_2]^+ \simeq [Co\ en_2Br_2]^+ < [Co\ en_2Cl_2]^+ \simeq [Co\ en_2NO_2Cl]^+ < [Co(NH_3)_4(NO_2)_2]^+ < [Co\ en(NH_3)_2Cl_2]^+$$

For the cis ions,

$$[Co\ en_2Cl_2]^+ < [Co\ en_2(NCS)_2]^+ < [Co\ en(NH_3)_2Cl_2]^+ \simeq [Co\ en_2NO_2Cl]^+ < [Co\ en_2(NO_2)_2]^+ < [Co(NH_3)_4(NO_2)_2]^+$$

A part of the present work was supported by a grant-in-aid from the Ministry of Education.

*Department of Chemistry*
*Faculty of Science*
*Kanazawa University*
*Kanazawa*

# *The Beckmann Rearrangement of 1, 2-Cyclohexane-dione Dioxime in Liquid Sulfur Dioxide*[1]

By Niichiro TOKURA, Ritsuro TADA and Kunio YOKOYAMA

(Received March 8, 1961)

The Beckmann rearrangement of 1, 2-diketone dioxime has scarcely been reported on except in the case of benzil dioximes[2]. In the present article the authors wish to reports on the Beckmann rearrangement of 1, 2-cyclohexanedione dioxime in liquid sulfur dioxide, which resulted in a variety of interesting products.

Several examples of the Beckmann rearrangement, in which the directions of the course of the rearrangement were affected by difference in the reagents applied or conditions used have been published. In a report of Brown, van Gulic and Schmid[3], for instance, the migratory aptitude of pivalophenone oxime was found to be largely dependent upon the nature of the reagent applied, the oxime being subjected to geometrical isomerization before rearrangement[4]. The present authors have also observed that the Beckmann rearrangement of 1, 6-cyclodecanedione dioxime yielded different products accoding to the different reagents used in the rearrangement. Such complicated results have also been reported by McLaren and Schacht[5], and Yukawa and his associates[6]. However, one of the anomalies during the rearrangement, the occurrence of the syn-anti isomerization of the oximes before the rearrangement, can be largely reduced as was reported in a recent article[7] if the reaction is conducted in liquid sulfur dioxide.

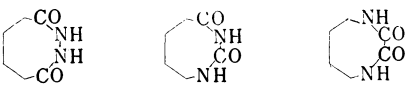
In a preceding paper[8], the present authors reported on their unsuccessful attempt at the Beckmann rearrangement of 1, 2-cyclohexanedione dioxime (I) with thionyl chloride in liquid sulfur dioxide. They obtained only a dehydrated product, cyclohexano[c]-1, 2, 5-oxadiazole (II) in a yield of 70 per cent.



I II

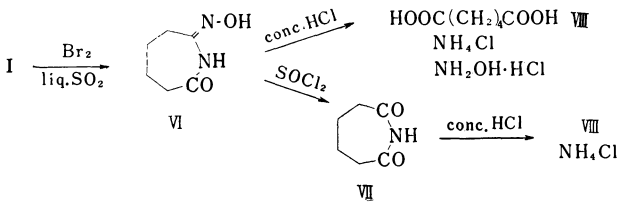
Although the reaction with thionyl chloride was unfruitful, however, the bromine in liquid sulfur dioxide and the sulfur trioxide in sulfur dioxide afforded the rearranged products with which the present paper is concerned.

As 1, 2-cyclohexanedione dioxime (I) has not been found to have geometrical isomers and as the various reagent examined in this material have given no symptom of the presence of geometrical isomers, the problem of the possible isomer was excluded in this experiment. In view of the authors' experience with the Beckmann rearrangement, it is interesting to examine the formation of the three possible cyclic acidamide III, IV, V or the mixture of these compounds in the reaction products. But the transformation to any of these three has not been observed.



III IV V

Bromine in liquid sulfur dioxide yielded a half-rearranged product as follows:




1) The Beckmann Rearrangement in Liquid Sulfur Dioxide. Part VIII.
2) J. Meisenheimer and W. Lamparter, *Ber.*, **57**, 276 (1924).
3) R. F. Brown, N. M. van Gulic and G. H. Schmid, *J. Am. Chem. Soc.*, **77**, 1094 (1955).
4) N. Tokura, R. Tada and K. Suzuki, This Bulletin, **32**, 654 (1958).
5) A. D. McLaren and R. E. Schacht, *J. Org. Chem.*, **14**, 254 (1949).
6) Y. Yukawa, "Jikken Kagaku Koza", Vol. 18, Maruzen, Tokyo (1958), p. 426.
7) R. Tada, Y. Masubuchi and N. Tokura, This Bulletin, **34**, 209 (1961).
8) Part VII of this series, This Bulletin, **34**, 270 (1961).

The product was contaminated with a large amount of brown resinous matter from which white crystalline substances VI were isolated by acetone extraction in a yield of 32 per cent. A very small amount of II was also found in the mixture. The substance VI, m. p. 155°C, was soluble in water, acid, base, ethyl alcohol and acetone respectively but was insoluble in ether, benzene and chloroform. When VI was subjected to hydrolysis with concentrated hydrochloric acid, adipic acid, ammonium chloride[9] and hydroxylamine hydrochloride[10] were identified in the reaction mixture; no hydrazine salt was found in the mixture[11], however, the infrared spectrum of VI also proved the presence of OH and NH (2900~3200 $cm^{-1}$, strong and broad) and carbonyl (1620~1600 $cm^{-1}$, strong) groups. Moreover, the NMR spectrum of VI in dimethylsulfoxide confirmed the presence of =NOH and =NH, as in Fig. 1[12]. The peak of the oximine group was consistent with that of cyclohexanoxime, and the very low and broader absorbancy in the higher field corresponded to that of the imino group.

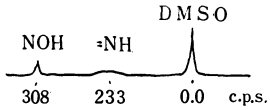



Fig. 1. NMR spectrum of VI in DMSO. c. p. s. was taken with that of DMSO as standard.

Thus the structure of VI was established as 1-aza-7-oximinocyclohepta-2-one. In order to effect the rearrangement of the remaining oximino group of VI, VI was further subjected to a reaction with thionyl chloride in ether. The resultant product seemed likely to be adipic imide (VII)[13], the oximino group being eliminated from VI without accepting further rearrangement. The hydrolysis of VII with concentrated hydrochloric acid afforded adipic acid (VIII) and ammonium chloride. The infrared spectrum of VII was agreeable with that of cyclic imide as reported by Vegstky et al.[14]

The attempted rearrangement with sulfur trioxide in liquid sulfur dioxide was accompanied by a large resinous matter. By extracting the viscous reaction mixture with ether, an orange oil (IX) was obtained. The oil boiled at 181~183°C/17 mmHg, and its yield was 23 per cent.

$$\mathrm{I} \xrightarrow[\text{liq. } SO_2]{SO_3} \underset{NH_2OH}{NC\text{-}(CH_2)_4\text{-}COOH} \xrightarrow{\text{conc.HCl}} \underset{\mathrm{IX}}{\mathrm{VIII}}$$

The compound IX was identified as δ-cyanovaleric acid from the elemental analysis, the infrared spectrum, the hydrolysis to adipic acid, the esterification and the saponification value of the ester. The present authors also found hydroxylamine in the residue of the reaction mixture by the diacetyl monoxime method[10]. Thus, the cleavage of I to IX seems likely to pass through an intermediate, 1,2-cyclohexanedione 2-monoxime (X), which might be derived through partial hydrolysis of an oximino group of I, the so-called Beckmann rearrangement of the second order being followed. An alternative explanation is also conceivable and will be discussed later.

## Experimental

**Materials.**—Commercial sulfur dioxide was dried with concentrated sulfuric acid[15] and distilled.

Bromine was dehydrated with concentrated sulfuric acid and distilled. Sulfur trioxide of extra pure grade was used without further purification. 1,2-Cyclohexanedione dioxime (I) was synthesized[8] from 2-halo-cyclohexanone by reacting with hydroxylamine in yields of 10 to 34 per cent.

**Infrared Spectrum.**—A Perkin Elmer model 21 infrared spectrophotomer was used.

**NMR Spectrum.**—A Varian Associates' type V-4300 (40 mc.) nuclear magnetic resonance spectrometer was used.

**Reaction of Bromine on I.**—The dioxime(I) (14.2 g.) and bromine (35.2 g.) were reacted in 150 ml. of liquid sulfur dioxide at room temperature for one hour. When the reaction was over, the solution was poured into ice-water, the sulfur dioxide was evaporated and the residue was extracted with ether. From the ether extract, colorless crystals were obtained after the condensation of the solution. This substance was identified as cyclohexano-[c]-1,2,5-oxadiazole (II), which had already been produced and confirmed by the reaction of thionyl chloride on I in liquid sulfur dioxide[8], by its m. p. and mixed m. p. of 25.5~26.0°C: the yield was 0.6 g. (4%). The residual solution was neutralized with sodium carbonate and extracted with chloroform. Seven grams of resinous material was obtained from the solution, but the nature of this material was obscure.

The residual solution of the chloroform extraction was condensed in vacuo and triturated with acetone. On the evaporation of acetone, 4.6 g. (32%) of colorless crystals resulted. This crystal, VI, melting at 155°C (from water or ethyl alcohol), was soluble in water, acid, base, ethyl alcohol and acetone respectively but was insoluble in ether, benzene and

9) By Nessler reagent.
10) W. Hirscher and J. A. Verboeff, *Chem. Abstr.*, **17**, 2845 (1923).
11) L. Szebelledy and V. Madis, ibid., **31**, 6128 (1937).
12) The NMR spectrum was taken by the courtesy of Prof. T. Isobe.
13) E. N. Zilbermann, *Chem. Abstr.*, **50**, 8458 (1956): H. K. Hall, Jr. and A. K. Schneider, *J. Am. Chem. Soc.*, **80**, 6411 (1958).
14) A. Vegstky, K. Harada and S. W. Fox, *J. Am. Chem. Soc.*, **80**, 336 (1958).
15) D. Murakami and N. Tokura, This Bulletin, **31**, 431 (1958).

chloroform. The elemental analysis showed no difference to the starting oxime I, suggesting that a rearrangement was undertaken in this reaction.

Found: C, 51.21; H, 6.85; N, 19.68. Calcd. for $C_6H_{10}O_2N_2$: C, 50.69; H, 7.07; N, 19.71%. IR $\nu_{max}^{KBr}$ 2900~3200 (strong and broad, -OH and =NH); 1660 (strong and broad, =CO) and 1620 weak, -C=N) $cm^{-1}$, respectively.

**Hydrolysis of VI.**—VI (2.0 g.) was refluxed for 2 hr. in concentrated hydrochloric acid. After the reaction, the colorless needles (III) so produced were filtered and recrystallized from ethyl alcohol, 1.1 g., m. p. 151~152°C. The mixed melting point with adipic acid showed no depression.

Found: C, 49.46: H, 6.94. Calcd. for $C_6H_{10}O_4$: C, 49.31: H, 6.90%.

The filtrate was evaporated to dryness. This residue contained ammonium chloride (Nessler test). Also hydroxylamine hydrochloride was identified[10]. No hydrazine salt was found in the residual mixture[11].

**Reaction of IV with Thionyl Chloride.**—VI(0.5 g.) was refluxed in ether (20 ml.) with thionyl chloride (0.5 g.) for fifteen minutes. The reaction mixture was poured into ice-water, and white powder (0.2 g.), m. p. 166.5°C., was yielded by the ethereal solution. This compound VII was assumed to be adipic acid imide from the elemental analysis, the infrared spectrum and the hydrolysis with concentrated hydrochloric acid to adipic acid (VIII), the melting point and the mixed melting point being 152°C.

Found: N, 1030, Calcd. for $C_6H_9O_2N$: N, 11.02%. IR $\nu_{max}^{KBr}$ 3200 and 3350, (strong, =NH), 1700 (=CO) and 2950 (=$CH_2$) $cm^{-1}$, respectively. From the reaction mixture of the hydrolysis, after the filtration of the afforded adipic acid, neither hydrazine nor hydroxylamine salt was identified by the procedure described above.

**Reaction of I with Sulfur Trioxide.**—I (7.1 g.) and sulfur trioxide (10.0 g.) were reacted in 100 ml. of sulfur dioxide for one hour at room temperature. The reaction mixture was poured into ice-water, after which the sulfur dioxide was allowed to evaporate and was then extracted with ether. The ethereal solution was washed with water, dried and evaporated. An orange-colored liquid (IX), boiling at 181~183°C/17 mmHg, $n_D^{17}=1.4452$, 1.6 g. (23%), was obtained and identified as δ-cyano-valeric acid, (literature[16], b. p. 158~160°C/5 mmHg, $n_D^{20}=1.4481$).

The residual solution after the extraction contained a large amount of resinous matter which could not be further examined.

Found: N, 10.53. Calcd. for $C_6H_9O_2N$: N, 11.02%. IR $\nu_{max}^{liq.}$, 3000~3300 (strong and broad, -OH), 2260 (medium, -CN) and 1700 (strong, =CO) $cm^{-1}$, respectively.

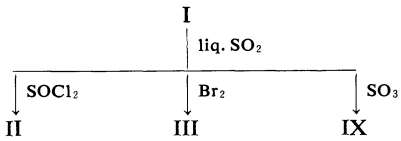
**Hydrolysis of IX**—IX(0.3 g.) was reacted with 3 ml. of concentrated hydrochloric acid by refluxing. On cooling of the reaction mixture, colorless needles were obtained in the mixture, which on admixture with adipic acid (VIII) showed no depression of the m. p. of 151~152°C.

**Esterification of IX.**—IX(2.0 g.) and two drops of concentrated sulfuric acid in 4 ml. of absolute ethyl alcohol were refluxed for 24 hr. The mixture was then mixed with water, and the separated oil was dried and distilled. An oil of b. p. 252~256°C 760 mmHg, (reportedly[16] 145~150°C/24 mmHg), was obtained. This oil was consistent with ethyl δ-cyano-valerate.

Found: C, 60.83; H, 8.37; N, 8.44, Calcd. for $C_8H_{13}O_2N$: C, 61.91; H, 8.44; N, 9.03%. Sapon. value, Found, 706.5, Calcd., 722.5.

## Discussion

When I was reacted with three different reagents, thionyl chloride, bromine and sulfur trioxide respectively, in liquid sulfur dioxide, for one hour at room temperature, three different products were obtained, viz., cyclohexano[c]-1, 2, 5-oxadiazole (II), 1-aza-7-oximino-cycloheptа-2-one (VI) and δ-cyano-valeric acid (IX) respectively, among which the first has been presented in a preceding paper[8].



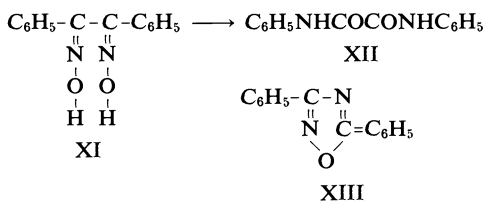

If the reactions were performed without sulfur dioxide, no such simple product was obtained. Thus, thionyl chloride yielded much resinous matter, and II was obtained in a yield of zero to ten per cent. Bromine afforded only nitrosobromo compound, the presence of which was recognized by the blue color formation. Sulfur trioxide also produced a large amount of resin. This means that the reaction in liquid sulfur dioxide was greatly favored by the assistance of the solvation of this solvent, which enabled the reaction to be carried out at a lower temperature and to avoid various side reactions.

The results obtained above may be useful to enhance our understanding of the mechanism of the Beckmann rearrangement in liquid sulfur dioxide. Not only were the three products different, but the features of the respective processes were entirely different.

They were a dehydrative condensation, a Beckmann rearrangement of one of the two oximino groups, and a ring cleavage reaction respectively. The Beckmann rearrangement of 1, 2-diphenyl-1, 2-dione dioxime (benzil dioxime) which reportedly consisted of three geometrical isomers, has already been reported[17]. According to Meisenheimer and Lamparten[2], the β-isomer of XI afforded oxanilide XII, both of the two oximino groups rearranging, whereas α- and γ-isomers yielded

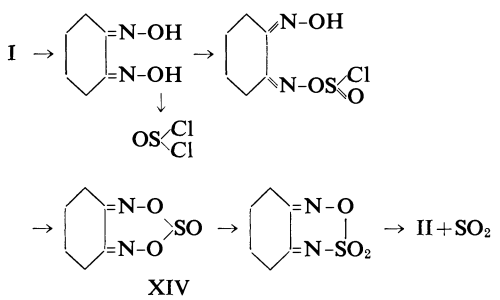
16) R. H. Wiley and H. S. Morgan, Jr., *J. Org. Chem.*, **15**, 800 (1950); W. Reppe, *Ann.*, **596**, 127 (1955).
17) a) K. Awers and V. Meyer. *Ber.*, **21**, 810 (1888). b) E. Beckmann and A. Koster, *Ann.*, **274**, 18 (1893). c) E. Gunther, *Ber.*, **21**, 516 (1888); *Ann.*, **257**, 276 (1889).

3, 5-diphenyl-1, 2, 4-oxadiazole (XIII), a product of one oximino group rearrangement followed by dehydration. The reagent used were thionyl chloride and phosphorus compounds.



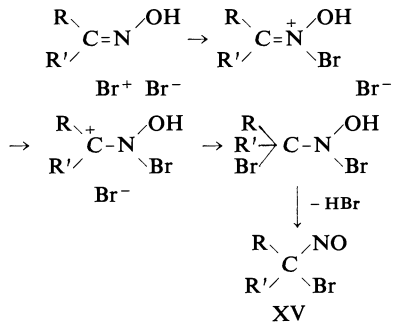

That a simple dehydration occurred by thionyl chloride from I to II indicates that the rate of the Beckmann rearrangement of I with thionyl chloride was much less than the rate of condensation with the same reagent in liquid sulfur dioxide. In such a cyclic dioxime as I, the steric impedence by the ring enlargement, if it arose, would be considerable. On the other hand, in the case of XI, no steric hindrance was anticipated, and the formation of azilinium cation favorable for the Beckmann rearrangement may be greatly assisted by the participation of the phenyl group.

The predominance of the condensation reaction between the two competitive reaction is a result of the nature of the reagent (thionyl chloride). A=N-O·SOCl group formed from a reaction between thionyl choride and a oximino group will easily produce a sulfite linkage XIV by reacting with another oximino group, for these two groups are occupying positions very close to each other. Consecutively, the formation of a sultone via the Bissinger rearrangement[18] and the conversion of the sulfite to II by elimination of the sulfur dioxide molecule would be undertaken. Very recently, Gillis[19]

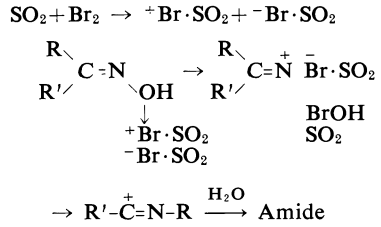



has reported the formation of tetrahydrofuran from 1, 4-tetramethylene glycol with thionyl chloride via the sulfite. The derivation of II from I closely resembles this furan formation.

Here, the behavior of bromine in liquid sulfur dioxide is very interesting. When the reagent is bromine only, without sulfur dioxide, the bromine cation will attack the nitrogen atom of the oxime:

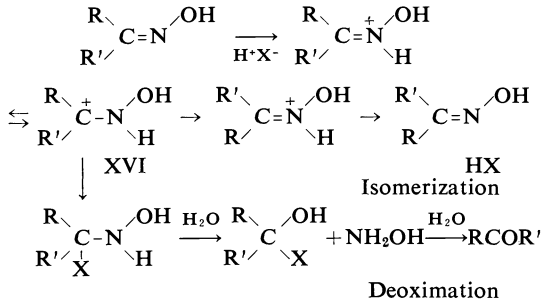



Producing a nitroso bromo compound XV which is characteristically blue in color. However, the bromine in sulfur dioxide[20] may attack the oxygen atom of the oxime, since the voluminous $SO_2$-solvated bromo-cation is liable to prefer the oxygen atom to the nitrogen atom; this would be followed by the rearrangement:




The reason why only one of the two oximino groups will accept the rearrangement is perhaps due to the steric hindrance.

Generally speaking, the attack of hydrogen acid causes some complex results in the attempted Beckmann rearrangement. The side reactions are the isomerization[5,21] of the oxime and the deoximation of the oxime (ketone formation)[21]. The origin of both arises from the same source, the formation of a carbonium ion, XVI:




18) W. Bissinger, F. E. King and C. W. Hamilton, *J. Am. Chem. Soc.*, **70**, 3940 (1948).
19) R. G. Gillis. *J. Org. Chem.*, **25**, 651 (1960).
20) N. Tokura, R. Asami and R. Tada, *J. Am. Chem. Soc.*, **79**, 3135 (1957).
21) R. Tada, Y. Masubuchi and N. Tokura, This Bulletin, **34**, 270 (1961).

There are many examples of carbonium ion formation from oxime with hydrogen acid, such as hydrochloric acid, sulfuric acid and hydrogen cyanide[21,22]. Such a carbonium ion (XVI) cannot undertake the Beckmann rearrangement. To carry out the rearrangement, an ion-pair formation

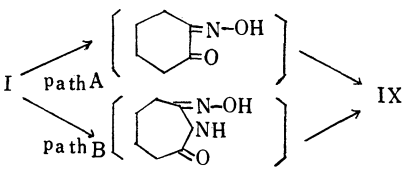
$$=N\text{-}O\text{-} \rightarrow =\overset{+}{N}\ \overset{-}{O}\text{-}$$

between the two atoms is necessary[23].

The cleavage of I to IX is presumed to pass through an intermediate, 1,2-cyclohexanedione monoxime (X), which may result from a partial deoximation of I, the so-called Beckmann rearrangement of the second order being followed (path A). A small amount of water remaining in the solvent (sulfur dioxide) may be responsible for the deoximation by serving as a source of the proton,

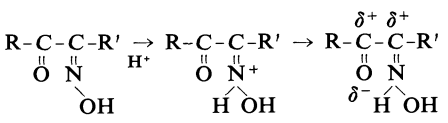
$$SO_3+H_2O+H^+ \rightarrow SO_4H^-$$

An alternate path B might be considered.



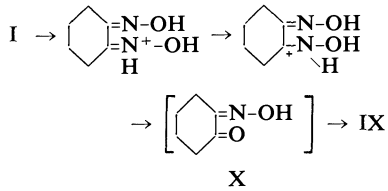

However, path B must be ruled out because this route cannot explain the presence of hydroxylamine in the reaction mixture.

The dioxime I has two oximino group sterically interferring with each other, and the elimination of one of the oximes would be a natural consequence. It is a plausible conclusion that I was cleaved to IX, via the stage of cyclohexanedione monoxime (X), the deoximation being effected by sulfuric acid mentioned above. As the result of the material balance of the IX formation, a large amount of resinous matter was recognized. Such a resinification by a dehydration reaction would supply enough water to make the proton source available for the deoximation. The Beckmann rearrangement of the second order, a well-discussed phenomenon[24], may be explained as:



$$\rightarrow R\cdot\overset{+}{C}O + R'CN \xrightarrow{OH^-} RCOOH + R'CN$$

Summarizing the above discussion, the formation of $\delta$-cyanovaleric acid (XI) may be visualized as:




## Summary

Three different reagents, thionyl chloride, bromine and sulfur trioxide in liquid sulfur dioxide were reacted on 1,2-cyclohexanedione dioxime to yield cyclohexano[c]-1,2,5-oxadiazole, 1-aza-7-oximinocyclohepta-2-one and $\delta$-cyanovaleric acid respectively. Only the bromine in liquid sulfur dioxdie effected the Beckmann rearrangement. Thionyl chloride caused a dehydrative condensation, as has been reported previously. Sulfur trioxide yielded a product resulting from a deoximative cleavage. The reasons for the different processes and the different products have been discussed.

The authors are grateful to Befu Chemical Industries Inc., for the donation of liquid sulfur dioxide.

*The Chemical Research Institute of Non-Aqueous Solutions*
*Tohoku University*
*Katahira-cho, Sendai*

22) O. L. Brady and E. P. Dunn, *J. Chem. Soc.*, **109**, 656 (1916); G. Munch, *Ber.*, **29**, 62 (1896).
23) M. Kuhara, Y. Toda, *Memoirs Col. Kyoto Univ.*, **2**, 387 (1910).
24) D. Murakami and N. Tokura, This Bulletin, **31**, 1044 (1958); R. T. Conley and F. A. Mikulski, *J. Org. Chem.*, **24**, 97 (1959); A. F. Ferris, ibid., **24**, 580 (1959).

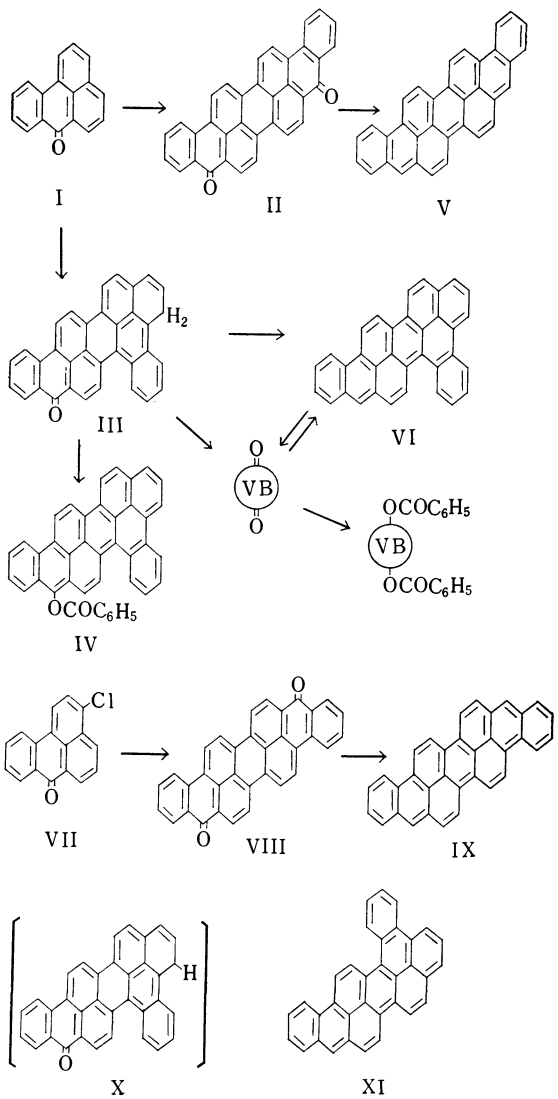
# *Studies of Violanthrone B. I. Reduction and Oxidation of Violanthrone B*[1]

By Junji AOKI

(Receivied March 18, 1961)

When benzanthrone (I) is fused with potassium hydroxide in the presence of phenol or sodium acetate, by its own condensation, violanthrone (II) is obtained; this substance is very useful as a vat dye. On the other hand, as a by-product, a black violet compound which is worthless as vat dye is obtained; this compound is barely vattable at 65~70°C. This worthless compound was found by the study of Maki and denoted as violanthrone B[2]. Further, he suggested III as its formula with one carbonyl group. Although this assumption has been partially confirmed by studies on the condensations of benzanthrone derivatives by Maki and Nagai[3], there remain many doubtful points. Furthermore, recently it has been found by Akamatu and Maekawa[4] that this substance was paramagnetic and that it may be a new radical compound to be known as formula X. Their studies are quite interesting and valuable in the field of the chemistry of this polynuclear system.

From the result of elementary analysis and the preparation of the leucobenzoate (IV) which was obtained by the author by the addition of benzoyl chloride to the vat solution, it has been found, however, that this substance has only one carbonyl group. Following the reduction technique of Clar[5], in which violanthrone A[6] was reduced to violanthrene A (V) with zinc dust in the mixed flux of zinc chloride and sodium chloride, the author obtained the reduction product from violanthrone B. This compound resembles violanthrene A, which shows a strong yellow green fluorescence in organic solvent and is green when dissolved in concentrated sulfuric acid. It is, however, evident that this substance is apparently different from violanthrene A; the reduced compound is more soluble than violanthrene A in organic solvent and the melting point of the former is 344°C (corr.), while that of the later is higher than 360°C[5,7]. In addition, this compound is not identical with isoviolanthrene (IX)[5] either, the reduction product of isoviolanthrone (VIII) prepared by




1) Read befroe the 13th Annual Meeting of the Chemical Society of Japan, April, 1960.

2) T. Maki, *J. Chem. Soc. Ind., Japan* (*Kôgyô Kwagaka Zasshi*), 35, 1441 (1932); *Chem. Abstr.*, 27, 1629 (1933).

3) T. Maki, ibid., 38, 1390 (1935); *Chem. Abstr.*, 30, 2008 (1936); T. Maki and A. Kikuchi, ibid., 43, 763 (1940); *Chem. Abstr.*, 35, 1783 (1941); Y. Nagai et al., ibid., 47, 529 (1944).

4) H. Akamatu and T. Maekawa, Presented at the 13th Annual Meeting of the Chemical Society of Japan, April, 1960.

5) E. Clar, *Ber.*, 72, 1648 (1939).

6) "A" is used to distinguish it from the B-compound.

7) E. Clar, *Ber.*, 76, 458 (1943).

the bimolecular self condensation of 3-chlorobenzanthrone (VII), because isoviolanthrene is yellow green rather than green when dissolved in concentrated sulfuric acid and melts at a temperature higher than 360°C[5,7]. From the results of his chemical analysis, the author has concluded that the reduction product is a new hydrocarbon having a "dibenzanthrene" type skeleton. We denote this hydrocarbon violanthrene B (VI).

When violanthrene A was oxidized with dilute sulfuric acid and potassium bichromate, the author obtained violanthrone A. In an effort to obtain violanthrone B, violanthrene B (VI) was oxidized, but violanthrone B (III) was not obtained. The oxidized product is readily vattable at 30°C and cotton is dyed in it a dark violet. The result of elementary analysis suggested that it may be a quinone of a dibenzanthrene type. This assumption was confirmed by the author, who synthesized its leucodibenzoate at m. p. 335~336°C (corr.).

However, he has found the more interesting fact that the quinone can also be prepared from violanthrone B (III) by a similar operation. Further, from this quinone violanthrene B (VI) was obtained again by zinc dust fusion.

In conclusion, it is reasonable to suppose that all derivatives from violanthrone B have the same polynuclear skeleton, but not those of violanthrene A and isoviolanthrene A.

On the other hand, it has been confirmed by the author that violanthrone B has only one carbonyl group, and further, it has been reported by Nagai et al. that the 6-position of benzanthrone contributes to the formation of the B-compound[3]. Consequently, the hypothetic skeleton (IV), submitted by Maki, coincides with the above facts, but the isomeric formula XI must also be re-considered for the same reason. A detailed discussion will be presented in a later report.

## Experimental

**Violanthrone A (II) and Violanthrone B (III).**—These substances were prepared by the operation stated in Maki's paper[2], but for the purpose of increasing the yield of B-compound, the condition of the alkali fusion was somewhat modified as below. Benzanthrone (I) (10.0 g.) was fused with 40 g. of 85% potassium hydroxide and 4.2 g. of phenol at 220°C for 30 min. (Ref. 2 : 81% potassium hydroxide, 12.4 g. of phenol, 1 hr.).

Violanthrone A was obtained as one product, vattable at 55°C and insoluble in chlorobenzene. Yield, 2.5 g. of violet black powder. The concentrated sulfuric acid solution shows a pure violet color.

The other product, which was barely vattable and insoluble in glacial acetic acid, was violanthrone B. Yield, 5.4 g. of violet black powder. It is soluble in concentrated sulfuric acid as a blue color[8].

Found: C, 91.47; H, 4.35. Calcd. for $C_{34}H_{18}O$ (III): C, 92.28; H, 4.10%.

**Leucobenzoate of Violanthrone B (IV).**—Violanthrone B (III) (0.50 g.) was vatted by heating with 10 g. of sodium hydroxide, 10 g. of sodium hydrosulfite and 200 ml. of water at 70°C and 5 g. of benzoyl chloride was added. The mtxture was shaked without heating for 2 hr. After being allowed to stand overnight, the precipitate was collected and washed neutral. Yield, 0.50 g. of dark brown powder. The product was recrystallized from xylene-petroleum ether, giving red brown needles, m. p. 327~328°C (uncorr.), 340~341°C (corr.). The product is soluble in organic solvent with a strong yellow green fluorescence and in concentrated sulfuric acid solution shows at first a blue color and then a blue green.

Found: C, 89.92; H, 4.19. Calcd. for $C_{41}H_{22}O_2$ (IV): C, 90.09; H, 4.06%.

**Violanthrene B (VI).**—Two gram of violanthrone B (III) in the form of fine powder, was kept with 2.0 g. of zinc dust in the mixed flux of 10 g. of zinc chloride and 2.0 g. of sodium chloride at 260°C for 20 min. Then the mixture was treated with 300 ml. of water and the insoluble material was filtered off. To remove the excess of zinc dust, it was suspended in 100 ml. of water and 30 ml. of concentrated hydrochloric acid was added. After being kept overnight, the insoluble was collected and washed neutral. The crude reduction product (1.8 g.) was sublimated in a high vaccum ($10^{-3}$~$10^{-4}$ mmHg) and recrystallized from 100 parts of *o*-dichlorobenzene, giving orange red needles, m. p. 328°C (uncorr.), 341°C (corr.). This product is soluble in organic solvent with a strong yellow green fluorescence, and in the concentrated sulfuric acid solution shows at first blue and then green, after which it changes no more.

Found: C, 95.56; H, 4.32. Calcd. for $C_{34}H_{18}$ (VI): C, 95.75; H, 4.25%.

**Violanthrene A (V).**—Synthesis was carried out by a method similar to that used for VI[9]. The crude product (1.8 g.) obtained from 2.0 g. of violanthrone A (II), was sublimated in high vaccum and refluxed with 100 g. of *o*-dichlorobenzene for 30 min. The small amount of soluble impurities was removed by hot filtration. Yield, 0.6 g. of brown red crystalline powder, m. p. 476~478°C (uncorr.)[10]. This substance is only with difficulty soluble in organic solvent and in a concentrated sulfuric acid solution shows green color.

**Isoviolanthrene A (IX).**—Synthesis was carried out by a method similar to that used for V. Yield, 32% from isoviolanthrone (VIII). Dark red crystalline powder, m. p. 506~508°C (uncorr.)[11]. The product is only with difficulty soluble in organic solvent and appears as a yellow green coloration in concentrated sulfuric acid.

**Oxidation of Violanthrene B.**—To a solution of

8) The sample was purified by means of chromatography on anhydrous sodium carbonate from *o*-dichlorobenzene.
9) Cf. also Ref. 5
10) Ref. 7, m. p. 478°C.
11) Ref. 7, m. p. 510°C.

1.00 g. of violanthrene B (VI) in 30 ml. of concentrated sulfuric acid was added, with cooling, 30 ml. of water. After cooling till the room temperature, 1.0 g. of potassium bichromate, which had been dissolved in 20 ml. of water, was added. The mixture was stirred for 3 hr. on a boiling water bath and, after being diluted with 300 ml. of water, was filtered. The unchanged VI was separated as the insoluble part by treating it with a 2% alkaline hydrosulfite solution at 30°C, and 0.95 g. of the oxidation product was obtained from the violet filtrate by air oxidation. The crude product, finely powdered, was boiled with 300 g. of *o*-dichlorobenzene with reflux for 2 hr., and insoluble impurities was removed by hot filtration. The filtrate was evaporated to a volume of about 100 ml. for crystallization. The crystal (0.65 g.) formed was recrystallized from chlorobenzene, giving black violet needles, melting point higher than 360°C. The product shows pure blue when dissolved in concentrated sulfuric acid and reddish violet in a hot organic solvent, but it is readily vattable at 30°C while III is with difficulty vatted even at 60°C.

Found: C, 88.74; H, 3.83. Calcd. for $C_{34}H_{16}O_2$; C, 89.46; H, 3.53%.

*Leucodibenzoate.* — The oxidation product (0.50 g.) was vatted by heating with 8 g. of sodium hydroxide, 10 g. of sodium hydrosulfite and 200 ml. of water at 50°C and 5.0 g. of benzoyl chloride was added. The mixture was shaked without heating for 2 hr. and allowed to stand overnight. The precipitate was then collected and the unchanged substance was removed by treating with an alkaline hydrosulfite solution as the insoluble part. The crude product (0.45 g.) was recrystallized repeatedly from *o*-dichlorobenzene-petroleum ether, giving orange brown needles, m. p. 322~323°C (uncorr.), 335~336°C (corr.). This product is only with difficulty soluble in alcohol, when dissolved in benzene, xylene and *o*-dichlorobenzene gives a strong yellow green fluorescence, and in a concentrated sulfuric acid solution gives a bluish green coloration.

Found: C, 85.96; H, 3.93. Calcd. for $C_{48}H_{26}O_4$: C, 86.47; H, 3.93%.

**Oxidation of Violanthrone B.**—By an operation similar to that used for VI, 2.00 g. of violanthrone B (III) was oxidized with 2.0 g. of potassium bichromate and diluted sulfuric acid, and 1.65 g. of crude product was obtained from an alkaline hydrosulfite vat as the soluble part (the insoluble, 0.30 g.). It was boiled with 300 g. of *o*-dichlorobenzene, and 1.00 g. of violet black needles of a melting point higher than 360°C were obtained from the filtrate after hot filtration. The product was easily vattable, was soluble in concentrated sulfuric acid, appearing as a pure blue color, and its absorption spectrum and leucobenzoate are identical with those of the oxidation product of violanthrene B.

*Reduction.* — By zinc dust fusion 0.20 g. of the above mentioned quinone was reduced. The crude product was purified by sublimation in high vacuum and recrystallization from *o*-dichlorobenzene. Yield, 0.06 g. of orange red needles, m. p. 326~328°C (uncorr.). This product was identical with violanthrene B (VI).

**Oxidation of Violanthrene A.**—By an operation similar to that used for VI, 1.00 g. of violanthrene A was oxidized with 1.0 g. of potassium bichromate and diluted sulfuric acid. The crude product was treated with 3% alkaline hydrosulfite solution at 60°C, and the unchanged substance was removed as the insoluble. From the red violet filtrate, 0.85 g. of the oxidation product was obtained. It was boiled with 100 g. of chlorobenzene for 1 hr., filtered and dried. Yield, 0.80 g. of violet black powder, melting point higher than 360°C. The product was soluble in concentrated sulfuric acid, giving a pure violet color, and, further, any other properties were also identical with those of violanthrone A (II) (Found: C, 89.11; H, 4.03%).

The author wishes to express his thanks to Professor Hideo Akamatu, Professor Hiroo Inokuchi and Professor Yoshio Nagai for their kind advice. He is also indebted to Mr. Shozo Masuda for carring out the analyses.

*Department of Chemistry*
*Facutly of Science*
*Toho University*
*Narashino, Chiba*

# *Studies of Violanthrone B. II. Reduction of Isoviolanthrone B*

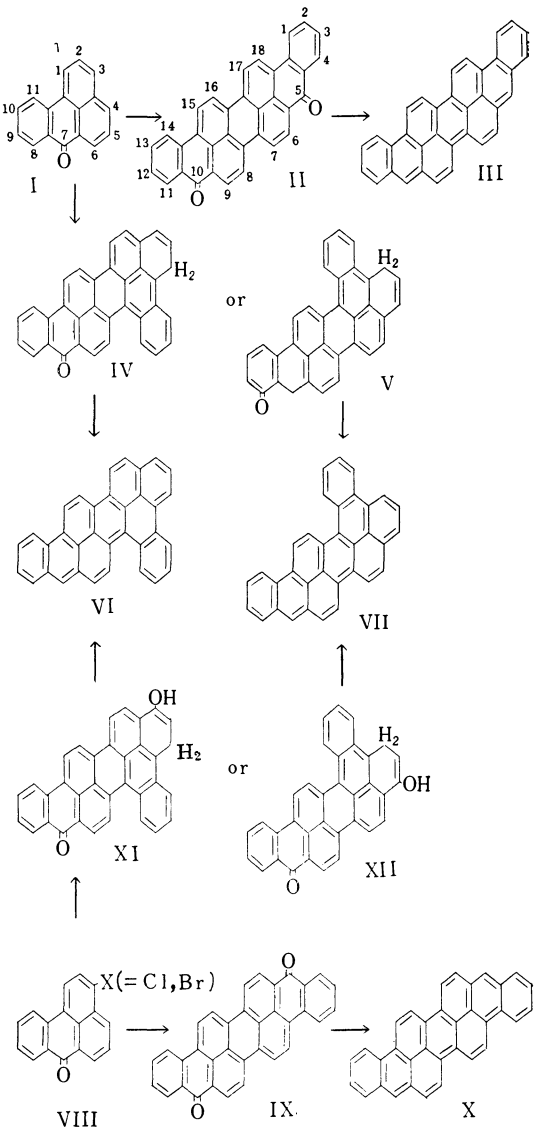
By Junji AOKI

(Received March 18, 1961)

As described in a previous paper[1], the reduction of violanthone B resulted in obtaining the new condensed aromatic hydrocarbon, violanthrene B. Generally, when the method of alkali fussion on benzanthrone (I) derivatives (except 3-position) is applied for the purpose of obtaining the vat dyes of the violanthron (II) series, the B-compound is by-produced with violanthrone derivatives. For example, 4, 11- and 1, 14-dimethoxyviolanthrone were prepared from 8- and 11-methoxybenzanthrone respectivery by alkali fusion, and B-compounds were also obtained[2]. Violanthrone B and these B-componds resemble each other in their vattability and in their coloration with concentrated sulfuric acid. It is, therefore, suggested that the B-compounds by-produced with A-compounds of the violanthrone A type may be derivatives of violanthrone B.

Further, Nagai and Masuda have reported that the 6-position of benzanthrone contributes to the formation of B-compound because the reaction of the alkali fusion of 6-phenylbenzanthrone produces A-compound, but not B-compound[3]. According to these facts, the formula VI or VII can be applied to the skeleton of B-compound, which has only one carbonyl group[4].

On the other hand, there is another type of B-compound, that by-produced with isoviolanthrone (IX) from 3-halogenobenzanthrone (VIII) by heating with alcoholic potassium hydroxide. This B-compound, which is as barely vattable as violanthrone B, has been denoted as isoviolanthrone B by Maki and Nagai[5], and they have suggested as the formula XI, in which the halogen atom was converted into the hydroxl group. In addition, Nagai et al. have reported that the reaction of the alcoholic alkali of 3-chloro-6-phenylbenzanthrone produces A-compound of the isoviolanthrone type, but not B-compound[3].




Therefore, although the formula (XI) appears feasible the isomeric formula (XII) may be also considered, as has been mentioned for violanthrone B[6].

The author has tried to reduce isoviolanthrone B to hydrocarbon by the method of

1) J. Aoki, This Bulletin, **34**, 1817 (1961).

2) T. Maki, *J. Chem. Soc. Ind., Japan*, **38**, 1390 (1935); *Chem. Abstr.*, **30**, 2008 (1936); T. Maki and A. Kikuchi, ibid., **43**, 763 (1940); *Chem. Abstr.*, **35**, 1783 (1941).

3) Y. Nagai and M. Masuda, *J. Chem. Soc. Ind., Japan*, **47**, 529 (1944).

4) Consequently, violanthrone B may be considered as having the formula IV or V; T. Maki has suggested IV as the formula.

5) T. Maki and Y. Nagai, *J. Chem. Soc. Ind. Japan*, **37**, 493 (1934); *Chem. Abstr.*, **28**, 5435 (1934).

6) These compounds may be considered free radical because of their paramagnetism; therefore, instead of formulas IV, V, XI and XII, those which take off one hydrogen atom should be preferred. See also Ref. 1.

TABLE I. PROPERTIES OF "DIBENZANTHRENES"

| | Violanthrene B | | Isoviolanthrene B | | Violanthrene A | | Isoviolanthrene A |
|---|---|---|---|---|---|---|---|
| Appearance | Orang red | | Deep red | | Red | | Dark red |
| M. p., °C | 344 | | 400~402 | | 478[7] | | 510[7] |
| Color in $H_2SO_4$ | Green | | Yellow green | | Green | | Yellow green |
| Solubility | | >[8] | | > | | > | |
| Alcohol | Insol. | | Insol. | | Insol. | | Insol. |
| Benzene | Hardly sol. | | Hardly sol. | | Hardly sol. | | Hardly sol. |
| *o*-Dichlorobenzene | Sol. in hot | | Sol. in hot | | Hardly sol. | | Hardly sol. |

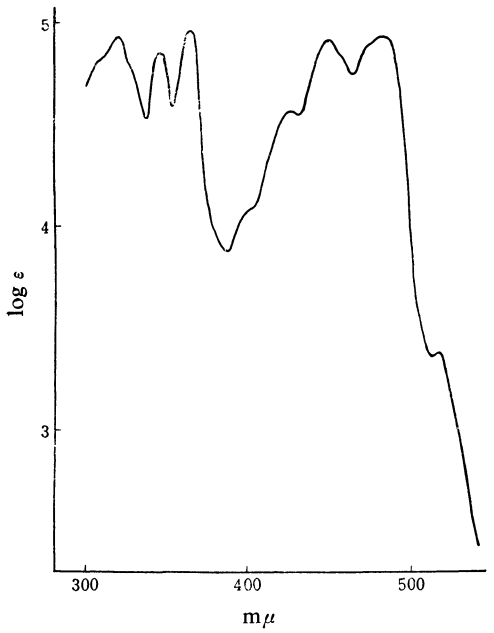



Fig. 1. Absorption spectrum of Violanthrene B (in benzene).

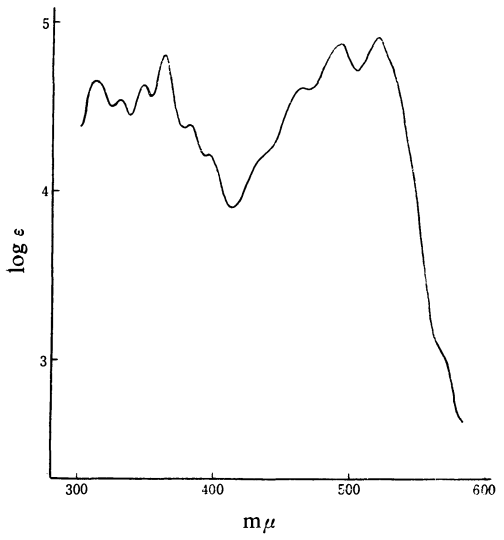



Fig. 2. Absorption spectrum of isoviolanthrene B (in benzene).

zinc dust fusion in order to find the structural formula of this compound. The hydrocarbon obtained from the above method recrystallized from *o*-dichlorobenzene in deep red needles. The meting point of this compound was 400~402°C (uncorr.), and its absorption spectrum was different from that of violanthrene B, as is shown in Figs. 1 and 2. In addition, the properties of this new hydrocarbon, which is called by the author isoviolanthrene B, are quite different from those of violanthrene B, violanthrene A (III) and also isoviolanthrene A (X), as is shown in Table I.

From these facts, we can draw the following conclusions: there are only two types of B-compound, with skeletons assumed to be the fosmulas VI and VII; one of them is violanthrene B and the other is isoviolanthrene B.

## Experimental

**Isoviolanthrone A (IX) and Isoviolanthrone B.**—A mixture of 40 g. of potassium hydroxide, 25 g. of phenol, 15 g. of ethanol and 10.0 g. of 3-chlorobenzanthrone was refluxed with stirring for 2 hr. Then the mixture was treated by the method described in Ref. 5. The yield of isoviolanthrone A was 3.2 g., and this substance is soluble in concentrated sulfuric acid, giving a blue green color. Isoviolanthrone B was obtained as the product, barely vattable and insoluble in glacial acetic acid. In the concentrated sulfuric acid solution it shows as a dark violet color. Yield, 3.0 g. of violet black powder. This sample was once more treated with an alkaline hydrosulfite solution, dissolved in hot chlorobenzene and, after hot filtration, deposited by concentrating the filtrate.

Found: C, 88.80; H, 3.58. Calcd. for $C_{34}H_{18}O_2$ (XI or XII): C, 89.06; H, 3.95%.

**Isoviolanthrene B.**—A fine powder of 1.00 g. of isoviolanthrone B was kept with 1.0 g. of zinc dust in the mixed flux of 5 g. of zinc chloride and 1 g. of sodium chloride at 260~280°C for 30 min. Then the mixture was treated with 300 ml. of water and the insoluble part filtered off. To remove the excess of zinc dust, it was suspended with 100 ml. of water, and 30 ml. of concentrated hydrochloric acid was added. After being kept overnight, the insoluble part was collected and washed neutral. The crude

7) E. Clar, *Ber.*, **76**, 456 (1943).
8) This symbol defined a solubilization power.

reduction product (0.80 g.) was sublimated in a high vacuum ($10^{-3}$~$10^{-4}$ mmHg), and recrystallized from *o*-dichlorobenzene, giving deep red fine needles, m. p. 400~402°C (uncorr.). This product is soluble in organic solvent, giving off a strong fluorescence, and in a concentrated sulfuric acid solution shows at first as green and then as a yellow green, after which it changed no more.

Found: C, 95.56; H, 4.34. Calcd. for $C_{34}H_{18}$ (VI or VII): C, 95.75; H, 4.25%.

The author wishes to express his thanks to Professor Hideo Akamatu, Professor Hiroo Inokuchi and Professor Yoshio Nagai for their kind advice. He is also indebted to Mr. Shozo Masuda for carrying out the analyses.

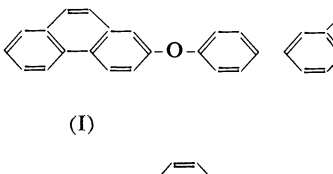
*Department of Chemistry*
*Faculty of Science*
*Toho University*
*Narashino, Chiba*

# *Synthesis of Phenanthryl Phenyl Ethers*

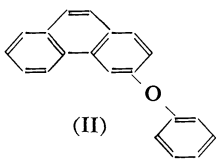
By Hajime SUZUMURA

(Received March 31, 1961)

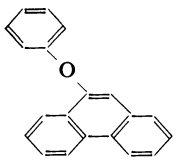
Searching for aromatic ethers which have high boiling points and thermal stability, derivatives of phenanthrene, 2- and 3-phenanthrylphenyl ethers (Formulas I and II respectively) were synthesized and their physical properties examined. Of the phenanthrylphenyl ethers, only a 9-phenyl isomer (Formule III) has hitherto been reported on the literature[1].



(I)



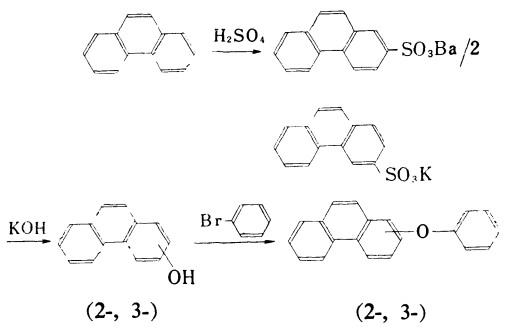
(II)



(III)

The author newly synthesized 2- and 3-phenyl ethers by the scheme shown below.

TABLE I




(2-, 3-) (2-, 3-)

1) R. L. Huang, *J. Chem. Soc.*, **1955**, 3295.

Purified phenanthrene was sulfonated[2], and a mixture of monosulfonates was fused with potassium hydroxide[3], yielding phenanthrols which were then condensed with bromobenzene to give the ethers. The properties of purified specimens are shown in Table II.

TABLE II. PHENANTHRYLPHENYL ETHERS

| Properties | Isomer 2- | Isomer 3- | Calcd. |
|---|---|---|---|
| Appearence | White needles | White needles | — |
| B. p., °C | 225( 1mmHg) | 220 (1 mmHg) | — |
| M. p., °C | 121~122 | 86~87 | — |
| Elementary analysis | | | |
| C, % | 88.69 | 89.16 | 88.86 |
| H, % | 5.00 | 5.39 | 5.22 |
| Trinitrobenzene complex | | | |
| M. p., °C | 133~134 | 111~112 | — |
| Appearence | Pale yellow needles | Pale yellow leaflets | — |
| N, % | 8.91 | 8.96 | 8.70 |

## Experimental

**Materials.** — *Phenanthrene.* — A sample supplied by Yawata Chemical Industry Co. was purified by fusion with potassium hydroxide, followed by vacuum distillation, recrystallization from ethanol and treatment with chromium trioxide; m. p. 97~98.5°C, reported 98.7~99.5°C[4].

*Bromobenzene.* — A commercial reagent was redistilled; $n_D^{20.5}$ 1.5598, reported $n_D^{20}$ 1.5602[5].

2) "Org. Synth.", Col. Vol. II (1955), p. 482.
3) Fieser, *J. Am. Chem. Soc.*, **51**, 2466 (1929).
4) J. Heilbron, "Dictionary of Org. Compds.", Vol. IV, Oxford University Press, New York (1953), p. 84.
5) Merck Index, 7th Edition, Merck & Co. Inc., Rahway, N. J. (1960), p. 168.

*Copper Powder.*—This was precipitated from an aqueous solution of $CuSO_4 \cdot 5H_2O$ by the addition of zinc granules and was washed with water, with dilute hydrochloric acid, and finally with ethanol.

*Sulfuric Acid, Potassium Hydroxide.*—Commercial reagent.

**Synthesis of 2- and 3-Phenanthrol.** — Purified phenanthrene (50 g.)* was sulfonated by the method described in the literature[2]. From the reaction mixture, less soluble mono-sulfonic acids were separated as sodium salts, leaving disulfonates in the filtrate. By recrystallizing sodium mono-sulfonates from water, the relatively insoluble 2-isomer was first obtained, which was further purified as barium salt. From the filtrate, by concentration and the addition of potassium chloride, potassium 3-sulfonate was obtained. 2-Ba-sulfonate; 14.1 g., 16% (reported 17~21%). 3-K-sulfonate; 17.6 g., 21% (reported 24~26%). Then the sulfonates were fused with potassium hydroxide. To potassium hydroxide (about 3 parts) melted in a nickel crucible at 290~300°C, barium or potassium sulfonate (1 part) was added gradually over a period of 20 min. by stirring; the heating was continued for a further 5 min. at 320~330°C. The mixture was then allowed to cool and was dissolved in water. The addition of hydrochloric acid to this solution yielded a precipitate which was filtered off.

The precipitate was redissolved in an aqueous solution of potassium hydroxide and filtered off to remove insoluble matter. By the neutralization of the filtrate, crude phenanthrols were obtained which were filtered off and recrystallized from a mixture of ligroin and ethanol. The results of the potassium hydroxide fusion are shown in Table III.

TABLE III

| Phenanthrene sulfonate | Amount g. | Phenanthrol Amount g. | Phenanthrol M. p. °C | Reported m. p. °C |
|---|---|---|---|---|
| 2-Ba | 14 | 5.5 | 162.7~167.7<br>166~168 (purified) | 168 |
| 3-K | 17 | 10.3 | 112.6~118.5<br>116.8~118.9 (purified) | 118~119 |

**Synthesis of 2-Phenanthryl Phenyl Ether.** — A mixture of 2-phenanthrol, potassium hydroxide bromobenzene and copper powder in a flask fitted with an air condenser was placed in an oil bath and heated. The cooled mixture was first treated with a 10% aqueous solution of potassium hydroxide to dissolve unreacted phenanthrol and was then extracted repeatedly with benzene. The combined extracts were concentrated and distilled in vacuo. The distillation apparatus employed was designed for distilling solid samples and equipped with a fractionating column (10 mm.×350 mm.) packed with stainless Dixon packing 2 mm. in diameter. The distillate, which was solid melting at about 110~116°C, was recrystallized 3 times from ethanol, yielding white needles. The experimental results of the condensation reaction are shown in Table IV.

* One tenth of the amount used in Ref. 2.

Found: C, 88.69; H, 5.00; mol. wt. (Rast), 273. Calcd. for $C_{20}H_{14}O$: C, 88.86; H, 5.22%; mol. wt. 270.

*Infrared Absorption Spectrum.*—The spectrum of 2-phenanthryl phenyl ether in carbon bisulfide is shown in Fig. 1. The band appearing at 825 $cm^{-1}$

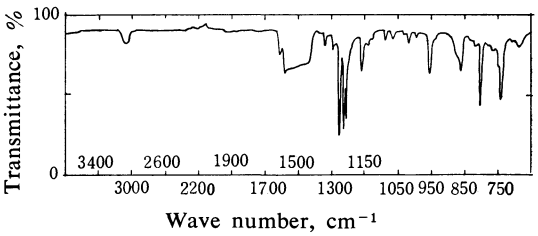



Fig. 1. 2-Phenanthryl phenyl ether.

corresponds to a 1,2,4-substitution in the benzene ring. This means a substitution in the 2- or 3-position of phenanthrene, which may be regarded as a substituted benzene. Similarly, because an absorption band at 807 $cm^{-1}$ which corresponds to a 1,2,3,4-substitution in benzene is absent, the 9- or 10-position of phenanthrene is not substituted. The absence of a strong absorption in the region of 752~753 $cm^{-1}$ shows that a 1,2,3-substitution in the benzene ring is not present; that is, there is no substitution in the 1- or 4-position of phenanthrene. The spectrum which shows characteristic absorptions of 2- or 3-substituted phenanthrene can be clearly distinguished from that of a 3-phenyl isomer, which will be described later. A band at 690 $cm^{-1}$ may be assigned to a phenoxy group. Phenoxynaphthalenes ($\alpha$, $\beta$), *p*-phenoxydiphenyl, and *p,p'*-diphenoxydiphenyl which the author prepared showed a medium absorption in the vicinity of this wave number.

*Ultraviolet Spectra.*—The spectra of the 2-phenyl as well as the 3-phenyl isomer are shown in Fig. 2.

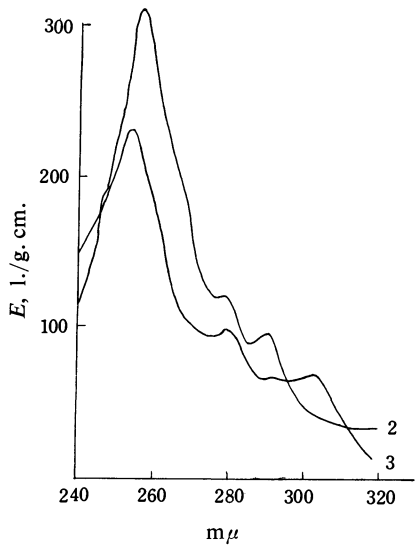



Fig. 2

2, 2-Phenyl isomer; 3, 3-Phenyl isomer

TABLE IV. 2-PHENANTHRYL PHENYL ETHER

| No. | 2-Phenanthrol[a] g. | Bromobenzene g. | KOH g. | Cu g. | Condition Temp. °C | Condition Time hr. | Distillate g. | Recrystallized Amount g. | Recrystallized M. p. °C | Recrystallized Yield[b] % |
|---|---|---|---|---|---|---|---|---|---|---|
| 1 | 4.2 | 3.1 | 1.3 | 0.2 | 150~200 | 2 1/3 | 3.1 | 1.6 | 120~121 | 27 |
| 2 | 1.1 | 2.0 | 0.35 | 0.05 | 170~185 | 3 5/6 | 0.89 | 0.45 | 120~121 | 29 |
| 3 | 4.2 | 5.9 | 1.3 | 0.2 | 140~200 | 5 | 4.5 | 2.50 | 121~122 | 43 |

a) M. p. of phenanthrol; Nos. 1 and 2, 162.7~167.7°C; No. 3, 166~168°C.
b) Mol. % based on 2-phenanthrol employed.

TABLE V. 3-PHENANTHRYL PHENYL ETHER

| No. | 3-Phenanthrol[a] g. | Bromobenzene g. | KOH g. | Cu g. | Condition Temp. °C | Condition Time hr. | Distillate g. | Recrystallized Amount g. | Recrystallized M. p. °C | Recrystallized Yield[b] % |
|---|---|---|---|---|---|---|---|---|---|---|
| 1 | 5.5 | 4.0 | 1.7 | 0.20 | 150~200 | 5 1/2 | 5.3 | 2.35 | 85~86 | 31 |
| 2 | 3.1 | 5.4 | 1.0 | 0.13 | 160~170 | 4 1/2 | 1.99 | 1.32 | 86~87 | 31 |
| 3 | 4.2 | 5.9 | 1.3 | 0.20 | 140~200 | 5 | 4.8 | 2.95 | 86~87 | 50 |

a) M. p. of 3-phenanthrol; Nos. 1 and 2, 112.6~118.5°C; No. 3, 116.8~118.9°C.
b) Mol. % based on 3-phenanthrol employed.

The absorption maxima are different from those of 2- or 3-alkyl phenanthrene.

*Solubility.*—It is only with difficulty soluble in cold ethanol, readily soluble in benzene, and insoluble in water.

*Trinitrobenzene Complex.*—This was prepared from 2-phenanthryl phenyl ether (86 mg.) and 72 mg. of trinitrobenzene in ethanol. Three recrystallizations from ethanol yielded 45 mg. of short yellow needles, which melted at 133~134°C.

Found: N, 8.91, Calcd. for $C_{26}H_{17}O_7N_3$; N, 8.70%.

**Synthesis of 3-Phenanthryl Phenyl Ether.**—The 3-phenyl isomer was prepared and purified in the same manner as in the case of the 2-phenyl isomer. The experimental results are shown in Table V.

Recrystallization from ethanol gave white needles which melted at 86~87°C.

Found: C, 89.16; H, 5.39; mol. wt. (Rast), 273. Calcd. for $C_{20}H_{14}O$: C, 88.86; H, 5.22%; mol. wt., 270.

*Infrared Spectrum.*—The spectrum in carbon disulfide is shown in Fig. 3.

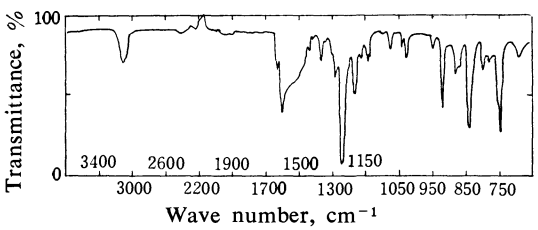



Fig. 3. 3-Phenanthryl phenyl ether.

A band at 690 $cm^{-1}$ corresponds to a phenoxyl group. Other absorption bands appearing in the finger print region are typical of 3-substituted phenanthrene, as a comparison with those of 3-ethylphenanthrene[6] shows:

| | Wave numbers, $cm^{-1}$ | | | | |
|---|---|---|---|---|---|
| 3-Phenanthryl phenyl ether | 880 | 865 | 840 | 798 | 747 |
| 3-Ethylphenanthrene | 881 | 864 | 839 | 800 | 746 |

*Ultraviolet Spectrum.*—The spectrum is shown in Fig. 2.

*Solubility.*—It is only with difficulty soluble in cold ethanol, moderately soluble in benzene, and insoluble in water.

*Trinitrobenzene Complex.*—This was prepared from ether (99 mg.) and trinitrobenzene (108 mg.) in ethanol. Three recrystallizations from ethanol yielded 73 mg. of a pale yellow adduct, m. p. 111~112°C.

Found: N, 8.96. Calcd. for $C_{26}H_{20}O_7N_3$, N, 8.70%.

The author is indebted to Professor Ryozo Goto of Kyoto University for his helpful discussions and for his criticisms of this work, and to Professor Sakujiro Kimura for his advice and encouragement.

*Tokyo Laboratory of Research Center*
*Yawata Chemical Industry Co.*
*Chuo-ku, Tokyo*

6) E. Ochiai, et al., *Pharm. Bull.*, 5, 113 (1957).

# *Studies on Isoprenoide. XIII. Transformation of Pinene by the Action of Boron Trifluoride*

By Kimiko NAGAI

(Received March 25, 1961)

The transformation in the reaction of various reagents upon pinenes have been investigated[1-4] in detail, and the existence of camphene has been observed in the conversion products of pinene in almost all cases. The author has been engaged in a series of experiments on the reaction of boron trifluoride, an electrophilic agent, upon terpenes. It has been reported[5] that the reaction of boron trifluoride upon terpenes produces mainly polymerized products; my experiments seen to verify this.

According to another paper[6] stating that isoborneol was produced by the reaction of glacial acetic acid upon camphene with a catalyst of boron trifluoride, the author has obtained bornyl acetate in a considerable yield in the reaction of glacial and anhydrous acetic acids upon $\alpha$-pinene with a catalyst of boron trifluoride, as has been formerly communicated[7].

Because in this reaction $\alpha$-pinene is isomerized to camphene by boron trifluoride ethyl ether complex and further is esterified[6], the isomerization of $\alpha$-pinene to camphene in the absence of glacial and anhydrous acetic acids was attempted. Namely, solutions of boron trifluoride ethyl ether complex in various solvents were prepared, $\alpha$-pinene was subjected to a reaction at room temperature with various amounts of catalyst and various reaction times, and the transformation of $\alpha$-pinene and the production of camphene were investigated, taking advantage of the infrared absorption spectrum and gas chromatography.

The determination of $\alpha$-pinene and camphene based on the infrared absorption spectrum has already been investigated by Kitajima, Takeshita et al.[8], who adopted 772 $cm^{-1}$ for $\alpha$-pinene and 667 $cm^{-1}$ for camphene as a characteristic absorption in the practice of estimation. The author adopted 1130 $cm^{-1}$ for $\alpha$-pinene and 1115 $cm^{-1}$ for camphene, made a calibration curve using $\alpha$-pinene purified by distillation, and diluted solutions of camphene 10~80 per cent, for which determination was carried out on the amount of $\alpha$-pinene and camphene in the reaction products catalyzed by boron trifluoride ethyl ether complex; at the same time, this result was compared with that of gas chromatography.

When a catalyst, boron trifluoride ethyl ether complex, was used with a solvent of ligroin or benzene, and also when it was directly applied to $\alpha$-pinene without the use of any solvents, violent heat generation and polymerization occurred, and the degree of heat generation and polymerization descending from ligroin through benzene to an absence of solvents.

When ethyl ether was used as a solvent, the generation of heat was hardly observed, and it was noted from the infrared absorption spectrum that by the action of boron trifluoride ethyl ether complex, $\alpha$-pinene is converted to camphene through the Wagner-Meerwein rearrangement and that the greater the extent of isomerization to camphene the larger the amount of boron trifluoride ethyl ether complex used and the longer the reaction time.

As the infrared absorption spectrum show peaks at 817 and 827 $cm^{-1}$, the existence of a group $\begin{matrix} R \\ R' \end{matrix}\!\!>\!C=C<\!\!\begin{matrix} R'' \\ H \end{matrix}$ is presumed, and hence the formation of polymers of $\alpha$-pinene is conceivable.

Reaction products in the solvent of benzene or ligroin for which no heat generation and polymerization appeared showed such infrared absorption spectra that, while the characteristic absorption (at 1130 $cm^{-1}$) was not observed, that for camphene was observed faintly at 1115 $cm^{-1}$ and those for end-methylene and *gem*-dimethyl radical were observed at 877 and 1660 $cm^{-1}$, and at 1363 and 1384 $cm^{-1}$ respectively. Gas chromatography of these reaction products showed a small peak corresponding to camphene; also in the case of solvents of benzene or ligroin, the formation of camphene was found, though in an extremely small amount.

In this reaction, the isomerization of $\alpha$-pinene into camphene by the action of boron

1) K. Ono, This Bulletin, **2**, 16, 207 (1927).
2) T. Kuwada, *J. Soc. Chem. Ind., Japan*, (*Kōgyo Kwagaku Zasshi*), **32**, 1154 (1929).
3) E. Schwent and K. Schmidt, D. R. Pat. 578569 (1934).
4) P. A. Mulany, C., II, 430 (1931).
5) M. Berthelot, *Ann. chim. phys.*, (3) **38**, 38 (1853).
6) I. G. Farbenindustrie, D. R. Pat. 589779 (1933).
7) K. Nagai, *Bull. Pharm. Kinki Univ.*, **3**, 11 (1960).
8) M. Kitajima and T. Takeshita, *Report of the Central Research Institute, The Monopoly Corporation*, **95**, 95 (1956).

trifluoride ethyl ether complex through the Wagner-Meerwein rearrangement was confirmed, and in the case of a violent reaction, although it almost polymerizes, the formation of a small amount of camphene was detected.

## Experimental

**Sample.** — α-Pinene and camphene purified by repeated distillation on metallic sodium were used. The physical constants of the samples are as follows: α-pinene b. p. 154.5~156°C, $d_4^{25}$ 0.8550, $n_D^{25}$ 1.4641; camphene b. p. 154~155°C, m. p. 47.0~47.5°C.

**The Calibration Curve of α-Pinene and Camphene.**—Camphene was diluted with α-pinene 10~80 per cent, and the characteristic absorption at 1130 and 1115 $cm^{-1}$ was selected for the infrared absorption spectra of α-pinene and camphene respectively; from the ratio of the above two absorptions, a calibration curve as seen in Fig. 1 was obtained.

TABLE I. RATIO OF ABSORPTION AT 1130 AND 1115 $cm^{-1}$

| α-Pinene % $I_1$ | Camphene % $I_2$ | $\log I_1/I_2$ |
|---|---|---|
| 100 | — | 0.5090 |
| 90 | 10 | 0.6256 |
| 80 | 20 | 0.7238 |
| 70 | 30 | 0.8443 |
| 60 | 40 | 1.0164 |
| 50 | 50 | 1.222 |
| 40 | 60 | 1.411 |
| 30 | 70 | 1.644 |
| 20 | 80 | 1.905 |

$I_1$: The height of the mininum point on the absorption band of α-pinene

$I_2$: The height of the minimum point on the absorption band of camphene

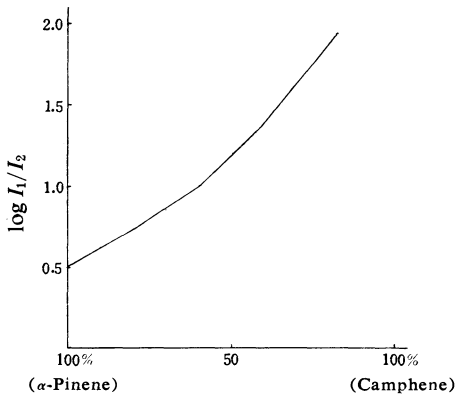



Fig. 1. Calibration curve of camphene and α-pinene.

**Reaction in the Solvent of Ethyl Ether.** — A mixture of α-pinene 10 ml. and ethyl ether 15 ml. was added to each 0.8, 1.5, 2.0 and 3.0 ml. of boron trifluoride ethyl ether complex and was allowed to react for 72 hr. at room temperature; after washing with 10% sodium carbonate and water, followed by drying, the reaction product was examined with the aid of the infrared absorption spectrum and gas chromatography. Figure 2 is the infrared absorption spectrum of the product obtained when α-pinene, camphene and 3.0 ml. of a catalyst were used. As shown from the calibration curve in Fig. 1, the yield of camphene is maximum, about 50 per cent, when 3.0 ml. of boron trifluoride ethyl ether complex was used, whereas in the reaction with 0.8 ml., the α-pinene remained almost unchanged.

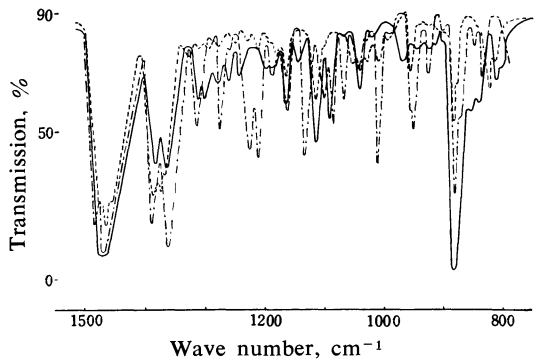



Fig. 2. Infrared absorption spectrum obtained by using α-pinene, camphene and 3.0 ml. catalyst.

——— Camphene ----- 3.0 ml. Catalyst
—·—· α-Pinene

TABLE II. ESTIMATION OF CAMPHENE ON THE BASIS OF INFRARED ABSORPTION SPECTRA OF REACTION PRODUCTS IN ETHYL ETHER

| Boron trifloride, ml. | Camphene % | Absorption coefficient |
|---|---|---|
| 0.8 | 10.0 | 0.529 |
| 1.5 | 41.0 | 1.029 |
| 2.0 | 46.2 | 1.127 |
| 3.0 | 50.0 | 1.214 |

ESTIMATION OF α-PINENE AND CAMPHENE BASED ON GAS CHROMATOGRAPHY

| Boron trifluoride, ml. | Camphene % | α-Pinene % |
|---|---|---|
| 0.8 | 12.1 | 80.9 |
| 1.5 | 44.2 | 29.7 |
| 2.0 | 44.0 | 16.9 |
| 3.0 | 52.9 | 10.6 |

P. E. G. 6000 (20 ml./min. 180°C, 0.25 kg./$cm^2$, 16 mV. 150 mA. 5 mm./min. He)

Moreover, the relation between the yield of camphene and the reaction time in the case of 3.0 ml. of boron trifluoride ethyl ether complex was investigated; the result is shown in Table III, from which it can be observed that a large amount of

TABLE III. RLATION BETWEEN THE YIELD OF CAMPHENE AND REACTION TIME

| | | | | |
|---|---|---|---|---|
| Infrared absorption spectrum | Reaction time, hr. | 24 | 48 | 72 |
| | Camphene % | 49.5 | 49.9 | 50.5 |
| | Absorption coefficient | 1.210 | 1.213 | 1.225 |
| Gas chromatography | Reaction time, hr. | 24 | 48 | 72 |
| | Camphene % | 50.9 | 51.2 | 51.5 |
| | $\alpha$-pinene, % | 12.8 | 12.4 | 10.6 |

camphene is formed in the case of an hour-long reaction.

**Reaction in the Solvent of Benzene and Ligroin.**—To 10 ml. of a sample, 15 ml. of both benzene and ligroin were added, and boron trifluoride ethyl ether complex was added to the benzene solution in amounts of 0.3, 0.5 and 1.0 ml. and to the ligroin solution in amounts of 1.5, 2.0 and 3.0 ml., and after reaction ceased, treatment similar to that described above was performed. In the case of these reactions, heat generation and polymerization occurred violently; when the amount of catalyst was small, the existence of camphene was observed, but $\alpha$-pinene was not, as shown from the data of the infrared absorption spectra and gas chromatography, although the estimation of the camphene formed was nevertheless difficult.

**Reaction Without Solvents.**—This reaction shows a remarkable heat generation and polymerization, yielding reddish-brown, viscous, oily substances; because the existence of $\alpha$-pinene was still observed only on the basis of the infrared absorption spectrum and gas chromatography, the estimation was not successful.

The author wishes to express her gratitude to Assistant Professor I. Ogura for his guidance and encouragement throughout this work, and her sincere thanks to Mr. K. Machida, Kyoto University, for his services in the measurement of the infrared absorption spectrum and to Mr. K. Matsushima of our University for his help in the analysis of gas chromatography.

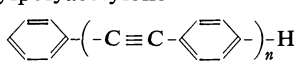
*Pharmaceutical Faculty*
*Kinki University*
*Fuse-shi, Osaka*

# *Alternant Conjugate Systems. I. Syntheses and Properties of Polytolans*

By Shōichi Misumi

(Received March 7, 1961)

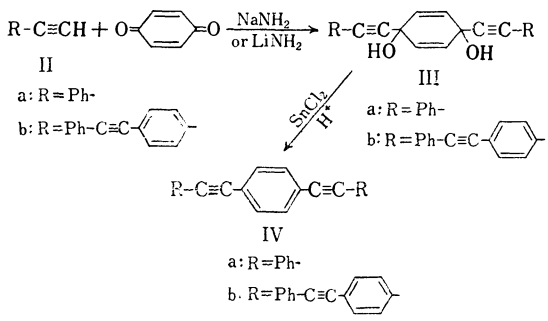
Alternative insertion of benzene nuclei between the triple bonds of the polyacetylenic chain of $\alpha,\omega$-diphenylpolyyne constitutes an interesting conjugate system, polytolan (I). The present author has investigated the syntheses of a series of polytolans (I; $n=2$, 3, 4) to compare their ultraviolet spectroscopic properties with those of polyphenylpolyene[1] and diphenylpolyacetylene.



I

The several methods[2-4] proposed for the synthesis of tolan all seem to be inadequate to the syntheses of the higher homologues owing to the poor solubility or the difficulty in the syntheses of the intermediates.

During the course of a study concerning the reaction of quinones with acetylenes, the author has found that polytolans having an even number of $n$ can be synthesized according to the following series of reactions. For example, the reaction of sodium phenylacetylide(IIa) in




1) S. Misumi and M. Kuwana, This Bulletin, 33, 711 (1960).

2) L. I. Smith and M. M. Falkof, "Org. Synth.", 22, 50 (1942); C. C. Price and C. E. Greene, *J. Polymer Sci.*, 6, 111 (1952); G. Drefahl and G. Plötner, *Chem. Ber.*, 91, 1280 (1958).

3) T. Curtius et al., ibid., 22, 2161 (1889); *J. prakt. Chem.*, [2] 44, 171 (1891); W. Schlenk et al., *Ann.*, 463, 76 (1928).

4) P. Lipp, *Ber.*, 56, 570 (1923); E. E. Harris et al., *J. Am. Chem. Soc.*, 48, 3144 (1926); G. H. Coleman et al., ibid., 56, 132 (1934); 58, 2310 (1936).

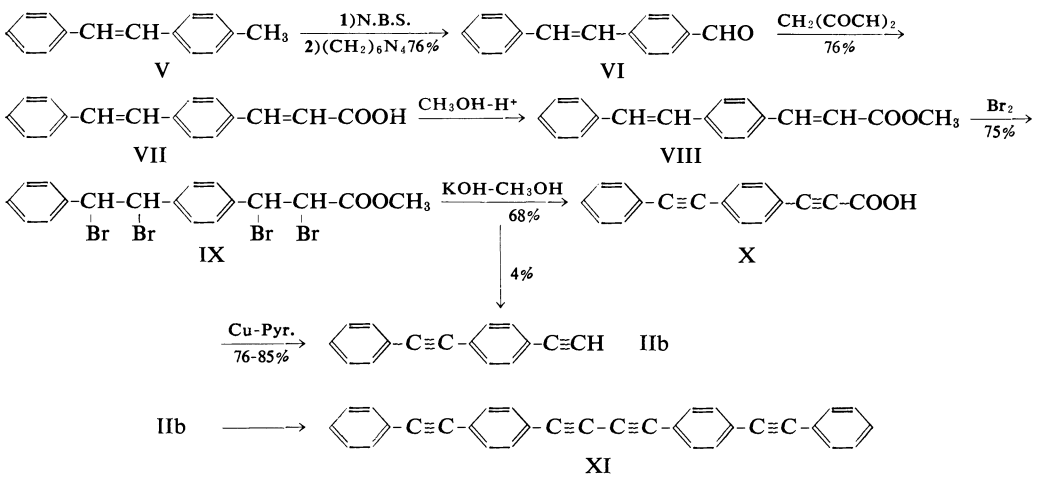
liquid ammonia with *p*-benzoquinone afforded the diacetylenic glycol (IIIa) in a yield of 31%. The reductive aromatization of IIIa with phosphorus diiodide or stannous chloride[5] resulted in the formation of distolan(IVa)[6]. Independently, IVa was synthesized by Ried according to essentially the same procedure[7]. The generalization of the reductive aromatization was achieved by his employing several kinds of quinones[7].

The present author has employed this method for the synthesis of tetrakistolan (I; $n=4$). The reaction of *p*-benzoquinone with the sodium salt of *p*-ethynyltolan (IIb) in liquid ammonia, in which IIb and its sodium salt are sparingly soluble, resulted in a recovery of the starting materials. As it was known that a lithium salt of an ethynyl compound has a larger solubility than a salt of other alkali metal[8], the reaction of the lithium salt of IIb with *p*-benzoquinone was carried out in dioxane, yielding tetra-acetylenic glycol(IIIb) in a yield of 13%. The reductive aromatization of IIIb afforded tetrakistolan (IVb) as light yellow needles with a green fluorescence. The solutions of IVb in various organic solvents exhibit an intense and characteristic violet fluorescence.

*p*-Ethynyltolan (IIb), which was used as a starting material for the synthesis of IVb, was synthesized according to the following series of reactions. A quantitative yield of the ester (VIII) was obtained by refluxing the suspension of *p*-styrylcinnamic acid (VII)[9] in methanol containing a catalytic amount of sulfuric acid. The dehydrobromination of the tetrabromide (IX) resulted in *p*-phenylethynyl-phenylpropiolic acid (X), together with a small amount of decarboxylated product (IIb). Several methods have been proposed for the decarboxylation of substituted phenylpropiolic acids[10-11], but the author has found that the acid (X) in pyridine or quinoline was smoothly decarboxylated to IIb in the presence of copper powder. Extension of the synthetic route of phenylacetylene[12] from cinnamic acid to styrylcinnamic acid (VII) was found to be unsuccessful owing to the poor solubility of the intermediate tetrabromide in various solvents.

*p*-Ethynyltolan (IIb) crystallizes in the form of colorless needles and gives amorphous yellow cuprous salt. Its mercuric acetylide was obtained in well-defined fine silky needles. As illustrated in Fig. 1, the ultraviolet spectrum of IIb was found to be closely related to tolan rather than to phenylacetylene, with a red-shift of ca. 15 mμ. The oxidative coupling of IIb according to Eglinton's method[13] afforded bis(*p*-phenylethynyl-phenyl)diacetylene (XI) as colorless plates. The disappearance of fine structure in the ultraviolet spectrum of XI as compared with that of diphenyldiacetylene is remarkable (Fig. 1).

Tristolan (I; $n=3$) was synthesized from




5) R. Kuhn et al., *Helv. Chim. Acta*, **11**, 87 (1928); *Ber.*, **71**, 783, 1510, 1889 (1938); **73**, 1410 (1940); *Chem. Ber.*, **84**, 566 (1951).

6) S. Misumi and M. Kuwana, presented at the 12th Annual Meeting of the Chemical Society of Japan, Kyoto, April, 1959.

7) W. Ried et al., *Chem. Ber.*, **90**, 2553 (1957); **91**, 2459 (1958); *Angew. Chem.*, **69**, 205, 614 (1957); *Naturwissenschaften*, **46**, 142 (1959).

8) B. B. Elsner and P. F. M. Paul, *J. Chem. Soc.*, **1951**, 893.

9) G. Drefahl and W. Hartrodt, *J. prakt. Chem.*, [4] **276**, 124 (1957).

10) K. Schofield and J. C. Simpson, *J. Chem. Soc.*, **1945**, 512; H. Gilman et al., *J. Am. Chem. Soc.*, **53**, 4192 (1931); J. A. Leroy, *Bull. soc. chim. France*, [3] **7**, 644 (1892).

11) W. Weltzien and F. Micheel, *Ann.*, **433**, 247 (1923); M. M. Otto, *J. Am. Chem. Soc.*, **56**, 1393 (1934).

12) J. V. Nef, *Ann.*, **308**, 264 (1899); J. C. Hessler, "Org. Synth." Col. Vol., I, 438 (1948).

13) G. Eglinton and A. G. Galbraith, *Chem. & Ind.*, **1956**, 737; *J. Chem. Soc.*, **1959**, 889.

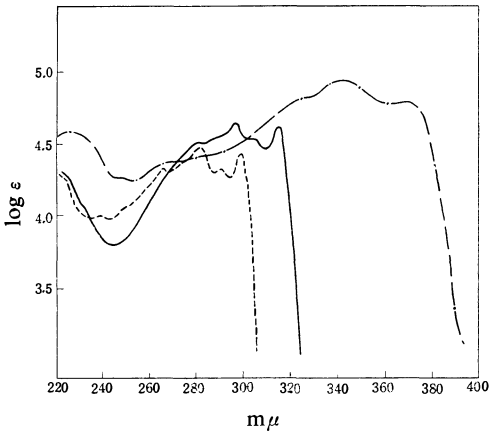



Fig. 1. The ultraviolet spectra of *p*-ethynyltolan (IIb, ——) and tolan (----) in *n*-hexane and bis(*p*-phenylethynylphenyl)-diacetylene (XI, —·—) in ethanol.

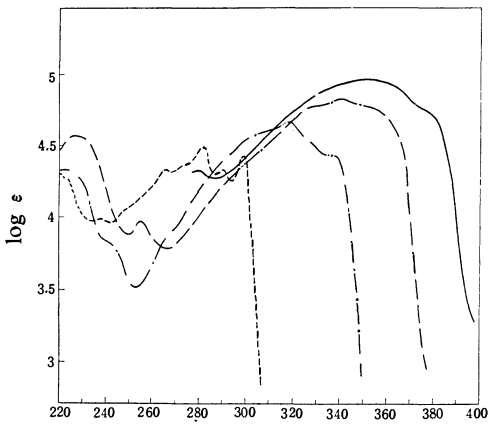



Fig. 2. The ultraviolet spectra of polytolans (I)
$n$=4, ——; $n$=3, —·—; $n$=2, —··—; $n$=1, ----

*p,p'*-distyrylstilbene[14] according to the procedure of Drefahl[2].

The ultraviolet spectra and the physical properties of these polytolans are presented in Fig. 2 and Table I. An examination of the ultraviolet spectra of polytolans indicates that an increase in the length of the conjugate system causes a displacement of the strongest absorption band towards a longer wavelength; this bathochromic displacement, however, becomes smaller for each additional $-C_6H_4-C\equiv C-$ grouping. Two empirical formulae ($\lambda=kn+\lambda_0$ or $\lambda=k\sqrt{n}+\lambda_0$) have been proposed to relate the number of double bonds in a conjugated chromophore group ($n$) with the wavelength of the absorption maximum ($\lambda$)[15], but the absorption maxima of polytolans could not be expressed by either of these empirical formulae, because the plot of the wavelength of the absorption maxima against $n$ or the square root of $n$ does not give a straight line, as is illustrated in Fig. 3.

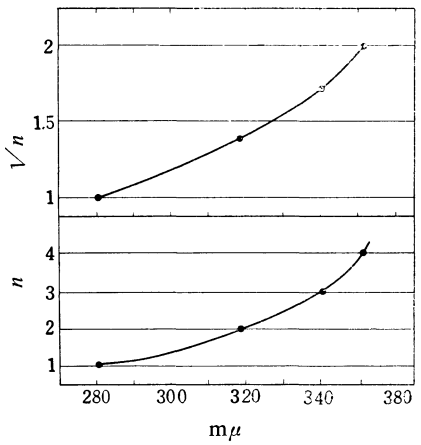



Fig. 3. Wavelength positions of the main absoption maxima plotted against number or $n\sqrt{n}$ of polytolans (I).

The spectra of tristolan (I; $n$=3) and tetrakistolan (I; $n$=4) showed absorption maxima at 256 and 279 mμ respectively. Similar maxima are also observed in the spectra of the corresponding ethylenic analogues. The occurrence of these bands can presumably be attributed to a higher order transition of the total chromophore, as is pointed out by Dale[16] and Zechmeister et al.[17].

The ultraviolet spectra of diphenylpolyacetylenes exhibit a regular bathochromic shift in accordance with the increase of the number of acetylenic linkage, also, the fine structure of the spectra becomes more and more distinct with the increase in the length of the conjugate system[18]. The same trend is also recognized in the case of diphenylpolyenes[19]. Kortüm attributed the increase in the fine structure of the spectra of diphenyl-polyyne and -polyene to the increase of the double bond character of single bonds in these conjugate systems. The increase in double bond character results

14) The synthesis of this substance will be reported on the following paper.

15) G. Schwarzenbach, *Z. Elektrochem.*, **47**, 40 (1941).
16) J. Dale, *Acta Chem. Scand.*, **8**, 1235 (1954).
17) L. Zechmeister, A. L. LeRosen, W. A. Schroeder, A. Polgár, and L. Pauling, *J. Am. Chem. Soc.*, **65**, 1940 (1943),
18) M. Nakagawa et al., *Proc. Japan Acad.*, **26**, 38, 43 (1950); *J. Chem. Soc. Japan, Pure. Chem. Sec.* (*Nippon Kagaku Zasshi*), **72**, 561, 993 (1951); H. H. Schlubach and V. Franzen, *Ann.*, **573**, 110 (1951); F. Bohlmann, *Chem. Ber.*, **84**, 785 (1951); **86**, 63 (1953); *Angew. Chem.*, **65**, 385 (1953).
19) K. W. Haussen, R. Kuhn and A. Smakula, *Z. physik. Chem.*, **B29**, 384 (1935).

Table I. Properties of polytolans and related compounds

| | M.p., °C | Fluorescence | | UV spectrum | |
|---|---|---|---|---|---|
| | | Solid | Solution | $\lambda_{max}$, mμ | Solvent |
| Distolan (I : $n$=2) | 181.5~182 | — | Light violet | 222, 318, 337 | a |
| Tristolan (I : $n$=3) | 283 ~285 | Light green | Violet | 226, 256, 325*, 340 | c |
| Tetrakistolan (I : $n$=4) | 307 ~312 | Light green | Intense violet | 279, 351, 378* | b |
| $p$-Ethynyltolan (IIb) | 90.5~91 | — | — | 279, 288*, 295, 303, 314 | a |
| (XI) | 229 ~229.5 | — | Violet | 225, 268*, 326*, 342, 368 | d |

* inflexion ; a : $n$-hexane, b : benzene, c : chloroform, d : 95% alcohol

in a fixation of the molecule in a uniplanar conformation and necessarily retards the torsional vibration of the molecule[20].

On the contrary, the fine structure in the spectra of polytolans gradually becomes obscure with the increase in the length of the alternant conjugate system. The distinct fine structure observed in the spectrum of tolan can be traced in that of distolan (IVa), but the spectra of tris- and tetrakis-tolan show only a weak inflection at the corresponding positions, as is illustrated in Fig. 2. The single bond length of the $C_6H_5$-C≡ grouping has been reported to be almost identical in the series of diphenylpolyyne, whereas a distinct contraction of the single bond length inserted between two acetylenic linkages was observed in the same series, as

Table II. Single bond lengths in diphenylpolyyne Ph-(C≡C)$_n$-Ph

| $n$ | Bond length of Ph-C≡ Å | Bond length of ≡C-C≡ Å | Ref. |
|---|---|---|---|
| 1 | 1.40 | — | 21 |
| 2 | 1.44 | 1.39 | 22 |
| 4 | 1.42 | 1.37, 1.33, 1.37 | 23 |
| 5 | 1.45 | 1.39, 1.33, 1.33, 1.39 | 23 |

is summarized in Table II. These results indicate that the single bond in the $C_6H_5$-C≡ grouping has a minor degree of multiple bond character as compared with the single bond in ≡C-C≡ grouping. Consequently, an insertion of the $p$-phenylene group in a position of single bond in a conjugate polyyne chain may cause an increase of torsional vibration about the single bond of the ≡C-$C_6H_4$-C≡ grouping. Also, the increase in the number of single bond with a minor multiple bond character may increase the transition energy of photoecxitation. The disappearance of the fine structure and the hypsochromic shift of absoption maxima in the spectra of polytolans as compared with those of diphenylpolyynes seem to be attributable to the above-mentioned two reasons. This inference is also cosistent with the fact that $p$-ethynyltolan and tolan show quite similar absorption curves (Fig. 1) and the fact that the fine structure which is observed in the spectrum of diphenyldiacetylene is almost lost in the absorption curve of bis($p$-phenylethynyl-phenyl)diacetylene (XI) (Fig. 1).

The ultraviolet spectrum of distolan reported by Drefahl[2] showed a strong inflection at ca. 350 mμ which could not be observed in the spectrum of the compound prepared by the author. The presence of inflection at this wavelength seems to arise from a contamination with the starting material, $p$-distyrylbenzene ($\lambda_{max}$ 350 mμ) or $p$-styryltolan ($\lambda_{max}$ 333 ; $\lambda_{infl.}$ 352 mμ).

## Experimental*

**1, 4-Bisphenylethynyl-2, 5-cyclohexadien-1, 4-diol (IIIa).**—To a solution of sodium amide (prepared from sodium, 3.8 g., 0.167 mol.) in liquid ammonia (100 ml.) was added dropwise phenylacetylene (17 g., 0.167 mol.) in dry ether (50 ml.). After stirring for 2 hr., $p$-benzoquinone (10 g., 0.093 mol.) in dry tetrahydrofuran (70 ml.) was dropped into the mixture over a period of 3 hr. A transient development of blue color was observed on the addition of the quinone, and the entire mixture gradually changed to a deep brown solution. Ammonia was evaporated after the addition of ammonium chloride, and the residual solid was extracted with ethyl acetate. The extract was thoroughly washed with water and dried. After removal of the solvent, the residue was dissolved in ethyl acetate-benzene and passed through a short column of alumina. The crude crystals obtained on concentrating the solvent were recrystallized from benzene to give IIIa, colorless leaflets, m. p. 176~177°C, yield 8.1 g. (31.2%). (Ried[7] reported a yield of 50~55% employing lithium amide.)

Found : C, 84.47 ; H, 5.04. Calcd. for $C_{22}H_{16}O_2$ : C, 84.59 ; H, 5.16%.

* All melting points are uncorrected.

20) G. Kortüm and G. Dreesen, *Chem. Ber.*, **84**, 182 (1951).
21) J. M. Robertson and I. Woodward, *Proc. Roy. Soc.*, **A 164**, 436 (1938).
22) E. H. Wiebenga, *Z. Krist.*, **102**, 193 (1940).
23) T. Watanabe, N. Masaki and H. Mitsuda, International Congress of the International Union of Cristallography, Cambridge, England, Aug., 1960.

IR max($cm^{-1}$) 3320, 3260($\nu_{OH}$), 2225($\nu_{C\equiv C}$), 1007($\delta_{OH}$).

***p*-Bis(phenylethynyl)benzene [Distolan] (I : n=2)**—A solution of stannous chloride dihydrate (1.0 g.) in concentrated hydrochloric acid (3.0 ml.) was added to a stirred solution of the glycol (IIIa, 388 mg.) in tetrahydrofuran (20 ml.), and the mixture was stirred for several hours at room temperature. After standing overnight, the reaction mixture was poured into water and extracted with benzene. The extract was washed with water and dried. After removal of the solvent, the residue was dissolved in light petroleum-benzene (1 : 1, 10 ml.). The solution was then chromatographed over alumina and eluted with the same solvent, resulting in crude crystals. This was recrystallized from dry ethanol, yielding IVa, m. p. 172~175°C, 115 mg. (33.1%). Sublimation of this material in vacuo (160~175°C/15 mmHg) afforded pure IVa, colorless needles.

Found: C, 95.12; H, 5.12. Calcd. for $C_{22}H_{14}$: C, 94.93; H, 5.07%.

IVa was also obtained in a yield of ca. 20% by a reductive aromatization of IIIa with phosphorus diiodide.

***p*-Bis(β-phenylethyl)benzene.**—IVa in dry tetrahydrofuran was catalytically reduced over palladium-charcoal (5%). After removal of the catalyst, the reduction product obtained by evaporating the solvent was recrystallized twice from ethanol to yield *p*-bis(β-phenylethyl)benzene, on colorless plates, m. p. 90.5~91°C.

Found: C, 92.59; H, 7.67. Calcd. for $C_{22}H_{22}$: C, 92.26; H, 7.74%.

***p*-Stilbenealdehyde(VI).**—VI was prepared according to the procedure of Drefahl[9] with slight modifications, m. p. 113~114°C., 76% yield (lit. value, m. p. 116~117°C.).

IR max.($cm^{-1}$) 1695($\nu_{C=O}$), 1205, 1165(-CHO), 968($\delta_{=CH-}$).

***p*-Styrylcinnamic Acid (VII).**—Stilbenealdehyde (VI, 30.2 g., 0.145 mol.) and malonic acid (31 g., 0.29 mol.) were dissolved in a mixture of pyridine (60 ml.) and piperidine (1.5 ml.). A vigorous evolution of carbon dioxide was observed when the solution was warmed to 60~65°C. The solution was kept at 100°C for 3 hr. and then refluxed for 2 hr. The cooled reaction mixture was poured onto crashed ice (300 g.) containing hydrochloric acid (100 ml.). The precipitate was then filtered and washed with water. Recrystallization of this material from acetic acid yielded VII, on lustrous light yellow plates, m. p. 255~256°C, 27.5 g. (76%) (lit. value, m. p. 256~258°C, 70%)[9].

IR max.($cm^{-1}$) 1685($\nu_{C=O}$), 1427, 1278(-COOH), 959($\delta_{=CH-}$).

**Methyl *p*-Styrylcinnamate (VIII).**—A few milliliters of concentrated sulfuric acid was added to a suspension of styrylcinnamic acid (VII, 20 g.) in methanol (600 ml.), and the mixture was refluxed for 10 hr. The crystals of the acid gradually changed to pale greenish yellow plates. The cooled reaction mixture was then filtered. The crystals obtained by concentrating the filtrate were combined with the first crop and recrystallized from carbon tetrachloride, resulting in VIII, on light yellow plates, m. p. 185.5~186°C, 20.4 g. (97%).

Found: C, 81.79; H, 6.18. Calcd. for $C_{18}H_{16}O_2$: C, 81.79; H, 6.10%.

UV max(mμ) 236(ε=8,000), 345(24,000)(in 95% ethanol)

IR max($cm^{-1}$)1717($\nu_{C=O}$), 1169, 1114(-$COOCH_3$), 980, 969, 961($\delta_{=CH-}$).

**Methyl *p*-Styrylcinnamate Tetrabromide (IX).**—Bromine (30.0 g., 0.19 mol.) in chloroform (30 ml.) was gradually added to a stirred solution of the ester (VIII, 20.4 g., 0.077 mol.) in chloroform (700 ml.) under cooling with running water. The large amount of crystals deposited made the agitation of the reaction mixture impossible after about two-thirds of bromine had been added. After all the bromine had been introduced, the mixture was warmed to 40°C to complete the reaction. The crystals were filtered and washed with a small amount of chloroform, yielding the tetrabromide, 33.8 g. (75%), m. p. 235~238°C (decomp.). Further recrystallization from acetic acid afforded a pure material, colorless scale-like crystals, m. p. 242°C (decomp.).

Found: Br, 54.25. Calcd. for $C_{18}H_{16}O_2Br_4$: Br, 54.74%.

***p*-Phenylethynyl-phenylpropiolic Acid (X).**—The tetrabromide (IX, 34 g., 0.058 mol.) was intimately mixed with finely powdered potassium hydroxide (90 g., 0.6 mol.) and absolute methanol (400 ml.) was added in one portion to the mixture. After the vigorous reaction had ceased, the mixture was refluxed for 8 to 10 hr. The cooled reaction mixture was poured into water (600 ml.), and the potassium propiolate deposited was filtered and washed with a small amount of water. The combined filtrate and washing were extracted with ether. The ethereal extract was washed with water and dried. The residue obtained by removing the solvent was dissolved in light petroleum (b. p. 60~70°C.) and passed through a short column of alumina. Recrystallization of the crude crystals which were obtained by concentrating the filtrate gave IIb, pale yellow needles, 0.5 g. (4.3 %), m. p. 87~89.5°C.

The above-mentioned potassium salt was dissolved in hot methanol (400 ml.) and treated with active charcoal. On acidification of the methanolic solution with concentrated hydrochloric acid, crude *p*-phenylethynyl-phenylpropiolic acid (X) was obtained as crystals, m. p. 200~203°C, 9.7 g. (68%). Further purification was carried out by repeating the precipitation of the acid (X) from the methanolic solution with the addition of water, while a decomposition was observed when a solution of the acid is heated, especially in the presence of active charcoal. The pure material melts at 206~207°C.

Found: C, 82.67; H, 4.15. Calcd. for $C_{17}H_{10}O_2$: C, 82.91; H, 4.09%.

IR max. ($cm^{-1}$) 2205($\nu_{C\equiv C}$), 1667($\nu_{C=O}$), 1440, 1295(-COOH).

***p*-Ethynyltolan (IIb).**—To a solution of the propiolic acid (X, 1 part) in pyridine (10 parts) was added copper powder (0.1 part). The evolution of carbon dioxide was observed immediately, and in a few minutes the reaction mixture began

to froth vigorously. After the vigorous reaction had subsided, the mixture was refluxed for 40~60 min. To the cooled reaction mixture was added light petroleum (b. p. 60~70°C), and copper powder was removed by filtration. The filtrate was washed repeatedly with 2 N hydrochloric acid and then with aqueous sodium hydroxide and water successively. Concentration of the dried filtrate resulted in light brown needles, m. p. 78~83°C (yield, 76~85%). The crude ethynyltolan thus obtained was purified through chromatography over alumina, as the crude material was contaminated with a small amount of the propiolic ester. Recrystallization of the eluate from light petroleum gave pure IIb.

Found: C, 94.72; H, 4.98. Calcd. for $C_{16}H_{10}$: C, 95.02; H, 500%.

IR max.($cm^{-1}$) 3260($\nu_{\equiv CH}$).

The mercuric acetylide which was prepared according to the method of Johnson[24] was recrystallized from ethanol-benzene, yielding silky long needles, m. p. 244~245°C.

IR max.($cm^{-1}$) 2150 ($\nu_{C\equiv C}$).

**Bis(*p*-phenylethynyl-phenyl)diacetylene (XI).**—Cupric acetate monohydrate (7.5 g.) was added to a solution of *p*-ethynyltolan (IIb, 0.5 g.) in dry pyridine (50 ml.). The mixture was stirred for 8 hr. at 60~75°C. The reation mixture was diluted with benzene (200 ml.) and washed with 2 N hydrochloric acid, aqueous sodium hydroxide and water successively. The benzene solution was dried and the solvent removed, yielding a red solid. The crude material was washed twice with a small amount of light petroleum. The light yellow crystals thus obtained were recrystallized twice from benzene to give pure XI, on colorless plates.

Found: C, 95.04; H, 4.61. Calcd. for $C_{32}H_{18}$: C, 95.49; H, 4.51%.

**1, 4-Bis(*p*-phenylethynyl-phenylethynyl)-2, 5-cyclohexadien-1, 4-diol (IIIb).**—Dry dioxane (50 ml.) was added to a solution of lithium amide (prepared from lithium, 0.1 g., 14.3 mmol.) in liquid ammonia, and the ammonia was evaporated, resulting in a light pink solution. Into this solution was stirred *p*-ethynyltolan (IIb, 3 g., 14.8 mmol.) in dry dioxane (10 ml.). The color of the solution gradually changed from yellow to a transparent dark brown. After warming to 50°C for 20 min., the mixture was refluxed for 10 min. to expel the remaining ammonia and then cooled to room temperature. Under vigorous stirring, a solution of *p*-benzoquinone (0.8 g., 7.5 mmol.) in dry dioxane (20 ml.) was slowly added to the mixture over a period of 4 hr. A transient development of blue color was observed, and the color of the mixture changed to brown, forming a large amount of precipitate. The reaction mixture was stirred for ca. 20 hr. at room temperature and then refluxed for 3 hr. The cooled reaction mixture was introduced into water (500 ml.) and extracted with ethyl acetate. The extract was washed with water, dried and chromatographed over alumina. The crystalline fractions were recrystallized from benzene, yielding the glycol (IIIb), in the form of fine, long silky needles, m. p. 248~250°C., 475 mg. (12.6%).

Found: C, 88.90; H, 4.72. Calcd. for $C_{38}H_{24}O_2$: C, 89.04; H, 4.72%.

IR max.($cm^{-1}$) 3580, 3460($\nu_{OH}$), 2230($\nu_{C\equiv C}$), 1025, 1000 ($\delta_{OH}$).

**1, 4-Bis (*p*-phenylethynyl-phenylethynyl) benzene [Tetrakistolan] (IVb).**—To a warm solution of the glycol (IIIb, 245 mg.) in ethyl acetate (30 ml.) was added a solution of stannous chloride dihydrate (1 g.) in acetic acid (2 ml.) and ethyl acetate (2 ml.). The immediate deposition of a light yellow precipitate was observed. The mixture was then refluxed for 4 hr. and cooled. The precipitate was filtered (172 mg.) and dissolved in ethyl acetate. The solution was passed through a short column of alumina, and the filtrate was dried by evaporation. The residue, after recrystallization from chlorobenzene, gave tetrakistolan (IVb), in the form of light greenish yellow needles with a green fluorescence.

Found: C, 95.06; H, 4.81. Calcd. for $C_{38}H_{22}$: C, 95.37; H, 4.63%.

The author wishes to express his hearty thanks to Professor Masazumi Nakagawa for his helpful guidance throughout this work. The cost of this research was partly defrayed from the Scientific Research Expenditure of the Ministry of Education, to which author's thanks are also due.

*Department of Chemistry*
*Faculty of Science*
*Osaka University*
*Kita-ku, Osaka*

24) J. R. Johnson and W. L. McEwen, *J. Am. Chem. Soc.*, **48**, 469 (1926).

# *Alternant Conjugate Systems. II. Syntheses of Stereoisomeric p-Distyrylbenzenes and Related Compounds**

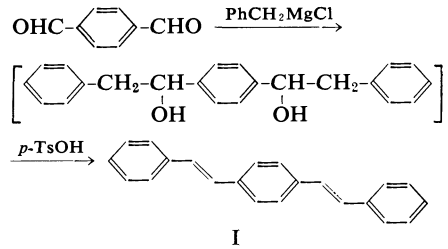
By Sōichi MISUMI, Motoyuki KUWANA, Kunie MURASHIMA and Masazumi NAKAGAWA

(Received March 7, 1961)

From a study of the ultraviolet absorption spectra of cis-trans isomeric carotenoids, Zechmeister and Pauling[1] have proposed a so-called "cis-peak rule" to correlate the molecular geometry with the spectrum. But the ultraviolet spectra of 1, 18-diphenyl-3, 7, 12, 16-tetramethyl-octadecanonaenes containing one or two sterically hindered cis-double bonds lack the cis-peak[2] which would be expected to appear according to the prediction of Zechmeister. Oroshnik[3] has also pointed out from his study of the ultraviolet spectra of sterically hindered retrovitamin A methyl ether and analogous compounds that the validity of Zechmeister's rule may be restricted to sterically unhindered cis-polyenes and that the spectra of hindered cis-polyenes cannot be explained by this rule alone.

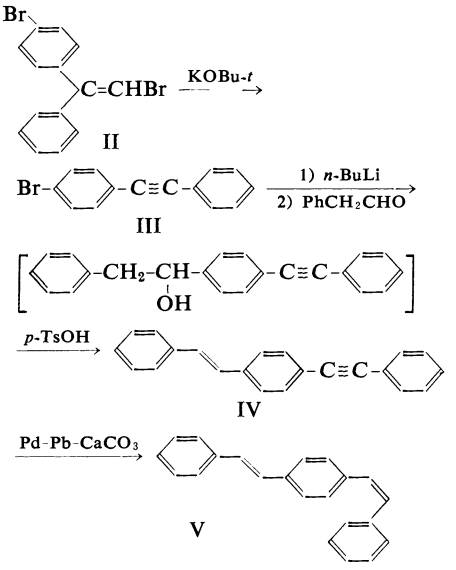
In order to examine the validity of Zechmeister's rule with regard to stilbene derivatives containing hindered cis-double bonds, the authors have carried out the syntheses of three stereoisomers of *p*-distyrylbenzene and related compounds. The present paper deals with the syntheses of these compounds; their spectroscopic properties will be discussed together with those of *p, p'*-distyrylstilbenes and related compounds in the following paper of this series.

Among the three possible geometrical isomers of *p*-distyrylbenzene, the trans, trans-isomer was prepared by Kaufmann as early as 1917[4]. Afterward, various methods of preparation of this compound have been proposed[5]. The present authors have synthesized the trans-trans compound I according to the following series of reactions.




I

It is well-known that the ethylenic compound obtained by a dehydrohalogenation or dehydration reaction contains only a small amount of cis-isomer and that the partial hydrogenation of an acetylenic compound over Lindlar's catalyst is regarded as the most practical method obtaining cis-ethylenic compound[6]. More recently, it has been reported in some cases that the Wittig reaction[7] affords cis-compound together with trans-isomer. The authors have found during the course of the synthetical studies of stilbene homologues that the Wittig reaction is feasible for the synthesis of cis-isomer. Therefore, the second isomer, the *trans, cis-p*-distyrylbenzene (V), was prepared by the above-mentioned two methods.




* For a preliminary announcement of this study, see This Bulletin, 33, 711 (1960).

1) L. Zechmeister, L. Pauling et al., *J. Am. Chem. Soc.*, 65, 1940 (1943); L. Zechmeister, *Chem. Revs.*, 34, 267 (1944); *Experientia*, 10, 1 (1954).

2) C. F. Garber, C. H. Eugster and P. Karrer, *Helv. Chim. Acta*, 35, 1580 (1952); 36, 562 (1953).

3) W. Oroshnik and A. D. Mebane, *J. Am. Chem. Soc.*, 76, 5719 (1954).

4) H. Kaufmann, *Ber.*, 50, 524 (1917).

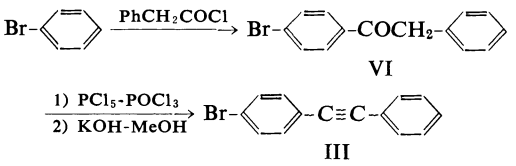
5) a) G. Drefahl and G. Plötner, *Chem. Ber.*, 91, 1274 (1958); b) J. Dale, *Acta Chem. Scand.*, 11, 971 (1957); c) K. Friedrich and H. G. Henning, *Chem Ber.*, 92, 2944 (1959); T. W. Campbell and R. N. McDonald, *J. Org. Chem.*, 24, 1246 (1959).

6) H. Lindlar, *Helv. Chim. Acta*, 35, 446 (1952).

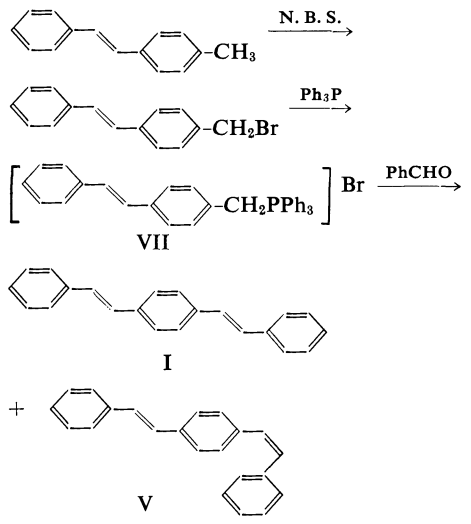
7) G. Wittig, *Angew. Chem.*, 71, 260 (1959).

The corresponding acetylenic analogue, *p*-styryltolan (IV), was synthesized according to the following scheme from *p*-bromotolan (III), which is prepared by means of a Fritsch-Buttenberg-Wiechell rearrangement[8] of *α*-*p*-bromophenyl-*β*-bromostyrene (II).

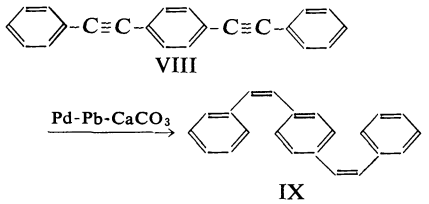
*p*-Bromotolan (III) was also obtained by a dehydrochlorination of the ketodichloride of *p*-bromodesoxybenzoin (VI). This method has, however, been found to be less advantageous owing to the low yield of the Friedel-Crafts reaction for the preparation of VI.



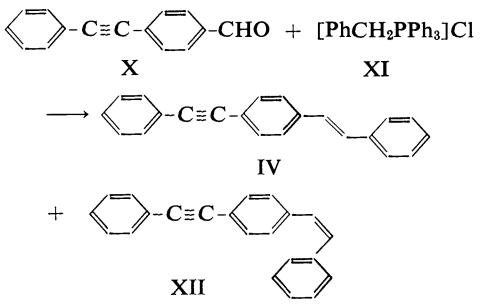

*p*-Bromomethylstilbene which was derived from *p*-methylstilbene was converted to phosphonium salt VII. The reaction of the salt VII with benzaldehyde yielded *trans*, *trans*-distyrylbenzene and *trans*, *cis*-distyrylbenzene (V) in about the same yield. The trans, cis-isomer V thus obtained was found to be identical




with the trans, cis-isomer derived from acetylenic analogue by partial hydrogenation.




The third isomer, *cis*, *cis*-*p*-distyrylbenzene (IX), was prepared by the double partial hydrogenation of *p*-bisphenylethynyl-benzene (VIII)[9] over Lindlar's catalyst*.




The reaction of tolanaldehyde (X)[10] with benzyltriphenylphosphonium chloride (XI) also gave *trans*-*p*-styryltolan (IV) and *cis*-*p*-styryltolan (XII) in about equal yields. The formation of an equal amount of cis-isomer was also observed in the Wittig reaction of other stilbene homologues, which experiments will be reported on in a following paper. The formation of a four-membered cycle in an intermediate stage of Wittig reaction is generally accepted, and the formation of cis- and trans-isomers in an almost equal yield seems to be rather peculiar on the basis of this hypothesis, since the intermediate of the cis-isomer is

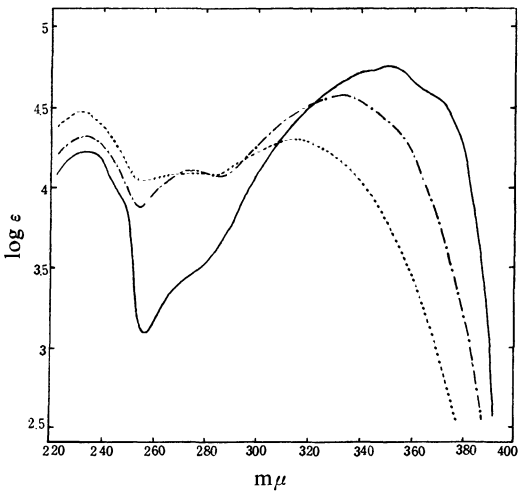



Fig. 1. The ultraviolet spectra of *p*-distyrylbenzenes in *n*-hexane.
*trans*, *trans*, ——; *trans*, *cis*, —·—·; *cis*, *cis*, – – –

8) W. P. Buttenberg, *Ann.*, **279**, 327 (1894); P. Lipp, *Ber.*, **56**, 570 (1923); G. H. Coleman et al., *J. Am. Chem. Soc.*, **56**, 132 (1934); **58**, 2310 (1936); M. Bouis, *Ann. Chim.*, [10] **9**, 402 (1928); A. A. Bothner-By, *J. Am. Chem. Soc.*, **77**, 3293 (1955).

9) S. Misumi, This Bulletin, **34**, 1827 (1961).

* Dale[5a] assigned the configuration of *trans*, *cis*-distyrylbenzene to a compound of m. p. about 95°C., which was isolated from the products of the photo-isomerization of trans, trans-isomer. However, the ultraviolet spectra of pure trans, cis- and cis, cis-compounds indicate that the compound of m. p. about 95°C is possibly a mixture of trans, cis- and cis, cis-isomers.

10) G. Drefahl and G. Plötner, *Chem. Ber.*, **93**, 990 (1960).

TABLE I. PROPERTIES OF *p*-DISTYRYLBENZENES AND RELATED COMPOUNDS

| | M. p., °C | UV spectrum, $\lambda_{max}(\varepsilon_{max})$, mμ | | | |
|---|---|---|---|---|---|
| *t*—*t* | 266 ~267 | 232 (16200) | | 350 (57000) | |
| *t*—*c* | 114 ~114.5 | 232 (20000) | 273 (12200) | 331 (36500) | |
| *c*—*c* | 86.5~ 87.5 | 232 (27600) | 270 (10900) | 314 (17700) | |
| A—A | 181.5~182 | 222 (20800) | | 318 (45400) | 337 (27000) |
| A—*t* | 211 ~211.5 | 230 (26600) | | 333 (55300) | |
| A—*c* | 78 ~ 78.5 | 227 (26800) | 271 (17700) | 312 (32900) | |

*t*, *c* and A denote *cis*-ethylenic, *trans*-ethylenic and acetylenic linkage, respectively.

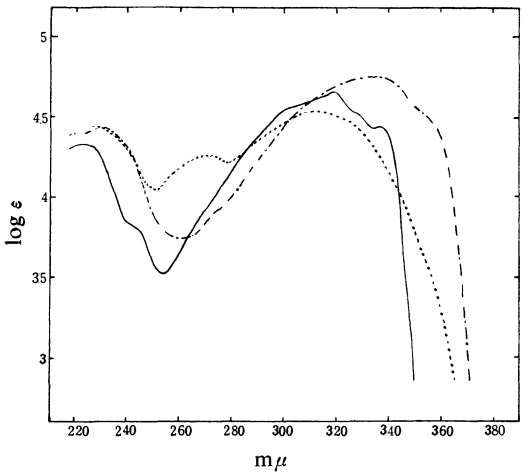



Fig. 2. The ultraviolet spectra of *p*-styryltolans (IV, *trans*, —·—·; XII, *cis*, ----) and distolan (VIII, ——) in *n*-hexane.

probably less stable than that of the trans-isomer owing to the steric interaction of two phenyl groups.

The ultraviolet spectra of the above-mentioned three stereoisomeric *p*-distyrylbenzenes and two *p*-styryltolans are presented in Figs. 1 and 2. The spectroscopic and physical properties of these compounds are summarized in Table I.

The shifts of the wavelength, where the absorption maxima of these compounds at the longest wavelength appear, represent an interesting feature. The introduction of a cis-double bond or an acetylenic bond instead of a trans-double bond caused a blue shift of ca. 18 and 16 mμ respectively. The absorption intensities of $\lambda_{max}$ at the longest wavelength of *trans-trans*, *trans*-acetylene and acetylene-acetylene compounds diminish with the increase in the amount of acetylenic linkage. Usually the absorption intensity of polyyne compound was found to be 2.6 fold as large as that of polyene compound. This phenomenon has been explained in terms of the larger number of π-electrons in triple bond and the linear geometry of polyyne compound[11]. As stated above, this is not valid for the absorption intensities of an alternant conjugate system of the styryltolan type. The decrease of absorption intensity by the introduction of aceylenic linkage seems to be attributable to an enhancement of the free rotation of the *p*-phenylene group, which may decrease the probability of transition of the full conjugate system.

The photoisomerizations and the discussions concerning the cis-peak of these compounds will be reported in the following paper together with those of the compounds of the distyrylstilbene series.

11) F. Bohlmann, *Angew. Chem.*, 65, 385 (1953).

## Experimental*

***trans, trans-p*-Distyrylbenzene (I).**—*a) From Terephthalaldehyde.*—To a stirred solution of benzylmagnesium chloride (from magnesium, 3.75 g. and benzyl chloride, 20.0 g., 0.158 mol.) in dry ether (100 ml.) was added dropwise terephthalaldehyde[12] (10.0 g., 0.075 mol.) in dry tetrahydrofuran (150 ml.); this mixture was refluxed for 3 hr. A saturated aqueous solution of ammonium chloride was added to the cooled mixture and the organic layer separated by decantation. The inorganic residue was extracted with ether and the extract combined with the organic layer. The solvent was distilled from the combined solution to give the crude glycol (27 g.). A solution of the crude glycol (25 g.) in dry toluene (220 ml.) containing *p*-toluenesulfonic acid (0.8 g.) was refluxed for 2 hr. The crystals deposited from the cooled reaction mixture were filtered and recrystallized from chlorobenzene, yielding *trans, trans-p*-distyrylbenzene (I), on light greenish yellow plates, m. p. 261~262.5°C. The viscous tarry material obtained by concentration of the mother liquor was treated with chlorobenzene, yielding a second crop of I. The crude material was repeatedly recrystallized from chlorobenzene to give I. The total yield was found to be 4.3 g. (22%). Further recrystallization from the same solvent afforded pure I, m. p. 266~267°C.

Found: C, 93.59; H, 6.76. Calcd. for $C_{22}H_{18}$: C, 93.57; H, 6.43%.

*b) From p-Styrylbenzyl-triphenylphosphonium Bromide (VII).*—I was obtained from VII together with *trans, cis-p*-distyrylbenzene (V). The details will be described in section b) on the preparation of V.

***p*-Bromotolan (III).**—The bromostyrene (II) was prepared from *p*-bromoacetophenone[13] via three

* All melting points are uncorrected.

12) J. M. Snell and A. Weissberger, "Org. Synth.", Col. Vol. I (1948), p. 109.

13) R. Adams and C. R. Noller, ibid., (1955), p. 788.

steps according to the method of Bothner-By[8] in a yield of 26%, trans-form, m. p. 105.5~106.5°C. A solution of potassium *tert*-butoxide in *tert*-butyl alcohol (from potassium, 3 g. and *tert*-butyl alcohol, 40 ml.) was stirred with the finely powdered *p*-bromostyrene (II, 17 g., 0.05 mol.), and the mixture was refluxed for 3 days. To the cooled reaction mixture, *tert*-butyl alcohol (180 ml.) and water (360 ml.) were added, precipitating a colorless solid. The solid was filtered, washed with water and dried. The recrystallization of solid from light petroleum yielded III, in the form of colorless plates, m. p. 82~83°C, 10.5 g. (83%).

Found: C, 65.81; H, 3.54; Br, 30.73. Calcd. for $C_{14}H_9Br$: C, 65.39; H, 3.53; Br, 31.07%.

***trans-p*-Styryltolan (IV).** — *a) From p-Bromotolan (III).*—A little excess of *n*-butyllithium in ether (prepared from *n*-butyl chloride and lithium, the concentration being estimated by titration with 0.1 N hydrochloric acid) was slowly stirred into a solution of *p*-bromotolan (10.3 g., 0.04 mol.) in dry ether (100 ml.) in an atmosphere of pure nitrogen, and the mixture was refluxed for 2.5 hr. To the resultant orange yellow solution of tolan-lithium was added phenylacetaldehyde (6 g., 0.05 mol., freshly prepared from the dimethylacetal) in dry ether (65 ml.) at room temperature. A gradual change of the orange yellow color of the mixture to a white suspension was observed. Then the mixture was refluxed for 3 hr. to complete the reaction. A slow stream of pure nitrogen was introduced continuously into the reaction flask throughout these operations. A saturated aqueous solution of ammonium chloride (5.5 g.) and water were successively added to the cooled reaction mixture. The organic layer was separated. The organic layer and the ethereal extract were combined, washed with water and dried. The orange-colored oily residue obtained on evaporating the solvent was dissolved in dry toluene (150 ml.) containing *p*-toluenesulfonic acid (0.5 g.). The solution was refluxed, and the water formed was removed continuously by means of a water-separator. The crystals deposited on cooling the mixture were filtered and the mother liquor concentrated, resulting in the deposition of a second crop of crystals. The combined crystals were recrystallized twice from benzene, yielding *trans-p*-styryltolan, in the form of colorless leaflets, m. p. 211~211.5°C, 3.5 g. (31%).

Found: C, 94.09; H, 5.83. Calcd. for $C_{22}H_{16}$: C, 94.25; H, 5.75%.

*b) From p-Tolanaldehyde (X) by Wittig Reaction.*—The reactions described below were carried out in a dark place. *p*-Tolanaldehyde[10] (1 g., 4.85 mmol.) and benzyltriphenylphosphonium chloride (2 g., 5.15 mmol., m. p. 313~315°C) were mixed with absolute ethanol (25 ml.). To the stirred suspension was added an excess of lithium ethoxide in absolute ethanol. After stirring for 8.5 hr. at room temperature, the deposited pale yellow solid (0.7 g., a mixture of *trans-p*-styryltolan and phosphonium salt) was filtered. The solid was dissolved in benzene and the solution passed through a column of alumina to remove the phosphonium salt. The crude crystals obtained on evaporating the filtrate were recrystallized from benzene, yielding *trans-p*-styryltolan, in the form of colorless leaflets, m. p. 210~211°C, 0.5 g. (35.7%); this was found to be identical with the specimen obtained by the above-mentioned method a) by mixed melting point determination.

***cis-p*-Styryltolan (XII).** — The following operations were carried out in a dark place. The above-mentioned mother liquor of the Wittig reaction was diluted with water, precipitating a mixture of a solid and a brown oily material. The precipitate was dissolved in light petroleum. The solution was passed through a column of alumina and eluted with the same solvent. A colorless solid (m. p. 76~78°C) obtained from the eluate was recrystallized from aqueous ethanol, giving *cis-p*-styryltolan (XII), m. p. 78~78.5°C, colorless needles, 0.6 g. (49.2%).

Found: C, 93.88; H, 5.69. Calcd. for $C_{22}H_{16}$: C, 94.25; H, 5.75%.

***trans, cis-p*-Distyrylbenzene (V).** — *a) Partial Reduction of trans-p-Styryltolan (IV).*—The following operations were carried out in a dark place. Hydrogenation of the styryltolan (IV, 0.1 g.) in tetrahydrofuran (20 ml.) over Lindlar's catalyst resulted in the uptake of ca. 1 mol. of hydrogen. After removal of the catalyst, the solvent was evaporated under a reduced pressure. The residue was mixed with hot ethanol. The hot mixture was filtered to remove a small amount of insoluble trans, trans-isomer. The crystals separated on cooling the filtrate were filtered promptly. The crystals were found to be pure trans, cis-isomer V, in the form of colorless plates, m. p. 114~114.5°C.

Found: C, 93.58; H, 6.44. Calcd. for $C_{22}H_{18}$: C, 93.57; H, 6.43%.

*b) From p-Styrylbenzyl-triphenylphosphonium Bromide (VII).*—The following reactions and operations were carried out in a dark place. The phosphonium salt (VII, 2 g., 3.74 mmol.) was added to a solution of benzaldehyde (0.4 g., 3.77 mmol.) in absolute ethanol (60 ml.). Into this suspension was stirred an excess of a solution of lithium ethoxide in absolute ethanol. The mixture was stirred for 3 hr. at room temperature, and the solid was filtered (filtrate A). The solid was digested with boiling ethanol (30 ml.) and the insoluble material (solid B) filtered. The filtrate was cooled to yield trans, cis-isomer (V), m. p. 113.5~114.5°C. This was combined with the second crop, which was obtained on diluting the filtrate A with water and recrystallized from ethanol, yielding pure trans, cis-isomer (V), in the form of colorless plates, m. p. 113.5~114.5°C, 340 mg. (32.3%). This substance showed no depression of the melting point on admixture with the specimen derived by the above-mentioned method a).

Recrystallization of the solid B from chlorobenzene yielded trans, trans-isomer I, in the form of light greenish yellow plates, m. p. 253°C, 370 mg. (35.1%). The mixed melting point determination of this substance with the specimen derived from terephthalaldehyde proved the identity.

Exposure of the mother liquor of recrystallization of trans, cis-isomer to direct sunlight resulted in a deposition of crystals. This crystals were found to

be identical with trans, trans-isomer I, m. p. 255°C, 44 mg. (4%).

The total yield of the Wittig reaction was found to be 754 mg. (71.5%).

***cis, cis-p*-Distyrylbenzene (IX).**—Two moles of hydrogen were absorbed in a period of 18 min. on the hydrogenation of a solution of *p*-bis(phenylethynyl)benzene (VIII, 80 mg.) in tetrahydrofuran (20 ml.) over Lindlar's catalyst. After removal of the catalyst, the solvent was distilled under reduced pressure, yielding crystals. Repeated recrystallization of the crystals from light petroleum afforded cis, cis-isomer IX, in the form of colorless leaflets, m. p. 86.5~87.5°C.

Found: C, 93.79; H, 6.60. Calcd. for $C_{22}H_{18}$: C, 93.57; H, 6.43%.

The cost of this research was partly defrayed by the Scientific Research Expenditure Fund of the Ministry of Education, to which the authors' thanks are due.

*Department of Chemistry*
*Faculty of Science*
*Osaka University*
*Kita-ku, Osaka*

# *Preparation and Absorption Spectra of the Cobalt(III) Complexes of Amino Acids*[1]

By Motoshichi MORI, Muraji SHIBATA, Eishin KYUNO and Mitsuhiro KANAYA

(Received March 3, 1961)

There are two isomers, $\alpha$ (violet) and $\beta$ (red), of trisglycinatocobalt(III). It has recently been ascertained from the absorption spectra by Shimura and Tsuchida[2] and also by Basolo et al.[3] that the more soluble $\alpha$-form is a trans-cis isomer and that the other is a cis-cis isomer. This assignment is supported theoretically by Nakamoto et al.[4] Furthermore, Shimura[5] came to the same conclusion with trisalaninato cobalt(III).

The present research has two main purposes: one is an investigation on the preparation of these kinds of complexes, and the other an approach to the structures of the complexes by comparing their absorption spectra with those of model compounds having cis-cis and trans-cis structures. In addition, the thermal stability and the infrared spectra of the complexes are studied.

## Experimental

**Preparation.**—i) *Method Using Cobalt(III) Hydroxide.*—This is essentially the same as the method of Ley and Winkler[6]. To a solution of the desired amino acid was added a slight excess of freshly prepared cobalt(III) hydroxide, and the mixture was heated on a water-bath until a dark red solution was obtained. The resultant solution was filtered once to remove unreacted hydroxide. The filtrate was evaporated on a water-bath almost to dryness. The residue was dissolved in a little hot water, and the solution was filtered, if necessary. On evaporating and then standing the solution, violet crystals of the $\alpha$-form were obtained. The corresponding $\beta$-form was contaminated with the $\alpha$-form, but the amount of contamination was very small. It was very easy to purify the $\alpha$-form because of the great difference between the solubilities of the two isomers. By this method the $\alpha$-isomers of glycine, *dl*-alanine and *l*-leucine were prepared with good yields. Therefore, this method may be recommended as a general method for the $\alpha$-isomer.

Found: Co, 20.7; N, 14.8. Calcd. for $\alpha$-[Co(gly)$_3$*]: Co, 20.9; N, 14.9%. Found: Co, 18.1; N, 12.8. Calcd. for $\alpha$-[Co(ala*)$_3$]: Co, 18.2; N, 13.0%. Found: Co, 11.8; N, 18.4. Calcd. for $\alpha$-[Co(leu*)$_3$]: Co, 12.8; N, 18.6%.

ii) *Method Using Hexamminecobalt(III) Chloride.*—This method was devised by us though a similar method was reported almost at the same time[7]; the principle is based on the following equation;

$$[Co(NH_3)_6]Cl_3 + 3NH_2CH_2COOH + 3KOH \rightarrow [Co(gly)_3] + 3KCl + 3H_2O + 6NH_3$$

A mixed solution of the desired amino acid with the hexamminecobalt(III) chloride was introduced

1) Part V: On the syntheses of metal complexes. Part IV. M. Mori, M. Shibata, E. Kyuno and Y. Okubo, This Bulletin, **31**, 940 (1958). Partly presented at the 11 th Annual Meeting of the Chemical Society of Japan, Tokyo, April, 1958.

2) Y. Shimura and R. Tsuchida, This Bulletin, **29**, 311 (1956).

3) F. Basolo, C. J. Ballhausen and J. Bjerrum, *Acta Chem. Scand.*, **9**, 810 (1955).

4) K. Nakamoto, J. Fujita, M. Kobayashi and R. Tsuchida, *J. Chem. Phys.*, **27**, 439 (1957).

5) Y. Shimura, This Bulletin, **31**, 173 (1958).

6) H. Ley and H. Winkler, *Ber.*, **42**, 3894 (1909).

* The following abbreviations are used: gly, $NH_2CH_2COO^-$; ala, $NH_2CH(CH_3)COO^-$; leu, $(CH_3)_2CHCH_2CH(NH_2)COO^-$.

7) R. G. Neville and G. Gorin, *J. Am. Chem. Soc.*, **78**, 4895 (1956).

into a round flask with an air condenser, and a slight excess of 3 N potassium hydroxide was added to the mixture. The whole was heated until some crystalline materials appeared in it (it took more than 1 hr.). On cooling the contents by holding the flask in running water, fine violet crystals of the $\beta$-form separated out. In this step the $\alpha$-form was not obtained even in traces, but it was produced with a poor yield on evaporating the mother liquor.

From the experiments with glycine, *dl*-alanine and *l*-leucine, it was found that this method was convenient for the preparation of the less soluble $\beta$-form.

Found: Co, 19.6; N, 13.8. Calcd. for $\beta$-[Co(gly)$_3$]: Co, 19.7; N, 14.0%. Found; Co, 18.5; N, 12.9. Calcd. for $\beta$-[Co(ala)$_3$]: Co, 18.2; N, 13.0%. Found: Co, 12.4; N, 8.8%; Calcd. for $\beta$-[Co(leu)$_3$]: Co, 12.6; N, 9.0%.

iii) *Method Using Potassium Tricarbonatocobaltate (III).*—The reaction to this method, which was also devised by us, is as follows:

$$K_3[Co(CO_3)_3]+3NH_2CH_2COOH+3CH_3COOH\rightarrow$$
$$[Co(gly)_3]+3CH_3COOK+3H_2O+3CO_2$$

A desired amino acid was poured into a green solution of tricarbonatocobaltate(III) prepared by the method described in a previous paper[8], and the mixture was warmed on a water-bath for a little while, whereupon the color of the solution changed from green to blue. Then, 6 N acetic acid was added dropwise until the evolution of carbon dioxide ceased and the color of the solution became red-viotet. After filtering the solution, the filtrate was allowed to stand for some time in the cold. Crystals of the less soluble $\beta$-form were deposited, and then the $\alpha$-form separated out on evaporating the mother liquor over sulfuric acid. This method was applied to the same materials as those in i) and ii), and $\alpha$ and $\beta$ isomers were obtained in about equal amounts.

iv) *Ammoniatriacetatoethylenediaminecobalt(III)*, [*Co en(ata*)*]·$H_2O$.—About 3 g. of the $\alpha$-K[Co(ata)(OH)(OH$_2$)]·2H$_2$O prepared by the method described in the previous paper[9] was suspended in 20 ml. of water, and 6 ml. of a 10% solution of ethylenediamine was added to the suspension. The mixture was warmed on a water-bath until a red-violet solution was obtained. On evaporating the resultant solution over sulfuric acid, dark violet crystals of the desired complex separated out gradually. Yield, about 3 g.

Found: Co, 17.8; N, 12.7. Calcd. for [Co en(ata)]·H$_2$O: Co, 18.1; N, 12.9%.

v) *Citratotriamminecobalt(III)*, [*Co*($NH_3$)$_3$*cit***]·$H_2O$.—About 5 g. of *cis-cis*-[Co(NH$_3$)$_3$(NO$_3$)$_3$] and 2 g. of potassium citrate were dissolved separately in a little hot water, and the solutions were mixed and warmed on a water-bath for a few minutes. Then, about three volumes of ethanol was added to the solution, whereupon a violet oily material went to the bottom. After removal of the material by a separating funnel, the solution was kept in a refrigerator until fine rosy crystals separated out. This was slightly hygroscopic. Yield, about 1.5 g.

Found: Co, 17.9; N, 12.7. Calcd. for [Co(NH$_3$)$_3$cit]·H$_2$O: Co, 18.6; N, 13.1%.

Of all the complexes prepared here, the ammoniatriacetatoethylenediamine- and the citratotriamminecobalt(III) are to be regarded as new complexes. The aqueous solutions of all the complexes are very stable against acids and heat. Their solubilities in water decrease in the order of the glycinato-, the alaninato- and the leucinato-complexes; while the leucinato-complex is soluble to a certain extent in ethanol, the glycinato-complex is sparingly soluble in it.

**Thermal Decomposition and Absorption Spectra.**—The thermal decomposition was performed by using a Shimadzu thermal-balance in the same manner as that described in a previous paper[9]. The absorption spectra in solution were measured by a Hitachi EPU spectrophotometer, and the infrared spectra were obtained with a Koken DS 201 infrared spectrophotometer equipped with sodium chloride optics.

## Results and Discussion

**Thermal Decomposition.**—The decomposition curves of the glycinato-, alaninato- and leucinato-complexes are shown in Figs. 1—2 in which the weight loss per formual weight was plotted against temperature. In the case of the $\beta$-glycinato-complex, there is a certain weight loss corresponding to one molecule of water at 100~150°C, but there is no such weight loss in the corresponding $\alpha$-complex. It has been believed that the $\alpha$-complex has two molecules of water of crystallization, but the compound obtained in the present study is anhydrous. The decompositions of both isomers begin at nearly 220°C, and the weight loss corresponding to three molecules of

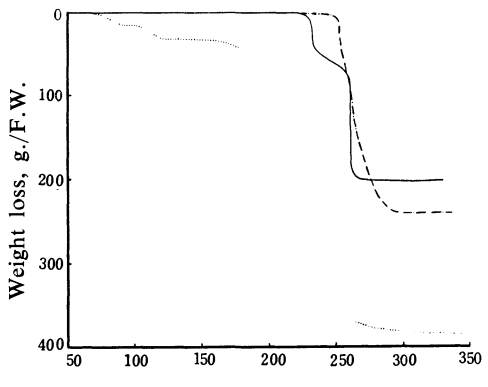



Fig. 1. Thermal decomposition curves of:
—— $\alpha$-[Co(gly)$_3$]
-·-· $\alpha$-[Co(ala)$_3$]
····· $\alpha$-[Co(leu)$_3$]·2H$_2$O

8) M. Mori, M. Shibata, E. Kyuno and T. Adachi, This Bulletin, 29, 883 (1956).
* Abbreviation ata stands for ammoniatriacetate ion.
9) M. Mori, M. Shibata, E. Kyuno and Y. Okubo, This Bulletin, 31, 940 (1958).
* Abbreviation cit stands for citrate ion.

ammonia is clearly observed at the first stage of decomposition. In the cases of the $\alpha$- and the $\beta$-alaninato-complex there is no evidence for the existence of water of crystallization and the decomposition temperatures are about 250°C. For the $\alpha$-isomer of the leucinato-complexes, the removal of water takes place in two steps and the total amounts correspond to $2H_2O$. On the other hand, the $\beta$-isomer may be anhydrous because no distinct weight loss is observed. The decomposition temperatures are in the neighborhood of 180°C. In general, it may be said that the $\alpha$-forms are less stable than the corresponding $\beta$-forms, though the difference in the decomposition temperature is not very large.

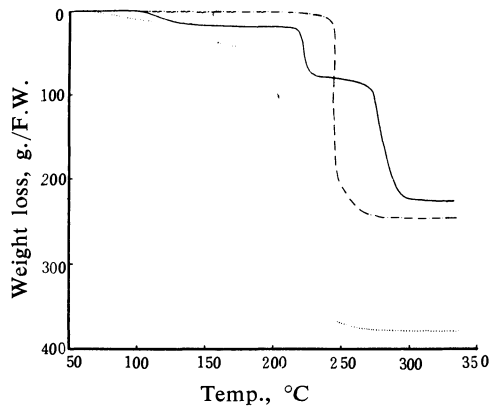



Fig. 2. Thermal decomposition curves of:
—— $\beta$-$[Co(gly)_3]\cdot H_2O$
-·-· $\beta$-$[Co(ala)_3]$
····· $\beta$-$[Co(leu)_3]$

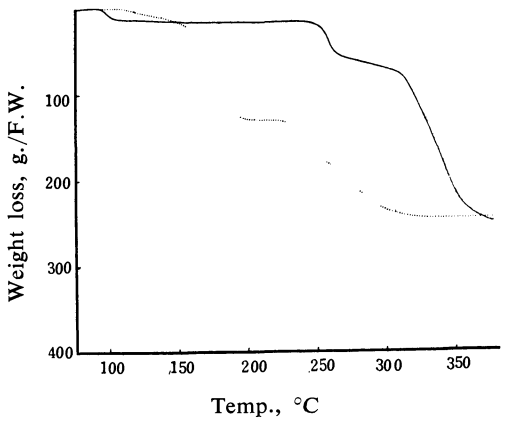



Fig. 3. Thermal decomposition curves of:
—— [Co en(ata)]$\cdot H_2O$
····· $[Co(NH_3)_3cit]\cdot H_2O$

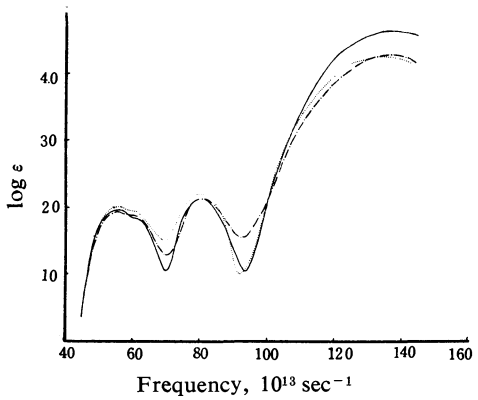



Fig. 4. Absorption spectra of:
—— $\alpha$-$[Co(gly)_3]$
-·-· $\alpha$-$[Co(ala)_3]$
····· $\alpha$-$[Co(leu)_3]\cdot H_2O$

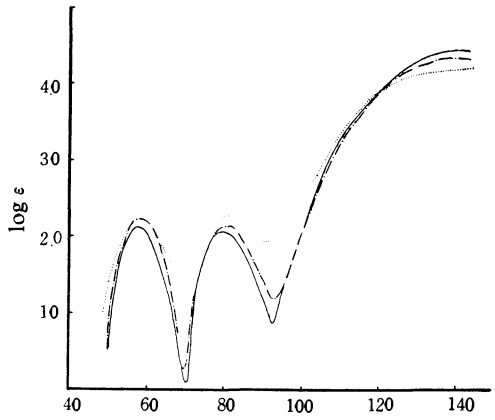



Fig. 5. Absorption spectra of:
—— $\beta$-$[Co(gly)_3]$
-·-· $\beta$-$[Co(ala)_3]$
····· $\beta$-$[Co(leu)_3]\cdot H_2O$

TABLE I. ABSORPTION MAXIMA AND log ε ($10^{13}$/sec.)

| | $\nu_1$ | log $\varepsilon_1$ | $\nu_2$ | log $\varepsilon_2$ | $\nu_3$ | log $\varepsilon_3$ | $\nu_{2\,calcd}$ | $\Delta$ |
|---|---|---|---|---|---|---|---|---|
| $\alpha$-$[Co(gly)_3]$ | 55.4 | 1.97 | 80.4 | 2.15 | 136.4 | 4.64 | 79.18 | +1.22 |
| $\alpha$-$[Co(ala)_3]$ | 55.6 | 1.96 | 80.7 | 2.16 | 135.8 | 4.34 | 79.42 | +1.28 |
| $\alpha$-$[Co(leu)_3]\cdot 2H_2O$ | 55.6 | 2.04 | 80.0 | 2.23 | 135.8 | 4.30 | 79.42 | +0.58 |
| $[Co\ en(ata)]\cdot H_2O$ | 57.5 | 2.20 | 82.0 | 2.24 | 133.9 | 4.59 | 81.68 | +0.32 |
| $\beta$-$[Co(gly)_3]\cdot H_2O$ | 57.7 | 2.16 | 79.6 | 2.08 | 140.2 | 4.45 | 81.92 | −2.32 |
| $\beta$-$[Co(ala)_3]$ | 58.0 | 2.22 | 80.4 | 2.21 | — | — | 82.27 | −1.87 |
| $\beta$-$[Co(leu)_3]\cdot H_2O$ | 58.0 | 2.27 | 80.4 | 2.26 | — | — | 82.27 | −1.87 |
| $[Co(NH_3)_3cit]\cdot H_2O$ | 56.4 | 1.58 | 79.8 | 1.92 | — | — | 80.37 | −0.57 |

TABLE II. INFRARED ABSORPTION

| Assignment | | α-[Co(gly)$_3$] | β-[Co(gly)$_3$] | α-[Co(ala)$_3$] | β-[Co(ala)$_3$] |
|---|---|---|---|---|---|
| | | | 3356(sh) | 3460(w) | |
| st | $NH_2$ | 3106(sh) | 3106(sh) | 3125(s) | 3096(sh) |
| | | | 1621(vs) | | 1634(vs) |
| st-a | $CO_2$ | 1618(vs) | 1585(vs) | 1629(vs) | 1582(vs) |
| st-s | $CO_2$ | 1351(sh) | 1350(sh) | 1344(sh) | 1344(sh) |
| d, w | $NH_2$ | 1299(m) | 1302(s) | 1282(s) | 1274(vs) |
| st-a | CCN | 1233(m) | 1205(s) | 1238(w) | 1250(w) |
| d, t | $CH_2$ | 1181(s) | 1174(s) | 1190(m) | 1190(m) |
| d, t | $NH_2$ | 1036(w) | 1030(w) | 1024(w) | 1028(w) |
| d, r | $CH_2$ | | | | |
| or d, r | $NH_2$ | 955(w) | 963(m) | — | — |
| st-s | CCN | 911(m) | 919(m) | 924(m) | 923(m) |
| d, r | $NH_2$ | 819(m) | 821(m) | 864(s) | 858(s) |
| or d, r | $CH_2$ | 778(w) | 776(m) | 821(w) | 821(sh) |
| | | | | 806(w) | 807(m) |
| | | | 759(w) | | |
| d | $CO_2$ | 753(m) | 755(w) | 763(w) | 761(w) |
| | | | | | 1124(sh) |
| ? | | 1133(s) | 1149(s) | 1126(s) | 1109(m) |

* K. Nakamura, *J. Chem. Soc. Japan, Pure Chem. Sec.* (*Nippon Kagaku Zasshi*), 80, 113 (1959). The abbreviations used in the first column of the table of assignments are: st, bond stretching vibration; d, deformation vibration; r, rocking vibration; w, wagging vibration; t, twisting vibration; ?, assignment uncertain; -s, symmetric vibration; -a, asymmetric vibra-

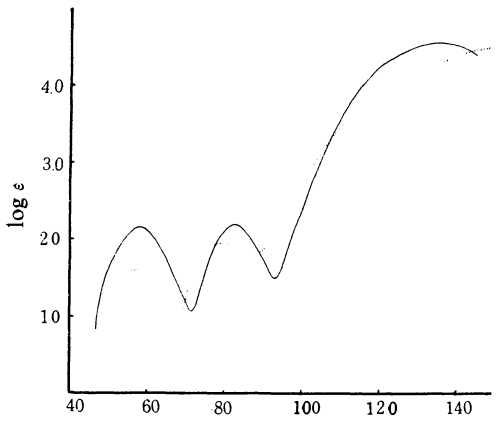



Fig. 6. Absorption spectra of:
—— [Co en(ata)]·$H_2O$
····· [Co$(NH_3)_3$cit]·$H_2O$

The decomosition curves for the ammoniatriacetato- and the citrato-complex are shown in Fig. 3. The former complex loses one molecule of water at a temperature below 100°C and begins to decompose at about 240°C. The latter is dehydrated at about 150°C and then decomposed when the temperature is raised.

**Visible and Ultraviolet Absorption Spectra.**— The absorption spectra of the α- and the β-forms are summarized in Figs. 4 and 5 respectively. The characteristic difference between them is seen in the first and the third bands; all of the first bands of the α-forms are more or less splitted, while those of the β-forms are normal and sharp. The third bands for the α-forms are sharper than those for the β-forms.

The absorption curves of the ammoniatriacetato- and the citrato-complex are shown in Fig. 6. The former complex has a somewhat split first band and a distinct third band, but the latter has a sharp first band and no maximum in the region of the third band.

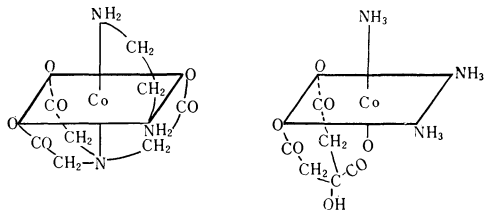
As mentioned above, the ammoniatriacetato-complex is taken as a model for the trans-cis configuration and the citrato-complex for the cis-cis configuration, because ammoniatriacetate ion acts as a tetradentate donor and citrate ion is a tridentate ligand; consequently the most probable structures of the two complexes are thought to be those given in Fig. 7. From the similarity of the absorption spectra, it may be concluded that all the α-forms have the trans-cis structure and the β-forms, the cis-cis. The same conclusion has been reached by others[2,3,5] but a somewhat different approach was adopted in our study.

The numerical data of the absorption spectra of these complexes are summarized in Table I; the absorption maxima for the second bands reveal a general relationship between the α- and β-isomers. In the last two columns of

BANDS($cm^{-1}$) FOR AMINOACIDS COMPLEXES

| α-[Co(leu)$_3$] | β-[Co(leu)$_3$] | [Co en(ata)]·$H_2O$ | [Co($NH_3$)$_3$cit]·$H_2O$ | $NH_2$-$CH_2$-COOH* |
|---|---|---|---|---|
| | | 3413(w) | 3425(sh) | |
| 3175(sh) | 3175(sh) | 3145(m) | 3175(sh) | |
| | 1639(vs) | | | |
| 1634(vs) | 1613(vs) | 1631(vs) | 1577(vs) | 1572(vs) |
| 1325(sh) | 1333( s ) | 1323(m) | 1328( s ) | 1412( s ) |
| 1299(m) | 1299(m) | 1266(m) | 1271(m) | 1133(m) |
| | | | | 1109(m) |
| 1235(w) | 1266(w) | 1229(w) | 1232( s ) | 1034( s ) |
| 1160(m) | 1190(w) | 1198(w) | 1170(w) | |
| 1073(w) | 1040(w) | 1059(m) | 1067( s ) | |
| 988(w) | 971(w) | 957(w) | 938(w) | 909(sh) |
| 926(w) | 924(w) | 913( s ) | 914(w) | 892( s ) |
| 847(m) | 843(m) | 849(sh) | 862( s ) | |
| 821(w) | 820(w) | | 820(sh) | |
| 794(w) | 777(w) | | | |
| 758(w) | 727( s ) | 758( s ) | 727( s ) | 696( s ) |
| 1127(w) | 1134(w) | 1152( s ) | 1140( s ) | |

tion. The abbreviation used in the body of the table of assignments to indicate the relative intensities of the absorption are; vs, very strong; s, strong; m, medium strong; w, weak; sh, shoulder.



[Co en(ata)] [Co($NH_3$)$_3$cit]

Fig. 7. Probable structures.

the table, the values calculated by a Sone's equation[10] and the differences ($\Delta$) of the calculated values from the observed maxima are given. All of the trans-cis isomers show positive difference and the cis-cis isomers, negative difference.

**Infrared Spectra.**—The numerical data of the infrared spectra are summarized in Table II, in which the assignment is carried out with reference to papers of Nakamura and others[11]. A distinctive difference between the absorption of α- and β-isomers is observed in the region of 1580~1630 $cm^{-1}$; there is only one peak for the α-isomer, but the β-isomer has two split absorption peaks. Among the isomers of the same type, the absorption maxima shifted to longer wavelengths in the following order: the leucinato-, the alaninato- and the glycinato-complexes.

**Preparation.**—It is very interesting that the methods mentioned in the Experimental section above have preferential properties for the production of cis-cis and trans-cis isomers; the cobalt(III) hydroxide method favors the trans-cis, the hexammine method is advantageous for the cis-cis, and the tricarbonato method gives both isomers in the about the same amount. Therefore, somewhat different mechanisms may be involved in these methods and perhaps in the formation of the isomers; the decisive factor is which of the nitrogen and oxygen atoms of the incoming donor attacks the objects first.

## Summary

Three different methods were investigated of the preparation of trisglycinato-, trisalaninato- and trisleucinato-cobalt(III). The method using cobalt(III) hydroxide is convenient for the α-form, the method using hexamminecobalt(III) salt is advantageous for the β-form, and the method using tricarbonatocobaltate(III) gives both forms of the complexes. In addition, two new isomers of [Co en(ata)]·$H_2O$ and [Co($NH_3$)$_3$cit]·$H_2O$ having trans-cis and cis-cis

10) K. Sone, *J. Chem. Soc. Japan, Pure Chem. Sec.* (*Nippon Kagaku Zasshi*), **71**, 270 (1950).
11) K. Nakamura, ibid., **80**, 113 (1959): S. Mizushima and I. Nakagawa, ibid., **80**, 124 (1959).

configurations with respect to the coordinated atoms were synthesized.

By comparing the visible and the ultraviolet absorption spectra, it was concluded that the $\alpha$-form is a trans-cis isomer and that the $\beta$-form is a cis-cis isomer. Thermal decomposition of the complexes was performed in order to estimate the water of crystallization and the stability. The infrared spectra of the complexes were also measured.

*Department of Chemistry*
*Faculty of Science*
*Kanazawa University*
*Kanazawa*

# *Studies on Metal Complex Species Using an Anion Exchange Resin. II. On the Adsorption of Silver from Nitrate Solution*

By Hirohiko WAKI

(Received January 16, 1961)

In the previous papers[1,2] the author has derived equations for determining the composition of a metal complex by use of an anion exchange resin and applied them to mercury-(II)-nitrate complex species. Silver is, as well as mercury, adsorbed on an anion exchange resin from solutions of various nitrates or nitric acid, though its adsorption is not strong. In this paper the adsorption of silver from nitrate solutions and nitric acid was studied and its form in the resin was determined by the previously reported method[1,2] as well as by a new method.

The adsorption of silver nitrate on an anion exchanger Dowex 1-X8 was examined and compared with that of alkali nitrates. Even alkali nitrates are taken up a little in the resin, but no appreciable difference in the adsorbability between sodium and potassium is evident, as shown in Fig. 1. The apparent adsorption of alkali metals may be considered merely as a permeation of dissociated normal salts. On the other hand, the adsorbed amount of silver nitrate is considerably larger than that of alkali nitrates.

This difference in the adsorbability between silver and alkali metals is remarkable when a small quantity of these elements is used in a nitric acid medium, as shown in Fig. 2. The

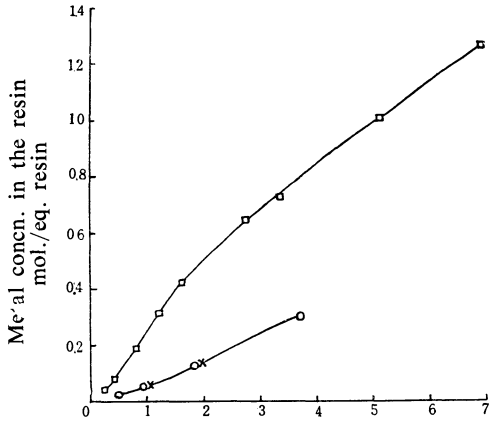



Fig. 1. Adsorption of Ag, Na and K from the solution of its nitrate only.
□ $AgNO_3$ ○ $NaNO_3$ × $KNO_3$

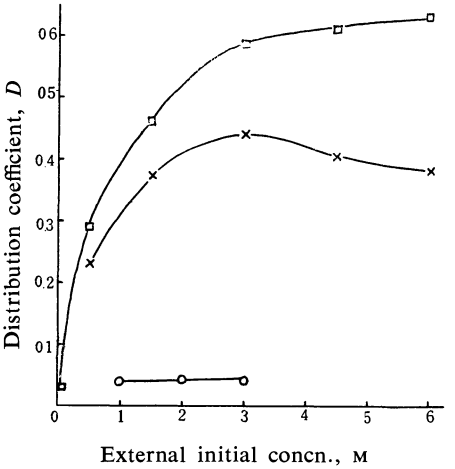



Fig. 2. Adsorption of Ag and Na in small quantity from nitrate solutions.
Metal: 0.1 mmol., Resin: 3 g., Solution: 8 ml.
□ Ag in $NaNO_3$ × Ag in $HNO_3$
○ Na in $HNO_3$

1) H. Waki, This Bulletin, 33, 1469 (1960).
2) H. Waki, ibid., 34, 829 (1961).

distribution coefficient of sodium is very small and scarcely increases at all with an increase in nitric acid concentration. On the other hand, the distribution coefficient of silver in nitric acid increases rapidly in the beginning, then gradually to a maximum near 3 M nitric acid and then decreases gradually. In sodium nitrate solution, the coefficient has no maximum and is somewhat greater than that in nitric acid. Although the coefficient is considerably smaller than that of mercury[1,2], it may be reasonable to consider that the adsorption of silver is not a simple permeation of the normal salt but is related to the formation of nitrate complex species.

However, silver ion does not appear to form any nitrate complex anion in an ordinary nitrate solution, since silver nitrate may be regarded as a kind of relatively strong electrolyte, as seen from the fact that the mean activity coefficient[3] of silver nitrate is similar to that of alkali nitrate, especially that of potassium nitrate and rubidium nitrate, and at the utmost the presence of undissociated silver nitrate[4] may be considered only in concentrated nitrate solution. Even if a slight quantity of the complex anion is present in the solution, it may be difficult to consider that the adsorption of silver takes place by a successive permeation of the complex, because it takes only a short time to reach the adsorption equilibrium. Accordingly, the adsorption of silver may be explained by its movement into the resin phase as silver ion $Ag^+$ and neutral species $AgNO_3^0$, followed by the conversion into a silver-nitrate complex in the resin phase.

For the purpose of determining the composition of a metal complex by use of an anion exchange resin, the distribution coefficient $D$ of a metal element was expressed as follows[1,2]:

$$\log D=\left(n-\frac{a}{b}\right)\log[X^{b-}]-\left(m-\frac{a}{b}\right)\log(X^{b-})+K+G \qquad (1)$$

where ( ) and [ ] indicate the concentrations in the solution phase and the resin phase, $m$ and $n$ represent the numbers of an anion $X^{b-}$ binding to one metal ion $M^{a+}$ in these phases, and $K$ and $G$ represent the terms containing the complex formation constants and the activity coefficients in both phases, respectively. When the metal is present as $M^{a+}$ in the solution, Eq. 1 may be written as follows:

$$\log D=\left(n-\frac{a}{b}\right)\log[X^{b-}]+\frac{a}{b}\log(X^{b-})+K+G \qquad (2)$$

if a similar assumption is made in a silver-nitrate system, the following equation is obtained.

$$\log D-\log(NO_3^-)=(n-1)\log[NO_3^-]+K+G \qquad (3)$$

**Experiment by the Addition of an Indifferent Anion.**—This experiment was carried out in a way similar to that in the mercury-nitrate system. Two grams of an anion exchanger Dowex 1-X8 (100~200 mesh) of nitrate form was mixed with 10 ml. of a solution containing 0.3 mmol. of silver nitrate and a series of mixtures of sodium nitrate and sodium perchlorate of various mixing ratios (total concentration is 3 M). After equilibrium is reached silver and nitrate in the resin were determined. Silver was analyzed titrimetrically with a potassium thiocyanate and nitrate spectrophotometrically at 300 mμ. The amounts of silver and nitrate in the solution were estimated by subtraction from their total amounts.

The ion concentrations in the resin phase were always represented as millimoles of the ion per milliequivalent of the resin. The distribution coefficient of silver was calculated as

$$D=\frac{\text{mmol. of Ag adsorbed per meq. of the resin}}{\text{mmol. of Ag per ml. of the soln.}}$$

After the nitrate concentration in the resin was corrected as in the case of mercury-nitrate, $\log D-\log(NO_3^-)$ was plotted against the logarithm of the nitrate ion concentration in the resin. As shown in Fig. 3, in the range where nitrate is predominant, the gradient of the curve is 0.9, which corresponds approximately to $n=2$. From this result, it may be recognized that most of the silver-nitrate complex adsorbed from 3 M sodium nitrate solution has the form of $Ag(NO_3)_2^-$.

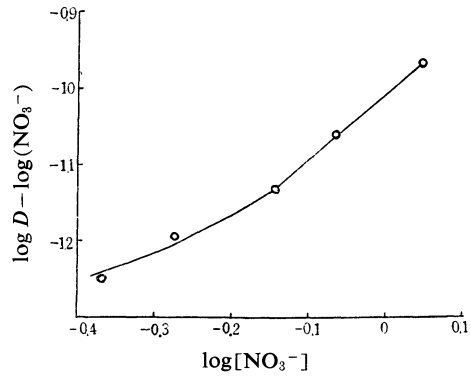



Fig. 3. Distribution coefficient of Ag as a function of the nitrate concentration in the resin phase. The measurements were carried out at the nitrate-rich range. Total concentration of the external solution is 3 M.

3) R. A. Robinson and R. H. Stokes, "Electrolyte Solutions", Butterworths Scientific Publications, London (1955).
4) J. Bjerrum, G. Schwarzenbach and L. G. Sillén, "Stability Constants. Part II Inorganic Ligands", London (1958).

TABLE I. EQUILIBRIUM DATA ON THE BATCH EXPERIMENT

A. 2 M Series Resin : 7.14 meq., Solution : 8 ml.

| Batch No. | 1 | 2 | 3 | 4 | 5 | 6 | 7 |
|---|---|---|---|---|---|---|---|
| $AgNO_3$ given, mmol. | 0.100 | 1.275 | 1.985 | 3.97 | 5.96 | 7.94 | 11.91 |
| $NaNO_3$ given, mmol. | 16.00 | 14.72 | 14.00 | 12.00 | 10.00 | 8.00 | 4.00 |
| (Ag) mmol./ml. | 0.00813 | 0.112 | 0.175 | 0.361 | 0.559 | 0.755 | 1.175 |
| [Ag] mmol./meq. | 0.00490 | 0.0536 | 0.0819 | 0.152 | 0.209 | 0.266 | 0.352 |
| $D$ ml./meq. | 0.603 | 0.481 | 0.468 | 0.420 | 0.373 | 0.352 | 0.299 |
| $(NO_3^-)$ mmol./ml. | 1.88 | 1.83 | 1.80 | 1.76 | 1.73 | 1.66 | 1.59 |
| $[NO_3]_t$ mmol./meq. | 1.15 | 1.19 | 1.22 | 1.27 | 1.30 | 1.37 | 1.45 |
| $\log D - \log(NO_3^-)$ | −0.494 | −0.581 | −0.585 | −0.622 | −0.666 | −0.673 | −0.726 |

B. 3 M Series Resin : 6.45 meq., Solution : 8 ml.

| Batch No. | 1 | 2 | 3 | 4 | 5 | 6 |
|---|---|---|---|---|---|---|
| $AgNO_3$ given, mmol. | 0.100 | 0.985 | 1.97 | 3.94 | 5.91 | 7.88 |
| $NaNO_3$ given, mmol. | 24.07 | 23.07 | 22.06 | 20.06 | 18.05 | 16.04 |
| (Ag) mmol./ml. | 0.00805 | 0.0838 | 0.171 | 0.349 | 0.539 | 0.733 |
| [Ag] mmol./meq. | 0.00552 | 0.0488 | 0.0938 | 0.178 | 0.247 | 0.313 |
| $D$ ml./meq. | 0.686 | 0.583 | 0.550 | 0.551 | 0.459 | 0.428 |
| $(NO_3^-)$ mmol./ml. | 2.83 | 2.78 | 2.75 | 2.70 | 2.69 | 2.62 |
| $[NO_3]_t$ mmol./meq. | 1.24 | 1.28 | 1.30 | 1.37 | 1.38 | 1.46 |
| $\log D - \log(NO_3^-)$ | −0.256 | −0.343 | −0.374 | −0.428 | −0.478 | −0.533 |

**Experiment by the Loading of the Complex.**— In determining the composition of a metal complex, a method in which the ratio of the adsorbed amount of the metal to the exchange capacity of the resin is determined after the resin is saturated with the metal complex anion, has often been employed[5]. This method is simple and reliable when the complex is stable and strongly adsorbed on an anion exchanger. However, it can not be used when the complex is unstable and not strongly adsorbed.

In view of this, a new loading method was studied by the present writer, which is based on Eq. 2. In the proposed method, instead of the addition of the indifferent anion, a greater amount of the same metal element is used to keep the ionic strength in the solution phase constant. The ligand ion concentration in the resin phase is therefore varied by the loading of the metal complex instead of an indifferent anion. Assuming that $MX_n^{(bn-a)-}$ is only one species for the resin phase, this concentration is expressed by

$$[X^{b-}] = [X]_t - n[MX_n^{(bn-a)-}] \quad (4)$$

where $[X]_t$ is the total ligand concentration irrespective of species. From Eq. 2 and Eq. 4 the following equation is obtained.

$$\log D = \left(n - \frac{a}{b}\right)\log([X]_t - n[MX_n^{(bn-a)-}]) + \frac{a}{b}\log(X^{b-}) + K + G \quad (5)$$

When a considerable amount of the metal is adsorbed, for the determination of $n$, $\log D/(X^{b-})^{a/b}$ can not be plotted against $\log[X^{b-}]$, because the second term in the right side of Eq. 4 can not be neglected and $n$ is unknown. Accordingly, in this case $\log D/(X^{b-})^{a/b}$ is plotted against $[MX_n^{(bn-a)-}]$ and the slope of the curve should be compared with that of the standard curves drawn by substituting 1, 2, 3, ……for $n$ in Eq. 5.

In a system of silver nitrate and sodium nitrate, Eq. 5 is written as follows:

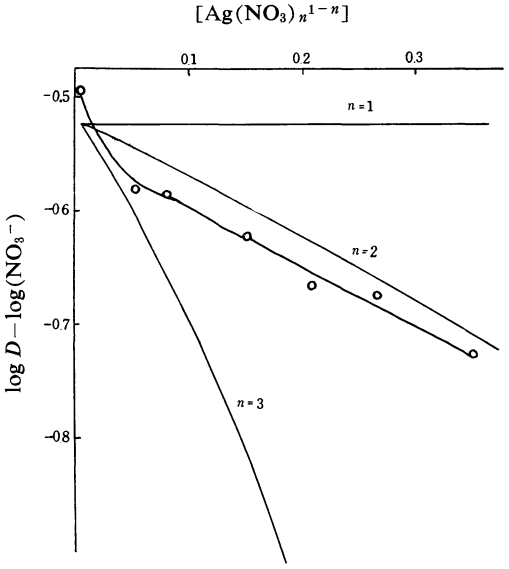



Fig. 4. Comparison with the standard curves in the system where the external initial concentration of $AgNO_3$+$NaNO_3$ is 2 M.
The standard curves are drawn in a position in which their gradients may compare with that of experimental curve.
-○- Measured —— Standard

5) For example, R. A. Horne, R. H. Holm and M. D. Meyers, *J. Phys. Chem.*, **61**, 1955 (1957).

$$\log D - \log(NO_3^-) = (n-1)\log([NO_3]_t - n[Ag(NO_3)_n^{(n-1)-}]) + K + G \quad (6)$$

The experiment was carried out by equilibrating 3 g. of an anion exchanger Dowex 1-X8 (100~200 mesh) of nitrate form with 10 ml. of a solution containing a series of mixtures of silver nitrate and sodium nitrate of various mixing ratios (total concentration is 2 M or 3 M), followed by determination of silver and nitrate in the solution phase. The silver concentration in each phase and the distribution coefficient were estimated in the same way as before. The nitrate in the solution was determined by titrating with a sodium hydroxide solution, after it was converted into nitric acid through a cation exchange column of hydrogen form. The amount of total nitrate in the resin was estimated by subtraction.

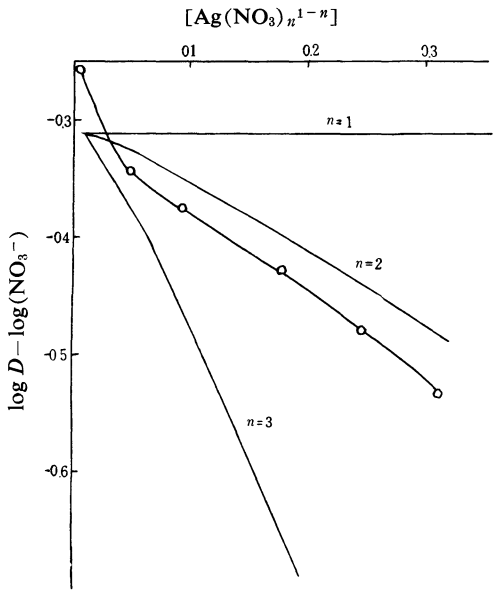



Fig. 5. Comparison with the standard curves in the system where the external initial concentration of $AgNO_3+NaNO_3$ is 3 M.
The standard curves are drawn in a position in which their gradients may compare with that of experimental curve.
-○- Measured —— Standard

The equilibrium data are tabulated in Table I and the curves for analysis are drawn in Fig. 4 and Fig. 5. Each slope of the curve is similar to that of the standard curve for $n=2$ in a wide range of the silver concentration except at a very low concentration. From this fact it may be considered that most silver in the resin phase exist as $Ag(NO_3)_2^-$ at the external nitrate concentration of about 2~3 M. This result is in agreement with that in the former experiment carried out by the addition of an indifferent anion. The high value of the gradient at the low concentration of silver is presumably due not to the presence of higher nitrate complexes, but to the inconstancy of the activity coefficient term in this region.

## Summary

1) It was found that silver was to some extent adsorbed on a strong base anion exchange resin from nitrate solutions. Its behavior was significantly different from that of alkali metals.

2) The equations derived in the previous paper were applied to a study of silver-nitrate complex. Starting from the same equation, two methods using either $NaNO_3+NaClO_4$ mixed media or the loading of the complex were employed, and the two results were in good agreement.

3) It was presumed that most silver in the resin exists as $Ag(NO_3)_2^-$ in neutral nitrate media where the external nitrate concentrations were about 2~3 M, although such anionic species may not be considered to exist in an ordinary nitrate solution.

The author wishes to express his sincere thanks to Professor Jun Yoshimura of Kyushu University for his guidance and encouragement. He also thanks Professor Hidetake Kakihana of Tokyo Technical University for his valuable suggestion.

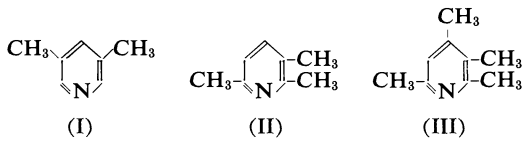
*Department of Chemistry*
*Faculty of Science*
*Kyushu University*
*Hakozaki, Fukuoka*

# *Separations of Lutidines, Collidines and 2, 3-Cyclopentenopyridines from Coal Tar Bases*

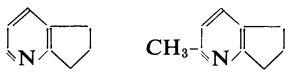
By Hajime SUZUMURA

(Received April 10, 1961)

In order to examine the tertiary amines in coal tar bases, especially in a forerunning of quinoline, methods of picrate and urea adduct formation, countercurrent extraction and chromatography were applied in order to effect the isolation of the bases. Selective separations could be carried out easily for some of the high boiling bases. From a fraction boiling at 170°C, 3, 5-lutidine[1] (I) was separated relatively easily as a zinc chloride adduct, and 2, 3-disubstituted pyridines such as 2, 3, 6-collidine[1] (II), 2, 3, 4, 6-tetramethylpyridine[2,3] (III), 2, 3-cyclopentenopyridine[2] (IV) and 2, 3-cyclopenteno-6-methylpyridine[3-5] (V) were isolated as

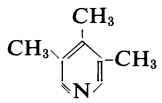


(I) (II) (III)



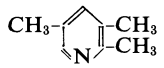
(IV) (V)

urea adducts from the fractions with corresponding boiling points. Furthermore, using a chromatographic column of cupric chloride-aluminum oxide which was effective for separations of pyridine, picolines and lutidines[6,7]



(VI)

2, 3-cyclopenteno-6-methylpyridine and 3, 4, 5-collidine[4,8-10] (VI) were separated. The latter was isolated for the first time from coal tar bases by the author[8]. With the same chromatographic column, 2, 3, 5-collidine[10] (VII) could also be separated and purified.



(VII)

The properties and physical constants of the bases which were separated are shown in the following tables.

## Experimental

**Materials.**—The materials used in the present investigation were all supplied by Yawata Chemical Industry Co.; their properties are shown below.

TABLE I. 3,5-LUTIDINE

| | B. p. °C | $d_4^{25}$ | M. p. of $B(HgCl_2)_2HCl$ °C | M. p. of picrate °C |
|---|---|---|---|---|
| Isolated | 171~172 | 0.9390 | 169~170 | 244~244.5 |
| Reported[1] | 171 | 0.9385 | 170 | 240 |

TABLE II. 2,3,6-COLLIDINE

| | B. p. °C | M. p. of picrate °C | $n_D^{25}$ |
|---|---|---|---|
| Isolated | 171~171.5 (uncorr.) | 147.4~148.4 | 1.5020 |
| Reported[1] | 172.8 | 148 | |

TABLE III. 2,3,4,6-TETRAMETHYLPYRIDINE

| | B. p. °C | $n_D^{25}$ | N % | M. p. of picrate °C | M. p. of picrolonate °C | Ultraviolet spectrum in cyclohexane $\lambda_{max}$ mμ | $\varepsilon_{max}$ |
|---|---|---|---|---|---|---|---|
| Isolated | 202.5 | 1.5088 | 10.35 | 122~122.5 | 226.4~226.9 | 266 | 3294 |
| Reported[2] | 203.3 | 1.5087 | (10.37)* | 122.5~123 | 225.5 | 266.5 | 3210 |

* Calcd.

1) T. Eguchi, This Bulletin, 3, 227 (1928).
2) P. Arnall, *J. Chem. Soc.*, **1954**, 4040.
3) S. Jifuku, S. Nakayama, H. Suzumura and M. Uemura, *J. Japan Tar Ind. Association*, **10**, 126 (1958).
4) P. Arnall, *J. Chem. Soc.*, **1958**, 1202.
5) S. Tanaka et al., *Japan Analyst* (*Bunseki Kagaku*), **6**, 281 (1957).
6) R. Vignes et al., *Compt. rend.*, **232**, 1419 (1951).
7) E. Funakubo, *J. Chem. Soc. Japan, Ind. Chem. Sec.* (*Kogyo Kagaku Zasshi*), **59**, 220 (1956).
8) Annual Meeting of Japan Tar Industry Association, October, 1956.
9) A. S. Bailey et al., *J. Chem. Soc.*, **1959**, 2554.
10) K. Tsuda et al., *Pharm. Bull.*, **1**, 283 (1953).

TABLE IV. 2,3-CYCLOPENTENOPYRIDINE

| | B. p. °C | $n_D^{25}$ | M. p. of picrate °C | M. p. of picrolonate °C | Ultraviolet spectrum $\lambda_{max}$ mμ | $\varepsilon_{max}$ |
|---|---|---|---|---|---|---|
| Isolated | 199.5 | 1.538 | 183.5～184 | 238.8 | 272 | 4090 |
| Reported[2] | 199.3～199.4 | 1.541 | 182～183 | 239 | | |

TABLE V. 2,3-CYCLOPENTENO-6-METHYLPYRIDINE

| | B. p. °C | F. p. °C | $n_D$ | M. p. of picrate °C | M. p. of picrolonate °C |
|---|---|---|---|---|---|
| Isolated | 210.5～211 | 35.0～35.7 | 1.527 (40°C) | 152.1～152.6 | 205.5～206.5 |
| Reported[4] | 211.9(761mmHg) | 31.8 | 1.5297(32.5°C) | 155 | 170 |
| Reported[5] | | 35·0 | | 152.8～153.1 | |

TABLE VI. 3,4,5-COLLIDINE

| | B. p. °C | M. p. °C | $d_4^t$ | $n_D$ | M. p. of picrate °C | M. p. of picrolonate °C | N % |
|---|---|---|---|---|---|---|---|
| Isolated | 210.3～210.8 | 32.6～35.6 | 0.955 (35°C) | 1.5115 (35°C) | 173.6～174.3 | 224 | 11.25 |
| Reported[4] | 211.4～211.5 (759 mmHg) | 36.8 | 0.947 (40°/20°C) | 1.5132 (37°C) | 178 | 232 | |
| Reported[9] | — | — | — | — | 174～175 | 228 | |
| Reported[10] | 205～207 | 10～13 | 0.9616 (15°C) | 1.5103 (15°C) | 174 | 188 | Calcd. 11.52 |

TABLE VII. 2,3,5-COLLIDINE

| | B. p. °C | $n_D^{25}$ | M. p. of chloroplatinate °C | M. p. of picrate °C |
|---|---|---|---|---|
| Isolated | 185～185.8 | 1.5045 | 211 | 184.5～185.2 |
| Reported[10] | 186.8 | 1.5057 | 212 | 184 |

TABLE VIII

Forerunning of quinoline ($S_1$)

Toluidine fraction
b. p. 199.8～202.2°C (28%)
↓
Tertiary amines (21%) ($T_3$)
↓ distilled
b. p. 183～189°C 32%
b. p. 200～201°C 17%

Xylidine fraction
b. p. 210.5～225°C (12%)
↓
Tertiary amines (50%) ($X_3$)
↓ distilled (30 mmHg)

| No. of fraction | Temp. of distillation °C | Yield* % |
|---|---|---|
| 2 | 95～ 96 | 8.8 |
| 3 | 96～100.5 | 13.2 |
| 4 | ～102 | 11.0 |
| 5 | ～104 | 8.0 |
| 6 | ～105 | 14.6 |
| 7 | ～108 | 17.2 |
| 8 | 108 | 13.0 |

* The yield in each step is based on an immediately preceding material.

TABLE IX. 2,3-CYCLOPENTENO-6-METHYLPYRIDINE

| No. of fraction | Urea adduct Amount g. | Urea adduct M. p. °C | Base recovered from urea adduct g. | Picrate Amount g. | Picrate M. p. °C |
|---|---|---|---|---|---|
| 7 | — | 86～129 | 1.4 | 0.35 | 149～150.5 |
| 8 | 2.4 | 88～129 | 1.3 | 0.80 | 150～150.5 |
| 9 | 2.6 | 88～129 | 1.3 | 0.90 | 150～150.5 |

TABLE X. 3,4,5-COLLIDINE AND 2,3-CYCLOPENTENO-6-METHYLPYRIDINE

| No. of band | 1 | 2 | 3 | 4 | 5 | 6 | 7 |
|---|---|---|---|---|---|---|---|
| Base recovered from each band, g. | 0.25 | 0.25 | 0.39 | 2.6 | 2.4 | 1.9 | 0.8 |
| M. p. of picrate, °C | 170.5~172.5 | 171~172 | | 150~151 | 150~151 | 192~195 | |
| Amount of picrate, g. | 0.7375 | 0.6425 | | 3.0 | 1.4 | 0.4 | |
| Compound | 3,4,5-Collidine | | | 2,3-Cyclopenteno-6-methylpyridine | | Unidentified | |

TABLE XI.

| No. of fraction | 1 | 2 | 3 | 4 |
|---|---|---|---|---|
| Amount, g. | 8.4 | 5.0 | 3.4 | 5.4 |
| $n_D^{25}$ | 1.5093 | 1.5094 | 1.5115 | 1.5201 |
| M. p.* of picrate, °C | 124~138 | 113~125 | 124~150 | 178~179 |

* After recrystallized twice from ethanol.

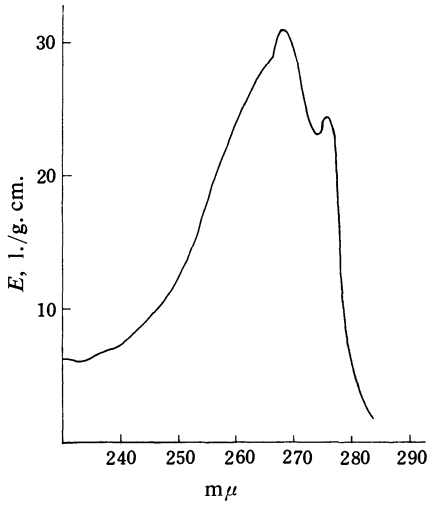



Fig. 1. 3,5-Lutidine in ethanol.

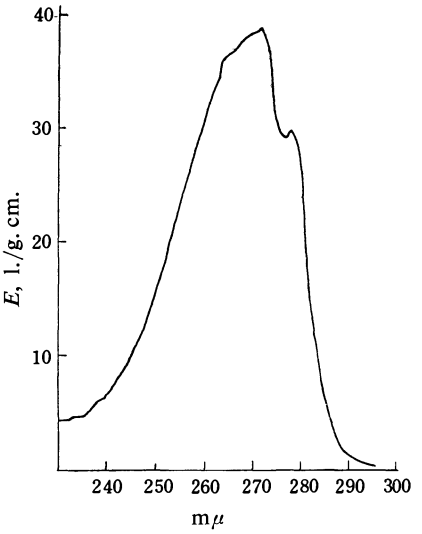



Fig. 3. 2,3-Cyclopentenopyridine.

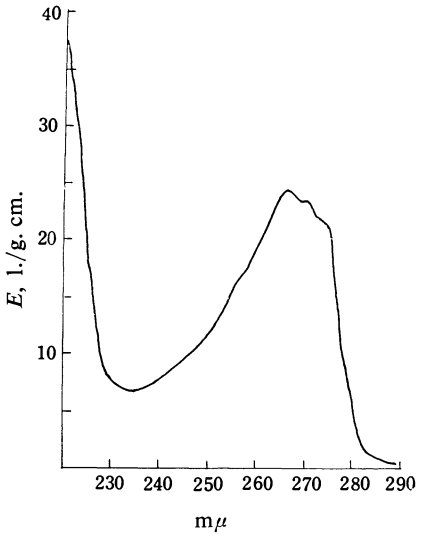



Fig. 2. 2,3,4,6-Tetramethylpyridine.

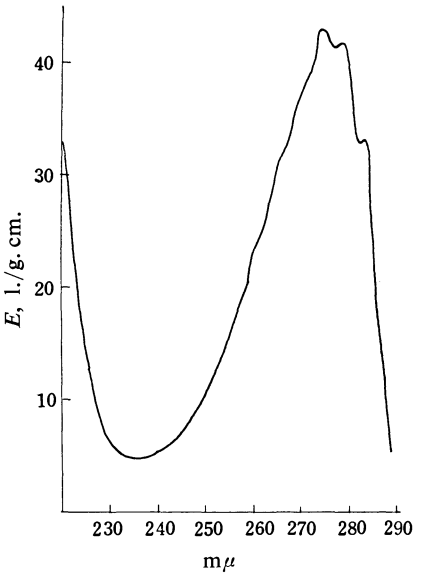



Fig. 4. 2,3-Cyclopenteno-6-methylpyridine.

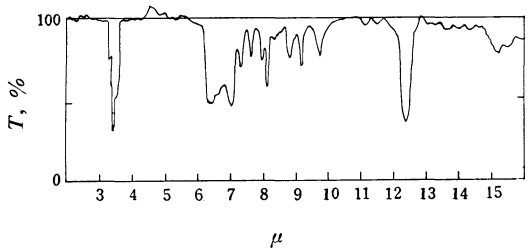



Fig. 5. 2,3-Cyclopenteno-6-methylpyridine.

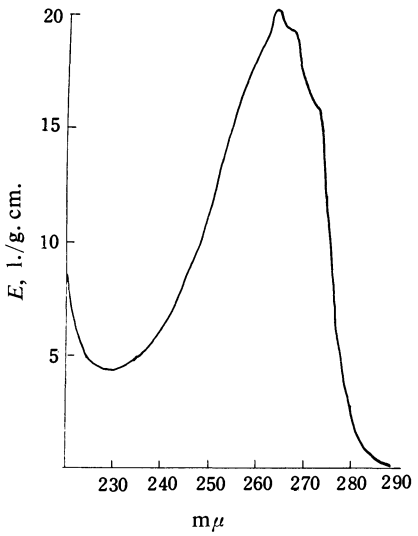



Fig. 6. 3,4,5-Collidine.

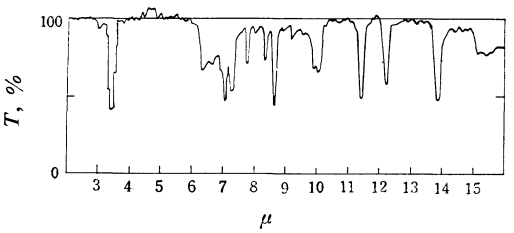



Fig. 7. 3,4,5-Collidine.

(1) Industrial grade collidine grade 1

| Sample | First drop | 10% | 50% | 90% | Dry point |
|---|---|---|---|---|---|
| A | 165.7 | 171.7 | 173 | 178 | 180 |
| B | 161.0 | 166.0 | 172 | 181 | 185 |

(2) Tertiary amines boiling at 200 and 210°C. A forerunning of quinoline (Fig. 8) was obtained when the crude quinoline was first extracted with sulfuric acid from the middle oil of coal tars and then fractionally distilled. Fractionating through a packed column 3 m. in height, this forerunning was separated into toluidine and xylidine fractions. Primary amines in these fractions were removed by acetylation, and the mixture of tertiary amines thus obtained was fractionally distilled as shown in Table VIII.

**Separation of 3, 5-Lutidine by Zinc Chloride.**— Industrial grade collidine grade 1 (Sample A) (1250

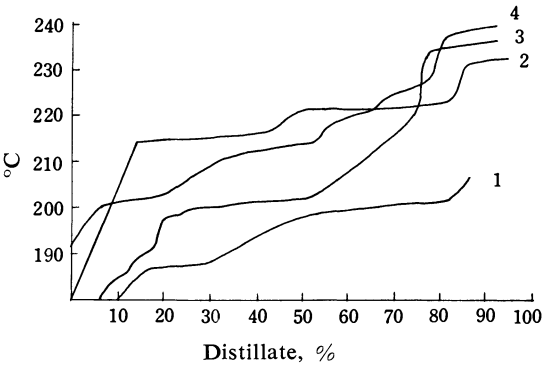



Fig. 8

1 $T_3$ ($S_1$)
2 $X_3$ ($S_1$)
3 Forerunning of quinoline ($S_1$)
4 $X_3$ ($S_4$)

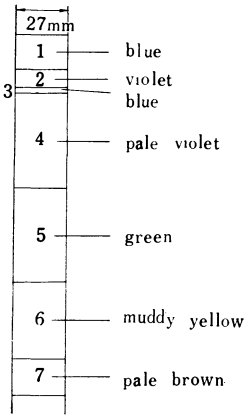



Fig. 9

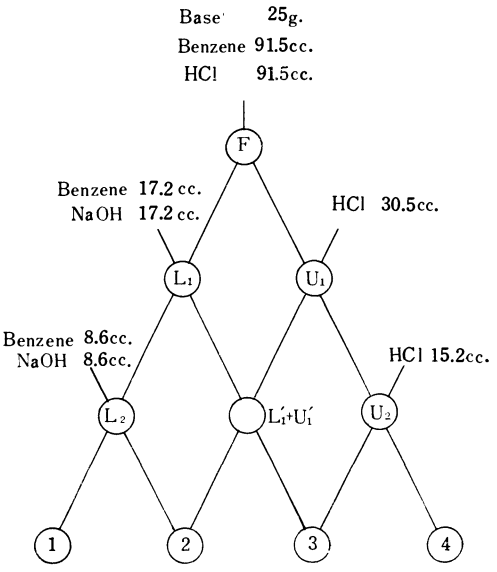



Fig. 10

cc.) was fractionated through a column 2 m. in height and packed with single turn helices, and a fraction boiling at 168~171°C (534 cc.) was obtained. When a 50% aqueous solution of zinc chloride was stirred into this fraction, a white adduct was precipitated which was washed with benzene to remove free bases and then steam-distilled. The distillate, on treatment with an aqueous solution of picric acid, gave crude picrates, m. p. 240°C, in about a 4% yield based on the fraction. The crude picrate (49 g.) was refluxed with 700 cc. of ethanol, yielding 42 g. of pure picrate, which was decomposed to give pure 3,5-lutidine.

**Separation by Urea-adduct.**—*Separation of 2,3,6-Collidine.*—One kilogram of Industrial grade collidine grade 1 (Sample B) was distilled into the following fractions:

| Fraction | up to 165°C | 165~167°C | 170~175°C |
|---|---|---|---|
| Amount, g. | 515 | 107 | 326 |

To the fraction boiling at 170~175°C (80 g.), a 50% aqueous solution of urea was added, and the resulting white adduct of m. p. 128~132°C was decomposed by steam distillation. A picrate (12 g.) melting at 147.4~148.4°C was obtained from the distillate. After being recrystallized once from ethanol, the picrate was decomposed, yielding 3.1 g. of pure 2,3,6-collidine.

*2,3,4,6-Tetramethylpyridine.*—To 16 g. of the fraction ($T_3$) boiling at 200~201°C, 43 g. of a 50% aqueous solution of urea was added, and the resulting adduct was washed with ether and decomposed by steam distillation to give a base (4.5 g.) boiling at 198°C. The picrate of this base, after three recrystallizations from ethanol, melted at 122~122.5°C. The base was also confirmed by picrolonate and ultraviolet absorption spectrum.

*2,3-Cyclopentenopyridine.*—To 36 g. of No. 3 fraction of $X_3$, a solution of urea (112 g.) in 50 cc. of water was added to form urea adduct, m. p. 124~132°C, which was decomposed, yielding 18 g. of basic material showing $n_D^{25}$ 1.5200. This was next purified as picrate, and after a recrystallization from ethanol picrate of 2,3-cyclopentenopyridine (21 g.) which melted at 178~179°C (uncorr.) was obtained. From the filtrate of urea adduct, 10 g. of the picrate of the base was recovered.

*2,3-Cyclopenteno-6-methylpyridine.*—To 5 g. of Nos. 8 and 9 fractions of $S_4$, 1 g. of a 60% aqueous solution of urea was added to yield an adduct from which 2,3-cyclopenteno-6-methylpyridine was recovered as picrate. The purified picrate did not show a melting point depression when admixed with an authentic sample. The results are shown in Table IX.

Similarly, from 50 g. of No. 9 fraction of $S_4$, 19.8 g. of picrate was obtained. The combined picrates were decomposed, yielding 7.45 g. of the free base with $n_D^{35}$ 1.5280. Bases which were recovered from the filtrate of the adduct boiled at 214°C and had $n_D^{20}$ 1.5270, and N content 10.31%.

**Chromatographic Separation.**—*Separation of 3,4,5-Collidine and 2,3-Cyclopenteno-6-methylpyridine.*—As Vignes used for the separation of pyridine, picolines and 2,6-lutidine[6], a mixture of cupric chloride (2 parts), aluminum chloride (25 parts), glycerol (6 parts) and distilled water (2 parts) was ground, dried at 50°C, and then used as an adsorbent in a chromatographic column. The adsorbent (190 g.) was packed in a column as shown in Fig. 9. No. 7 fraction (10.02 g.) from $X_3$, in Table VIII, was placed on a column and developed with 280 cc. of ether. After 5 hr., development was complete, giving various zones as shown in Fig. 9. From each zone, bases were recovered by the addition of an alkali, followed by steam distillation. While examining these bases as picrates, the author found that the bases of Nos. 4 and 5 mainly consisted of 2,3-cyclopenteno-6-methylpyridine, and a base of Nos. 1 and 2 whose picrate melted at 171~172°C (uncorr.) was identified as 3,4,5-collidine (Table X). A comparison of the properties of the base with those of the synthetic sample used in the identification of coal tar bases[10] is as follows: b.p. 210.3~210.8°C (reported 205~207°C), melting point of the picrate 173.6~174.3°C (reported 174°C), N content found 11.25% (Calcd. for $C_8H_{11}N$, 11.52%), molecular weight found 118 (Calcd. 121), and molar refractivity calculated from $d_4^{35}$ 0.9552 and $n_D^{35}$ 1.5115 38.1 (which is very close to the calculated values for collidines 38.6~38.8). The infrared spectrum in carbon disulfide and the ultraviolet spectrum in cyclohexane agreed with those of the literature cited. The base (0.4954 g.) was oxidized with 3.91 g. of potassium permanganate (used as a 2% aqueous solution) at 90°C over a period of 32 hr. Pyridine carboxylic acid was recovered as its copper salt; this was then decomposed by hydrogen sulfide to give the crude acid (0.0874 g.). After a recrystallization from water, pyridine carboxylic acid was obtained which melted with decomposition at 262.5°C (corr.).

Found: N, 5.8. Calcd. for $C_8H_5O_6N \cdot 3H_2O$: N, 5.3%.

*Separation of 2,3,5-Collidine.*—Separation of this base by picrate formation was reported in the literature, but the procedure of recrystallization was time-consuming. By using the chromatographic column described above, 2,3,5-collidine was separated easily. Bases of the fraction boiling at 183~190°C which remained in the solution after the solid urea adduct was removed were placed on the column and developed. A green zone was obtained, and from this zone was recovered a base whose picrate melted at 184~185°C and proved to be 2,3,5-collidine by the mixed melting point. Colors developed by other bases in this procedure are as follows: 3,5-lutidine (blue), 2,4,5-collidine (violet), 2,3,6-collidine (blue) and 2,3-cyclopentenopyridine (blue).

**Separation of 2,3-Cyclopentenopyridine by Countercurrent Extraction.**—2,3-Cyclopentenopyridine which was separated as urea adduct could also be separated by countercurrent extraction. The scheme of extraction, shown in Fig. 10, was similar to that described in the literature[11] using benzene and hydrochloric acid.

Using No. 2 fraction of $S_1$ as a feed, 2,3-cyclopentenopyridine was found to be concentrated in a fraction which was only with great difficulty soluble in the acid phase. The extraction was conducted

11) S. Tanaka et al., *Japan Analyst (Bunseki Kagaku)*, 5, 455, 513 (1956).

as shown in Fig. 10; bases were distributed between benzene and hydrochloric acid by shaking for 5 min. in a separatory funnel. The upper benzene layer $U_1$ was separated, hydrochloric acid (1 N) was added, and the extraction was repeated, forming upper $U_2$ and lower layer $U_1'$. To $L_1$, which was the lower layer of $U_1$, benzene and 1 N sodium hydroxide were added, and extraction was conducted to give $L_1'$ and $L_2$. $L_1'$ and $U_1'$ were combined and distributed between themselves. The extraction was continued until the 4 fractions shown in Fig. 10 were obtained. The amount, the refractive index and the melting point of the picrate of the base recovered from each fraction are shown in Table XI.

The basicity of the base was expected to decrease gradually from No. 1 to No. 4. From fraction No. 4 the picrate of 2,3-cyclopentenopyridine (4.5 g.) was separated and identified by mixed melting point with an authentic sample.

*Tokyo Laboratory of Research Center*
*Yawata Chemical Industry Co.*
*Chuo-ku, Tokyo*

# *The Raman Spectra of 1,3,5-Trichlorobenzene and 1,3,5-Trichlorobenzene-$d_3$*

By Shinnosuke SAËKI

(Received April 12, 1961)

A report on the infrared absorption spectra of ordinary and deuterated 1,3,5-trichlorobenzene has been previously presented by the author[1], but the Raman spectra of these substances have not yet been studied in detail. In this paper the Raman spectra of these substances are reported on, and the assignment of the observed Raman lines is presented, including that of the overtones and combinations.

As the molecule of 1,3,5-trichlorobenzene has a high symmetry, ten pairs of degenerate vibrations are contained in its thirty normal vibrations, and twenty fundamental frequencies are expected to be observed in the molecular spectra of this substance. Of these twenty frequencies, fourteen are active to the Raman effect.

Hitherto the assignments of the normal vibrations of the various aromatic derivatives have been made by collecting a large number of data for many similarly substituted benzenes and by comparing and systematizing these data. In the present report, instead of referring to the data of other substances, the assignment is determined by taking the spectra of both ordinary and deuterated substances, by applying the product rule, and by referring to the results of qualitative measurements of the depolarization ratios.

## Experimental

Commercial 1,3,5-trichlorobenzene was recrystallized from ethanol solution three times, and was then further purified by sublimation. Deuterated material was prepared by stirring the ordinary 1,3,5-trichlorobenzene with deuterated sulfuric acid for eight hours at 105°C. The reaction mixture was poured on ice and recrystallized from ethanol. The progress of substitution was checked by the infrared absorption spectrum after each substitution reaction, and the reaction was repeated until the strongest absorption band of $C_6HD_2Cl_3$ could hardly be recognized. It was found that the absorption bands of $C_6H_3Cl_3$ almost completely disappeared after the first reaction, and that three repetitions of the reaction were sufficient to complete the substitution reaction*.

The instrument used for the measurements was a Cary model 81 Raman spectrophotometer. The source was a mercury arc lamp of Toronto type; the dispersion of the grating was 4 Å/mm. at 5000 Å wavelength.

Raman spectra were taken of the solution in carbon tetrachloride (1 g. solute dissolved in 5 ml. solvent) and in methanol (0.5 g. solute dissolved in 5 ml. solvent) for both ordinary and deuterated substances. As the solubilities of the substances in methanol are not sufficiently large, it was impossible to make the concentration of both solutions equal.

The depolarization ratio was measured by surrounding the Raman tube by polaroid cylinders and by polarizing the exciting light in directions parallel and perpendicular to the axis of the Raman tube.

## Results

The observed Raman spectra are shown in Figs. 1—4. In the spectrum of the methanol solution of ordinary trichlorobenzene, as the base line rose gradually with increasing frequency, it was necessary to reset the zero

1) S. Saëki, This Bulletin, 33, 1024 (1960).

* The substance in which a given band originated was easily known by following the intensity changes of that band with the repetition of the substitution reactions.

suppression of the amplifier at 1800 $cm^{-1}$. Although the cause of the shift of the base line was not found, this gave rise to no obstacle for the measurement of the frequencies of Raman lines. In the figures, the peaks pointed out by the small arrows are due to the solvents or the source lamp (D line, 2602 $cm^{-1}$).

The frequencies and intensities of the observed lines are listed in Tables I and II. The intensities are shown for the spectra excited by the polarized lights in both directions (cross and parallel). The scale of the intensity is simply the height of a Raman line measured on the chart. The notation "masked" in the tables means that the line was not observed in that solution, being masked by a strong Raman line of the solvent, while it was observed in the other solution. The notation "unobserved" means that the line was not observed in that solution, while it was observed

TABLE I. RAMAN SPECTRUM OF 1,3,5-TRICHLOROBENZENE

| $\tilde{\nu}$ $cm^{-1}$ | Methanol soln. intensity | | $\tilde{\nu}$ $cm^{-1}$ | Carbon tetrachloride soln. intensity | | Depolarization ratio |
|---|---|---|---|---|---|---|
| | Cross | Parallel | | Cross | Parallel | |
| 188 | — | 17 | | Masked | | |
| 209 | + | 7 | | Masked | | |
| 373 | 26 | 9 | 374 | 42 | 14 | p. |
| 425 | 5 | 5 | | Unobserved | | |
| | Unobserved | | 526 | 1 | 1 | |
| 994 | 57 | 20 | 994 | 99 | 35 | p. |
| | Masked | | 1060 | 6 | 2 | p. |
| 1147 | 26 | 12 | 1146 | 38 | 15 | p. |
| | Masked | | 1536 | 10 | 3 | |
| 1565 | 12 | 15 | 1565 | 21 | 24 | dep. |
| | Unobserved | | 2150 | 1 | — | |
| | Unobserved | | 2211 | 3 | 0 | |
| | Unobserved | | 2263 | 3 | 1 | |
| 3076 | 17 | 15 | 3081 | 33 | 24 | dep. |
| 3130 | 3 | 0 | 3132 | 7 | 2 | p. |

TABLE II. RAMAN SPECTRUM OF 1,3,5-TRICHLOROBENZENE-$d_3$

| $\tilde{\nu}$ $cm^{-1}$ | Methanol soln. intensity | | $\tilde{\nu}$ $cm^{-1}$ | Carbon tetrachloride soln. intensity | | Depolarization ratio |
|---|---|---|---|---|---|---|
| | Cross | Parallel | | Cross | Parallel | |
| 188 | 70 | 70 | | Masked | | dep. |
| 374 | 38 | 14 | 373 | 63 | 21 | p. |
| 418 | 10 | 10 | 417 | — | 13 | dep. |
| 495 | 5 | 5 | 492 | — | sh. | |
| | Unobserved | | 711 | sh. | sh. | |
| 950 | 86 | 31 | 952 | 100 | 54 | p. |
| | Masked | | 993 | 21 | 6 | p. |
| | Masked | | 1058 | 4 | 1 | |
| 1144 | 18 | 8 | 1142 | 45 | 16 | p. |
| | Masked | | 1337 | 2 | 2 | |
| | Masked | | 1418 | 4 | 1 | |
| | Masked | | 1528 | + | — | |
| 1550 | 25 | 25 | 1548 | 47 | 43 | dep. |
| 1767 | 3 | 2 | | Unobserved | | |
| 1883 | 4 | 3 | | Unobserved | | |
| 2027 | 3 | 3 | | Unobserved | | |
| 2283 | — | 2 sh. | 2282 | sh. | 5 | |
| 2303 | 17 | 10 | 2303 | 41 | 25 | |
| | Unobserved | | 2389 | 2 | 2 | |
| | Unobserved | | 2537 | 6 | 3 | p. |
| | Unobserved | | 3079 | 2 | 2 | |
| | Unobserved | | 3094 | 3 | 2 | |

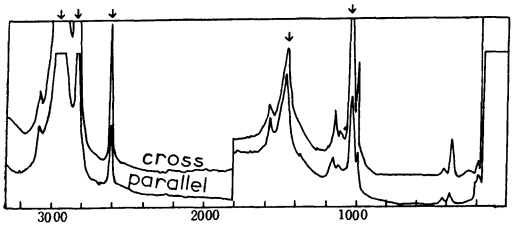



Fig. 1. Raman spectra of 1,3,5-trichlorobenzene (0.5 g. in 5 ml. methanol).

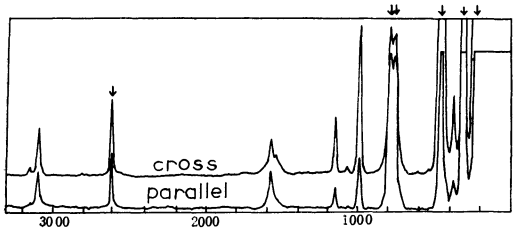



Fig. 2. Raman spectra of 1,3,5-trichlorobenzene (1 g. in 5 ml. carbon tetrachloride).

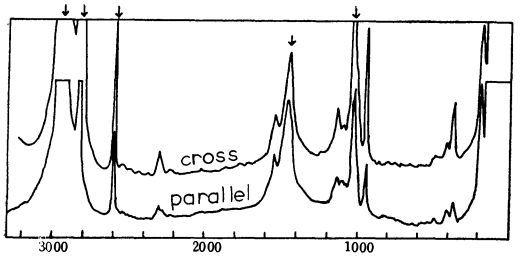



Fig. 3. Raman spectra of 1,3,5-trichlorobenzene-$d_3$ (0.5 g. in 5 ml. methanol).

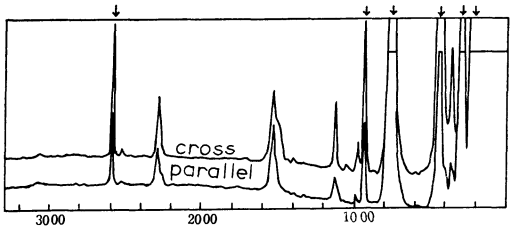



Fig. 4. Raman spectra of 1,3,5-trichlorobenzene-$d_3$ (1 g. in 5ml. carbon tetrachloride).

in the other solution. This inconstancy of observation might be due to the unequal concentrations or to different solvent effects in both solutions. In any case, it should be remembered that there might be a little ambiguity in such lines.

## Assignment

**1, 3, 5-Trichlorobenzene.**—*Species* $A_1'$. — It is universally known that the vibrations belonging to totally symmetric species give the most intense Raman lines. In the case of 1, 3, 5-trichlorobenzene, four normal vibrations belong to species $A_1'$, as is shown in Table III. The C-H stretching vibration is expected to appear about 3000 $cm^{-1}$, the breathing of the benzene ring is expected to appear about 1100 $cm^{-1}$ judging from the case of *p*-dichlorobenzene (which was reported on in our previous paper[2]), the C-Cl stretching vibration is expected to be observed in the region 700~800 $cm^{-1}$, and the deformation of the ring is expected to be observed at 300~400 $cm^{-1}$. From these estimations of the frequencies, four lines with remarkable intensities were selected from the observed Raman lines, that is, the lines at 3079, 1147, 994 and 374 $cm^{-1}$. However, as is seen in Table I, the line at 3079 $cm^{-1}$ was not very definitely polarized. In the vicinity of this line, another line was observed at 3130 $cm^{-1}$ which was apparently polarized. Therefore, it might be considered that this line corresponded to the C-H symmetric stretching vibration of the species $A_1'$ and that the above-mentioned line at 3079 $cm^{-1}$ corresponded to the C-H degenerate stretching vibration of the species E'. But this assignment conflicts with the empirical knowledge that a line belonging to a totally symmetric species is generally more intense than a line belonging to other species, and that the frequency of a degenerate stretching vibration of the C-H bonds is higher than that of a symmetric one as a general rule. Therefore, it seems to be more plausible to assign the line at 3079 $cm^{-1}$ to both degenerate and symmetric stretching vibrations of C-H bonds. Then the line at 3130 $cm^{-1}$ might well be explained as an overtone of the line at 1563 $cm^{-1}$ (e'), which will be discussed later.

The other three polarized lines were easily assigned to the other three normal vibrations

Table III. The normal modes of 1,3,5-trichlorobenzene

| Species | Mode |
|---|---|
| $A_1'$ | C-H or C-D stretching |
| | Ring breathing |
| | C-Cl stretching |
| | Ring deformation |
| E' | C-H or CD stretching |
| | Ring stretching |
| | Ring stretching |
| | C-H or C-D in-plane bending |
| | C-Cl stretching |
| | Ring in-plane deformation |
| | C-Cl in-plane bending |
| E'' | C-H or C-D out-of-plane bending |
| | Ring out-of-plane deformation |
| | C-Cl out-of-plane bending |

2) S. Saëki, ibid., 34, 1658 (1961).

TABLE IV. THE ASSIGNMENTS OF RAMAN LINES OF 1,3,5-TRICHLOROBENZENE

| Species | No. | $\tilde{\nu}$ $C_6H_3Cl_3$ | $\tilde{\nu}$ $C_6D_3Cl_3$ | Mode |
|---|---|---|---|---|
| | $\nu_1$ | 3079 | 2303 | C-H or C-D stretching |
| $A_1'$ | $\nu_2$ | 1147 | 1143 | Ring breathing |
| | $\nu_3$ | 994 | 951 | C-Cl stretching |
| | $\nu_4$ | 374 | 374 | Ring deformation |
| | $\nu_{11}$ | 3079 | 2303 | C-H or C-D stretching |
| | $\nu_{12}$ | 1565 | 1548 | Ring stretching |
| | $\nu_{13}$ | (1412) | 1337 | Ring stretching |
| E' | $\nu_{14}$ | (1103) | (843) | C-H or C-D in-plane bending |
| | $\nu_{15}$ | (814) | (795) | C-Cl stretching |
| | $\nu_{16}$ | 425 | 418 | Ring in-plane deformation |
| | $\nu_{17}$ | 209 or 188 ? | 188 ? | C-Cl in-plane bending |
| | $\nu_{18}$ | — | 711 | C-H or C-D out-of-plane bending |
| E'' | $\nu_{19}$ | 526 | 494 | Ring out-of-plane deformation |
| | $\nu_{20}$ | 188 ? | 188 ? | C-Cl out-of-plane bending |

N. B. The values in parentheses are the wave number which were observed in the infrared spectra.

of species $A_1'$, as is shown in Table IV. Since these lines had remarkable intensities, and no alternate lines were observed in their vicinities, the assignment was quite unambiguous. Although the frequency of the $\nu_3$, the C-Cl stretching vibration, to which the line at 994 $cm^{-1}$ was assigned, was a little higher than the expected value, it is nevertheless a quite probable value for such a vibration, considering the fact pointed out in our previous paper[3] that the strong coupling between the normal vibrations of such frequencies may often cause a large frequency shift from the empirically expected one. Consequently, this molecule might not have a normal vibration which could be called a C-Cl stretching vibration in its proper sense. However, at present such a vibration will be called a C-Cl stretching vibration for convenience.

*Species E'.* — Contrary to the easy assignment of the normal vibrations belonging to species $A_1'$, the assignment of the observed lines to the seven normal vibrations of this species was very difficult. Since the normal vibrations belonging to species E' are active in both the Raman and infrared spectra, the assignments would appear to be easily achieved by looking for the frequencies which were commonly observed in the Raman and infrared spectra. However, this could not be done so easily in practice. Actually only four frequencies were commonly observed in Raman and infrared spectra, that is, 3079 (3098), 1565 (1565), 1060 (1100 or 1055) and 425 (430). (in $cm^{-1}$. The frequencies put between parentheses are those observed in the infrared absorption spectrum in a gaseous state.) The fact that only four vibrations appeared commonly in both spectra, while seven were expected, suggested that the intensities of the Raman lines or the infrared absorption bands of the other three vibrations were to weak to be observed. But, on the other hand, the abovementioned four lines could definitely be assigned to species E'. However, the line at 1060 $cm^{-1}$ was somewhat questionable. Since the infrared absorption spectrum of the substance was measured in the gaseous state, the frequency of an observed band must be a little higher than that of the corresponding line observed in the Raman spectrum. From this consideration, it was not reasonable to consider the infrared absorption band at 1055 $cm^{-1}$ to correspond to the Raman line at 1060 $cm^{-1}$. And the other infrared band observed at 1103 $cm^{-1}$ seemed too high to be regarded as the corresponding band of this Raman line. Moreover, its depolarization ratio shown in Table I suggested that it belongs to species $A_1'$. These facts might rule out the assignment of the line at 1060 $cm^{-1}$ to the normal vibration of species E'.

As for the other three commonly observed frequencies, the line at 3079 $cm^{-1}$ was assigned to the degenerate stretching vibration of C-H bonds ($\nu_{11}$), as was mentioned above, and the line at 1565 $cm^{-1}$ was assigned to the stretching vibration of the benzene ring ($\nu_{12}$), and the line at 425 $cm^{-1}$ to the deformation vibration of the benzene ring ($\nu_{16}$), all with sufficient certainty.

As for the remaining four normal vibrations

3) S. Saëki, ibid., 33, 1021 (1960).

of this species ($\nu_{13}$, $\nu_{14}$, $\nu_{15}$ and $\nu_{17}$), the assignment of the lines was very difficult. The stretching vibration of the benzene ring, $\nu_{13}$, is empirically expected to appear in the frequency region 1400~1600 $cm^{-1}$. But, as is seen in Fig. 1 and in Table I, no Raman line was clearly observed in this region except for the line at 1565 $cm^{-1}$. A weak line observed only with difficulty at 1536 $cm^{-1}$ for the solution in carbon tetrachloride was polarized and had to be considered as an overtone or a combination belonging to species $A_1'$ (for example 1147 $(a_1')+374(a_1')$). As was already reported in our previous paper[1], the infrared absorption spectrum of this substance showed many intense absorption bands in this region of the spectrum (1412 (s), 1398 (m), 1384 (m) and 1341 (s)). The band at 1412 $cm^{-1}$ was especially clearly assigned to a fundamental because of its outstanding intensity. Consequently, although the Raman line was not observed, it appears to be plausible to assign this band to $\nu_{13}$.

The C-H in-plane bending vibration was expected to appear in the vicinity of 1000 $cm^{-1}$, where only the above-mentioned polarized line at 1060 $cm^{-1}$ was observed. In the infrared absorption spectrum[1], a remarkable band was observed at 1103 $cm^{-1}$ which showed a large frequency shift on the substitution for hydrogen atoms by deuterium atoms. Accordingly, we assigned this band to the C-H in-plane bending vibration ($\nu_{14}$).

As for the C-Cl stretching vibration $\nu_{15}$, since the coupling with other vibrational modes might shift its frequency from its usual value, as in the case of $\nu_3$, it would be necessary to examine it over a relatively wide region of frequency, such as 600~1000 $cm^{-1}$. However, no Raman line was found in spite of taking such an extremely wide region. In the infrared absorption spectrum, two intense bands were observed, that is, bands at 855 and 814 $cm^{-1}$. The former was clearly identified from the shape of its envelope* to be a band which did not belong to species E'. Consequently, the band at 814 $cm^{-1}$ was assigned to the C-Cl stretching vibration of species E' ($\nu_{15}$).

The C-Cl in-plane bending vibration $\nu_{17}$ was expected to be found about 200 $cm^{-1}$. In the neighborhood of 200 $cm^{-1}$ a remarkable line was observed at 188 $cm^{-1}$, and a less intense line was observed at 209 $cm^{-1}$. Since there exists another Raman active bending vibration of C-Cl bonds which belongs to species E'' (out-of-plane), the above-mentioned two observed Raman lines apparently originate in these two C-Cl bending vibrations. However, it was difficult to find the correspondence between these lines and these normal vibrations. It was imagined, by analogy to C-H vibrations, that the line of the higher frequency (209 $cm^{-1}$) might probably correspond to the in-plane bending vibration, and the lower one to the out-of-plane vibration. Of course, however, this was not certain.

*Species E''.*—Three out-of-plane normal vibrations belong to this species, as listed in Table III. To the C-Cl out-of-plane bending vibration $\nu_{20}$, as was mentioned above, either the line at 209 $cm^{-1}$ or the line at 188 $cm^{-1}$ —probably the latter—was to be assigned. The out-of-plane deformation vibration of the benzene ring $\nu_{19}$ was expected to be observed from 400 to 500 $cm^{-1}$, where a very weak and depolarized line was found at 526 $cm^{-1}$. Disregarding its low intensity, we assigned this line to $\nu_{19}$ for the following reasons: 1. An overtone or combination belonging to a species other than $A_1'$ might not appear in the spectrum with an observable intensity. 2. The frequency of this line (526 $cm^{-1}$) could not be derived by combining or multiplying the frequencies of other fundamentals. 3. The line at 1060 $cm^{-1}$ which was mentioned in previous paragraphs was well explained as the overtone of this line.

The C-H out-of-plane vibration $\nu_{18}$ was expected to appear in the vicinity of 800 $cm^{-1}$, but no corresponding Raman line was observed in this frequency region. This might be because the intensity of the line was probably too low to be observed.

*Overtones and Combinations.*—The overtones and combinations which have already been explained are as follows:

3132 $cm^{-1}$ $(A_1')$: 1565 $cm^{-1}$ $(e')\times 2$

1536 $cm^{-1}$ $(A_1')$: 1147 $cm^{-1}$ $(a_1')$
$+374$ $cm^{1}$ $(a_1')$ three weak lines

1060 $cm^{-1}$ $(A_1')$: 526 $cm^{-1}$ $(e'')\times 2$

In addition to these lines three weak lines were observed between 2100 and 2300 $cm^{-1}$, as is shown in Table I. Though two of these lines were easily explained as

2263 $cm^{-1}$ $(A_1')$: 1147 $cm^{-1}$ $(a_1')\times 2$

2211 $cm^{-1}$ $(A_1')$: 1103 $cm^{-1}$ $(e')\times 2$

the third line observed at 2150 $cm^{-1}$ was difficult to explain. It might probably originate. in a slight amount of impurity.

The assingment determined above is shown in Table IV.

**1, 3, 5-Trichlorobenzene-$d_3$.**—*Species $A_1'$.*—The strong and polarized Raman line at 2303 $cm^{-1}$

* Concerning the envelopes of the infrared absorption bands of these substances, a report will be presented soon.

was easily and definitely assigned to the symmetric stretching vibration of C-D bonds. The remaining three vibrations are the breathing and the deformation of the benzene ring, and the symmetric stretching of the C-Cl bonds, all of which are not much influenced by the substitution for hydrogen atoms by deuterium atoms. Therefore, these vibrations of deuterated 1, 3, 5-trichlorobenzene were expected to be observed at frequencies only a little lower than those of the corresponding lines of 1, 3, 5-trichlorobenzene, that is, at 1147, 994 and 374 $cm^{-1}$ respectively. In fact, as is shown in Table II, three strong and polarized lines were found at 1143, 951 and 374 $cm^{-1}$ in the Raman spectra of deuterated trichlorobenzene. So, the lines at 1143, 951 and 374 $cm^{-1}$ were unambiguously assigned to the ring breathing ($\nu_2$), C-Cl stretching ($\nu_3$) and ring deformation vibration ($\nu_4$) respectively. In the Raman spectrum of deuterated substance, a line was observed at 993 $cm^{-1}$ which appeared to correspond to the line at 994 $cm^{-1}$ of ordinary substance better than the line at 951 $cm^{-1}$ did. However, the requirement of fulfilling the product rule and the definite inferiority in the intensity of the line at 993 $cm^{-1}$ to the line at 951 $cm^{-1}$ ruled out the assignment of the former line to $\nu_3$. It seemed that this line should be explained as the overtone of the line at 492 $cm^{-1}$ ($e''$), which will be discussed later, just as the line at 1060 $cm^{-1}$ was the overtone of the line at 526 $cm^{-1}$ in the case of ordinary substance. Its unusually strong intensity might well be explained by the Fermi resonance with the line at 951 $cm^{-1}$.

*Species* $E'$. — As was done in the case of ordinary substance, four frequencies which were observed commonly in the Raman and infrared absorption spectra were picked up. These were 2303 (2310), 1548 (1560), 1337 (1342) and 418 (420) $cm^{-1}$. The line at 2303 $cm^{-1}$ was a polarized line and was already assigned to the C-D symmetric stretching vibration of species $A_1'$. In the neighborhood of this line was observed another weak depolarized line at 2282 $cm^{-1}$. It was difficult to determine which of these two lines was to be assigned to the C-D degenerate stretching vibration. However, since the line at 2282 $cm^{-1}$ might be explained as a combination, 952 ($a_1'$) + 1342 ($e'$, gaseous infrared band), the line at 2303 $cm^{-1}$ was assigned to the C-D degenerate stretching vibration, assuming that its frequency was equal to that of the symmetric vibration as in the case of trichlorobenzene.

The lines at 1548 and at 418 $cm^{-1}$ were assigned to the stretching and deformation vibrations of the benzene ring respectively. As these line definitely corresponded to the lines at 1565 and 425 $cm^{-1}$ of ordinary substance, there is no point of discussion in the assignment.

The line at 1337 $cm^{-1}$, though weak in Raman spectra, corresponded to the intense band at 1342 $cm^{-1}$ in the infrared absorption spectrum, and it was plausibly assigned to the stretching vibration of the ring, $\nu_{13}$, by taking account of its frequency and depolarization ratio. Other weak lines observed in its vicinity, that is, lines at 1528, 1455 and 1418 $cm^{-1}$, could not be assigned to $\nu_{13}$ from a consideration of their depolarization ratios and of correspondencies with the infrared absorption bands.

The remaining three vibrations are the in-plane bending vibration of C-D bonds, the stretching vibration and the in-plane bending vibration of C-Cl bonds. As the first two vibrations were not observed in the Raman spectra, probably because of their weak intensities, as in the case of trichlorobenzene, the frequencies of observed in the infrared spectrum had to be adopted. To the in-plane bending vibration of C-D bonds was assigned the absorption band at 843 $cm^{-1}$ observed in the infrared spectrum, for the corresponding band of the ordinary substance was observed at 1103 $cm^{-1}$. The absorption band at 799 $cm^{-1}$ was assigned to the C-Cl stretching vibration, because the band at 814 $cm^{-1}$ was assigned to the corresponding vibration of ordinary substance.

The in-plane bending vibration of C-Cl bonds was expected to be observed near 200 $cm^{-1}$, and only a remarkable line at 188 $cm^{-1}$ was observed in this region for deuterated substance. From both the intensity and the depolarization ratio, this line was considered to correspond to the line at 188 $cm^{-1}$ of ordinary substance, but it was not known at this point whether this line was to be assigned to the in-plane or to the out-of-plane vibration of C-Cl bonds. Concerning this alternate assignment, some discussion will be given later.

*Species* $E''$. — The frequency of the out-of-plane bending vibration of C-D bonds is estimated to be lower than 800 $cm^{-1}$, and a diffuse line was observed at 711 $cm^{-1}$ as a shoulder of a strong Raman line of the solvent in the spectrum of carbon tetrachloride solution of deuterated substance. This line seemed to be recognizable also in the methanol solution, but due to its low intensity it could not be clearly distinguished from the noise. However, a polarized line which seemed to correspond to the first harmonic of this vibration was observed at 1418 $cm^{-1}$. Since this line could not be explained as an overtone or as a combination of other vibrations, the line at 711 $cm^{-1}$ could be considered as a normal vibration.

It was apparent from the frequency and

the depolarization ratio that the line at 494 $cm^{-1}$ corresponds to the line at 526 $cm^{-1}$ of ordinary substance. Accordingly the line at 494 $cm^{-1}$ was assigned to the out-of-plane bending vibration of the benzene ring of deuterated substance.

As for the out-of-plane vibration of C-Cl bonds, the line at 188 $cm^{-1}$ might be assigned to it. However, as was mentioned above, it is difficult to determine whether this line is to be assigned to the in-plane or out-of-plane vibration of C-Cl bonds.

The above assignment is shown in Table IV.

*Overtones and Combinations.*—More overtones and combinations were observed in the spectra of deuterated substance than in that of ordinary substance. As was stated above, the line at 993 $cm^{-1}$ was explained as 495 ($e''$)×2, the line at 2282 $cm^{-1}$ as 952 ($a_1'$)+1337 ($e'$), and the line at 1418 $cm^{-1}$ as 711 ($e''$)×2. For the other observed Raman lines, the following explanations were possible:

1058: 535 ($a_2''$)×2

1455: ?

1528: 1337 ($e'$, from the infrared spectrum) +188 ($e'$ or $e''$)

1767: 1337 ($e'$)+418 ($e'$)

1883: 1143 ($a_1'$)+767 ($e'$) or 1337 ($e'$) +535 ($a_2''$)

2029: 1550 ($e'$)+841 ($e'$, from the infrared spectrum)

2537: 950 ($a_1'$)+1550 ($e'$)

3079, 3094: 1549 ($e'$)×2, 2303 ($a_1'$ and $e'$) +801 ($a_2''$)

Though the line observed at 1455 $cm^{-1}$ could not be well explained, the existence of such a line is quite natural, since the molecule has three normal vibrations belonging to species $A_2'$ which are active to neither the Raman nor the infrared spectrum. Some of the above-mentioned explanations of overtones and combinations were not consistent with the observed qualitative depolarization ratios* But this inconsistency might not be very significant. If too much confidence was put in the observed results of the depolarization ratio, it might sometimes lead to an erroneous assignment. However, it should be mentioned here that the above explanation of the overtones and combinations may not be absolutely correct because of the existence of the unobservable normal vibrations.

* For example, the combination of two fundamental vibrations belonging to species E′ brings out four vibrations belonging to species $A_1'$, $A_2'$ and E′ respectively, of which the one belonging to species $A_1'$ might have the highest intensity in Raman effect. Therefore, the depolarization ratio of the observed line corresponding to this combination has to be considerably small.

## Discussion

The product rule was applied to the assignment given above. For species $A_1'$, the ratio of the products of the frequencies of the ordinary and deuterated trichlorobenzenes was calculated from the observed frequencies, such as 1.401 in good agreement with the theoretical value 1.414, showing that the assignment was correct.

In species E′, it has previously been pointed out that the assignment of $\nu_{17}$ was somewhat questionable. The theoretical value of the ratio is 1.982. Assuming that the line at 209 $cm^{-1}$ of ordinary trichlorobenzene and the line at 188 $cm^{-1}$ of deuterated correspond to the in-plane bending vibrations of C-Cl bonds, $\nu_{17}$'s, the ratio calculated from the observed frequencies was 2.162, exceeding the theoretical value by about 9%. On the other hand, assuming that the line observed at 188 $cm^{-1}$ of both trichlorobenzenes corresponds to $\nu_{17}$, the calculated ratio was found to be 1.944, lower than the theoretical value by about 2%. This discrepancy of 2% could be expected from the accumulation of small errors in frequency measurements, from the shift of the fundamental lines due to Fermi reasonance, etc., but that of 9% had to be regarded as inexplicable and might suggest an erroneous assignment. Thus, it was decided that the lines at 188 $cm^{-1}$ in both substances had to be assigned to $\nu_{17}$. However, it should be mentioned here that, since there exists a possibility that an unobservably weak line corresponding to the line at 209 $cm^{-1}$ does exsist at a suitable frequency (about 205 $cm^{-1}$) in the spectrum of deuterated substance, the above assignment can not be considered absolutely correct.

For species E″, the theoretical value is 1.402. However, since $\nu_{18}$ (C-H out-of-plane bending vibration) of ordinary trichlorobenzene was not observed, the observed ratio could not be compared with the theoretical one. Accordingly, the above-mintioned question concerning the assignment of the C-Cl in-plane bending vibration could not be solved. However, if the frequency of $\nu_{20}$'s were assumed to be 188 $cm^{-1}$ for both ordinary and deuterated substances, the frequency of $\nu_{18}$ of ordinary substance could be calculated to be 936 $cm^{-1}$ by applying the product rule. However, as was stated in the previous paragraphs, no Raman line was observed in the neighborhood of this frequency.

**Summary**

The Raman spectra and the qualitative depolarization ratio of each line were observed for the solutions of 1, 3, 5-trichlorobenzene and 1, 3, 5-trichlorobenzene-$d_3$. The assignments of Raman active normal vibrations of these substances were carried out from the results of these measurements. The assignments for species $A_1'$ and $E'$ proved to be correct from the application of the product rule, showing a good accordance between theoretical and calculated ratios of products of the frequencies. However, the application of the product rule was impossible for species $E''$ because of unobserved frequencies.

The author would like to express his appreciation of the valuable advice given by Dr. Y. Mashiko.

*Government Chemical Industrial Research Institute, Tokyo*
*Shibuya-ku, Tokyo*

# *Raman Spectra of 1, 2, 4, 5-Tetrachlorobenzene and 1, 2, 4, 5-Tetrachlorobenzene-$d_2$*

By Shinnosuke SAËKI

(Received May 16, 1961)

Concerning the infrared absorption spectra of 1, 2, 4, 5-tetrachlorobenzene and 1, 2, 4, 5-tetrachlorobenzene-$d_2$, a report[1] was previously presented by the author in which tentative assigments were proposed for the observed infrared absorption bands. In this paper the Raman spectra of these substances will be presented, and the assignment of these observed lines will be discussed.

The Raman spectra of ordinary 1,2,4,5-tetrachlorobenzene have already been reported on by several investigators[2]. But all of their papers have been concerned with a group of similarly substituted benzenes, 1, 2, 4, 5-tetrachlorobenzene was treated simply as a member of this group. Consequently, the molecular spectra of 1, 2, 4, 5-tetrachlorobenzene itself do not appear to have been fully studied. In this paper, instead of adopting such an inductive method, the Raman spectrum was observed for deuterated as well as for ordinary 1, 2, 4, 5-tetrachlorobenzene, and the assignment was carried out by comparing the Raman spectra for both species of the substance.

Since the molecule contains four chlorine atoms, the normal vibrations were expected to be concentrated in a lower frequency region compared with those of *p*-dichlorobenzene and 1,3,5-trichlorobenzene, which have been studied in previous papers[3-6]. As the observation of low frequency vibrations is much easier in Raman effect than in infrared spectroscopy, the product rule can be applied more completely to Raman lines. However, since a Raman line belonging to a species other than the totally symmetric one generally has a relatively low intensity and can often escape observation, this might become a new obstacle for the assignment.

## Experimental and Results

Ordinary commercial 1,2,4,5-tetrachlorobenzene of extra pure grade was recrystallized from ethanol three times, and then further purified by sublimation.

The deuterated substance was prepared in the following way: 1,2,4,5-tetrachlorobenzene was stirred with deuterated sulfuric acid for eight hours at 150°C. The reaction mixture was then poured on ice and the precipitate filtered off and dried. The degree of substitution was checked by the infrared absorption spectrum after each substitution reaction, and the reaction was repeated until the strongest absorption band of $C_6HDCl_4$ could hardly be recognized. The obtained $C_6D_2Cl_4$ was purified in the same way as that of ordinary tetrachlorobenzene.

The Raman spectra were measured by using a Cary model 81 automatic recording spectrophotometer, and the qualitative depolarization ratios were measured by the two-exposure method, using polaroid cylinders.

The measurements were carried out for the solutions in carbon tetrachloride and in benzene.

Although the Raman spectra of *p*-dichlorobenzene and 1,3,5-trichlorobenzene were measured for the solutions in methanol and carbon tetrachloride[5,6], the solubility of 1,2,4,5-tetrachlorobenzene in

1) S. Saëki, This Bulletin, 34, 1552 (1961).
2) For example, J. W. Murray and D. H. Andrews, *J. Chem. Phys.*, 2, 119 (1934).
3) S. Saëki, This Bulletin, 33, 1021 (1960).
4) S. Saëki, ibid., 33, 1024 (1960).
5) S. Saëki, ibid., 34, 1658 (1961).
6) S. Saëki, ibid., 34, 1851 (1961).

methanol is so low that the spectra could not be measured in methanol solutions. Since the solubility of chlorobenzene decreases with the increasing number of chlorine atoms contained in the molecule, the concentrations of the sample solutions were not very high in this case. In the carbon tetrachloride solution, about 0.7 g. solute was dissolved in 5 ml. of solvent, while in the benzene solution about 0.6 g. solute was dissolved in 5 ml. of solvent. Irrespective of these low concentrations, the solute was not entirely dissolved at room temperature, and it was necessary to keep the Raman tube in the lamp compartment for almost an hour in order to dissolve the entire solute*.

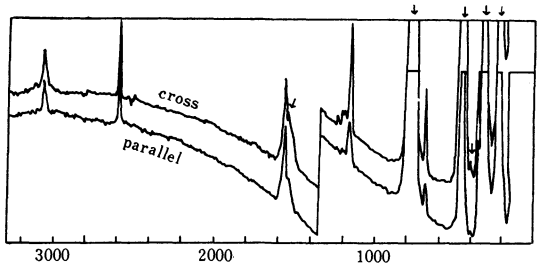


Fig. 1. Raman spectra of 1,2,4,5-tetrachlorobenzene (0.7 g. in 5 cc. carbon tetrachloride).

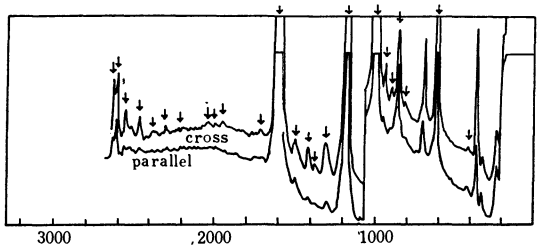


Fig. 2. Raman spectra of 1,2,4,5-tetrachlorobenzene (0.6 g. in 5 cc. benzene).

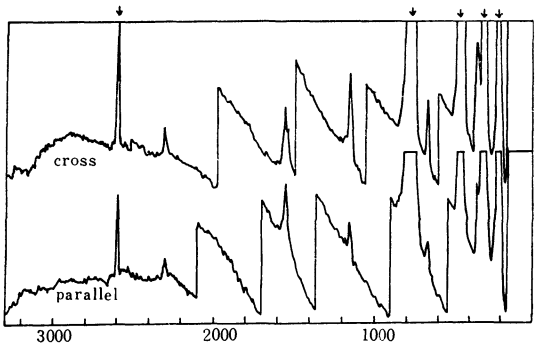


Fig. 3. Raman spectra of 1,2,4,5-tetrachlorobenzene-$d_2$ (0.5 g. in 4 cc. carbon tetrachloride).

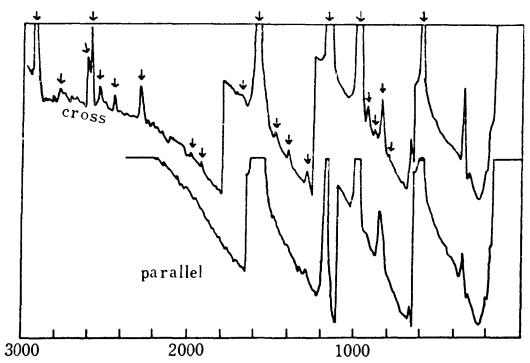


Fig. 4. Raman spectra of 1,2,4,5-tetrachlorobenzene-$d_2$ (0.6 g. in 5 cc. benzene).

TABLE I. RAMAN SPECTRUM OF 1,2,4,5-TETRACHLOROBENZENE

| Carbon tetrachloride solution | | | Benzene solution | | |
|---|---|---|---|---|---|
| | Intensity | | | Intensity | |
| $\tilde{\nu}$, $cm^{-1}$ | Cross | Parallel | $\tilde{\nu}$, $cm^{-1}$ | Cross | Parallel |
| | | | 184 | sh 1 | sh 1 |
| | | | 226 | 16 | 17 |
| | | | 314 | 10 | 12 |
| 350 | >70 | sh 22 | 352 | 84 | 38 |
| | | | 467 | 1 | — |
| | | | 509 | 2 | 2 |
| ca. 570 | 2 | — | 554 | 1 | — |
| 685 | 50 | 18 | 685 | 53 | 22 |
| 1162 | 72 | 27 | | | |
| 1190 | 7 | 6 | | | |
| 1206 | 10 | 5 | | | |
| 1236 | 3 | 3 | | | |
| ca. 1535 | + | — | | | |
| 1567 | 33 | 35 | | | |
| 2502 | 6 | 3 | | | |
| 3075 | 25 | 17 | | | |
| 3137 | 4 | — | | | |

TABLE II. RAMAN SPECTRUM OF 1,2,4,5-TETRACHLOROBENZENE-$d_2$

| Carbon tetrachloride solution | | | Benzene solution | | |
|---|---|---|---|---|---|
| | Intensity | | | Intensity | |
| $\tilde{\nu}$, $cm^{-1}$ | Cross | Parallel | $\tilde{\nu}$, $cm^{-1}$ | Cross | Parallel |
| | | | 184 | sh 2 | sh 4 |
| | | | 215 | sh 5 | sh 7 |
| | | | 315 | 6 | 7 |
| 351 | 63 | sh 20? | 351 | 49 | 22 |
| 667 | 41 | 16 | 665 | 34 | 14 |
| | | | 956 | sh 10 | |
| 1155 | 54 | 21 | | | |
| 1180 | 6 | 5 | | | |
| 1208 | 4 | + | | | |
| 1410 | 2? | — | | | |
| 1418 | 7 | 2 | | | |
| 1520 | 1? | sh + | | | |
| 1552 | 44 | 45 | | | |
| 1675 | 3? | — | | | |
| 2301 | 17 | 13 | | | |
| ca. 2500 | 6 | + | | | |

* The temperature was 36°C in the lamp compartment.

As the concentrations of the solutions were low, a relatively high gain was required for the measurements; consequently, the signal to noise ratio in the obtained spectra was about 25, a rather low value for this spectrometer. The obtained Raman spectra are shown in Figs. 1—4, where the noises could not be well represented because of the small sizes of the figures. The base line of each spectrum, especially of the spectra of deuterated substance, rose towards the higher frequency limit of the spectrum. This was probably due to a slight amount of resinous impurity, which was unavoidable in this case. The rapid rising of the base line made necessary its resetting at several frequencies, but it produced no obstruction to the measurement of the frequencies of Raman lines.

In the figures, the Raman lines marked with small arrows are those of the solvent or of the mercury arc lamp.

The observed Raman lines are listed in Tables I and II. In the tables, the intensities are simply represented by the heights of lines measured by the scale on the chart.

## Assignment

Since the 1, 2, 4, 5-tetrachlorobenzene molecule has the symmetry $V_h$, as does the *p*-dichlorobenzene molecule, fifteen of thirty normal vibrations are active to the Raman effect. Also, as this molecule has a center of symmetry, there is no vibration which is active in both the Raman effect and infrared absorption, according to the mutual exclusion law. The fifteen Raman active normal vibrations are classified as six vibrations belonging to species $A_g$ (in-plane), five to species $B_{3g}$ (in-plane), one to species $B_{1g}$ (out-of-plane), and three to species $B_{2g}$ (out-of-plane)*. These normal vibrations and their modes are shown in Table III.

TABLE III. SPECIES AND MODES OF NORMAL VIBRATIONS OF 1,2,4,5-TETRACHLOROBENZENE

| Species | No. | Mode |
|---|---|---|
| $A_g$ | $\nu_1$ | C-H or C-D stretching |
| | $\nu_2$ | Ring stretching |
| | $\nu_3$ | Ring stretching |
| | $\nu_4$ | C-Cl stretching |
| | $\nu_5$ | Ring deformation |
| | $\nu_6$ | C-Cl in-plane bending |
| $B_{1g}$ | $\nu_9$ | C-Cl out-of-plane bending |
| $B_{2g}$ | $\nu_{15}$ | C-H or C-D out-of-plane bending |
| | $\nu_{16}$ | Ring out-of-plane deformation |
| | $\nu_{17}$ | C-Cl out-of-plane bending |
| $B_{3g}$ | $\nu_{23}$ | Ring stretching |
| | $\nu_{24}$ | C-H or C-D in-plane bending |
| | $\nu_{25}$ | C-Cl stretching |
| | $\nu_{26}$ | Ring in-plane deformation |
| | $\nu_{27}$ | C-Cl in-plane bending |

* The x-axis was taken along the two-fold axis perpendicular to the molecular plane, and the z axis was taken along the line combining the two hydrogen atoms.

Sixteen Raman lines were observed for ordinary as well as for deuterated 1, 2, 4, 5-tetrachlorobenzene, but, considering their frequencies, some of them apparently do not correspond to normal vibrations. Therefore, it seems that some of the Raman active normal vibrations were not observed on account of very low frequencies or intensities.

**1, 2, 4, 5-Tetrachlorobenzene.** — *Species $A_g$.* — The six normal vibrations belonging to species $A_g$ are seen in Table III. In the spectra obtained, the polarized and strong lines were observed in the regions expected from their modes, except for $\nu_2$ and $\nu_6$ (see Figs. 1 and 2), and the following assignment was unambiguously decided upon: $\nu_1$: 3075 $cm^{-1}$, $\nu_3$: 1162 $cm^{-1}$, $\nu_4$: 685 $cm^{-1}$ and $\nu_5$: 350 $cm^{-1}$. Considering the high intensities and low depolarization ratios of these lines, no point of discussion exists in the above assignment.

In the region around 1500 $cm^{-1}$ where the ring stretching vibration was expected to appear, a remarkable line was observed at 1567 $cm^{-1}$. However, the large depolarization ratio of this line clearly showed itself to correspond to the ring stretching vibration of species $B_{3g}$. In addition to this line, a much weaker line was with difficulty observed at 1535 $cm^{-1}$ only in the carbon tetrachloride solution. As this line was observed as a shoulder of the Raman line of the solvent at 1550 $cm^{-1}$ only in the spectrum excited by perpendicularly polarized light, its accurate frequency was difficult to measure. However, it was clear that this was a polarized line, since it entirely disappeared when excited by parallelly polarized light.

It might be indeed unusual for a line belonging to species $A_g$ to show such a weak intensity, but since no other polarized line was found in this region, this line had to be considered to correspond to the totally symmetric ring stretching vibration.

As for the last vibration of species $A_g$, $\nu_6$, the in-plane bending vibration of the C-Cl bonds, two weak lines were observed near 200 $cm^{-1}$, one at 226 $cm^{-1}$ and the other at 184 $cm^{-1}$. In the carbon tetrachloride solution, these lines were masked by a strong line of the solvent, but in the benzene solution they were observed as a shoulder of the exciting line. However, neither of these lines could be assigned to $\nu_6$, for both of them had considerable depolarization ratios. Therefore, it was concluded that $\nu_6$ might have a lower frequency and be completely masked by the Rayleigh line. By estimating from the width of the Rayleigh line, the frequency should be lower than 175 $cm^{-1}$.

*Species $B_{1g}$.*—As is seen in Table III, the only vibration belonging to species $B_{1g}$ is the out-of-plane bending vibration of C-Cl bonds, $\nu_9$. As there are four Raman active bending vibrations of C-Cl bonds, that is, $\nu_6$, $\nu_9$, $\nu_{17}$ and $\nu_{27}$, it is very difficult to determine the assignment of the two observed lines at 184 and 226 $cm^{-1}$. However, these lines were shifted to 184 and 215 $cm^{-1}$ respectively, by the deuteration; this fact suggests that the line at 226 $cm^{-1}$ of ordinary tetrachlorobenzene could not correspond to $\nu_9$, which belongs to species $B_{1g}$, for the product rule requires that the ratio of the $\nu_9$'s of ordinary and deuterated tetrachlorobenzene be 1. Consequently, the conclusion was drawn that the vibration $\nu_9$ corresponds to the line at 184 $cm^{-1}$ or lies in the unobservable low frequency region.

*Species $B_{2g}$.*—Although the out-of-plane bending vibration of C-H bonds was expected to appear in the region from 800 to 1000 $cm^{-1}$, no Raman line was observed in this region, as is seen in Table I. Since the Raman active out-of-plane vibrations of C-H bonds were not observed in the spectrum of *p*-dichloro- and 1, 3, 5-trichlorobenzene, as was reported in the previous papers[2,3], it appeared to be unobservable, in this case also on account of its low intensity.

To the out-of-plane deformation vibration of the ring, $\nu_{16}$, the line at 314 $cm^{-1}$ could be assigned. However, since there is another ring deformation vibration belonging to species $B_{3g}$ ($\nu_{26}$), it seemed also possible to assign the line at 314 $cm^{-1}$ to it. However, this latter possibility must be ruled out for a reason which will be mentioned later.

As for the out-of-plane bending vibration of C-Cl bonds, $\nu_{17}$, it is possibly unobserved. However, provided that it were observed in the spectra, the line at 184 $cm^{-1}$ or 226 $cm^{-1}$ might be regarded as the corresponding line.

*Species $B_{3g}$.*—As the stretching vibration of the benzene ring, $\nu_{23}$, was expected to appear at about 1500 $cm^{-1}$, it was clear that the above-mentioned remarkable line at 1567 $cm^{-1}$ corresponded to this vibration. This assignment is consistent with the observed qualitative depolarization ratio.

In the region 1000~1200 $cm^{-1}$ where the in-plane bending vibration of C-H bonds, $\nu_{24}$, was expected to appear, two lines of medium intensity were observed at 1190 and 1206 $cm^{-1}$. Since the latter line was polarized, as is shown in Table I, the former was assigned to $\nu_{24}$.

Although the C-Cl stretching vibration, $\nu_{25}$, was expected to appear in the vicinity of 700 $cm^{-1}$, no line was observed in this region except the strong line at 685 $cm^{-1}$ which had already been assigned to $\nu_4$. But if lines are looked for over a wider frequency region, two weak lines are found at 509 and 554 $cm^{-1}$. Although the former was a little stronger than the latter, the latter combining with the line at 685 $cm^{-1}$ ($a_g$), gave a combination line at 1236 $cm^{-1}$ which could not be explained as any other combination. Therefore, the line at 554 $cm^{-1}$ was assigned to $\nu_{25}$.

To the in-plane deformation vibration of the benzene ring, $\nu_{26}$, either the line at 467 $cm^{-1}$ or at 509 $cm^{-1}$ might be assigned. It appeared to be a little strained to assign the line at 314 $cm^{-1}$ to $\nu_{26}$, for $\nu_{26}$ probably has a frequency higher than 351 $cm^{-1}$, which was the frequency of the totally symmetric in-plane deformation vibration of the benzene ring. However, since the lines at 467 and 509 $cm^{-1}$ were both very weak, it was difficult to determine which was to be assigned to $\nu_{26}$. If one was taken for the fundamental, the other had to be explained as an overtone or a combination. However, if necessary, both of them could be explained as an overtone or a combination, that is, $467=226$ ($b_{2g}$)$\times 2$ and $509=184$ ($b_{1g}$ or $b_{3g}$)$+314$ ($b_{2g}$).

However, there was another, more plausible explanation for the line at 509 $cm^{-1}$. As was reported in our previous paper[4], a strong absorption band was observed at 507 $cm^{-1}$ in the infrared absorption spectrum of this substance. Taking account of this fact, the Raman line at 509 $cm^{-1}$ was explained as the forbidden line which was brought out by the breakdown of the rule of mutual exclusion in solution. Since it is quite probable that the rule of mutual exclusion breaks down in the condensed system, the above explanation appeared to be the most plausible. Accordingly, the line at 467 $cm^{-1}$ was assigned to $\nu_{26}$.

For the C-Cl in-plane bending vibration, $\nu_{27}$, there were two lines to be assigned, that is, the lines at 184 $cm^{-1}$ and at 226 $cm^{-1}$. As has been mentioned above, it is impossible to determine definitely the assignment of these lines. It might as possibly be that $\nu_{27}$ was not observed as that $\nu_{27}$ corresponds to one of these two lines.

*Overtones and Combinations.*—There were five observed lines which were not assigned to the fundamentals, that is, the lines at 3137, 2502, 1236, 1206 and 509 $cm^{-1}$. The lines at 1236 and 509 $cm^{-1}$ have already been explained as 685 ($a_g$)$+554$ ($b_{3g}$) and as a forbidden line which was brought out by the breakdown of the mutual exclusion law respectively.

The line at 3137 $cm^{-1}$ was clearly explained as 1567 ($b_{3g}$)$\times 2$.

Although the lines at 2502 and 1206 $cm^{-1}$ were both polarized, these could be well explained neither as an overtone nor as a combination belonging to species $A_g$. Since these

two lines were observed also in the carbon tetrachloride solution of the deuterated substance, as is shown in Table II, they should be regarded as lines due to the slight impurity contained in the solvent. Although these lines were not observed in the Raman spectrum of the pure solvent, they might quite probably appear in the spectra of sample solutions because of the extremely high gain required on the measurement of the sample solutions. Thus, these lines were removed from discussion.

**1, 2, 4, 5-Tetrachlorobenzene-$d_2$.**—*Species $A_g$.*—The line at 2301 $cm^{-1}$ corresponded apparently to $\nu_1$, the stretching vibration of the C-D bonds. Although the depolarization ratio of this line was observed to be unusually high*, there was no other remarkable line in its vicinity. Since there is no other Raman active stretching vibration of C-D bonds, there is no room for doubting this assignment.

A very weak line observed at 1520 $cm^{-1}$ was assigned to $\nu_2$, for it was apparent from the frequency and the intensity that this line corresponds to the line at 1535 $cm^{-1}$ ($\nu_2$) of ordinary 1, 2, 4, 5-tetrachlorobenzene.

For $\nu_3 \sim \nu_5$, the assignment could unambiguously be determined, as is shown in Table IV. No line was observed for $\nu_6$. This might be because its frequency was too low to be observed, as in the case of ordinary substance. A combination line was observed at 1675 $cm^{-1}$ which could well be explained by assuming the frequency of $\nu_6$ to be 155 $cm^{-1}$, as will be shown later. But, of course, this was not strong enough support for assigning 155 $cm^{-1}$ to $\nu_6$.

*Species $B_{1g}$.*—Only $\nu_9$ belongs to this species. As was already mentioned, it is not certain that the frequency of this vibration is high enough to be observed. Provided that this vibration can be observed, the line at 184 $cm^{-1}$ could be assigned to it.

*Species $B_{2g}$.*—The C-D out-of-plane bending vibration of this species, $\nu_{15}$, was not observed as in the case of the ordinary substance.

To the deformation vibration of the ring, $\nu_{16}$, the line at 315 $cm^{-1}$ was assigned. Although it is impossible that the frequency of the deuterated substance is higher than that of the ordinary substance (314 $cm^{-1}$), this might be attributed to a slight error in the measurement of the frequency because of excessive noise.

As for $\nu_{17}$, the line at 184 $cm^{-1}$ might be assigned to it. However, the assignment for such C-Cl bending vibrations is not very certain for the reason which has already been stated in the case of ordinary tetrachlorobenzene.

* The measurement was repeated three times, and the high depolarization ratio was observed every time.

*Species $B_{3g}$.*—The line at 1552 $cm^{-1}$ was easily assigned to $\nu_{23}$, the stretching vibration of the ring.

As for $\nu_{24}$, since it was observed at 1190 $cm^{-1}$ in the case of the ordinary substance, it was expected to appear near 1000 $cm^{-1}$ in the deuterated substance. But in this region only a weak and diffuse line was observed at 956 $cm^{-1}$. Since, irrespective of its low depolarization ratio, this line could not be explained as an overtone or as a combination belonging to species $A_g$, it might be assigned to $\nu_{24}$. It will be seen later that this assignment facilitates the explanation of some combination lines.

Although $\nu_{25}$ and $\nu_{26}$ of ordinary tetrachlorobenzene were observed at 554 and 467 $cm^{-1}$ respectively, those of deuterated one were not observed.

As for $\nu_{27}$, since the line at 226 $cm^{-1}$ was assigned to it in the case of 1, 2, 4, 5-tetrachlorobenzene, the line at 215 $cm^{-1}$ should be assigned to it in the case of deuterated substance.

*Overtones and Combinations.*—There were six observed lines which were not assigned to the fundamentals, that is, 1180, 1208, 1410, 1448, 1675 and 2500 $cm^{-1}$. Of these six, the two lines at 1208 $cm^{-1}$ and 2500 $cm^{-1}$ should be regarded as lines of the impurity contained in the solvent (carbon tetrachloride), as was pointed out in the previous paragraphs, and removed from discussion.

The line at 1180 $cm^{-1}$ was explained as 956 ($b_{3g}$) + 215 ($b_{2g}$). The existence of this combination line appeared to justify not only the assignment of the weak line at 956 $cm^{-1}$ to a fundamental, but also the determination of species $B_{2g}$ for the fundamental line at 215 $cm^{-1}$. For, by assuming that this line corresponds to the fundamental of species $B_{3g}$ ($\nu_{27}$), the species of the combination line at 1180 $cm^{-1}$ should be $A_g$, while the observed depolarization ratio was relatively high. However, it should be mentioned here that the certainty of this determination of the species depends on the reliability of the measurement of the depolarization ratio.

The lines at 1410 and 1448 $cm^{-1}$ were well explained as the overtones of the infrared active fundamentals of 719 and 725 $cm^{-1}$ respectively. These two overtones might perhaps resonate and be shifted away from each other.

The line at 1675 $cm^{-1}$, with a low depolarization ratio, could not be explained as an overtone, but, provided that the frequency of the unobserved $\nu_6$ of species $A_g$ is 155 $cm^{-1}$, it can be explained as a combination, 1520 ($a_g$) + 155 ($a_g$).

The assignments determined above are shown in Table IV.

TABLE IV. THE ASSIGNMENTS OF RAMAN LINES OF ORDINARY AND DEUTERATED 1,2,4,5-TETRACHLOROBENZENE

| Species | No. | $\tilde{\nu}$ | | Mode |
|---|---|---|---|---|
| | | $C_6H_2Cl_4$ | $C_6D_2Cl_4$ | |
| $A_g$ | $\nu_1$ | 3075 | 2301 | C-H or C-D stretching |
| | $\nu_2$ | ca. 1535 | 1520 | Ring stretching |
| | $\nu_3$ | 1162 | 1155 | Ring stretching |
| | $\nu_4$ | 685 | 667 | C-Cl stretching |
| | $\nu_5$ | 351 | 351 | Ring in-plane deformation |
| | $\nu_6$ | — | — | C-Cl in-plane bending |
| $B_{1g}$ | $\nu_9$ | 184? | 184? | C-Cl out-of-plane bending |
| $B_{2g}$ | $\nu_{15}$ | — | — | C-H or C-D out-of-plane bending |
| | $\nu_{16}$ | 314 | 315 | Ring out-of-plane deformation |
| | $\nu_{17}$ | 226 | 215 | C-Cl out-of-plane bending |
| $B_{3g}$ | $\nu_{23}$ | 1567 | 1552 | Ring stretching |
| | $\nu_{24}$ | 1190 | 956 | C-H or C-D in-plane bending |
| | $\nu_{25}$ | 554 | — | C-Cl stretching |
| | $\nu_{26}$ | 467 | — | Ring in-plane deformation |
| | $\nu_{27}$ | 184? | 184? | C-Cl in-plane bending |

## Discussion

According to the product rule, the theoretical values of the product of the ratios of the frequencies for each substance are 1.414, 1, 1.393 and 1.408 for species $A_g$, $B_{1g}$, $B_{2g}$ and $B_{3g}$ respectively.

For species $A_g$, although the frequencies of $\nu_6$'s were observed for neither species of substance, these could with enough security be assumed to be nearly equal*. With this assumption, the ratio calculated from the observed frequencies for species $A_g$ was 1.394 in good accordance with the above-mentioned theoretical value, showing the correctness of the proposed assignment.

For species $B_{1g}$, the assignment was determined so that the product rule might be fulfilled.

For species $B_{2g}$, as the bending vibrations of C-H and C-D bonds were not observed, the application of the product rule was impossible.

For species $B_{3g}$, the application of the product rule was also impossible because, while all normal vibrations were observed for 1,2,4,5-tetrachlorobenzene (assuming that $\nu_{27}$ is 184 $cm^{-1}$), some of those for 1,2,4,5-tetrachlorobenzene-$d_2$ were not observed.

Generally speaking, in the case of 1,2,4,5-tetrachlorobenzene, it was difficult to observe Raman lines of low intensity because of its poor solubility to the solvents. Furthermore, it is impossible, because of the mutual exclusion law, to look for these unobserved normal frequencies in the infrared absorption spectrum. Consequently, for some of the normal vibrations of this substance, there was no way of knowing their frequencies; this fact prevented the application of the product rule to verify the proposed assignment for most of the species. However, the clear explanation of observed weak lines as overtones or combinations appears to suggest that the proposed assignments might be the most reliable one at present.

## Summary

The Raman spectra of 1,2,4,5-tetrachlorobenzene and 1,2,4,5-tetrachlorobenzene-$d_2$ were measured in their dissolved states in methanol and carbon tetrachloride. The depolarization ratio of each Raman line was also observed qualitatively by the two-exposure method, using polaroid cylinders. On the basis of these experimental results, the assignment of normal vibrations was determined. The verification of the proposed assignments by means of the product rule was impossible for most of the species because of some unobserved normal vibrations. But, for species $A_g$, good agreement was obtained between the theoretical and observed values of the product of the frequencies for each substance, and the correctness of the assignment was thus verified.

The author would like to thank Dr. Y. Mashiko for helpful comments in connection with this paper.

*Government Chemical Industrial Research Institute, Tokyo*
*Shibuya-ku, Tokyo*

* The fact that the normal vibrations with low frequency were scarcely influenced by the substitution for hydrogen atoms of deuterium ones has been seen in the cases of *p*-dichlorobenzene and 1,3,5-trichlorobenzene (Refs. 5 and 6).

# *Mass-spectrometric Study on Ionization and Dissociation of Formaldehyde, Acetaldehyde, Acetone and Ethyl Methyl Ketone by Electron Impact*

By Ichiro KANOMATA

(Received March 28, 1961)

The ionization and dissociation of ethyl alcohol[1,2] and diethyl ether[3] molecules caused by electron impact have previously been studied by the present author. It has been concluded that the ionization takes place by the removal of one of the lone pair electrons of the oxygen atom and that the bond energy additivity can be applied to the ionized dissociation of these molecules by considering the trivalent character of the $O^+$.

In this report, the ionization and dissociation of formaldehyde, acetaldehyde, acetone and ethyl methyl ketone molecules, each of which has an oxygen atom as in the case of alcohols and ethers, are discussed in relation to the determination of appearance potentials of the ions produced by electron impact. In the case of formaldehyde and acetaldehyde, Reed[4,5] previously carried out an appearance potential study for the purpose of determining the dissociation energies of $D$(H–CHO), $D$(H–CO) and $D(CH_3$–CHO) and the ionization potential of CHO radical. Further, Morrison et al.[6] reported the determination of the ionization potentials of these two molecules. A similar study was also made by Kambara[7] with acetone.

## Experimental

The mass-spectrometer[8] used for this study is of a 90° sector type ($r$=12 cm.). The appearance potentials (AP) of ions were determined by the retarding potential difference method[9] (RPD). The apparatus[10] is nearly identical with Fox's[11], and its details have been described[12]. The ionization potentials and uppor break points on the ionization efficiency curves of $N_2$, CO and Kr obtained in the present study agree well with Fox's results.

The ionization potential of argon (15.77 eV.) was used as a standard for parent ions, although, owing to the RPD method, such a standard was not necessary in as much as the ion source was clean. Appearance potentials of fragment ions were determined by referring to the appearance potentials of parent ions.

The samples were chemically pure. Formaldehyde was prepared through the thermal decomposition of the polymer, and other sample gases were used after dehydration by calcium chloride.

## Results

The appearance ratios of the ions produced by 75 eV. electron impact and their appearance potentials are shown in Tables I and II respectively. Some ionization efficiency curves are illustrated in Fig. 1. Owing to the RPD method, characterized by a narrow distribution (0.2 eV.) of electron energy, fine structures appear in the ionization efficiency curves.

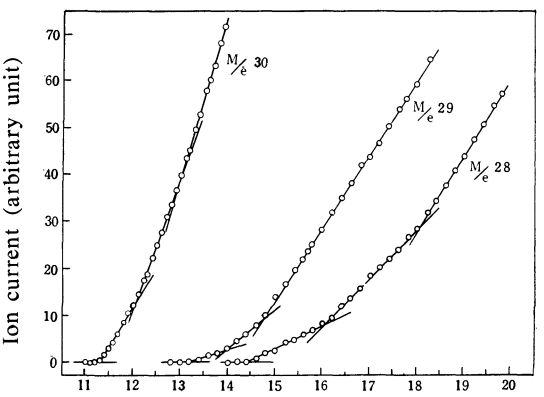



Fig. 1. Ionization efficiency curves of $HCHO^+$, $CHO^+$ and $CO^+$.

## Discussion

The production processes of ions are as follows:

*1) Formaldehyde*

**M/e=30** $HCHO^+$

The ion is a parent ion. Two distinct breaks exist in the ionization efficiency curve; the

1) T. Kambara and I. Kanomata, *Butsuri*, **4**, 71 (1949).
2) T. Kambara and I. Kanomata, *Hitachi Hyoron Rombun-shu*, No.7, 15 (1949).
3) I. Kanomata, This Bulletin, **34**, 1596 (1961).
4) R. E. Reed, *Trans. Faraday Soc.*, **53**, 1195 (1957).
5) R. E. Reed, ibid., **54**, 949 (1958).
6) H. Hurzeler, M. G. Inghram and J. D. Morrison, *J. Chem. Phys.*, **28**, 76 (1958).
7) T. Kambara, *J. Phys. Soc. Japan*, **5**, 84 (1950).
8) I. Kanomata, Y. Kaneko and T. Oguri, *Mass Spectroscopy*, No. 3, 12 (1954).
9) R. E. Fox, W. M. Hickam, T. Kjeldaas and D. J. Grove, *Phys. Rev.*, **84**, 859 (1951).
10) I. Kanomata, Y. Kaneko and T. Oguri, *Mass Spectroscopy*, No. 6, 46 (1956).
11) R. E. Fox et al., *Rev. Sci. Instr.*, **26**, 1101 (1955).
12) I. Kanomata, Y. Kaneko and T. Oguri, *J. Appl. Phys. Japan*, **30**, 502 (1961).

TABLE I. APPEARANCE RATIO

| M/e | Ion | Appearance ratio | | | |
|---|---|---|---|---|---|
| | | $(CH_3)(C_2H_5)CO$ | $(CH_3)_2CO$ | $CH_3CHO$ | HCHO |
| 72 | $C_4H_8O^+$ | 53.0 | | | |
| 58 | $C_3H_6O^+$ | | 37.4 | | |
| 57 | $C_3H_5O^+$ | 22.4 | 1.3 | | |
| 45 | $C_2H_5O^+$ | 0.5 | | | |
| 44 | $C_2H_4O^+$ | 2.4 | 2.3 | 64.5 | |
| 43 | $C_2H_3O^+$ | **100.0** | **100.0** | 37.8 | |
| 42 | $C_2H_2O^+$, $C_3H_6^+$ | 6.5 | 4.8 | 10.7 | |
| 41 | $C_2HO^+$, $C_3H_5^+$ | 2.4 | 2.4 | 4.8 | |
| 40 | $C_2O^+$, $C_3H_4^+$ | 1.2 | 1.3 | | |
| 39 | $C_3H_3^+$ | 4.3 | 3.7 | | |
| 38 | $C_3H_2^+$ | 2.4 | 1.8 | | |
| 37 | $C_3H^+$ | 2.3 | 1.4 | | |
| 30 | $CH_2O^+$ | 4.5 | | | 90 |
| 29 | $CHO^+$, $C_2H_5^+$ | 20.2 | 3.3 | **100.0** | **100** |
| 28 | $CO^+$, $C_2H_2^+$ | 7.4 | 14.6 | 13.4 | 29.8 |
| 27 | $C_2H_3^+$ | 5.4 | 4.8 | | |
| 26 | $C_2H_2^+$ | 1.3 | 3.1 | 7.1 | |
| 25 | $C_2H^+$ | | 7.7 | | |
| 16 | $CH_4^+$, $O^+$ | | | 7.0 | |
| 15 | $CH_3^+$ | 23.7 | 19.6 | 44.5 | |
| 14 | $CH_2^+$ | 5.1 | 2.7 | 16.0 | 5 |
| 13 | $CH^+$ | 1.6 | | 5.0 | 4 |
| 12 | $C^+$ | 1.7 | | | 3 |

TABLE II. APPEARANCE POTENTIAL (eV.)

| M/e | Ion | Appearance potential | | | |
|---|---|---|---|---|---|
| | | $(CH_3)(C_2H_5)CO$ | $(CH_3)_2CO$ | $CH_3CHO$ | HCHO |
| 72 | $(CH_3)(C_2H_5)CO^+$ | $9.88\pm0.03$, $10.5_3$ | | | |
| 58 | $(CH_3)_2CO^+$ | | $9.84\pm0.04$<br>$10.6_7\pm0.1$<br>$11.5_4\pm0.1$ | | |
| 57 | $C_2H_5CO^+$ | $10.81\pm0.04$, 12.0 | | | |
| 44 | $CH_3CHO^+$ | | | $10.31\pm0.04$<br>$11.2_4\pm0.1$<br>12.2 | |
| 43 | $CH_3CO^+$, $CH_2CHO^+$ | $11.10\pm0.03$, 12.4 | $10.94\pm0.04$<br>$11.9_4\pm0.1$<br>$12.9_4\pm0.1$ | $11.38\pm0.04$<br>$12.0_5\pm0.1$<br>$12.7\pm0.1$<br>$13.7\pm0.1$ | |
| 30 | | | | | $10.86\pm0.02$<br>$11.6_6\pm0.1$<br>$12.6_3\pm0.15$ |
| 29 | $C_2H_5^+$, $CHO^+$ | $12.71\pm0.03$, 15.2 | | $12.53\pm0.04$<br>$13.8\pm0.15$<br>$14.8\pm0.2$<br>$16.9\pm0.2$ | $12.90\pm0.07$<br>$13.6\pm0.1$<br>$14.2_5\pm0.1$ |
| 28 | $CO^+$, $C_2H_4^+$ | $14.4\pm0.2$, 15.6<br>17.4 | $14.6\pm0.2$<br>15.4<br>16.8 | $14.5_4\pm0.1$<br>15.3~15.6<br>$17.4\pm0.2$ | $14.1\pm0.05$<br>15.5~15.9<br>$18.3\pm0.3$ |
| 27 | $C_2H_3^+$ | | 16.9 | | |
| 15 | $CH_3^+$ | $15.4\pm0.2$ | $15.53\pm0.08$<br>$17.3\pm0.15$ | $14.8_2\pm0.05$ | |

energy values corresponding to the threshold and the breaks are $10.86\pm0.02$, $11.6_6\pm0.1$ and $12.6_3\pm0.15$ eV. respectively. Sugden and Price[13] determined the first, second and third ionization potentials of HCHO as $10.8\pm0.1$, $11.8\pm0.2$ and $13.1\pm0.2$ eV. respectively through the measurement of the total ion current produced by the impact of accelerated photo-electrons. The three values obtained by the present author may be expected to correspond to these ionization potentials.

The first ionization potential of 10.86 eV. agrees well with Reed's result of 10.85 eV. obtained by electron impact[4], with Watanabe's of 10.87 eV. by photon impact[14], and with the spectroscopic value of 10.88 eV.[15] It was pointed out by McMurry[16] in his report on absorption spectra that lone pair electrons of the oxygen atom in the molecule are at the highest occupied orbital. Therefore, the first ionization potential corresponds to the energy necessary for the removal of one of the lone pair electrons.

The second ionization potential of $11.6_6$ eV., on which there are very few data[13], may relate to the ionization caused by the removal of the $\pi$-electron of the C-O bond, as has been theoretically pointed out by Foster and Boys[17] and by Sugden.

The third ionization potential of $12.6_3$ eV. is thought to correspond to the removal of a $\sigma$-electron from the C-O bond, as has also been pointed out by Foster and Boys.

The values of the first ionization potentials of parent molecules of aldehyde and ketone obtained by the present author are listed in Table III with their dipole moments. It is shown that the ionization potentials decrease by 0.5 eV. in the order of HCHO, $CH_3CHO$ and $(CH_3)_2CO$, but that the ionization potential of $(CH_3)(C_2H_5)CO$ is a little larger than that of $(CH_3)_2CO$.

TABLE III. IONIZATION POTENTIAL AND DIPOLE MOMENT

| Molecule | Ionization potential, eV. | Dipole moment* ($D$) |
|---|---|---|
| HCHO | 10.86 | 2.27 |
| $CH_3CHO$ | 10.31 | 2.72 |
| $C_2H_5CHO$ | — | 2.73 |
| $(CH_3)_2CO$ | 9.84 | 2.85 |
| $(CH_3)(C_2H_5)CO$ | 9.88 | 2.79 |

* Dipole moment: Compiled by L. G. Wesson, a publication of the Technology press. M.I.T.

13) T. M. Sugden and W. C. Price, *Trans. Faraday Soc.*, **44**, 116 (1948).
14) K. Watanabe, *J. Chem. Phys.*, **26**, 542 (1957).
15) W. C. Price, ibid., **3**, 256 (1935).
16) H. L. McMurry, ibid., **9**, 231 (1941).
17) J. M. Foster and S. F. Boys, *Rev. Mod. Phys.*, **32**, 303 (1960).

The fact that ionization potentials decrease with the increase of the number of $CH_3$ group may be due to the effect of hyper-conjugation on the ionization of the oxygen atom. That is, it is considered, in general, that the hyper-conjugation effect is predominant when the carbon atom bound with the $CH_3$ group is in an $sp^2$ configuration. The fact that the ionization potential of ethyl methyl ketone is somewhat larger than that of acetone seems to indicate that the hyper-conjugation plays an important role in the present case.

These results closely relate to the change of the dipole moments of the molecules which can be explained by the hyper-conjugation. The ionization potential decreases with the increment of dipole moment.

**M/e=29** $H\text{-}C\equiv O^+$

Two breaks exist in the ionization efficiency curve of this ion. The values of the threshold and the breaks are 12.90, 13.6 and $14.2_5$ eV. respectively.

The appearace potential of the $R_1^+$ ion produced from the $R_1R_2$ molecule is expressed as follows when excess energy (excitation and kinetic energy of $R_1^+$ and/or $R_2$) is disregarded.

$$A(R_1^+)=I(R_1)+D(R_1-R_2)$$

If the ionization takes place by the removal of one of the lone pair electrons belonging to the oxygen atom in the molecule, the energy necessary for this reaction is 10.86 eV. By inserting the value of $D$(H-CHO) (79.3 kcal./mol. or 3.45 eV.) in the above equation, the ionization potential of $R_{29}$ is obtained as 9.45 eV. (12.9 eV.$-$3.45 eV.). This value is 1.4 eV. lower than the ionization potential of the formaldehyde molecule. This may be explained by the fact that the triple bond formation can be expected between C and $O^+$ in the ionized state of CHO, while, for the ionized state of formaldehyde, only the double bond can exist. That is, the formation of the triple bond brings the stabilization of 1.4 eV. on the $CHO^+$. The value of 1.4 eV. is considerably smaller than the stabilization energy of 2.35 eV. in the case of $H_2C=O^+-C_2H_5$ produced from diethyl ether[3].

The bond energy between C and O in formaldehyde is 144 kcal./mol.[18] If it is assumed that this bond energy is not affected by the ionization of the lone pair electron of the oxygen atom in the molecule, the total bond energy of $O^+$ in the $CHO^+$ is calculated as 176.2 kcal./mol. (144 kcal./mol. $+23.06\times1.4$ kcal./mol.).

18) Y. K. Syrkin and M. E. Dyatkina, "Structure of Molecules and the Chemical Bond", Interscience Publishers, New York.

The author has previously pointed out in his discussion of the ionized decomposition of diethyl ether[3] that the total bond energies of $O^+$ in $H_2C=O^+-C_2H_5$ and in $H-C\equiv O^+$ are 204 kcal./mol. and 183 kcal./mol. respectively. The present datum (176 kcal./mol.) agrees with the previous result (183 kcal./mol.) on the whole.

The reason why the energy of trivalence in the $H-C\equiv O^+$ is smaller than that in the $H_2C=O^+-C_2H_5$ is thought to be due to the fact that the former has a smaller number of resonance structures.

**M/e=28 $CO^+$**

The observed appearance potentials of this ion are 14.1±0.05, 15.5~15.9 and 18.3±0.3 eV. respectively.

The following two processes may be considered for the creation of $CO^+$ from formaldehyde:

$$HCHO+e \rightarrow CO^+ [19]+H_2+2e$$

$$HCHO+e \rightarrow CO^+ +2H+2e$$

The heat of reaction, or the appearance potential of $CO^+$, is calculated as 14.1 eV. for the former reaction and as 18.5 eV. for the latter. These values agree well with the appearance potentials obtained in the present work.

The break between 15.5~15.9 eV. in the ionization efficiency curve is vague; it sometimes appears, and sometimes it dose not. The value is close to the ionization potential of the nitrogen molecule, so it is thought that the break is due to the ionization of $N_2$, which exists as a background in the mass-spectrometer.

On the other hand, from the thermal decomposition experiments previously made by the present author, it has been found that HCHO is thermally unstable, that it decomposes easily to the CO molecule, and that the CHO radical can not be expected through the thermal decomposition. Therefore, it is also reasonable to consider that a part of formaldehyde gas thermally decomposes into CO gas on the tungsten filament of the ion source and that the CO molecule is ionized when it enters again into ionization chamber. According to this assumption, the first appearance potential of M/e=28 corresponds to the ionization potential of the CO molecule; the experimental result does not disagree with the above conclusion. In this case, the second breaks at 18.3 eV. may correspond to the excited state of the $CO^+$ ion.

19) F. H. Field and J. L. Franklin, "Electron Impact Phenomena and the Properties of Gaseous Ions", Academic Press Inc. Publishers, New York (1957).

*2) Acetaldehyde*

**M/e=44 $CH_3CHO^+$**

The observed value of 10.31 eV. is the first ionization potential of the acetaldehyde molecule. Two breaks exist, at $11.2_4$ and 12.2 eV. on the ionization efficiency curve.

Sugden and Price[13] have previously obtained observed values of 10.4±0.1, 11.3±0.1, 12.3±0.1 and 13.5±0.2 eV. through measurement of the total ionization current. The first three values agree well with the values of the present author. At the electron energy as large as 13.5 eV., the dissociation of molecular ion certainly takes place. So Sugden's method, which dealt with only the total ionization current, is unsuitable for the determination of the higher ionization potentials of the parent molecule.

As regards the classification of the ionization potentials of $CH_3CHO$, it is reasonable to consider, as in the case of $HCHO^+$, that 10.31 eV. corresponds to the energy necessary for the removal of one of the lone pair electrons of the oxygen atom in the molecule, that $11.2_4$ eV. is the energy needed for the removal of a $\pi$-electron in the C–O bond, and that 12.3 eV. is the energy needed for the removal of an $\sigma$-electron in the C–O bond in the molecule.

**M/e=43 $CH_3CO^+$ or $CH_2CHO^+$**

The appearance potential of this ion is 11.38 eV., and breaks exist at 12.1, 12.7 and 13.7 eV. The M/e=43 ion is produced by subtracting a hydrogen atom from the parent molecular ion. The bond dissociation energy of C–H in the aldehyde radical is thought to be smaller than that in the methyl radical; moreover, if a hydrogen atom is removed from the aldehyde radical, the stabilization of energy due to the formation of a triple bond of $O^+$ may take place. Accordingly it is reasonable to conclude that the hydrogen atom is removed from the aldehyde radical in the molecule. Thus, when relation $A(R43^+)=I(R43)+D(CH_3CO-H)$ and $D(CH_3CO-H)=3.48$ eV.[20] are used, $I(CH_3CO)$ is obtained as 7.90 eV.

This value is 2.41 eV. (55 kcal./mol.) smaller than the ionization potential of the parent molecule. It can be considered that the stabilization by 2.41 eV. takes place with the formation of a triple bond of $O^+$ in this ion. If it is assumed that the bond energy between C and O atoms in acetaldehyde is not affected by the ionization of one of the lone pair electrons of oxygen atom and that the bond energy additivity is applicable to such an ionic state, the total bond energy of $O^+$ in $CH_3C\equiv O^+$ is

20) J. S. Roberts and H. A. Skinner, *Trans. Faraday Soc.*, 45, 339 (1949).

obtained as 204.5 kcal./mol. (149.5+55 kcal.) by considering that the bond energy between C and O in acetaldehyde is 149.5 kcal.[18]

On the other hand, the total bond energy of $O^+$ in $CHO^+$ was calculated as 176 and 183 kcal. by the author, as has been described above. The increase of the stabilization in the $CH_3CO^+$ ion seems to be due to the resonance between different structures, for example, $H_3{\equiv}C{-}C{\equiv}O^+$ and $H^+H_2{=}C{=}O$.

As for the second and the third ionization potentials, no information has been obtained to interpret them.

**M/e=29** $CHO^+$

As $D(CH_3\text{-}CHO)$[20] is 71.5 kcal./mol. (3.10 eV.), $I(CHO)$ is calculated as 9.43 eV. from the observed appearance potential of the ion. This value agrees well with the value of $I(CHO)$ obtained from HCHO in this report, and it is only a little smaller than Reed's value of 9.87 eV.[4] In this case the stabilization energy is obtained as follows:

$I(CH_3CHO)-I(CHO)=0.88$ eV. (20.4 kcal./mol.). Therefore, the total bond energy of $O^+$ in $H{-}C{\equiv}O^+$, calculated under the assumptions described above, is 170 kcal./mol. (149.5 +20.4 kcal./mol.). This value should more closely agree with the 183 kcal./mol. obtained from diethyl ether and with the 176 kcal./mol. from formaldehyde. However, such a discrepancy among these values is unavoidable under these loose assumptions.

**M/e=28** $CO^+$ or $C_2H_4^+$

The ionization efficiency curve of M/e=28 has an uncertain break between 15.3~15.6 eV. and a rather distinct break at 17.4 eV. The heat of reactions, or the appearance potentials of $CO^+$ from $CH_3CHO$, are obtained, by considering the heat of the formation of $CO^+$ and of the other related molecules and radicals, as follows:

$$CH_3CHO+e \rightarrow CO^+ + CH_4 + 2e \qquad 13.8 \text{ eV.}$$
$$CH_3CHO+e \rightarrow CO^+ + CH_2 + H_2 + 2e \qquad 15.8 \text{ eV.}$$
$$CH_3CHO+e \rightarrow CO^+ + H + CH_3 + 2e \qquad 18.2 \text{ eV.}$$

The calculated values do not agree with the observed appearance potentials of the M/e=28 ion. However, as the appearance ratio of this ion is very small the influence of $N_2^+$ from the background in the mass-spectrometer could be expected to be greater, and so the apparent appearance potentials should also be greater than expected. By considering such a bad observing condition, the observed values may be said to correspond closely enough to the above-estimated reactions.

On the other hand, if the reaction is assumed as $CH_3CHO \rightarrow C_2H_4^+ + O$, the heat of reaction would be 15.3 eV.

**M/e=15** $CH_3^+$

The reaction to produce $CH_3^+$ is supposed as

$$CH_3CHO+e \rightarrow CH_3^+ [19] + CHO + 2e$$
or $$CH_3CHO+e \rightarrow CH_3^+ + CO + H + 2e$$

The ionization potential of $CH_3$ radical can be estimated from various data. The mean value of the data given from various ionized decompositions of organic compounds is 10.0 eV. Moreover, the energy for direct ionization of $CH_3$ radical is also 10.0 eV. If $I(CH_3)=10.0$ eV., $D(CH_3-CHO)=3.10$ eV.[20] and $D(H-CO)=1.13$ eV.[20], the heat of reaction for these processes is calculated as 13.10 eV. and 14.23 eV. respectively. The observed value agrees with the latter calculated value by assuming that the reaction has an excess energy of 0.6 eV.

*3) Acetone*

**M/e=58** $(CH_3)_2CO^+$

Two break points exist in the ionization efficiency curve. The values of the threshold and the break points are 9.84±0.04, $10.6_7$±0.1 and $11.5_4$±0.1 eV. respectively. It is thought that these values must be compared with Sugden and Price's values, 10.2±0.1, 11.3±0.1, 12.2±0.1 and 13.6±0.2 eV., which were obtained by the measurement of the total ionization current produced by the impact of accelerated photo-electrons. The discrepancy is large. Sugden's method seems, however, to be unsuitable for the determination of the higher ionization potentials of the parent molecule because of the formation of fragment ions. The first ionization potential of the molecule was determined as 9.92 and 9.89 eV. mass-spectrometrically, by Morrison et al.[21] and Omura et al.[22] respectively, as 9.69 eV. from the measurement of the total ionization current produced by photon impact by Watanabe[23], and as 9.705 eV. spectrometrically. It is reasonable that the first, second and third ionization potentials obtained are correlated, as in the case of formaldehyde, to the ionization of the lone pair electron of the oxygen atom, of the $\pi$-electron and of the $\sigma$-electron in the C-O bond respectively.

**M/e=43** $CH_3CO^+$

There are two breaks in the ionization efficiency curve. By considering that $D(CH_3-COCH_3)$ is 3.15 eV.[20], $I(CH_3CO)$ is obtained as

21) J. D. Morrison and A. J. C. Nicholson, *J. Chem. Phys.*, **20**, 1021 (1952).
22) I. Omura, K. Higasi and H. Baba, This Bulletin, **29**, 504 (1956).
23) K. Watanabe, *J. Chem. Phys.*, **26**, 542 (1957).

7.79 eV. from the relation of $I(CH_3CO) = A(CH_3CO^+) - D(CH_3-COCH_3)$. The value is 2.05 eV. smaller than the ionization potential of acetone. By assuming the structure of this ion as $CH_3C{\equiv}O^+$, in which the trivalency is satisfied, the value of 2.05 eV. is thought to be the stabilization energy through the formation of the triple bond.

The total bond energy of $O^+$ in the ion is calculated as 202 kcal./mol. by adopting 155 kcal./mol.[18] as the bond energy between C and O in acetone. The value 202 kcal./mol. agrees well with that calculated in the case of acetaldehyde.

**M/e=28** $CO^+$ or $C_2H_4^+$

The appearance ratio of this ion is small, and the influence of $N_2^+$ in background seems to be large, so the accuracy is not great. The heat of reaction for seven processes, which are all expected to produce M/e=28, is calculated as follows:

$(CH_3)_2CO+e \rightarrow CO^+$ [19] $+C_2H_6+2e$ 14.3 eV.

$(CH_3)_2CO+e \rightarrow CO^+ + H_2 + C_2H_4 + 2e$ 15.7 eV.

$(CH_3)_2CO+e \rightarrow CO^+ + 2(CH_3) + 2e$ 17.9 eV.

$(CH_3)_2CO+e \rightarrow C_2H_4^+$ [19] $+CO+H_2+2e$ 12.2 eV.

$(CH_3)_2CO+e \rightarrow C_2H_4^+ + HCHO + 2e$ 12.1 eV.

$(CH_3)_2CO+e \rightarrow C_2H_4^+ + CHO$[20] $+H+2e$ 15.5 eV.

$(CH_3)_2CO+e \rightarrow C_2H_4^+ + CO + 2H + 2e$ 16.6 eV.

However, a conclusion as to a process suitable for the production of the M/e 28 ion could not be obtained.

**M/e=27** $C_2H_3^+$

This ion must be $C_2H_3^+$. The calculated appearance potentials for this ion are as follows:

$(CH_3)_2CO+e \rightarrow C_2H_3^+$ [19] $+H_2+CHO+2e$ 14.3 eV.

$(CH_3)_2CO+e \rightarrow C_2H_3^+ + H + H_2 + CO + 2e$ 15.5 eV.

$(CH_3)_2CO+e \rightarrow C_2H_3^+ + 3H + CO + 2e$ 19.8 eV.

These values do not agree with the observed value. Therefore, the mechanism of the production of this ion can not be found.

**M/e=15** $CH_3^+$

The calculated appearance potentials of this ion are as follows:

$(CH_3)_2CO+e \rightarrow CH_3^+$ [19] $+CH_3CO$[20] $+2e$ 13.1 eV.

$(CH_3)_2CO+e \rightarrow CH_3^+ + CH_3 + CO + 2e$ 13.9 eV.

$(CH_3)_2CO+e \rightarrow CH_3^+ + CH + H_2 + CO + 2e$ 16.3 eV.

Accordingly, the second and the third reactions would be possible if the reactions take place with excess energies (kinetic and/or excitational energies) of 1.6 and 1.0 eV. respectively. In order to know the possible reactions conclusively, however, the kinetic energies of produced ions must be measured more precisely.

*4) Ethyl Methyl Ketone*

**M/e=72** $CH_3COC_2H_5^+$

There is a break in the ionization efficiency curve of this ion, and there seem to exist something like breaks above the first break point.

The first ionization potential is thought to be the energy by which the removal of one of the lone pair electrons of the O atom in the molecule takes place, as in the previous discussion of this report. The value obtained by the present author is a little larger than that of acetone. The fact is reasonably explained by assuming that hyper-conjugation is a little smaller in ethyl methyl ketone. This tendency was recognized also in a comparison of dipole moments.

**M/e=57** $C_2H_5CO^+$ or $CH_2CO^+CH_3$

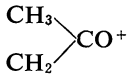
If this ion is assumed to be $C_2H_5CO^+$, the corresponding reaction is as follows:

$$CH_3COC_2H_5 + e \rightarrow C_2H_5CO^+ + CH_3 + 2e$$

Moreover, the structure of the ion produced should be $C_2H_5-C{\equiv}O^+$, which satisfies the trivalency as in the case of $HCO^+$ from formaldehyde and of $CH_3CO^+$ from acetaldehyde as well as acetone. $I(C_2H_5CO)$ is obtained as 7.66 eV. by use of the relations, $A(C_2H_5CO^+) = I(C_2H_5CO) + D(CH_3-COC_2H_5)$ and $D(CH_3-COC_2H_5) = 3.15$ eV[20]. This value is a little smaller than the value of $I(CH_3CO)$ obtained previously in this report.

From the value of $I(C_2H_5CO)$, the stabilization energy by the formation of triple bond of $O^+$ in this ion is calculated as 2.22 eV. (9.88 eV.−7.66 eV.). Hence, the total binding energy of $O^+$ in this ion is obtained as 206 kcal./mol. (157 kcal./mol.[18] + 23.06×2.22 kcal./mol.). This value agrees quite well with the

values for $CH_3C{\equiv}O^+$ obtained in the case of acetaldehyde and acetone.

On the other hand, if this ion is assumed to be  , the ionization potential of this ion is obtained as 7.20 eV., provided that the dissociation energy between C atoms in the ethyl radical in the molecule is assumed as 3.60 eV., which is the dissociation energy of ethane. However, in this case the stabilization due to the formation of the triple bond of $O^+$ in the ion can not take place. The value of 7.20 eV. is therefore thought to be as abnormally small as the ionization of the oxygen atom in the radical.

**M/e=43** $CH_3CO^+$

The assumed reaction for the production of this ion is as follows:

$$CH_3COC_2H_5+e \rightarrow CH_3CO^+ + C_2H_5 + 2e$$

$I(CH_3CO)$ is calculated as 7.97 eV. by the use of $D(CH_3CO-C_2H_5)=3.13$ eV.[20] This value of $I(CH_3CO)$ must, of course, agree with the values of $I(CH_3CO)$ in the cases of acetaldehyde and acetone. In this case also, by assuming 1.91 eV., which is the difference between this value and the ionization potential of the parent molecule, as the stabilization energy due to the formation of the triple bond of $O^+$ in the ion, 202 kcal. is obtained as total bond energy of the $O^+$ in the $CH_3$-$C{\equiv}O^+$ ion (157 kcal. $+23.06\times1.91$ kcal.). This also agrees quite well with the values previously described in this report. Furthermore, the heat of the formation of $CH_3CO^+$ is calculated, by using the value obtained above, as 174 kcal./mol. The value agrees well with the value cited above (cf. Ref. 19).

**M/e=29** $C_2H_5^+$ or $CHO^+$

If this ion is assumed to be $C_2H_5^+$, the heat of reaction, or the appearance potentials, are calculated as follows:

$$CH_3COC_2H_5+e \rightarrow C_2H_5^+ + CH_3CO + 2e \qquad 11.8\text{ eV.}$$

$$CH_3COC_2H_5+e \rightarrow C_2H_5^+ + CH_3 + CO + 2e \qquad 12.55\text{ eV.}$$

The second process seems to take place. In this case, the reaction by which the $CH_3CO$ radical is produced is impossible, as in the case of acetone.

On the other hand, if the ion is assumed to be $CHO^+$, energetically there is some possibility as follows:

$$CH_3COC_2H_5+e \rightarrow CHO^+ + C_3H_7 + 2e \qquad 12.1\text{ eV.}$$

$$CH_3COC_2H_5+e \rightarrow CHO^+ + C_2H_4 + CH_3 + 2e \qquad 13.2\text{ eV.}$$

**M/e=28** $CO^+$ or $C_2H_4^+$

As the appearance ratio of this ion is very small, a high degree of accuracy in measurement can not be expected. The heat of reaction for the following processes is calculated:

$$MeEtCO+e \rightarrow CO^+ + C_3H_8 + 2e \qquad 14.3\text{ eV.}$$

$$MeEtCO+e \rightarrow CO^+ + CH_4 + C_2H_4 + 2e \qquad 16.35\text{ eV.}$$

$$MeEtCO+e \rightarrow CO^+ + Me + Et + 2e \qquad 17.9\text{ eV.}$$

$$MeEtCO+e \rightarrow C_2H_4^+ + CH_4 + CO + 2e \qquad 11.65\text{ eV.}$$

$$MeEtCO+e \rightarrow C_2H_4^+ + CH_3CHO + 2e \qquad 11.8\text{ eV.}$$

$$MeEtCO+e \rightarrow C_2H_4^+ + CH_3 + CHO + 2e \qquad 14.9\text{ eV.}$$

$$MeEtCO+e \rightarrow C_2H_4^+ + CH_2 + H_2 + CO + 2e \qquad 11.6\text{ eV.}$$

If the second appearance potential of 15.6 eV. is rejected for the reason described previously in the discussion on the M/e=28 ion produced from formaldehyde, the first and the third processes will probably be possible.

**M/e=15** $CH_3^+$

The heat of the reaction of the following process is calculated as 15.05 eV.

$$CH_3COC_2H_5+e \rightarrow CH_3^+ + C_2H_5 + CO + 2e$$

The appearance potential of the $CH_3^+$ agrees with the above-calculated heat of reaction if the excess energy of 0.3 eV. is permitted in the above process.

On the other hand, if the reaction is assumed to be $CH_3COC_2H_5+e \rightarrow CH_3^+ + CH_3COCH_2+2e$, and the values of $I(CH_3)$ and $D(C\text{–}C)$ to be 10.0 eV. and 3.6 eV. respectively, the heat of the reaction of this process is obtained as 13.6 eV. This does not agree with the appearance potential.

The reason why the process through which $CH_3^+$ is produced from acetone has a relatively large excess energy, while the process through which $CH_3^+$ is produced from ethyl methyl ketone has a small excess energy, is not obvious.

*5) Heat of Formation of $CHO^+$, $CH_3CO^+$ and $C_2H_5CO^+$*

The appearance potential of an ion is the heat of the reaction by which the ion is formed if no excess energy is involved, and the process may be treated by the usual methods

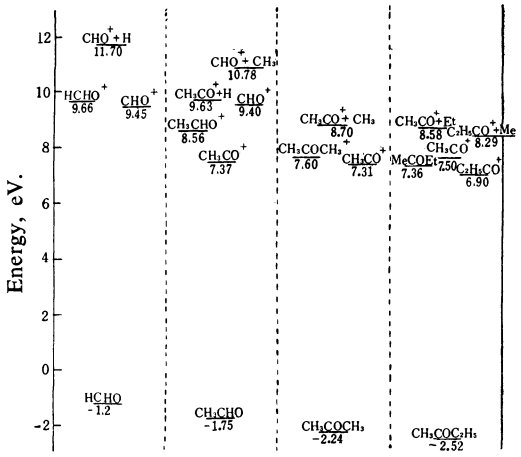



Fig. 2. Heat of formation of ions determined.

of thermochemistry. Thus, for the reaction $R_1R_2 \rightarrow R_1^+ + R_2$, the relation

$$A(R_1^+) = \Delta H_f(R_1^+) + \Delta H_f(R_2) - \Delta H_f(R_1R_2)$$

is given, provided that the reaction involves no excess energy.

By introducing the measured appearance potentials and the heat of formation of related molecules as well as radicals into the above relation, heats of formation of $CHO^+$, $CH_3CO^+$ and $C_2H_5CO^+$ are obtained, as shown in Fig. 2. The agreement between the heats of formation for the same ion produced from different molecules is very good, considering that the values are obtained through the appearance potential study.

## Summary

A study of the ionization and dissociation of formaldehyde, acetaldehyde, acetone and ethyl methyl ketone, all of which have an oxygen atom, was carried out through the appearance potential method. As appearance potentials were obtained by the retarding potential difference method, break points, which correspond to successively occurring ionization, appeared in the ionization efficiency curves of molecules and fragments. By considering the relation of energy, it is concluded that the ionization of the molecule takes place at first by the removal of one of the lone pair electrons of oxygen atom in the molecule, and that, in the formation of a fragment ion including an oxygen atom, dissociation takes place to create a triple bond, satisfying the trivalency of $O^+$ in the fragment ions.

The total bond energy of $O^+$ in $CH_3C{\equiv}O^+$ and $C_2H_5C{\equiv}O^+$ are calculated as about 200 kcal./mol., while in $HC{\equiv}O^+$ it is 170~180 kcal./mol. as in the case of diethyl ether reported previously. This fact may be explained by the number of resonance structures related.

The second and the third ionization potentials are thought to correspond to the removal of the $\pi$-electron and $\sigma$-electron in C-O bond respectively. The heat of formation of $CHO^+$, $CH_3CO^+$ and $C_2H_5CO^+$ are obtained from various reactions.

The author wishes to express his gratitude to Professor K. Kido and Professor T. Titani for their continual guidance and encouragement throughout this work, and to Professor K. Hirota of Osaka University and Professor S. Nagakura of the Institute for Solid State Physics, the University of Tokyo, for their kind advice and valuable discussion. He is also greatly indebted to Mr. Y. Kaneko and Mr. T. Oguri for their earnest co-operation.

*Department of Physics*
*Faculty of Science*
*Tokyo Metropolitan University*
*Setagaya-ku, Tokyo*

# SHORT COMMUNICATIONS

## *The Polymerization of γ-Methyl-L-glutamate-N-carboxyanhydride Initiated with Acetic Acid*

By Tôru OKUDA and Setsuji SAKURAI

(Received August 26, 1961)

The rate of polymerization of *N*-carboxyanhydrides (NCAs) of α-amino acids and the molecular weight of polypeptides formed vary widely with the characteristic of reaction medium and initiator[1-3]. We have found that for the polymerization of γ-methyl-L-glutamate-NCA, acetic acid which has little or no initiating ability in one solvent, does act as an initiator in another solvent. Thus, when the NCA was dissolved in chloroform ($1.07\times10^{-1}$ mol. $l^{-1}$) containing acetic acid ($5.35\times10^{-2}$ mol. $l^{-1}$), rapid polymerization occurred, and completed within 130 min., while in dioxane solution no appreciable reaction was observed. Addition of dioxane (10% by volume) to the chloroform solution of the NCA caused an induction period of approximate 70 min. and a depression in rate (See Fig. 1). The evolution of carbon dioxide upon dissolution of the NCA in acetic acid was much slower than in the system chloroform-acetic acid. From the reaction mixture in acetic acid we were able to isolate only terminal-free low molecular weight peptide, which, according to the results of elementary analysis and optical rotation in dichloroacetic acid, had no acetyl group and was composed of 3 units of γ-methyl-L-glutamate residue. Found: C, 47.1; H, 6.71; N, 9.53. Calcd. for $(C_6H_9O_3N)_3\cdot H_2O$: C, 48.3; H, 6.49; N, 9.40%. $[\alpha]_D^{23}=17°$ (*c* 1.9). So far, no other products such as acetylated derivatives, diketopiperazine or cyclic peptide have been detected.

The fact that the degree of polymerization of the final polymer obtained in the polymerization in chloroform is much higher ($[\eta]=0.98$, $\overline{DP}=500\sim600$) than that expected from the initial NCA-initiator ratio of 2 indicates that only a small part of acetic acid was utilized as a true initiator. Therefore, the behavior of acetic acid as an initiator in chloroform solution seems to resemble somewhat that of tertiary amine.

Fig. 2 shows that two successive propagation rates exist. Similar change in propagation rate was observed in polymerizations of other NCAs[3-8] and explained either by conformational change (random or β-form to α-helix)

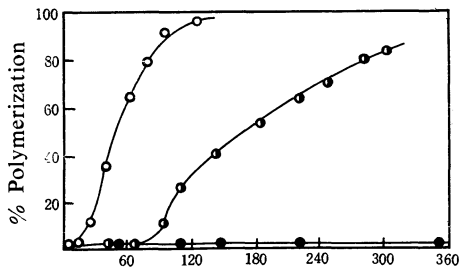



Fig. 1. Time-conversion curves for polymerization of γ-methyl-L-glutamate-NCA ($1.07\times10^{-1}$ mol. $l^{-1}$) indicated with acetic acid ($5.35\times10^{-2}$ mol. $l^{-1}$) in solution at 30°C.
—○—: In chloroform, —◑—: in chloroform-dioxane (9:1 by volume), —●—: in dioxane.

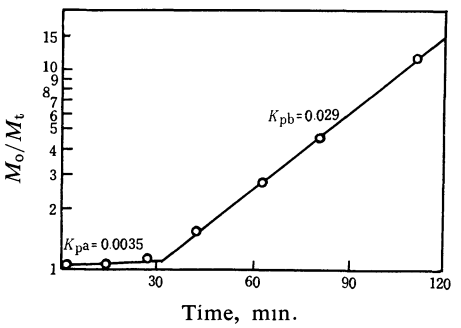



Fig. 2. The polymerization of γ-methyl-L-glutamate-NCA in chloroform at 30°C, initiated with acetic acid under the condition given in Fig. 1. The values of [NCA] initially and at time *t* are denoted by $M_0$ and $M_t$, respectively.

1) E. R. Blout and R. H. Karlson, *J. Am. Chem. Soc.*, **78**, 941 (1956).
2) C. H. Bamford, A. Elliott and W. E. Hanby, "Synthetic polypeptides", Academic Press Inc., New York, N. Y. (1956), p. 92.
3) R. D. Lundberg and P. Doty, *J. Am. Chem. Soc.*, **79**, 3961 (1957).
4) P. Doty and R. D. Lundberg, ibid., **78**, 4810 (1956).
5) T. Okuda, A. Akamatsu and Y. Takeda, unpublished data.
6) D. G. H. Ballard and C. H. Bamford, *J. Chem. Soc.*, **1959**, 1039.
7) H. Weingarten, *J. Am. Chem. Soc.*, **80**, 352 (1958).
8) J. D. Coombes and E. Katchalaski, ibid., **82**, 5280 (1960).

in the growing polypeptide chain[4,7], or by gel effect due to precipitation of polymer or gelation[6]. In the present case, after a slow propagation rate, when about one-tenth of the NCA had been consumed the propagation shifted to a faster rate. Since the average DP of the polymer was found to be 500~600, the transition occurred when the growing polypeptide chain had reached a $\overline{DP}=50\sim60$. Because this value exceeds the one necessary for the conformational transition of poly-$\gamma$-methyl-L-glutamate (15~25 residues[5]) the gel effect might be more responsible for occurrence of the two successive propagation rates.

We wish to express our thanks to Drs. H. Oeda and T. Yoshida for permission to publish the present work.

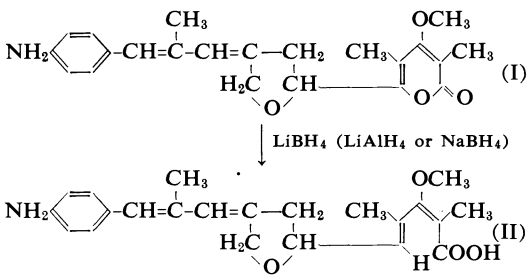
*Central Research Laboratory*
*Ajinomoto Co., Inc.*
*Kawasaki*

## *Reduction of α-Pyrones with Complex Metal Hydrides*

By Kiyoyuki YAMADA, Mitsuo ISHIZAKA and Yoshimasa HIRATA

(Received November 21, 1961)

During the course of the structural investigation of aureothin[1], we obtained several derivatives that were regarded as products of unusual reactions. One of the remarkable examples is "aminol H" (II) which was produced from isoaureothamine (I) by treatment with various complex metal hydrides[2].




In order to examine whether or not the occurrence of this rather unexpected reduction is due to the complexity of the other part of the molecule, reduction of simple α-pyrones with complex metal hydrides was carried out.

4, 6-Dimethyl-α-pyrone, when treated with lithium aluminum hydride in tetrahydrofuran, gave β-methylsorbic acid, m. p. 97°C[3] (Found: C, 67.00; H, 8.10. Calcd. for $C_7H_{10}O_2$: C, 66.46; H, 7.99%. Ultraviolet spectrum, $\lambda_{max}^{EtOH}$, 260 mμ, log ε, 4.0). Reduction of 4, 6-dimethyl-α-pyrone with lithium borohydride in a similar condition also gave the same acid, whereas no reaction took place with sodium borohydride.

Further, lithium aluminum hydride reduction of 4-methoxy-6-methyl-α-pyrone, which is a good model compound for isoaureothamine (I), yielded β-methoxysorbic acid (III) (m. p. 147~149°C (decomp.)[4]. Found: C, 59.17; H, 7.13. Calcd. for $C_7H_{10}O_3$: C, 59.14; H, 7.09%. Ultraviolet spectrum, $\lambda_{max}^{EtOH}$, 264 mμ, log ε, 4.1) and a neutral product (b. p. 101~104°C/16 mmHg. One methoxyl group. Ultraviolet spectrum; $\lambda_{max}^{EtOH}$, 239 mμ) which was shown to be identical with 3-methoxy-2, 4-hexadienol (IV) obtained from β-methoxysorbic acid by lithium aluminum hydride reduction.

The relative amounts of the two products, III and IV, are considerably dependent on the reaction conditions (temperature, manner of addition, etc.), the details of which will be reported elsewhere. Thus, it was established that generally the hydrogenolysis of the 1, 6-linkage of the α-pyrone ring occurs in the reduction using complex metal hydrides.

*Chemical Institute*
*Faculty of Science*
*Nagoya University*
*Chikusa-ku, Nagoya*

1) K. Yamada, H. Nakata and Y. Hirata, *J. Chem. Soc. Japan, Pure Chem. Sec. (Nippon Kagaku Zasshi)*, **81**, 340 (1960).

2) K. Yamada, T. Naito, K. Okuhara, H. Nakata and Y. Hirata, This Bulletin, 33, 1303 (1960).

3) H. Burton and C. K. Ingold, *J. Chem. Soc.*, **1929**, 2022; R. Kuhn and M. Hoffer, *Ber.*, **65**, 651 (1932).

4) E. R. H. Jones and M. C. Whiting, *J. Chem. Soc.*, **1949**, 1423; H. B. Henbest and E. R. H. Jones, ibid., **1950**, 3628.